REVIEW

The Effect of α-Linolenic Acid and Linoleic Acid on the Growth and Development of Formula-Fed Infants: A Systematic Review and Meta-analysis of Randomized Controlled Trials

Tuesday Udell[a], Robert A. Gibson[b], Maria Makrides[c],*, and the PUFA Study Group

[a]Department of Paediatrics & Child Health, Flinders University, Bedford Park, South Australia, 5042, Australia; [b]Child Nutrition Research Centre, Child Health Research Institute, Flinders Medical Centre, Bedford Park, South Australia, 5042, Australia; and [c]Child Nutrition Research Centre, Child Health Research Institute, and Department of Paediatrics, University of Adelaide, Women's & Children's Hospital, North Adelaide, South Australia, 5006, Australia

ABSTRACT: This systematic review and meta-analysis aimed to evaluate the effect of modifying 18-carbon PUFA [18-C PUFA: α-linolenic acid (ALA, 18:3n-3) and linoleic acid (LA, 18:2n-6)] in the diets of term and preterm infants on DHA (22:6n-3) status, growth, and developmental outcomes. Only randomized controlled trials (RCT) involving formula-fed term and preterm infants, in which the 18-C PUFA composition of the formula was changed and growth or developmental outcomes were measured, were included. Differences were presented as control (standard formula) and treatment (18-C PUFA-supplemented formula). Primary analyses for term infants were 4 and 12 mon and for preterm infants 37–42 and 57 wk postmenstrual age. Five RCT involving term infants and three RCT involving preterm infants were included in the systematic review. Infants fed ALA-supplemented formula had significantly higher plasma and erythrocyte phospholipid DHA levels than control infants. There was no effect of ALA supplementation on the growth of preterm infants. In term infants, ALA supplementation was associated with increased weight and length at 12 mon, which was at least 4 mon after the end of dietary intervention. Developmental indices of term infants did not differ between groups. There was a transient improvement in the retinal function of preterm infants fed ALA-supplemented diets compared with controls. The findings suggest that ALA-supplemented diets improve the DHA status of infants. Further studies are needed to provide convincing evidence regarding the effects of ALA supplementation of formula on infant growth and development.

Paper no. L9673 in *Lipids 40*, 1–11 (January 2005).

DHA (22:6n-3) is a major structural lipid of the brain and can be derived endogenously from α-linolenic acid (ALA, 18:3n-3).

The enhanced development of breast-fed infants relative to formula-fed infants is thought to be due, in part, to the presence of DHA in breast milk (1–3). In the past, infant formulas were not supplemented with DHA, and levels of its precursor, ALA, were low relative to the high levels of the n-6 FA linoleic acid (LA, 18:2n-6). This imbalance in formula fats in favor of LA was largely ignored until animal studies demonstrated that dietary insufficiency of ALA resulted in lower levels of DHA in the brain and retina and loss of visual function (4–6). These studies were the catalyst for clinical intervention trials of both preformed long-chain PUFA (20- and 22-carbon LCPUFA) and variations in the balance of ALA and LA to assess the effect on infant DHA status and visual and neurodevelopment. An early study involving preterm infants that investigated both strategies suggested that a dietary supply of n-3 LCPUFA was more effective than ALA enrichment in enhancing DHA status and visual function to levels comparable with those of breast-fed infants (7,8). Despite the preliminary nature of this pioneering trial, relatively little work has since focused on modifying 18-carbon PUFA (18-C PUFA: ALA and LA) blends in infant formulas as a strategy for increasing infant DHA status and improving developmental outcomes (9–15; Jensen, C.L., Chen, H., Prager, T.C., Fraley, J.K., Anderson, R.E., and Heird, W.C., unpublished report).

A systematic review of trials involving 18-C PUFA is important because levels of 18-C PUFA in formulas have varied over the last 20 yr with little direct evaluation. Meanwhile, formulas containing LCPUFA have become widely available but remain expensive, a possible barrier to their use by some population groups. There is a need to assess the efficacy of simply modifying 18-C PUFA blends on DHA status; function, as measured by cognitive and visual outcomes; and safety, as assessed by growth.

With this in mind, we undertook a systematic review and meta-analysis of randomized controlled trials (RCT) to determine the effect of 18-C PUFA-enriched formula on the growth and development of term and preterm infants. Our review included trials that varied the ALA and/or LA content of the formula. Primary outcomes were weight, length, head circumference, and indices of neurological development. We also examined the

treatment effect on plasma and erythrocyte phospholipid DHA, EPA (20:5n-3), and arachidonic acid (AA, 20:4n-6) levels.

METHODS

Search strategy. A search of the Cochrane Controlled Trials Register and MEDLINE using the key words: *infant AND formula* and one of the following—*linoleic acid, linolenic acid,* or *polyunsaturated fatty acids*—identified relevant trials. In MEDLINE, search limits were *randomized controlled trial* and *human*. Hand-searching of abstracts and conference proceedings was performed. The last literature search was completed in May 2004. Eight trials involving term infants and three trials involving preterm infants were identified as potentially eligible for inclusion and were retrieved for review.

(i) Selection of trials. Trials were eligible for inclusion if they had a randomized design, the ALA and/or LA level of the formula fat was varied but other nutrients in the formula remained the same, and growth or development were reported as an outcome measure. For trials involving term infants, the test formula was to have commenced within 14 d of birth, and the diet duration was at least 8 wk to allow the intervention to have an effect on tissue status. For trials involving preterm infants, the test formula was to have been fed for at least 3 wk based on the usual practice of not feeding preterm formula beyond hospital discharge. Infants consuming test diets that contained LCPUFA were excluded. From the eight RCT involving term infants, two were excluded because the test diet was commenced after the infants were 14 d old (16,17) and another because multiple nutrient components of the formula were modified (19). The five eligible RCT involving term infants were published in seven separate papers (9–13,19,20). The three RCT involving preterm infants were published in eight separate papers (7,8,14,15, 21–23; Jensen, C.L., Chen, H., Prager, T.C., Fraley, J.K., Anderson, R.E., and Heird, W.C., unpublished report).

(ii) Data abstraction and collection. Data abstraction forms were compiled and authors were contacted when published details were unclear. Where growth, development, or FA mean data were assessed but not published at designated time-points, these unpublished data were obtained from the investigators. Unpublished data were received for three trials involving term infants (10,11,13) and two trials involving preterm infants (22; Jensen, C.L., Chen, H., Prager, T.C., Fraley, J.K., Anderson, R.E., and Heird, W.C., unpublished report).

Statistical analysis. Primary analyses for trials involving term infants were made at 4 mon (a time when solid foods were traditionally introduced) and 12 mon of age (when formula feeding often ends). Where data were available, growth, development, and FA status at other time points were included to explore short- and long-term effects. Primary comparisons of trials involving preterm infants were made at 37–42 wk (term) and 57 wk postmenstrual age (PMA). Comparisons were also made at other assessment points where data were available. For trials that included more than two test diets, the control group was specified as the one most closely matching the LA-to-ALA

balance of that found in current commercially available formulas of around 10 to 1.

Meta-analyses were computed using the Metaview program available in Review-Manager 4.2 (Cochrane Collaboration). A fixed-effects model was used where there was no significant heterogeneity, whereas a random-effects model was used if significant heterogeneity existed. Each study was weighted in the meta-analysis according to the SD and the number of infants. Data were reported as weighted mean difference (WMD) with 95% confidence intervals (CI). In a supplementary analysis, mean FA data of term infants at 4 mon of age were plotted as a function of ALA levels in the test formulas (11,19). In the graphs, polynomial regression curves were fitted to the FA data and r^2 values reported.

RESULTS

Trials involving term infants. (i) Summary of included studies. Five trials involving term infants, conducted in North America ($n = 4$) and Australia ($n = 1$), were included in this review (9–13,19,20) (Table 1). Three trials intervened with formula enriched with ALA (between 3.2 and 4.8 wt%), thus also lowering the LA/ALA ratio (11–13,19,20), whereas two trials tested formula enriched with both LA (34 wt%) and ALA (5 wt%) and kept the LA/ALA ratio constant (9,10). None of the included trials tested reducing the LA level of the formula to lower the LA/ALA ratio. Variations in the balance of LA and ALA in the fats of the formulas were obtained through blending vegetable oils including coconut, corn, soy, canola, safflower, sunflower, and palm. The trial by Innis *et al.* (10) included four groups of formula-fed infants that were not included in the analysis because the test formulas contained DHA. The most commonly used developmental outcomes were visual function (9,11,13) and global neurodevelopment (11,13). Visual function was measured by Teller acuity cards (9), visual evoked potential (VEP) acuity (11), and VEP latency (to checkerboard patterns subtending a visual angle of 30-min arc) (11,13). Neurodevelopment was assessed by the Bayley Scales of Infant Development (BSID) First (11) or Second Edition (20). The BSID included both the mental developmental index and psychomotor developmental index. Other developmental assessments included the Clinical Adaptive Test (CAT), Clinical Linguistic and Auditory Milestone Scale (CLAMS), and Gross Motor Scale (GM) of the Revised Gesell Developmental Inventory (20). Developmental quotients (DQ) were determined for language development (CLAMS DQ), visual problem-solving ability (CAT DQ), overall cognition (the mean of CLAMS and CAT DQ), and gross motor development (GM DQ) (20). Growth was measured by standard procedures in all trials.

All trials reported a randomized design with two reporting adequate concealment of allocation (11,13,19,20). Makrides *et al.* (11) and Jensen *et al.* (13,19,20) reported blinding of both parents and trial staff. All trials had relatively small sample sizes. Innis *et al.* (9) reported <20% attrition of infants through to 3 mon of age, and Makrides *et al.* (11) reported <20% attrition through to 4 mon of age.

TABLE 1
Characteristics of Randomized Trials Involving Formula-Fed Term Infants

Trial	PUFA intervention[a]	Number of infants enrolled	Number of infants completing trial (attrition rate)	Growth assessment age (mon)	Neurodevelopment assessment	Visual function assessment[b]	FA assessment age (mon)	Comments[c]
Treatment: Increased ALA level while LA held constant								
Ponder *et al.*, 1992, USA, 2 sites (12)	C - LA/ALA, 31.4/0.8; T - LA/ALA, 34.2/4.8; diet duration = 2 mon	Not stated	Through to 2 mon: C = 14 (unknown) T = 11 (unknown)	0, 1, 2	Not assessed	Not assessed	0, 1, 2	Trial had BM reference group.
Makrides *et al.*, 2000, Australia, 2 sites (11)	C - LA/ALA, 16.9/1.7; T - LA/ALA, 16.6/3.3; diet duration = 8 mon	C = 36 T = 37	Through to 4 mon: C = 30 (17%) T = 30 (19%)	0, 1.5, 4, 8, 12, 24	BSID I (12,24)[d]	VEP_act (4,8) VEP_lat (4)	0, 1.5, 4, 8	Trial had BM reference group.
Jensen *et al.*, 1996 Jensen *et al.*, 1997 Voigt *et al.*, 2002, USA (13,19,20)	C - LA/ALA, 16.5/1.7 T1 - LA/ALA, 17.6/3.2 T2 - LA/ALA, 17.3/0.95 T3 - LA/ALA, 15.6/0.4; diet duration = 4 mon	C = 20 T1 = 20 T2 = 20 T3 = 20	Through to 4 mon: C = 16 (20%) T1 = 13 (35%) T2 = 17 (85%) T3 = 17 (85%)	0, 0.75, 2, 4, 8, 12	BSID II, CAT, CLAMS, GM (12)	VEP_lat (4, 8)	0, 0.75, 2, 4	Trial had BM reference group.
Treatment: Level of ALA + LA increased but LA/ALA ratio kept constant								
Innis *et al.*, 1996, USA, 4 sites (10)	C - LA/ALA, 20.5/2.1; T - LA/ALA, 34.2/4.8; diet duration = 4 mon	Not stated	Through to 4 mon: C = 21 (unknown) T = 16 (unknown)	0, 1, 2, 4	Not assessed	Not assessed	0, 1, 2, 4	Formulas with LCPUFA excluded. Trial had BM reference group.
Innis *et al.*, 1997, North America, 7 sites (9)	C-LA/ALA, 18.0/1.9; T-LA/ALA, 34.2/4.7; diet duration = 3 mon	C = 69 T = 70	Through to 3 mon: C = 59 (15%) T = 57 (19%)	0, 1, 2, 3	Not assessed	TAC (3)	0, 3	Trial had BM reference group.

[a]LA, linoleic acid (18:2n-6); ALA, α-linolenic acid (18:3n-3); C, standard infant formula (assigned as the control by the researchers); T, infant formula (assigned as the treatment by the researchers) supplemented with α-linolenic acid; LA and ALA values expressed as % total FA.
[b]Age (mon) in parentheses; TAC, Acuity Cards procedure from Teller Acuity Card Handbook; VEP_act, visual evoked potential (acuity); VEP_lat, visual evoked potential (latency); BSID I, Bayley Scales of Infant Development First Edition; BSID II, Bayley Scales of Infant Development Second Edition; CAT, Clinical Adaptive Test; CLAMS, Clinical Linguistic and Auditory Milestone Scale; GM, Gross Motor Scale of the Revised Gesell Developmental Inventory;
[c]BM, breast milk; DHA, 22:6n-3; LCPUFA, long-chain PUFA.
[d]Additional data, which were not published in the paper, were obtained from the author.

TABLE 2
Weight, Length and Head Circumference of Term Infants Fed ALA-Enriched Formulas Compared with Control

Outcome	Jensen et al. (13) treatment, control[a,b]	Makrides et al. (11) treatment, control[a,b]	Ponder et al. (12) treatment, control[a]	Total number of infants (treatment, control)	Mean difference [95% CI][c]	Z[d]
Weight (kg)						
2 mon	5.00(0.57), 5.13(0.50)	—	5.10(0.49), 5.15(0.53)	24, 30	−0.09[−0.37, 0.19]	0.63(0.53)
4 mon	6.21(0.64), 6.61(0.65)	6.64(0.74), 6.30(0.70)	—	43, 46	0.06[−0.23, 0.35][e]	0.43(0.67)
12 mon	9.43(0.92), 9.34(2.53)	10.34(1.21), 9.64(0.96)	—	39, 42	0.62[0.09, 1.15]	2.30(0.02)*
24 mon	—	12.97(1.29), 12.47(1.56)	—	22, 26	0.50[−0.31, 1.31]	1.22(0.22)
Length (cm)						
2 mon	57.0(2.5), 56.6(2.1)	—	56.5(2.0), 56.8(1.9)	24, 30	0.01[−1.13, 1.15]	0.02(0.98)
4 mon	61.9(2.8), 61.8(2.5)	62.8(2.4), 61.6(2.0)	—	43, 46	0.93[−0.03, 1.90]	1.90(0.06)
12 mon	75.9(3.1), 75.9(3.6)	77.0(2.9), 74.8(2.2)	—	39, 42	1.78[0.58, 2.97]	2.92(0.004)*
24 mon	—	88.9(3.3), 87.8(3.1)	—	23, 26	1.04[−0.76, 2.84]	1.13(0.26)
Head circumference (cm)						
2 mon	38.3(1.0), 38.3(1.2)	—	38.5(0.7), 38.9(1.5)	24, 30	−0.18[−0.77, 0.41]	0.60(0.55)
4 mon	40.8(1.1), 40.9(1.1)	41.8(1.0), 41.3(1.1)	—	43, 46	0.2[−0.15, 0.74]	1.29(0.20)
12 mon	—	47.1(1.2), 46.6(1.3)	—	28, 29	0.51[−0.13, 1.15]	1.57(0.12)
24 mon	—	49.6(1.2), 49.0(1.4)	—	22, 26	0.59[−0.14, 1.32]	1.59(0.11)

[a]Mean and SD.
[b]Some figures were taken from unpublished data.
[c]Fixed effects estimate of the weighted mean difference in growth between groups. Positive value indicates greater mean score for treatment group relative to control group.
[d]Test of overall effect of weighted mean difference; associated P value in parentheses. A P value < 0.05 is highlighted with an asterisk (*).
[e]Random effects estimate of the weighted mean difference in growth between groups. Positive value indicates greater mean score for treatment group relative to control group.

(ii) Trials involving enrichment with ALA. The trials of Jensen et al. (13,19,20), Makrides et al. (11), and Ponder et al. (12) tested the effect of enhancing the level of ALA while holding the level of LA constant. There were no significant differences in weight, length, and head circumference between groups except at 12 mon of age (Table 2). At this age the infants in the treatment group were longer (WMD: 1.78 cm, 95% CI: 0.58, 2.97; P = 0.004; n = 81) and heavier (WMD: 0.62 kg, 95% CI: 0.09, 1.15; P = 0.02; n = 81) than infants in the control group (Table 2). It is interesting to note that these effects were found at least 4 mon after dietary intervention had ceased, and infants were consuming sources of dietary FA from other milks and solids.

Despite randomization, the treatment group in Makrides et al. (11) was significantly heavier at birth than the control group. This had little effect on the pooled data, and no differences were seen between the birth weight of the control and treatment groups overall (WMD: 0.03 kg, 95% CI: –0.13, 0.18; P = 0.71; n = 122). At birth, there was also no difference in length (WMD: 0.34 cm, 95% CI: –0.21, 0.88; P = 0.23; n = 127) or head circumference (WMD: 0.04 cm, 95% CI: –0.38, 0.46; P = 0.85; n = 127) between groups.

Few infants were assessed for global neurodevelopmental outcomes, and there were no common assessments (Table 3). No difference could be detected between control and treatment groups for any outcome. There were also no differences in visual function between the groups at 4 or 8 mon of age as assessed by VEP latency and acuity (Table 3).

The level of DHA in plasma phospholipids of infants in the ALA-enriched group was consistently higher than in the con-trol group from 2 mon of age and higher in erythrocyte phospholipids from 4 mon of age (Table 4). In the supplementary analysis including all available data at 4 mon of age, increasing ALA dose was associated with increased levels of plasma and erythrocyte phospholipid DHA (Fig. 1). However, dietary ALA enrichment did not result in the DHA levels seen in breast-fed infants (Figs. 1A and 1B). ALA enrichment increased the level of plasma phospholipid EPA from 4 mon of age and erythrocyte phospholipid EPA from 2 mon of age (Table 4), and values reached those seen in breast-fed infants when ALA enrichment was approximately 3% of total FA (Figs. 1C and 1D). ALA supplementation lowered AA in plasma phospholipids at 2 mon of age and erythrocyte phospholipid AA levels at 4 mon of age compared with infants in the control group (Table 4). As dietary ALA increased, infant plasma and erythrocyte AA decreased (Figs. 1E and 1F). Erythrocyte AA levels of formula-fed infants matched those of breast-fed infants.

(iii) Trials involving enrichment with both ALA and LA. The data from the two included studies relating to growth, development, or LCPUFA status could not be combined because one trial did not measure outcomes after 3 mon (9). There were no differences in growth at 4 mon, visual acuity at 3 mon, or LC-PUFA status between the groups (Table 5).

Trials involving preterm infants. Summary of included studies. Three trials involving preterm infants conducted in North America (n = 2) and Europe (n = 1) were included in this systematic review (7,8,14,15,21–23; Jensen, C.L., Chen, H., Prager, T.C., Fraley, J.K., Anderson, R.E., and Heird, W.C., unpublished report) (Table 6). All trials involved enrichment of formula fats with ALA (2.0–3.2 wt%) relative to the control

TABLE 3
Developmental Outcomes of Term Infants Fed ALA-Enriched Formulas Compared with Control

Outcome	Voigt et al. (20) and Jensen et al. (13) treatment, control[a,b]	Makrides et al. (11) treatment, control[a,b]	Total number of infants (treatment, control)	Mean difference [95% CI][c]	Z[d]
Neurodevelopment[e]					
Bayley I MDI					
12 mon	—	111(13), 109(15)	28, 29	1.99[−5.45, 9.43]	0.52(0.60)
24 mon	—	106(20), 106(19)	24, 26	0.42[−10.45, 11.29]	
Bayley I PDI					
12 mon	—	97(18), 104(18)	28, 29	−6.55[−15.98, 2.88]	1.36(0.17)
24 mon	—	104(15), 108(18)	24, 26	−4.27[−13.52, 4.98]	0.90(0.37)
Bayley II MDI					
12 mon	101(11), 101(11)	—	11, 12	−0.50[−9.17, 8.17]	0.11(0.91)
Bayley II PDI					
12 mon	96(11), 94(12)	—	11, 12	2.70[−6.70, 12.10]	0.56(0.57)
CAT DQ					
12 mon	105(5), 106(7)	—	11, 12	−1.20[−5.92, 3.52]	0.50(0.62)
CLAMS DQ					
12 mon	100(9), 99(6)	—	11, 12	1.70[−4.43, 7.83]	0.54(0.59)
CAT/CLAMS DQ					
12 mon	103(6), 102(4)	—	11, 12	0.20[−3.87, 4.27]	0.10(0.92)
GM DQ					
12 mon	102(7), 99(9)	—	11, 12	3.30[−3.54, 10.14]	0.95(0.34)
Visual function					
Visual evoked potential latency					
4 mon	123(19), 131(9)	134(9), 135(10)	39, 41	−1.55[−6.16, 3.05]	0.66(0.51)
8 mon	116(13), 116(9)	—	11, 11	0.15[−9.02, 9.32]	0.03(0.97)
Visual evoked potential acuity					
4 mon	—	0.7(0.1), 0.8(0.1)	23, 23	−0.05[−0.12, 0.02]	1.41(0.16)
8 mon	—	0.4(0.2), 0.4(0.2)	17, 20	0.01[−0.13, 0.15]	0.14(0.89)

[a]Mean and SD.
[b]See footnote b in Table 2.
[c]Fixed effects estimate of the weighted mean difference in development between groups. Positive value indicates greater mean score for treatment group relative to control group.
[d]See footnote d in Table 2.
[e]Bayley I, Bayley Scales of Infant Development First Edition; Bayley II, Bayley Scales of Infant Development Second Edition; CAT DQ, visual problem-solving ability; CLAMS DQ, language development; CAT/CLAMS DQ, overall cognition; MDI, mental developmental indices; PDI, psychomotor developmental indices. For other abbreviations see Tables 1 and 2.

formula (0.5–1.0 wt%). The most recent trial reported that nutrient-enriched, postdischarge formula was included as part of the feeding regimen available to all randomized groups (Jensen, C.L., Chen, H., Prager, T.C., Fraley, J.K., Anderson, R.E., and Heird, W.C., unpublished report). Two trials assessed growth to 57 wk PMA, whereas the third trial assessed growth up to hospital discharge when infants were 37 wk PMA (Table 6). Uauy et al. (7,8,15,21–23) measured visual function by VEP acuity, electroretinogram (ERG), and forced-choice preferential looking (FPL) acuity, and Jensen et al. (Jensen, C.L., Chen, H., Prager, T.C., Fraley, J.K., Anderson, R.E., and Heird, W.C., unpublished report) measured VEP latency (at a 30-min arc).

All trials reported that infants were randomly allocated to formula groups, but only one reported adequate concealment of allocation (Jensen, C.L., Chen, H., Prager, T.C., Fraley, J.K., Anderson, R.E., and Heird, W.C., unpublished report). Two trials were double-blind (15, Jensen, C.L., Chen, H., Prager, T.C., Fraley, J.K., Anderson, R.E., and Heird, W.C., unpublished report). Billeaud et al. (14) reported <20% attrition of infants at the end of the study (37 wk PMA). Uauy et al. (7,8,15,21–23) and Jensen et al. (Jensen, C.L., Chen, H., Prager, T.C., Fraley,

J.K., Anderson, R.E., and Heird, W.C., unpublished report) reported >20% attrition at 57 wk PMA. There were no significant differences in gestational age at birth (control 31.2 ± 1.2 wk compared with treatment 30.8 ± 1.5 wk) or birth weight (control 1.5 ± 0.2 kg compared with treatment 1.4 ± 0.3 kg). There were no differences in weight, length, or head circumference between the groups through to 57 wk PMA (Table 7).

The included trials measured different aspects of visual function that could not be combined. ERG analysis of one study at 36 wk PMA showed that infants fed increased dietary ALA had more sensitive rod photo receptors (log k WMD: –0.34 scot td-sec, 95% CI: –0.59, –0.09; $P = 0.009$; $n = 43$) and could respond to lower light intensities (rod threshold WMD: –0.37 scot td-sec, 95% CI: –0.66, –0.08; $P = 0.01$; $n = 43$) than infants fed control formula (Table 8). Birch et al. (22) reported that the ALA-enriched group had significantly better FPL acuity than the control group ($P < 0.05$) at 57 wk PMA (mean data unavailable). One trial found no difference in VEP latency between groups (Table 8).

At term and 57 wk PMA, infants in the ALA-enriched group had higher plasma and erythrocyte phospholipid EPA and DHA

TABLE 4
Blood DHA, EPA, and Arachidonic Acid (AA) levels (% total FA) of Term Infants Fed ALA-Enriched Formulas Compared with Control

Outcome	Jensen et al. (20) treatment, control[a]	Makrides et al. (11) treatment, control[a,b]	Ponder et al. (12) treatment, control[a]	Total number of infants treatment, control	Mean difference [95% CI][c]	Z[d]
Plasma phospholipids						
DHA						
2 mon	2.25(0.66), 1.66(0.30)	—	2.80(0.10), 2.40(0.30)	24, 30	0.43[0.28, 0.58]	5.47(<0.00001)*
4 mon	1.72(0.66), 1.27(0.35)	2.39(0.38), 1.95(0.30)	—	43, 46	0.44[0.28, 0.60]	5.45(<0.00001)*
8 mon	—	2.40(0.49), 1.77(0.41)	—	25, 27	0.63[0.38, 0.88]	5.01(<0.00001)*
EPA						
2 mon	0.31(0.10), 0.16(0.06)	—	0.70(0.10), 0.20(0.10)	24, 30	0.32[−0.02, 0.67][e]	1.85(0.06)
4 mon	0.29(0.11), 0.15(0.08)	0.40(0.10), 0.26(0.11)	—	43, 46	0.14[0.10, 0.18]	6.43(<0.00001)*
8 mon	—	0.56(0.28), 0.27(0.11)	—	25, 25	0.29[0.17, 0.41]	4.82(<0.00001)*
AA						
2 mon	6.20(2.00), 6.60(1.30)	—	7.30(0.40), 8.80(0.40)	24, 30	−1.43[−1.74, −1.13]	9.18(<0.00001)*
4 mon	5.80(1.90), 6.20(1.40)	6.71(0.87), 6.91(0.92)	—	43, 46	−0.22[−0.65, 0.20]	1.03(0.30)
8 mon	—	8.03(1.47), 7.34(1.10)	—	25, 27	0.69[−0.02, 1.40]	1.90(0.06)
Erythrocyte phospholipids						
DHA						
2 mon	3.13(0.74), 2.47(0.70)	—	—	13, 16	0.66[0.13, 1.19]	2.45(0.01)*
4 mon	2.39(0.76), 1.73(0.51)	3.49(0.32), 3.03(0.35)	—	43, 46	0.48[0.32, 0.64]	5.90(<0.00001)*
8 mon	—	3.02(0.48), 2.36(0.30)	—	25, 26	0.66[0.44, 0.88]	5.86(<0.00001)*
EPA						
2 mon	0.30(0.06), 0.12(0.06)	—	—	13, 16	0.18[0.14, 0.22]	8.03(<0.00001)*
4 mon	0.34(0.05), 0.17(0.07)	0.43(0.07), 0.25(0.03)	—	43, 46	0.18[0.15, 0.20]	15.01(<0.00001)*
8 mon	—	0.51(0.15), 0.28(0.07)	—	25, 26	0.23[0.17, 0.29]	6.97(<0.00001)*
AA						
2 mon	15.10(1.10), 14.70(2.90)	—	—	13, 16	0.40[−1.14, 1.94]	0.51(0.61)
4 mon	16.60(1.50), 17.50(1.50)	14.05(0.72), 14.83(0.75)	—	43, 46	−0.79[−1.14, −0.44]	4.41(<0.0001)*
8 mon	—	14.48(0.92), 14.88(0.89)	—	25, 26	−0.40[−0.90, 0.10]	1.58(0.11)

[a]Mean and SD.
[b]See footnote b in Table 2.
[c]Fixed effects estimate of the weighted mean difference in FA between groups. Positive value indicates greater mean score for treatment group relative to control group.
[d]See footnote d in Table 2.
[e]Random effects estimate of the weighted mean difference in FA between groups. Positive value indicates greater mean score for treatment group relative to control group. For other abbreviations see Tables 1 and 2.

TABLE 5
Growth, Development and FA Status of Term Infants Fed Formulas Enriched with Both LA and ALA (LA:ALA constant) Compared with Control

Outcome	Innis et al. (10) treatment, control[a,b]	Innis et al. (9) treatment, control[a]	Total number of infants (treatment, control)	Mean difference [95% CI][c]	Z[d]
Growth at 4 mon					
Weight (kg)	6.44(1.08), 6.76(0.83)	—	16, 21	−0.32[−0.96, 0.32]	0.98(0.33)
Length (cm)	62.9(2.4), 63.7(3.2)	—	16, 20	−0.77[−2.60, 1.06]	0.82(0.41)
Head circumference (cm)	41.3(1.5), 41.5(1.3)	—	16, 20	−0.22[−1.17, 0.73]	0.45(0.65)
Development at 3 mon		—			
Preferential looking acuity	—	2.67(0.64), 2.51(0.50)	57, 59	0.16[−0.05, 0.37]	1.50(0.13)
Plasma phospholipids at 4 mon (wt%)					
DHA	1.90(0.69), 2.00(0.36)	—	12, 13	−0.10[−0.54, 0.34]	0.45(0.65)
AA	8.00(1.73), 8.60(1.44)	—	12, 13	−0.60[−1.85, 0.65]	0.94(0.35)
EPA	0.40(0.00), 0.40(0.00)	—	12, 13	—	—

[a]Mean and SD.
[b]See Table 2 for footnote b.
[c]Fixed effects estimate of the weighted mean difference between groups. Positive value indicates greater mean score for treatment group relative to control group.
[d]See Table 2 for footnote d. See Tables 1, 2, and 4 for abbreviations.
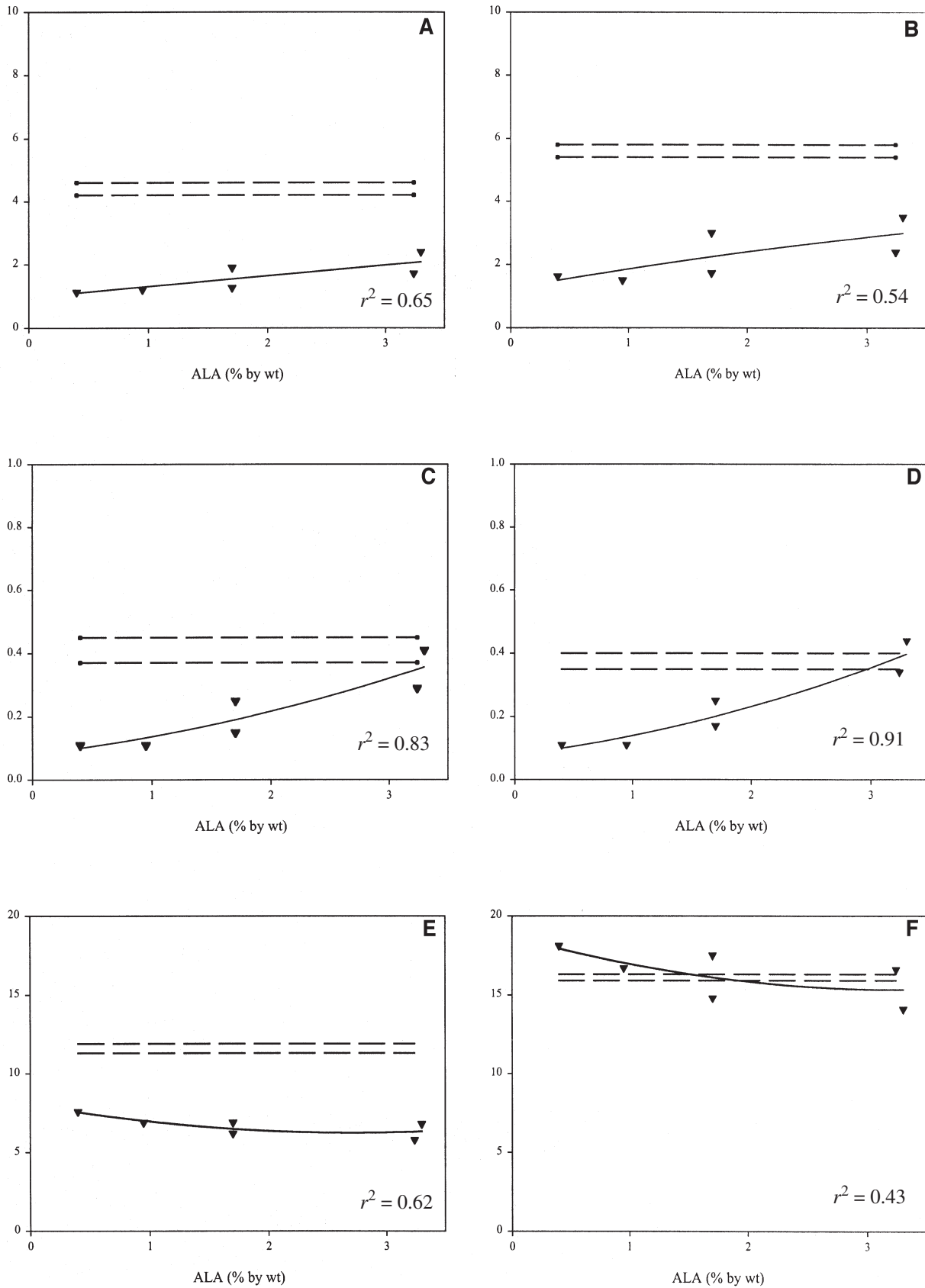
FIG. 1. Plasma and phospholipid DHA (22:6n-3), EPA (20:5n-3), and arachidonic acid (AA; 20:4n-6) levels (A, C, and E, respectively) and erythrocyte phospholipid DHA, EPA, and AA levels (B, D, and F, respectively) of formula-fed infants at 4 mon of age as a function of α-linolenic acid (ALA; 18:3n-3) in the test formulas from two trials involving term infants (▼) (11,20). The 95% confidence interval of plasma and erythrocyte phospholipid DHA, EPA, and AA levels of fully breast-fed Australian infants at 4 mon of age are shown (– – –) (11).

TABLE 6
Characteristics of Randomized Trials Involving Preterm Infants

Trial and location	Dietary intervention[a]	Number of infants enrolled	Number of infants completing trial (attrition rate)	Growth assessment age[b]	Neurodevelopment assessment	Visual function assessment[c]	FA assessment age[b]	Comments
Uauy and colleagues, 1990–1994, USA (7,8,15,21–23)	C - LA/ALA, 24.2/0.5; T - LA/ALA, 20.8/2.7; feeding until 57 wk PMA; no nutrient enrichment postdischarge	C = 25 T = 27	At 40 wk PMA: C = 18 (28%) T = 20 (26%) At 57 wk PMA: C = 13 (48%) T = 16 (41%)	34, 40, 48, 57	Not assessed	ERG (36, 57) FPL (57) VEP_act (36, 57, 66)	32, 36, 57	DHA formula group excluded. Trial had BM reference group.
Billeaud et al., 1997, France, 2 sites (14)	C - LA/ALA, 12.5/0.55; T - LA/ALA, 12.5/1.95; feeding until 37 wk PMA; no nutrient enrichment postdischarge	C = 32 T = 31	At 37 wk PMA: C = 31 (3%) T = 27 (13%)	D2, D15, 37	Not assessed	Not assessed	33, 35, 37	Trial had BM reference group.
Jensen et al., USA[d]	C - LA/ALA, 17.3/1.0; T - LA/ALA, 15.6/3.2; feeding until 57 wk PMA post discharge nutrient enrichment	C = 21 T = 21	At 57 wk PMA: C = 13 (38%) T = 16 (24%)	F, D, 43, 48, 57, 774	Not assessed	VEP_lat (57, 74)	F, D, 43, 48, 57, 74	Unpublished

[a]PMA, postmenstrual age; for other abbreviations see Table 1. Nutrient enrichment involves supplying extra protein and calories after 43 wk PMA; C, formula allocated as control; T, formula allocated as test; LA and ALA values expressed as % total FA.

[b]Weeks postmenstrual age; B, birth; D, discharge; F, full feeds; D2, the second day after the first significant formula intake; D15, the 15th day after the first significant formula intake .

[c]Age (wk PMA) in parentheses; ERG, electroretinogram; FPL, forced-choice preferential looking acuity.

[d]Jensen, C.L., Chen, H., Prager, T.C., Fraley, J.K., Anderson, R.E., and Heird, W.C., unpublished report.

TABLE 7
Weight, Length and Head Circumference of Preterm Infants Fed ALA-Enriched Formulas Compared with Control

Outcome	Billeaud *et al.* (14) (treatment, control)[a]	Uauy *et al.* (15) (treatment, control)[a]	Jensen *et al.* (treatment, control)[a,b]	Total number of infants (treatment control)	Mean difference [95% CI][c]	Z[d]
Weight (kg)						
37–42 wk PMA	2.51(0.31), 2.53(0.30)	3.04(0.41), 3.25(0.41)	—	47, 49	−0.07[−0.21, 0.06]	1.03(0.55)
48 wk PMA	—	4.64(0.58), 4.69(0.46)	4.33(0.50), 4.88(0.93)	36, 31	−0.18[−0.46, 0.11]	1.23(0.22)
57 wk PMA	—	6.05(0.75), 5.88(0.54)	5.56(0.61), 6.22(1.05)	32, 26	−0.12[−0.49, 0.26]	0.60(0.55)
Length (cm)						
37–42 wk PMA	46.0(2.0), 46.0(2.0)	48.5(2.2), 48.5(2.0)	—	47, 49	0.00[−0.82, 0.82]	0.00(1.00)
48 wk PMA	—	55.1(2.0), 55.4(1.9)	53.6(2.4), 53.5(2.9)	36, 31	−0.20[−1.25, 0.84]	0.38(0.70)
57 wk PMA	—	60.7(2.4), 60.5(2.1)	58.8(2.8), 59.4(3.1)	32, 26	−0.09[−1.40, 1.22]	0.13(0.89)
Head circumference (cm)						
37–42 wk PMA	33.0(1.0), 33.0(1.0)	34.8(1.3), 35.2(1.0)	—	47, 49	−0.13[−0.55, 0.29]	0.61(0.54)
48 wk PMA	—	38.7(1.4), 39.1(1.3)	38.0(1.4), 38.6(1.6)	36, 31	−0.49[−1.16, 0.19]	1.41(0.16)
57 wk PMA	—	41.2(1.3), 41.4(1.3)	40.8(1.9), 42.5(5.6)	32, 26	−0.32[−1.23, 0.59]	0.69(0.49)

[a]Mean and SD.
[b]All figures were taken from Jensen, C.L., Chen, H., Prager, T.C., Fraley, J.K., Anderson, R.E., and Heird, W.C., unpublished report.
[c]For footnote c see Table 2.
[d]For footnote d See Table 2.

than infants in the control group (Table 9). These higher blood levels of n-3 LCPUFA were associated with a reduction in plasma phospholipid AA at term but not at 57 wk PMA.

DISCUSSION

This systematic review and meta-analysis includes trials designed to modify 18-C PUFA in the diets of term and preterm infants in order to improve infant DHA status and assess the effects on growth and development. Our review is unique in that much of the data included were previously unpublished and were made available by the investigators. This maximized the amount of data available for the meta-analysis and decreased the risk of publication bias. However, the review only identified only five trials involving term infants and three trials involving preterm

infants. Although there are three possible dietary strategies to improve the availability of ALA for metabolism to DHA, most trials have simply assessed ALA enrichment without changing LA. Only two studies increased total 18-C PUFA, and no trials attempted to decrease dietary LA. The only studies to address the latter option were successful in improving DHA status but were not considered in this review because they were not randomized (24,25), and no growth or developmental outcome data were reported (25). The small number of trials was surprising given the intense interest in DHA, a major metabolite of ALA. It also highlighted the paucity and lack of commonality of data relating to visual and developmental outcomes.

There was no effect of dietary ALA enrichment on term infant growth except at 12 mon of age where infants consuming ALA-enriched formula were heavier and longer compared with

TABLE 8
Visual Development of Preterm Infants Fed ALA-Enriched Formulas Compared with Controls

Outcome	Birch *et al.* (23) (treatment, control)[a]	Jensen *et al.* (treatment, control)[a,b]	Total number of infants (treatment, control)	Mean difference [95% CI][c]	Z[d]
Retinal function					
ERG - rod log *k* (scot td-sec)					
36 wk PMA	1.39(0.55), 1.73(0.28)	—	24, 19	−0.34[−0.59, −0.09]	2.63(0.009)*
57 wk PMA	0.44(0.26), 0.53(0.22)	—	17, 12	−0.09[−0.27, 0.09]	1.01(0.31)
ERG - rod log threshold (scot td-sec)					
36 wk PMA	0.71(0.59), 1.08(0.37)	—	24, 19	−0.37[−0.66, −0.08]	2.51(0.01)*
57 wk PMA	−1.38(0.26), −1.32(0.20)	—	17, 12	−0.06[−0.23, 0.11]	0.70(0.48)
Visual function					
Visual evoked potential latency					
57 wk PMA	—	144(24), 139(13)	15, 13	5.40[−8.58, 19.38]	0.76(0.45)

[a]Mean and SD.
[b]All figures were taken from Jensen, C.L., Chen, H., Prager, T.C., Fraley, J.K., Anderson, R.E., and Heird, W.C., unpublished report.
[c]Fixed effects estimate of the weighted mean difference in development between groups. Positive value indicates greater mean score for treatment group relative to control group.
[d]For footnote d see Table 2.

TABLE 9
Blood DHA, EPA, and AA Levels (% total FA) of Preterm Infants Fed ALA-Enriched Formulas Compared with Control

Outcome	Billeaud et al. (14) (treatment, control)[a]	Uauy et al. (7) (treatment, control)[a]	Jensen et al. (15) (treatment, control)[a,b]	Total number of infants treatment, control	Mean difference [95% CI][c]	Z[d]
Plasma phospholipids						
DHA						
37–42 wk PMA[e]	2.27(0.82), 1.58(0.82)	—	—	25, 26	0.69[0.24, 1.14]	3.00(0.003)*
57 wk PMA	—	2.11(0.47), 0.84(0.37)	1.40(0.30), 1.00(0.40)	31, 26	0.77[0.57, 0.97][f]	7.57(<0.00001)*
EPA						
37--42 wk PMA	0.47(0.20), 0.20(0.15)	—	—	25, 26	0.27[0.17, 0.37]	5.44(<0.00001)*
57 wk PMA	—	0.60(0.23), 0.20(0.08)	0.34(0.15), 0.15(0.09)	31, 26	0.27[0.19, 0.34][c]	7.19(<0.00001)*
AA						
37–42 wk PMA	7.08(1.17), 7.99(1.17)	—	—	25, 26	−0.91[−1.55, −0.27]	2.78(0.005)*
57 wk PMA	—	5.26(1.29), 4.88(1.23)	5.40(1.50), 6.30(1.20)	31, 26	−0.21[−0.88, 0.47]	0.60(0.55)
Erythrocyte phospholipids						
DHA						
57 wk PMA	—	2.41(0.86), 1.15(0.77)	—	16, 13	1.26[0.67, 1.85]	4.16(<0.0001)*
EPA						
57 wk PMA	—	0.46(0.22), 0.24(0.11)	—	16, 13	0.22[0.10, 0.34]	3.50(0.0005)*
AA						
57 wk PMA	—	13.70(3.90), 14.00(1.90)	—	16, 13	−0.30[−2.47, 1.87]	0.27(0.79)

[a]Mean and SD.
[b]All figures were taken from unpublished data.
[c]Fixed effects estimate of the weighted mean difference in FA between groups. Positive value indicates greater mean score for treatment group relative to control group.
[d]For footnote d see Table 2.
[e]PMA, postmenstrual age.
[f]Random effects estimate of the weighted mean difference in FA between groups. Positive value indicates greater mean score for treatment group relative to control group.

control infants. This time point was at least 4 mon after dietary intervention had ceased. Furthermore, these findings may have been influenced by the unbalanced randomization in the trial conducted by Makrides et al. (11), which resulted in the ALA-enriched group being consistently heavier and longer at birth and throughout the dietary intervention. Although our meta-analysis showed no differences in weight, length, or head circumference at birth, the majority of 12-mon data were contributed by Makrides et al. (11). The limited data do not support the suggestion that perturbations in blood EPA and AA levels (induced by high-ALA diets) were associated with lower weight or length in term or preterm infants. In fact, the results showed no difference in weight, length, or head circumference even at the specific time-points where levels of erythrocyte AA were lower and EPA erythrocyte levels were higher in the ALA-enriched group compared with controls. Interestingly, the only study to suggest a negative effect of ALA supplementation on weight gain was observed between term infants fed high ALA (3.2 wt%, $n = 13$) and low ALA (0.4 wt%, less than the control group of 1.7 wt% used in this meta-analysis, $n = 17$) at one of four time-points assessed (13). That dietary ALA enrichment did not influence the growth of preterm infants raises questions in our minds as to the validity of the individual finding relating to the growth of term infants and highlights the limitations of single small trials and a meta-analysis performed on few trials with small sample sizes.

It has been suggested that term infants fed formula with at least 2% of total FA as ALA experience normal visual development, whereas such a level may be inadequate for preterm infants (26). The very limited developmental data available from this meta-analysis can throw no light on this issue since much of the data could not be combined and the limited sample sizes did not allow the detection of meaningful differences for most outcomes. Interestingly, the majority of data available were for VEP latency of term infants, and there were no group differences for this outcome. Visual development studies in preterm infants found those fed ALA-supplemented formula (2.7 wt%) had significantly increased retinal function at 36 wk PMA, but this effect was not sustained to 57 wk PMA. No trials of ALA enrichment assessed the neurodevelopment of preterm infants.

Pooled data indicate that infants consuming ALA-enriched diets had significantly increased levels of plasma and erythrocyte DHA compared with controls. However, the strategy of increasing ALA, without decreasing LA, was not effective in increasing formula-fed infant DHA levels to breast-fed infant levels but was effective in increasing EPA and decreasing AA levels. Two nonrandomized studies, not included in this review, aimed to increase infant DHA levels by lowering the LA content of the diet. Clark et al. (25) lowered formula LA to 3.5 wt%, maintained ALA at 1 wt%, and increased erythrocyte DHA levels but not to breast-fed infant levels. Courage et al. (24) assessed term infants fed evaporated milk with an LA/ALA ratio of 2.3:1 and showed increased erythrocyte PE DHA above formula-fed infants but again not to breast-fed infant levels. Trials are needed to address the relative benefits and risks of low-LA formulas.

Recommendations by international expert committees concerning the ALA content of formula have been made in the absence of an extensive database from randomized trials. This review has verified the need for further studies with long-term followup and large numbers of infants to ensure sufficient

statistical power to detect growth and developmental differences between dietary groups, should they exist. Practically, the findings from such trials will ensure that future recommendations regarding the 18-C PUFA levels for term and preterm infant formula will be more rigorous and evidence-based.

REFERENCES

1. Anderson, J.W., Johnstone, B.M., and Remley, D.T. (1999) Breast-Feeding and Cognitive Development: A Meta-analysis, *Am. J. Clin. Nutr. 70*, 525–535.
2. Birch, E., Birch, D., Hoffman, D., Hale, L., Everett, M., and Uauy, R. (1993) Breast-Feeding and Optimal Visual Development, *J. Pediatr. Ophthalmol. Strabismus 30*, 33–38.
3. Makrides, M., Neumann, M., Simmer, K., Pater, J., and Gibson, R.A. (1995) Are Long-Chain Polyunsaturated Fatty Acids Essential Nutrients in Infancy? *Lancet 345*, 1463–1468.
4. Neuringer, M., Connor, W.E., Lin, D.S., Barstad, L., and Luck, S. (1986) Biochemical and Functional Effects of Prenatal and Postnatal Omega-3 Fatty Acid Deficiency on Retina and Brain in Rhesus Monkeys, *Proc. Natl. Acad. Sci. USA 83*, 4021–4025.
5. Neuringer, M., Connor, W.E., Van Petten, C., and Barstad, L. (1984) Dietary Omega-3 Fatty Acid Deficiency and Visual Loss in Infant Rhesus Monkeys, *J. Clin. Invest. 73*, 272–276.
6. Anderson, R.E., Landis, D.J., and Dudley, P.A. (1976) Essential Fatty Acid Deficiency and Renewal of Rod Outer Segments in the Albino Rat, *Invest. Ophthalmol. 15*, 232–236.
7. Hoffman, D.R., and Uauy, R. (1992) Essentiality of Dietary Omega 3 Fatty Acids for Premature Infants: Plasma and Red Blood Cell Fatty Acid Composition, *Lipids 27*, 886–895.
8. Uauy, R.D., Birch, D.G., Birch, E.E., Tyson, J.E., and Hoffman, D.R. (1990) Effect of Dietary Omega-3 Fatty Acids on Retinal Function of Very-Low-Birth-Weight Neonates, *Pediatr. Res. 28*, 485–492.
9. Innis, S.M., Akrabawi, S.S., Diersen-Schade, D.A., Dobson, M.V., and Guy, D.G. (1997) Visual Acuity and Blood Lipids in Term Infants Fed Human Milk or Formulae, *Lipids 32*, 63–72.
10. Innis, S.M., Auestad, N., and Siegman, J.S. (1996) Blood Lipid Docosahexaenoic and Arachidonic Acid in Term Gestation Infants Fed Formulas with High Docosahexaenoic Acid, Low Eicosapentaenoic Acid Fish Oil, *Lipids 31*, 617–625.
11. Makrides, M., Neumann, M.A., Jeffrey, B., Lien, E.L., and Gibson, R.A. (2000) A Randomized Trial of Different Ratios of Linoleic to α-Linolenic Acid in the Diet of Term Infants: Effects on Visual Function and Growth, *Am. J. Clin. Nutr. 71*, 120–129.
12. Ponder, D.L., Innis, S.M., Benson, J.D., and Siegman, J.S. (1992) Docosahexaenoic Acid Status of Term Infants Fed Breast Milk or Infant Formula Containing Soy Oil or Corn Oil, *Pediatr. Res. 32*, 683–688.
13. Jensen, C.L., Prager, T.C., Fraley, J.K., Chen, H.M., Anderson, R.E., and Heird, W.C. (1997) Effect of Dietary Linoleic/α-Linolenic Acid Ratio on Growth and Visual Function of Term Infants, *J. Pediatr. 131*, 200–209.
14. Billeaud, C., Bougle, D., Sarda, P., Combe, N., Mazette, S., Babin, F., Entressangles, B., Descomps, B., Nouvelot, A., and Mendy, F. (1997) Effects of Preterm Infant Formula Supplementation with α-Linolenic Acid with a Linoleate/α-Linolenate Ratio of 6: A Multicentric Study, *Eur. J. Clin. Nutr. 51*, 520–526.
15. Uauy, R., Hoffman, D.R., Birch, E.E., Birch, D.G., Jameson, D.M., and Tyson, J. (1994) Safety and Efficacy of Omega-3 Fatty Acids in the Nutrition of Very Low Birth Weight Infants: Soy Oil and Marine Oil Supplementation of Formula, *J. Pediatr. 124*, 612–620.
16. Lapillonne, A., Jensen, C.L., Fraley, J.K., Clarke, S.D., and Heird, W.C. (2002) Effect of Various Linoleic Acid (LA) and α-Linolenic Acid (ALA) Intake on Growth, Energy Expenditure, and Body Composition of Term Infants, presented at the 5th Congress of the International Society for the Study of Fatty Acids and Lipids, Montréal, Canada, May 7–11.
17. Fuchs, G.J., Farris, R.P., DeWier, M., Hutchinson, S., Strada, R., and Suskind, R.M. (1994) Effect of Dietary Fat on Cardiovascular Risk Factors in Infancy, *Pediatrics 93*, 756–763.
18. Hayes, K.C., Pronczuk, A., Wood, R.A., and Guy, D.G. (1992) Modulation of Infant Formula Fat Profile Alters the Low-Density Lipoprotein/High-Density Lipoprotein Ratio and Plasma Fatty Acid Distribution Relative to Those with Breast-Feeding, *J. Pediatr. 120*, S109–S116.
19. Jensen, C.L., Chen, H.M., Fraley, J.K., Anderson, R.E., and Heird, W.C. (1996) Biochemical Effects of Dietary Linoleic/α-Linolenic Acid Ratio in Term Infants, *Lipids 31*, 107–113.
20. Voigt, R.G., Jensen, C.L., Fraley, J.K., Rozelle, J.C., Brown, F.R., and Heird, W.C. (2002) Relationship Between ω3 Long-Chain Polyunsaturated Fatty Acid Status During Early Infancy and Neurodevelopmental Status at 1 Year of Age, *J. Hum. Nutr. Diet. 15*, 111–120.
21. Uauy-Dagach, R., Mena, P., and Hoffman, D.R. (1994) Essential Fatty Acid Metabolism and Requirements for LBW Infants, *Acta Paediatr. Suppl. 405*, 78–85.
22. Birch, E.E., Birch, D.G., Hoffman, D.R., and Uauy, R. (1992) Dietary Essential Fatty Acid Supply and Visual Acuity Development, *Invest. Ophthalmol. Vis. Sci. 32*, 3242–3253.
23. Birch, D.G., Birch, E.E., Hoffman, D.R., and Uauy, R.D. (1992) Retinal Development in Very-Low-Birth-Weight Infants Fed Diets Differing in Omega-3 Fatty Acids, *Invest. Ophthalmol. Vis. Sci. 33*, 2365–2376.
24. Courage, M.L., McCloy, U.R., Herzberg, G.R., Andrews, W.L., Simmons, B.S., McDonald, A.C., Mercer, C.N., and Friel, J.K. (1998) Visual Acuity Development and Fatty Acid Composition of Erythrocytes in Full-Term Infants Fed Breast Milk, Commercial Formula, or Evaporated Milk, *J. Dev. Behav. Pediatr 19*, 9–17.
25. Clark, K.J., Makrides, M., Neumann, M.A., and Gibson, R.A. (1992) Determination of the Optimal Ratio of Linoleic Acid to α-Linolenic Acid in Infant Formulas, *J. Pediatr. 120*, S151–S158.
26. Heird, W.C., Prager, T.C., and Anderson, R.E. (1997) Docosahexaenoic Acid and the Development and Function of the Infant Retina, *Curr. Opin. Lipidol. 8*, 12–16.

Highly Unsaturated Fatty Acid Synthesis in Vertebrates: New Insights with the Cloning and Characterization of a Δ6 Desaturase of Atlantic Salmon

Xiaozhong Zheng, Douglas R. Tocher*, Cathryn A. Dickson, J. Gordon Bell, and Alan J. Teale

Institute of Aquaculture, University of Stirling, Stirling FK9 4LA, Scotland, United Kingdom

ABSTRACT: Fish are an important source of the n-3 highly unsaturated fatty acids (HUFA), eicosapentaenoic (EPA) and docosahexaenoic (DHA) acids that are crucial to the health of higher vertebrates. The synthesis of HUFA involves enzyme-mediated desaturation, and a Δ5 fatty acyl desaturase cDNA has been cloned from Atlantic salmon (*Salmo salar*) and functionally characterized previously. Here we report cloning and functional characterization of a Δ6 fatty acyl desaturase of Atlantic salmon and describe its genomic structure, tissue expression, and nutritional regulation. A salmon genomic library was screened with a salmon Δ5 desaturase cDNA and positive recombinant phage isolated and subcloned. The full-length cDNA for the putative fatty acyl desaturase was shown to comprise 2106 bp containing an open reading frame of 1365 bp specifying a protein of 454 amino acids (GenBank accession no. AY458652). The protein sequence included three histidine boxes, two transmembrane regions, and an N-terminal cytochrome b_5 domain containing the heme-binding motif HPGG, all of which are characteristic of microsomal fatty acid desaturases. Functional expression showed that this gene possessed predominantly Δ6 desaturase activity. Screening and sequence analysis of the genomic DNA of a single fish revealed that the Δ6 desaturase gene constituted 13 exons in 7965 bp of genomic DNA. Quantitative real-time PCR assay of gene expression in Atlantic salmon showed that both Δ6 and Δ5 fatty acyl desaturase genes, and a fatty acyl elongase gene, were highly expressed in intestine, liver, and brain, and less so in kidney, heart, gill, adipose tissue, muscle, and spleen. Furthermore, expression of both Δ6 and Δ5 fatty acyl desaturase genes in intestine, liver, red muscle, and adipose tissue was higher in salmon fed a diet containing vegetable oil than in fish fed a diet containing fish oil.

Paper no. L9602 in *Lipids 40*, 13–24 (January 2005).

Highly unsaturated fatty acids (HUFA), including arachidonate (20:4n-6), EPA (20:5n-3), and DHA (22:6n-3), are crucial to the health and normal development of higher vertebrates (1–3). Fish are the most important source of n-3 HUFA for humans, but with fisheries in decline, an increasing proportion of fish are being provided by rapidly expanding aquacul-

ture (4). Paradoxically, aquaculture is itself dependent on fisheries for the provision of fish meals and oils traditionally used in the feed formulations (5). Their use ensures the high nutritional quality of farmed fish through the high levels of n-3 HUFA that fish oil (FO) and fish meal provide. However, feed-grade fisheries have reached sustainable limits. Along with concern over organic contaminants in FO, this has dictated that alternatives to FO must be found if aquaculture is to continue to expand and supply more of the global demand for fish (6).

The only practical, sustainable alternative to FO is vegetable oils (VO), which are rich in C_{18} PUFA but devoid of the n-3 HUFA abundant in FO (7). Consequently, tissue FA compositions in fish fed VO are characterized by increased levels of C_{18} PUFA and decreased levels of n-3 HUFA, which may reduce their nutritional value to the human consumer (8). The extent to which fish can convert C_{18} PUFA to HUFA varies, associated with their complement of FA desaturase enzymes. Although Atlantic salmon (*Salmo salar* L.) are capable of producing DHA from 18:3n-3, and so express the necessary desaturase activities, the production is insufficient to maintain n-3 HUFA in fish fed VO at levels found in fish fed FO (9–11). Our primary hypothesis is that understanding the molecular basis of HUFA biosynthesis and its regulation in fish will enable us to optimize the activity of the pathway to ensure efficient and effective use of VO in aquaculture while maintaining the nutritional quality of farmed fish for the consumer.

Δ5 and Δ6 fatty acyl desaturases and elongases are critical enzymes in the pathways for the biosynthesis of HUFA. In recent years, significant progress has been made in characterizing FA desaturases involved in HUFA synthesis (12). Full-length cDNAs for Δ6 desaturases have been isolated from the filamentous fungus *Mortierella alpina* (13), the nematode *Caenorhabditis elegans* (14), rat (15), mouse and human (16). FA Δ5 desaturase genes have been isolated from *M. alpina* (17), *C. elegans* (18,19), and humans (20,21). Moreover, we have reported isolation of a cDNA of zebrafish (*Danio rerio*, GenBank accession no. AF309556) that has high similarity to mammalian Δ6 desaturase genes. Functional analysis by heterologous expression in the yeast *Saccharomyces cerevisiae* indicated that the zebrafish gene was unique in that the cDNA encoded an enzyme having both Δ6 and Δ5 desaturase activities (22). Putative FA desaturase cDNAs have now also been

isolated and cloned from rainbow trout (*Oncorhynchus mykiss*, GenBank accession no. AF301910) (23) and gilthead seabream (*Sparus aurata*, GenBank accession no. AY055749) (24). Functional analysis showed that these two desaturase genes, along with cDNAs recently cloned from common carp (*Cyprinus carpio*, GenBank accession no. AF309557) and turbot (*Psetta maximus*, GenBank accession no. AF301910) encoded basically unifunctional Δ6 FA desaturase enzymes responsible for the first and possibly rate-limiting step in the biosynthesis of HUFA from 18:3n-3 and 18:2n-6 (25). Recently, a full-length cDNA for a desaturase containing 1365 bp encoding 454 amino acid residues has been cloned from Atlantic salmon (GenBank accession no. AF478472). Functional analysis showed that this gene was primarily a Δ5 desaturase with virtually no Δ6 activity (26). Therefore, it was presumed that other FA desaturase genes should be present in Atlantic salmon.

The objectives of the study described here were, first, to clone and functionally characterize a Δ6 desaturase gene of Atlantic salmon; second, to describe its genomic structure; and third, to place it in evolutionary and physiological contexts. Therefore, we detail the exon/intron organization of a salmon Δ6 desaturase gene, describe the expression profile of both Δ6 and Δ5 fatty acyl desaturase and fatty acyl elongase genes in various tissues, and demonstrate nutritional regulation of the fatty acyl desaturase genes.

MATERIALS AND METHODS

Putative desaturase cloning and its genomic organization. An Atlantic salmon genomic DNA library constructed previously with the lambda FIX II/Xho I partial fill-in vector kit (Stratagene, La Jolla, CA) was probed with a full-length salmon Δ5 fatty acyl desaturase cDNA (GenBank accession no. AF478472). Inserts of positive recombinant phages were isolated and subcloned into the pBluescript KS II vector for sequencing (Stratagene). The full putative desaturase genomic nucleotide sequence was assembled using BioEdit, version 5.0.6 (Tom Hall, Department of Microbiology, North Carolina State University, Raleigh, NC).

Total RNA was extracted from liver tissue of Atlantic salmon fed a standard extruded diet based on fish meal and FO using TRIzol® reagent (GibcoBRL, Grand Island, NY). 3′-RACE (rapid amplification of cDNA ends) cDNA was synthesized using MMLV (Moloney murine leukemia virus) reverse transcriptase (Promega, Madison, WI) primed by the oligonucleotide, T7PolyT, 5′-TACGACTCATATAGGGCGT-GCAGTTTT TTTTTTTT-3′. The specific sense primer, D6P31, 5′-CAGGGGTGGGCCCGGTGGAGGGCTA-3′ was designed for 3′-RACE PCR based on the genomic sequence described above. This was used in conjunction with T7PolyT primer for the RACE PCR isolation of the salmon desaturase cDNA fragment predicted to contain the 3′ UTR (untranslated region). PCR amplification was performed using the Hotstar Taq master kit (Qiagen, Crowley, West Sussex, United Kingdom) and involved an initial denaturation step at 95°C for 15

min, followed by 30 cycles of denaturation at 95°C for 30 s, annealing at 58°C for 30 s, and extension at 72°C for 3 min. The final extension at 72°C was for 10 min. 5′-RACE-cDNA was synthesized using the SMART^TM RACE cDNA amplification kit (Clontech, Palo Alto, CA). The primer, SD6PPR3, 5′-GTCGCATTCCATCCCAATCC-3′ was designed according to the 3′-RACE PCR fragment sequence. This was used in conjunction with universal primer mix: long 5′-CTAATAC-GACTCACTATAGGGCAAGCAGTGGTACAACGGA-GT-3′ and short 5′-CTAATACGACTCACTATAGGGC-3′ to perform 5′-RACE PCR using high-fidelity DNA polymerase (Roche Diagnostics Ltd., Lewes, East Sussex, United Kingdom). Amplification involved an initial step at 95°C for 1 min and 70°C for 3 min, and four cycles of denaturation at 95°C for 15 s, annealing at 62°C for 1 min, and extension at 72°C for 1 min 30 s, followed by 27 cycles of denaturation at 95°C for 15 s, annealing at 56°C for 30 s and extension at 72°C for 1 min 30 s. The final extension at 72°C was for 10 min.

All RACE PCR products were cloned into the pBluescript KS II^+ vector for sequencing. The 3′ and 5′ RACE PCR fragment sequences were aligned to assemble the full nucleotide sequence of the putative desaturase cDNA using BioEdit, version 5.0.6. The assembled putative fatty acyl desaturase cDNA sequence and its genomic DNA sequence were aligned to assign consensus donor and acceptor splice recognition sequences.

Heterologous expression of desaturase open reading frames (ORF) in S. cerevisiae. PCR amplification was carried out to clone the salmon putative desaturase cDNA ORF. Sense primer, D6RF2, 5′-ATGGGGGGCGGAGGCCAGCA-GAATGATTCAG-3′, and antisense primer, D6RR1, 5′-AT-GCGATGGATTAAATCCCG –3′ (located in the 3′ UTR) were designed for first-round PCR after comparing nucleotide sequences of this putative cDNA and the Δ5 desaturase cDNA. Expression primers were designed for a second round of PCR. The sense primer, SalpYESFOR, 5′-CCCAAGCTTAC-TATGGGGGGCGGAGGCC-3′ contains a *HindIII* site (underlined) and antisense primer, SalPYESREV2, 5′- CCG-CTCGAGTCATTTATGGAGATATGCAT-3′ contains an *XhoI* site (underlined). PCR was performed using high-fidelity DNA polymerase (Roche Diagnostics Ltd.) following the manufacturer's instructions. Amplification involved an initial denaturation step at 95°C for 2 min, followed by 30 cycles of denaturation at 95°C for 30 s, annealing at 55°C for 30 s, and extension at 72°C for 2 min and 30 s followed by a final extension at 72°C for 10 min.

Following PCR, the DNA fragments were restricted with the appropriate enzymes, *HindIII* and *XhoI*, and ligated into the similarly digested yeast expression vector pYES2 (Invitrogen Ltd., Paisley, United Kingdom). Ligation products were then used to transform Top10F′ *Escherichia coli* competent cells (Invitrogen Ltd.), which were screened for the presence of recombinants. Transformation of the yeast *S. cerevisiae* (strain InvSc1) with the recombinant plasmids was carried out using the S.c.EasyComp Transformation Kit (Invitrogen Ltd.). Selection of yeast containing the desaturase/pYES2

constructs was on *S. cerevisiae* minimal medium (SCMM) minus uracil. Culture of the recombinant yeast was carried out in SCMM$^{-uracil}$ broth as described previously (22), using galactose induction of gene expression. Each culture was supplemented with one of the following PUFA substrates: α-linolenic acid (18:3n-3), linoleic acid (18:2n-6), eicosatetraenoic acid (20:4n-3), dihomo-γ-linoleic acid (20:3n-6), docosapentaenoic acid (22:5n-3), or docosatetraenoic acid (22:4n-6). PUFA were added to the yeast cultures at concentrations of 0.5 mM (C_{18}), 0.75 mM (C_{20}), and 1 mM (C_{22}), as uptake efficiency decreases with increasing chain length. Yeast cells were harvested, washed, and dried, and lipid was extracted by homogenization in chloroform/methanol (2:1, vol/vol) containing 0.01% BHT as antioxidant as described previously (22). FAME were prepared, extracted, purified by TLC, and analyzed by GC, all as described previously (22). The proportion of substrate FA converted to the longer-chain FA product was calculated from the gas chromatograms as 100 × [product area/(product area + substrate area)]. Unequivocal confirmation of FA products was obtained by GC–MS of the picolinyl derivatives as described in detail previously (22).

Salmon tissue RNA extraction and quantitative real-time PCR (qrtPCR). Tissue expression profiles and effects of diet were investigated in Atlantic salmon that had been fed one of two diets from the first feeding. The diets consisted of a control in which FO was the only added oil and an experimental diet in which 75% of the FO was replaced by a VO blend containing rapeseed, palm, and linseed oils in a 3.7:2:1 ratio. Both diets were fishmeal-based and contained 48% protein, 26% lipid, 7% moisture, and 8% ash as determined by proximate analyses. The FA compositions of the diets (6 mm pellet) are given in Table 1. The diets were prepared by the Nutreco Aquaculture Research Centre (Stavanger, Norway) and formulated to satisfy the nutritional requirements of salmonid fish (27).

Fish were sampled in November 2003, 6 mon after seawater transfer, following 18 mon on the diets, at which point the weights of the fish fed the FO and VO diets were 1250.0 ± 84.9 and 1280.0 ± 79.4 g, respectively. Eight fish per dietary treatment were sampled, and liver, brain, heart, kidney, gill, intestine (pyloric caeca), spleen, white and red muscle, and adipose tissue were collected, frozen immediately in liquid nitrogen, and subsequently stored at –80°C before extraction. Total RNA extraction was performed as described above. Five micrograms of total RNA was reverse-transcribed into cDNA using an MMLV reverse transcriptase first strand cDNA synthesis kit (Promega UK, Southampton, United Kingdom). Gene expression of the fatty acyl Δ6 and Δ5 desaturase, and fatty acyl elongase genes in tissue from individual salmon fed the different diets were studied by quantitative real-time PCR (qrt-PCR). β-Actin was used for normalization of mRNA levels. The PCR primers were designed according to Δ6 desaturase (accession no. AY458652), and the published Δ5 desaturase (accession no. AF478472), elongase (accession no. AY170327), and β-actin (accession no. AF012125) cDNA sequences. For the Δ6 desaturase, the for-

TABLE 1
FA Composition (percentage of total FA) of Diets^a

	FO	VO
14:0	6.1	2.4
16:0	14.7	16.0
18:0	2.8	3.3
Total saturated^b	24.3	21.9
16:1n-7^c	5.0	2.0
18:1n-9	13.5	35.2
18:1n-7	2.5	2.3
20:1n-9^d	10.4	3.6
22:1n-11^e	14.9	4.8
24:1n-9	0.7	0.3
Total monoenes	47.0	48.2
18:2n-6	4.0	11.8
20:4n-6	0.5	0.2
Total n-6 PUFA^f	5.1	12.2
18:3n-3	1.1	8.5
18:4n-3	2.4	0.8
20:4n-3	0.7	0.2
20:5n-3	6.7	2.8
22:5n-3	1.1	0.4
22:6n-3	10.4	4.5
Total n-3 PUFA^g	22.4	17.3
Total PUFA^h	28.7	29.9

^{a}Data are the means of two samples. FO, fish oil; VO, vegetable oil blend.
^{b}Totals contain 15:0 present at up to 0.5%.
^{c}Contains 16:1n-9.
^{d}Contains 20:1n-11 and 20:1n-7.
^{e}Contains 22:1n-9.
^{f}Totals contain 18:3n-6, 20:2n-6, 20:3n-6, and 22:5n-6 present at up to 0.2%.
^{g}Totals contain 20:3n-3 present at up to 0.1%.
^{h}Totals contain C_{16} PUFA.

ward primer was 5′-CCCCAGACGTTTGTGTCAG-3′, and the reverse primer was 5′-CCTGGATTGTTGCTTTGGAT-3′. For the Δ5 desaturase, the forward primer was 5′-GTGAATGGGGATCCATAGCA-3′, and the reverse primer was 5′-AAACGAACGGACAACCAGA-3′. For the elongase, the forward and reverse primers were 5′-TGATTTGTGTTCCAAATGGC-3′ and 5′-CTCATGACGGGAACCT CAAT-3′, respectively. For β-actin, 5′-ACATCAAGGAGAAGCTGTGC-3′ and 5′-GACAACGGAACCTCTCGTTA-3′ were the forward and reverse primers, respectively. PCR product sizes were 181, 192, 219, and 141 bp, respectively. The linearized plasmid DNA containing the target sequence for each gene was quantified to generate a standard curve of known copy number. Amplification of cDNA samples and DNA standards was carried out using a SYBR Green PCR kit (Qiagen) under the following conditions: 15 min denaturation at 95°C, 45 cycles of 15 s at 94°C, 15 s at 55°C, and 30 s at 72°C. This was followed by product melt to confirm single PCR products. Thermal cycling and fluorescence detection were conducted in a Rotor-Gene 3000 system (Corbett Research, Cambridge, United Kingdom). The copy numbers of the specific genes in the sample, normalized to total RNA, were used to compare expression levels between different tissues, and the ratios of copy numbers between the target genes

and β-actin were calculated and used to compare the gene expression levels in fish fed the two diets.

Sequence analysis. Nucleotide sequences were determined by standard dye terminator chemistry using a PerkinElmer ABI-377 DNA sequencer following the manufacturer's protocols (PerkinElmer, Applied Biosystems). Deduced amino acid sequences of desaturases from various species were aligned using ClustalX, and sequence phylogenies were predicted using the Neighbour Joining method (28). Confidence in the resulting phylogenetic tree branch topology was measured by bootstrapping through 1000 iterations.

Materials. Eicosatetraenoic (20:4n-3), docosapentaenoic (22:5n-3), and docosatetraenoic (22:4n-6) acids (all >98–99% pure) were purchased from Cayman Chemical Co. (Ann Arbor, MI). Linoleic (18:2n-6), α-linolenic (18:3n-3), and eicosatrienoic (20:3n-6) acids (all >99% pure), BHT, 1,1′-carbonyldiimidazole, 2,2-dimethoxypropane, FA-free BSA, galactose, 3-(hydroxymethyl) pyridine, HBSS, nitrogen base, raffinose, tergitol NP-40, and uracil dropout medium were obtained from Sigma Chemical Co. Ltd. (Dorset, United Kingdom). TLC (20 cm × 20 cm × 0.25 mm) plates precoated with silica gel 60 (without fluorescent indicator) were purchased from Merck (Darmstadt, Germany). All solvents were HPLC grade and were from Fisher Scientific (Loughborough, United Kingdom).

RESULTS

Sequence analyses. The full length of the putative salmon desaturase cDNA (mRNA), as determined by 5′- and 3′-RACE PCR, was shown to be 2106 bp, which included a 5′-UTR of 284 bp and a 3′-UTR of 457 bp. Sequencing revealed that the cDNA included an ORF of 1365 bp, which specified a protein of 454 amino acids (GenBank accession no. AY458652). The protein sequence included all the characteristic features of microsomal FA desaturases, including three histidine boxes and an N-terminal cytochrome b_5 domain containing the heme-binding motif, HPGG (Fig. 1). The protein sequence also contained two transmembrane regions. These features are similar to those of other FA desaturase genes including salmon Δ5 desaturase, the zebrafish Δ6/Δ5 desaturase, and the human Δ5 (GenBank accession no. AF126799) and Δ6 (GenBank accession no. AF199596) desaturases. However, the new salmon desaturase, like the salmon Δ5 desaturase and the rainbow trout Δ6 desaturase sequences, had an insertion of 10 amino acid residues at the N-terminal end.

A pairwise comparison was made between fish and human desaturase sequences. The amino acid sequence predicted by the salmon putative (Δ6) desaturase ORF shows 91% identity to the salmon Δ5 desaturase, and 94% identity to the trout Δ6 desaturase. The salmon cDNA shows 65% identity to that of the zebrafish Δ6/Δ5 desaturase, and 65 and 58% identity to the human Δ6 and Δ5 cDNAs, respectively.

A phylogenetic tree was constructed on the basis of the amino acid sequence alignments between the salmon fatty acyl desaturases and 15 other desaturases of fish and mammals (Fig. 2). The phylogenetic analysis clustered the new Atlantic salmon putative desaturase sequence with the Atlantic salmon Δ5 desaturase, rainbow trout Δ6 desaturase and other, as yet uncharacterized, masou (cherry) salmon (*Oncorhynchus masou*) desaturase genes, but closest to the trout Δ6 desaturase. The salmonid desaturases clustered more closely with turbot, sea bream, and tilapia (*Oreochromis nilotica*) desaturases than with carp Δ6 desaturase and zebrafish Δ5/Δ6 desaturase. All of the fish desaturase genes clustered together, and closer to the mammalian (mouse and human) Δ6 desaturases than to the mammalian Δ5 desaturases.

Functional characterization. The salmon desaturase cDNA was functionally characterized by determining the FA profiles of transformed *S. cerevisiae* containing either the pYES vector alone or the vector with the salmon desaturase cDNA insert, grown in the presence of a variety of potential FA substrates, including Δ6 substrates (18:2n-6 and 18:3n-3), Δ5 substrates (20:3n-6 and 20:4n-3), and Δ4 substrates (22:4n-6 and 22:5n-3). The FA composition of the yeast transformed with the vector alone showed the four main FA normally found in *S. cerevisiae*, namely 16:0, 16:1n-7, 18:0, and 18:1n-9, together with the exogenously derived FA. This is consistent with *S. cerevisiae* not possessing Δ5 or Δ6 FA desaturase activities (Figs. 3 and 4). The most prominent additional peaks were observed in the profiles of transformed yeast grown in the presence of the Δ6 desaturase substrates, 18:3n-3 and 18:2n-6 (Fig. 3). Based on GC retention time and confirmed by GC–MS, the additional peaks associated with the presence of the salmon desaturase cDNA were identified as 18:4n-3 (Fig. 3B) and 18:3n-6 (Fig. 3D), corresponding to the Δ6 desaturation products of 18:3n-3 and 18:2n-6, respectively. Approximately, 60.1% of 18:3n-3 was converted to 18:4n-3 and 14.4% of 18:2n-6 was converted to 18:3n-6 in yeast transformed with the salmon desaturase (Table 2). However, a very small additional peak representing desaturated FA product, as confirmed by GC–MS, was observed in the lipids of *S. cerevisiae* transformed with the desaturase cDNA when the transformed yeast was incubated with 20:4n-3 (Figs. 4A and 4B). About 2.3% of 20:4n-3 (n-3 Δ5 activity) was desaturated by the salmon clone, but no product of desaturation of the 20:3n-6 substrate was detected, indicating no significant n-6 Δ5 desaturase activity. The desaturase cDNA did not express any Δ4 desaturase activity as evidenced by the lack of any observable additional peaks representing desaturated products of 22:5n-3 or 22:4n-6 (data not shown). Overall, therefore, the results showed that the salmon desaturase cDNA-encoded enzyme was essentially a Δ6 fatty acyl desaturase, with only a very low level of Δ5 desaturase activity, and no Δ4 desaturase activity.

Genomic structure. The alignment of the Δ6 fatty acyl desaturase cDNA and the genomic sequences revealed 13 exons spanning 7965 bp of genomic DNA as illustrated in Table 3.

FA desaturase and elongase gene expression in salmon tissues. To identify which tissues were likely to contribute to HUFA synthesis in the Atlantic salmon, reverse transcription qrtPCR was used to examine the tissue distribution of Δ6 and

```
                                                              ****
Atlantic salmon D6   MGGGGQQMDSGEPAKGDRGGPGGGLGGSAVYTWEEVQRHSHRGDQWLVIDRKVYNITQWAKRHPGGIRVI  70
Atlantic salmon D5   MGGGGQQTESSEPAKGDGLEPDGGQGGSAVYTWEEVQRHSHRSDQWLVIDRKVYNITQWAKRHPGGIRVI  70
Rainbow trout D6     MGGGGQQTESSEPAKGDGVGPDGGRGGSAVYTWEEVQRHCHRSDKWLVIDRKVYNITQWAKRHPGGIRVI  70
Zebrafish D5/D6      MGGGGQQTDRITDTNG----------RFSSYTWEEVQRHTKHGDQWVVVERKVYNVSQWVRRHPGGLRIL  60
Human D6             MGKGGNQGEGAAEREVS----------VPTFSWEEIQRHNLRTDRWLVIDRKVYNITKWSIQHPGGQRVI  60
Human D5             MAPDPLAAETAAQGLTP----------RYFTWDEVAQRSGCEERWLVIDRKVYNISEFTRRHPGGSRVI  59

Atlantic salmon D6   SHFAGEDATDAFVAFHPNPNFVRKFLKPLLIGELAPTEPSQDHGKNAVLVQDFQALRNRVEREGLLRARP  140
Atlantic salmon D5   SHFAGEDATEAFSAFHLDANFVRKFLKPLLIGELAPTEPSQDHGKNAALVQDFQALRDHVEREGLLRARL  140
Rainbow trout D6     SHFAGEDATDAFVAFHPDPNFVRKFLKPLLIGELATTEPSQDHGKNAVLVQDFQALRDRVEREGLLRARP  140
Zebrafish D5/D6      GHYAGEDATEAFTAFHPNLQLVRKYLKPLLIGELEASEPSQDRQKNAALVEDFRALRERLEAEGCFKTQP  130
Human D6             GHYAGEDATDAFRAFHPDLEFVCKFLKPLLIGELAPEEPSQDHGKNSKITEDFRALRKTAEDMNLFKTNH  130
Human D5             SHYAGQDATDPFVAFHINKGLVRKYMNSLLIGELSPEQPSFEPTKNKELTDEFRELRATVERMGLMKANH  129

Atlantic salmon D6   LFFSLYLGHILLLEALALGLLWVWGTSWSLTLLCSLMLATSQSQAGWLQHDYGHLSVCKKSSWNHVLHKF  210
Atlantic salmon D5   LFFSLYLGHILLLEALALGLLWVWGTSWSLTLLCSLMLATSQAQAGWLQHDYGHLSVCKKSSWNHKLHKF  210
Rainbow trout D6     LFFSLYLGHILLLEALALGLLWVWGTSWSLTLLCSLMLATSQSQAGWLQHDYGHLSVCKTSSWNHVLHKF  210
Zebrafish D5/D6      LFFALHLGHILLLEAIAFMMVWYFGTGWINTLIVAVILATAQSQAGWLQHDFGHLSVFKTSGMNHLVHKF  200
Human D6             VFFLLLLAHIIALESIAWFTVFYFCNGWIPTLITAFVLATSQAQAGWLQHDYGHLSVYRKPKWNHLVHKF  200
Human D5             VFFLLYLHILLLDGAQWLTLWVFGTSFLPFLLCAVLLSAVQAQAGWLQHDFGHLSVFSTSKWNHLLHHF  199

Atlantic salmon D6   VIGHLKGASANWWNHRHFQHHAKPNVLSKDPDVNMLH-VFVLGDKQPVEYGIKKLKYMPYHHQHQYFFLI  279
Atlantic salmon D5   VIGHLKGASANWWNHRHFQHHAKPNVFRKDPDIMSLP-VFVLGDTQPVEYGIKKLKYMPYHHQHQYFFLI  279
Rainbow trout D6     VIGHLKGASANWWNHRHFQHHAKPNVSKDPDVNSLH-VFVLGDKQPVEYGIKKLKYMPYHHQHQYFFLI  279
Zebrafish D5/D6      VIGHLKGASAGWWNHRHFQHHAKPNIFRKDPDVNMLN-AFVVGNVQPVEYGVKKIDHLPYMHQHRYFFFI  269
Human D6             VIGHLKGASANWWNHRHFQHHAKPNIFHKDPDVNMLH-VFVLGEWQPIEYGKKKLKYLPYNHQHEYFFLI  269
Human D5             VIGHLKGAPASWWNHMHFQHHAKPNCFRKDPDINMHPFFFALGKILSVELGKQRKNYMPYNHQHRYFFLI  269

Atlantic salmon D6   GPPLLIPVFFTIQIEQTMFSQRNWVDLAWSMTFYLRFFCSYYPFFGFFGSVALITFVRFLESHWFVWVTQ  349
Atlantic salmon D5   GPPLIVPVFFNIQIFRTMFSQRDWVDLAWSMSFYLRFFCCYYPFFGFFGSVALISFVRFLESHWFVWVTQ  349
Rainbow trout D6     GPPLVIPVFFTIQIEQTMFSQRNWVDLAWAMTFYLRFFCCYYPFFGFFGSVALISFVRFLESHWFVWVTQ  349
Zebrafish D5/D6      GPPLLIPVYFQFQIFHNMISHGMWVDLLWCISYYVRYFLCYTQFYCVFWAIILFNFVRFMESHWFVWVTQ  339
Human D6             GPPLLIPMYFQYQIIMTMIVHKNWVDLAWAVSYYIRFFITYIPFYGILGALLFLNFIRFLESHWFVWVTQ  339
Human D5             GPPALLDLYFQWYIFYFVIQRKWVDLAWMITFYVVRFFLTYVVPLLCLKAFLGLFFIWRFLESMWFVWVTQ  339

Atlantic salmon D6   MNHLPMEIDHERHQDWLTMQLSGTCNIEQSTFNDWFSGHLNFQIEHHLFPTMPRHNYHLVAPLVRTLCEK  419
Atlantic salmon D5   MNHLPMEMDHERHQDWLTMQLSATCNIEQSTFNDWFSGHLNFQIEHHLFPTMPRHNYHLVAPLVRTLCEK  419
Rainbow trout D6     MNHLPMEIDHERHQDWLTMQLSATCNIEQSTFNDWFSGHLNFQIEHHLFPTMPRHNYHLVAPLVRALCEK  419
Zebrafish D5/D6      MSHIPMMIDYERNQDWLSMQLVATCNIEQSAFNDWFSGHLNFQIEHHLFPTVPRHNYWRAAPRVRALCEK  409
Human D6             MNHIVMEIDQEAYRDWFSSQLTATCNVEQSFFNDWFSGHLNFQIEHHLFPTMPRHMLHKIAPLVKSLCAK  409
Human D5             MNHIPMHIDHDRNMDWVSTQLQATCNVHKSAFNDWFSGHLNFQIEHHLFPTMPRHNYHKVAPLVQSLCAK  409

Atlantic salmon D6   HGIPYQVKTLQRAIIDVVRSLKKSGDLWLDAYLHK  454
Atlantic salmon D5   HGVPYQVKTLQKGMTDVVRSLKKSGDLWLDAYLHK  454
Rainbow trout D6     HGLPYQVKTLQRAIIDVVGSLKKSGDLWLDAYLHK  454
Zebrafish D5/D6      YGVRYQEKTLYGAFADIIRSLEKSGELWLDAYLNK  444
Human D6             HGIEYQEKPLLRALLDIIRSLKKSGKLWLDAYLHK  444
Human D5             HGIEYQSKPLLSAFADIIHSLKESGQLWLDAYLHQ  444
```
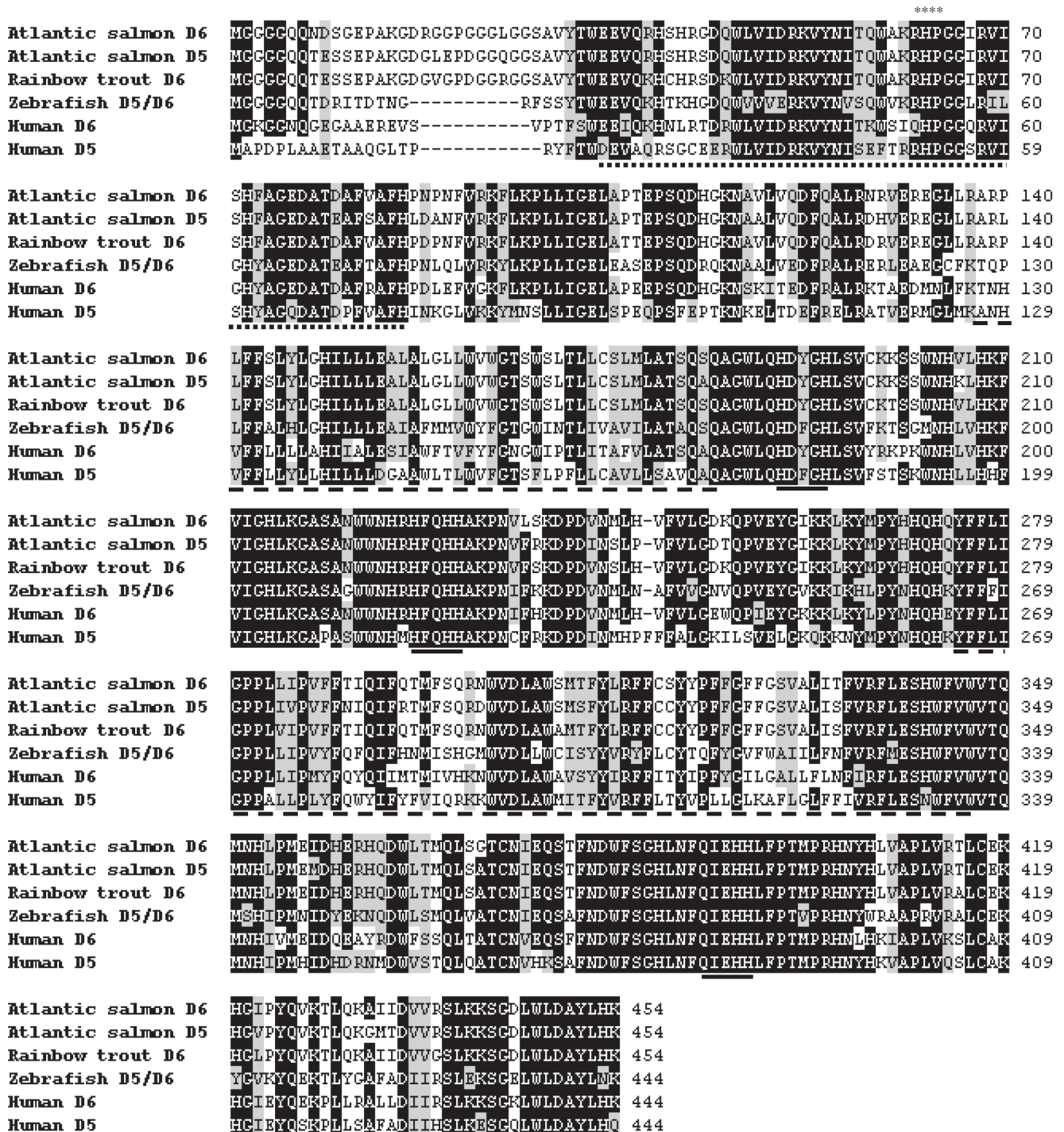
FIG. 1. Comparison of the deduced amino acid sequence of Δ6 and Δ5 polyunsaturated fatty acyl desaturases from Atlantic salmon with that of desaturases from trout, zebrafish, and humans. Identical residues are shaded black, and similar residues are shaded grey. Identity/similarity shading was based on the BLOSUM62 matrix, and the cutoff for shading was 75%. The cytochrome b_5-like domain is dot-underlined, the two transmembrane regions are dash-underlined, the three histidine-rich domains are solid underlined, and asterisks on the top mark the heme-binding motif, HPGG.

Δ5 fatty acyl desaturase and fatty acyl elongase mRNAs. The results showed that the three genes were expressed in all tissues examined, with the highest expression in terms of the absolute copy numbers (mean ± SD, $n = 8$) in intestine, followed by liver and brain (Fig. 5). In comparison with the Δ5 desaturase, the transcript copy abundance for the Δ6 desaturase was higher in these tissues with higher expression, but lower in tissues with lower expression, other than kidney. The transcript copy abundance for fatty acyl elongase was much lower than that for the Δ6 and Δ5 desaturases in all tissues.

The ratios of copy numbers between the target genes and β-actin were determined (means ± SD, $n = 4$), and the fold
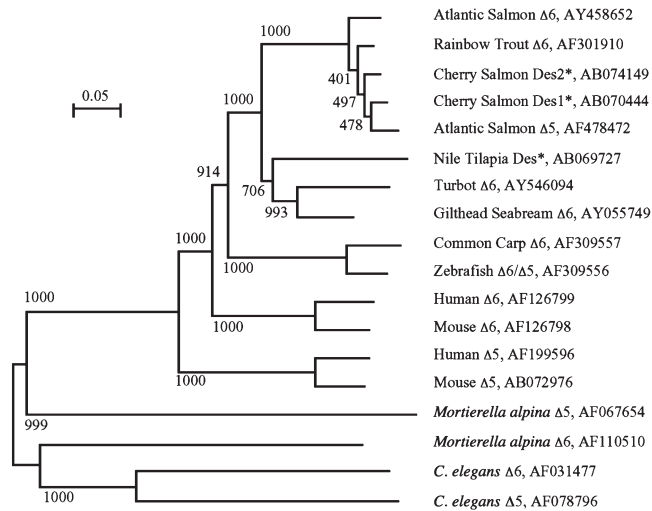
FIG. 2. Phylogenetic tree of Δ6 and Δ5 desaturases from salmon, and desaturases from other fish species (zebrafish, cherry salmon, rainbow trout, seabream, common carp, turbot, and tilapia), mammals (mouse and human), fungus (*Mortierella alpina*), and nematode (*Caenorhabditis elegans*). The tree was constructed using the Neighbour Joining method using *ClustalX* and *NJPLOT*. The horizontal branch length is proportional to the amino acid substitution rate per site. The numbers represent the frequencies with which the tree topology presented here was replicated after 1000 bootstrap iterations. Sequences marked with an asterisk are not functionally characterized.

difference between the mean value of target gene expression in the tissue of fish fed VO was calculated relative to the expression in tissues of fish fed FO (Fig. 6). The results revealed that Δ6 and Δ5 fatty acyl desaturase gene expression in liver and red muscle of fish fed VO was significantly increased compared with fish fed the FO diet, whereas the expression of both desaturases in heart and spleen, and Δ5 in gill and kidney was decreased in fish fed VO (Fig. 6). Expression of both desaturases in intestine and adipose tissue was also higher in fish fed VO, although with the high variation these effects were below the level of statistical significance. However, feeding VO decreased the expression of the fatty acyl elongase gene in most tissues, significantly so in heart, gill, brain, adipose, spleen, and kidney (Fig. 6).

DISCUSSION

Several fish desaturases have been cloned and functionally characterized in recent years. These are the bifunctional zebrafish enzyme showing both Δ6 and Δ5 desaturase activity (22), an Atlantic salmon desaturase that was shown to be predominantly an n-3 Δ5 desaturase (26), and common carp, rainbow trout, gilthead seabream, and turbot desaturases that were all shown to be predominantly Δ6 desaturases (25). The bifunctional nature of the Δ6/Δ5 desaturase of zebrafish suggested that it may be a prototypic or ancestral progenitor desaturase (22,29). But the subsequent characterization of several essentially unifunctional Δ6 fish desaturases and the salmon Δ5 desaturase indicates that the zebrafish enzyme might be atypical.
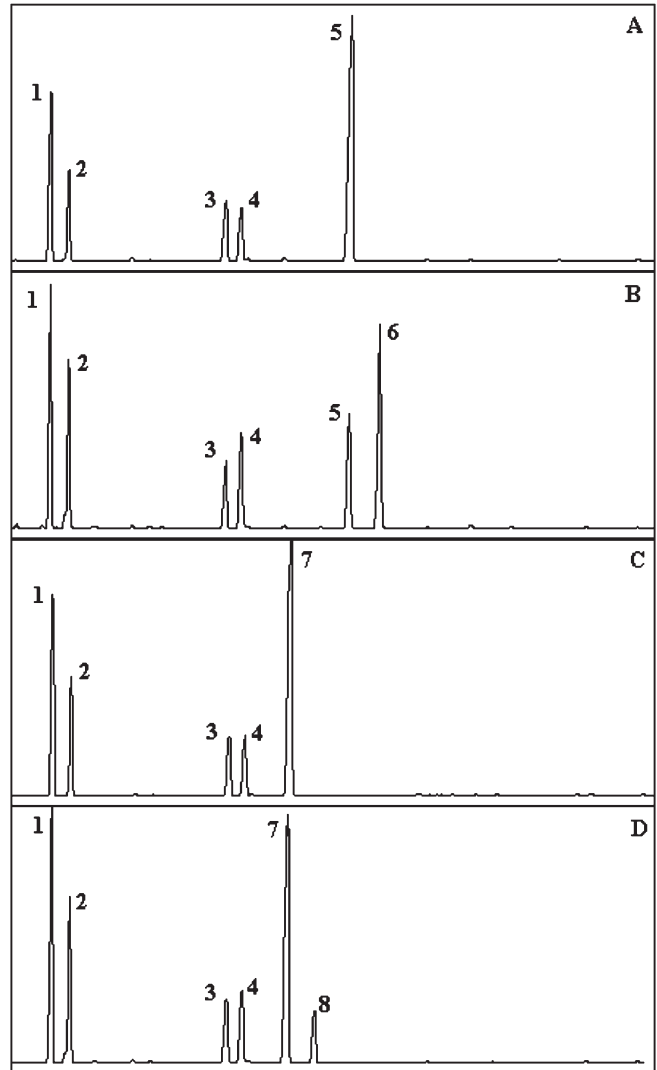
FIG. 3. Functional expression of the Atlantic salmon putative fatty acyl desaturase in transgenic yeast (*Saccharomyces cerevisiae*) grown in the presence of Δ6 substrates, 18:3n-3 and 18:2n-6. FA were extracted from yeast transformed with pYES vector without insert (A and C) or containing the putative FA desaturase cDNA insert (B and D). The first four peaks in panels A–D are the main endogenous FA of *S. cerevisiae*, namely, 16:0 (1), 16:1n-7 (2), 18:0 (3), and 18:1n-9 (with 18:1n-7 as shoulder) (4). Peak 5 in panels A and B, and peak 7 in panels C and D are the exogenously added substrate FA, 18:3n-3 and 18:2n-6, respectively. Peaks 6 and 8 in panels B and D were identified as the resultant desaturated products, namely, 18:4n-3 and 18:3n-6, respectively. Vertical axis, FID response; horizontal axis, retention time.

The study described here has further increased our knowledge of PUFA desaturases in fish. The cloning and functional characterization of a predominantly Δ6 desaturase gene makes the Atlantic salmon the first fish species to be shown to have separate and distinct genes for Δ6 and Δ5 desaturases, as reported previously for *C. elegans* (14,18,19) and humans (16,20,21). The salmon Δ6 desaturase clone also showed measurable, but very low, levels of Δ5 activity and thus was similar to other fish Δ6 desaturases of carp, trout, seabream,
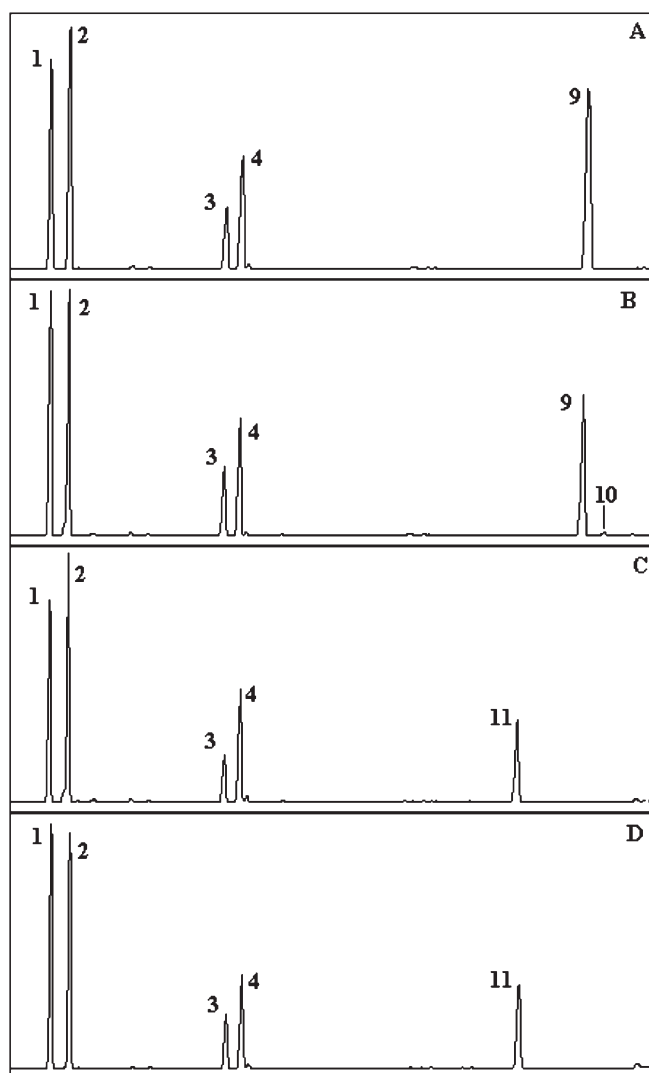
FIG. 4. Functional expression of the Atlantic salmon putative fatty acyl desaturase in transgenic yeast (*Saccharomyces cerevisiae*) grown in the presence of Δ5 substrates, 20:4n-3 and 20:3n-6. FA were extracted from yeast transformed with pYES vector without insert (A and C) or containing the putative FA desaturase cDNA insert (B and D). The first four peaks in panels A–D are as described in the caption to Figure 3. Peak 9 in panels A and B, and peak 11 in panels C and D are the exogenously added substrate FA, 20:4n-3 and 20:3n-6, respectively. Peak 10 in panel B was identified as the resultant desaturated product of 20:4n-3, namely, 20:5n-3. Vertical axis, FID response; horizontal axis, retention time.

TABLE 2

Functional Characterization of Salmon FA Desaturase cDNA Clone in the Yeast *Saccharomyces cerevisiae*

PUFA substrates	Products	Desaturase activity	Conversion rate[a] (%)
α-Linolenic acid (18:3n-3)	18:4n-3	Δ6	60.1
Linoleic acid (18:2n-6)	18:3n-6	Δ6	14.4
Eicosatetraenoic acid (20:4n-3)	20:5n-3	Δ5	2.3
Dihomo-γ-linolenic acid (20:3n-6)	20:4n-6	Δ5	0
Docosapentaenoic acid (22:5n-3)	22:6n-3	Δ4	0
Docosatetraenoic acid (22:4n-6)	22:5n-6	Δ4	0

[a]Conversion rates represent the proportion of substrate FA converted to the longer-chain FA product, calculated from the gas chromatograms as 100 × [product area/(product area + substrate area)].

TABLE 3

Exon and Intron Boundaries of Atlantic Salmon Δ6 Fatty Acyl Desaturase

Exon	Size (bp)	3′ splice acceptor	5′ splice donor	Intron size (bp)
1	25[a]		..AATATTGgtgagtg..	698
2	496[b]	..tttgcagCTGGCCC..	..TGCCACGgtcagta..	1127
3	111	..tttgtagGACGCAT..	..GAAAAATgtgagga..	744
4	198	..catacagGCAGTAC..	..GTCTCAGgtaccat..	228
5	102	..ctctcagTCCCAGG..	..CCTAAAGgtaggct..	345
6	126	..tttccagGGTGCCT..	..TGTAGAGgtagtta..	515
7	61	..attgcagTATGGTA..	..TTCCTCAgtaagtc..	128
8	77	..ctttcagTTGGACC..	..CTGGGTGgtgagat..	303
9	98	..tgtgaagGATCTGG..	..TCGTCAGgtaaagt..	161
10	97	..tatatagGTTTTTG..	..CATGCAGgtaacat..	1011
11	80	..gtcttagTTGAGTG..	..AACACCAgtaagtg..	383
12	126	..ctcccagTCTGTTT..	..TTGTCAGgtaagtg..	216
13	509[c]	..tctccagGTCACTG..		

[a]Exon is a 5′-untranslated region (5′-UTR)
[b]Exon includes a 5′-UTR of 259 bp.
[c]Exon includes a 3′-UTR of 457 bp.

and turbot (25). But, unlike the zebrafish desaturase, which showed very significant Δ5 desaturase activity at around 70% of the Δ6 activity (22), the n-3 Δ5 activity in the salmon cDNA product was only 3.8% of the Δ6 activity. It is likely that the level of Δ5 desaturase activity measured is of limited physiological significance.

The study described here also clearly showed that the salmon Δ6 desaturase has a marked preference for the n-3 substrate 18:3n-3 over the n-6 substrate 18:2n-6. A similar preference for n-3 FA substrates rather than n-6 substrates on heterologous expression in yeast was observed previously with the zebrafish Δ6/Δ5 desaturase, salmon Δ5 desaturase (22,26), and trout, seabream, carp, and turbot Δ6 desaturases (25). These data are consistent with earlier enzymological studies investigating the desaturation of ^{14}C-labeled FA substrates in primary hepatocytes (9), primary brain astrocytes (30), and established cell lines (31). Therefore, it appears that greater activity toward n-3 PUFA may be a characteristic of fish fatty acyl desaturases. In contrast, functional characterization of Δ6 desaturases of other organisms including nematodes, mammals, fungi, mosses, and higher plants failed to show a preference for either 18:3n-3 or 18:2n-6 substrates, although recently Δ6 desaturases have been identified in *Primula* sp. that have a preference for n-3 substrates (32). However, data of these kinds obtained from heterologous expression can be regarded as only semiquantitative, as there are likely to be differences between FA, for example, in their uptake into organisms such as yeasts (33).

The present study shows unequivocally that distinct Δ6 and Δ5 desaturase genes exist in Atlantic salmon, as is the case in humans, and possibly in mammals in general. However, the two salmon cDNAs are very similar in that the predicted amino acid sequence encoded by the Δ6 cDNA is 91%
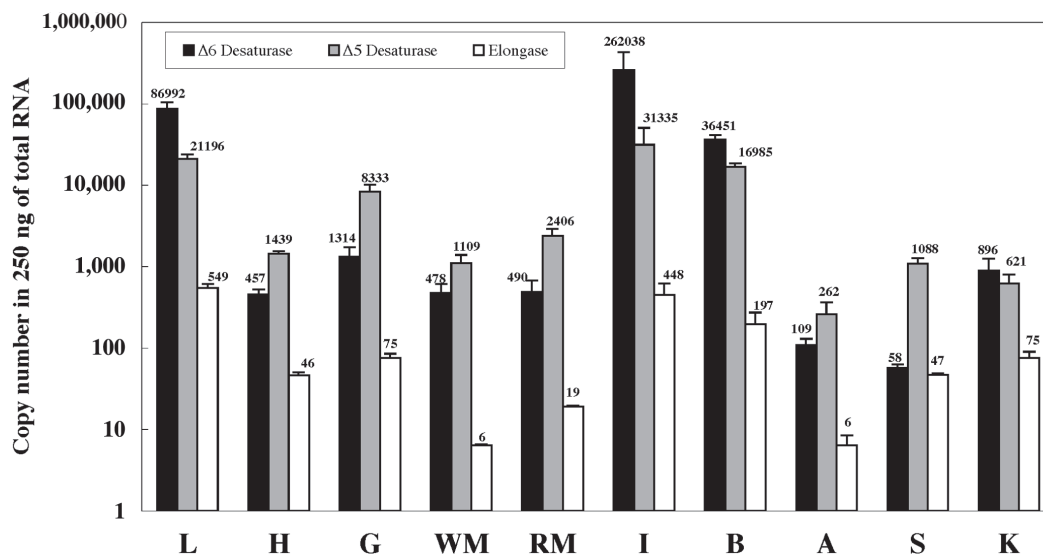
FIG. 5. Tissue distribution of FA Δ6 and Δ5 desaturase and elongase genes in Atlantic salmon. Transcript (mRNA) copy number was determined by quantitative real-time PCR (qrtPCR) as described in the Materials and Methods section. Results are expressed as the copy numbers in 250 ng of total RNA and are means ± SEM (*n* = 4). L, liver; H, heart; G, gill; WM, white muscle; RM, red muscle; I, intestine; B, brain; A, adipose; S, spleen; K, kidney.

identical with that encoded by the Δ5 desaturase cDNA. In contrast, in humans and *C. elegans*, the two functional Δ6 and Δ5 desaturases share an amino acid identity of only 62 (20) and 45% (19), respectively. Whether or not distinct Δ6 and Δ5 desaturase genes evolved from a common ancestral desaturase progenitor, these data suggest that the process occurred or began more recently in the evolution of Atlantic salmon than in the evolution of humans and *C. elegans*. In this regard, it is pertinent to note that the Atlantic salmon is partially tetraploid, with the tetraploidization event thought to have occurred 25–100 million years ago (34). However, evolution of desaturases in Atlantic salmon and in fish in general remains a subject for speculation. Study of further FA desaturase genes of fish are indicated, and certainly other desaturases are likely to be identified in fish species such as carp and trout, which have the ability to produce DHA from 18:3n-3 (35). But in marine species such as sea bream and turbot, the search for Δ5 desaturases will be particularly intriguing as these species lack the ability to produce EPA and DHA from 18:3n-3. This is attributed to deficiencies in Δ5 desaturation in sea bream, but to C_{18-20} elongation in turbot (36,37).

The salmon Δ6 desaturase showed no Δ4 desaturase activity, perhaps as expected based on the functional characterization of all fish and mammalian Δ6 and Δ5 desaturases reported to date (22,25,26,38). This is consistent with the hypothesis that the synthesis of DHA from EPA in both mammals and fish proceeds *via* elongation to 24:5n-3 followed by a Δ6 desaturation rather than *via* Δ4 desaturation of 22:5n-3 (35,39). Heterologous expression studies of human and rat Δ6 desaturases showed that the same enzymes are active on C_{18} and C_{24} FA (33,40) and that the bifunctional zebrafish desaturase was also capable of desaturating C_{24} FA (41). It will be interesting to determine the activities of all an-

imal Δ6 desaturases toward C_{24} FA substrates. In contrast to higher animals, production of DHA *via* a pathway including Δ4 desaturation appears to operate in some lower organisms such as *Thraustochytrium* sp. (42), and the algae *Euglena gracilis* (43) and *Pavlova lutheri* (44).

Genomic characterization showed that the salmon Δ6 desaturase comprised 13 exons, which is one more than that reported for the human Δ6 desaturase (45). The additional exon in the salmon gene is a small 25 bp exon at the extreme 5′ end. The remaining exons are homologous to the 12 exons in the human Δ6 desaturase, except that exon 2 of the salmon gene is 30 bp longer than exon 1 in the human gene, corresponding to the additional 10 amino acids found in most salmonid desaturases. However, the remaining exons are exactly the same size as their equivalents in the human gene, and splice and acceptor sites are interrupted at similar nucleotide positions, even though the lengths of the introns are quite different. In humans, there is evidence that the desaturase gene cluster has arisen by gene duplication. This is on the basis that the exon organization is nearly identical in the three family members, with each gene consisting of 12 exons and splice and acceptor sites interrupted at identical nucleotide positions within highly conserved codons (45). Further work on the genomic organization of fish desaturases may help to clarify the significance of the additional exon in salmon and the possible evolutionary history of desaturases, as sequence alignments alone are not conclusive (46).

The phylogenetic sequence analyses grouped the fish desaturases largely as expected based on classical phylogeny with the carp and zebrafish (Ostariophysi; cyprinids), trout and salmon (Salmoniformes; salmonidae), and tilapia, sea bream, and turbot (Acanthopterygia; cichlids, perciformes, and pleuronectiformes) appearing in three distinct clusters
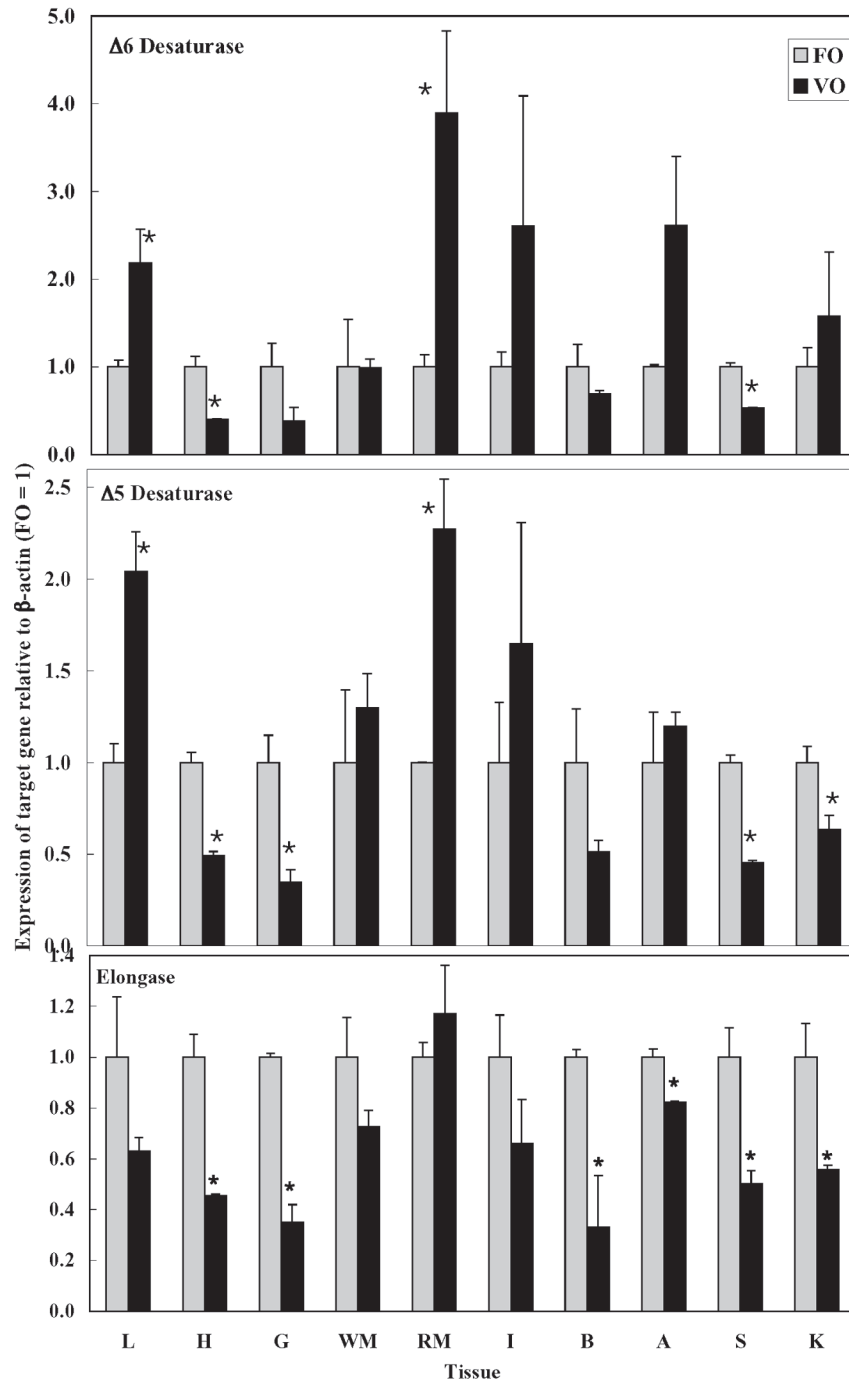
FIG. 6. Effect of dietary vegetable oil (VO) on the expression of FA Δ6 and Δ5 desaturase and elongase genes in tissues from Atlantic salmon. Transcript (mRNA) copy number was determined by qrtPCR as described in the Materials and Methods section. The ratios of copy numbers between the target genes and β-actin were calculated as means ± SEM ($n = 4$). Results are expressed as the fold differences by comparison of mean values in fish fed the vegetable oil diet compared with those in fish fed the fish oil (FO) diet (FO = 1). For other abbreviations see Figure 5. *Mean values for fish fed VO are significantly different ($P < 0.05$) from those for fish fed FO as determined by the Student t-test.

(47). However, the cloning of Atlantic salmon Δ6 desaturase revealed that both Δ6 and Δ5 desaturases in salmonids contain additional amino acids by comparison with those of other species, having chain lengths of 454 amino acids (or 452 as

in cherry salmon Des2) compared with 444 for the cyprinid (carp and zebrafish) and human desaturases (16,20,22,23,26). Furthermore, it has been reported that the desaturase cDNAs encode proteins of 445 amino acids in seabream (24) and turbot

(25), one more residue than in cyprinid and human desaturases. These data support our previous observation that differences in polypeptide length are not in these cases related to function (25).

qrtPCR revealed that the expression of fatty acyl desaturase genes was highest in intestine, liver, and brain and lower in heart, gill, white and red muscle, kidney, spleen, and adipose tissue. Previously, by using RT-PCR, it was shown that Δ6 desaturase of rainbow trout and sea bream was expressed in intestinal tissue (23,24). In the present study, salmon intestinal tissue had levels of Δ6 and Δ5 expression 3- and 1.5-fold greater than liver. Similarly, expression of Δ6 and Δ5 in intestine was 7.2- and 1.9-fold greater than in brain. Therefore, these results suggest that intestine, the first organ to encounter dietary FA, has the capacity to play an important role in the primary processing of dietary FA *via* desaturation. Cho *et al.* (20) reported that human liver expressed 4–5 times more Δ5 desaturase and 12 times more Δ6 desaturase than brain. Our results show that salmon liver contained 2.4 times more Δ6 desaturase mRNA than brain, and the Δ5 desaturase mRNA levels in liver and brain were similar. Regardless of which gene has the higher level of mRNA, the observation that all tissues investigated express detectable levels of Δ6 and Δ5 desaturase and elongase mRNAs is consistent with the important roles that desaturase and elongase enzymes play in maintaining cellular membrane HUFA. That intestine expressed such high levels of both Δ6 and Δ5 desaturase is consistent with data from *in vitro* enzyme assays in isolated enterocytes (48,49) and *in vivo* stable isotope studies (50,51), which have shown enterocytes and intestine to be sites of significant HUFA synthesis in salmonids. The level of Δ6 desaturase mRNA in highly expressing tissues was substantially greater than the amount of Δ5 desaturase mRNA, but the level of Δ6 desaturase mRNA in lower-expressing tissues was lower than the amount of Δ5 desaturase mRNA. In comparison, a study of the relative abundance of Δ6 and Δ5 desaturase mRNA in various human tissues revealed that the level of Δ6 desaturase mRNA in eight different tissues was significantly greater than the amount of Δ5 desaturase mRNA (20). This observation is particularly interesting because Δ6 is often considered the enzyme that catalyzes the rate-limiting step in the synthesis of HUFA (52).

The results of this study show that the expression of Δ6 and Δ5 FA desaturases is under nutritional regulation in Atlantic salmon. Thus, the expression of these genes is higher in liver and red muscle (and possibly intestine and adipose tissue) of salmon fed diets containing C_{18} PUFA-rich VO compared with fish fed diets containing HUFA-rich fish oil. Although Δ6 desaturase is regarded as the main rate-limiting step in the HUFA biosynthesis pathway, Δ5 desaturase is reported also to be under nutritional regulation in mammals (53). In a previous study, the expression and activity of fatty acyl elongase appeared to be nutritionally regulated in Atlantic salmon (54). That study showed that dietary linseed oil increased the expression of both Δ5 FA desaturase and elongase genes in salmon liver (54). Similar effects of dietary linseed oil had been reported previously, with the liver transcript level of Δ6 desaturase being higher in trout fed linseed oil than in trout fed FO (23). However, the present study showed that the expression and activity of the elongase decreased in most tissues of salmon fed diets containing the VO blend compared with fish fed diets containing FO. The precise reason for the different responses in elongase gene expression is unclear but may be related to differences in the FA profiles of the linseed oil and VO-blend diets. In the present trial, the total n-3 HUFA level in the diet in which the VO blend replaced 75% of the FO was over 8%, which compares well with 9% HUFA in the diet in the previous trial in which 25% of the FO was replaced by linseed oil, a level of replacement that did not increase elongase activity (54). Elongase activity was increased only by diets in which 50–100% of FO was replaced with linseed oil, resulting in much lower levels of n-3 HUFA (54).

In conclusion, the study reported here has identified and characterized a Δ6 desaturase gene in Atlantic salmon. It had measurable, but very low, levels of Δ5 desaturase activity. The salmon Δ6 desaturase gene comprises 13 exons, one more than the human Δ6 and Δ5 desaturases. Genes for Δ6 and Δ5 desaturases and elongases were expressed in various tissues of salmon, and highly expressed in liver, intestine, and brain. Both Δ6 and Δ5 desaturase gene expression in intestine, liver, red muscle, and adipose tissue were significantly increased in salmon fed VO compared with fish fed FO.

ACKNOWLEDGMENTS

REFERENCES

1. Simopoulos, A.P. (1989) Summary of the NATO Advanced Research Workshop on Dietary Omega 3 and Omega 6 Fatty Acids: Biological Effects and Nutritional Essentiality, *J. Nutr. 119*, 521–528.
2. Simopoulos, A.P. (1991) Omega-3 Fatty Acids in Health and Disease and in Growth and Development, *Am. J. Clin. Nutr. 54*, 438–463.
3. Lands, W.E. (1992) Biochemistry and Physiology of n-3 Fatty Acids, *FASEB J. 6*, 2530–2536.
4. Tidwell, J.H., and Allan, G.L. (2002) Fish as Food: Aquaculture's Contribution, *World Aquaculture 33*, 44–48.
5. Sargent, J.R., and Tacon, A. (1999) Development of Farmed Fish: A Nutritionally Necessary Alternative to Meat, *Proc. Nutr. Soc. 58*, 377–383.
6. Barlow, S. (2000) Fish Meal and Fish Oil: Sustainable Feed Ingredients for Aquafeeds, *Global Aquacult. Advocate 4*, 85–88.
7. Sargent, J.R., Tocher, D.R., and Bell, J.G. (2002) The Lipids, in *Fish Nutrition*, 3rd edn. (Halver, J.E., and Hardy, R.W., eds.), pp. 181–257, Academic Press, San Diego.
8. Bell, J.G., McEvoy, J., Tocher, D.R., McGhee, F., Campbell, P.J., and Sargent, J.R. (2001) Replacement of Fish Oil with Rape Seed Oil in Diets of Atlantic Salmon (*Salmos salar*) Affects Tissue

Lipid Compositions and Hepatocyte Fatty Acid Metabolism, *J. Nutr. 131*, 1535–1543.

9. Bell, J.G., Tocher, D.R., Farndale, B.M., Cox, D.I., McKinney, R.W., and Sargent, J.R. (1997) The Effect of Dietary Lipid on Polyunsaturated Fatty Acid Metabolism in Atlantic Salmon (*Salmo salar*) Undergoing Parr–Smolt Transformation, *Lipids 32*, 515–525.

10. Tocher, D.R., Bell, J.G., Henderson, R.J., McGhee, F., Mitchell, D., and Morris, P.C. (2000) The Effect of Dietary Linseed and Rapeseed Oils on Polyunsaturated Fatty Acid Metabolism in Atlantic Salmon (*Salmo salar*) Undergoing Parr–Smolt Transformation, *Fish Physiol. Biochem. 23*, 59–73.

11. Tocher, D.R., Bell, J.G., Dick, J.R., and Crampton, V.O. (2003) Effects of Vegetable Oil Diets on Atlantic Salmon Hepatocyte Desaturase Activities and Liver Fatty Acid Compositions, *Lipids 38*, 723–732.

12. Tocher, D.R., Leaver, M.J., and Hodgson, P.A. (1998). Recent Advances in the Biochemistry and Molecular Biology of Fatty Acyl Desaturases, *Prog. Lipid Res. 37*, 73–117.

13. Huang, Y.-S., Chaudhary, S., Thurmond, J., Bobik, E.G., Yuan, L., Chan, G.E., Kirchner, S.J., Mukerji, P., and Knutson, D.S. (1999) Cloning of Δ12- and Δ5-Desaturases from *Mortierella alpina* and Recombinant Production of γ-Linolenic Acid in *Saccharomyces cerevisiae*, *Lipids 34*, 649–659.

14. Napier, J.A., Hey, S.J., Lacey, D.J., and Shewry, P.R. (1998) Identification of a *Caenorhabditis elegans* Δ[6]-Fatty-Acid-Desaturase by Heterologous Expression in *Saccharomyces cerevisiae*, *Biochem. J. 330*, 611–614.

15. Aki, T., Shimada, Y., Inagaki, K., Higashimoto, H., Kawamoto, S., Shiget, S., Ono, K., and Suzuki, O. (1999) Molecular Cloning and Functional Characterization of Rat Δ-6 Fatty Acid Desaturase, *Biochem. Biophys. Res. Commun. 255*, 575–579.

16. Cho, H.P., Nakamura, M.T., and Clarke, S.D. (1999) Cloning, Expression and Nutritional Regulation of the Human Δ6 Desaturase, *J. Biol. Chem. 274*, 471–477.

17. Michaelson, L.V., Lazarus, C.M., Griffiths, G., Napier, J.A., and Stobart, A.K. (1998) Isolation of a Δ5 Fatty Acid Desaturase Gene from *Mortierella alpina*, *J. Biol. Chem. 273*, 19055–19059.

18. Michaelson, L.V., Napier, J.A., Lewis, M., Griffiths, G., Lazarus, C.M., and Stobart, A.K. (1998) Functional Identification of a Fatty Acid Δ5 Desaturase Gene from *Caenorhabditis elegans*, *FEBS Lett. 439*, 215–218.

19. Watts, J.L., and Browse, J. (1999) Isolation and Characterization of a Δ[5] Fatty Acid Desaturase from *Caenorhabditis elegans*, *Arch. Biochem. Biophys. 362*, 175–182.

20. Cho, H.P., Nakamura, M.T., and Clarke, S.D. (1999) Cloning, Expression and Nutritional Regulation of the Human Δ5 Desaturase, *J. Biol. Chem. 274*, 37335–37339.

21. Leonard, A.E., Kelder, B., Bobik, E.G., Chuang, L.-T., Parker-Barnes, J.M., Thurmond, J.M., Kroeger, P.E., Kopchick, J.J., Huang, Y.-S., and Mukerji, P. (2000) cDNA Cloning and Characterization of Human Δ5 Desaturase Involved in the Biosynthesis of Arachidonic Acid, *Biochem. J. 347*, 719–724.

22. Hastings, N., Agaba, M., Tocher, D.R., Leaver, M.J., Dick, J.R., Sargent, J.R., and Teale, A.J. (2001) A Vertebrate Fatty Acid Desaturase with Δ5 and Δ6 Activities, *Proc. Natl. Acad. Sci. USA 98*, 14304–14309.

23. Seiliez, I., Panserat, S., Kaushik, S., and Bergot, P. (2001) Cloning, Tissue Distribution and Nutritional Regulation of a Δ6-Desaturase-like Enzyme in Rainbow Trout, *Comp. Biochem. Physiol. 130B*, 83–93.

24. Seiliez, I., Panserat, S., Corraze, G., Kaushik, S., and Bergot, P. (2003) Cloning and Nutritional Regulation of a Δ6-Desaturase-like Enzyme in the Marine Teleost Gilthead Seabream (*Sparus aurata*), *Comp. Biochem. Physiol. 135B*, 449–460.

25. Zheng, X., Seiliez, I., Hastings, N., Tocher, D.R., Panserat, S., Dickson, C.A., Bergot, P., and Teale A.J. (2004) Characterisa-tion and Comparison of Fatty Acyl Δ6 Desaturase cDNAs from Freshwater and Marine Teleost Fish Species, *Comp. Biochem. Physiol. 139B*, 269–279.

26. Hastings, N., Agaba, M.K., Tocher, D.R., Zheng, X., Dickson, C.A., Dick, J.R., and Teale, A.J. (2004) Molecular Cloning and Functional Characterization of Fatty Acyl Desaturase and Elongase cDNAs Involved in the Production of Eicosapentaenoic and Docosahexaenoic Acids from α-Linolenic Acid in Atlantic Salmon (*Salmo salar*), *Mar. Biotechnol.*, in press.

27. U.S. National Research Council (1993) *Nutrient Requirements of Fish*, National Academy Press, Washington, DC.

28. Saitou, N., and Nei, M. (1987) The Neighbor-Joining Method. A New Method for Reconstructing Phylogenetic Trees, *Mol. Biol. Evol. 4*, 406–425.

29. Napier, J.A., Michaelson, L.V., and Sayanova, O. (2003) The Role of Cytochrome b_5 Fusion Desaturases in the Synthesis of Polyunsaturated Fatty Acids, *Prostaglandins Leukotrienes Essent. Fatty Acids 68*, 135–143.

30. Tocher, D.R., and Sargent, J.R. (1990) Incorporation into Phospholipid Classes and Metabolism *via* Desaturation and Elongation of Various ^{14}C-Labelled (n-3) and (n-6) Polyunsaturated Fatty Acids in Trout Astrocytes in Primary Culture, *J. Neurochem. 54*, 2118–2124.

31. Tocher, D.R., and Sargent, J.R. (1990) Effect of Temperature on the Incorporation into Phospholipid Classes and the Metabolism *via* Desaturation and Elongation of (n-3) and (n-6) Polyunsaturated Fatty Acids in Fish Cells in Culture, *Lipids 25*, 435–442.

32. Sayanova, O.V., Beaudoin, F., Michaelson, L.V., Shewry, P.R., and Napier, J.A. (2003) Identification of *Primula* Fatty Acid Δ6-Desaturases with n-3 Substrate Preferences, *FEBS Lett. 542*, 100–104.

33. De Antueno, R.J., Knickle, L.C., Smith, H., Elliot, M.L., Allen, S.J., Nwaka, S., and Winther, M.D. (2001) Activity of Human Δ5 and Δ6 Desaturases on Multiple n-3 and n-6 Polyunsaturated Fatty Acids, *FEBS Lett. 509*, 77–80.

34. Allendorf, F.W., and Thorgaard, G.H. (1984) Tetraploidy and the Evolution of Salmonid Fishes, in *Evolutionary Genetics of Fishes: Monographs in Evolutionary Biology* (Turner, B.J., ed.), pp. 1–53, Plenum Press, New York.

35. Tocher, D.R. (2003) Metabolism and Functions of Lipids and Fatty Acids in Teleost Fish, *Rev. Fisheries Sci. 11*, 107–184.

36. Tocher, D.R., and Ghioni, C. (1999) Fatty Acid Metabolism in Marine Fish: Low Activity of Δ5 Desaturation in Gilthead Sea Bream (*Sparus aurata*) Cells, *Lipids 34*, 433–440.

37. Ghioni, C., Tocher, D.R., Bell, M.V., Dick, J.R., and Sargent, J.R. (1999) Low C_{18} to C_{20} Fatty Acid Elongase Activity and Limited Conversion of Stearidonic Acid, 18:4n-3, to Eicosapentaenoic Acid, 20:5n-3, in a Cell Line from the Turbot, *Scophthalmus maximus*, *Biochim. Biophys. Acta 1437*, 170–181.

38. Pereira, S.L., Leonard, A.E., and Mukerji, P. (2003) Recent Advances in the Study of Fatty Acid Desaturases from Animals and Lower Eukaryotes, *Prostaglandins Leukotrienes Essent. Fatty Acids 68*, 97–106.

39. Wallis, J.G., Watts, J.L., and Browse, J. (2002) Polyunsaturated Fatty Acid Synthesis: What Will They Think of Next? *Trends Biochem. Sci. 27*, 467–473.

40. D'Andrea, S., Guillou, H., Jan, S., Catheline, D., Thibault, J.-N., Bouriel, M., Rioux, V., and Legrand, P. (2002) The Same Rat Δ6-Desaturase Not Only Acts on 18- but Also on 24-Carbon Fatty Acids in Very-Long-Chain Polyunsaturated Fatty Acid Biosynthesis, *Biochem. J. 364*, 49–55.

41. Tocher, D.R., Agaba, M., Hastings, N., and Teale, A.J. (2003) Biochemical and Molecular Studies of the Fatty Acid Desaturation Pathway in Fish, in *The Big Fish Bang—Proceedings of the 26th Annual Larval Fish Conference* (Browman, H.I., and Skiftesvik, A.B., eds.), pp. 211–227, Institute of Marine Nutrition, Bergen.

42. Qui, X., Hong, H., and MacKenzie, S.L. (2001) Identification of a Δ4 Fatty Acid Desaturase from *Thraustochytrium* sp. Involved in the Synthesis of Docosahexaenoic Acid by Heterologous Expression in *Saccharomyces cerevisiae* and *Brassica juncea*, *J. Biol. Chem. 276*, 31561–31566.

43. Meyer, A., Cirpus, P., Ott, C., Scheckler, R., Zahringer, U., and Heinz, E. (2003) Biosynthesis of Docosahexaenoic Acid in *Euglena gracilis*: Biochemical and Molecular Evidence for the Involvement of a Δ4-Fatty Acyl Group Desaturase, *Biochemistry 42*, 9779–9788.

44. Tonon, T., Harvey, D., Larson, T.R., and Graham, I.A. (2003) Identification of a Very Long Chain Polyunsaturated Fatty Acid Δ4-Desaturase from the Microalga *Pavlova lutheri*, *FEBS Lett. 553*, 440–444.

45. Marquardt, A., Stöhr, H., White, K., and Weber B.H.F. (2000) cDNA Cloning, Genomic Structure, and Chromosomal Localization of Three Members of the Human Fatty Acid Desaturase Family, *Genomics 66*, 175–183.

46. Sperling, P., Ternes, P., Zank, T.K., and Heinz, E. (2003) The Evolution of Desaturases, *Prostaglandins Leukotrienes Essent. Fatty Acids 68*, 73–95.

47. Nelson, J.S. (1994) *Fishes of the World*, 3rd edn., John Wiley & Sons, New York.

48. Tocher, D.R., Fonseca-Madrigal, J., Bell, J.G., Dick, J.R., Henderson, R.J., and Sargent, J.R. (2002) Effects of Diets Containing Linseed Oil on Fatty Acid Desaturation and Oxidation in Hepatocytes and Intestinal Enterocytes in Atlantic Salmon (*Salmo salar*), *Fish Physiol. Biochem. 26*, 157–170.

49. Tocher, D.R., Fonseca-Madrigal, J., Dick, J.R., Ng, W.-K., Bell, J.G., and Campbell, P.J. (2004) Effects of Diets Containing Palm Oil and Water Temperature on Fatty Acid Desaturation and Oxidation in Hepatocytes and Intestinal Enterocytes in Rainbow Trout (*Oncorhynchus mykiss*), *Comp. Biochem. Physiol. 137B*, 49–63.

50. Bell, M.V., Dick, J.R., and Porter A.E.A. (2001) Biosynthesis and Tissue Deposition of Docosahexaenoic Acid (22:6n-3) in Rainbow Trout (*Oncorhynchus mykiss*), *Lipids 36*, 1153–1159.

51. Bell, M.V., Dick, J.R., and Porter, A.E.A. (2003) Pyloric Ceca Are a Major Site of 22:6n-3 Synthesis in Rainbow Trout (*Oncorhynchus mykiss*), *Lipids 38*, 39–44.

52. Brenner, R.R. (1989) Factors Influencing Fatty Acid Chain Elongation and Desaturation, in *The Role of Fats in Human Nutrition* (Vergrosesen, A.J., and Crawford, M., eds.), 2nd edn., pp. 45–79, Academic Press, San Diego.

53. Brenner, R.R. (1981) Nutritional and Hormonal Factors Influencing Desaturation of Essential Fatty Acids, *Prog. Lipid Res. 20*, 41–47.

54. Zheng, X., Tocher, D.R., Dickson, C.A., Bell, J.G., and Teale, A.J. (2004) Effects of Diets Containing Vegetable Oil on Expression of Genes Involved in Polyunsaturated Fatty Acid Biosynthesis in Liver of Atlantic Salmon (*Salmo salar*), *Aquaculture 236*, 467–483.

Molecular Evidence That the Rate-Limiting Step for the Biosynthesis of Arachidonic Acid in *Mortierella alpina* Is at the Level of an Elongase

Seiki Takeno[a], Eiji Sakuradani[a], Shoichi Murata[a], Misa Inohara-Ochiai[b], Hiroshi Kawashima[c], Toshihiko Ashikari[b], and Sakayu Shimizu[a,*]

[a]Laboratory of Fermentation Physiology and Applied Microbiology, Division of Applied Life Sciences, Graduate School of Agriculture, Kyoto University, Kyoto 606-8502, Japan, and Institutes for [b]Advanced Technology and [c]Health Care Science, Suntory Ltd., Osaka 618-0001, Japan

ABSTRACT: The oil-producing fungus *Mortierella alpina* 1S-4 is an industrial strain for arachidonic acid (AA) production. To determine its physiological properties and to clarify the biosynthetic pathways for PUFA, heterologous and homologous gene expression systems were established in this fungus. The first trial was performed with an enhanced green fluorescent protein gene to assess the transformation efficiency for heterologous gene expression. As a result, strong fluorescence was observed in the spores of the obtained transformant, suggesting that the foreign gene was inherited by the spores. The next trial was performed with a homologous PUFA elongase (GLELOp) gene, this enzyme having been reported to catalyze the elongation of GLA (18:3n-6) to dihomo-γ-linolenic acid (20:3n-6), and to be the rate-limiting step of AA production. The FA composition of the transformant was different from that of the host strain: The GLA content was decreased whereas that of AA was increased. These data support the hypothesis that the GLELOp enzyme plays an important role in PUFA synthesis, and may indicate how to control PUFA biosynthesis.

Paper no. L9634 in *Lipids 40*, 25–30 (January 2005).

PUFA can serve as precursors of the eicosanoids of signaling molecules including prostaglandins, thromboxanes, and leukotrienes, and they also play important roles as structural components of membrane phospholipids (1,2). The principal PUFA that act as precursors for eicosanoid synthesis are dihomo-γ-linolenic acid (DGLA, 20:3n-6), arachidonic acid (AA, 20:4n-6), and EPA (20:5n-3). All mammals synthesize eicosanoids, which are involved in regulating inflammatory responses, reproductive function, immune responses, and blood pressure (3). Therefore, studies on PUFA biosynthesis are important in both the medical and pharmaceutical fields.

We found the filamentous fungus, *Mortierella alpina* 1S-4, to be a producer of PUFA-containing lipids (4). This species is unique in its capacity to produce C_{20} PUFA, such as DGLA, AA, and EPA. We have studied FA metabolism in this strain and succeeded in using it for the industrial production of AA

(5). Therefore, this fungus is a good model for analyzing a FA desaturation and/or elongation system from both fundamental and applied standpoints. A number of mutants derived from this fungus that show alterations in the FA synthetic pathways have been determined through analyses of the FA composition or accumulation.

Wynn and Ratledge (6) determined that the rate-limiting step for AA production is at the level of the elongation of GLA (18:3n-6) to DGLA (6). They also predicted that enhancement of the elongase activity would lead to an increase in AA production (6). In plants and mammals, it is believed that microsomal FA elongation is a four-step process comprising one condensation step, two reduction steps, and one dehydration step (7). Biochemical studies have provided indirect evidence that the reaction catalyzed by the condensing enzyme of the elongation system is rate-limiting (7–9). This enzyme regulates the substrate specificity in terms of the chain length and the degree of unsaturation of FA. Recently, the elongase responsible for the conversion of GLA to DGLA, designated as GLELO, was identified through expression studies on a *M. alpina* expression sequence tag library in yeast (10,11).

We have established a transformation system for this fungus (12) and have applied it to the study of PUFA production, especially AA. In this study, we succeeded in increasing AA production by *M. alpina* through metabolic engineering, namely, construction of a *M. alpina* strain over-expressing the GLELO gene: (i) As a first step, the enhanced green fluorescent protein (EGFP) gene was expressed in *M. alpina* 1S-4 to assess expression of two genes (*ura5* and *EGFP*), and (ii) GLELO cDNA was cloned and isolated from the strain, and then over-expressed in the same strain, hereby leading to increased AA production. This is the first report of the significant importance of the FA composition in an AA industrial strain, *M. alpina* 1S-4.

EXPERIMENTAL PROCEDURES

Enzymes and chemicals. Restriction enzymes and other DNA-modifying enzymes were obtained from Takara Bio Inc. (Shiga, Japan) and New England BioLabs (Beverly, MA). All other chemicals were of the highest purity commercially available.

Strains, media, and growth conditions. Mortierella alpina 1S-4 *ura5⁻* (13) was maintained on Potato Dextrose Agar

---

*To whom correspondence should be addressed.
E-mail: sim@kais.kyoto-u.ac.jp
Abbreviations: AA, arachidonic acid; DGLA, dihomo-γ-linolenic acid; EGFP, enhanced green fluorescent protein; GLELO, elongase responsible for conversion of GLA to DGLA.

medium (Difco, Detroit, MI) containing 5-fluoroorotic acid (0.5 mg/mL) and uracil (0.05 mg/mL). GY medium containing glucose and yeast extract was used for FA composition analyses. The composition of the GY medium depended on the kind of assay (see below). The compositions of the Czapek–Dox and SC media were given in a previous paper (13). For sporulation of the *ura5⁻* strain, uracil was added to the Czapek–Dox medium at 0.05 mg/mL. SC medium was used as the uracil-free synthetic medium for cultivation of the *ura5⁻* strains and the transformants. This synthetic medium was also used to maintain the transformants. Fungal strains were cultivated at 28°C with reciprocal shaking (120 strokes/min).

Preparation of genomic DNA and construction of a cDNA library. Preparation of genomic DNA of the *M. alpina* strain was performed according to the method described previously (14). Purification of mRNA and cDNA synthesis were also performed according to the methods described previously (15,16).

Isolation of GLELO cDNA of M. alpina 1S-4 and its expression in Aspergillus oryzae. Two primers were synthesized for amplification of the *M. alpina* 1S-4 GLELO cDNA by PCR with the following primers, designed on the basis of the nucleotide sequence of GLELOp of *M. alpina* ATCC 32221 (10): a sense primer, 5′-ATGGAGTCGATTGCGCAATTCCT-3′, and an anti-sense primer, 5′-TTACTGCAACTTCCTTGCCTTCTCCTT-3′. These primers were used in a Biometra T Gradient thermal cycler (Biometra GmbH, Göttingen, Germany) with a program of 1 min at 94°C, 1 min at 52.5°C, and 2 min at 72°C, for 35 cycles, followed by extension for 10 min at 72°C. The amplified 1.0-kb PCR product was cloned into the pT7Blue T-Vector (Novagen, Madison, WI) to construct pT7-GLELO, and then used to transform *Escherichia coli* DH5α. This clone was determined to encode a protein similar to GLELOp of *M. alpina* ATCC 32221 by DNA sequencing, as described below. Transformation of *A. oryzae* was performed by the method described by Gomi *et al.* (17) and Iimura *et al.* (18). A shuttle vector, pNGA142 (19), with the GLELO cDNA insert was used as the transformation vector for *A. oryzae*. Stable transformants were isolated by repeated sporulation on Czapek–Dox medium plates.

Construction of transformation vectors for the M. alpina 1S-4 ura5⁻ strain. Transformation vector pD4 (20), which was developed for the transformation of *M. alpina*, was kindly supplied by Prof. David B. Archer (University of Nottingham, United Kingdom). pD4 originally contained an expression unit composed of the histone H4.1 promoter, the modified *hpt* gene, and the *N*-(5′-phosphoribosyl)anthranilate isomerase (*trpC*) transcription terminator. The region from the promoter to the terminator was amplified using a forward primer, HisProFX (5′-TAC<u>GAATTC</u>A-AGCGAAAGAGAGATTATGAA-3′), and a reverse primer, TrpCRX (5′-GAA<u>GAATTC</u>CCTCTAAACAAGTGTACCTGT-3′), with pD4 as a template. The two primers contained an *Eco*RI restriction site (underlined). A modified pBluescript® II SK+ (Stratagene, La Jolla, CA) was prepared by deletion of its *Bam*HI site for convenient manipulation in further experiments. The approximately 2.7-kb PCR product was digested with *Eco*RI, followed by ligation into the modified pBluescript® II SK+ digested with *Eco*RI, and designated as pBlues-hpt.

Transformation vectors pDura5GFP and pDura5GLELO were constructed by modification of pDura5 developed as a transformation vector of the *M. alpina* 1S-4 *ura5⁻* strain (12). pDura5GFP is a vector for the expression system of the enhanced green fluorescent protein (EGFP) gene. An EGFP gene was amplified using a forward primer, GFPforward (5′-TCGCCA<u>CCATGG</u>TGAGCAAG-3′), and a reverse primer, GFPreverse (5′-CGC<u>GGATCC</u>TTTACTTGTA-3′), designed on the basis of the sequence of the EGFP gene on the pEGFP vector (Clontech Laboratories Inc., Palo Alto, CA) at an annealing temperature of 58°C with the pEGFP vector as a template. The GFPforward and GFP reverse primers contained *Nco*I and *Bam*HI restriction sites, respectively (underlined). The approximately 700-bp fragment digested with *Nco*I and *Bam*HI was ligated to pBlues-hpt digested with the same enzymes to remove the pre-existing *hpt* gene, resulting in the construction of a vector designated as pBlues-GFP. The EGFP gene expression unit obtained from pBlues-GFP on digestion with *Eco*RI was ligated to the *Eco*RI site of pDura5, resulting in the construction of pDura5GFP (Fig. 1).
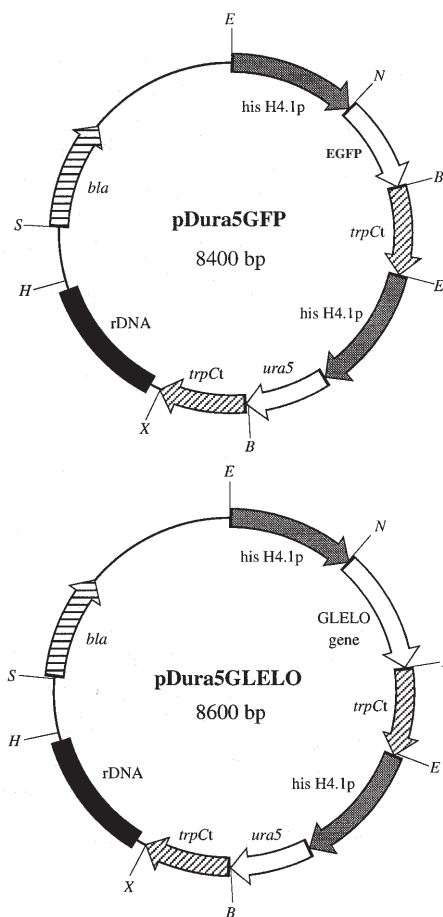
FIG. 1. Two transformation vectors for *Mortierella alpina* 1S-4 *ura5⁻* mutant. The details of each gene and the method for constructing these vectors are given in the Experimental Procedures section. Restriction sites: *E, Eco*RI; *N, Nco*I; *B, Bam*HI; *X, Xba*I; *H, Hin*dIII; *S, Ssp*I.

pDura5GLELO is a vector for expression of the GLELO gene. *Mortierella alpina* 1S-4 GLELO cDNA was amplified using a forward primer, GLELOF (5′-CA<u>CCATGG</u>AGTC-GATTGCGC-3′), and a reverse primer, GLELOR (5′-GT-<u>GGATCC</u>TTACTGCAACTTCCTTGCCTT-3′), at an annealing temperature of 54°C with the 1S-4 cDNA library as a template. The GLELOF and GLELOR primers contained *Nco*I and *Bam*HI sites, respectively (underlined). The approximately 1.0-kb PCR product was ligated to the pT7Blue T-Vector to construct pT7-GLELO. By following the same strategy as for the construction of pDura5GFP, pDura5GLELO was constructed (Fig. 1).

Transformation of the M. alpina 1S-4 ura5⁻ strain. Transformation of the *M. alpina* 1S-4 *ura5⁻* strain with pDura5GFP or pDura5GLELO was performed with a PDS-1000/He Particle Delivery System (Bio-Rad Laboratories Inc., Hercules, CA) as described previously (12).

Isolation of stable transformants and checking of transformation by PCR were performed by the methods described previously (12).

FA analyses. The *A. oryzae* recombinant transformed with the *M. alpina* 1S-4 GLELOp cDNA was inoculated into a test tube containing 5 mL GY medium containing 2% glucose and 1% yeast extract, and then cultivated at 28°C with reciprocal shaking (120 strokes/min) for 3–4 d. The spores or mycelia of *M. alpina* 1S-4 recombinants transformed with pDura5GLELO and the host cells were inoculated into 20-mL Erlenmeyer flasks containing 4 mL of GY medium containing 2 or 5% glucose, 1% yeast extract, and 0.05 mg/mL of uracil. The culture was performed at 28°C with reciprocal shaking (120 strokes/min) for the desired period. FA analysis was performed basically as described in the previous paper (21).

Nucleotide sequence accession numbers. The nucleotide sequences of the GLELO genomic gene cloned from *M. alpina* 1S-4 have been assigned DDBJ accession no. AB193123.

RESULTS AND DISCUSSION

Transformation of the M. alpina 1S-4 ura5⁻ strain with pDura5GFP. The first trial involved expression of the EGFP gene in the *M. alpina* 1S-4 *ura5⁻* strain using a homologous *ura5* gene-containing vector. This would directly demonstrate that a two-gene expression system is feasible, and that heterologous gene expression in *M. alpina*, which will lead to further applications, has been achieved. The EGFP gene was placed under the control of the same promoter and terminator as previously used for expression of the homologous *ura5* gene (12). On the basis of this idea, an EGFP-expression vector, pDura5GFP, was constructed and used for transformation of the *ura5⁻* strain. Transformation was successfully performed, and six stable transformants were selected from the 45 isolated. All the stable ones were determined to be transformed through vector insertion into the rDNA locus (data not shown). When both host cells (*ura5⁻* strain) and ones of the transformants were cultivated in various media and observed under a fluorescence microscope, strong fluorescence was detected, mainly in

TABLE 1
FA Compositions of *Aspergillus* Transformant MG-5[a]

	mol% of FA in the total FA of the cells[b]			
		Control strain		MG-5
FA	Control strain	(+ GLA)[c]	MG-5	(+ GLA)
16:0	17.4	9.9	14.0	11.8
18:0	5.8	2.7	5.2	4.1
18:1n-9	14.8	5.5	11.7	7.6
18:2n-6	56.8	30.0	63.8	43.4
GLA	—[d]	50.6	—	17.5
18:3n-3	5.1	1.4	1.4	1.5
20:2n-6	—	—	4.0	2.9
DGLA	—	—	—	11.2

[a]*A. oryzae* MG-5 strain, which was transformed with *Mortierella alpina* 1S-4 GLELO cDNA, and the control strain without the GLELO gene were grown at 28°C for 3–4 d in 5 mL of GY medium with reciprocal shaking (120 strokes/min).
[b]These values are the means of triplicate experiments.
[c]0.2% GLA methyl ester was added to the culture broth.
[d]—, not detected; DGLA, dihomo-γ-linolenic acid.

the outer part of the cells. To remove this fluorescence, protoplasts were prepared, but the resulting cells still had a strong fluorescence. Although these transformants seemed to show strong fluorescence in their cytoplasm, the observation could not be thought to be sufficient evidence that the EGFP gene was truly expressed.

How the self-fluorescence of this fungus is produced remains unclear, as it was impossible to detect the fluorescence from the EGFP protein precisely in the mycelial cells. On the other hand, when spores were observed under the fluorescence microscope, a strong fluorescence was detected only in those of the transformants (data not shown). This finding implies that the foreign gene could be inherited by both the daughter cells and spores and indicates that the EGFP and *ura5* genes were both successfully expressed in this fungus. Hence, we expected that the same strategies could be used for expression of genes involved in PUFA syntheses, leading to elucidation of FA metabolism and improvement of PUFA production.

Isolation and heterologous expression of the GLELO gene of M. alpina 1S-4. The gene encoding GLELOp, which catalyzes elongation of GLA to DGLA, has previously been cloned from *M. alpina* ATCC 32221 and characterized (10). To perform homologous expression of the GLELO gene, the GLELO cDNA of *M. alpina* 1S-4 was isolated. As a result, a fragment containing an open reading frame with a length of 957 bp, starting with an ATG codon and ending with a TAA codon, was isolated. The gene was suggested to encode a protein consisting of 318 amino acids with a M.W. of 37,000 (data not shown). A computer-aided homology search of the amino acid sequences of other proteins in a database revealed that the deduced amino acid sequence of the resultant gene exhibits 95.9% identity with that of the GLELOp of *M. alpina* ATCC 32221, and 33.5 and 32.5% identity with those of elongation of very long chain FA protein 2 (ELO2) of mouse and human, respectively (22,23). The amino acid sequence of GLELOp showed several regions of identity, including a common histidine box motif, with ELO2. A

TABLE 2
Comparison of FA Compositions of *M. alpina* 1S-4 Transformants[a]

Incubation period (d)	FA	mol% of FA in the total FA of the cells[b]		
		Host cell	Transformant #3	Transfomant #8
4	16:0	18.5	16.8	19.7
	18:0	5.7	5.4	7.0
	18:1n-9	28.2	27.8	27.3
	18:2n-6	9.9	10.2	9.0
	GLA	7.7	9.2	6.7
	DGLA	5.8	6.4	6.7
	AA	19.8	20.9	20.5
10	16:0	19.7	19.9	20.0
	18:0	6.4	7.12	6.5
	18:1n-9	30.6	24.9	32.1
	18:2n-6	8.7	8.5	8.4
	GLA	5.6	3.8	5.6
	DGLA	5.9	6.2	4.5
	AA	18.1	25.6	19.1

[a]Two *M. alpina* 1S-4 recombinants transformed with pDura5GLELO, #3 and #8, and host cells were grown at 28°C for 4 or 10 d in 4 mL of GY medium containing uracil under reciprocal shaking (120 strokes/min).
[b]These values are the means of triplicate experiments. AA, arachidonic acid; for other abbreviations see Table 1.

hydropathy plot (Kyte and Doolittle) of GLELOp indicated that this protein is hydrophobic in nature and contains several presumptive transmembrane domains (data not shown). Furthermore, functional analyses were also performed on gene expression in *A. oryzae* (Table 1). The *Mortierella alpina* 1S-4 GLELO cDNA was ligated to fungal expression vector pNGA142. In the resultant plasmid, designated as pGEGA10, expression of the cloned GLELOp gene was controlled by a glucoamylase promoter of *A. oryzae*. The FA composition of the selected *A. oryzae* transformant, MG-5, was different from that of the control strain without the GLELO gene: The new peak in the chromatogram of FAME from the transformant cultured in GY medium for 4 d exhibited a retention time identical to the FAME standard of 20:2n-6, which is produced through an elongase reaction on endogenous 18:2n-6. In the presence of exogenous GLA, a new peak of DGLA was observed only for the transformant, indicating conversion of GLA to DGLA at the rate of 39%, whereas the rate of conversion of endogenous 18:2n-6 to 20:2n-6 was 5.9%, and 18:1n-9 and 18:3n-3 were not converted to the corresponding 20-carbon PUFA at all. Another experiment indicated that exogenous 18:1n-12 was converted to 20:1n-12 with a conversion rate of 2.1% (data not shown). The GLELOp of *M. alpina* ATCC 32221 showed the same characteristics as that of *M. alpina* 1S-4 (10,11). Thus, the cDNA was determined to be the gene encoding GLELOp throughout this analysis.

It is generally believed that the elongation activity involves four distinct subunit enzymes: a condensing enzyme, two reductases, and a dehydrase. It is unlikely that one protein exhibits all four activities (11). Therefore, the elongase activity of GLELOp in the *Aspergillus* transformants is likely to arise from interaction with other endogenous components of *Aspergillus* elongase.

Transformation of M. alpina 1S-4 with pDura5GLELO. A transformation vector, pDura5GLELO (Fig. 1), was constructed

and used for transformation of the *ura5⁻* strain to over-express the GLELO gene. Out of the 36 transformants obtained, 9 were determined to be stable transformants with pDura5GLELO (data not shown). To investigate their properties, two transformants (#3 and #8) were cultivated in GY medium, containing 5% glucose, 1% yeast extract, and 0.05 mg/mL of uracil, for 4 or 10 d to investigate their FA compositions (Table 2). It was verified that complementation of *ura5* genes does not influence the FA composition of the host cells (data not shown). Transformant #8 showed the same FA composition as that of the host cells, regardless of the cultivation period. On the other hand, transformant #3 exhibited a different FA composition from that of the host cells: GLA, which serves as a substrate for GLELOp, was decreased and AA was increased. For further investigation, time course experiments were performed with transformant #3 and the host cells (Fig. 2). The accumulation of AA continued after 4 d in both strains, regardless of the culture conditions. With 5% glucose in the medium, AA content remained low in comparison with that with 2% glucose. Although this observation was in accordance with results previously reported, the AA productivity (mg/mL of culture broth) was proportional to the glucose concentration (data not shown) (4). In the case of 2% glucose (Figs. 2A and B), the AA content increased linearly after 4 d in the transformant but not in the host cells. Our previous report also stated that significant AA accumulation was observed in the stationary phase (5,24), and this phase is thought to correspond to the period after 4 d in the present experiment.

The final content of AA in the transformant was higher than that in the host cells. Hence, over-expression of the GLELO gene clearly occurred in this lipogenic phase rather than in the growth phases. With 5% glucose (Figs. 2C and 2D), differences in the FA profile appeared clearly: The AA content of transformant #3 increased more than that of the host cells after 5 d. The GLA content of the transformant cells remained lower than that of the host cells, especially after 4 d. The DGLA content increased at the beginning of cultivation and then decreased concomitantly with the increase in the AA content. The AA content of transformant #3 was 1.4-fold higher than that of the host cells at the end point. The significance of this increase can be appreciated from our previous efforts to enhance the productivity, which did not achieve such significant change. This major increase must therefore have resulted from the enzyme playing an important role in AA biosynthesis. In addition, the analysis of real-time quantitative PCR showed that the quantity of GLELO RNA in transformant #3 was 7.4-fold higher than that of the host strain on 4 d (data not shown). Therefore, the results obtained for stable transformant #3 must be directly due to GLELO gene expression.

In conclusion, GLELOp catalyzes the conversion of GLA to DGLA and serves as the rate-limiting step in AA production. As predicted by Wynn and Ratledge (6), AA productivity can be increased through enhancement of the enzyme activity. This is the first report that genetic manipulation led to an increase in AA production by an industrial oleaginous strain, *M. alpina* 1S-4.
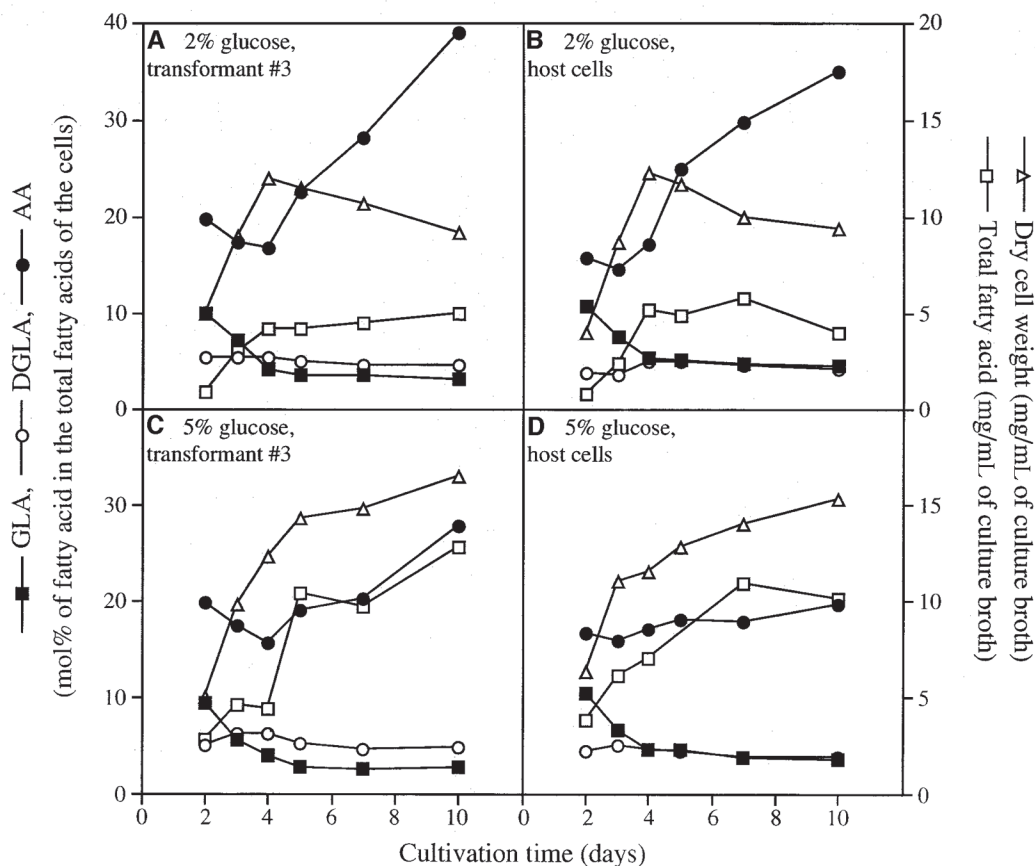
FIG. 2. Time courses of changes in the mycelial FA content in the GLELO-over-expressing *M. alpina* 1S-4 transformant and the host cells. All cultivations were started by inoculation of the respective spores and performed with reciprocal shaking (120 strokes/min) at 28°C. The culture conditions were as follows: (A, B) GY medium containing 2% glucose. (C, D) GY medium containing 5% glucose. All media also contained 1% yeast extract and 0.05 mg/mL uracil. The strains used were as follows: (A, C) transformant; (B, D) host cells. FA analysis was performed with total biomass obtained from each cultivation. The values are the means of triplicate experiments. DGLA, dihomo-γ-linolenic acid; AA, arachidonic acid.

ACKNOWLEDGMENTS

REFERENCES

1. Needleman, P., Turk, J., Jakschik, B.A., Morrison, A.R., and Lefkowith, J.B. (1986) Arachidonic Acid Metabolism, *Annu. Rev. Biochem. 55*, 69–102.
2. Smith, W.L., and Borgeat, P. (1985) The Eicosanoids: Prostaglandins, Thromboxanes, Leukotrienes, and Hydroxy-eicosaenoic Acids, in *Biochemistry of Lipids and Membranes* (Vance, D.E., and Vance, J.E., eds.), pp. 325–360, Benjamin/Cummings, Menlo Park, CA.
3. Horrobin, D.F. (1992) Nutritional and Medical Importance of γ-Linolenic Acid, *Prog. Lipid Res. 31*, 163–194.
4. Yamada, H., Shimizu, S., and Shinmen, Y. (1987) Production of Arachidonic Acid by *Mortierella elongata* 1S-5, *Agric. Biol. Chem. 51*, 785–790.
5. Shimizu, S., Ogawa, J., Kataoka, M., and Kobayashi, M. (1997) Screening of Novel Microbial Enzymes for the Production of Biologically and Chemically Useful Compounds, in *Advances in Biochemical Engineering/Biotechnology* (Schepter, T., ed.), Vol. 58, pp. 45–87, Springer-Verlag, Berlin.
6. Wynn, J.P., and Ratledge, C. (2000) Evidence That the Rate-Limiting Step for the Biosynthesis of Arachidonic Acid in *Mortierella alpina* Is at the Level of the 18:3 to 20:3 Elongase, *Microbiology 146*, 2325–2331.
7. Cinti, D.L., Cook, L., Nagi, M.N., and Suneja, S.K. (1992) The Fatty Acid Chain Elongation System of Mammalian Endoplasmic Reticulum, *Prog. Lipid Res. 31*, 1–51.
8. Bernert, J.T., Jr. , and Sprecher, H. (1977) An Analysis of Partial Reactions in the Overall Chain Elongation of Saturated and Unsaturated Fatty Acids by Rat Liver Microsomes, *J. Biol. Chem. 252*, 6736–6744.
9. Nugteren, D.H. (1965) The Enzymic Chain Elongation of Fatty Acids by Rat-Liver Microsomes, *Biochim. Biophys. Acta 106*, 280–290.
10. Parker-Barnes, J.M., Das, T., Bobik, E., Leonard, A.E., Thurmond, J.M., Chaung, L.T., Huang, Y.S., and Mukerji, P. (2000) Identification and Characterization of an Enzyme Involved in

the Elongation of n-6 and n-3 Polyunsaturated Fatty Acids, *Proc. Natl. Acad. Sci. USA 97*, 8284–8289.

11. Das, T., Thurmond, J.M., Bobik, E., Leonard, A.E., Parker-Barnes, J.M., Huang, Y.S., and Mukerji, P. (2000) Polyunsaturated Fatty Acid-Specific Elongation Enzymes, *Biochem. Soc. Trans*. *28*, 658–660.

12. Takeno, S., Sakuradani, E., Murata, S., Inohara-Ochiai, M., Kawashima, H., Ashikari, T., and Shimizu, S. (2004) Establishment of an Overall Transformation System for an Oil-Producing Filamentous Fungus, *Mortierella alpina* 1S-4, *Appl. Microbiol. Biotechnol.* *65*, 419–425.

13. Takeno, S., Sakuradani, E., Murata, S., Inohara-Ochiai, M., Kawashima, H., Ashikari, T., and Shimizu, S. (2004) Cloning and Sequencing of the *ura3* and *ura5* Genes, and Isolation and Characterization of Uracil Auxotrophs of the Fungus *Mortierella alpina* 1S-4, *Biosci. Biotechnol. Biochem.* *68*, 277–285.

14. Malardier, L., Daboussi, M.J., Julien, J., Roussel, F., Scazzocchio, C., and Brygoo, Y. (1989) Cloning of the Nitrate Reductase Gene (*niaD*) of *Aspergillus nidulans* and Its Use for Transformation of *Fusarium oxysporum*, *Gene 78*, 147–156.

15. Chomczynski, P., and Sacchi, N. (1987) Single-Step Method of RNA Isolation by Acid Guanidinium Thiocyanate–Phenol–Chloroform Extraction, *Anal. Biochem. 162*, 156–159.

16. Sakuradani, E., Kobayashi, M., and Shimizu, S. (1999) Δ9-Fatty Acid Desaturase from Arachidonic Acid-Producing Fungus. Unique Gene Sequence and Its Heterologous Expression in a Fungus, *Aspergillus*, *Eur. J. Biochem. 260*, 208–216.

17. Gomi, K., Iimura, Y., and Hara, S. (1987) Integrative Transformation of *Aspergillus oryzae* with a Plasmid Containing the *Aspergillus nidulans argB* Gene, *Agric. Biol. Chem. 51*, 2549–2555.

18. Iimura, Y., Gomi, K., Uzu, H., and Hara, S. (1987) Transformation of *Aspergillus oryzae* Through Plasmid-Mediated Complementation of the Methionine-Auxotrophic Mutation, *Agric. Biol. Chem. 51*, 323–328.

19. Sakuradani, E., Kobayashi, M., and Shimizu, S. (1999) Identification of an NADH-Cytochrome b_5 Reductase Gene from an Arachidonic Acid-Producing Fungus, *Mortierella alpina* 1S-4, by Sequencing of the Encoding cDNA and Heterologous Expression in a Fungus, *Aspergillus oryzae*, *Appl. Environ. Microbiol. 65*, 3873–3879.

20. Mackenzie, D.A., Wongwathanarat, P., Carter, A.T., and Archer, D.B. (2000) Isolation and Use of a Homologous Histone H4 Promoter and a Ribosomal DNA Region in a Transformation Vector for the Oil-Producing Fungus *Mortierella alpina*, *Appl. Environ. Microbiol. 66*, 4655–4661.

21. Sakuradani, E., Kobayashi, M., Ashikari, T., and Shimizu, S. (1999) Identification of Δ12-Fatty Acid Desaturase from Arachidonic Acid-Producing *Mortierella* Fungus by Heterologous Expression in the Yeast *Saccharomyces cerevisiae* and the Fungus *Aspergillus oryzae*, *Eur. J. Biochem. 261*, 812–820.

22. Tvrdik, P., Westerberg, R., Silve, S., Asadi, A., Jakobsson, A., Cannon, B., Loison, G., and Jacobsson, A. (2000) Role of a New Mammalian Gene Family in the Biosynthesis of Very Long Chain Fatty Acids and Sphingolipids, *J. Cell Biol. 149*, 707–717.

23. Ota, T., Suzuki, Y., Nishikawa, T., Otsuki, T., Sugiyama, T., Irie, R., Wakamatsu, A., Hayashi, K., Sato, H., Nagai, K., *et al.* (2004) Complete Sequencing and Characterization of 21,243 Full-Length Human cDNAs, *Nat. Genet. 36*, 40–45.

24. Shimizu, S., Kawashima, H., Akimoto, K., Shinmen, Y., and Yamada, H. (1989) Microbial Conversion of an Oil Containing α-Linolenic Acid to an Oil Containing Eicosapentaenoic Acid, *J. Am. Oil Chem. Soc. 66*, 342–347.

Over-expression of Hepatic Neutral Cytosolic Cholesteryl Ester Hydrolase in Mice Increases Free Cholesterol and Reduces Expression of HMG-CoAR, CYP27, and CYP7A1

Timothy B. Langston[a], Phillip B. Hylemon[b], and W.M. Grogan[a],*

Departments of [a]Biochemistry and Molecular Biophysics and [b]Microbiology and Immunology,
Medical College of Virginia Campus, Virginia Commonwealth University, Richmond, Virginia 23298

ABSTRACT: Hepatic neutral cytosolic cholesteryl ester hydrolase (hncCEH) is a key enzyme in the regulation of hepatic free cholesterol (FC). In examining the effects of over-expression of this enzyme on cholesterol homeostasis, mice were infected with a recombinant adenovirus construct (AdCEH) of the rat hncCEH cDNA driven by the human cytomegalovirus promoter. Cholesteryl esterase and p-nitrophenylcaprylate (PNPC) esterase activities were measured in liver postmitochondrial supernatants at 1, 3, 7, and 11 d after infection with AdCEH or a control virus expressing β-galactosidase (AdβGAL). The PNPC esterase activity of AdCEH mice peaked threefold higher than controls on day 2, declining on subsequent days. In contrast, cholesteryl esterase peaked eightfold higher than controls on day 3, indicating a shift in substrate selectivity of hncCEH. Hepatic FC peaked at 144% of controls, 7 d postinfection. The mRNAs for cholesterol 7α-hydroxylase, sterol 27-hydroxylase, and HMG-CoA reductase decreased to 47, 46, and 58% of controls, respectively, on day 7, coinciding with peak FC concentrations. Coinciding with increased cholesteryl esterase activity, hepatic esterified cholesterol dropped precipitously from day 3 onward, to 11% of controls by day 11. Hepatic TAG levels also declined, consistent with the reported TAG lipase activity of hncCEH. These results demonstrate elevation of FC and depletion of cholesteryl esters by over-expression of hncCEH, which were resistant to compensatory responses by other enzymes of cholesterol homeostasis.

Paper no. L9627 in *Lipids 40*, 31–38 (January 2005).

Free cholesterol (FC) is an essential component of membranes and an important determinant of their physicochemical properties. FC is also the precursor to bile acids, steroid hormones, and oxysterols that regulate pathways of lipid metabolism, including cholesterol biosynthesis (1–3). Indicative of the metabolic and regulatory significance of these roles, intracellular FC levels are maintained within relatively narrow ranges over a broad range of dietary intakes and metabolic states (4–7). Among the homeostatic processes contributing to this stability is the cycle of esterification with long-chain FA and hydrolysis of the resulting cholesteryl esters (CE) to regenerate metabolically active FC. The hydrolytic component of this CE cycle is catalyzed by the hepatic neutral cytosolic CE hydrolase (hncCEH), which has been cloned and characterized in this laboratory (8–11). The hncCEH is a broad-specificity carboxylesterase that hydrolyzes TAG (12) and water-soluble esters of p-nitrophenol, as well as CE (8,9,12). Similar to other enzymes in cholesterol metabolism, the hncCEH promoter has active sterol responsive elements that regulate hncCEH expression (10,13,14). Moreover, hncCEH mRNA, protein, and enzymatic activity are altered in response to perturbations of sterol flux, consistent with the hypothesis that hncCEH plays a significant role in cholesterol homeostasis (8,10,15).

Cholesterol homeostasis is maintained in the liver by regulation of the various input and output pathways for metabolism and transport. In addition to hncCEH, these include (i) ACAT, which catalyzes the esterification component of the CE cycle; (ii) HMG-CoA reductase (HMGCoAR), the rate-determining enzyme in the *de novo* synthesis of cholesterol; (iii) cholesterol 7α-hydroxylase (CYP7A1), and sterol 27-hydroxylase (CYP27), which catalyze the initial steps in the classic and alternative pathways, respectively, for bile acid synthesis; and (iv) lipoprotein synthesis, uptake, and degradation (16,17). The response of each of these to perturbations in the metabolically active cholesterol pools is the means by which the liver maintains cholesterol homeostasis.

Although a number of studies have examined the effects of perturbations of cholesterol homeostasis on hncCEH, the current studies were designed to determine the effects of over-expression of hncCEH on hepatic sterol metabolism and other key enzymes of cholesterol homeostasis. To this end, an adenoviral vector was constructed with a cytomegalovirus promoter to constitutively express hncCEH. We describe the validation of this construct in cell culture and mice and the effects of over-expression of hncCEH on hepatic lipid levels and mRNAs of several enzymes known to exhibit compensatory responses to altered sterol flux through the liver.

MATERIALS AND METHODS

Chemicals and supplies. Radionuclides were purchased from New England Nuclear (Boston, MA); p-nitrophenylcaprylate

*To whom correspondence should be addressed at Department of Biochemistry, Medical College of Virginia Campus, Virginia Commonwealth University, Richmond, VA 23298. E-mail: grogan@hsc.vcu.edu

Abbreviations: AdβGAL, adenovirus over-expressing β-galactosidase; AdCEH, adenovirus over-expressing cholesteryl ester hydrolase; CE, cholesteryl ester; CYP7A1, cholesterol 7α-hydroxylase; CYP27, sterol 27-hydroxylase; FC, free cholesterol; GAPDH, glyceraldehyde-3-phosphate-dehydrogenase; HMG-CoAR, HMG-CoA reductase; hncCEH, hepatic neutral cytosolic cholesteryl ester hydrolase; HSL, hormone-sensitive lipase; pfu, plaque-forming units; PNPC, p-nitrophenylcaprylate.

(PNPC) from Sigma Laboratories (St. Louis, MO); CsCl, tissue culture ware, and solvents from Fisher Scientific (Columbia, MD); and C57BL/6 mice from the National Cancer Institute (National Institutes of Health, Bethesda, MD). Mice were fed Teklad (Harlan, Indianapolis, IN) rodent diet *ad libitum* and then fasted for 12 h prior to sacrifice. Mice were maintained on an alternating 12-h light/12-h dark schedule. A single 100-µL injection of virus was administered *via* tail vein. Serum levels of liver enzymes, aspartate aminotransferase and alanine aminotransferase, were measured in animals infected with virus. Since these enzymes were elevated in some mice from each group, regardless of dose, construct, or level of expression (data not shown), weight was used as a discriminator. Mice losing >2% in body weight postinjection were excluded from these studies.

Construction of the transfer vector, viral purification, and plaque assay. The cDNA for hncCEH (9) was cut from pCR3-CEH using *XhoI*. The transfer vector, pSCT1, was digested with *SalI*, and hncCEH cDNA was ligated into the transfer vector through the complementary *XhoI/SalI* sites. Insertion of hncCEH cDNA was verified by restriction digestion and sequencing. Homologous recombination was performed by the Massey Cancer Center Adenoviral Core Facility to produce infectious particles. Several viral lines were selected for DNA isolation and sequencing. Because the poly-A signal of hncCEH was provided by the vector, the hncCEH mRNA was extended by approximately 200 bases during transcription from the viral genome. The elongated message allowed the hncCEH transcript to be distinguished from endogenous mRNAs for homologous mouse esterase in Northern blots using the full-length cDNA as a probe.

Virus was purified essentially as described by Gerard and Meidell (18). Fifty 180 cm^2 dishes were seeded with 293 cells at a density of 10%. Medium was changed every 48 h until cells were confluent. Confluent 293 cells were infected at MOI (multiplicity of infection) 200 for 24 h. The medium was then aspirated and replenished. Sixty hours after infection, floating cells were collected, pelleted, and immediately lysed by six freeze/thaw cycles (–80°C ethanol bath followed by 18°C water bath). Cellular debris was removed by centrifugation and the cleared viral lysate was layered over a discontinuous CsCl gradient (1.24–1.40 g/mL) in six Beckman Ultra-Clear tubes (14 × 89 mm). The tubes were centrifuged in an SW40 rotor at 155,000 × *g* for 2 h. The viral band was collected and layered onto a 1.33 g/mL continuous CsCl cushion in two Ultra-Clear tubes. The tubes were centrifuged in an SW40 rotor at 155,000 × *g* for 18 h. Occasionally, the virus would aggregate and, although the viral band was thick, these preparations were found to have very low titers. Preparations that aggregated were discarded. The viral band was collected and dialyzed in a Pierce dialyzer cassette with a 10,000-MW cutoff against 4 L of dialysis buffer [10 mM Tris, 1 mM MgCl$_2$, pH 7.4, and 10% (vol/vol) glycerol] at 4°C for 24 h. The solution was aliquotted into cryogenic vials, snap-frozen in liquid N$_2$ vapor, and stored at –80°C.

Plaque assays were performed on a small aliquot from the pure virus that was frozen separately. Confluent 293 cells in 25 cm^2 flasks were infected with aliquots of virus in serial dilutions and incubated overnight. Medium was removed and 4 mL of complete media with 1.25% agarose was added. After 4 d, 4 mL of agarose medium with 0.02% neutral red dye (AdCEH) or X-Gal (AdβGAL) was added and flasks were monitored for plaques for 10 more days.

Cell culture of human embryonic 293 cells. The 293 cells were cultured in DMEM with high glucose (4.5 g/mL), L-glutamine (0.292 g/mL), penicillin (100 U/mL), streptomycin (100 µg/mL), and 10% heat-inactivated FBS, in a humidified environment at 37°C with 5% CO$_2$.

Preparation of total RNA and Northern blot analysis. Total RNA from livers was prepared by CsCl pelleting (10). Aliquots with 2.5, 5, and 8 µg RNA from each mouse were electrophoresed on 1% agarose gels with formaldehyde. Northern blots were prepared using GeneScreen™ (NEN Life Science Products, Boston, MA) membranes as described previously (19). Blots were simultaneously hybridized to ^{32}P-labeled cDNAs of rat hncCEH and the internal loading standard, mouse glyceraldehyde-3-phosphate-dehydrogenase (GAPDH). Hybridizing bands were visualized by exposure on a phosphor K-screen (Bio-Rad, Hercules, CA) and the Molecular Imager FX system. Densitometry was performed using Quantity One software (Bio-Rad). Density values from bands hybridizing to hncCEH were normalized to GAPDH.

Lipid extraction and determination. Total lipids were extracted by the method of Bligh and Dyer (20). Extracts were dried under N$_2$ and resuspended in 1 mL isopropanol for lipid determination. Hepatic TAG were measured with the Sigma Diagnostics Triglyceride GPO-Trender kit; hepatic total cholesterol, with Sigma Diagnostics Infinity Cholesterol Reagent; and hepatic FC, with the Boehringer Mannheim (Indianapolis, IN) cholesterol kit using standards certified by suppliers. Esterified cholesterol was calculated by the difference between total cholesterol and FC.

Ribonuclease protection assay. Ribonuclease protection assays were performed as described previously using an Ambion RPA II system (Austin, TX) (21). The gel was dried and placed on film overnight at –80°C. Bands were quantified with a Molecular Dynamics densitometer and Bio-Rad Quantity One software. Values were normalized to cyclophilin.

Enzyme assays. Cholesteryl esterase activity was measured by hydrolysis of cholesteryl [1-^{14}C]oleate using the radiometric method of Ghosh and Grogan (22). hncCEH is a broad-specificity esterase that exhibits higher activity with water-soluble *p*-nitrophenyl esters than with lipophilic substrates. These esters provide a rapid and sensitive screen for catalytic activity. PNPC esterase activity was determined spectrophotometrically with PNPC as described earlier (12). PNPC hydrolysis was determined in 1 mL assay buffer with 1–200 µg protein. Two hundred nanomoles of PNPC was added to start the reaction, which was incubated for 1–15 min at 37°C. Absorbance was measured at 400 nm.

The β-galactosidase assay was started by addition of 150 µL of β-galactosidase substrate buffer (200 mM Na$_2$HPO$_4$, 2 mM MgCl$_2$, 100 mM β-mercaptoethanol, and 1.33 mg/mL *o*-nitro-

phenyl β-D-galactopyranoside) to 150 μL of sample (12). The reaction mixture was incubated at 37°C until the reaction was stopped with 500 μL of 1 M $NaHCO_3$. Absorbance was measured at 420 nm.

Statistical analysis. Data presented in Figures 4–6 and Table 1 are correlated; i.e., they are collected from the same set of mice. Data were analyzed for statistically significant differences using the unpaired *t*-test, testing for equal SD. A Welch correction was used for comparison of means with significant differences in SD.

RESULTS

Validation of adenoviral constructs in cell culture. hncCEH is a broad-specificity esterase that hydrolyzes the synthetic water-soluble substrate PNPC more efficiently than natural lipophilic substrates (12). Moreover, since earlier studies showed that cholesteryl esterase activity of hncCEH varied with its level of phosphorylation, PNPC-esterase activity provides a more reliable index for over-expression of this enzyme (12). Thus, PNPC-esterase was used in the initial screening for catalytic activity. To determine the effectiveness of the adenoviral constructs as expression vectors, PNPC-esterase and β-galactosidase activities were measured in COS-7 cells infected with AdCEH and control construct AdβGAL. As shown in Figure 1, β-galactosidase activity was 40-fold higher in AdβGAL controls than in AdCEH-infected cells, whereas PNPC-esterase activity of AdβGAL controls was not different from that of uninfected cells (0.779 μmol/h/mg protein). Thus, virus infection itself did not elevate PNPC-esterase activity in cell culture. In contrast, PNPC-esterase was 460-fold higher in AdCEH infected cells (358 μmol/h/mg protein) than in AdβGAL controls, whereas β-galactosidase was not elevated. Thus, elevated PNPC-esterase levels were attributed specifically to expression of the hncCEH cDNA.

Optimization of conditions for adenovirus expression in mice. Mice were injected with various doses of AdβGAL to optimize expression and determine maximum tolerated doses of virus. A dose of 10^{13} pfu (plaque-forming units) produced no β-galactosidase activity above saline-injected controls. Mice injected with 10^{14}, $10^{14.5}$, and 10^{15} pfu AdβGAL exhibited 2-, 8- and 83-fold higher β-galactosidase activities, respectively, than controls on day 3 postinjection (data not shown). All dosages were tolerated, except 10^{15} pfu, which was lethal to 40% of the mice. Whereas $10^{14.5}$ pfu produced an eightfold increase in activity without acute toxicity or weight loss (data not shown), this dosage was selected for subsequent studies. β-Galactosidase was then measured in the livers of mice at various times after injection with $10^{14.5}$ pfu AdβGAL. β-Galactosidase activity was 117-, 76- and 8-fold higher than saline-injected controls 1, 2, and 3 d postinfection, declining to control values by day 7 (data not shown).

Optimization of expression of hncCEH in mice. To determine a minimum dosage necessary for expression of hncCEH, the hncCEH mRNA was measured in total RNA extracts from livers of mice infected with various doses of AdCEH. As de-
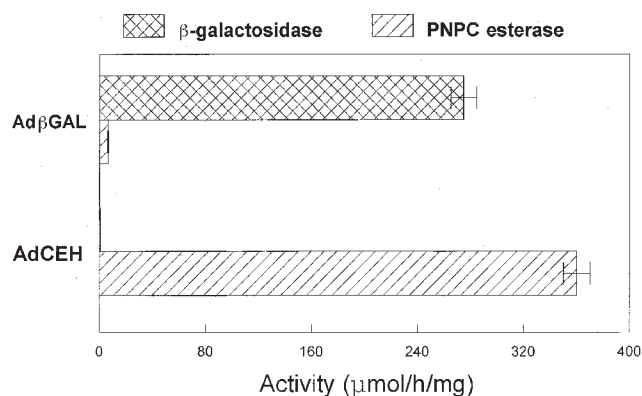

FIG. 1. *p*-Nitrophenylcaprylate (PNPC) esterase and β-galactosidase activities in postmitochondrial supernatants of COS-7 cells infected with AdCEH (adenovirus over-expressing cholesteryl ester hydrolase) or Adβ-GAL (adenovirus over-expressing β-galactosidase). Cells were infected at MOI (multiplicity of infection) 100, harvested 72 h postinfection, and assayed for both substrates. The controls were infected cells assayed for the activity that was not associated with the infecting virus. Activity is expressed as mean ± SEM for two different cultures at three protein concentrations, each in triplicate.

picted in Figure 2, the larger exogenous rat mRNA transcript of AdCEH was distinguishable from homologous endogenous mouse mRNA (23) that also hybridized with the hncCEH probe. The hncCEH mRNA was visible on Northern blots 3 d after infection with 10^{13} pfu (lanes 10–12), whereas only bands corresponding with endogenous carboxylesterases were visible at lower doses (lanes 1–9). Mice injected with AdβGAL expressed only the endogenous mRNA (data not shown). Thus, the well-tolerated dose $10^{14.5}$ pfu was well above the minimum necessary for expression of hncCEH mRNA.
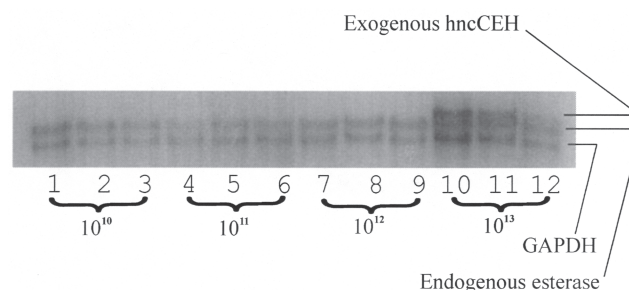
FIG. 2. Northern blot showing expression of hepatic neutral cytosolic cholesteryl ester hydrolase (hncCEH) mRNA in livers of mice injected with various doses of AdCEH. Mice were injected by tail vein with 1 × 10^{10} to 1 × 10^{13} plaque-forming units (pfu) AdCEH or AdβGAL (not shown). Livers were harvested and total RNA extracted 72 h after infection. Northern blots were probed with full-length hncCEH cDNA and glyceraldehyde-3-phosphate-dehydrogenase (GAPDH) (constitutive loading standard) probe as described in the Materials and Methods section. Rat trans gene (exogenous hncCEH) is 200 bp larger than homologous mouse transcript (endogenous hncCEH) due to inclusion of the viral poly A tail. Lanes 1–3: 1 × 10^{10}, Lanes 4–6: 1 × 10^{11}, Lanes 7–9: 1 × 10^{12}, Lanes 10–12: 1 × 10^{13}; three individual mice were used for each dosage. For abbreviations see Figure 1.
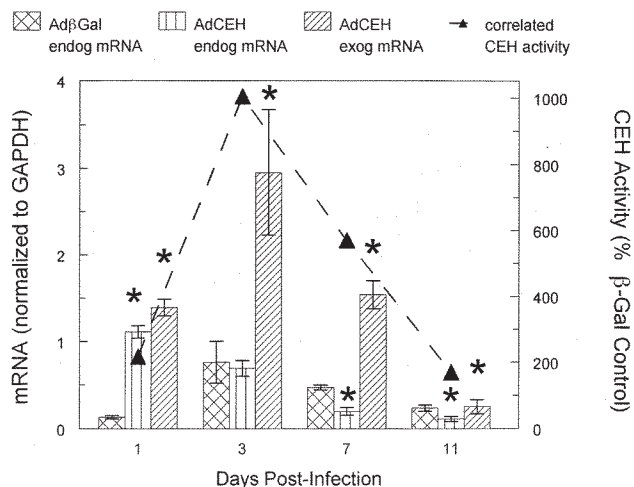
FIG. 3. Rat hncCEH (exog) and homologous mouse esterase (endog) mRNA in mice over-expressing hncCEH or control β-galactosidase. Mice were injected with $1 \times 10^{14.5}$ pfu AdCEH or AdβGAL. Livers were harvested at the indicated times and hncCEH mRNA or endogenous mouse esterase mRNA was measured and normalized to the loading standard GAPDH by quantitative Northern blot as described in the Materials and Methods section (see Fig. 2 for representative autoradiogram). Correlated cholesteryl esterase activities corresponding with the mRNA levels are graphed on the right axis as % AdβGAL control (- - -). Normalized activities are expressed as average ± SEM for three mice, except day 1, for which the AdCEH group contained two mice; (*) indicates $P < 0.05$. CEH, cholesteryl ester hydrolase; β-Gal, β-galactosidase; for other abbreviations see Figures 1 and 2.

Time course for expression of hncCEH in mice. Mice were injected with $10^{14.5}$ pfu AdCEH or AdβGAL, and livers were harvested at 1, 3, 7, and 11 d postinfection. The rat hncCEH (exogenous) and mouse endogenous mRNAs were measured by quantitative Northern blotting. As shown in Figure 3, hncCEH (exogenous) mRNA was present in AdCEH-infected mice on all days, whereas this transcript was absent from the AdβGAL controls. Three days after infection, hncCEH mRNA peaked fourfold higher than endogenous message but declined on subsequent days. Consistent with the function of hncCEH, cholesteryl esterase activity measured in the same liver samples (dotted line) correlated well with the hncCEH mRNA levels. Endogenous mRNA hybridizing with the cDNA for hncCEH was increased 24 h postinfection by AdCEH, possibly reflecting a transient increase in expression of the homologous mouse esterase-22 (23) not seen in AdβGAL controls. However, this increase in endogenous mRNA was not seen on day 3. By days 7 and 11, endogenous mRNA was significantly lower in the AdCEH-infected mice, suggesting a compensatory lowering of the homologous mouse esterase in response to elevated levels of hncCEH activity.

Both PNPC-esterase and cholesteryl esterase activities were measured in liver homogenates at 1, 2, 3, 7, and 11 d postinjection. As shown in Figure 4, PNPC-esterase activity was elevated by AdCEH within 24 h, peaked at 300% of controls on day 2, remained elevated through day 7, but declined to 62% of controls by day 11. In contrast, cholesteryl esterase activity
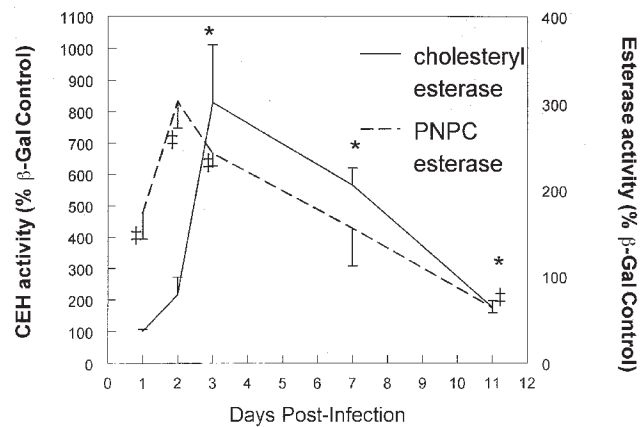
FIG. 4. Time course for expression of hepatic PNPC and cholesteryl esterase activities in mice infected with AdCEH or AdβGAL. Mice were injected by tail vein with $10^{14.5}$ pfu AdβGAL or AdCEH. Postmitochondrial supernatants were assayed for esterase activity using PNPC or cholesteryl $[1\text{-}^{14}C]$oleate. Assays were performed at two different protein concentrations, each in triplicate. Activity is expressed as % AdβGAL control ± SEM for three mice/group, except day 1, for which the AdCEH group contained two mice; (*) indicates different from controls, $P < 0.05$. For abbreviations see Figures 1 and 3.

was not significantly elevated until day 3, when it rose to 829% of controls. Cholesteryl esterase activity then declined gradually but remained 76% higher than controls on day 11. Thus, the two esterase activities followed somewhat different time courses of expression. It is possible that the lag in expression of cholesteryl esterase reflects protein kinase activation, which is not required for the expression of PNPC esterase activity by this enzyme (22).

Effects of hncCEH over-expression on liver cholesterol and TAG. As presented in Table 1, FC, the product of hncCEH, trended higher in AdCEH mice on all days postinjection. FC was 44% higher ($P < 0.03$) than AdβGAL controls on day 7, following a peak in hepatic cholesteryl esterase activity. Moreover, the mean FC was significantly higher than controls ($P < 0.02$, $n = 9$) when values were pooled for days 3, 7, and 11, the period of elevated cholesteryl esterase. Also consistent with the time course for cholesteryl esterase activity, hepatic esterified cholesterol was not significantly different from controls on days 1 and 3 but trended lower on day 7 and fell to 11% of control values by day 11 ($P < 0.02$). Thus, over-expression of hncCEH elevated hepatic FC and depleted esterified cholesterol, the physiological substrate for this enzyme. The associated depletion of esterified cholesterol most likely limited the elevation of FC on days 7 and 11 while cholesteryl esterase remained elevated. The two groups exhibited no significant differences in serum total cholesterol on any single day, although the pooled values for days 7 and 11 were slightly lower than controls (Table 1).

As reported earlier, hncCEH also hydrolyzes TAG *in vitro* and is activated by cAMP-dependent protein kinase, suggesting that this enzyme also functions as the hepatic hormone-sensitive TAG lipase (12,24,25). Consistent with such a functional role, hepatic TAG also dropped well below control levels in

TABLE 1
Effects of Hepatic Neutral Cytosolic CE Hydrolase (hncCEH) and β-Galactosidase Over-expression on Liver Lipids and Serum Cholesterol[a]

| | Liver lipid class (mg/g liver) | | | | |
| | Total | Free | Esterified | | Serum |
Day/treatment	cholesterol	cholesterol	cholesterol	TAG	cholesterol (mg/dL)
Infection + 1					
AdCEH	3.12 ± 0.30	2.33 ± 0.03	0.79 ± 0.33	38 ± 1	152 ± 16
AdβGAL	3.05 ± 0.09	2.16 ± 0.15	0.89 ± 0.24	19 ± 2	180 ± 22
Infection + 3					
AdCEH	2.00 ± 0.22	1.61 ± 0.18	0.38 ± 0.08	7.0 ± 1.1	128 ± 7
AdβGAL	1.62 ± 0.06	1.39 ± 0.12	0.23 ± 0.09	4.1 ± 0.3	120 ± 11
Infection + 7					
AdCEH	2.44 ± 0.22	2.17 ± 0.17**	0.27 ± 0.09	2.9 ± 0.5****	91 ± 3.0
AdβGAL	1.86 ± 0.03	1.51 ± 0.09	0.35 ± 0.05	17.8 ± 2.8	116 ± 3.5
Infection + 11					
AdCEH	1.95 ± 0.10	1.93 ± 0.10	0.02 ± 0.01***	8.2 ± 2.0	103 ± 0.05
AdβGAL	1.95 ± 0.04	1.80 ± 0.04	0.18 ± 0.05	14.0 ± 3.1	119 ± 15
Infection + 3-11					
AdCEH	2.13 ± 0.12*	1.91 ± 0.11***			
AdβGAL	1.81 ± 0.05	1.56 ± 0.07			
Infection + 7-11					
AdCEH	2.19 ± 0.15	2.05 ± 0.10****	0.14 ± 0.07	5.5 ± 1.5*****	96 ± 5*
AdβGAL	1.90 ± 0.03	1.64 ± 0.07	0.27 ± 0.05	15.9 ± 2.1	117 ± 5

[a]Mice were injected with $10^{14.5}$ pfu adenovirus over-expressing cholesteryl ester (CE) hydrolase (AdCEH) or control β-galactosidase (AdβGal). At the specified time postinjection, liver or serum lipid extracts from three mice/group were analyzed in triplicate for TAG and free and total cholesterol; esterified cholesterol was calculated as the difference, total cholesterol – free cholesterol. Values are means ± SEM. *Significantly different from AdβGAL controls, *$P < 0.005$; **$P < 0.03$; ***$P < 0.02$; ****$P < 0.01$; *****$P < 0.003$. Infection + 3-11 = mean of all values for days 3,7, and 11 ($n = 9$). Infection + 7-11 = mean of all values for days 7 and 11 ($n = 6$).

AdCEH-injected mice after day 3, following a pattern similar to that of CE (see Table 1). TAG were higher than controls in AdCEH-injected mice on days 1 and 3, prior to induction of cholesteryl esterase activity. However, the subsequent mobilization reduced TAG to 17% of control levels ($P < 0.01$) by day 7 and 35% of controls ($P < 0.003$) for the pools of all mice from days 7 and 11.

Effects of hncCEH over-expression on other hepatic enzymes of cholesterol homeostasis. The hepatic mRNAs for HMGCoAR, CYP7A1, and CYP27 were measured by ribonuclease protection assays in the same mice injected with AdCEH at time points corresponding with increased cholesteryl esterase activities and FC levels. As seen in Figure 5, mRNAs for all three enzymes were initially slightly higher than controls in AdCEH-injected mice, although this trend was significant only for CYP7A1 on day 1. Like the early elevations in endogenous carboxylesterase mRNA and TAG, this apparent elevation was modest in comparison with changes occurring at later time points and probably reflects transient perturbations of the system, since cholesteryl esterase activity was not expressed on day 1. Following the appearance of cholesteryl esterase activity and the resulting increase in hepatic free cholesterol, mRNAs for all three enzymes declined markedly and were significantly lower than controls in AdCEH mice on day 7. The resulting decline in mRNA levels from day 3 to day 7 was 46% for CYP27 and 47% for CYP7A1. Moreover, 44% higher FC

levels in AdCEH mice were accompanied by 42% lower HMGCoAR mRNA on day 7, consistent with the well-known feedback regulation of this enzyme (1,3).
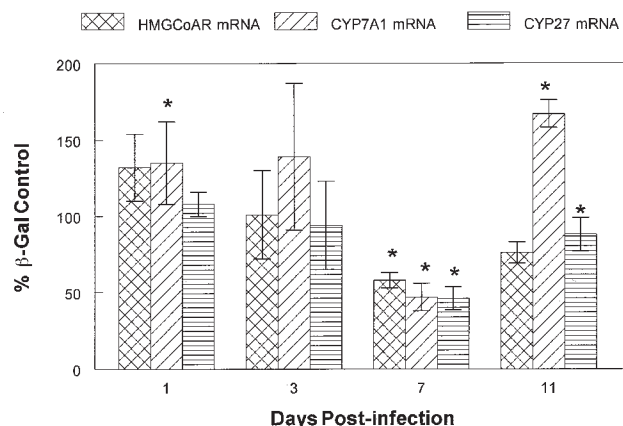
FIG. 5. Effects of hncCEH over expression on hepatic mRNAs for HMG-CoA reductase (HMGCoAR), cholesterol 7α-hydroxylase (CYP7A1), and sterol 27-hydroxylase (CYP27). Mice were injected by tail vein with $10^{14.5}$ pfu AdβGAL or AdCEH. Livers were harvested at the indicated times and total RNAs extracted for measurement of mRNAs by quantitative ribonuclease protection assays as detailed in the Materials and Methods section. Values represent mean % control ± SEM for three mice, except day 1 for which the AdCEH group contained two mice; (*) indicates $P < 0.05$. For other abbreviations see Figures 1 and 2.

DISCUSSION

As noted earlier, a number of studies have shown that hncCEH mRNA, enzyme protein, and catalytic activity are regulated in response to perturbations of cholesterol homeostasis that are known to result in altered sterol flux through the liver (8,10,11,13). However, the current study is the first to show that over-expression of hncCEH both perturbs hepatic lipid levels and produces predictable compensatory responses in other enzymes involved in regulation of cholesterol homeostasis. Both hncCEH mRNA (Fig. 3) and cholesteryl esterase activity (Fig. 4) were elevated in AdCEH mice after day 2, remaining three- and sixfold higher than AdβGal controls on day 7, by which time FC was elevated 44% over controls (Table 1). Although FC dropped thereafter, it is likely that this increase would have been greater and more sustained if these changes had not been accompanied by substantial depletion of the hepatic CE substrate pool (Table 1). Although mRNA for HMGCoAR, the rate-limiting step in cholesterol biosynthesis, decreased 42% from day 3 to day 7, which would tend to oppose the effects of hncCEH over-expression, this compensatory change did not prevent an increase in FC. Moreover, the initial enzymes in the acidic and neutral bile acid biosynthetic pathways were also suppressed on day 7. Although this is counterintuitive in terms of the expected effects on intracellular FC, it is nevertheless apparent that homeostatic responses did not fully compensate for the effects of hncCEH over-expression, even when CE were in limited supply. This underscores the importance of hncCEH in maintaining cholesterol homeostasis.

Whereas hncCEH hydrolyzes CE and TAG stores in the liver, hormone-sensitive lipase (HSL) is responsible for this activity in adipose, steroidogenic, and mammary tissues. Since hncCEH and HSL perform essentially the same function in different tissues, over-expression of hncCEH and HSL should produce similar effects. Escary *et al*. (26) used a plasmid vector to over-express HSL in lipid-laden adipocytes treated with an ACAT inhibitor and observed a two- to threefold increase in hydrolysis of CE (26). In that study, HSL over-expression resulted in almost complete hydrolysis of intracellular CE stores within 6 h. Whereas an ACAT inhibitor was required for depletion of CE stores in that study, in the current study, liver CE stores were almost completely depleted by over-expression of hncCEH (Table 1), without inhibition of ACAT. More recently, Okazaki *et al*. (27) used an adenovirus construct to over-express HSL in lipid-laden macrophage foam cells, which also resulted in depletion of CE stores. In those studies, increased CE hydrolysis was apparently compensated by increased cholesterol efflux, analogous to reverse cholesterol transport from the cells, preventing significant increases in cellular FC levels over a broad range of viral titers and CE levels. Although the liver also exports FC, it is apparent from the current study that neither of these processes in the bile and in serum lipoproteins compensated for the elevation in FC produced by over-expression of hncCEH (Table 1). To the contrary, the 18% reduction in serum cholesterol levels on days 7 and 11 could reflect decreased lipoprotein secretion resulting from depleted CE and TAG stores. Increased biliary cholesterol secretion remains a possible compensatory mechanism, although this was not measured in the current study.

Like HSL, hncCEH hydrolyzes TAG as well as CE (12). Sztalryd *et al*. (28) showed that over-expression of HSL in cultured adipocytes prevented accumulation of TAG. In the current study, over-expression of hncCEH was similarly associated with a substantial depletion of liver TAG *in vivo* (Table 1). Inasmuch as both enzymes are also activated by cyclic AMP-dependent protein kinase, these data suggest that hncCEH and HSL may play similar multifunctional roles in liver and extrahepatic tissues, respectively (22,29). However, unlike hncCEH, there is as yet no evidence that HSL plays a central regulatory role in cholesterol homeostasis (8,10,11,13).

As the hydrolytic component of the CE cycle in the liver, hncCEH promotes production of both FC and oxysterols, potent regulators of sterol and bile acid synthesis. To date, most studies have been focused on ACAT, the biosynthetic component of the CE cycle in the liver and most other tissues. Several investigators have used ACAT inhibitors to shift the balance toward net hydrolysis, relying on an unspecified endogenous CE hydrolase to mobilize endogenous CE (30–32). The resulting increases in FC were associated with decreased activity and mRNA for enzymes of cholesterol biosynthesis and increased activity and mRNA for CYP7A1, the rate-limiting enzyme in the acidic bile acid biosynthetic pathway. These investigators concluded that expansion of the FC pool provides both substrate and inducer for CYP7A1. This induction is mediated by increased oxysterol concentrations through the nuclear hormone receptor LXRα (liver X receptor α), which up-regulates transcription of the CYP7A1 gene (33,34). The role of oxysterols in suppressing enzymes of cholesterol biosynthesis is well documented (35,36).

Similar to the effects of ACAT inhibition, over-expression of hncCEH in the current study was accompanied by lower HMGCoAR levels on days 7 and 11, following peak cholesteryl esterase activity and coinciding with the highest levels of FC observed. Moreover, CYP7A1 mRNA was elevated on day 11, following several days of elevated cholesteryl esterase activity and a peak in FC levels. Paradoxically, both CYP7A1 and CYP27 mRNA levels were suppressed on day 7. This may reflect feedback inhibition of these pathways by transient overproduction of bile acids in response to increased FC levels (37). Both CYP7A1 and CYP27 are negatively regulated by cholate. Cholate not only decreases the stability of CYP27 mRNA but is also a ligand for the FXR (farnesoid X receptor), which stimulates expression of the negative regulatory factor SHP (small heterodimer partner), which in turn represses transcription of CYP7A1 (38–41). Although attempts were made to test this possibility by measuring biliary bile acids, variation between animals was too high to detect any trends (data not shown). Nevertheless, these data indicate that the capacity of bile acid biosynthetic pathways to compensate for mobilization of CE stores is limited by mechanisms that override the effects of intracellular FC. This is not unexpected, given the potential toxicity of bile acids (42).

ACKNOWLEDGMENTS

REFERENCES

1. Brown, J.S., and Goldstein, J.L. (1980) Multivalent Feedback Regulation of HMG CoA Reductase, a Control Mechanism Co-ordinating Isoprenoid Synthesis and Cell Growth, *J. Lipid Res. 21*, 505–517.

2. Schroepfer, G.J. (2000) Oxysterols: Modulators of Cholesterol Metabolism and Other Processes, *Physiol. Rev. 80,* 361–554.

3. Ness, G.C., and Chambers, C.M. (2000) Feedback and Hormonal Regulation of Hepatic 3-Hydroxy-3-methylglutaryl Coenzyme A Reductase: The Concept of Cholesterol Buffering Capacity, *Proc. Soc. Exp. Biol. Med. 224*, 8–19.

4. Erickson, S.K., Shrewsbury, M.A., Brools, C., and Myers, D.J. (1980) Rat Liver Acyl-Coenzyme A:Cholesterol Acyltransferase: Its Regulation *in vivo* and Some of Its Properties, *J. Lipid Res. 21*, 930–940.

5. Harry, D.S., Dini, M., and McIntyre, N. (1972) Effect of Cholesterol Feeding and Biliary Obstruction on Hepatic Cholesterol Biosynthesis in the Rat, *Biochim. Biophys. Acta 296*, 209–220.

6. Yap, P.M., and Tabas, I. (2001) Free Cholesterol Loading of Macrophage Is Associated with Widespread Mitochondrial Dysfunction and Activation of the Mitochondrial Apoptosis Pathway, *J. Biol. Chem. 276*, 42468–42476.

7. Tabas, I., Marathe, S., Kessler, G.A., Beatini, N., and Shiratori, Y. (1996) Evidence That the Initial Up-regulation of Phosphatidylcholine Biosynthesis in Free Cholesterol-Loaded Macrophages Is an Adaptive Response That Prevents Cholesterol-Induced Cellular Necrosis. Proposed Role of an Eventual Failure of This Response in Foam Cell Necrosis in Advanced Atherosclerosis. *J. Biol. Chem. 271*, 22773–22781.

8. Grogan, W.M., Bailey, M.L., Heuman, D.M., and Vlahcevic, Z.R. (1991) Effects of Perturbations in Hepatic Free and Esterified Cholesterol Pools on Bile Acid Synthesis, Cholesterol 7α-Hydroxylase, HMG-CoA Reductase, Acyl-CoA:Cholesterol Acyltransferase and Cytosolic Cholesteryl Ester Hydrolase, *Lipids 26*, 907–914.

9. Ghosh, S., Mallonee, D.H., Hylemon, P.B., and Grogan, W.M. (1995) Molecular Cloning and Expression of Rat Hepatic Neutral Cholesteryl Ester Hydrolase, *Biochim. Biophys. Acta 1259*, 305–312.

10. Ghosh, S., Natarajan, R., Pandak, W., Hylemon, P.B., and Grogan, W.M. (1998) Regulation of Hepatic Neutral Cholesteryl Ester Hydrolase by Hormones and Changes in Cholesterol Flux, *Am. J. Physiol. 274*, G662–G668.

11. Natarajan, R., Ghosh, S., and Grogan. W.M. (1998) Molecular Cloning of the Promoter for Rat Hepatic Neutral Cholesterol Ester Hydrolase: Evidence for Transcriptional Regulation by Sterols, *Biochem. Biophys. Res. Commun. 243* 349–355.

12. Natarajan, R., Ghosh, S., and Grogan, W.M. (1996) Catalytic Properties of the Purified Rat Cytosolic Cholesteryl Ester Hydrolase, *Biochem. Biophys. Res. Commun. 225*, 413–419.

13. Natarajan, R., Ghosh, S., and Grogan. W.M. (1999) Regulation of the Rat Neutral Cytosolic Cholesteryl Ester Hydrolase Promoter by Hormones and Sterols: A Role for Nuclear Factor-Y in the Sterol-Mediated Response, *J. Lipid Res. 40*, 2091–2098.

14. Osborne, T.F., and LaMorte, V.J. (1998) Molecular Aspects in Feedback Regulation of Gene Expression by Cholesterol in Mammalian Cells, *Methods 16*, 42–48.

15. Pandak, W.M., Schwarz, C., Hylemon, P.B., Mallonee, D., Valerie, K., Heuman, D.M., Fisher, R.A., Redford, K., and Vlahce-

vic, Z.R. (2001) Effects of CYP7A1 Overexpression on Cholesterol and Bile Acid Homeostasis, *Am. J. Physiol. Gastrointest. Liver Physiol. 281*, G878–G889.

16. Simons, K., and Ikonen, E. (2000) How Cells Handle Cholesterol, *Science 290*, 1721–1726.

17. Hylemon, P.B., Pandak, W.M., and Vlahcevic, Z.R. (2001) Regulation of Hepatic Cholesterol Homeostasis, in *Liver Biology and Pathobiology* (Arias, I.M., Boyer, J.L., Chisari, F.V., Fausto, N., Schachter, D.A., and Shafritz, D.A., eds., pp. 231–247, Lippincott Williams & Wilkins, New York.

18. Gerard, R.D., and Meidell, R.S. (1995) Adenovirus Vectors, in *DNA Cloning 4: Mammalian Systems* (Glover, D.M., and Hames, B.D., eds.), pp. 285–306, Oxford University Press, New York.

19. Natarajan, R., Ghosh, S., and Grogan, W.M. (1996) Age Related Changes in mRNA, Protein and Catalytic Activity of Hepatic Cholesterol Ester Hydrolase in Male Rats: Evidence for Transcriptional Regulation, *Biochim. Biophys. Acta 1302*, 153–156.

20. Bligh, E., and Dyer, W. (1959) A Rapid Method of Total Lipid Extraction and Purification, *Can. J. Biochem. Phys. 37*, 911–917.

21. Hylemon, P.B., Gurley, E.C., Stravitz, R.T., Litz, J.S., Pandak, W.M., Chiang, J.Y., and Vlahcevic, Z.R. (1992) Hormonal Regulation of Cholesterol 7 α-Hydroxylase mRNA Levels and Transcriptional Activity in Primary Rat Hepatocyte Cultures, *J. Biol. Chem. 267*, 16866–16871.

22. Ghosh, S., and Grogan, W.M. (1989) Activation of Rat Liver Cholesterol Ester Hydrolase by cAMP-Dependent Protein Kinase and Protein Kinase C, *Lipids 24*, 733–736.

23. Eisenhardt, E., and von Deimling, O. (1982). Interstrain Variation of Esterase-22, a New Isozyme of the House Mouse, *Comp. Biochem. Physiol. B 73*, 719–724.

24. Natarajan, R., Ghosh, S., and Grogan, W.M. (1996) Age-Related Changes in mRNA, Protein and Catalytic Activity of Hepatic Neutral Cholesterol Ester Hydrolase in Male Rats: Evidence for Transcriptional Regulation, *Biochim. Biophys. Acta 1302*, 153–158.

25. Natarajan, R., Ghosh, S., and Grogan, W.M. (1997) Age-Related Changes in Catalytic Activity, Enzyme Mass, mRNA, and Subcellular Distribution of Hepatic Neutral Cholesterol Ester Hydrolase in Female Rats, *Lipids 32*, 463–470.

26. Escary, J.L., Choy, H.A., Reue, K., and Schotz, M.C. (1998) Hormone-Sensitive Lipase Overexpression Increases Cholesteryl Ester Hydrolysis in Macrophage Foam Cells, *Arterioscler. Thromb. Vasc. Biol. 18*, 991–998.

27. Okazaki, H., Osuga, J., Tsukamoto, K., Isoo, N., Kitamine, T., Tamura, Y., Tomita, S., Sekiya, M., Yahagi, N., Iizuka, Y., Ohashi, K., *et al.* (2002) Elimination of Cholesterol Ester from Macrophage Foam Cells by Adenovirus-Mediated Gene Transfer of Hormone-Sensitive Lipase, *J. Biol. Chem. 277*, 31893–31899.

28. Sztalryd, C., Komaromy, M.C., and Kraemer, F.B. (1995) Overexpression of Hormone-Sensitive Lipase Prevents Triglyceride Accumulation in Adipocytes, *J. Clin. Invest. 95*, 2652–2661.

29. Khoo, J.C., Steinberg, D., Huang, J.J., and Vagelos, P.R. (1976) Triglyceride, Diglyceride, Monoglyceride, and Cholesterol Ester Hydrolases in Chicken Adipose Tissue Activated by Adenosine 3′:5′-Monophosphate-Dependent Protein Kinase. Chromatographic Resolution and Immunochemical Differentiation from Lipoprotein Lipase, *J. Biol. Chem. 251*, 2882–2890.

30. Post, S.M., Zoeteweij, J.P., Bos, M.H., deWit, E.C., Havinga, R., Kuipers, F., and Princen, H.M. (1999) Acyl-Coenzyme A:Cholesterol Acyltransferase Inhibitor, Avasimbe, Stimulates Bile Acid Synthesis and Cholesterol 7α-Hydroxylase in Cultured Rat Hepatocytes and *in vivo* in the Rat, *Hepatology 30*, 491–500.

31. Azuma, Y., Kawasaki, T., Ohno, K., Seto, J., Yamada, T., Yamasaki, M., and Nobuhara, Y. (1999) Effects of NTE-122, a Novel Acyl-CoA:Cholesterol Acyltransferase Inhibitor, on Cholesterol

Esterification and Lipid Secretion from Caco-2 Cells, and Cholesterol Absorption in Rats, *Jpn. J. Pharmacol. 80*, 81–84.

32. Murakami, S., Yamagishi, I., Sato, M., Tomisawa, K., Nara, Y., and Yamori, Y. (1997) ACAT Inhibitor HL-004 Accelerates the Regression of Hypercholesterolemia in Stroke-Prone Spontaneously Hypertensive Rats (SHRSP): Stimulation of Bile Acid Production by HL-004, *Atherosclerosis 133*, 97–104.

33. Lu, T.T., Makishima, M., Repa, J.J., Schoonjans, K., Kerr, T.A., Auwerx, J., and Mangelsdorf, D.J. (2000) Molecular Basis for Feedback Regulation of Bile Acid Synthesis by Nuclear Receptors, *Mol. Cell 6*, 507–515.

34. Peet, D.J., Turley, S.D., Ma, W.M., Janowski, B.A., Lobaccaro, J., Hammer, R.E., and Mangelsdorf, D.J. (1998) Cholesterol and Bile Acid Metabolism Are Impaired in Mice Lacking the Nuclear Oxysterol Receptor LXRα, *Cell 93*, 693–704.

35. Brown, A.J., and Jessup, W. (1999) Oxysterols and Atherosclerosis, *Atherosclerosis 142*, 1–28.

36. Smith, L.L., and Johnson, B.H. (1989) Biological Activities of Oxysterols, *Free Radic. Biol. Med. 7*, 285–332.

37. Stroup, D., Crestani, M., and Chiang, J.Y. (1991) Identification of a Bile Acid Response Element in the Cholesterol 7 α-Hydroxylase Gene CYP7A, *Am. J.Physiol. 273*, G508—G517.

38. Chen, W., and Chiang, J.Y.L. (2003) Regulation of Human Sterol 27-Hydroxylase Gene (*CYP27A1*) by Bile Acids and Hepatocyte Nuclear Factor 4α (HNF4α), *Gene 313*, 71–82.

39. Wang, L., Han, Y., Kim, C., Lee, Y., and Moore, D. (2003) Resistance of SHP-Null Mice to Bile Acid-Induced Liver Damage, *J. Biol. Chem. 278*, 44475–44481.

40. Li-Hawkins, J., Gafvels, M., Olin, M., Lund, E.G., Andersson, U., Schuster, G., Bjorkhem, I., Russell, D.W., and Eggertsen, G. (2002) Cholic Acid Mediates Negative Feedback Regulation on Bile Acid Synthesis in Mice, *J. Clin. Invest. 110*, 1191–1200.

41. Gupta, S., Stravitz, R.T., Dent, P., and Hylemon, P.B. (2001) Down Regulation of Cholesterol 7α-Hydroxylase (CYP7A1) Gene Expression by Bile Acids in Primary Rat Hepatocytes Is Mediated by the c-Jun N-Terminal Kinase Pathway, *J. Biol. Chem. 276*, 15816–15822.

42. Heuman, D.M., Pandak, W.M., Hylemon, P.B., and Vlahcevic, Z.R. (1991) Conjugates of Ursodeoxycholate Protect Against Cytotoxicity of More Hydrophobic Bile Salts: *In vitro* Studies in Rat Hepatocytes and Human Erythrocytes, *Hepatology 14*, 920—926.

β-Oxidation Capacity of Red and White Muscle and Liver in Atlantic Salmon (*Salmo salar* L.)—Effects of Increasing Dietary Rapeseed Oil and Olive Oil to Replace Capelin Oil

Ingunn Stubhaug*, Livar Frøyland, and Bente E. Torstensen

National Institute of Nutrition and Seafood Research (NIFES), Nordnes, 5817 Bergen, Norway

ABSTRACT: Post-smolt Atlantic salmon (*Salmo salar*) were fed six diets in which capelin oil was replaced with 0, 25, 50, 75, or 100% rapeseed oil (RO; low-erucic acid) or 50% olive oil (OO). The experimental diets were fed to single groups of Atlantic salmon for 42 wk, whereas the 100% capelin oil (0% RO) diet was fed in duplicate. The β-oxidation capacity of palmitoyl-CoA was determined, using a method optimized for salmon tissues, at the start of the experiment, after 21 wk (October), and after 42 wk (March) in red and white muscle and in liver. Red muscle showed the highest specific β-oxidation capacity, but when expressed as total β-oxidation capacity for the whole tissue, white muscle was the most important tissue for the β-oxidation of FA. From the initial to the final sampling, the β-oxidation capacity of white muscle increased significantly, whereas the β-oxidation capacity in liver decreased significantly. After 22 wk, white muscle exhibited an increased β-oxidation capacity when the dietary RO content was raised from 25 to 75%, with similar effects in red muscle and liver after 42 wk of feeding. The present results also show that the β-oxidation capacity increased with an increase in fish size.

Paper no. L9581 in *Lipids 40*, 39–47 (January 2005).

Lipids of marine origin have beneficial effects on human health, including the possible prevention of cardiac diseases (1,2). Farmed Atlantic salmon (*Salmo salar* L.) are normally fed a diet with a high lipid content, in which the lipids traditionally originate from other marine sources. Since the availability of marine lipid resources is declining, it is desirable to investigate the possibility of incorporating vegetable oil into fish feeds while maintaining fish welfare and the beneficial effects of fish consumption on human health. However, to monitor the possible effects of vegetable oils on fish welfare, increased knowledge regarding the basic mechanisms of lipid metabolism is needed.

Vegetable oils do not contain FA whose chain lengths exceed 18 carbons. Rapeseed oil (low-erucic acid) and olive oil have low levels of 18:3n-3, moderate levels of 18:2n-6, and high levels of 18:1n-9 compared with other vegetable oils. Marine oils typically have high levels of n-3 FA, containing 22:6n-3 (DHA) and 20:5n-3 (EPA) and monounsaturated FA (MUFA) with backbones exceeding 18 carbons in length such as 20:1n-9 and 22:1n-11.

β-Oxidation occurs in mitochondria and peroxisomes in both fish and mammals (3–7). In studies in which mitochondrial and peroxisomal β-oxidation have been measured separately, peroxisomal β-oxidation has been shown to constitute as much as 30% of total hepatic β-oxidation in *Notothenia gibberifrons*, an Antarctic cod (8), and 50% in Longhorn sculpins (*Myoxocephalus octodecimspinosus*) (9). A study measuring mitochondrial and peroxisomal β-oxidation in Atlantic salmon showed that 20 and 40% of the total β-oxidation capacity originated from peroxisomes in red and white muscle, respectively (10).

Previous studies have found that red muscle has the highest capacity for β-oxidation (10,11) and white muscle the lowest. In a study by Torstensen *et al.* (12), Atlantic salmon were fed diets in which capelin oil was replaced with either palm oil or oleic acid-enriched sunflower oil. Compared with the capelin oil diet, the diet containing palm oil exhibited lower digestibility, but no significant differences in β-oxidation in red muscle were found. Metabolic processes in fish, including lipid metabolism, are affected by season (13–15), temperature [reviewed by Guderley (16)], and fish size (10,17,18).

The aim of the present study was to investigate the effects on β-oxidation capacity due to an altered dietary lipid composition. In particular, the effect of increasing dietary levels of rapeseed oil (RO) and olive oil (OO) at the expense of capelin oil was studied. OO is a major component in the Mediterranean diet, which is known to have benefits for human health. RO and OO both have high levels of 18:1n-9; thus, a comparison between these two alternative oil sources was of interest. In addition, the method for measuring β-oxidation capacity was optimized for Atlantic salmon tissues.

MATERIALS AND METHODS

Raising conditions. The fish experiment was carried out at the Gildeskaal research station in Norway (67° North) from May 2001 to March 2002. Atlantic salmon with a mean initial weight of 142 ± 1 g were divided into 7 net pens of 125 m³,

with approximately 600 fish in each net pen. Biomass and mean fish weight in each of the net pens were determined by bulk weighing and were determined for all fish at each sampling. The diets were fed to satiation by hand, and any dead fish were removed daily and recorded. The fish were exposed to continuous light from December 22 to May 1. Before and after this period, the fish were exposed to natural light. The temperature was measured monthly and ranged from 4 to 15°C (see Ref. 19 for further details).

The diets were produced by Nutreco ARC (Stavanger, Norway) and were formulated to contain 450 g·kg^{-1} protein, 300 g·kg^{-1} lipid, 60 g·kg^{-1} moisture, 70 g·kg^{-1} ash, and 120 g·kg^{-1} nitrogen-free extract. The experimental diets had increasing levels of RO, 0, 25, 50, 75, and 100%, at the expense of capelin oil, and one diet in which 50% OO was added instead of capelin oil. The diets had complete vitamin and mineral contents. The 0% RO diet was fed to duplicate groups, whereas the other diets were fed to single groups in a regression design.

Sampling procedure and preparation of tissue homogenates. The fish were fasted 24 h prior to sampling. Fish were randomly selected and anesthetized with metomidate (7 g·L^{-1}; Norwegian Medicinal Depot, Oslo, Norway) before being killed by a blow to the head. Samples were taken at three stages during the experimental period: a first sampling in May (initial sampling), an intermediate sampling in October (22 wk), and a final sampling in March (42 wk).

For measurements of β-oxidation capacity (performed on-site), 15 fish were sampled and 5 fish were then pooled, yielding three subsamples from each net pen. Red and white muscle and liver were dissected out immediately. Red muscle was taken from a region starting at the dorsal fin and extending to the tail, and was dissected free from skin and white muscle. The portion of white muscle was taken from the "Norwegian quality cut" region, between the dorsal and ventral fins. Approximately 1 g of red and white muscle and liver were sampled from each fish (a total of 5 g for each subsample).

Samples from the red and white muscle and liver were then transferred to 50-mL plastic tubes containing 20 mL of buffer and were homogenized using an UltraTurrax homogenizer. The homogenization buffer contained 10 mM HEPES (all chemicals were obtained from Sigma Chemical Co., St. Louis, MO, unless otherwise stated), 1 mM EDTA, and 0.25 M sucrose (Merck KGaA, Darmstadt, Germany), and was adjusted to pH 7.4. The resulting homogenate was centrifuged at $1500 \times g$ for 10 min at 4°C. The postnuclear fractions (E-fractions), which contained mitochondria, peroxisomes, and other organelles, were collected. The E-fraction from each tissue sample was divided into three analytical parallels and one blank. An aliquot of the fraction was retained for protein determination and stored at –20°C until analyzed.

FA composition. The FA composition of total lipids in the experimental diets (stored at –20°C) was analyzed using methods described previously (20,21). The methyl esters were separated using a Trace 2000 gas chromatograph (Fison CE Instru-

ments, Milan, Italy; "cold on-column" injection, 60°C for 1 min at 25°C min^{-1}, 160°C for 28 min at 25°C min^{-1}, 190°C for 17 min at 25°C min^{-1}, and 220°C for 10 min), equipped with a 50-m CP-Sil 88 (Chrompack, Middelburg, The Netherlands) fused-silica capillary column (i.d., 0.32 mm) The FA were identified by retention times using standard mixtures of methyl esters (Nu-Chek-Prep, Elysian, MN), and the FA composition (wt%) was calculated using an integrator (TotalChrom software, Version 6.2, PerkinElmer Life and Analytical Sciences, Inc., Boston, MA), connected to the gas chromatograph. The content of FA per gram of diet was calculated using 19:0 methyl as the internal standard.

Enzyme activity. The rate of β-oxidation was measured for each of the three tissues using [1-^{14}C]palmitoyl-CoA as substrate. A buffer mix was made in two steps: A HEPES buffer adjusted to pH 8.1 (20 mM of HEPES with 125 mM of KCl (Merck KGaA) was first made and stored. On the day of the assay, the following components were added to 10 mL of the HEPES buffer: 1 mL of 10 mM EDTA, 1 mL of 250 mM MgCl$_2$ (Merck KgaA), 2 mL of 100 mM DL-DTT (DL-dithiothreitol), 150 μL of 20 mM NAD, 1 mL of 100 mM ADP, and 12.5 μL of 25 mM L-carnitine. The following volumes of E-fraction were then mixed with 250 μL of buffer mix in 10-mL plastic tubes: 30 μL for red muscle, 300 μL for white muscle, and 30 μL for liver (diluted 1:5 with homogenization buffer).

The tubes containing homogenized tissue and buffer mix (called the assay mix) were pre-incubated in a water bath at 20°C for 2 min before adding 5 μL of 1.5 mM [1-^{14}C]palmitoyl-CoA (0.4 kBq; American Radiolabeled Chemicals Inc., St. Louis, MO). The reaction was stopped after 10 min by adding 150 μL of 1.5 mM KOH (Merck KGaA). To bind nonoxidized FA, 25 μL of FA-free BSA (FAF-BSA; 100 mg·mL^{-1}) was added and the tubes were shaken. The BSA–FA complex was then precipitated by adding 500 μL of ice-cold 4 M HClO$_4$ (Merck KGaA). The tubes were centrifuged for 10 min at $2400 \times g$. A 500-μL aliquot of the supernatant, which then contained products from mitochondrial and peroxisomal β-oxidation, was added to 8 mL of scintillation cocktail (LumaSafe Plus^{TM}; Lumac·LSC, Groningen, The Netherlands). Disintegrations per minute (dpm) were measured in a scintillation counter (Packard 1900 TR liquid scintillation analyzer). One blank was made for each sample in the same way as for the analytical samples except that [1-^{14}C]palmitoyl-CoA was added after KOH had been added to the tubes. β-Oxidation capacity was expressed as the specific activity (Eq. 1) in the acid-soluble supernatant:

$$\text{specific activity} = \frac{\text{parallels} - \text{blank}}{\text{mg protein} \cdot \text{incubation time} \cdot \text{standard}} \cdot 100 \quad [1]$$

where parallels and blanks are expressed in dpm, incubation time in minutes, and standard is the specific activity of the radiolabeled FA added to the reaction (dpm·nmol^{-1}). The β-oxidation activity, expressed per minute per gram of wet tissue and per minute per tissue, is calculated as given in Equations 2 and 3:

$$\text{per g wet tissue} = \frac{[\text{Eq. 1}] \cdot \text{mg protein} \cdot \text{mL E-fraction}}{\text{g tissue used}} \quad [2]$$

$$\text{per tissue} = [\text{Eq. 2}] \cdot \text{mean fish weight} \cdot \text{tissue factor} \quad [3]$$

where a tissue factor of 0.6 was used for white muscle, 0.05 was used for red muscle, and 0.01 was used for liver (22).

Method optimization. Prior to conducting the fish experiment, the method of measuring β-oxidation capacity in tissue homogenates was improved from previously described methods (10,23). The improved method was tested for different protein concentrations (E-fractions) added to the buffer mix for all three tissues and with different pH in the buffer mix (adjustment of pH in the HEPES buffer). This was done to find a linear relationship between the velocity of the reaction and the protein concentration for all three tissues. For optimization of the method, Atlantic salmon raised at the Institute of Marine Research in Bergen, Norway, were used. The fish weighed 725 ± 205 g and were 41 ± 4 cm long. These fish were fed a commercial fish feed (Orion MP 400-60A; Skretting, Stavanger, Norway), which contained 430 g·kg^{-1} (crude) protein, 330 g·kg^{-1} lipids, 72 g·kg^{-1} ash, and 9 g·kg^{-1} fiber.

Tissue preparation and enzyme activity measurements were performed as described previously except that the pH of the initial buffer mix (chemicals added to the HEPES buffer) and the amount of E-fractions added to the buffer mix varied. The pH was measured using a pH meter (inoLab pH level 1; WTW, Weilheim, Germany).

Statistical analysis. Data from the method optimization were calculated using GraphPad Prism, version 4.0 (GraphPad Software, Inc., San Diego, CA). To create a curve-fitting plot for the data, a one-site binding equation for hyperbolic curves was used:

$$Y = \frac{B_{\max} \cdot X}{(K_d + X)} \quad [4]$$

where Y is the velocity measured in dpm, $B_{\max}$ is the maximal binding, K_d is the protein concentration (amount of enzyme) required to reach half binding, and X is the protein concentration. Data for the fish experiment were analyzed for statistical differences using the nonparametric Kruskal–Wallis method (Statistica, version 6.0; StatSoft Inc., Tulsa, OK), owing to the fact that subsamples were used in this experiment (24).

RESULTS

Method improvement. A linear relationship was found between milligrams of protein and amount of product produced (dpm) for all tissues (Fig. 1). Less protein had to be added to the assay for red muscle and for liver than in the original protocol to obtain linearity. The left panels of Figure 1 show the relationship between dpm and protein up to the point of saturation. The right panels of Figure 1 exhibit the linear portion of the curve. When the pH of the buffer increased, the velocity of the reaction increased, and the points followed a hyperbolic curve better than when a lower pH was used (Fig. 1, left panels). The

linear range for white muscle was from 0.6 to 4.5 mg protein, for red muscle the linear range was between 0.02 and 0.13 mg protein, and for liver the range was between 0.04 and 0.18 mg protein (Fig. 1, right panels).

The liver homogenate had the highest pH, 7.4 ± 0.3 (diluted E-fraction, 1 + 4), whereas the white muscle homogenate had the lowest pH, 6.29 ± 0.04. Red muscle homogenate had a pH of 6.8 ± 0.1. In the assay mix, the pH of white muscle increased from 6.5 to 6.7, for red muscle the pH increased from 6.0 to 7.0, and in the liver the pH increased from 5.5 to 6.7 with an increase in pH of the buffer.

Fish experiment. The mean weight of fish from the initial sampling to the final sampling increased from 146 ± 28 to 1572 ± 301 g, with a mean weight of 993 ± 213 g in the intermediate sampling. Mortalities were negligible throughout the experiment. The sampled fish were randomly selected and did not differ in mass from the bulk weighing of the fish (19). The FA composition of the different diets is given in Table 1. With increasing RO in the diet, the amount of dietary saturated FA and n-3 FA decreased. Within the n-3 FA, the amount of α-linolenic acid (18:3n-3) increased, whereas the levels of DHA and EPA decreased. Furthermore, total MUFA and total n-6 FA increased with increasing RO levels in the diet. The MUFA 18:1n-9 was the FA responsible for the increase of MUFA. The FA composition of the 50% OO diet group was most similar to that of the 50% RO diet group.

The total β-oxidation capacity (both mitochondrial and peroxisomal β-oxidation activity) of oxidized [1-^{14}C]palmitoyl-CoA (β-oxidation capacity) of red and white muscle and liver is presented in Figure 2. There was a significant increase in β-oxidation capacity in white muscle from May to March and a significant decrease in liver β-oxidation from May to October.

Within the sampling performed in October, the β-oxidation capacity in white muscle increased 1.7-fold when Atlantic salmon were fed 75% RO compared with 0% RO; however, this change was not statistically significant. Atlantic salmon fed 75% RO had a significantly higher β-oxidation capacity compared with Atlantic salmon fed 100% RO (Fig. 2, top panel). In the final sampling period, the differences between the dietary groups in white muscle β-oxidation were smaller than in October, although all the dietary groups increased their β-oxidation capacity compared with October, with the exception of the group fed the 75% RO diet.

Irrespective of diet, red muscle had the highest β-oxidation capacity of the tissues measured. There were no statistically significant differences between sample times or between dietary groups (Fig. 2, middle panel). However, the β-oxidation capacity between the dietary groups was more or less the same within each sample period, and the red muscle sampled in March showed a β-oxidation capacity similar to that of the white muscle sampled in October and to the liver sampled in March (Fig. 2, bottom panel). Fish fed 50% OO had the highest β-oxidation capacity in red muscle in October compared with the other dietary groups, showing a 1.6-fold increase compared with fish fed 0% RO. The β-oxidation capacity of red muscle was lower in March than in October.
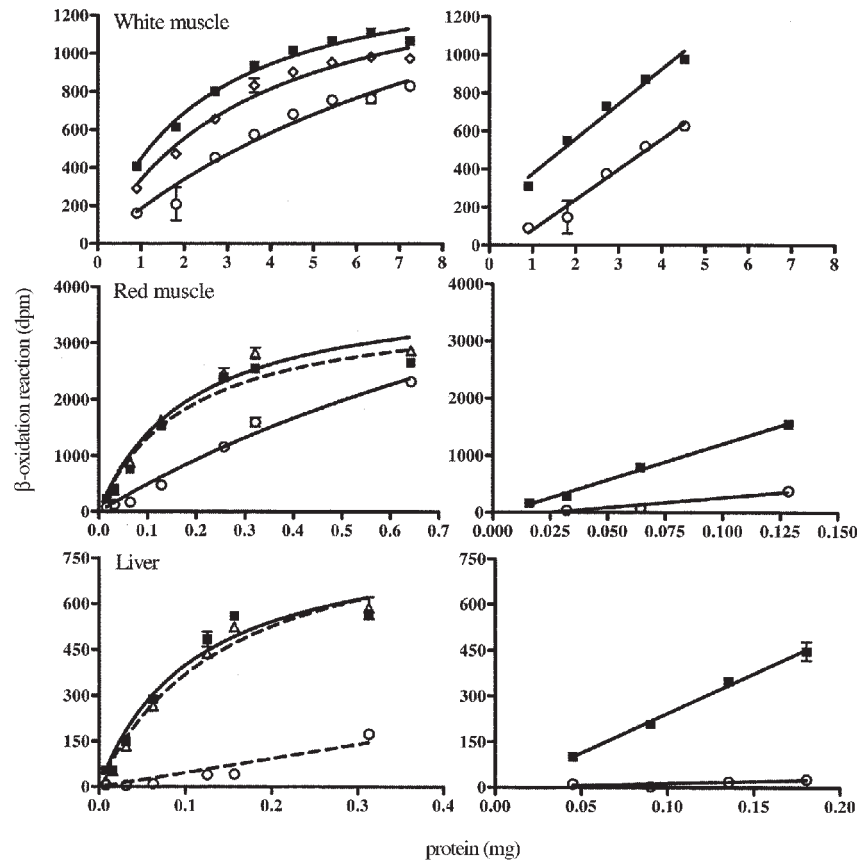
FIG. 1. The β-oxidation activity in white (top panels) and red (middle panels) muscle and in liver (bottom panels) homogenates using $[1-^{14}C]$palmitoyl-CoA as substrate. Increasing concentrations and different pH in the buffer were tested. The figures on the left side show the β-oxidation activity with increasing tissue concentrations up to the point of saturation between the substrate and protein. The figures on the right side show the β-oxidation activity within the linear range of the reaction. The activity is expressed as net disintegrations per minute (dpm). The different symbols relate to the pH of the HEPES buffer used in the buffer mix: pH 7.3 (○), 7.8 (◇), 8.1 (■), and 8.3 (△). Closed symbols indicate the preferred pH (see discussion for details). Each data point is the average of three parallel measurements, and the error bars show SD. The values on the *x*-axis for red muscle in the original protocol (middle left panel) are estimated, using a factor of 0.0083 between the protein values (mg) and volumes of E-fraction (postnuclear supernatant; μL) added on the basis of other experiments performed and the mean relationship between measured milligrams of protein and volume of the E-fraction.

In October the liver exhibited a significantly increased β-oxidation capacity in Atlantic salmon fed the 50% OO diet, compared with fish fed the 0% RO diet (Fig. 2, bottom panel). Data on livers of the other dietary groups in the October samples were lost due to a mistake in preparation of the assay buffer. There were no statistical differences in hepatic β-oxidation capacity between the dietary groups within the final sampling.

Figures 3 and 4 show the β-oxidation capacity for white and red muscle and for liver expressed per gram of tissue and per tissue (i.e., accounting for total tissue mass), respectively. When accounting for total tissue mass, white muscle had the highest β-oxidation capacity of the three tissues measured (Fig. 4). Liver, on the other hand, had the lowest β-oxidation capacity per tissue. The β-oxidation capacity in white muscle and in liver increased during the experimental period (Fig. 4). Irrespective of how the β-oxidation capacity was expressed, the pattern within a sample period or the relative changes between sample times did not change in the muscle. When expressing the data on a per-tissue basis (Fig. 4), there was an increased β-oxidation capacity in Atlantic salmon fed 0% RO in the initial sampling period compared with the other sampling times for all three tissues.

DISCUSSION

Method improvement. To enable measurement of the maximum β-oxidation activity (capacity) and to observe changes in the capacity of the β-oxidation reaction, it is necessary to find the range of tissue concentrations over which a linear relationship

TABLE 1
Dietary FA Composition (mg FA g^{-1} feed, w/w) of the Six Experimental Diets[a]

FA	0% RO	25% RO	50% RO	75% RO	100% RO	50% OO
14:0	14.4	10.8	8.5	5.1	1.0	7.2
16:0	25.0	21.6	21.0	17.9	13.7	24.9
18:0	2.1	2.6	3.3	3.8	4.1	4.1
Sum saturated	43.9	37.5	35.1	29.9	21.7	38.2
16:1n-9	0.5	0.5	0.4	—	—	0.4
16:1n-7	17.3	13.1	10.4	6.3	1.5	9.5
18:1n-9	24.1	48.5	76.2	101.5	128.6	79.1
18:1n-7	7.4	7.2	7.9	8.0	7.7	5.9
20:1n-11	0.9	0.6	0.7	0.6	—	0.6
20:1n-9	36.9	28.5	23.0	14.7	5.1	19.1
20:1n-7	1.5	0.9	0.7	0.5	—	0.7
22:1n-11	28.6	21.8	17.1	10.3	2.3	11.6
22:1n-9	4.4	3.5	3.0	2.2	1.2	2.3
Sum monoenes	123.0	125.6	140.3	144.5	146.9	130.0
18:2n-6	7.6	16.3	27.0	36.9	46.9	16.4
20:2n-6	0.5	0.5	—	—	—	—
20:4n-6	0.6	0.5	0.2	—	—	0.4
Sum n-6	8.7	17.3	27.2	36.9	46.9	16.8
18:3n-3	2.3	6.4	11.0	15.9	20.7	5.5
18:4n-3	6.1	4.7	3.7	2.2	0.4	3.1
20:4n-3	0.9	0.6	0.5	—	—	0.5
20:5n-3	12.6	9.7	8.0	5.1	1.7	6.9
22:5n-3	0.9	0.7	0.6	0.4	—	0.5
22:6n-3	10.0	8.0	7.1	5.0	2.5	6.2
Sum n-3	34.1	30.6	31.4	28.6	25.4	23.1
n-3/n-6	3.9	1.8	1.2	0.8	0.5	1.4
Sum total FA	215.5	215.1	235.4	239.9	240.9	212.2
Sum identified	210.1	212.0	234.0	239.9	240.9	208.1

[a]Data are presented as means (n = 2); when values are below 0.1, they are denoted by —. RO, rapeseed oil; OO, olive oil.

exists between tissue content and β-oxidation rate in Atlantic salmon tissues. Thus, the purpose of the current study was to determine experimentally the conditions under which the substrate and other co-factors were in excess and only the enzymes of β-oxidation were rate-limiting for red and white muscle and liver. A linear range was found for the three tissues tested.

Assay pH played a major role in obtaining reliable, reproducible results. If the pH of the assay mix was not near the enzymes' pH optimum, the functionality of the enzyme was reduced, and saturation of activity was not achieved (Fig. 1, pH 7.3). The rate of β-oxidation activity increased the most in liver when the pH was increased from pH 7.3 to 8.1, whereas the smallest increase was found in white muscle. Increasing the pH further for white muscle did not result in a better curve (data not shown). Based on this and the minor differences associated with raising the pH from 8.1 to 8.3, the optimal pH level in the HEPES buffer was set at 8.1. Salmonids use white muscle for fast swimming and red muscle for prolonged and sustainable swimming (25). During fast swimming (anaerobic work), the muscle produces lactic acid that acts to lower the pH in the muscle (26). This may indicate that enzymes in white muscle are adapted to function in a more acidic environment and therefore have a broader pH optimum. Alternatively, the observations reported here may be explained by white muscle having a higher buffering capacity compared with liver and red muscle.

Another methodological aspect that requires consideration is the production and possible escape of radiolabeled CO_2 from oxidized [1-^{14}C]palmitoyl-CoA. The last step in energy production results in ATP, H_2O, and CO_2. Intuitively, therefore, a measure of CO_2 production during the assay could be used to compensate for this potentially lost label and thus be used to calculate exact β-oxidation rates. However, it has previously been found that measuring only the [^{14}C]CO_2 production did not give satisfying results when estimating the [^{14}C]FA oxidation rate (27). Another study found that insignificant amounts of [^{14}C]CO_2 were produced during the β-oxidation reaction, even after 1 h of incubation (9). The reaction in the present study was run for 10 min; it may therefore be assumed that the amount of [^{14}C]CO_2 produced in the β-oxidation reaction was negligible.
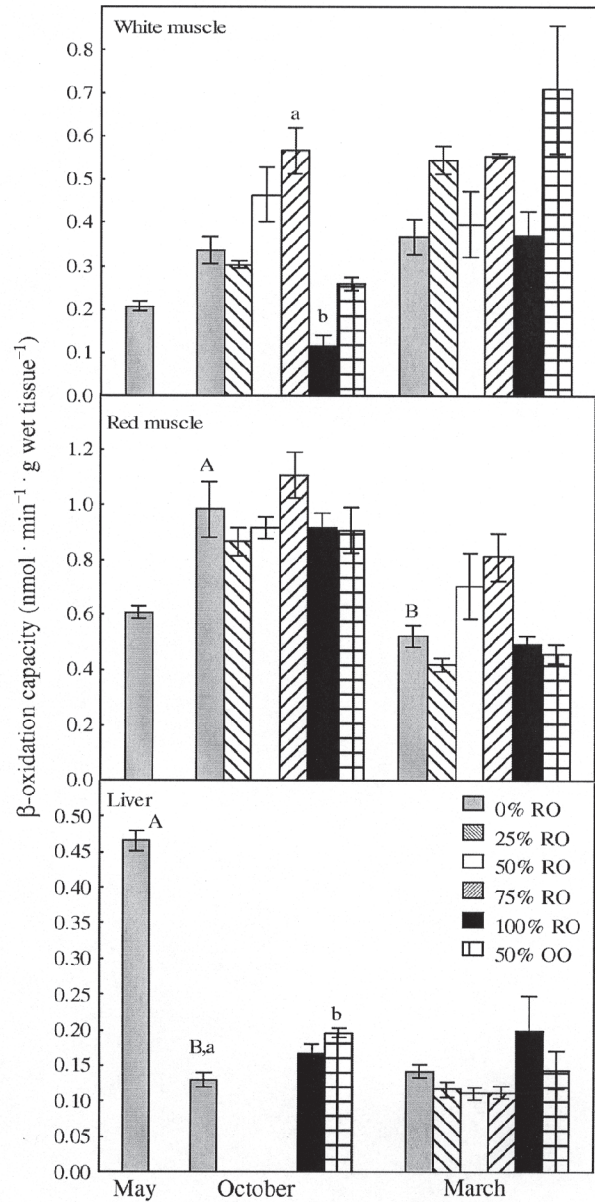
Fish experiment. Fish growth did not vary significantly among the dietary groups [details on growth parameters are given in Torstensen *et al.* (19)]. This result is in line with previous studies regarding the replacement of fish oil with vegetable
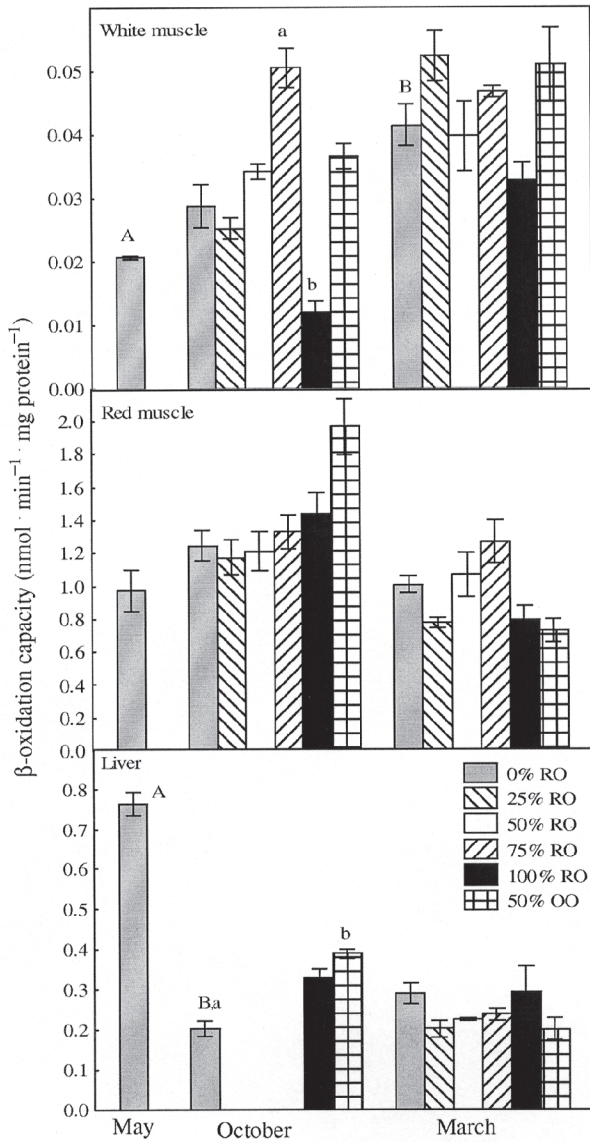
FIG. 2. β-Oxidation capacity, measured using [1-^{14}C]palmitoyl-CoA as substrate in white muscle, red muscle, and liver from post-smolt Atlantic salmon fed diets containing 0, 25, 50, 75, or 100% of the lipid content as rapeseed oil (RO) or 50% as olive oil (OO) to replace capelin oil for 42 wk (March). An intermediate sampling was performed after 22 wk (October). β-Oxidation capacity is expressed as nmol·min^{-1}·mg protein^{-1}. Data are presented as means ± SEM ($n = 3$). Capital letters indicate statistically significant differences between 0% RO for every sampling; small letters indicate differences within each sampling. No letters indicate no statistically significant differences. Data were analyzed using the nonparametric Kruskal–Wallis test. Note that the scaling on the *y*-axis differs between tissues.

FIG. 3. β-Oxidation capacity, measured using [1-^{14}C]palmitoyl-CoA as substrate in white muscle, red muscle, and liver from post-smolt Atlantic salmon fed diets containing 0, 25, 50, 75, or 100% of the lipid content as RO or 50% as OO to replace capelin oil for 42 wk (March). An intermediate sampling was performed after 22 wk (October). β-Oxidation capacity is expressed as nmol·min^{-1}· g wet tissue^{-1}. Data are presented as mean ± SEM ($n = 3$). Capital letters indicate statistically significant differences between 0% RO for every sampling; small letters indicate differences within each sampling. Data were analyzed using the nonparametric Kruskal–Wallis test. Note that the scaling on the *y*-axis differs between tissues. For abbreviations see Figure 2.

oils (12,28–30). FA composition was analyzed in red and white muscle and in liver in the present experiment and has been reported by Torstensen *et al.* (21). FA compositions of both types of muscle were highly reflective of the dietary FA compositions, which is in agreement with earlier findings (31–34).

In the present experiment, red muscle had the highest specific β-oxidation capacity, whereas white muscle had the lowest (Fig. 1). This is in agreement with earlier results (12,35). However,

when considering the total amount of energy produced by β-oxidation in the different tissues, white muscle is the most important tissue (Fig. 4), since white muscle makes up approximately 60% of the total body mass in Atlantic salmon (22). These results are also supported by previous studies (10,11).

All fish in the present experiment were fed a commercial feed
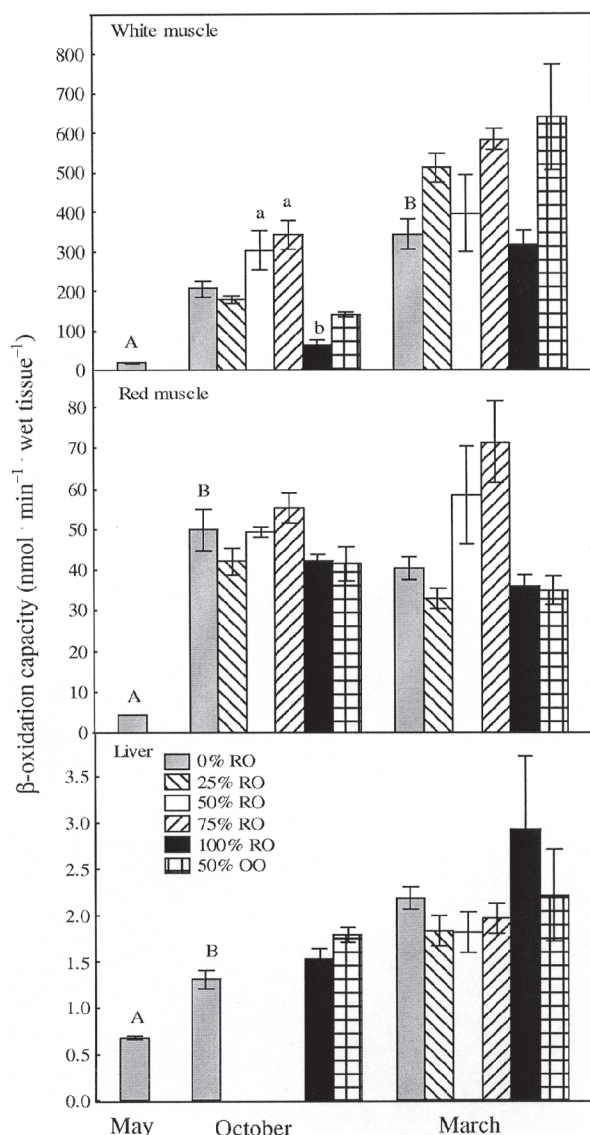
FIG. 4. β-Oxidation capacity, measured using [1-^{14}C]palmitoyl-CoA as substrate in white muscle, red muscle, and liver from post-smolt Atlantic salmon fed diets containing 0, 25, 50, 75, or 100% of the lipid content as RO or 50% as OO to replace capelin oil for 42 wk (March). An intermediate sampling was performed after 22 wk (October). β-Oxidation capacity is expressed as nmol·min^{-1}· wet tissue^{-1}. Data are presented as mean ± SEM ($n = 3$). Capital letters indicate statistically significant differences between 0% RO for every sampling; small letters indicate differences within each sampling. Data were analyzed using the nonparametric Kruskal–Wallis test. Note that the scaling on the *y*-axis differs between tissues. For abbreviations see Figure 2.

the initial and the intermediate sampling (Fig. 2, bottom panel). Red muscle showed no significant differences over the course of the experiment. It was reported earlier that β-oxidation capacity decreases with an increase in fish size (10,12). The results from the present study showed that the β-oxidation capacity in all three tissues increased with size, especially in the first growth phase after seawater transfer (Fig. 4; 0% RO). Kiessling *et al.* (17) did not find any differences in muscle 3-hydroxyacyl-CoA dehydrogenase activity, a key enzyme in β-oxidation, in the seawater phase. However, both the size of the fish (36) and the method for measuring β-oxidation capacity differed between these studies, and this may explain the variation between the two results. Since white and red muscle together constitute approximately 65% of the total body weight (22), it can therefore be concluded that the β-oxidation capacity in Atlantic salmon increased during growth.

The β-oxidation capacity in white muscle in Atlantic salmon was highest during winter (March), coinciding with the lowest temperature, whereas liver had the highest β-oxidation capacity in the spring (May; medium temperature). Earlier studies showed that the β-oxidation enzyme activity in muscle is affected by temperature [reviewed by Guderley (16)] and by season (13) and might increase during acclimatization to the cold. In the present experiment, the temperature varied from 7.7°C in May to 3.7°C in March to 9.7°C in October. The statistically significant increase in β-oxidation capacity seen in white muscle in March (Fig. 2) could therefore be due to acclimatization to lower temperatures. This increase was not observed for the other two tissues.

Three possible mechanisms may account for the increase in β-oxidation capacity: enhanced mitochondria or peroxisome content in the cells, increased enzyme content (e.g., increase in the volume of organelles), or a stimulation in the relative activity of the enzymes [reviewed by Reddy and Mannaerts (7)]. The increased β-oxidation capacity of white and red muscle from the 25% RO to the 75% RO dietary group in October, and of red muscle and liver in the final sampling period, indicated that there was a positive correlation between increasing RO content in the feed and β-oxidation capacity (Fig. 2). Thus, a single FA or a combination of FA that induced β-oxidation capacity might be present in the feed. Substrate preferences for the β-oxidation reaction have been found in both rainbow trout (37–39) and Atlantic salmon (38). It was previously shown that in rainbow trout red muscle mitochondria, MUFA, especially 16:1n-7, 18:1n-9, 22:1n-9, and 22:6n-3, were β-oxidized at the same rate, whereas 18:2n-6 and 18:3n-3 had lower β-oxidation rates (37). In a recent study (40), 50% of the 18:1n-9 or 20:5n-3 added to skeletal muscle cells was β-oxidized. In addition, 22:1n-11 is scarce in the phospholipids of fish biomembranes in spite of high dietary levels and is therefore thought to be a good substrate for β-oxidation (41). The increased β-oxidation capacity in white muscle with increasing dietary RO content could be due to the increased level of dietary MUFA that accompanied this diet. Although similar trends were observed in red muscle and in liver, there were no statistically significant effects. Similarly, in a study in which dietary capelin oil was

prior to the experiment. The main differences between the initial sampling period and the 0% RO diet group in the final sampling would reflect the combined effects of growth, ontogeny, temperature, light regime, and season. White muscle had a significantly increased β-oxidation capacity between the initial and final sampling, whereas liver had a decreased β-oxidation capacity over the same time period, with statistical differences noted between

replaced with 50 and 100% oleic acid-enriched sunflower oil and 100% palm oil, no significant differences in the β-oxidation capacity in Atlantic salmon red muscle were observed after 21 wk (12). Analysis of the FA composition of fish in the present study indicated a relatively low retention of 18:2n-6, 18:3n-3, and MUFA in white muscle (21). Additionally, EPA and DHA exhibited increased tissue retention with increasing dietary RO content, whereas 18:1n-9 and 18:2n-6 displayed decreased retention. It has been suggested in several studies that in fish, the FA present in excess are preferentially β-oxidized over those present in lower amounts (21,42). In the present study, the amount of both 18:2n-6 and 18:3n-3 increased with increasing dietary RO, coinciding with an increased β-oxidation capacity in white muscle in October, and in red muscle and liver in March. This result indicates that when 18:2n-6 and 18:3n-3 are fed in high concentrations, they become good substrates for the β-oxidation reaction and might even be inducers of the reaction in white muscle.

From the same sampled fish as those used in the present study, Torstensen *et al.* (19) showed that the lipid content decreased in October with increasing dietary RO and in the 50% OO diet. In addition, there was a tendency for lower fish growth with increasing diet RO and in the OO group in October (with no significant differences in growth of the sampled fish, data not shown). However, in March, differences in fish growth were masked by a decreased specific growth rate, and observed differences in lipid content in white muscle were smoothed out (19). The observed decline in lipid content in October (19) was not reflected by changes in β-oxidation capacity in the muscle (Fig. 2). Since the content of lipids depends on a number of factors in addition to their use for energy metabolism, it is likely that processes such as growth, absorption, and deposition of fat may better reflect the changes in lipid content. Another possibility for the decreased lipid content in white muscle was that a change in lipid deposition occurred that did not favor the storage of lipids in white muscle. Several studies have shown that lipid deposition in muscle is affected when Atlantic salmon are fed vegetable oil (29,30).

Increasing the dietary RO content from 75 to 100% resulted in an 8% increase in the specific β-oxidation capacity in red muscle, compared with a 75% decrease in white muscle in the October sampling period (Fig. 2). In the same dietary groups, the β-oxidation capacity decreased in both red and white muscle by 37 and 30%, respectively, in the March sampling. Thus, the FA composition of the 100% RO diet may not have favored β-oxidation in the muscles. When 50% of the capelin oil was replaced with OO, the effects of β-oxidation capacity were more or less the same as when the capelin oil was replaced with 50% RO (Fig. 2). However, there was an increased β-oxidation capacity in red muscle and in liver in October when Atlantic salmon were fed 50% OO, but this difference was not seen in March. If the growth of the fish had been greater over the last sampling period, then an improved β-oxidation capacity may have been seen.

Similar dietary effects on β-oxidation capacity in red and white muscle and in liver were observed when the data were expressed per gram of wet tissue or per gram of protein (Figs. 2, 3). This indicates that there were no differences in protein concentration between the samples. However, when the data were expressed as β-oxidation capacity per tissue, red muscle and liver exhibited different responses (Figs. 2, 4), indicating that tissue size is an important factor to consider when determining β-oxidation capacity, especially for the liver. In examining the three tissues measured in the present study, one can conclude that the tissues responded differently to diets, seasons, and growth. In addition, it is difficult to know which factor was most influential on the β-oxidation capacity. Further studies are therefore needed to understand more regarding the contribution of whole tissue to the overall lipid metabolism of fish, and what factors can be manipulated to maximize both the metabolism of aquacultural species and economic factors. White muscle is clearly an important tissue in this perspective.

ACKNOWLEDGMENTS

REFERENCES

1. Sanderson, P., Finnegan, Y.E., Williams, C.M., Calder, P.C., Burdge, G.C., Wootton, S.A., Griffin, B.A., Millward, D.J., Pegge, N.C., and Bemelmans, W.J.E. (2002) UK Food Standards Agency α-Linolenic Acid Workshop Report, *Br. J. Nutr.* *88*, 573–579.
2. Uauy, R., and Valenzuela, A. (2000) Marine Oils: The Health Benefits of n-3 Fatty Acids, *Nutrition 16*, 680–684.
3. Mannaerts, G.P., Debeer, L.J., Thomas, J., and De Schepper, P.J. (1979) Mitochondrial and Peroxisomal Fatty Acid Oxidation in Liver Homogenates and Isolated Hepatocytes from Control and Clofibrate-Treated Rats, *J. Biol. Chem. 11*, 4585–4595.
4. Small, G., and Connock, M. (1981) Palmitoyl-CoA Oxidase in Goldfish (*Carassius auratus*): Detection in Several Tissues and Subcellular Location in Intestinal Peroxisomes, *Comp. Biochem. Physiol. 68B*, 151–153.
5. Foerster, E.C., Fährenkemper, F., Rabe, U., Graf, P., and Sies, H. (1981) Peroxisomal Fatty Acid Oxidation as Detected by H_2O_2 Production in Intact Perfused Rat Liver, *Biochem. J. 196*, 705–712.
6. Gurr, M.I., and Harwood, J.L. (1991) *Lipid Biochemistry*, 4th edn., pp. 79–80, Chapman & Hall, London.
7. Reddy, J.K., and Mannaerts, G.P. (1994) Peroxisomal Lipid Metabolism, *Annu. Rev. Nutr. 14*, 343–370.
8. Crockett, E.L., and Sidell, B.D. (1993) Substrate Selectivities Differ for Hepatic Mitochondrial and Peroxisomal β-Oxidation in an Antarctic Fish, *Notothenia gibberifrons*, *Biochem. J. 289*, 427–433.
9. Crockett, E.L., and Sidell, B.D. (1993) Peroxisomal β-Oxidation Is a Significant Pathway for Catabolism of Fatty Acids in a Marine Teleost, *Am. J. Physiol. 264*, R1004–R1009.
10. Frøyland, L., Lie, Ø., and Berge, R.K. (2000) Mitochondrial and

Peroxisomal β-Oxidation Capacities in Various Tissues from Atlantic Salmon *Salmo salar*, *Aquacult. Nutr. 6*, 85–89.

11. Frøyland, L., Madsen, L., Eckhoff, K.M., Lie, Ø., and Berge, R.K. (1998) Carnitine Palmitoyltransferase I, Carnitine Palmitoyltransferase II, and Acyl-CoA Oxidase Activities in Atlantic Salmon (*Salmo salar*), *Lipids 33*, 923–930.

12. Torstensen, B.E., Lie, Ø., and Frøyland, L. (2000) Lipid Metabolism and Tissue Composition in Atlantic Salmon (*Salmo salar* L.)—Effects of Capelin Oil, Palm Oil, and Oleic Acid-Enriched Sunflower Oil as Dietary Lipid Sources, *Lipids 35*, 653–663.

13. Nordgarden, U., Torstensen, B.E., Frøyland, L., Hansen, T., and Hemre, G.I. (2003) Seasonally Changing Metabolism in Atlantic Salmon (*Salmo salar* L.) II—β-Oxidation Capacity and Fatty Acid Composition in Muscle Tissues and Plasma Lipoproteins, *Aquacult. Nutr. 9*, 295–303.

14. Guderley, H., St Pierre, J., Couture, P., and Hulbert, A.J. (1997) Plasticity of the Properties of Mitochondria from Rainbow Trout Red Muscle with Seasonal Acclimatization, *Fish. Physiol. Biochem. 16*, 531–541.

15. Thibault, M., Blier, P.U., and Guderley, H. (1997) Seasonal Variation of Muscle Metabolic Organization in Rainbow Trout (*Oncorhynchus mykiss*), *Fish. Physiol. Biochem. 16*, 139–155.

16. Guderley, H. (2004) Metabolic Responses to Low Temperature in Fish Muscle, *Biol. Rev. 79*, 409–427.

17. Kiessling, A., Kiessling, K.H., Storebakken, T., and Asgard, T. (1991) Changes in the Structure and Function of the Epaxial Muscle of Rainbow Trout (*Oncorhynchus mykiss*) in Relation to Ration and Age II. Activity of Key Enzymes in Energy Metabolism, *Aquaculture 93*, 357–372.

18. Atherton, W.D., and Aitken, A. (1970) Growth, Nitrogen Metabolism and Fat Metabolism in *Salmo gairdneri* Rich., *Comp. Biochem. Physiol. 36*, 719–747.

19. Torstensen, B.E., Frøyland, L., Ørnsrud, R., and Lie, Ø. (2004) Tailoring of a Cardioprotective Muscle Fatty Acid Composition of Atlantic Salmon (*Salmo salar*) Fed Vegetable Oil, *Food Chem. 87*, 567–580.

20. Lie, Ø., Lied, E., and Lambertsen, G. (1986) Liver Retention of Fat and of Fatty Acids in Cod (*Gadus morhua*) Fed Different Oils, *Aquaculture 59*, 187–196.

21. Torstensen, B.E., Frøyland, L., and Lie, Ø. (2004) Replacing Dietary Fish Oil with Increasing Levels of Rapeseed Oil and Olive Oil—Effects on Atlantic Salmon (*Salmo salar* L.) Tissue and Lipoprotein Lipid Composition and Lipogenic Enzyme Activities, *Aquacult. Nutr. 10*, 175–192.

22. Hamre, K., and Lie, Ø. (1995) α-Tocopherol Levels in Different Organs of Atlantic Salmon (*Salmo salar* L.)—Effect of Smoltification, Dietary Levels of n-3 Polyunsaturated Fatty Acids and Vitamin E, *Comp. Biochem. Physiol. 111A*, 547–554.

23. Frøyland, L., Asiedu, D.K., Vaagenes, H., Garras, A., Lie, Ø., Totland, G.K., and Berge, R.K. (1995) Tetradecylthioacetic Acid Incorporated into Very Low Density Lipoprotein: Changes in the Fatty Acid Composition and Reduced Plasma Lipids in Cholesterol-Fed Hamsters, *J. Lipid Res. 36*, 2529–2540.

24. Oppedal, F. (2002) Influences of Artificial Light on Atlantic Salmon (*Salmo salar* L.) in Seawater, Dr.Scient. Thesis, University of Bergen, Bergen, Norway, pp. 1–61.

25. Bone, Q. (1966) On Function of 2 Types of Myotomal Muscle Fibre in Elasmobranch Fish, *J. Mar. Biol. Assoc. UK 46*, 321–348.

26. Wokoma, A., and Johnston, I.A. (1981) Lactate Production at High Sustainable Cruising Speeds in Rainbow Trout (*Salmo gairdneri* Richardson), *J. Exp. Biol. 90*, 361–364.

27. Veerkamp, J.H., van Moerkerk, T.B., Glatz, J.F.C., Zuurveld, J.G.E.M., Jacobs, A.E.M., and Wagenmakers, A.J.M. (1986) $^{14}CO_2$ Production Is No Adequate Measure of [^{14}C]Fatty Acid Oxidation, *Biochem. Med. Metab. Biol. 35*, 248–259.

28. Bell, J.G., Tocher, D.R., Henderson, R.J., Dick, J.R., and Crampton, V.O. (2003) Altered Fatty Acid Compositions in Atlantic Salmon (*Salmo salar*) Fed Diets Containing Linseed and Rapeseed Oils Can Be Partially Restored by a Subsequent Fish Oil Finishing Diet, *J. Nutr. 133*, 2793–2801.

29. Bell, J.G., Henderson, R.J., Tocher, D.R., McGhee, F., Dick, J.R., Porter, A., Smullen, R.P., and Sargent, J.R. (2002) Substituting Fish Oil with Crude Palm Oil in the Diet of Atlantic Salmon (*Salmo salar*) Affects Muscle Fatty Acid Composition and Hepatic Fatty Acid Metabolism, *J. Nutr. 132*, 222–230.

30. Bell, J.G., McEvoy, J., Tocher, D.R., McGhee, F., Campbell, P.J., and Sargent, J.R. (2001) Replacement of Fish Oil with Rapeseed Oil in Diets of Atlantic Salmon (*Salmo salar*) Affects Tissue Lipid Compositions and Hepatocyte Fatty Acid Metabolism, *J. Nutr. 131*, 1535–1543.

31. Waagbø, R., Sandnes, K., Sandvin, A., and Lie, Ø. (1991) Feeding Three Levels of n-3 Polyunsaturated Fatty Acids at Two Levels of Vitamin E to Atlantic Salmon (*Salmo salar*). Growth and Chemical Composition, *Fisk. Dir. Skr., Ser. Ernæring 4*, 51–63.

32. Lie, Ø., Waagbø, R., and Sandnes, K. (1988) Growth and Chemical Composition of Adult Atlantic Salmon (*Salmo salar*) Fed Dry and Silage-Based Diets, *Aquaculture 69*, 343–353.

33. Bell, G.J., Henderson, J.R., Tocher, D.R., and Sargent, J.R. (2004) Replacement of Dietary Fish Oil with Increasing Levels of Linseed Oil: Modification of Flesh Fatty Acid Composition in Atlantic Salmon (*Salmo salar*) Using a Fish Oil Finishing Diet, *Lipids 39*, 223–232.

34. Torstensen, B. (2000) Transport and Metabolism of Lipids in Atlantic Salmon *Salmo salar* L., Dr.Scient. Thesis, University of Bergen, Bergen, Norway, pp. 3–43.

35. Henderson, R.J., and Tocher, D.R. (1987) The Lipid Composition and Biochemistry of Fresh water Fish, *Prog. Lipid. Res. 26*, 281–347.

36. Kiessling, A., Storebakken, T., Asgard, T., and Kiessling, K.H. (1991) Changes in the Structure and Function of the Epaxial Muscle of Rainbow Trout (*Oncorhynchus mykiss*) in Relation to Ration and Age I. Growth Dynamics, *Aquaculture 93*, 335–356.

37. Kiessling, K.H., and Kiessling, A. (1993) Selective Utilization of Fatty Acids in Rainbow Trout (*Oncorhynchus mykiss* Walbaum) Red Muscle Mitochondria, *Can. J. Zool. 71*, 248–251.

38. Egginton, S. (1996) Effect of Temperature on the Optimal Substrate for β-Oxidation, *J. Fish. Biol. 49*, 753–758.

39. Henderson, R.J., and Sargent, J.R. (1985) Chain-Length Specificities of Mitochondrial and Peroxisomal β-Oxidation of Fatty Acids in Livers of Rainbow Trout (*Salmo gairdneri*), *Comp. Biochem. Physiol. 82B*, 79–85.

40. Vegusdal, A., Østbye, T.K., Tran, T.N., Gjøen, T., and Ruyter, B. (2004) β-Oxidation, Esterification, and Secretion of Radiolabeled Fatty Acids in Cultivated Atlantic Salmon Skeletal Muscle Cells, *Lipids 39*, 649–658.

41. Henderson, R.J., and Sargent, J.R. (1981) Lipid Biosynthesis in Rainbow Trout, *Salmo gairdnerii*, Fed Diets of Differing Lipid Content, *Comp. Biochem. Physiol. 69C*, 31–37.

42. Torstensen, B.E., and Stubhaug, I. (2004) β-Oxidation of 18:3n-3 in Atlantic Salmon (*Salmo salar* L.) Hepatocytes Treated with Different Fatty Acids, *Lipids 39*, 153–160.

Sulfur-Substituted and α-Methylated Fatty Acids as Peroxisome Proliferator-Activated Receptor Activators

**Laila N. Larsen[a],*, Linda Granlund[b], Anne Kristin Holmeide[c],
Lars Skattebøl[c], Hilde Irene Nebb[b], and Jon Bremer[a]**

Institute of Basic Medical Sciences, Departments of [a]Biochemistry, [b]Nutrition, and [c]Chemistry, University of Oslo, Norway

ABSTRACT: FA with varying chain lengths and an α-methyl group and/or a sulfur in the β-position were tested as peroxisome proliferator-activated receptor (PPAR)α, -δ(β), and -γ ligands by transient transfection in COS-1 cells using chimeric receptor expression plasmids, containing cDNAs encoding the ligand-binding domain of PPARα, -δ, and -γ. For PPARα, an increasing activation was found with increasing chain length of the sulfur-substituted FA up to C_{14}-S acetic acid (tetradecylthioacetic acid = TTA). The derivatives were poor, and nonsignificant, activators of PPARδ. For PPARγ, activation increased with increasing chain length up to C_{16}-S acetic acid. A methyl group was introduced in the α-position of palmitic acid, TTA, EPA, DHA, *cis*9,*trans*11 CLA, and *trans*10,*cis*12 CLA. An increased activation of PPARα was obtained for the α-methyl derivatives compared with the unmethylated FA. This increase also resulted in increased expression of the two PPARα target genes acyl-CoA oxidase and liver FA-binding protein for α-methyl TTA, α-methyl EPA, and α-methyl DHA. Decreased or altered metabolism of these derivatives in the cells cannot be excluded. In conclusion, saturated FA with sulfur in the β-position and increasing carbon chain length from C_9-S acetic acid to C_{14}-S acetic acid have increasing effects as activators of PPARα and -γ in transfection assays. Furthermore, α-methyl FA derivatives of a saturated natural FA (palmitic acid), a sulfur-substituted FA (TTA), and PUFA (EPA, DHA, *c*9,*t*11 CLA, and *t*10,*c*12 CLA) are stronger PPARα activators than the unmethylated compounds.

Paper no. L9588 in *Lipids 40*, 49–57 (January 2005).

FA are key substrates in several metabolic pathways, and organisms have evolved complex mechanisms to maintain a proper balance between absorption, metabolism, and storage of FA. In mammals, several of these mechanisms involve nuclear transcription factors. The peroxisome proliferator-activated receptors (PPARs) belong to the nuclear receptor superfamily, which are activated by, e.g., FA and peroxisome proliferators. These receptors control the expression of genes regulating lipid and glucose metabolism as well as adipogenesis (1–4). The PPAR family consists of three subtypes encoded by separate genes: PPARα, PPARδ (also called hNUC1, PPARβ, or FAAR), and PPARγ1 and –γ2 (5–7). PPARα is expressed mainly in liver and kidney and to a lesser extent in skeletal muscle, heart, and intestine; PPARδ , in contrast, is expressed ubiquitously (8). PPARγ1 is expressed in various organs such as liver, heart, and muscle, whereas PPARγ2 is expressed almost exclusively in adipose tissue. All three PPARs form heterodimers with retinoid X receptor (RXR), and these heterodimers regulate expression of their target genes by binding to specific consensus DNA sequences, termed peroxisome proliferator-responsive elements (9,10).

Synthetic compounds that induce peroxisomal proliferation in rodents and hypolipidemic agents such as clofibrate and WY-14,643 have been shown to specifically bind to and activate PPARα (11,12). Saturated (11,13,14) and unsaturated FA [EPA (20:5n-3) and DHA (22:6n-3)] (11), branched-chain FA (15), and some eicosanoids (11,16) are among the natural ligands for PPARα. Unsaturated FA, 8(*S*)HETE, bezafibrate, eicosatetraynoic acid, and the synthetic compound GW501516 [2-methyl-4-((4-methyl-2-(4-trifluoromethylphenyl)-1,3-thiazol-5-yl)-methylsulfanyl)phenoxy-acetic acid] (12,17) bind to and activate PPARδ. Antidiabetic compounds of the thiazolidinedione class, a prostaglandin J_2 metabolite, and some unsaturated FA are PPARγ ligands (12,18–20).

Our group has been studying the effects and metabolism of 3-thia FA for many years. The 3-thia FA are metabolized by ω-oxidation followed by β-oxidation from the ω-end (21), and by sulfur oxidation to sulfoxide by flavine-containing monooxygenase (22). It has previously been shown that 3-thia FA derivatives and some unsaturated α-methyl FA induce peroxisomal β-oxidation in liver (23–25) and hepatoma cells (26). Furthermore, Madsen *et al*. (27) have published that tetradecylthioacetic acid (TTA) is a stronger ligand for PPARα than for PPARδ and -γ.

Phytanic acid (3,7,11,15- tetramethylhexadecanoic acid) is a branched-chain FA with one of its methyl groups in the β-position and is present in ruminant fats and meat. It is primarily degraded in peroxisomes by α-oxidation to pristanic acid (2,6,10,14-tetramethylpentadecanoic acid), which is a branched-chain FA with one of its methyl groups in the α-position. Zomer *et al*. (15) have shown that pristanic acid is a better ligand for PPARα than phytanic acid. Since branched-chain FA accumulate in a variety of inherited peroxisomal disorders (28,29), it is

*To whom correspondence should be addressed at Institute of Basic Medical Sciences, Department of Biochemistry, P.O. Box 1112, Blindern, University of Oslo, 0317 Oslo, Norway. E-mail: l.n.larsen@medisin.uio.no

Abbreviations: AcA, acetic acid; ACO, acyl-CoA oxidase 1; BRL 49653, rosiglitazone; HRMS, high-resolution MS; LBD, ligand-binding domain; L-FABP, liver-specific fatty acid-binding protein; PPAR, peroxisome proliferator-activated receptor; RXR, retinoid X receptor; TTA, tetradecylthioacetic acid (C_{14}-S acetic acid); UAS, upstream activating sequence; WY-14,643, pirinixic acid, also known as 4-chloro-6-(2,3-xylidino)-2-pyrimidinylthioacetic acid.

of interest to study the effects of these FA on activation of nuclear receptors.

CLA are a group of positional and geometric isomers of linoleic acid (18:2n-6) found in ruminant fat and dairy products (30). The predominant isomers in food and commercial CLA preparations are *cis*9,*trans*11 CLA (*c*9,*t*11 CLA) and *trans*10,*cis*12 CLA (*t*10,*c*12 CLA) (30). In animal studies, *t*10,*c*12 CLA has been shown to alter body composition by reducing body fat mass and increasing lean body mass (31). We showed that *t*10,*c*12 CLA prevents lipid accumulation in 3T3-L1 adipocytes, in part by acting as a PPARγ modulator (32). Furthermore, we recently showed that small structural changes in the *t*10,*c*12 CLA molecule (changing from *t*10,*c*12 to *t*10,*t*12 or introducing a methyl group in the α-position of *t*10,*c*12 CLA) totally abolish the lipid preventive effect observed for *t*10,*c*12 CLA (33).

In light of the aforementioned studies, it is clear that small changes in the molecular structure of FA have a great influence on their ability to activate the different PPAR subtypes.

The aim of this study was to investigate whether increasing the chain length and introducing an α-methyl group (Fig. 1) in different FA and derivatives affect their activation of the three PPAR subtypes.

MATERIALS AND METHODS

Materials. Lipofectamine™, FBS, fungizone, and penicillin/streptomycin were obtained from Invitrogen (Carlsbad, CA). Reporter Lysis buffer (Promega) was bought from AH Diagnostics (Aarhus, Denmark). Hybond-N+-membranes and the Megaprime DNA labeling system kit were purchased from Amersham Biosciences (Oslo, Norway). DMEM, Hams F10 medium, Williams E-medium, and EPA were from Sigma. The two CLA isomers (purity >90%) were gifts from Natural ASA (Hovdebygda, Norway); DHA (purity >90%) was a gift from Norsk Hydro (Oslo, Norway). α-Methyl- and α-ethyl EPA were synthesized as previously described (26). TTA was synthesized according to Spydevold and Bremer (25). α-Methyl TTA was prepared by the same procedure using thiolactic acid instead of thioacetic acid.

Synthesis of α-methyl FA. The NMR spectra were recorded in CDCl$_3$, with a Bruker Avance DPX 200 instrument or a Bruker Avance DPX 300 instrument. The IR spectra were obtained with a PerkinElmer 1310 IR spectrophotometer or a Nicolet Magna-IR 550 spectrometer. Mass spectra were recorded at 70 eV with a Fisons VG Pro spectrometer. All reactions were performed under a nitrogen or argon atmosphere.

(i) Esterification of CLA. To a solution of CLA (2.0 g, 7.1 mmol) in methanol (50 mL) was added one drop of concentrated H$_2$SO$_4$. The mixture was stirred overnight at room temperature. Hexane and water were added. The aqueous phase was collected and extracted with ether. The combined organic phase was washed with brine and water and then dried (MgSO$_4$). Filtration and evaporation under reduced pressure gave the methyl ester (2.1 g, 100%).
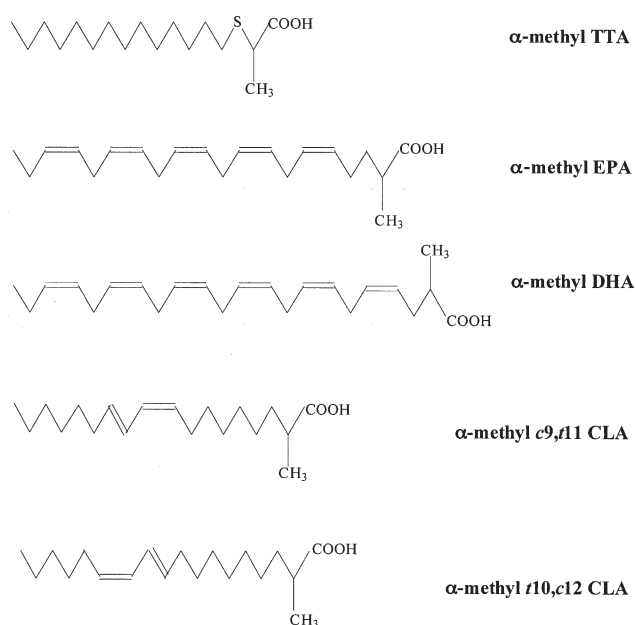
FIG. 1. Structural formulas of α-methyl tetradecylthioacetic acid (TTA), α-methyl EPA, α-methyl DHA, α-methyl *cis*9,*trans*11 CLA, and α-methyl *trans*10,*cis*12 CLA.

(ii) Methyl (9Z,11E)-octadecadienoate[1]. δ$_H$ (300 MHz): 0.85 (3H, *br t*, *J* = 6.5 Hz), 1.20–1.50 (16H, *m*), 1.59 (2H, *m*), 2.00–2.20 (4H, *m*), 2.26 (2H, *t*, *J* = 7.5 Hz), 3.62 (3H, *s*), 5.20–5.35 (1H, *m*), 5.61 (1H, *dt*, *J* = 15.0 Hz, *J* = 7.0 Hz), 5.89 (1H, *t*, *J* = 10.9 Hz), 6.24 (1H, *ddd*, *J* = 15.0 Hz, *J* = 10.9 Hz, *J* = 1.1 Hz); δ$_C$ (75 MHz): 13.99, 22.54, 24.84, 27.55, 28.84, 28.95, 29.02, 29.04, 29.31, 29.57, 31.67, 32.81, 33.97, 51.26, 125.51, 128.64, 129.73, 134.59, 174.09.

(iii) Methyl (10E,12Z)-octadecadienoate δ$_H$ (300 MHz): 0.86 (3H, *br t*, *J* = 6.6 Hz), 1.20–1.50 (16H, *m*), 1.59 (2H, *m*), 2.00–2.20 (4H, *m*), 2.27 (2H, *t*, *J* = 7.6 Hz), 3.64 (3H, *s*), 5.27 (1H, *dt*, *J* = 10.9 Hz, *J* = 7.6 Hz), 5.62 (1H, *dt*, *J* = 15.0 Hz, *J* = 7.0 Hz), 5.91 (1H, *t*, *J* = 10.9 Hz), 6.26 (1H, *ddd*, *J* =15.0 Hz, *J* = 10.9 Hz, *J* = 1.1 Hz); δ$_C$ (75 MHz): 14.02, 22.53, 24.91, 27.63, 29.11 (2 × CH$_2$), 29.16, 29.26, 29.34, 29.39, 31.46, 32.83, 34.07, 51.38, 125.63, 128.55, 130.09, 134.53, 174.27.

Preparation of α-methyl acids. General procedure. The procedure is based on a literature procedure (26). Butyllithium (1.2 equiv, 1.6 M in hexane) was added dropwise to a stirred solution of diisopropylamine (1.4 equiv) in dry THF (0.47 mmol/mL) under argon at –20°C. The mixture was stirred at –78°C for 45 min before dropwise addition of the methyl ester (1.0 equiv) in dry THF (0.17 mmol/mL). The mixture was stirred at –78°C for 30 min before addition of methyl iodide (1.6 equiv). The mixture was allowed to warm to –20°C over 1.5 h. The mixture was then poured into water, and the water phase was collected and extracted with hexane. The combined organic phase was washed

---

[1]The NMR spectrum of methyl (9Z,11*E*)-octadecadienoate has been published by Lie Ken Jie *et al.* (34–36). The spectral data for the olefinic protons and in particular the coupling constants differ in all their publications. Other published NMR spectra of the corresponding acid support our data (37,38).

with 1 M HCl, then water, and dried (MgSO$_4$). Filtration and evaporation under reduced pressure gave the ester. The α-methyl ester (1.0 equiv) was dissolved in ethanol (0.23 mmol/mL) at room temperature and added to a stirred solution of LiOH (7.4 equiv) in water (1.7 mmol/mL). The mixture was left stirring overnight. Water and hexane were added, and the organic phase was collected. The organic phase was washed with an aqueous LiOH solution (1.5 M). The water phase was acidified with 5% HCl to pH 2 and extracted with ether. The organic phase was washed with brine, then water, and dried (MgSO$_4$). Filtration and evaporation gave the acids.

(i) 2-Methyl (9Z,11E)-octadecadienoic acid (α-methyl c9,t11 CLA. The 2-methyl (9Z,11*E*)-octadecadienoic acid was obtained from methyl (9Z,11*E*)-octadecadienoate in 74% yield according to the general procedure. ν_{max} (film)/cm^{-1} 2926, 2855, 1706; δ_H (300 MHz): 0.86 (3H, *br t, J* = 6.7Hz), 1.15 (3H, *d, J* = 7.0 Hz), 1.20–1.50 (17H, *m*), 1.60–1.70 (1H, *m*), 2.00–2.20 (4H, *m*), 2.35–2.50 (1H, *m*), 5.20–5.35 (1H, *m*), 5.63 (1H, *dt, J* = 15.0 Hz, *J* = 7.0 Hz), 5.92 (1H, *t, J* = 10.9 Hz), 6.27 (1H, *ddd, J* = 15.0 Hz, *J* = 10.9, Hz, *J* = 1.0 Hz), 10.4–10.6 (1H, *br s*); δ_C (75 MHz): 14.07, 16.78, 22.60, 27.07, 27.62, 28.90, 29.04, 29.36 (2 × CH$_2$), 29.64, 31.72, 32.87, 33.48, 39.35, 125.55, 128.68, 129.86, 134.73, 183.40; *m/z* (EI) 294 (M$^+$, 63%), 95, 81, 67 (100) [high-resolution MS (HRMS): found 294.255499. C$_{19}$H$_{34}$O$_2$ requires 294.255881].

(ii) 2-Methyl (10E,12Z)-octadecadienoic acid (α-methyl t10,c12 CLA). The 2-methyl (10*E*,12*Z*)-octadecadienoic acid was obtained from the methyl (10*E*,12*Z*)-octadecadienoate in 80% yield according to the general procedure. ν_{max} (film)/cm^{-1} 2925, 2854, 1705; δ_H (300 MHz): 0.87 (3H, *br t, J* = 6.8 Hz), 1.16 (3H, *d, J* = 7.0 Hz), 1.20–1.50 (17H, *m*), 1.60–1.70 (1H, *m*), 2.00–2.20 (4H, *m*), 2.35–2.50 (1H, *m*), 5.28 (1H, *dt, J* = 10.9 Hz, *J* = 7.6 Hz), 5.63 (1H, *dt, J* = 15.0 Hz, *J* = 7.0 Hz), 5.92 (1H, *t, J* = 10.9 Hz), 6.27 (1H, *ddd, J* = 15.0 Hz, *J* = 10.9 Hz, *J* = 1.0 Hz), 10.4–10.6 (1H, *br s*); δ_C (75 MHz): 14.03, 16.78, 22.54, 27.11, 27.65, 29.14, 29.29, 29.36, 29.41, 29.42, 31.47, 32.84, 33.48, 39.38, 125.65, 128.58, 130.08, 134.53, 183.60; *m/z* (EI) 294 (M$^+$, 61%), 95, 81, 67 (100) (HRMS: found 294.254987. C$_{19}$H$_{34}$O$_2$ requires 294.255881).

(iii) 2-Methyldocosa-(all-Z)-4,7,10,13,16,19-hexaenoic acid (α-methyl DHA). The α-methyl DHA was obtained from DHA ethyl ester in 81% yield according to the general procedure, except that THF (2 mL/mmol ester) was added in the hydrolysis to increase the reaction rate. ν_{max} (film)/cm^{-1} 3013, 2966, 1708; δ_H (300 MHz): 0.96 (3H, *t, J* = 7.5 Hz), 1.18 (3H, *d, J* = 6.8 Hz), 2.06 (2H, *m*), 2.20–2.30 (1H, *m*), 2.35–2.55 (2H, *m*), 2.75–2.95 (10H, *m*), 5.25–5.55 (12H, *m*); δ_C (75 MHz) 14.25, 16.34, 20.55, 25.53, 26.63, 30.90, 39.41, 126.32, 127.01, 127.87, 127.98, 128.08, 128.11, 128.23, 128.56, 130.26, 132.03 (10 × CH), 128.27 (2 × CH), 182.37; *m/z* (CI) 343 (M + 1, 1.65%), 215, 93 (100) (HRMS: found M + 1 343.262563. C$_{23}$H$_{35}$O$_2$ requires 343.263706).

Cell cultures. COS-1 cells (ATCC no. CRL 1650) were cultured in DMEM supplemented with L-glutamine (2 mM), penicillin (50 U/mL), streptomycin (50 µg/mL), fungizone (2.5 µg/mL), and 10% inactivated FBS. The cells were incubated at 37°C in a humidified atmosphere of 5% CO$_2$ and 95% air and
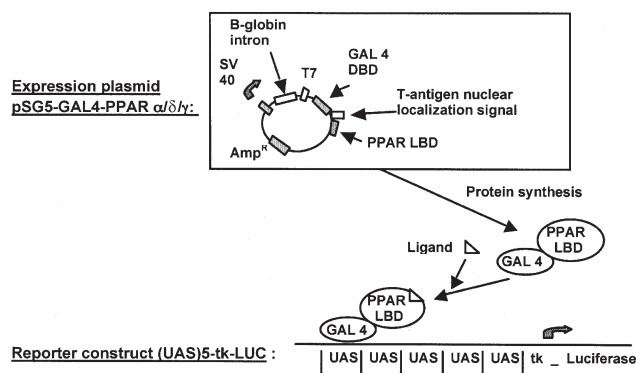
FIG. 2. Description of the transfection procedure. The ligand-binding domain (LBD) of peroxisome proliferator-activated receptors (PPAR)α/δ/γ was cloned together with GAL4 DNA-binding domain (DBD) into the pSG5 vector (Stratagene, LaJolla, CA). GAL4 is a yeast activator that controls the transcription of genes, and the regulation is exercised at the upstream activating sequence (UAS). The SV40 promoter ascertains transcription of the GAL4 DBD and PPAR LBD. Ligand binding to the PPAR LBD activates GAL4 DBD in a way that promotes binding to a UAS region on the reporter construct. Binding to the UAS region stimulates the tk promoter to drive luciferase (LUC) expression and thus increases the amounts of LUC enzyme. Up to five GAL4 DBD–PPAR LBD dimers can bind to the reporter construct at the same time, as regulated by the amount and affinity of the PPAR ligand.

used for transient transfections. Every third day, the cells in each flask were split into new flasks containing fresh media.

The establishment, cloning, and cell propagation of the 7800C1 Morris rat hepatoma cell line have been described by Richardson *et al.* (39). Growth conditions were described earlier (24).

Transfection. pSG5-GAL4-PPARα, pSG5-GAL4-PPARδ, and pSG5-GAL4-PPARγ chimera expression constructs containing the ligand-binding domain (LBD) of mouse PPARα, PPARδ, and PPARγ and the (UAS)$_5$-tk-LUC (where UAS = upstream activating sequence and LUC = luciferase) reporter construct (Fig. 2) were generous gifts from Dr. Krister Bamberg (Astra Zeneca, Mølndalen, Sweden).

Cells (1.5×10^5 COS-1) were plated in 30-mm tissue dishes (six-well plates), 1 d before transfection. Transient transfection by lipofection was performed as described by Invitrogen (Carlsbad, CA). Each well received 0.4 µg of the reporter construct (UAS)$_5$-tk-LUC, 0.8 µg pGL3-basic (Promega, Madison, WI), and 0.04 µg pSG5-GAL4-PPARα, pSG5-GAL4-PPARδ, or pSG5-GAL4-PPARγ. pGL3-basic, an empty vector, was added to obtain the recommended amount of total DNA per well and per µL Lipofectamine. Ligands or FA-free BSA (control) was added to the media 5 h after transfection. FA stock solutions (6 mM) were made on FA-free BSA (2.4 mM), and stored frozen. Unsaturated FA stock solutions were kept under argon to avoid oxidation. Transfected cells were maintained for 24 h before lysis by Reporter Lysis buffer. Binding of the FA to the LBD of PPAR activates GAL4 binding to UAS, which in turn stimulates the tk promoter to drive luciferase expression (Fig. 2). Luciferase activity was measured using a luminometer (TD-20/20 luminometer; Turner Designs, Sunnyvale, CA) and normalized against protein content. The PPARα and -γ constructs were used by our group in an earlier study (32).

*Protein content.* Protein content was measured by the Bio-Rad protein assay (Bio-Rad Laboratories, Hercules, CA).

RNA extraction and Northern blot analysis. Total RNA from 7800C1 Morris hepatoma cells was extracted with Ultraspec (Ultraspec RNA, Biotecx Laboratories, Inc., Houston, TX). For Northern analysis, the RNA samples (20 µg) were fractionated in 1.5% formaldehyde agarose gel by electrophoresis, and then transferred to nylon filters. The abundance of the transcript was determined by Northern hybridization using a specific cDNA probe for rat acyl CoA oxidase (ACO), rat liver-specific FA-binding protein (L-FABP), and the ribosomal protein L27 (ATCC #107385). Probes were obtained by PCR using the following primers: ACO Fwd, 5′-cacgcaatagttctggctca-3′; ACO Rev, 5′-gccattcgacattcttcgat-3′; L-FABP Fwd, 5′-tgggaaaggaaac-ctcattg-3′; L-FABP Rev, 5′-gccttgtctaaattctcttgctg-3′. The cDNA was labeled with (α-^{32}P)dCTP using the Megaprime DNA labeling system kit. L27 was used as control for equal loading.

Statistics. Results are presented as means ± SD. Significant differences were evaluated by Student's *t*-test, and the significance level was set at *P* < 0.05.

RESULTS

Saturated FA with a sulfur atom in the β-position as activators of PPARα and -γ. Transient transfections were done in COS-1 cells, according to the description in the Materials and Methods section and Figure 2. For the purpose of determining the most suitable concentration of FA/derivatives, concentration curves were made in the range of 1–100 µM. Based on these concentration curves, 10 and 50 µM were chosen as the most optimal concentrations for activation of PPARα and -γ, respectively. We found that saturated FA with sulfur in the β-position and increasing carbon chain length from C_9-S acetic acid (AcA) to C_{14}-S AcA (= TTA), had increasing effects as activators of the GAL4-PPARα and -γ chimera in the transfection assay (Fig. 3). Seventeenfold activation of PPARα was observed with C_{14}-S AcA, whereas derivatives with chain lengths above C_{14}-S AcA were poorer PPARα activators (Fig. 3A). Furthermore, the C_{15}-S – C_{18}-S AcA were stronger PPARγ-activators than C_{14}-S AcA (sixfold activation) with C_{16}-S AcA having the strongest effect (increasing the activation 10-fold) (Fig. 3B). The sulfur-substituted FA were poor activators of PPARδ, and we found no significant effect compared with the control. The results are therefore not shown.

Palmitic acid derivatives with sulfur in the β-position and/or α-methyl group, as activators of PPARα. Figure 4A shows that adding a methyl group in the α-position of palmitic acid increased its ligand-binding activity sevenfold, compared with palmitic acid, at 50 µM concentration (*P* < 0.05). Palmitic acid itself induced a twofold activation and seemed to be a poor activator of PPARα. Furthermore, C_{14}-S AcA (= TTA), which corresponds to palmitic acid with an additional sulfur in the β-position, was an even stronger PPARα activator than α-methyl palmitic acid (*P* < 0.05 at 0.5, 1, and 10 µM). Finally, palmitic acid with both an additional sulfur in the β-position and a methyl group in the α-position (α-methyl TTA) was a significantly stronger activator than TTA at concentrations of 0.5–50 µM

A

B
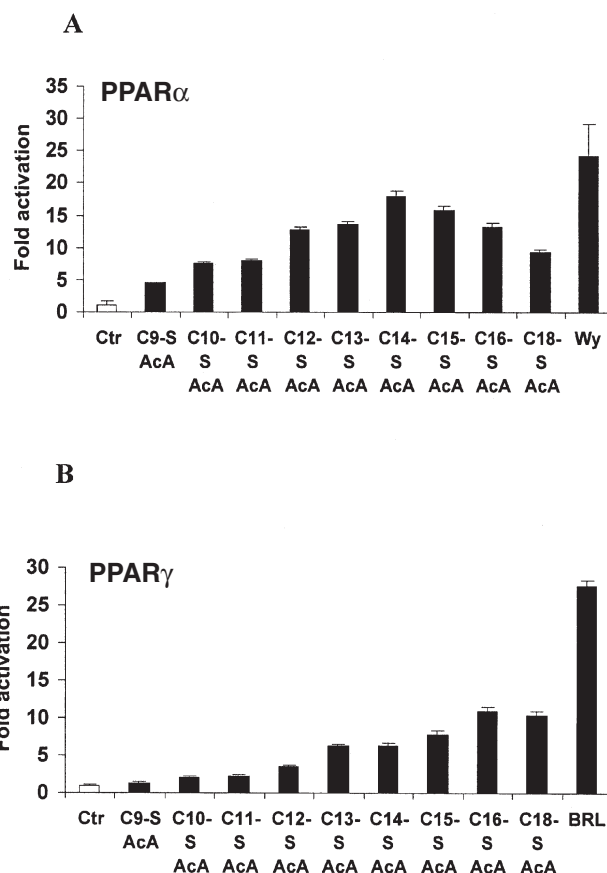
**FIG. 3.** FA derivatives with a sulfur atom in the β-position and varying chain length as activators of PPARα and PPARγ. COS-1 cells were transiently transfected by lipofection with a chimeric receptor expression plasmid, pSG5-GAL4-mPPARα (A) or -mPPARγ (B) and the reporter plasmid (UAS)$_5$-tk-LUC as described in the Materials and Methods section and Figure 2. The cells were treated with FA derivatives: (A) 10 µM or (B) 50 µM (10 µM BRL) for 24 h before cell harvesting. WY-14,643 and BRL 49653 were included since they are known activators of PPARα and PPARγ, respectively. Luciferase/protein ratios are expressed relative to luciferase/protein ratios in cotransfected cells stimulated with vehicle (BSA) as control (Ctr). The results represent the means ± SD of three experiments, each performed in triplicate. All derivatives activated PPARα and PPARγ significantly more than the control (*P* < 0.05). BRL 49653, rosiglitazone; WY-14,643, pirinixic acid, also known as 4-chloro-6-(2,3-xylidino)-2-pyrimidinylthioacetic acidd; AcA, acetic acid; for other abbreviations see Figure 2.

(*P* < 0.05). WY-14,643 was included in the test since it is a well-known PPARα ligand.

PUFA, with or without a methyl group in the α-position, as activators of PPARα. Since saturated FA with a methyl group on the α-carbon seemed to be stronger PPARα activators than the parent FA, we wanted to see if the same effect could be obtained by adding a methyl-group to the α-carbon of PUFA. α-Methyl derivatives of EPA (20:5n-3) and DHA (22:6n-3) were made and tested for their ability to activate the PPARα LBD in the transfection assay in COS-1 cells. As with saturated FA, PUFA with an α-methyl group activated PPARα more than the parent FA (*P* < 0.05) (Fig. 4B). The concentration of FA and derivatives in
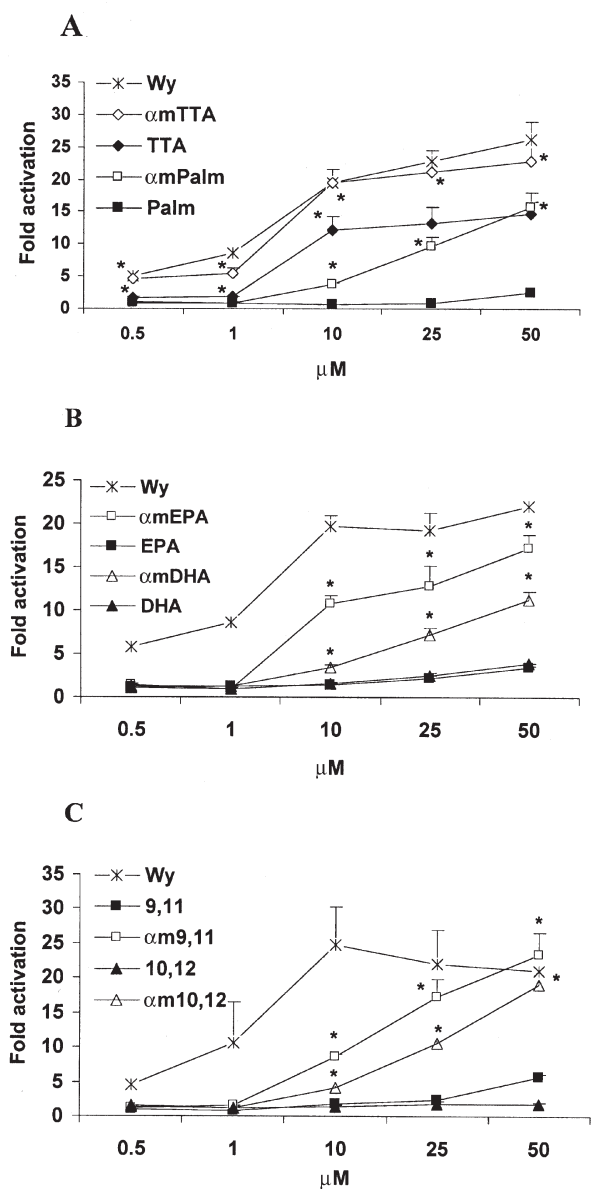
FIG. 4. Effects of increasing concentrations of FA and FA derivatives on activation of PPARα, compared with the known PPARα ligand, WY-14,643. COS-1 cells were transiently transfected by lipofection with a chimeric receptor expression plasmid, pSG5-GAL4-mPPARα, and the reporter plasmid (UAS)₅-tk-LUC as described in the Materials and Methods section and Figure 2. The cells were treated with WY-14,643 (Wy) and (A) α-methyl palmitic acid (αmPalm), palmitic acid (Palm), tetradecylthioacetic acid (TTA), and α-methyl tetradecylthioacetic acid (αmTTA); (B) EPA, α-methyl EPA (αmEPA), DHA, and α-methyl DHA (αmDHA); (C) *cis*9,*trans*11 CLA (9,11), α-methyl *cis*9,*trans*11CLA (αm9,11), *trans*10,*cis*12 CLA (10,12), α-methyl *trans*10,*cis*12CLA (αm10,12). Transfected cells were maintained for 24 h before harvesting. Luciferase activity was correlated to protein concentration. Results are presented as fold activation relative to luciferase/protein ratios in cotransfected cells stimulated with vehicle (BSA) as control and given as mean ± SD of three experiments, each performed in triplicate. One representative experiment is presented in A, B and C. Student's *t*-test was performed on the data, and an asterisk (*) indicates *P* < 0.05 for (A): values that were judged statistically different from the corresponding values in the immediately below curve (i.e., αmTTA vs. TTA, TTA vs. αmPalm, and αmPalm vs. Palm); (B) and (C): PPARα activation by α methyl derivatives significantly higher than PPARα activation by the unmethylated FA.
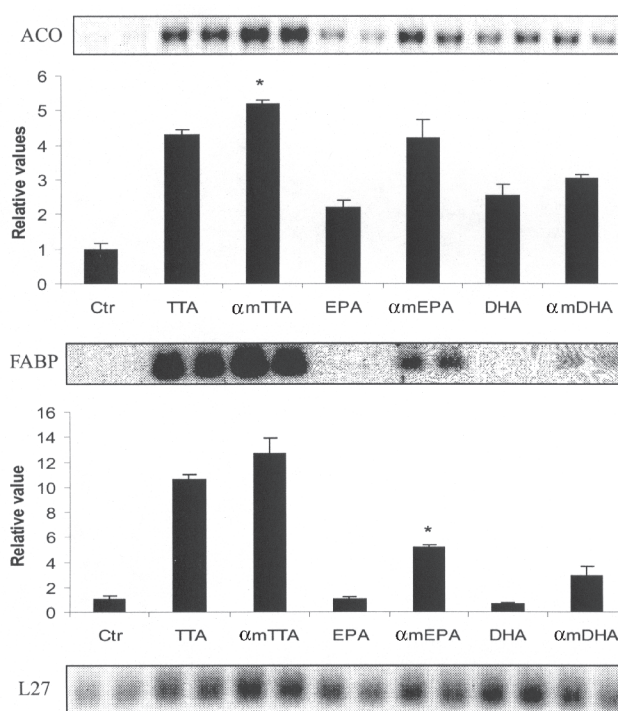
FIG. 5. Induction of PPARα-responsive genes. 7800C1 Morris hepatoma cells were treated with 50 μM FA/FA derivative, whereas control cells received BSA, for 24 h. RNA was extracted and applied (20 μg per lane) to nylon filters by gel electrophoresis and blotting. Filters were hybridized with ³²P-labeled cDNA for acyl-CoA oxidase (ACO), liver-specific FA-binding protein (L-FABP), and the ribosomal protein L27. The scans of the ACO and FABP mRNAs were calculated against scans of the L27 bands, which were examined in the same samples and used as a loading control. The values are presented relative to values obtained from cells stimulated with vehicle (BSA) as control, and given as the means ± SD of two experiments. Each experiment included two parallels per treatment. *Significantly (*P* ≤ 0.05) different from the corresponding unmethylated compound. For abbreviations see Figure 1.

the cell medium was increased from 0.5 to a saturating level at 50 μM. At 50 μM the PPARα activation was increased from 3- to 22-fold for α-methyl EPA compared with EPA and from 4- to 11-fold for α-methyl DHA compared with DHA. EPA and DHA and their α-methyl derivatives were tested as activators of PPARδ and -γ in the same way as for PPARα. Both derivatives were stronger activators of PPARδ and -γ than EPA and DHA, but the effects were not as strong as for PPARα (data not shown). EPA with an ethyl group in the α-position was made (26) and tested as a PPARα activator. It activated PPARα with equal strength as α-methyl EPA (data not shown).

In agreement with earlier studies, we found that *c*9,*t*11 CLA, and *t*10,*c*12 CLA were relatively weak PPARα activators (32), but *c*9,*t*11 CLA was a more efficacious PPARα activator than *t*10,*c*12 CLA (fivefold compared with twofold activation at 50 μM concentration). α-Methyl derivatives of the two CLA isomers were found to be stronger activators of PPARα than the parent CLA (*P* < 0.05) (Fig. 4C), with α-methyl *c*9,*t*11 CLA (23-fold activation) being a stronger activator than α-methyl *t*10,*c*12 CLA (19-fold activation). However, both derivatives were much weaker

activators than WY-14,643 at low concentrations. Also for PPARγ, the α-methyl CLA were found to be stronger PPARγ activators than the natural CLA but much weaker activators than the known PPARγ ligand, BRL 49653 (rosiglitazone) (data not shown). Because of the much lower effects of the derivatives as PPARγ activators compared with PPARα, we chose to focus on PPARα target genes in our next step in the present study.

Effects on PPARα target genes. To verify our results from the transfection studies in a more physiologic system, we tested the effects of FA derivatives on PPARα target genes. For this experiment 7800C1 Morris rat hepatoma cells were used. This cell line was used extensively in our earlier studies on lipid metabolism (24,25,40–43) and is well suited for this purpose. Rat and mouse PPARα LBD have a high degree of homology (44). Since no sign of toxic effects was observed at a ligand concentration of 50 μM in the medium, the cells were treated with 50 μM FA for 24 h, and gene expression of ACO and L-FABP were studied by Northern hybridization. Figure 5 shows that all of the ligands induced the transcription of the ACO-gene more than was obtained with vehicle (BSA) only (control). α-Methyl TTA, α-methyl EPA, and α-methyl DHA induced ACO gene expression more than TTA, EPA, and DHA, respectively, although only α-methyl TTA acted at a significant level ($P \leq 0.05$). As for ACO, the expression of FABP was increased after treatment with TTA, α-methyl TTA, α-methyl EPA, and α-methyl DHA, and the methylated FA had stronger effects than the corresponding unmethylated FA. However, no effect on transcription of the two PPARα-target genes was found for the two α-methyl CLA derivatives, compared with the parent FA and control (data not shown).

DISCUSSION

TTA is known to increase peroxisomal β-oxidation activity in rat hepatocytes and hepatoma cells (25). It has been shown to be a potent PPARα-ligand (11,14), inducing increased transcription of several PPARα-target genes (42), and to induce peroxisomal proliferation in rat liver cells (23,45). In this study we asked the question: Will the effects of FA with sulfur in the β-position vary with varying chain length?

We found that increasing the carbon chain length increased the luciferase activity in the transfection assays, indicating stronger PPARα and -γ activators. The FA derivatives C_{13}-S AcA – C_{15}-S AcA were the strongest PPARα activators, whereas C_{16}-S AcA was the strongest PPARγ activator. As a comparison, feeding studies have shown that the activity and mRNA level of the PPARα-responsive gene ACO increases as a function of chain length of 3-thia FA, with the effect of the C_{12}-, C_{13}-, C_{14}-, and C_{15}-S AcA being strongest (46,47). Xu and coworkers (14) have shown in competition assays that saturated FA containing 12 carbon atoms or fewer were unable to interact with the three PPARs. They also found that saturated FA with chain lengths from 14 to 16 carbon units bind to PPARα, bind more weakly to PPARδ, and fail to interact efficiently with PPARγ. Furthermore, saturated FA with chain lengths of 20 or more carbon units failed to bind well with any of the PPARs. These results correspond

well with our present results. Comparison of the values for palmitic acid as a PPARα activator at 10 μM (Fig. 4A) (unchanged luciferase activity) with C_{14}-S AcA (TTA) in the same figure (a 12× increase) shows that the sulfur-substituted FA are stronger activators than the comparable unmodified saturated FA. In studying the geometry and chemical composition of the PPAR ligand-binding cavity, the reason why some FA are better activators than others might be clearer: According to Cronet and coworkers (48), the structure of PPARα LBD is very similar to both PPARγ LBD and PPARδ LBD, about 60–65% identical. EPA, which is a PPARδ ligand, has a hydrophilic head group that forms hydrogen bonds to amino acids in the vicinity in the LBD cavity. Its long hydrophobic tail forms interactions with hydrophobic amino acids in other parts of the ligand-binding cavity (14). This could explain why shorter saturated FA do not activate PPARs, e.g., they cannot make sufficient hydrophobic interactions required for stable ligand binding. Another feature common to several of the peroxisome proliferators and PPARα activators is an oxygen atom in the β-position (49) that enters into hydrogen bond formation with a serine residue in the ligand- binding cavity (44). Both sulfur and oxygen atoms are capable of making hydrogen bonds with serine; hence WY-14,643, with a sulfur in the β-position, is a strong PPARα ligand (5). In comparison, all of the thia FA in this study have a sulfur in the β-position, which might explain the relatively strong activation compared with unmodified saturated FA.

Our next question was whether a methyl group in the α-position of saturated or unsaturated FA would have any influence on their properties as PPARα activators.

We found that adding one methyl group to the α-carbon of palmitic acid (= α-methyl palmitic acid) increased its PPARα activation significantly. Adding a sulfur in the β-position of palmitic acid (= TTA) increased the activation even more, and TTA had a significantly stronger effect than α-methyl palmitic acid. Introducing both an α-methyl group and a β-sulfur (= α-methyl TTA) increased the activation even further and significantly more than TTA. We also found that α-methylation of PUFA made them into stronger PPARα activators. The same effect is observed by moving a methyl group from a β- to an α-position of naturally occurring branched-chain FA such as phytanic and pristanic acid (15). As a comparison, clofibric acid and several other compounds known as strong peroxisome proliferators and PPARα activators also can be seen as carboxylic acids with one or two α-methyl group(s) (49). Altogether, our studies and studies by others might suggest the presence of a pocket for methyl groups as well as flexibility in the PPARα ligand-binding cavity, close to the binding site for the carboxylic group.

According to these hypotheses, α-methyl TTA fulfills the three criteria of having the required chain length, a sulfur that can make a hydrogen bond with the serine residue, and a methyl group that fits into the suggested pocket in the LBD of PPARα. α-Methyl TTA was found to be the strongest PPARα activator in this study next to WY-14,643.

In agreement with our results showing increased PPARα activation, α-methyl TTA, α-methyl EPA, and α-methyl DHA also showed increased mRNA levels of the PPARα target genes

ACO and L-FABP in 7800C1 Morris hepatoma cells. This corresponds well with our earlier *in vitro* studies, which showed that α-methyl EPA is incorporated into cell phospholipids and increases ACO activity in hepatoma cells more than EPA (26). To our knowledge, the effects of α-methyl DHA have not been studied before. The increased transcription of ACO by TTA, α-methyl TTA, EPA, α-methyl EPA, DHA, and α-methyl DHA compared with the control may indicate increased β-oxidation of FA. Also, in feeding experiments, α-methyl TTA is a stronger inducer of ACO than TTA (50). Earlier studies showed that TTA decreases serum TG and cholesterol concentrations in animals fed this derivative (51–53). Others have shown that α-methyl EPA decreases plasma TG values more than EPA when given to rats (54). α-Methyl EPA is also a stronger inhibitor of platelet aggregation than EPA, both *in vitro* (26) and *in vivo* (54).

In addition, we found that α-methyl EPA, α-methyl DHA, and α-methyl TTA increased the expression of L-FABP more than EPA, DHA, and TTA, respectively. L-FABP is a cytosolic protein that binds endogenous FA, including branched-chain FA (55) and long-chain PUFA (56). This protein is involved in the uptake and intracellular transport of FA to either peroxisomal membranes or to the nucleus (57) for activation of PPARs (58). Furthermore, phytanic acid is a transcriptional activator of L-FABP expression, and this effect is mediated by PPARα (55).

The α-methyl CLA did not increase the mRNA for the same two PPARα target genes. This indicates that PPAR activators do not always induce the transcription of PPAR-responsive genes. Coactivators and corepressors play important roles in the regulation of transcription and may be differently recruited by various PPAR activators (59,60). Also, the regulation of PPAR target genes in lipid homeostasis is likely to be the consequence of a complex interplay among multiple PPAR and RXR isoforms and the ligands to these receptors (4,9,10). Prohibition of the dimerization by different ligands will prevent transcription of the PPARα target genes. Further, the α-methyl CLA might be antagonists, occupying the LBD and preventing transcription of ACO and L-FABP. Finally, we also speculate on the probability that the metabolism of these derivatives in 7800C1 Morris hepatoma cells may be different from the metabolism of the other derivatives used in this study.

The delayed catabolism of 3-thia FA and α-methyl FA may contribute to the increased effects of these FA derivatives compared with their unmodified counterparts, as shown in this paper. The degradation of FA differs according to their chemistry. Saturated and unsaturated straight-chain FA with a chain length of 4–20 carbon atoms are β-oxidized in mitochondria, whereas longer FA (C_{20}–C_{24}) have to be chain-shortened by β-oxidation in peroxisomes. Introduction of a methyl group in the α-position of FA is sufficient to decrease its β-oxidation in mitochondria (61), leading to peroxisomal oxidation by a specific noninducible branched-chain fatty acyl-CoA oxidase (62). Substituting a sulfur atom at the β-position in the carbon chain of a saturated FA prevents normal β-oxidation of the FA derivative. In addition to decreased or altered metabolism, it also remains possible that these compounds have altered affinity for serum- or intracellular binding proteins, which in turn might influence their PPARα activation.

In conclusion, saturated FA with sulfur in the β-position and increasing carbon chain length until C_{14}-S acetic acid have increasing effects as activators of PPARα and -γ in transfection assays. Furthermore, α-methyl FA derivatives of the saturated natural FA palmitic acid, the sulfur-substituted FA TTA, and PUFA (EPA, DHA, *c*9,*t*11 CLA, and *t*10,*c*12 CLA) are stronger PPARα activators than the unmethylated compounds.

REFERENCES

1. Brun, R.P., and Spiegelman, B.M. (1997) PPARγ and the Molecular Control of Adipogenesis, *J. Endocrinol. 155*, 217–218.
2. Schoonjans, K., Staels, B., and Auwerx, J. (1996) Role of the Peroxisome Proliferator-Activated Receptor (PPAR) in Mediating the Effects of Fibrates and Fatty Acids on Gene Expression, *J. Lipid Res. 37*, 907–925.
3. Schoonjans, K., Martin, G., Staels, B., and Auwerx, J. (1997) Peroxisome Proliferator-Activated Receptors, Orphans with Ligands and Functions, *Curr. Opin. Lipidol. 8*, 159–166.
4. Sørensen, H.N., Treuter, E., and Gustafsson, J.Å. (1998) Regulation of Peroxisome Proliferator-Activated Receptors, *Vitam. Horm. 54*, 121–166.
5. Isseman, I., and Green, S. (1990) Activation of a Member of the Steroid Hormone Receptor Superfamily by Peroxisome Proliferators, *Nature 347*, 645–650.
6. Dreyer, C., Krey, G., Keller, H., Givel, F., Helftenbein, G., and Wahli, W. (1992) Control of the Peroxisomal β-Oxidation Pathway by a Novel Family of Nuclear Hormone Receptors, *Cell 68*, 879–887.
7. Kliewer, S.A., Forman, B.M., Blumberg, B., Ong, E.S., Borgmeyer, U., Mangelsdorf, D.J., Umesono, K., and Evans, R.M. (1994) Differential Expression and Activation of a Murine Peroxisomal Proliferator-Activated Receptor, *Proc. Natl. Acad. Sci. USA 91*, 7355–7359.
8. Braissant, O., Foufelle, F., Scotto, C., Dauca, M., and Wahli, W. (1996) Differential Expression of Peroxisome-Proliferator Activated Receptors (PPARs): Tissue Distribution of PPAR-α, -β, and -γ in the Adult Rat, *Endocrinology 137*, 354–366.
9. Keller, H., Dreyer, C., Medin, J., Mahoudi, A., Ozato, K., and Wahli, W. (1993) Fatty Acids and Retinoids Control Lipid Metabolism Through Activation of Peroxisome Proliferator-Activated Receptor–Retinoid X Receptor Heterodimers, *Proc. Natl. Acad. Sci. USA 90*, 2160–2164.
10. Kliewer, S.A., Umesono, K., Noonan, D.J., Heyman, R.A., and Evans, R.M. (1992) Convergence of 9-*cis* Retinoic Acid and Peroxisome Proliferator Signalling Pathways Through Heterodimer Formation of Their Receptors, *Nature 358*, 771–774.
11. Forman, B., Chen, J., and Evans, R.M. (1997) Hypolipidemic Drugs, Polyunsaturated Fatty Acids, and Eicosanoids Are Ligands for Peroxisome Proliferator-Activated Receptors α and δ, *Proc. Natl. Acad. Sci. USA 94*, 4312–4317.
12. Krey, G., Braissant, O., L'Horset, F., Kalkhoven, E., Perroud, M., Parker, M.G., and Wahli, W. (1997) Fatty Acids, Eicosanoids, and Hypolipidemic Agents Identified as Ligands of Peroxisome Proliferator-Activated Receptors by Coactivator-Dependent Receptor Ligand Assay, *Mol. Endocrinol. 11*, 779–791.
13. Forman, B.M., Chen, J., and Evans, R.M. (1996) The Peroxisome Proliferator-Activated Receptors: Ligands and Activators, *Ann. N.Y. Acad. Sci. 804*, 266–275.

14. Xu, H.E., Lambert, M.H., Montana, V.G., Parks, D.J., Blanchard, S.G., Brown, P.J., Sternbach, D.D., Lehmann, J.M., Wisely, G.B., Willson, T.M, *et al.* (1999) Molecular Recognition of Fatty Acids by Peroxisome Proliferator-Activated Receptors, *Mol. Cell 3*, 397–403.

15. Zomer, A.W.M., van der Burg, B., Jansen, G.A., Wanders, R.J.A., Poll-The, B.T., and van der Saag, P.T. (2000) Pristanic Acid and Phytanic Acid: Naturally Occurring Ligands for the Nuclear Receptor Peroxisome Proliferater-Activated Receptor α, *J. Lipid Res. 41*, 1801–1807.

16. Kliewer, S.A., Sundseth, S.S., Jones, S.A., Brown, P.J., Wisely, G.B., Koble, C.S., Devchand, P., Wahli, W., Willson, T.M., Lenhard, J.M., and Lehmann, J.M. (1997) Fatty Acids and Eicosanoids Regulate Gene Expression Through Direct Interactions with Peroxisome Proliferator-Activated Receptors α and γ, *Proc. Natl. Acad. Sci. USA 94*, 4318–4323.

17. Oliver, W.R., Shenk, J.L., Snaith, M.R., Russell, C.S., Plunket, K.D., Bodkin, N.L., Lewis, M.C., Winegar, D.A., Sznaidman, M.L., Lambert, M.H., *et al.* (2001) A Selective Peroxisome Proliferator-Activated Receptor Agonist Promotes Reverse Cholesterol Transport, *Proc. Natl. Acad. Sci. USA 98*, 5306–5311.

18. Forman, B.M., Tontonoz, P., Chen, J., Brun, R.P., Spiegelman, B.M., and Evans, R.M. (1995) 15-Deoxy-$\Delta^{12,14}$-Prostaglandin J_2 Is a Ligand for the Adipocyte Determination Factor PPARγ, *Cell 83*, 803–812.

19. Kliewer, S.A., Lenhard, J.M., Willson, T.M., Patel, I., Morris, D.C., and Lehmann, J.M. (1995) A Prostaglandin J_2 Metabolite Binds Peroxisome Proliferator-Activated Receptor γ and Promotes Adipocyte Differentiation, *Cell 83*, 813-819.

20. Lehmann, J.M., Moore, L.B., Smith-Oliver, T.A., Wilkinson, W.O., Willson, T.M., and Kliewer, S.A. (1995) An Antidiabetic Thiazolidinedione Is a High Affinity Ligand for Peroxisome Proliferator-Activated Receptor γ (PPARγ), *J. Biol. Chem. 270*, 12953–12956.

21. Bergseth, S., and Bremer, J. (1990) Alkylthioacetic Acids (3-thia fatty acids) Are Metabolized and Excreted As Shortened Dicarboxylic-Acids *in vivo*, *Biochim. Biophys. Acta 1044*, 237–242.

22. Hvattum, E., Bergseth, S., Pedersen, C.N., Bremer, J., Aarsland, A., and Berge, RK. (1991) Microsomal Oxidation of Dodecylthioacetic Acid (a 3-thia fatty acid) in Rat Liver, *Biochem. Pharmacol. 41*, 945–953.

23. Berge, RK., Aarsland, A., Kryvi, H., Bremer, J., and Aarsaether, N. (1989) Alkylthioacetic Acid (3-thia fatty acids)—A New Group of Non-β-oxidizable, Peroxisome-Inducing Fatty Acid Analogues. I. A Study on the Structural Requirements for Proliferation of Peroxisomes and Mitochondria in Rat Liver, *Biochim. Biophys. Acta 1004*, 345–356.

24. Norrheim, L., Sørensen, H., Gautvik, K.M., Bremer, J., and Spydevold, Ø. (1990) Synergistic Actions of Tetradecylthioacetic Acid (TTA) and Dexamethasone on Induction of the Peroxisomal β-Oxidation and on Growth Inhibition of Morris Hepatoma Cells. Both Effects Are Counteracted by Insulin, *Biochim. Biophys. Acta 1051*, 319–323.

25. Spydevold, O., and Bremer, J. (1989) Induction of Peroxisomal β-Oxidation in 7800 C1 Morris Hepatoma Cells in Steady State by Fatty Acids and Fatty Acid Analogues, *Biochim. Biophys. Acta 1003,* 72–79.

26. Larsen, L.N., Bremer, J., Flock, S., and Skattebol, L. (1998) α- and β-Alkyl-Substituted Eicosapentaenoic Acids: Incorporation into Phospholipids and Effects on Prostaglandin H Synthase and 5-Lipoxygenase, *Biochem. Pharmacol. 55,* 405–411.

27. Madsen, L., Guerre-Millo, M., Flindt, E.N., Berge, K., Tronstad, K.J., Bergene, E., Sebokova, E., Rustan, A.C., Jensen, J., Mandrup, S., *et al*. (2002) Tetradecylthioacetic Acid Prevents High Fat Diet Induced Adiposity and Insulin Resistance, *J. Lipid Res. 43*, 742–750.

28. Jansen, G.A., Ofman, R., Ferdinandusse, S., Ijlst, L., Muijsers, A.O., Skjeldal, O.H., Stokke, O., Jakobs, C., Besley, G.T., Wraith, J.E., and Wanders, R.J. (1997) Refsum Disease Is Caused by Mutations in the Phytanoyl-CoA Hydroxylase Gene, *Nat. Genet. 17*, 190–193.

29. Wanders, R.J.A., and Tager, J.M. (1998) Lipid Metabolism in Peroxisomes in Relation to Human Disease, *Mol. Aspects Med. 19*, 69–154.

30. Chin, S.F., Liu, W., Storkson, J.M., Ha, Y.L., and Pariza, M.W. (1992) Dietary Sources of Conjugated Dienoic Isomers of Linoleic Acid, a Newly Recognized Class of Anticarcinogens, *J. Food Compos. Anal. 5*, 185–197.

31. Park, Y., Storkson, J.M., Albright, K.J., Liu, W., and Pariza, M.W. (1999) Evidence That the *trans*-10,*cis*-12 Isomer of Conjugated Linoleic Acid Induces Body Composition Changes in Mice, *Lipids 34*, 235–241.

32. Granlund, L., Juvet, L.K., Pedersen, J.I., and Nebb, H.I. (2003) *Trans* 10,*cis* 12-Conjugated Linoleic Acid Prevents Triacylglycerol Accumulation in Adipocytes by Acting as a PPARγ Modulator, *J. Lipid Res. 44*, 1441–1452.

33. Granlund, L., Larsen, L.N., Nebb., H.I., and Pedersen, J.I., Effects of Structural Changes of Fatty Acids on Lipid Accumulation in Adipocytes and Primary Hepatocytes, *Biochim. Biophys. Acta*, in press.

34. Jie, M.S.F.L., Pasha, M.K., and Alam, M.S. (1997) Synthesis and Nuclear Magnetic Resonance Properties of All Geometrical Isomers of Conjugated Linoleic Acids, *Lipids 32*, 1041–1044.

35. Lie Ken Jie, M.S.F, Lam, C.N.W., Ho, J.C.M., and Lau, M.M.L. (2003) Epoxidation of a Conjugated Linoleic Acid Isomer, *Eur. J. Lipid Sci. Technol. 105*, 391–396.

36. Lie Ken Jie, M.S.F., Pasha, M.K., and Alam, M.S. (1999) Nuclear Magnetic Resonance Spectroscopic Analysis of Conjugated Linoleic Acid Esters, in *Advances in Conjugated Linoleic Acid Research, Volume 1* (Yurawecz, M.P., Mossoba, M.M., Kramer, J.K.G., Pariza, M.W., and Nelson, G.J., eds.) pp. 152–163, AOCS Press, Champaign.

37. Chen, C.-A., and Sih, C.J. (1998) Chemoenzymatic Synthesis of Conjugated Linoleic Acid, *J. Org. Chem. 63*, 9620–9621.

38. Chen, C.A., Lu, W., and Sih, C.J. (1999) Synthesis of 9*Z*,11*E*-Octadecadienoic and 10*E*,12*Z*-Octadecadienoic Acids, the Major Components of Conjugated Linoleic Acid, *Lipids 34*, 879–884.

39. Richardson, U.I., Snodgrass, P.J., Nuzum, C.T., and Tashjian, A.H., Jr. (1974) Establishment of a Clonal Strain of Hepatoma Cells Which Maintain in Culture the Five Enzymes of the Urea Cycle, *J. Cell. Physiol. 83,* 141–149.

40. Steineger, H.H., Sørensen, H.N., Tugwood, J.D., Skrede, S., Spydevold, O., and Gautvik, K.M. (1994) Dexamethasone and Insulin Demonstrate Marked and Opposite Regulation of the Steady-State mRNA Level of the Peroxisomal Proliferator-Activated Receptor (PPAR) in Hepatic Cells. Hormonal Modulation of Fatty-Acid-Induced Transcription, *Eur. J. Biochem. 225*, 967–974.

41. Sørensen, H.N., Hvattum, E., Paulssen, E.J., Gautvik, K.M., Bremer, J., and Spydevold, O. (1993) Induction of Peroxisomal Acyl-CoA Oxidase by 3-Thia Fatty Acid, in Hepatoma Cells and Hepatocytes in Culture Is Modified by Dexamethasone and Insulin, *Biochim. Biophys. Acta 1171*, 263–271.

42. Sørensen, H.N., Gautvik, K.M., Bremer, J., and Spydevold, O. (1992) Induction of the Three Peroxisomal β-Oxidation Enzymes Is Synergistically Regulated by Dexamethasone and Fatty Acids, and Counteracted by Insulin in Morris 7800C1 Hepatoma Cells in Culture, *Eur. J. Biochem. 208*, 705–711.

43. Wu, P., Skrede, S., Hvattum, E., and Bremer, J. (1993) Substrate and Hormone Regulation of Palmitoyl-CoA Synthetase in 7800 C1Morris Hepatoma Cells and Cultured Rat Hepatocytes, *Biochim. Biophys. Acta 1170*, 118–124.

44. Lewis, D.F.V., Jacobs, M.N., Dickins, M., and Lake, B.G. (2002) Molecular Modelling of the Peroxisome Proliferator-Activated Receptor α (PPARα) from Human, Rat and Mouse, Based on Homology with the Human PPARγ Crystal Structure, *Toxicol. in Vitro 16*, 275–280.

45. Berge, R.K., Aarsland, A., Kryvi, H., Bremer, J., and Aarsaether,

N. (1989) Alkylthio Acetic Acids (3-thia fatty acids)—A New Group of Non-β-oxidizable Peroxisome-Inducing Fatty Acid Analogues—II. Dose–Response Studies on Hepatic Peroxisomal- and Mitochondrial Changes and Long-Chain Fatty Acid Metabolizing Enzymes in Rats, *Biochem. Pharmacol. 38,* 3969–3979.

46. Frøyland, L., Madsen, L., Sjursen, W., Garras, A., Lie, Ø., Songstad, J., Rustan, A.C., and Berge, R.K. (1997) Effect of 3-Thia Fatty Acids on the Lipid Composition of Rat Liver, Lipoproteins, and Heart, *J. Lipid Res. 38,* 1522–1534.

47. Madsen, L., Garras, A., Asins, G., Serra, D., Hegardt, F.G., and Berge, R.K. (1999) Mitochondrial 3-Hydroxy-3-methylglutaryl Coenzyme A Synthase and Carnitine Palmitoyltransferase II as Potential Control Sites for Ketogenesis During Mitochondrion and Peroxisome Proliferation, *Biochem. Pharmacol. 57,* 1011–1019.

48. Cronet, P., Petersen, J.F.W., Folmer, R., Blomberg, N., Sjöblom, K., Karlsson, U., Lindstedt, E., and Bamberg, K. (2001) Structure of the PPARα and -γ Ligand Binding Domain in Complex with AZ 242: Ligand Selectivity and Agonist Activation in the PPAR Family, *Structure 9,* 699–706.

49. Lewis, D.F.V., and Lake, B.G. (1998) Molecular Modelling of the Rat Peroxisome Proliferator-Activated Receptor -α (rPPARα) by Homology with Human Retinoic Acid X Receptor α (hRXRα) and Investigation of Ligand Binding Interactions: QSARs, *Toxicol. in Vitro 12,* 619–632.

50. Vaagenes, H., Madsen, L., Dyrøy, E., Elholm, M., Stray-Pedersen, A., Frøyland, L., Lie, Ø., and Berge, R.K. (1999) Methylated Eicosapentaenoic Acid and Tetradecylthioacetic Acid: Effects on Fatty Acid Metabolism, *Biochem. Pharmacol. 58,* 1133–1143.

51. Aarsland, A., Aarsaether, N., Bremer, J., and Berge, R.K. (1989) Alkylthioacetic Acids (3-thia fatty acids) as Non-β-oxidizable Fatty Acid Analogues: A New Group of Hypolipidemic Drugs. III. Dissociation of Cholesterol- and Triglyceride-Lowering Effects and the Induction of Peroxisomal β-Oxidation, *J. Lipid Res. 30,* 1711–1718.

52. Asiedu, D.K., Skorve, J., Willumsen, N., Demoz, A., and Berge, R.K. (1993) Early Effects on Mitochondrial and Peroxisomal β-Oxidation by the Hypolipidemic 3-Thia Fatty Acids in Rat Livers, *Biochim. Biophys. Acta. 1166,* 73–76.

53. Skorve, J., Asiedu, D., Rustan, A.C., Drevon, C.A., al-Shurbaji, A., and Berge, R.K. (1990) Regulation of Fatty Acid Oxidation and Triglyceride and Phospholipid Metabolism by Hypolipidemic Sulfur-Substituted Fatty Acid Analogues, *J. Lipid Res. 31,* 1627–1635.

54. Willumsen, N., Vaagenes, H., Holmsen, H., and Berge, R.K. (1998) On the Effect of 2-Deuterium- and 2-Methyl-eicosapentaenoic Acid Derivatives on Triglycerides, Peroxisomal β-Oxidation and Platelet Aggregation in Rats, *Biochim. Biophys. Acta. 1369,* 193–203.

55. Wolfrum, C., Ellinghaus, P., Fobker, M., Seedorf, U., Assmann, G., Børchers, T., and Spener, F. (1999) Phytanic Acid Is Ligand and Transcriptional Activator of Murine Liver Fatty Acid Binding Protein, *J. Lipid Res. 40,* 708–714.

56. Norris, A.W., and Spector, A.A. (2002) Very Long Chain n-3 and n-6 Polyunsaturated Fatty Acids Bind Strongly to Liver Fatty Acid-Binding Protein, *J. Lipid Res. 43,* 646–653.

57. Huang, H., Starodub, O., McIntosh, A., Kier, A.B., and Schroeder, F. (2002) Liver Fatty Acid-Binding Protein Targets Fatty Acids to the Nucleus. Real Time Confocal and Multiphoton Fluorescence Imaging in Living Cells, *J. Biol. Chem. 277,* 29139–29151.

58. Wolfrum, C., Borrmann, C.M., Borchers, T., and Spener, F. (2001) Fatty Acids and Hypolipidemic Drugs Regulate Peroxisome Proliferator-Activated Receptors α- and γ-Mediated Gene Expression *via* Liver Fatty Acid Binding Protein: A Signaling Path to the Nucleus, *Proc. Natl. Acad. Sci. USA 98,* 2323–2328.

59. Jia, Y., Qi, C., Kashireddy, P., Surapureddi, S., Zhu, Y., Rao, M.S., Roith, D., Chambon, P., Gonzalez, F.J., and Reddi, J.K. (2004) Transcription Coactivator PBP, the Peroxisome Proliferator-Activated Receptor (PPAR)-Binding Protein, Is Required for PPARα-Regulated Gene Expression in Liver, *J. Biol. Chem. 279,* 24427–24434.

60. Stanley, T.B., Leesnitzer, L.M., Montana, V.G., Galardi, C.M., Lambert, M.H., Holt, J.A., Xy, H.E., Moore, L.B., Blanchard, S.G., and Stimmel, J.B. (2003) Subtype Specific Effects of Peroxisome Proliferator-Activated Receptor Ligands on Corepressor Affinity, *Biochemistry 42,* 9278–9287.

61. Singh, H., Beckman, K., and Poulos, A. (1994) Peroxisomal β-Oxidation of Branched Chain Fatty Acids in Rat Liver. Evidence That Carnitine Palmitoyltransferase I Prevents Transport of Branched Chain Fatty Acids into Mitochondria, *J. Biol. Chem. 269,* 9514–9520.

62. Van Veldhoven, P.P., Vanhoven, G., Vanhoutte, F., Dacremont, G., Parmentier, G., Eyssen, H.J., and Mannaerts, G.P. (1991) Identification and Purification of a Peroxisomal Branched Chain Fatty Acyl-CoA Oxidase, *J. Biol. Chem. 266,* 24676—24683.

High-Fat Diets Impede the Lowering Effect of Cyclosporine A on Rat Brain Lipids and Interact with the Expression of Apolipoproteins E and J

Pascale Montpied[a],*, Nicole Domingo[b], Michèle Senft[b], Henri Portugal[c], Pierre Petit[d], and Françoise Chanussot[b]

[a]Centre National de la Recherche Scientifique (CNRS) UMR 5191-Ecole Normale Supérieure–LSH, BP7000-69342 Lyon cedex, France, [b]Institut National de la Santé et de la Recherche Médicale (INSERM) Unité 476, Faculté de Médecine, 13385 Marseille cedex 5, France, [c]Laboratoire de Biochimie et Centre ARCOL (Comité Francais de Coordination des Recherches sur l'Athérosclérose et le Cholestérol), Hôpital Sainte Marguerite, 13009 Marseille, France, and [d]CNRS UMR 5094-Faculté de Pharmacie 34093 Montpellier, France

ABSTRACT: Cyclosporine A (CsA), a common immunosuppressive agent, produces hyperlipidemia and apolipoprotein profile alterations in plasma as well as neurological and psychiatric complications. In rats, 10 mg CsA/kg/d treatments for 3 wk induce alterations of the electroencephalogram, and of the blood and brain lipids. Using this model, we evaluated whether triacylglycerol (TG)- and lecithin (PC)-enriched diets, reported to decrease epileptic episodes (TG) and to improve memory, could modify the effects of CsA treatment on brain lipids and possibly change apolipoprotein (apo) E and apoJ gene expression. To evaluate this hypothesis, three groups of rats were treated for 3 wk with CsA and received a low-fat, PC, or TG diet. Three other groups were fed the above-mentioned diets and were treated with the CsA solvent. As a control, one group was fed only the low-fat diet. The CsA-mediated decreases in brain cholesterol and PC contents, under a low-fat diet, were eliminated by the TG and PC diets. These high-fat diets induced a global increase in hippocampal transcriptional activity, as revealed by elevated polyadenylated RNA levels. The apoE and apoJ mRNA levels in the cortex and hippocampus of rats receiving the solvent were not statistically different between the TG- and PC-enriched diets but showed important variations compared with the low-fat diet solvent-treated group. A differential effect between the two high-fat diets was observed in the hippocampus, resulting in a significant increase of the apoE to apoJ ratio with the PC diet. The balance between apoE and apoJ is presumed to be important in encephalopathic mechanisms, by its involvement through low levels of brain cholesterol and PC, that might be associated with mental disorders. Our results therefore suggest that diet enrichment with polyunsaturated fat might be beneficial during CsA therapy. However, if the high levels in PC used here are more beneficial on CsA peripheral side effects than similar enrichment in TG, this does not seem to be the case in the brain. Thus, lower levels in PC should be tested.

Paper no. L9375 in *Lipids 40*, 59–67 (January 2005).

*To whom correspondence should be addressed at CNRS UMR 5191, Ecole Normale Supérieure-LSH, 15, Parvis Descartes, BP7000-69342 Lyon-cedex, France. E-mail: Pascale.Montpied@ens-lsh.fr

Abbreviations: APF, Anionic Peptide Factor; apo, apolipoproteins; CNS, central nervous system; CsA, cyclosporine A; FA, fatty acid; PC, lecithin; PolyA+ RNA, polyadenylated RNA; SSC, standard sodium citrate; TG, triacylglycerol.

Cyclosporine A (CsA), a potent immunosuppressive drug, is used in the treatment of autoimmune disorders (1) and after transplantation. However, a number of side effects occur quite often (2,3). Hepatic and renal dysfunction are the most frequent, but neurological and psychiatric complications are described as well (4–8). Seizures, memory and mood impairments, or psychotic episodes (4,7) are reported and are probably related to a drug accumulation in the brain. Such accumulation results from a combination of several types of CsA-mediated tissue, cellular, and molecular alterations (9–12). At the blood–brain barrier level, vascular injuries associated with anatomic disruption (9) and a decrease in the expression of the P-glycoprotein have been described in patients (10) and in CsA-treated rodents (12). Some neuropathological symptoms seen in patients were reproduced in rats, such as preepileptic alterations of the electroencephalograms (EEG) previously reported after 2 wk of treatment (13). The rat model therefore provided the opportunity to characterize the cellular and molecular events associated with CsA-mediated neurological dysfunction. Accumulation of phosphorylated neurofilaments was observed in rats exposed to CsA (14). The preepileptic alterations of the EEG and the accumulation of insoluble material as neurofilaments are typical features in latent epilepsy and Alzheimer's disease, respectively, and are presumed to be related to the neuropathology observed (15,16). Nevertheless, even if the expected similarities with the animal model of Alzheimer's disease and epilepsy at the level of apolipoprotein expression have not yet been described (15,17–19), the observed alterations in brain lipid content suggest that some neuropathological mechanisms might be analogous between CsA-induced mental disorders and several human neurological or mental disorders (i.e., Alzheimer's, memory loss, depression, and suicide). Such changes have been suggested to be associated with decreases in brain cholesterol and abnormalities of lipid metabolism (20–22). Vegetable n-6 polyunsaturated soybean lecithin (phosphatidylcholine: PC), rich in n-6 PUFA, seems to be a suitable dietary supplement during immunosuppressive treatment with CsA since it has been shown to reduce hypercholesterolemia (23), as well as to improve memory and possibly Alzheimer's deficits (24–27). Dietary triacyglycerol (TG) supplements have no positive effect

on blood cholesterol in rats, but have also been shown to improve learning (28). In addition, the major known effect of dietary TG consists of positive effects on brain excitability used as "ketogenic diets" since the 1920s to decrease seizure frequency in refractory childhood epilepsy (29,30). Thus, we hypothesized in the present work that the content in the brain of unesterified cholesterol and PC, seen to be altered following CsA treatment, could be restored by an appropriate lipid enrichment of the diet, which might be helpful in preventing CsA-mediated neurological side effects.

MATERIALS AND METHODS

Animals. Male Wistar rats (255 ± 10 g) were fed low- or high-fat diets for 3 wk (Table 1). The daily dietary intakes were isoenergetic (390 kJ/d for high-fat diets and 380 kJ/d for the standard low-fat diet). Animals were divided into seven groups, each group comprising six rats. They received care in compliance with the guidelines of the Animal Research Committee (INSERM guidelines, approved by the Minister of Agriculture no. 107 150). One group did not receive any treatment and was fed the standard low-fat diet (control group C). Daily intraperitoneal injections (200 µL/kg/d) were performed for 3 wk in the six other groups fed either the low-fat diet, or high-fat diets consisting of either a 20% enriched soybean TG diet (TG group) or a 20% enriched soybean PC diet (PC group). The fatty acid (FA) composition was similar in the TG and PC groups: In both high-fat diets, the levels of the main FA were as follows (molar percentage): palmitic acid, 11.3%; oleic acid, 18.0%; linoleic acid, 59.0%; α-linolenic acid, 7.7%. In addition, the high-fat diets had a lower content of carbohydrates compared with the C group (starch, 140 and 240 g/kg; sucrose, 123 and 183 g/kg in the high-fat and C groups, respectively). Half of the treated animals received only a volume of the CsA solvent (S group), a sixfold dilution of Cremophor in 0.9% NaCl (Novartis, Rueil Malmaison, France). The other half re-ceived the same volume with 10 mg/kg/d of CsA (Novartis). After the 3-wk period, rats were anesthetized after an overnight fast by an intramuscular injection containing 20 mg/kg xylazine (Rompun; Bayer, Puteaux, France) and 15 mg/kg ketamine (Imalgène; Rhône Merieux, Lyon, France). Plasma and brain were recovered and stored at −80°C.

RNA analysis. Brains were thawed in ice-cold 0.12 M PBS, (pH 7.4) and dissected on ice. Cortices and hippocampi of each animal were weighed and homogenized separately in the amount of tri-instapur solution indicated by the supplier in order to have identical conditions of RNA extraction (Eurogentec, Seraing Belgium). A reliable polyadenylated RNA (poly A+) quantitative assay was used to assess the transcriptional activity in the cortex and the hippocampus of each animal in relation to possible effects of the treatments. The preparations of total RNA were used for dot blot analysis as described previously (31). Briefly, they were denatured in 150 µL of 20× SSC (standard sodium citrate 1× = 0.15 M NaCl/0.015 M sodium citrate, pH 7.2) for 5 min at 70°C and dot blotted under vacuum in a dot blot apparatus (Schleicher and Schuell, Keene, NH); the 150 ng (for polyA+ dosage) or 1200 ng [for apolipoprotein (ApoE) and apoJ mRNA quantifications) of total RNA loaded on the membrane was fixed at 80°C for 1 h. RNA dots prehybridized (TechneHybridiser HB-ID) at 45°C for 2 h in a phosphate hybridization buffer containing 250 mM Na_2HPO_4, 7% SDS, and 1% BSA fraction V, at pH 6.5, were then hybridized following removal of the used prehybridization solution in a solution containing the same ingredients plus 5×10^6 cpm/mL of the radioactive probe [or 10×10^6 cpm/mL in the case of the oligodeoxythymidyl (oligodT) probe, to have the appropriate molecular concentration]. Following overnight hybridization, membranes were washed twice at room temperature for 30 min in 250 mM Na_2HPO_4 and 1% SDS, and once at 45°C in 250 mM Na_2HPO_4 and 0.1% SDS. Autoradiograms of the membranes were obtained at different times of exposure to control for linearity with a standard liver mRNA loaded at

TABLE 1
Experimental Design

	IP injection		Diets		
	CsA[b]	Solvent[c]	Standard diet[d]	Soybean TG diet[e]	Soybean PC[f] diet
Group[a]	(µL/kg/d)	(µL/kg/d)	(UAR no. AO4, 4% total lipids)	(20% total lipids)	(20% total lipids)
C			40 g/d		
S		200	40 g/d		
TG-S		200		25 g/d	
PC-S		200			25 g/d
CsA	200		40 g/d		
TG-CsA	200			25 g/d	
PC-CsA	200				25 g/d

[a]C, naive control rats; S, solvent-treated rats; CsA, cyclosporine A (CsA)-treated rats; TG-S, triacylglycerol (TG)-enriched diet plus S-treated rats; TG-CsA, TG-enriched diet plus CsA-treated rats; PC-S, lecithin (PC)-enriched diet plus S-treated rats; PC-CsA, PC-enriched diet plus CsA-treated rats.
[b]10 mg/200 µL of CsA (Sandoz-Novartis, Rueil Malmaison, France). CsA was diluted by sixfold with 0.9% NaCl.
[c]The solvent of CsA was supplied by Sandoz; Cremophor containing ethanol, castor oil, and nitrogen was diluted sixfold in 0.9% NaCl.
[d]UAR (Villemoisson-sur-Orge, France).
[e]Société Française des oléagineux (St Laurent Blangy, France).
[f]Epikuron 200, containing more than 92% of purified soybean PC (Lucas Meyer, Chelles, France).

various concentrations. Optical density (O.D.) of each dot on the autoradiogram signals corresponding to total RNA from rat cerebral cortex or hippocampus and to a control dot allowed us to quantify the levels of expression of the mRNA species specifically hybridized with the labeled oligomeric sequence. For quantification of the poly A+, negative hybridization controls were made using various amounts of a mix containing rRNA and tRNA. No signal was detected up to 20 µg, an amount about 100 times above the amounts loaded on the experimental dots containing only a natural abundance of these RNA species. Densitometric measurements were obtained using Image 1.36 MacintoshII software (Wayne Rasband, National Institute of Mental Health, Bethesda, MD) following calibration with Kodak calibration step tablet 809ST601 as a standard. Unsaturated autoradiograms were measured from three independent hybridization experiments.

Synthesis and labeling of the probes. The oligodT template (19–24 mer) was purchased from Pharmacia (Piscataway, NJ). Oligomers used to probe apoE and apoJ mRNA species were customized by Eurogentec. Rat sequences for these messengers were obtained through Genbank (accession numbers J00705 and X13231, respectively, for apoE and apoJ). Oligonucleotide sequences were controlled for specificity and secondary structure using Oligo r 4.03 (primer analysis software; National Biosciences Inc., Plymouth, MN). ApoE and apoJ probes were complementary to the coding sequences from nucleotide 518 to 552 and from nucleotide 449 to 476, respectively.

The labeling of the probes was performed at 37°C using 50 units of terminal deoxytransferase (Eurogentec) (or 100 units for the oligodT probe) and 50 µCi (or 120 mCi for the oligodT probe) of ^{32}P dTTP (800 Ci/mmol; Amersham, Les Ulis, France). The 50-µL reaction mixture containing 10 pmol of oligomer (or 15 pmol of oligodT template, and 4 pmol of cold dTTP) was incubated for 20 min (or overnight in the case of the oligodT probe). The probes obtained were either tailed with an average of 4 to 8 nucleotides for the specific messenger probes or with an average of 20 to 30 nucleotides for the oligodT probe as seen on a 15% acrylamide gel.

Protein assay. The dosage of the plasmatic and brain protein contents was determined with a Pierce kit (Rockford, IL).

Lipid assays. TG concentrations were evaluated by the enzymatic method of Fossati and Prencipe (32); total and unesterified cholesterol, respectively, were measured by the enzymatic methods of Siedel *et al.* (33) and Stähler *et al.* (34); and PC was measured by an enzymatic method based on the presence of the choline moiety (35). Serum was used directly, and brain lipids were extracted by the method of Folch *et al* (36).

Analysis of plasmatic biological markers. Blood samples were taken at sacrifice after an overnight fast. Using the enzymatic assay described by Ziegenhorn *et al.* (37), the glucose level in each rat plasma was measured, as were the plasma activities of glutamic oxaloacetate transaminase and glutamic pyruvate transaminase (38). Plasma urea and uric acid concentrations were also measured with Boehringer kits (Boehringer, Paris, France).

The Anionic Peptide Factor (APF) was purified from rat HDL$_3$ isolated by sequential ultracentrifugation at density 1.21 and tangential ultracentrifugation (Filtron, Coignières, France). The supernatant was processed successively through 100–10-kDa hydrophobic membranes. Using the purified 7-kDa APF, ELISA assays were performed with a polyclonal antibody (MD 94) from immunized rabbits and a monoclonal antibody (MAB 32) from Balb/c mice. These two antibodies had been characterized previously and did not cross-react with apoA-I. The determinations of APF concentrations in the samples were of two types: (i) an ELISA with direct antigen binding, and (ii) an ELISA with competitive antigen displacement as described previously (39). The standard curve allowed us to detect APF concentrations ranging from 0.2 to 5 µg/mL.

Statistical analysis. All the results are expressed as the arithmetical means of each group with their SE. Significance was analyzed by a one-way ANOVA, and the differences between groups were evaluated according to Fisher's test at $P < 0.05$. All calculations were performed using StatView^{TM} SE and Graphics (Abacus Concepts, Inc., Berkeley, CA; version 19 for Macintosh computer).

RESULTS

Plasma analysis. (i) Biological markers for peripheral dysfunctions. Blood urea was significantly increased by CsA. A comparison between the S groups and the corresponding CsA-treated groups showed increases of 65, 40, and 91% ($P < 0.01$), respectively, in the low-fat, TG-enriched, and PC-enriched diet groups (Table 2). Uremic response was more limited with the TG-enriched diet, and the levels were not significantly higher than those measured in naïve C group rats. None of the CsA-treated groups had uremia levels indicating serious renal failure or damage, and there was no pathological risk to the brain or other organs.

None of the rats treated with CsA showed increases in transaminase blood activities (Table 2). Thus, there was no CsA-mediated liver cytotoxicity in any experimental groups. Hypoglycemia, which might have increased the encephalopathic mechanism (40,41), was not observed. Following one night of fasting, glycemia was higher in animals fed the TG-enriched diet (groups TG-S and TG-CsA) than in the other groups; however, this diet effect was moderate and the values remained in the physiological range.

(ii) Lipidemia. On the low-fat diets (groups C, S, and CsA), plasma TG, total cholesterol, and unesterified cholesterol were significantly increased in the group treated with CsA (Table 2). However, as previously reported (17), the plasma unesterified cholesterol was already increased by the solvent, whereas the other blood lipids were selectively increased by CsA. A significant ($P < 0.05$) 1.6-fold increase in the ratio of unesterified to total cholesterol blood content (Table 2) was found in both the solvent and the CsA groups fed the low-fat diet. Feeding the rats a TG- or PC-enriched diet (groups TG-S and PC-S) eliminated the solvent-mediated increase of the unesterified to total cholesterol ratio. Concomitantly, the TG- and PC-enriched diets

TABLE 2
Effect of CsA and Its Solvent on Plasmatic Parameters in Rats Fed a Low- or High-Fat Diet[a]

	Control	Solvent			CsA		
	Low-fat diet	Low-fat diet	High-fat diet		Low-fat diet	High-fat diet	
	C	S	TG-S	PC-S	CsA	TG-CsA	PC-CsA
Glu mmol/L[b]	13.8 ± 0.7	15.5 ± 0.7	21.8 ± 2.0[d,f]	14.0 ± 0.6	14.6 ± 1.1	21.5 ± 2.2[g,i]	12.6 ± 0.5
Urea mmol/L	8.6 ± 0.3	7.3 ± 0.2	7.5 ± 0.5	6.7 ± 0.4	12.1 ± 0.3[b,c]	10.5 ± 0.6[g,i,j]	12.8 ± 0.9[k]
Uric acid mmol/L	89.6 ± 8.1	45.4 ± 3.2[a]	79.8 ± 10.3[d]	63.7 ± 5.3	59.6 ± 6.4[b]	85.1 ± 9.9[g,i]	38.8 ± 3.6[k]
GPT IU/L	54.4 ± 6.1	51.0 ± 5.0	45.5 ± 3.0	40.8 ± 4.8	41.1 ± 5.0	60.6 ± 7.3[g,i]	26.1 ± 2.7[h,k]
GOT IU/L	152.9 ± 10.5	140.8 ± 14.7	191.8 ± 17.3[d,f]	149.5 ± 10.3	149.1 ± 12.9	151.1 ± 13.3[j]	125.9 ± 4.9
Protein g/L	55.3 ± 0.9	54.8 ± 0.6	51.4 ± 0.9[d]	50.0 ± 0.5[e]	52.8 ± 0.6[b]	51.4 ± 0.9[g,i]	47.4 ± 0.5[h,k]
APF µg/mL	5.60 ± 0.76	1.06 ± 0.06[a]	8.02 ± 1.02[d,f]	12.78 ± 0.90[e]	3.17 ± 0.51[b]	7.59 ± 0.66[g,i]	10.94 ± 0.74[h]
TC mmol/L[b]	1.23 ± 0.05	1.34 ± 0.05	1.62 ± 0.09[d,f]	2.04 ± 0.07[e]	1.64 ± 0.08[b,c]	1.59 ± 0.14[i]	2.25 ± 0.13[h]
EC mmol/L	1.01 ± 0.04	0.97 ± 0.04	1.30 ± 0.08[d,f]	1.58 ± 0.05[e]	1.19 ± 0.06[c]	1.27 ± 0.11[i]	1.70 ± 0.09[h]
UC mmol/L	0.21 ± 0.02	0.37 ± 0.02[a]	0.32 ± 0.04	0.47 ± 0.02[e]	0.46 ± 0.02[b]	0.32 ± 0.03[g]	0.55 ± 0.04[h,i]
UC/TC mol/mol	0.17 ± 0.02	0.28 ± 0.01[a]	0.20 ± 0.02[d]	0.23 ± 0.01[e]	0.28 ± 0.01[b]	0.20 ± 0.004[g,i]	0.24 ± 0.01[h]
TG mmol/L[b]	0.51 ± 0.06	0.47 ± 0.05	0.68 ± 0.11	0.61 ± 0.08	1.03 ± 0.10[b,c]	0.60 ± 0.10[g]	1.06 ± 0.10[i,k]

[a]Comparisons were made between the seven animal groups comprising the control group (C) of unlabeled animals, and the experimental groups receiving either 10 mg/kg/d of CsA or the CsA solvents with a low-fat or a TG- or PC-enriched diet. Results are expressed as means ± SE (n = 10 in groups C, S, and CSA; n = 8 in groups TG-S, TG-CsA, PC-S, and PC-CsA). Glu, glucose; GPT, glutamic pyruvate transaminase; GOT, glutamic oxaloacetate transaminase; TC, total cholesterol; EC, esterified cholesterol; UC, unesterified cholesterol; APF, Anionic Peptide Factor; for other abbreviations see Table 1. Significance of the data was evaluated by Fisher's test. The presence of a superscript lowercase letter after the values given for an experimental group indicates statistical significance of at least $P < 0.05$. The letters correspond to the following comparisons: [a]C vs. S; [b]C vs. CsA; [c]S vs. CsA; [d]S vs. TG-S; [e]S vs. PC-S; [f]TG-S vs. PC-S; [g]CsA vs. TG-CsA; [h]CsA vs. PC-CsA; [i]TG-CsA vs. PC-CsA; [j]TG-S vs. TG-CsA; [k]PC-S vs. PC-CsA.
[b]To convert mmol/L to mg/L, multiply Glu by 18, TC by 38.6, and TG by 88.5.

induced increases in total cholesterolemia of 18 ($P < 0.05$) and 34% ($P < 0.05$), respectively, without a parallel increase in the unesterified cholesterol plasma level in the TG-enriched diet, whereas in the PC-fed group, a 20% ($P < 0.05$) increase in the unesterified cholesterol level was also measured (Table 2). Concerning selective CsA-mediated increases in the concentrations of plasma total cholesterol and TG seen in the low-fat-fed rats, we observed that only the TG-enriched diet countered this drug effect. With the PC-enriched diet, the CsA-mediated increase in TG plasma levels was still observed, reaching 74% ($P < 0.05$) (Table 2). To further analyze the beneficial or detrimental aspects of lipidemia alterations observed in the various experimental groups, we measured the 7-kDa APF. This peptide was described previously as a minor apolipoprotein in HDL (HDL$_3$). With a low-fat diet, we observed an important solvent-mediated decrease in APF (Table 2). The two high-fat diets, and particularly the PC diet, drastically increased the plasma APF level. No change in the APF level was observed when the CsA treatment was added to the TG-enriched diet (group TG-CsA), whereas the APF level was significantly lowered by CsA in the PC-fed group. However, in this last group (group PC-CsA), the APF level remained significantly higher than in the two other CsA-treated groups (groups CsA and TG-CsA), and it was still significantly above the levels measured in the C group.

Brain lipid concentrations. Brain unesterified cholesterol levels were significantly higher in the groups fed high-fat diets (groups TG-S and PC-S) compared with the low-fat diet (group S) (Table 3); the TG- and PC-enriched diets produced increases of 25% ($P < 0.01$) and 16% ($P < 0.05$), respectively (Table 3). With the CsA-treatment, brain unesterified cholesterol remained above normal in rats fed the high-fat diets. There was a maximal effect of CsA with the low-fat diet, on the concentration of brain unesterified cholesterol inducing significantly

lower levels than normal. The effect was limited with the TG-enriched diet, inducing a 12% decrease compared with the S group fed the TG diet, and there was no effect with the PC-enriched diet (Table 3). The levels in the TG- and PC-fed groups were not significantly different.

TG were present at low concentrations in the brain. Their levels were unchanged in the CsA group fed the low-fat diet compared with the S group. When rats were fed the TG- and the PC-enriched diets, significant increases in brain TG levels were measured, reaching 54 and 31%, respectively, compared with the S group fed the low-fat diet. CsA administration significantly reduced the effect of the TG diet on the brain TG levels, whereas it had no effect when applied with the PC-enriched diet. A comparison of brain TG levels in the three groups treated with CsA showed that the two high-fat-fed groups had significantly higher brain TG levels.

As previously reported with a low-fat diet, the brain levels of PC in both the CsA and S groups showed a significant drug-related decrease. In the TG and PC groups receiving the solvent, the brain PC levels showed significant increases (by 54 and 17%, respectively) compared with the S group fed a low-fat diet. When the CsA treatment was applied to high-fat-fed animals, a lowering effect on brain PC was observed only in the TG-enriched diet group. In spite of this 23% decrease ($P < 0.01$), the PC levels remained 18% above the levels measured in the C group and 48% above the levels measured in the low-fat CsA-treated group. In the PC-enriched diet-fed group treated with CsA, the PC levels were 31% ($P < 0.05$) above the control, 54% above the levels measured in the CsA-treated group fed a low-fat diet, and 10% above the levels measured in the CsA-treated group fed a TG-enriched diet (Table 2).

Cortical and hippocampal global transcription. There were no significant differences in the cortical transcriptional steady

TABLE 3
Effect of CsA and Its Solvent on Brain Lipids in Rats Fed a Low- or High-Fat Diet[a]

	Control	Solvent			CsA		
	Low-fat diet	Low-fat diet	High-fat diet		Low-fat diet	High-fat diet	
	C	S	TG-S	PC-S	CsA	TG-CsA	PC-CsA
TG nmol/mg protein	30.0 ± 4.7	30.8 ± 2.2	47.5 ± 3.7[c]	40.3 ± 2.1	26.7 ± 1.4	37.5 ± 2.0[d]	36.1 ± 2.9[f]
UC nmol/mg protein	691.7 ± 53.7	627.6 ± 36.4	784.1 ± 36.8[c]	731.8 ± 55.1	554.6 ± 27.7[a]	696.6 ± 25.9[d]	756.5 ± 62.7[f]
PL nmol/mg protein	710.5 ± 58.9	733.5 ± 35.7	1128.3 ± 37.0[c]	861.9 ± 20.6[g]	616.0 ± 33.8[b]	864.6 ± 31.5[d,e]	933.1 ± 38.1[f]

[a]Comparisons were made between the seven animal groups comprising the control group (C) of unlabeled animals, and the experimental groups receiving either 10 mg/kg/d of CsA or the CsA solvent (S) under a low-fat or a TG- or PC-enriched diet. Results are expressed as means ± SE (n = 10 in groups C, S, and CsA; n = 8 in groups TG-S, TG-CsA, PC-S, and PC-CsA). PL, phospholipids; for other abbreviations see Tables 1 and 2. Significance of the data were evaluated by Fisher's test. Presence of a lowercase superscript letter after the values given for an experimental group indicates statistical significance of at least $P <$ 0.05. The letters correspond to the following comparisons: [a]C vs. CsA; [b]S vs. CsA; [c]S vs. TG-S; [d]CsA vs. TG-CsA; [e]TG-S vs. TG-CsA; [f]CsA vs. PC-CsA; [g]TG-S vs. PC-S.

state between the different groups. In contrast, in the hippocampus, the transcriptional activities in the two TG groups receiving either solvent or CsA were, respectively, 48% and 56.5% ($P <$ 0.05) above the activity measured in the C group. In all CsA-treated groups, increases in the transcriptional level were measured, and this effect in the PC-fed group brought the hippocampus polyA+ level up to 30% ($P <$ 0.05) above basal levels (data described only in the text).

ApoE gene expression. Significant treatment-dependent alterations of transcriptional activity were observed; therefore, it was more appropriate to evaluate the concentration of apoE mRNA species in the cortex and hippocampus using known values of the polyA+ RNA loaded for each preparation.

In the cortex, and even more so in the hippocampus, the effect of CsA on apoE gene expression was clearly dependent on the lipid contents of the diets. In rats fed the low-fat diet, there was no CsA-mediated alteration in apoE mRNA levels, whereas for the high-fat-fed rats, CsA influenced the regulation of apoE mRNA levels (Table 4). The latter were already modified by the TG-enriched diet, which had minor and opposite effects on the cortical and hippocampal apoE mRNA levels. In the S groups, the TG diet induced a nonsignificant increase of 17.5% and a decrease of 15%, respectively, in these brain areas, compared with the low-fat-fed rats. The CsA treatment applied with the TG-enriched diet nullified these effects,

mediating a significant (33%) cortical decrease and a 32% hippocampal increase in apoE mRNA expression. Compared with the TG-enriched diet, the PC-enriched diet produced a minor increase in cortical apoE gene expression (15%; nonsignificant) but had a much greater effect on hippocampal apoE mRNA levels, producing a decrease of 55%. When CsA treatment was applied with the PC-enriched diet, a cortical decrease was observed, but it did not reach significance (22%). In the hippocampus, a major CsA-mediated increase (51%) was measured, restoring the apoE mRNA to basal levels (Table 4).

Cortical and hippocampal apoJ gene expression. Compared with the low-fat diet, the TG-enriched diet group showed a significant (29%) increase in cortical apoJ mRNA expression and a significant (51%) decrease in hippocampal apoJ expression. Enrichment of the diet with PC produced a significant (34%) increase in cortical apoJ mRNA levels and a nonsignificant (29%) decrease in hippocampal levels (Table 4).

Compared with the rats fed the TG-enriched diet (group TG-S) or an PC-enriched diet (group PC-S), the rats receiving CsA with these two diets showed a drop in cortical apoJ mRNA expression: −45% ($P <$ 0.01) and −42% ($P <$ 0.01) for the TG- and PC-fed groups, respectively. In the hippocampus, the effects of the TG-enriched diets were eliminated by the drug treatment (*cf.* groups TG-S vs. TG-CsA), and a CsA-mediated increase in apoJ mRNA hippocampal expression was observed:

TABLE 4
Effect of CsA and Its Solvent on Brain Apolipoprotein (apo) E and apoJ mRNA in Rats Fed a Low- or High-Fat Diet[a]

mRNA		Control	Solvent			CsA		
		Low-fat diet	Low-fat diet	High-fat diet		Low-fat diet	High-fat diet	
species	O.D. U/A+	C	S	TG-S	PC-S	CsA	TG-CsA	PC-CsA
apoE	Cortex	480.6 ± 38.9	493.3 ± 38.9	582.8 ± 57.7	563.3 ± 56.2	486.7 ± 45.9	394.4 ± 52.7[c]	440.0 ± 53.7
	Hippocampus	577.5 ± 26.6	494.7 ± 50.9	419.9 ± 16.9	319.5 ± 79.1[b]	540.3 ± 44.4	615.3 ± 64.1[c]	482.4 ± 56.1
apoJ	Cortex	394.3 ± 27.3	467.0 ± 63.9	598.5 ± 46.9	614.2 ± 81.8	425.4 ± 59.1	412.4 ± 101.0	433.3 ± 54.8
	Hippocampus	316.2 ± 23.1	351.9 ± 24.3	232.8 ± 26.2[a]	272.5 ± 44.8	343.8 ± 28.9	367.5 ± 22.6[c]	245.8 ± 44.8[d,e]
apoE/apoJ ratio	Cortex	1.25 ± 0.10	1.19 ± 0.16	1.01 ± 0.15	0.93 ± 0.03	1.29 ± 0.16	1.06 ± 0.12	1.02 ± 0.07
	Hippocampus	1.88 ± 0.14	1.54 ± 0.26	1.90 ± 0.28	1.15 ± 0.09	1.63 ± 0.13	1.67 ± 0.13	2.16 ± 0.31[f]

[a]Comparisons were made between the seven animal groups comprising the control group (C) of unlabeled animals, and the experimental groups receiving either 10 mg/kg/d of CsA or the CsA solvent with a low-fat or a TG- or PC-enriched diet. Results are expressed as means ± SE (n = 10 in groups C, S, and CsA; n = 8 in groups TG-S, TG-CsA, PC-S, and PC-CsA). For abbreviations see Table 1. Significance of the data were evaluated by Fisher's test. Presence of a lowercase superscript letter after the values given for an experimental group indicates statistical significance of at least $P <$ 0.05. The letters correspond to the following comparisons: [a]S vs. TG-S; [b]S vs. PC-S; [c]TG-S vs. TG-CsA; [d]CsA vs. PC-CsA; [e]TG-CsA vs. PC-CsA; [f]PC-S vs. PC-CsA.

+58% ($P < 0.01$). In contrast, the CsA treatment further decreased apoJ mRNA expression when animals were fed the PC-enriched diet (groups PC-CsA vs. S), and the decrease reached –43% ($P < 0.01$) (Table 4).

DISCUSSION

TG- or PC-enriched diets have been used for their beneficial effects on central nervous system (CNS) functional disorders (24–30). The aim of this study was to determine whether these diets modified some aspects of the previously observed alterations of brain lipid metabolism in response to CsA treatment (17), and whether these diets might be useful in a preventive approach toward CsA-induced neurological and psychiatric disorders. Thus, we now report that these high-fat diets can compensate for the CsA-mediated decreases in brain unesterified cholesterol and PC concentrations observed in rats fed a low-fat diet. In addition, we observed the regulation of brain apolipoprotein gene expression by both the TG- and PC-enriched diets, and differential interactions of CsA treatment with these regulatory mechanisms, depending on the high-fat diet, the region of the brain and the apolipoprotein being considered.

Concerning nutritional aspects, there have been several studies showing that the metabolic effects of dietary PC are not only those of adding the effects of dietary TG to those of choline, but also are specific to the PC supplementation (23,42–45). When free choline was administered alone, the observed effects were not as profound as those of PC: First, there was no drastic and acute hypocholesterolemic effect, as with PC (42); second, unlike dietary PC, choline did not significantly increase the biliary phospholipid and cholesterol output (42). The anti-atherogenic effects of PC, characterized by a hypocholesterolemic effect and the reduction of the aortic fatty streak area in hypercholesterolemic animals, are in fact reduced following dietary ingestion of TG plus choline (43). Thus, the two types of diets, enriched in either PC or TG plus choline, are not equivalent in their metabolic effects. Finally, PC is more efficient in terms of its overall benefits to the health; in addition, it seems better able to manipulate brain choline homeostasis indirectly using the choline precursor rather than directly using choline administration (44–46). Thus, we have chosen to compare lipoprotein and lipid metabolism at the brain level after consumption of either a PC- or a TG-enriched diet.

CsA treatment administered at a dose of 10 mg/kg/d for 2 or 3 wk is known to produce hepatic alterations (47,48), increased lipidemia (49,50), and brain EEG abnormalities without convulsions (13), but major toxicity is not commonly observed. Indeed, in the experimental groups receiving the CsA treatment, none of the rats had behavioral abnormalities or health-threatening alterations of the peripheral toxicity markers whatever the diet considered. Consistent with previous reports on solvent cholestatic effects (47,48), we observed an increase in phospholipidemia and an alteration of the balance between total and unesterified cholesterol. When CsA was added, the known effect of CsA itself was observed, with additional hyperlipidemic responses in rats fed the low-fat diet. In contrast, we now report that the high-fat diets led to different alterations of lipidemia during CsA treatment. Feeding the rats with TG-enriched diet did not significantly modify lipidemia and prevented a CsA-induced increase in cholesterolemia. The PC-enriched diet by itself modified lipidemia, resulting in an increase in plasma TG, and mainly in total cholesterol. CsA treatment with this diet further increased total cholesterol and TG. It is interesting to note that both high-fat diets conferred a solvent effect on lipidemia. We also found a large and significant increase in plasma APF concentration. APF, a minor HDL_3 apolipoprotein component, was previously shown to be a carrier of unesterified cholesterol, stimulating reverse cholesterol transport from the plasma toward the liver and bile (51). With the PC-enriched diet, we observed that the hyperlipidemic responses to CsA were maintained. Cholesterolemia was further increased by CsA but was nevertheless associated with quite a high level of APF (10- and 2.75-fold higher than in the solvent- and CsA-treated low-fat-fed groups). Furthermore, the comparison of blood markers for cholesterol metabolism following CsA treatment showed a 1.2-fold increase in cholesterolemia without an increase in APF in the low-fat conditions and a 1.1-fold increase in cholesterolemia associated with a 12-fold increase in APF in the PC-enriched diet-fed group. Therefore, supplying high levels of dietary phospholipids might be a unique stimulus to better tissue and cellular disposal of cholesterol and to improve reverse cholesterol transport during the immunosuppressive treatment. These first results on peripheral lipid metabolism support the possibility of using high-fat diets to improve CsA-mediated CNS disorders. We have previously reported that the solvent had no effect on lipid metabolism in the brain, whereas CsA produced a lowering of unesterified cholesterol and phospholipid. This latter response contrasts with the brain cholesterol overloading and lipid release occurring in hypercholesterolemic and epileptic models, and might explain why there was no CsA-induced alteration in apoE and apoJ gene expression (17). These unchanged levels in apoE and apoJ mRNA species initially led us to suppose that CsA-induced neurological effects, compared with those described in other encephalopathies such as Alzheimer's disease and epilepsy, are not related to alterations in brain apolipoprotein expression. We thus hypothesized, first, that the low concentration of unesterified cholesterol and phospholipids in the brain could be involved in some of the memory impairment, depressive symptoms, or manic episodes described in CsA-treated patients (4,20,21,52,53). This is supported by the literature reporting correlations between increased risks for mental disorders and disturbances of cholesterol metabolism.

However, we are now reporting that with high-fat diets modifying the normal levels of apolipoprotein gene expression in untreated rats, CsA treatment led to modifications of the levels of apoE and apoJ brain mRNA, and the CsA-mediated decreases in brain phospholipids and unesterified cholesterol were nullified by the high-fat diets. In view of these results, it is possible to hypothesize that in the reported cases of psychiatric or neurological dysfunction seen with CsA treatment, either a reduction of brain lipids or an unbalanced expression

of apoE and apoJ, as seen in chronic epilepsy and in Alzheimer's disease, could be involved. Finally, it is important to focus on the differential effect of CsA on brain lipid concentrations and on cortical or hippocampal apolipoprotein expression under the two high-fat diets. On one hand, the TG-enriched diet did not suppress the CsA-mediated changes; rather it decreased the brain unesterified cholesterol and phospholipid contents but by itself produced an increase in these lipids that compensated for the drug effect. On the other hand, the PC-enriched diet suppressed CsA-mediated decreases in the two types of brain lipids but did not by itself change the levels of either the unesterified cholesterol or phospholipids.

In contrast with PC, dietary TG have not been used to improve neurological symptoms such as those observed in Alzheimer's disease, but rather to decrease the frequency of seizures in children suffering from refractory epilepsy (29,30); such high-fat diets act through the elevation of plasma ketones that produce beneficial effects on energy metabolism and neuronal excitability, and probably on detrimental glial activation in the brain (54). These findings are relevant, given that in our experimental high-fat diets, the level of carbohydrates was also decreased, as recommended in antiepileptic diets. Phospholipid diet supplements have been suggested to improve memory deficits and Alzheimer's dementia in humans as well as in animal models, and are believed to act by increasing phospholipid, and in particular PC, availability in the brain (24–27). In animals, however, memory improvement was reported with soy TG supplementation, and the increased brain phospholipid concentrations observed in our experiment in response to the TG-enriched diet might be related to these previous observations (28).

TG are much less abundant in the brain than are cholesterol and phospholipids, but their variation could be meaningful and was also evaluated. There was an increase in brain TG in response to the TG- or PC-enriched diets, whereas plasma TG remained stable, as already discussed. When the CsA treatment was applied to high-fat-fed animals, the brain TG content remained unaltered in the group fed the PC-enriched diet (for the low-fat diet group) and were decreased by the drug treatment in the TG-enriched diet-fed rats.

The effect of CsA on the lipid steady state in the brain appeared to be different in rats fed the low-fat, TG-enriched, or PC-enriched diet. It is possible to hypothesize that different pathological mechanisms involving various aspects of brain lipid metabolism might occur in different CsA-treated patients depending on their genetic or nutritional background. In patients having initially low lipid levels, it is possible that lipid enrichment of the diet might reverse neurological risk. PC-enrichment, already shown to be beneficial on CsA-induced hepatic alterations (47,48), appears superior since it blocks CsA-induced brain alterations rather than only compensating for these alterations, as did the TG-enriched diet. Alternatively, in patients already having a high level of brain apolipoprotein expression due to genetic or environmental causes, CsA treatment might produce modifications of apoE and apoJ expression, as also observed in treated rats fed high-fat diets. If prolonged, such a situation might increase encephalopathic risk. ApoE and

apoJ are supposed to be pro-amyloidogenic and anti-amyloidogenic, respectively (19,55). ApoE has a propensity to form fibrils, increasing the various forms of deposits described in brains of Alzheimer's patients. ApoJ is involved in the transport of the β-amyloid peptide responsible in part for the progression of Alzheimer's disease. It is believed that the balance between the two brain apolipoproteins is important in avoiding Alzheimer's disease and epilepsy (19,55). Feeding a diet highly enriched in lecithin might nevertheless produce a long-term unfavorable balance of apolipoproteins in the hippocampus. Amyloidogenic accumulation might occur in this structure known to be involved in some seizure initiation and memory, and high levels of cyclophillin might be expressed, with massive overexpression following seizures. In contrast, in the cortex, PC seemed to improve the ratio in favor of a better elimination of the amyloid component and to lessen the trend toward deposition of apoE. It is important to point out that a previous study showed better improvement of memory in a mouse model when using a 2% phospholipid-enrichment compared with an 8% enrichment (56). This suggests that a lower content of PC in the diet should be tolerated better than a 20% PC diet, and might restore a normal ratio between apoE and apoJ in the hippocampus.

In conclusion, dietary management might help to reduce some long-term side effects of CsA. An enrichment of the diet with soybean lipids might benefit several aspects of the neurological side effects of the drug. Both soybean TG and PC prevent CsA-induced decreases in unesterified cholesterol and phospholipid content of the brain. All these effects should be clarified in further studies to improve our ability to mediate pharmacological immunosuppression without risk to the CNS. However, testing a lower PC content in the diet would probably be better. This study provides a broad perspective on the use of nutritional lipids to alleviate the consequences of brain injury induced by a toxic substance and demonstrates that this approach could potentially prevent adverse side effects.

REFERENCES

1. Faulds, D., Goa, K.L., and Benfield, P. (1993) Cyclosporin: A Review of Its Pharmacodynamic and Pharmacokinetic Properties and Therapeutic Use in Immunoregulatory Disorders, *Drugs 45*, 953–1040.
2. Whiting, P.H., Thompson, A.W., and Simpson, J.G. (1985) Cyclosporine: Toxicity, Metabolism, and Drug Interactions: Implications from Animal Studies, *Transplant. Proc. 17*, 134–144.
3. Kahan, B.D. (1989) Cyclosporine, *New Engl. J. Med. 321*, 1725–1738.
4. Patchell, R.A. (1994) Neurological Complications of Organ Transplantation, *Ann. Neurol. 36*, 688–703.
5. Wasserstein, P.H., and Honig, L.S. (1996) Parkinsonism During Cyclosporine Treatment, *Bone Marrow Transplant. 18*, 649–650.
6. Gopal, A.K., Thorning, D.R., and Back, A.L. (1999) Fatal Outcome Due to Cyclosporine Neurotoxicity with Associated Pathological Findings, *Bone Marrow Transplant. 23*, 191–193.
7. Tauboll, E., Gerdts, R., and Gjerstad, L. (1998) Cyclosporin A and Brain Excitability Studied *in vitro, Epilepsia 39*, 687–691.
8. Bechstein, W.O. (2000) Neurotoxicity of Calcineurin Inhibitors: Impact and Clinical Management, *Transplant. Int. 13*, 313–326.

9. Bartynski, W.S., Grabb, B.C., Zeigler, Z., Lin, L., and Andrews, D.F. (1997) Watershed Imaging Features and Clinical Vascular Injury in Cyclosporin A Neurotoxicity, *J. Comput. Assist. Tomogr. 21*, 872–880.

10. Lum, B.L., Fisher, G.A., Brophy, N.A., Yahanda, A.M., Adler, K.M., Kaubisch, S., Halsey, J., and Sikic, B.I. (1993) Clinical Trials of Modulation of Multidrug Resistance. Pharmacokinetic and Pharmacodynamic Considerations, *Cancer 72*, 3502–3514.

11. Sakata, A., Tamai, I., Kawazu, K., Deguchi, Y., Ohnishi, T., Saheki, A., and Tsuji, A. (1994) *In vivo* Evidence for ATP-Dependent and P-Glycoprotein Mediated Transport of Cyclosporin A at the Blood Brain Barrier, *Biochem. Pharmacol. 48*, 1989–1992.

12. Schinkel, A.H., Wagenaar, E., Mol, C.A., and Van Deemter, L. (1996) P-Glycoprotein in Blood Brain Barrier of Mice Influences the Brain Penetration and the Pharmacological Activity of Many Drugs, *J. Clin. Invest. 97*, 2517–2524.

13. Racusen, L.C., Famiglio, L.M., Fivush, B.A., Olton, D.S., and Solez, K. (1988) Neurologic Abnormalities and Mortality in Rats Treated with Cyclosporine A, *Transplant. Proc. 20*, 934–936.

14. Tanaka, T., Takeda, M., Niigawa, H., Hariguchi, S., and Nishimura, T. (1993) Phosphorylated Neurofilament Accumulation in Neuronal Perikarya by Cyclosporin A Injection in Rat Brain, *Methods Find. Exp. Clin. Pharmacol. 15*, 77–87.

15. Montpied, P., De Bock, F., Lerner-Natoli, M., Bockäert, J., and Rondouin, G. (1999) Hippocampal Alterations of Apolipoprotein E and D mRNA Levels *in vivo* and *in vitro* Following Kainate Excitotoxicity, *Epilepsy Res. 35*, 135–146.

16. Shepherd, C.E., McCann, H., Thiel, E., and Halliday, G.M. (2002) Neurofilament-Immunoreactive Neurons in Alzheimer's Disease and Dementia with Lewy Bodies, *Neurobiol. Dis. 9*, 249–257.

17. Montpied, P., Batxelli, I., André, M., Portugal, H., Lairon, D., Bockäert, J., and Chanussot, F. (2003) Effects of Cyclosporine-A on Brain Lipids and Apolipoprotein E, J Gene Expression in Rats, *Neuroreport 14*, 573–576.

18. Montpied, P., De Bock, F., Baldy-Moulinier, M., and Rondouin, G. (1998) Alterations of Metallothionein II and Apolipoprotein J mRNA Levels in Kainate-Treated Rats, *Neuroreport 9*, 79–83.

19. Zlokovic, B.V. (1996) Cerebrovascular Transport of Alzheimer's Amyloid β and Apolipoproteins J and E: Possible Anti-amyloidogenic Role of the Blood–Brain Barrier, *Life Sci. 59*, 1483–1497.

20. Kim, J.M., Stewart, R., Shin, I.S., and Yoon, J.S. (2002) Low Cholesterol, Cognitive Function and Alzheimer's Disease in a Community Population with Cognitive Impairment, *J. Nutr. Health Aging 6*, 320–323.

21. Hawton, K., Cowen, P., Owens, D., Bond, A., and Elliott, M. (1993) Low Serum Cholesterol and Suicide, *Br. J. Psychiatry 162*, 818–825.

22. Muldoon, M.F., Ryan, C.M., Matthews, K.A., and Manuck, S.B. (1997) Serum Cholesterol and Intellectual Performance, *Psychosom. Med. 59*, 382–387.

23. Polichetti, E., Diaconescu, N., Lechène de la Porte, P., Malli, L., Portugal, H., Pauli, A.M., Lafont, H., Tuchweber, B., Yousef, I., and Chanussot, F. (1996) Cholesterol-Lowering Effect of Soybean Lecithin in Normolipidaemic Rats by Stimulation of Biliary Lipid Secretion, *Br. J. Nutr. 75*, 471–481.

24. Rosenberg, G.S., and Davis, K.L. (1982) The Use of Cholinergic Precursors in Neuropsychiatric Diseases, *Am. J. Clin. Nutr. 36*, 709–720.

25. Canty, D.J., and Zeisel, S.H. (1994) Lecithin and Choline in Human Health and Disease, *Nutr. Rev. 52*, 327–339.

26. Hung, M.C., Shibasaki, K., Yoshida, R., Sato, M., and Imaizumi, K. (2001) Learning Behaviour and Cerebral Protein Kinase C, Antioxidant Status, Lipid Composition in Senescence-Accelerated Mouse: Influence of a Phosphatidylcholine–Vitamin B_{12} Diet, *Br. J. Nutr. 86*, 163–171.

27. Magil, S.G., Zeisel, S.H., and Wurtman, R.J. (1981) Effects of Ingesting Soy or Egg Lecithins on Serum Choline, Brain Choline and Acetylcholine, *J. Nutr. 111*, 166–170.

28. Coscina, D.V., Yehuda, S., Dixon, L.M., Kish, S.J., and Leprohon-Greenwood, C.E. (1986) Learning Is Improved by Soybean Oil Diet in Rats, *Life Sci. 38*, 1789–1794.

29. Huttenlocher, P.R., Wilbourn, A.J., and Signore, J.M. (1971) Medium-Chain Triglycerides as Therapy for Intractable Childhood Epilepsy, *Neurology 21*, 1097–1103.

30. Woody, R.C., Brodie, M., Hampton, D.K., and Fiser, R.H., Jr. (1988) Corn Oil Ketogenic Diet for Children with Intractable Seizures, *J. Child Neurol. 3*, 21–24.

31. Montpied, P., Morrow, A.L., Karanian, J.W., Ginns, E.I., Martin, B.M., and Paul, S.M. (1991) Prolonged Ethanol Inhalation Decreases γ-Aminobutyric Acid A Receptor α Subunit mRNAs in the Rat Cerebral Cortex, *Mol. Pharmacol. 39*, 157–163.

32. Fossati, P., and Prencipe, L. (1982) Serum Triglycerides Determined Colorimetrically with an Enzyme That Produces Hydrogen Peroxide, *Clin. Chem. 28*, 2077–2080.

33. Siedel, J., Hagele, E.O., Ziegenhorn, J., and Wahlefeld, A.W. (1983) Reagent for the Enzymatic Determination of Serum Total Cholesterol with Improved Lipolytic Efficiency, *Clin. Chem. 29*, 1075–1080 .

34. Stähler, F., Gruber, W., Stinshoff, K., and Röschlau, P. (1977) A Practical Enzymatic Cholesterol Determination, *Med. Lab. 30*, 29–37.

35. Takayama, M., Itoh, S., Nagasaki T., and Tanimizu, I. (1977) A New Enzymatic Method for Determination of Serum Choline Containing Phospholipids, *Clin. Chim. Acta 79*, 93–98.

36. Folch, J., Lees, M., and Sloane Stanley, G.H. (1957) A Simple Method for the Isolation and Purification of Total Lipids from Animal Tissues, *J. Biol. Chem. 226*, 497–509.

37. Ziegenhorn, J., Neumann, U., Hagen, A., Bablok, W., and Strinshoff, K. (1977) Kinetic Enzymatic Method for Automated Determination of Glucose in Blood and Serum, *J. Clin. Chem. Clin. Biochem. 15*, 13–19.

38. Kessler, G., Morgenstern, S., Snyder, L., and Varady, R. (1975) Improved Point Assays for ALT and AST in Serum Using the Technicon SMAC High Speed Computer Controlled Biochemical Analyser to Eliminate the Common Errors Found in Enzyme Analysis, paper presented at the 9th International Congress for Clinical Chemistry, Toronto.

39. Domingo, N., Grosclaude, J., Bekaert, E.D., Chapman, M.J., Shimizu, S., Ayrault-Jarrier, M., Ostrow, J.D., and Lafont, H. (1992) Epitope Mapping of the Human Biliary Amphipathic Anionic Polypeptide (APF): Similarity with a Calcium-Binding Protein (CBP) Isolated from Gallstones and Bile and Immunologic Cross-Reactivity with Apolipoprotein A-I, *J. Lipid Res. 33*, 1419–1430.

40. Pedersen, W.A., Culmsee, C., Ziegler, D., Herman, J.P., and Mattson, M.P. (1999) Aberrant Stress Response Associated with Severe Hypoglycemia in a Transgenic Mouse Model of Alzheimer's Disease, *J. Mol. Neurosci. 13*, 159–165.

41. Yanagisawa, M., Planel, E., Ishiguro, K., and Fujita, S.C. (1999) Starvation Induces τ Hyperphosphorylation in Mouse Brain: Implications for Alzheimer's Disease, *FEBS Lett. 461*, 329–333.

42. Leblanc, M.J., Gavino, V., Perea, A., Yousef, I.M., Levy, E., and Tuchweber, B. (1998) The Role of Dietary Choline in the Beneficial Effects of Lecithin on the Secretion of Biliary Lipids in Rats, *Biochim. Biophys. Acta 1393*, 223–234.

43. Wilson, T.A., Meservey, C.M., and Nicolosi, R.J. (1998) Soy Lecithin Reduces Plasma Lipoprotein Cholesterol and Early Atherogenesis in Hypercholesterolemic Monkeys and Hamsters: Beyond Linoleate, *Atheroselerosis 140*, 147–153.

44. Klein, J., Koppen, A., and Loffelholz, K. (1998) Regulation of Free Choline in Rat Brain: Dietary and Pharmacological Manipulations, *Neurochem Int. 32*, 479–485.

45. Mastellone, I., Polichetti E., Grès, C., de la Maisonneuve, C.,

Domingo, N., Marin, V., Lorec, A.M., Farnarier, C., Portugal, H., Kaplanski, G., and Chanussot, F. (2000) Dietary Soybean Phosphatidylcholines Lower Lipidemia: Mechanisms at the Levels of Intestine, Endothelial Cell and Hepato-biliary Axis, *J. Nutr. Biochem. 11*, 461–466.

46. Polichetti, E., Janisson, A., Iovanna, C., Portugal, H., Mekki, N., Lorec, A.M., Pauli, A.M., Luna, A., Lairon, D., La Droitte, P., Lafont, H., and Chanussot, F. (1998) Stimulation of the apoA–I–High Density Lipoprotein System by Dietary Soyabean Lecithin in Humans, *J. Nutr. Biochem. 9*, 659–664.

47. Benkoël, L., Chanussot, F., Dodero, F., De La Maisonneuve, C., Lambert, R., Brisse, J., Delmas, M., and Chamlian, A. (1998) Modification of Ca^{2+},Mg^{2+}-ATPase and F-Actin Distribution in Hepatocytes of Cyclosporine A Treated Rats. Effect of Soybean Lecithin and Triacyglycerol, *Cell. Mol. Biol. 44*, 1221–1227.

48. Benkoël, L., Chanussot, F., Dodero, F., de la Maisonneuve, C., Lambert, R., Brisse, J., and Chamlian, A. (1999) Effect of Dietary Lipids on Hepatic Na^{+},K^{+}-ATPase in Cyclosporine A Treated Rats: Immunocytochemical Analysis of α1 Subunit by Confocal Laser Scanning Microscopy Imaging, *Dig. Dis. Sci. 44*, 1613–1619.

49. Schorn, T.F., Kliem, V., Bojanovski, M., Bojanovski, D., Repp, H., Bunzendahl, H., and Frei, U. (1991) Impact of Long Term Immunosuppression with Cyclosporin A on Serum Lipids in Stable Renal Transplant Recipients, *Transplant. Int. 4*, 92–95.

50. Espino, A., Lopez-Miranda, J., Blanco-Cerrada, J., Zambrana, J.L., Aumente, M.A., Paniagua, J.A., Blanco-Molina, A., Jimenez-Pereperez, J.A., Rodriguez, M., and Perez-Jimez, F.

(1995) The Effect of Cyclosporine and Methylprednisolone on Plasma Lipoprotein Levels in Rats, *J. Lab. Clin. Med. 125*, 222–227.

51. Martigne, M., Domingo, N., Chanussot, F., Nalbone, G., Lafont, H., and Hauton, J.C. (1988) Effect of the Bile Anionic Polypeptide Fraction on the Fate of Cholesterol Carried by the Liposomes in the Rat, *Proc. Soc. Exp. Biol. Med. 187*, 234–344.

52. Mulder, M., Ravid, R., Swaab, D.F., de Kloet, E.R., Haasdijk, E.D., Julk, J., van der Boom, J.J., and Havekes, L.M. (1998) Reduced Levels of Cholesterol, Phospholipids, and Fatty Acids in Cerebrospinal Fluid of Alzheimer Disease Patients Are Not Related to Apolipoprotein E4, *Alzheimer Dis. Assoc. Disord. 12*, 198–203.

53. Ellison, L.F., and Morrison, H.I. (2001) Low Serum Cholesterol Concentration and Risk of Suicide, *Epidemiology 12*, 168–172.

54. Stafstrom, C.E., and Bough, K.J. (2003) The Ketogenic Diet for the Treatment of Epilepsy: A Challenge for Nutritional Neuroscientists, *Nutr. Neurosci. 6*, 67–79.

55. Poirier, J. (2003) Apolipoprotein E and Cholesterol Metabolism in the pathogenesis and Treatment of Alzheimer's Disease, *Trends Mol. Med. 9*, 94–101.

56. Moriyama, T., Uezu, K., Matsumoto, Y., Chung, S.Y., Uezu, E., Miyagi, S., Uza, M., Masuda, Y., Kokubu, T., Tanaka, T., and Yamamoto, S. (1996) Effects of Dietary Phosphatidylcholine on Memory in Memory Deficient Mice with Low Brain Acetylcholine Concentration, *Life Sci. 58*, 111–118.

Restoration of Depressed Prostanoid-Induced Ileal Contraction in Spontaneously Hypertensive Rats by Dietary Fish Oil

Glen S. Patten*, Michael J. Adams, Julie A. Dallimore, Paul F. Rogers, David L. Topping, and Mahinda Y. Abeywardena

CSIRO Health Sciences & Nutrition, Adelaide, South Australia 5000, Australia

ABSTRACT: We have reported that dietary fish oil (FO) rich in n-3 PUFA modulates gut contractility. It was further demonstrated that the gut of spontaneously hypertensive rats (SHR) has a depressed contractility response to prostaglandins (PG) compared with normotensive Wistar-Kyoto (WKY) rats. We investigated whether feeding diets supplemented with n-3 PUFA increased gut contractility and restored the depressed prostanoid response in SHR gut. Thirteen-week-old SHR were fed diets containing fat at 5 g/100 g as coconut oil (CO), lard, canola oil containing 10% (w/w) n-3 FA as α-linolenic acid (18:3n-3), or FO (as HiDHA®, 22:6n-3) for 12 wk. A control WKY group was fed 5 g/100 g CO in the diet. As confirmed, the SHR CO group had a significantly lower gut response to PGE_2 and $PGF_{2\alpha}$ compared with the WKY CO group. Feeding FO increased the maximal contraction response to acetylcholine in the ileum compared with all diets and in the colon compared with lard, and restored the depressed response to PGE_2 and $PGF_{2\alpha}$ in the ileum but not the colon of SHR. FO feeding also led to a significant increase in gut total phospholipid n-3 PUFA as DHA (22:6n-3) with lower n-6 PUFA as arachidonic acid (20:4n-6). Canola feeding led to a small increase in ileal EPA (20:5n-3) and DHA and in colonic DHA without affecting contractility. However, there was no change in ileal membrane muscarinic binding properties due to FO feeding. This report confirms that dietary FO increases muscarinic- and eicosanoid receptor-induced contractility in ileum and that the depressed prostanoid response in SHR ileum, but not colon, is restored by tissue incorporation of DHA as the active nutrient.

Paper no. L9578 in *Lipids 40,* 69–79 (January 2005).

Increasing evidence is emerging from animal experiments and human epidemiological and clinical studies that dietary n-3 long-chain (LC) PUFA from marine sources are beneficial for bowel function, aid gut repair (1–3), and ameliorate inflammatory conditions, but this is yet to be translated into clinical practice (4). Results from our previous animal studies showed that dietary fish oil (FO) supplementation led to modified contractility properties of isolated gut tissue (5,6). For the guinea pig, a diet containing 3% tuna FO, and high in

DHA (22:6n-3), led to a lower voltage threshold to initiate contraction and a lower sensitivity to the isoprostane 8-*iso*-prostaglandin (PG) E_2 in the ileum with increased n-3 PUFA content in the tissue total phospholipid fraction (5). In a subsequent study, Sprague-Dawley rats were fed 10% FO rich in EPA (20:5n-3) (EPA/DHA, 17:11) (6). In this strain of rat, dietary FO supplementation led to an increased maximal contraction in the ileum, elicited by muscarinic and eicosanoid agonists, that was not observed for the colon. However, both ileum and colon had similar increases in tissue n-3 PUFA EPA, docosapentaenoic acid (DPA, 22:5n-3), and DHA (6). This tissue-specific difference was explained by possible differences of n-3 PUFA modulation of receptor subtype populations that have been described for many systems (7,8) or the different functionality of the small intestine compared with large bowel (9).

Our most recent study demonstrated that there were no marked effects of a large range of dietary saturated fat (SF) on rat ileal contractility, unlike that demonstrated for n-3 PUFA (6). However, there was a trend for depressed PGE_2 and $PGF_{2\alpha}$ contractility responses in the ileum and colon of spontaneously hypertensive rats (SHR) that was not evident for isoprostane, muscarinic, or angiotensin receptor systems (10). This trend of depressed prostanoid activity became significant when the groups fed the three levels of dietary fat were combined (10). The aims of the present study were to confirm a depressed prostanoid response in SHR gut compared with Wistar-Kyoto (WKY) rats and, if confirmation was made, to determine whether feeding FO containing high DHA or canola oil rich in n-3 PUFA as α-linolenic acid (ALA) increased the muscarinic receptor-induced response and restored the depressed prostanoid response in gut from SHR. We also investigated the effects of two autocoid peptides, angiotensin II and bradykinin, which have potent activity in smooth muscle cells and which are involved in pathophysiological conditions such as inflammation and hypertension (11,12).

MATERIALS AND METHODS

Animals and diets. Male SHR and WKY rats were purchased from Animal Resource Centre (Canning Vale, Western Australia, Australia) at 12 wk of age and housed in the small animal colony of CSIRO Health Sciences and Nutrition (HSN). The rats were fed standard commercial laboratory rat chow

containing approximately 5% fat (Glen Forrest Stockfeeders, Glen Forrest, Western Australia, Australia) and water *ad libitum* for 1 wk to acclimatize. They were subjected to a 12-h light/dark cycle at 23°C. The rats were housed and the experiment conducted with the approval of the CSIRO HSN animal ethics committee.

At 13 wk of age, the rats were separated into one dietary group of 12 WKY rats and four groups of 16 SHR, housed 3–5 per cage and fed synthetic diets *ad libitum* for 12 wk. To avoid oxidation, diets were stored at −20°C and changed daily. The isoenergetic semipurified diets were based on the AIN-93M diet (13) and contained (g/kg): casein, 180; mineral mix, 35; vitamin mix, 10; α-cellulose, 50; cornstarch, 580.7; L-cysteine, 1.8; choline chloride, 2.5; and sucrose, 90. In addition, the control diet contained 5% (50 g/kg) coconut oil (CO) (Meadow Lea Coconut Oil; Goodman Fielder Pty. Ltd., North Ryde, Sydney, New South Wales, Australia) for a WKY group and SHR group or 5% fat as lard (SF) (Chapman's; George Weston Foods Ltd., Thebarton, South Australia, Australia), 5% canola oil (Can) (Meadow Lea GOLD'N Canola Oil; Goodman Fielder Pty. Ltd.), or 5% FO (HiDHA®; Clover Corporation Ltd., Altona North, Victoria, Australia) for the three other SHR groups. The FA compositions of the diets are shown in Table 1.

Diet FA content. The FA content of the 5% fat-supplemented diets had a wide range of SF levels, with the CO and lard (SF) diets containing 89.4 and 47% compared with the FO and Can diets, which contained 37.7 and 8%, respectively. CO diet SF are predominantly from 10:0 to 16:0, whereas the lard fat is 16:0 to 18:0. The Can diet contained predominantly the plant-derived monosaturated FA oleic acid (18:1n-9) at 62% and the shorter n-3 PUFA, ALA (18:3n-3) at 10.5%. This contrasts with the FO (HiDHA®) diet, which contains

the LC PUFA EPA and DHA at 6.5 and 22.5% of FA, respectively. The n-6/n-3 ratios of the CO, SF, Can, and FO diets were 16.7, 13.3, 1.9, and 0.2, respectively (Table 1).

Blood pressure (BP) measurements. The BP of a subset of WKY and SHR was measured every 4 wk using the tail cuff method (14) in a 29°C cabinet with restraining tubes (models 805 and 815; IITC Inc., Life Science Instruments, Woodland Hills, CA) using a model 229 blood pressure amplifier/pump and recorded using model 31 blood pressure software version 2.34 (IITC Inc.).

Tissue collection. At the completion of the 12-wk feeding experiment, the rats were fasted overnight, weighed, anesthetized with Nembutal (sodium pentobarbitone, 60 mg/kg intraperitoneal), and then killed by exsanguination. The small intestine and colon were removed and prepared for physiologic recordings as described (5,6,10). Tissue samples were snap-frozen in liquid nitrogen at −80°C for later tissue total phospholipid FA analysis.

Total phospholipid FA analysis of ileal and colonic tissue. Small frozen sections (150 mg) of ileum or colon were ground in a glass homogenizer, total lipids were extracted in methanol/chloroform/water (2:4:1) and separated by TLC, and the FA were methylated and analyzed by GLC as described previously (5,6).

Physiologic recording of ileal and colonic contractility. Sections of the ileum, proximal colon, or distal colon (0.03–0.04 m) were secured in an organ chamber with buffer conditions, organ chamber mechanics, and contraction properties determined as described (5,6,10). Ileal and colonic tissue were run in parallel. Results are given as volts per gram of (gut) tissue (V/g).

Electrically induced contraction of colon. The colon was induced to contract by electrical stimulation at 60 V for 5 ms at 0.02 Hz using a Grass S48 stimulator (Astro-Med Inc., West Norwich, RI) *via* 10-mm circular stainless steel electrodes placed above and below the tissue. Maximal colonic contractions were reached at approximately 20 min, after which time the stimulator was turned off.

Contraction of quiescent ileum and colon. The gastrointestinal agonists were added sequentially to the bath containing ileal or colonic tissue. Dose–response curves were generated by cumulative addition of agonists added as a small bolus to the incubating tissue. Each agent was washed out from the bath after maximal contraction had been achieved and the tissue stabilized at baseline for 15 min before the addition of the next agonist (5,6,10).

Preparation of gut membrane fraction. Frozen gut tissue was coarsely ground by pestle and mortar under liquid nitrogen and taken up into ice-cold isolating medium (1:10, wt/vol) containing (in mM) 250 sucrose, 50 Tris, 1 EDTA, 1 $MgCl_2$, pH 7.4. The tissue was homogenized in 10 mL of the above medium by UltraTurrax® (Janke&Kunkel GmbH, Staufen, Germany) at setting 4 for 3 bursts for 10 s (15). The brei was filtered through several layers of wide-weave cheesecloth and centrifuged at $6000 \times g$ for 15 min in a J2-21 centrifuge (Beckman Instruments Co., Palo Alto, CA) at 4°C.

TABLE 1
FA Composition of Experimental Diets[a]

FA	CO[b]	SF	Can	FO
		g/100 g FA		
10:0	5.4	0.2	ND	ND
12:0	51.2	0.3	0.1	ND
14:0	19.4	2.1	0.4	4.0
16:0	10.3	26.4	5.3	23.2
18:0	3.2	16.9	2.1	6.6
18:1n-9	7.3	38.4	58.8	18.7
18:2n-6	3.0	10.6	20.8	4.4
18:3n-3	0.2	0.8	10.5	0.6
20:5n-3	ND	ND	0.2	6.5
22:5n-3	ND	ND	ND	1.2
22:6n-3	ND	ND	ND	22.4
Σ Saturated	89.4	47.0	8.0	37.7
Σ Monounsaturated	7.4	41.5	60.5	24.6
Σ Polyunsaturated	3.2	11.6	31.5	37.7
Σ n-6	3.0	10.7	20.8	6.4
Σ n-3	0.2	0.8	10.7	31.4
n-6/n-3	16.7	13.3	1.9	0.2

[a]Values are means of two samples performed in duplicate. Percentages were derived from the full FA set.
[b]Abbreviations: CO, coconut oil diet; SF, saturated fat (lard) diet; Can, canola oil diet; FO, fish oil diet; ND, not detected.

The supernatant was decanted and retained and the pellet resuspended in isolating medium and recentrifuged as before. The supernatants were combined and spun at $50,000 \times g$ for 30 min. The final pellet was resuspended in (mmol/L) 50 Tris, 1 EGTA, 10 MgCl$_2$, pH 7.4 assay buffer that contained protease inhibitors diluted into this buffer at 1:1000 (vol/vol). The stock protease inhibitor concentrations were (mg/mL, solvent): phenylmethylsulfonyl fluoride 17.4, DMSO; aprotinin 1, H$_2$O; iodoacetate 184, H$_2$O; and pepstatin A 1.37, DMSO (16). The final tissue concentration was approximately 5 mg/mL, and the stock solution was stored in aliquots at −80°C for muscarinic binding assays.

Muscarinic receptor binding assay. Receptor radio-ligand binding activity was determined in the gut membrane fraction $(6,000–50,000 \times g)$ with the nonselective tritiated muscarinic antagonist, quinuclidinyl benzylate ([^{3}H]QNB) (16). For saturation binding assays, membranes (approximately 100 µg protein/tube) were incubated with shaking in assay buffer with increasing concentrations of [^{3}H]QNB (specific activity 1.6 TBq/mmol; NEN, Sydney Australia) (0.05–2 nmol/L) at 30°C for 1 h. Preliminary experiments performed in triplicate (not shown) established that [^{3}H]QNB binding to the gut membrane preparation was linear between 20 and 200 µg protein and that at 100 µg protein per assay, maximal binding occurred by 40 min. The reaction was stopped *via* rapid filtration through Whatman GF/C glass fiber filters. After washing with 3×4 mL ice-cold assay buffer, filters were placed into vials and counted in 3 mL water-soluble scintillation cocktail (Aquasol-2; NEN Research Products) at about 50% efficiency. Nonspecific binding was measured in the presence of 10^{-6} mol/L atropine and did not exceed 15% of total binding.

Protein determination. Values for the gut membrane protein content were determined after solubilization in 0.1 M NaOH and 1% (wt/vol) SDS using BSA as standard (17).

Pharmacologic agents and suppliers. The pharmacological agents (concentration range in nmol/L used in organ bath or assay) and suppliers were as follows: acetylcholine (10–22,000), atropine sulfate (0.1–1,000), bradykinin (0.1–1,000), carbamylcholine chloride (carbachol) (10–22,000), and fine chemicals were from Sigma Chemical (Sydney, NSW, Australia); and PGF$_{2\alpha}$ (1–7,000), PGE$_2$ (1–7,000), and 8-*iso*-PGE$_2$ (10–7,000) were from Sapphire Bioscience (Crows Nest, NSW, Australia). For the ileum, the order of agonists was acetylcholine, angiotensin II, 8-*iso*-PGE$_2$, PGF$_{2\alpha}$, and PGE$_2$. Because the colon does not tolerate multiple additions well, the order of agonists after electrical stimulation was as follows: proximal colon: acetylcholine, angiotensin II, 8-*iso*-PGE$_2$; distal colon: carbachol, PGF$_{2\alpha}$, and PGE$_2$.

Data analysis. Data are shown as means ± SEM. Statistical evaluation was performed by ANOVA, with a Bonferroni multiple comparison post-test performed when the *F*-test was significant at $P < 0.05$ or by Student's *t*-test. The EC$_{50}$ (nmol/L) and maximal contraction (V/g of tissue) values, and maximal binding (B_{max}) and 50% of maximal binding (K_d) were determined from concentration-dose curves and satura-

tion binding isotherms using graph fits in GraphPad Prism 4.0 (GraphPad Software, San Diego, CA) with $R^2 > 0.99$.

RESULTS

Animal weights. The initial (13 wk) and final (25 wk) weights (g) of the experimental animal groups as mean ± SEM (*n*) were as follows: WKY CO, 276 ± 6, 414 ± 8 (12); SHR CO, 290 ± 5, 427 ± 8 (16); SHR SF, 294 ± 4, 419 ± 4 (16); SHR Can, 307 ± 5, 417 ± 4 (16); and SHR FO, 308 ± 4, 428 ± 6 (16). There was no significant difference between weights for WKY or SHR CO groups or between final or Δ (final minus initial) weights between SHR dietary groups.

Blood pressure. The initial (13 wk) and final (25 wk) systolic BP measurements (mm Hg) as mean ± SEM for $n = 6$–8 rats were as follows: WKY CO, 147 ± 3, 146 ± 5; SHR CO, 175 ± 4, 184 ± 4; SHR SF, 180 ±5, 187 ± 4; SHR Can, 174 ± 5, 195 ± 3; and SHR FO, 168 ± 5, 191 ± 4. The initial ($P < 0.05$) and final BP ($P < 0.001$) of the WKY group was significantly different from all SHR groups. There was no significant difference in BP between SHR dietary groups.

FA content of total phospholipids of ileum and colon. There were no major differences in the FA composition of ileum or colon in WKY and SHR groups fed CO diets with n-6/n-3 ratios of ileum 11.5 and 11.4 and colon 11.5 and 10.6, respectively. The shorter-chain saturated fats in the CO diet (10:0–14:0) were not incorporated into ileal or colonic tissue. The FA profiles of ileal and colonic tissue in the SHR fed CO or SF were similar. The major differences observed for the Can diet from the two saturated fat diets (CO and SF) were an increase in the n-3 content as DHA ($P < 0.05$), with a modest drop in the n-6/n-3 ratio in ileum to 7.9 and colon to 8.2. However, the FO diet dramatically increased the DHA content in both tissue types ($P < 0.001$) with resultant n-6/n-3 ratios of 2.3 and 1.7 ($P < 0.001$) at the expense of arachidonic acid (20:4n-6) and the total n-6 content ($P < 0.01$). With the FO diet (high in DHA), there was no detectable tissue phospholipid ALA or EPA (Tables 2, 3).

Electrically induced contraction of colon. There was no difference in electrically induced maximal contraction (V/g tissue) between WKY and SHR CO groups for the proximal or distal colon. For the SHR groups across the diets, there was an increase in the maximal contraction of the proximal colon in the FO group compared with the SF group ($P < 0.01$) that was not evident for the distal colon (Table 4).

Gastrointestinal agonist-induced contraction of ileum and colon from WKY and SHR fed the CO diet. The comparison of dose–response curves of WKY and SHR fed CO diets for agonist-induced contraction by PGF$_{2\alpha}$ and PGE$_2$ for ileum and colon is shown in Figure 1 with the calculated EC$_{50}$ (nmol/L) and maximal contraction (V/g tissue) values for all agonists shown in Table 5 for ileum and Table 6 for colon. For ileum, PGF$_{2\alpha}$ (Fig. 1A) produced a lower maximal contraction ($P < 0.003$) for SHR compared with WKY, and for PGE$_2$ (Fig. 1C) there was a lower maximal contraction ($P < 0.01$) and

TABLE 2
FA Levels of Total Phospholipid Fraction of Ileum from WKY and SHR Fed 5 g/100 g Fat-Supplemented Diets for 12 wk[a]

| FA | WKY | SHR | | | |
	CO	CO	SF	Can	FO
			g/100 g FA		
14:0	0.9 ± 0.3	0.8 ± 0.1[a]	0.2 ± 0.1[b]	0.1 ± 0.1[b]	ND
16:0	22.5 ± 0.4	24.6 ± 0.3	23.3 ± 0.5[a]	25.5 ± 0.9	26.4 ± 0.3[b]
18:0	20.0 ± 0.5	20.5 ± 0.1	22.4 ± 0.3	20.9 ± 0.8	20.3 ± 0.6
24:0	4.6 ± 0.2	6.0 ± 0.2[a]	5.9 ± 0.6[a,c]	3.4 ± 1.2	1.6 ± 0.3[b]
18:1n-9	17.8 ± 0.3	14.4 ± 0.2	13.1 ± 2.2	14.2 ± 1.2	13.1 ± 0.2
18:2n-6	5.8 ± 0.7	3.9 ± 0.2[a]	4.0 ± 0.1[a]	6.5 ± 0.6[b]	5.7 ± 0.2[b]
20:4n-6	21.0 ± 0.4	22.8 ± 0.4[a]	25.1 ± 0.8[a]	22.4 ± 1.3[a]	18.3 ± 0.2[b]
20:5n-3	ND	ND	ND	0.2 ± 0.1	ND
22:6n-3	1.5 ± 0.0	1.5 ± 0.0[a]	1.7 ± 0.2[a]	2.6 ± 0.1[b]	9.7 ± 0.2[c]
Σ Saturated	48.8 ± 0.7	52.8 ± 0.3	52.8 ± 0.7	50.9 ± 1.0	50.3 ± 1.4
Σ Monounsaturated	19.5 ± 0.4	16.2 ± 0.4	14.1 ± 0.6	15.1 ± 0.8	15.0 ± 0.7
Σ Polyunsaturated	30.7 ± 1.0	30.3 ± 0.2	32.8 ± 0.7	33.6 ± 1.7	34.2 ± 0.2
Σ n-6	28.2 ± 0.8	27.9 ± 0.2[a]	30.1 ± 0.6[a]	29.8 ± 1.5[a]	24.0 ± 0.2[b]
Σ n-3	2.5 ± 0.1	2.4 ± 0.0[a]	2.8 ± 0.2[a]	3.8 ± 0.1[b]	10.3 ± 0.2[c]
n-6/n-3	11.5 ± 0.1	11.4 ± 0.1[a]	11.1 ± 1.0[a]	7.9 ± 0.6[b]	2.3 ± 0.04[c]

[a]Values are means ± SEM for *n* = 4, derived from the full FA set. Means for a spontaneously hypertensive rat (SHR) tissue in a row with superscripts without a common letter differ; *P* < 0.05. WKY, Wistar-Kyoto rats; for other abbreviations see Table 1.

TABLE 3
FA Levels of Total Phospholipid Fraction of Colon from WKY and SHR Fed 5 g/100 g Fat-Supplemented Diets for 12 wk[a]

| FA | WKY | SHR | | | |
	CO	CO	SF	Can	FO
			g/100 g FA		
14:0	1.6 ± 0.1	1.0 ± 0.3	0.1 ± 0.1	0.3 ± 0.2	0.3 ± 0.2
16:0	31.2 ± 0.4	30.9 ± 0.5	30.3 ± 0.2	32.6 ± 0.7	31.2 ± 0.4
18:0	21.5 ± 0.4	19.9 ± 0.6	22.4 ± 0.2	21.4 ± 0.5	20.6 ± 0.4
24:0	1.3 ± 0.1	2.5 ± 1.1	1.1 ± 0.1	ND	1.6 ± 0.3
18:1n-9	16.2 ± 0.6	15.8 ± 0.2[a]	17.0 ± 0.3[b]	17.4 ± 0.3[b]	14.1 ± 0.2[c]
18:2n-6	2.9 ± 0.1	2.4 ± 0.1[a]	3.1 ± 0.2[a,c]	4.2 ± 0.2[b]	3.8 ± 0.2[b,c]
20:4n-6	21.3 ± 0.4	21.2 ± 0.5[a]	21.6 ± 0.5[a]	19.8 ± 0.5[a]	13.9 ± 0.4[b]
20:5n-3 (EPA)	ND	ND	ND	ND	ND
22:6n-3 (DHA)	1.9 ± 0.1	1.8 ± 0.1[a]	2.1 ± 0.1[a]	2.9 ± 0.1[b]	9.9 ± 0.2[c]
Σ Saturated	55.7 ± 0.4	55.4 ± 0.3	54.9 ± 0.2	54.6 ± 0.6	54.8 ± 0.6
Σ Monounsaturated	18.1 ± 0.7	17.3 ± 0.4[a]	18.1 ± 0.3[a]	18.1 ± 0.2[a]	15.5 ± 0.3[b]
Σ Polyunsaturated	26.1 ± 0.3	25.9 ± 0.6	26.8 ± 0.5	26.9 ± 0.6	27.9 ± 0.4
Σ n-6	24.2 ± 0.3	23.7 ± 0.5[a]	24.7 ± 0.4[a]	24.0 ± 0.5[a]	17.7 ± 0.4[b]
Σ n-3	2.1 ± 0.1	2.3 ± 0.2[a]	2.1 ± 0.1[a]	2.9 ± 0.1[b]	10.2 ± 0.1[c]
n-6/n-3	11.5 ± 0.5	10.6 ± 0.7[a]	12.0 ± 0.2[a]	8.2 ± 0.2[b]	1.7 ± 0.02[c]

[a]Values are mean ± SEM for *n* = 4. Percentages were derived from the full FA set. Means for an SHR tissue in a row with superscripts without a common letter differ; *P* < 0.05. For abbreviations see Tables 1 and 2.

TABLE 4
Effect of Electrically Driven Contraction on Colon from WKY and SHR Fed 5% Fat-Supplemented Diets for 12 wk[a]

| Tissue/Diet | WKY | SHR | | | |
	CO	CO	SF	Can	FO
			V/g		
Proximal colon	2.2 ± 0.2	2.3 ± 0.2	1.7 ± 0.2[a]	2.1 ± 0.2	2.9 ± 0.3[b]
Distal colon	2.1 ± 0.2	2.1 ± 0.2	2.1 ± 0.2	1.7 ± 0.2	2.1 ± 0.2

[a]Values are mean ± SEM for *n* = 12 for WKY and *n* = 16 for SHR. Means for an SHR tissue in a row with superscripts without a common letter differ; *P* < 0.01. For abbreviations see Tables 1 and 2.
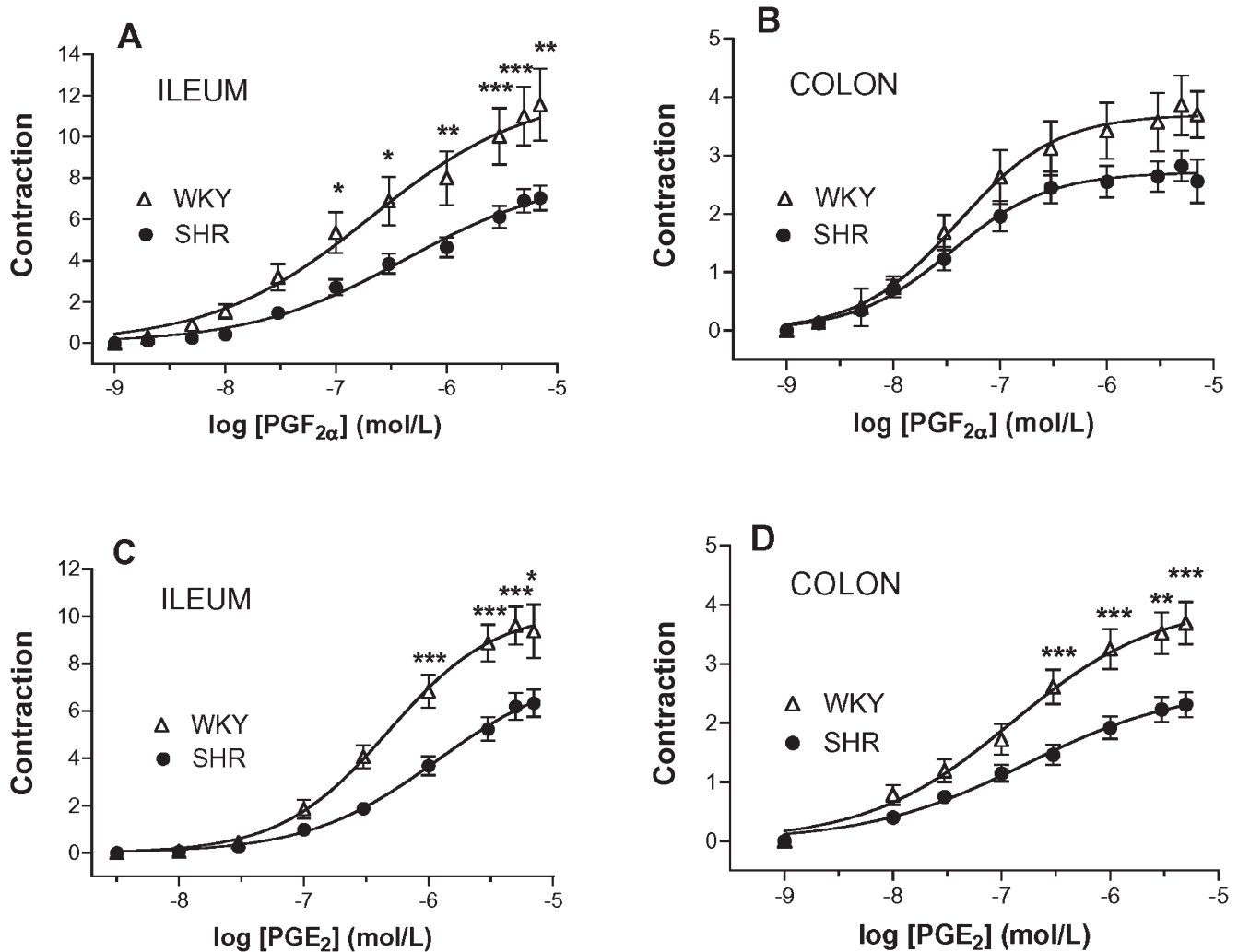
FIG. 1. Effects of prostaglandin $F_{2\alpha}$ ($PGF_{2\alpha}$) on the contraction of ileum (A) and colon (B) and PGE_2 on contraction of ileum (C) and colon (D) from Wistar Kyoto rats (WKY) ($\triangle$) and spontaneously hypertensive rats (SHR) ($\bullet$) fed a 5 g/100 g coconut oil (CO)-supplemented diet. The results are plotted as means ± SEM generated from pooled data for contractions from $n = 12$ WKY and $n = 16$ SHR individual pieces of ileum determined as voltage per gram of tissue (V/g). Significant differences for individual concentrations determined by Student's t-test with significance indicated as follows: $*P < 0.05$, $**P < 0.01$, $***P < 0.001$. The calculated EC_{50} (nmol/L) and maximal contraction (V/g tissue) values for $PGF_{2\alpha}$ and PGE_2 are shown in Table 5 for ileum and Table 6 for colon.

lower sensitivity ($P < 0.002$) for SHR compared with WKY. For the colon, the agonists $PGF_{2\alpha}$ (Fig. 1B) and PGE_2 (Fig. 1D) produced a lower maximal contraction of SHR compared with WKY ($P < 0.02$ and $P < 0.05$, respectively).

Gastrointestinal agonist-induced contraction of ileum and colon from SHR fed the CO, SF, Can, and FO diets. Comparison of the effects of experimental diets on SHR ileal and colonic tissue agonist-induced contraction is shown in Figures 2 and 3. The EC_{50} (nmol/L) and maximal contraction (V/g) values for ileal and colonic tissue are given in Tables 5 and 6, respectively. For ileum, acetylcholine (Fig. 2A), $PGF_{2\alpha}$ (Fig. 2E), and PGE_2 (Fig. 2F) produced higher maximal contraction in the FO group than in the other three dietary groups ($P < 0.01$). The FO group also had higher maximal contraction responses to angiotensin II compared with the SF group

($P < 0.05$) (Fig. 2B) and a higher maximal contraction response to bradykinin compared with the Can group ($P < 0.05$) (Fig. 2C) in ileum. Although there was a trend for increased contraction for 8-*iso*-PGE_2 by FO compared with the other dietary groups, it did not reach significance. For colon, in response to acetylcholine the FO group had higher maximal contraction compared with the SF group ($P < 0.001$) (Fig. 3A) and a higher sensitivity compared with the Can group ($P < 0.01$). The FO group also had a higher maximal contraction response to 8-*iso*-PGE_2 compared with SF ($P < 0.05$) (Fig. 3C) and Can ($P < 0.05$) groups and a higher sensitivity in response to carbachol compared with the SF group ($P < 0.05$) (Fig. 3D). There were no significant differences across the dietary groups for colon in response to angiotensin II, $PGF_{2\alpha}$, or PGE_2.

TABLE 5

EC$_{50}$ (nmol/L) and Maximal Contraction (V/g) Values Derived from Concentration–Response Curves for Agonists Applied to Ileum from WKY and SHR Fed 5 g/100 g Fat-Supplemented Diets for 12 wk[a]

Agonist		WKY CO	SHR CO	SHR SF	SHR Can	SHR FO
Acetylcholine	EC$_{50}$	1896 ± 269	2060 ± 296	1732 ± 463	2575 ± 638	1677 ± 246
	V/g	11.3 ± 1.8	9.2 ± 1.0[a]	7.5 ± 0.9[a]	8.8 ± 1.1[a]	14.2 ± 1.2[b]
Angiotensin II	EC$_{50}$	18.6 ± 9.7	7.4 ± 2.8	14.9 ± 6.0	4.5 ± 2.5	7.3 ± 3.8
	V/g	9.3 ± 1.0	9.4 ± 1.3	6.3 ± 1.1[a]	10.0 ± 1.4	11.3 ± 0.9[b]
Bradykinin	EC$_{50}$	25.9 ± 11.1	8.3 ± 1.9	19.7 ± 7.0	12.4 ± 4.5	11.4 ± 3.9
	V/g	10.1 ± 1.2	8.0 ± 1.0	8.2 ± 0.9	5.9 ± 0.8[a]	9.9 ± 1.0[b]
8-*iso*-PGE$_2$	EC$_{50}$	369 ± 59	477 ± 57	483 ± 51	455 ± 54	294 ± 33
	V/g	10.9 ± 0.6	10.3 ± 0.8	9.8 ± 0.7	9.9 ± 0.8	11.0 ± 0.8
PGF$_{2\alpha}$	EC$_{50}$	526 ± 126	568 ± 124	1079 ± 259	480 ± 138	585 ± 171
	V/g	13.0 ± 1.4	8.3 ± 0.6[a]	8.6 ± 0.7[a]	8.7 ± 0.7[a]	12.6 ± 0.8[b]
PGE$_2$	EC$_{50}$	560 ± 73	1366 ± 181	1511 ± 241	1085 ± 200	674 ± 117
	V/g	10.4 ± 0.9	7.2 ± 0.7[a]	7.4 ± 0.8[a]	8.1 ± 0.7[a]	12.5 ± 0.7[b]

[a]Values are mean ± SEM for $n = 16$ for acetylcholine, 8-*iso*-PGE$_2$, PGF$_{2\alpha}$, and PGE$_2$, and $n = 8$ for angiotensin II and bradykinin. Means for an SHR tissue in a row with superscripts without a common letter differ; $P < 0.05$. PG, prostaglandin; for other abbreviations see Tables 1 and 2.

TABLE 6

EC$_{50}$ (nmol/L) and Maximal Contraction (V/g) Values Derived from Concentration–Response Curves for Agonists Applied to Colon from WKY and SHR Fed 5 g/100 g Fat-Supplemented Diets for 12 wk[a]

| Agonist		WKY CO	SHR CO	SHR SF	SHR Can	SHR FO
Acetylcholine	EC$_{50}$	891 ± 154	1514 ± 208	1481 ± 310	2130 ± 354[a]	676 ± 156[b]
	V/g	5.7 ± 0.4	6.1 ± 0.4	4.8 ± 0.3[a]	6.0 ± 0.3	6.7 ± 0.3[b]
Angiotensin II	EC$_{50}$	0.3 ± 0.1	0.8 ± 0.3	1.8 ± 0.9	0.5 ± 0.2	1.5 ± 1.0
	V/g	5.7 ± 0.4	6.0 ± 0.4	4.2 ± 0.6	5.4 ± 0.2	6.3 ± 0.9
8-*iso*-PGE$_2$	EC$_{50}$	103 ± 17	174 ± 54	159 ± 39	136 ± 46	159 ± 50
	V/g	3.2 ± 0.3	3.9 ± 0.3	3.1 ± 0.3[a]	3.1 ± 0.2[a]	4.3 ± 0.3[b]
Carbachol	EC$_{50}$	815 ± 121	835 ± 81	1062 ± 91[a]	943 ± 120	664 ± 47[b]
	V/g	7.2 ± 0.6	6.4 ± 0.2	6.5 ± 0.3	6.6 ± 0.4	7.1 ± 0.4
PGF$_{2\alpha}$	EC$_{50}$	51 ± 8	66 ± 19	68 ± 16	88 ± 21	81 ± 17
	V/g	3.9 ± 0.5	2.8 ± 0.2	2.7 ± 0.2	2.5 ± 0.3	2.8 ± 0.2
PGE$_2$	EC$_{50}$	194 ± 54	307 ± 95	327 ± 67	426 ± 99	327 ± 67
	V/g	3.8 ± 0.4	2.5 ± 0.3	2.7 ± 0.3	2.7 ± 0.4	2.7 ± 0.3

[a]Values are mean ± SEM for $n = 16$ for acetylcholine, 8-*iso*-PGE$_2$, carbachol, PGF$_{2\alpha}$, and PGE$_2$, and $n = 8$ for angiotensin II. Means for a SHR tissue in a row with superscripts without a common letter differ; $P < 0.05$. Carbachol, carbamylcholine chloride; for other abbreviations see Tables 1, 2, and 5.

Muscarinic binding in ileal membrane preparations. The K_d (nmol/L) calculated for individual saturation binding isotherms for SF was $0.21 ± 0.01$ and for FO was $0.20 ± 0.003$ with maximal binding (B_{max}) (fmol/mg membrane protein) for SF of $540 ± 42$ and for FO of $457 ± 24$, which were not significantly different (Fig. 4). By comparison, the maximal contraction (V/g) for ileal tissue from the same SHR subset fed SF in response to acetylcholine was $6.4 ± 1.8$ compared with FO of $14.3 ± 2.1$ ($n = 5$) ($P < 0.02$) [see Fig. 2A and Table 5 for comparison of calculated EC$_{50}$ and maximal contraction (V/g) values compared across diets].

DISCUSSION

We have previously shown that dietary FO rich in EPA and DHA can increase the muscarinic- and eicosanoid-induced ileal responses in the normotensive Sprague-Dawley rat (6). This study investigated whether the recently observed depres-

sion in prostanoid-induced contraction in gut tissue of SHR (10) could be restored by n-3 PUFA from plant or fish sources. To test this, we fed 13-wk-old SHR diets supplemented with 5% as canola oil rich in ALA (18:3n-3) or as a fish oil fraction high in DHA (22:6n-3) with SF and CO as controls. In this study, there were no significant lowering effects on BP by n-3 PUFA feeding. Using animal models, a blood pressure lowering has previously been noted using both EPA and DHA mixtures, DHA alone, and Can (18–20). In those studies and other reports, the n-3 PUFA was delivered at the development stage of hypertension (3–7 wk) compared with 13 wk, the established stage of hypertension in this study (21). Dietary supplementation with LC n-3 PUFA diets delivered at 3 mon or later also have been found to lower SHR blood pressure when fed for a long term of 12–18 mon (22). In this study, the modulation of gut smooth muscle contractility by n-3 PUFA is discussed in relation to hypertension and other potentially related pathological conditions.
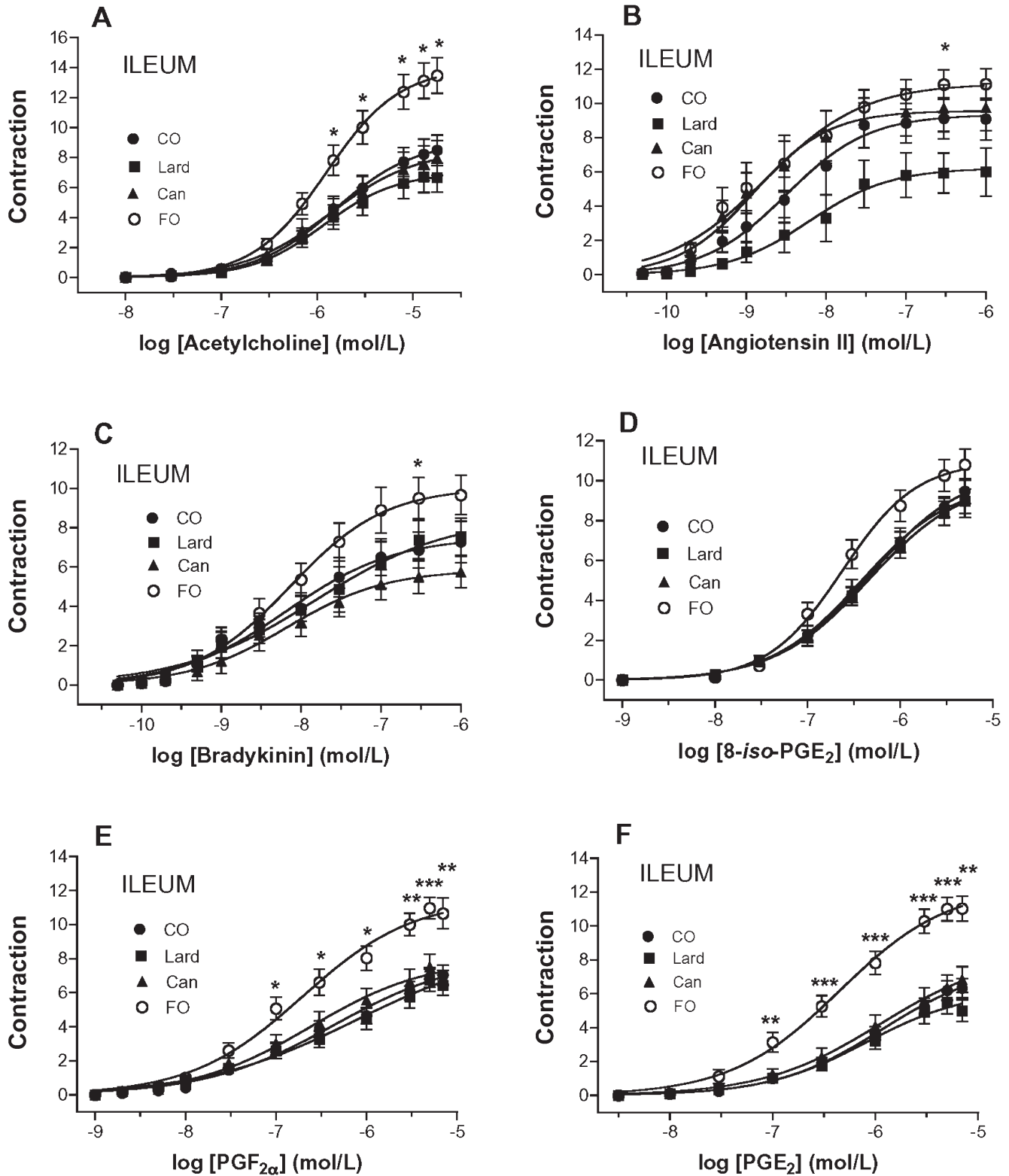
FIG. 2. Effects of acetylcholine (A), angiotensin II (B), bradykinin (C), 8-*iso*-PGE$_2$ (D), PGF$_{2\alpha}$ (E), and PGE$_2$ (F) on the contraction of ileum from SHR fed diets supplemented with 5 g/100 g coconut oil (CO) (●), lard (■), canola oil (Can) (▲), or fish oil (FO) (○). The results are plotted as means ± SEM generated from pooled data for contractions from *n* = 16 individual pieces of ileum determined as voltage per gram of tissue (V/g). Significant differences for individual concentrations determined by ANOVA with the Bonferroni post test indicated as follows: *$P < 0.05$, **$P < 0.01$, ***$P < 0.001$. Table 5 shows comparisons of the calculated EC$_{50}$ and maximal contraction (V/g) values for ileum for all agonists. For other abbreviations see Figure 1.
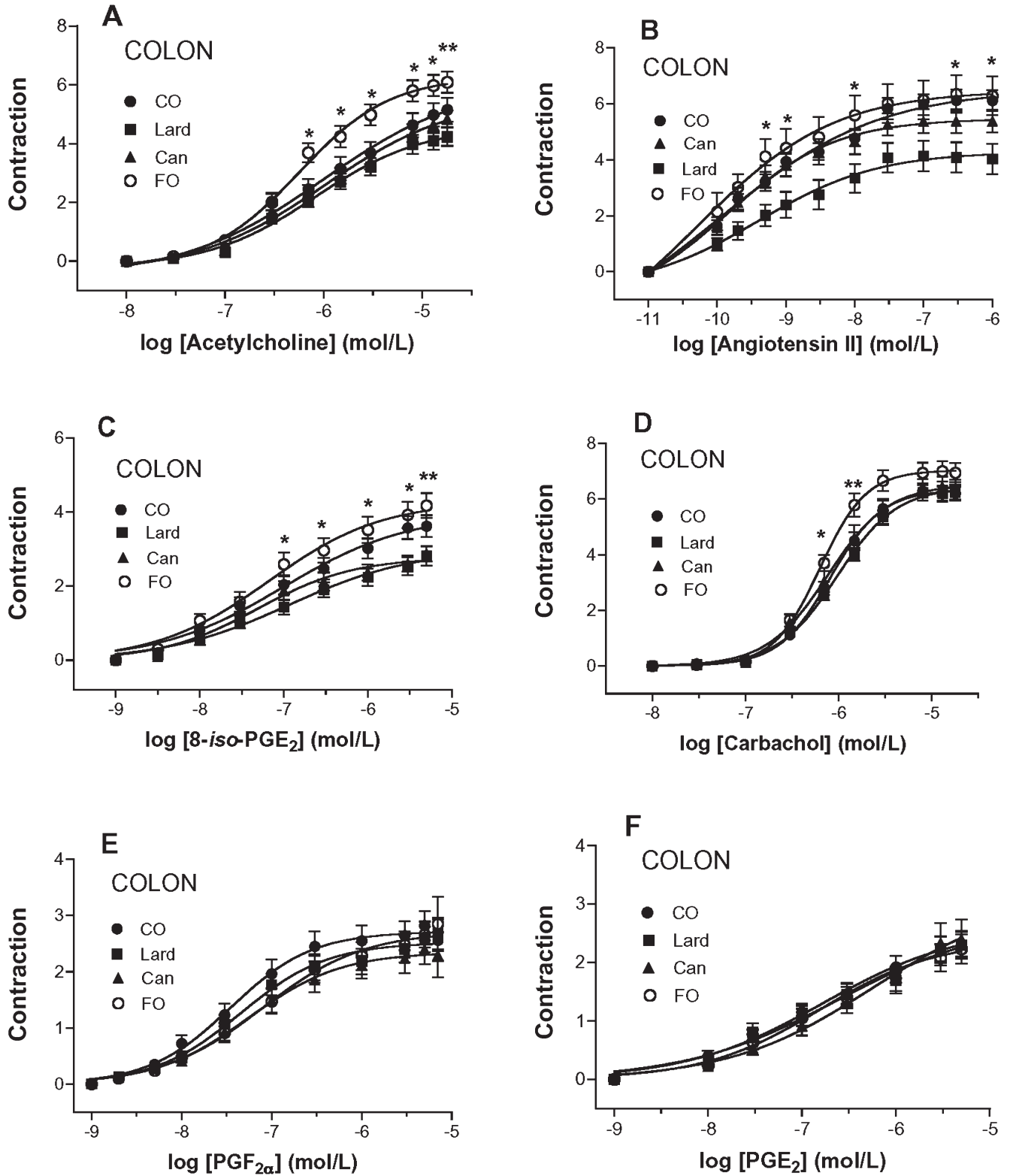
FIG. 3. Effects of acetylcholine (A), angiotensin II (B), 8-*iso*-PGE$_2$ (C) on proximal colon, and carbachol (D), PGF$_{2\alpha}$ (E), and PGE$_2$ (F) on distal colon contraction from SHR fed diets supplemented with 5 g/100 g coconut oil (CO) (●), lard (■), canola oil (Can) (▲), or fish oil (FO) (○). The results are plotted as means ± SEM generated from pooled data for contractions from n =16 SHR individual pieces of colon determined as voltage per gram of tissue (V/g). Significant differences for individual concentrations determined by Student's *t*-test with significance indicated as follows: *$P < 0.05$, **$P < 0.01$. Table 6 shows comparisons of the calculated EC$_{50}$ (nmol/L) and maximal contraction (V/g tissue) values for colon for all agonists.
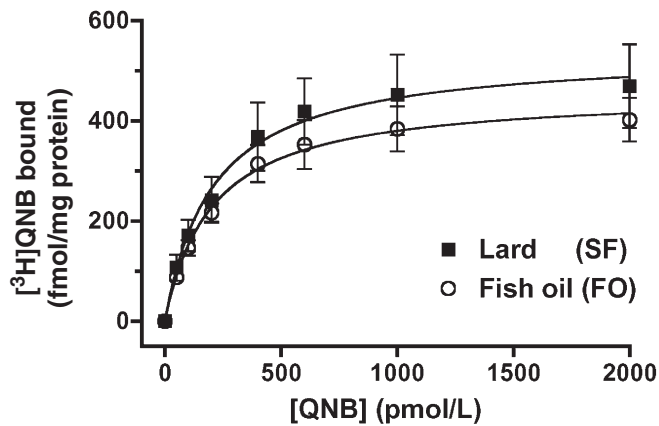
FIG. 4. Saturation binding isotherms for the tritiated muscarinic antagonist quinuclidynyl benzylate ([^{3}H]QNB) from the pooled data from ileal tissues from $n = 5$ SHR fed diets supplemented with 5 g/100 g fat as lard (SF) (■) or fish oil (FO) (○). Results are plotted at each concentration as mean ± SEM. Figure 2A shows acetylcholine dose curves for ileum from groups fed diets supplemented with 5 g/100 kg fat as coconut oil, lard, canola oil, or fish oil, and Table 5 shows comparisons of calculated EC_{50} and maximal contraction (V/g) values for ileum for acetylcholine and other agonists. There were no significant differences for K_d (concentration at half-maximal binding) or B_{max} (maximal binding) values for SHR ileum across SF or FO dietary groups. For other abbreviations see Figure 1.

First, it was established that SHR fed a diet of SF as CO exhibited a significantly depressed PGE_2 and $PGF_{2\alpha}$ response in ileum and colon compared with the WKY control group. This depressed response was not observed for muscarinic, isoprostane, or autocoid peptide agonists angiotensin II or bradykinin. We report here that the FO diet, with high DHA as the most likely active nutrient, restored the depressed prostanoid effect in ileal but not colonic tissue. This effect was not observed for the Can-supplemented diet rich in ALA that produced only a marginal increase in EPA and DHA in ileum and only DHA in colon. It is to be determined whether FO feeding alters the PG receptor properties of ileal and colonic tissue in a manner that may explain the differences in tissue reactivity. Functionally, the large intestine is primarily for drying and storage of digestive waste material, whereas the contractile properties influenced by n-3 PUFA in the ileum may not be translated to the distal bowel (6).

Using SHR, we have also confirmed that FO feeding resulted in higher maximal contraction responses to muscarinic and prostanoid agonists in the ileum that we previously demonstrated in normotensive Sprague-Dawley rats (6). We also investigated the effects of potent gastrointestinal peptide agonists. The first, angiotensin II, plays a key role in the renin–angiotensin system (23), especially as it relates to hypertension and the development of disease (24,25). The second, bradykinin, is a potent autocoid that can act on endogenous smooth muscle cells (11,12) and is also involved with gut pathophysiological conditions (18,24) and co-involved with the renin–angiotensin system (23). Both peptides lead to increased maximal contraction of ileum after FO dietary supplementation compared with SF or Can.

Electrically driven contraction of colon is predominantly induced by acetylcholine release (25), and we found a significant increase in maximal contraction in the proximal colon by FO feeding compared with the SF diet. This observation was supported by a significantly higher acetylcholine-induced contraction of proximal colon by the FO diet compared with the SF diet, but not by the muscarinic mimetic, carbachol, in the distal colon, although there was an increase in sensitivity. This observation was not seen for normotensive Sprague-Dawley rats in our previous study (6). However, we note that FO supplementation did not increase contractility due to angiotensin II or again to prostanoids in colon.

Dietary FO can affect membrane receptor properties of various systems in different tissues, such as the α- and β-adrenergic (7,26), angiotensin II (27), various eicosanoids (thromboxane A_2/PGH_2) (28), as well as insulin (29) and other G-protein-coupled systems (8). In an attempt to determine the mechanism of n-3 PUFA effects on gut contractility, we measured muscarinic binding properties of ileal membrane preparations to determine whether FO supplementation modified ileal receptor characteristics. Although FO feeding markedly increased ileal maximal contraction compared with an SF diet in response to acetylcholine, there was no change in the muscarinic receptor population. There may have been a change in muscarinic subtype (30), which we are now investigating. However, it may be that the n-3 PUFA modification is post receptor and the involvement of calcium handling is to be determined (21,31).

In previous FO feeding studies, guinea pigs received diets with 4.2% ALA, 1.5% EPA, and 5% DHA as fat that resulted in 2.1% ALA, 0.8% EPA, and 3.6% DHA as FA in the ileal phospholipid fraction from very low levels. This led to alterations in voltage- and isoprostane-induced sensitivity changes in ileal contractility measurements (5). The recent rat study involved feeding FO containing 1% ALA, 11% EPA, and 7% DHA as fat that resulted in 0% ALA, 9% EPA, and 7% DHA as rat ileal membrane FA (6). That n-3 PUFA ratio correlated with increased ileal muscarinic- and eicosanoid-induced contractility properties. The study described herein used a high-DHA FO source in the diet containing 1% ALA, 6.5% EPA, and 22% DHA as fat that resulted in 0% ALA, 0% EPA, and 10% DHA in ileal membrane FA. It is therefore postulated that DHA is the active nutrient involved in the physiological alterations to agonist-induced gut contractility. Can rich in ALA resulted in only a modest increase in tissue DHA levels with no effect on contractility. Incorporation of Can is animal- and tissue-type dependent and relies on the ability of the tissue to elongate and desaturate ALA to longer n-3 PUFA. However, it is also to be determined whether diets with very high ALA levels or diets rich in only EPA that markedly increased tissue n-3 PUFA levels manifest increased gut contractility.

There are advantages and disadvantages of various experimental models of bowel disease (32). Although patients with inflammatory bowel disease (IBD) rarely have hypertension (33), and Crohn's disease may be negatively correlated with BP (34), it may be suggested that the SHR model with depressed

prostanoid-induced contractility responses may mimic a moderate case of IBD. Models of chemically induced ileitis have revealed a hyporesponsiveness in receptor-mediated strength of contraction of circular muscle due to carbachol and histamine (35) and modulation of purinergic nerve activity (36). Additionally, intestinal inflammation induced by *Trichinella spiralis* infection led to functional and structural changes, characterized by a decreased response to electrical field stimulation (37). Finally, and in relation to this study, tissue concentration of prostanoids was markedly elevated and their receptor population altered in the tissue of animals and humans with intestinal inflammation (38).

Models of IBD including ileitis and ulcerative colitis (UC) have both tissue damage and altered contractility properties. Administration of human recombinant interleukin-11 in a trinitrobenzenesulfonic acid colitis rabbit model partially normalized changes in contractile properties toward receptor-specific (motilin, acetylcholine, substance P) and receptor-independent (KCl) stimuli (39) and also suppressed intestinal inflammation and reversed intestinal smooth muscle dysfunction (carbachol, KCl) in HLA-B27 transgenic rats (40). Chemical-induced colitis in rats (dextran sulfate sodium) and mice (dinitrobenzene sulfonic acid) has been improved by butyrate enema and dietary curcumin (component of the spice turmeric) proposed to be in part *via* the transcription factor, nuclear factor kappa B that is involved in the production of inflammatory chemokines (41).

Recent studies report that dietary FO results in suppressed production of proinflammatory cytokines (42). Trinitrobenzenesulfonic acid-treated rats with UC fed FO for 1 wk showed significantly less macroscopic and microscopic damage and lower biochemical and histochemical markers of tissue damage (alkaline phosphatase, myeloperoxidase, and PGE_2) (43). Results of human trials suggest that dietary FO supplementation may improve Crohn's disease (4). It is now reasonable to assume that n-3 PUFA may have a major role to play in IBD not only by reducing symptoms of tissue pathology but also by improving contractility and functionality. Small-animal IBD models may soon demonstrate this important duality of n-3 PUFA function. Transgenic technology has recently produced a mouse that can convert n-6 to n-3 FA and that has the potential to be genetically backcrossed with mouse disease models such as IBD to test the effects of n-3 PUFA on the pathogenesis and treatment of disease (44) and complement dietary studies without the use of pharmaceuticals (45).

REFERENCES

1. Lopez-Pedrosa, J.M., Ramirez, M., Torres, M.I., and Gil, A. (1999) Dietary Phospholipids Rich in Long-Chain Polyunsaturated Fatty Acids Improve the Repair of Small Intestine in Previously Malnourished Piglets, *J. Nutr. 129*, 1149–1155.
2. Mooney, M.A., Vaughn, D.M., Reinhart, G.A., Powers, R.D., Wright, J.C., Hoffman, C.E., Swaim, S.F., and Baker, H.J. (1998) Evaluation of the Effects of Omega-3 Fatty Acid-Containing Diets on the Inflammatory Stage of Wound Healing in Dogs, *Am. J. Vet. Res. 59*, 859–863.
3. Ruthig, D.J., and Meckling-Gill, A. (1999) Both (n-3) and (n-6) Fatty Acids Stimulate Wound Healing in the Rat Epithelial Cell Line, IEC-6, *J. Nutr. 129*, 1791–1798.
4. Campos, F.G., Waitzberg, D.L., Teixeira, M.G., Mucerino, D.R., Kiss, D.R., and Habr-Gama, A. (2003) Pharmacological Nutrition in Inflammatory Bowel Disease, *Nutr. Hosp. 18*, 57–64.
5. Patten, G.S., Bird, A.R., Topping, D.L., and Abeywardena, M.Y. (2002) Dietary Fish Oil Alters the Sensitivity of Guinea Pig Ileum to Electrically Driven Contractions and 8-*iso*-PGE$_2$, *Nutr. Res. 22*, 1413–1426.
6. Patten, G.S., Abeywardena, M.Y., McMurchie, E.J., and Jahangiri, A. (2002) Dietary Fish Oil Increases Acetylcholine- and Eicosanoid-Induced Contractility of Isolated Ileum, *J. Nutr. 132*, 2506–2513.
7. Reithmann, C., Scheininger, C., Bulgan, T., and Werdan, K. (1996) Exposure of the n-3 Polyunsaturated Fatty Acid Docosahexaenoic Acid Impairs α 1-Adrenoceptor-Mediated Contractile Responses and Inositol Phosphate Formation in Rat Cardiomyocytes, *Naunyn. Schmiedebergs Arch. Pharmacol. 354*, 109–119.
8. Mitchell, D.C., Niu, S.L., and Litman, B.J. (2003) DHA-Rich Phospholipids Optimize G-Protein-Coupled Signalling, *J. Pediatr. 143*, S80–S86.
9. Glebov, O.K., Rodriguez, L.M., Nakahara, K., Jenkins, J., Cliatt, J., Humby, C.J., DeNobile, J., Soballe, P., Simon, R., Wright, G., *et al.* (2003) Distinguishing Right from Left Colon by the Pattern of Gene Expression, *Cancer Epidemiol. Biomarkers Prev. 12*, 755–762.
10. Patten, G.S., Adams, M.J., Dallimore, J.A., and Abeywardena, M.Y. (2004) Depressed Prostanoid-Induced Contractility of Gut in Spontaneously Hypertensive Rat (SHR) Is Not Affected by Level of Dietary Fat, *J. Nutr. 134,* 2924–2929.
11. Hu, H.Z., Gao, N., Liu, S., Ren, J., Wang, X., Xia, Y., and Wood, J.D. (2004) Action of Bradykinin in the Submucosal Plexus of Guinea-Pig Intestine, *J. Pharmacol. Exp. Ther. 309*, 310–319.
12. Souza, D.G., Lomez, E.S., Pinho, V., Pesquero, J.B., Bader, M., Pesquero, J.L., and Teixeira, M.M. (2004) Role of Bradykinin B$_2$ and B$_1$ Receptors in the Local, Remote and Systemic Inflammatory Responses That Follow Intestinal Ischemia and Reperfusion Injury, *J. Immunol. 172*, 2542–2548.
13. Reeves, P.G., Nielsen, F.H., and Fahey, G.C., Jr. (1993) AIN-93 Diets for Laboratory Rodents: Final Report of the American Institute of Nutrition *ad hoc* Writing Committee on the Reformulation of the AIN-76A Rodent Diet, *J. Nutr. 123*, 1939–1951.
14. Pfeffer, J.M., Pfeffer, M.A., and Frohlich, E.D. (1971) Validity of an Indirect Tail-Cuff Method for Determining Systolic Arterial Pressure in Unanaesthetized Normotensive and Spontaneously Hypertensive Rats, *J. Clin. Med. 78*, 957–962.
15. McMurchie, E.J., Patten, G.S., McLennan, P.L., and Charnock, J.S. (1987) A Comparison of the Properties of the Cardiac β-Adrenergic Receptor Adenylyl Cyclase System in the Rat and the Marmoset Monkey, *Comp. Biochem. Physiol. 88B*, 989–998.
16. Alam, S.Q., Ren, Y.F., and Alam, B.S. (1988) [^{3}H]Forskolin- and [^{3}H]Dihydroalprenolol-Binding Sites and Adenylate Cyclase Activity in Heart of Rats Fed Diets Containing Different Oils, *Lipids 23*, 207–213.
17. Lowry, O.H., Rosebrough, N.R., Farr, A.L., and Randall, R. (1951) Protein Measurement with the Folin Phenol Reagent, *J. Biol. Chem. 193*, 265–275.
18. Chi, M.S., Ray, R.L., Williams D.C., Vander Tuig, M., and Galbreath, K. (1999) Effects of Dietary Fat on Blood Pressure and Plasma Lipids in Spontaneously Hypertensive Rats, *Nutr. Res. 19*, 917–925.
19. Aguila, M.B., Loureiro, C.C., da Rocha Pinheiro, A., and Mandarim-de-Lacerda, C.A. (2002) Lipid Metabolism in Rats

Fed Diets Containing Different Types of Lipids, *Arq. Bras. Cardiol. 78*, 32–38.

20. Engler, M.M., Engler, M.B., Pierson, D.M., Molteni, L.B., and Molteni, A. (2002) Effects of Docosahexaenoic Acid on Vascular Pathology and Reactivity in Hypertension, *Exp. Biol. Med. 228*, 299–307.

21. Triboulot, C., Hichami, A., Denys, A., and Khan, N.A. (2001) Dietary (n-3) Polyunsaturated Fatty Acids Exert Antihypertensive Effects by Modulating Calcium Signaling in T Cells of Rats, *J. Nutr. 131*, 2364–2369.

22. Bellinger-Germain, S., Poisson, J.P., and Narce, M. (2002) Antihypertensive Effects of Dietary Unsaturated FA Mixture in Spontaneously Hypertensive Rats, *Lipids 37*, 561–567.

23. Jackson, E.K., and Herzer, W.A. (2001) Regional Vascular Selectivity of Angiotensin II, *J. Pharmacol. Exp. Ther. 297*, 736–745.

24. Ganten, D., Paul, M., and Lang, R.E. (1991) The Role of Neuropeptides in Cardiovascular Regulation, *Cardiovasc. Drugs Ther. 5*, 119–130.

25. Stanton, M.P., Hengel, P.T., Southwell, B.R., Chow, C.W., Keck, J., Hutson, J., and Bornstein, J.C. (2003) Cholinergic Transmission to Colonic Circular Muscle of Children with Slow-Transit Constipation Is Unimpaired, but Transmission to NK2 Receptors Is Lacking, *Neurogastroenterol. Motil. 15*, 669–678.

26. Grynberg, A., Fournier, A., Sergiel, J.P., and Athias, P. (1996) Membrane Docosahexaenoic Acid vs. Eicosapentaenoic Acid and the Beating Function of the Cardiomyocytes and Its Regulation Through Adrenergic Receptors, *Lipids 31*, S205–S210.

27. Awad, A.B., Brown, G.P., Fink, C.S., and Helinski, J.D. (1993) Effect of Dietary Fat on Glomerular Lipid Composition and Angiotensin II Receptors, *Jpn. J. Physiol. 43*, 775–784.

28. Bayon, Y., Croset, M., Daveloose, D., Guerbette, F., Chirouze, V., Viret, J., Kader, J.-C., and Lagarde, M. (1995) Effect of Specific Phospholipid Molecular Species Incorporated in Human Platelet Membranes on Thromboxane A_2/Prostaglandin H_2 Receptors, *J. Lipid Res. 36*, 47–56.

29. Bhathena, S.J., Berlin, E., McClure, D., and Peters, R.C. (2001) Effects of Dietary Fats on Red Blood Cell Membrane Insulin Receptor in Normo- and Hypercholesterolemic Miniature Swine, *J. Nutr. Biochem. 12*, 529–535.

30. Sales, M.A., Sterin-Borda, L., Rodriguez, M., and Borda, E.S. (1997) Intracellular Signals Coupled to Different Rat Ileal Muscarinic Receptor Subtypes, *Cell. Signal. 9*, 373–378.

31. Engler, M.M., Engler, M.B., Pierson, D.M., Molteni, L.B., and Molteni, A. (2003) Effects of Docosahexaenoic Acid on Vascular Pathology and Reactivity in Hypertension, *Exp. Biol. Med. (Maywood) 228*, 299–307.

32. Stadnicki, A., and Colman, R.W. (2003) Experimental Models of Inflammatory Bowel Disease, *Arch. Immunol. Ther. Exp. (Warsz) 51*, 149–155.

33. Kuzmic, A.C., Kolacek, S., Brkljacic B., and Huzjak, N. (2001) Renal Artery Stenosis Associated with Crohn's Disease, *Pediatr. Nephrol. 16*, 371–373.

34. Koga, H., Iida, M., Matsumoto, T., Aoyagi, K., and Fujishima, K. (1996) Correlation Between Disease Activity and Arterial Blood Pressure in Crohn's Disease, *Eur. J. Gastroenterol. Hepatol. 8*, 787–791.

35. Marinolle, J.P., Garcia-Villar, R., Fioramonti, J., and Bueno, L. (1997) Altered Contractility of Circular and Longitudinal Muscle in TNBS-Inflamed Guinea Pig Ileum, *Am. J. Physiol. 35*, G1258–G1267.

36. De Man, J.G., Seerden, T.C., De Winter, B.Y., Van Marck, E.A., Herman, A.G., and Pelckmans, P.A. (2003) Alteration of the Purinergic Modulation of Enteric Neurotransmission in the Mouse Ileum During Chronic Intestinal Inflammation, *Br. J. Pharmacol. 139*, 172–184.

37. Tanovic, A., Jimenez, M., and Fernandez, E. (2002) Changes in Inhibitory Responses to Electrical Field Stimulation of Intestinal Smooth Muscle from *Trichinella spiralis* Infected Rats, *Life Sci. 26*, 3121–3126.

38. Cosme, R., Lublin, D., Takafuji, V., Lynch, K., and Roche, J.K. (2000) Prostanoids in Human Colonic Mucosa: Effects of Inflammation on PGE_2 Receptor Expression, *Human Immunol. 61*, 684–696.

39. Depoortere, I., Thijs, T., Van Assche, G., Keith, J.C., and Peeters, T.L. (2000) Dose Dependent Effects of Recombinant Human Interleukin-11 on Contractile Properties in Rabbit 2,4,6-Trinitrobenzene Sulfonic Acid Colitis, *J. Pharmacol. Exp. Ther. 294*, 983–990.

40. Greenwood-Van Meerveld, B., Venkova, K., and Keith, J.C. (2001) Recombinant Human Interleukin-11 Restores Smooth Muscle Function in the Jejunum and Colon of Human Leukocyte Antigen-B27 Rats with Intestinal Inflammation, *J. Pharmacol. Exp. Ther. 299*, 58–66.

41. Sahl, B., Assi, K., Templeman, V., Parhar K., Owen, D., Gomez-Munoz, A., and Jacobson, K. (2003) Curcumin Attenuates DNB-Induced Murine Colitis, *Am. J. Physiol. 285*, G235–G243.

42. Yaqoob, P. (2004) Fatty Acids and the Immune System: From Basic Science to Clinical Applications, *Proc. Nutr. Soc. 63*, 89–104.

43. Nieto, N., Torres, M.I., Rios, A., and Gill, A. (2002) Dietary Polyunsaturated Fatty Acids Improve Histological and Biochemical Alterations in Rats with Ulcerative Colitis, *J. Nutr. 132*, 11–19.

44. Kang, J.X., Wang, J., Wu, L., and Kang, Z.B. (2004) Fat-1 Mice Convert n-6 to n-3 Fatty Acids, *Nature 427*, 504.

45. Singh, V.P., Patil, C.S., Jain, N.K., Singh, A., and Kulkarni, S.K. (2003) Effect of Nimesulide on Acetic Acid- and Leukotriene-Induced Inflammatory Bowel Disease in Rats, *Prostaglandins Other Lipid Med. 71*, 163–175.

Dietary n-3 Polyunsaturated Fatty Acids Increase T-Lymphocyte Phospholipid Mass and Acyl-CoA Binding Protein Expression

Lauren W. Collison[a], Robert E. Collison[a], Eric J. Murphy[b], and Christopher A. Jolly[a,*]

[a]Division of Nutritional Sciences, The University of Texas at Austin, Austin, Texas 78712, and [b]Department of Pharmacology, Physiology and Therapeutics, The University of North Dakota, Grand Forks, North Dakota 58202-9037

ABSTRACT: Dietary flaxseed oil, which is enriched in α-linolenic acid, and fish oil, which is enriched in EPA and DHA, possess anti-inflammatory properties when compared with safflower oil, which is enriched in linoleic acid. The influence of flaxseed oil and fish oil feeding on lipid metabolism in T-lymphocytes is currently unknown. This study directly compared the effects of feeding safflower oil, flaxseed oil, and fish oil for 8 wk on splenic T-lymphocyte proliferation, phospholipid mass, and acyl-CoA binding protein expression in the rat. The data show that both flaxseed oil and fish oil increased acyl-CoA binding protein expression and phosphatidic acid mass in unstimulated T-lymphocytes when compared with safflower oil feeding. Fish oil feeding increased cardiolipin mass, whereas flaxseed oil had no effect. After stimulation, flaxseed oil and fish oil blunted T-lymphocyte interleukin-2 production and subsequent proliferation, which was associated with the lack of increased acyl-CoA binding protein expression. The results reported show evidence for a novel mechanism by which dietary flaxseed oil and fish oil suppress T-lymphocyte proliferation *via* changes in acyl-CoA binding protein expression and phospholipid mass.

Paper no. L9590 in *Lipids 40*, 81–87 (January 2005).

In general, the n-3 PUFA are considered to be anti-inflammatory, whereas the n-6 PUFA are considered to be pro-inflammatory (1,2). Some reports show that, within the n-3 series, dietary lipids such as fish oil, which is enriched in EPA and DHA, possess more potent anti-inflammatory properties than flaxseed oil, which is enriched in α-linolenic acid (α-LNA) (3,4). It is well known that one of the major targets of dietary n-3 PUFA is the T-lymphocyte, a cell that is important in determining the type and extent of an immune response (5). Several reports show that flaxseed oil (linseed oil) and fish oil may have a similar potency in inhibiting lymphocyte proliferation *ex vivo* (6,7). *In vivo*, feeding flaxseed oil can dramatically blunt the development of autoimmune disease in mice, a result that is similar to that seen in fish oil feeding (8).

Acyl-CoA binding protein (ACBP) is a 10 kDa intracellular protein that binds acyl-CoA with high affinity and is found in every tissue tested including the spleen (9,10). Several recent reports have shown that ACBP may be an important regulator of cell function. For example, depletion of ACBP in human cell lines inhibits proliferation (11) and blocks adipocyte differentiation (12). Furthermore, transformed colon cells have increased ACBP expression (13).In rat liver microsomes, one potential mechanism by which ACBP may regulate cell function is by increasing phosphatidic acid (PtdOH) biosynthesis (14). This is important because PtdOH is the precursor for all glycerophospholipids and TG. Recent evidence using liver mitochondria suggests that ACBP may be an important determinant in the positional distribution of FA within phospholipids (15). Although most studies indicate that ACBP may play a positive role in cell function, one report has shown that ACBP may be involved in increasing apoptosis (16).

To date, only one report has examined the impact of diet on ACBP expression; it was shown that a high-fat diet increased ACBP expression in the liver (17). The role of ACBP in T-lymphocyte function and the mechanism by which different dietary lipid types affect the expression of ACBP are currently unknown. Whereas the impact of dietary n-3 PUFA on T-lymphocyte FA composition is well known, the influence on phospholipid mass of flaxseed oil is relatively unexplored. Therefore, this study aimed to determine the impact of diets enriched in α-LNA (flaxseed) or EPA and DHA (fish oil) on ACBP protein expression and phospholipid mass in splenic T-lymphocytes.

MATERIALS AND METHODS

Animals. Male Sprague-Dawley rats (five per group) were randomly assigned to a safflower oil diet (Saff), flaxseed oil diet (Flax), or fish oil diet (Fish). Six-month-old rats, weighing roughly 500 g each, were housed two per cage in a 12-h light/12-h dark room and had free access to diets and water. Following 8 wks of feeding, rats were euthanized by CO_2 asphyxiation, and livers and spleens were aseptically harvested. All procedures were approved by the University of Texas Animal Use and Care Committee.

Diets. Diet ingredients were purchased from Dyets, Inc. (Bethelehem, PA), prepared fresh each week, and maintained at 4°C. Isocaloric diets were designed to meet the nutritional

Abbreviations: ACBP, acyl CoA binding protein AP-1, activating protein-1; LA, linoleic acid; α-LNA, α-linolenic acid; IL-2, interleukin-2; mtGPAT, mitochondrial glycerol-3-phosphate acyltransferase; MTT, 3-(4,5-dimethylthiazol-2-yl)-2,5-diphenyltetrazolium bromide; PL, phospholipids; PPARγ, peroxisomal proliferator-activated receptor γ; PtdOH, phosphatidic acid.

requirements of rats as determined by the American Institute of Nutrition (18). Diets contained (g/kg) 200 soy protein, 300 dextrose, 310 cornstarch, 35 cellulose, 100 lipid, 2 choline, 1.5 DL-methionine, 1.5 L-cysteine, 1.3 α-tocopherol, 1.2 γ-tocopherol, 1 TBHQ, 35 mineral mix (AIN-93M-MX), and 15 vitamin mix (AIN-93-VX). Detailed composition of the vitamin and mineral mix has been reported elsewhere (18). Rats were fed, 30 g/d, one of three semipurified diets differing only in lipid content: (i) 10% w/w safflower oil (Saff) enriched in α-linoleic acid (α-LA), (ii) 3% Saff plus 7% flaxseed oil (Flax) enriched in α-LNA, and (iii) 3% Saff plus 7% fish oil (Fish) enriched in EPA and DHA. Safflower, flaxseed, and fish (menhaden) oils were all purchased from Dyets, Inc. Saff was added to the Flax and Fish diets as a source of LA to prevent EFA deficiency. Two separate feeding trials were performed because all the experiments could not be obtained from one rat. Feeding trial 1 consisted of performing proliferation, interleukin-2 (IL-2) secretion, and phospholipid (PL) mass determinations. Feeding trial 2 consisted of performing proliferation (to ensure consistency between diet studies) and Western immunoblotting.

T-lymphocyte isolation and culture conditions. Sprague-Dawley rat splenic T-lymphocytes were isolated using negative selection Immulan columns (Biotecx, Inc., Houston, TX) per the manufacturer's instructions as previously described (19), yielding a 90% pure splenic T-lymphocyte population. Isolation by negative selection prevents the stimulation of the T-lymphocyte's receptor during the isolation procedure, as occurs with positive selection methods. T-lymphocytes were counted using a Cell-Dyn 900 Hematology Analyzer (Sequoia-Turner Corp., Mountainview, CA). T-lymphocytes, 25×10^6 cells per petri dish, were stimulated at 37°C for 30 min in pre-warmed complete culture media (10% heat-inactivated FBS plus 100 U/mL penicillin, 100 μg/mL streptomycin, 10 μM 2-mercaptoethanol, and 100 mM L-glutamine) with 10 μg/mL plate-bound anti-CD3 to mimic *in vivo* antigenic stimulation.

FA analysis. FA analysis was performed on the diet and liver samples. Liver samples were homogenized and washed with cold PBS prior to lipid extraction. Lipids were extracted from both diet and liver samples with *n*-hexane/2-propanol (3:2, vol/vol) (20). The lipid extracts were centrifuged at $800 \times g$ to pellet cellular debris. The lipid-containing supernatants were filtered through a 0.2-μm nylon filter, dried under nitrogen, and redissolved in methanol. The samples were converted to FAME using the method of Brockerhoff (21). Briefly, methanolic KOH was added, followed by 0.2 M aqueous H_2SO_4. The FAME were extracted by *n*-hexane, dried under nitrogen, and redissolved in *n*-hexane for cleanup by TLC. Cleanup was performed to remove glycerol or other nonmethylated lipids prior to analysis by GC. The samples were run in parallel with authentic FAME standards (Sigma, St. Louis, MO) on Silica 60G plates, prerun with acetone, with a toluene solvent system. FAME were visualized with a 0.1% 8-anilino-1-naphthalene-sulfonic acid salt solution under UV light, and the corresponding FAME bands were scraped and redissolved in methanol. The FAME were again extracted by *n*-hexane prior to separa-

tion by GLC. FAME were separated using a Varian 3900GC equipped with an FID and a Varian CP-Wax 52CB WCOT fused-silica 50 m × 0.32 mm column. The injector and detector temperatures were set to 200 and 270°C, respectively. The split ratio was 1:10, and helium was used as the carrier gas at a flow of 1.5 mL/min. The column temperature was initially set to 50°C, increased to 140°C at a rate of 20°C/min, held for 5 min, increased to 200°C at 4°C/min, increased to 240°C at 2°C/min, and held for 30 min. FAME standards, as well as a 17:0 internal standard, were used to establish relative retention times. Peak area data were collected and analyzed using Varian Star Chromatography Workstation Version 5.52 software.

Proliferation. T-lymphocyte proliferation was measured using the MTT [3-(4,5-dimethylthiazol-2-yl)-2,5-diphenyltetrazolium bromide] Cell Proliferation Assay as described by the manufacturer (American Type Cell Culture, Manassas, VA). A plastic 96-well plate was precoated with either anti-CD3 at a concentration of 0.01 μg/μL in $NaHCO_3$ or $NaHCO_3$ alone before addition of cells. The plate was incubated in a humidified incubator containing 5% CO_2 at 37°C for 4 h to facilitate binding of the antibody to the wells. Plates were washed with sterile PBS, and 1.5 million cells in 100 μL of cell culture media were added to their corresponding wells. Cells were incubated for 18 h at 37°C to induce proliferation. Then 20 μL MTT reagent was added to each well, mixed gently, and incubated for approximately 4 h. The cells were permeabilized with 100 μL of detergent and incubated at room temperature for 2 h. The plate was read at an absorbance of 570 nm, and absorbance values were background-corrected.

IL-2 secretion. IL-2 secretion into the culture media was measured using a commercially available IL-2 ELISA kit from R&D Systems (Minneapolis, MN). Stimulated and unstimulated cells, prepared as described above for proliferation studies, were pelleted and their supernatants collected. The ELISA was performed according to the manufacturer's instructions. IL-2 was quantified using IL-2 standards supplied by the manufacturer of the kit and then reading the absorbance at 415 nm using an UltraMarc plate reader (BioRad, Hercules, CA). All samples were run in duplicate and the average absorbances used for quantification.

PL mass analysis. Frozen T-lymphocytes were thawed and the lipids extracted by the addition of 2-propanol (1 mL) to the tube containing the cells. This was added to a test tube containing hexane (3 mL) and the original tube containing the cells rinsed with another aliquot of 2-propanol (22). This results in a quantitative single-phase extraction of cellular PL and neutral lipids (23,24). The single-phase extract was thoroughly mixed, and the residue pelleted by centrifugation. The lipid-containing organic fraction was removed and concentrated to dryness under nitrogen, and a known amount of solvent was added. The samples were quantitatively spotted on a heat-activated Whatman LK6 TLC plate and developed in a solvent system containing chloroform/methanol/acetic acid/water (60:30:3:1 by vol). Individual bands corresponding to commercially prepared standards were scraped into acid-washed tubes and analyzed for phosphorus content. Phosphorus content was calculated by

linear regression of a standard curve. A 1:1 ratio was used to convert phosphorus to PL values except for cardiolipin (2:1) because each PL contains only one phosphorus atom, except cardiolipin, which contains two phosphorus atoms (25).

The protein pellet was air-dried overnight and then incubated with 0.2 M KOH at 65°C overnight to resolubilize the proteins. Protein concentration was determined using a modified dye-binding assay with BSA for the standard curve (26).

Western immunoblotting. Stimulated or unstimulated T-lymphocytes were pelleted and lysed in 50 μL of lysis buffer containing 5 mM Tris·HCl, 10 mM EDTA, 0.15 M NaCl, 0.1% Tween 20, 1 μL/mL β-mercaptoethanol, and 7 μL/mL protease inhibitors, pH 7.4. Lysates were centrifuged, and the protein-containing supernatants were quantified using the BioRad Protein Assay. Protein was separated by SDS-PAGE using Bio-Rad's Kaleidoscope Prestained Standards for running standards. The protein was transferred onto PolyScreen polyvinylidene difluoride membranes (NEN Life Sciences, Boston, MA), and the membranes were blocked with 15 mL blocking solution containing 25 mM Tris·HCl, 0.125 M NaCl, 4% nonfat milk, 0.1% Tween 20, pH 8.0. Membranes were probed with antiACBP antibody (provided by Dr. Jens Knudsen). Bands were detected using an alkaline phosphatase-conjugated goat-anti-rabbit secondary antibody and CDP-Star chemiluminescence reagent (NEN Life Sciences). The membrane was visualized using autoradiography, and densitometry was performed using a BioRad Gel Documentation System. The data are presented as arbitrary units, which refer to the densitometric (density) values obtained by the gel documentation system. The membrane was also probed with an anti-cbl-b antibody to control for lane loading variation.

Statistical analysis. Data were analyzed using one-way ANOVA and significant differences determined using Tukey's multiple comparison test with GraphPad Prism software (San Diego, CA). A *P* value that was <0.05 was considered significantly different. An asterisk or different numbers of asterisks

represent a significant difference from any other group within that experiment. Pearson's correlation was used to determine the correlation between ACBP, cardiolipin mass, and T-lymphocyte proliferation and IL-2 production.

RESULTS

Diet and liver FA analysis. Table 1 shows that the Saff diet contained 78% of its total FA as LA, with undetectable levels of α-LNA, EPA, and DHA. There was no significant difference in the total weight of the liver lipid between the diet groups. The Flax diet contained 46% of its total FA as α-LNA and 28% as LA, whereas EPA and DHA were undetectable. The Fish diet contained 12% of its total FA as EPA, 12% as DHA, 22% as LA, and trace amounts of α-LNA. Table 2 shows the impact of feeding the different diets for 8 wk on the FA composition of the liver. Livers from animals fed the Flax diet contained significantly (*P* < 0.05) higher levels of LA (25%) when compared with the Saff (20%) or Fish (16%) diet groups. The Flax diet was the only diet that resulted in a significant accumulation of α-LNA in the liver. Both the Flax and Fish diets were equally effective

TABLE 1
FA Analysis of the Experimental Diets[a]

FA	Percent FA composition		
	Saff	Flax	Fish
Myristic acid (14:0)	—	—	8.56
Palmitic acid (16:0)	6.96	5.23	17.65
Palmitoleic acid (16:1)	—	—	10.00
Stearic acid (18:0)	1.65	2.00	2.52
Oleic acid (18:1)	13.48	17.01	12.25
Linoleic acid (18:2n-6)	77.91	28.81	22.58
Linolenic acid (18:3n-3)	—	46.96	1.62
EPA (20:5n-3)	—	—	12.30
DHA (22:6n-3)	—	—	12.52

[a]Saff, safflower oil diet; Flax, flaxseed oil diet; Fish, fish oil diet.

TABLE 2
Dietary n-3 PUFA Alter Liver FA Composition[a]

FA	Percent FA composition		
	Saff	Flax	Fish
Myristic acid (14:0)	0.52 ± 0.04	0.52 ± 0.03	0.70 ± 0.01
Palmitic acid (16:0)	23.41 ± 0.50	20.55 ± 0.24*	24.78 ± 0.42
Palmitoleic acid (16:1)	2.46 ± 0.41	1.78 ± 0.13	2.48 ± 0.07
Stearic acid (18:0)	14.42 ± 0.39	12.57 ± 0.24	13.74 ± 0.23
Elaidic acid (18:1*t*)	6.46 ± 0.71	9.81 ± 0.37*	5.01 ± 0.18
Oleic acid (18:1*c*)	3.41 ± 0.12	2.25 ± 0.06	2.64 ± 0.08
Linoleic acid (18:2n-6)	19.69 ± 1.03	24.85 ± 0.80*	15.96 ± 0.19**
γ-Linolenic acid (18:3n-6)	0.35 ± 0.04	0	0
α-Linolenic acid (18:3n-3)	0	6.85 ± 0.76*	0.38 ± 0.02
Eicosadienoic acid (20:2)	0.38 ± 0.03	0	0
Eicosatrienoic acid (20:3n-6)	0.95 ± 0.16	0.80 ± 0.05	0.91 ± 0.03
Arachidonic acid (20:4n-6)	24.44 ± 0.77	11.06 ± 0.38*	9.99 ± 0.21*
EPA (20:5n-3)	0	5.21 ± 0.17*	7.52 ± 0.21**
DHA (22:6n-3)	3.52 ± 0.27	3.76 ± 0.09	15.91 ± 0.37*

[a]For diet abbreviations see Table 1; *n* = 4 or 5; an asterisk or different numbers of asterisks represent a significant difference from any other group within that experiment.
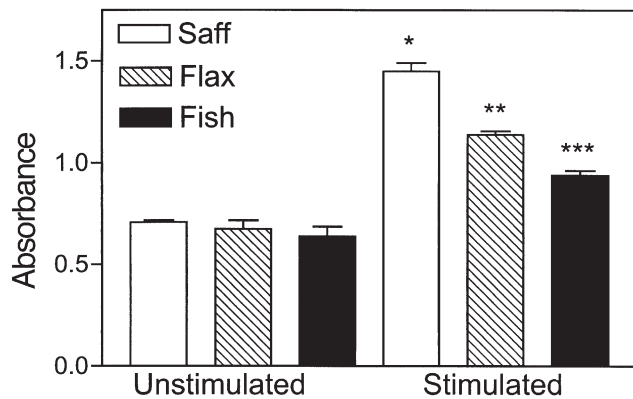
FIG. 1. Dietary flaxseed and fish oil differentially inhibit T-lymphocyte proliferation. Rats were fed a diet enriched in safflower oil (Saff), flaxseed oil (Flax), or fish oil (Fish) for 8 wk. Splenic T-lymphocytes were isolated and cultured with (Stimulated) or without (Unstimulated) anti-CD3 monoclonal antibody for 18 h. Proliferation was determined using the MTT [3-(4,5-dimethylthiazol-2-yl)-2,5-diphenyltetrazolium bromide] dye uptake test as described in the Materials and Methods section. Bars represent the mean ± SEM of five individual rats. Different numbers of asterisks represent a significant difference from any other group within that experiment.
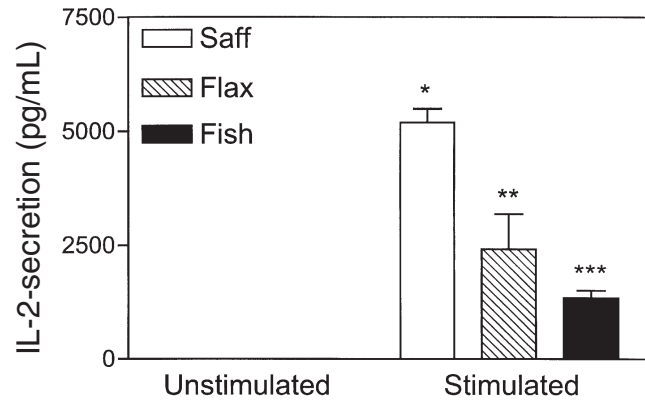
FIG. 2. Dietary flaxseed and fish oil inhibit T-lymphocyte interleukin-2 (IL-2) secretion. Rats were fed a diet enriched in safflower oil (Saff), flaxseed oil (Flax), or fish oil (Fish) for 8 wk. Splenic T-lymphocytes were isolated and cultured with (Stimulated) or without (Unstimulated) anti-CD3 monoclonal antibody as described in the caption for Figure 1. After 24 h, culture supernatants were collected and IL-2 was quantified using an ELISA kit as described in the Materials and Methods section. Bars represent the mean ± SEM of five individual rats. Different numbers of asterisks represent a significant difference from any other group within that experiment.

at reducing the arachidonic acid levels to 11 and 10%, respectively, when compared with the 24% found in the Saff group. The Flax and Fish diet groups contained similar levels of EPA, which was undetectable in the Saff diet group. The Fish diet group contained significantly ($P < 0.05$) more DHA (16%) than the Saff and Flax diet groups, which contained approximately 4% DHA.

T-lymphocyte function. Figure 1 shows that diet did not affect spontaneous splenic T-lymphocyte proliferation in the absence of the anti-CD3 stimuli. Addition of anti-CD3 antibody significantly ($P < 0.05$) increased T-lymphocyte proliferation, which was blunted by approximately 20 and 35% in the Flax and Fish diet groups, respectively. Figure 2 shows that, as would be expected, IL-2 is not secreted by the T-lymphocytes into the culture media in the absence of stimulation with anti-CD3. Addition of anti-CD3 antibody significantly ($P < 0.05$) increased T-lymphocyte IL-2 secretion, which was blunted by approximately 50 and 70% in the Flax and Fish diet groups, respectively.

Phospholipid mass in T-lymphocytes. Table 3 shows that diet did not have a significant effect on PE, PC, PI, PS, or sphingomyelin mass in splenic T-lymphocytes. The Fish diet group had significantly ($P < 0.05$) greater PtdOH mass (21 nmol/mg protein) when compared with the Saff and Flax diets, which had 13 and 7 nmol/mg protein, respectively. Fish and Flax feeding significantly ($P < 0.05$) increased cardiolipin mass to 15 and 7 nmol/mg protein, respectively, when compared with the 3 nmol/mg protein found in the Saff group.

ACBP expression in T-lymphocytes. Figure 3A shows the influence of stimulation and diet on ACBP expression in T-lymphocytes. Feeding fish oil almost doubled ACBP expression, whereas flaxseed oil feeding increased ACBP protein expression by 50% when compared with the Saff diet group in unstimulated T-lymphocytes. Stimulation increased ACBP expression by 25% but there was no significant effect of stimulation in the Flax diet group. In contrast, stimulation significantly ($P < 0.05$) decreased ACBP expression in the Fish diet group.

TABLE 3
Influence of Dietary n-3 PUFA on T-Lymphocyte Phospholipid Mass[a]

Phospholipid	Phospholipid composition (nmol/mg protein)		
	Saff	Flax	Fish
Cardiolipin (CL)	2.7 ± 2.3	7.1 ± 2.8**	14.6 ± 2.6*
Phosphatidic acid	13.2 ± 5.9	7.2 ± 3.9	21.1 ± 4.1*
Phosphatidylethanolamine	75.3 ± 8.4	72.5 ± 7.4	76.1 ± 3.8
Phosphatidylinositol	24.0 ± 2.5	18.9 ± 3.4	27.4 ± 3.9
Phosphatidylserine	29.7 ± 6.7	27.5 ± 3.4	34.1 ± 7.5
Phosphatidylcholine	175.4 ± 23.4	155.5 ± 16.8	172.2 ± 21.9
Sphingomyelin	148.5 ± 34.6	171.3 ± 26.5	149.2 ± 23.2
Total	468.8 ± 83.8	459.8 ± 64.1	494.8 ± 67.0

[a]For diet abbreviations see Table 1. An asterisk or different numbers of asterisks represent a significant difference from any other group within that experiment.
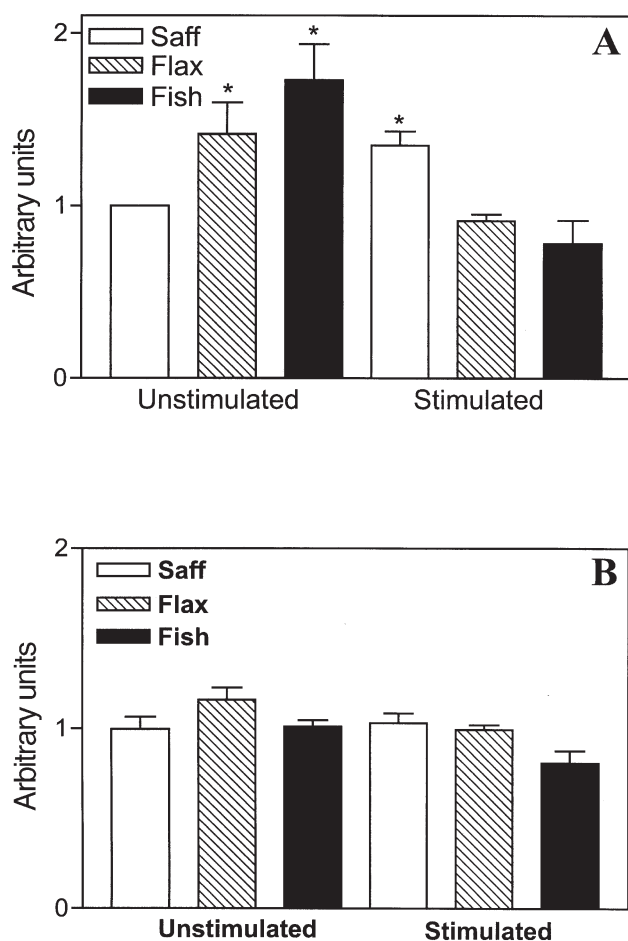
FIG. 3. Acyl-CoA binding protein (ACBP) expression is differentially regulated in resting and activated T-lymphocytes. Rats were fed a diet enriched in safflower oil (Saff), flaxseed oil (Flax), or fish oil (Fish) for 8 wk. Splenic T-lymphocytes were isolated and cultured with (Stimulated) or without (Unstimulated) anti-CD3 monoclonal antibody as described in the caption for Figure 1. After 30 min, T-lymphocytes were harvested and total cellular protein was extracted and subjected to Western immunoblotting for ACBP (A) or cbl-b (B) as described in the Materials and Methods section. Bars represent the mean ± SEM of 4 or 5 individual rats. An asterisk represents a significant difference from any other group within that experiment.

Figure 3B serves as lane-loading controls for Figure 3A since cbl-b expression is known to not change with CD3 stimulation (19). Overall, there was a significant positive correlation (0.864, $P < 0.001$) between diet, proliferation, and ACBP levels. There also was a significant negative correlation (−0.689, $P < 0.004$) between diet, ACBP levels, and cardiolipin mass.

DISCUSSION

Our results showing that both the Flax and Fish oil diets decreased liver arachidonic acid levels to the same extent are similar to those reported in the spleens of chickens (27), rats (28), and mice (29). These results are different from a previous report in which the feeding of canola oil, also enriched in α-LNA, did

not significantly affect arachidonic acid levels in the liver (30). The reason for this difference is most likely due to the fact that the authors fed the rats for only 6 d, whereas our study fed the rats for 8 wk. This is important because it explains how both Flax and Fish feeding reduces prostaglandin production to a similar extent in spleen lymphocytes (28). Decreasing arachidonic acid-derived prostaglandin production is a well-known mechanism by which n-3 PUFA are thought to regulate immune function. However, decreased prostaglandin production cannot be the primary mechanism by which the Flax and Fish diets inhibit T-lymphocyte function in our system because the Fish diet was more potent than the Flax diet at suppressing T-lymphocyte IL-2 secretion and subsequent proliferation. This explanation is supported by our findings that feeding arachidonic acid to mice did not affect splenic lymphocyte function (5).

The dietary Flax group had a higher LA content in their livers when compared with the Saff diet-fed group. This may be due to the conversion of LA to arachidonic acid in the Saff diet group, as suggested by the higher arachidonic acid content in the livers of the Saff diet group, which was not found in the Flax or Fish diet groups. The Flax diet group also had a slightly higher LA content than the Fish diet group, which may be due to the higher LA content in the Flax vs. the Fish diet. Interestingly, the livers of all three diet groups contained significant quantities of the *trans* FA elaidic acid. Elaidic acid was most likely already present in the livers prior to the start of the study and could have come from the commercial chow the rats were initially fed, since *trans* FA were not detected in the semipurified diets used in this study and rats cannot endogenously make *trans* FA.

The Flax and Fish diets selectively increased cardiolipin mass, whereas only the Fish diet increased PtdOH mass. Increasing cardiolipin mass suggests that the n-3 PUFA may be acting directly on the mitochondria since cardiolipin is found primarily in mitochondria. The ability of dietary n-3 PUFA to regulate mitochondrial cardiolipin FA unsaturation selectively has been shown in colonocytes and is correlated with increased caspase-3 activity, suggesting that the n-3 PUFA have antiproliferative effects (31). This is in agreement with our findings that the results of both Flax and Fish feeding are antiproliferative with respect to T-lymphocytes. Furthermore, the Fish diet, when compared with the Flax diet, was more potent at reducing T-lymphocyte proliferation and was also able to increase PtdOH mass, which is the immediate precursor PL to cardiolipin. This is the first study to report the impact of dietary n-3 PUFA feeding on T-lymphocyte phospholipid mass. The mechanism by which Fish and Flax diet feeding increases cardiolipin mass is unknown but may involve up-regulation of mitochondrial glycerol-3-phosphate acyltransferase (mtGPAT). The mtGPAT enzyme catalyzes the rate-limiting step in PtdOH biosynthesis (32) and is thus a likely target of dietary n-3 PUFA feeding. Indeed, mtGPAT gene expression was shown to be regulated by hormones, dietary starvation, and high carbohydrate feeding in liver and adipocytes (33). Specifically, n-3 PUFA feeding was shown to increase liver phospholipid mass, although an increase in mtGPAT activity was not observed (34). In another report, both n-3 and n-6 PUFA feeding increased mtGPAT activity in

rat liver (35). The reason for this discrepancy is most likely due to differences in dietary lipid levels fed and timing of tissue collection; however, these reports do set the precedent for n-3 PUFA feeding to alter mtGPAT activity and phospholipid mass. The influence of n-3 PUFA feeding on T-lymphocyte mtGPAT activity is currently unknown.

The increase in cardiolipin and PtdOH mass was correlated with increased ACBP expression, with the Fish diet being the most potent in unstimulated T-lymphocytes. This is consistent with evidence showing that ACBP can increase the activities of both the microsomal (36) and mitochondrial isoforms (15) of GPAT. The Flax and Fish diet feeding increased ACBP expression in unstimulated T-lymphocytes; however, Flax and Fish diet feeding prevented the increase in ACBP expression in stimulated T-lymphocytes. It is not unusual that the changes in ACBP in unstimulated T-lymphocytes did not have an impact on proliferation or IL-2 secretion in unstimulated cultures. T-lymphocytes do not proliferate or secrete IL-2 without appropriate antigenic stimulation (i.e., anti-CD3); therefore, it is not surprising that the increased ACBP expression in unstimulated cultures does not alter proliferation or IL-2 secretion. The differential influence of n-3 PUFA feeding may be related to how the ACBP gene is regulated. The ACBP promoter contains a binding site for activating protein-1 (AP-1), which is a fos/jun heterodimer, and peroxisomal proliferator-activated receptor γ (PPARγ) (37). Activation of the rat ACBP gene has been shown to occur in response to PPARγ in adipocytes (38). Recent evidence suggests that PPARγ may be a potent anti-inflammatory agent inhibiting T-lymphocyte proliferation (39,40). Since n-3 PUFA are PPARγ ligands, the increase in ACBP expression would be expected in T-lymphocytes. The lack of induction of ACBP expression in response to stimulation in Flax- and Fish-diet-fed rat T-lymphocytes may be due to reduced activation of the AP-1 transcription factor. It is well known that dietary n-3 PUFA feeding suppresses T-lymphocyte signal transduction (5). This study is the first report to show the rapid (i.e., 30-min) induction of ACBP expression, indicating that it may play an important role in cell function, as has been suggested by others (11–13).

In summary, we have shown that dietary n-3 PUFA increase cardiolipin and PtdOH mass in resting T-lymphocytes, which is correlated with increased ACBP expression. Furthermore, we have shown that ACBP expression can be increased following T-lymphocyte activation and that this response is blunted by dietary n-3 PUFA. Regulation of ACBP expression and phospholipid mass may be a novel mechanism by which dietary n-3 PUFA exert their anti-inflammatory effects on T-lymphocytes.

ACKNOWLEDGMENTS

REFERENCES

1. Chapkin, R.S., McMurray, D.N., and Jolly, C.A. (2000) Dietary n-3 Polyunsaturated Fatty Acids Modulate T-Lymphocyte Activation: Clinical Relevance in Treating Diseases of Chronic Inflammation, in *Nutrition and Immunology: Principles and Practice* (Gershwin, M.E., German, B.J., and Keen, C.L., eds.), pp. 121–134, Humana Press, Totowa.
2. Fernandes, G., and Jolly, C.A. (1998) Nutrition and Autoimmune Disease, *Nutr. Rev. 56*, S161–S169.
3. Thies, F., Nebe-von-Caron, G., Powell, J.R., Yaqoob, P., Newsholme, E.A., and Calder, P.C. (2001) Dietary Supplementation with Eicosapentaenoic Acid, but Not with Other Long-Chain n-3 or n-6 Polyunsaturated Fatty Acids, Decreases Natural Killer Cell Activity in Healthy Subjects Aged >55 y, *Am. J. Clin. Nutr. 73*, 539–548.
4. Fritsche, K.L., Cassity, N.A., and Huang, S.C. (1991) Effect of Dietary Fat Source on Antibody Production and Lymphocyte Proliferation in Chickens, *Poult. Sci. 70*, 611–617.
5. Jolly, C.A., Jiang, Y.H., Chapkin, R.S., and McMurray, D.N. (1997) Dietary (n-3) Polyunsaturated Fatty Acids Suppress Murine Lymphoproliferation, Interleukin-2 Secretion, and the Formation of Diacylglycerol and Ceramide, *J. Nutr. 127*, 37–43.
6. Wang, Y.W., Field, C.J., and Sim, J.S. (2000) Dietary Polyunsaturated Fatty Acids Alter Lymphocyte Subset Proportion and Proliferation, Serum Immunoglobulin G Concentration, and Immune Tissue Development in Chicks, *Poult. Sci. 79*, 1741–1748.
7. Brouard, C., and Pascaud, M. (1993) Modulation of Rat and Human Lymphocyte Function by n-6 and n-3 Polyunsaturated Fatty Acids and Acetylsalicylic Acid, *Ann. Nutr. Metab. 37*, 146–159.
8. Hall, A.V., Parbtani, A., Clark, W.F., Spanner, E., Keeney, M., Chin-Yee, I., Philbrick, D.J., and Holub, B.J. (1993) Abrogation of MRL/lpr Lupus Nephritis by Dietary Flaxseed. *Am. J. Kidney Dis. 22*, 326–332.
9. Gossett, R.E., Frolov, A.A., Roths, J.B., Behnke, W.D., Kier, A.B., and Schroeder, F. (1996) Acyl-CoA Binding Proteins: Multiplicity and Function, *Lipids 31*, 895–918.
10. Burgi, B., Lichtensteiger, W., and Schlumpf, M. (2000) Diazepam-Binding Inhibitor/Acyl-CoA-Binding Protein mRNA and Peripheral Benzodiazepine Receptor mRNA in Endocrine and Immune Tissues After Prenatal Diazepam Exposure of Male and Female Rats, *J. Endocrinol. 166*, 163–171.
11. Faergeman, N.J., and Knudsen, J. (2002) Acyl-CoA Binding Protein Is an Essential Protein in Mammalian Cell Lines, *Biochem. J. 368*, 679–682.
12. Mandrup, S., Sorensen, R.V., Helledie, T., Nohr, J., Baldursson, T., Gram, C., Knudsen, J., and Kristiansen, K. (1998) Inhibition of 3T3-L1 Adipocyte Differentiation by Expression of Acyl-CoA-Binding Protein Antisense RNA, *J. Biol. Chem. 273*, 23897–23903.
13. Gossett, R.E., Schroeder, F., Gunn, J.M., and Kier, A.B. (1997) Expression of Fatty Acyl-CoA Binding Proteins in Colon Cells: Response to Butyrate and Transformation, *Lipids 32*, 577–585.
14. Gossett, R.E., Edmondson, R.D., Jolly, C.A., Cho, T.H., Russell, D.H., Knudsen, J., Kier, A.B., and Schroeder, F. (1998) Structure and Function of Normal and Transformed Murine Acyl-CoA Binding Proteins, *Arch. Biochem. Biophys. 350,* 201–213.
15. Kannan, L., Knudsen, J., and Jolly, C.A. (2003) Aging and Acyl-CoA Binding Protein Alter Mitochondrial Glycerol-3-Phosphate Acyltransferase Activity, *Biochim. Biophys. Acta 1631*, 12–16.
16. Melloni, E., Averna, M., Salamino, F., Sparatore, B., Minafra, R., and Pontremoli, S. (2000) Acyl-CoA-Binding Protein Is a Potent m-Calpain Activator, *J. Biol. Chem. 275*, 82–86.
17. Bhuiyan, J., Pritchard, P.H., Pande, S.V., and Seccombe, D.W.

(1995) Effects of High-Fat Diet and Fasting on Levels of Acyl-Coenzyme A Binding Protein in Liver, Kidney, and Heart of Rat, *Metabolism 44*, 1185–1189.

18. Reeves, P.G., Nielsen, F.H., and Fahey, G.C., Jr. (1993) AIN-93 Purified Diets for Laboratory Rodents: Final Report of the American Institute of Nutrition *ad hoc* Writing Committee on the Reformulation of the AIN-76A Rodent Diet, *J. Nutr. 123*, 1939–1951.

19. Xu, Z., George, C., and Jolly, C.A. (2004) CD28 Activation Does Not Down-regulate Cbl-b Expression in Aged Rat T-Lymphocytes, *Mech. Ageing Dev. 125*, 595–602.

20. Murphy, E.J., Stiles, T., and Schroeder, F. (2000) Sterol Carrier Protein-2 Expression Alters Phospholipid Content and Fatty Acyl Composition in L-Cell Fibroblasts, *J. Lipid Res. 41*, 788–796.

21. Brockerhoff, H. (1975) Determination of the Positional Distribution of Fatty Acids in Glycerolipids, *Methods Enzymol. 35*, 315–325.

22. Murphy, E.J., Rosenberger, T.A., and Horrocks, L.A. (1997) Effects of Maturation on the Phospholipid and Phospholipid Fatty Acid Compositions in Primary Rat Cortical Astrocyte Cell Cultures, *Neurochem. Res. 22*, 1205–1213.

23. Saunders, R.D., and Horrocks, L.A. (1984) Simultaneous Extraction and Preparation for High-Performance Liquid Chromatography of Prostaglandins and Phospholipids, *Anal. Biochem. 143,* 71–75.

24. Hara, A., and Radin, N.S. (1978) Lipid Extraction of Tissues with a Low-Toxicity Solvent, *Anal. Biochem. 90*, 420–426.

25. Rouser, G., Siakotos, A., and Fleischer, S. (1969) Quantitative Analysis of Phospholipids by Thin Layer Chromatography and Phosphorus Analysis of Spots, *Lipids 13*, 85–86.

26. Bradford, M.M. (1976) A Rapid and Sensitive Method for the Quantitation of Microgram Quantities of Protein Utilizing the Principle of Protein-Dye Binding, *Anal. Biochem. 72*, 248–254.

27. Fritsche, K.L., Cassity, N.A., and Huang, S.C. (1991) Effect of Dietary Fats on the Fatty Acid Compositions of Serum and Immune Tissues in Chickens, *Poult. Sci. 70*, 1213–1222.

28. Fritsche, K.L., and Johnston, P.V. (1990) Effect of Dietary Omega-3 Fatty Acids on Cell-Mediated Cytotoxic Activity in BALB/c Mice, *Nutr. Res. 10,* 577–588.

29. Kleemann, R., Scott, F.W., Worz-Pagenstert, U., Nimal Ratnayake, W.M., and Kolb, H. (1998) Impact of Dietary Fat on Th1/Th2 Cytokine Gene Expression in the Pancreas and Gut of Diabetes-Prone BB Rats, *J. Autoimmun. 11*, 97–103.

30. Palombo, J.D., DeMichele, S.J., Boyce, P.J., Noursalehi, M., Forse, R.A., and Bistrian, B.R. (1998) Metabolism of Dietary α-Linolenic Acid vs. Eicosapentaenoic Acid in Rat Immune Cell Phospholipids During Endotoxemia, *Lipids 33*, 1099–1105.

31. Hong, M.Y., Chapkin, R.S., Barhoumi, R., Burghardt, R.C., Turner, N.D., Henderson, C.E., Sanders, L.M., Fan, Y.Y., Davidson, L.A., Murphy, M.E., *et al.* (2002) Fish Oil Increases Mitochondrial Phospholipid Unsaturation, Upregulating Reactive Oxygen Species and Apoptosis in Rat Colonocytes, *Carcinogenesis 23*, 1919–1925.

32. Dircks, L.K., and Sul, H.S. (1997) Mammalian Mitochondrial Glycerol-3-Phosphate Acyltransferase, *Biochim. Biophys. Acta 1348*, 17–26.

33. Coleman, R.A., Lewin, T.M., and Muoio, D.M. (2000) Physiological and Nutritional Regulation of Enzymes of Triacylglycerol Synthesis, *Annu. Rev. Nutr. 20*, 77–103.

34. Ikeda, I., Cha, J.Y., Yanagita, T., Nakatani, N., Oogami, K., Imaizumi, K., and Yazawa, K. (1998) Effects of Dietary α-Linolenic, Eicosapentaenoic and Docosahexaenoic Acids on Hepatic Lipogenesis and β-Oxidation in Rats, *Biosci. Biotechnol. Biochem. 62,* 675–680.

35. Wong, S.H., Nestel, P.J., Trimble, R.P., Storer, G.B., Illman, R.J. and Topping, D.L. (1984) The Adaptive Effects of Dietary Fish and Safflower Oil on Lipid and Lipoprotein Metabolism in Perfused Rat Liver, *Biochim. Biophys. Acta 792*, 103–109.

36. Jolly, C.A., Wilton, D.C., and Schroeder, F. (2000) Microsomal Fatty Acyl-CoA Transacylation and Hydrolysis: Fatty Acyl-CoA Species Dependent Modulation by Liver Fatty Acyl-CoA Binding Proteins, *Biochim. Biophys. Acta 1483*, 185–197.

37. Elholm, M., Bjerking, G., Knudsen, J., Kristiansen, K., and Mandrup, S. (1996) Regulatory Elements in the Promoter Region of the Rat Gene Encoding the Acyl-CoA-Binding Protein, *Gene 173*, 233–238.

38. Helledie, T., Grontved, L., Jensen, S.S., Kiilerich, P., Rietveld, L., Albrektsen, T., Boysen, M.S., Nohr, J., Larsen, L.K., Fleckner, J., *et al.* (2002) The Gene Encoding the Acyl-CoA-Binding Protein Is Activated by Peroxisome Proliferator-Activated Receptor γ Through an Intronic Response Element Functionally Conserved Between Humans and Rodents, *J. Biol. Chem. 277*, 26821–26830.

39. Daynes, R.A., and Jones, D.C. (2002) Emerging Roles of PPARs in Inflammation and Immunity, *Nat. Rev. Immunol. 2*, 748–759.

40. Harris, S.G., and Phipps, R.P. (2001) The Nuclear Receptor PPAR γ Is Expressed by Mouse T Lymphocytes and PPAR Gamma Agonists Induce Apoptosis, *Eur. J. Immunol. 31*, 1098–1105.

Milk Fat Synthesis Is Unaffected by Abomasal Infusion of the Conjugated Diene 18:3 Isomers *cis*-6,*trans*-10, *cis*-12 and *cis*-6,*trans*-8,*cis*-12

A. Sæbø[a], J.W. Perfield II[b], P. Delmonte[c], M.P. Yurawecz[c], P. Lawrence[d], J.T. Brenna[d], and D.E. Bauman[b],*

[a]Natural ASA, N-6160 Hovdebygda, Norway, [b]Department of Animal Science, Cornell University, Ithaca, New York 14853, [c]U.S. Food and Drug Administration, Center for Food Safety and Applied Nutrition, College Park, Maryland 20740, and [d]Division of Nutritional Sciences, Cornell University, Ithaca, New York 14853

ABSTRACT: It has been previously established that *trans*-10,*cis*-12 CLA is a potent inhibitor of milk fat synthesis. Although the mechanism of this action is not completely understood, it has been speculated that eicosanoid-like metabolites of this isomer formed by the activity of tissue desaturases may be responsible for its activity. The objective of this study was to investigate the effects of an enrichment containing an 18:3 conjugated diene, produced in the metabolism of *trans*-10,*cis*-12 CLA, on milk fat synthesis. Three rumen-fistulated Holstein cows (210 ± 8 d in milk) were randomly assigned in a 3 × 3 Latin square experiment. Treatments were (i) control, (ii) *trans*-10,*cis*-12 CLA supplement (2.1 g/d; positive control), (iii) enrichment providing two conjugated diene 18:3 isomers (2.6 g/d of *cis*-6,*trans*-10,*cis*-12 and 4.0 g/d of *cis*-6,*trans*-8,*cis*-12) and *trans*-10,*cis*-12 CLA (2.1 g/d). Treatments were abomasally infused for 5 d at 4-h intervals, and there was a 7-d interval between periods. Milk yield, dry matter intake, and milk protein yield were unaffected by treatments. In contrast, the *trans*-10,*cis*-12 CLA supplement reduced milk fat yield by 27%, whereas the supplement enriched with conjugated diene 18:3 isomers (treatment iii) had no effect on milk fat yield beyond that attributable to its *trans*-10,*cis*-12 CLA content. The transfer efficiency of *trans*-10,*cis*-12 CLA into milk fat was 25 and 24% for treatments ii and iii, respectively. At the same time, the abomasally infused conjugated diene 18:3 isomers were transferred to milk fat with an efficiency of 33 and 41% for *cis*-6,*trans*-10,*cis*-12 and *cis*-6,*trans*-8,*cis*-12 18:3, respectively. Overall, short-term abomasal infusion of the conjugated diene 18:3 isomers had no effect on milk fat synthesis, thereby offering no support for an involvement of metabolites of *trans*-10,*cis*-12 CLA in the regulation of milk fat synthesis.

Paper no. L9525 in *Lipids 40*, 89–95 (January 2005).

CLA have a number of biological effects, one of which involves the regulation of lipid metabolism. Supplementation of CLA has been shown to reduce milk fat content in lactating species including cows, pigs, and nursing women (1). Dietary CLA also reduces fat deposition in a number of animal growth models such as mice, rats, and pigs (2). Specifically, the *trans*-10,*cis*-12 CLA isomer is involved in the inhibition of milk fat synthesis (3) as well as the reduction of body fat accretion (4). However, the mechanism by which *trans*-10,*cis*-12 CLA effects lipid metabolism is not fully understood.

Many of the biological effects of PUFA can be attributed to FA intermediates formed during metabolism; a specific example is the formation of eicosanoids from n-3 and n-6 FA (5). Therefore, it is possible that the *trans*-10,*cis*-12 CLA isomer *per se* does not regulate lipid metabolism, but rather a specific FA formed during its metabolism may be responsible for the biological activity. Several of the proposed theories for the mechanisms of action of CLA involve their metabolism. These theories include: interfering with the synthesis and function of eicosanoids, the activation of peroxisome proliferator-activated receptor γ by metabolites of CLA isomers, and the ability of CLA metabolites to act as eicosanoids (6,7).

Metabolites of CLA isomers have been identified in CLA-supplemented animals (7,8), and the *trans*-10,*cis*-12 CLA isomer has been shown to be elongated and desaturated in a manner similar to linoleic acid (7–10). Although it has been postulated that *trans*-10,*cis*-12 CLA acts directly to alter lipid metabolism (1,11), the involvement of metabolites of *trans*-10,*cis*-12 CLA in the regulation of lipid metabolism has not been directly evaluated. In an attempt to better understand the role of CLA metabolites in situations where *trans*-10,*cis*-12 CLA causes a reduction in milk fat synthesis, an enrichment containing *cis*-6, *trans*-10,*cis*-12 18:3 was provided to dairy cows and effects on milk fat synthesis were examined. This partially conjugated triene is formed by Δ^6-desaturation in the initial step in the metabolism of *trans*-10,*cis*-12 CLA; following the example of Banni (7), we will refer to it as a conjugated diene 18:3 (CD 18:3).

EXPERIMENTAL PROCEDURES

The Cornell University Institutional Animal Care and Use Committee approved all procedures involving animals. Three rumen-fistulated lactating Holstein cows [210 ± 8 d in milk (DIM); mean ± SE] were randomly assigned in a 3 × 3 Latin square experiment. Cows were housed in tie stalls at the Cornell University Large Animal Teaching and Research Unit and

*To whom correspondence should be addressed at 262 Morrison Hall, Department of Animal Science, Cornell University, Ithaca, NY 14853-4801. E-mail: deb6@cornell.edu

Abbreviations: CD, conjugated diene; DIM, days in milk; DMI, dry matter intake; MS/MS, tandem MS.

TABLE 1
Ingredient and Chemical Composition of Diet

Composition	Concentration
Ingredient (% of dry matter)	
Alfalfa hay	54.1
Cracked corn	31.2
Expeller soybean meal	8.3
Cottonseed	3.1
Urea	0.3
Dicalcium phosphate	0.4
Salt	0.6
Vitamin and mineral mix[a]	2.0
Chemical analysis (% of dry matter)	
Crude protein	18.6
Crude fat	3.8
NDF[b]	35.2
ADF[c]	24.3
NE_L[d] (Mcal/kg dry matter)	1.57

[a]Contained 20.0% Cl, 18.0% Na, 12.0% Ca, 8.0% S, 7.5% Mg, 1.0% K, 0.48% Zn, 0.40% Mn, 0.29% Fe, 0.07% Cu, 0.01% P, 0.006% Co, 550 IU/g of vitamin A, 132 IU/g of vitamin D, and 297 IU/g of vitamin E.
[b]NDF = neutral detergent fiber.
[c]ADF = acid detergent fiber.
[d]NE_L = net energy of lactation.

TABLE 2
FA Profile of Conjugated FA Supplements[a]

FA (%)	10,12 CLA supplement	CD 18:3 supplement
16:0	<0.1	0.2
18:1 c-9	0.5	4.0
18:2 c-9,c-12	<0.1	16.9
CLA		
18:2 c-9,t-11	3.4	11.8
18:2 t-10,c-12	92.5	11.7
Other CLA	3.3	<0.1
Conjugated diene 18:3		
18:3 c-6,t-10,c-12	ND	14.6
18:3 c-6,t-8,c-12	ND	21.8
Other	<0.1	18.9

[a]Total compositions of supplements were determined using GC analysis, whereas HPLC and GC/MS/MS analysis were used to separate and identify the conjugated diene (CD) 18:3 isomers. ND = not detected.

fed a total mixed ration formulated to meet or exceed nutrient requirements for energy, protein, minerals, and vitamins (12) using the Cornell Net Carbohydrate and Protein System (13). Chopped alfalfa was the major forage component, with cracked corn as the major concentrate (Table 1). Cows were fed *ad libitum* with equal portions of feed offered at 0700 and 1900 h daily. Dry matter intake (DMI) was measured daily, and water was provided at all times.

Cows were milked at 0700 and 1900 h daily. Yield was determined and samples were taken from each milking. One aliquot was stored with preservative (bronopol tablet; D&F Control System, San Ramon, CA) at 4°C until it was analyzed for fat and protein content by IR spectroscopy (Dairy One, Ithaca, NY) using methods detailed by Bernal-Santos *et al.* (14). A second aliquot was stored without preservative at –20°C until analyzed for FA composition.

Ethanol was used as a carrier for the FA supplements, and infusates provided <100 mL/d of ethanol. Treatments were abomasal infusion of (i) ethanol (control), (ii) *trans*-10,*cis*-12 CLA (2.1 g/d; positive control), and (iii) enrichment providing two CD 18:3 isomers (2.6 g/d of *cis*-6,*trans*-10,*cis*-12 18:3 and 4.0 g/d of *cis*-6,*trans*-8,*cis*-12 18:3) plus *trans*-10,*cis*-12 CLA (2.1 g/d). The composition of the supplements (Natural ASA, Hovdebygda, Norway) is provided in Table 2. The CD 18:3 enrichment was made by a mild alkaline isomerization procedure of a concentrate of γ-linolenic acid. On isomerization of linoleic acid, this procedure yields approximately 50% each of *cis*-9,*trans*-11 and *trans*-10,*cis*-12 CLA, and less than 1% each of *cis-cis* and *trans-trans* isomers. The CD 18:3 supplement was therefore expected to contain predominantly *cis*-6, *trans*-8,*cis*-12 and *cis*-6,*trans*-10,*cis*-12 18:3 FA.

Identification of the specific CD 18:3 isomers present in the enrichment was accomplished by first isolating the FA by

HPLC and then determining their structure by GC/tandem MS (GC/MS/MS) analysis. HPLC fractionation and quantitative analysis of CD 18:3 were carried out using a Waters 2995 chromatographic system (Waters Associates, Milford, MA) equipped with a Waters 2695 PDA detector (acquiring 200–300 nm), and three ChromSpher 5 Lipids columns (each 4.6 mm i.d.; length 250 mm stainless steel; 5 µm particle size; Varian Inc., Walnut Creek, CA) in series maintained at 20°C. CD 18:3 were eluted with 50:50 (% by vol) hexane/0.4% acetonitrile in an isooctane mobile phase at 1.0 mL/min. Single chromatograms were extracted at 233 nm. After identifying the CLA isomers present in the CD 18:3 enrichment by comparison with reference material, the other two major peaks showing characteristic UV conjugated diene spectra were fractionated (Fig. 1). Once separated, fractions were subjected to acetontrile CI MS/MS as described in detail previously (15). Single-stage MS data revealed that the two FAME were indeed partially conjugated 18:3 FA based on the [M + 54 – 32]/[M + 54] ratios. MS/MS fragments for both CD 18:3 isomers were observed at *m/z* 276 and 232, establishing that double bonds were in the 6- and 12-positions, with an additional double bond internal to these positions. A fragment at *m/z* 222 showed that the internal double bond in one CD 18:3 isomer was in the 8-position, whereas a fragment at *m/z* 178 for the other isomer demonstrated the internal double bond was in the 10-position. The intensity of peaks was consistent with assignment for both FAME as *cis-trans-cis*. The two CD 18:3 isomers were thus assigned as *cis*-6,*trans*-10,*cis*-12 and *cis*-6,*trans*-8,*cis*-12.

Infusates were prepared from the same source each experimental period and stored under nitrogen gas at 4°C until they were infused during the experimental period. The *trans*-10,*cis*-12 CLA supplement and the CD 18:3 supplement treatments were targeted to provide an equal amount of *trans*-10,*cis*-12 CLA. Average amounts of CLA isomers provided by the treatments over the three infusion periods are presented in Table 3. Treatment periods were 5 d in duration, and treatments were abomasally infused six times a day at 4-h intervals. At each time point, equal volumes were infused into the abomasum *via* 0.5 cm (i.d.) polyvinyl chloride tubing that was passed through
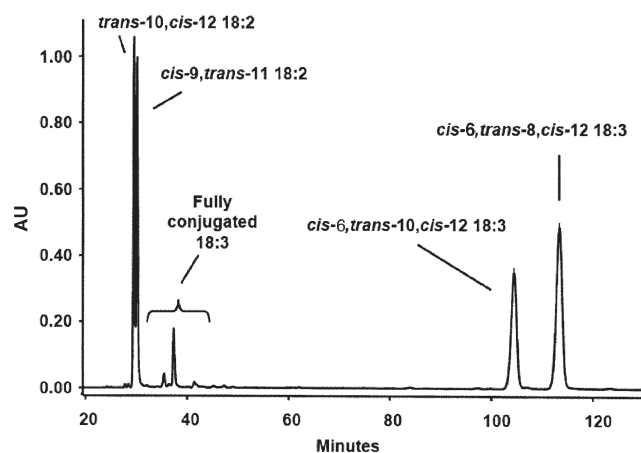
FIG. 1. Partial chromatogram demonstrating the HPLC separation of the two conjugated diene (CD) 18:3 isomers present in the CD 18:3 supplement.

the rumen fistula and sulcus omasi as described by Spires *et al.* (16). Abomasal infusion of supplements was used as a convenient experimental means to prevent rumen biohydrogenation of the PUFA contained in the supplements and to accurately account for the quantity of FA supplied by the different treatments. Treatment periods were followed by a 7-d washout to minimize carryover effects in the next treatment period.

FA analysis. Milk fat was extracted using the method of Hara and Radin (17), and FAME were prepared by base-catalyzed transmethylation according to Christie (18) with modifications by Chouinard *et al.* (19). FAME were quantified using a gas chromatograph (GC system HP 6890+; Hewlett Packard, Wilmington, DE) equipped with a CP-SIL 88 fused-silica capillary column [100 m × 0.25 mm (i.d.) with 0.2-µm film thickness; Varian, Inc.]. GC conditions were as described previously (20). FA peaks were identified using pure methyl ester standards (Nu-Chek-Prep, Elysian, MN). Additional standards for CLA isomers were obtained from Natural ASA, and a butter oil reference standard (CRM 164; Commission of the European Community Bureau of References, Brussels, Belgium) was

TABLE 3
Quantities of FA Provided by Abomasal Infusion of Supplements[a]

| FA (g/d)	10,12 CLA supplement	CD 18:3 supplement
16:0	<0.1	<0.1
18:1 *c*-9	0.1	0.7
18:2 *c*-9,*c*-12	<0.1	3.0
CLA		
18:2 *c*-9,*t*-11	<0.1	2.1
18:2 *t*-10,*c*-12	2.1	2.1
Other CLA	<0.1	<0.1
CD 18:3		
18:3 *c*-6,t-10,*c*-12		2.6
18:3 *c*-6,t-8,*c*-12		4.0
Other	<0.1	3.4

[a]For abbreviation see Table 2.

used to determine recoveries and correction factors for individual FA. In addition, a milk fat sample from each cow receiving the CD 18:3 supplement was analyzed by HPLC using the conditions stated previously to determine the percentages of the two CD 18:3 isomers present in the single peak identified by GC.

Statistical analysis. Data were statistically analyzed as a 3×3 Latin square design using the PROC MIXED procedure of SAS (21) with the model: $Y_{ijk} = \mu + T_i + R_j + C_k + E_{ijk}$ where Y_{ijk} is observation, μ is overall mean, T_i is treatment ($i = 1, 2,$ and 3), R_j is period ($j = 1, 2,$ and 3), C_k is cow ($k = 1, 2,$ and 3), and E_{ijk} is residual error. Values presented are least square means and significance was set at $P < 0.05$.

RESULTS AND DISCUSSION

The metabolism of CLA to conjugated intermediates has been shown in mice (22), rats (10,23–25), and lambs (26). *Trans*-10,*cis*-12 CLA is a potent inhibitor of milk fat synthesis. and its metabolism involves an initial desaturation by Δ^6-desaturase to give a CD 18:3, followed by an elongation and desaturation producing CD 20:3 and CD 20:4, respectively (Fig. 2). These can be further metabolized in the same manner as linoleic acid to eicosanoid-like compounds. In the present study, we examined the effect of a CD 18:3 enrichment containing *cis*-6,*trans*-10,*cis*-12 to determine whether this metabolite of *trans*-10,*cis*-12 CLA was involved in the mechanism of the regulation of milk fat synthesis. Owing to the lack of pure *cis*-6,*trans*-10,*cis*-12 18:3, a FA enrichment was used that also contained a second CD 18:3 isomer (*cis*-6,*trans*-8,*cis*-12) as well as *trans*-10,*cis*-12 CLA. The *trans*-10,*cis*-12 CLA supplement (positive control treatment) and the CD 18:3 supplement were supplied in quantities so that each provided 2.1 g/d of *trans*-10,*cis*-12 CLA. This dose of *trans*-10,*cis*-12 CLA is far less than the
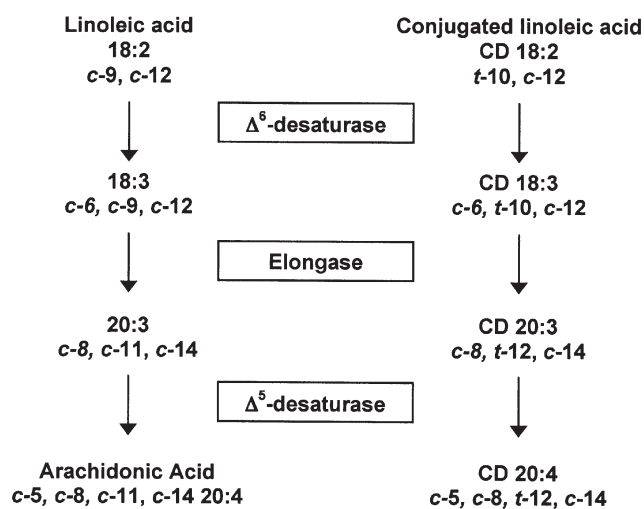
FIG. 2. Metabolic pathway for the desaturation and elongation of linoleic acid and *trans*-10,*cis*-12 CLA. Adapted from Banni (7). For abbreviation see Figure 1.

TABLE 4
Performance of Lactating Dairy Cows During Abomasal Infusions[a]

Variable		Control	10,12 CLA Supplement	CD 18:3 Supplement	SEM	P^b
			Treatment			
Dry matter intake (kg/d)		23.3	21.8	21.3	1.1	0.50
Milk (kg/d)		24.4	25.9	25.3	1.2	0.24
Milk fat						
	%	3.11[a]	2.11[b]	2.25[b]	0.10	<0.001
	kg/d	0.766[a]	0.546[b]	0.568[b]	0.057	0.01
Milk protein						
	%	2.68	2.72	2.76	0.13	0.27
	g/d	0.649	0.701	0.699	0.039	0.17

[a]Values represent an average of day 5 of abomasal infusion of FA supplements.
[b]Statistical probability of treatment effects. Means within a row with different superscripts differ.

amount (~10 g/d) required to achieve nadir for the reduction in milk fat yield based on the dose–response relationships described previously (27). Therefore, if the mechanism of action for *trans*-10,*cis*-12 CLA is due to this initial metabolite (*cis*-6,*trans*-10,*cis*-12 18:3) or the formation of subsequent metabolites, additional milk fat depression should have occurred in the treatment group receiving the CD 18:3 supplement. This was not observed, and overall the treatment groups receiving the *trans*-10,*cis*-12 CLA supplement and the CD 18:3 supplement had similar reductions in milk fat content and milk fat yield (Table 4). Further, the magnitude of the reductions in milk fat yield observed for the *trans*-10,*cis*-12 CLA supplement and CD 18:3 supplement is consistent with results previously reported for abomasal infusion of pure *trans*-10,*cis*-12 CLA (27,28).

The temporal pattern for milk fat yield illustrated a progressive reduction for cows receiving the FA supplements, while no change in milk fat yield was observed for the control (Fig. 3). On termination of the supplements, milk fat yield returned to normal for both the *trans*-10,*cis*-12 CLA and CD 18:3 treatment groups. In contrast to effects on milk fat, FA supplements had no effect on DMI, milk yield, or milk protein (Table 4). The lack of change in these variables is consistent with other studies that have abomasally infused CLA isomers and observed a reduction in milk fat synthesis (3,19,27–32).

The FA composition of the milk fat from the three treatment groups is presented in Table 5. The observed decrease in milk fat yield for the positive control and the CD 18:3 treatments was the result of reductions in most FA. Milk FA composition was shifted owing to a greater reduction of *de novo* synthesized FA, resulting in a relative increase in the proportion of preformed long-chain FA. Shifts in milk fat composition are comparable to results previously observed in studies in which CLA caused a reduction in milk fat synthesis (3,19,28–33). Consistent within these studies was a reduced secretion of all milk FA, with a greater reduction of the FA containing ≤16 carbons resulting in a proportional increase of the FA of >16 carbons.

Partial chromatograms of representative milk fat samples from the three treatment groups depicting the elution of the CLA and partially conjugated 18:3 isomers are shown in Fig-

ure 4. The partially conjugated 18:3 isomers present in the CD 18:3 supplement eluted as a single peak under our GC conditions, and this peak was not present in the milk fat of either the control or *trans*-10,*cis*-12 CLA treatment groups (Fig. 4). Clearly, the CD 18:3 isomers were taken up by the mammary gland and incorporated into milk fat. Milk fat from each cow receiving the CD 18:3 supplement was further analyzed by HPLC and GC/MS/MS to determine the isomer mixture in the single CD 18:3 peak identified by GC analysis. Based on these analyses, 35% of the peak was *cis*-6,*trans*-10,*cis*-12 18:3, and the other 65% was *cis*-6,*trans*-8,*cis*-12 18:3. By using these values, it was determined that the abomasally infused dose was transferred to milk fat with an efficiency of 33% for *cis*-6,*trans*-10,*cis*-12 18:3 and 41% for *cis*-6,*trans*-8,*cis*-12 18:3. Milk fat content of the *trans*-10,*cis*-12 CLA isomer was at the limit of detection in the control group. However, as expected, a similar increase in the milk fat content of this isomer was observed when cows received the *trans*-10,*cis*-12 CLA supplement
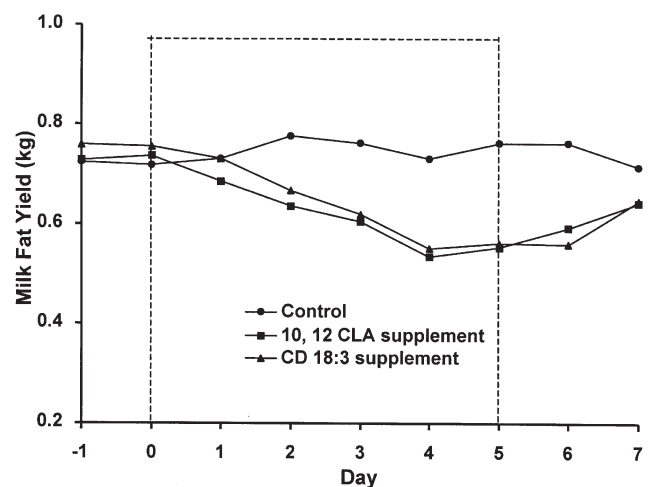
FIG. 3. Temporal pattern of milk fat yield during abomasal infusion of FA supplements. Infusions were for 5 d and are indicated by the dotted lines. Values represent means from three cows; SEM = 0.06 kg/d.

TABLE 5
Composition of Milk Fat During Abomasal Infusions[a]

FA (%)	Control	10-12 CLA Supplement	CD 18:3 Supplement	SEM	P^b
4:0	5.03	5.00	4.94	0.45	0.93
6:0	1.95[a]	1.52[b]	1.64[b]	0.13	<0.001
8:0	0.91[a]	0.64[b]	0.73[c]	0.06	<0.001
10:0	1.81[a]	1.34[b]	1.46[c]	0.11	<0.001
12:0	2.01[a]	1.73[b]	1.82[c]	0.10	<0.001
14:0	9.07[a]	8.36[b]	8.37[b]	0.34	<0.001
14:1	0.79[a]	0.68[b]	0.69[b]	0.12	0.03
15:0	0.89[c]	0.97[a]	0.94[b]	0.02	<0.001
16:0	25.65[a]	23.53[b]	22.90[b]	0.72	<0.001
16:1	1.14	1.06	1.02	0.07	0.22
17:0	0.52[b]	0.61[a]	0.59[a]	0.02	<0.001
18:0	13.43	14.20	14.16	0.79	0.15
18:1 *t*-6-8	0.36[c]	0.44[a]	0.39[b]	0.01	<0.001
18:1 *t*-9	0.31[b]	0.34[a]	0.34[a]	0.02	0.01
18:1 *t*-10	0.48	0.50	0.51	0.04	0.36
18:1 *t*-11	1.58	1.68	1.72	0.17	0.15
18:1 *t*-12	0.56	0.57	0.56	0.03	0.81
18:1 *c*-9	26.93[b]	29.48[a]	28.94[a]	1.14	<0.001
18:2 *c*-9,*c*-12	2.83[c]	3.35[b]	3.72[a]	0.25	<0.001
18:2 *c*-9,*t*-11	0.65[b]	0.67[b]	0.85[a]	0.07	<0.001
18:2 *t*-10,*c*-12	<0.01[b]	0.11[a]	0.10[a]	0.003	<0.001
18:3 *c*-9,*c*-12,*c*-15	0.39[b]	0.42[b]	0.46[a]	0.02	0.005
18:3 *c*-6,*t*-10,*c*-12	<0.01[b]	<0.01[b]	0.17[a]	0.01	<0.001
18:3 *c*-6,*t*-8,*c*-12	<0.01[b]	<0.01[b]	0.32[a]	0.01	<0.001
20:0	0.11	0.11	0.11	0.01	0.69
Other	2.61	2.70	2.68	0.06	0.41
Summation by source[c]					
<C_{16}	22.46[a]	20.24[b]	20.58[b]	1.03	<0.001
C_{16} + $C_{16:1}$	26.79[a]	24.58[b]	23.92[b]	0.77	<0.001
>C_{16}	50.75[b]	55.17[a]	55.48[a]	1.73	<0.001
Desaturase index					
14:1/14:0	0.09	0.08	0.08	0.01	0.67
16:1/16:0	0.04	0.04	0.04	0.002	0.85
18:1/18:0	2.04	2.08	2.05	0.15	0.86
*c*9,*t*11 CLA/18:1 *t*11	0.42[b]	0.40[b]	0.49[a]	0.02	<0.001

[a]Values represent an average of day 5 of abomasal infusion of FA supplements.
[b]Statistical probability of treatment effects. Means within a row with different superscripts differ.
[c]FA <C_{16} originate from *de novo* synthesis, FA >C_{16} are preformed FA taken up by the mammary gland, and C_{16} + $C_{16:1}$ FA come from both *de novo* and preformed sources.

(0.11% of total FA) and the CD 18:3 supplement (0.10% of total FA) (Table 5). These increases reflect similar transfer efficiencies for the *trans*-10,*cis*-12 CLA isomer into milk fat from the *trans*-10,*cis*-12 CLA supplement (mean = 25%, range = 20–29%) and the CD 18:3 supplement (mean = 24%, range = 19–27%). In a summary of six studies, de Veth *et al*. (27) reported an average transfer efficiency of 22% for abomasally infused *trans*-10,*cis*-12 CLA. Thus, the transfer of *trans*-10,*cis*-12 CLA into milk fat is less than that observed for the two CD 18:3 isomers. This difference cannot be accounted for by the metabolism of *trans*-10,*cis*-12 CLA to *cis*-6,*trans*-10,*cis*-12 18:3, because this partially conjugated 18:3 isomer was not present in the milk fat of the control or the treatment group receiving the *trans*-10,*cis*-12 CLA supplement (Fig. 4).

The desaturase index comprises four ratios of FA that represent a proxy for the Δ^9-desaturase enzyme in the mammary gland (1). These ratios were not different among treatment groups, with the exception of an increase in the ratio of *cis*-9,*trans*-11 CLA to *trans*-11 18:1 observed when cows received the CD 18:3 supplement (Table 5). This increase was expected due to the presence of *cis*-9,*trans*-11 CLA isomer in the CD 18:3 supplement (Table 2), which resulted in an increase of this CLA isomer in milk fat (Table 5). Previous studies involving growing rodents have demonstrated that the *trans*-10,*cis*-12 CLA isomer affects both enzyme activity and gene expression for Δ^9-desaturase (34). High doses of *trans*-10,*cis*-12 CLA have also been noted to alter the milk fat desaturase index in dairy cows (1,35). However, the present study is similar to others
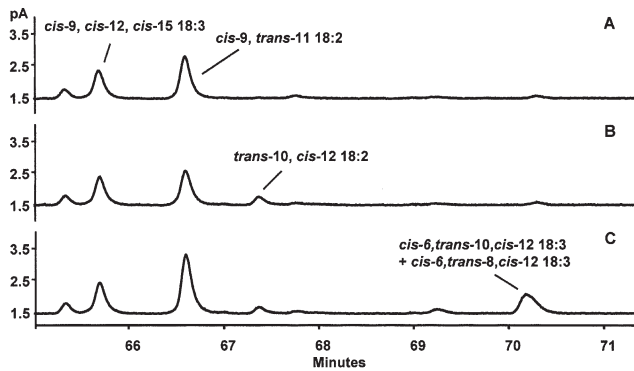
FIG. 4. Partial gas chromatogram of milk fat from cows that had received treatments involving control (A), *trans*-10,*cis*-12 CLA supplement (B), and CD 18:3 supplement (mixture of *cis*-6,*trans*-10,*cis*-12 18:3 and cis-6,*trans*-8,*cis*-12 18:3, plus *trans*-10,*cis*-12 CLA) (C). For abbreviation see Figure 1.

in that low doses of *trans*-10,*cis*-12 CLA do not alter the desaturase index in the milk fat (14,28).

Overall, abomasal infusion of *trans*-10,*cis*-12 CLA caused a reduction in milk fat synthesis that was consistent with previous studies. A greater reduction in milk fat synthesis was not observed for the treatment group receiving the CD 18:3 supplement. This indicates that despite being taken up and incorporated into milk fat, neither the Δ^6 desaturation product of *trans*-10,*cis*-12 CLA (*cis*-6,*trans*-10,*cis*-12 18:3) nor the other CD 18:3 isomer present in the supplement (*cis*-6,*trans*-8,*cis*-12 18:3) had any effect on milk fat synthesis. Therefore, these data support a mechanism of action for *trans*-10,*cis*-12 CLA involving this specific isomer, *per se*, in the reduction of milk fat synthesis, and they provide no support that the mechanism involves a metabolite of *trans*-10,*cis*-12 CLA.

ACKNOWLEDGMENTS

REFERENCES

1. Bauman, D.E., Corl, B.A., and Peterson, D.G. (2003) Biology of Conjugated Linoleic Acid Acids in Ruminants, in *Advances in Conjugated Linoleic Acid Research* (Sébédio, J.-L., Christie, W.W., and Adlof, R.O., eds.), Vol. 2, pp. 146–173, AOCS Press, Champaign.
2. Wang, Y., and Jones, P.J. (2004) Dietary Conjugated Linoleic Acid and Body Composition, *Am. J. Clin. Nutr. 79*, 1153S–1158S.
3. Baumgard, L.H., Corl, B.A., Dwyer, D.A., Sæbø, A., and Bauman, D.E. (2000) Identification of the Conjugated Linoleic Acid Isomer That Inhibits Milk Fat Synthesis, *Am. J. Physiol. Regul. Integr. Comp. Physiol. 278*, R179–R184.
4. Park, Y., Storkson, J.M., Albright, K.J., Liu, W., and Pariza, M.W. (1999) Evidence That the *trans*-10,*cis*-12 Isomer of Conjugated Linoleic Acid Induces Body Composition Changes in Mice, *Lipids 34*, 235–241.
5. Jump, D.B., and Clarke, S.D. (1999) Regulation of Gene Expression by Dietary Fat, *Annu. Rev. Nutr. 19*, 63–90.
6. Belury, M.A. (2002) Dietary Conjugated Linoleic Acid in Health: Physiological Effects and Mechanisms of Action, *Annu. Rev. Nutr. 22*, 505–531.
7. Banni, S. (2002) Conjugated Linoleic Acid Metabolism, *Curr. Opin. Lipidol. 13*, 261–266.
8. Sébédio, J.-L., Chardigny, J.M., and Berdeaux, O. (2003) Metabolism of Conjugated Linoleic Acids, in *Advances in Conjugated Linoleic Acid Research* (Sébédio, J.-L., Christie, W.W., and Adlof, R.O., eds.), Vol. 2, pp. 259–266, AOCS Press, Champaign.
9. Sébédio, J.-L. (1999) Conjugated Linoleic Acid Metabolites in Rats, in *Advances in Conjugated Linoleic Acid Research* (Yurawecz, M.P., Mossoba, M.M., Kramer, J.K.G., Pariza, M.W., and Nelson, G.J., eds.), Vol. 1, pp. 319–326, AOCS Press, Champaign.
10. Gruffat, D., De La Torre, A., Chardigny, J.M., Durand, D., Loreau, O., Sébédio, J.-L., and Bauchart, D. (2003) *In vitro* Comparison of Hepatic Metabolism of 9*cis*-11*trans* and 10*trans*-12*cis* isomers of CLA in the Rat, *Lipids 38*, 157–163.
11. Pariza, M.W., Park, Y., Xu, X., Ntambi, J.M., and Kang, K. (2003) Speculation on the Mechanisms of Action of Conjugated Linoleic Acid, in *Advances in Conjugated Linoleic Acid Research* (Sébédio, J.-L., Christie, W.W., and Adlof, R.O., eds.), Vol. 2, pp. 251–258, AOCS Press, Champaign.
12. National Research Council (2001) *Nutrient Requirements of Dairy Cattle*, 7th rev. edn., National Academy of Sciences, Washington, DC.
13. Fox, D.G., Tedeschi, L.O., Tylutki, T.P., Russell, J.B., Van Amburgh, M.E., Chase, L.E., Pell, A.N., and Overton, T.R. (2004) The Cornell Net Carbohydrate and Protein System Model for Evaluating Herd Nutrition and Nutrient Excretion, *Anim. Feed Sci. Technol. 112*, 29–78.
14. Bernal-Santos, G., Perfield, J.W., Barbano, D.M., Bauman, D.E., and Overton, T.R. (2003) Production Responses of Dairy Cows to Dietary Supplementation with Conjugated Linoleic Acid (CLA) During the Transition Period and Early Lactation, *J. Dairy Sci. 86*, 3218–3228.
15. Michaud, A.L., Yurawecz, M.P., Delmonte, P., Corl, B.A., Bauman, D.E., and Brenna, J.T. (2003) Identification and Characterization of Conjugated Fatty Acid Methyl Esters of Mixed Double Bond Geometry by Acetonitrile Chemical Ionization Tandem Mass Spectrometry, *Anal. Chem. 75*, 4925–4930.
16. Spires, H.R., Clark, J.H., Derrig, R.G., and Davis, C.L. (1975) Milk Production and Nitrogen Utilization in Response to Postruminal Infusion of Sodium Caseinate in Lactating Cows, *J. Nutr. 105*, 1111–1121.
17. Hara, A., and Radin, N.S. (1978) Lipid Extraction of Tissues with a Low-Toxicity Solvent, *Anal. Biochem. 90*, 420–426.
18. Christie, W.W. (1982) A Simple Procedure for Rapid Transmethylation of Glycerolipids and Cholesteryl Esters, *J. Lipid Res. 23*, 1072–1075.
19. Chouinard, P.Y., Corneau, L., Barbano, D.M., Metzger, L.E., and Bauman, D.E. (1999) Conjugated Linoleic Acids Alter Milk Fatty Acid Composition and Inhibit Milk Fat Secretion in Dairy Cows, *J. Nutr. 129*, 1579–1584.
20. Perfield, J.W., II, Bernal-Santos, G., Overton, T.R., and Bauman, D.E. (2002) Effects of Dietary Supplementation of Rumen-

Protected Conjugated Linoleic Acid in Dairy Cows During Established Lactation, *J. Dairy Sci. 85*, 2609–2617.

21. SAS Institute, Inc. (1992) SAS Technical Report P-229, SAS/STAT Software: Changes and Enhancements, Release 6.07, SAS Institute, Cary, NC.

22. Belury, M.A., and Kempa-Steczko, A. (1997) Conjugated Linoleic Acid Modulates Hepatic Lipid Composition in Mice, *Lipids 32*, 199–204.

23. Banni, S., Day, B.W., Evans, R.W., Corongiu, F.P., and Lombardi, B. (1995) Detection of Conjugated Diene Isomers of Linoleic Acid in Liver Lipids of Rats Fed a Choline-Devoid Diet Indicates That the Diet Does Not Cause Lipoperoxidation, *Nutr. Biochem. 6*, 281–289.

24. Sébédio, J.-L., Juaneda, P., Dobson, G., Ramilison, I., Martin, J.C., Chardigny, J.M., and Christie, W.W. (1997) Metabolites of Conjugated Isomers of Linoleic Acid (CLA) in the Rat, *Biochim. Biophys. Acta 1345*, 5–10.

25. Sébédio, J.-L., Angioni, E., Chardigny, J.M., Grégoire, S., Juanéda, P., and Berdeaux, O. (2001) The Effect of Conjugated Linoleic Acid Isomers on Fatty Acid Profiles of Liver and Adipose Tissues and Their Conversion to Isomers of 16:2 and 18:3 Conjugated Fatty Acids in Rats, *Lipids 36*, 575–582.

26. Banni, S., Carta, G., Contini, M.S., Angioni, E., Deiana, M., Dessi, M.A., Melis, M.P., and Corongiu, F.P. (1996) Characterization of Conjugated Diene Fatty Acids in Milk, Dairy Products, and Lamb Tissues, *J. Nutr. Biochem. 7*, 150–155.

27. de Veth, M.J., Griinari, J.M., Pfeiffer, A.M., and Bauman, D.E. (2004) Effect of CLA on Milk Fat Synthesis in Dairy Cows: Comparison of Inhibition by Methyl Esters and Free Fatty Acids, and Relationships Among Studies, *Lipids 39*, 365–372.

28. Peterson, D.G., Baumgard, L.H., and Bauman, D.E. (2002) Short Communication: Milk Fat Response to Low Doses of *trans*-10,*cis*-12 Conjugated Linoleic Acid (CLA), *J. Dairy Sci. 85*, 1764–1766.

29. Baumgard, L.H., Sangster, J.K., and Bauman, D.E. (2001) Milk Fat Synthesis in Dairy Cows Is Progressively Reduced by Increasing Supplemental Amounts of *trans*-10,*cis*-12 Conjugated Linoleic Acid (CLA), *J. Nutr. 131*, 1764–1769.

30. Chouinard, P.Y., Corneau, L., Sæbø, A., and Bauman, D.E. (1999) Milk Yield and Composition During Abomasal Infusion of Conjugated Linoleic Acids in Dairy Cows, *J. Dairy Sci. 82*, 2737–2745.

31. Loor, J.J., and Herbein, J.H. (2003) Reduced Fatty Acid Synthesis and Desaturation Due to Exogenous *trans*10,*cis*12-CLA in Cows Fed Oleic or Linoleic Oil, *J. Dairy Sci. 86*, 1354–1369.

32. Perfield, J.W., II, Sæbø, A., and Bauman, D.E. (2004) Use of Conjugated Linoleic Acid (CLA) Enrichments to Examine the Effects of *trans*-8,*cis*-10 CLA, and *cis*-11,*trans*-13 CLA on Milk-Fat Synthesis, *J. Dairy Sci. 87*, 1196–1202.

33. Mackle, T.R., Kay, J.K., Auldist, M.J., McGibbon, A.K.H., Philpott, B.A., Baumgard, L.H., and Bauman, D.E. (2003) Effects of Abomasal Infusion of Conjugated Linoleic Acid on Milk Fat Concentration and Yield from Pasture-Fed Dairy Cows, *J. Dairy Sci. 86*, 644–652.

34. Lee, K.N., Pariza, M.W., and Ntambi, J.M. (1998) Conjugated Linoleic Acid Decreases Hepatic Stearoyl-CoA Desaturase mRNA Expression, *Biochem. Biophys. Res. Commun. 248*, 817–821.

35. Park, Y., Storkson, J.M., Ntambi, J.M., Cook, M.E., Sih, C.J., and Pariza, M.W. (2000) Inhibition of Hepatic Stearoyl-CoA Desaturase Activity by *trans*-10,*cis*-12 Conjugated Linoleic Acid and Its Derivatives, *Biochim. Biophys. Acta 1486*, 285–292.

GC–MS Structural Characterization of Fatty Acids from Marine Aerobic Anoxygenic Phototrophic Bacteria

J.-F. Rontani[a,*], S. Christodoulou[a], and M. Koblizek[b,c]

[a]Laboratoire de Microbiologie de Géochimie et d'Ecologie Marines (UMR 6117), 13288 Marseille, France,
[b]Institute of Microbiology, 379 81 Trebon, Czech Republic, and [c]Institute of Physical Biology,
University of South Bohemia, Nove Hrady, Czech Republic

ABSTRACT: The FA composition of 12 strains of marine aerobic anoxygenic phototrophic bacteria belonging to the genera *Erythrobacter, Roseobacter*, and *Citromicrobium* was investigated. GC–MS analyses of different types of derivatives were performed to determine the structures of the main FA present in these organisms. All the analyzed strains contained the relatively rare 11-methyloctadec-12-enoic acid, and three contained 12-methyloctadec-11-enoic acid, which has apparently never been reported before. High amounts of the very unusual octadeca-5,11-dienoic acid were present in 9 of the 12 strains analyzed. A FA containing a furan ring was detected in three strains. Analytical data indicated that this FA was 10,13-epoxy-11-methyloctadeca-10,12-dienoic acid. A very interesting enzymatic peroxidation of the allylic carbon 10 of *cis*-vaccenic acid was observed in three strains. Deuterium labeling and GC–MS analyses enabled us to demonstrate that this enzymatic process involves the initial dioxygenase-mediated formation of 10-hydroperoxyoctadec-11(*cis*)-enoic acid, which is then isomerized to 10-hydroperoxyoctadec-11(*trans*)-enoic acid and converted to the corresponding hydroxyacids and oxoacids. Different biosynthetic pathways were proposed for these different compounds.

Paper no. L9671 in *Lipids 40*, 97–108 (January 2005).

It has long been known that various forms of bacteriochlorophyll (BChl) are present in prokaryotes, which perform anoxygenic photosynthesis under anaerobic conditions. In 1978, however, BChl *a* was detected in three strains of obligate aerobic bacteria (1,2). Since then, several strains of aerobic bacteria containing BChl *a* have been reported [for reviews see Shimada (3) and Yurkov and Beatty (4)]. The novel aspect of this increasingly large group of bacteria is that they are strict aerobes unable to grow under anaerobiosis. Apparently, these organisms, which are widely known as aerobic anoxygenic phototrophs (AAP) (4), might represent an evolutionary transient phase from anaerobic phototrophs to aerobic heterotrophs (3).

Until recently, AAP were thought to be confined only to specialized niches such as the surface of seaweed, coastal sands, cyanobacterial mats, and water in high tidal zones (5,6). However, in 1999, a significant activity of anoxygenic photosynthesis was discovered in the open ocean by BChl *a* fluorescence emission measurement and was attributed to the presence of AAP (7). Later, the presence of AAP was reported from the euphotic zone of various marine environments (8–11).

Little is known about AAP diversity. All the marine AAP isolates reported to date have been classified as members of four genera: *Erythrobacter*, *Roseobacter*, *Citromicrobium*, and *Roseibium* (6,12–15). Phylogenetically, the *Erythrobacter* and *Citromicrobium* genera belong to the Sphingomonadaceae family (α-4 subclass of the *Proteobacteria*), and the *Roseobacter* and *Roseibium* genera belong to the Rhodobacteriaceae family (α-3 subclass of the *Proteobacteria*).

In the present work, we analyzed the lipid composition of several isolates of marine AAP belonging to the *Erythrobacter*, *Roseobacter*, and *Citromicrobium* genera. The structures of FA were determined by GC–MS analysis of different derivatives.

MATERIALS AND METHODS

Organisms. Twelve strains containing functional bacterial photosynthetic reaction centers were isolated from diverse marine environments (Table 1). Isolation and characterization of these strains were described previously (10,15). The isolates were grown under fully aerobic conditions exposed to a light–dark cycle (12/12 h) at 23°C. The cultures were inoculated into Erlenmeyer flasks containing an organic enriched seawater medium supplemented with 0.5 g peptone and 0.1 g yeast extract per liter (15). The cells were harvested in a stationary phase by centrifugation at $10,000 \times g$.

Alkaline hydrolysis. Saponification was carried out on approximately 15 mg (dry weight) of wet cells of AAP; 25 mL of water, 25 mL of methanol, and 2.8 g of potassium hydroxide were added and the mixture was saponified by refluxing for 2 h. The content of the flask was acidified with hydrochloric acid (pH 1) after cooling and was subsequently extracted three times with dichloromethane. The combined dichloromethane extracts were dried over anhydrous Na_2SO_4, filtered, and concentrated by rotary evaporation at 40°C to give the total solvent-extractable lipid compounds.

Acidic hydrolysis. The residues obtained after alkaline hydrolysis were treated with 2 M HCl by refluxing for 4 h. After cooling, the reaction mixture was extracted three times with dichloromethane. The combined extracts were then dried over

TABLE 1
Genus and Origin of the Different Strains of Aerobic Anoxygenic Phototrophs (AAP) Analyzed

Strain	Genus	Origin	Temperature (°C)	Depth (m)
NAP1	*Erythrobacter*	NW Atlantic (39°36′N, 72°27′W)	12	0
MG3	*Erythrobacter*	SE Atlantic/W Indian (41°06′S, 19°25′E)	16	0
AT8	*Erythrobacter*	NE Pacific (48°15′N, 128°19′W)	16	0
BA13	*Erythrobacter*	SE Atlantic (48°33′N, 129°53′W)	16	22
B20	*Erythrobacter*	The Baltic Sea (55°17′N, 18°55′E)	18	0
COL2P	*Roseobacter*	Mediterranean coast (42°28′N, 3°11′E)	23	0
SYOP2	*Roseobacter*	Australia, Sydney coast	18	0
B09	*Roseobacter*	The Baltic Sea (59°39′N, 24°9′E)	17	0
B11	*Roseobacter*	The Baltic Sea (59°22′N, 22°36′E)	16	0
BS110	*Roseobacter*	Bosphorus (41°12.8′N, 29°07.4′E)	14	62
BS36	*Roseobacter*	The Black Sea (45°42.7′N, 31°05.7′E)	16	5
CV44	*Citromicrobium*	Central Atlantic (22°45′N, 46°04′W)	25	100

anhydrous Na_2SO_4, filtered, and concentrated by rotary evaporation at 40°C.

Lipid extraction. Approximately 15 mg (dry weight) of wet cells of AAP were extracted ultrasonically with chloroform/methanol/water (1:2:0.8, by vol) (16). Chloroform and deionized water were added to the combined extracts to obtain the final chloroform/methanol/water ratio of 1:1:0.9 (by vol) to initiate phase separation. The lipids were recovered in the lower chloroform phase, which was dried over anhydrous Na_2SO_4, filtered, and concentrated by rotary evaporation at 40°C.

Reduction. Reduction of allylic hydroperoxyacids and oxoacids to alcohols was performed in methanol (25 mL) by excess $NaBH_4$ or $NaBD_4$ (10 mg per 1 mg of extract). The mixture was agitated for 30 min at 20°C using magnetic stirring (17). After reduction, water and KOH were added and saponification was carried out as described in the *Alkaline hydrolysis* section.

Acetylation. Extracts were taken up in a mixture of 300 µL pyridine and acetic anhydride (2:1, vol/vol). The mixture was incubated overnight at 50°C and then evaporated to dryness under nitrogen. Under these conditions, hydroperoxides are quantitatively transformed to the corresponding ketones (18). After acetylation, saponification was carried out as described in the *Alkaline hydrolysis* section.

Osmium tetroxide oxidation. Lipid extracts and OsO_4 (1:2, w/w) were added to a pyridine/dioxane mixture (1:8, vol/vol; 5 mL) and incubated for 1 h at room temperature. Then 6 mL of Na_2SO_3 suspension (8.5 mL of 16% Na_2SO_3 in water/methanol, 8.5:2.5, vol/vol) was added and the mixture was again incubated for 1.5 h. The resulting mixture was gently acidified (pH 3) with HCl and extracted three times with dichloromethane (5 mL). The combined dichloromethane extracts were subsequently dried over anhydrous Na_2SO_4, filtered, and concentrated.

Formation of pyrrolidide derivatives. Lipid extracts were taken up in 2 mL of BF_3/methanol (14%) and heated at 80°C for 1 h. After cooling, an excess of water was added, and methyl esters were extracted three times with hexane, dried over anhydrous Na_2SO_4, filtered, and concentrated using rotary evaporation. The methyl esters obtained were dissolved in

1 mL of pyrrolidine. Then 0.1 mL of acetic acid was added and the mixture was heated at 100°C for 1 h. The excess pyrrolidine was removed under a stream of nitrogen at 50°C, and the residue was taken up in hexane/diethyl ether (1:1, vol/vol; 8 mL) and washed three times with water (4-mL portions). The organic phase was dried over anhydrous Na_2SO_4, filtered, and evaporated to obtain the required pyrrolidide derivatives.

Catalytic hydrogenation. Lipid extracts were hydrogenated overnight under magnetic stirring in methanol with $Pd/CaCO_3$ (10–20 mg/mg of extract) (Aldrich, St. Quentin Fallavier, France) as a catalyst. After hydrogenation, the catalyst was removed by filtration and the filtrate was concentrated by rotary evaporation.

Silylation. After evaporation of the solvent, each residue was taken up in 300 µL of a mixture of anhydrous pyridine and bis(trimethylsilyl)trifluoroacetamide (BSTFA) (Supelco, St. Quentin Fallavier, France) (2:1, vol/vol) and silylated for 1 h at 50°C. After evaporation to dryness under nitrogen, the residue was redissolved in ethyl acetate (2 mL/mg) and BSTFA (0.1 mL) and then analyzed by GC–MS.

GC–MS analysis. GC–EIMS analyses (under EI) were carried out with a HP 5890 Series II Plus gas chromatograph connected to an HP 5972 mass spectrometer. The following operating conditions were used: 30 m × 0.25 mm (i.d.) column coated with SolGel-1 (SGE, Ringwood, Australia; film thickness, 0.25 µm); oven temperature programmed from 60 to 130°C at a rate of 30°C min^{-1} and then from 250 to 300°C at 4°C min^{-1}; carrier gas (He) maintained at 1.04 bar until the end of the temperature program and then programmed from 1.04 to 1.5 bar at a rate of 0.04 bar min^{-1}; injector (on-column with retention gap) temperature, 50°C; electron energy, 70 eV; source temperature, 170°C; cycle time, 1.5 s.

Structural assignments were based on interpretation of the MS fragmentations and confirmed by comparison of retention times and mass spectra with those of authentic compounds when these were available.

Analyses of a blank treatment without cells and of AAP grown on glutamate (instead of yeast extract) were done in parallel to check for possible contamination.

TABLE 2
FA Compositions of the Different Strains of AAP Analyzed[a]

Acids	NAP1	MG3	AT8	BA13	B20	CV44	COL2P	SYOP2	B09	B11	BS110	BS36
Saturates												
12:0							3.6				0.1	
14:0	1.3	3.0	1.3	4.4	1.8	1.0	0.7	2.1	1.4	0.6	0.6	0.7
15:0	1.0	1.7	2.6	2.7	0.9	0.4	0.3	0.8	0.4	0.3	0.2	0.2
16:0	7.3	14.1	7.9	17.2	9.0	5.7	10.6	12.6	8.8	6.0	10.2	4.5
17:0	1.3	0.5	1.0	0.8	0.3	0.1	0.8	0.3	0.4	0.1	0.1	0.2
18:0	1.5	4.6	2.8	6.4	3.3	0.6	2.1	9.4	9.0	0.8	1.6	3.8
Monounsaturates												
12:1n-7									1.1	2.1		
16:1n-7	2.0	2.6	1.2	2.3	1.6	1.2	0.6	0.5	0.4	0.9	2.8	1.0
17:1n-8	2.2	0.3	1.5	0.5	0.5	Traces[b]					Traces	
17:1n-6	1.4	0.1	0.9	0.1	5.9	0.4					0.2	
18:1n-7	65.0	45.2	51.0	41.7	70.1	63.4	62.8	48.4	56.7	59.7	24.8	75.0
19:1n-8	1.8		0.4	0.4								
Polyunsaturates												
18:2n-7,13	9.4	7.8	12.9	9.2			c	12.3	6.8	11.4		5.4
Branched												
Me11,18:1n-6	3.1	10.5	9.8	7.1	Traces	10.9	2.8	9.4	10.1	10.5	3.0	4.7
Me12,18:1n-7	Traces		1.7	0.9								
Unknown							1.1			7.3		
Cyclic												
11,12-cyclo-18:0	Traces		Traces	0.4		0.1	3.4				25.1	
Furanoid							1.9				8.2	0.3
Hydroxyacids												
14:0 (2-OH)	0.5	5.8	1.5	2.6	1.6	4.0					1.4	
15:0 (2-OH)	0.5	0.6	2.4	1.5	0.8	Traces					0.4	
16:0 (2-OH)	0.4	0.4	0.3	0.3	3.1	11.9	4.1				6.4	
14:1n-7 (2-OH)											0.4	
16:1n-7 (2-OH)											2.2	
18:1n-7 (2-OH)											1.0	
10:0 (3-OH)							0.3			1.0	5.9	
12:0 (3-OH)							3.9		0.2	Traces	1.6	
13:0 (3-OH)											0.3	
14:0 (3-OH)							0.6					
12:1 (3-OH)									2.2	4.6		3.0
18:1n-9 (10-OH) *cis*		1.0									1.2	Traces
18:1n-9 (10-OH) *trans*		Traces									0.1	Traces

[a]For genera and origins of the bacterial strains see Table 1. See Table 1 for other abbreviation.
[b]<0.1%.
[c]Detected in cultures grown on glutamate.

RESULTS AND DISCUSSION

Saturated FA. The FA compositions of the different strains analyzed are summarized in Table 2. AAP contained a standard pattern of saturated FA ranging from C_{12} to C_{18}, which were rather uninformative. We failed to detect significant amounts of C_{15} and C_{17} branched saturated FA, which is in a good agreement with the well-known lack of such FA in most of the Gram-negative bacteria (19,20).

Monounsaturated FA. In EI mass spectra of monounsaturated FA methyl or trimethylsilyl esters, no feature permits the double bond to be located, because the double bond can migrate when the alkyl chain is ionized in the mass spectrometer. This phenomenon appeared to be particularly prominent in the case of branched FA (21). To avoid the migration problem, it was necessary to prepare specific derivatives of unsaturated FA that "fixed" the double bond. Two methods were used: OsO_4 oxidation (22) and pyrrolidide formation (23). The OsO_4 method involves the formation of diols by stereospecific oxidation of double bonds and subsequent analyses of the silylated diols by GC–MS. The position of the double bond can be deduced from the mass fragmentation patterns of these derivatized compounds. Pyrrolidide derivatives were chosen for this study since: (i) they are prepared under relatively mild conditions, (ii) they are stable chemically, and (iii) they are well suited to the structural characterization of branched unsaturated FA.

The AAP strains investigated contained monounsaturated FA ranging from C_{12} to C_{19} and were dominated by octadec-11(*cis*)-enoic acid (*cis*-vaccenic acid) (Table 2). Two interesting branched 19:1 FA were detected: the 11-methyloctadec-12-enoic and the 12-methyloctadec-11-enoic acids. The mass spectra of the bis-trimethylsilyloxy and pyrrolidide derivatives of the 11-methyloctadec-12-enoic acid are shown in Figure 1. The mass spectrum of the bis-trimethylsilyloxy derivative (obtained after OsO_4 oxidation of the double bond and subsequent silylation), exhibited two strong fragment ions at *m/z* 173 and

A

B
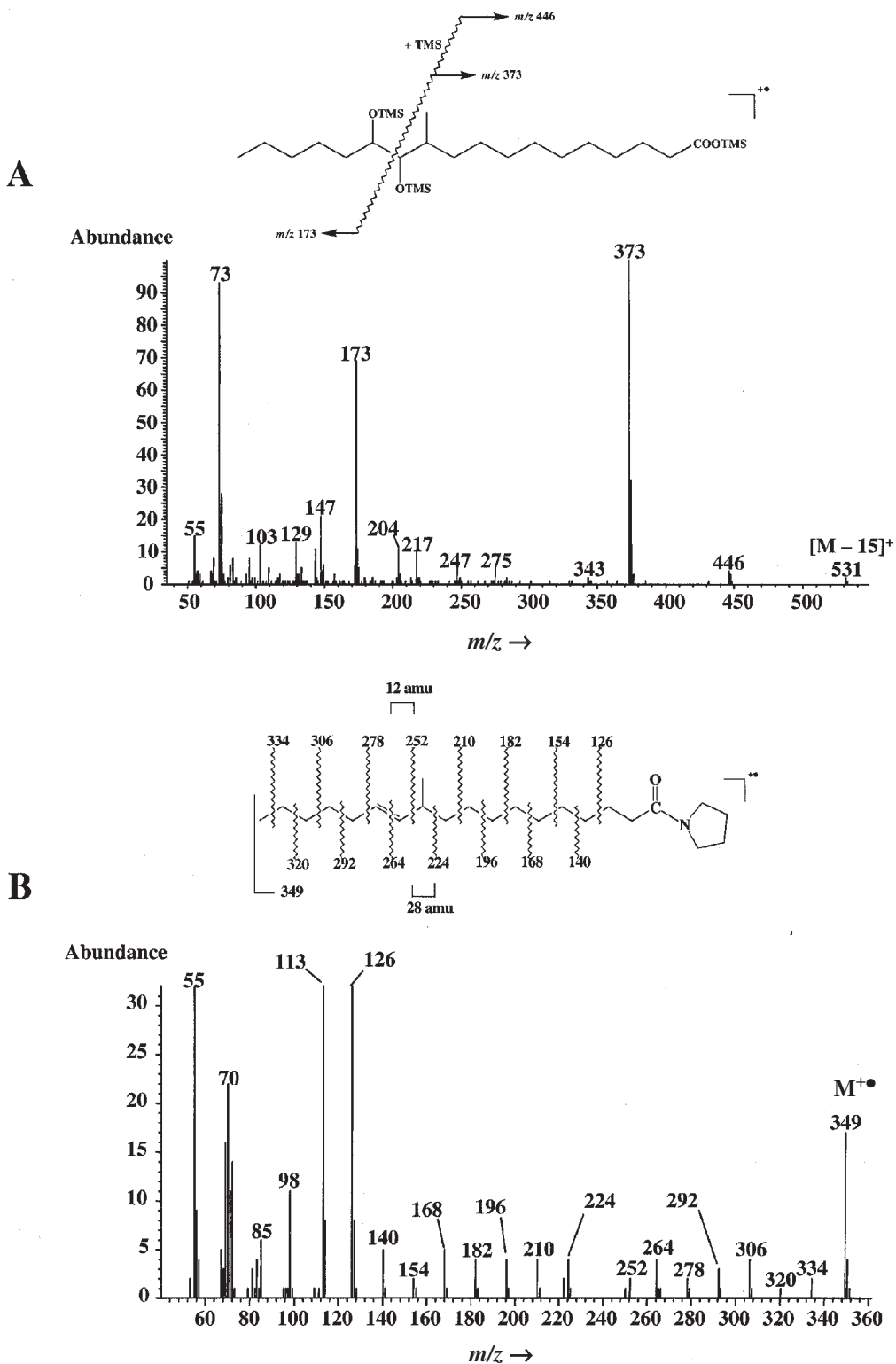
FIG. 1. EI mass spectra of the silylated OsO$_4$ (A) and pyrrolidide (B) derivatives of 11-methyloctadec-12-enoic acid. TMS, trimethylsilyl.

373 resulting from the cleavage of the bond between the two carbon atoms bearing the trimethylsilyloxy groups (Fig. 1A). This proved the presence of a double bond in position 12 in the parent FA. The useful ion at *m/z* 446 resulting from trimethyl-silyl transfer toward the carboxylic group (24,25) confirmed that the fragment ion at *m/z* 373 contained the carboxylic group. In the mass spectrum of the pyrrolidide derivative (Fig. 1B), the gap of 28 amu between *m/z* 224 and 252 localized the methyl
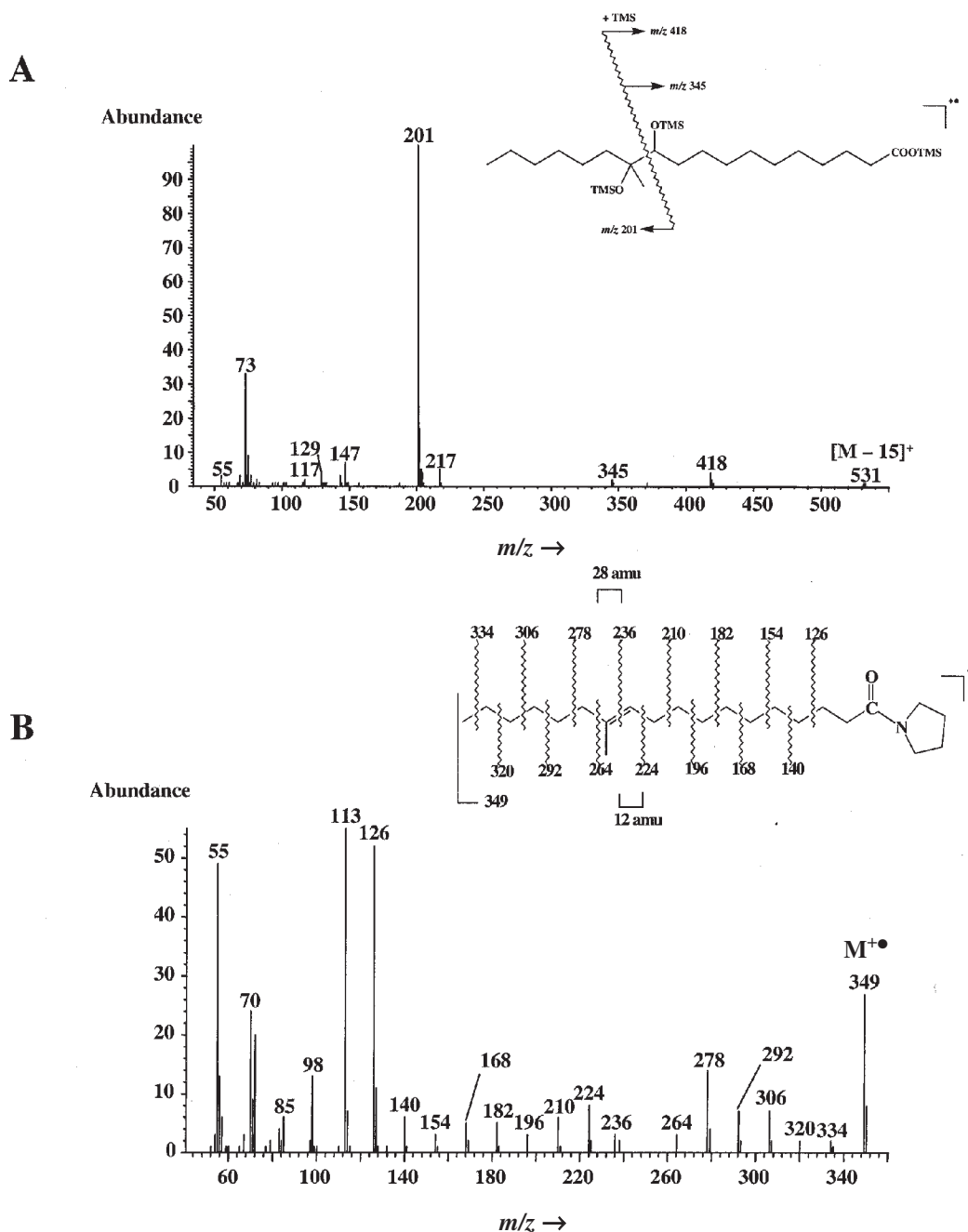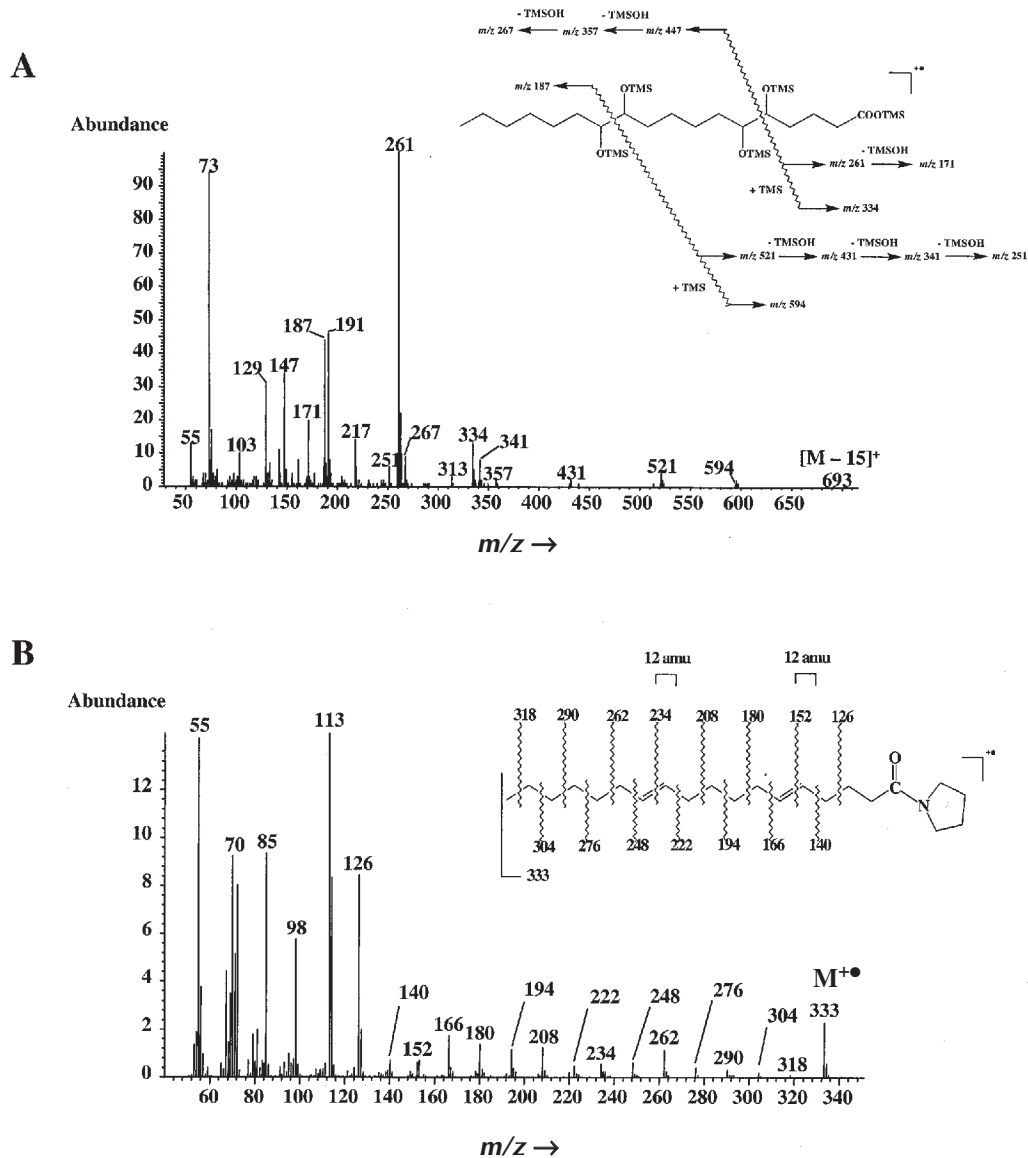
FIG. 2. EI mass spectra of the silylated OsO_4 (A) and pyrrolidide (B) derivatives of 12-methyloctadec-11-enoic acid. For abbreviation see Figure 1.

branch on the carbon C11 (26), whereas the gap of 12 amu between m/z 252 and 264 confirmed the presence of the double bond in position 12. Indeed, if an interval of 12 amu, instead of the regular 14, was observed between the most intense peaks of clusters of fragments containing n and n – 1 carbon atoms of the acid moiety, the double bond was located between carbon n and n + 1 in the molecule (23). 12-Methyloctadec-11-enoic acid was also identified from the mass spectra of its bis-trimethylsilyloxy and pyrrolidide derivatives (Fig. 2). In the mass spectrum of the pyrrolidide derivative (Fig. 2B), the gap

of 12 amu between m/z 224 and 236 showed a double bond in position 11, whereas the gap of 28 amu between m/z 236 and 264 localized the methyl branch on the carbon C12. This assignment was also supported by the presence of fragment ions at m/z 201 (base peak), 345, and 418 in the mass spectrum of the bis-trimethylsilyloxy derivative (Fig. 2A).

11-Methyloctadec-12-enoic acid was present in all the AAP strains analyzed (Table 2). This acid was previously detected in other bacteria such as mycobacteria (27), *Shewanella putrefaciens* (28), *Thiobacillus* (29), *Thiohalocapsa halophila*, and

A

B

FIG. 3. EI mass spectra of the silylated OsO$_4$ (A) and pyrrolidide (B) derivatives of octadeca-5,11-dienoic acid. For abbreviation see Figure 1.

Halochromatium salexigens (Rontani, J.-F., unpublished data). It seems to be a FA typical of bacteria. In contrast, 12-methyloctadec-11-enoic acid was found in only three strains of AAP (Table 2). To our knowledge, this compound has never been reported before.

PUFA. Small amounts of octadeca-9,12-dienoic acid (linoleic acid) were detected in all the strains of AAP analyzed. This result is very surprising, since it is generally believed that bacteria are unable to synthesize methylene-interrupted PUFA (19). After careful examination, it appeared that this acid resulted from contamination during the analytical treatment.

Nine of the 12 strains of AAP analyzed contained a significant proportion of the unusual octadeca-5,11-dienoic acid (Table 2). The mass spectra of the tetra-trimethylsilyloxy and

pyrrolidide derivatives of this acid are shown in Figure 3. The presence of double bonds in positions 5 and 11 is well supported by the intense fragment ions at *m/z* 187, 261, and 334 observed in the mass spectrum of the tetra-trimethylsilyloxy derivative (Fig. 3A) and by the gaps of 12 amu between *m/z* 140 and 152 and between *m/z* 222 and 234 in the mass spectrum of the pyrrolidide derivative (Fig. 3B).

Octadeca-5,11-dienoic acid was previously found in the seed oil of some gymnosperms, e.g., *Ginkgo biloba* (30), and occasionally in sponge lipids (Christie, W.W., unpublished results), always as a minor component. To our knowledge, the presence of this unusual FA has never been reported in phytoplankton (31–34) or in anaerobic photosynthetic bacteria (35). Even though this acid was not detected in all the strains analyzed
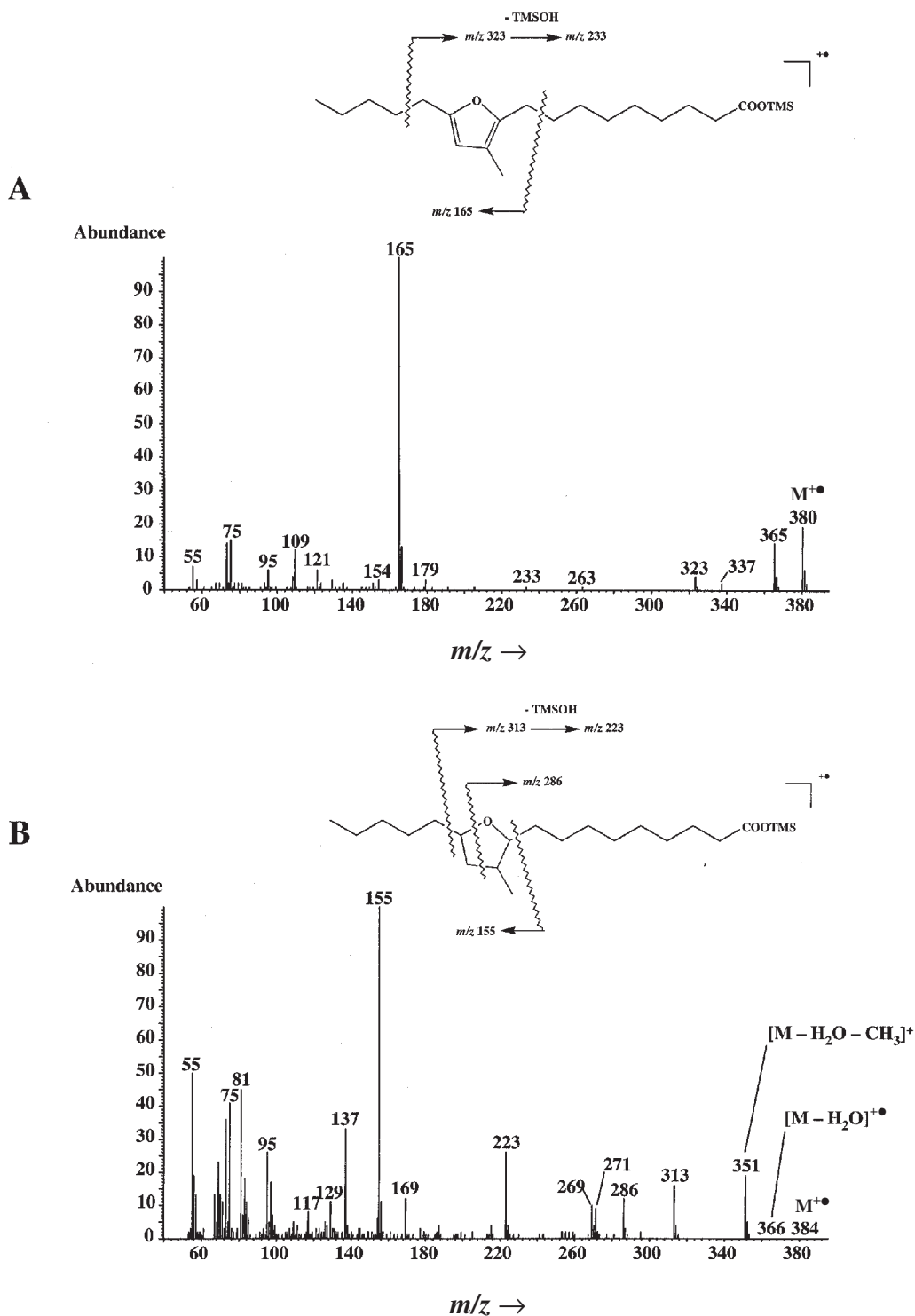
FIG. 4. EI mass spectra of silylated 10,13-epoxy-11-methyloctadeca-10,12-dienoic (A) and 10,13-epoxy-11-methyl-octadecanoic (B) acids. For abbreviation see Figure 1.

(Table 2), it could constitute a useful indicator of the presence of AAP because of its relative abundance in these organisms.

Cyclic FA. 11,12-Methyleneoctadecanoic acid (lactobacillic acid) was detected in six strains of AAP (Table 2). A particularly high proportion was present in the strain BS110. This cyclopropane FA has been differentiated from its corresponding olefinic isomers after catalytic hydrogenation (36). The first step in the biosynthesis of the cyclopropane ring in a FA is similar to that for certain methyl-branched FA, and involves initial addition of a methyl group from *S*-adenosylmethionine to a double bond and subsequent loss of a proton. Thus, lactobacillic acid must be formed by the addition of a methylene group

A

Retention time (min) →

B

Retention time (min) →
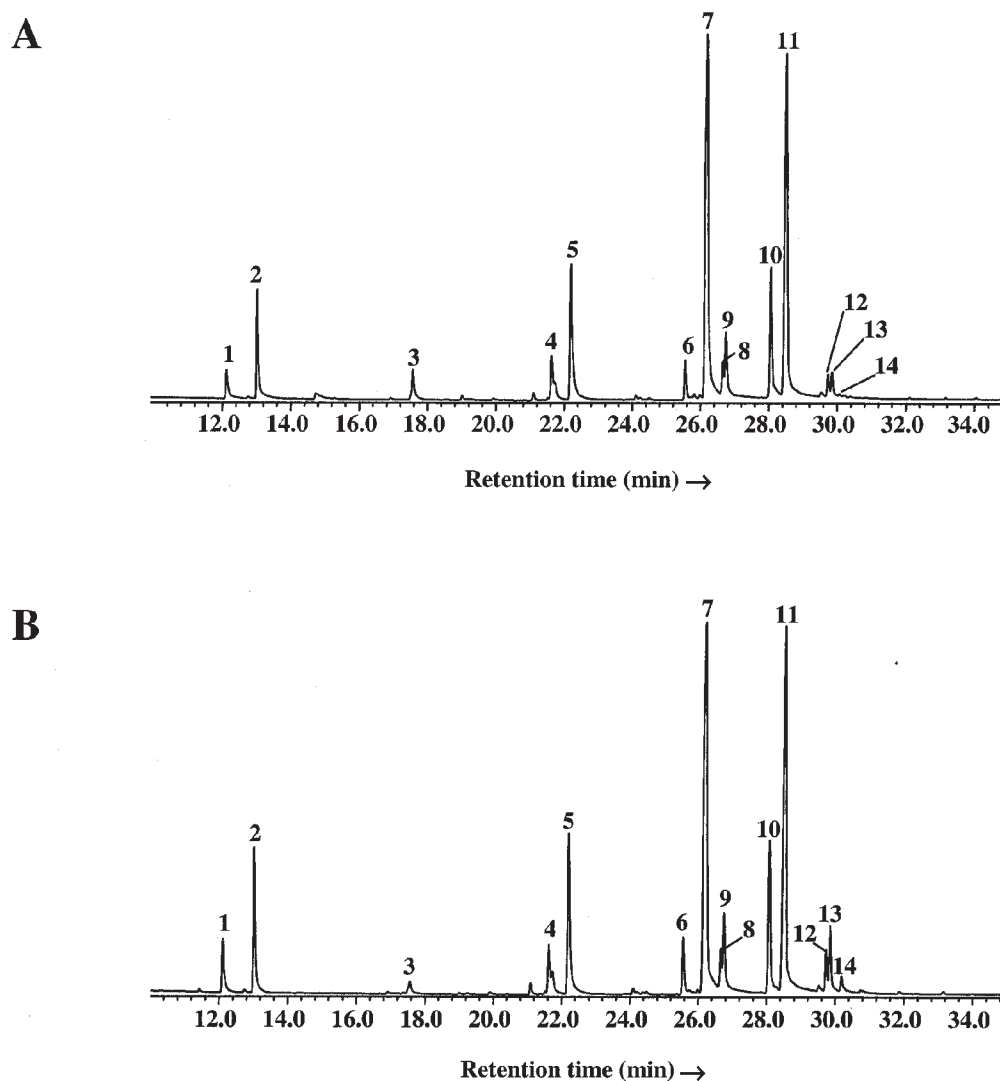
FIG. 5. Total ion current chromatogram of the silylated total lipid extract of the strain BS110 before (A) and after (B) NaBH$_4$ reduction. 1, Dodec-5-enoic acid; 2, 3-hydroxydecanoic acid; 3, 3-hydroxydodecanoic acid; 4, hexadec-9-enoic acid + 2-hydroxypentadecanoic acid; 5, hexadecanoic acid; 6, 2-hydroxyhexadec-9-enoic acid; 7, *cis*-vaccenic acid + 2-hydroxyhexadecanoic acid; 8, octadecanoic acid; 9, 11-methyloctadec-12-enoic acid; 10, 10,13-epoxy-11-methyloctadeca-10,12-dienoic acid; 11, 11,12-methyleneoctadecanoic acid; 12, 2-hydroxyoctadec-11-enoic acid; 13, 10-hydroxyoctadec-11(*cis*)-enoic acid; 14, 10-hydroxyoctadec-11(*trans*)-enoic acid.

across the double bond of *cis*-vaccenic acid. This acid has been found in a wide range of bacterial species of many different types, both Gram-negative and Gram-positive, from strict anaerobes to obligate aerobes.

A furan FA, 10,13-epoxy-11-methyloctadeca-10,12-dienoic acid, was detected in the strains BS110, BS36, and COL2P (Table 2). The mass spectrum of this silylated FA is shown in Figure 4A. Allylic cleavage of the alkylcarboxylic chain at the furan ring produced the base peak at *m/z* 165, whereas allylic cleavage of the alkyl chain yielded a fragment ion at *m/z* 323. The furan ring itself gave rise to a fragment ion at *m/z* 109 characteristic of trisubstituted furan acids (37). The position of the methyl group was determined after hydrogenation (in the presence of Pd as catalyst) (Fig. 4B), thanks to the THF-specific ring cleavage at *m/z* 286 enabling the unambiguous localization of the methyl substituent (38).

10,13-Epoxy-11-methyloctadeca-10,12-dienoic acid was previously detected in several strains of marine bacteria (*S. putrefasciens, Listonella anguillarum, Marinomonas communis, Pseudomonas fluorescens, Enterobacter agglomerans*) (28,37). A very interesting biosynthetic pathway of this acid starting from *cis*-vaccenic acid was proposed by Shirasaka *et al.* (28). The first step of this pathway is thought to be the formation of 11-methyloctadec-12-enoic acid through methylation of *cis*-vaccenic acid; 11-methyloctadeca-10,12-dienoic acid is then produced through desaturation. The next step involves a lipoxygenase-type oxidation, followed by ring closure. The involvement of such a process in BS110, BS36, and COL2P is well supported by the presence of relatively high proportions of 11-methyloctadec-12-enoic acid in these three strains (Table 2). However, the intermediate 11-methyloctadeca-10,12-dienoic acid, which was previously detected by Shirasaka *et al.* (28), has not been observed in these strains.
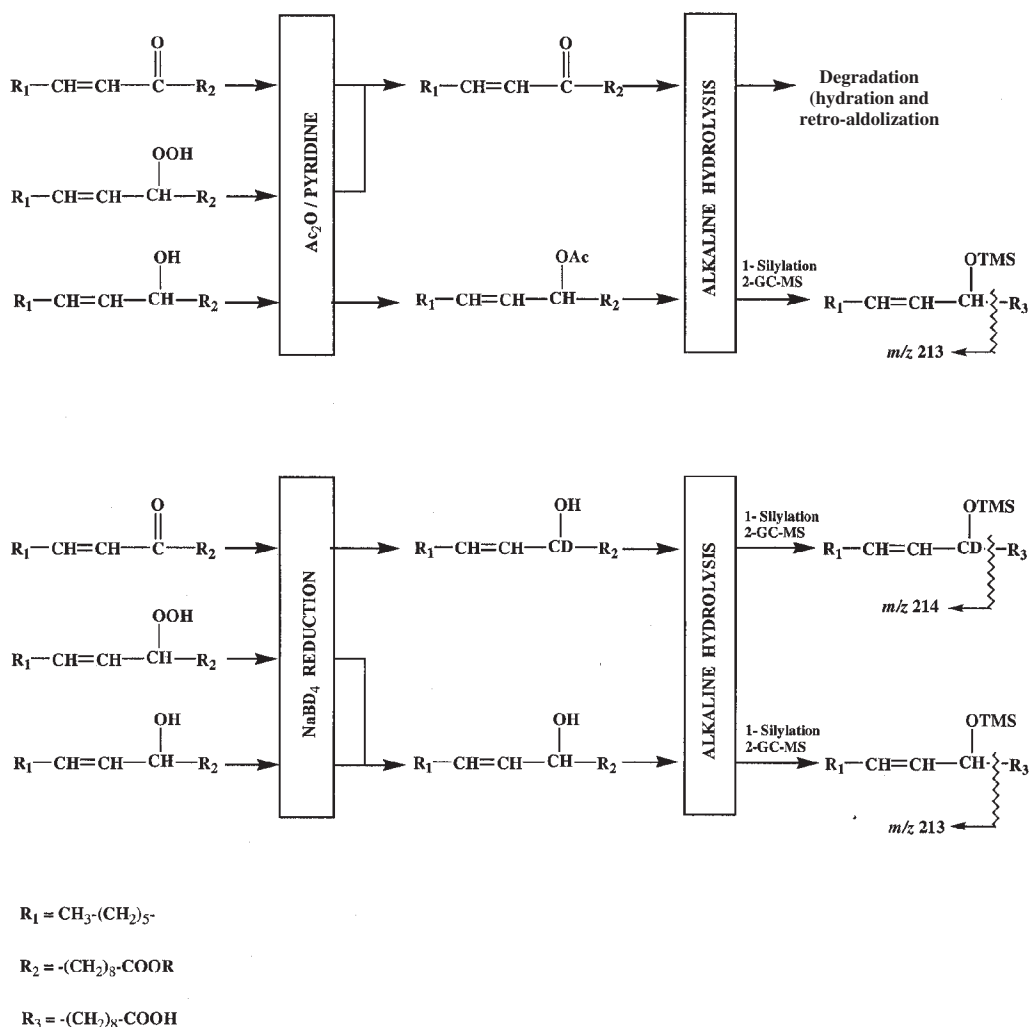
FIG. 6. Characterization of allylic hydroperoxy, hydroxy-, and oxoacids after parallel acetylation and NaBD$_4$ reduction. For abbreviation see Figure 1.

Hydroxyacids. Sphingomonadaceae are generally characterized by the presence of sphingolipids and 2-hydroxyacids and by the lack of 3-hydroxyacids (39). Indeed, all the tested *Erythrobacter-* and *Citromicrobium*-related strains belonging to the Sphingomonadaceae family contain 2-hydroxytetradecanoic, 2-hydroxypentadecanoic, and 2-hydroxyhexadecanoic acids (Table 2). The content of 2-hydroxyacids increases significantly when the acidic hydrolysis is carried out after saponification. This suggests that these compounds are components of sphingolipidic structures linked to sphingosine by amide bonds, which are only partially hydrolyzed during saponification. It is interesting to note that the hydrolysis of these amide bonds is induced during the natural senescence of AAP, when a significant increase in the 2-hydroxyacid content occurs (40).

3-Hydroxyacids were present only in *Roseobacter*-related AAP (Table 2). These compounds, which are typically produced as intermediates in the β-oxidation of monocarboxylic acids,

constitute a classical component of the cell wall lipopolysaccharides of several Gram-negative bacteria (35,41). Interestingly, the *Roseobacter*-related strains COL2P and BS110, in addition to 3-hydroxyacids, also contained 2-hydroxyacids (Table 2).

Cis and *trans* 10-hydroxyoctadec-11-enoic acids were detected in the strains MG3, BS36, and BS110 (Fig. 5, Table 2). The mass spectra of their silylated derivatives were described previously (42). They exhibited a strong fragment ion at *m/z* 213 corresponding to the cleavage at the carbon-bearing –OSiMe$_3$ group. Determination of *cis-* and *trans-*isomers was based on comparison of the retention times with standards. A similar regiospecific oxygenation of the allylic carbon 10 of *cis*-vaccenic acid has been observed previously in senescent cells of the halophilic purple sulfur bacterium *Thiohalocapsa halophila* incubated under aerobic conditions in the dark (42). This enzymatic process was attributed to the involvement of a lipoxygenase. Lipoxygenases are nonheme iron-containing dioxygenases that catalyze the addition of molecular oxygen to
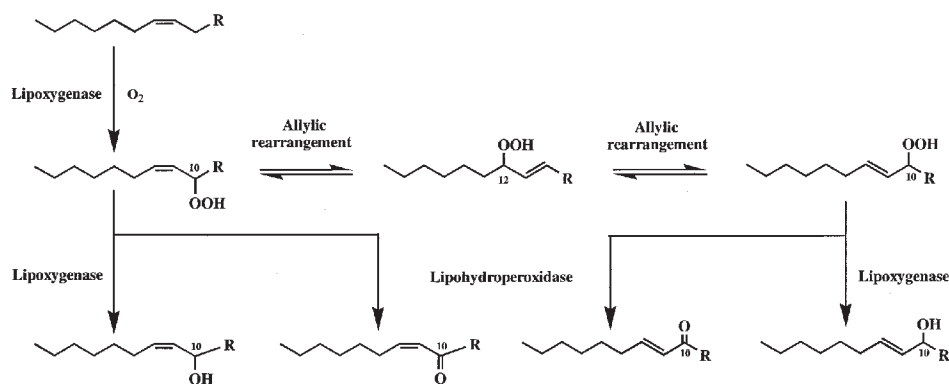
FIG. 7. Proposed pathways for the enzymatic oxygenation of *cis*-vaccenic acid in the strains BS110, BS36, and MG3.

PUFA with a (*cis,cis*)-1,4-pentadiene system to give an unsaturated FA hydroperoxide (43). Lipoxygenases may also catalyze the oxygenation of monounsaturated FA such as oleic (44–47), octadec-*cis*-12-enoic (47), or *cis*-vaccenic (42) acid. These processes afford mainly hydroxy-, hydroperoxy-, or oxoacids. Lipoxygenases are widely distributed in plants, fungi, and animals (48). Recently, these enzymes were also detected in bacteria (45,49). The presence of lipoxygenase in the strains BS110 and BS36 is consistent with their relatively high content of furan FA (Table 2). The amounts of *cis* and *trans* 10-hydroxyoctadec-11-enoic acids increased considerably when the samples were reduced with NaBH$_4$ before the alkaline hydrolysis (Fig. 5). Some tests involving deuterium labeling, acetylation, and GC–MS analyses (Fig. 6) were carried out to determine whether this additional production of hydroxyacids resulted from the reduction of the corresponding hydroperoxy- or oxoacids during the treatment. The organic extracts were divided into two fractions. One part was reduced by NaBD$_4$ and saponified, whereas the other was first acetylated (to dehydrate the hydroperoxides to ketones) and then saponified. Comparison of the amounts of unlabeled hydroxyacids present after acetylation (naturally occurring hydroxyacids) and after reduction (naturally occurring + hydroperoxide reduction-derived hydroxyacids) allowed us to estimate the proportion of hydroperoxyacids and hydroxyacids present in the samples, whereas quantification of the deuterated hydroxyacids after reduction (thanks to the fragment ion at *m/z* 214) (Fig. 6) corresponded to the amount of oxoacids. The allylic oxoacids could not be characterized directly since these compounds do not survive alkaline hydrolysis and are cleaved after hydration and retro-aldol reactions (50). These tests cannot be carried out on the strain BS36 since 10-hydroxyoctadec-11-enoic acids were present in only trace amounts in this strain (Table 2). The results obtained proved that strains BS110 and MG3 contained hydroperoxyacids, oxoacids, and hydroxyacids (Table 3). The presence of significant proportions of hydroperoxides is very surprising since they are extremely cytotoxic and cause dam-

age to membranes and proteins in particular (51). Several enzymatic processes causing further reactions of the hydroperoxides and avoiding their accumulation have been described previously. These processes involve: (i) reduction to the corresponding hydroxyacids (51), (ii) homolytic cleavage of the O–O bond resulting in the formation of oxoacids (48), (iii) dehydration to allene oxides and subsequent hydrolysis of these unstable intermediates (52), and (iv) direct cleavage of the hydroperoxides to aldehydes and oxoacids (53). Only the first two degradation processes seem to act significantly in the strains BS110 and MG3. The reduction of hydroperoxyacids to the corresponding hydroxyacids is generally attributed to the lipoxygenases themselves (51), whereas the breakdown of hydroperoxyacids to oxoacids is induced by lipohydroperoxidases (48). Similar to enzymatic conversion, the hydroperoxides formed may also undergo chemical decomposition under mild conditions. The majority of these decomposition reactions involve free radicals and are promoted by heat, photolysis, metal ions, and metalloproteins. The products of these reactions are similar to those of enzymatic transformations or are either homologs or isomers of the enzymatically produced compounds (48). The quite distinct proportions of hydroperoxyacids, hydroxyacids, and oxoacids observed in the case of the

TABLE 3
Relative Proportions (%) of 10-Hydroperoxyoctadec-11-enoic Acids and Their Degradative Hydroxyacids and Oxoacids in the Strains BS110 and MG3

Compound	BS110	MG3
10-Hydroperoxyoctadec-11(*cis*)-enoic acid	35	35
10-Hydroxyoctadec-11(*cis*)-enoic acid	40	45
10-Oxooctadec-11(*cis*)-enoic acid	25	20
10-Hydroperoxyoctadec-11(*trans*)-enoic acid	20	—[a]
10-Hydroxyoctadec-11(*trans*)-enoic acid	15	—
10-Oxooctadec-11(*trans*)-enoic acid	65	—

[a]Not determined (only trace amounts). For genera and origins of the bacterial strains see Table 1.

cis and *trans* isomers (Table 3) allowed us to exclude the involvement of such abiotic processes during the degradation of *cis* and *trans* 10-hydroperoxyoctadec-11-enoic acid. Allylic hydroperoxides may also undergo highly stereoselective free radical allylic rearrangement (54). These processes, which can act on both *cis* and *trans* allylic hydroperoxides, afford only *trans* configurations (54). The detection of trace amounts of 12-hydroperoxyoctadec-10(*trans*)-enoic acid and its corresponding hydroxyacid and oxoacid in BS110 and MG3 strongly suggests that isomerization of 10-hydroperoxyoctadec-11(*cis*)-enoic acid results from such a rearrangement (Fig. 7).

In conclusion, the FA composition of AAP is characterized by saturated and monounsaturated FA ranging from C_{12} to C_{18} and from C_{12} to C_{19}, respectively, with *cis*-vaccenic acid as the major component. All the AAP analyzed contained the relatively rare 11-methyloctadec-12-enoic acid. This acid was previously detected in some marine bacteria (27–29). It seems to be a typical bacterial FA. The strains NAP1, AT8, and BA13 contained small amounts of the 12-methyloctadec-11-enoic acid, which apparently has never been reported before.

The presence of relatively high proportions of the octadec-5,11-dienoic acid in 9 of the 12 strains of AAP analyzed is very surprising since bacteria usually do not contain PUFA. This unusual acid could constitute a useful indicator of the presence of AAP in the marine environment.

An interesting regiospecific enzymatic peroxidation of the allylic carbon 10 of *cis*-vaccenic acid was observed in the strains BS110, BS36, and MG3. A similar oxidation process was previously described in the case of the purple sulfur bacterium *Thiohalocapsa halophila* (42) and attributed to the involvement of a lipoxygenase. This enzymatic attack of *cis*-vaccenic acid seems to be a characteristic of some (aerobic and anaerobic) phototrophic bacteria. The presence of a lipoxygenase in AAP is well supported by the detection of significant amounts of a furan FA, the 10,13-epoxy-11-methyloctadeca-10,12-dienoic acid in the strains BS110, BS36, and COL2P.

All the strains analyzed belonging to the *Erythrobacter* and *Citromicrobium* genera contained 2-hydroxyacids linked by amide bonds in sphingolipidic structures. These compounds are released during the natural senescence of these organisms. In contrast, all the *Roseobacter*-like strains contained 3-hydroxyacids.

ACKNOWLEDGMENTS

REFERENCES

1. Sato, K. (1978) Bacteriochlorophyll Formation by Facultative Methylotrophs, *Protaminobacter rubber* and *Pseudomonas* AM1, *FEBS Lett. 85*, 207–210.

2. Harashima, K., Shiba, T., Totsuka, T., Shimidu, U., and Taga, N. (1978) Occurrence of Bacteriochlorophyll-*a* in a Strain of an Aerobic Heterotrophic Bacterium, *Agric. Biol. Chem. 42*, 1627–1628.

3. Shimada, K. (1995) Aerobic Anoxygenic Phototrophs, in *Anoxygenic Photosynthetic Bacteria* (Blankenship, R.E., Madigan, M.T., and Bauer, C.E., eds.), p. 105–122, Kluwer Academic, Dordrecht, The Netherlands.

4. Yurkov, V.V., and Beatty, J.T. (1998) Aerobic Anoxygenic Phototrophic Bacteria, *Microbiol. Mol. Biol. Rev. 62*, 695–724.

5. Shiba, T., Simidu, U., and Taga, N. (1979) Distribution of Aerobic Bacteria Which Contain Bacteriochlorophyll-*a*, *Appl. Environ. Microbiol. 38*, 43–45.

6. Shiba, T. (1991) *Roseobacter litoralis* gen. nov., sp. nov. and *Roseobacter denitrificans* sp. nov., Aerobic Pink-Pigmented Bacteria Which Contain Bacteriochlorophyll-*a*, *Syst. Appl. Microbiol. 14*, 140–145.

7. Kolber, Z.S., Van Dover, C.L., Niederman, R.A., and Falkowski, P.G. (2000) Bacterial Photosynthesis in Surface Waters of the Open Ocean, *Nature 407*, 177–179.

8. Kolber, Z.S., Plumley, F.G., Lang, A.S., Beatty, J.T., Blankenship, R.E., VanDover, C.L., Vetriani, C., Koblizek, M., Rathgeber, C., and Falkowski, P.G. (2001) Contribution of Aerobic Photoheterotrophic Bacteria to the Carbon Cycle in the Ocean, *Science 292*, 2492–2495.

9. Goericke, R. (2002) Bacteriochlorophyll-*a* in the Ocean: Is Anoxygenic Bacterial Photosynthesis Important? *Limnol. Oceanogr. 47*, 290–295.

10. Koblízek, M., Falkowski, P.G., and Kolber, Z.S. (2005) Diversity and Distribution of Photosynthetic Bacteria in the Black Sea, *Deep Sea Res. II*, in press.

11. Koblízek, M., Ston-Egiert, J., Sagan, S., and Kolber, Z. (2004) Diel Changes in Bacteriochlorophyll-*a* Concentration Suggest Rapid Bacterioplankton Cycling in the Baltic Sea, *FEMS Microbiol Ecol. 51*, 353–361.

12. Shiba, T., and Simidu, U. (1982) *Erythrobacter longus* gen. nov., sp. nov., an Aerobic Bacterium Which Contains Bacteriochlorophyll-*a, Int. J. Syst. Bacteriol. 32*, 211–217.

13. Nishimura, Y., Muroga, Y., Saito, S., Shiba, T., Takamiya, K., and Shioi, Y. (1994) DNA Relatedness and Chemotaxonomic Feature of Aerobic Bacteriochlorophyll-Containing Bacteria Isolated from Coasts of Australia, *J. Gen. Appl. Microbiol. 40*, 287–296.

14. Suzuki, T., Muroga, Y., Takahama, M., and Nishimura, Y. (2000) *Roseibium denhamense* gen. nov., sp. nov. and *Roseibium hamelinense* sp. nov., Aerobic Bacteriochlorophyll-Containing Bacteria Isolated from the East and West Coasts of Australia, *Int. J. Syst. Bacteriol. 50*, 2151–2156.

15. Koblizek, M., Béjà, O., Bidigare, R.R., Christensen, S., Benetiz-Nelson, B., Vetriani, C., Kolber, M.K., and Falkowski, P.G. (2003) Isolation and Characterization of *Erythrobacter* sp. Strains from the Upper Ocean, *Arch. Microbiol. 180*, 327–338.

16. Volkman, J.K., Farmer, C.L., Barrett, S.M., and Sikes, E.L. (1997) Unusual Dihydroxysterols as Chemotaxonomic Markers for Microalgae from the Order Pavlovales (Haptophyceae), *J. Phycol. 33*, 1016–1023.

17. Marchand, D., and Rontani, J.-F. (2003) Visible Light-Induced Oxidation of Lipid Components of Purple Sulphur Bacteria: A Significant Process in Microbial Mats, *Org. Geochem. 34*, 61–79.

18. Mihara, S., and Tateba, H. (1986) Photosensitized Oxygenation Reactions of Phytol and Its Derivatives, *J. Org. Chem. 51*, 1142–1144.

19. Harwood, J.L., and Russell, N.L. (1984) *Lipids in Plants and Microbes*, pp. 1–162, Allen & Unwin, London.

20. Wilkinson, S.G. (1988) Gram-Negative Bacteria, in *Microbial Lipids* (Ratledge, C., and Wilkinson, S.G., eds.), pp. 299–488, Alden Press, London.

21. Rontani, J.-F., and Aubert, C. (2003) Electron Ionization Mass Spectral Fragmentation of C_{19} Isoprenoid Aldehydes and Carboxylic Acid Methyl and Trimethylsilyl Esters, *Rapid Commun. Mass Spectrom. 17*, 949–956.

22. McCloskey, J.A., and McClelland, M.J. (1965) Mass Spectra of *O*-Isopropylidene Derivatives of Unsaturated Fatty Esters, *J. Am. Chem. Soc. 87*, 5090–5093.

23. Andersson, B.A., Christie, W.W., and Holman, R.T. (1974) Mass Spectrometric Determination of Positions of Double Bonds in Polyunsaturated Fatty Acid Pyrrolidides, *Lipids 10*, 215–219.

24. Capella, P., and Zorzut, C.M. (1968) Determination of Double Bond Position in Monounsaturated Fatty Acid Esters by Mass Spectrometry of Their Trimethylsilyloxy Derivatives, *Anal. Chem. 40*, 1458–1463.

25. de Leeuw, J.W., van der Meer, J.W., Rijpstra, W.I.C., and Schenck, P.A. (1980) On the Occurrence and Structural Identification of Long Chain Ketones and Hydrocarbons in Sediments, in *Advances in Organic Geochemistry 1979* (Douglas, A.G., and Maxwell, J.R., eds.), pp. 211–217, Pergamon Press, Oxford.

26. Andersson, B.A., and Holman, R.T. (1975) Mass Spectrometric Localization of Methyl Branching in Fatty Acids Using Acylpyrrolidines, *Lipids 10*, 716–718.

27. Couderc, F. (1995) Gas Chromatography/Tandem Mass Spectrometry as an Analytical Tool for the Identification of Fatty Acids, *Lipids 30*, 691–699.

28. Shirasaka, N., Nishi, K., and Shimizu, S. (1997) Biosynthesis of Furan Fatty Acids (F-acids) by a Marine Bacterium, *Shewanella putrefaciens*, *Biochim. Biophys. Acta 1346*, 253–260.

29. Kerger, B.D., Nichols, P.D., Antworth, C.P., Sand, W., Bock, E., Cox, J.C., Langworthy, T.A., and White, D.C. (1986) Signature Fatty Acids in the Polar Lipids of Acid-Producing *Thiobacillus* spp.: Methoxy, Cyclopropyl, α-Hydroxy-Cyclopropyl and Branched and Normal Monoenoic Fatty Acids, *FEMS Microbiol. Ecol. 38*, 67–77.

30. Wolff, R.L., Christie, W.W., and Marpeau, A.M. (1999) Reinvestigation of the Polymethylene-Interrupted 18:2 and 20:2 Acids of *Ginkgo biloba* Seed Lipids, *J. Oil Am. Chem. Soc. 76*, 273–277.

31. Volkman, J.K., Jeffrey, S.W.J., Nichols, P.D., Rogers, G.I., and Garland, C.D. (1989) Fatty Acid and Lipid Composition of 10 Species of Microalgae Used in Mariculture, *J. Exp. Mar. Biol. Ecol. 128*, 219–240.

32. Viso, A.-C., and Marty, J.-C. (1993) Fatty Acids from 28 Marine Microalgae, *Phytochemistry 34*, 1521–1533.

33. Volkman, J.K., Barrett, S.M., Blackburn, S.I., Mansour, M.P., Sikes, E.L., and Gelin, F. (1998) Microalgal Biomarkers: A Review of Recent Research Developments, *Org. Geochem. 29*, 1163–1179.

34. Reuss, N., and Poulsen, L.K. (2002) Evaluation of Fatty Acids as Biomarkers for a Natural Plankton Community. A Field Study of a Spring Bloom and a Post-bloom Period of West Greenland, *Mar. Biol. 141*, 423–434.

35. Imhoff, J.F., and Bias-Imhoff, U. (1995) Lipids, Quinones and Fatty Acids of Anoxygenic Phototrophic Bacteria, in *Anoxygenic Photosynthetic Bacteria* (Blankenship, R.E., Madigan, M.T. and Bauer, C.E., eds.), pp. 179–205, Kluwer Academic, Dordrecht, The Netherlands.

36. McCloskey, J.A. (1969) Mass Spectrometry of Lipids and Steroids, *Methods Enzymol. 14*, 382–450.

37. Shirasaka, N., Nishi, K., and Shimizu, S. (1995) Occurrence of a Furan Fatty Acid in Marine Bacteria, *Biochim. Biophys. Acta 1258*, 225–227.

38. Scheinkönig, J., Hannemann, K., and Spiteller, G. (1995) Methylation of the β-Positions of the Furan Ring in F-acids, *Biochim. Biophys. Acta 1254*, 73–76.

39. Busse, H.J., Kämpfer, P., and Denner, E.B.M. (1999) Chemotaxonomic Characterization of *Sphingomonas*, *J. Ind. Microbiol. Biotechnol. 23*, 242–251.

40. Rontani, J.-F., Koblizek, M., Beker, B., Bonin, P., and Kolber, Z. (2003) On the Origin of *cis*-Vaccenic Acid Photodegradation Products in the Marine Environment, *Lipids 38*, 1085–1092.

41. Klok, J., Baas, M., Cox, H.C., de Leeuw, J.W., Rijpstra, W.I.C., and Schenck, P.A. (1988) The Mode of Occurrence of Lipids in a Namibian Shelf Diatomaceous Ooze with Emphasis on the β-Hydroxy Fatty Acids, *Org. Geochem. 12*, 75–80.

42. Marchand, D., Grossi, V., Hirschler-Réa, A., and Rontani, J.-F. (2002) Regiospecific Enzymatic Oxygenation of *cis*-Vaccenic Acid During Aerobic Senescence of the Halophilic Purple Sulfur Bacterium *Thiohalocapsa halophila*, *Lipids 37*, 541–548.

43. Kühn, H., Schewe, T., and Rapoport, S.M. (1986) The Stereochemistry of the Reactions of Lipoxygenases and Their Metabolites. Proposed Nomenclature of Lipoxygenases and Related Enzymes, *Adv. Enzymol. 58*, 273–311.

44. Wang, T., Yu, W.G., and Powell, W.S. (1992) Formation of Monohydroxy Derivatives of Arachidonic Acid, Linoleic Acid, and Oleic Acid During Oxidation of Low Density Lipoprotein by Copper Ions and Endothelial Cells, *J. Lipid Res. 33*, 525–537.

45. Guerrero, A., Casals, I., Busquets, M., Leon, Y., and Manresa, A. (1997) Oxidation of Oleic Acid to (*E*)-10-Hydroperoxy-8-octadecenoic and (*E*)-10-Hydroxy-8-octadecenoic Acids by *Pseudomonas* sp. 42A2, *Biochim. Biophys. Acta 1347*, 75–81.

46. Oliw, E.H., Su, C., Skogstrom, T., and Benthin, G. (1998) Analysis of Novel Hydroperoxides and Other Metabolites of Oleic, Linoleic, and Linolenic Acids by Liquid Chromatography–Mass Spectrometry, *Lipids 33*, 843–852.

47. Clapp, C.H., Senchak, S.E., Stover, T.J., Potter, T.C., Findeis, P.M., and Novak, M.J. (2001) Soybean Lipoxygenase-Mediated Oxygenation of Monounsaturated Fatty Acids to Enones, *J. Am. Chem. Soc. 123*, 747–748.

48. Schewe, T., Rapoport, S.M., and Kühn, H. (1986) Enzymology and Physiology of Reticulocyte Lipoxygenase: Comparison with Other Lipoxygenases, *Adv. Enzymol. 58*, 191–272.

50. Marchand, D., and Rontani, J.-F. (2001) Characterisation of Photooxidation and Autoxidation Products of Phytoplanktonic Monounsaturated Fatty Acids in Marine Particulate Matter and Recent Sediments, *Org. Geochem. 32*, 287–304.

51. Galliard, T., and Chan, H.W.–S. (1980) Lipoxygenases, in *The Biochemistry of Plants: A Comprehensive Treatise* (Stumpf, P.K., and Conn, E.E., eds.), Vol. 4, pp. 131–161, Academic Press, New York.

52. Hamberg, M. (1987) Mechanism of Corn Hydroperoxide Isomerase: Detection of 12,13(*S*)-Oxido-9(*Z*),11-octadecadienoic Acid, *Biochim. Biophys. Acta 920*, 76–84.

53. Galliard, T., Matthew, J.A., Fishwick, M.J., and Wright, A.J. (1976) The Enzymatic Degradation of Lipids Resulting from Physical Disruption of Cucumber (*Cucumis sativus*) Fruit, *Phytochemistry 15*, 1647–1650.

54. Porter, N.A., Caldwell, S.E., and Mills, K.A. (1995) Mechanisms of Free Radical Oxidation of Unsaturated Lipids, *Lipids 30*, 277–290.

COMMUNICATION

Preparation and Fractionation of Conjugated Trienes from α-Linolenic Acid and Their Growth-Inhibitory Effects on Human Tumor Cells and Fibroblasts

Miki Igarashi and Teruo Miyazawa*

Laboratory of Food & Biodynamic Chemistry, Graduate School of Agricultural
Science, Tohoku University, Sendai 981-8555, Japan

ABSTRACT: Conjugated α-linolenic acid (CLnA) was prepared from α-linolenic acid (9,12,15-18:3n-3, LnA) by alkaline treatment; we fractionated CLnA into three peaks by reversed-phase column-HPLC as evidenced by monitoring absorbance at 205, 235, and 268 nm. Peak I was a conjugated dienoic FA derived from LnA, whereas Peaks II and III were conjugated trienoic LnA. Proton NMR analysis showed that Peak III consisted of the all-*trans* isomer. The methylated Peak III was further divided into five peaks (Peaks IV–VIII) by silver ion column-HPLC. Peak V, a major constituent in the Peak III fraction, was identified as conjugated 10*t*,12*t*,14*t*-LnA by GC-EIMS and ^{1}H NMR analysis. Peaks III and V, which consisted of conjugated all-*trans* trienoic LnA, had stronger growth-inhibitory effects on human tumor cell lines than the other collected peaks and strongly induced lipid peroxidation as compared with Peaks I, II, and LnA. We propose that conjugated all-*trans* trienoic FA have the strongest growth-inhibitory effect among the conjugated trienoic acids and conjugated dienoic acids produced by alkaline treatment of α-LnA, and that this effect is mediated by lipid peroxidation.

Paper no. L9522 in *Lipids 40*, 109–113 (January 2005).

Conjugated FA can be prepared from nonconjugated FA by alkaline treatment (1). A conjugated FA frequently used for research is conjugated linoleic acid (CLA), which is prepared from linoleic acid (18:2n-6) or linoleic acid-rich oils such as safflower oil by alkaline treatment (2–4). We have also reported that conjugated FA can be prepared from α-linolenic acid (18:3n-3, LnA), EPA (20:5n-3), and DHA (22:6n-3) by alkaline treatment (5,6). However, alkaline treatment yields a mixture of geometrical and positional isomers (1,6). For example, alkaline treatment of linoleic acid produces mainly 9*c*,11*t*- and 10*t*,12*c*-CLA (1,2), whereas alkaline treatment of LnA produces a mixture of conjugated dienes and trienes termed conjugated α-linolenic acid (CLnA) (6,7).

CLnA, conjugated EPA, and conjugated DHA prepared by alkaline treatment are more cytotoxic against human tumor cells than their nonconjugated counterparts and CLA (6). Moreover, the conjugated FA that have an absorbance maximum at 268 nm (conjugated trienes) are more strongly cytotoxic than the conjugated FA with an absorbance maximum at 235 nm (conjugated dienes) (6) or 315 nm (conjugated tetraenes) (5). Therefore, a conjugated trienoic acid may be more cytotoxic than conjugated dienoic and tetraenoic acids prepared from the same FA.

Some reports have indicated that 10*t*,12*c*-CLA, but not 9*c*,11*t*-CLA, is the active cytotoxic compound in CLA prepared by alkaline treatment (8–10). Al-Madaney *et al.* (11) suggested that 9*c*,11*c*-CLA increases the formation of thromboxane B$_2$ compared with other CLA isomers. Thus, we proposed that the cytotoxic efficacy of CLnA, conjugated EPA, and conjugated DHA depends on their geometrical and positional chemical structures.

In this study, we investigated the geometrical and positional chemical structures of CLnA isomers after their formation by alkaline treatment and their abilities to inhibit the growth of tumor cells.

MATERIALS AND METHODS

Preparation of CLnA by alkaline treatment. LnA (10 mg; a gift from Bizen Chemical, Okayama, Japan) was added to 1 mL of 21% potassium hydroxide/ethylene glycol (KOH/EG, wt/vol) solution in a test tube (10-mL volume) (1,5,6). Nitrogen gas was bubbled into the mixture, after which the tube was sealed with a screw cap and allowed to stand for 10 min at 180°C. The reaction mixture was then cooled, and 1 mL of methanol and 2 mL of 6 N HCl were added. After dilution with 2 mL of distilled water, the conjugated FA was extracted with 5 mL of hexane. The hexane extract was washed with 3 mL of 30% methanol and 3 mL of distilled water before being dried under a nitrogen gas stream. The CLnA preparation was stored at –20°C after being purged with nitrogen gas. UV/vis spectrophotometric analysis of the conjugated FA was performed with a spectrophotometer (Shimadzu UV-2400P; Shimadzu Corporation, Kyoto, Japan). Spectrophotometric readings confirmed the formation of the conjugated FA of dienes (235 nm) and trienes (268 nm) (1,12).

Reversed-phase column-HPLC fractionation. CLnA was dissolved in acetonitrile, and this solution was fractionated by
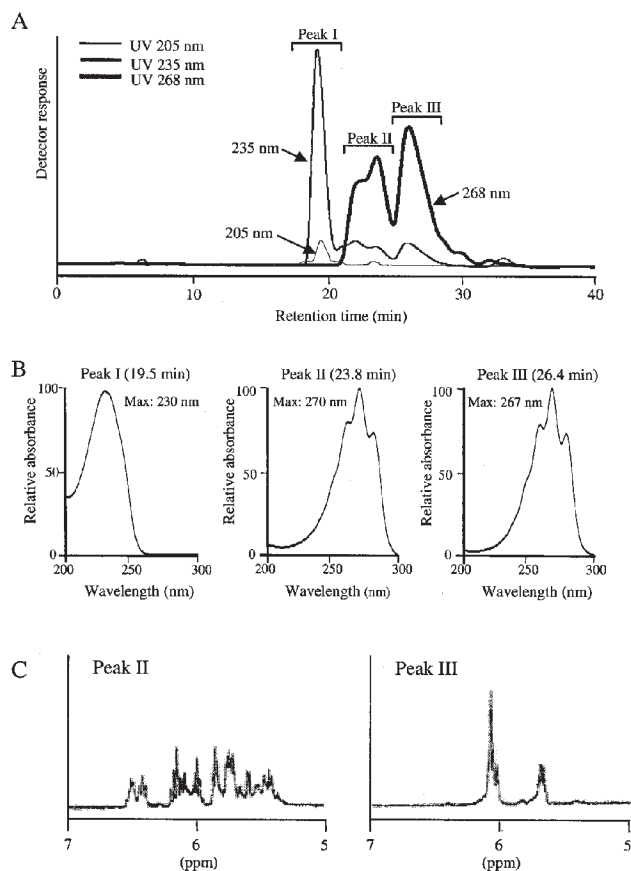
FIG. 1. Reversed-phase HPLC chromatogram of conjugated α-linolenic acid prepared using a 21% KOH solution for 10 min (A), UV spectra of the HPLC-separated peaks (B), and ^{1}H NMR spectra at 500 MHz of Peaks II and III (C).

reversed-phase column-HPLC using a pump (880-PU; Jasco, Inc., Tokyo, Japan) with a diode array detector (SPD-M10AVP; Shimadzu Corporation). The reversed-phase column was Inertsil ODS 10 (10 μm particle size, 4.6 × 250 mm; GL Sciences, Inc., Tokyo, Japan) fitted with a guard column containing similar ODS packing material (9.5 × 50 mm). The mobile phase was acetonitrile/water (70:30, vol/vol), and the flow rate was 1.5 mL/min. Detection was at 205 nm, 235 nm (conjugated diene), and 268 nm (conjugated triene). Typical chromatograms of CLnA and the spectra of peaks are shown in Figure 1A. Peaks I–III were collected individually and dried completely under nitrogen gas.

Silver ion column-HPLC fractionation. Peak III was methylated with 14% BF$_3$/methanol (Wako Pure Chemicals Industries, Ltd., Osaka, Japan) at room temperature for 30 min (13,14). The methylated FA was then dissolved in hexane, and this solution was fractionated using silver-ion HPLC and a diode array detector. The silver ion column-HPLC (Ag$^+$-HPLC) column was ChromSpher Lipids (5 μm particle size, 4.6 × 250 mm; Chrompack, Bridgewater, NJ). The mobile phase was hexane/acetonitrile (100:0.15, vol/vol), and the flow rate was 1.0 mL/min. Detection was at 268 nm (conjugated triene). A typical

chromatogram is shown in Figure 2A. Peaks IV–VIII were collected and dried completely under nitrogen gas.

GC-EIMS. The FAME fractions IV to VIII were hydrolyzed to their FFA with a 0.2 N KOH solution at 40°C for 90 min. The FA were then converted to 4,4-dimethyloxazoline (DMOX) derivatives (15). The GC-EIMS analysis was performed as described previously (4).

NMR spectroscopy. The FFA were dissolved in acetonitrile-d_3 (ICN Pharmaceuticals, Inc., Costa Mesa, CA) at a concentration of 1.0 mg/mL. Proton NMR (^{1}H NMR) spectroscopy was performed on a Varian Unity INOVA 500 (500 MHz) (Varian, Inc., Palo Alto, CA).

Cell cultures. Human tumor cells (DLD-1, HepG2, A549, MCF-7, and MKN-7) were obtained from the Cell Resource Center for Biochemical Research at Tohoku University (Sendai, Japan). Human fibroblasts (MRC-5, TIG-103, and KMS-6) were purchased from the Human Science Research Resources Bank (Osaka, Japan). The cells were cultured as described previously (5,6).

MTT [3-(4,5-dimethylthiazol-2-yl)-2,5-diphenyltetrazolium bromide] dye reduction assay. To examine the growth-inhibitory effect of conjugated FA on human tumor cells and fibroblasts, we performed the MTT dye reduction assay (5,6). Briefly, stock solutions of FA were prepared in ethanol at a concentration of 25 mM. The FA were diluted to the final concentrations of 25 μM in RPMI 1640 (for tumor cells; Sigma, St. Louis, MO) or MEM (for fibroblasts; Sigma) supplemented with 0.5% BSA (these served as the test media). Control cells were exposed to test medium supplemented with 0.1% ethanol. The α- and β-eleostearic acids used were purified from tung oil by reversed-phase column-HPLC (4).

Determination of TBARS. The semiconfluent cells seeded in a 60-mm diameter dish were cultured in test media containing FA. After incubation for 24 h, DLD-1 cells were assayed for the amount of TBARS as a conventional index for lipid peroxidation according to the method of Gavino *et al.* (16).

Statistical analysis. Statistical comparisons among several groups were made using one-way ANOVA, followed by the Newman–Keuls test for multiple comparisons among the groups. The Student's *t*-test was used for comparisons between two groups. Differences were considered significant at $P < 0.05$.

RESULTS AND DISCUSSION

CLnA prepared by alkaline treatment was separated into three peaks by reversed-phase column-HPLC with monitoring at 205, 235, and 268 nm. The chromatogram is shown in Figure 1A; the retention times for Peaks I, II, and III were at 19.5, 23.8, and 26.4 min, respectively. These peaks showed maximal absorption at 230, 270, and 267 nm, respectively (Fig. 1B). These results suggest that Peak I contains conjugated dienoic LnA (LnA, which is monoconjugated plus one isolated double bond), whereas Peaks II and III consist of conjugated trienoic LnA. From the 10 mg LnA initially used for alkaline isomerization, 70% was converted to conjugated FA (6). The yield for Peaks I, II, and III was 2.1, 2.3, and 2.0 mg, respectively. The ^{1}H NMR signals arising from
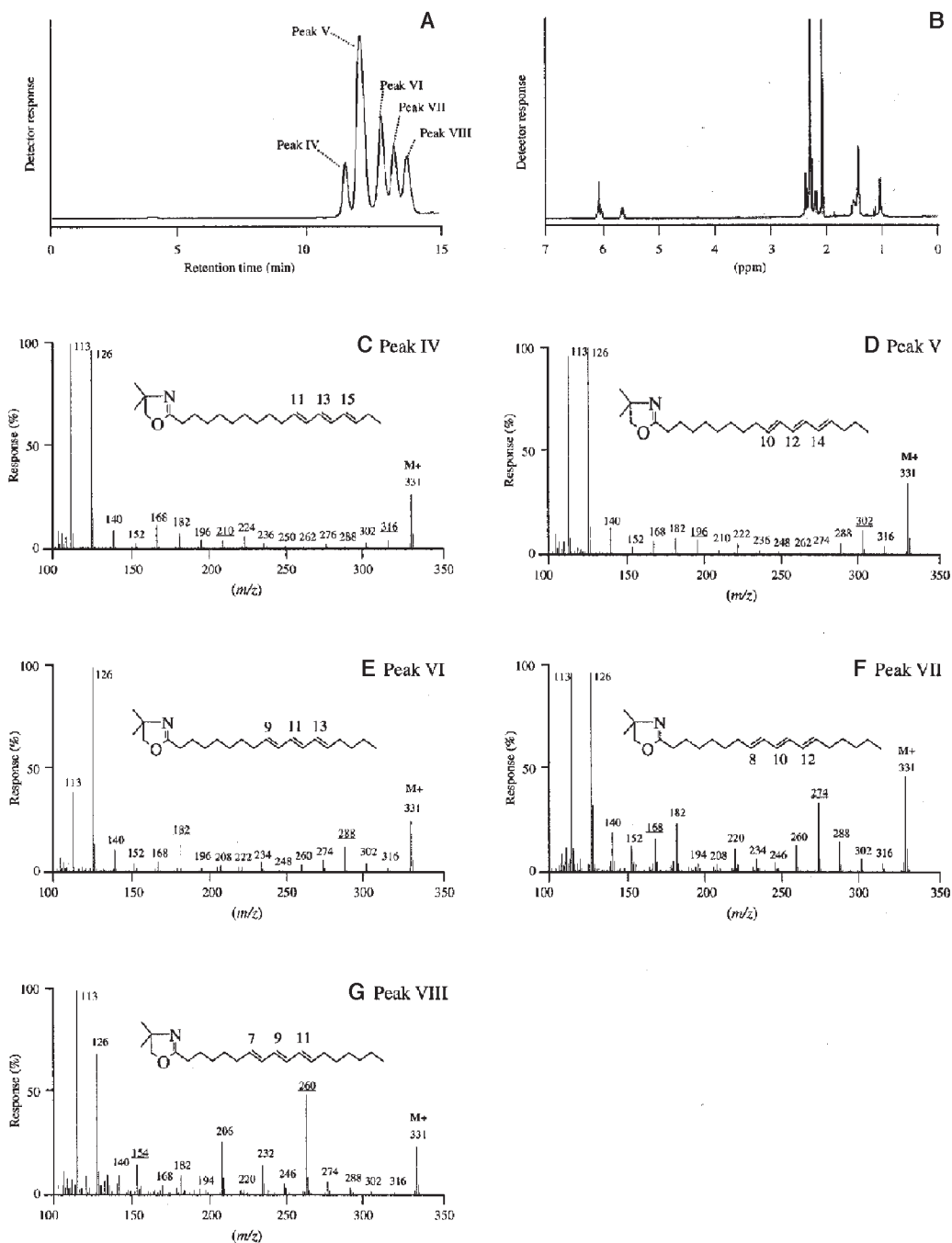
FIG. 2. Ag⁺-HPLC chromatogram of methylated Peak III (A), ¹H NMR spectrum at 500 MHz of Peak V (B), and GC-EIMS spectra of the 4,4-dimethyloxazoline derivatives of Peaks IV (C), V (D), VI (E), VII (F), and VIII (G). Allylic cleavage fragments are underlined.

Peaks II and III were also examined. The olefinic proton signal (5.5–6.5 ppm) reveals the geometrical configuration of the conjugated double bond. On the basis of comparison with the spectra of commercial α- and β-eleostearic acids (data not shown; Larodan Fine Chemicals AB, Malmo, Sweden), and of previous reports (17,18), it appears Peak III was composed of all-*trans*

isomers (Fig. 1C) whereas Peak II consisted of several *trans* and *cis* isomers (mono-*cis*, di-*trans* CLnA; di-*cis*, mono-*trans* CLnA; and all-*cis* CLnA) (Fig. 1C).

Methylated Peak III (which consists of all-*trans* isomers, as determined by ¹H NMR) was separated into five peaks by Ag⁺-HPLC by monitoring the eluate at 265 nm. The fractions were:

TABLE 1
Growth-Inhibitory Effects of Conjugated α-Linolenic Acids on Human Tumor Cell Lines and Fibroblasts[a]

FA	Human tumor cell lines[b]					Human fibroblasts[c]		
	DLD-1	HepG2	A549	MCF-7	MKN-7	TIG-103	MRC-5	KMS-6
	Viable cells (% of control)							
Control	100 ± 3	100 ± 4	100 ± 7	100 ± 2	100 ± 12	100 ± 2	100 ± 3	100 ± 2
LnA	81 ± 5*	94 ± 5	87 ± 4	87 ± 1**	85 ± 5	92 ± 3	86 ± 2	102 ± 3
CLnA[d]	61 ± 2***	77 ± 4**	82 ± 5	95 ± 2	90 ± 6	112 ± 3	90 ± 5	108 ± 1
Peak I	64 ± 2**	91 ± 1	87 ± 3	86 ± 2***	85 ± 3	92 ± 2	88 ± 3	91 ± 2
Peak II	44 ± 1**	86 ± 2*	64 ± 2**	70 ± 3***	55 ± 5*	104 ± 3	92 ± 2	100 ± 2
Peak III	10 ± 1***	30 ± 2***	3 ± 0.1***	53 ± 1***	4 ± 0.2***	57 ± 4***	69 ± 4***	83 ± 2***
α-ESA[e]	41 ± 1***					105 ± 3	115 ± 3	108 ± 3
β-ESA	35 ± 1***					75 ± 1*	114 ± 4	75 ± 3*

[a]Cells were incubated for 24 h after supplementation of FA at a concentration of 25 μM. The percentage of cell numbers incubated with control medium for 24 h was treated as 100%. Values are mean ± SE ($n = 6$). *$P < 0.05$, **$P < 0.01$, and ***$P < 0.001$ compared with the control.
[b]DLD-1, colorectal adenocarcinoma; HepG2, hepatoma; A549, lung adenocarcinoma; MCF-7, breast adenocarcinoma; MKN-7, tubular adenocarcinoma.
[c]MRC-5, male lung (JCRB0521; TIG-103, female skin (JCRB0528); KMS-6 female embryonal (JCRB0432).
[d]CLnA, conjugated α-linolenic acid prepared with 21% KOH solution for 10 min.
[e]ESA, eleostearic acid.

Peak IV 9.1%, Peak V 45.1%, Peak VI 17.9%, Peak VII 16.3%, Peak VIII 11.6% (Fig. 2A). After the fractionation, each peak was hydrolyzed to their FFA. Peak V consisted of 0.8 mg obtained from the original starting material of 10 mg LnA. The DMOX derivatives of each of the five peaks were similarly prepared and analyzed by GC-EIMS (4,15). Figure 2D shows the GC-EIMS spectra of the DMOX derivative of Peak V. The spectrum exhibited a molecular ion at m/z 331, and allylic cleavages of the fatty acyl chain at m/z 196 and 302. The mass spectrum exhibited mass differences of 12 mass units between m/z 210 and 222, between m/z 236 and 248, and between m/z 262 and 274, indicating that this was a conjugated triene (Fig. 2D). Peak V was consistent with the structure 10t,12t,14t-CLnA (Fig. 2D). The structural confirmation of all the other peaks was determined in the same way. Peaks IV, VI, VII, and VIII were therefore assigned the structures 11t,13t,15t-CLnA (Fig. 2C), 9t,11t,13t-CLnA (Fig. 2E), 8t,10t,12t-CLnA (Fig. 2F), and 7t,9t,11t-CLnA (Fig. 2G), respectively. Spitzer *et al.* (7) previously reported that 10,12,14-CLnA and 9,11,13-CLnA were detected when CLnA was prepared with a 6.5% KOH/EG solution.

We examined the growth-inhibitory effects of each peak that had been collected by reversed-phase column-HPLC and Ag⁺-HPLC on five human tumor cell lines (DLD-1, HepG2, A549, MCF-7, and MKN-7) and three human fibroblast lines (TIG-103, MRC-5 and KMS-6) (Table 1). At a concentration of 25 μM, Peak III (all-*trans* conjugated triene) had the strongest growth-inhibitory effect on tumor cell lines compared with Peaks I and II. The growth-inhibitory effect of Peak III on DLD-1 was shown to be dose- (data not shown; 0–100 μM) and time-dependent (data not shown; from 0 to 24 h). Thus, the all-*trans* conjugated trienoic FA appears to have a strong growth-inhibitory effect on human tumor cell lines. The growth-inhibitory effect of Peak V (10t,12t,14t-CLnA) on DLD-1 was at the same level as that of Peak III, and was stronger than that of β-eleostearic acid (9t,11t,13t-octadecatrienoic acid purified from tung oil). Moreover, β-eleostearic

acid had a higher growth-inhibitory effect compared with α-eleostearic acid (9c,11t,13t-octadecatrienoic acid purified from tung oil). It was shown previously that 10t,12c-CLA is the active CLA isomer rather than 9c,11t-CLA (8–10). Thus, the differences in the growth-inhibitory effects of conjugated trienoic acids appear to be related to specific geometric and positional isomers. The all-*trans* conjugated trienoic acids we tested (Peak III and β-eleostearic acid) also showed growth-inhibitory effects in human fibroblasts.

We previously reported that conjugated EPA and DHA induce apoptosis *via* lipid peroxidation (5). We thus tested the ability of the different isolated conjugated FA to induce lipid peroxidation by assaying for TBARS levels. The level of TBARS for Peak V (10t,12t,14t-CLnA) in the culture was greater compared with Peaks I–III after 24 h incubation (Fig. 3). Moreover, β-eleostearic acid induced more lipid peroxidation than α-eleostearic acid (Fig. 3). These results suggest that
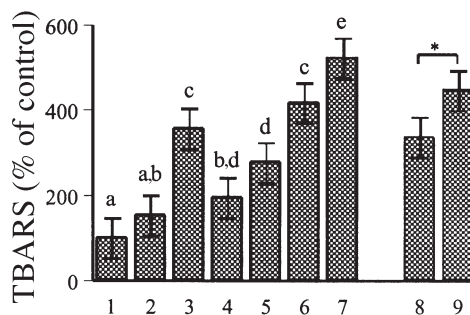
FIG. 3. TBARS formation in DLD-1 cells supplemented with conjugated α-linolenic acids. DLD-1 cells were incubated for 24 h with 25 μM of each FA. Values not sharing a common superscript letter (a–e) are significantly different by the Newman–Keuls test. *, $P < 0.05$ by Student's t-test. Values shown are the mean ± SE ($n = 4$ or 5). (1) Control; (2) α-linolenic acid; (3) conjugated α-linolenic acid prepared with alkaline solution; (4) Peak I; (5) Peak II; (6) Peak III; (7) Peak V; (8), α-eleostearic acid; (9) β-eleostearic acid.

all-*trans* trienoic CLnA induces lipid peroxidation compared with the other geometrical isomers, and that CLnA generated by alkaline treatment induces lipid peroxidation, which ultimately inhibits cell growth.

Recently, we reported that tung oil, which is rich in α-eleostearic acid, lacked toxicity and was better at decreasing tumor tissue weight in DLD-1-transplanted mice than CLA (17). This suggests that conjugated trienoic acid, especially conjugated all-*trans* isomers, may be developed into anticancer drugs of broad utility.

REFERENCES

1. Association of Official Analytical Chemists (1990) Acids (polyunsaturated) in Oil and Fats, in *Official Methods of Analysis of the Association of Official Analytical Chemists* (Helrich, K., ed.), pp. 960–963, Association of Official Analytical Chemists, Arlington.
2. Ha, Y.L., Grimm, N.K., and Pariza, M.W. (1987) Anticarcinogens from Fried Ground Beef: Heat-Altered Derivatives of Linoleic Acid, *Carcinogenesis 8*, 1881–1887.
3. Ip, C., Chin, S.F., Scimeca, J.A., and Pariza, M.W. (1991) Mammary Cancer Prevention by Conjugated Dienoic Derivative of Linoleic Acid, *Cancer Res. 51*, 6118–6124.
4. Tsuzuki, T., Igarashi, M., Komai, M., and Miyazawa, T. (2003) Significant Occurrence of 9,11-Conjugated Linoleic Acid (18:2, n-7) in the Liver and Plasma Lipids of Rats Fed 9,11,13-Eleostearic Acid (18:3, n-5)-Supplemented Diet, *J. Nutr. Sci. Vitaminol. 49*, 195–200.
5. Igarashi, M., and Miyazawa, T. (2000) Do Conjugated Eicosapentaenoic Acid and Conjugated Docosahexaenoic Acid Induce Apoptosis *via* Lipid Peroxidation in Cultured Human Tumor Cells? *Biochem. Biophys. Res. Commun. 270*, 649–656.
6. Igarashi, M., and Miyazawa, T. (2000) Newly Recognized Cytotoxic Effect of Conjugated Trienoic Fatty Acids on Cultured Human Tumor Cells, *Cancer Lett. 148*, 173–179.
7. Spitzer, V., Marx, F., and Pfeilsticker, K. (1994) Electron Impact Mass Spectra of the Oxazoline Derivatives of Some Conjugated Diene and Triene C_{18} Fatty Acids, *J, Am. Oil Chem. Soc. 71*, 873–876.
8. Kang, K., Liu, W., Albright, K.J., Park, Y., and Pariza, M.W. (2003) *Trans*-10,*cis*-12 CLA Inhibits Differentiation of 3T3-L1 Adipocytes and Decreases PPARγ Expression, *Biochem. Biophys. Res. Commun. 303*, 795–799.
9. Yamasaki, M., Chujo, H., Koga, Y., Oishi, A., Rikimaru, T., Shimada, M., Sugimachi, K., Tachibana, H., and Yamada, K. (2002) Potent Cytotoxic Effect of the *trans*10,*cis*12 Isomer of Conjugated Linoleic Acid on Rat Hepatoma dRLh-84 Cells, *Cancer Lett. 188*, 171–180.
10. Choi, Y., Park, Y., Pariza, M.W., and Ntambi, J.M. (2001) Regulation of Stearoyl-CoA DesaturaseActivity by the *trans*-10,*cis*-12 Isomer of Conjugated Linoleic Acid in HepG2 Cells, *Biochem. Biophys. Res. Commun. 284*, 689–693.
11. Al-Madaney, M.M., Kramer, J.K.G., Deng, Z., and Vanderhoek, J.Y. (2003) Effects of Lipid-Esterified Conjugated Linoleic Acid Isomers on Platelet Function: Evidence for Stimulation of Platelet Phospholipase Activity, *Biochim. Biophy. Acta 635,* 75–82.
12. Pitt, G.A.J., and Morton, R.A. (1957) Ultra-violet Spectrophotometry of Fatty Acids, *Prog. Chem. Fats Other Lipids 4*, 227–278
13. American Oil Chemists' Society (1973, revised to 1990) Fatty Acid Composition by GLC: Marine Oils, in *Official Methods and Recommended Practices of the American Oil Chemists' Society* (Firestone, D., ed.), Champaign, IL, Method Ce 1b-89.
14. Igarashi, M., Tsuzuki, T., Kambe, T., and Miyazawa, T. (2004) Recommended Methods of Fatty Acid Methylester Preparation for Conjugated Dienes and Trienes in Food and Biological Samples, *J. Nutr. Sci. Vitaminol. 50*, 121–128.
15. Fay, L., and Richli, U. (1991) Location of Double Bonds in Polyunsaturated Fatty Acids by Gas Chromatography–Mass Spectrometry After 4, 4-Dimethyloxazoline Derivatization, *J. Chromatogr. A 541*, 89–98.
16. Gavino, V.C., Miller, J.S., Ikharebha, S.O., Milo, G.E., and Cornwell, D.G. (1981) Effect of Polyunsaturated Fatty Acids and Antioxidants on Lipid Peroxidation in Tissue Cultures, *J. Lipid Res. 22*, 763–769.
17. Conacher, H.B.S., Gunstone, F.D., Hornby, G.M., and Padley, F.B. (1969) Glyceride Studies: Part IX: Intraglyceride Distribution of Vernolic Acid and of Five Conjugated Octadienoic Acids in Seed Glycerides, *Lipids 5,* 434–441.
18. Suzuki, O., Hashimoto, T., Hayamizu, K., and Yamamoto, O. (1969) Studies on the Nuclear Magnetic Spectra of Olefinic Protons of Conjugated Fatty Acid Methyl Esters, *Lipids 5*, 457–462.
19. Tsuzuki, T., Tokuyama, Y., Igarashi, M., and Miyazawa, T. (2004) Tumor Growth Suppression by α-Eleostearic Acid, a Linolenic Acid Isomer with a Conjugated Triene System, *via* Lipid Peroxidation. *Carcinogenesis 25*, 1417–1425.

n-3 Fatty Acid Enrichment of Edible Tissue of Poultry: A Review

C. Rymer* and D.I. Givens

Nutritional Sciences Research Unit, Department of Agriculture, University of Reading, Reading, RG6 6AR, United Kingdom

ABSTRACT: There is clear evidence of the nutritional benefits of consuming long-chain n-3 PUFA, which are found predominantly in oily fish. However, oily fish consumption, particularly in the United Kingdom, is declining, as is the consumption of all meats with the exception of poultry, which has increased in consumption by 73% in the last 30 yr. This pattern, if less marked, is reflected throughout Europe, and therefore one means of increasing long-chain n-3 PUFA consumption would be to increase the long-chain n-3 PUFA content in the edible tissues of poultry. This review considers the feasibility of doing this, concentrating particularly on chickens and turkeys. It begins by summarizing the benefits to human health of consuming greater quantities of n-3 FA and the sources of n-3 PUFA in the human diet. The literature on altering the FA composition of poultry meat is then reviewed, and the factors affecting the incorporation of n-3 PUFA into edible tissues of poultry are investigated. The concentration of α-linolenic acid (ALA) in the edible tissues of poultry is readily increased by increasing the concentration of ALA in the birds' diet (particularly meat with skin, and dark meat to a greater extent than white meat). The concentration of EPA in both white and dark meat is also increased when the birds' diet is supplemented with EPA, although supplementing the diet with the precursor (ALA) does not result in a noticeable increase in EPA content in the edible tissues. Although supplementing the birds' diets with relatively high concentrations of DHA does result in an increased concentration of DHA in the tissues, the relationship between dietary and tissue concentrations of DHA is much weaker than that observed with ALA and EPA. The impact that altering the FA composition of edible poultry tissue may have on the organoleptic and storage qualities of poultry products is also considered.

Paper no. L9582 in *Lipids 40*, 121–130 (February 2005).

The role of n-3 FA in the prevention of coronary heart disease and, in the case of 22:6n-3 (DHA), as a vital component in the retina and the membrane phospholipids of the brain is well established. Emken and his colleagues (1) demonstrated that 20:5n-3 (EPA) and DHA can be produced in humans by the sequential elongation and desaturation of 18:3n-3 (α-linolenic acid, ALA), but the rates of these conversions are low (1–3) and appear to be more limited in young men than young women (4–7), suggesting that DHA synthesis may be up-regulated in situations where there may be a greater demand for DHA, such as to meet the possible needs of a fetus or neonate. It has been suggested that this poor conversion of ALA to DHA is the result of an ancient diet that was rich in DHA, which reduced an evolutionary need to maintain an active conversion apparatus (8). Infants are able to convert ALA to DHA (9–11), but the requirements for DHA in the neonate are extremely high. A review by Salem *et al.* in 2001 (12) concluded (on the evidence of brain and retinal function in preterm and term infants fed either breast milk or formula that was supplemented or otherwise with long-chain PUFA) that it would be prudent to ensure preformed DHA was included in the infant diet.

In the adult, the conversion of ALA to DHA may not meet the long-term demand for DHA in diabetics, as the activity of Δ-5 and Δ-6 desaturases is reduced in the diabetic state (13). Alcohol also inhibits the activity of Δ-5 and Δ-6 desaturase and reduces the concentration of long-chain n-3 PUFA in the tissues (14). The competition for Δ6 desaturase in the conversion of ALA to 18:4n-3 and 18:2n-6 (linoleic acid, LA) to 18:3n-6 (γ-linolenic acid) means that diets with high n-6 FA contents can reduce n-3 FA conversion by as much as 40% (1). Since Western diets typically have a high ratio of n-6/n-3 FA, the conversion of ALA to DHA is likely to be compromised. The need for an adequate intake of ALA, with an appropriate balance of n-6/n-3 FA, is therefore well recognized, and the inclusion of preformed DHA in circumstances where the conversion of ALA to DHA may be insufficient is acknowledged.

SOURCES OF N-3 PUFA

ALA is found in certain seed oils (such as linseed and canola) and green vegetables. Dietary sources of both EPA and DHA are confined almost entirely to fish products. Adequate intakes of EPA and DHA may be achieved by consuming two portions of fish each week, and of these portions one should be of oily fish (15). However, fish consumption in the United Kingdom is very low, as is the proportion of the population that eat fish (16), and this pattern is reflected throughout northern Europe. Clearly, other sources of n-3 PUFA need to be developed if the northern European population is to achieve the recommended intakes of these EFA. One approach is to incorporate microencapsulated n-3 PUFA into "standard" foods. The other is to alter the FA composition of foods that make a significant contribution to fat intake. A survey of European diets revealed that 26% of total fat intake came from dairy products, and meat and meat products accounted for 21% (17). A review of experiments that investigated the potential of enhancing the EPA and DHA content of bovine milk by altering the cow's diet con-

*To whom correspondence should be addressed at Nutritional Sciences Research Unit, School of Agriculture, Policy and Development, University of Reading, P.O. Box 237, Reading, RG6 6AR, UK.
E-mail: c.rymer@reading.ac.uk

Abbreviations: ALA, α-linolenic acid; LA, linoleic acid; PI, peroxidizability index.

cluded that this approach had only limited success (18), but there may be possible advantages to increasing the n-3 PUFA content of meat. Poultry meat accounts for 41% of the consumption of meat and meat products in the United Kingdom (19) and so is potentially a valuable route for increasing the intake of long-chain n-3 PUFA. The objective of this review is to consider the factors that affect the efficiency with which dietary n-3 PUFA is incorporated into the edible tissues of poultry.

POULTRY AS A SOURCE OF N-3 PUFA

Compared with mammals, the n-3 PUFA content of skeletal muscle in birds is lower and that of n-6 higher (20), and when birds are fed typical diets, the concentrations of n-3 PUFA in their edible tissues are relatively low (21). Of the n-3 PUFA that are present, ALA is concentrated in the TAG fraction, whereas EPA and DHA are more prevalent in the phospholipid fraction (21). White (breast) meat is the most popular poultry meat, but although its lipids are rich in phospholipids, and so relatively rich in EPA and DHA, dark (leg) meat and skin are the richest sources of all n-3 FA because of the higher lipid content of these tissues (Table 1).

In a study of nine species of birds (fed different diets and managed independently), the concentration of DHA in skeletal muscle phospholipids was negatively related to body size (20). It was suggested that smaller species of birds, with their higher metabolic rates, required higher concentrations of DHA to help maintain sodium and calcium pumps. This might suggest that, when fed similar diets, turkeys would have a lower DHA content in their edible tissues than would broilers.

No direct comparisons between chickens and turkeys of the n-3 PUFA content of their edible tissues could be found in the literature. However, two studies (22,23) in which similar diets were fed estimated the n-3 PUFA content of edible tissues in chickens and turkeys, respectively. In these studies, n-3 PUFA-rich oils were added to the birds' diets, but the results summarized in Table 2 relate to the control diets. However, even in

these diets, fishmeal was added as a protein source (as is widely done in the industry), and this feedstuff would also supply some n-3 PUFA to the birds' diets. It is clear from these data that dark meat is a richer source of ALA than is white meat, although there is little difference between the white and dark meats in terms of their longer-chain n-3 PUFA contents. Turkeys appear to be a richer source of ALA than chickens, and females had a higher ALA content in their meat than did males. The long-chain n-3 PUFA content of chicken meat (white or dark) and turkey white meat was similar, despite the higher fishmeal content of the turkeys' diet (49.5 g/kg fishmeal vs. 40 g/kg redfish meal for the broilers). This observation may support the notion that smaller birds have inherently higher DHA contents in their muscles than do larger birds (20). However, the turkey dark meat had a much higher long-chain n-3 PUFA and ALA content than did the other tissues. This partly reflects the higher lipid content of dark meat compared with white meat, and the high long-chain n-3 PUFA content of turkey dark meat may also be a result of the higher fishmeal content of the turkeys' diet compared with the broilers' diet. Clearly this area requires further research.

ENHANCEMENT OF N-3 PUFA CONTENT OF POULTRY MEAT

The FA composition of both pigs and poultry can in theory be relatively easily modified by dietary means. As early as 1963, it was noted that the FA compositions of broilers' breast, thigh, and skin tissues were similar to those of the broilers' diet (24), and in the 1960s Neudoerffer and Lea demonstrated that feeding fish oil to turkeys increased the concentrations of EPA and DHA in the depot fat (25) and muscle lipids (26) of the turkeys. Consequently, it is possible to increase the proportion of n-3 PUFA substantially in both eggs and the edible tissues of pigs and poultry (21,27–30). Much work has been done to enhance the n-3 PUFA content of poultry meat by dietary means, and this can result in nutritionally meaningful intakes of n-3 PUFA

TABLE 1
Lipid Content and Composition, and FA Composition of Different Edible Tissues in Poultry Fed a Standard Diet[a]

	Edible tissue		
	White meat	Dark meat	Skin
Lipid content (wt% fresh tissue)	0.9	2.2	30.3
Lipid composition (wt% total lipid)			
TAG	43	83	100
Phospholipid	55	16	Trace
FA composition			
(% total FA)			
ALA	0.5	0.7	1.0
EPA	0.9	0.5	0.1
DHA	1.8	1.0	0.1
(mg/100 g edible tissue)			
ALA	4.5	15.5	304
EPA	6.3	13.3	122
DHA	16.2	22.0	31

[a]Data from Reference 21. ALA. α-linolenic acid. Trace < 0.5%.

TABLE 2
FA Composition of Broiler and Turkey Meat When Birds Were Fed Diets Containing 40–50 g/kg Fishmeal[a]

| Meat | Species | Sex | Lipid content (g/kg) | FA composition[a] | | | |
| | | | | % FA | | mg/100 g meat | |
				ALA	EPA + DHA	ALA	EPA + DHA
White	Chicken	Male	9	0.4	5.4	3.6	48.5
		Female	10	0.5	4.5	5.0	45.1
	Turkey	Male	7	0.8	7.3	5.6	51.1
		Female	7	1.1	6.4	7.7	44.7
Dark	Chicken	Male	19	0.6	2.6	11.4	49.5
		Female	20	0.6	2.6	12.0	52.0
	Turkey	Male	22	1.5	3.9	33.1	85.8
		Female	24	2.2	3.0	52.7	72.0

[a]References 22, 23. For abbreviation see Table 1.

by people who consume these products (31). There are some drawbacks to this practice, most notably the reduced shelf life of the products (29,32), and the negative effect that n-3 PUFA enrichment appears to have on the organoleptic qualities of poultry meat (21,26,27,33).

It is relatively easy to measurably increase the ALA content of poultry meat by supplementing the diet with feeds rich in ALA. Such feeds typically include oilseeds such as linseed or canola. As ALA is associated more with the TAG rather than the phospholipids, most of the ALA that is found in edible tissues accumulates in the dark meat and skin. A number of authors have reported the proportionate response of increased ALA content in edible tissues to increasing dietary concentrations of ALA (22,23,31–44). These data are presented in Figure 1 to illustrate the responses observed across a range of different experiments, and also analyzed by linear regression; the relationships that were observed are summarized in Table 3 and illustrated in Figure 1.

The response of the ALA content of skinless white meat (in turkeys or broilers) to increasing dietary ALA concentration is poor. However, strong relationships were observed between dietary ALA content and the ALA content of meat with skin, be it white or dark. The response of the ALA content of skinless dark meat (both in turkeys and broilers) to increasing dietary ALA content was intermediate. This is understandable, as it is the skin and to a lesser extent the dark meat that has the highest lipid content and the greater proportion of TAG (in which ALA accumulates). These therefore are the tissues that respond most to increased dietary ALA with an increased tissue concentration of ALA. Most of the data in Figure 1 were collected from experiments on broilers, and so although the regression coefficients between dietary ALA content and turkey tissue ALA content are high (0.986–0.993), these are primarily a reflection of the very few, but well spaced, data points that were included in the regressions. A much more rigorous comparison is needed to determine whether real differences exist between broilers and turkeys in terms of their response to increasing dietary ALA concentrations.

One of the few direct comparisons between turkeys and chickens found that young (between 1 and 3 wk of age) turkeys were more efficient at digesting saturated fats than were young chickens (45). This difference between the two species disappeared at 3 wk of age, and there was much less of a difference when unsaturated lipids were fed. The digestibility of dietary lipids that are designed to enhance the n-3 PUFA content of the meat is therefore not likely to be significantly different between finishing turkeys and chickens.

No difference between different breeds or sexes of chicken in their response to dietary PUFA was identified (21,31). Very few data in Figure 1 were collected from male broilers, as birds were either analyzed as a mixed sex group, or females were used instead. However, the data in Figure 2 have been segregated into male and female broilers to illustrate the response in dark meat ALA concentration to increasing dietary ALA concentration. Although the regression slope with the male birds appears slightly steeper than that of the females, the confidence intervals of the two coefficients overlap and there is no evidence of any difference between the sexes in
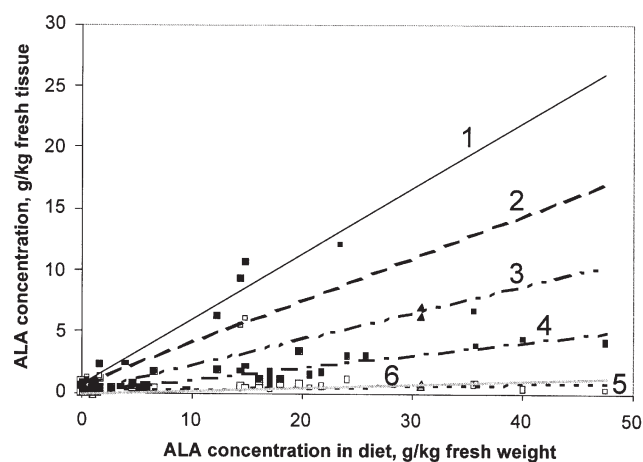
FIG. 1. Effect of increasing dietary concentrations of α-linolenic acid (ALA) on the concentration of ALA in the edible tissues of poultry meat. Line 5, (○) skinless, white broiler meat ($R^2 = 0.309$); Line 4, (●) skinless dark broiler meat ($R^2 = 0.772$); Line 2, (□) white broiler meat with skin ($R^2 = 0.995$); Line 1, (■) dark broiler meat with skin ($R^2 = 0.963$); Line 6, (△) white (skinless) turkey meat ($R^2 = 0.986$); Line 3, (▲) dark (skinless) turkey meat ($R^2 = 0.993$).

TABLE 3
Relationship Between Dietary Concentration of ALA and the Concentration of ALA in the Edible Tissues of Poultry

Tissue	Constant	Coefficient for dietary ALA concentration[a]	R^2 (%)	P	s
Broilers					
Skinless white meat	0.189	0.015	30.9	0.000	0.267
Skinless dark meat	0.079	0.104	77.2	0.000	0.634
White meat with skin	0.777	0.343	99.5	0.002	0.223
Dark meat with skin	0.790	0.528	96.3	0.000	0.856
Turkeys					
Skinless white meat	0.038	0.025	98.6	0.000	0.044
Skinless dark meat	0.158	0.216	99.3	0.000	0.263

[a]Expressed as g/kg fresh weight. For abbreviation see Table 1.

terms of their response. This may be a reflection of the physiological immaturity of broilers when they are slaughtered, and it is possible that the adult birds might show a sex difference in their response to dietary ALA. However, since the vast majority of table chickens are slaughtered before they reach puberty, any such differences are unlikely to be of practical importance.

The source of ALA may affect the efficiency with which it is incorporated into body tissues, perhaps because of the presence of other antinutritional factors in the oil's source, or the interaction with other nutrients in the diet. A number of confounding factors in the responses to increasing dietary ALA content with different ALA sources are illustrated in Figure 3 and summarized in Table 4. However, one can see that there is no real relationship between dietary and tissue ALA concentration when fish oil is fed, mainly because of the very low ALA content of fish oil. The data do show that the richest source of dietary ALA, and therefore the most effective means of increasing the ALA content of edible poultry tissues, is linseed oil. From these data, there is no clear evidence of oil source affecting the efficiency with which ALA is incorporated into body tissue. Data presented by Ajuyah *et al.* (34), however, do show that the physical form in which the oil is presented may affect the tissue ALA content of birds that consume the oil. These authors observed that feeding a reconstituted mixture of the extracted oilseed meal and free oil resulted in significantly higher ALA contents in both white and dark meat for linseed, but there was no significant difference with canola. These results illustrate that the efficiency with which dietary ALA is transferred from the diet to the edible tissues of poultry is affected by the digestibility of the feed. Certain oilseeds (for example, linseed, but not apparently canola) require some processing to ensure that broilers consuming the seed are able to digest and absorb the oil supplied.

EPA

There is a generally linear relationship between the concentration of EPA in the diet and the EPA content of edible tissues (Fig. 4), although there is considerable variation in the response
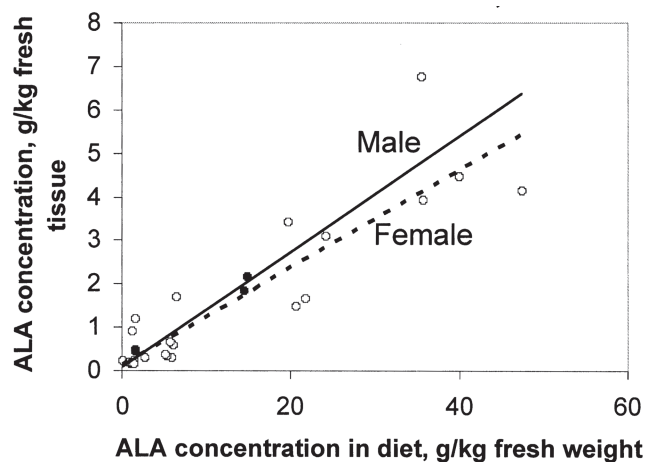
FIG. 2. The effect of broiler sex on the ALA content of dark meat in response to increasing dietary concentrations of ALA. (—) (●) Male (R^2 = 0.971, slope = 0.133 ± 0.0094); (----); (○) female (R^2 = 0.819, slope = 0.112 ± 0.0108). For abbreviation see Figure 1.
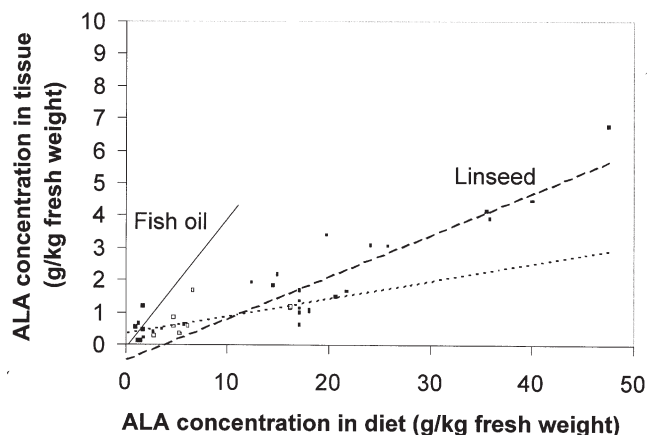
FIG. 3. The effect of different oil sources on the relationship between increasing dietary ALA concentration and the concentration of ALA in the dark meat of broilers. (●) Fish oil, R^2 = 0.102; (■) linseed oil, R^2 = 0.674; (○) canola oil, R^2 = 0.315.

TABLE 4
Regression Statistics for the Relationships Between Increasing Dietary ALA Concentrations from Different Oil Sources and the ALA Concentration in Dark Broiler Meat[a]

Source	Constant	Coefficient	R^2 (%)	P	s
Fish oil	−0.201	0.405	10.2	0.338	0.337
Linseed	−0.224	0.117	67.4	0.000	0.936
Canola	0.374	0.054	31.5	0.116	0.425

[a]For abbreviation see Table 1.

with low dietary EPA contents. The two data points that indicate a very high response to dietary EPA content are from Komprda *et al*. (23) where EPA and DHA were not distinguished from each other, and these points therefore illustrate the tissue response in terms of total EPA + DHA concentration. Much of the tissue EPA content in these instances could therefore in fact be DHA. No clear distinctions could be made between meat with and without skin, but this was mostly because of insufficient data ($n = 4$ for white meat with skin). However, since EPA is concentrated in the phospholipids and the skin lipids are predominantly TAG, the contribution that skin would make to the EPA content of edible tissues would be small. This is in contrast to what was observed with ALA, because of the accumulation of ALA that occurs in TAG. There was also no marked difference between white and dark meats in their EPA content, suggesting that white meat (the more popular of the two) is as good a source of EPA as is dark meat.
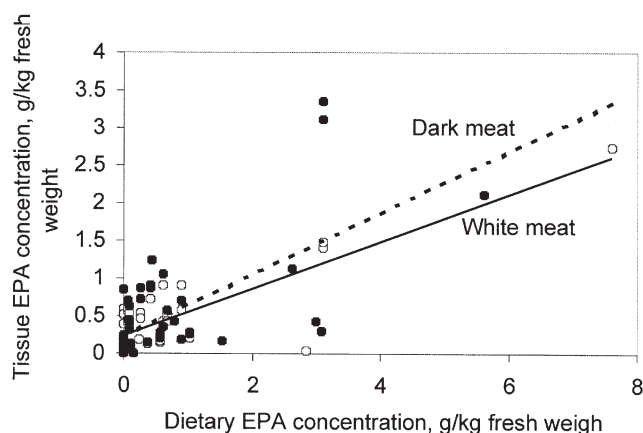
The relationship between dietary and tissue EPA content is described by Equations 1 and 2:

$$[EPA]_{white\ meat} = 0.219 + 0.311[EPA]_{diet} \qquad [1]$$

$R^2 = 0.671$, $s = 0.284$, $P = 0.000$; and

$$[EPA]_{dark\ meat} = 0.231 + 0.408[EPA]_{diet} \qquad [2]$$

$R^2 = 0.448$, $s = 0.497$, $P = 0.000$, where $[EPA]_{white\ meat}$, $[EPA]_{dark\ meat}$, $[EPA]_{diet}$ are the concentrations (g/kg fresh

weight) of EPA in the white meat, dark meat, and diet, respectively.

EPA in the tissues may come from either the direct incorporation of dietary EPA or the conversion of dietary ALA to EPA by the bird. When the diet is supplemented with terrestrial sources of n-3 PUFA, this is the only means by which EPA may accumulate in the tissues, since the EPA content of terrestrial plant oils is negligible. In Figure 5, the concentration of dietary ALA has been plotted against tissue EPA concentration. There is at best a very weak relationship between dietary ALA content and tissue EPA content, illustrating that supplementing the poultry diet with ALA (the potential precursor of EPA) does not enhance the EPA content of edible poultry tissues to any nutritionally meaningful extent (23,27,28,42,44). There is evidence that dietary ALA supplementation does result in conversion of ALA to EPA by the bird, but the EPA that is synthesized accumulates in the liver rather than the edible tissues (46). There were relatively high concentrations of EPA with some diets that had very low ALA contents (Fig. 5), because of the inclusion of fishmeal as a protein source in these diets, which would also supply a dietary source of EPA.

DHA

The increase in the DHA content of poultry lipids, particularly in breast muscle, following the addition of fish oils or marine algae to poultry diets is well established (21,22,25–27,29,41,43,47). However, the clear linear relationship between the n-3 FA concentration in the diet and the corresponding n-3 FA content of edible tissues that was observed with ALA and EPA is not evident for DHA (Fig. 6). Relatively high
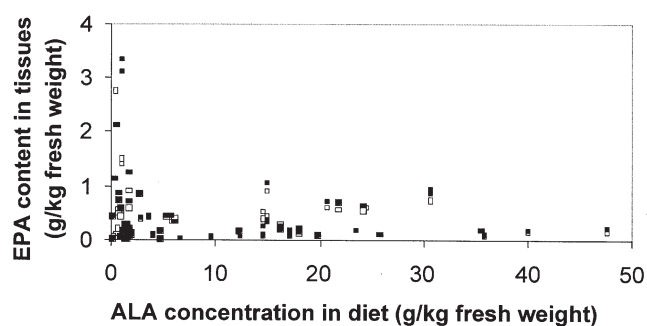
FIG. 4. Relationship between the concentration of EPA in the diet and the concentration of EPA in the edible tissues of poultry meat. (○—) White meat, $R^2 = 0.671$; (●----) dark meat, $R^2 = 0.448$.

FIG. 5. Relationship between ALA concentration in the diet and EPA content in the edible tissues of poultry. (○) White meat, $R^2 = 0.0002$; (●) dark meat, $R^2 = 0.010$.
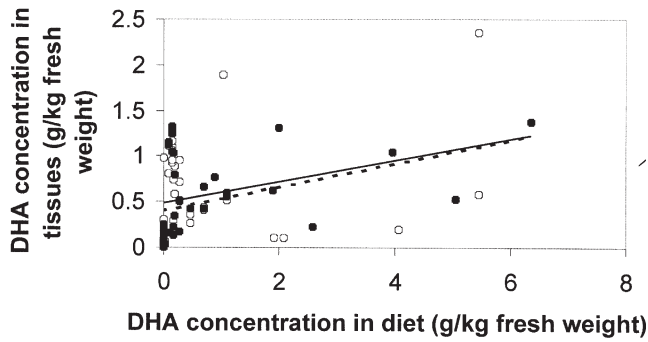
FIG. 6. Relationship between DHA concentration in the diet and DHA content in the edible tissues of poultry. (○—) White meat, $R^2 = 0.093$; (●----) dark meat, $R^2 = 0.143$.

intakes of DHA (achieved by high inclusion rates of fish oil or fishmeal) show a more obvious relationship (Fig. 7), but the regression statistics for these relationships are much weaker than the corresponding relationships observed for EPA. The equations describing the relationships between DHA content in the diet and in white and dark meat are as follows:

$$[DHA]_{white\ meat} = 0.420 + 0.173[DHA]_{diet} \qquad [3]$$

$R^2 = 0.158$, $s = 0.6558$, $P = 0.179$, and

$$[DHA]_{dark\ meat} = 0.442 + 0.109[DHA]_{diet} \qquad [4]$$

$R^2 = 0.344$, $s = 0.288$, $P = 0.017$, where $[DHA]_{white\ meat}$, $[DHA]_{dark\ meat}$, and $[DHA]_{diet}$ are the concentrations (g/kg fresh weight) of DHA in the white meat, dark meat, and diet respectively.

It is evident from Figure 6 that, even when the diet contains little or no DHA, some DHA is to be found in the edible tissues of poultry (albeit at very low concentrations), and more would
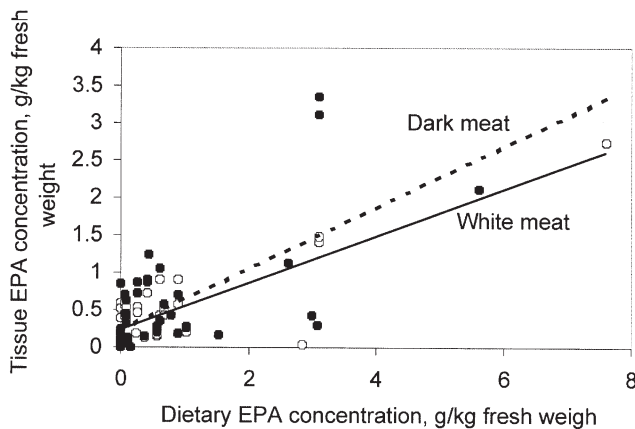

FIG. 7. Relationship between DHA concentration in the diet and DHA content in the edible tissues of poultry when the diets are supplemented with marine oils or meals. (○—) White meat, $R^2 = 0.158$; (●----) dark meat, $R^2 = 0.344$.
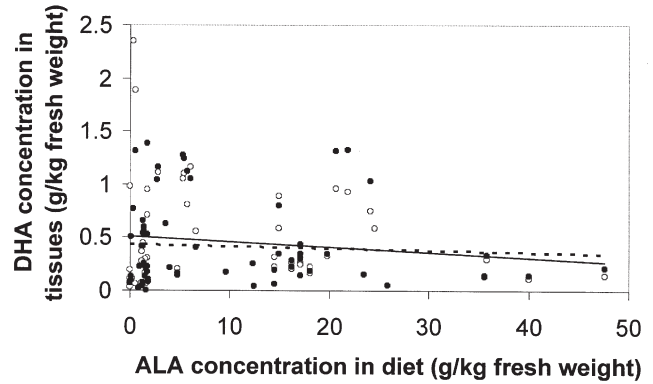

FIG. 8. Relationship between ALA concentration in the diet and DHA content in the edible tissues of poultry. (○—) White meat, $R^2 = 0.016$; (●----) dark meat, $R^2 = 0.003$.

be found in their brain and nervous system. Birds are able to synthesize DHA, but increasing the supply of substrate (ALA) by increasing the ALA content of the diet clearly does not result in an increase in the DHA content of the edible tissues (Fig. 8). Indeed, it would almost appear that high ALA concentrations in the diet reduce the accumulation of DHA in the tissues. This lack of relationship between ALA intake and edible tissue DHA content may be because the DHA that is synthesized is not then partitioned to skeletal muscle (42), being accumulated in the liver instead (46); or it could be that, as in the human, an increase in ALA supply does not result in an increase in DHA synthesis but rather an increase in β-oxidation of ALA (48) or an accumulation of ALA in the tissues (49). In conclusion, it is evident that dietary modifications can increase the DHA content of the edible tissues of poultry, but the magnitude of the response and the factors that affect that response are unclear.

OXIDATIVE STABILITY AND ORGANOLEPTIC QUALITY OF N-3 PUFA-ENRICHED POULTRY MEAT

Unsaturated lipids readily undergo oxidation to produce peroxides and aldehydes that are responsible for the reduction in storage quality that is often associated with poultry meat with an enhanced PUFA content (21,29). The oxidative stability of unsaturated lipids decreases as their degree of unsaturation increases, and so poultry meat with an enhanced ALA content will be more susceptible to oxidation than poultry meat with a similar concentration of LA. The peroxidizability index (PI) of a lipid reflects the relative rate of peroxidation of each FA (50), and is calculated from Equation 5 (51):

$$PI = (\%monoenoic \times 0.025) + (\%dienoic \times 1) + (\%trienoic \times 2) + (\%tetraenoic \times 4) + (\%pentaenoic \times 6) + (\%hexaenoic \times 8) \quad [5]$$

From this equation, it is clear that poultry meat with a higher concentration of ALA compared with LA will be more susceptible to oxidation, and also that poultry meat with an enhanced concentration of EPA and DHA will be particularly susceptible to oxidative damage. The balance of volatile compounds pro-

duced from the oxidative breakdown of n-3 FA produces the fishy aroma and off-taste that is characteristic of meat from poultry that have been fed n-3 FA (26,50,52), although if the oxidation process can be limited or halted then the meat should remain acceptable for human consumption. Indeed, Moran (53) concluded from his review of the literature that the FA composition of fat in lean tissue had minimal effect on the organoleptic qualities of meat once peroxidation products had been eliminated.

Synthetic antioxidants such as BHA or BHT that may be added to the diet can help prevent oxidation of unsaturated dietary lipids, at least prior to consumption. Small amounts of these antioxidants may then be found in the birds' tissues (54), which may then reduce the rate of oxidation of the lipid in the meat (54,55). At lower inclusion rates of BHT, however (0.05 g/kg compared with 0.8 g/kg), the protective action of dietary BHT did not extend to the meat (37). The use of α-tocopherol as an antioxidant is effective at reducing the oxidation of unsaturated lipids in meat, thereby preventing or delaying the onset of off-flavors (32,52), and it appears that there is a concerted action in the tissues to protect n-3 PUFA, with α-tocopherol being an excellent protector of these FA (56). Supplementing birds' diets with α-tocopherol (beyond their nutritional requirements) does appear to be an effective means of increasing the oxidative stability and organoleptic acceptability of poultry meat with enhanced concentrations of n-3 PUFA (32,52,56).

Meat from poultry fed oxidized oils (as a result of heat treatment or other spoilage) appears to be particularly susceptible to oxidation (37,54), but it is not clear from the literature whether this is because of an increased consumption of peroxides and other oxidation markers, which then increase the rate of peroxidation of PUFA in meat tissue (and deplete the stores of α-tocopherol and other antioxidants), or whether heated oils that are incorporated into muscle tissue are more prone to oxidation than fresh oils. Supplementing diets containing oxidized oils with α-tocopherol reduced the rate of oxidation of the meat (37,52). However it is clearly preferable to ensure when feeding lipids with a high PI (as is the case when trying to increase the concentration of ALA, EPA, or DHA in poultry meat) that the dietary lipids used have not been subjected to heating or other pro-oxidative processes, while also ensuring that the birds' diet is supplemented with α-tocopherol to maintain the oxidative stability of the meat (56).

The method of cooking may also affect the flavor of meat from chickens fed fish oil. No unusual tastes were observed in chickens fed 20 g/kg cod liver oil when their meat was fried and served warm, but a fishy flavor became apparent when the meat cooled, and a definite unpleasant flavor was observed when the chicken was stewed or roasted (57). The susceptibility of different tissues to the development of off-flavors is also variable. The higher degree of unsaturation in white meat lipids compared with dark meat means that the lipids in white meat are more susceptible to oxidation (52,58), particularly as it is the phospholipid fraction (more concentrated in the white meat than the dark meat) that is the main contributor to the development of oxidation products (58). However, the higher fat content of dark meat compared with white meat means that oxidation and the development of off-flavors occur more quickly in dark meat compared with white meat (32,50,58). A treatment that resulted in breast meat with an acceptable flavor and high long-chain n-3 PUFA content also produced wings that were unacceptable (33). Although thighs and wings are less commercially valuable than breast meat, such a treatment would clearly have a negative impact on the whole-carcass market (33). Poultry meat with enhanced long-chain n-3 FA contents may also be more liable to the development of a warmed-over flavor, which results from the rapid onset of rancidity in cooked meat during short-term refrigerated storage (59). Although the concentration of oxidation markers in freshly cooked chicken meat from broilers fed up to 120 g/kg fishmeal was not significantly different from that of meat from birds fed no fishmeal, noticeable differences were observed after 4 d of refrigerated storage (52). In a separate (unpublished) study of the experiment reported by Ratnayake *et al.* (22), this was associated after just 2 d with the development of off-flavors in the warmed-over meat from birds supplemented with 120 g/kg fishmeal (60).

In attempting to reduce the development of off-flavors in n-3 FA-enhanced poultry meat, many studies have focused on reducing or removing fish oils from the poultry diet for varying periods of time before slaughter (41). Although this has often been effective in making the product more acceptable to consumers, it also has the effect of reducing the n-3 PUFA content of the poultry meat. This approach therefore needs to find a balance between maximizing n-3 PUFA content of edible tissues and maintaining an acceptable taste in the product. When using fish oils to increase the long-chain n-3 PUFA content of poultry meat, Leskanich and Noble (21) recommended that only high-quality (i.e., unoxidized) materials should be used, the amount of fish oil or fishmeal in the diet should be limited (to 10 and 120 g/kg, respectively), and supplementary antioxidants should be included in the diet.

The feeding of marine algae rather than fish oil can result in enhanced tissue EPA and DHA content, but without some of the problems associated with off-flavors. This is probably because the oil droplets in algae are encapsulated within the algal cell and this protects them, at least in part, from oxidative deterioration (38). It is also possible that the algae contain more natural antioxidants than fish oil. However, when broiler diets were supplemented with fish oil or with natural golden marine algae, a reduction in the flavor score was still observed although this was less marked with the algae supplement (38). In human nutrition, an alternative means of consuming n-3 FA is to microencapsulate them and then include them in other foods. This greatly increases their shelf life and palatability while also maintaining their bio-availability (61). It is possible that processed products containing poultry meat could incorporate microencapsulated n-3 FA, although the whole chicken and whole turkey market could not benefit in this way. An alternative approach may be to include microencapsulated fish oils in poultry diets. This would ensure that the lipids absorbed by the birds were not oxidized, which would in itself reduce the development of off-flavors, but the meat itself would still need protection from oxidation occurring during storage.

CONCLUSIONS

In adult humans, the conversion of ALA to EPA is limited, and the further conversion to DHA appears to be marginal at best. Increasing ALA intake does not increase the concentration of EPA and DHA in the circulation, and there is no clear evidence that it reduces any of the risk factors associated with coronary heat disease. There is clearly a need for preformed EPA and DHA in the human diet, but the intake of fish (the principal source of EPA and DHA) is extremely low in northern European diets.

When poultry are fed typical diets, their n-3 PUFA content is low, with no evidence of any differences between sexes and genotypes of different species of poultry. There may be some differences between different poultry species, although no clear comparisons could be found in the literature. However, in two separate experiments in which broilers and turkeys had been fed broadly similar diets, the ALA content of turkey meat was greater than that of broiler meat. There was little difference in the total EPA and DHA content of the broiler meat (both white and dark) compared with turkey white meat, but the concentration of these FA in turkey dark meat appeared to be greater. Dark meat is a relatively rich source of ALA, whereas EPA and DHA accumulate in the white meat. However, the low lipid content of white meat compared with dark meat results in the concentration of EPA and DHA in white and dark meats being broadly similar.

Increasing the concentration of n-3 PUFA in poultry diets results in an increase in the n-3 PUFA content of poultry meat. Including feeds such as linseed in the diet increases the diet's ALA content, whereas marine sources (fish oil, fishmeal, or marine algae) increase the diet's EPA and DHA content. Linear relationships between diet ALA concentration and the ALA content of edible poultry tissues were observed, particularly for dark meat with skin. Skinless white meat had only a poor relationship between diet and tissue ALA content. There was no evidence of bird sex or genotype affecting these relationships, and data were insufficient to make a comparison between species. However, one study suggested that the response to increased ALA content may be lower in turkey white meat, but greater in turkey dark meat compared with the corresponding tissues in broilers.

The EPA content of poultry meat was increased by feeding marine products (fishmeal, fish oil, and marine algae), and a linear relationship between the concentration of EPA in the diet and in both white and dark meat was observed. However, feeding ALA did not cause a noticeable increase in EPA content, suggesting that, as with humans, an increased supply of substrate (ALA) did not induce an increased synthesis of product (EPA). Some DHA was found in the edible tissues of poultry even when no DHA was fed, but the concentrations were low. The DHA content of edible poultry tissues was increased when DHA was included in the diet (from marine products), but there was no clear relationship between diet and tissue in terms of their respective DHA contents.

Feeding marine products to poultry will increase their long-chain n-3 PUFA content, but the oxidative stability of the meat will decrease as a result. This has negative effects on both the shelf life and the flavor of the meat. These shortcomings may be overcome by ensuring that only good-quality materials are used, by limiting the inclusion rate of fish oil or fishmeal in the diet, and by including antioxidants such as α-tocopherol in the diet at supranutritional concentrations (100 IU/kg). This can then result in nutritionally meaningful amounts of long-chain n-3 PUFA being delivered from the edible tissues of poultry and could have beneficial effects on the health of consumers.

ACKNOWLEDGMENTS

REFERENCES

1. Emken, E.A., Adlof, R.O., and Gulley, R.M. (1994) Dietary Linoleic Acid Influences Desaturation and Acylation of Deuterium-Labeled Linoleic and Linolenic Acids in Young Adult Males, *Biochim. Biophys. Acta 1213*, 277–288.
2. Ghafoorunissa, S.A. (1998) Requirements of Dietary Fats to Meet Nutritional Needs and Prevent the Risk of Atherosclerosis—An Indian Perspective, *Indian J. Med. Res. 108*, 191–202.
3. Gerster, H. (1998) Can Adults Adequately Convert α-Linolenic Acid (18:3 n-3) to Eicosapentaenoic Acid (20:5n-3) and Docosahexaenoic Acid (22:6n-3)? *Int. J. Vitam. Nutr. Res. 68*, 159–173.
4. Burdge, G. (2004) α-Linolenic Acid Metabolism in Men and Women: Nutritional and Biological Implications, *Curr. Opin. Clin. Nutr. Metab. Care ., 7*, 137–144.
5. Burdge, G.C., and Wootton, S.A. (2002). Conversion of α-Linolenic Acid to Eicosapentaenoic, Docosapentaenoic and Docosahexaenoic Acids in Young Women, *Br. J. Nutr. 88*, 411–421.
6. Burdge, G.C., Jones, A.E., and Wootton, S.A. (2002) Eicosapentaenoic and Docosapentaenoic Acids Are the Principal Products of α-Linolenic Acid Metabolism in Young Men, *Br. J. Nutr. 88*, 355–364.
7. Smit, E.N., Fokkema, M.R., Boersma, E.R., and Muskiet, F.A. (2003) Higher Erythrocyte 22:6n-3 and 22:5n-6, and Lower 22:5n-3 Suggest Higher Δ-4-Desaturation Capacity in Women of Childbearing Age, *Br. J. Nutr. 89*, 739–740.
8. Muskiet, F.A.J., Fokkema, M.R., Schaafsma, A., Boersma, E.R., and Crawford, M.A. (2004) Is Docosahexaenoic Acid (DHA) Essential? Lessons from DHA Status Regulation, Our Ancient Diet, Epidemiology and Randomized Controlled Trials, *J. Nutr. 134*, 183–186.
9. Salem, N., Jr., Wegher, B., Mena, P., and Uauy, R. (1996) Arachidonic and Docosahexaenoic Acids Are Biosynthesized from Their 18-Carbon Precursors in Human Infants, *Proc. Natl. Acad. Sci. USA 93*, 49–54.
10. Sauerwald, T.U., Hachey, D.L., Jensen, C.L., Chen, H., Anderson, R.E., and Heird, W.C. (1996) Effect of Dietary α-Linolenic Acid Intake on Incorporation of Docosahexaenoic and Arachidonic Acids into Plasma Phospholipids of Term Infants, *Lipids 31* (Suppl.), S131–S135.
11. Innis, S.M., Sprecher, H., Hachey, D., Edmond, J., and Anderson, R.E. (1999) Neonatal Polyunsaturated Fatty Acid Metabolism, *Lipids 34*, 139–149.
12. Salem, N., Jr., Litman, B., Kim, H.-Y., and Gawrisch, K. (2001) Mechanisms of Action of Docosahexaenoic Acid in the Nervous System, *Lipids 36*, 945–959.

13. Pehowich, D.J. (1998) Dietary n-3 Fatty Acids Alter Angiotensin-Induced Contraction and 1,2-Diacylglycerol Fatty Acid Composition in Thoracic Aortas from Diabetic Rats, *Prostaglandins Leukot. Essent. Fatty Acids 58*, 301–309.

14. Nervi, A.M., Peluffo, R.O., and Brenner, R.R. (1980) Effects of Ethanol Administration on Fatty Acid Desaturation, *Lipids 15*, 263–268.

15. Department of Health (1994) *Department of Heath Report on Health and Social Subjects No. 46. Nutritional Aspects of Cardiovascular Disease*, Report of the Cardiovascular Review Group Committee on Medical Aspects of Food Policy, 186 pp., HMSO London.

16. Lovegrove, J.A., Brooks, C.N., Murphy, M.C., Gould, B.J., and Williams, C.M. (1997) Use of Manufactured Foods Enriched with Fish Oils as a Means of Increasing Long-Chain n-3 Polyunsaturated Fatty Acid Intake, *Br. J. Nutr. 78*, 223–236.

17. Hulshof, K.F.A.M., van Erp-Baart, M.A., Anttolainen, M., Becker, W., Church, S.M., Couet, C., Hermann-Kunz, E., Kesteloot, H., Leth, T., Martins, I., *et al.* (1999) Intake of Fatty Acids in Western Europe with Emphasis on *trans* Fatty Acids: The Transfair Study, *Eur. J. Clin. Nutr. 53*, 143–157.

18. Rymer, C., Givens, D.I., and Wahle, K.W.J. (2003). Dietary Strategies for Increasing Docosahexaenoic Acids (DHA) and Eicosapentaenoic Acid (EPA) Concentrations in Bovine Milk, A Review, *Nutr. Abs. Ser. Rev. B., Livestock Feeds and Feeding 73*, 9R–25R.

19. DEFRA (2001) *National Food Survey 2000: Annual Report on Food Expenditure, Consumption and Nutrient Intakes*, 214 pp, Stationery Office, London.

20. Hulbert, A.J., Faulks, S., Buttemer, W.A., and Else, P.L. (2002). Acyl Composition of Muscle Membranes Varies with Body Size in Birds, *J. Exp. Biol. 205*, 3561–3569.

21. Leskanich, C.O., and Noble, R.C. (1997) Manipulation of the n-3 Polyunsaturated Fatty Acid Composition of Avian Eggs and Meat, *Worlds Poult. Sci. J. 53*, 155–183.

22. Ratnayake, W.M.N., Ackman, R.G., and Hulan, H.W. (1989) Effect of Redfish Meal Enriched Diets on the Taste and n-3 PUFA of 42-Day-Old Broiler Chickens, *J. Sci. Food Agric. 49*, 59–74.

23. Komprda, T., Zelenka, J., Bakaj, P., Kladroba, D., Blazkova, E. and Fajmonova, E. (2002) Cholesterol and Fatty Acid Content in Meat of Turkeys Fed Diets with Sunflower, Linseed or Fish Oil, *Arch. Geflügelkd. 67*, 65–75.

24. Marion, J.E., and Woodroof, J.G. (1963) The Fatty Acid Composition of Breast, Thigh and Skin Tissues of Chicken Broilers as Influenced by Dietary Fats, *Poult. Sci. 48*, 1202–1207.

25. Neudoerffer, T.S., and Lea, C.H. (1966) Effects of Dietary Fish Oil on the Composition and Stability of Turkey Depot Fat, *Br. J. Nutr. 20*, 581–594.

26. Neudoerffer, T.S., and Lea, C.H. (1967) Effects of Dietary Polyunsaturated Fatty Acids on the Composition of the Individual Lipids of Turkey Breast and Leg Muscle, *Br. J. Nutr. 21*, 691–714.

27. Hargis, P.S., and van Elswyk, M.E. (1993) Manipulating the Fatty-Acid Composition of Poultry Meat and Eggs for the Health Conscious Consumer, *Worlds Poult. Sci. J. 49*, 251–264.

28. Jakobsen, K. (1999) Dietary Modifications of Animal Fats: Status and Future Perspectives, *Fett/Lipid 101*, 475–483.

29. Manilla, H.A., and Husvéth, F. (1999) n-3 Fatty Acid Enrichment and Oxidative Stability of Broiler Chicken (a review), *Acta Aliment. 28*, 235–249.

30. Mourot, J., and Hermier, D. (2001) Lipids in Monogastric Animal Meat, *Reprod. Nutr. Dev. 41*, 109–118.

31. Hulan, H.W., Ackman, R.G., Ratnayake, W.M.N., and Proudfoot, F.G. (1988) Omega-3 Fatty Acid Levels and Performance of Broiler Chickens Fed Redfish Meal or Redfish Oil, *Can. J. Anim. Sci. 68*, 533–547.

32. Nam, K.-T., Lee, H.-A., Min, B.-S., and Kang, C.-W. (1997) Influence of Dietary Supplementation with Linseed and Vitamin E on Fatty Acids, α-Tocopherol and Lipid Peroxidation in Muscles of Broiler Chicks, *Anim. Feed Sci. Technol. 66*, 149–158.

33. Gonzalez-Esquerra, R., and Leeson, S. (2000) Effects of Menhaden Oil and Flaxseed in Broiler Diets on Sensory Quality and Lipid Composition of Poultry Meat, *Br. Poult. Sci. 41*, 481–488.

34. Ajuyah, A.O., Lee K.H., Hardin, R.T., and Sim, J.S. (1991) Influence of Dietary Full-Fat Seeds and Oils on Total Lipid, Cholesterol and Fatty-Acid Composition of Broiler Meats, *Can. J. Anim. Sci. 71*, 1011–1019.

35. Ajuyah, A.O., Hardin, R.T., Cheung, K., and Sim, J.S. (1992) Yield, Lipid, Cholesterol and Fatty-Acid Composition of Spent Hens Fed Full-Fat Oil Seeds and Fish-Meal Diets, *J. Food Sci. 57*, 338–341.

36. Chanmugan, P., Boudreau, M., Bouette, T., Park, R.S., Hebert, J., Berrio, L., and Hwang, D.H. (1992) Incorporation of Different Types of n-3 Fatty Acids into Tissue Lipids of Poultry, *Poult. Sci. 71*, 516–521.

37. Sheehy, P.J.A., Morrissey, P.A., and Flynn, A. (1993) Influence of Heated Vegetable-Oils and α-Tocopheryl Acetate Supplementation on α-Tocopherol, Fatty-Acids and Lipid-Peroxidation in Chicken Muscle, *Br. Poult. Sci. 34*, 367–381.

38. Mooney, J.W., Hirschler, E.M., Kennedy, A.K., Sams, A.R., and van Elswyk, M.E. (1998) Lipid and Flavour Quality of Stored Breast Meat from Broilers Fed Marine Algae, *J. Sci. Food Agric. 78*, 134–140.

39. Nitsan, Z., Mokady, S., and Sukenik, A. (1999) Enrichment of Poultry Products with ω3 Fatty Acids by Dietary Supplementation with the Alga *Nannochloropsis* and Mantur Oil, *J. Agric. Food Chem. 47*, 5127–5132.

40. Krasicka, B., Kulasek, G.W., Swierczewska, E., and Orzechowski, A. (2000) Body Gains and Fatty Acid Composition in Carcasses of Broilers Fed Diets Enriched with Full-Fat Rapeseed and/or Flaxseed, *Arch. Geflügelkd. 64*, 61–69.

41. López-Ferrer, S., Baucells, M.D., Barroeta, A.C., and Grashorn, M.A. (2001) n-3 Enrichment of Chicken Meat. 1. Use of Very Long-Chain Fatty Acids in Chicken Diets and Their Influence on Meat Quality: Fish Oil, *Poult. Sci. 80*, 741–752.

42. López-Ferrer, S., Baucells, M.D., Barroeta, A.C., Galobart, J., and Grashorn, M.A. (2001) n-3 Enrichment of Chicken Meat. 2. Use of Precursors of Long-Chain Polyunsaturated Fatty Acids: Linseed Oil, *Poult. Sci. 80*, 753–761.

43. Howe, P.R.C., Downing, J.A., Grenyer, B.F.S., Grigonis-Deane, E.M., and Bryden, L. (2002) Tuna Fishmeal as a Source of DHA for n-3 PUFA Enrichment of Pork, Chicken, and Eggs, *Lipids 37*, 1067–1076.

44. Özpinar, H., Kahraman, R., Abas, I., Kutay, H.C., Eseceli, H., and Grashorn, M.A. (2003) Effect of Dietary Fat Source on n-3 Fatty Acid Enrichment of Broiler Meat, *Arch. Geflügelkd. 67*, 57–64.

45. Mossab, A., Hallouis, J.M., and Lessire, M. (2000) Utilization of Soybean Oil and Tallow in Young Turkeys Compared with Young Chickens, *Poult. Sci. 79*, 1326–1331.

46. Ajuyah, A.O., Hardin, R.T. and Sim, J.S. (1993) Studies on Canola Seed in Turkey Grower Diet: Effects on ω-3 Fatty Acid Composition of Breast Meat, Breast Skin and Selected Organs, *Can. J. Anim. Sci. 73*, 177-181.

47. González-Esquerra, R. and Leeson, S. (2001) Alternatives for Enrichment of Eggs and Chicken Meat with Omega-3 Fatty Acids, *Can. J. Anim. Sci. 81*, 295–305.

48. Vermunt, S.H.F., Mensink, R.P., Simonis, M.G., and Hornstra, G. (2000) Effects of Dietary α-Linolenic Acid on the Conversion and Oxidation of ^{13}C-α-Linolenic Acid, *Lipids 35*, 137–142.

49. Burdge, G.C., Finnegan, Y.E., Minihane, A.M., Williams, C.M., and Wootton, S.A. (2003) Effect of Altered Dietary *n*-3 Fatty

Acid Intake upon Plasma Lipid Fatty Acid Composition, Conversion of [¹³C]α-Linolenic Acid to Longer-Chain Fatty Acids and Partitioning Towards β-Oxidation in Older Men, *Br. J. Nutr. 90*, 311–321.

50. Meynier, A., Genot, C., and Gandemer, G. (1999) Oxidation of Muscle Phospholipids in Relation to Their Fatty Acid Composition with Emphasis on Volatile Compounds, *J. Sci. Food Agric. 79*, 797–804.

51. Arakawa, K., and Sagai, M. (1986) Species Differences in Lipid Peroxide Levels in Lung Tissue and Investigation of Their Determining Factors, *Lipids 21*, 769–775.

52. O'Keefe, S.F., Proudfoot, F.G., and Ackman, R.G. (1995) Lipid Oxidation in Meats of Omega-3 Fatty-Acid Enriched Broiler Chickens, *Food Res. Intl. 28*, 417–424.

53. Moran, E.T., Jr. (1996) Fat Modification of Animal Products for Human Consumption, *Anim. Feed Sci. Technol. 58*, 91–99.

54. Asghar, A., Lin, C.F., Gray, J.I., Buckley, D.J., Booren, A.M., Crackel, R.L., and Flegal, C.J. (1989) Influence of Oxidised Dietary Oil and Antioxidant Supplementation on Membrane-Bound Lipid Stability in Broiler Meat, *Br. Poult. Sci. 30*, 815–823.

55. Lin, C.F., Asghar, A., Gray, J.I., Buckly, D.J., Booren, A.M., Crackel, R.L., and Flegal, C.J. (1989) Effects of Oxidised Dietary Oil and Antioxidant Supplementation on Broiler Growth and Meat Stability, *Br. Poult. Sci. 30*, 855–864.

56. Jahan, K., Paterson, A. and Spickett, C.M. (2004) Fatty Acid Composition, Antioxidants and Lipid Oxidation in Chicken Breasts from Different Production Regimes, *Intl. J. Food Sci., Technol. 39*, 443–453.

57. Carrick, C.W., and Hauge, S.M. (1926) The Effect of Cod-Liver Oil upon Flavor in Poultry Meat, *Poult. Sci. 5*, 213–215.

58. Pikul, J., Leszczynski, D.E., and Kummerow, F.A. (1984) Relative Role of Phospholipids, Triacylglycerols, and Cholesterol Esters on Malonaldehyde Formation in Fat Extracted from Chicken Meat, *J. Food Sci. 49*, 704-708.

59. Wilson, B.R., Pearson, A.M., and Shorland, F.B. (1976) Effect of Total Lipids and Phospholipids on Warmed-Over Flavor in Red and White Muscle from Several Species as Measured by Thiobarbituric Acid Analysis, *J. Agric. Food Chem. 24*, 7–11.

60. Poste, L.M. (1990) A Sensory Perspective of Effects of Feeds on Flavor in Meats: Poultry Meats, *J. Anim. Sci. 68*, 4414–4420.

61. Schrooyen, P.M.M., van der Meer, R., and De Kruif, C.G. (2001) Microencapsulation: Its Application in Nutrition, *Proc. Nutr. Soc. 60*, 475–479.

ARTICLES

Maternal Dietary Conjugated Linoleic Acid Alters Hepatic Triacylglycerol and Tissue Fatty Acids in Hatched Chicks

Gita Cherian*, Wu Ai, and Mary P. Goeger

Department of Animal Sciences, Oregon State University, Corvallis, Oregon, 97331-6702

ABSTRACT: The effects of feeding CLA to hens on newly hatched chick hepatic and carcass lipid content, liver TAG accumulation, and FA incorporation in chick tissues such as liver, heart, brain, and adipose were studied. These tissues were selected owing to their respective roles in lipid assimilation (liver), as a major oxidation site (heart), as a site enriched with long-chain polyunsaturates for function (brain), and as a storage depot (adipose). Eggs with no, low, or high levels of CLA were produced by feeding hens a corn–soybean meal–basal diet containing 3% (w/w) corn oil (Control), 2.5% corn oil + 0.5% CLA oil (CLA1), or 2% corn oil + 1.0% CLA oil (CLA2). The egg yolk content of total CLA was 0.0, 1.0, and 2.6% for Control, CLA1, and CLA2, respectively ($P < 0.05$). Maternal dietary CLA resulted in a decrease in chick carcass total fat ($P < 0.05$). Liver tissue of CLA2 chicks had the lowest fat content ($P < 0.05$). The liver TAG content was 8.2, 5.8, and 5.1 mg/g for Control, CLA1, and CLA2 chicks, respectively ($P < 0.05$). The chicks hatched from CLA1 and CLA2 incorporated higher levels of *cis*-9,*trans*-11 CLA in the liver, plasma, adipose, and brain than Control ($P < 0.05$). The content of 18:0 was higher in the liver, plasma, adipose, and brain of CLA1 and CLA2 than Control ($P < 0.05$), but no difference was observed in the 18:0 content of heart tissue. A significant reduction in 18:1 was observed in the liver, plasma, adipose, heart, and brain of CLA1 and CLA2 chicks ($P < 0.05$). DHA (22:6n-3) was reduced in the heart and brain of CLA1 and CLA2 chicks ($P < 0.05$). No difference was observed in carcass weight, dry matter, or ash content of chicks ($P > 0.05$). The hatchabilities of fertile eggs were 78, 34, and 38% for Control, CLA1, and CLA2, respectively ($P < 0.05$). The early dead chicks were higher in CLA1 and CLA2 than Control (18 and 32% compared with 9% for Control), and alive but not hatched chicks were 15 and 19% for CLA1 and CLA2, compared with 8% for Control ($P < 0.05$). Maternal supplementation with CLA leads to a reduction in hatchability, liver TAG, and carcass total fat in newly hatched chicks.

Paper no. L9648 in *Lipids 40*, 131–136 (February 2005).

CLA have received considerable attention for their potential to repartition body mass in growing animals (1–3) and for their suggested health-promoting effects (4–6). CLA is a collective term used for a group of positional and geometric dienoic isomers of essential linoleic acid (18:2n-6). Among the CLA isomers, *cis*-9,*trans*-11 (*c*9,*t*11) and *trans*-10,*cis*-12 (*t*10,*c*12) are the predominant ones found in foods of ruminant origins where they are synthesized by rumen microbes. Because a major proportion of fat in the U.S. diet is of animal origin, feeding strategies have been adopted to increase the content of CLA in foods of ruminant as well as nonruminant origin, such as pork, chicken eggs, and meat (7–9), because of the possible health-promoting properties of CLA (4–6).

Enriching eggs with up to 14.8% CLA has been reported through manipulation of the diets of laying hen (10). CLA incorporation in eggs resulted in a significant increase in saturated FA (SFA) (16:0, 18:0) with a concomitant reduction in monounsaturated FA (MUFA) (16:1, 18:1n-9) (10,11). However, feeding CLA had little effect on the total fat content of egg. Yolk fat is primarily TAG (68%) and phospholipids (28%). During the 21-d incubation period, the chicken embryo utilizes over 80% of the yolk fat for energy production, for formation of fat stores, and for synthesis of membrane phospholipids (12,13). The yolk-derived lipids are reassembled into TAG-rich lipoproteins by the endodermal cells of the yolk sac membrane (12). Tissue maturation in the embryo is also dependent on the incorporation of highly characteristic FA profiles into cell membrane phospholipids. Recent studies suggest that phospholipids containing long-chain n-6 and n-3 PUFA are involved in many cellular signaling mechanisms such as cardiac rhythm, neurotransmission, and photoreception (14). Therefore, FA delivery, partitioning, and tissue uptake during incubation affects embryonic health and hatchability. Adverse effects of yolk CLA on hatchability (15), yolk absorption and reduction in chick VLDL TAG were reported (16). Because the CLA composition of egg yolk can be manipulated by diet, the CLA-modified egg is a useful research tool for studying the role of maternal dietary CLA on lipid metabolism in the progeny. Given that CLA are known to have significant effects on lipid partitioning in mammals, it is important to evaluate the extent to which supplementation of CLA during development through maternal supply (yolk) influences FA composition and TAG allocation in hatched chicks. The objectives of the present study were to investigate the effects of feeding CLA to hens on chick hepatic and carcass lipid content, liver TAG accumulation, and FA incorporation into chick tissues such as liver, heart, brain, and adipose. These tissues were selected because of

---

their respective roles in lipid assimilation (liver), oxidation (heart), functional long-chain PUFA incorporation (brain), and storage (adipose).

MATERIALS AND METHODS

These experiments were reviewed by the Oregon State University Animal Care and Use Committee to ensure adherence to Animal Care Guidelines.

Maternal diet and egg enrichment of CLA. Eggs with different levels of CLA were obtained by feeding New Hampshire breeder hens a corn–soybean meal-based diet containing 3% corn oil (Control), 2.5% corn oil + 0.5% CLA oil (CLA1), and 2% corn oil + 1% CLA oil (CLA2). All the diets were isoenergetic (2900 kcal/kg feed) and isonitrogenous (16% crude protein). The FA composition of the diets is shown in Table 1. Corn oil was purchased from a local market. The CLA oil containing 75% FFA oil was donated from a commercial source (CLA One®; Pharmanutrients, Lake Bluff, IL) and was made of approximately equal amounts of *c*9,*t*11 and *t*10,*c*12. The other FA in the CLA oil were 16:0 (4.4%), 18:0 (2.8%), 18:1 (15.4%), and 18:2 n-6 (1.8%). The diets were mixed weekly and were stored in a cold room (4°C) in airtight containers. The experimental diets were fed to hens (*n* = 30; 10 per treatment) for a period of 6 wk. The birds were kept individually in cages and were maintained on a 16:8 light/dark photoperiod and standard conditions of temperature and ventilation as per Oregon State University Poultry Farm standard operating procedures. Water and feed were provided *ad libitum.*

Sample collection. After 5 wk on experimental diet, hens were artificially inseminated with 0.05 mL of pooled semen collected immediately before insemination. Eggs were gathered for 10 d after insemination and were held in a cold room at 65°F (18.3°C). All eggs were warmed to room temperature before setting in the incubator. All the eggs were distributed randomly in the incubator. A total of 180 eggs (60 eggs per treatment) were incubated at 37°C and 85% RH. Hatching

times were observed from day 21 onward in the morning and evening. The hatched chicks from all treatments were counted in the early morning of Day 22. The eggs that did not hatch were removed from the incubator and were also counted. The eggs were broken open and the number of embryos that were dead or pips (i.e., alive and pipped through the shell, but not free of the shell) were also counted. The hatched chicks (five per treatment) were sacrificed, and heart, adipose, liver, and blood (1 mL) were collected. From the remaining hatched chicks five were taken for proximate analysis. All samples were stored at −80°C and were analyzed within 2 mon of collection.

Carcass pressure cooking. The carcasses were autoclaved individually in pyrex beakers at 121°C (15 psi) for 2.5 h. When cool, the contents of each beaker were homogenized in a 4-L Waring heavy-duty laboratory blender on high speed (20,000 rpm) for 5 min. The resulting slurry was taken for lipid and proximate analysis according to methods of the Association of Official Analytical Chemists (17).

Lipid analyses. Total lipids were extracted from feed, egg yolk, liver, heart, adipose, plasma, and carcass slurry by the method of Folch *et al.* (18). About 1 g of yolk, feed, carcass slurry, adipose, or whole tissues (heart, brain, liver) was weighed into a screw-capped test tube with 18 mL of chloroform/methanol (2:1, vol/vol), and homogenized with a polytron (Type PT10/35; Brinkman Instruments, Westbury, NY) for 15 to 20 s at high speed. After an overnight incubation at 4°C, 4 mL of 0.88% sodium chloride solution was added and mixed. The phases were separated by centrifugation, and the lower chloroform layer was collected for lipid and FA analysis. Total lipids were determined gravimetrically for liver, egg yolk, and carcass. The lipid extract (2 mL) was taken into a 16-mL screw-capped glass tube and dried in a block heater at 39°C under a gentle stream of nitrogen. The dried lipids were resolubilized in 2 mL of boron trifluoride/methanol (10% w/w) and were heated in a 95–100°C water bath for 60 min and FAME were prepared. The FAME were separated and quantified by GC.

Analysis of FA composition was performed with an HP 6890 gas chromatograph (Hewlett-Packard Co., Wilmington, DE) equipped with an autosampler, FID, and fused-silica capillary column, 100 m × 0.25 mm × 0.2 µm film thickness (SP-2560; Supelco, Bellefonte, PA). Sample (2 µL) was injected with helium as a carrier gas onto the column programmed for ramped oven temperatures (initial temperature was 110°C, held for 0.5 min, then ramped at 20°C/min to 200°C and held for 50 min, then ramped at 10°C/min to 230°C and held for 5.0 min). Inlet and detector temperatures were both 250°C (12). Peak areas and percentages were calculated using Hewlett-Packard ChemStation software. FAME were identified by comparison with retention times of authentic standards (Matreya, Pleasant Gap, PA). FA values and total lipids are expressed as weight percentages.

Liver TAG were estimated by adapting an enzyme-based procedure with a colorimetric end point, originally developed for serum as reported earlier (19). The liver tissue total lipid extract served as substrate. A glycerol standard (G1394-5ML;

TABLE 1
Major FA Composition (%) of Maternal Diets

Dietary treatments[a]

FA	Control	CLA1	CLA 2
14:0	0.1 ± 0.0	0.1 ± 0.0	0.1 ± 0.0
16:0	13.5 ± 0.7	13.3 ± 0.1	13.2 ± 0.1
18:0	1.9 ± 0.1	1.9 ± 0.1	1.9 ± 0.1
18:1	25.4 ± 0.8	24.0 ± 0.6	23.4 ± 0.7
18:2	56.8 ± 0.3	52.8 ± 0.1	49.1 ± 0.2
18:3n-3	2.4 ± 0.0	2.4 ± 0.1	2.2 ± 0.1
Cis-9,*trans*-11 CLA	0.0 ± 0	2.6 ± 0.0	4.7 ± 0.1
Trans-10,*cis*-12 CLA	0.0 ± 0	2.9 ± 0.0	5.3 ± 0.2
Total SFA	15.5 ± 0.5	15.3 ± 0.2	15.2 ± 0.3
Total MUFA	25.4 ± 0.6	23.9 ± 0.1	23.5 ± 0.2
Total CLA	0.0 ± 0.0	5.6 ± 0.1	10.0 ± 0.1
Total n-6 PUFA	56.7 ± 0.3	52.8 ± 0.1	49.1 ± 0.4
Total n-3 PUFA	2.4 ± 0.0	2.4 ± 0.1	2.2 ± 0.1

[a]Control diet contained 3% corn oil. CLA1 and CLA2 represent corn oil + 0.5% CLA or corn oil + 1% CLA, respectively. SFA, saturated FA; MUFA, monounsaturated FA.

Sigma Chemical, St. Louis, MO) was used for calibration of the assay, and Accutrol normal control serum (A2034-1VL; Sigma Chemical) for quality control.

Statistical analysis. The effects of maternal diet on carcass lipids, hepatic and plasma lipids, TAG, and FA were analyzed by ANOVA using SAS (version 8.2) (SAS Institute, Cary, NC) (20). Student–Newman–Keuls multiple range test (21) was used to compare differences among treatment means ($P < 0.05$). Mean values and SEM are reported.

RESULTS AND DISCUSSION

All the diets were isoenergetic, isonitrogenous, and had added 3% oil, which was within the limits of energy and protein supplied to breeder hens. Addition of CLA oil altered the $c9,t11$ and $t10,c12$ content of the diets (Table 1). CLA were present only in the CLA-supplemented diets (CLA1 and CLA2) and consisted of both $c9,t11$ and $t10,c12$. Incorporating CLA oil in the diet resulted in a significant increase in $c9,t11$ and $t10,c12$ content of eggs (Fig. 1A). The content of total CLA was 1.0 and 2.6%, respectively, in CLA1 and CLA2 eggs. Inclusion of CLA also resulted in an increase in SFA (16:0, 18:0) with a concomitant reduction in MUFA (18:1) resulting in an increase in SFA/MUFA ratio in CLA1 and CLA2 eggs (Fig. 1B). These results also corroborate our previous reported results and those of others (10,11). This decrease in MUFA may be due to inhibition of the expression of the stearoyl-CoA desaturase-1 (SCD-1) enzyme that converts 16:0 and 18:0 to 16:1 and 18:1 by CLA, respectively (22). Inclusion of CLA did not alter the total lipid content of egg, which was 30.6, 31.2, and 29.9 for Control, CLA1, and CLA2, eggs, respectively ($P > 0.05$).

Liver lipids, TAG, and FA. A significant effect of dietary CLA on hepatic total lipid was noted. Livers of chicks hatched from hens fed CLA2 were lower in total lipids than Control chicks ($P < 0.05$) (Fig. 2A). The decrease in liver lipids by yolk CLA could be the consequence of a higher oxidation rate of these FA as reported in mice fed $t10,c12$ CLA (23). The decrease in liver lipids was associated with a decrease in hepatic TAG concentration in both CLA1 and CLA2 chicks ($P < 0.05$) (Table 2). To our knowledge, effects of maternal dietary CLA on liver TAG concentrations in hatched chicks have not been previously reported. Transfer of lipids and fat-soluble nutrients from the egg yolk to the embryonic liver is accomplished by TAG-rich lipoproteins through the yolk sac membrane (24). The percentage of TAG in VLDL particles has been reported to be lower in chicks hatched from hens fed CLA (16). These researchers also observed a reduction in remnant yolk in the chicks hatched from hens fed CLA, suggesting that CLA enrichment in the yolk leads to either an impairment in yolk lipid removal or hepatic tissue TAG accretion during the incubation period. Since yolk TAG is the main source of energy for avian embryos, a lack of mobilization or an impairment in absorption may affect chick health. In our study, the percentages of early dead chicks were higher in CLA1 and CLA2 than Control (18 and 32% compared with 9% for Control), and alive but not hatched (pipped) chicks were 15 and 19% for CLA1 and
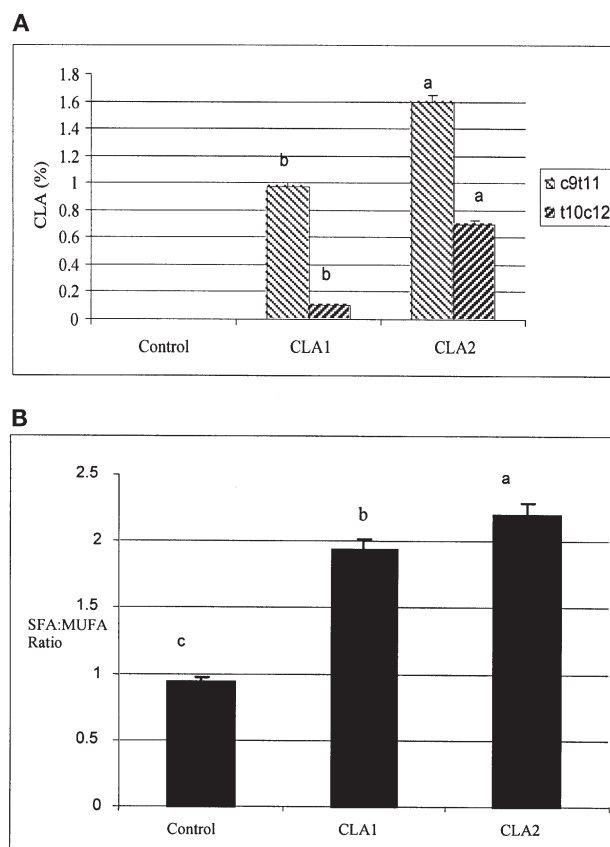
FIG. 1. CLA isomers (%) (A) and total saturated to monounsaturated ratio (B) in the egg yolk from breeder hens fed diets containing 0.0, 0.5%, or 1.0% CLA. [a–c]Means with different superscripts differ significantly for each bar ($P < 0.05$) ($n = 5$). Control diet contained 3% corn oil. CLA1 and CLA2 represent 2.5% corn oil + 0.5% CLA or 2% corn oil +1% CLA.

CLA2 compared with 8% for Control. The hatchabilities of fertile eggs were 78, 34, and 38% for Control, CLA1, and CLA2, respectively ($P < 0.05$). CLA have been reported to accumulate in the liver mitochondrial matrix affecting the oxidation of other FA (23). Because the avian embryo derives 90% of its energy from oxidation of FA, a reduced energy source may lead to embryonic death or an increase in live but not hatched chicks, as noted in our study.

An increase in egg yolk CLA resulted in a dramatic change in the chick liver SFA and MUFA content (Table 2). A significant increase in 18:0 with a concomitant decrease in 18:1 was observed in CLA1 and CLA2 chicks. The inhibitory action of CLA on SCD-1, the enzyme capable of converting 18:0 to 18:1, has been reported (22). In the present study, yolk and liver 18:0 was significantly higher in the CLA1 and CLA2 groups, indicating the inhibitory action of maternal CLA on SCD-1. An alteration of Δ-6 desaturase in chick liver due to an altered n-6/n-3 FA ratio in the maternal diet has been reported (25). These results suggest that maternal FA may have a profound effect on liver enzyme activities affecting unsaturated FA metabolism during avian embryonic development. Total CLA
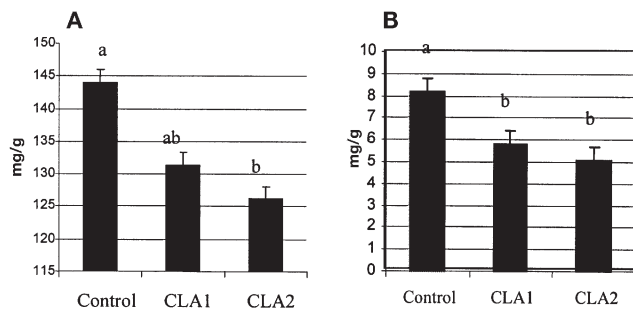
FIG. 2. Hepatic total lipid (A) and TAG (B) content of newly hatched chicks from breeder hens fed diets with or without CLA. [a–b]Means with different superscripts differ significantly ($P < 0.05$) ($n = 5$). Control diet contained 3% corn oil. CLA1 and CLA2 represent 2.5% corn oil + 0.5% CLA or 2% corn oil +1% CLA.

were higher in the liver of CLA2 chicks. The *c9,t*11 isomer was the predominant isomer and was higher ($P < 0.05$) in livers from CLA1 and CLA2 chicks (Table 2). In addition to the changes in SFA and MUFA, the content of 18:2n-6 and total n-6 FA was higher in CLA1 and CLA2 chicks ($P < 0.05$). The level of DHA (22:6n-3) was lower in CLA2 chicks ($P < 0.05$).

The FA composition of chick plasma, adipose, heart, and brain tissue is shown in Tables 3 and 4. Stearic acid (18:0) was increased significantly in the plasma and brain of CLA1 and CLA2 chicks compared with the Control (Table 3). However, no difference was observed in the heart tissue content of 18:0 in CLA1 and CLA2, suggesting that the activities of SCD-1 in chickens may be tissue-specific. Consistent with findings in the liver, 18:1 was significantly reduced in the plasma, heart, and brain tissue of CLA1 and CLA2 chicks (Tables 3 and 4). Inclu-

TABLE 2
Major FA Composition (%) of Newly Hatched Chick Liver Total Lipids

FA	Dietary treatments[a]		
	Control	CLA1	CLA2
14:0	0.60 ± 0.0[b]	0.91 ± 0.0[a]	0.99 ± 0.0[a]
16:0	10.2 ± 0.8	9.8 ± 0.8	9.6 ± 0.9
16:1	1.0 ± 0.3	0.8 ± 0.1	0.8 ± 0.1
18:0	11.1 ± 1.0[b]	14.9 ±1.0[a]	15.3 ± 1.2[a]
18:1 n-9	49.1 ± 3.6[a]	36.5 ± 2.0[b]	33.7 ± 3.1[b]
18:2 n-6	16.4 ± 0.7[c]	24.1 ± 1.2[b]	25.8 ± 1.2[a]
18:3 n-3	0.0 ± 0.0[c]	0.5 ± 0.0[b]	0.6 ± 0.0[a]
20:4 n-6	8.0 ± 1.0	8.3 ± 0.4	7.8 ± 1.1
Cis-9,*trans*-11 CLA	0.0 ± 0.0[c]	0.7 ± 0.1[b]	1.6 ± 0.1[a]
Trans-10,*cis*-12 CLA	0.0 ± 0.0[b]	0.0 ± 0.0[b]	0.3 ± 0.2[a]
22:4 n-6	0.1 ± 0.2	0.4 ± 0.2	0.4 ± 0.2
22:5 n-6	1.2 ± 0.2	1.1 ± 0.1	1.0 ± 0.2
22:6 n-3	2.3 ± 0.4[a]	1.8 ± 0.3[ab]	1.4 ± 0.4[b]
Total SFA	21.2 ±1.4[b]	24.7 ± 1.6[a]	25.2 ± 2.1[a]
Total MUFA	50.5 ± 3.5[a]	38.1 ± 2.0[b]	35.5 ± 2.8[b]
Total n-6 PUFA	25.9 ± 2.0[b]	34.1 ± 1.3[a]	35.3 ± 0.7[a]
Total n-3 PUFA	2.3 ± 0.4	2.3 ± 0.3	2.2 ± 0.4

[a]Control diet contained 3% corn oil. CLA1 and CLA2 represent 2.5% corn oil + 0.5% CLA or 2% corn oil +1% CLA. [a–c]Means ± SD with different superscripts within a row differ significantly ($P < 0.05$) ($n = 5$). For abbreviations see Table 1.

TABLE 3
Major FA Composition (%) of Newly Hatched Chick Plasma and Adipose Tissue[a]

FA	Dietary treatments		
	Control	CLA1	CLA2
	Plasma		
14:0	0.3 ± 0.0	0.3 ± 0.0	0.3 ± 0.0
16:0	19.7 ± 1.2	20.2 ± 1.3	21.1 ± 1.1
16:1	0.9 ± 0.5	1.0 ± 0.2	0.8 ± 0.2
18:0	11.9 ± 0.8[b]	14.5 ± 0.4[a]	15.1 ± 0.9[a]
18:1 n-9	30.1 ± 1.4[a]	20.8 ± 1.3[b]	18.6 ± 1.5[c]
18:2 n-6	25.4 ± 0.9[b]	31.1 ± 1.8[a]	33.8 ± 1.1[a]
20:4 n-6	9.3 ± 1.0[a]	9.3 ± 1.3[a]	6.8 ± 1.7[b]
Cis-9,*trans*-11 CLA	0.0 ± 0.0[b]	0.5 ± 0.1[a]	0.7 ± 0.1[a]
Trans-10,*cis*-12 CLA	0.0 ± 0	0.0 ± 0	0.1 ± 0.0
22:5 n-6	0.6 ± 0.1	0.8 ± 0.1	0.6 ± 0.2
22:6 n-3	0.6 ± 0.3	0.6 ± 0.2	0.2 ± 0.0
Total SFA	32.2 ± 1.1[c]	34.9 ± 1.7[ab]	36.7 ± 0.2[a]
Total MUFA	31.9 ± 2.4[a]	22.4 ± 1.1[b]	20.4 ± 2.1[b]
Total n-6 PUFA	35.4 ±1.3[b]	41.2 ± 1.6[a]	41.4 ± 0.9[a]
Total n-3 PUFA	0.6 ± 0.1[b]	1.4 ± 0.1[a]	0.9 ± 0.1[a]
Total CLA	0.0 ± 0[c]	0.5 ± 0.1[b]	0.8 ± 0.1[a]
	Adipose		
14:0	0.8 ± 0.0[b]	0.9 ± 0.1[ab]	0.9 ± 0.1[a]
16:0	28.9 ± 0.3[c]	31.8 ± 0.8[b]	32.7 ± 0.6[a]
16:1	2.1 ± 0.2[a]	1.0 ± 0.2[b]	0.3 ± 0.3[c]
18:0	7.0 ± 0.6[c]	9.4 ± 0.7[b]	10.8 ± 0.3[a]
18:1 n-9	35.2 ± 1.6[a]	21.4 ± 0.6[b]	18.8 ± 0.4[c]
18:2 n-6	24.0 ± 1.2[b]	33.1 ± 0.8[a]	32.5 ± 0.6[a]
18:3 n-3	0.3 ± 0.2[b]	0.9 ± 0.1[a]	1.0 ± 0.1[a]
20:4 n-6	1.5 ± 0.2[a]	0.9 ± 0.1[b]	0.6 ± 0.1[b]
Cis-9,*trans*-11 CLA	0.0 ± 0[c]	0.7 ± 0[b]	1.4 ± 0[a]
Trans-10,*cis*12 CLA	0.0 ± 0[c]	0.3 ± 0[b]	0.8 ± 0.1[a]
Total SFA	36.7 ± 0.6[c]	42.1 ± 1.4[b]	44.5 ± 1.0[a]
Total MUFA	37.4 ± 1.8[a]	22.3 ± 0.6[b]	19.1 ± 0.6[c]
Total n-6 PUFA	25.5 ± 1.4[b]	34.0 ± 0.9[a]	33.1 ± 0.7[a]
Total n-3 PUFA	0.4 ± 0[b]	0.9 ± 0[a]	0.9 ± 0[a]

[a]Control diet contained 3% corn oil. CLA1 and CLA2 represent 2.5% corn oil + 0.5% CLA or 2% corn oil + 1% CLA. [a–c]Means ± SD with different superscripts within a row differ significantly ($P < 0.05$) (n = 5). For abbreviations see Table 1.

sion of CLA also resulted in a significant increase in linoleic acid (18:2 n-6) in CLA1 and CLA2 chicks in the plasma, heart, and brain. The enrichment of total CLA due to maternal diet in the order of magnitude was adipose > liver > plasma > brain. No CLA was detected in the heart tissue. The contents of long-chain n-6 PUFA such as arachidonic acid (20:4n-6), 22:4n-6, and 22:5n-6 were higher in the brain tissue of CLA1 and CLA2 chicks than in Control chicks ($P < 0.05$). However, DHA (22:6n-3) was lower in the heart and brain tissue of CLA1 and CLA2 chicks by maternal supplementation of CLA than in control chicks ($P < 0.05$). Although an adverse effect of yolk CLA on hatchability has been reported (15), very few studies have investigated the role of egg CLA during avian embryonic development. The alteration of n-6 and n-3 FA observed in the chick tissues in the current study may also affect eicosanoid metabolism in these tissues. Feeding CLA has been reported to reduce the levels of brain prostaglandin E_2 in mice (26). The decrease in the concentration of 18:1 and the altered SFA/MUFA ratio, along with impaired eicosanoid metabolism

TABLE 4
Major FA Composition (%) of Newly Hatched Chick Heart and Brain Tissue[a]

FA	Control	CLA1	CLA2
		Dietary treatments	
		Heart	
14:0	0.0 ± 0.0	0.1 ± 0.0	0.1 ± 0.0
16:0	20.9 ± 0.9	21.5 ± 1.0	22.7 ± 0.9
16:1	2.4 ± 0.2	3.1 ± 0.2	2.9 ± 0.8
18:0	20.6 ± 1.1	19.8 ± 0.9	21.1 ± 1.1
18:1 n-9	14.1 ± 1.3[a]	11.0 ± 1.1[b]	9.9 ± 0.4[b]
18:2 n-6	12.3 ± 0.8[b]	19.1 ± 1.2[a]	17.3 ± 0.9[a]
20:2 n-6	0.1 ± 0.0	0.0 ± 0.0	0.0 ± 0.0
20:4 n-6	21.2 ± 0.5	19.7 ± 0.9	20.3 ± 0.8
22:4 n-6	0.1 ± 0.0[a]	0.0 ± 0.0[b]	0.0 ± 0.0[b]
22:5 n-6	1.5 ± 0.5	1.3 ± 0.2	1.2 ± 0.3
22:6 n-3	2.5 ± 0.1[a]	1.6 ± 0.2[b]	1.5 ± 0.2[b]
Total SFA	43.3 ± 1.5	43.0 ± 1.2	45.6 ± 1.4
Total MUFA	17.0 ± 1.9[a]	14.1 ± 0.6[b]	12.9 ± 1.2[b]
Total n-6 PUFA	37.2 ± 0.6	41.3 ± 0.6	39.8 ± 0.9
Total n-3 PUFA	2.5 ± 0.1[a]	1.6 ± 0.4[b]	1.7 ± 0.2[b]
		Brain	
14:0	0.5 ± 0.0	0.5 ± 0.0	0.5 ± 0.0
16:0DMA	3.2 ± 0.1	3.3 ± 0.1	3.2 ± 0.9
16:0	30.4 ± 0.5	30.4 ± 0.8	29.7 ± 3.2
16:1	4.4 ± 0.2[b]	4.6 ± 0.3[b]	5.1 ± 1.4[a]
18:0	16.9 ± 0.4[b]	17.9 ± 0.2[a]	18.3 ± 2.5[a]
18:1 n-9	14.3 ± 0.4[a]	11.6 ± 0.4[b]	10.5 ± 0.3[c]
18:2 n-6	2.1 ± 0.1[c]	3.1 ± 0.2[b]	3.7 ± 0.4[a]
20:1n-9	0.4 ± 0.0[a]	0.2 ± 0.2[b]	0.2 ± 0.1[b]
20:2 n-6	0.5 ± 0.1[c]	0.9 ± 0.1[b]	1.1 ± 1.3[a]
20:3 n-6	0.3 ± 0.0	0.3 ± 0.0	0.3 ± 0.1
20:4 n-6	9.8 ± 0.2[b]	10.6 ± 0.4[a]	10.6 ± 1.5[a]
20:5 n-3	0.0 ± 0.1[b]	0.0 ± 0.1[b]	0.3 ± 0.1[a]
22:0	0.2 ± 0[ab]	0.1 ± 0[b]	0.3 ± 0.1[a]
22:4 n-6	2.0 ± 0.1[c]	2.2 ± 0.1[b]	2.4 ± 0.2[a]
Cis-9,trans-11 CLA	0.0 ± 0.0[b]	0.1 ± 0.1[b]	0.5 ± 0.2[a]
22:5 n-6	2.9 ± 0.4[b]	3.6 ± 0.2[a]	3.6 ± 0.5[a]
22:5 n-3	0.1 ± 0.1[c]	0.4 ± 0.0[b]	0.6 ± 0.1[a]
22:6 n-3	10.6 ± 0.4[a]	9.5 ± 0.3[b]	8.6 ± 0.6[b]
24:1	0.0 ± 0	0.3 ± 0.1	0.2 ± 0.1

[a]Control diet contained 3% corn oil. CLA1 and CLA2 represent 2.5% corn oil +0.5% CLA or 2% corn oil + 1% CLA. [a–c]Means ± SD with different superscripts within a row differ significantly ($P < 0.05$) ($n = 5$). For abbreviations, see Table 1. Total SFA also includes 16:0 dimethylacetal (DMA) and 18:0 DMA. Total MUFA includes 16:1, 18:1, 20:1, and 24:1.

through alteration in n-6 and n-3 FA ratio, may all contribute to embryonic health and survival in CLA-enriched eggs.

Enrichment of yolk with CLA did not affect the carcass weight, carcass dry matter, or ash content (Table 5). However, chick carcasses from CLA1 and CLA2 were lower in total fat than in Control ($P < 0.05$). The carcass fat for CLA2 chicks was 26% less than Control chicks. Latour *et al*. (16) reported an increase in the retention of remnant yolk in chicks hatched from eggs containing CLA. Inhibition of yolk fat absorption or transfer through the yolk sac or an increase in oxidation may contribute to the reduced fat accumulation in CLA1 and CLA2 chicks. The beneficial effect of CLA in reducing body fat mass has attracted great attention and has been reported in various species (2,3). Feeding CLA at 2 or 3% has been associated with reduced carcass fat in broilers (27). The moisture and ash contents of chick carcasses in our study were not affected by ma-

TABLE 5
Carcass Characteristics of Newly Hatched Chicks Hatched from Breeder Hens Fed Diets with or without CLA[a]

	Control	CLA1	CLA2
		Dietary treatments	
Carcass weight (g)	36.0 ± 0.6	35.1 ± 0.9	34.1 ± 0.8
Carcass total fat (%)	6.1 ± 0.9[a]	5.1 ± 0.8[b]	4.5 ± 0.3[b]
Carcass dry matter (%)	25.7 ± 1.6	28.1 ± 3.9	27.1 ± 0.7
Carcass ash (%)	2.5 ± 0.2	2.6 ± 0.3	2.5 ± 0.3

[a]Control diet contained 3% corn oil. CLA1 and CLA2 represent 2.5% corn oil + 0.5% CLA or 2% corn oil + 1% CLA. [a–b]Means ± SD with different superscripts within a row differ significantly ($P < 0.05$) ($n = 5$).

ternal dietary CLA, in agreement with studies reported in broiler chickens fed diets containing 2 or 3% CLA (27).

Poor hatchability and an increase in culls are major economic losses to hatching egg producers. Owing to the current interest in increasing the CLA content of ruminant and non-ruminant foods, fats and FA from rendered sources may enter the livestock and avian feed chain. Inclusion of such rendered fat in the diets of breeder birds and egg-laying species may affect the health of the progeny. The results from the present study demonstrating that increasing yolk CLA alters lipid metabolism in chicks suggest that further investigations are needed on the use of CLA in breeder animal feeding and also on the long-term clinical use of CLA supplementation in lactating women.

ACKNOWLEDGMENTS

REFERENCES

1. Pariza, M.W., Park, Y., and Cook, M.E. (2001) The Biologically Active Isomers of Conjugated Linoleic Acid, *Prog. Lipid Res. 4,* 283–298.
2. DeLany, J.P., Blohm, P., Truett, A.A., Scimeca, J.A., and West, D.B. (1999) Conjugated Linoleic Acid Rapidly Reduces Body Fat Content in Mice Without Affecting Energy Intake, *Am. J. Physiol. 276,* R1172–R1179.
3. Belury, M.M., and Kempa-Stezko, A. (1997) Conjugated Linoleic Acid Modulates Hepatic Lipid Composition in Mice, *Lipids 32,* 199–204.
4. Belury, M.A. (2002) Dietary Conjugated Linoleic Acid in Health: Physiological Effects and Mechanisms of Action, *Annu Rev. Nutr. 22,* 505–531.
5. Belury, M.A. (2002) Inhibition of Carcinogenesis by Conjugated Linoleic Acids: Potential Mechanisms of Action, *J. Nutr. 13,* 2995–2998.
6. Ip, C., Banni, S., Angioni, E., Carta, G., McGinley, J., Thompson., H.J., Barbano, D., and Bauman, D. (1999) Conjugated Linoleic Acid-Enriched Butterfat Alters Mammary Gland Morphogenesis and Reduces Cancer Risk in Rats, *J. Nutr. 12,* 2135–2142.
7. Mir, P.S., McAllister, T.A., Scott. S., Aalhus, J.L., Baron, V., McCartney, D., Charmley, E., Goonewardene, L., Basarab, J.,

Okine, E., *et al.* (2004) Conjugated Linoleic Acid-Enriched Beef Production, *Am. J. Clin. Nutr. 79(6),* 1207S–1211S.

8. Dugan, M.E.R., Alhus, J.L., and Kramer, J.K.G. (2004) Conjugated Linoleic Acid Pork Research, *Am. J. Clin. Nutr. 79(6),* 1212S–1216S.

9. Cherian, G. (2002) Lipid Modification Strategies and Nutritionally Functional Poultry Foods. Food Science and Product Technology. Ch 4. In *Food Science and Product Technology* (Nakano, T., and Ozimek, L., eds.) pp. 77–72. Research Sign Post, India.

10. Du, M., Ahn, D.U., and Sell, J.L. (1999) Effect of Dietary Conjugated Linoleic Acid on the Composition of Egg Yolk Lipids, *Poultry Sci. 7,* 1639–1645.

11. Cherian, G., Holsonbake, T.B., Goeger, M.P., and Bildfell, R. (2002) Dietary CLA Alters Yolk and Tissue FA Composition and Hepatic Histopathology of Laying Hens, *Lipids 37(8),* 751–757.

12. Noble, R.C., and Cocchi, M. (1990) Lipid Metabolism in the Neonatal Chicken, *Prog. Lipid Res. 29,* 107–140.

13. Cherian, G., Gopalakrishnan, N., Akiba, Y., and Sim, J.S. (1997) Effects of Maternal Dietary 18:3 n-3 Acids on the Accretion of Long Chain Polyunsaturated Fatty Acids in the Tissue of Developing Chick Embryo, *Biol. Neonate 72,* 165–174.

14. Salem, N., Litman, B., Kim, H.Y., and Gawrisch, K. (2001) Mechanisms of Action of Docosahexaenoic Acid in the Nervous System, *Lipids 36,* 945–959.

15. Aydin, R., Pariza, M.W., and Cook, M.E. (2001) Olive Oil Prevents the Adverse Effects of Dietary Conjugated Linoleic Acid on Chick Hatchability and Egg Quality, *J. Nutr. 13,* 800–806.

16. Latour, M.A., Devitt, A.A., Meunier, R.A., Stewart, J.J., and Watkins, B.A. (2000) Effects of Conjugated Linoleic Acid. 1. Fatty Acid Modification of Yolks and Neonatal Fatty Acid Metabolism, *Poultry Sci. 78,* 817–821.

17. Association of Official Analytical Chemists (1980) *Official Methods of Analysis*. 13th edn., Association of Official Analytical Chemists, Washington, DC.

18. Folch, J., Lees, M., and Sloane-Stanley, G.H. (1957) A Simple Method for the Isolation and Purification of Total Lipids from Animal Tissues, *J. Biol. Chem. 226,* 497–507.

19. Cherian, G., and Goeger, M.P. (2004) Hepatic Lipid Characteristics and Histopathology of Laying Hens Fed CLA or n-3 Fatty Acids, *Lipids 39,* 31–36.

20. SAS Institute (2001) *SAS User's Guide. Statistics*, Release 8.2 SAS Institute Inc, Cary, NC.

21. Steel, R.G.D., and Torrie, J.H. (1980) *Principles and Procedures of Statistics: A Biometrical Approach*, 2nd edn., McGraw-Hill, Toronto.

22. Sessler, A.M., and Ntambi, J.M. (1998) Polyunsaturated Fatty Acid Regulation of Gene Expression, *J. Nutr. 128,* 923–926.

23. Degrace, P., Demizieux, L., Gresti, J., Chardigny, J.M., Sébédio, J.L., and Clouet, P. (2004) Hepatic Steatosis Is Not Due to Impaired Fatty Acid Oxidation Capacities in C57BL/6J Mice Fed the Conjugated *trans*-10,*cis*-12-Isomer of Linoleic Acid, *J. Nutr. 134,* 861–867.

24. Lazier, C.B., Wiktorowicz, M., DiMattia, G.E., Gordon, G.A., Binder, R., and Williams, D.L. (1994) Apolipoprotein (apo)B and Apo II Gene Expression Are Both Estrogen-Responsive in Chick Embryo Liver but Only Apo II Is Estrogen-Responsive in Kidney, *Mol. Cell. Endocrinol. 106,* 187–194.

25. Cherian, G., and J.S. Sim. (2001) Maternal Dietary α-Linolenic Acid (18:3n-3) Alters n-3 Polyunsaturated Fatty Acid Metabolism and Liver Enzyme Activity in Hatched Chicks, *Poult. Sci. 80,* 901–905.

26. Nakanishi, T., Koutoku, T., Kawahara, S., Murai, A., Furuse, M., Nakanishi, T., Koutoku, T., Kawahara, S., Murai, A., and Furuse, M. (2003) Dietary Conjugated Linoleic Acid Reduces Cerebral Prostaglandin E(2) in Mice, *Neurosci. Lett. 1, 341(2),* 135–138.

27. Du, M., and Ahn, D.U. (2002) Effect of Dietary Conjugated Linoleic Acids on the Growth Rate of Live Birds and on the Abdominal Fat Content and Quality of Broiler Meat, *Poult. Sci. 81,* 428–433.

Effects of Specific CLA Isomers on Plasma Fatty Acid Profile and Expression of Desaturases in Humans

Myriam A.M.A. Thijssen[a,]*, Corinne Malpuech-Brugère[b], Stéphane Gregoire[c], Jean Michel Chardigny[c], Jean Louis Sébédio[c], and Ronald P. Mensink[a]

[a]Department of Human Biology, Maastricht University, Maastricht, The Netherlands, [b]Unité du Métabolisme Protéino-Energétique, Institut National de la Recherche Agronomique (INRA), Clermont Ferrand, France, and [c]Unité de Nutrition Lipidique, INRA, Dijon, France

ABSTRACT: Human studies suggest that CLA changes metabolism, possibly through effects on mRNA expression of desaturase and elongase enzymes. In this respect, differential effects of the two most common dietary CLA isomers, *cis*-9,*trans*-11 (*c*9,*t*11) and *trans*-10,*cis*-12 (*t*10,*c*12) CLA, have hardly been studied. We therefore gave 25 healthy, overweight men and women daily for 6 wk a drinkable dairy product containing 3 g of oil that was rich in oleic acid. For the next 18 wk, the control group ($n = 7$) continued to use this product, whereas the second ($n = 9$) and third groups ($n = 9$) received products with 3 g of purified *c*9,*t*11 CLA or *t*10,*c*12 CLA. For each gram of *c*9,*t*11 CLA consumed, the proportion in plasma phospholipids increased by 0.26%. For *t*10,*c*12 CLA, this value was 0.20%. The *t*10,*c*12 CLA isomer increased plasma TAG levels of conjugated 18:3, whereas *c*9,*t*11 CLA increased those of both conjugated 18:3 and 20:3. In plasma phospholipids, the $\Delta 9$ desaturation index of 18:0 (18:1n-9/18:0) was decreased by *t*10,*c*12 CLA ($P = 0.03$ for diet effects), and the $\Delta 6$ desaturation index [(18:3n-6 + 20:3n-6)/18:2n-6] was decreased by both CLA isomers ($P < 0.01$ for diet effects). The $\Delta 5$ desaturation index (20:4n-6/20:3n-6) and the $\Delta 9$ desaturation index of 16:0 (16:1n-7/16:0) were not affected. No effects were seen on mRNA expression of desaturases and elongase in peripheral blood mononuclear cells (PBMC). We therefore conclude that incorporation of *c*9,*t*11 and *t*10,*c*12 CLA into plasma lipids reflects dietary intakes. Compared with oleic acid, $\Delta 9$ and $\Delta 6$ desaturation indices in plasma phospholipids are decreased after consumption of *c*9,*t*11 or *t*10,*c*12 CLA. Effects on desaturation indices were, however, not reflected by changes at the transcriptional level for the various desaturases and elongase enzymes in PBMC.

Paper no. L9653 in *Lipids 40*, 137–145 (February 2005).

CLA refers to a group of positional and geometrical isomers of linoleic acid containing conjugated double bonds. *Cis*-9,*trans*-11 (*c*9,*t*11) CLA is the most common CLA isomer in nature and is present in ruminant products, whereas commercially available capsules enriched with CLA also contain other isomers such as *trans*-10,*cis*-12 (*t*10,*c*12) CLA (1). Because of their postulated health benefits (2,3), dietary supplements with CLA are now widely available. To explain these health effects, several mechanisms have been proposed, including regulation of genes coding for enzymes known to modulate lipid and FA metabolism, such as desaturases (2,4).

Desaturases are involved in the formation of long-chain metabolites from precursor FA such as stearic, linoleic, and α-linolenic acids. Studies in mice and rats have indeed reported that CLA, mainly the *t*10,*c*12 isomer, suppressed $\Delta 9$ desaturase mRNA expression or enzyme activity (5–7). Moreover, the *c*9,*t*11 isomer decreased $\Delta 6$ desaturase activity in liver microsomes (5). In cell culture studies, effects of *t*10,*c*12 CLA on $\Delta 9$ desaturase activity were confirmed in a human hepatoma-derived cell line (HepG2) (8,9). However, effects of *c*9,*t*11 CLA on desaturase activities are inconsistent (8,9). Furthermore, effects of both CLA isomers at the mRNA expression level of desaturases have hardly been studied. Because desaturation products play an important role in many processes including eicosanoid production, lipid metabolism, and immune function (2,3), inhibition of desaturation may influence health. Most human studies, however, have been carried out using a mixture of CLA isomers and have not focused on specific effects of the major CLA isomers (10–12). Isomer-specific effects of CLA, as observed in animal studies, may explain conflicting results in humans (4,13). Therefore, to examine whether *c*9,*t*11 CLA and *t*10,*c*12 CLA affect desaturation differently in humans, we investigated the effects of these two CLA isomers on the FA compositions of plasma phospholipids (PL), cholesteryl esters (CE), and TAG. In addition, effects on mRNA expression of $\Delta 9$, $\Delta 6$, and $\Delta 5$ desaturases and of elongase by peripheral blood mononuclear cells (PBMC) were studied. Recently, the human $\Delta 5$ (14), $\Delta 6$ (15), and $\Delta 9$ (16) desaturase and elongase (17) genes have been characterized, and reverse transcription quantitative PCR (RT-qPCR) were developed based upon the desaturase and elongase gene sequences.

EXPERIMENTAL PROCEDURES

Subjects. Healthy male and female volunteers were recruited *via* advertisements in local newspapers. Interested people were informed about the purposes and requirements of the study and

---

---

had to give their written informed consent before they entered the screening procedure. This procedure consisted of two fasting blood samples for analysis of serum lipids and lipoproteins, hematological parameters, C-reactive protein, and liver and kidney functions, measurement of blood pressure, and collection of a morning urine specimen for analysis of glucose. Participants had to meet all of the eligibility criteria: aged 35–65 yr, body mass index between 25 and 30 kg/m^2, diastolic blood pressure below 95 mmHg and systolic blood pressure below 160 mmHg, fasting serum total cholesterol concentrations less than 7.0 mmol/L, serum TAG concentrations below 3.0 mmol/L, and plasma glucose below 6.0 mmol/L. Furthermore, subjects were apparently healthy as indicated by a medical questionnaire, not pregnant, and weight stable during the past 3 mon; had no history of atherosclerotic disease or malignancy within the past 5 yr, normal liver and kidney function, no glycosuria or anemia, no abuse of drugs or alcohol, and no use of any medication known to affect lipid or glucose metabolism. Blood donation or participation in another biomedical trial was not allowed within 4 wk before the start of the study or during the study.

The Medical Ethics Committee of Maastricht University approved the study protocol. This study was part of a multicenter study as reported elsewhere (18). For 25 subjects of the placebo group and the high-dose CLA groups of the Maastricht cohort, desaturase expression in PBMC and FA compositions of plasma lipids were analyzed. During the screening period, their body mass indexes ranged from 24.4 to 30.5 kg/m^2 (mean 27.4 kg/m^2). The subjects' fasting serum lipid levels ranged from 3.2 to 6.8 mmol/L for total cholesterol (mean 5.0 mmol/L), from 0.8 to 2.8 mmol/L for HDL cholesterol (mean 1.2 mmol/L), and from 0.4 to 2.4 mmol/L for TAG (mean 1.2 mmol/L).

Study design. The study had a randomized, double-blind, placebo-controlled, parallel design. During the first 6 wk of the trial (run-in period), all volunteers consumed daily a dietary supplement providing 3 g of high-oleic sunflower oil (placebo). After the run-in period, subjects were randomly allocated to one of the three treatment groups. For the next 18 wk of the study (intervention period), one group ($n = 7$) continued to consume the placebo dairy product daily. The second ($n = 9$) and third ($n = 9$) groups consumed the dairy product with 3 g of purified *c*9,*t*11 CLA or 3 g of *t*10,*c*12 CLA, respectively.

Dietary supplements containing CLA were provided as an acidified drinkable dairy product produced by Danone (Palaiseau, France) as described earlier (18). The two different isomers of CLA, *c*9,*t*11 CLA and *t*10,*c*12 CLA, were incorporated as a TAG in the dairy drinks and were produced by Natural Lipids Ltd. (Hovdebygda, Norway). Different flavors were added to the products. The placebo product used during the run-in period had a different flavor from the one used during the intervention period. Bottles were packaged in boxes of 14.

Participants consumed one bottle daily (100 mL) of this dietary supplement between lunch and dinner. In a diary, participants had to record the daily time of consumption of the supplements and to note any signs of illness, medication used, alcohol consumption, and any deviations from the study protocol. Subjects were urged not to change their habitual diet, level of physical exercise, smoking habits, or use of alcohol during the study. Volunteers visited the university at least once every 2 wk to receive a new supply of supplements. Supplements that were left over had to be returned and were counted as a measure of compliance. Compliance was also checked by analysis of the FA composition of plasma PL. Furthermore, at each visit a dietitian checked the diary.

Blood sampling. Blood samples were obtained at the end of the run-in period (week 6) and at the end of the intervention period (week 24) after an overnight fast. Moreover, participants were instructed not to use alcohol during the previous day and not to smoke on the morning before blood sampling. Venous blood was sampled using a vacutainer system with the volunteer in a recumbent position. For RNA isolation from PBMC, blood was collected into two EDTA tubes and kept on ice until leukocyte isolation. In addition, one EDTA tube was collected to obtain plasma for analysis of the FA composition of plasma lipids. This tube was centrifuged within 1 h after venipuncture at $3500 \times g$ for 30 min at 4°C. Plasma samples were snap-frozen in liquid nitrogen and stored at –80°C.

Leukocyte isolation. PBMC were isolated from blood by gradient centrifugation using Lymphoprep (Nycomed Ltd., Birmingham, United Kingdom). Before isolation of PBMC, blood was diluted by addition of an equal volume of Hanks' balanced salt solution (HBSS; Gibco BRL, Life Technologies, Breda, The Netherlands). Then 2 vol of diluted blood was layered over 1 vol of Lymphoprep in a 50-mL centrifuge tube (Greiner Bio-One, Alphen a/d Rijn, The Netherlands). After centrifugation at $800 \times g$ for 30 min at 4°C, the interphase containing PBMC was transferred into a new 50-mL centrifuge tube. PBMC were washed with an equal volume of HBSS and centrifuged for 10 min at $250 \times g$ at 4°C. The cell pellet was resuspended in 1.5 mL Trizol reagent (Gibco BRL, Gaithersburg, MD) and transferred into an RNase-free 2 mL tube (Eppendorf, Hamburg, Germany).

RNA preparation. Total RNA from PBMC was prepared according to the manufacturer's instructions of the Trizol reagent (Gibco BRL). Briefly, 300 μL chloroform was added to separate phases. After incubation for 2–3 min at room temperature and centrifugation for 15 min at $12,000 \times g$ (4°C), the water phase, containing the RNA, was pipetted into a clean RNase-free tube. Then, the RNA was precipitated by addition of 750 μL isopropanol. After incubation for 20 min at –80°C and centrifugation for 10 min at $12,000 \times g$ (4°C), the RNA pellet was washed twice with 75% ethanol. In each washing step, the samples were centrifuged for 5 min at $7,500 \times g$ (4°C). Finally, RNA was dried and dissolved in 50 μL RNase-free water by incubation at 55–60°C for 10 min. Subsequently, both RNA samples were pooled and further purified using the RNeasy Mini Kit (Qiagen, Leusden, The Netherlands). During this purification procedure, RNA was treated on-column with DNase (RNase-free DNase set; Qiagen) as described in the manufacturer's protocol. Before storage at –80°C, the RNA concentrations were measured spectrophotometrically at 260 nm. All RNA preparations must have an A260/A280 ratio of >1.8 to ensure RNA purity.

cDNA synthesis. Aliquots of 350 ng of total cellular RNA were reverse-transcribed. All samples were denatured for 5 min at 85°C. Reverse transcription of RNA was performed in 40 µL RT mixture containing first strand buffer, 10 mM DTT, 400 U Moloney mouse murine leukemia reverse transcriptase, 20 U ribonuclease inhibitor (all provided by Gibco BRL), 5 µM random hexamers (Applied Biosystems, Nieuwerkerk a/d Ijssel, The Netherlands), and 375 µM deoxynucleotides (Amersham Pharmacia Biotech, Woerden, The Netherlands). After hexanucleotides had been annealed for 10 min at 22°C, cDNA synthesis was performed for 90 min at 37°C, followed by an enzyme inactivation step for 3 min at 95°C. Finally, cDNA was rapidly chilled to 4°C and stored at –20°C until use.

RT-qPCR. A RT-qPCR protocol was developed for the quantification of the human housekeeping gene β-actin and desaturase and elongase enzymes. Primers and probe for the desaturase and elongase assays were derived from Genbank sequence NM_013402 for Δ5 desaturase (FA desaturase 1), NM_004265 for Δ6 desaturase (FA desaturase 2), NM_005063 for Δ9 desaturase (stearoyl-CoA desaturase), and NM_021814 for elongase (ELOVL5) using Primer Express 1.5 software (Applied Biosystems). To prevent pseudogene amplification of Δ9 desaturase, a minor groove binder (MGB) probe was developed to anneal specifically to the cDNA strand of the functional gene. Primer and probe sequences for β-actin were identical to those described by Kreuzer *et al.* (19) and those for Δ6 desaturase similar as described by Leonard *et al.* (20). All probes were dual-labeled with a fluorescent FAM (6-carboxyfluorescein) reporter dye at the 5′ end and a TAMRA (6-carboxytetramethylrhodamine) quencher dye (or a nonfluorescent quencher and MGB for Δ9 desaturase) at the 3′ end. Primer and probe sequences are listed in Table 1.

Thirty-five nanograms of cDNA was amplified in a total reaction volume of 25 µL containing 12.5 µL universal master mix (Applied Biosystems), 7.5 pmol of each primer, and 5 pmol probe. PCR reactions were performed in an optical 96-well reaction plate (Applied Biosystems) on an ABI PRISM 7000 Sequence Detection System (Applied Biosystems). PCR cycling conditions were: 2 min at 50°C for optimal AmpErase UNG enzyme activity and 10 min at 95°C to activate the polymerase enzyme, followed by 45 two-step cycles of 95°C for 15 s and 60°C for 60 s. Fluorescence intensity of all wells was monitored every cycle. The number of PCR cycles to reach the fluorescence (Rn) threshold value is the cycle threshold (Ct) and is presented by the system. The Ct value for each sample is proportional to the log of the initial amount of target cDNA copies. Relative mRNA quantification was performed using the comparative ΔΔCt method (21). Moreover, to check PCR efficiencies, on every plate calibration curves for all different assays were constructed using five different dilutions of a cDNA standard (8.75 ng/µL) made from a human RNA pool.

FA composition of lipids. Analyses of FA compositions of plasma PL at the end of the run-in and experimental periods and of CE and TAG at the end of the experimental period was performed as previously described by Sébédio *et al.* (22). Briefly, plasma lipids were extracted using a mixture of chloroform and methanol (2:1, vol/vol) (23). Lipid classes were then fractionated into PL, CE, and TAG using NH_2 cartridges (Phase Separation Products, Saint Quentin en Yvelines, France) (24). After esterification and transmethylation of FA, the resultant FAME were analyzed by GLC using an HP 5890 series II gas chromatograph (Hewlett-Packard, Palo Alto, CA) equipped with a CP-Sil 88 capillary column (100 m × 0.25 µm i.d., 0.2 µm film thickness; Chrompack, Middelburg, The Netherlands) and an FID (25). The detection limit was 0.01% (w/w).

Statistics. Effects of the experimental products were examined by ANOVA using the general linear model (GLM) procedure of the SPSS 11 package for Mac OS X. When the analyses indicated a significant effect of diet ($P < 0.05$), the diets were compared pair-wise. *P*-Values were corrected for three-group comparisons by the Bonferroni correction. Confidence intervals (CI, 95%) were calculated for the differences between the diets. Values are presented as means ± SD. Pearson correlations were determined by pairwise comparisons between parameters. A probability level (*P*-value) of less than 0.05 was considered statistically significant.

TABLE 1
Primer and Probe Sequences for Reverse Transcription Quantitative PCR

Target sequence	Primer or probe	Sequence (5′-3′)	Amplicon length (bp)
β-Actin	β-Actin forward	agc ctc gcc ttt gcc ga	176
	β-Actin reverse	ccg ccg ccc gtc cac acc cgc c	
	β-Actin probe	ctg gtg cct ggg gcg	
Δ5 Desaturase	Δ5 Desaturase forward	ggt gta caa cat cag cga gtt ca	148
	Δ5 Desaturase reverse	aat cag gag aga gtt cat ata ctt ctt cac	
	Δ5 Desaturase probe	cag gat gcc acg gat ccc ttt gtg	
Δ6 Desaturase	Δ6 Desaturase forward	tgg caa tgg ctg gat tcc ta	65
	Δ6 Desaturase reverse	cag ctt ggg cct gag agg t	
	Δ6 Desaturase probe	cct cat cac ggc ctt gtt cct tgc	
Δ9 Desaturase	Δ9 Desaturase forward	gcc ctg tat ggg atc act ttg a	108
	Δ9 Desaturase reverse	acg atg agc tcc tgc tgt tat g	
	Δ9 Desaturase probe	cta cct gca agt tct aca	
Elongase	Elongase forward	aac agg agt atg gga agg caa a	86
	Elongase reverse	gga cac gga taa tct tca tat ctg att	
	Elongase probe	ctt ctg tca ggg cac acg cac cg	

TABLE 2
Incorporation of CLA Isomers and Their Metabolites into Plasma Phospholipids at the End of the Run-in Period and at the End of the Experimental Period

FA	Run-in period[a,b]			Experimental period[a,b]		
	Placebo	c9,t11	t10,c12	Placebo	c9,t11	t10,c12
			% of total FA (w/w)			
	n = 6	n = 8	n = 6	n = 6	n = 8	n = 6
c9,t11	0.15 ± 0.06	0.11 ± 0.05	0.11 ± 0.04	0.16 ± 0.05[a]	0.88 ± 0.40[b]	0.22 ± 0.06[a]
t10,c12	ND[a]	ND	ND	ND[a]	0.03 ± 0.05[a]	0.61 ± 0.27[b]
c,c CLA	ND	ND	ND	ND[a]	0.01 ± 0.00[b]	ND[a]
t,t CLA	ND	ND	ND	ND[a]	0.02 ± 0.01[b]	0.02 ± 0.01[b]
t11 18:1	0.34 ± 0.11	0.34 ± 0.13	0.27 ± 0.10	0.31 ± 0.11	0.25 ± 0.07	0.23 ± 0.02
Conjugated 18:3	ND	ND	ND	ND	ND	ND
Conjugated 20:3	ND	ND	ND	ND	ND	ND

[a]Values are means ± SD. ND, not detectable (<0.01%). For statistical analysis, ND values were set at zero.
[b]Values in a row without a common roman superscript differ from each other ($P < 0.017$).

RESULTS

Twenty-two of the 25 subjects completed the study protocol. Two men withdrew during the run-in period and one woman from the t10,c12 group during the experimental period. Moreover, results of two women (one woman from the c9,t11 and one woman from the t10,c12 group) were excluded from statistical analyses, because no chromatograms were available. In addition, for one man from the c9,t11 group the isolated RNA concentration was too low to measure mRNA levels reliably.

Incorporation of CLA isomers and their metabolites into plasma lipid classes. Dietary adherence to the CLA supplements was confirmed by the presence of the individual CLA isomers in plasma PL, CE, and TAG (Tables 2 and 3). As shown in Table 2, the c9,t11 CLA isomer was already present in plasma PL during the run-in period, owing to its presence in the habitual diets of the subjects. When consuming 3 g of the individual CLA isomers, the proportion of c9,t11 CLA in PL increased by 0.77%—from 0.11 to 0.88%—in the c9,t11 group, whereas the proportion of t10,c12 CLA increased from 0.00 to 0.61% in the t10,c12 group. Metabolites of the CLA isomers, the 18:3 and 20:3 conjugated isomers, were only detected in TAG (Table 3). The proportion of the conjugated 18:3 isomer

($P < 0.001$ for diet effects) was increased in the t10,c12-supplemented group ($P < 0.001$) relative to both other groups, whereas that of the conjugated 20:3 isomer ($P = 0.011$ for diet effects) was higher in the c9,t11 group ($P < 0.01$), relative to the placebo group and t10,c12 group. Moreover, proportions of vaccenic acid (t11 18:1), a precursor for the synthesis of c9,t11 CLA, in TAG ($P = 0.044$ for diet effects) was significantly decreased in the c9,t11 group ($P = 0.017$) and tended to decrease in the t10,c12 group ($P = 0.061$) relative to the placebo group.

Positive associations were observed between the proportions of c9,t11 CLA in PL with those in CE and TAG ($r = 0.944$, $P < 0.001$ and $r = 0.901$, $P < 0.001$, respectively). Similar associations were found between the proportions of t10,c12 CLA in PL with those in CE and TAG ($r = 0.987$, $P < 0.001$ and $r = 0.968$, $P < 0.001$, respectively).

FA compositions of plasma lipid classes. At baseline, only the proportion of Mead acid (20:3n-9) in PL was significantly different between the three diet groups ($P = 0.048$ for differences between the three groups). Supplementation of CLA isomers resulted in decreases in the proportions of oleic acid (18:1n-9), 16:1n-9, 20:3n-9, and dihomo-γ-linolenic acid (20:3n-6) in one or more plasma lipid classes (Tables 4 and 5). Although these decreases were more pronounced in the t10,c12

TABLE 3
Incorporation of CLA Isomers and Their Metabolites into Plasma Cholesteryl Esters and TAG at the End of the Experimental Period

FA	Cholesteryl esters[a,b]			TAG[a,b]		
	Placebo	c9,t11	t10,c12	Placebo	c9,t11	t10,c12
			% of total FA (w/w)			
	n = 6	n = 7	n = 6	n = 6	n = 7	n = 6
c9,t11	0.12 ± 0.05[a]	0.61 ± 0.24[b]	0.16 ± 0.05[a]	0.34 ± 0.09[a]	1.16 ± 0.33[b]	0.42 ± 0.13[a]
t10,c12	ND[a]	0.04 ± 0.02[a]	0.42 ± 0.18[b]	ND[a]	0.06 ± 0.02[a]	0.53 ± 0.27[b]
c,c CLA	ND[a]	0.02 ± 0.01[b]	ND[a]	ND[a]	0.02 ± 0.02[b]	0.01 ± 0.01[a]
t,t CLA	ND[a]	0.03 ± 0.01[b]	0.02 ± 0.01[b]	ND[a]	0.04 ± 0.02[b]	0.03 ± 0.01[b]
t11 18:1	ND	ND	ND	1.55 ± 0.83[a]	0.81 ± 0.29[b]	0.97 ± 0.05[a,b]
Conjugated 18:3	ND[a]	ND[a]	0.03 ± 0.01[b]	ND[a]	0.05 ± 0.04[a]	0.20 ± 0.12[b]
Conjugated 20:3	ND	ND	ND	ND[a]	0.03 ± 0.03[b]	0.00 ± 0.00[a]

[a]Values are means ± SD. ND, not detectable (<0.01%). For statistical analysis, ND were set at zero.
[b]For each lipid class, values in a row without a common roman superscript differ from each other ($P < 0.017$).

TABLE 4
FA Composition of Plasma Phospholipids at the End of the Run-in Period and at the End of the Experimental Period

FA	Run-in period[a,b]			Experimental period[a,b]		
	Placebo	$c9,t11$	$t10,c12$	Placebo	$c9,t11$	$t10,c12$
			% of total FA (w/w)			
	$n = 6$	$n = 8$	$n = 6$	$n = 6$	$n = 8$	$n = 6$
16:0	28.73 ± 1.24	28.53 ± 1.67	27.98 ± 0.95	28.51 ± 1.71	28.05 ± 1.68	28.32 ± 1.38
16:1n-9	0.24 ± 0.04	0.22 ± 0.04	0.20 ± 0.01	0.24 ± 0.03[a]	0.20 ± 0.03[b]	0.18 ± 0.03[b]
16:1n-7	0.64 ± 0.19	0.67 ± 0.27	0.54 ± 0.13	0.66 ± 0.19	0.58 ± 0.21	0.45 ± 0.05
18:0	15.42 ± 0.50	15.20 ± 1.11	14.62 ± 1.57	14.99 ± 0.74	15.11 ± 0.72	15.21 ± 0.84
18:1n-9	10.80 ± 1.13	11.24 ± 1.58	9.51 ± 1.22	10.75 ± 1.62	9.77 ± 0.69	9.01 ± 1.09
18:1n-7	1.53 ± 0.24	1.45 ± 0.17	1.38 ± 0.16	1.40 ± 0.17	1.44 ± 0.25	1.29 ± 0.16
18:2n-6	21.12 ± 2.25	22.12 ± 2.58	22.31 ± 1.61	20.97 ± 2.03	22.21 ± 2.49	23.50 ± 1.96
18:3n-6	0.09 ± 0.05	0.11 ± 0.05	0.09 ± 0.05	0.10 ± 0.03	0.08 ± 0.06	0.03 ± 0.04
18:3n-3	0.19 ± 0.04	0.21 ± 0.07	0.14 ± 0.03	0.22 ± 0.02	0.23 ± 0.07	0.22 ± 0.07
20:3n-9	0.25 ± 0.14[a]	0.14 ± 0.03[b]	0.14 ± 0.04[b]	0.22 ± 0.09[a]	0.12 ± 0.04[b]	0.10 ± 0.03[b]
20:3n-6	3.81 ± 0.85	3.10 ± 0.91	3.66 ± 0.71	3.93 ± 0.67[a]	2.91 ± 0.96[b]	2.65 ± 0.40[b]
20:4n-6	9.98 ± 1.35	9.61 ± 1.95	11.37 ± 0.51	10.35 ± 2.15	10.51 ± 1.54	10.50 ± 1.60
20:5n-3	0.89 ± 0.42	0.95 ± 0.38	0.99 ± 0.41	0.94 ± 0.34	0.96 ± 0.50	0.91 ± 0.46
22:4n-6	0.38 ± 0.05	0.33 ± 0.09	0.38 ± 0.12	0.41 ± 0.02	0.40 ± 0.07	0.42 ± 0.16
22:5n-6	0.18 ± 0.03	0.13 ± 0.04	0.16 ± 0.05	0.20 ± 0.03	0.16 ± 0.03	0.19 ± 0.08
22:5n-3	0.90 ± 0.16	0.82 ± 0.18	0.95 ± 0.09	0.96 ± 0.15	1.01 ± 0.17	1.01 ± 0.19
22:6n-3	2.40 ± 0.48	2.85 ± 0.59	3.42 ± 0.90	2.79 ± 0.93	3.34 ± 0.95	3.10 ± 0.90

[a]Values are means ± SD.
[b]Values in a row without a common roman superscript differ from each other ($P < 0.017$).

group, differences between the two CLA groups never reached statistical significance. The decreases were compensated for by increases in linoleic acid (18:2n-6) and CLA. In CE ($P = 0.029$ for diet effects), the proportions of 18:2n-6 were higher in the $t10,c12$ CLA group than in the $c9,t11$ CLA ($P = 0.044$) and the placebo group ($P = 0.011$). Moreover, in TAG ($P = 0.017$ for diet effects), proportions of 18:2n-6 were higher in both CLA

intervention groups ($P = 0.038$ for $c9,t11$ and $P < 0.01$ for $t10,c12$) than in the placebo group.

Effects of individual CLA isomers on desaturation indices and mRNA expressions. From the FA compositions of PL, CE, and TAG, the ratio of 20:4n-6/20:3n-6 was calculated as an index for $\Delta5$ desaturation, the ratio of (18:3n-6 + 20:3n-6)/18:2n-6 for $\Delta6$ desaturation, and the ratios of 16:1n-7/16:0

TABLE 5
FA Composition of Plasma Cholesteryl Esters and TAG at the End of the Experimental Period

| FA	Cholesteryl esters[a,b]			TAG[a,b]		
	Placebo	$c9,t11$	$t10,c12$	Placebo	$c9,t11$	$t10,c12$
			% of total FA (w/w)			
	$n = 6$	$n = 7$	$n = 6$	$n = 6$	$n = 7$	$n = 6$
16:0	10.82 ± 1.02	10.81 ± 0.98	9.89 ± 0.79	29.00 ± 4.14	28.52 ± 4.49	25.84 ± 2.54
16:1n-9	0.50 ± 0.12[a]	0.40 ± 0.11[a,b]	0.32 ± 0.04[b]	0.96 ± 0.14	0.81 ± 0.22	0.83 ± 0.09
16:1n-7	3.30 ± 1.20	2.74 ± 1.12	2.12 ± 0.34	4.26 ± 0.87	3.68 ± 1.20	3.28 ± 0.62
18:0	0.60 ± 0.36	0.78 ± 0.14	0.75 ± 0.16	4.12 ± 0.96	4.26 ± 0.99	3.72 ± 0.57
18:1n-9	20.07 ± 2.14[a]	18.21 ± 1.53[a,b]	16.98 ± 2.19[b]	36.76 ± 2.48	33.18 ± 4.27	34.51 ± 4.30
18:1n-7	1.10 ± 0.39	1.49 ± 0.43	1.11 ± 0.33	3.17 ± 0.79	2.74 ± 0.48	3.00 ± 0.27
18:2n-6	51.29 ± 4.83[a]	52.84 ± 2.96[a]	57.18 ± 2.62[b]	12.37 ± 4.39[a]	16.67 ± 3.52[b]	18.68 ± 1.85[b]
18:3n-6	1.23 ± 0.45	1.06 ± 0.40	0.83 ± 0.34	0.30 ± 0.15	0.32 ± 0.13	0.34 ± 0.24
18:3n-3	0.63 ± 0.07	0.64 ± 0.10	0.61 ± 0.15	0.98 ± 0.44	0.96 ± 0.25	1.30 ± 0.49
20:3n-9	0.07 ± 0.05	0.05 ± 0.01	0.03 ± 0.01	0.15 ± 0.07	0.13 ± 0.04	0.12 ± 0.07
20:3n-6	0.92 ± 0.15[a]	0.67 ± 0.21[b]	0.61 ± 0.09[b]	0.23 ± 0.04	0.25 ± 0.08	0.24 ± 0.07
20:4n-6	7.09 ± 2.19	7.30 ± 0.82	7.01 ± 1.10	1.04 ± 0.38	1.54 ± 0.56	1.37 ± 0.41
20:5n-3	0.98 ± 0.57	1.11 ± 0.58	0.81 ± 0.38	0.17 ± 0.07	0.27 ± 0.18	0.24 ± 0.11
22:4n-6	ND	ND	ND	0.13 ± 0.04	0.15 ± 0.03	0.18 ± 0.07
22:5n-6	ND	ND	ND	0.08 ± 0.02	0.07 ± 0.02	0.10 ± 0.05
22:5n-3	ND	ND	ND	0.29 ± 0.09	0.38 ± 0.21	0.43 ± 0.10
22:6n-3	0.45 ± 0.19	0.55 ± 0.21	0.51 ± 0.16	0.38 ± 0.16	0.67 ± 0.37	0.69 ± 0.28

[a]Values are means ± SD. ND, not detectable (<0.01%).
[b]For each lipid class, values in a row without a common roman superscript differ from each other ($P < 0.017$).
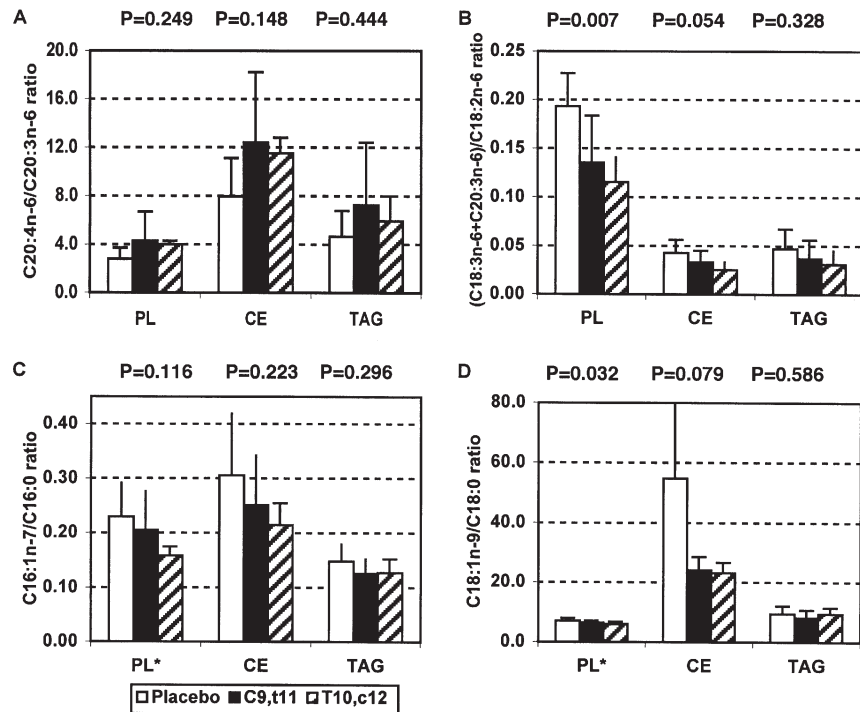
FIG. 1. Effects of placebo, *c*9,*t*11, and *t*10,*c*12 CLA on (A) Δ5 (20:4n-6/20:3n-6), (B) Δ6 [(18:3n-6 + 20:3n-6)/18:2n-6] and (C,D) Δ9 (16:1n-7/16:0 and 18:1n-9/18:0) desaturation indices. Values are means ± SD. *n* = 6 in the placebo group, *n* = 7 in the *c*9,*t*11 group for cholesteryl ester (CE) and TAG, *n* = 8 for phospholipids (PL), and *n* = 6 in the *t*10,*c*12. *Δ9 Desaturation indices in PL are multiplied by 10, because indices are very low owing to the high abundance of saturated FA in PL.

and of 18:1n-9/18:0 for Δ9 desaturation (Fig. 1). With respect to the Δ5 and Δ6 desaturation indices, comparable patterns were seen in all three lipid classes. The Δ5 desaturation index was slightly higher in both CLA groups than in the placebo group, but differences between groups did not reach statistical significance ($P = 0.249$ in PL, $P = 0.148$ in CE, $P = 0.444$ in TAG for diet effects). The Δ6 desaturation index in PL was significantly decreased in both CLA groups ($P < 0.01$ for diet effects). Compared with the placebo group, the decrease in the *c*9,*t*11 group was 0.06 ($P = 0.013$, 95% confidence interval (CI) for the difference: –0.102 to –0.014) and in the *t*10,*c*12 group 0.08 ($P < 0.01$, 95% CI for the difference: –0.125 to –0.031). This change nearly reached statistical significance in CE ($P = 0.054$ for diet effects), but not in TAG ($P = 0.328$ for diet effects). Also for the Δ9 desaturation index, dietary effects were observed. Compared with the placebo group, the 18:1n-9/18:0 ratio in PL ($P = 0.032$ for diet effects) was significantly decreased in the *t*10,*c*12 CLA-supplemented group ($P = 0.010$, 95% CI for the difference: –0.232 to –0.010) and tended to decrease in the *c*9,*t*11 group ($P = 0.102$, 95% CI for the difference: –0.172 to 0.036). In CE, effects on the same index nearly reached statistical significance ($P = 0.079$ for diet effects), and both CLA isomers tended to decrease the Δ9 desaturation index relative to the placebo ($P = 0.048$ for *c*9,*t*11 CLA, 95% CI for the difference: –68.85 to 7.65 and $P = 0.050$ for *t*10,*c*12 CLA, 95% CI for the difference: –71.17 to 8.22). In contrast, intervention groups did not differ significantly in their effects on the Δ9 desaturation index when calculated as 16:1n-7/16:0 ($P = 0.116$ in PL, $P = 0.223$ in CE, $P = 0.296$ in TAG).

mRNA expression of Δ5, Δ6, and Δ9 desaturases and elongase did not differ between the three intervention groups (Fig. 2). *P*-Values for diet effects were, respectively, 0.914 for Δ5 desaturase, 0.563 for Δ6 desaturase, 0.234 for Δ9 desaturase, and 0.807 for elongase. The various desaturation indices in PL, CE, and TAG were not correlated with their respective mRNA levels.
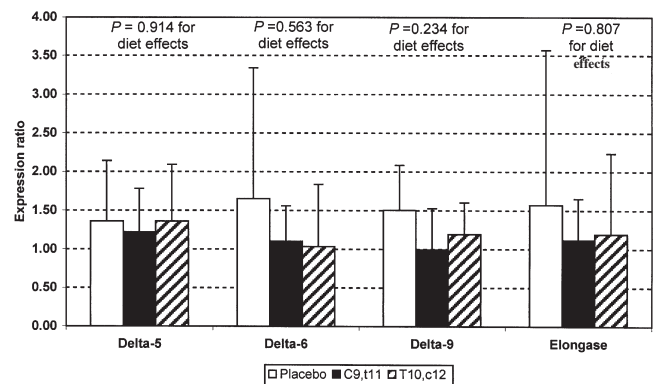
FIG. 2. Effects of placebo, *c*9,*t*11, and *t*10,*c*12 CLA on Δ5, Δ6, and Δ9 desaturase and elongase expression ratios. Values (means ± SD) are obtained using TaqMan procedures (comparative cycle threshold method) and are normalized to the housekeeping gene β-actin and relative to the run-in period. No statistically significant differences were observed between treatments. All samples were analyzed in duplicate. *n* = 6 in the placebo group, *n* = 7 in the *c*9,*t*11 group, and *n* = 6 in the *t*10,*c*12 group.

DISCUSSION

In this study we evaluated the effects of *c*9,*t*11 CLA and *t*10,*c*12 CLA, the two most common CLA isomers in the diet, on the FA compositions of plasma PL, CE, and TAG. As these effects may be mediated through effects of CLA on desaturase activity, we also studied effects on mRNA expression of Δ5, Δ6, and Δ9 desaturases and elongase by PBMC. Our results suggest that *c*9,*t*11 CLA and *t*10,*c*12 CLA affect the FA composition of plasma lipid classes differently but do not change mRNA expression of desaturases or elongase in PBMC.

Both *c*9,*t*11 CLA and *t*10,*c*12 CLA were incorporated into plasma PL, CE, and TAG. Based on the proportional increases in PL, it can be estimated that each gram of *c*9,*t*11 CLA in the diet increases its proportion in PL by 0.26%. For *t*10,*c*12 CLA, this estimate is 0.20%. These values are in good agreement with those of a recent study in which healthy men received each CLA isomer in increasing doses from 0.00 to 0.6 to 1.2 to 2.4 g per day (26). In that study, both isomers were incorporated in a dose-dependent manner into plasma PC and CE, and into total lipids of PBMC. In plasma PC, the proportions of *c*9,*t*11 CLA increased from 0.21 to 0.32 to 0.52 to 0.79% in PC, or on average 0.25% per g of *c*9,*t*11 CLA. Similarly, for *t*10,*c*12 CLA it can be calculated that for each gram increase in the diet, the increase in PC was 0.17%. These estimates agree very well with our values. Moreover, these findings are in accordance with studies in rats and mice, in which incorporation of *c*9,*t*11 CLA into lipid fractions was also slightly higher than that of *t*10,*c*12 CLA (27,28).

Because *c*9,*t*11 CLA—not the *t*10,*c*12 CLA isomer—was already present in plasma PL after the run-in period, this CLA isomer should have been provided by the habitual diet. By assuming a linear relationship between the intake of *c*9,*t*11 CLA and its incorporation into plasma PL (26), it can be calculated that the habitual diet of our subjects should have provided daily about 430 mg of *c*9,*t*11 CLA. This is much higher than the mean estimated intake of 200 mg in the Netherlands Cohort Study (29). In other Western countries, comparable dietary CLA intakes were observed (30). Foods that provide the *c*9,*t*11 CLA isomer are ruminant products such as meat, cheese, milk, and yogurt, in which *c*9,*t*11 CLA accounts for 75–90% of total CLA (1). Part of the discrepancy between our estimates and these studies can be explained by the fact that methods to assess dietary intakes underestimate real intakes (30). However, the largest part may be explained by the conversion of vaccenic acid (*t*11 18:1) into *c*9,*t*11 CLA *in vivo*, as observed in several human studies (31,32). If one assumes a conversion rate of 19% of *t*11 18:1 into *c*9,*t*11 CLA (32), a habitual daily intake of approximately 1200 mg of *t*11 18:1 is necessary to explain a difference of 230 mg in *c*9,*t*11 CLA intake. In the Netherlands Cohort Study, daily intake of *t*11 18:1 was 700–800 mg (29). Thus, our data on *c*9,*t*11 CLA levels in plasma PL after the run-in period can be explained by habitual intakes of this isomer and by the conversion of *t*11 18:1 into *c*9,*t*11 CLA.

The FA composition of plasma TAG suggested that the *t*10,*c*12 CLA isomer was mainly converted into the conjugated 18:3 metabolite, whereas supplementation with the *c*9,*t*11 CLA isomer increased both 18:3 and 20:3 CLA metabolites, though to a lesser extent. Similar results have been observed in rats (28). This might suggest a blockade of the elongation step by *t*10,*c*12 CLA, which we could not, however, demonstrate at the mRNA expression level in PBMC. It is also possible that the conjugated 18:3 metabolite of *t*10,*c*12 CLA has a lower affinity for elongase than the conjugated 18:3 metabolite of *c*9,*t*11 CLA.

In contrast to several other studies (10,11), CLA supplementation significantly changed the FA compositions of plasma PL, TAG, and CE. In general, proportions of 18:1n-9, 16:1n-9, 20:3n-9, and 20:3n-6 acids decreased at the expense of CLA and 18:2n-6. These effects were more pronounced in the *t*10,*c*12 CLA group than in the *c*9,*t*11 CLA-supplemented group, although differences between the two CLA groups did not reach statistical significance. Smedman and Vessby (12) found comparable effects on the FA composition of serum PL in humans consuming 4.2 g of CLA isomers (*c*9,*t*11/*t*10,*c*12 as 50:50) per day for 12 wk. In addition, in that study proportions of stearic (18:0), γ-linoleic (18:3n-6), docosatetraenoic (22:4n-6), and docosapentaenoic (22:5n-3) acids increased and that of palmitic acid (16:0) decreased. It is possible that the intervention periods of 4 wk (11) or 45 d (10) were too short to change the composition of plasma lipids. Surprisingly, in our study proportions of linoleic acid increased. Thus, linoleic acid was not displaced by CLA in plasma lipids as suggested earlier (12). Because linoleic acid is an EFA and is not produced endogenously, this effect might suggest a decrease in Δ6 desaturation. However, unlike some other studies (5,9,11), we did not find decreased proportions of longer-chain metabolites of linoleic acid including arachidonic acid, which is an important precursor for eicosanoids.

With respect to the Δ9 desaturation index, our data confirmed those of Smedman and Vessby (12). In their study, a daily supplement of 4.2 g of a mixture of CLA isomers resulted in a decreased Δ9 desaturation index (12). Although the Δ9 desaturation index in that study was only calculated from the conversion of 18:0 into 18:1n-9, we calculated it also from the conversion of 16:0 into 16:1n-7. However, only the 18:1n-9/18:0 ratio was significantly reduced in PL by the *t*10,*c*12 CLA isomer. This may indicate that the preferred substrate of Δ9 desaturase is 18:0 rather than 16:0, as also is suggested by stable-isotope studies in humans (33,34). In addition, 16:0 is preferentially elongated instead of Δ9- desaturated (34). Also in cell culture (8,9) and animal studies (5–7), the *t*10,*c*12 CLA isomer inhibited Δ9 desaturase activity. In contrast, the *c*9,*t*11 CLA isomer did not affect Δ9 desaturase activity in all these studies, except for one. In a human hepatoma-derived cell line (HepG2 cells), the *c*9,*t*11 CLA isomer slightly decreased Δ9 desaturase activity when added at nonphysiological concentrations (9).

As for a mixture of CLA isomers (12), the Δ6 desaturation index was decreased by *c*9,*t*11 as well as by *t*10,*c*12 CLA. In contrast, in HepG2 cells *t*10,*c*12 CLA, but not *c*9,*t*11 CLA, suppressed Δ6 desaturation (9). Furthermore, in hepatic rat microsomes *c*9,*t*11 CLA decreased the Δ6 desaturation of linoleic

acid, but not that of α-linolenic acid. In that study, $t10,c12$ CLA decreased the Δ6 desaturation of linoleic acid only at the highest concentration (5). Taken together, whereas *in vitro* effects of the individual CLA isomers on Δ6 desaturation are rather inconsistent, *in vivo* both CLA isomers seem to decrease Δ6 desaturation activity in humans. Unlike Smedman and Vessby (12), who reported an increase in the Δ5 desaturation index, we found no effect on this index. In contrast, in HepG2 cells, $t10,c12$ CLA even suppressed Δ5 desaturation (9). Therefore, effects of the individual CLA isomers on Δ5 desaturase activities are until now rather inconsistent and clearly deserve further exploration.

No effects of the $t10,c12$ and $c9,t11$ CLA isomers on mRNA expression in PBMC were evident. Only a few studies have evaluated the effects of CLA on mRNA expression of desaturases before (7,8). In mice that were fed a mixture of CLA isomers, other isomers than $c9,t11$ CLA were held responsible for the inhibitory effect on stearoyl-CoA desaturase gene 1 mRNA expression (7). However, in cell culture studies, Choi *et al.* (8) found that the $t10,c12$ and $c9,t11$ CLA isomers did not influence mRNA expression in human-derived HepG2 cells. In that study, $t10,c12$ CLA decreased Δ9 desaturase activity but did not change desaturase protein levels. Hence, $t10,c12$ CLA might regulate the activity of Δ9 desaturase without any effect at the transcriptional level.

To quantify mRNA expression ratios of the Δ5, Δ6, and Δ9 desaturases and elongase we developed RT-qPCR assays. With this method, the PCR product is already accurately detected during the PCR amplification, which is less time-consuming and laborious than conventional PCR techniques because no post-PCR handling is required. Although assays for Δ5, Δ6 desaturase, and elongase were easily developed, for Δ9 desaturase or stearoyl-CoA desaturase a pseudogene has been reported (16), which called for additional precautions. Instead of the more regular dual-labeled probes, we therefore used an MGB probe, which is more specific to the target sequence and does not anneal to the pseudogene sequence. These assays can easily be used in large-scale human studies. Tissue accessibility, however, remains a problem. We chose to analyze desaturase expression in PBMC, as liver tissue is for obvious reasons difficult to obtain. Although for some genes a correlation between liver and PBMC mRNA levels has been demonstrated (35), it is still unknown whether mRNA expression ratios of Δ5, Δ6, and Δ9 desaturases and elongase in PBMC are representative for those in the liver. This may also explain the lack of effects of the two CLA isomers on mRNA expression. Future studies should therefore concentrate to validate molecular signatures (e.g., mRNA, protein, and metabolic profiles) in PBMC as a marker for other, less accessible tissues and organs.

In conclusion, incorporation of the individual CLA isomers, $c9,t11$ and $t10,c12$, into plasma lipids (PL, CE, and TAG) reflects dietary intakes. Compared with oleic acid, Δ9 and Δ6 desaturation indices in plasma PL are decreased after consumption of $c9,t11$ or $t10,c12$ CLA. Effects on desaturation indices, however, were not reflected by changes at the transcriptional level for the various desaturases and elongase enzymes in PBMC.

REFERENCES

1. Chin, S.F., Liu, W., Storkson, J.M., Ha, Y.L., and Pariza, M.W. (1992) Dietary Sources of Conjugated Dienoic Isomers of Linoleic Acid, a Newly Recognized Class of Anticarcinogens, *J. Food Compos. Anal. 5,* 185–197.
2. Belury, M.A. (2002) Dietary Conjugated Linoleic Acid in Health: Physiological Effects and Mechanisms of Action, *Annu. Rev. Nutr. 22,* 505–531.
3. Pariza, M.W., Park, Y., and Cook, M.E. (2001) The Biologically Active Isomers of Conjugated Linoleic Acid, *Prog. Lipid Res. 40,* 283–298.
4. Evans, M., Brown, J., and McIntosh, M. (2002) Isomer-Specific Effects of Conjugated Linoleic Acid (CLA) on Adiposity and Lipid Metabolism, *J. Nutr. Biochem. 13,* 508.
5. Bretillon, L., Chardigny, J.M., Gregoire, S., Berdeaux, O., and Sébédio, J.L. (1999) Effects of Conjugated Linoleic Acid Isomers on the Hepatic Microsomal Desaturation Activities *in vitro*, *Lipids 34,* 965–969.
6. Park, Y., Storkson, J.M., Ntambi, J.M., Cook, M.E., Sih, C.J., and Pariza, M.W. (2000) Inhibition of Hepatic Stearoyl-CoA Desaturase Activity by *trans*-10, *cis*-12 Conjugated Linoleic Acid and Its Derivatives, *Biochim. Biophys. Acta 1486,* 285–292.
7. Lee, K.N., Pariza, M.W., and Ntambi, J.M. (1998) Conjugated Linoleic Acid Decreases Hepatic Stearoyl-CoA Desaturase mRNA Expression, *Biochem. Biophys. Res. Commun. 248,* 817–821.
8. Choi, Y., Park, Y., Pariza, M.W., and Ntambi, J.M. (2001) Regulation of Stearoyl-CoA Desaturase Activity by the *trans*-10,*cis*-12 Isomer of Conjugated Linoleic Acid in HepG2 Cells, *Biochem. Biophys. Res. Commun. 284,* 689–693.
9. Eder, K., Slomma, N., and Becker, K. (2002) *Trans*-10,*cis*-12 Conjugated Linoleic Acid Suppresses the Desaturation of Linoleic and α-Linolenic Acids in HepG2 Cells, *J. Nutr. 132,* 1115–1121.
10. Petridou, A., Mougios, V., and Sagredos, A. (2003) Supplementation with CLA: Isomer Incorporation into Serum Lipids and Effect on Body Fat of Women, *Lipids 38,* 805-811.
11. Mougios, V., Matsakas, A., Petridou, A., Ring, S., Sagredos, A., Melissopoulou, A., Tsigilis, N., and Nikolaidis, M. (2001) Effect of Supplementation with Conjugated Linoleic Acid on Human Serum Lipids and Body Fat, *J. Nutr. Biochem. 12,* 585–594.
12. Smedman, A., and Vessby, B. (2001) Conjugated Linoleic Acid Supplementation in Humans—Metabolic Effects, *Lipids 36,* 773–781.
13. Terpstra, A.H. (2004) Effect of Conjugated Linoleic Acid on Body Composition and Plasma Lipids in Humans: An Overview of the Literature, *Am. J. Clin. Nutr. 79,* 352–361.
14. Cho, H.P., Nakamura, M., and Clarke, S.D. (1999) Cloning, Expression, and Fatty Acid Regulation of the Human Δ-5 Desaturase, *J. Biol. Chem. 274,* 37335–37339.
15. Cho, H.P., Nakamura, M.T., and Clarke, S.D. (1999) Cloning,

Expression, and Nutritional Regulation of the Mammalian Δ-6 Desaturase, *J. Biol. Chem. 274,* 471–477.

16. Zhang, L., Ge, L., Parimoo, S., Stenn, K., and Prouty, S.M. (1999) Human Stearoyl-CoA Desaturase: Alternative Transcripts Generated from a Single Gene by Usage of Tandem Polyadenylation Sites, *Biochem. J. 340,* 255–264.

17. Leonard, A.E., Bobik, E.G., Dorado, J., Kroeger, P.E., Chuang, L.T., Thurmond, J.M., Parker-Barnes, J.M., Das, T., Huang, Y.S., and Mukerji, P. (2000) Cloning of a Human cDNA Encoding a Novel Enzyme Involved in the Elongation of Long-Chain Polyunsaturated Fatty Acids, *Biochem. J. 350*, 765–770.

18. Malpuech-Brugere, C., Verboeket-Van De Venne, W.P., Mensink, R.P., Arnal, M.A., Morio, B., Brandolini, M., Sæbø, A., Lassel, T.S., Chardigny, J.M., Sébédio, J.L., and Beaufrere, B. (2004) Effects of Two Conjugated Linoleic Acid Isomers on Body Fat Mass in Overweight Humans, *Obes. Res. 12,* 591–598.

19. Kreuzer, K.A., Lass, U., Landt, O., Nitsche, A., Laser, J., Ellerbrok, H., Pauli, G., Huhn, D., and Schmidt, C.A. (1999) Highly Sensitive and Specific Fluorescence Reverse Transcription-PCR Assay for the Pseudogene-Free Detection of β-Actin Transcripts As Quantitative Reference, *Clin. Chem. 45,* 297–300.

20. Leonard, A.E., Kelder, B., Bobik, E.G., Chuang, L.T., Parker-Barnes, J.M., Thurmond, J.M., Kroeger, P.E., Kopchick, J.J., Huang, Y.S., and Mukerji, P. (2000) cDNA Cloning and Characterization of Human Δ^5-Desaturase Involved in the Biosynthesis of Arachidonic Acid, *Biochem. J. 347,* 719–724.

21. Applied Biosystems (1997) *Relative Quantitation of Gene Expression, ABI PRISM 7700 Sequence Detection System—User Bulletin #2,* pp. 1–36, Applied Biosystems, Nieuwerkerk a/d Ijssel, The Netherlands.

22. Sébédio, J.L., Juanéda, P., Dobson, G., Ramilison, I., Martin, J.C., Chardigny, J.M., and Christie, W.W. (1997) Metabolites of Conjugated Isomers of Linoleic Acid (CLA) in the Rat, *Biochim. Biophys. Acta 1345,* 5–10.

23. Folch, J., Lees, M., and Sloane Stanley, G.H. (1957) A Simple Method for the Isolation and Purification of Total Lipids from Animal Tissues, *J. Biol. Chem. 226,* 497–509.

24. Kaluzny, M.A., Duncan, L.A., Merritt, M.V., and Epps, D.E. (1985) Rapid Separation of Lipid Classes in High Yield and Purity Using Bonded Phase Columns, *J. Lipid Res. 26,* 135–140.

25. Sébédio, J.L., Juanéda, P., Gregoire, S., Chardigny, J.M., Martin, J.C., and Ginies, C. (1999) Geometry of Conjugated Double Bonds of CLA Isomers in a Commercial Mixture and in Their Hepatic 20:4 Metabolites, *Lipids 34,* 1319–1325.

26. Burdge, G.C., Lupoli, B., Russell, J.J., Tricon, S., Kew, S., Banerjee, T., Shingfield, K.J., Beever, D.E., Grimble, R.F., Williams, C.M., *et al.* (2004) Incorporation of *cis*-9,*trans*-11 or *trans*-10,*cis*-12 Conjugated Linoleic Acid into Plasma and Cellular Lipids in Healthy Men, *J. Lipid Res. 45,* 736–741.

27. Kelley, D.S., Bartolini, G.L., Warren, J.M., Simon, V.A., Mackey, B.E., and Erickson, K.L. (2004) Contrasting Effects of *t*10,*c*12- and *c*9,*t*11-Conjugated Linoleic Acid Isomers on the Fatty Acid Profiles of Mouse Liver Lipids, *Lipids 39,* 135–141.

28. Sébédio, J.L., Angioni, E., Chardigny, J.M., Gregoire, S., Juanéda, P., and Berdeaux, O. (2001) The Effect of Conjugated Linoleic Acid Isomers on Fatty Acid Profiles of Liver and Adipose Tissues and Their Conversion to Isomers of 16:2 and 18:3 Conjugated Fatty Acids in Rats, *Lipids 36,* 575–582.

29. Voorrips, L.E., Brants, H.A., Kardinaal, A.F., Hiddink, G.J., van den Brandt, P.A., and Goldbohm, R.A. (2002) Intake of Conjugated Linoleic Acid, Fat, and Other Fatty Acids in Relation to Postmenopausal Breast Cancer: The Netherlands Cohort Study on Diet and Cancer, *Am. J. Clin. Nutr. 76,* 873–882.

30. Ritzenthaler, K.L., McGuire, M.K., Falen, R., Shultz, T.D., Dasgupta, N., and McGuire, M.A. (2001) Estimation of Conjugated Linoleic Acid Intake by Written Dietary Assessment Methodologies Underestimates Actual Intake Evaluated by Food Duplicate Methodology, *J. Nutr. 131,* 1548–1554.

31. Adlof, R.O., Duval, S., and Emken, E.A. (2000) Biosynthesis of Conjugated Linoleic Acid in Humans, *Lipids 35,* 131–135.

32. Turpeinen, A.M., Mutanen, M., Aro, A., Salminen, I., Basu, S., Palmquist, D.L., and Griinari, J.M. (2002) Bioconversion of Vaccenic Acid to Conjugated Linoleic Acid in Humans, *Am. J. Clin. Nutr. 76,* 504–510.

33. Emken, E.A. (1994) Metabolism of Dietary Stearic Acid Relative to Other Fatty Acids in Human Subjects, *Am. J. Clin. Nutr. 60,* 1023S–1028S.

34. Rhee, S.K., Kayani, A.J., Ciszek, A., and Brenna, J.T. (1997) Desaturation and Interconversion of Dietary Stearic and Palmitic Acids in Human Plasma and Lipoproteins, *Am. J. Clin. Nutr. 65,* 451–458.

35. Powell, E.E., and Kroon, P.A. (1994) Low Density Lipoprotein Receptor and 3-Hydroxy-3-methylglutaryl Coenzyme A Reductase Gene Expression in Human Mononuclear Leukocytes Is Regulated Coordinately and Parallels Gene Expression in Human Liver, *J. Clin. Invest. 93,* 2168–2174.

Synthesis of the Conjugated Trienes 5*E*,7*E*,9*E*,14*Z*,17*Z*-Eicosapentaenoic Acid and 5*Z*,7*E*,9*E*,14*Z*,17*Z*-Eicosapentaenoic Acid, and Their Induction of Apoptosis in DLD-1 Colorectal Adenocarcinoma Cells

Tsuyoshi Tsuzuki[a], Kazumi Tanaka[a], Shigefumi Kuwahara[b], and Teruo Miyazawa[a,*]

[a]Food & Biodynamic Chemistry Laboratory, Graduate School of Agricultural Science, Tohoku University, Sendai 981-8555, Japan, and [b]Laboratory of Applied Bioorganic Chemistry, Graduate School of Agricultural Science, Tohoku University, Sendai 981-8555, Japan

ABSTRACT: During the course of our recent study on the anti-tumor effect of conjugated eicosapentaenoic acids (CEPA), we found that acid mixtures prepared by treating EPA with KOH in ethylene glycol induced potent apoptotic cell death in human tumor cells via membrane phospholipid peroxidation. Interestingly, the KOH-treated CEPA mixtures were more cytotoxic than EPA and CLA and had no effect on normal human fibroblast cells. To identify the specific cytotoxic FA in the CEPA mixture, we synthesized possible candidates for the active species. Here, we report the synthesis of (5*E*,7*E*,9*E*,14*Z*,17*Z*)-5,7,9,14,17-eicosapentaenoic acid (E-CEPA) and its 5-(*Z*) isomer (Z-CEPA), both of which are conjugated trienes that exist naturally in red algae (*Ptilota filicina* J. Agardh). E-CEPA and Z-CEPA were synthesized from methyl 5-oxopentanoate in six steps, using three types of Wittig reactions as the key steps. Next, we examined the cytotoxicity of E-CEPA and Z-CEPA in human tumor cells and confirmed their bioactivity. Both E-CEPA and Z-CEPA had a strong cytotoxic reaction in tumor cells, and this effect occurred through induction of apoptosis.

Paper no. L9599 in *Lipids* 40, 147–154 (February 2005).

Conjugated FA is a generic term for FA with conjugated double bond systems, as exemplified by CLA (1). Several CLA isomers exist as a result of positional and geometrical isomerism of the conjugated double bonds, and the major naturally occurring CLA isomer is referred to as 9*Z*,11*E*-18:2 (Scheme 1). CLA was first reported to have an anticarcinogenic effect, and subsequently various other physiological effects have been shown, including an antiarteriosclerotic effect and a role in regulation of lipid metabolism (1–5). These activities of CLA are associated with its conjugated double bond system. CLA is found naturally, especially ruminant fats such as beef tallow and milk fat (1). However, the CLA level in these foodstuffs is around 1% (w/w), and hence natural fats can-

not be used as health-promoting CLA-containing supplements. Therefore, at present, oils that include CLA are prepared from alkali isomerization of vegetable oils such as safflower oil, and these products are marketed as health supplements.

Conjugated FA other than CLA exist in nature. Seed oils of certain plants include conjugated triene FA, such as α-eleostearic acid (9*Z*,11*E*,13*E*-18:3) and calendic acid (8*E*,10*E*,12*Z*-18:3), at levels of 30 to 80% (w/w) (6,7), and seaweeds such as red and green algae contain conjugated EPA (CEPA; 5*E*,7*E*,9*E*,14*Z*,17*Z*-20:5 and 5*Z*,7*E*,9*E*,14*Z*,17*Z*-20:5) (Scheme 1) (8). We are particularly interested in seeds and algae that contain conjugated FA, and we have studied the properties of these materials extensively (9–16). During the course of our recent study on the antitumor effect of CEPA *in vivo* and *in vitro*, we found that acid mixtures prepared by treating all-(*Z*)-5,8,11,14,17-eicosapentaenoic acid (EPA, Scheme 1) with KOH in ethylene glycol under a number of different reaction conditions induced potent apoptotic cell death in several kinds of tumor cells, through membrane phospholipid peroxi-
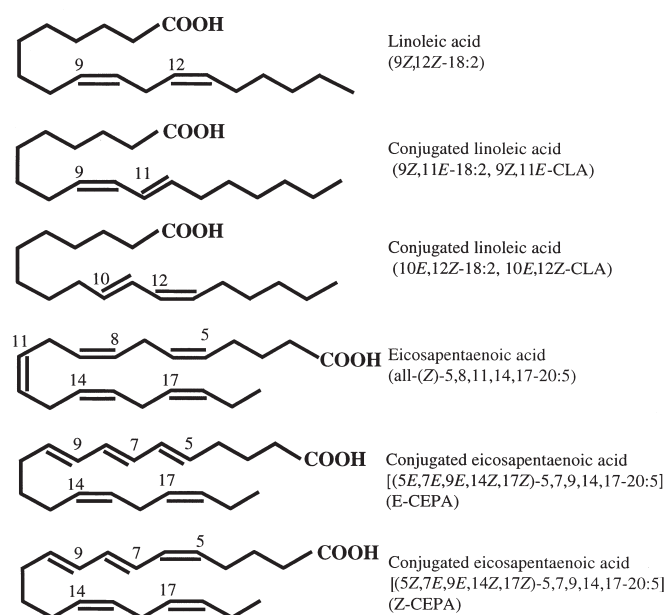
*To whom correspondence should be addressed at Food & Biodynamic Chemistry Laboratory, Graduate School of Life Science and Agriculture, Tohoku University, Tsutsumidori-Amamiyamachi 1-1, Aobaku, Sendai 981-8555, Japan. E-mail: miyazawa@biochem.tohoku.ac.jp

Abbreviations: CEPA, conjugated eicosapentaenoic acid; DIBAL, diisobutylaluminum hydride; E-CEPA, (5E,7E,9E,14Z,17Z)-5,7,9,14,17-eicosapentaenoic acid; HR, high resolution; KHMDS, KN[Si(CH$_3$)$_3$]$_2$; Z-CEPA, 5-Z isomer of E-CEPA.
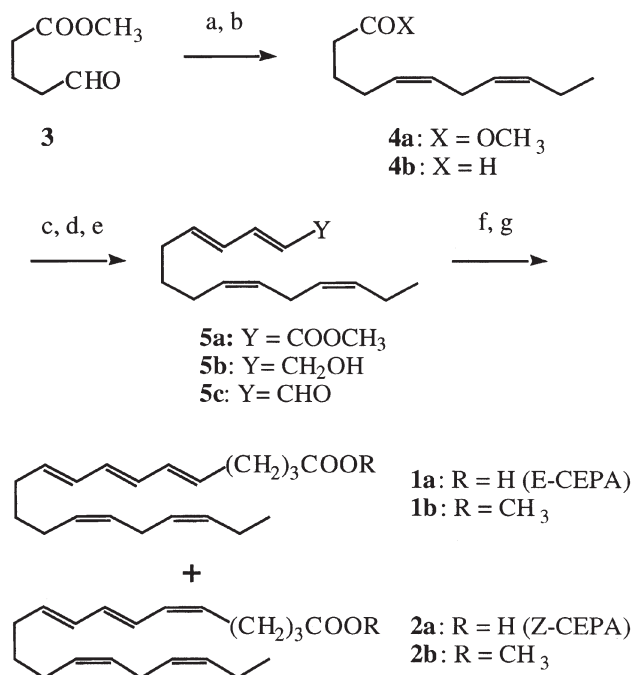
SCHEME 1

FIG. 1. Synthetic scheme for Z-CEPA and E-CEPA. Reagents, (a) $CH_2(CH_2PPh_3)_2 \cdot 2Br$, KHMDS, THF, propanal, then **3** (32%); (b) DIBAL, CH_2Cl_2 (64%); (c) $(EtO)_2P(O)CH_2CH=CHCO_2CH_3$, LiOH, THF (46%); (d) DIBAL, CH_2Cl_2, (80%); (e) MnO_2, CH_2Cl_2 (79%); (f) $Ph_3P(CH_2)_4CO_2H \cdot Br$, LiHMDS, THF; then CH_2N_2, ether (**1b**, 44%; **2b**, 28%). Z-CEPA, conjugated EPA [5Z,7E,9E,14Z,17Z)-5,7,9,14,17-20:5]; E-CEPA, conjugated EPA [(5E,7E,9E,14Z,17Z)-5,7,9,14,17-20:5]; HMDS, hexamethyl phosphoramide; DIBAL, diisobutylaluminum hydride; KHMDS, $KN[Si(CH_3)_3]_2$.

dation (9,12). Interestingly, the KOH-treated mixtures were more cytotoxic than the EPA mixture itself but had no effect on normal human fibroblast cell lines. UV spectroscopic analysis of the KOH-treated mixtures showed that they contained various conjugated diene, triene, tetraene, and pentaene FA, which were present at various ratios, depending on the reaction conditions used. Among these mixtures, the one containing a higher amount of conjugated triene FA (UV λ_{max}: 268 nm) exhibited the highest cytotoxicity, suggesting that the most important component for cytotoxicity may be an EPA containing a conjugated triene structure.

To identify the specific cytotoxic FA, we have synthesized possible candidates for the active species. Here, we report the synthesis of (5E,7E,9E,14Z,17Z)-5,7,9,14,17-eicosapentaenoic acid (E-CEPA, Scheme 1) and its 5-(Z)- isomer (Z-CEPA, Scheme. 1), which both exist naturally in the red alga (*Ptilota filicina* J. Agardh). We then examined the cytotoxicity of these molecules in human tumor cells and confirmed that both isomers have strong bioactivity.

EXPERIMENTAL PROCEDURES

Synthesis of E-CEPA and Z-CEPA (Fig. 1). Methyl 5-oxopentanoate (**3**) was prepared in two steps from δ-valerolactone, according to the literature method (17). Methyl (5Z,8Z)-5,8-undecadienoate (**4a**) was prepared by a one-pot double-Wittig protocol developed by Pohnert and Boland (18). $KN[Si(CH_3)_2]_2$, abbrevi-

ated as KHMDS (0.5 M in toluene, 50 mL, 25 mmol), was added dropwise to a stirred suspension of 1,3-propanediylbis(triphenylphosphonium) dibromide (9.00 g, 12.3 mmol) in THF (120 mL) at –78°C under a nitrogen atmosphere. The mixture was allowed to warm to room temperature gradually over 2 h and stirred for an additional 30 min. Hexamethyl phosphoramide (6 mL) was added to the mixture, and the resulting homogeneous orange solution was recooled to –78°C. Propanal (1.00 mL, 14.0 mmol) was added dropwise to the solution, and the mixture was allowed to warm to 0°C over 2 h, stirred for an additional 30 min, and then recooled to –78°C. A solution of **3** (1.00 g, 7.70 mmol) in THF (15 mL) was added dropwise to the reaction mixture, and the mixture was allowed to warm gradually to room temperature. After being quenched with a saturated aqueous NH_4Cl solution, the mixture was extracted with ether. The extract was washed with brine, dried (using $MgSO_4$), and concentrated *in vacuo*. The residue was chromatographed over SiO_2 (150 g, elution with a 90:1 hexane/ethyl acetate mixture) to give **4a**.

Reduction of **4a** with diisobutylaluminum hydride (DIBAL) gave (5Z,8Z)-5,8-undecadienal (**4b**), which was then subjected to a four-carbon elongation reaction using methyl (E)-4-(diethoxyphosphoryl)but-2-enoate (19). DIBAL (0.95 M in hexane, 13.6 mL, 12.9 mmol) was added dropwise to a stirred solution of **4a** (2.40 g, 12.3 mmol) in CH_2Cl_2 (70 mL) at –78°C. After 30 min, the reaction mixture was quenched with a saturated aqueous NH_4Cl solution, and allowed to warm gradually to room temperature. Celite® was added to the mixture, and the resulting slurry was filtered through a Celite pad. The filtrate was dried (using $MgSO_4$) and concentrated *in vacuo*. The residue was chromatographed over SiO_2 (45 g, elution with a 100:1 hexane/ethyl acetate mixture) to give **4b**.

A mixture of **4b** (1.00 g, 6.00 mmol), methyl (E)-4-(diethoxyphosphoryl)but-2-enoate (6.70 mmol, 1.60 g). and $LiOH \cdot H_2O$ (275 mg, 6.70 mmol) in THF (50 mL) containing pulverized 4 Å molecular sieves (6.5 g) was stirred at reflux temperature for 14 h. The reaction mixture was filtered through a Celite pad, and the filtrate was concentrated *in vacuo*. The residue was chromatographed over SiO_2 (75 g, elution with a 40:1 hexane/ethyl acetate mixture) to give methyl (2E,4E,9Z,12Z)-2,4,9,12-pentadecatetraenoate (**5a**). DIBAL (0.95 M in hexane, 1.1 mL, 1.05 mmol) was added dropwise to a stirred solution of **5a** (120 mg, 0.5 mmol) in CH_2Cl_2 (8 mL) at –78°C. After 30 min, the mixture was worked up in a similar manner to that described for the preparation of **4b** to give (2E,4E,9Z,12Z)-2,4,9,12-pentadecatetraenol (**5b**) after SiO_2 chromatographic purification (5 g, elution with a 5:1 hexane/ethyl acetate mixture).

A mixture of **5b** (584 mg, 2.65 mmol) and MnO_2 (chemically treated, 8 g; Wako Pure Chemical Industries, Ltd., Tokyo, Japan) in CH_2Cl_2 (250 mL) was sonicated with a sonic cleaner (Honda Ultrasonic Cleaner W221) for 4 h at room temperature. The mixture was filtered through a pad of Celite, and the filtrate was concentrated *in vacuo* to give (2E,4E,9Z,12Z)-2,4,9,12-pentadecatetraenal (**5c**). Butyllithium (1.58 M in hexane, 0.30 mL, 0.47 mmol) was added dropwise to a stirred solution of 1,1,1,3,3,3-hexamethyldisilazane (80 mg, 0.50 mmol) in THF (2 mL) at 0°C, and the mixture was stirred for 20 min. The resulting solution was added

dropwise to a suspension of (4-carboxybutyl)triphenylphosphonium bromide (100 mg, 0.225 mmol) in THF (1 mL) at room temperature, and the mixture was stirred for 30 min, giving an orange solution. A solution of **5c** (50 mg, 0.2 mmol) in THF (0.5 mL) was added to the orange solution at room temperature. After being stirred for 30 min, the mixture was quenched with a saturated aqueous oxalic acid solution (1 mL) and extracted with ether. The extract, which contained (5*E*,7*E*,9*E*,14*Z*,17*Z*)-5,7,9,14,17-eicosapentaenoic acid (**1a**) and (5*Z*,7*E*,9*E*,14*Z*,17*Z*)-5,7,9,14,17-eicosapentaenoic acid (**2a**), was treated with an ethereal diazomethane (prepared from *N*-nitroso-*N*-methylurea) to give a mixture of methyl (5*E*,7*E*,9*E*,14*Z*,17*Z*)-5,7,9,14,17-eicosapentaenoate (**1b**) and methyl (5*Z*,7*E*,9*E*,14*Z*,17*Z*)-5,7,9,14,17-eicosapentaenoate (**2b**) after concentration *in vacuo*.

The mixture was repeatedly chromatographed over SiO_2 (25 g silica gel 60, 230–400 mesh; Merck, Darmstadt, Germany; elution with a 50:1 hexane/ether mixture) to give **1b** and **2b**. Two conjugated EPA methyl esters (**1b** and **2b**) were isolated using HPLC, based on the method we used before (16). Two CEPA methyl esters were dissolved in hexane, and this solution was fractionated by normal-phase HPLC using an 880-PU pump (Jasco, Inc., Tokyo, Japan) with an SPD-M10AVP detector (Shimadzu, Kyoto, Japan). A ChromSpher Lipids column impregnated with silver (5 μm particle size, 4.6 × 250 mm; Chrompack, Bridgewater, NJ) was used. A hexane/acetonitrile (100:0.15, vol/vol) mobile phase was used, and the flow rate was 1.0 mL/min. Detection was at 270 nm (FAME with a conjugated triene). A substance showing a large peak at 270 nm was repeatedly fractionated, and the two fractions collected (**1b** and **2b**) were purified. The collected fractions were dried completely under nitrogen gas.

IR spectra were measured as films, using a JASCO IR Report-100 spectrometer. ^{1}H NMR spectra were recorded in $CDCl_3$ (Wako Pure Chemicals Industries, Ltd., Osaka, Japan) with tetramethylsilane as an internal standard, using a Varian Gemini 2000 spectrometer (300 MHz) or a Varian UNITYplus-500 spectrometer (500 MHz). Mass spectra were obtained with a JEOL JMS-700 spectrometer operating in EI mode. Merck silica gel 60 (70–230 mesh) was used for silica gel column chromatography, unless otherwise stated. UV/vis spectrophotometric analysis of the conjugated EPA methyl esters was performed with a Shimadzu UV-2400P instrument. Geometric isomerism of the conjugated double bonds was distinguished easily using ^{13}C NMR under ^{13}C NMR conditions similar to those we have previously reported (16). Conjugated EPA methyl esters were dissolved in $CDCl_3$ at a concentration of 1 mg/mL. The ^{13}C NMR spectra were recorded on a Varian Unity 600 spectrometer (Varian, Inc., Palo Alto, CA) operating at 150 MHz.

Materials for cell culture. RPMI 1640 medium (containing 0.3 mg/mL L-glutamine and 2.0 mg/mL sodium bicarbonate) and all-(*Z*)-5,8,11,14,17- EPA were obtained from Sigma (St. Louis, MO). FBS was purchased from Dainippon Pharmaceutical (Osaka, Japan). Penicillin and streptomycin were products of Gibco BRL (Rockville, MD). 9*Z*,11*E*-CLA (99% purity) and 10*E*,12*Z*-CLA (99% purity) were obtained from Cayman Chemical Co. (Ann Arbor, MI).

Preparation of conjugated EPA (Mix-CEPA). In our previous study, CEPA (a FA with a conjugated trienoic structure) had the strongest cytotoxic effect compared with CLA, conjugated linolenic acid, and conjugated DHA (9,12). In the current study, CEPA was prepared from EPA by alkaline isomerization, using the previously reported method (9,12,20), and the initial product is henceforth referred to as mix-CEPA. The CEPA concentrate was stored at –20°C after being purged with nitrogen gas. UV/vis spectrophotometric analysis of the conjugated FA was performed with a Shimadzu UV-2400PC, and confirmed the presence of conjugated FA containing dienes (absorption maximum at 235 nm), trienes (268 nm), tetraenes (315 nm), pentaenes (345 nm), and hexaenes (375 nm) (21). The CEPA oil (Mix-CEPA) used in the subsequent experiments consisted of 57.6% conjugated dienes, 34.5% conjugated trienes, 6.7% conjugated tetraenes, and 1.2% conjugated pentaenes.

Cells and cell cultures. DLD-1 (colorectal adenocarcinoma), HepG2 (hepatoma), A549 (lung adenocarcinoma), and HL-60 (acute promyelocytic leukemia) human tumor cells were obtained from the Cell Resource Center for Biochemical Research at Tohoku University (Sendai, Japan). All tumor cells were cultured in RPMI 1640 medium (containing 0.3 mg/mL L-glutamine and 2.0 mg/mL sodium bicarbonate) supplemented with 10% FBS, 100 units/mL penicillin, and 100 mg/mL streptomycin. Cells were maintained at 37°C in a humidified atmosphere of 95% air and 5% CO_2.

Cell viability test using CLA and CEPA. Cell viability was assessed by the WST-1 method (13,22). The cells (DLD-1, HepG2, A549, and HL-60) were seeded onto 96-well culture plates at a density of 1×10^5 cells/well in 100 μL RPMI-1640 containing 10% FBS. Stock solutions of 9*Z*,11*E*-CLA, 10*E*,12*Z*-CLA, Mix-CEPA, E-CEPA (**1a**) and Z-EPA (**2a**) were prepared in ethanol at concentrations of 100 mM. For these experiments, the FA were prepared from the stock solution and diluted to final concentrations of 0–20 μM in FBS-free RPMI-1640. The final concentration of ethanol never exceeded 0.1% (vol/vol). After incubation for 24 h at 37°C, the cells were placed in 100 μL of fresh FBS-free RPMI-1640 medium with various concentrations of the FA. After 24, 10 μL of WST-1 solution was added to each well to evaluate cell viability. After incubation for 3 h at 37°C, cell viability was measured using a microplate reader (Model 550; Bio-Rad, Tokyo, Japan) at a wavelength of 450 nm and a reference wavelength of 655 nm.

Fluorescence dye staining analysis in DLD-1 cells (apoptosis assay) (9). DLD-1 cells were seeded on coverslips treated with ethanol (control), 2.5 mM E-CEPA, or 2.5 mM Z-CEPA for 24 h. After incubation, cells were washed in PBS and fixed in 4% formaldehyde. The fixed cells were stained for nuclei with Hoechst 33342 (1 μg/mL in PBS) for 10 min, washed in PBS, and mounted using 50% glycerol. The stained cells were observed by IX-FLA fluorescence microscopy (Olympus, Tokyo, Japan). Apoptotic cells were identified based on brightness due to condensed chromatin.

DNA fragmentation ladder assay in DLD-1 cells (apoptosis assay) (12,13). DLD-1 cells (1×10^5/mL) were seeded onto 10-cm dishes treated with ethanol (control), 2.5 μM E-CEPA, or 2.5 μM Z-CEPA for 24 h, and then transferred into a glass tube. Cells were suspended in lysis buffer (5 mM Tris, 20 mM EDTA, 0.5% Triton X-100, pH 8.0) and incubated for 30 min at 4°C. After

incubation, the tube was spun at $17,400 \times g$ for 20 min to separate the intact chromatin from the DNA fragments. Following centrifugation, 2 µL of RNase A (1 mg/mL; Sigma) was added to the supernatant, and the mixture was incubated at 37°C for 1 h. Proteinase K (2 µL; 1 mg/mL; Sigma) was then added, and incubation was continued for an additional 1 h. DNA was precipitated with a mixture of 20 µL of 5 M NaCl and 120 µL of 2-propanol overnight at –20°C. Following centrifugation, pellets were air-dried and dissolved in 20 µL of TE buffer (10 mM Tris and 1 mM EDTA, pH 7.4). Extracted DNA was separated by electrophoresis in a 2.0% agarose gel at 100 V in a pH 8.4 buffer containing 90 mM Tris, 90 mM boric acid, and 2 mM EDTA. Each gel was stained with ethidium bromide and photographed under UV light.

Statistics. Statistical analysis was performed using a one-way ANOVA, followed by a Newman–Keuls test for multiple comparisons among several groups. A difference was considered to be significant at $P < 0.05$.

RESULTS

Synthesis of Z-CEPA and E-CEPA (Fig. 1). The synthesis began with preparation of homoconjugated diene **4a** by the one-pot double-Wittig protocol developed by Pohnert and Boland (18). According to the reported procedure, the bis-ylide obtained by treating 1,3-propanediylbis(triphenylphosphonium) dibromide with 2 equiv of KHMDS was allowed to react sequentially with propanal and methyl 5-oxopentanoate (**3**) to give 487 mg (32 %) of **4a**. IR ν_{max} cm^{-1}: 3000 (*m*), 1740 (*s*); ^{1}H NMR (300 MHz, CDCl$_3$) δ: 0.97 (3H, *t*, *J* = 7.6 Hz, 11-H$_3$), 1.71 (2H, *qui*, *J* = 7.3 Hz, 3-H$_2$), 2.01–2.15 (4H, *m*, 4-H$_2$, 10-H$_2$), 2.33 (2H, *t*, *J* = 7.3 Hz, 2-H$_2$), 2.77 (2H, *t*, *J* = 6.5 Hz, 7-H$_2$), 3.67 (3H, *s*, OCH$_3$), 5.22–5.46 (4H, *m*, 5-H, 6-H, 8-H, 9-H); HR-EIMS *m/z* (M$^+$): calcd. for C$_{12}$H$_{20}$O, 196.1464; found, 196.1463.

Reduction of **4a** with DIBAL gave 1.30 g (64%) of **4b**, IR ν_{max} cm^{-1}: 3000 (*m*), 2710 (*s*), 1720 (*s*); ^{1}H NMR (300 MHz, CDCl$_3$) δ: 0.97 (3H, *t*, *J* = 7.4 Hz, 11-H$_3$), 1.71 (2H, *qui*, *J* = 7.3 Hz, 3-H$_2$), 2.01–2.16 (4H, *m*, 4-H$_2$, 10-H$_2$), 2.45 (2H, *td*, *J* = 7.3, 1.7 Hz, 2-H$_2$), 2.77 (2H, *t*, *J* = 6.7 Hz, 7-H$_2$), 5.23–5.47 (4H, *m*, 5-H, 6-H, 8-H, 9-H), 9.78 (1H, *t*, *J* = 1.7 Hz, 1-H). HR-EIMS *m/z* (M$^+$): calcd. for C$_{11}$H$_{18}$O, 166.1357; found, 166.1359. Compound **4b** was then subjected to a four-carbon elongation reaction using methyl (*E*)-4-(diethoxyphosphoryl)but-2-enoate. Reduction of **4b** gave 684 mg (46%) of **5a**, IR ν_{max} cm^{-1}: 3000 (*m*), 1720 (*vs*), 1640 (*s*); ^{1}H NMR (300 MHz, CDCl$_3$) δ: 0.97 (3H, *t*, *J* = 7.6 Hz, 15-H$_3$), 1.51 (2H, *qui*, *J* = 7.4 Hz, 7-H$_2$), 2.01–2.13 (4H, *m*, 8-H$_2$, 14-H$_2$), 2.19 (2H, *q*, *J* = 7.4 Hz, 6-H$_2$), 2.77 (2H, *t*, *J* = 6.5 Hz, 11-H$_2$), 3.74 (3H, *s*, OCH$_3$), 5.24–5.44 (4H, *m*, 9-H, 10-H, 12-H, 13-H), 5.79 (1H, *d*, *J* = 15.7 Hz, 2-H), 6.07–6.24 (2H, *m*, 4-H, 5-H), 7.27 (1H, *dd*, *J* = 15.4, 10.2 Hz, 3-H). HR-EIMS *m/z* (M$^+$): calcd. for C$_{16}$H$_{24}$O$_2$, 248.1776; found, 248.1778.

The resulting tetraene-ester (**5a**) was converted in a conventional manner into aldehyde **5c** *via* alcohol **5b**. Reduction of **5a** gave 85 mg (80%) of **5b**, IR ν_{max} cm^{-1}: 3350 (*m*), 3000 (*m*), 980 (*s*); ^{1}H NMR (300 MHz, CDCl$_3$) δ: 0.97 (3H, *t*, *J* = 7.6 Hz, 15-H$_3$), 1.28 (1H, *br*, OH), 1.46 (2H, *qui*, *J* = 7.4 Hz, 7-H$_2$), 2.02–2.14 (6H, *m*, 6-H$_2$, 8-H$_2$, 14-H$_2$), 2.77 (2H, *t*, *J* = 5.9 Hz, 11-H$_2$), 4.17
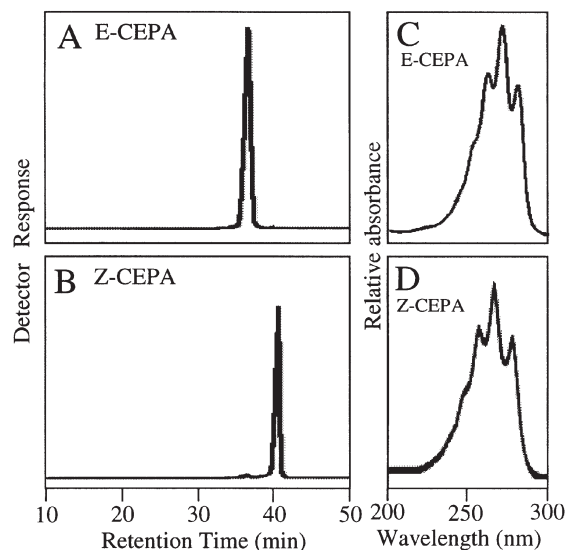
FIG. 2. HPLC chromatograms and UV absorption spectra of two synthetic conjugated EPA (CEPA) methyl esters. Two synthetic CEPA were separated with HPLC. The flow-rate was 1 mL/min with a hexane/acetonitrile (100:0.15) mobile phase, and detection at 270 nm (FAME with a conjugated triene). (A) HPLC chromatogram of E-CEPA methyl ester (retention time 36–37 min); (B) HPLC chromatograms of Z-CEPA methyl ester (retention time 39–41 min); (C) UV absorption spectrum of E-CEPA methyl ester (λ_{max} = 258, 268, 279); (D) UV absorption spectrum of Z-CEPA methyl ester (λ_{max} = 256, 266, 275). For abbreviations see Figure 1.

(2H, *d*, *J* = 5.5 Hz, 1-H$_2$), 5.26–5.44 (4H, *m*, 9-H, 10-H, 12-H, 13-H), 5.66–5.78 (2H, *m*, 2-H, 5-H), 6.06 (1H, *dd*, *J* = 15.1, 10.4 Hz, 4-H), 6.23 (1H, *dd*, *J* = 15.1, 10.4 Hz, 3-H). HR-EIMS *m/z* (M$^+$): calcd. for C$_{15}$H$_{24}$O, 220.1827; found, 220.1827.

Oxidation of **5b** gave 456 mg (79%) of **5c**, IR ν_{max} cm^{-1}: 2720 (*w*), 1680 (*s*), 1635 (*s*), 980 (*m*); ^{1}H NMR (300 MHz, CDCl$_3$) δ: 0.97 (3H, *t*, *J* = 7.6 Hz, 15-H$_3$), 1.54 (2H, *qui*, *J* = 7.0 Hz, 7-H$_2$), 2.04–2.14 (4H, *m*, 8-H$_2$, 14-H$_2$), 2.24 (2H, *q*, *J* = 7.0 Hz, 6-H$_2$), 2.77 (2H, *t*, *J* = 6.6 Hz, 11-H$_2$), 5.29 (1H, *dt*, *J* = 10.3, 7.0 Hz, 9-H), 5.34–5.43 (3H, *m*, 10-H, 12-H, 13-H), 6.08 (1H, *dd*, *J* = 15.3, 8.0 Hz, 2-H), 6.28 (1H, *dt*, *J* = 15.3, 7.0 Hz, 5-H), 6.33 (1H, *dd*, *J* = 15.3, 10.4 Hz, 4-H), 7.09 (1H, *dd*, *J* = 15.3, 10.4 Hz, 3-H), 9.54 (1H, *d*, *J* = 8.0 Hz, 1-H). HR-EIMS *m/z* (M$^+$): calcd. for C$_{15}$H$_{22}$O, 218.1671; found, 218.1676.

Finally, an (*E*)-selective Wittig olefination of **5c** with (4-carboxybutyl)triphenylphosphonium bromide gave a mixture of **1a** and **2a** (23). Since the spectroscopic characterization of the acids had been conducted in their methyl ester forms, the acid mixture was immediately treated with diazomethane to furnish 28 mg (44%) of **1b** and 14 mg (22%) of **2b** after chromatographic purification (Figs. 2A, 2B). **1b**: IR ν_{max} cm^{-1}: 3000 (*s*), 1740 (*s*), 1650 (*w*), 1640 (*w*), 1240 (*m*), 1200 (*m*), 1165 (*m*), 995 (*s*); ^{1}H NMR (CDCl$_3$) δ: 0.97 (3H, *t*, *J* = 7.6 Hz, 20-H$_3$), 1.46 (2H, *qui*, *J* = 7.6 Hz, 12-H$_2$), 1.73 (2H, *qui*, *J* = 7.3 Hz, 3-H$_2$), 2.02–2.15 (8H, *m*, 4-H$_2$, 11-H$_2$, 13-H$_2$, 19-H$_2$), 2.31 (2H, *t*, *J* = 7.3 Hz, 2-H$_2$), 2.77 (2H, *br t*, *J* = 5.9, 16-H$_2$), 3.66 (3H, *s*, OCH$_3$), 5.24–5.42 (4H, *m*, 14-H, 15-H, 17-H, 18-H), 5.61(1H, *dt*, *J* = 14.2, 7.2 Hz, 5-H), 5.67 (1H, *dt*, *J* = 14.5, 7.3 Hz, 10-H), 6.01–6.11 (4H, *m*, 6-H, 7-H, 8-H, 9-
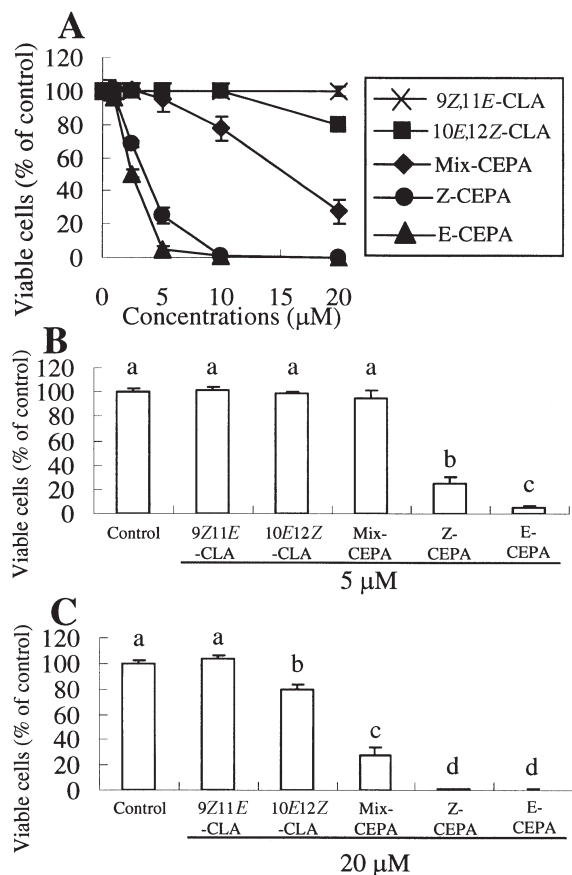
FIG. 3. Cell viability test using 9*Z*,11*E*-CLA, 10*E*,12*Z*-CLA, Mix-CEPA, Z-CEPA, and E-CEPA in DLD-1 cells (A–C). DLD-1 cells were incubated for 24 h after treatment with each FA. (A) DLD-1 cells were incubated after treatment with 0–20 μM FA. (B) DLD-1 cells were incubated after treatment with ethanol (control) and 5 μM FA. (C) DLD-1 cells were incubated after treatment with ethanol (control) and 20 μM FA. Values are shown as the mean ± SD (*n* = 6). a,b,c,d: values with different superscripts are significantly different at *P* < 0.05. For abbreviations see Figure 1.

FIG. 4. Apoptosis assay (fluorescence dye staining analysis and DNA fragmentation ladder analysis) using Z-CEPA and E-CEPA in DLD-1 cells (A-E). Fluorescence dye staining analysis of DLD-1 cells treated with ethanol (control, A), 2.5 μM Z-CEPA (B), and 2.5 μM E-CEPA (C). Cells were incubated for 24 h after treatment with CEPA. Magnification: 100×. (D) Fluorescence dye staining analysis of DLD-1 cells treated with 2.5 μM Z-CEPA. Cells were incubated for 24 h after supplementation of Z-CEPA. Magnification: 200×. The arrows indicate apoptotic cells. (E) DNA fragmentation ladder analysis of DLD-1 cells treated with CEPA. Agarose gel electrophoresis of low-M.W. DNA extracted from DLD-1 cells. DLD-1 cells were exposed to ethanol (control), 2.5 μM Z-CEPA, or 2.5 μM E-CEPA. M: M.W. markers. For abbreviations see Figure 1.

H); high resolution (HR)-FABMS *m/z* ([M + 1]$^+$): calcd. for $C_{21}H_{33}O_2$, 317.2480; found, 317.2480; UV (MeOH) λ_{max} = 258, 268, 279 (Fig. 2C); ^{13}C NMR (CDCl$_3$) δ: 174.01 (C-1), 33.36 (C-2), 24.52 (C-3), 32.08 (C-4), 132.62 (C-5), 131.32 (C-6), 130.64 (C-7), 131.45 (C-8), 130.57 (C-9), 134.34 (C-10), 32.35 (C-11), 29.23 (C-12), 26.68 (C-13), 129.61 (C-14), 128.49 (C-15), 25.55 (C-16), 127.31 (C-17), 131.85 (C-18), 20.55 (C-19), 14.31 (C-20), 51.49 (COOCH$_3$). **2b**: IR ν$_{max}$ cm^{-1}: 3000 (*s*), 1740 (*s*), 1650 (*w*), 1640 (*w*), 1240 (*m*), 1205 (*m*), 1170 (*m*), 995 (*m*), 965 (*w*); ^{1}H NMR (CDCl$_3$) δ: 0.97 (3H, *t*, *J* = 7.6 Hz, 20-H$_3$), 1.46 (2H, *qui*, *J* = 7.6 Hz, 12-H$_2$), 1.73 (2H, *qui*, *J* = 7.3 Hz, 3-H$_2$), 2.04–2.15 (6H, *m*, 11-H$_2$, 13-H$_2$, 19-H$_2$), 2.23 (2H, *q*, *J* = 7.5 Hz, 4-H$_2$), 2.33 (2H, *t*, *J* = 7.4 Hz, 2-H$_2$), 2.77 (2H, *br t*, *J* = 6.0 Hz, 16-H$_2$), 3.67 (3H, *s*, OCH$_3$), 5.25–5.42 (5H, *m*,5-H, 14-H, 15-H, 17-H, 18-H), 5.71 (1H, *dt*, *J* = 14.4, 7.2 Hz, 10-H), 6.04 (1H, *br t*, *J* = 11.4 Hz, 6-H), 6.10 (1H, *dd*, *J* = 14.4, 11.0 Hz, 9-H), 6.18 (1H, *dd*, *J* = 14.5, 11.0 Hz, 8-H), 6.35 (1H, *dd*, *J* = 14.5, 11.4 Hz, 7-H); HR-FABMS *m/z* ([M + 1]$^+$): calcd. for $C_{21}H_{33}O_2$, 317.2480; found, 317.2481; UV (MeOH) λ_{max} = 256, 266, 275 (Fig. 2D); ^{13}C NMR (CDCl$_3$) δ:

174.02 (C-1), 33.37 (C-2), 24.82 (C-3), 27.08 (C-4), 130.77 (C-5), 129.77 (C-6), 125.75 (C-7), 130.79 (C-8), 130.19 (C-9), 135.10 (C-10), 32.36 (C-11), 29.23 (C-12), 26.68 (C-13), 129.60 (C-14), 128.48 (C-15), 25.57 (C-16), 127.31 (C-17), 131.82 (C-18), 20.55 (C-19), 14.30 (C-20), 51.48 (COOCH$_3$).

The UV, ^{1}H NMR, and ^{13}C NMR spectral data for **1b** and **2b** were identical to the respective authentic data (8).

Cell viability test using E-CEPA and Z-CEPA in DLD-1 cells. The cytotoxicity of the synthetic CEPA isomers (E-CEPA and Z-CEPA) was examined in comparison with that of Mix-CEPA and CLA. DLD-1 cells were treated with 0 to 20 μM of five FA (9*Z*,11*E*-CLA, 10*E*,12*Z*-CLA, Mix-CEPA, E-CEPA, or Z-CEPA) at a purity of 99%, and cell viability 24 h after administration was measured using the WST-1 method. E-CEPA and Z-CEPA showed dose-dependent cytotoxicity reactions in DLD-1 cells, and these effects were stronger than those of CLA and Mix-CEPA (Fig. 3A). After administration of Z-CEPA and E-CEPA at a dose of 5 μM, the cell survival rates were 25 and 5%, respectively, compared with the control (Figs. 3A, 3B). Compared with Z-CEPA, E-CEPA showed a stronger cytotoxicity reaction in DLD-1 cells. After administration of 10*E*,12*Z*-CLA and Mix-CEPA at a dose of 20 μM, the cell survival rates were 80 and 27%, respectively, compared with the control (Figs. 3A, 3C). Hence, Mix-CEPA showed a stronger cytotoxicity reaction in DLD-1 cells, compared with 10*E*,12*Z*-CLA. Compound 9*Z*,11*E*-CLA at a dose of 20 μM did not show a cyto-
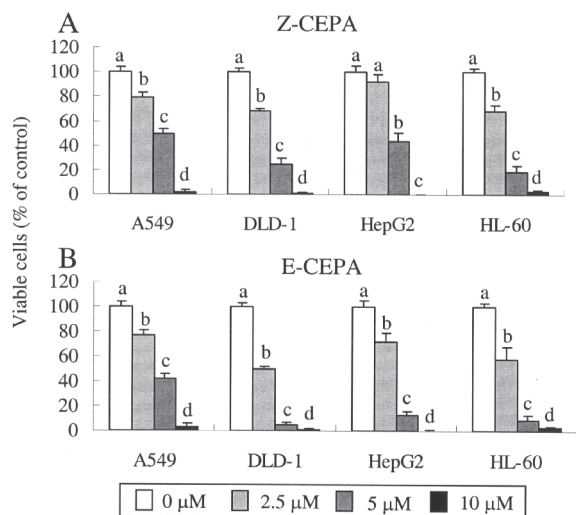
FIG. 5. Cell viability test using Z-CEPA (A) and E-CEPA (B) in various human tumor cells. Human tumor cells (A549, DLD-1, HepG2, HL-60 cells) were incubated for 24 h after treatment with FA. Values are shown as the mean ± SD (*n* = 6). a,b,c,d: values with different superscripts are significantly different at *P* < 0.05. For abbreviations see Figure 1.

toxicity reaction in DLD-1 cells (Fig. 3). The Mix-CEPA, Z-CEPA, and E-CEPA concentrations for 50% suppression of cell viability were approximately 15, 3, and 2.5 µM, respectively. Hence, the order of cytotoxicity reaction in DLD-1 cells was E-CEPA > Z-CEPA > Mix-CEPA > 10*E*,12*Z*-CLA > 9*Z*.11*E*-CLA.

Apoptosis assays (fluorescence dye staining analysis and DNA fragmentation ladder analysis) in DLD-1 cells. To characterize the mechanism of cell death, cytological alterations and cellular DNA degradation were analyzed. DLD-1 cell death caused by E-CEPA and Z-CEPA was accompanied by marked changes in cellular morphology. Nuclear condensation and brightness were observed by fluorescent microscopy in Hoechst 33342-stained cells treated with E-CEPA and Z-CEPA, compared with cells treated with ethanol only (Fig. 4A–D), and treatment of DLD-1 cells with 2.5 µM E-CEPA or Z-CEPA resulted in a DNA fragmentation ladder (Fig. 4E). Hence, it was shown that E-CEPA and Z-CEPA induced apoptosis in DLD-1 cells.

Cell viability test using E-CEPA and Z-CEPA in various human tumor cells. The cytotoxicity of the CEPA isomers was examined in three other human tumor cell lines (HepG2, A549, and HL-60), in addition to DLD-1 cells. Both E-CEPA and Z-CEPA showed strong dose-dependent cytotoxicity reactions in all the cultured human tumor cells examined (Fig. 5), with these effects being particularly strong in DLD-1 and HL-60 cells, compared with A549 and HepG2 cells.

DISCUSSION

In this study, we have synthesized two naturally occurring CEPA isomers and examined their cytotoxicity reaction in human tumor cells, compared with that of CLA. Consequently, we confirmed that E-CEPA and Z-CEPA, both of which contain a conjugated triene system, have a strong cytotoxicity reaction in tumor cells and that this occurs through induction of apoptosis. As far as we are aware, this is the first study to verify the cytotoxicity reaction of a naturally occurring CEPA.

We previously reported that CEPA has some potentially interesting physiological effects (9,12). However, in those studies, we used CEPA prepared by alkaline isomerization, and the CEPA was therefore a mixture of several isomers. At present, it is difficult to identify all of these isomers, and it is possible that some isomers produced by alkaline isomerization have little antitumor effect and may even have harmful side reactions . Therefore, the bioactivity of each isomer needs to be investigated. CEPA isomers such as 5*Z*,7*E*,9*E*,14*Z*,17*Z*–20:5 and 5*E*,7*E*,9*E*,14*Z*,17*Z*–20:5 (Scheme 1) are found in red algae (8), but the amounts of these molecules are extremely small and it is very difficult to extract and purify CEPA from red algae. Hence, synthesis of these molecules provides an alternative approach, and in this study we succeeded in the synthesis of two CEPA isomers, beginning from δ-valerolactone (Figs. 1, 2). The UV, ^{1}H NMR, and ^{13}C NMR spectral data of the synthetic CEPA isomers (E-CEPA and Z-CEPA) were identical to the respective authentic data (8).

Most CLA in nature is in the form of 9*Z*,11*E*-CLA (1). However, natural sources contain only a small amount of CLA, and therefore CLA used experimentally is generally prepared from linoleic acid by alkali isomerization, which gives a mixture of two isomers: 9*Z*,11*E*-CLA and 10*E*,12*Z*-CLA (Scheme 1). Several studies have shown an antitumor effect of the CLA mixture prepared by alkali isomerization (1,4,5), but it was only recently verified in a comparative study of the isomers that 9*Z*,11*E*-CLA had little effect and 10*E*,12*Z*-CLA, the minor component in nature, had a strong effect (24). This result was confirmed in the current study, which showed that 10*E*,12*Z*-CLA had a stronger cytotoxic effect than 9*Z*,11*E*-CLA (Fig. 3). In evaluating the cytotoxic effect of synthesized CEPA (E-CEPA and Z-CEPA) in tumor cells, 9*Z*,11*E*-CLA, 10*E*,12*Z*-CLA and Mix-CEPA (a CEPA mixture prepared from EPA by alkali isomerization) were used as positive controls. The results showed that E-CEPA and Z-CEPA had an extremely strong cytotoxic effect in tumor cells, compared with the CLA (Fig. 3). Therefore, both E-CEPA and Z-CEPA, which have a stronger physiological effect than CLA, are expected to be effective as physiologically active lipids.

The results also showed that E-CEPA and Z-CEPA had an extremely strong cytotoxic effect in tumor cells, compared with Mix-CEPA (Fig. 3). Mix-CEPA contains many structural isomers, and it is likely that some isomers that are only weakly bioactive are present in Mix-CEPA. We have previously clarified that conjugated FA with a conjugated triene system have a far stronger cytotoxicity reaction than conjugated FA with a conjugated diene system (13). The content of Mix-CEPA includes 58% conjugated diene FA and 35% conjugated triene FA, whereas the synthetic CEPA isomers contain only a conjugated triene system, perhaps accounting for the stronger activity of E-CEPA and Z-CEPA.

The synthetic CEPA isomers were observed to promote nuclear condensation and DNA fragmentation in DLD-1 cells, indicating induction of apoptosis (Fig. 4). This suggests that synthetic CEPA is safe, because apoptosis, and not necrosis, was induced in

the cancer cells. Furthermore, the synthetic CEPA isomers showed strong cytotoxicity reaction not only in the DLD-1 colorectal cancer cells but also in pulmonary carcinoma, hepatoma, and leukemia cells (Fig. 5). Therefore, it is anticipated that the synthetic CEPA will act on various carcinomas. E-CEPA, which contains an all-(E) conjugated triene structure, showed stronger cytotoxicity reaction than Z-CEPA, in which the conjugated triene structure contains both E and Z unsaturation configurations (Scheme 1; Figs. 3, 5). Hence, geometrical isomerism can influence the bioactivity of conjugated triene FA, and it appears that an all-(E) configuration leads to a stronger cytotoxicity reaction.

The mechanisms reportedly underlying the antitumor effects of FA include lipid peroxidation, modulation of eicosanoid production by changes in FA composition, and changes in membrane fluidity (25). Some studies have suggested that lipid peroxidation itself induces apoptosis and suppression of cell viability (26–33), and we have previously reported that some conjugated FA with a conjugated triene system can induce apoptosis in tumor cells *via* lipid peroxidation. It is likely that synthetic CEPA also induces apoptosis through lipid peroxidation. Hence the use of CEPA in food and medicine has considerable potential, once its safety is confirmed in animal studies and clinical trials.

ACKNOWLEDGMENT

REFERENCES

1. Ha, Y.L., Grimm, M.W., and Pariza, M.W. (1987) Anticarcinogens from Fried Ground Beef: Heat-Altered Derivatives of Linoleic Acid, *Carcinogenesis 8*, 1881–1887.
2. Lee, K.N., Kritchevsky, D., and Pariza, M.W. (1994) Conjugated Linoleic Acid and Atherosclerosis in Rabbits, *Atherosclerosis 108*, 19–25.
3. Park, Y., Albright, K.J., Storkson, J.M., Liu, W., Cook, M.E., and Pariza, M.W. (1999) Changes in Body Composition in Mice During Feeding and Withdrawal of Conjugated Linoleic Acid, *Lipids 34*, 243–248.
4. Ip, C., Chin, S.F., Scimeca, J.A., and Pariza, M.W. (1991) Mammary Tumor Prevention by Conjugated Dienoic Derivative of Linoleic Acid, *Cancer Res. 51*, 6118–6124.
5. Igarashi, M., and Miyazawa, T. (2001) The Growth Inhibitory Effect of Conjugated Linoleic Acid on a Human Hepatoma Cell Line, HepG2, Is Induced by a Change in Fatty Acid Metabolism, but Not the Facilitation of Lipid Peroxidation in the Cells, *Biochim. Biophys. Acta. 1530*, 162—171.
6. Hopkins, Y. (1972) Fatty Acids with Conjugated Unsaturation, in *Topics in Lipid Chemistry* (Gunstone, F.D., ed.), pp. 37–87, ELEK Science, London.
7. Badami, R.C., and Patil, K.B. (1981) Structure and Occurrence of Unusual Fatty Acids in Minor Seed Oils, *Prog. Lipid Res. 19*, 119–153.
8. Lopez, A., and Gerwick, W.H. (1987) Two New Icosapentaenoic Acids from the Temperate Red Seaweed *Ptilota filicina* J. Agardh, *Lipids 22*, 190–194.
9. Igarashi, M., and Miyazawa, T. (2000) Do Conjugated Eicosapentaenoic Acid and Conjugated Docosahexaenoic Acid Induce Apoptosis *via* Lipid Peroxidation in Cultured Human Tumor Cells? *Biochem. Biophys. Res. Commun. 270*, 649–656.
10. Igarashi, M., and Miyazawa, T. (2000) Newly Recognized Cytotoxic Effect of Conjugated Trienoic Fatty Acids on Cultured Human Tumor Cells, *Cancer Lett. 148*, 173–179.
11. Tsuzuki, T., Igarashi, M., Komai, M., and Miyazawa, T. (2003) A Metabolic Conversion of 9,11,13-Eleostearic Acid (18:3) to 9,11-Conjugated Linoleic Acid (18:2) in the Rat, *J. Nutr. Sci. Vitaminol. 49*, 195–200.
12. Tsuzuki, T., Igarashi, M., and Miyazawa, T. (2004) Conjugated Eicosapentanoic Acid (EPA) Inhibits Transplanted Tumor Growth *via* Membrane Lipid Peroxidation in Nude Mice, *J. Nutr. 134*, 1162–1166.
13. Tsuzuki, T., Tokuyama, Y., Igarashi, M., and Miyazawa, T. (2004) Tumor Growth Suppression by α-Eleostearic Acid, a Linolenic Acid Isomer with a Conjugated Triene System, *via* Lipid Peroxidation, *Carcinogenesis 25*, 1417–1425.
14. Igarashi, M., Tsuzuki, T., Kambe, T., and Miyazawa, T. (2004) Recommended Methods of Fatty Acid Methylester Preparation for Conjugated Dienes and Trienes in Food and Biological Samples, *J. Nutr. Sci. Vitaminol. 50*, 121–128.
15. Tsuzuki, T., Igarashi, M., Iwata, T., Yamauchi-Sato, Y., Yamamoto, T., Ogita, K., Suzuki, T., and Miyazawa, T. (2004) Oxidation Rate of Conjugated Linoleic Acid and Conjugated Linolenic Acid Is Slowed by Triacylglycerol Esterification and α-Tocopherol, *Lipids 39*, 475–480.
16. Tsuzuki, T., Tokuyama, Y., Igarashi, M., Nakagawa, K., Ohsaki, Y., Komai, M., and Miyazawa, T. (2004) α-Eleostearic Acid (9Z11E13E-18:3) Is Quickly Converted to Conjugated Linoleic Acid (9Z11E-18:2) in Rats, *J. Nutr. 134*, 2634–2639.
17. Fleming, I., and Higgins, D. (1998) Stereocontrol in Organic Synthesis Using Silicon-Containing Compounds. A Synthesis of (±)-Carbacyclin Analogue with the Geometry of the Exocyclic Double Bond Controlled by the Protodesilylation of Allylsilane, *Perkin Trans. 1*, 2673–2678.
18. Pohnert, G., and Boland, W. (2000) Highly Efficient One-Pot Double-Wittig Approach to Unsymmetrical (1Z,4Z,7Z)-Homoconjugated Trienes, *Eur. J. Org. Chem. 2000*, 1821–1826.
19. Heintzelman, G.R., Fang, W.-K., Keen, S.P., Wallace, G.A., and Weinreb, S.M. (2002) Stereoselective Total Syntheses and Assignment of Stereochemistry of the Freshwater Cyanobacterial Hepatotoxins Cylindrospermopsin and 7-Epicylindrospermopsin, *J. Am. Chem. Soc. 124*, 3939–3945.
20. Helrich, K. (1990) Acids (polyunsaturated) in Oil and Fats, in *Official Methods of Analysis of the Association of Official Analytical Chemists*, pp. 960–963, Arlington.
21. Pitt, G.A.J., and Morton, R.A. (1957) Ultra-violet Spectrophotometry of Fatty Acids, *Prog. Chem. Fats Other Lipids 4*, 227–278.
22. Ishiyama, M., Tominaga, H., Shiga, M., Sasamoto, K., Ohkura, Y., and Ueno, K. (1996) A Combined Assay of Cell Viability and *in vitro* Cytotoxicity with a Highly Water-Soluble Tetrazolium Salt, Neutral Red and Crystal Violet, *Biol. Pharm. Bull. 19*, 1518–1520.
23. Gapinski, D.M., Roman, C.R., Rinkema, L.E., and Fleisch, J.H. (1988) Leukotriene Receptor Antagonists. 4. Synthesis and Leukotriene D4/E4 Receptor Antagonist Activity of 4-(Alkyl)acetophenone Derivatives, *J. Med. Chem. 31*, 172–175.
24. Miller, A., Stanton, C., and Devery, R. (2002) *Cis* 9,*trans* 11- and *trans* 10,*cis* 12-Conjugated Linoleic Acid Isomers Induce Apoptosis in Cultured SW480 Cells, *Anticancer Res. 22 (6C)*, 3879–3887.
25. Cave, W.T., Jr. (1991) Dietary n-3 (ω-3) Polyunsaturated Fatty Acid Effects on Animal Tumorigenesis, *FASEB J. 5*, 2160–2166.
26. Esterbauer, H. (1993) Cytotoxicity and Genotoxicity of Lipid-Oxidation Products, *Am. J. Clin. Nutr., 57*, 779S–786S.
27. Grune, T., Siems, W.G., Zollner, H., and Esterbauer, H. (1994) Metabolism of 4-Hydroxynonenal, a Cytotoxic Lipid Peroxida-

tion Product, in Ehrlich Mouse Ascites Cells at Different Proliferation Stages, *Cancer Res. 54*, 5231–5235.

28. Sandstrom, P.A., Tebbey, P.W., Van Cleave, S., and Buttke, T.M. (1994) Lipid Hydroperoxides Induce Apoptosis in T Cells Displaying a HIV-Associated Glutathione Peroxidase Deficiency. *J. Biol. Chem. 269*, 798–801.

29. Sandstrom, P.A., Pardi, D., Tebbey, P.W., Dudek, R.W., Terrian, D.M., Folks, T.M., and Buttke, T.M. (1995) Lipid Hydroperoxide-Induced Apoptosis: Lack of Inhibition by Bcl-2 Over-expression, *FEBS Lett. 365*, 66–70.

30. Aoshima, H., Satoh, T., Sakai, N., Yamada, M., Enokiko, Y., Ikeuchi, T., and Hatanaka, H. (1997) Generation of Free Radicals During Lipid Hydroperoxide-Triggered Apoptosis in PC12h Cells, *Biochim. Biophys. Acta, 1345*, 35–42.

31. Ji, C., Rouzer, C.A., Marnett, L.J., and Pietenpol, J.A. (1998) Induction of Cell Cycle Arrest by the Endogenous Product of Lipid Peroxidation, Malondialdehyde, *Carcinogenesis 19*, 1275–1283.

32. Cheeseman, K.H., Collins, M., Proudfoot, K., Slater, T.F., Burton, G.W., Webb, A.C., and Ingold, K.U. (1986) Studies on Lipid Peroxidation in Normal and Tumor Tissues, *Biochem. J. 235*, 507–514.

33. Tisdale, M., and Mahmoud, M.B. (1983) Activities of Free Radical Metabolizing Enzymes in Tumors, *Br. J. Cancer 47*, 809–812.

Production and Protein Kinase C Activation of Diacylglycerols Containing Polymethylene-Interrupted PUFA

Jun-ichi Morishige, Yoshimichi Takai, Kaoru Hirano, Tamotsu Tanaka*, and Kiyoshi Satouchi

Department of Applied Biological Science, Fukuyama University, Fukuyama 729-0292, Japan

ABSTRACT: Sciadonic acid (20:3, Δ-5c,11c,14c) is a polymethylene-interrupted PUFA (PMI-PUFA) that is present in conifer seeds and known to be incorporated into animal cells and to accumulate in membrane PI as a substitute for arachidonate. In this study, we investigated whether PI having sciadonate could serve as source of DAG that could activate protein kinase C (PKC). When Swiss 3T3 cells cultured with sciadonic acid were stimulated with 100 nM of bombesin, 1-stearoyl-2-sciadonoyl-glycerol (G) and 1-stearoyl-2-arachidonoyl-G were produced. The net increments of these two molecular species of DAG reflected the levels of the two molecular species in the PI in the cells. When cells cultured with juniperonic acid (20:4, Δ-5c,11c,14c,17c) were stimulated, 1-stearoyl-2-juniperonoyl-G was produced in proportion to the level of this molecular species in PI in the cells. We also examined PKC activation by synthetic DAG using a partially purified PKC fraction from rat brain and found that both 1-stearoyl-2-sciadonoyl-G and 1-stearoyl-2-juniperonoyl-G could activate PKC comparably to 1-stearoyl-2-arachidonoyl-G. These results indicate that 1-stearoyl-PI having these C_{20} PMI-PUFA residues can serve as sources of potential signaling molecules.

Paper no. L9613 in *Lipids* **40**, 155–162 (February 2005).

The alignment of the double bonds of typical PUFA, such as arachidonic acid (AA) and EPA, are interrupted by one methylene group. However, the alignment of the double bonds in some PUFA are interrupted by two or more methylenes. The PUFA with this characteristic alignment of double bonds are categorized as nonmethylene-interrupted PUFA or as polymethylene-interrupted-PUFA (PMI-PUFA). PMI-PUFA, such as pinolenic acid (18:3, Δ-5,9,12), sciadonic acid (20:3, Δ-5,11,14; SciA), and juniperonic acid (20:4, Δ-5,11,14,17; JA), have been shown to exist widely in coniferous plants (1-4). Currently, conifer seed oils are not directly used as dietary oils, but some kinds of conifer seeds are consumed in some countries, such as Italy, Korea, and Japan. Pasquier *et al.* (5) proposed that conifer seeds be considered as a potential source of dietary oil because dietary conifer seed oils have shown substantial lipid-lowering potential in experimental animals (6,7).

PMI-PUFA are known to serve as substrates for enzymes of glycerolipid biosynthesis and FA oxidation (8). The incorpora-tion of PMI-PUFA into membrane phospholipids of animal cells in both *in vivo* and *in vitro* experiments has been reported (5,6,9–13). Our recent investigation demonstrated that SciA (lacking the Δ8 double bond of AA) and JA (lacking the Δ8 double bond of EPA) (Scheme 1) were metabolized in a manner similar to AA and EPA, respectively, in the process of acylation to phospholipids in HepG2 cells (13). We also demonstrated that SciA is an effective substitute for arachidonate of PI in HepG2 cells (12). The *in vivo* accumulation of sciadonate in hepatic PI of mice has been demonstrated using *Platycladus orientalis* (*Biota orientalis*) seed oil, which contains only 2.9% SciA (9,10).

A well-known characteristic of PI in mammalian cells is an abundance of arachidonate. At the molecular level, PI has been reported to be composed mainly of 1-stearoyl-2-arachidonoyl species in various organs and cells of mammals (14–19). Since inositolphospholipid is a main source of DAG in cell signaling, the predominant molecular species of DAG produced during the early response to agonistic stimulation is 1-stearoyl-2-arachidonoyl-glycerol (-G) (20). Therefore, the replacement of arachidonate in membrane PI with a PMI-PUFA residue implies structural modification of the source of signaling molecules. In this study, we investigated whether molecular species of PI having a PMI-PUFA residue could serve as source of DAG. Such information is helpful for better understanding the
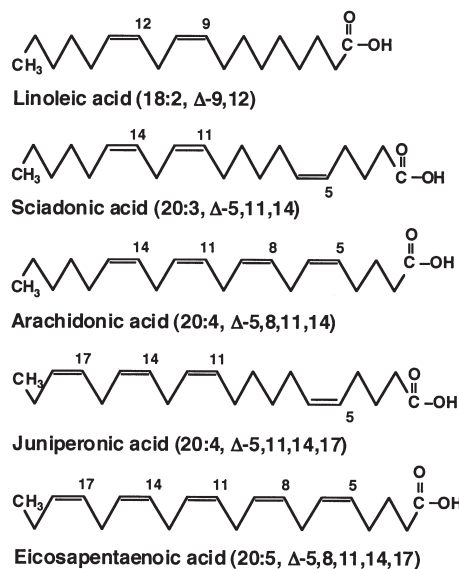
Linoleic acid (18:2, Δ-9,12)

Sciadonic acid (20:3, Δ-5,11,14)

Arachidonic acid (20:4, Δ-5,8,11,14)

Juniperonic acid (20:4, Δ-5,11,14,17)

Eicosapentaenoic acid (20:5, Δ-5,8,11,14,17)

SCHEME 1

metabolic fate of dietary PMI-PUFA and the mechanisms of the beneficial effects of PMI-PUFA-containing conifer seeds used as a traditional Chinese medicine (21). For this purpose, we conducted experiments using Swiss 3T3 cells, a well-documented cell line in the research on inositolphospholipid signaling. We also examined the efficacies of activation of protein kinase C (PKC) by synthetic DAG homologs including PMI-PUFA-containing molecular species.

MATERIALS AND METHODS

Materials. Dulbecco's modified Eagle's medium (DMEM), penicillin, streptomycin, and FBS were obtained from Gibco BRL and Life Technologies, Inc. (Rockville, MD). Essentially FA-free BSA, 1-stearoyl-2-lyso-*sn*-glycero-3-phosphocholine, bombesin, phospholipase C (PLC) (from *Bacillus cereus*), myelin basic protein from bovine brain, and histone from calf thymus were obtained from Sigma Chemical Co. (St. Louis, MO). AA, EPA, and linoleic acid were purchased from Serdary Research Laboratories (London, Ontario, Canada). [γ-^{32}P]ATP (3,000 Ci/mmol) was obtained from PerkinElmer Life Sciences, Inc. (Boston, MA). Biota and umbrella pine seeds were purchased from a nursery. The seeds were milled in methanol, and lipids were extracted by the method of Folch *et al.* (22). The lipid extract of the seeds was dissolved in 5% methanolic HCl, and FAME were prepared (23). SciA and JA were purified using argentation-TLC from FAME prepared from umbrella pine and biota seeds, respectively (23), and used after saponification. The purities of these PMI-PUFA were checked by GC and were over 98%. The double-bond positions of purified PMI-PUFA were confirmed by GC–MS, as described in Reference 23. All other reagents were of reagent grade.

Cell culture and analysis of cellular lipids. Swiss 3T3 cells obtained from the American Type Culture Collection (Manassas, VA) were plated in 100-mm plastic dishes at 4×10^5 cells/dish, and maintained in 10 mL of DMEM containing 10% FBS in a humidified atmosphere of 10% CO$_2$, 90% air at 37°C. After they had grown to confluence, 50 µM of FA was added to the cell cultures three times (12, 24, and 48 h before harvest) as a BSA complex (24). The cells were washed with PBS and harvested by trypsinization. The lipids of the cells were extracted by the method of Bligh and Dyer (25). The PI of the Swiss 3T3 cells was isolated from the lipid extract by 2-D TLC using chloroform/methanol/28% ammonia (65:35:5, by vol) for the first solvent system and chloroform/acetone/methanol/acetic acid/water (50:20:10:13:5, by vol) for second solvent system. The FA composition of the PI was analyzed by GC (Shimadzu GC-14A; Shimadzu, Kyoto, Japan) equipped with a capillary column coated with CBP 20 (0.25 µm film, 30 m length; Shimadzu) as FAME obtained by transmethylesterification (23). The carrier gas was nitrogen. The temperature of the injection/FID was set at 250°C. The initial column temperature was set at 170°C and then raised to 225°C at 5°C/min. The molecular species of the PI was determined by HPLC as a 1,2-DAG-dinitrobenzoyl derivative (DAG-DNB). A portion of the PI was hydrolyzed with PLC from *B. cereus*, and the result-

ing DAG was reacted with 3,5-DNB-chloride (26). The DAG-DNB formed was purified by TLC using hexane/diethyl ether (70:30, vol/vol) as the solvent system and analyzed by HPLC (Tosoh CCPD, Tokyo, Japan) equipped with a 0.45×25 cm Inertsil ODS-2 column (GL Science Inc., Tokyo, Japan) using acetonitrile/isopropanol (80:20, vol/vol) as the eluent (13). The molecular species of PC of Swiss 3T3 cells was analyzed as a DNB derivative by a similar method. To assign each peak, the eluate corresponding to each molecular species peak was collected, and direct FA analysis of each fraction was conducted by GC after transmethylesterification of DAG-DNB as described above. The trypan blue exclusion test showed that there was no significant difference in cell viability among the cells cultured with various PUFA.

DAG-production assay. Swiss 3T3 cells cultured with various FA (linoleic acid, SciA, JA, or EPA) were washed, harvested and suspended in a buffer consisting of 20 mM HEPES (pH 7.4), 115 mM NaCl, 5.4 mM KCl, 0.8 mM MgCl$_2$, 1.8 mM CaCl$_2$, and 13.8 mM glucose (buffer A) at density of 1×10^6 cells/mL. After 3 min of preincubation, the suspension (4 mL) of cells was incubated with 100 nM bombesin for 10 s under continuous stirring at 37°C. Then, the cell suspension was mixed with 15 mL of a mixture of chloroform/methanol (1:2, vol/vol) and 540 pmol of 1,2-distearoyl-G as an internal standard, and sonicated for 30 s. Lipids were extracted by the method of Bligh and Dyer (25). The 1,2-DAG was isolated from the lipid extract by TLC using hexane/diethyl ether/acetic acid (20:80:1, by vol) as the solvent system. The purified 1,2-DAG was converted to DAG-DNB and analyzed by HPLC as described above. Peaks in the chromatograms were assigned from the data obtained in the molecular species analyses of PC and PI of Swiss 3T3 cells. Amounts of each molecular species of DAG were determined based on the peak area relative to that of the DNB-derivative of 1,2-distearoyl-G as the internal standard.

Synthesis of DAG. DAG for PKC assay were prepared by hydrolysis of synthetic PC with PLC (27). Briefly, AA, SciA, JA, or EPA was converted to its respective fatty acyl chloride by treatment with oxalyl chloride at 4°C for 3 h in the dark. 1-Stearoyl-2-lyso-*sn*-glycero-3-phosphocholine suspended in dry hexamethylphosphoric triamide was allowed to react with the fatty acyl chloride at 4°C for 24 h in the dark. The resultant PC was purified by TLC using chloroform/methanol/water (65:35:6, by vol) as the solvent system. The purities of the PC having SciA or JA, novel PC synthesized in this study, were confirmed by matrix-assisted laser desorption/ionization time-of-flight MS in a Voyager DE STR (Applied Biosystems, Framingham, MA,) using 2,5-dihydroxybenzoic acid as a matrix (28). 1-Stearoyl-2-sciadonoyl-PC and 1-stearoyl-2-juniperonoyl-PC gave a set of three intense signals of [M + H]$^+$, [M + Na]$^+$, and [M + K]$^+$ at *m/z* 812.6, 834.6, and 850.6 (sciadonoyl-PC) and *m/z* 810.6, 832.6, and 848.6 (juniperonoyl-PC), respectively. DAG was obtained by digestion of the PC with PLC from *B. cereus*. The resultant DAG was used for PKC assay after purification by TLC using hexane/diethyl ether/acetic acid (20:80:1, by vol) as the solvent system. The amount of DAG was determined by GC using heptadecanoic acid as the internal standard.

Preparation of PKC fraction. The PKC fraction was prepared from rat brain soluble fractions (29). Male Wistar rats (250 g body weight) were anesthetized with diethyl ether and sacrificed by decapitation. The whole brains (1.5–1.6 g each) from eight rats were homogenized in a Potter-Elvehjem glass-Teflon homogenizer with 160 mL of buffer consisting of 25 mM Tris-HCl (pH 7.5), 50 mM 2-mercaptoethanol, 2 mM EGTA, 1 mM PMSF, and 0.25 M sucrose. The homogenate was centrifuged for 90 min at $75,000 \times g$. The supernatant was applied to a DEAE-cellulofine column (2.5×11 cm; Seikagaku Kogyo, Tokyo, Japan), which was equilibrated beforehand with a buffer consisting of 25 mM Tris-HCl (pH 7.5), 50 mM 2-mercaptoethanol, and 2 mM EGTA (buffer B). After washing the column with 200 mL of buffer B at a flow rate of 0.7 mL/min, proteins retained in the column were eluted by the application of 400 mL of a linear NaCl gradient (0–400 mM) in buffer B at a flow rate of 0.5 mL/min. The eluate was fractionated (7 mL each), and the absorbance at 280 nm and PKC activities of each fraction were measured as described below.

PKC assay. 1-Stearoyl-2-oleoyl-*sn*-glycero-3-phosphoserine (PS) (62.5 nmol) and DAG (15.5 nmol) in a mixture of chloroform/methanol (1:1,vol/vol) were placed in a round-bottomed tube, and the solvents were removed under reduced pressure in a rotary evaporator. The resulting thin films of mixed lipids were suspended in 1 mL of 125 mM Tris-HCl buffer (pH 7.4) by vortexing. The suspension was then sonicated for 1 min in a bath-type sonicator (200 W, 42 kHz) at 25°C. A PKC assay was conducted with the resulting lipid vesicles. The reaction mixture (50 μL) contained 25 mM Tris-HCl (pH 7.4), 5 mM $MgCl_2$, 1 μM $CaCl_2$, 25 μg of calf thymus histone, 10 μM $[\gamma$-$^{32}P]ATP$ (0.5 μCi), lipid vesicles (12.5 μM PS and 3.1 μM DAG), and 3 μg protein of the PKC fraction. In the experiment using myelin basic protein from bovine brain (25 μg) as the PKC substrate, 1.5 μg protein of the PKC fraction was used. The reaction was started by addition of the PKC fraction. After incubation for 5 min at 30°C, the reaction was terminated by addition of 20 mM ATP (50 μL), and 50 μL of the mixture was spotted on P-81 ion-exchange paper (Whatman). The paper was washed three times with 75 mM phosphoric acid solution and dried for 1 h at 80°C. The radioactivity of the phosphorylated proteins that were adsorbed on the paper was measured by liquid scintillation counting.

RESULTS

Bombesin-induced DAG-production in Swiss 3T3 cells cultured with various PUFA. Bombesin has been reported to be a potent stimulator that induces biphasic DAG generation (30). In a time-course experiment using Swiss 3T3 cells labeled with $[^3H]AA$, the highest DAG production was observed at 10 s of incubation with 100 nM of bombesin (data not shown). Therefore, the DAG-production assay of Swiss 3T3 cells cultured with or without (control) various PUFA was conducted in this condition. The amounts of each DAG molecular species were determined by HPLC using 1,2-distearoyl-G as the internal standard (Figs. 1,2). Although the FA profile of PI in animal

tissues shows an abundance of arachidonate, the PI of the control cells had molecular species containing not only AA but also oleic acid (18:1, Δ-9) and Mead acid (20:3, Δ-5,8,11; MA) (Table 1). The abundance of n-9 series unsaturated FA in membrane lipids indicated that the cells without FA supplementation were in a condition of FA deficiency and that MA compensated for the AA deficiency in PI. The DAG-production assay revealed that both 1-stearoyl-2-arachidonoyl-G and 1-stearoyl-G containing MA increased markedly in control cells stimulated with bombesin (Fig. 1). The net increments of 1-stearoyl-2-arachidonoyl-G and 1-stearoyl-G containing MA were calculated to be 115 and 78 pmol/4×10^6 cells, respectively (Fig. 2). The ratio of the amounts of these DAG (approximately 1:1) reflected the abundance of corresponding molecular species in the PI (22 and 20%, respectively) of control cells (Table 1). We confirmed here that DAG produced under our assay conditions were PI-derived, because both AA and MA were scarcely detected in the PC of the control cells (data not shown). Similar experimental results using Swiss 3T3 cells have been reported by Pettitt and Wakelam (31).

When the cells were cultured with linoleic acid, the level of 1-stearoyl-2-arachidonoyl-PI increased markedly (64%) (Table 1). Consistent with changes in the molecular species composition of PI, only the molecular species 1-stearoyl-2-arachidonoyl-G increased, from 76 to 209 pmol/4×10^6 cells, upon the stimulation with bombesin (Figs. 1,2).

As seen in HepG2 cells (13), SciA was available as an acyl group of PI in Swiss 3T3 cells. As a result, 1-stearoyl-2-sciadonoyl-PI emerged in place of 1,2-dioleoyl-PI and 1-stearoyl-PI containing MA (Table 1). The HPLC analysis of DAG-DNB prepared from cells cultured with SciA showed that the levels of 1-stearoyl-2-arachidonoyl-G and the mixture of 1-stearoyl-2-sciadonoyl-G + 1,2-dipalmitoyl-G increased on bombesin stimulation (Figs. 1,2). Almost all the increments in the level of the latter mixed DAG were considered attributable to the increase in the amount of 1-stearoyl-2-sciadonoyl-G, because 1,2-dipalmitoyl species did not exist in the PI of SciA-supplemented cells, and the level of 1,2-dipalmitoyl-G in other cells was not changed much by agonistic stimulation. Accordingly, the net increment of 1-stearoyl-2-sciadonoyl-G could be estimated as 98 pmol/4×10^6 cells, which was approximately twice the increment of 1-stearoyl-2-arachidonoyl-G (54 pmol/4×10^6 cells). The relative amounts of these DAG reflected the abundance of corresponding molecular species in PI (22 and 38%, respectively) in the cells cultured with SciA. This result indicated that PI having sciadonate is used as a source of DAG equally to PI having arachidonate.

Like SciA, JA was extensively acylated to PI in Swiss 3T3 cells. As a result, 1-stearoyl-2-juniperonoyl-PI constituted 42% of the total molecular species of PI (Table 1). When the cells were stimulated with bombesin, two molecular species of DAG, namely 1-stearoyl-2-arachidonoyl-G and 1-stearoyl-2-juniperonoyl-G, were produced (Figs. 1,2). The net increments of these DAG were calculated to be 46 and 87 pmol/4×10^6 cells, respectively. The ratio of the amounts of these DAG (approximately 1:2) reflected the abundance of corresponding mo-
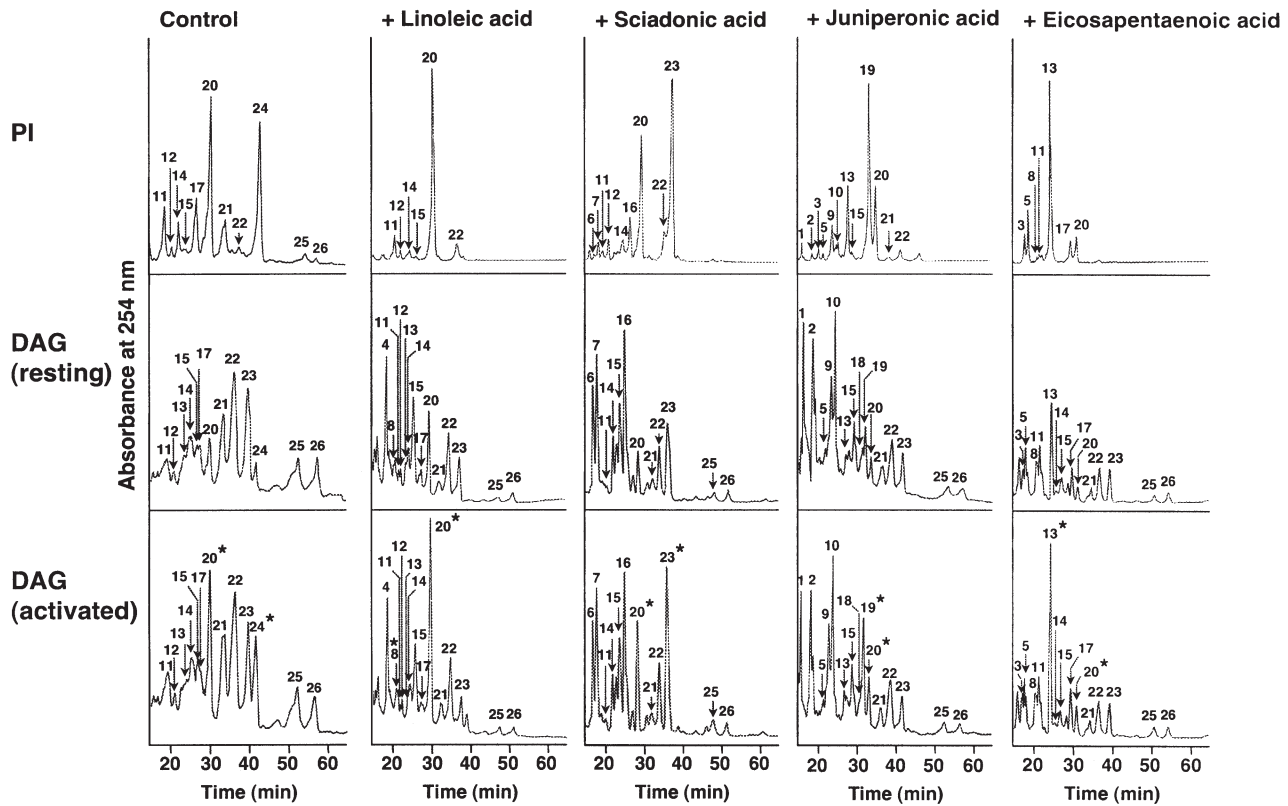
FIG. 1. HPLC of dinitrobenzoyl (DNB) derivatives of PI and DAG obtained from Swiss 3T3 cells cultured with or without PUFA. Swiss 3T3 cells cultured without fa (control) or with 50 μM PUFA were incubated with (activated) or without (resting) 100 nM of bombesin for 10 s. The lipids were extracted after addition of 1,2-distearoyl-glycerol (-G) as an internal standard. The isolated DAG was converted to a DNB derivative and analyzed by HPLC. The DNB derivative of 1,2-distearoyl-G was eluted at 80 min. HPLC of the DNB derivative of PI isolated from the resting cells is also shown. Peaks observed in the molecular species analysis of PI and PC were assigned by direct analysis with GC after transmethylesterification. From these data, peaks in the chromatograms of DAG were assigned. The numbers above peaks correspond to the peak numbers of molecular species shown in Table 1 and Figure 2. An asterisk (*) indicates significantly increased from resting cells.

lecular species in the PI (15 and 42%, respectively) in the cells cultured with JA (Table 1).

Similar experiments were conducted with EPA. 1-Stearoyl-2-eicosapentaenoyl-PI was the predominant molecular species (53%) of PI in cells cultured with EPA (Table 1). In these cells, 1-stearoyl-2-arachidonoyl-PI constituted only 9% of the total molecular species of PI. Consistent with this profile of the molecular species of PI, the predominant molecular species of DAG produced due to the stimulation was 1-stearoyl-2-eicosapentaenoyl-G. The increments of 1-stearoyl-2-arachidonoyl-G and 1-stearoyl-2-eicosapentaenoyl-G were estimated to be 16 and 99 pmol/4×10^6 cells, respectively (Figs. 1,2). The relative productions of these DAG (approximately 1:6) were in good agreement with the abundance of each molecular species in PI in the cells.

Activation of PKC by synthetic DAG homologs. We examined the efficacies of PKC activation by DAG having PMI-PUFA residues (Table 2). Because of the low activity of the enzyme, efficacies of PKC activation by different DAG could not be determined using commercially obtained PKC. Therefore, the enzyme fraction used here was prepared from rat brain cytosol using DEAE ion-exchange coumn chromatography by the method reported by Inagaki *et al.* (29). The fraction with the

highest PKC activity was eluted from the column at 150 mM NaCl and used for the PKC assay after appropriate dilution. This PKC fraction has been shown to contain cPKC as major isoenzymes (32). In fact, the PKC activity was found to be highly dependent on cofactors (Figs. 3A,B): It required >10 μM PS, >6 μM 1-stearoyl-2-arachidonoyl-G, and >1 μM Ca^{2+}. On the basis of these results, the assay was conducted in the presence of 12.5 μM of PS, 3.1 μM of synthetic DAG, and 1 μM of Ca^{2+}. The potencies of DAG for PKC activation were examined using histone or myelin basic protein as the substrate (Table 2). Although actual PKC activities were higher in the experiments with myelin basic protein than those with histone in all DAG species, the relative potencies of DAG were essentially similar with both substrates. The DAG with the highest potency for activation of the PKC fraction was 1-stearoyl-2-arachidonoyl-G. In contrast, DAG having a palmitoyl (*sn*-1) or linoleoyl group (*sn*-2) were poor activators, indicating that the structural requirement of DAG for PKC activation could be determined under our assay condition. The levels of PKC activation by both 1-stearoyl-2-sciadonoyl-G and 1-stearoyl-2-juniperonoyl-G were comparable to that by 1-stearoyl-2-arachidonoyl-G. We also prepared mixed DAG vesicles containing 1-stearoyl-2-arachidonoyl-G and 1-stearoyl-G having C_{20}
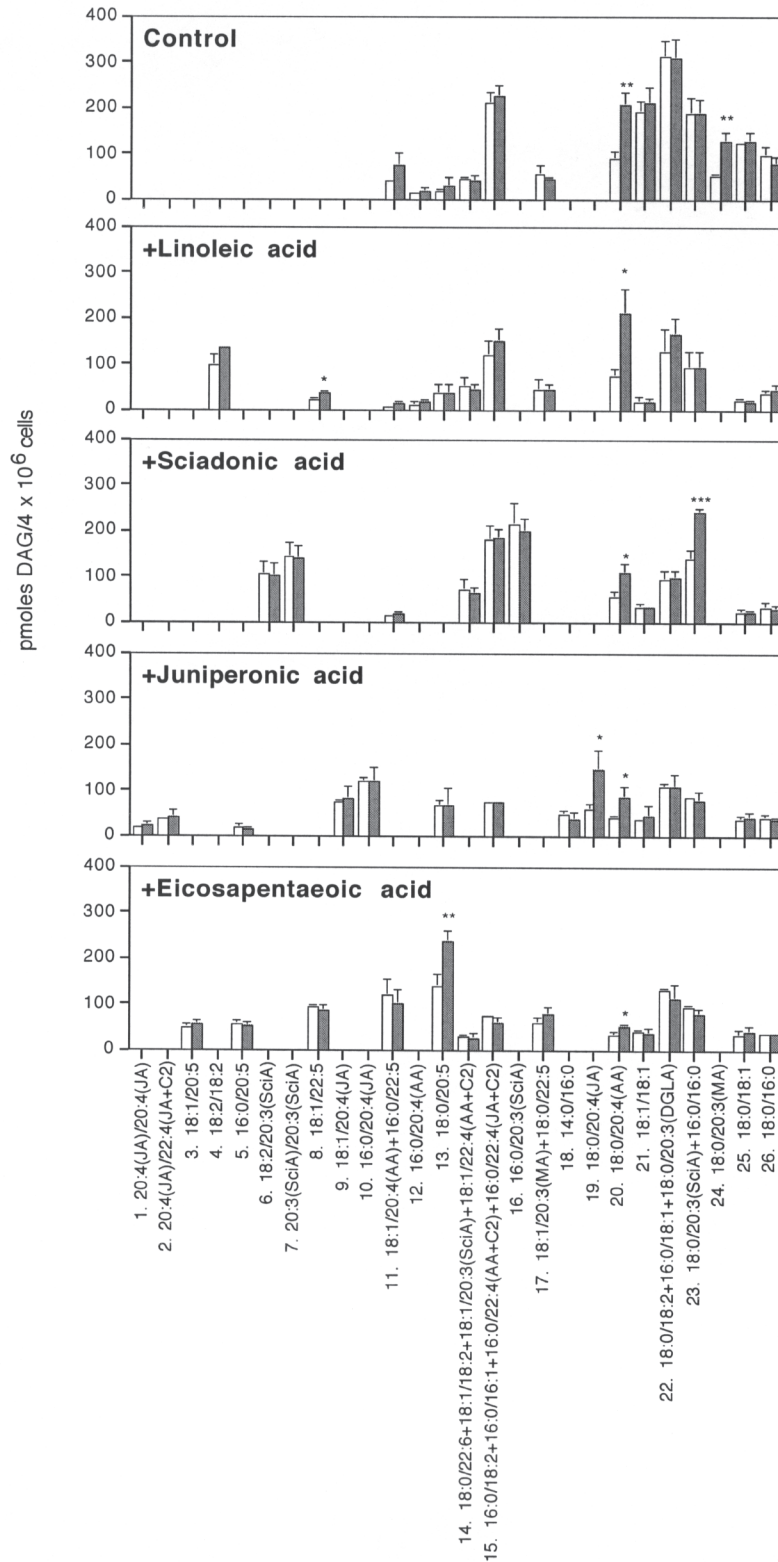
FIG. 2. Bombesin-induced DAG-production in Swiss 3T3 cells cultured with various PUFA. Swiss 3T3 cells cultured without or with 50 μM PUFA were incubated with (hatched bar) or without (open bar) 100 nM bombesin for 10 s. DAG isolated from the cells were analyzed by HPLC as shown in Figure 1, and the amounts of each DAG were determined on the basis of the peak area relative to that of DNB of 1,2-distearoyl-G as internal standard. Values are expressed as pmol/4 × 10^6 cells ± SD from three independent experiments. JA, juniperonic acid; SciA, sciadonic acid; AA, arachidonic acid; MA, Mead acid; DGLA, dihomo-γ-linolenic acid; +C2, chain-elongated metabolite. For other abbreviation see Figure 1. *, **, ***Significantly different from resting cells using Student's *t*-test (*$P < 0.05$, **$P < 0.01$, ***$P < 0.001$).

TABLE 1
Molecular Species of PI in Swiss 3T3 Cells Cultured with Various PUFA[a]

No.	Molecular species	Control	Linoleic acid	Sciadonic acid	Juniperonic acid	Eicosapentaenoic acid
				Cells cultured in the presence of:		
				%		
1.	20:4(JA)/20:4(JA)	N.D.[a]	N.D.	N.D.	2.4 ± 1.1	N.D.
2.	20:4(JA)/22:4(JA+C2)	N.D.	N.D.	N.D.	1.2 ± 0	N.D.
3.	18:1/20:5	N.D.	N.D.	N.D.	1.4 ± 1.0	6.5 ± 2.4
4.	18:2/18:2	N.D.	N.D.	N.D.	N.D.	N.D.
5.	16:0/20:5	N.D.	N.D.	N.D.	1.2 ± 0.1	8.0 ± 3.4
6.	18:2/20:3(SciA)	N.D.	N.D.	1.1 ± 0.3	N.D.	N.D.
7.	20:3(SciA)/20:3(SciA)	N.D.	N.D.	3.0 ± 0.8	N.D.	N.D.
8.	18:1/22:5	N.D.	N.D.	N.D.	N.D.	3.2 ± 2.5
9.	18:1/20:4(JA)	N.D.	N.D.	N.D.	6.5 ± 1.2	N.D.
10.	16:0/20:4(JA)	N.D.	N.D.	N.D.	7.8 ± 1.6	N.D.
11.	18:1/20:4(AA) +16:0/22:5	7.4 ± 0.7	6.4 ± 1.8	2.0 ± 1.0	N.D.	2.1 ± 0.3
12.	16:0/20:4(AA)	1.6 ± 0.3	3.5 ± 1.0	2.3 ± 0.9	N.D.	N.D.
13.	18:0/20:5	N.D.	N.D.	N.D.	10.3 ± 3.9	53.0 ± 2.4
14.	18:0/22:6+18:1/18:2 +18:1/20:3(SciA) +18:1/22:4(AA+C2)	3.9 ± 0.6	4.7 ± 0.5	7.6 ± 1.7	N.D.	N.D.
15.	16:0/18:2+16:0/16:1 +16:0/22:4(AA+C2) +16:0/22:4(JA+C2)	2.7 ± 0.5	1.2 ± 0.3	N.D.	1.7 ± 0.4	N.D.
16.	16:0/20:3(SciA)	N.D.	N.D.	6.5 ± 2.5	N.D.	N.D.
17.	18:1/20:3(MA) +18:0/22:5	8.8 ± 1.6	N.D.	N.D.	N.D.	8.5 ± 1.2
18.	14:0/16:0	N.D.	N.D.	N.D.	N.D.	N.D.
19.	18:0/20:4(JA)	N.D.	N.D.	N.D.	42.3 ± 5.2	N.D.
20.	18:0/20:4(AA)	22.0 ± 4.9	63.7 ± 4.7	22.1 ± 3.7	14.5 ± 0.1	8.9 ± 1.5
21.	18:1/18:1	9.9 ± 3.9	N.D.	N.D.	0.8 ± 0.7	N.D.
22.	18:0/18:2+16:0/18:1 +18:0/20:3(DGLA)	3.4 ± 2.1	7.0 ± 0.7	6.1 ± 0.8	3.7 ± 0.4	N.D.
23.[b]	18:0/20:3(SciA)	N.D.	N.D.	38.4 ± 2.6	N.D.	N.D.
24.	18:0/20:3(MA)	20.2 ± 2.9	N.D.	N.D.	N.D.	N.D.
25.	18:0/18:1	3.2 ± 1.2	N.D.	N.D.	N.D.	N.D.
26.	18:0/16:0	1.1 ± 0.4	N.D.	N.D.	N.D.	N.D.

[a]The peak number corresponds to the number of molecular species shown in Figures 1 and 2. Values are percentages of the total molecular species, means ± SD (three or four harvests of cells). AA, arachidonic acid; SciA, sciadonic acid; JA, juniperonic acid; MA, Mead acid; DGLA, dihomo-γ-linolenic acid; +C2, chain-elongated metabolite. N.D., not detected.
[b]Judging from the GC analysis, peak 23 did not contain 16:0/16:0 at significant concentration.

PMI-PUFA residue at a molar ratio 1:1 and used them for PKC assay. The results showed that the relative potencies of the mixture of 1-stearoyl-2-arachidonoyl-G and 1-stearoyl-2-sciadonoyl-G, and the mixture of 1-stearoyl-2-arachidonoyl-G and 1-stearoyl-2-juniperonoyl-G were 100 and 91%, respectively, compared with that of 1-stearoyl-2-arachidonoyl-G alone. These results indicated that the potencies of 1-stearoyl-G having C_{20} PMI-PUFA residues are comparable to that of 1-stearoyl-2-arachidonoyl-G.

DISCUSSION

Previously, we demonstrated that SciA, an n-6 series C_{20} PMI-PUFA, is an effective substitute for AA residue of PI in HepG2 cells (12,13). The accumulation of SciA in PI has been observed in mice fed biota seed oil, which contains 2.9% SciA (9,10). In this study using Swiss 3T3 cells, supplementation of SciA to cells caused enrichment of newly formed 1-stearoyl-2-sciadonoyl-PI, which was the most abundant molecular species in PI (38%) (Table 1). Although our previous study with HepG2

cells showed that neither JA nor EPA accumulated in PI at levels similar to SciA (13), these n-3 PUFA were effectively acylated to PI in Swiss 3T3 cells (Table 1). The reason for the difference in the metabolic behaviors of these n-3 PUFA in HepG2 cells and Swiss 3T3 cells is unknown, but it might be ascribed to differences in the substrate specificity of enzymes, such as acyl CoA:1-acyl-2-lyso-PI acyltransferase, CoA-dependent transacylase, and enzymes involved in the phosphoinositide cycle, responsible for biosynthesis of PI in the respective cell lines. In any event, supplementation of SciA and JA to Swiss 3T3 cells modified the molecular species composition of PI extensively.

A portion of PI in the membrane is metabolized by PI 4-kinase and PI 5-kinase. The resulting PIP_2 is hydrolyzed by activated PLC in response to the agonistic stimulation. Our results indicated that 1-stearoyl-2-sciadonoyl-PI is sequentially metabolized by these PI-kinases and PLC in a similar manner to 1-stearoyl-2-arachidonoyl-PI, because 1-stearoyl-2-sciadonoyl-G and 1-stearoyl-2-arachidonoyl-G were produced in response to stimulation with bombesin in proportion to the level of each molecular species in PI of the cells cultured with SciA. This was

TABLE 2
Efficacy of PKC Activation of Various DAG[a]

DAG molecular species	PKC activity	
	Histone	Myelin basic protein
	nmol/mg protein (%)	
18:0/20:4(AA)	13.5 ± 1.3 (100)	37.0 ± 3.0 (100)
18:0/20:3(SciA)	12.5 ± 0.5 (93)	35.8 ± 2.0 (97)
18:0/20:4(JA)	12.7 ± 1.4 (94)	34.7 ± 2.8 (94)
18:0/20:5	11.1 ± 0.5[b] (82)	30.7 ± 2.8[b] (83)
18:1/18:1	10.8 ± 0.7[b] (80)	35.8 ± 2.6 (97)
18:0/18:2	11.6 ± 0.5[b] (86)	25.3 ± 1.7[b] (68)
16:0/18:1	9.3 ± 0.9[b] (69)	28.1 ± 1.9[b] (76)
16:0/18:2	9.0 ± 0.7[b] (67)	28.9 ± 1.4[b] (78)
16:0/20:4(AA)	10.3 ± 0.7[b] (76)	28.8 ± 1.6[b] (78)

[a]Protein kinase C (PKC) assay was conducted in the presence of $CaCl_2$ (1 µM), PS (12.5 µM), DAG (3.1 µM), and calf thymus histone (25 µg/0.05 mL) or bovine brain myelin basic protein (25 µg/0.05 mL) as described in the Materials and Methods section. The partially purified PKC fraction from rat brain (3 and 1.5 µg protein/0.05 mL) was used for the experiments with histone and myelin basic protein, respectively. Data are expressed as nmol per 5 min per mg protein, means ± SD, from three to ten independent assays. Values in parentheses are the percentage of PKC activity with 1-stearoyl-2-arachidonoyl-glycerol. For abbreviations see Table 1.
[b]Significantly different from 1-stearoyl-2-arachidonoyl-glycerol using Student's t-test, $P < 0.001$.

also the case for the 1-stearoyl-2-juniperonoyl-PI. From these observations, it is possible to conclude that 1-stearoyl-PI containing these C_{20} PMI-PUFA localize at the cell membrane in a manner similar to 1-stearoyl-2-arachidonoyl-PI, and that PI-kinases and PLC in Swiss 3T3 cells do not discriminate the structural differences between AA residue and SciA or JA residue in inositolphospholipids.

In this study, we showed that the most potent activator of the PKC fraction was 1-stearoyl-2-arachidonoyl-G, the predominant molecular species in PI in various organs and mammalian cells (14–19). Although the level of activation of the PKC fraction by 1-stearoyl-2-eicosapentaenoyl-G was somewhat lower than that by 1-stearoyl-2-arachidonoyl-G, as re-

ported by Marignani *et al*. (33) and Madani *et al*. (34), both 1-stearoyl-2-sciadonoyl-G and 1-stearoyl-2-juniperonoyl-G activated the PKC fraction comparably to 1-stearoyl-2-arachidonoyl-G. The activation of PKC in living cell is a complicated process. The specific anchoring protein (35) and free PUFA (36) are reported to mediate PKC translocation, and its phosphorylation modulates the activity of PKC (37). Because our data on PKC activation are limited to the *in vitro* condition, the possibilities that processes of translocation of PKC or interaction with the PKC substrate are affected in the cells treated with PMI-PUFA cannot be ruled out, but the results presented above indicate that the PKC used in our assay do not discriminate the structural difference between the arachidonate and C_{20} PMI-PUFA residues in DAG molecules.

In conclusion, we found that PI having sciadonate or juniperonate are converted to DAG with similar efficacy as PI having arachidonate. The resulting DAG having these C_{20} PMI-PUFA residues were shown to be potent activators for the PKC fraction. It is thus possible to consider that PI having these C_{20} PMI-PUFA residues can serve as sources of potential signaling molecules.

FIG. 3. Characterization of protein kinase C (PKC) fraction obtained from rat brain cytosol. The PKC fraction was prepared from rat brain cytosol by DEAE ion-exchange column chromatography. PKC activity was measured using the fraction (3 µg protein/0.05 mL) with the highest PKC activity in the presence of 12.5 µM PS, 1 µM $CaCl_2$ and various concentrations of 1-stearoyl-2-arachidonoyl-G (A), or in the presence of 1.55 µM 1-stearoyl-2-arachidonoyl-G, 1 µM $CaCl_2$, and various concentrations of PS (B). In both experiments, calf thymus histone (25 µg/0.05 mL) was used as the PKC substrate. Data are expressed as nmol per 5 min per mg protein, means ± SD, from experiments performed in duplicate. For other abbreviation see Figure 1.

ACKNOWLEDGMENTS

REFERENCES

1. Smith, C.R., Jr. (1970) Occurrence of Unusual Fatty Acids in Plants, in *Progress in Chemistry of Fats and Other Lipids* (Holman, R.T., ed.), Vol. 11, Part 1, pp. 137–177, Pergamon Press, London.
2. Takagi, T., and Itabashi, Y. (1982) *cis*-5-Olefinic Unusual Fatty Acids in Seed Lipids of Gymnospermae and Their Distribution in Triacylglycerols, *Lipids 17*, 716–723.

3. Wolff, R.L. (1998) Sources of 5,11,14-20:3 (Sciadonic) Acid, a Structural Analog of Arachidonic Acid, *J. Am. Oil. Chem. Soc. 75*, 1901-1902.

4. Wolff, R.L., Deluc, L.G., and Marpeau A.M. (1996) Conifer Seeds: Oil Content and Fatty Acid Composition, *J. Am. Oil. Chem. Soc. 73*, 765–771.

5. Pasquier, E., Ratnayake, W.M.N., and Wolff, R.L. (2001) Effects of Δ5 Polyunsaturated Fatty Acids of Maritime Pine (*Pinus pinaster*) Seed Oil on the Fatty Acid Profile of the Developing Brain of Rats, *Lipids 36*, 567–574.

6. Ikeda, I., Oka, T., Koba, K., Sugano, M., and Lie Ken Jie, M.S.F. (1992) 5*c*,11*c*,14*c*-Eicosatrienoic Acid and 5*c*,11*c*, 14*c*,17*c*-Eicosatetraenoic Acid of *Biota orientalis* Seed Oil Affect Lipid Metabolism in the Rat, *Lipids 27*, 500–504.

7. Asset, G., Staels, B., Wolff, R.L., Bauge, E., Madj, Z., Fruchart, J-C., and Dallongeville, J. (1999) Effects of *Pinus pinaster* and *Pinus koraiensis* Seed Oil Supplementation on Lipoprotein Metabolism in the Rat, *Lipids 34*, 39–44.

8. Ide, T., Murata, M., and Sugano, M. (1995) Octadecatrienoic Acids as the Substrates for the Key Enzymes in Glycerolipid Biosynthesis and Fatty Acid Oxidation in Rat Liver, *Lipids 30*, 755–762.

9. Berger, A., and German, J. B. (1991) Extensive Incorporation of Dietary Δ-5,11,14 Eicosatrienoate into the Phosphatidylinositol Pool, *Biochim. Biophys. Acta 1085*, 371–376.

10. Berger, A., Fenz, R., and German, J.B. (1993) Incorporation of Dietary 5,11,14-Icosatrienoate into Various Mouse Phospholipid Classes and Tissues, *J. Nutr. Biochem. 4*, 409–419.

11. Chen, Q., Yin, F.Q., and Sprecher, H. (2000) The Questionable Role of a Microsomal Δ8 Acyl-CoA-Dependent Desaturase in the Biosynthesis of Polyunsaturated Fatty Acids, *Lipids 35*, 871–879.

12. Tanaka, T., Takimoto, T., Morishige, J., Kikuta, Y., Sugiura, T., and Satouchi, K. (1999) Non-Methylene-Interrupted Polyunsaturated Fatty Acids: Effective Substitute for Arachidonate of Phosphatidylinositol, *Biochem. Biophys. Res. Commun. 264*, 683–688.

13. Tanaka, T., Morishige, J., Takimoto, T., Takai, Y., and Satouchi, K. (2001) Metabolic Characterization of Sciadonic Acid (5*c*,11*c*,14*c*-Eicosatrienoic acid) as an Effective Substitute for Arachidonate of Phosphatidylinositol, *Eur. J. Biochem. 268*, 4928–4939.

14. Kurvinen, J.-P., Kuksis, A., Sinclair, A.J., Abedin, L., and Kallio, H. (2000) The Effect of Low α-Linolenic Acid Diet on Glycerophospholipid Molecular Species in Guinea Pig Brain, *Lipids 35*, 1001–1009.

15. Jungalwala, F.B., Evans, J.E., and McCluer, R.H. (1984) Compositional and Molecular Species Analysis of Phospholipids by High Performance Liquid Chromatography Coupled with Chemical Ionization Mass Spectrometry, *J. Lipid Res. 25*, 738–749.

16. Patton, G.M., Fasulo, J.M., and Robins, S.J. (1982) Separation of Phospholipids and Individual Molecular Species of Phospholipids by High-Performance Liquid Chromatography, *J. Lipid Res. 23*, 190–196.

17. Takamura, H., Narita, H., Park, H.J., Tanaka, K., Matsuura, T., and Kito, M. (1987) Differential Hydrolysis of Phospholipid Molecular Species During Activation of Human Platelets with Thrombin and Collagen, *J. Biol. Chem. 262*, 2262–2269.

18. Takamura, H., Kasai, H., Arita, H., and Kito, M. (1990) Phospholipid Molecular Species in Human Umbilical Artery and Vein Endothelial Cells, *J. Lipid Res. 31*, 709–717.

19. Nakagawa, Y., Sugiura, T., and Waku, K. (1985) The Molecular Species Composition of Diacyl-, Alkylacyl- and Alkenylacylglycerophospholipids in Rabbit Alveolar Macrophages. High Amounts of 1-*O*-Hexadecyl-2-arachidonoyl Molecular Species in Alkylacylglycerophosphocholine, *Biochim. Biophys. Acta 833*, 323–329.

20. Mauco, G., Dangelmaier, C.A., and Smith, J.B. (1984) Inositol Lipids, Phosphatidate and Diacylglycerol Share Stearoylarachi-donoylglycerol as a Common Backbone in Thrombin-stimulated Human Platelets, *Biochem. J. 224*, 933–940.

21. Nishiyama, N., Chu, P.J., and Saito, H. (1995) Beneficial Effects of Biota, a Traditional Chinese Herbal Medicine, on Learning Impairment Induced by Basal Forebrain-Lesion in Mice, *Biol. Pharm. Bull. 18*, 1513–1517.

22. Folch, J., Lees, M., and Sloane-Stanley, G.H. (1957) A Simple Method for the Isolation and Purification of Total Lipids from Animal Tissues, *J. Biol. Chem. 226*, 497–509.

23. Tanaka, T., Shibata, K., Hino, H., Murashita, T., Kayama, M., and Satouchi, K. (1997) Purification and Gas Chromatographic–Mass Spectrometric Characterization of Non-Methylene Interrupted Fatty Acid Incorporated in Rat Liver, *J. Chromatogr. B 700*, 1–8.

24. Chen, Q., and Nilsson, Å. (1993) Desaturation and Chain Elongation of *n*-3 and *n*-6 Polyunsaturated Fatty Acids in the Human CaCo-2 Cell Line, *Biochim. Biophys. Acta 1166*, 193–201.

25. Bligh, E.G., and Dyer, W.J. (1959) A Rapid Method of Total Lipid Extraction and Purification, *Can. J. Biochem. Physiol. 37*, 911–917.

26. Kito, M., Takamura, H., Narita, H., and Urade, R. (1985) A Sensitive Method for Quantitative Analysis of Phospholipid Molecular Species by High-Performance Liquid Chromatography, *J. Biochem.* (Tokyo) *98*, 327–331.

27. Tanaka, T., Minamino, H., Unezaki, S., Tsukatani, H., and Tokumura, A. (1993) Formation of Platelet-Activating Factor-like Phospholipids by Fe^{2+}/Ascorbate/EDTA-Induced Lipid Peroxidation, *Biochim. Biophys. Acta 1166*, 264–274.

28. Hirano, K., Itoh, T., Morihara, H., Tanaka, T., and Satouchi, K. (1998) Cytosolic Lysophosphatidylcholine/Transacylase in the Production of Dipolyunsaturated Phosphatidylcholine in Bonito Muscle, *FEBS Lett. 437*, 193–196.

29. Inagaki, M., Watanabe, M., and Hidaka, H. (1985) *N*-(2-Aminoethyl)-5-isoquinolinesulfonamide, a Newly Synthesized Protein Kinase Inhibitor, Functions as a Ligand in Affinity Chromatography, *J. Biol. Chem. 260*, 2922–2925.

30. Cook, S.J., Palmer, S., Plevin, R., and Wakelam, M.J.O. (1990) Mass Measurement of Inositol 1,4,5-Trisphosphate and *sn*-1,2-Diacylglycerol in Bombesin-Stimulated Swiss 3T3 Mouse Fibroblasts, *Biochem. J. 265*, 617–620.

31. Pettitt, T.R., and Wakelam, M.J.O. (1993) Bombesin Stimulates Distinct Time-dependent Changes in the *sn*-1,2-Diradylglycerol Molecular Species Profile from Swiss 3T3 Fibroblasts as Analysed by 3,5-Dinitrobenzoyl Derivatization and h.p.l.c. Separation, *Biochem. J. 289*, 487–495.

32. Ohno, S., Kawasaki, H., Imajoh, S., Suzuki, K., Inagaki, M., Yokokura, H., Sakoh, T., and Hidaka, H. (1987) Tissue-specific Expression of Three Distinct Types of Rabbit Protein Kinase C, *Nature 325*, 161–166.

33. Marignani, P.A., Epand, R.M., and Sebaldt, R.J. (1996) Acyl Chain Dependence of Diacylglycerol Activation of Protein Kinase C Activity *in vitro, Biochem. Biophys. Res. Commun. 225*, 469–473.

34. Madani, S., Hichami, A., Legrand, A., Belleville, J., and Khan, N.A. (2001) Implication of Acyl Chain of Diacylglycerols in Activation of Different Isoforms of Protein Kinase C, *FASEB J. 15*, 2595–2601.

35. Mochly-Rosen, D., and Gordon, A.S. (1998) Anchoring Protein for Protein Kinase C: A Means for Isozyme Selectivity, *FASEB J. 12*, 35–42.

36. O'Flaherty, J.T., Chadwell, B.A., Kearns, M.W., Sergeant, S., and Daniel. L.W. (2001) Protein Kinase C Translocation Responses to Low Concentrations of Arachidonic Acid, *J. Biol. Chem. 276*, 24743–24750.

37. Keranen, L.M., Dutil, E.M., and Newton, A.C. (1995) Protein Kinase C is Regulated in vivo by Three Functionally Distinct Phosphorylations, *Curr. Biol. 5*, 1394—1403.

Decreased Serum Adiponectin in Adolescents and Young Adults with Familial Primary Hypercholesterolemia

Lian-Yu Lin[a], Chiau-Suong Liau[a], Wei-Shiung Yang[b], and Ta-Chen Su[a,c,]*

Divisions of [a]Cardiology and [b]Endocrinology & Metabolism, Department of Internal Medicine, National Taiwan University Hospital, Taipei, Taiwan, and [c]Institute of Industrial Hygiene and Occupational Medicine, College of Public Health, National Taiwan University, Taipei, Taiwan

ABSTRACT: Decreased serum adiponectin is associated with dyslipidemia. However, serum adiponectin status has never before been studied in patients with familial-related severe primary hypercholesterolemia (FRSPH). The aim of this study is to measure serum adiponectin level in a group of young patients with FRSPH and determine its correlation with insulin-resistant status. Twenty-three patients with FRSPH [average LDL-cholesterol (LDL-C) = 250.8 (190–610) mg/dL] without clinical manifestations of metabolic syndrome as well as 46 healthy (control) adolescents and young adults (<30 yr old) were included. The serum adiponectin, fasting sugar, insulin, lipids, systolic and diastolic blood pressure (SBP and DBP), and anthropometrical indices such as body mass index and waist circumference were obtained. The homeostasis model assessment (HOMA) was calculated to estimate the insulin resistant status. Compared with healthy controls, patients with FRSPH had a significantly lower mean serum adiponectin level (7.7 ± 1.8 µg/mL vs. 10.1 ± 4.3 µg/mL, $P = 0.013$). After adjustment for HOMA and associated covariates, multiple linear regression analysis showed that patients with FRSPH are significantly associated with hypoadiponectinemia. Compared with healthy controls, patients with FRSPH had a significantly lower mean serum adiponectin level (7.7 ± 1.8 µg/mL vs. 10.1 ± 4.3 µg/mL, $P = 0.013$). After adjustment for HOMA and associated covariates, multiple linear regression analysis showed that patients with FRSPH are significantly associated with hypoadiponectinemia. The serum adiponectin levels are lower in young patients with FRSPH without clinical manifestations of metabolic syndrome. The mechanism of hypoadiponectinemia in patients with FRSPH is probably independent of insulin resistance.

Paper no. L9652 in *Lipids 40*, 163–167 (February 2005).

Adipose tissue is now known not to be simply an inert storage depot for lipids but rather an important endocrine organ that plays a key role for the control of energy homeostasis through secretion of a variety of hormones and cytokines called adipocytokines (1). Adiponectin, an adipocytokine that is abundantly expressed in adipose tissue, has been associated with systemic insulin sensitivity both *in vivo* and *in vitro* (2–4). Clinical observations also have shown that serum adiponectin is reduced in patients with obesity, type 2 diabetes, coronary artery diseases (CHD), and hypertension (5–7), and all of them are closely related to insulin resistance.

In addition to hypertension and diabetes mellitus (DM), dyslipidemia was closely related to decreased serum adiponectin (6,8). Hotta *et al.* (6) observed a significant negative correlation between serum adiponectin and TG levels and a positive correlation between adiponectin and HDL-cholesterol (HDL-C) levels in type 2 DM (6). Matsubara *et al.* (8) extended this finding by demonstrating similar correlations in nondiabetic female subjects. The mechanism underlying the observed close association may be attributable to insulin resistance and/or hyperinsulinemia (2–4,8), a main component of metabolic syndrome. One proposed mechanism is that adiponectin decreases circulating FFA by increasing FA oxidation muscle (2,9). This results in decreased TG content in muscle, which has been associated with improved insulin sensitivity (10). In addition, liver FFA influx also is decreased in the presence of adiponectin, which might lead to decreased hepatic TG content and improve hepatic insulin sensitivity and reduce glucose output (2).

Familial-related severe primary hypercholesterolemia (FRSPH) is associated with excessive cardiovascular mortality and morbidity (11). Recently, it has been demonstrated that decreased plasma adiponectin levels are associated with CHD and with CHD risk (6,12). It is of great interest to measure the adiponectin levels in this population. Because older patients often have unhealthy physical conditions that are closely related to insulin resistance, such as hypertension, obesity, and diabetes, we tested the hypothesis of decreased adiponectin levels in a group of young patients with FRSPH and without comorbidities of metabolic syndrome. The aim of this study is to compare serum adiponectin level in young patients with FRSPH and matched healthy controls and to determine its correlation with insulin-resistant status and lipid profile.

SUBJECTS AND METHODS

Subjects. We studied a total of 23 FRSPH adolescents and young adults (<30 yr old) who were recruited for familial

*To whom correspondence should be addressed at Departments of Internal Medicine and Occupational Medicine and Industrial Hygiene, National Taiwan University Hospital and Medical College of National Taiwan University, 7, Chung-Shan South Road, Taipei, Taiwan 100.
E-mail: tachensu@ha.mc.ntu.edu.tw

Abbreviations: BMI, body mass index; BP, blood pressure; CHD, coronary artery diseases; DBP, diastolic blood pressure; DM, diabetes mellitus; FH, familial hypercholesterolemia; FRSPH, familial-related severe primary hypercholesterolemia; HDL-C, HDL cholesterol; HOMA, homeostasis model assessment; hs-CRP, high-sensitive C-reactive protein; LDL-C, LDL cholesterol; SBP, systolic blood pressure; WC, waist circumference.

hypercholesterolemia screening (FH) during 2002 at the lipid clinic of National Taiwan University Hospital. These patients were diagnosed to have FRSPH on the basis of having LDL-cholesterol (LDL-C) levels in themselves and in two or more first-degree relatives that were above 190 mg/dL and/or the presence of tendinous xanthomas within the kindred. Subjects having serum levels of HDL-C and TG in the normal range, and subjects with any etiologies of secondary hyperlipidemia, such as nephritic syndrome, obstructive liver disease, hypothyroidism, DM, or use of drugs affecting lipid levels were excluded. The genetic basis of FRSPH is heterogeneous and is associated not only with a high number of different LDL receptor gene mutations and other genetic abnormalities but also with differences in frequencies of specific mutations between populations. Thus, in the absence of genetic confirmation, we defined our study subjects as having FRSPH but as not having FH. However, about half of them had strong evidence of pathognomonic stigmata, namely, tuberous xanthoma or tendinous xanthoma of FH, and their LDL-C levels all were above 95th percentile for sex and age. Another age- and gender-matched 57 healthy controls, whose LDL-C levels were <130 mg/dL, were recruited from the healthy examination. Subjects with a history of hypertension, DM, and cardiovascular diseases or with serum creatinine over 1.5 mg/dl, serum TG over 150 mg/dL, resting blood pressure (BP) at or above 130/85 mmHg, or fasting plasma sugar over 110 mg/dL were excluded in this study. All subjects received a detailed medical history review and physical examination. Subjects' weight and height as well as their waist circumference (WC) were also obtained. The body mass index (BMI) was calculated by dividing the weight in kilograms by the square of the height in meters. The systolic BP (SBP) and diastolic BP (DBP) readings were recorded to the nearest 2 mmHg as the mean of two measurements by mercury sphygmomanometer with the subjects seated.

Serum markers. A venous blood sample was taken from subjects after an overnight fast of 12 h for measuring plasma glucose, insulin, TG, total cholesterol, LDL-C, and HDL-C by an autoanalyzer (Hitachi 7250 Special; Hitachi, Tokyo, Japan). Serum insulin level was measured by using a Microparticle Enzyme immunoassay (AxSYM Insulin; Abbott Diagnostic Division, Tokyo, Japan), and the insulin resistance index derived by homeostasis model assessment (HOMA) was as previously described (13). Serum high sensitive C-reactive protein (hs-CRP) and adiponectin were measured by using a chemiluminescent enzyme-labeled immunometric assay (Immulite C-Reactive Protein; Diagnostic Products Co., Los Angeles, CA) and a quantitative sandwich enzyme-linked immunoassay (Quantikine Human Adiponectin/Acrp30 Immunoassay; R&D, Minneapolis, MN), respectively. The protocol was reviewed and approved by the Ethical Committee of the National Taiwan University Hospital and institutional review board.

Statistics. Data were presented as means and SD, unless indicated otherwise. Log transformation was performed for variables with significant deviation from normal distribution before further analyses. All statistical analyses were performed using the SPSS/PC statistical program (version 10.0 for Windows; SPSS, Inc., Chicago, IL). The continuous variables between patients and healthy controls were compared by Student's *t*-test whereas the category parameters were by Mann–Whitney U test. The correlations between the adiponectin level and other variables were tested by Pearson's correlation. Multiple linear regression models were performed using serum adiponectin levels as the dependent variable and using age, gender, BMI, WC residuals (after adjustment for BMI), HOMA, mean BP, TG, and HDL-C as independent variables. Adjusted R^2 values were used to estimate the variance explained in each model.

RESULTS

As shown in Table 1, the mean serum LDL-C level was 250.8 (190–610) mg/dL in FRSPH and 99.4 (30.0–130.0) mg/dL in healthy controls. Patients with FRSPH had a significantly lower mean serum adiponectin level compared with healthy controls (7.7 ± 1.8 vs. 10.1 ± 4.13 µg/mL, *P*-value = 0.013). Except for the serum TG levels (*P* = 0.048), we also found that other demographic and clinical characteristics were not significantly different between the two groups. For small study populations, we used several linear regression models to adjust potential confounding factors. After the adjustment of other covariates (see Table 2), patients with FRSPH still had a significantly lower mean serum adiponectin level.

Correlation analysis between the serum adiponectin levels and other covariates were performed in patients with FRSPH, healthy controls, and total study populations. As demonstrated in Table 3, the serum adiponectin levels generally were negatively correlated with DBP, BMI, and the levels TG, hs-CRP, and HOMA, and were positively associated with the serum HDL-C levels, suggesting that within each group, factors considered to be part of metabolic syndrome were closely associated with serum adiponectin levels.

DISCUSSION

The present study demonstrated that serum adiponectin is decreased in young patients with FRSPH and without clinical manifestations of metabolic syndrome. Although the mechanism responsible for hypoadiponectinemia in FRSPH is still unclear, it indeed deserved further studies.

FH is a common autosomal dominant disorder in which LDL clearance from the circulation is impaired. In the absence of other causes of insulin resistance, patients with FH have been shown to have normal fasting insulin levels and not to be insulin resistant (14). Adiponectin has been negatively correlated with serum TG and positively correlated with serum HDL-C both in patients with dyslipidemia and in healthy adolescents (6,8,15). Interestingly, our present study found that in young FRSPH subjects with extreme serum LDL-C levels, the serum adiponectin levels were lower regardless of the adjustment of other insulin sensitivity markers. These observations indicate that the correlation between hypercholesterolemia and

TABLE 1
Demographic and Clinical Characteristics of the Study Subjects[a]

Variables	FRSPH $n = 23$	Healthy controls $n = 46$	
LDL-C, mg/dL	250.8 (190–610)	99.4 (30.0–130)	P
Age (yr)	19.7 ± 5.8	19.9 ± 4.7	0.868
Gender (male/female)	12/11	24/22	0.998
Body mass index (kg/m^2)	20.3 ± 3.3	21.4 ± 3.9	0.246
Waist circumference (cm)	71.9 ± 9.9	73.7 ± 11.2	0.520
Systolic BP (mmHg)	105.4 ± 13.7	102.2 ± 13.8	0.368
Diastolic BP (mmHg)	67.1 ± 10.4	68.4 ± 9.8	0.624
Fasting glucose (mg/dL)	84.2 ± 7.1	86.0 ± 5.7	0.358
Fasting insulin (mU/L)	6.9 ± 3.8	7.9 ± 4.9	0.393
HOMA-IR	1.4 ± 0.8	1.7 ± 1.0	0.329
Cholesterol (mg/dL)	339.5 ± 101.1	179.6 ± 26.5	<0.001
HDL-C (mg/dL)	53.2 ± 7.2	54.9 ± 8.7	0.418
TG (mg/dL)	88.3 ± 26.5	74.8 ± 26.3	0.048
hs-CRP (mg/dL)	0.14 ± 0.32	0.16 ± 0.6	0.905
Adiponectin (mg/mL)	7.7 ± 1.8	10.1 ± 4.3	0.013

[a]Abbreviations: FRSPH, familial-related severe primary hypercholesterolemia; BP, blood pressure; HOMA-IR, insulin resistance index derived by homeostasis model assessment; HDL-C, HDL-cholesterol; LDL-C, LDL-cholesterol; hs-CRP, high-sensitive C-reactive protein.

hypoadiponectinemia may be mediated through a pathway that is independent of insulin resistance. It is well known that cytokines such as TNF-α and interleukin-6 can inhibit the secretion of adiponectin from adipocytes (17–20). It is possible that the cytokines elicited by extreme hypercholesterolemia (21–23) may result in decreased adiponectin secretion in patients with FRSPH.

Table 2 revealed a consistent negative association of FRSPH with serum adiponectin levels after multiple linear regression analysis in different models, which corroborated the current hypothesis in this study. However, although both HDL-C and TG were found to be associated with serum adiponectin levels as in previous studies, we are the first to demonstrate the significant negative association between FRSPH and serum adiponectin levels. Thus, all the evidence and inferences should be under careful scrutiny.

In FH, early CHD is a complex trait that results from a large monogenic component of susceptibility that is due to extremely high levels of LDL-C (24). However, the mecha-

nism beyond LDL-C and the possible association with metabolic trait of adiponectin have never been reported. The finding of low adiponectin in these patients may have additive effects in increasing cardiovascular disease risk. In addition to its metabolic effects, adiponectin was found to protect vessels from damage through various mechanisms. It was demonstrated that adiponectin could inhibit monocyte adhesion to endothelial cells (25,26) and transformation of macrophages to foam cells (27). In one *in vivo* study, adiponectin-deficient mice exhibited excessive vascular remodeling following acute injury (28). In another mouse atherosclerosis model, enhanced adiponectin expression reduced atherosclerotic changes (29). It was also demonstrated that adiponectin directly stimulated the production of nitric oxide, an important mediator that regulates vascular tone and function (30). In one recent report, high plasma adiponectin concentrations were associated with lower risk of myocardial infarction in men, and this relationship could be only partly explained by differences in blood lipids and was independent of inflammation

TABLE 2
Multiple Linear Regression Models Showing Regression Coefficients and P-Value, Using Serum Adiponectin Levels (log transformed) As the Dependent Variable, with Other Covariates As Independent Variables[a]

	Model 1	Model 2	Model 3	Model 4
Age (yr)	−0.058 (0.618)	−0.004 (0.975)	−0.015 (0.906)	0.045 (0.263)
Gender	0.261 (0.038)	0.349 (0.006)	0.231 (0.082)	0.294 (0.033)
FRSPH	−0.260 (0.035)	−0.243 (0.035)	−0.301 (0.015)	−0.304 (0.015)
Log-HDL-C	0.251 (0.046)	0.275 (0.024)	0.164 (0.218)	0.192 (0.151)
Log-TG	−0.102 (0.445)	−0.090 (0.461)	−0.156 (0.216)	−0.106 (0.432)
Log-HOMA	−0.118 (0.343)			0.011 (0.937)
Mean BP		−0.265 (0.035)		−0.272 (0.056)
Log-BMI			−0.178 (0.176)	−0.096 (0.494)
Waist residuals			0.124 (0.315)	0.141 (0.254)
R^2	0.160	0.210	0.180	0.206

[a]R^2, adjusted R^2 of the model. BMI, body mass index; for other abbreviations see Table 1.

TABLE 3
Correlation Coefficients of Serum Adiponectin Levels (log transformed), vs. Associated Covariates in These Adolescents and Young Adults[a] (n = 69)

Variables	FRSPH (n = 23) C.C. (P value)	Controls (n = 46) C.C. (P value)	Total (n = 69) C.C. (P value)
Age (yr)	−0.073 (0.741)	−0.227 (0.128)	−0.161 (0.187)
Systolic BP (mmHg)	−0.308 (0.153)	−0.101 (0.505)	−0.178 (0.143)
Diastolic BP (mmHg)	−0.511 (0.013)	−0.175 (0.245)	−0.230 (0.058)
Log-BMI	−0.453 (0.030)	−0.201 (0.179)	−0.202 (0.096)
Log-Waist circumference	−0.340 (0.121)	−0.085 (0.585)	−0.112 (0.370)
Log-Cholesterol	0.378 (0.075)	−0.064 (0.673)	−0.212 (0.081)
Log-LDL-C	0.361 (0.091)	−0.056 (0.711)	−0.223 (0.065)
Log-HDL-C	0.447 (0.032)	0.158 (0.295)	0.239 (0.047)
Log-TG	−0.413 (0.050)	−0.076 (0.615)	−0.224 (0.065)
Log-Fasting glucose	0.076 (0.729)	0.026 (0.864)	0.084 (0.492)
Log-Fasting insulin	−0.585 (0.004)	−0.073 (0.630)	−0.165 (0.179)
Log-HOMA-IR	−0.553 (0.008)	−0.069 (0.650)	−0.151 (0.220)
Log-hs-CRP	−0.083 (0.715)	−0.397 (0.007)	−0.299 (0.014)

[a]C.C., correlation coefficient; for other abbreviations see Tables 1 and 2.

and glycemic status (12). In addition to the standard lipid-lowering medication, it is possible that agents or methods that can increase serum adiponectin might help in inhibiting the development of cardiovascular diseases.

REFERENCES

1. Chandran, M., Phillips, S.A., Ciaraldi, T., and Henry R.R. (2003) Adiponectin: More Than Just Another Fat Cell Hormone? *Diabetes Care 260*, 2442–2450.
2. Yamauchi, T., Kamon, J., Waki, H., Terauchi, Y., Kubota, N., Hara, K., Mori, Y., Ide, T., Murakami, K., Tsuboyama-Kasaoka, N., *et al.* (2001) The Fat Derived Hormone Adiponectin Reverses Insulin Resistance Associated with Both Lipoatrophy and Obesity *Nat. Med. 7*, 941–946.
3. Fasshauer, M., Klein, J., Neumann, S., Eszlinger, M., and Paschke, R. (2001) Adiponectin Gene Expression Is Inhibited by Beta Adrenergic Stimulation *Via* Protein Kinase A in 3T3-L1 Adipocytes, *FEBS Lett. 507*, 142–146.
4. Kubota, N., Terauchi, Y., Yamauchi, T., Kubota, T., Moroi, M., Matsui, J., Eto, K., Yamashita, T., Kamon, J., Satoh, H., *et al.* (2002) Disruption of Adiponectin Causes Insulin Resistance and Neointimal Formation, *J. Biol. Chem. 277*, 25863–25866.
5. Arita, Y., Kihara, S., Ouchi, N., Takahashi, M., Maeda, K., Miyagawa, J., Hotta, K., Shimomura, I., Nakamura, T., Miyaoka, K., *et al.* (1999) Paradoxical Decrease of an Adipose-Specific Protein: Adiponectin in Obesity, *Biochem. Biophys. Res. Commun. 257*, 79–83.
6. Hotta, K., Funahashi, T., Arita, Y., Takahashi, M., Matsuda, M., Okamoto, Y., Iwahashi, H., Kuriyama, H., Ouchi, N., Maeda, K., *et al.* (2000) Plasma Concentrations of a Novel, Adipose-Specific Protein, Adiponectin, in Type 2 Diabetic Patients, *Arterioscler. Thromb. Vasc. Biol. 20*, 1595–1599.
7. Adamczak, M., Wiecek, A., Funahashi, T., Chudek, J., Kokot, F., and Matsuzawa, Y. (2003) Decreased Plasma Adiponectin Concentration in Patients with Essential Hypertension, *Am. J. Hypertens. 16*, 72–75.
8. Matsubara, M., Maruoka, S., and Katayose, S. (2002) Decreased Plasma Adiponectin Concentrations in Women with Dyslipidemia, *J. Clin. Endocrinol. Metab. 87*, 2764–2769.
9. Fruebis, J., Tsao, T.S., Javorschi, S., Ebbets-Reed, D., Erickson, M.R., Yen, F.T., Bihain, B.E., and Lodish, H.F. (2001) Proteolytic Cleavage Product of 30-kDa Adipocyte Complement-Related Protein Increases Fatty Acid Oxidation in Muscle and Causes Weight Loss in Mice, *Proc. Natl. Acad. Sci. USA. 98*, 2005–2010.
10. Boden, G., and Shulman, G.I. (2002) Free Fatty Acids in Obesity and Type 2 Diabetes: Defining Their Role in the Development of Insulin Resistance and β-Cell Dysfunction, *Eur. J. Clin. Invest. 32* (Suppl. 3), 14–23.
11. Wiegman, A., Rodenburg, J. de Jongh, S., Defesche, J.C., Bakker, H.D., Kastelein, J.J., Sijbrands, E.J. (2003) Family History and Cardiovascular Risk in Familial Hypercholesterolemia: Data in More Than 1000 Children, *Circulation 107*, 1473–1478.
12. Pischon, T., Girman, C.J., Hotamisligil G.S., Rifai N., Hu, F.B., and Rimm, E.B. (2004) Plasma Adiponectin Levels and Risk of Myocardial Infarction in Men, *JAMA 291*, 1730–1737.
13. Haffner, S.M., Miettinen, H., and Stern, M.P. (1997) The Homeostasis Model in the San Antonio Heart Study, *Diabetes Care 20*, 1087–1092.
14. Raal, F.J., Panz, V.R., Pilcher, G.J., and Joffe, B.I. (1999) Atherosclerosis Seems Not to Be Associated with Hyperinsulinaemia in Patients with Familial Hypercholesterolaemia, *J. Intern. Med. 246*, 75–80.
15. Huang, K.C., Lue, B.H., Yen, R.F., Shen, C.G., Ho, S.R., Tai, T.Y., and Yang, W.S. (2004) Plasma Adiponectin Levels and Metabolic Factors in Nondiabetic Adolescents, *Obes. Res. 12*, 119–124.
16. Weyer, C., Funahashi, T., Tanaka, S., Hotta, K., Matsuzawa, Y., Pratley, R.E., and Tataranni, P.A. (2001) Hypoadiponectinemia in Obesity and Type 2 Diabetes: Close Association with Insulin Resistance and Hyperinsulinemia, *J. Clin. Endocrinol. Metab. 86*, 1930–1935.
17. Fasshauer, M., Kralisch, S., Klier, M., Lossner, U., Bluher, M., Klein, J., and Paschke, R. (2003) Adiponectin Gene Expression and Secretion Is Inhibited by Interleukin-6 in 3T3-L1 Adipocytes, *Biochem. Biophys. Res. Commun. 301*, 1045–1050.
18. Ruan, H., and Lodish, H.F. (2003) Insulin Resistance in Adipose Tissue: Direct and Indirect Effects of Tumor Necrosis Factor-α, *Cytokine Growth Factor Rev. 14*, 447–455.
19. Lihn, A.S., Richelsen, B., Pedersen, S.B., Haugaard, S.B., Rathje, G.S., Madsbad, S., and Andersen, O. (2003) Increased Expression of TNF-α, IL-6, and IL-8 in HALS: Implications for Reduced Adiponectin Expression and Plasma Levels, *Am. J. Physiol. Endocrinol. Metab. 285*, E1072–E1080.
20. Bruun, J.M., Lihn, A.S., Verdich, C., Pedersen, S.B., Toubro, S., Astrup, A., and Richelsen, B. (2003) Regulation of

Adiponectin by Adipose Tissue-Derived Cytokines: *in vivo* and *in vitro* Investigations in Humans, *Am. J. Physiol. Endocrinol. Metab. 285*, E527—E533.

21. Sampietro, T., Tuoni, M., Ferdeghini, M., Ciardi, A., Marraccini, P., Prontera, C., Sassi, G., Taddei, M., and Bionda, A. (1997) Plasma Cholesterol Regulates Soluble Cell Adhesion Molecule Expression in Familial Hypercholesterolemia, *Circulation 96*, 1381–1385.

22. Mizia-Stec, K., Zahorska-Markiewicz, B., Mandecki, T., Janowska, J., Szulc, A., Jastrzekbska-Maj, E., and Gasior Z. (2003) Hyperlipidaemias and Serum Cytokines in Patients with Coronary Artery Disease, *Acta Cardiol. 58*, 9–15.

23. Holven, K.B., Myhre, A.M., Aukrust, P., Hagve, T.A., Ose, L., and Nenseter, M.S. (2003) Patients with Familial Hypercholesterolaemia Show Enhanced Spontaneous Chemokine Release from Peripheral Blood Mononuclear Cells *ex vivo*. Dependency of Xanthomas/Xanthelasms, Smoking and Gender, *Eur. Heart J. 24*, 1756–1762.

24. Hegele, R.A. (2002) Environmental Modulation of Atherosclerosis End Points in Familial Hypercholesterolemia, *Atheroscler. Suppl. 2*, 5–7.

25. Ouchi, N., Kihara, S., Arita, Y., Maeda, K., Kuriyama, H., Okamoto, Y., Hotta, K., Nishida, M., Takahashi, M., Nakamura, T., *et al.* (1999) Novel Modulator for Endothelial Adhesion Molecules; Adipocyte-Derived Plasma Protein, Adiponectin, *Circulation 100*, 2473–2476.

26. Okamoto, Y., Arita, Y., Nishida, M., Muraguchi, M., Ouchi, N., Takahashi, M., Igura, T., Inui, Y., Kihara, S., Nakamura, T., *et al.* (2000) An Adipocyte-Derived Plasma Protein, Adiponectin, Adheres to Injured Vascular Wall, *Horm. Metab. Res. 32*, 47–50.

27. Ouchi, N., Kihara, S, Arita, Y., Nishida, M., Matsuyama, A., Okamoto, Y., Ishigami, M., Kuriyama, H., Kishida, K., Nishizawa, H., *et al.* (2001) Adipocyte-Derived Plasma Protein, Adiponectin, Suppresses Lipid Accumulation and Class A Scavenger Receptor Expression in Human Monocyte-Derived Macrophages, *Circulation 103*, 1057–1063.

28. Matsuda, M., Shimomura, I., Sata, M., Arita, Y., Nishida, M., Maeda, N., Kumada, M., Okamoto, Y., Nagaretani, H., Nishizawa, H., *et al.* (2002) Role of Adiponectin in Preventing Vascular Stenosis. The Missing Link of Adipo-vascular Axis, *J. Biol. Chem. 277*, 37487–37491.

29. Okamoto, Y.. Kihara, S., Ouchi, N., Nishida, M., Arita, Y., Kumada, M., Ohashi, K., Sakai, N., Shimomura, I., Kobayashi, H., *et al.* (2002) Adiponectin Reduces Atherosclerosis in Apolipoprotein E-Deficient Mice, *Circulation 106*, 2767–2770.

30. Ouchi, N., Kobayashi, H., Kihara, S., Kumada, M., Sato, K., Inoue, T., Funahashi, T., and Walsh, K. (2004) Adiponectin Stimulates Angiogenesis by Promoting Cross-Talk Between AMP-Activated Protein Kinase and Akt Signaling in Endothelial Cells, *J. Biol. Chem. 279*, 1304–1309.

Effects of a Diet High in Plant Sterols, Vegetable Proteins, and Viscous Fibers (Dietary Portfolio) on Circulating Sterol Levels and Red Cell Fragility in Hypercholesterolemic Subjects

Peter J. Jones[a], Mahmoud Raeini-Sarjaz[a], David J.A. Jenkins[b,c,d,e,*], Cyril W.C. Kendall[b,d], Edward Vidgen[b,d], Elke A. Trautwein[h], Karen G. Lapsley[i], Augustine Marchie[b,d], Stephen C. Cunnane[b], and Philip W. Connelly[c,f,g]

[a]School of Dietetics and Human Nutrition, McGill University, Montréal, Qúebec; [b]Clinical Nutrition & Risk Factor Modification Center and [c]Department of Medicine, Division of Endocrinology and Metabolism, St. Michael's Hospital, Toronto, Ontario; Departments of [d]Nutritional Sciences, [e]Medicine, [f]Biochemistry, and [g]Laboratory Medicine and Pathobiology, Faculty of Medicine, University of Toronto, Toronto, Ontario, Canada M5S 3E2; [h]Unilever Health Institute, Unilever R&D Vlaardingen, The Netherlands; and [i]The Almond Board of California, Modesto, California, 95354

ABSTRACT: Plant sterols, soy proteins, viscous fibers, and nuts are advised for cholesterol reduction, but their combined effect on plant sterol absorption has never been tested. We assessed their combined action on serum sterols in hyperlipidemic subjects who were following low-saturated fat diets before starting the study and who returned to these diets post-test. The 1-month test (combination) diet was high in plant sterols (1 g/1,000 kcal), soy protein (23 g/1,000 kcal), viscous fiber (9 g/1,000 kcal), and almonds (14 g/1000 kcal). Fasting blood was obtained for serum lipids and sterols, and erythrocytes were obtained for fragility prior to and at 2-wk intervals during the study. The combination diet raised serum campesterol concentrations by 50% and β-sitosterol by 27%, although these changes were not significant after Bonferroni correction; near-maximal rises were found by the end of the first week, but no change was found in red cell fragility despite a 29% reduction in the LDL cholesterol level. No significant associations were observed between changes in red cell fragility and blood lipids or sterols. We conclude that plant sterols had a minimal impact on serum sterol concentrations or red cell fragility in hyperlipidemic subjects on diets that greatly reduced their serum lipids.

Paper no. L9398 in *Lipids 40*, 169–174 (February 2005).

Plant sterols have been shown to lower serum LDL cholesterol (1–3) by 8–12% in the absence of other dietary modifications (e.g., vs. low-fat diets) in a meta-analysis by Law (4). Despite broad acceptance of the safety of plant sterols by most Western countries, concerns have been raised that absorption of plant sterols may have adverse consequences, possibly by modifying cell membrane fragility resulting from the displacement of cholesterol (5). Few data are available from human studies concerning the influence of dietary sterols on membrane fragility and serum sterols, especially using diets that result in marked reductions in serum cholesterol levels (6,7). We therefore assessed the effect on serum plant sterols of diets high in other cholesterol-lowering dietary components. These components, which included viscous fiber (8–11), soy protein (12,13), and almonds in

combination (dietary portfolio), have been shown to produce a marked reduction in serum cholesterol (6,7). The specific objective was to assess whether a plant sterol-enriched diet, combined with other agents known to reduce circulating cholesterol levels, would result in a change in cell membrane fragility and circulating plant sterol and lipid concentrations in hyperlipidemic individuals.

EXPERIMENTAL PROCEDURES

Subjects. Thirteen subjects (7 men and 6 postmenopausal women), aged (mean ± SE) 65 ± 3 yr (median 64 yr; range 43–84 yr); body mass index 25.6 ± 0.9 kg/m^2 (median 26.1 kg/m^2; range 20.6–30.7 kg/m^2); baseline LDL cholesterol 4.22 ± 0.11 mmol/L (median 4.27 mmol/L; range 3.51–4.99 mmol/L) were recruited from patients attending the Risk Factor Modification Center, St. Michael's Hospital. All subjects had taken part in previous dietary studies, were experienced in following dietary protocols and previously had had raised LDL cholesterol levels (>4.1 mmol/L) (14). At the time of the study, 5 subjects had raised LDL cholesterol levels, one subject had raised TG levels (>2.30 mmol/L, range 0.7–5.1 mmol/L), 3 subjects had both raised LDL cholesterol and TG levels, one subject had a low HDL cholesterol concentration (<0.9 mmol/L), and 3 subjects had blood lipids in the normal range (14). None of the subjects had a history of diabetes, renal disease, or liver disease, and none were taking medications known to influence serum lipids. One subject completed only 3 wk and withdrew because of dyspepsia associated with a *Helicobacter pylori* infection requiring antibiotic therapy.

Dietary advice on low-saturated fat (<7% dietary calories) and low-cholesterol diets (<200 mg/d) had been reinforced on at least two occasions over the previous year, and at entry to the study, 6 subjects had recorded diets with <7% (total energy) saturated fat and 9 subjects had followed diets with <200 mg/d cholesterol.

Study protocol. Subjects were followed on their own low-saturated fat therapeutic diets for 1 wk prior to the start of the study, and for an additional 2 wk after the study on return to their low-saturated fat therapeutic diets. During the middle 4

*To whom correspondence should be addressed at Clinical Nutrition and Risk Factor Modification Center, St. Michael's Hospital, 61 Queen St. East, Toronto, Ontario, Canada, M5C 2T2. E-mail: cyril.kendall@utoronto.ca

TABLE 1
Calculated Macronutrient Intakes (mean + SE) During the Run-in, Test, and Run-out Phases of the Portfolio Study

	Run-in (*n* = 12)	Portfolio diet (mean weeks 2–4, *n* = 13)	Run-out (week 6, *n* = 12)
Energy (kcal/d)	1,703 ± 120	1,999 ± 118	1,703 ± 104
Total protein (% of protein)	17.3 ± 0.8	22.4 ± 0.5	18.1 ± 0.8
Vegetable protein	48.7 ± 3.5	96.8 ± 0.2	39.1 ± 2.8
Available carbohydrate (% of energy)	52.9 ± 2.8	50.6 ± 0.6	58.2 ± 1.3
Total dietary fiber (g/1,000 kcal)	17.1 ± 1.9	30.7 ± 1.0	17.8 ± 1.8
Total fat (% of energy)[a]	28.3 ± 2.5	27.0 ± 0.8	22.7 ± 1.5
SFA	7.7 ± 0.7	4.3 ± 0.1	6.2 ± 0.7
MUFA	11.9 ± 1.6	11.8 ± 0.5	9.0 ± 0.7
PUFA	6.0 ± 0.4	9.9 ± 0.2	5.3 ± 0.5
Dietary cholesterol (mg/1,000 kcal)	99 ± 13	10 ± 3	79 ± 9
Alcohol (% of energy)	1.5 ± 0.5	0.2 ± 0.1	1.0 ± 0.4
Satiety (–3 to +3)[b]	1.3 ± 0.2	2.9 ± 0.2	1.3 ± 0.3

[a]SFA, saturated FA; MUFA, monounsaturated FA; PUFA, polyunsaturated FA.
[b]Satiety: –3, extreme hunger; +3, extremely full.

wk, subjects followed a combination diet in which all foods were provided with the exception of fresh fruit and most vegetables. Blood samples and body weights were obtained after 12-h overnight fasts at weekly intervals and at week 2 of the washout. Seven-day weighed diet histories were obtained for the week prior to and for 2 wk following the combination diet. Completed menu checklists were returned at weekly intervals during the 4-wk combination diet period.

The study was approved by the Ethics Committee of the University of Toronto and St. Michael's Hospital, and informed consent was obtained from the subjects.

Diets. Diets eaten before and after the 4-wk combination diet were the subjects' routine therapeutic low-fat diets, which approximated National Cholesterol Education Program Step 2 guidelines (<7% energy from saturated fat and <200 mg/d dietary cholesterol) (Table 1) (14). Subjects were provided with self-taring electronic scales and asked to weigh all food items consumed during the study period. During the combination diet period, all foods consumed by the subjects were provided at weekly clinic visits with the exception of fruit and low-calorie vegetables (i.e., non-starch-containing vegetables), which subjects were instructed to obtain from their local stores. Subjects were provided with a 7-d rotating menu plan, including specified fruits and vegetables, on which they checked off each item as it was eaten and confirmed the weight of the foods. The same menu plan was used for all subjects but was modified to suit individual preferences, providing the goals for viscous fiber, soy protein, plant sterols, and almond consumption were met. For ease of consumption, where possible, items were prescribed in whole units.

The aim of the combination diet (dietary portfolio) was to provide 1 g of plant sterols per 1,000 kcal as an enriched margarine. The Unilever margarine contained approximately 46% sitosterol, 26% campesterol, 19% stigmasterol, 2.7% brassicasterol, 1.3% sitostanol, 0.8% campestanol, and 0.8% avenasterol, with the remainder made up of various other plant sterols. The Unilever margarine provided 12% plant sterol (w/w). Two

grams of plant sterol was contained in 25 g of margarine, for 82 kcal. In addition, the diet supplied 8.2 g of viscous fiber per 1,000 kcal from oats, barley, and psyllium and 22.7 g of soy protein per 1,000 kcal as soy milk or meat analogs. Raw, unblanched almonds also provided vegetable protein (2.9 g/1,000 kcal). Emphasis was placed on eggplant and okra as additional sources of viscous fiber (0.55 g/1,000 kcal and 0.67 g/1,000 kcal, respectively). Thus, 200 g of eggplant and 100 g of okra were prescribed to be eaten on a 2,000-kcal diet each day. Diets were provided at a targeted intake to maintain body weight based on estimated caloric requirements (15).

Compliance was assessed from the completed weekly checklists and from the return of uneaten food items.

Analyses. Serum lipid data were reported previously (6). All samples were stored at –70°C prior to analysis. Sera for plant sterol analysis were unavailable for one subject, and an additional 3 subjects were missing one or both week 1 and week 3 samples. As also mentioned earlier, one subject dropped out at week 3. Plant sterols and cholesterol in serum and membrane were measured by GLC (HP 5890 Series II; Hewlett-Packard, Palo Alto, CA). Briefly, 5α-cholestane was added to each sample as an internal standard. Samples were saponified with 0.5 M methanol-KOH for 1 h at 100°C, and sterols were extracted using petroleum ether and injected into the gas–liquid chromatograph. The column temperature was 285°C. Isothermal running conditions (oven temperature 285°C) were maintained for 42 min. The injector and detector were set at 300 and 310°C, respectively. The carrier gas (helium) flow rate was 1.2 mL/min with the inlet splitter set at 100:1. Individual plant sterols and cholesterol were identified using authentic standards (Sigma-Aldrich Canada Ltd., Oakville, Ontario). The CV in the plant sterol measurement was 4% (16). Serum was analyzed according to the Lipid Research Clinics' protocol (17) for total cholesterol, TG, and HDL cholesterol, after dextran sulfate–magnesium chloride precipitation (18). Levels of LDL cholesterol were calculated (19). Serum apolipoprotein A-l and B were measured

by nephelometry (20). All samples from a given individual wer-analyzed in the same batch.

Red cell fragility was assessed on fresh red cells collected in vacutainer tubes containing EDTA (Becton Dickinson, Mississauga, Ontario). Packed red cells (0.02 mL) were added to 2 mL unbuffered saline covering the range of sodium chloride concentrations from 0.20 to 0.70 g/L in 0.05 g/L increments. After 1 h, the cells were centrifuged at $1,000 \times g$ at room temperature for 5 min and the supernatant was read at 540 nm (21). Data are presented as unadjusted O.D. readings and as adjusted percentages of the maximum O.D. obtained for both tests combined. The adjusted values were used to calculate the saline concentration that corresponded to the 50% hemolysis value. The p50 value for red cell hemolysis (50% hemolysis value) was calculated, assuming a linear response between the two consecutive O.D. readings spanning the half-point of the maximum hemolysis recorded for the subject. For each subject, the maximum O.D. (maximum hemolysis) obtained from both tests combined represented the 100% hemolysis value for that subject. Preliminary data on red cell fragility expressed as 50% hemolysis were reported previously (6).

Diets were analyzed using a program based on USDA data (22) with additional data on foods analyzed in the laboratory for protein, total fat, and dietary fiber using AOAC methods (23). FA were analyzed by GLC (24). Additional dietary fiber values were obtained from the tables of Anderson and Bridges (25).

Statistical analysis. The results were expressed as means ± SE. The significance of the differences between the pretreatment diet, combination diet, and post-treatment diet was assessed by the least squares means test with the Tukey–Kramer adjustment for multiplicity of simultaneous comparisons (PROC MIXED/SAS 8.2) (26). The model used had the treatment value as the response variable and the week and interaction term diet by sex as main effects and a random term corresponding to subject nested within sex. Student's paired *t*-test (two-tailed) was used to assess the significance of the percentage change from pretreatment.

With the present subject numbers for red cell fragility, assuming a SD of effect of 3.4%, a 3% difference could be detected as significant ($P < 0.05$). Likewise, assuming a SD of effect of 0.015 g/100 mL, a difference of 0.013 g/100 mL should be detected as significant.

The concentration required to obtain 50% hemolysis was determined assuming a linear response between consecutive observations. For each subject, the maximal O.D. obtained from both tests combined represented the 100% hemolysis value for that subject. A Pearson correlation analysis was used to assess relations between plant sterol measurements and other measurements. A Bonferroni adjustment was also made to the significance levels to allow for the multiple comparisons (26). Six largely independent primary measures were recognized: change in red cell fragility, serum campesterol and β-sitosterol, and LDL cholesterol, HDL cholesterol, and TG.

RESULTS

Demographics and compliance. Throughout the period of observation, subjects tended to lose weight: [–0.10 ± 0.05 kg/wk ($P = 0.127$) over the combination diet, and –0.2 ± 0.05 kg/wk ($P = 0.001$) during the run-out phase]. In the majority of subjects, compliance in terms of caloric intake was good, with 92.5 ± 2.9% of the calories prescribed being consumed.

Serum plant sterols. Serum plant sterol concentrations tended to increase over the 1-mon combination diet (Fig. 1). Serum campesterol concentrations increased by 50 ± 15% from baseline for weeks 2–4; the respective increase for serum sitosterol was 27 ± 14% (Table 2). For campesterol, the unadjusted rise was significant ($P = 0.007$) but disappeared after Bonferroni correction ($P = 0.139$).

Serum lipids. Full details of the blood lipid responses were reported previously (6). Significant reductions in blood lipids were seen at the end of the combination diet compared with the run-in and run-out periods (Table 2). From baseline, reductions were seen in LDL cholesterol (29.0 ± 2.7%, $P < 0.001$), apolipoprotein B (24.3 ± 2.0%, $P < 0.001$), and the total/HDL cholesterol ratio (19.8 ± 2.9%, $P = 0.004$).

Red cell fragility. No significant difference was seen in red cell fragility between the pretreatment and week 4 of the com-
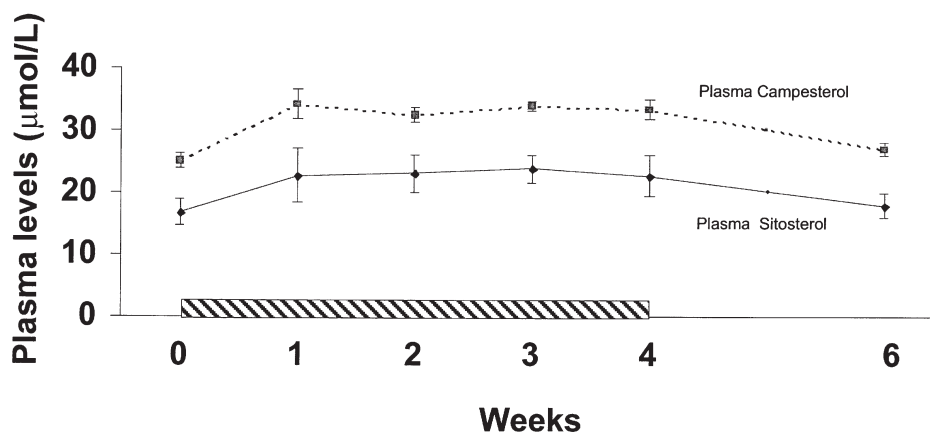
FIG. 1. Mean plasma values for campesterol and sitosterol over 6 wk in 7 subjects. (hatched bar) Administration period of sterols. Plant sterol data were unavailable for one subject, an additional subject dropped out prior to the week 4 sample, and 3 subjects were lacking one or both week 1 and week 3 samples.

TABLE 2
Blood Lipids[a] and Apolipoproteins at Baseline and on the Combination Diet

	Baseline (week 0)	Mean treatment[b] (weeks 2–4)	P[c]
Cholesterol[d] (mmol/L)			
Total-C	6.46 ± 0.21	5.01 ± 0.20	<0.001
LDL-C	4.22 ± 0.11	3.01 ± 0.17	<0.001
HDL-C	1.37 ± 0.11	1.34 ± 0.11	0.992
TG[d] (mmol/L)	1.92 ± 0.35	1.45 ± 0.18	0.984
Apolipoproteins[e] (g/L)			
ApoA-1	1.70 ± 0.07	1.61 ± 0.08	0.334
ApoB	1.32 ± 0.05	1.01 ± 0.05	<0.001
Ratios			
Total-C/HDL-C	5.06 ± 0.41	4.00 ± 0.30	0.004
LDL-C/HDL-C	3.31 ± 0.26	2.45 ± 0.24	<0.001
ApoB/apoA-1	0.80 ± 0.05	0.64 ± 0.05	0.004

[a]Blood lipid results have been published in full elsewhere (6). Total-C, total cholesterol; LDL-C, LDL cholesterol; HDL-C, HDL cholesterol.
[b]Treatment values represent the mean of weeks 2, 3, and 4.
[c]P values after Bonferroni correction.
[d]To convert cholesterol and TG to mg/dL, multiply by 38.67 and 88.57, respectively.
[e]To convert apolipoprotein A-1 and B values to mg/dL, multiply by 100.

bination diet (saline concentration for 50% hemolysis, 0.436 ± 0.007 g/100 mL vs. 0.441 ± 0.006 g/100 mL, $P = 0.223$, unadjusted, $P = 0.734$ adjusted). No significant differences between mean pre- and postcombination diet values were seen at any time point when expressed as unadjusted O.D. readings at 540 nm (Fig. 2A) or as percent hemolysis, where the highest O.D. value for each individual was taken as 100% for that individual (Fig. 2B).

Relation of plant sterols to other measurements. No significant associations were seen between change in serum sterols and red cell fragility (serum campesterol, $r = -0.09$, $P = 0.803$; sitosterol $r = 0.12$, $P = 0.717$). The negative values indicate the tendency of a reduced fragility (reduced saline concentration for hemolysis) with increasing plant sterols, although no associations were significant.

For serum sterols, an association was seen at baseline between plasma sitosterol and total cholesterol ($r = 0.72$, $P = 0.008$), LDL cholesterol ($r = 0.83$, $P = 0.001$), and apolipoprotein B ($r = 0.91$, $P < 0.001$). No relation was seen between changes in serum sterols and blood lipids.

DISCUSSION

Supplementation with plant sterols in a diet that also contained high levels of viscous fibers, soy protein, and almonds produced large reductions in serum lipids but was associated with only relatively small increases in plasma sterol concentrations. There has been concern that significant increases in plasma sterols may result in modification of membrane lipids with the exclusion of cholesterol and that this change would increase membrane fragility (5). The present data indicate that the small changes in serum lipids do not relate significantly to red cell osmotic fragility.

The absence of effect on red cell fragility indices examined opposes recent findings in rats suggesting that diets high in
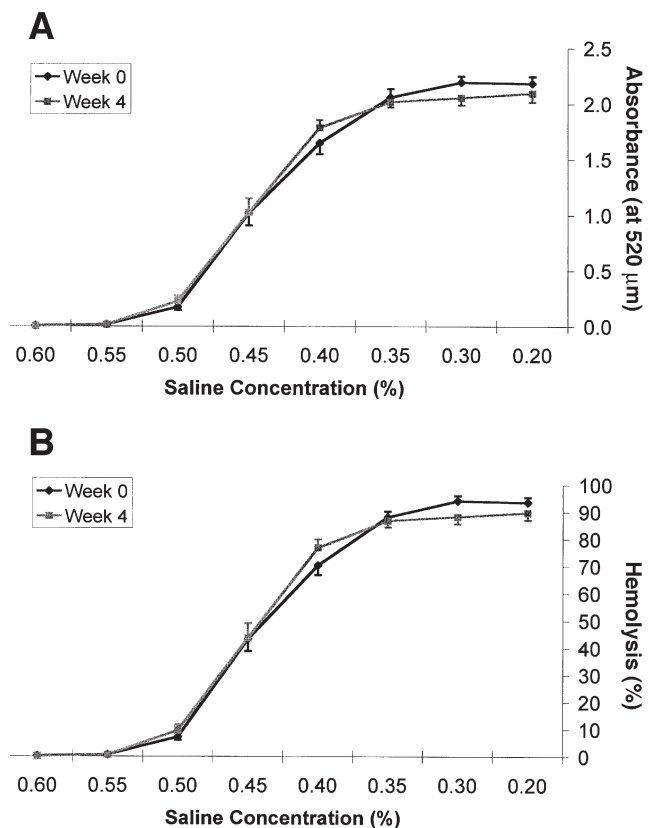
FIG. 2. (A) Osmotic fragility of red blood cells from subjects at baseline (week 0) and week 4 of the combination diet after 6 h of exposure to varying saline concentrations. Data are presented as unadjusted O.D. readings. (B) Osmotic fragility of red blood cells from subjects at baseline (week 0) and week 4 of the combination diet after 6 h of exposure to varying saline concentrations. Data are presented as the percentage of hemolysis, with the maximal O.D. reading obtained for each subject representing 100% hemolysis.

plant sterols may increase the predisposition to hemorrhagic events (5). Clearly, more effort is required to define the real risk of hemorrhagic sequelae in the use of plant sterols as cholesterol-lowering agents at the levels provided in functional foods.

Components used in this combination diet were based on the hypothesis that during the course of human evolution, the diet was likely to have been high in vegetable proteins, dietary fiber, and plant sterols. All these components have now been recognized to lower serum cholesterol (1–3,8–13, 27, 28). Vegetable protein as soy (13), viscous dietary fiber, oats (27), psyllium (10), and, most recently, plant sterols (4) have received FDA approval for health claims for coronary heart disease risk reduction. These components, together with almonds (29,30), which may combine several cholesterol-lowering components, were the focus of the present diet.

In a previous study an attempt was made to reconstruct diets that may have been eaten at an earlier stage in human evolution by using plant foods readily available in the supermarket (31). The plant sterol intake on this "Myocene," or 4–7 million-year-old, diet was 1 g/d for men, indicating that historically high plant sterol intakes may have been associated with diets high in fiber and vegetable protein (31). The cholesterol lowering achieved with this evolutionary model diet was of a magnitude similar to that seen in the present study, in which the diet was high in the same active ingredients.

It is possible that almonds and viscous fiber in the present diet may have protective effects on red cell fragility and that adverse effects of plant sterols may have been masked. However, there are no data on the effects of nuts or viscous fiber on red cell fragility. Equally, it could be argued that nuts, which are good sources of plant sterols, might be expected to add to any adverse effect of the sterol margarine if such existed and that this might be compounded by viscous fiber, which further reduces serum cholesterol levels, possibly increasing the stiffness of the membrane and increasing the risk of hemolysis. Nevertheless, these points are purely speculative since no significant change in hemolysis was observed.

It is also possible that 4 wk was not long enough to demonstrate more subtle changes in red cell hemolysis since the red cell half-life in humans is 25–35 d for a mean life span of 120 d (32). In the rat the red cell half-life is of the order of 19 d with a life span of 60 d (33). In this situation, 1-mon studies might be more appropriate; however, this was the time frame used in rat studies that showed increased hemolysis with plant sterols by 4–5% (5). Based on studies of spontaneously hypertensive rats (5), it has been suggested that increased plant sterol intakes, especially from canola oil, may increase the risk of hemorrhagic stroke (5). This effect is thought to be due to increased cell membrane fragility (5,21) secondary to displacement of cholesterol by plant sterols in the membrane. However, the similar survival of olive oil-fed and corn-oil fed spontaneously hypertensive rats leaves questions remaining as to the role of phytosterol intakes in this process. Also, we found no relation between serum plant sterol levels and red cell osmotic fragility. A good relation, however, has been observed between plasma and membrane plant sterols in a study involving hypercholes-

terolemic children (34). Furthermore, there was no significant association between the change in concentration of plasma sterols and red cell fragility, although our subject numbers are small. These data add support to the general acceptance of plant sterol-enriched margarine for use by the public. An additional reason why the present study demonstrated no difference in red cell fragility may relate to the lack of sensitivity of the test itself. Pre-incubated erythrocytes are more sensitive indicators of red cell fragility than fresh erythrocytes, especially in situations of pathologically increased fragility (35). However, the rat studies demonstrating the ill effects of plant sterols did not use pre-incubated cells. Our study therefore endeavored to use the same type of analysis to allow direct comparison.

Were plant sterol consumption to be restricted, then the guidelines promoting increased intakes of fruit, vegetables, whole-grain cereals, legumes, and unhydrogenated vegetable oils would need to be revised. Such diets deliver appreciable amounts of plant sterols, and it could be argued that, from the evolutionary perspective, these are the diets to which we have adapted in the context of high-fiber, vegetable protein, and plant sterol intakes. The lack of these plant food components results in unacceptable levels of serum cholesterol that will qualify a significant proportion of the adult population for cholesterol-lowering medications (14).

In conclusion, high plant sterol intakes in the context of high-fiber vegetable protein diets have only a small effect on serum plant sterol concentrations despite large reductions in serum lipids. Moreover, high plant sterol-containing diets do not alter red cell fragility, a finding that should be examined further, given the recently reported promotion of hemorrhagic events by plant sterols in rats.

ACKNOWLEDGMENTS

REFERENCES

1. Jones, P.J., Ntanios, F.Y., Raeini-Sarjaz, M., and Vanstone, C.A. (1999) Cholesterol-Lowering Efficacy of a Sitostanol-Containing Phytosterol Mixture with a Prudent Diet in Hyperlipidemic Men, *Am. J. Clin. Nutr. 69*, 1144–1150.
2. Miettinen, T.A., Puska, P., Gylling, H., Vanhanen, H., and Vartiainen, E. (1995) Reduction of Serum Cholesterol with Sitostanol-Ester Margarine in a Mildly Hypercholesterolemic Population, *N. Engl. J. Med. 333*, 1308–1312.
3. Lees, A.M., Mok, H.Y., Lees, R.S., McCluskey, M.A., and Grundy, S.M. (1977) Plant Sterols as Cholesterol-Lowering Agents: Clinical Trials in Patients with Hypercholesterolemia and Studies of Sterol Balance, *Atherosclerosis 28,* 325–338.

4. Law, M. (2000) Plant Sterol and Stanol Margarines and Health, *Br. Med. J. 320*, 861–864.

5. Ratnayake, W.M., L'Abbe, M.R., Mueller, R., Hayward, S., Plouffe, L., Hollywood, R., and Trick, K. (2000) Vegetable Oils High in Phytosterols Make Erythrocytes Less Deformable and Shorten the Life Span of Stroke-Prone Spontaneously Hypertensive Rats, *J. Nutr. 130*, 1166–1178.

6. Jenkins, D.J., Kendall, C.W., Faulkner, D., Vidgen, E., Trautwein, E.A., Parker, T.L., Marchie, A., Koumbridis, G., Lapsley, K.G., Josse, R.G., *et al.* (2002) A Dietary Portfolio Approach to Cholesterol Reduction: Combined Effects of Plant Sterols, Vegetable Proteins, and Viscous Fibers in Hypercholesterolemia, *Metabolism 51*, 1596-1604.

7. Jenkins, D.J., Kendall, C.W., Marchie, A., Faulkner, D.A., Wong, J.M., de Souza, R., Emam, A., Parker, T.L., Vidgen, E., Lapsley, K.G., *et al.* (2003) Effects of a Dietary Portfolio of Cholesterol-Lowering Foods vs Lovastatin on Serum Lipids and C-Reactive Protein, *JAMA 290*, 502–510.

8. Jenkins, D.J., Wolever, T.M., Rao, A.V., Hegele, R.A., Mitchell, S.J., Ransom, T.P., Boctor, D.L., Spadafora, P.J., Jenkins, A.L., and Mehling, C. (1993) Effect on Blood Lipids of Very High Intakes of Fiber in Diets Low in Saturated Fat and Cholesterol, *N. Engl. J. Med. 329*, 21–26.

9. U.S. Food and Drug Administration (1998) Food Labeling: Health Claims; Soluble Fiber from Certain Foods and Coronary Heart Disease, FDA, Rockville, MD, Docket No. 96P-0338.

10. Anderson, J.W., Allgood, L.D., Lawrence, A., Altringer, L.A., Jerdack, G.R., Hengehold, D.A., and Morel, J.G. (2000) Cholesterol-Lowering Effects of Psyllium Intake Adjunctive to Diet Therapy in Men and Women with Hypercholesterolemia: Meta-analysis of 8 Controlled Trials, *Am. J. Clin. Nutr. 71*, 472–479.

11. Brown, L., Rosner, B., Willett, W.W., and Sacks, F.M. (1999) Cholesterol-Lowering Effects of Dietary Fiber: A Meta-analysis, *Am. J. Clin. Nutr. 69*, 30–42.

12. Anderson, J.W., Johnstone, B.M., and Cook-Newell, M.E. (1995) Meta-analysis of the Effects of Soy Protein Intake on Serum Lipids, *N. Engl. J. Med. 333*, 276–282.

13. U.S. Food and Drug Administration. (1999) FDA Final Rule for Food Labelling: Health Claims: Soy Protein and Coronary Heart Disease, *Fed. Regist. 64*, 57699–57733.

14. Expert Panel on Detection, Evaluation, and Treatment of High Blood Cholesterol in Adults (2001) Executive Summary of the Third Report of the National Cholesterol Education Program (NCEP) Expert Panel on Detection, Evaluation, and Treatment of High Blood Cholesterol in Adults (Adult Treatment Panel III), *JAMA 285*, 2486–2497.

15. Lipid Research Clinics (1982) Population Studies Data Book. Volume II: The Prevalence Study-Nutrient Intake, U.S. Government Printing Office, Washington, DC, U.S. Department of Health and Human Services Publication no. (NIH) 82-2014.

16. Jones, P.J., Raeini-Sarjaz, M., Ntanios, F.Y., Vanstone, C.A., Feng, J.Y., and Parsons, W.E. (2000) Modulation of Plasma Lipid Levels and Cholesterol Kinetics by Phytosterol Versus Phytostanol Esters, *J. Lipid Res. 41*, 697–705.

17. Lipid Research Clinics (1982) *Manual of Laboratory Operations: Lipid and Lipoprotein Analysis*, revised, U.S. Government Printing Office, Washington, DC, U.S. Department of Health and Human Services Publication no. (NIH) 75-678.

18. Warnick, G.R., Benderson, J., and Albers, J.J. (1982) Dextran Sulfate-Mg^{2+} Precipitation Procedure for Quantitation of High-Density-Lipoprotein Cholesterol, *Clin. Chem. 28*, 1379–1388.

19. Friedewald, W.T., Levy, R.I., and Fredrickson, D.S. (1972) Estimation of the Concentration of Low-Density Lipoprotein Cholesterol in Plasma, Without Use of the Preparative Ultracentrifuge, *Clin. Chem. 18*, 499–502.

20. Fink, P.C., Romer, M., Haeckel, R., Fateh-Moghadam, A., Delanghe, J., Gressner, A.M., and Dubs, R.W. (1989) Measurement of Proteins with the Behring Nephelometer. A Multicentre Evaluation, *J. Clin. Chem. Biochem. 27*, 261–276.

21. Naito, Y., Konishi, C., and Ohara, N. (2000) Blood Coagulation and Osmolar Tolerance of Erythrocytes in Stroke-Prone Spontaneously Hypertensive Rats Given Rapeseed Oil or Soybean Oil as the Only Dietary Fat, *Toxicol. Lett. 117*, 209–215.

22. The Agricultural Research Service (1992) *Composition of Foods, Agriculture Handbook No. 8*. U.S. Department of Agriculture, Washington, DC.

23. Association of Official Analytical Chemists (1980) *AOAC Official Methods of Analysis*, AOAC, Washington, DC.

24. Cunnane, S.C., Hamadeh, M.J., Liede, A.C., Thompson, L.U., Wolever, T.M., and Jenkins, D.J. (1995) Nutritional Attributes of Traditional Flaxseed in Healthy Young Adults, *Am. J. Clin. Nutr. 61*, 62–68.

25. Anderson, J.W., and Bridges, S.R. (1988) Dietary Fiber Content of Selected Foods, *Am. J. Clin. Nutr. 47*, 440–447.

26. SAS Institute (1997) *SAS/STAT User's Guide*, edn. 6.12, SAS Institute, Cary, NC.

27. U.S. Food and Drug Administration (2001) *Food Labeling: Health Claims; Soluble Fiber from Whole Oats and Risk of Coronary Heart Disease*, pp. 15343–15344, FDA, Rockville, MD, Docket No. 95P-0197.

28. Olson, B.H., Anderson, S.M., Becker, M.P., Anderson, J.W., Hunninghake, D.B., Jenkins, D.J., LaRosa, J.C., Rippe, J.M., Roberts, D.C., Stoy, D.B., *et al*. Psyllium-Enriched Cereals Lower Blood Total Cholesterol and LDL Cholesterol, but Not HDL Cholesterol, in Hypercholesterolemic Adults: Results of a Meta-analysis, *J. Nutr. 127*, 1973–1980.

29. Jenkins, D.J., Kendall, C.W., Marchie, A., Parker, T.L., Connelly, P.W., Qian, W., Haight, J.S., Faulker, D., Vidgen, E., Lapsley, K.G., and Spiller, G.A. (2002) Dose Response of Almonds on Coronary Heart Disease Risk Factors: Blood Lipids, Oxidized Low-Density Lipoproteins, Lipoprotein(a), Homocysteine, and Pulmonary Nitric Oxide: A Randomized, Controlled, Crossover Trial, *Circulation 106*, 1327–1332.

30. Spiller, G.A., Jenkins, D.A., Bosello, O., Gates, J.E., Cragen, L.N., and Bruce, B. (1998) Nuts and Plasma Lipids: An Almond-Based Diet Lowers LDL-C While Preserving HDL-C, *J. Am. Coll. Nutr. 17*, 285–290.

31. Jenkins, D.J., Kendall, C.W., Popovich, D.G., Vidgen, E., Mehling, C.C., Vuksan, V., Ransom, T.P., Rao, A.V., Rosenberg-Zand, R., Tariq, N., *et al.* (2001) Effect of a Very-High-Fiber Vegetable, Fruit, and Nut Diet on Serum Lipids and Colonic Function, *Metabolism 50*, 494–503.

32. International Committee for Standardization in Haematology (1971) Recommended Methods for Radioisotope Red-Cell Survival Studies. A Report by the ICSH Panel on Diagnostic Applications of Radioisotopes in Haematology, *Br. J. Haematol. 21*, 241–250.

33. Goodman, J.W., and Smith, L.H. (1961) Erythrocyte Life Span in Normal Mice and in Radiation Bone Marrow Chimeras, *Am. J. Physiol. 200*, 764–770.

34. Ketomaki, A.M., Gylling, H., Antikainen, M., Siimes, M.A., and Miettinen, T.A. (2003) Red Cell and Plasma Plant Sterols Are Related During Consumption of Plant Stanol and Sterol Ester Spreads in Children with Hypercholesterolemia, *J. Pediatr. 142*, 524–531.

35. Young, L.E., Izzo, M.J., and Platzer, R.F. (1951) Hereditary Spherocytosis. I. Clinical, Hematologic and Genetic Features in 28 Cases, with Particular Reference to the Osmotic and Mechanical Fragility of Incubated Erythrocytes, *Blood 6*, 1073.

Effects of a Water-Soluble Phytostanol Ester on Plasma Cholesterol Levels and Red Blood Cell Fragility in Hamsters

Naoyuki Ebine, Xiaoming Jia, Isabelle Demonty, Yanwen Wang, and Peter J.H. Jones*

School of Dietetics and Human Nutrition, Macdonald Campus of McGill
University, Ste. Anne de Bellevue, Québec, Canada H9X 3V9

ABSTRACT: The aim of this study was to assess the efficacy of a novel water-soluble phytostanol analog, disodium ascorbyl phytostanyl phosphates (DAPP), on plasma lipid levels and red blood cell fragility in hamsters fed atherogenic diets. For 5 wk, 50 male Golden Syrian hamsters were fed a semipurified diet without added cholesterol (noncholesterol, group 1), or a semipurified diet with 0.25% cholesterol (cholesterol-control, group 2). Groups 3–5 were fed the cholesterol-control diet with an addition of 1% phytostanols (diet 3), 0.71% DAPP (DAPP 0.7%, diet 4), or 1.43% DAPP (DAPP 1.4%, diet 5). Diets 4 and 5 provided 0.5 and 1% phytostanols, respectively. Supplementation of 0.71 and 1.43% DAPP decreased plasma total cholesterol concentrations by 34 ($P < 0.001$) and 46% ($P < 0.001$), respectively, in comparison with the cholesterol-control group, whereas free stanols reduced ($P = 0.007$) plasma cholesterol concentrations by 14%. Similarly, non-HDL-cholesterol concentrations were reduced by 39 ($P < 0.001$) and 54% ($P < 0.001$) in hamsters supplemented with DAPP 0.7% and DAPP 1.4%, respectively, relative to the cholesterol-control group. The hypocholesterolemic effect of DAPP 1.4% was threefold stronger than that of free stanols. In hamsters supplemented with DAPP 1.4%, plasma TG concentrations were 45% lower ($P = 0.018$) than in cholesterol-control-fed hamsters, whereas no such beneficial effect was observed in the free stanol group. Erythrocyte fragility was unaffected by DAPP or free phytostanols. Results of the current study demonstrate that DAPP lowers cholesterol more efficiently than free stanols, without an adverse effect on erythrocyte fragility in hamsters.

Paper no. L9517 in *Lipids 40*, 175–180 (February 2005).

The cholesterol-lowering effects of plant sterols have been well established (1–4). Meta-analyses have shown that dietary supplementation of plant sterols can reduce plasma LDL cholesterol levels by 8–12% in humans (4,5). The cholesterol-lowering effects of plant sterols reportedly result from the inhibition of dietary cholesterol absorption and biliary cholesterol reabsorption by inhibiting cholesterol incorporation into micelles in the intestine (2,6–8).

Through the process of hydrogenation, plant sterols are converted to plant stanols (also called phytostanols), which are ab-

sorbed at a negligible level (9,10). Based on previous data in animal and human studies, free plant stanols are believed to be more effective than free sterols in lowering plasma cholesterol (9–17). Esterification of free plant sterols and stanols with fat-soluble compounds, such as FA, increases their fat solubility. Several studies have demonstrated that the esterification of plant sterols with long-chain FA increases fat solubility, resulting in an increased suspension of plant sterols in the dietary fats or oils (5,8,18). In addition, some human trials comparing plant sterol esters with plant stanol esters have demonstrated that sterol esters and stanol esters appear to be roughly equivalent in their cholesterol-lowering efficacy (6,7,19–21). Progressively, the solubility and physical state of plant sterols and stanols appear to be determining factors in their cholesterol-lowering efficiency (22).

More recently, a water-soluble analog of phytostanols, disodium ascorbyl phytostanyl phosphates (DAPP), was developed through chemical modifications (23,24). DAPP were produced by covalently linking ascorbate to the *sn*-3 position of the phytostanol *via* a phosphodiester bond. The two major components of DAPP are disodium ascorbyl campestanyl phosphate and disodium ascorbyl sitostanyl phosphate. Results from a study in apolipoprotein E knockout mice showed that DAPP was more efficient in lowering cholesterol than the unesterified stanols (24). However, there have been no comparative studies on the effects of DAPP and unesterified stanols in wild-type animal models in which circulating cholesterol levels are increased by feeding atherogenic diets.

The ingestion of plant sterols is associated with increased plant sterol levels in red blood cell (RBC) membranes (25). Studies in hyperlipidemic, otherwise healthy individuals have shown no detrimental effect of plant sterols on RBC fragility in humans (25–27). However, a recent animal study suggested that plant sterols may decrease RBC deformability and life span in spontaneously hypertensive rats (28), raising the question of whether dietary supplementation with plant sterols or stanols is safe. Therefore, the present study was undertaken to compare the cholesterol-lowering efficacy of a water-soluble stanol analog (DAPP) and its parent compound, free stanols, and to determine their impacts on RBC fragility in hamsters fed atherogenic diets.

MATERIALS AND METHODS

Animals and diets. Fifty male Golden Syrian hamsters weighing 90–110 g (Charles River Laboratories, Montréal, Québec,

---

*To whom correspondence should be addressed at School of Dietetics and Human Nutrition, Macdonald Campus of McGill University, 21,111 Lakeshore, Ste. Anne de Bellevue, Québec, Canada H9X 3V9.
E-mail: peter.jones@mcgill.ca

Current address of fourth author: Institute for Nutrisciences and Health, National Research Council, 93 Mount Edward Road, Charlottetown, PEI, Canada C1A 5T1.

Abbreviations: ABC, ATP-binding cassette; DAPP, disodium ascorbyl phytostanyl phosphates; RBC, red blood cell; SHRSP, stroke-prone spontaneously hypertensive rat.

Canada) were randomly divided into 5 groups. Animals were housed individually in stainless-steel colony cages with a 12 h (light)/12 h (dark) light cycle. The room temperature was set at 20 ± 1°C. After a 2-wk acclimatization period on the regular rodent chow (Charles River Laboratories), animals were randomly assigned into 5 groups and fed experimental diets for 5 wk. Groups 1 and 2 were fed a semipurified diet without cholesterol (noncholesterol) and with 0.25% cholesterol (cholesterol-control), respectively. Groups 3–5 were fed the cholesterol-control diet, with an addition of 1% (w/w) of unesterified phytostanol (stanol), 0.71% of DAPP (DAPP 0.7%), or 1.43% of DAPP (DAPP 1.4%), respectively. Diets DAPP 0.7% and DAPP 1.4% were designed to provide 0.5% and 1% of free phytostanols (parent phytostanols), respectively, based on the M.W. of the phytostanols and DAPP. DAPP contained 65% (w/w) sitostanol and 35% campestanol. Unesterified phytostanols and DAPP were provided by Forbes Medi-Tech Inc. (Vancouver, British Columbia, Canada). All diets contained 5% fat provided in the form of a mix of beef tallow and safflower oil to yield a polyunsaturated to saturated FA ratio of 0.4.

The compositions of the diets are presented in Table 1. The experiment was reviewed and approved by the Animal Care and Research Ethics Committee of McGill University and was conducted in accordance with the guidelines of the Canadian Council on Animal Care.

Blood sample collection and plasma cholesterol analyses. After 5 wk of feeding on the experimental diets, hamsters were fasted overnight prior to anesthetization with halothane. Blood samples were collected by decapitation into tubes containing EDTA and placed on ice. Plasma and RBC were separated by centrifugation at $350 \times g$ rpm for 15 min. Plasma samples were stored at −80°C until analyses. Plasma total, HDL, and non-HDL cholesterol, as well as TG concentrations, were measured in duplicate by enzymatic methods (Roche Diagnostics, Laval, Québec, Canada) (29,30). HDL cholesterol was measured after precipitation of apolipoprotein B containing lipoproteins with dextran sulfate and magnesium chloride (31). Since the Friede-

wald equation (32) may not be applicable to hamsters, non-HDL cholesterol was used instead of LDL cholesterol; this was calculated by subtracting HDL cholesterol from total cholesterol.

Measurement of RBC fragility. RBC fragility was measured using fresh RBC collected in vacutainer tubes containing EDTA. An aliquot of 0.2 mL RBC was added to 2 mL unbuffered saline solution with a sodium chloride concentration ranging from 0.20 to 0.60%. After 1 h, the cells were centrifuged at $210 \times g$ for 5 min at room temperature. The supernatants were collected and measured for absorbance at 520 nm (33). The saline concentration for 50% hemolysis was calculated and considered as the median osmotic fragility. The concentration required to obtain 50% hemolysis was determined by assuming that a linear response existed between consecutive observations.

Data analysis and statistics. Results are expressed as means ± SEM, and a *P* value of <0.05 was considered significant. Data were subjected to an ANOVA using the general linear model procedure of the Statistical Analysis System (SAS Institute, Cary, NC) to determine the main treatment effects. When a significant effect was detected, Duncan's New Multiple Range test was performed to identify differences among treatment groups. The relationships between plasma cholesterol concentrations and the median osmotic RBC fragility were tested using Pearson's correlation coefficients.

RESULTS

Body weight and food consumption. No significant difference was observed in final body weight among the treatment groups after 5 wk of feeding. However, hamsters fed DAPP 1.4% had relatively lower final body weights compared with other groups, although the difference was not statistically significant. Similarly, there were no significant differences among the groups in average or total food consumption during the 5-wk period.

Plasma lipid concentrations. Effects of the experimental diets on plasma total, HDL, and non-HDL cholesterol levels are

TABLE 1
Composition of Experimental Diets[a]

Diet (% w/w)	Nonchol	Chol-control	Stanol	DAPP 0.7%	DAPP 1.4%
Casein	20.0	20.0	19.8	19.8	19.8
Cornstarch	28.0	28.0	27.7	27.7	27.7
Sucrose	36.3	36.0	35.6	35.6	35.6
Beef tallow/safflower oil	5.0	5.0	5.0	5.0	5.0
Cellulose	5.0	5.0	4.9	4.9	4.9
DL-Methionine	0.5	0.5	0.5	0.5	0.5
Mineral mixture	4	4	4	4	4
Vitamin mixture	1	1	1	1	1
Choline bitartrate	0.2	0.2	0.2	0.2	0.2
Butylated hydroxytoluene	0.02	0.02	0.02	0.02	0.02
Cholesterol	—	0.25	0.25	0.25	0.25
Phytostanols	—	—	1.0	—	—
DAPP	—	—	—	0.71[b]	1.43[b]

[a]Nonchol, control diet without added cholesterol; Chol-control, control diet with 0.25% added cholesterol; Stanol, chol-control with 1% added phytostanols; DAPP (disodium ascorbyl phytostanyl phosphates), chol-cholesterol with added DAPP.
[b]DAPP 0.7% and DAPP 1.4% contained 0.5 and 1.0% unesterified phytostanols, respectively.
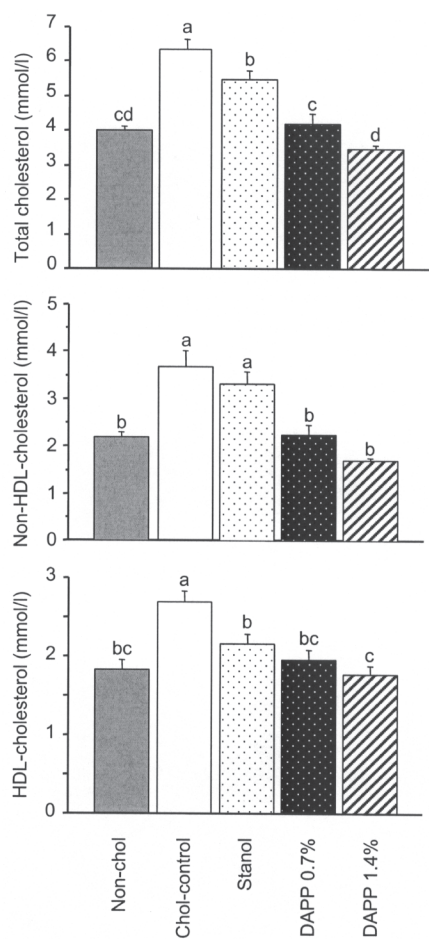
FIG. 1. Effects of phytostanols and their water-soluble analogs on plasma total cholesterol, non-HDL cholesterol, and HDL cholesterol levels in hamsters. Data are expressed as means and SEM (n = 10). Bars carrying different superscripts are significantly different (P < 0.05). Non-chol, control diet without added cholesterol; Chol-control, control diet with 0.25% added cholesterol; Stanol, chol-control with 1% added phytostanols; DAPP 0.7%, chol-cholesterol with 0.71% added disodium ascorbyl phytostanyl phosphates; DAPP 1.4%, chol-cholesterol with 1.43% added disodium ascorbyl phytostanyl phosphates.

shown in Figure 1. In hamsters fed DAPP 0.7% and DAPP 1.4%, total cholesterol was reduced by 34 (P < 0.001) and 47% (P < 0.001), respectively, in comparison with the cholesterol-control group, and these values were similar to the noncholesterol group. Similarly, non-HDL cholesterol levels in hamsters supplemented with DAPP 0.7% and DAPP 1.4% were 39 (P < 0.001) and 54% (P < 0.001) lower, respectively, than in those fed the cholesterol-control diet. The stanol diet lowered (P = 0.007)

total cholesterol by 14% relative to the cholesterol-control diet. HDL cholesterol levels were lower in the two DAPP (P < 0.001) and stanol (P = 0.005) groups in comparison with the cholesterol-control group, and the values were similar with the noncholesterol group. However, changes in HDL cholesterol levels after feeding the DAPP and stanol diets were not reflected by changes in total cholesterol/HDL cholesterol and non-HDL cholesterol/HDL cholesterol ratios, which were decreased in the DAPP 1.4% group compared with the cholesterol-control (P = 0.028) and stanol groups (P = 0.006) (data not shown).

Effects of diet treatments on plasma TG concentrations are shown in Table 2. Although the free stanol diet did not affect plasma TG concentrations in comparison with the cholesterol-control diet, DAPP 1.4% reduced TG concentrations by 45% (P = 0.018) compared with the cholesterol-control group. Additionally, plasma TG concentrations were decreased by 42 (P = 0.022) and 49% (P = 0.004), respectively, in hamsters fed DAPP 0.7% and DAPP 1.4% compared with hamsters fed the free stanol diet.

RBC fragility. The saline concentration associated with the median osmotic fragility was (in %) 0.481 ± 0.004, 0.467 ± 0.007, 0.489 ± 0.007, 0.486 ± 0.005, and 0.478 ± 0.009 in DAPP 0.7%, DAPP 1.4%, stanols, cholesterol-control, and noncholesterol, respectively. There were no differences among the treatment groups. Likewise, there was no significant difference in RBC fragility across the treatment groups at any saline concentration (Fig. 2). Positive correlations were observed between the median osmotic fragility (%) and plasma total cholesterol (mmol/L) (r = 0.44, P = 0.003) and non-HDL cholesterol concentrations (r = 0.43, P = 0.004).

DISCUSSION

This is the first study to show a more potent hypocholesterolemic effect from DAPP compared with unesterified phytostanols in non-gene-treated animals with diet-induced higher circulating cholesterol levels. In hamsters fed DAPP, a strong cholesterol-lowering effect was observed, which resulted in total and non-HDL cholesterol levels similar to those observed in hamsters fed the noncholesterol diet. The DAPP diet showed a stronger hypocholesterolemic effect than the stanol diet, with a dose-dependent response being observed. Similar to the current finding, the cholesterol-lowering effect of DAPP on circulating cholesterol levels has been reported in other animal studies. For example, gerbils given 1 and 2% (w/w) DAPP in the diet, or 2 and 4% DAPP in drinking water had decreased total and LDL cholesterol levels (23,34). Recently, Lukic *et al.* (24) reported that in comparison with the control diet, a 4-wk administration of DAPP

TABLE 2
Effects of Phytostanols and Their Water-Soluble Analogs on Plasma TG Concentrations in Hamsters[a]

Diet	TG (mmol/L)	Diet[b]	TG (mmol/L)
Nonchol	4.50 ± 0.34[a,b,c]	DAPP 0.7%	3.64 ± 0.46[b,c]
Chol-control	5.88 ± 0.66[a,b]	DAPP 1.4%	3.23 ± 0.30[c]
Stanol	6.30 ± 0.96[a]		

[a]Values are mean ± SEM (n = 10 per group). Values carrying different superscripts (a–c) are significantly different (P < 0.05). For diet descriptions, see Table 1.
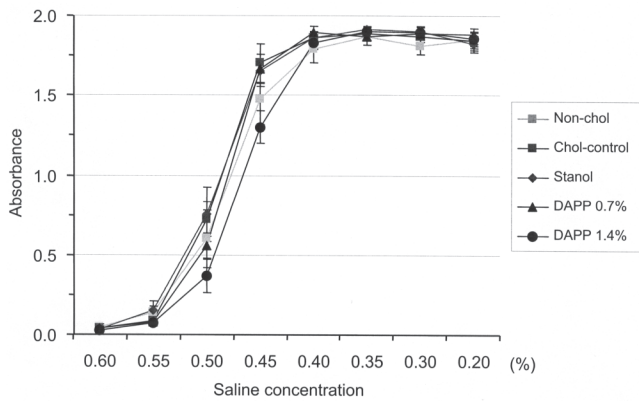
FIG. 2. Effects of phytostanols and their water-soluble analogs on red blood cell fragility in hamsters. Data are expressed as means and SEM (*n* = 9, except the chol-control group, where *n* = 7). For diet descriptions, see Figure 1.

at a dose as low as 0.5% reduced total cholesterol concentrations by approximately 75% in cholesterol-fed apolipoprotein E knockout mice.

Inhibition of cholesterol absorption from the intestine is a well-established mechanism through which plant sterols/stanols lower plasma cholesterol concentrations (2,35–39). DAPP has been shown to reduce cholesterol absorption in rats in a dose-dependent manner (40). The current study showed a stronger hypocholesterolemic effect from DAPP than from the corresponding unesterified stanols, despite the same amount of stanols being provided in the DAPP 1.4% and stanols groups. The effects of the individual components of DAPP on circulating cholesterol levels were examined previously only in apolipoprotein E-deficient mice (24). Those results indicated that DAPP resulted in an extreme lowering of total cholesterol concentrations in that model, whereas less favorable effects were observed with a mixture of ascorbic acid and unesterified stanols. Results of the present study, together with previous ones, suggest that the esterification of stanols with ascorbic acid is responsible for the increased hypocholesterolemic effect of DAPP relative to unesterified stanols. The present results also suggest that increasing the water solubility of plant stanols could be an approach to reducing the effective dose of plant sterols or stanols in lowering blood lipids.

Currently, the mechanism of action of DAPP on cholesterol absorption is not fully understood. A widely accepted explanation is that sterols and stanols compete with cholesterol in the intestine during their incorporation into micelles and thus decrease cholesterol uptake by enterocytes (40). In an *in vitro* study, DAPP decreased cholesterol accumulation in Caco-2 cells, suggesting that DAPP may modify some extracellular mechanisms of cholesterol influx and efflux (41). Most recently, Wasan *et al.* (42) observed that DAPP reduced the accumulation of cholesterol in cultured rat small intestinal crypt cells and speculated that DAPP might inhibit the interaction of cholesterol or cholesterol micelles with the receptors of enterocytes or act as an antagonist of cholesterol influx channels. Transporters of the ATP-binding cassette (ABC) family appear to play important roles in regulating cholesterol absorption and excretion (43,44). Support-

ive data were obtained by Berge *et al.* (45) that the increased accumulation of dietary cholesterol in subjects with autosomal recessive disorder was caused by mutations in the adjacent region of ABCG5 and ABCG8 genes. More studies are required to define the roles of ABCG5 and ABCG8 in the inhibition of cholesterol absorption by plant sterols and stanols.

A few studies have examined the potential TG-lowering effect of DAPP. When gerbils were given DAPP at concentration of 4% dissolved in the drinking water for 8 wk, TG concentrations were reduced compared with controls that did not receive DAPP (34). However, this effect was not observed in another study in which gerbils were fed 2% of DAPP for 4 wk (23). In a study conducted in apolipoprotein E knockout mice, plasma TG were reduced after feeding a 2% DAPP diet for 4 and 8 wk, respectively, in comparison with the control group, whereas no difference was observed after 12 wk (24). In the current study, we observed that DAPP was effective at lower concentrations in decreasing plasma TG levels compared with the cholesterol-control diets, as well as the unesterified phytostanol diet, whereas unesterified stanols showed no effect. In addition to the DAPP 1.4% group, although not statistically significant, the DAPP 0.7% group showed lower average TG levels in comparison with the noncholesterol-control group, implying the existence of a hypolipidemic effect of DAPP. The mechanisms through which DAPP lowers plasma TG are currently unknown. Further studies are required to verify the TG-lowering actions of DAPP and to elucidate the underlying mechanisms.

It has been suggested that plant sterols/stanols may increase the risk of hemorrhagic stroke, based on studies in stroke-prone spontaneously hypertensive rats (SHRSP) (28,46). In these hypertensive animals, when 0.2% (w/w) plant sterols were administered in their diets, decreased erythrocyte deformability was detected by using an ektacytometer, which can measure relatively minor alterations in RBC membrane rigidity, internal viscosity, and the ratio of surface area to volume (28). However, the osmotic fragility test detected no detrimental effects in the present animal model even though a higher dose of plant stanols (1%) was applied. Using the same method applied in the present study, Jenkins *et al.* (26) reported no significant changes in RBC fragility in humans after 4 wk of a low saturated fat diet enriched with plant sterols, soy protein, and viscous fibers. In addition, this research group illustrated constant results on fragility in another recent study (27). Hendriks *et al.* (25) reported that increased plant sterol concentrations in RBC membrane after long-term (1-yr) consumption of a plant sterol ester-enriched spread did not affect RBC deformability, which was measured by a method similar to that described in the study of SHRSP. Therefore, it is possible that the results obtained in SHRSP cannot be readily extrapolated to healthy animals or to other species. A significant decrease in the intestinal mRNA expressions of ABCG5 and ABCG8, which are involved in the selective transport of dietary sterols in the intestine, has been reported in SHRSP compared with Wistar rats (47). Results of this study suggest that the unfavorable effects on enterocytes observed in the SHRSP following supplementation of plant sterols are due to the increased absorption of plant sterols in this species. The present data, obtained in hypercholes-

terolemic, otherwise healthy animals, and the observations previously done in humans suggest that the use of plant stanols as food-based cholesterol-lowering agents may not be associated with an increased risk of hemorrhagic stroke for the general population. However, more effort is warranted to evaluate the risk of hemorrhagic sequelae with plant sterols or stanols used at the levels provided in functional foods. The incubated fragility test is one of the most sensitive measurements for detecting subtle changes in fragility (48,49). Since the adverse effects of plant sterols and stanols on RBC fragility are small, the incubated fragility test might be beneficial for detecting minor changes induced by dietary manipulation.

In the present study, positive correlations have been observed between the median osmotic fragility and plasma total cholesterol and non-HDL cholesterol concentrations, indicating that lowered plasma cholesterols have the potential to fortify RBC membranes against osmotic stimulation. Replacement of a part of the cholesterol with plant sterols in erythrocyte membranes has been shown to cause adverse events on RBC deformability and results in a decreased life span in spontaneously hypertensive rats (28). In contrast, a recent study that provided 0.5% cholesterol diets to Wistar rats suggested that erythrocytes become more fragile in animals with high plasma cholesterol concentrations; when cholesterol-lowering agents were added to the diet, the fragility of the RBC was partially reversed (50). Correlations observed in the present study between osmotic fragility and plasma cholesterol levels appear to support the latter observation. Plant sterols have been reported to alter plasma cholesterols as well as RBC cholesterol simultaneously in spontaneously hypertensive rats (28,46). High plasma cholesterol has been demonstrated to increase RBC fragility; therefore, plant sterols may have positive effects on RBC fragility, since sterols lower plasma cholesterol. However, plant sterols may also have unfavorable effects on RBC deformability, since sterols lower RBC cholesterol, which is essential for membrane integrity. In view of the fact that plant sterols may have either beneficial or detrimental effects on RBC fragility, this may account for the differing results seen in previous studies (25–28).

In conclusion, the results of the present study demonstrate that the esterification of plant stanols with a water-soluble compound, such as ascorbic acid, increases their cholesterol-lowering efficacy in hamsters fed atherogenic diets. DAPP could therefore offer a more efficient treatment alternative to hypercholesterolemic subjects than the other existing forms such as stanol esters with FA and free stanols. The findings of the current study also suggest that ascorbyl phytostanyl phosphate has potential for treating hypertriglyceridemia. The absence of a detrimental effect of DAPP on RBC fragility indicates that dietary supplementation with DAPP at the dose used in the current study may not be a trigger of plant sterol-induced adverse events on erythrocyte homeostasis.

ACKNOWLEDGMENTS

REFERENCES

1. Ling, W.H., and Jones, P.J.H. (1995) Enhanced Efficacy of Sitostanol-Containing Versus Sitostanol-Free Phytosterol Mixtures in Altering Lipoprotein Cholesterol Levels and Synthesis in Rats, *Atherosclerosis 118*, 319–331.
2. Ntanios, F.Y., and Jones, P.J.H. (1999) Dietary Sitostanol Reciprocally Influences Cholesterol Absorption and Biosynthesis in Hamsters and Rabbits, *Atherosclerosis 143*, 341–351.
3. Jones, P.J.H., and Raeini-Sarjaz, M. (2001) Plant Sterols and Their Derivatives: The Current Spread of Results, *Nutr. Rev. 59*, 21–24.
4. Katan, M.B., Grundy, S.M., Jones, P., Law, M., Miettinen, T., and Paoletti, R. (2003) Efficacy and Safety of Plant Stanols and Sterols in the Management of Blood Cholesterol Levels, *Mayo. Clin. Proc. 78*, 965–978.
5. Law, M.R. (2000) Plant Sterol and Stanol Margarine and Health, *Br. Med. J. 320*, 861–864.
6. Jones, P.J.H., Raeini-Sarjaz, M., Ntanios, F.Y., Vanstone, C.A., Feng, J.Y., and Parsons, W.E. (2000) Modulation of Plasma Lipid Levels and Cholesterol Kinetics by Phytosterol Versus Phytostanol Esters, *J. Lipid Res. 41*, 697–705.
7. Normen, L., Dutta, P., Lia, A., and Andersson, H. (2000) Soy Sterol Esters and β-Sitostanol Ester as Inhibitors of Cholesterol Absorption in Human Small Bowel, *Am. J. Clin. Nutr. 71*, 908–913.
8. Lichtenstein, A.H., and Deckelbaum, R.J. (2001) AHA Science Advisory: Stanol/Sterol Ester Containing Foods and Blood Cholesterol Levels: A Statement for Health Care Professionals from the Nutrition Committee of the Council on Nutrition, Physical Activity, and Metabolism of the American Heart Association, *Circulation 103*, 1177–1179.
9. Sugano, M., Morioka, H., and Ikeda, I. (1977) A Comparison of Hypocholesterolemic Activity of β-Sitosterol and β-Sitostanol in Rats, *J. Nutr. 107*, 2011–2019.
10. Heinemann, T., Kullak-Ublick, G.A., Pietruck, B., and von Bergmann, K. (1991) Mechanisms of Action of Plant Sterols on Inhibition of Cholesterol Absorption. Comparison of Sitosterol and Sitostanol, *Eur. J. Clin. Pharmacol. 40*, S59–S63.
11. Sugano, M., Kamo, F., Ikeda, I., and Morioka, H. (1976) Lipid-Lowering Activity of Phytostanols in Rats, *Atherosclerosis 24*, 301–309.
12. Ikeda, I., Kawasaki, A., Samezima, K., and Sugano, M. (1981) Antihypercholesterolemic Activity of β-Sitostanol in Rabbits, *J. Nutr. Sci. Vitaminol. 27*, 243–251.
13. Heinemann, T., Leiss, O., and von Bergmann, K. (1986) Effect of Low-Dose Sitostanol on Serum Cholesterol in Patients with Hypercholesterolemia, *Atherosclerosis 61*, 219–223.
14. Heinemann, T., Pietruck, B., Kullak-Ublick, G., and von Bergmann, K. (1988) Comparison of Sitosterol and Sitostanol on Inhibition of Intestinal Cholesterol Absorption, *Agents Actions Suppl. 26*, 117–122.
15. Becker, M., Staab, D., and von Bergmann K. (1993) Treatment of Severe Familial Hypercholesterolemia in Childhood with Sitosterol and Sitostanol, *J. Pediatr. 122*, 292–296.
16. Vanhanen, H.T., Blomqvist, S., Ehnholm, C., Hyvonen, M., Jauhiainen, M., Torstila, I., and Miettinen, T.A. (1993) Serum Cholesterol, Cholesterol Precursors, and Plant Sterols in Hypercholesterolemic Subjects with Different ApoE Phenotypes During Dietary Sitostanol Ester Treatment, *J. Lipid Res. 34*, 1535–1544.
17. Ntanios, F.Y., and Jones P.J.H. (1998) Effects of Variable Dietary Sitostanol Concentrations on Plasma Lipid Profile and Phytosterol Metabolism in Hamsters, *Biochim. Biophys. Acta 1390*, 237–244.
18. Ostlund, R.E., Jr. (2002) Phytosterols in Human Nutrition, *Annu. Rev. Nutr. 22*, 533–549.
19. Weststrate, J.A., and Meijer, G.W. (1998) Plant Sterol-Enriched

Margarines and Reduction of Plasma Total- and LDL-Cholesterol Concentrations in Normocholesterolaemic and Mildly Hypercholesterolaemic Subjects, *Eur. J. Clin. Nutr. 52*, 334–343.

20. Hallikainen, M.A., Sarkkinen, E.S., Gylling, H., Erkkila, A.T., and Uusitupa, M.I. (2000) Comparison of the Effects of Plant Sterol Ester and Plant Stanol Ester-Enriched Margarines in Lowering Serum Cholesterol Concentrations in Hypercholesterolaemic Subjects on a Low-Fat Diet, *Eur. J. Clin. Nutr. 54*, 715–725.

21. Noakes, M., Clifton, P., Ntanios, F., Shrapnel, W., Record, I., and McInerney, J. (2002) An Increase in Dietary Carotenoids When Consuming Plant Sterols or Stanols Is Effective in Maintaining Plasma Carotenoid Concentrations, *Am. J. Clin. Nutr. 75*, 79–86.

22. Moreau, R.A., Whitaker, B.D., and Hicks, K.B. (2002) Phytosterols, Phytostanols, and Their Conjugates in Foods: Structural Diversity, Quantitative Analysis, and Health-Promoting Uses, *Prog. Lipid Res. 41*, 457–500.

23. Wasan, K.M., Najafi, S., Peteherych, K.D., and Pritchard, P.H. (2001) Effects of Novel Hydrophilic Phytostanol Analog on Plasma Lipids Concentrations in Gerbils, *J. Pharm. Sci. 90*, 1795–1799.

24. Lukic, T., Wasan, K.M., Zamfir, D., Moghadasian, M.H., and Pritchard, P.H. (2003) Disodium Ascorbyl Phytostanyl Phosphate Reduces Plasma Cholesterol Concentrations and Atherosclerotic Lesion Formation in Apolipoprotein E-Deficient Mice, *Metabolism 52*, 425–431.

25. Hendriks, H.F., Brink, E.J., Meijer, G.W., Princen, H.M., and Ntanios, F.Y. (2003) Safety of Long-Term Consumption of Plant Sterol Esters-Enriched Spread, *Eur. J. Clin. Nutr. 57*, 681–692.

26. Jenkins, D.J., Kendall, C.W., Faulkner, D., Vidgen, E., Trautwein, E.A., Parker, T.L., Marchie, A., Koumbridis, G., Lapsley, K.G., Josse, R.G., *et al.* (2002) A Dietary Portfolio Approach to Cholesterol Reduction: Combined Effects of Plant Sterols, Vegetable Proteins, and Viscous Fibers in Hypercholesterolemia, *Metabolism 51*, 1596–1604.

27. Jenkins, D.J., Kendall, C.W., Marchie, A., Faulkner, D., Vidgen, E., Lapsley, K.G., Trautwein, E.A., Parker, T.L., Josse, R.G., Leiter, L.A., and Connelly, P.W. (2003) The Effect of Combining Plant Sterols, Soy Protein, Viscous Fibers, and Almonds in Treating Hypercholesterolemia, *Metabolism 52*, 1478–1483.

28. Ratnayake, W.M., L'Abbe, M.R., Mueller, R., Hayward, S., Plouffe, L., Hollywood, R., and Trick, K. (2000) Vegetable Oils High in Phytosterols Make Erythrocytes Less Deformable and Shorten the Life Span of Stroke-Prone Spontaneously Hypertensive Rats, *J. Nutr. 130*, 1166–1178.

29. Lipid Research Clinics. (1982) *Manual of Laboratory Operations. Lipid and Lipoprotein Analysis*, U.S. Government Printing Office, Washington, DC, U.S. Department of Health and Human Services Publication no. (NIH) 75–678.

30. Kohlmeier, M. (1986) Direct Enzymic Measurement of Glycerides in Serum and in Lipoprotein Fractions. *Clin. Chem. 32*, 63–66.

31. Warnick, G.R., Benderson, J., and Albers, J.J. (1982) Dextran Sulfate-Mg^{2+} Precipitation Procedure for Quantitation of High-Density-Lipoprotein Cholesterol, *Clin. Chem. 28*, 1379–1388.

32. Friedewald, W.T., Levy, R.I., and Fredrickson, D.S. (1972) Estimation of the Concentration of Low-Density Lipoprotein Cholesterol in Plasma, Without Use of the Preparative Ultracentrifuge, *Clin. Chem. 18*, 499–502.

33. Naito, Y., Konishi, C., and Ohara, N. (2000) Blood Coagulation and Osmolar Tolerance of Erythrocytes in Stroke-Prone Spontaneously Hypertensive Rats Given Rapeseed Oil or Soybean Oil as the Only Dietary Fat, *Toxicol. Lett. 117*, 209–215.

34. Wasan, K.M., Najafi, S., Wong, J., and Kwong, M. (2001) Assessing Plasma Lipid Levels, Body Weight, and Hepatic and Renal Toxicity Following Chronic Oral Administration of a Water-Soluble Phytostanol Compound, FM-VP4, to Gerbils, *J. Pharm. Pharm. Sci. 4*, 228–234.

35. Heinemann, T., Axtmann, G., and von Bergmann, K. (1993) Comparison of Intestinal Absorption of Cholesterol with Different Plant Sterols in Man, *Eur. J. Clin. Invest. 23*, 827–831.

36. Ikeda, I., and Sugano, M. (1998) Inhibition of Cholesterol Absorption by Plant Sterols for Mass Intervention, *Curr. Opin. Lipidol. 9*, 527–531.

37. Jones, P.J.H. (1999) Cholesterol-Lowering Action of Plant Sterols, *Curr. Atheroscler. Rep. 1*, 230–235.

38. Plat, J., and Mensink, R.P. (2001) Effects of Plant Sterols and Stanols on Lipid Metabolism and Cardiovascular Risk, *Nutr. Metab. Cardiovasc. Dis. 11*, 31–40.

39. de Jong, A., Plat, J., and Mensink, R.P. (2003) Metabolic Effects of Plant Sterols and Stanols (review), *J. Nutr. Biochem. 14*, 362–369.

40. Wasan, K.M., Peteherych, K.D., and Najafi, S. (2001) Assessing the Plasma Pharmacokinetics, Tissue Distribution, Excretion and Effects on Cholesterol Pharmacokinetics of a Novel Hydrophilic Compound, FM-VP4, Following Administration to Rats, *J. Pharm. Pharm. Sci. 4*, 207–216.

41. Ramaswamy, M., Yau, E., Wasan, K.M., Boulanger, K.D., Li, M., and Pritchard, P.H. (2002) Influence of Phytostanol Phosphoryl Ascorbate, FM-VP4, on Pancreatic Lipase Activity and Cholesterol Accumulation Within Caco-2 Cells, *J. Pharm. Pharm. Sci. 5,* 29–38.

42. Wasan, K.M., Yau, E., Boulanger, K.D., Ramswamy, M., and Pritchard, P.H. (2003) Effects of Disodium Ascorbyl Phytostanol Phosphates (FM-VP4) on Cholesterol Accumulation Within Rat Intestinal Cells, *AAPS PharmSci 5*, Article 6.

43. Schmitz, G., Langmann, T., and Heimerl, S. (2001) Role of ABCG1 and Other ABCG Family Members in Lipid Metabolism, *J. Lipid Res. 42*, 1513–1520.

44. Ordovas, J.M., and Tai, E.S. (2002) The Babel of the ABCs: Novel Transporters Involved in the Regulation of Sterol Absorption and Excretion, *Nutr. Rev. 60*, 30–33.

45. Berge, K.E., Tian, H., Graf, G.A., Yu, L., Grishin, N.V., Schultz, J., Kwiterovich, P., Shan, B., Barnes, R., and Hobbs, H.H. (2000) Accumulation of Dietary Cholesterol in Sitosterolemia Caused by Mutations in Adjacent ABC Transporters, *Science 290*, 1771–1775.

46. Ratnayake, W.M., Plouffe, L., L'Abbe, M.R., Trick, K., Mueller, R., and Hayward, S. (2003) Comparative Health Effects of Margarines Fortified with Plant Sterols and Stanols on a Rat Model for Hemorrhagic Stroke, *Lipids 38*, 1237–1247.

47. Ogawa, H., Yamamoto, K., Kamisako, T., and Meguro, T. (2003) Phytosterol Additives Increase Blood Pressure and Promote Stroke Onset in Salt-Loaded Stroke-Prone Spontaneously Hypertensive Rats, *Clin. Exp. Pharmacol. Physiol. 30*, 919–924.

48. Young, L.E., Izzo, M.J., and Platzer, R.F. (1951) Hereditary Spherocytosis. I. Clinical, Hematologic and Genetic Features in 28 Cases, with Particular Reference to the Osmotic and Mechanical Fragility of Incubated Erythrocytes, *Blood 6*, 1073–1098.

49. Langley, G.R., and Felderhof, C.H. (1968) Atypical Autohemolysis in Hereditary Spherocytosis as a Reflection of Two Cell Populations: Relationship of Cell Lipids to Conditioning by the Spleen, *Blood 32*, 569–585.

50. Kempaiah, R.K., and Srinivasan, K. (2002) Integrity of Erythrocytes of Hypercholesterolemic Rats During Spices Treatment, *Mol. Cell. Biochem. 236*, 155–161.

A Comparison of the Effect of Medium- vs. Long-Chain Triglycerides on the *in vitro* Solubilization of Cholesterol and/or Phytosterol into Mixed Micelles

Anna von Bonsdorff-Nikander[a,*], Leena Christiansen[a], Laura Huikko[b], Anna-Maija Lampi[b], Vieno Piironen[b], Jouko Yliruusi[a,c], and Ann Marie Kaukonen[c]

[a]Division of Pharmaceutical Technology, Faculty of Pharmacy, [b]Department of Applied Chemistry and Microbiology, Division of Food Chemistry, and [c]Viikki Drug Discovery Technology Center (DDTC), Faculty of Pharmacy, FIN-00014 University of Helsinki, Finland

ABSTRACT: Despite clinical evidence of the cholesterol-lowering effects of phytosterols, the exact mechanisms involved are still unclear. Displacement of cholesterol by phytosterols from mixed micelles, which is due to their greater hydrophobicity, is one of the hypotheses for the lumenal effects contributing to the reduction of intestinal cholesterol absorption. In this study a dynamic *in vitro* lipolysis method was used to examine the solubilization behavior of cholesterol and/or phytosterols during lipolysis to probe the efficacy of cholesterol displacement from mixed micelles by phytosterols. The effects of lipid chain length on sterol solubilization were studied by using microcrystalline suspensions containing 17% phytosterol or cholesterol, formulated in long-chain TG (LCT) and medium-chain TG (MCT). When digesting cholesterol suspended in LCT, the entire cholesterol dose was incorporated into the micellar phase. For the cholesterol formulation suspended in MCT, 50.3% of the initial dose was recovered in the micelles. Under the respective conditions, we observed lower solubilization of phytosterols than of cholesterol (roughly fourfold). Only 25% of the initial phytosterol dose was solubilized from suspensions formulated with LCT, and 13% was solubilized from MCT formulations. Co-administration of phytosterol and cholesterol suspensions showed a significant reduction of cholesterol solubilization, particularly when dosed in MCT, with ~25% of the cholesterol dose solubilized. Insignificant amounts of cholesterol were displaced by phytosterols when cholesterol was presolubilized in the mixed micelles. The results show that, compared with LCT, mixed micelles containing MCT lipolysis products have a reduced solubilizing capacity for cholesterol, which adds to the effectiveness of the phytosterols in displacing cholesterol. This suggests potential benefits of using medium chain length lipids in cholesterol-lowering phytosterol products.

Paper no. L9616 in *Lipids* 40, 181–190 (February 2005).

Since the early 1950s, the cholesterol-lowering properties of phytosterols in humans have been known (1). In plants, sterols are always present as a mixture, and they have the same func-tion as cholesterol in animals: They are essential components of cell membranes (2,3). When consumed at a level of 1–3 g/d, an LDL cholesterol-lowering effect of up to 10% can be achieved (4,5). Thus, today phytosterols are incorporated into a wide variety of food products, referred to as functional foods. The intake of phytosterols from natural sources in the Western diet is at levels of approximately 100–500 mg/d (6–8).

Cholesterol enters the intestinal tract from two major sources, typically two-thirds from biliary secretion and one-third from dietary sources (9,10). Phytosterols are structurally related to cholesterol but differ from cholesterol only in their unsaturation level and/or side-chain configuration. However, less than 2% of the ingested phytosterols are absorbed in humans and other mammals, considerably less than the absorption of cholesterol, which can be up to 60% (11). Furthermore, the amount of absorption varies among the individual phytosterols depending on both the sterol nucleus and the length of the side chain (7,12). The most prevalent phytosterol, sitosterol, has an absorption value of 0.5%, whereas sitostanol, without the double bond in the sterol nucleus, has the lowest value, at 0.04% (11).

Although phytosterols are absorbed less efficiently than cholesterol, their lumenal processing is similar to that of cholesterol and is intimately connected to the overall process of lipid digestion (e.g., 134). Because of the hydrophobicity of phytosterols, solubilization into intestinal mixed micelles is a prerequisite for reaching the site of absorption, the extent of which is greatly enhanced in the presence of products of TG digestion (MG and FA) (13,15). As a result of micellar solubilization, the diffusion of sterols is improved through the unstirred water layer at the intestinal brush border.

Presently, the cholesterol-lowering effects of phytosterols are attributed to both luminal- and enterocyte-based processes, but their exact mechanisms, relative extent, and importance still need further investigation. Recent findings link cholesterol absorption to active influx and efflux sterol transporters in the enterocytes, whereas the lumenal effects of phytosterols have mainly been based on their greater hydrophobicity, which imparts a greater affinity for mixed micelles during fat digestion (7,16,17). Thus, they may displace dietary and intestinal cholesterol from the micelles, thereby reducing the solubilization

of intestinal cholesterol. Some evidence of the exclusion of cholesterol from mixed micelles has been presented in a static (nondigesting) solubilization study utilizing mixed micelles composed of bile salts (BS), phospholipids (PL), and long-chain MG and FA (18). However, no studies incorporating the lipolysis process or the effect of lipid chain length have previously been published.

For lipophilic or hydrophobic drugs, improved oral absorption after postprandial administration or when formulated with lipids is mainly attributed to the increased solubilizing capacity of the intestinal BS/PL mixed micelles afforded by the incorporation of lipolysis products (MG and FA) and/or lipidic excipients (19–21). Similar to the sterols, solubilization of poorly water-soluble drugs into intestinal mixed micelles will greatly facilitate their transfer to the site of absorption. The mechanistic aspects of drug solubilization during lipolysis have been examined in several recent studies using an *in vitro* digestion method, which incorporates the dynamics of the lipolysis process. Although a simplification of the *in vivo* situation, the *in vitro* method has shown its usefulness in predicting the relative effectiveness of different lipid formulations *in vivo* (22–25). One of the major findings of these studies, as well as accompanying studies on the solubilizing capacity of colloidal species produced (26), was the understanding that medium chain length (C_8–C_{10}) lipids may be less suitable for co-administration with highly lipophilic drugs since the MG and FA produced thereof form smaller mixed micelles compared with lipids of longer chain lengths (C_{14}–C_{18}), thereby having lower solubilizing capacity and providing reduced benefits for oral absorption.

In the current study, the dynamic *in vitro* digestion method was used to examine the solubilization behavior of cholesterol and/or phytosterols during lipolysis to probe the efficacy of cholesterol displacement from mixed micelles by phytosterols. The effects of lipid chain length on the solubilization capacity and displacement of cholesterol were studied by using sterol suspensions formulated in long-chain TG (LCT) or medium-chain TG (MCT). To use formulations with relevance *in vivo*, the suspensions were prepared according to the method previously developed to produce a cholesterol-lowering microcrystalline phytosterol suspension in oil (27,28). This suspension,

formulated in rapeseed oil, has been shown to reduce plasma total and LDL cholesterol concentrations in a clinical study (5).

EXPERIMENTAL PROCEDURES

Materials. Phytosterol was purchased as β-sitosterol (≥78.5% β-sitosterol, 8.7% campesterol, 10% β-sitostanol, and 1% campestanol) from Merck (Darmstadt, Germany), and cholesterol (>99%) was from Sigma Chemical Co. (St. Louis, MO). Soybean oil (SBO, LCT; ≥85% linoleic, oleic, and linolenic acid) was a Sigma product and Captex 355 (MCT; ≥95% caprylic and capric acid) was a product from Abitech Corporation (Janesville, WI). More detailed FA compositions of SBO and Captex 355 can be found in Kaukonen *et al.* (23). Sodium taurodeoxycholate (NaTDC) (Sigma Chemical Co.), egg lecithin, Lipoid E 80 (approximately 81.8% PC; Lipoid GmbH, Ludwigshafen, Germany), and chloroform (Rathburn Chemicals Ltd., Walkerburn, Scotland) were used in the preparation of mixed micelles. The lipolysis buffer contained Trizma® maleate, sodium chloride, sodium hydroxide, and sodium azide, all obtained from Sigma, and calcium chloride dihydrate from Riedel-de-Haën (Seelze, Germany). Water was obtained from a Milli-Q (Millipore, Milford, MA) water purification system. Pancreatin from porcine pancreas (8× USP specifications activity) was a Sigma product, and 4-bromophenylboronic acid (BPBA) was purchased from Aldrich Chemical Co. (St. Louis, MO). Sodium hydroxide (1 M, Fixanal®; Riedel-de-Haën) was used to prepare a 0.2 M NaOH titration solution.

Preparation of phytosterol and cholesterol suspensions. The suspensions were prepared by heating phytosterol (see Table 1 for the individual phytosterol concentrations determined) or cholesterol and either SBO or Captex 355 in a vessel while stirring. The phytosterol or cholesterol was dissolved at about 100°C, and a clear solution was formed (27,28). After cooling to about 90°C, purified water at the same temperature was added to the suspension containing phytosterol. The vessel was immediately immersed in ice, and the suspension was stirred until it had reached at least room temperature (+25°C). The phytosterol suspension contained 17% (w/w) phytosterol, 70% MCT or LCT oil and 13% water, whereas the cholesterol sus-

TABLE 1
Sterol Composition and Physicochemical Parameters

	Sterol composition in suspension (%)	mW (g/mol)	cLog P[a]	Log P[b]	Aqueous solubility[b] [µM]
β-Sitosterol	76.3	414.7	10.73	9.63	0.005
β-Sitostanol	13.7	416.4	11.10		
Campesterol	8.1	400.7	10.20	9.31	
Campestanol	1.1	402.7	10.56		
Stigmasterol	0.3	412.7	10.21	8.97	
Δ5-Avenasterol	Below detection	412.7	10.33		
Cholesterol	>99	386.7	9.85	8.53	0.032

[a]Calculated using Advanced Chemistry Development (ACD/Labs, Toronto, Ontario) software, Solaris V4.67.
[b]From Reference 39.

TABLE 2
Aqueous Phase Concentrations of Phytosterols (PS) and Cholesterol (CH) After 60 min Digestion of 50 mg Long-Chain TG (LCT) or Medium-Chain TG (MCT)

	Fed micelles		Fasted micelles		Cholesterol micelles (fed)	
	Phytosterol content in aqueous phase (distribution %)	Cholesterol content in aqueous phase (distribution %)	Phytosterol content in aqueous phase (distribution %)	Cholesterol content in aqueous phase (distribution %)	Phytosterol content in aqueous phase (distribution %)	Cholesterol content in aqueous phase (distribution %)
Sterol dose in LCT						
15 µmol CH		100		100		
14 µmol PS	25.0[a]				24.2 ± 1.9[b]	96.1 ± 3.7
28 µmol PS	15.9[a]				28.0[a]	100[a]
14 µmol PS and						
15 µmol CH	20.4 ± 2.3	85.8 ± 11.8[b]	30.1± 6.7[b]	87.9 ± 11.0[b]		
Sterol dose in MCT						
15 µmol CH		50.3 ± 1.5		39.7 ± 1.8		
14 µmol PS	12.9[a]				15.6 ± 0.5[b]	95.6 ± 3.8
28 µmol PH	7.2[a]				5.8[a]	97.1
14 µmol PS and						
15 µmol CH	15.5 ± 2.3	24.4 ± 3.1[b]	11.1 ± 6.1[b]	18.4 ± 4.7[b]		

[a]$n = 1$.
[b]Statistically significant difference ($P < 0.05$) between corresponding LCT and MCT values.

pension contained 17% cholesterol and 83% MCT or LCT oil. The suspension preparation was validated by analysis of the sterol content in triplicate. The variation in the presumed sterol content of the suspensions was 102.2% (SD ± 3.0, $n = 3$) for cholesterol and 98.3% (SD ± 4.7, $n = 3$) for phytosterols.

In vitro lipid digestion. The *in vitro* lipolysis experiments were conducted in the same manner as those described earlier (22,23,29,30). Cholesterol and/or phytosterol suspensions were dispersed in 9 mL of BS/PL mixed micelles prepared in a pH 7.5 buffer (50 mM Trizma maleate, 150 mM NaCl, 5 mM CaCl$_2$). All digests contained a total of 50 mg of LCT (6 mM) or MCT (10 mM), i.e., 25 mg of pure TG was added when only cholesterol or phytosterol suspensions were studied. Two levels of BS/PL concentrations were used to represent fed-state (20 mM NaTDC/5 mM PC) or fasted-state (5 mM NaTDC/1.25 mM PC) small intestinal conditions (31–33). Phytosterol was dosed at either 14 or 28 µmol, whereas cholesterol was dosed at 15 µmol. The fed micelles contained 0.08 mM cholesterol, because of residual cholesterol in the egg lecithin, but are referred to as cholesterol-free in the text. Cholesterol-loaded micelles with 1.5 mM cholesterol were also used to simulate the presence of endogenous or presolubilized cholesterol (a total of 15 µmol in 10 mL) under fed-state conditions (32,33). Lipolysis experiments were performed at 37°C in a stirred and thermostated glass vessel and were initiated by the addition of 1 mL of a 20% pancreatin suspension (1 g of pancreatin to 5 mL of digestion buffer). The lipolysis was performed over 60 min using a pH-Stat titration unit (Radiometer, Copenhagen, Denmark) that maintained the pH at 7.5. The FA produced by TG lipolysis were titrated with 0.2 M NaOH. At the end of each experiment, a lipolysis inhibitor (50 µL of 0.5 M BPBA in methanol) was added to the digestion mixture to stop further digestion. Two 4-mL aliquots of the postdigestion mixtures were then ultracentrifuged in polyallomer centrifuge tubes (34 min at 37°C and 300,000 × g) to separate the digests into an oil phase, an aqueous phase, and a precipitated pellet. The aqueous phase was aspirated into a syringe by penetrating the side of the tube and was transferred into glass vials. Finally, the samples were dried overnight in a lyophilizer (LyoPro 3000 freeze dryer; Heto, Allerød, Denmark) before analyzing by GC. *t*-Tests (SigmaStat 2.0; SYSTAT Software Inc., Point Richmond, CA) were performed on assayed sterol concentrations in the micellar phases to statistically compare the results between the MCT and LCT systems. These results are presented in Table 2.

Phytosterol solubility determination. Solubility was determined by adding anhydrous phytosterol crystals (dried over night at 80°C, 0% RH) to the aqueous phase obtained after *in vitro* lipolysis of 50 mg of LCT or MCT in fed-state micelles preloaded with 1.5 mM cholesterol. A total of four digests were performed (for both MCT and LCT) to obtain the aqueous phase after separation by ultracentrifugation. Solid phytosterol was added (1 mg phytosterol/1 mL aqueous phase; total volume ~7 mL), after which the samples were incubated at +37°C for the entire period of the solubility studies and vortexed periodically. Sterol concentrations were analyzed by GC from samples taken at the start of the experiment and after 6, 24, 48, and 120 h incubation. The samples (0.5 mL) were filtered (13-mm syringe filter with a 0.2-µm polyvinylidene difluoride membrane) prior to determination, and the filtrate was collected for analysis. To assess the potential loss of solubilized sterol by filtration, aqueous-phase samples from digests containing both cholesterol and phytosterols were analyzed prior to and post filtration. The loss of sterols was ≤1.7 %. No apparent physical or visual changes were observed during the solubility study.

Sample preparation and GC analysis of sterols. Sterols were analyzed after alkaline hydrolysis of the samples by a GC method using an internal standard for quantification as pre-

sented earlier (34,35). The dried samples were suspended in 1 mL water and the internal standard was added (0.2 mg dihydrocholesterol, ≈95%; Sigma-Aldrich). The samples were subjected to alkaline hydrolysis (35), the unsaponifiable lipid fractions were purified using a SiOH cartridge (Bond Elut, 500 mg; Varian, Harbor City, CA), and sterols in aliquots of one-tenth of the sterol fraction were converted to trimethylsilyl ethers (TMS) (34). The TMS sterols were dissolved in 200 µL of heptane before analysis by GC.

An Agilent Technologies 6890N Network GC system gas chromatograph equipped with an autosampler, on-column 7683 Series injector, and FID (300°C) was used. The column was a RTX®-5w/INTEGRA fused-silica column [diphenyl and dimethyl polysiloxane (5:95), 60 m × 0.32 mm i.d., 0.1-µm film with 10-m Integra-Guard column; Restek Corp., Bellefonte, PA). GC analysis of the TMS sterols was performed as described earlier (34). An in-house reference sample (rapeseed oil) was used to monitor the analytical level each day. The CV was 1.86% for total sterol concentration and 2.12% for β-sitosterol (*n* = 19). GC separation and quantification were monitored daily by injecting a sterol standard mixture containing dihydrocholesterol, cholesterol, and stigmasterol. The determination limit of sterols in a sample after the sample preparation procedure was 5 µg.

RESULTS

Across all systems studied, the digestion of MCT and LCT was essentially complete after 60 min with no oily layer remaining after centrifugation. The only exception was when digesting LCT in the presence of fasted mixed micelles. In this case, it was possible to distinguish a few minute oil droplets in addition to the aqueous- and pellet-phase postultracentrifugation. A 50-mg dose of lipids was used to produce similar endpoints of digestion with the two lipids where practically all of the digestion products were likely to be incorporated into mixed micelles (24,26). This enabled comparison of the two systems on more equal terms with regard to the solubilizing capacity of the colloidal phases formed. Although fed-state conditions might be considered more relevant, fasted-state conditions were also studied to probe the effects of the BS/PL level on solubilization. This was warranted, not only by the wide range of BS/PL levels determined in aspirates from different subjects (31–33), but also because reduced gall bladder emptying has been observed after ingestion of MCT lipids (31).

Solubilization of cholesterol or phytosterols into mixed micelles during lipolysis. Digestion experiments with LCT or MCT lipids containing either cholesterol or phytosterol were conducted to establish their individual solubilization behavior. Under fed-state conditions, the solubilization of cholesterol from the LCT suspension formulation into the micelles was markedly different compared with the formulation containing MCT (Fig. 1A and Table 2). When digesting cholesterol suspended in LCT, the entire cholesterol dose (*n* = 3) was incorporated into the micellar phase. For the MCT suspension formulation of cholesterol, only 50.3% (±1.5%, *n* = 3) of the initial cholesterol dose was recovered in the micellar phase. A

reduction in the BS/PL concentration (fasted state) did not diminish cholesterol solubilization in the LCT system, and the entire cholesterol dose was again solubilized into the mixed micellar phase. On the other hand, cholesterol solubilization into fasted mixed micelles containing MCT digestion products decreased significantly (39.7 ± 1.8%, *n* = 3) compared with the corresponding event in the fed state.

Phytosterol solubilization was determined using fed-state mixed micelles (Fig. 1B, Table 2). As with cholesterol, phytosterols were incorporated into the mixed micellar phase but to a substantially lower degree than the cholesterol. Only 25% of the initial phytosterol dose was solubilized from suspensions containing LCT, and only 13% was solubilized from MCT formulations. However, the relative solubilizing capacity of the LCT and MCT systems was comparable to that observed with cholesterol. For MCT suspensions, increasing the phytosterol dose from 14 to 28 µmol led to a slight increase in the concentration of solubilized phytosterol (163 vs. 183 µM), as only 7% of the higher phytosterol dose was incorporated into the micelles. A more distinct increase in the concentration of solubilized phytosterol (329 vs. 452 µM) could be observed from the suspension prepared in LCT; however, not more than 15.9% of the phytosterol dose was solubilized at the higher dose.

Solubilization of co-administered cholesterol and phytosterols into mixed micelles during lipolysis. Digestion of co-administered phytosterol and cholesterol suspensions in either LCT or MCT was performed to simulate dietary intake of both sterols and to study the capacity of phytosterol to reduce cholesterol solubilization. The amounts of lipid and individual sterols were identical to those of the digests presented in the previous section.

When LCT suspensions were used under fed-state conditions, the extent of cholesterol solubilization in the micelles decreased to 85.8% (± 11.8%, *n* = 3) (Fig. 2, Table 2). The solubilization was not affected by a decline in the BS concentration (87.9 ± 11.0%, *n* = 3). A more significant decrease of cholesterol solubilization in mixed micelles was observed when co-administering phytosterol and cholesterol suspended in MCT. In the fed state, the content of cholesterol in micelles decreased to 24.4% (± 3.1, *n* = 3) of the initial cholesterol dose and was even lower in the fasted state (18.4, ± 4.7%, *n* = 3). The results indicate that when cholesterol and phytosterols are simultaneously present during lipid digestion, less cholesterol will be solubilized by the mixed micelles. However, it would seem that phytosterols together with MCT act as a more efficient limiting factor in the micelles' capacity to solubilize cholesterol.

Solubilization of phytosterols into cholesterol-loaded mixed micelles. Micelles preloaded with cholesterol represent a truer system than micelles without, since some cholesterol, as an integral component of bile, will be presolubilized in the intestinal mixed micelles under *in vivo* conditions (18,32). The preloaded fed-state micelles contained 1.5 mM cholesterol (15 µmol in 10 mL), which is within the range of concentrations observed in small intestinal aspirates after ingestion of a test meal (32,33). Phytosterols were administered as described previously at a dose of 14 µmol.

The phytosterols, administered as either MCT or LCT suspen-
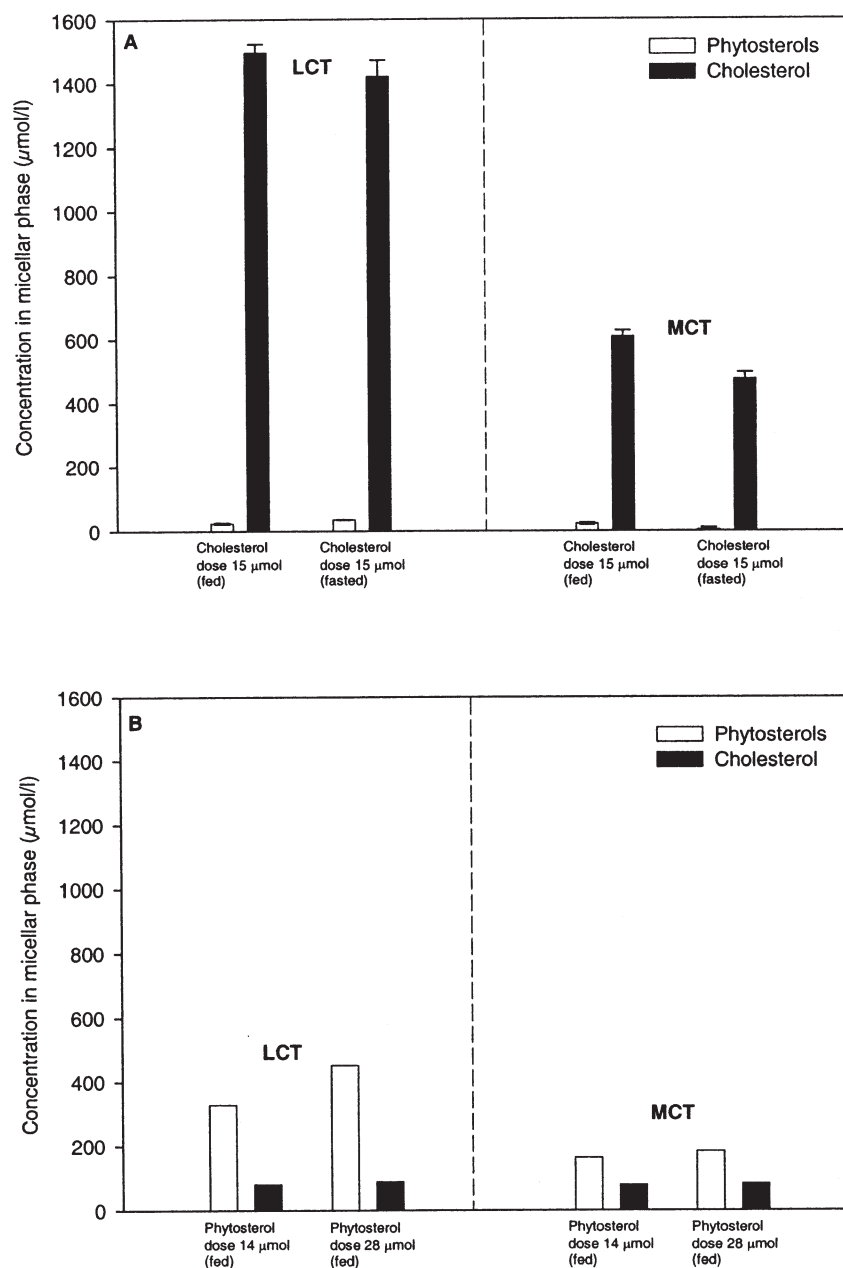
FIG. 1. The impact of lipid chain length on the micellar solubilization of sterols during lipid digestion. The sterols were administered with a total of 50 mg of either long-chain TG (LCT) or medium-chain TG (MCT). (A) Solubilization of cholesterol (dose 15 μmol) into mixed micelles under a fed state [20 mM sodium taurodeoxycholate (NaTDC)/5 mM PC] or a fasted state (5 mM NaTDC/1.25 mM PC) ($n = 3$). (B) Solubilization of phytosterols (dose either 14 μmol or 28 μmol) into mixed micelles under a fed state ($n = 1$). Error bars represent SD.

sions, were solubilized into the cholesterol-loaded micelles to an extent similar to that during digestion with the cholesterol-free micelles (Figs. 3 and 1B, Table 2). Again, the solubilization of phytosterols suspended in LCT was more effective ($24.2 \pm 1.9\%$, $n = 3$) compared with the MCT-based suspension ($15.6 \pm 0.5\%$, $n = 3$). However, the incorporation of phytosterols into the cholesterol-preloaded mixed micelles did not significantly decrease the cho-

lesterol content. The cholesterol content in the micellar phase was 95.6% ($\pm 3.8\%$, $n = 3$) of the administered dose when phytosterols suspended in MCT were digested, and a similar cholesterol content was achieved with the LCT formulation ($96.1 \pm 3.7\%$, $n = 3$). A twofold increase in the phytosterol dose (28 μmol) did not further reduce the cholesterol content in the micelles (see Table 2).

Phytosterol solubility in MCT and LCT postdigestion
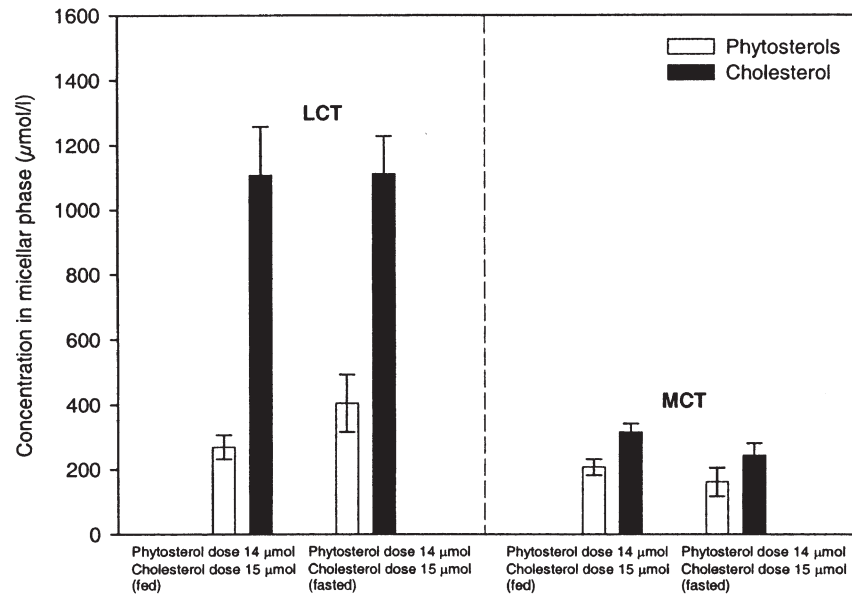
FIG. 2. Solubilization of co-administered phytosterol and cholesterol into mixed micelles. The sterol suspensions contained a total of 50 mg of either LCT or MCT. The bile salt (BS)/phospholipids (PL) concentration levels were 20 mM NaTDC/5 mM PC (fed state) or 5 mM NaTDC/1.25 mM PC (fasted state) ($n = 3$). For other abbreviations see Figure 1. Error bars represent SD.

phases. The solubility of phytosterols was determined in MCT and LCT postdigestion aqueous phases obtained with cholesterol-loaded micelles. This was done to further probe the validity of the results showing little displacement of presolubilized cholesterol by phytosterol suspensions during lipolysis.

An increase in the phytosterol concentration was observed as a function of time for both MCT and LCT mixed micellar phases (Fig. 4). At 120 h, the solubilization of phytosterol into the micelles was 119 μM (± 38, $n = 3$) for the MCT phase (Fig. 4A), compared with 392 μM (± 21, $n = 3$) for the LCT phase (Fig. 4B). These results emphasize the efficacy of the lipolysis process, since approximately the same amount of phytosterol was incor-
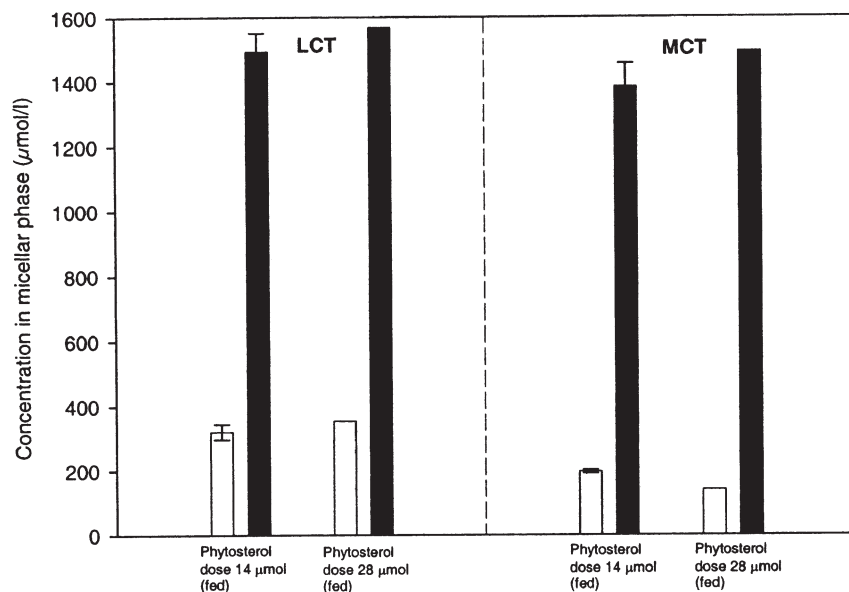
FIG. 3. Solubilization of phytosterol (dose either 14 μmol or 28 μmol) into micelles preloaded with 1.5 mM cholesterol. Phytosterols were administered with 50 mg of either LCT or MCT. The BS/PL concentration level was 20 mM NaTDC/5 mM PC (fed state) ($n = 3$). For abbreviations see Figures 1 and 2. Error bars represent SD.
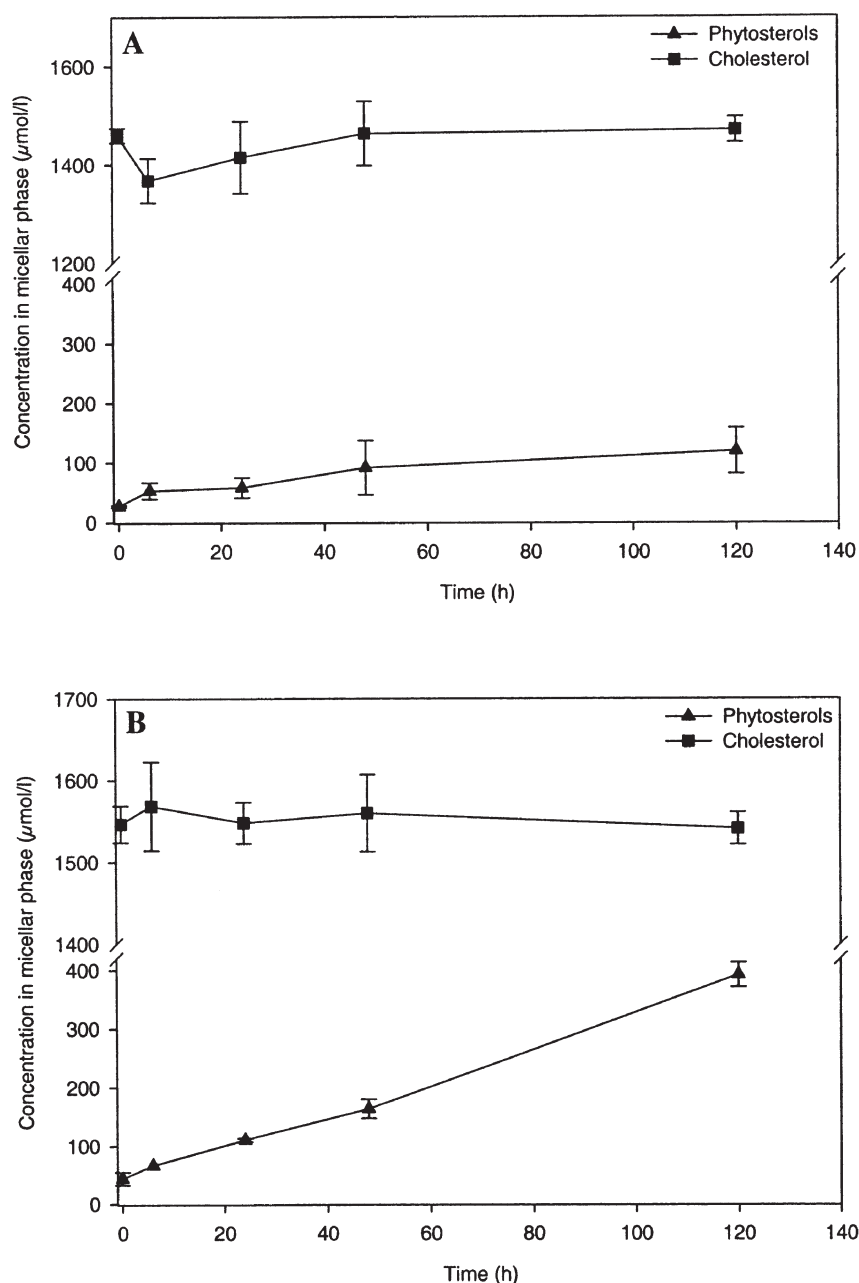
FIG. 4. Phytosterol solubility (+37°C, up to 120 h) in the mixed micellar phase obtained after *in vitro* lipolysis of 50 mg of (A) MCT or (B) LCT in fed-state micelles (20mM NaTDC/5mM PC) preloaded with 1.5 mM cholesterol (*n* = 4). For abbreviations see Figure 1. Error bars represent SD.

porated into the micelles during 120 h as during 1 h of lipolysis (see Fig. 1B).

Congruent with the lipolysis results, the solubilization of phytosterols into the micelles did not affect the content of cholesterol significantly. The cholesterol content in the micelles containing MCT digestion products varied (during 120 h) from 1367 (± 45, *n* = 3) to 1470 µM (± 26, *n* = 3), whereas the content in the LCT digestion phase varied from 1541 (± 20, *n* = 3) to 1568 µM (± 54,

n = 3) during the same time interval. These results suggest that presolubilized cholesterol may be difficult to displace.

Worth mentioning is that equilibrium sterol solubilities were not achieved with certainty during this study. Phytosterol concentrations sampled at 120 h were significantly higher than those at 48 h, which was more pronounced in samples from LCT micellar solutions (an increase of 139%) compared with MCT samples (30%, respectively).

DISCUSSION

For cholesterol, the crucial step in its lumenal processing is solubilization into mixed micelles, a prerequisite for the transport toward the brush border membrane. Previous *in vitro* studies have shown that very lipophilic drugs, with high log *P* (e.g., halofantrine, log *P* 8.86) are solubilized better into mixed micelles containing digestion products of LCT, whereas lower log *P* drugs (e.g., griseofulvin, log *P* 2.18) favor the systems containing medium-chain FA (23,26). Subsequent *in vivo* studies support these findings and give credence to the use of the dynamic *in vitro* lipolysis method as a predictive model of intestinal solubilization processes (24,25). Table 1 demonstrates log *P* values for all the sterols present in this study. If our results are consistent with the preceding findings, the high log *P* values suggest that incorporating sterols into mixed micelles containing long-chain FA is more efficient. This *in vitro* lipolysis study was performed to probe the above hypothesis on sterol solubilization and to further examine whether phytosterols are able to displace cholesterol from mixed micelles during lipid digestion. The experimental conditions were designed according to the previous studies producing *in vitro–in vivo* correlations (24).

We found, indeed, that the mixed-micellar phase containing digestion products of LCT was able to incorporate significantly higher amounts of cholesterol than that obtained after digestion of MCT (Fig. 1A). Replacing the long chain length (C_{14}–C_{18}) TG with one containing medium chain length (C_8–C_{10}) FA decreased the amount of solubilized cholesterol by 50% in the aqueous phase. Interestingly, comparable trends have been observed *in vivo*. Kritchevsky and Tepper (36) reported a similar reduction in serum total cholesterol concentration following ingestion of MCT compared with LCT in rats. Similarly, they stated that the cholesterol level was reduced by 50% of the initial amount in liver and serum when rats were fed MCT instead of coconut or corn oil. Notably, rats are not the ideal model when evaluating lipid digestion, since bile secretion in the rat is continuous and not food dependent as in humans (24). However, similar results were also obtained when Borel *et al.* (37) compared the effect of MCT and LCT on the bioavailability of fat-soluble β-carotene (log *P* 15.5) in humans. They found β-carotene plasma levels to be markedly diminished when administered together with MCT instead of LCT. These results, together with the results on lipophilic drugs (24,25), indicate that the less efficient *in vitro* solubilization of sterols provided by MCT digestion products may have relevance for *in vivo* absorption.

Regardless of lipid chain length, the amount of cholesterol solubilized into the micelles was roughly fourfold compared with that of phytosterols in the respective system (Table 2), with the individual phytosterols solubilized in proportion to their respective quantity in the solid (see Table 1). In contrast, results from a static dissolution study using simulated mixed micelles reported similar solubilization for cholesterol and β-sitosterol but showed reduced solubilization for sitostanol (18). With increasing hydrophobicity (see Table 1 for log *P* values

and aqueous solubility), the micellar solubilizing capacity for phytosterols is reduced compared with cholesterol (38). However, the relative benefits derived from solubilization also increase with increasing hydrophobicity, thereby affording the more hydrophobic phytosterols a higher affinity to the micelles (39). The selectivity for sterol hydrophobicity will depend on the hydrophilicity of the BS, i.e., on the number of hydroxyl groups and conjugating moiety (38,39). This may explain our dissimilar results as the dihydroxy BS in the present study (NaTDC) are likely to be more selective than the BS mixture used by Mel'nikov *et al.* (18).

Co-administration of phytosterol and cholesterol, particularly when suspended in MCT, showed a significant reduction of solubilized cholesterol in digests using cholesterol-free micelles (Fig. 2, Table 2). As was previously mentioned, the entire cholesterol dose administered was solubilized into mixed micelles containing LCT digestion products (see *Solubilization of cholesterol or phytosterols into mixed micelles during lipolysis* section). The amount of cholesterol solubilized into the micellar phase was reduced to 50.3% (±1.5%, *n* = 3) when digested with MCT. When MCT suspensions of phytosterols and cholesterol were co-administered, the solubilization of cholesterol into the mixed micelles containing MCT digestion products was further reduced to 24.4% (±3.1%, *n* = 3) of the administered dose.

The effects observed during MCT digestion of co-administered sterols are in excess of that observed with LCT, where reduction of cholesterol solubilization was 14.2%. These results are in agreement with the results and hypothesis presented by previous authors stating that the presence of phytosterols will reduce the micellar solubilization of cholesterol because of the limited solubilizing capacity of the mixed micelles or thermodynamic preferences (18). The lower solubilizing capacity for highly lipophilic compounds of the mixed micelles from MCT digests, compared with those of LCT lipids, would therefore further exacerbate the situation (24–26).

Despite the promising results with co-administered sterols, we were practically unable to displace presolubilized cholesterol during digestion in either the MCT or LCT system (Fig. 3); these results were supported by the solubility studies (Fig. 4). Potential reasons for this are the extent of micellar saturation, the lack of solid cholesterol to promote precipitation, and the time span of the experiment. Mel'nikov *et al.* (18) showed that phytosterols and β-stanols were able to compete with and displace preloaded cholesterol from mixed micelles containing long-chain FA, provided the micelles were loaded with sufficient amounts of cholesterol. Even in the presence of solid cholesterol, phytosterols were able to displace cholesterol from the mixed micelles only when the preloaded micelles were saturated (1.0 mM), whereas both cholesterol and phytosterols were incorporated into micelles at lower preloading (0.2 mM). Maximal displacement was obtained progressively over several hours of incubation. The cholesterol dose (1.5 mM) in the present study, although higher than that producing cholesterol precipitation in the study by Mel'nikov *et al.*, may not have been high enough to form saturated micelles because of higher

concentrations of the lipolysis products. An additional factor includes the dynamic processing during lipid digestion, which may promote supersaturation of colloidal (especially vesicular) structures (22–25). This would contribute to the lack of difference observed between the MCT and LCT lipids, as the presence of presolubilized cholesterol is likely to promote and stabilize vesicular structures, which for MCT systems would impart a relatively higher impact on the solubilizing capacity (26).

In a previous study Plat *et al*. (40), stated that consumption of 2.5 g of phytosterols in either one or three meals during the day was equally effective in lowering plasma LDL cholesterol levels. This suggests that phytosterols might also affect cholesterol absorption through other than lumenal mechanisms, e.g., through effects on the enterocyte level. A specific protein in jejunal enterocytes, called Niemann–Pick C1 L1 (NPC1L1), was recently found to facilitate cholesterol absorption through the brush border membrane (41). Similarly, NPC1L1 seems to play an important role in the intestinal influx of phytosterol. The ATP-binding cassette (ABC) transporters ABCG5, ABCG8, and ABCA1 are involved in the transport of excess sterol from the enterocytes back into the intestine (42,43). These transport systems appear to be unable to differentiate between cholesterol and phytosterols, whereby an increased amount of phytosterols in the intestine or in the enterocytes would increase the amount of cholesterol excreted (44,45). However, effects of phytosterol on the lumenal processing of cholesterol may also contribute to the findings of Plat *et al*. (40). In view of the high amount of phytosterol ingested in one dose, it is likely that much of the phytosterol would remain unsolubilized and precipitate in the intestine, later to be resolubilized when food is again ingested. In this way, phytosterols would be reintroduced into the solubilization process of cholesterol during lipolysis of the ingested lipids contained in the food. This kind of resolubilization process has been suggested to account for the observed double peaking in plasma concentration–time profiles with halofantrine, which is a highly lipophilic, poorly water-soluble drug (46).

The present study showed that cholesterol solubilization into mixed micelles is reduced in the presence of MCT digestion products and that phytosterols formulated in MCT could reduce cholesterol amounts even further and in excess of that observed with LCT systems. These interesting *in vitro* results raise questions about the potential benefits of medium chain length lipids in cholesterol-lowering phytosterol products. Today, approximately 95% of the ingested fat is LCT, although MCT should pose little or no risk from toxicity when consumed as a dietary supplement at levels up to 15% of the daily dietary calories or about 50% of the total daily dietary fats (47,48). However, potential risks for increased serum TG concentrations should be recognized at high levels of MCT (48,49). The *in vitro* lipolysis model is a fairly new method used to simulate the intestinal dissolution conditions in humans (22–25,30,50). Although the method has shown promising predictive capacity, the complex dynamic composition of fluids *in vivo*, especially during the fed state, is difficult to simulate and warrants additional experiments (both *in vitro* and *in vivo*) to probe this hypothesis further.

REFERENCES

1. Pollak, O.J. (1953) Successful Prevention of Experimental Hypercholesterolemia and Cholesterol Atherosclerosis in the Rabbit, *Circulation 12*, 696–701.
2. Hartman, M.A. (1998) Plant Sterols and Membrane Environment, *Trends Plant Sci. 3*, 170–175.
3. Quilez, J., Garcia-Lorda, P., and Salas-Salvado, J. (2003) Potential Uses and Benefits of Phytosterols in Diet: Present Situation and Future Directions, *Clin. Nutr. 22*, 343–351.
4. Katan, M.B., Grundy, S.M., Jones, P., Law, M., Miettinen, T., Paoletti, R., and Stresa Workshop Participants (2003) Efficacy and Safety of Plant Stanols and Sterols in the Management of Blood Cholesterol Levels, *Mayo Clin. Proc. 78*, 965–978.
5. Christiansen, L.I., Lähteenmäki, P.L.A., Mannelin, M.R., Seppänen-Laakso, T.E., Hiltunen, R.V.K., and Yliruusi, J.K. (2001) Cholesterol-Lowering Effect of Spreads Enriched with Microcrystalline Plant Sterols in Hypercholesterolemic Subjects, *Eur. J. Nutr. 40(2)*, 66–73.
6. Lu, K., Lee, M.-H., and Patel, S.B. (2001) Dietary Cholesterol Absorption: More Than Just Bile, *Trends Endocrinol. Metab. 12*, 314–320.
7. Clifton, P. (2002) Plant Sterols and Stanols—Comparison and Contrasts. Sterols Versus Stanols in Cholesterol-Lowering: Is There a Difference? *Atheroscler. Suppl. 3(3)*, 5–9.
8. Valsta, L.M., Lemström, A., Ovaskainen, M.-L., Lampi, A.-M., Toivo, J., Korhonen, T., and Piironen, V. (2004) Estimation of Plant Sterol and Cholesterol Intake in Finland: Quality of New Values and Their Effect on Intake, *Br. J. Nutr. 92*, 671–678.
9. Wilson, M.D., and Rudel, L.L. (1994) Review of Cholesterol Absorption with Emphasis on Dietary and Biliary Cholesterol, *J. Lipid Res. 35*, 943–955.
10. Trautwein, E.A., Duchateau, G.S., Lin, Y., Mel'nikov, S.M., Molhuizen, H.O.F., and Ntanios, F.Y. (2003) Proposed Mechanism of Cholesterol-Lowering Action of Plant Sterols, *Eur. J. Lipid Sci. Technol. 105*, 171–185.
11. Ostlund, R.E., Jr., McGill, J.B., Zeng, C.-M., Covey, D.F., Stearns, J., Stenson, W.F., and Spilburg C.A. (2002) Gastrointestinal Absorption and Plasma Kinetics of Soy Δ^5-Phytosterols and Phytostanols in Humans, *Am. J. Physiol. Endocrinol. Metab. 282*, E911–E916.
12. Heinemann, T., Kullak-Ublick, G.-A., Pietruck, B., and von Bergman, K. (1991) Mechanism of Action of Plant Sterols in Inhibition of Cholesterol Absorption. Comparison of Sitosterol and Sitostanol, *Eur. J. Clin. Pharmacol. 40* (Suppl. 1), S59–S63.
13. Ros, E. (2000) Intestinal Absorption of Triglyceride and Cholesterol. Dietary and Pharmacological Inhibition to Reduce Cardiovascular Risk, *Atherosclerosis 151*, 257–279.
14. Carey, M.C., and Small, D.M. (1970) The Characteristics of Mixed Micellar Solutions with Particular Reference to Bile, *Am. J. Med. 49(11)*, 590–608.
15. Moghadasian, M.H., and Frohlich, J.J. (2000) Effects of Dietary Phytosterols on Cholesterol Metabolism and Atherosclerosis: Clinical and Experimental Evidence, *Am. J. Med. 107*, 588–594.
16. Ikeda, I., and Sugano, M. (1983) Some Aspects of Mechanism of Inhibition of Cholesterol Absorption by β-Sitosterol, *Biochim. Biophys. Acta 732*, 651–658.
17. Ling, W.H., and Jones, P.J.H. (1995) Enhanced Efficacy of Sitostanol-Containing Versus Sitostanol-Free Phytosterol Mixtures in Altering Lipoprotein Cholesterol Levels and Synthesis in Rats, *Atherosclerosis 118*, 319–331.
18. Mel'nikov, S.M., Seijen ten Hoorn, J.W.M., and Eijkelenboom, A.P.A.M. (2004) Effect of Phytosterols and Phytostanols on the Solubilization of Cholesterol by Dietary Mixed Micelles: An *in vitro* Study, *Chem. Phys. Lipids 127*, 121–141.
19. Humberstone, A.J., and Charman, W.N. (1997) Lipid Based Vehi-

cles for the Oral Delivery of Poorly Water Soluble Drugs, *Adv. Drug Delivery Rev. 25*, 103–128.

20. MacGregor, K.J., Embleton, J.K., Lacy, J.E., Perry, A.P., Solomon, L.J., Seager, H., and Pouton, C.W. (1997) Influence of Lipolysis on Drug Absorption from the Gastro-intestinal Tract, *Adv. Drug Delivery Rev. 25*, 33–46.

21. Porter, C.J.H., and Charman, W.N. (2001) *In vitro* Assessment of Oral Lipid Based Formulations, *Adv. Drug Delivery Rev. 50*, S127–S147.

22. Kaukonen, A.M., Boyd, B.J., Charman, W.N., and Porter, C.J.H. (2004) Drug Solubilization Behaviour During *in vitro* Digestion of Suspension Formulations of Poorly Water-Soluble Drugs in Triglyceride Lipids, *Pharm. Res. 21*, 254–260.

23. Kaukonen, A.M., Boyd, B.J., Porter, C.J.H., and Charman, W.N. (2004) Drug Solubilization Behavior During *in vitro* Digestion of Simple Triglyceride Lipid Solution Formulations, *Pharm. Res. 21*, 245–253.

24. Porter, C.J.H., Kaukonen, A.M., Taillard-Bertschinger, A., Boyd, B.J., O'Connor, J.M., Edwards, G.E., and Charman, W.N. (2004) Use of *in vitro* Lipid Digestion Data to Explain the *in vivo* Performance of Triglyceride-Based Oral Lipid Formulations of Poorly Water-Soluble Drugs: Studies with Halofantrine, *J. Pharm. Sci. 93*, 1110–1121.

25. Porter, C.J.H., Kaukonen, A.M., Boyd, B.J., Edwards, G.E., and Charman, W.N. (2004) Susceptibility to Lipase-Mediated Digestion Reduces the Oral Bioavailability of Danazol After Administration as a Medium-Chain Lipid-Based Microemulsion Formulation, *Pharm. Res. 21*, 1405–1412.

26. Kossena, G.K., Boyd, B.J., Porter, C.J.H., and Charman, W.N. (2003) Separation and Characterisation of the Colloidal Phases Produced on Digestion of Common Formulation Lipids and Assessment of Their Impact on the Apparent Solubility of Selected Poorly Water Soluble Drugs, *J. Pharm. Sci. 92*, 634–648.

27. Christiansen, L.I., Rantanen, J.T., von Bonsdorff, A.K., Karjalainen, M.A., and Yliruusi, J.K. (2002) A Novel Method of Producing a Microcrystalline β-Sitosterol Suspension in Oil, *Eur. J. Pharm. Sci. 15*, 261–269.

28. von Bonsdorff-Nikander, A., Rantanen, J., Christiansen, L., and Yliruusi, J.K. (2003) Optimizing the Crystal Size and Habit of β-Sitosterol in Suspension, *AAPS PharmSciTech 4*, 349–356.

29. Sek, L., Porter, C.J.H., and Charman, W.N. (2001) Characterisation and Quantification of Medium Chain and Long Chain Triglycerides and Their *in vitro* Digestion Products, by HPTLC Coupled with *in situ* Densitometric Analysis, *J. Pharm. Biomed. Anal. 25*, 651–661.

30. Sek, L., Porter, C.J.H., Kaukonen, A.M., and Charman, W.N. (2002) Evaluation of the *in-vitro* Digestion Profiles of Long and Medium Chain Glycerides and the Phase Behaviour of Their Lipolytic Products, *J. Pharm. Pharmacol. 54*, 29–41.

31. Ladas, S.D., Isaacs, P.E.T., Murphy, G.M., and Sladen, G.E. (1984) Comparison of the Effects of Medium and Long Chain Triglyceride Containing Liquid Meals on Gall Bladder and Small Intestinal Function in Normal Man, *Gut 25*, 405–411.

32. Hernell, O., Staggers, J.E., and Carey, M.C. (1990) Physical-chemical Behavior of Dietary and Biliary Lipids During Intestinal Digestion and Absorption. 2. Phase Analysis and Aggregation States of Lumenal Lipids During Duodenal Fat Digestion in Healthy Adult Human Beings, *Biochemistry 29*, 2041–2056.

33. Armand, M., Borel, P., Pasquier, B., Dubois, C., Senft, M., Andre, M., Peyrot, J., Salducci, J., and Lairon, D. (1996) Physicochemical Characteristics of Emulsions During Fat Digestion in Human Stomach and Duodenum, *Am. J. Physiol. 271*, G172–G183.

34. Piironen, V., Toivo, J., and Lampi, A.-M. (2002) Plant Sterols in Cereals and Cereal Products, *Cereal Chem. 79*, 148–154.

35. Soupas, L., Juntunen, L., Lampi, A.-M., and Piironen, V. (2004) Effects of Sterol Structure, Temperature, and Lipid Medium on Phytosterol Oxidation, *J. Agric. Food Chem. 52*, 6485–6491.

36. Kritchevsky, D., and Tepper, S.A. (1965) Influence of Medium-Chain Triglyceride (MCT) on Cholesterol Metabolism in Rats, *J. Nutr. 86*, 67–72.

37. Borel, P., Tyssandier, V., Mekki, N., Grolier, P., Rochette, Y., Alexandre-Gouabau, M.C., Lairon, D., and Azaïs-Braesco, V. (1998) Chylomicron β-Carotene and Retinyl Palmitate Responses Are Dramatically Diminished when Men Ingest β-Carotene with Medium-Chain Rather than Long-Chain Triglyserides, *J. Nutr. 128*, 1361–1367.

38. Armstrong, M., and Carey, M. (1987) Thermodynamic and Molecular Determinants of Sterol Solubilities in Bile Salt Micelles, *J. Lipid Res. 28*, 1144–1155.

39. Wiedmann, T.S., and Kamel, L. (2002) Examination of the Solubilization of Drugs by Bile Salt Micelles, *J. Pharm. Sci. 91*, 1743–1764.

40. Plat, J., van Onselen, E.N.M., van Heugten, M.M.A., and Mensink, R.P. (2000) Effects on Serum Lipids, Lipoproteins and Fat Soluble Antioxidant Concentrations of Consumption Frequency of Margarines and Shortenings Enriched with Plant Stanol Esters, *Eur. J. Clin. Nutr. 54*, 671–677.

41. Altmann, S.W., Davis, H.R., Zhu, L., Yao, X., Hoos, L.M., Tetzloff, G., Iyer, S.N., Maquire, M., Golovko, A., Zeng, M., *et al.* (2004) Niemann–Pick C1 Like 1 Protein Is Critical for Intestinal Cholesterol Absorption, *Science 303*, 1201–1204.

42. Berge, K.E., Tian, H., Graf, G.A., Yu, L., Grishin, N.V., Schultz, J., Kwiterovich, P., Shan, B., Barnes, R., and Hobbs, H.H. (2000) Accumulation of Dietary Cholesterol in Sitosterolemia Caused by Mutations in Adjacent ABC Transporters, *Science 290*, 1771–1775.

43. Chen, H.C. (2001) Molecular Mechanisms of Sterol Absorption, *J. Nutr. 131*, 2603–2605.

44. Davis, H.R., Zhu, L.-J., Hoos, L.M., Tetzloff, G., Maquire, M., Liu, J., Yao, X., Iyer, S.P.N., Lam, M.-H., Lund, E.G., *et al.* (2004) Niemann–Pick C1 Like 1 (NPC1L1) Is the Intestinal Phytosterol and Cholesterol Transporter and Key Modulator of Whole-Body Cholesterol Homeostasis, *J. Biol. Chem. 279*, 33586–33592.

45. Ostlund, R.E., Jr. (2004) Phytosterols and Cholesterol Metabolism, *Curr. Opin. Lipidol. 15*, 37–41.

46. Porter, C.J.H., Kaukonen, A.M., Taillardat-Bertschinger, A., Boyd, B.J., O'Connor, J.M., Edwards, G.A., and Charman, W.N. (2003) Use of *in vitro* Digestion Data to Explain the *in vivo* Performance of Triglyceride-Based Oral Lipid Formulations of Poorly Water-Soluble Drugs: Studies with Halofantrine, *J. Pharm. Sci. 93*, 1110–1121.

47. Embleton, J.K., and Pouton, C.W. (1997) Structure and Function of Gastro-intestinal Lipases, *Adv. Drug Delivery Rev. 25*, 15–32.

48. Traul, K.A., Driedger, A., Ingle, D.L., and Nakhasi, D. (2000) Review of the Toxicologic Properties of Medium-Chain Triglycerides, *Food Chem. Toxicol. 38*, 79–98.

49. Hill, J.O., Peters, J.C., Swift, L.L., Yang, D., Sharp, T., Abumrad, N., and Greene, H.L. (1990) Changes in Blood Lipids During Six Days of Overfeeding with Medium or Long Chain Triglycerides, *J. Lipid Res. 31*, 407–416.

50. Zangenberg, N.H., Mullertz, A., Gjelstrup Kristensen, H., and Hovgaard, L. (2001) A Dynamic *in vitro* Lipolysis Model—II. Evaluation of the Model, *Eur. J. Pharm. Sci. 14*, 237–244.

A Study on the Causes for the Elevated n-3 Fatty Acids in Cows' Milk of Alpine Origin

Florian Leiber, Michael Kreuzer*, Daniel Nigg,
Hans-Rudolf Wettstein, and Martin Richard Leo Scheeder

Institute of Animal Science, Swiss Federal Institute of Technology (ETH), Zurich, Switzerland

ABSTRACT: The influence of grass-only diets either from ryegrass-dominated lowland pastures (400 m above sea level) or botanically diverse alpine pastures (2000 m) on the FA profile of milk was investigated using three groups of six Brown Swiss cows each. Two groups were fed grass-only on pasture (P) or freshly harvested in barn (B), both for two experimental periods in the lowlands and, consecutively, two periods on the alp. Group C served as the control, receiving a silage-concentrate diet and permanently staying in the lowlands. Effects of vegetation stage or pasture vs. barn feeding on milk fat composition were negligible. Compared with the control, α-linolenic acid (18:3n-3) consumption was elevated in groups P and B (79%; $P < 0.001$) during the lowland periods but decreased on the alp to the level of C owing to feed intake depression and lower 18:3n-3 concentration in the alpine forage. Average 18:3n-3 contents of milk fat were higher in groups P and B than in C by 33% ($P < 0.01$) at low and by 96% ($P < 0.001$) at high altitude, indicating that 18:3n-3 levels in milk were to some extent independent of 18:3n-3 consumption. The *cis*-9,*trans*-11 CLA content in milk of grass-fed cows was higher compared with C but lower for the alpine vs. lowland periods whereas the *trans*-11,*cis*-13 isomer further increased with altitude. Long-chain n-3 FA and phytanic acid increased while arachidonic acid decreased with grass-only feeding, but none of them responded to altitude. Grass-only feeding increased milk α-tocopherol concentration by 86 and 134% at low and high altitude ($P < 0.001$), respectively. Changes in the ruminal ecosystem due to energy shortage or specific secondary plant metabolites are discussed as possible causes for the high 18:3n-3 concentrations in alpine milk.

Paper no. L9566 in *Lipids 40*, 191–202 (February 2005).

Recently, elevated contents of beneficial functional FA in cows' milk and cheese derived from alpine grazing systems were reported (1–4). Increased contents of n-3 PUFA and an improved ratio of n-3 to n-6 PUFA in milk of cows grazing on alpine pastures were shown (3,5). It was even hypothesized that a relation between high levels of α-linolenic acid (18:3n-3) in alpine cheese and a favorable cardiovascular health status of the alpine population may exist (4). Generally, n-3 PUFA are known to be essential for human health, and problems may arise if they are consumed in too low a proportion relative to n-6 FA (6). Furthermore, the content of CLA (18:2 *cis*-9,*trans*-11 isomer), a FA that also has shown potential to benefit human health (7), was found to be clearly enriched in milk (3) or cheese (1,2) from alpine production systems compared with those from intensive lowland production. Additionally, the proportion of short- and medium-chain saturated FA (SFA), which are supposed to increase the risk of cardiovascular diseases (8), was found to be markedly lower in milk and milk products originating from cows grazing high alpine pastures (2,4,5).

Milk fat derived from cows grazing high alpine pastures therefore seems to have a considerably higher dietetic value than conventional milk, but the reasons for these differences are still unclear. To our knowledge, in previous studies the individual factors of the alpine sojourn of cows potentially affecting milk fat composition were never differentiated, and diets fed in the lowlands for control were either not specified or not restricted to herbage-only, as is usual practice in Swiss alpine dairy systems. Known mechanisms influencing the FA profile in lowland milk are (i) the basic effect of grazing and the related body fat mobilization (9,10) as well as influences of the herbage's botanical composition (10,11), (ii) the degree of usage of concentrates, in particular wheat, barley, and maize in the diets, which mainly contribute SFA, 18:1, and 18:2n-6 but very little 18:3n-3 (10,12,13), and (iii) the effect of herbage conservation (13–15). These factors could also contribute to the differences in composition between common lowland milk and milk from alpine pastures. It is, however, still unclear whether, in addition, specific plants (16), the 18:3n-3 content of the alpine flora (3,17) and even the hypoxic environment *per se* (4) are responsible for the typically high contents of CLA and n-3 PUFA of alpine milk products. Otherwise, the "alpine paradox" (4) would actually be a general phenomenon of feeding grass at any altitude and mainly reflect the difference from mixed, often maize-based, diet types. The objective of the present study was to determine experimentally the factors responsible for the composition of milk fat of cows consuming grass at high altitude. Comparisons included grass-only vs. mixed diets in the lowland, high altitude vs. lowland grazing of the cows, pasture vs. indoor feeding, and young vs. mature swards.

EXPERIMENTAL PROCEDURES

Animals. Eighteen Brown Swiss cows, having been 94 (65 to 127) d into their second lactation at the beginning of the experiment, were blocked by calving date and allocated to three groups (P, pasture group; B, barn-fed group; C, control group) with minimal between-group variance for energy-corrected milk yield, milk protein, and milk fat percentage. Average milk yield, at the start of the experiment, was 21.7, 22.2, and 22.3 kg/d for groups P, B, and C, respectively. The corresponding average contents per kilogram of milk were 43.6, 42.0, and 41.4 g fat; 30.3, 31.1, and 31.8 g protein; and 50.6, 50.4, and 49.1 g lactose, respectively.

Experimental schedule. Six subperiods (S0 to S5) were defined. Each subperiod lasted for 21 d, and intensive sampling was always done during the respective third week. All data and data points in the figures refer to the average values of these intensive sampling weeks within each subperiod. The first part of the experiment took place at the ETH research station Chamau in central Switzerland at 400 m above sea level. During the baseline subperiod (S0) all cows were tethered in a barn and fed a mixed control diet. During the "lowland period," comprising the two subperiods S1 and S2, group P was turned out to pasture for 24 h/d, while groups B and C remained in the barn. Group B was fed only freshly harvested grass *ad libitum*, and group C remained on the control diet. After S2, all cows were kept in the barn again until the alpine vegetation was ready for grazing and harvest. During this time, groups P and B stayed on the grass-only diet at *ad libitum* access. At the end of this transition period, which lasted for 28 d, just before and after the transport to the alpine location, additional milk samples were taken. These samples provided the additional data points in Figures 3 to 6. For the "alpine period," Groups P and B were transported to the alpine ETH research station Alp Weissenstein located at 2000 m above sea level in the Eastern Swiss alps. Half of the group P and B cows were switched to the respective other group in order to counterbalance possible residual effects of the previous treatment. This balanced rearrangement of groups P and B is indicated in the figures by the dotted line. Group C remained in the lowlands and continued to serve as control group. Like the lowland period, the alpine period consisted of two subperiods (S3 and S4). S5 as a final baseline evaluation was carried out with all cows kept in the lowland barn again and fed the control diet.

During the intensive sampling weeks, milk yield was recorded and proportionate milk samples of each cow and each milking were obtained. The samples were frozen at −20°C immediately after sampling. Cows were weighed and blood samples were taken at days 2 and 6 within each sampling week. Two feed samples were drawn every day in each group during the sampling weeks of the subperiods. An aliquot of each feed sample was dried at 60°C for 48 h, and a second was frozen at −20°. Feces were sampled once a day from each animal and frozen. Later, all samples were defrosted, pooled per sampling week (feed) or per animal and sampling week (feces), and then dried and ground through a 0.75-mm sieve for analy-sis. Feed intake was measured daily for cows kept in barn. On pasture, feed samples were obtained mimicking the selection behavior of the cows for at least 3 h distributed over the whole daytime, and feed intake was calculated using the double-alkane technique (18). As the source for the synthetic marker alkanes (C_{32} and C_{36}), controlled release alkane capsules (CRC; Captec, Auckland, New Zealand) were introduced into the rumen of the cows 8 d prior to each sampling week. Odd-chain alkanes (C_{31} and C_{33}) in feed were used as internal markers. The actual alkane recovery rates in feces were determined with the known feed intake of the group B cows that had also received CRC.

Diets. S1 started at the earliest possible vegetation stage of the first growth; S2 followed 3 wk later on a now more mature sward. The same principle was followed for S3 and S4 at the alpine location. The lowland areas were intensively managed leys with regular manure fertilization. The alpine pasture was native and not fertilized. The botanical composition was visually estimated in the standing sward within each sampling week in eight systematically distributed 9-m^2 plots (four per pasture and harvest paddock, respectively) according to the method of Braun-Blanquet (19). The main species characteristics of the experimental sites are shown in Table 1. The analyzed nutrient and FA composition of the experimental feeds is listed in Table 2. Data for individual vegetation stages are not displayed since vegetation stage effects on milk fat composition were found to be not significant.

Herbage for group B was harvested daily in the early morning from paddocks adjoining those grazed by group P cows; the two were similar in botanical composition. It was then kept tightly packed to avoid any possible losses of FA by wilting of the forage (15). The control diet contained hay, ryegrass silage, and maize silage in proportions of 0.1:0.6:0.3 on a dry-matter (DM) basis, was provided *ad libitum*, and was supplemented by concentrates according to milk yield. The two commercial concentrates used contained rumen-protected fat (Table 2), which made up 410 g/kg of total dietary FA in the control diet. The cows of all groups had *ad libitum* access to NaCl and a nonvitaminized mineral mix (Ca:P = 2:1; Nährkosan, Büron, Switzerland) during the whole experiment.

Analysis. Frozen milk samples were defrosted and pooled per cow and sampling week. After direct transesterification, according to Suter *et al.* (20), the FAME were extracted with *n*-heptane and then separated and quantified with GC using a Sil 88 column (100 m × 0.25 mm, 0.2 μm; Varian Inc, Darmstadt, Germany) on an HP 6890 (Hewlett-Packard, Wilmington, DE). Hydrogen flow was 1.5 mL/min; 0.5 mL of *n*-heptane containing the FAME was injected on column. The temperature program was: 60°C for 5 min; increase by 14°C/min up to 165°C; 2°C/min up to 225°C; isothermal for another 15 min. Temperature program and peak identification were adapted from Collomb and Bühler (21) with some modifications. The peaks for 16:1*trans* and 20:1*trans* may contain some branched-chain FA (22). They were therefore only included in the calculation of total FAME and not separately shown in the tables. The applied chromatographic method also is not able to separate *trans-*

TABLE 1
Frequent Plant Species in the Lowland and the Alpine Pastures Used in the Experiment

	Estimated proportions of total ground covering[a]		
	>10%	4–10%	1–4%
Lowland site (16 plots)			
Monocotyledonae (77%)			
Total species found: 9	*Lolium multiflorum, Poa trivialis, Lolium perenne*	*Poa annua*	*Festuca pratense, Poa pratense*
Leguminosae (6%)			
Total species found: 2		*Trifolium repens*	*Trifolium pratense*
Dicotyledonae (except Leguminosae) (16%)			
Total species found: 8	*Taraxacum officinale*		*Rumex obtusifolius, Ranunculus repens, Bellis perennis*
Alpine site (16 plots)			
Monocotyledonae (36%)			
Total species found: 14	*Festuca rubra*	*Trisetum flavescens, Phleum alpinum, Poa alpina, Festuca pratense*	*Poa trivialis, Nardus stricta, Poa pratense*
Leguminosae (23%)			
Total species found: 11	*Trifolium pratense*	*Trifolium montanum*	*Trifolium repens, Trifolium badii, Lotus* spp., *Trifolium nivale*
Dicotyledonae (except Leguminosae) (40%)			
Total species found: 46		*Rumex arifolius, Alchemilla vulgaris, Taraxacum officinale*	*Peucedaneum osthrutium, Ranunculus montanus, Ranunculus acer, Achillea stricta, Carum carvi, Chaero phyllum cicutaria, Campanula scheuchzeri, Crepis aurea, Veronica chamaedrys, Plantago alpina, Leontodon hispidus*

[a]Visually estimated according to the method of Braun-Blanquet (19).

8,*cis*-10 and *trans*-7,*cis*-9 from the major *cis*-9,*trans*-11 CLA-isomer as well as *trans*-11,*cis*-13 from *cis*-9,*cis*-11 (3,23). However, the concentration of the *trans*-7,*cis*-9 isomer has been described to be about 100-fold lower than the *cis*-9,*trans*-11 isomer in milk, and changes due to (alpine) feeding occurred on a rather low level (3,24). Proportions of and effects on *trans*-8,*cis*-10 are even lower than for *trans*-7,*cis*-9 (24). Thus, we conclude that any distortion of the effect on the *cis*-9,*trans*-11 isomer is small, although it might be slightly biased because both of these minor isomers are likely to increase with altitude of the site where the dairy cows are kept (24). Similarly, the *cis*-9,*cis*-11 isomer, coeluting with the *trans*-11,*cis*-13 isomer, seems to be present only in traces if at all (24; Collomb, M., personal communication); we therefore refer to this peak as *trans*-11,*cis*-13. Response factors were determined using BCR 164 standard milk fat (Certified Reference Material; EC Reference Materials, Brussels, Belgium) as a reference. The milk fat content measured with a standard NIR procedure (Milkoscan 4000; Foss, Höganäs, Sweden) closely correlated with the amount of total FAME obtained with GC (r^2 = 0.93). Phytanic acid (3,7,11,15-tetramethylhexadecanoic acid) was separated and quantified in the milk samples of S2 and S3 and in the samples drawn directly before and after transfer to the alp, using an

RTX225 column (30 m × 0.32 mm, 0.5 µm; Restek Corporation, Bellefonte, PA). Injection volume was 1 µL in a 30:1 split modus at 240°C. Hydrogen flow was 4.0 mL/min. The temperature program was 140°C for 2 min, ramp 5°C/min up to 215°C, isothermal for 5 min.

Lipids from feeds were extracted by accelerated solvent extraction (ASE 200; Dionex Corp., Sunnyvale CA) using hexane/isopropanol (2:1 vol/vol) and transformed into FAME according to Wettstein *et al.* (25). FAME were dissolved in hexane and analyzed with GC on a Supelcowax™-10 column (30 m × 0.32 mm, 0.25 µm; Supelco Inc., Bellefonte, PA) after split injection (1:30) at 270°C. The injection volume was 2 µL; hydrogen flow was 2.2 mL/min. The temperature program was 160°C for 1 min, ramp 20°C/min up to 190°C, ramp 7°C/min up to 230°C; isotherm at 230°C for 4 min, ramp 20°C/min up to 250°C, isotherm for 4 min.

Tocopherols in milk were analyzed after saponification with KOH with normal-phase HPLC on a Merck-Hitachi system with UV detection (La Chrom; Darmstadt, Germany) according to Rettenmaier and Schüepp (26). The β-, γ-, and δ-tocopherols were always below the detection limit.

Feed contents of DM and nitrogen (N × 6.25 = crude protein) were analyzed with standard methods as described previ-

TABLE 2
Nutrient and FA Contents of Feeds Used in the Experiment[a]

	Origin	Dry matter (DM) (g/kg)	NE$_L$[b] (MJ/kg)	Crude protein (g/kg)	Total FA	SFA[c]	18:1Δ11	18:1Δ9	18:2n-6	18:3n-3
							FA (g/kg DM)			
Green forages[d]										
Pasture	Lowland	190 ± 13	6.12 ± 0.46	142 ± 4	16.2 ± 3.7	2.86 ± 0.60	0.065 ± 0.029	0.470 ± 0.288	2.91 ± 1.16	9.06 ± 1.61
Harvest	Lowland	177 ± 24	6.11 ± 0.54	137 ± 8	14.8 ± 2.7	2.77 ± 0.47	0.057 ± 0.019	0.343 ± 0.177	2.61 ± 1.01	8.27 ± 0.87
Pasture	Alpine	190 ± 4	5.57 ± 0.41	138 ± 8	12.2 ± 2.4	2.77 ± 0.33	0.066 ± 0.012	0.616 ± 0.037	2.35 ± 0.42	5.72 ± 1.45
Harvest	Alpine	186 ± 25	5.63 ± 0.28	138 ± 8	13.4 ± 2.4	2.93 ± 0.37	0.069 ± 0.004	0.646 ± 0.004	2.63 ± 0.34	6.29 ± 1.50
Components of the mixed diet[d]										
Hay	Lowland	770 ± 14	5.62 ± 0.02	178 ± 1	18.4 ± 0.1	4.64 ± 0.09	0.085 ± 0.000	0.439 ± 0.003	2.90 ± 0.03	9.12 ± 0.19
Grass silage	Lowland	514 ± 43	5.32 ± 0.03	168 ± 0	19.0 ± 0.3	4.40 ± 0.19	0.080 ± 0.006	0.669 ± 0.043	3.19 ± 0.11	9.58 ± 0.33
Maize silage	Lowland	334 ± 11	6.33 ± 0.01	62 ± 0	22.8 ± 0.2	4.57 ± 0.06	0.205 ± 0.004	6.103 ± 0.177	11.20 ± 0.20	0.59 ± 0.01
Energy concentrate[e]	Lowland	854 ± 2	7.45 ± 0.05	151 ± 4	61.3 ± 1.6	44.79 ± 1.54	0.335 ± 0.016	5.587 ± 0.324	9.70 ± 0.70	0.78 ± 0.02
Protein concentrate[f]	Lowland	860 ± 0	7.75 ± 0.05	423 ± 6	59.1 ± 0.6	46.23 ± 0.55	0.275 ± 0.006	4.229 ± 0.366	7.68 ± 0.47	0.57 ± 0.09

[a]Means ± SD.
[b]NE$_L$: net energy for lactation, calculated based on formula of RAP (28).
[c]SFA: saturated FA (sum of 10:0 through 24:0).
[d]Average of two subperiods with two samples per subperiod; each sample pooled from 7 d.
[e]g/kg DM: wheat, 300; barley, 190; wheat bran, 150; oats, 120; straw meal, 50; maize, 50; crystalline fat (rumen-protected; Alikon, Bützberg, Switzerland), 40; maize gluten, 30; molasses, 30; canola cake, 20; sugar beet pulp, 20.
[f]g/kg DM: soybean meal, 480; maize gluten, 220; straw meal, 60; wheat, 40; crystalline fat, 40; sugar beet pulp, 40; molasses, 30; wheat bran, 10.

ously (27). Contents of net energy for lactation were calculated based on the equations used in the official Swiss feed evaluation (28). Plasma metabolites and insulin were analyzed with standard assays. Plasma insulin was measured with a radioimmunoassay kit (No. 1064 1401; Pharmacia, Uppsala, Sweden). Plasma concentrations of nonesterified FA (NEFA), β-hydroxybutyrate (BHB), glucose, and urea were analyzed on a COBAS-MIRA chemistry analyzer (Roche, Basel, Switzerland), with the following assays: NEFA with NEFA-C WA 994-75409 (Wako, Neuss, Germany), BHB with product 310-A (Sigma, Buchs, Switzerland), glucose with assay No. 1447513 and urea with assay No. 1489364 (both Roche).

Statistics. Data were evaluated with three mixed models by SAS V8.2e (PROC MIXED; SAS Institute, Cary, NC;). Model 1 included group (P, B, or C) and calving date (classified in three blocks of similar calving date) as fixed factors. Animal was included as random effect, and the individual baseline (S0) values were used as a covariate. The least squares (LS) means and all significances of the group × period interaction, shown in Tables 3 and 4, are based on model 1. The same model, but without the covariate S0, was used to obtain LS means of all subperiods (including S0) for the illustration in the figures. A third model was applied for the calculation of the altitude and the vegetation stage effects, considering vegetation stage (two classes: young or mature) and main period (lowland or alps) as additional fixed effects. Group C, for which feed and altitude remained unchanged, was excluded from the calculations with model 3.

RESULTS

Feed intake and metabolic energy supply. During the lowland period, the DM intake of the grass-only fed cows was lower than in cows of group C [significantly for group P ($P < 0.05$) and as a tendency for group B ($P < 0.1$); Table 3]. Nevertheless, the calculated net energy intake of B and P cows did not differ significantly from C cows during the lowland period (Fig. 1A), and milk yield decreased only slightly (Fig. 2B). However, unlike C cows, P and B cows lost weight from S0 to S1 ($P < 0.05$; Fig. 2A), and all blood plasma metabolites indicated a certain catabolic state (Table 3). In the alpine period (S3 and S4), DM intake in groups P and B decreased ($P < 0.001$) compared with the lowland period and with C cows, and net energy intake was reduced by approximately one-third ($P < 0.01$). Accordingly, milk yield markedly decreased when cows were transferred to the alpine location ($P < 0.001$; Fig. 2). Although body weight did not further decline, plasma levels of BHB ($P < 0.001$) and NEFA ($P < 0.001$) still increased and plasma glucose ($P < 0.05$) and insulin ($P < 0.001$) further decreased during the alpine sojourn of the cows (Table 3).

FA intake. In S1 and S2, individual FA consumption of the grass-only fed cows differed from that of the C cows (Table 3) since lowland grass had clearly higher levels of 18:3n-3 but much lower levels of SFA, monounsaturated FA, and 18:2n-6 than the control diet (*cf.* Table 2). Thus, 18:3n-3 was the main dietary FA for groups P and B, whereas for group C, 16:0 and

TABLE 3
Daily Intake and Metabolic Traits of Cows During the Experimental Periods[a]

Group	Lowland period (avg. of S1 and S2)			Alpine period (avg. of S3 and S4)			SE[b]	Significances		
	Control	Barn	Pasture	Control	Barn	Pasture		Group[c]	Period (altitude)[d]	Group × period[c]
Intake (per cow per day)[e,f]										
DM (kg)	18.2[a]	16.9[a,b]	16.4[b]	18.3[a]	13.8[c]	13.7[c]	0.52	<0.001	<0.001	<0.01
FA (g)										
Total FA	597	238*	254*	580	169*	161*	19.3	<0.001	<0.001	NS[h]
Saturated FA	342.9	45.5*	46.5*	325.3	38.2*	37.5*	14.70	<0.001	<0.001	NS
18:1Δ9	56.3	5.74*	8.05*	54.9	8.54*	8.34*	1.695	<0.001	<0.01	NS
18:1Δ11	3.26	0.97*	1.11*	3.17	0.93*	0.93*	0.112	<0.001	<0.05	NS
18:2n-6	114.0	44.4*	49.0*	112.3	34.7*	32.9*	3.37	<0.001	<0.001	NS
18:3n-3	80.4[b]	138.2[a]	148.5[a]	83.3[b]	82.8[b]	79.8[b]	5.53	<0.001	<0.001	<0.001
Blood plasma concentrations[e,f]										
BHB[g] (mmol/L)	477[d]	667[c]	638[c,d]	510[c,d]	921[b]	1119[a]	35.0	<0.001	<0.001	<0.01
NEFA[g] (mmol/L)	93[c]	64[c]	137[b]	60[c]	94[c]	203[a]	18.0	<0.001	<0.05	<0.05
Glucose (mmol/L)	3.23	3.20	3.02*	3.19	2.92*	2.92*	0.057	<0.05	<0.01	NS
Insulin (pmol/L)	71.2	55.0*	37.1*	66.9	30.2*	24.1*	3.99	<0.001	<0.001	NS

[a]n = 12 per group and period.
[b]Standard error of groups.
[c]Evaluated by model 1.
[d]Evaluated by model 3 (without control).
[e]Superscript roman letters a–d indicate significant differences ($P < 0.05$) between group × period interaction means according to model 1.
[f]Values marked with asterisks are significantly different ($P < 0.05$) from the respective control group value according to model 1.
[g]BHB, β-hydroxybutyrate; NEFA, nonesterified FA.
[h]NS, not significant; for other abbreviation see Table 2.

18:0, originating from the concentrates, and 18:1 and 18:2n-6, coming from both the concentrates and the maize silage, were the major dietary FA. In the alpine period, the total FA content of the herbage tended to be lower ($P < 0.1$; t-test) than during the lowland period (Table 2). Additionally, the 18:3n-3 proportion of total FA in the herbage declined ($P < 0.01$; t-test). This resulted in a reduced intake of total FA and 18:3n-3 by 23 and 43%, respectively, in the alpine compared with the lowland period for both P and B ($P < 0.001$; Table 3 and Fig. 1B).

Fat content and saturated FA in milk. The fat content in milk was not affected by the grass-only diets in the lowlands but (with concomitantly decreased milk yields) it increased in group P ($P < 0.001$) and in group B ($P < 0.1$) after transport to the alps. With the start of grass feeding in S1, the proportion of the even-chain SFA 6:0 through 14:0 in total milk FAME of groups P and B initially increased ($P < 0.001$). From subperiod S2 on, there was an almost linear decrease in the proportions of these FA in total FAME and in the milk of the P and B cows, with the values finally decreasing below the levels of control group (representatively shown for 10:0 and 12:0 in Fig. 3). Figure 3 illustrates that this was a continuous decline that, to a considerable extent, had already taken place before the transfer to the alpine site. In S5, the concentration of 6:0 through 14:0 returned to the baseline values represented by the C cows. During the lowland period, a decrease in the proportion of 16:0 as part of the total FAME occurred with the herbage-only diets (P cows: $P < 0.01$; B cows: $P < 0.05$) compared with the control diet (C), whereas 17:0 moderately increased ($P < 0.05$ for both groups) and the proportion of 18:0 remained unaffected. With

the alpine sojourn of P and B groups, the 18:0 proportion of total FAME significantly increased whereas those of 16:0 and 17:0 were not affected by the location.

18:1 FA in milk. Among the identified 18:1 *trans* isomers, the 18:1*trans*-10/*trans*-11 proportions of total FAME increased ($P < 0.001$) with lowland grass-only diets by more than 3.3-fold, whereas the 18:1*trans*-4-*trans*-9 isomers were moderately reduced, particularly in group B ($P < 0.01$), compared with C cows (Table 4). During the alpine period, compared with the lowland values in groups P and B, the double-peak comprising 18:1*trans*-11 (*trans*-vaccenic acid) clearly decreased, whereas the concentration of the 18:1*trans*-4 to *trans*-9 in total FAME significantly increased. The proportion of 18:1*cis*-9, as the dominating 18:1, remained unaffected by the grass-only diets in the lowlands but was elevated at high altitude by 32% ($P < 0.001$) compared with the lowland values in P and B cows.

CLA in milk. All identified CLA isomers increased markedly as a proportion of the total FAME when grass-only diets were fed in groups P and B ($P < 0.001$; Table 4). Accordingly, during the lowland periods, the proportion of the main isomer, 18:2 *cis*-9,*trans*-11, was on average 1.9-fold higher in milk fat of P and B cows than in the milk of C cows. From S0 to S1, CLA increased in both P and B cows ($P < 0.001$); from S1 to S2 a further increase occurred only in P cows ($P < 0.05$). This was the reason for the significant difference between P and B cows in the lowland period ($P < 0.01$; Table 4, Fig. 4). During the alpine sojourn, the concentration of the main CLA isomer, 18:2 *cis*-9,*trans*-11, in total FAME decreased ($P < 0.01$), whereas the 18:2 *trans*-11,*cis*-13 isomer significantly increased in the P and B groups

TABLE 4
FA Content of Milk, FA Profile of Milk Fat, and α-Tocopherol Content of Milk[a]

Group	Lowland period (avg. of S1 and S2)			Alpine period (avg. of S3 and S4)			SE[b]	Significances		
	Control	Barn	Pasture	Control	Barn	Pasture		Group[c]	Period (altitude)[d]	Group × period[c]
Total FAME[e] (g/L)	41.1[b]	43.8[a,b]	41.3[b]	40.1[b]	46.0[a,b]	47.0[a]	1.76	NS[i]	<0.001	<0.05
FA[e,f] (g/100 g FAME)										
4:0	3.48[b]	3.48[b]	3.55[b]	3.26[c]	3.89[a]	3.55[b]	0.071	<0.05	<0.01	<0.001
6:0	2.37[b]	2.55[a]	2.55[a]	2.19[c]	2.17[c]	2.04[d]	0.033	NS	<0.001	<0.01
8:0	1.31[b]	1.52[a]	1.53[a]	1.21[c]	1.06[d]	1.02[d]	0.020	NS	<0.001	<0.001
10:0	2.74[b]	3.46[a]	3.54[a]	2.53[b]	1.91[c]	1.95[c]	0.011	NS	<0.001	<0.001
12:0	3.14[b]	4.04[a]	3.85[a]	3.00[b]	2.23[c]	2.09[c]	0.067	NS	<0.001	<0.001
14:0	10.7[b]	12.1[a]	11.5[a,b]	10.8[b]	9.5[c]	8.5[d]	0.25	<0.05	<0.001	<0.001
16:0	34.0	29.3*	25.3*	33.7	29.5*	25.4*	0.79	<0.001	NS	NS
17:0	0.627[c]	0.875[a]	0.843[a,b]	0.642[c]	0.811[b]	0.843[a,b]	0.0089	<0.001	<0.05	<0.05
18:0	10.2[b,c]	9.3[c]	10.1[b,c]	9.4[c]	10.4[b]	11.8[a]	0.25	<0.01	<0.001	<0.001
18:1t4-t8	0.249[b]	0.185[c]	0.236[b,c]	0.238[b,c]	0.285[a,b]	0.313[a]	0.0161	NS	<0.001	<0.01
18:1t9	0.426[a,b]	0.309[c]	0.328[b,c]	0.422[a,b]	0.450[a]	0.469[a]	0.0256	NS	<0.001	0.05
18:1t10-11	0.84[d]	3.34[a]	4.01[a]	0.73[d]	2.37[c]	3.12[b]	0.219	<0.001	<0.001	<0.05
18:1t12	0.182	0.191	0.185	0.166	0.187	0.177	0.0090	NS	NS	NS
18:1c9	18.8[b,c]	16.4[c]	18.3[c]	20.2[b,c]	21.6[a,b]	24.1[a]	0.88	NS	<0.001	<0.001
18:1c11	0.477	0.399	0.460	0.541	0.576	0.653	0.0371	NS	<0.001	NS
18:1c12	0.160	0.092*	0.095*	0.174	0.101*	0.117*	0.0042	<0.001	<0.001	NS
18:2c9,t11[g]	0.529[c]	1.370[b]	1.705[a]	0.551[c]	1.163[b]	1.340[b]	0.098	<0.001	<0.01	<0.05
18:2t9,t11	0.041	0.082*	0.088*	0.045	0.077*	0.085*	0.0032	<0.001	NS	NS
18:2t10,c12	0.038[c]	0.046[b]	0.044[b,c]	0.041[b,c]	0.042[b,c]	0.051[a]	0.0020	<0.05	NS	<0.05
18:2t11,c13[h]	0.020[c]	0.073[b]	0.073[b]	0.020[c]	0.102[a]	0.114[a]	0.0072	<0.001	<0.001	<0.05
18:2n-6	1.38[b]	0.84[c]	0.94[c]	1.31[b]	1.42[b]	1.57[a]	0.040	<0.01	<0.001	<0.001
18:2c9,c15	0.033[c]	0.049[b]	0.047[b]	0.032[c]	0.050[b]	0.054[a]	0.0011	<0.001	<0.01	<0.05
18:3n-6	0.028[a]	0.021[b]	0.021[b]	0.029[a]	0.017[c]	0.018[c]	0.0009	<0.001	<0.001	<0.05
18:3n-3	0.495[d]	0.619[c]	0.703[c]	0.536[d]	0.950[b]	1.146[a]	0.030	<0.001	<0.001	<0.001
20:0	0.162[b]	0.136[c]	0.139[c]	0.171[b]	0.183[a,b]	0.200[a]	0.0054	NS	<0.001	<0.001
20:4n-6	0.077	0.071	0.066*	0.083	0.073*	0.066*	0.0020	<0.001	NS	NS
20:5n-3	0.060	0.073*	0.083*	0.065	0.083*	0.083*	0.0038	<0.001	NS	NS
22:5n-3	0.078	0.113*	0.109*	0.085	0.118*	0.120*	0.0048	<0.001	NS	NS
22:6n-3	ND	0.009*	0.009*	ND	0.010*	0.009*	0.002	<0.001	NS	NS
Total n-3	0.81[d]	1.32[c]	1.43[c]	0.85[d]	1.64[b]	1.98[a]	0.056	<0.001	<0.001	<0.001
Total n-6	2.18[b]	1.62[c]	1.77[c]	2.11[b]	2.16[b]	2.36[a]	0.056	<0.05	<0.001	<0.001
n-6/n-3[f]	2.71	1.24*	1.24*	2.54	1.32*	1.21*	0.067	<0.001	NS	NS
α-Tocopherol[f] (mg/L)	0.75	1.42*	1.37*	0.67	1.57*	1.57*	0.041	<0.001	<0.05	NS

[a]n = 12 per group and period.
[b]Standard error of groups.
[c]Evaluated by model 1.
[d]Evaluated by model 3 (without control).
[e]Superscript roman letters indicate significant differences ($P < 0.05$) between group × period interaction means according to model 1.
[f]Values marked with asterisks are significantly different ($P < 0.05$) from the respective control group value according to model 1.
[g]Including the *trans*-8,*cis*-10 and *trans*-7,*cis*-9 isomers.
[h]Possibly including traces of the *cis*-9,*cis*-11 isomer.
[i]NS, not significant; ND, not detected.

($P < 0.001$). In S5, the CLA concentration and secretion returned to the baseline value (Fig. 4).

Linolenic acid in milk. Whereas the γ-linolenic acid (18:3n-6) proportion of total FAME decreased with grass-only diets ($P < 0.01$) in the lowland period, the concentration of α-linolenic acid (18:3n-3) increased by 34% ($P < 0.001$; Table 4). Slightly lower 18:3n-3 proportions were observed for B cows compared with P cows ($P < 0.01$) and for S2 compared with S1 ($P < 0.05$; Fig. 5). After transfer to the alpine site, 18:3n-3 proportions of total FAME of pastured cows (group P) were 0.63-fold higher compared with the respective lowland levels

($P < 0.001$) and 1.14-fold higher than the value found in the C group ($P < 0.001$). The increase in B cows was less pronounced. The analysis of the milk samples obtained directly before and after the transfer to the alps showed that the increase of 18:3n-3 proportion was a direct response to the alpine sojourn rather than a continuous time effect of grass feeding (Fig. 5). In contrast to the proportionate values, the absolute daily 18:3n-3 secretion with milk remained unaffected by feeding grass to cows kept in barn. The pastured cows still showed a significantly higher daily 18:3n-3 secretion in the lowlands ($P < 0.01$) and at the alpine site ($P < 0.001$) compared with the
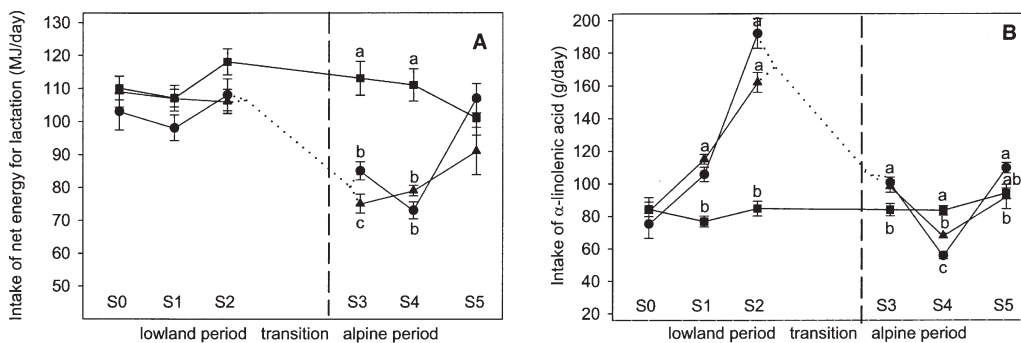
FIG. 1. Average intake of net energy and α-linolenic acid throughout the entire experiment. S0 and S5 baseline subperiods; S1 and S2, lowland subperiods; S3 and S4 alpine subperiods. ● Pasture group; ▲ indoor grass group; ■ control group; n = 6 per group. Dotted lines indicate that half of the cows were switched between pasture and indoor group. Dashed lines mark the day of transport of the grass-fed cows to the alpine location. Error bars represent SE. Different superscripts indicate significant group differences at $P < 0.05$.
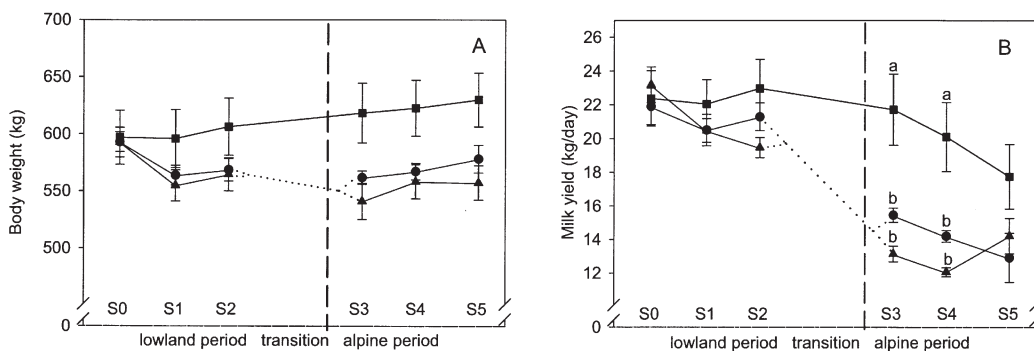
FIG. 2. Average body weight and milk yield throughout the entire experiment. S0 and S5 baseline subperiods; S1 and S2, lowland subperiods; S3 and S4 alpine subperiods. ● Pasture group; ▲ indoor grass group; ■ control group; n = 6 per group. Dotted lines indicate that half of the cows were switched between pasture and indoor group. Dashed lines mark the day of transport of the grass-fed cows to the alpine location. Error bars represent SE. Different superscripts indicate significant group differences at $P < 0.05$.
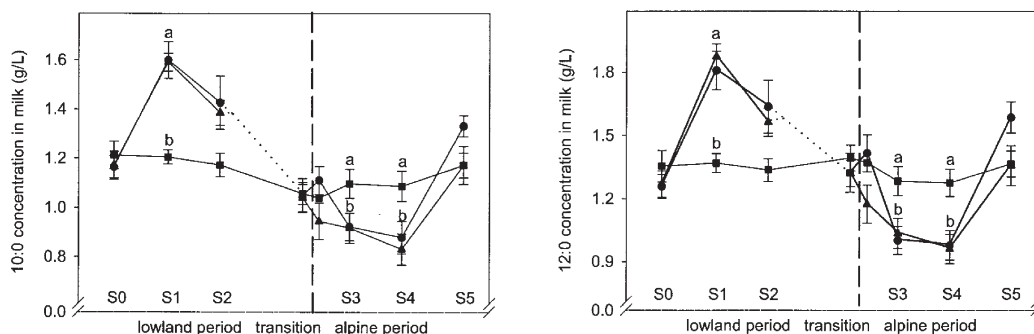
FIG. 3. Concentrations of medium-chain saturated FA in milk throughout the entire experiment. S0 and S5 baseline subperiods; S1 and S2, lowland subperiods; S3 and S4 alpine subperiods. ● Pasture group; ▲ indoor grass group; ■ control group; n = 6 per group. Dotted lines indicate that half of the cows were switched between pasture and indoor group. Dashed lines mark the day of transport of the grass-fed cows to the alpine location. Error bars represent SE. Different superscripts indicate significant group differences at $P < 0.05$.
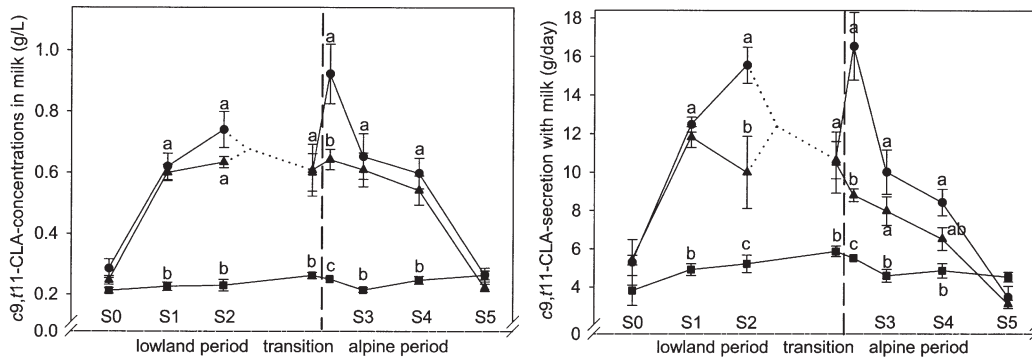
FIG. 4. Milk concentrations and daily excretion of CLA (18:2c9,t11) throughout the entire experiment. S0 and S5 baseline subperiods; S1 and S2, lowland subperiods; S3 and S4 alpine subperiods. ● Pasture group; ▲ indoor grass group; ■ control group; n = 6 per group. Dotted lines indicate that half of the cows were switched between pasture and indoor group. Dashed lines mark the day of transport of the grass-fed cows to the alpine location. Error bars represent SE. Different superscripts indicate significant group differences at *P* < 0.05.

FIG. 5. Milk concentrations and daily excretion of α-linolenic acid (18:3n-3) throughout the entire experiment. S0 and S5 baseline subperiods; S1 and S2, lowland subperiods; S3 and S4 alpine subperiods. ● Pasture group; ▲, indoor grass group; ■ control group; n = 6 per group. Dotted lines indicate that half of the cows were switched between pasture and indoor group. Dashed lines mark the day of transport of the grass-fed cows to the alpine location. Error bars represent SE. Different superscripts indicate significant group differences at *P* < 0.05.
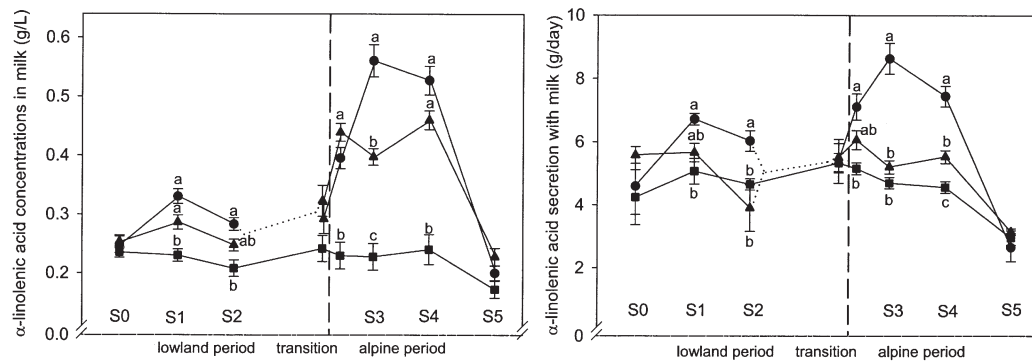
control cows. In S5, 18:3n-3 concentration returned to the baseline value (Fig. 5).

Long-chain PUFA in milk. Concentrations of the long-chain n-3 PUFA (EPA, 20:5n-3; docosapentaenoic acid, 22:5n-3; DHA, 22:6n-3) were higher in milk samples of the grass-only groups than in C cows (*P* < 0.01), whereas 20:4n-6 (arachidonic acid) was somewhat lower in P and B cows (Table 4). The ratio of all n-6/n-3 PUFA was diminished by half in P and B compared with C. The long-chain PUFA responded neither to the alpine sojourn (Table 4) nor to the stage of vegetation (data not shown).

Phytanic acid. Phytanic acid concentration in milk fat, which was analyzed in a smaller subset of samples (S2, transition period, and S3), was markedly higher with grass-only feeding compared with the control diet (*P* < 0.001; Fig. 6). There was a slight, but not significant, additional increase with alpine sojourn.

α-Tocopherol. The α-tocopherol concentration was 0.86- and 1.31-fold higher in milk of P and B cows than that of C

cows during the lowland and the alpine period, respectively (*P* < 0.001; Table 4). In S5, the values of the previously grass-fed groups dropped nearly to the baseline level (from 1.57 mg/L in S4 to 0.95 mg/L in S5; the baseline value in S0 had been 0.79 mg/L for P and B on average).

DISCUSSION

Impact of feeding grass only on milk FA profile. In the lowland period, turnout to pasture and the concurrent start of feeding only grass in the barn did not markedly change the net energy intake relative to controls but clearly altered the amount and composition of the ingested lipids and the FA composition of the milk lipids. The intake of SFA, 18:1, and 18:2n-6 declined for groups P and B in the lowlands, since the concentrates and the included rumen-protected fat, maize, and cereals were no longer available. In turn, 18:3n-3-intake was nearly doubled (Fig. 1).

Among the unsaturated FA, 18:3n-3 is one of those most
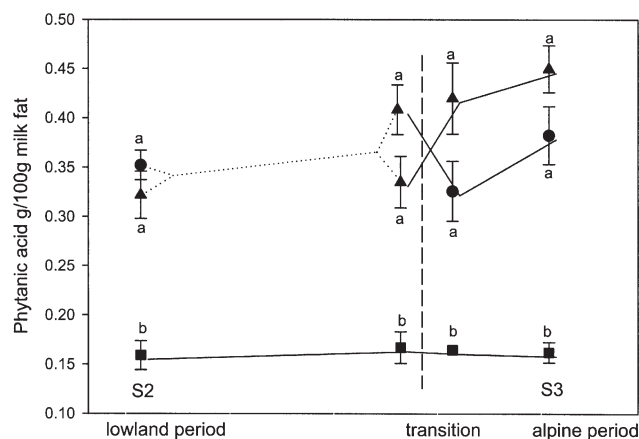
FIG. 6. Phytanic acid concentration in milk fat. S2, lowland period; S3, alpine period. ● Pasture group; ▲ indoor grass group; ■ control group; n = 6 per group. Dotted lines indicate that half of the cows were switched between pasture and indoor group. Dashed line marks the day of transport of grass-fed cows to the alpine location. Error bars represent SE. Different superscripts indicate significant differences at $P < 0.05$.

susceptible to ruminal biohydrogenation (29). Up to 99% of the dietary 18:3n-3 can be partially or completely hydrogenated (30). Main derivatives of 18:3n-3 biohydrogenation are 18:1*trans*-11 and 18:0 (31), which are partly desaturated at the Δ9 position to *cis*-9,*trans*-11 CLA and 18:1*cis*-9, respectively, in the mammary gland (32). As a consequence, under normal ruminal conditions, the high proportion of 18:3n-3 in grass-only diets explains the elevated contents of CLA and 18:1*trans*-11 in milk fat as also found in the current study (Fig. 4, Table 4). However, the increase of *cis*-9,*trans*-11 CLA during lowland grazing in our case was even more pronounced than in other studies (3,10,11,33). We did not find a substantial reduction of CLA in milk fat when harvested grass was fed instead of grazing, as has been previously described by Elgersma *et al.* (34), but this is probably a problem related to the wilting during storage (15), which we had carefully avoided.

The small proportion of 18:3n-3 passing by the rumen may appear in milk in its native form or in the form of endogenous derivatives (20:5n-3, 22:5n-3, and 22:6n-3; 35). Accordingly, all 20- and 22n-3 PUFA were higher in the milk fat of grass-only fed cows compared with the control. However, the moderate increase of these n-3 PUFA proportion found in milk fat in the lowland period of the present study (Table 4) did not reflect the massive increase in 18:3n-3 intake of cows fed only grass (Fig. 1; Table 3). This underlines the high extent and relevance of the biohydrogenation of 18:3n-3 during the lowland period. We assume that the supply of fermentable energy during this period was sufficiently high to support extensive biohydrogenation. Furthermore, mobilized body fat, as indicated by the decrease in body weight (Fig. 2) and the significantly higher NEFA concentration in plasma of the pasture group (Table 3), may have contributed to the 18:3n-3 in milk fat (36). Thus, the actual recovery of ingested 18:3n-3 in the milk can be assumed to be even lower than the apparent recovery.

The relatively sharp increase in the proportion of 6:0 to 14:0

in milk of P and B cows at the beginning of the lowland period (Fig. 3) may be explained by a shift in ruminal production from propionate to acetate, when all concentrates were withdrawn since acetate is the substrate for the FA *de novo* synthesis in the mammary gland. The subsequent continuously decreasing amount of medium-chain SFA might have been a result of a decreased energy intake and mobilization of body fat stores at the expense of *de novo* synthesis. However, as a moderate decrease of these medium-chain SFA also occurred in the control group, which was not exposed to dietary changes, a general effect linked to the progression of lactation may be assumed.

Impact of feeding alpine grass on the milk FA profile. Unlike Kraft *et al.* (3), we found that *cis*-9,*trans*-11 CLA and 18:1*trans*-11 concentrations in milk fat were not further elevated when P and B cows received alpine instead of lowland grass (Fig. 4). These are not necessarily conflicting results, because other influencing factors apart from alpine effects cannot be excluded, since Kraft *et al.* (3) compared milk from different herds. Ferlay *et al.* (12) found a considerable reduction of CLA after 3 wk of alpine grazing and related this to the stage of plant development (17). In the present experiment, no corresponding effect of stage of vegetation occurred at any experimental site (Fig. 4). In contrast to what was indicated by the results of Fievez *et al.* (11), there was also no noticeable effect of forage biodiversity on the CLA concentration. Thus, feeding only grass, irrespective of site and vegetative stage, may *per se* be a main contributor to high *cis*-9,*trans*-11 CLA proportions in milk fat. Whereas the main isomer, *cis*-9,*trans*-11, slightly declined owing to alpine feeding, the *trans*-11,*cis*-13 isomer was further increased, making it an interesting marker and potential target of experiments elucidating its possible physiological effects.

The 18:3n-3 contents of forages were described to decrease with maturation of the grass (37). In the present study, this was also found in the alpine grass (6.81 vs. 4.13 g 18:3n-3/kg DM for young vs. mature grass) but not in the lowlands (6.76 vs. 9.01 g 18:3n-3/kg DM). Furthermore, *Lolium perenne* and *Trifolium repens*, two of the dominant species in the lowland pasture (Table 1), contain far higher contents of 18:3n-3 than many other grasses and legumes (37). The absence of these species and the on-average higher maturity of the alpine forages (27) may at least partly explain the lower 18:3n-3 proportion in total FAME of the alpine grass. Together with alpine-specific anorexia of the cows (27), this drastically decreased 18:3n-3 intake (Fig. 1). In contrast to this, the most surprising and, with respect to human nutrition, most important effect of the alpine sojourn was the sharp increase of 18:3n-3 concentrations in milk fat, which in our case was definitely not related to the 18:3n-3 supply from food as suggested elsewhere (3,17).

Three hypotheses will be discussed here that could explain, alone or in combination, this discrepancy between intake of 18:3n-3 and its concentration in milk fat. One hypothesis (i) is that body fat mobilization with a preference for 18:3n-3 took place as a result of the energy deficiency associated with high altitude. The other hypotheses are that ruminal biohydrogenation activity was reduced by either energy deficiency (ii) or specific

secondary plant ingredients that inhibit ruminal microbes (iii). The fact that less than 10% of 18:3n-3 escapes biohydrogenation in the rumen (30) makes it likely that even small changes in the ruminal ecosystem, influencing hydrogenating microbes, may have large effects on the amount of 18:3n-3 available at the duodenum.

(i) Metabolic energy deficiency related to altitude. One key issue might be the decrease in energy intake of the cows transferred to the alpine site. Although cows partially reduced the energy deficit by a sharp decline in milk yield, as found in previous studies (27,38), there were several indications of a persisting metabolic energy deficit such as decreased plasma glucose and insulin levels and increased body fat mobilization (as indicated by elevated plasma NEFA and BHB levels). Mobilization of body fat depots is typical for cows kept in high alpine regions (27,39), and a preferential release of 18-PUFA from body fat was observed in undernourished ruminants (36). This would suggest that the elevated 18:3n-3 concentrations in the milk fat obtained in the alpine period (Fig. 5) could originate at least partially from body fat. This hypothesis is underlined by the fact that 18:3n-3 was even more highly concentrated in the P cows because grazing activity is assumed to cause additional energy expenditure in this hypoxic and uneven environment (38). The differences in plasma BHB and NEFA concentrations between the P and the B group during the alpine period further support this explanation. The higher proportion of 18:1*cis*-9 in the alpine milk vs. control and of the milk from P vs. B cows also fits this hypothesis, because 18:1*cis*-9, the major FA in depot fat, is likely to be released from body stores.

(ii) Ruminal energy deficiency. Kelly *et al.* (33) considered ruminal ecosystem changes to be responsible for alterations in PUFA proportions of milk fat. In our study, in response to the nutritional energy deficiency during the alpine period in groups P and B (here: lack of fermentable organic matter), the rumen microbial capacity for biohydrogenation may have been reduced and more 18:3n-3 could have remained available for absorption. This would explain the negative response of *cis*-9,*trans*-11 CLA and 18:1*trans*-11 to alpine sojourn on the one hand and the positive response of 18:3n-3 on the other hand, which was found when comparing lowland and alpine milk samples derived from the grass-fed cows in our experiment (Table 4; Figs. 4 and 5). Milk of cows having restricted access to pasture was reported to have lower 18:3n-3 and increased 18:1*trans*-11 and *cis*-9,*trans*-11 CLA proportions when the animals were supplemented with grain (10). Also, Sasaki *et al.* (30) reported an increase of ruminal biohydrogenation of 18:3n-3 in sheep from 93 to 99% when a roughage-only diet was supplemented with concentrate at 400 g/kg. This supports the assumption of fermentable organic matter being one key factor for milk FA profile.

Both the mobilization hypothesis and the hypothesis of a reduced ruminal biohydrogenation are based on the presence of a serious energy deficiency during high-altitude grazing, which is underlined by many variables concerning performance and metabolic profile. Data are consistent with those of Agenäs *et al.* (9) where, at turnout to pasture, an impaired energy balance

of the cows was associated with elevated 18:3n-3 concentrations in milk.

(iii) Inhibition of ruminal biohydrogenation by dietary components. Another explanation, which would rely on a specific high-alpine phenomenon, is the assumption that typically high concentrations of secondary plant ingredients, such as polyphenols and terpenoids (40,41) as well as others, may inhibit hydrogenating microorganisms in the rumen. Tannins were shown to inhibit several strains of *Butyrivibrio fibrisolvens* (42), one of the most important biohydrogenating ruminal bacteria species (31). On the other hand, the findings of Dewhurst *et al.* (43) that 18:3n-3 biohydrogenation was reduced when feeding *Trifolium pratense* instead of *T. repens* suggest that plant constituents other than tannins also may influence biohydrogenation. In the present study, *T. pratense* was the most abundant legume in the alpine pasture but made up only 1.6% of the lowland forage. We assume that a complex interaction of different factors determines CLA and 18:3n-3 concentrations in milk rather than a monofactorial alpine mechanism. This implies that CLA and 18:3n-3 may be variable across milks from different alpine origins, which also may explain part of the differences between studies.

All hypotheses discussed to explain the higher 18:3n-3 concentrations in alpine pasture-derived milk fat would include the expectation of enhanced 20:5n-3 (EPA) and 22:6n-3 (DHA) content too, as 18:3n-3 can be converted to some extent into these FA in mammals (35). Although all 20- and 22n-3 PUFA were significantly higher in milk of groups P and B compared with group C and thus showed a diet effect, no additional effect of the alpine sojourn was found. It can be speculated that the maximal transfer rate was already reached at the 18:3n-3 concentration met in the lowlands by groups P and B. Furthermore, the transfer of PUFA from blood into milk also has to be considered: In particular, 20 and 22n-3 PUFA are reported to be preferentially bound to phospholipids in lipoproteins and therefore are hardly cleaved by lipoprotein lipases in the mammary gland. This could explain the low transfer rate into milk (44). The answer to the question—Which are the limiting factors of EPA and DHA synthesis and secretion?—is not yet clear (44), but it seems relevant to examine this question, since these n-3 PUFA are of an even higher specificity and importance for human health than 18:3n-3 (35).

Phytanic acid. This branched-chain 20:0 FA, being present in the plasma lipids of cows in proportions as high as 130 g/kg total FA (45), was strongly discriminated for by the mammary gland and was found in milk fat in concentrations between 10 and 500 mg/kg (46). The markedly increased values that were reached on pasture in the present study are at the upper limit of the literature values for butter as reviewed by Brown *et al.* (46). Similar to CLA, phytanic acid is supposed to act as a gene transcription factor and is assumed to exert antidiabetic effects (47). However, in this context a general risk of consuming higher amounts of phytanic acid for Refsum's disease patients, who suffer from inherited disorders of peroxisomal α-oxidation (48), must be considered.

α-Tocopherol. A reduced oxidative stability may be a prob-

lem in PUFA-rich milk lipids (49), including technological, flavor-related, and human health aspects. Our results indicate that pasture in any form obviously provides high amounts of α-tocopherol for milk synthesis and that its concentration is even higher in milk derived from alpine pasture. The α-tocopherol concentrations in pasture-derived milk were much higher than the minima suggested by Al-Mabruk *et al.* (49) to ensure a favorable oxidative stability of milk. According to Jensen *et al.* (50), α-tocopherol is actively secreted into the milk, and its daily amounts excreted with milk remain constant at levels between 20 and 30 mg/d. Indeed, in the grass-only fed cows, the absolute excretion of α-tocopherol per day with milk was on average higher during the lowland than during the alpine period. Thus, the significantly higher concentrations in milk produced during the alpine period were mainly a consequence of the reduced milk yield. On the other hand, the control cows on average did not reach a level of 20 mg α-tocopherol excretion per day, suggesting that the supply with this diet was too low to reach the naturally determined range.

General implications. Concerning high CLA and n-3 PUFA contents, a low n-6/n-3 ratio, and low concentrations of SFA, the alpine milk in this study, as in previous studies, constituted a more favorable FA pattern than conventionally produced lowland milk (2,3,8). However, levels of *cis*-9,*trans*-11-CLA were not different from milk obtained with lowland grazing, even though this pasture was intensively managed and poor in species diversity. We therefore conclude that the effects on this CLA isomer and on 18:1*trans*-FA are linked to grazing in general rather than being the result of a specific alpine pasture effect. In agreement with Kraft *et al.* (3), the same seems to hold true for the long-chain PUFA (20:5, 22:5, and 22:6 n-3). The situation is obviously different for 18:3n-3, which was markedly elevated by the alpine conditions, thus confirming previous findings (3,4). However, the real nature of the alpine grazing effect on 18:3n-3 concentration in milk still has to be elucidated. Where specific plant constituents are one of the major reasons affecting CLA and n-3 PUFA contents, strategies to increase 18:3n-3 further would be applicable also for lowland milk production systems. Where energy deficiency is the major driving factor, there would be only a very limited potential since a conflict would arise between product quality and animal welfare.

ACKNOWLEDGMENTS

REFERENCES

1. Innocente, N., Praturlon, D., and Corradini, C. (2002) Fatty Acid Profile of Cheese Produced with Milk from Cows Grazing on Mountain Pastures, *Ital. J. Food Sci. 3*, 217–224.
2. Zeppa, G., Giordano, M., Gerbi, V., and Arlorio, M. (2003) Fatty Acid Composition of Piedmont "Ossolano" Cheese, *Lait 83,* 167–173.
3. Kraft, J., Collomb, M., Möckel, P., Sieber, R., and Jahreis, G. (2003) Differences in CLA Isomer Distribution of Cow's Milk Lipids, *Lipids 38,* 657–664.
4. Hauswirth, C.B., Scheeder, M.R.L., and Beer, J.H. (2004) High Omega-3 Fatty Acid Content in Alpine Cheese—The Basis for an Alpine Paradox, *Circulation 109*, 103–107.
5. Bianchi, M., Fortina, R., Battaglini, L., Mimosi, A., Lussiana, C., and Ighina, A. (2003) Characterisation of Milk Production in Some Alpine Valleys of Piemonte, *Ital. J. Anim. Sci. 2*, 305–307.
6. Simopoulos, A.P. (2002) The Importance of the Ratio of Omega-3/Omega-6 Essential Fatty Acids, *Biomed. Pharmacother. 56*, 365–379.
7. Belury, M.A. (2002) Dietary Conjugated Linoleic Acid in Health: Physiological Effects and Mechanisms of Action, *Annu. Rev. Nutr. 22,* 505–531.
8. Nakamura, T., Azuma, A., Kuribayashi, T., Sugihara, H., Okuda, S., and Nakagawa, M. (2003) Serum Fatty Acid Levels, Dietary Style and Coronary Heart Disease in Three Neighbouring Areas in Japan: The Kumihama Study, *Br. J. Nutr. 89*, 267–272.
9. Agenäs, S., Holtenius, K., Griinari, M., and Burstedt, E. (2002) Effects of Turnout to Pasture and Dietary Fat Supplementation on Milk Fat Composition and Conjugated Linoleic Acid in Dairy Cows, *Acta Agric. Scand. 52A*, 25–33.
10. Wijesundera, C., Shen, Z., Wales, W.J., and Dalley, D.E. (2003) Effect of Cereal Grain and Fibre Supplements on the Fatty Acid Composition of Milk Fat of Grazing Dairy Cows in Early Lactation, *J. Dairy Res. 70,* 257–265.
11. Fievez, V., Vlaeminck, B., Raes, K., Chow, T.T., De Smet, S., Demeyer, D., and Bruinenberg, M.H. (2002) Dietary and Milk Fatty Acid Composition in Relation to the Use of Forages from Semi-natural Grasslands, *Grassl. Sci. Eur. 7*, 558–559.
12. Ferlay, A., Martin, B., Pradel, P., Capitan, P., Coulon, J.B., and Chilliard, Y. (2002) Effect of the Nature of Forages on Cow Milk Fatty Acids Having a Positive Role on Human Health, *Grassl. Sci. Eur. 7*, 556–557.
13. Chilliard, Y., Ferlay, A., and Doreau, M. (2001) Effect of Different Types of Forages, Animal Fat or Marine Oils in Cow's Diet on Milk Fat Secretion and Composition, Especially Conjugated Linoleic Acid (CLA) and Polyunsaturated Fatty Acids, *Livest. Prod. Sci. 70*, 31–48.
14. Boufaied, H., Chouinard, P.Y., Tremblay, G.F., Petit, H.V., Michaud, R., and Belanger, G. (2003) Fatty Acids in Forages. II. *In vitro* Ruminal Biohydrogenation of Linolenic and Linoleic Acids from Timothy, *Can. J. Anim. Sci. 83*, 513–522.
15. Dewhurst, R.J., Moorby, J.M., Scollan, N.D., Tweed, J.K.S., and Humphreys, M.O. (2002) Effects of a Stay-Green Trait on the Concentrations and Stability of Fatty Acids in Perennial Ryegrass, *Grass Forage Sci. 57*, 360–366.
16. Collomb, M., Bütikofer, U., Sieber, R., Jeangros, B., and Bosset, J.-O. (2002) Correlation Between Fatty Acids in Cows' Milk Fat Produced in the Lowlands, Mountains and Highlands of Switzerland and Botanical Composition of the Fodder, *Int. Dairy J. 12*, 661–666.
17. Martin, B., Fedele, V., Ferlay, A., Grolier, P., Rock, E., Gruffat, D., and Chilliard, Y. (2004) Effects of Grass-Based Diets on the Content of Micronutrients and Fatty Acids in Bovine and Caprine Dairy Products, *Grassl. Sci. Eur. 9*, 876–886.
18. Berry, N.R., Scheeder, M.R.L., Sutter, F., Kröber, T.F., and Kreuzer, M. (2000) The Accuracy of Intake Estimation Based on the Use of Alkane Controlled-Release Capsules and Faeces Grab Sampling in Cows, *Ann. Zootech. 49*, 3–13.
19. Braun-Blanquet, J. (1964) *Pflanzensoziologie*, 3rd edn., Springer Verlag, Vienna.

20. Suter, B., Grob, K., and Pacciarelli, B. (1997) Determination of Fat Content and Fatty Acid Composition Through 1-min Transesterification in the Food Sample; Principles, *Z. Lebensm. Unters. Forsch. A 204*, 252–258.

21. Collomb, M., and Bühler, T. (2000) Analyse de la composition en acides gras de la graisse de lait, *Mitt. Lebensm. Hyg. 91*, 306–332.

22. Wolff, R.L., and Precht, D. (2002) A Critique of 50-m CP-Sil 88 Capillary Columns Used Alone to Assess *trans*-Unsaturated Fatty Acids in Foods: The Case of the TRANSFAIR Study, *Lipids 37*, 627–629.

23. Kramer, J.K.G., Blackadar, C.B. and Zhou, J. (2002) Evaluation of Two GC Columns (60-m SUPELCOWAX 10 and 100-m CP Sil 88) for Analysis of Milkfat with Emphasis on CLA, 18:1, 18:2 and 18:3 Isomers, and Short- and Long-Chain FA, *Lipids 37*, 823–835.

24. Collomb, M., Sieber, R., and Bütikofer, U. (2004) CLA Isomers in Milk Fat from Cows Fed Diets with High Levels of Unsaturated Fatty Acids, *Lipids 39*, 355–364.

25. Wettstein, H.-R., Scheeder, M.R.L., Sutter, F., and Kreuzer, M. (2001) Effect of Lecithins Partly Replacing Rumen-Protected Fat on Fatty Acid Digestion and Composition of Cow Milk, *Eur. J. Lipid Sci. Technol. 103*, 12–22.

26. Rettenmaier, R., and Schüep, W. (1992) Determination of Vitamins A and E in Liver Tissue, *Int. J. Vitam. Nutr. Res. 62*, 312–317.

27. Leiber, F., Kreuzer, M., Jörg, B., Leuenberger, H., and Wettstein, H.-R. (2004) Contribution of Altitude and Alpine Origin of Forage to the Influence of Alpine Sojourn of Cows on Intake, Nitrogen Conversion, Metabolic Stress and Milk Synthesis, *Anim. Sci. 78*, 451–466.

28. RAP (Station federale de recherches en production animále) (1999) *Fütterungsempfehlungen und Nährwerttabellen für Wiederkäuer*, 4th edn., Landwirtschaftliche Lehrmittelzentrale, Zollikofen, Switzerland.

29. Wachira, A.M., Sinclair, L.A., Wilkinson, R.G., Hallett, K., Enser, M., and Wood, J.D. (2000) Rumen Biohydrogenation of n-3 Polyunsaturated Fatty Acids and Their Effects on Microbial Efficiency and Nutrient Digestibility in Sheep, *J. Agric. Sci. 135*, 419–428.

30. Sasaki, H., Horiguchi, K., and Takahashi, T. (2001) Effects of Different Concentrate and Roughage Ratios on Ruminal Balance of Long-Chain Fatty Acids in Sheep, *Asian-Austral. J. Anim. Sci. 14*, 960–965.

31. Song, M.K. (2000) Fatty Acid Metabolism by Rumen Microorganisms, *Asian-Austral. J. Anim. Sci. 13*, 137–148.

32. Griinari, J.M., Corl, B.A. Lacy, S.H., Chouinard, P.Y., Nurmela, K.V.V., and Bauman, D.E. (2000) Conjugated Linoleic Acid Is Synthesized Endogenously in Lactating Dairy Cows by Δ9-Desaturase. *J. Nutr. 130*, 2285–2291.

33. Kelly, M.L., Kolver, E.S., Baumann, D.E., van Amburgh, M.E., and Muller, L.D. (1998) Effect of Intake of Pasture on Concentrations of Conjugated Linoleic Acid in Milk of Lactating Cows, *J. Dairy Sci. 81*, 1630–1636.

34. Elgersma, A., Ellen, G., and Tamminga, S. (2004) Rapid Decline of Contents of Beneficial Omega-7 Fatty Acids in Milk from Grazing Cows with Decreasing Herbage Allowance, *Grassl. Sci Eur. 9*, 1136–1138.

35. Sinclair, A.J., Attar-Bashi, N.M., and Li, D. (2002) What Is the Role of α-Linolenic Acid for Mammals? *Lipids 37*, 1113–1123.

36. Soppela, P., and Nieminen, M. (2002) Effect of Moderate Wintertime Undernutrition on Fatty Acid Composition of Adipose Tissues of Reindeer (*Rangifer tarandus tarandus* L.), *Comp. Biochem. Physiol. A 132*, 403–409.

37. Boufaied, H., Chouinard, P.Y., Tremblay, G.F., Petit, H.V., Michaud, R., and Belanger, G. (2003) Fatty Acids in Forages. I. Factors Affecting Concentrations, *Can. J. Anim. Sci. 83*, 501–511.

38. Christen, R.E., Kunz, P.L., Langhans, W., Leuenberger, H., Sutter, F., and Kreuzer, M. (1996) Productivity, Requirements and Efficiency of Feed and Nitrogen Utilization of Grass-fed Early Lactating Cows Exposed to High Alpine Conditions, *J. Anim. Physiol. Anim. Nutr. 76*, 22–35.

39. Kreuzer, M., Langhans, W., Sutter, F., Christen, R.E., Leuenberger, H., and Kunz, P.L. (1998) Metabolic Response of Early Lactating Cows Exposed to Transport and High Altitude Grazing Conditions, *Anim. Sci. 67*, 237–248.

40. Barry, T.N., and McNabb, W.C. (1999) The Implications of Condensed Tannins on the Nutritive Value of Temperate Forages Fed to Ruminants, *Br. J. Nutr. 81*, 263–272.

41. Mariaca, R.G., Berger, T.F.H., Gauch, R., Imhof, M.I., Jeangros, B., and Bosset, J.O. (1997) Occurrence of Volatile Mono- and Sesquiterpenoids in Highland and Lowland Plant Species as Possible Precursors for Flavor Compounds in Milk and Dairy Products, *J. Agric. Food Chem. 45*, 4423–4434.

42. Min, B.R., Barry, T.N., Attwood, G.T., and McNabb, W.C. (2003) The Effect of Condensed Tannins on the Nutrition and Health of Ruminants Fed Fresh Temperate Forages: A Review, *Anim. Feed Sci. Technol. 106*, 3–19.

43. Dewhurst, R.J., Evans, R.T., Scollan, N.D., Moorby, J.M., Merry, R.J., and Wilkins, R.J. (2003) Comparison of Grass and Legume Silages for Milk Production. 2. *In vivo* and *in sacco* Evaluations of Rumen Function, *J. Dairy Sci. 86*, 2612–2621.

44. Offer, N.W., Mardsen, M., Dixon, J., Speake, B.K., and Thacker, F.E. (1999) Effect of Dietary Fat Supplements on Levels of n-3 Poly-unsaturated Fatty Acids, *trans* Acids and Conjugated Linoleic Acid in Bovine Milk, *Anim. Sci. 69*, 613–625.

45. Lough, A.K. (1977) The Phytanic Acid Contents of the Lipids of Bovine Tissues and Milk, *Lipids 12*, 115–119.

46. Brown, P.J., Mei, G., Gibberd, F.B., Burston, D., Mayne, P.D., McClinchy, J.E., and Sidey, M. (1993) Diet and Refsum's Disease. The Determination of Phytanic Acid and Phytol in Certain Foods and the Application of This Knowledge to the Choice of Suitable Convenience Foods for Patients with Refsum's Disease, *J. Hum. Nutr. Diet. 6*, 295–305.

47. McCarty, M.F. (2001) The Chlorophyll Metabolite Phytanic Acid Is a Natural Rexinoid—Potential for Treatment and Prevention of Diabetes, *Med. Hypoth. 56*, 217–219.

48. Mukherji, M., Schofield, C.J., Wierzbicki, A.S., Jansen, G.A., Wanders, R.J.A., and Lloyd, M.D. (2003) The Chemical Biology of Branched-chain Lipid Metabolism, *Prog. Lipid Res. 42*, 359–376.

49. Al-Mabruk, R.M., Beck, M.F.G., and Dewhurst, R.J. (2004) Effects of Silage Species and Supplemental Vitamin E on the Oxidative Stability of Milk, *J. Dairy Sci. 87*, 406–412.

50. Jensen, S.K., Johannsen, A.K.B., and Hermansen, J.E. (1999) Quantitative Secretion and Maximal Secretion Capacity of Retinol, β-Carotene and α-Tocopherol into Cows' Milk, *J. Dairy Res. 66*, 511–522.

METHODS

Quantitative Determination of Total Lipid Hydroperoxides by a Flow Injection Analysis System

Jeong-Ho Sohn, Yusuke Taki, Hideki Ushio, and Toshiaki Ohshima*

Department of Food Science and Technology, Tokyo University of Marine Science
and Technology, Konan 4, Minato-ku, Tokyo 108-8477, Japan

ABSTRACT: A flow injection analysis (FIA) system coupled with a fluorescence detection system using diphenyl-1-pyrenylphosphine (DPPP) was developed as a highly sensitive and reproducible quantitative method of total lipid hydroperoxide analysis. Fluorescence analysis of DPPP oxide generated by the reaction of lipid hydroperoxides with DPPP enabled a quantitative determination of the total amount of lipid hydroperoxides. Use of 1-myristoyl-2-(12-((7-nitro-2-1,3-benzoxadiazol-4-yl)amino) dodecanoyl)-sn-glycero-3-phosphocholine as the internal standard improved the sensitivity and reproducibility of the analysis. Several commercially available edible oils, including soybean oil, rapeseed oil, olive oil, corn oil, canola oil, safflower oil, mixed vegetable oils, cod liver oil, and sardine oil were analyzed by the FIA system for the quantitative determination of total lipid hydroperoxides. The minimal amounts of sample oils required were 50 µg of soybean oil (PV = 2.71 meq/kg) and 3 mg of sardine oil (PV = 0.38 meq/kg) for a single injection. Thus, sensitivity was sufficient for the detection of a small amount and/or low concentration of hydroperoxides in common edible oils. The recovery of sample oils for the FIA system ranged between 87.2 ± 2.6% and 102 ± 5.1% when PV ranged between 0.38 and 58.8 meq/kg. The CV in the analyses of soybean oil (PV = 3.25 meq/kg), cod liver oil (PV = 6.71 meq/kg), rapeseed oil (PV = 12.3 meq/kg), and sardine oil (PV = 63.8 meq/kg) were 4.31, 5.66, 8.27, and 11.2%, respectively, demonstrating sufficient reproducibility of the FIA system for the determination of lipid hydroperoxides. The squared correlation (r^2) between the FIA system and the official AOCS iodometric titration method in a linear regression analysis was estimated at 0.9976 within the range of 0.35–77.8 meq/kg of PV (n = 42). Thus, the FIA system provided satisfactory detection limits, recovery, and reproducibility. The FIA system was further applied to evaluate changes in the total amounts of lipid hydroperoxides in fish muscle stored on ice.

Paper no. L9651 in *Lipids 40*, 203–209 (February 2005).

Lipid oxidation occurring in food is a major cause of quality deterioration in flavor, texture, consistency, and appearance. It is also a decisive factor in the causes of aging and some diseases (1). Since lipid oxidation is one of the most important problems in food chemistry, a great deal of research has been devoted to its mechanisms and the development of effective antioxidants. Although various methods have been proposed to measure hydroperoxides, the instability and diversity of hydroperoxides in a complex food system becomes a hindrance to an accurate and simple analysis. The widely accepted iodometric titration (2,3) and the enzymatic assay (4) have inherent problems such as sensitivity, selectivity, and interference with contaminants. It is therefore very important and necessary to develop more efficient analytical methods to evaluate lipid peroxidation in complex food systems.

In the analysis of hydroperoxides by HPLC, quantitative determination by UV light absorption at around 235 nm is based on the oxidation reaction of the conjugated double bond of the lipid (5). However, with respect to applications evaluating the early stage of lipid oxidation, there are problems involving specificity and detection sensitivity. In response to these problems, Yamada *et al.* (6) used an electrochemical detection method that utilized the redox potential of hydroperoxides to detect the primary lipid peroxidation product. However, the detection sensitivity was inadequate to analyze trace amounts of lipid hydroperoxides. One solution to this problem involves a postcolumn chemiluminescence detection based on luminol or isoluminol oxidation during the reaction of hydroperoxide and cytochrome C (7,8). Some applications to biological systems also have been reported (9–11). Generally, nonpolar solvent systems based on *n*-hexane are used in HPLC for the separation of hydroperoxide positional isomers (12). However, a postcolumn reaction of luminol to luminol oxide progresses only under aqueous alkaline conditions (9). Therefore, the number and types of organic solvents used for the mobile phase are relatively limited, since hydrophobic nonpolar solvent mixtures do not mix well with hydrophilic luminol reagents in a postcolumn reaction coil.

Diphenyl-1-pyrenylphosphine (DPPP) is a fluorescence reagent that reacts specifically with various lipid hydroperoxides to form DPPP oxide, even in the presence of lipid alcohols. The DPPP oxide is excited at 352 nm of UV light and gives the emission wavelength (λ_{em}) of 380 nm. The DPPP solution has been confirmed as having sufficient stability by holding it at –25°C in the dark. The stability of DPPP itself has been maintained for more than 20 mon at 5°C in the dark (13). This reaction progresses in different types of solvents (14). A few applications of this system have already been reported for the analyses of hydroperoxides of TAG, cholesterol, cholesterol esters, and phospholipids in biological systems (15–20). This method has also been applied to analyze the distributions of

---

*To whom correspondence should be addressed.
E-mail: tohshima@s.kaiyodai.ac.jp

Abbreviations: DPPP, diphenyl-1-pyrenylphosphine; FIA, flow injection analysis; NBD-labeled PC, 1-myristoyl-2(12-((7-nitro-2-1,3-benzoxadiazol-4-yl)amino)dodecanoyl)-sn-glycero-3-phosphocholine.
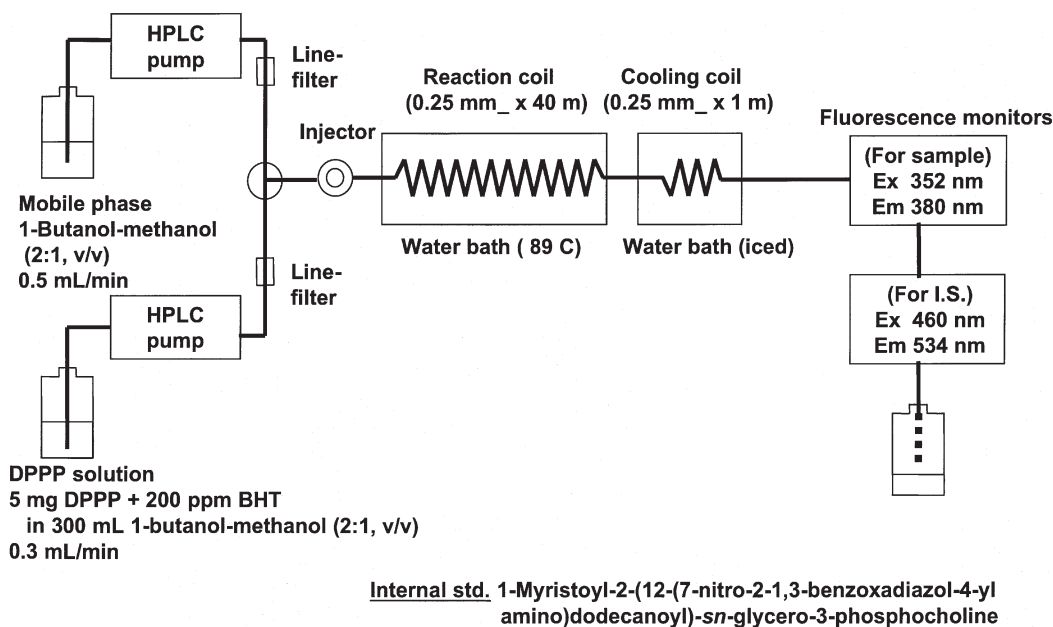
FIG. 1. A system diagram for flow injection analyses of total lipid hydroperoxides. BHT, butylated hydroxytoluene; DPPP, diphenyl-1-pyrenylphosphine; I.S., internal standard.

hydroperoxide isomers of FAME (21–24). However, since various lipid classes coexist in food, separating and analyzing each hydroperoxide with a different chemical structure is complicated. Therefore, a simultaneous method that can determine total lipid hydroperoxides in food and other complex systems is required.

The aim of this study was to establish an accurate and simple analytical methodology that could enable the quantitative determination of total amounts of lipid hydroperoxides in complex food systems. For the analytical method proposed in this study, an HPLC separation column was replaced by a stainless-steel reaction coil, and an appropriate internal standard was introduced to facilitate study of the total lipid hydroperoxide contents.

MATERIALS AND METHODS

Chemicals and materials. DPPP was purchased from Dojindo Laboratories Co., Ltd. (Kumamoto, Japan). BHT was purchased from Tokyo Kasei Kogyo Co., Ltd. (Tokyo, Japan). 1-Myristoyl-2-(12-((7-nitro-2-1,3-benzoxadiazol-4-yl)amino)dodecanoyl)-*sn*-glycero-3-phosphocholine (NBD-labeled PC) was purchased from Avanti Polar Lipids, Inc. (Alabaster, AL). Methanol of HPLC grade from Kokusan Chemical Co., Ltd. (Tokyo, Japan) and 1-butanol from Kishida Chemical Co., Ltd. (Osaka, Japan) were used after degassing. All other chemicals were of analytical grade.

Commercially available soybean oil (Miyazawa Yakuhin Co., Ltd., Tokyo, Japan), rapeseed oil (Yamahiko Hayasi Co., Tokyo, Japan), olive oil, corn oil, canola oil, safflower oil (Ajinomoto Co., Inc., Tokyo, Japan), mixed vegetable oils (Nisshin Oillio Ltd., Tokyo, Japan), cod liver oil (Toho Co., Tokyo,

Japan), and sardine oil (extracted and purified in the laboratory) were used as sample oils. Briefly, sardine oil was extracted by the Bligh and Dyer procedure (25) and purified by open column chromatography (72 cm length × 6 cm i.d.) on Spherical silica gel 60 40–50 μm, Kanto Chemical Co. Inc., Tokyo, Japan) using *n*-hexane followed by 5% (vol/vol) diethyl ether in *n*-hexane as the eluates.

The flow injection analysis (FIA) system. A diagram of the FIA system with a fluorescence detection system using DPPP is illustrated in Figure 1. The mobile phase (a mixture of 200 mL of 1-butanol and 100 mL of methanol) was passed through a Shimadzu model LC-9A HPLC pump (Kyoto, Japan) at a flow rate of 0.5 mL/min and subsequently transferred to a stainless-steel reaction coil (0.25 mm i.d. × 40 m) immersed in a water bath (NTT-1400; Eyela, Tokyo, Japan) controlled at 89°C. The nonfluorescent DPPP reagent reacted with lipid hydroperoxides to produce fluorescent DPPP oxide quantitatively in the coil. After the reaction, the eluent from the coil was cooled by passing it through a short stainless-steel coil (0.25 mm i.d. × 1 m) immersed in an ice-water bath. At the inlet of the reaction coil, a DPPP solution (5 mg of DPPP and 100 mg of BHT dissolved in a mixture of 200 mL of 1-butanol and 100 mL of methanol) was pumped with a Shimadzu model LC-10AS (Kyoto, Japan) and mixed with the eluent from the column in a T-connector. The DPPP solution, which was kept in a brown bottle on ice in the dark, was pumped at a flow rate of 0.3 mL/min. The fluorescence intensity of the DPPP oxides was monitored at 352 nm of excitation wavelength (λ_{ex}) and at 380 nm of λ_{em} with a Shimadzu model RF 535 fluorescence detector. The NBD-labeled PC used as an internal standard was monitored at 460 nm of λ_{ex} and at 534 nm of λ_{em} with a Shimadzu model RF-10A fluorescence detector, which was set in

the flow line behind the first fluorescence detector. The fluorescence intensity signals were integrated with two Shimadzu Chromatopac C-R6A chromatographic integrators. The injection volume was 20 μL, and all samples were analyzed in triplicate.

To find the most appropriate flow rates for the mobile phase as well as the DPPP solution, a mixture of 0.03 mg of sardine oil (PV = 82 meq/kg) and the internal standard (4.82 nmol) was dissolved in 10 mL of chloroform and introduced into the FIA system. Flow rates of the mobile phase and DPPP solution were increased stepwise from 0.2 to 0.8 mL/min and from 0.03 to 0.5 mL/min, respectively.

To evaluate the effects of the reaction coil temperature, each of the 20-μL portions containing 0.2, 0.4, or 0.6 mg of rapeseed oil (PV = 4.0 meq/kg) as well as 9.64 pmol of NBD-labeled PC was injected separately into the FIA system at the range of 60 to 90°C.

Calibration curve. A calibration curve was used to determine total lipid hydroperoxides with the FIA system in cod liver oils with different degrees of peroxidation. Five solutions with different mixing ratios (0.2:1.0, 0.5:1.0, 1.0:1.0, 2.0:1.0, and 3.0:1.0, mL/mL) of cod liver oil (PV = 22.3 meq/kg, 1.0330 g oil/10 mL chloroform) and the internal standard (4.82 nmol/mL methanol) were prepared quantitatively. Each solution was made up to 10 mL by chloroform, and each 20-μL portion was injected separately into the FIA system in triplicate.

Determination of PV. PV of the oils were determined by iodometric titration according to AOCS Official Method Cd 8-53 (2).

Fish sample preparation. Cultured live yellowtail (*Seriola quinqueradiata*) was obtained from a Misaki fishing port in Kanagawa, Japan. The yellowtail were sacrificed and immediately stored on ice during 1 h of transportation to the laboratory. The fish muscle specimen was separated into dorsal, ventral, and dark muscle. The separated muscle was thoroughly minced with a model MK-K50 cooking cutter (National, Tokyo, Japan) and stored on ice in polyethylene bags.

A 5-g portion of the fish muscle was extracted and purified according to the method of Bligh and Dyer (25). A 1-mL solution of NBD-labeled PC (4.82 nmol/mL in methanol) was added as an internal standard prior to homogenization. The homogenate was centrifuged at $1700 \times g$ for 8 min at 4°C. The lower layer was dehydrated by anhydrous sodium sulfate and filtered through a membrane filter (PTFE 0.20 μm; Advantec Toyo Roshi Kaisha, Ltd., Tokyo, Japan), and the filtrate thus obtained was made up to 10 mL by chloroform. A 20-μL portion of the sample solution containing 9.64 pmol of the internal standard was injected into the FIA system to determine the total lipid hydroperoxides.

Statistics. Measurements of hydroperoxide contents were carried out in triplicate and are represented as the mean ± SD. Student's *t*-test (26) was used to distinguish significant differences among the mean values. A statistically significant difference was selected at $P < 0.01$. A simple linear regression was calculated from the calibration curve, and the correlation between hydroperoxide contents obtained by the FIA system and the iodometric titration method was evaluated.

RESULTS AND DISCUSSION

Flow rates. Effects of the flow rates of the mobile phase and DPPP solution on peak areas are shown in Figure 2. The peak area ratios of the oil decreased gradually with the increase in flow rate of the mobile phase. Higher sensitivities in the detection of lipid hydroperoxides were obtained by reducing the flow rates; however, flow rates below 0.3 mL/min caused the constant flow by the pump to decline (Fig. 2B). On the other hand, the peak area ratios increased gradually with an increase in the flow rate of the DPPP solution up to 0.3 mL/min and plateaued at flow rates over 0.4 mL/min (Fig. 2B). Thus, the flow rates of the mobile phase and DPPP solution were set at 0.5 mL/min and 0.3 mL/min, respectively, to obtain sharp peaks and stable baselines on the chromatograms.

Reaction temperature. Changes in the peak area ratios were plotted in terms of the temperature of the reaction coil and are illustrated in Figure 3. For all the lines with different amounts of hydroperoxides injected, the peak area ratios increased gradually with an increase in reaction temperature. Indeed, the peak area ratios obtained at reaction temperatures of 70, 80, and 90°C were 138–141, 183–191, and 250–253%, respectively, of those obtained at 60°C. When the reaction temperature was increased to 90°C, the peak area ratios did not plateau and still tended to increase. The baselines of DPPP oxide and NBD-labeled PC on the chromatograms, however, became remarkably unstable at temperatures over 91°C due to solvent boiling. From the results of these preliminary examinations, the reaction
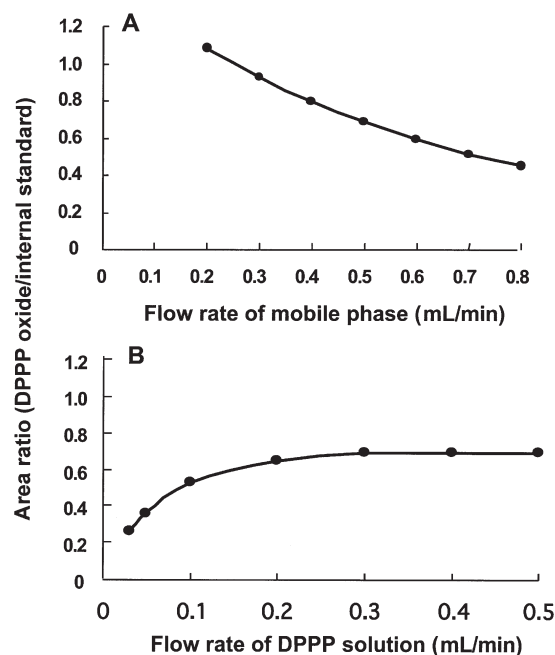
FIG. 2. Effects of flow rates of the mobile phase (A) and the DPPP solution (B) on the peak area ratios of sardine oil with a PV of 82 meq/kg. A 20-μL portion of a sardine oil/chloroform solution (1.5 mg/mL) containing 9.64 pmol of 1-myristoyl-2(12-((7-nitro-2-1,3-benzoxadiazol-4-yl)amino)dodecanoyl)-*sn*-glycero-3-phosphocholine (NBD-labeled PC) was injected into the FIA system at a reaction coil temperature of 89°C. For other abbreviation see Figure 1.

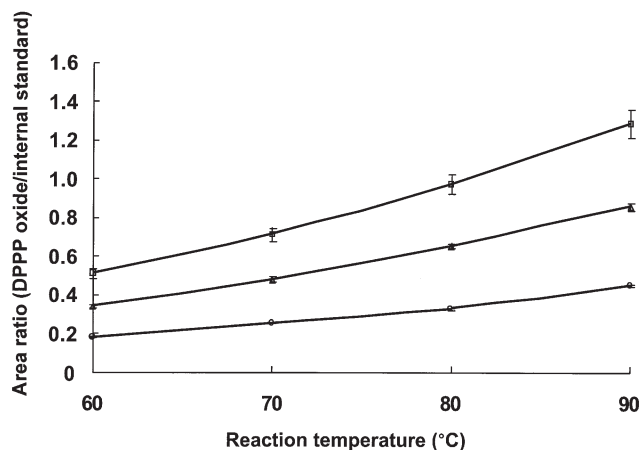**FIG. 3.** Effects of reaction coil temperature on the peak area ratios of DPPP oxide and NBD-labeled PC used as an internal standard. Twenty-microliter portions containing 0.2 (-○-), 0.4 (-△-), or 0.6 mg (-□-) of rapeseed oils (PV = 4.0 meq/kg) were injected separately.

temperature was set at 89°C to obtain the highest reaction efficiency under the present experimental conditions.

The FIA system. Several organic solvents, including chloroform, ethanol, methanol, acetone, benzene, diethyl ether, and *n*-hexane, were investigated to find suitable injection solvents for the FIA system. All injected solvents other than *n*-hexane had no effects on the fluctuation in intensity and provided no peaks on the baseline of the chromatogram. However, certain solvent characteristics, such as the toxicity of methanol and benzene, the insolubility of phospholipids in acetone and ethanol, and the flammability of diethyl ether, made certain injection solvents unsuitable for the FIA system. *n*-Hexane represented a small peak on the chromatogram when monitored at 352 nm of λ_{ex} and at 380 nm of λ_{em}. The effects of *n*-hexane on the peak signals of the sample were not negligible, especially for the analyses of small amounts and/or low concentrations of hydroperoxides in the lipid samples. From these results, we concluded that chloroform was the most suitable solvent for the FIA system (Fig. 4A). Additionally, the effects of radical trapping agents such as BHT and α-tocopherol on the fluorescence detection system were investigated. A chloroform solution of 200 ppm BHT or 200 ppm α-tocopherol showed no influence on the chromatogram (data not shown) as reported previously (22,27).

The primary fluorescence spectra of the DPPP oxide and the internal standard ranged between 360 and 410 nm and between 500 and 560 nm, respectively (data not shown), suggesting that no interference occurred in excited fluorescence intensities between the DPPP oxide and the internal standard.

The chromatograms of fish oil and the internal standard were monitored at the most suitable flow rates of the mobile phase (0.5 mL/min) and the DPPP solution (0.3 mL/min) as shown in Figures 4B and 4C, respectively. The retention times of DPPP oxide and the internal standard were approximately 3.2 and 3.3 min, respectively. Thus, the total lipid hydroperoxides of the sample were determined as a single peak in a short
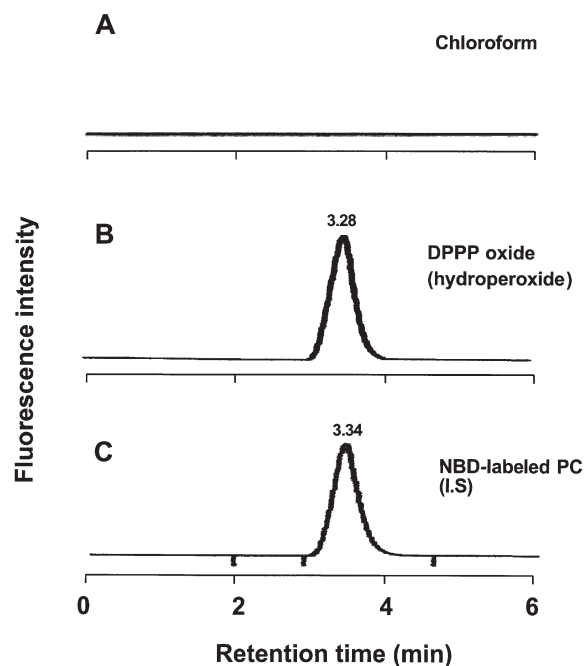
FIG. 4. Typical chromatograms obtained by the FIA system. (A) Chloroform as an injection solvent; (B) DPPP oxide reacted with total lipid hydroperoxide in the total lipid extracted from ordinary muscle of yellowtail (ca. 0.8 mg oil/injection); (C) NBD-labeled PC used as an internal standard (9.64 pmol/injection).

time. These results indicate that the FIA system is a rapid and simple method for the determination of hydroperoxides in lipids compared with the traditional iodometric determination.

Calibration curve. A calibration curve for the determination of total lipid hydroperoxides is shown in Figure 5. A linear relationship was obtained, with a squared correlation (r^2) of 0.9977 between the peak area ratios and the molar ratios of DPPP oxide peak areas and NBD-labeled PC. The minimal detectable amount of total hydroperoxides on the calibration curve was 24.0 pmol per injection.

Reproducibility and recovery. To obtain reproducibility in the quantitative determination of hydroperoxides with the FIA system, the hydroperoxide contents of several commercially available edible oils were analyzed in replicate, as summarized in Table 1. The CV for soybean oil, rapeseed oil, cod liver oil, and sardine oil were 4.31, 8.27, 5.66, and 11.2%, respectively, suggesting that the FIA system provided satisfactory reproducibility for the quantitative determination of lipid hydroperoxides.

Recoveries of authentic cumene hydroperoxides previously added to several edible oils were measured, as shown in Table 2. Recoveries ranged between 87.2 and 102%, suggesting that the FIA system provided sufficient recovery and reproducibility for the determination of total lipid hydroperoxides in edible oils.

Application to commercially available edible oils. The FIA system was applied to the quantitative determination of total lipid hydroperoxides in commercially available edible oils, including
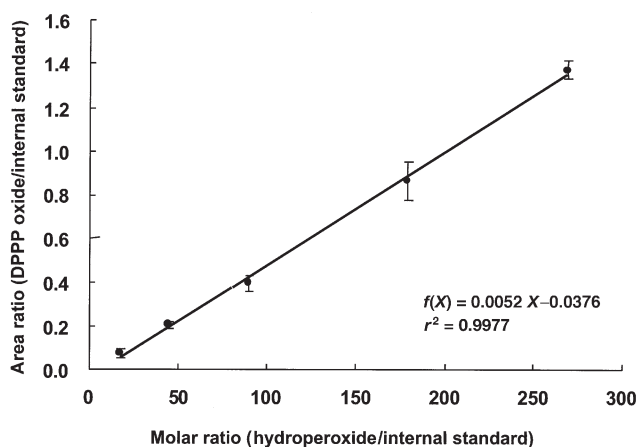
FIG. 5. A simple linear regression curve between the area ratios (DPPP oxide/NBD-labeled PC) and the molar ratios (cod liver oil hydroperoxide/NBD-labeled PC). The minimal detectable amount of total hydroperoxide on the calibration curve was 24.0 pmol of hydroperoxide per an injection.

soybean, rapeseed, olive, corn, canola, safflower, mixed vegetable, cod liver, and sardine oils. The hydroperoxide contents determined by the FIA system were compared with those determined by the official AOCS iodometric titration method, as shown in Figure 6. The simple linear regression curve, with $r^2 = 0.9976$ ($n = 42$) between the hydroperoxide contents determined by the FIA system and the iodometric titration method, suggested that the FIA system could be used not only as a practical alternative to the iodometric titration method but also as more sensitive and specific methodology for the quantitative determination of trace amounts of lipid hydroperoxides.

Application to muscle lipids. Changes in total lipid hydroperoxides in the muscle of cultured yellowtail during iced storage were measured with the FIA system and are illustrated in Figure 7. Although the total lipid hydroperoxide contents in the ventral and dorsal muscle were low and remained unchanged, those in the dark muscle contained significantly higher amounts of total hydroperoxides ($P < 0.01$) compared with those of the ventral and dorsal muscle throughout the storage time up to 4 d. These results coincided well with those obtained by Nakamura *et al.* (28), who reported that the PV of dark muscle were higher than ordinary muscle in wild yellowtail. The total lipid hydroperoxide content became sixfold that of the ventral and dorsal muscle after 4 d of storage, suggesting that the rate of lipid oxidation in the edible part of whole muscle is mainly due to the high lipid oxidation rate in the dark muscle. The off-flavor caused by rancidity in the dark muscle was confirmed after 3 d (data not shown) in this particular case, suggesting that lipid hydroperoxide contents determined by the FIA system offer an alternative oxidative index that is more sensitive than sensory evaluation.

In the case of muscle foods with lipid contents of less than 1%, such as flatfish muscle, 500–1000 g of muscle would be required to extract 5–10 g of total lipids, which would be a minimal amount for one iodometric titration for hydroperoxide determination. For the analyses in triplicate, at least 1500–3000 g of muscle would be required. The FIA system required less than 1 g of muscle for an accurate and reproducible determination of lipid hydroperoxide contents. Indeed, the present study showed that the lipid hydroperoxide content in the ordinary muscle of yellowtail with a total lipid content of 8% was approximately 200 neq/5 g muscle just after the fish were sacrificed; the hydroperoxide content of lipids was 0.5 meq/kg. To obtain the hydroperoxide content of ordinary yellowtail muscle by the iodometric titration method, approximately 120 g of ordinary muscle would be required for one titration trial, which is a disadvantage of the iodometric method. In comparison, the FIA system required only 5 g of muscle for a single determination. In particular, the present FIA system showed sufficient sensitivity and reproducibility to evaluate the early stage of oxidization of lean fish muscle.

TABLE 1
Reproducibility of Total Lipid Hydroperoxides by the Flow Injection Analysis (FIA) System

	Soybean oil	Cod liver oil	Rapeseed oil	Sardine oil
Mean[a] (meq/kg)	3.25	6.71	12.3	63.8
SD[b]	0.14	0.38	1.02	7.17
CV (%)	4.31	5.66	8.27	11.2

[a]$n = 10$ in all cases for all samples.
[b]SD of mean for all samples.

TABLE 2
Recovery of Total Lipid Hydroperoxides for the FIA System

	Hydroperoxides (nmol/g oil)			
Oil (PV)	Found[a] ($n = 3$)	Added[b]	Found in total ($n = 10$)	Recovery
Rapeseed oil (7.54 meq/kg)	7,540 ± 117	2,530	9,556 ± 603	94.9 ± 6.0
Sardine oil (0.38 meq/kg)	382 ± 39	2,726	3,189 ± 157	102.6 ± 5.1
Rapeseed oil (11.4 meq/kg)	11,413 ± 454	2,353	13,036 ± 1,172	94.7 ± 8.5
Sardine oil (58.8 meq/kg)	58,880 ± 2,382	2,471	53,498 ± 1,577	87.2 ± 2.6

[a]Mean ± SD. For abbreviation see Table 1.
[b]Added: cumene hydroperoxide added to oils.
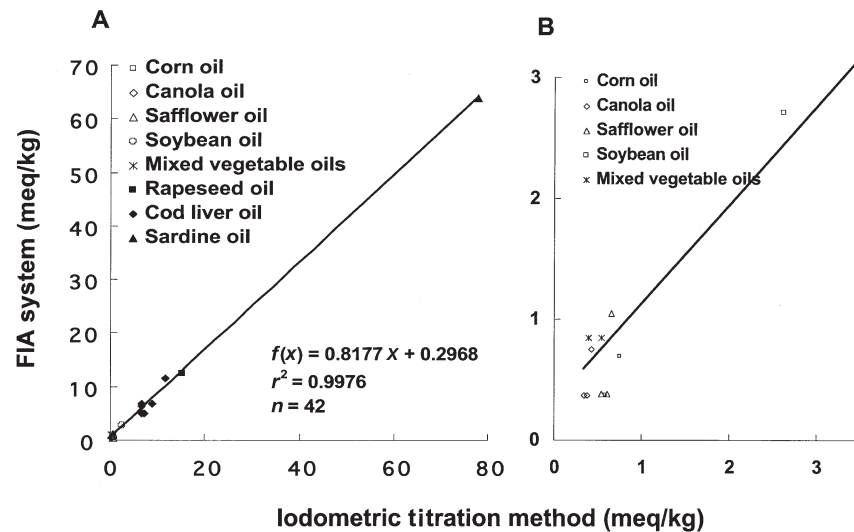
FIG. 6. Relationship between the total lipid hydroperoxide contents determined by the proposed FIA system and those obtained by the iodometric titration method. (A) in a wide range of PV between 0 and 80 meq/kg; (B) in a narrow range of PV between 0 and 3.2 meq/kg.

Although the iodometric titration method has been widely used to determine hydroperoxide contents, it may be unreliable at very low oxidation levels, i.e., <1 meq/kg, because of interference by molecular oxygen, the reaction of liberated iodine with other components, and uncertainty in the titration endpoint. Moreover, to determine the hydroperoxide content in edible oils with PV between 1 and 10 meq/kg, 5–10 g of oils would be required for a traditional iodometric titration. In contrast, in the FIA system the actual amount of soybean oil required was only 0.05 mg when the hydroperoxide content of the oil was 2.7 ± 0.24 meq/kg ($n = 15$). In a practical analysis with the FIA system, however, approximately 10 mg of oil would be enough for accurate weighing of the oil.

In summary, in the proposed FIA system quantitative determination of total lipid hydroperoxides was accomplished with high reproducibility, even at extremely low hydroperoxide concentrations, not only in refined fats and oils but also in oils in foods and foodstuffs.

ACKNOWLEDGMENTS

REFERENCES

1. Halliwell, B., and Gutteridge, J.M.C. (1999) Free Radicals, Other Reactive Species and Disease, in *Free Radicals in Biology and Medicine*, 3rd edn. (edited by Halliwell, B., and Gutteridge, J.M.C.), pp. 617–783, Oxford University Press, Oxford.
2. AOCS (1993) *Official and Methods and Recommended Practices of the American Oil Chemists' Society*, 4th edn., AOCS Press, Champaign, Method Cd 8-53.
3. Asakawa, T., and Matsushita, S. (1980) A Colorimetric Microdetermination of Peroxide Values Utilizing Aluminum Chloride as the Catalyst, *Lipids 15*, 965–967.
4. Marshall, P.J., Warso, M.A., and Lands, W.E. (1981) Selective Microdetermination of Lipid Hydroperoxides, *Anal. Biochem. 154*, 191–199.
5. Hara, S., Nemoto, K., Yamada, H., and Totani, Y. (1988) HPLC Analysis of Lipid Peroxides, POV Determination of Autoxidation Triglycerides, *J. Jpn. Oil Chem. Soc. 37*, 541–545.
6. Yamada, Y., Terao, J., and Matsushita, S. (1987) Electrochemical Detection of Phospholipid Hydroperoxides in Reverse-Phase High Performance Liquid Chromatography, *Lipids 22*, 125–128.
7. Yamamoto, Y., Brodsky, M.H., Baker, J.C., and Ames, B.N. (1987) Detection and Characterization of Lipid Hydroperoxides at Picomole Levels by High-Performance Liquid Chromatography, *Anal. Chem. 160*, 7–13.
8. Miyazawa, T., Yasuda, K., and Fujimoto, K. (1987) Chemilu-
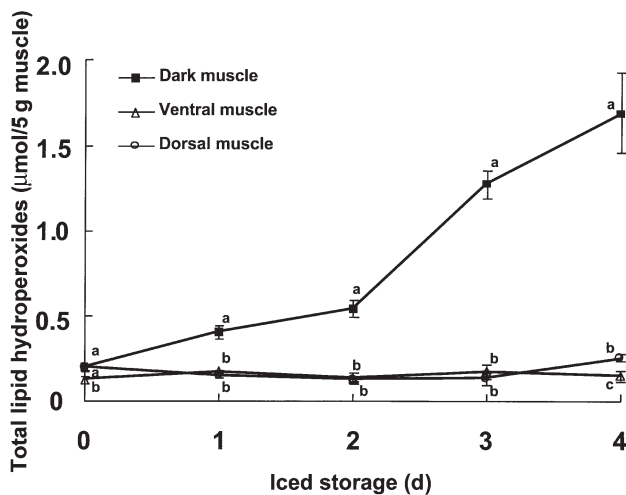
FIG. 7. Changes in total lipid hydroperoxide determined by the FIA system in yellowtail muscles during iced storage. For each muscles in the same storage days, values with different superscripts (a-c) are significantly different ($P < 0.01$)

minescence High Performance Liquid Chromatography of Phosphatidylcholine Hydroperoxide, *Anal. Lett. 20*, 915–925.

9. Yamamoto, Y., and Niki, E. (1989) Presence of Cholesteryl Ester Hydroperoxide in Human Blood Plasma, Biochem. *Biophys. Res. Commun. 165*, 989–993.

10. Miyazawa, T. (1989) Determination of Phospholipid Hydroperoxides in Human Blood Plasma by a Chemiluminescence-HPLC Assay, *Free Radic. Biol. Med. 7*, 209–217.

11. Miyazawa, T., Suzuki, T., Fujimoto, K., and Yasuda, K. (1992) Chemiluminescent Simultaneous Determination of Phosphatidylcholine Hydroperoxide and Phosphatidylethanolamine Hydroperoxide in the Liver and Brain of the Rat, *J. Lipid Res. 33*, 1051–1059.

12. Chan, H.W.S., and Levett, G. (1977) Autoxidation of Methyl Linoleate. Separation and Analysis of Isomeric Mixtures of Methyl Linoleate Hydroperoxides and Methyl Hydroxylinoleates, *Lipids 12*, 99–104.

13. Akasaka, K., Ohrui, H., and Meguro, H. (1988) Fluorometric Determination of Lipid Hydroperoxides with Phosphine Reagents, *Nippon Nogei Kagaku Kaishi 62*, 1487–1490.

14. Akasaka, K., Suzuki, T., Ohrui, H., and Meguro, H. (1987) Study on Aromatic Phosphines for Novel Fluorometry of Hydroperoxides (II). The Determination of Lipid Hydroperoxides with Diphenyl-1-Pyrenylphosphine, *Anal. Lett. 20*, 797–907.

15. Akasaka, K., Ohrui, H., and Meguro, H. (1993) Determination of Triacylglycerol and Cholesterol Ester Hydroperoxides in Human Plasma by High-Performance Liquid Chromatography with Fluorometric Postcolumn Detection, *J. Chromatogr. 617*, 205–211.

16. Akasaka, K., Ohrui, H., and Meguro, H. (1994) Measurement of Cholesterol Hydroperoxides of High and Combined Low and Very Low Lipoprotein in Human Plasma, *Biosci. Biotech. Biochem. 58*, 396–399.

17. Akasaka, K., Ohata, A., Ohrui, H., and Meguro, H. (1995) Automatic Determination of Hydroperoxides of Phosphatidylcholine and Phosphatidylethanolamine in Human Plasma, *J. Chromatogr. 665*, 37–43.

18. Kaewsrithong, J., Qiau, D.-F., Ohshima, T., Ushio, H., Yamanaka H., and Koizumi, C. (2000) Unusual Levels of Phosphatidylcholine Hydroperoxide in Plasma, Red Blood Cell, and Livers of Aromatic Fish, *Fisheries Sci. 66*, 768–775.

19. Kaewsrithong, J., Ohshima, T., and Ushio, H. (2001) Seasonal Variation of Phosphatidylcholine Hydroperoxides in Blood of Sweet Smelt *Plecogrossus altivelis, Comp. Biochem. Physiol. 130B*, 33—42.

20. Kaewsrithong, J., Ohshima, T., Ushio, H., Nagasaka, R., Maita, M., and Sawada, M. (2001) Effects of an Excess Dose of Dietary α-Tocopherol on Hydroperoxide Accumulation and Erythrocyte Osmotic Fragility of Sweet Smelt *Plecogrossus altivelis* (Temminck et Schlegel), *Aquaculture Res. 32*, 191–198.

21. Ohshima, T., Hopia, A., German, B.J., and Frankel, E.N. (1996) Determination of Hydroperoxides and Structures by High-Performance Liquid Chromatography with Post-column Detection with Diphenyl-1-pyrenylphosphine, *Lipids 31*, 1091–1096.

22. Ohshima, T., Ushio, H., and Koizumi, C. (1997) Analysis of Polyunsaturated Fatty Acid Isomers Hydroperoxides by High-Performance Liquid Chromatography with Post-column Fluorescence Detection, in *Flavor and Chemistry of Seafoods* (Shahidi, F., and Cadwallader, K.R., eds.), ACS Symposium Series 674, pp. 198–217, American Chemical Society, Washington, DC.

23. Wang, X.-H., Ohshima, T., Ushio H., and Koizumi, C. (1999) Proportion of Geometrical Hydroperoxide Isomers Generated by Radical Oxidation of Methyl Linoleate in Homogeneous Solution and in Aqueous Emulsion, Lipids 34, 675–679.

24. Wang, X.-H., Ushio, H., and Ohshima, T. (2003) Distributions of Hydroperoxide Positional Isomers Generated by Oxidation of 1-Palmitoyl-2-arachidonyl-*sn*-glycero-3-phosphocholine in Liposomes and in Methanol Solution, *Lipids 38*, 65–72.

25. Bligh, E.G., and Dyer, W.J. (1959) A Rapid Method of Total Lipid Extraction and Purification, *Can. J. Biochem. Physiol. 37*, 911–917.

26. Box, G.E.P., Hunter, W.G., and Hunter, J.S. (1978) *Statistics for Experimenters*, pp. 21–56, John Wiley & Sons, New York.

27. Akasaka, K., and Ohrui, H. (2000) Development of Phosphine Reagents for the High-Performance Liquid Chromatographic-Fluorometric Determination of Lipid Hydroperoxides, *J. Chromatogr. 881*, 159–170.

28. Nakamura, T., Tanaka, R., Higo, Y., Taira, K., and Takeda, T. (1998) Lipid Peroxide Levels in Tissues of Live Fish, *Fisheries Sci. 64*, 617–620.

sn-Position Determination of Phospholipid-Linked Fatty Acids Derived from Erythrocytes by Liquid Chromatography Electrospray Ionization Ion-Trap Mass Spectrometry

Christopher Beermann*, Michael Möbius, Nadine Winterling, Joachim J. Schmitt, and Günther Boehm

Numico Research Germany, D-61381 Friedrichsdorf, Germany

ABSTRACT: The *sn*-position of FA in membrane lipids has an influence on the physiological function of cells, is predictive for diseases, and therefore is useful for diagnostics. The current study compares the compositions of acyl chain substituents in the *sn*-1 and *sn*-2 positions of the glycerol backbones of phospholipids derived from human erythrocytes by using RP-HPLC coupled with on-line electrospray ionization ion trap MS. Preferential loss of the acyl group in the *sn*-1 position was used to determine the degree of regiospecific preference exhibited by the phospholipid molecules. The identities of the molecular species and the positions of the acyl substituents were identified using product-ion spectra of major precursor ions selected from the mass spectra averaged across peaks in the total ion chromatogram. Saturated FA were found to be located mainly in the *sn*-1 position of the glycerol backbones of erythrocyte phospholipids, whereas PUFA were found primarily in the *sn*-2 position. All measured phospholipids revealed palmitic acid (16:0) at the *sn*-1 position. Linoleic acid (18:2n-6) and arachidonic acid (20:4n-6) were found to be attached exclusively to the *sn*-2 position of the backbone, whereas eicosadienoic (20:2n-6) and eicosatrienoic acid (20:3n-9) occurred in both positions of the backbone of PC. Oleic (18:1n-9), linoleic (18:2n-6), and octadecatrienoic (18:3) acids of PE and PS were linked to both positions. Lignoceric acid (24:1n-9) was found to be strictly localized at the *sn*-2 position, whereas nervonic (24:1n-9) acid of PS was associated with both positions of the backbone. A detailed analysis of the blood cell membrane lipids by MS might be helpful to characterize postprandial kinetics of pharmacological or dietary lipid applications, as well as environmental influences on cell membranes.

Paper no. L9604 in *Lipids 40*, 211–218 (February 2005).

The membrane lipids of human red blood cells consist mainly of cholesterol (Chol), glycerophospholipids, sphingomyelin (SM), and glycosphingolipids. Each glycerophospholipid possesses a distinctive FA composition distributed between the *sn*-1 or *sn*-2 position and determined by acyltransferases during biosynthesis. The ester linkage in a phospholipid may be re-placed by a vinyl ether linkage to form a plasmalogen, or one FA may be lost altogether, which results in a lysophospholipid (1). However, the alkylacyl and alkenylacyl species of choline and ethanolamime phosphatides are not part of the present study. The *sn*-position of FA is important to characterize the physiological function of lipids integrated into cellular membranes. Besides, it indicates condition, state, and dysfunction of cells. In this study, the regiospecificity of FA of membrane lipids derived from human erythrocytes is determined by LC coupled with MS for routine measurements. The *sn*-position of FA of phospholipids has a significant impact on membrane function, cell signaling, and substrate specificity of enzymes. Unfavorable distribution of the *sn*-positions of FA is associated with several diseases including sickle cell anemia. In this case, the erythrocyte membrane contains more saturated and mononounsaturated FA, but less PUFA at the *sn*-2 position, which affects cation balance, membrane phospholipid asymmetry, and hypercoagulability (2). SM and Chol have been found to segregate into self-assembled domains referred to as membrane rafts, which act as the physiological surroundings for intrinsic membrane proteins. These lipid rafts are obviously important for the activity of growth factors, membrane-associated enzymes (3), receptor–ligand interactions, and cell signaling (4). A higher degree of unsaturation in FA of PE in the *sn*-2 position is thought to influence physical characteristics of lipid rafts (5). Therefore, signal transduction through the membrane might be influenced by the alkyl-chain properties of membrane lipids. In addition, it has been demonstrated by Brooks *et al.* (6) that thermal stress in carp liver microsomes induces specific alterations in the distribution of the *sn*-position in mononounsaturated and polyunsaturated FA of phospholipids (6).

The heterogeneous enzyme class of phospholipase A2 (PLA-2) hydrolyzes FA from the *sn*-2 position of membrane phospholipids. PUFA, which are located in this position, have been described to be precursors of hormone-like multifunctional eicosanoids. Thus, the PLA-2 substrate specificity is involved in platelet aggregation (7), cell cycle progression (8), and inflammatory immune response (9), which reveal the importance of the *sn*-position of FA. A prolonged stimulation of PLA-2 has been hypothesized to decrease membrane integrity found in the neurodegenerative Alzheimer's disease (10).

Several studies have shown that the FA composition of

---

*To whom correspondence should be addressed at Numico Research Germany. E-mail: milupa.research@T-online.de

Abbreviations: CGC, capillary gas chromatography; Chol, cholesterol; ESI, electrospray ionization; FAB, fast atom bombardment; ITMS, ion trap MS; MS[n], sequenced MS; PLA-2 phospholipase A2; RP, reversed-phase; RT, retention time; SIC, selected ion chromatogram; SM, sphingomyelin; TIC, total ion chromatogram.

blood and organs, such as heart or liver, can be influenced by nutritional or pharmacological lipid applications (9). The postprandial kinetics of the applied FA are reflected by alterations of the FA composition of plasma and red blood cells. Plasma-derived FFA are actively incorporated into lysophosphatides of erythrocytes and usually appear in the *sn*-2 position of the glycerol (1). The specific *sn*-positions of FA present in pharmacological or dietary lipid applications have been found to determine the digestibility in the gastrointestinal tract, the absorption by intestinal enterocytes, lipoprotein transport pathways of the portal or lymph system, and the incorporation and distribution into body organs and cellular membranes (11). Therefore, the *sn*-position of FA of the target organ represents an important parameter in characterizing the physiological efficiency of the applied active FA.

Apart from the common method used to determine the *sn*-position of FA linked to phospholipids, which involves specific enzymatic digestion and subsequent LC or GC analysis (12), various MS methods are currently available. For structural analysis of phosphatidyldiacylglycerols of erythrocytes, fast atom bombardment (FAB) (13), matrix-assisted laser desorption/ionization time of flight (14), and electrospray ionization (ESI) techniques with triple-quadrupole tandem (15) as well as ion trap MS (ITMS) detections (16) have been applied. These procedures differ considerably with regard to sample application (range of M.W. and polarity), ion fragmentation, and detection sensitivity. ESI is described as a soft ionization technology compared with chemical or electronic ionization and is therefore feasible to characterize amphiphilic molecules. Kerwin *et al.* (17) identified glycerophospholipid and SM species by generating H^+-ions of the polar phosphoryl group and $RCOO^-$-ions of the acyl constituents with ESI-MS (17). This technique provides the fragmentation of defined parent ions and a detailed molecular structural analysis *via* sequenced MS (MS^n) experiments (18,19). Marzilli *et al.* (20) described a structural characterization of TAG using ESI sources and MS^n experiments with ITMS detection. This determination is based on the formation of *sn*-position-specific acyl product ions and on acylketene moieties, which are subject to collision voltage within MS^3 experiments. The ratio of the signal intensities of the distinct fragment ions has been used to distinguish between the first and second position. Likewise, this preferential acyl group cleavage from the *sn*-1 position of phospholipids might be applicable to determine the regiospecificity of phospholipids with distinct ion fragmentation by MS^n experiments and ITMS. The current study successfully characterized the *sn*-position of FA linked to phospholipids derived from erythrocytes. The lipid class separation was carried out by normal-phase HPLC combined with ESI–ITMS on-line coupled with a low-flow-rate reversed-phase (RP)-HPLC within one step (LC/ESI-ITMS).

MATERIALS AND METHODS

Erythrocytes. Fresh venous blood samples from healthy volunteers were collected in heparin-coated tubes. The samples were pooled and centrifuged at $1500 \times g$ for 10 min to separate erythrocytes and plasma.

Total lipid extraction of polar lipids. The erythrocytes were disintegrated according to the method of Rose and Oaklander (21). One volume equivalent of distilled water was added to an aliquot of erythrocytes. After 15 min incubation time, 5.5 vol equiv of isopropanol (–20°C) were added dropwise while stirring. This was followed by the addition of 3.5 vol equiv chloroform, to achieve a water/isopropanol/ $CHCl_3$ ratio of 2:11:7. The solution was centrifuged for 20 min at $2000 \times g$. The supernatant was evaporated with nitrogen to dryness. The lipids were extracted with chloroform/methanol/distilled water (10:10:9, by vol) according to Bligh and Dyer (22).

Separation of phospholipids and fractionation by HPLC. The phospholipid classes were separated by HPLC and fractionated *via* automatic fractionation sampling (23). An aliquot of the lipid extract was dissolved in chloroform/methanol (1:1, vol/vol) at a concentration of 0.5–2.5 mg/mL. The lipid class separation was completed with an HPLC Alliance 2695 Separation module from Waters (Waters GmbH, Eschborn, Germany) coupled with a PL-ELS 1000 evaporative light scattering detection system (Polymer Laboratories, Darmstadt, Germany). The detection was established at 100°C for the nebulizer and 100°C for the evaporator. For the lipid class separation, a polyvinyl alcohol chemically bound stationary phase PVA Sil column (5 µm, 250×4 mm) (YMC Europe, Schermbeck, Germany) was used.

The eluent system corresponded to that of Christie (24): A, *n*-hexane/*tert*-methylbutylether (98:2; vol/vol); B, isopropanol/acetonitrile/chloroform/acetic acid (84:8:8:0.025; by vol); C, isopropanol/water (twice-distilled)/triethylamine (50:50:0.2, by vol). All applied solvents were of HPLC-grade or supra-solvent quality (Merck Eurolab, Darmstadt, Germany). The solvent-gradient system was as follows: 0–1 min A/B/C (%) 98:2:0, 1–5 min A/B/C (%) 80:20:0, 5–20 min A/B/C (%) 42:52:6, 20–27 min A/B/C (%) 32:52:16, 27–30 min A/B/C 30:54:16, 30–33 min A/B/C (%) 30:70:0, 33–40 min A/B/C (%) 98:2:0. The flow rate was 1 mL/min. The distinct lipid classes were characterized by retention time (RT).

The distinct lipid species were collected with an automatic fraction-sampler from Waters by peak signal recognition. The fractions were collected in 5 mL screw-cap-closure glass tubes.

Determination of the sn-position of FA linked to phospholipids by LC/ESI-ITMS. The analysis of the *sn*-position was acquired on the LC MS system LCQ Deca (ThermoFinnigan, San Jose, CA). The distinct phospholipid fractions (10–80 µg/fraction) were separated into the molecular species by RP chromatography using a C18 RP column, Thermo Hypersil C18 200×1 mm (ThermoFinnigan). The eluent system corresponded to the one described by Patton (25): isocratic: 20 mM formic acid in methanol/water/acetonitrile (90.5:7:2.5, by vol) at a flow rate of 80 µL/min. All solvents used were of HPLC grade or supra-solvent quality (Merck Eurolab). The liquid chromatograph was coupled to the mass spectrum spectrometer with an on-line ESI source. The tip voltage was set at 4.5 kV in the positive mode. The capillary voltage was 40 V, the capillary temperature

was held at 200°C. The ion collision energy in the MS^n experiments was adjusted to between 30 and 35%. The mass range was set between 200 and 1200 Da. The total measurement time was 60 min. The following standards were used: 2-oleyl-1-palmitoyl-*sn*-glycero-3-phosphocholine, 1-oleyl-2-palmitoyl-*sn*-glycero-3-phosphocholine, 2-oleyl-1-palmitoyl-*sn*-glycero-3-phosphoethanol-amine (all Sigma-Aldrich Chemie GmbH, Taufkirchen, Germany), and 2-oleyl-1-palmitoyl-*sn*-glycero-3-phosphoserine (Avanti Polar Lipids Inc., Alabaster, AL).

FAME analysis by capillary gas chromatography (CGC). The separated fractions of the HPLC fractionation were evaporated with nitrogen to dryness. For the derivatization, the samples were dissolved in 2 mL methanol/hexane (4:1, vol/vol) plus 0.5% pyrogallol and were methylated according to Lepage and Roy (26) with 200 µL acetylchloride at 100°C, 1 h; 5 mL 6% K_2CO_3 was added, and the resultant mixture was centrifuged for 10 min at $2200 \times g$. The upper hexane phase containing the FAME was removed and dried with Na_2SO_4.

The FAME were analyzed by CGC performed on the Varian Chrompack LS 32 system (Varian Chrompack, Middelburg, The Netherlands) fitted with a cold split/splitless injector to prevent FA discrimination. A chemically bound 50% cyanopropyl-methylpolysiloxane capillary column DB23, 40 m Fisons (Varian Chrompack) was used for the separation of FA species. The chromatographic conditions were as follows: injector (PTV): 65 to 270°C, split ratio 15:1, carrier gas: helium at a 40 cm/s flow rate. The signals were identified by an FID at 280°C. FA were identified according to their RT. The column oven temperatures were as follows: initial temperature: 60°C for 0.1 min; from 60 to 180°C at 40°C/min; 180°C for 2

min; from 180 to 210°C at 2°C/min; 210°C for 3 min; from 210 to 240°C at 3°C/min; 240°C for 10 min.

RESULTS AND DISCUSSION

The membrane lipid composition of blood cells, such as thrombocytes, leucocytes and erythrocytes, is correlated to cell structure, maturation state, function, and activity. Kew *et al.* (27) have suggested that the FA composition of immune cells mainly determines immune response variations. The activation of monocytes and macrophages has been found to correlate with alterations in the composition of membrane phospholipids (28). Besides, volume and reactivity of platelets are influenced by the FA composition of the membrane (29). Within the physiological homeostasis of blood cell membranes, the composition of polar lipids and associated FA reflects the plasma FA composition, which has been shown to be directly influenced by the diet, several diseases, and other environmental FA (9).

In this study, the pooled membrane lipids of erythrocytes derived from healthy volunteers were characterized by HPLC analysis. The erythrocyte membranes predominantly contained Chol, PA, PE, PC, PI, PS, as well as SM. This result essentially corresponds to the current literature. However, no phospholipid lysoforms could be detected, as previously found by Cooper (1) (Fig. 1). The alkylacyl and alkenylacyl species of choline and ethanolamine phosphatides, which have been described to make up a major part of the erythrocyte membrane, were not part of the present study (1). To characterize the FA composition of distinct phospholipid classes, the glycerylphospholipids of the erythrocytes were fractionated. Louis *et al.* (30) have
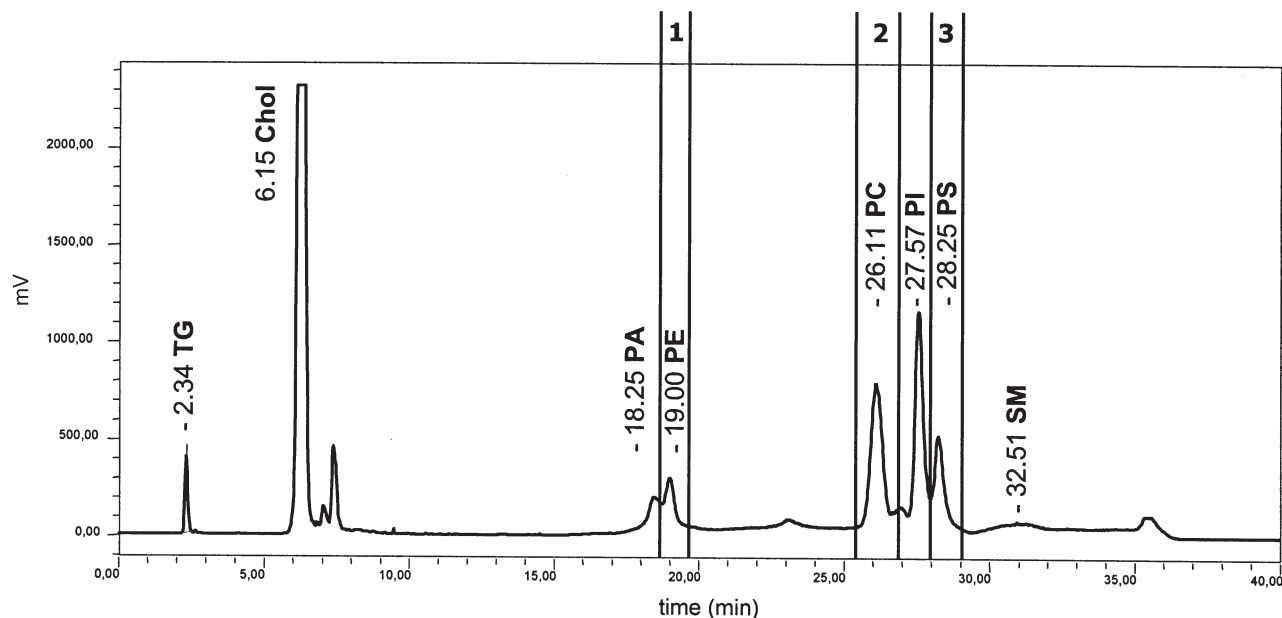
FIG. 1. HPLC separation and fractionation of membrane lipids from human erythrocytes. For separation, a polyvinylalcohol chemically bonded stationary phase was used. Eluent gradient A, *n*-hexane/*tert*-methylbutylether (vol/vol) 98:2; B, isopropanol/acetonitrile/chloroform/acetic acid (by vol) 84:8:8:0.025; C, isopropanol/distilled water/triethylamine (by vol) 50:50:0.2 at a flow rate of 1 mL/min. The samples were measured by evaporated light scattering detection. Chol, cholesterol; SM, sphingomyelin; TG, triacylglycerol.

TABLE 1
FA Composition and Regiospecificity of Integrated FA of Distinct Lipid Species of Human Erythrocytes[a]

|	Total	PC		PE		PS	
		FA	sn-1/sn-2	FA	sn-1/sn-2	FA	sn-1/sn-2
14:0	0.5	0.6		0.8		3.2	
15:0	0.2	0.2		0.3		0.3	
16:0	26.1	29.0	16:0/18:1n-9	27.9	16:0/18:1n-9	19.6	16:0/18:1n-9
16:1n-7	0.4		16:0/18:2n-6	0.4	16:0/18:2n-6	0.6	16:0/18:2n-6
17:0	0.5	0.5	16:0/20:2n-6	0.5	16:0/18:3	0.6	16:0/18:3n-6
17:1n-7	0.04	0.04	16:0/20:3n-6	0.3			16:0/24:0
18:0	15.8	14.3	16:0/20:4n-6	12.6		7.9	16:0/24:1n-9
18:1n-7/-9	13.8	21.4		21.2	18:1n-9/16:0	7.1	18:1n-9/16:0
18:2n-6	8.1	11.0		2.0	18:2n-6/16:0	3.6	18:2n-6/16:0
18:3n-6	0.2	0.8		2.0		1.5	
18:3n-3	0.1	0.05		0.5		2.9	18:3/16:0
20:0	0.6	0.08		0.6		0.9	
20:1n-9	0.3	0.5		0.7			
20:2n-6	0.2	0.4	20:2n-6/16:0	0.09			
20:3n-6	1.3	1.7	20:3n-6/16:0	0.2		0.3	
20:4n-6	9.4	5.3		1.2		1.3	
20:5n-3	0.4	0.2					
22:0	2.4	0.2		1.8		5.2	
22:1n-9	0.05	8.7		15.6		6.4	
22:4n-6	2.0	0.7		0.4		0.2	
22:5n-3	0.3	0.5		0.1		0.2	
22:5n-6	0.4	0.1				0.2	
22:6n-3	3.0	1.1		0.3		0.9	
23:0	0.4	0.1				1.0	
24:0	7.5	0.2		3.6		12.8	24:0/16:0
24:1n-9	5.7	0.2		3.4		12.0	
SAFA	52.0	46.2		50.0		60.2	
MUFA	21.8	31.2		41.6		26.3	
PUFA	25.8	22.2		7.2		11.3	

[a]The FA composition was measured by FAME capillary gas chromatographic analysis. Data are presented in weight percentage (wt%). The regiospecificity was analyzed by LC–electrospray ionization–MS. SAFA, saturated FA; MUFA, monounsaturated FA.

shown that saturated and monounsaturated FA are predominant (30). In our study, the total FA composition of erythrocyte lipids was dominated by palmitic acid, (16:0) stearic acid (18:0), lignoceric acid (24:0), and oleic acid (18:1n-9). PUFA of the n-6 family, such as linoleic acid (18:2n-6), arachidonic acid (20:4n-6), and adrenic acid (22:4n-6), predominate compared with the content of α-linolenic (18:3n-3), stearidonic (20:4n-3), eicosapentaenoic (20:5n-3), docosapentaenoic (22:5n-3) and docosahexaenoic (22:6n-3) acids of the n-3 family (Table 1). Likewise, a heterogeneous distribution of FA within the distinct lipid classes of erythrocytes could be detected. This study focused on three different membrane phospholipids: (i) PC as the major membrane phospholipid of erythrocytes, which roughly reflects the total FA pattern of erythrocyte lipids; and (ii) PE and (iii) PS, which are considerably different from PC. The analysis revealed that palmitic and oleic acids are mainly linked to PC and PE, which is in accordance with the current literature (1). Whereas PS is rich in lignoceric and nervonic (24:1n-9) acids, erucic acid (22:1n-9) is highly associated with PE. In comparison, PUFA were predominantly associated with PC, whereas saturated FA were mainly associated with PS.

In the next step, the sn-positions of FA linked to glycerol were determined by MS[n] experiments. The location of double bonds of associated FA is not detectable via LC/ITMS. Therefore, the n-3, n-6, and n-9 families were concluded from the CGC analysis of the respective FA. To prove whether it is possible to differentiate the identity and sn-position of acyl substituents of asymmetrical phospholipids with ESI-ITMS, two PC standards with an identical but asymmetrical FA composition were measured (Fig. 2). The asymmetrical oleyl-palmitoyl-phosphocholine standards revealed the same mass per charge (m/z) value of 760. The MS–MS experiments of 760 Da indicated that both standards were fragmented into the same pattern: (m/z) values 577, 522, 504, 478, and 495. The ratio between the 504 Da (M – palmitic acid) and 478 Da (M – oleic acid) fragments could be used to distinguish between the first and second position. As the sn-1 position is preferentially cleaved from the glycerol backbone, the minor ion signal indicated the sn-2 position, whereas the dominating ion signal indicated the sn-1 position in a ratio of 2:1. As already described by Hsu and Turk (31), the cleavage of the ester linkage between FA and glycerol leads to the formation of the acid ion (RCOOH[+]) and the ketene ion (RCHCO[+]), which could be identified additionally (Fig. 2).
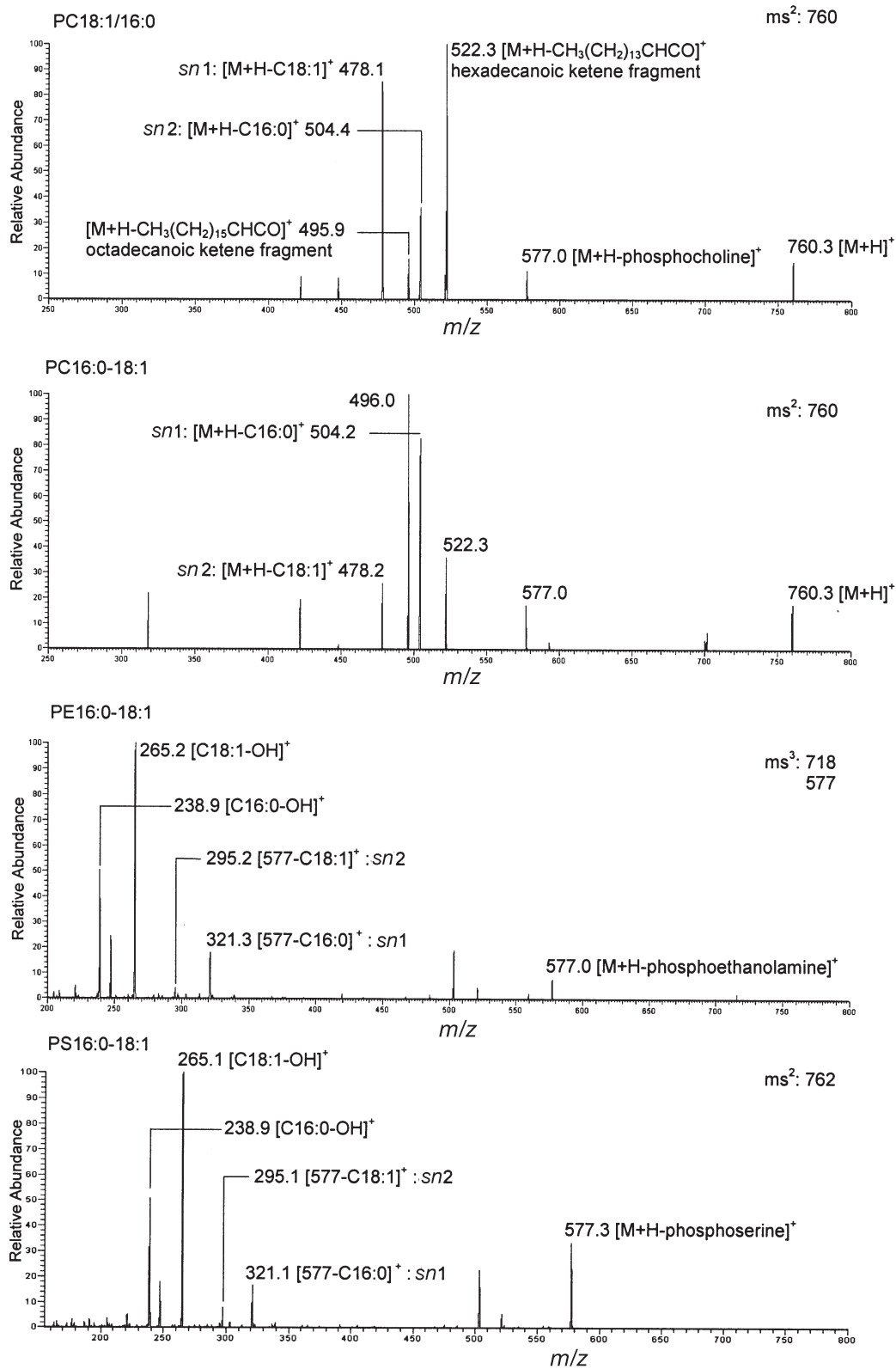
FIG. 2. Determination of the sn-position of asymmetrical PC, PE, and PS standards by electrospray ionization sequenced MS (ESI-MS^n). Mass spectra were acquired on an MS system with an on-line ESI source. The tip voltage was set at 4.5 kV in the positive mode. The ion collision energy in the MS^n experiments was adjusted between 30 and 35%. The data are presented as mass per charge (*m/z*).

In contrast to PC, the polar group of PE did influence the MS–MS fragmentation pattern, possibly owing to electron shifts induced by the amino group *via* communicating covalent bindings. Thus, no valid ratio between the ion signals indicating the *sn*-positions could be established. However, the functional head group disappeared from the 2-oleyl-1-palmitoyl-PE within the MS^3 experiment, based on the 718 Da ion signal. As a result, the 577 Da (M – phosphoethanolamine) fragment ion enabled the determination of the *sn*-positions. Again, the ratio of 2:1 between 321.3 Da (M – palmitic acid) for the *sn*-1 position and 295.2 Da (M – oleic acid) for the *sn*-2 position was demonstrated. The 238 (palmitic acid + OH) and 265 Da (olecic acid – OH) ions indicated the cleaved FA. The polar head group of the PS-standard 2-oleyl-1-palmitoyl-PS did not affect the fragmentation pattern within the MS–MS experiment. The parent ion of 762 Da disintegrated into 577 Da (M – phosphoserine), 321 Da (M – palmitic acid), and 295 Da (M – oleic acid) ions. With the ratio of 2:1 between the 321 Da fragment for the *sn*-1 position and the 295 Da fragment for the *sn*-2 position, it was possible to distinguish between the *sn*-positions. Likewise, the 238 Da fragment (palmitic acid – OH) and the 265 Da fragment (oleic acid – OH) indicated the cleaved FA.

Although various studies such as that by Han (32) described triple quadrupole applications with direct infusion into the ESI source, the distinct phospholipid classes of the native erythrocyte matrix used in this study resulted in inadequate ionization patterns. These patterns are insufficient for MS^n measurement with ITMS if the sample is directly applied with a syringe pump. This might be due to an ion overload of the ion trap that competes with the analyte ion signal and therefore impairs adequate signal recognition with this technique. Thus, the *sn*-position of FA associated with PC, PE, and PS was analyzed by coupling the MS measurement with RP LC to separate the different molecular phospholipid species. The total ion chromatogram (TIC) was scanned manually or automatically (triple play modus) within a mass range of 700–1500 Da, to select specific ion signals. After that, sequenced MS^n experiments based on the selected ions were established to identify molecular species and the position of the acyl substituents (Fig. 3).

The TIC of the PC fraction revealed five different and two asymmetrical molecular species with RT of 31.1–32.8, 32.9–39.0, 39.1–43.1, 49.1–55.1, and 55.2–60 min, which is illustrated by the selected ion chromatogram (SIC) of 758, 760, 782, 784, and 786 Da (Fig. 3). For instance, the MS–MS experiment with the 784 Da parent ion indicated a ratio of 1:1 between the 478.3 Da (M – eicosatrienoic acid) and 528 Da (M – palmitic acid) fragments. Asymmetrical FA distribution between the *sn*-1 and *sn*-2 position explains this ratio. Again, (+18 Da) fragments accompanied the signals that declared the respective *sn*-position. In contrast to the fragmentation pattern of the PC-standard (Fig. 2), a fragment ion of 725 Da (M – 59 Da) arose from native PC, which indicates the loss of the choline-fragment $[M + H – N(CH_3)_3]^+$. This different fragmentation pattern might be due to the associated FA, which differ in length and degree of saturation. The MS–MS experiments of the PC fractions derived from erythrocytes confirm that the

linkage energy of acyl substituents and the glycerol backbone is associated with the molecular structure of FA. The higher the degree of unsaturation of FA, the more energy is needed for MS^n fragmentation. Analyses of neutral lipids with FAB/MS and ESI/MS of the triple quadrupole type have demonstrated that the specific loss of FA is reduced when the chain length and number of double bonds increase (15,33). However, in this study the *sn*-position of FA was measurable in a range of length and degree of saturation between 16:0 and 20:4, which might be due to the polarity of phospholipids and the ion trap detection. In general, the FA distribution of PC showed mainly palmitic acid in the *sn*-2 position, and oleic, linoleic, and arachidonic acids exclusively in the *sn*-2 position. Eicosadienoic and eicosatrienoic acids were an exception, because they were associated with both positions (Table 1). This distribution seems to correspond to the physiological demands. For instance, palmitic acid as a structural membrane element is located in the *sn*-1 position, whereas arachidonic acid, which as a substrate for PLA-2 is necessary for the eicosanoid metabolic pathway (9), is located in the *sn*-2 position.

Likewise, palmitic acid of PE and PS was predominantly linked to the *sn*-1 position, whereas oleic, linoleic, and octadecatrienoic (18:3) acids were linked to both positions. Lignoceric acid of PS was strictly located in the *sn*-2 position, but nervonic acid was associated with both positions.

Although ESI-coupled RP-HPLC is always a compromise with regard to chromatographic and ionization requirements, the separation of the fractionated lipid classes is sufficient to produce distinct molecular species for subsequent MS^n experiments. The distribution of the *sn*-position of FA associated with PC and PS was directly measurable in the positive mode as well as in the negative mode (data not shown) *via* MS–MS. However, the determination of the *sn*-position of FA associated with PE required MS^3. Although 10–80 μg of the phospholipid fraction was applied onto the RP-HPLC column, minor molecular species of the membrane lipid spectrum with FA of up to 8 wt% were not detectable, owing to limited signal intensities of TIC and SIC. With regard to necessary amounts of sample and the corresponding measurement intensity, the LC/ESI-ITMS analysis of the *sn*-position is not comparable to the enzyme/CGC analysis, but is a reproducible method for routine determination of the *sn*-position of physiologically relevant, nonmodified phospholipid species. Apart from the aperture of the spraying needle and the applied voltage, the ionization by ESI depends on the spray and droplet size (34). Micro- or nano ESI techniques using low liquid flow rates to produce an accurate spray with a small droplet shape have been described and offer feasible possibilities to ionize polar lipids effectively (35,36). Therefore, the next steps to improve analytical sensitivity of this chromatography–MS application should be a down-scale to micro- or nano ESI with flow rates between 2 and 20 μL/min.

These results demonstrate that ESI-ITMS is a strategy that can be used for the direct structural determination of phospholipids derived from native matrices. A detailed analysis of the blood cell membrane lipids using LC coupled with ITMS
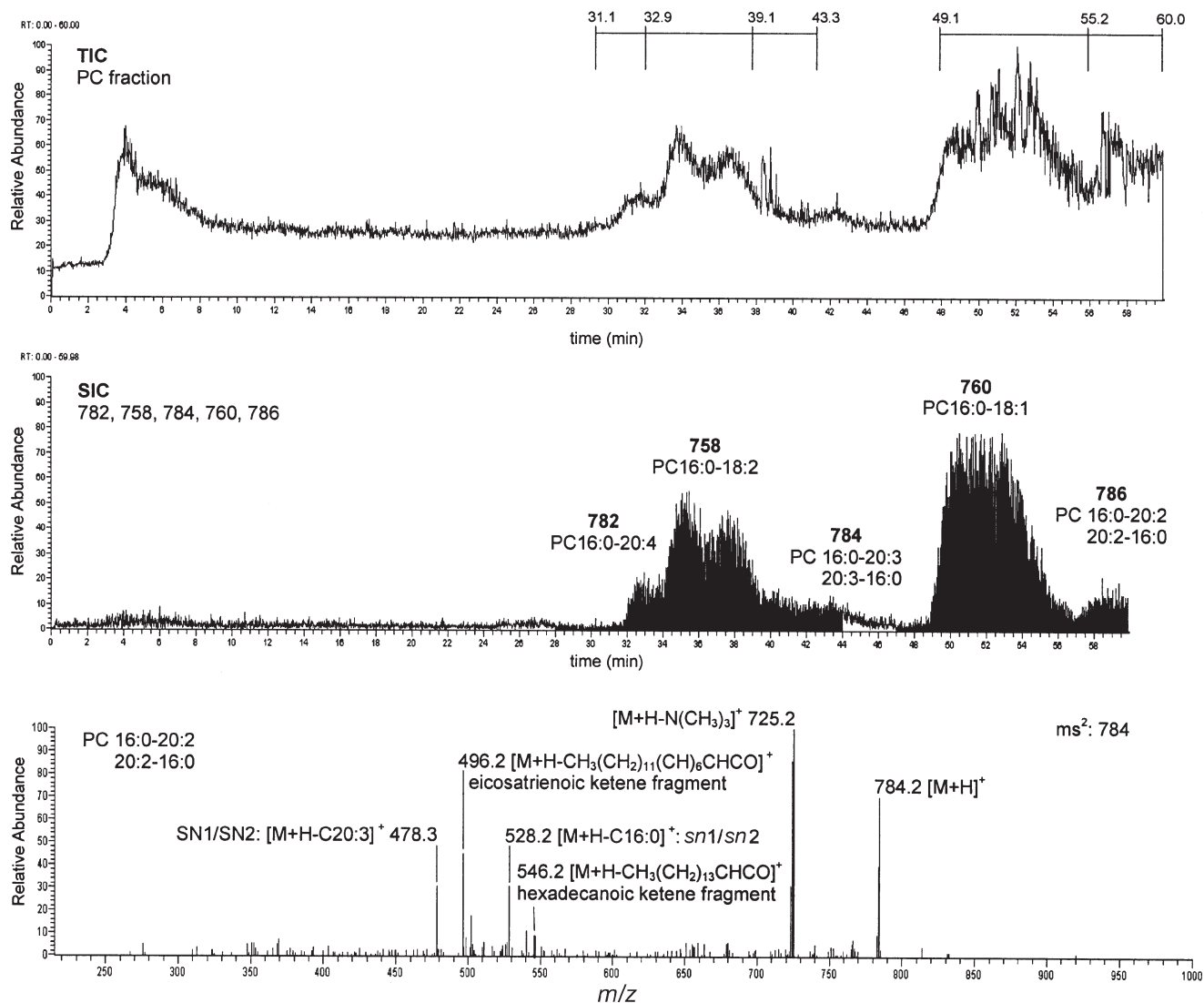
FIG. 3. Determination of the sn-position of PC from human erythrocytes by RP-HPLC coupled with ESI-MS[n]. For the LC, a stationary C18 reversed-phase column was used. Isocratic eluent: 20 mM formic acid in methanol/water/acetonitrile 90.5:7:2.5 (by vol) at a flow rate of 80 µL/min. The separation of phospholipid species is presented as a total ion chromatogram (TIC) and a selected ion chromatogram (SIC). The mass spectra were acquired on an MS system with an on-line ESI source. The tip voltage was set at 4.5 kV in the positive mode. The capillary voltage was 40 V, the capillary temperature was held at 200°C. The ion collision energy in the MS[n] experiments was adjusted to between 30 and 35%. The data are presented as m/z. For other abbreviations, see Figure 2.

might be helpful for diagnostic issues and dietary applications, in order to control or characterize environmental influences.

REFERENCES

1. Cooper, R.A. (1970) Lipids of Human Red Cell Membrane: Normal Composition and Variability in Disease, *Semin. Hematol. 7*, 296–322.

2. Connor, W.E., Lin, D.S., Thomas, G., Ey, F., DeLoughery, T., and Zhu, N. (1997) Abnormal Phospholipid Molecular Species of Erythrocytes in Sickle Cell Anemia, *J. Lipid Res. 38*, 2516–2528.

3. Van Meer, G., and Lisman, Q. (2002) Sphingolipid Transport: Rafts and Translocators, *J. Biol. Chem. 277*, 25855–25858.

4. Perry, D.K., and Hannun, Y.A. (1998) The Role of Ceramide in Cell Signaling, *Biochim. Biophys. Acta 1436*, 233-243.

5. Shaikh, S.R., Dumaual, A.C., LoCassio, D., Siddiqui, R.A., and Stillwell, W. (2003) Acyl Chain Unsaturation in PEs Modulates Phase Separation from Lipid Raft Molecules, *Biochem. Biophys. Res. Commun. 311*, 793796.

6. Brooks, S., Clark, G.T., Wright, S.M., Truemann, R.J., Postle, A.D., Cossins, A.R., and Maclean, N.M. (2002) Electrospray Ionization Mass Spectrometric Analysis of Lipid Restructuring in the Carp (*Cyprinus carpio* L.) During Cold Acclimation, *J. Exp. Biol. 205*, 3989–3997.

7. Takayama, K., Kudo, I., Kim, D.K., Nagata, K., Nozawa, Y., and Inoue, K. (1991) Purification and Characterization of Human Platelet Phospholipase A2 Which Preferentially Hydrolyzes an Arachidonyl Residue, *FEBS Lett. 282*, 326–330.

8. Boonstra, J., and Rossum, G.S. van (2003) The Role of Cytosolic Phospholipase A2 in Cell Cycle Progression, *Prog. Cell Cycle Res. 5*, 181–190.

9. Calder, P.C., and Deckelbaum, R.J. (1999) Dietary Lipids: More Than Just a Source of Calories, *Curr. Opin. Clin. Nutr. Metab. Care 2*, 105–107.

10. Farooqui, A.A., Yang, H.C., and Horrocks, L. (1997) Involvement of Phospholipase A2 in Neurodegeneration, *Neurochem. Int. 30*, 517–522.

11. Tso, P., Karlstad, M.D., Bistrain, B.R., and DeMichele, S.J. (1995) Intestinal Digestion, Absorption, and Transport of Structured Triglycerides and Cholesterol in Rats, *Am. J. Physiol. 268*, 568–577.

12. Christie, W.W., *Lipid Analysis*, 2nd edn., Pergamon Press, Elmsford, New York, 1982.

13. Egge, H., Peter-Kalalinic, J., and Hanfland, P. (1984) Structure Analysis of Glycosphingolipids Using Fast Atom Bombardment (FAB) Techniques, *Adv. Exp. Med. Biol. 174*, 55–63.

14. Al-Saad, K.A., Siems, W.F., Hill, H.H., Zabrouskov, V., and Knowles N.R. (2003) Structural Analysis of Phosphatidylcholines by Post-Source Decay Matrix-Assisted Laser Desorption/Ionization Time-of-Flight Mass Spectrometry, *J. Am. Soc. Mass Spectrom. 14*, 373–382.

15. Han, X., and Gross, R.W. (1994) Electrospray Ionization Mass Spectrometric Analysis of Human Erythrocyte Plasma Membrane Phospholipids, *Proc. Natl. Acad. Sci. USA 91*, 10635–10639.

16. Ekroos, K., Ejsing, C.S., Bahr, U., Karas, M., Simons, K., and Shevchenko, A. (2003) Charting Molecular Composition of Phosphatidylcholines by Fatty Acid Scanning and Ion Trap MS^3 Fragmentation, *J. Lipid Res. 44*, 2181–2192.

17. Kerwin, J.L., Tuininga, A.R., and Ericsson, L.H. (1994) Identification of Molecular Species of Glycerophospholipids and Sphingomyelin Using Electrospray Mass Spectrometry, *J. Lipid Res. 35*, 1102–1114.

18. Wilm, M., and Mann, M. (1996) Analytical Properties of the Nanoelectrospray Ion Source, *Anal. Chem. 68*, 1–8.

19. Creaser, C.S., and Stygall, J.W. (1998) Recent Developments in Analytical Ion Trap Mass Spectrometry, *Trends Anal. Chem. 17*, 583–593.

20. Marzilli, L.A., Fay, L.B., Dionisi, F., and Vouros, P. (2003) Structural Characterization of Triacylglycerols Using Electrospray Ionization-MS^n Ion-Trap MS, *J. Am. Oil Chem. Soc. 80*, 195–202.

21. Rose, H.G., and Oaklander, M. (1965) Improved Procedure for the Extraction of Lipids from Erythrocytes, *J. Lipid Res. 63*, 428–431.

22. Bligh, E.G., and Dyer, W.J. (1959) A Rapid Method of Total Lipid Extraction and Purification, *Can. J. Biochem. Physiol. 37*, 911–917.

23. Beermann, C., Green, A., Möbius, M., Schmitt, J.J., and Boehm, G. (2003) Lipid Class Separation by HPLC of Seed Lipid Compositions from Different *Brassica napus* L. Varieties, *J. Am Oil Chem. Soc. 80*, 747–753.

24. Christie, W.W. (1995) Separation of Lipid Classes from Plant Tissues by High-Performance Liquid Chromatography on Chemically Bonded Stationary Phases, *J. High. Resolut. Chromatogr. 18*, 97–100.

25. Patton, G.M., Fasulo, J.M., and Robins, S.J (1982) Separation of Phospholipids and Individual Molecular Species of Phospholipids by High-Performance Liquid Chromatography, *J. Lipid Res. 23*, 190–196.

26. Lepage, G., and Roy, C.C. (1984) Improved Recovery of Fatty Acids Through Direct Transesterification Without Prior Extraction or Purification, *J. Lipid Res. 25*, 1391–1396.

27. Kew, S., Banerjee, T., Minihane, A.M., Finnegan, Y.E., Williams, C.M., and Calder, P.C. (2003) Relation Between the Fatty Acid Composition of Peripheral Blood Mononuclear Cells and Measures of Immune Cell Function in Healthy, Free-Living Subjects Aged 25–72 y, *Am. J. Clin. Nutr. 77,* 1278–1286.

28. Schmid, B., Finnen, M.J., Harwood, J.L., and Jackson, S.K. (2003) Acylation of Lysophosphatidylcholine Plays a Key Role in the Response of Monocytes to Lipopolysaccharide, *Eur. J. Biochem. 270*, 2782–2788.

29. Li, D., Turner, A., and Sinclair, A.J. (2002) Relationship Between Platelet Phospholipid FA and Mean Platelet Volume in Healthy Men, *Lipids 37*, 901–906.

30. Louis, R.A., and Justice, J.B., Jr. (1985) Fatty Acid Composition of Human Erythrocyte Membranes by Capillary Gas Chromatography–Mass Spectrometry, *J. Chromatogr. 342*, 1–12.

31. Hsu, F.F., and Turk, J. (2000) Charge-Remote and Charge-Driven Fragmentation Processes in Diacyl Glycerophosphoethanolamine Upon Low-Energy Collision Activation: A Mechanistic Proposal, *J. Am. Soc. Mass Spectrom. 11*, 892–899.

32. Han, X., Abendschein, D.R., Kelley, J.G., and Gross, R.W. (2000) Diabetes-Induced Changes in Specific Lipid Molecular Species in Rat Myocardium, *Biochem. J. 352*, 79–89.

33. Hartvigsen, K., Ravandi, A., Bukhave, K., Holmer, G., and Kuksis, A. (2001) Regiospecific Analysis of Neutral Ether Lipids by Liquid Chromatography/Electrospray Ionization/Single Quadrupole Mass Spectrometry: Validation with Synthetic Compounds, *J. Mass Spectrom. 36,* 1116–1124.

34. Schmidt, A., Karas, M., and Dülcks, T. (2003) Effect of Different Solution Flow Rates on Analyte Ion Signals in Nano-ESI MS, or: When Does ESI Turn into Nano-ESI? *J. Am. Soc. Mass Spectrom. 14*, 492–500.

35. Friedl, C.H., Lochnit, G., Geyer, R., Karas, M., and Bahr, U. (2000) Structural Elucidation of Zwitterionic Sugar Cores from Glycosphingolipids by Nanoelectrospray Ionization–Ion-Trap Mass Spectrometry, *Anal. Biochem. 284*, 279–287.

36. Schneiter, R., Brügger, B., Sandhoff, R., Zellnig, G., Leber, A., Lampl, M., Athenstaedt, K., Hrastnik, C., Eder, S., Daum, G., *et al.* (1999) Electrospray Ionization Tandem Mass Spectrometry (ESI-MS/MS) Analysis of the Lipid Molecular Species Composition of Yeast Subcellular Membranes Reveals Acyl Chain-Based Sorting/Remodeling of Distinct Molecular Species en Route to the Plasma Membrane, *J. Cell. Biol. 146*, 741–754.

Astonishing Diversity of Natural Surfactants: 2. Polyether Glycosidic Ionophores and Macrocyclic Glycosides

Valery M. Dembitsky*

Department of Organic Chemistry and School of Pharmacy, Hebrew University, Jerusalem, Israel

ABSTRACT: Polyether glycosidic ionophores and macrocyclic glycosides are of great interest, especially for the medicinal and pharmaceutical industries. These biologically active natural surfactants are good prospects for the future chemical preparation of compounds useful as antibiotics, anticancer agents, or in industry. More than 300 interesting and unusual natural surfactants are described in this review article, including their chemical structures and biological activities.

Paper no. L9676 in *Lipids 40,* 219–248 (March 2005).

The diversity of natural surfactants and their biomedical activity has recently been partly reviewed in some articles (1–6) and books (7–10). Polyether glycosidic ionophores and macrocyclic glycosides are a large group of structurally related polyketide natural surfactants (2,11–13). The polyether glycosidic ionophores are characterized by multiple tetrahydrofuran and tetrahydropyrane (or more) rings connected by aliphatic bridges, direct C–C linkage, or spiro-linkages, and they also contain one or more sugar moieties. Other features include a free carboxyl function, many lower alkyl groups, and a variety of functional oxygen groups. These structural features enable the molecule to form a cyclic conformation with the oxygen functions at the center and the alkyl groups on the outer surface. Accordingly, this conformation results in lipid solubility, even for the salt forms, enabling transport of cations across lipid membranes (14–16). The term ionophore was first used by Pressman *et al.* to describe compounds that can transport ions across artificial or natural membranes (17). The polyethers

*Address correspondence at Department of Organic Chemistry, P.O. Box 39231, Hebrew University, Jerusalem 91391, Israel.
E-mail: dvalery@cc.huji.ac.il or devalery@gmail.com

Abbreviations: EC_{50}, the median effect concentration, being a statistically-derived concentration of a substance that can be expected to cause (i) an adverse reaction in 50% of organisms or (ii) a 50% reduction in growth or in the growth rate of organisms; ED_{50} (effective dose$_{50}$), the amount of material required to produce a specified effect in 50% of an animal population; GI, growth inhibition; GI_{50}, the concentration needed to reduce the growth of treated cells to half that of untreated (i.e., control) cells; HSV-1, herpes simplex virus type 1; IC, inhibitory concentration; IC_{50}, concentration at which growth or activity is inhibited by 50% (applies to ligand and growth inhibition); %ILS, percent increase in life span; LC_{50} for drugs with a cytotoxic effect, the concentration of drug at which 50% of cells die (a 50% reduction in the measured protein at the end of the drug treatment as compared with that at the beginning); LD_{50}, (lethal dose$_{50}$), the dose of a chemical that kills 50% of a sample population; log IC (log EC), IC (or EC) in a log 10 scale (a log 10 scale is frequently used when *x* values are a serial dilution, as a better estimate of the SE is obtained); log GI_{50}, log concentrations that reduced cell growth to 50% of the level at the start of the experiment; $log_{10} RC_{50}$, root elongation half inhibition concentration (mol/L) in logarithmic form; LD, lethal dose; LD_{50}, the dose at which 50% of test subjects die; LPS, lipopolysaccharide; MIC, minimal inhibitory concentration; RC_{50}, concentration at which there is a 50% reduction in the number of offspring as compared with controls; TRAP, tartrate-resistant acid phosphatase; VZV, varicella-zoster virus.

are sometimes referred to as carboxylic acid ionophores to distinguish some antibiotics from other compounds showing ionophoretic activity (18,19). Individual polyether ionophores exhibit varying specificities for cations (20,21).

Many macrolide glycosides are well-established antimicrobial agents in both clinical and veterinary medicine (22–25). These agents can be administered orally and are generally used to treat infections in the respiratory tract, skin and soft tissues, and genital tract caused by Gram-positive organisms, such as *Mycoplasma* species, and by certain susceptible Gram-negative and anaerobic bacteria (26–28).

The macrolide class is large and structurally diverse (2,12,29–31). Macrolides are produced by the fermentation of microorganisms and/or are found in marine invertebrates, such as sponges, bryozoa, or marine cyanobacteria, and in dinoflagellate species belonging to the genera *Amphidinium*, *Gambierdiscus*, *Prymnesium,* and *Protoceratium* (32–34). Additionally, structural modifications using both chemical and microbiological means have yielded biologically active semisynthetic derivatives. The term macrolide was introduced in 1957 by Woodward (35) to denote the class of substances produced by *Streptomyces* species containing a macrocyclic lactone ring. The generalized structure is a highly substituted monocyclic lactone (aglycone) to which is attached one or more saccharides glycosidically linked to hydroxyl groups on either the aglycone or another saccharide (12,30). The aglycones are derived *via* similar polyketide biosynthetic pathways and thus share many structural features in terms of pattern and stereochemistry of substituents (36, and references cited). Traditional macrolide antibiotics are divided into three families according to the size of the aglycone, which can be 12-, 14-, or 16-membered, but more recently macrolides with 30–72-membered macrolactone glycosides have been isolated (2,12,29–31). Because one or more amino sugars are usually present, these compounds are basic and can form acid addition salts. In addition, one or more neutral sugars are often present. The saccharides share some common features: They tend to be highly deoxygenated and N- and/or O-methylated, and the amino groups are located at either position 3 or 4. The most common macrocyclic glycosides are given below.

POLYETHER GLYCOSIDIC IONOPHORES

Ionophores are used as food antibiotics throughout the world in the beef and poultry industries. The efficiency of cattle production is increased by altering rumen fermentation and controlling the protozoa that cause coccidiosis. Ionophores act by

interrupting the transmembrane movement and intracellular equilibrium of ions in certain classes of bacteria and protozoa that inhabit the gastrointestinal tract. The actions of ionophores provide a competitive advantage for certain microbes at the expense of others (37).

More than 100 polyether ionophores have been discovered from microorganisms, marine invertebrates, and algal species, and only some compounds contain sugar(s) (38–42).

SIMPLE GLYCOSIDIC POLYETHERS

Some simple glycosidic ionophores were isolated nearly 30 years ago from fungi belonging to the order Hyphomycetes. In 1977, Traxler and coworkers (43–45) reported the isolation and characterization of a family of novel antifungal antibiotics, named papulacandins A, B, C, D **1–3**, and **6a**, from *Papularia sphaerosperma*, with *in vitro* activity against *Candida albicans* and other yeasts. In general these compounds showed acceptable inhibition of β-1,3-glucan synthase and whole-cell activity, although little or no efficacy in animal models was found (46–48). Papulacandins A, B, and C contain a spirocyclic diglycoside and two unsaturated FA, linked as esters to two hydroxyl groups of the diglycosides. Papulacandin D, a monosaccharide relative, is the simplest member of the family (44,45,48). The common opportunistic infection in AIDS patients, *Pneumocystis carinii* pneumonia, has been effectively overcome by newer members of the papulacandin family, Mer-WF3010 **4** and L-687-781 **5** (49–51). Papulacandin D, which lacks the short FA and the galactose residue, exhibits antifungal activity; hence, less complex molecules may result in enhanced biological activity or provide a better understanding of the elements required for activity. Saricandin **6** has been isolated from the pathogenic fungus *Fusarium* sp. (52).

dinoflagellates belonging to the genus *Amphidinium* (53–55). Colopsinol A **7**, a novel polyhydroxyl compound, has been isolated from the cultured marine dinoflagellate *Amphidinium* sp. (strain number Y-5). Colopsinol A **7** is the first member of a new class of polyketide natural products possessing a gentiobioside moiety and a sulfate ester. The polyketide aglycone consisted of a C_{56}-linear aliphatic chain with one exo-methylene and two methyl branches as well as two ketones, five hydroxyl groups, and a tetrahydropyran and two epoxide rings (53). Colopsinol A **7** inhibited DNA polymerases α and β, and colopsinol C **10** exhibited cytotoxicity (53,54). Colopsinol E **8** exhibited cytotoxicity against L1210 murine leukemia cells [IC_{50} value (concentration at which growth or activity is inhibited by 50%) = 7 μg/mL], whereas colopsinol D **11** showed less cytotoxicity (IC_{50}, 20 μg/mL) (55,56).

7 Colopsinol A, R =
8 Colopsinol E, R = H

9 Colopsinol B, R = H
10 Colopsinol C, R =

11 Colopsinol D

1 Papulacandin A, R =
2 Papulacandin B, R =
3 Papulacandin C, R =
4 Mer-WF3010, R =
5 L-687,781, R =

6 Saricandin

6a Papulacandin D

Simple glycosidic ionophores, colopsinols A–E **7–11**, have also recently been discovered from different strains of marine
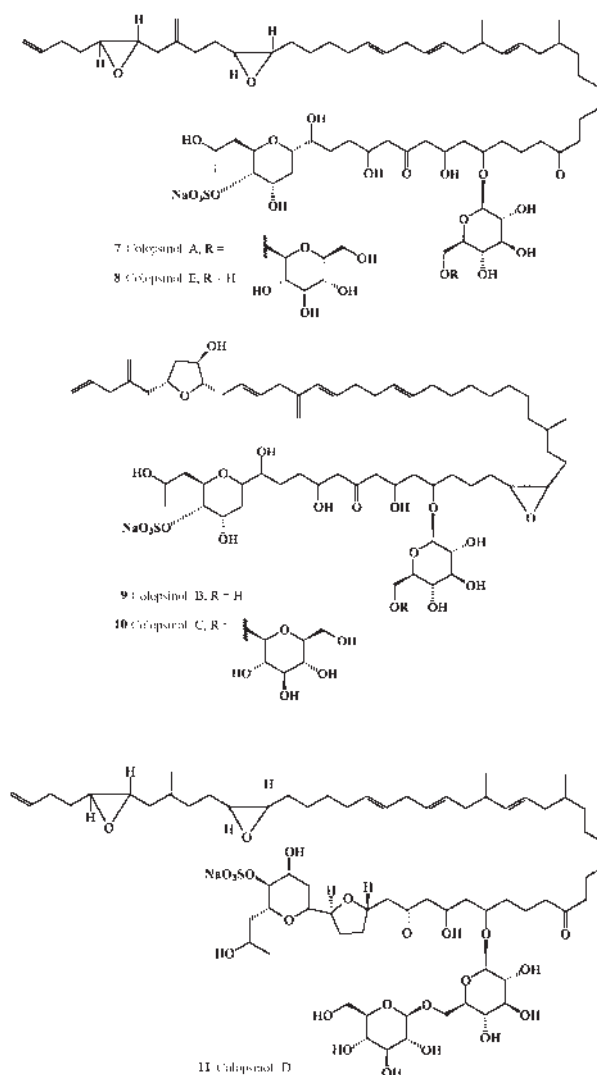
LIPOPHILIC POLYETHER GLYCOSIDES

Streptomycetes produce a wide variety of commercially important polyketide compounds, including the well-known macrolide, polyene, and polyether antibiotics that exhibit antibacterial, antifungal, anthelminthic, antitumor, and immuno-

suppressive activities. Biosynthesis of these antibiotics is catalyzed by a large family of polyketide synthases using malonyl-CoA, methylmalonyl-CoA, and ethylmalonyl-CoA as extender units for building the polyketide backbone (57–60).

Maduramicin **12**, known as antibiotic X-14868A, a novel ionophore that contains an unusual dimethoxy sugar, has been isolated from *Actinomadura yumaensis*, and its biosynthesis was reported (11,41,61,62). The biosynthesis of α- and β-maduramicin in a culture has been studied using ^{13}C-, ^{14}C-, and ^{18}O-labeled precursors. The results are consistent with the initial formation of a triene, which is converted to maduramicin by cyclization of the triepoxide.

Lenoremycin **13** and the closely related metabolites dianemycin, leuseramycin, and moyukamycin are pentacyclic ethers containing a second tetrahydropyran–tetrahydrofuran spiroketal in place of the more commonly occurring pair of tetrahydrofuran rings typical of monensin, and are produced by *Streptomyces hygroscopicus* X-14540 (63). Biosynthesis of lenoremycin was reported by Cane and Hubbard (64).

Carriomycin **14**, a polyether antibiotic, was isolated from culture broth of *S. hygroscopicus* strain T-42082. It is active against Gram-positive bacteria, several fungi, yeasts, and mycoplasma, and it is also coccidiostatic (65). Carriomycin, lonomycin, and etheromycin efficiently transported K$^+$, Rb$^+$, and Na$^+$ through a CCl$_4$ barrier. These antibiotics caused a massive release of K$^+$, Rb$^+$, or Na$^+$, but not of Li$^+$ and Cs$^+$, from mitochondria previously loaded with these cations by valinomycin or monazomycin. Carriomycin is a monovalent cation-selective ionophore (66), as are lonomycin and etheromycin.

K-41 **15**, known as A32887 and antibiotic RP37454, is produced by *S. hygroscopicus* (67). This antibiotic was characterized as a polycyclic polyether compound and was active against Gram-positive bacteria. K-41A **16** and two other new pentacyclic polyethers are produced by a marine bacterium belonging to the order Actinomycetales (68).
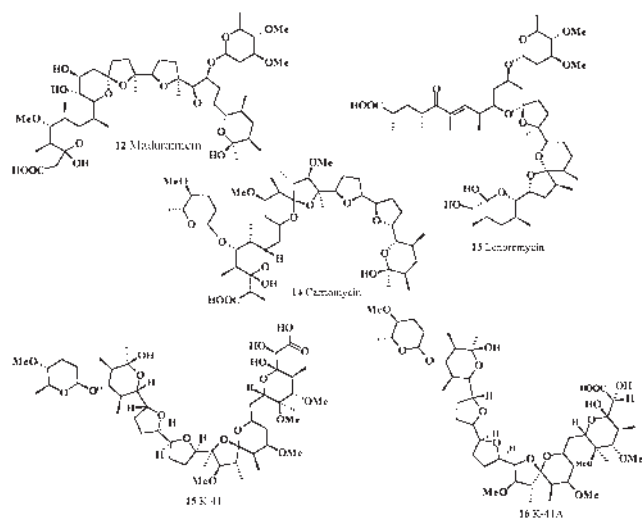
Two antibiotics, SF2324 **17** and SF2370, produced by *Actinomadura roseorura* (69,70), and an unusual ionophore, LL-C23201γ **18**, were isolated after fermentation from *Streptomyces olivaceo-griseus* sp. nov. (71). Both antibiotics showed antibacterial and anticoccidial activities. The natural antibiotic A80789 **19**, which is used in cattle feeds and is related to lonomycin A, was isolated from *S. hygroscopicus* (72). A new polyether antibiotic, CP-82009 **20**, closely related to septamycin **21**, was isolated by solvent extraction from the fermentation broth of *Actinomadura* sp. (ATCC 53676). CP-82009 is among the most potent anticoccidial agents known, effectively controlling the *Eimeria* species that are the major causative agents of chicken coccidiosis at doses of 5 mg/kg or less in feed. It is also active *in vitro* against certain Gram-positive bacteria, as well as the spirochete *Serpulina (Treponema) hyodysenteriae* (73).
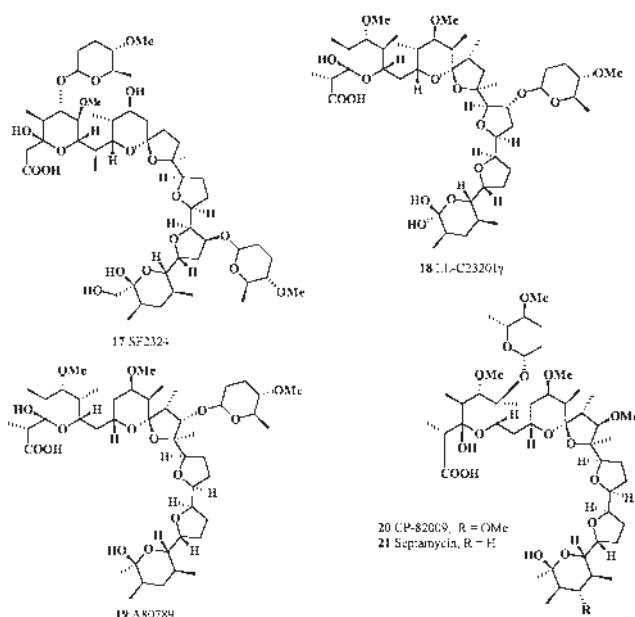
Unusual and rare polyethers with spiroketal moieties, everninomicins B, C, and D **22–24**, are a new class of oligosaccharide antibiotics (74–78) produced by *Micromonospora carbonacea* that possess highly potent activity against Gram-positive bacteria. More important, everninomicins demonstrate antibacterial activity both *in vitro* and *in vivo* against multiply resistant strains of methicillin-resistant *Staphylococcus aureus* and vancomycin-resistant enterococci (79,80). The major component, Ziracin (SCH 27899) **25**, demonstrated potent activity against Gram-positive bacteria both *in vitro* and *in vivo* including multiply resistant strains of methicillin-resistant *S. aureus* and vancomycin-resistant *Enterococcus faecalis*. A new member of the everninomicin family of compounds, Sch 58761 **26**, was isolated from the fermentation broth of *M. carbonaceae* (81).
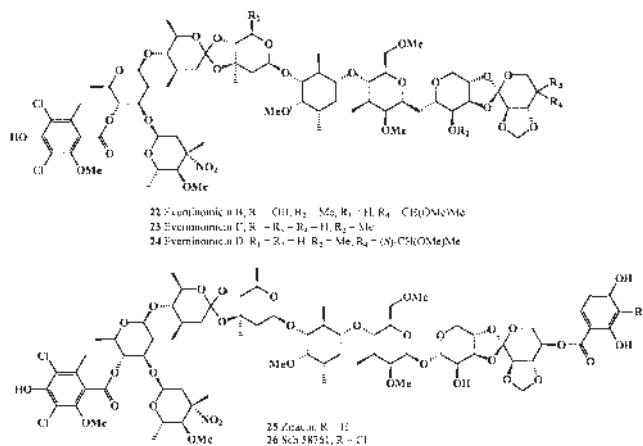
A novel everninomicin, Sch 49088 **27**, containing an unusual hydroxylamino-ether sugar with activity against methicillin-resistant *Staphylococci*, also has been isolated from *M. carbonacea* (82). A new oligosaccharide antibiotic, everninomicin-6 (EV-6) **28**, resembled everninomicin D quite closely except for the absence of the nitrosugar and the replacement on ring G of the CH_2OMe group with a CH_2OH group; it was isolated from *M. carbonacea* (83).
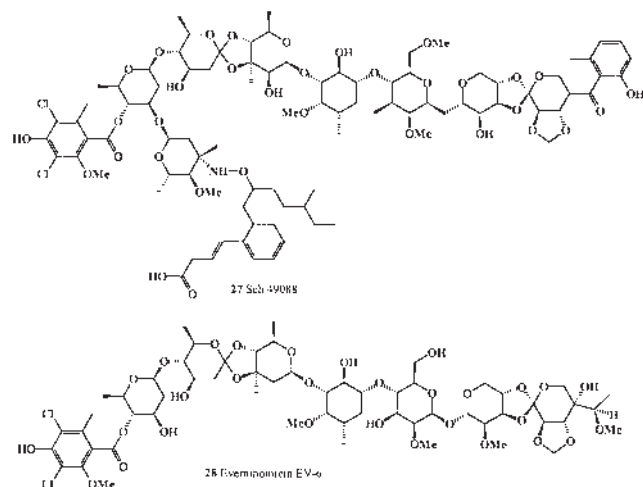
Four polyether antibiotics, **29**–**32**, isolated from a hitherto undescribed *Nocardia* culture (strain X-14868), were reported by Hoffman-La Roche in 1983 (84,85). Biological profiling revealed that all four compounds are moderately active against Gram-positive bacteria. Polyether **29** is active against *Serpulina hyodysenteriae*, and both **29** and **30** are potent anticoccidial agents *in vivo* vs. *Eimeria tenella*. CP-60993 **33**, having a

moderate activity against Gram-positive bacteria, was isolated in 1990 from the fermentation broth of a culture of *S. hygroscopicus* ATCC 39305 (86,87). Endusamycin **34** (known as CP-63517) was first identified from a new strain of *Streptomyces endus* subsp. *aureus* ATCC 39574 (88). Endusamycin **34** demonstrates an excellent spectrum of Gram-positive antibacterial and anticoccidial activities, both *in vitro* and *in vivo*. CP-80219 **35** demonstrated good activity against Gram-positive bacteria, as well as antiserpulina activity vs. *S. hyodysenteriae* (89).
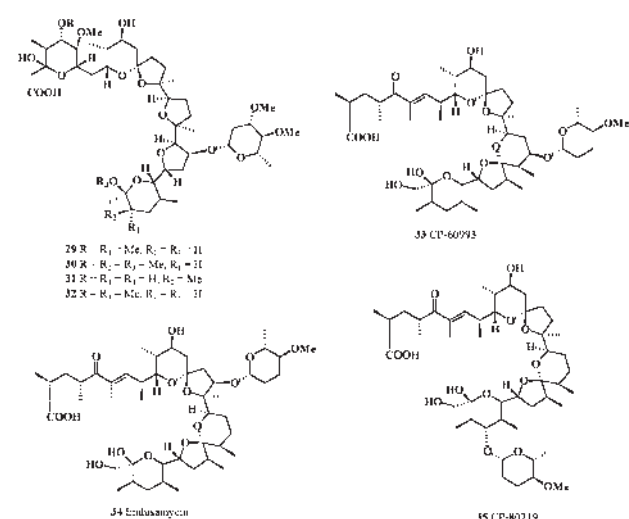
Screening the extract from *S. hygroscopicus* TM-581 has led to the discovery of the dianemycin **36** analog moyukamycin (90). Originally isolated from a culture of *Streptomyces* sp. X-14931, this ionophore demonstrated *in vitro* activity against Gram-positive microorganisms such as cocci, bacilli, mycobacteria, molds, and yeasts. It also showed activity against a mixed *Eimeria* infection (91). Isodianemycin **37** has demonstrated antibacterial properties comparable to the original antibiotic dianemycin (92).

Maduramycin **38** and the 12-methylportmicin ionophore CP-84657 **39** both have been isolated from a fermentation broth of *Actinomadura* sp. ATCC 53708. One similar to ionophore **39** was isolated from *A. fibrosa* and named A82810 (93). Polyether **39** is among the most potent anticoccidial agents known, effectively controlling the major *Eimeria* species (*E. tenella, E. acervulina, E. maxima*, and *E. necatrix*) responsible for avian coccidiosis at doses of 5 mg/kg or less in feed. This compound is also active against certain Gram-positive bacteria *in vitro* as well as the spirochete *S. hyodysenteriae*, the causative agent in swine dysentery (94,95). The ionophores W341C **40** and CP-120509 **41** (96) were produced by *Streptomyces* W341 (57).
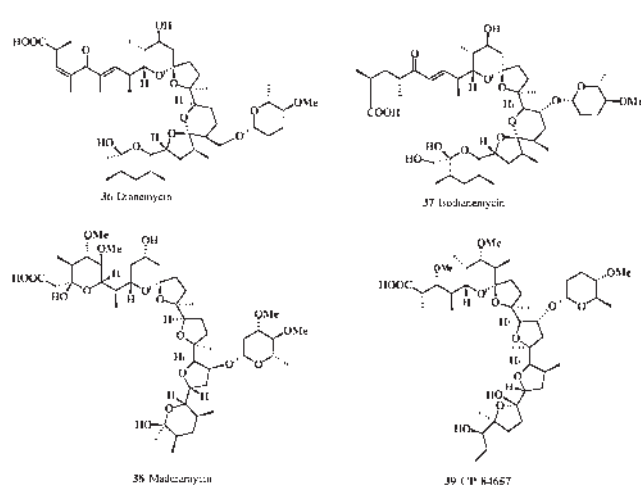
Antibiotic 6016 **42**, produced by the fermentation of *Streptomyces albus* 6016, was isolated as its sodium salt (97). Fermentation of *Actinomadura roseorufa* Huang sp. nov. ATCC 39697 produces UK-58852 **43** together with minor amounts of CP-70228 **44** and CP-70828 **45** (98,99). Treatment of **43** with *para*-toluenesulfonic acid in acetonitrile/water yielded a mixture of two compounds, including semduramicin **46**. This compound, also known as UK-61689, was obtained by fermentation of a mutant of the *A. roseorufa* and shows activity against both *E. tenella* and *E. maxima* (100). CP-91243 **47** and CP-91244 **48**, along with **45**, were isolated from a mutant of *A. roseorufa* ATCC 53666 (101).

HIGHLY OXYGENATED LIPOPHILIC TOXINS

New antitumor compounds named protoceratins I (without sugar), II **53**, III **52**, and IV **54** have recently been isolated from culture broths of the dinoflagellate *Protoceratium* cf. *reticulatum* (107). Isolated compounds showed extremely potent cytotoxicity against human tumor cell lines. The major principle, protoceratin I, proved to be identical with 2-homoyessotoxin, a well-known shellfish toxin. Protoceratins II **53**, III **52**, and IV **54** were determined to be di-, mono-, and triarabinosides of protoceratin I (without sugar), respectively.

Etheromycin **49**, produced by *Streptomyces* C20-12 FERM P-2736 and *S. hygroscopicus* ATCC 31050 (57,102), and the new 3-*O*-methylseptamycin **50** (analog of **21**) have recently been discovered by Mülhaupt (103). Polyether ionophore **51**, named nanchangmycin, was discovered by Chinese scientists (104–106); it was produced by *Streptomyces nanchangensis* (NS3226), and showed insecticidal activities.

Prymnesium parvum (Division Haptophyta, Class Prymnesiophyceae, Family Haptophyceae) is a unicellular red tide microalga that blooms in marine and brackish water and causes massive fish kills worldwide (108,109). Ichthyotoxins with very surprising structures, prymnesin-1 **55** and prymnesin-2 **56**, have been isolated from *P. parvum* (110,111). The prymnesins are highly oxygenated lipophilic toxins reminiscent of dinoflagellate toxins such as ciguatoxin, brevetoxin, maitotoxin, and palytoxin. The C_{90} carbon (!) skeleton has no carbon

branching except for one methyl group. Five contiguous ether rings resemble those of the dinoflagellate toxins. Prymnesins **55** and **56** contain multiple functional groups such as conjugated double and triple bonds, chlorine atoms, an amino group, and glycosidic residues, including the uncommon L-xylose. They are the major hemolytic and ichthyotoxic agents in the red tide microalga *P. parvum* (112), with **56** causing 50% hemolysis of a 1% suspension of canine red blood cells at 0.5 nM. The lethality of **56** on the freshwater fish *Tanichthys albonubes* was comparable to that of brevetoxin; the ichthyotoxicity was markedly enhanced by Ca^{2+} and by a slight elevation of pH. The LC_{50} (concentration of drug at which 50% of cells die) in a Ca^{2+}-free medium (pH 7.0) was 300 nM, and in the presence of 2 mM Ca^{2+} (pH 8.0) it was 3 nM (112).
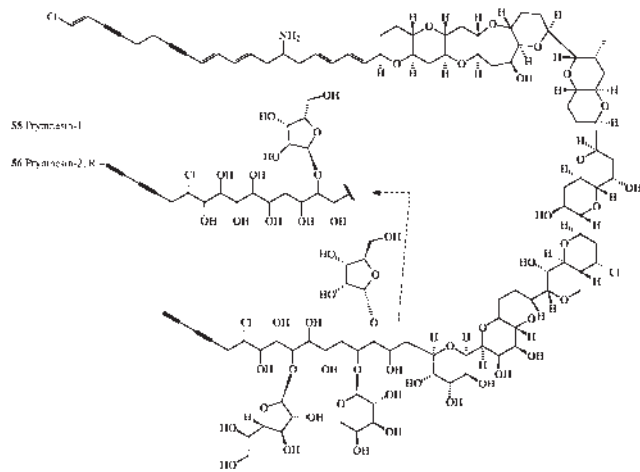
MACROCYCLIC GLYCOSIDES

Many FA glucosides in lactone form, named macrolides (or macrocyclic glycosides), have been isolated from bacteria, lower invertebrates, and/or fungi (2,3,5,9,12,13,18,26,29, 30,32,34,113,114). Some macrocyclic glycosides were found in plants (115). At present, more than 100 microbial products continue to be used clinically as antibiotics, antitumor agents, and agrichemicals (3,30,32). The importance of these compounds in medicine has served to underscore their importance in pharmacology, chemistry, and industry. Throughout the years, extensive chemical programs have been developed worldwide to synthesize these compounds and to understand the structural foundations for their bioactivity. Still today, massive efforts are underway in the pharmaceutical industry to explore soil bacterial fermentation products. These studies continue to show exciting results. Examples of such polyketides include erythromycin (antibacterial), nystatin (antifungal), avermectin (antiparasitic), rapamycin (immunosuppressant), daunorubicin (antitumor), and many others (12,13,29,113,114).

SIMPLE DIARYLHEPTANOID GLYCOSIDES

Diarylheptanoids are a family of natural plant metabolites whose characteristic structural feature is the presence of two hydroxylated aromatic rings tethered by a linear seven-carbon chain. They can be further divided into three subgroups, namely, linear and biaryl macrocycles (**57–61**) and *m,p*-cyclophane (**62–68**) (115). Evidence has accumulated suggesting that the linear diarylheptanoids are the biogenetic precursors of the macrocyclic congeners **57–61** and **62–68** (116–118).

Many new simple diarylheptanoids and their glycosides, named acerogenin and aceroside, were isolated from the stem bark of *Acer nikoense, A. griseum*, and *A. triflorum* (119). Three new cyclic diarylheptanoids, acerosides B1 **57** and B2 **58** and aceroketoside **59**, were isolated together with 20 known compounds from a Japanese folk medicine, the stem bark of *A. nikoense*. The principal diarylheptanoid constituents were found to exhibit inhibitory activity on nitric oxide (NO) production in lipopolysaccharide-activated macrophages (120). The stem bark of the Aceraceae plant *A. nikoense*, which is indigenous to Japan, has been used as a folk medicine for hepatic disorders and eye diseases. It has been reported that the biphenyl-type diarylheptanoids from *Myrica rubra* showed inhibitory activities on the release of β-hexosaminidase from RBL-2H3 cells (121) and on NO production in lipopolysaccharide (LPS)-activated macrophages (122). Macrocyclic diaryl ether heptanoids as ovalifoliolatins A and B from the Indian tree *Boswellia ovalifoliolata* also showed antibacterial activity against the Gram-negative bacteria *Chromobacterium violaceum* (ATCC #12472), *Klebsiella aerogenes* (ATCC #15380), *Pseudomonas aeroginosa* (ATCC #25619), and *Pseudomonas fluorescens* (ATCC #13525) and against the Gram-positive bacteria *S. aureus* (ATCC #9144), *Bacillus subtilis* (ATCC #6051), and *Bacillus sphaericus* (ATCC #14577) (123). Aceroside I **60** and IV **61** were isolated from *A. nikoense* (119).
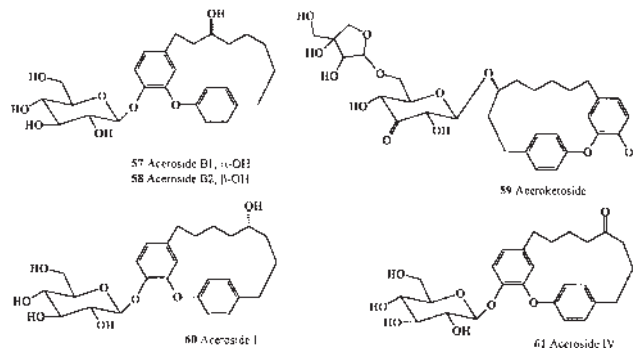
Myricanols **62**, **65**, and **66**; myricanone **63**; neomyricanone **64**; myricanene A **67** and B **68**; and their five new glycosides were isolated from the stem bark of Chinese *M. rubra*, and myricanone and galeon from the stem of *Myrica gale* var. *tomentosa* (121). The Myricaceae plant *M. rubra* is widely distributed in China, Taiwan, Japan, and Korea. The bark of *M. rubra* (Myricae cortex) has been used locally as an astringent, antidote, and antidiarrheic in Japanese folk medicine and also has been used externally for burns and skin diseases in Chinese traditional medicine. Biphenyl-type diarylheptanoids showed inhibitory activities on the release of β-hexosaminidase from RBL-2H3 cells and on NO production in LPS-activated macrophages (121).

62 Myricanol

63 Myricanone, R = O, R₁ = H,H
64 Neomyricanone, R = H,H, R₁ = O

65 (−)-S-Myricanol, 11-α-OH
66 Myricanol Glycoside, 11β-OH

67 Myricanene A

68 Myricanene B
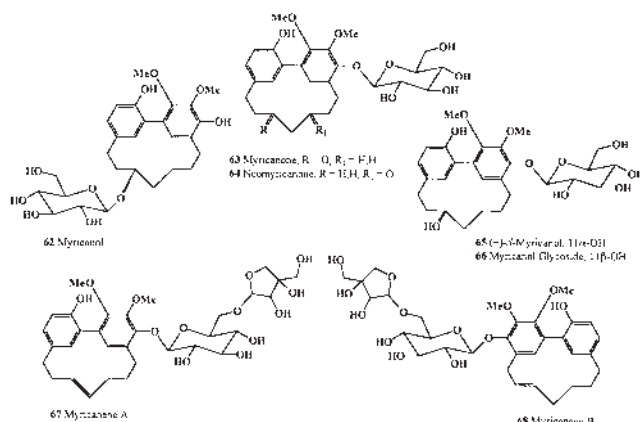
DIMERIC MACROCYCLIC GLYCOSIDES

Dimeric macrolide glycosides are a rare group of biologically active compounds produced by some microorganisms and marine sponges (2). The elaiophylin **69** and two new methyl derivatives **70** and **71** were isolated from the mycelium cake of *Streptomyces* strains HKI-0113 and HKI-0114. Elaiophylin **69**, with C-2 symmetry was originally isolated from *Streptomyces melanosporus* (124), later as azalomycin B from *S. hygroscopicus* var. *azalomyceticus* (125) and also from *Streptomyces violaceoniger* (Tu 905) (126). It is now available in large quantities by fermentation of other naturally high-producing *Streptomyces* spp., for example, strains DSM-4137 and DSM-3816. Elaiophylin **69** is known to be active as an antibacterial and antihelminthic; to have antitumor and immunosuppressant properties; and to inhibit NO synthesis (127, and references cited).

Halichoblelide **72**, a novel macrolide with potent cytotoxicity against tumor cells in culture, has been isolated from a strain of *S. hygroscopicus* originally separated from the marine fish *Halichoeres bleekeri* (128). Halichoblelide exhibited potent cytotoxic activity against the murine P388 cell line [ED$_{50}$ (effective dose$_{50}$, the amount of material required to produce a specified effect in 50% of an animal population) 0.63 µg] and 39 human cancer cell lines (BSY-1, NCI-H522, MKN74, and others). The tested mean value of log GI$_{50}$ (log concentrations that reduced cell growth to 50% of the level at the start of the experiment) over all cell lines appeared to be −5.25.
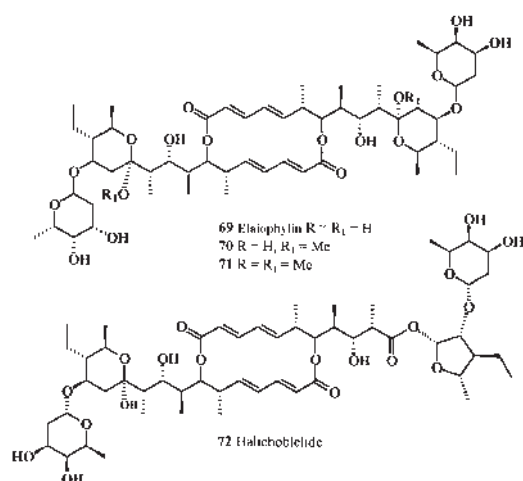
Clavosolides A–D **73**–**76**, dimeric macrolides incorporating cyclopropyl, tetrahydropyranyl, and glycosidic ring systems, were isolated from the cytotoxic extract of a Philippines collection of the marine sponge *Myriastra clavosa* (129). Clavosolides A **73** and B **74** also were recently reported metabolites from *M. clavosa* (130). The dimeric monoterpenoid glycoside **77** was isolated from the aqueous ethanol extract of the whole plants of *Dicliptera riparia* (131). The dimeric secoiridoid glycoside lisianthoside **78** was isolated from plant *Lisianthius jefensis* (Gentianaceae) (132).

73 Clavosolide A, R = R₁ = R₂ = Me
74 Clavosolide B, R = R₁ = Me, R₂ = H
75 Clavosolide C, R = R₂ = Me, R₁ = H
76 Clavosolide D, R = H, R₁ = R₂ = Me

77 Dicliripariside A

78 Lisianthoside
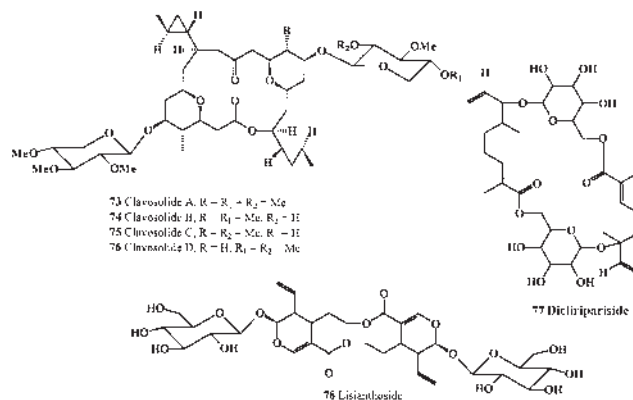
Pakistolides A **79** and B **80**, novel dimeric β-(glucosyloxy)benzoates were isolated from the Pakistani tree *Berchemia pakistanica* belonging to the genus *Berchemia* (Rhamnaceae), which comprises *ca.* 10 species scattered throughout the tropics of Asia, Africa, and America (133). The roots and stems of *Berchemia* species are traditionally used for the treatment of gallstones, liver diseases, neuralgia, and stomach cramps in Japan, and also are used in traditional Chinese medicine as an antipyretic, a diuretic, and for the treatment of rheumatism and lumbago (134). Both **79** and **80** showed high lipoxygenase inhibition activity and promising potential to inhibit lipoxygenase *in vivo*. They also were found to have inhibitory activity against β-glucosidase (133).

69 Elaiophylin R = R₁ = H
70 R = H, R₁ = Me
71 R = R₁ = Me

72 Halichoblelide

79 Pakistolide A

80 Pakistolide B
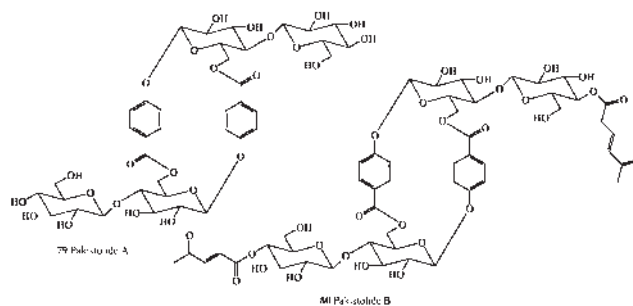
More than 160 macrocyclic hydrolyzable tannins were hitherto known (135,136), along with oenotheins, cuphiins, eugeniflorins, camellins, and woodfordins, which have been isolated from the genera *Oenothera* (137), *Cuphea* (138), *Eugenia* (139), *Gordonia* (140), and *Woodfordia* (141). Structures of these dimeric compounds are similar to **81**–**84**, and they constitute an important class of oligomers with unique macrocyclic

structures. Many of these compounds showed antitumor activity, inhibition of DNA topoisomerase II, and induced apoptosis in K562 cells (136). The antitumor activities of four macrocyclic hydrolyzable tannin dimers, cuphiin D1 **81**, cuphiin D2 **82**, woodfordin C **83**, and oenothein B **84**, isolated from *Cuphea hyssopifolia* (Lythraceae), were studied (142). All compounds significantly inhibited the growth of the human carcinoma cell lines KB, HeLa, DU-145, and Hep 3B and the leukemia cell line HL-60, and they showed less cytotoxicity than adriamycin against a normal cell line (WISH). All four compounds inhibited the viability of S-180 tumor cells in an *in vitro* assay and an *in vivo* S-180 tumor-bearing ICR mouse model. Oenothein B **83** demonstrated the greatest cytotoxicity (IC_{50} = 11.4 µg/mL) against S-180 tumor cells in culture, whereas cuphiin D1 **81** resulted in the greatest increase in survival of S-180 tumor-bearing mice [ILS (increase in life span) = 84.1%]. These findings suggest not only that the antitumor effects of these compounds are related to their cytotoxicity on carcinoma cell lines but also that they depended on a host-mediated mechanism; they may therefore have potential for antitumor applications (142). Cuphiin D1 **81** induced cytotoxicity in HL-60 cells, and the IC_{50} was 16 µM after 36 h of treatment; it also inhibited Bcl-2 expression in the HL-60 cells and induced apoptosis (143).
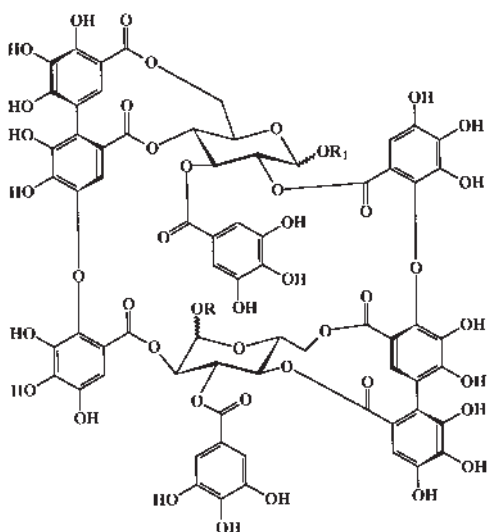
81 Cuphiin D1, R = α-galloyl, R_1 = β-galloyl
82 Cuphiin D2, R = H, R_1 = β-galloyl
83 Woodfordin C, R = α-galloyl, R_1 = H
84 Oenothein B, R = R_1 = H

Two new cyclic compounds with long-chain fatty acyl esters, glucolipsin A **85** and B **86**, were isolated from the butanol extracts of *Streptomyces purpurogeniscleroticus* WC71634 and *Nocardia vaccinii* WC65712, respectively (144). Glucolipsins A **85** and B **86** relieved the inhibition of glucokinase by FAC (fatty acyl CoA) with RC_{50} values (i.e., concentration at which there is a 50% reduction in the number of offspring as compared with controls; log10 RC_{50}, root elongation half inhibition concentration [mol/L] in logarithmic form) of 5.4 and 4.6 µM.

Streptomyces microflavus strain 2445 produced the major

product fattiviracin FV-8 **87**, which consists of four glucose and two trihydroxy FA residues (145). Fattiviracin FV-8, purified from the culture broth of *S. microflavus*, showed potent antiviral activities against HIV type 1 (HIV-1), herpes simplex virus type 1 (HSV-1), varicella-zoster virus (VZV), and influenza viruses A and B (146).
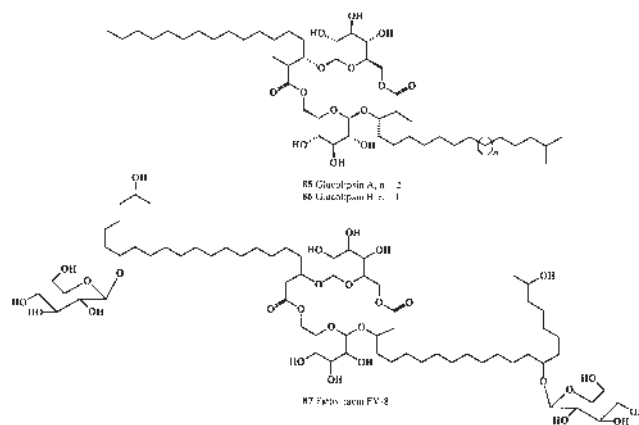
The actinomycete strain *Kibdelosporangium albatum* R761-7 (ATCC 55061) produced new antiviral antibiotics, cycloviracins B1 **88** and B2. They showed weak activity against Gram-positive bacteria and potent antiviral activity against HSV-1 (147,148). A novel antiherpetic agent, fattiviracin A1, was isolated from the culture broth of strain no. 2445, identified as *S. microflavus* (149). The structure of fattiviracin A1 is a new macrocyclic diester consisting of four D-glucose units and two (C_{24} and C_{33}) hydroxy FA. It is closely related to the cycloviracins B1 **88** and B2 but differs from these known compounds in both the length of its side chain and the sugar moiety. Fattiviracin A1 showed potent antiviral activities against HSV-1, VZV, influenza virus A, and HIV-1. It showed no cytotoxicity against Vero cells. Fattiviracin A1 exhibited no significant antibacterial or antifungal activities. Treatment of HSV-1 with fattiviracin A1 decreased its infectivity to Vero cells. The mechanism of its antiviral activity may be due to inactivation of the viral particles and inhibition of viral entry into the host cells (150).
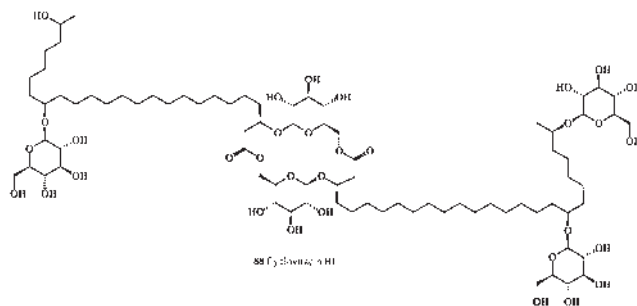
Macroviracins **89–96** are a new class of macrocyclic compounds that were isolated from the mycelium extracts of *Streptomyces* sp. BA-2836,1 and were classified into eight types of congeners (A–D) by the length (C_{22} or C_{24}) of the constitutive

FA. These natural products exhibit a powerful antiviral activity against HSV-1 and VZV, and their potency is reported to be 10 times that of acyclovir. Structurally, macroviracins are related to sugar-FA lactones such as cycloviracins and fattiviracins, and differ remarkably in the size of the macrocyclic ring systems (151,152).

89 Macroviracin A, n = n₂ = 1
90 Macroviracin B1, n = n₁ = 1, n₂ = 2
91 Macroviracin B2, n = 2, n₁ = 1, n₂ = 2
92 Macroviracin B3, n = 2, n₁ = n₂ = 1
93 Macroviracin C1, n = 1, n₁ = n₂ = 2
94 Macroviracin C2, n = n₂ = 2, n₁ = 1
95 Macroviracin C3, n = n₁ = 2, n₂ = 1
96 Macroviracin D, n = n₁ = n₂ = 2
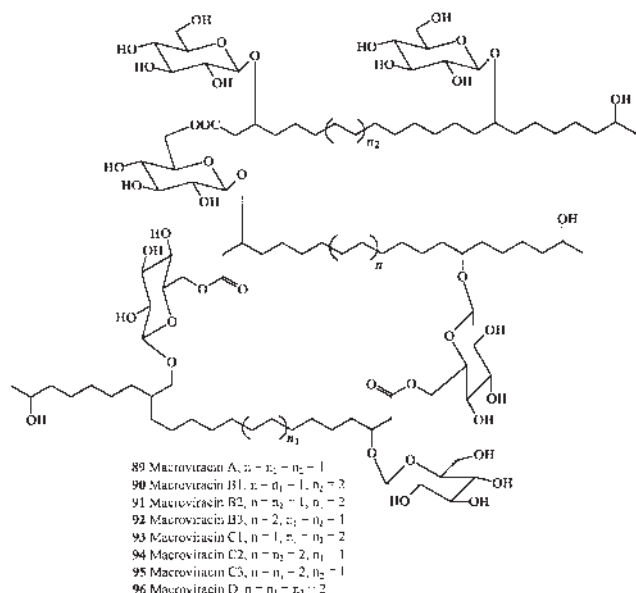
HYBRID MACROCYCLIC GLYCOSIDES

Hybrid macrocyclic glycosides are usually FA macrolactones or their derivatives bearing one or more (rare) sugar(s) and produced by microorganisms, lower invertebrates, microalgae, fungi, and/or plant species (2). Hybrid macrocyclic glycosides also can be formed with many other substituents.

10–13-MEMBERED RING GLYCOSIDIC MACROLIDES

A few 10-membered ring macrolide glycosides are found in nature. Thus, the leaves of a small tree *Gonocaryum calleryanum* (family Icaciaceae), named Balotangginto, has afforded new secoiridoid glycosides acylated with 2,3-dihydroxy-2-methylbutanoic acid, three of which (**97a–c**) have a novel 10-membered dilactone ring (153). *Gonocaryum calleryanum* is mainly distributed from Indonesia to Taiwan. Its leaves are used in Philippine folk medicine for the treatment of stomach diseases (154). More recently, Chan *et al.* (155) of the Taiwan Medicinal College isolated **97a** and **97b** from leaves, branches, stems, and root bark from the same species (*G. calleryanum*) grown in the southern part of Taiwan.

The novel highly cytotoxic metabolites apicularen A and apicularen B **98** were isolated in a screening of the myxobacterial genus *Chondromyces* (156). The structure of the apicularens A and B was characterized by a salicylic acid residue as part of a 10-membered lactone, which bears an acylenamine side chain. Apicularens are present in nearly every strain of *C. apiculatus*, *C. pediculatus*, *C. lanuginosus,* and *C. robustus*. Apicularen B **98** was identified as 11-*O*-(2-*N*-acetamido-2-

deoxy-β-D-gluco-pyranosyl)apicularen. According to feeding experiments with ¹³C-labeled acetates, glycine, and methionine, apicularens A and B are acetate-derived polyketides containing a glycine residue as precursor of the enamine. The glycoside apicularen B showed weak antimicrobial activity against Gram-positive bacteria, e.g., *Micrococcus luteus* [minimal inhibitory concentration (MIC) 12.5 µg/mL] and *Corynebacterium fascians* (MIC 25 µg/mL), and moderate cytotoxic activity, with IC_{50} values between 0.2 and 1.2 µg/mL with nine different human cancer cell lines, including the multidrug-resistant line KB-V1 (157).

97a Gonocaryoside A, R = Me
97b Gonocaryoside B, R = H

98 Apicularen B

97c Gonocaryoside C
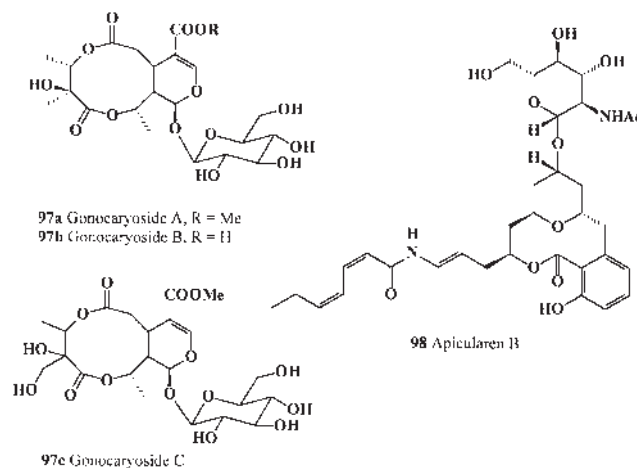
Two novel 10-membered ring chlorinated glycosidic macrolides, latrunculinosides A **99a** and B **99b**, containing substituted 2-oxecanones (decalactones) were isolated from the marine sponge *Latrunculia corticata* (158). Both glycosides contain unusual saccharides such as β-D-olivose, β-L-digitoxose, β-L-amicetose, and β-D-oliose. These compounds gave positive results in antifeeding assays (for goldfish), **99a** 1.7 µg/mL and **99b** 3.3 µg/mL, respectively (158).

99a Latrunculinoside A

99b Latrunculinoside B
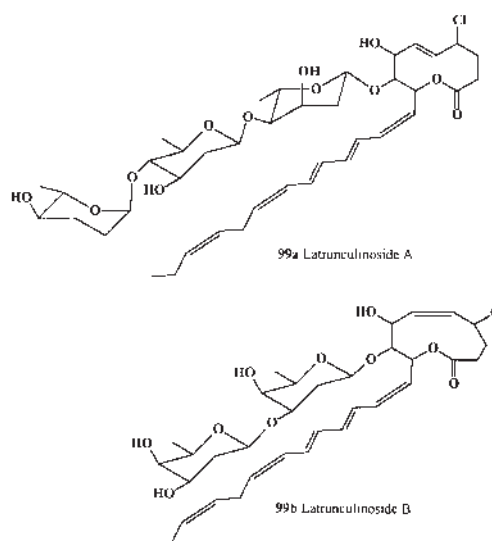
The 10–12-membered ring macrocyclic compounds, tannin derivatives **100a–f**, and **102a,b** have been isolated from

the aerial parts of *Cunonia macrophylla* (an endemic Cunoni-aceae, New Caledonia) (159), *Pelargonium reniforme* (Berlin, Germany) (160), *Tellima grandiflora* (fringe cups, Saxifragaceae, Germany) (161), and from fruits of *Punica granatum* (California) (162).

Furosin **100f** was isolated from the whole plant of *Euphorbia helioscopia* (Euphorbiaceae), collected at Cheongju City (Korea); this hydrolyzable tannin markedly decreased the differentiation of both murine bone marrow mononuclear cells and Raw264.7 cells into osteoclasts, as revealed by the reduced number of tartrate-resistant acid phosphatase (TRAP)-positive multinucleated cells and decreased TRAP activity (163). A gallotannin-containing fraction of *Phyllanthus amarus* and the isolated ellagitannins corilagin **100c** and geraniin (isomer of furosin **100f**) were the most potent mediators of antiviral activities. The *P. amarus*-derived preparations blocked the interaction of HIV-1 gp120 with its primary cellular receptor CD4 at an IC$_{50}$ of 2.65 (water/alcohol extract) to 0.48 µg/mL (geraniin). Inhibition was also evident for the HIV-1 enzymes integrase (0.48–0.16 µg/mL), reverse transcriptase (8.17–2.53 µg/mL), and protease (21.80–6.28 µg/mL) (164,165). Corilagin **100c** also has shown antimicrobial activity against human bacterial pathogens (*S. aureus*, *Corynebacterium accolans*), a plant pathogen (*Erwinia carotovora*), and a human pathogenic yeast (*C. albicans*) (159).

100a R = galloyl

100b R = galloyl

100c R = α-galloyl
100d R = β-galloyl

100e R = galloyl

100f Furosin, R = galloyl
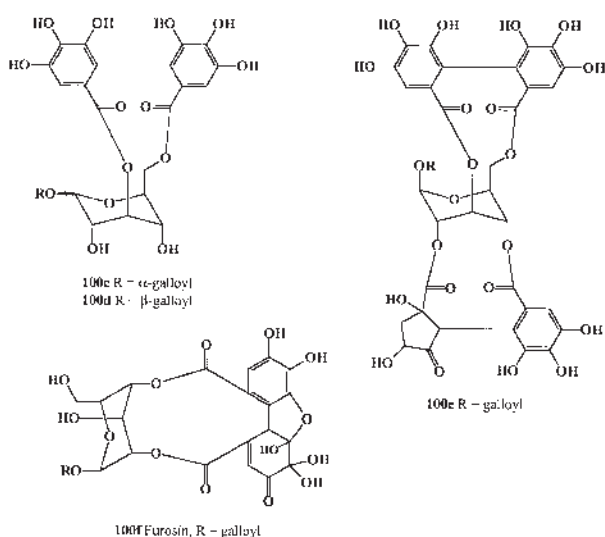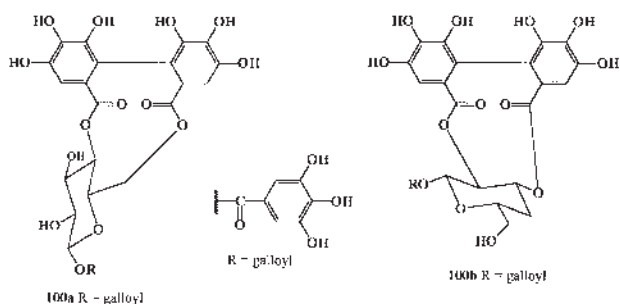
Cornusiin E **101** isolated from *Tellima grandiflora* was catalyzed by an oxygen-dependent laccase-type phenol oxidase (161). Punicalagins **102a,b** are major polyphenols of *Punica granatum* (162), and their hydrolyzed derivatives punicalin and

2-*O*-galloylpunicalin, from *Terminalia triflora* leaves, showed inhibitory activity against an HIV-1 reverse transcriptase; punicalin showed an IC$_{50}$ of 0.11 µg/mL and 2-*O*-galloylpunicalin an IC$_{50}$ of 0.10 µg/mL (165).

101 Cornusiin E, R = galloyl

102a Punicalagin, R = α-OH
102b Punicalagin, R = β-OH
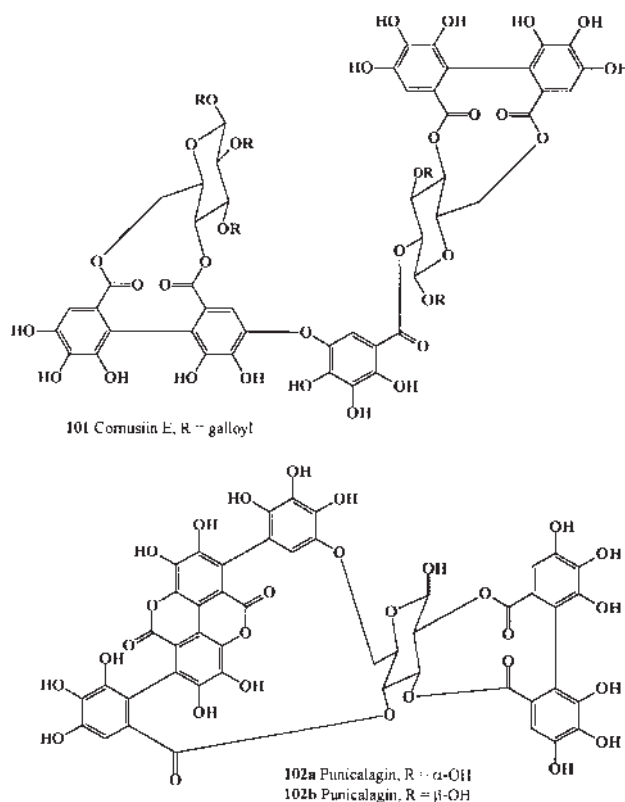
A few glycosidic macrolides having a 12-membered ring system also are found in nature. Thus, methymycin **103**, neomethymycin **104**, and YC-17 **105** were found in culture broths of a *Streptomyces* species (166–168). A new macrolide, **106**, named novamethymycin, was similar to compounds **103**–**105** and was isolated from *S. venezuelae* (169).

The spinosyns **107**–**112** are novel macrolides produced by *Saccharopolyspora spinosa* (170). Spinosyns are comprised of a tetracyclic macrolide containing forosamine and tri-*O*-methyl rhamnose, with different degrees of methylation on the polyketide or deoxysugars (171–173). The two major factors in the *S. spinosa* fermentation, spinosyn A **107** and spinosyn D **108**, differ from each other by a single methyl substituent at position 6 of the polyketide. Spinosad, a combination of spinosyn A and spinosyn D, is marketed by Dow AgroSciences for the control of agricultural insect pests. Spinosads are highly effective against target insects and have an excellent environmental and mammalian toxicological profile (174–176). Cloning and analysis of the spinosad biosynthetic gene cluster of *S. spinosa* have recently been reported (177). Novel spinosyns, **113**–**118**, have been prepared by biotransformation using a genetically engineered strain of *Saccharopolyspora erythraea*, in which the β-D-forosamine moiety in glycosidic linkage to the hydroxy group at C-17 was replaced by α-L-mycarose (178). Lepicidin A **119** was isolated in 1990 from the fermentation broth of the soil microbe *S. spinosa* by Eli Lilly Co. (179). Lepicidin A exhibits insecticidal activity, particularly against *Lepidoptera* larvae.

This group of antibiotics is characterized by excellent antibacterial activity, particularly against Gram-positive bacteria. Macrolides can be defined and distinguished from the other groups of antibiotics by the unique feature of their chemical structure. They are polyfunctional macrocyclic lactones, and the majority of them contain at least one amino sugar moiety, which is the cause of the basicity of the molecules.

103 Methymycin, R = OH, R₁ = H
104 Neomethymycin, R = H, R₁ = OH
105 YC 17, R = R₁ = H
106 Novamethymycin, R = R₁ = OH

107 Spinosyn A, R = H, R₁ = R₂ = R₃ = Me
108 Spinosyn D, R = R₁ = R₂ = R₃ = Me
109 R = R₁ = H, R₂ = R₃ = Me
110 R = R₃ = H, R₁ = R₂ = Me
111 R = R₃ = H, R₁ = R₂ = Me
112 R = R₂ = R₁ = H, R = Me

113 R = R₂ = H
114 R = Me, R₂ = H
115 R = H, R₁ = L-Mycarose
116 R = Me, R₁ = L-Mycarose
117 R = H, R₁ = D-Glc
118 R = Me, R₁ = D-Glc

119 (+)-Lepicidin A
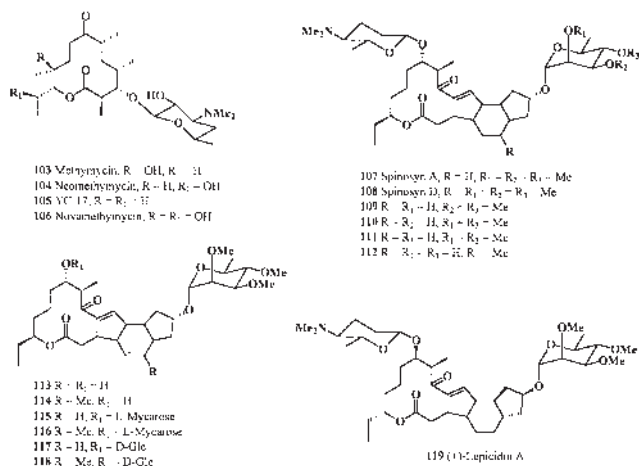
Two new cytotoxic macrolide glycosides, auriside A **120** and auriside B **121**, have recently been isolated from the Japanese sea hare *Dolabella auricularia* (180). Both aurisides showed cytotoxicity against HeLa S$_3$ cells, with IC$_{50}$ values of 0.17 and 1.2 µg/mL, respectively.

A glycosidic macrolide having a structure similar to aurisides, lyngbouilloside **122**, was characterized from the marine cyanobacterium *Lyngbya bouillonii*, collected in Papua New Guinea. Lyngbouilloside was modestly cytotoxic to neuroblastoma cells (IC$_{50}$ value of 17 µM) (181). Also, a new glycoside macrolide termed lyngbyaloside B **123** was isolated from a Palauan collection of the marine cyanobacterium *Lyngbya* sp. and exhibited slight cytotoxicity (182).

Callipeltoside A **124**, B **125**, and C **126**, bioactive marine glycoside macrolides, were isolated from the marine sponge *Callipelta* sp. (183). Callipeltose A **124** was found to protect against HIV virus infection *in vitro* (184) and also showed activity in cytotoxic assays against KB and P388 cells.

120 Auriside A, R =

121 Auriside B, R =

122 Lyngbouilloside

123 Lyngbyaloside B

124 Callipeltoside A, R
125 Callipeltoside B, R₁
126 Callipeltoside C, R₂
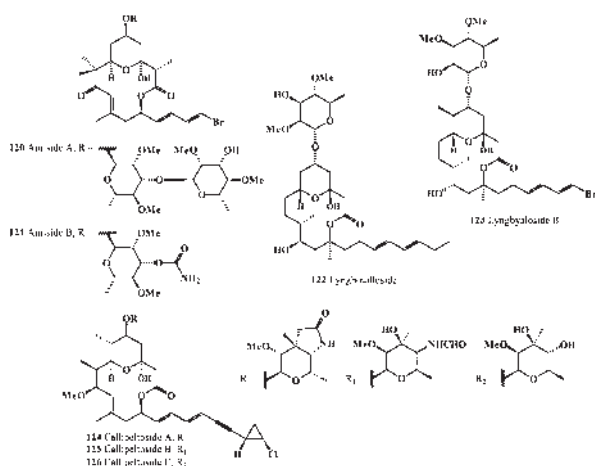
The macrolide polycavernoside A **127a** is a toxic metabolite produced by the marine red alga *Polycavernosa tsudi* (formerly *Gracilaria edulis*) (185). More recently, another four polycavernosides, A2 **127b**, A3 **127c**, B **128a**, and B2 **128b**, were also found in the same alga *P. tsudi* (186).

New antibiotics named decatromicins A **129** and B **130** were isolated from the culture broth of *Actinomadura* sp. MK73-NF4 (187,188). Decatromicins A and B inhibited the growth of Gram-positive bacteria, including methicillin-resistant *S. aureus* (187). These antibiotics are closely related to pyrrolosporin A **131**. Pyrrolosporin A **131**, new macrolide antitumor antibiotic possessing an unusual spiro-α-acyltetronic acid moiety, was isolated from the fermentation broth of *Micromonospora* sp. strain C39217-R109-7 (189). Pyrrolosporin A **131** showed antimicrobial activity against Gram-positive bacteria, was weakly active against Gram-negative bacteria, and prolonged the life span of mice inoculated with P388 leukemia cells (190).

127a Polycavernoside A, R = OH, R₁ = OMe
127b Polycavernoside A2, R = R₁ = OH
127c Polycavernoside A3, R = R₁ = OMe
128a Polycavernoside B, R = OMe, R₁ = OH
128b Polycavernoside B2, R = OMe, R₁ = OAc

129 Decatromicin A, R = H
130 Decatromicin B, R = Cl

131 Pyrrolosporin A
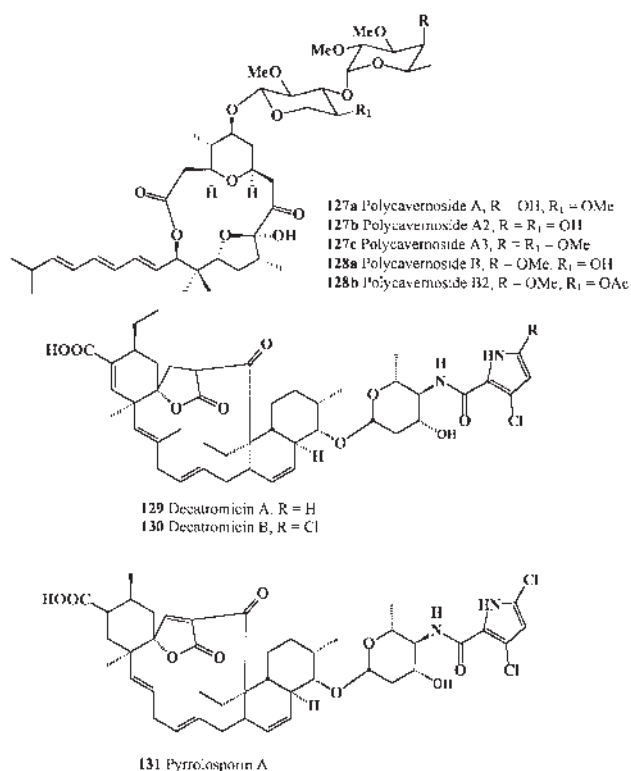
14-MEMBERED RING GLYCOSIDIC MACROLIDES

The 14-membered ring glycosidic macrolides represent a large group of natural compounds. Biologically active antibiotics, lactone glycosides named erythromycins A **132**, B **133**, C **134**, D **135**, F **136**, and E **137** have been isolated from *Streptomyces erythreus* (191–193) and *Nocardia* species (194,195). Oleandomycin **138** and oleandomycin Y **139** were produced by *Streptomyces antibioticus* (196–198). Pikromycin **140**, narbomycin **141**, and 5-*O*-mycaminosyl-narbonolide **142** were isolated from *Streptomyces felleus* (199,200) and *Streptomyces narbonensis* (201). 10,11-Dihydropikromycin **143** and kayamicin **144** were produced by *S. narbonensis* (202). Tri-*O*-

acetyloleandomycin **145** and erythromycin esters **146–149** also have been isolated from *Streptomyces* sp. (203–206).
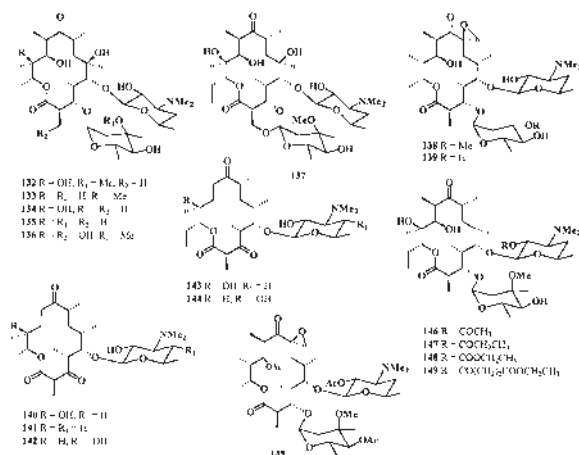
Megalomicin A **150**, B **151**, C₁ **152**, C₂ **153**, and XK-41-B₂ **154** were obtained for the first time from *Micromonospora megalomicea* (207) and were later isolated from culture broths of *Micromonospora inositola* (208,209). 3″-*O*-Demethyl-2″,3″-anhydrolankamycin **155**, lankamycin **156**, kujimycin A **157**, 15-dehydrolankamycin **158**, 15-*O*-(4-*O*-acetyllar-canosyl)-lankamycin **159**, and 23672-RP **160** belonging to the lankamycin/kujimycin group have been isolated from *Streptomyces violaceoniger* and *Streptomyces spinichromogenes* (210–217). The brominated glycosidic macrolide lyngbyalo-side **160a** is produced by the marine cyanobacterium *Lyngbya bouillonii* (218).
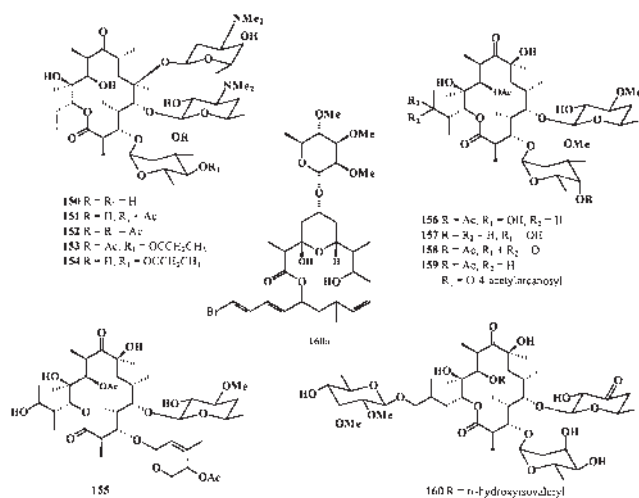
A new class of potent antifungal agents that comprise a 14-membered macrocyclic lactam ring attached to a sugar flu-virucin B1 **163** (also known as Sch 38516) and B2 **164** (Sch 38518) have been isolated from *Actinomadura vulgaris* subsp. *lanata* (219,220). Fluvirucin B1 was active against *Candida* sp. (MIC 0.91 µg/mL), and it also exhibited activity against the influenza A virus. More recently, the 14-membered lactams flu-virucins A1 **161**, A2 **162**, B1 **163**, B2 **164**, B3, B4, and B5 (with common aglycon like B1) have been isolated from dif-

ferent strains of actinomycetes, have been shown to be active against the influenza A virus, and belong to the same family of compounds (221–223). The morphology, chemotaxonomy, and cultural and physiological characteristics of the five strains of actinomycetes that produce antiviral antibiotics, fluvirucin con-geners, have been studied. All strains have meso-2,6-di-aminopimelic acid in the cell wall. Four strains, Q464-31, L407-5, R359-5, and R516-16, belong to the maduromycetes since they have madurose in the whole cell. The remaining one strain, R869-90, has rhamnose but no madurose and was a no-cardioform actinomycete. These five strains were classified and designated as follows: Strain Q464-31 (fluvirucin A1 producer) was *Microtetraspora tyrrhenii* sp. nov. (group of *Actinomadura pusilla*), and strain L407-5 (fluvirucin B2 producer) was a maduromycete. Strain R359-5 (fluvirucin B1 producer) was *Microtetraspora pusilla* (group of *A. pusilla*). Strain R869-90 (fluvirucin A2 producer) was *Saccharothrix mutabilis*, and strain R516-16 (fluvirucins B2, B3, B4, and B5 producer) was a maduromycete (224). Also, fluvirucin B2 from *Streptomyces* sp. MJ677-72F5 was found to inhibit PI-specific phospholipase C (225).
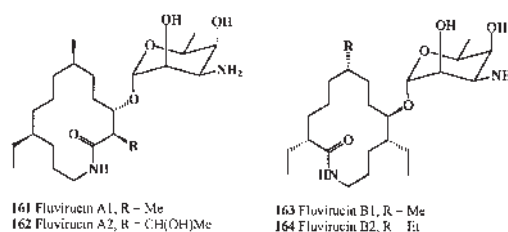
15-MEMBERED RING MACROLIDES

Two antibiotics containing the sugar leucanicidin **165** and 19-*O*-methylleucanicidin **166** are potent inhibitors of larval devel-opment in the parasitic nematode *Haemonchus contortus* (226), and they have been isolated from *Streptomyces* isolates A233, A239, and A240.

A new 15-membered macrocyclic glycolipid lactone, cus-cutic resinoside A **167**, was isolated from the seeds of *Cuscuta chinensis* (Convolvulaceae), which showed potency for stimu-lating MCF-7 cell proliferation. The compound significantly stimulated not only MCF-7 cell proliferation but also T47D human breast cancer cells at a concentration of 10 µM (227).
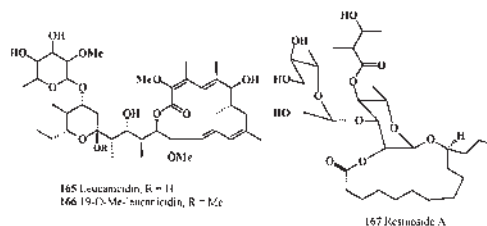
16-MEMBERED RING GLYCOSIDIC MACROLIDES

The 16-membered ring as well as the 14-membered ring macrolides are also a large group of natural macrocyclic com-pounds produced by microorganisms and lower invertebrates.

The avermectins **168–179** are a family of naturally occurring macrocyclic lactones with exceedingly high activity against helminths and arthropods (228,229). A primary fermentation product of S*treptomyces avermitilis*, avermectin B1 **170**, is an important and widely used agricultural pesticide (230). Although compound **168** is extremely effective against mites, it is much less effective against nematodes, especially the cabbage looper, the corn earworm, and the southern armyworm (230). The level of activity against these species is insufficient to justify commercial development for these uses. A mixture of naturally occurring avermectins significantly suppressed the growth of the ascites Ehrlich carcinoma and P388 lympholeukemia and the solid Ehrlich and 755 carcinomata (231).
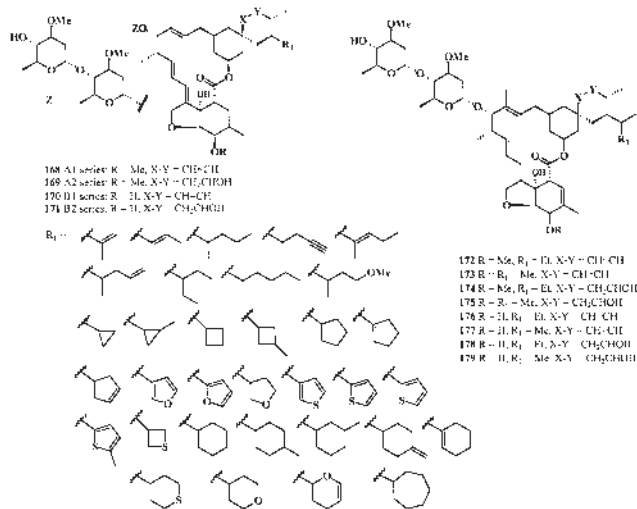
Two novel unusual flavonol epimeric macrocyclic derivatives, **180** and **181**, have been isolated from the wild water lily *Nymphaea lotus* (232). This is the first report of such a macrocycle from any source. *Nymphaea lotus* is widespread on the Nile River and its tributaries in central and southern Sudan. Throughout this region, the roots of the plant are usually cooked as a starchy vegetable, whereas the roots and particularly the leaves have been used in traditional Sudanese medicine as a remedy for dysentery, to treat tumors (233), and as an antibacterial (234).

180 Nympholide A

181 Nympholide B
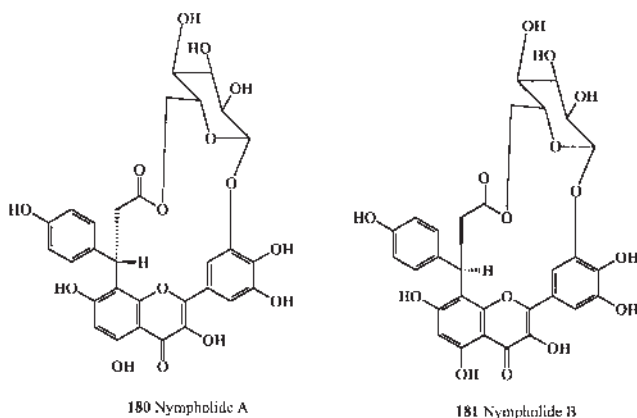
The spiramicins antibiotics **182–188** were isolated from culture broths of *Streptomyces ambofaciens* (235–238). High-speed countercurrent chromatography was successfully applied to the separation of spiramycin types I, II, and III (239). The tylosin group antibiotics **189–195** and related compounds **196–199** were produced by microorganisms *Streptomyces fradie* (240–242), and *S. hygroscopicus* (243).
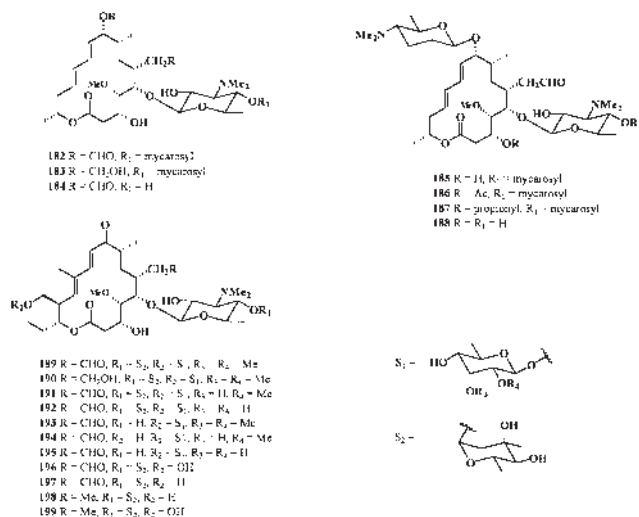
A series of leucomycins, A$_1$ **200**, A$_5$ **201**, A$_7$ **202**, A$_9$ **203**, V **204**, A$_3$ (= josamycin) **205**, A$_4$ **206**, A$_6$ **207**, A$_8$ **208**, U **209**, platenomicin A$_1$ **210**, medicamycin A$_2$ **211**, medicamycin A$_1$ (= espinomycin A$_1$; platenomycin B$_1$) **212**, platenomycin C$_2$ (= espinomycin A$_3$) **213**, DHP **214**, espinomycin A$_2$ **215**, and platenomycin A$_0$ **216** have been isolated from *Streptoverticillium (Streptomyces) kitasatoensis* (232). A$_3$ (= josamycin) **205** also was obtained from culture broths of *Streptoverticillium (Streptomyces)* var. *josamyceticus* (233). Antibiotics containing epoxy groups (positions 12,13), named maridomycin I (= platenomycin C$_3$) **217**, VII **218**, III (= platenomycin C$_1$) **219**, V **220**, II (= platenomycin C$_4$) **221**, IV **222**, and VI **223**, were obtained from culture broths of *S. hygroscopicus* (244–252). Compounds **224–229** also have been isolated from culture broths of *S. hygroscopicus* (253).
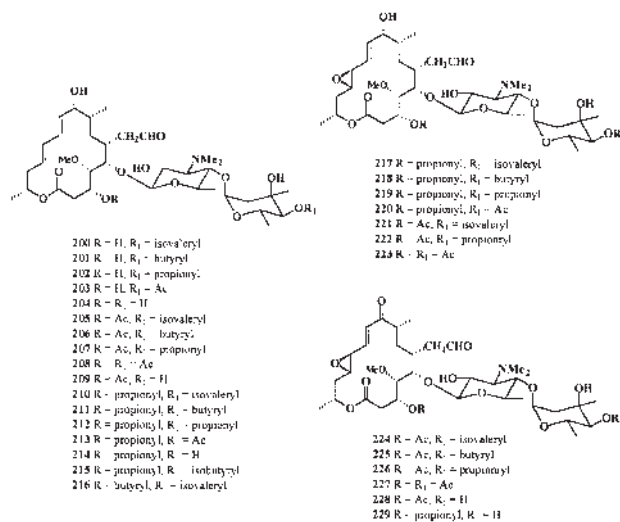
Some related 16-membered ring macrolides containing an amino sugar, such as carbomycin B **230**, platenomycin W$_1$ **231**, platenomycin W$_2$ **232**, niddamycin **233**, midecamycin A$_4$ **234**, midecamycin A$_3$ **235**, DOA **236**, and DOP **237**, have been obtained from *Streptomyces platensis* subsp. *malvinus* (253–258). A

series designated by abbreviations (SF-837 and its derivatives A_1–A_4) were obtained from another strain of *Streptomyces mycarofaciens* (259–263), whereas niddamycin **233** was produced by culture broths of *Streptomyces djakatensis* (264). Other macrolides have a 12,13-epoxide. Acumycin **238** was isolated from culture broths of *Streptomyces griseoflavus* (265). The same compound was isolated from culture broths of *Streptomyces fradiae* var. *acinicolor* and designated cirramycin B **238**. A6888C (cirramycin F-1) **239** and cirramycin F-2 **240** were produced by *Streptomyces flocculus* (266), whereas the closely related macrolide M119-A **241** was produced by an alkalophilic actinomycete (267). Similar derivatives with additional methoxyglycosides include angolamycin **242**, isolated from *Streptomyces eurythermus* (268), and staphcoccomycin **243**, produced by culture broths of *Streptomyces* sp. AS-NG-16 (269).

244 R – CHO, R_1 – O·I,R_2 – H
245 R – CHO, R_1   R_2   H
246 R – CHO, R_1   H, R_2   OH
247 R – CH_2OH, R   R_2   H
248 R – Me, R_1   R_2 – H
249 R – R_1   R_2 – H

250 R – CHO, R   R_1 – OH
251 R – CHO, R – OH, R_2   H
252 R – CHO, R   H, R_2 – OH
253 R – CHO, R_2 – R_2 – H
254 R – CH_2OH, R_1   H, R_2   OH
255 R – CH_2OH, R_1   R_2   H
256 R – Me, R_1   R_2   H
257 R – Me, R   R_2 – H
258 R – Me, R_2 – H, R_2   OH

259 R – H, R_1   Me, R_2 – H
260 R – R_1 – Me, R_2   H
261 R – H, R_1 – Me, R_2 – OH
262 R   R_1   R_2 – H
263 R_2   H

264 R – R – Me, R_2 – H
265 R – R   Me, R_2 – OH
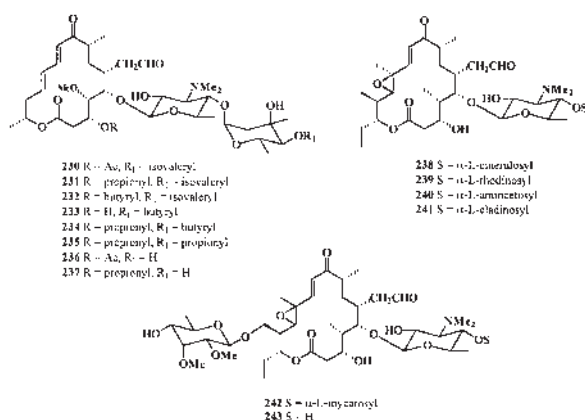
Cirramycin A_1 **244** was obtained from culture broths of *Streptomyces cirratus* (270–272). Rosaramicin **245**, formerly rosamicin, was produced by *Micromonospora rosaria* and shown to be 4'-deoxycirramycin A_1 (273,274). Structures of four related compounds produced by *Micromonospora capillata* (275,276), including izenamicin A_3 **246**, juvenimicin A_4 **247**, M-4365 A_1 **248**, and juvenimicin A_2 **249**, are shown below. Hydrolysis of both neutral sugars from tylosin yielded 5-*O*-mecaminosyl-tylonolide (OMT, **250**) (277). Analogous hydrolysis of mycarose from DMOT, GS-77-3, and GS-77-1 yielded compounds **251**–**258** (278–280). A series named mycinamicines I–VII, **259**–**265**, respectively, have been isolated from culture broths of *Micromonospora griseorubida* (281–284).
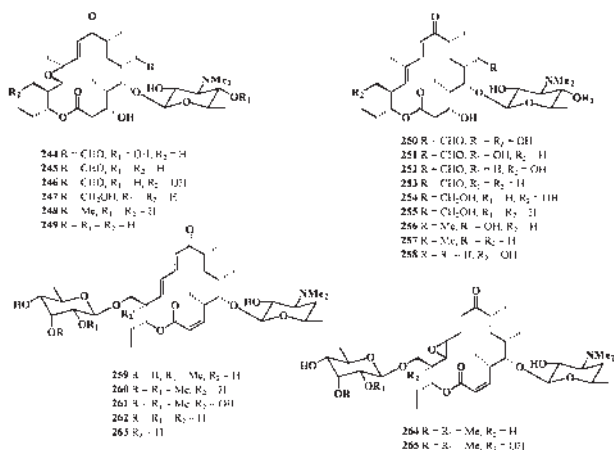
Three antibiotics having a similar structure, chalcomycin **266** (285–287), neutramycin **267** (288–290), and CP-70-662 **268** (291), are produced by *Streptomyces bikiniensis, S. rimosus*, and *S. hirsutus,* respectively. Aldgamycin F **269**, G **270** (also known as 8-deoxyaldgamycin F), and E **271** have been isolated from culture broths of *S. lavendulae* (292) and *S. avidinii* (293), and swalpamycin **272** was isolated from *S. anandii* subsp. *swalpus* (294,295).

266 R – Me, 3, – OH
267 R – H, R_3 – OH
268 R – Me, 3, – H

269 R – OH
270 R   H

271

272
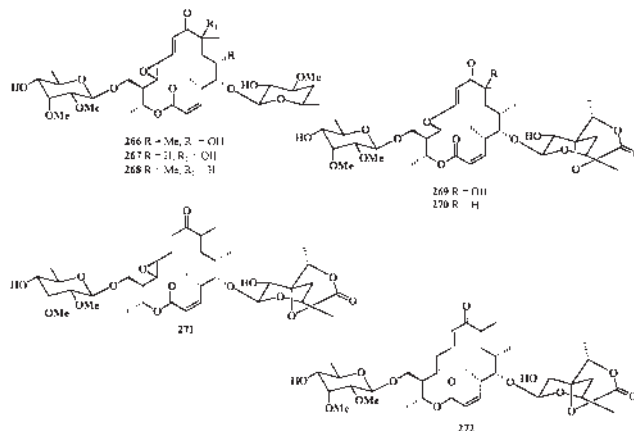
17–28-MEMBERED RING MACROCYCLIC GLYCOSIDES

A novel 17-membered ring macrolide named versipelostatin **273**, a metabolite of *Streptomyces versipellis* 4083-SVS6, was isolated as a GRP78 molecular chaperone down-regulator (296). GRP78 acts as a molecular chaperone in the endoplasmic reticulum by associating transiently with incipient proteins to facilitate protein folding (297). Overexpression of GRP78 enables solid tumor cells to grow in hypoxic and glucose-starved conditions, which is the characteristic circumstance of the core of a solid tumor (298). Biosynthesis of versipelostatin also was reported (299).

A new 18-membered ring resin glycoside, mammoside A **274**, and three resin-glycosides, named mammosides B, H1, and H2, were isolated from the tuber of *Merremia mammosa* (Convolvulaceae) (300). The antifungal macrocyclic lactone antibiotic, irumamycin **275**, was found in the culture broth of *Streptomyces subflavus* subsp. *irumaensis* nov. subsp. (301). More recently, irumamycin **275** and two analogs, **275a,b**, were produced by newly isolated *Streptomyces* sp. strain US80 (302). Irumamycin and the two analogs showed antimicrobial activities against Gram-positive and Gram-negative bacteria (*Escherichia coli* ATCC 8739, *Micrococcus luteus* LB 14110, *Bacillus subtilis* ATCC 6633, and *S. aureus* ATCC 6538). All three pure compounds, **275** and **275a,b**, inhibited growth of the two filamentous fungi (*Verticillium dahliae*, *Fusarium* sp.) and *Candida tropicalis* R2 CIP203; the highest antifungal activity was shown by irumamycin **275** (302).

Concanamycin A **276** and related compounds B and C were isolated from the mycelium of *Streptomyces diastatochromogenes* S-45 as effective inhibitors of concanavalin A-stimulated proliferation of mouse splenic lymphocytes (303). They repre-

sent a new class of 18-membered macrolide antibiotics and are biologically active *in vitro* against several fungi and yeasts, but not bacteria. Concanamycin A, the main component, has been identified with the antifungal antibiotics folimycin and A-661-I; it is a potent and specific ATPase inhibitor (304).

273 Versipelostatin

274 Mammnoside A

275 Irumamycin, R =

275a X-14952 B, R =

275b 17-OH-Verturicin A, R =

276 Concanamycin A
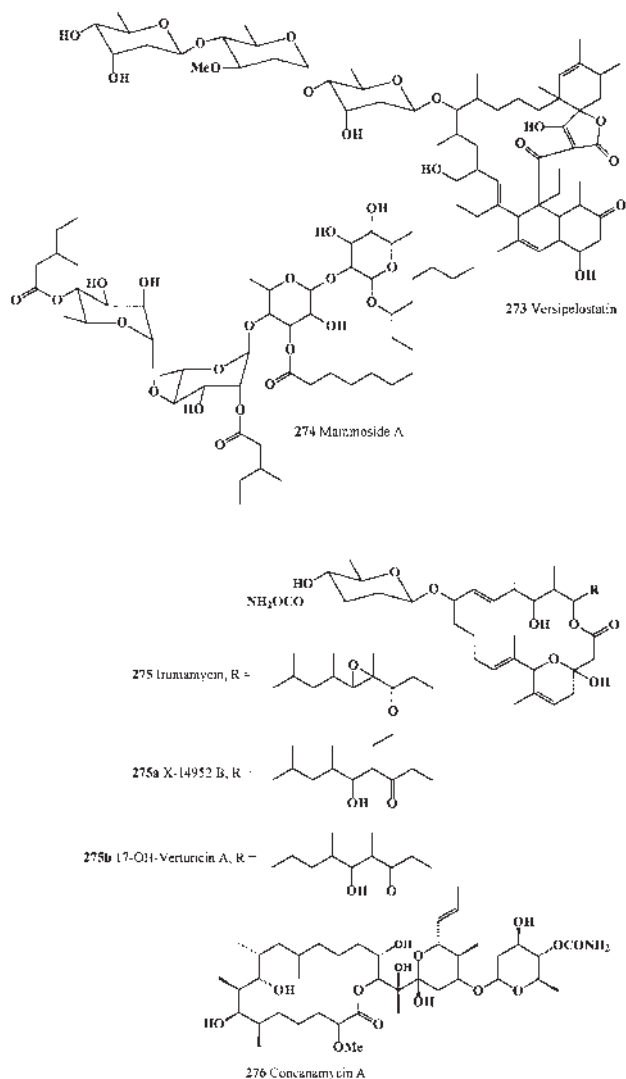
The tiacumicins are a group of 18-membered macrolide antibiotics originally isolated from the fermentation broth of *Dactylosporangium aurantiacum* subsp. *hamdenensis* (305–310). Tiacumicin B **277a**, the major antibiotic component produced by this culture, contains an unsaturated 18-membered macrolide ring with a seven-carbon sugar at carbon 11 and a 6-deoxysugar at carbon 20. This compound is apparently identical to one of the lipiarmycins, a previously described group of lipiarmycin antibiotics, **277c,d**, produced by *Actinoplanes deccanensis*, and to clostomicin B1, an antibiotic from *Micromonospora echinospora* (309). Tiacumicin C **277b** differs

in the position of butyrate esterification on the seven-carbon sugar. Tiacumicin C appears to be identical to clostomicin B2, a member of the clostomicin complex isolated from *M. echinospora* (309). Tiacumicins B **277a** and C **277b** showed *in vitro* activity against 15 strains of *Clostridium difficile* (MIC 0.12 μg/mL for B, and 0.25 μg/mL for C) (309,310).

277a Tiacumicin B, R = COC(CH₂)₂, R₁ = H
277b Tiacumicin C, R = H, R₂ = COC(CH₂)₂

277c Lipiarmycin A3, R = Et
277d Lipiarmycin A4, R = Me
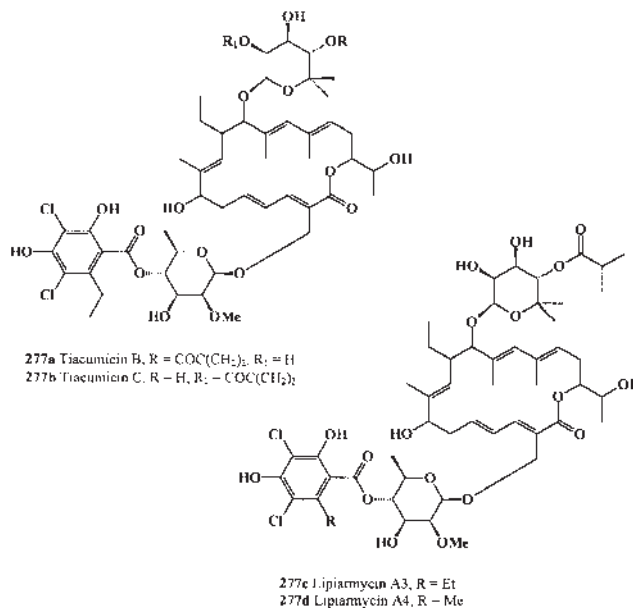
The first macrocyclic anthocyanin pigment was discovered in 1998 by Bloor (311). He examined flowers of the red/mauve carnation (*Dianthus caryophyllus*) cultivars 'Kortina Chanel' and 'Purple Torres' grown in New Zealand and found them to contain the unique macrocyclic anthocyanin pigment **278a**, a malylated cyanidin 3,5-diglucoside in which the malyl group is linked to both sugars (311). More recently, **278a** and **278b** were isolated from the same plant grown in Japan (312). Macrocyclic compound **278b** also was found in the 'Cyclamen Red' (or pink) flowers from Italy, France, and The Netherlands ('Red Rox') (313). The modified violet carnation cultivars 'Moondust' and 'Moonshadow' (*Dianthus caryophyllus*) produce a cyclic delphinidin type anthocyanin elphinidin, **279** (314). A new antitumor antibiotic (against human colon carcinoma Co-3), vicenistatin **280**, was isolated from the culture broth of *Streptomyces* sp. HC34 and is a unique 20-membered macrocylic lactam with a novel amino sugar vicenisamine (315).

A new antifungal 24-membered polyene macrolide, tetrin **281**, and the related compounds tetrins A **282** and B **283**, and tetramycins A **284** and B **285** have been isolated from *Streptomyces* sp. GK9244 (316). Maduralide **286**, a novel macrolide possessing a 24-membered ring, was isolated from a marine actinomycete grown in liquid culture (317).

288a Anthocyanin, R = OH, R₁ = H
288b R, R₁ = H
279 Elphinidin, R = R₁ = OH

280 Vicenistatin

281 X,Y = O, R = R₁ = Me, R₂ = H
282 X = OH, Y = H, R = R₁ = Me, R₂ = H
283 X = Y = OH, R = R₁ = Me, R₂ = H
284 X = OH, Y = H, R = Me, R₁ = Et, R₂ = H
285 X,Y = O, R = R₁ = Me, R₂ = Ac

286 Maduralide
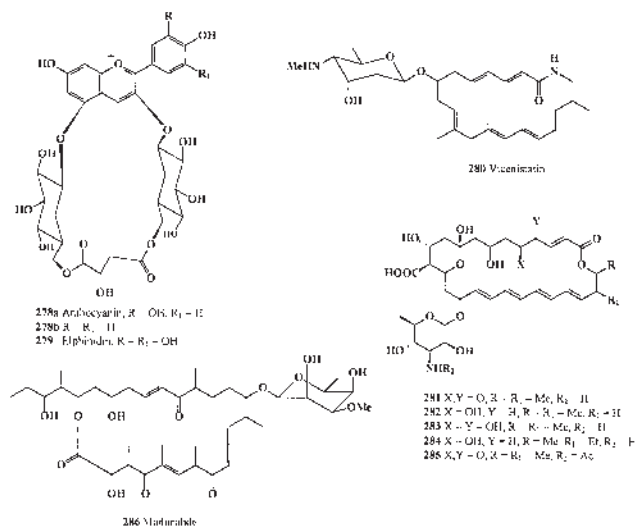
Pimaricin **287** and the analog de-epoxy-pimaricin **288** are 24-member ring lactone antifungal antibiotics (318) produced by *Streptomyces natalensis* ATCC 27448, which is widely used in the food industry to prevent mold contamination on cheese and other nonsterile foods (319,320). The anti-inflammatory pentaene 28-membered ring lactones eurocidins C, D **289**, and E have been isolated from the culture broth of *Streptoverticillium eurocidicum* IFO 13491 as the inhibitors (321–323). Eurocidins C and E do not contain sugar moieties in their structure.

287 Pimaricin

288 De-epoxy-pimaricin

289 Eurocidin D
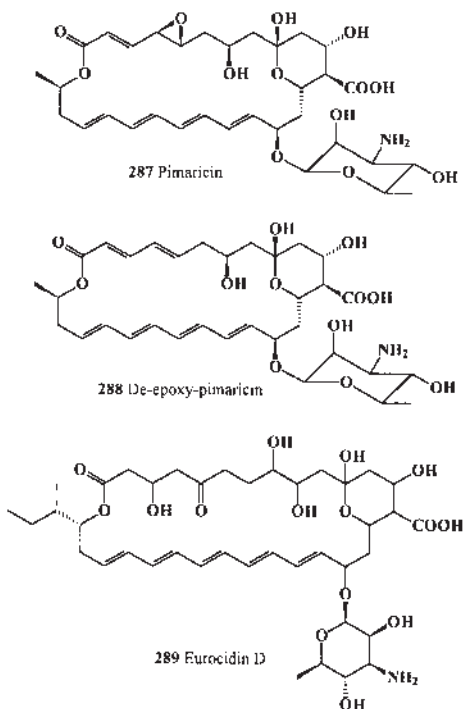
30–72-MEMBERED RING MACROCYCLIC GLYCOSIDES

A new macrolide lactone antifungal antibiotic, brasilinolide A **290**, was isolated from the fermentation broth of *Nocardia* sp. IFM 0406. The producer was identified as *Nocardia brasiliensis* (324,325). This macrolide was active only against *Aspergillus niger* but not against other fungi including yeasts or other filamentous fungi and bacteria. Brasilinolide A also showed an immunosuppressant activity in the mixed lymphocyte reaction with an IC_{50} of 0.625 µg mL^{-1}. More recently, brasilinolides B **290a** and C **290b** were isolated from *N. brasiliensis* and from *N. brasiliensis* strain IFM0406 (326). The **290b** showed cytotoxicity against murine lymphoma P388 cells (IC_{50} 8.3 µg/mL), whereas **290** was not cytotoxic at IC_{50} 100 µg/mL.

290 Brasilinolide A, R = COCH₂COOH, R₁ = COC₄H₉
290a Brasilinolide B, R = COC(C₄H₉)COOMe, R₁ = Me
290b Brasilinolide C, R = R₁ = H
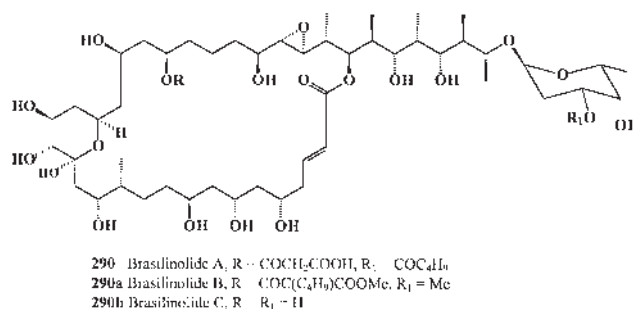
The new, highly complex chlorinated pyrrole-containing macrolide colubricidin A **291** was isolated from the fermentation broth of a new *Streptomyces* sp. LL-C13122 (327). It showed nematocidal activity against *Caenorhabditis elegans* and also demonstrated potent activity against Gram-positive bacteria.

291 Colubricidin A
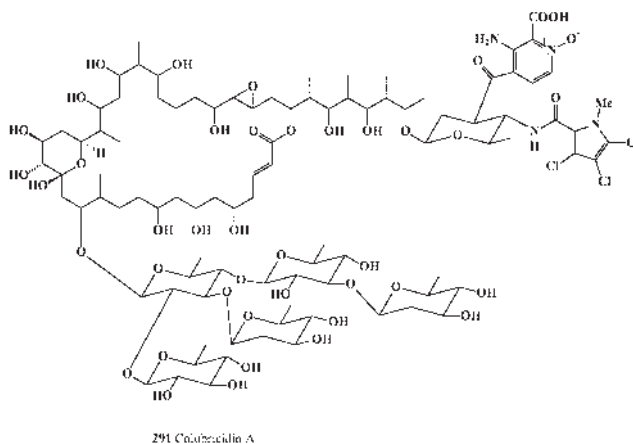
The polyene macrolide antibiotic nystatin **292** produced by *Streptomyces noursei* ATCC 11455 is an important antifungal agent. The nystatin molecule contains a polyketide moiety represented by a macrolactone ring to which the deoxy sugar mycosamine is attached (328). The biosynthetic pathway of nystatin has been elucidated (328).

Amphotericin B **293**, the first commercially significant antifungal drug, has been available for more than 30 years and was described by Oura *et al*. (329). According to the National Library of Medicine (Bethesda, MD), more than 13,000 experimental and review articles have been published on amphotericin B **293** during the last 30 years. This polyene macrolide antifungal agent continues to play a major role in the treatment of systemic fungal infections, despite the introduction of newer agents such as the azoles. Because of the proven efficacy of amphotericin B and the increasing number of indications for antifungal agents, an extensive review of this drug has been published (330). This paper discusses the clinical uses of amphotericin B, including its application in AIDS-related fungal infections, in neutropenic cancer patients who are persistently febrile, and in infections of the central nervous system, lungs, peritoneum, genitourinary system, eyes, and skin. The paper also reviews the drug's adverse reactions, with a discussion of administration techniques that may reduce these reactions, and its spectrum of activity, pharmacokinetics, and dosage and administration (330).

Candicidin **294**, an aromatic heptaene antibiotic produced by *Streptomyces griseus* IMRU 3570, was discovered by Lechevalier (331) and named antibiotic C135, although it was renamed candicidin because of its strong activity against species of *Candida*. Candicidin was used to treat vaginal candidiasis (332–334) and prostatic hyperplasia (335).

292 Nystatin

293 Amphotericin B

294 Candicidin D
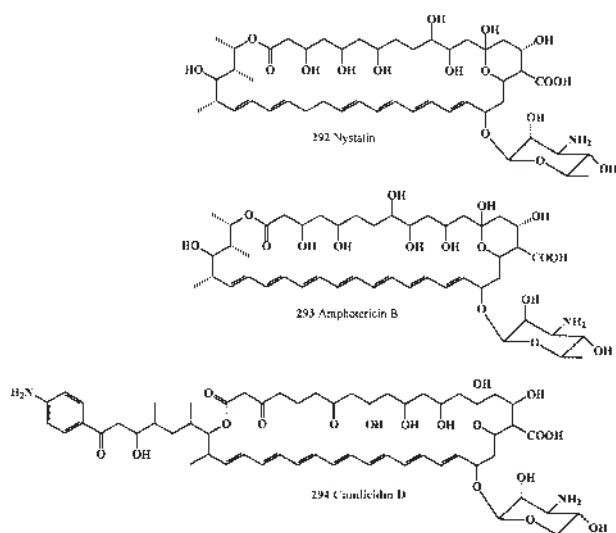
A few 42-membered macrolactone glycosides have been isolated from the microorganisms. Oasomycin B **295** contains α-D-mannose at the 22 carbon atom produced by *Streptoverticillium baldacci* subsp. *netropse* (strain FH-S 1625) (336), as

do desertomycin A **296** and B **297**. Oasomycin B **295** and desertomycins **296** and **297** vary in the side chains located at carbon atom 41 and in the α-1-*O*-linked D-mannose moiety attached to carbon atom 22. Desertomycin A **296** exhibits selective antifungal and broad antibacterial activity *in vitro* as well as considerable cytotoxic effects. The acute toxicity in mice was reported to be in the range of 1–12 mg/kg [LD_{50} (dose at which 50% of test subjects die) = 1.5 mg/kg s.c. (337) and 12 mg/kg p.o. (338)]. Mathemycins A **298** and B **299**, new antifungal macrolactone glycosides, have been isolated from *Actinomycete* species (339–341). The compounds of **298** and **299** show moderate *in vitro* activity against the following phytopathogens, with minimum active concentration values of 62.5 mg/L: *Fusarium culmorum, Alternaria mali, Botrytis cirea, Pellicularia sasaki, Leptosphaeria nodorum, Pyricularia oryzae, Pseudocercosporella herpotrichoides*, and *Phytophthora infestans*.

295 Oasomycin B

296 Desertomycin A, R = H
297 Desertomycin B, R = (C−NH)NH₂
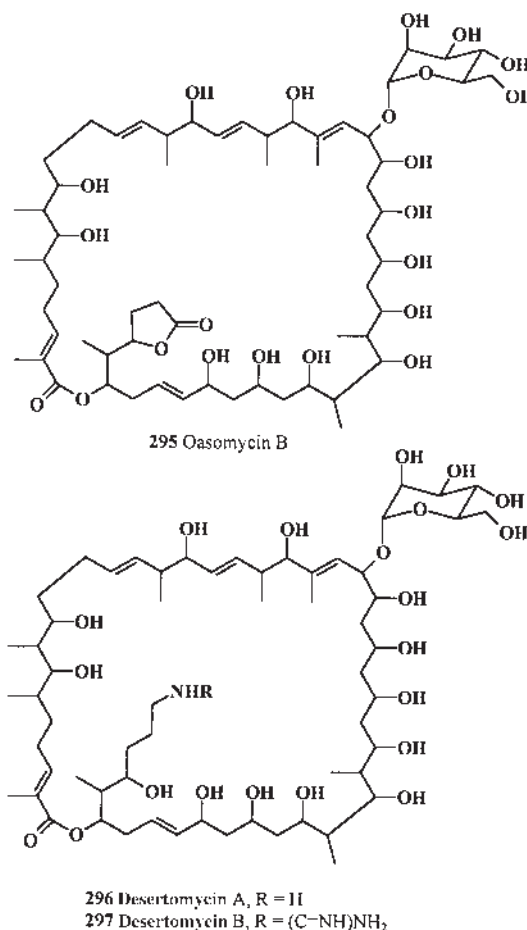
A unique new 52-membered ring cyclic β-glucan, α-cyclosophorohexadecaose **300**, was purified from cultures of *Xanthomonas campestris* (342).
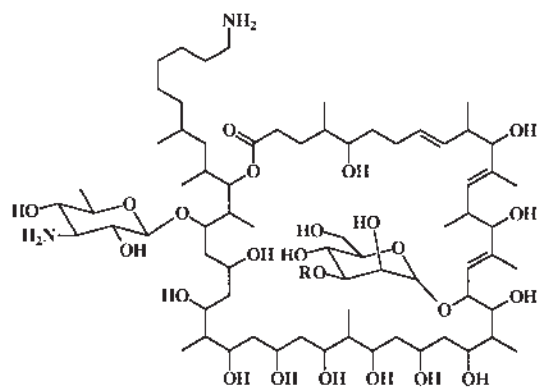
298 Mathemycin A, R = H
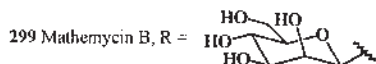
299 Mathemycin B, R =

Archaebacteria thrive in environments characterized by anaerobiosis, saturated salt, and both high and low extremes of temperature and pH. The bulk of their membrane lipids are polar, characterized by the archaeal structural features typified by ether linkage of the glycerol backbone to isoprenoid chains of constant length, often fully saturated, and with *sn*-2,3 stereochemistry opposite that of glycerolipids of bacteria and eukarya (343). Molecular species of C_{40} isoprenoid chains, having different numbers of cyclopentane rings, were detected in the ether core lipid of *Thermoplasma acidophilum* (344,345). The average cyclization number of the hydrocarbon chains in the lipids increased with increasing growth temperatures. Two neutral glycolipids, **301** and **302**, isolated from *T. acidophilum* provide examples of the unusual 72-membered ring macrocyclic structures of archaebacteria lipids. The same glycolipids are produced by some other archaebacteria (343).
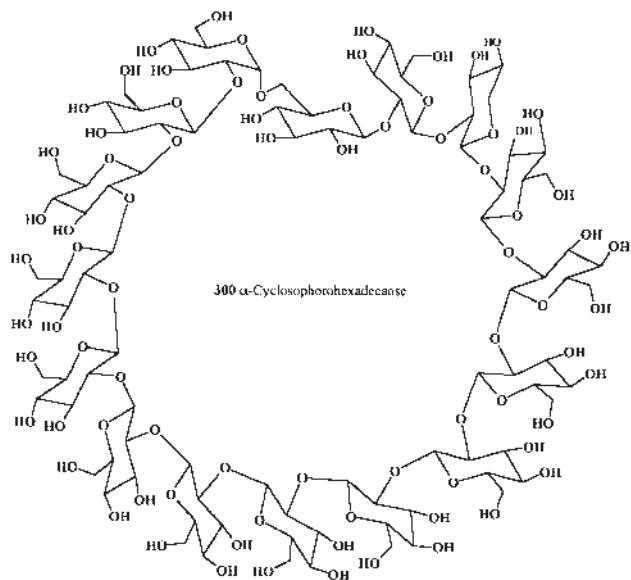
300 α-Cyclosophorohexadecaose
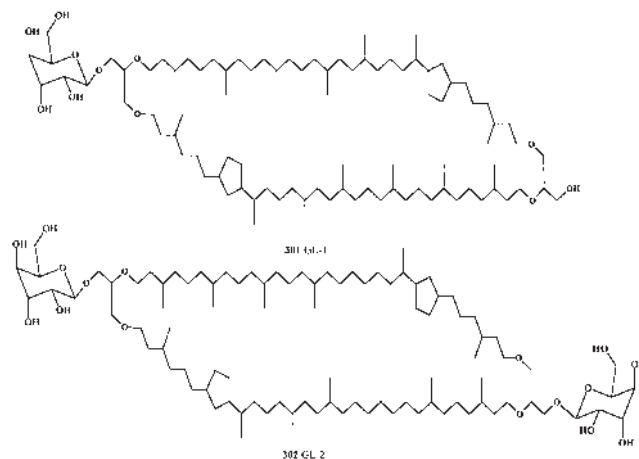
UNUSUAL BOLAFORM AMPHIPHILES

Bolaform amphiphilic compounds exhibit diverse surface activities, biodegradability, reactivity, and antimicrobial properties (346). Bola-amphiphiles are molecules with two polar head groups separated by one or more hydrophobic spacer groups; three general types can be identified (see Fig. 1). The polar groups include glycerol and related polyols and are connected to the hydrophobic chain through ether, acetal, ester, and amide links (347). Compounds of type A can form micelles or monolayer lipid vesicles for a range of variants in the structure, but more complex behavior has been observed for bis(azacrown ether) bola-amphiphiles (micelle or multilamellar vesicle formation depending on the length of the spacer group) (348). Compounds with polyhydroxy head groups act as gelling agents in water by forming fiber-like aggregates (349); similar rods and tubules are formed by self-assembly of bola-amphiphiles with amino acid and ammonium functionalities as the head groups (350). One interesting property of many bola-amphiphiles is their capacity to become incorporated into lipid membranes. Depending on its structure, the bola-amphiphile can act either as a membrane-disrupting agent (351,352) or as a membrane stabilizer (353). Most studies of bola-amphiphiles that interact with membranes involve either pseudomacrocyclic type B or macrocyclic type C structures. These are analogs of the lipid constituents of the highly stable membranes from archaebacteria (see structures **301** and **302**). These bacterial membranes are made up of macrocyclic lipids (type C) with two polyisoprenoid spacer groups attached to the glycerol head groups by ether linkages (354). The nondenaturing properties of bolaform amphiphilic compounds, sugar-based nonionic surfactants, may provide interesting advantages for these compounds in cosmetic, pharmaceutical, and food applications.

The novel pseudomacrocyclic bola-amphiphilic (type B) compounds **303** and **304** have been synthesized (355,356), as
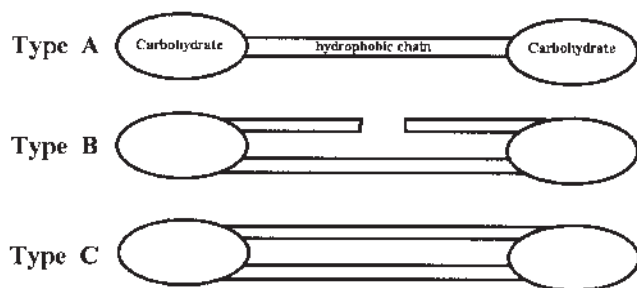
FIG. 1. Basic structures of bolaform surfactants: Type A, single-chain bolaform; Type B, pseudomacrocyclic bolaform; Type C, macrocyclic bolaform.

have galactose-based (type C) macrocyclic surfactant **305** analogs of archaeobacterial membrane components (356). Compound **305** and the pseudomacrocyclic bolaforms **303** and **304** display interesting new surface tension properties; they are insoluble in water and undergo monolayer compression.
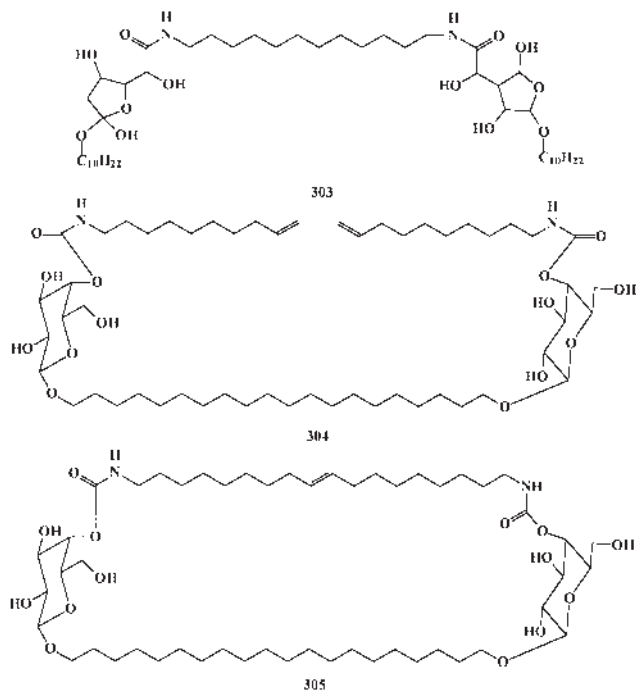
Macrocyclic compounds such as porphyrins, their analogs and derivatives have been widely used as photosensitizers in photodynamic therapy for cancer diseases (357–360). The photosensitizer **306**, 3,12,13,22-tetraethyl-8,17-bis[(2-amino-2-deoxy-α,β-D-glucopyranose)-carbonylethyl]-2,7,18,23-tetra-methyl-sapphyrin, has been synthesized (361), and the biolocalization and photochemical properties of this sapphyrin **306** have been investigated (361). This photosensitizer absorbs in the far visible region, shows good tumor localization, and demonstrates a significantly larger absolute and relative tumor to normal tissue ratio (ratio T/N; amount in tumor, 330 μg g^{-1} wet tissue, T/N = 19.0). Raman spectroscopic studies indicate that the monomerized photosensitizer **306** effectively damaged BSA and calf thymus DNA after light excitation under the con-

ditions of a large excess of this macromolecule. Porphyrin derivatives with eight sugars, **307** and **308**, with activity against some cancer cells, also were synthesized (362).
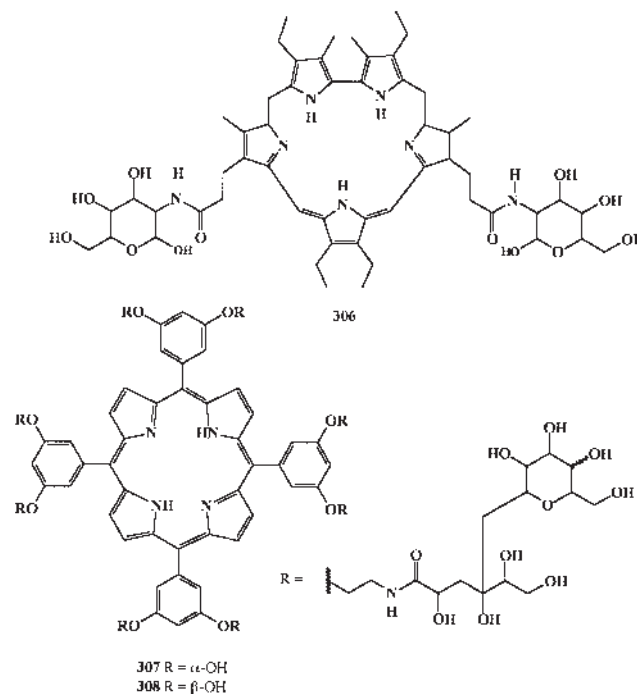
Fujimoto *et al.* (362) also synthesized the new biologically active saccharide-coated macrocycles **309** and **310**, and found that rat hepatoma cells bind a calixarene having two galactoses on each of its four aromatic rings. Spleen cells lacking specific galactoside receptors did not bind this calixerene, nor did rat hepatoma cells bind the calixarene substituted with glucose instead of galactose. The more effective analogs **311–315**, with two galacto-calixarene macrocycles covalently joined by a long spacer and belonging to type B bolaform surfactants, were synthesized by Menger and co-workers (363); the authors proposed that the new bolaforms **311–315** might "glycotarget" a group of cancer cells and thereby interconnect them for therapeutic purposes.
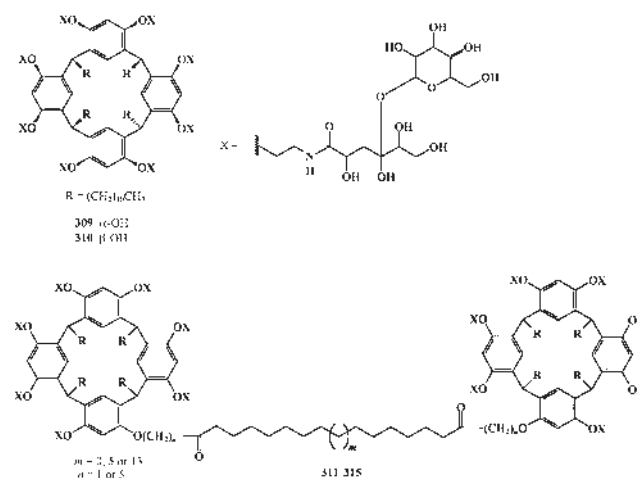
Over the last 50 years, a great number of new therapeutic agents have been discovered. However, in spite of the unquestionable advances in pharmacotherapy, it is calculated that a satisfactory treatment has yet to be developed for two out of every three diseases. This is the case for numerous forms of cancer and viral or heart diseases. The need for new, more specific. and better adapted medicines is greater each day. We have reviewed more than 300 natural glycoside-containing compounds, and some of them and/or their synthetic derivatives could eventually be used as potent therapeutic agents. The marine environment constitutes a vast potential source of new bioactive molecules. One of the most interesting groups of substances of marine origin, from the pharmacological point of view, is that of the acyclic or cyclic polyethers, which generally present a great diversity in size and potent biological activities.

With the examples of recent product innovations from bolaform chemistry and the successful development of synthetic capabilities and biologically potent products, the potential for drug development in this area also has been demonstrated. Combining novel marine and terrestial raw materials, as well as deriving new synthetic methods to form new products, will also be a challenge for research and development in the future, as will be the development of products for polymer or composite applications. Extensive basic investigations, especially regarding the use of new natural surfactant derivatives, can be expected in the near future.

REFERENCES

1. Dembitsky, V.M. (2005) Astonishing Diversity of Natural Surfactants. 1. Glycosides of Fatty Acids and Alcohols, *Lipids 39*, 933–953.
2. Dembitsky, V.M. (2004) Chemistry and Biodiversity of Biologically Active Natural Glycosides, *Chem. Biodivers. 1*, 673–781.
3. Kren, V., and Martinkova, L. (2001) Glycosides in Medicine: The Role of Glycosidic Residue in Biological Activity, *Curr. Med. Chem. 8*, 1303–1328.
4. Kingston, W. (2004) Streptomycin, Schatz v. Waksman, and the Balance of Credit for Discovery, *J. Hist. Med. Allied Sci. 59*, 441–462.
5. Ng, A.W., Wasan, K.M., and Lopez-Berestein, G. (2003) Development of Liposomal Polyene Antibiotics: An Historical Perspective, *J. Pharm. Pharm. Sci. 6*, 67–83.
6. Casnati, A., Sansone, F., and Ungaro, R. (2003) Peptido- and Glycocalixarenes: Playing with Hydrogen Bonds Around Hydrophobic Cavities, *Acc. Chem. Res. 36*, 246–254.
7. Sener, B. (ed.) (2002) *Biodiversity: Biomolecular Aspects of Biodiversity and Innovative Utilization*, Kluwer Academic/Plenum, New York.
8. Ernst, B., Hart, G.W., and Sinaÿ, P. (eds.) (2000) *Carbohydrates in Chemistry and Biology*, Wiley-VCH, Weinheim.
9. Satoshi, O. (ed.) (2002) *Macrolide Antibiotics: Chemistry, Biology, and Practice*, Amsterdam, Academic Press.
10. Rosen, M.J. (2004) *Surfactants and Interfacial Phenomena*, 3rd edn., John Wiley & Sons, New York.
11. Robinson, J.A. (1991) Chemical and Biochemical Aspects of Polyether–Ionophore Antibiotic Biosynthesis, *Prog. Chem. Org. Nat. Prod. 58*, 1–82.
12. Kirst, H.A. (1992) Macrolides, in *Encyclopedia of Chemical Technology*, 4th edn. (Howe-Grant, M., ed.), Vol. 3, pp. 169–213, John Wiley & Sons, New York.
13. Crandell, L.W., and Hamill, R.L. (1992) Antibiotics, Polyenes, in *Encyclopedia of Chemical Technology*, 4th edn. (Howe-Grant, M., ed.), Vol. 3, pp. 307–311, John Wiley & Sons, New York.
14. Szabo, G. (1981) Structural Aspects of Ionophore Function, *Fed. Proc. 40*, 2196–2201.
15. Krasne, S., and Eisenman, G. (1976) Influence of Molecular Variations of Ionophore and Lipid on the Selective Ion Permeability of Membranes: I. Tetranactin and the Methylation of Nonactin-type Carriers, *J. Membr. Biol. 30*, 1–44.
16. Szabo, G., Eisenman, G., Laprade, R., Ciani, S.M., and Krasne, S. (1973) Experimentally Observed Effects of Carriers on the Electrical Properties of Bilayer Membranes—Equilibrium Domain. With a Contribution on the Molecular Basis of Ion Selectivity, *Membranes 2*, 179–328.
17. Pressman, B.C., Harris, E.J., Jagger, W.S., and Johnson, J.M. (1967) Antibiotic-Mediated Transport of Alkali Ions Across Lipid Barriers, *Proc. Natl. Acad. Sci. USA 58*, 1949–1956.
18. Matsuoka, M., and Sasaki, T. (2004) Inactivation of Macrolides by Producers and Pathogens, *Curr. Drug Targets Infect. Disord. 4*, 217–240.
19. Goldman, R.C., and Scaglione, F. (2004) The Macrolide–Bacterium Interaction and Its Biological Basis, *Curr. Drug Targets Infect. Disord. 4*, 241–260.
20. Wheeler, J.J., Veiro, J.A., and Cullis, P.R. (1994) Ionophore-Mediated Loading of Ca^{2+} into Large Unilamellar Vesicles in Response to Transmembrane pH Gradients, *Mol. Membr. Biol. 11*, 151–157.
21. Somani, P., Kabell, G.G., Saini, R.K., and Hester, R.K. (1980) The Effect of Monensin, a Na^+-Selective Carboxylic Ionophore, on Coronary Circulation, *Adv Myocardiol. 2*, 435–447.
22. Maravic, G. (2004) Macrolide Resistance Based on the Erm-Mediated rRNA Methylation, *Curr. Drug Targets Infect. Disord. 4*, 193–202.
23. Budanov, S.V., and Vasil'ev, A.N. (2004) Clarithromycin: Specific Features of Antimicrobial Spectrum and Clinical Use, *Antibiot. Khimioter. (Russian) 49*, 19–25.
24. Gotfried, M.H. (2004) Appropriate Outpatient Macrolide Use in Community-Acquired Pneumonia, *J. Am. Acad. Nurse Pract. 16*, 146–150.
25. Gotfried, M.H. (2003) Clarithromycin (Biaxin) Extended-Release Tablet: A Therapeutic Review, *Expert Rev. Anti Infect. Ther. 1*, 9–20.
26. Cazzola, M., Matera, M.G., and Blasi, F. (2004) Macrolide and Occult Infection in Asthma, *Curr. Opin. Pulm. Med. 10*, 7–14.
27. Neher, J.O., and Morton, J.R. (2004) What Is the Best Macrolide for Atypical Pneumonia? *J. Fam. Pract. 53*, 229–230.
28. Hammerschla g, M.R. (2003) Pneumonia Due to *Chlamydia pneumoniae* in Children: Epidemiology, Diagnosis, and Treatment, *Pediatr. Pulmonol. 36*, 384–390.
29. Satoshi, O. (ed.) (2002) *Macrolide Antibiotics: Chemistry, Biology, and Practice*, Academic Press, Amsterdam.
30. Schönfeld, W., and Kirst, H.A. (eds.) (2002) *Macrolide Antibiotics*, Birkhauser Verlag.
31. Burja, A.M., Banaigs, B., Abou-Mansour, E., Burgess, J.G., and Wright, P.C. (2001) Marine Cyanobacteria—A Prolific Source of Natural Products, *Tetrahedron 57*, 9347–9377.
32. Shimizu, Y. (2000) Microalgae as a Drug Source, in *Drugs from the Sea* (Fusetani, N., ed.), pp. 30–45, Karger, Basel.
33. Kobayashi, J., and Ishibashi, M. (1999) Marine Natural Products and Marine Chemical Ecology, in *Comprehensive Natural Products Chemistry* (Mori, K., ed.), Vol. 8, pp. 415–649, Elsevier, Amsterdam.
34. Shimizu, Y. (1996) Microalgal Metabolites: A New Perspective, *Annu. Rev. Microbiol. 50*, 431–465.

35. Woodward, R.B. (1957) Struktur und Biogenese der Macrolide: Eine neue Klasse von Naturstoffen, *Angew. Chem. 69*, 50–62.

36. Moore, B.S., and Hopke, J.N. (2001) Discovery of a New Bacterial Polyketide Biosynthetic Pathway, *Chembiochem. 2*, 35–38.

37. McGuffey, R.K., Richardson, L.F., and Wilkinson, J.I.D. (2001) Ionophores for Dairy Cattle: Current Status and Future Outlook, *J. Dairy Sci. 84, Suppl.*, E194–E203.

38. O'Hagan, D. (1991) *The Polyketide Metabolites*, Ellis Horwood, Chichester, United Kingdom.

39. Dutton, C.J., Banks, B.J., and Cooper, C.B. (1995) Polyether Ionophores, *Nat. Prod. Rep. 12*, 165–181.

40. Murata, M., and Yasumoto, T. (2000) The Structure Elucidation and Biological Activities of High Molecular Weight Algal Toxins: Maitotoxin, Prymnesins and Zooxanthellatoxins, *Nat. Prod. Rep. 17*, 293–314.

41. Rein, K.S., and Borrone, J. (1999) Polyketides from Dinoflagellates: Origins, Pharmacology and Biosynthesis, *Comp. Biochem. Physiol. 124B*, 117–131.

42. Faul, M.M., and Huff, B.E. (2000) Strategy and Methodology Development for the Total Synthesis of Polyether Ionophore Antibiotics, *Chem. Rev. 100*, 2407–2473.

43. Traxler, P., Gruner, J., and Auden, J.A.L. (1977) Papulacandins, A New Family of Antibiotics with Antifungal Activity, I. Fermentation, Isolation, Chemical and Biological Characterization of Papulacandins A, B, C, D and E, *J. Antibiot. 30*, 289–296.

44. Traxler, P., Fritz, H., and Richter, W.J. (1977) On the Structure of Papulacandin B, a New Antibiotic with Antifungal Activity, *Helv. Chim. Acta 60*, 578–584.

45. Traxler, P., Fritz, H., Fuhrer, H., and Richter, W.J. (1980) Papulacandins, a New Family of Antibiotics with Antifungal Activity. Structures of Papulacandins A, B, C and D, *J. Antibiot. 33*, 967–978.

46. Onishi, J., Meinz, M., Thompson, J., Curotto, J., Dreikorn, S., Rosenbach, M., Douglas, C., Abruzzo, G., Flattery, A., Kong, L., *et al.* (2000) Discovery of Novel Antifungal (1,3)-β-D-Glucan Synthase Inhibitors, *Antimicrob. Agents Chemother. 44*, 368–377.

47. Debono, M., and Gordee, R.S. (1994) Antibiotics That Inhibit Fungal Cell Wall Development, *Annu. Rev. Microbiol. 48*, 471–497.

48. Rommele, G., Traxler, P., and Wehrli, W. (1983) Papulacandins: The Relationship Between Chemical Structure and Effect on Glucan Synthesis in Yeast, *J. Antibiot. 36*, 1539–1542.

49. Kaneto, R., Chiba, H., Agematu, H., Shibamoto, N., Yoshioka, T., Nishada, H., and Okamoto, M. (1993) Mer-WF3010, a New Member of the Papulacandin Family. I. Fermentation, Isolation and Characterization, *J. Antibiot. 46,* 247–250.

50. Chiba, H., Kaneto, R., Agematu, H., Shibamoto, N., Yoshioka, T., Nishida, H., and Okamoto, R. (1993) Mer-WF3010, a New Member of the Papulacandin Family. II. Structure Determination, *J. Antibiot. 46*, 356–358.

51. Van Middlesworth, F., Omstead, M.N., Schmatz, D., Bartizal, K., Fromtling, R., Bills, G., Nollstadt, K., Honeycutt, S., Zweerink, M., Garrity, G., and Wilson, K. (1991) L-687,781, A New Member of the Papulacandin Family of β-1,3-D-Glucan Synthesis Inhibitors. 2. Fermentation, Isolation, and Biological Activity, *J. Antibiot. 44*, 45–51.

52. Chen, R.H., Tennant, S., Frost, D., O'Beirne, M.J., Karwowski, J.P., Humphrey, P.E., Malmberg, L.H., Choi, W., Brandt, K.D., West, P., *et al.* (1996) Discovery of Saricandin, a Novel Papulacandin, from a *Fusarium* Species, *J. Antibiot. 49*, 596–598.

53. Kobayashi, J., Kubota, T., Takahashi, M., Ishibashi, M., Tsuda, M., and Naoki, H. (1999) Colopsinol A, a Novel Polyhydroxyl Metabolite from Marine Dinoflagellate *Amphidinium* sp., *J. Org. Chem. 64,* 1478–1482.

54. Kubota, T., Tsuda, M., Takahashi, M., Ishibashi, M., Naoki, H., and Kobayashi, J. (1999) Colopsinols B and C, New Long Chain Polyhydroxy Compounds from Cultured Marine Dinoflagellate *Amphidinium* sp., *J. Chem. Soc.*, *Perkin Trans. 1*, 3483–3487.

55. Kubota, T., Tsuda, M., Takahashi, M., Ishibashi, M., Oka, S., and Kobayashi, J. (2000) Colopsinols D and E, New Polyhydroxyl Linear Carbon Chain Compounds from Marine Dinoflagellate *Amphidinium* sp.*, Chem. Pharm. Bull. 48*, 1447–1451.

56. Mayer, A.M.S., and Gustafson, K.R. (2003) Marine Pharmacology in 2000: Antitumor and Cytotoxic Compounds, *Int. J. Cancer 105*, 291–299.

57. Westley, J.W. (1977) Polyether Antibiotics: Versatile Carboxylic Acid Ionophores Produced by *Streptomyces*, *Adv. Appl. Microbiol. 22*, 177–223.

58. Westley, J.W. (ed.) (1982) *Polyether Antibiotics: Naturally Occurring Acid Ionophores, Biology*, Marcel Dekker, New York.

59. Hopwood, D.A. (1997) Genetic Contributions to Understanding Polyketide Synthases, *Chem. Rev. 97*, 2465–2497.

60. Katz, L., and McDaniel, R. (1999) Novel Macrolides Through Genetic Engineering, *Med. Res. Rev. 19*, 543–558.

61. Tsou, H.R., Rajan, S., Fiala, R., Mowery, P.C., Bullock, M.W., Borders, D.B., James, J.C., Martin, J.H., and Morton, G.O. (1984) Biosynthesis of the Antibiotic Maduramicin. Origin of the Carbon and Oxygen Atoms as well as the ^{13}C NMR Assignments, *J. Antibiot. 37*, 1651–1663.

62. Tsou, H.R., Rajan, S., Chang, T.T., Fiala, R.R., Stockton, G.W., and Bullock, M.W. (1987) The Utilization of Molecular Oxygen During the Biosynthesis of Maduramicin, *J. Antibiot. 40*, 94–99.

63. Mizoue, K., Seto, H., Mizutani, T., Yamagishi, M., Kawashima, A., Omura, S., Ozeki, M., and Otake, N. (1980) Studies on the Ionophorous Antibiotics. XXV. The Assignments of the ^{13}C-NMR Spectra of Dianemycin and Lenoremycin, *J. Antibiot. 33*, 144–156.

64. Cane, D.E., and Hubbard, B.R. (1987) Polyether Biosynthesis. 3. Origin of the Carbon Skeleton and Oxygen Atoms of Lenoremycin, *J. Am. Chem. Soc. 109*, 6533–6535.

65. Imada, A., Nozaki, Y., Hasegawa, T., Mizuta, E., Igarasi, S., and Yoneda, M. (1978) Carriomycin, a New Polyether Antibiotic Produced by *Streptomyces hygroscopicus, J. Antibiot. 31*, 7–14.

66. Mitani, M., and Otake, N. (1978) Studies on the Ionophorous Antibiotics. XV. The Monovalent Cation Selective Ionophorous Activities of Carriomycin, Lonomycin and Etheromycin, *J. Antibiot. 31*, 750–755.

67. Tsuji, N., Nagashima, K., Kobayashi, M., Wakisaka, Y., and Kawamura, Y. (1976) Two New Antibiotics, A-218 and K-41. Isolation and Characterization, *J. Antibiot. 29*, 10–14.

68. Cheng, X.C., Jensen, P.R., and Fenical, W. (1999) Arenaric Acid, a New Pentacyclic Polyether Produced by a Marine Bacterium (Actinomycetales), *J. Nat. Prod. 62*, 605–607.

69. Sassaki, T. (1985) A New Antibiotic SF2324 Produced by *Actinomadura*, Japanese Patent Application 60130394.

70. Sezaki, M., Sasaki, T., Nakazawa, T., Takeda, U., Iwata, M., Watanabe, T., Koyama, M., Kai, F., Shomura, T., and Kojima, M. (1985) A New Antibiotic SF-2370 Produced by *Actinomadura, J. Antibiot. 38*, 1437–1439.

71. Labeda, D.P., Goodman, J.J., and Martin, J.H.E.J. (1986) Antibiotic LL-C23201-γ, U.S. Patent Application 4628046.

72. Bull, A.T., Goodfellow, M., and Slater, J.H. (1992) Biodiversity as a Source of Innovation in Biotechnology, *Annu. Rev. Microbiol. 46*, 219–246.

73. Dirlam, J.P., Belton, A.M., Bordner, J., Cullen, W.P., Huang,

L.H., Kojima, Y., Maeda, H., Nishiyama, S., Oscarson, J.R., Ricketts, A.P., *et al.* (1992) CP-82,009, a Potent Polyether Anticoccidial Related to Septamycin and Produced by *Actinomadura* sp., *J. Antibiot. 45*, 331–340.

74. Wright, D.E. (1979) The Oorthosomycins, a New Family of Antibiotics, *Tetrahedron 35*, 1207–1237.

75. Girijavallabhan, V.M., and Ganguly, A.K. (1992) Antibiotics, in *Kirk–Othmer Encyclopedia of Chemical Technology*, 4th edn., Vol. 3, pp. 259–266, John Wiley & Sons, New York.

76. Ganguly, A.K., and Saksena, A.K. (1975) Structure of Everninomicin B, *J. Antibiot. 28*, 707–709.

77. Ganguly, A.K., Sarre, O.Z., Greeves, D., and Morton, J. (1975) Structure of Everninomicin D-1, *J. Am. Chem. Soc. 97*, 1982–1985.

78. Ganguly, A.K., Pramanik, B., Chan, T.M., Sarre, O.Z., Liu, Y.-T., Morton, J., and Girijavallabhan, V. (1989) The Structure of New Oligosaccharide Antibiotics, 13-384 Component-1 and Component-5, *Heterocycles 28*, 83–88.

79. Wang, E., Simard, M., Bergeron, Y., Beauchamp, D., and Bergeron, M.G. (2000) *In vivo* Activity and Pharmacokinetics of Ziracin (SCH27899), a New Long-Acting Everninomicin Antibiotic, in a Murine Model of Penicillin-Susceptible or Penicillin-Resistant Pneumococcal Pneumonia, *Antimicrob. Agents Chemother. 44*, 1010–1018.

80. Linden, P.K., and Miller, C.B. (1999) Vancomycin Resistant Enterococci: The Clinical Effect of a Common Nosocomial Pathogen, *Diagnost. Microbiol. Infect. Disease 33*, 113–120.

81. Chu, M., Mierza, R., Patel, M., Jenkins, J., Das, P., Pramanik, B., and Chan, T.-M. (2000) A Novel Everninomicin Antibiotic Active Against Multidrug-Resistant Bacteria, *Tetrahedron Lett. 41*, 6689–6693.

82. Saksena, A.K., Jao, E., Murphy, B., Schumacher, D., Chan, T.M., Puar, M.S., Jenkins, J.K., Maloney, D., Cordero, M., Pramanik, B.N., *et al.* (1998) Structure Elucidation of Sch 49088, a Novel Everninomicin Antibiotic Containing an Unusual Hydroxylamino-Ether Sugar, Everhydroxylaminose, *Tetrahedron Lett. 39*, 8441–8444.

83. Bartner, P., Pramanik, B.N., Saksena, A.K., Liu, Y.-H., Das, P.R., Sarre, O., and Ganguly, A.K. (1997) Structure Elucidation of Everninomicin-6, a New Oligosaccharide Antibiotic, by Chemical Degradation and FAB-MS Methods, *J. Am. Soc. Mass Spectrom. 8*, 1134–1140.

84. Liu, C.M., Hermann, T.E., Downey, A., La, B., Prosser, T., Schildknecht, E., Palleroni, N.J., Westley, J.W., and Miller, P.A. (1983) Novel Polyether Antibiotics X-14868A, B, C, and D Produced by a *Nocardia*. Discovery, Fermentation, Biological as well as Ionophore Properties and Taxonomy of the Producing Culture, *J. Antibiot. 36*, 343–350.

85. Liu, C.M., Prosser, T., and Westley, J. (1985) Antibiotic X-14934A, U.S. Patent Application 4,510,317.

86. Cullen, W.P., Bordner, J., Huang, L.H., Moshier, P.M., Oscarson, J.R., Presseau, L.A., Ware, R.S., Whipple, E.B., Kojima, Y., and Maeda, H. (1990) CP-60,993, a New Dianemycin-like Ionophore Produced by *Streptomyces hygroscopicus* ATCC 39305: Fermentation, Isolation and Characterization, *J. Ind. Microbiol. 5*, 365–374.

87. Celmer, W.D., Cullen, W.P., Maeda, H., Ruddock, J.C., and Tone, J. (1987) 19-Epi-dianemycin as an Anticoccidial and Antibacterial Agent, U.S. Patent Application 4707493.

88. Oscarson, J.R., Bordner, J., Celmer, W.D., Cullen, W.P., Huang, L.H., Maeda, H., Moshier, P.M., Nishiyama, S., Presseau, L., Shibakawa, R., and Tone, J. (1989) Endusamycin, a Novel Polycyclic Ether Antibiotic Produced by a Strain of *Streptomyces endus* subsp. *aureus*, *J. Antibiot. 42*, 37–48.

89. Dirlam, J.P., Presseau-Linabury, L., and Koss, D.A. (1990) The Structure of CP-80,219, a New Polyether Antibiotic Related to Dianemycin, *J. Antibiot. 43*, 727–730.

90. Nakayama, H., Seto, H., Otake, N., Yamaguchi, M., Kawashima, A., Mizutani, T., and Omura, S. (1985) Studies on the Ionophorous Antibiotics. 28. Moyukamycin, a New Glycosylated Polyether Antibiotic, *J. Antibiot. 38*, 1433–1436.

91. Westley, J.W., Liu, C.M., Sello, L.H., Troupe, N., Blount, J.F., Chiu, A.M., Todaro, L.J., Miller, P.A., and Liu, M. (1984) Isolation and Characterization of Antibiotic X-14931A, the Naturally Occurring 19-Deoxyaglycone of Dianemycin, *J. Antibiot. 37*, 813–815.

92. Hauske, J.R., and Kostek, G. (1989) Structure Elucidation of a New Polyether Antibiotic *iso*-Dianemycin, *J. Org. Chem. 54*, 3500–3504.

93. Kawada, M., Sumi, S., Umezawa, K., Inouye, S., Sawa, T., and Seto, H. (1992) Circumvention of Multidrug Resistance in Human Carcinoma KB Cells by Polyether Antibiotics, *J. Antibiot. 45*, 556–562.

94. Dirlam, J.P., Belton, A.M., Bordner, J., Cullen, W.P., Huang, L.H., Kojiima, Y., Maeda, H., Hishida, H., Nishiyama, S., Oscarson, J.R., Rickets, A.P., Sakakibara, T., Tone, J., and Tsukuda, K. (1990) CP-84,657, a Potent Polyether Anticoccidial Related to Portmicin and Produced by *Actinomadura* sp., *J. Antibiot. 43*, 668–679.

95. Ricketts, A.P., Dirlam, J.P., and Shively, J.E. (1992) Anticoccidial Efficacy and Chicken Toleration of Potent New Polyether Ionophores. 2. The Portmicin Relative CP-84,657, *Poultry Sci. 71*, 1631–1636.

96. Dirlam, J.P., Bordner, J., Chang, S.P., Grizzuti, A., Nelson, H., Tynan, E.J., and Whipple, E.B. (1992) The Isolation and Structure of CP-120,509, a New Polyether Antibiotic Related to Semduramicin and Produced by Mutants of *Actinomadura roseorufa*, *J. Antibiot. 45*, 1544–1548.

97. Kusakabe, Y., Mitsuoka, S., Omuro, Y., Seino, A., Arika, T., and Iwakaya, Y. (1979) Antibiotic of CP-120,509, Japanese Patent Application 7984576.

98. Cullen, W.P., Celmer, W.D., Chappel, L.R., Huang, L.H., Jefferson, M.T., Ishiguro, M., Maeda, H., Nishiyama, S., Oscarson, J.R., Shibakawa, R., and Tone, J. (1988) CP-61,405, a Novel Polycyclic Pyrrolether Antibiotic Produced by *Streptomyces routienii huang* sp. nov., *J. Industr. Microbiol. 2*, 349–357.

99. Glazer, E.A., Koss, D.A., Olson, J.A., Ricketts, A.P., Schaaf, T.K., and Wiscount, R.J., Jr. (1992) Synthetic Modification of a Novel Microbial Ionophore—Exploration of Anticoccidial Structure–Activity Relationships, *J. Med. Chem. 35*, 1839–1844.

100. Ricketts, A.P., Glazer, E.A., Migaki, T.T., and Olson, J.A. (1992) Anticoccidial Efficacy of Semduramicin in Battery Studies with Laboratory Isolates of Coccidia, *Poultry Sci. 71*, 98–103.

101. Tynan, E.J., Nelson, T.H., Davies, R.A., and Wernau, W.C. (1992) The Production of Semduramicin by Direct Fermentation, *J. Antibiot. 45*, 813–815.

102. Dobler, M. (1981) *Ionophores and Their Structures,* p. 379, John Wiley & Sons, New York.

103. Mulhaupt, T. (2003). Isolierung und Strukturafklarung von Sekundarmetaboliten aus marinen Microorganismen nach biologischen und chemischen Gesichtspunkten, Ph.D. Dissertation, Ludwig-Maximilians Universitat, Munchen, Germany.

104. Sun, Y., Zhou, X., Liu, J., Bao, K., Zhang, G., Tu, G., Kieser, T., and Deng, Z. (2002) *Streptomyces nanchangensis*, a Producer of the Insecticidal Polyether Antibiotic Nanchangmycin and the Antiparasitic Macrolide Meilingmycin, Contains Multiple Polyketide Gene Clusters, *Microbiology 148*, 361–371.

105. Sun, Y.H., Zhou, X.F., Tu, G.Q., and Deng, Z.X. (2002) Determination of Nanchangmycin and Meilingmycin by High Performance Liquid Chromatography, *Se Pu (in Chinese) 20*, 43–45.

106. Sun, Y., Zhou, X., Dong, H., Tu, G., Wang, M., Wang, B., and

Deng, Z. (2003) A Complete Gene Cluster from *Streptomyces nanchangensis* NS3226 Encoding Biosynthesis of the Polyether Ionophore Nanchangmycin, *Chem. Biol. 10*, 431–441.

107. Konishi, M., Yang, X., Li, B., Fairchild, C.R., and Shimizu, Y. (2004) Highly Cytotoxic Metabolites from the Culture Supernatant of the Temperate Dinoflagellate *Protoceratium* cf. *reticulatum*, *J. Nat. Prod. 67*, 1309–1313.

108. Graneli, E., and Johansson, N. (2003) Increase in the Production of Allelopathic Substances by *Prymnesium parvum* Cells Grown Under N- or P-Deficient Conditions, *Harmful Algae 2*, 135–145.

109. Yasumoto, T. (2001) The Chemistry and Biological Function of Natural Marine Toxins, *Chem. Rec. 1*, 228–242.

110. Igarashi, T., Satake, M., and Yasumoto, T. (1996) Prymnesin-2: A Potent Ichthyotoxic and Hemolytic Glycoside Isolated from the Red Tide Alga *Prymnesium parvum*, *J. Am. Chem. Soc. 118*, 479–480.

111. Igarashi, T., Satake, M., and Yasumoto, T. (1999) Structures and Partial Stereochemical Assignments for Prymnesin-1 and Prymnesin-2: Potent Hemolytic and Ichthyotoxic Glycosides Isolated from the Red Tide Alga *Prymnesium parvum*, *J. Am. Chem. Soc. 121*, 8499–8511.

112. Igarashi, T., Aritake, S., and Yasumoto, T. (1998) Biological Activities of Prymnesin-2 Isolated from a Red Tide Alga *Prymnesium parvum, Nat. Toxins. 6*, 35–41.

113. Hamilton-Miller, J.M.T. (1973) Chemistry and Biology of the Polyene Macrolide Antibiotics, *Bacteriol. Rev. 37*, 166–196.

114. Fenical, W. (1993) Chemical Studies of Marine Bacteria: Developing a New Resource, *Chem. Rev. 93*, 1673–1683.

115. Keseru, G.M., and di Nogra, M. (1995) The Chemistry of Natural Diarylheptanoids, in *Studies in Natural Products Chemistry* (Atta-ur-Rahman, ed.), Vol. 17, pp. 357–394, Elsevier Science, New York.

116. Roughley, P.J., and Whiting, D.A. (1971) Diarylheptanoids: The Problems of the Biosynthesis, *Tetrahedron Lett.,* 3741–3746.

117. Roughley, P.J., and Whiting, D.A. (1973) Experiments in the Biosynthesis of Curcumin, *J. Chem. Soc., Perkin Trans 1*, 2379–2388.

118. Inoue, T., Kenmochi, N., Furukawa, N., and Fujita, M. (1987) Biosynthesis of Acerogenin A, a Diarylheptanoid from *Acer nikoense, Phytochemistry 26*, 1409–1411.

119. Inoue, T. (1993) Constituents of *Acer nikoense* and *Myrica rubra*. On Diarylheptanoids, *Yakugaku Zasshi (in Japanese) 113*, 181–197.

120. Morikawa, T., Tao, J., Toguchida, I., Matsuda, H., and Yoshikawa, M. (2003) Structures of New Cyclic Diarylheptanoids and Inhibitors of Nitric Oxide Production from Japanese Folk Medicine *Acer nikoense*, *J. Nat. Prod. 66,* 86–91.

121. Matsuda, H., Morikawa, T., Tao, J., Ueda, K., and Yoshikawa, M. (2002) Bioactive Constituents of Chinese Natural Medicines. VII. Inhibitors of Degranulation in RBL-2H3 Cells and Absolute Stereostructures of Three New Diarylheptanoid Glycosides from the Bark of *Myrica rubra*, *Chem. Pharm. Bull. 50*, 208–215.

122. Tao, J., Morikawa, M., Toguchida, I., Ando, S., Matsuda, H., and Yoshikawa, M. (2002) Inhibitors of Nitric Oxide Production from the Bark of *Myrica rubra*: Structures of New Biphenyl Type Diarylheptanoid Glycosides and Taraxerane Type Triterpene, *Bioorg. Med. Chem. 10*, 4005–4012.

123. Lakshmi Niranjan Reddy, V., Ravinder, K., Srinivasulu, M., Venkateshwar Goud, T., Malla Reddy, S., Srujankumar, D., Prabhakar Rao, T., Suryanarayana Murty, U., and Venkateswarlu, Y. (2003) Two New Macrocyclic Diaryl Ether Heptanoids from *Boswellia ovalifoliolata*, *Chem. Pharm. Bull. 51*, 1081–1084.

124. Arcamone, F.M., Bertazzoli, C., Ghione, M., and Scotti, T.

(1959) Melanosporin and Elaiophylin, New Antibiotics from *Streptomyces melanosporus* (*Sive melanosporofaciens*) sp., *Gion. Microbiol. 7*, 207–216.

125. Arai, M. (1960) Azalomycins B and F, Two New Antibiotics II. Properties and Isolation, *J. Antibiot. 13*, 46–50.

126. Fiedler, H.P., Worner, W., Zahner, H., Kaiser, H.P., Keller-Schierlein, W., and Muller, A. (1981) Metabolic Products of Microorganisms. 200. Isolation and Characterisation of Niphithricins A and B, and Elaiophylin, Antibiotics Produced by *Streptomyces violaceoniger*, *J. Antibiot. 34*, 1107–1118.

127. Haydock, S.F., Mironenko, T., Ghoorahoo, H.I., and Leadlay, P.F. (2004) The Putative Elaiophylin Biosynthetic Gene Cluster in *Streptomyces* sp. DSM4137 Is Adjacent to Genes Encoding Adenosylcobalamin-Dependent Methylmalonyl CoA Mutase and to Genes for Synthesis of Cobalamin, *J. Biotechnol. 113*, 55–68.

128. Yamada, T., Minoura, K., and Numata, A. (2002) Halichoblelide, a Potent Cytotoxic Macrolide from a *Streptomyces* Species Separated from a Marine Fish, *Tetrahedron Lett. 43*, 1721–1724.

129. Erickson, K.L., Gustafson, K.R., Pannell, L.K., Beutler, J.A., and Boyd, M.R. (2002) New Dimeric Macrolide Glycosides from the Marine Sponge *Myriastra clavosa, J. Nat. Prod. 65,* 1303–1306.

130. Rao, M.R., and Faulkner, D.J. (2002) Clavosolides A and B, Dimeric Macrolides from the Philippines Sponge *Myriastra clavosa, J. Nat. Prod. 65*, 386–388.

131. Luo, Y., Feng, C., Tian, Y., and Zhang, G. (2002) Glycosides from *Dicliptera riparia*, *Phytochemistry 61*, 449–454.

132. Hamburger, M., Hostettmann, M., Stoeckli-Evans, H., Solis, P.N., Gupta, M.P., and Hostettmann, K. (1990) A Novel Type of Dimeric Secoiridoid Glycoside from *Lisianthius jefensis* Robyns et Elias, *Chim. Acta 73*, 1845–1852.

133. Mukhtara, N., Malik, A., Riaza, N., Iqbala, K., Tareen, R.B., Khana, S.N., Nawaza, S.A., Siddiquia, J., and Iqbal Choudharya, M.I. (2004) Pakistolides A and B, Novel Enzyme Inhibitory and Antioxidant Dimeric 4-(Glucosyloxy)benzoates from *Berchemia pakistanica, Helv. Chim. Acta 87*, 416–424.

134. Inoshiri, S., Sasaki, M., Kohda, H., Otsuka, H., and Yamasaki, K. (1987) Aromatic Glycosides from *Berchemia racemosa*, *Phytochemistry 26*, 2811–2814.

135. Okuda, T., Yoshida, T., and Hatano, T. (1993) Classification of Oligomeric Hydrolysable Tannins and Specificity of Their Occurrence in Plants, *Phytochemistry 32*, 507–521.

136. Yoshida, T., Hatano, T., and Ito, H. (2000) Chemistry and Function of Vegetable Polyphenols with High Molecular Weights, *Biofactors 13*, 121–125.

137. Chen, L.-G., Yen, K.-Y., Yang, L.-L., Hatano, T., Okuda, T., and Yoshida, T. (1999) Macrocyclic Ellagitannin Dimers, Cuphiins D_1 and D_2, and Accompanying Tannins from *Cuphea hyssopifolia, Phytochemistry 50*, 307–312.

138. Lee, M.H., Chiou, J.F., Yen, K.Y., Yang, L.L., Yen, K.Y., Hatano, T., Yoshida, T., and Okuda, T. (1997) Two Macrocyclic Hydrolysable Tannin Dimers from *Eugenia uniflora, Phytochemistry 44*, 1343–1349.

139. Yoshida, T., Chou, T., Shing, T., and Okuta, T. (1995) Oenotheins D, F and G, Hydrolysable Tannin Dimers from *Oenothera laciniata, Phytochemistry 40*, 565–561.

140. Yoshida, T., Chou, T., Haba, K., Okano, Y., Shingu, T., Miyamoto, K., Koshiura, R., and Okuda, T. (1989) Camelliin B and Nobotanin I, Macrocyclic Ellagitannin Dimers and Related Dimers, and Their Antitumor Activity, *Chem. Pharm. Bull. 37*, 3174–3176.

141. Yoshida, T., Chou, T., Matsuda, M., Yasuhara, T., Yazaki, K., Hatano, T., Nitta, A., and Okuda, T. (1991) Woodfordin D and Oenothein A, Trimeric Hydrolyzable Tannins of Macro-Ring Structure with Antitumor Activity, *Chem. Pharm. Bull. (Tokyo) 39*, 1157–1162.

142. Wang, C.C., Chen, L.G., and Yang, L.L. (1999) Antitumor Activity of Four Macrocyclic Ellagitannins from *Cuphea hyssopifolia, Cancer Lett. 140*, 195–200.

143. Wang, C.C., Chen, L.G., and Yang, L.L. (2000) Cuphiin D$_1$, the Macrocyclic Hydrolyzable Tannin Induced Apoptosis in HL-60 Cell Line, *Cancer Lett. 149*, 77–83.

144. Qian-Cutrone, J., Ueki, T., Huang, S., Mookhtiar, K.A., Ezekiel, R., Kalinowski, S.S., Brown, K.S., Golik, J., Lowe, S., Pirnik, D.M., *et al*. (1999) Glucolipsin A and B, Two New Glucokinase Activators Produced by *Streptomyces purpurogeniscleroticus* and *Nocardia vaccinii*, *J. Antibiot. 52*, 245–255.

145. Habib, E.S., Yokomizo, K., Suzuki, K., and Uyeda, M. (2001) Biosynthesis of Fattiviracin FV-8, an Antiviral Agent, *Biosci. Biotechnol. Biochem. 65*, 861–864.

146. Habib, E.S., Yokomizo, K., Nagao, K., Harada, S., and Uyeda, M. (2001) Antiviral Aactivity of Fattiviracin FV-8 Against Human Immunodeficiency Virus Type 1 (HIV-1), *Biosci. Biotechnol. Biochem. 65*, 683–685.

147. Tsunakawa, M., Komiyama, N., Tenmyo, O., Tomita, K., Kawano, K., Kotake, C., Konishi, M., and Oki, T. (1992) New Antiviral Antibiotics, Cycloviracins B1 and B2. I. Production, Isolation, Physico-chemical Properties and Biological Activity, *J. Antibiot. 45*, 1467–1471.

148. Tsunakawa, M., Kotake, C., Yamasaki, T., Moriyama, T., Konishi, M., and Oki, T. (1992) New Antiviral Antibiotics, Cycloviracins B1 and B2. II. Structure Determination, *J. Antibiot. 45*, 1472–1480.

149. Uyeda, M., Yokomizo, K., Miyamoto, Y., and Habib, E.E. (1998) Fattiviracin A1, a Novel Antiherpetic Agent Produced by *Streptomyces microflavus* Strain No. 2445. I. Taxonomy, Fermentation, Isolation, Physico-chemical Properties and Structure Elucidation, *J. Antibiot. 51*, 823–828.

150. Yokomizo, K., Miyamoto, Y., Nagao, K., Kumagae, E., Habib, E.S., Suzuki, K., Harada, S., and Uyeda, M. (1998) Fattiviracin A1, a Novel Antiviral Agent Produced by *Streptomyces microflavus* Strain No. 2445. II. Biological Properties, *J. Antibiot. 51*, 1035–1039.

151. Hyodo, T., Tsuchiya, Y., Sekine, A., and Amano, T. (1999) A Novel Antiviral Agent Produced by *Streptomyces*, Japanese Kokai Tokkyo Koho, Japanese Patent Application 11246587.

152. Takahashi, S., Hosoya, M., Koshino, H., and Nakata, T. (2003) Determination of Absolute Structure of Macroviracins by Chemical Synthesis, *Org. Lett. 5*, 1555–1558.

153. Kaneko, T., Sakamoto, M., Ohtani, K., Ito, A., Kasai, R., Yamasaki, K., and Padorina, W.G. (1995) Secoiridoid and Flavonoid Glycosides from *Gonocaryum calleryanum*, *Phytochemistry 39*, 115–120.

154. Mabberley, D.J. (1997) *The Plants-Book, a Portable Dictionary of the Vascular Plant*s, Oxford University Press, Oxford.

155. Chan, Y.Y., Leu, Y.L., Lin, F.W., Li, C.Y., Wu, Y.C., Shi, L.S., Liou, M.J., and Wu, T.S (1998) A Secoiridoid and Other Constituents of *Gonocaryum calleryanum*, *Phytochemistry 47*, 1073–1077.

156. Jansen, R., Kunze, B., Reichenbach, H., and Höfle, G. (2000) Antibiotics from Gliding Bacteria, LXXXVI. Apicularen A and B, Cytotoxic 10-Membered Lactones with a Novel Mechanism of Action from *Chondromyces* Species (Myxobacteria): Isolation, Structure Elucidation, and Biosynthesis, *Eur. J. Org. Chem. 6*, 913–919.

157. Kunze, B., Jansen, R., Sasse, F., Hofle, G., and Reichenbach. H. (1998) Apicularens A and B, New Cytostatic Macrolides from *Chondromyces* Species (Myxobacteria): Production, Physico-chemical and Biological Properties, *J. Antibiot. 51*, 1075–1080.

158. Rezanka, T., and Dembitsky, V.M. (2003) Ten Membered Substituted Cyclic 2-Oxecanone (decalactone) Derivatives from *Latrunculia corticata*, a Red Sea Sponge, *Eur. J. Org. Chem.*, 2144–2152.

159. Fogliani, B., Raharivelomanana, P., Bianchini, J.-P., Bouraïma-Madjèbi, S., and Hnawia, E. (2005) Bioactive Ellagitannins from *Cunonia macrophylla*, an Endemic Cunoniaceae from New Caledonia, *Phytochemistry 66*, 241–247.

160. Latté, K.P., and Kolodziej, H. (2000) Pelargoniins, New Ellagitannins from *Pelargonium reniforme*, *Phytochemistry 54*, 701–708.

161. Niemetz, R., Schilling, G., and Gross, G.G. (2003) Biosynthesis of the Dimeric Ellagitannin, Cornusiin E, in *Tellima grandiflora*, *Phytochemistry 64*, 109–114.

162. Seeram, N., Lee, R., Hardy, M., and Heber, D. (2005) Rapid Large Scale Purification of Ellagitannins from Pomegranate Husk, a By-product of the Commercial Juice Industry, *Separat. Purific. Technol. 41*, 49–55.

163. Park, E.K., Kim, M.S., Lee, S.H., Kim, K.H., Park, J.-Y., Kim, T.-H., Lee, I.-S., Woo, J.-T., Jung, J.-C., Shin, H.-I. *et al*. (2004) Furosin, an Ellagitannin, Suppresses RANKL-Induced Osteoclast Differentiation and Function Through Inhibition of MAP Kinase Activation and Actin Ring Formation, *Biochem. Biophys. Res. Commun. 325*, 1472–1480.

164. Notka, F., Meier, G., and Wagner, R. (2004) Concerted Inhibitory Activities of *Phyllanthus amarus* on HIV Replication *in vitro* and *ex vivo*, *Antiviral Res. 64,* 93–102.

165. Martino, V., Morales, J., Martínez-Irujo, J.J., Font, M., Monge, A., and Coussio, J. (2004) Two Ellagitannins from the Leaves of *Terminalia triflora* with Inhibitory Activity on HIV-1 Reverse Transcriptase, *Phytother. Res. 18*, 667–669.

166. Dutcher, J.D. (1963) Chemistry of the Amino Sugars Derived from Antibiotic Substances, *Adv. Carbohyd. Chem. 18*, 259–308.

167. Djerassi, C., and Halpern, O. (1957) The Structure of the Antibiotic Neomethymicin, *J. Am. Chem. Soc. 79*, 2022–2023.

168. Djerassi, C., and Halpern, O. (1958) Macrolide Antibiotics. VII. The Structure of Neomethymicin, *Tetrahedron 3*, 255–268.

169. Hong, J.S.J., Park, S.H., Choi, C.Y., Sohng, J.K., and Yoon, Y.J. (2004) New Olivosyl Derivatives of Methymycin/Pikromycin from an Engineered Strain of *Streptomyces venezuelae*, *FEMS Microbiol. Lett. 238*, 391–399.

170. Mertz, F.P., and Yao, R.C. (1990) *Saccharopolyspora spinosa* sp. nov. Isolated from Soil Collected in a Sugar Mill Rum Still, *Int. J. Syst. Bacteriol. 40*, 34–39.

171. Kirst, H.A., Michel, K.H., Martin, J.W., Creemer, L.C., Chio, E.H., Yao, R.C., Nakatsukasa, W.M., Boeck, L., Occolowitz, J.L., Paschal, J.W., *et al.* (1991) A83543A-D, Unique Fermentation Derived Tetracyclic Macrolides, *Tetrahedron Lett. 32*, 4839–4842.

172. De Amicis, C.V., Dripps, J.E., Hatten, C.J., and Karr, L. (1997) Physical and Biological Properties of the Spynosins: Novel Macrolide Pest-Control Agents from Fermentation, in *Phytochemicals for Pest Control* (Hedin, P.A., Hollingworth, R.M., Masler, E.P., Miyamoto, J., and Thompson, D.G., eds.), ACS Symposium Series 658, pp. 144–154, American Chemical Society, Washington, DC.

173. Kirst, H.A., Michel, K.H., Mynderse, J.S., Chio, E.H., Yao, R.C., Nakatsukasa, W.M., Boeck, L., Occolowitz, J.L., Paschal, J.W., Deeter, J.B., and Thompson, G.D. (1992) Discovery, Isolation, and Structure Elucidation of a Family of Structurally Unique Fermentation Derived Tetracyclic Macrolides, in *Synthesis and Chemistry of Agrochemicals III* (Baker, D.R., Fenyes, J.G., and Stevens, J.J., eds.), pp. 214–225, American Chemical Society, Washington, DC.

174. Sparks, T.C., Crouse, G.D., and Durst, G. (2001) Natural Products as Insecticides: The Biology, Biochemistry, and Quantitative Structure–Activity Relationships of Spinosyns and Spinosoids, *Pest Management Sci. 57*, 896–905.

175. Sparks, T.C., Thompson, G.D., Kirst, H.A., Hertline, M.B., Larson, L.L., Worden, T.V., and Thibault, S.T. (1998) Biological Activity of the Spinosyns, New Fermentation Derived Insect Control Agents, on Tobacco Budworm (Lepidoptera, Noctuidae) Larvae, *J. Econ. Entomol. 91*, 1277–1283.

176. Thompson, G.D., Dutton, R., and Sparks, T.C. (2000) Spinosad—A Case Study: An Example from a Natural Products Discovery Programme, *Pest Management Sci. 56*, 696–702.

177. Waldron, C., Matsushima, P., Rosteck, P.R., Jr., Broughton, M.C., Turner, J., Madduri, K., Crawford, K.P., Merlo, D.J., and Baltz, R.H. (2001) Cloning and Analysis of the Spinosad Biosynthetic Gene Cluster of *Saccharopolyspora spinosa*, *Chem. Biol. 8*, 487–499.

178. Gaisser, S., Martin, C.J., Wilkinson, B., Sheridan, R.M., Lill, R.E., Weston, A.J., Ready, S.J., Waldron, C., Crouse, G.D., Leadlay, P.F., and Staunton, J. (2002) Engineered Biosynthesis of Novel Spinosyns Bearing Altered Deoxyhexose Substituents, *Chem. Commun.*, 618–619.

179. Boeck, L., Chio, H., Eaton, T., Godfrey, O., Michel, K., Nakatsukasa, W., and Yao, R. (Eli Lilly). (1990) Lepicidin A from the Soil Microbe *Saccharopolyspora spinosa*, European Patent Application EP375 316; *Chem. Abstr. 114*, 80066 (1991).

180. Sone, H., Kigoshi, H., and Yamada, K. (1996) Aurisides A and B, Cytotoxic Macrolide Glycosides from the Japanese Sea Hare *Dolabella auricularia, J. Org. Chem. 61*, 8956–8960.

181. Tan, L.T., Marquez, B.L., and Gerwick, W.H. (2002) Lyngbouilloside, a Novel Glycosidic Macrolide from the Marine Cyanobacterium *Lyngbya bouillonii, J. Nat. Prod. 65*, 925–928.

182. Luesch, H., Yoshida, W.Y., Harrigan, G.G., Doom, J.P., Moore, R.E., and Paul, V.J. (2002) Lyngbyaloside B, a New Glycoside Macrolide from a Palauan Marine Cyanobacterium, *Lyngbya* sp., *J. Nat. Prod. 65*, 1945–1948.

183. Zampella, A., D'Auria, M.V., and Minale, L. (1997) Callipeltosides B and C, Two Novel Cytotoxic Glycoside Macrolides from a Marine Lithistida Sponge *Callipelta* sp., *Tetrahedron 53*, 3243–3248.

184. Zampella, A., D'Auria, M.V., Minale, L., Debitus, C., and Roussakis, C. (1996) Callipeltoside A: A Cytotoxic Aminodeoxy Sugar-Containing Macrolide of a New Type from the Marine Lithistida Sponge *Callipelta* sp., *J. Am. Chem. Soc. 118*, 11085–11088.

185. Yotsu-Yamada, M., Haddock, R.L., and Yasumoto, T. (1993) Polycavernoside A—A Novel Glycosidic Macrolide from the Red Alga *Polycavernosa tsudai* (*Gracilaria edulis*), *J. Am. Chem. Soc. 115,* 1147–1148.

186. Yotsu-Yamada, M., Seki, T., Paul, V., Hideo, H., and Yasumoto, T. (1995) 4 New Analogs of Polycavernoside A, *Tetrahedron Lett. 36*, 5563–5566.

187. Momose, I., Iinuma, H., Kinoshita, N., Momose, Y., Kunimoto, S., Hamada, M., and Takeuchi, T. (1999) Decatromicins A and B, New Antibiotics Produced by *Actinomadura* sp. MK73-NF4. I. Taxonomy, Isolation, Physico-chemical Properties and Biological Activities, *J. Antibiot. 52*, 781–786.

188. Momose, I., Hirosawa, S., Nakamura, H., Naganawa, H., Iinuma, H., Ikeda, D., and Takeuchi, T. (1999) Decatromicins A and B, New Antibiotics Produced by *Actinomadura* sp. MK73-NF4. II. Structure Determination, *J. Antibiot. 52*, 787–796.

189. Schroeder, D.R., Colson, K.L., Klohr, S.E., Lee, M.S., Matson, J.A., Brinen, L.S., and Clardy, J. (1996) Pyrrolosporin A, a New Antitumor Antibiotic from *Micromonospora* sp. C39217-R109-7. 2. Isolation, Physico-chemical Properties, Spectroscopic Study and X-Ray Analysis, *J. Antibiot. 49*, 865–872.

190. Lam, K.S., Hesler, G.A., Gustavson, D.R., Berry, R.L., Tomita, K., MacBeth, J.L., Ross, J., Miller, D., and Forenza, S. (1996) Pyrrolosporin A, a New Antitumor Antibiotic from *Micromonospora* sp. C39217-R109-7. 1. Taxonomy of Producing Organism, Fermentation and Biological Activity, *J. Antibiot. 49*, 860–864.

191. McGuire, J.M., Bunch, R.L., Anderson, R.C., Doaz, H.E., Flyun, E.H., Powell, H.M., and Smith, J.W. (1952) Ilotycin, a New Antibiotic, *Schweiz. Med. Wochenschr. 82*, 1064–1065.

192. Wiley, P.F., Gale, R., Pettinga, C.W., and Gerzon, K. (1957) Erythromycin. XII. The Isolation, Properties and Partial Structure of Erythromycin C, *J. Am. Chem. Soc. 79*, 6074–6077.

193. Maier, J., Martin, J.R., Egan, R.S., and Corcoran, J.W. (1977) Antibiotic Glycosides. 8. Erythromycin D, a New Macrolide Antibiotic, *J. Am. Chem. Soc. 99*, 1620–1622.

194. Martin, J.R., Devault, R.L., Sinclair, A.C., Stanaszek, R.S., and Johnson, P. (1982) A New Naturally Occurring Erythromycin: Erythromycin F, *J. Antibiot. 35*, 426–430.

195. Cachet, T., Roets, E., Hoogmartens, J., and Van Der Haeghe, H. (1975) Extension of the Erythromycin Biosynthetic Pathway: Isolation and Structure of Erythromycin E, *Tetrahedron 31*, 1985–1989.

196. Celmer, W.D., and Sobin, B.A. (1956) The Isolation of Two Synergistic Antibiotics from a Single Fermentation Source, *Antibiot. Annu. 1955–1956*, 437–441.

197. Celmer, W.D., Els, H., and Murai, K. (1958) Oleandomycin Derivatives, Preparation and Characterization, *Antibiot. Ann. 1957–1958*, 476–483.

198. Celmer, W.D. (1971) Stereochemical Problems in Macrolide Antibiotics, *Pure Appl. Chem. 28*, 413–453.

199. Brockmann, H. (1963) Anthracyclinones and Anthracyclines (rhodomycinone, pyrromycinone and their glycosides), *Fortschr. Chem. Org. Naturst. (in German) 21*, 121–182.

200. Brockmann, H., and Pfennig, N. (1953) The Production of Actinomycin by Counter Current Partition, *Hoppe Seylers Z. Physiol. Chem. 292*, 77–88.

201. Corbaz, R., Ettlinger, L., Kellerschierlein, W., and Zahner, H. (1957) Systematology of Actinomycetes. I. Streptomycetes with Rhodomycin-like Pigments, *Arch. Mikrobiol. (in German) 25*, 325–332.

202. Majer, J., McAlpine, J.B., Egan, R.S., and Corcoran, J.W. (1976) Antibiotic Glycosides. VII 10,11-Dihydropicromycin: Another Metabolite of *Streptomyces venezuelae*, *J. Antibiot. 29*, 769–770.

203. Stephens, V.C., Conine, J.W., and Murphy, H.W. (1959) Esters of Erythromycin. IV. Alkyl Sulfate Salts, *J. Am. Pharm. Assoc. 48*, 620–622.

204. Stephens, V.C., and Conine, J.W. (1959) Esters of Erythromycin. III. Esters of Low Molecular Weight Aliphatic Acids, *Antibiot Annu. 1958–1959*, 346–353.

205. Clark, R.K., Jr., Fricke, H.H., and Lanius, B. (1957) The Purification of Synnematin B by Ion Exchange Resins, *Antibiot. Annu. 1956–1957*, 749–754.

206. Philippon, A., Cluzel, R., and Soussy, C.J. (1995) Azithromycin: Critical Points, *Pathol Biol (Paris) (in French) 43*, 488–497.

207. Marquez, J., Murawski, A., Wagman, G.H., Jaret, R.S., and Reimann, H. (1969) Isolation, Purification and Preliminary Characterization of Megalomicin, *J. Antibiot. 22*, 259–264.

208. Takasawa, S., Kawamoto, I., Okachi, R., Machida, Y., and Nara, T. (1974) A New Antibiotic, XK-46, *J. Antibiot. 27*, 502–506.

209. Wagman, G.H., and Weinstein, M.J. (1980) Antibiotic from *Micromonospora*, *Annu. Rev. Microbiol. 34*, 537–557.

210. Egan, R.S., and Martin, J.R. (1970) Structure of Lankamycin, *J. Am. Chem. Soc. 92*, 4129–4130.

211. Muntwyler, R., and Keller-Schierlein, W. (1972) Metabolic Products of Microorganisms. Stereochemistry of Lankamycin, *Helv. Chim. Acta (in German) 55*, 460–467.

212. Roncari, G., and Keller-Schierlein, W. (1966) Metabolic Products of Microorganisms, *Helv. Chim. Acta (in German) 49*, 705–711.

213. Namiki, S., Omura, S., Nakayoshi, H., and Sawada, J. (1969) Studies on the Antibiotics from *Streptomyces spinichromogenes* var. *kujimyceticus*. I. Taxonomic and Fermentation Studies with *Streptomyces spinichromogenes* var. *kujimyceticus*, *J. Antibiot. 22*, 494–499.

214. Omura, S., Muro, T., Namiki, S., Shibata, M., Sawada, and J. (1969) Studies on the Antibiotics from *Streptomyces spinichromogenes* var. *kujimyceticus*. 3. The Structure of Kujimycin A and Kujimycin B, *J. Antibiot. 22*, 629–634.

215. Martin, J.R., Egan, R.S., Goldstein, A.W., Mueller, S.L., Kellerschierlein, W., Mitscher, L.A., and Foltz, R.L. (1976) 3′-De-*O*-methyl-2′,3′-anhydro-lankamycin, a New Macrolide Antibiotic from *Streptomyces violaceoniger*, *Helv. Chim. Acta 59*, 1886–1894.

216. Martin, J.R., Egan, R.S., Goldstein, A.W., Stanaszek, R.S., Tadanier, J. and Kellerschierlein, W. (1977) Minor Lankamycin-Related Antibiotics from *Streptomyces violaceoniger*, *Helv. Chim. Acta 60*, 2559–2565.

217. Arnoux, B., Pascard, C., Raynaud, L., and Lunel, J. (1980) 23672 RP, a New Macrolide Antibiotic from *Streptomyces chryseus*. Mass Spectrometry Study and X-Ray Structure Determination, *J. Am. Chem. Soc. 102*, 3605–3608.

218. Klein, D., Braekman, J.C., Daloze, D., Hoffmann, L., and Demoulin, V. (1997) Lyngbyaloside, a Novel 2,3,4-Tri-*O*-methyl-6-deoxy-α-mannopyranoside Macrolide from *Lyngbya bouillonii* (Cyanobacteria), *J. Nat. Prod. 60*, 1057–1059.

219. Hegde, V.R., Patel, M.G., Gullo, V.P., Ganguly, A.K., Sarre, O., Puar, M.S., and McPhail, A.T. (1990) Macrolactams: A New Class of Antifungal Agents, *J. Am. Chem. Soc. 112*, 6403–6405.

220. Hegde, V.R., Patel, M.G., Gullo, V.P., and Puar, M.S. (1991) SCH-38518 and SCH-39185—2 Novel Macrolactam Antifungals, *J. Chem. Soc. Chem. Commun.*, 810–812.

221. Naruse, N., Tenmyo, O., Kawano, K., Tomita, K., Ohgusa, N., Miyaki, T., Konishi, M., and Oki, T. (1991) Fluvirucin-A1, Fluvirucin-A2, Fluvirucin-B1, Fluvirucin-B2, Fluvirucin-B3, Fluvirucin-B4, and Fluvirucin-B5, New Antibiotics Active Against Influenza A Virus. 1. Production, Isolation, Chemical Properties and Biological Activities, *J. Antibiot. 44*, 733–740.

222. Naruse, N., Tsuno, T., Sawada, Y., Konishi, M., and Oki, T. (1991) Fluvirucin-A1, Fluvirucin-A2, Fluvirucin-B1, Fluvirucin-B2, Fluvirucin-B3, Fluvirucin-B4, and Fluvirucin-B5, New Antibiotics Active Against Influenza A Virus. 2. Structure Determination, *J. Antibiot. 44*, 741–755.

223. Naruse, N., Konishi, M., Oki, T., Inouye, Y., and Kakisawa H. (1991) Fluvirucin-A1, Fluvirucin-A2, Fluvirucin-B1, Fluvirucin-B2, Fluvirucin-B3, Fluvirucin-B4 and Fluvirucin-B5, New Antibiotics Active Against Influenza A Virus. 3. The Stereochemistry and Absolute Configuration of Fluvirucin-A1, *J. Antibiot. 44*, 756–761.

224. Tomita, K., Oda, N., Hoshino, Y., Ohkusa, N., and Chikazawa, H. (1991) Fluvirucin-A1, Fluvirucin-A2, Fluvirucin-B1, Fluvirucin-B2, Fluvirucin-B3, Fluvirucin-B4 and Fluvirucin-B5, New Antibiotics Active Against Influenza-A Virus. 4. Taxonomy of the Producing Organisms, *J. Antibiot. 44*, 940–948.

225. Ui, H., Imoto, M., and Umezawa, K. (1995) Inhibition of Phosphatidylinositol Specific Phospholipase C Activity by Fluvirucin B2, *J. Antibiot. 48*, 387–390.

226. Lacey, E., Gill, J.H., Power, M.L., Rickards, R.W., O'Shea, M.G., and Rothshild, J.M. (1995) Bafilolides, Potent Inhibitors of the Motility and Development of the Free-Living Stages of Parasitic Nematodes, *Int. J. Parasitol. 25*, 349–357.

227. Umehara, K., Nemoto, K., Ohkubo, T., Miyase, T., Degawa, M., and Noguchi, H. (2004) Isolation of a New 15-Membered Macrocyclic Glycolipid Lactone, Cuscutic Resinoside A from the Seeds of *Cuscuta chinensis*: A Stimulator of Breast Cancer Cell Proliferation, *Planta Med. 70*, 299–304.

228. Yates, D.M., Portillo, V., and Wolstenholme, A.J. (2003) The Avermectin Receptors of *Haemonchus contortus* and *Caenorhabditis elegans*, *Int. J. Parasitol. 33*, 1183–1193.

229. Wilson, M.L. (1993) Avermectins in Arthropod Vector Management—Prospects and Pitfalls, *Parasitol. Today 9*, 83–87.

230. Yen, T.H., and Lin, J.L. (2004) Acute Poisoning with Emamectin Benzoate, *J. Toxicol. Clin. Toxicol. 42*, 657–661.

231. Drinyaev, V.A., Mosin, V.A., Kruglyak, E.B., Novik, T.S., Sterlina, T.S., Ermakova, N.V., Kublik, L.N., Levitman, M.K., Shaposhnikova, V.V., and Korystov, Y.N. (2004) Antitumor Effect of Avermectins, *Eur. J. Pharmacol. 501*, 19–23.

232. Elegami, A.A., Bates, C., Gray, A.I., Mackay, S.P., Skellern, G.G., and Waigh, R.D. (2003) Two Very Unusual Macrocyclic Flavonoids from the Water Lily *Nymphaea lotus*, *Phytochemistry 63*, 727–731.

233. El Ghazali, G.E.B., El Tohami, M.S., and Elegami, A.A. (1994) *Medicinal Plants of the White Nile Provinces*, pp. 76–90, Khartoum University Press, Khartoum, Sudan.

234. Elegami, A.A., Almagboul, A.Z., Omer, M.E.A., and El Tohami, M.S. (2001) Sudanese Plants Used in Folkloric Medicine: Screening for Antibacterial Activity. Part X, *Fitoterapia 72*, 810–817.

235. Cosar, C. (1956) Study of Acute Toxicity of Spiramycin in Mice and Its Activity in Experimental Infections of the Same, *Therapie (in French) 11*, 324–328.

236. Chain, E.B. (1958) Chemistry and Biochemistry of Antibiotics, *Annu. Rev. Biochem. 27*, 167–222.

237. Sugimoto, C., Mitani, K., Nakazawa, M., Sekizaki, T., Terakado, N., and Isayama, Y. (1983) *In vitro* Susceptibility of *Haemophilus somnus* to 33 Antimicrobial Agents, *Antimicrob. Agents Chemother. 23*, 163–165.

238. Lounes, A., Lebrihi, A., Benslimane, C., Lefrebrve, G., and Germain, P. (1995) Effect of Nitrogen/Carbon Ratio on the Specific Production Rate of Spiramicin by *Streptomyces ambofaciens, Process Biochem. 31*, 13–20.

239. Oka, H., Harada, K., Suzuki, M., and Ito, Y. (2000) Separation of Spiramycin Components Using High-Speed Counter-Current Chromatography, *J. Chromatogr. 903*, 93–98.

240. Stark, W.M., Daily, W.A., and McGuire, J.M. (1961) A Fermentation Study of the Biosynthesis of Tylosin in Synthetic Media, *Rend. Ist. Super. Sanita 1*, 340–354.

241. Hamil, R.L., Haney, M.E., Stamper, M., and Wiley, P.F. (1961) Tylosin, a New Antibiotic. II. Isolation, Properties, and Preparation of Desmycosin, a Microbiologically Active Degradation Product, *Antibiot. Chemother. 11,* 328–334.

242. Baltz, R.H., Seno, E.T., Stonessifer, J., and Wild, G.M. (1983) Biosynthesis of the Macrolide Antibiotic Tylosin. A Preferred Pathway from Tylactone to Tylosin, *J. Antibiot. 36*, 131–141.

243. Grafe, U., Bocker, H., Reinhardt, G., Tkocz, H., and Thrum, H. (1973) Biosynthesis of the Macrolide Antibiotic A 6599 by *Streptomyces hydroscopicus* JA 6599 and Activity of the NADP-Dependent Metabolism, *Z. Allg. Mikrobiol. (in German) 13*, 115–129.

244. Hata, T., Yamamoto, H., Matsumae, A., and Ito, S. (1953) Leucomycin, a New Antibiotic, *J. Antibiot. 6*, 87–89.

245. Osono, T., Oka, Y., Watanabe, S., Okami, Y., and Ishida, H. (1967) A New Antibiotic, Josamycin I. Isolation and Physicochemical Characteristics, *J. Antibiot. 20*, 174–180.

246. Muroi, M., Izawa, M., and Kishi, T. (1972) Structures of Maridomycin 1,3,4,5 and 6 Macrolide Antibiotics, *Experientia 28*, 129–131.

247. Muroi, M., Izawa, M., Ono, H., Higashide, E., and Kishi, T. (1972) Isolation of Maridomycins and Structure of Maridomycin II, *Experientia 28*, 501–502.

248. Muroi, M., Izawa, M., Ono, H., Higashide, E., and Kishi, T. (1972) Isolation of Maridomycins and Structure of Maridomycin II, *Experientia 28*, 878–880.

249. Ono, H., Hasegawa, T., Higashide, E., and Shibata, M. (1973) Maridomycin, a New Macrolide Antibiotic. I. Taxonomy and Fermentation, *J. Antibiot. 26*, 191–198.

250. Muroi, M., Izawa, M., Asai, M., Kishi, T., and Mizuno, K. (1973) Maridomycin, a New Macrolide Antibiotic. II. Isolation and Characterization, *J. Antibiot. 26*, 199–205.

251. Muroi, M., Izawa, M., and Kishi, T. (1976) Maridomycin, a New Macrolide Antibiotic. X. The Structure of Maridomycin II, *Chem. Pharm. Bull. 24*, 450–462.

252. Muroi, M., Izawa, M., and Kishi, T. (1976) Maridomycin, a New Macrolide Antibiotic. XI. The Structures of Maridomycin Components, *Chem. Pharm. Bull. 24*, 463–478.

253. Suzuki, M., Takamori, I., Kinumaki, A., Sugawara, Y., and Okuda, T. (1971) The Structures of Antibiotics YL-704 A and B, *Tetrahedron Lett. 12*, 435–438.

254. Suzuki, M., Takamori, I., Kinumaki, A., Sugawara, Y., and Okuda, T. (1971) The Structure of Antibiotics YL-704 C1, C2 and W1, *J. Antibiot. 24*, 904–906.

255. Umino, K., Takeda, N., Ito, Y., and Okuda, T. (1974) Studies on Pentenomycins. II. The Structures of Pentenomycin I and II, New Antibiotics, *Chem. Pharm. Bull. 22*, 1233–1238.

256. Kinumaki, A., Takamori, I., Sugawara, Y., Nagahama, N., Suzuki, M., Egawa, Y., Sakuraza, M., and Okuda, T. (1974) Studies on the Macrolide Antibiotic YL-704 Complex. 2. The Structures of New Macrolide Antibiotics YL-704 A1 and B1, *J. Antibiot. 27*, 102–107.

257. Kinumaki, A., Takamori, I., Sugawara, Y., Suzuki, M., and Okuda, T. (1974) Studies on the Macrolide Antibiotic YL-704 Complex. 3. The Structures of New Macrolide Antibiotics YL-704 A1 and B1, *J. Antibiot. 27*, 107–116.

258. Kinumaki, A., Takamori, I., Sugawara, Y., Suzuki, M., and Okuda, T. (1974) Studies on the Macrolide Antibiotic YL-704 Complex. 4. The Structures of New Macrolide Antibiotics YL-704 A1 and B1, *J. Antibiot. 27*, 117–126.

259. Niida, T., Tsuruoka, T., Ezaki, N., Sugawara, Y., Akita, E., and Inouye, S. (1971) A New Antibiotic, SF-837, *J. Antibiot. 24*, 319–320.

260. Inouye, S., Tsuruoka, T., Shomura, T., Ezaki, N., and Niida, T. (1971) Studies on Antibiotic SF-837, a New Antibiotic. II. Chemical Structure of Antibiotic SF-837, *J. Antibiot. 24*, 460–475.

261. Omoto, S., Inouye, S., and Niida, T. (1971) Separation of Aminoglycosidic Antibiotics by Gas–Liquid Chromatography, *J. Antibiot. 24*, 430–434.

262. Inouye, S., Shomura, T., Tsuruoka, T., Omoto, S., and Niida, T. (1972) Isolation and Structure of Two Metabolites of a Macrolide Antibiotic, SF-837 Substance, *Chem. Pharm. Bull. 20*, 2366–2371.

263. Tsuruoka, T., Inouye, S., Shomura, T., Ezaki, N., and Niida, T. (1971) Studies on Antibiotic SF-837, a New Antibiotic. IV. Structures of Antibiotics SF-837 A2, A3 and A4, *J. Antibiot. 24*, 526–536.

264. Huber, G., Wallhaeusser, K.H., Fries, L., Steigler, A., and Weidenmueller, H.L. (1962) Niddamycin, a New Macrolide Antibiotic, *Arzneimittelforschung (in German) 12*, 1191–1195.

265. Masamune, S., Bates, G.S., and Corcoran, J.W. (1977) Macrolides. Recent Progress in Chemistry and Biochemistry, *Angew. Chem. Int. Ed. Eng. 16*, 585–607.

266. Sawada, Y., Tsuno, T., Miyaki, T., Naito, T., and Oki, T. (1989) New Cirramycin Family Antibiotics F-1 and F-2. Selection of Producer Mutants, Fermentation, Isolation, Structural Elucidation and Antibacterial Activity, *J. Antibiot. 42*, 242–253.

267. Tanba, H., Kawasaki, T., Mitadera, Y., Soga, H., Shinkai, H., Otsuki, N., Sakakibara, M., and Tatsuta, K. (1988) M119-A, A Novel Macrolide Antibiotic, *Jpn. J. Antibiot. (in Japanese) 41*, 604–605.

268. Brufani, M., and Keller-Schierlein, W. (1966) Metabolic Products of Microorganisms, 54. On the Sugar Building Stones of Angolamycin: L-Mycarose, D-Mycinose and D-Angolosamine, *Helv. Chim. Acta (in German) 49*, 1962–1970.

269. Shimi, I.R., Shoukry, S., and Ali, F.T. (1979) Staphcoccomycin, a New Basic Macrolide Antibiotic, *J. Antibiot. 32*, 1248–1255.

270. Koshiyama, H., Okanishi, M., Ohmori, T., Miyaki, T., Tsukiura, H., Matsuzaki, M., and Kawaguchi, H. (1963) Cirramycin, a New Antibiotic, *J. Antibiot. 16*, 59–66.

271. Koshiyama, H., Tsukiura, H., Fujisawa, K., Konishi, M., and Hatori, M. (1969) Studies on Cirramycin A1. I. Isolation and Characterization of Cirramycin A1, *J. Antibiot. 22*, 61–64.

272. Tsukiura, H., Konishi, M., Saka, M., Naito, T., and Kawaguchi, H. (1969) Studies on Cirramycin A1. 3. Structure of Cirramycin A1, *J. Antibiot. 22*, 89–99.

273. Wagman, G.H., Waitz, J.A., Marquez, J., Murawaski, A., Oden, E.M., Testa, R.T., and Weinstein, M.J. (1972) A New Micromonospora Produced Macrolide Antibiotic, Rosamicin, *J. Antibiot. 25*, 641–646.

274. Puar, M.S., and Schumacher, D. (1990) Novel Macrolides from *Micromonospora rosaria*, *J. Antibiot. 43*, 1497–1501.

275. Furumai, T., Maezawa, I., Matsuzawa, N., Yano, S., Yamaguchi, T., Takeda, K., and Okuda, T. (1977) Macrolide Antibiotics M-4365 Produced by Micromonospora. I. Taxonomy, Production, Isolation, Characterization and Properties, *J. Antibiot. 30*, 443–449.

276. Kinumaki, A., Harada, K., Suzuki, T., Suzuki, M., and Okuda, T. (1977) Macrolide Antibiotics M-4365 Produced by Micromonospora. II. Chemical Structures, *J. Antibiot. 30*, 450–454.

277. Morin, R.B., Gorman, M., Hamil, R.L., and Demarco, P.V. (1970) The Structure of Tylosin, *Tetrahedron Lett. 11*, 4737–4740.

278. Baltz, R.H., and Seno, E.T. (1981) Properties of *Streptomyces fradiae* Mutants Blocked in Biosynthesis of the Macrolide Antibiotic Tylosin, *Antimicrob. Agents Chemother. 20*, 214–225.

279. Kirst, H.A., Wild, G.M., Baltz, R.H., Seno, E.T., Hamill, R.L., Paschal, J.W., and Dorman, D.E. (1983) Elucidation of Structure of Novel Macrolide Antibiotics Produced by Mutant Strains of *Streptomyces fradiae*, *J. Antibiot. 36*, 376–382.

280. Kirst, H.A., Wild, G.M., Baltz, R.H., Hamill, R.L., Ott, J.L., Counter, F.T., and Ose, E.E. (1982) Structure–Activity Studies Among 16-Membered Macrolide Antibiotics Related to Tylosin, *J. Antibiot. 35*, 1675–1682.

281. Hayashi, M., Kinoshita, K., Sudate, Y., Satoi, S., Sakakibara, H., Harada, K., and Suzuki, M. (1983) Mycinamicins, New Macrolide Antibiotics. VII. Structures of Minor Components, Mycinamicin VI and VII, *J. Antibiot. 36*, 175–178.

282. Satoi, S., Muto, N., Hayashi, M., Fujii, T., and Otani, M. (1980) Mycinamicins, New Macrolide Antibiotics. I. Taxonomy, Production, Isolation, Characterization and Properties, *J. Antibiot. 33*, 364–376.

283. Hayashi, M., Ohno, M., Katsumata, S., Satoi, S., Harada, K.I., Takeda, M., and Suzuki, M. (1981) Mycinamicins, New Macrolide Antibiotics. IV. Structure of Mycinamicin III, *J. Antibiot. 34*, 276–281.

284. Kinoshita, K., Satoi, S., Hayashi, M., Harada, K., Suzuki, M., and Nakatsu, K. (1985) Mycinamicins, New Macrolide Antibiotics. VIII. Chemical Degradation and Absolute Configuration of Mycinamicins, *J. Antibiot. (Tokyo) 38*, 522–526.

285. Woo, P.W.K., Dion, H.W., and Bartz, Q.R. (1961) Chemistry of Chalcose, a 3-Methoxy-4,6-dideoxyhexose, *J. Am. Chem. Soc. 83*, 3352–3353.

286. Woo, P.W.K., Dion, H.W., and Bartz, Q.R. (1962) A Degradation Product of Chalcomycin: 2,4-Dimethyl-3-chalcosyloxy-6-oxoheptanoic Acid, *J. Am. Chem. Soc. 84*, 1512–1513.

287. Woo, P.W.K., Dion, H.W., and Johnson, L.F. (1962) The Stereochemistry of Chalcose, A Degradation Product of Chalcomycin, *J. Am. Chem. Soc. 84*, 1066–1067.

288. Lefemine, D.V., Barbatschi, F., Dann, M., Thomas, S.O., Kunstmann, M.P., Mitscher, L.A., and Bohonos, N. (1963) Neutramycin, a New Neutral Macrolide Antibiotic, *Antimicrob. Agents Chemother. 9*, 41–44.

289. Kunstmann, M.P., and Mitscher, L.A. (1965) Some Additional Observations on the Chemical Nature of Neutramycin, *Experientia 21*, 372–373.

290. Mitscher, L.A., and Kunstmann, M.P. (1969) The Structure of Neutramycin, *Experientia 25*, 12–13.

291. Hauske, J.R., Dibrino, J., Guadliana, M., and Kostek, G. (1986) Structure Elucidation of a New Neutral Macrolide Antibiotic, *J. Org. Chem. 51*, 2808–2814.

292. Kunstmann, M.P., Mitscher, L.A., and Patterson, E.L. (1964) Aldgamycin E, a New Neutral Macrolide Antibiotic, *Antimicrob. Agents Chemother. 10*, 87–90.

293. Mizobuchi, S., Mochizuki, J., Soga, H., Tanba, H., and Inoue, H. (1986) Aldgamycin G, a New Macrolide Antibiotic, *J. Antibiot. 39*, 1776–1778.

294. Chatterjee, S., Reddy, G.C.S., Franco, C.M.M., Rupp, R.H., Ganguli, B.N., Fehlhaber, H.W., and Kogler, H. (1987) Swalpamycin, a New Macrolide Antibiotic. II. Structure Elucidation, *J. Antibiot. 40*, 1368–1374.

295. Franco, C.M.M., Gandli, J.N., Chatterjee, S., and Ganguli, B.N. (1987) Swalpamycin, a New Macrolide Antibiotic. I. Taxonomy of the Producing Organism, Fermentation, Isolation and Biological Activity, *J. Antibiot. 40*, 1361–1367.

296. Park, H.-R., Furihata, K., Hayakawa, Y., and Shin-ya, K. (2002) Versipelostatin, a Novel GRP78/Bip Molecular Chaperone Down-regulator of Microbial Origin, *Tetrahedron Lett. 43*, 6941–6945.

297. Roy, B., and Lee, A.S. (1999) The Mammalian Endoplasmic Reticulum Stress Response Element Consists of an Evolutionarily Conserved Tripartite Structure and Interacts with a Novel Stress-Inducible Complex, *Nucleic Acids Res. 27*, 1437–1443.

298. Sausville, E.A. (2004) Versipelostatin: Unfolding an Unsweetened Death, *J. Natl. Cancer Instit. 96*, 1266–1267.

299. Chijiwa, S., Park, H.-R., Furihata, K., Ogata, M., Endo, T., Kuzuyama, T., Hayakawa, Y., and Shin-ya, K. (2003) Biosynthetic Studies of Versipelostatin, a Novel 17-Membered α-Tetronic Acid Involved Macrocyclic Compound Isolated from *Streptomyces versipellis*, *Tetrahedron Lett. 44*, 5897–5900.

300. Kitagawa, I., Ohashi, K., Baek, N.I., Sakagami, M., Yoshikawa, M., and Shibuya, H. (1997) Indonesian Medicinal Plants. XIX. 1) Chemical Structures of Four Additional Resin Glycosides, Mammosides A, B, H1, and H2, from the Tuber of *Merremia mammosa* (Convolvulaceae), *Chem. Pharm. Bull. 45*, 786–794.

301. Omura, S., Tanaka, Y., Nakagawa, A., Iwai, Y., Inoue, M., and Tanaka, H. (1982) Irumamycin, a New Antibiotic Active Against Phytopathogenic Fungi, *J. Antibiot. 35*, 256–257.

302. Fourati-Ben Fguira, L., Fotso, S., Ben Ameur-Mehdi, R., Mellouli, L., and Laatsch, H. (2005) Purification and Structure Elucidation of Antifungal and Antibacterial Activities of Newly Isolated *Streptomyces* sp. strain US80, *Res. Microbiol.*, in press.

303. Kinashi, H., Someno, K., and Sakaguchi, K. (1984) Isolation and Characterization of Concanamycins A, B and C, *J. Antibiot. 37*, 1333–1343.

304. Malikova, M., Shi, J., and Kandror, K.V. (2004) V-type ATPase Is Involved in Biogenesis of GLUT4 Vesicles, *Am. J. Physiol. Endocrinol. Metab. 287*, E547–E552.

305. Hochlowski, J.E., Swanson, S.J., Ranfranz, L.M., Whittern, D.N., Buko, A.M., and McAlpine, J.B. (1987) Tiacumicins, a Novel Complex of 18-Membered Macrolide Antibiotics. II. Isolation and Structure Determination, *J. Antibiot. 40*, 575–588.

306. Theriault, R.J., Karwowski, J.P., Jackson, M., Girolami, R.L., Sunga, G.N., Vojtko, C.M., and Coen, L.J. (1987) Tiacumicins, a Novel Complex of 18-Membered Macrolide Antibiotics. I. Taxonomy, Fermentation and Antibacterial Activity, *J. Antibiot. 40*, 567–574.

307. Coronelli, C., White, R.J., Lancini, G.C., and Parenti, F. (1975) Lipiarmycin, A New Antibiotic from Actinoplanes. II. Isolation, Chemical Biological and Biochemical Characterization, *J. Antibiot. 28*, 253–259.

308. Parenti, F., Pagan, H., and Beretta, G. (1975) Lipiarmycin, a New Antibiotic from Actinoplanes. I. Description of the Producer Strain and Fermentation Studies, *J. Antibiot. 28*, 247–252.

309. Omura, S., Imamura, N., Oiwa, R., Kuga, H., Iwata, R., Masuma, R., and Iwai, Y. (1986) Clostomicins, New Antibiotics Produced by *Micromonospora echinospora* subsp. *armeniaca* subsp. nov. I. Production, Isolation and Physicochemical and Biological Properties, *J. Antibiot. 39*, 1407–1412.

310. Sergio, S., Pirali, G., White, R., and Parenti, F. (1975) Lipiarmycin, a New Antibiotic from Actinoplanes. III. Mechanism of Action, *J. Antibiot. 28*, 543–549.

311. Bloor, S.J. (1998) A Macrocyclic Anthocyanin from Red/Mauve Carnation Flowers, *Phytochemistry 49*, 225–228.

312. Nakayama, M., Koshioka, M., Yoshida, H., Kan, Y., Fukui, Y., Koike, A., and Yamaguchi, M.-A. (2000) Cyclic Malyl Anthocyanins in *Dianthus caryophyllus*, *Phytochemistry 55*, 937–939.

313. Gonnet, J.-F., and Fenet, B. (2000) "Cyclamen Red" Colors Based on a Macrocyclic Anthocyanin in Carnation Flowers, *J. Agric. Food Chem. 48*, 22–26.

314. Fukui, Y., Tanaka, Y., Kusumi, T., Iwashita, T., and Nomoto, K. (2003) A Rationale for the Shift in Colour Towards Blue in Transgenic Carnation Flowers Expressing the Flavonoid 3′,5′-Hydroxylase Gene, *Phytochemistry 63*, 15–23.

315. Shindo, K., Kamishohara, M., Odagawa, A., Matsuoka, M., and Kawai, H. (1993) Vicenistatin, a Novel 20-Membered Macrocyclic Lactam Antitumor Antibiotic, *J. Antibiot. 46*, 1076–1081.

316. Ryu, G., Choi, W.C., Hwang, S., Yeo, W.H., Lee, C.S., and Kim, S.K. (1999) Tetrin C, a New Glycosylated Polyene Macrolide Antibiotic Produced by *Streptomyces* sp. GK9244, *J. Nat. Prod. 62*, 917–919.

317. Pathirana, C., Tapiolas, D., Jensen, P.R., Dwight, R., and Fenical, W. (1991) Structure Determination of Maduralide: A New 24-Membered Ring Macrolide Glycoside Produced by a Marine Bacterium (Actinomycetales), *Tetrahedron Lett. 32*, 2323–2326.

318. Struyk, A.P., Hoette, I., Drost, G., Waisvisz, J.M., Van Eek, T., and Hoogerheide, J.C. (1957) Pimaricin, a New Antifungal Antibiotic, *Antibiot. Annu. 5*, 878–885.

319. Gil, J.A., and Martin, J.F. (1997) Polyene Antibiotics, in *Biotechnology of Antibiotics*, 2nd edn. (Strohl, W.R., ed.), pp. 551–576, Marcel Dekker, New York.

320. Mendes, M.V., Recio, E., Fouces, R., Luiten, R., Martín, J.F., and Aparicio, J.F. (2001) Engineered Biosynthesis of Novel Polyenes: A Pimaricin Derivative Produced by Targeted Gene Disruption in *Streptomyces natalensis*, *Chem. Biol. 8*, 635–644.

321. Okami, Y., Utahara, R., Nakamura, S., and Umezawa, H. (1954) Studies on Antibiotic Actinomycetes. IX. On Streptomyces Producing a New Antifungal Substance Mediocidin and Antifungal Substances of Fungicidin–Rimocidin–Chromin Group, Eurocidin Group and Trichomycin–Ascosin–Candicidin Group, *J. Antibiot. 7*, 98–103.

322. Osato, T., Ueda, M., Fukuyama, S., Yagishita, K., Okami, Y., and Umezawa, H. (1955) Production of Tertiomycin (a new antibiotic substance), Azomycin and Eurocidin by *S. eurocidicus*, *J. Antibiot. 8*, 105–109.

323. Nakagomi, K., Takeuchi, M., Tanaka, H., Tomizuka, N., and Nakajima, T. (1990) Studies on Inhibitors of Rat Mast Cell Degranulation Produced by Microorganisms. I. Screening of Microorganisms, and Isolation and Physico-chemical Properties of Eurocidins C, D and E, *J. Antibiot. (Tokyo) 43*, 462–469.

324. Tanaka, Y., Komaki, H., Yazawa, K., Mikami, Y., Nemoto, A., Tojyo, T., Kadowaki, K., Shigemori, H., and Kobayashi, J. (1997) Brasilinolide A, a New Macrolide Antibiotic Produced by *Nocardia brasiliensis*: Producing Strain, Isolation and Biological Activity, *J. Antibiot. 50*, 1036–1041.

325. Mikami, Y., Komaki, H., Imai, T., Yazawa, K., Nemoto, A., Tanaka, Y., and Graefe, U. (2000) A New Antifungal Macrolide Component, Brasilinolide B, Produced by *Nocardia brasiliensis, J. Antibiot. 53*, 70–74.

326. Komatsu, K., Tsuda, M., Tanaka, Y., Mikami, Y., and Kobayashi, J. (2004) Absolute Stereochemistry of Immunosuppressive Macrolide Brasilinolide A and Its New Congener Brasilinolide C, *J. Org. Chem. 69*, 1535–1541.

327. Kong, F., Liu, D.Q., Nietsche, J., Tischler, M., and Carter, G.T. (1999) Colubricidin A, a Novel Macrolide Antibiotic from a *Streptomyces* sp., *Tetrahedron Lett. 40*, 9219–9223.

328. Brautaset, T., Sekurova, O.N., Sletta, H., Ellingsen, T.E., Strøm, A.R., Valla, S., and Zotchev, S.B. (2000) Biosynthesis of the Polyene Antifungal Antibiotic Nystatin in *Streptomyces noursei* ATCC 11455: Analysis of the Gene Cluster and Deduction of the Biosynthetic Pathway, *Chem. Biol. 7*, 395–403.

329. Oura, M., Sternberg, T.H., and Wright, E.T. (1955–1956) A New Antifungal Antibiotic, Amphotericin B, *Antibiot. Annu. 3*, 566–573.

330. Gallis, H.A., Drew, R.H., and Pickard, W.W. (1990) Amphotericin B: 30 Years of Clinical Experience, *Rev. Infect. Dis. 12*, 308–329.

331. Lechevalier, H. (1953) Fungicidal Antibiotics, Produced by Actinomycetes, Candicidin, *Presse Med. 61*, 1327–1328.

332. Roberts, C.L., and Sullivan, J.J. (1965) Moniliasis. The Use of Candicidin Vaginal Ointment for Treatment, *Calif. Med. 103*, 109–111.

333. Friedel, H.J. (1966) Candicidin, a New Vaginal Monilicide. A Test Series, *MD State Med. J. 15*, 36–37.

334. Kivinen, S., Tarkkila, T., Laakso, L., Laakso, K. (1979) Short-Term Topical Treatment of Vulvovaginal Candidiasis with the Combination of 5-Fluorocytosine and Candicidin, *Curr. Med. Res. Opin. 6*, 88–92.

335. Jensen, K.M., and Madsen, P.O. (1983) Candicidin Treatment of Prostatism: A Prospective Double-Blind Placebo-Controlled Study, *Urol. Res. 11*, 7–10.

336. Grabley, S., Kretzschmar, G., Mayer, M., Philipps, S., Thiericke, R., Wink, R., and Zeeck, A. (1993) Secondary Metabolites by Chemical-Screening. 2. Oasomycins, New Macrolactones of the Desertomycin Family, *Liebigs Ann. Chem. 5*, 573–579.

337. Dolak, L.A., Reusser, F., Baczynskyj, L., Mizsak, S.A., Hannon, B.R., and Castle, T.M. (1983) Desertomycin: Purification and Physical-Chemical Properties, *J. Antibiot. 36*, 13–19.

338. Uri, J.V. (1986) Desertomycin—A Potentially Interesting Antibiotic (a review), *Acta Microbiol. Hung. 33*, 271–283.

339. Mukhopadhyay, T., Nadkarni, S.R., Bhat, R.G., Gupte, S.V., Ganguli, B.N., Petry, S., and Kogler, H. (1999) Mathemycin B, a New Antifungal Macrolactone from Actinomycete Species HIL Y-8620959, *J. Nat. Prod. 62*, 889–890.

340. Mukhopadhyay, T., Vijayakumer, E.K.S., Nadkarni, S.R., Fehlhader, H.W., Kogler, H., and Petry, S. (1998) Mathemycin A, a New Antifungal Macrolactone from *Actinomycete* sp. HIL Y-8620959—II. Structure Elucidation, *J. Antibiot. 51*, 582–585.

341. Nadkarni, S.R., Mukhopadhyay, T., Bhat, R.G., Gupte, S.V., Ganguli, B.N., and Sachse, B. (1998) Mathemycin A, a New Antifungal Macrolactone from *Actinomycete* sp. HIL Y-8620959—I. Fermentation, Isolation, Physico-chemical Properties and Biological Activities, *J. Antibiot. 51*, 579–581.

342. York, W.S. (1995) A Conformational Model for Cyclic β-(1→2)-Linked Glucans Based on NMR Analysis of the β-Glucans Produced by *Xanthomonas campestris, Carbohydr. Res. 278*, 205–225.

343. Kates, M., Kushner, D.J., and Matheson, A.T. (eds.) (1993) *The Biochemistry of Archaea*, Elsevier, New York.

344. Uda, I., Sugai, A., Itoh, Y.H., and Itoh, T. (2001) Variation in Molecular Species of Polar Lipids from *Thermoplasma acidophilum* Depends on Growth Temperature, *Lipids 36*, 103–105.

345. Uda, I., Sugai, A., Kon, K., Ando, S., Itoh, Y.H., and Itoh, T. (1999) Isolation and Characterization of Novel Neutral Glycolipids from *Thermoplasma acidophilum, Biochim. Biophys. Acta 1439*, 363–370.

346. Matsumura, S., Imai, K., Yoshikawa, S., Kawada, K., and Uchirobi, T. (1990) Bola-form Amphiphilic Compounds: Their Surface Activities, Biodegradability, and Antimicrobial Properties, *J. Am. Oil Chem. Soc. 67*, 996–1001.

347. Müllerfahrnow, A., Saenger, W., Fritsch, D., Schneider, P., and Fuhrhop, J.-H. (1993) Molecular and Crystal Structure of the Bola-Amphiphile *n*-[8-(D-gluconamido)octyl]-D-gluconamide, *Carbohydr. Res. 242*, 11–20.

348. Munoz, S., Mallen, J., Nakano, A., Chen, Z., Gay, I., Echegoyen, L., and Gokel, G.W. (1993) Ultrathin Monolayer Lipid Membranes from a New Family of Crown Ether-Based Bola-Amphiphiles, *J. Am. Chem. Soc. 115*, 1705–1711.

349. Newkome, G.R., Moorefield, C.N., Baker, G.R., Behera, R.K., Escamilla, G.H., and Saunders, M.J. (1992) Chemistry of Micelles. 16. Supramolecular Self-Assemblies of 2-Directional Cascade Molecules—Automorphogenesis, *Angew. Chem., Int. Ed. Engl. 31*, 917–919.

350. Fuhrhop, J.-H., Spiroski, D., and Boettcher, C. (1993) Molecular Monolayer Rods and Tubules Made of α-(L-lysine),ω-(amino) Bolaamphiphiles, *J. Am. Chem. Soc. 115*, 1600–1601.

351. Jayasuriya, N., Bosak, S., and Regen, S.L. (1990) Design, Synthesis, and Activity of Membrane-Disrupting Bolaphiles, *J. Am.Chem. Soc. 112*, 5844–5850.

352. Jayasuriya, N., Bosak, S., and Regen, S.L. (1990) Supramolecular Surfactants: Polymerized Bolaphiles Exhibiting Extraordinarily High Membrane-Disrupting Activity, *J. Am. Chem. Soc. 112*, 5851–5854.

353. Moss, R.A., and Li, J.-M. (1992) Bilayer-Bridging Bolaamphiphilic Lipids, *J. Am. Chem. Soc. 114*, 9227–9229.

354. Yamauchi, K., and Kinoshita, M. (1993) Highly Stable Lipid-Membranes from Archaebacterial Extremophiles, *Prog. Polym. Sci. 18*, 763–804.

355. Bertho, J.-N., Coué, A., Ewing, D.F., Goodby, J.W., Letellier, P., Mackenzie, G., and Plusquellec, D. (1997) Novel Sugar Bola-Amphiphiles with a Pseudo Macrocyclic Structure, *Carbohydrate Res. 300*, 341–346.

356. Satgé, C., Granet, R., Verneuil, B., Champavier, Y., and Krausz, P. (2004) Synthesis and Properties of New Bolaform and Macrocyclic Galactose-Based Surfactants Obtained by Olefin Metathesis, *Carbohydrate Res. 339*, 1243–1254.

357. Nyman, E.S., and Hynninen, P.H. (2004) Research Advanced in the Use of Tetrapyrrolic Photosensitizers for Photodynamic Therapy, *J. Photochem. Photobiol. B: Biol. 73*, 1–28.

358. Sessler, J.L., and Miller, R.A. (2000) Texaphyrins: New Drugs with Diverse Clinical Applications in Radiation and Photodynamic Therapy, *Biochem. Pharmacol. 59*, 733–739.

359. Sharman, W.M., Allen, C.M., Van Lier, A.E., and Van Lier, J.E. (1999) Photodynamic Therapeutics: Basic Principles and Clinical Applications, *Drug Discov. Today 4*, 507–517.

360. Dolphin, D. (1994) Photomedicine and Photodynamic Therapy, *Can. J. Chem. 72*, 1005–1013.

361. Synytsya, A., Král, V., Blechová, M., and Volka, K. (2004) Biolocalisation and Photochemical Properties of Two Novel Macrocyclic Photosensitisers: A Spectroscopic Study, *J. Photochem. Photobiol. B: Biol. 74*, 73–84.

362. Fujimoto, K., Miyata, T., and Aoyama, Y. (2000) Saccharide-Directed Cell Recognition and Molecular Delivery Using Macrocyclic Saccharide Clusters: Masking of Hydrophobicity to Enhance the Saccharide Specificity, *J. Am. Chem. Soc. 122,* 3558–3559.

363. Menger, F.M., Bian, J., Sizova, E., Martinson, D.E., and Seredyuk, V.A. (2004) Bolaforms with Fourteen Galactose Units: A Proposed Site-Directed Cohesion of Cancer Cells, *Org. Lett. 6*, 261–264.

ARTICLES

Novel Oxylipins Formed from Docosahexaenoic Acid by Potato Lipoxygenase—10(*S*)-Hydroxydocosahexaenoic Acid and 10,20-Dihydroxydocosahexaenoic Acid

Igor A. Butovich*, Mats Hamberg, and Olof Rådmark

Division of Physiological Chemistry II, Department of Medical Biochemistry
and Biophysics, Karolinska Institute, S-171 77, Stockholm, Sweden

ABSTRACT: Potato tuber lipoxygenase (ptLOX) has been shown to catalyze the aerobic formation of at least four major oxygenated derivatives of DHA. Two of the products—7,17(*S*)- and 10,17(*S*)-dihydro(pero)xy-DHA [7,17- and 10,17-diH(P)DHA]—were formed from soybean 15-LOX-derived 17(*S*)-hydro(pero)xy-DHA [17(*S*)-H(P)DHA], whereas two novel oxylipin compounds—10(*S*)-hydro(pero)xy-DHA and 10,20-dihydro(pero)xy-DHA [10(*S*)-H(P)DHA and 10,20-diH(P)DHA, respectively]—were the major direct products of DHA oxidation by ptLOX. The reactions proceeded relatively slowly but could be stimulated by catalytic amounts of SDS. Micromolar concentrations of 10(*S*)-HPDHA effectively abolished the kinetic lag period of ptLOX activation. Enzymatic activity with DHA or 17(*S*)-HPDHA as substrate was about 8% of that with linoleic acid—a standard natural ptLOX substrate—whereas 17(*S*)-HDHA was converted at a rate of ~1%. The enzyme was relatively unstable and quickly inactivated during the reaction with DHA on with 17(*S*)-HPDHA (first-order kinetic constant of inactivation $k_{in} = 1.5 \pm 0.3$ min^{-1}), but not with 17(*S*)-HDHA. Both 7,17- and 10,20-diH(P)DHA were clearly products of double oxygenation catalyzed by soybean 15-LOX and/or ptLOX. Our observation that ptLOX could convert 17-HDHA to 10,17-diH(P)DHA indicates that this dihydroxylated derivative of DHA also can be formed *via* a double lipoxygenation mechanism.

Paper no. L9683 in *Lipids 40*, 249–257 (March 2005).

Potato tuber lipoxygenase (ptLOX, EC 1.14.18.1) has been shown to catalyze oxygenation of a range of PUFA (1–4) as well as some of their derivatives, e.g., linoleic acid methyl ester (5), glyceryl ester (6), and linoleyl alcohol (7,8). The reactions proceed in micellar solutions with maximal reaction rates at pH values slightly below neutrality, typically 6.3 to 6.5. Under these conditions, ptLOX substrates—PUFA and their derivatives—are poorly soluble and tend to aggregate quickly. To make the reaction mixtures more thermodynamically stable and homogeneous, it was proposed to include in the reaction mixtures small amounts of the nonionic detergent Lubrol PX (5,9–11) or a similar compound, the monododecyl ether of decaethylene glycol ($C_{12}E_{10}$) (6–8). The rates of the dioxygenation reactions were greatly enhanced in the presence of certain acidic amphiphilic compounds (activators) (6–8,10,11; and references therein). The product profile was not noticeably affected by inclusion of the activators (5,6,8). Under these conditions, ptLOX formed several positional and geometrical isomers of the oxygenated products, which occurred partly owing to the dual (normal and inverse) orientation of the substrate molecule in the enzyme's catalytic center, and partly because of enzyme-triggered nonenzymatic reactions (6,8). It was found that inclusion of free-radical scavengers [e.g., TEMPO (2,2,6,6-tetramethyl-1-piperidinyloxy)] in the reaction mixtures substantially increased the optical purity of the oxygenation products by suppressing nonenzymatic free-radical chain reactions (6,8).

Recently, several DHA oxygenation products have been identified, including mono-, di- and trihydro(pero)xy-DHA (4,12–14)], a common feature of which is oxygenation at C17 of DHA. This group of compounds was termed "resolvins" because they were formed during the resolution phase of an acute inflammatory response, after treatment of experimental animals and cells with acetylsalicylic acid (ASA) and DHA. The mechanism of formation of some of them, *e.g.*, 7,17(*R*)-dihydroperoxydocosahexaenoic acid [7,17(*R*)-diHPDHA], was postulated to start with oxygenation of DHA by cyclooxygenase-2 acetylated with ASA (4,12), although in a recent paper it was proposed that a LOX-catalyzed formation of 17(*S*)-HPDHA could also be a starting point in making 10,17(*S*)-dihydroxy DHA (diHDHA) (14). The same group found that many of these singly, doubly, and triply oxygenated compounds could also be formed in "one-pot reactions" of DHA oxidation catalyzed by ptLOX and soybean 15-LOX (4,12). However, no detailed information on the reactions was provided.

In this report, we describe two novel oxylipins formed from DHA by ptLOX, as well as further studies on the conversion by ptLOX of soybean 15-LOX-derived 17(*S*)-HPDHA and 17(*S*)-HDHA.

*To whom correspondence should be addressed at Department of Ophthalmology, University of Texas Southwestern Medical Center at Dallas, 5323 Harry Hines Blvd., Dallas, TX 75390-9057.
E-mail: Igor.Butovich@UTSouthwestern.edu

EXPERIMENTAL PROCEDURES

DHA was purchased from Nu-Chek-Prep (Elysian, MN). Soybean 15-LOX type 1-B (100 KU/mg solid; activity measured as described by the manufacturer) was a product of Sigma-Aldrich (Stockholm, Sweden). Potato LOX was purchased from Cayman Chemical (Ann Arbor, MI) and according to the manufacturer's data was 98% pure. The purity of the protein was retested by SDS-PAGE. The enzyme produced a single band on a 10–15% gradient gel on a PhastSystem (Pharmacia-LKB) with Coomassie® brilliant blue G-250 staining. For preparative synthesis of lipid metabolites, semipurified ptLOX from locally grown potato tubers was used. (In preliminary experiments, the purity of the enzyme preparations was shown to have no effect on the product profile of DHA oxidation.) Other compounds were purchased from Sigma-Aldrich. A Waters Spherisorb Si 5 µm 3.2 × 250 mm straight-phase HPLC (SP-HPLC) column was a product of Supelco (Bellefonte, PA). A Chiralcel OB-H 4.6 × 250 mm chiral column was manufactured by Daicel Chemical Industries, Ltd. (Tokyo, Japan). HPLC-grade solvents were obtained from Rathburn Chemical Ltd. (Walkerburn, Scotland). A Hewlett-Packard HPLC system equipped with a 1040A diode-array detector and Chem-Station software was used in chromatographic experiments.

Enzymatic oxidation of DHA by soybean 15-LOX. Soybean 15-LOX-catalyzed oxidation of DHA resulting in formation of 17(*S*)-HPDHA was described earlier (15). In our modified procedure, virtually 100% conversion of DHA into 17(*S*)-HPDHA was obtained. Briefly, a 10-mL aliquot of 100 µM DHA dissolved in aerated 0.05 M sodium borate buffer (pH 9.0) was mixed with ~100 µg soybean 15-LOX and left at 4°C for 10 min under constant stirring. To convert the newly formed hydroperoxide(s) of DHA into the corresponding hydroxides, a solution of $NaBH_4$ in 1 M NaOH was added to the reaction mixture at the end of the incubation period (final concentration of the reducing agent, 0.5 mg/mL), and the mixture was left for another 15 min at 4°C under gentle stirring (foaming!). The reaction was then stopped, and the excess of $NaBH_4$ was decomposed by adding 0.1 mL of glacial acetic acid after which the mixture was allowed to stand on ice for another 15 min. When the target product was 17(*S*)-HPDHA, the reduction step was omitted from the procedure. Finally, the product was passed through a 500-mg Supelco Discovery C18 solid-phase extraction cartridge in accordance with the manufacturer's recommendations, the cartridge was washed with distilled water, and the products were eluted with absolute ethanol. After evaporation of the solvent, 17(*S*)-HDHA was redissolved in absolute ethanol and stored at –20°C under argon for a week without noticeable degradation of the sample. The extent of reduction was monitored by SP-HPLC analysis of the products in a hexane/2-propanol/acetic acid (989:10:1, by vol) solvent mixture as described below. Under these conditions, 17-HDHA had a shorter retention time (RT) than 17-HPDHA.

Enzymatic oxidation of DHA by ptLOX. The reactions were performed essentially as described before for linoleyl alcohol (7,8) and 1-monolinoleoyl glycerol (6). For preparative-scale

synthesis of DHA metabolites, the reaction mixture was composed of 100 µM DHA, 0.02% $C_{12}E_{10}$, 100 µM SDS, and 1 mM TEMPO dissolved in 10 mL of aerated 0.05 M MES-NaOH buffer with pH 6.3. The reaction was started by adding ~2 U of ptLOX [1 U was defined as the amount of enzyme that catalyzed formation of 1 µmol of 9(*S*)-hydroperoxyoctadecadienoic acid (HPODE)/min with linoleic acid (LA) as substrate], and the mixture was incubated for 15 min at 4°C under constant stirring. At the end of the incubation period, the reaction was stopped with acetic acid; the products were extracted as described above for soybean 15-LOX products, redissolved in absolute ethanol, and stored at –20°C under argon. For kinetic experiments performed spectrophotometrically as described earlier for other LOX substrates (5,6,8,9), TEMPO was excluded from the mixture because its high absorptivity interfered with UV analysis, and the total volume of the reaction mixture typically was 0.5 mL. The reactions were carried out in quartz spectrophotometric cells at room temperature (23 ± 1°C). The reactions were started by adding enzyme aliquots followed by vigorous mixing of the solution with a pipette and were monitored at 238 (for conjugated dienes) or 272 nm (for conjugated trienes, see below). Molar absorption coefficients (ε_m) of the conjugated dienes and trienes formed during the reaction were assumed to be 25,000 $M^{-1} cm^{-1}$ (16) and 40,000 $M^{-1} cm^{-1}$ (estimate), respectively.

Enzymatic synthesis of 7,17- and 10,17-diH(P)DHA. The doubly oxygenated metabolites of DHA were prepared using the procedure described above for DHA by incubating either 17(*S*)-HDHA or 17(*S*)-HPDHA (100 µM final concentration) with ~2 U of ptLOX.

SP-HPLC on silica gel. Crude product mixtures were analyzed chromatographically on a Waters Spherisorb Si 5 µm 3.2 × 250 mm SP-HPLC column. Detection of the eluted peaks was performed simultaneously at 236 (conjugated dienes) and 270 nm (conjugated trienes). Monohydroxylated FA were eluted by a hexane/2-propanol/acetic acid (989:10:1, by vol) solvent mixture at a flow rate of 1 mL/min, whereas dihydroxylated acids were separated in a hexane/2-propanol/acetic acid (979:20:1, by vol) mixture at the same flow rate, unless indicated otherwise. The individual fractions of oxygenated DHA metabolites were collected manually, and their purities were rechecked under the same conditions.

GC–MS. The isolated fractions of individual lipids were subjected to catalytic hydrogenation with H_2 over PtO_2 (15). Then the samples were trimethylsilylated with a trimethylchlorosilane/pyridine mixture and evaporated under vacuum; the residue was redissolved in a small volume of dry hexane and then analyzed by GC–MS. A Hewlett-Packard model 5970 mass selective detector connected to a Hewlett-Packard model 5890 gas chromatograph was used for GC–MS. A capillary column of 5% phenylmethylsiloxane (length, 12 m; film thickness, 0.33 µm; carrier gas, helium) was used. The temperature was raised from 120 to 260°C at a rate of 10°C/min.

GLC. GLC was carried out with a Hewlett-Packard model 5890 gas chromatograph equipped with an FID and a methylsilicone capillary column (length, 25 m; film thickness, 0.33

μm; carrier gas, helium). The column temperature was raised 2°C/min starting at 190°C.

Steric analysis of the products. Determination of the absolute configuration of allylic alcohol groups in LOX-generated metabolites was carried out by GLC analysis of (−)-menthoxycarbonyl (MC) derivatives of short-chain esters formed upon oxidative ozonolysis (17). The analyte (10 μg or less) was derivatized by treatment with (−)-menthoxycarbonyl chloride (20 μmol; Aldrich) in a mixture of toluene (30 μL) and dry pyridine (5 μL) at 23°C for 1 h. The reaction mixture was subjected to TLC using a solvent system of ethyl acetate/hexane (5:95, vol/vol). A broad zone of silica gel corresponding to R_f 0.6–0.8 was scraped off and eluted with distilled diethyl ether. The MC derivative thus eluted was dissolved in 0.5 mL of chloroform, cooled to −20°C, and exposed to a stream of ozone/oxygen (1:9, vol/vol) for 30 s. Solvent was removed under argon and the residue treated with 0.1 mL of peracetic acid at 40°C for 15 h. The residue obtained following evaporation of the reagent was treated with diazomethane and analyzed by GLC and GC–MS using a reference sample of the MC derivative of dimethyl (±)-malate. Under the conditions used, MC derivatives of 2(*S*)-hydroxyesters or diesters elute at shorter RT compared with those of the corresponding 2(*R*)-hydroxy derivatives.

The mono- and dihydroxylated DHA (methyl esters) were also analyzed on a Chiralcel OB-H chiral column. The monohydroxylated derivatives were eluted with hexane/2-propanol (99:1, vol/vol) solvent mixture, whereas dihydroxylated compounds were analyzed in a hexane/2-propanol (80:20, vol/vol) solvent mixture, both at a flow rate of 1 mL/min. Peaks were detected at 236 and/or 270 nm.

RESULTS

Oxidation of DHA. Under aerobic conditions, ptLOX transformed DHA into a compound with a λ_{max} at 238 nm, indicative of a 1,4-pentadiene to 1,3-conjugated diene transformation usually associated with LOX-catalyzed monooxygenation of unsaturated FA (Fig. 1A). Then the catalytic activity of the enzyme was determined spectrophotometrically by monitoring the progress curves of the reaction at 238 nm. Under similar conditions, ptLOX activity with DHA as substrate was found to be ~7.5% of that with LA. Unlike the reaction with LA, ptLOX-catalyzed oxygenation of DHA stopped long before the FA and molecular oxygen had been depleted, thus giving a relatively low product yield (Fig. 1B, curve **a**). When equal aliquots of active enzyme were added to the same reaction mixture, the reaction proceeded with reaction rates and product yields approaching those of the first incubation (Fig. 1B, curves **b** and **c**). The yield of the lipid oxidation product was proportional to the amount of the enzyme added: a 3-fold increase in the initial enzyme concentration in the reaction mixture led to a ~2.8-fold increase in the product formation. Also, the same patterns of enzyme inactivation/inhibition during reaction, and of reaction restoration with fresh enzyme, were observed at higher enzyme concentrations (data not shown). The kinetics
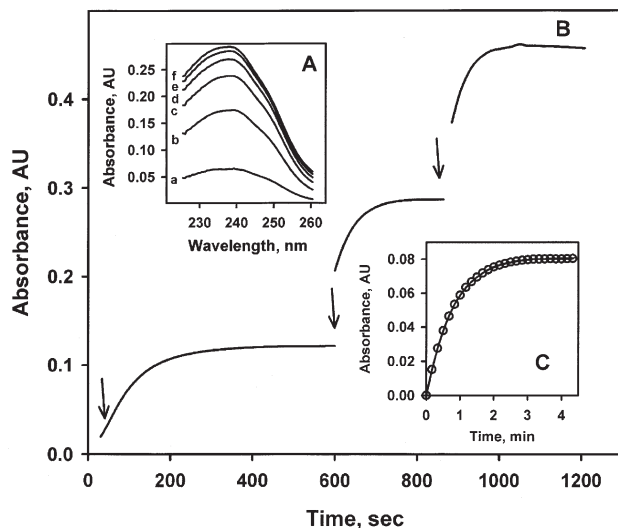
FIG. 1. Oxidation of DHA by potato tuber lipoxygenase (ptLOX). (A) Formation of the conjugated dienes during oxidation of 100 μM DHA by ptLOX. Experimental conditions: as described in the Experimental Procedures section. The reaction was initiated by adding 5 μL of ptLOX stock solution. Spectra **a** to **f** were recorded at 30-s intervals. (B) Kinetic curves of DHA oxidation by ptLOX. Experimental conditions: as described in the Experimental Procedures section. Substrate: 100 μM DHA. The reaction was initiated by adding 2.5 μL of ptLOX stock solution. Absorbance was measured at 238 nm. Arrows indicate the time points when equal ptLOX aliquots were added. (C) Reaction inactivation of ptLOX on oxidation of 100 μM DHA. Open circles: experimental points. Solid line: kinetic curve computed using Equation 1 and the following parameters: $V_0 = 0.10398$ AU/min; $k_{in} = 1.28$ min^{-1}.

of ptLOX inactivation during oxidation of DHA was investigated in more detail. A previously described mathematical approach (18; and references therein) was applied to determine an apparent first-order kinetic constant of ptLOX inactivation during the reaction (k_{in}). We thus found that the progress curve of 100 μM DHA oxidation by ptLOX in the presence of 5 μM 10-HPDHA [added to eliminate the well-known lag period of the enzyme activation (5,6,8,9,19) was adequately described by a simple reaction inactivation equation:

$$P_t = \frac{V_0}{k_{in}} \times (1 - e^{-k_{in} \times t}) \qquad [1]$$

where P_t is the product concentration (in absorbance units, AU) at time t, and V_0 is the initial reaction rate (Fig. 1C). The values of V_0 and k_{in} were found to be 0.104 AU/min and 1.28 min^{-1}, respectively (as $\varepsilon_{238} = 25,000$ M$^{-1} \times$ cm^{-1}, the rate of 0.104 AU/min translates into ~4.2 μM of product/min). A 3-fold increase in the initial concentration of ptLOX led to a 3.5 ± 0.5 fold increase in the V_0 and a concurrent increase in k_{in} to ~1.8 min^{-1}. According to Equation 1, when $t \to \infty$, then $P_t \to V_0/k_{in} = P_{lim}$, i.e., the product yield at the end of the catalytic reaction in which an enzyme undergoes fast inactivation. Simple calculations of the reaction yield using the values determined for V_0 and k_{in} showed that a 3-fold increase in the initial enzyme concentration should give a 2.6-fold increase in the product formation, which is close to the value obtained experimentally (2.8).

Oxidative conversion of 17(S)-H(P)DHA. During incubation of 17(S)-HPDHA with ptLOX, the hydroperoxide was effectively transformed into another product, which had a UV-spectrum of a 1,3,5-conjugated triene with clear maxima at 272 and 280 nm (Fig. 2). The increase in the optical density in the region from 260 to 280 nm was accompanied by a simultaneous decrease in the absorbance at λ 238 nm. A single isosbestic point (λ 251 nm) has been found in the electronic spectra of the reaction mixture taken while the reaction progressed (Fig. 2), which is indicative of a direct transformation of 1,3-conjugated diene into 1,3,5-conjugated triene (Scheme 1):

SCHEME 1

In a manner similar to the oxidation of DHA, a rapid loss of the enzymatic activity with k_{in} = 1 min^{-1} was observed during the reaction with 17(S)-HPDHA (data not shown). The observed reaction rate was ~8.3% of that with LA as substrate (Table 1).

17(S)-HDHA was converted by ptLOX into a new product possessing a similar electronic spectrum with a triplet 260, 270, and 280 nm and an isosbestic point at 250 nm (Fig. 3). The reaction rate of 17(S)-HDHA conversion was noticeably slower than that of 17(S)-HPDHA, but the former reaction eventually gave a comparable, or even higher, yield of the triene(s) owing to a much slower enzyme inactivation/inhibition (Fig. 4). The

TABLE 1
Comparison of the Activity of ptLOX with Various Substrates[a]

Substrate 100 μM	Product formed	Analytical wave-length, nm	Activity[b], %	k_{in}, min^{-1}
Linoleic acid	9(S)-HPODE	234	100	0.2[c]
DHA	Hydroperoxy-DHA	238	7.6	1.5 ± 0.3
17(S)-HPDHA	Triene(s)	272	8.3	~1
17(S)-HDHA	Triene(s)	272	1	NA

[a]ptLox, potato tuber lipoxygenase; 9(S)-HPODE, 9(S)-hydroperoxyoctadecadienoic acid; 17(S)-H(P)DHA, 17(S)-hydro(pero)xy-DHA; NA, not available. [b]When calculating the activity of ptLOX with different substrates, ε_{238} = 25,000 M^{-1} × cm^{-1} and ε_{272} = 40,000 M^{-1} × cm^{-1} were used. Composition of the reaction mixture was as follows: 0.5 mL of 0.1 mM substrate, 0.1 mM SDS, 0.02% (wt/vol) monododecyl ether of decaethylene glycol (C$_{12}$E$_{10}$), 0.05 M MES/NaOH buffer pH 6.3, ambient temperature (23 ± 1°C). [c]From Reference 9.

value of k_{in} could not be computed because of the complex form of the kinetic curve. Interestingly, a noticeable lag period of ptLOX activation was observed with 17(S)-HDHA as substrate because the reaction achieved its maximal rate only after 12 min into the reaction (Fig. 4, inset). The lag was visible on both the progress curves—17(S)-HDHA decomposition and the conjugated triene formation—and was virtually nonexistent in the case of 17(S)-HPDHA (Fig. 2, inset).

Characterization of the oxygenated products. For elucidation of the molecular structures of the main products of DHA oxidation, the lipids were extracted and analyzed by SP-HPLC and GC–MS. A typical chromatogram of the products of DHA oxidation (Fig. 5) showed two major products (compounds **I** and **II**), with considerably different retention times on a silica gel column. The UV spectrum of the less polar compound **I** with λ_{max} 236 nm is typical for monohydroxylated PUFA, whereas the much more polar compound **II**, dissolved in the mobile phase, showed a less common electronic spectrum (Fig. 5, inset) with two maxima at 224 and 242 nm (A$_{224}$/A$_{242}$ = 1.37). To ensure that the UV spectrum of compound **II** was not a superposition of spectra of two different co-eluting substances, compound **II** was rechromatographed in several hexane/2-propanol/acetic acid mixtures either in the form of a free acid or methyl ester (data not shown). It was concluded that compound **II** indeed possessed the electronic absorption spectrum depicted in Figure 5. Interestingly, the same sample of purified compound **II** dissolved in ethanol showed a somewhat different UV spectrum with a primary maximum at about 243 nm and a secondary maximum (or a shoulder) at 224 nm with A$_{224}$/A$_{243}$ = 0.7.

Compounds **I** and **II** were isolated by SP-HPLC and, after catalytic hydrogenation and trimethylsilylation, subjected to EI GC–MS analysis. A total ion chromatogram of compound I (Fig. 6A) revealed the presence of one major peak with an RT of ~16.1 min. The fragmentation pattern of the di-trimethylsilyl (di-TMS) derivative of the totally hydrogenated compound **I** showed three prominent fragments with *m/z* 73, 271, and 331, and less intense fragments 469 and 485 (Fig. 6B). All the major fragments were shown to coelute as a single peak if plotted as a single ion monitoring chromatogram

FIG. 2. ptLOX-catalyzed conversion of 100 μM 17-hydroperoxy DHA (17-HPDHA) into a conjugated triene. Experimental conditions: as described in the Experimental Procedures section for DHA. The reaction was initiated by adding 10 μL of ptLOX stock solution. Spectra **a** to **e** were recorded at 1-min intervals. Inset: Kinetic curves of ptLOX-catalyzed conversion of 100 μM 17-HPDHA recorded at 238 and 272 nm. For other abbreviation see Figure 1.

FIG. 3. ptLOX-catalyzed conversion of 100 μM 17-hydroxy DHA (17-HDHA) into a conjugated triene. Experimental conditions: as described in the Experimental Procedures section for DHA. The reaction was initiated by adding 20 μL of ptLOX stock solution. Spectra **a** to **d** were recorded at 2-min intervals. For other abbreviation see Figure 1.
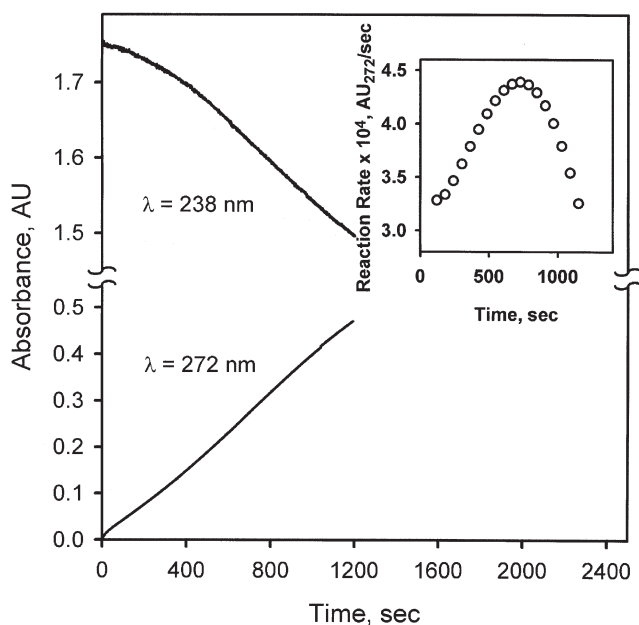
FIG. 4. Kinetic curves of ptLOX-catalyzed conversion of 17-HDHA recorded at 238 and 272 nm. Experimental conditions: See the Experimental Procedures section and Figure 2. The reaction was initiated by adding 10 μL of ptLOX stock solution. Inset: The dependency of the reaction rate of 17(*S*)-HDHA transformation by ptLOX on the reaction time. The data were taken from the main portion of this figure, numerically differentiated, and plotted as reaction rate vs. time. For abbreviations see Figures 1 and 3.
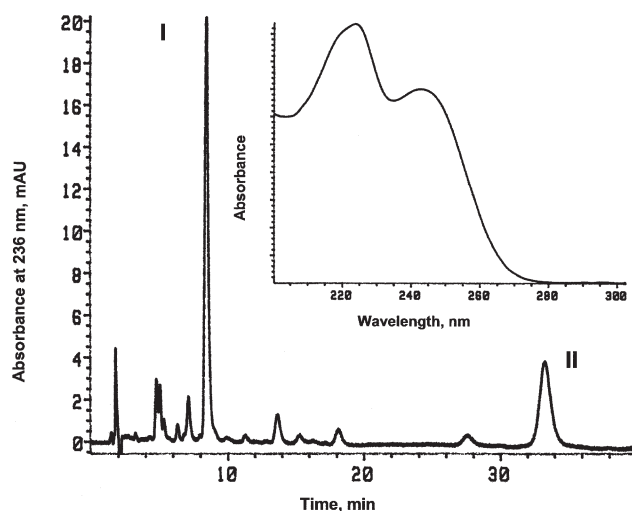
FIG. 5. Straight-phase HPLC (SP-HPLC) analysis of the DHA lipoxygenation products. Inset: a UV spectrum of compound **II** taken during the HPLC analysis.

(Fig. 6C). These data provide strong evidence that the compound in hand is fully hydrogenated diTMS-10-HDHA (M.W. 500.9), whereas the starting compound **I** is 10-HDHA.

Fully trimethylsilylated and hydrogenated compound **II** produced characteristic fragments with *m/z* 73, 117 (minor), 131, 331, 359, and 469 (Fig. 7). The following assignments of the common fragments were made: *m/z* 73 − Si(CH$_3$)$_3$, 117 − COOSi(CH$_3$)$_3$, 131 − CH$_3$CH$_2$CHOSi(CH$_3$)$_3$, 469 − (588 − TMSiOH − CH$_2$CH$_3$), M.W. 589.1, exact mass 588.4. The rest of the fragments are depicted in Figure 7. These data, in combination with the fragmentation pattern of the same compound **II** treated with diazomethane prior to trimethylsilylation (*m/z* 73, 131, 273, 359, and 515, data not shown) proved that it is a C$_{22}$ FA with two hydroxyls at carbons 10 and 20, i.e., 10,20-diHDHA.

To determine whether 10-HDHA had been formed as a single optical isomer, it was converted into the methyl ester and analyzed by HPLC on a chiral column as described in the Experimental Procedures section. The compound eluted as a single major peak (>90%) with an RT of 26 min in hexane/2-propanol (99:1, vol/vol, flow rate 1 mL/min) and a minor (<10%) component with a longer RT of 30.2 min. The determination of the absolute stereochemistry of 10-HDHA was performed by its oxidative ozonolysis of its MC-derivative as described earlier for 9- and 13-hydroxyoctadecadienoic acids (17). The enzymatically formed 10-HDHA gave a single product peak, which coeluted with the MC derivative of dimethyl (*S*)-malate. Therefore, the configuration of the hydroxyl at the carbon atom number 10 is *(S)*, and the major monooxygenated product of ptLOX oxidation of DHA is 10(*S*)-HPDHA.

10,20-DiHDHA was eluted as a single peak on a Chiralcel OB-H column in solvent mixtures of hexane/2-propanol (90:10, vol/vol; flow rate 1 mL/min; RT 31.5 min: and 80:20, vol/vol; flow rate 1 mL/min; RT 13.5 min). No traces of other compounds were detected, suggesting that 10,20-diHDHA
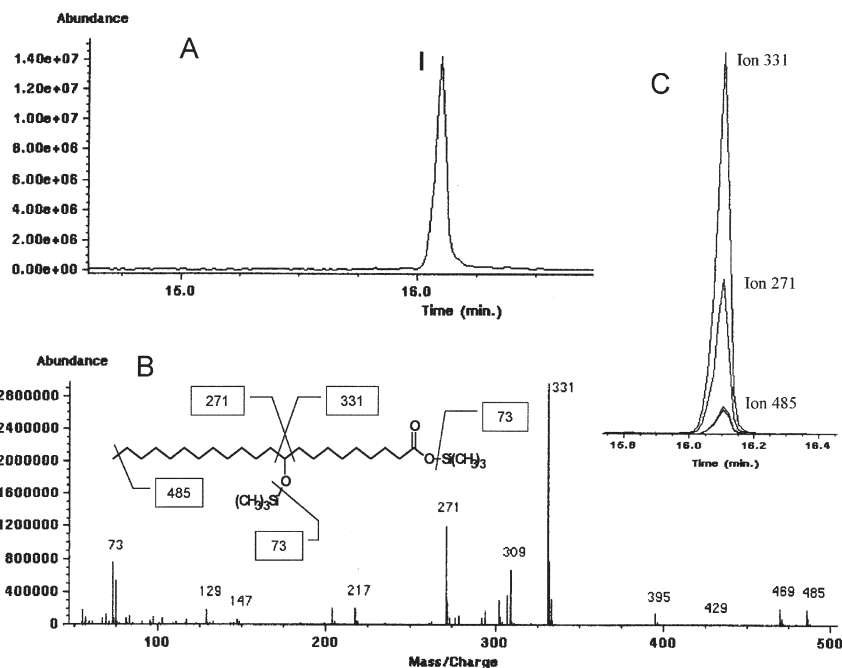
FIG. 6. GC–MS analysis of compound **I** after hydrogenation with H_2/PtO_2 and trimethylsilylation. (A) Total ion chromatograph (TIC); (B) electron impact MS (EI MS) fragmentation pattern; (C) single ion monitoring chromatogram: ions with *m/z* ratios of 271, 331, and 485 were monitored.
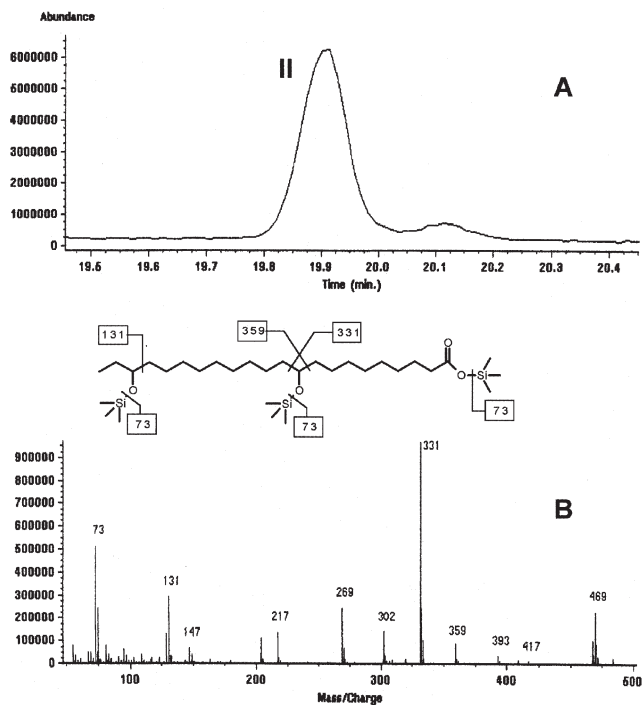
FIG. 7. GC–MS analysis of compound **II** after hydrogenation with H_2/PtO_2 and trimethylsilylation. (A) TIC of compound **II** and (B) its EI MS fragmentation pattern. For abbreviations see Figure 6.

was present as a single stereoisomer. The absolute stereochemistry of the hydroxyl group at C20 remains to be determined.

In the reaction of ptLOX with 17(*S*)-HPDHA, there were three major product peaks detected after reduction of the product mixture with $NaBH_4$ (compounds **III**, **IV**, and **V**; Figs. 8A and 8B). Compound **III** was positively identified as 17(*S*)-HDHA. The UV spectrum of the less polar compound **IV** (Fig. 8C) was virtually identical to that of 10,20-diHDHA (Fig. 5), whereas compound **V** (Figs. 8B and 8D) was identified as a conjugated triene with λ_{max} 260, 270, and 280 nm. GC–MS analysis of the hydrogenated TMS derivative of compound **IV** revealed characteristic fragments with *m/z* ratios of 73, 173, 289, 402, 427, 517, and 573, which were indicative of a triTMS derivative of fully hydrogenated 7,17-diHDHA. The corresponding derivative of compound **V** produced fragments 73, 173, 331, 359, 427, 517, and 573 (M.W. 589.1, exact mass 588.4), suggesting that it was 10,17-diHDHA.

10,17-DiHDHA was also found as a major metabolite in the lipid product mixture obtained by incubating 17-HDHA and ptLOX followed by reduction of the reaction products with $NaBH_4$ (compound **V**, Fig. 9). Interestingly, with 17-HDHA as substrate, production of 7,17-diHDHA (compound **IV**) was considerably reduced (but still present) compared with the experiments with 17-HPDHA (compare Figs. 9A and 8A). The molecular structures of the DHA metabolites are presented in Scheme 2.
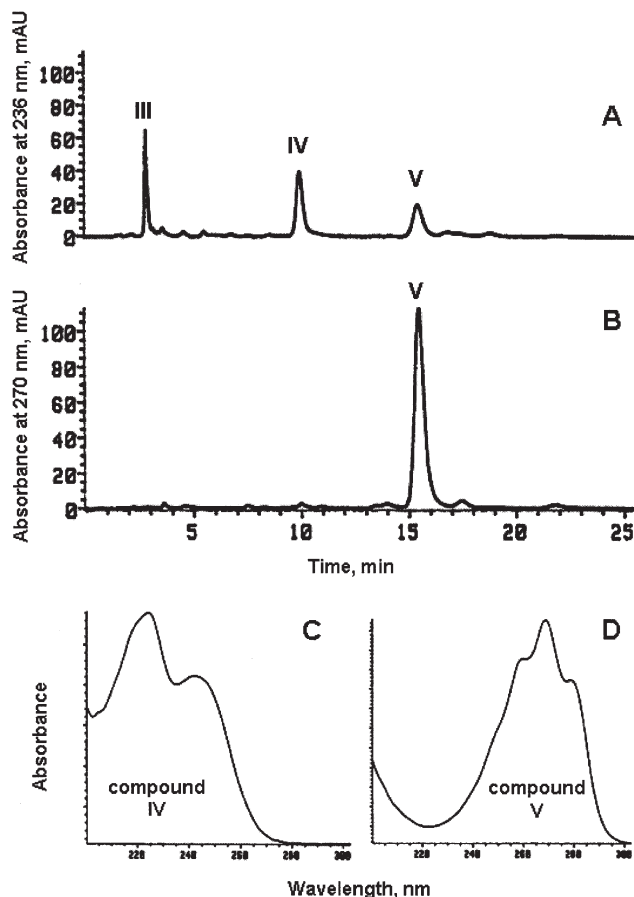
FIG. 8. SP-HPLC analysis of 17(*S*)-HPDHA lipoxygenation products. Analytical wavelengths: (A) 236 nm; (B) 270 nm. Panels C and D: UV spectra of compounds **IV** and **V**. For abbreviations see Figures 2 and 5.

DISCUSSION

Under aerobic conditions in a mixed micellar solution composed of a nonionic detergent $C_{12}E_{10}$, SDS, and DHA, ptLOX oxidized DHA at a rate of ~8% of that with LA as substrate, which makes DHA a relatively poor substrate for ptLOX. Nevertheless, the enzymatic activity was high enough to generate sufficient amounts of the reaction products. Noticeable was the fast enzyme inactivation/inhibition during the reaction with the rate constant of inactivation of 1 to 2 min^{-1}, the reasons for which are yet not known. Interestingly, transformation of 17(*S*)-HPDHA into 10,17-diH(P)DHA proceeded quickly but also caused rapid loss of the enzymatic activity, whereas in the reaction with 17(*S*)-HDHA, ptLOX was much more stable, although the reaction was slower and was accompanied by a noticeable lag period. There is no doubt that the differences in kinetics were caused by the presence of the hydroperoxy group in 17(*S*)-HPDHA that may serve as a ptLOX activator that readily converts the "resting" ferrous form of ptLOX into a catalytically active ferric form (19), thus minimizing the catalytic lag and, in certain cases, enhancing the apparent activity of LOX (20). On the contrary, 17(*S*)-HDHA, being unable to convert Fe^{2+} to Fe^{3+}, was expectedly a poorer substrate in terms of the reaction rate.
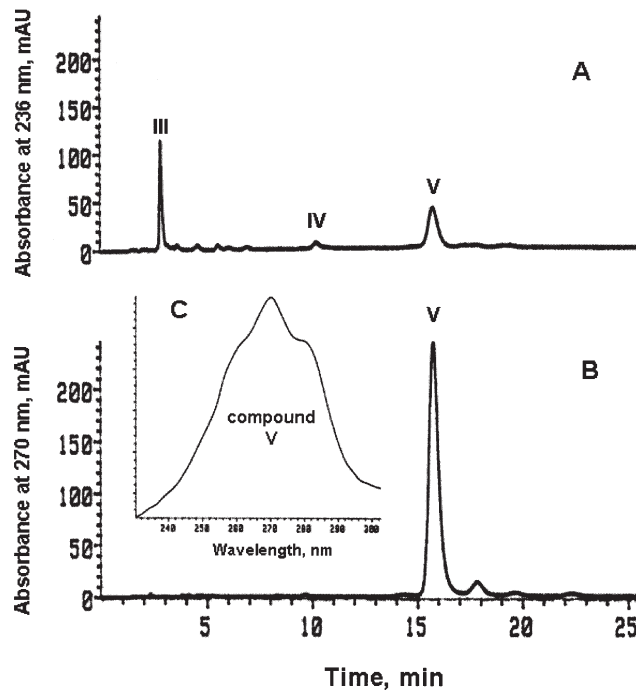
FIG. 9. SP-HPLC analysis of 17(*S*)-HDHA lipoxygenation products. Analytical wavelengths: (A) 236 nm; (B) 270 nm. Inset: UV spectrum of compound **V**. For abbreviations see Figures 3 and 5.

Oxygenation of DHA catalyzed by ptLOX generated two novel oxylipins—10(*S*)-H(P)DHA and a doubly oxygenated product 10,20-diH(P)DHA. Oxygenation of DHA at C10 was shown to proceed stereospecifically to yield the 10(*S*)-hydroperoxide of DHA. The absolute stereochemistry of 10,20-diH(P)DHA remains to be determined, but based on the stereospecificity of DHA oxygenation, it is reasonable to assume that in 10,20-diH(P)DHA the hydro(pero)xy group at C10 position has the (*S*)-configuration too. Since no 20-H(P)DHA was identified among the products [although ptLOX produced several minor metabolites with elution times close to the one for 10-H(P)DHA], oxygenation of DHA at C10 seems to be the first step in making 10,20-diH(P)DHA, followed by the secondary
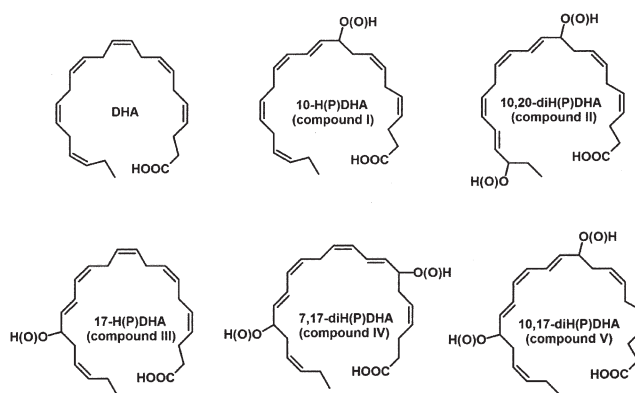
SCHEME 2

reaction at C20. The latter would necessitate abstraction of a hydrogen atom from the methylene C18.

In the ptLOX-catalyzed reaction, which involves formation of a carbon-centered free radical, hydrogen abstraction at C12 is followed by isomerization of the radical to C10 and its reaction with molecular oxygen at this position (Scheme 3):

SCHEME 3
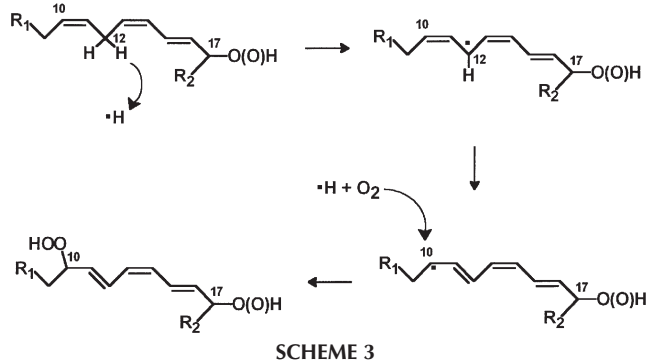
When conversion of 17(*S*)-H(P)DHA into 10,17(*S*)-diHDHA was described previously, it was proposed that 17-HPDHA is converted into 10,17-diHDHA with *trans,trans,cis*-geometry of the conjugated double bonds by an LOX-like activity *via* an epoxidation/isomerization reaction (13). Our observation that 10,17-HDHA can also be formed from 17-HDHA by ptLOX points toward a different reaction mechanism (i.e., double lipoxygenation), with likely *trans,cis,trans*-geometry of the conjugated double bonds. An interesting result was the UV spectra of 7,17- and 10,20-diHDHA recorded during HPLC experiments (Figs. 5 and 8C). The splitting of the λ_{max} was most likely caused by the presence of the following fragment present in both compounds (Scheme 4):

SCHEME 4
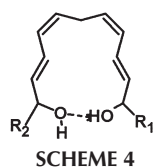
In nonpolar solvents such as the HPLC mixtures used in this study, interaction of the two polar hydroxy groups by an *intramolecular* hydrogen bond could be facilitated by solvophobic effects of hexane. Indicatively, the very same sample of 10,20-diHDHA, after being dissolved in a much more polar solvent (ethanol), showed a reversed UV spectrum with a primary absorption maximum at 243 nm and a suppressed maximum (or shoulder) at 224 nm. This solvatochromic effect is probably due to the ability of the alcohol to form hydrogen bonds with the hydroxyl groups of 10,20-diHDHA thus partly disrupting the intramolecular hydrogen bond postulated in Scheme 4. Though theoretically possible, an interaction of two or more molecules of 7,17- or 10,20-diHDA through formation of *intermolecular* hydrogen bonds seems unlikely because the effect would be concentration-dependent, which was not the case. A direct involvement of the carboxyl group of the dihydroxylated compounds is also implausible because (i) the methyl ester derivatives showed the same spectral properties as the free acids, and (ii) the distances between the carboxyl group and the hydroxyls of 7,17- and 10,20-diHDHA differ from compound to compound without affecting their spectra. Thus, the UV maximum with λ_{max} of 224 nm is, probably, characteristic of the structure presented in Scheme 4, whereas the second maximum of 243 nm is related to the same compound with disrupted intramolecular hydrogen bond. Both forms seem to coexist in equilibrium, which depends on the ability of the solvent to form hydrogen bonds with the hydroxyl groups of 7,17- and 10,20-diHDHA. It is noteworthy that a similarly split spectrum (with a secondary maximum at 226 nm and a primary maximum at 243 nm) was previously described for an arachidonic acid metabolite formed by double lipoxygenation (5,15-dihydroxyeicosatetraenoic acid) (21–26), although no explanation for it was provided.

In summary, ptLOX has been shown to catalyze formation of at least four major oxygenated derivatives of DHA. Two of these—7,17- and 10,17-diH(P)DHA—were formed from the
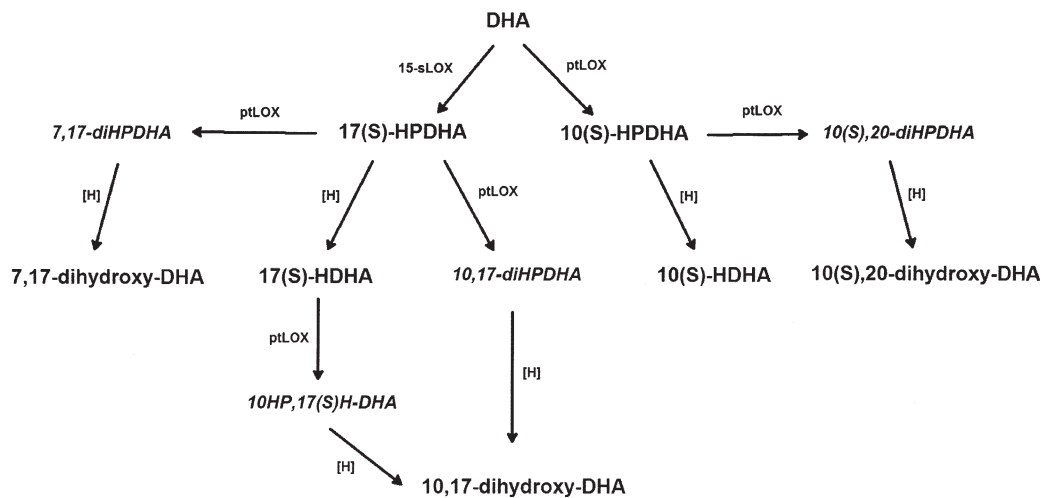
SCHEME 5

soybean 15-LOX product 17(*S*)-H(P)DHA, whereas two novel compounds—10(S)-HPDHA and 10,20-diH(P)DHA—were direct ptLOX products of DHA oxidation (see Schemes 2 and 5). PUFA of the n-3 class have effects in normal physiology and disease (27,28). Some of these effects may be due to metabolites formed by LOX-catalyzed reactions, such as the docosanoids formed from DHA (29). As described here, DHA metabolites can be generated in substantial amounts using plant LOX for use in further studies of (patho)physiological effects of these oxygenated FA in human cells and tissues.

ACKNOWLEDGMENTS

REFERENCES

1. Galliard, T., and Phillips, D.R. (1971) Lipoxygenase from Potato Tubers. Partial Purification and Properties of an Enzyme That Specifically Oxygenates the 9-Position of Linoleic Acid, *Biochem. J. 124*, 431–438.

2. Shimizu, T., Rådmark, O., and Samuelsson, B. (1984) Enzyme with Dual Lipoxygenase Activities Catalyzes Leukotriene A$_4$ Synthesis from Arachidonic Acid, *Proc. Natl. Acad. Sci. USA 81*, 689–693.

3. Reddy, C.C., Bertler, C., and Hammarström, S. (1990) Conversion of Dihomo-γ-linolenic Acid to Mono- and Dihydroxy Acids by Potato Lipoxygenase: Evidence for the Formation of 8,9-Leukotriene A$_3$, *Arch. Biochem. Biophys. 279*, 211–217.

4. Hong, S., Gronert, K., Devchand, P.R., Moussignac, R.L., and Serhan, C.N. (2003) Novel Docosatrienes and 17S-Resolvins Generated from Docosahexaenoic Acid in Murine Brain, Human Blood, and Glial Cells. Autacoids in Anti-inflammation, *J. Biol. Chem. 278*, 14677–14687.

5. Butovich, I.A., Tsys, E.V., and Mogilevich, T.V. (1992) Oxidation of Linoleic Acid and Methyl Linoleate by Potato and Soybean Lipoxygenases: A Comparative Study, *Biokhimiya 57*, 1472–1480.

6. Butovich, I.A., and Reddy, C.C. (2001) Enzyme-Catalyzed and Enzyme-Triggered Pathways in Dioxygenation of 1-Monolinoleoyl-*rac*-glycerol by Potato Tuber Lipoxygenase, *Biochim. Biophys. Acta 1546*, 379–398.

7. Butovich, I.A., Lukyanova, S.M., and Reddy, C.C. (1998) Oxidation of Linoleyl Alcohol by Potato Tuber Lipoxygenase: Possible Mechanism and the Role of Carboxylic Group in Substrate Binding, *Biochem. Biophys. Commun. 249*, 344–349.

8. Butovich, I.A., Luk'yanova, S.M., and Reddy, C.C. (2000) Oxidation of Linoleyl Alcohol by Potato Tuber Lipoxygenase: Kinetics and Positional, Stereo, and Geometrical (*cis, trans*) Specificity of the Reaction, *Arch. Biochem. Biophys. 378*, 65–77.

9. Butovich, I.A., and Kukhar, V.P. (1989) Potato 5-Lipoxygenase. Kinetics of Linoleic Acid Oxidation, *Ukr. Biokhim. Zh. 61*, 106–108.

10. Butovich, I.A., and Kukhar, V.P. (1991) Amphiphilic Aliphatic Acids—Activators of 5-Lipoxygenase. The Adsorption–Micellar Regulatory Mechanism, *Dokl. Akad. Nauk SSSR 316*, 1486–1490.

11. Butovich, I.A., Soloshonok, V.A., Solodenko, V.A., and Kukhar,V.P. (1990) Activation of 5-Lipoxygenase by Lipophilic *n*-Alkyl-Containing Acids—An Allosteric Process, *Bioorg. Khim. 16*, 270–271.

12. Serhan, C.N., Hong S., Gronert, K., Colgan, S.P., Devchand, P.R., Mirick, G., and Moussignac, R.L. (2002) Resolvins: A Family of Bioactive Products of Omega-3 Fatty Acid Transformation Circuits Initiated by Aspirin Treatment That Counter Proinflammation Signals, *J. Exp. Med. 196*, 1025–1037.

13. Serhan, C.N., Arita, M., Hong, S., and Gotlinger, K. (2004) Resolvins, Docosatrienes, and Neuroprotectins, Novel Omega-3 Derived Mediators, and Their Endogenous Aspirin-Triggered Epimers, *Lipids 39*, 1125–1132.

14. Serhan, C.N. (2005) Novel ω-3-Derived Local Mediators in Anti-inflammation and Resolution, *Pharm. Therapeut. 105*, 7–21.

15. Hamberg, M., and Samuelsson, B. (1967) On the Specificity of the Oxygenation of Unsaturated Fatty Acids Catalyzed by Soybean Lipoxidase, *J. Biol. Chem. 242*, 5329–5335.

16. Gibian, M.J., and Vandenberg, P. (1987) Product Yield in Oxygenation of Linoleate by Soybean Lipoxygenase: The Value of the Molar Extinction Coefficient in the Spectrophotometric Assay, *Anal. Biochem. 163*, 343–349.

17. Hamberg, M. (1971) Steric Analysis of Hydroperoxides Formed by Lipoxygenase Oxygenation of Linoleic Acid, *Anal. Biochem. 43*, 515–526.

18. Roy, A.B. (1978) The Sulfatase of Ox Liver. XXI: Kinetic Studies of the Substrate-Induced Inactivation of Sulphatase A, *Biochim. Biophys. Acta 526*, 489–506.

19. Butovich, I.A., and Reddy, C.C. (2002) Inhibition of Potato Lipoxygenase by Linoleyl Hydroxamic Acid: Kinetic and EPR Spectral Evidence for a Two-Step Reaction, *Biochem. J. 365*, 865–871.

20. Schilstra, M.J., Veldink, G.A., and Vliegenthart, J.F. (1994) The Dioxygenation Rate in Lipoxygenase Catalysis Is Determined by the Amount of Iron(III) Lipoxygenase in Solution, *Biochemistry 33*, 3974–3979.

21. Bild, G.S., Ramadoss, C.S., Lim, S., and Axelrod, B. (1977) Double Dioxygenation of Arachidonic Acid by Soybean Lipoxygenase-1, *Biochem. Biophys. Res. Commun. 74*, 949–954.

22. Van Os, C.P.A., Rijke-Schilder, G.P.M., Van Halbeek, H., Verhagen, J., and Vliegenthart, J.F.G. (1981) Double Dioxygenation of Arachidonic Acid by Soybean Lipoxygenase-1. Kinetics and Regio–Stereo Specificities of the Reaction Steps, *Biochim. Biophys. Acta 663*, 177–193.

23. Maas, R.L., Turk, J., Oates, J.A., and Brash, A.R. (1982) Formation of a Novel Dihydroxy Acid from Arachidonic Acid by Lipoxygenase-Catalyzed Double Oxygenation in Rat Mononuclear Cells and Human Leukocytes, *J. Biol. Chem. 257*, 7056–7067.

24. Schwenk, U., Morita, E., Engel, R., and Christophers, E. (1992) Identification of 5-Oxo-15-hydroxy-6,8,11,13-eicosatetraenoic Acid as a Novel and Potent Human Eosinophil Chemotactic Eicosanoid, *J. Biol. Chem. 267*, 12482–12488.

25. Petrich, K., Ludwig, P., Kühn, H., and Schewe, T. (1996) The Suppression of 5-Lipoxygenation of Arachidonic Acid in Human Polymorphonuclear Leukocytes by the 15-Lipoxygenase Product (15*S*)-Hydroxy-(5Z,8Z,11Z,13*E*)-eicosatetraenoic Acid: Structure–Activity Relationship and Mechanism of Action, *Biochem. J. 314*, 911–916.

26. Chavis, C., Vachier, I., Chanez, P., Bousquet, J., and Godard, P. (1996) 5(*S*),15(*S*)-Dihydroxyeicosatetraenoic Acid and Lipoxin Generation in Human Polymorphonuclear Cells: Dual Specificity of 5-Lipoxygenase Towards Endogenous and Exogenous Precursors, *J. Exp. Med. 183*, 1633–1643.

27. Jump, D.B. (2002) The Biochemistry of n-3 Polyunsaturated Fatty Acids, *J. Biol Chem. 277*, 8755–8758.

28. De Caterina, R. (2003) Antiarrhythmic Effects of Omega-3 Fatty Acids: From Epidemiology to Bedside, *American Heart J. 146*, 420–430.

29. Marcheselli, V.M., Hong, S., Lukiw, W.J., Tian, X.H., Gronert, K., Musto, A., Hardy, M., Gimenez, J.M., Chiang, N., Serhan, C.N., and Bazan, N.G. (2003) Novel Docosanoids Inhibit Brain Ischemia–Reperfusion-Mediated Leukocyte Infiltration and Proinflammatory Gene Expression, *J. Biol. Chem. 278*, 43807–43817.

Effect of Homocysteine, Folates, and Cobalamin on Endothelial Cell- and Copper-Induced LDL Oxidation

Ana María Ronco*, Argelia Garrido, Miguel N. Llanos,
Carlos Guerrero-Bosagna, Daniela Tamayo, and Sandra Hirsch

Instituto de Nutrición y Tecnología de los Alimentos (INTA), Universidad de Chile, Casilla 138-11, Santiago, Chile

ABSTRACT: Oxidation of LDL contributes to endothelial dysfunction and atherosclerosis. This process could be associated with hyperhomocysteinemia, a condition that can be reduced after folic acid treatment. Because a reduction in LDL oxidation may improve endothelial function, we studied the effect of some vitamins (folic acid, 5-methyltetrahydrofolic acid, and vitamin B-12) on LDL oxidation, either in the presence or absence of homocysteine. For this purpose, two *in vitro* systems were used: an endothelial cell-catalyzed LDL oxidation system and a cell-free copper-initiated LDL oxidation system. The kinetics of copper-catalyzed LDL oxidation was determined by continuous monitoring of the production of conjugated dienes in the reaction medium. TBARS production, a parameter of lipid peroxidation, was also evaluated. In both *in vitro* systems, only 5-methyltetrahydrofolic acid was able to decrease TBARS production in a concentration-dependent manner, independently of the presence or absence of homocysteine. In the copper-induced LDL oxidation system, vitamin B-12 and 5-methyltetrahydrofolic acid increased the lag time of conjugated diene production by 25 and 47%, respectively, suggesting that both vitamins in this system had antioxidant properties. Folic acid was unable to show antioxidant properties when included in either *in vitro* system. The results demonstrate that 5-methyltetrahydrofolic acid and vitamin B-12 are important protective agents against LDL oxidative modifications.

Paper no. L9644 in *Lipids 40*, 259–264 (March 2005).

LDL are susceptible to oxidation by the vascular wall cells, which contributes to the initiation of endothelial dysfunction (1,2). This condition is a key process in atherosclerosis and has been reported in chronic mild fasting hyperhomocysteinemia (3). The mechanism associated with homocysteine (Hcy)-induced endothelial dysfunction is probably mediated by oxidative stress, leading to increased levels of oxidized LDL (3,4). Hcy, a thiol-containing amino acid derived from the demethylation of dietary methionine, may generate partially reduced reactive oxygen species that are able to stimulate the lipid peroxidation involved in the atherosclerotic process (5). In this process, oxidatively modified LDL may play an important role in endocytosis *via* the macrophage scavenger receptor (2).

The plasma Hcy level in humans is determined by genetic and nutritional factors and is inversely related to the levels of some vitamins such as B-6, B-12, and folic acid (6). These vitamins are necessary for the metabolic remethylation and transsulfuration pathways during Hcy synthesis (3).

Bellamy *et al.* (7) demonstrated that folic acid supplementation reduces plasma levels of Hcy and improves endothelium-dependent vasodilation. On the other hand, recent findings reported by our group showed that hyperhomocysteinemia was not associated with vascular reactivity and oxidative stress in subjects with normal serum folate concentrations (8). The administration of 5-methyltetrahydrofolate (5-MTHF), the active form of folic acid, improved endothelial function in hypercholesterolemic subjects not presenting vascular disease (9). Furthermore, oral folic acid prolonged the lag time of LDL oxidation in children with chronic renal failure (10). In cultured human endothelial cells, 5-MTHF has intrinsic antioxidant actions caused by reducing intracellular production of superoxides (11). In addition, folate has been shown to reduce the susceptibility of LDL to oxidation *in vitro* (12).

Considering that conditions decreasing LDL oxidation could be related to an improvement of endothelial function, the main aim of the present work was to evaluate whether vitamins (folates or vitamin B-12), either in the absence or presence of Hcy, are able to modify LDL oxidation. For this purpose, two *in vitro* systems were used: a cell-free copper-catalyzed system and a human umbilical vein endothelial cell (HUVEC)-mediated oxidative modification of LDL.

MATERIALS AND METHODS

Chemicals. DL-Hcy (95% purity; 2 amino-4-mercaptobutyric acid), folic acid (pteroyl-L-glutamic acid), 5-methyltetrahydrofolic acid (5-methyl-5,6,7,8-tetrahydropteroyl-L-glutamic acid disodium salt), and vitamin B-12 (cyanocobalamin) were from Sigma (St. Louis, MO).

Isolation of LDL. LDL from healthy volunteers were isolated from freshly prepared EDTA-plasma by sequential ultracentrifugation in the density range of 1.019–1.063 g/mL (13) and subsequent dialysis against PBS, pH 7.4, for 24 h; the LDL was used immediately after the dialysis procedure. To determine LDL protein concentration, the BioRad Protein Assay (Bio-Rad Laboratories, Hercules, CA) was used.

HUVEC cultures. HUVEC were isolated from recently

---

*To whom correspondence should be addressed at Laboratorio de Hormonas y Receptores, INTA, Universidad de Chile, Casilla 138-11, Santiago, Chile. E-mail: amronco@inta.cl

Abbreviations: Hcy, homocysteine; HUVEC, human umbilical vein endothelial cell; 5-MTHF, 5-methyltetrahydrofolate; THF, tetrahydrofolate.

A.M. RONCO *ET AL.*

TABLE 1
Effect of Vitamin B-12, Folic Acid, and 5-Methyltetrahydrofolate (5-MTHF) on the Lag Time and Oxidation Rate of Conjugated Diene Production During Copper-Induced LDL Oxidation[a]

Treatment	Lag time (% of control)	Oxidation rate (% of control)
Control (Cu^{2+})	100	100
Vitamin B-12 (10 µmol/L)	125.5 ± 15.3*	66.2 ± 14.2*
Folic acid (10 µmol/L)	108.2 ± 10.2	95.0 ± 9.3
5-MTHF (10 µmol/L)	147.0 ± 19.6*	105.3 ± 7.6

[a]An asterisk (*) indicates $P < 0.01$.

delivered umbilical cords after treatment with collagenase. Cells were grown in M-199 supplemented with 20% FBS (Gibco, Invitrogen Corp., Carlsbad, CA) and 15 µg/mL of endothelial cell growth supplement until confluence. Dishes were trypsinized and cultured until passage 6 to 8 (14).

Kinetics of copper-catalyzed LDL oxidation. Recently dialyzed LDL (50 µg) was incubated at 37°C in PBS, pH 7.4, containing 5 µmol/L CuSO$_4$ in the absence (control) or presence of folic acid (10 µmol/L), vitamin B-12 (10 µmol/L), or 5-MTHF (10 µmol/L). The kinetics of Cu^{2+}-catalyzed LDL oxidation was followed by determining the changes in absorbance at 234 nm every 10 min for 230 min in a Shimadzu UV-160A spectrophotometer. Appropriate reagent blanks were used. Lag times (min) of conjugated diene formation (nmol/mL) were determined (15). The slopes from the curves obtained in the kinetic studies represent the oxidation rates of conjugated diene production.

Kinetics of TBARS production. LDL (100 µg/mL) were incubated at 37°C for 30, 60, and 120 min with 5 µmol/L CuSO$_4$ in PBS (1 mL final volume) in the presence of Hcy (15 or 100 µmol/L) and different 5-MTHF concentrations. At the indicated times, cold TCA was added to the tubes (5% final concentration). After centrifugation, the solution was assayed for lipid peroxides by measuring TBARS in the presence of 0.67% thiobarbituric acid and 40 µmol/L BHT. After boiling for 20 min, absorbance was measured at 530 nm. Results were expressed as TBARS production (nmol/mg LDL) using the appropriate standard solution of 1,1,1,1,-tetraethoxypropane (a malondialdehyde analog) and a molar extinction coefficient of $1.56 \times 10^5 \text{ M}^{-1}\text{cm}^{-1}$ (16).

HUVEC-mediated LDL oxidation. Human endothelial cells (3×10^5) were treated with Hcy (15 or 100 µmol/L) and 100 µg/mL LDL in the absence or presence of folic acid (100 µmol/L), vitamin B-12 (100 µmol/L), or 5-MTHF (100 µmol/L) in M-199 medium without phenol red. After 24 h, the medium was collected and assayed for lipid peroxidation by measuring TBARS as described in the preceding section.

Statistical methods. Data were analyzed using the Sigma Stat program (version 2002; Systat Software Inc., Richmond, CA). Results were expressed as the mean ± SD. Statistical differences involving multiple treatments were determined by Friedman ANOVA and the Kruskal–Wallis nonparametric tests. When treatment differences were revealed by those tests, the differences between individual treatments were determined with Dunn's *post hoc* test. The observed slopes and lag time
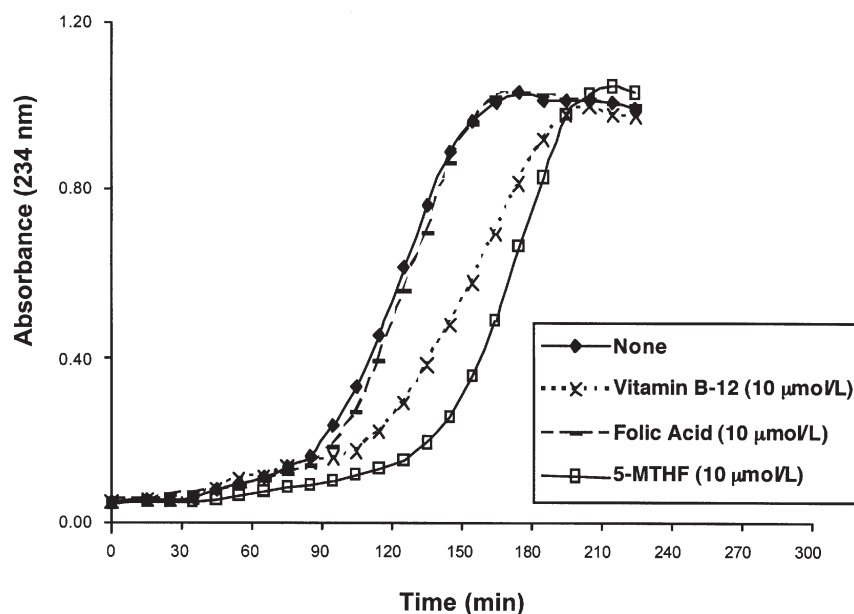
FIG. 1. Formation of conjugated dienes during copper-initiated oxidation of LDL: effect of folic acid, vitamin B-12, and 5-methyltetrahydrofolate (5-MTHF). LDL (50 µg/mL) was incubated at 37°C in PBS containing 5 µmol/L CuSO$_4$ and folic acid (10 µmol/L), vitamin B-12 (10 µmol/L), or 5-MTHF (10 µmol/L). Changes in absorbance at 234 nm were measured every 10 min for 230 min as described in the Materials and Methods section. Values are means of duplicates from one of three representative experiments.

TABLE 2
Effect of Different Doses of Homocysteine (Hcy) and 5-MTHF on TBARS (nmol/mg LDL) Formed During Copper-Initiated LDL Oxidation[a]

Treatment	Incubation time (min)		
	30	60	120
Control	8.5 ± 1.2	22.8 ± 2.5	73.2 ± 5.8
Hcy (15 µmol/L)	8.8 ± 1.3	9.4 ± 1.4*	10.0 ± 0.5*
Hcy (100 µmol/L)	7.2 ± 0.3	8.8 ± 0.8*	9.1 ± 0.7*
5-MTHF (10 µmol/L)	9.8 ± 1.2	12.7 ± 1.0*	75.4 ± 5.6
5-MTHF (50 µmol/L)	6.0 ± 1.3	13.5 ± 1.4*	15.3 ± 0.5*
5-MTHF (100 µmol/L)	8.9 ± 1.1	11.2 ± 1.5*	17.3 ± 1.2*

[a]An asterisk (*) indicates $P < 0.01$. For other abbreviation see Table 1.

values, expressed as percentages of control, were compared with results of the nonparametric chi-square test (Table 1). Significances are reported at $P \leq 0.05$.

RESULTS

Copper-catalyzed LDL oxidation. The kinetics of Cu^{2+}-catalyzed oxidation of LDL was followed spectrophotometrically at 234 nm to determine the lag time for conjugated diene formation. Furthermore, LDL oxidation rates were calculated, as assessed by the slope of diene formation (Fig. 1). As expected, when copper was used to initiate oxidation, increasing incubation times produced sequential elevations of the O.D. of the reaction mixtures. Figure 1 shows that only vitamin B-12 and 5-MTHF delayed conjugated diene formation, by 25 and 47%, respectively, indicating that both compounds had antioxidant properties. Folic acid did not show antioxidant properties (Fig. 1, Table 1). Interestingly, vitamin B-12, in addition to significantly increasing the lag time, also greatly reduced the oxidation rate (Table 1). In the cell-free system, the kinetics of TBARS production was followed for 2 h at 30 min intervals; as usual, Cu^{2+} was used to catalyze LDL oxidation (Table 2). Production of TBARS was highly reduced when Hcy (15 or 100 µmol/L) was added to the incubation media, an effect significant after 60 min of incubation and maintained for at least 120 min. A reduced production of TBARS also was obtained when 50 or 100 µmol/L of 5-MTHF was added to the LDL oxidation system (Table 2). This effect was observed after 60 min of incubation and was maintained for 120 min. The reduced TBARS production obtained with the lower concentration of 5-MTHF tested (10 µmol/L) was evident until 60 min of incubation, after which TBARS production reached levels similar to those observed in the control group at 2 h of incubation (Table 2).

Cell-catalyzed LDL oxidation. When HUVEC were incubated in the absence of Hcy with control buffer, folic acid, or vitamin B-12 for 24 h, there were no differences in cell-initiated LDL oxidation, as assessed by TBARS production measurements. TBARS values were in the range of 35–40 nmol/mg LDL in all the aforementioned experimental conditions (Fig. 2). Conversely, TBARS production was dramatically decreased

to approximately 6 nmol/mg LDL when cells were incubated with 100 µmol/L 5-MTHF either in the presence or absence of Hcy.
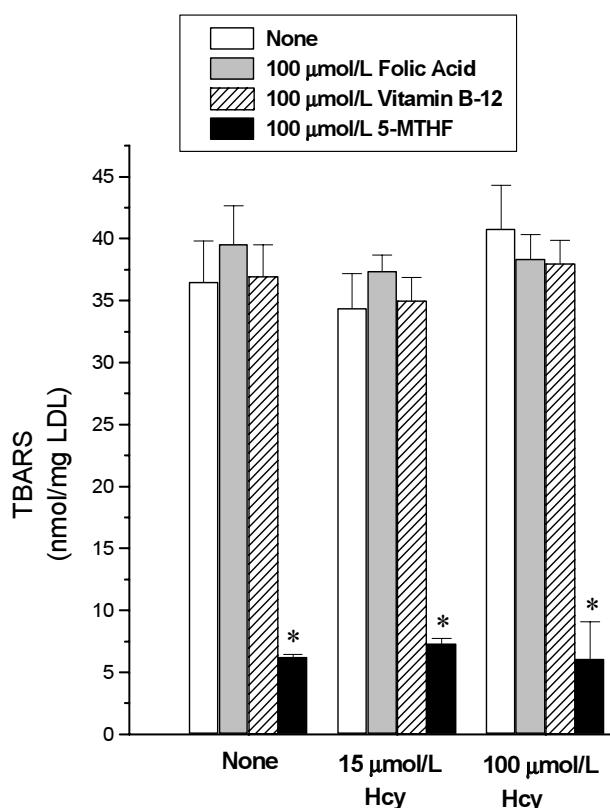
FIG. 2. TBARS production during human endothelial cell-catalyzed oxidation of LDL. Effect of folic acid, vitamin B-12, and 5-MTHF in the presence or absence of homocysteine (Hcy). Human endothelial cells (3 × 10^{5}) were incubated with LDL (100 µg/mL) at 37°C for 24 h in the presence or absence of 15 or 100 µmol/L of Hcy and folic acid (100 µmol/L), vitamin B-12 (100 µmol/L), or 5-MTHF (100 µmol/L). TBARS production in the incubation media was determined as described in the Materials and Methods section. Data are expressed in nmol/mg LDL and are given as means ± SD of three separate experiments with different cell cultures (passage 3 to 6). *$P < 0.05$. For other abbreviation see Figure 1.

DISCUSSION

This study demonstrates for the first time a protective effect of 5-MTHF against *in vitro* HUVEC-catalyzed oxidation of LDL. We also demonstrate here a vitamin B-12-mediated protection against LDL oxidation; however, this effect was evident only in the copper-induced LDL oxidation system and not in the HUVEC-mediated oxidation of LDL. Furthermore, the vitamin B-12 antioxidant effect was manifested not only by increased lag times of conjugated diene production but also by reduced LDL oxidation rates. These unexpected results are difficult to explain, but it is quite possible that they are related mainly to the structural forms of vitamin B-12, which may present different oxidation states of the cobalt atom bonded to the molecule (17,18). We suggest here that the cyanocobalamin—a cob(III)alamin—used in this study, may generate "base-off" cobalamin species in water solutions (where the dimethylbenzimidazol ligand axially coordinated to cobalt is detached by protonation to the nitrogen imidazol). Base-off configuration has a tendency to change the cobalt coordination number from six to five and even to four [Co(III), Co(II), and Co(I), respectively] (19–21). Thus, the cobalt present in cyanocobalamin solutions may have +1 (I), +2 (II), and +3 (III) oxidation states. All these chemical species may participate in redox reactions involving Co(III/II) and Co(II/I) couples with different redox potentials (22). According to these antecedents, cyanocobalamin in solution may show a dynamic equilibrium among different chemical species: cob(I)alamin, cob(II)alamin, and cob(III)alamin. The presence of Cu^{2+} in the incubations as the initiator of LDL oxidation could, in our case, affect cob(I)-/cob(II)-/cob(III)alamin equilibrium to preferentially increase the cob(III)alamin oxidized form. These sequential redox reactions should also transform Cu^{2+} to Cu^{1+} to some extent. Since the low-oxidation-state copper ion is not an inducer of lipoperoxidation, the presence of this ion should not result in LDL oxidation. Thus, in our *in vitro* system vitamin B-12 might participate in sequential redox reactions that, as a result, reduce Cu^{2+} to Cu^{1+}, a condition that obviously avoids LDL oxidation. Therefore, vitamin B-12 is able to protect LDL indirectly against Cu^{2+}-initiated oxidation as a consequence of its ability to reduce Cu^{2+} to Cu^{1+}. This hypothesis could explain the lack of antioxidant effect of cyanocobalamin in the HUVEC-initiated LDL oxidation system and also the reduced copper-induced oxidation rate of LDL, an effect not elicited by 5-MTHF. This effect of cyanocobalamin could be of physiological relevance, having a therapeutic potential in several pathologies involving alterations in transition metal homeostasis and redox activity conducive to the development of neurodegenerative disorders (18,23). In addition, of main interest could be the clinical use of the most reduced forms of vitamin B-12 [cob(I)alamin], such as methylcobalamin and adenosylcobalamin (17).

In both *in vitro* oxidation systems, 5-MTHF was capable of protecting against LDL oxidation, an effect evidenced by decreased TBARS production in the incubation media. These results agree with previously published data demonstrating that 5-MTHF was able to produce a potent protective effect on the copper-mediated oxidation of LDL (12). Nevertheless, folic acid was unable to protect LDL, indicating no antioxidant properties of this folate form and suggesting that this last compound was not converted to 5-MTHF in HUVEC. Nevertheless, it is worth mentioning that most dietary folates are converted to 5-MTHF (the main circulating form of folates) in the intestinal cells (24).

Rezk *et al*. (25) recently reported that folic acid has a poor antioxidant activity in peroxynitrite scavenging and lipid peroxidation inhibition. Conversely, fully reduced folate forms such as tetrahydrofolate (THF) and 5-MTHF showed the higher antioxidant activities (25). The antioxidant activity of folates could mainly reside in the pterin moiety, being optimal when it is fully reduced. The reduced pterin moiety may have electron-donating effects that are likely involved in the antioxidant activity of THF and 5-MTHF (25,26). The antioxidant potency of 5-MTHF also may be enhanced by the methyl group present at the 5-amino group, which is able to increase the electron-donating effect of the group. This may explain the high antioxidant activity of 5-MTHF against LDL oxidation found in the present study. Although we observed an inhibition of TBARS production with 10 μmol/L 5-MTHF, this concentration was not high enough to support antioxidant activity during the whole incubation time (Table 2). In addition, the absence of a significant difference in the protective effect when 50 or 100 μmol/L of 5-MTHF was added indicates that, under our experimental conditions, a maximum protective effect could be reached in a range of concentrations greater than 10 and equal to or less than 50 μmol/L.

The relevance of these *in vitro* observations could be unclear, because the usual plasma concentration for folates is in the low nanomolar range (9), and we used relatively high concentrations of 5-MTHF in our experiments. However, is important to note that red-cell folates rise to the micromolar range after 5 mg of oral supplementation of folic acid (27).

The 5-MTHF antioxidant effect was independent of Hcy concentration, thus discarding the involvement of indirect actions of Hcy on free radical-induced oxidation of LDL. Although in this study intracellular oxidative stress was not evaluated, the lowering effects of 5-MTHF on TBARS production, together with previous results showing reduced levels of superoxide ions in 5-MTHF-treated endothelial cells (11), suggest that the 5-MTHF antioxidant effect could be related to decreased levels of intracellular reactive oxygen species (28).

This study also demonstrates that pathophysiological noncytotoxic Hcy concentrations have no effect on TBARS production in the endothelial cell system. The lack of oxidative effect of Hcy is in accordance with our previous clinical findings in mild hyperhomocysteinemic subjects (8). When copper ions were used to initiate oxidation, 15 and 100 μmol/L of Hcy reduced the generation of lipid peroxides after 60–120 min of incubation. The protective antioxidant effect of Hcy may be explained by its free radical-scavenging properties due to the presence of thiol groups, which are more evident at higher Hcy concentrations and lower incubation periods (29). The similar

inhibitory effect on TBARS production with 15 or 100 μmol/L Hcy revealed that a plateau could have been reached even with the lowest Hcy concentration used, indicating that at those incubation times, lower concentrations of Hcy should have been sufficient to reduce the copper-induced oxidative effects on LDL lipids. A previous study reported a mild increase and a decrease in lipid peroxide and TBARS production when low (6 and 25 μmol/L) or high (>100 μmol/L) Hcy concentrations, respectively, were added to a copper-induced LDL oxidation system (29). Nevertheless, in our cell-free system, 15 μmol/L of Hcy protected against LDL oxidation; this apparent discrepancy may be explained by the different incubation times used in both studies.

A protective effect of Hcy (>25 μmol/L) in a mononuclear cell system for at least 6 h of incubation was described previously (1); however, in our HUVEC-initiated LDL oxidation system, Hcy was unable to protect against LDL oxidation. Discrepancies between those results and ours could be attributable to the different cells used and to the possible oxidation of Hcy to homocystine due to the longer incubation time of our experiments (24 h). Although pro-oxidant properties of Hcy were shown previously, the experimental conditions were completely different from the ones in this study (30).

Several *in vitro* studies have demonstrated that Hcy can alter the vasoactive properties of cultured endothelial cells by impairing the production or bioavailability of some cellular mediators (31–33). However, those results were obtained with >200 μmol/L Hcy in the culture medium, a concentration that, although not deleterious for endothelial cell survival, may affect cell function (31). Since the Hcy concentrations added to the culture media were similar to those commonly found in hyperhomocysteinemic subjects (≥15 μmol/L) (8), it is suggested here that, under mild hyperhomocysteinemia, Hcy may be unable to alter LDL oxidation and perhaps other cell mediators within the endothelium.

In summary, the main results presented in this study permit us to postulate that 5-MTHF protects against oxidative modifications of LDL in endothelial cells, an effect independent of Hcy concentration. This 5-MTHF-mediated antioxidant effect may be related to a decreased oxidative stress status in endothelial cells. The finding showing the antioxidant activity of cyanocobalamin could have relevant therapeutic potential in alterations in transition metal homeostasis and redox activity conducive to several degenerative disorders and may suggest priority for the clinical use of the most reduced vitamin B-12 forms.

ACKNOWLEDGMENTS

REFERENCES

1. Sparrow, C.P., and Olszewski, A. (1993) Cellular Oxidation of Low Density Lipoprotein Is Caused by Thiol Production in Media Containing Transition Metal Ions, *J. Lipid Res. 3*, 1219–1228.
2. Witztum, J.L., and Steinberg, D. (1991) Role of Oxidized Low Density Lipoprotein in Atherogenesis, *J. Clin. Invest. 88*, 1785–1792.
3. Olszewski, A., and McCully, K. (1993) Homocysteine Metabolism and the Oxidative Modification of Protein and Lipids, *Free Radical Biol. Med. 14*, 683–693.
4. Ventura, P., Panini, R., Verlato, C., Scarpetta, G., and Salvioli, G. (2000) Peroxidation Indices and Total Antioxidant Capacity in Plasma During Hyperhomocysteinemia Induced by Methionine, *Metabolism 49*, 225–228.
5. Jocelyn, P.C. (1972) *Biochemistry of the SH Group: The Occurrence, Chemical Properties, Metabolism and Biological Function of Thiols and Disulphides*, pp. 84 –115, Academic Press, New York.
6. Hankey, G.J., and Eikelboom, J.W. (1999) Homocysteine and Vascular Disease, *Lancet 35*, 407–413.
7. Bellamy, M.F., McDowell, I.F., Ramsey, M.W., Brownlee, M., Newcombe, R.G., and Lewis, M.J. (1999) Oral Folate Enhances Endothelial Function in Hyperhomocysteinaemic Subjects *Eur. J. Clin. Invest. 29*, 659–662.
8. Hirsch, S., Ronco, A.M., Vasquez, M., de la Maza, M.P., Garrido, A., Barrera, G., Gattas, V., Glasinovic, A., Leiva, L., and Bunout, D. (2004) Hyperhomocysteinemia in Healthy Young Men and Elderly Men with Normal Serum Folate Concentration Is Not Associated with Poor Vascular Reactivity or Oxidative Stress, *J. Nutr. 134*, 1832–1835.
9. Verhaar, M.C., Wever, R.M., Kastelein, J.J., van Dam, T., Koomans, H.A., and Rabelink, T.J. (1998) 5-Methyltetrahydrofolate, the Active Form of Folic Acid, Restores Endothelial Function in Familial Hypercholesterolemia, *Circulation 97*, 237–241.
10. Bennett-Richards, K., Kattenhorn, M., Donald, A., Oakley, G., Varghese, Z., Rees, L., and Deanfield, J.E. (2002) Does Oral Folic Acid Lower Total Homocysteine Levels and Improve Endothelial Function in Children with Chronic Renal Failure? *Circulation 105*, 1810–1815.
11. Stroes, E.S., van Faassen, E.E., Yo, M., Martasek, P., Boer, P., Govers, R., and Rabelink, T.J. (2000) Folic Acid Reverts Dysfunction of Endothelial Nitric Oxide Synthase, *Circ. Res. 86*, 1129–1134.
12. Nakano, E., Higgins, J.A., and Powers, H.J. (2001) Folate Protects Against Oxidative Modification of Human LDL, *Br. J. Nutr. 86*, 637–639.
13. Havel, R.J., Eder, H.A., and Bradgon, H.F. (1955) The Distribution and Chemical Composition of Ultracentrifugally Separated Lipoproteins in Human Serum, *J. Clin. Invest. 34*, 1345–1352.
14. Terramani, T.T., Eton, D., Bui, P.A., Wang, Y., Weaver, F.A., and Yu, H. (2000) Human Macrovascular Endothelial Cells: Optimization of Culture Conditions, *In Vitro Cell. Dev. Biol.–Animal 36*, 125–132.
15. Esterbauer, H., Striegl, G., Puhl, H., and Rotheneder, M. (1989) Continuous Monitoring of *in vitro* Oxidation of Human Low Density Lipoprotein, *Free Radical Res. Commun. 6*, 67–75.
16. Lapenna, D., Ciofani, G., Pierdomenico, S.D., Giamberardino, M.A., and Cuccurullo, F. (2001) Reaction Conditions Affecting the Relationship Between Thiobarbituric Acid Reactivity and Lipid Peroxides in Human Plasma, *Free Radical Biol. Med. 31*, 331–335.
17. Kelly, G. (1997) The Coenzyme Forms of Vitamin B12: Toward an Understanding of Their Therapeutic Potential, *Altern. Med. Rev*. 2, 459–471.
18. McCaddon, A., Regland, B., Hudson, P., and Davies, G. (2002) Functional Vitamin B_{12} Deficiency and Alzheimer Disease, *Neurology 58*, 1395–1399.
19. Wirt, M.D., Sagi, I., and Chance, M.R. (1992) Formation of a

Square Planar Co(I)B12 Intermediate. Implications for Enzyme Catalysis, *Biophys. J. 63*, 412–417.

20. Wirt, M.D., and Chance, M.R. (1993) Temperature Dependent Coordination Effects in Base-off Adenosyl and Methylcobalamin by X-ray Edge Spectroscopy, *J. Inorg. Biochem. 49*, 265–273.

21. Van Doorslaer, S., Jeschke, G., Epel, B., Goldfard, D., Eichel, R.A., Krautler, B., and Schweiger, A. (2003) Axial Solvent Co-ordination in "Base-off" Cob(II)alamin and Related Co(II)-cor-rinates Revealed by 2D-EPR, *J. Am. Chem. Soc. 125*, 5915–5927.

22. Chemaly, S.M., Jack, L.A., Yellowlees, L.J., Harper, P.L., Heeg, B., and Pratt, J.M. (2004) Vitamin B12 as an Allosteric Cofactor: Dual Fluorescence, Hysteresis, Oscillations and the Selection of Corrin over Porphyrin, *Dalton Trans. 21*, 2125–2134.

23. Moreira, P.I., Siedlak, S.L., Aliev, G., Zhu, X., Cash, A.D., Smith, M.M., and Perry, G. (2004) Oxidative Stress Mechanisms and Potential Therapeutics in Alzheimer Disease, *J. Neural Transm.*, DOI 10.1007/s00702-004-0242-8 (published on-line December 7, 2004).

24. Pentieva, K., McNulty, H., Reichert, R., Ward, M., Strain, J.J., McKillop, D.J., McPartlin, J.M., Connolly, E., Molloy, A., Kramer, K., and Scott, J. (2004) The Short-Term Bioavailabilities of [6*S*]-5-Methyltetrahydrofolate and Folic Acid Are Equivalent in Men, *J. Nutr. 13*, 580–585.

25. Rezk, B.M., Haenen, G., van der Vijgh, W.J.F., and Bast, A. (2003) Tetrahydrofolate and 5-Methyltetrahydrofolate Are Folates with High Antioxidant Activity. Identification of the Antioxidant Pharmacophore, *FEBS Lett. 555*, 601–605.

26. Heijnen, C.G., Haenen, G.R., Oostveen, R.M., Stalpers, E.M., and Bast, A. (2002) Protection of Flavonoids Against Lipid Per-oxidation: The Structure–Activity Relationship Revisited, *Free Radical Res. 36*, 575–581.

27. Verhaar, M.C., Wever, R., Kastelein, J., Loon, D., Milstien, S., Koomans, H.A., and Rabelink, T.J. (1999). Effects of Oral Folic Acid on Endothelial Function in Familial Hypercholesterolemia, *Circulation 100*, 335–338.

28. Doshi, S.N., McDowell, I.F., Moat, S.J., Lang, D., Newcombe, R.G., Kredan, M.B., Lewis, M.J., and Goodfellow, J. (2001) Folate Improves Endothelial Function in Coronary Artery Disease: An Effect Mediated by Reduction of Intracellular Superoxide? *Arterioscler. Thromb. Vasc. Biol. 21*, 1196–1202.

29. Halvorsen, B., Brude, I., Drevon, C.A., Nysom, J., Ose, L., Christiansen, E.N., and Nenseter, M.S. (1996) Effect of Homo-cysteine on Copper Ion-Catalyzed, Azo Compound-Initiated and Mononuclear Cell-Mediated Oxidative Modification of Low Density Lipoprotein, *J. Lipid Res. 37*, 1591–1600.

30. Hirano, K.T., Ogihara, M.M., Yasuda, H., Tamai, N., Kawa-mura, N., and Mino, M. (1994) Homocysteine Induces Iron-Cat-alyzed Lipid Peroxidation of Low Density Lipoprotein That Is Prevented by α-Tocopherol, *Free Radical Res. 21*, 267–276.

31. Demuth, K., Atger, V., Borderie, D., Benoit, M.O., Sauvaget, D., Lotersztajn, S., and Moatti, N. (1999) Homocysteine De-creases Endothelin-1 Production by Cultured Human Endothe-lial Cells, *Eur. J. Biochem. 263*, 367–376.

32. Zhang, X., Li, H., Jin, H., Ebin, Z., Brodsky, S., and Goligorsky, M.S. (2000) Effects of Homocysteine on Endothelial Nitric Oxide Production, *Am. J. Physiol Renal Physiol. 279,* F671–F678.

33. Wang, J., Dudman, N.P., and Wilcken, D.E. (1993) Effects of Homocysteine and Related Compounds on Prostacyclin Produc-tion by Cultured Human Vascular Endothelial Cells, *Thromb. Haemostasis 70*, 1047–1052.

Dietary Conjugated Linoleic Acid Increases Endurance Capacity and Fat Oxidation in Mice During Exercise

Wataru Mizunoya, Satoshi Haramizu, Tetsuro Shibakusa, Yuki Okabe, and Tohru Fushiki*

Laboratory of Nutrition Chemistry, Division of Food Science and Biotechnology,
Graduate School of Agriculture, Kyoto University, Kyoto 606-8502, Japan

ABSTRACT: Ingestion of CLA activates β-oxidation and causes loss of body fat in rodents. We investigated the effects of dietary CLA on endurance capacity and energy metabolism during exercise in mice. Five-week-old male BALB/c mice were fed a control diet containing 1.0% linoleic acid or a diet containing 0.5% CLA that replaced an equivalent amount of linoleic acid for 1 wk. The maximum swimming time until fatigue was significantly higher in the CLA-fed group than in the control group. During treadmill running, the respiratory exchange ratio was significantly lower in the CLA-fed group, but oxygen consumption did not differ significantly between groups, suggesting that FA contributed more as an energy substrate in the CLA-fed mice. The muscle lipoprotein lipase activity was significantly higher in the CLA-fed group than in the control group. These results suggest that CLA ingestion increases endurance exercise capacity by promoting fat oxidation during exercise.

Paper no. L9626 in *Lipids 40*, 265–271 (March 2005).

CLA refers to a group of positional and geometric isomers derived from linoleic acid (LA). CLA is found in foods such as ruminant meats, pasteurized dairy products, and processed cheeses (1–3). Dietary CLA has many potential health benefits, such as reducing fat mass and the risk of carcinogenesis (4–8) and atherosclerosis (9,10).

Ingesting CLA for several weeks can reduce body fat content. For example, a CLA-supplemented diet (0.5–1.5% CLA) decreases adipose tissue mass in mice (11–13). The metabolic rate is higher in mice fed a CLA-supplemented diet than in mice fed a control diet for six (13) to eight weeks (14); similar results have been reported in rats (15). We previously demonstrated that a single oral administration of CLA increases serum concentrations of catecholamines and FFA, fat oxidation, and energy expenditure in mice (16). Others have reported that CLA enhances the β-oxidation of FA acids in various tissues, assessed by measuring the activity of carnitine palmitoyltransferase (CPT), the rate-limiting enzyme of the mitochondrial β-oxidation system (12,17). These results suggest that CLA reduces body fat levels by enhancing fat oxidation.

One important effect of endurance exercise training is the sparing of muscle glycogen stores during exercise through an increased ability of skeletal muscle to oxidize fat (18,19). This suggests that enhancing fat oxidation decreases carbohydrate consumption by the muscle (especially muscle glycogen) and increases endurance capacity. For example, oral administration of capsaicin increases the endurance capacity of mice by enhancing the secretion of catecholamines and the use of FA as a substrate (20). We speculated that CLA, which enhances fat oxidation, might increase endurance exercise performance. To our knowledge, no research has reported the effects of CLA on endurance exercise performance. The purpose of this study was to investigate the possible benefits of CLA as a dietary supplement to increase endurance exercise performance.

MATERIALS AND METHODS

Animals and diets. Five-week-old male BALB/c mice (Japan Shizuoka Laboratory Center, Hamamatsu, Japan) were used. The mice were housed in standard cages (33 × 23 × 12 cm) under controlled conditions of temperature (22 ± 0.5°C), RH (50%), and lighting (lights on 1800–0600 h). They were given free access to water and a control diet (1.0% LA) or a diet containing 0.5% CLA incorporated into the diet by replacing an equivalent amount (w/w) of LA. Table 1 shows the composition of the experimental diets based on the AIN-76 formulation containing CLA. This composition was described fully in our previous report (14). Food intake was recorded every 2 d. The care and treatment of the experimental animals conformed to

TABLE 1
Composition of Experimental Diets[a]

Ingredient (g/kg)	Group	
	Control	CLA
Casein	195.8	195.8
L-Methionine	3.0	3.0
Cornstarch	665.3	665.3
Soybean oil	30.0	30.0
CLA	0.0	5.0
LA	10.0	5.0
Cellulose	50.0	50.0
Mineral mix	35.0	35.0
Vitamin mix	10.0	10.0
(±)-α-Tocopherol	0.5	0.5
TBHQ	0.5	0.5

[a]LA, linoleic acid.

the Kyoto University guidelines for ethical treatment of laboratory animals.

Materials. We used unesterified safflower LA in the control diet and synthesized CLA from unesterified safflower LA, both of which were synthesized from safflower oil and analyzed by Rinoru Oil Mills Co., Ltd. (Tokyo, Japan). The composition of samples was 17.4% palmitic acid, 2.3% stearic acid, 6.5% oleic acid, and 73.5% LA or CLA. The composition of CLA was analyzed by GC and determined to consist of 34.0% *cis*-9,*trans*-11 and *trans*-9,*cis*-11 CLA; 35.1% *trans*-10,*cis*-12 CLA; 2.5% *cis*-9,*trans*-11 and *cis*-10,*cis*-12 CLA; and 1.9% *trans*-9,*trans*-11 and *trans*-10,*trans*-12 CLA.

Maximum swimming time. In the first week, 5-wk-old BALB/c mice (*n* = 32) were made to swim for 30 min in a current with a flow rate of 5 L/min twice on two consecutive days to accustom them to swimming. The baseline swimming time to exhaustion was measured at a flow rate of 7 L/min on three occasions every 2 d. We calculated the means and SD of the three maximum swimming times and selected SD values of 10 min or less. We then eliminated the mice with the longest or the shortest mean maximum swimming times, until the final SD values approached 20% of the means. Finally, we selected 16 mice from the original 32 according to these criteria and divided them into two groups, a CLA-fed group and a control group, with equivalent average swimming times. Details of these methods have been described in a previous report (21). Mice were fasted for 2 h before the measurement of maximum swimming time. All mice were provided the control diet during the first week. In the second week, all mice, including nonexercised (sedentary) mice, were provided with the CLA diet or control diet for 1 wk and swam to exhaustion at a flow rate of 7 L/min to measure the maximum swimming time.

Organ weights and energy substrates. Mice were killed by decapitation immediately after swimming to exhaustion, with nonexercised control mice killed at the same time. Blood was rapidly collected from the neck. The gastrocnemius and quadriceps muscles; epididymal, perirenal, and inguinal fat; brown adipose tissue; and liver, heart, spleen, and kidneys were removed and weighed. The gastrocnemius and quadriceps muscles and liver were rapidly frozen in liquid nitrogen and stored at −80°C for subsequent analysis of tissue glycogen concentration and muscle lipoprotein lipase (LPL) activity. The muscle and liver glycogen contents were measured spectrophotometrically using enzymatic techniques as described elsewhere (22). Serum was obtained by centrifugation ($740 \times g$ for 10 min) and stored at −70°C until analyzed. Serum concentrations of glucose (Glucose-ARII; Wako Pure Chemical Industries, Osaka, Japan), FFA (NEFA C Test Wako; Wako Pure Chemical Industries), TG (Triglyceride G Test Wako; Wako Pure Chemical Industries), and ketone bodies (Ketone Test; Sanwa Chemical Institute, Nagoya, Japan) were measured using commercial kits.

Respiratory gas analysis. The mice not used for measuring the maximal swimming time were made to run for 30 min at 21 m/min twice during the week before the experiment to accustom them to the treadmill. This speed elicited about 60% of maximal oxygen consumption in our pilot experiment and was assumed to represent a moderate level of exercise that slightly exceeded the animals' lactic acid threshold. We selected 12 mice from the 16 nonswimmers by eliminating those mice with the highest and lowest body weights. Six days after assigning all mice to their respective groups, these mice were placed in a treadmill chamber and made to run for 42 min. The initial running speed was 6 m/min for 2 min, and the speed was increased 3 m/min every 2 min until reaching 21 m/min, after which it remained constant for 30 min. Respiratory gas was monitored throughout the run.

Apparatus. The system used to measure the swimming time to exhaustion was an adjustable-current swimming apparatus for mice. The details have been described previously (23). Briefly, an acrylic plastic pool ($90 \times 45 \times 45$ cm) was filled with water to a depth of 38 cm, the current was generated with a pump (type C-P60H; Hitachi, Tokyo, Japan), and the water temperature was maintained precisely at 34°C with an electric heater. This swimming apparatus has been used previously to evaluate the effects of food and nutrients such as capsaicin (20), an overdose of caffeine (23), hydroxycitrate (24), Nanpao® (25), and medium-chain TG (26).

The gas analyzer used to assess metabolic rate consisted of CO_2 and O_2 analyzers (model RL-600; Alco System, Tokyo, Japan), and a switching system (model ANI6-A-S; Alco System) to sample gas from each metabolic chamber. Mice were separated into two groups, and each mouse was placed in a metabolic chamber designed to measure respiratory gas. The details of the methods have been described in a previous report (24). Briefly, room air was pumped through the chambers, and expired air was dried in a thin cotton column and then directed to an O_2/CO_2 analyzer. The amounts of oxidized fat and carbohydrate were estimated from the oxygen consumption and respiratory exchange ratio (RER) values using the RL-600 software. Details of the equations have been described elsewhere (24). Data for each chamber were collected every 2 min.

The running system was a treadmill (model Simplex II; Columbus Instruments, Columbus, OH) apparatus for mice. The system consisted of three running lanes of equal dimensions ($28.8 \times 4.7 \times 4$ cm); each lane was encased in a metabolic chamber with an inside volume of ~1000 cm^3. An electric fan was used to mix the air. The system independently monitored respiratory gases for one to three mice.

Measurement of muscle LPL activity. The muscle LPL activity was measured using a fluorescent method described elsewhere (27). Samples (40–60 mg) of skeletal muscle (quadriceps) were ground in liquid nitrogen and incubated in 400 µL of Krebs–Ringer solution, 10 mM Tris-HCl buffer (pH 8.4) containing 150 mM NaCl, 2 mM EDTA, 1 g/100 mL of BSA, and 5 U (100 mg/L) heparin (28), with gentle shaking at 25°C. After 30 min, the tissue was removed from the medium by centrifugation for 5 min ($8,300 \times g$), and the supernatant was used to measure LPL activity using a commercial kit that includes a nonfluorescent substrate emulsion that becomes intensely fluorescent upon interaction with LPL (Roar Biomedical, New York, NY). The total protein content of each sample was measured by the Bradford method with Coomassie brilliant blue
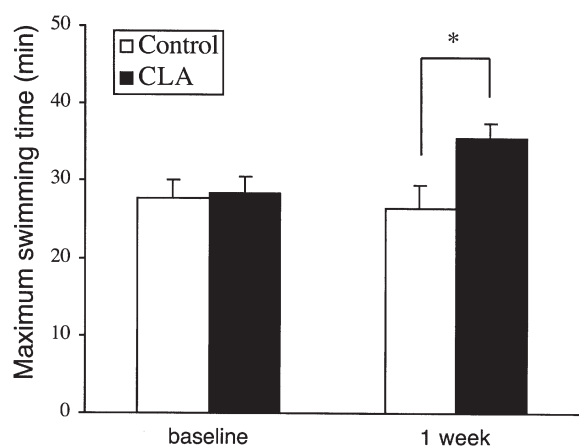
FIG. 1. The maximum swimming time to fatigue in BALB/c mice measured at baseline and after 1 wk. Mice were fed either a diet containing 0.5% CLA or a control diet for 1 wk. Values are means ± SE for eight mice. Swimming capacity was measured at a flow rate of 7 L/min. *Significant difference between groups (*P* < 0.05, unpaired Student's *t*-test).

solution. LPL activity was assessed relative to the protein content of the tissue.

Statistical analysis. Data are expressed as means ± SEM. Student's *t*-test was used to compare the two dietary groups after dietary intervention. Analyses were performed with the StatView software package (Macintosh Version J 5.0; Abacus Concepts, Berkeley, CA); *P* < 0.05 was accepted as significant.

RESULTS

Food intake did not differ significantly between the two dietary groups. The accumulated 7-d food intake was 24.8 ± 1.5 g/mouse (3.5 g/mouse per day) in the CLA-fed group and 25.4 ± 1.4 g (3.6 g/mouse per day) in the control group. Swimming endurance did not differ significantly between the control and CLA-fed groups before the start of dietary intervention (Fig.

1). After 1 wk of the control diet or the diet containing 0.5% CLA, swimming endurance capacity was significantly higher, by 25%, in CLA-fed mice than in control mice (Fig. 1). The maximal swimming time of the control group was similar before and after dietary intervention.

Oxygen consumption during running did not differ between the two dietary groups (Fig. 2A). The RER increased throughout the first 20 min and then decreased in both groups and was significantly lower in CLA-fed mice than in control mice (Fig. 2B). Fat oxidation, calculated from the RER and oxygen consumption, was consistently higher in the CLA group than in the control group (Fig. 3A). Carbohydrate oxidation during the 42-min run was lower in the CLA group than in the control group (Fig. 3B).

Sedentary mice were included as an indicator of the nonexercised, resting state. The body weight of sedentary mice did not change significantly after the week of dietary intervention. The weights of adipose tissue from various sites, including epididymal fat, perirenal fat, inguinal fat, and brown adipose tissue, were significantly lower in the sedentary CLA-fed mice than in the sedentary control mice (Table 2). Similar trends (i.e., lower adipose tissue weights in CLA-fed mice) were observed in mice sacrificed after swimming to fatigue (data not shown). In sedentary mice, serum glucose concentrations did not differ significantly between the two dietary groups. The serum concentrations of FFA and ketone bodies were significantly lower, and serum TG concentration tended to be lower in the sedentary CLA group than in the sedentary control group (Table 3). Similar trends (i.e., lower concentrations of FFA, ketone bodies, and TG) were observed in CLA-fed mice sacrificed after swimming to fatigue, but these values did not differ significantly. After swimming to fatigue, the serum glucose concentrations of the control and CLA-fed groups were higher than in their respective sedentary groups, and the serum concentrations of FFA, ketone bodies, and TG were significantly higher in the CLA-fed mice than in the CLA-fed sedentary
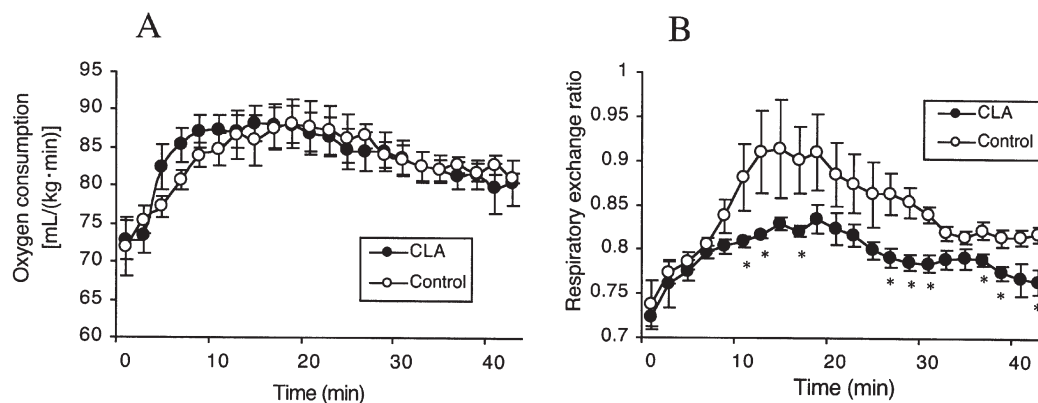
FIG. 2. Oxygen consumption (A) and respiratory exchange ratio (B) during treadmill running in BALB/c mice fed the 0.5% CLA-containing diet for 6 d. Values are means ± SE for 5–7 mice that ran in the treadmill chamber for 42 min. The initial running speed was 6 m/min, and speed was increased 3 m/min every 2 min until it reached 21 m/min, after which it remained constant. *Significant difference between groups (*P* < 0.05, unpaired Student's *t*-test).
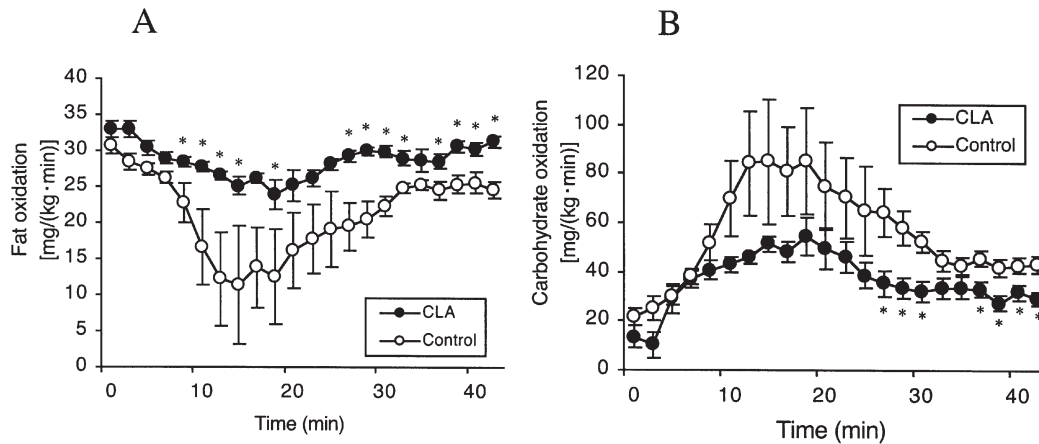
FIG. 3. Fat oxidation (A) and carbohydrate oxidation (B) during treadmill running in BALB/c mice fed the 0.5% CLA-containing diet for 6 d. Values are means ± SE for 5–7 mice that ran in the treadmill chamber for 42 min. The initial running speed was 6 m/min, and speed was increased 3 m/min every 2 min until it reached 21 m/min, after which it remained constant. Fat and carbohydrate oxidation were calculated from the respiratory exchange ratio and oxygen consumption (24). *Significant difference between groups ($P < 0.05$, unpaired Student's *t*-test).

group. The concentrations of liver and gastrocnemius muscle glycogen did not differ between dietary groups in the sedentary mice or in the exercised mice (Table 4).

LPL activity was measured to determine whether CLA feeding increased fat oxidation in skeletal muscle. LPL activity in skeletal muscle was significantly higher after swimming to fatigue in the CLA group than in the control group (Fig. 4); LPL activity also tended to be higher in the sedentary CLA-fed mice than in the sedentary control mice (data not shown).

DISCUSSION

Previous studies (11–13) demonstrated that CLA supplementation causes weight loss in rodents; we reported previously that CLA supplementation decreases body weight and adipose tissue weight in a dose-dependent manner (14). These changes appear to be independent of diet and have been found with high-fat and high-carbohydrate diets (13). This reduction in body fat is not related to energy intake (29,30). It has been speculated that the reduction in fat mass reflects an increase in energy expenditure and fat oxidation (12). Our previous study showed that oxygen consumption increased in mice fed a diet containing 1.0% CLA for 8 wk (14). Several investigators have reported that CLA enhances CPT activity in some tissues, indicating a greater efficiency of FA oxidation. Greater CPT activity in skeletal muscle (12,17), brown adipose tissue, and liver (17) may inhibit TG storage in adipose tissue and decrease fat accumulation. A previous study showed that a single oral administration of CLA increased both fat oxidation and oxygen consumption in mice (16).

During moderate-intensity exercise, muscle uses circulating FFA, extramuscular glucose, muscle TG, and muscle glycogen as substrates (31–33). The amount of glycogen stored in working muscles is an important determinant of endurance exercise capacity (34). Increased fat utilization during endurance exer-

cise improves endurance capacity by sparing muscle glycogen stores (35,36). For example, caffeine elevates the plasma concentration of FFA and decreases the rate of glycogen depletion during exercise, enhancing fat oxidation and decreasing muscle glycogen utilization (37). We found that 1 wk of the CLA diet significantly increased endurance capacity in mice. To determine whether enhanced fat use caused the increase in endurance capacity, we analyzed the respiratory gas of mice running in the treadmill chamber. Analysis of respiratory gas enables one to evaluate energy metabolism continuously during exercise. As expected, during running, estimated fat oxidation was higher and estimated carbohydrate oxidation lower in the CLA group than in the control group (Fig. 3). These data suggest that the increase in endurance capacity was caused by enhanced fat utilization during exercise. We did not examine the muscle glycogen concentration continuously during exercise because it was difficult to include enough swimming mice in this protocol. However, two studies have reported increased en-

TABLE 2
Body Weight and Organ Weights in Mice Fed 0.5% CLA-Containing Diet or the Control Diet for 1 wk[a]

Variable (g)	Control	CLA
Body weight	22.9 ± 0.5	22.7 ± 0.6
Gastrocnemius	0.244 ± 0.007	0.252 ± 0.006
Quadriceps	0.354 ± 0.006	0.367 ± 0.012
Liver	1.217 ± 0.048	1.318 ± 0.038
Heart	0.119 ± 0.004	0.123 ± 0.004
Spleen	0.098 ± 0.005	0.099 ± 0.005
Kidney	0.383 ± 0.016	0.393 ± 0.009
Perirenal fat	0.170 ± 0.014	0.064 ± 0.003*
Epididymal fat	0.351 ± 0.022	0.175 ± 0.009*
Brown adipose tissue	0.085 ± 0.003	0.061 ± 0.005*
Inguinal fat	0.237 ± 0.018	0.099 ± 0.012*

[a]Values are means ± SE for 7–9 mice. *Significantly different from control group ($P < 0.05$).

TABLE 3
Serum Concentrations of Substrates in Mice Fed 0.5% CLA-Containing Diet or the Control Diet for 1 wk[a]

	Sedentary		Swimming to Fatigue	
	Control	CLA	Control	CLA
Glucose (mg/dL)	153.4 ± 4.2	172.3 ± 2.8	$199.5 \pm 2.8^{\dagger}$	$222.4 \pm 2.8^{\dagger}$
FFA (mEq/L)	1.23 ± 0.05	$0.78 \pm 0.03^*$	1.22 ± 0.02	$1.08 \pm 0.02^{\dagger}$
Ketone body (mg/dL)	369.3 ± 30.4	$135.5 \pm 19.89^*$	381.4 ± 12.4	$288.5 \pm 10.2^{\dagger}$
TG (mg/dL)	160.6 ± 6.4	131.5 ± 3.5	195.4 ± 6.6	$186.3 \pm 4.2^{\dagger}$

[a]Values are means ± SE for 7–8 mice. *Significantly different from each control group ($P < 0.05$). [†]Significantly different between sedentary and swimming to fatigue in the same group ($P < 0.05$).

TABLE 4
Gastrocnemius Muscle and Liver Glycogen Concentrations in Mice Fed 0.5% CLA-Containing Diet or the Control Diet for 1 wk[a]

	Sedentary		Swimming to fatigue	
Tissue concentration (mg/g)	Control	CLA	Control	CLA
Gastrocnemius	3.348 ± 0.381	3.063 ± 0.260	2.392 ± 0.165	2.687 ± 0.376
Liver	53.56 ± 2.49	52.48 ± 3.85	41.71 ± 3.10	42.63 ± 2.17

[a]Values are means ± SE for 7–9 mice.

durance swimming capacity after feeding capsaicin (20) and hydroxycitric acid (24), and both proposed that the increased endurance capacity might be caused by increased fat utilization during exercise, which spared muscle glycogen. We believe that CLA produced a similar effect in our study.

The blood lactic acid threshold correlates with the exercise intensity that produces excess lactic acid and reflects increasing reliance on carbohydrate utilization, because lactic acid is produced only by anaerobic glycolysis. The blood pH is constantly adjusted within a relatively narrow range, and carbon dioxide is liberated from carbonate in the blood, which helps maintain pH when lactic acid accumulates in the blood during intense exercise. The liberated carbon dioxide is expired from the lungs, increasing the RER. RER was lower during exercise in the CLA group than in the control group, indicating greater use of FFA and less of carbohydrate as a substrate; we speculate that blood lactic acid concentration was also lower during exercise in the CLA group.

The mechanism responsible for the enhanced fat oxidation induced by CLA remains unclear. LPL activity was significantly higher in the CLA group than in the control group. Blood TG is hydrolyzed by LPL in the muscle capillaries, releasing FA that are taken up by skeletal muscle. LPL activity in skeletal muscle increases after exercise training (38). Several investigators have reported that CLA enhances CPT activity (12,17). In addition, increased muscle LPL activity may play a role in enhanced FA oxidation in skeletal muscle. Previous studies have shown that CLA inhibits LPL activity in a dose-dependent manner in 3T3-L1 adipocytes (12) and that LPL activity in adipose tissue decreases in mice fed CLA for 4 d (39). It has been suggested that LPL is regulated independently in various tissues; for example, Ong *et al*. (40) reported that exercise training increased LPL activity in skeletal muscle but not

in adipose tissue and heart. Our results, showing an increase in LPL activity in skeletal muscle in the CLA group, are consistent with those obtained in adipose tissue. It is possible that CLA inhibits lipogenesis in adipose tissue and promotes fat oxidation in skeletal muscle.

In this study, the serum concentration of ketone bodies was lower in the sedentary CLA group than in the sedentary control group (Table 3). Ketone bodies are produced in the liver from FA and oxidized in extrahepatic tissue; enhanced oxidation of ketone bodies in the extrahepatic tissue in the CLA group might be responsible for the CLA-mediated reduction of the serum concentration of ketone bodies. Similarly, the serum
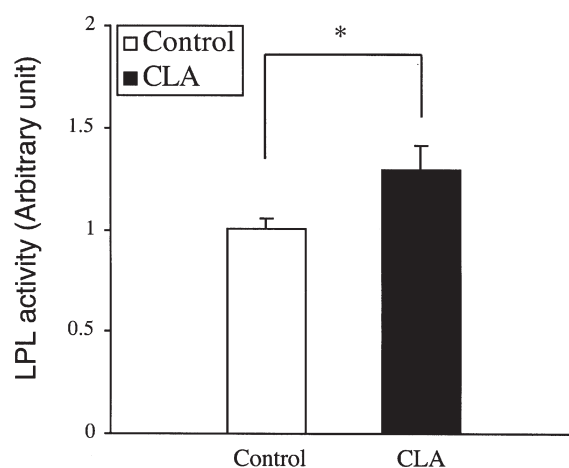
FIG. 4. Muscle lipoprotein lipase (LPL) activity after swimming to fatigue in BALB/c mice fed the 0.5% CLA-containing diet for 1 wk. Values are means ± SE for 6–7 mice. *Significant difference between groups ($P < 0.05$, unpaired Student's *t*-test).

concentration of FFA was lower in the sedentary CLA group than in the sedentary control group. Our data are consistent with those from a previous report, which speculated that the lower serum concentration of FFA might have been caused by decreased adipose tissue mass in the CLA group (15).

Several isomers of CLA act as high-affinity ligands and activators of peroxisome proliferator-activated receptor (PPAR)α (41). CLA may stimulate fat oxidation by inducing PPARα, which plays an important role in fat metabolism. PPARα regulates acyl-CoA oxidase, cytochrome P4504A1, and liver FA-binding protein (42), which may activate the oxidation of body fat. However, dietary CLA reduces adipose tissue weight and induces some PPAR-responsive genes in liver to a similar extent in PPARα-null mice fed a diet containing CLA and in wild-type mice (43). It is possible that CLA modulates fat metabolism *via* mechanisms involving other isoforms of PPAR. For example, it has been reported that CLA increases PPARγ mRNA in adipose tissue (44).

There appears to be an isomer-specific effect of CLA. The *trans*-10,*cis*-12 CLA isomer is much more effective at lowering adipose tissue mass than the *cis*-9,*trans*-11 CLA isomer in mice (45) and rats (15), and *trans*-10,*cis*-12 CLA appears to be the effective isomer for modulating gene expression in cultured 3T3-L1 preadipocytes (46). To ensure consistency between studies, we used the same mixture of CLA in this study as in our previous experiments (14,16). It is possible that our results are due to the *trans*-10,*cis*-12 CLA contained in the mixture.

In humans, the effects of CLA on weight loss are inconclusive at present (47–50), most likely because the dosages of CLA relative to body weight were lower in human than in animal studies. Our dosage was 0.9 g/kg, and the dosage used in other studies on mice was about 1.0 g/kg, whereas the highest reported dosage in humans was 6.8 g/d (0.075 g/kg body weight) (47). Thus, CLA might not reach the effective dosage in humans. However, two studies have shown that these doses were adequate to increase insulin resistance, lipid peroxidation, and inflammation in humans (51,52). In human studies, supplementation with high doses should be conducted carefully until further information becomes available on the effects and adverse side effects of CLA. It is also possible that the effectiveness differs between isomers according to species because the mechanism underlying the action of CLA is not clearly known. Furthermore, Ohnuki *et al.* (16) suggested that CLA enhances sympathetic nervous activity and energy metabolism. The marked effects of CLA in rodent models could arise *via* activation of brown adipose tissue by enhanced sympathetic nervous activity, an effect that would not occur in older humans. At present, we cannot rule out brown adipose tissue as a cause of weight loss in CLA-fed rodents.

In summary, feeding mice a diet containing 0.5% CLA for 6 to 7 d increased endurance exercise capacity and fat oxidation and reduced RER and carbohydrate utilization during exercise. Muscle LPL activity increased in CLA-fed mice, suggesting that LPL plays a role in enhancing FA oxidation. These results suggest that the increase in endurance capacity induced by CLA feeding in mice might be explained by the promotion of fat oxidation during exercise.

REFERENCES

1. Chin, S.F., Liu, W., Storkson, J.M., Ha, Y.L., and Pariza, M.W. (1992) Dietary Sources of Conjugated Dienoic Isomers of Linoleic Acid, a Newly Recognized Class of Anticarcinogens, *J. Food Comp. Anal. 5*, 185–197.
2. Ha, Y.L., Grimm, N.K., and Pariza, M.W. (1987) Anticarcinogens from Fried Ground Beef: Heat-Altered Derivatives of Linoleic Acid, *Carcinogenesis 8*, 1881–1887.
3. Ha, Y.L., Grimm, N.K., and Pariza, M.W. (1989) Newly Recognized Anticarcinogenic Fatty Acids: Identification and Quantification in Natural and Processed Cheeses, *J. Agric. Food Chem. 37*, 75–81.
4. Chew, B.P., Wong, T.S., Shultz, T.D., and Magnuson, N.S. (1997) Effects of Conjugated Dienoic Derivatives of Linoleic Acid and Beta-Carotene in Modulating Lymphocyte and Macrophage Function, *Anticancer Res. 17*, 1099–1106.
5. Ip, C., Scimeca, J., and Thompson, H.J. (1994) Conjugated Linoleic Acid: A Powerful Anticarcinogen from Animal Fat Sources, *Cancer 74*, 1050–1054.
6. Ip, C., Singh, M., Thompson, H.J., and Scimeca, J.A. (1994) Conjugated Linoleic Acid Suppresses Mammary Carcinogenesis and Proliferative Activity of the Mammary Gland in the Rat, *Cancer Res. 54*, 1212–1215.
7. Shultz, T.D., Chew, B.P., and Seaman, W.R. (1992) Differential Stimulatory and Inhibitory Responses of Human MCF-7 Breast Cancer Cells to Linoleic Acid and Conjugated Linoleic Acid in Culture, *Anticancer Res. 12*, 2143–2145.
8. Visonneau, S., Cesano, A., Tepper, S.A., Scimeca, J.A., Santoli, D., and Kritchevsky, D. (1997) Conjugated Linoleic Acid Suppresses the Growth of Human Breast Adenocarcinoma Cells in SCID Mice, *Anticancer Res. 17*, 969–973.
9. Lee, K.N., Kritchevsky, D., and Pariza, M.W. (1994) Conjugated Linoleic Acid and Atherosclerosis in Rabbits, *Atherosclerosis 108*, 19–25.
10. Nicolosi, R.J., Rogers, E.J., Kritchevsky, D., Scimeca, J.A., and Huth, P.J. (1997) Dietary Conjugated Linoleic Acid Reduces Plasma Lipoproteins and Early Aortic Atherosclerosis in Hypercholesterolemic Hamsters, *Artery 22*, 266–277.
11. Belury, M.A., and Kempa-Steczko, A. (1997) Conjugated Linoleic Acid Modulates Hepatic Lipid Composition in Mice, *Lipids 32*, 199–204.
12. Park, Y., Albright, K.J., Liu, W., Storkson, J.M., Cook, M.E., and Pariza, M.W. (1997) Effect of Conjugated Linoleic Acid on Body Composition in Mice, *Lipids 32*, 853–858.
13. West, D.B., Delany, J.P., Camet, P.M., Blohm, F., Truett, A.A., and Scimeca, J. (1998) Effects of Conjugated Linoleic Acid on Body Fat and Energy Metabolism in the Mouse, *Am. J. Physiol. 275*, R667–R672.
14. Ohnuki, K., Haramizu, S., Ishihara, K., and Fushiki, T. (2001) Increased Energy Metabolism and Suppressed Body Fat Accumulation in Mice by a Low Concentration of Conjugated Linoleic Acid, *Biosci. Biotechnol. Biochem. 65*, 2200–2204.
15. Nagao, K., Wang, Y.M., Inoue, N., Han, S.Y., Buang, Y., Noda, T., Kouda, N., Okamatsu, H., and Yanagita, T. (2003) The 10*trans*,12*cis* Isomer of Conjugated Linoleic Acid Promotes Energy Metabolism in OLETF Rats, *Nutrition 19*, 652–656.
16. Ohnuki, K., Haramizu, S., Oki, K., Ishihara, K., and Fushiki, T. (2001) A Single Oral Administration of Conjugated Linoleic Acid Enhanced Energy Metabolism in Mice, *Lipids 36*, 583–587.
17. Rahman, S.M., Wang, Y., Yotsumoto, H., Cha, J., Han, S., Inoue, S., and Yanagita, T. (2001) Effects of Conjugated Linoleic Acid on Serum Leptin Concentration, Body-Fat Accumulation, and β-Oxidation of Fatty Acid in OLETF Rats, *Nutrition 17*, 385–390.
18. Maughan, R.J. (1998) The Sports Drink as a Functional Food: Formulations for Successful Performance, *Proc. Nutr. Soc. 57*, 15–23.

19. Williams, C. (1998) Dietary Macro- and Micronutrient Requirements of Endurance Athletes, *Proc. Nutr. Soc. 57*, 1–8.

20. Kim, K.M., Kawada, T., Ishihara, K., Inoue, K., and Fushiki, T. (1997) Increase in Swimming Endurance Capacity of Mice by Capsaicin-Induced Adrenal Catecholamine Secretion, *Biosci. Biotechnol. Biochem. 61*, 1718–1723.

21. Mizunoya, W., Oyaizu, S., Ishihara, K., and Fushiki, T. (2002) Protocol for Measuring the Endurance Capacity of Mice in an Adjustable-Current Swimming Pool, *Biosci. Biotechnol. Biochem. 66*, 1133–1136.

22. Hassid, W.Z., and Abraham, S. (1957) Chemical Procedure for Analysis of Polysaccharides: Determination of Glycogen and Starch, *Methods Enzymol. 3*, 34–37.

23. Matsumoto, K., Ishihara, K., Tanaka, K., Inoue, K., and Fushiki, T. (1996) An Adjustable-Current Swimming Pool for the Evaluation of Endurance Capacity of Mice, *J. Appl. Physiol. 81*, 1843–1849.

24. Ishihara, K., Oyaizu, S., Onuki, K., Lim, K., and Fushiki, T. (2000) Chronic (−)-Hydroxycitrate Administration Spares Carbohydrate Utilization and Promotes Lipid Oxidation During Exercise in Mice, *J. Nutr. 130*, 2990–2995.

25. Saito, M., Ishihara, K., Onuki, K., Inoue, K., and Fushiki, T. (1998) Effects of Nanpao®, a Mixture of 31 Chinese Crude Drugs, on Increasing Endurance Exercise Performance of Swimming Mice, *Nat. Med. 52*, 14–21.

26. Fushiki, T., Matsumoto, K., Inoue, K., Kawada, T., and Sugimoto, E. (1995) Swimming Endurance Capacity of Mice Is Increased by Chronic Consumption of Medium-Chain Triglycerides, *J. Nutr. 125*, 531–539.

27. Yamazaki, H., Arai, M., Matsumura, S., Inoue, K., and Fushiki, T. (2002) Intracranial Administration of Transforming Growth Factor-β3 Increases Fat Oxidation in Rats, *Am. J. Physiol. 283*, E536–E544.

28. Taskinen, M.R., Nikkila, E.A., Huttunen, J.K., and Hilden, H. (1980) A Micromethod for Assay of Lipoprotein Lipase Activity in Needle Biopsy Samples of Human Adipose Tissue and Skeletal Muscle, *Clin. Chim. Acta 104*, 107–117.

29. DeLany, J.P., Blohm, F., Truett, A.A., Scimeca, J.A., and West, D.B. (1999) Conjugated Linoleic Acid Rapidly Reduces Body Fat Content in Mice Without Affecting Energy Intake, *Am. J. Physiol. 276*, R1172–R1179.

30. West, D.B., Blohm, F.Y., Truett, A.A., and DeLany, J.P. (2000) Conjugated Linoleic Acid Persistently Increases Total Energy Expenditure in AKR/J Mice Without Increasing Uncoupling Protein Gene Expression, *J. Nutr. 130*, 2471–2477.

31. Ahlborg, G., Felig, P., Hagenfeldt, L., Hendler, R., and Wahren, J. (1974) Substrate Turnover During Prolonged Exercise in Man. Splanchnic and Leg Metabolism of Glucose, Free Fatty Acids, and Amino Acids, *J. Clin. Invest. 53*, 1080–1090.

32. Coyle, E.F. (1995) Substrate Utilization During Exercise in Active People, *Am. J. Clin. Nutr. 61*, 968S–979S.

33. Wahren, J., Felig, P., Ahlborg, G., and Jorfeldt, L. (1971) Glucose Metabolism During Leg Exercise in Man, *J. Clin. Invest. 50*, 2715–2725.

34. Bergstrom, J., Hermansen, L., Hultman, E., and Saltin, B. (1967) Diet, Muscle Glycogen and Physical Performance, *Acta Physiol. Scand. 71*, 140–150.

35. Miller, W.C., Bryce, G.R., and Conlee, R.K. (1984) Adaptations to a High-Fat Diet That Increase Exercise Endurance in Male Rats, *J. Appl. Physiol. 56*, 78–83.

36. Nakamura, M., Brown, J., and Miller, W. C. (1998) Glycogen Depletion Patterns in Trained Rats Adapted to a High-Fat or High-Carbohydrate Diet, *Int. J. Sports Med. 19*, 419–424.

37. Spriet, L.L., MacLean, D.A., Dyck, D.J., Hultman, E.,

Cederblad, G., and Graham, T.E. (1992) Caffeine Ingestion and Muscle Metabolism During Prolonged Exercise in Humans, *Am. J. Physiol. 262*, E891–E898.

38. Kiens, B., and Lithell, H. (1989) Lipoprotein Metabolism Influenced by Training-Induced Changes in Human Skeletal Muscle, *J. Clin. Invest. 83*, 558–564.

39. Xu, X., Storkson, J., Kim, S., Sugimoto, K., Park, Y., and Pariza, M.W. (2003) Short-Term Intake of Conjugated Linoleic Acid Inhibits Lipoprotein Lipase and Glucose Metabolism but Does Not Enhance Lipolysis in Mouse Adipose Tissue, *J. Nutr. 133*, 663–667.

40. Ong, J.M., Simsolo, R.B., Saghizadeh, M., Goers, J.W., and Kern, P.A. (1995) Effects of Exercise Training and Feeding on Lipoprotein Lipase Gene Expression in Adipose Tissue, Heart, and Skeletal Muscle of the Rat, *Metabolism 44*, 1596–1605.

41. Moya-Camarena, S.Y., Vanden Heuvel, J.P., Blanchard, S.G., Leesnitzer, L.A., and Belury, M.A. (1999) Conjugated Linoleic Acid Is a Potent Naturally Occurring Ligand and Activator of PPARα, *J. Lipid. Res. 40*, 1426–1433.

42. Schoonjans, K., Staels, B., and Auwerx, J. (1996) The Peroxisome Proliferator Activated Receptors (PPARs) and Their Effects on Lipid Metabolism and Adipocyte Differentiation, *Biochim. Biophys. Acta 1302*, 93–109.

43. Peters, J.M., Park, Y., Gonzalez, F.J., and Pariza, M.W. (2001) Influence of Conjugated Linoleic Acid on Body Composition and Target Gene Expression in Peroxisome Proliferator-Activated Receptor α-Null Mice, *Biochim. Biophys. Acta 1533*, 233–242.

44. McNeel, R.L., Smith, E.O., and Mersmann, H.J. (2003) Isomers of Conjugated Linoleic Acid Modulate Human Preadipocyte Differentiation, *In Vitro Cell Dev. Biol. Anim. 39*, 375–382.

45. Park, Y., Storkson, J.M., Albright, K.J., Liu, W., and Pariza, M.W. (1999) Evidence That the *trans*-10,*cis*-12 Isomer of Conjugated Linoleic Acid Induces Body Composition Changes in Mice, *Lipids 34*, 235–241.

46. Kang, K., Liu, W., Albright, K.J., Park, Y., and Pariza, M.W. (2003) *trans*-10,*cis*-12 CLA Inhibits Differentiation of 3t3-L1 Adipocytes and Decreases PPAR γ Expression, *Biochem. Biophys. Res. Commun. 303*, 795–799.

47. Blankson, H., Stakkestad, J.A., Fagertun, H., Thom, E., Wadstein, J., and Gudmundsen, O. (2000) Conjugated Linoleic Acid Reduces Body Fat Mass in Overweight and Obese Humans, *J. Nutr. 130*, 2943–2948.

48. Mougios, V., Matsakas, A., Petridou, A., Ring, S., Sagredos, A., Melissopoulou, A., Tsigilis, N., and Nikolaidis, M. (2001) Effect of Supplementation with Conjugated Linoleic Acid on Human Serum Lipids and Body Fat, *J. Nutr. Biochem. 12*, 585–594.

49. Zambell, K.L., Keim, N.L., Van Loan, M.D., Gale, B., Benito, P., Kelley, D.S., and Nelson, G.J. (2000) Conjugated Linoleic Acid Supplementation in Humans: Effects on Body Composition and Energy Expenditure, *Lipids 35*, 777–782.

50. Zambell, K.L., Horn, W.F., and Keim, N.L. (2001) Conjugated Linoleic Acid Supplementation in Humans: Effects on Fatty Acid and Glycerol Kinetics, *Lipids 36*, 767–772.

51. Smedman, A., Vessby, B., and Basu, S. (2004) Isomer-Specific Effects of Conjugated Linoleic Acid on Lipid Peroxidation in Humans: Regulation by α-Tocopherol and Cyclo-oxygenase-2 Inhibitor, *Clin. Sci. (London) 106*, 67–73.

52. Riserus, U., Smedman, A., Basu, S., and Vessby, B. (2004) Metabolic Effects of Conjugated Linoleic Acid in Humans: The Swedish Experience, *Am. J. Clin. Nutr. 79*, 1146S–1148S.

Size and Number of Lymph Particles Measured by a Particle Sizer During Absorption of Structured Oils in Rats

Trine Porsgaard*, Jirí Kánský, Sarah Mason, and Huiling Mu

BioCentrum-DTU and Center for Advanced Food Studies (LMC),
Technical University of Denmark, 2800 Lyngby, Denmark

ABSTRACT: Chylomicrons transport absorbed fat from the intestine to the circulation. During dietary fat absorption, the chylomicrons become larger in diameter, and in some studies an increase in chylomicron number has been observed as well. In the present study, we compared particle size and number in rat lymph following administration of four different oils. We administered fish oil, medium-chain TAG (MCT), and two structured oils differing in intramolecular structure, with either medium-chain FA in the outer positions of the TAG and long-chain n-3 PUFA in the *sn*-2 position (MLM oil) or with the reverse structure (LML oil), to lymph-cannulated rats and collected lymph in fractions for the following 8 h. Chylomicron size was measured by a particle size analyzer immediately after collection, and from these data the number of chylomicrons present was estimated. The number of particles in lymph increased during the absorption of oils containing long-chain PUFA (MLM, LML, and fish oil), whereas it was not affected by administration of MCT. The FA from MCT were probably absorbed *via* the portal vein; therefore, only a small number of particles were measured in lymph. When comparing the two structured oils, we observed a tendency toward a higher number of particles after LML administration, although the difference was not statistically significant. The highest number of particles after administration of all oils was observed in the size intervals 53–80 and 80–121 nm and probably represented small chylomicrons. Thus, the FA composition influenced the number of particles in lymph during absorption, whereas TAG structure had only a minor influence.

Paper no. L9665 in *Lipids 40*, 273–279 (March 2005).

Chylomicrons are the transport vehicles for intestinally absorbed fat, and the FA composition of the chylomicrons reflects the FA composition of dietary fat. During absorption, chylomicrons are formed in the enterocytes, are released to the lymphatics, and then enter the circulation. Chylomicron formation can be regulated through changes in the size and number of particles secreted to the lymph. Some studies suggest that chylomicron size depends mainly on the amount of fat absorbed and transported to the lymphatics, and that during fat absorption the particles increase in diameter (1–3). Hayashi *et al.* (2) observed that infusion of triolein in rats increased the size but not the number of chylomicrons produced by the small intestine. The size of the chylomicrons formed during absorption may be influenced by the degree of saturation of the dietary fats, since studies have shown that absorption of unsaturated fats produces larger chylomicrons compared with absorption of saturated fats (1,4,5). Some studies have suggested an influence on chylomicron number during absorption of dietary fat as well. Kalogeris and Story (4) suggested that feeding different fat sources influences the number of chylomicrons produced, since they observed a greater phospholipid output in rat lymph during infusion of butter oil compared with infusion of corn oil. Degrace *et al.* (6) observed that chylomicrons were large after administration of a bolus of corn oil to lymph-cannulated rats and were small and more numerous after cod liver oil administration. This means that diverse results have been obtained regarding the size and number of chylomicrons produced during absorption.

Differences in the FA composition and structure as well as differences in the size of chylomicrons in response to dietary lipids affect the clearance of these TAG-rich lipoproteins in plasma (1,7–9), and this may further influence the extent of the postprandial lipemia. Zilversmith (10) suggested that raised levels of chylomicrons and chylomicron remnants, which circulate following a meal, play a role in the development of atherosclerosis. Furthermore, Levy *et al.* (1) suggested that large chylomicrons are removed faster than smaller ones. This fast removal could be the reason for the low plasma TAG level observed after feeding diets rich in unsaturated fats, since unsaturated FA give rise to large chylomicrons. Contrary to this result, Martins *et al.* (8) found that when a similar number of particles were injected into rats, the small particles were removed faster than the large particles. These differences may be the result of differences in experimental design.

The effect on chylomicron composition, size, and number of differences in intramolecular structure of dietary TAG has been investigated in several studies. Aoe *et al.* (11) showed that the positional distribution of FA influenced the size and composition of chylomicrons in rats but not the number of chylomicrons during absorption. In contrast to this study, Carvajal *et al.* (12) observed no effect of different dietary TAG structures on chylomicron size. Previously performed studies on lymphatic absorption of structured lipids showed that the TAG structure influenced the absorption of dietary lipids (13–15) and thereby may influence the clearance of chylomicrons from circulation.

---

*To whom correspondence should be addressed at BioCentrum-DTU, Biochemistry and Nutrition, Technical University of Denmark, Søltofts Plads, Building 224, DK-2800 Lyngby, Denmark. E-mail: tpo@biocentrum.dtu.dk
Abbreviations: LML, specific structured TAG (M = medium-chain FA, L = long-chain FA); MCT, medium-chain TAG; MLM, specific structured TAG (M = medium-chain FA, L = long-chain FA).

The aim of the present study was to compare the size and number of lymph particles produced during absorption of a bolus of structured TAG containing decanoic acid (10:0) and n-3 PUFA of marine origin. Animal and human feeding studies have revealed that the intake of diets rich in n-3 PUFA has important effects on postprandial lipemia and lipoprotein metabolism, as reviewed by Harris (16). Two structured TAG were produced by enzymatic interesterification, giving rise to TAG with different intramolecular structures, and the impact of these structures on lymph particle size and number was compared with the impact of fish oil and a medium-chain TAG (MCT). The absorption of oils was followed for 8 h with frequent collection of lymph fractions. In most studies involving chylomicron size determinations, the usual approach has been to examine the lymph particles by electron microscopy followed by measurements of particle diameter (1,5,6,11,12). In the present study, we analyzed the lymph fractions immediately after collection using a particle sizer (Mastersizer 2000; Malvern Instruments, Malvern, Worcestershire, United Kingdom). The laser diffraction technique is rapid and can measure many particles, thereby reducing the time for analysis by severalfold in comparison with electron microscopy. The particle sizer determined the drop size distribution based on the scattering pattern produced by particles moving through the path of a laser beam. From the particle size and lymph volume, the number of particles in each fraction was calculated. We are not aware of this technique being used to determine the size of lymph particles, and this could be an area to pursue further. However, Leuschner *et al.* (17) reported good agreement between a laser light-scattering method using a Malvern Mastersizer and a scanning transmission electron microscopy method used to measure particle size distributions of *Bacillus* spore suspensions with a median size of 900 nm.

MATERIALS AND METHODS

Experimental oils. Fish oil was purchased from Aarhus United A/S (Aarhus, Denmark), and MCT was from Grünau GmbH Illertissen (Illertissen, Germany). Two specific structured oils were produced by enzymatic interesterification. MLM (where M = medium-chain FA and L = long-chain FA) was made by a specific reaction between enriched fish oil (Epax 4510 TG; Pronova Biocare a.s., Lysaker, Norway) and 10:0 (Henkel Kimianika Sdn. Bhd., Selangor, Malaysia) catalyzed by Lipozyme RM IM (Novozymes, Bagsværd, Denmark), resulting in regiospecific TAG with n-3 PUFA mainly in the *sn*-2 position. LML was produced by a specific reaction between tri-10:0 (Grünau GmbH Illertissen) and ethyl esters produced from marine oils (Epax 6000 EE containing ~60% n-3 FA; Pronova Biocare) catalyzed by Lipozyme RM IM, resulting in regiospecific TAG with n-3 PUFA mainly in the *sn*-1,3 positions. The interesterifications were performed in a packed-bed reactor, and the products were purified by short-path distillation (18,19). The FA composition of TAG and the structure of TAG represented by the FA composition in *sn*-2 MAG (Table 1) were measured as described previously (20).

Housing of animals. Male Specific Pathogen-Free Wistar rats (Taconic M&B, Ll. Skensved, Denmark) were housed two per plastic cage in a temperature- (21°C) and humidity- (50%) controlled environment on a 12 h/12 h light/dark cycle with a standard nonpurified diet (Altromin No. 1324; Chr. Petersen A/S, Ringsted, Denmark) and with water freely available. They were acclimatized to the housing conditions for 10 d before surgery and weighed 250–310 g at the time of surgery. The experiment was approved by the Danish Committee for Animal Experiments.

TABLE 1
FA Composition in TAG and in *sn*-2 MAG of Oils (mol%)[a]

FA	MLM		LML		MCT		Fish oil	
	TAG	*sn*-2	TAG	*sn*-2	TAG	*sn*-2	TAG	*sn*-2
8:0	0.7	0.3	2.0	2.0	62.2	59.7	—	—
10:0	41.5	11.2	38.2	60.5	36.2	39.2	—	—
14:0	0.3	0.7	0.3	0.3	—	—	8.5	12.6
16:0	2.4	6.3	1.2	1.3	—	—	18.0	22.3
16:1	1.0	2.6	0.5	0.6	—	—	6.9	7.4
18:0	2.3	6.6	2.9	3.1	—	—	2.1	0.5
18:1n-9	4.1	9.7	5.7	5.9	—	—	12.6	7.4
18:1n-7	2.3	5.1	2.0	1.9	—	—	2.2	0.8
18:2n-6	0.5	1.1	0.6	0.6	—	—	2.9	3.0
18:3n-3	0.4	0.9	0.7	0.6	—	—	3.3	3.1
18:4n-3	2.5	3.5	0.7	0.2	—	—	4.3	4.3
20:1	1.9	3.8	1.8	2.0	—	—	7.1	2.2
20:4n-3	1.1	1.5	1.1	0.3	—	—	0.8	0.7
20:5n-3	27.1	34.6	23.4	12.2	—	—	7.6	9.2
22:1	2.6	4.2	2.6	1.6	—	—	10.2	3.0
22:5n-3	1.2	1.4	3.2	2.4	—	—	0.8	1.5
22:6n-3	7.0	4.2	13.1	4.5	—	—	11.2	21.4
Others	1.1	2.3	—	—	1.6	1.1	1.5	0.6

[a]Values are the mean of two determinations for FA composition and three determinations for *sn*-2 MAG. A dash (—) means not detected. 20:1 includes the isomers of n-9 and n-7, whereas 22:1 includes the isomers of n-11 and n-9.

Surgery of rats. Rats were anesthetized i.m. with a Zoletil mixture (0.06 mL/100 g; The Royal Veterinary and Agricultural University, Copenhagen, Denmark) and were subjected to cannulation of the main mesenteric lymph duct (21) with a clear vinyl tube (o.d. 0.8 mm, i.d. 0.5 mm; Critchley Electrical Products, New South Wales, Australia). A silicone feeding tube (o.d. 3.0 mm, i.d. 1.0 mm; Polystan, Værløse, Denmark) was inserted into the fundus region of the stomach and fixed with a purse-string suture. After surgery, the rats were placed in individual restraining cages at 25°C (22) with tap water freely available but without food and with a steady infusion of saline–glucose (0.15 M NaCl, 0.004 M KCl, and 0.28 M glucose) at 2 mL/h through the feeding tube. After surgery, the rats were given 0.05 mL of antidote (atipamezol hydrochloride, 5 mg/mL; Antisedan, Orion, Espoo, Finland). To reduce pain and stress, the rats received 0.3 mL of Rimadyl (carprofen, 50 mg/mL, diluted 1:10 with sterile water; Pfizer, Ballerup, Denmark) and 0.2 mL of Stesolid (diazepam, 5 mg/mL; Dumex-Alpharma A/S, Copenhagen, Denmark) after the operation and then regularly during the experiment.

Collection of lymph and administration of oil. Lymph collection was initiated in the afternoon after the operation, and an overnight fraction of lymph [with 0.7 mL of a 10% (wt/vol) Na$_2$ EDTA solution (E. Merck, Darmstadt, Germany) added to prevent coagulation] was collected to obtain a baseline fraction. In the morning on the first postoperative day, a sonicated emulsion of 0.5 mL of oil and 0.5 mL of a solution containing 20 mM taurocholate (Sigma, St. Louis, MO) and 10 mg/mL choline (Sigma) in distilled water was given as a bolus injection through the feeding tube followed by 0.5 mL of saline, and the infusion of saline–glucose was continued at 2 mL/h. Lymph was collected in tubes containing 100 or 200 μL of the EDTA solution in the following fractions: 0–2, 2–3, 3–4, 4–6, and 6–8 h after oil administration. Immediately after collection, the samples were analyzed by a particle sizer.

Particle-sizing procedure. Lymph samples were analyzed using a Mastersizer 2000 (Malvern Instruments Ltd.) with both the red light source (a helium–neon laser) and the blue solid-state light source. Dispersed droplets and particles in the size range of 20 nm to 2,000 μm can be measured, which is suitable for chylomicrons that have an expected size range of between 40 and 300 nm. The measured light-scattering pattern is assumed to come from spherical droplets, which is not a limitation in this case since the chylomicrons were expected to be spherical. The general purpose analysis model for unimodal drop size distributions was selected. A refractive index of 1.33 was used for the dispersant (distilled water); the particle refractive index was 1.470 and the absorption value was 0.01, which are the values for milk fat. The measurement procedure was as follows: First, 100 mL of distilled water was added to the Hydro SM dispersing unit, the stirrer was set at 2,500 rpm, and background calibration with water was initiated. Lymph fractions were weighed, and the entire fraction (4 or 10 mL for baseline fractions) was added and stirred for 1 min before beginning measurements. Three measurements were made on a sample as it circulated in the Hydro SM unit to confirm that the

size distribution of the sample did not change with time during measurement.

Calculation of particle number. Chylomicron samples of between 1 and 4 mL were dispersed in 100 mL of water for measurement in the Mastersizer 2000. The sizer measured a volume concentration, c, which was equal to the volume of particles in the measurement system divided by the total volume of liquid in the system. The volume of particles present can be calculated using Equation 1:

$$V_P = c(V_1 + V_2) \qquad [1]$$

where V_P is the volume occupied by the particles in the system, V_1 is the volume of the sample aliquot containing the chylomicrons that was added to the sizer, and V_2 is the volume of water used to disperse the sample. Volume $V_1 = V_P + V_m$, where V_m is the volume of the saline and EDTA solution mixture in which the particles are suspended.

The sizer also measures the volume fraction, R_i, of particles with an average diameter D_i present in size interval i. The volume of particles in size interval i is

$$V_i = R_i V_P \qquad [2]$$

whereas for spherical particles it is

$$V_i = N_i \pi D_i^3/6 \qquad [3]$$

where N_i is the number of particles present in that size interval. Combining Equations 1, 2, and 3 gives

$$N_i = (6R_i/\pi D_i^3)c(V_1 + V_2) \qquad [4]$$

For these experiments, V_2 was 100 mL (±2 mL), and V_1 was between 1.00 and 4.00 mL. The weight of the sample aliquot containing the chylomicrons in grams was set equal to its volume in milliliters when using Equation 4, since the fraction of chylomicrons in the sample aliquot was less than 2% by volume. The total number of particles in the sample is the sum of the number of particles present within each individual size interval.

Since samples were collected over time periods of either 1 or 2 h, the number of particles measured was standardized to a time interval of 1 h for all comparisons.

Statistics. Data represent the mean ± SEM of 5 rats in each group. Differences in lymph flow between the baseline and maximum flow rate in the different groups were tested using a *t*-test. To test differences between groups in the total number of lymph particles and in the number of particles in different size intervals, one-way ANOVA with Tukey's multiple comparison post test was performed using GraphPad Prism, version 3.02 (GraphPad software, San Diego, CA).

RESULTS

Particle size distribution curve. An example of a particle size distribution curve obtained from the Mastersizer instrument
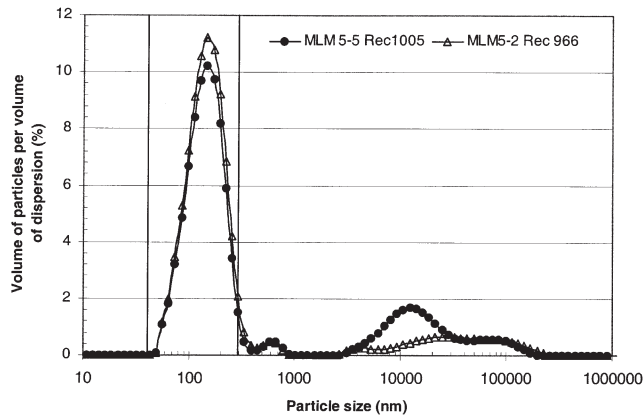
FIG. 1. Particle size distribution curve in lymph after administration of MLM (specific structured TAG, where M = medium-chain FA and L = long-chain FA) as obtained from the Mastersizer instrument (Malvern Instruments Ltd., Malvern, Worcestershire, United Kingdom). Volume percentage is plotted as a function of particle size in nanometers. The vertical lines indicate the focus region for further analysis. The coding refers to animal 5, fraction number 2 or 5, along with a measurement reference code.

FIG. 2. Total particle number in lymph in relation to the fraction after administration of MLM, LML (specific structured TAG, where M = medium-chain FA and L = long-chain FA), medium-chain TAG (MCT), or fish oil. Data represent mean ± SEM.

after administration of MLM oil is shown in Figure 1. The major peak was in the interval 40–1,000 nm, representing lipoproteins in the lymph. In some measurements we also observed a much smaller but broader peak in the size interval 10,000–100,000 nm representing cells. Since this peak did not interfere with the size measurements of the lipoproteins, we decided not to use a centrifugation step to remove the cells and thereby kept the method as simple as possible.

FA composition of TAG and in the sn-2 position of oils. The MLM and LML oils had almost the same content of major FA in the TAG, with 40 mol% of 10:0 and 34–36 mol% of long-chain n-3 PUFA (EPA, 20:5n-3, and DHA, 22:6n-3), but the structure represented by the FA in the *sn*-2 position of TAG differed, with high contents of 20:5n-3 and 22:6n-3 in the MLM oil and a high content of 10:0 in the LML oil (Table 1). MCT contained octanoic acid (8:0) and 10:0, and the fish oil had high contents of palmitic acid (16:0), oleic acid (18:1n-9), 20:5n-3, and 22:6n-3 with enrichment of the n-3 PUFA in the *sn*-2 position.

Lymph flow. Lymph flow at the baseline represented by lymph collected during the night following surgery, where rats were in the fasting state, was 1.5 ± 0.1 mL/h for all rats with no differences between groups. As a result of fat administration, the lymph flow increased significantly ($P < 0.05$) compared with the baseline flow. Maximum flow rates were observed in the fraction at 0–2 h for MLM, MCT, and fish oil, with values reaching 2.4 ± 0.2, 2.0 ± 0.3, and 2.5 ± 0.3 mL/h, respectively, whereas the maximum flow rate after LML administration was in the fraction at 2–3 h, reaching a value of 2.7 ± 0.2 mL/h.

Particle size and numbers in lymph. Although slight differences in particle size distribution were observed among the four oils, the difference in *c* differed greatly, indicating that the number of particles collected in the different fractions differed. Therefore, the volume distribution was converted to a number distribution, and the number of particles in the different frac-

tions collected was calculated as described in the Materials and Methods section. In the baseline fractions, the total number of particles was between 1.0^{14} and 1.2^{14} (Fig. 2). Compared with the number at baseline, the number of particles following fat administration increased severalfold for the MLM, LML, and fish oil groups, whereas MCT administration resulted only in a small, nonsignificant increase in particle number. The highest number of lymph particles after fish oil administration was observed in the 2–3 h fraction, after MLM and LML administration in the 3–4 h fraction, and after MCT administration in the 4–6 h fraction. In most fractions, except baseline and 0–2 h, the total number of particles after MCT administration was significantly lower compared with the other fats ($P < 0.05$). The highest number of particles was observed after LML administration, although this number was not significantly different from those after MLM and fish oil administration.
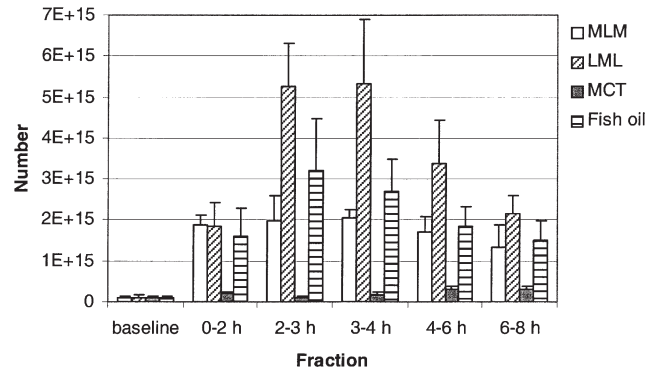
The number of particles in each size interval was very low for all four oils in the baseline fraction (Fig. 3). Following lipid administration, the number in each size interval increased dramatically within the first 2 h after MLM administration, more slowly after LML and fish oil administration, and even more slowly after MCT administration; the highest number was reached in the last two fractions from 4 to 8 h. Lipid absorption resulted primarily in increases in particle numbers in the size intervals 53–80 and 80–121 nm and in minor increases in the other size intervals. No particles were observed with sizes larger than 270 nm. Administration of MCT resulted in very few particles of sizes of 158–182 and 182–270 nm, whereas the other oils led to increases in the number of particles in the intervals of larger particle size as well.

DISCUSSION

Our results suggest that the number of particles in lymph increased during the absorption of lipids containing long-chain PUFA, but not during administration of MCT. Lipids containing long- and medium-chain FA positioned differently on the TAG molecule gave similar numbers of lymph particles,
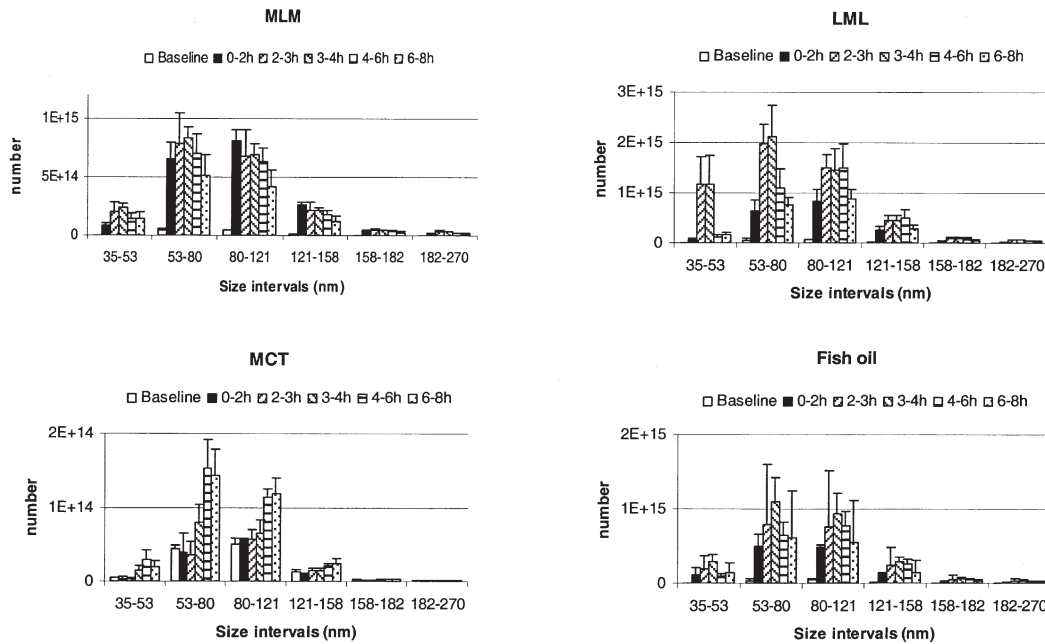
FIG. 3. Number of particles in different size intervals and in the different fractions after administration of MLM, LML, MCT, or fish oil, respectively. Data represent mean ± SEM. Notice the different scales in the four figures. For abbreviations see Figures 1 and 2.

although there was a tendency toward a higher number with the LML oil compared with the MLM oil. The highest number of particles was observed in the size intervals of 53–80 and 80–121 nm. The size of lymph particles was easily measured by a particle sizer immediately after collection. This method was fast and without time-consuming sample preparation.

Dietary TAG are hydrolyzed in the intestinal tract by the preduodenal lipases and the pancreatic lipase into *sn*-2 MAG and FFA (23,24). The hydrolysis products are absorbed into the enterocytes, with high conservation of the FA located in the *sn*-2 position of the dietary fat (25). In the enterocytes, the *sn*-2 MAG are reesterified with FA of exogenous and endogenous origin to form a new population of TAG; these are packed into chylomicrons and secreted to the lymph. Because of the high polarity of short- and medium-chain FA, the low affinity for the cytosolic FA-binding proteins, and the low activation to CoA esters, these are primarily absorbed *via* the portal vein for oxidation in the liver (26), with less absorption through the lymphatic system as the chain length of the FA becomes shorter (27). The MCT used in this study contained 62 mol% 8:0 and 36 mol% 10:0. With this FA composition, it was expected that the oil would primarily be absorbed *via* the portal vein (26,27), and this was probably the reason we did not observe an increase in number of lymph particles following administration of MCT. Although no obvious maximum number of lymph particles was observed after MCT administration, the highest number occurred in the last two fractions that were collected in the experiment. The *sn*-2 MAG from the hydrolysis of MCT were absorbed into the enterocytes for TAG resynthesis, whereas the FFA primarily were led to the portal vein; this may have caused a shortage of FA for TAG resynthesis in the enterocytes. There-

fore, endogenous FA stores had to be mobilized before TAG resynthesis could take place, and this may be the cause for the delay in the maximum number of lymph particles after MCT administration.

Structured TAG may combine the advantages of the easily digested and absorbed MCT with the delivery of different PUFA with specific effects in the body. In the present study, we combined medium-chain FA with n-3 PUFA of marine origin. A high intake of n-3 PUFA has been correlated with beneficial effects on the plasma lipid profile, leading to a low incidence of coronary heart disease (16,28). Furthermore, n-3 PUFA were shown to influence brain and visual development during infancy (29) and to have immunomodulatory effects (30). The interest in these effects has led to studies on the potential benefits of structured TAG containing n-3 PUFA. In the present study, we compared the effects of MLM and LML structured lipids with n-3 PUFA on lymph particle size and number. Both oils resulted in increases in the number of particles during absorption, and there was a tendency toward a higher number of particles following LML administration. Because of the structure of MLM, we expected that parts of the medium-chain FA hydrolyzed from the outer positions of the TAG would be absorbed *via* the portal vein and therefore result in less FFA for resynthesis in the enterocytes, and thus in a lower number of lymph particles compared with LML. Furthermore, a shortage of FFA for the resynthesis of TAG after MLM administration could explain why the maximum number of lymph particles was not observed before the 3–4 h fraction. The maximum number of particles was observed in the same fraction after LML administration. The tendency for acyl migration is higher when medium-chain FA are located in the *sn*-2 position of TAG

(13) compared with long-chain FA in the *sn*-2 position (25). This could lead to a shortage of *sn*-2 MAG, which would delay TAG resynthesis in the enterocytes. Fish oil was enriched with n-3 PUFA in the *sn*-2 position, which caused the structure to resemble MLM more than it resembled LML, whereas the overall FA composition differed due to the high content of medium-chain FA in the MLM oil. The maximum number of particles appeared in an earlier fraction after fish oil administration compared with administration of MLM and LML. We have investigated the *in vitro* rate of pancreatic lipase hydrolysis and the lymphatic absorption of these three oils, and have observed a faster hydrolysis and a faster absorption of fish oil compared with the two structured oils (Porsgaard, T., Xu, X., Göttsche, J., and Mu, H., unpublished report), which correlates well with the earlier time for the maximum number of particles observed after fish oil administration in the present study. The number of particles observed after fish oil administration was between the numbers observed after MLM and LML administration although it was not significantly different from either.

VLDL (diameter 30–90 nm) are the predominant lipoproteins secreted by the intestine during the fasting state. After fat ingestion, the secretion of chylomicrons is induced and the diameter of chylomicrons in the postprandial state is between 40 and 300 nm (2,5,11,12) depending on the nature of the administered fats. Tso *et al*. (31) suggested that chylomicron synthesis is induced during fat absorption because at high FA concentrations, the VLDL secreted is saturated. In the present study, the highest number of particles in the fasting state was found in the size intervals of 53–80 and 80–121 nm. They probably represented mostly VLDL particles. During fat absorption, increases in particle numbers were observed in all size intervals after administering all four oils but especially in the intervals of 53–80 and 80–121 nm. Since we did not separate the lymph particles into chylomicrons and VLDL, we may conclude either that we observed an increase in the number of VLDL particles in the absorptive state or that the absorption of the administered fats resulted in increases in the number of small chylomicrons. Kalogeris and Story (5) measured the mean diameters of lymph chylomicrons isolated by ultracentrifugation between 87 and 112 nm after infusion in rats of corn, butter, and olive oil, which were sizes close to those measured in our experiment. Levy *et al*. (1) found that the diameter of chylomicrons isolated after MCT administration (60 nm) was smaller compared with the diameter of chylomicrons isolated after safflower (185 nm) and coconut oil (140 nm) administration. Therefore, we conclude that administration of structured oils as well as fish oil and MCT under the experimental conditions applied in this study primarily resulted in increases in the numbers of small chylomicrons. Although we also observed increases in the larger size intervals, we measured increases in the numbers rather than increases in the sizes during absorption of the administered oils. This is in contrast to what was observed by Hayashi *et al*. (2), in which triolein absorption led to the expansion of chylomicron size instead of increases in the number of secreted chylomicrons. Differences in experimental conditions could be a reason for this discrepancy, since Hayashi

et al. used an 8-h intraduodenal infusion of lipid and followed the absorption during and after establishing steady-state TAG transport, whereas we followed the absorption of a single bolus of oil. On the contrary, this cannot be the entire story, since Kalogeris and Story (4) observed differences in chylomicron size as well as in number after using experimental conditions similar to those of Hayashi *et al*. Degrace *et al*. (6) suggested that the size and number of chylomicrons secreted during absorption depends on the time involved in absorption of the individual fats, and thereby also the length of the small intestine that is involved in the absorption process.

Few other studies have investigated the effect of structured lipids on chylomicron size and number. Carvajal *et al*. (12) performed experiments with MLM and LML structured oils containing medium-chain FA and linoleic acid (18:2n-6). Rats were fed experimental diets containing the structured oils for 3 wk followed by lymph collection. No effect from differences in intramolecular structures was found in lymph lipid output, lipid composition of the chylomicrons, or particle size. The particle size was slightly higher (120–140 nm) than we measured. Aoe *et al*. (11) compared the effect of positional distribution of dioleoyl-palmitoyl glycerol on chylomicron transport, composition, and size in rats and observed that the mean diameter of chylomicrons was larger after an infusion of 1,3-dioleoyl-2-palmitoyl glycerol compared with 1,2-dioleoyl-3-palmitoyl glycerol. On the basis of the experiments performed with structured oils, no overall conclusion can be drawn on whether the intramolecular structure of dietary TAG influences the size and number of chylomicrons produced during absorption and therefore also whether the structured oils influence postprandial lipemia differently.

ACKNOWLEDGMENTS

REFERENCES

1. Levy, E., Roy, C.C., Goldstein, R., Bar-On, H., and Ziv, E. (1991) Metabolic Fate of Chylomicrons Obtained from Rats Maintained on Diets Varying in Fatty Acid Composition, *J. Am. Coll. Nutr. 10*, 69–78.
2. Hayashi, H., Fujimoto, K., Cardelli, J.A., Nutting, D.F., Bergstedt, S., and Tso, P. (1990) Fat Feeding Increases Size, but Not Number, of Chylomicrons Produced by Small Intestine, *Am. J. Physiol. 259*, G709–G719.
3. Daher, C.F., Baroody, G.M., and Howland, R.J. (2003) Effect of a Surfactant, Tween 80, on the Formation and Secretion of Chylomicrons in the Rat, *Food Chem. Toxicol. 41*, 575–582.
4. Kalogeris, T.J., and Story, J.A. (1992) Lymph Chylomicron Size Is Modified by Fat Saturation in Rats, *J. Nutr. 122*, 1634–1642.
5. Kalogeris, T.J., and Story, J.A. (1992) Lymph Chylomicron Composition and Size Are Modified by Level of Intestinally Infused Cholesterol and Triglyceride Source in Rats, *J. Nutr. 122*, 1045–1055.

6. Degrace, P., Caselli, C., Rayo, J.M., and Bernard, A. (1996) Intestinal Lymph Absorption of Butter, Corn Oil, Cod Liver Oil, Menhaden Oil, and Eicosapentaenoic and Docosahexaenoic Acid Ethyl Esters in Rats, *Lipids 31*, 405–414.

7. Christensen, M.S., Mortimer, B.-C., Høy, C.-E., and Redgrave, T.G. (1995) Clearance of Chylomicrons Following Fish Oil and Seal Oil Feeding, *Nutr. Res. 15*, 359–368.

8. Martins, I.J., Mortimer, B.-C., Miller, J., and Redgrave, T.G. (1996) Effects of Particle Size and Number on the Plasma Clearance of Chylomicrons and Remnants, *J. Lipid Res. 37*, 2696–2705.

9. Redgrave, T.G., Kodali, D.R., and Small, D.M. (1988) The Effect of Triacyl-*sn*-glycerol Structure on the Metabolism of Chylomicrons and Triacylglycerol-rich Emulsions in the Rat, *J. Biol. Chem. 263*, 5118–5123.

10. Zilversmith, D.B. (1995) Atherogenic Nature of Triglycerides, Postprandial Lipidemia, and Triglyceride-rich Remnant Lipoproteins, *Clin. Chem. 41*, 153–158.

11. Aoe, S., Yamamura, J.-I., Matsuyama, H., Hase, M., Shiota, M., and Miura, S. (1997) The Positional Distribution of Dioleoyl-palmitoyl Glycerol Influences Lymph Chylomicron Transport, Composition and Size in Rats, *J. Nutr. 127*, 1269–1273.

12. Carvajal, O., Nakayama, M., Kishi, T., Sato, M., Ikeda, I., Sugano, M., and Imaizumi, K. (2000) Effect of Medium-Chain Fatty Acid Positional Distribution in Dietary Triacylglycerol on Lymphatic Lipid Transport and Chylomicron Composition in Rats, *Lipids 35*, 1345–1351.

13. Jensen, M.M., Christensen, M.S., and Høy, C.-E. (1994) Intestinal Absorption of Octanoic, Decanoic, and Linoleic Acids: Effect of Triglyceride Structure, *Ann. Nutr. Metab. 38*, 104–116.

14. Christensen, M.S., Høy, C.-E., Becker, C.C., and Redgrave, T.G. (1995) Intestinal Absorption and Lymphatic Transport of Eicosapentaenoic (EPA), Docosahexaenoic (DHA), and Decanoic Acids: Dependence on Intramolecular Triacylglycerol Structure, *Am. J. Clin. Nutr. 61*, 56–61.

15. Straarup, E.M., and Høy, C.-E. (2000) Structured Lipids Improve Fat Absorption in Normal and Malabsorbing Rats, *J. Nutr. 130*, 2802–2808.

16. Harris, W.S. (1989) Fish Oils and Plasma Lipid and Lipoprotein Metabolism in Humans: A Critical Review, *J. Lipid Res. 30*, 785–807.

17. Leuschner, R.G.K., Weaver, A.C., and Lillford, P.J. (1999) Rapid Particle Size Distribution Analysis of *Bacillus* Spore Suspensions, *Colloids Surf. B, Biointerfaces 13*, 47–57.

18. Xu, X. (2000) Enzymatic Production of Structured Lipids: Process Reactions and Acyl Migration, *inform 11*, 1121–1129.

19. Xu, X., Balchen, S., Høy, C.-E., and Adler-Nissen, J. (1998) Production of Specific-Structured Lipids by Enzymatic Interesterification in a Pilot Continuous Enzyme Bed Reactor, *J. Am. Oil Chem. Soc. 75*, 1573–1579.

20. Porsgaard, T., and Høy, C.-E. (2000) Lymphatic Transport in Rats of Several Dietary Fats Differing in Fatty Acid Profile and Triacylglycerol Structure, *J. Nutr. 130*, 1619–1624.

21. Bollman, J.L., Cain, J.C., and Grindley, J.H. (1948) Techniques for the Collection of Lymph from the Liver, Small Intestine, or Thoracic Duct of the Rat, *J. Lab. Clin. Med. 33*, 1349–1352.

22. Bollman, J.L. (1948) A Cage Which Limits the Activity of Rats, *J. Lab. Clin. Med. 33*, 1348.

23. Hamosh, M. (1990) Lingual and Gastric Lipases, *Nutrition 6*, 421–428.

24. Mattson, F.H., and Volpenhein, R.A. (1964) The Digestion and Absorption of Triglycerides, *J. Biol. Chem. 239*, 2772–2777.

25. Åkesson, B., Gronowitz, S., Herslof, B., and Ohlson, R. (1978) Absorption of Synthetic, Stereochmically Defined Acylglycerols in the Rat, *Lipids 13*, 338–343.

26. Bernard, A., and Carlier, H. (1991) Absorption and Intestinal Catabolism of Fatty Acids in the Rat: Effect of Chain Length and Unsaturation, *Exp. Physiol. 76*, 445–455.

27. Mu, H., and Høy, C.-E. (2000) Effects of Different Medium-Chain Fatty Acids on Intestinal Absorption of Structured Triacylglycerols, *Lipids 35*, 83–89.

28. Kris-Etherton, P.M., Harris, W.S., and Appel, L.J. (2002) Fish Consumption, Fish Oil, Omega-3 Fatty Acids, and Cardiovascular Disease, *Circulation 106*, 2747–2757.

29. Uauy, R., Hoffman, D.R., Peirano, P., Birch, D.G., and Birch, E.E. (2001) Essential Fatty Acids in Visual and Brain Development, *Lipids 36*, 885–895.

30. Calder, P.C., Yaqoob, P., Thies, F., Wallace, F.A., and Miles, E.A. (2002) Fatty Acids and Lymphocyte Functions, *Br. J. Nutr. 87*, S31–S48.

31. Tso, P., Lindström, M.B., and Borgström, B. (1987) Factors Regulating the Formation of Chylomicrons and Very-Low-Density Lipoproteins by the Rat Small Intestine, *Biochim. Biophys. Acta 922*, 304–313.

Metabolites of Dietary Triacylglycerol and Diacylglycerol During the Digestion Process in Rats

Noriko Osaki[a], Shinichi Meguro[a], Noriyuki Yajima[a], Noboru Matsuo[b], Ichiro Tokimitsu[a,*], and Hiroyuki Shimasaki[c]

[a]Biological Science Laboratories, Kao Corporation, Tochigi 321-3497, Japan, [b]Health Care Products Research Laboratories No. 1, Kao Corporation, Tokyo 131-8501, Japan, and [c]Department of Biochemistry, Teikyo University School of Medicine, Tokyo 173-8605, Japan

ABSTRACT: The present study investigated the metabolic fate of dietary TAG and DAG and also their digestion products in the stomach and small intestine. A diet containing 10% TAG or DAG oil, enriched in 1,3-DAG, was fed to Wistar rats *ad libitum* for 9 d. After 18 h of fasting, each diet was re-fed *ad libitum* for 1 h. The weights of the contents of the stomach and small intestine were measured, and the acylglycerol and FFA levels were analyzed by GC at 0, 1, and 4 h after the 1-h re-feeding. The amounts of re-fed diet ingested and the gastric and small intestinal content were not different between the two diet groups. In the TAG diet group, the main products were TAG and DAG, especially 1(3),2-DAG. In addition, 1,3-DAG and 1(3)-MAG were present in the stomach, and the 1,3-DAG levels increased over time after the re-feeding period. In the DAG diet group, the main products in the stomach were DAG, MAG, FFA, and TAG. There were significantly greater amounts of 1,3-DAG, 1(3)-MAG, and FFA in the DAG diet group in the stomach compared with the TAG diet group. The amount of FFA in the stomach relative to the amount of ingested TAG plus DAG in the DAG diet group was higher than that in the TAG diet group. Acylglycerol and FFA levels were considerably lower in the small intestine than in the stomach. These results indicate that, in the stomach, where acyl migration might occur, the digestion products were already different between TAG and DAG oil ingestion, and that DAG might be more readily digested by lingual lipase compared with TAG. Furthermore, almost all of the dietary lipid was absorbed, irrespective of the structure of the acylglycerol present in the small intestine.

Paper no. L9593 in *Lipids 40*, 281–286 (March 2005).

Although the majority of the digestion of dietary lipids is completed in the small intestine, the digestion starts in the stomach. From 10 to 30% of ingested lipid is digested in the stomach by gastric lipase, and, as a result, gastric lipid digestion has an important role in humans (1,2), especially in neonates and in patients with cystic fibrosis or pancreatitis (3–6). In rats, the digestion of lipids in the stomach is catalyzed by lingual lipase (7–11), which has considerable homology with the amino acid sequence of human gastric lipase (12,13). This enzyme preferentially cleaves the ester bonds at the *sn*-3 position relative to the *sn*-1 position under acidic conditions (pH 3.0 to 6.5) (7,8).

Hamosh *et al*. (11) measured gastric TAG levels after feeding a diet containing corn oil to rats *ad libitum* for 10 or 20 min. They reported that approximately 20 and 29% of the ingested TAG was digested after 10- and 20-min feeding periods, respectively. Lai and Ney (14) reported that the gastric TAG levels were approximately 38 to 50%, 12 to 17%, and 2 to 4% of the ingested TAG at 2, 5, and 9 h, respectively, after a diet containing corn oil or palm oil was fed to rats. In these studies, only changes in the ingested TAG levels were determined, and changes in makeup of digestion products (DAG, MAG, and FFA) were not investigated. Differences in the rate and extent of digestion of lipids by gastric and pancreatic lipases depend on the nature of the FA present. Medium-chain TAG that contain FA such as octanoic and decanoic acids were reported to be digested more rapidly than long-chain TAG (15). However, differences in the digestion of lipids with respect to the number and position of FA attached to the glycerol backbone have not been examined extensively.

TAG constitutes the greater portion of dietary lipids of animal and vegetable origin as a high energy source, whereas DAG, a type of natural structured lipid contained in many edible oils and fats, makes up a few to approximately 10% of the dietary lipids from animals and vegetables (16,17). A dietary DAG oil rich in 1,3-DAG decreases serum TAG levels (18,19), prevents postprandial hyperlipidemia (20–22), and suppresses visceral fat accumulation (23–26) in animals and humans in comparison with TAG oil with a similar FA composition. Taguchi *et al*. (27) also reported that the absorption coefficient of DAG oil was 96%, similar to that of TAG oil. However, a detailed understanding of the digestion products of DAG oil compared with TAG oil is limited.

In this study, we administered a diet containing TAG or DAG oil with a similar FA composition to rats and investigated the metabolic features of the dietary lipids, which differed in structure, by analyzing the digestion products in the stomach and small intestine, the main locations where digestion occurs.

EXPERIMENTAL PROCEDURES

Test oil. TAG oil was prepared by mixing rapeseed oil, safflower oil, and perilla oil to conform to the FA composition of DAG oil. DAG oil was prepared by esterifying glycerol with FFA from rapeseed oil and soybean oil by the method of

---

*To whom correspondence should be addressed at Biological Science Laboratories, Kao Corporation, 2606 Akabane, Ichikai, Haga, Tochigi, 321-3497 Japan. E-mail: tokimitsu.ichirou@kao.co.jp
Abbreviation: HSL, hormone-sensitive lipase.

TABLE 1
FA and Acylglycerol Compositions of TAG Oil and DAG Oil

Component	TAG	DAG
FA	g/100 g total FA	
14:0	0.1	0
16:0	5.4	3.1
16:1	0.2	0
18:0	2.0	1.2
18:1	37.1	39.2
18:2	46.0	47.5
18:3	7.3	8.6
20:0	0.5	0.2
20:1	0.9	0.2
22:0	0.2	0
22:1	0.1	0
Acylglycerols	g/100 g oil	
TAG	97.7	13.8
DAG	2.3	85.8
1(3),2-DAG	1.1	27.9
1,3-DAG	1.2	57.9
MAG	0	0.4

Huge-Jensen *et al.* (28). The FA and acylglycerol composition of each oil, as analyzed by GC, is shown in Table 1. The FA composition of the TAG oil was very similar to that of the DAG oil. The DAG concentration of the DAG oil was 85.8 g/100 g and the ratio of 1(3),2- to 1,3-DAG was 32.5:67.5.

Diet. The test diet contained 10 g/100 g of either TAG or DAG oil. Ingredients other than the test oil were casein (20 g/100 g), cellulose (4 g/100 g), AIN-76 mineral mixture (29) (4 g/100 g), AIN-76 vitamin mixture (29) (1 g/100 g), and potato starch (61 g/100 g). Each diet was prepared in one batch for the entire experimental period and was stored at 5°C.

Animals and experimental design. Male Wistar rats (7 wk old, 189 ± 7.8 g), obtained from CLEA Japan (Tokyo, Japan), were housed in metal cages and had free access to commercial rodent diet CE-2 (CLEA Japan) and drinking water. They were maintained in a temperature-controlled environment (23 ± 2°C) under a 12-h light/dark cycle. After a 7-d acclimatization period, they were divided into two groups so that the body weight of each group was approximately equal and transferred to individual metabolic cages. The rats in one group were fed the TAG oil diet, and the others were fed the DAG oil diet (TAG diet group and DAG diet group, respectively) for 9 d to accustom the animals to eating each test diet. Food intake was recorded every 3 or 4 d. The body weights of all rats were recorded at day 1 and 9. After ingestion of the test diets for 9 d, the rats were fasted for 18 h and then re-fed each diet *ad libitum* for 1 h. At the defined time points, 0, 1, and 4 h after re-feeding the test diets, the rats were anesthetized with diethyl ether and killed by withdrawing blood from the abdominal aorta. The stomach and small intestine (60 cm from the pylorus) were removed and washed three times with 5 mL of ice-cold 150 mM NaCl, respectively. Each content was mixed with 15 mL of ethanol and stored at −70°C until measurement. The groups that were killed at 0, 1, and 4 h after re-feeding of the

test diets are referred to hereafter as the 0 h, 1 h, and 4 h groups, respectively. The group that was not re-fed is referred to as the fasting group. The animal experiments were performed with the approval of the Ethics Committee for Experimental Animals of the Kao Corporation.

Lipid extraction. The lipids were extracted from aliquots of the freeze-dried gastric and small intestinal contents homogenized using a mortar, and a chloroform solution of pentadecanoic acid methyl ester (Sigma Chemical Co., St. Louis, MO), as an internal standard, was added using a modification of the method of Folch *et al.* (30).

Lipids analysis by GC. The lipid contents of the extracted total lipids were analyzed by GC. The lipids were purified using Sep-Pak silica (Waters, Milford, MA). The lipids were silylated with trimethylchlorosilane TMSI-H (GL Science, Tokyo, Japan) by a modification of the American Oil Chemists' Society official method (31) and the method of Taguchi *et al.* (27). The trimethylsilyl esters dissolved in hexane were separated on a GC-18A gas chromatograph (Shimadzu, Kyoto, Japan) connected to a FID and fitted with a DB-1 capillary column (15 m × 0.25 mm × 0.1 µm; J&W Scientific, Folsom, CA). Operating conditions were: initial temperature, 80°C; rate of temperature increase, 10°C/min; final temperature, 335°C (held for 44.5 min); injection and detector temperature, 350°C; carrier gas, helium at 1.78 mL/min. Peak detection was performed using a GC work station CLASS-GC 10 (Shimadzu) programmed for peak identification.

Materials for GC. Palmitic, stearic, oleic, linoleic, and linolenic acids as the FFA standards, 1-monooleoyl-glycerol as the 1(3)-MAG standard, and 2-monooleoyl-glycerol as the 2-MAG standard were purchased from Sigma Chemical Co. 1-Oleoyl-2-palmitoyl-glycerol and 1-oleoyl-3-palmitoyl-glycerol were purchased from Funakoshi (Tokyo, Japan). 1,2-Dioleoyl-glycerol and 1,3-dioleoyl-glycerol were purchased from Sigma Chemical Co. 1-Oleoyl-2-palmitoyl-glycerol and 1,2-dioleoyl-glycerol were used as the 1(3),2-DAG standards, 1-oleoyl-3-palmitoyl-glycerol and 1,3-dioleoyl-glycerol were used as the 1,3-DAG standards. 1,3-Dioleoyl-2-palmitoyl-glycerol, from Sigma Chemical Co, and trioleoyl-glycerol, from Wako (Osaka, Japan) were used as the TAG standards.

Statistical analyses. Data are expressed as the means ± SD. Statistical significance of the differences ($P < 0.05$) between the two diet groups were determined by Student's *t*-test and a two-way ANOVA using StatView for Windows version 5.0 (SAS Institute, Inc., Cary, NC).

RESULTS AND DISCUSSION

Food intake and body weight. The amounts of food intake in the TAG and DAG diet groups for 9 d were 152.1 ± 9.2 and 147.7 ± 10 g/rat, respectively. Body weights of the fasting, 0, 1, and 4 h groups in the TAG diet group after ingestion for 9 d were 234.2 ± 10.2, 247.6 ± 7.5, 236.7 ± 9.7, and 248.5 ± 6.5 g, respectively. The values for the fasting, 0, 1, and 4 h groups in the DAG diet group after ingestion for 9 d were 234.2 ± 8.9, 240.8 ± 6.4, 235.9 ± 12.8, and 244.5 ± 11.5 g, respectively. The

TABLE 2
Amounts of Gastric and Small Intestinal Contents[a] (dry wt)

Tissue	Test group	TAG diet group		DAG diet group	
		(g/stomach)	(%)[b]	(g/stomach)	(%)
	Fasting	0.16 ± 0.12		0.15 ± 0.04	
Stomach	0 h	3.81 ± 1.24	(87.8 ± 7.8)	4.43 ± 1.60	(87.7 ± 18.9)
	1 h	2.77 ± 1.81	(63.3 ± 12.9)	2.74 ± 1.06	(64.0 ± 17.2)
	4 h	1.82 ± 0.82	(34.1 ± 9.3)	1.53 ± 0.71	(34.1 ± 4.8)
		(g/intestine)	(%)	(g/intestine)	(%)
	Fasting	0.16 ± 0.12		0.15 ± 0.04	
Small intestine	0 h	0.22 ± 0.03	(5.4 ± 2.2)	0.20 ± 0.05	(4.1 ± 1.5)
	1 h	0.27 ± 0.13	(7.1 ± 3.2)	0.28 ± 0.07	(7.1 ± 1.6)
	4 h	0.22 ± 0.07	(4.5 ± 1.7)	0.21 ± 0.04	(4.2 ± 1.1)

[a]Values are the mean ± SD ($n = 7$).
[b]Mean ± SD are shown as percentages of the amounts of ingested test diet for 1 h.

amounts of food intake during the re-feeding period (for 1 h) of the 0, 1, and 4 h groups in the TAG diet group after 18 h of fasting were 4.3 ± 1.2, 4.1 ± 1.9, and 4.7 ± 1.2 g, respectively. The values for 0, 1, and 4 h groups in the DAG diet group after 18 h of fasting were 5.0 ± 1.4, 4.1 ± 1.1, and 5.0 ± 1.3 g, respectively. There were no differences at any point between the two diet groups in the amounts of food consumed for 9 d, body weights, and amounts of food intake during the re-feeding period . All rats remained healthy during the study period.

Gastric/intestinal contents. The dried gastric and small intestinal (60 cm from the pylorus) contents at 0, 1, and 4 h after the re-feeding period in the TAG and DAG diet groups and the fasting group are shown in Table 2. The gastric contents decreased over time after the re-feeding period in both the TAG and DAG diet groups. At 4 h after the re-feeding period, the gastric contents in the TAG and DAG diet groups were 34.1 ± 9.3 and 34.1 ± 4.8% of the weight of the re-fed diet, respectively. In the two diet groups, the small intestinal contents were

highest at 1 h after the re-feeding period. At 1 h after the re-feeding period, the small intestinal contents in the TAG and DAG diet groups were 7.1 ± 3.2 and 7.1 ± 1.6% of the weight of the re-fed diet, respectively. There were no differences in the gastric and small intestinal contents between the two diet groups.

Acylglycerols and FFA in the gastric content. Acylglycerol and FFA levels in the gastric contents of the TAG and DAG diet groups are shown in Table 3. The gastric contents in the fasting group were small, and there were no differences in the acylglycerol and FFA levels between the two diet groups.

In the TAG diet group, the main products were TAG and DAG, especially 1(3),2-DAG. The TAG and 1(3),2-DAG levels decreased over time after the re-feeding period, whereas the 1,3-DAG level increased over time after the re-feeding period. The 1(3)-MAG, 2-MAG, and FFA levels were highest at 1 h after the re-feeding period. The TAG intakes, which were calculated from the food intake and the TAG content in the TAG

TABLE 3
Amounts of Acylglycerols and FFA in the Stomach[a] (mg/gastric content)

	Test group	TAG[b]	1(3),2-DAG[c]	1,3-DAG[d]	1(3)-MAG[e]	2-MAG[f]	FFA[g]	FFA/ingested TAG + DAG (%)[h]
	Fasting	0.06 ± 0.12	0.00 ± 0.01	ND	0.01 ± 0.03	0.07 ± 0.17	0.05 ± 0.14	—
TAG diet group	0 h	218.85 ± 97.38	51.98 ± 14.58	0.54 ± 0.70	0.63 ± 0.83	4.15 ± 2.41	12.09 ± 5.49	2.72 ± 1.05
	1 h	154.89 ± 73.09	46.86 ± 24.49	8.71 ± 6.94	1.22 ± 0.83	4.38 ± 2.41	20.07 ± 11.38	4.44 ± 1.60
	4 h	154.85 ± 50.94	32.53 ± 9.86	16.89 ± 8.71	0.90 ± 0.50	0.92 ± 1.08	13.84 ± 5.30	2.46 ± 0.69
	Fasting	0.14 ± 0.20	ND	ND	0.06 ± 0.16	0.04 ± 0.08	0.18 ± 0.47	—
DAG diet group	0 h	67.94 ± 49.18**	78.58 ± 39.05	127.48 ± 59.02**	16.78 ± 7.88**	6.99 ± 4.03	26.19 ± 22.85	4.62 ± 2.96
	1 h	42.45 ± 17.76**	49.49 ± 15.81	85.33 ± 33.11***	11.24 ± 3.75***	5.97 ± 3.22	23.70 ± 7.96	5.57 ± 1.02
	4 h	28.67 ± 6.85***	44.39 ± 13.01	71.87 ± 17.35**	9.25 ± 3.09**	4.19 ± 1.88*	20.12 ± 4.56*	3.64 ± 0.65**
Two-way ANOVA	Diet	<0.0001	NS	<0.0001	<0.0001	=0.0037	=0.0251	=0.017
	Time	<0.0001	<0.0001	<0.0001	<0.0001	<0.0001	<0.0001	=0.028
	Diet × time	=0.0014	NS	<0.0001	<0.0001	NS	NS	NS

[a]Values are means ± SD ($n = 7$). ND, not determined; NS, not significant. Significantly different from TAG diet group: *$P < 0.05$; **$P < 0.01$; ***$P < 0.001$.
[b]TAG standard.
[c]1(3),2-DAG standard.
[d]1,3-DAG standard.
[e]1(3)-MAG standard.
[f]2-MAG standard.
[g]FFA standard.
[h]Gastric FFA contents relative to the amount of ingested fat (sum of TAG + DAG).

TABLE 4
Amounts of Acylglycerols and FFA in the Small Intestine[a] (mg/small intestinal content)

	Test group	TAG[b]	1(3),2-DAG[c]	1,3-DAG[d]	1(3)-MAG[e]	2-MAG[f]	FFA
	Fasting	ND	0.01 ± 0.02	ND	ND	0.01 ± 0.02	0.16 ± 0.24
TAG diet	0 h	0.26 ± 0.24	0.25 ± 0.11	0.14 ± 0.09	ND	0.07 ± 0.06	0.75 ± 1.17
group	1 h	0.30 ± 0.44	0.15 ± 0.15	0.03 ± 0.06	ND	0.15 ± 0.10	0.52 ± 0.53
	4 h	0.04 ± 0.07	0.09 ± 0.13	0.03 ± 0.04	ND	0.04 ± 0.06	1.33 ± 1.57
	Fasting	ND	0.02 ± 0.03	ND	ND	0.02 ± 0.03	0.06 ± 0.15
DAG diet	0 h	1.11 ± 0.60*	0.29 ± 0.08	0.18 ± 0.08	0.03 ± 0.02	0.06 ± 0.04	1.78 ± 1.64
group	1 h	0.48 ± 0.60	0.20 ± 0.19	0.13 ± 0.19	ND	0.06 ± 0.06	0.73 ± 0.70
	4 h	0.10 ± 0.10	0.10 ± 0.05	0.01 ± 0.02	ND	ND	1.06 ± 0.92
	Diet	= 0.0047	NS	NS	NS	NS	NS
Two-way	Time	<0.0001	<0.0001	<0.0001	NS	= 0.0013	= 0.0135
ANOVA	Diet × time	= 0.0132	NS	NS	NS	NS	NS

[a]For footnotes see Table 3.

diet, were 452 ± 126, 430 ± 199, and 540 ± 110 mg/rat in the 0, 1, and 4 h groups, respectively. The TAG levels in the gastric contents in the TAG diet group were 219 ± 97, 155 ± 73, and 155 ± 51 mg/rat in the 0, 1, and 4 h groups, amounting to 47 ± 9, 36 ± 5, and 28 ± 6% of the TAG intakes, respectively. Lai and Ney (14) reported that the gastric TAG levels were approximately 38 to 50% and 12 to 17% of the TAG intakes at 2 and 5 h, respectively, after a diet containing 16% corn oil was fed to rats. Therefore, the results of the present study were consistent with those of Lai and Ney. TAG is digested into DAG, MAG, or FFA by lingual lipase or gastric lipase under acidic conditions (pH 3.0–6.5) (1,2,11). The main products of digestion of TAG in the stomach include 1,2-DAG and 2-MAG, since these lipases preferentially cleave the ester bond at the *sn*-3 position relative to the *sn*-1 position (7,8). In the present study, DAG and MAG, detected in the stomach of the TAG diet group were mainly 1(3),2-DAG and 2-MAG, as has been previously reported (8); in addition, 1,3-DAG and 1(3)-MAG digestion products were present. It is noteworthy that the 1,3-DAG levels increased over time after the re-feeding period. This finding raises the possibility that 1(3),2-DAG, a digestion product of TAG, might have been converted to 1,3-DAG in the stomach under acidic conditions as the result of acyl migration, as heat and acid treatment promotes the migration of acyl groups in the DAG molecule (32). Meanwhile, 1(3)-MAG might be produced as a digestion product of 1,3-DAG.

In the DAG diet group, the main products were DAG, MAG, FFA, and TAG. The TAG, 1(3),2-DAG, 1,3-DAG, 1(3)-MAG, 2-MAG, and FFA levels decreased over time after the re-feeding period. There were no differences in the 1(3),2-DAG level in the gastric contents between the TAG diet group and the DAG diet group. The 1,3-DAG and 1(3)-MAG levels in the DAG diet group were higher than those in the TAG diet group. The levels of 2-MAG and FFA, and the gastric FFA contents relative to the amount of ingested fat (TAG plus DAG) in the DAG diet group were higher than those in the TAG diet group. Murase *et al*. (25) and Kondo *et al*. (33) reported that the levels of 1(3)-MAG and FFA, as digestion products in the small intestinal lumen after the administration of a 1,3-[carboxyl-^{14}C]DAG emulsion into the small intestine, were higher than those after the administration of a [carboxyl-^{14}C]TAG

emulsion. The data presented herein confirm 1(3)-MAG and FFA as metabolic features of DAG oil, also in the stomach, in the case of rats fed a DAG diet. We hypothesize that the 1(3)-MAG levels in the DAG diet group were higher than those in the TAG diet group because an ester bond in 1,3-DAG, a major constituent of the DAG diet, was cleaved at the *sn*-3 position by lingual lipase, as was demonstrated for TAG (7,8). The FFA levels and the gastric FFA contents relative to the amount of ingested fat [FFA/ingested TAG plus DAG (%)] in the DAG diet group were higher than those in the TAG diet group. These findings indicate that DAG might be more readily digested by lipase compared with TAG in the stomach. The rate constant (k_1) in the first step, in which TAG is digested into 1(3),2-DAG and FFA by pancreatic lipase, was lower than that (k_2) in the second step, in which 1(3),2-DAG is digested into 2-MAG and FFA, suggesting that pancreatic lipase more markedly promotes digestion of DAG (34). In adipose tissue, hormone-sensitive lipase (HSL) has a high affinity for DAG compared with TAG (35). To our knowledge, there are no analogous reports of differences between lingual and gastric lipase; however, the results reported herein suggest that lingual and gastric lipase promote the preferential digestion of DAG rather than the digestion of TAG, as demonstrated for pancreatic lipase and HSL.

Acylglycerols and FFA in the small intestinal content. The acylglycerol and FFA levels in the small intestinal contents of the TAG and DAG diet groups are shown in Table 4. In the fasting group, there were no differences between the two diet groups in the acylglycerol and FFA levels in the small intestinal contents. Nor were there differences in the 1(3),2-DAG, 1,3-DAG, 1(3)-MAG, 2-MAG, and FFA levels between the two diet groups. The TAG level in the DAG diet group was significantly higher than that in the TAG diet group at 0 h after the re-feeding period; however, there were no differences at 1 and 4 h after the re-feeding period. As just above, DAG might be more readily digested by lipase compared with TAG in the stomach. Thus, in the DAG diet group, the digestion of TAG in the presence of DAG might be delayed compared with DAG digestion, and the TAG content in the small intestine might be transiently higher than that in the TAG diet group. In both the TAG and DAG diet groups, the acylglycerol and FFA levels in the small intestine were markedly lower than those in the stomach. The amounts of

acylglycerols plus FFA in the small intestinal contents were 0.4% or less of the amounts of ingested TAG or DAG oil. Lai and Ney (14) reported that the amount of TAG in the small intestinal contents was less than 0.7% of the total amount of ingested TAG oil. Therefore, the results of the present study are consistent with those reported by Lai and Ney. Our results also demonstrated that both TAG and DAG oils are nearly completely digested and absorbed in the small intestine.

Our results suggest that, in the stomach of the rat, acyl migration from 1,2-DAG to 1,3-DAG may occur and the digestion products of TAG and DAG oil ingestion are different. Moreover, DAG oil is more readily digested than TAG oil. Therefore, DAG oil might be useful for neonates with underdeveloped digestion and absorption, and patients with cystic fibrosis or pancreatitis.

REFERENCES

1. Armand, M., Borel, P., Dubois, C., Senft, M., Peyrot, J., Salducci, J., Lafont, H., and Lairon, D. (1994) Characterization of Emulsions and Lipolysis of Dietary Lipids in the Human Stomach, *Am. J. Physiol. 266*, G372–G381.
2. Armand, M., Borel, P., Pasquier, B., Dubois, C., Senft, M., Andre, M., Peyrot, J., Salducci, J., and Lairon, D. (1996) Physicochemical Characteristics of Emulsions During Fat Digestion in Human Stomach and Duodenum, *Am. J. Physiol. 271*, G172–G183.
3. Hamosh, M. (1979) A Review. Fat Digestion in the Newborn: Role of Lingual Lipase and Preduodenal Digestion, *Pediatr. Res. 13*, 615–622.
4. Hamosh, M. (1996) Digestion in the Newborn, *Clin. Perinatol. 23*, 191–209.
5. Muller, D.P. (1982) Disorders of Lipid Absorption, *Clin. Gastroenterol. 11*, 119–140.
6. Balasubramanian, K., Zentler-Munro, P.L., Batten, J.C., and Northfield, T.C. (1992) Increased Intragastric Acid-Resistant Lipase Activity and Lipolysis in Pancreatic Steatorrhoea due to Cystic Fibrosis, *Pancreas 7*, 305–310.
7. Staggers, J.E., Frost, S.C., and Wells, M.A. (1981) Studies on Fat Digestion, Absorption, and Transport in the Suckling Rat. III. Composition of Bile and Evidence for Enterohepatic Circulation of Bile Salts, *J. Lipid Res. 23*, 1143–1151.
8. Paltauf, F., Esfandi, F., and Holasek, A. (1974) Stereospecificity of Lipases. Enzymic Hydrolysis of Enantiomeric Alkyl Diacylglycerols by Lipoprotein Lipase, Lingual Lipase and Pancreatic Lipase, *FEBS Lett. 40*, 119–123.
9. Hamosh, M., Ganot, D., and Hamosh, P. (1979) Rat Lingual Lipase. Characteristics of Enzyme Activity, *J. Biol. Chem. 254*, 12121–12125.
10. DeNigris, S.J., Hamosh, M., Kasbekar, D.K., Lee, T.C., and Hamosh, P. (1988) Lingual and Gastric Lipases: Species Differences in the Origin of Prepancreatic Digestive Lipases and in the Localization of Gastric Lipase, *Biochim. Biophys. Acta 959*, 38–45.
11. Hamosh, M., and Scow, R.O. (1973) Lingual Lipase and Its Role in the Digestion of Dietary Lipid, *J. Clin. Invest. 52*, 88–95.
12. Bodmer, M.W., Angal, S., Yarranton, G.T., Harris, T.J., Lyons, A., King, D.J., Pieroni, G., Riviere, C., Verger, R., and Lowe, P.A. (1987) Molecular Cloning of a Human Gastric Lipase and Expression of the Enzyme in Yeast, *Biochim. Biophys. Acta 909*, 237–244.
13. Docherty, A.J., Bodmer, M.W., Angal, S., Verger, R., Riviere, C., Lowe, P.A., Lyons, A., Emtage, J.S., and Harris, T.J. (1985) Molecular Cloning and Nucleotide Sequence of Rat Lingual Lipase cDNA, *Nucleic Acids Res. 13*, 1891–1903.
14. Lai, H.C., and Ney, D.M. (1998) Gastric Digestion Modifies Absorption of Butterfat into Lymph Chylomicrons in Rats, *J. Nutr. 128*, 2403–2410.
15. Bach, A.C., and Babayan, V.K. (1982) Medium-Chain Triglycerides: An Update, *Am. J. Clin. Nutr. 36*, 950–962.
16. D'Alonzo, R.P., Kozarek, W.J., and Wade, R.L. (1982) Glyceride Composition of Processed Fats and Oils as Determined by Glass Capillary Gas Chromatography, *J. Am. Oil Chem. Soc. 59*, 292–295.
17. Abdel-Nabey, A.A., Shehata, A.A.Y., Ragab, M.H., and Rosell, J.B. (1992) Glycerides of Cottonseed Oils from Egyptian and Other Varieties, *Riv. Ital. Sostanze Grasse 69*, 443–447.
18. Hara, K., Onizawa, K., Honda, H., Otsuji, K., Ide, T., and Murata, M. (1993) Dietary Diacylglycerol-Dependent Reduction in Serum Triacylglycerol Concentration in Rats, *Ann. Nutr. Metab. 37*, 185–191.
19. Yamamoto, K., Asakawa, H., Tokunaga, K., Watanabe, H., Matsuo, N., Tokimitsu, I., and Yagi, N. (2001) Long-Term Ingestion of Dietary Diacylglycerol Lowers Serum Triacylglycerol in Type II Diabetic Patients with Hypertriglyceridemia, *J. Nutr. 131*, 3204–3207.
20. Murata, M., Hara, K., and Ide, T. (1994) Alteration by Diacylglycerols of the Transport and Fatty Acid Composition of Lymph Chylomicrons in Rats, *Biosci. Biotechnol. Biochem. 58*, 1416–1419.
21. Taguchi, H., Watanabe, H., Onizawa, K., Nagao, T., Gotoh, N., Yasukawa, T., Tsushima, R., Shimasaki, H., and Itakura, H. (2000) Double-Blind Controlled Study on the Effects of Dietary Diacylglycerol on Postprandial Serum and Chylomicron Triacylglycerol Responses in Healthy Humans, *J. Am. Coll. Nutr. 19*, 789–796.
22. Tada, N., Watanabe, H., Matsuo, N., Tokimitsu, I., and Okazaki, M. (2001) Dynamics of Postprandial Remnant-like Lipoprotein Particles in Serum After Loading of Diacylglycerols, *Clin. Chim. Acta 311*, 109–117.
23. Nagao, T., Watanabe, H., Goto, N., Onizawa, K., Taguchi, H., Matsuo, N., Yasukawa, T., Tsushima, R., Shimasaki, H., and Itakura, H. (2000) Dietary Diacylglycerol Suppresses Accumulation of Body Fat Compared to Triacylglycerol in Men in a Double-Blind Controlled Trial, *J. Nutr. 130*, 792–797.
24. Murase, T., Mizuno, T., Omachi, T., Onizawa, K., Komine, Y., Kondo, H., Hase, T., and Tokimitsu, I. (2001) Dietary Diacylglycerol Suppresses High Fat and High Sucrose Diet-Induced Body Fat Accumulation in C57BL/6J Mice, *J. Lipid Res. 42*, 372–378.
25. Murase, T., Aoki, M., Wakisaka, T., Hase, T., and Tokimitsu, I. (2002) Anti-obesity Effect of Dietary Diacylglycerol in C57BL/6J Mice: Dietary Diacylglycerol Stimulates Intestinal Lipid Metabolism, *J. Lipid Res. 43*, 1312–1319.
26. Maki, K.C., Davidson, M.H., Tsushima, R., Matsuo, N., Tokimitsu, I., Umporowicz, D.M., Dicklin, M.R., Foster, G.S., Ingram, K.A., Anderson, B.D., *et al.* (2002) Consumption of Diacylglycerol Oil as Part of a Reduced-Energy Diet Enhances Loss of Body Weight and Fat in Comparison with Consumption of a Triacylglycerol Control Oil, *Am. J. Clin. Nutr. 76*, 1230–1236.
27. Taguchi, H., Nagao, T., Watanabe, H., Onizawa, K., Matsuo, N., Tokimitsu, I., and Itakura, H. (2001) Energy Value and Digestibility of Dietary Oil Containing Mainly 1,3-Diacylglycerol Are Similar to Those of Triacylglycerol, *Lipids 36*, 379–382.
28. Huge-Jensen, B., Galluzzo, D.R., and Jensen, R.G. (1988) Studies on Free and Immobilized Lipases from *Mucor miehei*, *J. Am. Oil Chem. Soc. 65*, 905–910.
29. American Institute of Nutrition (1997) Report of the American Institute of Nutrition *ad hoc* Committee on Standards for Nutritional Studies, *J. Nutr. 107*, 1340–1348.
30. Folch, J., Lees, M., and Sloane Stanley, G.H. (1957) A Simple

Method for the Isolation and Purification of Total Lipids from Animal Tissues, *J. Biol. Chem. 226*, 497–509.

31. AOCS (1997) *Official Methods and Recommended Practices of AOCS*, 5th edn., AOCS Press, Champaign, IL, Method Cd 11b-91.

32. Crossley, A., Freeman, I.P., Hudson, J.F. and Pierce, J.H. (1959) Acyl Migration in Diglycerides, *J. Chem. Soc*. *152*, 760–764.

33. Kondo, H., Hase, T., Murase, T., and Tokimitsu, I. (2003) Digestion and Assimilation Features of Dietary DAG in the Rat Small Intestine, *Lipids 38*, 25–30.

34. Lykidis, A., Mougios, V., and Arzoglou, P. (1995) Kinetics of the Two-Step Hydrolysis of Triacylglycerol by Pancreatic Lipases, *Eur. J. Biochem. 230*, 892–898.

35. Kraemer, F.B., and Shen, W.J. (2002) Hormone-Sensitive Lipase: Control of Intracellular Tri-(di-)acylglycerol and Cholesteryl Ester Hydrolysis, *J. Lipid Res*. *43*, 1585–1594.

Tissue-Dependent Alterations in Lipid Mass in Mice Lacking Glycerol Kinase

Mikhail Y. Golovko[a], Johnathan T. Hovda[a], Zong-Jin Cai[c], William J. Craigen[c], and Eric J. Murphy[a,b,*]

Departments of [a]Pharmacology, Physiology, and Therapeutics and [b]Chemistry, University of North Dakota, Grand Forks, North Dakota 58202-9037, and [c]Departments of Molecular and Human Genetics and Pediatrics, Baylor College of Medicine, Houston, Texas 77030

ABSTRACT: Glycerol kinase (ATP:glycerol-3-phosphotransferase, EC 2.7.1.30, glycerokinase) (Gyk) has a central role in plasma glycerol extraction and utilization by tissues for lipid biosynthesis. Gyk deficiency causes various phenotypic changes ranging from asymptomatic hyperglycerolemia to a severe metabolic disorder with growth and psychomotor retardation. To better understand the potential role of Gyk in tissue lipid metabolism, we determined phospholipid (PL), cholesterol (Chol), and triacylglycerol (TG) mass in a number of tissues from mice lacking Gyk. We report a tissue-dependent response to Gyk gene deletion. Tissues with elevated total PL mass (brain, kidney, muscle) were characterized by the increased mass of ethanolamine glycerophospholipids (EtnGpl), choline glycerophospholipids, and phosphatidylserine (PtdSer). In heart, lipid changes were characterized by a reduction in total PL, including decreased EtnGpl, phosphatidylinositol, and PtdSer mass and decreased TG and FFA mass. In parallel with tissue PL alterations, tissue Chol was also changed, maintaining a normal Chol/PL ratio. Under conditions of Gyk deficiency, we speculate that glycerol-3-phosphate and lipid production is maintained *via* alternative biosynthesis, including glycolysis, glyceroneogenesis, or by direct acylation of glycerol in brain, muscle, kidney, and liver, but not in heart.

Paper no. L9641 in *Lipids 40*, 287–293 (March 2005).

In mammals, the main sources of glycerol are either triacylglycerol (TG) hydrolysis in tissues or direct synthesis *via* glyceroneogenesis (1). Once inside the cell, glycerol is immediately phosphorylated by glycerol kinase (Gyk), thereby targeting glycerol to different metabolic pathways and maintaining an inward gradient for glycerol flux (2). The importance of glycerol in mammals is demonstrated by a high turnover rate of whole-body glycerol, which is equivalent to that for glucose (3–5). The bulk of total glycerol is used by liver and kidney (6), whereas the remainder of the glycerol is used by nonhepatic, nonrenal tissues, including muscle (7), brain (8,9), heart, and adipose tissue (10). The predominant use of glycerol in tissue is for TG and phospholipid (PL) biosynthesis (1,7,9,11,12). For example, in liver the half-life of glycerol is 0.5 h for TG and several hours for PL (13). The half-life of glycerol in brain PC is 3 d (14), and 5 d in the total lipid fraction (15). Glycerol can also be used for glucose and amino acid synthesis (8), accounting for up to 20–25% of total glucose production (4,16). Further, it can also be directly oxidized to CO_2, representing 3–10% of total body CO_2 output (3), and it can be used for formation of a hydrogen shuttle system in mitochondria (17).

Because Gyk has a central role in plasma glycerol extraction and utilization by tissues, its activity could be critical for the formation of membrane PL and deposited lipids, such as TG, as well as for carbohydrate homeostasis and energy production by tissues. X-Linked Gyk deficiency in humans causes various phenotypic changes ranging from asymptomatic hyperglycerolemia to a severe metabolic disorder with growth and psychomotor retardation (18). Gyk deficiency may be associated with Duchenne muscular dystrophy and congenital adrenal hypoplasia as part of a contiguous gene deletion syndrome (18). In contrast, a number of intragenic mutations at the Gyk locus have been reported in humans with isolated Gyk deficiency (19–22); however, the biochemical effects of Gyk deficiency on multiple metabolic pathways remain unknown.

To study the physiological role of Gyk and the pathophysiology of Gyk deficiency, we previously generated Gyk-deficient mice by gene-targeted deletion (23). In contrast to Gyk-deficient humans, the affected males die 3–4 d after birth and are characterized by normal plasma glucose, 80-fold elevation in plasma glycerol level, and a 3-fold elevation of plasma FFA. Further, these mice demonstrate induction of gluconeogenic genes, probably *via* elevated glucocorticoids. Others have observed that Gyk deficiency inhibits glycerol utilization in PL and TG biosynthesis (24), confirming the importance of Gyk in lipid metabolism.

To better understand the potential role of Gyk on tissue lipid metabolism, we determined PL mass and composition. In addition, cholesterol (Chol), FFA, and TG mass were measured in these tissues. We report tissue-dependent differences in response to loss of Gyk activity. In parallel with alteration in PL mass, Chol mass was also changed, maintaining a normal Chol/PL ratio. In the absence of Gyk-produced glycerol-3-phosphate (Gro-3-P), we speculate that lipid production is maintained *via* alternative biosynthesis, including glycolysis

---

*To whom correspondence should be addressed at Department of Pharmacology, Physiology and Therapeutics, School of Medicine and Health Sciences, University of North Dakota, 501 N. Columbia Rd., Room 3700, Grand Forks, ND 58202-9037. E-mail: emurphy@medicine.nodak.edu

Abbreviations: Chol, cholesterol; CerPCho, sphingomyelin; ChoGpl, choline glycerophospholipids; Gyk, glycerol kinase; Gro-3-P, glycerol-3-phosphate; EtnGpl, ethanolamine glycerophospholipids; PL, phospholipids; PtdSer, phosphatidylserine; PtdIns, phosphatidylinositol; TG, triacylglycerol.

and glyceroneogenesis, or by direct acylation of glycerol in brain, muscle, kidney, and liver, but not in heart.

MATERIALS AND METHODS

Animals. X-Linked Gyk-deficient mice were generated by gene targeting in embryonic stem cells (23). Male pups were killed on postnatal day 2 and tissues were collected by dissection followed by snap-freezing in liquid nitrogen. The genotypes of the mice were then determined by a PCR-based assay, and male littermates with an intact Gyk gene served as controls. All studies were performed following approval by the Baylor College of Medicine institutional animal use review committee.

Tissue lipid extraction. Frozen tissue was pulverized under liquid nitrogen temperatures. Lipids from the tissue powder were extracted using a Tenbroeck tissue homogenizer and *n*-hexane/2-propanol (3:2, vol/vol) (25,26). Briefly, tissue was homogenized in 1.8 mL *n*-hexane/2-propanol (3:2, vol/vol) per 0.1 g tissue and quantitatively transferred to a test tube, using an additional 3 mL of *n*-hexane/2-propanol (3:2, vol/vol) per 0.1 g tissue to rinse the homogenizer. The protein-containing residue was pelleted by centrifugation.

Sample preparation for analysis. Lipid extracts were prepared for separation by HPLC by reducing the sample volume under a stream of nitrogen and filtering the samples through a 0.2 µm Nylon filter (Rainin, Emeryville, CA). The filtered sample was then dried to completeness and redissolved in a known volume of HPLC-grade *n*-hexane/2-propanol (3:2, vol/vol) for PL separation and in *n*-hexane/2-propanol/acetic acid (98.7:1.2:0.1, by vol) for neutral lipid separation.

PL mass determination. The PL were separated by HPLC using a gradient of *n*-hexane/2-propanol (3:2 vol/vol) and *n*-hexane/2-propanol/water (56.7:37.8:5.5, by vol) as previously described (27,28). This method gives baseline resolution of all the major classes of PL. The eluant absorbance was monitored at 205 nm. Individual PL mass was determined by assay of lipid phosphorus (29).

Chol mass determination. The neutral lipid-containing fraction was collected during the PL separation described above. The neutral lipids were separated using a binary solvent system consisting of *n*-hexane/2-propanol/acetic acid (98.7:1.2:0.1, by vol) and *n*-hexane (30,31). The eluant absorbance was monitored at 205 nm. Chol concentration was determined based on a Chol (Nu-Chek-Prep, Elysian, MN) standard curve.

FFA analysis. FFA fraction from the neutral lipid separation described above was subjected to acid-catalyzed esterification (32), and FFA were analyzed by GLC.

TG mass determination. PL and neutral lipids were separated by liquid column chromatography, using activated silicic acid (Clarkson Chemical Company, Inc., Williamsport, PA) as the stationary phase (33). Neutral lipids were eluted with 10 vol of chloroform/methanol (58:1 vol/vol), and PL were eluted with 10 vol of methanol. The collected neutral lipid fraction was separated by HPLC as described above. The eluent was monitored by a light-scattering detector, and TG mass was determined by using a standard curve from commercially pur-

chased standards (Nu-Chek-Prep). TG mass was converted from grams to moles using the M.W. for tristearoylglycerol.

Total PL FA composition. The PL fraction was collected after liquid column chromatography as described above. PL were subjected to base-catalyzed transesterification (34) and analyzed by GLC.

HPLC. The HPLC system consisted of a Selectosil column (5 µm, 4.6 × 250 mm; Phenomenex, Torrance, CA), a Beckman 126 pump (Fullerton, CA), and a Beckman 166 UV/Vis detector or ELSD (model 301; ESA Inc., Chelmsford, MA).

GLC. The gas–liquid chromatograph (model 14A; Shimadzu, Kyoto, Japan) was equipped with a capillary column (SP 2330; 30 m × 0.32 mm i.d.; Supelco, Bellefonte, PA) and an FID. FA were quantified using a standard curve from commercially purchased standards (Nu-Chek-Prep), and 17:0 was the internal standard.

Protein assay. Proteins were measured using a modified dye-binding assay (35). The dried protein residue from the lipid extract was digested overnight in 0.2 M KOH at 65°C. After digestion, aliquots were used to measure the protein concentration by converting absorbance to concentration using BSA as a standard.

Statistics. Statistical analysis was done using a one-way ANOVA combined with a Tukey–Kramer *post hoc* test using Instat II (Graphpad, San Diego, CA). Statistical significance was defined as <0.05.

RESULTS

The total PL mass of brain, heart, liver, kidney, and muscle of wild-type males, and Gyk-deficient hemizygous males are presented in Table 1. In brain, kidney, and muscle of affected males, the total PL mass was elevated 1.3-fold in each tissue. In contrast, the PL mass was decreased 24% in heart tissue of Gyk-deficient males, whereas liver tissue PL mass was not statistically different between groups.

The changes in Chol mass in brain, heart, liver, kidney, and muscle tissues of Gyk-deficient animals are presented in Table 1. Similar to total PL mass, the Chol mass was increased 1.5-fold in brain and 1.6-fold in muscle of affected males. Chol mass was not significantly changed in heart, liver, and kidney between groups. Despite dramatic changes in total PL in brain, heart, muscle, and kidney and in Chol in brain and muscle, the Chol/PL ratio was not affected in Gyk-deficient mice (Table 1).

We have previously shown that Gyk-deficient mice exhibit an 80-fold increase in plasma glycerol (23). High plasma glycerol is excreted in the urine, which leads to osmotic diuresis, salt loss, and dehydration (36). To test the hypothesis that the changes in PL concentration in some tissues are the result of tissue dehydration, we measured protein mass in the tissues. There were no statistically significant differences between groups in protein mass per gram of wet tissue (data not shown).

The individual PL class mass was determined for each tissue (Table 2). All Gyk-deficient tissues with elevated total PL mass, i.e., brain, kidney, muscle, are characterized by an

TABLE 1
Total Phospholipid (PL) and Cholesterol Mass, and Cholesterol/Total PL Ratio in Gyk-Deficient Mice[a]

		Cholesterol μmol/g ww	Total PL μmol/g ww	Cholesterol/total PL
Brain	+/o	12.4 ± 2.5 (4)	20.1 ± 1.9 (4)	0.62 ± 0.15 (4)
	–/o	16.2 ± 1.9* (4)	25.3 ± 1.4* (4)	0.62 ± 0.04 (4)
Heart	+/o	5.0 ± 0.9 (4)	14.4 ± 0.6 (4)	0.34 ± 0.06 (4)
	–/o	4.7 ± 0.9 (5)	10.9 ± 1.9* (5)	0.44 ± 0.11 (5)
Liver	+/o	6.0 ± 0.9 (3)	19.0 ± 2.8 (3)	0.32 ± 0.05 (3)
	–/o	6.3 ± 0.4 (4)	21.6 ± 3.1 (4)	0.30 ± 0.05 (4)
Kidney	+/o	11.1 ± 1.5 (4)	11.5 ± 2.0 (4)	0.99 ± 0.23 (4)
	–/o	10.4 ± 2.8 (4)	14.3 ± 0.6* (4)	0.72 ± 0.22 (4)
Muscle	+/o	3.0 ± 0.9 (4)	9.6 ± 0.9 (4)	0.31 ± 0.09 (4)
	–/o	4.8 ± 0.9* (4)	12.8 ± 1.5* (4)	0.38 ± 0.10 (4)

[a]Values are expressed as means ± SD. The numbers in parentheses indicate the number of samples tested. *$P < 0.05$. Gyk, glycerol kinase; ww, wet weight; +/o, tissues from wild-type male mice; –/o, tissues from knockout male mice.

elevation in individual PL masses; and in the heart, the decrease of total PL mass paralleled the decrease in individual PL masses (Table 2).

In brains of affected males, EtnGpl, PtdSer, and ChoGpl masses were elevated 1.3-, 1.4-, and 1.2-fold, respectively (Table 2), but PL composition was not different between groups (data not shown).

In muscles of affected males, EtnGpl and ChoGpl masses also were elevated 1.3- and 1.4-fold, respectively (Table 2), but PL composition was not different between groups (data not shown).

In kidney samples of Gyk-deficient males, PtdSer mass was elevated 1.5-fold (Table 2), and PL composition was not different between groups (data not shown).

In contrast to other tissues examined, heart EtnGpl, PtdSer, and phosphatidylinositol (PtdIns) masses were decreased 23, 43, and 26%, respectively, in affected males (Table 2). The mole composition of PL also was altered, with PtdIns decreased by 23%, as compared with wild-type animals (data not shown).

In liver, there were no differences in individual PL mass or distribution (Table 2 and data not shown).

In culture systems, Gyk deficiency decreases glycerol incorporation into TG (24). Also, the plasma FFA mass is increased threefold in Gyk-deficient mice (23). To determine the effect of Gyk deficiency on the tissue neutral lipid mass, TG and FFA masses were determined for brain (tissue with elevated PL mass), liver (tissue with unaffected PL), and heart (tissue with decreased PL mass) (Table 3). The changes in TG mass were consistent with those observed for PL. In brain, TG mass was increased 1.4-fold, in liver TG mass was unaffected, and in heart TG mass was decreased 84%. FFA mass in heart was also decreased 56% (Table 3), consistent with PL mass decreases in hearts of affected males.

The potential that Gyk deficiency could alter the FA composition of total brain and liver PL was also determined. No changes in brain and liver PL FA composition were found between groups (Table 4), indicating that there were no preferences in the FA entering PL.

TABLE 2
Individual PL Masses[a] **in Tissues from Gyk-Deficient Mice**

	Brain, μmol/g ww		Heart, μmol/g ww		Liver, μmol/g ww		Kidney, μmol/g ww		Muscle, μmol/g ww	
	+/o	–/o	+/o	–/o	+/o	–/o	+/o	–/o	+/o	–/o
EtnGpl	5.5 ± 1.2	7.3 ± 0.5*	4.3 ± 0.1	3.3 ± 0.4*	5.2 ± 0.7	6.0 ± 1.1	2.8 ± 0.6	3.4 ± 0.4	2.3 ± 0.4	3.0 ± 0.6*
LysoPtdEtn	0.4 ± 0.4	0.2 ± 0.0	0.2 ± 0.3	0.0 ± 0.0	0.1 ± 0.0	0.1 ± 0.0	0.1 ± 0.1	0.3 ± 0.1	0.3 ± 0.1	0.5 ± 0.1
PtdIns	0.8 ± 0.4	0.9 ± 0.1	0.8 ± 0.1	0.5 ± 0.1*	1.3 ± 0.3	1.6 ± 0.3	0.8 ± 0.2	0.9 ± 0.2	0.6 ± 0.1	0.8 ± 0.2
PtdSer	2.0 ± 0.5	2.8 ± 0.3*	0.7 ± 0.1	0.5 ± 0.1*	0.9 ± 0.1	1.0 ± 0.2	0.9 ± 0.2	1.3 ± 0.3*	0.7 ± 0.2	1.0 ± 0.2
ChoGpl	10.4 ± 0.7	12.7 ± 0.4*	6.9 ± 0.4	5.5 ± 1.3	10.4 ± 1.8	11.6 ± 2.0	5.3 ± 1.1	6.3 ± 0.7	4.6 ± 0.7	6.3 ± 0.7*
CerPCho	0.6 ± 0.3	0.8 ± 0.2	1.1 ± 0.2	0.8 ± 0.2	0.9 ± 0.04	0.9 ± 0.3	1.2 ± 0.1	1.5 ± 0.3	0.7 ± 0.2	0.8 ± 0.1
LysoPtdCho	0.4 ± 0.2	0.6 ± 0.4	0.4 ± 0.2	0.3 ± 0.1	0.2 ± 0.0	0.4 ± 0.2	0.4 ± 0.1	0.5 ± 0.1	0.5 ± 0.3	0.4 ± 0.1
n[b]	4	4	4	5	3	4	4	4	4	4

[a]Values are expressed as means ± SD. *$P < 0.05$.
[b]n, number of samples tested; EtnGpl, ethanolamine glycerophospholipids; lysoPtdEtn, lysophosphatidylethanolamine; PtdIns, phosphatidylinositol; PtdSer, phosphatidylserine; ChoGpl, choline glycerophospholipid; CerPCho, sphingomyelin; lysoPtdCho, lysophosphatidylcholine; for other abbreviations see Table 1.

TABLE 3
Individual TG and FFA Mass in Tissues from Gyk-Deficient Mice[a]

	TG, μmol/g ww		FFA, nmol/g ww	
	+/o	–/o	+/o	–/o
Brain	0.3 ± 0.0 (5)	0.4 ± 0.1* (5)	32 ± 5 (3)	47 ± 17 (3)
Heart	2.2 ± 0.2 (3)	0.4 ± 0.1* (3)	216 ± 23 (3)	96 ± 21* (3)
Liver	33.7 ± 12.0 (4)	15.1 ± 14.7 (4)	183 ± 63 (3)	243 ± 43 (3)
Kidney			204 ± 16 (3)	201 ± 78 (3)
Muscle			53 ± 34 (3)	46 ± 6 (3)

[a]Values are expressed as means ± SD. The numbers in parentheses indicate the number of samples tested. *$P < 0.05$. For abbreviations see Table 1.

DISCUSSION

Glycerol has a significant role in lipid biosynthesis, but this role is not limited to tissues with the highest Gyk activity (kidney and liver); it is also important in muscle (7), in brain (9,37), and to a lesser extent in heart (37,38). Gyk catalyzes the initial reaction of glycerol utilization by tissues, making it an important participant in lipid synthesis. For instance, in fibroblasts from humans with Gyk deficiency, the targeting of glycerol for use in PL and TG biosynthesis is decreased 98%, but the utilization of glucose for PL and TG biosynthesis is not affected (24). In Gyk-deficient mice, the esterification of glycerol is also disrupted, as demonstrated by an observed 80-fold hyperglycerolemia and a 3-fold elevation of plasma FFA (23). Collectively, these results suggest that Gyk deficiency could lead to decreased tissue PL mass. To address this question, we determined tissue lipid mass from Gyk-deficient mice to provide greater insight into the role of Gyk in lipid biosynthesis.

In contrast to the putative role for Gyk in PL biosynthesis, the mass of total PL and the mass of some individual PL were increased in brain, kidney, and muscle from affected males (Tables 1 and 2) or else were unaffected, as in liver (Tables 1 and

2). The changes in TG mass in brain, liver, and heart were consistent with those observed for PL. Several explanations may account for the observed increase in PL mass in kidney and muscle, and in PL and TG in brain of Gyk-deficient mice.

In Gyk-deficient mice, it would be reasonable that the lack of Gro-3-P production from free glycerol is compensated for by alternative mechanisms of Gro-3-P formation and lipid synthesis in kidney, muscle, brain, liver, and, to a lesser extent, in heart. Several compensatory mechanisms are possible. Gro-3-P production may be maintained from glucose *via* glycolysis, or from pyruvate (lactate) and from glycogenic amino acids *via* glyconeogenesis, also referred to as glyceroneogenesis (1). These routes lead to increased dihydroxyacetone phosphate production. Dihydroxyacetone phosphate can be directly acylated, reduced, and then used for glycerolipid or TG formation or reduced to Gro-3-P and then used for lipid synthesis (39).

The glyceroneogenesis pathway has an important role in the liver and muscle and possibly in other organs. It contributes up to 65% of the glycerolipids secreted by liver (1) and from 52 (fed animals) to 70% (fasted animals) of Gro-3-P used for lipid synthesis in muscle (40). It is noteworthy that in soleus muscle, which has a low rate of glucose utilization, the contribution of

TABLE 4
PL and FA Composition in Brain and Liver[a] **from Gyk-Deficient Mice**

	Brain, mol%		Liver, mol%	
	+/o	–/o	+/o	–/o
16:0	34.5 ± 0.6	34.2 ± 0.5	24.2 ± 2.1	23.8 ± 2.0
16:1	2.6 ± 0.4	2.5 ± 0.3	0.8 ± 0.3	0.6 ± 0.2
18:0	16.7 ± 0.3	17.0 ± 0.2	18.5 ± 2.1	16.2 ± 2.9
18:1n-9/n-11	15.2 ± 0.4	15.0 ± 0.8	7.5 ± 0.8	6.8 ± 1.8
18:1n-7	3.3 ± 0.2	3.3 ± 0.4	1.1 ± 0.4	0.9 ± 0.5
18:2n-6	0.8 ± 0.2	1.0 ± 0.3	11.7 ± 1.9	14.3 ± 3.7
18:3n-3	0.1 ± 0.1	0.1 ± 0.1	0.0 ± 0.0	0.0 ± 0.0
20:1n-9	0.3 ± 0.0	0.3 ± 0.1	0.0 ± 0.0	0.0 ± 0.0
20:2n-6	0.0 ± 0.1	0.1 ± 0.1	0.4 ± 0.2	0.4 ± 0.1
20:3n-6	0.3 ± 0.2	0.2 ± 0.2	1.1 ± 0.4	1.2 ± 0.1
20:4n-6	10.2 ± 0.4	10.4 ± 0.6	14.3 ± 1.3	14.6 ± 1.9
22:2n-6	0.0 ± 0.1	0.0 ± 0.0	0.8 ± 0.2	0.8 ± 0.5
22:4n-6	2.2 ± 0.2	2.1 ± 0.1	0.5 ± 0.1	0.5 ± 0.1
22:5n-6	0.1 ± 0.1	0.3 ± 0.3	0.2 ± 0.2	0.3 ± 0.3
22:5n-3	0.0 ± 0.0	0.2 ± 0.2	0.8 ± 0.3	1.2 ± 0.5
22:6n-3	13.5 ± 0.4	13.5 ± 0.2	17.9 ± 1.9	18.1 ± 1.6
n	3	5	4	4

[a]Values are expressed as means ± SD. *$P < 0.05$. For abbreviations see Tables 1 and 2.

glucose to Gro-3-$\underline{P}$ formation is significantly lower than in quadriceps, which has a higher rate of glucose utilization (40). This suggests that tissues with a low rate of glucose utilization may have a lower capability of maintaining Gro-3-$\underline{P}$ production through the use of glucose. This observation could explain, at least in part, the decrease of PL and TG in the heart of Gyk-deficient mice. As the glycolytic flux, measured as pyruvate production, in heart (20 $\mu mol \times min^{-1} \times g^{-1}$ tissue) is 4- to 14-fold lower than in muscle (41), brain (42,43), and kidney (44), the requirements for heart Gro-3-$\underline{P}$ may not be well compensated for by the use of glucose in Gyk-deficient mice, whereas in brain, kidney, and muscle such a compensation is a reasonable expectation.

If it is true that the lack of Gro-3-$\underline{P}$ production from glycerol is compensated for by glucose utilization under Gyk-deficient conditions, then the rate of glucose utilization, and possibly production, should be increased in Gyk-deficient tissues. In humans, the Gyk deficiency may be accompanied by hypoglycemia (18), perhaps reflecting the increased use of plasma glucose. Hypoglycemia is also observed in mice deficient in dihydroxyacetone-phosphate dehydrogenases (36). In Gyk-deficient mice, the glucose concentration did not differ significantly from the control values (23); however, the amount of corticosterone was increased threefold and the activity of the gluconeogenic enzyme phosphoenolpyruvate carboxykinase was increased 2.7-fold (23). This simultaneous increase in glucose production by tissues stimulated by corticosterone provides a potential source of glucose or its precursors for Gro-3-$\underline{P}$ synthesis.

Alternatively, lipid synthesis in Gyk-deficient conditions could use glycerol that is directly acylated (45). The direct acylation of glycerol occurs when Gyk is inhibited or at high glycerol concentrations (2 mM) (45). We speculate that this non-physiological pathway is less regulated and, under conditions of excess substrate availability, leads to increased PL and TG synthesis in brain, kidney, and muscle.

However, in liver the PL and TG masses were unaffected and in heart they were decreased (Tables 1–3). These results support the contention that osmotic diuresis does not account for the increase in PL mass. This observation may reflect limited glycerol availability for heart tissue. Because the acylation of glycerol is regulated by its tissue availability (45), the direct acylation pathway for PL synthesis may not be compensated for in tissues with limited capability to transport glycerol through the plasma membrane. The movement of alcohols across cell membranes is regulated by aquaporin/aquaglyceroporin channels (2,8). Some aquaglyceroporin channels, such as the glycerol intrinsic protein, are widely expressed in different mammalian tissues, including muscle, kidney, and brain, but not in heart and liver (46). Heart and liver express abundant aquaporin channels (AQP8), which are not permeable to glycerol (46); however, liver expresses the specific aquaglyceroporin channel AQP9 (37). The lack of glycerol-permeable channels in heart may limit glycerol flux, thereby decreasing the capability of heart to use glycerol for lipid synthesis *via* direct acylation. As heart TG are an important reserve of the tissue FFA used for energy supply (47–49), the dramatic 84% decrease in heart TG could significantly alter heart energy metabolism. This assumption is consistent with 56% decrease in FFA mass observed in heart of affected males (Table 3).

The activation of direct acylation could explain, in part, the observed increase of the main glycerophospholipid species, i.e., ChoGpl, EtnGpl, and PtdSer, in brain and muscle, and PtdSer in kidney, whereas PtdIns was not affected in Gyk-deficient mice (Table 2). The Kennedy pathway for ChoGpl, EtnGpl, and PtdSer synthesis requires DAG (50–52), which can be easily synthesized *via* a direct acylation pathway. In contrast, PtdIns synthesis requires PA as a direct precursor (53), the formation of which from glycerol would be limited in Gyk-deficient tissues.

In Gyk-deficient mouse tissues, the Chol mass was altered in parallel with PL mass (Table 1). As a result, the Chol/PL ratio was not disturbed. This is of great importance, as alterations in the Chol/PL ratio could lead to significant changes in membrane biophysical properties and lead to various cellular dysfunctions (54–56). Thus, changes in the Chol level in Gyk-deficient tissues could act as a protective mechanism against PL alterations, similar to what is observed in other pathophysiological conditions (57).

In summary, three groups of tissues could be selected according to their response to Gyk deficiency conditions: tissues with increased total PL mass (brain, muscle, and kidney); decreased total PL mass (heart); or unaffected total PL mass (liver). In parallel with PL alterations, Chol was also changed, maintaining a normal Chol/PL ratio. Tissues with elevated total PL mass (brain, kidney, muscle) were characterized by an increased mass of some individual glycerophospholipids (EtnGpl, ChoGpl, PtdSer). Other glycerophospholipid species, including PtdIns, were not affected in these tissues. Under conditions of Gyk deficiency, we speculate that production of Gro-3-$\underline{P}$ and lipid is maintained *via* alternative biosynthesis, including glycolysis and glyceroneogenesis, or by direct acylation of glycerol in brain, muscle, kidney, and liver, but not in heart.

ACKNOWLEDGMENTS

REFERENCES

1. Reshef, L., Olswang, Y., Cassuto, H., Blum, B., Croniger, C.M., Kalhan, S.C., Tilghman, S.M., and Hanson, R.W. (2003) Glyceroneogenesis and the Triglyceride/Fatty Acid Cycle, *J. Biol. Chem. 278*, 30413–30416.
2. Stroud, R.M., Savage, D., Miercke, L.J.W., Lee, J.K., Khademi, S., and Harries, W. (2003) Selectivity and Conductance Among the Glycerol and Water Conducting Aquaporine Family of Channels, *FEBS Lett. 555*, 79–84.
3. Bortz, W.M., Paul, P., Haff, A.C., and Holmes, W.L. (1972) Glycerol Turnover and Oxidation in Man, *J. Clin. Invest. 51*, 1537–1546.
4. Baba, H., Zhang, X.J., and Wolfe, R.R. (1995) Glycerol Gluconeogenesis in Fasting Humans, *Nutrition 11*, 149–153.

5. Agteresch, H.J., Leij-Halfwerk, S., Van Den Berg, J.W., Hordijk-Luijk, C.H., Wilson, J.H., and Dagnelie, P.C. (2000) Effects of ATP Infusion on Glucose Turnover and Gluconeogenesis in Patients with Advanced Non-small-cell Lung Cancer, *Clin. Sci. (London) 98*, 689–695.

6. Previs, S.F., Martin, S.K., Hazey, J.W., Soloviev, M.V., Keating, A.P., Lucas, D., David, F., Koshy, J., Kirschenbaum, D.W., Tserng, K.Y., and Brunengraber, H. (1996) Contributions of Liver and Kidneys to Glycerol Production and Utilization in the Dog, *Am. J. Physiol. 271*, E1118–E1124.

7. Guo, Z., and Jensen, M.D. (1999) Blood Glycerol Is an Important Precursor for Intramuscular Triacylglycerol Synthesis, *J. Biol. Chem. 274*, 23702–23706.

8. Nguyen, N.H., Brathe, A., and Hassel, B. (2003) Neuronal Uptake and Metabolism of Glycerol and the Neuronal Expression of Mitochondrial Glycerol-3-phosphate Dehydrogenase, *J. Neurochem. 85*, 831–842.

9. Pascual de Bazan, H.E., and Bazan, N.G. (1976) Phospholipid Composition and [14C]Glycerol Incorporation into Glycerolipids of Toad Retina and Brain, *J. Neurochem. 27*, 1051–1057.

10. Robinson, J., and Newsholme, E.A. (1967) Glycerol Kinase Activities in Rat Heart and Adipose Tissue, *Biochem. J. 104*, 2C–4C.

11. Wolfe, R.R., Klein, S., Carraro, F., and Weber, J.M. (1990) Role of Triglyceride-Fatty Acid Cycle in Controlling Fat Metabolism in Humans During and After Exercise, *Am. J. Physiol. 258*, E382–E389.

12. Carmaniu, S., and Herrera, E. (1980) Comparative Utilization *in vivo* of [U-14C]Glycerol, [2-3H]Glycerol, [U-14C]Glucose and [1-14C]Palmitate in the Rat, *Arch. Int. Physiol. Biochim. 88*, 255–263.

13. Glaumann, H., Bergstrand, A., and Ericsson, J.L. (1975) Studies on the Synthesis and Intracellular Transport of Lipoprotein Particles in Rat Liver, *J. Cell Biol. 64*, 356–377.

14. Abdel-Latif, A.A., and Smith, J.P. (1970) *In vivo* Incorporation of Choline, Glycerol and Orthophosphate into Lecithin and Other Phospholipids of Subcellular Fractions of Rat Cerebrum, *Biochim. Biophys. Acta 218*, 134–140.

15. Lapetina, E.G., Rodriguez de Lores Arnaiz, G., and De Robertis, E. (1969) Turnover Rates for Glycerol, Acetate and Orthophosphate in Phospholipids of the Rat Cerebral Cortex, *Biochim. Biophys. Acta 176*, 643–646.

16. Peroni, O., Large, V., Odeon, M., and Beylot, M. (1996) Measuring Glycerol Turnover, Gluconeogenesis from Glycerol, and Total Gluconeogenesis with [2-13C] Glycerol: Role of the Infusion-Sampling Mode, *Metabolism 45*, 897–901.

17. Lumeng, L., Bremer, J., and Davis, E.J. (1976) Suppression of the Mitochondrial Oxidation of (−)-Palmitylcarnitine by the Malate-Aspartate and α-Glycerophosphate Shuttles, *J. Biol. Chem. 251*, 277–284.

18. McCabe, E.R.B. (2001) Disorders of Glycerol Metabolism, in *The Metabolic and Molecular Bases of Inherited Disease* (Scriver, C., Beaudet, A.L., Sly, W.S., Valle, D., Childs, B., Kinzler, K.W., and Vogelstein, B., eds.), 8th edn., pp. 2217–2237, McGraw-Hill, New York.

19. Walker, A.P., Muscatelli, F., Stafford, A.N., Chelly, J., Dahl, N., Blomquist, H.K., Delanghe, J., Willems, P.J., Steinmann, B., and Monaco, A.P. (1996) Mutations and Phenotype in Isolated Glycerol Kinase Deficiency, *Am. J. Hum. Genet. 58*, 1205–1211.

20. Dipple, K.M., Zhang, Y.-H., Huang, B.-L., McCabe, L.L., Dallongeville, J., Inokuchi, T., Kimura, M., Marx, H.J., Roederer, G.O., Shih, V., Yamaguchi, S., Yoshida, I., and McCabe, E.R.B. (2001) Glycerol Kinase Deficiency: Evidence for Complexity in a Single Gene Disorder, *Hum. Genet. 109*, 55–62.

21. Hellerud, C., Burlina, A., Gabelli, C., Ellis, J.R., Nyholm, P.G., and Lindstedt, S. (2003) Glycerol Metabolism and the Determination of Triglycerides—Clinical, Biochemical and Molecular Findings in Six Subjects, *Clin. Chem. Lab. Med. 41*, 46–55.

22. Hellerud, C., Adamowicz, M., Jurkiewicz, D., Taybert, J., Kubalska, J., Ciara, E., Popowska, E., Ellis, J.R., Lindstedt, S., and Pronicak, E. (2003) Clinical Heterogeneity and Molecular Findings in Five Polish Patients with Glycerol Kinase Deficiency: Investigation of Two Splice Site Mutations with Computerized Splice Junction Analysis and Xp21 Gene-Specific mRNA Analysis, *Mol. Genet. Metab. 79*, 149–159.

23. Mahbubul Huq, A.H., Lovell, R.S., Ou, C.-N., Beaudet, A.L., and Craigen, W.J. (1997) X-Linked Glycerol Kinase Deficiency in the Mouse Leads to Growth Retardation, Altered Fat Metabolism, Autonomous Glucocorticoid Secretion and Neonatal Death, *Hum. Mol. Genet. 6*, 1803–1809.

24. Bartley, J.A., and Ward, R. (1985) Glycerol Kinase Deficiency Inhibits Glycerol Utilization in Phosphoglyceride and Triacylglycerol Biosynthesis, *Pediatr. Res. 19*, 313–314.

25. Hara, A., and Radin, N.S. (1978) Lipid Extraction of Tissues with a Low-Toxicity Solvent, *Anal. Biochem. 90*, 420–426.

26. Saunders, R.D., and Horrocks, L.A. (1984) Simultaneous Extraction and Preparation for HPLC of Prostaglandins and Phospholipids, *Anal. Biochem. 143*, 71–75.

27. Dugan, L.L., Demediuk, P., Pendley, C.E., II, and Horrocks, L.A. (1986) Separation of Phospholipids by High Pressure Liquid Chromatography: All Major Classes Including Ethanolamine and Choline Plasmalogens, and Most Minor Classes, Including Lysophosphatidylethanolamine, *J. Chromatogr. 378*, 317–327.

28. Murphy, E.J., Stephens, R., Jurkowitz-Alexander, M., and Horrocks, L.A. (1993) Acidic Hydrolysis of Plasmalogens Followed by High-Performance Liquid Chromatography, *Lipids 28*, 565–568.

29. Rouser, G., Siakotos, A., and Fleischer, S. (1969) Quantitative Analysis of Phospholipids by Thin Layer Chromatography and Phosphorus Analysis of Spots, *Lipids 1*, 85–86.

30. Murphy, E.J., Prows, D.R., Jefferson, J.R., and Schroeder, F. (1996) Liver Fatty Acid Binding Protein Expression in Transfected Fibroblasts Stimulates Fatty Acid Uptake and Metabolism, *Biochim. Biophys. Acta 1301*, 191–196.

31. Murphy, E.J., Rosenberger, T.A., and Horrocks, L.A. (1996) Separation of Neutral Lipids by High Performance Liquid Chromatography: Quantification by Ultraviolet, Light Scattering and Fluorescent Detectors, *J. Chromatogr. B 685*, 9–14.

32. Akesson, B., Elovsson, J., and Arvidsson, G. (1970) Initial Incorporation into Rat Liver Glycerolipids of Intraportally Injected [3H]Glycerol, *Biochim. Biophys. Acta 210*, 15–27.

33. Murphy, E.J., and Schroeder, F. (1997) Sterol Carrier Protein-2 Mediated Cholesterol Esterification in Transfected L-Cell Fibroblasts, *Biochim. Biophys. Acta 1345*, 283–292.

34. Brockerhoff, H. (1975) Determination of the Positional Distribution of Fatty Acids in Glycerolipids, *Methods Enzymol. 35*, 315–325.

35. Bradford, M. (1976) A Rapid and Sensitive Method for the Quantitation of Microgram Quantities of Protein Utilizing the Principle of Protein–Dye Binding, *Anal. Biochem. 72*, 248–254.

36. Brown, L.J., Kosa, R.A., Marshall, L., Kozak, L.P., and MacDonald, M.J. (2002) Lethal Hypoglycemic Ketosis and Glyceroluria in Mice Lacking Both the Mitochondrial and the Cytosolic Glycerol Phosphate Dehydrogenases, *J. Biol. Chem. 277*, 32899–32904.

37. Custo, G., Corazzi, L., Mastrofini, P., and Arienti, G. (1987) Glycerol Incorporation into Brain Lipids in Rat Pups Born to Ethanol-Intoxicated Dams, *Neurochem. Res. 12*, 469–473.

38. Tardi, P.G., Man, R.Y., and Choy, P.C. (1992) The Effect of Methyl-Lidocaine on the Biosynthesis of Phospholipids *de novo* in the Isolated Hamster Heart, *Biochem. J. 285*, 161–166.

39. Athenstaedt, K., and Daum, G. (1999) Phosphatidic Acid, a Key Intermediate in Lipid Metabolism, *Eur. J. Biochem. 266*, 1–16.

40. Watford, M. (2000) Functional Glycerol Kinase Activity and the Possibility of a Major Role for Glyceroneogenesis in Mammalian Skeletal Muscle, *Nutr. Rev. 58*, 145–148.

41. Crabtree, B., and Newsholme, E.A. (1972) The Activities of Phosphorylase, Hexokinase, Phosphofructokinase, Lactate Dehydrogenase and the Glycerol 3-Phosphate Dehydrogenases in Muscles from Vertebrates and Invertebrates, *Biochem. J. 126*, 49–58.

42. Duelli, R., Maurer, M.H., Staudt, R., Heiland, S., Duembgen, L., and Kuschinsky, W. (2000) Increased Cerebral Glucose Utilization and Decreased Glucose Transporter Glut1 During Chronic Hyperglycemia in Rat Brain, *Brain Res. 858*, 338–347.

43. Sokoloff, L., Reivich, M., Kennedy, C., Des Roisiers, M.H., Patlak, C.S., Pettigrew, K.D., Sakurada, O., and Shinohara, M. (1977) The [^{14}C]Deoxyglucose Method for the Measurement of Local Cerebral Glucose Utilization: Theory, Procedure, and Normal Values in the Conscious and Anesthetized Albino Rat, *J. Neurochem. 28*, 897–916.

44. Garcia-Salguero, L., and Lupianez, J.A. (1989) Metabolic Adaptation of the Renal Carbohydrate Metabolism. II. Effects of a High Carbohydrate Diet on the Gluconeogenic and Glycolytic Fluxes in the Proximal and Distal Renal Tubules, *Mol. Cell. Biochem. 85*, 91–100.

45. Lee, D.P., Deonarine, A.S., Kienetz, M., Zhu, Q., Skrzypczak, M., Chan, M., and Choy, P.C. (2001) A Novel Pathway for Lipid Biosynthesis: The Direct Acylation of Glycerol, *J. Lipid Res. 42*, 1979–1986.

46. Ma, T., Yang, B., and Verkman, A.S. (1997) Cloning of a Novel Water and Urea-Permeable Aquaporin from Mouse Expressed Strongly in Colon, Placenta, Liver, and Heart, *Biochem. Biophys. Res. Commun. 240*, 324–328.

47. DeGrella, R.F., and Light, R.J. (1980) Uptake and Metabolism of Fatty Acids by Dispersed Adult Rat Heart Myocytes. I. Kinetics of Homologous Fatty Acids, *J. Biol. Chem. 255*, 9731–9738.

48. Klein, M.S., Goldstein, R.A., Welch, M.J., and Sobel, B.E. (1979) External Assessment of Myocardial Metabolism with [^{11}C]Palmitate in Rabbit Hearts, *Am. J. Physiol. 237*, H51–H57.

49. Tamboli, A., O'Looney, P., Vander Maten, M., and Vahouny, G.V. (1983) Comparative Metabolism of Free and Esterified Fatty Acids by the Perfused Rat Heart and Rat Cardiac Myocytes, *Biochim. Biophys. Acta 750*, 404–410.

50. McMaster, C.R., and Bell, R.M. (1997) CDP-Choline:1,2-Diacylglycerol Cholinephosphotransferase, *Biochim. Biophys. Acta 1348*, 100–110.

51. McMaster, C.R., and Bell, R.M. (1997) CDP-Ethanolamine:1,2-Diacylglycerol Ethanolaminephosphotransferase, *Biochim. Biophys. Acta 1348*, 117–123.

52. Araki, W., and Wurtman, R.J. (1998) How Is Membrane Phospholipid Biosynthesis Controlled in Neural Tissues? *J. Neurosci. Res. 51*, 667–674.

53. Heacock, A.M., and Agranoff, B.W. (1997) CDP-Diacylglycerol Synthase from Mammalian Tissues, *Biochim. Biophys. Acta 1348*, 166–172.

54. Schroeder, F., Frolov, A.A., Murphy, E.J., Atshaves, B.P., Pu, L., Wood, W.G., Foxworth, W.B., and Kier, A.B. (1996) Recent Advances in Membrane Cholesterol Domain Dynamics and Intracellular Cholesterol Trafficking, *Proc. Soc. Exp. Biol. Med. 213*, 150–177.

55. Wood, W.G., Schroeder, F., Avdulov, N.A., Chochina, S.V., and Igbauboa, U. (1999) Recent Advances in Brain Cholesterol Dynamics: Transport, Domains, and Alzheimer's Disease, *Lipids 34*, 225–234.

56. Petrovich, D.R., Finkelstein, S., Waring, A.J., and Farber, J.L. (1984) Liver Ischemia Increases the Molecular Order of Microsomal Membranes by Increasing the Cholesterol-to-Phospholipid Ratio, *J. Biol. Chem. 259*, 13217–13223.

57. Murphy, E.J., Schapiro, M.B., Rapoport, S.I., and Shetty, H.U. (2000) Phospholipid Composition and Levels Are Altered in Down Syndrome Brain, *Brain Res. 867*, 9–18.

Vaccenic Acid Metabolism in the Liver of Rat and Bovine

Dominique Gruffat[a],*, Anne De La Torre[a], Jean-Michel Chardigny[b],
Denys Durand[a], Olivier Loreau[c], and Dominique Bauchart[a]

[a]Institut National de la Recherche Agronomique (INRA), Research Unit on Herbivores, Nutrients and Metabolisms Group,
63122 Saint Genès-Champanelle, France, [b]INRA Dijon, Lipid Nutrition Unit, 21065 Dijon, France,
and [c]Commissariat à l'Energie Atomique, Saclay, 91191 Gif/Yvette Cedex, France

ABSTRACT: Hepatic metabolism of vaccenic acid (VA), especially its conversion into CLA, was studied in the bovine (ruminant species that synthesizes CLA) and in the rat (model for nonruminant) by using the *in vitro* technique of liver explants. Liver tissue samples were collected from fed animals (5 male Wistar rats and 5 Charolais steers) and incubated at 37°C for 17 h under an atmosphere of 95% O_2/5% CO_2 in medium supplemented with 0.75 mM of FA mixture and with 55 µM [1-^{14}C]VA. VA uptake was about sixfold lower in bovine than in rat liver slices ($P <$ 0.01). For both species, VA that was oxidized to partial oxidation products represented about 20% of VA incorporated by cells. The chemical structure of VA was not modified in bovine liver cells, whereas in rat liver cells, 3.2% of VA was converted into 16:0 and only 0.33% into CLA. The extent of esterification of VA was similar for both animal species (70–80% of incorporated VA). Secretion of VA as part of VLDL particles was very low and similar in rat and bovine liver (around 0.07% of incorporated VA). In conclusion, characteristics of the hepatic metabolism of VA were similar for rat and bovine animals, the liver not being involved in tissue VA conversion into CLA in spite of its high capacity for FA desaturation especially in the rat. This indicates that endogenous synthesis of CLA should take place exclusively in peripheral tissues.

Paper no. L9672 in *Lipids* 40, 295–301 (March 2005).

Trans FA (TFA) are mainly found in ruminant fats (dairy products, bovine and lamb meat) as a result of the hydrogenation and trans isomerization chain reaction of dietary PUFA by rumen bacteria. They are also found in shortenings and table spreads, produced by industrial catalytic hydrogenation of vegetable oils. *Trans* positional isomers in fats originating from industrial hydrogenation, where a mixture of isomers is found, differ somewhat from those in fats derived from ruminant fermentation, which result in a predominance of vaccenic acid (VA, 18:1 *trans*11) (1). Evidence suggests potentially adverse effects of TFA on the risk of coronary heart disease (2,3). However, VA is also a precursor of CLA, which is believed to possess important beneficial properties for human health, as suggested from experiments using different animal models (4). Conversion by desaturation of VA to CLA takes place in tissues of ruminants where the Δ9-desaturase enzyme (EC

1.14.99.5) is expressed, i.e., mammary gland in the lactating ruminant and adipose tissue in the growing ruminant (5,6). Moreover, endogenous synthesis of CLA from VA, based on the increase of CLA concentration in either serum, adipose tissue, or milk observed with diets supplemented with VA, also has been shown in mice (7,8), rats (9,10), pigs (11), and humans (12–14).

In considering suggested properties of VA, which may be either deleterious (risks of coronary heart disease) or beneficial (precursor of CLA), it is important to determine with precision the metabolic fate of VA in the ruminant (as a species that produces CLA) and the rat (as an animal model of nonruminant species). Among the different tissues and organs that are involved in FA metabolism, the liver appears to play a central role in lipid metabolism (15). Indeed, once in the liver, FA can be either extensively or partially oxidized in mitochondria to produce energy and generate CO_2 and ketone bodies, or esterified into triacylglycerols (TG), phospholipids (PL), and cholesterol esters in the cytoplasm. The alternative fate of TG in the liver is their exportation in the blood circulation as part of particles of VLDL (15,16). Previous studies using the *in vitro* method of incubated liver slices have demonstrated that hepatic FA metabolism varies with either the nature of FA (17,18) or the animal species (19). No data are available on hepatic metabolism of TFA except for a study by Guzman *et al.* (20), who have shown that elaidic acid is preferentially oxidized in rat hepatocytes, whereas oleic acid is preferentially esterified, indicating that double bond configuration of FA may also affect the metabolic fate of FA.

In this context, the aim of our study was to compare, by using the *in vitro* method of incubated liver slices, characteristics of hepatic metabolism of VA in the bovine with that of the rat. For this purpose, we determined the relative intensity of the different successive pathways of the hepatic VA metabolism, i.e., uptake, oxidation, bioconversion, and esterification, and finally its secretion as part of VLDL particles.

EXPERIMENTAL PROCEDURES

Chemicals and materials. The medium for incubation of liver slices (RPMI-1640), BSA free of FA, glutamine (300 mg/L), FA, and an antibiotic-antimycotic cocktail (penicillin, 100 U/mL; streptomycin, 0.1 mg/mL; amphoterine B 0.25 µg/mL) were purchased from Sigma Chemical (St. Louis, MO). Tri [9,10 ^{3}H]olein (185 MBq/mL) and 1,2 dipalmitoyl L-3-phos-

phatidyl[*N*-methyl-^{3}H]choline (37 MBq/mL) were purchased from Amersham International (Bucks, United Kingdom). [1-^{14}C]VA (1.97 GBq/mmol) was graciously provided by the Atomic Energy Centre (Saclay, Gif/Yvette, France). Hyamine hydroxide was purchased from ICN Biochemicals (Irvine, CA). Perchloric acid and organic solvents (chloroform, methanol, propanol, diethyl ether, acetic acid) were purchased from Polylabo (Paris, France). Ready Safe® scintillation cocktail was purchased from Beckman Instruments (Fullerton, CA). Plastic Petri dishes for organ culture were purchased from Beckton Dickinson (Cockeysville, MD). Plastic center wells were purchased from Kontes (Vineland, NJ) and aminopropyl-activated silica Sep-Pak® cartridges were purchased from Waters (Milford, MA).

Tissue preparation and liver slice incubation. All experiments were conducted in a manner compatible with national legislation on animal care (Certificate of Authorisation to Experiment on Living Animal no. 7740, Ministry of Agriculture and Fish Products, Paris, France). Five male Wistar rats (age 16 ± 1 wk) were fed *ad libitum* a standard chow diet and allowed free access to water. In the same way, five Charolais steers (age 25 ± 1 mon; live weight 713 ± 39 kg) were fed a conventional diet (hay and cereal concentrate, 45 and 55% dry matter, respectively). Liver tissue samples were taken from rats under general anesthesia (diethyl ether) and from steers just after slaughtering. Then liver samples were quickly rinsed of blood in an ice-cold saline solution (NaCl, 9 g/L), connective tissue was trimmed, and liver samples were cut into 0.5-mm slices. Approximately 200-mg portions of fresh liver were placed on stainless grids positioned either on a plastic organ culture Petri dish (for quantification of FA bioconversion, esterification, and secretion) or in a 25-mL flask equipped with suspended plastic wells (for measurement of specific CO_2 production) in the presence of RPMI-1640 medium (0.9 mL per dish and 1.4 mL per flask) supplemented with the antibiotic-antimycotic cocktail. Liver samples were placed under a water-saturated atmosphere (95% O_2 and 5% CO_2) for 3 h at 37°C to deplete hepatic cells with intracellular FA. The medium was then replaced with similar fresh medium containing a mixture of FA (21) representative in composition and concentration of bovine plasma nonesterified FA [0.75 mM final concentration, which consisted of caprylic acid (16 µM), capric acid (16 µM), myristic acid (58 µM), palmitic acid (200 µM), stearic acid (220 µM), oleic acid (213 µM), and linoleic acid (26 µM)] in addition to [1-^{14}C]VA (55 µM) complexed with BSA (FA/albumin molar ratio 4:1). Kinetic experiments have been performed to verify the correct viability of liver slices until 24 h (17). Consequently, liver slice incubations were stopped after 17 h of labeling: Briefly, media (2.5 mL) were collected and liver slices were washed with 2 mL of buffered solution (KCl, 0.4 g/L; Na_2HPO_4, 0.60 g/L; NaH_2PO_4, 0.2 g/L; pH 7.4; and D-glucose 2 g/L) before their homogenization with a Dounce homogenizer in 2 mL of 0.25 mM Tris-HCl (pH 8.0) and 50 mM NaCl (pH 8.0).

Determination of FA oxidation. CO_2 excreted in the atmosphere by liver cells was complexed with hyamine hydroxide

(500 µL) placed into suspended plastic center wells inside flasks at the beginning of the incubation as described earlier (19). After 17 h of incubation, wells were introduced into scintillation vials containing 4 mL of Ready Safe scintillation cocktail for radioactivity quantification. The production of ketone bodies was estimated according to the method of Graulet *et al.* (19). Briefly, cell homogenates (250 µL) and media (500 µL) were treated for 20 min at 4°C with ice-cold perchloric acid (0.2 mM final). After centrifugation for 20 min at 4°C at 1,850 $\times g$, an aliquot of supernatant containing the acid-soluble products (ASP) (mainly ketone bodies) was introduced into a scintillation vial and the radioactivity was counted.

Determination of FA bioconversion. Total liver lipids were extracted according to the method of Folch *et al.* (22), and their corresponding FA were liberated and methylated by transmethylation at room temperature according to the method of Christie *et al.* (23). FAME containing [^{14}C]FAME were analyzed by GLC using an HP 5890 series II gas chromatograph (Hewlett-Packard, Palo Alto, CA), equipped with a splitless injector and a fused Stabilwax wide-bore silica column (60 m × 0.53 mm i.d.; 0.50 µm film thickness; Restek, Evry, France). The outflow from the column was split between an FID (10%) and a copper oxide oven heated at 700°C to transform the [^{14}C]FA into $^{14}CO_2$ (90%). Radioactivity was quantified with a radiodetector (GC-RAM) (Lablogic, Sheffield, United Kingdom) by counting $^{14}CO_2$ after its mixing with a 9:1 ratio of argon/methane, as previously described (24). Data were computed using Laura software (Lablogic).

Determination of FA esterification into neutral and polar lipids. Total liver lipids were extracted according to the method of Folch *et al.* (22) after addition of a standard (nonradioactive) liver homogenate (850 µL containing approximately 10 mg of lipids) as a lipid carrier and of [^{3}H]trioleylglycerol (67 Bq) and [^{3}H]PC (100 Bq) as internal TG and PL standards (19). Neutral and polar lipids were separated by affinity-LC with aminopropyl-activated silica Sep-Pak® cartridge according to Kaluzny *et al.* (25). They were directly collected into scintillation vials, evaporated to dryness under an air stream, and counted for radioactivity.

Hepatic secretion of VLDL. Newly secreted [^{14}C]VLDL were purified by ultracentrifugation according to Graulet *et al.* (19). Hence, the medium (3 mL) previously supplemented with purified plasma bovine VLDL (0.3 mg of VLDL-TG per 12-mL tube) as a carrier for VLDL during ultracentrifugation was adjusted to the density of 1.063 g/L with potassium bromide and overlaid with 9 mL of saline solution. VLDL particles were isolated by ultracentrifugal flotation at $100,000 \times g$ for 16 h at 15°C in a Kontron Centrikon T-2060 ultracentrifuge equipped with a TST 41-14 rotor (Kontron, Zürich, Switzerland). Two milliliters was collected at the top of each tube and recentrifuged under the same conditions, except that pure albumin (50 mg/tube) was added to remove traces of free [^{14}C]FA adsorbed onto VLDL particles. Finally, purified VLDL (2.5 mL) were counted for radioactivity in scintillation vials.

Statistical analysis. Values are expressed as means ± SEM for the five independent experiments per each animal species.

Comparison of means between animal species was tested by using the Student's *t*-test for unpaired data.

RESULTS

VA uptake. The amount of VA taken up by the hepatocytes of rat and bovine animals (expressed in nmol per g fresh tissue) corresponded to the sum of FA incorporated into the hepatic lipids (neutral and polar lipids) plus FA oxidized into ASP in the homogenate plus FA oxidized to CO_2 and subsequently excreted to the atmosphere. After 17 h of incubation, hepatic uptake of VA by bovine hepatocytes was 17.8% of that by rat hepatocytes (15.2 vs. 85.5 nmol/g of fresh liver, $P < 0.001$) (Fig. 1A). A similar result was observed when the intensity of VA uptake was expressed as the percentage of radioactivity introduced in the incubation medium (Fig. 1B).

VA oxidation. The extent of β-oxidation, calculated as the ratio of total oxidation products (sum of ASP and CO_2) to total incorporated VA in hepatocytes, was similar in bovine and in rat liver slices (Table 1). It corresponded to about 28 and 19% of VA incorporated by cells for bovine and rat hepatocytes, respectively. Oxidation of VA led for the most part to the production of ASP (>90% total oxidized VA) in both species. This partial oxidation, expressed as the percentage of oxidized VA, constituted a greater portion of that oxidized in the bovine than in the rat hepatocytes (+8.5%, $P < 0.01$). In the same way, in spite of the slow rate of VA total oxidation (determined as the amount of [^{14}C]CO_2 excreted) in both species (<10% total oxidized VA), total oxidation of VA into CO_2 in the bovine liver, expressed as a percentage of oxidized VA, was one-fifth that of rat liver ($P < 0.01$) (Table 1).

*Bioconversion of VA.* Total lipids were extracted from liver homogenates after 17 h of incubation. Their FA composition was determined by GLC analysis and their relative radioactivity quantified by a radiodetector. In our experimental conditions, VA was not converted by desaturation into higher unsaturated FA or CLA isomers by bovine hepatocytes (Fig. 2A). In contrast, in rat hepatocytes (Fig. 2B), a low quantity of VA was converted into CLA 9*cis*,11*trans* (0.33 ± 0.19% of total VA). Moreover, radioactivity was also recovered in 16:0 but at a higher extent (3.2 ± 2% of total incorporated radioactivity). These new labeled FA were identified according to the similarity of their respective retention times with those of corresponding standards.

VA esterification. The extent of VA esterification (expressed as a percentage of FA converted into neutral and polar lipids out of total VA incorporated into cells), which was similar for the two species, corresponded to about 72 and 81% of VA incorporated by bovine and rat hepatocytes, respectively (Table 2). VA was preferentially esterified into polar lipids by the bovine liver (56.5% of esterified VA, $P < 0.05$) and, conversely, into neutral lipids by the rat liver (61.1% of esterified VA, $P < 0.05$).

VA secretion as part of VLDL particles. The extent of VA secretion as part of VLDL particles by the liver slices for 17 h (Fig. 3A) was very low for both species. This secretion by bovine liver was less than 20% ($P < 0.02$) that of rat liver (0.012 vs. 0.066 nmol of secreted VA/g fresh tissue, respectively). However, when expressed as the percentage of VA taken up by the hepatic cells, VA secreted as part of VLDL particles was not significantly different between the two animal species (Fig. 3B) (0.067 and 0.085% for bovine and rat liver, respectively).

DISCUSSION

The specific metabolism of VA, especially how it is channeled toward the esterification, oxidation, or bioconversion pathways in tissues or organs (more precisely, in the liver), is not documented in spite of the importance of VA availability to peripheral tissues, especially as a precursor of CLA. Moreover, the liver might be directly implicated in the synthesis of CLA from VA due to its high desaturase activity. In this context, our study
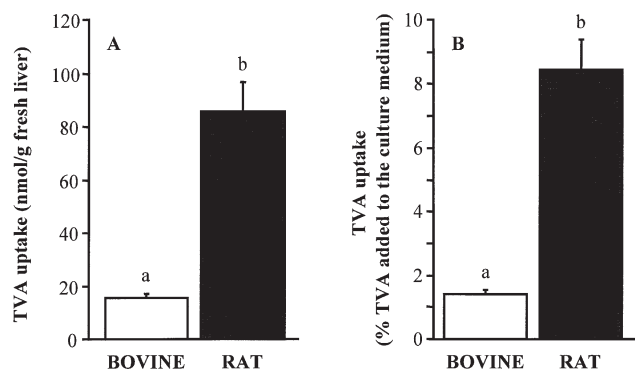
FIG. 1. Uptake of vaccenic acid (VA) by bovine and rat liver slices. Liver slices from bovine and rat were incubated in medium containing a mixture of FA (0.75 mM) and 55 µM [1-^{14}C]VA for 17 h. Uptake of VA by liver slices was calculated as the sum of VA converted into CO_2 and into acid-soluble products, and incorporated into total cellular lipids after 17 h of incubation. Values are expressed per g of fresh liver (A) or as the percentage of VA introduced in culture medium (B). TVA, *trans*-vaccenic acid. Data are means ± SE of 5 animals per group. ^{a,b}Mean values with unlike superscript letters were significantly different using Student's *t*-test ($P < 0.01$).

TABLE 1
Oxidation of Vaccenic Acid (VA) into Acid-Soluble Products (ASP) and CO_2 in Rat and Bovine Liver Slices^a

	Bovine^b	Rat^b
Extent of VA oxidation (% of VA incorporated by cells)	28.03 ± 3.09	19.06 ± 4.18
Production of acid-soluble products (% of oxidized VA equivalents)	98.12 ± 0.53	90.38 ± 1.89*
Production of CO_2 (% of oxidized VA equivalents)	1.88 ± 0.53	9.62 ± 1.89*

^{a}Liver slices from bovine and rat were incubated for 17 h in a medium containing [1-^{14}C]VA. The extent of oxidation was calculated as the ratio of total oxidation products (sum of ASP and CO_2) to total VA incorporated into liver explants. ASP produced by liver slices were purified from cell homogenate and medium by perchloric acid treatment, and secreted CO_2 was complexed into hyamine hydroxide.
^{b}Data are means ± SEM of 5 animals per group. The significance of differences between species was tested by Student's *t*-test. *$P < 0.01$.
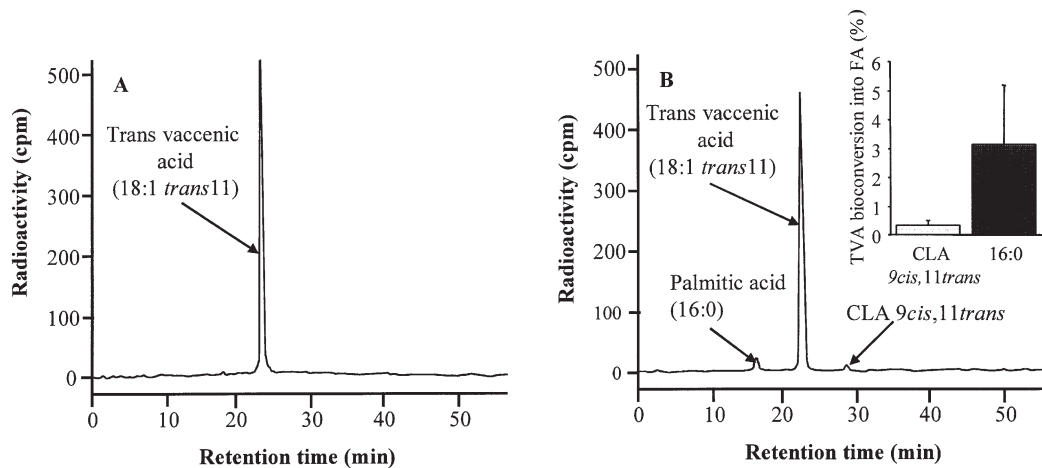
FIG. 2. Representative radiochromatograms of [^{14}C]VA bioconversion into other FA in bovine and rat liver slices. Liver slices from bovine (A) and rat (B) were incubated in medium containing a mixture of FA (0.75 mM) and 55 μM [1-^{14}C]VA for 17 h. Cellular lipids were extracted, transformed into methyl esters, and analyzed by GLC. The outflow from the column was split between an FID (10%) and a copper oxide oven to transform the labeled FA into ^{14}CO$_2$ (90%). The radioactivity was determined with a radiodetector by counting ^{14}CO$_2$. The proportions of radioactivity recovered in other FA were calculated as the ratio between the radioactivity corresponding to the metabolite and the sum of the radioactivity present in peaks of VA plus their corresponding metabolite. For abbreviation see Figure 1.

is the first that investigates, by using the *in vitro* method of incubated liver slices, the specificity of VA metabolism in the liver of the bovine (a species that produces CLA) and the rat (an animal model for monogastrics).

In our experimental conditions, the lower VA uptake by liver of the bovine compared with that of the rat confirmed previous data with oleate in calf and rat liver slices (19). Uptake of long-chain FA across the plasma membrane is known to involve two mechanisms: a passive diffusion through the membrane bilayer (26) and a protein-facilitated transfer (27). However, Bojesen and Bojesen (28) have proposed a third mechanism of FA diffusion in protein-defined annular lipid domains that is not carrier-mediated. These authors showed that binding and membrane transfer rates of PUFA in sheep red cells were less than half of those measured for human red cells, probably because of the difference between species in composition of membranes. Nevertheless, higher VA uptake by rat liver slices compared with that of bovine might be attributable to a higher rate of intracellular FA utilization (oxidation, esterification) increasing cellular needs (26), to more efficient or more numerous FA transporters (27), or to differences in membrane composition between rat and bovine hepatocytes.

Once in hepatocytes, VA catabolism was determined by the production of ^{14}CO$_2$ and ^{14}C-ASP from [1-^{14}C]VA. The use of [1-^{14}C]VA might be limiting to describe VA catabolism since it only reflected the initial rate of oxidation contrary to the use of [U-^{14}C]VA. However, the aim of the present work was not to describe VA catabolism exhaustively but rather to describe VA behavior in the liver and its channel toward the different metabolic pathways. Moreover, Chatzidakis and Otto (29) previously demonstrated that the use of [1-^{14}C]FA gave data quite similar to [U-^{14}C]FA, being therefore a good choice for studies

of FA oxidation in cells. The catabolism of FA in the liver is mostly directed toward the synthesis of ketone bodies for energy utilization by tissues (30) as shown in the present study in which products of VA oxidation were dominated by ASP (more than 90% of total oxidation products). The proportion of VA oxidized to CO$_2$, although minor, differed between the rat and the bovine liver, as previously reported by Reid and Husbands (31), who showed that the rate of oleate oxidation to CO$_2$ was twofold higher in hepatic mitochondria of rat than in that of sheep, and by Kleppe *et al.* (32), who reported that oxidation of oleate to CO$_2$ was three- to fourfold lower in goat compared with rat hepatocytes. This difference can be attributed to a lower capacity of the Krebs cycle relative to that of the β-oxidation pathway in large mammals (such as bovine) than in rats

TABLE 2
Esterification of VA into Phospholipids and Neutral Lipids in Rat and Bovine Liver Slices[a]

	Bovine[b]	Rat[b]
Extent of VA esterification (% of VA incorporated by cells)	72.0 ± 3.09	80.9 ± 4.18
Production of phospholipids (% of esterified VA equivalents)	56.5 ± 6.77	39.0 ± 2.78*
Production of neutral lipids (% of esterified VA equivalents)	43.5 ± 6.77	61.0 ± 2.78*

[a]Bovine and rat liver slices were incubated for 17 h in a medium containing [1-^{14}C]VA. Esterification rate was calculated as the ratio of total esterification (sum of neutral and polar lipids) to total VA incorporated into liver explants. Total lipids from homogenate were extracted with chloroform/methanol (2:1), and the different lipid classes were separated on aminopropyl-activated silica cartridges.
[b]Data are means ± SEM of 5 animals per group. The significance of differences between species was tested by Student's *t*-test. *$P < 0.05$. For abbreviation see Table 1.
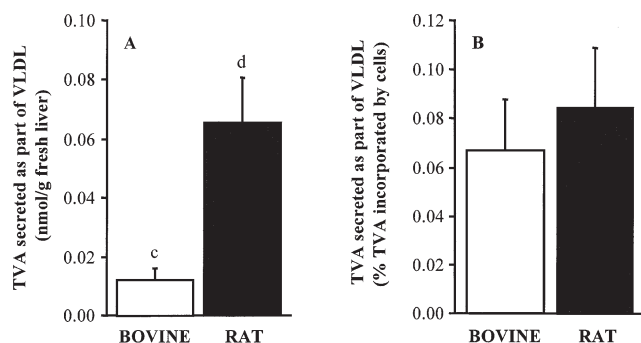
FIG. 3. Secretion of VA as part of lipids in VLDL particles by bovine and rat liver slices. Liver slices from bovine and rat were incubated in medium containing a mixture of FA (0.75 mM) and 55 μM [1-^{14}C]VA for 17 h. VLDL were purified by ultracentrifugal flotation. Values were expressed per g fresh liver (A) or as percentage of VA incorporated into liver slices (B). Data are means ± SE of 5 animals per group. For abbreviation see Figure 1. ^{c,d}Mean values with unlike superscript letters were significantly different using the Student's *t*-test ($P < 0.02$).

in relation to a lower energy requirement of the liver in large-sized than in small-sized animals (33). However, the proportion of VA readily oxidized by bovine and rat liver slices was similar in both species (around 20%) and was similar to that of oleate as determined by the same methodology in the preruminant calf and the rat (18,19). It can be concluded that differences noted in intensity of VA oxidation between species were directly linked with differences in VA uptake. However, the only study in rat describing characteristics of *trans* FA metabolism in hepatocytes showed that elaidic acid (18:1 Δ9*trans*) was oxidized to a greater extent than oleic acid (18:1 Δ9*cis*) (80 vs. 60% of metabolized FA) (20). Discrepancies between the two studies could be explained either by differences in the chemical structure of *trans* FA (18:1 Δ11*trans* vs. 18:1 Δ9*trans*) or, more probably, by differences in the incubation conditions of *trans* FA (elaidic acid was added alone into the medium whereas VA was added with a mixture of FA similar to bovine plasma nonesterified FA to simulate *in vivo* physiological conditions). In the study of Guzman *et al.* (20), the addition of elaidic acid alone to the medium might explain its high rate of oxidation since it represented the only energy source provided to hepatocytes.

The lack of VA bioconversion into more desaturated or elongated derivatives such as CLA in both species was not expected since several studies had reported an endogenous production of *cis*9,*trans*11 CLA from VA (5,6,9,10). Synthesis of CLA from VA is clearly catalyzed by the Δ9-desaturase, as demonstrated by using different specific stimulators or inhibitors of the activity of this enzyme (5,6). In rodents, the Δ9-desaturase is predominantly located in the liver (34), and Pollard *et al.* (35) demonstrated that VA was efficiently desaturated in the rat liver microsomes by Δ9-desaturation. In contrast, in growing and lactating ruminants, Δ9-desaturase is mainly present in the adipose tissues and the mammary gland, respectively (36,37) although Ward *et al.* (37) recently demonstrated the presence of a significant amount of Δ9-desaturase

transcripts in the liver of ovine. Moreover, Chang *et al.* (38) showed that a high-fat diet induced Δ9-desaturase activity in ruminant liver. The lack of VA bioconversion in the present study might be explained by the difference between our experimental conditions and those of Pollard *et al.* (35). Indeed, the mixed FA added to the medium, and therefore potentially available for hepatocytes, contained preferred substrates (16:0, 18:0) for the Δ9-desaturase leading to production of oleic and palmitoleic acids, respectively (39). Moreover, the *ex vivo* system was chosen to preserve the normal architecture of the liver tissue, to avoid dedifferentiation of hepatocytes, and finally, to preserve the regulatory effect as under *in vivo* conditions (40). It was not the case for the study of Pollard *et al.* (35) using isolated rat liver microsomal systems of which activities of other cellular constituents were excluded. Consequently, the rat liver would have a low capacity to convert VA into CLA, and adipose tissue would be the major site of endogenous synthesis of CLA, as previously proposed by Santora *et al.* (8) in mice and by Bauchart *et al.* (41) in bovine.

Surprisingly, a small but nonnegligible part of the ^{14}C VA was recovered as ^{14}C 16:0 in the rat liver slices (3.2% of incorporated VA). It has been demonstrated that *trans* FA may undergo partial β-oxidation in peroxisomes (20), a process in which FA are shortened by two carbon atoms per cycle. The shortened FA may escape from the peroxisomes and be further metabolized in the mitochondria or incorporated into different lipid classes. Thus, 16:0 may be produced by peroxisomal β-oxidation. Further, the ^{14}C-acetate released from peroxisomes could be reincorporated into 16:0 by *de novo* synthesis (42). Similar catabolic processes have already been demonstrated in the liver of rat in the case of mono-*trans* isomers of linoleic and α-linolenic acids (43) and of CLA (44,45), and in the liver of preruminant calf fed a coconut oil-based milk diet rich in 12:0 and 14:0 (42).

Differences in the way of esterification of VA and metabolites between rat (into neutral lipids) and bovine (into polar lipids) have not previously been reported. However, the slight differences observed between animal species were in agreement with previous data showing a preferential esterification of oleate into polar lipids in the bovine liver (De La Torre, A., Gruffat, D., Chardigny, J.M., Durand, D., and Bauchart, D., unpublished data) and into the neutral lipids in the rat liver (18).

The extent of secretion of VA incorporated into TG as part of VLDL particles by both bovine and rat liver slices was, in intensity, rather low in our experimental conditions (less than 0.1% of VA incorporated into cells), which is in agreement with the fact that newly synthesized TG represented only a small part (4 to 13%) of lipids secreted by the liver as parts of VLDL (46). Neosynthesized TG are stored primary in cytosolic droplets from which they enter into a hydrolysis/esterification cycle to return to the endoplasmic reticulum for VLDL assembly (47). Therefore, it is not excluded that, in our experimental conditions, the time of incubation for liver slices would be too short to allow the return of a significant amount of TG to the secretion pool. Differences between species of VA secretion intensity probably resulted from differences in VA uptake rather

than in capacity to secrete VA in VLDL since no difference was noted when results were expressed as the percentage of VA incorporated by cells.

In conclusion, the *in vitro* model of liver slices allows us to compare the main metabolic pathways of VA in bovine and rat animals. We clearly demonstrated that the hepatic metabolism of VA was not significantly different between the two animal species since differences in intensity of the different metabolic pathways of VA were directly linked to differences in uptake efficiency of VA between these two animal species. It is important to note that VA was not converted into CLA by the liver of either species. The extrahepatic sites for endogenous synthesis of CLA included adipose tissue, as suggested by an *in vivo* experiment with mice given a VA supplement, which showed a large incorporation of CLA from VA into lipids in adipose tissue (8). Indeed metabolic experiments using adipose tissue slices would be necessary to verify this hypothesis.

ACKNOWLEDGMENTS

REFERENCES

1. Fritsche, J., and Steinhart, H. (1998) Analysis, Occurrence and Physiological Properties of *trans* Fatty Acids (TFA) with Particular Emphasis on Conjugated Linoleic Acid Isomers (CLA)—A Review, *Fette Lipid 100*, 190–210.
2. Koletzko, B., and Decsi, T. (1997) Metabolic Aspects of *trans* Fatty Acids, *Clin. Nutr. 16*, 229–237.
3. Lichtenstein, A.H. (2000) *Trans* Fatty Acids and Cardiovascular Disease Risk, *Curr. Opin. Lipidol. 11*, 37–42.
4. Pariza, M.W. (2004) Perspective on the Safety and Effectiveness of Conjugated Linoleic Acid, *Am. J. Clin. Nutr. 79* (Suppl.), 1132S–1136S.
5. Griinari, J.M., Corl, B.A., Lacy, S.H., Chouinard, P.Y., Nurmela, K.V.V., and Bauman, D.E. (2000) Conjugated Linoleic Acid Is Synthesized Endogenously in Lactating Dairy Cows by Δ9-Desaturase, *J. Nutr. 130*, 2285–2291.
6. Corl, B.A., Baumgard, L.H., Dwyer, D.A., Griinari, J.M., Phillips, B.S., and Bauman, D.E. (2001) The Role of Δ9-Desaturase in the Production of *cis*-9,*trans*-11 CLA, *J. Nutr. Biochem. 12*, 622–630.
7. Loor, J.J., Lin, X., and Herbein, J.H. (2002) Dietary *trans*-Vaccenic Acid (*trans*11-18:1) Increases Concentration of *cis*9,*trans*11-Conjugated Linoleic Acid (rumenic acid) in Tissues of Lactating Mice and Suckling Pups, *Reprod. Nutr. Dev. 42*, 85–99.
8. Santora, J.E., Palmquist, D.L., and Roehrig, K.L. (2000) *Trans*-Vaccenic Acid Is Desaturated to Conjugated Linoleic Acid in Mice, *J. Nutr. 130*, 208–215.
9. Ip, C., Banni, S., Angioni, E., Carta, G., McGinley, J., Thompson, H.J., Barbano, D., and Bauman, D. (1999) Conjugated Linoleic Acid-Enriched Butter Fat Alters Mammary Gland Morphogenesis and Reduces Cancer Risk in Rats, *J. Nutr. 129*, 2135–2142.
10. Banni, S., Angioni, E., Murru, E., Carta, G., Melis, M.P., Bauman, D., Dong, Y., and Ip, C. (2001) Vaccenic Acid Feeding Increases Tissue Levels of Conjugated Linoleic Acid and Suppresses Development of Malignant Lesions in Rat Mammary Gland, *Nutr. Cancer 41*, 91–97.
11. Gläser, K.R., Wenk, C., and Scheeder, M.R.L. (2002) Effects of Feeding Pigs Increasing Levels of C18:1 *trans* Fatty Acids on Fatty Acid Composition of Backfat and Intramuscular Fat as Well as Backfat Firmness, *Arch. Anim. Nutr. 56*, 117–130.
12. Salminen, I., Mutanen, M., Jauhiainen, M., and Aro, A. (1998) Dietary *trans* Fatty Acids Increase Conjugated Linoleic Acid Levels in Human Serum, *J. Nutr. Biochem. 9*, 93–98.
13. Adlof, R.O., Duval, S., and Emken, E.A. (2000) Biosynthesis of Conjugated Linoleic Acid in Humans, *Lipids 35*, 131–135.
14. Turpeinen, A.M., Mutanen, M., Aro, A., Salminen, I., Basu, S., Palmquist, D.L., and Griinari, J.M. (2002) Bioconversion of Vaccenic Acid to Conjugated Linoleic Acid in Humans, *Am. J. Clin. Nutr. 76*, 504–510.
15. Gruffat, D., Durand, D., Graulet, B., and Bauchart, D. (1996) Regulation of VLDL Synthesis and Secretion in the Liver, *Reprod. Nutr. Dev. 36*, 375–389.
16. Bauchart, D., Gruffat, D., and Durand, D. (1996) Lipid Absorption and Hepatic Metabolism in Ruminants, *Proc. Nutr. Soc. 55*, 39–47.
17. Graulet, B., Gruffat-Mouty, D., Durand, D., and Bauchart, D. (2000) Effects of Milk Diets Containing Beef Tallow or Coconut Oil on the Fatty Acid Metabolism of Liver Slices from Preruminant Calves, *Br. J. Nutr. 84*, 309–318.
18. Gruffat, D., De La Torre, A., Chardigny, J.M., Durand, D., Loreau, O., Sébédio, J.L., and Bauchart, D. (2003) *In vitro* Comparison of Hepatic Metabolism of 9*cis*-11*trans* and 10*trans*-12*cis* Isomers of CLA in the Rat, *Lipids 38*, 157–163.
19. Graulet, B., Gruffat, D., Durand, D., and Bauchart, D. (1998) Fatty Acid Metabolism and Very Low Density Lipoprotein Secretion in Liver Slices from Rats and Preruminant Calves, *J. Biochem. 124*, 1212–1219.
20. Guzman, M., Klein, W., Gomez del Pulgar, T., and Geelen, M.J.H. (1999) Metabolism of *trans* Fatty Acids by Hepatocytes, *Lipids 34*, 381–386.
21. Chilliard, Y., Bauchart, D., and Barnouin, J. (1984) Determination of Plasma Non-esterified Fatty Acids in Herbivores and Man: A Comparison of Value Obtained by Manual or Automatic Chromatographic, Titrimetric, Colorimetric and Enzymatic Methods, *Reprod. Nutr. Develop. 24*, 469–482.
22. Folch, J., Lees, M., and Sloane-Stanley, G.H.S. (1957) A Simple Method for the Isolation and Purification of Total Lipids from Animal Tissues, *J. Biol. Chem. 226*, 497–509.
23. Christie, W.W., Sébédio, J.L., and Juanéda, P. (2001) A Practical Guide to the Analysis of Conjugated Linoleic Acid, *inform 12*, 147–152.
24. Bretillon, J., Chardigny, J.M., Grégoire, S., Berdeaux, O., and Sébédio, J.L. (1999) Effects of Conjugated Linoleic Acid Isomers on the Hepatic Microsomal Desaturation Activities *in vitro*, *Lipids 34*, 965–969.
25. Kaluzny, M.A., Rode, L.M., Meritt, M.V., and Epps, D.E. (1985) Rapid Separation of Lipid Classes in High Yield and Purity Using Bonded Phase Columns, *J. Lipid Res. 26*, 135–140.
26. Zakim, D. (1996) Fatty Acids Enter Cells by Simple Diffusion, *Proc. Soc. Exp. Biol. Med. 212*, 5–14.
27. Hajri, T., and Abumrad, N.A. (2002) Fatty Acid Transport Across Membranes: Relevance to Nutrition and Metabolic Pathology, *Annu. Rev. Nutr. 22*, 383–415.
28. Bojesen, I.N., and Bojesen, E. (1999) Sheep Erythrocyte Membrane Binding and Transfer of Long-Chain Fatty Acids, *J. Membr. Biol. 171*, 141–149.
29. Chatzidakis, C., and Otto, D.A. (1987) Labeled Oxidation Products from [1-^{14}C], [U-^{14}C] and [16-^{14}C]-Palmitate in Hepatocytes and Mitochondria, *Lipids 22*, 620–626.
30. Eaton, S., and Bartlett, K. (1999) Tissue Specific Differences in Intramitochondrial Control of β-Oxidation, *Adv. Exp. Med. Biol. 466*, 161–168.
31. Reid, J.C.W., and Husbands, D.R. (1985) Oxidative Metabolism of Long-Chain Fatty Acids in Mitochondria from Sheep and Rat Liver, *Biochem. J. 225*, 233–237.

32. Kleppe, B.R., Aiello, R.J., Grummer, R.R., and Armentano, L.E. (1988) Triglyceride Accumulation and Very Low-Density Lipoprotein Secretion by Rat and Goat Hepatocytes *in vitro*, *J. Dairy Sci. 71*, 1813–1822.

33. Piot, C., Veerkamp, J.H., Bauchart, D., and Hocquette, J.F. (1998) Contribution of Mitochondria and Peroxisomes to Palmitate Oxidation in Rat and Bovine Tissues, *Comp. Biochem. Physiol. 121*, 185–194.

34. Ntambi, J.M. (1995) The Regulation of Stearoyl-CoA Desaturase (SCD), *Prog. Lipid Res. 34*, 139–150.

35. Pollard, M.R., Gunstone, F.D., James, A.T., and Morris, L.J. (1980) Desaturation of Positional and Geometric Isomers of Monoenoic Fatty Acids by Microsomal Preparations from Rat Liver, *Lipids 15*, 306–314.

36. St. John, L.C., Lunt, D.K., and Smith, S.B. (1991) Fatty Acid Elongation and Desaturation Enzyme Activities of Bovine Liver and Subcutaneous Adipose Tissue Microsome, *J. Anim. Sci. 69*, 1064–1073.

37. Ward, R.J., Travers, M.T., Richards, S.E., Vernon, R.G., Salter, A.M., Buttery, P.J., and Barber, M.C. (1998) Stearoyl-CoA Desaturase mRNA Is Transcribed from a Single Gene in the Ovine Genome, *Biochim. Biophys. Acta 1391*, 145–156.

38. Chang, J.H., Lunt, D.K., and Smith, S.B. (1992) Fatty Acid Composition and Fatty Acid Elongase and Stearoyl-CoA Desaturase Activities in Tissues of Steers Fed High Oleate Sunflower Seed, *J. Nutr. 122*, 2074–2080.

39. Ntambi, J.M. (1999) Regulation of Stearoyl CoA Desaturase by Polyunsaturated Fatty Acids and Cholesterol, *J. Lipid Res. 40*, 1549–1558.

40. Olinga, P., Meijer, D.K.F., Soloff, M.J.H., and Groothuis, G.M.M. (1997) Liver Slices in *in vitro* Pharmacotoxicology with Special Reference to the Use of Human Liver Tissue, *Toxicol. in vitro 12*, 77–100.

41. Bauchart, D., De La Torre, A., Durand, D., Gruffat, D., and Peyron, A. (2002) L'Apport de Graine de Lin Riche en Acide Linolénique Favorise le Dépôt de CLA Principalement dans les Triglycérides du Muscle chez le Bouvillon, *Proceedings 9èmes Journées des Sciences du Muscle et Technologie de la Viande*, pp. 73–74, Clermont-Fd., France.

42. Bauchart, D., Durand, D., Gruffat-Mouty, D., Piot, C., Graulet, B., Chilliard, Y., and Hocquette, J.F. (1999) Transport Sanguin et Métabolisme Tissulaire des Lipides chez le Veau de Boucherie, *INRA Prod. Anim. 12*, 273–285.

43. Bretillon, L., Chardigny, J.M., Noël, J.P., and Sébédio, J.L. (1998) Desaturation and Chain Elongation of [1-^{14}C]Mono-*trans* Isomers of Linoleic and α-Linolenic Acids in Perfused Rat Liver, *J. Lipid Res. 39*, 2228–2239.

44. Sébédio, J.L., Angioni, E., Chardigny, J.M., Grégoire, S., Juanéda, P., and Berdeaux, O. (2001) The Effect of Conjugated Linoleic Acid Isomers on Fatty Acid Profiles of Liver and Adipose Tissues and Their Conversion to Isomers of 16:2 and 18:3 Conjugated Fatty Acids in Rats, *Lipids 36*, 575–582.

45. Banni, S., Petroni, A., Blasevich, M., Carta, G., Angioni, E., Murru, E., Day, B.W., Melis, M.P., Spada, S., and Ip, C. (2004) Detection of Conjugated C16 PUFAs in Rat Tissues as Possible Partial β-Oxidation Products of Naturally Occurring Conjugated Linoleic Acid and Its Metabolites, *Biochim. Biophys. Acta 1682*, 120–127.

46. Gibbons, G.F., and Wiggins, D. (1995) Intracellular Triacylglycerol Lipase: Its Role in the Assembly of Hepatic Very-Low-Density Lipoprotein (VLDL), *Adv. Enzyme Regul. 35*, 179–198.

47. Gibbons, G.F., Bartlett, S.M., Sparks, C.E., and Sparks, J.D. (1992) Extracellular Fatty Acids Are Not Utilized Directly for the Synthesis of Very-Low Density Lipoprotein in Primary Cultures of Rat Hepatocytes, *Biochem. J. 287*, 749–753.

Anticancer Activity and Possible Mode of Action of 4-*O*-Podophyllotoxinyl 12-Hydroxyl-octadec-*Z*-9-enoate

Guoyi Ma[a], Shabana I. Khan[a], Jamal Mustafa[a], Larry A. Walker[a,b], and Ikhlas A. Khan[a,c,]*

[a]National Center for Natural Products Research, Research Institute of Pharmaceutical Sciences, and Departments of [b]Pharmacology and [c]Pharmacognosy, School of Pharmacy, University of Mississippi, University, Mississippi 38677

ABSTRACT: 4-*O*-Podophyllotoxinyl 12-hydroxyl-octadec-*Z*-9-enoate (PHEFE) is a structurally novel FA analog of podophyllotoxin. In the present study, *in vitro* effects of PHEFE on a panel of 60 human tumor cell lines and its potential modes of anticancer action were investigated. PHEFE exhibited strong growth-inhibitory action in a number of solid tumor cells *in vitro*. It did not inhibit tubulin polymerization as podophyllotoxin does; rather, it inhibited the catalytic activity of topoisomerase II. Flow cytometry and staining assay with 4,6-diamidine-2-phenylindole dihydrochloride showed that PHEFE blocked the cell cycle at the G_2/M phase and induced apoptosis in HL-60 cells. These analyses suggest that PHEFE has promising anticancer characteristics that differ from podophyllotoxin and etoposide.

Paper no. L9621 in *Lipids 40*, 303–308 (March 2005).

The present generation of antineoplastic agents offers limited therapeutic benefits for most human malignancies, and the problem of resistance compromises the effectiveness of these drugs. Thus, there is a continuing need for identification and development of new agents with novel mechanisms of action and improved therapeutic potential. Although empirical evaluation of clinical efficacy remains the cornerstone for the clinical development of novel agents, an understanding of the mechanism of action of putative new antineoplastic agents is an area of profound importance.

Podophyllotoxin (Fig. 1), the bioactive principle of genus *Podophyllum*, is known for its potent antitumor activity (1,2). It functions as a mitotic inhibitor by binding reversibly to tubulin and inhibiting microtubule assembly (2,3). The main deficiency of podophyllotoxin is its lack of selectivity against tumor cells, which greatly restricts its clinical utility. Numerous synthetic approaches have been undertaken to develop analogs of podophyllotoxin, resulting in a growing number of compounds with improved therapeutic indices. Extensive studies have permitted the clinical development of two widely used glycosylated semisynthetic derivatives, etoposide and teniposide. They inhibit the essential enzyme DNA topoisomerase II (Topo II) by stabilizing the cleavage complex that results in DNA damage (3–5). Although etoposide and teniposide are known to be useful against various types of tumors, the problems of drug resistance, myelosuppression, and low bioavailability have limited their therapeutic application. New podophyllotoxin derivatives that possess altered pharmacological profiles and different antitumor mechanisms of action could expand the utility of this class. Recently, we reported an efficient and high-yielding method for synthesis of C_4-FA analogs of podophyllotoxin, as well as preliminary investigations of *in vitro* anticancer activity (6). Out of these 10 analogs, eight compounds demonstrated significant growth inhibition in four human solid tumor (SK-MEL, KB, BT-549, SK-OV-3) and leukemia (HL-60) cells with IC_{50} values ranging from 0.07 to 4.0 µM but did not inhibit growth of noncancerous VERO cells, unlike podophyllotoxin, which showed an IC_{50} of 0.55 µM for VERO cells. This suggested their mechanism of action may be different from that of podophyllotoxin. The IC_{50} for the most active derivative, 4-*O*-podophyllotoxinyl 12-hydroxyl-octadec-*Z*-9-enoate (PHEFE) ranged from 0.07 to 0.3 µM (6). With this view, efforts were directed to exploring the anticancer activity of one of these structurally novel compounds, the most active derivative, PHEFE (Fig. 1), against the National Cancer Institute's (NCI's) 60 human tumor cell lines screening panel. To understand the mode of action for anticancer activity, we also studied the effect of PHEFE on microtubule assembly, topoisomerases, cell cycle, and apoptosis in HL-60 cells. Here, we report the findings of these investigations.

MATERIALS AND METHODS

Chemicals and reagents. PHEFE was synthesized as described previously (6). Cell culture reagents were purchased from Quality Biological, Inc. (Gaithersburg, MD), except for FBS, which was purchased from Atlanta Biochemical, Inc. (Atlanta, GA). 4,6-Diamidine-2-phenylindole dihydrochloride (DAPI) and all other reagents were obtained from Sigma (St. Louis, MO). Lyophilized tubulin was purchased from Cytoskeleton Inc. (Denver, CO). Purified human topoisomerase enzymes and kinetoplast DNA (kDNA) were purchased from TopoGen Inc. (Columbus, OH).

Cell lines and cultures. HL-60 promyelocytic leukemia cells from the American Type Culture Collection (ATCC; Rockville, MD) were grown in RPMI 1640 medium supplemented with 10% FBS, 2 mM L-glutamine, and 10, 000 U/mL penicillin G
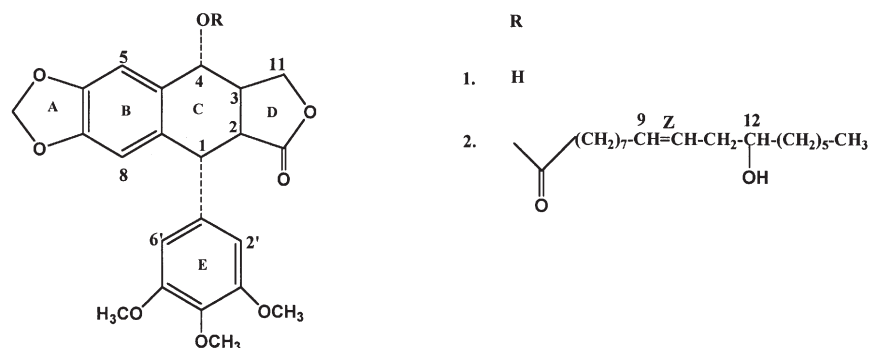
FIG. 1. Chemical structure of podophyllotoxin (**1**) and 4-*O*-podophyllotoxinyl 12-hydroxyl-octadec-Z-9-enoate (PHEFE) (**2**).

sodium in an atmosphere of 95% humidity and 5% CO_2 at 37°C. The details of cell lines used in the NCI anticancer drug discovery program are available at http://dtp.nci.nih.gov.

Evaluation of in vitro antitumor activity. Antitumor activity of PHEFE was determined at NCI through the antitumor screening program that consists of a panel of 60 human tumor cell lines (7). The activity was tested at a minimum of five concentrations at 10-fold dilutions (0.01 to 100 μM). Cells were exposed to the drug for 48 h, and the cell viability was determined by sulforhodamine B protein assay (http://dtp.nci.nih.gov). The activity is reported in terms of GI_{50} (concentration that causes a growth inhibition of 50%).

Microtubule polymerization assay. The assay for microtubule polymerization was performed in Corning Costar 96-well plates using CytoDYNAMIX Screen from Cytoskeleton Inc. Bovine brain tubulin used in the assay contained 90% tubulin and 10% microtubule-associated proteins. The lyophilized tubulin was reconstituted to 2 mg/mL in G-PEM buffer consisting of 80 mM Pipes [piperazine-*N*,*N*′-bis(2-ethanesulfonic acid)] sesquisodium salt, 2 mM $MgCl_2$, 0.5 mM EGTA, and 1 mM GTP, pH 6.9. When 100 μL of reconstituted tubulin is pipetted to a well of a prewarmed plate, it polymerizes efficiently at 37°C. Tubulin polymerization is measured by recording the increase in absorbance at 340 nm for 30 min on a Bio-Tek PowerWaveXS (Bio-Tek Instruments, Inc., Winooski, VT) plate reader. Taxol (10 μM) and podophyllotoxin (10 μM) were included as known ligands (stabilizer and inhibitor, respectively) for tubulin polymerization. PHEFE was tested up to a concentration of 25 μM using a stock of 5 mM in DMSO. The final DMSO concentration was 0.5% in the assay and did not affect the rate of tubulin assembly.

Assay for inhibition of topoisomerase II. (i) Catalytic activity. Measurement of the catalytic activity of Topo II was based on the conversion of kDNA to decatenated kDNA. The assay was performed in a total volume of 20 μL containing 200 ng kDNA, test compound, and 2 units of Topo II in assay buffer (50 mM Tris-HCl, pH 8.0, 120 mM KCl, 10 mM $MgCl_2$, 0.5 mM ATP, 0.5 mM DTT, and 30 μg/mL BSA). The mixture was incubated at 37°C for 30 min, and the reaction was terminated by the addition of 4 μL of stop buffer [5% sarkosyl (*n*-lauroyl-

sarcosine, sodium salt), 0.125% bromophenol blue, 25% glycerol]. DNA was analyzed by electrophoresis on 1% agarose gel in TAE buffer (40 mM Tris-acetate, 2 mM EDTA, pH 8.5). Ethidium bromide (0.5 μg/mL) was added to the agarose gel and running buffer. After destaining with water, the gel was photographed on a Gel Doc system, and DNA was quantified by densitometric analysis using NIH Image 1.52. One unit of enzyme is defined as the amount of enzyme that can decatenate 200 ng of kDNA in 30 min at 37°C. Enzyme activity was measured in terms of the percentage of substrate kDNA converted to product (decatenated kDNA). The concentration of the test compound (PHEFE) that prevented 50% of the substrate from being converted to the product (IC_{50}) was calculated.

(ii) Cleavage assay. The assay was performed as just given with 4 units of Topo II in the cleavage buffer (30 mM Tris-HCl, pH 7.6, 120 mM NaCl, 8.0 mM $MgCl_2$, 3.0 mM ATP, and 15 mM β-mercaptoethanol). The reaction was terminated by addition of 2 μL SDS (10%) followed by addition of Proteinase K (50 μg/mL; Sigma Chemical) and further incubation at 37°C for 30 min. The loading buffer (10×) was added, and DNA was extracted with an equal volume of CIA (chloroform/isoamyl alcohol, 24:1). DNA was analyzed by electrophoresis and photodocumented as already described. Cleavage buffer is optimized to detect formation of cleavage complexes, and the decatenation activity is less robust in this buffer. Including ethidium bromide in the gel and buffer allows clear resolution of cleavage products and detection of linear DNA.

Cell cycle analysis. Cell cycle analysis of HL-60 cells was performed using flow cytometry. HL-60 cells were treated with vehicle, PHEFE (0.5 μM), or podophyllotoxin (0.02 μM) for 0–48 h. The cells ($2–4 \times 10^5$) were harvested and then washed with ice-cold PBS, followed by the immediate addition of 1 mL of ice-cold 70% ethanol. After fixation overnight at 4°C, cells were washed twice with PBS again, treated with RNase A (40 μg/mL) for 10 min, and stained with propidium iodide (50 μg/mL) for 15 min. Flow cytometry analysis was performed on a Becton Dickinson FACScan equipped with Becton Dickinson CELL Quest software.

Morphological assessment of cell death. Exponentially growing HL-60 cells were treated with vehicle, PHEFE (0.5

μM), or podophyllotoxin (0.02 μM) for 48 h. The cells were harvested by centrifugation and washed three times with PBS and fixed in a solution of 3.7% formaldehyde and then in methanol for 10 min each. Fixed cells were stained with 4 μg/mL of DAPI for 10 min. The nuclear morphology of cells was observed using a Nikon Universal Condenser C-CU fluorescence microscope equipped with a 100× oil immersion objective and UV-2A filter cubes. Images were acquired with Kodak camera tools-DC 290 and digitized using IPLab Spectrum (Scanalytics, Fairfax, VA) software.

All assays described were performed at least in duplicate, and the representative data are shown in the figures and table.

RESULTS

Anticancer activity against a panel of 60 human cancer cell lines in vitro. The growth-inhibitory activities of PHEFE against a panel of human cancer cell lines were evaluated in the NCI disease-oriented anticancer drug screen program. PHEFE inhibited the growth of a number of cancer cell lines tested in a concentration-dependent manner. However, there were significant differences in the sensitivity of these cells to PHEFE. Table1 lists the GI_{50} values of PHEFE in comparison with the GI_{50} values of etoposide. It can be seen that non-small-cell lung cancer NCI-H522, melanoma UACC-257, and breast cancer MDA-MB-435 cells were the most sensitive ($GI_{50} < 0.01$ μM), followed by non-small-cell lung cancer NCI-H23, colon cancer HCT-116, HT29 and KM12, CNS cancer SF-295, melanoma M14 and SK-MEL-2, renal cancer ACHN and SN12C, and breast cancer MDA-MB-231/ATCC cells (GI_{50} values ranging from 0.04 to 0.96 μM). Several other cells listed in Table 1 were moderately sensitive to PHEFE (GI_{50} values 1.17 to 8.95 μM) whereas some were least sensitive ($GI_{50} > 100$ μM). The pattern of sensitivity of cell lines was different for etoposide (VP-16), and compared with etoposide, a higher sensitivity of various cell lines to PHEFE was observed. However, prostate cancer and leukemia cells (except K562) were more sensitive to etoposide than PHEFE. Among solid tumors, cells most sensitive to PHEFE were not sensitive to etopside, e.g., NCI-H522, UACC-257, and MDA-MB-435.

Effect of PHEFE on tubulin polymerization. To explore the mechanism of anticancer action of PHEFE, we assessed the effect of PHEFE on tubulin polymerization *in vitro* and compared that result with the known ligands podophyllotoxin and taxol. As shown in Figure 2, PHEFE did not inhibit or stimulate the rate and extent of tubulin polymerization. However, as expected, podophyllotoxin inhibited and taxol stimulated tubulin polymerization. Thus, the anticancer action of PHEFE does not involve interaction with tubulin and does not resemble that of its parent compound podophyllotoxin.

Inhibition of topoisomerases. To study whether the cytotoxic action of PHEFE is also associated with inhibition of topoisomerases, the effects of PHEFE on human DNA Topo I and II were investigated. The activity of Topo I was not affected by PHEFE (data not shown). It inhibited Topo II-mediated decatenation of kDNA (catalytic activity of Topo II), as

TABLE 1
Anticancer Activity of PHEFE in Comparison with Etoposide[a]

Disease types	Cell lines	GI_{50} (μM) PHEFE	Etoposide
Leukemia	HL-60 (TB)	3.73	0.79
	K-562	3.36	12.59
	MOLT-4	8.95	0.50
	RPMI-8226	3.33	2.00
	SR	1.44	0.20
Non-small-cell lung cancer	A549/ATCC	5.59	3.98
	EKVX	3.42	25.12
	HOP-62	1.17	2.00
	HOP-92	>100	10.0
	NCI-H23	0.34	6.31
	NCI-H332M	>100	79.43
	NCI-H460	3.00	0.50
	NCI-H522	<0.01	6.31
Colon cancer	COLO 205	3.64	39.81
	HCT-116	0.76	12.59
	HCT-15	3.42	15.85
	HT29	0.63	31.62
	KM12	0.12	19.95
	SW-620	1.87	6.31
CNS cancer	SF-268	2.30	7.94
	SF-295	0.24	6.31
	SNB-19	>100	6.31
	SNB-75	>100	12.59
	U251	3.04	3.16
Melanoma	LOX IMVI	3.30	2.51
	MALME-3M	>100	10.0
	M14	0.04	0.79
	SK-MEL-2	0.87	19.95
	SK-MEL-28	>100	19.95
	SK-MEL-5	1.91	5.01
	UACC-257	<0.01	39.81
	UACC-62	>100	6.31
Ovarian cancer	IGROVI	4.08	31.62
	OVCAR-3	6.50	39.81
	OVCAR-4	7.63	>100
	OVCAR-8	2.46	12.59
	SK-OV-3	45.7	15.85
Renal cancer	786-0	2.49	1.26
	ACHN	0.96	0.79
	CAKI-1	3.48	3.98
	SN12C	0.49	5.01
	TK-10	>100	5.01
	UO-31	2.53	39.81
Prostate cancer	PC-3	1.24	0.63
	DU-145	3.52	0.79
Breast cancer	MCF7	2.46	2.00
	NCI/ADR-RES	1.40	63.10
	MDA-MB-231/ATCC	0.52	1.58
	MDA-MB-435	<0.01	31.62
	T-47D	>100	1.00

[a]PHEFE, 4-*O*-podophyllotoxinyl 12-hydroxy-octadec-*Z*-9-enoate; CNS, central nervous system. GI_{50}, concentration required to achieve 50% growth inhibition.

shown in Figure 3A (lanes 6–8), in a dose-dependent manner (90, 70, and 5% inhibition at 70, 14, and 2.8 μM). An IC_{50} of 10 μM was computed from the dose curve (Fig. 3B). Podophyllotoxin did not affect the decatenation activity of Topo II (Fig. 3A, lanes 3–5). In the cleavage assay, PHEFE did not show any cleavage complex stabilization activity (lanes 4–6 in Fig. 4)
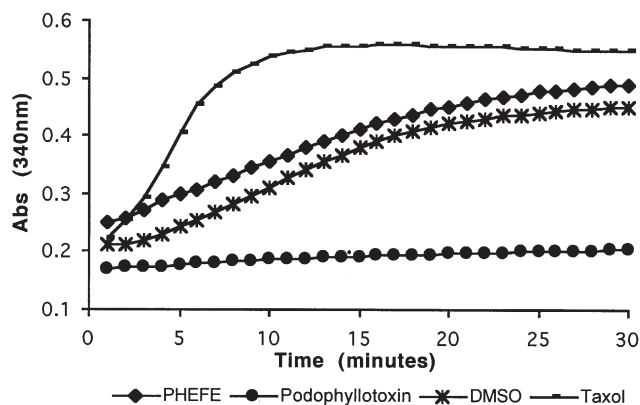
FIG. 2. Effect of PHEFE on tubulin polymerization. Tubulin polymerization of purified bovine brain was determined in presence of PHEFE (25 µM), podophyllotoxin (10 µM), and taxol (10 µM) as described in the Materials and Methods section. The extent of tubulin polymerization ($A_{340 \text{ nm}}$) is plotted as a function of time.

A

B
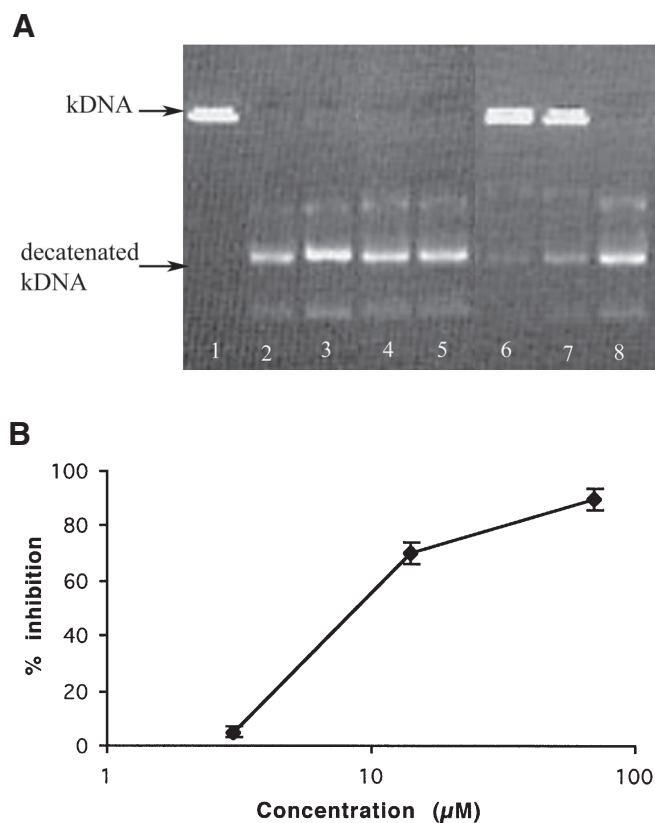
FIG. 3. Topoisomerase (Topo) II assay. (A) Determination of catalytic activity. Kinetoplast DNA (kDNA: 200 ng) was incubated with 2 units of Topo II in assay buffer with and without test drugs. Reaction was stopped and DNA was analyzed on agarose gel as described in the Material and Methods section. Lane 1: Substrate control (no enzyme); lane 2: Topo II activity without drug (DMSO control); lanes 3–5 and 6–8: Topo II activity in presence of podophyllotoxin and PHEFE (70, 14, and 2.8 µM, respectively). (B) Inhibition of catalytic activity of Topo II by PHEFE. Percent inhibition was calculated after quantifying the DNA bands. Error bar reflects the mean ± SEM of two determinations. For other abbreviation see Figure 1.
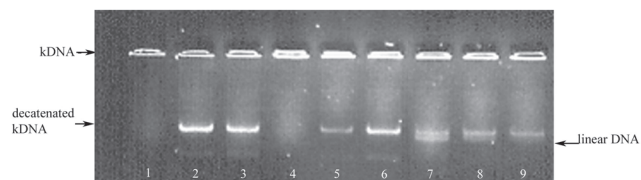
FIG. 4. Topo II assay: Determination of cleavage complex stabilization activity. Kinetoplast DNA (kDNA: 200 ng) was incubated with 4 units of Topo II in cleavage buffer with and without test drugs. The reaction was stopped with SDS and Proteinase K; after extraction with chloroform/isoamyl alcohol (24:1), DNA was analyzed on agarose gel as described in the Materials and Methods section. Lane 1: Substrate control (no enzyme); lane 2: kDNA and Topo II without drug (DMSO control); lane 3: kDNA, Topo II, and podophyllotoxin (70 µM), lanes 4–6: kDNA, Topo II, and PHEFE (70, 14, 2.8 µM); lanes 7–9: kDNA, Topo II, and etoposide (50, 25, and 12.5 µM). For other abbreviations see Figures 1 and 3.

and did not result in the formation of linear DNA as seen with etoposide (lanes 7 and 8 in Fig. 4). On the basis of these results, it is clear that PHEFE does not resemble podophyllotoxin (Fig. 3A) or etoposide (Fig. 4) with regard to its action on Topo II.

Induction of cell cycle arrest. To investigate the effects on cell cycle arrest, we examined the effects in HL-60 leukemia cells. As shown in Figure 5, at 6 h after the treatment with 0.5 µM of PHEFE, the cells began to arrest in the G_2/M phase of the cell accompanied by reduction of G_0/G_1 cycle. After 12 h, the majority of the surviving cells were in $G_2/M$ phase. At 24 h after treatment, the cells showed fragmented DNA (hypodiploids, HD) smaller than that of G_1 phase cells associated with apoptotic cell death. By 48 h, most cells had reached G_2/M and died. Likewise, podophyllotoxin treatment (0.02 mM) also arrested HL-60 cells at the G_2/M phase.

Induction of apoptosis. It is well established that prolonged cell cycle arrest leads to programmed cell death (apoptosis) (8,9). Therefore, we also tested the apoptosis-inducing ability of PHEFE in HL-60 cells by DAPI staining assay. As shown in Figure 6, after 48 h exposure, PHEFE (0.5 µM) induced extensive nuclear condensation and fragmentation in HL-60 cells, indicating that apoptosis was induced as a result of PHEFE treatment. Podophyllotoxin (0.02 µM) also induced apoptosis in HL-60 cells.

DISCUSSION

PHEFE is a C_4 α-bifunctional (12-hydroxyl-Z-9-ene) FA analog of podophyllotoxin. Our preliminary study showed that PHEFE suppressed the growth of a panel of five human cancer cells (SK-MEL, KB, BT-549, SK-OV-3, and HL-60) without affecting the growth of normal cells (6), suggesting that PHEFE might have a different molecular mechanism by which antitumor activity is achieved. In a continuation of this work, we further examined the anticancer activity of PHEFE on a broader panel of 60 tumor cells available at NCI (Table 1). The result demonstrated that PHEFE significantly inhibited the growth of a number of human tumor cells in a concentration-
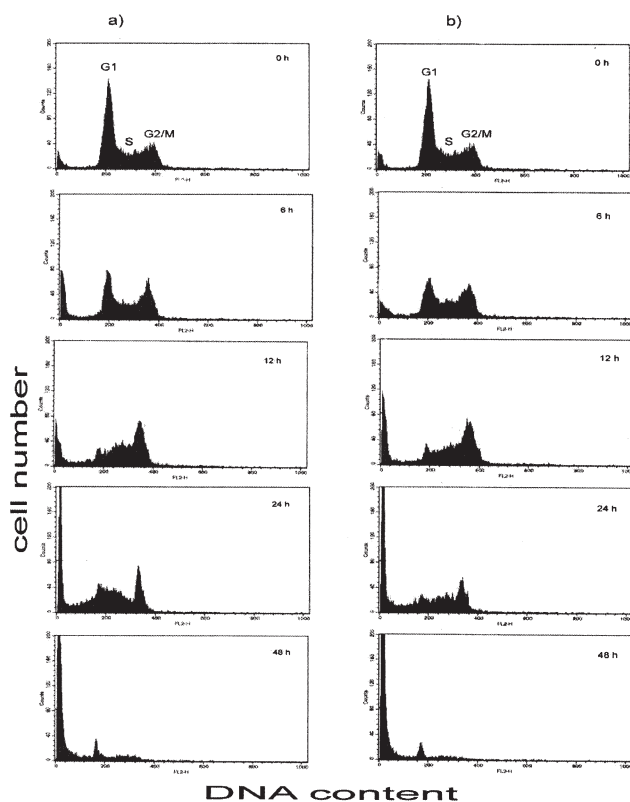
FIG. 5. Effects of PHEFE (a) and podophyllotoxin (b) on cell cycle arrest in HL-60 cells. HL-60 cells in log phase growth were incubated with 0.5 μM PHEFE or 0. 02 μM podophyllotoxin for 0–48 h. Samples were taken at the times indicated in each panel for flow cytometric cell cycle analysis as described in the Materials and Methods section. Data shown represent relative numbers of cells (*y* axis) as a function of fluorescence intensity (*x* axis). For abbreviation see Figure 1.

FIG. 6. Induction of apoptosis by PHEFE in HL-60 cells. HL-60 cells were exposed to vehicle (a), 0.5 μM PHEFE (b), or 0.02 μM podophyllotoxin (c) for 48 h. Cells were harvested and washed with ice-cold PBS, followed by fixation in 3.7% formaldehyde and methanol. Fixed cells were incubated with 4 μg/mL of 4,6-diamidine-2-phenylindole dihydrochloride, and nuclear morphology was examined by using a fluorescent microscope. Arrows indicate apoptotic cells with condensed and fragmented nuclei.

dependent manner. Non-small-cell lung cancer NCI-H522, melanoma UACC-257, and breast cancer MDA-MB-435 cells were highly sensitive to this compound ($GI_{50} < 0.01$ μM), suggesting that PHEFE may turn out to be active against non-small-cell lung cancer, melanoma, and breast cancers. After comparison with etoposide, it was interesting to note that the pattern of sensitivity of the cells to PHEFE was not similar to etoposide. This is indicative of a different mode of action. Action of PHEFE on tubulin and Topo II also indicated that this compound does not resemble podophyllotoxin or etoposide in affecting these targets. It is well recognized that solid tumors are hard to treat, as they metastasize and develop resistance toward chemotherapy and radiation (10). PHEFE showed more potent anticancer activity against solid tumors than leukemia, which may be beneficial in the treatment of solid tumors. It is worth further exploring the potential of PHEFE to develop it as a possible new chemotherapeutic agent.

Since FA-derived podophyllotoxin molecules are a relatively new class of compounds (6,11,12), the molecular targets by which they exert antitumor activity have not yet been studied. In this report, we investigated the effects of the C_4-mono FA analog, PHEFE, on tubulin polymerization, topoisomerase activity, cell cycle progression, and apoptosis for the first time.

Microtubules are cytoskeletal structures formed by highly dynamic assemblies of tubulin heterodimers, and they play a crucial role in many biological processes, including mitosis, intracellular transport, exocytosis, and cell growth. An essential function of microtubules is to partition duplicated chromosomes into daughter cells during cell division. Microtubule dynamics are dramatically increased during mitosis and are very sensitive to interferences, thereby constituting an important target in cancer chemotherapy (2). The mechanism by which podophyllotoxin blocks cell division is known to be related to its inhibition of microtubule assembly in the mitotic apparatus (2,13). Unlike podophyllotoxin and a variety of its C_4 analogs (2), PHEFE did not inhibit tubulin polymerization. This observation suggests a unique profile of anticancer activity for PHEFE, involving mechanisms unrelated to inhibition of tubulin polymerization.

Topoisomerases are cellular enzymes that are intricately involved in maintaining the topographic structure of circular DNA during translation, transcription, and mitosis (14,15). These enzymes are well known as targets for a number of anticancer drugs (16–18). Catalytic Topo II inhibitors such as aclarubicin, merbarone, novobiocin, MST-16, ICRF-187, and ICRF-193 are emerging as an interesting new class of compounds in cancer

therapy for a variety of reasons (17,18). PHEFE inhibited the catalytic activity of Topo II without showing any cleavage complex stabilization effects. This effect is different from that observed for the epipodophyllotoxin analogs (βC-4, epimers) etoposide and teniposide, which are known to act *via* Topo II cleavage complex stabilization (16). Therefore, PHEFE may be a candidate of pharmaceutical significance, because of its α-stereochemistry at C-4 and its interaction with Topo II, similar to the class of catalytic inhibitors (17,18). In cell cycle analysis, both PHEFE and podophyllotoxin block the cell cycle at the G_2/M phase. However, the mechanism of action by which they induce cell cycle arrest is different. Podophyllotoxin blocks cell cycle progression in association with inhibition of tubulin polymerization, whereas PHEFE lacks the tubulin inhibition but elicits G_2/M blockage in association with inhibition of Topo II. The IC_{50} for Topo II inhibition (10 μM) is much higher than the concentration required to induce cell cycle arrest and apoptosis (0.5 μM). This suggests that, in addition to Topo II inhibition, another cellular mechanism or mechanisms may also be involved in the cytotoxic action of PHEFE.

The mode of cell death induced by PHEFE and podophyllotoxin was further investigated by DAPI staining assay. There are two known mechanisms of cell death: necrosis and apoptosis. Necrosis is usually considered to result from physical injury. Apoptosis is a deliberate and genetically controlled cellular response to developmental and environmental stimuli; it is characterized by cell shrinkage and chromatin condensation, followed by fragmentation of nuclear components (19). Selective induction of apoptosis in cancer cells or malignant tissues represents an efficient strategy for cancer chemotherapy. In this study, apoptosis was detected within 48 h of drug treatment by DAPI staining assay at cytotoxic concentrations. PHEFE and podophyllotoxin induced extensive nuclear condensation and DNA fragmentation. The results of studies by flow cytometry show that there was extensive HD debris, perhaps from apoptotic cells. These investigations indicate that PHEFE and podophyllotoxin, although displaying distinct pharmacological properties, both induce cellular responses that lead to induction of apoptosis.

Unlike podophyllotoxin, etoposide, and teniposide, PHEFE neither inhibited microtubulin polymerization nor stabilized the cleavage complex of DNA Topo II. Rather, it inhibited the catalytic activity of Topo II. The overall effect of PHEFE also resulted in cell cycle arrest and apoptosis.

ACKNOWLEDGMENTS

REFERENCES

1. Gordaliza, M., Castro, M.A., del Corral, J.M., and Feliciano, A.S. (2000) Antitumor Properties of Podophyllotoxin and Related Compounds, *Curr. Pharm. Des. 6,* 1811–1839.
2. Shi, Q., Chen, K.C., Morrist-Natschke, S.L., and Lee K.H. (1998) Recent Progress in the Development of Tubulin Inhibitors as Antimitotic Antitumor Agents, *Curr. Pharm. Des. 4*, 219–248.
3. Cragg, G., and Suffness, M. (1988) Metabolism of Plant-Derived Anticancer Agents, *Pharmac. Ther. 37*, 425–461.
4. Sinha, B.K., and Myers, C.E. (1984) Irreversible Binding of Etoposide (VP-16-213) to Deoxyribonucleic Acid and Proteins, *Biochem. Pharmacol. 33*, 3725–3728.
5. Haim, N., Nemec, J., Roman, J., and Sinha, B.K. (1987) *In vitro* Metabolism of Etoposide (VP-16- 213) by Liver Microsomes and Irreversible Binding of Reactive Intermediates to Microsomal Proteins, *Biochem. Pharmacol. 36*, 327–336.
6. Mustafa, J., Khan, S.I., Ma, G., Walker, L.A., and Khan I.A. (2004) Synthesis and Anticancer Activities of Fatty Acid Analogs of Podophyllotoxin, *Lipids 39*, 167–172.
7. Boyd, M.R., and Paull, K.D. (1995) Some Practical Considerations and Applications of the National Cancer Institute *in vitro* Anticancer Drug Discovery Screen, *Drug Devel. Res. 34*, 91–109.
8. Lock, R.B., and Ross, W.E. (1987) DNA Topoisomerases in Cancer Therapy, *Anticancer Drug Des. 2*, 151–164.
9. McPherson, J.P., and Goldenberg, G.J. (1998). Induction of Apoptosis by Deregulated Expression of DNA Topoisomerase IIα, *Cancer Res. 58*, 4519–4524.
10. Welsh, S.J., and Powis, G. (2003) Hypoxia Inducible Factor as a Cancer Drug Target, *Curr. Cancer Drug Targets 3*, 391–405.
11. Nagao, Y., Mustafa, J., Sano, S., Ochiai, M., Tazuko, T., and Shigeru, T. (1991) Different Mechanism of Action of Long Chain Fatty Acid Esters of Podophyllotoxin and Esters of Epipodophyllotoxin Against P388 Lymphocytic Leukemia in Mice, *Med. Chem. Res. 1*, 295–299.
12. Lie Ken Jie, M.S.F., Mustafa, J., and Pasha, M.K. (1999) Synthesis and Spectral Characteristics of Some Unusual Fatty Esters of Podophyllotoxin, *Chem. Phys. Lipids 100*, 165–170.
13. Sakurai, H., Miki, T., Imakura, Y., Shibuya, M., and Lee, K.H. (1991) Metal- and Photo-Induced Cleavage of DNA by Podophyllotoxin, Etoposide, and Their Related Compounds, *Mol. Pharmacol. 40*, 965–973.
14. Holm, C., Goto, T., Wang, J.C., and Botstein, D. (1985) DNA Topoisomerase II Is Required at the Time of Mitosis in Yeast, *Cell 41,* 553–563.
15. Watt, P.M., and Hickson, I.D. (1994) Structure and Function of Type II Topoisomerases, *Biochem. J. 303*, 681–695.
16. Wang, H.K., Morris-Natschke, S.L., and Lee, K.H. (1997) Recent Advances in the Discovery and Development of Topoisomerase Inhibitors as Antitumor Agents, *Med. Res. Rev. 4,* 367–425.
17. Larsen A.K., Escargueil, A.E., and Skladanowski, A. (2003) Catalytic Topoisomerase II Inhibitors in Cancer Therapy, *Pharmacol. Ther. 99*, 167–181.
18. Tanabe, K., Ikegami, Y., Ishida, R., and Andoh, T. (1991) Inhibition of Topoisomerase II by Antitumor Agents Bis(2,6-dioxopiperazine) Derivatives, *Cancer Res. 51,* 4903–4908.
19. Binder, C., and Hiddemann, W. (1994) Programmed Cell Death: Many Questions Still to Be Answered, *Ann. Hematol. 69*, 45–55.

Distribution of Polyunsaturated Fatty Acids Including Conjugated Linoleic Acids in Total and Subcellular Fractions from Healthy and Cancerous Parts of Human Kidneys

Kristina Hoffmann[a], Jörg Blaudszun[b], Claus Brunken[c],
Wilhelm-Wolfgang Höpker[b], Roland Tauber[c], and Hans Steinhart[a,*]

[a]Institute of Biochemistry and Food Chemistry, University of Hamburg, 20146 Hamburg, Germany, and
Departments of [b]Pathology and [c]Urology, General Hospital Barmbek, 22291 Hamburg, Germany

ABSTRACT: Differences in the FA composition of subcellular fractions from healthy and cancerous kidney tissues from the same patients were examined. Only minor differences in CLA content were found between the healthy and the cancerous tissue portions. Regarding the distribution pattern, CLA incorporation into nuclei and cytosol was significantly higher than incorporation into plasma membranes and mitochondria, which could be correlated to the neutral lipid content of these fractions. The subcellular distribution pattern of CLA was similar to that observed with monounsaturated FA but unlike that found with 18:2n-6, which underlines the different physiological properties of CLA and 18:2n-6. Because PUFA have been suggested to have an effect on cancer risk, the contents of n-3 and n-6 PUFA were determined in kidney and renal cell carcinoma (RCC). The 18:2n-6 content and Δ^5 desaturase activity were significantly lower, and the 18:3n-6, 20:3n-6, and 20:5n-3 contents and Δ^6 desaturase activity were significantly higher in RCC than in healthy renal tissue, indicating a changed PUFA metabolism in RCC. Previous research has suggested that CLA inhibits the elongation and desaturation of 18:2n-6 into 20:4n-6. In that case, one might speculate that a diet enriched in CLA would be a useful tool in preventing RCC. However, the involvement of CLA in preventing renal cancer could not be demonstrated definitively from the design of this experiment. Further understanding of the cause and/or consequence of the difference in FA metabolism may lead to a better understanding of RCC.

Paper no. L9605 in *Lipids 40*, 309–315 (March 2005).

CLA describes a group of positional and stereochemical isomers of 18:2n-6 that contain two conjugated double bonds. CLA can be found in natural food sources, such as dairy products or the meat of ruminant animals (1). At the end of the 1980s, CLA was found to possess anticarcinogenic properties, and nowadays the anticarcinogenic effect of CLA is well known from several *in vivo* and *in vitro* studies (2,3). However, the mechanism(s) of the anticarcinogenic effect of CLA have not yet been clarified, although several studies have shown that diets containing CLA are associated with altered phospholipid-associated FA metabolism and eicosanoid formation (4,5).

The existing data suggest that dietary CLA might also be used in humans for the prevention of cancer, and the feasibility of increasing the CLA content of food is already being considered to increase the CLA intake in humans (6). In spite of such potential, few studies are available that deal with the association between CLA and cancer in humans. In 2000 Aro *et al.* (7) examined the relationship between dietary or serum CLA in women and the risk of breast cancer. They found dietary or serum CLA to be significantly lower in cancer cases than in controls, suggesting a protective effect of CLA on breast cancer risk, but only in postmenopausal patients. In contrast, a cohort study, carried out in 2002, estimated dietary intake of CLA to be associated with increased risk of breast cancer in postmenopausal patients (8). The correlation between CLA and cancers other than breast cancer in humans has not been examined so far.

Renal cell cancer (RCC) is responsible for about 2% of all cancer deaths in developed countries and represents 80–85% of all tumors of the kidney. The risk of RCC is known to be influenced by many environmental factors, such as tobacco smoking, elevated body mass index (BMI), a few medical conditions, and a family history of the disease. Furthermore, many dietary factors have been considered in relation to RCC. Vegetables, fruit, vitamin C, and carotenoids have shown protective effects, whereas meat and milk products have been risk factors; however, the findings have not been uniform (9).

In the present study, differences in the FA composition of subcellular fractions from healthy and affected kidney tissues from the same patients were examined. In detail, the contents of CLA isomers and the long-chain n-6 and n-3 FA, which are involved in eicosanoid biosynthesis, were determined and the appropriate ratios for the calculation of Δ^9, Δ^6, and Δ^5 desaturase and elongase activities were formed. Several studies have already focused on the incorporation of CLA into individual tissue lipid classes (10,11). Only a few studies, however, have dealt with the distribution of CLA in cell organelles (12,13), and no study has reported on the distribution of CLA in cell organelles in human tissues. The intracellular distribution of CLA is of interest because it could provide valuable clues to potential biochemical target sites.

MATERIALS AND METHODS

Tissue procurement. Patients with a clinical diagnosis of renal cancer underwent surgical resection of their tumors at the Department of Urology, General Hospital Barmbek, Hamburg. All patients had a radical nephrectomy of the involved kidney and gave written consent to a protocol approved by the ethics commission of the Hamburg Medical Association. A piece of cancerous tissue and a piece of healthy renal tissue were removed from the nephrectomy specimen for study immediately following resection. Tissue sectioning was performed by a pathologist in the Department of Pathology, General Hospital Barmbek, Hamburg, so as not to compromise the histological diagnosis. Samples were snap-frozen in liquid nitrogen and stored at −80°C until analyzed.

Cell fractionation. Tissue specimens were fractionated into nuclear, mitochondrial, plasma membrane, and cytosolic fractions as described previously (14). Briefly, tissue specimens were suspended in a 10-fold volume of homogenization medium (0.25 M sucrose, 0.01 M Tris-HCl, 1 mM EDTA, pH 7.5) and homogenized, first in an UltraTurrax homogenizer for 5 s and then in a Potter–Elvehjem homogenizer with six up-and-down strokes of a Teflon pestle. The homogenate was filtered through a coarse metal sieve and was centrifuged at 1,000 × *g* for 10 min. The crude pellet, representing the nuclear fraction, was resuspended in 1.38 M sucrose and purified by centrifugation at 40,000 × *g* for 80 min. After separation of the crude nuclear fraction, the supernatant fluid was centrifuged at 39,000 × *g* for 45 min to sediment mitochondria and plasma membranes. The 39,000 × *g* supernatant was regarded as the cytosolic fraction. To separate the plasma membranes from the mitochondria, the pellet was resuspended in 1.38 M sucrose and homogenized in a Potter–Elvehjem homogenizer with three up-and-down strokes. Sucrose (0.25 M) was loaded on top of the suspension and the resulting discontinuous gradient was centrifuged at 57,000 × *g* for 90 min. The plasma membranes appeared as a band at the sucrose interface, and the mitochondria were in the bottom pellet.

To determine the purity of the subcellular fractions, the activities of marker enzymes were measured. Succinate dehydrogenase was used as a marker for mitochondria, alkaline phosphatase for plasma membranes, acid phosphatase for lysosomes, NADPH-cytochrome c reductase for microsomes, lactate dehydrogenase for cytosol, and catalase for peroxisomes. All these assays were carried out as described previously (15–18). For calculation of enzyme activities, the protein contents of tissue homogenates and subcellular fractions were measured by the method of Bradford (19). All fractions were highly enriched in their corresponding marker enzymes. The fraction designated the cytosolic fraction contained not only cytosol but also microsomes and lysosomes.

Lipid analysis. Lipids were isolated from whole tissue homogenates as well as from cell fractions by extracting them twice with dichloromethane/methanol (2:1, vol/vol) and once with hexane. Subsequently, FAME were generated by derivatization of the lipid extract with 5% potassium methoxide in methanol (Merck-Schuchardt, Hohenbrunn, Germany) at 60°C for 15 min according to the method of Pfalzgraf *et al.* (20). The pattern of total FAME was analyzed by GC (Hewlett-Packard GC system 6890 with FID, Waldbronn, Germany) using a CP-Sil 88 capillary column (100 m × 0.25 mm i.d. with a 0.2-µm film thickness; Chrompack, Middelburg, The Netherlands). The following three-step temperature run was used to separate FAME: initial 70°C, held 3 min; 8°C/min to 180°C, held 10 min; 3°C/min to 235°C, held 10 min. The inlet temperature was 200°C and the detector temperature was 260°C. A 2-µL volume was injected at a split ratio of 10:1. Hydrogen was used as the carrier gas at 1.5 mL/min.

CLA isomer distribution was determined by silver ion HPLC analysis (21). Separation was carried out with a Waters 515 HPLC system (Waters, Milford, MA) equipped with a photodiode array detector 996. Two silver-loaded Chromspher 5 Lipids columns (Chrompack), 5-mm particle size, 250 × 4.6 mm, were used series-wound with a mobile phase of hexane/acetonitrile (100:0.5, vol/vol) at a flow rate of 1 mL/min. Because of their conjugated double bonds, CLA isomers could be detected at 234 nm, whereas unconjugated unsaturated FA absorbed at 200 nm.

FAME standards, including a mixture of CLA isomers, were used to identify and quantify sample FAME (Sigma Chemical Co., Deisenhofen, Germany).

Statistical analysis. All data are expressed as mean ± SD. Statistical comparisons between healthy renal tissue and RCC were made using Student's two-tailed *t*-test for paired values ($P < 0.05$). One-way ANOVA with Scheffé, Student–Newman–Keuls, and Tukey-B as *post hoc* tests were used to determine significant differences in FA distribution between the subcellular fractions ($P < 0.05$). All statistics were performed using SPSS Statistical Software, version 11.5.2.1 (SPSS Inc., Chicago, IL).

RESULTS

All 23 patients studied had RCC. Table 1 shows clinical characteristics of the tumors. Three patients suffered additional diseases, namely, alimentary adiposity, family hyperlipidemia, or type 2 diabetes. Two patients were smokers. All patients, male and female, were born between 1921 and 1957 and had a mean BMI of 25.95 ± 2.85. All clinical and anthropomorphic data were collected at the Departments of Urology and Pathology, General Hospital Barmbek (Hamburg, Germany).

CLA content was readily detected in the total lipid extracts of healthy human renal tissue and RCC as well as in nuclear, mitochondrial, plasma membrane, and cytosolic fractions of these tissues (Fig. 1). For kidney, CLA incorporation was significantly higher in nuclei and cytosol compared with total lipid extract, plasma membranes, and mitochondria. For RCC, similar CLA contents were measured, with the exception of plasma membranes. The CLA content in plasma membranes of RCC was significantly higher than in plasma membranes of healthy renal tissue (0.33 ± 0.18 and 0.21 ± 0.06%, respectively). No further differences in total CLA content between the two types of tissue were detected.

TABLE 1
Clinical Characteristics of the Renal Cell Carcinoma Studied

WHO (UICC)[a] classification	Number of patients ($n = 23$)	WHO (UICC) classification	Number of patients ($n = 23$)
Primary tumor		Histological grading	
pT1	3	GI	1
pT2	2	GII	16
pT3	1	GII	6
pT3a	9	Staging (Robson)	
pT3b	6	I	4
pT4	2	II	1
Regional lymph nodes		III	15
pNx	16	IV	3
pN0	6		
pN2	1		
Distant metastasis			
pMx	22		
pM1	1		

[a]WHO, World Health Organization; UICC, Union Internationale Contra Cancrum.

The distribution pattern of the monounsaturated FA (MUFA) 14:1*cis*9, 16:1*cis*9, 18:1*cis*9, 20:1*cis*11, 22:1*cis*13, and 24:1*cis*15 in sum in the subcellular fractions was similar to the distribution pattern observed with total CLA and unlike that found with 18:2n-6 (Figs. 2, 3). The 18:2n-6 content was highest in mitochondria and lowest in total lipid extracts of both types of tissue. The MUFA content was significantly lower in the nuclear, cytosolic, and plasma membrane subcellular fractions of healthy compared with RCC tissues, whereas 18:2n-6 was significantly lower in total lipid extracts and significantly higher in the nuclear fraction of RCC.

The individual CLA isomers present in these tissues are shown in Figure 4. The *cis*9,*trans*11-CLA was shown to be the prominent CLA isomer in healthy renal tissue as well as in RCC with more than 80% of total CLA. A significant difference between the two types of tissues was detected only for *cis*11,*trans*13-CLA; the content was higher in RCC than in healthy renal tissue (2.67 ± 1.39 and $1.49 \pm 0.70\%$, respectively).

In addition to the CLA contents, the total FA profiles were determined; 16:0, 18:0, 18:1*cis*9, 18:2n-6, and 20:4n-6 were found to be the major FA in all subcellular fractions from both types of kidney tissue studied (data not shown). In detail, we examined the contents of the long-chain n-6 (18:2n-6, 18:3n-6, 20:3n-6, and 20:4n-6) and n-3 PUFA (18:3n-3, 20:5n-3, and 22:6n-3) (Fig. 5A– C).

The appropriate product/precursor ratios were calculated for Δ^9, Δ^6, and Δ^5 desaturase and elongase activities (Figs. 6A, 6B). For Δ^9 desaturase activity, the ratio Δ^9-MUFA (14:1*cis*9, 16:1*cis*9, and 18:1*cis*9)/saturated FA (SFA) (14:0, 16:0, and 18:0), for Δ^6 desaturase activity the ratio 18:3n-6/18:2n-6, for elongase activity the ratio 20:3n-6/18:3n-6, and for Δ^5 desaturase activity the ratio 20:4n-6/20:3n-6 were calculated.

Significant differences were observed for 18:2n-6, 18:3n-6, 20:3n-6, 20:5n-3, Δ^6 desaturase, and Δ^5 desaturase activities, with 18:2n-6 content (13.73 ± 1.78 and $14.7 \pm 2.04\%$, respectively) and Δ^5 desaturase activity being lower, and with 18:3n-6 (0.12 ± 0.08 and $0.04 \pm 0.02\%$, respectively), 20:3n-6 ($1.71 \pm$
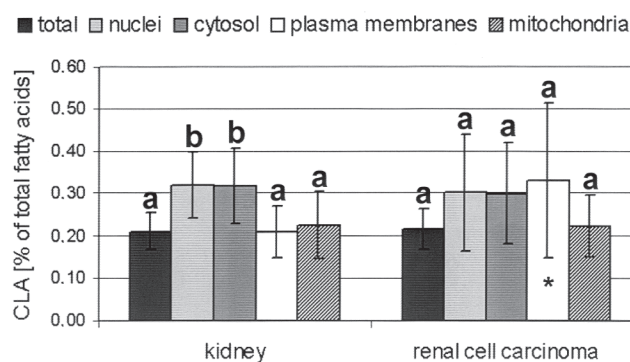
FIG. 1. CLA content in tissue samples of human kidney and renal cell carcinoma as well as in their subcellular fractions. Values are means ± SD ($n = 23$). Columns marked with different letters within one kind of tissue are significantly different ($P < 0.05$). (*), Corresponding healthy and cancerous tissues were significantly different at $P < 0.05$.
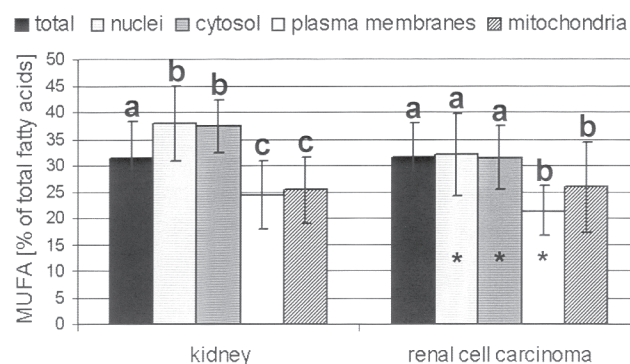
FIG. 2. Content of the monounsaturated FA (MUFA) 14:1*cis*9, 16:1*cis*9, 18:1*cis*9, 20:1*cis*11, 22:1*cis*13, and 24:1*cis*15 in sum in tissue samples of human kidney and renal cell carcinoma as well as in their subcellular fractions. Values are means ± SD ($n = 23$). Columns marked with different letters within one kind of tissue are significantly different ($P < 0.05$). (*), Corresponding healthy and cancerous tissues were significantly different at $P < 0.05$.
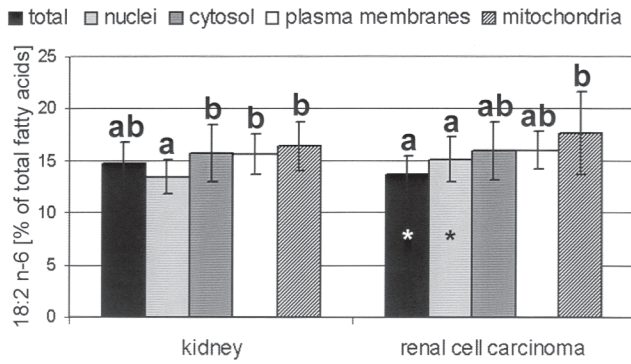
FIG. 3. 18:2n-6 content in tissue samples of human kidney and renal cell carcinoma as well as in their subcellular fractions. Values are means ± SD (*n* = 23). Columns marked with different letters within one kind of tissue are significantly different (*P* < 0.05). (*), Corresponding healthy and cancerous tissues were significantly different at *P* < 0.05.

0.50 and 1.10 ± 0.38%, respectively), and 20:5n-3 contents (0.36 ± 0.20 and 0.24 ± 0.16%, respectively) and Δ^6 desaturase activity being higher in RCC than in healthy renal tissue. The 20:4n-6 content (12.82 ± 4.18 and 15.12 ± 5.84%, respectively) and the elongase activity tended to be lower, whereas the 22:6n-3 content (1.79 ± 1.27 and 1.23 ± 0.70%, respectively) tended to be higher in RCC than in healthy renal tissue, but the differences were not significant. No differences at all between cancerous and healthy tissue were found for the 18:3n-3 content (0.50 ± 0.21 and 0.45 ± 0.17%, respectively) and Δ^9 desaturase activity.

DISCUSSION

Several studies dealing with the incorporation and distribution of CLA into different types of animal tissue are described in the literature (10,11,22–24). Unfortunately, the results of animal studies cannot easily be assigned to humans because of species and age differences. For this reason, studies on humans are indispensable. The present study is a first step to providing valuable clues to potential biochemical target sites of CLA in human renal
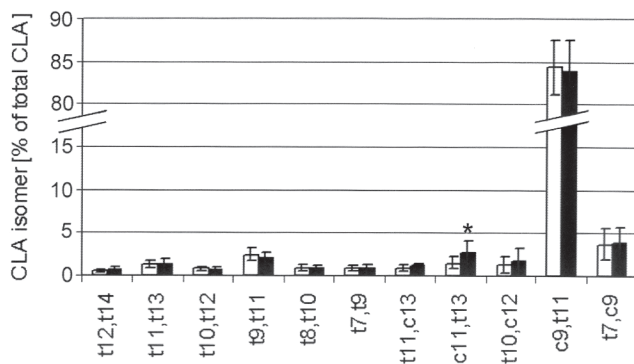
FIG. 4. Contents of CLA isomers in tissue samples of human kidney (white column) and renal cell carcinoma (black column). Values are means ± SD (*n* = 23). (*), Corresponding healthy and cancerous tissues were significantly different at *P* < 0.05.
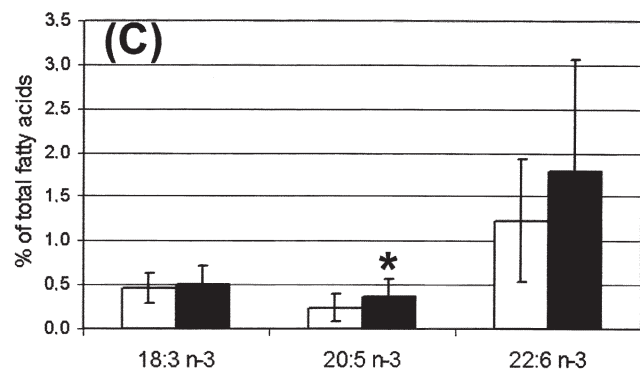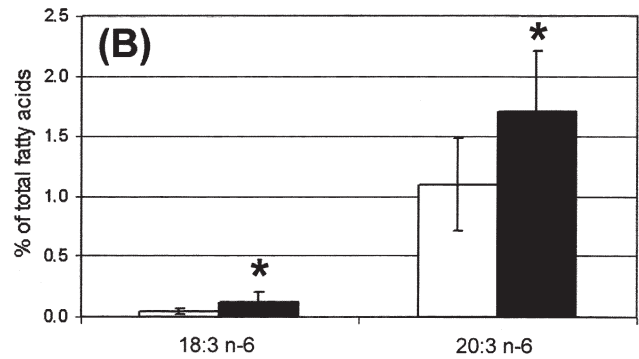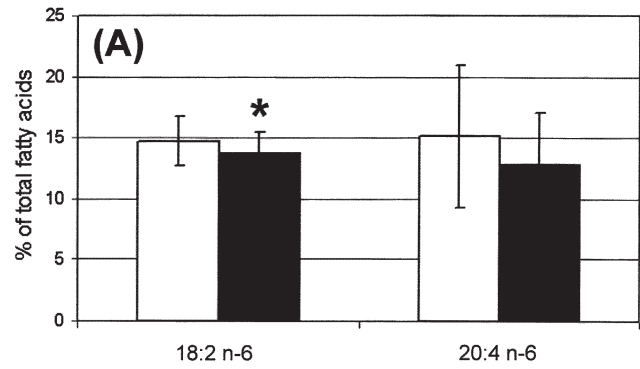
FIG. 5. Contents of (A) 18:2n-6 and 20:4n-6, (B) 18:3n-6 and 20:3n-6, and (C) 18:3n-3, 20:5n-3, and 22:6n-3 in tissue samples of human kidney (white column) and renal cell carcinoma (black column). Values are means ± SD (*n* = 23). (*), Corresponding healthy and cancerous tissues were significantly different at *P* < 0.05.

cancer by comparing the subcellular distribution of CLA in healthy and cancerous tissue samples from the same patients. The study design is limited by missing information on dietary intake values, and there is no comparison of true healthy vs. cancerous kidney tissues. However, as human tissues can be acquired only as waste products accruing at operations, systematic nutritional studies on human cancer are impossible. The examination of healthy and cancerous tissue samples from the same patients offered the possibility of comparing paired tissue samples with the same nutritional status. And even within this limited experimental design, significant differences in FA distribution were found between healthy and cancerous renal tissue, which emphasizes the importance of these results.
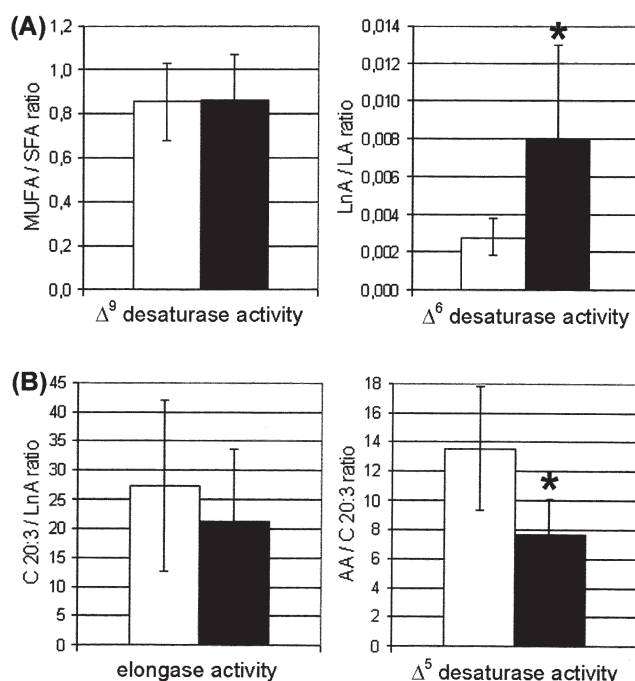
FIG. 6. Activity of (A) Δ^9 and Δ^6 desaturase and (B) elongase and Δ^5 desaturase in tissue samples of human kidney (white column) and renal cell carcinoma (black column). Values are means ± SD (n = 23). (*), Corresponding healthy and cancerous tissues were significantly different at $P < 0.05$. SFA, saturated FA; LA, linoleic acid; LnA, linolenic acid; AA, arachidonic acid; for other abbreviation see Figure 2.

The variation in CLA content between healthy and cancerous kidney tissue was generally very small. No significant difference in total CLA content between renal tissue and RCC could be observed. This result is in accordance with the results of Chajès *et al.* (25), who found no significant difference in mean CLA levels between patients with invasive breast carcinoma and patients with benign breast pathologies. However, Lavillonnière and Bougnoux (26) showed that the CLA content of breast tissue was higher in women with benign disease than in women with carcinoma of the breast.

Because of these contradictory results, the aim of this study was to examine the content of CLA in cancerous tissues more thoroughly. Therefore, total CLA content was measured not only in human RCC and the corresponding unaffected renal tissue of human tumor-bearing kidneys, but also in subcellular fractions of these tissues.

The distribution of CLA over cell organelles is only rarely described in the literature. Demarée *et al.* (12) found that more than 50% less CLA is incorporated into microsomes than into membrane fractions (containing plasma membranes, nuclei, and mitochondria) and nonmembrane fractions (containing nonpolar lipids) of adipose tissue and longissimus muscle of postweanling pigs. Because the microsomes are mainly part of the cytosolic fraction (14) and it was shown that CLA is incorporated best into nuclei and cytosol and significantly less into plasma membranes and mitochondria of renal tissue, the results of Demarée *et al.* (12) are in disagreement with this study.

Banni *et al.* (11) found that CLA is preferentially incorpo-

rated into neutral lipids. Therefore, it is of interest to discuss whether the CLA levels were higher in subcellular fractions containing higher levels of neutral lipids compared with phospholipids. For mitochondria, all values reported for total lipids as the percentage of dry weight and the proportion as phospholipids are in relatively good agreement. It is clear that pig and beef heart and mouse and rat liver mitochondria all have very similar total lipid contents (about 27%) and that about 90% of the total lipids are phospholipids (27). Nuclei have not been studied adequately for total lipid content. A value of 11% was reported for rat liver nuclei, and phospholipids were found to represent only about 3% of the dry weight of a pure preparation of nuclei (27). For plasma membranes, total lipid values of 30.5 and 32.8% were reported for rat and mouse liver, respectively, of which 60.0 and 55.0%, respectively, comprised phospholipids (28). Therefore, the neutral lipid content is much higher in nuclei than in mitochondria and plasma membranes, which explains the preferential incorporation of CLA into nuclei compared with mitochondria and plasma membranes. No data on the neutral lipid content of cytosolic fractions are reported in the literature.

Van Hoeven and Emmelot (28) found increased contents of neutral lipids in hepatoma plasma membranes from mice and rats compared with normal liver plasma membranes. That might explain the significant enhancement of CLA content in the plasma membranes from RCC in comparison with healthy renal tissue. However, no data have been reported in the literature on the lipid class composition of RCC plasma membranes.

The subcellular distribution of CLA was compared with the distribution patterns of 18:2n-6 and the MUFA 14:1*cis*9, 16:1*cis*9, 18:1*cis*9, 20:1*cis*11, 22:1*cis*13, and 24:1*cis*15 in sum. We found that CLA and MUFA were similarly distributed, which is easily explained by the stereochemical structure of CLA. The most prominent CLA isomers in renal tissue and RCC are the *cis*,*trans* and *trans*,*cis* isomers, respectively. *Trans* unsaturated FA show a stereochemical structure similar to that of SFA; consequently, *cis*,*trans* and *trans*,*cis* unsaturated FA show a stereochemical structure similar to that of *cis*-MUFA. The subcellular distribution of 18:2n-6 is different from that of CLA, supporting the results of Banni *et al.* (11), who found that 18:2n-6 is distributed mainly in phospholipids, whereas CLA is incorporated primarily in the neutral lipids of rat liver. Therefore, the different cellular distributions of CLA and 18:2n-6 underline the different physiological properties of these two FA.

In addition, the incorporation of single CLA isomers was examined. No marked differences were found between healthy and cancerous renal tissues. Only the content of the *cis*11,*trans*13-CLA isomer was slightly, but significantly, increased in RCC. *Cis*11,*trans*13-CLA is one of the CLA isomers that is found mainly in commercial CLA preparations (29,30). It differs from the opposite 11,13-CLA geometric isomer *trans*11,*cis*13-CLA, which is generally present in natural dairy fats (31). However, Fritsche *et al.* (32) also reported on the occurrence of *cis*11,*trans*13-CLA in beef samples. Kramer *et al.* (33) examined the distribution of CLA isomers in tissue lipid classes of pigs fed a commercial CLA mixture. They found a

preferential accumulation of *cis*11,*trans*13-CLA in cardiac lipids compared with liver lipids, inner back fat, and omental fat. No data on kidney lipids have been reported, but the occurrence of *cis*11,*trans*13-CLA in kidney and RCC lipids might be due to a comparable accumulation of this isomer from trace amounts in foods, as observed for cardiac lipids.

In addition to CLA, total lipid profiles were determined. As discussed previously, marked variations in FA contents between the subcellular fractions of the two types of kidney tissue studied were detectable (14). However, because of variations between different kinds of tissues and species, no general statement on the characteristic FA profiles of single subcellular fractions was possible. The goal of the present study was a detailed, statistical examination of the n-3 PUFA 18:3n-3, 20:5n-3, and 22:6n-3 and the n-6 PUFA 18:2n-6, 18:3n-6, 20:3n-6, and 20:4n-6 in kidney and RCC, as PUFA have been suggested to have an effect on cancer risk by increasing the formation of eicosanoids in the tumor tissue (34). The contents of the n-6 PUFA measured were in good agreement with the results of Geers *et al*. (35), who analyzed the phospholipid composition of nephromas and the unaffected cortex of 15 tumor-bearing human kidneys. They found 18:2n-6 (11.1 ± 2.7 and 15.3 ± 1.5%, respectively) to be significantly decreased; 20:4n-6 + 22:1 (11.1 ± 3.7 and 14.9 ± 4%, respectively) tended to be decreased; and 20:3n-6 + 22:0 (3.9 ± 2.0 and 3.1 ± 0.5%, respectively) tended to be increased in the nephromas. No data on the contents of n-3 PUFA in renal tissue samples are reported in the literature.

The differences determined in n-3 and n-6 FA distribution and the resulting differences in desaturase and elongase activities between healthy renal tissue and RCC indicate a changed PUFA metabolism in RCC. No literature so far has linked n-3 and n-6 metabolism and RCC *via* its role as an eicosanoid precursor, but an abnormal cholesterol metabolism is described, which leads to the speculation that not only cholesterol metabolism but also other FA metabolic pathways may be abnormal (36). Furthermore, there is already evidence linking PUFA metabolism and breast cancer (7) or prostate cancer, another urological cancer (37). The greater 18:3n-6/18:2n-6 ratio but lower 20:3n-6/18:3n-6 and 20:4n-6/20:3n-6 ratios calculated in this study lead to the assumption that the low 20:4n-6 levels may be a result of decreased elongase and Δ^5 desaturase activities. Another explanation for the lower RCC contents of 20:4n-6 as well as 20:5n-3, substrates for the synthesis of eicosanoids by cyclooxygenase or lipoxygenase, might be an increased production of eicosanoids, which has previously been postulated for prostate cancer (37) and which has already been shown for breast cancer (38).

Further understanding of the cause and/or consequence of the differences in FA metabolism between healthy renal tissue and RCC may lead to a better understanding of RCC. Banni *et al*. (4) suggested that CLA inhibits the elongation and desaturation of 18:2n-6 into 20:4n-6. In that case, one might speculate that a diet enriched in CLA is a useful tool in preventing RCC. However, differences in CLA content and isomer distribution between healthy and cancerous kidney tissues from the same patients appeared to be minimal in the present study. Therefore, the involvement of CLA in preventing cancer of the kidneys cannot be definitively demonstrated from the design of this experiment.

Tavani and La Vecchia have shown that meat and milk products are risk factors in RCC (9). Results from studies on the association between consumption of dairy products and risk of breast cancer have been controversial. Some studies have found a significant inverse association, some a significant positive association, and some no association (39). Possible reasons for the discrepancy include different effects by different components of diary products. CLA, alone or together with other ingredients of dairy products, may be a factor that is responsible for a positive effect. This view is supported by the anticarcinogenic effects of CLA observed in experimental animal studies. On the other hand, a high consumption of processed meat and poultry, as reflected in an increased proportion of 20:4n-6 in serum FA, may increase the risk of breast cancer or RCC. Another possible explanation for the lack of an association between the intake of foods rich in CLA, such as ruminant products, and the occurrence of RCC is that the amount of CLA stored in human tissues may be too low to induce any protective effect on tumor development. CLA remains at a level at which inhibition of tumor growth has never been documented in animals.

ACKNOWLEDGMENT

REFERENCES

1. Fritsche, J., and Steinhart, H. (1998) Amounts of Conjugated Linoleic Acid (CLA) in German Foods and Evaluation of Daily Intake, *Z. Lebensm.-Unters.-Forsch. A 206*, 77–82.

2. Ip, C., Banni, S., Angioni, E., Carta, G., McGinley, J., Thompson, H.J., Barbano, D., and Bauman, D. (1999) Conjugated Linoleic Acid-Enriched Butter Fat Alters Mammary Gland Morphogenesis and Reduces Cancer Risk in Rats, *J. Nutr. 129*, 2135–2142.

3. Palombo, J.D., Ganguly, A., Bistrian, B.R., and Menard, M.P. (2002) The Antiproliferative Effects of Biologically Active Isomers of Conjugated Linoleic Acid on Human Colorectal and Prostatic Cancer Cells, *Cancer Lett. 177*, 163–172.

4. Banni, S., Angioni, E., Casu, V., Melis, M.P., Carta, G., Corongiu, F.P., Thompson, H., and Ip, C. (1999) Decrease in Linoleic Acid Metabolites as a Potential Mechanism in Cancer Risk Reduction by Conjugated Linoleic Acid, *Carcinogenesis 20*, 1019–1024.

5. Kavanaugh, C.J., Liu, K.L., and Belury, M.A. (1999) Effect of Dietary Conjugated Linoleic Acid on Phorbol Ester-Induced PGE(2) Production and Hyperplasia in Mouse Epidermis, *Nutr. Cancer 33*, 132–138.

6. O'Shea, M., Lawless, F., Stanton, C., and Devery, R. (1998) Conjugated Linoleic Acid in Bovine Milk Fat: A Food-Based Approach to Cancer Prevention, *Trends Food Sci. Technol. 9*, 192–196.

7. Aro, A., Mannisto, S., Salminen, I., Ovaskainen, M.L., Kataja, V., and Uusitupa, M. (2000) Inverse Association Between Dietary and Serum Conjugated Linoleic Acid and Risk of Breast

Cancer in Postmenopausal Women, *Nutr. Cancer 38*, 151–157.

8. Voorrips, L.E., Brants, H.A.M., Kardinaal, A.F.M., Hiddink, G.J., van den Brandt, P.A., and Goldbohm, R.A. (2002) Intake of Conjugated Linoleic Acid, Fat, and Other Fatty Acids in Relation to Postmenopausal Breast Cancer: The Netherlands Cohort Study on Diet and Cancer, *Am. J. Clin. Nutr. 76*, 873–882.

9. Tavani, A., and La Vecchia, C. (1997) Epidemiology of Renal-Cell Carcinoma, *J. Nephrol. 10*, 93–106.

10. Sugano, M., Tsujita, A., Yamasaki, M., Yamada, K., Ikeda, I., and Kritchevsky, D. (1997) Lymphatic Recovery, Tissue Distribution, and Metabolic Effects of Conjugated Linoleic Acid in Rats, *J. Nutr. Biochem. 8*, 38–43.

11. Banni, S., Carta, G., Angioni, E. Murru, E., Scanu, P., Melis, M.P., Bauman, D.E., Fischer, S.M., and Ip, C. (2001) Distribution of Conjugated Linoleic Acid and Metabolites in Different Lipid Fractions in the Rat Liver, *J. Lipid Res. 42*, 1056–1061.

12. Demarée, S.R., Gilbert, C.D., Mersmann, H.J., and Smith, S.B. (2002) Conjugated Linoleic Acid Differentially Modifies Fatty Acid Composition in Subcellular Fractions of Muscle and Adipose Tissue but Not Adiposity of Postweanling Pigs, *J. Nutr. 132*, 3272–3279.

13. Demizieux, L., Degrace, P., Gresti, J., Loreau, O., Noel, J.P., Chardigny, J.M., Sébédio, J.L., and Clouet, P. (2002) Conjugated Linoleic Acid Isomers in Mitochondria: Evidence for an Alteration of Fatty Acid Oxidation, *J. Lipid Res. 43*, 2112–2122.

14. Hoffmann, K., Blaudzsun, J., Brunken, C., Höpker, W.-W., Tauber, R., and Steinhart, H., New Application of a Subcellular Fractionation Method to Kidney and Testis for the Determination of Conjugated Linoleic Acid in Selected Cell Organelles of Healthy and Cancerous Human Tissues, *Anal. Bioanal. Chem.*, in press.

15. Mackler, P., Collip, P.J., Duncan, H.M., Rao, N.A., and Huennekens, F.M. (1962) An Electron Transport Particle from Yeast: Purification and Properties, *J. Biol. Chem. 237*, 2968–2974.

16. Cohen, G., Dembiec, D., and Marcus, J. (1970) Measurement of Catalase Activity in Tissue Extracts, *Anal. Bichem. 34*, 30–38.

17. Williams, C.H., and Kamin, H. (1962) Microsomal Triphosphopyridine Nucleotide-Cytochrome c Reductase of Liver, *J. Biol. Chem. 237*, 587–595.

18. Bergmeyer, H.U. (1970) *Methoden der enzymatischen Analyse*, 2nd edn., Verlag Chemie, Weinheim.

19. Bradford, M.M. (1976) A Rapid and Sensitive Method for the Quantitation of Microgram Quantities of Protein Utilizing the Principle of Protein-Dye Binding, *Anal. Biochem. 72*, 248–254.

20. Pfalzgraf, A., Timm, M., and Steinhart, H. (1994) Gehalte von *trans*-Fettsäuren in Lebensmitteln, *Z. Ernährungswiss. 33*, 24–43.

21. Sehat, N., Yurawecz, M.P., Roach, J.A.G., Mossoba, M.M., Kramer, J.K.G., and Ku, Y. (1998) Silver-Ion High-Performance Liquid Chromatographic Separation and Identification of Conjugated Linoleic Acid Isomers, *Lipids 33*, 217–221.

22. Yang, L., Yeung, S.Y.V., Huang, Y., Wang, H.Q., and Chen, Z.-Y. (2002) Preferential Incorporation of *trans,trans*-Conjugated Linoleic Acid Isomers into the Liver of Suckling Rats, *Br. J. Nutr. 87*, 253–260.

23. Chardigny, J.M., Hasselwander, O., Genty, M., Kraemer, K., Ptock, A., and Sébédio, J.L. (2003) Effect of Conjugated FA on Feed Intake, Body Composition, and Liver FA in Mice, *Lipids 38*, 895–902.

24. Kelley, D.S., Bartolini, G.L., Warren, J.M., Simon, V.A., Mackey, B.E., and Erickson, K.L. (2004) Contrasting Effects of *t*10,*c*12- and *c*9,*t*11-Conjugated Linoleic Acid Isomers on the Fatty Acid Profiles of Mouse Liver Lipids, *Lipids 39*, 135–141.

25. Chajès, V., Lavillonnière, F., Ferrari, P., Jourdan, M.-L., Pinault, M., Maillard, V., Sébédio, J.-L., and Bougnoux, P. (2002) Conjugated Linoleic Acid Content in Breast Adipose Tissue Is Not Associated with the Relative Risk of Breast Cancer in a Population of French Patients, *Cancer Epidemiol. Biomarkers Prev. 11*, 672–673.

26. Lavillonnière, F., and Bougnoux, P. (1999) Conjugated Linoleic Acid (CLA) and the Risk of Breast Cancer, in *Advances in Conjugated Linoleic Acid Research* (Yurawecz, M.P., Mossoba, M.M., Kramer, J.K.G., Pariza, M.W., and Nelson, G.J., eds.), Vol. 1, pp. 276–282, AOCS Press, Champaign, IL.

27. Fleischer, S., and Rouser, G. (1965) Lipids of Subcellular Particles, *J. Am. Oil Chem. Soc. 42*, 588–607.

28. Van Hoeven, R.P., and Emmelot, P. (1972) Lipid Class Composition of Plasma Membranes Isolated from Rat and Mouse Liver and Hepatomas, *J. Membr. Biol. 9*, 105–126.

29. Sehat, N., Yurawecz, M.P., Roach, J.A.G., Mossoba, M.M., Kramer, J.K.G., and Ku, Y. (1998) Silver-Ion High-Performance Liquid Chromatographic Separation and Identification of Conjugated Linoleic Acid Isomers, *Lipids 33*, 217–221.

30. Sehat, N., Rickert, R., Mossoba, M.M., Kramer, J.K.G., Yurawecz, M.P., Roach, J.A.G., Adlof, R.O., Morehouse, K.M., Fritsche, J., Eulitz, K.D., Steinhart, H., and Ku, Y. (1999) Improved Separation of Conjugated Fatty Acid Methyl Esters by Silver-Ion High-Performance Liquid Chromatography, *Lipids 34*, 407–413.

31. Kraft, J., Collomb, M., Moeckel, P., Sieber, R., and Jahreis, G. (2003) Differences in CLA Isomer Distribution of Cow's Milk Lipids, *Lipids 38*, 657–664.

32. Fritsche, J., Fritsche, S., Solomon, M.B., Mossoba, M.M., Yurawecz, M.P., Morehouse, K., and Ku, Y. (2000) Quantitative Determination of Conjugated Linoleic Acid Isomers in Beef Fat, *Eur. J. Lipid Sci. Technol. 102*, 667–672.

33. Kramer, J.K.G., Sehat, N., Dugan, M.E.R., Mossoba, M.M., Yurawecz, M.P., Roach, J.A.G., Eulitz, K., Aalhus, J.L., Schaefer, A.L., and Ku, Y. (1998) Distributions of Conjugated Linoleic Acid (CLA) Isomers in Tissue Lipid Classes of Pigs Fed a Commercial CLA Mixture Determined by Gas Chromatography and Silver Ion-High-Performance Liquid Chromatography, *Lipids 33*, 549–558.

34. Bartsch, H., Nair, J., and Owen, R.W. (1999) Dietary Polyunsaturated Fatty Acids and Cancers of the Breast and Colorectum: Emerging Evidence for Their Role as Risk Modifiers, *Carcinogenesis 20*, 2209–2218.

35. Geers, R., Christophe, A., Matthys, F., Verdonk, G., and Popelier, G. (1977) Phospholipid Analysis of Nephromas and Unaffected Cortex of Tumour-Bearing Human Kidneys, *Biochem. Soc. Trans. 5*, 1167–1169.

36. Gebhard, R.L., Clayman, R.V., Prigge, W.F., Figenshau, R., Staley, N.A., Reesey, C., and Bear, A. (1987) Abnormal Cholesterol Metabolism in Renal Clear Cell Carcinoma, *J. Lipid Res. 28*, 1177–1184.

37. Faas, F.H., Dang, A.Q., White, J., Schaefer, R.F., and Johnson, D.E. (2003) Decreased Prostatic Arachidonic Acid in Human Prostatic Carcinoma, *BJU Int. 92*, 551–554.

38. Rose, D.P., and Connolly, J.M. (1990) Effects of Fatty Acids and Inhibitors of Eicosanoid Synthesis on the Growth of a Human Breast Cancer Cell Line in Culture, *Cancer Res. 50*, 7139–7144.

39. Knekt, P., and Järvinen, R. (1999) Intake of Dairy Products and Breast Cancer Risk, in *Advances in Conjugated Linoleic Acid Research* (Yurawecz, M.P., Mossoba, M.M., Kramer, J.K.G., Pariza, M.W., and Nelson, G.J., eds.), Vol. 1, pp. 444–470, AOCS Press, Champaign, IL.

Identification of Δ^7 Phytosterols and Phytosteryl Glucosides in the Wood and Bark of Several *Acacia* Species

Carmen S.R. Freire, Dora S.C. Coelho, Nuno M. Santos, Armando J.D. Silvestre*, and Carlos Pascoal Neto

Center for Research in Ceramics and Composite Materials (CICECO)
and Department of Chemistry, University of Aveiro, 3810-193 Aveiro, Portugal

ABSTRACT: The wood and bark of four *Acacia* species growing in Portugal, namely, *A. longifolia, A. dealbata, A. melanoxylon,* and *A. retinodes*, were investigated for their sterol content. The lipids fractions of the different wood and bark samples were isolated, and the sterols were identified and quantified by GC–MS. Two Δ^7 sterols, specifically, spinasterol and dihydrospinasterol, were the main sterols found in considerable amounts, particularly in wood tissues (more than 0.5 g/kg of dry wood in the case of *A. melanoxylon* and *A. retinodes*). The corresponding unusual steryl glucosides were also identified in significant amounts in the wood and bark extracts.

Paper no. L9682 in *Lipids 40,* 317–322 (March 2005).

Sterols are a very important group of lipidic compounds because of their broad range of biological functions and activities. In the Plant Kingdom, a large number of sterols (phytosterols) have been identified, of which the Δ^5 sterols, such as β-sitosterol (stigmasta-5-en-3-β-ol) and stigmasterol, are the most abundant (1,2). The homologous Δ^7 sterols, spinasterol and dihydrospinasterol (stigmastadien-7,22*E*-3-β-ol and stigmasta-7-en-3-β-ol, respectively), are the major components of only a few plant families, e.g., Caryophylaceae and Cactaceae (2). Furthermore, phytosterols can occur in free form, esterified with FA and aromatic acids, or as glucosides (2).

Phytosterols play a key role in stabilizing the cell membranes in plants (as cholesterol does in animals). Moreover, their beneficial effects on human health (3), of which the reduction of blood cholesterol level is the most well known, have been recognized for many years. However, the most significant advances in this field, and particularly in the use of phytosterols as ingredients in functional foods, have been made in the last decade (3). Currently, a wide range of functional foods supplemented with phytosterols are available on the market (4), leading to an increasing demand for abundant sources of these natural products.

Acacia trees are not cultivated in Portugal; however, they represent the main invasive plant species of the Portuguese pine and eucalyptus forests, as well as of the coastal dune systems (5). Every year a large number of *Acacia* trees are harvested to avoid the propagation of these exotic species, leading to the production of considerable amounts of biomass that are mainly used for domestic energy production. The wood and bark of these exotic species could represent a renewable source of fine chemicals. In fact, a large number of publications have been published describing the composition of *Acacia* species, and the most relevant results have recently been reviewed (6). However, only a few publications discuss the sterol composition of specific *Acacia* species (7–10). Since information on the chemical composition of *Acacia* species growing in Portugal is still lacking, we set out to characterize the most relevant species, namely, *A. longifolia*, *A. dealbata*, *A. melanoxylon*, and *A. retinodes*.

In the present work, the different *Acacia* wood and bark lipids were isolated by Soxhlet extraction and characterized by GC–MS. We report, for the first time, the identification of considerably high amounts of the less common Δ^7 sterols, namely, spinasterol and dihydrospinasterol, and the corresponding glucosides in the lipidic extracts of the wood and bark of the main *Acacia* species growing in Portugal.

MATERIALS AND METHODS

Samples. *Acacia* wood and bark samples were randomly sampled from 6 to 8 trees growing in the forests of the region of Aveiro, Portugal, at the end of May 2004. Samples were collected from the stem 1 m above the ground. Wood and bark samples were air-dried for 2 wk and then ground and sieved, and the granulometric fractions of 40–60 mesh were used for analysis.

Extraction of lipids from wood and bark samples. Three powdered aliquots (20 g) of each sample were Soxhlet extracted with dichloromethane for 8 h. The solvent was evaporated to dryness and the lipophilic extracts were weighed. The results were expressed as a percentage of dry wood or bark.

GC–MS analysis and quantification of the lipophilic extracts. (i) Extract derivatization. Prior to GC–MS analysis, approximately 20 mg of each dried extract was trimethylsilylated according to a known procedure (11): The residue was dissolved in 250 µL of dry pyridine, and compounds containing carboxyl and hydroxyl groups were converted into trimethylsilyl (TMS) esters and ethers, respectively, by adding 250 µL of bis(trimethylsilyl)trifluoroacetamide (BSTFA) and 50 µL of trimethylchlorosilane (TMSCl). After the mixture had stood at 70°C for 30 min, the derivatized extracts were analyzed by GC–MS.

*To whom correspondence should be addressed. E-mail: armsil@dq.ua.pt

Abbreviations: BSTFA, bis(trimethylsilyl)trifluoroacetamide; IS, internal standard; TMS, trimethylsilyl; TMSCl, trimethylchlorosilane.

(ii) GC–MS analysis procedure. Free sterols were analyzed and quantified in a Trace 2000 Series gas chromatograph equipped with a Finnigan Trace MS mass spectrometer, using helium as carrier gas (35 cm/s), and a J&W DB-1 capillary column (30 m × 0.32 mm i.d., 0.25 µm film thickness; J&W Scientific, Folsom, CA). The chromatographic conditions were as follows: initial temperature, 80°C; temperature rate, 4°C/min; final temperature, 285°C; injector temperature, 290°C; transfer-line temperature, 290°C; split ratio, 1:100.

Steryl glucosides were analyzed and quantified by GC–MS using a shorter length J&W DB-1 capillary column (15 m × 0.32 mm i.d., 0.25 µm film thickness). The chromatographic conditions were as follows (11): initial temperature, 100°C for 3 min; temperature rate, 5°C/min; final temperature, 340°C for 12 min; injector temperature, 320°C; transfer-line temperature, 290°C; split ratio, 1:100.

(iii) Identification and quantification of free sterols and steryl glucosides. Compounds were identified as TMS derivatives by comparing their mass spectra with the GC–MS spectral library, with data from the literature, and in some cases by injection of standards. For quantitative analysis, GC–MS was calibrated with the pure reference compounds stigmasterol and β-sitosteryl glucoside relative to tetracosane, the internal standard used. The respective multiplication factors needed to obtain correct quantification of the peak areas were calculated as an average of six GC–MS runs. All bark and wood extracts were injected in triplicate.

Mass spectra of Δ^7 steryl glucosides (TMS derivatives). Spinasteryl glucoside: 73 (14.8), 147 (7.1), 204 (100), 217 (13.8), 255 (3.1) 305 (1.4), 361 (2.7), 395 (7.4), 513 (4.0), 667 (0.5), 757 (0.5). Dihydrospinasteryl glucoside: 73 (10.1), 147 (7.2), 204 (100), 217 (13.2), 255 (1.2), 305 (1.3), 361 (1.8), 397 (12.9), 515 (3.5), 669 (0.5), 759 (0.5).

Chemicals. Stigmasterol (95% purity) and tetracosane (99% purity), BSTFA (99% purity), TMSCl (99% purity), dichloromethane (analytical grade), and pyridine (analytical grade) were supplied by Sigma Chemicals Co. (Madrid, Spain). Pyridine was dried by distillation over sodium hydroxide. Pure sitosteryl glucoside was isolated from a plant extract enriched in this steryl glucoside (12).

RESULTS AND DISCUSSION

The different *Acacia* species studied here, *A. longifolia*, *A. dealbata*, *A. melanoxylon*, and *A. retinodes*, presented similar wood lipid contents (Table 1), 0.3–0.5% of dry wood weight, which are values of the same order as those previously reported for *A. mangium* (10). The lipids contents of the bark samples (0.9–2.7%) were also very similar between the different *Acacia* species (Table 1); however, they were generally considerably higher that those found in the corresponding woods.

The GC–MS analysis of the lipophilic extracts of the four *Acacia* woods showed that they had very similar compositions, with FA and sterols as the main components (Fig. 1). Steryl glucosides were also found in all wood extracts, although in lower amounts. In addition, we found steryl esters, MG, and

TABLE 1
Lipidic Fraction (dichloromethane extractives) Yields (%, dry basis) of the Four *Acacia* Wood and Bark Samples

	Wood	Bark
A. longifolia	0.31 ± 0.01	0.92 ± 0.01
A. dealbata	0.36 ± 0.03	2.00 ± 0.06
A. melanoxylon	0.50 ± 0.03	2.04 ± 0.06
A. retinodes	0.31 ± 0.01	2.71 ± 0.09

long-chain alcohols among the minor components of the *Acacia* wood extracts.

Compositions of the *Acacia* bark extracts were similar; however, in these extracts long-chain fatty alcohols and MG were major components, along with FA and alcohols (Fig. 1). Therefore, the GC–MS chromatograms of the bark lipophilic extractives were much more complex than those observed for the corresponding wood extracts (Fig. 1). From a practical point of view, this could represent a disadvantage when considering the isolation of particular components.

Free sterols. As shown in Table 2, free sterols were more abundant in *Acacia* woods than in the corresponding bark tissues. *Acacia melanoxylon* and *A. retinodes* woods, in particular, contained notable amounts of these compounds (more than 500 mg of free sterols/kg of dry wood). These results were in good agreement with those published for *A. mangium* and *A. crassicarpa* (10). However, in these species, such high amounts of free sterols were found only in heartwood tissues (10). Bark samples contained around 200–300 mg of sterols/kg of dry bark.

Two Δ^7 sterols, namely, spinasterol and dihydrospinasterol (Fig. 2), were the main sterols identified in the wood and bark extracts of *A. dealbata*, *A. melanoxylon*, and *A. retinodes* (Table 2); on the other hand, *A. longifolia* contained similar amounts of the homologous Δ^5 (stigmasterol and β-sitosterol) and Δ^7 (spinasterol and dihydrospinasterol) sterols (Figs. 1 and 2, Table 2). As mentioned, these sterols have been reported previously in other *Acacia* species (7,8,10). However, the simultaneous occurrence of Δ^5 and Δ^7 sterols is quite unusual in woody plants. Campesterol, stigmastanol, and β-sitostanol also were found in some wood and bark samples but as minor components.

The sterols referred to here were identified based on their characteristic retention times (11) and on well-documented fragmentation patterns of their TMS derivatives (13,14). The homologous Δ^5 and Δ^7 sterols were easily distinguished by MS: (i) The ion $[M -129]^+$ was the characteristic base peak of the TMS derivatives of Δ^5 sterols, whereas it was absent from the mass spectra of the Δ^7 sterols; (ii) Δ^7 sterols, in particular the monounsaturated ones, in general presented a strong molecular ion and lost their lateral chain much more easily, leading to a characteristic intense peak at *m/z* 255.

Steryl glucosides. The steryl glucosides present in the lipidic fraction of *Acacia* woods and barks accounted for 31.5–159.0 mg/kg of dry wood and 146.0–352.6 mg/kg of dry bark (Table 3). Although it is commonly accepted that complete extraction of steryl glucosides requires more polar solvents (15), a recent
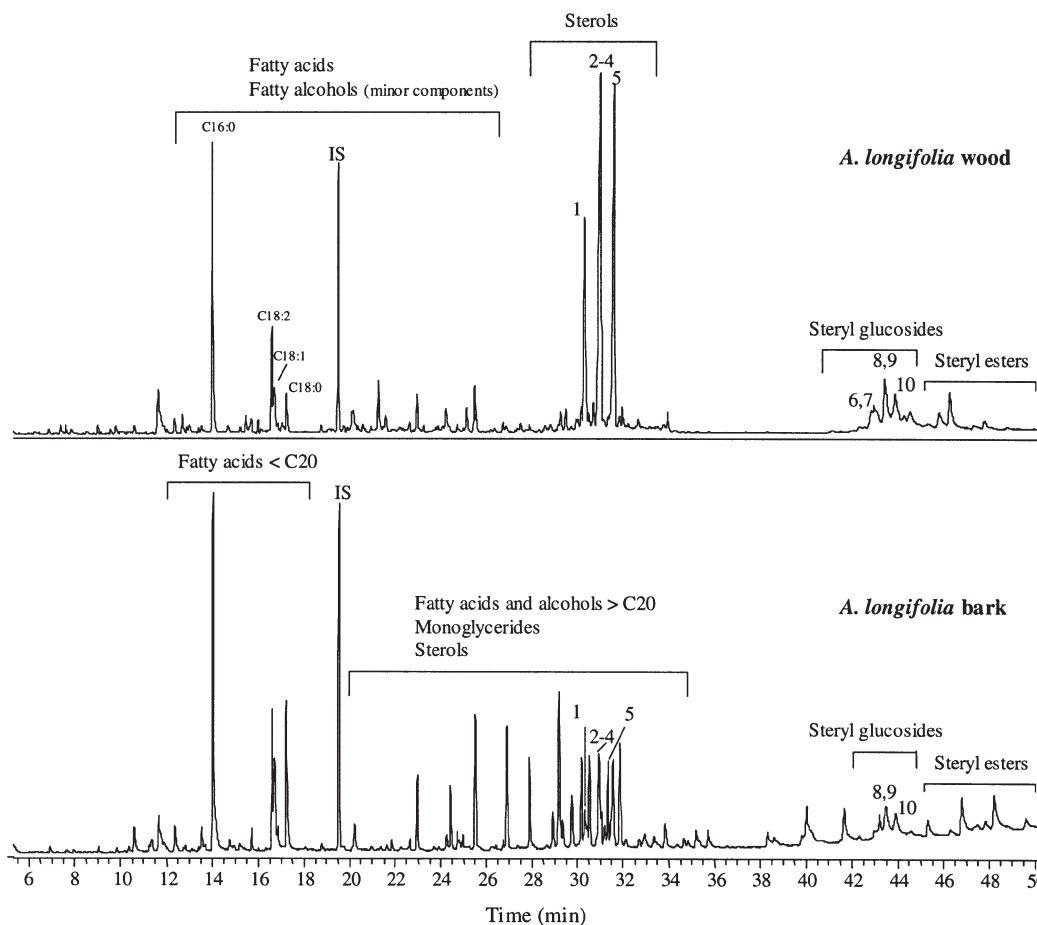
FIG. 1. GC–MS chromatograms, obtained with a 15-m DB-1 capillary column (J&W Scientific, Folsom, CA), of the lipidic fraction extracts of the *Acacia longifolia* wood and bark. 16:0, palmitic acid; 18:2, linoleic acid; 18:1, oleic acid; 18:0, stearic acid; IS, internal standard; 1, stigmasterol; 2, spinasterol; 3, β-sitosterol; 4, β-sitostanol; 5, dihydrospinasterol; 6, campesteryl glucoside; 7, stigmasteryl glucoside; 8, spinasteryl glucoside; 9, β-sitosteryl glucoside; 10, dihydrospinasteryl glucoside.

publication showed that similar yields could be obtained with dichloromethane (16); and in the case of woody plants, we observed that after extraction with dichloromethane, only small amounts of steryl glucosides (less than 3%) remained in the sample (12,17). Therefore, these values are expected to be representative of the total content of steryl glucosides of the different *Acacia* wood and bark tissues.

As observed with free sterols, the Δ⁷ steryl glucosides, that is, spinasteryl glucoside and dihydrospinasteryl glucoside, were identified in *A. dealbata*, *A. melanoxylon*, and *A. retin-*

TABLE 2
Free Sterols Identified in Acacia Wood and Bark Lipidic Fractions (mg/kg of the plant fraction dry weight)[a]

	t_R	*A. longifolia*		*A. dealbata*		*A. melanoxylon*		*A. retinodes*	
		Wood	Bark	Wood	Bark	Wood	Bark	Wood	Bark
Campesterol	54.64	4.34	—	—	—	—	—	—	—
Stigmasterol	55.11	60.8	40.3	—	—	—	—	—	—
Stigmastanol	55.27	8.73	—	—	—	—	—	—	—
Spinasterol	55.97	127.7*	111.2*	171.9	145.5	325.6	95.8	358.6	191.7
β-Sitosterol		—	—	—	—	—	—	—	—
β-Sitostanol	56.12	24.6	43.5	18.5	—	20.6	13.9	7.43	—
Dihydrospinasterol	56.81	108.9	125.9	190.6	113.9	274.5	102.9	285.6	92.2
Total		335.07	320.9	381.0	259.4	620.7	212.6	651.63	283.9

[a]Obtained with a 30-m DB-1 column (J&W Scientific, Folsom, CA). (Note that this column is different from that used in Fig. 1.) *Sum of the abundances of co-eluting spinasterol and β-sitosterol. t_R, retention time (min). A dash indicates "not detected."

R= H, β-Sitosterol
R=glc, Sitosteryl glucoside

R= H, Stigmasterol
R=glc, Stigmasteryl glucoside

R= H, Dihydrospinasterol
R=glc, Dihydrospinasteryl glucoside

R= H, Spinasterol
R=glc, Spinasteryl glucoside
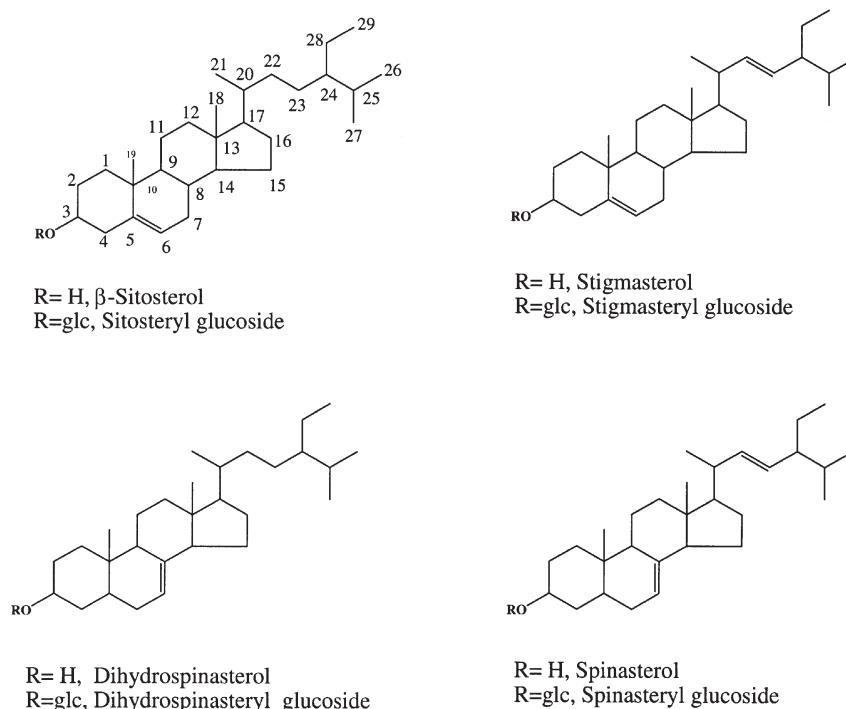
FIG. 2. Structures of the main phytosterols and steryl glucosides identified on the lipophilic fraction of the *Acacia* woods and barks studied here. glc, glucose moiety.

odes wood and bark lipids (Figs. 1, 2), whereas a mixture of the homologous Δ^5 and Δ^7 steryl glucosides was found in the wood and bark lipophilic extracts of *A. longifolia* (Figs. 1, 2). To our knowledge, steryl glucosides have not been reported previously as *Acacia* wood and bark components, although spinasteryl glucoside and dihydrospinasteryl glucoside have been reported as components of *A. concinna* seed pods (18). In addition, steryl glucosides are not common components of woody plants, although spinasteryl glucoside has been reported as a component of *Albizia julibrissin* bark (19).

Steryl glucosides were also identified by GC–MS as TMS derivatives based on their characteristic fragmentation patterns (12,15,20). However, the mass spectra of the TMS derivatives of Δ^5 and Δ^7 steryl glucosides were very similar: The molecular ions were not observed, but their M.W. could be determined based on the mass of the $[M - 15]^+$, $[M - 15 - 90]^+$, and $[M - 15 - 90 - 90]^+$ ions. Cleavage of the sterol 3-C–O bond with charge retention on the sterol portion produced intense ions corresponding to the sterol moiety, that is, 383 for campesteryl glucoside, 395 for stigmasteryl and spinasteryl glucosides, and 397 for β-sitosteryl glucoside and dihydrospinasteryl glucosides, respectively. Finally, charge retention on the monosaccharide portion and cleavage of the C–O-glucosidic bond gave characteristic ions of the hexoses at *m/z* 451, 361, 217, 204, and 147. Furthermore, the ion at *m/z* 204 was very prominent, which is an indication of the hexose pyranoside configuration (19).

The distinction between the homologous Δ^5 and Δ^7 steryl glucosides was then established based on previous knowledge

TABLE 3
Steryl Glucosides Identified in *Acacia* Wood and Bark Lipidic Fractions (mg/kg of the plant fraction dry weight)[a]

	t_R	*A. longifolia*		*A. dealbata*		*A. melanoxylon*		*A. retinodes*	
		Wood	Bark	Wood	Bark	Wood	Bark	Wood	Bark
Campesteryl glucoside	42.70	35.7*	—	—	—	—	—	—	—
Stigmasteryl glucoside	42.94		—	—	—	—	—	—	—
Spinasteryl glucoside	43.42	44.4**	88.2**	11.9	186.4	80.3	170.5	59.3	—
Sitosteryl glucoside				—	—	—	—	—	—
Dihydrospinasteryl glucoside	43.90	29.6	57.8	19.6	166.2	78.7	92.0	66.4	—
Total		109.7	146.0	31.5	352.6	159.0	262.5	125.7	—

[a]Obtained with a 15-m DB-1 column (J&W Scientific, Folsom, CA). (Note that these are the same column and chromatographic conditions as shown in Fig. 1.) *Sum of the abundances of partially overlying campesteryl glucoside and stigmasteryl glucoside; **sum of the abundances of co-eluting sitosteryl glucoside and spinasteryl glucoside. t_R, retention time (min). A dash indicates "not detected."

of the retention times of Δ^5 steryl glucosides (12) and on the co-injection of a sample enriched in these compounds (12), assuming that they presented the same profile as that observed with the corresponding free sterols. Therefore, the Δ^7 steryl glucosides, spinasteryl glucoside, and dihydrospinasteryl glucoside eluted after the corresponding Δ^5 steryl glucosides, stigmasteryl glucoside, and β-sitosteryl glucoside.

Steryl esters were detected only in the wood and bark of *A. longifolia*. The peaks assigned to steryl esters (Fig. 1) showed characteristic retention times and fragmentations of this group of compounds (21). However, the presence of some other unexpected fragments suggests that such peaks co-eluted with other components and therefore unambiguous identification was not possible.

Finally, acylsteryl glucosides, normally detected together with steryl glucoside, were not found in the present study, although they could have been detected easily under the experimental conditions used (17,20).

In conclusion, the wood and bark of the *Acacia* species investigated were rich natural sources of bioactive sterols, particularly of the Δ^7 sterols spinasterol and dihydrospinasterol (which can be easily isolated by simple solvent extraction), as well as of the corresponding steryl glucosides. A wide variety of biological activities have been attributed to these sterols. The effect of spinasterol on reducing plasma and liver cholesterol levels has been recognized for many years (22). The antitumorigenic potential of spinasterol also was demonstrated previously (23), and more recently, spinasterol was found to have considerable therapeutic potential in modulating the development and/or progression of diabetic nephropathy (24). On the other hand, dihydrospinasterol showed a potent inhibitory effect on the Epstein–Barr virus early antigen (25), whereas its glucoside exhibited anticarcinogenic and cytotoxic potential (26).

ACKNOWLEDGMENTS

REFERENCES

1. Nes, W.R. (1989) Steroids, in *Natural Products of Woody Plants II* (Rowe, J.W., ed.), pp. 808–842, Springer-Verlag, New York.
2. Nes, W.R. (1977) The Biochemistry of Plant Sterols, *Adv. Lipid Res. 15*, 233–324.
3. Quílez, J., García-Lorda, P., and Salas-Salvadó, J. (2003) Potential Uses and Benefits of Phytosterols in Diet: Present Situation and Future Direction, *Clin. Nutr. 22*, 343–351.
4. Hicks, K.B., and Moreau, R.A. (2001) Phytosterols and Phytostanols: Functional Food Cholesterol Busters, *Food Technol. 55*, 63–67.
5. Marchante, H., Marchante, E., and Freitas, H. (2003) Invasion of the Portuguese Dune Ecosystems by the Exotic Species *Acacia longifolia* (Andrews) Willd: Effects at the Community Level, in *Plant Invasions: Ecological Threats and Management Solutions* (Child, L.E., Brock, J.H., Brundu, G., Prach, K., Pysek, P., Wade, P.M., and Williamson, M., eds.), pp. 75–85, Backhuys Publishers, Leiden, The Netherlands.
6. Seigler, D.S. (2003) Phytochemistry of *Acacia—sensu lato*, *Biochem. Syst. Ecol. 31*, 845–873.
7. Clark-Lewis, J.W., and Dainis, I. (1967). The Phytosterols from *Acacia* Species: α-Spinasterol and Stigmast-7-enol, *Aust. J. Chem. 20*, 1961–1974.
8. Mahato, S.B., Pal, B.C., and Price, K.R. (1989). Structure of Acaciaside, a Triterpenoid Trisaccharide from *Acacia auriculiformis*, *Phytochemistry 28,* 207–210.
9. Pech, G.G., Brito, W.F., Mena G.J., and Quijano, L. (2002) Constituents of *Acacia cedilloi* and *Acacia gaumeri*. Revised Structure and Complete NMR Assignments of Resinone, *Z. Natur. C-A-J. Biosci. 57*, 773–776.
10. Pohjamo, S., Willfor, S., and Holmbom, B. (2004) Wood Resin in *Acacia mangium* and *Acacia crassicarpa* Wood and Knots, *Appita J.*, in press.
11. Freire, C.S.R., Silvestre, A.J.D., and Pascoal Neto, C. (2002) Identification of New Hydroxy Fatty Acids and Ferulic Acid Esters in the Wood of *Eucalyptus globulus*, *Holzforschung 56*, 143–149.
12. Oliveira, L., Freire, C.S.R., Silvestre, A.J.D., Cordeiro, N., Torres, I., and Evtuguin, D. (2004) Steryl Glucosides from Banana Plant *Musa acuminata* Colla var. *Cavendish*, *Ind. Crops Prod.*, in press.
13. Combaut, G. (1986) GC–MS of Plant Sterols Analysis, in *Gas Chromatography/Mass Spectrometry* (Linskens, H.F., and Jackson, J.F., eds.), pp. 121–133, Springer-Verlag, Berlin.
14. Rahier, A., and Benveniste, P. (1989) Mass Spectral Identification of Phytosterols, in *Analysis of Sterols and Other Biologically Significant Steroids* (Nes, W.D., and Parish, E.J., eds.), pp. 223–250, Academic Press, San Diego.
15. Moreau, A.M., Powell, M.J., and Singh V. (2003) Pressurized Liquid Extraction of Polar and Nonpolar Lipids in Corn and Oats with Hexane, Methylene Chloride, Isopropanol, and Ethanol, *J. Am. Oil Chem. Soc. 80,* 1063–1067.
16. Freire, C.S.R., Silvestre, A.J.D., Pascoal Neto, C., Domingues, P., and Silva, A.M.S. (2004) New Glucosides in the Wood and Bark of *Eucalyptus globulus* and Kraft Pulps. *Holzforschung 58*, 501–503.
17. Gafur, M.A., Obata, T., Kiuchi, F., and Tsuda, Y. (1997) *Acacia concinna* Saponins. I. Structures of Prosapogenols Concinnosides A–F, Isolated from the Alkaline Hydrolysate of the Highly Polar Saponin Fraction, *Chem. Pharm. Bull. 45*, 620–625.
18. Duke, J.A. (1992) *Handbook of Phytochemical Constituents of GRAS Herbs and Other Economic Plants*, CRC Press, Boca Raton, FL.
19. Grunwald, C., and Huang, L.-S. (1989) Analysis of Steryl Glycosides, in *Analysis of Sterols and Other Biologically Significant Steroids* (Nes, W.D., and Parish, E.J., eds.), pp. 49–60, Academic Press, San Diego.
20. Gutiérrez, A., and del Río, J.C. (2001) Gas Chromatography/Mass Spectrometry Demonstration of Steryl Glycosides in Eucalypt Wood, Kraft Pulp and Process Liquids, *Rapid Commun. Mass Spectrom. 15*, 2515–2520.
21. Serreqi, A.N., Leone, R., del Rio, L.F., Mei, S., Fernandez, M., and Breuil, C. (2000) Identification and Quantification of Important Steryl Esters in Aspen Wood, *J. Am. Oil Chem. Soc. 77*, 413–418.
22. Uchida, K., Mizuno, H., Hirota, K., Takeda, K., Takeuchi, N., and Ishikawa, Y. (1983) Effects of Spinasterol and Sitosterol on Plasma and Liver Cholesterol Levels and Biliary and Fecal Sterol and Bile-Acid Excretions in Mice, *Jpn. J. Pharmacol. 33*, 103–112.
23. Villasenor, I.M., and Domingo, A.P. (2000) Anticarcinogenicity Potential of Spinasterol Isolated from Squash Flowers, *Teratog. Carcinog. Mutagen. 20*, 99–105.

24. Jeong, S.I., Kim, K.J., Choi, M.K., Keum, K.S., Lee, S., Ahn, S.H., Back, S.H., Song, J.H., Ju, Y.S., Choi, B.K., and Jung, K.Y. (2004) α-Spinasterol Isolated from the Root of *Phytolacca americana* and Its Pharmacological Property on Diabetic Nephropathy, *Planta Med. 70*, 736–739.
25. Iwatsuki, K., Akihisa, T., Tokuda, H., Ukiya, M., Higashihara, H., Mukainaka, T., Iizuka, M., Hayashi, Y., Kimura, Y., and Nishino, H. (2003) Sterol Ferulates, Sterols, and 5-Alk(en)yl-resorcinols from Wheat, Rye, and Corn Bran and Their Inhibitory Effects on Epstein–Barr Virus Activation, *J. Agric. Food Chem. 51*, 6683–6688.
26. Arisawa, M., Kinghorn, A.D., Cordell, G.A., Phoebe, C.H., and Fansworth, N.R. (1985) Plant Anticancer Agents. XXXVI. Schottenol Glucoside from *Baccharis coridifolia* and *Ipomopsis aggregata*, *Planta Med. 6*, 544–545.

METHOD

Foam Fractionation of Exo-lipases from a Growing Fungus (*Pleurotus sapidus*)

Diana Linke[a], Holger Zorn[a], Birte Gerken[b], Harun Parlar[b], and Ralf G. Berger[a,*]

[a]Universität Hannover, Institut für Lebensmittelchemie, D-30453 Hannover, Germany, and [b]TU München, Lehrstuhl für Chemisch-Technische Analyse und Chemische Lebensmitteltechnologie, D-85354 Freising, Germany

ABSTRACT: Active lipases were isolated from the culture supernatant of the basidiomycetous fungus *Pleurotus sapidus* by foam fractionation. The pH value, the gas flow, and the foaming period were systematically varied to optimize the transport of the enzymes into the foam phase. On a 70-mL scale, a maximum recovery of hydrolytic activity of 95% was obtained at pH 7.0 and 60 mL N_2 min^{-1} after 50 min. The procedure, with minor modifications, was also applicable to native pellet cultures of *P. sapidus*. The same recovery of 95% was achieved, with purification and enrichment factors of 11.6 and 28.0, respectively.

Paper no. L9684 in *Lipids 40*, 323–327 (March 2005).

Foam fractionation belongs to the group of adsorptive bubble separation techniques. As bubbles rise through a liquid phase that contains the target solute, the most surface-active molecules preferentially adsorb onto the interfacial area. Bubbles leaving the surface of the feed solution carry both adsorbed compound and bulk liquid into the emerging column of foam. The interstitial liquid drains back along the lamella of the bubbles and returns nonadsorbed solutes to the retentate. The emerging foam does not reach a thermodynamic equilibrium; it becomes drier, shows coalescence, and finally collapses into a liquid foamate. Because of the high surface-to-volume ratio of a foam, the foamate is enriched in the surface-active target compound. Ostwald (1) investigated foam fractionation for the isolation of natural compounds and attained patent protection of this technology as early as 1920. In recent years, foam fractionation has been increasingly researched for the separation of surface-active, low-molecular-mass compounds from diluted aqueous solutions (2,3). As amphiphilic species, proteins are foaming agents, and several researchers have used foam fractionation successfully for the isolation of β-casein and plant storage proteins (4,5). However, by adsorption of a protein onto the anisotropic gas–liquid interface, partial unfolding of the tertiary structure may occur, resulting in a decrease or loss of bioactivity (6,7). Generally, the ability to develop a stable foam depends on the surface properties of the protein molecules (8). With increasing hydrophobicity, the surface tension of the solution decreases and the concentration of the target protein in the foam is increased (9,10). The dynamics of foam formation, foam structure, and foam properties are affected by a number of operational parameters, e.g., gas flow rate (11). Mathematical models of foam fractionation processes have been compiled by Du *et al.* (3) and Suzuki and Maruyama (12).

Typically, lipases are bipolar molecules distinguished by an interfacial mode of catalytic action (13), which may render them particularly suitable for isolation by foam fractionation. In submerged cultures of fungi, some of the lipases are secreted into the growth medium (14,15). This suggests their immediate separation by a batch-type foaming of the nutrient medium. In this study, lipases were produced by the basidiomycete *Pleurotus sapidus*, using Tween 80 as an inducer, and were isolated from either the clear supernatant or the pellet suspension culture.

METHODS

Chemicals. Tris hydrochloride and agarose were obtained from Roth (Karlsruhe, Germany); manganese sulfate monohydrate, ammonium nitrate, BSA, and dipotassium hydrogen phosphate were from Fluka (Seelze, Germany); D-(+)-glucose monohydrate, L-asparagine monohydrate, yeast extract, potassium dihydrogen phosphate, sodium hydroxide, hydrochloric acid, Coomassie Brilliant Blue G-250, and EDTA were from Merck (Darmstadt, Germany); Tween 80, magnesium sulfate, ferrous(III) chloride × $6H_2O$, calcium chloride × $2H_2O$, sodium chloride, and copper sulfate × $7H_2O$ were from Riedel-de Haën (Seelze, Germany); and zinc sulfate × $7H_2O$ and phenolphthalein were from J.T.Baker B.V. (Deventer, The Netherlands). Ethanol (96%) was from Kraul & Wilkening und Stelling (Hannover, Germany). High-purity water was prepared with an E-pure water purification system (Barnstead, Dubuque, IA).

Cultivation and lipase production. Mycelia of *P. sapidus* [8266 DSM (Deutsche Sammlung von Mikroorganismen und Zellkulturen)] were maintained on 1.5% agar plates with standard nutrient liquid (SNL) medium according to Zorn *et al.* (15). Precultures of *P. sapidus* were prepared from a mycelial block (1 cm^2) as inoculum, which was excised from the agar plate and placed in a 300-mL Erlenmeyer flask containing 100 mL of SNL medium. After treatment with an UltraTurrax homogenizer (Janke & Kunkel, Staufen, Germany), the fungal culture was incubated for 7 d at 150 rpm and 24°C. For the production of lipase, three different main cultures were prepared in 500-mL Erlenmeyer flasks containing 250 mL SNL, 250 mL

SNL without glucose, and 250 mL mineral salt medium by transferring 20 mL of the preculture into each flask (15). The secretion of lipase into the medium was induced by addition of 0.4% (vol/vol) Tween 80 to the main cultures, which were then incubated at 150 rpm and 24°C. At the time of maximal lipase activity, the supernatant was separated from the mycelium by filtration under reduced pressure (filter paper #595; Schleicher & Schuell, Dassel, Germany). Media and equipment were autoclaved prior to use, and sterile techniques were applied throughout the procedures.

Protein determination. Protein concentration was determined according to Lowry *et al.* (16) using BSA as a standard.

Lipase assay. Hydrolytic activity was quantified by monitoring the FFA resulting from the hydrolysis of Tween 80 by a titrimetric assay. Samples were adjusted to pH 7.0 with 0.1 M NaOH or 0.1 M HCl. The reaction mixture containing 2.16 g of Tween 80, 5 mL of 50 mM Tris/HCl buffer, pH 7.0, and 2 mL of test solution were incubated in a water bath at 37°C and 160 rpm for 15 to 60 min depending on enzyme activity. The reaction was terminated by adding 5 mL of ethanol. Blanks were prepared with an inactivated enzyme solution. The FFA were titrated with 50 mM NaOH using 2% ethanolic phenolphthalein as an indicator. The lipase activity was calculated from the difference between the blank and the sample. One unit of enzyme was defined as 1 μmol of FFA released per minute under the specified conditions.

Isoelectric focusing (IEF) and lipase activity staining. IEF PAGE was performed on a Multiphor II system (Pharmacia LKB) using Servalyt^{TM} Precotes^{TM} precast gels with an immobilized pH gradient of pH 3 to 6 (Serva, Heidelberg, Germany). The isoelectric point (pI) of the lipase was estimated using a low-pI (2.8 to 6.5) calibration kit (Amersham Biosciences, Freiburg, Germany). Gels were silver stained. For activity staining, a Tween 80–agarose-overlay gel was developed. Agarose (2%) was dissolved in a solution of 0.004 mg mL^{-1} Tris and 0.0125 mg mL^{-1} NaCl under boiling. Equivalent volumes of 0.5 mg mL^{-1} Tween 80 and 0.01 mg mL^{-1} CaCl$_2$ were added, and the pH was adjusted to 7.0 using 0.01 N NaOH. After focusing, the IEF gel was incubated on the Tween 80–agarose overlay at 37°C for 3.5 h, and the overlay gel was covered with 0.1 N NaOH to visualize the hydrolytic activity.

Configuration of equipment and experimental procedure for foam fractionation. The foaming device consisted of a cylindrical glass chamber (length, 18 cm; diameter, 3 cm) with a porous frit (P3, porosity 16 to 40 μm), a column (length, 27 cm; diameter, 1.6 cm), a glass bowl (250 mL, 7.7 cm equatorial diameter, or 500 mL, 9.5 cm equatorial diameter), a horseshoe bend, and a receiving flask (Fig. 1). Experiments were carried out with 70 mL of enzyme solution. Nitrogen was passed through the frit, and the rising foam collapsed in the receiver. Samples for protein and activity analyses were taken from the initial solution, from the foamed sample solution (retentate), and from the liquefied foam.

Calculations. The following calculations were made for each foam fractionation:
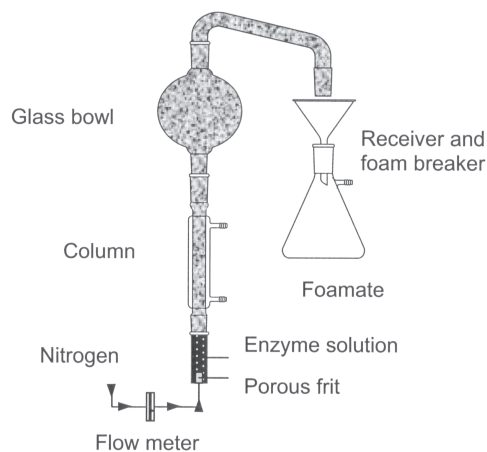
FIG. 1. Scheme of the foam fractionation device.

recovery of protein (RP) =

$$\frac{\text{mass of protein (mg) in the liquefied foam}}{\text{mass of protein (mg) in the initial solution}} \times 100\% \qquad [1]$$

recovery of activity (Ra) =

$$\frac{\text{activity (U) in the liquefied foam}}{\text{activity (U) in the initial solution}} \times 100\% \qquad [2]$$

purification factor (P) =

$$\frac{\text{specific activity (U mg}^{-1}\text{) in the liquefied foam}}{\text{specific activity (U mg}^{-1}\text{) in the initial solution}} \qquad [3]$$

enrichment factor (E) =

$$\frac{\text{activity (U mL}^{-1}\text{) in the liquefied foam}}{\text{activity (U mL}^{-1}\text{) in the initial solution}} \qquad [4]$$

All quantitative data represent average values of at least duplicate analyses.

RESULTS

Influence of medium composition on extracellular lipase activity. The extracellular lipase activity of *P. sapidus* cultures containing different carbon sources was determined over a period of 7 d. The highest hydrolytic activity (312 U L^{-1}) was observed after 5 d in SNL medium without glucose (Fig. 2). This supernatant was used for foam fractionation as described in the following section.

Foam fractionation of lipases from the culture supernatant. The Rp and Ra were examined at varying pH values of the enzyme-containing solutions. The following parameters were held constant: 40 mL N$_2$ min^{-1}, 50-min foaming period, 24°C. The pH was adjusted from 5.0 to 8.0 with 0.1 N NaOH or 0.1 N HCl, respectively. The optimal pH value was 7.0, where 54% of activity was received in the foam, and the loss of activity during the fractionation process was about 5%. The minimal recovery in the foam and a loss of activity of 28% were observed at pH 8.0
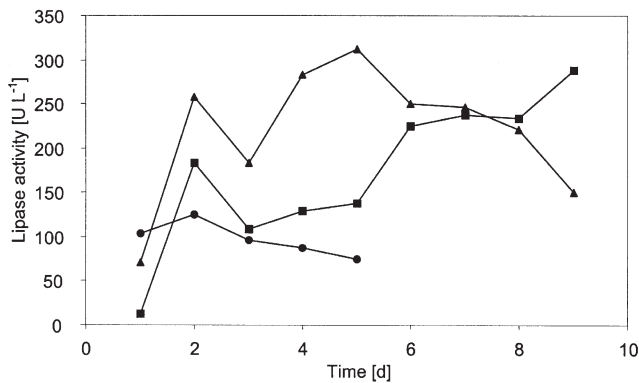
FIG. 2. Lipase production as affected by the carbon source. Standard nutrient liquid (SNL) medium containing 3% (wt/vol) glucose and 0.4% (vol/vol) Tween 80 (●) (solution became highly viscous after 5 d); SNL without glucose but 0.4% (vol/vol) Tween 80 (▲); mineral salt medium with 0.4% (vol/vol) Tween 80 (■).

(Fig. 3). The kinetics of enzyme transport into the foam phase was investigated over a period of 90 min. A foaming period of 50 min gave the highest Ra. By increasing the gas flow to 60 mL min^{-1}, the recovery of hydrolytic activity rose to 95% (Fig. 4). A marginal loss of total activity (2.8%) was observed, i.e., 2.2% of activity remained in the retentate. P was calculated as 2.9, and E was 3.3.

Foam fractionation of the native pellet culture. When a native suspension culture of *P. sapidus* was submitted to the foaming procedure, most of the mycelium pellets remained in the retentate. Some smaller pellets rose up with the foam and were easily separated using a suction filter funnel. The recovery of hydrolytic activity in the liquefied, cell-free foam was 93%, with a loss of total activity of 6%. P was estimated as 3.0 and E was 3.8. To observe the kinetics of transport of lipases during the foaming period, samples were drawn every 5 min, and the liquefied samples were tested for activity on a Tween 80–agarose gel. Hydrolytic activity was detectable in each of the foam fractions, but no quantitative analyses were performed.

To increase the E and P of foam fractionation of the suspension culture, the volume of the glass bowl was doubled to 500

FIG. 4. Recovery of lipase activity in the foam phase after foam fractionation from culture supernatant as a function of flow rate (pH 7.0, 50 min, 24°C, 250-mL glass bowl).

mL. The aging foam became drier due to the increased drainage effect. As a result, the E and P were significantly enhanced (Fig. 5).

DISCUSSION

Separation of active lipases. Foam systems consist of a thin liquid film including a gas phase (10,17). The two phases are separated by a thin interfacial region to which amphiphilic solutes may adsorb. It has been common academic opinion that adsorption of an enzyme onto an interface comes along with denaturation (18). Betancor *et al.* (19) successfully prevented enzyme inactivation by coating the enzyme surface using a hydrophilic shell of dextran-aldehyde. In the present study, no modifications of the protein structure were necessary to separate active lipases from growing cultures of *P. sapidus* (Fig. 2) by foam fractionation.

pH dependence. Surface activity, stability, and packaging at the gas–liquid interface of a protein are maximal at its pI (20–22). Accordingly, transport of the target protein into the foam phase should be most efficient at its pI. However, the maximal transport of the lipase of *P. sapidus* was observed at pH 7.0 (Fig. 3), far from the pI of the native isoenzymes (4.5 to 5.4), and only about 3 to 6% of the catalytic activity of the enzymes was lost during the process (Fig. 4).

FIG. 3. Recovery of lipase activity in the foam after foam fractionation from culture supernatant as a function of pH (50 min, 40 mL N$_2$ min^{-1}, 24°C, 250-mL glass bowl).

FIG. 5. Recovery of activity (Ra) and total protein (Rp), purification factor (P), and enrichment factor (E) of foam fractionation from native suspension cultures of *Pleurotus sapidus* (pH 7.0, 50 min, 24°C, 500-mL glass bowl).

Liu *et al.* (23) accumulated about 40% of trypsin and about 50% of catalase activity from aqueous solutions into the foam. In the absence of a detergent, recoveries depended on the type of sparging gas used rather than on the actual pH value. In the present experiments, however, the loss of total hydrolytic activity increased with an increasing distance from the pH optimum (Fig. 3).

Effect of Tween 80. As mentioned, the optimal pH value for the separation process was 7.0 and not the pI. This is explained by residual amounts of the lipase inducer, Tween 80, in the feed solution. The detergent may have formed associations with the enzyme molecules possessing deviating apparent pI values. Proteins are generally less surface active than low-molecular-mass detergents, such as polyoxyethylene sorbitan monostearate, because of the high free energy levels of protein coverage of the interface (8). The addition of Tween 80 to processed foods, such as bakery products and ice cream, is common in Europe (EU Declaration Numbers E491 to E495) and in other countries worldwide. Looking at the low absolute concentration of technical enzymes, a carryover into processed foods may be tolerable.

Gas flow. Gas flow was identified as another quantifiable parameter of the foaming process. Flow rates of 6 mL min^{-1} resulted in a distinct degradation of β-glucosidase (24). Lipases in the present study were more shear tolerant, as indicated by the quantitative transport of the hydrolytic activity at a gas flow rate of 60 mL min^{-1} (Fig. 4).

Design of the foam fractionation device. Foam drainage and competition for the interface determine the E of a protein and hence the overall efficiency of the separation. Whereas the population of molecules at the interface depends on chemical parameters, such as concentration, hydrophobicity, diffusivity, and conformational flexibility (10), the drainage (or kinetic stability) of a foam can be affected by processing parameters, such as flow rate, and by the design of the foaming device. As in previous work on low-molecular-mass compounds (5), lengthening the height of the foaming column was inefficient. Doubling the volume of the glass bowl improved the E and P (Fig. 5). Under the conditions chosen, the process time was long enough to allow for adequate drainage of the interstitial liquid and short enough to minimize protein residence and unfolding at the interface. Because the liquid film of the lamella drained continuously, the final volume of the liquefied foam was much smaller than the volume of the feed phase.

Comparison with alternative processes. Conventional purification processes of two lipase isoforms of *Candida rugosa* (Lip1 and Lip2) by precipitation, hydropho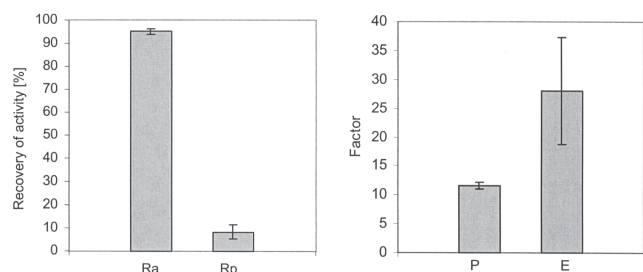bic interaction chromatography, dialysis, and anionic exchange chromatography recovered 45% of Lip1, with P of 5.3, and 4.7% of Lip2, with P of 4.1 (25). Yadav *et al.* (26) purified a lipase from *Aspergillus terreus* in five steps with a yield of 18% and a P of 11.9. The present experiments yielded lipase recoveries of 95% of total activity, with P of 11.6. Because an increase in hydrophobicity leads to a corresponding increase in protein adsorption onto the gas–liquid interface, the results indicate that fungal lipases appear to possess sufficient hydrophobic moi-

eties to be suitable for a separation by foam fractionation. In line with this consideration, Fernandes *et al.* (9) attached a hydrophobic fusion tag (Trp-Pro)$_4$ to a recombinant cutinase from *Fusarium solani pisi* and achieved higher recoveries in the foam (98%) as compared with the wild-type cutinase (52%). Thus, foam fractionation of fungal lipases offers potential as a valuable component of novel purification schemes.

Competing Interests Statement

The authors declare that they have no competing financial interests.

REFERENCES

1. Ostwald, W. (1920) Verfahren zum Verdampfen von Flüssigkeiten, Patentschrift Nr. 327976, Klasse 12a, Gruppe 2, Reichspatentamt.
2. Britten M., and Lavoie, L. (1992) Foaming Properties of Proteins as Affected by Concentration, *J. Food Sci. 57*, 1219–1222.
3. Du, L., Loha, V., and Tanner, R.D. (2000) Modeling a Protein Foam Fractionation Process, *Appl. Biochem. Biotechnol. 84–86*, 1087–1099.
4. Brown, A.K., Kaul, A., and Varley, J. (1999) Continuous Foaming for Protein Recovery: Part I. Recovery of β-Casein, *Biotechnol. Bioeng. 62*, 278–290.
5. Parlar, H., Gschwendtner, O., Anschütz, A., Leupold, G., and Görg, A. (2001) Influence of Selected Parameters on the Isoelectric Adsorptive Bubble Separation (IABS) of Potato Proteins, *Adv. Food Sci. 23*, 2–10.
6. Schügerl, K. (2000) Recovery of Proteins and Microorganism from Cultivation Media by Foam Flotation, *Adv. Biochem. Eng. Biotechnol. 68*, 191–233.
7. Belitz, H.-D., Grosch, W., and Schieberle, P. (2004) *Food Chemistry*, 3rd rev. edn., pp. 61–62, Springer Verlag, Berlin.
8. Damodaran, S. (1997) Protein-Stabilized Foams and Emulsions, in *Food Proteins and Their Applications* (Damodaran, S., and Paraf, A., eds.), pp. 57–110, Marcel Dekker, New York.
9. Fernandes, S., Mattiasson, B., and Hatti-Kaul, R. (2002) Recovery of Recombinant Cutinase Using Detergent Foam, *Biotechnol. Prog. 18*, 116–123.
10. Lockwood, C.E., Bummer, P.M., and Jay, M. (1997) Purification of Proteins Using Foam Fractionation, *Pharm. Res. 14*, 1511–1515.
11. Varley, J., Brown, A.K., Boyd, J.W.R., Dodd, P.W., and Gallagher, S. (2004) Dynamic Multi-point Measurement of Foam Behaviour for a Continuous Fermentation over a Range of Key Process Variables, *Biochem. Eng. J. 20*, 61–72.
12. Suzuki, A., and Maruyama, H. (2001) Influence of Liquid Properties and Operating Variables on Enrichment Ratio in Nonfoaming and Foaming Adsorptive Bubble Separation Techniques, *J. Colloid Sci. 238*, 54–61.
13. Arreguín-Espinosa, R., Arreguín, B., and Gonzáles, C. (2000) Purification and Properties of a Lipase from *Cephaloleia presignis* (Coleoptera, Chrysomelidae), *Biotechnol. Appl. Biochem. 31*, 239–244.

14. Freire, D.M., Teles, E.M.F., Bon, E.P.S., and Sant' Anna, G.L. (1997) Lipase Production by *Penicillium restrictum* in a Bench-Scale Fermenter, *Appl. Biochem. Biotechnol. 63–65*, 409–421.

15. Zorn, H., Breithaupt, D.E., Takenberg, M., Schwack, W., and Berger, R.G. (2003) Enzymatic Hydrolysis of Carotenoid Esters of Marigold Flowers (*Tagetes erecta* L.) and Red Paprika (*Capsicum annuum* L.) by Commercial Lipases and *Pleurotus sapidus* Extracellular Lipase, *Enzyme Microbiol. Technol. 32*, 623–628.

16. Lowry, O.H., Rosebrough, N.J., Farr, A.L., and Randall, R.J. (1951) Protein Measurement with the Folin Phenol Reagent, *J. Biol. Chem. 193*, 265–275.

17. Schramm, L.L., and Wassmuth, F. (1994) Foams: Basic Principles, in *Foams: Fundamentals and Applications in Petroleum Industry* (Schramm, L.L., ed.), *Adv. Chem. 242*, pp. 3–45, American Chemical Society, Washington, DC.

18. Cumper, C.W.N., and Alexander, A.E. (1950) The Surface Chemistry of Proteins, *Trans. Faraday Soc. 46*, 235–253.

19. Betancor, L., López-Gallego, F., Hidalgo, A., Alonso-Morales, N., Fuentes, M., Fernández-Lafuente, R., and Guisán, J. (2004) Prevention of Interfacial Inactivation of Enzymes by Coating the Enzyme Surface with Dextran-Aldehyde, *J. Biotechnol. 110*, 201–207.

20. DeSouza, A.H.G., Tanner, R.D., and Effler, W.T. (1991) The Effect of pH and Gas Composition on the Bubble Fractionation of Proteins, *Appl. Biochem. Biotechnol. 28/29*, 655–666.

21. Charm, S.E., Morningstar, J., Matteo, C.C., and Paltiel, B. (1966) The Separation and Purification of Enzymes Through Foaming, *Anal. Biochem. 15*, 498–508.

22. Noel, J., Prokop, A., and Tanner, R.D. (2002) Foam Fractionation of a Dilute Solution of Bovine Lactoferrin, *Appl. Biochem. Biotechnol. 98–100*, 395–402.

23. Liu, Z., Liu, Z., Wang, D., Ding, F., and Yuan, N. (1998) On the Denaturation of Enzymes in the Process of Foam Fractionation, *Bioseparation 7*, 167–174.

24. Burapatana, V., Prokop, A., and Tanner, R.D. (2004) Degeneration of β-Glucosidase Activity in a Foam Fractionation Process, *Appl. Biochem. Biotechnol. 113–116*, 619–625.

25. Linko, Y.-Y., and Wu, X.Y. (1996) Biocatalytic Production of Useful Esters by Two Forms of Lipase from *Candida rugosa*, *J. Chem. Tech. Biotechnol. 65*, 163–170.

26. Yadav, R.P., Saxena, R.K., Gupta, R., and Davidson, W.S. (1998) Purification and Characterization of a Regiospecific Lipase from *Aspergillus terreus*, *Biotechnol. Appl. Biochem. 28*, 243–249.

ARTICLES

Associations Between Apolipoprotein E Genotype and Circulating F$_2$-Isoprostane Levels in Humans

Marion Dietrich[a], Youqing Hu[a], Gladys Block[a], Estibaliz Olano[b], Lester Packer[c], Jason D. Morrow[d], Mark Hudes[e], Gulbahar Abdukeyum[b], Gerald Rimbach[f], and Anne M. Minihane[b,*]

[a]School of Public Health, University of California, Berkeley, California, [b]Hugh Sinclair Unit of Human Nutrition, University of Reading, Reading, United Kingdom, [c]Department of Molecular Pharmacology and Toxicology, School of Pharmacy, University of Southern California, Los Angeles, California, [d]Vanderbilt University, Division of Clinical Pharmacology, Nashville, Tennessee, [e]Department of Nutritional Sciences, University of California, Berkeley, California, and [f]Institute of Human Nutrition and Food Science, Christian Albrechts University, Kiel, Germany

ABSTRACT: Apolipoprotein E (apoE), an important determinant of plasma lipoprotein metabolism, has three common alleles (ε2, ε3, and ε4). Population studies have shown that the risk of diseases characterized by oxidative damage, such as coronary heart disease and Alzheimer's disease, is significantly higher in ε4 carriers. We evaluated the association between apoE genotypes and plasma F$_2$-isoprostane levels, an index of lipid peroxidation, in humans. Two hundred seventy-four healthy subjects (104 males, 170 females; 46.9 ± 13.0 yr; 200 whites, 74 blacks; 81 nonsmokers, 64 passive smokers, and 129 active smokers) recruited for a randomized clinical antioxidant intervention trial were included in this analysis. ApoE genotype was determined by PCR and restriction enzyme digestion. Free plasma F$_2$-isoprostane was measured by GC–MS. Genotype groups were compared using multiple regression analysis with adjustment for sex, age, race, smoking status, body mass index, plasma ascorbic acid, and β-carotene. Subjects with ε3/ε4 and ε4/ε4 genotype (ε4-carriers) and with ε2/ε3 and ε3/ε3 (non-ε4-carriers) were pooled for analysis. In subjects with high cholesterol levels (total cholesterol above 200 mg/dl), plasma F$_2$-isoprostane levels were 29% higher in ε4 carriers than in non-ε4-carriers ($P = 0.0056$). High-cholesterol subjects that are ε4 carriers have significantly higher levels of lipid peroxidation as assessed by circulating F$_2$-isoprostane levels.

Paper no. L9670 in *Lipids 40,* 329–334 (April 2005).

Apolipoprotein E (apoE) genotype is recognized as a determinant of cardiovascular disease and Alzheimer's disease (AD) risk (1–5). The majority of the apoE protein is produced by the liver and is traditionally known as a mediator of lipoprotein metabolism in both hepatic and extrahepatic tissue (6,7). In the circulation, it is found as an integral component of chylomicrons (CM), VLDL, and HDL. In addition to being centrally involved in lipoprotein metabolism, new localized roles for apoE in cardiovascular biology have recently been identified (8,9).

Point mutations in the gene locus for apoE, located on the long arm of chromosome 19, result in changes in the primary structure of the 299-amino acid protein end product with Arg/Cys substitutions at positions 112 and 158 (apoε2 Cys 112 Cys 158, apoε3 Cys 112 Arg 158, apoε4 Arg 112 Arg 158). In all populations, the ε3 allele is the most frequent. Apoε3 homozygotes (ε3/ε3), apoε2 heterozygotes and homozygotes (ε2/ε3, ε2/ε2), and ε4 heterozygotes and homozygotes (ε3/ε4, ε4/ε4) constitute approximately 55–70, 5–15, and 20–35%, respectively, of North American and European populations (10,11). Numerous observation studies have confirmed that chronic diseases such as coronary heart disease (CHD), stroke, and AD are significantly higher in ε4 carriers (1–5). In a meta-analysis of 10 published studies, Wilson and co-workers (1) reported odds ratios (OR) of CHD of 0.76–2.44 for clinical CHD associated with carrying the ε4 allele relative to the common ε3/ε3 genotype. Furthermore, apoE genotype is highly predictive of maturity-onset AD. In a community-based study involving 6,000 AD patients, the OR for AD was 3.2 and 14.9 in ε3/ε4 and ε4/ε4 (1–3% of Westernized populations), respectively, when individuals were compared with matched controls (ε3/ε3) (4). These differences in disease risk have traditionally been attributed to higher circulating LDL cholesterol (LDLC) levels in the apoε4 subgroups, which are thought to be due to the combined effects of reduced hepatic LDL-receptor expression, increased VLDL to LDL conversion, and an increased utilization of dietary cholesterol (12–14) in this subgroup. However, it is unlikely that the 3–8% higher LDLC observed in apoε4 carriers (14,15) is solely responsible for the increased CHD and AD incidence.

It is well recognized that free radical-mediated oxidative stress is involved in both the initiation and progression of many chronic diseases (16–19). Sources of oxidative stress include exogenous factors such as cigarette smoke or UV light exposure as well as endogenous sources such as reactive oxygen/nitrogen species (ROS/RNS) produced during normal physiological processes including phagocytosis and oxidative phosphorylation (18).

We hypothesize that the pathogenesis of these oxidative stress-associated diseases may be attributable in part to a differential antioxidant capacity of the endogenous apoE isoforms. Reduced antioxidant function of apoε4 has previously been described in *in vitro*, cell culture, animal, and *ex vivo*

models of AD (20–22). Studies in mice have shown that F_2-isoprostanes, a lipid peroxidation biomarker of oxidative stress, are increased in the brains of apoE-deficient mice (22), indicating that apoE may be associated with oxidant/antioxidant balance *in vivo*. Studies in Alzheimer patients showed that lipid peroxidation was significantly elevated in tissues of subjects who are homozygous for the ε4 allele compared with ε3/ε3 cases and controls (23). However, the impact of apoE genotype on oxidative stress status in nondiseased, apparently healthy individuals is largely unknown and is the subject of the current investigation.

SUBJECTS AND METHODS

Subjects (81 nonsmokers, 64 passive smokers, and 129 active smokers) were enrolled in an intervention study on the effect of antioxidant supplements on oxidative damage in active and passive smokers (24). The study was conducted in Berkeley and Oakland, California, between 1998 and 1999, and was approved by the institutional review boards of the University of California, Berkeley, and of Kaiser Permanente. Exclusion criteria for participation in the study were reported consumption of ≥4 servings of fruit and vegetables per day; intake of more than 2 alcoholic drinks per day; a history of alcohol problems less than 1 year ago; pregnancy; use of blood-thinning drugs; a history of hemochromatosis, kidney stones, or any other kidney problems, hepatitis, diabetes, or HIV infection; and cancer, stroke, or heart attack within the past 5 years. The detailed design of the antioxidant intervention study on active smokers and passive smokers is described elsewhere (24,25). Baseline plasma samples from the intervention study were used for this analysis.

Clinical protocols. Blood samples were obtained from all participants after an overnight 12-h fast. Venous blood was drawn into EDTA vacutainers and centrifuged at 5°C for 10 min at $1200 \times g$. Plasma isolation and freezing of samples (−70°C) was conducted within 1 h of taking the sample. Plasma measures included carotenoids, ascorbic acid, α- and γ-tocopherol, cholesterol, LDLC, HDL cholesterol, triglycerides (TG), transferrin saturation, C-reactive protein, malondialdehyde, F_2-isoprostanes, and cotinine. All participants completed the 1998 version of the Block food-frequency questionnaire. Other data obtained included body mass index (BMI), blood pressure, and alcohol intake.

Laboratory measurements. (i) Measurement of F_2-isoprostanes in plasma. Free F_2-isoprostane levels in plasma were quantified, after purification and derivatization, by selected ion monitoring GC/negative ion chemical ionization-MS employing $[^2H_4]8$-iso-$PGF_{2\alpha}$ as an internal standard. Compounds were analyzed as pentafluorobenzyl ester and trimethylsilyl ether derivatives by monitoring the M − 181 ions (*m/z* 569 Da for endogenous F_2-isoprostane and *m/z* 573 Da for $[^2H_4]8$-iso-$PGF_{2\alpha}$). This assay has an intra-individual variability precision of ±6% and an accuracy of 96% as measured by using an internal standard. Interday variability is <6% (26).

(ii) Measurement of apoE genotype. Genomic DNA was isolated from buffy coat using the QIAamp DNA Blood Mini Kit protocol (Qiagen Ltd., Crawley, United Kingdom), followed by PCR to amplify specific sequences of DNA as described earlier (14). ApoE genotype was identified by restriction enzyme digestion with PAGE used to separate the PCR fragments. Individual genotypes were characterized from the fragment patterns.

(iii) Plasma analysis. Carotenoids were measured by RP-HPLC (27). Ascorbic acid was determined spectrophotometrically using 2,4-dinitrophenylhydrazine as a chromogen (28). Concentrations of cotinine were determined by GC with nitrogen-phosphorus detection (29,30). Total cholesterol and TG levels were measured by end point spectroscopy (Sigma-Aldrich, St. Louis, MO).

Statistical analysis. Statistical analyses were conducted using SAS Version 8.2 (Cary, NC). Subjects with ε3/ε4 and ε4/ε4 genotypes were pooled due to small sample size in the ε4/ε4 genotype group. Non-ε4 subjects (ε2/ε3, ε3/ε3) were pooled to serve as the reference group. Subjects with ε2/ε4 genotype were excluded due to small sample size (*n* = 5). Subjects of race other than white and black were also excluded owing to the small sample size. Multiple regression analysis was conducted with the dependent variable plasma F_2-isoprostanes log-transformed. Variables examined as potential covariates included sex, race, age, BMI, smoking status, plasma vitamin C, α-tocopherol, γ-tocopherol, β-carotene, HDL cholesterol, LDLC, total cholesterol, TG, and cotinine levels. Potential effect modification was examined, including interactions of genotype with baseline plasma antioxidant levels, sex, race, total cholesterol, and LDLC. In Tables 2 and 3 the data are dichotomized by total cholesterol above and below 200 mg/dL.

RESULTS

One hundred four male and 170 female subjects were included in the analysis, with a mean (±SD) age of 46.9 ± 13.0 yr. In Table 1, apoε4 carriers (*n* = 73) and noncarriers (*n* = 201) were compared. No significant differences at *P* < 0.05 between these two groups were evident for any of the outcomes measured. However, the expected trends toward higher LDLC and total cholesterol in ε4 carriers were observed, although the 5–7% intergroup differences did not reach statistical significance.

While examining effect modification, a significant interaction between apoE genotype and plasma total cholesterol levels was found (*P* = 0.014). Therefore, subsequent stratification analysis was performed on the subgroups with circulating cholesterol levels above or below the clinical standard of total cholesterol (200 mg/dL). The subject characteristics were similar for the high and low cholesterol group (data not shown).

As shown in Table 2 and Figure 1, the apoε4 genotype was significantly associated with higher plasma F_2-isoprostane levels among high-cholesterol subjects (*P* = 0.0056), with 29% higher levels evident in this subgroup. Cholesterol, TG, and the lipid-soluble antioxidant vitamins α- and γ-tocopherol were investigated as possible covariates. They were not significantly

TABLE 1
Baseline Characteristics for All Subjects, and by Apolipoprotein (apoE) Genotype

| | | ApoE genotype | | |
| | All subjects | ε3/ε4 and ε4/ε4 | ε2/ε3 and ε3/ε3 | |
Subject characteristics	(n = 274)	(n = 73)	(n = 201)	P value
Sex				
Male	104	31	73	0.354
Female	170	42	128	
Race				
White	200	47	153	0.053
Black	74	26	48	
Current smoking status				
Nonsmoker	81	19	62	0.176
Passive smoker	64	13	51	
Smoker	129	41	88	
Body mass index (kg/m^2)				
Normal weight (<25)	94	24	70	0.296
Overweight (25–29.9)	101	32	69	
Obese (≥30)	79	17	62	
Age (yr)	46.9 (13.0)[a]	45.7 (12.5)	47.1 (13.3)	0.431
Plasma measures[b]				
F$_2$-isoprostanes[c] (pmol/L)	129.2 (70.1)	133.7 (72.5)	127.9 (70.4)	0.546
Ascorbic acid (mg/dL)	0.96 (0.45)	0.93 (0.48)	0.97 (0.44)	0.575
β-Carotene (μg/dL)	16.3 (17.0)	14.9 (12.3)	16.8 (18.6)	0.332
Cholesterol (mg/dL)	197.1 (44.1)	204.6 (49.0)	194.4 (41.9)	0.091
TG (mg/dL)	115.8 (69.5)	121.7 (70.8)	113.7 (69.8)	0.400
HDLC (mg/dL)	41.6 (12.3)	41.5 (14.3)	41.6 (11.4)	0.980
LDLC (mg/dL)	132.4 (38.9)	138.7 (43.4)	130.1 (36.6)	0.104
α-Tocopherol (mg/dL)	1.5 (0.6)	1.6 (0.7)	1.5 (0.6)	0.183
γ-Tocopherol (mg/dL)	0.28 (0.15)	0.30 (0.19)	0.27 (0.14)	0.231

[a]Means (SD).
[b]Plasma values shown are unadjusted for covariates.
[c]Arithmetic means. LDLC, LDL cholesterol; HDLC, HDL cholesterol.

TABLE 2
Adjusted Mean F$_2$-Isoprostane Levels by Genotype in Subjects with Plasma Total Cholesterol Above 200 mg/dL (n = 112)

Factor	Adjusted[a] mean F$_2$-isoprostane level (pmol/L)	F statistic[b]	P value[c]
ApoE genotype		8.02	0.0056
ε3/ε4 and ε4/ε4	115.7 (98.4, 136.1)		
ε2/ε3 and ε3/ε3	89.8 (80.3, 100.5)		
Sex		12.84	0.0005
Age		0.73	0.3957
Race		17.93	<0.0001
Current smoking status		4.72	0.0109
Body mass index		7.78	0.0007
Plasma ascorbic acid		10.33	0.0018
Plasma β-carotene		17.49	<0.0001

[a]Adjusted for the other variables shown.
[b]The F statistic measures the contribution of each variable to the prediction of plasma F$_2$-isoprostane levels.
[c]The P value represents the result after adjustment for all the other variables shown, performed by multiple regression analysis.
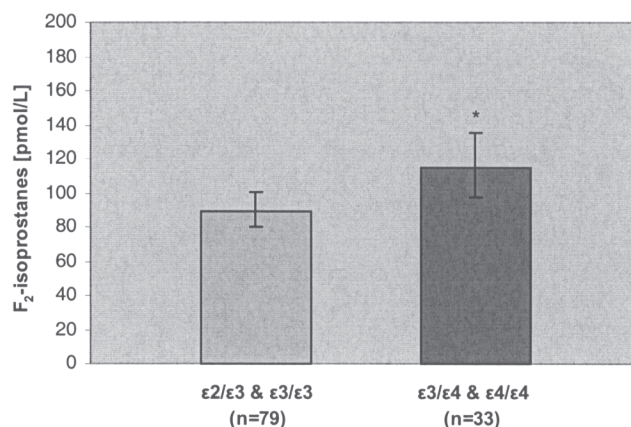
FIG. 1. Plasma F$_2$-isoprostane levels by genotype in subjects with plasma total cholesterol above 200 mg/dL. These are adjusted means (±SE); *significantly different: P = 0.0056.

TABLE 3
Adjusted Mean F$_2$-Isoprostane Levels by Genotype in Subjects with Plasma Total Cholesterol Below 200 mg/dL (n = 162)

Factor	Adjusted[a] mean F$_2$-isoprostane level (pmol/L)	F statistic[b]	P value[c]
ApoE genotype		0.72	0.3987
ε3/ε4 and ε4/ε4	99.5 (86.5, 114.5)		
ε2/ε3 and ε3/ε3	106.6 (97.1, 117.0)		
Sex		19.05	<0.0001
Age		0.00	0.9649
Race		14.69	0.0002
Current smoking status		3.72	0.0265
Body mass index		4.37	0.0143
Plasma ascorbic acid		9.39	0.0026
Plasma β-carotene		5.31	0.0225

[a]Adjusted for the other variables shown.
[b]The *F* statistic measures the contribution of each variable to the prediction of plasma F$_2$-isoprostane levels.
[c]The *P* value represents the result after adjustment for all the other variables shown, performed by multiple regression analysis.

associated with the dependent variable F$_2$-isoprostanes and therefore not included in the model, with inclusion/exclusion having little effect on the overall apoE/isoprostane relationship (data not shown).

No statistically significant association was observed between apoE genotype and F$_2$-isoprostane levels in individuals with a cholesterol level <200 mg/dL (P = 0.3987, Table 3). In addition, strong significant independent associations between sex, race, smoking status, BMI, plasma ascorbic acid, β-carotene, and circulating F$_2$-isoprostane were observed in both cholesterol subgroups. This has been previously reported by our group (31).

DISCUSSION

The effect of apoE genotype on LDL cholesterol cannot alone explain the differences in AD and CHD risk between ε4 carriers and the ε2 and ε3 subgroups. In advanced atherogenesis, a significant proportion of total apoE is produced by macrophages within the arterial lining (32). It is speculated that any differences in the antioxidant capacity of the apoE isoforms within the antioxidant-depleted, transition metal-rich environment of the vascular intima, which is rich in free radical-producing inflammatory cells, could make a significant contribution to atherogenesis.

In the current investigation, circulating levels of F$_2$-isoprostanes were used as an index of oxidative stress and lipid peroxidation. F$_2$-Isoprostanes have been widely used as a sensitive and specific marker of lipid peroxidation with significantly higher levels evident in CHD patients compared with matched controls (33). Specifically, levels have been shown to increase with advancing age, smoking, hypercholesterolemia, and diabetes (34–39). Furthermore, in addition to serving as an oxidative marker, F$_2$-isoprostanes exert direct proatherogenic proinflammatory properties and have been shown to act as vasoconstrictors and to stimulate platelet activation (33).

Our finding of higher plasma F$_2$-isoprostane levels in hy-

percholesterolemic individuals was consistent with earlier findings (38,39). For example, in the study of Davi and coworkers (39), a greater than twofold higher F$_2$-isoprostane level was evident in hypercholesterolemic subjects compared with age- and sex-matched controls. In the current study, a significant negative association between plasma β-carotene and F$_2$-isoprostane levels (P < 0.0001) as well as between plasma vitamin C and F$_2$-isoprostane levels was observed in the high-cholesterol group (P = 0.0018). This finding is consistent with previously published studies (31,40–42).

In individuals with a circulating cholesterol level below 200 mg/dL, apoE genotype did not emerge as an independent determinant of lipid peroxidation. However, in those subjects with total cholesterol above 200 mg/dL, a 29% higher F$_2$-isoprostane level was evident in apoε4 carriers relative to noncarriers. Differences in levels of lipid peroxidation between the apoE subgroups may be attributable to differences in the antioxidant activities of the apoE isoforms.

The antioxidant capacity of the apoE protein was first investigated with respect to neuronal damage in AD. In 1996, Miyata and Smith (21) investigated the antioxidant potential of the apoE isoforms with respect to their ability to protect against rat neuronal B12 cell death on exposure to hydrogen peroxide (H$_2$O$_2$). At physiological concentrations, all three apoE proteins significantly reduced H$_2$O$_2$-induced cell death, in the following order, ε2 > ε3 > ε4, with the ε2 protein being approximately twofold more effective compared with ε4 (21). Subsequent *in vitro* assays were consistent with the initial cellular work, with the authors indicating that differences in antioxidant capacity were attributable to the differential ability of the protein to bind transition metal ions. Consistent with these findings are data that demonstrate a differential *in vitro* oxidation of recombinant apoE using the myeloperoxidase system, with apoε4 being more susceptible than apoε3, which is in turn more susceptible than apoε2 (20). Furthermore, basal and activated oxidative damage and lipid peroxide levels in the following order, ε4 > ε3 > ε2, were evident in the postmortem brains of AD patients (23).

Evidence regarding the contribution of the apoE isoform to oxidative stress and of its implications for localized events in the artery wall that contribute to atherogenesis is limited. In the Northwick Park Heart Study II (NHPSII), following correction of the data for blood lipids and other known risk factors, Humphries and coworkers (43) speculated that the 2.79-fold increased risk of CHD events in ε4 smokers relative to the non-smoking combined group, with OR of 0.85 and 1.47 observed in ε2 carriers and ε3 homozygotes, respectively, may be due to the differential antioxidant capacity of the apoE protein isoforms. Although no direct evidence was provided by the authors, the data were suggestive of an exacerbation of oxidative stress in smokers by the apoε4 phenotype relative to the ε3 and ε2 smoking groups.

It is speculated that apoE isoform differences in antioxidant capacity could be attributable to a change in the tertiary configuration of the metal binding site of the protein. The mature 299-amino acid protein consists of an amino acid (residues 20–165)

and a carboxyl (225–299) terminal (NT and CT) separated by a hinge region, which in relation to lipoprotein metabolism are responsible for the ligand and lipid binding, respectively (44,45). The 3-D structure of the NT domain consists of four helix bundles, within which is thought to lie the tetrahedral metal-binding peptide sequence (46). It is speculated that variations in the Arg and Cys content of the isoforms lead to conformational changes in the protein structure owing to disruption in salt bridge formation (47), which could alter the metal-binding capacity. Likewise, although all three isoforms contain eight methionine residues, an apoE-specific protein conformational change may result in differences in exposure of methionine residues in the ε2, ε3, and ε4 isoforms. Methionine has been shown to act as an internal antioxidant within proteins (48). For example, the methionine residues of apoA1 and A2 have been shown to make a significant contribution to a reduction in hydroperoxides associated with human HDL (49). Furthermore, variations in the number of cysteine residues, with ε2, ε3, and ε4 having 2, 1, and 0, respectively, may contribute to variations in levels of lipid peroxidation products.

The current study provides data demonstrating greater lipid peroxidation in individuals with an apoε4 genotype (20–35% of U.S. and European populations). It contributes to the limited available evidence that the increased risk of chronic disease associated with an apoε4 genotype is in part attributable to an imbalance in oxidant/antioxidant homeostasis. It is likely that in hypercholesterolemic groups with an apoε4 genotype, and in particular smokers, antioxidant therapy, such as for example increased vitamin C intakes, may negate in part the increased CHD risk in these individuals.

ACKNOWLEDGMENTS

REFERENCES

1. Wilson, P.W.F., Schaefer, E.J., Larson, M.G., and Ordovas, J.M. (1996) Apolipoprotein E Alleles and Risk of Coronary Disease, *Arterioscler. Thromb. Vascular Biol. 16*, 1250–1255.
2. Eichner, J.E., Dunn, S.T., Perveen, G., Thompson, D.M., Stewart, K.E., and Stroehla, B.C. (2002) Apolipoprotein E Polymorphism and Cardiovascular Disease: A HuGE Review, *Am. J. Epidemiol. 155*, 487–495.
3. Gerdes, L.U., Gerdes, C., Kervinen, K., Savolainen, M., Klausen, I.C., Hansen, P.S., Kesaniemi, Y.A., and Faergeman, O. (2000) The Apolipoprotein ε4 Allele Determines Prognosis and the Effect on Prognosis of Simvastatin on Survivors of Myocardial Infarction: A Substudy of the Scandinavian Simvastatin Survival Study, *Circulation 101*, 1366–1371.
4. Farrer, L.A., Cupples, L.A., Haines, J.L., Hyman, B., Kukull, W.A., Mayeux, R., Myers, R.H., Pericak-Vance, M.A., and van Dujin, C.M. (1997) Effects of Age, Sex, and Ethnicity on the Association Between Apolipoprotein E Genotype and Alzheimer Disease. A Meta-analysis. ApoE and Alzheimer Disease Meta-analysis Consortium, *JAMA 278*, 1349–1356.
5. Poirier, J., Davignon, J., Bouthillier, D., Kogan, S., Bertrand, P.,

and Gauthier, S. (1993) Apolipoprotein E Polymorphism and Alzheimer's Disease (1993) *Lancet 342*, 697–699.
6. Havel, J.H., and King, J.P. (1989) Lipoprotein and Lipid Metabolism Disorders. Introduction: Structure and Metabolism of Plasma Lipoproteins, in *The Metabolic Basis of Inherited Disease* (Scriver, C.R., Beaudet, A.L., Sly, W.S., and Valle, D., eds.), 6th edn., McGraw-Hill, New York, p. 1215.
7. Beisiegel, U., Weber, W., Ihrke, G., Herz, J., and Stanley, K.K. (1989) The LDL-Receptor-Related Protein, LRP, Is an Apolipoprotein E-Binding Protein, *Nature 341*, 162–164.
8. Mahley, R.W., and Rall, S.C., Jr. (2000) Apolipoprotein E: Far More Than a Lipid Transport Protein, *Annu. Rev. Genomics Hum. Genetics 1*, 507–537.
9. Curtiss, L.K., and Boisvert, W.A. (2000) Apolipoprotein E and Atherosclerosis, *Curr. Opin. Lipidol. 11*, 243–251.
10. Lahoz, C., Schaefer, E.J., Cupples, A., Wilson, P.W.F., Levy, D., Osgood, D., Parpos, S., and Pedro-Botet, J. (2001) Apolipoprotein E Genotype and Cardiovascular Disease in the Framingham Heart Study, *Atherosclerosis 154*, 529–537.
11. Schiele, F., De Bacquer, D., Vincent-Viry, M., Beisiegel, U., Ehnholm, C., Evans, A., Kafatos, A., Martins, M.C., Sans, S., Sass, C., *et al.* (2000) The ApoEurope Group. Apolipoprotein E Serum Concentrations and Polymorphism in Six European Countries: The ApoEurope Project, *Atherosclerosis 152*, 475–488.
12. Welty, F.K., Lichtenstein, A.H., Barrett, P.H., Jenner, J.L., Dolnikowski, G.G., and Schaefer, E.J. (2000) Effects of ApoE Genotype on ApoB-48 and ApoB-100 Kinetics with Stable Isotopes in Humans, *Arterioscler. Thromb. Vasc. Biol. 20*, 1807–1810.
13. Boerwinkle, E., and Sing, C.F. (1987) The Use of Measured Genotype Information in the Analysis of Quantitative Phenotypes in Man: II. The Role of the Apolipoprotein E Polymorphism in Determining Levels, Variability, and Covariability of Cholesterol, Betalipoprotein, and Triglycerides in a Sample of Unrelated Individuals, *Am. J. Med. Genet. 27*, 567–582.
14. Minihane, A.M., Khan, S., Leigh-Firbank, E.C., Talmud, P., Wright, J.W., Murphy, M.C., Griffin, B.A., and Williams, C.M. (2000) ApoE Polymorphism and Fish Oil Supplementation in Subjects with an Atherogenic Lipoprotein Phenotype, *Arterioscler. Thromb. Vasc. Biol. 20*, 1990–1997.
15. Boer, J.M., Ehnholm, C., Menzel, H.J., Havekes, L.M., Rosseneu, M., O'Reilly, D.S., and Tiret, L.. (1997) Interactions Between Lifestyle-Related Factors and the ApoE Polymorphism on Plasma Lipids and Apolipoproteins. The EARS Study. European Atherosclerosis Research Study, *Arterioscler. Thromb. Vas. Biol. 17*, 1675–1681.
16. Halliwell, B., and Gutteridge, J.M. (1990) *Free Radicals in Biology and Medicine,* Clarendon Press, Oxford, United Kingdom.
17. Christen, Y. (2000) Oxidative Stress and Alzheimer Disease, *Am. J. Clin. Nutr. 71*, 621S–629S.
18. Halliwell, B. (1994) Free Radicals and Antioxidants: A Personal View, *Nutr. Rev. 1*, 253–265.
19. Schippling, S., Kontush, A., Arlt, S., Buhmann, C., Sturenburg, H.J., Mann, U., Muler-Thomsen, T., and Beisiegel, U. (2000) Increased Lipoprotein Oxidation in Alzheimer's Disease, *Free Radic. Biol. Med. 28*, 351–360.
20. Jolivalt, C., Leininger-Muller, B., Bertrand, P., Herber, R., Christen, Y., and Siest, G. (2000) Differential Oxidation of Apolipoprotein E Isoforms and Interaction with Phospholipids, *Free Radic. Biol. Med. 28*, 129–140.
21. Miyata, M., and Smith, J.D. (1996) Apolipoprotein E Allele-Specific Antioxidant Activity and Effects on Cytotoxicity by Oxidative Insults and β-Amyloid Peptides, *Nat. Genet. 14*, 55–61.
22. Pratico, D., Rokach, J., and Tangirala, R.K. (1999) Brains of

Aged Apolipoprotein E-Deficient Mice Have Increased Levels of F$_2$-Isoprostanes, *in vivo* Markers of Lipid Peroxidation, *J. Neurochem. 73*, 736–741.

23. Ramassamy, C., Averill, D., Beffert, U., Bastianetto, S., Theroux, L., Lussier-Cacan, S., Cohn, J.S., Christen, Y., Davignon, J., *et al.* (1999) Oxidative Damage and Protection by Antioxidants in the Frontal Cortex of Alzheimer's Disease Is Related to the Apolipoprotein E Genotype, *Free Radic. Biol. Med. 27*, 544–553.

24. Dietrich, M., Block, G., Hudes, M., Morrow, J.D., Norkus, E.P., Traber, M.G., Cross, C.E., and Packer, L. (2002) Antioxidant Supplementation Decreases F(2)-Isoprostanes in Plasma of Smokers, *Cancer Epidemiol. Biomarkers Prev. 11*, 7–13.

25. Dietrich, M., Block, G., Benowitz, N.L., Morrow, J.D., Hudes, M., Jacob, P., III, Norkus, E.P., and Packer, L. (2003) Vitamin C Supplementation Decreases Oxidative Stress Biomarker F$_2$-Isoprostanes in Plasma of Nonsmokers Exposed to Environmental Tobacco Smoke, *Nutr. Cancer 45*, 176–184.

26. Morrow, J.D., and Roberts, L.J., II (1999) Mass Spectrometric Quantification of F$_2$-Isoprostanes in Biological Fluids and Tissues as Measure of Oxidant Stress, *Methods Enzymol. 300*, 3–12.

27. Sowell, A.L., Huff, D.L., Yeager, P.R., Caudill, S.P., and Gunter, E.W. (1994) Retinol, α-Tocopherol, Lutein/Zeaxanthin, β-Cryptoxanthin, Lycopene, α-Carotene, *trans*-β-Carotene, and Four Retinyl Esters in Serum Determined Simultaneously by Reversed-Phase HPLC with Multiwavelength Detection, *Clin. Chem. 40*, 411–416.

28. Otles, S. (1995) Comparative Determination of Ascorbic Acid in Bass (*Morone lebrax*) Liver by HPLC and DNPH Methods, *Int. J. Food Sci. Nutr. 46*, 229–232.

29. Jacob, P.I., Wilson, M., and Benowitz, N.L. (1981) Improved Gas Chromatographic Method for the Determination of Nicotine and Cotinine in Biologic Fluids, *J. Chromatogr. 222*, 61–70.

30. Jacob, P.I., Yu, L., Wilson, M., and Benowitz, N.L. (1991) Selected Ion Monitoring Method for Determination of Nicotine, Cotinine and Deuterium-Labeled Analogs: Absence of an Isotope Effect in the Clearance of (*S*)-Nicotine-3′,3′-d$_2$ in Humans, *Biol. Mass Spectrom. 20*, 247–252.

31. Block, G., Dietrich, M., Norkus, E.P., Morrow, J.D., Hudes, M., Caan, B., and Packer, L. (2002) Factors Associated with Oxidative Stress in Human Populations, *Am. J. Epidemiol. 156*, 274–285.

32. Mazzone T. (1996) Apolipoprotein E Secretion by Macrophages: Its Potential Physiological Functions, *Curr. Opin. Lipidol. 14*, 55–61.

33. Patrono, C., and Fitzgerald, G.A. (1997) Isoprostanes: Potential Markers of Oxidative Stress in Atherothrombotic Disease, *Arterioscler. Thromb. Vasc. Biol. 17*, 2309–2315.

34. Ide, T., Hsutsui, H., Ohashi, N., Hayashidani, S., Suematsu, N., Tschihashi, M., Tamai, H., and Takeshita, A. (2002) Greater Oxidative Stress in Healthy Young Men Compared with Premenopausal Women, *Arterioscler. Thromb. Vasc. Biol. 22*, 438–442.

35. Morrow, J.D., Frei, B., Longmire, A.W., Gaziano, J.M., Lynch, S.M., Shyr, Y., Strauss, W.E., Oates, J.A., and Roberts, L.J., II (1995) Increase in Circulating Products of Lipid Peroxidation (F$_2$-isoprostanes) in Smokers: Smoking as a Cause of Oxidative Damage, *New Engl. J. Med. 332*, 1198–1203.

36. Chehne, F., Oguogho, A., Lupattelli, G., Budinsky, A.C., Palumbo, B., and Sinzinger, H. (2001) Increase of Isoprostane 8-Epi-PGF(2α) After Restarting Smoking, *Prostaglandins Leukot. Essent. Fatty Acids 64*, 307–310.

37. Davi, G., Alessandrini, P., Mezzetti, A., Minotti, G., Bucciarelli, T., Costantini, F., Cipollone, F., Bon, G.B., Ciabattoni, G., and Patrono, C. (1999) *In vivo* Formation of 8-Iso-prostaglandin F$_{2\alpha}$ and Platelet Activation in Diabetes Mellitus: Effects of Improved Metabolic Control and Vitamin E Supplementation, *Circulation 99*, 224–229.

38. Reilly, M.P., Pratico, D., Delanty, N., DiMinno, G., Tremoli, E., Rader, D., Kapoor, S., Rokach, J., Lawson, J., and FitzGerald, G.A. (1998) Increased Formation of Distinct F$_2$-Isoprostanes in Hypercholesterolemia, *Circulation 98*, 2822–2828.

39. Davi, G., Alessandrini, P., Mezzetti, A., Minotti, G., Bucciarelli, T., Costantini, F., Cipollone, F., Bon, G.B., Ciabattoni, G., and Patrono, C. (1997) *In vivo* Formation of 8-Epi-prostaglandin F$_2$ Is Increased in Hypercholesterolemia, *Arterioscler. Thromb. Vasc. Biol. 17*, 3230–3235.

40. Mayne, S.T., Walter, M., Cartmel, B., Goodwin, W.J., Jr., and Blumberg, J. (2004) Supplemental β-Carotene, Smoking and Urinary F$_2$-Isoprostane Excretion in Patients with Prior Early Stage Head and Neck Cancer, *Nutr. Cancer 49*, 1–6.

41. Wendland, B.E., Aghdassi, E., Tam, C., Carrier, J., Steinhart, A.H., Wolman, S.L., Baron, D., and Allard, J.P. (2001) Lipid Peroxidation and Plasma Antioxidant Micronutrients in Crohn Disease, *Am. J. Clin. Nutr. 74*, 259–264.

42. Aghdassi, E., and Allard, J.P. (2000) Breath Alkanes as a Marker of Oxidative Stress in Different Clinical Conditions, *Free Radic. Biol. Med. 28*, 880–886.

43. Humphries, S.E., Talmud, P.J., Hawe, E., Bolla, M., Day, I.N.M., and Miller, G.J. (2001) Apolipoprotein ε4 and Coronary Heart Disease in Middle-Aged Men Who Smoke: A Prospective Study, *Lancet 358*, 115–119.

44. Morrow, J.A., Segall, M.L., Lund-Katz, S., Phillips, M.C., Knapp, M., Rupp, B., and Weisgraber, K.H. (2000) Differences in Stability Among the Human Apolipoprotein E Isoforms Determined by the Amino-Terminal Domain, *Biochemistry 39*, 11657–11666.

45. Dong, L.M., and Weisgraber, K.H. (1996) Human Apolipoprotein ε4 Domain Interaction. Arginine 61 and Glutamic Acid 255 Interact to Direct the Preference for Very Low Density Lipoproteins, *J. Biol. Chem. 271*, 19053–19057.

46. Regan, L. (1995) Protein Design: Novel Metal Binding Sites, *Trends Biochem. Sci. 20*, 280–285.

47. Wilson, C., Wardell, M.R., Weisgraber, K.H., Mahley, R.W., and Agard, D.A. (1991) Three-Dimensional Structure of the LDL Receptor-Binding Domain of Human Apolipoprotein E, *Science 252*, 1817–1822.

48. Levine, R.L., Mosini, L., Berlett, B.S., and Stadtman, E.R. (1996) Methionine Residues as Endogenous Antioxidants in Proteins, *Proc. Nat. Acad. Sci. 93*, 15036–15040.

49. Garner, B., Waldeck, A.R., Witting, P.K., Rye, K.A., and Stocker, R. (1998) Oxidation of High Density Lipoproteins. II. Evidence for Direct Reduction of Lipid Hydroperoxides by Methionine Residues of Apolipoprotein A1 and AII, *J. Biol. Chem. 273*, 6088–6095.

Alterations of the Lipid Profile After 7.5 Years of Low-Dose Antioxidant Supplementation in the SU.VI.MAX Study

Serge Hercberg[a,b,*], Sandrine Bertrais[a], Sébastien Czernichow[a], Nathalie Noisette[a], Pilar Galan[a], Adèle Jaouen[a], Jean Tichet[c], Serge Briancon[d], Alain Favier[e,f], Louise Mennen[a], and Anne-Marie Roussel[g]

[a]U557 Institut National de la Santé et de la Recherche Médicale (INSERM) [Unité Mixte de Recherche (UMR) INSERM/Institut National de la Recherche Agronomique (INRA)/Conservatoire National des Arts et Métiers (CNAM)], Institut Scientifique et Technique de la Nutrition et de l'Alimentation/CNAM, Paris, France; [b]Unité de Surveillance et d'Epidémiologie Nutritionnelle (USEN), Institut de Veille Sanitaire InVS/CNAM, Paris, France; [c]Institut Régional de la Santé (IRSA), Tours, France; [d]Ecole de Santé Publique, Epidémiologie clinique, E1 3444, Faculté de Médecine, CHU Nancy, France; [e]Laboratoire Lésions des Acides Nucléiques, UMR CNRS-CEA-UJF 5046, Grenoble, France; [f]Département de Biologie intégrée, CHU La Tronche, Grenoble, France; and [g]Laboratoire Nutrition, Vieillissement et Maladies Cardiovasculaires, EA 4736, UJF, UFR de Pharmacie, La Tronche, Grenoble France

ABSTRACT: Antioxidant micronutrients have been reported to be associated with an improvement in the blood profile, but the results are not consistent. The aim of the present study was to assess the effects of antioxidant supplementation on changes in the serum lipid profile of adult participants in the SU.VI.MAX study. French adults (n = 12,741: 7,713 females aged 35–60 yr, and 5,028 males aged 45–60 yr) received daily antioxidant supplementation (120 mg vitamin C, 30 mg vitamin E, 6 mg β-carotene, 100 μg selenium, and 20 mg zinc) or a matching placebo. Median follow-up time was 7.5 yr. After 7.5 yr, no effect of supplementation on total cholesterol was observed in men or women after adjusting for baseline total cholesterol levels and lipid-lowering medications. The prevalence of hypercholesterolemia (≥6.5 mmol/L) showed a trend toward being higher in women who received supplements compared with those who received the placebo (P = 0.06). In both sexes, the group receiving supplements exhibited higher mean serum TG concentrations than did the placebo group (P = 0.06 in men; P = 0.05 in women). The prevalence of hypertriglyceridemia (≥2.3 mmol/L) was also significantly higher in men who received supplements (P = 0.03), but not in women. Our results suggest than long-term daily supplementation with low doses of β-carotene, vitamins C and E, selenium, and zinc does not result in an improved lipid profile and could even adversely affect some blood lipids, possibly with a higher risk of hyperlipidemia in women.

Paper no. L9659 in *Lipids 40*, 335–342 (April 2005).

The SU.VI.MAX study is a randomized, double-blind, placebo-controlled primary prevention trial that showed—in a middle-aged French population presumably free of cardiovascular disease (CVD) and of cancer at baseline—that daily low-dose antioxidant vitamin and trace element supplementation for 7.5 years lowered the total incidence of cancer in men, but not in women (1). No effect on the incidence of CVD was found in either gender. However, preclinical studies suggested that a diet rich in various compounds with antioxidant properties inhibited the atherogenic process (2). Moreover, numerous large prospective studies have shown significant inverse associations between overall mortality (3) and cardiovascular events (4), and antioxidant status and intake. Several mechanistic hypotheses suggest that antioxidants play a role in the inhibition of atherogenic processes (5). However, the primary prevention trials and most of the secondary prevention trials that have evaluated the effect of different antioxidant supplements on CVD (6–10) have been unable to detect any beneficial effects, as in the SU.VI.MAX study, and two of these (8,9) have even suggested harmful effects on cardiovascular events.

In fact, the beneficial effects of antioxidants in preventing CVD are still open to debate, since different mechanisms have been proposed whereby antioxidant nutrients could decrease or increase the risk of CVD (11).

The hypothesis of the protective effect of antioxidants is supported by the fact they can inhibit the oxidation of LDL cholesterol, a particularly atherogenic molecule (11). Antioxidant micronutrients (vitamins and trace elements) also are reportedly associated with an improved blood profile, but these results are not consistent (12) since β-carotene and zinc are suspected of affecting the serum lipid profile adversely (13,14). Moreover, most of the antioxidant supplementation trials testing the impact on circulating lipid concentrations have been short term, have involved a small number of participants, and have presented some methodological limitations.

Therefore, the aim of the present work was to investigate the relationship between antioxidant status and lipid profile, and to assess the effects of supplementation with nutritional doses of antioxidant vitamins and trace elements on total, LDL, and HDL cholesterol and TG levels after 7.5 yr of follow-up in the SU.VI.MAX trial.

EXPERIMENTAL PROCEDURES

Subjects and methods. Details concerning the study rationale, design, methods, and participant characteristics have been reported previously (1,15). In brief, 12,741 French adults (7,713 females aged 35–60 yr and 5,028 males aged 45–60 yr) were randomly allocated to receive either a combination of antioxidants [120 mg vitamin C, 30 mg vitamin E (all-*rac*-α-tocopherol), 6 mg β-carotene, 100 μg selenium (as selenium-enriched yeast), and 20 mg zinc (as gluconate)] or a matching placebo in a single daily capsule. Eligibility criteria were lack of diseases likely to hinder active participation or threaten 5-yr survival, acceptance of the possibility of receiving a placebo and of the implications of participation, lack of regular supplementation with any of the vitamins or trace elements in the supplement, and absence of extreme beliefs or behaviors regarding diet. The median follow-up time was 7.54 yr.

The protocol was approved by a medical ethics committee and the national committee for the protection of privacy and civil liberties.

Educational level, smoking status, menopausal status, and contraceptive use were obtained from a questionnaire at baseline. Level of education was coded in three categories according to the highest certification obtained (primary school, high school, university, or equivalent).

Blood samples were obtained in Vacutainer tubes (Becton Dickinson, Le Pont de Claix, France) after a 12-h fast at inclusion and at the last check-up after 7.5 yr of follow-up (antioxidant markers were measured, at 7.5 yr, on only a randomized subsample of 1,400 subjects).

All biochemical measurements were performed in a central laboratory. Vitamin C status was evaluated by serum ascorbic acid determination using an automated method based on the continuous flow principle. Serum β-carotene and tocopherol levels were measured by HPLC. Serum zinc was determined by flame atomic absorption spectrometry, and serum selenium was measured by electrothermal atomic absorption spectrometry with a Zeeman effect.

Total cholesterol and TG were assayed using an enzymatic method [at baseline, Technicon Dax 24, Bayer Diagnostics (Tarreytown, NY), and 7.5 yr later, Advia 1650, Bayer Diagnostics]. CV for cholesterol and TG assays were 0.7 and 1.4%, respectively. HDL cholesterol was measured only at the end of the study (CV = 1.3%). The LDL cholesterol concentration was computed with the Friedewald formula only for subjects who had a TG value ≤4 mmol/L (350 mg/dL). Among the 12,741 subjects, 739 (5.8%) withdrew consent during the study (6.7% of women, and 4.4% of men); 343 (5.4%) were in the intervention group (mean follow-up time ± SD: 2.0 ± 1.5 yr), and 396 (6.2%) were in the placebo group (mean follow-up time ± SD: 1.9 ± 1.5 yr). Seven hundred thirty-six subjects (5.8%) were lost to follow-up (6.0% for women, and 5.5% of men) for various reasons: 367 in the intervention group (follow-up time: 5.1 ± 2.2 yr) and 369 in the placebo group (follow-up time: 5.0 ± 2.3 yr). No differences in the percentage of subjects lost to follow-up or who withdrew consent were observed between groups within each gender. There were no differences in capsule consumption between the groups (mean percentage of capsules taken: 79% in each). Data are presented from the intention-to-treat analysis; the results were unchanged with a per-protocol analysis on subjects who took either >75 or >90% of the supplements assigned.

Statistical methods. All analyses comparing the placebo and the intervention groups were performed by intention-to-treat, separately in men and women. Baseline and end-trial characteristics of the two groups were compared by Student's *t*-test and the chi-square test where appropriate. Results are expressed as percentages or means ± SD. Because of the skewed distributions for TG, β-carotene, and vitamin C values, these variables were logarithmically transformed, and geometric means as well as 95% confidence intervals are presented. Relationships between lipid and antioxidant concentrations at baseline, after adjustment for use of lipid-lowering medications, were assessed by computing partial Spearman rank correlation coefficients. We calculated sex-specific tertiles of baseline antioxidant levels in the placebo group and performed analyses of covariance (ANCOVA) with tests for linear trend, in both the placebo and intervention groups, according to these tertiles. Means ± SD are presented, after adjustment for lipid medication use at the end of the study. Data were processed on an Alpha-VMS system, and a specific database was developed using Statistical Analysis System software, version 8.2 (SAS Institute Inc., Cary, NC).

RESULTS

Characteristics of participants and the relationship between serum antioxidant concentrations and lipid profile at baseline. Baseline characteristics are presented in Table 1. In both men and women, the placebo and the intervention group did not differ in terms of age; smoking habits; contraception use and menopausal status; body mass index; and serum values of antioxidants, vitamins, and trace elements, except that in women the intervention group had a slightly lower level of serum zinc ($P = 0.05$) and a higher level of education ($P = 0.02$) compared with those in the placebo group ($P = 0.02$). A significantly higher level of serum cholesterol ($P < 0.04$) was found in women taking supplements, and a lower percentage of subjects taking lipid-lowering medications was observed at baseline ($P < 0.02$). Conversely, a higher mean level of apolipoprotein (apo) A-1 ($P = 0.02$) and a higher percentage of lipid-lowering medications ($P < 0.002$) were found in men taking supplements compared with those in the placebo group.

Correlation coefficients between baseline lipid markers and baseline serum values of antioxidant status, after taking into account the use of lipid-lowering medications, are presented in Table 2. In both sexes, serum β-carotene was positively correlated with total cholesterol and apoA-1 (and with apoB in women) and negatively correlated with TG. Serum vitamin C was not significantly related to total cholesterol, but was inversely correlated with TG and was positively correlated with apoA-1 (and in men, inversely correlated with apoB). Serum

TABLE 1
Baseline Characteristics of the Subjects[a]

	Men			Women		
	Placebo (n = 2508)	Intervention (n = 2520)	P	Placebo (n = 3869)	Intervention (n = 3844)	P
Age (yr)	51.8 ± 4.7	51.8 ± 4.6	0.95	47.1 ± 6.6	47.2 ± 6.6	0.80
Educational level: n (%)						
Primary school	612 (24.9)	570 (23.1)		741 (19.7)	713 (19.1)	
High school	865 (35.3)	899 (36.4)		1532 (40.8)	1429 (38.2)	
University or equivalent	976 (39.8)	1002 (40.5)	0.30	1484 (39.5)	1596 (42.7)	0.02
Smoking status: n (%)						
Nonsmokers	828 (34.5)	812 (33.7)		2022 (54.8)	2001 (54.6)	
Previous smokers	1206 (50.2)	1229 (50.9)		1076 (29.1)	1061 (28.9)	
Current smokers	368 (15.3)	372 (15.4)	0.83	595 (16.1)	606 (16.5)	0.89
Contraception: n (%)						
No				1413 (51.7)	1405 (51.7)	
Oral				507 (18.6)	471 (17.3)	
Intrauterine device				812 (29.7)	843 (32.0)	0.39
Menopausal: n (%)				951 (25.5)	950 (25.5)	0.97
Body mass index (kg/m^2)	25.6 ± 3.2	25.6 ± 3.3	0.84	23.5 ± 4.0	23.3 ± 3.9	0.07
Serum β-carotene[b] (μmol/L)	0.37 (0.36, 0.38)	0.37 (0.36, 0.38)	0.78	0.55 (0.54, 0.57)	0.56 (0.54, 0.57)	0.75
Serum α-tocopherol (μmol/L)	32.2 ± 8.5	32.3 ± 8.3	0.85	30.9 ± 7.5	31.1 ± 7.8	0.46
Serum vitamin C[b] (μg/mL)	7.84 (7.66, 8.03)	7.68 (7.50, 7.86)	0.23	9.58 (9.44, 9.73)	9.61 (9.46, 9.76)	0.78
Serum selenium (μmol/L)	1.13 ± 0.20	1.14 ± 0.20	0.07	1.08 ± 0.19	1.09 ± 0.19	0.28
Serum zinc (μmol/L)	13.5 ± 1.9	13.5 ± 1.8	0.79	12.9 ± 1.9	12.8 ± 1.8	0.05
Fasting blood glucose (mmol/L)	6.00 ± 0.98	5.98 ± 1.05	0.63	5.53 ± 0.75	5.53 ± 0.80	0.76
Total cholesterol (mmol/L)	6.19 ± 0.99	6.21 ± 1.03	0.66	5.87 ± 1.03	5.92 ± 1.03	0.04
Total cholesterol ≥ 6.5 mmol/L: n (%)	888 (35.4)	912 (36.2)	0.56	940 (24.3)	985 (25.6)	0.18
TG[b] (mmol/L)	1.20 (1.17, 1.22)	1.21 (1.19, 1.24)	0.40	0.81 (0.80, 0.82)	0.80 (0.79, 0.81)	0.41
TG ≥ 2.3 mmol/L: n (%)	275 (11.0)	301 (11.9)	0.27	77 (2.0)	87 (2.3)	0.41
apoA-1 (g/L)	1.54 ± 0.23	1.52 ± 0.23	0.02	1.69 ± 0.26	1.70 ± 0.26	0.51
apoB (g/L)	1.20 ± 0.25	1.21 ± 0.27	0.11	1.03 ± 0.24	1.04 ± 0.24	0.17
Use of lipid-lowering drugs at baseline: n (%)	181 (7.4)	243 (9.8)	0.002	146 (3.9)	109 (2.9)	0.02

[a]Values in italics represent statistical significance.
[b]Geometric means (95% confidence intervals) because of skewed distributions. apo, apolipoprotein.

α-tocopherol, serum zinc, and serum selenium levels were positively correlated with all lipid markers in both sexes (except for TG and selenium).

Changes in lipid profile according to baseline antioxidant status in the placebo group. Table 3 presents changes in the serum total cholesterol and TG levels in the placebo group after 7.5 yr of follow-up, adjusted for use of lipid-lowering drugs and after exclusion of subjects taking lipid-lowering medications at baseline.

In both men and women, an overall significant decrease in total cholesterol levels and a significant increase in serum TG was observed. The decrease in total cholesterol was significantly more pronounced in women in the highest tertile for baseline serum concentrations of β-carotene, α-tocopherol, selenium, and zinc, and no linear trend was observed with baseline serum vitamin C levels. In men, similar trends were observed, although these were significant only for serum α-tocopherol and zinc.

Conversely, for TG, the highest increase was observed in women in the highest tertile for serum β-carotene and serum selenium and in the lowest tertile for serum vitamin E. For vitamin E, the trend was the same in men.

Effect of antioxidant supplementation on antioxidant markers and lipid profile. Serum β-carotene; vitamins C and E; zinc;

selenium; total, HDL, and LDL cholesterol; and TG concentrations, at 7.5 yr, in the supplemented and placebo groups are presented in Table 4. Statistically significant differences were observed between the intervention and placebo groups for all antioxidants markers at 7.5 yr. In women, we observed a slightly significant difference in mean total serum cholesterol in the group of women receiving supplements (P = 0.05); however, this difference disappeared after adjusting for lipid-lowering medications and baseline total cholesterol level (P = 0.37). HDL cholesterol was significantly lower in women receiving supplements, but not in men. No significant difference was observed for LDL cholesterol. The prevalence of hypercholesterolemia (≥6.5 mmol/L) was higher in women receiving supplements than in the placebo group (P = 0.06). No difference between the two groups was observed in men.

Concerning serum TG, the group receiving supplements exhibited a higher mean serum concentration, even after adjustment (P = 0.06 in men, and P = 0.05 in women). The percentage of hypertriglyceridemia (≥2.3 mmol/L) was significantly higher only in men receiving supplements (P = 0.03). The percentage of subjects taking lipid-lowering medications at the end of the intervention was significantly higher in men receiving supplements (P = 0.02).

TABLE 2
Partial[a] Spearman Rank Correlation Coefficients Between Antioxidants and Blood Lipids at Baseline

	Total cholesterol	TG	apoA-1	apoB	β-Carotene	α-Tocopherol	Vitamin C	Selenium
Men								
TG	0.32	1						
	<0.0001							
apoA-1	0.21	−0.27	1					
	<0.0001	*<0.0001*						
apoB	0.85	0.45	−0.08	1				
	<0.0001	*<0.0001*	*<0.0001*					
β-Carotene	0.09	−0.20	0.08	0.01	1			
	<0.0001	*<0.0001*	*<0.0001*	*0.51*				
α-Tocopherol	0.48	0.29	0.14	0.43	0.20	1		
	<0.0001	*<0.0001*	*<0.0001*	*<0.0001*	*<0.0001*			
Vitamin C	−0.02	−0.11	0.05	−0.06	0.22	0.05	1	
	0.18	*<0.0001*	*0.005*	*0.002*	*<0.0001*	*0.008*		
Selenium	0.10	−0.02	0.11	0.07	0.004	0.05	0.01	1
	<0.0001	*0.29*	*<0.0001*	*<0.0001*	*0.82*	*0.01*	*0.42*	
Zinc	0.09	0.07	0.05	0.11	−0.006	0.05	0.02	0.07
	<0.0001	*0.0002*	*0.01*	*<0.0001*	*0.72*	*0.005*	*0.36*	*<0.0001*
Women								
TG	0.31	1						
	<0.0001							
apoA-1	0.29	−0.03	1					
	<0.0001	*0.02*						
apoB	0.85	0.37	−0.02	1				
	<0.0001	*<0.0001*	*0.16*					
β-Carotene	0.19	−0.16	0.09	0.12	1			
	<0.0001	*<0.0001*	*<0.0001*	*<0.0001*				
α-Tocopherol	0.49	0.22	0.25	0.40	0.31	1		
	<0.0001	*<0.0001*	*<0.0001*	*<0.0001*	*<0.0001*			
Vitamin C	0.01	−0.07	0.07	−0.002	0.19	0.08	1	
	0.32	*<0.0001*	*<0.0001*	*0.90*	*<0.0001*	*<0.0001*		
Selenium	0.12	0.01	0.13	0.10	0.008	0.08	0.03	1
	<0.0001	*0.39*	*<0.0001*	*<0.0001*	*0.57*	*<0.0001*	*0.04*	
Zinc	0.09	0.06	0.05	0.10	0.001	0.02	0.006	0.07
	<0.0001	*<0.0001*	*0.0006*	*<0.0001*	*0.94*	*0.21*	*0.68*	*<0.0001*

[a]Adjusted for use of lipid-lowering drugs at baseline. Values in italics represent statistical significance. For abbreviation see Table 1.

DISCUSSION

Dietary antioxidants are suggested to protect against lipid peroxidation (5). Many observational studies have shown that a high dietary intake or high blood concentration of antioxidant vitamins is associated with a reduced risk of CVD (3,4). However, randomized controlled studies investigating the clinical use of antioxidant supplementation to prevent CVD have provided conflicting, even disappointing, results (16). In the SU.VI.MAX study, after 7.5 yr of supplementation with a combination of nutritional doses of antioxidants, no major effect was seen on the incidence of ischemic CVD. The purpose of the present analysis was to determine the effect of this supplementation on modifiable risk factors for atherosclerotic CVD, such as blood lipids.

After 7.5 yr of follow-up, we observed an overall significant decrease in total cholesterol levels and a significant increase in serum TG in the placebo group (adjusted for the use of lipid-lowering drugs at the end of the study). This may be related to the fact that at baseline, we screened all subjects and detected

hypercholesterolemia in 36% of men and 26% of women. Because they were under the care of the heath services, they may have decreased their cholesterol concentrations by modifying their lifestyles or adapting their drug use. The screening detected hypertriglyceridemia at baseline to a lesser extent than hypercholesterolemia (11.7% in men, and 2.2% in women), and the potential effect of hypotriglyceridemic treatment in decreasing the mean TG concentration in serum might consequently have been less obvious at the end of the study.

The main findings presented here show that long-term supplementation with a combination of β-carotene, vitamins C and E, zinc, and selenium is associated with an increase in serum TG in men and women, and with a higher percentage of hypertriglyceridemia in men. The increase in serum TG was slight but significant and still led to mean values in the physiological range; its biological or pathological significance is unknown.

The changes in total cholesterol concentration were less obvious. In women receiving supplements, we observed an increase in total cholesterol, but this alteration disappeared after adjusting for lipid-lowering medications and baseline total cholesterol

TABLE 3
**Mean (± SD) and Adjusted[a] (%) Values of Cholesterol and TG at Baseline
and After 7.5 yr of Follow-up in the Placebo Group**

	Cholesterol		TG	
	Men	Women	Men	Women
Mean ± SD at baseline	6.17 ± 0.99	5.85 ± 1.02	1.18 (1.15, 1.21)[b]	0.80 (0.79, 0.81)[b]
Mean ± SD after 7.5 yr following	5.66 ± 0.90	5.62 ± 0.89	1.09 (1.06, 1.12)[b]	0.87 (0.86, 0.89)[b]
Change after 7.5 yr (%)	−6.9 ± 14.1	−3.0 ± 14.7	4.33 ± 1.28	19.27 ± 1.21
P	<0.0001	<0.0001	0.0005	<0.0001
Variations after 7.5 yr according to baseline levels of serum values of antioxidant markers				
Tertiles for serum β-carotene				
Highest	−7.4 ± 0.6	−4.4 ± 0.5	6.2 ± 2.2	24.6 ± 2.1
Middle	−6.7 ± 0.7	−2.6 ± 0.5	4.5 ± 2.3	20.0 ± 2.1
Lowest	−6.4 ± 0.7	−1.9 ± 0.6	2.1 ± 2.4	12.7 ± 2.1
P for trend	*0.24*	*0.001*	*0.21*	*0.0001*
Tertiles for serum α-tocopherol				
Highest	−9.9 ± 0.6	−6.7 ± 0.5	−0.4 ± 2.3	14.1 ± 2.2
Middle	−6.7 ± 0.6	−2.4 ± 0.5	4.8 ± 2.3	21.4 ± 2.2
Lowest	−4.0 ± 0.6	−0.2 ± 0.5	8.5 ± 2.3	23.3 ± 2.2
P for trend	*<0.0001*	*<0.0001*	*0.01*	*0.003*
Tertiles for vitamin C				
Highest	−7.2 ± 0.6	−3.3 ± 0.6	2.4 ± 2.4	23.2 ± 2.4
Middle	−6.9 ± 0.7	−2.7 ± 0.6	6.1 ± 2.5	20.9 ± 2.4
Lowest	−6.7 ± 0.7	−2.2 ± 0.6	4.2 ± 2.6	17.6 ± 2.5
P for trend	*0.61*	*0.18*	*0.61*	*0.10*
Tertiles for serum selenium				
Highest	7.6 ± 0.6	−4.5 ± 0.5	6.3 ± 2.3	23.1 ± 2.0
Middle	−6.6 ± 0.6	−2.2 ± 0.5	1.9 ± 2.2	18.0 ± 2.2
Lowest	−6.4 ± 0.6	−2.1 ± 0.5	5.1 ± 2.1	17.3 ± 2.0
P for trend	*0.16*	*0.001*	*0.72*	*0.04*
Tertiles for serum zinc				
Highest	−7.9 ± 0.6	−4.3 ± 0.5	3.1 ± 2.2	17.1 ± 2.0
Middle	−6.8 ± 0.6	−2.6 ± 0.5	4.9 ± 2.1	21.6 ± 2.1
Lowest	−5.8 ± 0.6	−1.7 ± 0.5	5.1 ± 2.3	19.9 ± 2.1
P for trend	*0.01*	*0.0004*	*0.52*	*0.35*

[a]Adjusted for use of lipid-lowering drugs at the end of the study. Values in italics represent statistical significance.
[b]Geometric means (95% confidence intervals) because of skewed distributions.

level. HDL cholesterol was significantly lower in women receiving supplements, but not in men, and the prevalence of hypercholesterolemia also was higher. At the end of intervention, the percentage of subjects taking lipid-lowering medications was significantly higher in the group of men receiving supplements.

The relationship between lipid metabolism and antioxidant status is supported by a substantial body of data. The majority of published data on this topic are concerned with lipid metabolism and vitamin C status. Animal experiments have shown that marginal vitamin C deficiency in guinea pigs increases plasma and tissue cholesterol levels, and that vitamin C supplementation decreases cholesterol levels in guinea pigs, rabbits, and vitamin C-dependent rats fed an atherogenic diet (17). But results of human studies, both observational and experimental, are less consistent than those of their animal counterparts. In several observational studies, plasma ascorbic acid and vitamin C intakes were positively associated with HDL cholesterol concentrations (18,19) and apoA-1, and were inversely associated with total cholesterol (20), but other studies did not demonstrate such associations (21). Few intervention trials using antioxidant nutrients alone or in pairs have been performed, but until now, most of them have consistently shown no significant effect on serum total cholesterol, HDL cholesterol, or TG levels with either β-carotene (22,23), vitamin C (12,24), a combination of vitamins C and E (25), or vitamins C and E associated with β-carotene supplementation (26). However, most of these trials have presented flaws, such as a low statistical power, failure to blind treatment, or nonrandom allocation of supplements. Furthermore, they have included a small number of participants (10 to 440 subjects) or short-term supplementation (most from 3 wk to 12 mon; only a few had a long follow-up), and some have been concerned with specific patients. None of these studies have pointed out an adverse effect of vitamin C consumption at nutritional doses on lipid profiles at the level given in the SU.VI.MAX study. Hence, nutritional doses of vitamin C cannot be suspected to increase TG in serum, and an optimal nutritional intake of these nutrients, by consuming an adequate amount of fruits and vegetables, must always be encouraged.

Our subjects also received 30 mg/d of α-tocopherol in the supplement. This is more than twofold the usual dietary recommendations, and given the dietary mean intakes of vitamin

TABLE 4
Antioxidant and Lipid Levels of Subjects After 7.5 yr of Follow-up[a]

	Men			Women		
	Placebo (*n* = 2508)	Intervention (*n* = 2520)	*P*	Placebo (*n* = 3869)	Intervention (*n* = 3844)	*P*
β-Carotene (μmol/L)	0.62 ± 0.42	1.10 ± 0.72	*<0.001*	1.06 ± 0.74	1.71 ± 1.03	*<0.001*
α-Tocopherol (μmol/L)	30.0 ± 6.9	33.7 ± 8.2	*<0.001*	29.3 ± 6.2	32.4 ± 7.1	*<0.001*
Vitamin C (μg/mL)	9.4 ± 3.7	11.4 ± 3.0	*<0.001*	11.0 ± 3.7	12.9 ± 3.2	*<0.001*
Selenium (μmol/L)	1.30 ± 0.20	2.15 ± 0.43	*<0.001*	1.26 ± 0.23	1 .84 ± 0.36	*<0.001*
Zinc (μmol/L)	11.5 ± 1.5	13.5 ± 3.8	*<0.05*	11.5 ± 1.2	12.2 ± 1.5	*<0.05*
Total cholesterol (mmol/L)						
Crude	5.66 ± 0.90	5.65 ± 0.88	*0.64*	5.63 ± 0.89	5.68 ± 0.96	*0.05*
Adjusted[b]	5.66 ± 0.02	5.65 ± 0.02	*0.57*	5.65 ± 0.02	5.67 ± 0.02	*0.37*
Total cholesterol ≥ 6.5 mmol/L	273 (10.9%)	269 (10.7%)	*0.81*	377 (9.7%)	425 (11.1%)	*0.06*
TG[c] (mmol/L)						
Crude	1.11 (1.08, 1.13)	1.15 (1.12, 1.18)	*0.02*	0.88 (0.86, 0.89)	0.89 (0.87, 0.90)	*0.36*
Adjusted[b]	1.11 (1.09, 1.14)	1.14 (1.12, 1.17)	*0.06*	0.87 (0.86, 0.89)	0.89 (0.88, 0.90)	*0.05*
TG ≥ 2.3 mmol/L	100 (4.0%)	133 (5.3%)	*0.03*	44 (1.1%)	47 (1.2%)	*0.73*
HDL cholesterol (mmol/L)						
Crude	1.41 ± 0.35	1.39 ± 0.34	*0.02*	1.71 ± 0.41	1.72 ± 0.39	*0.76*
Adjusted	1.41 ± 0.01	1.39 ± 0.01	*0.03*	1.71 ± 0.01	1.72 ± 0.01	*0.81*
HDL cholesterol < 0.9 mmol/L	864 (34.4%)	837 (33.2%)	*0.35*	1487 (38.4%)	1398 (36.4%)	*0.06*
LDL cholesterol[d] (mmol/L)						
Crude	3.63 ± 0.83	3.63 ± 0.80	*0.82*	3.45 ± 0.83	3.48 ± 0.87	*0.32*
Adjusted	3.63 ± 0.02	3.63 ± 0.02	*0.97*	3.45 ± 0.02	3.48 ± 0.02	*0.32*
LDL cholesterol ≥ 4.1 mmol/L	426 (17.0%)	423 (16.8%)	*0.85*	469 (12.1%)	515 (13.4%)	*0.09*
Use of lipid-lowering drugs at end of study (%)	12.6%	15.0%	*0.02*	6.6%	6.1%	*0.33*

[a]Values in italics represent statistical significance.
[b]Adjusted for use of lipid-lowering drugs at the end of the study and baseline level.
[c]Geometric means (95% confidence intervals) because of skewed distributions.
[d]Calculated using the Friedewald formula.

E in our population, it can be postulated that the supplemented group exhibited a total daily intake of around 40 mg/d of vitamin E. This important supply, over a long period of time, could be partly responsible for an adaptive mechanism involving a stimulation of VLDL synthesis and TG metabolism, with an increase in the transport and incorporation of vitamin E in membranes and lipoproteins. A synergistic effect with β-carotene cannot be totally ruled out, and β-carotene might be implicated in deleterious effects on TG. The hypothesis of a specific role of β-carotene (alone or stimulated by vitamin E) is consistent with data from a subsample of 52 participants in the CARET study (14). In this randomized cancer chemoprevention trial, long-term supplementation with 30 mg of β-carotene and 25,000 IU retinyl palmitate showed a nonsignificant increase in serum TG levels during the supplementation period, and a decrease in serum TG levels 10 months after the intervention was discontinued.

In our supplement, there were also antioxidant trace elements, and lipid metabolism may be further modulated by trace element status. Suboptimal intakes of zinc and selenium are associated with modified lipid and lipoprotein profiles and increased risk factors for CVD and diabetes (27,28). In addition

to several antioxidants present in LDL particles, selenium acts against oxidative processes, and there is no evidence of an adverse effect of selenium on the lipid profile. It has been demonstrated that selenium deficiencies negatively influence cholesterol metabolism and contribute to LDL oxidation (29). Moreover, the membrane-bound form of the enzyme GPx can efficiently reduce hydroperoxides in the phospholipids and cholesterol esters associated with LDL and HDL cholesterol (30). Other animal studies showed that endothelial function is impaired in selenium-deficient hypercholesterolemic rats (31). Results from interventional studies involving selenium and lipids are scarce. A slight improvement in the serum lipoprotein profile was reported in subjects with a low initial selenium status who received selenium yeast tablets (96 μg/d) for 2 wk (32), and in the elderly, supplementation with 100 μg/d of selenium resulted in a decreased malondialdehyde plasma level and decreased TG levels (33). In the present study, in addition to daily dietary intakes, the supplemental amount of zinc led to daily zinc intakes that could be estimated around 30 mg/d. At this dose, no deleterious effects have been reported on immunity, antioxidant function, and enzymatic activities. Zinc supplementation, at pharmacological doses (160 to 300 mg/d or

even 30 to 60 mg/d), resulted in lower HDL cholesterol in healthy adults, which may be related to the negative effects on copper status (34). The antagonistic association between copper and zinc is also thought to be partly responsible for numerous metabolic abnormalities, including hypercholesterolemia (35).

Data on the impact of pharmacological doses of zinc on lipid metabolism are scarce and controversial. Two randomized studies with zinc showed a decrease in HDL cholesterol or total cholesterol (36,37), and four showed no change in the lipid profile (38–41). Among the three nonrandomized studies, one showed undesirable changes in HDL and LDL cholesterol (42), another (43) showed no effect on the lipid profile, and the third (44) showed an increase in HDL cholesterol and a decrease in LDL cholesterol 8 wk after supplementation with zinc was stopped. Cross-sectional studies also have produced inconsistent results. In a study of 152 men, aged 57 to 76 yr, the correlation coefficients for serum zinc with total cholesterol or HDL cholesterol were near zero (45). Similarly, a study of 186 volunteers, with ages ranging from 15 to 67 yr, reported no association between serum zinc and serum lipid levels (46). More recently, in a large population sample of adults aged 20 to 80 yr in Belgium, a significant positive relationship was shown between serum zinc levels and both total cholesterol and the "antiatherogenic" HDL cholesterol (47).

The slight increase in TG serum levels we observed in our study could also possibly be due to zinc-induced leptin production. Whereas zinc deficiency results in decreased leptinemia (48), zinc supplementation induces an increase in leptin activity, which is known to increase the efflux of FA from adipocytes (49).

Our results suggest than long-term combined antioxidant supplementation with β-carotene, vitamins C and E, selenium, and zinc is not associated with an improvement in the lipid profile. This observation is consistent with the lack of effect of such supplementation on the incidence of CVD in our population. The observed increase in the TG levels of subjects receiving supplements is slight, but it can be considered an adverse and unexpected effect. It may be hypothetized that supranutritional amounts of zinc and vitamin E could activate adaptive mechanisms and lipogenesis. Interactions with other dietary factors, especially β-carotene, cannot be totally ruled out. Consideration of these data are important, since they underline that long-term supplementation, even at low doses, results in adaptive mechanisms and modified metabolism, especially with supranutritional doses of zinc and vitamin E.

ACKNOWLEDGMENTS

REFERENCES

1. Hercberg, S., Galan, P., Preziosi, P., Bertrais, S., Mennen, L., Malvy, D., Roussel, A.M., Favier, A., and Briançon, S. (2004) The SU.VI.MAX Study: A Randomised, Placebo-Controlled Trial of the Health Effects of Antioxidant Vitamins and Minerals, *Arch. Intern. Med. 164*, 2335–2342.

2. Prasad, K., and Kaira, J. (1993) Oxygen Free Radicals and Hypercholesterolemic Atherosclerotic Heart Disease, *N. Engl. J. Med. 125*, 958–973.

3. Losonczy, K.G., Harris, T.G., and Havlik, R.J. (1996) Vitamin E and Vitamin C Supplement Use and Risk of All-Cause and Coronary Heart Disease Mortality in Older Persons: The Established Population for Epidemiologic Studies of the Elderly, *Am. J. Clin. Nutr. 64*, 190–196.

4. Rimm, E.B., Stampfer, M.J., Ascherio, A., Giovannucci, E., Colditz, G.A., and Willett, W.C. (1993) Vitamin E Consumption and the Risk of Coronary Heart Disease in Men, *N. Engl. J. Med. 328*, 1450–1456.

5. Jialal, I., and Devaraj, S. (1996) The Role of Oxidized Low Density Lipoprotein in Atherogenesis, *J. Nutr. 126* (Suppl.), 1053S–1057S.

6. Hennekens, C.H., Buring, J.E., Manson, J.E., Stampfer, M., Rosner, B., Cook, N.R., Belanger, C., LaMotte, F., Gaziano, J.M., Ridker, P.M., *et al.* (1996) Lack of Effect of Long-Term Supplementation with β-Carotene on the Incidence of Malignant Neoplasms and Cardiovascular Disease, *N. Engl. J. Med. 334*, 1145–1149.

7. Lee, I.M., Cook, N.R., Manson, J.E., Buring, J.E., and Hennekens, C.H. (1999) β-Carotene Supplementation and Incidence of Cancer and Cardiovascular Disease: The Women's Health Study, *J. Natl. Cancer Inst. 24*, 2102–2106.

8. The α-Tocopherol, β-Carotene Cancer Prevention Study Group. (1994) The Effect of Vitamin E and β-Carotene on the Incidence of Lung Cancer and Other Cancers in Male Smokers, *N. Engl. J. Med. 330*, 1029–1035.

9. Omenn, G.S., Goodman, G.E., Thorquist, M.D., Balmes, J., Cullen, M.R., Glass, A., Keogh, J.P., Meyskens, F.L., Valaxis, B., James, P.H., *et al.* (1996) Effects of a Combination of β-Carotene and Vitamin A on Lung Cancer and Cardiovascular Disease, *N. Engl. J. Med. 334*, 1150–1155.

10. Blot, W.J., Li, J.Y., Taylor, P.R., Guo, W., Dawsey, S., Wang, G.Q., Yang, C.S., Zhang, S.F., Gail, M., Li, G.Y., *et al.* (1993) Nutrition Intervention Trials in Linxian, China: Supplementation with Specific Vitamin/Mineral Combinations, Cancer Incidence, and Disease-Specific Mortality in the General Population, *J. Natl. Cancer Inst. 85*, 1483–1492.

11. Berliner, J.A., Navab, M., Fogelman, A.M., Frank, J.S., Demer, L.L., Edwards, P.A., Watson, A.D., and Lusis, A.J. (1995) Arteriosclerosis: Basic Mechanism, Oxidation, Inflammation, and Genetics, *Circulation 91*, 2488–2496.

12. Kim, M.K., Sasaki, S., Sasazuki, S., Okubo, S., Hayashi, M., and Tsugane, S. (2004) Long-Term Vitamin C Supplementation Has No Markedly Favourable Effect on Serum Lipids in Middle-Aged Japanese Subjects, *Br. J. Nutr. 91*, 80–90.

13. Hiller, R., Seigel, D., Sperduto, R.D., Blair, N., Burton, T.C., Farber, M.D., Gradoudas, E.S., Gunter, E.W., Hallar, J., Seddon, J.M., Sowell, A.L., Yannuzzi, L.A., and The Eye Disease Case-Control Study Group (1995). Serum Zinc and Serum Lipid Profiles in 778 Adults, *Ann. Epidemiol. 5*, 490–496.

14. Redlich, C.A., Chung, J.S., Cullen, M.R., Blaner, W.S., Van Bennekum, A.M., and Berglund, L. (1999) Effect of Long-Term β-Carotene and Vitamin A on Serum Cholesterol and Triglyceride Levels Among Participants in the Carotene and Retinol Efficacy Trial (CARET), *Atherosclerosis 145*, 425–432.

15. Hercberg, S., Preziosi, P., Briançon, S., Galan, P., Paul-

Dauphin, A., Malvy, D., Roussel, A.M., and Favier, A. (1998) A Primary Prevention Trial of Nutritional Doses of Antioxidant Vitamins and Minerals on Cardiovascular Diseases and Cancers in General Population: The SU.VI.MAX Study. Design, Methods and Participant Characteristics, *Control. Clin. Trials 19*, 336–351.

16. Vivekananthan, D.P., Penn, M.S., Sapp, S.K., Hsu, A., and Jopol, E.J. (2003) Use of Antioxidant Vitamins for the Prevention of Cardiovascular Disease: Meta-analysis of Randomised Trials, *Lancet 361*, 2017–2023.

17. Hemilä, H. (1992) Vitamin C and Plasma Cholesterol, *Crit. Rev. Food Sci. Nutr. 32*, 33–57.

18. Dallal, G.E., Choi, E., Jacques, P., Schaefer, E.J., and Jacob, R.A. (1989) Ascorbic Acid, HDL Cholesterol, and Apoprotein A-I in the Elderly, *J. Am. Coll. Nutr. 8*, 69–74.

19. Hallfrisch, J., Singh, V.N., Muller, C., Baldwin, H., Bannon, M.E., and Andres, R. (1994) High Plasma Vitamin C Associated with Increased Plasma LDL and HDL$_2$-Cholesterol, *Am. J. Clin. Nutr. 60*, 100–105.

20. Jacques, P.F. (1992) Relationships of Vitamin C Status to Cholesterol and Blood Pressure, *Ann. N.Y. Acad. Sci. 669*, 205–214.

21. Elwood, P.C., Hughes, R.E., and Hurley, R.J. (1970) Ascorbic Acid and Serum-Cholesterol, *Lancet 2*, 1197.

22. Nierenberg, D.W., Bayrd, G.T., and Stukel, T.A. (1991) Lack of Effect of Chronic Administration of Oral β-Carotene on Serum Cholesterol and Triglyceride Concentrations, *Am. J. Clin. Nutr. 53*, 652–654.

23. Ribaya-Mercato, J.D., Ordovas, J.M., and Russell, R.M. (1995) Effect of β-Carotene Supplementation on the Concentrations and Distribution of Carotenoids, Vitamin E, Vitamin A, and Cholesterol in Plasma Lipoprotein and Non-lipoprotein Fractions in Healthy Older Women, *J. Am. Coll. Nutr. 14*, 614–620.

24. Jacques, P.F., Sulsky, S.I., Perrone, G.E., Jenner, J., and Schaefer, E.J. (1995) Effect of Vitamin C Supplementation on Lipoprotein Cholesterol, Apolipoprotein, and Triglyceride Concentrations, *Ann. Epidemiol. 5*, 52–59.

25. Salonen, R.M., Nyyssonen, K., Kaikkonen, J., Porkkala-Sarataho, E., Voutilainen, S., Rissanen, T.H., Tuomainen, T.P., Valkonen, V.P., Ristonmaa, U., Lakka, H.M., *et al.* (2003) Antioxidant Supplementation in Atherosclerosis Prevention Study. Six-Year Effect of Combined Vitamin C and E Supplementation on Atherosclerotic Progression: The Antioxidant Supplementation in Atherosclerosis Prevention (ASAP) Study, *Circulation 25*, 947–953.

26. Miller, E.R., Appel, L.J., Levander, O.A., and Levine, D.M. (1997) The Effect of Antioxidant Vitamin Supplementation on Traditional Cardiovascular Risk Factors, *J. Cardiovasc. Risk 4*, 19–24.

27. Henning, B., Toborek, M., McClain, C.J., and Diana, J. (1996) Nutritional Implications of Zinc in Vascular Endothelial Cell Metabolism, *J. Am. Coll. Nutr. 15*, 345–348.

28. Roussel, A.M., Kerkeni, A., Majoub, S., Zouari, N., Matheau, J.M., and Anderson, R.A. (2003) Beneficial Effects of Zinc Supplementation on Lipid Peroxidation in Tunisian People with Type 2 Diabetes Mellitus, *J. Am. Coll. Nutr. 22*, 316–321.

29. Nève, J. (1996) Selenium as a Risk Factor for Cardiovascular Diseases, *J. Cardiovasc. Risk 3*, 42–47.

30. Takahashi, K., Avissar, N., Within, J., and Cohen, H.J. (1987) Purification and Characterization of Human Plasma Glutathione Peroxidase: A Selenoprotein Distinct from the Known Cellular Enzyme, *Arch. Biochem. Biophys. 256*, 677–686.

31. Stone, W.L., Stewart, M.E., Nicholas, C., and Pavuluri, S. (1986) Effects of Dietary Selenium and Vitamin E on Plasma Lipoprotein Cholesterol Levels in Male Rats, *Ann. Nutr. Metab. 30*, 94–103.

32. Luoma, P.V., Sotianemi, E.A., Korpela, A.H., and Kumpulainen, J. (1984) Serum Selenium, Glutathione Peroxidase Activity and High Density Lipoprotein Cholesterol. Effect of Selenium Supplementation, *Res. Commun. Chem. Pathol. Pharmacol. 46*, 469–472.

33. Nève, J. (1993) Rôle essentiel et indications cliniques du sélénium, *Méd. Hyg. 51*, 741–746.

34. He, J., Tell, G.S., Tang, Y.C., Mo, P.S., and He, G.Q. (1992) Relation of Serum Zinc and Copper to Lipids and Lipoproteins: The Yi People Study, *Am. Coll. Nutr. 11*, 74–78.

35. Klevay, L.M. (1973) Hypercholesteremia in Rats Produced by an Increase in the Ratio of Zinc to Copper Ingested, *Am. J. Clin. Nutr. 26*, 1060–1068.

36. Hooper, P.L., Visconti, L., Garry, P.J., and Hohnson, G.E. (1980) Zinc Lowers High-Density Lipoprotein-Cholesterol Levels, *JAMA 244*, 1960–1961.

37. Black, M.R., Medeiros, D.M., Brunett, E., and Welke, R. (1988) Zinc Supplements and Serum Lipids in Young Adult White Males, *Am. J. Clin. Nutr. 47*, 970–975.

38. Freeland-Graves, J.H., Friedman, B.J., Han, W.H., Shorey, R.L., and Young, R. (1982) Effect of Zinc Supplementation on Plasma High-Density Lipoprotein, Cholesterol and Zinc, *Am. J. Clin. Nutr. 35*, 988–992.

39. Bodgen, J.D., Oleske, J.M., and Lavenhar, M.A. (1988) Zinc and Immunocompetence in Elderly People: Effects of Zinc Supplementation for 3 Months, *Am. J. Clin. Nutr. 48*, 655–663.

40. Crouse, S.F., Hooper, P.L., Atterbom, H.A., and Papenfusz, R.L. (1984) Zinc Ingestion and Lipoprotein Values in Sedentary and Endurance-Trained Men, *JAMA 252*, 785–787.

41. Samman, S., and Roberts, D.C.K. (1986) Zinc Supplements Reduce Plasma LDL-Cholesterol in Females, *Proc. Nutr. Soc. Aust. 11*, 98–101.

42. Chandra, R.K. (1984) Excessive Intake of Zinc Impairs Immune Responses, *JAMA 252*, 1443–1446.

43. Pachotikarn, C., Medeiros, D.M., and Windham, F. (1985) Effect of Oral Zinc Supplementation upon Plasma Lipids, Blood Pressure, and Other Variables in Young Adult White Males, *Nutr. Rep. Int. 32*, 373–382.

44. Goodwin, J.S., Hunt, W.C., Hooper, P., and Garry, P.J. (1985) Relationship Between Zinc Intake, Physical Activity, and Blood Levels of High-Density Lipoprotein Cholesterol in a Healthy Elderly Population, *Metabolism 34*, 519–523.

45. Kromhout, D., Wibowo, A.A., Herber, R.F., Dalderup, L.M., Heerdink, H., de Lezenne Coulander, C., and Zielhuis, R.L. (1985) Trace Metals and Coronary Heart Disease Risk Indicators in 152 Elderly Men (the Zutphen Study), *Am. J. Epidemiol. 122*, 378–385.

46. Fischer, P.W.F., and Collins, M.W. (1983) Relationship Between Serum Zinc and Copper and Risk Factors Associated with Cardiovascular Disease [Letter], *Am. J. Clin. Nutr. 34*, 595–596.

47. Thijs, L., Staessen, J., and Amery, A. (1992) Determinants of Serum Zinc in a Random Sample of Four Belgian Towns with Different Degrees of Environmental Exposure to Cadmium, *Environ. Health Perspect. 98*, 251–258.

48. Chen, M.D., Sony, Y.M., and Lin, P.Y. (2000) Zinc May Be a Mediator of Leptin Production in Humans, *Life Sci. 66*, 3143–3149.

49. Steinberger, J., Steffen, L., Jacobs, D.R., Jr., Moran, A., Hong, C.P., and Sinaiko, A.R. (2003) Relation of Leptin to Insulin Resistance Syndrome in Children, *Obes. Res. 11*, 1124–1130.

The Impact of Age, Body Mass Index, and Fish Intake on the EPA and DHA Content of Human Erythrocytes

Scott A. Sands, Kimberly J. Reid, Sheryl L. Windsor, and William S. Harris*

Mid America Heart Institute, Saint Luke's Hospital, Kansas City, Missouri 64111,
and the Department of Medicine, University of Missouri–Kansas City, Kansas City, Missouri 64108

ABSTRACT: n-3 FA are beneficial for cardiovascular health, reducing platelet aggregation, TG levels, and the risk of sudden death from myocardial infarction. The percentage of EPA + DHA in red blood cells (RBC), also known as the Omega-3 Index, has recently been proposed as a risk marker for death from coronary heart disease (CHD). The purpose of this study was to begin to explore the factors that can influence RBC EPA + DHA. We collected information on the number of servings of tuna or nonfried fish consumed per month, as well as on age, gender, ethnicity, smoking status, the presence of diabetes, and body mass index (BMI) in 163 adults in Kansas City who were not taking fish oil supplements. The average RBC EPA + DHA in this population was 4.9 ± 2.1%. On a multivariate analysis, four factors significantly and independently influenced the Omega-3 Index: fish servings, age, BMI, and diabetes. The Index increased by 0.24 units with each additional monthly serving of tuna or nonfried fish ($P < 0.0001$), and by 0.5 units for each additional decade in age ($P < 0.0001$). The Index was 1.13% units lower in subjects with diabetes ($P = 0.015$) and decreased by 0.3% units with each 3-unit increase in BMI ($P = 0.001$). Gender or smoking status had no effect, and the univariate relationship with ethnicity vanished after controlling for fish intake. Given the importance of n-3 FA in influencing risk for death from CHD, further studies are warranted to delineate the nondietary factors that influence RBC EPA + DHA content.

Paper no. L9662 in *Lipids 40*, 343–347 (April 2005).

The n-3 FA EPA and DHA are known to have cardioprotective effects (1). Some of these effects include a reduction of platelet aggregation (2,3) and serum TG levels (4), and an increased heart rate variability (5), the latter being predictive of a lower risk of mortality due to cardiac arrhythmia (6). In the GISSI-Prevenzione study (7), n-3 FA supplementation produced a 20% reduction in total mortality and a 45% reduction in relative risk for sudden cardiac death, consistent with a reduced risk for arrhythmias. Because of these and other findings, the American Heart Association (AHA) now recommends that patients with known coronary heart disease (CHD) consume about 1 g/d of EPA + DHA. For individuals without known CHD, the AHA recommends at least two servings/wk of (preferably oily) fish to reduce the risk of cardio-

vascular disease (1). This would equate to approximately 500 mg/d of EPA + DHA.

The percentage of EPA + DHA in the red blood cell (RBC) membranes is a well-known biomarker of long-chain n-3 FA intake. Recently termed the "Omega-3 Index," it has been proposed as a new risk marker for CHD death (8). The RBC EPA + DHA has been shown to be responsive to increased intakes of n-3 FA (8), a valid surrogate for human myocardial n-3 content (9), and to be strongly associated with reduced risk of sudden cardiac death (10,11). Based on these previous studies, an RBC EPA + DHA of 8% or above has been proposed as a target cardioprotective level (8). The EPA + DHA content of RBC membranes varies across populations, presumably as a function of fish intake. Levels are generally low in Europeans (12,13), Americans (14,15), and Canadians (16), and high in Japanese (17) and Norwegians (18). Factors other than diet that may influence the incorporation of EPA + DHA in RBC have not been systematically investigated. The purpose of this study was to estimate average values for RBC EPA + DHA in a sample of adults from a Midwestern U.S. city, and to begin exploring the effects of gender, age, body mass index (BMI), ethnicity, smoking status, and the presence of diabetes on RBC EPA + DHA independent of fish intake.

MATERIALS AND METHODS

Volunteer selection. Healthy men and women between the ages of 20 and 80 from the Kansas City Metropolitan area were invited to participate in this study. Although generally healthy individuals were sought, those with self-reported, well-controlled type 1 or type 2 diabetes mellitus qualified as well. Individuals reporting consumption of fish oil supplements were excluded. The demographic information collected included age, gender, height, weight, ethnicity, smoking, diabetes, and the number of servings of tuna or nonfried fish consumed per month (hereafter referred to as "fish intake"). Weekly fish intake was calculated based on the reported monthly intake. The intake of tuna or nonfried fish was specifically queried because the answer to this question proved to be a powerful predictor of risk for death from ischemic heart disease in the Cardiovascular Health Study (19). Hence, we sought to determine whether it would correlate with RBC EPA + DHA. The protocol was approved by the Saint Luke's Hospital Institutional Review Board, and informed, written consent was obtained.

Laboratory methods. The sum of the EPA and the DHA, expressed as a percentage of total RBC FA, was measured as described previously (8). Briefly, blood was collected in EDTA, and the RBC pellet was isolated by centrifugation. After discarding the plasma and buffy coat, RBC were frozen at –70°C. The RBC pellet was warmed to room temperature, and an aliquot was extracted with isopropanol and hexane (each containing 50 mg/L of the antioxidant BHT). The lipid extract was dried under nitrogen and methylated for 10 min at 100°C with BF_3–methanol (Sigma, St. Louis, MO). After cooling, the FAME were extracted with hexane after the addition of water. The sample was again dried under nitrogen, reconstituted with hexane, and analyzed by flame ionization GC (Shimadzu GC-14A; Shimadzu Corporation, Kyoto, Japan) using a capillary column (SUPELCOWAX 10, 30 m length, 0.32 mm i.d., 0.25 µm film thickness; Supelco, Bellefonte, PA). FA were identified by comparison with known standards, and FA composition was reported as the weight percentage of total FA.

Statistical analysis. Univariate regression and one-way ANOVA models were used to determine the effects of each patient characteristic on RBC EPA + DHA. Analysis of covariance (ANCOVA) was used to determine the effect of fish consumption on RBC EPA + DHA after considering other possible influences (age, BMI, diabetes, gender, race, smoking). Nonlinear relationships were explored by testing quadratic terms in the ANCOVA models. Model assumptions were checked and verified. A critical alpha level of 0.05 was used to determine significance, and all significance tests were two-tailed. All data were analyzed using SAS, version 8.02 (SAS Institute, Cary, NC).

RESULTS

The study population included 163 individuals, 74 males and 89 females [Caucasian, 134 (82%); African American, 13 (8%); Hispanic, 10 (6%); Native American, Asian, East Indian, Arabic, 6 (3.6%)], with an average (±SD) age of 48 ± 15 yr (ages 20–29, 24; ages 30–39, 27; ages 40–49, 36; ages 50–59, 35; 60 and above, 41). Other study population characteristics were as follows: BMI, 26.2 ± 4.8 (range 18–47); servings per

month of tuna and nonfried fish, 4.2 ± 4.2 (range 0–30); smokers, 13 (8%); persons with diabetes, 13 (8%). The mean (±SD) RBC EPA + DHA was 4.9 ± 2.1%, with a range of 1.7 to 12.4% (Fig. 1). RBC EPA + DHA was below 8% in 91% of the sample and below 4% in 44% of the sample (Fig. 1).

Of the seven patient characteristics examined, five (all but gender and smoking status) proved to be significant predictors of RBC EPA + DHA on a univariate analysis (Table 1). On a multivariate analysis, ethnicity ceased to be a predictor, leaving BMI, age, diabetes, and fish intake as independent predictors. From Table 1, one can see that every additional 10 yr of age increased RBC EPA + DHA by 0.5 units, that each 3-unit rise in BMI decreased the Omega-3 Index by 0.3 units, and that the presence of diabetes was associated with a 1.13-unit decrease in RBC EPA + DHA. For every reported monthly serving of tuna or other nonfried fish, RBC EPA + DHA increased by 0.24 units. The relationships between reported fish intake (by frequency category and continuously) and the Omega-3 Index are presented in Figures 2 and 3. In both cases, there was a highly significant positive relationship between intake and this biomarker.

Although overall, men and women did not have significantly different unadjusted values for RBC EPA + DHA (5.0 ± 1.9 vs. 4.7 ± 2.2, *P* = 0.25), an examination of the male–female difference by decade suggested that women tended to have slightly higher levels than men (except for the 30s; Fig.
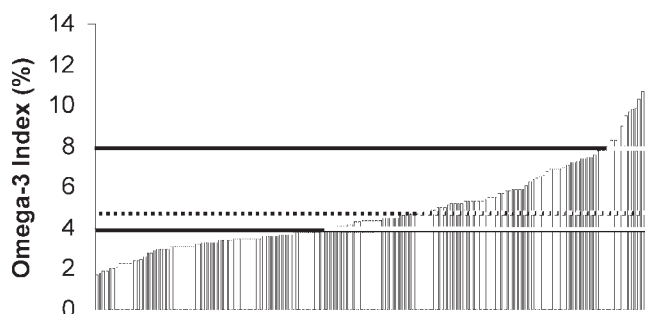
FIG. 1. Distribution of the percentage of red blood cell (RBC) EPA + DHA values (Omega-3 Index) in the study population. Lines at 8% and 4% indicate proposed low- and high-risk horizons, respectively, and the dotted line at 4.9% is the population average.

TABLE 1
Red Blood Cell EPA + DHA Model Results

Independent variable	Univariate[a]				Multivariate[b]			
	Estimate	Lower 95% CI	Upper 95% CI	*P*-value	Estimate	Lower 95% CI	Upper 95% CI	*P*-value
Fish servings	0.30	0.24	0.36	<0.0001	0.24	0.18	0.29	<0.0001
Age (10 yr)	0.53	0.33	0.73	<0.0001	0.49	0.33	0.66	<0.0001
BMI (3 units)	−0.40	−0.59	−0.21	<0.0001	−0.31	−0.46	−0.16	<0.0001
Diabetes	−1.15	−2.32	0.01	0.053	−1.13	−2.04	−0.22	0.0153
Female	0.37	−0.27	1.01	0.251	−0.28	−0.75	0.20	0.2473
Caucasian	1.07	0.25	1.89	0.011	0.47	−0.12	1.06	0.1160
Smoker	−0.20	−1.38	0.98	0.739	0.39	−0.44	1.22	0.3509

[a]Regression and ANOVA results.
[b]Multivariate regression and analysis of covariance results. CI, confidence inteval; BMI, body mass index.
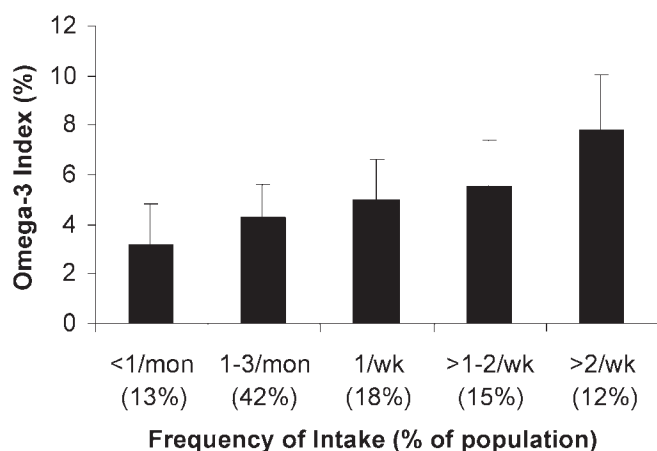
FIG. 2. Percentage of RBC EPA + DHA (Omega-3 Index) by category of reported consumption of tuna or nonfried fish per month. Groups differed by ANOVA ($P < 0.0001$), with the highest RBC EPA + DHA group differing significantly from all others ($P < 0.05$) and the second highest differing from the first ($P < 0.05$) by Tukey's *post hoc* test. The percentage of the population falling into each intake group is given in parentheses. For abbreviation see Figure 1.
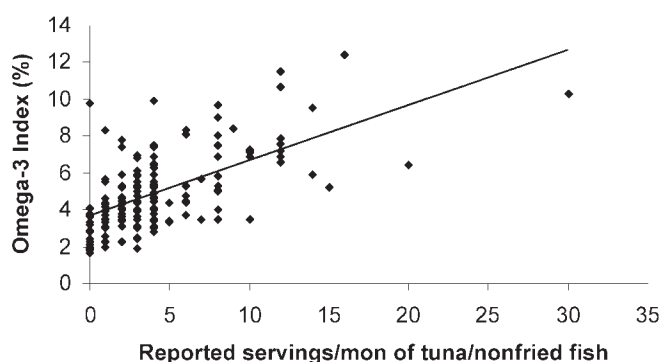
FIG. 3. The continuous relationship between the percentage of RBC EPA + DHA (Omega-3 Index) and reported monthly intake of tuna and nonfried fish. $R = 0.61$, $P < 0.0001$. For abbreviation see Figure 1.

4). On the multivariate analysis (which included a variety of relevant covariates), women did not have higher levels of RBC EPA + DHA (Table 1).

DISCUSSION

The average RBC EPA + DHA in this sample of 163 individuals not taking n-3 FA supplements was 4.9%. This value is well below the proposed 8% target value associated with a significantly reduced risk of CHD death; consistent with past reports (8), it is close to the high-risk value of 4% that has recently been proposed. RBC EPA + DHA varied by over sevenfold in this sample. Although we assumed that much of this variance was due to differences in fish intake, other factors influencing the Omega-3 Index had not been examined previously.

The number of servings of oily fish consumed per month did indeed have a major effect on long-chain n-3 FA blood
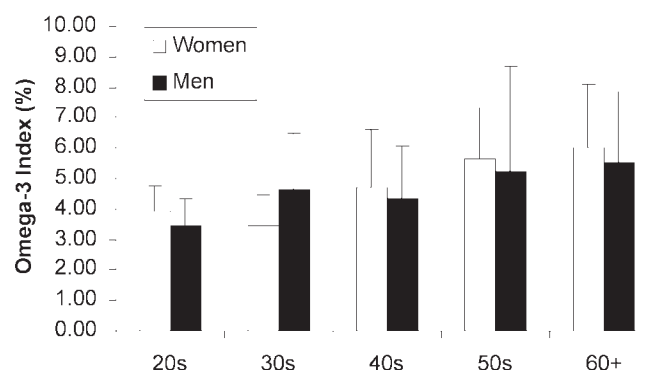
FIG. 4. Percentage of RBC EPA + DHA (Omega-3 Index) as a function of sex within age categories by univariate analysis. Male–female differences within categories were not significantly different. For abbreviation see Figure 1.

levels (Figs. 2 and 3). This was, of course, expected and suggests that simply inquiring about the number of tuna or nonfried fish meals a patient is consuming on a monthly basis will provide a reasonable estimate of his or her RBC EPA + DHA. This finding confirms what has already been shown with n-3 FA capsules, i.e., that the EPA + DHA content of RBC membranes is a valid reflection of n-3 FA intake (8).

Age was an independent predictor of RBC EPA + DHA, even after adjusting for fish intake. Interestingly, older rats have been reported to have higher cardiac DHA levels than younger rats fed the same diet (20). A similar association between age and plasma phospholipid n-3 FA content was observed in three separate populations in Quebec—the James Bay Cree, the Inuit of Nunavik, and individuals living in and around Quebec City (21–23). These authors attributed this relationship to the fact that older people traditionally consume more fish than younger individuals, but they did not report fish intake or adjust for it (23). One could speculate that older individuals may consume more α-linolenic acid or may convert it to longer-chain n-3 FA more readily than younger people. In addition, the rise in RBC EPA + DHA with age could reflect an increasingly slower turnover of n-3 FA in tissues. More studies in humans are needed to explore these possibilities.

An increase in BMI was associated with decreasing proportions of EPA + DHA in human erythrocyte membranes, again independent of reported frequency of fish intake. A simplistic interpretation of this observation may be that since fish is not typically served on a body-weight basis, obese individuals would consume a smaller "dose" of fish per unit of body weight than leaner individuals. This could lead to a lower concentration of long-chain n-3 FA in the larger total lipid pool. Alternatively, Cazzola *et al.* (24) recently showed that RBC from obese individuals are more susceptible to oxidative stress. They also found, as we did, a lower n-3 FA content in RBC membranes. Hence, the lower n-3 FA content could be secondary to increased oxidative processes characteristic of the obese state.

It has recently been reported that women may have a greater capacity to synthesize long-chain n-3 FA from short-

chain n-3 FA (25), and they tend to have higher plasma n-3 FA levels than men (26–28). This may reflect their physiological need to provide preformed DHA to the developing fetus. In light of these observations, we expected the women in our survey to have higher proportions of EPA + DHA in RBC membranes than the men. A trend toward this was seen in the univariate analysis, but the trend was reversed when other covariates were considered. Hence, sex alone does not appear to be a determinant of RBC EPA + DHA. Larger studies with greater power will be needed to examine this relationship.

The number of subjects who smoked, were diabetic, or were members of minority groups was small; thus, conclusions from these subgroups are only suggestive. In this study, smoking was not associated with reduced levels of EPA + DHA in RBC. This is in agreement with some studies (22,26) but not others (27,29). The presence of diabetes was associated with reduced RBC EPA + DHA values, in agreement with some studies (30) but not others (30–32). The inhibition of Δ6- and Δ5-desaturases (the enzymes responsible for converting α-linolenic acid to long-chain n-3 FA) in the diabetic state has been reported (33), but whether it applies in type 2 as well as type 1 diabetes is not clear. Ethnicity (i.e., not Caucasian) ceased to be a significant predictor of RBC EPA + DHA in the multivariate analysis. In other words, the lower RBC EPA + DHA seen in the non-Caucasian groups was likely the result of their generally being younger, heavier, and less likely to consume fish than the Caucasian group.

The RBC EPA + DHA, as measured here, may not be comparable to that reported by other workers for several reasons. First, in an effort to focus on the FA composition of the glycerophospholipids (and to exclude those from RBC sphingolipids), we methylated the lipid extract for 10, not 45, min. This also made the assay quicker to perform, which has obvious advantages in a clinical setting. Second, our method included one freeze–thaw cycle. This was shown in preliminary experiments to reduce the EPA + DHA content by about 10% compared with fresh RBC, but no further loss was noted with two or three freeze–thaw cycles. Since we anticipate that samples from most future research projects (i.e., large, prospective randomized trials with hard cardiovascular disease events as end points) will have been frozen at baseline, we chose to include this step in the routine assay so that cut-points identified with these frozen samples will be applicable in the clinical setting as well. Finally, myriad GC variables, pre- and postprocessing, known and unknown, conspire to almost guarantee significant laboratory-to-laboratory (and instrument-to-instrument) variability in an assay that is based on percent composition.

In conclusion, the content of EPA + DHA in human RBC membranes is a valid marker of the intake of long-chain n-3 FA from tuna and other nonfried fish. In addition, at least two factors besides n-3 FA intake appear to influence their incorporation into RBC membranes: age and BMI, with a suggestion that diabetes may also have an effect. Further studies are warranted to define the other factors that influence this emerging CHD risk factor more carefully.

ACKNOWLEDGMENTS

Disclaimer

W.S.H. holds a minority interest in OmegaMetrix, LLC, a company that offers a test for RBC EPA + DHA.

REFERENCES

1. Kris-Etherton, P.M., Harris, W.S., and Appel, L.J. (2002) Fish Consumption, Fish Oil, n-3 Fatty Acids, and Cardiovascular Disease, *Circulation 106*, 2747–2757.
2. Knapp, H.R. (1997) Dietary Fatty Acids in Human Thrombosis and Hemostasis, *Am. J. Clin. Nutr. 65* (Suppl.), 1687S–1698S.
3. Mori, T.A., Vandongen, R., Mahanian, F., and Douglas, A. (1992) Plasma Lipid Levels and Platelet and Neutrophil Function in Patients with Vascular Disease Following Fish Oil and Olive Oil Supplementation, *Metabolism 41*, 1059–1067.
4. Harris, W.S. (1997) n-3 Fatty Acids and Serum Lipoproteins: Human Studies, *Am. J. Clin. Nutr. 65* (Suppl.), 1645S–1654S.
5. Christensen, J.H., Skou, H.A., Fog, L., Hansen, V.E., Vesterlund, T., Dyerberg, J., Toft, E., and Schmidt, E.B. (2001) Marine n-3 Fatty Acids, Wine Intake, and Heart Rate Variability in Patients Referred for Coronary Angiography, *Circulation 103*, 651–657.
6. Huikuri, H.V., Castellanos, A., and Myerberg, R.J. (2001) Sudden Death Due to Cardiac Arrhythmias, *N. Engl. J. Med. 345*, 1473–1482.
7. GISSI-Prevenzione Investigators (1999) Dietary Supplementation with n-3 Polyunsaturated Fatty Acids and Vitamin E in 11,324 Patients with Myocardial Infarction: Results of the GISSI-Prevenzione Trial, *Lancet 354*, 447–455.
8. Harris, W.S., and von Schacky, C. (2004) RBC EPA + DHA: A New Risk Factor for Sudden Cardiac Death? *Prev. Med. 39*, 212–220.
9. Harris, W.S., Sands, S.A., Windsor, S.L., Ali, H.A., Stevens, T.L., Magalski, A., Porter, C.B., and Borkon, A.M. (2004) n-3 Fatty Acids in Cardiac Biopsies from Heart Transplant Patients: Correlation with Erythrocytes and Response to Supplementation, *Circulation 110*, 1645–1649.
10. Siscovick, D.S., Raghunathan, T.E., King, I., Weinmann, S., Wicklund, K.G., Albright, J., Bovbjerg, V., Arbogast, P., Smith, H., Kushi, L.H., *et al.* (1995) Dietary Intake and Cell Membrane Levels of Long-Chain n-3 Polyunsaturated Fatty Acids and the Risk of Primary Cardiac Arrest, *J. Am. Med. Assoc. 274*, 1363–1367.
11. Albert, C.M., Campos, H., Stampfer, M.J., Ridker, P.M., Manson, J.E., Willett, W.C., and Ma, J. (2002) Blood Levels of Long-Chain n-3 Fatty Acids and the Risk of Sudden Death, *N. Engl. J. Med. 346*, 1113–1118.
12. Palozza, P., Sgarlata, E., Luberto, C., Piccioni, E., Anti, M., Marra, G., Armelao, F., Franceschelli, P., and Bartoli, G.M. (1996) n-3 Fatty Acids Induce Oxidative Modifications in Human Erythrocytes Depending on Dose and Duration of Dietary Supplementation, *Am. J. Clin. Nutr. 64*, 297–304.
13. Lund, E.K., Harvey, L.J., Ladha, S., Clark, D.C., and Johnson, I.T. (1999) Effects of Dietary Fish Oil Supplementation on the Phospholipid Composition and Fluidity of Cell Membranes from Human Volunteers, *Ann. Nutr. Metab. 43*, 290–300.
14. Berlin, E., Bhathena, S.J., Judd, J.T., Nair, P.P., Peters, R.C., Bhagavan, H.N., Ballard-Barbash, R., and Taylor, P.R. (1992)

Effects of n-3 Fatty Acid and Vitamin E Supplementation on Erythrocyte Membrane Fluidity, Tocopherols, Insulin Binding, and Lipid Composition in Adult Men, *J. Nutr. Biochem. 3*, 392–400.

15. Francois, C.A., Connor, S.L., Bolewicz, L.C., and Connor, W.E. (2003) Supplementing Lactating Women with Flaxseed Oil Does Not Increase Docosahexaenoic Acid in Their Milk, *Am. J. Clin. Nutr. 77*, 226–233.

16. Mills, D.E., Murthy, M., and Galey, W.R. (1995) Dietary Fatty Acids, Membrane Transport, and Oxidative Sensitivity in Human Erythrocytes, *Lipids 30*, 657–663.

17. Kamada, T., Yamashita, T., Baba, Y., Kai, M., Setoyama, S., Chuman, Y., and Otsuji, S. (1986) Dietary Sardine Oil Increases Erythrocyte Membrane Fluidity in Diabetic Patients, *Diabetes 35*, 604–611.

18. Flaten, H., Hostmark, A.T., Kierulf, P., Lystad, E., Trygg, K., Bjerkedal, T., and Osland, A. (1990) Fish-Oil Concentrate: Effects on Variables Related to Cardiovascular Disease, *Am. J. Clin. Nutr. 52*, 300–306.

19. Mozaffarian, D., Lemaitre, R.N., Kuller, L.H., Burke, G.L., Tracy, R.P., and Siscovick, D.S. (2003) Cardiac Benefits of Fish Consumption May Depend on the Type of Fish Meal Consumed: The Cardiovascular Health Study, *Circulation 107*, 1372–1377.

20. Gudbjarnason, S. (1989) Dynamics of n-3 and n-6 Fatty Acids in Phospholipids of Heart Muscle, *J. Intern. Med. 225* (Suppl. 1), 117–128.

21. Dewailly, E., Blanchet, C., Gingras, S., Lemieux, S., Sauve, L., Bergeron, J., and Holub, B.J. (2001) Relations Between n-3 Fatty Acid Status and Cardiovascular Disease Risk Factors Among Quebecers, *Am. J. Clin. Nutr. 74*, 603–611.

22. Dewailly, E., Blanchet, C., Lemieux, S., Sauve, L., Gingras, S., Ayotte, P., and Holub, B.J. (2001) n-3 Fatty Acids and Cardiovascular Disease Risk Factors Among the Inuit of Nunavik, *Am. J. Clin. Nutr. 74*, 464–473.

23. Dewailly, E., Blanchet, C., Gingras, S., Lemieux, S., and Holub, B.J. (2002) Cardiovascular Disease Risk Factors and n-3 Fatty Acid Status in the Adult Population of James Bay Cree, *Am. J. Clin. Nutr. 76*, 85–92.

24. Cazzola, R., Rondanelli, M., Russo-Volpe, S., Ferrari, E., and Cestaro, B. (2004) Decreased Membrane Fluidity and Altered Susceptibility to Peroxidation and Lipid Composition in Over-weight and Obese Female Erythrocytes, *J. Lipid Res. 45*, 1846–1851.

25. Burdge, G.C., and Wootton, S.A. (2002) Conversion of α-Linolenic Acid to Eicosapentaenoic, Docosapentaenoic and Docosahexaenoic Acids in Young Women, *Br. J. Nutr. 88*, 411–420.

26. Kuriki, K., Nagaya, T., Tokudome, Y., Imaeda, N., Fujiwara, N., Sato, J., Goto, C., Ikeda, M., Maki, S., Tajima, K., and Tokudome, S. (2003) Plasma Concentrations of (n-3) Highly Unsaturated Fatty Acids Are Good Biomarkers of Relative Dietary Fatty Acid Intakes: A Cross-Sectional Study, *J. Nutr. 133*, 3643–3650.

27. Hibbeln, J.R., Makino, K.K., Martin, C.E., Dickerson, F., Boronow, J., and Fenton, W.S. (2003) Smoking, Gender, and Dietary Influences on Erythrocyte Essential Fatty Acid Composition Among Patients with Schizophrenia or Schizoaffective Disorder, *Biol. Psychiatry 53*, 431–441.

28. Giltay, E.J., Gooren, L.J., Toorians, A.W., Katan, M.B., and Zock, P.L. (2004) Docosahexaenoic Acid Concentrations Are Higher in Women Than in Men Because of Estrogenic Effects, *Am. J. Clin. Nutr. 80*, 1167–1174.

29. Simon, J.A., Fong, J., Bernert, J.T., Jr., and Browner, W.S. (1996) Relation of Smoking and Alcohol Consumption to Serum Fatty Acids, *Am. J. Epidemiol. 144*, 325–334.

30. Seigneur, M., Freyburger, G., Gin, H., Claverie, M., Lardeau, D., Lacape, G., LeMoigne, F., Crockett, R., and Boisseau, M.R. (1994) Serum Fatty Acid Profiles in Type I and Type II Diabetes: Metabolic Alterations of Fatty Acids of the Main Serum Lipids, *Diabetes Res. Clin. Pract. 23*, 169–177.

31. Pelikanova, T., Kohout, M., Valek, J., Base, J., and Stefka, Z. (1991) Fatty Acid Composition of Serum Lipids and Erythrocyte Membranes in Type 2 (non-insulin-dependent) Diabetic Men, *Metabolism 40*, 175–180.

32. Clore, J.N., Allred, J., White, D., Li, J., and Stillman, J. (2002) The Role of Plasma Fatty Acid Composition in Endogenous Glucose Production in Patients with Type 2 Diabetes Mellitus, *Metabolism 51*, 1471–1477.

33. Brenner, R.R. (2003) Hormonal Modulation of Δ6 and Δ5 Desaturases: Case of Diabetes, *Prostaglandins Leukot. Essent. Fatty Acids 68*, 151–162.

Triacylglycerol Hydroperoxides Not Detected in Pig Small Intestinal Epithelial Cells After a Diet Rich in Oxidized Triacylglycerols

Jukka-Pekka Suomela[a,*], **Markku Ahotupa**[b], **and Heikki Kallio**[a]

Departments of [a]Biochemistry and Food Chemistry and [b]Biomedicine, University of Turku, FI-20014 Turku, Finland

ABSTRACT: The presence of TAG hydroperoxides in the epithelial cells of the small intestines in growing pigs was studied after they had consumed a diet rich in either nonoxidized or oxidized sunflower seed oil (PV in oils, 1 and 190 mequiv O_2/kg, respectively). To obtain molecular-level information on the oxidized TAG structures, a new approach based on TLC and HPLC-electrospray ionization-MS was used in the analysis of the samples. TAG hydroperoxides were not detected in the small intestinal mucosa or adipose tissue of either group, whereas TAG hydroxides, ketones, and epoxides were detected in all samples. The results suggest that dietary TAG hydroperoxides do not lead to the appearance of these molecules in the tissues.

Paper no. L9660 in *Lipids 40*, 349–353 (April 2005).

Various studies suggest that oxidized FA within dietary lipids increase the oxidation level of human lipoproteins (1–3). Thus, it seems that the oxidized lipids are absorbed in the small intestine and/or they initiate a cascade of subsequent reactions that result in the increased oxidation of lipoproteins. It is unclear, however, in what degree different types of lipid oxidation products survive from mouth to small intestine and beyond, and whether all forms of oxidized lipids are absorbed.

The studies of Kanner and Lapidot (4) suggest that human stomach fluid, having a low pH, may be a good medium for food lipid peroxidation. On the other hand, in studies performed in rats by Kanazawa and Ashida (5,6), linoleic acid hydroperoxides did not reach the small intestine when dosed intragastrically at moderate levels as such or as trilinoleoylglycerol hydroperoxides. Only when very high doses (200 μmol or more) of linoleic acid hydroperoxides were used was partial transport to the small intestine observed. In the stomach, trilinoleoylglycerol hydroperoxides were broken down to linoleic acid hydroperoxides and hydroxides. Pure linoleic acid hydroperoxides given intragastrically were decomposed to hydroxides, epoxyketones, and aldehydes. Only aldehydes entered the small intestine when moderate levels of hydroperoxides were used. Aldehydes also seemed to be partly absorbed into the body.

If lipid hydroperoxides, either originating from diet or formed in the gastrointestinal tract (4,7), are present in the

small intestine, then they seem to be effectively removed by glutathione peroxidase under normal conditions. However, the hydroperoxides may be transported into lymph in conditions where the supply of glutathione is limited (8,9).

To study the effect of diet on the presence of FA hydroperoxides in tissue TAG, we investigated the small intestine mucosa and the adipose tissue of growing pigs after a 2-wk period of consuming a diet rich in either nonoxidized or oxidized sunflower seed oil. An approach based on TLC and HPLC-electrospray ionization (ESI)-MS was used in the analysis of the oxidized tissue lipids (10).

MATERIALS AND METHODS

Chemicals and reagents. 3-Chloroperoxybenzoic acid, triphenyl phosphine, and activated manganese dioxide (MnO_2) were obtained from Aldrich Chemical Co. (Milwaukee, WI). Reagents were of reagent grade or better quality. All solvents were of chromatography or reagent grade and were purchased from local suppliers. HPLC standard (G-1) containing synthetic monoacid TAG was obtained from Nu-Chek-Prep, Inc. (Elysian, MN). Synthetic 1,3-distearoyl-2-oleoyl-*sn*-glycerol was obtained from Sigma Chemical Co. (St. Louis, MO). 1,3-Didocosanoyl-2-oleoyl-*sn*-glycerol and 1-linoleoyl-2-oleoyl-3-palmitoyl-*sn*-glycerol were obtained from Larodan Fine Chemicals AB (Malmö, Sweden).

Preparation of reference compounds. The oxidized derivatives of synthetic TAG were prepared as described earlier (10). TAG hydroperoxides were prepared by photosensitized oxidation. TAG (10–20 mg) was added to 3 mL of methylene blue solution (0.1 mM methylene blue in dichloromethane) in a test tube that was placed in an ice bath under a 250 W photographer's lamp for 28 h. The distance between the sample solution and the lamp was approximately 20 cm. Hydroperoxides were purified by TLC as described below.

Animals and diets. The study plan was approved by the Test Animal Committee of MTT Agrifood Research Finland. Growing pigs (castrated boars) were used in the study. For 2 wk, two groups of three pigs (groups 1 and 2) were fed a diet (Table 1) containing 16% nonoxidized or oxidized sunflower seed oil. The average weight of the animals (average age 11 wk) was 28.1 ± 3.5 kg at the beginning of the feeding period and 39.5 ± 4.3 kg at the end of the period. The oil of group 1 was not oxidized (PV, 1 mequiv O_2/kg), whereas the oil of

---

*To whom correspondence should be addressed. E-mail: jusuom@utu.fi

Abbreviations: ACN:DB, acyl carbon number:number of double bonds; ESI, electrospray ionization.

TABLE 1
Composition of the Feed of the Pigs[a]

Component	g/kg feed	Component	g/kg feed
Barley	395.4	Monocalcium phosphate	8.3
Granulated soy[b]	384.6	Murovit-Selen-E[c]	23.2
Sunflower seed oil	160.0	Mineral-vitamin mix[d]	17.1
Feeding lime	11.5		

[a]Total energy from fat: 1530–1650 kcal/kg feed.
[b]Contains 3.4–6.8% fat.
[c]In kg of feed: 0.2 mg Se; 81 IU vitamin E.
[d]In kg of feed: 3.0 g Ca; 1.1 g P; 0.7 g Mg; 4.3 g NaCl; 135 mg Fe; 29 mg Cu; 0.4 mg Se; 119 mg Zn; 31 mg Mn; 0.3 mg I; 6806 IU vitamin A; 681 IU vitamin D; 65 mg vitamin E; 2.4 mg vitamin K; 2.5 mg vitamin B_1; 6.1 mg vitamin B_2; 3.6 mg vitamin B_6; 0.03 mg vitamin B_{12}; 0.3 mg biotin; 18.4 mg pantotenic acid; 27 mg niacin; 4.3 mg folic acid.

TABLE 2
FA Compositions of the Oils Fed to Pigs[a]

FA	Oil 1[b]	Oil 2[c]
16:0	5.8	6.0
18:0	3.5	3.6
18:1n-9	25.3	26.0
18:1n-7	0.6	0.6
18:2n-6	63.4	62.2
18:3n-3	0.1	0.1
20:0	0.2	0.2
20:1n-9	0.2	0.2
22:0	0.7	0.7
24:0	0.2	0.2

[a]Results expressed as percentage of total FA.
[b]PV, 1 mequiv O_2/kg oil.
[c]PV, 190 mequiv O_2/kg oil.

group 2 was oxidized in a convection oven at 60°C until a PV of 190 mequiv O_2/kg was reached. The PV determinations were made according to the AOCS Official Method Cd 8-53 (11). The vitamin E contents of the oils were as follows: group 1, 550 mg/kg; group 2, 103 mg/kg. The vitamin E determinations were made according to IUPAC 2.432 method (12). FA compositions of the oils (Table 2) were determined as described below.

The pigs were fed twice a day. During the first week, the pigs were fed 200 g oil/d and during the second week 230 g oil/d. Because of the high fat load, the pigs were fed in total 161 mg vitamin E/kg feed, not including vitamin E from the oils (Table 1).

Sample preparation. Pigs were killed 2–3 h after the last meal (half of the daily dose). An approximately 40-cm length of small intestine was detached at a distance of 80–200 cm from the beginning of the small intestine, the distance depending on the progress of intestinal contents. After the ends were tied, the detached intestinal portion was placed into a box containing physiological salt solution at 0°C. Later, the portion was split in the longitudinal direction. The contents were removed and the piece was rinsed with tepid water. The epithelial cells were scraped off the intestinal wall, and the lipids were extracted using chloroform/methanol (2:1, vol/vol).

Also, a small portion of adipose tissue was detached from the neck after slaughter. The lipids of the tissue were extracted using chloroform/methanol (2:1, vol/vol).

Purification of TAG and their oxidation products. For FA analysis, the TAG of small intestinal mucosa and adipose tissue were purified using Sep-Pak® (Milford, MA) prepacked silica columns (13). Normal-phase TLC was used to purify the oxidation products of the reference compounds and of the tissue TAG (14). Heptane/di-isopropyl ether/acetic acid (60:40:4, by vol) solution was used as the mobile eluent. Samples were applied to silica G-plates. The TAG band (R_f typically 0.59) and/or the fractions containing the oxidized TAG molecules (below the TAG band) were scraped off the plates. The lipids were recovered from the silica gel by extraction with chloroform/methanol (2:1, vol/vol). The extracts were washed with distilled water. TAG and their oxidation products were detected in UV light after spraying with 2,7-dichlorofluorescein.

FA analysis. The FAME of TAG were prepared by sodium methoxide-catalyzed transesterification (15). Methyl esters were dissolved in hexane and analyzed by GC (PerkinElmer AutoSystem, Norwalk, CT) using a DB-23 column (30 m × 0.32 mm i.d., 0.25 µm film thickness; Agilent Technologies, Palo Alto, CA). The instrument was equipped with an FID.

Analysis of samples by HPLC-ESI-MS. The oxidation products of TAG were separated by RP-HPLC (10). The HPLC system consisted of a Hitachi (Tokyo, Japan) L-6200 Intelligent Pump with a Discovery® HS C18 column (250 × 4.6 mm i.d.; Supelco Inc., Bellefonte, PA). The column was eluted at 0.85 mL/min and a linear gradient was used: 20% 2-propanol in methanol was changed to 80% 2-propanol in 20 min. The final composition was held for 10 min. Eighty-five percent of the effluent (0.72 mL/min) was led to a Sedex 75 (S.E.D.E.R.E., Alfortville, France) ELSD. An evaporation temperature of 70°C and nebulizer gas (air) pressure of 2.7 bar were used in the ELSD. Fifteen percent of the effluent (0.13 mL/min) was led to a Finnigan MAT TSQ 700 triple quadrupole mass spectrometer (Finnigan, San Jose, CA) equipped with a nebulizer-assisted electrospray interface. Full-scan MS spectra were collected in positive ionization mode (*m/z* 450–1100). The electrospray voltage used was +4.5 kV.

Statistical analysis. SPSS 12.0 for Windows (Chicago, IL) was used for data analysis. The comparison of FA compositions was carried out with independent samples *t*-test and Mann–Whitney U-test.

RESULTS AND DISCUSSION

The FA compositions of the TAG extracted from the small intestinal mucosa of the pigs are presented in Table 3. The TAG represent mainly the reassembled molecules formed inside the epithelial cells. Minor amounts of the TAG may also originate from the luminal side of the cells, representing molecules not broken down by gastric and pancreatic lipases and not detached by rinsing. As expected, the FA compositions reflected to a large degree those of the dietary sunflower seed oils. However, the relative amounts of 16:0 were higher and those of 18:1n-9 were lower in the mucosa of both groups compared with the test oils. In group 2, but not in group 1, the relative amount of mucosal 18:2n-6 seemed to be lower compared with the corresponding test oil.

TABLE 3
FA Compositions of the Small Intestine Mucosal TAG[a]

FA	Group 1[b]	Group 2[c]
16:0	8.2 ± 0.1	9.4 ± 0.5
16:1n-7	0.0 ± 0.0	0.3 ± 0.1
18:0	3.6 ± 0.1	5.0 ± 0.6
18:1n-9	22.5 ± 0.2	23.6 ± 0.1
18:1n-7	0.7 ± 0.0	0.8 ± 0.1
18:2n-6	63.4 ± 0.2	58.2 ± 0.0
18:3n-3	0.8 ± 0.1	0.7 ± 0.1
20:0	0.0 ± 0.1	0.2 ± 0.2
20:1n-9	0.1 ± 0.1	0.1 ± 0.1
20:4n-6	0.7 ± 0.3	1.0 ± 0.0

[a]Results expressed as percentage of total FA (mean ± SD).
[b]$n = 3$.
[c]$n = 2$.

The relative amounts of 16:0, 18:0, and 18:1n-9 seemed to be higher and the relative amounts of 18:2n-6 lower in group 2 and test oil 2 compared with group 1 and test oil 1, respectively (Table 3). However, the differences were larger in the mucosal FA compared with the test oil FA. None of the differences between groups 1 and 2 reached statistical significance, evidently because of small group sizes. We were able to analyze all three mucosal samples of group 1, but only two samples of group 2. In spite of this, it seems likely that the differences in mucosal TAG FA composition between the groups were caused by different dietary oils.

The relative amount of 16:0 appeared to be slightly higher and that of 18:2n-6 slightly lower in the adipose tissue of group 2 compared with group 1 (Table 4). This indicates an effect of test oil autoxidation on adipose tissue FA composition.

The oxidized TAG molecules were detected by extracting peaks of a specific m/z value from the MS chromatograms of HPLC runs (Fig. 1). Only sodium adduct ions were formed from the molecules in the positive ionization mode, which simplified identification. If the retention time for a peak of an m/z value suggested a certain type of oxidation product and a particular FA composition, and a homologous series of ions was found in the chromatogram, this was regarded as evidence of a certain molecular structure (10).

TABLE 4
FA Compositions of the Adipose Tissue TAG[a]

FA	Group 1[b]	Group 2[b]
14:0	1.0 ± 0.2	1.1 ± 0.1
16:0	19.1 ± 0.9	20.6 ± 1.4
16:1n-7	3.0 ± 0.8	3.0 ± 1.1
18:0	8.6 ± 1.3	8.6 ± 1.5
18:1n-9	37.0 ± 4.6	37.6 ± 1.5
18:1n-7	2.8 ± 0.1	3.0 ± 0.3
18:2n-6	24.8 ± 4.9	22.6 ± 2.3
18:3n-3	0.8 ± 0.1	0.8 ± 0.1
20:0	0.1 ± 0.0	0.1 ± 0.0
20:1n-9	0.7 ± 0.2	0.7 ± 0.1
20:2n-6	0.7 ± 0.1	0.7 ± 0.1
20:4n-6	0.5 ± 0.0	0.4 ± 0.1
Others	0.9 ± 0.1	0.7 ± 0.2

[a]Results expressed as percentage of total FA (mean ± SD).
[b]$n = 3$.
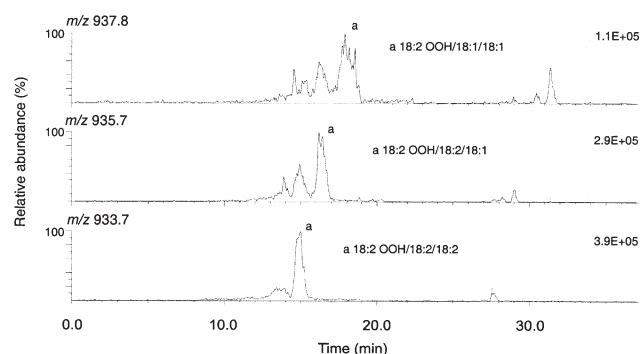
FIG. 1. Ion chromatograms showing the major TAG hydroperoxide species of the oxidized sunflower seed oil (PV, 190 mequiv O_2/kg). Molecular ions ($[M + Na]^+$) with an acyl carbon number of 54 are shown.

The molecular ions of the reference compounds containing a hydroperoxide group could be detected in mass chromatograms as simultaneously appearing peaks with a difference of 18 mass units, which helped in the identification of such molecules. The phenomenon was due to a cleavage of H_2O in the ion source.

In the oxidized test oil, TAG monohydroperoxides were the major class of oxidized TAG. The monohydroperoxides that were detected were formed from TAG with ACN:DB (acyl carbon number:number of double bonds) 52:2, 52:3, 52:4, 54:3, 54:4, 54:5, and 54:6. Dihydroperoxides were formed from TAG with ACN:DB 52:4, 54:6, and 54:5. However, these TAG hydroperoxides were not detected in the mucosa or the adipose tissue samples, neither as such nor as a combination of hydroperoxy and oxo/epoxy groups. This indicates an absence of these molecules in the tissue TAG, or a considerable decrease in their level compared with the oxidized sunflower seed oil. In taking the sensitivity of the instrumentation into consideration, the decrease was estimated to be at least 80% in the case of monohydroperoxides.

TAG hydroxides, ketones, and epoxides were detected in the tissue samples of both groups (Tables 5 and 6). No core aldehydes were detected. The same oxidized TAG molecular species were detected in both groups. Differences in the relative amounts of oxidized molecules could not be analyzed because of the small number of samples and, in case of mucosal samples, the overlapping of different acylglycerols and their derivatives in ELSD chromatograms. In our lipoprotein study (16) in which the same oils were employed, the amount of oxidized TAG (no hydroperoxides detected) was significantly higher in the lipoproteins of pigs fed the oxidized oil compared with the nonoxidized oil. Nonetheless, the same oxidized TAG molecular species were present in the lipoproteins of both groups.

It is interesting that TAG hydroxides, ketones, and epoxides were also detected in both the nonoxidized and oxidized test oils, although only traces of hydroperoxides were seen in the nonoxidized oil. These findings indicate that our method sensitively detects the secondary oxidation products of TAG present in different matrices.

TABLE 5
Postulated Structures of the Oxidized TAG Molecules Found in the Small Intestine Mucosal Samples[a]

ACN[b]	Hydroxides	Epoxides	Ketones
52	18:3 OH/18:2/16:0	18:2 epoxy/18:2/16:0	18:2 keto/18:2/16:0
	18:2 OH/18:2/16:0	18:2 epoxy/18:1/16:0	18:2 keto/18:1/16:0
	18:2 OH/18:1/16:0	18:1 epoxy/18:2/16:0	18:1 keto/18:2/16:0
	18:1 OH/18:2/16:0	18:1 epoxy/18:1/16:0	18:1 keto/18:1/16:0
	18:1 OH/18:1/16:0[c]	18:1 epoxy/18:0/16:0[c]	18:1 keto/18:0/16:0[c]
		18:0 epoxy/18:1/16:0[c]	18:0 keto/18:1/16:0[c]
54	18:3 OH/18:2/18:2	18:3 epoxy/18:2/18:2	18:3 keto/18:2/18:2
	18:2 OH/18:2/18:2	18:2 epoxy/18:2/18:2	18:2 keto/18:2/18:2
	18:2 OH/18:2/18:1	18:2 epoxy/18:2/18:1	18:2 keto/18:2/18:1
	18:1 OH/18:2/18:2	18:1 epoxy/18:2/18:2	18:1 keto/18:2/18:2
	18:2 OH/18:1/18:1	18:2 epoxy/18:1/18:1	18:2 keto/18:1/18:1
	18:1 OH/18:2/18:1	18:1 epoxy/18:2/18:1	18:1 keto/18:2/18:1
		18:1 epoxy/18:1/18:1	18:1 keto/18:1/18:1

[a]The most probable molecular structures based on *m/z* values, TAG FA compositions, and the assumption that the most unsaturated FA is oxidized; regioisomers are not distinguished.
[b]Acyl carbon number of the molecule.
[c]Uncertain/very weak peak in the chromatogram.

TABLE 6
Postulated Structures of the Oxidized TAG Molecules Found in the Adipose Tissue Samples[a]

ACN[b]	Hydroxides	Epoxides	Ketones
50	18:2 OH/16:1/16:0[c]	18:2 epoxy/16:1/16:0	18:2 keto/16:1/16:0
	18:2 OH/16:0/16:0[c]	18:2 epoxy/16:0/16:0	18:2 keto/16:0/16:0
	18:1 OH/16:0/16:0[c]	18:1 epoxy/16:0/16:0	18:1 keto/16:0/16:0
52	18:3 OH/18:2/16:0[c]	18:2 epoxy/18:2/16:0[c]	18:2 keto/18:2/16:0
	18:2 OH/18:2/16:0[c]	18:2 epoxy/18:1/16:0[c]	18:2 keto/18:1/16:0
	18:2 OH/18:1/16:0[c]	18:1 epoxy/18:2/16:0[c]	18:1 keto/18:2/16:0
	18:1 OH/18:2/16:0[c]	18:1 epoxy/18:1/16:0[c]	18:1 keto/18:1/16:0
	18:1 OH/18:1/16:0[c]	18:1 epoxy/18:0/16:0[c]	18:1 keto/18:0/16:0
		18:0 epoxy/18:1/16:0[c]	18:0 keto/18:1/16:0
54	18:2 OH/18:2/18:2	18:2 epoxy/18:2/18:2	18:2 keto/18:2/18:2
	18:2 OH/18:2/18:1	18:2 epoxy/18:2/18:1	18:2 keto/18:2/18:1
	18:1 OH/18:2/18:2	18:1 epoxy/18:2/18:2	18:1 keto/18:2/18:2
	18:2 OH/18:1/18:1	18:2 epoxy/18:1/18:1	18:2 keto/18:1/18:1
	18:1 OH/18:2/18:1	18:1 epoxy/18:2/18:1	18:1 keto/18:2/18:1
	18:1 OH/18:1/18:1	18:1 epoxy/18:1/18:1	18:1 keto/18:1/18:1
		18:1 epoxy/18:1/18:0	18:1 keto/18:1/18:0

[a]The most probable molecular structures based on *m/z* values, TAG FA compositions, and the assumption that the most unsaturated FA is oxidized; regioisomers are not distinguished.
[b]Acyl carbon number of the molecule.
[c]Uncertain/very weak peak in the chromatogram.

It is noteworthy that our HPLC system was not optimized for the analysis of TAG trihydroperoxides and other equally polar TAG oxidation products. Also, the possibility that some decomposition of hydroperoxy structures had occurred during sample preparation cannot be excluded. However, in our studies, TAG hydroperoxides have been observed to be relatively stable during extraction procedures, TLC, and HPLC runs.

Our results suggest an effective degradation of hydroperoxides before and/or during the reassembly of TAG molecules in the epithelial cells of small intestinal mucosa. The findings are in line with the results of Kanazawa and Ashida (5,6), which showed a very limited transport of hydroperoxides into the small intestine. The results obtained from a limited number of samples encourage further research on the physiological consequences of dietary fat oxidation, which is an area currently not too well understood.

REFERENCES

1. Naruszewicz, M., Wozny, E., Mirkiewicz, E., Nowicka, G., and Szostak, W.B. (1987) The Effect of Thermally Oxidized Soya Bean Oil on Metabolism of Chylomicrons—Increased Uptake and Degradation of Oxidized Chylomicrons in Cultured Mouse Macrophages, *Atherosclerosis 66,* 45–53.
2. Staprans, I., Rapp, J.H., Pan, X.M., Kim, K.Y., and Feingold, K.R. (1994) Oxidized Lipids in the Diet Are a Source of Oxidized Lipid in Chylomicrons of Human Serum, *Arterioscler. Thromb. 14,* 1900–1905.
3. Staprans, I., Hardman, D.A., Pan, X.M., and Feingold, K.R. (1999) Effect of Oxidized Lipids in the Diet on Oxidized Lipid Levels in Postprandial Serum Chylomicrons of Diabetic Patients, *Diabetes Care 22,* 300–306.
4. Kanner, J., and Lapidot, T. (2001) The Stomach as a Bioreactor: Dietary Lipid Peroxidation in the Gastric Fluid and the Effects of Plant-Derived Antioxidants, *Free Radic. Biol. Med. 31,* 1388–1395.
5. Kanazawa, K., and Ashida, H. (1998) Catabolic Fate of Dietary Trilinoleoylglycerol Hydroperoxides in Rat Gastrointestines, *Biochim. Biophys. Acta 1393,* 336–348.
6. Kanazawa, K., and Ashida, H. (1998) Dietary Hydroperoxides of Linoleic Acid Decompose to Aldehydes in Stomach Before Being Absorbed into the Body, *Biochim. Biophys. Acta 1393,* 349–361.
7. Ursini, F., Zamburlini, A., Cazzolato, G., Maiorino, M., Bon, G.B., and Sevanian, A. (1998) Postprandial Plasma Lipid Hydroperoxides: A Possible Link Between Diet and Atherosclerosis, *Free Radic. Biol. Med. 25,* 250–252.
8. Aw, T.Y., Williams, M.W., and Gray, L. (1992) Absorption and Lymphatic Transport of Peroxidized Lipids by Rat Small-Intestine *in vivo*: Role of Mucosal GSH, *Am. J. Physiol. 262,* G99–G106.
9. Aw, T.Y., and Williams, M.W. (1992) Intestinal Absorption and Lymphatic Transport of Peroxidized Lipids in Rats—Effect of Exogenous GSH, *Am. J. Physiol. 263,* G665–G672.
10. Suomela, J.-P., Ahotupa, M., Sjövall, O., Kurvinen, J.-P., and Kallio, H. (2004) New Approach to the Analysis of Oxidized Triacylglycerols in Lipoproteins, *Lipids 39,* 507–512.
11. AOCS (1997) *Official Methods and Recommended Practices of the AOCS,* 5th edn., AOCS Press, Champaign, IL.
12. IUPAC (1987) *Standard Methods for the Analysis of Oils, Fats and Derivatives,* 7th edn., Blackwell Science, Oxford, United Kingdom.
13. Hamilton, J.G., and Comai, K. (1988) Rapid Separation of Neutral Lipids, Free Fatty Acids and Polar Lipids Using Prepacked Silica Sep-Pak Columns, *Lipids 23,* 1146–1149.
14. Skipski, V.P., and Barclay, M. (1969) Thin-Layer Chromatography, *Methods Enzymol. 14,* 542–548.
15. Christie, W.W. (1982) A Simple Procedure for Rapid Transmethylation of Glycerolipids and Cholesteryl Esters, *J. Lipid Res. 23,* 1072–1075.
16. Suomela, J.-P., Ahotupa, M., and Kallio, H. (2005) Triacylglycerol Oxidation in Pig Lipoproteins After a Diet Rich in Oxidized Sunflower Seed Oil, *Lipids*, in press.

Gas Chromatography–Chemical Ionization–Mass Spectrometric Fatty Acid Analysis of a Commercial Supercritical Carbon Dioxide Lipid Extract from New Zealand Green-Lipped Mussel (*Perna canaliculus*)

Christopher J. Wolyniak[a], J. Thomas Brenna[a], Karen J. Murphy[b], and Andrew J. Sinclair[c,*]

[a]Division of Nutritional Sciences, Savage Hall, Cornell University, Ithaca, New York,
[b]Child Health Research Institute, Bedford Park, South Australia 5042, Australia,
and [c]Department of Food Science, RMIT University, Melbourne, Victoria 3001, Australia

ABSTRACT: Supercritical fluid extracts of New Zealand green-lipped mussels (NZGLM) have been suggested to have therapeutic properties related to their oil components. The large number of minor FA in NZGLM extract was characterized by a GC–CIMS/MS method that excels at identification of double-bond positions in FAME. The extract contained five major lipid classes: sterol esters, TAG, FFA, sterols, and polar lipids. The total FA content of the lipid extract was 0.664 g/mL. Fifty-three unsaturated FA (UFA) were fully identified, of which 37 were PUFA, and a further 21 UFA were detected for which concentrations were too low for assignment of double-bond positions. There were 17 saturated FA, with 14:0, 16:0, and 18:0 present in the greatest concentration. The 10 n-3 PUFA detected included 20:5n-3 and 22:6n-3, the two main n-3 FA; n-3 PUFA at low concentrations were 18:3, 18:4, 20:3, 20:4, 21:5, 22:5, 24:6, and 28:8. There were 43 UFA from the n-4, n-5, n-6, n-7, n-8, n-9, n-10, n-11 families, with 16:2n-4, 16:1n-5, 18:1n-5, 18:2n-6, 20:4n-6, 16:1n-7, 20:1n-7, 16:1n-9, 18:1n-9, and 20:1n-9 being the most abundant. In general, we estimated that FAME concentrations greater than 0.05% (w/w) were sufficient to assign double-bond positions. In total, 91 FA were detected in an extract of the NZGLM, whereas previous studies of fresh flesh from the NZGLM had reported identification of 42 FA. These data demonstrate a remarkable diversity of NZGLM FA.

Paper no. L9596 in *Lipids 40*, 355–360 (April 2005).

The New Zealand green-lipped mussel (NZGLM), *Perna canaliculus*, is a bivalve native marine mussel from the mollusc family Mytilidae that is found in the deep-sea beds in the Hauraki Gulf in New Zealand's North Island waters (1). It is distinguishable from other bivalve species by the presence of a bright green stripe around the posterior ventral margin of the shell and its distinctive green lip, which is visible on the inside of the shell.

For a number of years, it has been claimed that preparations from the NZGLM have therapeutic value in the treatment of inflammatory conditions including arthritis (2) and asthma (3). Animal studies suggest a reduction in adjuvant-induced polyarthritis, collagen-induced arthritis, or carageenan-induced footpad edema when treated with extracts from the NZGLM (4,5). Two commercial products from the NZGLM have been produced. One is a stabilized freeze-dried powder extract known as Seatone® (MacLab, Abbotsford, Victoria, Australia); the other is a supercritical carbon dioxide oil extract from the freeze-dried stabilized powder, sold in capsules after the addition of olive oil and vitamin E, that is known as Lyprinol® (Pharmalink International, Queensland, Australia).

A recently developed CI–tandem MS (CI–MS/MS) method using acetonitrile reagent gas enables identification of the number and position of double bonds in FAME (6,7). In this method, acetonitrile self-reacts to produce the reagent (1-methyleneimino)-1-ethenylium of mass 54 *via* a previously described mechanism (8). The CI reaction yields diagnostic ions of $[M + 54]^+$, MH^+, $[MH - 32]^+$, and $[MH - 32 - 18]^+$, which are used to identify carbon chain length and number of double bonds. The $[M + 54]^+$ ion is isolated for MS^2 analysis, where fragmentation patterns vary depending on the number of double bonds. In monoenes, cleavage takes place at bonds allylic to the double bond; dienes exhibit fragmentation vinylic to the double bonds. For higher-order polyenes, cleavage is at sites vinylic to the second double bond from each end of the carbon chain. The two diagnostic ions, previously designated α (ester-containing) and ω (terminal methyl-containing), were used to identify the location of the double bonds within the FAME (7). Since full identification is possible using the highly predictable fragments, FA standards are not needed, and less common FA are readily identified. The advantages of this method have been discussed previously (7). This identification method has been used in several studies identifying FA within a sample, including those present at less than 1% (w/w), in bovine milk fat (9), mouse liver, primate brain (7), and other marine oils (10). The aim of the present study was to examine the FA in the main lipids found in the lipid extract from the NZGLM.

MATERIALS AND METHODS

The extract from NZGLM was obtained from McFarlane Marketing (Melbourne, Australia). Briefly, to obtain the lipid extract, mussels were harvested, crushed and stabilized, and centrifuged; the supernatant extract from the mussels was frozen and then freeze-dried. The lipids from the freeze-dried powder were extracted in commercial quantities by supercritical CO_2.

TLC. TLC was used to separate individual neutral lipid classes [polar lipids (PL), TAG, FFA, sterols (ST), and sterol esters (SE)] using a solvent system of hexane/diethyl ether/glacial acetic acid (60:17:0.1). Individual fractions from TLC separation were transmethylated with BF_3 (14%) for 10 min at 100°C. A complete oil sample plus an internal standard of tricosanoic acid (23:0) was treated similarly to the TLC fractions. Following methylation, heptane and a saturated NaCl solution were then added to the mixture. The organic layer containing FAME was then removed for analysis. *Instrumentation.* In all analyses, a Varian Saturn 2000 ion trap mass spectrometer coupled to a Varian 3400 gas chromatograph (GC) equipped with a Varian 8200 autoinjector (Varian, Walnut Creek, CA) was used. The column was an SGE Chromatography Supplies (Austin, TX) BPX-70 (0.32 mm × 0.25 μm × 60 m). The GC oven temperature was ramped from 60 to 170°C at 50°C/min, held for 5 min, ramped to 200°C at 4°C/min, held for 5 min, ramped to 255°C at 49°C/min, and held for 9.18 min.

Analysis to determine FA identities was conducted using CI–MS with acetonitrile as the CI reagent. The "CI Auto" option in the software with the following CI parameters was used: CI storage level = 22.0 *m/z*, ejection amplitude = 8.0 V, background mass = 65 *m/z*, maximum ionization time = 2500 μs, maximum reaction time = 100 ms, target total ion chromatogram = 5000 counts, and prescan ionization time = 100 μs. Additional mass spectrometer parameters were: emission current = 20 μA; mass defect = 116 mmu/100 u; trap temperature = 175°C; manifold temperature = 45°C; transfer line temperature = 200°C; axial modulation = 3.6 V. Through CI–MS, the chain length and number of double bonds were determined. In CI–MS/MS with acetonitrile, the $[M + 54]^+$ ion is trapped and then forms two diagnostic ions used to determine the location of the double bond (7).

Percent composition and concentrations of FA were determined through EI–MS. Samples were run in triplicate and peaks were integrated using Varian Saturn GC–MS Workstation software, version 5.2.1. In these runs, each FA had a different ionization efficiency, resulting in peak areas not proportional to their concentration. To compensate for this, an equal-weight FAME mixture, 68A (Nu-Chek-Prep, Elysian, MN), was run along with samples to generate instrumental response factors. Response factors for all FA in the sample were based on comparable FA in the 68A mixture. For FA not included in 68A, the response factor was interpolated from those directly calculated. Factors used in interpolation include: number of carbons, number of double bonds, and location of the double bond relative to the end of the chain. All factors were normalized relative to 16:0. The raw peak area was multiplied by the appropriate response factor to generate peak areas proportional to the amount of FA in the sample. The adjusted peak areas were used to determine the percent composition of the FA in the sample. Concentrations were determined based on the known concentration of the internal standard added to the original sample.

RESULTS

The lipid extract contained five major fractions as separated by TLC, which corresponded to SE, TAG, FFA, ST, and PL. The total FA content of the lipid extract, derived from the analysis of the total FA, amounted to 664 mg/mL of the sample; SE was present at 41.4% (230 mg/mL); TAG, 7.7% (43 mg/mL); FFA, 46.8% (260 mg/mL); and PL, 4.1% (23 mg/mL). The identity of the bands between ST and PL has not been established; however, they may be partial glycerides. In contrast to this commercial extract, the lipid extract of fresh NZGLM contains 57–62% phospholipids (11).

Table 1 shows all FA revealed from analysis, including 70 fully identified FA and 21 for which it was not possible to assign the identification of the position of the double bonds. Eighteen unresolved FA pairs were present. Seventeen saturated FA were identified, the main ones being 14:0, 16:0, and 18:0. There were 10 n-3 PUFA identified, including EPA and DHA as the two main n-3 PUFA. Other n-3 PUFA included 18:3, 18:4, 20:3, 20:4, 21:5, 22:5, 24:6, and 28:8.

Forty-three UFA from the n-4, n-5, n-6, n-7, n-8, n-9, n-10, families were also identified, with 16:2n-4, 16:1n-5, 18:1n-5, 18:2n-6, 20:4n-6, 16:1n-7, 20:1n-7, 16:1n-9, 18:1n-9, and 20:1n-9 being the most abundant FA in these six families.

Eighteen FA pairs could not be separated by this technique. The two most abundant were 20:5/20:4n-3 and 22:2/22:4. It was not possible to assign the position of double bonds in 21 FA. The reason for this was their low proportion, in general less than 0.05% (w/w), in the total mixture. The 20:5 present in the unresolved peak was an unidentified isomer, separate from the major, fully resolved component, 20:5n-3.

Of the 91 FA reported, only 16 represented more than 1% of the total FA. In decreasing order of abundance, these were EPA, 16:0, DHA, 14:0, 16:1n-7, 18:0, 18:1n-5, 18:4n-3, 18:2n-6, 20:4n-6, 18:3n-3, 16:1n-5, 20:1n-9, 18:1n-9, 15:0, and 16:1n-9.

The FA of the four main FA-containing fractions were also analyzed, as shown in Table 2. The proportion of the main FA in these fractions was not the same, with the most obvious differences being for 14:0, which varied from 5.29% of PL FA to 8.72% of FFA; 16:0, which varied from 12.27% of PL FA to 23.04% of FFA; 20:5n-3, which varied from 16.89% for TAG to 26.91% for PL FA; and 22:6n-3, which varied from 11.40% for TAG to 18.44% for PL FA. In terms of FA composition, the FFA and TAG FA were the most similar of the four fractions.

TABLE 1
FA Composition and Concentration of the Total Lipids from a Lipid Extract of the New Zealand Green-Lipped Mussel[a]

FA	Weight %	mg/mL oil	FA	Weight %	mg/mL oil
12:0	0.07 ± 0.01	0.45 ± 0.03	15:1n-9	0.01 ± 0.01	0.08 ± 0.07
14:0	0.04 ± 0.00	0.25 ± 0.02	18:1n-9	1.24 ± 0.23	8.18 ± 1.50
14:0	0.00 ± 0.00	0.01 ± 0.01	20:1n-9	1.60 ± 0.09	10.6 ± 0.6
14:0	8.42 ± 0.14	55.7 ± 1.1	22:1n-9	0.01 ± 0.00	0.07 ± 0.01
15:0	1.05 ± 0.01	6.96 ± 0.09			
16:0	18.4 ± 0.2	122 ± 2	16:1n-10	0.43 ± 0.01	2.82 ± 0.06
17:0	0.13 ± 0.03	0.84 ± 0.16			
17:0	0.78 ± 0.02	5.17 ± 0.08	14:1n-7/15:0	0.07 ± 0.01	0.43 ± 0.05
18:0	3.34 ± 0.05	22.1 ± 0.3	15:0/15:1	0.08 ± 0.00	0.54 ± 0.02
20:0	0.05 ± 0.00	0.35 ± 0.02	15:1n-6/16:0	0.11 ± 0.00	0.74 ± 0.01
22:0	0.04 ± 0.00	0.25 ± 0.03	16:1n-9,7,5	10.3 ± 0.2	68.1 ± 1.6
			17:1n-9,11/16:2n-7	0.00 ± 0.00	0.00 ± 0.00
18:3n-3	1.61 ± 0.04	10.7 ± 0.2	16:2n-6/17:0	0.02 ± 0.01	0.16 ± 0.06
18:4n-3	2.70 ± 0.17	17.8 ± 1.1	17:1n-7,5	0.01 ± 0.00	0.08 ± 0.01
20:3n-3	0.05 ± 0.01	0.35 ± 0.09	17:1n-7,8	0.03 ± 0.00	0.16 ± 0.02
20:5n-3	21.2 ± 0.4	140 ± 3	18:0/17:1n-6	0.19 ± 0.00	1.23 ± 0.02
21:5n-3	0.52 ± 0.02	3.45 ± 0.10	16:3n-4/17:1n-4	0.18 ± 0.01	1.19 ± 0.04
22:5n-3	0.70 ± 0.02	4.64 ± 0.13	18:1n-11,9	0.14 ± 0.01	0.94 ± 0.04
22:6n-3	13.1 ± 0.1	86.5 ± 0.8	18:2n-6/19:1	1.74 ± 0.03	11.5 ± 0.1
24:6n-3	0.25 ± 0.02	1.66 ± 0.13	19:1n-9,8/18:3n-6	0.14 ± 0.00	0.92 ± 0.01
28:8n-3	0.18 ± 0.03	1.20 ± 0.17	20:2/19:4n-5	0.07 ± 0.01	0.43 ± 0.04
			20:3/21:1	0.18 ± 0.00	1.19 ± 0.03
16:2n-4	0.87 ± 0.00	5.75 ± 0.03	20:5/20:4n-3	0.43 ± 0.02	2.85 ± 0.12
18:2n-4	0.36 ± 0.01	2.38 ± 0.08	22:2/22:4	0.40 ± 0.02	2.64 ± 0.10
18:3n-4	0.25 ± 0.01	1.64 ± 0.03	22:5n-6/24:0	0.18 ± 0.01	1.16 ± 0.08
18:4n-4	0.00 ± 0.00	0.01 ± 0.00			
			12:1	0.01 ± 0.00	0.07 ± 0.03
14:1n-5	0.02 ± 0.00	0.10 ± 0.02	14:1	0.03 ± 0.00	0.18 ± 0.01
18:1n-5	3.15 ± 0.03	20.9 ± 0.3	15:1	0.00 ± 0.00	0.00 ± 0.00
			18:1	0.01 ± 0.00	0.05 ± 0.02
20:2n-6	0.37 ± 0.01	2.46 ± 0.06	18:1	0.04 ± 0.00	0.27 ± 0.01
20:3n-6	0.19 ± 0.01	1.22 ± 0.03	20:2	0.60 ± 0.04	4.00 ± 0.22
20:4n-6	1.73 ± 0.09	11.5 ± 0.6	22:1	0.00 ± 0.00	0.03 ± 0.00
22:4n-6	0.16 ± 0.01	1.03 ± 0.09	22:3	0.20 ± 0.01	1.35 ± 0.03
			22:3	0.37 ± 0.02	2.45 ± 0.10
18:1n-7	0.13 ± 0.00	0.86 ± 0.02	24:1	0.04 ± 0.04	0.26 ± 0.29
18:2n-7	0.03 ± 0.01	0.22 ± 0.07	22:5	0.03 ± 0.00	0.16 ± 0.01
19:1n-7	0.26 ± 0.01	1.69 ± 0.06	24:4	0.01 ± 0.01	0.09 ± 0.03
20:1n-7	0.90 ± 0.03	5.93 ± 0.18	24:5	0.10 ± 0.03	0.68 ± 0.17

[a]Results shown as mean ± SD of triplicate determinations.

DISCUSSION

The gas phase derivatization reaction developed in our laboratory (7) allowed for the more detailed FA profile. Previous analysis of fresh NZGLM flesh by nonpolar GC identified 42 FA, of which 16 accounted for greater than 1% of total FA (11). In the current analysis, no FA unique to the NZGLM were found. However, several less common FA were observed in the sample, including 14:1n-5, 14:1n-7, 15:1n-9, 16:2n-4, 16:3n-4, 17:1n-4, 17:1n-5, 17:1n-7, 17:1n-9, 17:1n-11, 18:2n-4, 18:3n-4, 18:4n-4, 19:1n-7, 19:4n-5, and 21:5n-3. The presence of these particular FA is consistent with previous analyses of FA in marine life, including the mussel species *Mytilus galloprovincialis* (12,13). There is no record of these FA appearing in mammals or other terrestrial species. As with previous occurrences of these FA, they appeared as a minor fraction of the total FA found and were present at less than 1% of the total lipid composition. Other samples have

also been analyzed using this method to find minor FA components. Samples from golden algae (*Schizochytrium* sp.), primate brain white matter, and mouse liver were examined, and all showed a number of minor components (7).

In the analysis of saturated FA, four were found to appear in multiple peaks: 14:0 (3 peaks), 15:0 (3 peaks), 16:0 (3 peaks), 17:0 (3 peaks). This occurrence is most likely the result of branched-chain FA including isoprenoid FA, with different isomers being resolved in the chromatographic analysis. Our method applies only to UFA since reaction with a double bond is required; thus, chain branching in saturated FA cannot be established. Murphy *et al.* (11) reported three branched-chain FA in fresh samples of the NZGLM (4,8,12-trimethyl tetradecanoic acid, *i*17:0, *i*18:0).

Omega-3 (n-3) FA made up a significant amount of the FA in the sample, with 40% of all FA being in this category. DHA and EPA accounted for 84% of the n-3 PUFA. EPA and DHA are also present in high amounts in other species, including

TABLE 2
FA Composition (%) of the Different Fractions from the TLC-Fractionated Lipid Extract from the New Zealand Green-Lipped Mussel[a]

FA	Polar lipids	FFA	TAG	Sterol esters
12:0	0.17 ± 0.00	0.09 ± 0.01	0.07 ± 0.02	0.19 ± 0.01
14:0	0.06 ± 0.00	0.03 ± 0.00	0.02 ± 0.01	0.07 ± 0.00
14:0	0.01 ± 0.00	0.00 ± 0.00	0.00 ± 0.00	0.03 ± 0.00
14:0	5.34 ± 0.21	8.80 ± 0.24	7.18 ± 0.10	7.44 ± 0.19
15:0	0.59 ± 0.00	1.11 ± 0.04	0.83 ± 0.01	0.79 ± 0.00
16:0	12.37 ± 0.02	23.24 ± 0.41	20.90 ± 0.26	15.86 ± 0.13
17:0	0.11 ± 0.01	0.11 ± 0.00	0.14 ± 0.00	0.11 ± 0.01
17:0	0.38 ± 0.01	0.74 ± 0.03	0.86 ± 0.01	0.52 ± 0.00
18:0	2.16 ± 0.02	4.00 ± 0.03	5.67 ± 0.06	3.11 ± 0.05
20:0	0.04 ± 0.00	0.04 ± 0.00	0.10 ± 0.00	0.05 ± 0.00
22:0	0.05 ± 0.00	0.02 ± 0.00	0.05 ± 0.00	0.04 ± 0.00
18:3n-3	1.94 ± 0.03	1.59 ± 0.01	1.26 ± 0.07	1.71 ± 0.01
18:4n-3	4.38 ± 0.04	2.50 ± 0.11	2.03 ± 0.07	3.69 ± 0.08
20:3n-3	0.05 ± 0.00	0.05 ± 0.00	0.06 ± 0.00	0.02 ± 0.00
20:5n-3	27.13 ± 0.03	19.26 ± 0.28	16.69 ± 0.20	22.13 ± 0.19
21:5n-3	0.73 ± 0.02	0.45 ± 0.00	0.41 ± 0.01	0.56 ± 0.02
22:5n-3	0.88 ± 0.02	0.65 ± 0.01	0.71 ± 0.01	0.77 ± 0.01
22:6n-3	18.60 ± 0.17	11.94 ± 0.09	11.27 ± 0.27	14.66 ± 0.14
24:6n-3	0.13 ± 0.01	0.10 ± 0.01	0.11 ± 0.01	0.16 ± 0.01
28:8n-3	0.10 ± 0.00	0.06 ± 0.00	0.06 ± 0.01	0.07 ± 0.01
16:2n-4	0.87 ± 0.01	0.78 ± 0.03	0.64 ± 0.02	0.75 ± 0.00
18:2n-4	0.34 ± 0.01	0.32 ± 0.01	0.33 ± 0.01	0.37 ± 0.00
18:3n-4	0.19 ± 0.00	0.17 ± 0.01	0.05 ± 0.01	0.16 ± 0.01
18:4n-4	0.03 ± 0.00	0.01 ± 0.00	0.03 ± 0.00	0.04 ± 0.00
14:1n-5	0.01 ± 0.00	0.01 ± 0.00	0.01 ± 0.00	0.01 ± 0.00
18:1n-5	2.06 ± 0.03	2.31 ± 0.07	2.43 ± 0.01	2.51 ± 0.04
20:2n-6	0.34 ± 0.01	0.37 ± 0.01	0.46 ± 0.00	0.42 ± 0.01
20:3n-6	0.22 ± 0.00	0.18 ± 0.01	0.24 ± 0.01	0.22 ± 0.00
20:4n-6	1.87 ± 0.02	1.86 ± 0.02	1.54 ± 0.04	1.74 ± 0.03
22:4n-6	0.16 ± 0.00	0.16 ± 0.00	0.20 ± 0.01	0.18 ± 0.01
18:1n-7	0.10 ± 0.00	0.13 ± 0.00	0.06 ± 0.02	0.13 ± 0.00
18:2n-7	0.02 ± 0.00	0.01 ± 0.00	1.11 ± 0.09	0.01 ± 0.00
19:1n-7	0.09 ± 0.15	0.00 ± 0.00	0.13 ± 0.11	0.00 ± 0.00
20:1n-7	0.69 ± 0.03	0.79 ± 0.03	1.16 ± 0.04	0.93 ± 0.03
15:1n-9	0.05 ± 0.01	0.02 ± 0.00	0.12 ± 0.01	0.19 ± 0.01
18:1n-9	1.06 ± 0.01	0.94 ± 0.05	1.35 ± 0.05	1.43 ± 0.01
20:1n-9	0.97 ± 0.03	1.29 ± 0.05	2.11 ± 0.08	1.47 ± 0.03
22:1n-9	0.00 ± 0.00	0.00 ± 0.00	0.00 ± 0.00	0.01 ± 0.00
16:1n-10	0.48 ± 0.02	0.42 ± 0.01	0.66 ± 0.01	0.63 ± 0.01
14:1n-7/15:0	0.06 ± 0.00	0.07 ± 0.01	0.07 ± 0.00	0.06 ± 0.01
15:0/15:1	0.06 ± 0.00	0.08 ± 0.00	0.10 ± 0.00	0.07 ± 0.00
15:1n-6/16:0	0.07 ± 0.01	0.11 ± 0.01	0.10 ± 0.01	0.08 ± 0.00
16:1n-9,7,5	10.54 ± 0.09	10.62 ± 0.21	11.88 ± 0.30	11.63 ± 0.09
17:1n-9,11/16:2n-7	0.03 ± 0.00	0.03 ± 0.00	0.03 ± 0.01	0.05 ± 0.00
16:2n-6/17:0	0.01 ± 0.00	0.01 ± 0.00	0.79 ± 0.01	0.00 ± 0.00
17:1n-7,5	0.01 ± 0.00	0.01 ± 0.00	0.29 ± 0.00	0.01 ± 0.00
17:1n-7,8	0.02 ± 0.00	0.02 ± 0.00	0.02 ± 0.00	0.03 ± 0.00
18:0/17:1n-6	0.16 ± 0.00	0.14 ± 0.01	0.24 ± 0.01	0.17 ± 0.00

(continued)

the bivalves *Ostrea lutaria* and *Crassostrea gigas*; in another New Zealand mollusc, *M. canaliculus,* DHA and EPA account for 85% of n-3 FA (14).

The very long chain FA 28:8n-3 was also found in this sample. This FA was discovered in dinoflagellate oils (10,15), as well as the in the Tasmanian blue mussel (*M. edulis)* (11). It has been

TABLE 2 (*continued*)
FA Composition (%) of the Different Fractions from the TLC-Fractionated Lipid Extract from the New Zealand Green-Lipped Mussel[a]

FA	Polar lipids	FFA	TAG	Sterol esters
16:3n-4/17:1n-4	0.18 ± 0.01	0.14 ± 0.00	0.15 ± 0.01	0.17 ± 0.00
18:1n-11,9	0.09 ± 0.00	0.12 ± 0.01	0.21 ± 0.00	0.15 ± 0.00
18:2n-6/19:1	1.73 ± 0.02	1.73 ± 0.03	1.72 ± 0.07	1.75 ± 0.02
19:1n-9,8/18:3n-6	0.18 ± 0.00	0.17 ± 0.01	0.19 ± 0.01	0.17 ± 0.01
20:2/19:4n-5	0.05 ± 0.00	0.01 ± 0.00	0.02 ± 0.00	0.21 ± 0.00
20:3/21:1	0.11 ± 0.00	0.12 ± 0.00	0.11 ± 0.01	0.11 ± 0.00
20:5/20:4n-3	0.38 ± 0.01	0.28 ± 0.01	0.23 ± 0.00	0.28 ± 0.00
22:2/22:4	0.31 ± 0.01	0.37 ± 0.01	1.05 ± 0.02	0.68 ± 0.01
22:5n-6/24:0	0.13 ± 0.01	0.12 ± 0.00	0.12 ± 0.01	0.13 ± 0.00
12:1	0.03 ± 0.00	0.04 ± 0.00	0.02 ± 0.01	0.04 ± 0.00
14:1	0.03 ± 0.01	0.03 ± 0.01	0.04 ± 0.01	0.01 ± 0.01
15:1	0.00 ± 0.00	0.00 ± 0.00	0.00 ± 0.00	0.00 ± 0.00
18:1	0.00 ± 0.00	0.00 ± 0.00	0.00 ± 0.00	0.00 ± 0.00
18:1	0.02 ± 0.00	0.03 ± 0.00	0.01 ± 0.01	0.03 ± 0.00
20:2	0.46 ± 0.01	0.56 ± 0.02	0.83 ± 0.03	0.78 ± 0.00
22:1	0.01 ± 0.00	0.01 ± 0.00	0.00 ± 0.00	0.00 ± 0.00
22:3	0.04 ± 0.01	0.39 ± 0.01	0.60 ± 0.01	0.03 ± 0.02
22:3	0.45 ± 0.02	0.18 ± 0.16	0.14 ± 0.12	0.11 ± 0.19
24:1	0.00 ± 0.00	0.00 ± 0.00	0.00 ± 0.00	0.01 ± 0.00
22:5	0.01 ± 0.00	0.01 ± 0.00	0.01 ± 0.01	0.01 ± 0.00
24:4	0.02 ± 0.00	0.01 ± 0.00	0.01 ± 0.00	0.02 ± 0.01
24:5	0.02 ± 0.00	0.01 ± 0.00	0.01 ± 0.00	0.01 ± 0.01

[a]Results shown as mean ± SD of triplicate determinations.

suggested that the presence of 28:8n-3 in the mussel species is dietary in origin, with algae being a source (15). Since its recent discovery, it has been detected in marine oils but not in tissues of terrestrial mammals. Because it is 4-5 desaturated, 28:8n-3 is a structural analog of 22:6n-3; however, no physiological properties have yet been reported for this FA in mammals.

The technique used for this analysis allowed for a more detailed FA profile of the analyte. Previously, FA were quantified using GC–FID, and the GC–MS method used here was used only for qualitative determination of FA. Through the use of EI–MS, the amount of the various FA was determined. Response factors for the various FA were more difficult to determine. However, this method is advantageous also in that a smaller sample amount is required for analysis. In decreasing the sample concentration, GC resolution increased, permitting the observation of those FA present in small amounts, especially those present at less than 1% of the whole sample. Full identification was still not possible for some FA present in low concentrations owing to inefficient ionization or reaction with the CI reagent. In these cases, the amount of [M + 54]$^+$ ion formed was not enough to allow for proper MS–MS analysis.

ACKNOWLEDGMENTS

REFERENCES

1. Goode, J., and Willson, C. (1990) *Seafood of Australia and New Zealand. A Comprehensive Guide to Its Preparation and Cooking*, Angus & Robertson, Melbourne, Australia.

2. Cho, S.H., Jung, Y.B., Seong, S.C., Park, H.B., Byun, K.Y., Lee, D.C., Song, E.K., and Son, J.H. (2003) Clinical Efficacy and Safety of Lyprinol, a Patented Extract from New Zealand Green-Lipped Mussel (*Perna canaliculus*) in Patients with Osteoarthritis of the Hip and Knee: A Multicenter 2-Month Clinical Trial, *Allerg. Immunol. (Paris) 35,* 212–216.

3. Emelyanov, A., Fedoseev, G., Krasnoschekova, O., Abulimity, A., Trendeleva, T., and Barnes, P.J.. (2002) Treatment of Asthma with Lipid Extract of New Zealand Green-Lipped Mussel: A Randomized Clinical Trial, *Eur. Respir. J. 20,* 596–600.

4. Whitehouse, M.W., Macrides, T.A., Kalafatis, N., Betts, W.H., Haynes, D.R., and Broadbent, J. (1997) Anti-inflammatory Activity of a Lipid Fraction (Lyprinol®) from the N.Z. Green-Lipped Mussel, *Inflammopharmacology 5,* 237–246.

5. Kosuge, T., Tsugi, K., Ishida, H., and Yamaguchi, T. (1986) Isolation of an Anti-histaminic Substance from Green-Lipped Mussel (*Perna canaliculus*), *Chem. Pharm. Bull. 34,* 4825–4828.

6. Van Pelt, C.K., and Brenna, J.T. (1999) Acetonitrile Chemical Ionization Tandem Mass Spectrometry to Locate Double Bonds in Polyunsaturated Fatty Acid Methyl Esters, *Anal. Chem. 71,* 1981–1989.

7. Michaud, A.L., Diau, G.Y., Abril, R., and Brenna, J.T. (2002) Double Bond Localization in Minor Homoallylic Fatty Acid Methyl Esters Using Acetonitrile Chemical Ionization Tandem Mass Spectrometry, *Anal. Biochem. 307,* 348–360.

8. Van Pelt, C.K., Carpenter, B.K., and Brenna, J.T. (1999) Studies of Structure and Mechanism in Acetonitrile Chemical Ionization Tandem Mass Spectrometry of Polyunsaturated Fatty Acid Methyl Esters, *J. Am. Soc. Mass Spectrom. 10,* 1253–1262.

9. Michaud, A.L., Yurawecz, M.P., Delmonte, P., Corl, B.A., Bauman, D.E., and Brenna, J.T. (2003) Identification and Characterization of Conjugated Fatty Acid Methyl Esters of Mixed Double Bond Geometry by Acetonitrile Chemical Ionization Tandem Mass Spectrometry, *Anal. Chem. 75,* 4925–4930.

10. Van Pelt, C.K., Huang, M.C., Tschanz, C.L., and Brenna, J.T. (1999) An Octaene Fatty Acid, 4,7,10,13,16,19,22,25-Octa-

cosaoctaenoic Acid (28:8n-3), Found in Marine Oils, *J. Lipid Res. 40*, 1501–1505.

11. Murphy, K.J., Mooney, B.D., Nichols, P.D., Mann, N.J., and Sinclair, A.J. (2002) Lipid, FA, and Sterol Composition of New Zealand Green-Lipped Mussel (*Perna canaliculus*) and Tasmanian Blue Mussel (*Mytilus edulis*), *Lipids 37,* 587–595.

12. Garrido, J.L., and Medina, I. (2002) Identification of Minor Fatty Acids in Mussels (*Mytilus galloprovincialis*) by GC–MS of Their 2-Alkenyl-4,4-dimethyloxazoline Derivatives, *Anal. Chim. Acta 465,* 409–416.

13. Ackman, R.G., and Tocher, C.S. (1968) Marine Phytoplankter Fatty Acids, *J. Fish. Res. Bd. Canada 25,* 1603–1620.

14. Nichols, P.D., Virtue, P., Mooney, B.D., Elliott, N.G., and Yearsley, G.K. (1998) Seafood, the Good Food. The Oil Content and Composition of Australian Commercial Fishes, Shellfishes and Crustaceans. FRDC Project 95/122. Guide prepared for the Fisheries Research and Development Corporation, Canberra, Australia.

15. Mansour, M.P., Volkman, J.K., Holdsworth, D.G., Jackson, A.E., and Blackburn, S.I. (1999) Very-long-chain (C_{28}) Highly Unsaturated Fatty Acids in Marine Dinoflagellates, *Phytochemistry 50,* 541–548.

Fatty Acids in Must Prepared from 11 Grapes Grown in Japan: Comparison with Wine and Effect on Fatty Acid Ethyl Ester Formation

Keita Yunoki[a,b], Yoshiro Yasui[c], Shuji Hirose[c], and Masao Ohnishi[a,b,]*

[a]United Graduate School of Agriculture Sciences, Iwate University, Morioka, Iwate 020-8550, Japan, [b]Department of Bioresource Science, Obihiro University of Agriculture and Veterinary Medicine, Inada, Obihiro, Hokkaido 080-8555, Japan, and [c]Tokachi-Ikeda Research Institute for Viticulture and Enology, Tokachi-Ikeda, Hokkaido 083-0002, Japan

ABSTRACT: FA components of 11 musts made from grape cultivars grown for making red wine in various regions of Japan and of wines made from the musts were compared to elucidate variety-dependent characteristics and to clarify their effect on FA ethyl ester (FAEE) formation in wine. Sixteen FA with carbon chain lengths from 12 to 26 were detected in all musts, with palmitic, linoleic, and linolenic acids generally predominating. Higher levels of linoleic acid were found in musts from a cold region (Hokkaido), and higher levels of oleic acid occurred in musts from a warm region (Honshu). Moreover, the unsaturation indexes (1.31–1.56) of five grape musts from the cold region showed significant differences among varieties, corresponding to the grapevines' degree of cryotolerance. The FA levels (610–6,610 nmol/100 mL) of all wines were extremely low (1.2–12.8%) compared with those of must, but the FA compositions were similar to those of must. Additionally, significant amounts of FAEE, possibly derived from yeast activity, were found in wines by using a solid-phase extraction method. The amounts of FAEE in wine significantly differed among samples (245–904 nmol/100 mL) and were inversely correlated with the percentage of linoleic acid in musts ($R = -0.883$). Thus, higher linoleic acid levels in must may be related to lower FAEE formation by yeast.

Paper no. L9646 in *Lipids 40,* 361–367 (April 2005).

Although lipid moieties derived from grapes and microbes exist in wine (1,2), there has been little research on the lipid components of wine compared with studies of other alcoholic beverages such as sake, beer, and whisky made from grains. The lipid components of rice used for making sake were found to correlate strongly with sake quality (3,4). Therefore, the relationship between the lipids in raw materials and yeast-mediated aroma formation, including esters, during alcoholic fermentation would be of particular interest in wine making.

As for the lipid-related components of wine, some research has detected only carotenoids and aroma components such as higher alcohols and esters (5–7). However, we recently reported that the FA composition of 12 commercial red wines differed with production method, grape harvest area, and aging

duration (8). Moreover, when changes in FA levels during wine production were investigated, high FA levels that were noted in must (29.5 mg/100 mL) declined to less than 4% by the bottled wine stage, accompanied by a decreased unsaturated FA proportion (8). In this study, the FA characteristics of 11 musts harvested in Japan, differing in both cultivation areas and grape varieties, were investigated, particularly with respect to whether the FA values may be useful as a way to identify the grape growing region and to variety-dependent characteristics such as cryotolerance. Moreover, we examined the wine after alcoholic fermentation to clarify the relationship between the FA levels of must and the formation of fatty acid ethyl ester (FAEE), an important flavor compound in wine.

MATERIALS AND METHODS

Must and wine samples. Eleven grape samples (approximately 10 kg each), listed in Table 1, were used in 2002 for wine production at Tokachi-Ikeda Research Institute for Viticulture and Enology (Ikeda, Hokkaido, Japan). The musts (nos. 1–5) from five grape varieties grown in Hokkaido in 2001 and 2003 also were analyzed. Three samples (nos. 6, 7, and 10), two samples (nos. 8 and 11) and sample no. 9 were kindly donated by the National Research Institute of Brewing (Higashihiroshima, Japan), University of Yamanashi (Kofu, Japan), and Asahi-machi-wine (Yamagata, Japan), respectively. Must was obtained from a free run of destemmed and crushed grapes prior to alcoholic fermentation. Alcoholic fermentation was carried out using a commercial yeast (Lalvin EC1118; Lallemand Inc., Montréal, Canada), at 25°C. Wine was at the stage after the first racking, subsequent to alcoholic fermentation (at 1 mon from must and before malo-lactic fermentation). The samples were immediately frozen at −30°C after sampling, and were stored at this temperature until analysis. Samples obtained were immediately subjected to general analysis and lipid extraction.

Grape varieties used in this study were collected from the northern part of Japan, in Hokkaido, to the southwestern part of Japan, in Hiroshima (Fig. 1). Since Hokkaido is located close to the northern limit of grape cultivation in Japan (around latitude 43°), where minimum temperatures can reach −30°C in winter, common grape varieties do not survive (9). Therefore, grape varieties for vinification were bred

*To whom correspondence should be addressed at Obihiro University of Agriculture and Veterinary Medicine, Inada, Obihiro, Hokkaido 080-8555, Japan. E-mail: mohnishi@obihiro.ac.jp

Abbreviation: FAEE, fatty acid ethyl ester.

TABLE 1
General Components in Musts and in Wines After Alcoholic Fermentation

Variety	Harvest area	Air temperature (°C)	Must Sugar (%)	Must pH	Must Total acidity	Wine Specific gravity	Wine alcohol (%,v/v)	Wine pH	Wine Total acidity
1 Kiyomi	Hokkaido	62.7	15.0	3.1	14.5	0.997	11.1	3.4	11.7
2 Kiyomai	Hokkaido	62.7	20.6	2.8	19.1	0.999	10.5	3.3	13.4
3 Yamasachi	Hokkaido	62.7	20.1	2.9	16.3	0.999	11.1	3.2	13.6
4 Wild grape	Hokkaido	62.7	10.2	2.7	33.5	1.000	11.2	3.1	18.3
5 Zweigeltrebe	Hokkaido	70.5	18.6	3.1	8.8	0.994	11.8	3.4	8.3
6 Muscat Bailey A	Shimane	95.7	19.2	3.8	4.8	0.995	12.0	3.8	6.6
7 Muscat Bailey A	Hiroshima	95.2	15.9	3.4	7.3	0.993	11.8	3.6	8.2
8 Muscat Bailey A	Yamanashi	98.0	16.9	3.5	5.0	0.993	12.0	3.5	7.2
9 Muscat Bailey A	Yamagata	84.8	18.6	3.4	7.9	0.994	11.5	3.4	9.1
10 Merlot	Hiroshima	95.2	16.4	3.4	7.9	0.994	12.0	3.4	7.3
11 Cabernet Sauvignon	Yamanashi	98.0	19.4	3.4	7.3	0.996	11.8	3.5	9.1

[a]Air temperature means the summation of average air temperature of four months from June to September.
[b]Total acidity (mL) was estimated as the tartaric acid equivalent.

with high cryotolerance (samples 2 and 3) by using the cross-breeding method with *Vitis vinifera* and wild grape (*V. amurensis* Rupr.; sample 4).

The cryotolerance of the five grapevines grown in Hokkaido was greatest in wild grape, followed by Kiyomai ≅ Yamasachi, Kiyomi, and lowest in Zweigeltrebe (9). Total acidity in musts ranged from 4.8 to 33.5; musts from grapes grown in the cold region (Hokkaido) showed particularly higher values, from 8.8 to 33.5, compared with those of the other six samples (Table 1). Wild grape, with a notably high cryotolerance, exhibited the highest total acidity value (33.5), estimated as tartaric acid equivalent. However, the differences in cultivation areas led to significant differences in total acidities (4.8–7.9), even in the same variety such as Muscat Bailey A (samples nos. 6–9).

General analysis of must and wine. The specific gravity, sugar contents, pH, and total acidity were analyzed according to the Official Method of the Japan National Tax Administration (10).

FA analysis. Lipophilic components were extracted from must and wine with a mixture of chloroform and methanol, and were then reacted with methanolic 5% HCl for 2 h at 95°C to prepare FAME, as described previously (8). The FAME were analyzed using a Shimadzu GC-2010 gas–liquid chromatograph equipped with a hydrogen FID and a capillary column of CP-SIL 88 (50 m × 0.25 mm i.d., film thickness 0.2 mm; GL Science, Tokyo, Japan). The column was programmed from 80 to 180°C at 15°C/min, then increased to 220°C at 2°C/min, and finally held for 10 min. Nitrogen was used as the carrier gas, and the injector and detector temperatures were maintained at 210 and 210°C, respectively. Tridecanoic acid was used as an internal standard for quantitative analyses. To identify FAME, GC–MS was conducted using a Shimadzu QP-2010 gas chromatograph–mass spectrometer equipped with the same capillary column that was used for GC. Helium was used as the carrier gas, the injector temperature was maintained at 240°C, and the ionizing energy was 70 eV.

Analysis of the FAEE by solid-phase extraction and GC–MS. The FAEE component of wine was separated using a

solid-phase extraction method (11). Briefly, a cartridge (LiChrolut EN 200 mg/3 mL; Merck, Darmstadt, Germany) was rinsed with 4 mL dichloromethane, 4 mL methanol, and finally 4 mL 12% ethanol. Wine (50 mL) was centrifuged at $1,500 \times g$ for 15 min. After transferring the supernatant, the pellet was washed with 25 mL of 12% ethanol (vol/vol) and separated by centrifugation. The combined supernatant was loaded into the preconditioned cartridge, approximately 2 mL/min. Then the sorbent was dried by letting air pass through it using an aspirator for 10 min and eluted with 1.3 mL hexane/diethyl ether (9:1, vol/vol). Five microliters of ethyl tridecylate solution (1 mg/mL hexane) as an internal standard and an appropriate amount of anhydrous Na_2SO_4 were added to the eluted sample. FAEE was analyzed using GC–MS for the FA analysis. The column temperature was initially 40°C for 5 min, then programmed from 40 to 70°C at 4°C/min, and finally at 8°C/min to 230°C, and held for 5 min. The reproducibility

FIG. 1. Grape harvesting areas in Japan. The winery where the samples were prepared is in the Tokachi district of Hokkaido. Numbers represent degrees north of the equator.

TABLE 2
FA Compositions (mol% ± SD) in Musts Made from Grapes Grown in Japan

FA	Harvest area[a] 1	2	3	4	5	6	7	8	9	10	11
12:0	0.2 ± 0.0	0.1 ± 0.1	0.1 ± 0.1	0.1 ± 0.1	0.1 ± 0.1	0.3 ± 0.1	0.3 ± 0.0	0.3 ± 0.0	0.4 ± 0.0	0.2 ± 0.1	0.2 ± 0.1
14:0	0.3 ± 0.0	0.4 ± 0.2	0.2 ± 0.1	0.4 ± 0.2	0.5 ± 0.2	0.8 ± 0.0	0.6 ± 0.0	0.7 ± 0.0	0.7 ± 0.4	0.5 ± 0.1	0.5 ± 0.2
16:0	26.8 ± 0.9	26.0 ± 0.4	27.0 ± 0.3	21.6 ± 0.5	26.2 ± 1.0	25.8 ± 0.5	25.4 ± 0.8	25.0 ± 0.7	23.3 ± 0.2	30.1 ± 0.3	29.8 ± 0.2
16:1(7)	<0.1 ± 0.1	0.1 ± 0.1	0.1 ± 0.1	0.1 ± 0.1	0.1 ± 0.1	0.2 ± 0.0	0.2 ± 0.0	0.2 ± 0.0	0.2 ± 0.0	0.2 ± 0.0	0.2 ± 0.1
16:1(9)	0.6 ± 0.4	0.5 ± 0.0	0.3 ± 0.2	0.5 ± 0.1	0.2 ± 0.2	0.2 ± 0.0	0.4 ± 0.0	0.4 ± 0.1	1.1 ± 0.1	0.5 ± 0.0	0.4 ± 0.0
18:0	2.3 ± 0.1	2.2 ± 0.1	1.9 ± 0.4	1.9 ± 0.3	3.1 ± 1.6	4.5 ± 0.1	2.9 ± 0.0	2.4 ± 0.1	2.9 ± 0.1	3.4 ± 0.1	2.5 ± 0.3
18:1(9)	4.2 ± 0.3	6.4 ± 0.2	5.2 ± 0.5	5.5 ± 0.9	6.8 ± 0.8	21.0 ± 0.2	20.3 ± 0.3	13.7 ± 0.1	21.3 ± 1.3	17.1 ± 0.2	8.1 ± 0.1
18:1(11)	0.6 ± 0.0	0.9 ± 0.0	0.9 ± 0.1	0.7 ± 0.0	0.9 ± 0.1	0.9 ± 0.1	0.8 ± 0.1	1.0 ± 0.0	1.0 ± 0.0	0.6 ± 0.1	0.9 ± 0.0
18:2(9,12)	45.1 ± 0.4	40.3 ± 0.4	42.2 ± 0.8	44.7 ± 1.3	47.4 ± 3.0	26.6 ± 0.2	29.3 ± 0.5	34.5 ± 0.3	29.8 ± 0.3	27.0 ± 0.3	37.4 ± 0.6
18:3(9,12,15)	14.4 ± 0.2	18.7 ± 0.4	17.2 ± 0.0	20.5 ± 0.4	9.2 ± 0.4	14.2 ± 0.1	14.6 ± 0.2	14.9 ± 0.1	13.0 ± 0.1	14.8 ± 0.3	13.3 ± 0.1
20:0	0.8 ± 0.0	0.7 ± 0.0	0.7 ± 0.0	0.5 ± 0.0	1.1 ± 0.1	1.2 ± 0.0	0.8 ± 0.0	0.9 ± 0.1	1.0 ± 0.1	0.9 ± 0.0	1.0 ± 0.1
22:0	2.0 ± 0.1	2.0 ± 0.1	2.0 ± 0.1	1.5 ± 0.1	2.2 ± 0.0	2.4 ± 0.1	2.0 ± 0.1	2.9 ± 0.1	2.6 ± 0.1	2.0 ± 0.0	2.3 ± 0.0
23:0	0.7 ± 0.6	0.6 ± 0.2	1.1 ± 0.2	1.1 ± 0.0	1.0 ± 0.1	0.4 ± 0.1	0.7 ± 0.3	1.1 ± 0.2	1.1 ± 0.6	1.0 ± 0.4	0.8 ± 0.1
24:0	0.9 ± 0.2	0.8 ± 0.0	0.8 ± 0.0	0.7 ± 0.1	0.7 ± 0.0	0.8 ± 0.2	0.9 ± 0.0	1.1 ± 0.1	1.0 ± 0.2	0.9 ± 0.0	1.2 ± 0.1
25:0	0.6 ± 0.5	<0.1 ± 0.1	0.1 ± 0.1	0.1 ± 0.1	0.1 ± 0.1	0.1 ± 0.1	0.1 ± 0.0	0.1 ± 0.0	0.1 ± 0.0	0.1 ± 0.0	0.3 ± 0.1
26:0	0.5 ± 0.1	0.3 ± 0.0	0.2 ± 0.2	0.1 ± 0.1	0.4 ± 0.1	0.6 ± 0.5	0.7 ± 0.0	0.8 ± 0.0	0.5 ± 0.0	0.7 ± 0.2	1.1 ± 0.2
Total acyls[b]	658 ± 88	824 ± 175	566 ± 129	662 ± 76	385 ± 77	421 ± 81	360 ± 60	305 ± 15	323 ± 39	399 ± 44	364 ± 46
ΣSFA/ΣUFA[c]	0.54 ± 0.02	0.50 ± 0.02	0.52 ± 0.01	0.39 ± 0.02	0.55 ± 0.07	0.58 ± 0.01	0.52 ± 0.02	0.55 ± 0.01	0.51 ± 0.03	0.66 ± 0.02	0.66 ± 0.01
UI[d]	1.39 ± 0.02	1.45 ± 0.02	1.43 ± 0.01	1.58 ± 0.03	1.30 ± 0.07	1.18 ± <0.01	1.24 ± 0.02	1.29 ± 0.01	1.22 ± 0.01	1.17 ± 0.02	1.24 ± 0.01

[a]For harvest area see Table 1.
[b]($\times 10^2$ nmol/100 mL)
[c]ΣSFA = Σ saturated FA; ΣUFA = Σ unsaturated FA.
[d]Unsaturation index = (Σmi · ni)/100, where mi is the percentage of each FA and ni is the number of C–C double bonds in each FA i.

of the method was determined by using standard ethyl butyrate, ethyl caprate, ethyl palmitate, ethyl oleate, and ethyl linoleate in a model wine solution, which contained 0.75 g/100 mL tartaric acid and 12% ethanol at pH 3.5 in distilled water. The recoveries of the five compounds ranged from 92 to 97%.

Statistical analysis. All data for lipid analyses are presented as averages from at least three independent experiments, along with the SD. Statistical significance was evaluated by ANOVA and tested by Scheffé analysis. For all statistical analyses, significance was established at $P < 0.05$, $P < 0.01$, and $P < 0.001$.

RESULTS

FA in must. Total FA concentrations ranged from 30,500 to 82,400 nmol/100 mL in the musts (Table 2). Considerable amounts of FA were detected in four samples (Kiyomi, Kiyomai, Yamasachi, and wild grape) from cryotolerant grapes grown in Hokkaido; concentrations were 56,600 to 82,400 nmol/100 mL. Sixteen FA with carbon chain lengths from 12 to 26 were detected in all samples (Table 2). Palmitic, linoleic, and linolenic acids were generally present as major components at 21.6 to 30.1%, 26.6 to 47.4%, and 9.2 to 20.5%, respectively. However, linoleic acid proportions showed significant differences among the samples, being particularly higher in five must samples from Hokkaido compared with those from other regions. Oleic acid was also one of the major FA, with levels at 13.7 to 21.3% in four Muscat Bailey A samples (nos. 6–9) and one Merlot sample (no. 10).

Unsaturation indexes, indicating the degree of FA unsatura-

tion (Table 2), ranged from 1.30 to 1.58 for five must samples (nos. 1–5) grown in Hokkaido; these values were higher than those in musts prepared from grapes grown in lower latitudes (1.18–1.29). Moreover, among the five grapes grown in Hokkaido, the order of the unsaturation indexes in must was identical to the level of cryotolerance (Table 2). Wild grape (sample no. 4), with the highest cryotolerance, showed the highest unsaturation index (1.58), whereas Zweigeltrebe (sample no. 5), with the lowest cryotolerance, showed the lowest value (1.30). It thus follows that the FA compositions of musts, derived from grapes from the same cultivation area, have individual specific profiles related to their variety-dependent characteristics. To confirm this, the FA compositions of five grape musts grown in Hokkaido from 2001 to 2003 were compared (Fig. 2). The unsaturation indexes over 3 yr showed significant differences among the five varieties tested.

Comparison of FA components between musts and wines. Total FA concentrations in wines (after the first racking subsequent to alcoholic fermentation) ranged from 610 to 6,610 nmol/100 mL (Table 3), markedly lower than the must stage (Table 2) for all samples tested. This decrease compared with must was least at 87.2% for sample no. 9 and was highest, at 98.1%, for sample no. 5. There was also a positive correlation ($R = 0.775$, $P < 0.01$) between the total acyl concentrations of each must sample and wine sample (Fig. 3).

As for the FA components of wine, 10:0 (capric acid) was detected as a new component (0.9–4.9%), in addition to 16 other FA with carbon chain lengths from 12 to 26 (all being already present in must). Of those, palmitic and linoleic acids
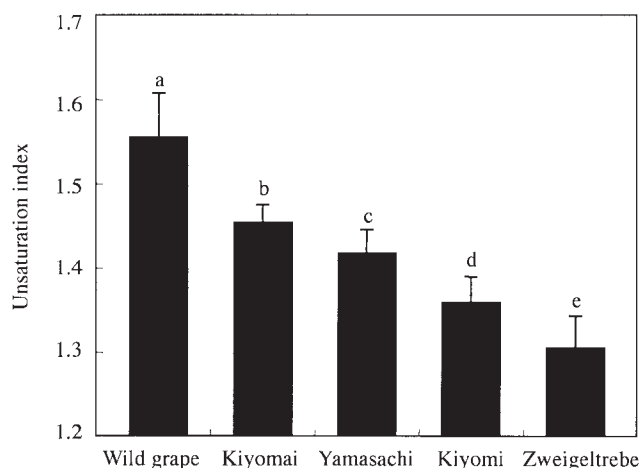
FIG. 2. Annual comparison of unsaturation indexes of FA in musts of five black grape varieties grown in Hokkaido for 3 yr. Unsaturation index means $(\Sigma m i \cdot n i)/100$, where m*i* is the percentage of each FA and n*i* is the number of C–C double bonds in each FA *i*. Data are represented as means ± SD. Different superscript letters indicate significant differences. The order of the cryotolerance strength of the grapevines is as follows: wild grape > Kiyomai ≅ Yamasachi > Kiyomi > Zweigeltrebe.

were generally predominant at 26.7–37.5% and 12.1–35.6%, respectively, in all samples (Table 3). High proportions of oleic acid, as well as both palmitic and linoleic acids, at 11.0 to 18.6%, were detected in wines made from grapes harvested in regions outside Hokkaido (nos. 6–11). Moreover, there were differences in the *cis*-9-palmitoleic acid compositions between wines from Hokkaido (nos. 1–5) and other wines, with the lat-

ter being notably higher at 4.8 to 11.0%. From must to wine, the relative proportions of PUFA, including linoleic and linolenic acids, decreased (the former at 4.9 to 28.3%, the latter at 4.8 to 10.6%), whereas those of saturated FA, including palmitic and stearic acids, increased (the former at 0.7 to 12.1%, the latter at 4.1 to 10.9%). In accordance with these changes, the wine unsaturation indexes ranged from 0.59 to 1.05, indicating that the degree of FA unsaturation decreased after alcoholic fermentation. The proportions of medium-chain FA, such as lauric and myristic acids, in each wine sample were higher than those in musts, although this difference was not significant.

The relationships between musts and wines were evaluated with respect to their proportions of palmitic, oleic, linoleic, and linolenic acids. Strong positive correlations ($R = 0.922$ for oleic acid, $R = 0.738$ for linoleic acid, and $R = 0.770$ for linolenic acid) were found for the latter three components, but not for palmitic acid (Fig. 4). The FA characteristics of wine were therefore similar to those of must, although FA concentrations and compositions were changed from the must stage by the alcoholic fermentation of the grapes.

Analysis of FAEE in wine. A hexane/diethyl ether (9:1, vol/vol)-eluted fraction was prepared from wine made from the Kiyomi grape using the solid-phase extraction method, then analyzed by capillary GC–MS (Fig. 5). When fragment ions of m/z 88, characteristic of FAEE, were monitored, 13 FAEE, from ethyl butyrate (peak 1) to ethyl linolenate (peak 13), as well as ethyl tridecylate (peak 6, used as an internal standard) were detected. In addition, a large peak with a retention time of ~13 min was judged to be isoamyl alcohol by comparison of
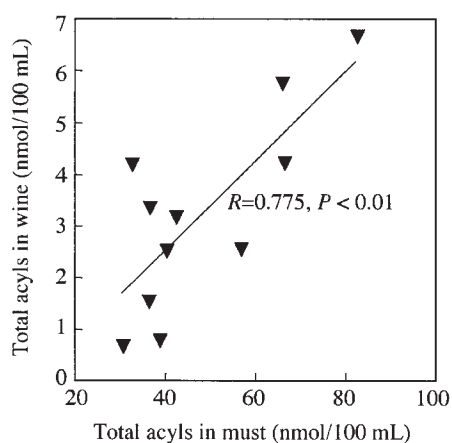
TABLE 3
FA Compositions (mol% ± SD) in Wines After Alcoholic Fermentation

FA	Harvest area[a]										
	1	2	3	4	5	6	7	8	9	10	11
10:0	1.1 ± 0.1	1.6 ± 0.5	1.1 ± 0.5	0.9 ± 0.3	4.9 ± 3.0	1.3 ± 0.1	0.9 ± 0.2	1.8 ± 1.8	2.1 ± 0.2	1.4 ± 0.6	1.3 ± 0.7
12:0	1.3 ± 0.1	1.9 ± 0.2	2.3 ± 0.9	1.5 ± 0.4	5.4 ± 0.7	1.4 ± 0.2	1.7 ± 0.0	2.8 ± 0.9	2.3 ± 0.3	1.5 ± 0.0	1.3 ± 0.3
14:0	1.1 ± 0.2	1.9 ± 0.3	2.1 ± 0.6	1.3 ± 0.2	4.6 ± 0.5	1.3 ± 0.1	1.9 ± 0.0	2.6 ± 0.8	1.7 ± 0.3	1.3 ± 0.1	1.1 ± 0.0
16:0	30.4 ± 1.6	26.7 ± 1.5	31.2 ± 2.3	28.0 ± 3.2	33.4 ± 4.0	30.7 ± 1.1	37.5 ± 1.5	30.0 ± 0.4	29.7 ± 1.6	33.8 ± 1.3	32.4 ± 1.1
16:1(7)	0.2 ± 0.2	0.4 ± 0.2	0.5 ± 0.5	0.5 ± 0.2	1.8 ± 0.6	0.4 ± 0.1	0.2 ± 0.2	0.6 ± 0.6	0.3 ± 0.2	0.3 ± 0.1	0.2 ± 0.2
16:1(9)	0.6 ± 0.3	0.8 ± 0.3	1.1 ± 0.9	1.1 ± 0.1	1.8 ± 0.5	6.0 ± 0.2	4.8 ± 0.5	7.4 ± 0.3	11.0 ± 0.0	10.0 ± 0.1	8.0 ± 0.4
18:0	8.3 ± 0.8	7.6 ± 0.5	9.6 ± 0.5	7.4 ± 0.7	11.0 ± 1.7	10.9 ± 0.8	13.8 ± 0.3	11.5 ± 0.1	7.0 ± 0.3	10.7 ± 0.5	7.2 ± 0.2
18:1(9)	5.0 ± 0.2	7.6 ± 0.6	5.8 ± 1.3	8.1 ± 0.4	8.6 ± 0.3	18.6 ± 0.2	13.9 ± 0.2	15.5 ± 0.1	15.6 ± 0.4	16.4 ± 0.4	11.0 ± 0.2
18:1(11)	0.6 ± 0.1	0.7 ± 0.0	0.9 ± 0.2	0.7 ± 0.0	0.4 ± 0.4	0.5 ± 0.4	0.7 ± 0.0	0.5 ± 0.5	0.8 ± 0.1	0.9 ± 0.1	1.0 ± 0.1
18:2(9,12)	35.6 ± 2.7	35.4 ± 0.5	25.6 ± 0.5	31.9 ± 2.9	19.1 ± 4.3	15.5 ± 0.2	13.1 ± 0.1	13.2 ± 0.6	17.0 ± 0.7	12.1 ± 0.0	21.3 ± 1.1
18:3(9,12,15)	7.3 ± 0.6	8.1 ± 1.1	8.4 ± 1.6	10.2 ± 1.6	2.8 ± 1.0	8.3 ± 0.2	6.6 ± 0.3	5.8 ± 0.2	8.2 ± 0.5	6.6 ± 0.3	8.1 ± 0.6
20:0	1.2 ± 0.1	1.0 ± 0.0	1.2 ± 0.1	0.8 ± 0.2	1.1 ± 0.4	1.1 ± 0.0	0.8 ± 0.0	1.0 ± 0.0	0.8 ± 0.0	0.7 ± 0.1	1.0 ± 0.0
22:0	3.0 ± 0.2	2.6 ± 0.1	3.9 ± 0.8	2.7 ± 0.3	1.8 ± 0.6	2.2 ± 0.2	1.6 ± 0.1	3.0 ± 0.0	2.0 ± 0.1	1.5 ± 0.1	2.5 ± 0.1
23:0	1.0 ± 0.2	1.1 ± 0.4	2.5 ± 1.1	2.2 ± 1.2	0.4 ± 0.7	0.2 ± 0.1	1.0 ± 0.1	1.3 ± 0.4	0.3 ± 0.0	1.4 ± 0.5	0.8 ± 0.1
24:0	1.8 ± 0.5	1.4 ± 0.2	2.5 ± 1.0	1.8 ± 0.7	1.6 ± 0.1	0.9 ± 0.2	0.8 ± 0.1	1.4 ± 0.0	0.7 ± 0.1	0.7 ± 0.0	1.3 ± 0.0
25:0	0.3 ± 0.2	0.3 ± 0.4	0.6 ± 0.2	0.3 ± 0.4	0.2 ± 0.2	0.1 ± 0.1	0.1 ± 0.1	0.7 ± 0.1	0.1 ± 0.0	0.1 ± 0.1	0.3 ± 0.1
26:0	1.2 ± 0.2	0.9 ± 0.2	0.7 ± 0.2	0.6 ± 0.2	1.1 ± 0.3	0.6 ± 0.0	0.6 ± 0.1	0.9 ± 0.1	0.4 ± 0.0	0.6 ± 0.0	1.2 ± 0.1
Total acyls[b]	5,706 ± 740	6,608 ± 922	2,503 ± 447	4,164 ± 679	723 ± 126	3,126 ± 576	1,497 ± 670	610 ± 25	4,135 ± 571	2,461 ± 211	3,304 ± 799
ΣFA/ΣUFA[c]	1.03 ± 0.12	0.89 ± 0.04	1.36 ± 0.11	0.90 ± 0.17	1.90 ± 0.46	1.03 ± 0.01	1.54 ± 0.09	1.33 ± 0.10	0.89 ± 0.04	1.16 ± 0.05	1.02 ± 0.09
UI[c]	1.00 ± 0.07	1.05 ± 0.04	0.85 ± 0.04	1.05 ± 0.11	0.59 ± 0.11	0.81 ± 0.01	0.66 ± 0.02	0.68 ± 0.03	0.86 ± 0.03	0.72 ± 0.02	0.87 ± 0.04

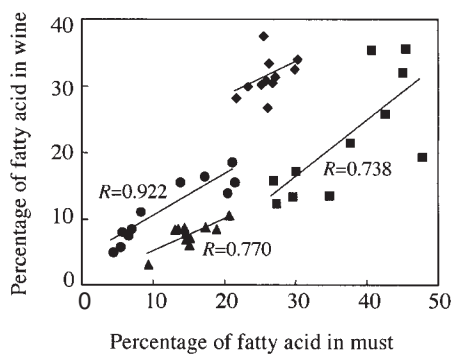[a]For harvest area see Table 1.
[b](nmol/100 mL).
[c]For abbreviations see Table 2.

FIG. 3. Correlation of total acyl concentration between must and wine. Data are represented as means of triplicate analyses.

FIG. 5. (A) Total ion chromatograms (TIC) and (B) mass chromatograms of FA ethyl esters from wine (Kiyomi) determined by a combination of solid-phase extraction and GC–MS. Peaks 1, 2, 3, 4, 5, 6, 7, 8, 9, 10, 11, 12, and 13 correspond to ethyl esters of 4:0, 6:0, 8:0, 10:0, 12:0, 13:0, 14:0, 16:0, 16:1, 18:0, 18:1, 18:2, and 18:3, respectively.
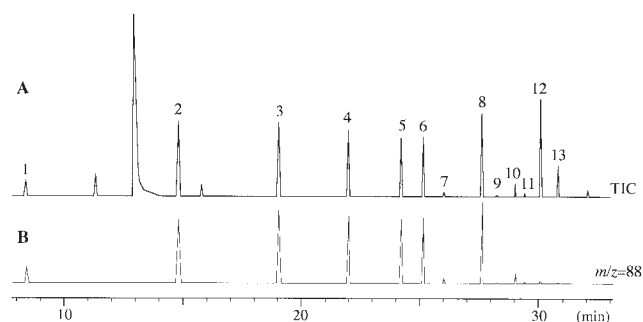
its mass spectrum and retention time with the standard compound.

Values for FAEE in each wine are shown in Table 4. Total amounts of FAEE ranged from 245 to 904 nmol/100 mL, with all Muscat Bailey A samples (nos. 6–9) showing high amounts (565–904 nmol/100 mL). Low amounts of FAEE were detected in wines produced from grapes grown in the cold region (nos. 1–5), compared with those from the other regions. When the effects of FA components in must on FAEE concentrations were examined, a strong negative correlation ($R = -0.882$, $P < 0.001$) was identified between the percentage of linoleic acid in must and the FAEE concentration in wine. This may suggest that the high linoleic acid proportion of the lipid constituents of must inhibit FAEE formation by yeast during alcoholic fermentation.

Ethyl butyrate, ethyl caproate, ethyl caprylate, and ethyl caprate were present as major FAEE, at 7.7 to 13.1%, 27.1 to 45.8%, 14.4 to 36.8%, and 6.5 to 9.7%, respectively (Table 4). Characteristically high levels of ethyl 9-palmitoleate and oleate were present in sample 10 (Merlot) at 11.8 and 4.4%, respec-

tively, whereas ethyl palmitate and ethyl linoleate were present in sample 1 (Kiyomi) at 10.0 and 13.6%, respectively. In addition, ethyl decenoate was detected in six samples including Kiyomai, although it was not detected in wine prepared from the Kiyomi grape (Fig. 5).

DISCUSSION

It was recently reported that palmitic, myristic, and lauric acids were the major FA in 12 commercial red wines, and that differences in wine production methods and grape cultivation regions (different countries, including Japan) could possibly influence the FA compositions of red wine (8). In the present study, the FA composition of grape musts from various cultivation areas in Japan and their wines were compared for the first time. The FA composition of Muscat Bailey A musts differed according to the area where the grapes were grown (Table 2), even though they were from the same variety. Alberto *et al.* (12) previously reported on the FA composition in must from Cabernet Sauvignon. Linoleic (20.6%), stearic (15.7%), and oleic acids (10.9%) were present as major FA. But for the most part, this differed considerably from the Cabernet Sauvignon (sample no. 11) used in this study. This discrepancy also may be due to differences in the cultivation areas. On the other hand, the unsaturation indexes of musts made from grapes grown in Hokkaido were higher than those in samples from the other regions, which means that the FA composition of grapes could change with different temperatures during maturation. Since the characteristics of the FA compositions of musts were also partially reflected in red wines after alcoholic fermentation (Fig. 4), FA analysis of wine may possibly be used as one of the parameters to determine grape harvest areas. The unsaturation indexes of must were found to differ significantly among the five varieties, possibly in relation to the different cryotolerance levels of the grape vines. Thus, the higher levels observed in musts from Hokkaido appear to be related to the greater cryotolerance of grapevines grown in Hokkaido (also observed in grape inner bark) (13).

FIG. 4. Correlation of FA composition between must and wine. ◆, ●, ■, and ▲ indicate 16:0, 18:1, 18:2, and 18:3, respectively. Data are represented as means of triplicate analyses. Probability values are less than 0.01, except for 16:0.

TABLE 4
FA Ethyl Ester Compositions (mol% ± SD) in Wines After Alcoholic Fermentation, as Estimated by the Solid-Phase Extraction Method

FA	Harvest area[a]										
	1	2	3	4	5	6	7	8	9	10	11
4:0	10.1 ± 4.5	9.3 ± 2.3	10.1 ± 1.1	11.3 ± 3.1	13.1 ± 2.1	10.5 ± 0.4	13.0 ± 0.6	11.9 ± 1.5	10.0 ± 1.5	10.9 ± 3.0	7.7 ± 3.3
6:0	27.1 ± 1.7	27.9 ± 4.0	35.2 ± 5.5	28.1 ± 1.4	45.8 ± 1.4	29.3 ± 0.8	34.3 ± 0.7	37.0 ± 0.7	27.6 ± 2.5	28.7 ± 4.1	29.5 ± 1.0
8:0	14.4 ± 0.8	22.8 ± 1.2	29.3 ± 1.7	21.2 ± 1.9	30.0 ± 3.2	28.7 ± 0.3	30.2 ± 3.5	38.9 ± 1.9	36.8 ± 4.3	22.3 ± 3.8	30.5 ± 1.3
10:0	8.3 ± 0.5	9.7 ± 1.1	9.6 ± 1.2	9.2 ± 0.8	7.4 ± 0.5	8.7 ± 0.0	7.5 ± 0.4	7.2 ± 0.3	9.0 ± 0.6	6.5 ± 0.1	8.1 ± 0.9
10:1(9)	0.0 ± 0.0	1.8 ± 0.6	0.6 ± 1.0	0.0 ± 0.0	0.0 ± 0.0	0.8 ± 0.1	0.3 ± 0.3	0.6 ± 0.5	2.0 ± 0.3	0.0 ± 0.0	0.0 ± 0.0
12:0	9.1 ± 0.4	6.2 ± 1.2	4.6 ± 1.4	7.2 ± 2.5	2.8 ± 1.3	3.5 ± 0.3	2.6 ± 0.1	0.7 ± 0.6	2.8 ± 0.4	3.0 ± 0.2	1.7 ± 0.7
14:0	0.3 ± 0.6	2.4 ± 2.3	0.3 ± 0.5	0.4 ± 0.4	0.0 ± 0.0	0.7 ± 0.5	0.4 ± 0.4	0.2 ± 0.3	0.1 ± 0.2	0.2 ± 0.2	0.3 ± 0.5
16:0	10.0 ± 1.5	7.8 ± 1.9	4.7 ± 0.9	7.3 ± 0.5	1.0 ± 0.8	5.0 ± 1.6	4.4 ± 2.5	1.1 ± 0.4	1.9 ± 0.5	5.1 ± 2.3	7.9 ± 3.3
16:1(9)	0.2 ± 0.3	0.0 ± 0.0	0.0 ± 0.0	0.5 ± 0.5	0.0 ± 0.0	5.3 ± 0.3	2.9 ± 0.7	1.4 ± 0.1	4.9 ± 1.7	11.8 ± 4.4	5.2 ± 2.8
18:0	2.1 ± 0.2	0.8 ± 0.8	0.6 ± 0.7	1.5 ± 0.3	0.0 ± 0.0	1.0 ± 0.3	0.8 ± 0.4	0.2 ± 0.4	0.4 ± 0.3	0.8 ± 0.4	1.2 ± 0.6
18:1(9)	0.7 ± 1.2	0.6 ± 0.6	0.5 ± 0.8	1.5 ± 0.4	0.0 ± 0.0	2.6 ± 0.1	0.9 ± 0.3	0.3 ± 0.5	1.0 ± 0.8	4.4 ± 1.6	2.0 ± 0.3
18:2(9,12)	13.6 ± 1.6	7.8 ± 0.6	3.8 ± 0.3	8.0 ± 0.6	0.0 ± 0.0	2.9 ± 0.2	1.7 ± 0.5	0.5 ± 0.4	2.2 ± 0.7	4.2 ± 2.0	4.3 ± 1.5
18:3(9,12,15)	3.9 ± 0.3	2.8 ± 0.3	1.0 ± 0.8	3.8 ± 0.7	0.0 ± 0.0	0.9 ± 0.9	1.0 ± 0.3	0.0 ± 0.0	1.2 ± 0.4	2.2 ± 0.3	1.6 ± 0.8
Total acyls[b]	294 ± 16	293 ± 12	329 ± 32	297 ± 39	245 ± 29	857 ± 6	904 ± 25	565 ± 9	784 ± 40	528 ± 51	390 ± 35

[a]For harvest area see Table 1.
[b](nmol/100 mL).

However, FA concentrations in all wines were lower than those in their must stages, which agrees with our previous study comparing the FA compositions of must and wine from the Kiyomi variety (8). We assumed that most of the lipophilic components of the wines tested would no longer be present through lees removal after alcoholic fermentation. We determined from the results that the FA levels in must decreased to 1/10 following filtration through a 0.45-μm filter compared with prefiltration levels (data not shown). A high proportion of *cis*-9-palmitoleic acid was present in wine samples nos. 6 to 11 compared with that in wines from Hokkaido (nos. 1–5). This may possibly indicate that *cis*-9-palmitoleic acid formation by yeast is inhibited by the high linoleic acid levels in musts from grapes grown in the cold region (14,15). Thus, it was clear that the differences in the FA compositions of musts influenced the FA components of the resulting wines.

Since the levels of medium-chain FA, such as capric acid, and *cis*-9-palmitoleic acid (probably produced by yeast) had increased in the wines, we tried to examine the FAEE that were produced during alcoholic fermentation. Although the FAEE is one of the lipid components of wine, the ethyl esters of lower FA cannot be recovered by the processes of washing and concentrating in the general lipid extraction method. These components therefore generally have been analyzed together with many other flavor components (16,17). However, it became clear that FA esters could be determined more easily by directly analyzing 50-mL wine samples using a combination of solid-phase extraction and capillary GC–MS rather than using the headspace method. The decrease in FA concentrations from the must stage to the wine stage as well as the FAEE compositions of wine (Tables 3, 4) differed among wines (samples nos. 1–5) prepared by the same wine production methods. It was assumed that differences in the FA compositions of the starting materials would influence yeast (*Saccharomyces cerevisiae*) growth, FA *de novo* synthesis, and enzymatic activity concerned with ethyl

ester formation (3,14,15,18,19). Therefore, low levels of FAEE (Table 4) were present in wines produced from grapes grown in Hokkaido, which contained much more linoleic acid (Table 2), corresponding to the negative correlation observed between the proportion of linoleic acid added to the yeast culture medium and the amount of isoamyl acetate formation (3). The linoleic acid included in the medium was directly incorporated into yeast cellular lipids such as PC, one of the major components of biomembrane lipids (3,15). Consequently, it was assumed that FA *de novo* synthesis in yeast was inhibited, which caused decreased levels of FAEE formation (3).

Linoleic acid and its ethyl ester, undesirable in "shochu" and beer manufacture because they cause an off-flavor (20,21), would not have an adverse influence on wine quality because PUFA derived from grapes are removed from wine mainly as lees during the wine-making process. Conversely, the PUFA released from grape cells appear to enhance the yeast's tolerance to alcohol and to low temperatures during and after fermentation, which is expected to increase aroma compounds by low-temperature fermentation (22).

REFERENCES

1. Jackson, R.S. (1993) *Wine Science: Principles and Applications*, pp. 60, 206, and 249, Academic Press, San Diego.
2. Morrison, W.R. (1978) *Cereal Lipids* (Pomeranz, Y., ed.), Vol. 2, pp. 311–315, American Association of Cereal Chemists, St. Paul, MN.
3. Ishikawa, T., and Yoshizawa, K. (1979) Effects of Cellular Fatty

Acids on the Formation of Flavor Esters by Saké Yeast, *Agric. Biol. Chem. 43*, 45–53.

4. Ishikawa, T., and Yoshizawa, K. (1978) Lipids of Rice-*koji* and Their Contribution to Saké Flavor, *Hakkokogaku* (in Japanese) *56*, 24–30.

5. de Pinho, P.G., Silva Ferreira, A.C., Mendes Pinto, M., Benitez, J.G., and Hogg, T.A. (2001) Determination of Carotenoid Profiles in Grapes, Musts, and Fortified Wines from Douro Varieties of *Vitis vinifera*, *J. Agric. Food Chem. 49*, 5484–5488.

6. Nykänen, L. (1986) Formation and Occurrence of Flavor Compounds in Wine and Distilled Alcoholic Beverages, *Am. J. Enol. Vitic. 37*, 84–96.

7. Baumes, R., Cordonnier, R., Nitz, S., and Drawert, F. (1986) Identification and Determination of Volatile Constituents in Wines from Different Vine Cultivars, *J. Sci. Food Agric. 37*, 927–943.

8. Yunoki, K., Tanji, M., Murakami, Y., Yasui, Y., Hirose, S., and Ohnishi, M. (2004) Fatty Acid Compositions of Commercial Red Wines, *Biosci. Biotechnol. Biochem. 68*, 2623–2626.

9. Kawaguchi, M., Imai, H., Naoe, M., Yasui, Y., and Ohnishi, M. (2000) Cerebrosides in Grapevine Leaves: Distinct Composition of Sphingoid Bases Among the Grapevine Species Having Different Tolerances to Freezing Temperature, *Biosci. Biotechnol. Biochem. 64*, 1271–1273.

10. Takahashi, T. (1993) *The Official Method of the National Tax Administration* (in Japanese), 4th edn., The Japan Brewery Association, Tokyo.

11. Lopez, R., Aznar, M., Cacho, J., and Ferreira, V. (2002) Determination of Minor and Trace Volatile Compounds in Wine by Solid-Phase Extraction and Gas Chromatography with Mass Spectrometric Detection, *J. Chromatogr. A 966*, 167–177.

12. Alberto, M., Jacques, B., and Alain, B. (1993) Fatty Acids from Lipid Fractions of Leaves and Different Tissues of Cabernet Sauvignon Grapes, *Am. J. Enol. Vitic. 44*, 180–186.

13. Kawaguchi, M., Ogiso, H., Ohnishi, M., and Ito, S. (1994) Breeding of a Cold-Resistant Grape Variety, *ASEV Jpn. Rep.* (in Japanese) *5*, 185–188.

14. Meyer, K.H., and Schweizer, E. (1976) Control of Fatty Acid Synthetase Levels by Exogenous Long-Chain Fatty Acids in the Yeasts *Candida lipolytica* and *Saccharomyces cerevisiae*, *Eur. J. Biochem. 65*, 317–324.

15. Fujii, T., Kobayashi, O., Yoshimoto, H., Furukawa, S., and Tamai. Y. (1997) Effect of Aeration and Unsaturated Fatty Acids on Expression of the *Saccharomyces cerevisiae* Alcohol Acetyltransferase Gene, *Appl. Environ. Microbiol. 63*, 910–915.

16. Marengo, E., Aceto, M., and Maurino, V. (2001) Classification of Nebbiolo-Based Wines from Piedmont (Italy) by Means of Solid-Phase Microextraction–Gas Chromatography–Mass Spectrometry of Volatile Compounds, *J. Chromatogr. A. 943*, 123–137.

17. Francioli, S., Torrens, J., Riu-Aumatell, M., Lopez-Tamames, E., and Buxaderas, S. (2003) Volatile Compounds by SPME-GC as Age Markers of Sparkling Wines, *Am. J. Enol. Vitic. 54*, 158–162.

18. Yoshioka, K., and Hashimoto, M. (1983) Ester Formation by Alcohol Acetyltransferase from Brewers' Yeast, *Agric. Biol. Chem. 45*, 2183–2190.

19. Lilly, M., Lambrechts, M.G., and Pretorius, I.S. (2000) Effect of Increased Yeast Alcohol Acetyltransferase Activity on Flavor Profiles of Wine and Distillates, *Appl. Environ. Microbiol. 66*, 744–753.

20. Esterbauer, H., and Schauenstein, E. (1977) Isomeric Trihydroxy-octadecenoic Acids in Beer: Evidence for Their Presence and Quantitative Determination (author's translation), *Z. Lebensm. Unters. Forsch. 164*, 255–259.

21. Nishiya, T., Aramaki, I., and Sugama, S. (1978) Separation of Identification of Ethyl Azelate Semialdehyde, Which Contributes to the Rancid Odor of Traditional Shôchû, *Hakkokogaku* (in Japanese) *56*, 182–187.

22. Torija, M.J., Beltran, G., Novo, M., Poblet, M., Guillamon, J.M., Mas, A., and Rozes, N. (2003) Effects of Fermentation Temperature and *Saccharomyces* Species on the Cell Fatty Acid Composition and Presence of Volatile Compounds in Wine, *Int. J. Food Microbiol. 85*, 127–136.

Lipid Characterization of Seed Oils from High-Palmitic, Low-Palmitoleic, and Very High-Stearic Acid Sunflower Lines

María J. Serrano-Vega, Enrique Martínez-Force, and Rafael Garcés*

Instituto de la Grasa, Consejo Superior de Investigaciónes Científicas (CSIC), 41012 Sevilla, Spain

ABSTRACT: Information obtained in recent years regarding the enzymes involved in FA synthesis can now be applied to develop novel sunflower lines by incorporating enzymes with specific characteristics into lines with a defined background. We have generated three highly saturated mutant lines in this way and characterized their FA content. The new high-palmitic, low-palmitoleic lines CAS-18 and CAS-25, the latter on a high-oleic background, have been selected from the high-stearic mutant CAS-3 by introducing a deficient stearic acid desaturase in a high-palmitic background from the previously developed mutant lines CAS-5 and CAS-12, respectively. As such, the desaturation of palmitic acid and the synthesis of palmitoleic acid and its derivatives (asclepic and palmitolinoleic acids) were reduced in these high-palmitic lines, increasing the stearic acid content. Likewise, introducing a FA thioesterase from a high-palmitic line (e.g., CAS-5) into the high-stearic CAS-3 increased the stearic acid content from 27 to 32% in the new high-stearic line CAS-31. As previously described in high-palmitic lines, high growth temperatures did not reduce the linoleic acid content of the oil. Furthermore, the FA composition of TAG, DAG, and phospholipids was modified in these lines. Besides a high degree of saturation, the TAG from these new vegetable oils have a low content of saturated FA in the sn-2 position. The α asymmetric coefficient obtained also indicates that the saturated FA are asymmetrically distributed within the TAG molecules. Indeed, the disaturated TAG content rose from 31.8 to 48.2%. These values of disaturated TAG are the highest to date in a temperate oilseed.

Paper no. L9698 in *Lipids 40*, 369–374 (April 2005).

The synthesis of FA in oilseeds up to the length of oleic acid occurs within the plastid. The enzymatic complex FA synthase I (FAS I) synthesizes up to the palmitoyl-acyl carrier protein (ACP), whereas FA synthase II (FAS II) elongates the palmitoyl-ACP to stearoyl-ACP. Finally, the stearoyl-ACP desaturase (SAD) introduces the first double bond into the molecule to produce oleoyl-ACP. The acyl-ACP are hydrolyzed by the action of the acyl-ACP thioesterases (TE), FatA or FatB, which have distinct preferences for unsaturated or saturated acyl-ACP, respectively. Nascent free FA are then exported to the cytoplasm and used as acyl-CoA for the syn-

thesis of glycerolipids in oilseeds, mainly TAG. In general, palmitic, stearic, and oleic acids are the main FA synthesized within the plastid in oilseeds, although later on oleic acid can then be desaturated, elongated, and so on.

Recently, some highly saturated sunflower mutant lines were generated by mutagenesis in an attempt to increase genetic variability (1,2). When the seed lipids from these mutant lines were analyzed, an increase in saturated FA content was observed, particularly in the TAG (3). From these mutants, two independent high palmitic acid lines were selected, both containing around 30% palmitic acid. Whereas one of these is on a standard high linoleic acid background (CAS-5), the other one is on a high oleic acid background (CAS-12). As a consequence, the seeds of these lines accumulated some palmitoleic (16:1n-7) and asclepic (18:1n-7) acids. Furthermore, the CAS-5 mutant also accumulated palmitolinoleic acid (16:2n-4). At least three partially recessive genes are responsible for the production of high quantities of palmitic FA in these mutants (4). Biochemical characterization of these mutants showed that the keto-acyl synthase II (KASII), an enzyme of the FAS II complex, was less active than the standard sunflower KASII. At the same time, an increase in TE activity on saturated FA was observed (5). The reduction in KASII activity led to an increase of palmitoyl-ACP production within the plastid, whereas the increase in TE activity on saturated FA promoted hydrolysis of the palmitoyl-ACP and subsequent export into the cytoplasm. On the other hand, some palmitoyl-ACP is desaturated within the plastid to palmitoleoyl-ACP owing to the activity of SAD, and this palmitoleoyl-ACP can be elongated to ascleployl-ACP by the action of the FAS II. Both these FA can then be exported into the cytoplasm where palmitoleic acid is converted to palmitolinoleic acid in the case of CAS-5 (5). Another highly saturated sunflower mutant with a high stearic acid content in the seed oil (CAS-3) was also obtained by mutagenesis (1). In this case, two partial dominant genes control the characteristic accumulation of FA (6). Biochemical characterization of this line identified a deficiency in the SAD activity and an increase in TE activity toward stearoyl-ACP that was responsible for this new trait (7). This mutant did not show any side effects due to the increase in its intraplastidial stearoyl-ACP content.

By considering all the available biochemical information and the channeling model proposed for the intraplastidial FA biosynthesis in the sunflower (8), we have generated a

*To whom correspondence should be addressed at Instituto de la Grasa, CSIC, Av. Padre García Tejero, 4, 41012 Sevilla, Spain. E-mail: rgarces@ig.csic.es

Abbreviations: ACP, acyl carrier protein; FAS I and II, FA synthase I and II; KASII, keto-acyl synthase II; SAD, stearoyl-ACP desaturase; TE, thioesterase.

hypothesis to further increase the saturated FA content of recombinant lines obtained from these initial mutants. For example, the introduction of the mutated SAD gene from the CAS-3 line into high-palmitic lines should reduce the amount of palmitoleic, asclepic, and palmitolinoleic acids that accumulate in the storage oil. Similarly, if the different TE activities described in both mutants depend on independent genes and are complementary, then an increase in saturated FA content would be expected when both activities are brought together. In this paper we characterize new lines obtained by crossing high-palmitic and high-stearic lines in accordance with this hypothesis.

EXPERIMENTAL PROCEDURES

Plant material. Sunflower seeds (*Helianthus annuus* L.) from the mutant lines CAS-5 and CAS-12 with high palmitic acid content, and the CAS-3 line with high stearic acid content were used in this work (1,2). The control seeds with a normal FA composition were from the public line RHA-274, from the USDA. The new sunflower lines described here were obtained by crossing high-palmitic and high-stearic acid mutants and selecting the lines of interest. Plants were cultivated in growth chambers at 25/15°C (day/night) cycles or at the temperatures indicated. A 16-h photoperiod was used with a photon flux density of 300 µmol $E \cdot m^{-2} \cdot s^{-1}$.

Lipid extraction and separation. About 500 mg of peeled seeds were ground in a screw-capped glass tube (10×13 mm) with a pestle and sand. The total lipids were extracted and separated by TLC on 0.25-mm-thick silica gel plates that were developed with hexane/ethyl ether/formic acid (75:25:1, by vol). The TLC plates were partially covered with a glass plate and exposed to iodine vapor. Unexposed TAG, DAG, and phospholipid fractions were scraped off the plates and eluted from the silica with chloroform/methanol (1:2, vol/vol). To determine their FA composition, phospholipids were further separated either on TLC silica gel plates developed with chloroform/methanol/acetic acid/H_2O (85:15:10:3.5, by vol) or on $(NH_4)_2SO_4$-impregnated silica gel plates developed with acetone/benzene/H_2O (90:30:10, by vol; 9). Individual polar lipids were identified by comparison with commercial standards, developed at the same time on the same TLC plate, and scraped off the plates.

Lipase hydrolysis. For positional analysis of FA in TAG, 10 mg of purified TAG was hydrolyzed with 2 mg pancreatic lipase in 1 mL of buffer containing 1 M Tris pH 8, 0.1 mL $CaCl_2$ (22%), and 0.25 mL deoxycholate (0.1%) (10). When approximately 60% of the TAG had been hydrolyzed (1–2 min), the reaction was stopped by adding 0.5 mL of 6 N HCl and the lipids were extracted three times with 1.5 mL ethyl ether. The reaction products were separated by TLC as indicated above. The FFA and *sn*-2-MAG bands, representing positions *sn*-(1+3) and *sn*-2 of TAG, respectively, were scraped off the plate and transmethylated. The FA composition of the original TAG was compared with that which remained after partial hydrolysis.

Lipid analysis. Isolated acyl lipids were converted to FAME from the isolated lipids by heating the samples at 80°C for 1 h in a 3-mL solution of methanol/toluene/H_2SO_4 (88:10:2, by vol; 11). After cooling, 1 mL of heptane was added and mixed. The FAME were recovered from the upper phase, then separated and quantified using a Hewlett-Packard 5890A gas chromatograph with a Supelco SP-2380 capillary column of fused silica (30 m length; 0.32 mm i.d.; 0.20 µm film thickness; Bellefonte, PA). Hydrogen was used as the carrier gas. The FA were identified by comparison with known standards and quantified with a hydrogen FID.

TAG species were separated and quantified by GLC using a Hewlett-Packard 6890 gas chromatograph with a Quadrex aluminum-clad bonded methyl 65% phenyl silicone 15M, 400-65HT-15-0.1F column (New Haven, CT). The TAG were identified and quantified by correcting the data for the relative FID response (12). After holding for 5 min, the oven temperature was ramped from 340 to 355°C at 1°C/min, the detector and injector temperatures were 400°C, and the split ratio was 1:100. Hydrogen was used as carrier gas, the linear rate being 31 cm/s.

The distribution of saturated FA in the external positions of TAG, *sn*-1 and *sn*-3, was calculated as the coefficient of asymmetry as previously developed (13). This coefficient was determined as the α of the TAG of the type SatUnsSat/SatUnsUns ($\alpha_{SUU/SUS}$) as we recommended for vegetable oils with a low content of saturated FA in the *sn*-2 position (13). An α value of 0.5 indicates that saturated FA are distributed equally between the *sn*-1 and *sn*-3 TAG stereochemical positions.

RESULTS AND DISCUSSION

FA composition of the oils. The FA composition of three recombinant lines, CAS-18, CAS-25, and CAS-31, was determined and is shown in Table 1.The CAS-18 and CAS-25 lines were selected from crosses of the high-stearic mutant CAS-3 with the high-palmitic mutants CAS-5 and CAS-12, respectively, keeping the high-palmitic background. These plants had inherited the low SAD activity from CAS-3 and consequently, had lower palmitoleic, asclepic, and palmitolinoleic acid contents. The CAS-31 line was obtained from the cross between CAS-3 and CAS-5, keeping the high-stearic background, and the efficient TE activity on saturated FA in this line increased the stearic and palmitic acid contents with respect to CAS-3. The FA composition of the RHA-274 control line and the parental lines, CAS-3, CAS-5, and CAS-12, are also shown (Table 1).

Thus, as proposed in our hypothesis, it appears that recombinant lines with reduced palmitoleic, asclepic, and palmitolinoleic acid contents could be selected by crossing the CAS-5 and CAS-12 with the CAS-3 line. In these plants, the palmitoleic acid content was reduced from 5.1 and 7.4% to 1.4 and 2.1%, respectively, whereas the asclepic acid content was reduced from 3.4 and 3.9% to 1.4 and 2.3%. It was no longer possible to detect palmitolinoleic acid in either CAS-18 or CAS-25. On the other hand, and as expected from the reduced

TABLE 1
FA Composition of Oils from the Newly Selected Recombinant Lines CAS-18, CAS-25, and CAS-31, as Well as in the Standard Control and Mutant Parental Lines, at Normal Growth Temperature (25/15°C)[a]

Sunflower line	FA composition (mol%)								
	16:0	16:1	16:2	18:0	18:1n-9	18:1n-7	18:2	20:0	22:0
RHA-274	5.9 ± 0.3	—	—	5.1 ± 0.4	36.6 ± 0.5	—	50.6 ± 0.6	0.7 ± 0.1	1.1 ± 0.1
CAS-3	7.4 ± 0.9	—	—	27.1 ± 2.2	16.1 ± 1.2	—	46.3 ± 3.4	1.5 ± 0.2	1.5 ± 0.3
CAS-5	34.7 ± 0.9	5.1 ± 0.7	0.6 ± 0.1	2.6 ± 0.2	6.9 ± 0.7	3.4 ± 0.6	45.1 ± 0.9	0.5 ± 0.1	1.0 ± 0.1
CAS-12	31.7 ± 1.7	7.4 ± 1.0	—	2.0 ± 0.3	50.5 ± 1.9	3.9 ± 0.5	2.7 ± 0.6	0.5 ± 0.1	1.3 ± 0.2
CAS-18	33.2 ± 1.2	1.4 ± 0.1	—	11.4 ± 1.2	4.0 ± 0.7	1.4 ± 0.1	45.8 ± 0.5	1.2 ± 0.1	1.5 ± 0.1
CAS-25	30.1 ± 0.6	2.1 ± 0.2	—	6.8 ± 0.1	45.8 ± 0.7	2.3 ± 0.3	10.2 ± 0.3	1.0 ± 0.1	1.6 ± 0.1
CAS-31	8.8 ± 0.4	—	—	31.9 ± 2.6	16.2 ± 1.6	—	39.2 ± 1.5	1.9 ± 0.4	1.8 ± 0.2

[a]Mean ± SD of three independent experiments. —, <0.5%.

SAD activity, the stearic acid content increased in both lines to as much as 11.4 and 6.8%, respectively.

The CAS-31 recombinant line had more stearic acid than the parental CAS-3 line. Moreover, a slight increase in the palmitic acid content was observed after improving the TE activity on saturated FA with respect to that from CAS-5. These FA represented 31.9 and 8.8% of the total FA respectively, compared with 27.1 and 7.4% in CAS-3. As the result of competition for substrate between the TE from CAS-5 and the FAS II from CAS-3, and according to the channeling proposal for FA biosynthesis within the sunflower plastid (8), a small increase in palmitic acid would be expected. Similar results were also found in other lipids, as will be shown shortly.

DAG and TAG components. The FA composition of the TAG of these sunflower oils was similar to the FA composition in the corresponding oils (see Table 2). Given that 95% of the oil's content is made up of TAG, this is not an unexpected result. DAG are precursors in the synthesis of TAG, but they are found in only minor amounts in the oil with respect to the TAG. The saturated FA content in the DAG was lower than in TAG, but we assumed that if they have a similar behavior to the neutral lipids in most vegetable oils, then saturated FA would be found in only the *sn*-1 position. To confirm that these TAG behaved as normal vegetable oil TAG, we analyzed the FA composition at positions *sn*-2 and *sn*-(1+3) of the purified TAG by partial hydrolysis using lipase (Table 3). In spite of the very high content of saturated FA in the TAG, the content of saturated FA in position *sn*-2 was very low, between 1.4 and 2.0% of the total saturated FA content. This figure was even lower than expected because in

CAS-31 TAG, stearic acid was elevated to 6.3-fold of that found in the control line RHA-274, from 31.9 to 5.1%, but in the *sn*-2 position only a 3.8-fold change was observed, from 1.5 to 0.4% (3). No very long chain FA, behenic and arachidic acids, were detected at the *sn*-2 position in these oils. The *sn*-(1+3) positions were mainly occupied by saturated FA, between 42.2 and 49.3%, around 20-fold that in the *sn*-2 position. As expected, the main unsaturated FA in the *sn*-2 position of the high-oleic line CAS-25 was oleic acid (76.4%), and in CAS-18 and CAS-31 linoleic acid represented 90.9 and 71.7%, respectively. Palmitoleic and asclepic acids are atypically distributed since, despite being unsaturated, they are mainly found at positions *sn*-(1+3). This suggests that the *sn*-2 lysophosphatidylcholine acyltransferase shows a higher specificity for oleic and linoleic acids than for saturated FA. All these data together suggest that these specialty oils are more similar to cacao butter (also called cocoa butter) than to saturated animal fats, indicating that they probably have good nutritional properties and are more healthful than animal or chemically modified vegetable fats (14,15).

TAG species. TAG are made up of three FA bound to a glycerol backbone. Two different oils with a similar FA composition could have different TAG compositions. As a consequence, the TAG composition of an oil provides more information than the FA composition. Indeed, the concept that oils are made up of TAG and not just FFA is very important. The TAG composition of these new oils can be seen in Table 4. The most important characteristic of these oils is the very high levels of disaturated TAG, whereas these are minor components or present in only trace amounts in normal sunflower

TABLE 2
FA Composition of TAG and DAG of the Novel Recombinant CAS-18, CAS-25, and CAS-31 Mutant Lines[a]

Line		FA composition (mol%)					
		16:0	16:1	18:0	18:1n-9	18:1n-7	18:2
CAS-18	TAG	33.6 ± 0.5	1.4 ± 0.2	11.0 ± 1.0	5.2 ± 0.7	1.2 ± 0.2	47.6 ± 1.4
	DAG	28.1 ± 1.2	1.3 ± 0.2	8.2 ± 0.6	8.8 ± 0.9	1.1 ± 0.2	52.5 ± 3.4
CAS-25	TAG	31.9 ± 1.2	2.8 ± 0.3	5.0 ± 0.3	52.3 ± 3.3	2.4 ± 0.2	5.6 ± 0.8
	DAG	16.6 ± 1.5	1.7 ± 0.1	3.0 ± 0.2	66.0 ± 4.5	3.9 ± 0.3	8.8 ± 1.0
CAS-31	TAG	8.8 ± 0.7	—	29.2 ± 2.1	12.6 ± 0.8	—	49.3 ± 1.7
	DAG	13.4 ± 0.9	—	22.1 ± 0.6	10.9 ± 1.2	—	53.6 ± 2.3

[a]Mean and SD of three independent experiments. —, <0.5%.

TABLE 3
FA Composition of *sn*-(1+3) and *sn*-2 Stereochemical Positions of TAG from CAS-18, CAS-25, and CAS-31 Mutants[a]

Sunflower line	Position	FA composition (mol%)							
		16:0	16:1	18:0	18:1n-9	18:1n-7	18:2	20:0	22:0
CAS-18	*sn*-(1+3)	49.3 ± 3.1	1.2 ± 0.1	20.2 ± 2.0	2.3 ± 0.2	1.5 ± 0.2	21.9 ± 0.8	1.5 ± 0.2	2.1 ± 0.2
	sn-2	1.6 ± 0.1	0.8 ± 0.1	0.7 ± 0.1	5.6 ± 0.4	0.4 ± 0.1	90.9 ± 4.4	—	—
CAS-25	*sn*-(1+3)	44.2 ± 2.3	2.5 ± 0.1	9.5 ± 0.6	30.5 ± 0.9	2.7 ± 0.4	6.7 ± 0.4	1.5 ± 0.1	2.4 ± 0.2
	sn-2	2.0 ± 0.3	1.4 ± 0.1	1.4 ± 0.1	76.4 ± 1.6	1.6 ± 0.2	17.2 ± 1.1	—	—
CAS-31	*sn*-1+3	9.1 ± 0.2	—	42.2 ± 2.2	9.4 ± 0.7	—	35.9 ± 2.2	1.9 ± 0.2	1.5 ± 0.1
	sn-2	1.2 ± 0.1	—	1.5 ± 0.5	25.6 ± 0.9	—	71.7 ± 1.7	—	—

[a]Mean and SD of three independent experiments. —, <0.5%.

oils (12). In the oil from the high-linoleic-, high-palmitic-, low-palmitoleic-derived sunflower line CAS-18, PLP and PLS are the main TAG species (where P = palmitic, L = linoleic, and S = stearic acid). These TAG species made up

TABLE 4
TAG Composition of Oils from Mutant CAS-18, CAS-25, and CAS-31 Seeds Measured Using a High-Temperature GC–FID Method[a]

	CAS-18	CAS-25	CAS-31
PPoP	0.3 ± 0.1	0.2 ± 0.1	
POP	2.2 ± 0.1	20.2 ± 0.8	0.5 ± 0.2
PPoO		5.5 ± 0.5	
PLP	25.1 ± 2.5	[a,b]	1.0 ± 0.2
PPoL	2.1 ± 0.3	0.3 ± 0.2	
POS	1.1 ± 0.1	8.3 ± 0.7	3.1 ± 0.6
POO		30.9 ± 2.8	0.7 ± 0.1
POAs		3.4 ± 0.3	
PLS	14.5 ± 1.1		8.1 ± 0.7
PoOO		9.2 ± 1.1	
POL	3.8 ± 0.3	[a,b]	3.4 ± 0.3
PAsL	2.5 ± 0.2		
PLL	26.2 ± 2.4	0.9 ± 0.2	4.2 ± 0.6
PoLL	0.3 ± 0.1		
SOS		1.7 ± 0.2	5.6 ± 0.5
SOO		7.7 ± 0.2	3.0 ± 0.2
SLS	3.1 ± 0.2		15.3 ± 1.4
OOO		4.1 ± 0.6	
OOAs		2.8 ± 0.3	
SOL	1.1 ± 0.3		13.5 ± 1.0
OOL		1.5 ± 0.2	1.4 ± 0.1
SLL	8.7 ± 0.7		21.2 ± 1.6
OLL	0.6 ± 0.1		3.9 ± 0.3
AsLL	0.4 ± 0.1		
LLL	4.4 ± 0.3		3.6 ± 0.2
SLA			2.1 ± 0.3
OLA			1.2 ± 0.1
POB		1.4 ± 0.2	
OOA		0.8 ± 0.1	1.1 ± 0.1
SOA			
PLB	1.5 ± 0.1		
LLA	0.6 ± 0.1		1.3 ± 0.1
OOB		1.3 ± 0.1	0.3 ± 0.1
SOB			1.3 ± 0.2
SLB	0.4 ± 0.2		1.2 ± 0.2
OLB			1.2 ± 0.1
LLB	0.6 ± 0.1		1.7 ± 0.1

[a]Mean and SD of threee independent experiments. —, <0.2%.
[b]These peaks did not separate and are included in the upper identification number. A, arachidic acid; As, asclepic acid; B, behenic acid; L, linoleic acid; O, oleic acid; P, palmitic acid; Po, palmitoleic acid; S, stearic acid.

25.1 and 14.5% of the total TAG content in this line as opposed to the 14.5 and 4.2% contributed in the corresponding parental line CAS-5 (12). In the high-oleic-, high-palmitic-, low-palmitoleic-derived line CAS-25, the main disaturated TAG species were POP and POS (where O = oleic acid), which corresponded to 20.2 and 8.3%. In the parental CAS-12 line, these TAG species represented 19.4 and 2.4% of the total TAG. In both the CAS-18 and CAS-25 lines, there was a considerable reduction in the TAG species containing palmitoleic and asclepic acids. This was expected given their lower representation in the oils of these lines with respect to the parental lines. Another common characteristic was the increase in PLS and POS, respectively, as a consequence of the increase of stearic acid.

In the high-linoleic, high-stearic CAS-31 there was a very important increase in PLS and SLS, from 6.8 to 8.1% and from 12.0 to 15.3%, respectively, when compared with the parental CAS-3 line (12). This was due to the increase in the stearic acid content and to a lesser extent, to the small increase in palmitic acid.

These new lines demonstrate an important increase with respect to their parental and standard sunflower lines in both saturated FA and in TAG with two saturated FA. The total disaturated TAG content was 31.8% in CAS-25, 39.3% in CAS-31, and 48.2% in CAS-18, this latter line probably constituting the temperate seed oil with the highest disaturated TAG content established to date. It has previously been shown that saturated FA are not symmetrically distributed between the *sn*-1 and *sn*-3 stereochemical positions in TAG molecules, and an asymmetrical α coefficient has been proposed to calculate this asymmetry (13). The calculated α SatUnsSat/SatUnsUns is that which is recommended for vegetable oils with a low content of saturated FA in the *sn*-2 position (13). Thus, to estimate this asymmetry in the new oils, we determined their α coefficient. The α for saturated TAG of the high-palmitic line CAS-18 was 0.42, higher than the 0.38 found in high-stearic line CAS-31, since their saturated FA are more symmetrically distributed. These results suggest that the acyltransferases involved in TAG biosynthesis have a different selectivity for palmitic or stearic acid. A similar effect was found when comparing the high-linoleic and high-oleic lines, for which the α coefficient for CAS-25 was 0.35. The smaller α value in the high-oleic lines is most likely related to the specificity of the acyltransferases.

Influence of the growth temperature. In previous studies, the content of linoleic acid in the high-palmitic line CAS-5 did not show big variations at different growth temperatures, even at a 30/20°C day/night growth temperature (16). This effect was not found in the high-stearic lines, such as CAS-3, or in the standard control lines. To determine whether these new very-high-palmitic lines behave in a similar fashion, the high-palmitic CAS-18 line and the high-palmitic, high-oleic CAS-25 line were grown at three different temperatures (Table 5). At high temperatures, the amount of linoleic acid produced by the CAS-18 line increased from 47.1 to 50.0%, reminiscent of the behavior of the high-palmitic CAS-5 sunflower mutants. A similar effect was found in the CAS-25 line with respect to oleic acid, which was coupled with a slight reduction in their linoleic acid content at a high growth temperature. This probably reflects the origin of this line from a high oleic acid background, which induces a behavior distinct from that of CAS-18. Nevertheless, the palmitic acid contents of all lines were similar and independent of the growth temperature. Furthermore, no differences were found among any other FA analyzed in these oils. This phenomenon may reflect the fact that membranes with a high palmitic acid content are always rigid and need to maximize their unsaturated linoleic acid content to maintain their membrane fluidity, a behavior that it is not found in the high-stearic lines (16).

Phospholipids. The FA composition of the main phospholipids in the seeds of these sunflower lines is shown in Table 6: PC, PI, and PE. As the sunflower seed is not a photosynthetic tissue, only small amounts of galactolipids accumulate. All phospholipids in these lines contain high levels of saturated FA, more than in standard control lines and even more than the highly saturated parental lines (3). The saturated FA content in PI was close to 50% in all the recombinant lines: 47.1% in CAS-18, 43.1% in CAS-25, and 45.3% in CAS-31. These values are similar to those that have been found for PI isolated from other sunflower lines (3). The contents of the other main phospholipids, PE and PC, were more variable, but always with a high level of saturated FA that reflected the principal saturated FA found in each line.

This study substantiates that biochemical data obtained from the analysis of sunflower mutant lines are important tools to guide the selection of new mutants with modified FA composition. In CAS-18 and CAS-25 lines, thanks to the introduction of a mutated SAD from the high-stearic line CAS-3, it has been possible to reduce the amount of palmitoleic, asclepic, and palmitolinoleic acids. In a similar way, the introduction of a TE activity that acts well on saturated FA in the new CAS-31 line elevated the stearic acid content in the oil up to 32%, improving the already high-stearic line CAS-3. These results confirm all previous biochemical findings regarding the association between SAD and TE in the generation of the mutant phenotypes of CAS-3, CAS-5, and CAS-12. Finally, by characterizing the lipids from these lines, we highlight the importance of the TAG composition and the asymmetric α coefficient for the saturated FA in these TAG.

ACKNOWLEDGMENTS

TABLE 5
FA Composition of CAS-18 and CAS-25 Seeds, Grown at Low (20/10°C), Medium (25/15°C), and High (30/20°C) Temperatures[a]

Sunflower line	Temperature (°)	16:0	16:1	18:0	18:1n-9	18:1n-7	18:2	20:0	22:0	18:2/18:1n-9
CAS-18	20/10	32.8 ± 1.8	1.9 ± 0.2	9.0 ± 1.0	4.7 ± 0.1	1.6 ± 0.1	47.1 ± 1.1	0.9 ± 0.1	1.8 ± 0.1	10.0
	25/15	31.6 ± 2.0	1.8 ± 0.1	9.5 ± 0.9	4.7 ± 0.4	1.7 ± 0.1	47.8 ± 1.3	0.9 ± 0.1	1.8 ± 0.2	10.2
	30/20	31.3 ± 1.6	2.1 ± 0.1	7.6 ± 0.9	4.7 ± 0.1	2.0 ± 0.1	50.0 ± 0.9	0.8 ± 0.1	1.5 ± 0.2	10.6
CAS-25	20/10	29.1 ± 1.0	2.4 ± 0.2	6.4 ± 0.7	47.2 ± 1.5	1.7 ± 0.1	9.1 ± 1.1	1.1 ± 0.4	1.6 ± 0.3	0.2
	25/15	30.3 ± 0.6	2.2 ± 0.1	6.9 ± 0.4	46.9 ± 1.2	2.5 ± 0.2	8.7 ± 1.0	0.9 ± 0.1	1.5 ± 0.1	0.2
	30/20	29.7 ± 0.7	2.9 ± 0.2	6.0 ± 0.9	51.1 ± 1.0	2.5 ± 0.3	6.6 ± 0.8	0.7 ± 0.1	1.4 ± 0.3	0.1

[a]Mean and SD of seeds from six different capitula.

TABLE 6
FA Composition of Main Seed Phospholipids[a]

Sunflower line	Lipid	FA composition (mol%)				
		16:0	16:1	18:0	18:1[b]	18:2
CAS-18	PI	38.2 ± 0.6	0.2 ± 0.07	8.9 ± 0.2	5.9 ± 0.4	46.8 ± 0.9
	PC	27.1 ± 0.3	1.1 ± 0.07	6.0 ± 0.1	8.7 ± 0.7	57.2 ± 1.3
	PE	30.4 ± 0.6	0.9 ± 0.1	3.8 ± 0.1	5.5 ± 0.6	59.4 ± 1.5
CAS-25	PI	35.8 ± 1.1	0.4 ± 0.1	7.3 ± 1.1	39.4 ± 2.6	17.3 ± 0.8
	PC	14.8 ± 0.6	1.2 ± 0.1	2.6 ± 0.1	68.6 ± 1.1	12.8 ± 0.5
	PE	21.8 ± 0.5	1.1 ± 0.1	2.3 ± 0.4	59.3 ± 1.3	15.5 ± 1.2
CAS-31	PI	20.0 ± 1.1	—[c]	25.3 ± 1.7	6.9 ± 1.1	47.8 ± 2.5
	PC	13.4 ± 0.5	—	19.8 ± 0.6	11.4 ± 0.4	55.4 ± 1.9
	PE	14.1 ± 0.4	—	14.4 ± 0.6	8.0 ± 0.3	63.5 ± 2.1

[a]Mean and SD of three independent experiments.
[b]Sum of 18:1n-9 and 18:1n-7 acids.
[c]—, <0.2%.

REFERENCES

1. Osorio, J., Fernández-Martínez, J.M., Mancha, M., and Garcés, R. (1995) Mutant Sunflower with High Concentration of Saturated Fatty Acids in the Oil, *Crop Sci. 33*, 739–742.

2. Fernández-Martínez, J.M., Mancha, M., Osorio, J., and Garcés, R. (1997) Sunflower Mutant Containing High Levels of Palmitic Acid in High Oleic Background, *Euphytica 97*, 113–116.

3. Álvarez-Ortega, R., Cantisán, S., Martínez-Force, E., and Garcés, R. (1997) Characterization of Polar and Nonpolar Seed Lipid Classes from Highly Saturated Fatty Acid Sunflower Mutants, *Lipids 32*, 833–837.

4. Pérez-Vich, B., Fernández, J., Garcés, R., and Fernández-Martínez, J.M. (1999) Inheritance of High Palmitic Acid Content in the Seed Oil of Sunflower Mutant CAS-5, *Theor. Appl. Genet. 98*, 496–501.

5. Martínez-Force, E., Álvarez-Ortega, R., and Garcés, R. (1999) Enzymatic Characterization of High Palmitic Sunflower (*Helianthus annuus* L.) Mutants, *Planta 207*, 533–538.

6. Pérez-Vich, B., Garcés, R., and Fernández-Martínez, J.M. (1999) Genetic Control of High Stearic Acid Content in the Seed Oil of Sunflower Mutant CAS-3, *Theor. Appl. Genet. 99*, 663–669.

7. Cantisán, S., Martínez-Force, E., and Garcés, R. (2000) Enzymatic Studies of High Stearic Acid Sunflower Seed Mutants, *Plant Physiol. Biochem. 38*, 377–382.

8. Martínez-Force, E., and Garcés, R. (2002) Dynamic Channelling During *de novo* FA Biosynthesis in *Helianthus annuus* Seeds, *Plant Physiol. Biochem. 40*, 383–391.

9. Khan, M., and Williams, J.P. (1997) Improved Thin-Layer Chromatography Methods for the Separation of Major Phospholipids and Glycolipids from Plant Lipid Extracts and Phosphatidyl Glycerol and Bis(monoacylglyceryl) Phosphate from Animal Lipid Extract, *J. Chromatogr. 140*, 179–185.

10. Mancha, M., and Vázquez, A. (1970) Transformación de los glicéridos durante la maduración de la aceituna. III. Distribución de los ácidos grasos en los triglicéridos, *Grasas Aceites 21*, 127–131.

11. Garcés, R., and Mancha, M. (1993) One-Step Lipid Extraction and Fatty Acid Methyl Esters Preparation from Fresh Plant Tissues, *Anal. Biochem. 211*, 139–143.

12. Fernández-Moya, V., Martínez-Force, E., and Garcés, R. (2000) Identification of Triacylglycerol Species from High-Saturated Sunflower (*Helianthus annuus* L.) Mutants, *J. Agric. Food Chem. 48*, 764–769.

13. Martínez-Force, E., Ruiz-López, N., and Garcés, R. (2004) The Determination of the Asymmetrical Stereochemical Distribution of Fatty Acids in Triacylglycerols, *Anal. Biochem. 334*, 175–182.

14. Renaud, S.C., Ruf, J.C., and Petithory, D. (1995) The Positional Distribution of Fatty Acids in Palm Oil and Lard Influences Their Biologic Effects in Rats, *J. Nutr. 125*, 229–237.

15. Kelly, F.D., Sinclair, A.J., Mann, N.J., Turner, A.H., Abedin, L., and Li, D. (2001) A Stearic Acid-Rich Diet Improves Thrombogenic and Atherogenic Risk Factor Profiles in Healthy Males, *Eur. J. Clin. Nutr. 55*, 88–96.

16. Martínez-Force, E., Álvarez-Ortega, R., Cantisán, S., and Garcés, R. (1998) Fatty Acid Composition in Developing High Saturated Sunflower (*Helianthus annuus* L.) Seeds: Maturation Changes and Temperature Effect, *J. Agric. Food Chem. 46*, 3577–3582.

Synthesis and *in vitro* Cytotoxic Activity of N-, F-, and S-Ether Derivatives of Podophyllotoxin Fatty Acid Adducts

Jamal Mustafa[a], Shabana I. Khan[a], Guoyi Ma[a],
Larry A. Walker[a,b], and Ikhlas A. Khan[a,b,*]

[a]National Center for Natural Product Research, Research Institute of Pharmaceutical Sciences, [b]Department of Pharmacology,
and [c]Department of Pharmacognocy, School of Pharmacy, University of Mississippi, University, Mississippi 38677

ABSTRACT: This paper represents the first synthesis, spectroscopic characterization, and antitumor evaluation of F-, N-, and S-containing $C_4\alpha$-FA derivatives of podophyllotoxin. In a synthetic strategy, a FA unit of 4-*O*-podophyllotoxinyl 12-hydroxy-octadec-*Z*-9-enoate **2**, a derivative of podophyllotoxin, was functionalized at the C-12 position by incorporating the F atom and N-containing moieties. The FA olefin (*Z*, C-9/C-10) of **2** was hydrogenated to produce a derivative possessing a hydroxy function (C-12) on a saturated C_{18} FA chain. In another synthetic strategy, two *S*-ethers of podophyllotoxin ($C_4\alpha$) were synthesized from a terminal unsaturated FA analog, 4-*O*-podophyllotoxinyl undec-10-enoate. Syntheses were achieved through effective synthetic procedures; ^{1}H NMR, ^{13}C NMR, IR, and high-resolution mass data proved excellent tools to characterize these derivatives. *In vitro* antitumor activity was investigated against a panel of five human neoplastic cell lines, SK-MEL (malignant, melanoma), KB (epidermal carcinoma, oral), BT-549 (ductal carcinoma, breast), SK-OV-3 (ovary carcinoma), and HL-60 (human leukemia). Keeping in view the severe lack of tumor selectivity of podophyllotoxin over normal cells, we assayed new analogs against noncancerous mammalian VERO (African green monkey kidney fibroblast) cell lines to gauge their extent of toxicity. Several of these compounds showed excellent moderation of antitumor activity. In general, we found excellent growth inhibition against the human leukemia cell line (HL-60), particularly for the analogs containing *S*-ethers and carbamates. None of the compounds were toxic to normal cell lines.

Paper no. L9656 in *Lipids 40*, 375–382 (April 2005).

Chemotherapy involves the administration of specific anticancer therapeutic chemicals to cancer patients (1,2). Because of physiological similarities between cancerous and noncancerous cells, the clinical efficacy of most anticancer drugs is limited by varying degrees of toxicity toward normal cells (3). The undesired side effects result from the lack of selectivity and the appearance of acquired resistance (2). Like most antineoplastic agents, the natural product podophyllotoxin **1** (4,5) also lacks tumor selectivity, which limits its clinical utility for cancer chemotherapy and that of many of its related products (6,7). Alterations of its
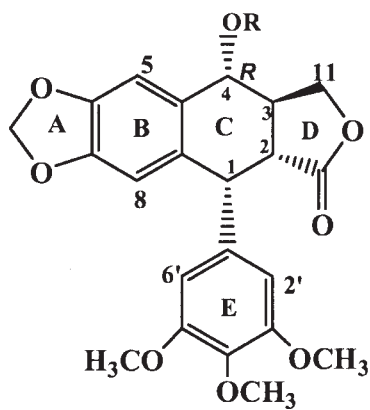
structure have yielded two semisynthetic derivatives, etoposide and teniposide, which are in clinical use (5,7,8). Drug resistance, metabolic inactivation, myelosuppression, and bioavailability have greatly undermined the clinical applications of these two drugs (5,9,10). Approaches to facilitate tumor-selective chemotherapy have been the topic of recent investigations (3,11).

Current trends in the treatment of human cancers favor drug combinations that result in improved responses, where the contributions of a variety of FA have been proved highly significant (12,13). A number of FA are part of our diet; therefore, nutritional dietary supplements highly enriched in certain FA have been suggested to prevent the side effects of cancer therapy (13,14). That certain TG and FA have the potential to prevent or inhibit carcinogenesis has been proposed (15–18). FA substituents on podophyllotoxin **1** may lead to analogs with enhanced cytotoxicity, but this strategy has not yet been explored except in a few studies (19,20). We recently demonstrated the efficient synthesis of a series of FA-based $C_4\alpha$-derivatives of **1** and their significant *in vitro* selectivity for inhibiting the growth of cancer cells over normal ones (21–23). One of these compounds, 4-*O*-podophyllotoxinyl 12-hydroxy-octadec-*Z*-9-enoate **2**, has been assayed *in vitro* against a panel of 60 human cancer cell lines at the National Cancer Institute (NCI) under a drug discovery program. Data produced by NCI for **2** have shown strong tumor inhibition activity against a wide spectrum of cancer cell lines (23). Our preliminary studies have indicated a mode of antitumor action for **2** that differs from podophyllotoxin, etoposide, and teniposide (23). These results encouraged the present work, which is directed toward the synthesis of $C_4\alpha$-FA analogs of **1** possessing F, N, and S and evaluation of their *in vitro* anticancer activity.

Here, we report the first synthesis of $C_4\alpha$-FA analogs of podophyllotoxin **1** containing the F and N atoms, obtained by chemical transformations of the hydroxy group present at the C-12 position on the FA chain of compound **2**. Further, this communication also presents the first synthesis of $C_4\alpha$-*S*-ether (thioether) FA analogs of **1**. A total of eight unusually functionalized FA derivatives of podophyllotoxin were synthesized (Scheme 1), and spectroscopic data established their chemical structures. The novel $C_4\alpha$-FA analogs were assayed for their *in vitro* antitumor activity against a panel of four human solid tumor cell lines, SK-MEL, KB, BT-549, SK-OV-3, and one human leukemia cell line, HL-60. To compare their tumor selectivity over normal cell lines, VERO cells were also included.
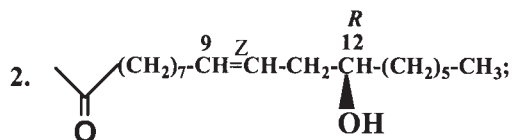
R

1. H;

2. $(CH_2)_7$-CH=CH-CH$_2$-CH-$(CH_2)_5$-CH$_3$; (positions 9 Z, R 12, OH)

3. $(CH_2)_7$-CH$_2$CH$_2$CH$_2$-CH-$(CH_2)_5$-CH$_3$ (R 12, OH)

4. $(CH_2)_7$-CH=CH-CH$_2$-CH-$(CH_2)_5$-CH$_3$; (9 Z, R/S 12, F)

5. $(CH_2)_7$-CH=CH-CH$_2$-CH-$(CH_2)_5$-CH$_3$; (9 Z, R 12)

6. $(CH_2)_7$-CH=CH-CH$_2$-CH-$(CH_2)_5$-CH$_3$; (9 Z, R 12)

7. $(CH_2)_7$-CH=CH-CH$_2$-CH-$(CH_2)_5$-CH$_3$; (9 Z, R 12)

8. $(CH_2)_7$-CH=CH-CH$_2$-CH-$(CH_2)_5$-CH$_3$; (9 Z, R 12)

9. $(CH_2)_8$CH=CH$_2$; (10)

10. $(CH_2)_8$CH$_2$CH$_2$-S-CH$_2$CH$_2$-OH ; (11, 2')

11. $(CH_2)_8$CH$_2$CH$_2$-S-CH$_2$-CH-CH$_2$-OH (11, 2', OH)
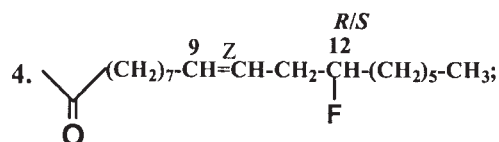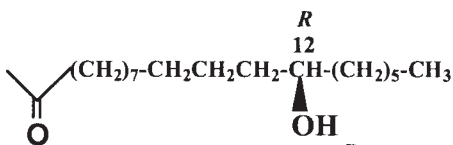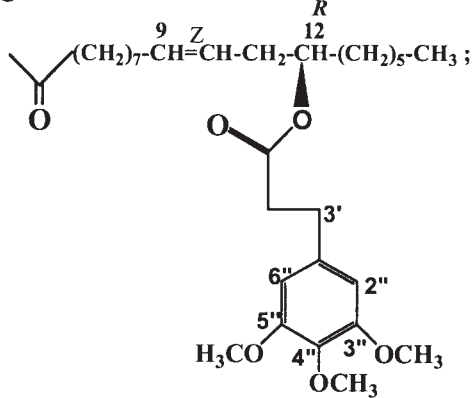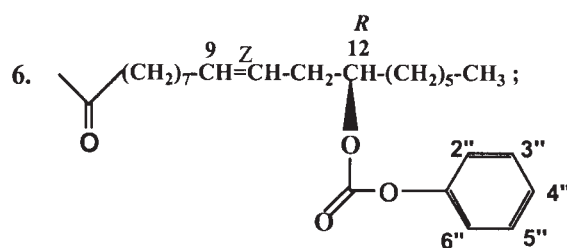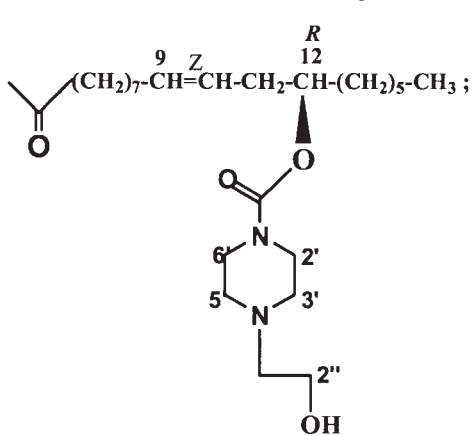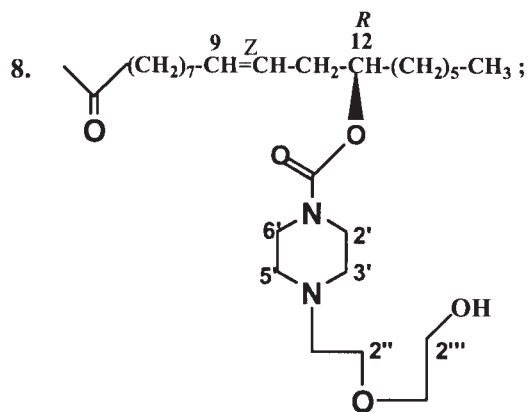
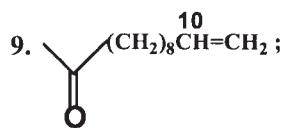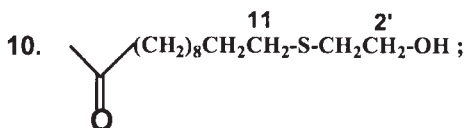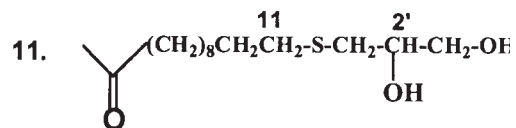**SCHEME 1**

EXPERIMENTAL PROCEDURES

The synthesis of 4-*O*-podophyllotoxinyl 12-hydroxy-octadec-*Z*-9-enoate **2** and all the experimental procedures used are as described previously (21). The palladium (10% on activated carbon powder, standard, reduced, normally 50% water wet) was purchased from Alfa Aesar (Ward Hill, MA). All other reagents were obtained from Aldrich Chemicals (Milwaukee, WI) and used without further purification.

(i) 4-O-Podophyllotoxinyl 12-hydroxy-octadecanoate 3. Compound **2** (100 mg) was dissolved in ethyl acetate (20 mL), and 10% Pd/C (10 mg) was added and hydrogenated for 8 h under a pressure of 45 psi. The solution was filtered and rotary-evaporated under reduced pressure at 20°C. The crude material was passed through a silica gel column (J.T.Baker, Phillipsburg, NJ; *n*-hexane/ethyl acetate, 1:1, vol/vol; R_f: 0.70) to obtain a sticky and viscous colorless oily form of **3** (yield: 99%). IR (CHCl$_3$, cm^{-1}): 3530, 1776, 1735, 1586, 1506, 1483, 1419, 1240, and 1122; ^{1}H NMR (CDCl$_3$, δ_H): 0.87 (*t*, *J* = 7.0 Hz, terminal methyl of the FA chain, 3H), 1.36–1.26 (*br m*, 11 × C$\underline{H}_2$ groups of the FA methylene chain, 22H), 1.40 (*m*, 11-C$\underline{H}_2$, 13-C$\underline{H}_2$, 4H), 1.68 (*m*, 2H), 2.43 (*m*, 2-C$\underline{H}_2$, 2H), 3.58 (*m*, 12-C$\underline{H}$-OH, 1H); ^{13}C NMR (CDCl$_3$, δ_C): 14.47 (C-18), 23.00 (C-17), 25.39 (C-16), 26.02, 29.61, 29.79, 29.96, 30.08 (C-11 & C-13), 32.23, 34.78 (C-2), 174.09 (ester carbonyl, C-1). The various resonances originating from the podophyllotoxin nucleus were as follows: ring A: δ_H 5.98 (*d*, *J* = 2.50 Hz, 1H) and 5.99 (*d*, *J* = 2.50 Hz, 1H), δ_C 101.97; ring B: δ_H 6.54 (*s*, 8-H), δ_C 110.09 (C-8); δ_H 6.76 (*s*, 5-H, 1H), δ_C 107.38 (C-5); ring C: δ_H 4.61 (*d*, $J_{1,2}$ = 4.50 Hz, 1-H, 1H), δ_C 44.29 (C-1); δ_H 2.92 (*dd*, $J_{1,2}$ = 4.60 Hz, $J_{2,3}$ =14.60 Hz, 2-H, 1H), δ_C 39.17 (C-2); δ_H 2.83 (*m*, 3-H, 1H), δ_C 45.95 (C-3); δ_H 5.89 (*d*, $J_{3,4}$ = 8.70 Hz, 4-H, 1H), δ_C 73.76 (C-4); ring D: two protons of 11-C$\underline{H}_2$ signals split into two, δ_H 4.23 (*t*, *J* = 10.0 Hz, 11-H, 1H) and δ_H 4.35 (*dd*, *J* = 7.0 Hz, *J* = 7.0 Hz, 11-H, 1H), δ_C 71.81 (C-11); ring E: δ_H 3.76 (*s*, 3′-H, 3′C-OC$\underline{H}_3$, 5′-H, 5′C-OC$\underline{H}_3$, 6H), 56.51 (C-3′, C-5′); δ_H 3.82 (*s*, 4′-H, 4′C-OC$\underline{H}_3$, 3H), δ_C 61.12 (C-4′); δ_H 6.40 (*s*, 2′-H, 6′-H, 2H), δ_C 108.49 (C-2′, C-6′); quaternary carbons of podophyllotoxin: 128.83, 132.72, 135.23, 137.52, 147.97, 148.49, 153.01, and 174.66 (lactone carbonyl in the D ring of podophyllotoxin); EI-MS found [M + H] 697.3952; C$_{40}$H$_{57}$O$_{10}$ [M + H]$^+$ requires 697.39517.

(ii) 4-O-Podophyllotoxinyl 12-fluoro-octadec-Z-9-enoate 4. Compound **2** (0.24 mmol) was dissolved in dry methylene chloride (3 mL) and to this solution, diethylaminosulfur trifluoride (DAST) (0.24 mmol) was added at −78°C (dry ice/acetone) under nitrogen. The reaction was warmed to room temperature and stirred for 1 h. Progress of the reaction was monitored by TLC. The complete conversion of **2** into the desired product was achieved in 1 h. The reaction mixture was diluted with methylene chloride (10 mL), washed with brine and water, dried over Na$_2$SO$_4$, and concentrated to dryness under reduced pressure at 20°C to obtain a crude reaction product. A silica gel flash column (*n*-hexane/ethyl acetate, 2:1, vol/vol; R_f: 0.90) was used to purify **4**. The isolated yield of a colorless, viscous oily product was 98.5%. IR (CHCl$_3$, cm^{-1}): 1777, 1732, 1587,

1481, 1420, 1329, 1235, 1125, 1038, 1000, 931, 862, and 772; ^{1}H NMR (CDCl$_3$, δ_H): 0.86 (*t*, *J* = 6.50 Hz, terminal methyl of the FA chain, 3H), 1.48 (*br m*, 8-C$\underline{H}_2$ was merged, 8 × C$\underline{H}_2$ groups of the FA methylene chain, 18H), 1.66–1.56 (*m*, 3-C$\underline{H}_2$, 13-C$\underline{H}_2$, 4H), 2.00 (*m*, 11-C$\underline{H}_2$, 2H), 2.38 (*m*, 2-C$\underline{H}_2$, 2H), 3.71 (*m*, 12-C$\underline{H}$-F, 1H), 5.40 (*m*, 9-H, 1H), 5.47 (*m*, 10-H, 1H); ^{13}C NMR (CDCl$_3$, δ_C): 14.49 (C-18), 23.04 (C-17), 25.36 (C-3), 25.51 (C-8), 29.55, 29.71, 32.25, 34.73 (C-2), 35.60 (C-11), 97.85 (C-12), 125.81 (C-9),132.78 (C-10), and 174.06 (ester carbonyl, C-1); EI-MS found [M + Na] 719.3576; C$_{40}$H$_{53}$O$_9$FNa [M + Na]$^+$ requires 719.3571.

(iii) 4-O-Podophyllotoxinyl 12-[3′-(3″, 4″, 5″-trimethoxy-phenyl)propionyloxy]octadec-Z-9-enoate 5. Equimolar amounts of 3-(3,4,5-trimethoxyphenyl)propionic acid and **2** were reacted to produce **5** by a method adopted earlier (21). The isolated (*n*-hexane/ethyl acetate, 1:1, vol/vol, R_f: 1.0) yield of this viscous colorless oil was 99%. IR (CHCl$_3$, cm^{-1}): 1779, 1733, 1587, 1464, 1235, 1123, and 1001; ^{1}H NMR (CDCl$_3$, δ_H): 0.90 (*t*, *J* = 7.0 Hz, terminal methyl of the FA chain, 3H), 1.34–1.27 (*br m*, 8 × C$\underline{H}_2$ groups of the FA methylene chain, 16H), 1.54 (*m*, 2H), 1.70 (*m*, 2H), 2.03 (*m*, 8-C$\underline{H}_2$, 2H), 2.31 (*m*, 2H), 2.42 (*m*, 2-C$\underline{H}_2$, 2H), 2.62 (*m*, 3′-C$\underline{H}_2$, 2H), 2.83 (*m*, 11-C$\underline{H}_2$, 2H), 2.97–2.91 (*m*, 2-H of podophyllotoxin, 2′-C$\underline{H}_2$, 3H), 4.91 (*m*, 12-H, 1H), 5.32 (*m*, 9-H, 1H), 5.46 (*m*, 10-H, 1H); ^{13}C NMR (CDCl$_3$, δ_C): 14.46 (C-18), 22.97 (C-17), 25.41, 25.71, 27.72 (C-8), 29.52, 29.91, 31.83, 32.11, 32.33 (C-3′), 33.01 (C-11), 34.74 (C-2), 36.64 (C-2′), 74.53 (C-12), 124.63 (C-9), 132.71 (C-10). Two ester carbonyls appeared at δ_C 172.96 (C-1′) and 174.10 (C-1). The NMR signals associated with two sets of three methoxy groups were as follows: δ_H 3.78 (*s*, 6H) and 3.83 (*s*, 6H) for 3′OC$\underline{H}_3$, 5′OC$\underline{H}_3$, 3″OC$\underline{H}_3$, and 5″OC$\underline{H}_3$; correlations at δ_C 56.43, 56.52 for C-3′, C-5′, C-3″ and C-5″; 3.86 (*s*, 6H) for 4′OC$\underline{H}_3$ and 4″OC$\underline{H}_3$; correlations at δ_C 61.14, and 61.21 (C-4′, C-4″). The equivalent aromatic protons 2′-H and 6′-H (podophyllotoxin ring E) appeared at δ_H 6.41 (*s*) and correlated at δ_C 108.50. Similar protons (2″-H and 6″-H) of the trimethoxyphenyl propionate moiety were deshielded to appear slightly downfield at δ_H 6.44 (*s*) and correlated at δ_C 105.56 (C-2″, C-6″). The quaternary carbons of both podophyllotoxin and the trimethoxyphenyl propionate moiety were recorded at δ_C 128.0, 132.91, 135.25, 136.80, 137.52, 147.98, 148.50, 153.02, 153.60; EI-MS found [M + H] 917.4676; C$_{52}$H$_{69}$O$_{14}$ [M + H]$^+$ requires 917.4687.

(iv) 4-O-Podophyllotoxinyl 12-(phenoxycarbonyloxy)oc-tadec-Z-9-enoate 6. First pyridine (1.80 mmol) and then phenyl chloroformate (1.80 mmol) were added to a dry methylene chloride (10 mL) solution of **2** (0.75 mmol) under a nitrogen atmosphere with stirring at 0°C. The reaction mixture turned yellow as soon as the phenyl chloroformate was added, and this was allowed to stir at room temperature. Phenoxy ester formation was completed in 30 min as revealed by TLC. After the usual workup, a crude product was obtained, which on purification by silica gel column chromatography (*n*-hexane/ethyl acetate, 1:1, vol/vol; R_f: 1.0) produced **6** as a yellowish oil. The isolated yield was 98.5%. IR (CHCl$_3$, cm^{-1}): 1755, 1731, 1588, 1483, 1329, 1243, 1210, 1125, 1036, 999, and 866; ^{1}H NMR

(CDCl$_3$, δ$_H$): 0.87 (*t*, *J* = 6.80 Hz, terminal methyl of the FA chain, 3H), 1.31–1.28 (*br m*, 8 × C$\underline{H}_2$ groups of the FA methylene chain, 16H), 1.64 (*m*, 4H), 2.05 (*m*, 8-C$\underline{H}_2$, 2H), 2.23 (*m*, 2-C$\underline{H}_2$, 11-C$\underline{H}_2$, 4H), 4.79 (*m*, 12-H, 1H), 5.38 (*m*, 9-H, 1H), 5.54 (*m*, 10-H, 1H), 7.15 (*m*, 3′′-H and 5′′-H, two *meta* protons, 2H), 7.22 (*m*, 4′′-H, one *para* proton, 1H), and 7.36 (*m*, 2′′-H and 6′′-H, two *ortho* protons, 2H); ^{13}C NMR (CDCl$_3$, δ$_C$): 14.43 (C-18), 22.93 (C-17), 25.34, 25.61, 27.68 (C-8), 29.46, 29.84, 32.06, 32.27, 33.89 (C-11), 34.69 (C-2), 79.85 (C-12), 121.43 (C-2′′, C-6′′), 124.04 (C-4′′), 126.19 (C-9), 129.75 (C-3′′, C-5′′), 132.71 (C-10), 133.58 (C-1′′, quaternary carbon), 152.97 (phenoxy carbonyl at C-12 of the FA), and 174.02 (ester carbonyl, C-1); EI-MS found [M + H] 815.3976; C$_{47}$H$_{59}$O$_{12}$ [M + H]$^+$ requires 815.40065.

(v) 4-O-Podophyllotoxinyl 12-[4′-(2′′-hydroxyethyl)piperazinecarbonyloxy]octadec-Z-9-enoate **7**. To a solution of **6** (1 mmol) in dry methylene chloride (5 mL) was added 1-(2-hydroxyethyl)piperazine (2 mmol) under nitrogen. After being stirred at room temperature for 24 h, the reaction mixture was diluted with methylene dichloride (10 mL), washed with brine and water, and dried. The organic layer was rotary-evaporated, and the viscous residue was chromatographed on a silica gel column (ethyl acetate/methanol, 9:1, vol/vol, *R$_f$*: 0.70) to afford a viscous colorless and sticky oily product, **7**, in 90% isolated yield. IR (CHCl$_3$, cm^{-1}): 3472, 1773, 1733, 1692, 1589, 1459, 1425, 1240, 1127, 1036, and 872; ^{1}H NMR (CDCl$_3$, δ$_H$): 0.88 (*t*, *J* = 6.30 Hz, terminal methyl of the FA chain, 3H), 1.32–1.28 (*br m*, 17-C$\underline{H}_2$, 7-C$\underline{H}_2$, 6 × C$\underline{H}_2$ groups of the FA methylene chain, 16H), 1.60 (*m*, 3-C$\underline{H}_2$, 13-C$\underline{H}_2$, 4H), 2.01 (*m*, 8-C$\underline{H}_2$, 2H), 2.23 (*m*, 2-C$\underline{H}_2$, 2H), 2.31 (*m*, 11-C$\underline{H}_2$, 2H), 2.55 (*m*, 3′-C$\underline{H}_2$, 5′-C$\underline{H}_2$, 4H), 2.62 (*t*, *J* = 5.22 Hz, 2′′-C$\underline{H}_2$, 2H), 2.96 (*m*, 2′-C$\underline{H}_2$, 6′-C$\underline{H}_2$, 4H), 3.68 (*t*, *J* = 5.22 Hz, 2′′-C$\underline{H}_2$, 2H), 3.53 (unresolved signal, D$_2$O exchangeable, O$\underline{H}$, 1H), 4.78 (*m*, 12-H, 1H), 5.36 (*m*, 9-H, 1H), 5.47 (*m*, 10-H, 1H); ^{13}C NMR (CDCl$_3$, δ$_C$): 14.43 (C-18), 22.94 (C-17), 25.22 (C-3), 25.73, 27.73 (C-8), 29.47, 29.56, 29.91, 32.12 (C-13), 32.51 (C-11), 34.14 (C-2), 40.24 (C-2′, C-6′), 53.15 (C-3′, C-5′), 58.10 (C-2′′), 59.99 (C-1′′), 75.65 (C-12), 126.84 (C-9), 132.71 (C-11), 155.60 (carbamate carbonyl attached to C-12 of the FA), and 173.75 (ester carbonyl, C-1); EI-MS found [M + H] 851.4689; C$_{47}$H$_{67}$O$_{12}$N$_2$ [M + H]$^+$ requires 851.4694.

(vi) 4-O-Podophyllotoxinyl 12-{4′-[2′′-(hydroxyethoxy)-ethyl]piperazinecarbonyloxy} octadec-Z-9-enoate **8**. The procedure was the same as described for **7** except that 1-[2-(2-hydroxyethoxy)ethyl] piperazine was used as a reagent. A colorless, viscous, and sticky oily, **8**, was obtained in 92% yield on isolation (ethyl acetate/methanol, 9:1, vol/vol, *R$_f$*: 0.60). IR (CHCl$_3$, cm^{-1}): 3450, 1774, 1731, 1692, 1589, 1459, 1425, 1244, 1126, 1037, 930, 867, and 733; ^{1}H NMR (CDCl$_3$, δ$_H$): 0.84 (*t*, *J* = 6.80 Hz, terminal methyl of the FA chain, 3H), 1.31–1.23 (*br m*, 6 × C$\underline{H}_2$ groups of the FA methylene chain, 12H), 1.52 (*m*, 3-C$\underline{H}_2$, 17-C$\underline{H}_2$, 4H), 1.64 (*m*, 13-C$\underline{H}_2$, 2H), 1.98 (*m*, 8-C$\underline{H}_2$, 2H), 2.21 (*m*, 2H), 2.24 (*m*, 11-C$\underline{H}_2$, 2H), 2.40 (*m*, 2-C$\underline{H}_2$, 2H), 2.51 (*m*, 3′-C$\underline{H}_2$, 5′-C$\underline{H}_2$, 4H), 2.61 (*m*, 1′′-C$\underline{H}_2$, 2H), 3.51 (*m*, 2′-C$\underline{H}_2$, 6′-C$\underline{H}_2$, 4H), 3.58 (*m*, 1′′′-C$\underline{H}_2$, 2H), 3.65 (*m*, 2′′-C$\underline{H}_2$, 2′′′-C$\underline{H}_2$, 4H), 3.72 (unresolved signal,

D$_2$O exchangeable, O$\underline{H}$, 1H), 4.73 (*m*, 12-H, 1H), 5.33 (*m*, 9-H, 1H), 5.41 (*m*, 10-H, 1H); ^{13}C NMR (CDCl$_3$, δ$_C$): 14.06 (C-18), 22.60 (C-17), 25.29 (C-3), 27.32 (C-8), 29.17, 29.50, 32.11 (C-13), 34.23 (C-2), 43.71 (C-2′, C-6′), 53.11 (C-3′, C-5′), 57.93 (C-1′′), 61.75 (C-2′′′), 67.23 (C-2′), 72.43 (C-1′′′), 75.21 (C-12), 126.42 (C-9), 132.30 (C-10), 155.25 (carbamate carbonyl attached to C-12 of the FA), and 173.42 (ester carbonyl, C-1); EI-MS found [M + H] 895.4909; C$_{49}$H$_{71}$O$_{13}$N$_2$ [M + H]$^+$ requires 895.4956.

(vii) 4-O-Podophyllotoxinyl undec-10-enoate **9**. Compound **9** was prepared by the reaction of podophyllotoxin and undec-10-enoic acid; the method is described in an earlier publication (21). Isolated (*n*-hexane/ethyl acetate, 1:1 vol/vol, *R$_f$*: 1.0) yield of a colorless oil was 99%. IR (CHCl$_3$, cm^{-1}): 1777, 1732, 1640, 1481, 1377, 1330, 1236, 1125, 997, and 862; ^{1}H NMR (CDCl$_3$, δ$_H$): 1.36–1.22 (*br m*, 4 × C$\underline{H}_2$ groups of FA methylene chain, 8H), 1.65 (*m*, 2H), 2.03 (*m*, 3-C$\underline{H}_2$, 9-C$\underline{H}_2$, 4H), 2.42 (*m*, 2-C$\underline{H}_2$, 2H), 4.94 (*m*, 11-C$\underline{H}_2$, 2H), 5.81 (*m*, 10-H, 1H); ^{13}C NMR (CDCl$_3$, δ$_C$): 24.50, 27.11, 28.85, 29.05, 29.15, 29.28, 33.77, 34.39 (C-2), 38.77, 114.29 (C-11), 139.15 (C-10), and 173.71 (ester carbonyl, C-1); EI-MS found [M + H] 581.2721; C$_{33}$H$_{41}$O$_9$ [M + H]$^+$ requires 581.2750.

(viii) 4-O-Podophyllotoxinyl 11-(2′-hydroxyethylthio)undecanoate **10**. 2-Mercaptoethanol (1.20 mmol) is added to a stirred solution of **9** (1 mmol) in dry methylene chloride (5 mL) and stirring is continued for 24 h under nitrogen at room temperature. Methylene chloride was rotary-evaporated, and silica gel chromatography (*n*-hexane/ethyl acetate, 1:1, vol/vol, *R$_f$*: 0.80) of the residue gave a colorless and sticky oily form of **10**. The isolated yield was recorded as 95%. IR (CHCl$_3$, cm^{-1}): 3507, 1778, 1733, 1588, 1484, 1420, 1331, 1239, 1171, 1127, 1038, 999, 866, and 735; ^{1}H NMR (CDCl$_3$, δ$_H$): 1.32–1.26 (*br m*, 6 × C$\underline{H}_2$ groups of the FA methylene chain, 12H), 1.55 (*m*, 2H), 1.65 (*m*, 2H), 2.25 (unresolved signal, O$\underline{H}$, D$_2$O exchangeable, 1H), 2.40 (*m*, 2-C$\underline{H}_2$, 2H), 2.51 (*t*, *J* = 7.60 Hz, 11-C$\underline{H}_2$, 2H), 2.68 (*t*, *J* = 6.0 Hz, 1′-C$\underline{H}_2$, 2H), 3.68 (*t*, *J* = 6.0 Hz, 2′-C$\underline{H}_2$, 2H); ^{13}C NMR (CDCl$_3$, δ$_C$): 24.96, 28.76, 29.12, 29.16, 29.31, 29.37, 29.70, 31.69, 33.87, 34.35 (C-2), 35.12 (C-1′), 60.40 (C-2′), and 173.74 (ester carbonyl, C-1); EI-MS found [M + Na] 681.2713; C$_{35}$H$_{46}$O$_{10}$SNa [M + Na]$^+$ requires 681.2709.

(ix) 4-O-Podophyllotoxinyl 11-(2′,3′-dihydroxypropylthio)-undecanoate **11**. To a stirred solution of **9** (1 mmol) in dry methylene chloride (5 mL) was added 3-mercapto-1,2-propanediol (1.20 mmol) under a nitrogen atmosphere. The reaction mixture was stirred at room temperature for 24 h. The organic solvent was rotary-evaporated, and the crude product was purified on a silica gel column (J.T.Baker; *n*-hexane/ethyl acetate, 1:2, vol/vol, *R$_f$*: 0.70) to produce **11**. The isolated yield of the viscous, colorless, and sticky oily product was 91%. IR (CHCl$_3$, cm^{-1}): 3425, 1776, 1731, 1653, 1588, 1481, 1419, 1236, 1169, 1124, 1038, and 864; ^{1}H NMR (CDCl$_3$, δ$_H$): 1.30–1.23 (*br m*, 6 × C$\underline{H}_2$ groups of the FA methylene chain, 12H), 1.55 (*m*, 2H), 1.65 (*m*, 2H), 2.45 (*m*, 2-C$\underline{H}_2$, 2H), 2.52 (*m*, 11-C$\underline{H}_2$, 2H), 2.62 (unresolved signal, D$_2$O exchangeable, 2 × O$\underline{H}$), 2.76 (*m*, 1′-C$\underline{H}_2$, 2H), 3.54 (*m*, one of the protons of 3′-C$\underline{H}_2$, 1H), 3.70 (*m*, second proton of 3′-C$\underline{H}_2$, 1H), 3.77 (*m*,

2′-H, 1H); ^{13}C NMR (CDCl$_3$, δ$_C$): 25.0, 28.98, 29.33, 29.32, 29.38, 29.52, 29.60, 29.89, 32.60 (C-11), 34.60 (C-2), 36.10 (C-1′), 65.63 (C-3′), 70.25 (C-2′), and 173.95 (ester carbonyl, C-1); EI-MS found [M + H] 689.3010; C$_{36}$H$_{49}$O$_{11}$S [M + H]$^+$ requires 689.2995.

Assay for in vitro anticancer activity. Compounds **1–11** were tested for their *in vitro* anticancer activity against a panel of human cancer cell lines, including SK-MEL (malignant, melanoma), KB (epidermal carcinoma, oral), BT-549 (ductal carcinoma, breast), SK-OV-3 (ovary carcinoma) and HL-60 (human leukemia) as well as for cytotoxicity in noncancerous VERO cells (African green monkey kidney fibroblast) as described previously (21). The highest concentration tested was 15 μM, and DMSO (0.5%) was used as a solvent control.

RESULTS AND DISCUSSION

Previous research (24–26) has suggested that FA in general, and PUFA in particular, have preventive and therapeutic potential against cancer. Results of our previous cytotoxicity studies on podophyllotoxin derivatives (C$_4$α-FA) involving natural FA of varying degrees of unsaturation, ω-hydroxyl FA, and 12-hydroxy-Z-9-ene FA demonstrated tumor selectivity over normal cells *in vitro* (21–23). A number of studies have concluded that chemically modified FA molecules possess more specific and potent biological activity with possible changes in their therapeutic targets (27). The present work is based on the chemically transformed FA analogs of podophyllotoxin **1**.

As part of our search for potential analogs of **1**, functionalities on FA side chains of an anticancer candidate, 4-*O*-podophyllotoxinyl 12-hydroxy-octadec-Z-9-enoate **2**, were chemically modified to generate first F- and N-containing analogs and then other products, 4-*O*-podophyllotoxinyl 12-hydroxy-octadecanoate **3**, 4-*O*-podophyllotoxinyl 12-fluoro-octadec-Z-9-enoate **4**, 4-*O*-podophyllotoxinyl 12-[3′-(3″,4″,5″-trimethoxyphenyl) propionyloxy]octadec-Z-9-enoate **5**, 4-*O*-podophyllotoxinyl 12-(phenoxycarbonyloxy)octadec-Z-9-enoate **6**, 4-*O*-podophyllotoxinyl 12-[4′-(2″-hydroxyethyl)-piperazinecarbonyloxy]octadec-Z-9-enoate **7**, and 4-*O*-podophyllotoxinyl 12-{4′-[2″-(hydroxyethoxy)ethyl]piperazinecarbonyloxy}octadec-Z-9-enoate **8** (Scheme 1) by adopting different synthetic strategies.

Compounds **3–5** were obtained directly from **2** by hydrogenation of the FA Z-double bond (C-9/10) *via* substitution of the FA 12C–OH by the F atom and by using the FA 12C–OH to esterify the carboxylic acid of a trimethoxy aromatic acid, respectively. The formation of podophyllotoxin FA carbamates **7** and **8** at C-12 of the FA chain was achieved in two steps: first, the conversion of **2** into its phenoxy ester **6**, followed by the reaction of **6** with two different functional piperazines.

Two *S*-ethers (thioethers), 4-*O*-podophyllotoxinyl 11-(2′-hydroxyethylthio)undecanoate **10** and 4-*O*-podophyllotoxinyl 11-(2′,3′-dihydroxypropylthio)undecanoate **11**, were synthesized from a new molecule, 4-*O*-podophyllotoxinyl undec-10-enoate **9** (Scheme 1). The hydroxy group (C$_4$α) of podophyllotoxin **1** was esterified with undec-10-enoic acid to give **9**

(Scheme 1). The chemical structures of **3–11** were established with the help of their spectroscopic data. In signals associated with the FA, with podophyllotoxin, and in compounds **5–8**, **10**, and **11**, with additional signals arising from the introduction of aromatic rings, N- and S-possessing moieties were adequately assigned in their respective IR, ^{1}H NMR, and ^{13}C NMR spectra and were confirmed by ^{13}C–^{1}H COSY correlation and distortionless enhancement by polarization transfer 135, 90, and 45 techniques. The high-resolution mass (electrospray ionization) spectral studies confirmed their elemental composition. A detailed spectroscopic characterization of **2** was discussed previously (21). Full spectroscopic values of **3** are given in the Experimental Procedures section because of its close structural resemblance to **2**. The NMR resonances related to the podophyllotoxin nucleus in the remaining compounds, **4–11**, were omitted as no appreciable difference was detected between these values and the ones we reported previously (21,22) for C$_4$α-FA derivatives.

The *Z*-double bond (C-9/10) in the FA side chain of compound **2** was hydrogenated under 45 psi (10% Pd/C) and yielded **3** as a completely hydrogenated product in high purity, as confirmed by its NMR analysis. The GLC and NMR spectra of aliquots taken at different time periods monitor the progress of the reaction and show the time required for complete hydrogenation. The reaction was repeated three times under similar reaction conditions, and the average time for complete hydrogenation of Z-9-ene was 8 h, when olefin signals were no longer detected in the NMR spectrum of the product.

The 12-fluoro derivative **4** was synthesized by fluorinating 12-C–OH of **2** with an equimolar amount of both **2** and DAST (source of fluorine) at −78°C under nitrogen for 1 h. The reaction proceeded cleanly under mild reaction conditions and produced only the desired product **4**. Compound **2** contained one trimethoxyphenyl group in its podophyllotoxin nucleus (ring E), and we introduced a second such moiety at C-12 in the FA chain to study the anticancer activity of the new molecule. The carboxylic acid group of 3-(3,4,5-trimethoxyphenyl)propionic acid was esterified with the 12-hydroxy group of **2** with dicyclohexylcarbodiimide (DCC)/dimethyl aminopyridine (DMAP) to achieve a quantitative amount of ditrimethoxy-phenyl-containing compound **5**. Podophyllotoxin C$_4$α-FA carbamates **7** and **8** were formed through phenoxy ester **6**, which was readily prepared quantitatively by treating **2** under anhydrous conditions with phenyl chloroformate and pyridine first at 0°C and then at room temperature for 30 min. A methylene chloride solution of phenoxy ester **6** was treated with 2 equiv of 1-(2-hydroxyethyl)piperazine under nitrogen at room temperature for 24 h to produce **7**. The chemical composition of compound **7** consisted of three nuclei. The FA formed an ester bond at C$_4$α of podophyllotoxin, and hydroxyethylpiperazine formed a carbamate at C-12 on the FA chain. Similarly, compound **8** was prepared when a solution of **6** was stirred with 2 equiv of 1-[2-(2-hydroxyethoxy)ethyl]piperazine at room temperature for 24 h. Compound **8** was slightly more functionalized than **7**. The spectroscopic data of this molecule were almost similar to **7** as far as the NMR signals related to the podophyllotoxin and FA

units were concerned, but differed in signals related to the piperazine moieties.

4-*O*-Podophyllotoxinyl undec-10-enoate **9** was used as an intermediate for synthesis of the S-ether analogs **10** and **11** and formed readily when DCC/DMAP were used to esterify the 4α-hydroxy group of **1** with the carboxylic acid group of FA, undec-10-enoic acid. The terminal double bond (C-11/10) in the FA side chain of **9** underwent an efficient addition reaction at C-11 when treated with a slight excess of 2-mercaptoethanol to give a saturated thioether-incorporated analog, **10**. The chemical composition of the FA part of **10** was very similar to the ω-hydroxy FA except that this FA contained an S atom to form a thioether moiety. Similarly, when compound **9** was reacted with 3-mercapto-1,2-propanediol, an addition reaction at C-11 afforded a saturated *S*-ether FA analog **11** of podophyllotoxin. Compound **11** possessed a FA that was bifunctional, as it had a vicinal diol (C-2′, C-3′) function beside a thioether group present at C-11 of the FA chain.

Configurations of two stereogenic/chiral centers, at which reactions occurred, are depicted in Scheme 1. The stereochemistry of both stereogenic centers, C-4 of podophyllotoxin and C-12 of the FA chain in compound **5**, at which coupling reactions took place, was retained. The reaction mechanism shows that the coupling reactions did not alter the configurations of the stereogenic centers (21,22). Similarly, the *R*-configuration at C-4 of the podophyllotoxin was retained in compounds **2–11**. The *R*-configuration of the stereogenic center (C-12) in the hydrogenated product **3** remained intact because three different groups and the lone hydrogen atom attached to it retained their respective priorities as those in compound **2**. According to the sequence rule, a change in the priorities of substituents changes the absolute configuration of the stereogenic center even without its participation in a reaction. It is well established that the fluorinating reagents, particularly DAST, replace the hydroxy group with fluorine stereospecifically to produce a product of

inverted configuration with the highest optical purity (28–30). Compound **4** might have the inversion of an *R*- to *S*-configuration at C-12 to which the fluorine is bonded. Since stereochemistry was not studied, we preferred to show the bonding of fluorine at C-12 as a mixture of isomers (Scheme 1). The phenoxy ester, **6**, was formed from compound **2** when the lone pair of electrons on the oxygen of the hydroxy group of the stereogenic carbon (C-12) attacked the carbonyl carbon of the phenyl chloroformate. This explains the retention of the *R*-configuration at C-12, as shown in Scheme 1. The retention of the R-configuration at C-12 in carbamates **7** and **8** was attributed to noninvolvement of the stereogenic carbon in the reaction, as these products were formed through the reactions of the carbonyl carbon of the phenoxy ester moiety of **6** with piperazines.

In vitro anticancer activity. Compounds **3–11** were assayed *in vitro* against four human solid tumors—SK-MEL (malignant, melanoma), KB (epidermal carcinoma, oral), BT-549 (ductal carcinoma, breast), and SK-OV-3 (ovary carcinoma)—and human leukemia (HL-60) and noncancerous VERO (African green monkey kidney fibroblast) cell lines. Their growth inhibition activities are listed in Table 1. Compounds **3–5** were chemically modified products of **2** and lacked a methylene-interrupted hydroxy-*Z*-ene (12-hydroxy-Z-9-ene) system in their FA side-chain moiety. Results of cytotoxicity testing indicated that probably the "12-hydroxy-Z-ene" system was important for these compounds to be active against the present panel of human neoplastic cell lines. Saturation of *Z*-unsaturation (C-9/C-10) in the FA chain of **2** decreased the activity of **3** against all four solid tumor cell lines. However, increased activity was recorded in HL-60 cells as compared with **2**. Similarly, a loss of activity against solid tumors was observed when the C-12 hydroxy group was substituted by the F atom in compound **4**, whereas almost the same potency against HL-60 was maintained. The loss of activity against certain cell lines may be attributed to inversion of the configuration at the stereogenic

TABLE 1
Cytotoxicity of Compounds in a Panel of Cancer Cell Lines and Kidney Fibroblast Cells[a]

Compounds[a]	Cancer cell lines					Kidney fibroblast
	SK-MEL	KB	BT-549	SK-OV-3	HL-60	VERO cells
1	0.22	0.24	0.36	0.19	0.01	0.55
2	0.45	1.26	4.76	0.17	0.66	NA
3	8.12	NA	7.50	10.64	0.22	NA
4	NA	NA	NA	NA	0.73	NA
5	NA	NA	NA	NA	NA	NA
6	NA	NA	NA	NA	NA	NA
7	0.72	2.4	1.2	0.84	0.58	NA
8	1.87	2.2	2.53	0.77	0.55	NA
9	NA	0.93	1.33	NA	0.08	NA
10	0.30	0.45	0.30	0.30	0.10	NA
11	2.9	0.35	0.81	NA	0.07	NA
Paclitaxel	0.72	0.77	0.70	1.08	0.0019	NA
Doxorubicin	2.7	2.55	1.87	2.0	0.012	NA

[a]Values are IC_{50} in μM.
[b]The highest concentration tested was 15 μM. IC_{50}, concentration that causes 50% growth inhibition; NA, not active; SK-MEL, human malignant melanoma; KB, human epidermal carcinoma, oral; BT-549, human ductal carcinoma, breast; SK-OV-3, human ovary carcinoma; HL-60, human leukemia; VERO, monkey kidney fibroblast. Paclitaxel and doxorubicin were used as positive controls.

center (C-12) or to the optical impurity of **4**. The FA carbamate (at C-12) derivatives **7** and **8** were uniformly active throughout five cancer cell lines, although they were more effective toward the HL-60-like compounds **2–4**. Compound **5** was inactive against all cell lines despite the presence of an additional 3,4,5-trimethoxy aromatic functionality (at C-12) in addition to one that was already in the main podophyllotoxin structure.

Compound **9** possessed a terminal unsaturated (11:1) FA chain at $C_4\alpha$ of the podophyllotoxin and was the first monoene FA analog that was found to be active against two solid tumor cell lines, KB and BT-549. It showed significantly high growth inhibition activity in the HL-60 (leukemia) cell line. Earlier investigations on the derivatives of FA internal *Z*-monoenes (20:1, Δ^{11}) *in vitro* against similar cell lines (21) and *in vivo* (18:1, Δ^9) against P388 lymphocytic leukemia (19) have failed to report any anticancer activity. The FA *S*-ether analogs **10** and **11**, derived from **9**, showed promising activities against all five cancer cell lines, except that **11** was not active against ovary carcinoma (SK-OV-3) cells. Analog **10** was functionalized with a FA moiety (C_{11}) at $C_4\alpha$ of podophyllotoxin, which has a close resemblance to the chemical structure of ω-hydroxy FA, and its extent of growth inhibition was the same as that recorded for a C_{10} ω-hydroxy FA $C_4\alpha$-analog against the same panel of human cancer cell lines (21). Both **10** and **11** were excellent growth inhibitors of HL-60 (leukemia cells). Unlike podophyllotoxin **1**, none of its new derivatives (2–11) were toxic toward normal mammalian cells. The present *in vitro* evaluation revealed that structural modifications of **2**, even by incorporation of the F atom or N-containing moieties and FA thioether derivatives, resulted in analogs that were nontoxic to noncancerous VERO cells (Table 1). This feature places these products into the class of anticancer agents that possess selectivity toward cancer cells over normal cells.

The main problem of podophyllotoxin and many of its analogs, which has substantially reduced their therapeutic usefulness, is their scant selectivity, because these molecules target both cancer and normal cells alike. This study involving FA-derived products has indicated promising results to address this problem at the present stage of *in vitro* testing. Further investigation of these molecules may provide useful leads in the development of new and effective pharmaceutical products.

ACKNOWLEDGMENTS

REFERENCES

1. Kauffman, J.M., and Foye, W.O. (1981) Cancer Chemotherapy, in *Principles of Medicinal Chemistry* (Foye, W.O., ed.), pp. 837–861, Lea and Febiger, Philadelphia.
2. Haskel, C.M. (1990) Principles of Cancer Chemotherapy, in *Cancer Treatment* (Haskel, C.M., ed.), pp. 27–52, W.B. Saunders, Philadelphia.
3. Xi, C.W., and Wang, P.G. (2003) Glucuronides in Anti-cancer Therapy, *Curr. Med. Chem.—Anti-cancer Agents 3*, 139–150.
4. Gordaliza, M., Castro, M.A., Miguel del Correl, J.M., and Feliciano, A.S. (2000) Antitumor Properties of Podophyllotoxin and Related Compounds, *Curr. Pharm. Design 6*, 1811–1839.
5. Damayanthi, Y., and Lown, J.W. (1998) Podophyllotoxins: Current Status and Recent Developments, *Curr. Med. Chem. 5*, 205–252.
6. Jardine, I. (1980) Podophyllotoxin, in *Anticancer Agents Based on Natural Product Models* (Cassady, J.M., and Douras, J.D., eds.), pp. 319–351, Academic Press, New York.
7. Keller-Juslen, C., Kuhn, M., Stahelin, H., and von Wartburg, A. (1971) Synthesis and Antimitotic Activity of Glycosidic Lignan Derivatives Related to Podophyllotoxin, *J. Med. Chem. 14*, 936–940.
8. Issell, B.F., Muggia, F.M., and Carter, S.K. (eds.) (1984) *Etoposide (VP-16): Current Status and New Developments,* Academic Press, New York.
9. van Maanen, J.M.S., Retel, J., De Vries, J., and Pinedo, H.M. (1988) Mechanism of Action of the Antitumor Drug Etoposide, *J. Natl. Cancer Inst. 80*, 1526–1533.
10. Lee, K.H. (1999) Novel Anticancer Agents from Higher Plants, *Med. Res. Rev. 19*, 569–596.
11. Murdter, T.E., Sperker, B., Kivisto, K.T., McClellan, M., Fritz, P., Friedel, G., Linder, A., Bosslet, K., Toomes, H., Dierkesmann, R., and Kroemer, H.K. (1997) Enhanced Uptake of Doxorubicin into Bronchial Carcinoma: β-Glucuronidase Mediates Release of Doxorubicin from Glucuronide Prodrug (HMR 1826) at the Tumor Site, *Cancer Res. 57*, 2440–2445.
12. Menendez, J.A., Ropero, S., Lupu, R., and Colomer, R. (2004) ω-6 Polyunsaturated Fatty Acid γ-Linolenic Acid (18:3n-6) Enhances Docetaxel (Taxotere) Cytotoxicity in Human Breast Carcinoma Cells: Relationship to Lipid Peroxidation and HER-2/neu Expression, *Oncol. Rep. 11*, 1241–1252.
13. Moyer, M.P., Hardman, W.E., and Cameron, I. (2003) Accelerated Action Fatty Acid (AAFA) Promotes Health of Normal Tissues and Minimizes the Toxic Side Effects of Chemotherapy, U.S. Patent Application 2002-102907 200220322, Priority: US 2001-278138, 27 pp.
14. Hardman, W.E., Cameron, I.L., and Moyer, M.P. (2001) Fatty Acids to Minimize Cancer Therapy Side Effects, PCT Intl. Application WO 99-US16666 19990722, 31 pp.
15. Larsson, S.C., Kumlin, M., Ingelman-Sundberg, M., and Wolk, A. (2004) Dietary Long-Chain n-3 Fatty Acids for the Prevention of Cancer: A Review of Potential Mechanisms, *Am. J. Clin. Nutr. 79*, 935–945.
16. Conklin, K.A. (2002) Dietary Polyunsaturated Fatty Acid: Impact on Cancer Chemotherapy and Radiation, *Altern. Med. Rev. 7 (1)*, 4–21.
17. Bougnoux, P. (1999) n-3 Polyunsaturated Fatty Acids and Cancer, *Curr. Opin. Clin. Nutr. Metabol. Care 2*, 121–126.
18. Berge, R. (2002) Fatty Acid Analogues for the Treatment of Cancer, PCT Intl. Application WO 2001-NO301 20010713, 31 pp.
19. Nagao, Y., Mustafa, J., Sano, S., Ochiai, M., Tazuko, T., and Shigeru, T. (1991) Different Mechanism of Action of Long Chain Fatty Acid Esters of Podophyllotoxin and Esters of Epipodophyllotoxin Against P388 Lymphocytic Leukemia in Mice, *Med. Chem. Res. 1*, 295–299.
20. Lie Ken Jie, M.S.F., Mustafa, J., and Pasha, M.K. (1999) Synthesis and Spectral Characteristics of Some Unusual Fatty Esters of Podophyllotoxin, *Chem. Phys. Lipids 100*, 165–170.
21. Mustafa, J., Khan, S.I., Ma, G., Walker, L.A., and Khan, I.A. (2004) Synthesis and Anticancer Activities of Fatty Acid Analogs of Podophyllotoxin, *Lipids 39*, 167–172.

22. Mustafa, J., Khan, S.I., Ma, G., Walker, L.A., and Khan, I.A. (2004) Synthesis, Spectroscopic and Biological Studies of Novel Estolides Derived from Antitumor Active 4-*O*-Podophyl-lotoxinyl 12-Hydroxyl Octadec-*Z*-9-enoate, *Lipids 39*, 659–666.

23. Ma, G., Khan, S.I., Mustafa, J., Walker, L.A., and Khan, I.A. (2005) Anticancer Activity and Possible Mode of Action of 4-*O*-Podophyllotoxinyl 12-Hydroxyl-octadec-*Z*-9-enoate, *Lipids 40*, 303–308.

24. Field, C.J., and Schley, P.D. (2004) Evidence for Potential Mechanisms for the Effect of Conjugated Linoleic Acid on Tumor Metabolism and Immune Function: Lessons from n-3 Fatty Acids, *Am. J. Clin. Nutr. 79 (6* Suppl.*)*, 1190S–1198S.

25. Akihisa, T., Tokuda, H., Ogata, M., Ukiya, M., Iizuka, M., Suzuki, T., Metori, K., Shimizu, N., and Nishino, H. (2004) Cancer Chemopreventive Effects of Polyunsaturated Fatty Acids, *Cancer Lett. 205*, 9–13.

26. Fearon, K.C.H. (2002) The Anticancer and Anticachectic Effects of n-3 Fatty Acids, *Clin. Nutr. 21* (Suppl. 2), S73–S77.

27. Tronstad, K.J., Berge, K., Berge, R.K., and Bruserud, O. (2003) Modified Fatty Acids and Their Possible Therapeutic Targets in Malignant Diseases, *Expert Opin. Ther. Targets 7*, 663–677.

28. Stelzer, U., and Effenberger, F. (1993) Preparation of (*S*)-Fluoronitriles, *Tetrahedron Asymm. 4*, 161–164.

29. Focella, A., Bizzarro, F., and Exon, C. (1991) Simple Stereospecific Syntheses of (*R*)-Fluorohexanoic Acid Ethyl Ester, *Synth. Commun. 21*, 2165–2170.

30. Leroy, J., Hebert, E., and Wakselman, C. (1979) Maximum Optical Rotation of 2-Fluorooctane? Survey of Fluorinating Reagents, *J. Org. Chem. 44*, 3406–3408.

METHODS

The Bottom-Up Solution to the Triacylglycerol Lipidome Using Atmospheric Pressure Chemical Ionization Mass Spectrometry

William Craig Byrdwell*

Department of Chemistry & Biochemistry, Florida Atlantic University, Boca Raton, Florida 33431

ABSTRACT: Presented here is an approach to representing the data from atmospheric pressure chemical ionization (APCI) mass spectrometry (MS) of triacylglycerols (TAG) using a set of one, two, or three Critical Ratios. These Critical Ratios may be used directly to provide structural information concerning the regioisomeric composition of the triacylglycerols (TAG), and about the degree of unsaturation in the TAG. An AAA-type, or Type I, TAG has only one Critical Ratio, the ratio of the protonated molecule, $[M + H]^+$, to the DAG fragment ion, $[AA]^+$. The Critical Ratio for a Type I TAG is $[MH]^+/\Sigma[DAG]^+$, and the mass spectrum of a Type I TAG can be reproduced from only this one ratio. An ABA/AAB/BAA, or Type II, TAG has two Critical Ratios, the $[MH]^+/\Sigma[DAG]^+$ ratio and the $[AA]^+/[AB]^+$ ratio. The $[AA]^+/[AB]^+$ ratio for a single TAG or TAG mixture can be compared with the $[AA]^+/[AB]^+$ ratios of pure regioisomeric standards, and the percentage of each regioisomer can be estimated. The abundance of the protonated molecule and the abundances of the two $[DAG]^+$ fragment ions can be calculated from the two Critical Ratios for a Type II TAG. To calculate the abundances, the Critical Ratios are processed through the Bottom-Up Solution to the TAG lipidome. First, Critical Limits are calculated from the Critical Ratios, and then the Critical Ratios are classified into Cases by comparison with the Critical Limits. Once the Case classification is known, the equation for the abundance of each ion in the mass spectrum is given by the Bottom-Up Solution. A Type III TAG has three different FA and three Critical Ratios. The $[MH]^+/\Sigma[DAG]^+$ ratio is the first Critical Ratio, the $[AC]^+/([AB]^+ + [BC]^+)$ ratio is the second Critical Ratio, and the $[BC]^+/[AB]^+$ ratio is the third Critical Ratio. The second critical ratio for a Type III TAG can be compared with regioisomeric standards to provide an estimate of the percentage composition of the regioisomers. The three Critical Ratios for a Type III TAG can be processed through the Bottom-Up Solution to calculate the four ion abundances that make up the APCI-MS mass spectrum. The Critical Ratios constitute a reduced data set that provides more information in fewer values than the raw abundances.

Paper no. L9524 in *Lipids* **40**, 383–417 (April 2005).

Work over the last decade has proved that HPLC combined with atmospheric pressure chemical ionization (APCI) MS is

*Address correspondence at Department of Chemistry & Biochemistry, Florida Atlantic University, 777 Glades Rd., P.O. Box 3091, Boca Raton, FL 33431. E-mail: byrdwell@fau.edu

Abbreviations: APCI, atmospheric pressure chemical ionization; BUS, Bottom-Up Solution; CID, collision-induced dissociation; EIC, extracted ion chromatogram; ESI, electrospray ionization; ITMS, ion-trap MS; L, linoleic acid; Ln, linolenic acid; O, oleic acid; P, palmitic acid; RP, reversed-phase; S, stearic acid; SFC, supercritical fluid chromatography; TIC, total ion current chromatogram; TSQ, triple-stage quadrupole.

an instrumental technique capable of accomplishing qualitative and quantitative analyses of complex mixtures of many classes of lipids. HPLC/APCI-MS is useful for qualitative and/or quantitative analysis of FA (1–4), TAG (5–11), phospholipids (12–16), ceramides (17), carotenoids (18–22), steroids (23–25), and others. Reviews of the applications of APCI-MS for lipid analysis have been published in recent years (26–29).

An important aspect of TAG analysis is the determination of the positional placement of the FA on the glycerol backbone (30). Plants synthesize lipids with structural specificity, namely, saturated FA are most often preferentially located on the *sn*-1 and *sn*-3 positions of the glycerol backbone, and PUFA are preferentially found in the *sn*-2 position. TAG are metabolized by enzymes in the human digestive system with structural specificity, with FA in the *sn*-1 and *sn*-3 positions being removed from the glycerol backbone first. Furthermore, enzymatic synthesis of TAG can be used to produce structured TAG with particular FA located in regiospecific locations (31). Therefore, knowledge of the composition of molecular species in a mixture of TAG, and of the regioisomeric configurations of selected TAG for which standards are available, could provide valuable information to be considered in the planning of dietary, nutritional, metabolic, and related studies. It has been demonstrated by a growing literature precedent that APCI-MS, preceded by a variety of HPLC or supercritical fluid chromatography (SFC) techniques, or simply by direct infusion, provides much of the information sought by those engaged in dietary studies of natural and/or synthetic TAG.

We have been interested in the qualitative and quantitative analysis of TAG. In 1995, we reported the first applications of reversed-phase (RP)-HPLC/APCI-MS to a mixture of synthetic TAG (6). In that initial work, we described basic characteristics of APCI-MS mass spectra of TAG and showed that APCI-MS mass spectra of TAG molecules exhibited primarily two types of ions. One is the protonated molecule and the other is DAG-like ions. We noted that the amount of the protonated molecule depends on the number of sites of unsaturation in the molecule. TAG with more sites of unsaturation form larger protonated molecule abundances (and small $[DAG]^+$ abundances), whereas those TAG with few sites of unsaturation form only small abundances of the protonated molecule (and large abundances of $[DAG]^+$). In summary, the abundance of the protonated molecule in a mass spectrum obtained by APCI-MS is proportional to (increases with) the amount of unsaturation in a TAG molecule and is inversely proportional to the abundances

of the [DAG]+ fragment ions. Although proportional in some way, the relationship between the degree of unsaturation and the abundance of the protonated molecule is not simply linear. The nature of the relationship remains to be characterized.

APCI-MS of TAG

Early reports. Shortly after the first report (6), we studied several qualitative applications of RP-HPLC/APCI-MS to TAG in normal and genetically modified seed oils (32) and in industrial seed oils containing epoxide and alkyne functional groups (33). We went on to study the quantitative analysis of TAG using response factors and have presented these results in several reports (7,34,35).

Meanwhile, other researchers used APCI-MS for qualitative analysis of TAG, with an emphasis on the identification of regioisomers. Laakso and Voutilainen (8) used silver-ion (argentation) chromatography with APCI-MS for analysis of 10 structurally specific regioisomers of TAG. The authors combined the partial separation of isomers of polyunsaturated TAG by the silver-loaded column with the detection ability of APCI-MS. The authors presented data for several di-acid TAG, which contain two different FA, A and B, to form three possible TAG regioisomers: ABA, AAB, or BAA. The authors showed that the DAG-like fragment ions, [DAG]+, seen in the APCI-MS mass spectrum of a di-acid TAG were formed in proportions that were other than statistically expected, which led to the understanding that the ratio of the abundances of the fragment ions, [AA]+/[AB]+, can be correlated with the identities of specific regioisomers. They showed that the [DAG]+ fragment ion formed by the loss of the FA chain in the *sn*-2 position was less abundant than the [DAG]+ formed by loss of the *sn*-1 or *sn*-3 FA. This demonstrated that the relative amounts of the fragment ions could potentially be used to identify the positional isomers present in a mixture of TAG. Also in 1996, Laakso (36) applied RP-HPLC/APCI-MS to the analysis of berry oils. Although the chromatographic behavior of the isomeric TAG was reversed on the RP column compared with the silver-loaded column, the APCI-MS mass spectra exhibited the same trends as described above. Manninen and Laakso (37) later applied SFC coupled with APCI-MS for analysis of regioisomers in berry oils.

In 1996, Mottram and Evershed (10) also demonstrated that the loss of the acyl chain from the *sn*-1 or *sn*-3 position was energetically favored over loss from the *sn*-2 position. These authors, in collaboration with other colleagues, went on to report the identities of regioisomers in a variety of vegetable oils (11) and in animal fats (38). Both Mottram and Evershed and colleagues (10,11,38), and Laakso and coworkers (8,36,37) reported several important qualitative trends. First, they agreed that the DAG-like ion, [DAG]+, formed by loss of the FA chain in the *sn*-2 position was less abundant than the [DAG]+ formed by loss of the *sn*-1 or *sn*-3 FA for di-acid TAG. Mottram and Evershed (10) were the first to mention that the APCI-MS mass spectrum of a TAG having three different FA, a tri-acid TAG, showed three [DAG]+ fragments, and that the [DAG]+ ion that had the lowest abundance was the *sn*-1,3 [DAG]+ fragment formed by loss of

the *sn*-2 FA chain. A TAG having three different FA is referred to as an ABC TAG; alternatively, it is termed a Type III TAG. Unless further specified, an ABC-type TAG can have six possible structures: ABC, BAC, BCA, CBA, CAB, and ACB. However, the *sn*-1 and *sn*-3 regioisomers cannot be distinguished by on-line APCI-MS without derivatization. To simplify reference to ABC-type TAG, they can be considered as ABC, BAC and BCA, with the understanding that the *sn*-1 and *sn*-3 positions can be reversed. So simply referring to a TAG as ABC cannot be assumed to represent one specific regioisomer having A at *sn*-1, B at *sn*-2, and C at *sn*-3. Because of the inherent ambiguity in the label ABC, we refer to this type of TAG as a Type III TAG herein, because no regiospecificity is inherently implied, and thus there is no inherent ambiguity.

The results of Laakso (36), Laakso and Voutilainen (8), Mottram, Evershed, and colleagues (10,11,38), and Laakso and Manninen (9) revealed that the [DAG]+ fragment ions formed by the loss of the *sn*-2 FA had the lowest abundance of the [DAG]+ fragment ions. Thus, the specific *sn*-1,3 [DAG]+ fragment could be identified. They also indicated that no preference for the *sn*-1 vs. *sn*-3 positions on the glycerol backbone of the TAG was observed. A preference was reported by Laakso and Voutilainen (8), Manninen and Laakso (37), and Laakso (36) that indicated that, for PUFA, a closer proximity of the double bonds to the glycerol backbone led to a larger abundance of the fragment formed by loss of the PUFA than when the double bonds were further away. Specifically, when γ-linolenic (n-6) acid (Ln) was compared with α-Ln (n-3), the former showed a more abundant [*sn*-1,3-DAG]+ fragment ion than the latter when the PUFA was in the *sn*-2 position.

Herein, when the APCI-MS data are used to specify the regiospecific structure of a TAG, the name of the TAG is placed in bold, as in **OPS**, compared with OPS, POS, or PSO (where S = stearic acid, P = palmitic acid, and O = oleic acid). This indicates that the *sn*-1,3 [DAG]+ (e.g., [**OS**]+) has been identified by its minimal abundance in an APCI-MS mass spectrum. Of course, these are also equal to **SPO**, compared with SPO, SOP, or OSP, all else being equal. This will be discussed further below.

Statistical and nonstatistical considerations for Type II TAG. A TAG having two different FA chains is referred to herein as a Type II TAG. It is also referred to as an ABA/AAB TAG. Of course, this is equal to ABA/BAA. These possibilities can also be referred to as ABA/(AAB/BAA). Since Type II TAG have two of one FA, A, and one of the other FA, B, there is a likelihood of 2/3 (= 66.67% statistical probability) that any [DAG]+ fragment would contain one A FA combined with a B FA, which would give either an [AB]+ or [BA]+ fragment ion, which are two possibilities with equivalent mass, in contrast to [AA]+. Since the [AB]+ and [BA]+ ions have the same mass, they are indistinguishable by APCI-MS, so these two ions may be considered as a single group and should represent 66.67% of the abundances of all [DAG]+ fragment ions, all else being equal. On the other hand, there is a 1/3 chance (= 33.33% statistical probability) that any [DAG]+ that is observed would contain two A FA, which would give the [AA]+ fragment, out of the three possible [DAG]+ fragment structures.

Statistical considerations can be used for determining what relative abundances of the [DAG]$^+$ fragment ions could be expected in an APCI-MS mass spectrum of a TAG. Based solely on statistical considerations, all Type II TAG contain two A FA and one B FA and so should give a ratio of abundances [AA]$^+$/([AB]$^+$ + [BA]$^+$) equal to (1/3)/(2/3) = 1/2, or 0.5. Regardless of their absolute abundances, from 100% to less than 1.00%, the ratio of the abundances of the [AA]$^+$ and [AB]$^+$ fragment ion *m/z* values should be 0.5. Observed conditions can lead to nonstatistical abundances of [AA]$^+$ and [AB]$^+$ [DAG]$^+$ fragment ions in APCI-MS mass spectra.

The [AA]$^+$ ion that is observed at a given *m/z* value will represent [*sn*-1,3-AA]$^+$, [*sn*-1,2-AA]$^+$, and [*sn*-2,3-AA]$^+$. Similarly, the [AB]$^+$ ion at a particular *m/z* value will represent [*sn*-1,3-AB]$^+$, [*sn*-1,2-AB]$^+$, and [*sn*-2,3-AB]$^+$, and also [*sn*-1,3-BA]$^+$, [*sn*-1,2-BA]$^+$, and [*sn*-2,3-BA]$^+$.

By using APCI-MS mass spectra of the pure regioisomers of *sn*-1,3 ABA TAG vs. *sn*-1,2 AAB TAG, it has been shown that the abundance of the [DAG]$^+$ fragment ion formed as [*sn*-1,3-AA]$^+$ from [**ABA** + H]$^+$ is smaller than that formed as [*sn*-1,2-AA]$^+$ from [**AAB** + H]$^+$, even though these ions are expected with equal statistical probability. Mottram and Evershed (10) and Hsu and Turk (39) mentioned that this indicated that the formation of the [*sn*-1,3-AA]$^+$ ion was energetically disfavored, because it involves loss of the *sn*-2 FA instead of one of the more labile *sn*-1 or *sn*-3 chains. Hsu and Turk (39), who used electrospray ionization (ESI) MS of TAG as their lithiated adducts, proposed that the *sn*-1 and *sn*-3 chains are promoted to leave by participation of the labile α-hydrogens of the neighboring FA. They suggest that the α-hydrogens of the middle FA are more labile than the α-hydrogens of the *sn*-1 or *sn*-3 chains and so help the *sn*-1 or *sn*-3 chains to leave more readily. Regardless of the specific mechanism that is assumed to operate, the observed ratios of [AA]$^+$/[AB]$^+$ are different for the different pure isomers of regiospecific TAG.

Table 1 shows the [AA]$^+$/[AB]$^+$ ratios for a variety of pure isomers, most of them commercially available. It is notable that the [AA]$^+$/[AB]$^+$ ratios of the two isomers are not equal for any

TABLE 1
Fragment Ratios Reported by Various Authors for Regiospecific Analysis by APCI-MS[a]

Authors[b]	Ionization method	AAB	[AA]$^+$/[AB]$^+$	ABA	[*sn*-1,3-AA]$^+$/ [*sn*-1,2- or *sn*-2,3-AB]$^+$
LV	APCI	PPO	0.89	POP	0.34
ME	APCI	PPO	0.95 ± 0.30	POP	0.20 ± 0.08
BN	APCI	PPO	0.87	POP	0.29
BN	ESI	PPO	0.68	POP	0.23
ML	APCI	PPO	0.79	POP	0.41
FHAFD	APCI	PPO	2.07[c]	POP	0.22
LV	APCI	OOP	0.70	OPO	0.09
BN	APCI	OOP	0.51	OPO	0.17
BN	ESI	OOP	0.67	OPO	0.24
ML	APCI	OOP	0.48	OPO	0.16
FHAFD	APCI	OOP	0.43	OPO	0.07
LV	APCI	OOLn (n-6)	1.97[c]	OLnO (n-6)	0.90[c]
ML	APCI	OOLn (n-6)	1.29[c]	OLnO (n-6)	0.63
L	APCI			OLnO (n-3)	0.17
L	APCI			OLnO (n-6)	0.64
LV	APCI	PPL	0.76		
ML	APCI	PPL	0.70		
FHAFD	APCI	PPL	2.99[c]	PLP	0.40
LV	APCI			SLS	0.38
ML	APCI			SLS	0.41
LV	APCI	SSP	0.56		
FHAFD	APCI	PPS	0.94	PSP	0.15
FHAFD	APCI	PPA	10.64[c]	PAP	1.56[c]
FHAFD	APCI	AAP	0.09	APA	0.02
BN	APCI	OOS	0.54		
BN	ESI	OOS	0.64		
FHAFD	APCI	OOS	0.44	OSO	0.11
ME	APCI	SSO	1.07 ± 0.16	SOS	0.29 ± 0.12
L	APCI	SSO	1.33[c]		
FHAFD	APCI	SSO	1.81[c]	SOS	0.26
L	APCI	LLO	1.24[c]		
JJF	APCI	LLO	0.7028	LOL	0.2289
FHAFD	APCI	LLS	1.52[c]	LSL	0.37

[a]Ratio of the abundances of [AA]$^+$ to [AB]$^+$ in AAB and ABA TAG.
[b]LV: Laakso and Voutilainen (8); ME: Mottram and Evershed (10); BN: Byrdwell and Neff (43); ML: Manninen and Laakso (SFC/APCI-MS) (37); L: Laakso (36); JJF: Jakab, Jablonkai, and Forgacs (42); FHAFD: Fauconnot, Hau, Aeschlimann, Fay, and Dionisi (40).
[c]Much higher than expected statistically. APCI, atmospheric pressure chemical ionization; SFC, supercritical fluid chromatography; P, palmitic acid; S, stearic acid; O, oleic acid; Ln, linolenic acid; A, arachidonic acid.

TAG. The two pure isomers each give different characteristic ion abundance ratios [AA]⁺/[AB]⁺, and these are almost all at nonstatistically expected ratios. The variation of the [AA]⁺/[AB]⁺ ratio with different regioisomers demonstrates that the positional placement of the FA on the glycerol backbone exerts a nonstatistical effect on the abundances of the ions formed by APCI-MS.

When comparing APCI-MS spectra of TAG, one must differentiate between (i) the APCI-MS mass spectrum of an individual TAG with unknown regiospecificity; (ii) the APCI-MS mass spectrum of a pure positional isomer of a TAG; (iii) a mass spectrum of a mixture of pure positional isomers; (iv) a mass spectrum of mixtures of several isomers in synthetic mixtures; and (v) mass spectra of combinations of TAG in natural mixtures. Knowing the type of sample being examined is essential to proper use of the [AA]⁺/[AB]⁺ ratio obtained from the sample. The actual [AA]⁺/[AB]⁺ ratio observed for any TAG or mixture of TAG is due to nonstatistical effects acting in combination with the expected ratio of 0.5. When considering the variety of pure TAG and TAG mixtures, the nonstatistical effects on the [AA]⁺/[AB]⁺ ratio can include: (i) differences in composition from 100% isomers to combinations of TAG regioisomers in TAG mixtures; (ii) formation of the *sn*-1,3 isomer, which is energetically disfavored under APCI-MS conditions, leading to a lower [AA]⁺/[AB]⁺ ratio when [AA]⁺ is the *sn*-1,3 isomer; and (iii) a disparity in the amount of unsaturation in FA A vs. B, and (iv) differences in the positions of the sites of unsaturation in the FA chains.

Characterization of the relationship between the identities of TAG structures and the [DAG]⁺ fragment ions in the APCI-MS mass spectra of TAG has been the subject of primarily qualitative investigations of regioisomers of TAG. Such studies have shown that each of the foregoing categories of TAG and TAG mixtures gives different [AA]⁺/[AB]⁺ ratios, based on the structure(s) of the TAG. Pure regioisomers give [AA]⁺/[AB]⁺ ratios that represent the upper and lower boundaries of the [AA]⁺/[AB]⁺ ratio that should be obtained by any mixture of regioisomers of a particular TAG.

Using APCI-MS mass spectra for qualitative analysis of TAG regioisomers. As mentioned, Laakso and Voutilainen (8), Mottram and Evershed and colleagues (10,11), and Laakso (36) showed that the [DAG]⁺ fragment ions formed by the loss of the *sn*-2 FA chain have the lowest abundance of the [DAG]⁺ fragment ions. The APCI-MS mass spectra of pure TAG isomers reported by the above authors demonstrated that the ion abundances and, more conveniently, the ratio of the ion abundances, [AA]⁺/[AB]⁺, are expected to change with the regioisomeric composition of a mixture of TAG regioisomers. These authors reported that if the FA A chains in an ABA/AAB/BAA TAG are located in the *sn*-1,3 positions, i.e., [*sn*-1,3-AA]⁺, the [DAG]⁺ fragment ion has a lower abundance than the 0.5 ratio statistically expected.

This tendency was used by Laakso (36) and Manninen and Laakso (37) to describe, in a semiquantitative way, the compositions of regioisomers in natural berry and other oils. This represented an early attempt at quantitative analysis of the relative

amounts of regioisomers. These articles described another interesting observation that must be taken into consideration. They showed that the positions of the double bonds in polyunsaturated TAG had a substantial impact on the relative abundances of [AA]⁺ and [AB]⁺ fragment ions. This trend can clearly be seen in Table 1 by comparing the [AA]⁺/[AB]⁺ ratios of the O(n-6)LnO and O(n-3)LnO regioisomers [where O = oleic acid, (n-6)Ln = γ-linolenic acid, and (n-3)Ln = α-linolenic acid]. The O(n-3)LnO isomer has a low [AA]⁺/[AB]⁺ ratio (= 0.17) typical of most pure *sn*-1,3 isomers. On the other hand, the O(n-6)LnO isomer has [AA]⁺/[AB]⁺ ratios (= 0.63 to 0.90) that are higher than the 0.5 that is statistically expected, and the OO(n-6)Ln isomer gives an even higher [AA]⁺/[AB]⁺ ratio. Observations such as these constitute the trends that can be correlated with certain ratios.

In addition to the observations previously mentioned, Table 1 shows several other trends. First, every ABA TAG gave an [AA]⁺/[AB]⁺ ratio that was smaller than the ratio from the corresponding AAB TAG. This, of course, reflects the fact that the loss of *sn*-2 chain is energetically disfavored. When the [AA]⁺ corresponds to the *sn*-1,3 isomer, its abundance is diminished. Another trend is that the [AA]⁺/[AB]⁺ ratio for almost all *sn*-1,3 isomers, ABA, is substantially below the statistically expected value of 0.5. The isomer that contained the (n-6)Ln was the exception to this trend. It can also be seen in Table 1 that most, but not all, AAB isomers gave [AA]⁺/[AB]⁺ ratios larger than the statistically expected value of 0.5. Hence, the [AA]⁺/[AB]⁺ ratio may by more useful for identifying some AAB TAG (e.g., PPO, where P = palmitic acid) than others (e.g., OOP).

Recent articles allow us to move toward a more numeric and quantitative method for analysis of TAG regioisomers. Articles cited below describe approaches that have been demonstrated to be useful to obtain a quantitative estimation of the percentage compositions of any regioisomers for which calibration standards are available. However, three other qualitative considerations should be mentioned. First, the [DAG]⁺ fragment ions that are produced by APCI-MS are isobaric with a normal intact DAG minus a water group. In the process of leaving, the R$_x$COO that is lost from a TAG in the APCI source takes the glycerol oxygen with it to form an [M + H − RCOOH]⁺ ion. These same [DAG]⁺ fragment ions are formed during ESI-MS/MS of TAG. According to Hsu and Turk (39), who performed deuterium-labeled experiments on lithiated TAG by ESI-MS, the carbonyl oxygen of the FA neighboring the one that is lost carries out nucleophilic attack on the glycerol carbon atom that contains the leaving group, forming a five- or six-membered ring, with the participation of the α-hydrogen of the ring-attached FA chain.

Second, plants produce TAG with regiospecificity as well as single enantiomers of asymmetric TAG having the L configuration. TAG that are produced by the chemical interesterification of glycerol and FA, such as the 35-TAG mixture used as an example herein, are a mixture of enantiomers.

Third, the integrated areas under the ion chromatograms of the [M + H]⁺ ion and of [DAG]⁺ fragment ions over a specific time range can be used to produce a mass spectrum that appears

the same as an averaged mass spectrum across the same time range. Since all [DAG]$^+$ fragments originate in the APCI source, all fragments that occur from a particular TAG must occur at the retention time associated with that TAG. So integrated areas under ion chromatograms corresponding to the fragments will be in the same proportions as the ion abundances in an averaged mass spectrum across the same time range. Therefore, quantitative estimation of the regioisomeric composition based on the [AA]$^+$/[AB]$^+$ ratio can use either integrated areas under ion chromatograms or abundances in an average mass spectrum across the chromatographic peak. The method for the quantitative analysis of TAG molecular species that we developed and have reported extensively before (7,34,35) uses the areas under ion chromatograms for quantitative analysis of TAG molecular species. These same data will also be used to construct the [AA]$^+$/[AB]$^+$ ratio and other ratios presented herein. Fauconnot *et al.* (40) also used areas under ion chromatograms for quantitative analysis of TAG regioisomers. The areas under the peaks of the [M + H]$^+$ and [DAG]$^+$ fragment ions determined by APCI-MS were used to calculate the Critical Ratios given in Table 2.

Using APCI-MS mass spectra for quantitative analysis of TAG regioisomers. In 2003, Byrdwell (29) cited the need for improved methods for quantitative analysis of regioisomers. In discussing the quantification of TAG positional isomers, he said:

A comprehensive study using the greatest possible number of positional isomers with disparate amounts of unsaturation needs to be undertaken for both APCI-MS and ESI-MS/MS. In our initial work, we did not address this issue because we felt that it would require lengthy quantification of the abundances of DAG fragment ions from a large series of standards to address the issue adequately. We believed that the proper approach would be to perform APCI-MS of a wide range of structured lipids, determine the ratios of DAG fragment ions that are produced, and then interpolate between the ratios for the 1,2- versus the 1,3- isomers to get a quantitative estimation of the relative amounts of each of these isomers in real samples. Unfortunately, only a limited number of structured lipids are commercially available, so full treatment of this subject will require synthesis of an array of structured lipids, followed by their analysis. Until then, great care must be exercised in using APCI-MS for positional isomer identification, especially for polyunsaturated TAG (41).

A recent article by Jakab, Jablonkai, and Forgacs (42) constitutes the first example of the process described above. Jakab *et al.* (42) described the use of APCI-MS for analysis of mixtures of pure positional isomers of LOL/LLO (where L = linoleic acid). They demonstrated that a calibration curve could be constructed that plotted the ratio of abundances of [DAG]$^+$ fragment ions vs. the percentage of the LLO isomer (the LOL isomer percentage could just as easily be plotted). This calibra-

tion curve, reproduced in Figure 1, accomplished quantification of the relationship between the abundances of ions in APCI-MS mass spectra and, more specifically, the ratio of abundances, [AA]$^+$/[AB]$^+$ (i.e., [LL]$^+$/[LO]$^+$), to the relative amount of the **ABA** isomer, i.e., the LOL isomer.

The equation shown by Jakab *et al.* (42) and seen in Figure 1 is the least-squares best-fit line equation, based on 11 mixtures representing the concentration range from 0% LOL/(LLO + OLL) to 100% LOL/(LLO + OLL). Of course, 0% LOL represents 100% (LLO + OLL), and, conversely, 100% LOL represents 0% (LLO + OLL). Any mixture of TAG should contain an amount of the ABA isomer somewhere between 0 and 100%, so this calibration line should apply to any mixture of these TAG, to correlate the amount of the [*sn*-1,3-AA]$^+$ isomer with the [AA]$^+$/[AB]$^+$ ratio.

These authors (42) simplified the complex situation mentioned by Byrdwell (41) by examining only the two isomers of one TAG. Nevertheless, they clearly demonstrated that the approach—of determining the DAG fragment ratios for a series of standard solutions and then interpolating the ratio of positional isomers from the DAG fragment ratios of actual samples—is effective for determining the relative amounts of two isomers. Of course, every TAG for which positional isomers are to be determined requires isomeric standards and multiple solutions of each standard pair of isomers to be quantified. As Figure 1 shows, Jakab *et al.* (42) used 11 solutions to cover the range from 0 to 100%, inclusive, by 10% increments. Five replicate measurements of each of these standard solutions represent at least 55 experiments that were performed to produce the calibration line shown in Figure 1. These experiments would need to include a larger number of pure regiospecific standards to be more widely applicable. Nevertheless, the approach taken by Jakab *et al.* (42) appears to be the most appropriate approach for accurate quantitative estimation of the relative amounts of regioisomers.

The full set of standard solutions serves to demonstrate that there is an approximately linear relationship ($r^2 = 0.9884$) between the [AA]$^+$/[AB]$^+$ ratio and the percent composition of regioisomers. One could say that the [AA]$^+$/[AB]$^+$ ratio can be used as a Critical Ratio for the determination of the percentage composition of mixtures of regioisomeric standards. Therefore, the question arises: Can this accurate quantitative analysis of TAG regioisomers be accomplished with fewer experimental data? Can one derive the same or similar results from a less extensive set of experiments? If so, then this would be an advantage. The first simplification would be to construct a line directly between the two end points of the line. This is experimentally equal to determining only the mass spectra and therefore the [AA]$^+$/[AB]$^+$ ratios for 100% pure **LLO** (0% **LOL**) and for 100% pure **LOL** (0% **LLO**). The equation for the line formed between the two average ($n = 5$) end point values in Figure 1 can be compared with the line formed by the least-squares best-fit line end points.

For instance, in the data presented by Jakab *et al.* (42), the observed extremes had average [AA]$^+$/[AB]$^+$ ratios of 0.7028 and 0.2289, for 100% **LLO** (= 0% **LOL**) and 100% **LOL** (= 0%

TABLE 2
TAG Composition and Critical Ratios from the Synthetic 35-TAG Mixture[a], Determined by APCI-MS (three replicates)

ECN	TAG	Statistical % comp.	Adjusted APCI-MS	$[M + H]^+/\Sigma[DAG]^+$	±SD	$[AA]^+/[AB]^+$	±SD	±SD2	$[BC]^+/[AB]^+$	±SD
48	PPP	0.84	0.75	0.00	0.00					
54	SSS	0.94	0.82	0.00	0.00					
48	OOO	0.85	0.88	3.24	0.39					
42	LLL	0.77	0.78	120.07	12.40					
36	LnLnLn	0.62	0.78	222.80	22.45					
50	PSP/PPS	2.62	2.40	0.00	0.00	49.26	0.84	0.84		
48	POP/PPO	2.54	2.49	0.55	0.12	65.28	2.35	2.35		
46	PLP/PPL	2.45	2.87	0.40	0.28	84.11	2.45	2.45		
44	PLnP/PPLn	2.28	2.53	12.81	2.34	69.94	3.11	3.11		
52	SPS/SSP	2.72	2.44	0.00	0.00	40.91	3.31	3.31		
52	SOS/SSO	2.73	2.48	0.45	0.04	75.14	2.78	2.78		
50	SLS/SSL	2.64	2.96	0.42	0.12	82.89	2.08	2.08		
48	SLnS/SSLn	2.45	2.75	9.59	1.12	60.98	3.16	3.16		
48	OPO/OOP	2.55	2.72	1.89	0.19	36.12	1.42	1.42		
50	OSO/OOS	2.65	2.76	1.12	0.32	39.82	1.73	1.73		
46	OLO/OOL	2.47	2.54	11.93	1.12	50.10	2.20	2.20		
44	OLnO/OOLn	2.30	2.27	36.94	3.35	41.62	2.52	2.52		
44	LPL/LLP	2.38	2.00	27.64	8.83	88.84	9.62	9.62		
46	LSL/LLS	2.47	2.29	43.47	8.73	76.07	8.61	8.61		
44	LOL/LLO	2.39	2.33	44.44	9.15	74.62	7.01	7.01		
40	LLnL/LLLn	2.15	2.21	101.35	36.30	51.97	17.86	3.70		
40	LnPLn/LnLnP	2.06	1.94	101.33	24.18	74.69	17.68	13.63		
42	LnSLn/LnLnS	2.13	1.96	61.31	12.99	95.10	20.10	10.10		
40	LnOLn/LnLnO	2.07	2.26	101.34	43.98	83.80	34.13	9.97		
38	LnLLn/LnLnL	2.00	2.15	128.01	26.00	64.08	12.94	5.77		
50	OPS	5.27	5.11	0.47	0.09	37.64	2.06		69.79	2.12
48	SPL	5.09	5.89	0.46	0.11	35.39	2.50		59.43	2.95
46	SPLn	4.73	5.42	9.28	1.57	39.78	2.36		76.70	3.46
46	LOP	4.93	4.57	6.44	1.33	40.39	2.10		98.27	2.51
44	LnOP	4.59	4.60	27.18	7.84	42.00	4.41		91.76	5.68
42	LnLP	4.43	3.78	48.86	18.13	36.71	13.38		73.38	23.84
48	LOS	5.11	5.72	7.45	0.87	43.86	2.99		85.70	4.63
46	OLnS	4.75	4.38	19.95	5.10	42.47	1.97		89.53	2.14
44	LnLS	4.59	4.00	45.35	14.32	38.65	11.15		78.57	20.52
42	LLnO	4.45	4.20	56.61	24.69	40.18	16.88		77.66	26.09
	Sum	100.01	100.03			$= [AC]^+/([AB]^+ + [BC]^+)$				

[a]ECN, equivalent carbon number = # carbon atoms in FA chains – (2 × # sites of unsaturation); Ln, 18:3, linolenic acid; L, 18:2, linoleic acid; O, 18:1, oleic acid; S, 18:0, stearic acid; P, 16:0, palmitic acid. The statistical composition is the composition calculated based on the FA composition. The adjusted APCI-MS composition is the composition determined by three replicate chromatographic runs, adjusted using response factors calculated from the FA composition (35). SD2, simple standard deviation of the three numberic $[AA]^+/[AB]$ ratio values. For other abbreviations see Table 1.

LLO), respectively. These values are shown in Table 1. Similarly, each set of $[AA]^+/[AB]^+$ ratios of TAG positional isomers in Table 1 defines the range of DAG fragment ion ratios that should be encountered in APCI-MS (as well as some ESI-MS) mass spectra of TAG. An equation of the line that approximately describes the $[AA]^+/[AB]^+$ ratio for any combination of TAG positional isomers can be constructed from these two end points. If one puts the line in Figure 1 in the form of $y = mx + b$, then $y = ([AA]^+/[AB]^+) = m \cdot (\% \textbf{LOL}) + b$. In this equation, b would equal the $([AA]^+/[AB]^+)$ ratio at 0% **LOL**. In terms of x and y, the coordinates of the two end points would be (0% **LOL**, $([AA]^+/[AB]^+)_{AAB}$) and (100% **LOL**, $([AA]^+/[AB]^+)_{ABA}$), where the subscripts represent the $([AA]^+/[AB]^+)$ ratios of pure standards of AAB and ABA, i.e., **LLO** (= 0% **LOL**) and **LOL**, which would be explicitly: (0%, 0.7028), (100%, 0.2289). The equation of the line constructed from these end points would be: $m = (\Delta y)/(\Delta x) = (y_2 - y_1)/(x_2 - x_1) = ((([AA]^+/[AB]^+)_{ABA} -$

$([AA]^+/[AB]^+)_{AAB}))/(100 - 0)$ and $b = ([AA]^+/[AB]^+)_{AAB}$. In terms of the data reported by Jakab *et al.* (42), this gives: $m = (\Delta y)/(\Delta x) = (y_2 - y_1)/(x_2 - x_1) = ((([LL]^+/[OL]^+)_{LOL}) - ([LL]^+/[OL]^+)_{LLO}))/(100 - 0) = (0.2289 - 0.7028)/(100 - 0) = (-0.4739)/(100) = -0.004739$; and $b = ([LL]^+/[OL]^+)_{LLO} = 0.7028$. From this line comes the relationship:

$$\left(\frac{[LL]^+}{[LO]^+}\right) = (-0.004739)\cdot(\%\textbf{LOL}) + 0.7028$$

This equation can be seen to be in the general form:

$$\left(\frac{[AA]^+}{[AB]^+}\right)_{Obs} = \left(\left(\frac{[AA]^+}{[AB]^+}\right)_{ABA} - \left(\frac{[AA]^+}{[AB]^+}\right)_{AAB}\right)\cdot\left(\frac{\%\textbf{ABA}}{100}\right) + \left(\frac{[AA]^+}{[AB]^+}\right)_{AAB} \quad [1]$$

To get a line with a positive slope, the y values, $([AA]^+/[AB]^+)$, can be arranged from lowest to highest, which means that the x values should be put in terms of % LLO to make x also go from low to high as $([AA]^+/[AB]^+)$ goes from low to high. The
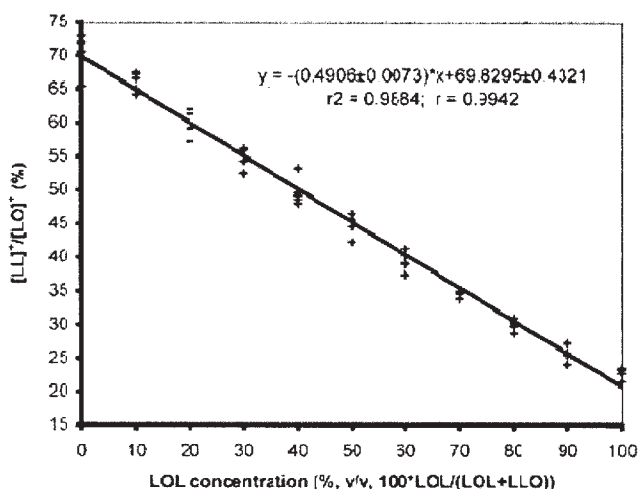
FIG. 1. Ratio of the $[LL]^+$ and $[LO]^+$ fragment ions (%) in mixtures of LOL and LLO at various percentages (calibration curve). L, linoleic acid; O, oleic acid. From A. Jakab, I. Jablonkai, and E. Forgacs, *Rapid Commun. Mass Spectrom. 17*, 2295–2302 (2003). Copyright John Wiley & Sons Ltd. Reprinted with permission.

equivalent points that would give a positive slope would be: $(x_1, y_1), (x_2, y_2) = (0\% \text{ LLO}, ([AA]^+/[AB]^+)_{ABA})$, (100% LLO, $([AA]^+/[AB]^+)_{AAB})$, or (0, 0.2289), (100, 0.7028). In terms of the average end point data by Jakab *et al*. (42), this would be a line having the equation:

$$\left(\frac{[LL]^+}{[LO]^+}\right) = (0.004739) \cdot (\% \text{ \textbf{LLO}}) + 0.2289$$

This equation can be written in a general form as:

$$\left(\frac{[AA]^+}{[AB]^+}\right)_{Obs} = \left(\left(\frac{[AA]^+}{[AB]^+}\right)_{AAB} - \left(\frac{[AA]^+}{[AB]^+}\right)_{ABA}\right) \cdot \left(\frac{\%\textbf{AAB}}{100}\right) + \left(\frac{[AA]^+}{[AB]^+}\right)_{ABA} \quad [2]$$

One can solve Equations 1 and 2 for the following relationships.

One may rearrange Equation 1 (and multiply by $(-1)/(-1)$) to solve for the % **ABA** as follows:

$$(\% \textbf{ABA}) = \left[\frac{\left(\frac{[AA]^+}{[AB]^+}\right)_{AAB} - \left(\frac{[AA]^+}{[AB]^+}\right)_{Obs}}{\left(\frac{[AA]^+}{[AB]^+}\right)_{AAB} - \left(\frac{[AA]^+}{[AB]^+}\right)_{ABA}}\right] x100 \quad [3]$$

Similarly, one may rearrange Equation 2 to solve for the % **AAB** as follows:

$$(\% \textbf{AAB}) = \left[\frac{\left(\frac{[AA]^+}{[AB]^+}\right)_{Obs} - \left(\frac{[AA]^+}{[AB]^+}\right)_{ABA}}{\left(\frac{[AA]^+}{[AB]^+}\right)_{AAB} - \left(\frac{[AA]^+}{[AB]^+}\right)_{ABA}}\right] x100 \quad [4]$$

And these two percentages share the relationship that % **LOL** + % LLO (= **LLO** + **OLL**) = 100%.

Therefore, whenever one percentage is known, % ABA or % AAB, the other may be known as % AAB (= % **AAB** + % **BAA**) = 100 − % **ABA** or % **ABA** = 100 − % AAB, respectively.

Equations 3 and 4 allow the direct calculation of the percentage composition of either one regiospecific isomer, % **ABA**, or the sum of two isomers, % AAB (= % **AAB** + % **BAA**). Of course, the $([AA]^+/[AB]^+)$ ratios of pure known standards of each individual TAG must be determined for each TAG for which quantification is sought. These $([AA]^+/[AB]^+)$ ratios of pure known standards potentially can be tabulated. We have compiled the $([AA]^+/[AB]^+)$ ratios of pure known standards before and have noted the references that allow the instrument type and conditions under which these values were obtained to be determined. If a researcher has a similar instrument and obtains $([AA]^+/[AB]^+)$ ratios of pure known standards on his or her instrument that are similar to those of the tabulated values, then these results lend credibility to the possibility that tabulated values might be helpful in assessing the percentages of regioisomers in a TAG mixture of unknown composition. The minimal approach to linear interpolation would require the analysis of two pure regioisomeric standards, and then the $([AA]^+/[AB]^+)_{Obs}$ ratio of a mixture of unknown regioisomeric content might be interpolated between the $([AA]^+/[AB]^+)$ ratios obtained for pure isomers, and a quantitative estimate of the % **ABA** or % AAB could be obtained with relative ease.

For example, Table 1 shows the ratio of $[PP]^+/([PO]^+,[OP]^+)$, which is more simply referred to as the $[PP]^+/[PO]^+$ ratios for two commercially available regiospecific isomers, POP and PPO. Four out of five authors using APCI-MS have reported low values for the $[PP]^+/[PO]^+ = [AA]^+/[AB]^+$ ratio, in the range of 0.20 to 0.34 (8,10,40,43). Three of four of those authors reported $[AA]^+/[AB]^+$ ratios between 0.87 and 0.95 for pure PPO, by APCI-MS. The fourth example of POP/PPO data in Table 1 had a higher $[AA]^+/[AB]^+$ ratio for POP (= 0.41) and a lower value for PPO (= 0.79) (37). Our reports and those of many others have been obtained on TSQ 700 and 7000 tandem triple-stage quadrupole instruments. The data by Fauconnot *et al*. (40) included in Table 1 were obtained on a tandem sector quadrupole instrument with a Z-spray interface. Unlike collision-induced dissociation (CID), which exhibits differences between TSQ and ion-trap MS (ITMS) instruments in fragment ions formed, full-scan APCI-MS mass spectra on a TSQ instrument can appear nearly identical to an APCI-MS mass spectrum obtained on an ITMS instrument. The reason for this is that fragmentation occurs in the ionization source, so the $[DAG]^+$ fragment ions are formed before they reach the first or subsequent mass analyzers, whether quadrupole or ion trap. In fact, the APCI ionization heads on the TSQ 700 and LCQ Deca instruments in our laboratory are nearly identical and have interchangeable parts but are not themselves interchangeable between instruments. This is in contrast to CID, which exhibits different ratios of fragment ions in TSQ vs. ITMS instruments. Hsu and Turk (44) reviewed the mechanisms of fragmentation of phospholipids and TAG by ESI-MS/MS in their recent book chapter.

The equations above, which are based on only two pure regioisomers, must be compared with the more accurate line described by the full set of standards analyzed by Jakab *et al*. (42). The equation for the best-fit line given in Figure 1 is $y = 0.4906 \cdot x + 69.83$, but the y axis gives $[AA]^+/[AB]^+$ as a percentage. The

equation of the line for the $[AA]^+/[AB]^+$ as a pure ratio (not a percentage) would therefore be:

$$\left(\frac{[LL]^+}{[LO]^+}\right) = (-0.004906) \cdot (\% \, \textbf{LOL}) + 0.6983$$

The best-fit line gives an $([AA]^+/[AB]^+)$ ratio of 0.6983 for 0% LOL and 0.2077 for 100% LOL.

These best-fit values for the pure positional isomers can be inserted into Equation 3 to give the following equation:

$$(\% \, \textbf{LOL}) = \left(\frac{0.6983 - \left(\frac{[AA]^+}{[AB]^+}\right)_{Obs}}{0.6983 - 0.2077}\right) x100$$

This can be used to calculate the % LOL from the $([AA]^+/[AB]^+)_{Obs}$ ratio for a mixture. For instance, a hypothetical $[AA]^+/[AB]^+$ ratio of 0.5348 would give a calculated % LOL of 33.33%. This is the $[AA]^+/[AB]^+$ ratio that would be expected from a statistically randomly distributed combination of two FA, L and O, onto the three possible positions of the glycerol backbone of a TAG, on the instrument and under the conditions reported by Jakab *et al.* (42). Thus, nonstatistical influences on the abundances of the $[DAG]^+$ fragments formed shift the $[AA]^+/[AB]^+$ ratio from the statistically expected value of 0.5 to a hypothetical $[AA]^+/[AB]^+$ ratio of 0.5348, calculated from the best-fit line using 11 standard solutions.

For comparison, the equation based only on the average values of the two pure standards, given in the form of Equation 3 above, is:

$$(\% \, \textbf{LOL}) = \left(\frac{0.7028 - \left(\frac{[AA]^+}{[AB]^+}\right)_{Obs}}{0.7028 - 0.2289}\right) x100$$

This equation gives a calculated % LOL of 35.45% from the same $([AA]^+/[AB]^+)_{Obs}$ ratio of 0.5438. Although this is not identical to the 33.33% obtained from the best-fit line made from 11 standards, it is a good approximation of the more accurate value and can be obtained with only two authentic standards, instead of a large number of mixtures containing various compositions. Certainly in the range 0 to 100%, narrowing the composition down to 35.45% LOL would represent a good approximation of 33.33%, but with much less data required. Of course, if greater accuracy is required for a particular application, more standards can be analyzed, and the same equations can be used with the slope and intercept calculated from the best-fit line.

The above equations allow one to quantify the relative amounts of positional isomers in a mixture. It is expected that the $[AA]^+/[AB]^+$ ratios of a greater variety of regiospecific isomers will be reported and compared, and this method will be applied to a greater variety of TAG mixtures. These equations also demonstrate the utility of the $[AA]^+/[AB]^+$ ratio for determination of the regiospecific composition of a TAG mixture. This ratio allows one to move from qualitative analysis of TAG to a more quantitative approximation of the composition of TAG regioisomers.

Even more recently, another article appeared that describes the linear relationship between the abundances of $[AA]^+$ and $[AB]^+$ fragments and the compositions of known standard mixtures of TAG regioisomers. Fauconnot *et al.* (40) reported calibration curves for regioisomers of seven pairs of Type II TAG standards. The authors showed the growing importance of the $[AA]^+/[AB]^+$ ratio in their statement: "Identification of the major regioisomers of an AAB/ABA pair of TGs was shown to be enabled by comparing the ratios of abundances of $c(AA^+)/c(AB^+)$ with the statistically expected value of 0.5."

In their calibration curves, though, they plotted what they called the *regioisomeric purity*, r_{AA}, which they defined as:

$$r_{AA} = \frac{100\% c(AA^+)}{c(AA^+) + c(AB^+)}$$

This equation can be shown to be equivalent to

$$r_{AA} = \frac{1}{1 + \frac{1}{\frac{(AA^+)}{(AB^+)}}} x100$$

It is much more convenient and useful to use the ratio $[AA]^+/[AB]^+$ directly. This is a simpler ratio, which can be used directly with Equations 3 and 4 to calculate the relative percentages of the regioisomers. This is also the approach used by Jakab *et al.* (42). Nevertheless, the data by Fauconnot *et al.* (40) also demonstrated the linear relationship between the $[AA]^+/[AB]^+$ ratio and the percent composition of the regioisomers.

CONSTRUCTION OF THE CRITICAL RATIOS

Construction and use of the $[AA]^+/[AB]^+$ ratio for a Type II TAG. If the APCI-MS or ESI-MS mass spectrum of a Type II TAG exhibits a ratio of ion abundances other than 0.50, then it is due to nonstatistical influences. Several of the nonstatistical influences already have been mentioned, but another nonstatistical influence that has been observed deserves further discussion. Laakso and Voutilainen (8), Manninen and Laakso (37), and Laakso (36) reported results for the effect of unsaturation on the abundances of $[DAG]^+$ fragment ions and showed that O(n-3)LnO behaved much like a normal, less unsaturated TAG, by exhibiting a low $[AA]^+/[AB]^+$ ratio of 0.17 (Table 1), owing primarily to the well-reported effect of being the $[DAG]^+$ fragment formed by loss of the *sn*-2 chain. Conversely, they showed that when the double bonds were closer to the carbonyl end of the chain, i.e., n-6 vs. n-3, a much greater amount of the $[sn\text{-}1,3\text{-}AA]^+$ fragment was formed, which led to a larger $[AA]^+/[AB]^+$ ratio, which had a larger value than the 0.5 that was statistically expected. The authors attributed the difference in the n-6 polyunsaturated TAG to the fact that the proximity of the double bonds to the carbonyl end of the chain helped make the PUFA a better leaving group. This made the polyunsaturated group, even in the *sn*-2 position, easily lost. This was reflected in the higher $[AA]^+/[AB]^+$ ratio for all of the n-6 FA, which, for the ABA isomer, was higher than statistically expected, and which, for the

AAB/BAA isomers, was higher than 1. Thus, more information could potentially be derived from the [AA]$^+$/[AB]$^+$ ratio.

The only reported [AA]$^+$/[AB]$^+$ ratio greater than 1 for a pure synthetic [*sn*-1,3-AA]$^+$ isomer was for *sn*-1,3-PAP (di-palmitoyl, arachidonyl TAG, 16:0, 20:4, 16:0) by Fauconnot *et al.* (40), seen in Table 1. The authors used an instrument with a Z-spray interface, whereas most other reports were based on data from ThermoFinnigan TSQ or LCQ instruments. Several values obtained on this instrument and shown in Table 1 were higher than the values obtained by other instruments, and many were much higher than the statistically expected value of 0.5. A notable exception was the TAG regioisomer pair APA/AAP. These both gave a virtually nonexistent [AA]$^+$ ion, the di-arachidonyl [DAG]$^+$ fragment, apparently because the arachidonic chain is lost so easily that two of them cannot both re-main attached. Arachidonic acid is an n-6 FA, like the (n-6)Ln in the OLnO/OOLn pair that Laakso and Voutilainen (8) and Manninen and Laakso (37) reported. The proposition that n-6 arachidonic acid is more easily lost would also explain why the [AA]$^+$/[AB]$^+$ ratios of the PAP/PPA isomer standards were much higher than statistically expected. If the arachidonic chain is lost easily from the TAG PAP because it is an n-6 FA, this would explain why a higher than expected abundance of the [PP]$^+$, dipalmitoyl DAG fragment ion, was observed. This again demonstrates that the [AA]$^+$/[AB]$^+$ Critical Ratio can be used to correlate observations in mass spectra with structural characteristics.

Another benefit to constructing the [AA]$^+$/[AB]$^+$ ratio is that two abundances, [AA]$^+$ and [AB]$^+$, which are two separate numbers, can now be represented by only one number, the nu-meric ratio [AA]$^+$/[AB]$^+$. It will be demonstrated that, using the [AA]$^+$/[AB]$^+$ Critical Ratio, both abundances can be accu-rately reconstructed from this one number when classified cor-rectly. This means that the same amount of information can be conveyed in less space, one number instead of two. When this number and one other number are processed through the Bot-tom-Up Solution (BUS), the complete mass spectrum of a Type II TAG can be reproduced and would exhibit two [DAG]$^+$ frag-ment ion abundances, [AA]$^+$ and [AB]$^+$, and a protonated mol-ecule abundance, for three abundances. These three ions con-stitute all of the primary peaks that provide the M.W. and DAG fragment structural information. The [AA]$^+$/[AB]$^+$ ratio can be used to store two of the three numbers for that mass spectrum as one ratio. Then a second ratio is used to provide the third value, and the relationship between the third value and the first two. The second ratio is the [MH]$^+$/Σ[DAG]$^+$ ratio, which pro-vides information for the value of [M + H]$^+$ and its relationship to [AA]$^+$ and [AB]$^+$. This ratio will be discussed shortly. Masses for each of these ions are specified by the *m/z* value from which came each peak area integrated over time. The known masses are compared with tabulated values, and all pos-sible identities for each mass are known, including isobaric species. Chromatographic information is used with the mass information to identify and differentiate isobaric species (7,34,35).

The [AA]$^+$/[AB]$^+$ ratio as provided at face value can be used

in Equations 3 and 4 to provide direct information regarding the percent compositions of regioisomers, compared with stan-dard solutions. This Critical Ratio, along with one other num-ber (the [MH]$^+$/Σ[DAG]$^+$ ratio), can be used with the BUS to accurately reproduce the exact three abundances that represent the mass spectrum. These characteristics of the BUS—of sav-ing space and providing more information in fewer values— will be seen with the other Critical Ratios as well. All Critical Ratios provide more information than the raw abundances, but the raw abundances can be reconstructed at will by processing them through the BUS.

Construction of the [MH]$^+$/Σ[DAG]$^+$ ratio for all TAG. During the preparation of a recent review (45), Byrdwell sought quantifiable numerical values that could be related to observed mass spectrometric fragmentation characteristics. Some empirically determined Critical Ratios were sought that could be used to describe, in a more quantitative way, the char-acteristics that were ascribed to APCI-MS mass spectra in that chapter. Among the fragmentation characteristics was the de-pendence of the abundance of the protonated molecule, [M + H]$^+$ or [MH]$^+$, on the amount of unsaturation in the TAG FA. TAG containing numerous sites of unsaturation have a proton-ated molecule, [M + H]$^+$ as the base peak, whereas TAG with fewer sites of unsaturation give a [DAG]$^+$ fragment as the base peak. Saturated TAG give a [DAG]$^+$ fragment as the base peak, with no or practically no [M + H]$^+$ abundance. This depen-dence of [M + H]$^+$ abundance on the amount of unsaturation often has been noted and was observed in our first report on the HPLC/APCI-MS analysis of TAG (6). Since that first report, we have sought ways to describe this undefined relationship in a qualitative or quantitative way. In 1997 (34), the relationship between the ratio of the abundance of the [M + H]$^+$ ion of a TAG to the sum of all ions, [M + H]$^+$ plus [DAG]$^+$, was mod-eled as using:

$$\frac{[TAG]^+}{[TAG]^+ + \Sigma[DAG]^+}$$

An equation was shown, referred to as *the TAG quotient 1/3 power fit*, that was an approximate representation of the curve described when this ratio was plotted vs. the number of sites of unsaturation in the TAG. This ratio has now been calculated to equal the following:

$$\frac{[TAG]^+}{[TAG]^+ + \Sigma[DAG]^+} = \frac{1}{1 + \dfrac{1}{\dfrac{[TAG]^+}{\Sigma[DAG]^+}}}$$

It is simpler, and is preferred, to use the [MH]$^+$/Σ[DAG]$^+$ ratio instead of the inverse of its inverse.

The ratio of the TAG protonated molecule, [TAG + H]$^+$, [M + H]$^+$, or [MH]$^+$, to Σ[DAG]$^+$ is referred to in the BUS as the [MH]$^+$/Σ[DAG]$^+$ ratio.

One important aspect of the relationship between the [M + H]$^+$ ion and the sum of the [DAG]$^+$ fragment ions is that they are inverses: When one goes up, the other goes down. This dependence is not linear, but it is inverse in some way. Since

one value goes up and one goes down, the ratio of these two values highlights, or accentuates, the dependence of $[M + H]^+$ on the degree of unsaturation. This ratio will show more movement in its numeric value than the abundance alone as the number of sites of unsaturation changes, since the ratio contains two abundances that have an inverse relationship. Therefore, the dependence of the abundance of the protonated molecule, $[M + H]^+$, on the degree of unsaturation is best reflected in the ratio of the protonated molecule, $[MH]^+$, to the sum of the DAG fragment ion abundances, $\Sigma[DAG]^+$, to give $[MH]^+/\Sigma[DAG]^+$. This ratio can be used as a Critical Ratio to provide information regarding the number of sites of unsaturation in the molecule, which determines whether the $[M + H]^+$ or a $[DAG]^+$ is the base peak. TAG containing numerous sites of unsaturation have an $[MH]^+/\Sigma[DAG]^+$ larger than 1, and thus have a $[M + H]^+$ base peak. TAG with few sites of unsaturation have a low $[MH]^+/\Sigma[DAG]^+$ ratio, and a $[DAG]^+$ base peak. Saturated TAG are expected to have an $[MH]^+/\Sigma[DAG]^+$ ratio of zero, because they often give no $[M + H]^+$ ion.

An important aspect of the BUS construct is that the Critical Ratios are chosen, or constructed, based on observations in APCI-MS mass spectra, and keep them from going to catastrophic values. It has been observed that the $[M + H]^+$ ion can be zero for saturated TAG, so if this number were alone in the denominator of a ratio, then the ratio would take a value of 1/0 for saturated TAG and would become unsolvable. Since it is known that the $[M + H]^+$ ion goes to zero for some TAG, but that $\Sigma[DAG]^+$ never goes to zero, one can choose to calculate the $[MH]^+/\Sigma[DAG]^+$ ratio instead of the $\Sigma[DAG]^+/[MH]^+$ ratio, so that the number that can go to zero is in the numerator. Thus, judicious selection of the ratio that is constructed can keep the system completely bounded in all observed circumstances. The $[MH]^+/\Sigma[DAG]^+$ ratio can be classified into one of two cases: $[MH]^+/\Sigma[DAG]^+ \leq 1$, or $[MH]^+/\Sigma[DAG]^+ > 1$. The case when $[MH]^+/\Sigma[DAG]^+ = 0$ is a subset of the case when $[MH]^+/\Sigma[DAG]^+ \leq 1$, so a special case for $[M + H]^+ = 0$ is not required. Therefore, selecting the $[MH]^+/\Sigma[DAG]^+$ ratio as the Critical Ratio to represent the abundance of the $[M + H]^+$ ion and its relationship to the $[DAG]^+$ fragment ions is the better choice, because it leads to a simpler construct, which requires only two cases and remains bounded in all observed circumstances. In all instances, the Critical Ratios, which are the primary elements in the BUS construct, have been chosen to be as simple as possible and yet still convey more information in fewer variables than the raw mass spectrum.

There is another consideration and guiding principle that is inherent in the BUS. Since the BUS is a construct based on data from MS, it inherently incorporates and reflects the two important rules for data from MS: (i) All relative abundances are limited to a maximum individual value of 100%, and (ii) one ion abundance must be 100%. Since the tallest peak in a mass spectrum is normalized to 100%, one peak always represents 100%. The BUS ensures that all calculated values are less than or equal to 100%, since this is the limit imposed by MS. And the BUS determines which peak is the tallest and establishes it as

100%. Of course, 100 per*cent* (one hundred per hundred) as a pure ratio is 1.00. The Critical Limits within the BUS are what keep all values limited to being within the two rules imposed by MS. The value of 1.00 for several of the ratios also has other inherent meanings that provide structural information regarding the TAG (for instance, if $[AA]^+/[AB]^+ > 1$ for a Type II TAG, this provides structural information regarding the identity of the regioisomers).

For a Type II TAG, only the first two Critical Ratios mentioned earlier are necessary to specify the appearance of the mass spectrum. The $[AA]^+/[AB]^+$ ratio is used at face value in Equations 3 and 4 to provide information on the composition of the regioisomers of the TAG. The other Critical Ratio, $[MH]^+/\Sigma[DAG]^+$, may be used to provide insight into the degree of unsaturation in the TAG. These two numbers, the two Critical Ratios for a Type II TAG, provide more information in fewer values than the three raw abundances that constitute the raw mass spectrum. The mass spectrum of a Type III TAG contains four primary peaks and so requires three critical ratios. However, the $[MH]^+/\Sigma[DAG]^+$ ratio provides the same kind of information about a Type III TAG as it does for a Type II TAG. The $[MH]^+/\Sigma[DAG]^+$ ratio provides information to correlate the total amount of unsaturation in the three FA to the abundance of the protonated molecule. For a Type I TAG, the mass spectrum contains only two peaks, which are the $[M + H]^+$ peak and one single $[DAG]^+$ fragment ion. For a Type I TAG, the BUS requires only the $[MH]^+/\Sigma[DAG]^+$ ratio to reproduce the mass spectrum, and it also provides information regarding the number of sites of unsaturation in the TAG molecular species. This critical ratio provides information regarding the abundance of the $[M + H]^+$ ion, when properly classified, and also provides information to relate the abundance of this ion to the $[DAG]^+$. So with the $[MH]^+/\Sigma[DAG]^+$ ratio, as with the $[AA]^+/[AB]^+$ ratio already discussed, more information is provided in this Critical Ratio than in the raw abundances. The proper selection of the complete set of Critical Ratios for Types I, II, and III TAG, of which the first Critical Ratio is the $[MH]^+/\Sigma[DAG]^+$ ratio, allows the BUS to be completely self-contained and to operate within the rules imposed by MS in all observed circumstances.

Construction of the $[AC]^+/([AB]^+ + [BC]^+)$ ratio for a Type III TAG. A Type III TAG has three different FA, ABC, and these produce three possible $[DAG]^+$ fragment ions, $[AB]^+$, $[BC]^+$, and $[AC]^+$. These fragment ions may contain A, B, and C in any combination of *sn*-1, *sn*-2, and *sn*-3 positions, and in a randomized mixture, these are observed to be statistically distributed throughout all positions (7). Statistically speaking, the abundances of all three ions, $[AB]^+$, $[BC]^+$, and $[AC]^+$, should be identical in the absence of nonstatistical influences. However, fragment ions are not observed with equal abundance in APCI-MS or ESI-MS/MS mass spectra. It has been observed (10,11) that the abundance of the ion formed from loss of the FA in the *sn*-2 position, which gives the $[sn-1,3-AC]^+$ fragment, is the lowest of the three possible $[DAG]^+$ fragment ions. With this rule, all Type III TAG could be categorized, and the identities of the FA in the *sn*-2 position known. All four possibilities for the

A and C FA with B still remain: $[sn\text{-}1,2\text{-}AB]^+$ and $[sn\text{-}2,3\text{-}BC]^+$ or $[sn\text{-}1,2\text{-}CB]^+$ and $[sn\text{-}2,3\text{-}BA]^+$. But the $[sn\text{-}1,3\text{-}AC]^+$ isomer can be identified as the ion with the lowest abundance, so a piece of structural information may be known from the ion having the lowest abundance.

For simplicity, the isobaric $[sn\text{-}1,3\text{-}AC]^+$ or $[sn\text{-}1,3\text{-}CA]^+$ regioisomers are usually referred to more briefly as $[sn\text{-}1,3\text{-}AC]^+$, with the understanding that APCI-MS cannot distinguish between the $[sn\text{-}1,3\text{-}AC]^+$ and $[sn\text{-}1,3\text{-}CA]^+$ isomers, and so both possibilities are always implied herein. By putting the $[sn\text{-}1,3\text{-}AC]^+$ abundance alone in the numerator of the second Critical Ratio of the Type III TAG (the $[MH]^+/\Sigma[DAG]^+$ ratio is the first Critical Ratio for all TAG), the second Critical Ratio can be used to reflect the trend in the $[sn\text{-}1,3\text{-}AC]^+$ abundance with regioisomeric structure. This is analogous to the way the $[AA]^+/[AB]^+$ ratio is used to provide structural information for a Type II TAG, except the means for quantitative analysis of the regioisomers of Type III TAG have not yet been developed as thoroughly as the quantification of Type II TAG has (see Jakab *et al.* (42) and Eqs. 3 and 4).

Thus, the Critical Ratio $[AC]^+/([AB]^+ + [BC]^+)$ for a Type III TAG first provides a piece of information, which is the identity of the $[sn\text{-}1,3\text{-}AC]^+$ isomer, and then allows the abundance of the $[sn\text{-}1,3\text{-}AC]^+$ isomer to be calculated, when properly classified by the Critical Limits. This Critical Ratio also contains information to relate the $[AC]^+$ ion abundance to the two other ions that make up the mass spectrum.

In a complex mixture of TAG, the complete identification of all TAG molecular species requires the chromatographic information provided by the on-line separation, in addition to the masses provided by APCI-MS, to differentiate the many isobaric molecular species having overlapping masses, such as $[OO]^+$ and $[SL]^+$, $[OL]^+$ and $[SLn]^+$, etc. $[OO]^+$ and $[SL]^+$ are separated by a good chromatographic method (35), and so these can be differentiated and the characteristic Critical Ratios for each TAG molecular species can be constructed.

For a Type III TAG, if all FA in a TAG were distributed statistically and there was no influence by different levels of unsaturation or preferential loss, then the $[AC]^+$, $[AB]^+$, and $[BC]^+$ fragment abundances should all be equal, and the $[AC]^+/([AB]^+ + [BC]^+)$ ratio would be 0.5. An $[AC]^+/([AB]^+ + [BC]^+)$ ratio other than 0.5 indicates that nonstatistical influences are affecting the abundances. An $[AC]^+/([AB]^+ + [BC]^+)$ ratio greater than 1 would certainly indicate a preference for $[AC]^+$. According to literature precedent, one should be able to identify the $[sn\text{-}1,3\text{-}AC]^+$ fragment as the fragment with the lowest $[AC]^+/([AB]^+ + [BC]^+)$ ratio, and thus have a substantial piece of information regarding the TAG, which came from just this one Critical Ratio. Thus, one should choose to construct the $[AC]^+/([AB]^+ + [BC]^+)$ ratio using the smallest abundance in the numerator, since this has been correlated (10,11) with being the $[sn\text{-}1,3\text{-}AC]^+$ isomer.

Throughout this work, the identities of A, B, and C are irrespective of mass but reflect only the regioisomeric position of the FA on the backbone. This is analogous to the Type II TAG, in which, for OPO, the FA represented by A, out of ABA, has

a larger mass than the FA in the B position. On the other hand, in POP, the A FA has a mass that is lower than the FA in the B position. ABC refers to the regioisomeric positions of FA, when properly assigned, whereas the identities of the $[DAG]^+$ are characterized first by mass, then by their chromatographic elution at that mass, and then by comparison with tabulated masses (11). With this approach, the A and C can be identified and labeled specifically, and the FA in the $sn\text{-}2$ position can be identified.

With the FA in the $sn\text{-}2$ position known, the identities of the FA in the $sn\text{-}1$ and $sn\text{-}3$ positions are known to constitute the isobaric $[DAG]^+$ fragment possibilities, $[sn\text{-}1,2\text{-}AB]^+$ and $[sn\text{-}2,3\text{-}BC]^+$, or $[sn\text{-}1,2\text{-}BA]^+$ and $[sn\text{-}2,3\text{-}CB]^+$. No definitive trend has yet been reported to distinguish between $[sn\text{-}1,2\text{-}AB]^+$ and $[sn\text{-}2,3\text{-}BA]^+$ or between $[sn\text{-}2,3\text{-}BC]^+$ and $[sn\text{-}1,2\text{-}CB]^+$. It is reasonable to expect that, after the $[AC]^+/([AB]^+ + [BC]^+)$ ratios of a sufficient number of Type III TAG have been tabulated, trends in this ratio will be observable and will be correlated with the regioisomeric structures of the TAG.

The literature precedent for APCI-MS analysis of Type III TAG is currently based on a limited number of observations (10,11). Because of this, the ability to use the $[AC]^+/([AB]^+ + [BC]^+)$ ratio for identification of regioisomers in complex mixtures of TAG has not yet been developed. Also, not all nonstatistical influences have been characterized. The influence of the number of double bonds and their positions in the fatty chain (n-6 vs. n-3) has already been discussed herein in detail for a Type II TAG, and so it is reasonable to expect that similar trends, relating increased levels of polyunsaturation to increased abundances of ions containing the FA with more double bonds, will be observed for Type III TAG. Furthermore, the positions of the double bonds were shown to have an influence on Type II TAG, as discussed herein, so the positions of the double bonds in the FA of Type III TAG could also be expected to exert an influence on the abundances of ions observed in APCI-MS mass spectra. If the $[AC]^+/([AB]^+ + [BC]^+)$ ratios of numerous Type III TAG from different mixtures of TAG having known compositions of regioisomers are accumulated and tabulated (as is done with Type II TAG), it may be possible to move toward a more quantitative interpretation of this Critical Ratio. For now, some expected and probably some unexpected nonstatistical influences remain to be characterized. Regardless of how specifically information from this Critical Ratio can be derived at this time, it is clear that the $[AC]^+/([AB]^+ + [BC]^+)$ ratio as a single number already provides more information than the raw abundance alone. The $[AC]^+$ abundance must be compared with the other abundances to know whether it is the smallest and whether it is therefore the $[sn\text{-}1\text{-}AC]^+$. The abundance does not provide the desired information if used by itself. It provides the desired information regarding the regiospecific identity of the ion exhibiting that abundance only if it is taken as a ratio to the other ions. As with the other Critical Ratios, the numerator provides the abundance of one ion directly, when classified correctly in the BUS, and the ratio provides information to relate this ion to the other ions.

So while it remains to be further characterized, this Critical

Ratio as a single numeric value for a Type III TAG provides not only the same, but more information, when used with the BUS, than the original raw abundance of [AC]$^+$ as a single number.

Construction of the [BC]$^+$/[AB]$^+$ ratio. No distinctive preference for the [*sn*-1,2-AB]$^+$ position compared with the [*sn*-2,3-BC]$^+$ position has been reported using APCI-MS data. There appears to be minimal difference energetically, in an APCI source, between loss of the FA in the *sn*-1 position and loss of the FA in the *sn*-3 position. Nevertheless, if there is any *sn*-1,2 vs. *sn*-2,3 preference, this would be reflected in the ratio [BC]$^+$/[AB]$^+$, if [BC]$^+$ is the abundance of the *sn*-2,3 isomer and [AB]$^+$ is the abundance of the *sn*-1,2 isomer, regardless of mass. The ratio [BC]$^+$/[AB]$^+$ would constitute the Critical Ratio necessary to specify any [*sn*-1,2-AB]$^+$ vs. [*sn*-2,3-BC]$^+$ preference (or vice versa). Based on previous reports, at this time no observed trends that correlate regioisomeric structures of Type III TAG with different amounts of unsaturation in the [*sn*-1,2-AB]$^+$ vs. [*sn*-2,3-BC]$^+$ FA can be cited. However, several expected trends can be discussed.

Just as was observed with Types I and II TAG, the amount of unsaturation in the FA should have an influence on the abundances of the [DAG]$^+$ fragment ions that contain the FA. Since there appears to be minimal influence due to the regioisomeric position of the FA in the TAG at the *sn*-1,2 vs. *sn*-2,3 positions, the degree of unsaturation in the fragment [AB]$^+$, compared with the unsaturation in [BC]$^+$, may exhibit a greater influence on the [BC]$^+$/[AB]$^+$ ratio than the unreported influence due to the regioisomeric identity. Of course, the locations and number of the double bonds were of primary importance in determining the effect of the double bonds on the ion abundances for Type II TAG and therefore should be expected to exert a similar influence on Type III TAG that contain PUFA.

Although the amount of information that can be derived from the [BC]$^+$/[AB]$^+$ ratio is currently limited, it does provide one piece of information at face value. This information is found by comparing the [BC]$^+$/[AB]$^+$ ratio to its inherent Critical Value of 1. If the [BC]$^+$/[AB]$^+$ ratio is greater than 1, the [BC]$^+$ ion is larger than [AB]$^+$ ion, but if this third Critical Ratio for a Type III TAG is less than 1, [AB]$^+$ is larger than [BC]$^+$. It can be seen that this third Critical Ratio for a Type III TAG can be used with the BUS, which incorporates the rules of MS, to provide the two numerical values that are the raw abundances of the [BC]$^+$ and [AB]$^+$ fragment ions from the one numerical value. Thus, this Critical Ratio provides the same information (two abundances) in less space (one number instead of two) than the raw abundances. Whether more information can be derived from this ratio will be determined by future reports.

Summary of the construction of the Critical Ratios. The Critical Ratios just described can be constructed and directly interpreted at face value to provide information regarding structural trends. These ratios provide a method for visualizing trends that is more direct than using the raw abundances alone. The trends are not as apparent in the raw data as they are in the Critical Ratios. Therefore, is it useful to construct these Critical Ratios as an aid to qualitative analysis of TAG.

Not only do these Critical Ratios highlight structural trends, but also they constitute a reduced data set from which the mass spectrum of any TAG can be reconstructed in its entirety. The Critical Ratios can be used with inherent Critical Values and calculated Critical Limits to classify all TAG into Cases. The Case into which a TAG is classified provides all of the equations necessary to calculate the abundances of every ion in the mass spectrum as well as the sum of all ions. This report will present the basic equations that encompass every structural possibility within the TAG Lipidome. The solution to the *Triacylglycerol Lipidome* comes in the form of the Critical Ratios operated into the BUS, to accomplish the classification of the TAG into the proper Cases, based on the Critical Values and Critical Limits. The ratios are applied with an interpretation matrix that provides structural information from the Critical Ratios as they operate through the Critical Values and Critical Limits. Once a TAG is properly classified by its Critical Ratios, the Case indicates the correct equations to use for the solution of all ion abundances. This combination of Critical Ratios with Critical Values and Critical Limits used to define the Cases, along with the interpretation matrix and the equations for each Case constitutes the BUS to the TAG Lipidome. This solution allows the primary ions in the mass spectrum of any TAG to be reproduced, and the Critical Ratios can be used for a quantitative description for the set of structural possibilities exhibited by the TAG.

Method for quantitative analysis based on ion abundances determined by APCI-MS. During the routine processing of data from LC/APCI-MS using the quantitative method of Byrdwell *et al*. (7,34,35), the area under every peak is integrated in every extracted ion chromatogram (EIC) of each *m/z* value for every [DAG]$^+$ fragment ion and protonated molecule, [M + H]$^+$. The peaks that gave the areas of [DAG]$^+$ fragment ions and protonated molecules, [M + H]$^+$, that come from a particular TAG must elute at the same specific retention time, since they come from the same TAG. Therefore, the areas under the fragment ion and protonated molecule chromatographic peaks constitute an average mass spectrum across the retention time window used for integration. The average mass spectrum is calculated as the normalized percent composition of the areas of the fragment ions and the protonated molecule across the integrated chromatographic retention time window for a particular TAG. Small differences in retention times at the beginning and end of the fragment peaks have no substantial impact on the integrated area of each peak. The integrated areas provide a good representation of the mass spectrum averaged across a chromatographic peak. Typical ion chromatograms that are integrated to give peak areas are shown and discussed in the subsequent section entitled Implementation of the BUS. All solutions provided herein work equally well on an average mass spectrum that is produced from integrated peak areas or from manual qualitative analysis, or from a single mass spectrum manually acquired. Of course, there is some variability in abundances between single replicate mass spectra, and this variability is greater for TAG present at low levels. Whichever abundances

are used to produce the Critical Ratios, the mass spectrum from which they come is exactly reproduced by the BUS.

As mentioned, the first Critical Ratio is the ratio of the percent abundance of the protonated molecule as a ratio to the sum of all [DAG]⁺ fragment ions:

$$\text{Critical Ratio 1} = \left(\frac{[MH]^+}{\sum [DAG]^+} \right) \qquad [5]$$

Table 2 lists the Critical Ratios for a 35-TAG mixture of synthetic TAG. The critical ratios are listed as a percentage simply for the most convenient display of four (or five) significant figures, with up to two decimal places. This is the same method of representation that Jakab *et al.* (42) used in their analysis of the [AA]⁺/[AB]⁺ ratio for characterization of mixtures of LOL/LLO. It is important to realize that the Critical Ratios as percentages must be converted to pure ratios (fractions), by dividing by 100, before they are used in the equations below. Throughout the following discussion, all ratios are expressed in pure fraction form, not percentage form. As a fraction, 100% equals 1.00, so 1.00 is the upper limit in the equations below. In the spreadsheet formulas used for the automated implementation of the BUS, the division of the ratio by 100 is incorporated into the formulas.

As already discussed, the first Critical Ratio can be used to define the overall unsaturation of a molecule. It is well known that saturated TAG have a [MH]⁺/Σ[DAG]⁺ ratio that is either very low or zero. The polyunsaturated TAG have large values of the [MH]⁺/Σ[DAG]⁺ ratio. The [MH]⁺/Σ[DAG]⁺ ratio for OOO is a very low value of 0.0324, and so for this Type I TAG (a mono-acid TAG), a [DAG]⁺ is the base peak, and the protonated molecule abundance is simply the [MH]⁺/Σ[DAG]⁺ ratio, expressed as a percentage, 3.24%. For LLL and LnLnLn, the large [MH]⁺/Σ[DAG]⁺ ratio indicates that [M + H]⁺ is the base peak, and the [DAG]⁺ abundance is easily calculated from the inverse of the [MH]⁺/Σ[DAG]⁺ ratio.

The second Critical Ratio depends on whether the molecule is a Type II or Type III TAG. For a Type II TAG, the second Critical Ratio is [AA]⁺/[AB]⁺. For a Type III TAG, the second Critical Ratio is ([AC]⁺/([AB]⁺ + [BC]⁺)):

Type II :
$$\text{Critical Ratio 2} = \left(\frac{[AA]^+}{[AB]^+} \right) \qquad [6a]$$

Type III :
$$\text{Critical Ratio 2} = \left(\frac{[AC]^+}{([AB]^+ + [BC]^+)} \right) \qquad [6b]$$

This second Critical Ratio has an obvious relationship to the positional preference of a TAG. It is expected that the ([AA]⁺/[AB]⁺) ratio should always be less than 1, unless there is a strong [AA]⁺ positional preference. Likewise, the ratio ([AC]⁺/([AB]⁺ + [BC]⁺)) should be less than 1 unless there is a strong [AC]⁺ positional preference. But the degree of unsaturation in the [AB]⁺ or [AC]⁺ fragment also has an effect on this ratio. Deconstruction of the second Critical Ratio of an ABC TAG into the two components of positional preference and de-

gree of unsaturation remains to be accomplished. For now, this ratio can simply be compared to positional isomer standards.

The third Critical Ratio is only observed from Type III TAG. It is the ratio of [BC]⁺/[AB]⁺, or the ratio of the *sn*-2,3 [DAG]⁺ to the *sn*-1,2 [DAG]⁺. For now, it is assumed that there is no particular preference between these two, but evidence at a future date may allow quantification of a preference for the *sn*-1,2 [DAG]⁺ peak over the *sn*-2,3 [DAG]⁺ peak or vice versa. All else being equal, a [BC]⁺/[AB]⁺ of ≤1 is used herein as the default assumption (assume [AB]⁺ ≥ [BC]⁺). The reason for this is discussed shortly. In the absence of any preference or assumption, the [BC]⁺/[AB]⁺ ratio may be less than one or greater than 1 with equal statistical probability, thereby giving an equal probability of Case 5 or Case 6.

THE BUS

The BUS for a Type I TAG. Now that the critical ratios have been defined, it is useful to examine the visualization approach that led to the definition of the Cases. Figure 2 shows the appearance of idealized APCI-MS mass spectra of TAG. The axes in these figures have a maximum value of 1, representing 100% as a pure ratio. AAA TAG are shown first in this figure.

Since an AAA TAG has only one [DAG]⁺ and the [M + H]⁺, it is obvious that the Critical Value that determines which peak is the base peak occurs when both [AA]⁺ and [MH]⁺ have their maximal values, and [MH]⁺/Σ[DAG]⁺ is equal to 1. The Critical Value for an AAA TAG is depicted in the upper right panel of Figure 2, Part I. From this Critical Value of [MH]⁺/Σ[DAG]⁺ = 1, if the [MH]⁺ were to diminish by the least amount, the [MH]⁺/Σ[DAG]⁺ ratio would be less than 1 and [AA]⁺ would be the base peak. This is referred to as Case 1, and the solution would use the equation shown in Scheme 1, Part I, for Case 1.

On the other hand, if the [DAG]⁺ were to diminish by the least amount, then the [MH]⁺/Σ[DAG]⁺ ratio would be larger than 1 and [M + H]⁺ would be the base peak. This is referred to as Case 2, and the solution would use the equation listed in Scheme 1, Part I, for Case 2. No other Critical Limit is necessary to specify the Case for a Type I TAG. Once the case has been specified, the actual percentages of [M + H]⁺ and the [AA]⁺ abundances are given by the equations in Scheme 1, Part I, for either the Case 1 solution [AA]⁺ base peak) or the Case 2 solution [M + H]⁺ base peak). The value of 1 serves as a Critical Value for all Types I, II, and III TAG. If the [MH]⁺/Σ[DAG]⁺ ratio is greater than 1 for any TAG, this automatically means that [M + H]⁺ is the base peak and specifies a Case 2 solution. More generally, if any Critical Ratio has a value greater than 1, the numerator is automatically the largest peak of the peaks used to construct the ratio.

Using a Type I TAG as an example, the pattern in the equations in the BUS can now be described. The sum of all ions can be referred to as the Σ(I⁺) for any TAG. For a Type I TAG, the sum of all ions, Σ(I⁺), is simply equal to the sum of the protonated molecule ion and the single [DAG]⁺ fragment ion, Σ([MH]⁺ + [DAG]⁺). Thus, Σ(I⁺) = Σ([MH]⁺ + [DAG]⁺). Similarly, the sum of all ions for any TAG is equal to the sum

I) 'AAA' TAG   Critical value = 1.0   **Critical Value :**

Case 1 $[AA]^+$ $[MH]^+$

Case 2 $[MH]^+$ $[AA]^+$

$[AA]^+$ $[MH]^+$

$$\frac{[MH]^+}{\sum[DAG]^+} = \frac{100\%}{100\%} = \frac{1.00}{1.00} = 1$$

II) 'ABA/AAB' TAG   Critical value = 0.5

Case 1.0 $\Sigma[DAG]^+$ $[MH]^+$

Case 3 $[AB]^+$ $[AA]^+$

Case 2.0 $[MH]^+$ $\Sigma[DAG]^+$

Case 4 $[AA]^+$ $[AB]^+$

III) 'ABC' TAG   Critical value = 0.33

Case 1.0 $\Sigma[DAG]^+$ $[MH]^+$

Case 3.0 (Σ_2) $[AC]^+$

Case 5 $[AB]^+$ $[BC]^+$

Case 2.0 $[MH]^+$ $\Sigma[DAG]^+$

Case 4.0 $[AC]^+$ (Σ_2)

Case 6 $[BC]^+$ $[AB]^+$

Critical Values :

Case *n.n* $\Sigma[DAG]^+$ $[MH]^+$

$$\frac{[MH]^+}{\sum[DAG]^+} = \frac{100\%}{200\%} = 1/2$$

Case *n.n.n* $\Sigma[DAG]^+$ $[MH]^+$

$$\frac{[MH]^+}{\sum[DAG]^+} = \frac{100\%}{300\%} = 1/3$$

Critical Limits :

Case *n.3* $\Sigma[DAG]^+$ $[AB]^+$ $[MH]^+$ $[AA]^+$

$$\frac{[MH]^+}{\sum[DAG]^+} = \frac{1}{1+\frac{[AA]^+}{[AB]^+}}$$

Case *n.4.n* $\Sigma[DAG]^+$ $[AC]^+[MH]^+$

$$\frac{[MH]^+}{\sum[DAG]^+} = \frac{1}{1+\frac{1}{\frac{[AC]^+}{([AB]^+ +[BC]^+)}}}$$

FIG. 2. Generalized representations of mass spectra used to calculate Critical Ratios. Also, generalized mass spectra that demonstrate Critical Values and Critical Limits are shown.

of the protonated molecule plus the sum of the $[DAG]^+$ fragment ions: $\Sigma(I^+) = \Sigma([MH]^+ + \Sigma[DAG]^+)$. The BUS for a Type I TAG shows that if the $[MH]^+/\Sigma[DAG]^+$ ratio is less than the Critical Value of 1, then the solution obeys Case 1. According to Case 1, the $[DAG]^+$ fragment is the base peak and has an abundance of 100% (= 1.00 as a pure ratio). In such a case, the sum of the ions $\Sigma(I^+)$ is $(1 + ([MH]^+/\Sigma[DAG]^+))$. For instance, OOO has an $[MH]^+/\Sigma[DAG]^+$ ratio of 0.0324. This ratio is less than 1, so OOO is solved using Case 1.

Classifying this TAG as a Case 1 TAG first provides a piece of information, which is that the $[DAG]^+$ fragment is the base peak, and then it provides the equation to use to calculate the abundance of the $[M + H]^+$ ion. The percent abundance of the

$[M + H]^+$ ion is given by $([MH]^+/\Sigma[DAG]^+) \times 100$, as shown in Scheme 1 Part I, or $(0.0324 \times 100) = 3.24\%$. Then the sum of all ions is $\Sigma(I^+) = \Sigma([DAG]^+ + [MH]^+) = 100\% + 3.24\% = 103.24\%$, which is 1.0324 as a pure ratio. Thus, for this Case 1 TAG, the following equivalences are true:

$$\sum(I^+) = \sum\left([MH]^+ + [DAG]^+\right) = \left(1 + \left(\frac{[MH]^+}{\sum[DAG]^+}\right)\right) = (1+.0324) = 1.0324, \text{ or } = 103.24\%$$

On the other hand, a TAG such as LLL has an $[MH]^+/\Sigma[DAG]^+$ ratio of 1.2007. This is greater than 1, and so Scheme 1, Part I, shows that this would be classified as a Case 2 solution. This classification immediately provides a piece of information, which is that the protonated molecule, $[M + H]^+$, is the base

peak, and then it provides the equation used to calculate the abundance of the [DAG]$^+$ fragment ion. The [DAG]$^+$ ion abundance (%) is given by $(1/([MH]^+/\Sigma[DAG]^+)) \times 100$, or $(1/1.2007) \times 100$, which equals 0.8328×100, or 83.28%. Thus, the base peak is known by the classification process, and the other abundance is given by the equation dictated by the classified BUS. The sum of the ions in the mass spectrum is $100 + 83.28\% = 183.28\%$, or 1.8328 as a pure ratio. The second solution can be seen to give the following equivalences:

$$\sum(I^+) = \sum([MH]^+ + [DAG]^+) = \left(1 + \frac{1}{\dfrac{[MH]^+}{\sum[DAG]^+}}\right) = \left(1 + \frac{1}{1.2007}\right) = 1.8328 \text{, or } = 183.28\%$$

There are only two possible solutions for a Type I TAG, and these may be summarized by the equivalence:

$$\sum(I^+) = \sum([MH]^+ + [DAG]^+) = \left\{\underset{\text{Case 1}}{\left(1 + \left(\frac{[MH]^+}{[DAG]^+}\right)\right)} \text{ or } \underset{\text{Case 2}}{\left(1 + \frac{1}{\left(\frac{[MH]^+}{[DAG]^+}\right)}\right)}\right\}$$

This equation shows that the sum of all ions is equal to the sum of the protonated molecule plus the one [DAG]$^+$ fragment ion, and this is equal to one of two possibilities, depending on whether it is a Case 1 or a Case 2 solution, as determined by whether the [MH]$^+$/Σ[DAG]$^+$ ratio is less than the Critical Value of 1 or larger than 1. Scheme 1, Part I, shows the equivalence just given. The foregoing two examples, for OOO and LLL, demonstrate that this equivalence is true for Type I TAG having an [MH]$^+$/Σ[DAG]$^+$ ratio less than 1 (OOO), or a ratio greater than 1 (LLL).

The BUS for a Type II TAG. For Types II and III TAG, a [MH]$^+$/Σ[DAG]$^+$ ratio greater than 1 certainly indicates that [M + H]$^+$ is the base peak, but an [MH]$^+$/Σ[DAG]$^+$ ratio less than 1 does not, by itself, indicate that [M + H]$^+$ is not the base peak. Thus, for Types II and III TAG, an [MH]$^+$/Σ[DAG]$^+$ ratio greater than 1 is sufficient, but not necessary, to define [M + H]$^+$ as the base peak for any TAG. Types II and III TAG have other Critical Values inherent in the construction of the ratios. The same logic demonstrated for AAA TAG of setting all peaks equal to 1 at the Critical Value and comparing the observed Critical Ratio to this Critical Value to determine the identity of the base peak is also applicable to Types II and III TAG.

The Critical Value for a Type II TAG is depicted in the fourth panel down in Figure 2. At the Critical Value for a Type II TAG, the [M + H]$^+$ and both [DAG]$^+$ have their maximum values of 1.00, or 100%. This circumstance is rarely, if ever, actually observed, but it serves as an inherent arithmetic equivalence point for TAG that fragment to produce two different [DAG]$^+$ ions. For any Type I, II, or III TAG, the Critical Value, at which all ions, $\Sigma(I^+)$, are at their maximum values, produces the limit that represents the minimum [MH]$^+$/Σ[DAG]$^+$ ratio that the TAG could have and still give a protonated molecule, [MH]$^+$. At the Critical Value for the [MH]$^+$/Σ[DAG]$^+$ ratio, if any [DAG]$^+$ fragment were to decrease by the least amount, the Σ[DAG]$^+$ would decrease, and the [MH]$^+$/Σ[DAG]$^+$ ratio would increase, and so this value represents the minimum of the ratio. If the [M + H]$^+$ abundance were to decrease by the least amount, it would not be the base peak, and so a piece of information would be known.

I) 'AAA' TAG

Critical Value = 1

$$\sum_1(I^+) = \sum_1([MH]^+ + [DAG]^+) = \underset{\text{Case 1}}{\left(1 + \left(\frac{[MH]^+}{\sum[DAG]^+}\right)_*\right)} \quad or \quad \underset{\text{Case 2}}{\left(1 + \frac{1}{\left(\frac{[MH]^+}{\sum[DAG]^+}\right)_*}\right)}$$

$$\left(\frac{[MH]^+}{\sum[DAG]^+}\right) \overset{?}{<} 1 \xrightarrow{\;Y\;} \text{Case 1} \quad \text{the } [DAG]^+ = 100\ \% \text{ (base peak)}$$

$$\downarrow N$$

$$\% [M + H]^+ = \left(\frac{[MH]^+}{\sum[DAG]^+}\right) x100$$

Case 2

$\% [M+H]^+ = 100\ \%$ (base peak)

$$\% [DAG]^+ = \frac{1}{\left(\frac{[MH]^+}{\sum[DAG]^+}\right)} x100$$
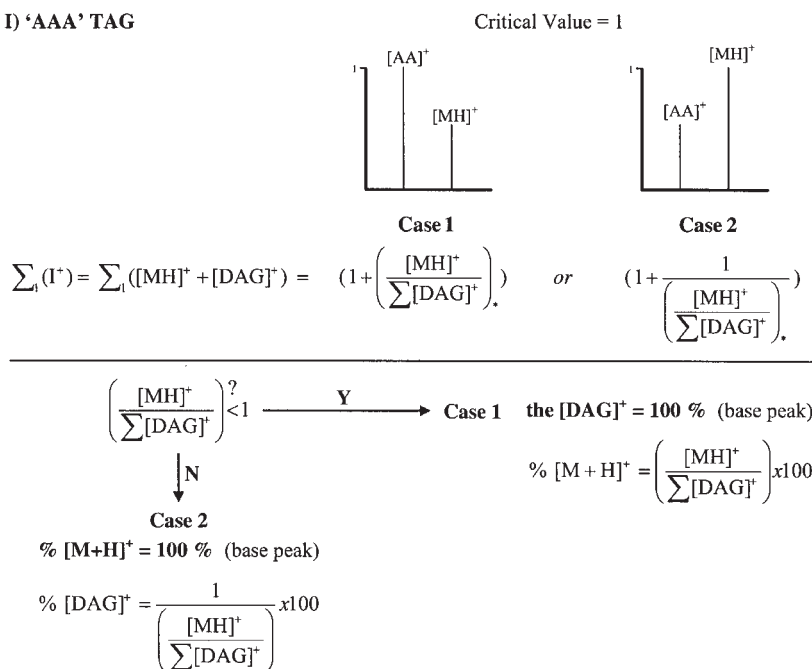
SCHEME 1, PART I. Equations to calculate the relative abundances of the [M + H]$^+$ and the [DAG]$^+$ fragment ion for an AAA TAG using the [MH]$^+$/Σ[DAG]$^+$ Critical Ratio from atmospheric pressure chemical ionization (APCI)-MS data (Table 2).

The Critical Value of the $[MH]^+/\Sigma[DAG]^+$ ratio for a Type II TAG, or ABA/AAB TAG, is 1/2, or 0.5, as shown in the fourth panel down in Figure 2. A mass spectrum with a $[MH]^+/\Sigma[DAG]^+$ ratio less than the Critical Value cannot have a protonated molecule base peak. But a $[MH]^+/\Sigma[DAG]^+$ ratio greater than the Critical Value does not immediately indicate that the protonated molecule is the base peak. The Critical Ratio must be further tested with another limit to determine whether the $[M + H]^+$ is the base peak. The Critical Value serves as the lower limit for the possibility of having a protonated molecule base peak. If the $[MH]^+/\Sigma[DAG]^+$ ratio is greater than the Critical Value, then the next limit to which it is compared is the Critical Limit, discussed next, which is the limit of the $[MH]^+/\Sigma[DAG]^+$ ratio, based on actual $[DAG]^+$ abundances, that defines whether the $[M + H]^+$ is the base peak or a $[DAG]^+$.

The Critical Limit for a Type II TAG. The Critical Limit for a Type II TAG makes use of the inherent limitations imposed by the MS construct, within which all abundances must operate. If it is known by classification that a TAG is Case 1, then a $[DAG]^+$ is known to be the base peak, and, for a Type II TAG, the possibilities for the base peak are narrowed down to two: (i) $[AB]^+$ is larger than $[AA]^+$, and so $[AB]^+$ is the base peak and has an abundance of 100%; or (ii) $[AA]^+$ is larger than $[AB]^+$, and so $[AA]^+$ is the base peak and has an abundance of 100%. In the first case, $[AB]^+$ is larger than $[AA]^+$, and so $[AB]^+$ is 100%, or is 1.00 as a pure ratio; thus, since $[AB]^+ = 1$, $[AA]^+/[AB]^+$ becomes equal to $[AA]^+/(1)$, and so $[AA]^+ = [AA]^+/[AB]^+$. In this case, the sum of the $[DAG]^+$ fragment ions is $[AB]^+ + [AA]^+ = (1.0000 + [AA]^+/[AB]^+)$. This may be summarized as:

$$\Sigma[DAG]^+(\text{ratio}) = \left(1.0000 + \frac{[AA]^+}{[AB]^+}\right) \quad or \quad \Sigma[DAG]^+(\%) = \left(1.0000 + \frac{[AA]^+}{[AB]^+}\right)x100$$

For instance, in the case of OOP, Table 2 gives an $[AA]^+/[AB]^+$ ratio of 0.3612, and since this value is less than 1, it is classified as Case 3. Along with the knowledge of the fact that there is a $[DAG]^+$ base peak, from classifying the $[MH]^+/\Sigma[DAG]^+$ ratio as Case 1, a Case 1.3 solution is dictated. In this case, $[AB]^+ = 100\%$, and so $[AA]^+ = ([AA]^+/[AB]^+) \times 100 = 0.3612 \times 100 = 36.12\%$. Then the sum of the $[DAG]^+$ ions is $1.0000 + 0.3612 = 1.3612$ as a ratio, or 136.12% as percent abundance.

On the other hand, if the ratio $[AA]^+/[AB]^+$ is greater than 1, and so is a Case 1.4 solution, then $[AA]^+$ is the base peak and has an abundance of 100% (= 1.0000). Then, since $[AA]^+ = 1$, $[AB]^+ = (1/[AA]^+/[AB]^+)) = (1/(1)/[AB]^+))$. This may be summarized as follows:

$$\Sigma[DAG]^+(\text{ratio}) = \left(1.0000 + \frac{1}{\frac{[AA]^+}{[AB]^+}}\right) \quad or \quad \Sigma[DAG]^+(\%) = \left(1.0000 + \frac{1}{\frac{[AA]^+}{[AB]^+}}\right)x100$$

Of course, since loss of the B chain in an **ABA** TAG is energetically disfavored, the $[sn\text{-}1\text{-}AA]^+$ fragment is expected and is normally observed to have a low abundance. It is most often observed as a ratio that is not only less than 1, but is often less than the 0.5 that is statistically expected. And so an $[AA]^+/[AB]^+$ ratio greater than 1 normally provides a piece of information, which is that there is a strong nonstatistical influence. This influence may be due to a structural characteristic of the FA (amount and location of unsaturation), which renders the $sn\text{-}2$ FA easily lost and gives an $[AA]^+/[AB]^+$ ratio that is larger than expected. Other nonstatistical influences may be involved that have not yet been elucidated.

To summarize the two preceding pairs of equations, if the Type II TAG is Case 1, then one of the $[DAG]^+$, $[AA]^+$ or $[AB]^+$, would be 1.00, and the sum of the $[DAG]^+$ fragment ions could be calculated as one of either of two possibilities:

$$\Sigma[DAG]^+ = \Sigma([AA]^+ + [AB]^+) = \left\{ 1 + \frac{[AA]^+}{[AB]^+} \quad or \quad 1 + \frac{1}{\frac{[AA]^+}{[AB]^+}} \right\}$$
$$\text{Case 3} \qquad\qquad \text{Case 4}$$

On the other hand, if the $[MH]^+/\Sigma[DAG]^+$ ratio is greater than the Critical Limit, then it would be a Case 2 solution, and the $[M + H]^+$ is the base peak. The equations for the $[AA]^+$ and $[AB]^+$ percent relative abundances would then be calculated using the inverses of the preceding two equations. These equations appear in the denominator of the Case 2 solutions. Likewise, these equations for the $\Sigma[DAG]^+$ appear as the denominator of the Critical Limit for a Type II TAG. At this Critical Limit, one of the $[DAG]^+$ fragment ions is 100%, or 1.00, and the other is less than 100%, based on its proper proportion, as given by either the $[AA]^+/[AB]^+$ ratio (Case 3), or $1/([AA]^+/[AB]^+)$ (Case 4). At this Critical Limit, $[MH]^+$ is also 100%, because it is the numerator of the ratio, $[MH]^+/\Sigma[DAG]^+$, for which this is the Critical Limit. The Critical Limit for a Type II TAG is pictured in the fifth (bottom) panel of Figure 2. In the hypothetical spectrum shown, one $[DAG]^+$ fragment is 1 and $[MH]^+$ is 1. From this point, if the $[MH]^+$ were to decrease by the least amount, the $[DAG]^+$ would be the base peak, whereas if the $[DAG]^+$ were to decrease by the least amount, the $[MH]^+$ would be the base peak. Hence, based on a particular $[AA]^+/[AB]^+$ ratio, the Critical Limit is the point that determines whether $[MH]^+$ or a $[DAG]^+$ is the base peak. The Critical Limit, with $[MH]^+ = 1$ and a $[DAG]^+ = 1$, is shown in Figure 2 and can be summarized in this equation:

$$\left(\frac{[MH]^+}{\Sigma[DAG]^+}\right)_{\substack{Critical \\ Limit}} = \frac{1}{1 + \frac{[AA]^+}{[AB]^+}} \quad or \quad \frac{1}{1 + \frac{1}{\frac{[AA]^+}{[AB]^+}}}$$
$$\text{Case } n.3 \qquad\qquad \text{Case } n.4$$

The area bounded by the equation set in the BUS for a Type II TAG can be envisioned as the structure shown in Figure 3, where the primary vertical axis is the $[MH]^+/\Sigma[DAG]^+$ ratio. The axis needs only to go to 1 in the figure, since anything above 1 automatically means an $[MH]^+$ base peak, and then the $\Sigma[DAG]^+$ is given by $1/[MH]^+/\Sigma[DAG]^+$, the inverse of the $[MH]^+/\Sigma[DAG]^+$ ratio. The $[MH]^+/\Sigma[DAG]^+$ ratio for a Type
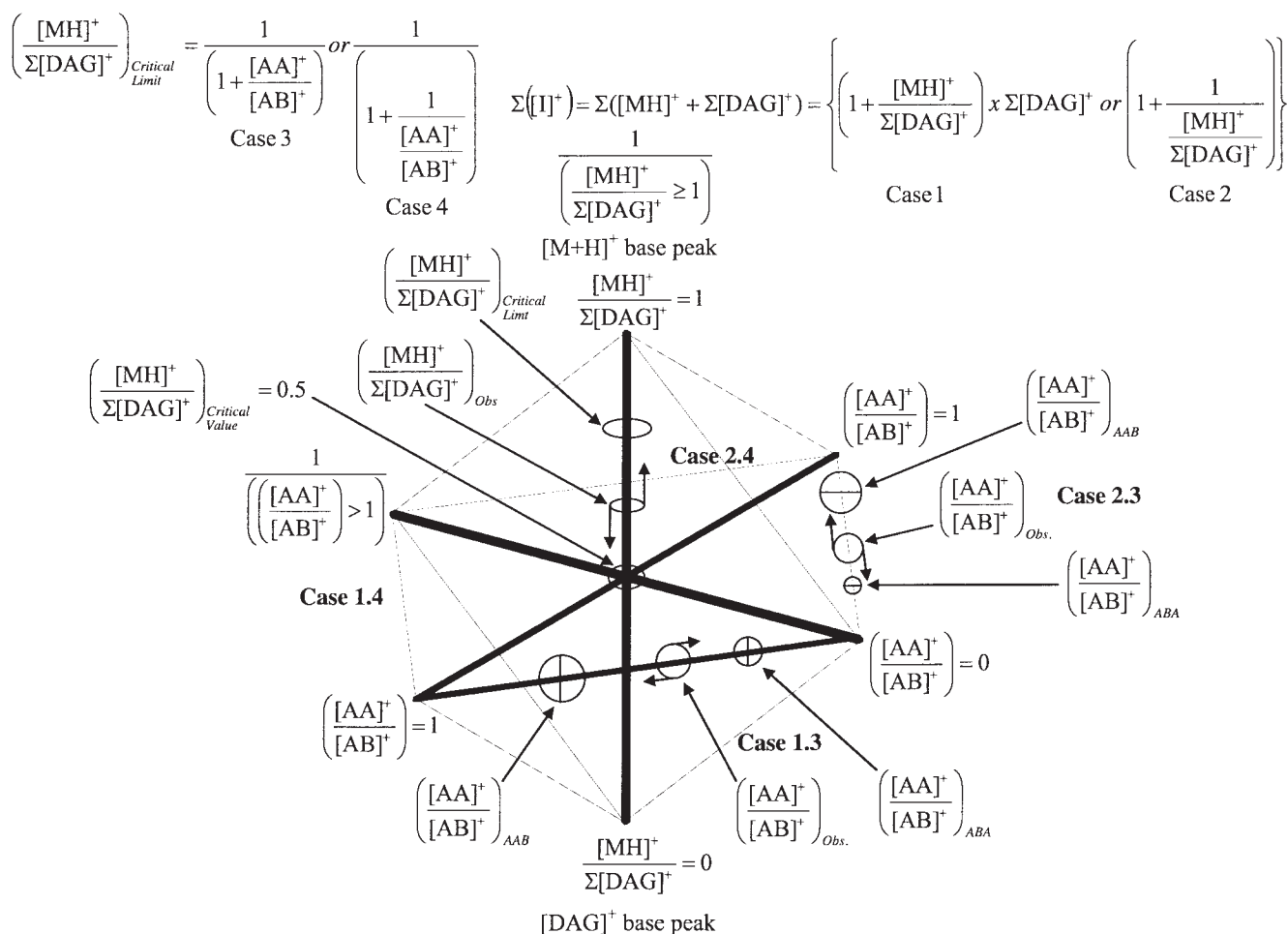
FIG. 3. The shape of the Triacylglycerol Lipidome for a Type II TAG. The Critical Value and the Critical Limit determine whether the [M + H]$^+$ or a [DAG]$^+$ fragment is the base peak. The [AA]$^+$/[AB]$^+$ ratio can be compared with regioisomeric standards for quantitative analysis of the amounts of regioisomers of calibrated TAG. The statistically expected value for the [AA]$^+$/[AB]$^+$ Critical Ratio = 1/2 = 0.5, Case 1.3 and Case 2.3, is not shown on the equatorial axis.

II TAG has an inherent Critical Value = 0.5, which is the minimum [MH]$^+$/Σ[DAG]$^+$ ratio that a TAG could have and still give an [MH]$^+$ base peak. This Critical Value of 0.5 is inherent in the MS construct pertaining to TAG. The Critical Value can be seen at the intersection of the vertical and equatorial axes in Figure 3. At the Critical Value, both of the [DAG]$^+$ were set to 100% to calculate the minimum possible [MH]$^+$/Σ[DAG]$^+$ ratio that could possibly give an [MH]$^+$ base peak. In real circumstances, [AA]$^+$ and [AB]$^+$ are rarely both equal to 100%, as they are at the theoretical Critical Value. In the rare case where [AA]$^+$ exactly equals [AB]$^+$ (whether 100% or not), either Case 3 or Case 4 could be used for the solution. The "less than" sign is used for Cases 1, 3, and 5, to produce a decision, but at the Critical Values and Critical Limits both Cases are equal.

The Critical Limit for a Type II TAG occurs when the larger of the two [DAG]$^+$ fragment ions is set to 100%, and the [MH]$^+$ is set to 100%, such that a decrease in either value will determine the base peak. The Critical Limit is based on the maximum hy-

pothetical Σ[DAG]$^+$ that could be obtained by an observed [AA]$^+$/[AB]$^+$ ratio. In real circumstances, the [AA]$^+$/[AB]$^+$ ratio that is observed is often less than the statistically expected value of 0.5, because of the trends already discussed regarding formation of the [sn-1,3-AA]$^+$ fragment in the APCI-MS source. For instance, the Critical Limit for the Type II TAG OPO/OOP can be calculated using the [AA]$^+$/[AB]$^+$ ratio of 0.3612 from Table 2, as follows: *Critical Limit* = 1/(1 + 0.3612) = 1/1.3612 = 0.7346. Of course, in the case of OPO/OOP, the [MH]$^+$/Σ[DAG]$^+$ could be seen to be less than the Critical Value of 0.5, so construction of the Critical Limit would not be necessary to classify it as Case 1, if classifying it manually. In contrast, if the observed [MH]$^+$/Σ[DAG]$^+$ ratio is greater than or equal to the Critical Limit, then it is Case 2, so the [MH]$^+$ is equal to 100%. For instance, the Critical Limit for the Type II TAG LnSLn/LnLnS can be calculated using the [AA]$^+$/[AB]$^+$ ratio of 0.9510 from Table 2 as follows: *Critical Limit* = 1/(1 + 0.9510) = 0.5126. This Critical Limit for LnSLn/LnLnS is seen in Table 3. The observed [MH]$^+$/Σ[DAG]$^+$ ratio from this TAG, given in

TABLE 3
Calculated Critical Values and Critical Limits[a] Used with the Bottom-Up Solution to Calculate Ion Abundances from Critical Ratios Determined by APCI-MS

TAG	Critical Value	Critical Limit 1	Critical Limit 2	Case		
PPP	1.00			1		
SSS	1.00			1		
OOO	1.00			1		
LLL	1.00			2		
LnLnLn	1.00			2		
PSP/PPS	0.50	67.00		1	3	
POP/PPO	0.50	60.50		1	3	
PLP/PPL	0.50	54.32		1	3	
PLnP/PPLn	0.50	58.84		1	3	
SPS/SSP	0.50	70.97		1	3	
SOS/SSO	0.50	57.10		1	3	
SLS/SSL	0.50	54.68		1	3	
SLnS/SSLn	0.50	62.12		1	3	
OPO/OOP	0.50	73.46		1	3	
OSO/OOS	0.50	71.52		1	3	
OLO/OOL	0.50	66.62		1	3	
OLnO/OOLn	0.50	70.61		1	3	
LPL/LLP	0.50	52.95		1	3	
LSL/LLS	0.50	56.80		1	3	
LOL/LLO	0.50	57.27		1	3	
LLnL/LLLn	0.50	65.80		2	3	
LnPLn/LnLnP	0.50	57.24		2	3	
LnSLn/LnLnS	0.50	51.26		2	3	
LnOLn/LnLnO	0.50	54.41		2	3	
LnLLn/LnLnL	0.50	60.95		2	3	
OPS	0.33	42.79	58.90	1	3	5
SPL	0.33	46.33	62.72	1	3	5
SPLn	0.33	40.49	56.59	1	3	5
LOP	0.33	35.93	50.44	1	3	5
LnOP	0.33	36.72	52.15	1	3	5
LnLP	0.33	42.19	57.68	2	3	5
LOS	0.33	37.43	53.85	1	3	5
OLnS	0.33	37.03	52.76	1	3	5
LnLS	0.33	40.39	56.00	2	3	5
LLnO	0.33	40.15	56.29	2	3	5

[a]The Critical Limit is given as a percentage to two decimal places but is used as a pure ratio. For abbreviations see Table 1.

Table 2, is 0.6131. Since the observed $[MH]^+/\Sigma[DAG]^+$ ratio is greater than the Critical Limit, it is classified as Case 2, and this ratio indicates that this TAG gave an $[MH]^+$ base peak. The $[DAG]^+$ abundances then are calculated using the Case 2.3 equations given in the BUS. The Critical Limit is seen as the upper circular limit on the main axis in Figure 3.

Two notes must be considered regarding the Critical Limit for a Type II TAG: First, in the automated spreadsheet implementation given below, only the Critical Limit is calculated and used, because it is sufficient to classify Case 1 or 2. The Critical Value for a Type II TAG is not required in the automated implementation. Second, in the rare case where the $[MH]^+/\Sigma[DAG]^+$ ratio exactly equals the Critical Limit, either a Case 1 or a Case 2 solution may be used.

During the process of calculating the Critical Limit and classifying the base peak as Case 1 or Case 2, the identity of Case 3 or Case 4 is found. For Case 1.n, when Case 3 or 4 is known, the $\Sigma[DAG]^+$ can be calculated using the Critical Ratio $[AA]^+/[AB]^+$

or its inverse, $1/[AA]^+/[AB]^+$. For all Cases, the observed $([AA]^+/[AB]^+)_{Obs}$ ratio of the sample can be compared with the $[AA]^+/[AB]^+$ ratios of regiospecific standards through Equations 3 and 4 above. The linear interpolation of the $([AA]^+/[AB]^+)_{Obs}$ ratio, between the $[AA]^+/[AB]^+$ ratios of standards, $([AA]^+/[AB]^+)_{ABA}$ and $([AA]^+/[AB]^+)_{AAB}$, is depicted on the equatorial lines in Figure 3. The circles around the equatorial lines represent the $([AA]^+/[AB]^+)_{Obs}$ ratios of pure regioisomeric standards, such as those given in Table 1. Figure 3 shows $([AA]^+/[AB]^+)_{Obs}$ ratios between 0 and 1, which is the most common case. This is the Case 1.3 or Case 2.3 solution. The BUS works equally well for $([AA]^+/[AB]^+)_{Obs}$ ratios greater than 1, and those instances give a Case 1.4 or Case 2.4 solution. The BUS does not depend on the linear interpolation given by Equations 3 or 4. The use of the $([AA]^+/[AB]^+)_{Obs}$ ratio for calculation of the regioisomeric composition is separate from the BUS.

The equations in the BUS can be demonstrated using the data from the synthetic mixture of 35 TAG made from five FA

II) 'AAB/ABA' TAG   Critical value = 0.5

Case 1.0 $\Sigma[DAG]^+$ $[MH]^+$

Case 2.0 $[MH]^+$ $\Sigma[DAG]^+$

Case 3 $[AB]^+$ $[AA]^+$

Case 4 $[AA]^+$ $[AB]^+$

$$\left(\frac{[MH]^+}{\sum[DAG]^+}\right) \overset{?}{<} 1$$

N   **Y**

Case 2.0
% [M+H]⁺ = 100 % (base peak) $\overset{Y}{\longleftarrow}$ $\left(\dfrac{[MH]^+}{\sum[DAG]^+}\right) \overset{?}{\geq} Critical\ Limit$ $\overset{Y}{\longleftarrow}$ $\left(\dfrac{[MH]^+}{\sum[DAG]^+}\right) \overset{?}{\geq} Critical\ Value$

if $\left(\dfrac{[AA]^+}{[AB]^+}\right) < 1.0$ (usual):

$Limit = \dfrac{1}{1+\left(\dfrac{[AA]^+}{[AB]^+}\right)}$ **Case n.3**

if $\left(\dfrac{[AA]^+}{[AB]^+}\right) \geq 1.0$ (unusual)[†]:

$Limit = \dfrac{1}{1+\left(\dfrac{1}{\dfrac{[AA]^+}{[AB]^+}}\right)}$ **Case n.4**

[†]Implies strong [AA]⁺ preference or large difference in FA unsat.

N   **N**

Case 1.0
a [DAG]⁺ = 100 % (base peak)

$\left(\dfrac{[AA]^+}{[AB]^+}\right) \overset{?}{<} 1.0$ (usual) $\overset{Y}{\longrightarrow}$ **Case 1.3**

% [AB]⁺ = 100 % (base peak)

$\% [AA]^+ = \left(\dfrac{[AA]^+}{[AB]^+}\right) x 100$

$\% [M+H]^+ = \left(\dfrac{[MH]^+}{\sum[DAG]^+}\right)\left(1+\dfrac{[AA]^+}{[AB]^+}\right) x 100$

Case 2.0
% [M+H]⁺ = 100 % (base peak)

$\left(\dfrac{[AA]^+}{[AB]^+}\right) \overset{?}{<} 1.0$ (usual) $\overset{Y}{\longrightarrow}$ **Case 2.3** $[AA]^+ < [AB]^+$

N[†]

Case 2.4[†]
$[AA]^+ \geq [AB]^+$

Same for Both Cases:

$\%[AB]^+ = \dfrac{1}{\left(\dfrac{[MH]^+}{\sum[DAG]^+}\right)\left(1+\left(\dfrac{[AA]^+}{[AB]^+}\right)\right)} x 100$

$\%[AA]^+ = \dfrac{1}{\left(\dfrac{[MH]^+}{\sum[DAG]^+}\right)\left(1+\dfrac{1}{\dfrac{[AA]^+}{[AB]^+}}\right)} x 100$

N[†]

Case 1.4[†]
% [AA]⁺ = 100 % (base peak)

$\%[AB]^+ = \dfrac{1}{\left(\dfrac{[AA]^+}{[AB]^+}\right)} x 100$

$\% [M+H]^+ = \left(\dfrac{[MH]^+}{\sum[DAG]^+}\right)\left(1+\dfrac{1}{\dfrac{[AA]^+}{[AB]^+}}\right) x 100$

SCHEME 1, PART II. Equations to calculate the relative abundances of the $[M + H]^+$ and $[DAG]^+$ fragment ions for ABA/AAB TAG using Critical Ratios from APCI-MS data (Table 2). For abbreviation see Scheme 1, Part I.

randomly distributed among the three positions on the glycerol backbone, given in Table 2. For example, this synthetic mixture contains oleic, palmitic, linoleic, linolenic, and stearic acids, so the TAG made from these FA include POP, for which standards of pure regioisomers have been run on the same instrument, as given in Table 1. The Type II TAG POP/PPO from the synthetic mixture gave the $([AA]^+/[AB]^+)_{Obs}$ ratio of 0.6528 in Table 2, as a pure ratio, and an $[MH]^+/\Sigma[DAG]^+$ ratio of

0.0055, as a pure ratio. These ratios are processed through the BUS, Scheme 1, Part II, as follows: the $[MH]^+/\Sigma[DAG]^+$ ratio is less than 1 and is also less than the Critical Value of 0.5. This allows classification of the solution for this TAG as being a Case 1 solution. There is no need to construct the Critical Limit, because the $[MH]^+/\Sigma[DAG]^+$ ratio is less than the Critical Value. Nevertheless, the Critical Limit can still be calculated as an example. For instance, the $([AA]^+/[AB]^+)_{Obs}$ ratio

of 0.6528 for POP/PPO in Table 1 is less than 1, so it indicates a case *n*.3 solution. The Critical Limit can be calculated as:

$$\left(\frac{[MH]^+}{\Sigma[DAG]^+}\right)_{\substack{Critical \\ Limit}} = \frac{1}{1+\dfrac{[AA]^+}{[AB]^+}} = \frac{1}{1+0.6528} = 0.6050$$

As expected, the $[MH]^+/\Sigma[DAG]^+$ ratio is less than the Critical Limit, so the solution for this TAG is categorized as a Case 1.3 solution. The Case 1.3 solution indicates that $[AB]^+$ is the base peak, equaling 100%, and the percent $[AA]^+$ is given as $[AA]^+ = (([AA]^+/[AB]^+)_{Obs} \times 100)$ ratio, or $0.6528 \times 100 = 65.28\%$. Finally, the $[MH]^+$ is calculated as $[MH]^+ (\%) = ([MH]^+/\Sigma[DAG]^+) \times (1 + 1/([AA]^+/[AB]^+)_{Obs}) \times 100 = (0.0055)(1 + 0.6528) \times 100 = 0.91\%$ abundance. This abundance is seen in the tabulated mass spectral data in Table 4. This small abundance is exactly as expected from a TAG with only one site of unsaturation. It can be seen from this example that the three abundances that make up the mass spectrum can be calculated from only the two Critical Ratios. Other example solutions are shown below.

As these examples demonstrate, the two Critical Ratios for a Type II TAG can be used to calculate the three abundances of the ions in the mass spectrum. Then the second Critical Ratio may also provide information regarding the percentage composition of regioisomers in the mixture. When the $([AA]^+/[AB]^+)_{Obs}$ ratio of 0.6528 for POP/PPO from the synthetic TAG mixture is inserted into Equation 3, with the ratios $([AA]^+/[AB]^+)_{ABA} = 0.29$ and $([AA]^+/[AB]^+)_{AAB} = 0.87$ for the pure regioisomeric standards from Table 1 [based on the report of Byrdwell and Neff (43)], the calculated % ABA is given as:

$$\%ABA = \frac{\left(\dfrac{[AA]^+}{[AB]^+}\right)_{AAB} - \left(\dfrac{[AA]^+}{[AB]^+}\right)_{Obs}}{\left(\dfrac{[AA]^+}{[AB]^+}\right)_{AAB} - \left(\dfrac{[AA]^+}{[AB]^+}\right)_{ABA}} x100 = \frac{0.87 - 0.6528}{0.87 - 0.29} x100 = 37.45\%$$
$$\text{from}$$
$$\text{Table 1}$$

This calculation indicates that the mixture appears to contain 37.45% POP. Since the FA in this mixture are statistically distributed among all possible positions on the glycerol backbone, the POP isomer would be expected to be present in an amount equal to one-third, or 33%, with PPO and OPP making up the other two-thirds. This synthetic mixture had previously been subjected to lipase hydrolysis, and it was determined that the FA were approximately statistically distributed (7), so it is not surprising that the $[AA]^+/[AB]^+)_{Obs}$ ratio for the POP in the synthetic mixture gives a percentage that is close to the expected value of 33%, even using tabulated values for regioisomeric standards. It must be noted that the tabulated values were obtained on the same instrument. Of course, when accurate quantification is sought, fresh standards should be analyzed. From the preceding discussion and examples below, one can see that, by using the Critical Ratios, the BUS provides the abundances that make up the mass spectrum, and one of the Critical Ratios may provide additional information regarding the composition of regioisomers.

The BUS for a Type III TAG. As already discussed, Type II TAG have a Critical Value and a Critical Limit for the $[MH]^+/\Sigma[DAG]^+$ ratio, which determine the identity of the base peak. Also, the number 1 serves as the Critical Value for the $[AA]^+/[AB]^+$ ratio to determine whether $[AA]^+$ or $[AB]^+$ is larger. Type III TAG have a Critical Value and a Critical Limit for the $[MH]^+/\Sigma[DAG]^+$ ratio, and a Critical Value and

TABLE 4
Spreadsheet Formulas for the Implementation of the Bottom-Up Solution[a]

The spreadsheet formulas, listed by TAG type, are as follows:

Type I:
$[MH]^+$: = IF(Q2=**1**,(E2),(100))
$[AA]^+$: = IF(Q2=**1**,(100),(100/(E2/100)))

Type II:
$[MH]^+$: = IF(Q7=**1**,(IF(R7=**3**,(E7*(1+(G7/100))),(E7*(1+(100/G7))))),(100))
$[AA]^+$: = IF(Q7=**1**,IF(R7=**3**,G7,100),(100/((E7/100)*(1+(1/(G7/100))))))
$[AB]^+$: = IF(Q7=**1**,IF(R7=**3**,100,G7),(100/((E7/100)*(1+(G7/100)))))

Type III:
$[MH]^+$: = IF(Q27=**1**,IF(R27=**3**,(IF(S27=**5**,(E27*(1+(G27/100))*(1+(I27/100))),(E27*(1+(G27/100))*(1+(100/I27))))),(E27*(1+(100/G27)))),100)
$[AC]^+$: = IF(Q27=**1**,IF(R27=**3**,(IF(S27=**5**,(G27*(1+(I27/100))),(G27*(1+(100/I27))))),(100)),(100/((E27/100)*(1+(100/G27)))))
$[AB]^+$: = IF(Q27=**1**,(IF(R27=**3**,(IF(S27=**5**,(100),(100/(I27/100)))),(1/((G27/100)*(1+(I27/100)))))),(100/((E27/100)*(1+(G27/100))*(1+(I27/100)))))
$[BC]^+$: = IF(Q27=**1**,(IF(R27=**3**,(IF(S27=**5**,((I27/100)*100),(100))),(1/((G27/100)*(1+(100/I27)))))),(100/((E27/100)*(1+(G27/100))*(1+(100/I27)))))

[a]Assume the columns in Table 2 were labeled A through J, and the rows were numbered from 1 to 37; then the Critical Ratios would be in columns E, G, and I, and the data would be in rows 2 to 36. Imagine the Case classification in Table 3 is in columns Q, R, and S, with the same rows as Table 2.
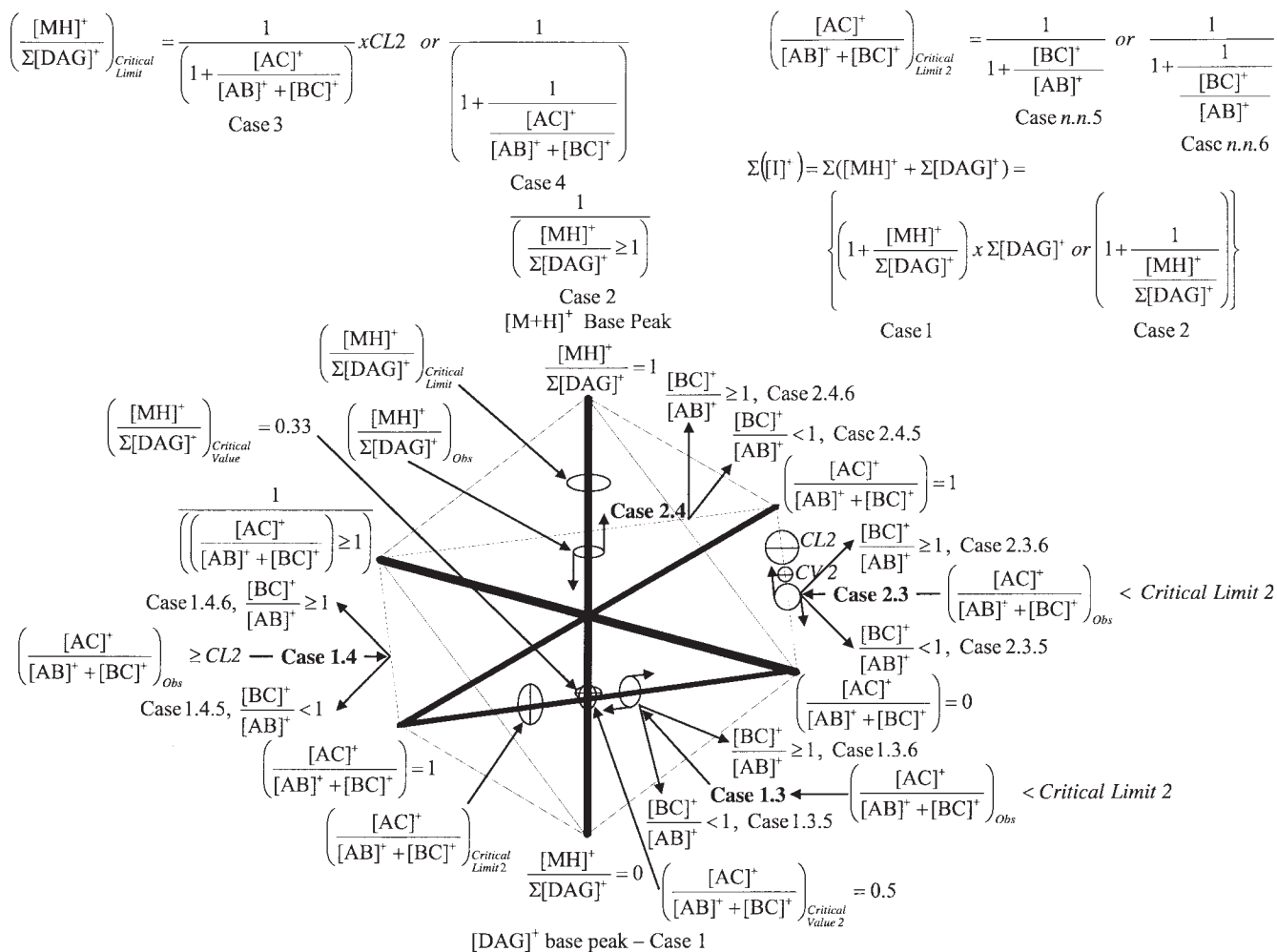
$$\left(\frac{[MH]^+}{\Sigma[DAG]^+}\right)_{\substack{Critical \\ Limit}} = \frac{1}{\left(1 + \frac{[AC]^+}{[AB]^+ + [BC]^+}\right)} x CL2 \quad or \quad \frac{1}{\left(1 + \frac{1}{\frac{[AC]^+}{[AB]^+ + [BC]^+}}\right)}$$

Case 3   Case 4

$$\left(\frac{[AC]^+}{[AB]^+ + [BC]^+}\right)_{\substack{Critical \\ Limit\ 2}} = \frac{1}{1 + \frac{[BC]^+}{[AB]^+}} \quad or \quad \frac{1}{1 + \frac{1}{\frac{[BC]^+}{[AB]^+}}}$$

Case n.n.5   Case n.n.6

$$\frac{1}{\left(\frac{[MH]^+}{\Sigma[DAG]^+} \geq 1\right)}$$

Case 2
[M+H]$^+$ Base Peak

$$\Sigma([I]^+) = \Sigma([MH]^+ + \Sigma[DAG]^+) =$$

$$\left\{ \left(1 + \frac{[MH]^+}{\Sigma[DAG]^+}\right) x \Sigma[DAG]^+ \quad or \quad \left(1 + \frac{1}{\frac{[MH]^+}{\Sigma[DAG]^+}}\right) \right\}$$

Case 1   Case 2

FIG. 4. The Shape of the Triacylglycerol Lipidome for a Type III TAG.

a Critical Limit for the $[AC]^+/([AB]^+ + [BC]^+)$ ratio, and the value 1 serves as the Critical Value for the $[BC]^+/[AB]^+$ ratio.

The first Critical Value for a Type III TAG is the Critical Value for the $[MH]^+/\Sigma[DAG]^+$ ratio, based on all ions being equal to 1. The Critical Value for the $[MH]^+/\Sigma[DAG]^+$ ratio of a Type III TAG is depicted in the right side of the fourth panel down in Figure 2. The Critical Value of the $[MH]^+/\Sigma[DAG]^+$ ratio for an ABC TAG is 1/3, or 0.33, as shown in Figure 2. A TAG with an $[MH]^+/\Sigma[DAG]^+$ ratio less than the Critical Value cannot have a protonated molecule base peak. The Critical Value for the $[MH]^+/\Sigma[DAG]^+$ ratio is depicted as the lower horizontal ring on the vertical axis in Figure 4. The Critical Values of TAG are inherent values based on the definition of the scale (= 100%) and do not depend on a particular Critical Ratio. An $[MH]^+/\Sigma[DAG]^+$ ratio greater than the Critical Value does not immediately indicate a protonated molecule base peak. The Critical Ratio must be further tested with another limit to determine whether the $[M + H]^+$ is the base peak. As with Type II TAG, the Critical Value serves as the lower limit for the possibility of having a protonated molecule base peak. The $[MH]^+/\Sigma[DAG]^+$ ratio may be above the Critical Value, yet still

not be the base peak, since the Critical Value is based on all $[DAG]^+$ being at their maximum values, which is not usually the case. A Critical Limit, on the other hand, is based on observed Critical Ratios from data. Critical Limits used for Type III TAG, including the limit of the $[MH]^+/\Sigma[DAG]^+$ ratio that defines whether the $[M + H]^+$ is the base peak, are discussed below.

(i) Critical Limit 1 for a Type III TAG. Critical Limit 1 is used to determine whether the $[M + H]^+$ or a $[DAG]^+$ fragment ion is the base peak. Just as the $[AA]^+/[AB]^+$ ratio for a Type II TAG was used to calculate the Critical Limit for a Type II TAG, the $[AC]^+/([AB]^+ + [BC]^+)$ ratio is used in an analogous way to calculate Critical Limit 1 for a Type III TAG. The $[AC]^+/([AB]^+ + [BC]^+)$ ratio is similar to the $[AA]^+/[AB]^+$ ratio in another way, which is that both have a statistically expected value of 0.5. The $[AC]^+$ fragment is one of three possible $[DAG]^+$ fragments, and is taken as a ratio to the other two, so the ratio $[AC]^+/([AB]^+ + [BC]^+)$ has a statistically expected value of 1/2, or 0.5. Also in an analogous way, the $[AC]^+/([AB]^+ + [BC]^+)$ ratio defines the Case 3 and Case 4 possibilities for a Type III TAG, as the $[AA]^+/[AB]^+$ ratio did for

A)

$$\frac{[MH]^+}{\sum[DAG]^+} = \frac{100}{95} = \frac{20}{19}$$

$$\frac{[AA]^+}{[AB]^+} = \frac{40}{55} = \frac{8}{11}$$

e.g.- LnPLn/LnLnP

$$\frac{[MH]^+}{\sum[DAG]^+} > 1, \quad \text{so} \ [MH]^+ = 100\% \ \text{and Case } \mathbf{2}.n$$

$$\text{Critical Limit} = \frac{1}{1+\frac{8}{11}} = \frac{1}{\frac{19}{11}} = \frac{11}{19} = 0.579$$

$$\left(\text{Not Used since} \ \frac{[MH]^+}{\sum[DAG]^+} > 1\right)$$

$$\frac{[AA]^+}{[AB]^+} < 1, \ \text{so Case } 2.\mathbf{3}$$

Case 2.3

$$\%[AB]^+ = \frac{1}{\left(\frac{20}{19}\right)\left(1+\frac{8}{11}\right)} \times 100 = \frac{1}{\left(\frac{20}{19}\right)\left(\frac{19}{11}\right)} \times 100 = \frac{1}{\frac{20}{11}} \times 100 = \frac{11}{20} \times 100 = 11 \times 5 = 55\%$$

$$\%[AA] = \frac{1}{\left(\frac{20}{19}\right)\left(1+\frac{1}{\frac{8}{11}}\right)} \times 100 = \frac{1}{\left(\frac{20}{19}\right)\left(1+\frac{11}{8}\right)} \times 100 = \frac{1}{\left(\frac{20}{19}\right)\left(\frac{19}{8}\right)} \times 100 = \frac{1}{\frac{20}{8}} \times 100 = \frac{8}{20} \times 100 = 8 \times 5 = 40\%$$

B)

$$\frac{[MH]^+}{\sum[DAG]^+} = \frac{100}{145} = \frac{20}{29}$$

$$\frac{[AA]^+}{[AB]^+} = \frac{75}{70} = \frac{15}{14}$$

$$\text{Critical Limit} = \frac{1}{1+\left(\frac{1}{\frac{15}{14}}\right)} = \frac{1}{1+\frac{14}{15}} = \frac{1}{\frac{29}{15}} = \frac{15}{29} = .517$$

$$\frac{[MH]^+}{\sum[DAG]^+}\left(=\frac{20}{29}\right) \geq \text{Critical Limit}\left(=\frac{15}{29}\right),$$

$$\text{so} \ [M+H]^+ = 100\% \ \text{and Case } \mathbf{2}.n$$

$$\frac{[AA]^+}{[AB]^+} \geq 1, \ \text{so Case } 2.\mathbf{4}$$

Case 2.4

$$\%[AB]^+ = \frac{1}{\left(\frac{20}{29}\right)\left(1+\frac{15}{14}\right)} \times 100 = \frac{1}{\left(\frac{20}{29}\right)\left(\frac{29}{14}\right)} \times 100 = \frac{1}{\frac{20}{14}} \times 100 = \frac{14}{20} \times 100 = 14 \times 5 = 70\%$$

$$\%[AA]^+ = \frac{1}{\left(\frac{20}{29}\right)\left(1+\frac{1}{\frac{15}{14}}\right)} \times 100 = \frac{1}{\left(\frac{20}{29}\right)\left(1+\frac{14}{15}\right)} \times 100 = \frac{1}{\left(\frac{20}{29}\right)\left(\frac{29}{15}\right)} \times 100 = \frac{1}{\frac{20}{15}} \times 100 = \frac{15}{20} \times 100 = 15 \times 5 = 75\%$$

Continued

FIG. 5. Examples of the Bottom-Up Solution (BUS) to the Triacylglycerol Lipidome, using abundances to the nearest 5%.

the Type II TAG. Because of these similarities, the shape of the area bounded by the $[MH]^+/\Sigma[DAG]^+$ ratio and the $[AC]^+/([AB]^+ + [BC]^+)$ ratio, which are the first two Critical Ratios for a Type III TAG, is similar to the shape of the Type II TAG Lipidome pictured in Figure 3. In the diagram of the shape of the Lipidome for a Type III TAG, the $[AC]^+/([AB]^+ +$

$[BC]^+)$ ratio is on the equatorial axis instead of the $[AA]^+/[AB]^+$ ratio, as shown in Figure 4.

The $[AC]^+/([AB]^+ + [BC]^+)$ ratio has a Critical Value of 0.5 that represents the minimum value that the ratio can have and still have an $[AC]^+$ abundance larger than or equal to the $[AB]^+$ and $[BC]^+$ abundances. If the $[AC]^+/([AB]^+ + [BC]^+)$ ratio has

C)

$$\frac{[MH]^+}{\sum[DAG]^+} = \frac{100}{200} = \frac{1}{2}$$

$$\frac{[AC]^+}{([AB]^+ + [BC]^+)} = \frac{55}{145} = \frac{11}{29}$$

$$\frac{[BC]^+}{[AB]^+} = \frac{60}{85} = \frac{12}{17}$$

e.g.- LnLP

$\frac{[BC]^+}{[AB]^+} < 1$, so Case *n.n.***5**

$$\text{Critical Limit 2} = \frac{1}{1 + \frac{12}{17}} = \frac{1}{\frac{29}{17}} = \frac{17}{29}$$

$\frac{[AC]^+}{([AB]^+ + [BC]^+)} < C_{L2}$, so Case *n.***3**.*n*

$$\text{Critical Limit 1} = \frac{1}{1 + \frac{11}{29}} x C_{L2} = \frac{1}{\frac{40}{29}} x \frac{17}{29} = \frac{29}{40} x \frac{17}{29} = \frac{17}{40}$$

$$\frac{[MH]^+}{\sum[DAG]^+} \overset{?}{\geq} CL1: \frac{1}{2} \overset{?}{\geq} \frac{17}{40}: \quad \text{YES, so Case } \mathbf{2}.n.n$$
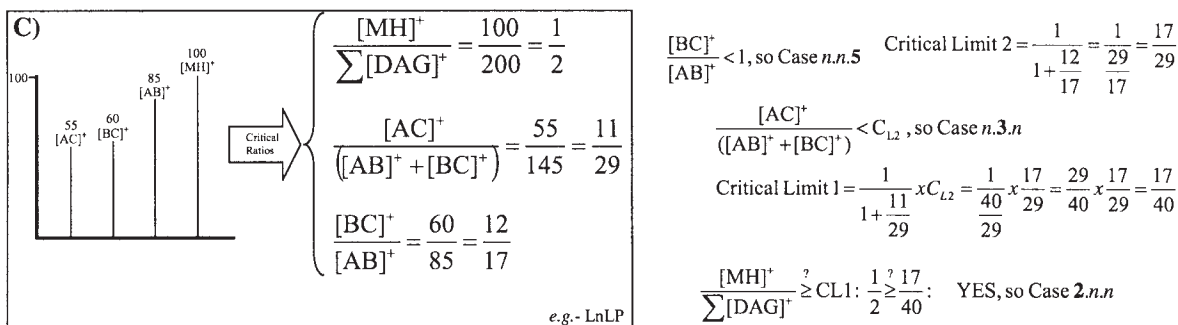
Therefore: Case 2.3.5

Case 2.3.5

Case 2, so [M+H]⁺ = 100 % (base peak)

$$\%[AC]^+ = \frac{1}{\left(\frac{1}{2}\right)\left(1 + \frac{1}{\frac{11}{29}}\right)} x100 = \frac{1}{\left(\frac{1}{2}\right)\left(1 + \frac{29}{11}\right)} x100 = \frac{1}{\left(\frac{1}{2}\right)\left(\frac{40}{11}\right)} x100 = \frac{1}{\frac{20}{11}} x100 = \frac{11}{20} x100 = 55\%$$

$$\%[AB]^+ = \frac{1}{\left(\frac{1}{2}\right)\left(1 + \frac{11}{29}\right)\left(1 + \frac{12}{17}\right)} x100 = \frac{1}{\left(\frac{1}{2}\right)\left(\frac{40}{29}\right)\left(\frac{29}{17}\right)} x100 = \frac{1}{\frac{40}{34}} x100 = \frac{17}{20} x100 = 17x5 = 85\%$$

$$\%[BC]^+ = \frac{1}{\left(\frac{1}{2}\right)\left(1 + \frac{11}{29}\right)\left(1 + \frac{1}{\frac{12}{17}}\right)} x100 = \frac{1}{\left(\frac{1}{2}\right)\left(\frac{40}{29}\right)\left(1 + \frac{17}{12}\right)} x100 = \frac{1}{\left(\frac{1}{2}\right)\left(\frac{40}{29}\right)\left(\frac{29}{12}\right)} x100 = \frac{1}{\frac{40}{24}} x100 = \frac{3}{5} x100 = 60\%$$

D)

$$\frac{[MH]^+}{\sum[DAG]^+} = \frac{20}{265} = \frac{4}{53}$$

$$\frac{[AC]^+}{([AB]^+ + [BC]^+)} = \frac{80}{185} = \frac{16}{37}$$

$$\frac{[BC]^+}{[AB]^+} = \frac{85}{100} = \frac{17}{20}$$

e.g.- LOS

$\frac{[BC]^+}{[AB]^+} < 1$, so Case *n.n.***5**

$$\text{Critical Limit 2} = \frac{1}{1 + \frac{17}{20}} = \frac{1}{\frac{37}{20}} = \frac{20}{37}$$

$\frac{[AC]^+}{([AB]^+ + [BC]^+)} < C_{L2}$, so Case *n.***3**.*n*

$$\text{Critical Limit 1} = \frac{1}{1 + \frac{16}{37}} x C_{L2} = \frac{1}{\frac{53}{37}} x \frac{20}{37} = \frac{37}{53} x \frac{20}{37} = \frac{20}{53}$$

$$\frac{[MH]^+}{\sum[DAG]^+} \overset{?}{\geq} CL1: \frac{4}{53} \overset{?}{\geq} \frac{20}{53}: \quad \text{NO, so Case } \mathbf{1}.n.n$$

Therefore: Case 1.3.5

Case 1.3.5

Case 1.3.5, so [AB]⁺ = 100 % (base peak)

$$\%[BC]^+ = \frac{17}{20} x100 = 17x5 = 85\%$$

$$\%[AC]^+ = \left(\frac{16}{37}\right)\left(1 + \frac{17}{20}\right)x100 = \left(\frac{16}{37}\right)\left(\frac{37}{20}\right)x100 = \frac{16}{20} x100 = 16x5 = 80\%$$

$$\%[MH]^+ = \left(\frac{4}{53}\right)\left(1 + \frac{16}{37}\right)\left(1 + \frac{17}{20}\right)x100 = \left(\frac{4}{53}\right)\left(\frac{53}{37}\right)\left(\frac{37}{20}\right)x100 = \frac{4}{20} x100 = 4x5 = 20\%$$

Continued

FIG. 5. (Continued)

E)

$$\frac{[MH]^+}{\sum[DAG]^+} = \frac{25}{250} = \frac{1}{10}$$

$$\frac{[AC]^+}{([AB]^+ + [BC]^+)} = \frac{70}{180} = \frac{7}{18}$$

$$\frac{[BC]^+}{[AB]^+} = \frac{100}{80} = \frac{5}{4}$$

$\frac{[BC]^+}{[AB]^+} > 1$, so Case $n.n.\mathbf{6}$ Critical Limit 2 $= \dfrac{1}{1+\dfrac{1}{\dfrac{5}{4}}} = \dfrac{1}{\dfrac{9}{5}} = \dfrac{5}{9}$

$\dfrac{[AC]^+}{([AB]^+ + [BC]^+)} < C_{L2}$, so Case $n.\mathbf{3}.n$

Critical Limit 1 $= \dfrac{1}{1+\dfrac{7}{18}} \times C_{L2} = \dfrac{1}{\dfrac{25}{18}} \times \dfrac{5}{9} = \dfrac{18}{25} \times \dfrac{5}{9} = \dfrac{2}{5}$

$\dfrac{[MH]^+}{\sum[DAG]^+} \overset{?}{\geq} CL1: \quad \dfrac{1}{10} \overset{?}{\geq} \dfrac{2}{5}: \quad$ NO, so Case $\mathbf{1}.n.n$
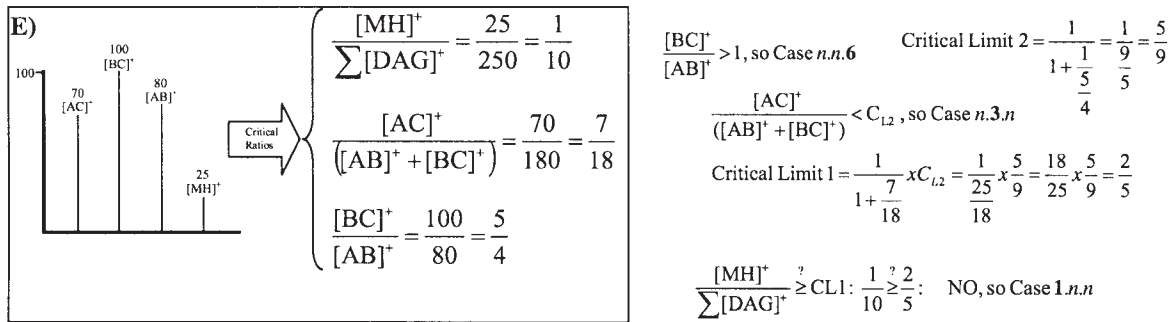
Therefore: Case 1.3.6

Case 1.3.6

Case 1.3.6, so $[BC]^+ = 100\,\%$ (base peak)

$$\%[AB]^+ = \frac{1}{\left(\dfrac{5}{4}\right)} x100 = \frac{4}{5} x100 = 4 x 20 = 80\%$$

$$\%[AC]^+ = \left(\frac{7}{18}\right)\left(1+\frac{1}{\dfrac{5}{4}}\right) x100 = \left(\frac{7}{18}\right)\left(\frac{9}{5}\right) x100 = \frac{7}{10} x100 = 70\%$$

$$\%[M+H]^+ = \left(\frac{1}{10}\right)\left(1+\frac{7}{18}\right)\left(1+\frac{1}{\dfrac{5}{4}}\right) x100 = \left(\frac{1}{10}\right)\left(\frac{25}{18}\right)\left(\frac{9}{5}\right) x100 = \frac{5}{20} x100 = 5 x 5 = 25\%$$

F)

$$\frac{[MH]^+}{\sum[DAG]^+} = \frac{70}{270} = \frac{7}{27}$$

$$\frac{[AC]^+}{([AB]^+ + [BC]^+)} = \frac{100}{170} = \frac{10}{17}$$

$$\frac{[BC]^+}{[AB]^+} = \frac{90}{80} = \frac{9}{8}$$

$\frac{[BC]^+}{[AB]^+} > 1$, so Case $n.n.\mathbf{6}$ Critical Limit 2 $= \dfrac{1}{1+\dfrac{1}{\dfrac{9}{8}}} = \dfrac{1}{\dfrac{17}{9}} = \dfrac{9}{17}$

$\dfrac{[AC]^+}{([AB]^+ + [BC]^+)} > C_{L2}$, so Case $n.\mathbf{4}.n$

Critical Limit 1 $= \dfrac{1}{1+\dfrac{1}{\left(\dfrac{10}{17}\right)}} = \dfrac{1}{\dfrac{27}{10}} = \dfrac{10}{27}$

$\dfrac{[MH]^+}{\sum[DAG]^+} \overset{?}{\geq} CL1: \quad \dfrac{7}{27} \overset{?}{\geq} \dfrac{10}{27}: \quad$ NO, so Case $\mathbf{1}.n.n$
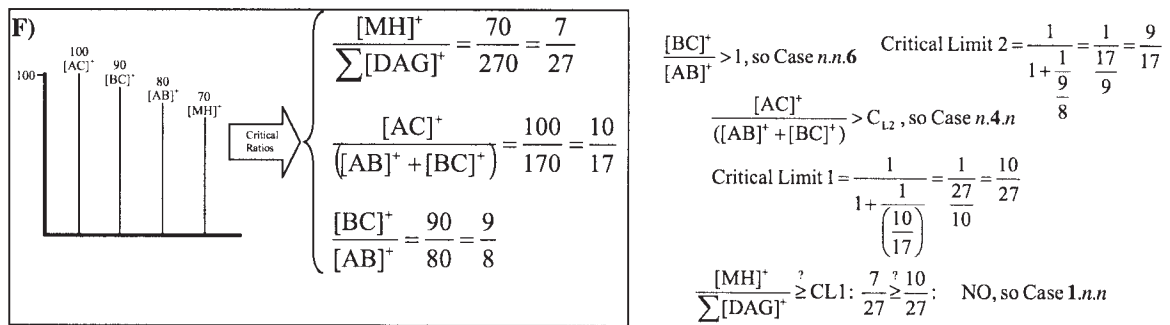
Therefore: Case 1.4.6

Case 1.4.6

Case 1.**4**.n, so $[AC]^+ = 100\,\%$ (base peak)

$$\%[M+H]^+ = \left(\frac{7}{27}\right)\left(1+\frac{1}{\dfrac{10}{17}}\right) x100 = \left(\frac{7}{27}\right)\left(\frac{27}{10}\right) x100 = \frac{7}{10} x100 = 70\%$$

$$\%[AB]^+ = \frac{1}{\left(\dfrac{10}{17}\right)\left(1+\dfrac{9}{8}\right)} x100 = \frac{1}{\left(\dfrac{10}{17}\right)\left(\dfrac{17}{8}\right)} x100 = \frac{1}{\dfrac{10}{8}} x100 = \frac{8}{10} x100 = 80\%$$

$$\%[BC]^+ = \frac{1}{\left(\dfrac{10}{17}\right)\left(1+\dfrac{1}{\dfrac{9}{8}}\right)} x100 = \frac{1}{\left(\dfrac{10}{17}\right)\left(\dfrac{17}{9}\right)} x100 = \frac{1}{\dfrac{10}{9}} x100 = \frac{9}{10} x100 = 90\%$$

FIG. 5. (Continued)

a value less than 0.5, then $[AC]^+$ must be smaller than $[AB]^+$ or $[BC]^+$, and so is a Case $n.3.n$ solution. Coincidentally, this second Critical Value for a Type III TAG also equals the statistically expected value of this Critical Ratio. The Critical Value of this Critical Ratio is seen in Scheme 1, Part III, and it is shown as Critical Value 2 on the equatorial axis in Figure 4.

If the ratio $[AC]^+/([AB]^+ + [BC]^+)$ is greater than 1, then $[AC]^+$ is automatically known to be larger than $[AB]^+$ and $[BC]^+$, and Critical Limit 1 can be constructed based only on $[AC]^+/([AB]^+ + [BC]^+)$. Furthermore, if $[AC]^+/([AB]^+ + [BC]^+)$ is greater than 1, this indicates a Case $n.4.n$ solution. For a Case $n.4.n$ solution, the value of Critical Limit 1 is given as:

$$\text{Critical Limit}\,1 = \frac{1}{1 + \frac{1}{\left(\frac{[AC]^+}{([AB]^+ + [BC]^+)}\right)}} \quad [7]$$

When the solution is classified as Case $n.4.n$ solution, $[AC]^+ = 100\%\ (= 1.00)$ at Critical Limit 1, because it is larger than $[AB]^+$ and $[BC]^+$, and so it is the peak against which the $[M + H]^+$ must be compared to determine the base peak. This is shown in the bottom panel of Figure 2.

When the $[AC]^+/([AB]^+ + [BC]^+)$ ratio is less than 1 but greater than 0.5, it must be compared with Critical Limit 2 to determine whether it is Case 3 or Case 4. The equation for Critical Limit 2 requires the use of the $[BC]^+/[AB]^+$ ratio, and so this ratio is first classified as either Case 5, in which the $[BC]^+/[AB]^+$ ratio is < 1, or Case 6, in which the $[BC]^+/[AB]^+$ ratio is ≥ 1. Knowing the Case for the third Critical Ratio for a Type III TAG allows Critical Limit 2 for the TAG to be calculated, which is:

$$\left(\frac{[AC]^+}{[AB]^+ + [BC]^+}\right)_{\substack{Critical \\ Limit\,2}} = \frac{1}{1 + \frac{[BC]^+}{[AB]^+}} \ or\ \frac{1}{1 + \frac{1}{\frac{[BC]^+}{[AB]^+}}}$$

$$\text{Case 5} \qquad\qquad \text{Case 6}$$

Then, to fully calculate Critical Limit 1 for a Case $n.3.n$ Type III TAG, both Critical Ratio 2 and Critical Ratio 3 are used. The complete equation for Critical Limit 1 for a Case $n.3.n$ solution is given as follows:

For Case 5:

$$\left(\frac{[MH]^+}{\Sigma[DAG]^+}\right)_{\substack{Critical \\ Limit\,1}} = \frac{1}{1 + \frac{[AC]^+}{[AB]^+ + [BC]^+}} \times \frac{1}{1 - \frac{[BC]^+}{[AB]^+}} = \frac{1}{\left(1 + \frac{[AC]^+}{[AB]^+ - [BC]^+}\right)\left(1 + \frac{[BC]^+}{[AB]^+}\right)} = \frac{1}{1 + \frac{[AC]^+}{[AB]^+ + [BC]^+}} \times CL2$$

or, for Case 6:

$$\left(\frac{[MH]^+}{\Sigma[DAG]^+}\right)_{\substack{Critical \\ Limit\,1}} = \frac{1}{1 - \frac{[AC]^+}{[AB]^+ + [BC]^+}} \times \frac{1}{1 - \frac{1}{\frac{[BC]^-}{[AB]^+}}} = \frac{1}{\left(1 - \frac{[AC]^+}{[AB]^+ + [BC]^+}\right)\left(1 + \frac{1}{\frac{[BC]^-}{[AB]^+}}\right)} = \frac{1}{1 + \frac{[AC]^+}{[AB]^+ - [BC]^+}} \times CL2$$

(ii) Critical Limit 2 for a Type III TAG. As seen above, Critical Limit 2 is necessary to calculate Critical Limit 1 when the $[AC]^+/([AB]^+ + [BC]^+)$ ratio is Case 3. This is the statistically expected normal circumstance. As already mentioned, the statistically expected $[AC]^+/([AB]^+ + [BC]^+)$ ratio is 0.5. To determine whether the $[AC]^+$ abundance is less than $[AB]^+$ or $[BC]^+$, or whether it is greater than $[AB]^+$ and $[BC]^+$, the $[AC]^+/([AB]^+ + [BC]^+)$ ratio must be compared with Critical Limit 2. This determines whether $[AC]^+/([AB]^+ + [BC]^+)$ obeys a Case 3.0 or a Case 4.0 solution. Critical Limit 2, in turn, depends on whether the third Critical Ratio, $[BC]^+/[AB]^+$, is greater than or less than 1.

Critical Limit 2 is calculated as follows:

$$\text{if}\left(\frac{[BC]^+}{[AB]^-}\right) < 1.0, \text{then } Critical\ Limit\ 2 = \frac{1}{1 + \frac{[BC]^-}{[AB]^+}}, \text{Else } Critical\ Limit\ 2 = \frac{1}{1 + \frac{1}{\left(\frac{[BC]^-}{[AB]^-}\right)}} \quad [8]$$

$$\text{Case } n.n.5 \qquad\qquad \text{Case } n.n.6$$

When this *Critical Limit 2* has been calculated, it is then used to calculate *Critical Limit 1*:

$$\text{if}\left(\frac{[AC]^-}{([AB]^+ + [BC]^-)}\right) < Critical\ Limit\ 2, \text{then } Critical\ Limit\ 1 = \frac{1}{1 + \left(\frac{[AC]^+}{([AB]^- + [BC]^-)}\right)} \times Critical\ Limit\ 2;$$

$$\text{Else } Critical\ Limit\ 1 = \frac{1}{1 + \frac{1}{\left(\frac{[AC]'}{([AB]^- + [BC]')}\right)}} \quad [9]$$

Critical Limit 1 is used to specify whether $[M + H]^+$ is the base peak, which determines either Case 1.0 or Case 2.0. Critical Limit 2 is used to specify whether $[AC]^+$ is larger than $[AB]^+$ and $[BC]^+$, which specifies either Case 3.0 or 4.0. The $[BC]^+/[AB]^+$ ratio alone (<1 or ≥1) specifies either Case 5 or 6. Thus, the complete Case classification can be given by comparison of the three Critical Ratios to Critical Limit 1, Critical Limit 2, and 1 (= Critical Value 3).

Once the Case has been classified, the complete set of equations necessary to calculate the abundance of every ion is given in Scheme 1, Part IIIA or IIIB, for the Case 1 or Case 2 solutions, respectively. Up to five specific values can be calculated from three Critical Ratios: (i) the abundance of the protonated molecule, (ii) the abundances of each of the three $[DAG]^+$ fragment ions, and (iii) the sum of all the ions. Three critical ratios are required to specify the four primary ions in an APCI-MS mass spectrum of an ABC-type TAG, plus the sum of all ions. Only two critical ratios are required to fully describe the three primary ions in the mass spectrum of an ABA/AAB-type TAG. Four specific values may be calculated for the mass spectrum of a Type II TAG: (i) the abundance of the protonated molecule, (ii) the abundances of each of the two $[DAG]^+$ fragment ions, $[AA]^+$ and $[AB]^+$, and (iii) the sum of all ions. Only one single Critical Ratio is necessary to describe an AAA, or Type I TAG. That one ratio specifies that one peak is the base peak and the other is a ratio to the first, and the sum of the ions is then given.

III) 'ABC' TAG   Critical Value = 0.33

$$\left(\frac{[MH]^+}{\sum[DAG]^+}\right)\overset{?}{<}1$$

N ← → Y

Case 2.0
% [M+H]$^+$ = 100 % (base peak) $\overset{Y}{\longleftarrow}$ $\left(\dfrac{[MH]^+}{\sum[DAG]^+}\right)\overset{?}{\geq}$ Critical Limit 1 $\overset{Y}{\longleftarrow}$ $\left(\dfrac{[MH]^+}{\sum[DAG]^+}\right)\overset{?}{\geq}$ Critical Value

$$\text{if}\left(\frac{[AC]^+}{([AB]^++[BC]^+)}\right)<C_{L2}: Critical\ Limit\ 1=\frac{1}{1+\left(\frac{[AC]^+}{([AB]^++[BC]^+)}\right)}xC_{L2}\ ;\ Else^\dagger Critical\ Limit\ 1=\frac{1}{1+\frac{1}{\left(\frac{[AC]^+}{([AB]^++[BC]^+)}\right)}}$$

Case n.3.n   Case n.4.n
†Implies strong [AC]$^+$ preference

N ↓   N ↓

Case 2.0
% [M+H]$^+$ = 100 % (base peak)
See Scheme 1, Part III_B

Case 1.0
a [DAG]$^+$ = 100 % (base peak)

$$\left(\frac{[AC]^+}{([AB]^++[BC]^+)}\right)\overset{?}{<}1.0$$

N† ← → Y

Case 1.4†
% [AC]$^+$ = 100 % (base peak) $\overset{Y^\dagger}{\longleftarrow}$ $\left(\dfrac{[AC]^+}{([AB]^++[BC]^+)}\right)\overset{?}{\geq}$ Critical Limit 2 $\overset{Y}{\longleftarrow}$ $\left(\dfrac{[AC]^+}{([AB]^++[BC]^+)}\right)\overset{?}{\geq}0.5$

N

$$\% [MH]^+=\left(\frac{[MH]^+}{\sum[DAG]^+}\right)\left(1+\frac{1}{\left(\frac{[AC]^+}{([AB]^++[BC]^+)}\right)}\right)x100$$

$$\text{if}\left(\frac{[BC]^+}{[AB]^+}\right)<1.0: Critical\ Limit\ 2=\frac{1}{1+\left(\frac{[BC]^+}{[AB]^+}\right)}$$
Case n.n.5
$$Else\ Critical\ Limit\ 2=\frac{1}{1+\frac{1}{\left(\frac{[BC]^+}{[AB]^+}\right)}}$$
Case n.n.6

$$\left(\frac{[BC]^+}{[AB]^+}\right)\overset{?}{<}1.0\ \overset{Y}{\longrightarrow}\ \text{Case 1.4.5}\quad [BC]^+ < [AB]^+$$

Case 1.3

Same for Both Cases:

$$\%[AB]^+=\frac{1}{\left(\frac{[AC]^+}{([AB]^++[BC]^+)}\right)\left(1+\frac{[BC]^+}{[AB]^+}\right)}x100$$

Case 1.3.5 $\overset{Y}{\longleftarrow}$ $\left(\dfrac{[BC]^+}{[AB]^+}\right)\overset{?}{<}1.0$

% [AB]$^+$ = 100 % (base peak)

$$\%[BC]^+=\left(\frac{[BC]^+}{[AB]^+}\right)x100$$

N ↓

Case 1.4.6
[BC]$^+$ ≥ [AB]$^+$

$$\%[BC]^+=\frac{1}{\left(\frac{[AC]^+}{([AB]^++[BC]^+)}\right)\left(1+\frac{1}{\frac{[BC]^+}{[AB]^+}}\right)}x100$$

$$\%[AC]^+=\left(\frac{[AC]^+}{([AB]^++[BC]^+)}\right)\left(1+\frac{[BC]^+}{[AB]^+}\right)x100$$

$$\%[MH]^+=\left(\frac{[MH]^+}{\sum[DAG]^+}\right)\left(1+\frac{[AC]^+}{([AB]^++[BC]^+)}\right)\left(1+\frac{[BC]^+}{[AB]^+}\right)x100$$

N

$$\%[AC]^+=\left(\frac{[AC]^+}{([AB]^++[BC]^+)}\right)\left(1+\frac{1}{\frac{[BC]^+}{[AB]^+}}\right)x100$$

$$\%[AB]^+=\frac{1}{\left(\frac{[BC]^+}{[AB]^+}\right)}x100$$

Case 1.3.6
% [BC]$^+$ = 100 % (base peak)

$$\%[MH]^+=\left(\frac{[MH]^+}{\sum[DAG]^+}\right)\left(1+\frac{[AC]^+}{([AB]^++[BC]^+)}\right)\left(1+\frac{1}{\frac{[BC]^+}{[AB]^+}}\right)x100$$

SCHEME 1, PART IIIA. Equations to calculate the relative abundances of the [M + H]$^+$ and [DAG]$^+$ fragment ions for Type III TAG (= ABC), Case 1.n.n, using Critical Ratios from APCI-MS data (Table 2). For abbreviation see Scheme 1, Part I.

IMPLEMENTATION OF THE BUS

The Critical Ratios are the key elements of the BUS to the TAG Lipidome. During the process of investigating the relationships between the Critical Ratios and the structural information that they provide, it was observed that the Critical Ratios contained all of the information necessary to reconstruct the mass spectrum from which they came. Thus, the starting point for the BUS for TAG is the construction of the Critical Ratios for the TAG. The reasons for the identities of the Critical Ratios were given in the section entitled Construction of the Critical Ratios. The Critical Ratios may be constructed from abundances or areas in several ways. They may be constructed either from the abundances from a single mass spectrum or from an averaged mass spectrum obtained by averaging individual mass spectra over time from data obtained by infusion of an analyte solution

III) 'ABC' TAG Critical Value = 0.33

$$\left(\frac{[MH]^+}{\sum[DAG]^+}\right)\overset{?}{<}1$$

N ────────────── Y

Case 2.0
% [M+H]$^+$ = 100 % (base peak) $\overset{Y}{\longleftarrow}$ $\left(\frac{[MH]^+}{\sum[DAG]^+}\right)\overset{?}{\geq} Critical\ Limit\ 1$ $\overset{Y}{\longleftarrow}$ $\left(\frac{[MH]^+}{\sum[DAG]^+}\right)\overset{?}{\geq} Critical\ Value$

$$if\left(\frac{[AC]^+}{([AB]^+ +[BC]^+)}\right)< C_{L2}: Critical\ Limit\ 1 = \frac{1}{1+\left(\frac{[AC]^+}{([AB]^+ +[BC]^+)}\right)} xC_{L2}; \ Else^\dagger\ Critical\ Limit\ 1 = \frac{1}{1+\frac{1}{\left(\frac{[AC]^+}{([AB]^+ +[BC]^+)}\right)}}$$
Case n.3.n   **Case n.4.n**
†Implies strong [AC]$^+$ preference

N ↓   N ↓

Case 2.0
% [M+H]$^+$ = 100 % (base peak)

$$\%[AC]^+ = \frac{1}{\left(\frac{[MH]^+}{\sum[DAG]^+}\right)\left(1+\frac{1}{\left(\frac{[AC]^+}{([AB]^+ +[BC]^+)}\right)}\right)} x100$$

Case 1.0
a [DAG]$^+$ = 100 % (base peak)
See Scheme 1, Part III_A

$$if\left(\frac{[BC]^+}{[AB]^+}\right)<1.0: Critical\ Limit\ 2 = \frac{1}{1+\left(\frac{[BC]^+}{[AB]^+}\right)}$$
Case n.n.5
$$Else\ Critical\ Limit\ 2 = \frac{1}{1+\frac{1}{\left(\frac{[BC]^+}{[AB]^+}\right)}}$$
Case n.n.6

$$\left(\frac{[AC]^+}{([AB]^+ +[BC]^+)}\right)\overset{?}{<}1.0$$

N† ────────────── Y

Case 2.4†
% [AC]$^+$ ≥ ([AB]$^+$ and [BC]$^+$) $\overset{Y^\dagger}{\longleftarrow}$ $\left(\frac{[AC]^+}{([AB]^+ +[BC]^+)}\right)\overset{?}{\geq} Critical\ Limit\ 2$ $\overset{Y}{\longleftarrow}$ $\left(\frac{[AC]^+}{([AB]^+ +[BC]^+)}\right)\overset{?}{\geq}0.5$

$\left(\frac{[BC]^+}{[AB]^+}\right)\overset{?}{<}1.0 \overset{Y}{\longrightarrow}$ **Case 2.4.5**
     [BC]$^+$ < [AB]$^+$

N ↓

Case 2.4.6
[BC]$^+$ ≥ [AB]$^+$

N ↓ (from Critical Limit 2)

Case 2.3
% [AC]$^+$ < ([AB]$^+$ or [BC]$^+$)

$\left(\frac{[BC]^+}{[AB]^+}\right)\overset{?}{<}1.0 \overset{Y}{\longrightarrow}$ **Case 2.3.5**
     [BC]$^+$ < [AB]$^+$

N ↓

Case 2.3.6
[BC]$^+$ ≥ [AB]$^+$

Same for All 2.n.n Cases:

$$\%[AB]^+ = \frac{1}{\left(\frac{[MH]^+}{\sum[DAG]^+}\right)\left(1+\frac{[AC]^+}{[AB]^+ +[BC]^+}\right)\left(1+\frac{[BC]^+}{[AB]^+}\right)} x100$$

$$\%[BC]^+ = \frac{1}{\left(\frac{[MH]^+}{\sum[DAG]^+}\right)\left(1+\frac{[AC]^+}{[AB]^+ +[BC]^+}\right)\left(1+\frac{1}{\frac{[BC]^+}{[AB]^+}}\right)} x100$$

SCHEME 1, PART IIIB. Equations to calculate the relative abundances of [M + H]+ and [DAG]$^+$ fragment ions for Type III TAG (= ABC), Case 2.*n.n*, using Critical Ratios from APCI-MS data (Table 2). For abbreviation see Scheme 1, Part I.

at a constant rate, or from data by injection of analyte into an infused solvent flow. Further still, the mass spectrum used to construct the Critical Ratios may be an averaged-in-time mass spectrum across a chromatographic peak, or it may be constructed from the integrated-in-time normalized relative area abundances. For mass spectra across a chromatographic peak, the abundances are different in the middle, front, and back portions of the peak, as was mentioned by Mottram *et al.* (11) and in a recent review (45). For Type II TAG, it appears that the regioisomers may be partially separated across the breadth of the

peak. Construction of the Critical Ratios for the first, middle, and last portions of the chromatographic peaks may help to make more trends apparent. For polyunsaturated TAG, the [AA]$^+$/[AB]$^+$ ratio is higher than other TAG and is often greater than 1.

The averaged mass spectrum across a chromatographic peak shows all ions eluted at that particular time. Similarly, a plot of the areas under integrated peaks in ion chromatograms at a particular retention time, normalized to 1 (or 100%), appears the same as a mass spectrum averaged across that time window. The

averaged mass spectrum of each TAG of the 35-TAG mixture given in Table 5 is an average of the three sets of mass spectra given by the (abundance × time) integrated peak areas of each of three chromatographic runs, in which complete chromatographic resolution was achieved between almost all TAG molecular species. Peaks that appear to overlap in the total ion current chromatogram (TIC) are resolved in ion chromatograms of [DAG]$^+$ fragments that are extracted out of the TIC, to form extracted ion chromatograms (EIC). Any overlapped peaks are apportioned as has been described previously (7,34). In the data set used herein, the only chromatographic peak that required apportionment was the P peak of OL and the O peak of SLn in the *m/z* 601.5 EIC, marked with an asterisk in Figure 6E. In whichever manner the percent relative abundances are obtained that represent the mass spectrum, the Critical Ratios can be calculated from the abundances or areas. One need not convert integrated peak areas to percent relative abundances, since the critical ratios can be calculated directly from the integrated areas as long as they are properly grouped by retention time for each TAG. However,

when averaging several runs, calculations should be based on normalized area percentages.

Error propagation in the Critical Ratios must be mentioned. In Table 2, the SD are not simply the SD of the three numerically calculated ratio values. Since the Critical Ratios are ratios of average abundances that each have a SD, error propagation is more correctly calculated as the square root of the sum of the squares of the percent relative SD of the abundances involved in the construction of the ratios. Table 2 shows the SD calculated in this way. When a ratio has been shown to have a linear relationship, such as the [AA]$^+$/[AB]$^+$ ratio for regioisomers, it may be appropriate to express the simpler SD in the ratio itself. In Table 2, the simple SD of the three numeric [AA]$^+$/[AB]$^+$ ratio values has been shown as SD2. In most cases, the peak that is the base peak in an averaged mass spectrum is the base peak in each of the averaged spectra, and so that abundance has a 0% SD from spectrum to spectrum. In the cases of highly unsaturated TAG, the error expressed as the square root of the sum of the squares of the SD of the abundances was larger than for TAG containing

TABLE 5
Percent Relative Ion Abundances Calculated from the Critical Ratios in Table 2, Using the Bottom-Up Solution in Scheme 1, Implemented by the Formulas in Table 4[a]

TAG	[MH]$^+$	[AA]$^+$ or [AC]$^+$	[AB]$^+$	[BC]$^+$	ΣI%
PPP	0.00	100.00			100.00
SSS	0.00	100.00			100.00
OOO	3.24	100.00			103.24
LLL	100.00	83.28			183.28
LnLnLn	100.00	44.88			144.88
PSP/PPS	0.00	49.26	100.00		149.26
POP/PPO	0.91	65.28	100.00		166.19
PLP/PPL	0.74	84.11	100.00		184.85
PLnP/PPLn	21.77	69.94	100.00		191.71
SPS/SSP	0.00	40.91	100.00		140.91
SOS/SSO	0.79	75.14	100.00		175.93
SLS/SSL	0.77	82.89	100.00		183.66
SLnS/SSLn	15.44	60.98	100.00		176.42
OPO/OOP	2.57	36.12	100.00		138.69
OSO/OOS	1.57	39.82	100.00		141.39
OLO/OOL	17.91	50.10	100.00		168.01
OLnO/OOLn	52.31	41.62	100.00		193.93
LPL/LLP	52.20	88.84	100.00		241.04
LSL/LLS	76.54	76.07	100.00		252.61
LOL/LLO	77.60	74.62	100.00		252.22
LLnL/LLLn	100.00	33.74	64.93		198.67
LnPLn/LnLnP	100.00	42.19	56.49		198.69
LnSLn/LnLnS	100.00	79.50	83.60		263.11
LnOLn/LnLnO	100.00	44.99	53.69		198.68
LnLLn/LnLnL	100.00	30.51	47.61		178.12
OPS	1.10	63.91	100.00	69.79	234.80
SPL	0.99	56.42	100.00	59.43	216.85
SPLn	22.92	70.29	100.00	76.70	269.91
LOP	17.93	80.08	100.00	98.27	296.28
LnOP	74.01	80.54	100.00	91.76	346.31
LnLP	100.00	54.96	86.35	63.36	304.67
LOS	19.90	81.45	100.00	85.70	287.05
OLnS	53.87	80.49	100.00	89.53	323.89
LnLS	100.00	61.47	89.06	69.98	320.51
LLnO	100.00	50.63	70.93	55.08	276.65

[a]This is an exact reproduction of the average mass spectrum obtained as an average of three chromatographic runs. I, ion abundance; for other abbreviations see Table 1.

FA with fewer sites of unsaturation. TAG. Although the approach used to obtain an averaged mass spectrum affects the SD of the abundances, the BUS does not depend on the approach used to obtain the mass spectrum.

Figures 5A through 5F show examples of mass spectra and the construction of the Critical Ratios. For Type II TAG, the $[AA]^+/[AB]^+$ ratio can be used to assess the amounts of regioisomers; so instead of providing abundances, which would then need to be converted into the ratio that is compared to regioisomeric standards, one could provide the desired ratio directly, along with one or two other ratios, which constitute the set of Critical Ratios. These ratios can be tabulated in fewer values than the raw abundances. The ratios therefore are a more efficient means of storing information. They provide more information in fewer values.

Automated spreadsheet implementation of the BUS starts with the classification of the Critical Ratios into Cases. The classification can be accomplished using only the Critical Limits. The Critical Values do not need to be used in the automated implementation. If the columns in Table 2 were labeled A through J, and the rows were numbered from 1 to 37, then the Critical Ratios would be in columns E, G, and I, and the data would be in rows 2 to 36. Based on Table 2 numbered as mentioned, the following formulas allow the calculation of the Critical Limits:

Type II: J7: =
   IF(G7<100,(100/(1+(G7/100))),(100/(1+(100/G7))))
                                                   Critical Limit

Type III: J27: =
   IF(G27<M27,(100/(1+(G27/100))*(M27/100)),(100/(1+
   (100/G27))))
                                                   Critical Limit 1

M27: = IF(I27<100,(100/(1+(I27/100))),(100/(1+(100/I27))))
                                                   Critical Limit 2

G7–36: = Critical Ratio $[AA]^+/[AB]^+$ (Type II TAG)
   or $[AC]^+/([AA]^+ + [AB]^+)$ (Type III)

I27–36: = Critical Ratio $[BC]^+/AB]^+$ (Type III TAG)

These formulas are the implementation of the equations for the Critical Limits that were given in the closed boxes in Scheme I, Parts II and III, and in Equations 7–9. These formulas may be pasted down the column for all TAG of each type, to automatically calculate the Critical Limits for all TAG. Notice that Critical Limit 1 for a Type III TAG depends on Critical Limit 2.

Notice that the formula for Critical Limit 2 for a Type III TAG is in the same form as the formula for the one Critical Limit of a Type II TAG. Once the Critical Limits have been calculated, then the Case classification can also be automated. The Critical Limits calculated from the Critical Ratios in Table 2 are given in Table 3, along with the Critical Values. Examples in the preceding text and in Figure 5 demonstrate calculation of the Critical Limit.

In the spreadsheet implementation for Type I TAG, the $[MH]^+/\Sigma[DAG]^+$ ratio is simply compared with 1, so the classification is =IF(E2<100,**1**,**2**), where **1** and **2** are Case 1 and Case 2. For both Types II and III TAG, the $[MH]^+/\Sigma[DAG]^+$ ratio is compared with the first Critical Limit (formulas just shown) and is given by: =IF(E7<J7,**1**,**2**), where **1** and **2** are Case 1 and Case 2, with the Critical Limit in column J. Next, Case 3 and Case 4 are determined. For the Type II TAG, the $[AA]^+/[AB]^+$ ratio is simply compared with 1, so the classification formula is: =IF(G7<100,**3**,**4**), where **3** and **4** are Case 3 and Case 4. For a Type III TAG, the $[AC]^+/([AB]^++[BC]^+)$ ratio is compared with Critical Limit 2, so the classification formula is: =IF(G27<M27,**3**,**4**), where Critical Limit 2 is in column M. Finally, Case 5 and Case 6 are determined. The $[BC]^+/[AB]^+$ ratio is simply compared with 1 for this determination, so the classification formula in spreadsheet notation is =IF(G27<100,**5**,**6**).

From these formulas, the TAG are classified into their complete Case classifications. The case classifications for the 35-TAG mixture, for which Critical Ratios are given in Table 2, are shown in Table 3. Once they are classified, the solution equations are given in Scheme 1 of the BUS. Since they may not be obvious and might seem daunting at first, the formulas will be given here by which the entire BUS can be implemented. This actually requires only a few nested spreadsheet formulas. To exemplify this, imagine that the case classification in Table 3 is in columns Q, R, and S of the same spreadsheet as that envisioned for Table 2. Keeping the same row numbers (2 through 36), the following formulas use the Cases defined in Table 3 with the Critical Ratios given in Table 2 to calculate the abundances of all ions in the original mass spectra.

In the implementation in a spreadsheet, the comparison of the $[MH]^+/\Sigma[DAG]^+$ ratio to 1 and to its Critical Value can be skipped, since the Critical Limits are sufficient to determine which peak is the base peak. The comparison with 1 and with the Critical Value is done when the BUS is being used manually (not in a spreadsheet), to accomplish the case classification of the TAG with these simple values if possible, to save time and avoid calculation of the more complicated Critical Limit(s).

When the spreadsheet is used, the formulas given above can be typed in and then pasted down the column, so calculation of the Critical Limits requires minimal effort. Therefore, these formulas for the Critical Limits can be used without first testing the $[MH]^+/\Sigma[DAG]^+$ ratio with the Critical Value and 1.

Similarly, for a Type III TAG, Critical Limit 1 depends on Critical Limit 2. Since the spreadsheet calculates both of these values easily from the formulas for the Critical Limits given, Critical Limit 2 is easily determined without first testing the $[AC]^+/([AB]^+ + [BC]^+)$ ratio using its Critical Value of 0.5. The $[AC]^+/([AB]^+ + [BC]^+)$ ratio can simply be compared with Critical Limit 2 using the automated classification formulas just given, to arrive at the Case classification for Case 3 or Case 4.

Thus, the whole Critical Limit calculation process is accomplished with only the three formulas given, and these are used with the Critical Ratios to accomplish the complete Case
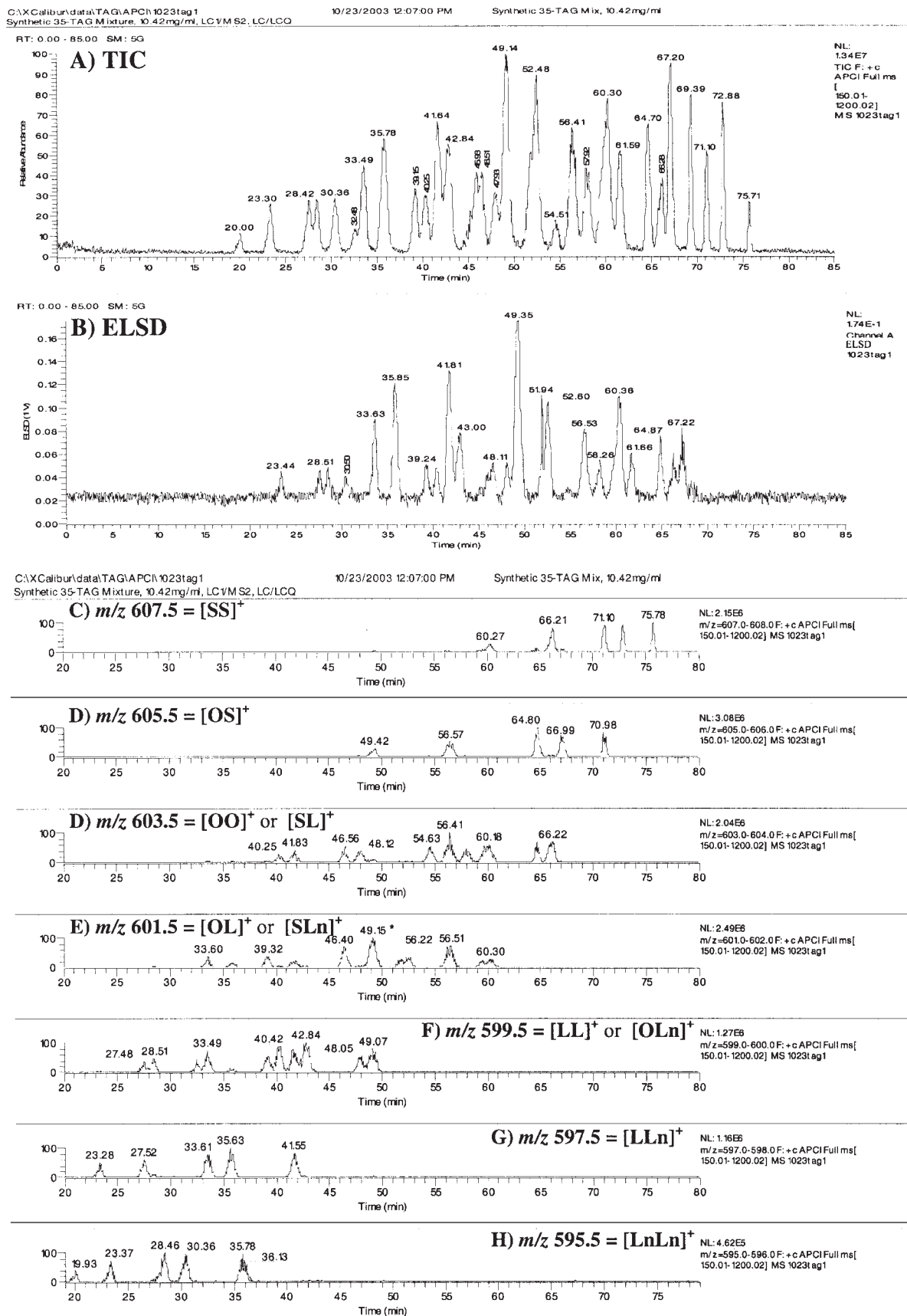
FIG. 6. Total ion current chromatogram (TIC), evaporative light-scattering detector (ELSD) chromatogram, and extracted ion chromatograms (EIC) of [DAG]+ fragment ion masses. S, stearic acid; Ln, linolenic acid; for other abbreviations see Figure 1.

classification of the TAG. Once the Case classification is accomplished, the BUS shows which equations to use to calculate the ion abundances for every TAG of every case. In looking at Scheme 1, it might appear difficult to implement the system of equations given in the BUS. However, the whole solution for every TAG can be implemented in only nine formulas that contain nested "if (*x*, then *y*, else *z*)" spreadsheet formulas, in which *x* is the case classification given in Table 3. There are nine types of $[MH]^+$ or $[DAG]^+$ fragment ions that can be produced from a Type I, II, or III TAG. The nine spreadsheet formulas necessary to calculate the abundance of every possible ion are provided in Table 4. These can be entered into the spreadsheet and then pasted down the column for each TAG type. Since there are only two possible cases for each Critical Ratio, the "if (*x*, then *y*, else *z*)" statement can be tested using Cases **1**, **3**, and **5** as *x*, and if any of the tests fails, then the inherent "else *z*" is the Case **2**, **4**, or **6** solution, respectively, by default. This is why, for a Type III TAG, only the values **1**, **3**, and **5** appear at the beginning of each "if (*x*, then *y*, else *z*)" statement. Notice in Table 4 that, for a Type III TAG, the "if (*x*, then *y*, else *z*)" statements are nested three levels deep, whereas for a Type II TAG, they are nested two levels deep. The spreadsheet formulas in Table 4 allow the abundances for every $[MH]^+$ ion and $[DAG]^+$ fragment from every TAG to be calculated based on the Critical Ratios tabulated in Table 2, using the Critical Limits and Case classification shown in Table 3. The abundances calculated from the spreadsheet formulas in Table 4 are given in Table 5.

Table 5 represents an average mass spectrum obtained from three chromatographic runs. The average mass spectrum was used to calculate the Critical Ratios. The values in Table 5 were calculated from the Critical Ratios in Table 2 processed through the equations in Table 4 and are exactly equal to the average mass spectrum to the number of significant figures given. In the spreadsheet, where many decimal places can be kept, the BUS reproduces the original mass spectrum to as many decimal places as desired. Figure 5 demonstrates that when theoretical Critical Ratios with infinite precision (perfect integer ratios) are used, the abundances are calculated with infinite precision. The abundances calculated and shown in Table 5, which are given by the BUS using the Critical Ratios in Table 2, are an exact reproduction of the average mass spectrum obtained from the average of three chromatographic runs, to two decimal places. The reproduced mass spectrum in Table 5 gives the Critical Ratios shown in Table 2. It should be noted that, since the abundances calculated from the BUS, shown in Table 5, required rounding to two decimal places, rounding error would occur each time the spectrum is reproduced from the Critical Ratios of a reproduced spectrum. In situations where the Critical Ratios are pure integer ratios, as shown in Figure 5, there is no error; and the Critical Ratios can be used to calculate the reproduced mass spectrum, and the Critical Ratios from the reproduced mass spectrum give the exact same Critical Ratios, with infinite precision. Just like the average mass spectra shown in Table 5, the abundances that

make up any individual APCI-MS mass spectrum can be exactly reproduced by the BUS. The Critical Ratios for any individual mass spectrum are processed through the BUS, and the abundances from which they came are reproduced to as many significant figures as were given for the Critical Ratios.

The structural trends that have been reported, as discussed in the foregoing sections, make up part of the Interpretation Matrix that is used to interpret information from the Critical Ratios. But the Interpretation Matrix is also used, if literature precedent has been reported, to make structural assignments that affect the Critical Ratios. The structural trends can be seen in the way the fragment ions are arranged in Table 5. It has already been discussed that the statistically expected $[AA]^+/[AB]^+$ ratio is 0.5. Thus, the $[AA]^+$ ion abundance is always expected to be smaller than the $[AB]^+$ abundance. It can be seen in Table 5 that the $[AA]^+$ ion abundance (identified as the $[AA]^+$ fragment by *m/z* value) is smaller than the $[AB]^+$ abundance for every TAG. With Type II TAG, there is no selection to be made regarding the identities of A and B, because whichever $[DAG]^+$ fragment has two of the same FA is the $[AA]^+$ fragment, and whichever $[DAG]^+$ fragment has two different FA is the $[AB]^+$. The 35-TAG mixture theoretically has equimolar amounts of regioisomers, since the FA are randomly distributed.

Based on linear interpolation of the $([AA]^+/[AB]^+)_{Obs}$ ratio between the $([AA]^+/[AB]^+)_{ABA}$ and $([AA]^+/[AB]^+)_{AAB}$ ratios of pure standards, the $[AA]^+/[AB]^+$ ratio for the 35-TAG mixture should give an $[AA]^+/[AB]^+$ ratio that is ~1/3 of the way between the $[AA]^+/[AB]^+$ ratio of the ABA isomer and the $[AA]^+/[AB]^+$ ratio of the AAB/BAA isomer pair. The $[AA]^+/[AB]^+$ ratios of many TAG regioisomers have not yet been reported. Table 2 represents one point, obtained from a randomized mixture, on the line interpolated between the two regioisomeric standards. The $[AA]^+/[AB]^+$ ratios in Table 2 theoretically represent approximately the one-third (1/3) point on the line interpolated between the $[AA]^+/[AB]^+$ ratios of the ABA isomer and the AAB/BAA isomer pair. As already mentioned, the 35-TAG synthetic mixture for which Critical Ratios were given in Table 2 represents a mixture of regioisomers, and each of these is present as a racemic mixture of enantiomers.

The $[AA]^+/[AB]^+$ ratios in Table 2 show that the TAG that contained the diolein DAG combined with a saturated FA had some of the lowest $[AA]^+/[AB]^+$ ratios. Polyunsaturated TAG, containing linoleic and linolenic acids, gave the highest $[AA]^+/[AB]^+$ ratios, especially from the TAG containing one saturated FA. Perhaps construction of the $[AA]^+/[AB]^+$ ratios from a larger number of TAG mixtures and TAG standards will lead to a greater understanding of the effects of unsaturation in the FA, and of the regioisomeric placement of the FA, on the relative abundances of the $[DAG]^+$ fragment ions formed from Type II TAG.

Unlike Type II TAG, for Type III TAG the identities of the FA A, B, and C are not automatically known. However, the trends reported from APCI-MS data provide information to be able to classify the FA and deduce the structure of $[AC]^+$ and

therefore to know the identity of the B FA in the *sn*-2 position. As discussed in the preceding sections, the *sn*-1,3 [DAG]$^+$ fragment has been reported to be energetically disfavored, and has been reported to exist in the least abundance (10,11) of the three [DAG]$^+$ fragments that come from a Type III TAG. Based on this reported trend, the abundances of Type III TAG in Table 5 have been arranged such that the [AC]$^+$ fragment is selected as the peak with the lowest abundance. Aligning the identity of [AC]$^+$ as the ion with the smallest abundance implies that it is the [*sn*-1,3-AC]$^+$ fragment. For instance, for OPS, the lowest [DAG]$^+$ abundance was observed from the [OS]$^+$ fragment (=[SO]$^+$), so the [OS]$^+$ fragment is labeled as the [AC]$^+$ fragment. In this way, the previous structural trends that have been reported for TAG can be used for identification of at least one of the three possible regioisomers for a Type III TAG. Before constructing the Critical Ratios (such as in Table 2), the lowest [DAG]$^+$ abundance should be properly identified as [AC]$^+$, so that the [AC]$^+$/([AB]$^+$ + [BC]$^+$) ratio will have its minimum value when the [AC]$^+$ fragment is properly assigned. Of course, the equations of the BUS operate properly whether the ions have been assigned properly or not, but proper construction of the Critical Ratios allows additional structural information to be derived and trends observed. In Table 5, one can observe that all [AC]$^+$ fragments have the lowest abundances of the three [DAG]$^+$ fragments for each TAG. However, the trend reported for Type III TAG was based on a limited number of Type III TAG; therefore, this trend needs to be further verified with additional Type III TAG standards. Regardless of how the Critical Ratios are used to derive regiospecific structural information, the BUS works with all values of all Critical Ratios.

No definitive trend has been reported for [AB]$^+$ vs. [BC]$^+$ fragments. All else being equal, the [AB]$^+$ vs. [BC]$^+$ fragments are interchangeable. Thus, it is equally likely that a TAG could represent a Case 5 vs. a Case 6 solution. In the absence of a definitive trend, the data can be used to try to elucidate any subtle trends that may not be readily apparent. If one chooses to set the [BC]$^+$ fragment equal to the smaller of the two possible abundances for [AB]$^+$ or [BC]$^+$, then perhaps the ratios will indicate some structural trends. For instance, in Table 5, the [BC]$^+$ fragment is chosen so that the [BC]$^+$ fragment is smaller than abundances for [AB]$^+$. By doing this, one can observe that every Type III TAG in the mixture that has less than two saturated FA had the least saturated chain in the C, or *sn*-3, position. Seven of the ten Type III TAG in the 35-TAG mixture had one or no saturated FA. All seven of these TAG gave a lower abundance for the [BC]$^+$ fragment than the [AB]$^+$ fragment when the single saturate or monounsaturate (for LLnO) was in the *sn*-3 position. Of course, the *sn*-1 and *sn*-3 positions could be reversed, and all Type III TAG would have the [BC]$^+$ fragment larger than the [AB]$^+$ fragment. But whichever way they are labeled, it reveals a trend that the [DAG]$^+$ fragment with more unsaturation is the larger fragment, in most cases, giving a [BC]$^+$/[AB]$^+$ ratio less than one, when the unsaturated TAG is labeled as the A, or *sn*-1, FA. Additional data from regioisomeric standards of Type III TAG will reveal which is the correct assignment. With the BUS, the mechanism, or the construct, is now in place to be able to

more easily identify and interpret structural trends, as they are reflected in the abundances of the [DAG]$^+$ fragment ions in APCI-MS mass spectra, and the Critical Ratios made from the raw abundances. Regardless of whether the [BC]$^+$ fragment is less than the [AC]$^+$ fragment or vice versa, the BUS accurately calculates the abundances of each ion whether the [BC]$^+$/[AB]$^+$ ratio is larger than 1 or less than 1.

In a way analogous to proteomics, the sum of all possible species and structures of lipid molecules may referred to as the *lipidome*, and the study of the lipidome is referred to as *lipidomics* (46). The sum of all possible structures of TAG may be referred to as the TAG Lipidome. There is not a single TAG that cannot be represented by its Critical Ratios, and from these Critical Ratios, all abundances of ions may be reproduced. Thus, Scheme 1 represents the complete boundary to the solution of the TAG Lipidome, based on data from APCI-MS mass spectra. There is no TAG that cannot be represented within this construct. The structural trends that have just been mentioned, which were correlated to values or trends in the Critical Ratios, constitute the Interpretation Matrix that is part of the BUS. These correlations are not written here in a single table but have been discussed in detail. In the future, further information may be added to the Interpretation Matrix to allow a preference for [BC]$^+$ vs. [AB]$^+$ to be further described, or other information may be added to allow more information to be interpreted from the Critical Ratios. But, whereas this may provide incremental additional information, the essential construct of the BUS to the TAG Lipidome is complete in its entirety as given in Scheme 1, and the mass spectrum of any TAG may be reproduced from its equations. The BUS constitutes the first full solution to the TAG Lipidome.

FUTURE DIRECTIONS

Critical Ratios and their use in the BUS have been demonstrated using APCI-MS of TAG. This solution is also applicable to data obtained by ESI-MS. Since ESI-MS produces mostly the protonated molecule, with small abundances of [DAG]$^+$ fragment ions, the [MH]$^+$/Σ[DAG]$^+$ ratio is, of course, higher for ESI-MS data, but as long as the Σ[DAG]$^+$ is nonzero, the BUS may be applied to the same Critical Ratios calculated from ESI-MS data as from APCI-MS data. Alternatively, since ESI-MS mass spectra never give a zero abundance of protonated molecule (whereas APCI-MS spectra do), the completely bounded solution to the TAG lipidome by ESI-MS would best be constructed using the (Σ[DAG]$^+$/[MH]$^+$) ratio. This will give essentially the same construct as the TAG lipidome by APCI-MS, but with the (Σ[DAG]$^+$/[MH]$^+$) ratio having an inverse relationship to the [MH]$^+$/Σ[DAG]$^+$ ratio. Nevertheless, as long as the Σ[DAG]$^+$ fragments is not zero, the same set of ions (an [MH]$^+$ and up to three [DAG]$^+$ fragment ions) can be used with the BUS for TAG analysis by ESI-MS as was used for analysis by APCI-MS. Furthermore, as several values obtained by ESI-MS in Table 1 show, the [AA]$^+$/[AB]$^+$ ratio obtained by ESI-MS may be useful for characterization of the regioisomers, just like the [AA]$^+$/[AB]$^+$ ratio obtained by APCI-MS.

Glycerophospholipids have some structural similarity to TAG, because both classes of molecules have a three-carbon glycerol backbone. This similarity is seen in the mass spectra of glycerophospholipids. Most glycerophospholipids produce a protonated molecule and one [DAG]⁺ fragment, which is the same type of DAG fragment that is produced by TAG. It should be obvious that these two ions could be represented by the ([MH]⁺/[DAG]⁺) ratio, and the abundances of the two ions could be found using Scheme 1, Part I, just like a Type I TAG. Furthermore, glycerophospholipids produce fragments ions by loss of one fatty acyl chain as either an acid or a ketene (44). Phospholipid fragments containing one FA, formed by loss of one fatty acyl chain as an acid or a ketene (44), are analogous to the [AA]⁺ or [AB]⁺ fragments from a Type II TAG, in that the fragments provide information to allow identification of regioisomers. It will be a very straightforward extension of the BUS to construct Critical Ratios from phospholipids and process them through a solution that will be very similar to this original BUS, but that will be customized to identify the ions observed from phospholipids.

This solution to the TAG lipidome was referred to as the BUS because it was accomplished through manual solutions to every possible case. Once the complete solution was accomplished, trends within the equations were observed, and the mathematical function behind those equations was developed. The new function that describes all possible combinations of two variables (abundances) interacting with each other is defined as the Unit Simulacrum. Once the patterns within the equations were recognized and the equations behind the equations were found, two more mathematically equivalent solutions to the TAG lipidome were produced, which are referred to as the term-wise simulacrum solution and the nested simulacrum solution. Since these other solutions were arrived at by using the equations behind the equations, it may be said that these solutions were developed using a "top-down" approach. These other solutions will be presented in another report. The masses of the fragments have not been discussed, since they are constant and are dictated by the identity of the TAG. For instance, it is automatically known that the TAG POL will produce a [PO]⁺ fragment having *m/z* 577.5, a [PL]⁺ fragment having *m/z* 575.5, an [OL]⁺ fragment having *m/z* 601.5, and a [POL + H]⁺ ion having *m/z* 857.8. These *m/z* values do not change and so do not need to be reiterated. It is the abundances of the protonated molecule and the [DAG]⁺ fragment ions that change and that are affected by unsaturation and by positional placement of the FA on the glycerol backbone. It is these structural features that the Critical Ratios elucidate. As demonstrated, these Critical Ratios can then be used to reconstruct the appearance of the APCI-MS mass spectrum of any TAG.

CONCLUSION

The BUS represents the first complete solution to the TAG lipidome. Critical Ratios have been defined that, used by themselves, provide direct information regarding the structural characteristics of TAG (e.g., amount of unsaturation and positional

isomer distribution). Furthermore, these Critical Ratios constitute a reduced data set from which the mass spectrum of any TAG can be reproduced in its entirety. This reduced data set has potential advantages for storage of library spectra. Normally, the abundances of all four ions in the mass spectrum of a TAG would be presented in tabular form to represent a mass spectrum. In using the BUS, only three pieces of data are required (the three Critical Ratios). This represents a saving of 25% (three values needed instead of four) for ABC TAG. For ABA/AAB TAG, only two critical ratios are necessary to provide all of the information necessary to reproduce the mass spectrum, compared with three abundance values that would be used to tabulate the spectrum. This constitutes a data storage reduction by 33% (two values needed instead of three) for ABA/AAB TAG. Since only one critical ratio is necessary to describe the mass spectral abundances of an AAA TAG completely, the BUS provides a 50% saving in data storage space required (one value needed instead of two). The benefit of reduced data storage requirements is in addition to the benefits of being able to use the Critical Ratios directly to determine the distribution of regioisomers and the degree of unsaturation.

In the past, articles often presented tabulated abundances of mass spectral ions (8,32,33,36,37), which could later be used to calculate the ratio of [AA]⁺/[AB]⁺ abundances to allow the positional isomer preference to be assessed (45). It has now been demonstrated that it is possible to list Critical Ratios that can be used directly to provide structural information (e.g., assessing the degree of unsaturation or assigning positional isomers) and that constitute a reduced data set that uses fewer values and therefore takes less space than conventional tabulated mass spectra. It has been demonstrated that the mass spectrum of any TAG can be reproduced from the Critical Ratios using the BUS, which uses Critical Values and Critical Limits, and an Interpretation Matrix, to define the Case of a TAG. Once the Case of the TAG is defined, the exact equations used to calculate the abundance of every ion in the mass spectrum are given by the BUS. Finally, all of the spreadsheet formulas that are necessary to implement the BUS have been provided. For the automated spreadsheet implementation, the following spreadsheet formulas are given: three formulas for Critical Limits, five formulas for the Case classification process, and nine formulas to calculate every possible [MH]⁺ or [DAG]⁺ fragment, which represent the primary ions in an APCI-MS mass spectrum, for a Type I, II, or III TAG.

REFERENCES

1. Kusaka, T., Ikeda, M., Nakano, H., and Numajiri, Y. (1988) Liquid Chromatography/Mass Spectrometry of Fatty Acids as Their Anilides, *J. Biochem. 104*, 495–497.
2. Kusaka, T., and Ikeda, M. (1992) Liquid Chromatography–Mass Spectrometry of Hydroperoxy Fatty Acids (in Japanese), *Proc. Jpn. Soc. Biomed. Mass Spectrom. 17*, 167–170.
3. Kusaka, T., and Ikeda, M. (1993) Liquid Chromatography–Mass Spectrometry of Fatty Acids Including Hydroxy and Hydroperoxy Acids as Their 3-Methyl-7-methoxy-1,4-benzoxazin-2-one Derivatives, *J. Chromatogr. 639*, 165–173.
4. Banni, S., Day, B.W., Evans, R.W., Corongiu, F.P., and Lom-

bardi, B. (1994) Liquid Chromatographic–Mass Spectrometric Analysis of Conjugated Diene Fatty Acids in a Partially Hydrogenated Fat, *J. Am. Oil Chem. Soc. 71*, 1321–1325.

5. Tyrefors, L.N., Moulder, R.X., and Markides, K.E. (1993) Interface for Open Tubular Column Supercritical Fluid Chromatography/Atmospheric Pressure Chemical Ionization Mass Spectrometry, *Anal. Chem. 65*, 2835–2840.

6. Byrdwell, W.C., and Emken, E.A. (1995) Analysis of Triglycerides Using Atmospheric Pressure Chemical Ionization Mass Spectrometry, *Lipids 30*, 173–175.

7. Byrdwell, W.C., Emken, E.A., Neff, W.E., and Adlof, R.O. (1996) Quantitative Analysis of Triglycerides Using Atmospheric Pressure Chemical Ionization–Mass Spectrometry, *Lipids 31*, 919–935.

8. Laakso, P., and Voutilainen, P. (1996) Analysis of Triacylglycerols by Silver-Ion High-Performance Liquid Chromatography–Atmospheric Pressure Chemical Ionization Mass Spectrometry, *Lipids 31*, 1311–1322.

9. Laakso, P., and Manninen, P. (1997) Identification of Milk Fat Triacylglycerols by Capillary Supercritical Fluid Chromatography–Atmospheric Pressure Chemical Ionization Mass Spectrometry, *Lipids 32*, 1285–1295.

10. Mottram, H.R., and Evershed, R.P. (1996) Structure Analysis of Triacylglycerol Positional Isomers Using Atmospheric Pressure Chemical Ionisation Mass Spectrometry, *Tetrahedron Lett. 37*, 8593–8596.

11. Mottram, H.R., Woodbury, S.E., and Evershed, R.P. (1997) Identification of Triacylglycerol Positional Isomers Present in Vegetable Oils by High Performance Liquid Chromatography/Atmospheric Pressure Chemical Ionization Mass Spectrometry, *Rapid Commun. Mass Spectrom. 11*, 1240–1252.

12. Byrdwell, W.C., and Borchman, D. (1997) Liquid Chromatography/Mass Spectrometric Characterization and Dihydrosphingomyelin of Human Lens Membranes, *Ophthal. Res. 29*, 191–206.

13. Karlsson, A.A., Michelsen, P., and Odham, G. (1998) Molecular Species of Sphingomyelin: Determination by High-Performance Liquid Chromatography/Mass Spectrometry with Electrospray and High-Performance Liquid Chromatography/Tandem Mass Spectrometry with Atmospheric Pressure Chemical Ionization, *J. Mass Spectrom. 33*, 1192–1198.

14. Qiu, D.F., Xiao, X.Y., Walton, T.J., Games, M.P.L., and Games, D.E. (1999) High-Performance Liquid Chromatography/Atmospheric Pressure Chemical Ionization Mass Spectrometry of Phospholipids in *Natronobacterium magadii*, *Eur. Mass Spectrom. 5*, 151–156.

15. Carrier, A., Parent, J., and Dupuis, S. (2000) Quantitation and Characterization of Phospholipids in Pharmaceutical Formulations by Liquid Chromatography–Mass Spectrometry, *J. Chromatogr. A 876*, 97–109.

16. Dobson, G., and Deighton, N. (2001) Analysis of Phospholipid Molecular Species by Liquid Chromatography–Atmospheric Pressure Chemical Ionisation Mass Spectrometry of Diacylglycerol Nicotinates, *Chem. Phys. Lipids 111*, 1–17.

17. Couch, L.H., Churchwell, M.I., Doerge, D.R., Tolleson, W.H., and Howard, P.C. (1997) Identification of Ceramides in Human Cells Using Liquid Chromatography with Detection by Atmospheric Pressure Chemical Ionization Mass Spectrometry, *Rapid Commun. Mass Spectrom. 11*, 504–512.

18. Van Breemen, R.B., Huang, C.R., Tan, Y., Sander, L.C., and Schilling, A.B. (1996) Liquid Chromatography/Mass Spectrometry of Carotenoids Using Atmospheric Pressure Chemical Ionization, *J. Mass Spectrom. 31*, 975–981.

19. Van Breeman, R.B., Xu, X., Viana, M.A., Chen, L., Stacewicz-Sapuntzakis, M., Duncan, C., Bowen, P.E., and Sharifi, R. (2002) Liquid Chromatography–Mass Spectrometry of *cis*- and all-*trans*-Lycopene in Human Serum and Prostate Tissue After Dietary Supplementation with Tomato Sauce, *J. Agric. Food Chem. 50*, 2214–2219.

20. Clarke, P.A., Barnes, K.A., Startin, J.R., Ibe, F.I., and Shepherd, M.J. (1996) High Performance Liquid Chromatography/Atmospheric Pressure Chemical Ionization–Mass Spectrometry for the Determination of Carotenoids, *Rapid Commun. Mass Spectrom. 10*, 1781–1785.

21. Hagiwara, T., Yasuno, T., Funayama, K., and Suzuki, S. (1997) Determination of Lycopene, α-Carotene and β-Carotene in Vegetable Juice by Liquid Chromatography/Atmospheric Pressure Chemical Ionization–Mass Spectrometry, *J. Food Hyg. Soc. Jpn. 38*, 211–218.

22. Hagiwara, T., Yasuno, T., Funayama, K., and Suzuki, S. (1998) Determination of Lycopene, α-Carotene and β-Carotene in Serum by Liquid Chromatography–Atmospheric Pressure Chemical Ionization Mass Spectrometry with Selected Ion Monitoring, *J. Chromatogr. B 708*, 67–73.

23. Kobayashi, Y., Saiki, K., and Watanabe, F. (1993) Characteristics of Mass Fragmentation of Steroids by Atmospheric Pressure Chemical Ionization Mass Spectrometry, *Biol. Pharmacolog. Bull. 16*, 1175–1178.

24. Ma, Y.C., and Kim, H.Y. (1997) Determination of Steroids by Liquid Chromatography/Mass Spectrometry, *J. Am. Soc. Mass Spectrom. 8*, 1010–1020.

25. Joos, P.E., and van Ryckeghem, M. (1999) Liquid Chromatography–Tandem Mass Spectrometry of Some Anabolic Steroids, *Anal. Chem. 71*, 4701–4710.

26. Byrdwell, W.C. (1998) APCI-MS for Lipid Analysis, *INFORM 9*, 986–997.

27. Byrdwell, W.C. (2001) Atmospheric Pressure Chemical Ionization Mass Spectrometry for Analysis of Lipids, *Lipids 36*, 327–346.

28. Laakso, P. (2002) Mass Spectrometry of Triacylglycerols, *Eur. J. Lipid Sci. Technol. 104*, 43–49.

29. Byrdwell, W.C. (2003) APCI-MS in Lipid Analysis, in *Advances in Lipid Methodology—Five* (Adlof, R.O., ed.), pp. 171–253, The Oily Press, Bridgwater, England.

30. Laakso, P. (1996) Analysis of Triacylglycerols—Approaching the Molecular Composition of Natural Mixtures, *Food Rev. Intt. 12*, 199–250.

31. Iwasaki, Y., and Yamane, T. (2000) Enzymatic Synthesis of Structured Lipids, *J. Mol. Catal. B: Enz. 10*, 129–140.

32. Neff, W.E., and Byrdwell, W.C. (1995) Soybean Oil Triacylglycerol Analysis by Reversed-Phase High-Performance Liquid Chromatography Coupled with Atmospheric Pressure Chemical Ionization Mass Spectrometry, *J. Am. Oil Chem. Soc. 72*, 1185–1191.

33. Neff, W.E., and Byrdwell, W.C. (1995) Triacylglycerol Analysis by High Performance Liquid Chromatography–Atmospheric Pressure Chemical Ionization Mass Spectrometry: *Crepis alpina* and *Vernonia galamensis* Seed Oils, *J. Liq. Chromatogr. Rel. Technol. 18*, 4165–4181.

34. Byrdwell, W.C., and Neff, W.E. (1997) Qualitative and Quantitative Analysis of Triacylglycerols Using Atmospheric Pressure Chemical Ionization Mass Spectrometry, in *New Techniques and Applications in Lipid Analysis* (McDonald, R.E., and Mossoba, M.M., eds.), pp. 45–80, AOCS Press, Champaign.

35. Byrdwell, W.C., Neff, W.E., and List, G.R. (2001) Triacylglycerol Analysis of Potential Margarine Base Stocks by High Performance Liquid Chromatography with Atmospheric Pressure Chemical Ionization Mass Spectrometry and Flame Ionization Detection, *J. Agric. Food Chem. 49*, 446–457.

36. Laakso, P. (1997) Characterization of α- and γ-Linolenic Acid Oils by Reversed-Phase High-Performance Liquid Chromatography–Atmospheric Pressure Chemical Ionization Mass Spectrometry, *J. Am. Oil Chem. Soc. 74*, 1291–1300.

37. Manninen, P., and Laakso, P. (1997) Capillary Supercritical Fluid Chromatography Atmospheric Pressure Chemical Ioniza-

tion Mass Spectrometry of Triacylglycerols in Berry Oils, *J. Am. Oil Chem. Soc. 74*, 1089–1098.

38. Mottram, H.R., Crossman, Z.M., and Evershed, R.P. (2001) Regiospecific Characterisation of the Triacylglycerols in Animal Fats Using High Performance Liquid Chromatography–Atmospheric Pressure Chemical Ionisation Mass Spectrometry, *Analyst 126*, 1018–1024.

39. Hsu , F.F., and Turk, J. (1999) Structural Characterization of Triacylglycerols as Lithiated Adducts by Electrospray Ionization Mass Spectrometry Using Low-Energy Collisionally Activated Dissociation on a Triple Stage Quadrupole Instrument, *J. Am. Soc. Mass Spectrom. 10*, 587–599.

40. Fauconnot, L., Hau, J., Aeschlimann, J.M., Fay, L.B., and Dionisi, F. (2004) Quantitative Analysis of Triacylglycerol Regioisomers in Fats and Oils Using Reversed-Phase High-Performance Liquid Chromatography and Atmospheric Pressure Chemical Ionization Mass Spectrometry, *Rapid Commun. Mass Spectrom. 18*, 218–224.

41. Byrdwell, W.C. (2003) APCI-MS in Lipid Analysis, in *Advances in Lipid Methodology–Five* (Adlof, R.E., ed.), p. 200, The Oily Press, Bridgwater, England.

42. Jakab, A., Jablonkai, I. and Forgacs, E. (2003) Quantification of the Ratio of Positional Isomer Dilinoleoyl-oleoyl Glycerols in Vegetable Oils, *Rapid Commun. Mass Spectrom. 17*, 2295–2302.

43. Byrdwell, W.C., and Neff, W.E. (2002) Dual Parallel Electrospray Ionization and Atmospheric Pressure Chemical Ionization Mass Spectrometry (MS), MS/MS and MS/MS/MS for the Analysis of Triacylglycerols and Triacylglycerol Oxidation Products, *Rapid Commun. Mass Spectrom. 16*, 300–319.

44. Hsu, F.F., and Turk, J. (2005) Electrospray Ionization with Low-Energy Collisionally Activated Dissociation Tandem Mass Spectrometry of Complex Lipids: Structural Characterization and Mechanisms of Fragmentation, in *Modern Methods for Lipid Analysis by Liquid Chromatography/Mass Spectrometry and Related Techniques (*Byrdwell, W.C., ed.), pp. 61–178, AOCS Press, Champaign.

45. Byrdwell, W.C. (2005) Qualitative and Quantitative Analysis of Triacylglycerols by Atmospheric Pressure Ionization (APCI and ESI) Mass Spectrometry Techniques, in *Modern Methods for Lipid Analysis by Liquid Chromatography/Mass Spectrometry and Related Techniques* (Byrdwell, W.C., ed.), pp. 298–412, AOCS Press, Champaign.

46. Han, X., and Gross, R.W., Toward Total Cellular Lipidome Analysis by ESI Mass Spectrometry from a Crude Lipid Extract, in *Modern Methods for Lipid Analysis by Liquid Chromatography/Mass Spectrometry and Related Techniques* (Byrdwell, W.C., ed.), pp. 488–509, AOCS Press, Champaign.

Gas Chromatographic Quantification of Fatty Acid Methyl Esters: Flame Ionization Detection vs. Electron Impact Mass Spectrometry

Eric D. Dodds[a], Mark R. McCoy[a,d], Lorrie D. Rea[c,d], and John M. Kennish[a,b,]*

[a]Applied Science, Engineering, and Technology Laboratory and [b]Department of Chemistry, University of Alaska Anchorage, Anchorage, Alaska 99508, [c]Environment and Natural Resources Institute, University of Alaska Anchorage, Anchorage, Alaska 99501, and [d]Alaska Department of Fish and Game, Physiological Ecology Laboratory, Anchorage, Alaska 99518

ABSTRACT: The determination of FAME by GC is among the most commonplace analyses in lipid research. Quantification of FAME by GC with FID has been effectively performed for some time, whereas detection with MS has been used chiefly for qualitative analysis of FAME. Nonetheless, the sensitivity and selectivity of MS methods advocate a quantitative role for GC–MS in FAME analysis—an approach that would be particularly advantageous for FAME determination in complex biological samples, where spectrometric confirmation of analytes is advisable. To assess the utility of GC–MS methods for FAME quantification, a comparative study of GC–FID and GC–MS methods has been conducted. FAME in prepared solutions as well as a biological standard reference material were analyzed by GC–FID and GC–MS methods using both ion trap and quadrupole MS systems. Quantification by MS, based on total ion counts and processing of selected ions, was investigated for FAME ionized by electron impact. Instrument precision, detection limits, calibration behavior, and response factors were investigated for each approach, and quantitative results obtained by each technique were compared. Although there were a number of characteristic differences between the MS methods and FID with respect to FAME analysis, the quantitative performance of GC–MS compared satisfactorily with that of GC–FID. The capacity to combine spectrometric examination and quantitative determination advances GC–MS as a powerful alternative to GC–FID for FAME analysis.

Paper no. L9654 in *Lipids* 40, 419–428 (April 2005)

The first of many important advances in the early development of GLC for analytical purposes was the separation and determination of FA reported by James and Martin in 1952 (1). Soon after, the analytical separation of FAME by vapor-phase chromatography was described by Cropper and Heywood (2). Since then, the characterization of FA composition by esterification to FAME and subsequent determination by GC has become one of the most widely performed analyses in lipid research laboratories and has found broad application to biochemical, biomedical, microbiological, agricultural, and ecological research.

Presently, a large number of lipid analysts use the FID to measure FAME separated by GC. Although FID has proven to be a robust tool for FAME determination, the lack of any selectivity can limit the usefulness of this detector when applied to complicated samples, since only instrument response and retention time information may be gathered. Owing in large part to this limitation, misidentification of FAME in the presence of contaminants, artifacts, or coeluting compounds is still of concern when using FID (3–5). Thus, much work has been done to maximize the usefulness of retention time for FAME identification through methods such as retention time locking, retention time prediction, and the dependence of retention time on FAME equivalent chain lengths (6–8); however, FAME identities assigned by such methods are generally considered tentative (9). Hence, FID analysis of complex biological extracts may prove inadequate in some situations, particularly for FAME of relatively low abundance (10).

With the coupling of MS methods to GC, much has been accomplished in the area of qualitative characterization of FAME mixtures. Since GC–MS provides spectrometric information on separated compounds, it provides a means of analyte selectivity; thus, detection with MS also represents a potentially powerful tool for quantitative analysis of FAME, especially in the presence of a convoluted biochemical background. Despite the prospective benefits of GC–MS methodologies for quantitative FAME analysis, the more familiar FID is still favored in many laboratories, particularly among lipid specialists.

GC–MS offers a host of tools for qualitative characterization of FA. For example, standard 70 eV EI ionization of picolinyl, dimethyloxazoline, pyrrolidide, pentafluorodimethylsilyl, and trimethylsilyl derivatives of FA has been extensively studied for the purpose of structural determination (11–17). EI ionization of these less common FA derivatives yields fragments of diagnostic value in locating the positions of branching and in some cases the positions of unsaturation in FA (although the geometric configuration of the double bond is not forthcoming).

The simplest method of FAME quantification by EI–MS may be carried out by monitoring a range of mass-to-charge (*m/z*) values that will encompass the fragments expected of the analytes, then determining amount based on integration of

peaks in the total ion count (TIC) chromatogram. If the identity and retention time of a given analyte have been established, the sensitivity and specificity of EI–MS can be extended through the use of selective ion monitoring (SIM), which involves the exclusive acquisition of a specified ion or group of ions during a given time frame. When SIM is used in concert with EI, an analyte peak area can be measured reliably regardless of high background or coeluting peaks, provided that ions unique to the analyte are monitored. Ideally, a fragment or fragments of relatively high abundance and characteristic *m/z* would be monitored. When entire mass spectra are acquired, benefits similar to those offered by SIM may be gained through quantification based on only a subset of the acquired ions extracted from the TIC. This selected ion extraction (SIE) allows complete spectra to be recorded and permits the exclusion of undesirable masses for purposes of quantification. Both approaches generally involve the use of relatively few ions for quantification; thus, significant numbers of analyte ions are disregarded and a corresponding loss of signal is experienced. Nonetheless, the net result is an enhancement of the signal-to-noise ratio by elimination of most nonanalyte response from the signal.

An investigation of the performance of FID vs. MS in quantifying FAME separated by GC has not been conducted since the work of Koza *et al.* in 1989 (18). These authors compared FID response factors (RF) of FAME with those obtained using EI in quadrupole (QP) as well as sector-type mass spectrometers. Unfortunately, only seven FAME were examined, none of which was polyunsaturated. In addition, the study provided no

information to users of ion trap (IT) MS systems (since this form of MS was still a relatively recent development at that time). Limits of detection (LOD), calibration behavior, and reproducibility of the instrumental methods were not addressed.

The present study provides a comparison of GC–FID and GC–MS techniques for quantitative FAME analysis. Using both IT and QP MS systems, quantification methods based on the TIC and selected ion techniques were applied to FAME ionized by EI. LOD, calibration characteristics, RF, and method precision for determination of a broad range of FAME were assessed by analysis of standard mixtures with each detection method. To determine the applicability of each approach to the analysis of a biological sample, FAME were prepared from a standard reference fish tissue homogenate with certified values for a group of individual FA [NIST Standard Reference Material (SRM) 1946] (19).

EXPERIMENTAL PROCEDURES

Calibration standards. A series of standard mixtures, including all FAME listed in Table 1, was prepared in residue analysis-grade hexane (EM Science, Gibbstown, NJ). These FAME were selected for calibration because of their prevalence in the tissues of fish and marine animals. The FAME were obtained from Sigma-Aldrich (St. Louis, MO), Supelco (Bellefonte, PA), Matreya (State College, PA), and Nu-Chek-Prep (Elysian, MN), and were of the highest purity available. For each level of calibration, all FAME were present at equal concentrations,

TABLE 1
Analyte FAME Present in the Calibration Standards and Their Order of Elution[a]

Elution order	FAME carbon numer	Systematic name	Common name
1	14:0	Tetradecanoic acid, methyl ester	Methyl myristate
2	16:0	Hexadecanoic acid, methyl ester	Methyl palmitate
3	16:1n-7	*cis*-9-Hexadecenoic acid, methyl ester	Methyl palmitoleate
4	17:0	Heptadecanoic acid, methyl ester	Methyl margarate
5	18:0	Octadecanoic acid, methyl ester	Methyl stearate
6	18:1n-9	*cis*-9-Octadecenoic acid, methyl ester	Methyl oleate
7	18:1n-7	*cis*-11-Octadecenoic acid, methyl ester	Methyl *cis*-vaccenate
8	18:2n-6	*cis,cis*-9,12-Octadecadienoic acid, methyl ester	Methyl linoleate
10	18:3n-3	*cis,cis,cis*-9,12,15-Octadecatrienoic acid, methyl ester	Methyl linolenate
9	19:0	Nonadecanoic acid, methyl ester	None
11	20:0	Eicosanoic acid, methyl ester	Methyl arachidate
12	20:1n-9	*cis*-11-Eicosenoic acid, methyl ester	Methyl gondoate
13	20:2n-6	*cis,cis*-11,14-Eicosadienoic acid, methyl ester	None
15	20:4n-6	*cis,cis,cis,cis*-5,8,11,14-Eicosatetraenoic acid, methyl ester	Methyl arachadonate
17	20:5n-3	*cis,cis,cis,cis,cis*-5,8,11,14,17-Eicosapentaenoic acid, methyl ester	EPA, methyl ester
14	21:0	Heneicosanoic acid, methyl ester	None
16	22:0	Docosanoic acid, methyl ester	Methyl behenate
18	22:1n-9	*cis*-13-Docosenoic acid, methyl ester	Methyl erucate
19	22:4n-6	*cis,cis,cis,cis*-7,10,13,16-Docosatetraenoic acid, methyl ester	Methyl adrenate
20	22:5n-3	*cis,cis,cis,cis,cis*-7,10,13,16,19-Docosapentenoic acid, methyl ester	DPA, methyl ester
21	22:6n-3	*cis,cis,cis,cis,cis,cis*-4,7,10,13,16,19-Docosahexaenoic acid, methyl ester	DHA, methyl ester

[a]The FAME of 21:0 was added pre-analysis as an internal standard.

ranging from 0.02 to 100.0 μg/mL across the series. As an internal standard, 21:0 FAME was added to each mixture at a concentration of 50.0 μg/mL. All standards were analyzed in quadruplicate by GC–FID and each of the GC–MS methods.

RF standard. A commercially available standard mixture of 37 FAME (Supelco) was used in the determination of RF. The original solution was diluted 10-fold to give a final concentration of 1.0 mg/mL total FAME. The RF standard was also spiked with the FAME of 21:0 to obtain a 50.0 μg/mL internal standard concentration. This preparation was then analyzed in quadruplicate by GC–FID and all GC–MS methods under study.

NIST SRM. The NIST SRM 1946 (Gaithersburg, MD), Lake Superior fish tissue homogenate, was used to evaluate the usefulness of each method in analysis of a realistic sample (19). The tissue homogenate was extracted using a Dionex ASE 200 accelerated solvent extractor (Sunnyvale, CA) (20). Conditions similar to those previously described for lipid extraction were used (21–27).

To prepare for extraction, the sample was removed from −80°C storage and allowed to thaw. A 100-mg portion of the tissue homogenate was weighed and combined with approximately 1 g hydromatrix drying agent (Varian, Walnut Creek, CA). The tissue and hydromatrix mixture were transferred to an 11-mL stainless steel extraction cell fitted with three cellulose filters, and additional hydromatrix was added to fill the cell. The sample was then extracted with 60% chloroform/40% methanol (obtained, respectively, from EM Science and Fisher Scientific, Fair Lawn, NJ) at 100°C and 13.8 MPa. Two static extraction cycles were carried out, each 5 min in duration. Both extraction solvents were residue-analysis grade and were treated with 100 mg/L BHT as an antioxidant (Sigma). The crude extract was dried by pouring it through a sintered glass funnel containing several grams of anhydrous sodium sulfate (J.T.Baker, Phillipsburg, NJ). This was followed by thorough rinsing of the funnel with chloroform. The pooled dried extract and rinsing were then concentrated to approximately 1 mL under a stream of nitrogen using a TurboVap apparatus set at a bath temperature of 50°C (Zymark, Hopkinton, MA). The extract concentrate was transferred to a round-bottomed reaction vessel, and the remaining solvent was evaporated by impinging with nitrogen. The recovered lipids were reconstituted in 1 mL 0.5 M methanolic KOH (VWR, West Chester, PA) and hydrolyzed at 80°C for 30 min. Once the reaction mixture had cooled to room temperature, 1 mL of freshly opened 10% BF_3 in methanol was added (Supelco). Transesterification was performed at 100°C for 10 min. After cooling, 1 mL of distilled water and 2 mL of hexane were added to the sample with vortexing. Following phase separation, the organic phase was collected and transferred to a new vessel. The solvent exchange was repeated with a fresh 2-mL portion of hexane. The recovered organic phases were pooled, spiked with the methyl ester of 21:0 to result in a final concentration of 50.0 μg/mL, and diluted to a total final volume of 10 mL with hexane. This sample was analyzed in quadruplicate by each detection method.

Instrumentation, chromatography, and detection methods. FID analyses were performed with an HP 5890 Series II Plus GC–FID system (Hewlett-Packard, Palo Alto, CA). The detector temperature was held at 300°C, and the flame was maintained with 30 mL/min H_2 and 300 mL/min air. Helium was used as the detector auxiliary gas at a flow of 30 mL/min. The same GC system was also used for QP EI-MS analyses by equipping the GC instrument described above with an HP 5970 MS. IT EI-MS analyses were carried out on a Varian CP-3800 GC equipped with a Varian Saturn 2200 MS. A 10-min solvent delay was applied to all detection methods. On both GC instruments, chromatography was carried out using a 60 m × 0.25 mm DB-23 capillary column with a film thickness of 0.25 μm (Agilent Technologies, Wilmington, DE). Helium was used as the carrier gas at a flow rate of 1.0 mL/min with constant flow compensation. GC inlets were held at a temperature of 300°C, and MS transfer lines were maintained at a temperature of 250°C. Sample injections of 1 μL were performed without split for 30 s, followed by a 10:1 split ratio for the remainder of the analysis. The oven temperature was programmed from 125 to 240°C at a rate of 3°C/min with a final hold of 1.67 min (the total analysis time was 40.00 min).

IT GC–MS was carried out using 70 eV EI, and these data were evaluated using both TIC and SIE. Additionally, QP GC–MS with 70 eV EI was carried out in full-scan acquisition (with quantification based on the TIC) as well as in SIM mode. All mass spectra were acquired over the *m/z* range of 40—400 except during SIM. A dwell time of 100 ms was used for all SIM ions. Ions acquired during QP-SIM or processed in IT-SIE are listed in Table 2. In all cases, the three most abundant ions were monitored (SIM) or extracted (SIE) from the complete spectrum.

RESULTS

Reproducibility, calibration, and LOD. Typical chromatograms of a FAME calibration standard obtained by each instrumental approach are shown in Figure 1. Although retention times and chromatographic resolution are slightly different among the methods (likely owing to the differing inlets, detector interfaces, and column ages involved), all analytes eluted under comparable conditions regardless of the instrument involved.

To compare the precision of each detection technique, the mean area ratio (AR) of each analyte FAME with respect to the internal standard was calculated based on the quadruplicate analyses of a FAME standard of intermediate concentration (10 μg/mL). The variability about each mean was computed and expressed as the relative SD (RSD). These results are provided in Table 3 for a representative suite of FAME. The greatest reproducibility was consistently achieved with detection by FID and QP-SIM, with both techniques giving AR with variabilities of less than 1% RSD for most FAME. Notable gains in precision were afforded by QP-SIM as compared with QP-TIC (on average, about 0.9% RSD as compared with about 3% RSD); however, this degree of precision enhancement was not fully realized when IT-SIE was compared with IT-TIC. Although

| FAME | Quantification ions (m/z) | |
	QP-SIM	IT-SIE
12:0	43 + 74 + 87	43 + 74 + 87
13:0	43 + 74 + 87	43 + 74 + 87
14:0	43 + 74 + 87	43 + 74 + 87
14:1n-9	41 + 55 + 74	41 + 55 + 67
15:0	43 + 74 + 87	43 + 74 + 87
15:1n-5	41 + 55 + 74	41 + 55 + 67
16:0	43 + 74 + 87	43 + 74 + 87
16:1n-7	41 + 55 + 69	41 + 55 + 67
17:0	43 + 74 + 87	43 + 74 + 87
17:1n-7	41 + 55 + 69	41 + 55 + 67
18:0	43 + 74 + 87	43 + 74 + 87
18:1n-9 *trans*	41 + 55 + 69	41 + 55 + 67
18:1n-9 *cis*	41 + 55 + 69	41 + 55 + 67
18:1n-7	41 + 55 + 69	41 + 55 + 67
18:2n-6 *trans*	41 + 55 + 67	67 + 81 + 95
18:2n-6 *cis*	41 + 55 + 67	67 + 81 + 95
18:3n-6	41 + 67 + 79	67 + 79 + 93
18:3n-3	41 + 67 + 79	67 + 79 + 93
19:0	43 + 74 + 87	43 + 74 + 87
20:0	43 + 74 + 87	43 + 74 + 87
20:1n-9	41 + 55 + 69	41 + 55 + 69
20:2n-6	41 + 55 + 67	67 + 81 + 95
20:3n-6	41 + 67 + 79	67 + 79 + 83
20:3n-3	41 + 67 + 79	67 + 79 + 93
20:4n-6	41 + 67 + 79	67 + 79 + 91
20:5n-3	41 + 79 + 91	67 + 79 + 91
21:0	43 + 74 + 87	43 + 74 + 87
22:0	43 + 74 + 87	43 + 74 + 87
22:1n-9	41 + 55 + 69	41 + 55 + 69
22:2n-6	41 + 55 + 67	67 + 81 + 95
22:4n-6	41 + 67 + 79	67 + 79 + 91
22:5n-3	41 + 67 + 79	67 + 79 + 91
22:6n-3	67 + 79 + 91	67 + 79 + 91
23:0	43 + 74 + 87	43 + 74 + 87
24:0	43 + 74 + 87	43 + 74 + 87
24:1n-9	43 + 79 + 91	41 + 55 + 69

[a]FAME listed here but absent from Table 1 were unique to the response factor standard. SIM, selective ion monitoring; SIE, selected ion extraction; QP, quadrupole; IT, ion trap.

there are obvious differences in the response reproducibilities among the different detection methods, essentially all of the results in Table 3 fall within a range of only a few percent RSD.

For each quantification method, calibration curves for all FAME were compiled by plotting the mean AR for the quadruplicate analyses as a function of FAME concentration. As a representative example, the calibration curves for the 18:0 FAME are shown in Figure 2. Whereas the FID exhibited a linear response over the entire concentration range examined, each of the MS methods was characteristically nonlinear to varying degrees. The MS method typically yielding the most nearly linear calibrations was QP-MS, where the range of linear response was extended with the use of SIM. The IT-MS methods demonstrated more pronounced departures from linearity under most conditions. This was not unexpected, as ion losses are well known to occur as a consequence of space charging when ions are present in the trap at high concentration. For quantification in subsequent experiments, a quadratic regression was used to

establish the nonlinear calibrations, whereas linear regressions were used for calibration where appropriate.

The LOD was calculated for each calibrated FAME, based on linear regression analysis of the AR vs. FAME concentration relationship. In this context, the LOD expressed in terms of instrumental response, LOD_R, is given by:

$$LOD_R = b + 3s_b \quad [1]$$

where b is the y-intercept of the linear regression line and s_b is the SE of the intercept (28). Rewriting Equation 1 to give LOD in terms of analyte concentration, LOD_C, and making the approximation that b approaches zero (which was, in fact, observed in practice), we have:

$$LOD_c = \frac{3s_b}{m} \quad [2]$$

where m is the slope of the linear fit. Since second-order regression was used to fit a number of the MS calibrations, the LOD for all FAME were based on first-order regression of the low concentration portions of all standard curves (i.e., the first four standard levels detectable by a given method), a region in which linear response was observed regardless of detection method.

The resultant LOD values for a number of analyte FAME are given in terms of both solution concentration and the corresponding number of picomoles (Table 4). Each of the quantification methods is fully capable of detecting low-picomole amounts of a variety of FAME. Detection of subpicomole quantities of almost all the FAME in Table 4 is readily accomplished by FID, with remarkably similar LOD observed for all FAME considered; in general, however, MS quantification methods proved to have LOD that were more sensitive to the identity of the FAME being detected. Of the MS-based quantification methods, QP-TIC generally had the highest LOD; however, when this instrument was operated in SIM mode, LOD were much improved (by as much as a factor of five), rivaling those of any other method. Figure 3 serves to underscore the advantage of quantification by SIM as opposed to TIC when using the QP instrument. For the IT instrument, however, similar improvements in LOD were not achieved in SIE vs. TIC modes. Thus, whereas quantification based on SIE in this case yields marginal improvement in LOD as compared with the TIC and still allows full-scan mass spectra to be acquired, SIM offers much more significant improvements in the LOD while precluding the acquisition of full-scan mass spectra.

RF. To investigate the response dependence of each method on the number of unsaturations as well as the FAME carbon number, the mean response of each analyte with respect to the internal standard was used to calculate the analyte RF according to Equation 3:

$$RF_a = \frac{R_a C_s}{R_s C_a} \quad [3]$$

where the RF of an analyte (RF_a) is given in terms of the analyte response (R_a), the internal standard response (R_s), and the
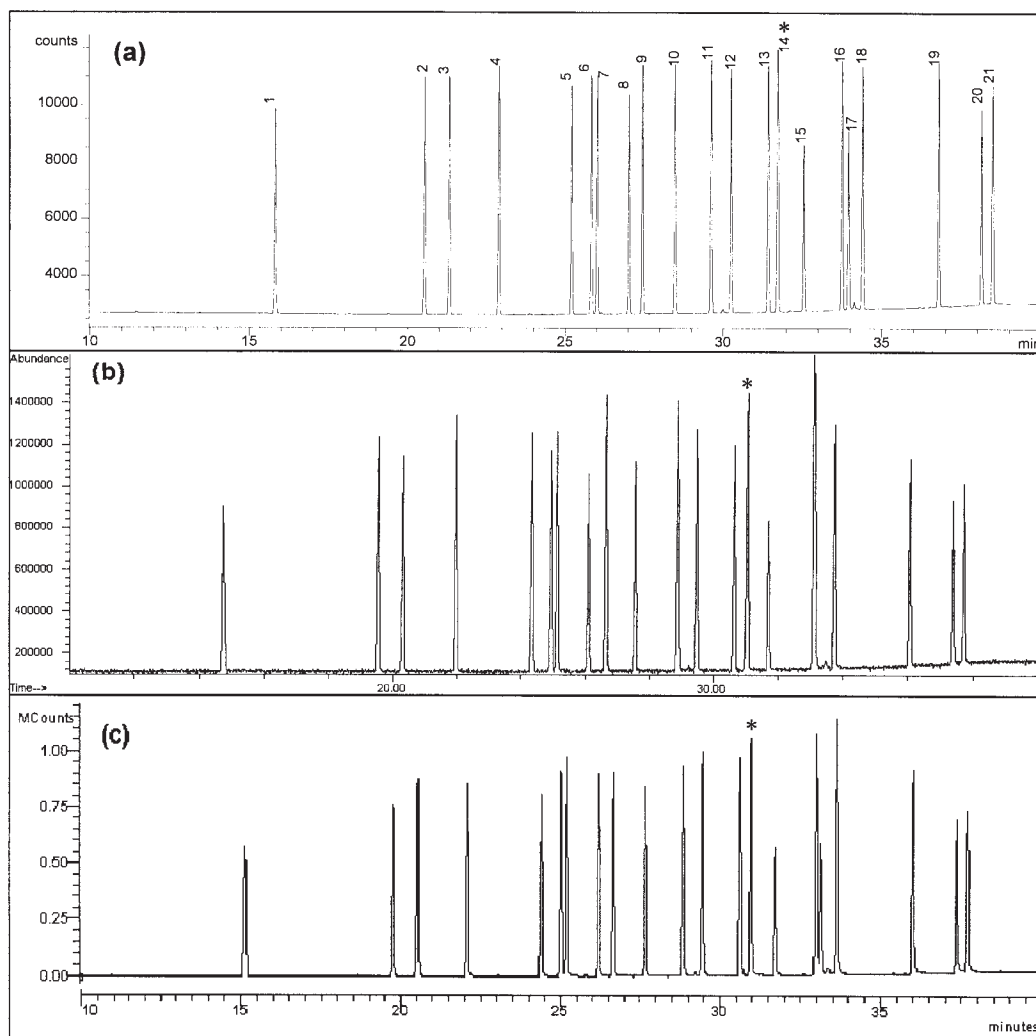
FIG. 1. Gas chromatograms of a FAME calibration standard with detection by FID (a), quadrupole (QP) MS (b), and ion trap (IT) MS (c). For (b) and (c), the total ion counts (TIC) are shown for m/z 40–400. All FAME were present at 50.0 μg/mL. The peaks numbered in (a) correspond to the compounds listed in Table 1. The same order of elution applies to (b) and (c). The internal standard is labeled with an asterisk.

concentrations of the analyte and the internal standard (C_a and C_s, respectively). RF for a representative sampling of FAME are shown for each instrumental approach in Figure 4.

An often-held assumption among lipid analysts is that, in an FID chromatogram, the peak area of an analyte FAME (A_{FAME}) divided by the total peak area of all FAME (ΣA_{FAME}) is equal to the ratio of the corresponding analyte FA mass (m_{FA}) to the total mass of FA present in the sample (Σm_{FA}):

$$\frac{A_{FAME}}{\Sigma A_{FAME}} = \frac{m_{FA}}{\Sigma m_{FA}} \qquad [4]$$

This statement is clearly based on a number of assumptions, not the least of which is that for the FID, the relative responses toward all FAME are equal. The present results, however, are in agreement with a number of contrary findings that attest to the questionable legitimacy of Equation 4 (29–31). That the

FID responses toward all FAME cannot be assumed equivalent may be argued strictly in terms of the mechanism of detection. In FID, the production of CHO^+ ions, which are collected by the cathode and thus generate the detected current, is proportional to the number of carbon–hydrogen bonds introduced to the flame. Since carbonyl carbons are not FID susceptible, it would follow that for an equal mass of two different FAME, the FAME of lower carbon number would have the smaller RF owing to a higher proportion of FID-inactive carbon. Hence, the FID RF for FAME are expected to depend on both the carbon number and the number of unsaturations of the analyte FAME in question. The FID RF shown in Figure 4 reinforce this point, clearly illustrating the predicted relationships. In practice, a number of additional factors prevent the FAME area percentage from equating to mass percentage; for example, injector bias results in a lesser percentage of more volatile com-

TABLE 3
Reproducibility of FAME Response by the Various Methods[a]

FAME	FID Mean AR	FID RSD (%)	QP-TIC Mean AR	QP-TIC RSD (%)	QP-SIM Mean AR	QP-SIM RSD (%)	IT-TIC Mean AR	IT-TIC RSD (%)	IT-SIE Mean AR	IT-SIE RSD (%)
14:0	0.154	1.26	0.146	2.44	0.181	0.67	0.155	3.94	0.272	3.01
16:0	0.165	0.79	0.151	4.29	0.180	0.66	0.179	4.22	0.276	3.74
16:1n-7	0.165	0.44	0.130	2.14	0.089	0.34	0.180	4.03	0.103	3.84
18:0	0.163	0.62	0.151	3.88	0.167	0.87	0.182	3.14	0.251	2.97
18:1n-9	0.171	0.62	0.135	2.95	0.085	0.96	0.194	3.82	0.159	3.52
18:2n-6	0.159	0.55	0.112	2.98	0.074	1.10	0.171	4.19	0.215	3.22
18:3n-3	0.171	0.22	0.108	3.33	0.077	0.99	0.160	3.71	0.176	3.45
22:1n-9	0.180	0.55	0.146	2.27	0.092	0.39	0.163	0.98	0.126	2.34
22:4n-6	0.179	0.46	0.107	3.54	0.070	1.14	0.131	2.85	0.130	0.13
22:5n-3	0.136	2.18	0.072	5.34	0.052	1.34	0.084	6.66	0.101	2.44
22:6n-3	0.158	2.10	0.083	2.23	0.061	1.69	0.102	3.76	0.118	1.58

[a]In all cases, the mean area ratio (AR) vs. the internal standard and relative standard deviation (RSD) of the AR are based on quadruplicate analyses of a 10 µg/mL standard FAME mixture. TIC, total ion counts; for other abbreviations see Table 2.

pounds being successfully loaded on-column (9,30,32). This phenomenon was likely responsible for the reduced FID RF for the 20:0 FAME seen in Figure 4(a).

Unsurprisingly, the MS detectors also have RF that are sensitive to the identity of the analyte, albeit in these cases the relationships between RF and carbon number or unsaturation number are more varied. The QP RF, for example, showed relatively little variability as a function of carbon number and had less scatter than FID; in the case of QP-SIM, the RF were reproduced with exceptional precision. The QP RF, however, experienced a steep reduction with the addition of even a single double bond, with additional but smaller reductions following with additional degrees of unsaturation. The only significant difference between QP-TIC and QP-SIM appeared to be a matter of precision. For IT-TIC, as in FID, the RF were directly proportional to carbon number and were diminished with increasing unsaturation number, although the range of RF was broader (about 0.6 to 1.1 for IT-SIE as opposed to a range of roughly 1.0 to 1.2 for FID). The RF for IT-SIE, though, did not

appear to be predictably dictated by either carbon number or degrees of unsaturation. Interestingly, the same ions were extracted to produce the IT-SIE data as were monitored by QP-SIM, but very different trends in RF were observed, illustrating the impact that continuously sorted ions (QP-SIM) vs. selected extraction of trapped and sequentially released ions (IT-SIE) can exert upon quantification.

NIST SRM. The analyte concentrations determined in the quadruplicate analyses of the NIST SRM extract were averaged, and the FA quantities were expressed in terms of the TG mass percentage in tissue such that direct comparison of the present results with the standard reference values reported by NIST was possible. These results for each detection technique are summarized in Figure 5. For the majority of the analytes (of which the NIST-certified FA are shown in Fig. 5), most FID and MS results were found to be in good agreement with the NIST SRM values (i.e., to within the SE of the measurements).

The procedure used for extraction of the SRM was significantly different from that used by NIST to characterize the

TABLE 4
Limits of Detection (LOD) for a Suite of the Standard FAME as Determined by the Various Methods of Analysis[a]

FAME	FID LOD (µg/mL)	FID LOD (pmol)	QP-TIC LOD (µg/mL)	QP-TIC LOD (pmol)	QP-SIM LOD (µg/mL)	QP-SIM LOD (pmol)	IT-TIC LOD (µg/mL)	IT-TIC LOD (pmol)	IT-SIE LOD (µg/mL)	IT-SIE LOD (pmol)
14:0	0.12	0.50	0.61	2.52	0.11	0.45	0.20	0.83	0.09	0.37
16:0	0.05	0.19	0.47	1.74	0.16	0.59	0.20	0.74	0.08	0.30
16:1n-7	0.11	0.41	0.86	3.21	0.18	0.67	0.23	0.86	0.15	0.56
18:0	0.13	0.44	0.64	2.15	0.21	0.70	0.19	0.64	0.09	0.30
18:1n-9	0.16	0.54	0.56	1.89	0.23	0.78	0.32	1.08	0.17	0.57
18:1n-7	0.15	0.51	0.58	1.96	0.23	0.78	0.34	1.15	0.81	2.74
18:2n-6	0.13	0.44	0.92	3.13	0.25	0.85	0.28	0.95	0.20	0.68
18:3n-3	0.14	0.48	1.15	3.94	0.27	0.92	0.24	0.82	0.19	0.65
20:0	0.15	0.46	0.40	1.23	0.23	0.71	0.26	0.80	0.15	0.46
20:1n-9	0.12	0.37	0.52	1.60	0.24	0.74	0.38	1.17	0.18	0.56
20:2n-6	0.11	0.34	0.47	1.46	0.24	0.75	0.40	1.24	0.19	0.59
22:1n-9	0.14	0.40	0.81	2.30	0.20	0.57	0.53	1.51	0.23	0.65
22:4n-6	0.32	0.92	0.65	1.88	0.20	0.58	0.44	1.27	0.42	1.21
22:5n-3	0.24	0.70	0.85	2.47	0.22	0.64	0.50	1.45	0.55	1.60
22:6n-3	0.54	1.58	0.21	0.61	0.25	0.73	0.78	2.28	0.52	1.52

[a]For abbreviations see Table 2.
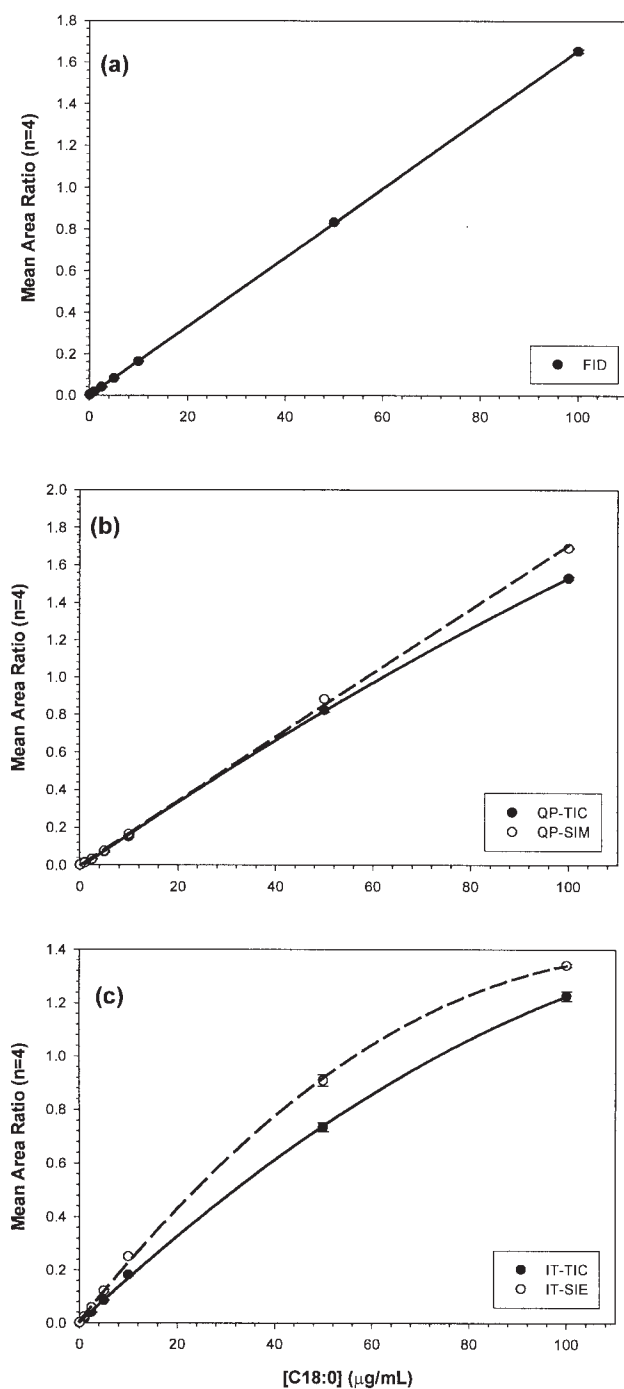
FIG. 2. Calibration curves for the 18:0 FAME as determined by FID (a), QP-MS (b), and IT-MS (c). Error bars, where large enough to be visible, represent the SD. SIM, selective ion monitoring; SIE, selected ion extraction; for other abbreviations see Figure 1.

sample. The present method made use of high-pressure, high-temperature accelerated solvent extraction with chloroform/methanol, employing less than 20 mL of solvent to extract 100 mg of tissue homogenate in roughly 20 min. By contrast, the SRM values were determined by 18–24 h Soxhlet extractions of 2.5 g tissue homogenate samples with hexane/acetone. Although the performance of accelerated solvent extraction for lipid extraction has been addressed elsewhere and deemed sat-

isfactory (21–27), these different approaches may be partly responsible for some of the minor discrepancies between the present results and the NIST SRM certified values; however, since the same extract was analyzed by all methods, the results are indeed suitable for direct comparison among the various quantification methods.

Overall, these results demonstrate that appropriately chosen and properly calibrated MS detection methods are capable of producing accurate quantitative results for FAME in a biological sample that are of comparable quality to those produced by the more traditional FID.

DISCUSSION

The present findings demonstrate that, although FID and various MS techniques exhibit distinct behavior where response to FAME for quantification is concerned, the use of calibration with internal standardization allows the application of MS to quantitative FAME analysis with adequate precision, low LOD, and accurate quantitative results. The hallmarks of FID performance in FAME quantification include a broad range of linear response, excellent precision, and subpicomole LOD. Of course, the main limitation of this detector is that the response is nonspecific and provides no information on the identity of the analyte.

Overall, the best MS performance was obtained using the QP instrument operated in SIM mode. Although some selectivity was afforded by virtue of the monitoring of selected ions, the ability to acquire complete mass spectra was precluded. Whereas this may be satisfactory for quantitative analysis of well-characterized samples, samples of unknown FAME composition should be screened with full-scan MS prior to SIM analysis for quantification. QP-SIM allowed better linearity of response and better precision when compared with acquisition of TIC on the same instrument and when compared with the IT instrument. Subpicomole LOD were also obtainable in SIM mode, a marginal improvement in the TIC LOD (typically, a few picomoles). Even so, it should be noted that the majority of these results occur within a rather small range regardless of detection method, with each method being capable of a level of performance that is acceptable for many applications.

The response of the IT instrument was less linear and, as has been reported, gave slightly different spectra from those produced using QP instruments (33). The main advantage of the IT instrument was that acquisition of full-scan mass spectra (IT-TIC) gave better quantitative performance than the QP-TIC; thus, although QP-SIM offered the best MS performance overall, IT-TIC was superior to QP-TIC for quantification with full-scan acquisition. The IT-MS analysis also afforded the ability to collect full spectra, yet still offered the capability to extract ions for a given analyte later if enhanced signal-to-noise was needed. Indeed, SIE of FAME chromatograms did allow some improvement in LOD and method precision.

These results also support the need for rigorous calibration, irrespective of the detection method chosen. Whereas appropriate calibration is particularly critical for MS work, the assumption of uniform FID RF is also inadequate for precise
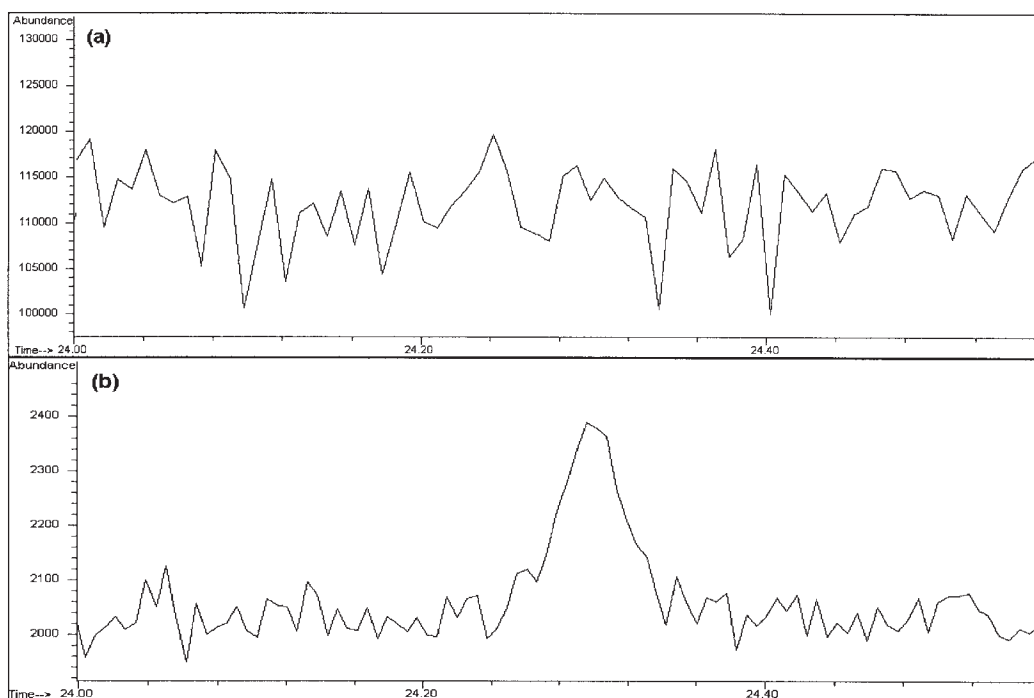
FIG. 3. Expanded chromatograms at the retention time of 18:0 FAME with detection by QP-MS showing the TIC (a) and SIM of *m/z* 43 + 74 + 87 (b). Approximately 20 pg of the 18:0 FAME was injected in both cases. For abbreviations see Figures 1 and 2.

quantitative work. If this approach is used, determinant errors are introduced that may be significant depending on the application.

The sensitivity and selectivity of GC–MS make it an advantageous platform for FAME quantification, despite its obvious absence from discussions on FAME quantification in even relatively recent reviews on the subject of FA analysis (9,29,34). In addition to providing several acceptable options for quantification of FAME, GC–MS offers two powerful advantages over FID: the ability to confirm the identity of analytes based on spectral information in addition to retention time, and the ability to separate peaks from a noisy background or coeluting peaks if unique ions are available. These characteristics, taken together with good quantitative performance and the widespread availability of GC–MS instruments such as those described here, offer compelling motivation to predict that GC–MS will eventually become a far more widely exploited alternative to GC-FID for FAME analysis, both quantitative and qualitative.

ACKNOWLEDGMENTS

REFERENCES

1. James, A.T., and Martin, A.J.P. (1952) Gas–Liquid Partition Chromatography: The Separation and Micro-estimation of Volatile Fatty Acids from Formic Acid to Dodecanoic Acid, *Biochem. J. 50*, 679–690.
2. Cropper, F.R., and Heywood, A. (1953) Analytical Separation of the Methyl Esters of the C_{12}–C_{22} Fatty Acids by Vapour-Phase Chromatography, *Nature 172*, 1101–1102.
3. Ackman, R.G. (1990) Misidentification of Fatty Acid Methyl Ester Peaks in Liquid Canola Shortening, *J. Am. Oil Chem. Soc. 67*, 1028.
4. Hawrysh, Z.J., Shand, P.J., Lin, C., Tokarska, B., and Hardin, R.T. (1990) Efficacy of Tertiary Butylhydroquinone on the Storage and Heat Stability of Liquid Canola Shortening, *J. Am. Oil Chem. Soc. 67*, 585–590.
5. Johnson, A.R., Fogerty, A.C., Hood, R.L., Kozuharov, S., and Ford, G.L. (1976) Gas–Liquid Chromatography of Ethyl Ester Artifacts Formed During the Preparation of Fatty Acid Methyl Esters, *J. Lipid Res. 17*, 431–432.
6. David, F., Sandra, P., and Wylie, P.L. (2002) Improving Analysis of Fatty Acid Methyl Esters Using Retention Time Locked Methods and Retention Time Databases, Agilent Technologies Application Note 5988-5871EN, Palo Alto, CA.
7. Torres, A.G., Trugo, N.M.F., and Trugo, L.C. (2002) Mathematical Method for the Prediction of Retention Times of Fatty Acid Methyl Esters in Temperature-Programmed Capillary Gas Chromatography, *J. Agric. Food Chem. 50*, 4156–4163.
8. Mjos, S.A. (2003) Identification of Fatty Acids in Gas Chromatography by Application of Different Temperature Programs on a Single Capillary Column, *J. Chromatogr. A 1015*, 151–161.
9. Eder, K. (1995) Gas Chromatographic Analysis of Fatty Acid Methyl Esters, *J. Chromatogr. B 671*, 113–131.
10. Roach, J.A.G., Yurawecz, M.P., Kramer, J.K.G., Mossoba,
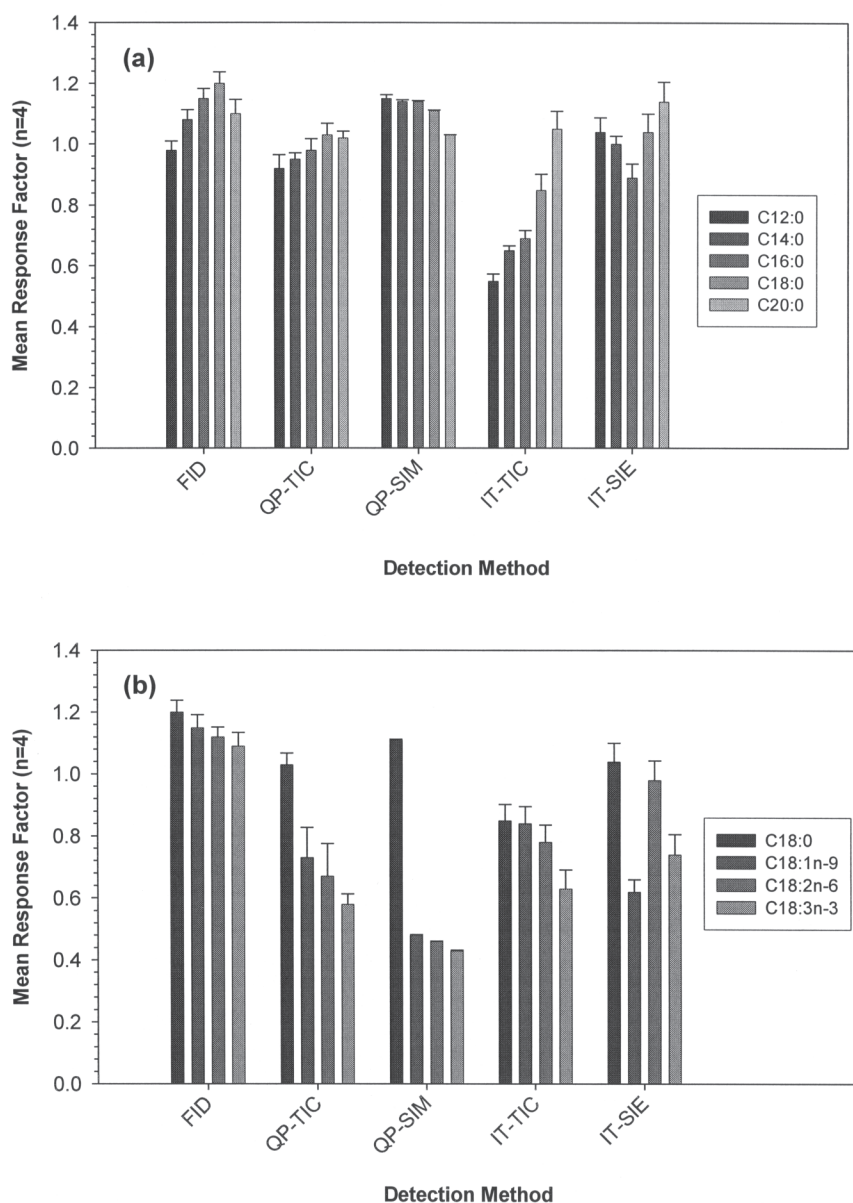
FIG. 4. Response factors for a series of saturated FAME (a) and a series of unsaturated FAME (b) as determined by each detection method. Error bars represent the SD. For abbreviations see Figure 2.

M.M., Eulitz, K., and Ku, Y. (2000) Gas Chromatography–High Resolution Selected-Ion Mass Spectrometric Identification of Trace 21:0 and 20:2 Fatty Acids Eluting with Conjugated Linoleic Acid Isomers, *Lipids 35*, 797–802.

11. Janssen, G., and Parmentier, G. (1978) Determination of Double Bond Positions in Fatty Acids with Conjugated Double Bonds, *Biomed. Mass Spectrom. 5*, 439–443.

12. Christie, W.W., Brechany, E.Y., Johnson, S.B., and Holman, R.T. (1986) A Comparison of Pyrrolidide and Picolinyl Ester Derivatives for the Identification of Fatty Acids in Natural Samples by Gas Chromatography–Mass Spectrometry, *Lipids 21*, 657–661.

13. Christie, W.W., Brechany, E.Y., and Holman, R.T. (1987) Mass Spectra of the Picolinyl Esters of Isomeric Mono- and Dienoic Fatty Acids, *Lipids 22*, 224–228.

14. Harvey, D.J. (1998) Picolinyl Esters for the Structural Determination of Fatty Acids by GC/MS, *Mol. Biotechnol. 10*, 251–260.

15. Christie, W.W. (1998) Gas Chromatography–Mass Spectrome-

try Methods for Structural Analysis of Fatty Acids, *Lipids 33*, 343–353.

16. Choi, M.H., and Chung, B.C. (2000) Diagnostic Fragmentation of Saturated and Unsaturated Fatty Acids by Gas Chromatography–Mass Spectrometry with Pentafluorophenyldimethylsilyl Derivatization, *Anal. Biochem. 277*, 271–273.

17. Hamilton, J.T., and Christie, W.W. (2000) Mechanisms for Ion Formation During the Electron Impact–Mass Spectrometry of Picolinyl Ester and 4,4-Dimethyloxazoline Derivatives of Fatty Acids, *Chem. Phys. Lipids 105*, 93–104.

18. Koza, T., Rezanka, T., and Wurst, M. (1989) Quantitative Analysis of Fatty Acid Methyl Esters by Capillary Gas Chromatography with Flame-Ionization Detection: Quadrupole and Sector Mass Spectrometer, *Folia Microbiol. 34*, 165–169.

19. May, W.E., and Rumble, J. (2002) Certificate of Analysis, Standard Reference Material 1946, Lake Superior Fish Tissue, National Institute of Standards and Technology, Gaithersburg, MD.
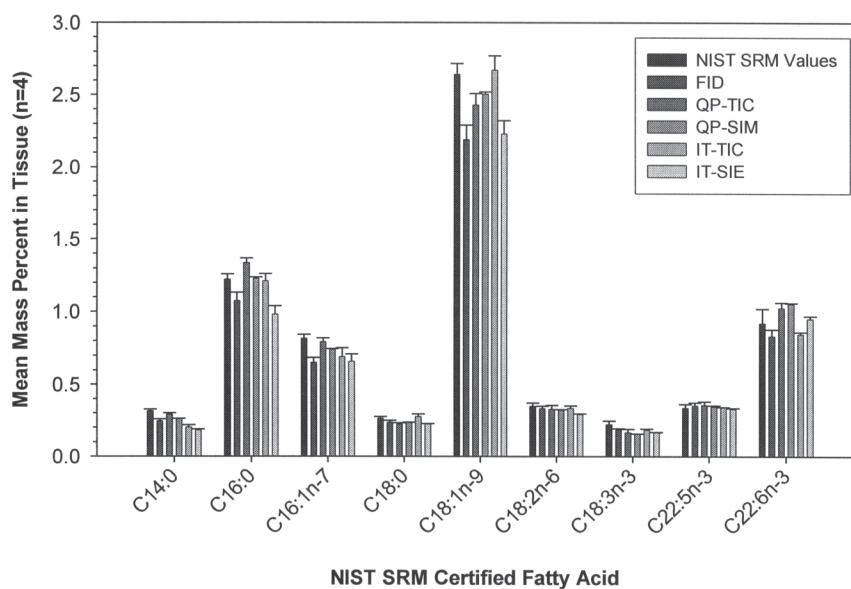
FIG. 5. Mean mass percentage (as TG) of representative certified FA in the NIST Standard Reference Material (SRM) 1946 as determined by each method. Error bars represent the SD, except for those associated with the NIST SRM values; for these values, the error bars represent the uncertainties reported by NIST. For other abbreviations see Figure 2.

20. Richter, B.E., Jones, B.A., Ezzell, J.L., Porter, N.L., Avdalovic, N., and Pohl, C. (1996) Accelerated Solvent Extraction: A Technique for Sample Preparation, *Anal. Chem. 68*, 1033–1039.
21. Schafer, K. (1998) Accelerated Solvent Extraction of Lipids for Determining the Fatty Acid Composition of Biological Material, *Anal. Chim. Acta 358*, 69–77.
22. Boselli, E., Velazco, V., Caboni, M.F., and Lercker, G. (2001) Pressurized Liquid Extraction of Lipids for the Determination of Oxysterols in Egg-Containing Food, *J. Chromatogr. A 917*, 239–244.
23. Richardson, R.K. (2001) Determination of Fat in Dairy Products Using Pressurized Solvent Extraction, *J. Assoc. Off. Anal. Chem. Int. 84*, 1522–1533.
24. Moreau, R.A., Powell, M.J., and Singh, V. (2003) Pressurized Liquid Extraction of Polar and Nonpolar Lipids in Corn and Oats with Hexane, Methylene Chloride, Isopropanol, and Ethanol, *J. Am. Oil Chem. Soc. 80*, 1063–1067.
25. Toschi, T.G., Bendini, A., Ricci, A., and Lercker, G. (2003) Pressurized Solvent Extraction of Total Lipids in Poultry Meat, *Food Chem. 83*, 551–555.
26. Zhuang, W., McKague, B., Reeve, D., and Carrey, J. (2004) A Comparative Evaluation of Accelerated Solvent Extraction and Polytron Extraction for Quantification of Lipids and Extractable Organochlorine in Fish, *Chemosphere 54*, 467–480.
27. Dodds, E.D., McCoy, M.R., Geldenhuys, A., Rea, L.D., and Kennish, J.M. (2004) Microscale Recovery of Total Lipids from Fish Tissue by Accelerated Solvent Extraction, *J. Am. Oil Chem. Soc. 81*, 835–840.

28. Miller, J.N., and Miller, J.C. (2000) *Statistics and Chemometrics for Analytical Chemistry*, 4th edn., pp. 120–123, Pearson Education, Essex.
29. Ackman, R.G. (2002) The Gas Chromatograph in Practical Analyses of Common and Uncommon Fatty Acids for the 21st Century, *Anal. Chim. Acta 465*, 175–192.
30. Ulberth, F., Gabernig, R.G., and Schrammel, F. (1999) Flame-Ionization Detector Response to Methyl, Ethyl, Propyl, and Butyl Esters of Fatty Acids, *J. Am. Oil Chem. Soc. 76*, 263–266.
31. Ackman, R.G., and Sipos, J.C. (1964) Application of Specific Response Factors in the Gas Chromatographic Analysis of Methyl Esters of Fatty Acids with Flame Ionization Detectors, *J. Am. Oil Chem. Soc. 41*, 377–378.
32. Craske, J.D., and Bannon, C.D. (1987) Gas Liquid Chromatography Analysis of the Fatty Acid Composition of Fats and Oils: A Total System for High Accuracy, *J. Am. Oil Chem. Soc. 64*, 1413–1417.
33. Horman, I., and Traitler, H. (1989) Routine Gas Chromatographic/Mass Spectrometric Analysis of Fatty Acid Methyl Esters Using the Ion Trap Detector, *Biomed. Environ. Mass Spectrom. 18*, 1016–1022.
34. Seppanen-Laakso, T., Laakso, I., and Hiltunen, R. (2002) Analysis of Fatty Acids by Gas Chromatography, and Its Relevance to Research on Health and Nutrition, *Anal. Chim. Acta 465*, 39–62.

Application of Supercritical Fluid Chromatography in the Quantitative Analysis of Minor Components (carotenes, vitamin E, sterols, and squalene) from Palm Oil

Yuen May Choo[a],*, **Mei Han Ng[a], Ah Ngan Ma[a],**
Cheng Hock Chuah[b], and Mohd. Ali Hashim[c]

[a]Malaysian Palm Oil Board (MPOB), No. 6, Persiaran Institusi, Bandar Baru Bangi, 43000 Kajang, Selangor, Malaysia, and Departments of [b]Chemistry and [c]Chemical Engineering, University of Malaya, Kuala Lumpur, Malaysia

ABSTRACT: The application of supercritical fluid chromatography (SFC) coupled with a UV variable-wavelength detector to isolate the minor components (carotenes, vitamin E, sterols, and squalene) in crude palm oil (CPO) and the residual oil from palm-pressed fiber is reported. SFC is a good technique for the isolation and analysis of these compounds from the sources mentioned. The carotenes, vitamin E, sterols, and squalene were isolated in less than 20 min. The individual vitamin E isomers present in palm oil were also isolated into their respective components, α-tocopherol, α-tocotrienol, γ-tocopherol, γ-tocotrienol, and δ-tocotrienol. Calibration of all the minor components of palm as well as the individual components of palm vitamin E was carried out and was found to be comparable to those analyzed by other established analytical methods.

Paper no. L9679 in *Lipids 40*, 429–432 (April 2005).

Crude palm oil (CPO) consists of mainly glycerides (TG, >90%; DG, 2–7%; and MG, <1%), FFA (3–5%), and about 1% minor components such as carotenoids (500–700 ppm), vitamin E (600–1000 ppm), sterols (250–620 ppm), and squalene (200–600 ppm) (1). These minor components are also present in palm fiber oil (PFO) but in a much higher concentration: carotenoids (4000–6000 ppm), vitamin E (2000–4000 ppm), sterols (4000–6500 ppm) (2). All these components have important physiological properties, such as being antioxidative, anticareinogenic, and hypocholesterolemic (3–12).

Various chromatographic and analytical techniques have been reported for the isolation and analysis of these minor components: vitamin E by HPLC using fluorescence detection, squalene and sterols by GC-FID after saponification, and total carotenes by UV-vis spectrophotometry (5,13–16). Chromatographic isolations, e.g., by HPLC and GC, of similar compounds from sources other than palm oil also have been reported (5,13–16).

Although supercritical fluid chromatography (SFC) was reported more than 20 years ago, its advantages have only recently been realized. The unique properties of supercritical fluid as a mobile phase in SFC overcome the difficulties of solute thermal instability and volatility encountered in GC and also shorten the relatively longer analysis times of HPLC separations (17). The comparatively lower operating temperature of SFC over GC gives the advantage of preserving the heat-labile compounds in palm oil. Thus, the deterioration of minor components in palm oil caused by thermal degradation can be minimized or avoided. The growth in popularity of SFC as an analytical tool has been slow because some technical deficiencies, such as injection methods, flow restrictors, and interfaces between the supercritical fluid chromatograph and detectors, needed be addressed before it could be more widely used.

Although the SFC of carotenes, vitamin E, and sterols has been reported in the past, it should be noted that most of these separations were carried out using model mixtures, thereby eliminating interference from other compounds that would be present should a real sample matrix be used (18,19). Moreover, successful SFC separations of real samples also differed from one type of oilseed to another, as the types of minor components present were not similar. In addition, the choice of a capillary or packed column influences the choice for SFC as a separation tool. Packed-column SFC has only recently gained popularity because of the rapid development of packed-column technologies in recent years.

The detection of solutes from SFC separations has been reported using detectors such as flame ionization, NMR, evaporative light-scattering, and IR (17–19). However, a UV variable-wavelength detector was chosen in this study, as the λ_{max} of the solutes indicates the identity of the minor components eluted. This is because the minor components in palm absorb UV at different wavelengths: carotenes at 446 nm, vitamin E at 291 nm, sterols at 220 nm, and squalene at 220 nm.

Previously, Ng and fellow researchers (20) reported the SFC separation of tocols from palm oil using both silica and diol columns. To date, a successful single SFC separation of carotenes, vitamin E, sterols, and squalene from any real sample matrix has not been reported. This paper now reports the SFC separation and quantification of these four minor oilseed components from both CPO and PFO.

*To whom correspondence should be addressed.
E-mail: Choo@mpob.gov.my

Abbreviations: CPO, crude palm oil; PFO, palm fiber oil; SFC, supercritical fluid chromatography;

EXPERIMENTAL PROCEDURES

Apparatus. A JASCO Model SUPER-200 SFC system with a UV-970 variable-wavelength UV/vis detector equipped with high-pressure flow cells was used.

Materials. CPO was obtained from Keck Seng (Malaysia) Berhad (Johor, Malaysia). Palm pressed fiber was obtained from the MPOB Experimental Mill (Negri Sembilan, Malaysia). The fiber was extracted for its oil by soaking it in hexane for 16 h.

All solvents used were of either chromatography or analytical grade and were purchased from Merck (Darmstadt, Germany), J.T.Baker (Phillipsburg, NJ), or HmBG (Hamburg, Germany). Solvents used for chromatography were degassed before use. CO_2 (99.995%) was purchased from Malaysian Oxygen Berhad (Kuala Lumpur, Malaysia).

Squalene, β-carotene, β-sitosterol, and α-tocopherol standards were purchased from Sigma-Aldrich (St. Louis, MO). Tocotrienol standards were obtained from Calbiochem (San Diego, CA).

Preparation of the unsaponifiable sample. Approximately 5 g of CPO was saponified with 5 mL of 50% ethanolic KOH and 1 g of pyrogallol (which acts as an antioxidant) by heating it in the dark under nitrogen flushing using a steam bath for 1 h. The saponified sample was then cooled to room temperature and extracted using a 50-mL portion of a single-phase system of 10% distilled water in *n*-hexane until the supernatant turned colorless. The pooled hexane extracts were washed with 50-mL portions of 10% ethanol in distilled water until the washed water turned neutral. The extract was then taken to dryness using a rotary evaporator and was further dried under vacuum.

The same saponification procedure was repeated using 3 g of PFO.

The yield of unsaponifiable sample from 5 g of CPO was 0.1 g, or 2%, whereas the yield from 3 g of PFO was 0.08 g, or 2.7%. Each unsaponifiable sample from CPO and PFO was dissolved in dichloromethane and injected into a supercritical fluid chromatograph, a high-performance liquid chromatograph, or a gas chromatograph after silylation for further analysis of sterols. Wavelengths for the detection of minor components were: carotenes, 446 nm; vitamin E, 291 nm; sterols, 220 nm; and squalene, 220 nm.

SFC. SFC was carried out using a 5-μm, 4.6 × 250 mm LiChrosorb® 60A Silica analytical column (Merck), with a flow rate of 3.12 mL/min CO_2 with 4% ethanol as entrainer under 180 kg/cm² pressure at 50°C. The loop at the injector port was 20 μL.

HPLC. Analysis of vitamin E was also carried out using HPLC coupled with a fluorescence detector (λ_{ex}: 295 nm; λ_{em}: 325 nm) to compare the results obtained by SFC. A LiChrosorb® 60A Silica analytical column (Merck), 4.6 mm i.d. × 250 mm length, was used. The mobile phase was hexane/THF/isopropanol (1000:60:4) at 1 mL/min.

GC. Results obtained from the analysis of squalene and sterols using SFC were compared with those obtained using a known GC method. Samples for GC analyses were prepared by adding 0.3 mL of 30% *N,O*-bis(trimethylsilyl) trifluoro-acetamide in dichloromethane to a weighed sample (*ca.* 0.02 g). The solution was brought up to 1.5 mL using dichloromethane. Thereafter, the sample mixture was heated at 60°C for 2 h before injection into the gas chromatograph-FID.

A Hewlett-Packard 5890 Series II Plus gas–liquid chromatograph was used. The column used was an SGE 15 m × 0.32 mm i.d. BPX5 0.25 μm capillary column (SGE, Melbourne, Australia); the initial oven temperature was set at 100°C for 1 min and increased to 400°C at the rate of 10°C/min. The injector and detector temperatures were set at 370°C. The oven equilibrium time was 3 min under a pressure of 6.60 psi. The carrier gas (helium) was set at flow velocity ranges of 1.99–2 mL/min/cm/s. The range of split ratio between the compressed air and H_2 gas was 0.0–1.

Quantification of carotene, vitamin E, sterols, and squalene. Standard curves of the vitamin E standards (α-tocopherol, α-tocotrienol, γ-tocopherol, γ-tocotrienol, and δ-tocotrienol) were obtained by injecting different concentrations of the standard into the supercritical fluid chromatograph. Peak areas were obtained, and calibration graphs were then plotted.

Similar steps were applied for the squalene and sterols, which were calibrated as β-sitosterol. Statistical data from the analysis were obtained based on the results of 15 repetitive analyses.

The total carotene content was confirmed using the established method of UV-vis spectrophotometry, by which its spectra and absorbance were obtained at 446 nm.

RESULTS AND DISCUSSION

The isolation of minor components of palm using SFC is a more straightforward method than other procedures. Conventional analyses of palm minor components are tedious, as different techniques such as UV-vis spectrophotometry, HPLC, and GC are necessary to quantify all four minor components of palm in just one sample. Because different analyses require different sample preparations, such as silylation, to convert the nonvolatile compounds to their more volatile derivatives for GC analyses, the whole procedure is time-consuming and labor-intensive. Using SFC, sample preparation, which takes less than 5 min, is carried out only once, thus saving time and labor. Moreover, isolation of the minor components of palm oil by SFC can be accomplished in less than 20 min (Fig. 1). This is much shorter than HPLC and GC, which takes 45 min to complete.

Figure 1 shows the SFC chromatograms of carotenes, vitamin E, sterols, and squalene in CPO and PFO, respectively. Squalene was eluted first, as observed at a wavelength of 220 nm. The amounts of squalene in CPO and PFO were 600 ± 10 and 1730 ± 30 ppm, respectively. The results obtained by the SFC analysis were comparable to those obtained by GC.

Carotenes were eluted as total carotenes, as observed at 446 nm. This was chosen as the wavelength of palm carotenes since it corresponds to the wavelength with maximal absorption in the UV. The amount of carotenes in palm oil was calibrated as
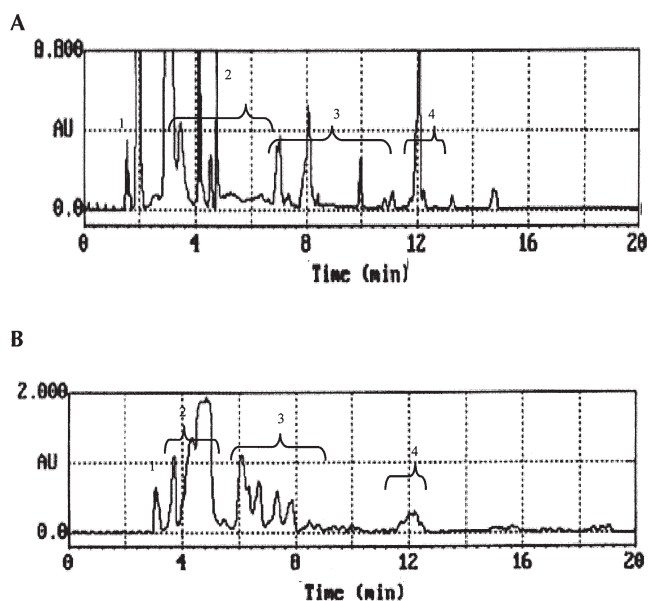
FIG. 1. Supercritical fluid chromatogram of crude palm oil (CPO) and palm fiber oil (PFO) unsaponifiable matter at 210 nm. CPO (A) and PFO (B) unsaponifiable matter was separated by supercritical fluid chromatography (SFC) with a LiChrosorb® 60A Silica column (4.6 mm i.d. × 250 mm length; Merck, Darmstadt, Germany) at 180 kg/cm² and 50°C. The compounds separated were: 1, squalene; 2, carotenes; 3, vitamin E; and 4, sterols.
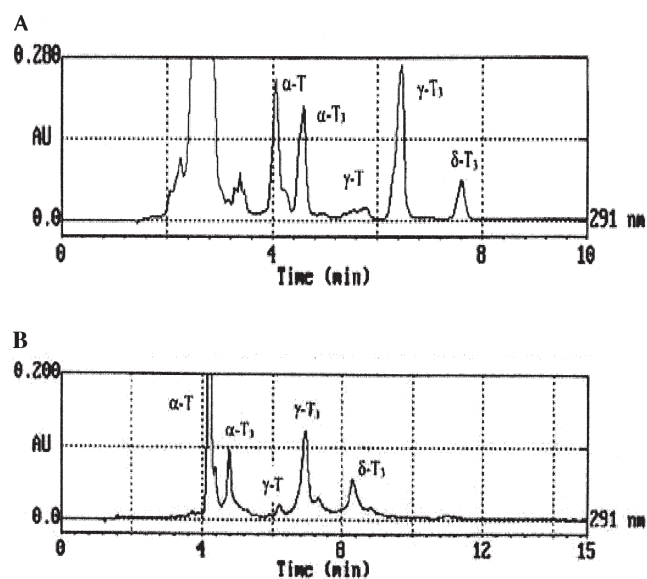
FIG. 2. Supercritical fluid chromatogram of vitamin E in CPO and PFO at 291 nm. Vitamin E in CPO (A) and PFO (B) was separated by SFC with a LiChrosorb 60A Silica column (4.6 mm i.d. × 250 mm length; Merck) at 180 kg/cm² and 50°C. α-T, α-tocopherol; α-T₃, α-tocotrienol; γ-T, γ-tocopherol; γ-T₃, γ-tocotrienol, and δ-T₃, δ-tocotrienol. For other abbreviations see Figure 1.

total β-carotene since it is the major carotene present in palm oil. The total carotenes in CPO were 550 ± 10 ppm, whereas they were 2400 ± 30 ppm in PFO. Using UV-vis spectrometry, the total carotenes in CPO and PFO were 600 ± 20 and 2290 ± 190 ppm, respectively. These results are in agreement with the results obtained by SFC.

Since vitamin E isomers have their maximal absorbance (fluorescence) at 291 nm, this wavelength was chosen for quantification of the vitamin E isomers. At 291 nm, the vitamin E isomers in palm oil were separated into five components, with α-tocopherol as the first vitamin E isomer to be eluted, followed by α-tocotrienol, γ-tocopherol, and γ-tocotrienol, with δ-tocotrienol as the last. Figure 2 shows the SFC chromatograms of vitamin E isomers in the CPO and PFO unsaponifiable samples at 290 nm. The concentrations of the five types of

vitamin E isomers detected in CPO and PFO are presented in Table 1 and compared with HPLC analyses. There was a distinct difference in the concentrations of the vitamin E isomers analyzed by SFC and HPLC. Analyses carried out using SFC gave higher concentrations than those by HPLC. This can be attributed to the fact that in HPLC, vitamin E is destroyed due to prolonged exposure to organic solvents. Because SFC uses supercritical carbon dioxide (SC-CO₂) as the mobile phase, the oxidation of minor components of palm (especially vitamin E isomers) is avoided because SC-CO₂ is nondestructive. Other organic solvents used with HPLC or other chromatographic methods have been shown to degrade the tocols.

Sterols were the last to be eluted by SFC and were quantified as total β-sitosterol, as this is the major sterol present in palm oil. The concentrations of total sterols in CPO and PFO

TABLE 1
Concentration of Vitamin E in Unsaponifiable Samples of Crude Palm Oil (CPO) and Palm Fiber Oil (PFO)[a]

	Concentration (ppm) recovered from			
	SFC		HPLC	
	PFO	CPO	PFO	CPO
α-Tocopherol	1260 ± 50	300 ± 40	1250 ± 70	310 ± 70
α-Tocotrienol	260 ± 10	230 ± 20	230 ± 40	240 ± 5
γ-Tocopherol	80 ± 5	20 ± 5	100 ± 20	10 ± 10
γ-Tocotrienol	480 ± 30	540 ± 30	350 ± 30	460 ± 30
δ-Tocotrienol	200 ± 50	90 ± 10	160 ± 10	100 ± 70
Total	2280 ± 145	1180 ± 105	2090 ± 170	1120 ± 185

[a]Results obtained by calibration with authentic standards using both supercritical fluid chromatography (SFC) and HPLC.

TABLE 2
Concentration of Individual Sterols Analyzed by GC^a

	Concentration (ppm)	
	CPO	PFO
Cholesterol	60	620
Stigmasterol	30	340
β-Sitosterol	60	300
Campesterol	80	990
Total	230	2250

^{a}Breakdown of the sterol composition of CPO and PFO as analyzed by GC. In contrast, the composition of sterols for SFC is reported in this paper as total sterols. For abbreviations see Table 1.

were 180 ± 10 and 2410 ± 50 ppm, respectively. GC-FID is an established method for the quantification of sterols by which the individual sterols can be calibrated (2). Table 2 shows GC results for the quantification of individual sterols. The results obtained by SFC for the determination of total sterols were comparable to those obtained by GC.

In conclusion, SFC can be applied for the isolation of minor components of palm oil, as SFC results for the isolation of these compounds are comparable to those obtained by known methods.

ACKNOWLEDGMENTS

REFERENCES

1. Goh, S.H., Choo, Y.M., and Ong, A.S.H. (1985) Minor Constituents of Palm Oil, *J. Am. Oil Chem. Soc. 62*, 237–240.
2. Choo, Y.M., Yap, S.C., Ooi, C.K., Ma, A.N., Goh, S.H., and Ong, A.S.H. (1996) Recovered Oil from Palm-Pressed Fiber: A Good Source of Natural Carotenoids, Vitamin E, and Sterols, *J. Am. Oil Chem. Soc. 73*, 599–602.
3. Yu, W., Zhao, Y., Xue, Z., Jin, H., and Wang, D. (2001) The Antioxidant Properties of Lycopene Concentrate Extracted from Tomato Paste, *J. Am. Oil Chem. Soc. 78*, 697–701.
4. Martinez-Valverde, I., Periago, M.J., Provan, G., and Chesson, A. (2002) Phenolic Compounds, Lycopene and Antioxidant Activity in Commercial Varieties of Tomato (*Lycopersicum esculentum*), *J. Sci. Food Agric. 82*, 323–330.
5. Qureshi, A.A., Mo, H.B., Packer, L., and Peterson, D.M. (2000) Isolation and Identification of Novel Tocotrienols from Rice Bran with Hypocholesterolemic, Antioxidant and Antitumor Properties, *J. Agric. Food Chem. 48*, 3130–3140.
6. Canfield, L.M. (1995) β-Carotenoid Metabolites: Potential Importance to Human Health, *Malaysian Oil Sci. Technol. 4 (1)*, 43–46.
7. Ashfaq, M.K., Zuberi, H.S., and Waqar, M.A. (2001) Vitamin E and β-Carotene Affect Anticancer Immunity: *In vitro* and *in vivo* Studies, in *2001 PORIM International Conference*, Malaysian Palm Oil Board, Kuala Lumpur, Malaysia.
8. Goh, S.H., Hew, N.F., Norhanom, A.E., and Yadar, M.C. (1994) Inhibition of Tumour Growth Promotion by Various Palm Oil Tocotrienols, *Int. J. Cancer 57*, 529–531.
9. Guthrie, N., Nesaretnam, K., Chambers, A.F., and Carroll, K.K. (1993) Inhibition of Breast Cancer Cell Growth by Tocotrienols, *FASEB J. 7*, A70.
10. Farquhar, J.W. (1996) Plant Sterols: Their Biological Effects in Humans, in *Handbook of Lipids in Human Nutrition*, CRC Press, Boca Raton, FL, pp. 101–105.
11. Nesaretnam, K., Kor, H.T., Ganesan, J., Chong, Y.H., Sundram, K., and Gapor, A. (1992) The Effect of Vitamin E Tocotrienols from Palm Oil on Chemically-Induced Mammary Carcinogenesis in Female Rats, *Nutr. Res. 12*, 63–75.
12. Tay, B.Y.P., and Choo, Y.M. (2000) Valuable Minor Constituents of Commercial Red Palm Olein: Carotenoids, Vitamin E, Ubiquinones and Sterols, *J. Oil Palm Res. 12 (1)*, 14–24.
13. Villén, J., Blanch, G.P., del Castillo, M.L.R., and Herraiz, M. (1998) Rapid and Simultaneous Analysis of Free Sterols, Tocopherols, and Squalene in Edible Oils by Coupled Reversed-Phase Liquid Chromatography–Gas Chromatography, *J. Agric. Food Chem. 46*, 1419–1422.
14. Boven, M.V., Daenens, P., Maes, K., and Cokelaere, M. (1997) Content and Composition of Free Sterols and Free Fatty Alcohols in Jojoba Oil, *J. Agric. Food Chem. 45*, 1180–1184.
15. Senorans, F.J., Villen, J., Tabera, J., and Herraiz, M. (1998) Simplex Optimization of the Direct Analysis of Free Sterols in Sunflower Oil by On-line Coupled Reversed Phase Liquid Chromatography–Gas Chromatography, *J. Agric. Food Chem. 46*, 1022–1026.
16. Senorans, F.J., Tabera, J., and Herraiz, M. (1996) Rapid Separation of Free Sterols in Edible Oils by On-line Coupled Reversed Phase Liquid Chromatography–Gas Chromatography, *J. Agric. Food Chem. 44*, 3189–3192.
17. Smith, R.M. (ed.) (1993) *Supercritical Fluid Chromatography*, RSC Chromatography Monographs, Royal Society of Chemistry, London.
18. King, J.W., and List, G.R. (1996) *Supercritical Fluid Technology in Oil and Lipid Chemistry*, AOCS Press, Champaign.
19. Laakso, P. (1992) Supercritical Fluid Chromatography of Lipids, in *Advances in Lipid Methodology–One* (Christie, W.W., ed.), Oily Press, Dundee, Scotland, pp. 81–120.
20. Ng, M.H., Choo, Y.M., Ma, A.N., Chuah, C.H., and Hashim, M.A. (2004) Isolation of Palm Tocols Using Supercritical Fluid Chromatography, *J. Chromatogr. Sci. 42*, 536–539.

COMMUNICATION

Antioxidant-Restricted Diet Reduces Plasma Nonesterified Fatty Acids in Trained Athletes

Trent A. Watson[a], Robert J. Blake[a], Robin Callister[b], and Manohar L. Garg[a],*

[a]Nutrition & Dietetics, School of Health Sciences, and [b]Human Physiology, School of Biomedical Science, University of Newcastle, New South Wales, 2308, Australia

ABSTRACT: Nonesterified FA (NEFA) are a major fuel source for humans at rest and during moderate exercise. The effect of dietary antioxidant restriction on plasma NEFA levels and exercise performance in trained athletes was examined. Seventeen athletes followed a 2-wk restricted-antioxidant (R-AO) diet, which resulted in a threefold reduction in antioxidant intake (ascorbic acid, 139 to 49 mg; β-carotene, 5093 to 1142 μg) and a significant ($P = 0.001$) reduction in the plasma NEFA. The amount and types of fat consumed were not different between the R-AO and habitual diets. Exercise time to exhaustion was not affected by the R-AO diet, but rating of perceived exertion (RPE) was significantly ($P = 0.03$) elevated. The increase in RPE may have occurred as a result of the R-AO diet and subsequent reduction in plasma NEFA; however, further research is required to confirm this conclusion.

Paper no. L9675 in *Lipids* 40, 433–435 (April 2005).

Nonesterified FA (NEFA) are a major fuel source for humans at rest and during exercise (1–4). Thus, a reduced availability of NEFA may influence exercise performance (5). A number of factors are known to influence an individual's available FA and ability to oxidize them as a fuel. These include exercise intensity and duration (4,6), training status (7,8), total and lean body weight (9), and diet.

Dietary intakes of fat and carbohydrate are known to influence plasma NEFA (10) and fat oxidation rates (11), which is where most researchers have focused their attention.

We previously reported that a restricted-antioxidant (R-AO) diet increases oxidative stress and increases the rating of perceived exertion (RPE) of athletes completing a 30 min submaximal run (12). Since NEFA has a significant role in exercise metabolism, the present study examined the effects of an R-AO diet and subsequent increase in oxidative stress on plasma NEFA levels and exercise performance in trained athletes.

EXPERIMENTAL PROCEDURES

Subjects. Healthy, well-trained male endurance-running athletes ($n = 17$) were recruited to participate in the study. All subjects were between 18 and 35 yr, were nonsmokers, and for at least 3 mon before the study had not taken any vitamin or mineral supplements or medication. The study was approved by the Human Research Ethics Committee of the University of Newcastle.

Study design. The study design has been described in detail previously (12). Briefly, subjects were required to attend the laboratory on three occasions. During the first visit, height, weight, skinfold thickness, and maximal oxygen uptake (VO$_2$max) were measured. The VO$_2$max was conducted using an incremental treadmill test to exhaustion. Before visits two and three, subjects completed a 4-d weighed-food record. Subjects followed their habitual (H-AO) diets prior to visit two and a restricted-antioxidant (R-AO) diet for 2 wk between visits two and three. During visits two and three, subjects were required to undertake a running test to exhaustion (30 min 60% VO$_2$ max, incremental to exhaustion) and provided blood samples for analysis of plasma NEFA. Four blood samples were collected: (i) at rest, (ii) after 30 min of submaximal exercise, (iii) immediately post high-intensity exhaustive exercise, and (iv) after 1 h of recovery. Time to exhaustion and Borgs RPE (13) were also measured.

The R-AO diet required participants to limit fruit and vegetables to one and two servings per day, respectively, and to avoid other foods high in antioxidants including tea, offal meat, wheat germ oil, and cod liver oil. Record *et al.* (14) used this protocol and reduced plasma concentrations of antioxidants in a 2-wk period. Participants in the present study were also encouraged to replace whole-grain breads and cereals with more processed varieties and to avoid antioxidant additives in processed foods.

NEFA analysis. NEFA were determined using the method established by Welz *et al.* (15). To 75 μL of plasma was added 2.5 mL of methanol/toluene (50:1 vol/vol) along with 75 μL of 21:0 free acid (0.04 mg/mL) as an internal standard, and then vortexed vigorously. To promote methylation, samples were incubated at 25°C for 45 min; this mixture was vortexed vigorously for 5 min, and then 1.25 mL of 6% K$_2$CO$_3$ was slowly added to stop the reaction. Hexane (75 μL) was added to the sample, which was then vortexed for 2 min and centrifuged at $3000 \times g$ at 4°C for 10 min to facilitate separation of layers. The latter two processes were conducted a second time to ensure the separation of layers. The upper hexane layer (approximately 100 μL) containing the FAME was then transferred to a 2-mL glass vial, containing a 200-μL high-recovery insert, and crimp-sealed with a Teflon-lined cap for subsequent analysis by GC using a 30 m × 0.25 mm (DB-225) fused carbon-silica

*To whom correspondence should be addressed at University of Newcastle, Callaghan, NSW, 2308, Australia. E-mail: manohar.garg@newcastle.edu.au

Abbreviations: H-AO, habitual-antioxidant; NEFA, nonesterified FA; R-AO, restricted-antioxidant; RPE, rating of perceived exhaustion.

column, coated with cyanopropylphenyl (J&W Scientific, Folsom, CA).

Statistical analysis. FA data were analyzed by repeated-measures analysis using the PROC MIXED model of SAS (1996; SAS Institute, Cary, NC). The MIXED model procedure was used to account for covariation within and between subjects over time (16). The MIXED model procedure of SAS provides a range of covariance structures to model for covariation. Once the covariance structure was modeled, inferences about fixed effects were established as generalized least squares (LS) means and SE estimates for intervention and time differences (16). The study has a power of 80% to detect differences in means. Statistical significance was set at $P \leq 0.05$.

RESULTS

Seventeen subjects completed the study; one athlete withdrew prior to the second visit because of injury. Subject physical characteristics, dietary intake, F_2-isoprostane levels, antioxidant biomarkers, and physical performance indicators have been reported previously (12).

Plasma concentrations of NEFA and the saturated, n-6, and n-3 PUFA components of the NEFA fractions were all significantly lower following the 2-wk R-AO diet when compared with the H-AO diet (Fig. 1) and were inversely correlated with plasma free F_2-isoprostanes (Table 1). Monunsaturated FA in the NEFA fraction tended to be lower on the R-AO diet but did not reach significance, nor were they significantly correlated with plasma free F_2-isoprostane. Plasma concentrations of NEFA tended to increase following the 30-min submaximal exercise period, then fall toward resting levels after exhaustive exercise, and increase again after 1 h of recovery. Although many individual FA in the NEFA fraction changed significantly as a result of exercise, this was not enough for exercise to affect the total plasma NEFA fraction significantly.

TABLE 1
Correlation Between Plasma Free F_2-Isoprostanes and Nonesterified FA (NEFA) Fractions

NEFA	r value	P-value
Total	−0.196	0.022
Saturated	−0.226	0.009
Monounsaturated	−0.043	0.621
Polyunsaturated		
n-6	−0.313	0.000
n-3	−0.210	0.015

DISCUSSION

The aim of this study was to examine the effect of an R-AO diet on plasma FA at rest and during exercise. The reduction in intake of antioxidant-rich foods resulted in a significant reduction in plasma NEFA concentration at rest, following 30 min of submaximal exercise, at exhaustion, and following 1 h of recovery when compared with the H-AO diet. The exercise protocol alone did not appear to have any significant effect on plasma NEFA concentrations, and no interaction effects were observed. Time-to-exhaustion was not affected by the reduction in NEFA, but the RPE was significantly increased during the exercise test when following the R-AO diet compared with the H-AO diet.

As previously reported (12), the R-AO diet resulted in a threefold reduction in ascorbic acid and β-carotene intakes. Energy, protein, carbohydrate, and fat intakes remained unchanged between the R-AO and H-AO diet, which excludes total carbohydrate and fat (type and amount) intakes of athletes that are known to influence plasma NEFA (17). Fasting, caffeine ingestion, and various supplements including L-carnitine, medium-chain TG, and long-chain TG have been shown to influence plasma NEFA (5). None of the subjects were taking these supplements, and the caffeine intake was not affected by the R-AO protocol. This leaves the reduction in dietary antioxidants on the R-AO diet as a single variable that could influence NEFA.

It is often thought that any intervention that increases FA availability in circulation has the potential to increase fat oxidation, slow the rate of glycogen use, and improve endurance exercise performance (5). On the contrary, reduced FA availability would be expected to have the opposite effect. FA availability is not the only factor to affect fat oxidation, which could explain why the majority of studies that have manipulated FA availability in plasma, including the present study, have not observed variations in exercise time to exhaustion (for review, see Ref. 5). Other factors that alter NEFA availability include NEFA movement across the muscle membrane, regulation of muscle TG lipase activity, and regulation of NEFA across the mitochondrial membranes (2). Exercise time-to-exhaustion as a performance measure also may lack the sensitivity to determine performance changes, which may explain why significant changes are not observed, particularly in a short-duration exercise protocol such as that used in the present study.

The present study does not explain the mechanism for the reduction in plasma NEFA following consumption of the

FIG. 1. Plasma nonesterified FA (NEFA) fractions following consumption of a restricted antioxidant diet in athletes at rest. Values reported as least squares means (SE of LS means). *$P < 0.001$. SFA, saturated FA; MUFA, monounsaturated FA; LS, least squares.

R-AO diet for 2 wk. However, we previously showed that the R-AO diet increased plasma concentrations of F_2-isoprostanes indicating that the balance of antioxidants and pro-oxidants had tipped in favor of the latter, which leaves the pro-oxidants to react with plasma molecules such as NEFA, consequently reducing their concentration (12). This is supported by the finding that the F_2-isoprostane value is inversely correlated with plasma NEFA. NEFA has previously been suggested to inhibit peroxidation of lipid membranes, thus acting like an antioxidant (18). In the presence of the reduction in antioxidant intake when consuming the R-AO diet, NEFA itself may have functioned as an antioxidant.

There is also a possibility that the inverse correlation between F_2-isoprostanes and NEFA could be explained by an indirect mechanism. Insulin levels (and insulin-mediated glucose uptake) are positively correlated ($r = 0.51$, $P < 0.004$) with free radical generation (19). Insulin is known to be a primary regulator of adipose tissue lipolysis and also FA re-esterification by reducing lipolysis and increasing re-esterification (17). Plasma NEFA concentrations may be reduced as a consequence of the increase in oxidative stress, which could in turn increase circulating insulin, a potent inhibitor of NEFA release from adipose tissue. Indeed, in the absence of insulin level measurements, there is not enough evidence in the present study to suggest that the proposed mechanism above is valid and thus merits further investigation.

It is also more likely that altered FA availability only has application in long-duration endurance-based exercise because of its substantial abundance when compared with carbohydrate, and the relative contribution of fat as a fuel is highest during low to moderate exercise intensities. The significantly elevated RPE score when subjects followed the R-AO diet in the present study indicates that their perception of effort to complete the 30-min submaximal run was increased on the R-AO diet compared with the H-AO diet protocol. It may be argued that an athlete with a heightened perception of effort is more likely to suffer performance detriment as the duration of exercise is increased.

The findings from this study suggest that the R-AO diet reduces plasma NEFA concentrations. However, further investigations are required to confirm the findings and further elucidate whether our proposed mechanisms are plausible. This will provide answers to the questions of whether antioxidants have a significant effect on fat oxidation and whether a reduction in plasma NEFA concentration has the potential to reduce the use of FA as a fuel for exercise to subsequently affect exercise performance.

REFERENCES

1. Jensen, M.D. (2003) Fate of Fatty Acids at Rest and During Exercise: Regulatory Mechanisms, *Acta Physiol. Scand. 178*, 385–390.
2. Spriet, L.L. (2002) Regulation of Skeletal Muscle Fat Oxidation During Exercise in Humans, *Med. Sci. Sports Exerc. 34*, 1477–1484.
3. van Loon, L.J., Greenhaff, P.L., Constantin-Teodosiu, D., Saris, W.H., and Wagenmakers, A.J. (2001) The Effects of Increasing Exercise Intensity on Muscle Fuel Utilisation in Humans, *J. Physiol. 536 (Pt. 1),* 295–304.
4. Romijn, J.A., Coyle, E.F., Sidossis, L.S., Gastaldelli, A., Horowitz, J.F., Endert, E., and Wolfe, R.R. (1993) Regulation of Endogenous Fat and Carbohydrate Metabolism in Relation to Exercise Intensity and Duration, *Am. J. Physiol. 265 (3, Pt. 1),* E380–E391.
5. Hawley, J.A. (2002) Effect of Increased Fat Availability on Metabolism and Exercise Capacity, *Med. Sci. Sports Exerc. 34*, 1485–1491.
6. Jones, N.L., Heigenhauser, G.J., Kuksis, A., Matsos, C.G., Sutton, J.R., and Toews, C.J. (1980) Fat Metabolism in Heavy Exercise, *Clin. Sci. (London) 59*, 469–478.
7. Kiens, B., Essen-Gustavsson, B., Christensen, N.J., and Saltin, B. (1993) Skeletal Muscle Substrate Utilization During Submaximal Exercise in Man: Effect of Endurance Training, *J. Physiol. 469*, 459–478.
8. Martin, W.H., III, Dalsky, G.P., Hurley, B.F., Matthews, D.E., Bier, D.M., Hagberg, J.M., Rogers, M.A., King, D.S., and Holloszy, J.O. (1993) Effect of Endurance Training on Plasma Free Fatty Acid Turnover and Oxidation During Exercise, *Am. J. Physiol. 265 (5, Pt. 1),* E708–E714.
9. Venables, M.C., Achten, J., Ring, C., and Jeukendrup, A.E. (2003) Fat Oxidation During Exercise Has Stronger Links to Physical Activity and VO$_2$max Than Body Fat, *Med. Sci. Sports Exerc. 35(5),* S25.
10. Pitsiladis, Y.P., Smith, I., and Maughan, R.J. (1999) Increased Fat Availability Enhances the Capacity of Trained Individuals to Perform Prolonged Exercise, *Med. Sci. Sports Exerc. 31*, 1570–1579.
11. Stepto, N.K., Carey, A.L., Staudacher, H.M., Cummings, N.K., Burke, L.M., and Hawley, J.A. (2002) Effect of Short-Term Fat Adaptation on High-Intensity Training, *Med. Sci. Sports Exerc. 34*, 449–455.
12. Watson, T.A., Callister, R., Taylor, R.D., Sibbritt, D.W., MacDonald-Wicks, L.K., and Garg, M.L. (2005) Antioxidant Restriction and Oxidative Stress in Short-Duration Exhaustive Exercise, *Med. Sci. Sports Exerc. 37*, 63–71.
13. Borg, G. (1970) Perceived Exertion as an Indicator of Somatic Stress, *Scand. J. Rehabil. Med. 2*, 92–98.
14. Record, I.R., Dreosti, I.E., and McInerney, J.K. (2001) Changes in Plasma Antioxidant Status Following Consumption of Diets High or Low in Fruit and Vegetables or Following Dietary Supplementation with an Antioxidant Mixture, *Br. J. Nutr. 85*, 459–464.
15. Welz, W., Sattler, W., Leis, H.J., and Malle, E. (1990) Rapid Analysis of Non-esterified Fatty Acids as Methyl Esters from Different Biological Specimens by Gas Chromatography After One-Step Esterification, *J. Chromatogr. 526*, 319–329.
16. Littell, R.C., Pendergast, J., and Natarajan, R. (2000) Modelling Covariance Structure in the Analysis of Repeated Measures Data, *Stat. Med. 19*, 1793–1819.
17. Achten, J., and Jeukendrup, A.E. (2004) Optimizing Fat Oxidation Through Exercise and Diet, *Nutrition 20*, 716–727.
18. Balasubramanian, K.A., Nalini, S., and Manohar, M. (1992) Nonesterified Fatty Acids and Lipid Peroxidation, *Mol. Cell. Biochem. 111*, 131–135.
19. Paolisso, G., D'Amore, A., Volpe, C., Balbi, V., Saccomanno, F., Galzerano, D., Giugliano, D., Varricchio, M., and D'Onofrio, F. (1994) Evidence for a Relationship Between Oxidative Stress and Insulin Action on Non-Insulin-Dependent (Type II) Diabetic Patients, *Metabolism 43*, 1426–1429.

ARTICLES

Triacylglycerol Oxidation in Pig Lipoproteins After a Diet Rich in Oxidized Sunflower Seed Oil

Jukka-Pekka Suomela[a,*], Markku Ahotupa[b], and Heikki Kallio[a]

Departments of [a]Biochemistry and Food Chemistry and [b]Biomedicine, University of Turku, FI-20014 Turku, Finland

ABSTRACT: The effects of two sunflower seed oil diets differing in oxidation levels (PV in oils 1 and 190 mequiv O_2/kg) on lipoprotein TAG and total lipid oxidation were investigated in growing pigs. For 2 wk, two groups of 10 pigs were fed either of the diets, after which blood samples were collected. A method based on RP-HPLC and electrospray ionization-MS was used for the analysis of oxidized TAG molecules in chylomicrons and VLDL. The baseline diene conjugation method was used for the estimation of *in vivo* levels of lipoprotein lipid oxidation. TAG molecules with a hydroxy, an epoxy, or a keto group attached to a FA, as well as TAG core aldehydes were detected in the samples. Typically, lipoprotein TAG and total lipids were more oxidized in the pigs fed on the oxidized oil compared with those fed on nonoxidized oil. Oxidation of dietary fat was thus reflected in the lipoprotein oxidation, which confirmed our earlier findings.

Paper no. L9695 in *Lipids* 40, 437–444 (May 2005).

Studies suggest that oxidized dietary lipids increase the oxidation level of chylomicrons and VLDL (1–3). In addition to oxidized LDL, which has a central role in atherogenesis, oxidized chylomicrons and their remnants also seem to be potentially atherogenic (4–7). Oxidation of chylomicrons results in particles that may serve as a substrate for scavenger receptors (7). Chylomicrons and their remnants may associate with arterial tissue with even greater efficiency than LDL (8).

Thus far, studies of the dietary effects on lipoprotein oxidation at the molecular level have been scarce. Also, there are only a few methods for direct measurement of lipoprotein oxidation (9). In our previous studies (3,10), we used a novel approach based on HPLC-electrospray ionization (ESI)-MS and baseline diene conjugation (BDC) methods to investigate lipid oxidation in human LDL (10) and in different pig lipoproteins (3). HPLC-ESI-MS was applied to the analysis of the oxidized TAG molecules. The BDC method was used to evaluate the oxidation levels of the samples. New information on the oxidized TAG molecules of lipoproteins was obtained. The results of the pig study (3) also suggested that oxidized dietary fat, in comparison with nonoxidized dietary fat, has an increasing effect on lipoprotein total lipid and TAG oxidation.

In the present study, we applied the approach described above to investigate the effects of oxidized dietary sunflower seed oil on the oxidation of pig lipoproteins. The group sizes were larger compared with the earlier pig study (3), and only two diet groups were compared with each other. Detailed information on lipoprotein total lipid and TAG oxidation as well as on the molecular structures of oxidized chylomicron and VLDL TAG was obtained. The results confirmed the conclusions drawn in the earlier pig study (3) and also gave more detailed information on the level of lipoprotein lipid oxidation.

MATERIALS AND METHODS

Chemicals and reagents. 3-Chloroperoxybenzoic acid, triphenyl phosphine and activated manganese dioxide (MnO_2) were obtained from Aldrich Chemical Co. (Milwaukee, WI). Reagents were of reagent grade or better quality. All solvents were of chromatography or reagent grade and were purchased from local suppliers. HPLC standard (G-1) containing synthetic monoacid TAG was obtained from Nu-Chek-Prep, Inc. (Elysian, MN). Synthetic 1,3-distearoyl-2-oleoyl-*sn*-glycerol was obtained from Sigma Chemical Co. (St. Louis, MO). 1,3-Didocosanoyl-2-oleoyl-*sn*-glycerol and 1-linoleoyl-2-oleoyl-3-palmitoyl-*sn*-glycerol were obtained from Larodan Fine Chemicals AB (Malmö, Sweden).

Preparation of reference compounds. The oxidized derivatives of synthetic TAG were prepared as described earlier (3,10) and purified by TLC as described below.

Animals and diets. The study plan was approved by the Test Animal Committee of MTT Agrifood Research Finland.

TABLE 1
Composition of the Feed of the Pigs[a]

Component	g/kg feed
Barley	395.4
Granulated soy[b]	384.6
Sunflower seed oil	160.0
Feeding lime	11.5
Monocalcium phosphate	8.3
Murovit-Selen-E[c]	23.2
Mineral-vitamin mix[d]	17.1

[a]Total energy from fat: 1530–1650 kcal/kg feed.
[b]Contains 3.4–6.8% fat.
[c]In kg of feed: 0.2 mg Se; 81 IU vitamin E.
[d]In kg of feed: 3.0 g Ca; 1.1 g P; 0.7 g Mg; 4.3 g NaCl; 135 mg Fe; 29 mg Cu; 0.4 mg Se; 119 mg Zn; 31 mg Mn; 0.3 mg I; 6806 IU vitamin A; 681 IU vitamin D; 65 mg vitamin E; 2.4 mg vitamin K; 2.5 mg vitamin B_1; 6.1 mg vitamin B_2; 3.6 mg vitamin B_6; 0.03 mg vitamin B_{12}; 0.3 mg biotin; 18.4 mg pantothenic acid; 27 mg niacin; 4.3 mg folic acid.

*To whom correspondence should be addressed. E-mail: jusuom@utu.fi

Abbreviations: ACN:DB, acyl carbon number:number of double bonds; BDC, baseline diene conjugation; ESI, electrospray ionization.

TABLE 2
FA Compositions of the Oils Fed to Pigs[a]

FA	Oil 1[b]	Oil 2[c]
16:0	5.8	6.0
18:0	3.5	3.6
18:1n-9	25.3	26.0
18:1n-7	0.6	0.6
18:2n-6	63.4	62.2
18:3n-3	0.1	0.1
20:0	0.2	0.2
20:1n-9	0.2	0.2
22:0	0.7	0.7
24:0	0.2	0.2

[a]Results expressed as percentage of total FA.
[b]PV 1 mequiv O_2/kg oil.
[c]PV 190 mequiv O_2/kg oil.

Twenty growing pigs (castrated boars) were used in the study. For 2 wk, two groups of 10 pigs (groups 1 and 2) were fed a diet (Table 1) containing 16% sunflower seed oil varying in oxidation levels. The average weight of the animals was 25.3 ± 1.9 kg (mean ± SD) at the beginning of the feeding period and 39.1 ± 4.1 kg at the end of the period. The oil of group 1 was not oxidized (PV 1 mequiv O_2/kg), whereas the oil of group 2 was oxidized in convection ovens at 60°C until the PV of 190 mequiv O_2/kg was reached. The PV determinations were made according to the AOCS official method Cd 8-53 (11) and could be expressed as millimoles of FA hydroperoxide groups per kilogram of oil. This method does not assay oxidized FA other than hydroperoxides. The vitamin E contents of the oils were as follows: group 1, 550 mg/kg; group 2, 103 mg/kg. The vitamin E determinations were made according to IUPAC 2.432 method (12). FA compositions of the oils (Table 2) were determined as described below.

The pigs were fed twice a day. During the first week, the pigs were fed 200 g oil/d and during the second week 230 g oil/d. Because of the high fat load, the pigs were fed in total 161 mg vitamin E/kg feed, not including vitamin E from the oils (Table 1). The level of vitamin E supplementation was based on the guidelines of MTT Agrifood Research Finland.

Sample preparation. Chylomicrons and VLDL were assumed to reach their highest levels during the first 4 h after a meal. Blood samples were obtained by venipuncture from the jugular vein at 3 and 4 h (time points 1 and 2, respectively) after the last meal (half of the daily dose). The blood was collected into tubes containing EDTA as an anticoagulant. Plasma was separated from cells by centrifugation at 3000 × *g* for 15 min. Chylomicrons and VLDL were separated from plasma by ultracentrifugation, and LDL were directly precipitated from EDTA plasma by buffered heparin as described (9,13). Lipids were extracted from plasma and lipoproteins using chloroform/methanol.

Purification of TAG and their oxidation products. For FA analysis, the TAG of chylomicrons and VLDL were purified using Sep-Pak® prepacked silica columns (Waters, Milford, MA) (14). Normal-phase TLC without added antioxidants was used to purify the reference compounds and the oxida-

tion products of chylomicron and VLDL TAG (15). Heptane/di-isopropyl ether/acetic acid (60:40:4, by vol) solution was used as the mobile eluent. Samples were applied to silica G plates. Resolved components were scraped off the plates and were recovered from the silica gel by extraction with chloroform/methanol (2:1, vol/vol). When TLC was applied to the lipoprotein lipid samples, two fractions below the TAG band were scraped from the plate (TAG band, R_f = 0.59; fraction 1, R_f = 0.30–0.50; fraction 2, R_f = 0.10–0.30). The fractions contained the oxidized TAG molecules (3). The extracts were washed with distilled water. TAG and their hydroxy, hydroperoxy, oxo, and epoxy derivatives were detected in UV light after spraying with 2,7-dichlorofluorescein (15).

FA analysis. The FAME of TAG were prepared by sodium methoxide-catalyzed transesterification (16). Methyl esters were dissolved in hexane and analyzed by GC (PerkinElmer AutoSystem, Norwalk, CT) using a DB-23 column (30 m × 0.32 mm i.d., 0.25 µm film thickness; Agilent Technologies, Palo Alto, CA). The instrument was equipped with an FID.

Analysis of samples by HPLC-ELSD and HPLC-ESI-MS. TAG and their oxidation products were separated by RP-HPLC. The HPLC system consisted of a Hitachi (Tokyo, Japan) L-6200 Intelligent Pump with a Discovery® HS C18 column (250 mm × 4.6 mm i.d.; Supelco Inc., Bellefonte, PA). The column was eluted at 0.85 mL/min and a linear gradient was used: 20% 2-propanol in methanol was changed to 80% 2-propanol in 20 min. The final composition was held for 10 min. Eighty-five percent of the effluent (0.72 mL/min) was led to a Sedex 75 (S.E.D.E.R.E., Alfortville, France) ELSD. An evaporation temperature of 70°C and nebulizer gas (air) pressure of 2.7 bar were used in the ELSD. Fifteen percent of the effluent (0.13 mL/min) was led to a Finnigan MAT TSQ 700 triple quadrupole mass spectrometer (Finnigan, San Jose, CA) equipped with a nebulizer-assisted electrospray interface. Full-scan MS spectra were collected in positive (*m/z* 450–1100) ionization mode. The electrospray voltage used was +4.5 kV.

Determination of the oxidation level of plasma and lipoproteins. For the estimation of total lipid oxidation by the baseline level of diene conjugation in plasma and lipoproteins, extracted lipids of plasma, chylomicrons, VLDL, and LDL were dissolved in cyclohexane and analyzed spectrophotometrically at 234 nm. Absorbance units were converted to molar units using the molar extinction coefficient $2.95 × 10^4$ M^{-1} cm^{-1}. The results were expressed as micromoles conjugated dienes in a liter of plasma to have an estimation of the actual level of oxidized lipoproteins in circulation (17). The proportions of oxidized TAG molecules were estimated by HPLC using the conditions described above. The estimations were based on the ELSD chromatograms of the HPLC runs in which an internal standard was used. The response of ELSD to the injected amount of a reference compound (10) was tested before the estimations were made.

Statistical analysis. SPSS 12.0 for Windows (Chicago, IL) was used for data analysis. Independent samples *t*-test and

Mann–Whitney U-test were used to compare the BDC values and FA compositions of the different pig groups.

RESULTS

FA compositions of the TAG of chylomicrons and VLDL are listed in Tables 3 and 4, respectively. As in our earlier study (3), the lipoproteins reflected to a large degree the FA compositions of the test oils. However, chylomicron and VLDL TAG contained more 16:0 (palmitic acid) and 18:3n-3 (α-linolenic acid), and less 18:1n-9 (oleic acid) than the corresponding test oils. Fat derived from soy at least partly explains these differences. VLDL TAG also seemed to contain less 18:2n-6 (linoleic acid) than the test oils. In chylomicron and VLDL TAG of group 2, the relative amount of 18:1n-9 appeared to be higher and that of 18:2n-6 lower compared with the TAG of group 1, as could be expected based on the FA compositions of the test oils. In VLDL TAG, 18:3n-6 (γ-linolenic acid) was present in notable amounts, which indicated incorporation of endogenous γ-linolenic acid into VLDL.

Elution factors determined by Sjövall *et al.* (18) and our group (10) for HPLC were used in the identification of TAG oxidation products after their applicability was confirmed for the present HPLC column. Several oxidation products of TAG were detected in the TLC fractions of chylomicron and VLDL lipids. The oxidized structures were found by extracting peaks of specific *m/z* values from the MS chromatograms of HPLC runs (Fig. 1) (10). Only sodium adduct ions were formed from the molecules in positive ion mode.

The postulated molecular structures of the oxidized TAG of chylomicrons and VLDL are listed in Table 5. In most oxidation products detected, oxidation had occurred in only one of the FA of a TAG molecule. These products consisted of TAG molecules with a hydroxy, an epoxy, or a keto group attached to a FA, and of TAG core aldehydes. Typically, the oxidation products were formed from TAG with ACN:DB (acyl carbon number:number of double bonds) 52:2, 52:3, 52:4, 54:3, 54:4, 54:5, and 54:6. In the present study, TAG core aldehydes were identified as such, not derivatives, in positive ion mode. The aldehydic [M + Na]$^+$ ions were observed to be

TABLE 3
FA Compositions of the TAG of Pig Chylomicrons[a]

FA	Time point 3 h	
	Group 1[b]	Group 2
16:0	7.5 ± 0.6	7.2 ± 0.4
16:1n-7	0.1 ± 0.0[a]	0.1 ± 0.0[b]
18:0	3.2 ± 0.4	3.4 ± 0.3
18:1n-9	23.7 ± 0.8[a]	25.2 ± 0.7[b]
18:1n-7	0.7 ± 0.0	0.8 ± 0.0
18:2n-6	62.4 ± 0.9[a]	61.1 ± 0.7[b]
18:3n-6	0.1 ± 0.0[a]	0.0 ± 0.1[b]
18:3n-3	0.6 ± 0.2	0.5 ± 0.1
20:0	0.1 ± 0.0	0.1 ± 0.0
20:1n-9	0.2 ± 0.0	0.2 ± 0.0
20:2n-6	0.1 ± 0.0	0.1 ± 0.0
20:4n-6	0.7 ± 0.1	0.8 ± 0.2
22:0	0.1 ± 0.1	0.2 ± 0.1
Others	0.3 ± 0.0	0.2 ± 0.1

FA	Time point 4 h	
	Group 1	Group 2
16:0	7.5 ± 0.7	7.3 ± 0.5
16:1n-7	0.1 ± 0.0	0.1 ± 0.0
18:0	3.3 ± 0.6	3.4 ± 0.3
18:1n-9	23.6 ± 1.0[a]	24.9 ± 0.6[b]
18:1n-7	0.7 ± 0.1	0.7 ± 0.0
18:2n-6	62.4 ± 1.6	61.3 ± 0.8
18:3n-6	0.1 ± 0.1	0.0 ± 0.1
18:3n-3	0.7 ± 0.2	0.6 ± 0.1
20:0	0.1 ± 0.1	0.1 ± 0.1
20:1n-9	0.2 ± 0.0[a]	0.2 ± 0.0[b]
20:2n-6	0.1 ± 0.1	0.1 ± 0.0
20:4n-6	0.8 ± 0.1	0.8 ± 0.2
22:0	0.2 ± 0.1	0.1 ± 0.1
Others	0.2 ± 0.1	0.1 ± 0.1

[a]Results expressed as percentage of total FA (mean ± SD, *n* = 10). Different superscript roman letters indicate significant differences between diet groups (*P* < 0.05).
[b]*n* = 8.

TABLE 4
FA Compositions of the TAG of Pig VLDL[a]

FA	Time point 3 h	
	Group 1[b]	Group 2
14:0	0.3 ± 0.1[a]	0.2 ± 0.1[b]
16:0	6.9 ± 1.4	6.4 ± 1.0
16:1n-7	0.3 ± 0.1	0.2 ± 0.1
18:0	2.6 ± 0.3	2.7 ± 0.3
18:1n-9	21.7 ± 0.8[a]	22.8 ± 0.4[b]
18:1n-7	0.7 ± 0.2	0.7 ± 0.2
18:2n-6	61.2 ± 2.0	60.4 ± 1.7
18:3n-6	2.0 ± 0.6	1.8 ± 0.5
18:3n-3	0.6 ± 0.1	0.6 ± 0.1
20:1n-9	0.2 ± 0.0[a]	0.2 ± 0.0[b]
20:2n-6	0.4 ± 0.1	0.5 ± 0.1
20:3n-6	0.3 ± 0.1	0.4 ± 0.1
20:4n-6	2.4 ± 0.5	2.7 ± 0.6
Others	0.3 ± 0.1	0.4 ± 0.1

FA	Time point 4 h	
	Group 1	Group 2
14:0	0.3 ± 0.1	0.3 ± 0.1
16:0	6.9 ± 1.4	6.6 ± 1.1
16:1n-7	0.3 ± 0.1	0.2 ± 0.1
18:0	2.8 ± 0.7	3.0 ± 0.4
18:1n-9	21.6 ± 0.9[a]	22.6 ± 0.6[b]
18:1n-7	0.7 ± 0.1	0.7 ± 0.2
18:2n-6	60.7 ± 2.8	59.8 ± 2.2
18:3n-6	1.8 ± 0.4	1.6 ± 0.5
18:3n-3	0.6 ± 0.2	0.6 ± 0.1
20:1n-9	0.2 ± 0.0	0.2 ± 0.1
20:2n-6	0.5 ± 0.1	0.5 ± 0.1
20:3n-6	0.3 ± 0.1	0.4 ± 0.1
20:4n-6	2.8 ± 0.5	3.1 ± 1.0
Others	0.4 ± 0.2	0.4 ± 0.2

[a]Results expressed as percentage of total FA (mean ± SD). Different superscript roman letters indicate significant differences at each time point between diet groups (*P* < 0.05).
[b]*n* = 8.
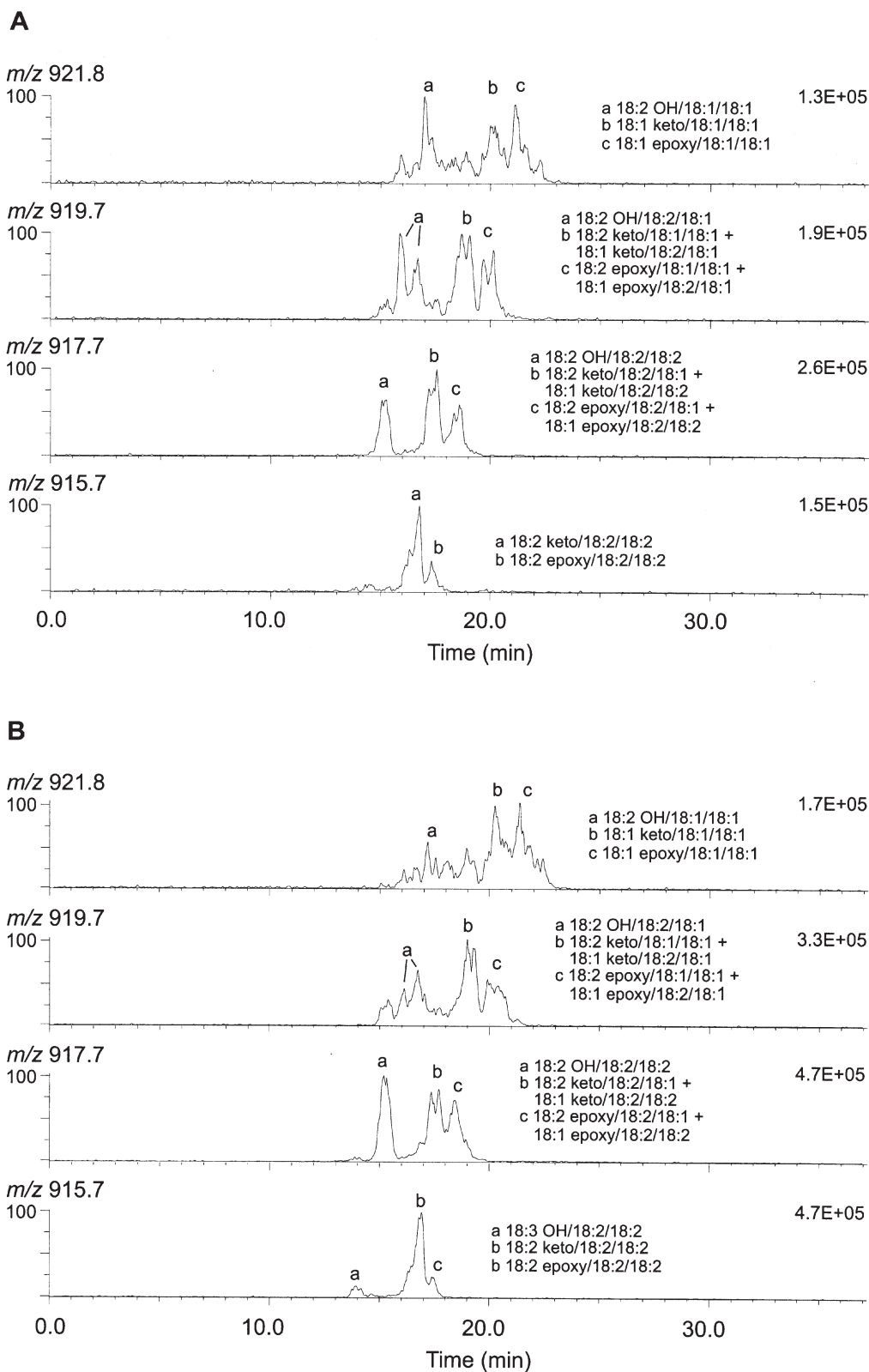
FIG. 1. Ion chromatograms showing the oxidized TAG molecules of pig chylomicrons. Postulated molecular structures (not regioisomers) are included in the chromatograms. TAG of 54 acyl carbons with a hydroxy, a keto, or an epoxy group attached to a FA in a sample representing group 1 (A) and group 2 (B). PV of the sunflower seed oil used in feed: group 1, 1 mequiv O$_2$/kg; group 2, 190 mequiv O$_2$/kg. Molecules detected as [M + Na]$^+$ ions.

TABLE 5
Postulated Structures of the Oxidized TAG Molecules Found in the Chylomicron and VLDL Samples[a]

ACN[b]	Hydroxides	Epoxides	Ketones	Aldehydes
50	18:1 epoxy/16:0/16:0[e]	18:2 keto/16:0/16:0[e]		
	18:1 epoxy/16:0/16:0[e]	18:1 keto/16:0/16:0[e]		
	18:0 epoxy/16:0/16:0[e]	18:0 keto/16:0/16:0[e]		
52	18:3 OH/18:2/16:0[c]	18:2 epoxy/18:2/16:0[c]	18:3 keto/18:2/16:0	9:0 ALD/18:2/16:0[c]
	18:2 OH/18:2/16:0	18:2 epoxy/18:1/16:0	18:2 keto/18:2/16:0	
	18:2 OH/18:1/16:0	18:1 epoxy/18:2/16:0	18:2 keto/18:1/16:0	
	18:1 OH/18:1/16:0	18:1 epoxy/18:1/16:0	18:1 keto/18:2/16:0	
	18:1 OH/18:0/16:0[c]	18:1 epoxy/18:0/16:0	18:1 keto/18:1/16:0	
		18:0 epoxy/18:1/16:0	18:1 keto/18:0/16:0	
			18:0 keto/18:1/16:0	
54	18:3 OH/18:2/18:2[c]	18:2 epoxy/18:2/18:2[c]	18:3 keto/18:2/18:2	8:0 ALD/18:2/18:2[c,d]
	18:2 OH/18:2/18:2	18:2 epoxy/18:2/18:1	18:2 keto/18:2/18:2	9:0 ALD/18:2/18:2 (45:4 ALD)
	18:2 OH/18:2/18:1	18:1 epoxy/18:2/18:2	18:2 keto/18:2/18:1	9:0 ALD/18:2/18:1 (45:3 ALD)
	18:2 OH/18:1/18:1	18:2 epoxy/18:1/18:1	18:1 keto/18:2/18:2	9:0 ALD/18:1/18:1 (45:2 ALD)[c]
	18:1 OH/18:1/18:1	18:1 epoxy/18:2/18:1	18:2 keto/18:1/18:1	12:1 ALD/18:2/18:2[c]
	18:2 OH/18:2 OH/18:2[f]	18:1 epoxy/18:1/18:1	18:1 keto/18:2/18:1	12:1 ALD/18:2/18:1[c]
		18:1 epoxy/18:1/18:0	18:1 keto/18:1/18:1	45:4 ALD + OH/epoxy/keto
		18:0 epoxy/18:1/18:1	18:1 keto/18:1/18:0	45:3 ALD + OH/epoxy/keto
			18:0 keto/18:1/18:1	45:2 ALD + epoxy/keto[c]
56	20:4 OH/18:2/18:2[d]	20:4 epoxy/18:2/18:1[d]	20:4 keto/18:2/18:2[d]	
	20:4 OH/18:2/18:1[d]	20:3 epoxy/18:2/18:2[d]	20:4 keto/18:2/18:1[d]	
			20:3 keto/18:2/18:2[d]	
			20:4 keto/18:1/18:1[d]	
			20:3 keto/18:2/18:1[d]	

[a]The most probable molecular structures based on *m/z* values, TAG FA compositions, and the assumption that the most unsaturated FA is oxidized; regioisomers are not distinguished. Molecules were detected as $[M + Na]^+$ ions. ALD, aldehyde.
[b]Acyl carbon number of the original TAG molecule.
[c]Uncertain/very weak peak in chromatogram.
[d]Detected mostly in chylomicron samples, group 2.
[e]Detected mostly in chylomicron samples.
[f]Detected in the samples of group 2.

partly transformed to $[M + Na + 32]^+$ adduct ions in our ion source, possibly indicating formation of hemiacetal structures within the molecules (Sjövall, O., personal communication). The phenomenon helped in the detection and identification of the core aldehydes.

Most of the oxidized TAG molecular structures were found in all samples at both time points. However, the peaks representing the TAG hydroxides/epoxides/ketones of 54 or 56 acyl carbons and the peaks representing the TAG core aldehydes of 45 carbons with a hydroxy/epoxy/keto group attached to the molecule were stronger in group 2 compared with group 1 (Table 5, Fig. 1). An exception was the ion representing the structure 18:2 OH/18:1/18:1 (postulated), which was stronger in group 1. The ratio of the structure 18:2 keto/18:2/18:2 (ACN:DB 54:6) to the structures 18:2 keto/18:2/18:1 + 18:1 keto/18:2/18:2 (ACN:DB 54:5) seemed to be higher in group 2 compared with group 1 (Fig. 1).

TAG epoxides and ketones may have formed so that the number of double bonds did not change (e.g., conversion of hydroperoxide to a ketone by dehydration) or so that one double bond was lost (formation of an epoxide or a ketone at a site of unsaturation) (19). In the epoxides formed from TAG

with ACN:DB 54:6 or 52:4, oxygen seems to have been added mainly at the site of a double bond, leading to the loss of the double bond. The assumption is based on the intensities of the extracted peaks in the MS chromatograms (Fig. 1) and the FA composition of the TAG (Tables 3 and 4).

In the oxidized test oil, TAG monohydroperoxides were the major class of oxidized TAG. Monohydroperoxides detected were formed from TAG with ACN:DB 52:2, 52:3, 52:4, 54:3, 54:4, 54:5, and 54:6. Dihydroperoxides were formed from TAG with ACN:DB 52:4, 54:6, and 54:5. The hydroperoxy TAG molecules were partly fragmented in the ion source (cleavage of H_2O), which helped in the identification of such molecules.

However, TAG hydroperoxides could not be detected in the lipoprotein samples, neither as such nor as a combination of hydroperoxy and oxo/epoxy groups. This is in accordance with our earlier studies (3,10), and indicates an absence of these molecules in the lipoprotein TAG, or a considerable decrease in the level of them compared with the oxidized sunflower seed oil.

Figure 2 shows the BDC values of plasma (total lipid BDC) and separate lipoproteins. The BDC method is sensi-

A

B

C

D
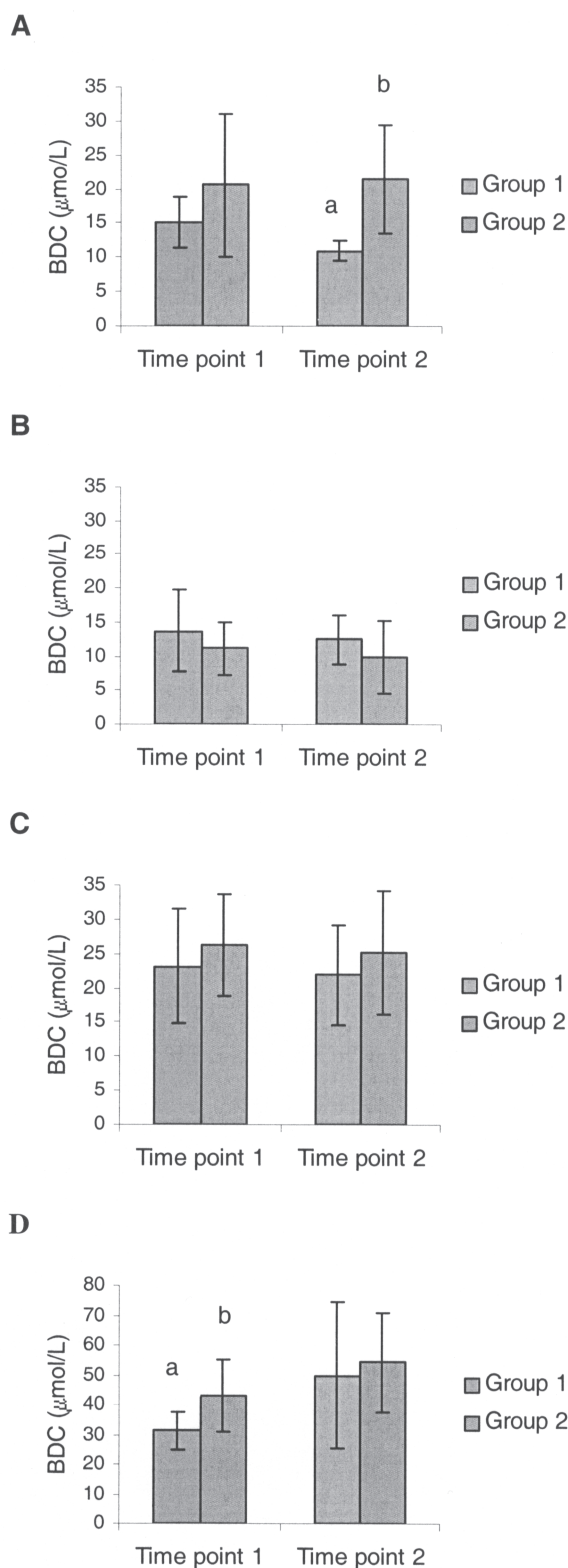
FIG. 2. Baseline diene conjugation (BDC) values (µmol/L plasma) of chylomicron (A), VLDL (B), LDL (C), and plasma (D) lipids. Time point 1, 3 h; time point 2, 4 h after the last test meal. Different letters indicate significant differences between the diet groups ($P < 0.05$). PV of the sunflower seed oil used in feed: group 1, 1 mequiv O_2/kg; group 2, 190 mequiv O_2/kg.

TABLE 6
Estimated Proportions of Oxidized TAG Molecules in the Total Lipids of the Test Oils and Lipoproteins Determined by ELSD[a]

	Group 1[b]		Group 2[c]	
Oil	0.0			6.4
Chylomicrons			Chylomicrons	
Time point 3 h	0.8 ± 0.7[a]		Time point 3 h	2.0 ± 0.6[b]
Time point 4 h	0.8 ± 0.9[a]		Time point 4 h	2.4 ± 0.7[b]
VLDL			VLDL	
Time point 3 h	0.1 ± 0.1		Time point 3 h	0.2 ± 0.2
Time point 4 h	0.1 ± 0.1[a]		Time point 4 h	0.2 ± 0.1[b]

[a]Results expressed as g/100 g of total lipids (mean ± SD, $n = 7$–10). Different superscript roman letters indicate significant differences between diet groups ($P < 0.05$).
[b]PV of the sunflower seed oil used in feed: 1 mequiv O_2/kg.
[c]PV of the sunflower seed oil used in feed: 190 mequiv O_2/kg.

tive, the normal level of conjugated dienes in lipoproteins being at least 10 times higher than the detection limit of the method. The amount of conjugated dienes appeared to be somewhat higher in plasma, chylomicrons, and LDL of group 2 compared with group 1. The differences were statistically significant in the plasma of time point 1 and in the chylomicrons of time point 2. In the VLDL of group 1, the amount of conjugated dienes seemed to be higher compared with group 2. However, these differences were not statistically significant.

The estimated proportions of oxidized TAG molecules in the total lipids of the test oils, chylomicrons, and VLDL are listed in Table 6. The oxidized molecules include all the oxidized TAG species that were detectable in HPLC-ELSD chromatograms. In the oxidized test oil, the TAG hydroperoxides could not be distinguished from secondary oxidation products because of overlapping peaks. However, based on MS chromatograms, the amount of the other oxidation products seemed to be small compared with TAG hydroperoxides.

Some samples could not be analyzed by HPLC owing to a small amount of sample provided. The results show that the proportion of oxidized TAG molecules was remarkably higher in the chylomicrons of group 2 compared with group 1. The proportion of the molecules in the VLDL of group 2 also seemed to be higher compared with group 1.

DISCUSSION

Our results demonstrate an effect of dietary lipid oxidation on lipoprotein oxidation level. Thus, it seems that the oxidized TAG are absorbed in the small intestine, and/or they initiate a cascade of subsequent oxidation reactions that result in the increased oxidation of lipoproteins and their TAG molecules.

It is noteworthy that the oxidized test oil contained less vitamin E than the nonoxidized oil, resulting in lower total vitamin E content in the feed containing the oxidized oil compared with the feed containing the nonoxidized oil (177 vs. 249 mg/kg feed, respectively).

TAG make a contribution of almost 30% to the diene conjugation of LDL (Ahotupa, M., and Viikari, J., unpublished results), a lipoprotein class containing considerably less TAG than chylomicrons and VLDL. Thus, oxidized TAG molecules are expected to have a major contribution to the total lipid oxidation of lipoproteins, particularly chylomicrons and VLDL. This is supported by the present results (Table 6).

TAG hydroperoxides could be detected in neither the chylomicron nor the VLDL samples. This is in accordance with our earlier pig study (3) and the observation that only small amounts of unmodified hydroperoxy lipids are found in tissue and blood samples (20,21). Studies by Kanazawa *et al.* (22,23) and by our group (24) suggest that dietary FA hydroperoxides ingested in moderate amounts may not survive in the gastrointestinal tract. If so, unmodified dietary TAG hydroperoxides are not transported into lipoproteins. Oxidation of formerly unmodified TAG molecules takes place in plasma to some extent (10), but we hypothesize that the TAG oxidation products found in plasma lipoproteins are partly formed from hydroperoxides in the gastrointestinal tract and possibly further modified in plasma.

The possibility that some decomposition of hydroperoxy structures had occurred during sample preparation cannot be excluded. However, in our studies, TAG hydroperoxides have been relatively stable during extraction procedures, TLC, and HPLC runs.

Lipoproteins rich in TAG seem to be important factors in the induction of atherogenesis (25), which could at least partly be explained by oxidized TAG molecules. As in our previous study (3), TAG hydroxides were present in the chylomicrons and VLDL. Linoleic acid hydroxides are found in atherosclerotic plaques, and they have been found to be endogenous activators and ligands of peroxisome proliferator activated receptor protein γ, which promotes monocyte/macrophage differentiation and uptake of oxidized LDL (20,26,27). Thus, lipoprotein TAG hydroxides could have an influence on atherogenesis (20).

The present results give further evidence on the effect of dietary fat oxidation on lipoprotein oxidation. Most of the results were in line with our earlier study (3) in which smaller pig groups were used. The results obtained by the BDC method suggest that plasma, chylomicron, and LDL lipids of group 2 were more oxidized compared with group 1. It was also shown that the chylomicron and VLDL samples of group 2 contained more oxidized TAG molecules than the samples of group 1. Our results suggest that the level of dietary fat oxidation is reflected in the level of lipoprotein oxidation.

ACKNOWLEDGMENTS

REFERENCES

1. Staprans, I., Rapp, J.H., Pan, X.M., Kim, K.Y., and Feingold, K.R. (1994) Oxidized Lipids in the Diet Are a Source of Oxidized Lipid in Chylomicrons of Human Serum, *Arterioscler. Thromb. 14,* 1900–1905.
2. Staprans, I., Rapp, J.H., Pan, X.M., and Feingold, K.R. (1996) Oxidized Lipids in the Diet are Incorporated by the Liver into Very Low Density Lipoprotein in Rats, *J. Lipid Res. 37,* 420–430.
3. Suomela, J.-P., Ahotupa, M., Sjövall, O., Kurvinen, J.-P., and Kallio, H. (2004) Diet and Lipoprotein Oxidation: Analysis of Oxidized Triacylglycerols in Pig Lipoproteins, *Lipids 39,* 639–647.
4. Grieve, D.J., Avella, M.A., Elliott, J., and Botham, K.M. (2000) The Interaction Between Oxidised Chylomicron Remnants and the Aorta of Rats Fed a Normocholesterolaemic or Hypercholesterolaemic Diet, *J. Vasc. Res. 37,* 265–275.
5. Napolitano, M., Rivabene, R., Avella, M., Amicone, L., Tripodi, M., Botham, K.M., and Bravo, E. (2001) Oxidation Affects the Regulation of Hepatic Lipid Synthesis by Chylomicron Remnants, *Free Radic. Biol. Med. 30,* 506–515.
6. Naruszewicz, M., Wozny, E., Mirkiewicz, E., Nowicka, G., and Szostak, W.B. (1987) The Effect of Thermally Oxidized Soya Bean Oil on Metabolism of Chylomicrons—Increased Uptake and Degradation of Oxidized Chylomicrons in Cultured Mouse Macrophages, *Atherosclerosis 66,* 45–53.
7. Umeda, Y., Redgrave, T.G., Mortimer, B.C., and Mamo, J.C.L. (1995) Kinetics and Uptake *in vivo* of Oxidatively Modified Lymph Chylomicrons, *Am. J. Physiol. 31,* G709–G716.
8. Mamo, J.C.L., and Wheeler, J.R. (1994) Chylomicrons or Their Remnants Penetrate Rabbit Thoracic Aorta as Efficiently as Smaller Macromolecules Including Low Density Lipoprotein, High Density Lipoprotein and Albumin, *Coron. Artery Dis. 5,* 695–705.
9. Ahotupa, M., Marniemi, J., Lehtimäki, T., Talvinen, K., Raitakari, O.T., Vasankari, T., Viikari, J., Luoma, J., and Ylä-Herttuala, S. (1998) Baseline Diene Conjugation in LDL Lipids as a Direct Measure of *in vivo* LDL Oxidation, *Clin. Biochem. 31,* 257–261.
10. Suomela, J.-P., Ahotupa, M., Sjövall, O., Kurvinen, J.-P., and Kallio, H. (2004) New Approach to the Analysis of Oxidized Triacylglycerols in Lipoproteins, *Lipids 39,* 507–512.
11. AOCS (1997) *Official Methods and Recommended Practices of the AOCS,* 5th edn., AOCS Press, Champaign.
12. IUPAC (1987) *Standard Methods for the Analysis of Oils, Fats and Derivatives,* 7th edn., Blackwell Science, Oxford, United Kingdom.
13. Ågren, J.J., Vidgren, H.M., Valve, R.S., Laakso, M., and Uusitupa, M. (2001) Postprandial Responses of Individual Fatty Acids in Subjects Homozygous for the Threonine- or Alanine-Encoding Allele in Codon 54 of the Intestinal Fatty Acid Binding Protein 2 Gene, *Am. J. Clin. Nutr. 73,* 31–35.
14. Hamilton, J.G., and Comai, K. (1988) Rapid Separation of Neutral Lipids, Free Fatty Acids and Polar Lipids Using Prepacked Silica Sep-Pak Columns, *Lipids 23,* 1146–1149.
15. Skipski, V.P., and Barclay, M. (1969) Thin-Layer Chromatography, *Methods Enzymol. 14,* 542–548.
16. Christie, W.W. (1982) A Simple Procedure for Rapid Transmethylation of Glycerolipids and Cholesteryl Esters, *J. Lipid Res. 23,* 1072–1075.
17. Ahotupa, M., Ruutu, M., and Mäntyla, E. (1996) Simple Methods of Quantifying Oxidation Products and Antioxidant Poten-

tial of Low Density Lipoproteins, *Clin. Biochem. 29,* 139–144.

18. Sjövall, O., Kuksis, A., Marai, L., and Myher, J.J. (1997) Elution Factors of Synthetic Oxotriacylglycerols as an Aid in Identification of Peroxidized Natural Triacylglycerols by Reverse-Phase High-Performance Liquid Chromatography with Electrospray Mass Spectrometry, *Lipids 32,* 1211–1218.

19. Neff, W.E., and Byrdwell, W.C. (1998) Characterization of Model Triacylglycerol (triolein, trilinolein and trilinolenin) Autoxidation Products *via* High-Performance Liquid Chromatography Coupled with Atmospheric Pressure Chemical Ionization Mass Spectrometry, *J. Chromatogr. A 818,* 169–186.

20. Spiteller, G. (1998) Linoleic Acid Peroxidation—The Dominant Lipid Peroxidation Process in Low Density Lipoprotein—and Its Relationship to Chronic Diseases, *Chem. Phys. Lipids 95,* 105–162.

21. Adachi, J., Yoshioka, N., Funae, R., Nagasaki, Y., Naito, T., and Ueno, Y. (2004) Phosphatidylcholine Hydroperoxide Levels in Human Plasma Are Lower Than Previously Reported, *Lipids 39,* 891–896.

22. Kanazawa, K., and Ashida, H. (1998) Catabolic Fate of Dietary Trilinoleoylglycerol Hydroperoxides in Rat Gastrointestines, *Biochim. Biophys. Acta 1393,* 336–348.

23. Kanazawa, K., and Ashida, H. (1998) Dietary Hydroperoxides of Linoleic Acid Decompose to Aldehydes in Stomach Before Being Absorbed into the Body, *Biochim. Biophys. Acta 1393,* 349–361.

24. Suomela, J.-P., Ahotupa, M., and Kallio, H (2005) Triacylglycerol Hydroperoxides Not Detected in Pig Small Intestinal Epithelial Cells After a Diet Rich in Oxidized Triacylglycerols, *Lipids 40,* 349–353.

25. Hamsten, A. (1993) Lipids as a Coronary Risk Factor—Analysis of Hyperlipemias, *Postgrad. Med. J. 69,* S8–S11.

26. Nagy, L., Tontonoz, P., Alvarez, J.G.A., Chen, H.W., and Evans, R.M. (1998) Oxidized LDL Regulates Macrophage Gene Expression Through Ligand Activation of PPAR γ, *Cell 93,* 229–240.

27. Tontonez, P., Nagy, L., Alvarez, J.G.A., Thomazy, V.A., and Evans, R.M. (1998) PPAR-γ Promotes Monocyte/Macrophage Differentiation and Uptake of Oxidized LDL, *Cell 93,* 241–252.

Changes in the Milk and Cheese Fat Composition of Ewes Fed Commercial Supplements Containing Linseed with Special Reference to the CLA Content and Isomer Composition

Pilar Luna, Javier Fontecha, Manuela Juárez, and Miguel Angel de la Fuente*

Instituto del Frío (Consejo Superior de Investigaciónes Científicas), José Antonio Novais 10, 28040 Madrid, Spain

ABSTRACT: A study was carried out to increase the CLA contents in ewes' milk fat under field conditions by dietary means and to investigate the extent of the changes and consequences for milk processing and cheese quality. During a 3-mon period, ewes' bulk milk samples were collected every week from two different herds. For the first 4 wk the ewes were fed a conventional diet. Then the following 6 wk a supplement enriched in α-linolenate (whole linseed) was incorporated into the ovine diet. Finally, in the last 3 wk the feeding was the same as in the first 4 wk. The FA profile in milk fat was monitored by GC, and the distribution of CLA isomers was thoroughly tested by combining GC–MS of 4,4-dimethyloxazoline derivatives (DMOX) with silver ion-HPLC (Ag$^+$-HPLC) of FAME. Reconstructed mass spectral profiles of CLA characteristic ions from DMOX were used to identify positional isomers, and Ag$^+$-HPLC was used to quantify them. An increase in total CLA in milk fat was observed, and total CLA remained elevated during the weeks of enriched α-linolenate feeding. In our experimental conditions there was a linear relationship between *trans*-vaccenic acid (*trans*-11-octadecenoic acid; *trans*-11 18:1) and 9-*cis*,11-*trans* CLA in ewes' milk fat. Concerning the CLA isomer profile, increases in the 11,13- and 12,14-18:2 positional isomers were considerable when linseed was included in the diet. Organoleptic characteristics of cheeses made with CLA-enriched milk did not substantially differ from those made with nonsupplemented ewes' milk. CLA total content and isomer profile did not change during ripening.

Paper no. L9567 in *Lipids 40*, 445–454 (May 2005).

CLA is a mixture of positional and geometric isomers of linoleic acid (18:2), which contains a conjugated double-bond system. In animal models, CLA exhibits several health-promoting attributes, including anticarcinogenic and antiatherogenic activities. Natural dietary sources of CLA are mainly milk fat contained in foods, such as whole milk, butter, and cheese. The quantitatively predominant CLA isomer in milk is the 9-*cis*,11-*trans* isomer, also called rumenic acid (RA), and it has been implicated as the most important isomer in terms of biological activity. The 10-*trans*,12-*cis* isomer seems to be the isomer responsible for reducing body fat content and might be the most active one, but its natural occurrence is low. More recently, other isomers have been found to be even more powerful than RA against human breast cancer cells (9-*cis*,11-*cis*) (1) or to exhibit greater cytotoxicity against gastric cancer cells (9-*trans*,11-*trans*) (2). However, their presence in lipids from ruminant products is reported less.

The CLA content in dairy products is affected by many factors during every stage from the field to the table, including raw material production, processing, aging, storage, and food preparation (3,4). Animal feeding strategies for CLA enrichment of milk have been reviewed, and diets with seed/oil supplements rich in PUFA that provide lipid substrates for the production of RA or *trans*-11 18:1 (*trans*-vaccenic acid, TVA) have proved to be effective (3,4). A number of studies have reported the effects of linseed or linseed oil on milk FA composition in dairy cows (5–12). In addition to enhancing CLA content, the dietary changes with linseed also result in milk fat containing a lower proportion of saturated FA and greater amounts of monounsaturated FA and PUFA.

The most significant changes in milk fat quality relate to rheological properties, which influence numerous aspects of the nature and quality of cheeses and other manufactured dairy products (13). The effects of processing conditions, storage, and aging on the CLA content of various types of dairy products are not very clear. As regards cheeses, reports and reviews present results for individual varieties, often in the belief that CLA levels may vary as a result of different processing conditions. These effects are likely to be small, and variations in CLA levels are similar to the levels in the starting milk (14–16). However, other studies have detected changes in the CLA levels or new isomers in ripened cheeses (17–20), and it is hypothesized that biohydrogenation of linolenic acid in cheese could lead to the formation of CLA isomers as intermediates.

Production of ewes' milk is of economic importance in a number of countries, especially those in the Mediterranean region and Middle East, where it is mainly used to produce a variety of cheeses. While it is accepted that hardly any studies have reported the effects of seed/oil supplements on ovine milk FA composition, and with one exception (21) a detailed characterization of the CLA isomer profile has been supplied, the evidence to support differences in lipid metabolism between ruminants is rather limited. Thus, changes in FA pro-

---

file of ovine milk fat should not substantially differ from the pattern previously described for cows' milk. If there are differences between ruminants, then goats appear to be the exception rather than ewes or cows (22).

Most of the works on ovine dairy products are limited to quantifying the most prominent peak assigned to CLA as FAME by means of GC. However, the CLA isomer mixtures in milk are complex, and no single technique can resolve all isomers. In recent years, different procedures have been used to elucidate CLA isomers. The majority of them have been quantified by silver-ion HPLC (Ag^{+}-HPLC) (18,23–25). GC–MS has been shown to be the most powerful tool for identifying them (18,26). A more complete qualitative and quantitative analysis involves applying both techniques, especially when GC is coupled to MS to provide structural information. A detailed positional analysis of the double bonds of FA subsequently can be performed using one of several FA derivatives other than FAME, such as 4,4-dimethyloxazoline (DMOX), that already are applied in different food materials. High-resolution MS with a selected ion-recording technique makes it possible to distinguish CLA from interfering FA and discriminate among the different isomers.

This experiment was carried out to enhance CLA levels in ewes' milk fat under field conditions by dietary means (commercial supplement enriched in linseed, SEL) and to investigate the extent of the changes and consequences for milk processing and cheese quality. The dietary intervention chosen could lead to changes in the FA composition in ewes' milk fat, and it would be useful to know how this could affect the characteristics of the cheese produced from this milk. Furthermore, it would mean that it was possible to see how the FA composition, particularly the amount and proportion of specific CLA isomers, would develop during the processing and aging of the cheese. Research on this topic, assisted by the analytical tools already mentioned, could lead to the development of natural, consumer-acceptable strategies and processing systems to produce CLA and dairy foods of proven quality with enhanced healthful properties.

MATERIALS AND METHODS

Feeding experiments. Briefly the study dealt with the impact of a diet supplemented with α-linolenate on the FA composition of the ewes' bulk milk fat. The experiment was performed from December to March with two representative herds of 330 and 300 lactating ewes of Assaf breed located in two different places in the Madrid region (Spain). All ewes were housed in dairy barns, and they had free access to water and appropriate bedding.

The study was conducted over a 13-wk period. Bulk milk samples were collected at weekly intervals during the milking period from both herds. Samples were taken from the storage tanks containing milk from the whole herd. During the first 4 wk both herds were offered a mixture *ad libitum* consisting of dehydrated alfalfa (45% of dry matter), corn (15% of dry matter), beet pulp (10% of dry matter), cotton seed

(13% of dry matter), and Lactovejina 100 (17% of dry matter), a commercial supplement from Cargill España S.A (Madrid, Spain). After 4 wk, Lactovejina 100 was replaced with Lactovejina 100 Tech (Cargill España S.A.), a supplement enriched in whole linseed. From weeks 5 to10 both herds were fed *ad libitum*, and their diets included Lactovejina 100 Tech (17% of dry matter). Finally, in the last 3 wk, the feeding was the same as in the first 4 wk. The chemical composition of both supplements is shown in Table 1, and total lipid contents were 4.7 and 5.8% in diets with Lactovejina 100 and Lactovejina 100 Tech, respectively.

Cheese-making experiments. The bulk milk of both herds, collected separately in the last weeks of both feeding periods, at 4 wk (control diet) and at 10 wk (SEL diets) from the starting point, was used for cheese making. Cheeses from each batch were made in a pilot plant as follows: 50 L of raw milk was heated to 32°C, and rennet was added to curdle the milk. No starter culture was added for cheese making because raw milk was used. After the milk had clotted (30 min), the curd was cut to the size of a hazelnut and then the vat temperature was gradually increased to 36–37°C at a rate of 1°C/3 min. At the same time, the curd was stirred to remove the whey and favor grain aggregation. Curds were placed into 3-kg molds and pressed in a horizontal pneumatic press until the pH was about 5.5. Cheeses were salted in brine (20° Baume) at 10°C for 12 h and then transferred to a ripening room where they remained at a temperature of approximately 13–14°C and ~85% RH for 120 d. Samples at 30, 60, and 120 d were taken from each batch for chemical analysis. A total of 5 cheeses were obtained from each batch.

Milk and cheese chemical analyses. Fat, protein, and total solids in milk were measured with a MilkoScan FT-6000 (Foss Electric, Barcelona, Spain). Total solids and fat in cheeses were determined according to the International Dairy Federation (IDF) standards (27,28).

(i) Lipid extraction and FA derivatization. Milk and cheese fat extraction was carried out according to the International Standards Organization (ISO; 29). The fat residue extracted was stored in amber vials, exposed to a stream of N_2 and

TABLE 1
Chemical Composition of Lactovejina 100 and Lactovejina 100 Tech[a]

Component	(weight %)	
	Lactovejina 100	Lactovejina 100 Tech
Moisture	13.20	10.77
Protein	20.00	20.00
Fat	5.71	12.23
Ash	7.73	7.79
Calcium	1.00	1.00
Phosphorus	0.53	0.55
Palmitic acid	0.41	0.73
Stearic acid	0.05	0.31
Oleic acid	0.97	2.22
Linoleic acid	2.46	2.95
α-Linolenic acid	0.15	5.00

[a]Lactovejina 100, a commercial feed supplement; Lactovejina 100 Tech, a supplement enriched in whole linseed; both from Cargill España S.A (Madrid, Spain).

frozen at −20°C until analysis. FAME were prepared by base-catalyzed methanolysis of the glycerides (KOH in methanol) as described in ISO (30). The preparation of DMOX derivatives from FAME was based on the Fay and Richli (31) procedure.

(ii) Ag⁺-HPLC. Ag⁺-HPLC separation of CLA methyl esters was carried out using a high-performance liquid chromatograph (Series 1100; Agilent Technologies, Palo Alto, CA) equipped with a photodiode array detector operated at 234 and 205 nm. Three ChromSpher 5 Lipid analytical columns (4.6 mm i.d. × 250 mm stainless steel; 5 μm particle size; Varian) were connected in series. The mobile phase was 0.1% acetonitrile in hexane and operated isocratically at a flow rate of 1.0 mL/min. The flow was initiated 0.5 h prior to the sample injection and the injection volume was 10 μL. To identify positional isomers a mixture (*cis*-9 *trans*-11, *trans*-8 *cis*-10, *cis-11 trans*-13, *trans*-10 *cis*-12 18:2 and small amounts of a variety of *cis-cis* and *trans-trans* 18:2 isomers) and pure CLA methyl ester isomers (*cis*-9 *trans*-11 and *trans*-10 *cis*-12 18:2) were purchased from Nu-Chek-Prep. Inc. (Elysian, MN).

(iii) GC–FID and GC–MS analyses. Milk and cheese FA contents were determined by GC–FID after conversion to FAME. FAME were analyzed on a PerkinElmer chromatograph (model 8420; Beaconsfield, United Kingdom) with an FID. FA were separated by using a CP-Sil 88 fused-silica capillary column (100 m × 0.25 mm i.d. × 0.2 μm film thickness; Chrompack, Middelburg, The Netherlands). The column was held at 70°C for 4 min after injection, temperature-programmed at 13°C/min to 175°C, held there for 27 min, and then temperature-programmed at 4°C/min to 215°C and held there for 36 min. Helium was the carrier gas with a column inlet pressure set at 214 KPa and a split ratio of 1:20. Injection volume was 0.2 μL. To obtain response factors, an anhydrous milk fat (reference material CRM-164) obtained from the European Commission (Brussels, Belgium), consisting of known amounts of FA, was used.

CLA DMOX derivatives were separated with the same column on an Agilent GC chromatograph (model 6890N) connected to an Agilent mass spectrometer detector (MS 5973N). The filament trap current was 400 μA at 70 eV. A 1-μL solution of DMOX derivatives was injected under the following conditions: initial oven temperature was 75°C for 2 min after injection, then temperature-programmed at 5°C/min to 180°C, held there for 30 min, and then temperature-programmed at 5°C to 220°C and held there for 30 min. The column inlet pressure was set at 197 KPa in a splitless injection system. To create other CLA isomers, standards from Nu-Chek-Prep described above were isomerized using I_2 (23), then converted to DMOX derivatives and used to identify CLA isomers by GC–MS.

Cheese sensory analysis. The sensory test was carried out following IDF recommendations (32) by a trained group of panelists (accustomed to consuming this type of cheese), consisting of staff from our Institute (15 tasters minimum). Cheeses were sampled and tested at 60 and 90 d of ripening.

A wedge (1-cm thick) was cut from the block of cheese and the rind was removed. All analyses were rated on a 10-point scale. The attributes analyzed were appearance, aroma strength, taste strength, texture, and general acceptability. The possible presence of certain features responsible for negative aspects in flavor and aroma were also evaluated. The SPSS package (SPSS 11.0 for Windows; SPSS Inc., Chicago, IL) was used for statistical analysis of these results. Variance analysis was performed to establish the effectiveness and significance level for $P \leq 0.05$.

RESULTS AND DISCUSSION

Milk yield and composition. To draw conclusions about the effects of diet on animal performance would require data from individual animals. However, descriptive data on average milk yield and composition can also be important for studies if the bulk raw milk is going to be used to manufacture cheese and other dairy products. Milk yields from both ewe herds were recorded daily during the entire period of the study. The mean daily milk yields per ewe were 2.5 and 2 L in herds 1 and 2, respectively. These volumes remained constant and did not decrease during the 3 mon that were monitored. Figure 1 shows the development of fat and protein concentration measured weekly for 3 mon in both herds. As can be seen, fat percentages decreased slightly during the period monitored, whereas the protein content remained stable.

FA composition of milk. The FA profile of ewes' milk fat was altered by the feed, and the development of the major FA content was similar for both herds during the period monitored (Fig. 2, Table 2). The proportions of saturated FA from 8:0 to 16:0 decreased with the SEL diet, whereas 4:0 and 6:0 hardly varied. Lipid supplementation with α-linolenic acid increased the 18:0 and 18:3 percentage as well as most of the 18:1 and 18:2 and isomers (Fig. 2, Table 2). Ewes' milk fat contained very small amounts of C_{20} and C_{22} PUFA, which were identified by using GC–MS. The most prominent PUFA
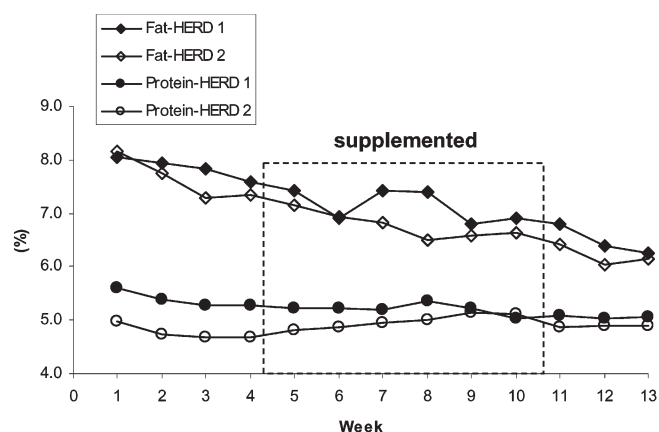
FIG. 1. Temporal pattern (% of total milk) of fat and protein content of bulk milk in two ewe herds fed a diet enriched in α-linolenic acid. During the treatment period (broken lines) a supplement enriched in linseed was added.
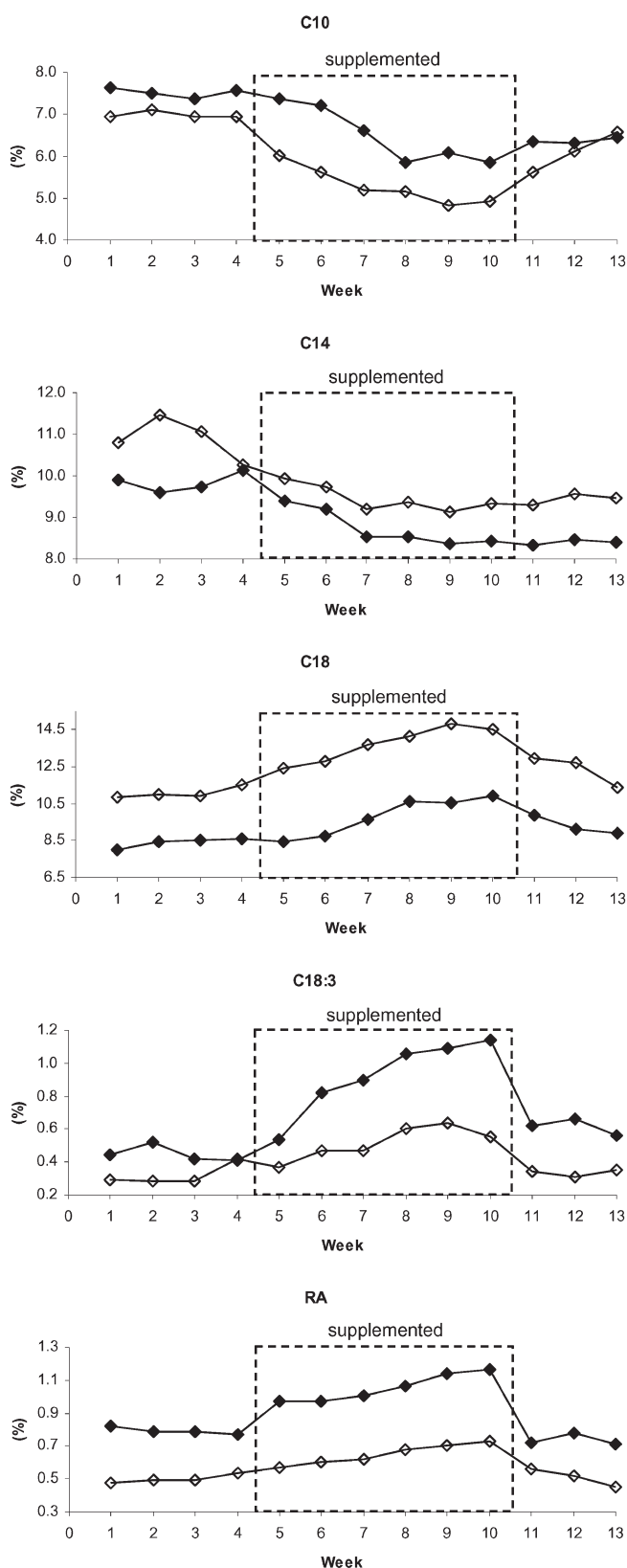
FIG. 2. Temporal pattern (% of total FA) of 10:0, 14:0, 18:0, α-linolenic acid (18:3), and rumenic acid (RA) of milk fat from ewes fed a diet enriched in α-linolenic acid. During the treatment period (broken lines), a supplement enriched in linseed was added. Herd 1 (♦), herd 2 (◇).

present were 20:4, 20:5 (EPA), and 22:5 (Table 2), whereas 22:6 (DHA) was absent. These percentages did not change when the diet was enriched in α-linolenic acid.

Although it is not possible to draw conclusions from bulk milk samples from 300 animals, since individual variability should be studied, these results seem to confirm the established theories developed from research studies with cows' milk when the livestock were fed different dietary supplements enriched in oilseed (3,4). The inclusion of long-chain FA in the diet reduces the concentration of medium-chain saturated FA in the milk mainly by inhibiting mammary *de novo* FA synthesis. Increases in the proportion of 18:0, 18:1, and 18:2 isomers would be associated with biohydrogenation activity in the rumen, which is stimulated by feeding with PUFA-enriched lipids. Nevertheless, the process of biohydrogenation in the rumen seemed to be limited, because noticeable amounts of α-linolenic acid contents escaped hydrogenation and increased the amounts of this FA in the milk fat of herds fed SEL. The proportion of α-linolenic acid in ewes' milk shifted from an average of 0.45 and 0.29% in the first weeks to 1.10 and 0.63% in both herds, respectively, at the end of the period of feeding with the supplement. The fact that there was a higher proportion of α-linolenic acid in milk when linseeds were added than when linseed oil was used could be due to partial protection by whole linseed against biohydrogenation because of the localization of oil in the seed. Oil is released slowly from seeds in the rumen and has relatively less probability of biohydrogenating than free oil (8,10).

Particularly remarkable was the rise in the *trans*-11 *cis*-15 18:2 level in the milk fat of ewes fed SEL (Table 2). *Trans*-11 *cis*-15 18:2 was first recognized as the main intermediate in the ruminal hydrogenation of α-linolenic acid *in vitro* and has also been confirmed recently in studies *in vivo* (33) as the major 18:2 isomer produced during hydrogenation of α-linolenic acid in the rumen. This pathway involves an initial isomerization to a conjugated triene (*cis*-9 *trans*-11 *cis*-15 18:3), followed by reductions in the double bonds at carbons 9, 15, and 11 to yield *trans*-11 *cis*-15 18:2, *trans*-11 18:1, then 18:0, respectively.

The analysis of PUFA is important considering present-day efforts to increase the n-3 FA content in milk fat. Two of the most important n-3 PUFA (EPA and DHA) usually have a very low level in traditional dairy diets (<0.1% of total FAME). DHA, for instance, is present only in trace amounts in milk fat unless the ruminant diet contains marine products. Consequently, the very low amounts of n-3 PUFA found in the present study came as no surprise.

RA and TVA relationship. RA content in milk fat was greater in ewes fed SEL than when they were fed the control diet (Fig. 2). Mean levels of RA in the first 4 wk were stable (0.80 and 0.50% in herds 1 and 2, respectively). With the new diet, levels rose in both herds. Finally, after SEL was eliminated from the diet, RA content dropped to its original values. In our experimental conditions, a high correlation of RA with TVA ($R^2 = 0.93$) was found in ewes' milk fat (Fig. 3). A

TABLE 2
FA Composition (% of total FAME) of Milk Fat from Ewes Fed the Control Diet (CD), Supplement Enriched in Linseed (LIN), and Cheeses at 1, 2, and 4 mon of Ripening Made from the Milk of Animals Fed a Supplement Enriched in Linseed

FA	Milk		Cheese		
	CD	LIN	1 mon	2 mon	4 mon
4:0	3.76 ± 0.38	3.68 ± 0.53	3.74 ± 0.42	3.72 ± 0.56	3.70 ± 0.47
6:0	3.13 ± 0.13	2.78 ± 0.14	2.76 ± 0.18	2.81 ± 0.16	2.70 ± 0.12
8:0	2.62 ± 0.04	2.22 ± 0.10	2.20 ± 0.11	2.24 ± 0.14	2.22 ± 0.30
9:0	0.06 ± 0.01	0.05 ± 0.01	0.05 ± 0.01	0.05 ± 0.01	0.06 ± 0.01
10:0	7.42 ± 0.11	5.95 ± 0.20	5.94 ± 0.19	5.98 ± 0.25	5.97 ± 0.32
10:1	0.29 ± 0.01	0.21 ± 0.01	0.21 ± 0.01	0.21 ± 0.01	0.21 ± 0.01
12:0	3.73 ± 0.05	3.02 ± 0.06	3.02 ± 0.05	3.03 ± 0.07	2.99 ± 0.07
13:0	0.12 ± 0.01	0.09 ± 0.01	0.09 ± 0.01	0.10 ± 0.01	0.09 ± 0.01
14:0 iso	0.06 ± 0.01	0.06 ± 0.01	0.06 ± 0.01	0.07 ± 0.01	0.06 ± 0.01
14:0	9.30 ± 0.19	8.07 ± 0.15	8.09 ± 0.16	8.05 ± 0.15	8.03 ± 0.21
15:0 iso	0.15 ± 0.01	0.15 ± 0.01	0.16 ± 0.01	0.16 ± 0.01	0.15 ± 0.01
15:0 anteiso	0.28 ± 0.01	0.31 ± 0.01	0.31 ± 0.01	0.31 ± 0.01	0.31 ± 0.01
14:1	0.16 ± 0.01	0.10 ± 0.01	0.10 ± 0.01	0.10 ± 0.01	0.10 ± 0.01
15:0	0.78 ± 0.02	0.72 ± 0.02	0.72 ± 0.02	0.71 ± 0.02	0.71 ± 0.02
15:1	0.08 ± 0.01	0.07 ± 0.01	0.07 ± 0.01	0.07 ± 0.01	0.07 ± 0.01
16:0 iso	0.25 ± 0.01	0.25 ± 0.01	0.25 ± 0.01	0.25 ± 0.01	0.24 ± 0.01
16:0	28.34 ± 0.33	24.95 ± 0.26	25.01 ± 0.34	24.79 ± 0.24	24.88 ± 0.54
17:0 iso	0.45 ± 0.01	0.57 ± 0.03	0.57 ± 0.03	0.57 ± 0.03	0.55 ± 0.02
17:0 anteiso	0.23 ± 0.01	0.28 ± 0.01	0.29 ± 0.03	0.28 ± 0.01	0.27 ± 0.01
16:1	1.25 ± 0.02	1.08 ± 0.02	1.08 ± 0.02	1.09 ± 0.03	1.07 ± 0.04
17:0	0.58 ± 0.02	0.59 ± 0.01	0.59 ± 0.01	0.58 ± 0.02	0.57 ± 0.01
17:1	0.15 ± 0.01	0.14 ± 0.01	0.14 ± 0.01	0.14 ± 0.01	0.14 ± 0.01
18:0	8.12 ± 0.13	10.50 ± 0.18	10.58 ± 0.10	10.37 ± 0.13	10.55 ± 0.39
18:1 (6-8 trans)	0.25 ± 0.02	0.29 ± 0.02	0.30 ± 0.03	0.30 ± 0.02	0.31 ± 0.04
18:1 (9 trans)	0.33 ± 0.04	0.37 ± 0.04	0.35 ± 0.02	0.34 ± 0.04	0.34 ± 0.05
18:1 (10 trans)	1.17 ± 0.03	1.60 ± 0.05	1.65 ± 0.07	1.74 ± 0.04	1.60 ± 0.09
18:1 (11 trans)	2.39 ± 0.06	3.62 ± 0.10	3.64 ± 0.10	3.54 ± 0.07	3.71 ± 0.13
18:1 (9-11 cis) + (12-15 trans)	17.65 ± 0.26	20.12 ± 0.43	19.87 ± 0.15	20.20 ± 0.26	20.07 ± 0.81
18:1 (12-13 cis)	0.46 ± 0.01	0.65 ± 0.01	0.66 ± 0.01	0.66 ± 0.01	0.65 ± 0.02
18:1 (16 trans + 14 cis)	0.25 ± 0.01	0.42 ± 0.01	0.42 ± 0.01	0.42 ± 0.01	0.43 ± 0.01
18:1 (15 cis) +19:0	0.16 ± 0.01	0.29 ± 0.01	0.29 ± 0.01	0.29 ± 0.01	0.29 ± 0.01
18:2 (9 trans, 12 trans) + (9 cis,13 trans)	0.28 ± 0.01	0.44 ± 0.01	0.44 ± 0.01	0.44 ± 0.01	0.43 ± 0.01
18:2 (8 trans, 13 cis + 9 cis,12 trans)	0.15 ± 0.01	0.20 ± 0.01	0.20 ± 0.01	0.20 ± 0.01	0.20 ± 0.01
18:2 (11 trans,15 cis)	0.03 ± 0.01	0.21 ± 0.02	0.21 ± 0.02	0.21 ± 0.02	0.20 ± 0.02
18:2 (9 cis,12 cis)	3.28 ± 0.13	2.84 ± 0.10	2.81 ± 0.08	2.84 ± 0.10	2.79 ± 0.07
20:0	0.17 ± 0.01	0.18 ± 0.01	0.18 ± 0.01	0.17 ± 0.01	0.18 ± 0.01
18:3	0.49 ± 0.01	1.05 ± 0.01	1.04 ± 0.01	1.05 ± 0.01	1.06 ± 0.03
CLA	0.80 ± 0.01	1.02 ± 0.01	1.01 ± 0.01	1.02 ± 0.01	1.02 ± 0.03
22:0	0.07 ± 0.01	0.07 ± 0.01	0.07 ± 0.01	0.06 ± 0.01	0.07 ± 0.01
20:4	0.18 ± 0.01	0.15 ± 0.01	0.15 ± 0.01	0.15 ± 0.01	0.15 ± 0.01
20:5	0.05 ± 0.01	0.06 ± 0.01	0.05 ± 0.01	0.06 ± 0.01	0.05 ± 0.01
22:5	0.06 ± 0.01	0.07 ± 0.01	0.07 ± 0.01	0.07 ± 0.01	0.04 ± 0.03
Other FA	0.47	0.51	0.56	0.56	0.76

product–precursor relationship of CLA with TVA in the ewes' rumen was suggested by Noble *et al*. (34), indicating that the TVA accumulated in the ewes' rumen could be used for postruminal synthesis of CLA, which might be more important quantitatively than CLA ruminal synthesis. Investigations to establish the importance of endogenous synthesis of CLA in ewes' body fat (35) found a correlation between TVA and RA concentrations in different tissues, and the accumulation of RA appeared to be far greater in the liver. Daniel *et al*. (35) highlighted the predominance of endogenous synthesis as the source of RA in ewes and also stressed the critical role of Δ-9 desaturase in the biology of CLA in this ruminant. However, information on the mammary gland or milk fat was not supplied.

The results of this study support the idea that dietary α-linolenic acid could also be a valuable means for increasing RA in ewes' milk. Although ewes and cows' response to lipid feeding might not be exactly the same, the effects of α-linolenic acid supplementation should not be very different between these species. Nonetheless, increases in CLA contents were modest in comparison with some previous studies on cows' milk, in which other types of seeds were used. The reasons could be the predominant pathways of biohydrogenation of dietary α-linolenic and linoleic acids in the rumen. Supplementation of linoleic acid appears to have an advantage over supplementation of α-linolenic acid, probably because it contributes to increased production of both CLA and TVA in the rumen, the latter of which ultimately becomes the
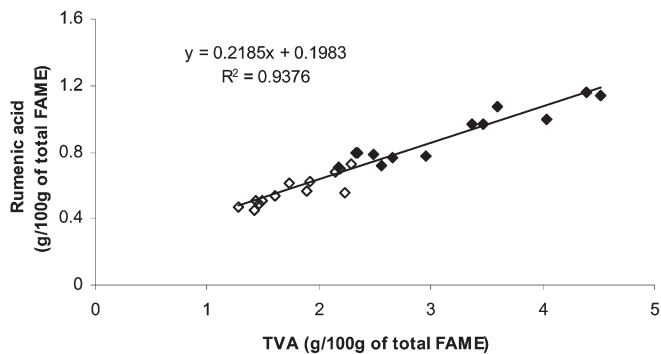
FIG. 3. Relationship between rumenic acid (9-*cis* 11-*trans* 18:2) and *trans*-vaccenic acid (11-*trans* 18:1, TVA) in ewes' milk fat from two herds (g/100 g of total FAME). Herd 1 (◆), herd 2 (◇).

substrate for CLA synthesis by Δ-9 desaturase in the mammary gland, whereas α-linolenic acid contributes to TVA only during its biohydrogenations (4). Feeding linseed results in great production of ruminal TVA, which could be subsequently used by the mammary gland for RA synthesis (33).

CLA isomer profile. The effect of diet on milk fat CLA is largely accounted for by a change in the concentration of RA, but other isomers can play an important role. The major positional isomer determined by Ag⁺-HPLC was 9,11 (*cis/trans* plus *trans/cis*), and 7,9 (*cis/trans* plus *trans/cis*) was the second most relevant peak with percentages about 80–85 and 6–8% of total CLA, respectively. RA abundance would be consistent with the relative importance of the endogenous synthesis of *cis*-9 *trans*-11 CLA from TVA by Δ-9 desaturase. Similarly, *trans*-7 *cis*-9 CLA would be produced from *trans*-7 18:1 by the same enzyme (36–38).

Figure 4 represents the relative concentration determined by Ag⁺-HPLC of minor CLA isomers and their development during the period of study. Noticeable increases in 12,14 and 11,13 (*cis-trans/trans-cis* and *trans-trans*) CLA were observed when linseed was added to the diet. Analysis by GC–MS of DMOX derivatives confirmed the increases in some of these isomers (Fig. 5). Three peaks emerged in the time of elution corresponding to *trans*-12 *trans*-14, *trans*-11 *trans*-13, and *trans*-11 *cis*-13 18:2, and their mass spectra (Fig. 6) were similar to the 11,13 and 12,14 positional isomer spectra previously described (26).

Only limited data are available on the effects of diet on the distribution of individual CLA isomers, but it seems that dietary supplements high in α-linolenic acid may increase the relative proportion of 11,13 and 12,14 positional isomers (21,39,40). Kraft *et al.* (24) hypothesized that the CLA isomers *trans*-11 *cis*-13 and *trans*-11 *trans*-13 18:2 are formed in large quantities as a result of grazing mountain pasture, which is rich in α-linolenic acid. As explained earlier, the pathway for the hydrogenation of α-linolenic acid in the rumen involves an initial isomerization in which the double bond at the carbon-12 position is transferred to the carbon-11 position to form *cis*-9 *trans*-11 *cis*-15 18:3, which is then reduced at both *cis* bonds to produce TVA through *trans*-11 *cis*-
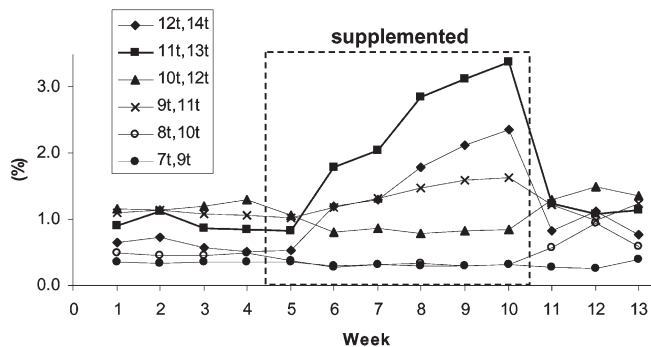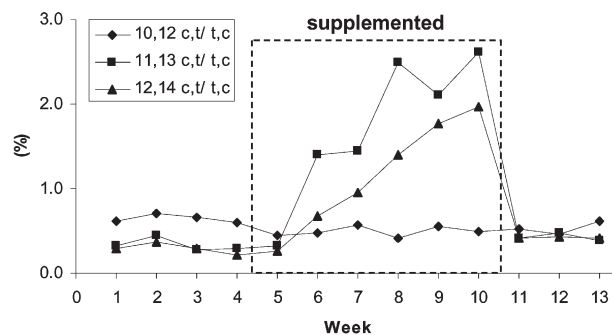
FIG. 4. Development of CLA isomer contents (% of total CLA) determined by silver-ion HPLC in milk fat of ewes fed a diet enriched in α-linolenic acid. The treatment period (broken lines) involved a 6-wk addition of a supplement enriched in linseed.
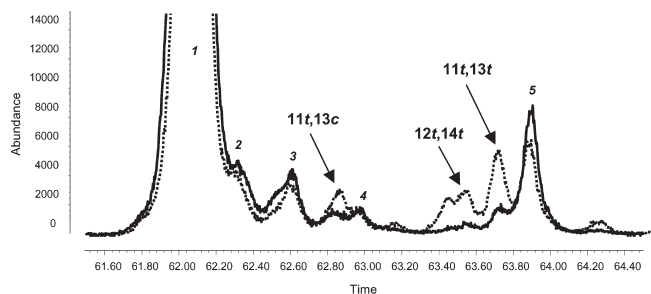
FIG. 5. Profiles by GC–MS of CLA dimethyloxazoline derivatives of milk fat from ewes fed a control diet (solid line) and a diet enriched in α-linolenic acid (dotted line) obtained by high-resolution selected-ion recording at *m/z* 333. **1:** 9-*cis* 11-*trans* 18:2 + 7,9 18:2. **2:** 9-*trans* 11-*cis* 18:2. **3:** 10-*trans* 12-*cis* 18:2. **4:** 9-*cis* 11-*cis* 18:2. **5:** 10-*trans* 12-*trans* 18:2 + 9-*trans* 11-*trans* 18:2.

15 18:2 as an intermediate (33,41). Kraft *et al.* (24) argued that the *trans*-11 double bond was the most stable *trans*-bond found among the 18:1 isomers and among the CLA isomers in ruminal fermentation. They proposed the existence of three different CLA isomers having a *trans*-11 double bond in milk: *cis*-9 *trans*-11 from bacterial synthesis in the rumen (*via* linoleic acid) plus mammary gland desaturation, and *trans*-11 *trans*-13 and *trans*-11 *cis*-13, both of bacterial origin in the rumen from α-linolenic acid as an indirect precursor. Thus, the increases in *trans*-11 *trans*-13 and *trans*-11 *cis*-13 18:2
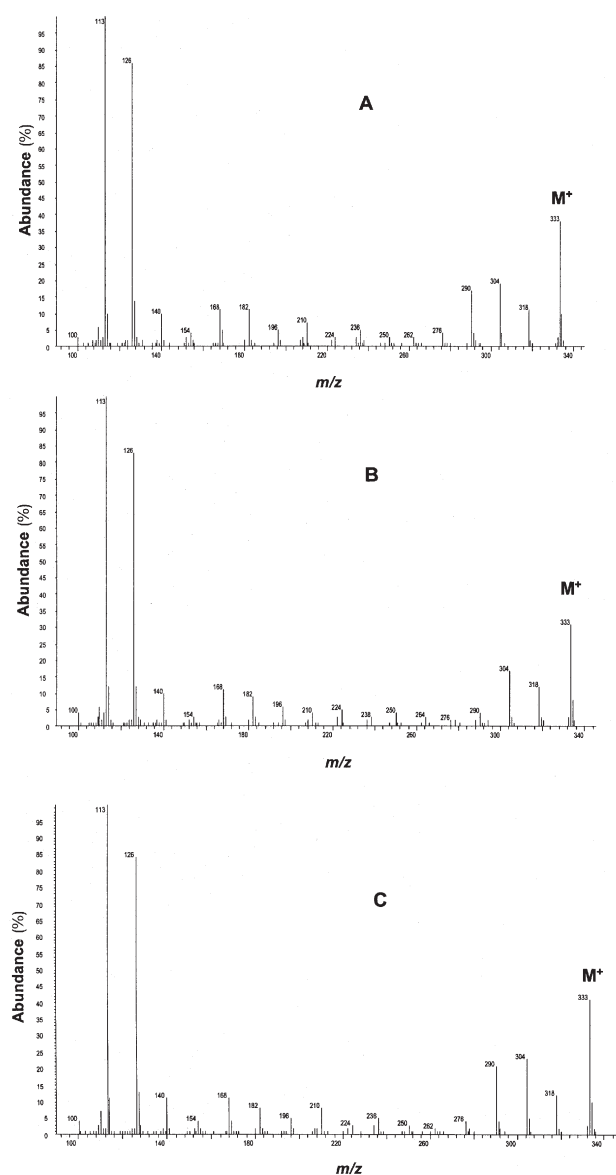
FIG. 6. Mass spectra of the peak labeled in Figure 5 as 11-*trans* 13-*cis* 18:2 (A), 12-*trans* 14-*trans* 18:2 (B), and 11-*trans* 13-*trans* 18:2 (C) corresponding to dimethyloxazoline derivatives of the milk fat of ewes fed a diet enriched in α-linolenic acid.

TABLE 3
Relative Composition (% of total CLA) Determined by Silver-Ion HPLC of CLA Isomers in Ewes' Raw Milk Fat from Animals Fed with a Linseed Enriched Supplement and in Cheeses Made from That Milk After 1, 2, and 4 mon of Ripening

		Cheese		
Isomer	Milk	1 mon	2 mon	4 mon
		(%)		
trans/trans				
12,14	2.05 ± 0.15	2.05 ± 0.13	2.11 ± 0.05	2.25 ± 0.06
11,13	3.11 ± 0.07	3.12 ± 0.06	3.10 ± 0.03	3.34 ± 0.01
10,12	0.69 ± 0.16	0.71 ± 0.17	0.77 ± 0.06	0.81 ± 0.08
9,11	1.50 ± 0.10	1.54 ± 0.09	1.59 ± 0.05	1.64 ± 0.07
8,10	0.38 ± 0.04	0.37 ± 0.02	0.41 ± 0.04	0.38 ± 0.08
7,9	0.41 ± 0.01	0.40 ± 0.01	0.44 ± 0.06	0.39 ± 0.05
cis/trans + *trans/cis*				
12,14	1.76 ± 0.07	1.74 ± 0.05	1.66 ± 0.11	1.75 ± 0.15
11,13	2.26 ± 0.12	2.23 ± 0.05	2.21 ± 0.01	2.23 ± 0.12
10,12	0.56 ± 0.01	0.58 ± 0.01	0.59 ± 0.06	0.58 ± 0.17
9,11	80.44 ± 0.47	80.49 ± 0.50	80.25 ± 0.25	79.85 ± 0.59
7,9	6.02 ± 0.06	6.00 ± 0.02	6.02 ± 0.12	5.98 ± 0.07

isomers found in the present study would be consistent with the results reported for the milk fat of cows grazed in alpine conditions (21,24). Nevertheless, the pathway from the *trans*-11 *cis*-15 18:2 to *trans*-11 *cis*-13 and *trans*-11 *trans*-13 18:2 isomers and the biological significance of these isomers are unclear and still have not been established.

With regard to other minor isomers, amounts of *trans*-10 *cis*-12 18:2 in the samples studied were low, less than 0.75% of total CLA isomers (Fig. 4, Table 3), and values did not change throughout the 3 mon of monitoring. As explanation, *trans*-10 *cis*-12 18:2 in the rumen would be formed from a linoleic but not from an α-linolenic acid pathway, as occurred for the *cis*-9 *trans*-11 isomer of CLA (41). Furthermore, since *cis*-12 desaturase activity has not been detected in the mam-

mary gland or other ruminant tissues, *trans*-10 18:1, formed in the rumen by biohydrogenation of different PUFA and absorbed from the intestine, would not be transformed endogenously to *trans*-10 *cis*-12 18:2.

With respect to *cis/cis* isomers, which are undetectable by UV-HPLC, small amounts were found in the ewe sample. The mass spectrum of the 9,11 positional isomer was detected just at the elution time of 9-*cis* 11-*cis* 18:2 when FA were derivatized to DMOX and analyzed by GC–MS. However, traces of other *cis/cis* isomers were not so clear. Concerning the rest of the CLA isomers found at low levels, no changes were observed when the supplement was added to the diet. These minor isomers seem to originate in the rumen (38). It has been suggested that ruminal bacteria possess several specific *cis*, *trans* isomerases that cause a wide range of these isomers and subsequently help produce a wide range of *trans*-18:1 FA in milk (36,41). Nonetheless, the biological significance of minor *trans*-18:1 isomers is still not well known and the pathways to their formation must be elucidated.

Development of CLA composition during cheese ripening. Mean fat content in cheeses made from the milk of ewes fed SEL was 58% (referring to total solid) and did not change during the ripening period. Nor were there alterations in proportions of major FA and total CLA after 4 mon. As can be seen in Table 2, FA profile hardly changed during the ripening period. After 4 mon, the levels of total CLA and other potentially healthful FA were steady. The effect on CLA content of converting milk to cheese and the subsequent aging and/or storage is controversial. Oxidative reactions could cause destruction of double bond systems, thus potentially reducing CLA levels. It could be argued that because CLA contains a conjugated double bond system, it would be more sensitive to oxidation or isomerization than linoleic or α-linolenic acid, and longer ripening times should show lower CLA content owing to the longer period of air exposure and fermenta-

tion time, which increases radical-mediated oxidation. The fact that no changes were observed in the PUFA profile during ripening (Table 2) seems to indicate that oxidation processes would not take place in these cheeses and that the original raw milk FA profile would not be altered.

The results of the present study coincide with previous research on different kinds of cheeses. No detrimental changes in the CLA content were observed during Mozzarella (14), Emmental (15), or Edam manufacture (16). However, other studies reported modifications in the FA profile and CLA content of Cheddar-type cheeses as a result of the processing (20). These changes were attributed to differences in lipid metabolism of the starter cultures, reflecting the activity of certain bacterial strains, such as lactic acid bacteria and propionibacteria, that are capable of converting linoleic acid to CLA *in vitro* (42,43).

The development of individual CLA isomers during cheese aging as determined by Ag^+-HPLC is shown in Table 3. Most of these isomers were previously reported in different types of cheeses (18,19,25). Considerable changes as a consequence of ripening were not observed, and only slight increases in some *trans/trans* isomers were noticed. Gnädig *et al.* (15) also showed a small increase in the content of the total *trans/trans* CLA isomers during Emmental cheese ripening. By carrying out studies of DMOX derivatives with GC–MS, it was possible to detect variable amounts of the different 9,11 18:2 geometric isomers (*trans/cis, cis/cis*, and *trans/trans*). However, it was not possible to do a reliable quantification and monitor the development of these isomers during the ripening period. The *cis*-9 *cis*-11 isomer co-elutes with C_{21} by GC and in the same area as oleic acid by Ag^+-HPLC, whereas *trans*-9 *cis*-11 18:2 was only resolved from RA when DMOX GC–MS was used. Werner *et al.* (17) also found that concentrations of individual CLA isomers (*cis*-9 *trans*-11, *cis*-9 *cis*-11, *trans*-9 *trans*-11/*trans*-10 *trans*-12) were different among cheeses with different ages. These authors attributed such differences in cheese to cultures and processing conditions. However, monitoring of CLA isomers from raw milk to aged cheese was not carried out.

Overall, the changes in CLA content and FA profile during cheese processing were small under the conditions studied. Such minor changes may not be of great significance. Since the processing of milk into cheese did not substantially alter the CLA content, the ideal solution for achieving cheeses with high concentrations of CLA would be to produce ewes' milk with a high CLA content.

Cheese sensory analysis. Table 4 shows the results of the sensory analysis of the cheeses, made with ewes' milk from the herds fed and not fed the supplement, at 2 and 3 mon of ripening. Scores for the sensory attributes—appearance, taste, and acceptability—did not differ among the samples, and there were no significant differences ($P \leq 0.05$) for cheeses made from the milk of ewes fed SEL. Although aroma and texture scores for cheeses manufactured from CLA-enriched milk at 2 mon of ripening were slightly lower than for cheeses prepared with bulk milk from ewe herds fed without SEL,

TABLE 4
Mean Scores of Sensory Attributes (on a 10-point scale) for Two Batches of Cheeses Made from Ewes' Raw Milk Fat from Animals Fed a Control Diet (CD) and a Diet Enriched in α-Linolenic Acid (LIN) at 2 and 3 mon of Ripening[a]

	2 mon		3 mon	
	CD	LIN	CD	LIN
Appearance	6.5 ± 0.7^a	6.7 ± 1.2^a	6.7 ± 1.2^a	6.0 ± 0.8^a
Aroma	6.7 ± 1.1^a	5.6 ± 1.3^a	5.6 ± 1.4^a	5.6 ± 1.0^a
Taste	5.4 ± 1.5^a	5.6 ± 1.3^a	4.8 ± 1.8^a	6.0 ± 0.9^a
Texture	6.5 ± 0.9^a	5.5 ± 1.0^a	5.7 ± 1.3^a	5.9 ± 0.9^a
General acceptability	5.7 ± 1.3^a	5.6 ± 1.2^a	5.6 ± 1.6^a	5.7 ± 0.9^a

[a]Values in the same row without a common superscript letter were significantly different: $P \leq 0.05$.

such differences were not significant. Furthermore, at 3 mon of ripening both values were similar. Finally, no strange flavors or odors were detected in the study.

Previous descriptive sensory analyses in dairy products high in PUFA and/or CLA do not supply definitive evidence. The impact of fortification with CLA on the properties of fluid milk and butter revealed that these products could exhibit different organoleptic characteristics (44,45), and their acceptance by consumers could be affected. However, in a more recent study (46), untrained panelists were unable to detect flavor differences initially and over time in milk with high CLA and TVA levels. For cheese, there are fewer studies. CLA-enriched milk was used successfully to manufacture Edam cheese with a softer texture and with acceptable organoleptic properties (16). Although in the current study no gritty characteristics were observed in cheeses made with milk from ewe herds fed SEL, increases in CLA and PUFA were small in comparison with amounts reported by Ryhänen *et al.* (16). Thus more research would be needed in this field to confirm the present findings and provide a full picture.

Commercial SEL addition to ovine diet under field conditions could be one way of increasing CLA content in milk fat. In the conditions assayed, minimum effects on the bulk milk yield and composition were observed. An additional advantage is the new FA profile. Other FA, potentially beneficial for human health, apart from RA, such as TVA and 18:3, increased in the milk fat of ewes fed supplemented diets. A decrease in the proportion of medium-chain saturated FA would also enhance the nutritional value of the milk. The changes observed in the CLA isomer profile do not apparently affect the nutritional properties of milk fat.

Overall, FA profile did not change during cheese making. The CLA content in ripened cheeses was comparable with the starting material, and no losses of potentially healthful FA were detected during processing. Finally, cheeses made with milk from linseed-supplemented diets exhibited sensory properties similar to the control products. Thus feeding with these supplements would not represent a hurdle for consumer acceptance of the final product. This could be an alternative way of obtaining dairy products from ewes' milk with added nutritional value.

ACKNOWLEDGMENTS

REFERENCES

1. Tanmahasamut, P., Liu, J., Hendry, L.B., and Sidell, N. (2004) Conjugated Linoleic Acid Blocks Estrogen Signaling in Human Breast Cancer Cells, *J. Nutr. 134*, 674–680.
2. Park, S.J., Park, C.W., Kim, S.J., Kim, J.K., Kim, Y.R., Kim, Y.S., and Ha, Y.L. (2003) Divergent Cytotoxic Effects of Conjugated Linoleic Acid Isomers on NCI-N87 Cells, in *Food Factors in Health Promotion and Disease Prevention* (Shahidi, F., Ho, C.-T., Watanabe, S., and Osawa, T., eds.), Symposium Series, Vol. 851, pp. 113–118, American Chemical Society, Washington, DC.
3. Khanal, R.C., and Olson, K.C. (2004) Factors Affecting Conjugated Linoleic Acid (CLA) Content in Milk, Meat, and Egg: A Review, *Pakistan J. Nutr. 3*, 82–98.
4. Stanton, C., Murphy, J., McGrath, E., and Devery, R. (2003) Animal Feeding Strategies for Conjugated Linoleic Acid Enrichment of Milk, in *Advances in Conjugated Linoleic Acid Research Volume 2* (Sébédio, J.L., Christie, W.W., and Adlof, R., eds.), pp. 123–145, AOCS Press, Champaign.
5. Kelly, M.L., Berry, J.R., Dwyer, D.A., Griinari, J.M., Chouinard, P.Y., Van Amburgh, M.E., and Bauman, D.E. (1997) Dietary Fatty Acid Sources Affect Conjugated Linoleic Acid Concentrations in Milk from Lactating Dairy Cows, *J. Nutr. 128*, 881–885.
6. Offer, N.W., Marsden, M., Dixon, J., Speake, B.K., and Thacker, F.E. (1999) Effect of Dietary Fat Supplements on Levels of n-3 Poly-unsaturated Fatty Acids, *trans* Acids and Conjugated Linoleic Acid in Bovine Milk, *Anim. Sci. 69*, 613–625.
7. Offer, N.W., Marsden, M., and Phipps, R.H. (2001) Effect of Oil Supplementation of a Diet Containing a High Concentration of Starch on Levels of *trans* Fatty Acids and Conjugated Linoleic Acids in Bovine Milk, *Anim. Sci. 73*, 533–540.
8. Dhiman, T.R., Satter, L.D., Pariza, M.W., Galli, M.P., Albright, K., and Tolosa, M.X. (2000) Conjugated Linoleic Acid (CLA) Content of Milk from Cows Offered Diets Rich in Linoleic and Linolenic Acid, *J. Dairy Sci. 83*, 1016–1027.
9. Lock, A.L., and Garnsworthy, P.C. (2002) Independent Effects of Dietary Linoleic and Linolenic Fatty Acids on the Conjugated Linoleic Acid Content of Cows' Milk, *Anim. Sci. 74*, 163–176.
10. Secchiari, P., Antongiovanni, M., Mele, M., Serra, A., Buccioni, A., Ferruzzi, G., Paoletti, F., and Petacchi, F. (2003). Effect of Kind of Dietary Fat on the Quality of Milk Fat from Italian Friesian Cows, *Livest. Prod. Sci. 83*, 43–52.
11. Deaville, E.R., Givens, D.I., and Blake, J.S. (2004) Dietary Supplements of Whole Linseed and Vitamin E to Increase Levels of α-Linolenic Acid and Vitamin E in Bovine Milk, *Anim. Res. 53*, 3–12.
12. Collomb, M., Sollberger, H., Bütikofer, U., Sieber, R., Stoll, W., and Schaeren, W. (2004) Impact of a Basal Diet of Hay and Fodder Beet Supplemented with Rapeseed, Linseed and Sunflowerseed on the Fatty Acid Composition of Milk Fat, *Int. Dairy J. 14*, 549–559.
13. Palmquist, D.L., Beaulieu, A.D., and Barbano, D.M. (1993) Feed and Animal Factors Influencing Milk-Fat Composition, *J. Dairy Sci. 76*, 1753–1771.
14. Dhiman, T.R., Helmink, E.D., McMahon, D.J., Fife, R.L., and Pariza, M.W. (1999) Conjugated Linoleic Acid Content of Milk and Cheese from Cows Fed Extruded Oilseeds, *J. Dairy Sci. 82*, 412–419.
15. Gnädig, S., Chamba, J.F., Perreard, E., Chappaz, S., Chardigny, J.M., Rickert, R., Steinhart, H., and Sébédio, J.L. (2004) Influence of Manufacturing Conditions on the Conjugated Linoleic Acid Content and the Isomer Composition in Ripened French Emmental Cheese, *J. Dairy Res. 71*, 1–5.
16. Ryhänen, E.L., Tallavaara, K., Griinari, J.M., Jaakkola, S., Mantere-Alhonen, S., and Shingfield, K.J. (2005) Production of Conjugated Linoleic Acid Enriched Milk and Dairy Products from Cows Receiving Grass Silage Supplemented with a Cereal-Based Concentrate Containing Rapeseed Oil, *Int. Dairy J. 15*, 207–217.
17. Werner, S.A., Luedecke, L.O., and Shultz, T.D. (1992) Determination of Conjugated Linoleic Acid Content and Isomer Distribution in Three Cheddar-Type Cheeses: Effects of Cheese Cultures, Processing and Aging, *J. Agric. Food Chem. 40*, 1817–1821.
18. Sehat, N., Kramer, J.K.G., Mossoba, M.M., Yurawecz, M.P., Roach J.A.G., Eulitz, K., Morehouse, K.M., and Ku, Y. (1998) Identification of Conjugated Linoleic Acid Isomers in Cheese by Gas Chromatography, Silver Ion High-Performance Liquid Chromatography and Mass Spectral Reconstructed Ion Profiles. Comparison of Chromatographic Elution Sequences, *Lipids 33*, 963–971.
19. Lavillonière, F., Martin, J.C., Bougnoux, P., and Sébédio, J.L. (1998) Analysis of Conjugated Linoleic Acid Isomers and Content in French Cheeses, *J. Am. Oil Chem. Soc. 75*, 343–352.
20. Lin, H., Boyston, T.D., Luedecke, L.O., and Shultz, T.D. (1999) Conjugated Linoleic Acid Content of Cheddar-Type Cheeses as Affected by Processing, *J. Food Sci. 64*, 874–878.
21. Collomb, M., Sieber, R., and Bütikofer, U. (2004) CLA Isomers In Milk Fat from Cows Fed Diets with High Levels of Unsaturated Fatty Acids, *Lipids 39*, 355–364.
22. Chilliard, Y., and Ferlay, A. (2004) Dietary Lipids and Forages Interactions on Cow and Goat Milk Fatty Acid Composition and Sensory Properties, *Reprod. Nutr. Dev. 44*, 467–492.
23. Eulitz, K., Yurawecz, M.P., Sehat, N., Fritsche, J., Roach, J.A.G., Mossoba, M.M., Kramer, J.K.G., Adlof, R.O., and Ku, Y. (1999) Preparation, Separation, and Confirmation of the Eight Geometrical *cis/trans* Conjugated Linoleic Acid Isomers 8,10- Through 11,13-18:2, *Lipids 34*, 873–877.
24. Kraft, J., Collomb, M., Möckel, P., Sieber, R., and Jahreis, G. (2003) Differences in CLA Isomer Distribution of Cows' Milk Lipids, *Lipids 38*, 657–664.
25. Rickert, R., Steinhart, H., Fritsche, J., Sehat, N., Yurawecz, M.P., Mossoba, M.M., Roach, J.A.G., Eulitz, K., Ku, Y., and Kramer, J.K.G (1999) Enhanced Resolution of Conjugated Linoleic Acid Isomers by Tandem-Column Silver-Ion High Performance Liquid Chromatography, *J. High Resolut. Chromatogr. 22*, 144–148.
26. Roach, J.A.G. (1999) Identification of CLA Isomers in Food and Biological Extracts by Mass Spectrometry, in *Advances in Conjugated Linoleic Acid, Volume 1* (Yurawecz, M.P., Mossoba, M.M., Kramer, J.K.G., Pariza, M.W., and Nelson, G.J., eds.), pp. 126–140, AOCS Press, Champaign.
27. IDF (International Dairy Federation) (1982) Determination of the Total Solid Content. FIL-IDF Standard no. 4A:1982, Brussels, Belgium.
28. IDF (International Dairy Federation) (1986) Determination of Fat Content. FIL-IDF Standard no. 5B:1986, Brussels, Belgium.
29. ISO (International Organization for Standardization) (2001)

Milk and Milk Products—Extraction Methods for Lipids and Li-posoluble Compounds, *International Standard ISO 14156-IDF 172:2001.*

30. ISO (International Organization for Standardization) (2002) Milk Fat—Preparation of Fatty Acid Methyl Esters, *International Standard ISO 15884-IDF 182:2002.*

31. Fay, L., and Richli, U. (1991) Location of Double Bonds in Polyunsaturated Fatty Acids by Gas Chromatography–Mass Spectrometry After 4,4-Dimethyloxazoline Derivatization, *J. Chromatogr. 541*, 89–98.

32. IDF (International Dairy Federation) (1987) Sensory Evaluation of Dairy Products, FIL-IDF Standard no. 99A, Brussels, Belgium.

33. Loor, J.J., Bandara, A.B.P.A., and Herbein, J.H. (2002) Characterization of 18:1 and 18:2 Isomers Produced During Microbial Biohydrogenation of Unsaturated Fatty Acids from Canola and Soya Bean Oil in the Rumen of Lactating Cows, *J. Anim. Physiol. Anim. Nutr. 86*, 422–432.

34. Noble, R.C., Moore, J.H., and Harfoot, C.G. (1974) Observations on the Pattern of Esterified and Unesterified Linoleic Acid in the Rumen, *Br. J. Nutr. 31*, 99–108.

35. Daniel, Z.C.T.R., Wynn, R.J., Salter, A.M., and Buttery, P.J. (2004) Differing Effects of Forage and Concentrate Diets on the Oleic Acid and Conjugated Linoleic Acid Content of Sheep Tissues: The Role of Stearoyl-CoA Desaturase, *J. Anim. Sci. 82*, 747–758.

36. Bauman, D.E., Corl, B.A., and Peterson, D.G. (2003) The Biology of Conjugated Acids in Ruminants, in *Advances in Conjugated Linoleic Acid Research*, *Volume 2* (Sebédio, J.L., Christie, W.W., and Adlof, R., eds.), pp. 146–173, AOCS Press, Champaign.

37. Griinari, J.M., Corl, B.A., Lacy, S.H., Chouinard, P.Y., Nurmela, K.V.V., and Bauman, D.E. (2000) Conjugated Linoleic Acid Is Synthesized Endogenously in Lactating Dairy Cows by Δ^9-Desaturase, *J. Nutr. 130*, 2285–2291.

38. Piperova, L.S., Sampugna, J., Teter, B.B., Kalscheur, K.F., Yu-rawecz, M.P., Ku, Y., Morehouse, K.M., and Erdman, R.A. (2002) Duodenal and Milk *trans* Octadecenoic Acid and Conjugated Linoleic Acid (CLA) Isomers Indicate That Postabsorptive Synthesis Is the Predominant Source of *cis*-9 Containing CLA in Lactating Dairy Cows, *J. Nutr. 132*, 1235–1241.

39. Griinari, J.M., Bauman, D.E., Chilliard, Y., Perajoki, P., and Nurmela, K. (2000) Dietary Influences on Conjugated Linoleic Acids (CLA) in Bovine Milk Fat, *3rd Meeting of the European Section of the AOCS*, June 18–21, Helsinki, p. 87.

40. Griinari, J.M., and Shingfield, K.J. (2002) Effect of Diet on Milk Fat *trans* Fatty Acid and CLA Isomer Composition in Ruminants, *Abstract of the 93rd AOCS Annual Meeting and Expo*, Abstract S2, AOCS Press, Champaign.

41. Khanal, R.C., and Dhiman, T.R. (2004) Biosynthesis of Conjugated Linoleic Acid (CLA): A Review, *Pakistan J. Nutr. 3*, 72–81.

42. Kishino, S., Ogawa, J., Omura, Y., Matsumura, K., and Shimizu, S. (2002) Conjugated Linoleic Acid Production from Linoleic Acid by Lactic Acid Bacteria, *J. Am. Oil Chem. Soc. 79*, 159–163.

43. Rainio, A., Vahvaselkä, M., Suomalainen, T., and Laakso, S. (2002). Production of Conjugated Linoleic Acid by *Propionibacterium freudenreichii* ssp. *shermanii, Lait 82*, 91–101.

44. Campbell, W., Drake, M.A., and Larick, D.K. (2003) The Impact of Fortification with Conjugated Linoleic Acid (CLA) on the Quality of Fluid Milk, *J. Dairy Sci. 86*, 43–51.

45. Baer, R.J., Ryali, J., Schingoethe, D.J., Kasperson, K.M., Donovan, D.C., Hippen, A.R., and Franklin, S.T. (2001) Composition and Properties of Milk and Butter from Cows Fed Fish Oil, *J. Dairy Sci. 84*, 345–353.

46. Lynch, J.M., Lock, A.L., Dwyer, D.A., Noorbakhsh, R., Barbano, D.M., and Bauman, D.E. (2005). Flavor and Stability of Pasteurized Milk with Elevated Levels of Conjugated Linoleic Acid and Vaccenic Acid, *J. Dairy Sci. 88*, 489—498.

Dietary Fatty Acids Regulate Cholesterol Induction of Liver CYP7α1 Expression and Bile Acid Production

Yan Li, Meng Jun Hou, Jing Ma, Zhi Hong Tang, Hui Lian Zhu, and Wen Hua Ling*

Department of Clinical Nutrition, Sun Yat-sen University (Northern Campus),
Guangzhou, 510080, People's Republic of China

ABSTRACT: In the present study we investigated the effects of dietary fats containing predominantly PUFA, monounsaturated FA (MUFA), or saturated FA (SFA) on lipid profile and liver cholesterol 7α-hydroxylase (CYP7α1) mRNA expression and bile acid production in C57BL/6J mice. The animals ($n = 75$) were randomly divided into five groups and fed a basic chow diet (AIN-93G) (BC diet), a chow diet with 1 g/100 g of cholesterol (Chol diet), a chow diet with 1 g/100 g of cholesterol and 14 g/100 g of safflower oil (Chol + PUFA diet), a chow diet with 1 g/100 g of cholesterol and olive oil (Chol + MUFA diet), or a chow diet with 1 g/100 g of cholesterol and myristic acid (Chol + SFA diet) for 6 wk. The results showed that the Chol + SFA diet decreased CYP7α1 gene expression and bile acid pool size, resulting in increased blood and liver cholesterol levels. Addition of PUFA and MUFA to a 1% cholesterol diet increased the bile acid pool production or bile acid excretion and simultaneously decreased liver cholesterol accumulation despite decreased CYP7α1 mRNA expression. The results indicate that the decreased bile acid pool size induced by the SFA diet is related to inhibition of the liver CYP7α1 gene expression, but an increased bile acid pool size and improved cholesterol homeostasis are disassociated from the liver CYP7α1 gene expression.

Paper no. L9639 in *Lipids 40*, 455–462 (May 2005).

The role of high blood cholesterol as an important factor in advancing atherosclerosis is now widely accepted. The role of diet in modifying blood cholesterol concentrations is also generally recognized. Dietary cholesterol and saturated FA (SFA) increase total cholesterol (TC) concentrations in circulation, whereas PUFA generally reduce and monounsaturated FA (MUFA) have a little or no effect on plasma cholesterol concentrations. Whole-body cholesterol homeostasis is controlled by many factors including absorption of dietary cholesterol, metabolism of plasma cholesterol, *de novo* cholesterol synthe-

sis, cellular uptake of cholesterol, and excretion of cholesterol into bile acids. The mechanisms by which dietary FA influence blood cholesterol are not fully defined.

Removal of excess cholesterol from the body by the formation of bile acids in the liver is very important for maintaining cholesterol homeostasis. Cholesterol 7α-hydroxylase (CYP7α1) is the first and rate-limiting enzyme of bile acid synthesis in the liver (1). Thus, the activity of CYP7α1 can have a major impact on the overall catabolism of excess cholesterol. Epidemiological studies and animal experiments suggest that lower CYP7α1 activity or CYP7α1 gene deficiency is related to hypercholesterolemia and the accumulation of cholesterol in liver. Mutation in the CYP7α1 gene may lead to high LDL-cholesterol (LDL-C) level and cardiovascular disease, and enhancement of CYP7α1 activity may decrease serum LDL-C effectively (2–6).

The level of CYP7α1 is regulated by various factors including nutrients, bile acid back to the liver from the intestine *via* the enterohepatic circulation process, and others. The regulation usually occurs at the level of transcription. Recently, some of the factors that regulate transcription of this gene have been described (7). Hydrophobic bile acids have a relatively strong inhibitory effect on this enzyme. Among dietary nutrients, cholesterol increases the expression of CYP7α1 mRNA (8–10), and other dietary fats or FA also play a role in modulation of CYP7α1 activity and mRNA expression. Cheema *et al.* in 1997 (11) reported that cholesterol status does not necessarily determine the amount of CYP7α1 mRNA, suggesting that other dietary fats are important factors in the regulatory potential of dietary cholesterol on CYP7α1 gene expression. The role of different FA in the ability of dietary cholesterol to stimulate liver CYP7α1 mRNA abundance and protein content and to regulate total bile acid synthesis has not been fully investigated.

The mechanisms by which dietary fat or FA affect cholesterol-induced bile acid synthesis and CYP7α1 activity or gene expression are complex and have not been elucidated so far. Evidence from some studies indicates that FA does not directly bind to CYP7α1 (12,13); the pathway of different FA that regulate CYP7α1 is worthy of further investigation.

The present study investigated the effects of dietary fats containing predominantly PUFA, MUFA, or SFA on the ability

of dietary cholesterol to regulate liver CYP7α1 mRNA abundance and bile acid synthesis.

MATERIALS AND METHODS

Animals and diets. Seventy-five female mice (C57BL/6J) from the animal center of Sun Yat-sen University were used in the experiments. The animals were bred and maintained under conventional housing conditions, and all procedures were followed in accordance with the approved protocol for use of experimental animals set by the standing committee on animal care at Sun Yet-sen University. The animals were randomly divided into five groups of 15 animals and fed for 6 wk with one of the following: a normal chow diet (AIN-93G formulation) (14) (BC group); a chow diet containing 1 g/100 g cholesterol (Chol diet); a chow diet with 1 g/100 g of cholesterol and 14 g/100 g of safflower oil (Chol + PUFA diet); a chow diet with 1 g/100 g of cholesterol and olive oil (Chol + MUFA diet); or a chow diet with 1 g/100 g of cholesterol and myristic acid (Chol + SFA diet). Linseed oil (1 g/100 g) was also added to Chol + PUFA, Chol + MUFA and Chol + SFA diets to ensure an adequate source of n-3 FA (15). The composition of the diets is shown in Table 1. The nutritional ingredients including casein, mineral mixture, and vitamin mixture were all purchased from Harlan Teklad (Madison, WI). Myristic acid and linseed oil were purchased from Sigma (St. Louis, MO). The FA composition was determined by GLC (Table 2). The animals were given free access to food and water. Samples of serum, liver, small intestine and its whole content were collected after 6 wk. Serum was frozen at −20°C, and the tissue samples were kept in liquid nitrogen. The total energy intake in food or body weight gained in the animals of the BC group was less than that of four test groups; however, no differences in the intake of energy or body weight gained among the four test groups was observed throughout the duration of the study (data not shown).

Serum lipids. Blood samples were obtained by retro-orbital bleeding under ether anesthesia, and serum was separated by centrifugation. Serum TC, LDL-C, and HDL-cholesterol (HDL-C) were measured using a Hitachi Automatic Analyzer (Tokyo, Japan). Serum TC was determined by a cholesterol esterase and cholesterol oxidase assay (16), and the concentrations of HDL-C were assayed by the same method after removing LDL-C and VLDL cholesterol with magnesium dextran sulfate. Serum LDL concentrations were calculated according to the Friedwald *et al.* formula (17), which assumes that circulating VLDL consists of 80% TG and 20% cholesterol.

Serum FA. The levels of serum FA were determined by capillary GC after extraction by methanol and hexane (4:1, vol/vol) and transesterification directly in a one-step reaction (18). The relative amount of each FA (g/100 g) was quantified. Serum levels of SFA, MUFA, and PUFA were calculated.

Hepatic cholesterol level. Liver was removed immediately and rinsed with cold PBS after the animal had been sacrificed, then dried, minced, and weighed before extracting the lipids by the method of Folch *et al.* (19). The TC content in liver was determined by using an enzymatic fluorometric assay based on a modification of the previously described methods (20). The samples were run in duplicate. All values are expressed as µmol/g tissue per animal.

Bile acid pool. The entire small intestine and its contents, along with the bulk of the liver and the gallbladder, were homogenized and combined, then extracted with isopropanol. The total bile acid content of the extract was taken to dryness and resuspended in an appropriate volume of methanol. Bile acids were quantified using the method of Bianchini *et al.* (21).

Preparation of liver microsomes. Liver microsomes were obtained using a modification of the method of Cheema *et al.* (11). Samples of frozen livers (100–500 mg) were minced in 1 mL of ice-cold buffer containing 0.3 mol/L sucrose, 1 mmol/L EDTA, 50 mmol/L KF, 50 mmol/L KC1, 5 mmol/L DTT, 0.1

TABLE 1
Dietary Formulation of Mice in Different Dietary Groups[a]

Ingredient (g/kg)	Groups				
	Basic chow (BC)	Chol	Chol + PUFA	Chol + MUFA	Chol + SFA
Cornstarch	397.486	391.62	341	341	341
Casein	200	200	200	200	200
Dextrinized cornstarch	132	129.77	113	113	113
Sucrose	100	98.1	85.3	85.3	85.3
Soybean oil	70	70	—	—	—
Safflower oil	—	—	140	—	—
Olive oil	—	—	—	140	—
Myristic acid	—	—	—	—	140
Linseed oil	—	—	10	10	10
Cholesterol	—	10	10	10	10
Fiber	50	50	50	50	50
Mineral mixture (AIN-93G-MX)	35	35	35	35	35
Vitamin mixture (AIN-93-VX)	10	10	10	10	10
L-Cysteine	3	3	3	3	3
Choline bitartrate	2.5	2.5	2.5	2.5	2.5
TBHQ	0.014	0.014	0.014	0.014	0.014

[a]Chol, cholesterol; MUFA, monounsaturated FA; SFA, saturated FA.

TABLE 2
FA Composition of Oil Used[a] (% total FA, wt/wt)

FA	Safflower oil	Olive oil	Myristic acid	Soybean oil	Linseed oil
8:0	ND	ND	ND	ND	ND
10:0	ND	ND	ND	ND	ND
12:0	ND	ND	ND	ND	ND
14:0	ND	ND	94.89	ND	ND
16:0	5.00	11.34	1.21	10.42	5.31
16:1	ND	0.65	ND	0.42	0.17
18:0	2.33	2.83	0.17	4.11	3.42
18:1	10.53	78.21	0.14	20.41	21.48
18:2n-6	78.37	5.83	0.61	54.56	14.94
18:3n-3	0.26	ND	0.83	7.61	36.81
18:4n-3	ND	ND	ND	0.38	ND
20:0	0.40	ND	ND	0.39	0.35
20:1	ND	ND	ND	0.10	0.47
20:4n-6	ND	ND	ND	ND	0.22
20:5n-3	ND	ND	ND	ND	ND
22:0	0.34	ND	ND	0.42	0.14
22:1	0.30	ND	ND	0.31	0.26
22:6n-3	ND	ND	ND	ND	ND
Others	2.47	1.14	2.15	0.88	16.41
ΣSFA	10.34	14.17	96.27	15.34	9.22
ΣMUFA	10.83	78.86	0.14	24.24	22.38
ΣPUFA	78.63	5.83	0.23	62.55	51.97

[a]Abbreviations used: ΣSFA, sum of SFA; ΣMUFA, sum of MUFA; ND, not detectable (<0.005%); for other abreviations see Table 1.

mol/L K_2HPO_4 (pH 7.4), and then disrupted in a 2-mL Potter-Elvehjem homogenizer. Homogenates were centrifuged at 9,000 × g at 4°C. The supernatant was centrifuged for 70 min at 110,000 × g in a SW-60 rotor (Beckman Instruments) at 4°C. The microsomal pellet from the second spin was resuspended in 1 mL of buffer containing 0.1 mol/L K_2HPO_4 (pH 7.4), 1 mmol/L EDTA, 50 mmol/L KF, 5 mmol/L DTT, and 50 mmol/L KCl. Aliquots of liver microsomes (60–70 mg/mL) were then rapidly frozen in liquid nitrogen and stored at −80°C until assayed.

Assay for CYP7α1 mRNA by RT-PCR. Total RNA was extracted from liver by using a reagent kit according to the manufacturer's instructions (Sangon, Shanghai, China). RNA was reverse-transcribed from 5 µg of total RNA in a final volume of 20 µL using the kit RT-PCR (Sangon). The reaction was stopped by heating the samples at 70°C for 10 min. cDNA was subjected to DNA amplification by PCR (22) using 2 units of Tag DNA polymerase and both primer pairs complementary to murine CYP7α1 cDNA, PPARα cDNA, and actin cDNA, at a final concentration of 0.4 µmol/L of each primer. The reaction was predenaturated at 94°C for 4 min. The amplification cycle (denaturing at 94°C for 30 s, annealing at 56°C for 45 s, and extending at 72°C for 45 min) was repeated 35 times and followed by a final extension for 10 min at 72°C. The primers for CYP7α1 were 5′-CCTTGGGACGTTTTCCTGCT-3′ (sense) and 5′-GCGCTCTTTGATTTAGGAAG-3′ (antisense). The expected product length was 515 bp. The primers for the "housekeeping gene" β-actin were 5′-GGACTCCTATGTGGGTGACGAGG-3′ (sense) and 5′-GGGAGAGCATAGCCCTCGTAGAT-3′ (antisense). The expected product length was 366 bp. Final PCR products were separated on 2% agarose gel and detected by ethidium bromide staining. Semiquantitative estimation was done by com-paring the amount of mRNA expression of CYP7α1 with β-actin.

Assay for CYP7α1 protein by Western blot. CYP7α1 protein was analyzed by immunoblotting with the anti-CYP7α1 antibody. Protein extracts of the liver microsome were prepared, and protein concentration was determined by using a Bio-Rad kit. Immunoblot analysis was performed using a modification of the method described by *Liang et al.* (23). Briefly, microsomal polypeptides (50 µg of protein) were loaded on 10% SDS-PAGE (Bio-Rad Laboratories, Hercules, CA), and the separated proteins were electrophoretically transferred to polyvinylidene difluoride membranes at 100 V for 90 min. The membrane was blocked in Tris-buffered saline with 0.1% Tween 20 and 5% nonfat milk and probed with the goat polyclonal antibody to CYP7α1 (1:800) (Santa Cruz Biotechnology, Santa Cruz, CA) overnight at 4°C, followed by a rabbit anti-goat conjugated horseradish peroxidase IgG (1:10,000) (Santa Cruz Biotechnology). Specific protein bands were revealed by enhanced chemiluminescence and visualized by the exposure to autoradiographic film.

Statistical analysis. Results are expressed as means ± SD. Data were analyzed by one-way ANOVA coupled with the Student–Newman–Keuls multiple comparison test. Differences were considered significant if $P < 0.05$. SPSS 11.0 software (Chicago, IL) was used for all statistical analyses.

RESULTS

Body weights and food intake. The amount of food consumption by the mice was recorded daily and did not significantly differ between the diet groups throughout the 6-wk feeding period. The

TABLE 3
Serum Lipid Concentrations in Mice Fed Different Diets[a]

Groups	TC (mmol/L)	LDL-C (mmol/L)	HDL-C (mmol/L)	LDL-C/HDL-C
BC	2.43 ± 0.11	0.35 ± 0.036	1.81 ± 0.11	0.20 ± 0.02
Chol	3.24 ± 0.09○	0.59 ± 0.023○	1.80 ± 0.07	0.33 ± 0.01○
Chol + PUFA	4.11 ± 0.14○,△,☆	0.58 ± 0.022○,☆	2.59 ±0.121○,△,☆	0.23 ± 0.01○,△,☆
Chol + MUFA	3.26 ± 0.20○,☆	0.63 ± 0.024○,△,☆	1.58 ± 0.068○,△,☆	0.40 ± 0.02○,△,☆
Chol + SFA	5.04 ± 0.14○,△	1.48 ± 0.05○,△	1.85 ± 0.06	0.73 ± 0.02○,△

[a]Results shown are means ± SD, $n = 10$. ○, $P < 0.001$ vs. BC group; △, $P < 0.05$ vs. Chol group; ☆, $P < 0.001$ vs. Chol + SFA group. TC, total cholesterol; LDL-C, LDL-cholesterol; HDL-C, HDL-cholesterol; BC, basic chow; for other abbreviations see Tables 1 and 2.

body weights of the animals did not significantly differ among the different dietary groups at the beginning. At the end of the feeding period, the body weight of mice fed BC diet was significantly lower than that of mice fed other diets, and there were no significant differences among Chol, SFA + Chol, PUFA + Chol, and MUFA + Chol dietary groups (data not shown).

Serum lipid profile. Addition of 1% cholesterol to the chow diet induced hypercholesterolemia, and addition of different types of FA with cholesterol further modified the plasma cholesterol levels (Table 3). As compared with the 1% cholesterol diet, supplementation of PUFA significantly decreased the serum levels of LDL-C and the LDL-C/HDL-C ratio, but increased the serum level of TC by 27% ($P < 0.001$) and that of HDL-C by 44% ($P < 0.001$). MUFA reduced serum HDL-C by 6.7% ($P < 0.05$) and elevated LDL-C by 12% ($P < 0.001$) and

the LDL-C/HDL-C ratio by 21% ($P < 0.001$), but had no influence on serum TC. SFA increased serum TC, LDL-C, and the LDL-C/HDL-C ratio by 56 ($P < 0.001$), 150 ($P < 0.001$), and 120% ($P < 0.001$), respectively. The mice fed the Chol + SFA diet had the highest LDL-C level and LDL-C/HDL-C ratio as compared with the other groups ($P < 0.001$) (Table 3).

Cholesterol accumulation in liver. Addition of cholesterol to diets increased the hepatic TC accumulation in all diet groups as compared with the BC diet ($P < 0.001$) (Fig. 1). Supplementation with SFA doubled the liver cholesterol content as compared with the 1% cholesterol diet alone ($P < 0.001$) and resulted in the highest level of liver cholesterol among the diet groups ($P < 0.001$). Accumulation of cholesterol in livers of mice fed Chol + PUFA and Chol + MUFA diets was reduced by 40 ($P < 0.001$) and 25% ($P < 0.001$), respectively, as compared with the mice fed cholesterol alone ($P < 0.001$). There was a significant difference in liver cholesterol levels between the Chol + PUFA and the Chol + MUFA groups ($P < 0.001$).

Bile acid pool. Addition of 1% cholesterol to the BC diet increased the bile acid pool size by 52% as compared with that of the BC diet ($P < 0.001$) (Fig. 2). When different FA were added to a cholesterol-supplemented diet, the response in bile acid pool size was variable. The bile acid pool size of mice fed the Chol + SFA diet decreased by 54% ($P < 0.001$) compared with mice fed the Chol diet; animals consuming the Chol + SFA diet had the lowest bile acid pool size among the different dietary groups ($P < 0.001$). The bile acid pool size in mice fed Chol + PUFA and Chol + MUFA diets increased by 26 ($P < 0.001$) and 48%, respectively, compared with mice fed a cholesterol diet alone ($P < 0.001$).

CYP7α1 mRNA expression and CYP7α1 protein content in liver. To investigate whether different diets cause an alteration of CYP7α1 mRNA, a reverse transcriptase-PCR analysis for total mRNA samples extracted from the liver was performed, and β-actin was used as housekeeping gene. The results showed that the highest level of CYP7α1 mRNA was expressed in the liver of mice fed Chol diet ($P < 0.001$). Consumption of Chol + PUFA or Chol + MUFA diets decreased the expression of CYP7α1 mRNA by 43 and 50%, respectively, compared with mice fed cholesterol alone ($P < 0.001$ and $P < 0.001$, respectively). The expression of CYP7α1 mRNA of the liver in mice fed Chol + SFA was only 16% ($P < 0.001$) of that of mice fed the Chol diet, and it was the lowest among the groups ($P < 0.001$) (Fig. 3A).
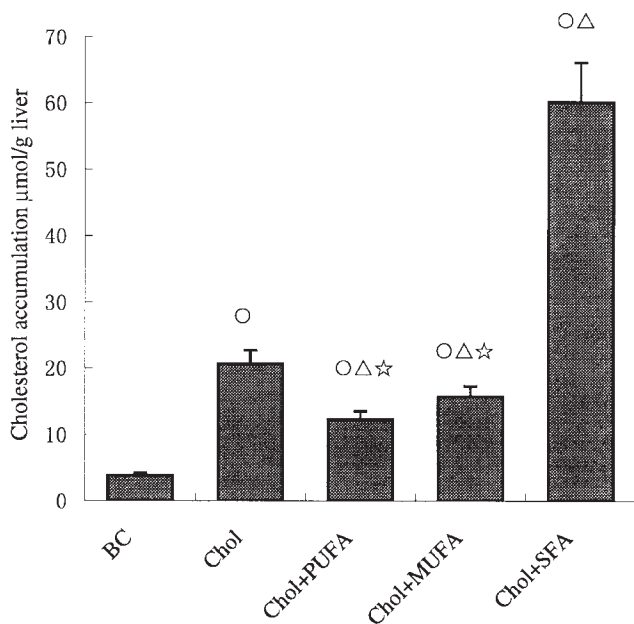
FIG. 1. Hepatic cholesterol concentrations in mice fed diets containing cholesterol and different fats. Cholesterol accumulation in livers was quantified as described in the Materials and Methods section. The differences among the groups were analyzed by one-way ANOVA coupled with LSD-*t* multiple comparison test. Values are expressed as means ± SD, $n = 8$. ○, $P < 0.001$ vs. BC group; △, $P < 0.001$ vs. Chol group; ☆, $P < 0.001$ vs. Chol + SFA group. BC, basic chow; MUFA, monounsaturated FA; SFA, saturated FA.
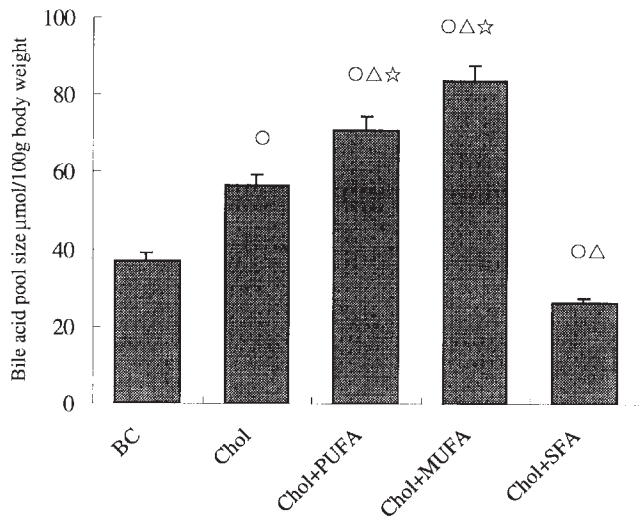
FIG. 2. Bile acid pool size in mice fed diets containing cholesterol and different fats. The bile acid pool size in mice was assayed as described in the Materials and Methods section. The differences among the groups were analyzed by one-way ANOVA coupled with LSD-t multiple comparison test. Values are means ± SD, $n = 7$. ○, $P < 0.001$ vs. BC group; △, $P < 0.001$ vs, Chol group; ☆, $P < 0.001$ vs. Chol + SFA group. For abbreviations see Figure 1.

Figure 3B shows that feeding of the cholesterol diet elevated liver CYP7α1 protein content by 48% compared with the BC group ($P < 0.001$), whereas feeding of the Chol + PUFA, Chol + MUFA, or Chol + SFA diets decreased CYP7α1 protein content by 29 ($P < 0.001$), 31 ($P < 0.001$), and 45% ($P < 0.001$), respectively, as compared with mice fed cholesterol alone. The mice fed Chol + SFA diet had the lowest content among the groups ($P < 0.001$).

DISCUSSION

All diets containing cholesterol in the present study induced hypercholesterolemia, but the response of blood lipids to the addition of different dietary FA to 1% cholesterol diet varied. The striking aspect in these results was that when PUFA was added to the Chol diet, the serum TC was significantly increased, although the increased fraction was mainly in the HDL-C. The effects of MUFA or SFA on serum cholesterol levels were similar to those found previously (24–28). Compared with cholesterol diet feeding, the Chol + MUFA diet produced the same serum TC, but significantly increased the LDLC/HDL-C ratio, meaning that MUFA does not affect the total serum cholesterol level but increases the distribution of cholesterol in LDL-C. The Chol + SFA diet resulted in higher ($P < 0.001$) serum TC and LDL-C/HDL-C (Table 3). In addition, the dietary cholesterol plus FA changed the accumulation of cholesterol in the liver. Liver cholesterol in mice fed the Chol + SFA diet was the highest among the groups, and was three, four, and five times more than that in mice fed Chol, Chol + MUFA, and Chol + PUFA diets, respectively (Fig. 1). Together, the changes of lipid profile in blood and cholesterol accumula-

tion in the liver following addition of SFA to the diet increased the risk of atherosclerosis. Dietary PUFA showed a beneficial effect, indicated by the increasing HDL concentration. MUFA did not cause a beneficial change by improving the lipid profile, as has been reported by others (29,30) because it increased serum LDL concentration.

In the present study, feeding a diet containing SFA and cholesterol for 6 wk reduced the bile acid pool size; consumption of diets containing MUFA and PUFA increased the pool size as compared with cholesterol alone. In previous study by Cheema *et al.* (11), feeding the SFA diet for 3 wk to mice induced the highest level of bile acids in gallbladder bile as compared with PUFA and MUFA diets. The different lengths of the feeding period could explain the discrepancy in results between our study and the report of Cheema *et al*. Synthesis of bile acid is affected by many factors, such as blood lipid profile, CYP7α1 activity, and bile acid feedback. It is possible that bile acid synthesis during a period of 3 wk of feeding of FA is different from that for 6 wk. A longer feeding period may better reflect the real impact of FA on bile acid synthesis. Secondly, Cheema *et al*. measured bile acid level in gallbladder bile, which does not represent the bile acid pool size that we measured.

Cholesterol degradation to bile acids occurs *via* "classic" (or neutral) and "alternative" (or acidic) bile acid biosynthetic pathways. The classic or neutral pathway, common to all mammals, is initiated by CYP7α1, an enzyme located in the endoplasmic reticulum. The rate of cholesterol degradation to bile acids is controlled in part by the enzyme CYP7α1, which catalyzes the initial step in the pathway of bile acid synthesis that is responsible for more than 50% of bile acid formation (31,32). CYP7α1 activity is controlled by a variety of hormonal and nutritional factors. On the basis of the fact that a positive correlation between CYP7α1 mRNA and CYP7α1 activity has been illustrated by many studies (11,33), we assayed the CYP7α1 mRNA expression to examine the influence of different dietary FA on the liver CYP7α1 activity. The stimulation of murine CYP7α1 gene expression by dietary cholesterol is well documented (34,35). In the present study we also confirm that CYP7α1 mRNA and protein abundance increased in response to a 1% cholesterol supplementation of the diet.

Dietary fats are known to modify the whole-body cholesterol homeostasis; the mechanism proposed is related to the regulation on CYP7α1 (1,24–28). Feeding 1% cholesterol increased CYP7α1 gene expression; however, addition of dietary FA to the cholesterol-enriched semipurified diets did not result in a further increase of CYP7α1 mRNA and protein abundance. The addition of PUFA, MUFA, and SFA to a 1% cholesterol diet all caused a significant reduction in both CYP7α1 mRNA and protein abundance as compared with a 1% cholesterol diet. The Chol + SFA diet caused the lowest expression of CYP7α1 mRNA among the groups (Fig. 3). Although the majority of studies have documented induction of CYP7α1 mRNA in response to dietary PUFA and suppression in response to dietary SFA, the reports on CYP7α1 mRNA in response to MUFA have not been unanimous (11,36). It has been

A

B
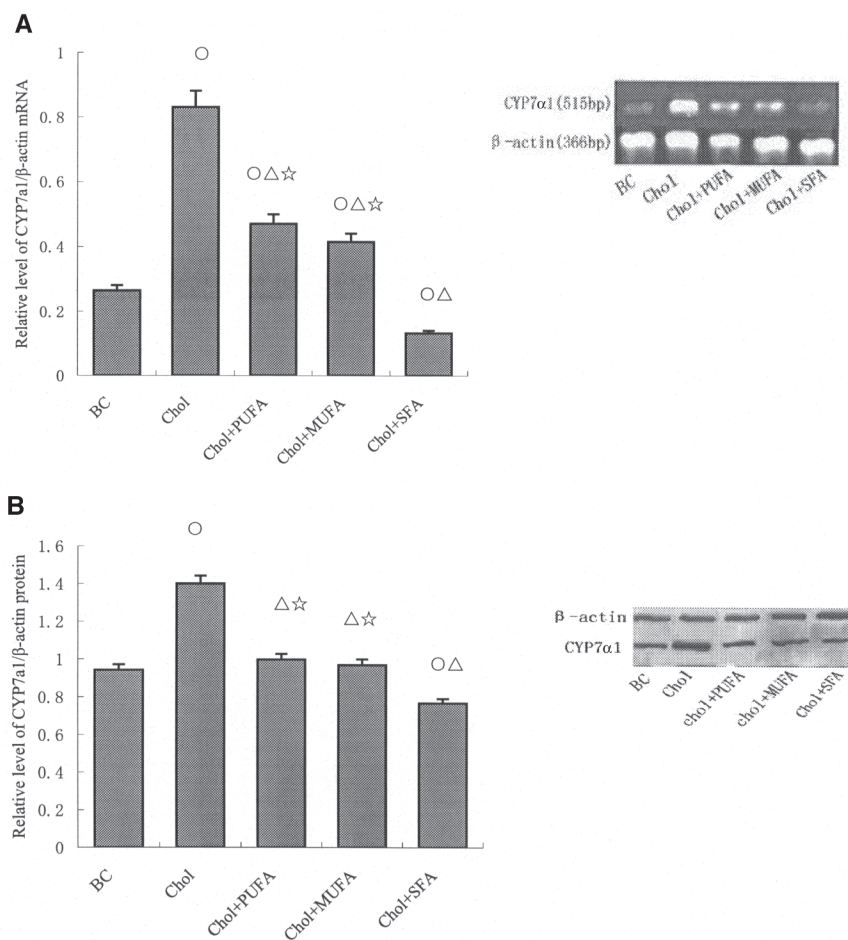
FIG. 3. Cholesterol 7α-hydroxylase (CYP7α1) mRNA (A) and protein (B) abundance in the liver microsome of mice fed diets containing cholesterol and different fats. The CYP7α1 mRNA and protein abundance were quantified as described in the Materials and Methods section. The levels of CYP7α1 mRNA (protein) were calculated as the ratio of CYP7α1 to β-actin mRNA (protein). The differences among the groups were analyzed by one-way ANOVA coupled with LSD-*t* multiple comparison test. Values are means ± SD, *n* = 5. ○, $P < 0.001$ vs. BC group; △, $P < 0.001$ vs. Chol group; ☆, $P < 0.001$ vs. Chol + SFA group. For other abbreviations see Figure 1.

reported that SFA directly inhibit CYP7α1 activity, which is related to the decrease of bile acid synthesis and smaller bile acid pool size (11). The alteration of pool size of bile acid induced by SFA diet is associated with the level of CYP7α1 mRNA. The SFA diet significantly decreased both the bile acid pool size and CYP7α1 mRNA expression (Fig. 2). The most striking aspect of the present results is that levels of CYP7α1 mRNA expression did not correlate with the variation of bile acid pool size in mice fed PUFA and MUFA diets. Addition of PUFA or MUFA to 1% cholesterol-supplemented diet led to a significant increase in the bile acid pool but decreased CYP7α1 mRNA expression.

Although several recent studies challenge the notion that the regulation of CYP7α1 is a major determinant of plasma cholesterol responsiveness, the regulation of bile acid biosynthesis by CYP7α1 behavior is quite different between mouse and human (33,37). The human CYP7α1 gene is not stimulated by dietary cholesterol in transgenic mice. In contrast, CYP7α1 gene expression is responsive to dietary cholesterol in the mouse (33). Bile acid synthesis exhibits negative feedback regulation *via* inhibition of the transcription of the CYP7α1 gene and a decrease in the enzymatic activity of CYP7α1 (38–40). The mechanism includes: "bile acid response element (BARE)" (41); activation of protein kinase C (42), which in turn activates farnesoid X receptor (FXR) (43,44); and cytokines (45). The fact that the SFA diet caused the lowest CYP7α1 mRNA expression and bile acid pool size among the groups suggested that SFA may directly inhibit the liver CYP7α1 through the BARE pathway. This result is consistent with a study (45) that suggested that dietary saturated fats retard excretion of dietary cholesterol as compared with PUFA and MUFA. However, the levels of CYP7α1 mRNA and protein decreased, whereas, contrary to expectation, the bile acid pool size increased in the mice fed Chol + PUFA or Chol +

MUFA diet. The effects of PUFA and MUFA on bile acid biosynthesis may consist of positive and negative pathways. PUFA and MUFA may directly exert stimulatory influence on CYP7α1 expression (11,36), which in turn promotes bile acid formation. However, bile acids back to the liver via the process of enterohepatic circulation inhibit CYP7α1 expression. It has been proposed that the bile acid pool size is the major regulator of CYP7α1 activity (46). When the feedback inhibition effect by bile acid overrides the induction by cholesterol and FA, the integrated outcome is the decrease of CYP7α1 mRNA expression. Tiemann *et al.* (46) demonstrated that long-term feeding of dietary cholesterol increases bile acid pool size despite decreased enzyme activity in mice. Thus, in the present study, the lower CYP7α1 mRNA expression in mice fed Chol + PUFA or Chol + MUFA may result mostly from the feedback inhibition of bile acids back to the liver rather than direct inhibition from PUFA or MUFA.

As already mentioned, the alternative (acidic) bile acid biosynthesis is also an important mechanism for maintenance of cholesterol homeostasis in animals (31). The acidic pathway initiated by CYP27α1 converts cholesterol to 27-hydroxycholesterol and cholestenoic acid. The acidic pathway may be considered as a reverse cholesterol transport process for removing excess cholesterol from the peripheral tissue to the liver for conversion to bile acids and thus may protect humans from developing atherosclerosis (47). It is possible that the high blood cholesterol concentration induced by dietary cholesterol and FA may promote the pathway of acidic bile acid biosynthesis, thus enlarging the bile acid pool size. Consequently, the increase of bile acid going back to the liver *via* the enterohepatic circulation process exerts an inhibitory role on CYP7α1 mRNA expression. However, it was reported that the alternate pathway of bile acid synthesis is not regulated by dietary cholesterol (35). How the high plasma lipid profile stimulates acidic bile acid biosynthesis remains unclear and needs further elucidation.

In conclusion, the present study found that diets containing SFA in addition to cholesterol decreased CYP7α1 gene expression and bile acid pool size, resulting in increased blood cholesterol and LDL concentrations. The addition of PUFA and MUFA to a cholesterol-supplemented diet increased bile acid pool production or bile acid excretion despite decreased CYP7α1 mRNA expression, which is beneficial in maintaining cholesterol homeostasis. The different dietary FA may play different roles in cholesterol removal or bile acid production *via* CYP7α1 or other pathways.

ACKNOWLEDGMENTS

REFERENCES

1. Russell, D.W., and Setchell, K.D. (1992) Bile Acid Biosynthesis, *Biochemistry 31*, 4737–4749.
2. Pullinger, C.R., Eng, C., Salen, G., Shefer, S., Batta, A.K., Erickson, S.K., Verhagen, A., Rivera, C.R., Mulvihill, S.J., Malloy, M.J., and Kane, J.P. (2002) Human Cholesterol 7α-Hydroxylase (CYP7α1) Deficiency Has a Hypercholesterolemic Phenotype, *J. Clin. Invest. 110*, 109–117.
3. Couture, P., Otvos, J.D., Cupples, L.A., Wilson, P.W., Schaefer, E.J., and Ordovas, J.M. (1999) Association of the A-204C Polymorphism in the Cholesterol 7α-Hydroxylase Gene with Variations in Plasma Low Density Lipoprotein Cholesterol Levels in the Framingham Offspring Study, *J. Lipid Res. 40*, 1883–1889.
4. Hegele, R.A., Wang, J., Harris, S.B., Brunt, J.H., Young, T.K., Hanley, A.J., Zinman, B., Connelly, P.W., and Anderson, C.M. (2001) Variable Association Between Genetic Variation in the CYP7 Gene Promoter and Plasma Lipoproteins in Three Canadian Populations, *Atherosclerosis 154*, 579–587.
5. Spady, D.K., Cuthbert, J.A., Willard, M.N., and Meidell, R.S. (1998) Overexpression of Cholesterol 7α-Hydroxylase (CYP7α) in Mice Lacking the Low Density Lipoprotein (LDL) Receptor Gene. LDL Transport and Plasma LDL Concentrations Are Reduced, *J. Biol. Chem. 273*, 126–132.
6. Pandak, W.M., Schwarz, C., Hylemon, P.B., Mallonee, D., Valerie, K., Heuman, D.M., Fisher, R.A., Redford, K., and Vlahcevic, Z.R. (2001) Effects of CYP7α1 Overexpression on Cholesterol and Bile Acid Homeostasis, *Am. J. Physiol. Gastrointest. Liver Physiol. 281*, G878–G889.
7. Vlahcevic, Z.R., Pandak, W.M., and Stravitz, R.T. (1999) Regulation of Bile Acid Biosynthesis, *Gastroenterol. Clin. North Am. 28*, 1–25.
8. Pawar, A., Botolin, D., Mangelsdorf, D.J., and Jump, D.B. (2003) The Role of Liver X Receptor-α in the Fatty Acid Regulation of Hepatic Gene Expression, *J. Biol. Chem. 278*, 40736–40743.
9. Gupta, S., Pandak, W.M., and Hylemon, P.B. (2002) LXR α Is the Dominant Regulator of CYP7α1 Transcription, *Biochem. Biophys. Res. Commun. 293*, 338–343.
10. Goodwin, B., Watson, M.A., Kim, H., Miao, J., Kemper, J.K., and Kliewer, S.A. (2003) Differential Regulation of Rat and Human CYP7α1 by the Nuclear Oxysterol Receptor Liver X Receptor-α *Mol. Endocrinol. 17*, 386–394.
11. Cheema, S.K., Cikaluk, D., and Agellon, L.B. (1997) Dietary Fats Modulate the Regulatory Potential of Dietary Cholesterol on Cholesterol 7 α-Hydroxylase Gene Expression, *J. Lipid Res. 38*, 315–323.
12. Nagao, K., Sato, M., Takenaka, M., Ando, M., Iwamoto, M., and Imaizumi, K. (2001) Feeding Unsaponifiable Compounds from Rice Bran Oil Does Not Alter Hepatic mRNA Abundance for Cholesterol Metabolism-Related Proteins in Hypercholesterolemic Rats, *Biosci. Biotechnol. Biochem. 65*, 371–377.
13. Bravo, E., Flora, L., Cantafora, A., De Luca, V., Tripodi, M., Avella, M., and Botham, K.M. (1998) The Influence of Dietary Saturated and Unsaturated Fat on Hepatic Cholesterol Metabolism and the Biliary Excretion of Chylomicron Cholesterol in the Rat, *Biochim. Biophys. Acta 1390*, 134–148.
14. Reeves, P.G., Nielsen, F.H., and Fahey, G.C. (1993) AIN-93 Purified Diets for Laboratory Rodents; Final Report of the American Institute of Nutrition *ad hoc* Writing Committee on the Reformulation of the AIN-76A Rodent Diet, *J. Nutr. 123*, 1939–1951.
15. Field, C.J., Toyomizu, M., and Clandinin, M.T. (1989) Relationship Between Dietary Fat, Adipocyte Membrane Composition and Insulin Binding in the Rat, *J. Nutr. 119*, 1483–1489.
16. Allain, C.C., Poon, L.S., Chan, C.S.G., Richmond, W., and Fu, P.C. (1974) Enzymatic Determination of Total Serum Cholesterol, *Clin. Chem. 20*, 740–745.
17. Friedewald, W.T., Levy, R.I., and Frederickson, D.S. (1972) Estimation of the Concentration of Low-Density Lipoprotein Cholesterol in Plasma Without Use of the Preparative Ultracentrifuge, *Clin. Chem. 18*, 499–502.

18. Lepage, G., and Roy, C.C. (1986) Direct Transesterification of All Classes of Lipids in a One-Step Reaction, *J. Lipid Res. 27*, 114–120.

19. Folch, J., Lees, M., and Sloane Stanley, G.H. (1957) A Simple Method for the Isolation and Purification of Total Lipids from Animal Tissues, *J. Biol. Chem. 226*, 497–509.

20. Gamble, W., Vaughan, M., Kruth, H.S., and Avigan, J. (1978) Procedure for Determination of Free Cholesterol in Micro- or Nanogram Amounts Suitable for Studies with Cultured Cells, *J. Lipid Res. 19*, 1068–1070.

21. Bianchini, F., Caderni, G., Dolara, P., Fantetti, L., and Kriebel, D. (1989) Effect of Dietary Fat, Starch and Cellulose on Fecal Bile Acids in Mice, *J. Nutr. 119*, 1617–1624.

22. Colle, J.H., Falanga, P.B., Singer, M., Hevin, B., and Milon, G. (1997) Quantitation of Messenger RNA by Competitive RT-PCR: A Simplified Read Out Assay, *J. Immunol. Methods 210*, 175–184.

23. Liang, K.H., Oveisi, F., and Vaziri, N.D. (1996) Gene Expression of Hepatic Cholesterol 7 α-Hydroxylase in the Course of Puromycin-Induced Nephrosis, *Kidney Int. 49*, 855–860.

24. Marckmann, P., Sandstrom, B., and Jespersen, J. (1990) Effects of Total Fat Content and Fatty Acid Composition in Diet on Factor VII Coagulant Activity and Blood Lipids, *Atherosclerosis 80*, 227–233.

25. Mott, G.E., Jackson, E.M., McMahan, C.A., and McGill, H.C., Jr. (1992) Dietary Cholesterol and Type of Fat Differentially Affect Cholesterol Metabolism and Atherosclerosis in Baboons, *J. Nutr. 122*, 1397–1406.

26. Rudel, L.L., Haines, J.L., and Sawyer, J.K. (1990) Effects on Plasma Lipoproteins of Monounsaturated, Saturated, and Polyunsaturated Fatty Acids in the Diet of African Green Monkeys, *J. Lipid Res. 31*, 1873–1882.

27. Fukushima, M., Shimada, K., Ohashi, E., Saitoh, H., Sonoyama, K., Sekikawa, M., and Nakano, M. (2001) Investigation of Gene Expressions Related to Cholesterol Metabolism in Rats Fed Diets Enriched in n-6 or n-3 Fatty Acid with a Cholesterol After Long-Term Feeding Using Quantitative-Competitive RT-PCR Analysis, *J. Nutr. Sci. Vitaminol. (Tokyo) 47*, 228–235.

28. Ramjiganesh, T., Roy, S., Freake, H.C., McIntyre, J.C., and Fernandez, M.L. (2002) Corn Fiber Oil Lowers Plasma Cholesterol by Altering Hepatic Cholesterol Metabolism and Up-regulating LDL Receptors in Guinea Pigs, *J. Nutr. 132*, 335–340.

29. Kris-Etherton, P.M., Pearson, T.A., Wan, Y., Hargrove, R.L., Moriarty, K., Fishell, V., and Etherton, T.D. (1999) High-Monounsaturated Fatty Acid Diets Lower Both Plasma Cholesterol and Triacylglycerol Concentrations, *Am. J. Clin. Nutr. 70*, 1009–1015.

30. Colette, C., Percheron, C., Pares-Herbute N., Michel, F., Pham, T.C., Brillant, L., Descomps, B., and Monnier, L. (2003) Exchanging Carbohydrates for Monounsaturated Fats in Energy-Restricted Diets: Effects on Metabolic Profile and Other Cardiovascular Risk Factors, *Int. J. Obes. Relat. Metab. Disord. 27*, 648–656.

31. Vlahcevic, Z.R., Stravitz, R.T., Heuman, D.M., Hylemon, P.B., and Pandak, W.M. (1997) Quantitative Estimations of the Contribution of Different Bile Acid Pathways to Total Bile Acid Synthesis in the Rat, *Gastroenterology 113*, 1949–1957.

32. Cooper, A.D. (1997) Bile Salt Biosynthesis: An Alternate Synthetic Pathway Joins the Mainstream, *Gastroenterology 113*, 2005–2008.

33. Agellon, L.B., Drover, V.A., Cheema, S.K., Gbaguidi, G.F., and Walsh, A. (2002) Dietary Cholesterol Fails to Stimulate the Human Cholesterol 7α-Hydroxylase Gene (CYP7α1) in Transgenic Mice, *J. Biol. Chem. 277*, 20131–20134.

34. Peet, D.J., Turley, S.D., Ma, W., Janowski, B.A., Lobaccaro, J.M., Hammer, R.E., and Mangelsdorf, D.J. (1998) Cholesterol and Bile Acid Metabolism Are Impaired in Mice Lacking the Nuclear Oxysterol Receptor LXR α, *Cell 93*, 693–704.

35. Schwarz, M., Russell, D.W., Dietschy, J.M., and Turley, S.D. (2001) Alternate Pathways of Bile Acid Synthesis in the Cholesterol 7α-Hydroxylase Knockout Mouse Are Not Upregulated by Either Cholesterol or Cholestyramine Feeding, *J. Lipid Res. 42*, 1594–1603.

36. Cheema, S.K., and Agellon, L.B. (1999) Metabolism of Cholesterol Is Altered in the Liver of C3H mice Fed Fats Enriched with Different C-18 Fatty Acids, *J. Nutr. 129*, 1718–1724.

37. Chen, J.Y., Levy-Wilson, B., Goodart, S., and Cooper, A.D. (2002) Mice Expressing the Human CYP7α1 Gene in the Mouse CYP7α1 Knock-Out Background Lack Induction of CYP7α1 Expression by Cholesterol Feeding and Have Increased Hypercholesterolemia When Fed a High Fat Diet, *J. Biol. Chem. 277*, 42588–42595.

38. Shefer, S., Hauser, S., Bekersky, I., and Mosbach, E.H. (1970) Biochemical Site of Regulation of Bile Acid Biosynthesis in the Rat, *J. Lipid Res. 11*, 404–411.

39. Pandak, W.M., Li, Y.C., Chiang, J.Y., Studer, E.J., Gurley, E.C., Heuman, D.M., Vlahcevic, Z.R., and Hylemon, P.B. (1991) Regulation of Cholesterol 7 α-Hydroxylase mRNA and Transcriptional Activity by Taurocholate and Cholesterol in the Chronic Biliary Diverted Rat, *J. Biol. Chem. 266*, 3416–3421.

40. Spady, D.K., Cuthbert, J.A., Willard, M.N., and Meidell, R.S. (1996) Feedback Regulation of Hepatic 7α-Hydroxylase Expression by Bile Salts in the Hamster, *J. Biol. Chem. 271*, 18623–18631.

41. Stravitz, R.T., Vlahcevic, Z.R., Gurley, E.C., and Hylemon, P.B. (1995) Repression of Cholesterol 7 α-Hydroxylase Transcription by Bile Acids Is Mediated Through Protein Kinase C in Primary Cultures of Rat Hepatocytes, *J. Lipid Res. 36*, 1359–1369.

42. Makishima, M., Okamoto, A.Y., Repa, J.J., Tu, H., Learned, R.M., Luk, A., Hull, M.V., Lustig, K.D., Mangelsdorf, D.J., and Shan, B. (1999) Identification of a Nuclear Receptor for Bile Acids, *Science 284*, 1362–1365.

43. Wang, H., Chen, J., Hollister, K., Sowers, L.C., and Forman, B.M. (1999) Endogenous Bile Acids Are Ligands for the Nuclear Receptor FXR/BAR, *Mol. Cell 3*, 543–553.

44. Miyake, J.H., Wang, S.L., and Davis, R.A. (2000) Bile Acid Induction of Cytokine Expression by Macrophages Correlates with Repression of Hepatic Cholesterol 7α-Hydroxylase, *J. Biol. Chem. 275*, 21805–21808.

45. Bravo, E., Flora, L., Cantafora, A., De Luca, V., Tripodi, M., Avella, M., and Botham, K.M. (1998) The Influence of Dietary Saturated and Unsaturated Fat on Hepatic Cholesterol Metabolism and the Biliary Excretion of Chylomicron Cholesterol in the Rat, *Biochim. Biophys. Acta 1390*, 134–148.

46. Tiemann, M., Han, Z., Soccio, R., Bollineni, J., Shefer, S., Sehayek, E., and Breslow, J.L. (2004) Cholesterol Feeding of Mice Expressing Cholesterol 7α-Hydroxylase Increases Bile Acid Pool Size Despite Decreased Enzyme Activity, *Proc. Natl. Acad. Sci. USA 101*, 1846–1851.

47. Chiang, J.Y. (2003) Bile Acid Regulation of Hepatic Physiology: III. Bile Acids and Nuclear Receptors, *Am. J. Physiol. Gastrointest. Liver Physiol. 284*, G349–G356.

Regulation of Palmitoyl-CoA Chain Elongation by Clofibric Acid in the Liver of Zucker fa/fa Rats

Tomoaki Toyama[a], Naomi Kudo[a,*], Atsushi Mitsumoto[b], and Yoichi Kawashima[a]

[a]Faculty of Pharmaceutical Sciences, Josai University, Saitama 350-0295, Japan, and [b]Faculty of Pharmaceutical Sciences, Josai International University, Chiba 283-8555, Japan

ABSTRACT: The regulation of palmitoyl-CoA chain elongation (PCE) by clofibric acid [2-(4-chlorophenoxy)-2-methylpropionic acid] was investigated in comparison with stearoyl-CoA desaturase (SCD) in the liver of obese Zucker fa/fa rats. The proportion of oleic acid in the hepatic lipids of Zucker obese rats is 2.7 times higher than that of lean littermates. The activities of PCE and SCD in the liver of Zucker obese rats were markedly higher than in lean rats, and the hepatic uptake of 2-deoxyglucose (2-DG) was also higher in Zucker obese rats compared with lean rats. The increased activities of SCD and PCE in Zucker obese rats were due to the enhanced expression of mRNA of both SCD1 and rat FA elongase 2 (rELO2), but not SCD2 or rELO1. The proportion of oleic acid in the liver was significantly increased by the administration of clofibric acid to Zucker obese rats, and the hepatic PCE activity and rELO2 mRNA expression, but not the SCD activity or SCD1 mRNA expression, were increased in response to clofibric acid treatment. By contrast, the activities of both PCE and SCD and the mRNA expression of SCD1 and rELO2 in the liver were increased by the treatment of Zucker lean rats with clofibric acid. Multiple regression analysis, which was performed to determine the relationships involving PCE activity, SCD activity, and the proportion of oleic acid, revealed that the three parameters were significantly correlated and that the standardized partial regression coefficient of PCE was higher than that of SCD. These results indicate that oleic acid is synthesized by the concerted action of PCE and SCD and that PCE plays a crucial role in the formation of oleic acid when Zucker fa/fa rats are given clofibric acid.

Paper no. L9702 in *Lipids 40*, 463–470 (May 2005).

Oleic acid is a major component of TG for storing energy and an important constituent of phospholipids for maintaining membrane function in mammals. Recently, the secretion of VLDL has been shown to be highly dependent on oleic acid production in the liver (1). Moreover, oleic acid is involved in the differentiation of neurons (2,3), regulation of appetite (4), and the development of obesity (5) and metabolic diseases such as atherosclerosis (6). The biosynthesis of oleic acid from palmitic acid involves sequential reactions catalyzed by palmitoyl-CoA chain elongase (PCE) and stearoyl-CoA desaturase (SCD) (7). PCE and SCD are induced by carbohydrates (8), refeeding after fasting (9,10), and peroxisome proliferators, such as clofibric acid [2-(4-chlorophenoxy)-2-methylpropionic acid], diethylhexylphthalate, and perfluorooctanoic acid (7,11,12). Based on these findings, it has been postulated that PCE is regulated by mechanisms similar to SCD. However, on the basis of an experiment in which the effects of carbohydrate and clofibric acid on PCE and SCD were examined in the liver of Wistar rats, we concluded that PCE is regulated in a manner different from that of SCD. Thus, the effects of clofibric acid on the activities of PCE and SCD in oleic acid formation in animals under a variety of physiological conditions are of interest.

Lipogenesis in the liver of genetically obese Zucker fa/fa rats is enhanced, resulting in excessive fat accretion and elevated plasma levels of TG compared with their nonobese littermates (13,14). The proportion of oleic acid in the hepatic lipids of obese Zucker rats is much higher than that of lean rats (15). It seems likely therefore that the formation of oleic acid is not governed by normal regulation in the liver of obese Zucker rats. However, no information is available on the activity of PCE and its regulation in the liver of obese and lean Zucker rats. Treatment of obese Zucker rats with fenofibrate, a clofibric acid analog, has been demonstrated to increase the proportion of oleic acid in hepatic lipids (13) but there is little information about the response of PCE and SCD to fibrates.

The aims of the present work are (i) to identify the genes responsible for PCE and SCD expression in the liver of lean and obese Zucker rats, (ii) to study the effects of clofibric acid on the expression of the genes responsible for PCE and SCD in the liver of Zucker rats, and (iii) to investigate the role of PCE, in comparison with SCD, in oleic acid formation in the liver of Zucker rats.

MATERIALS AND METHODS

Materials. [2-^{14}C]Malonyl-CoA (55 Ci/mol) and 2-deoxy-[1-^{14}C]glucose (2-[^{14}C]DG, 55 Ci/mol) were purchased from American Radiolabeled Chemicals, Inc. (St. Louis, MO); D-[2-^{3}H]mannitol (20 Ci/mmol) was from MP Biochemicals Inc. (Irvine, CA). Stearoyl-CoA, palmitoyl-CoA, malonyl-CoA, clofibric acid, and BSA were purchased from Sigma (St. Louis, MO); NADH and NADPH were from Oriental Yeast

*To whom correspondence should be addressed at Faculty of Pharmaceutical Sciences, Josai University, Keyakidai 1-1, Sakado, Saitama 350-0295, Japan.
E-mail: naokudo@josai.ac.jp

Abbreviations: AOX, acyl-CoA oxidase; clofibric acid, 2-(4-chlorophenoxy)-2-methylpropionic acid; 2-DG, 2-deoxyglucose; rELO, rat FA elongase; PCE, palmitoyl-CoA chain elongase; SA, specific radioactivity; SCD, stearoyl-CoA desaturase.

Co. (Tokyo, Japan); nonadecanoic acid was from Nu-Chek-Prep Inc. (Elysian, MN). All other chemicals used were of analytical grade.

Animals. Male obese Zucker fa/fa rats and their lean littermates aged 11 wk were purchased from Charles River Japan (Tokyo, Japan). Rats were fed on a standard chow (CE-2) (Clea Japan, Tokyo, Japan) *ad libitum* and allowed free access to water. Rats aged 15 wk were given a subcutaneous injection of clofibric acid at a dose of 100 mg/kg body weight twice a day for 7 d. Blood was obtained from the descending vena cava under diethylether anesthesia, and then their livers were removed and perfused with ice-cold 0.9% (wt/vol) aqueous NaCl. Part of the livers was frozen in liquid nitrogen and stored at -80°C for preparation of total RNA while another part of the livers was homogenized with 4 vol of 0.25 M sucrose/1.0 mM EDTA/10 mM Tris-HCl (pH 7.4) in a Potter glass-Teflon homogenizer. An aliquot of the homogenates was frozen in liquid nitrogen and stored at –80°C for lipid analysis and assay for peroxisomal acyl-CoA oxidase (AOX). The remaining homogenates were centrifuged at $18,000 \times g$ for 20 min, and the supernatant was recentrifuged under the same conditions. The supernatant was centrifuged at $105,000 \times g$ for 60 min. The pellet was resuspended in 0.25 M sucrose/0.1 mM EDTA/10 mM Tris-HCl (pH 7.4) and recentrifuged under the same conditions. The resulting pellet was resuspended in a small volume of 0.25 M sucrose/0.1 mM EDTA/10 mM Tris-HCl (pH 7.4) and used as an enzyme source (microsomes). All of these operations were carried out at 0–4°C. Protein concentrations were determined by the method of Lowry *et al.* (16) using BSA as a standard. All animal studies complied with the institutional board for animal studies, Josai University.

Enzyme assays. SCD activity was estimated spectrophotometrically as the stearoyl-CoA-stimulated re-oxidation of NADH-reduced cytochrome b_5 (17). The assay for the microsomal chain elongation of palmitoyl-CoA was performed by measuring the incorporation of [2-^{14}C]malonyl-CoA into palmitoyl-CoA (8). AOX was assayed by measuring palmitoyl-CoA-dependent H_2O_2 production according to the method of Small *et al.* (18) as previously described (8).

RNA extraction and real-time quantitative PCR. Total RNA was prepared from the livers of rats using an RNeasy kit (Qiagen, Hilden, Germany). RNA was quantified spectrophotometrically based on the absorption at 260 nm. Complementary DNA was prepared from the total RNA with avian myeloblastosis virus (AMV) reverse transcriptase (Takara, Tokyo, Japan). The specific primer sets for SCD1, SCD2, rat FA elongase 1 (rELO1), and rELO2 were designed using Primer Express 2.0 software (Applied Biosystems, Foster City, CA) (Table 1). The specific primer set for β-actin was used as described by Zhang *et al.* (19). PCR amplification was carried out using QuantiTect SYBR Green PCR master mix (Qiagen) with 300 nM primers. The amplification and detection were performed with an iCycler IQ real-time detection system (Bio-Rad, Richmond, CA). PCR conditions were a 15-min denaturation step at 95°C followed by 40 cycles of 15 s denaturation at 94°C, 30 s annealing at 57°C, and 30 s extension at 72°C. Reverse transcriptase-PCR products were analyzed by electrophoresis on ethidium bromide-stained agarose to ensure that a single amplicon of the expected size was indeed obtained. To measure PCR efficiency, serial dilutions of reverse transcribed RNA (0.1 to 100 ng) were amplified, and a line was obtained by plotting cycle threshold (C_T) values as a function of the starting reverse-transcribed RNA, the slope of which was used for an efficiency calculation using the formula $E = 10^{|(1/\text{slope})| - 1}$ (20). The quantity of any given gene, expressed as the value relative to the amount in the lean rats, was calculated after determination of the difference between the C_T of the given gene A and that of the calibrator gene B (β-actin) in the obese rats or clofibric acid-treated rats ($\Delta C_{T1} = C_{T1A} - C_{T1B}$) and lean rats ($\Delta C_{T0} = C_{T0A} - C_{T0B}$) using the $2^{-\Delta\Delta CT(1-0)}$ formula (20).

2-Deoxyglucose (2-DG) uptake. 2-DG uptake was measured according to Rajkumar *et al.* (21). In this procedure, rats were fasted for 12 h and then anesthetized by an intraperitoneal injection of pentobarbital (50 mg/kg body weight). A polyethylene catheter was placed in the right jugular vein, and then 2-[^{14}C]DG (9 μCi/rat) and D-[2-^{3}H]mannitol (90 mCi/rat) were injected through the catheter. D-[2-^{3}H]Mannitol was used to measure the extracellular spaces. For the determination of the decay of the specific radioactivity of 2-DG in blood, 200-mL blood samples were collected at 3, 5, 10, 20, 30, and 40 min after the injection of 2-[^{14}C]DG. The radioactivity in plasma was determined with a liquid scintillation

TABLE 1
Sequences of Specific Primers Employed

Gene[a]	Product size (bp)	GenBank Accession No.		Primers (5′-3′)
SCD1	123	J02585	Sense	TGTTCGTCAGCACCTTCTTG
			Antisense	GGATGTTCTCCCGAGATTGA
SCD2	94	AB032243	Sense	TGCACCCCCAGACACTTGTAA
			Antisense	GGATGCATGGAAACGCCATA
rELO1	117	AB071985	Sense	GCTTCATCCACGTCCTCATGT
			Antisense	TCAGCACAAACTGGACCAGCT
rELO2	381	AB071986	Sense	AGAACACGTAGCGACTCCGAA
			Antisense	CAAACGCGTAAGCCCAGAAT
β-Actin	220	V01217	Sense	TGCAGAAGGAGATTACTGCC
			Antisense	CGCAGCTCAGTAACAGTCC

[a]SCD, stearoyl-CoA desaturase; rELO, rat FA elongase.

counter (LSC-5100; Aloka, Tokyo, Japan), and the glucose concentration was measured with a glucometer (Glucocard; Aventis Pharma Japan, Tokyo, Japan). On completion of blood sampling, rats were killed and the livers rapidly removed. A small portion (about 200 μg) of each tissue was removed, frozen in liquid nitrogen, and kept frozen at –80°C for subsequent analysis. These tissues were digested at 70°C for 30 min in 0.5 mL of 1 M NaOH, followed by the addition of 0.5 mL 1 M HCl. Then 1 mL of 6% HClO$_4$ was added to the neutralized solution (200 mL) and, after centrifugation, an aliquot of the supernatant was used for the determination of radioactivity after the addition of 10 mL scintillation cocktail (EcoLite; ICN Biomedicals, Irvine, CA) in a scintillation counter. Protein concentrations were determined by BCA protein assay (Pierce, Rockford, IL). Calculation of 2-DG uptakerate was carried out using Equation 1:

$$2-\text{DG uptake} = \frac{(2-[^{14}C]DG)_t}{\int_0^{40} \text{SA } dt} \qquad [1]$$

where 2-[^{14}C]DG is the radioactivity (expressed as dpm per mg protein) taken up by the liver; t is time (min); and SA is the specific radioactivity of the glucose pool expressed as dpm per nmol of plasma glucose. The 2-[^{14}C]DG uptake derived from these data reflects the net glucose uptake over the 40 min period. Extracellular spaces were calculated using the formula: Extracellular spaces = (D-[2-^{3}H]mannitol)$_{liver}$/(D-[2-^{3}H]mannitol)$_{plasma}$, where (D-[2-^{3}H]mannitol)$_{liver}$ and (D-[2-^{3}H]mannitol)$_{plasma}$ represent mannitol concentrations in tissue and plasma, respectively (22).

Lipid analyses. For quantification of FA, a known amount of nonadecanoic acid was added to liver homogenates as an internal standard. Total lipid was extracted from the liver homogenates by the method of Bligh and Dyer (23). After the extract was taken to dryness in a stream of nitrogen, 1 mL of 10% KOH/90% methanol was added, and then the mixture was heated at 80°C for 60 min to allow saponification to take place. Nonsaponified lipids were removed by extracting three times with 3 mL hexane. After the addition of 1 mL of 6 M HCl, FFA were extracted three times with 3 mL of hexane. The combined extracts were taken to dryness, and methanolic BF$_3$ (15%, wt/vol) was added to the residue and the mixture heated at 100°C for 10 min. The FAME formed were extracted with hexane and subjected to GLC analysis as previously described (8).

Statistical analyses. Statistical significance between clofibric acid-treated and untreated rats or between Zucker lean and obese rats was analyzed by Student's *t*-test or Welch's test after applying the *F*-test for two means. Linear or multiple regression analyses were performed to evaluate the correlation between two or three parameters, respectively (24).

RESULTS

Activities and mRNA expression of both PCE and SCD in the liver of Zucker lean and obese rats. The activities of PCE and SCD in hepatic microsomes were measured in Zucker lean and obese rats. The activities of PCE and SCD were approximately 3 and 5 times higher, respectively, in the obese rats than in their lean littermates (Fig. 1). The mRNA expression of two rELO genes, rELO1 and rELO2 (25), and two SCD genes, SCD1 (26) and SCD2 (27), were determined in the liver of Zucker lean and obese rats. The hepatic mRNA expression of rELO2 and SCD1 in the liver of Zucker obese rats was markedly higher than that of lean littermates, whereas no significant difference was observed in the mRNA expression of either rELO1 or SCD2 between lean and obese rats (Fig. 2).
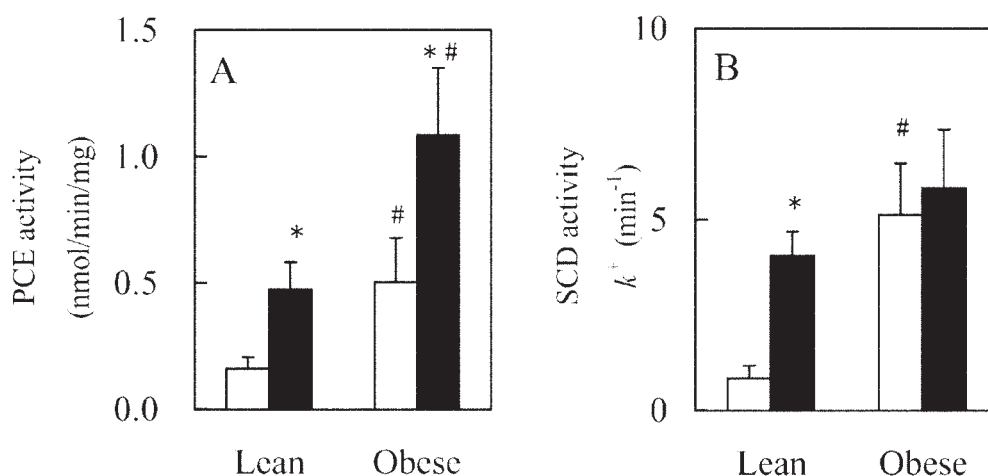
FIG. 1. Palmitoyl-CoA chain elongase (PCE) and stearoyl-CoA desaturase (SCD) activities in the liver of Zucker lean and obese rats, with or without clofibric acid. Rats were given subcutaneous injections of clofibric acid twice a day for 7 d. Microsomes were prepared from the rats, and the activities of PCE (A) and SCD (B) were determined. In (B), k^+ is the rate constant for steroyl-CoA-dependent reoxidation of NADH-reduced cytochrome b_5. Open bars and solid bars represent clofibric acid untreated rats and clofibric acid-treated rats, respectively. Values are means ± SD for four rats. *Differences from clofibric acid-untreated rats were statistically significant (*P* < 0.05). #Differences between lean and obese rats were statistically significant (*P* < 0.05).

Effects of clofibric acid on PCE and SCD activities and mRNA expression in the liver of Zucker lean and obese rats. The administration of clofibric acid to the lean rats increased the activities of PCE and SCD 3.0 and 4.9 times, respectively (Fig. 1). The treatment of the obese rats with clofibric acid further increased PCE activity, whereas SCD activity did not increase in response to clofibric acid treatment (Fig. 1). The administration of clofibric acid to Zucker lean rats increased the levels of mRNA for rELO2 and SCD1 5.1 and 2.8 times, respectively (Fig. 2B,C). However, there were no significant changes in the expression of either rELO1 or SCD 2 in lean rats following administration of clofibric acid (Fig. 2A,D). The treatments of Zucker obese rats with clofibric acid further increased the expression of rELO2 mRNA (Fig. 2B), as was observed with PCE activity (Fig. 1A), but the expression of SCD1 mRNA was unaffected (Fig. 2C). To confirm that the effect of clofibric acid on the liver of Zucker obese rats was sufficient to induce peroxisome proliferator-responsive enzymes, the effects of clofibric acid on liver weight and

AOX activity were determined (Table 2). In response to clofibric acid administration, there was a marked increase in AOX activity in both lean and obese rats. No significant difference was observed in AOX activity between lean and obese rats following treatment with clofibric acid. The liver weight of Zucker obese rats was 2.3 times greater than that of lean rats, and treatment with clofibric acid increased the liver weight of lean rats but not obese rats.

Proportion of hepatic oleic acid in Zucker lean and obese rats, with or without treatment with clofibric acid. Figure 3 shows the effects of clofibric acid administration on the proportion of oleic acid in hepatic lipids. The proportion of oleic acid in the hepatic lipids of Zucker obese rats was 2.7 times higher than that of the lean rats. The treatments of lean and obese rats with clofibric acid increased the proportion of oleic acid 2.0 and 1.4 times, respectively.

Effects of clofibric acid treatment on hepatic glucose uptake in vivo. Table 3 shows the effects of clofibric acid treatment on hepatic 2-DG uptake and the extracellular spaces in
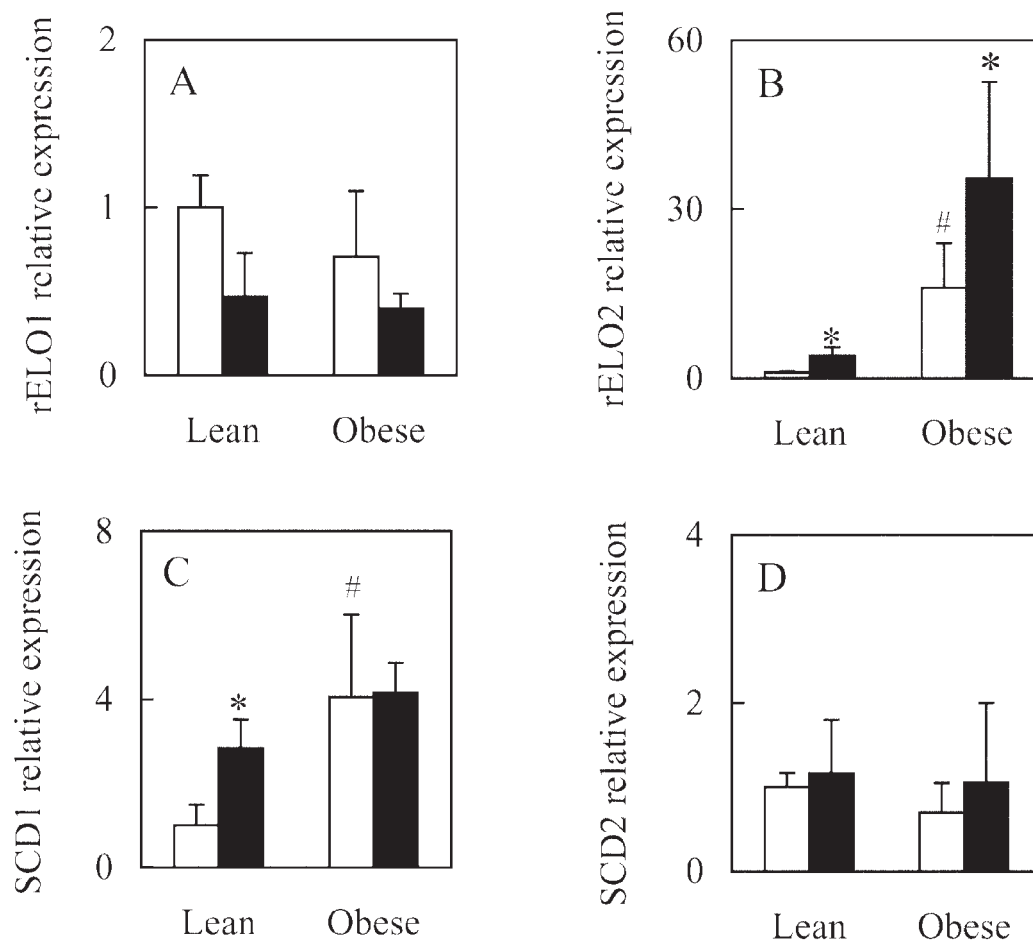
FIG. 2. mRNA expression of PCE and SCD in the liver of Zucker lean and obese rats, with or without clofibric acid. mRNA levels of rat FA elongase 1 (rELO1) (A), rELO2 (B), SCD1 (C), and SCD2 (D) were determined in the liver of Zucker lean and obese rats with or without clofibric acid treatment, using real-time reverse transcriptase-PCR and normalized by the expression of β-actin. The data are expressed as the relative mRNA level compared with the average expression level in Zucker lean rats (=1). Open bars and solid bars represent clofibric acid-unreated rats and clofibric acid-treated rats, respectively. Values are means ± SD for four rats. *Differences from clofibric acid-untreated rats were statistically significant ($P < 0.05$). #Differences between lean and obese rats were statistically significant ($P < 0.05$). For other abbreviations see Figure 1.

TABLE 2
Effects of Clofibric Acid on Liver Weight and AOX Activity in the Liver of Zucker Rats[a]

Phenotype	Clofibric acid	Body weight (g)	Liver weight (g)	AOX activity (nmol/min/mg)
Lean	–	390 ± 15	14.4 ± 0.7	3.7 ± 0.1
	+	370 ± 5.5*	18.1 ± 0.5	32.8 ± 2.0*
Obese	–	590 ± 8.8[#]	33.5 ± 2.4[#]	4.9 ± 0.6
	+	601 ± 12[#]	39.5 ± 5.2[#]	33.7 ± 2.8*

[a]Rats were given a subcutaneous injection of clofibric acid twice a day for 7 d at a dose of 100 mg/kg body weight. Values are means ± SD for four rats. *Differences from clofibric acid-untreated rats were statistically significant ($P < 0.05$). [#]Differences between lean and obese rats were statistically significant ($P < 0.05$). AOX, acyl-CoA oxidase; clofibric acid, 2-(4-chlorophenoxy)-2-methylpropionic acid.

Zucker rats. The blood glucose levels of the animals in the fed state were not significantly different between lean and obese rats, irrespective of clofibric acid treatment (data not shown). The decay in the specific radioactivity of 2-[^{14}C]DG in plasma was similar in all the experimental groups (data not shown), and the hepatic extracellular spaces were unaffected by the treatment with clofibric acid. The uptake of 2-DG by the liver in obese rats was 1.8 times higher than that in lean rats. Clofibric acid treatment did not affect the hepatic uptake of 2-DG in either lean or obese rats.

Relationship between the activity of PCE or SCD and the proportion of oleic acid in the liver. Linear regression analyses were carried out to examine the relationship between the proportion of oleic acid and the activity of either PCE or SCD in the liver. One regression line between the proportion of oleic acid and PCE activity was obtained for 16 sets of data from Figures 1 and 3, with a high correlation being seen be-

tween the two parameters ($r^2 = 0.728$, $P < 0.001$). Similarly, a high correlation was observed between the proportion of oleic acid and SCD activity ($r^2 = 0.647$, $P < 0.001$). The relative contribution of PCE and SCD to the proportion of oleic acid was determined by multiple linear regression analysis. The 16 sets of data from Figures 1 and 3 revealed a significant correlation among the three parameters ($r^2 = 0.748$, $P < 0.001$) (Table 4). The standardized partial regression coefficient between the proportion of oleic acid and PCE activity was 0.60 ($P < 0.05$), whereas that between the proportion of oleic acid and SCD activity was 0.29, with a partial correlation not achieving statistical significance ($P = 0.298$).

DISCUSSION

Increased activity of PCE and increased proportion of oleic acid in the liver of Zucker obese rats. In agreement with previous findings (13), the present study confirmed that the proportion of oleic acid in hepatic lipids of Zucker obese rats is much greater than that of their lean littermates. So far, an elevated activity of hepatic SCD is believed to be responsible for the increased proportion of oleic acid in the liver of Zucker obese rats (28); we also demonstrated the enhanced hepatic activity of SCD in obese rats. The biosynthesis of oleic acid from palmitic acid involves sequential reactions catalyzed by PCE and then SCD (7). Moreover, our recent study came to the conclusion that PCE plays a more important role than SCD in the physiological regulation of oleic acid biosynthesis in the liver of Wistar rats (8). No information, however, is available about the role of PCE in oleic acid formation in Zucker obese rats. The present study shows that the activity of not only SCD but also PCE in the liver is markedly higher in Zucker obese rats compared with lean rats. The possibility that the increased proportion of oleic acid following clofibric acid treatment is due to degradation of erucic acid (22:1n-9) is ruled out since the hepatic level of erucic acid was less than the detection limit in the liver of any animals tested. To our knowledge, this is the first evidence showing that Zucker obese rats exhibit an elevated PCE activity in the liver. Recently, two FA elongases, which catalyze the chain elongation of palmitoyl-CoA, rELO1, and rELO2, were cloned in rat liver (25). Moreover, four isoforms of SCD (SCD1, SCD2, SCD3, and SCD4) have been identified (26,27,29,30), and
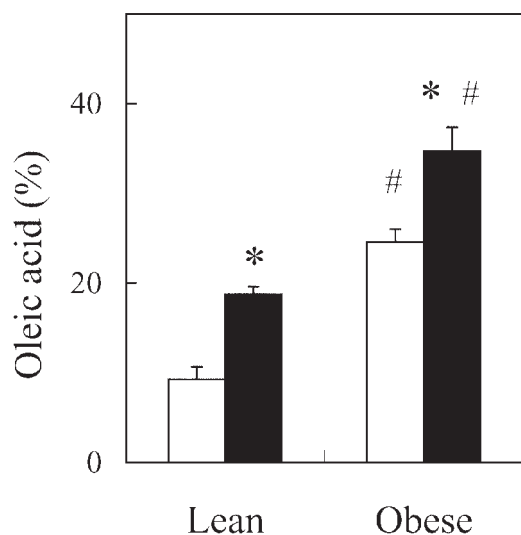
FIG. 3. Effects of clofibric acid administration on the proportion of oleic acid in hepatic lipids of Zucker lean and obese rats. Rats were given a subcutaneous injection of clofibric acid twice a day for 7 d. The FA composition of hepatic lipids of Zucker obese and lean rats was analyzed. Open bars and solid bars represent clofibric acid-untreated rats and clofibric acid-treated rats, respectively. Values are means ± SD for four rats. *Differences from clofibric acid-untreated rats were statistically significant ($P < 0.05$). [#]Differences between lean and obese rats were statistically significant ($P < 0.05$).

TABLE 3
Effects of Clofibric Acid on Hepatic 2-DG Uptake and Extracellular Spaces in Zucker Rats[a]

Phenotype	Clofibric acid	2-DG uptake (nmol/min/mg protein)	Extracellular spaces (mL/mg protein)
Lean	−	0.24 ± 0.01	1.8 ± 0.15
	+	0.21 ± 0.03	2.1 ± 0.67
Obese	−	0.43 ± 0.09[#]	2.0 ± 0.53
	+	0.39 ± 0.09[#]	1.5 ± 0.13

[a]Rats were given a subcutaneous injection of clofibric acid twice a day for 7 d at a dose of 100 mg/kg body weight. Values are means ± SD for four to five rats. [#]Differences between lean and obese rats were statistically significant ($P < 0.05$). 2-DG, 2-deoxyglucose; for other abbreviation see Table 2.

SCD1 and SCD2 were shown to be expressed in the liver of rats (26,31). The present study shows a considerable increase in the mRNA expression of rELO2 and SCD1, but not rELO1 or SCD2, in the liver of Zucker obese rats. It seems likely therefore that the elevated expression of rELO2 and SCD1 is responsible for the enhanced activities of PCE and SCD in the liver of Zucker obese rats, respectively, leading to the higher proportion of oleic acid. The present results strongly suggest that, compared with rELO2 and SCD1, neither rELO1 nor SCD2 plays a physiologically important role in the increased formation of oleic acid in the liver of Zucker obese rats.

Both PCE and SCD are considered to be regulated by transcriptional factors, such as peroxisome proliferator-activated receptor-α (32, 33) and sterol regulatory element binding protein-1 (34,35). However, recent studies have shown that carbohydrate induces PCE and SCD activity *via* a pathway that is independent of peroxisome proliferator-activated receptor-α (8) and that fructose increases the expression of SCD1 mRNA in the liver of sterol regulatory element binding protein-1c knockout mice (36). In addition to these facts, our previous study showed that carbohydrate regulates PCE activity in the liver of Wistar rats (8). These findings, taken together, suggest the possible involvement of carbohydrate in the regulation of PCE and SCD in the liver of Zucker obese rats. In fact, the present study shows that the hepatic uptake of 2-DG in Zucker obese rats is significantly greater than that in lean rats. It seems plausible therefore that the elevated hepatic uptake of glucose is responsible for the increase in the activities of PCE and SCD in the liver of Zucker obese rats. The Zucker obese rat has been shown to be deficient in leptin receptors (37), and the leptin-mediated signal is considered to produce

down-regulation of SCD expression (5). It seems likely therefore that the higher expression of PCE and SCD in Zucker obese rats is due to the loss of leptin signals in the liver. However, the relationship between glucose uptake and leptin remains to be clarified.

Induction of PCE by clofibric acid. Treatment of Wistar rats with clofibric acid markedly induces both PCE and SCD in the liver (8). However, in Zucker obese rats, there is no information about how clofibric acid affects the activity and gene expression of both PCE and SCD. The present study demonstrated that the proportion of oleic acid in the liver was significantly increased by the administration of clofibric acid to Zucker obese rats and that treatment with clofibric acid increased hepatic PCE activity and rELO2 mRNA expression, but not SCD activity or SCD1 mRNA expression. By contrast, the activities of both PCE and SCD are increased in response to clofibric acid treatment in the liver of Zucker lean rats. The increase in the activities of SCD and PCE is due to the elevated levels of mRNA expression of both rELO2 and SCD1. Both rELO1 and SCD2 exhibit no response to clofibric acid in the liver of both Zucker lean and obese rats. It should also be noted that PCE activity was additively induced by treating Zucker obese rats with clofibric acid, whereas SCD was not induced. Since clofibric acid induces AOX and SCD activity *via* peroxisome proliferator-activated receptor-α activation (32,38) and AOX is induced to the same extent in the liver of both Zucker lean and obese rats, the lack of induction of SCD by clofibric acid in Zucker obese rats seems not to be due to a peroxisome proliferator-activated receptor--α defect in the liver. To date, PCE and SCD have been considered to be regulated through common factors, such as carbohydrates (8), refeeding after fasting (9,10), and peroxisome proliferators (11,39,40). Our present results indicate the possibility that the mechanism of PCE regulation differs somewhat from that of SCD (8). Since hepatic glucose uptake is not changed by treating Zucker lean and obese rats with clofibric acid, it seems unlikely that clofibric acid regulates PCE activity *via* a change in the hepatic uptake of glucose.

Role of PCE in the formation of oleic acid. Our previous study suggested that PCE plays an important role in the formation of oleic acid in the liver of Wistar rats (8). In the present study, multiple regression analysis, which was performed to determine the relationship among the activities of PCE, SCD and the proportion of oleic acid, revealed that the stan-

TABLE 4
Relative Contribution of PCE and SCD to the Proportion of Oleic Acid in the Liver of Zucker Rats[a]

Independent variable	Standardized partial correlation coefficient	P
PCE	0.604	<0.05
SCD	0.290	0.298

[a]Multiple linear regression analysis was performed on the 16 sets of mean data from Figures 1 and 3. From the PCE activity, the SCD activity, and the proportion of oleic acid, a single linear regression line was obtained: $Y = 0.60X_1 + 0.29X_2$; Y, proportion of oleic acid; X_1, PCE activity; X_2, SCD activity; $r^2 = 0.748$; $P < 0.001$. PCE, palmitoyl-CoA chain elongase; for other abbreviation see Table 1.

dardized partial regression coefficient of PCE was higher than that of SCD. This result strongly suggests that the contribution of PCE to the regulation of the proportion of oleic acid is greater than that of SCD in the liver of Zucker rats treated with clofibric acid. The conclusion, which the present study has reached, is the same as the conclusion of our previous study using Wistar rats as experimental animals (8).

Thus, oleic acid is synthesized by the concerted action of PCE and SCD, and PCE plays an important role in the formation of oleic acid in the liver. Clofibric acid increases oleic acid formation *via* the induction of rELO2 in the liver of Zucker obese rats.

ACKNOWLEDGMENT

REFERENCES

1. Legrand, P., Catheline, D., Fichot, M.C., and Lemarchal, P. (1997) Inhibiting Δ9-Desaturase Activity Impairs Triacylglycerol Secretion in Cultured Chicken Hepatocytes, *J. Nutr. 127*, 249–256.
2. Tabernero, A., Lavado, E.M., Granda, B., Velasco, A., and Medina, J.M. (2001) Neuronal Differentiation Is Triggered by Oleic Acid Synthesized and Released by Astrocytes, *J. Neurochem. 79*, 606–616.
3. Granda, B., Tabernero, A., Tello, V., and Medina, J.M. (2003) Oleic Acid Induces GAP-43 Expression Through a Protein Kinase C-Mediated Mechanism That Is Independent of NGF but Synergistic with NT-3 and NT-4/5, *Brain Res. 988*, 1–8.
4. Obici, S., Feng, Z., Morgan, K., Stein, D., Karkanias, G., and Rossetti, L. (2002) Central Administration of Oleic Acid Inhibits Glucose Production and Food Intake, *Diabetes 51*, 271–275.
5. Cohen, P., Miyazaki, M., Socci, N.D., Hagge-Greenberg, A., Liedtke, W., Soukas, A.A., Sharma, R., Hudgins, L.C., Ntambi, J.M., and Friedman, J.M. (2002) Role for Stearoyl-CoA Desaturase-1 in Leptin-Mediated Weight Loss, *Science 297*, 240–243.
6. Massaro, M., and De Caterina, R. (2002) Vasculoprotective Effects of Oleic Acid: Epidemiological Background and Direct Vascular Antiatherogenic Properties, *Nutr. Metab. Cardiovasc. Dis. 12*, 42–51.
7. Cinti, D.L., Cook, L., Nagi, M.N., and Suneja, S.K. (1992) The Fatty Acid Chain Elongation System of Mammalian Endoplasmic Reticulum, *Prog. Lipid Res. 31*, 1–51.
8. Kudo, N., Toyama, T., Mitsumoto, A., and Kawashima, Y. (2003) Regulation by Carbohydrate and Clofibric Acid of Palmitoyl-CoA Chain Elongation in the Liver of Rats, *Lipids 38*, 531–537.
9. Oshino, N., and Sato, R. (1972) The Dietary Control of the Microsomal Stearyl CoA Desaturation Enzyme System in Rat Liver, *Arch. Biochem. Biophys. 149*, 369–377.
10. Sprecher, H. (1974) The Influence of Dietary Alterations, Fasting and Competitive Interactions on the Microsomal Chain Elongation of Fatty Acids, *Biochim. Biophys. Acta 360*, 113–123.
11. Alegret, M., Cerqueda, E., Ferrando, R., Vazquez, M., Sanchez, R.M., Adzet, T., Merlos, M., and Laguna, J.C. (1995) Selective Modification of Rat Hepatic Microsomal Fatty Acid Chain Elongation and Desaturation by Fibrates: Relationship with Peroxisome Proliferation, *Br. J. Pharmacol. 114*, 1351–1358.
12. Toyama, T., Kudo, N., Mitsumoto, A., and Kawashima, Y.

13. (2004) Effects of Perfluorocarboxylic Acids on the Activities of Acyl-CoA Elongations *in vivo* and *in vitro*, *Chem. Biol. Interact. 150*, 189–198.
13. Olivier, P., Plancke, M.O., Theret, N., Marzin, D., Clavey, V., and Fruchart, J.C. (1988) Effects of Fenofibrate on Lipoprotein Metabolism and Fatty Acid Distribution in Zucker Rats, *Atherosclerosis 74*, 15–21.
14. Bray, G.A. (1977) The Zucker-Fatty Rat: A Review, *Fed. Proc. 36*, 148–153.
15. Zucker, L.M. (1972) Fat Mobilization *in vitro* and *in vivo* in the Genetically Obese Zucker Rat "Fatty," *J. Lipid Res. 13*, 234–243.
16. Lowry, O.H., Rosebrough, N.J., Farr, A.L., and Randall, R.J. (1951) Protein Measurement with the Folin Phenol Reagent, *J. Biol. Chem. 193*, 265–275.
17. Oshino, N., Imai, Y., and Sato, R. (1971) A Function of Cytochrome B5 in Fatty Acid Desaturation by Rat Liver Microsomes, *J. Biochem. (Tokyo) 69*, 155–167.
18. Small, G.M., Burdett, K., and Connock, M.J. (1985) A Sensitive Spectrophotometric Assay for Peroxisomal Acyl-CoA Oxidase, *Biochem. J. 227*, 205–210.
19. Zhang, J., Chrysis, D., and Underwood, L.E. (1998) Reduction of Hepatic Insulin-Like Growth Factor I (IGF-I) Messenger Ribonucleic Acid (mRNA) During Fasting Is Associated with Diminished Splicing of IGF-I Pre-mRNA and Decreased Stability of Cytoplasmic IGF-I mRNA, *Endocrinology 139*, 4523–4530.
20. Anonymous (1997) User Bulletin #2: Relative Quantitation of Gene Expression, Applied Biosystems, Foster City, CA.
21. Rajkumar, K., Krsek, M., Dheen, S.T., and Murphy, L.J. (1996) Impaired Glucose Homeostasis in Insulin-Like Growth Factor Binding Protein-1 Transgenic Mice, *J. Clin. Invest. 98*, 1818–1825.
22. Cieslar, J., Huang, M.T., and Dobson, G.P. (1998) Tissue Spaces in Rat Heart, Liver, and Skeletal Muscle *in vivo*, *Am. J. Physiol. 275*, R1530–R1536.
23. Bligh, E.G., and Dyer, W.J. (1959) A Rapid Method of Total Lipid Extraction and Purification, *Can. J. Biochem. Physiol. 37*, 911–917.
24. Zar, J.H. (1984) *Biostatistical Analysis*, 2nd edn., pp. 328-346, Prentice-Hall Inc., Englewood Cliffs, New Jersey.
25. Inagaki, K., Aki, T., Fukuda, Y., Kawamoto, S., Shigeta, S., Ono, K., and Suzuki, O. (2002) Identification and Expression of a Rat Fatty Acid Elongase Involved in the Biosynthesis of C18 Fatty Acids, *Biosci. Biotechnol. Biochem. 66*, 613–621.
26. Thiede, M.A., Ozols, J., and Strittmatter, P. (1986) Construction and Sequence of cDNA for Rat Liver Stearyl Coenzyme A Desaturase, *J. Biol. Chem. 261*, 13230–13235.
27. Kaestner, K.H., Ntambi, J.M., Kelly, T.J., Jr., and Lane, M.D. (1989) Differentiation-Induced Gene Expression in 3t3-L1 Preadipocytes. A Second Differentially Expressed Gene Encoding Stearoyl-CoA Desaturase, *J. Biol. Chem. 264*, 14755–14761.
28. Wahle, K.W. (1974) Fatty Acid Composition and Desaturase Activity of Tissues of the Congenitally Obese Zucker Rat, *Comp. Biochem. Physiol. B 48*, 565–574.
29. Zheng, Y., Prouty, S.M., Harmon, A., Sundberg, J.P., Stenn, K.S., and Parimoo, S. (2001) Scd3—A Novel Gene of the Stearoyl-CoA Desaturase Family with Restricted Expression in Skin, *Genomics 71*, 182–191.
30. Miyazaki, M., Jacobson, M.J., Man, W.C., Cohen, P., Asilmaz, E., Friedman, J.M., and Ntambi, J.M. (2003) Identification and Characterization of Murine SCD4, a Novel Heart-specific Stearoyl-CoA Desaturase Isoform Regulated by Leptin and Dietary Factors, *J. Biol. Chem. 278*, 33904–33911.
31. Kakuma, T., Lee, Y., and Unger, R.H. (2002) Effects of Leptin, Troglitazone, and Dietary Fat on Stearoyl CoA Desaturase, *Biochem. Biophys. Res. Commun. 297*, 1259–1263.
32. Desvergne, B., and Wahli, W. (1999) Peroxisome Proliferator-

Activated Receptors: Nuclear Control of Metabolism, *Endocr. Rev. 20*, 649–688.

33. Kawashima, Y., and Kozuka, H. (1985) Regulation of Palmitoyl-CoA Chain Elongation and Linoleoyl-CoA Chain Elongation in Rat Liver Microsomes and the Differential Effects of Peroxisome Proliferators, Insulin and Thyroid Hormone, *Biochim. Biophys. Acta 834*, 118–123.

34. Foufelle, F., and Ferre, P. (2002) New Perspectives in the Regulation of Hepatic Glycolytic and Lipogenic Genes by Insulin and Glucose: A Role for the Transcription Factor Sterol Regulatory Element Binding Protein-1c, *Biochem. J. 366*, 377–391.

35. Matsuzaka, T., Shimano, H., Yahagi, N., Yoshikawa, T., Amemiya-Kudo, M., Hasty, A.H., Okazaki, H., Tamura, Y., Iizuka, Y., Ohashi, K., *et al.* (2002) Cloning and Characterization of a Mammalian Fatty Acyl-CoA Elongase as a Lipogenic Enzyme Regulated by SREBPs, *J. Lipid. Res. 43*, 911–920.

36. Miyazaki, M., Dobrzyn, A., Man, W.C., Chu, K., Sampath, H., Kim, H.J., and Ntambi, J.M. (2004) Stearoyl-CoA Desaturase 1 Gene Expression Is Necessary for Fructose-Mediated Induction of Lipogenic Gene Expression by Sterol Regulatory Element-Binding Protein-1c-Dependent and -Independent Mechanisms,

J. Biol. Chem. 279, 25164–25171.

37. Iida, M., Murakami, T., Ishida, K., Mizuno, A., Kuwajima, M., and Shima, K. (1996) Phenotype-Linked Amino Acid Alteration in Leptin Receptor cDNA from Zucker Fatty (*fa/fa*) Rat, *Biochem. Biophys. Res. Commun. 222*, 19–26.

38. Lazarow, P.B., and De Duve, C. (1976) A Fatty Acyl-CoA Oxidizing System in Rat Liver Peroxisomes; Enhancement by Clofibrate, a Hypolipidemic Drug, *Proc. Natl. Acad. Sci. USA 73*, 2043–2046.

39. Kawashima, Y., Hanioka, N., Matsumura, M., and Kozuka, H. (1983) Induction of Microsomal Stearoyl-CoA Desaturation by the Administration of Various Peroxisome Proliferators, *Biochim. Biophys. Acta 752*, 259–264.

40. Kawashima, Y., and Kozuka, H. (1985) Regulation of Palmitoyl-CoA Chain Elongation and Linoleoyl-CoA Chain Elongation in Rat Liver Microsomes and the Differential Effects of Peroxisome Proliferators, Insulin and Thyroid Hormone, *Biochim. Biophys. Acta 834*, 118–123.

A Carbohydrate-Rich Diet Reduces LDL Size in QQ Homozygotes for the Gln192Arg Polymorphism of the Paraoxonase 1 Gene

J. Delgado-Lista, F. Perez-Jimenez, E. Gavilan, C. Marin, F. Fuentes, R.A. Fernandez-Puebla,
P. Perez-Martinez, J.A. Paniagua, C. Aguilera, and J. Lopez-Miranda*

Lipid and Arteriosclerosis Research Unit, Department of Medicine, Hospital Universitario Reina Sofía,
School of Medicine, University of Córdoba, 14004 Córdoba, Spain

ABSTRACT: Paraoxonase 1 (PON 1) is an esterase with antioxidant properties that is present in HDL. Gln192Arg polymorphism (also named Q192R or Q/R) of the PON 1 gene that encodes this protein defines two alleles (Q and R). The R allele has been associated with higher cardiovascular risk. LDL size and susceptibility to oxidation also have been identified as cardiovascular risk factors. Our objective was to determine whether genetic variations in the Gln192Arg polymorphism influence LDL size and susceptibility to oxidation after the consumption of diets with different fat content. In our experiments, the participants ($n = 98$) underwent three 4-wk diets—one, saturated fat-enriched (SAT); another, monounsaturated fat-enriched (MONO); and a third, carbohydrate-enriched (CHO). We observed that LDL were smaller in the QQ group after the CHO diet vs. the SAT ($P < 0.01$) and MONO diets ($P < 0.03$). No differences in LDL size were found in QR/RR subjects. When we analyzed lag time of oxidation of LDL, we found that when carriers of the R allele (QR/RR) received the MONO diet, the lag period of LDL oxidation was longer as compared with the CHO diet. Otherwise, we found no differences in QQ homozygotes when we evaluated the lag time of oxidation of LDL after the three diets. These results suggest that the Gln192Arg polymorphism of the paraoxonase gene influences LDL size and susceptibility to oxidation in response to diet.

Paper no. L9680 in *Lipids 40*, 471–476 (May 2005).

The pathogenesis of atherosclerosis is multifactorial and is a result of the interaction of various environmental and genetic factors. Among these, genes encoding proteins related to lipid metabolism may play a significant role. One of these genes is responsible for encoding paraoxonase 1(PON 1), an HDL-associated esterase. It reduces the accumulation of lipoperoxides and destroys biologically active lipids that are present in minimally oxidized LDL, which is why an antiatherogenic role has been attributed to it (1,2). Recent data suggest the importance of nutritional factors in the regulation of its enzymatic activity (3). Among these, saturated FA (SAFA) or food rich in oxidized products decreases postprandial paraoxonase activity (4,5), whereas oleic acid increases it (6). In the PON 1 gene there are several polymorphisms related to changes in the activity of the enzyme. One of them is PON 1 Gln192Arg, which has two genetic variations (Q and R alleles). Q is the more prevalent form. The frequency of R varies among different populations, but an average frequency of 0.70 for Q and 0.30 for R alleles can be estimated. This frequency of alleles conforms to 55% QQ, 45% QR, and10% RR genotypes (7); Q allele (the more prevalent form) carriers produce an enzyme with a greater antioxidant capacity and a lower risk of coronary heart disease (CHD); on the other hand, the mutation that changes glutamine to arginine (R allele) has been identified as a possible independent risk factor for CHD in certain populations (8–10). A recent meta-analysis that included 43 case–control studies and 23,998 participants estimated the relative risk per allele of R allele for CHD as 1.12 (95% confidence interval 1.07–1.16). Nevertheless, the authors of that work (11) found a high variability in their results. A possible explanation of this variation could be the existence of environmental factors (such as diet) that would interfere with their results.

Diet plays an important role in the development of atherosclerosis. Saturated diets, high in SAFA, increase the formation of atherosclerotic plaques. Two diets have been proposed to slow the progress of this entity. One of them is a low-fat, high-carbohydrate (CHO) Diet. The other is the so-called Mediterranean diet, characterized by 33–40% energy intake as fat, mainly from monounsaturated FA (MUFA) from olive oil (16–29% energy), and a high intake of fruit, vegetables, grain, and fish and low consumption of meat, most of it in the form of poultry (12–14).

Small, dense LDL particles have an increased susceptibility to oxidative modification and elevated atherogenic properties (15). Because HDL prevents LDL oxidation, mainly by the effect of the PON 1 enzyme, we wanted to establish whether the existence of polymorphisms in the PON gene interacts with diet to influence two interrelated features of LDL: the size of the particles and their susceptibility to oxidative modifications.

MATERIALS AND METHODS

Subjects of the study. Both the study protocol and the subjects have been described previously (16). The volunteers (*n* = 98), 30 women and 68 men, ranged between 18 and 49 yr of age. All supplied a clinical history and underwent a medical examination, with no evidence of any chronic illness (such as cardiac, hepatic, renal, or thyroid dysfunction), obesity [defined as body mass index (BMI) ≥30 kg/m^2] or unusually high levels of physical activity. None had a family history of early onset coronary disease or had consumed substances that might interfere with plasma lipid levels in the 6 mon before the start of the study. Mean initial BMI remained constant at 22.6 ± 3.2 kg/m^2 throughout the study, with oscillations of less than 1%. To calculate individual daily energy requirements, the participants were asked, before the start of the experimental periods, to record in a diary their physical activity and diet for a full week. They were also encouraged to maintain their lifestyle and normal levels of physical activity and to note any event that could affect the outcome of the study, such as stress, any changes in smoking habits, or changes in the consumption of alcohol or foods not included in the experimental design. All the studies were carried out at the Lipids Research Unit of the Reina Sofía University Hospital (Córdoba, Spain), following the approval of the study protocol by the Human Investigation Review Committee of this institution.

Design and diets in the study. The study design included an initial 28-d period, during which all the subjects consumed a diet rich in SAFA (SAT phase), and whose composition as percentages of energy was: 15 protein, 47 carbohydrates, and 38 fats (of which 20% were SAFA, 6% PUFA, and 12% MUFA). During the next 28-d phase, and under a randomized crossover design, 49 subjects were given a Mediterranean MUFA-enriched diet (MONO phase), composed of: 15% protein, 47% carbohydrates, and 38% fat (<10% SAFA, 6% PUFA, 22% MUFA). During the third 4-wk period, they consumed a low-fat, high-carbohydrate diet (CHO) diet (17), which contained 15% protein, 55% carbohydrates and less than 30% fat (<10% SAFA, 6% PUFA, 12% MUFA). The remaining participants were given the carbohydrate diet (CHO) followed by the Mediterranean diet (MONO). The assignment of volunteers to this sequence was randomized, following a 1:1 ratio. Dietary cholesterol content remained constant throughout all three phases. Eighty percent of the MUFA in the MONO diet was obtained from extra virgin olive oil (*Olea europea* species). Carbohydrate consumption in the CHO period consisted of biscuits, bread, and jam. The source of saturated fat during the SAT phase was butter and palm oil.

Body weight was measured twice weekly.

Tables of food values from the United States and Europe (18,19) were used to calculate food composition and to design the menus for each dietary phase. During each experimental period 14 menus, prepared with regular solid foods, were used in rotation. All the meals, under the direct supervision of a qualified dietitian, were prepared and served in the

hospital. Dietary compliance was evaluated by examining the food diaries. Duplicate samples from each menu were collected and stored at −70°C. Protein, fat, and carbohydrate contents of each diet were analyzed using standard methods.

Blood sampling and biochemical determinations. Venous blood was collected from the subjects in EDTA-containing tubes (1 g/L) after a 12-h overnight fast, both at the beginning of the study and at the end of each dietary period. Plasma was then isolated from the samples obtained by centrifugation (2500 × *g* for 10 min at 4°C). All analyses, except the one for TG, were performed at the end of the study on samples stored at −70°C, to minimize assay variability. Plasma TG and cholesterol concentrations were measured using standard enzymatic methods (20,21). HDL cholesterol was measured using phosphotungstic acid-MgCl$_2$, after precipitation of apolipoprotein B (apo B)-containing lipoproteins (22). Quality controls were applied to every measurement using commercial kits (Precinorm; Precilip; Boehringer Mannheim, Mannheim, Germany). LDL cholesterol levels were calculated using the Friedewald formula (23). Apo A-I and apo B were determined by turbidimetry (24).

LDL isolation. LDL was isolated from fresh plasma samples by sequential ultracentrifugation with a Beckman model LE-70 ultracentrifuge with a type NVT65 rotor (Beckman, Palo Alto, CA) for 2 h at 405,000 × *g* and 4°C.

Determination of LDL particle size. The predominant peak particle diameter (LDL size) was measured in serum samples with polyacrylamide gradient gel electrophoresis (2 to 16% gradient) as previously described (25). The resulting gels were scanned and analyzed with the Scion Image for Windows (Scion Corporation, Frederick, MD) program. The LDL size of the subjects was determined by interpolating LDL migration on a regression curve of pattern size (in nm) vs. migration.

LDL particle oxidation. LDL oxidation was performed *in vitro* by adding Cu^{2+} (to a final concentration of 10 μmol/L) to 50 μg of LDL in 500 μL of PBS. Oxidation kinetics was analyzed by monitoring diene absorbance changes at 234 nm at 37°C for 200 min at 5-min intervals, in a UV/vis spectrophotometer (Beckman DU 640), following the technique described by Esterbauer *et al.* (26). The lag time (time before onset of the exponential phase of the LDL oxidation curve, expressed in minutes) was calculated as an indirect marker of the onset of LDL particle lipoperoxidation.

Genotype determination of the PON-1 polymorphism. DNA was extracted from the samples stored at −20°C in 10 mL Na-EDTA tubes. Codon 192 genotypes in the PON 1 gene were identified by a combination of PCR followed by digestion of the Alw-1 enzyme, as described by Humbert *et al.* (27). The PCR reactive mixture contained not only the genomic DNA but also MgCl$_2$, 4 dNTP (deoxy nucleotide 5′-triphosphate), buffer solution, DNA Taq polymerase, and the following oligonucleotide primer sequence: E1, 5′-TATTGTTGCTGTGGGAC-CTGAG-3′; and E2, 5′-CACGCTAAACCCAAATACATCTC-3′. The denaturation phase of the DNA sequence was achieved after 4 min at 95°C, followed by 30 denaturation cycles (30 s

at 95°C), annealing (30 s at 59°C), and extension (45 s at 72°C). Ten microliters of the 99 bp PCR product as mixed with the restrictive endonuclease *Alw-1* in a total volume of 15 μL for its enzymatic digestion. After incubating the mixture for over 4 h at 37°C, the digested DNA was isolated by electrophoresis onto an 8% nondenaturing polyacrylamide gel (2 h at 150 V). Bands were visualized using silver staining. The R genotype (Arginine) contains a unique restriction site, which results in 66 and 33 bp products, whereas the Q genotype (glutamine) does not cut, and its bands are located 99 bp away.

Statistical analysis. We made a stratified analysis based on the PON 1 Gln192Arg polymorphism. Population was distributed into two groups (QQ homozygotes, $n = 58$; QR/RR, $n = 40$). QR and RR were studied together owing to the small size of the RR group. Data were tested for statistical significance by ANOVA for repeated measures. When statistical significance was found, the Tukey's *post hoc* comparison test was used to identify group differences. A probability value less than 0.05 was considered significant. All data presented in text and tables are expressed as means ± S.E. The Statistical Package for the Social Sciences (SPSS) 11.0 (Chicago, IL) was used for the statistical comparisons.

RESULTS

Relative frequency of QQ homozygotes and QR/RR subjects, as well as participants' baseline characteristics according to genotype, are shown in Table 1. No differences were found between the two groups, QQ and QR/RR, in terms of age, BMI, or lipid and apo levels.

When evaluating the effect of the PON 1 Gln192Arg polymorphism on LDL particle size, we found no differences between different genotypes following the same diet. Nevertheless, we found that LDL were smaller in size in the QQ group after the consumption of CHO-rich diet as compared with the SAT- and MONO-rich diet (Table 2). In contrast, no differences in LDL size were found in QR/RR subjects after the three diets.

When studying LDL resistance to oxidation, we saw no differences between subjects when analyzing QQ vs. QR/RR groups for the same diet. Otherwise, we observed that replacing the SAT-enriched diet with the MONO-enriched diet improved resistance to oxidation, regardless of the Gln192Arg genotype. Likewise, QR/RR subjects presented a higher resistance to LDL oxidation after the MONO-enriched diet than after the CHO-enriched diet. This result was not observed with QQ homozygotes (Table 3).

With respect to plasma lipid levels after the consumption of the three diets, we observed that the Q/R polymorphism exerted no effect on the lipid level changes induced by the different diets. According to previous knowledge, consumption of the SAT-enriched diet increased levels of total cholesterol, LDL, and HDL in comparison with the CHO-enriched diet; similarly, consumption of the SAT-enriched diet increased levels of total cholesterol and LDL but not HDL in comparison with consumption of the MONO-enriched diet (Table 4).

TABLE 1
Baseline Characteristics of Participants at Study Onset[a], According to the Gln192Arg Polymorphism (Q/R) of PON 1

	QQ	QR/RR	*P* value
Number (%)	58 (59.2)	40 (40.8)	
Age (yr)	21.6 ± 2.1	21.4 ± 1.6	0.606
BMI (kg/m^2)	22.9 ± 3.1	22.3 ± 3.3	0.353
TC (mmol/L)	4.18 ± 0.67	3.97 ± 0.59	0.132
LDL (mmol/L)	2.49 ± 0.66	2.24 ± 0.58	0.215
HDL (mmol/L)	1.29 ± 0.35	1.27 ± 0.34	0.748
TG (mg/dL)	0.96 ± 0.52	0.91 ± 0.43	0.623
ApoA-1 (g/L)	0.13 ± 0.27	0.13 ± 0.24	0.569
Apo B (g/L)	0.67 ± 0.16	0.65 ± 0.12	0.389

[a]PON 1, paraoxonase 1; BMI, body mass index; TC, total cholesterol; ApoA-1 and B, apolipoproteins A-1 and B.

TABLE 2
LDL Size[a] (nm) [mean (SE)]

G	Diet	LDL size (nm)
QQ	SAT	25.95 (0.11)[a]
	CHO	25.77 (0.09)[b]
	MONO	25.91 (0.11)[a]
QR/RR	SAT	25.86 (0.13)[a]
	CHO	25.86 (0.11)[a]
	MONO	25.96 (0.13)[a]
P	Genotype	0.922
	Diet	0.043
	Interaction	0.288

[a]Values with different superscript letters are statistically different. Differences between SAT and CHO in QQ are at a level of $P = 0.01$ and between MONO and CHO in QQ are $P = 0.025$). G, genotype; SAT, saturated FA-enriched diet; CHO, carbohydrate-enriched diet; MONO, monounsaturated FA-enriched diet.

DISCUSSION

Our results show that a high-CHO diet induces the formation of smaller LDL than high-fat diets in carriers of the QQ genotype for the Q192R polymorphism (also called Gln192Arg) of the PON 1 gene, but not in carriers of the QR/RR genotypes. The presence of an R allele (genotypes QR/RR) increases LDL resistance to oxidation when a high-CHO diet is replaced isocalorically by MONO. Furthermore, R carriers,

TABLE 3
LDL Oxidation Lag Time[a] (min) [mean (SE)]

G	Diet	Lag time (min)
QQ	SAT	44.69 (3.88)[a]
	CHO	48.12 (3.38)[a,b]
	MONO	52.59 (3.55)[b]
QR/RR	SAT	44.90 (4.73)[a]
	CHO	45.41 (4.12)[a]
	MONO	55.79 (4.33)[b]
P	Genotype	0.963
	Diet	0.001
	Interaction	0.445

[a]Values with different letters are statistically different. Differences between MONO and SAT in QQ are at a level of $P = 0.03$. Differences between MONO and SAT in QR/RR are at $P = 0.02$, and between MONO and CHO in QR/RR are $P = 0.005$. For abbreviations see Table 2.

TABLE 4
Lipid Fractions Concentration*a* (mmol/L) After Each Diet According to Gln192Arg Polymorphism (Q/R) [mean (SD)]

G	Diet	Chol.	TG	LDL	HDL
QQ	SAT	4.26 (0.65)	0.81 (0.34)	2.62 (0.61)	1.25 (0.31)
	CHO	3.73 (0.62)	0.80 (0.36)	2.21 (0.58)	1.14 (0.27)
	MONO	3.77 (0.63)	0.77 (0.31)	2.22 (0.59)	1.19 (0.30)
QR/	SAT	4.14 (0.51)	0.84 (0.41)	2.52 (0.53)	1.23 (0.24)
RR	CHO	3.55 (0.51)	0.84 (0.33)	2.05 (0.45)	1.11 (0.22)
	MONO	3.62 (0.53)	0.83 (0.41)	2.07 (0.48)	1.19 (0.28)
P	Genotype	0.188	0.676	0.176	0.741
	Diet	0.0001	0.267	0.0001	0.0001
	Interaction	0.719	0.980	0.733	0.586

*a*Chol, cholesterol; for other abbreviations see Tables 2 and 3.

although they show no difference in LDL size in the CHO diet, benefit from changing from this diet to MONO, as it increases the resistance of their LDL to oxidation.

Data were obtained from an intervention study based on a baseline diet, followed by two diets administered using a randomized crossover design, in young normolipemic subjects. The rigorous control of the dietary protocol makes these data particularly significant. As described earlier, we observed an increase in LDL *in vitro* oxidation lag time during the consumption of a MONO-enriched diet as compared with SAT- and CHO-enriched diets, regardless of the PON genotype.

We previously reported other gene–diet interactions in lipid metabolism-related genes. Apo E has an important role in the metabolism of TG-rich lipoproteins. Genetic variations in the promoter region of apo E defines three alleles: E3, E4, and E2. It is known that people who carry E4 and E2 alleles in their apo E genotype show different lipid responses to diet from persons who are homozygous for the most prevalent form, E3. We have recently shown a direct relation between apo E genetic alleles and LDL size response to diet (28). To avoid confusing factors, we selected only E3E3 homozygotes in this study (29–32).

The relationship between the Q192R polymorphism and lipid response to different types of diets in humans is little known. In experiments with animals atherogenic diets have been found to decrease PON 1 activity, whereas a MONO-enriched diet or polyphenols increase it (33). In a study carried out on healthy women, a low-vegetable diet decreased PON 1 activity. The presence of the R allele in the Q192R polymorphism was thought to be responsible for a more marked decrease in this activity and in HDL reduction (34). However, as noted above, we observed no difference in the lipid response of the different genotypes to changes in dietary fat composition.

The Q192R polymorphism of PON 1 gene has two alleles, the Q allele, which carries a glutamine molecule at position 192, and the R allele, which carries arginine. The presence of the R allele previously has been associated with a higher cardiovascular risk, although evidence to support this view remains incomplete (8,11,35,36). This allele determines the production of PON, conferring it with a greater ability to metabolize paraoxon; this artificial substrate, which is not naturally present in humans, has been used in experimental studies to evaluate enzyme activity, although the clinical importance of

this ability is not clear. The enzyme activity metabolizing paraoxon seems to increase according to the following pattern: QQ < QR < RR (37).

On the other hand, several studies have shown that the Q allele has a greater antioxidant ability than the R allele, owing to its higher esterase and peroxidase activities (38,39).

Earlier work indicated that a low-fat diet induced a decrease in LDL particle size in the general population (15). In our study, QQ subjects followed this trend, but not QR/RR. On the other hand, R carriers showed a greater resistance of LDL to oxidation after consumption of the MONO-enriched diet compared with SAT- and CHO-enriched diets. No data about the polymorphism of PON 1 or LDL lag time in response to diet have been reported, but a study by Tomás *et al*. (40) revealed that a high oleic oil diet improves HDL cholesterol levels and PON 1 activity in carriers of the R allele (39). Furthermore Kuremoto *et al*. (41) recently associated the R/R genotype in Japanese (another population typically consuming a highly unsaturated fat diet) with lower LDL and HDL oxidation and lower risk of coronary disease. Our findings support the idea that carriers of QQ and QR do not have the same response to diet with respect to LDL. QQ subjects decreased their LDL particle size when exposed to a CHO-enriched diet. This effect has been previously shown in a general population not genotyped for PON 1. Nevertheless, QR/RR did not show this decrease in the present study. On the other hand, we found a more prolonged LDL oxidation lag time after consumption of the MONO diet compared with CHO diet only for QR/RR, and not for QQ. Although further research is needed, we hypothesize that PON 1 increases its function in R carriers following consumption of a MONO-enriched diet, and so LDL resistance to oxidation increases in these persons. In agreement with this hypothesis, it has been proposed before that an oleic acid-rich diet gives protection against lipoprotein oxidation, particularly in men carrying one or two R alleles and that increasing the amount of oleic acid in the diet of R carriers should reduce the risk of atherosclerosis (40).

The influence of the Q192R polymorphism as an isolated factor for absolute coronary disease risk is thought to be slight, although it could become clinically significant when combined with other environmental risk factors, such as diet (42).

REFERENCES

1. Mackness, M.I., Arrol, S., and Durrington, P.N. (1991) Paraoxonase Prevents Accumulation of Lipoperoxides in Low-Density Lipoprotein, *FEBS Lett. 286*, 152–154.

2. Watson, A.D., Berliner, J.A., Hama, S.Y., La Du, B.N., Faull, K.F., Fogelman, A.M., and Navab, M. (1995) Protective Effect of High Density Lipoprotein Associated Paraoxonase. Inhibition of the Biological Activity of Minimally Oxidized Low Density Lipoprotein, *J. Clin. Invest. 96*, 2882–2891.

3. Mackness, B., Mackness, M.I., Durrington, P.N., Arrol, S., Evans, A.E., McMaster, D., Ferrieres, J., Ruidavets, J.B., Williams, N.R., and Howard, A.N. (2000) Paraoxonase Activity in Two Healthy Populations with Differing Rates of Coronary Heart Disease, *Eur. J. Clin. Invest. 30*, 4–10.

4. Sutherland, W.H., Walker, R.J., de Jong, S.A., van Rij, A.M., Phillips, V., and Walker, H.L. (1999) Reduced Postprandial Serum Paraoxonase Activity After a Meal Rich in Used Cooking Fat, *Arterioscler. Thromb. Vasc. Biol. 19*. 1340–1347.

5. Neuman, M.P., Neuman, H.R., Durante Costas, F., Barrera, V. Tavella, M., Peterson, G., Veroni, H., and Neuman, J. (2000) Postprandial Increase of Lipid Peroxide Products Parallel Reduction of Antioxidant Enzyme Properties, *Atheroscler. 151*, 262.

6. Kudchodkar, B.J., Lacko, A.G., Dory, L., and Fungwe, T.V. (2000) Dietary Fat Modulates Serum Paraoxonase 1 Activity in Rats, *J. Nutr. 130*, 2427–2433.

7. Scacchi, R., Corbo, R.M., Rickards, O., and De Stefano, G.F. (2003) New Data on the World Distribution of Paraoxonase (PON1 Gln 192 → Arg) Gene Frequencies, *Hum. Biol. 75*, 365–373.

8. Serrato, M., and Marian, A.J. (1995) A Variant of Human Paraoxonase/Arylesterase (HUMPONA) Gene Is a Risk Factor for Coronary Artery Disease, *J. Clin. Invest. 96*, 3005–3008.

9. Mackness, B., Mackness, M.I., Arrol, S., Turkie, W., and Durrington, P.N. (1998) Effect of the Human Serum Paraoxonase 55 and 192 Genetic Polymorphisms on the Protection by High Density Lipoprotein Against Low Density Lipoprotein Oxidative Modification, *FEBS Lett. 423*, 57–60.

10. Mackness, M.I., Mackness, B., Durrington, P.N., Connelly, P.W., and Hegele, R.A. (1996) Paraoxonase: Biochemistry, Genetics and Relationship to Plasma Lipoproteins, *Curr. Opin. Lipidol. 7*, 69–76.

11. Wheeler, J.G., Keavney, B.D., Watkins, H., Collins, R., and Danesh, J. (2004) Four Paraoxonase Gene Polymorphisms in 11212 Cases of Coronary Heart Disease and 12786 Controls: Meta-Analysis of 43 Studies, *Lancet 363*, 689–695.

12. Perez-Jimenez, F., Lopez-Miranda, J., and Mata, P. (2002) Protective Effect of Dietary Monounsaturated Fat on Arteriosclerosis: Beyond Cholesterol, *Atherosclerosis 163*, 385–398.

13. National Cholesterol Education Program (NCEP) Expert Panel on Detection, Evaluation, and Treatment of High Blood Cholesterol in Adults (Adult Treatment Panel III) (2002) Third Report of the National Cholesterol Education Program (NCEP) Expert Panel on Detection, Evaluation, and Treatment of High Blood Cholesterol in Adults (Adult Treatment Panel III) Final Report, *Circulation 106*, 3143–3421.

14. Willett, W.C., Sacks, F., Trichopoulou, A., Drescher, G., Ferro-Luzzi, A., Helsing, E., and Trichopoulos, D. (1995) Mediterranean Diet Pyramid: A Cultural Model for Healthy Eating, *Am. J. Clin. Nutr. 61*, 1402S–1406S.

15. Desroches, S., and Lamarche, B. (2004) Diet and Low-Density Lipoprotein Particle Size, *Curr. Atheroscler. Rep. 6*, 453–460.

16. Perez-Martinez, P., Ordovas, J.M., Lopez-Miranda, J., Gomez, P., Marin, C., Moreno, J., Fuentes, F., Fernandez de la Puebla, R.A., and Perez-Jimenez, F. (2003) Polymorphism Exon 1 Variant at the Locus of the Scavenger Receptor Class B Type I Gene: Influence on Plasma LDL Cholesterol in Healthy Subjects During the Consumption of Diets with Different Fat Contents, *Am. J. Clin. Nutr. 77*, 809–813.

17. National Cholesterol Education Program (NCEP). (1994) Second Report of the Expert Panel on Detection, Evaluation, and Treatment of High Blood Cholesterol in Adults (Adult Treatment Panel II), *Circulation 89*, 1333–1445.

18. Human Nutrition Information Service, U.S. Department of Agriculture (1987) Composition of Foods, *Agriculture Handbook No. 8*, U.S. Government Printing Office, Washington, DC.

19. Varela, G. (1980) *Tablas de Composicion de Alimentos*, Consejo Superior de Investigaciónes Científicas, Madrid.

20. Allain, C.C., Poon, L.S., Chan, C.S., Richmond, W., and Fu, P.C. (1974) Enzymatic Determination of Total Serum Cholesterol, *Clin. Chem. 20*, 470–475.

21. Fossati, P., and Prencipe, L. (1982) Serum Triglycerides Determined Colorimetrically with an Enzyme That Produces Hydrogen Peroxide, *Clin. Chem. 28*, 2077–2080.

22. Assmann, G., Schriewer, H., Schmitz, G., and Hagele, E.O. (1983) Quantification of High-Density-Lipoprotein Cholesterol by Precipitation with Phosphotungstic Acid/MgCl$_2$, *Clin. Chem. 29*, 2026–2030.

23. Friedewald, W.T., Levy, R.I., and Fredrickson, D.S. (1972) Estimation of the Concentration of Low-Density Lipoprotein Cholesterol in Plasma, Without Use of the Preparative Ultracentrifuge, *Clin. Chem. 18*, 499–502.

24. Riepponen, P., Marniemi, J., and Rautaoja, T., (1987) Immunoturbidimetric Determination of Apolipoproteins A-1 and B in Serum, *Scand. J. Clin. Lab. Invest. 47*, 739–744.

25. Krauss, R., and Blanche, P. (1992) Detection and Quantification of LDL Subfractions, *Curr. Opin. Lipidol. 3*, 377 (1992).

26. Esterbauer, H., Striegl, G., Puhl, H., and Rotheneder, M. (1989) Continuous Monitoring of *in vitro* Oxidation of Human Low Density Lipoprotein, *Free Radic. Res. Commun. 6*, 67–75.

27. Humbert, R., Adler, D.A., Disteche, C.M., Hassett, C., Omiecinski, C.J., and Furlong, C.E. (1993) The Molecular Basis of the Human Serum Paraoxonase Activity Polymorphism, *Nat. Genet. 3*, 73–76.

28. Moreno, J.A., Perez-Jimenez, F., Martin, C., Gomez, P., Perez-Martinez, P., Moreno, R., Bellido, C., Fuentes, F., and Lopez-Miranda, J. (2004) The Effect of Dietary Fat on LDL Size Is Influenced by Apolipoprotein E Genotype in Healthy Subjects, *J. Nutr. 134*, 2517–2522.

29. Gonzalez-Amieva, A., Lopez-Miranda, J., Fuentes, F., Castro, P., Marin, C., Lopez-Granados, A., Valles, F., and Perez-Jimenez, F. (2000) Genetic Variations of the Apolipoprotein E Gene Determine the Plasma Triglyceride Levels After Heart Transplantation, *J. Heart Lung Transplant. 19*, 765–770.

30. Ordovas, J.M., Lopez-Miranda, J., Mata, P., Perez-Jimenez, F., Lichtenstein, A.H., and Schaefer, E.J. (1995) Gene–Diet Interaction in Determining Plasma Lipid Response to Dietary Intervention, *Atherosclerosis 118 (Suppl.)*, S11–S27.

31. Ordovas, J.M., Lopez-Miranda, J., Perez-Jimenez, F., Rodriguez, C., Park, J.S., Cole, T., and Schaefer, E.J. (1995) Effect of Apolipoprotein E and A-IV Phenotypes on the Low Density Lipoprotein Response to HMG CoA Reductase Inhibitor Therapy, *Atherosclerosis 113*, 157–166.

32. Lopez-Miranda, J., Ordovas, J.M., Mata, P., Lichtenstein, A.H., Clevidence, B., Judd, J.T., and Schaefer, E.J. (1994) Effect of Apolipoprotein E Phenotype on Diet-Induced Lowering of Plasma Low Density Lipoprotein Cholesterol, *J. Lipid Res. 35*, 1965–1975.

33. Mackness, M.I., Mackness, B., and Durrington, P.N. (2002) Paraoxonase and Coronary Heart Disease, *Atheroscler. Suppl. 3*, 49–55.

34. Rantala, M., Silaste, M.L., Tuominen, A., Kaikkonen, J., Salonen, J.T., Alfthan, G., Aro, A., and Kesaniemi, Y.A. (2002) Dietary Modifications and Gene Polymorphisms Alter Serum Paraoxonase Activity in Healthy Women, *J. Nutr. 132*, 3012–3017.

35. Sanghera, D.K., Aston, C.E., Saha, N., and Kamboh, M.I. (1998) DNA Polymorphisms in Two Paraoxonase Genes (PON1

and PON2) Are Associated with the Risk of Coronary Heart Disease, *Am. J. Hum. Genet. 62*, 36–44.

36. Herrmann, S.M., Blanc, H., Poirier, O., Arveiler, D., Luc, G., Evans, A., Marques-Vidal, P., Bard, J.M., and Cambien, F. (1996) The Gln/Arg Polymorphism of Human Paraoxonase (PON 192) Is Not Related to Myocardial Infarction in the ECTIM Study, *Atherosclerosis 126*, 299–303.

37. Ikeda, Y., Suehiro, T., Ohsaki, F., Arii, K., Kumon, Y., and Hashimoto, K. (2003) Relationships Between Polymorphisms of the Human Serum Paraoxonase Gene and Insulin Sensitivity in Japanese Patients with Type 2 Diabetes, *Diabetes Res. Clin. Pract. 60*, 79–85.

38. Aviram, M., Billecke, S., Sorenson, R., Bisgaier, C., Newton, R., Rosenblat, M., Erogul, J., Hsu, C., Dunlop, C., and La Du, B. (1998) Paraoxonase Active Site Required for Protection Against LDL Oxidation Involves Its Free Sulfhydryl Group and Is Different from That Required for Its Arylesterase/Paraoxonase Activities: Selective Action of Human Paraoxonase Allozymes Q and R, *Arterioscler. Thromb. Vasc. Biol. 18*, 1617–1624 (1998).

39. Mackness, B., Durrington, P.N., and Mackness, M.I. (1999) Polymorphisms of Paraoxonase Genes and Low-Density Lipoprotein Lipid Peroxidation, *Lancet 353*, 468–469.

40. Tomás, M., Senti, M., Elosua, R., Vila, J., Sala, J., Masia, R., and Marrugat, J. (2001) Interaction Between the Gln-Arg 192 Variants of the Paraoxonase Gene and Oleic Acid Intake as a Determinant of High-Density Lipoprotein Cholesterol and Paraoxonase Activity, *Eur. J. Pharmacol. 432*, 121–128.

4l. Kuremoto, K., Watanabe, Y., Ohmura, H., Shimada, K., Mokuno, H., and Daida, H. (2003) R/R Genotype of Human Paraoxonase (PON1) Is More Protective Against Lipoprotein Oxidation and Coronary Artery Disease in Japanese Subjects, *J. Atheroscler. Thromb. 10*, 85–92.

42. Robertson, K.S., Hawe, E., Miller, G.J., Talmud, P.J., and Humphries, S.E. (2003) Human Paraoxonase Gene Cluster Polymorphisms as Predictors of Coronary Heart Disease Risk in the Prospective Northwick Park Heart Study II, *Biochim. Biophys. Acta 1639*, 203–212 (2003).

Effect of 18:1n-9, 20:5n-3, and 22:6n-3 on Lipid Accumulation and Secretion by Atlantic Salmon Hepatocytes

A. Vegusdal[a,*], T. Gjøen[b], R.K. Berge[c], M.S. Thomassen[a], and B. Ruyter[a]

[a]AKVAFORSK, Institute of Aquaculture Research, NO-1432 Ås, Norway, [b]Department of Microbiology, Institute of Pharmacy, University of Oslo, NO-0316 Oslo, Norway, and [c]Department of Clinical Biology, Division of Biochemistry, Haukeland University Hospital, University of Bergen, NO-5021, Bergen, Norway

ABSTRACT: We have studied the effects of dietary FA on the accumulation and secretion of [³H]glycerolipids by salmon hepatocytes in culture. Atlantic salmon were fed diets supplemented with either 100% soybean oil (SO) or 100% fish oil (FO), and grew from an initial weight of 113 ± 5 g to a final weight of 338 ± 19 g. Hepatocytes were isolated from both dietary groups and incubated with [³H]glycerol in an FA-free medium; a medium supplemented with 0.75 mM of one of three FA—18:1n-9, 20:5n-3, or 22:6n-3—or a medium supplemented with 0.75 mM of the sulfur-substituted FA analog tetradecylthioacetic acid (TTA), which cannot undergo β-oxidation. Incubations were allowed to proceed for 1, 2, 6, or 24 h. The rate of the secretion of radioactive glycerolipids with no FA added was 36% lower from hepatocytes isolated from fish fed the FO diet than it was from hepatocytes isolated from fish fed the SO diet. Hepatocytes incubated with 18:1n-9 secreted more [³H]TAG than when incubated with no FA, whereas hepatocytes incubated with 20:5n-3 or TTA secreted less labeled TAG than when incubated with no FA. This observation was independent of the feeding group. Hepatocytes incubated with 22:6n-3 secreted the highest amounts of total [³H]glycerolipids compared with the other treatments, owing to increased secretion of phospholipids and mono- and diacylglycerols (MDG). In contrast, the same amounts of [³H]TAG were secreted from these cells as from cells incubated in an FA-free medium. The lipid-lowering effect of FO is thus independent of 22:6n-3, showing that 20:5n-3 is the FA that is responsible for the lipid-lowering effect. The ratio of TAG to MDG in lipids secreted from hepatocytes to which 20:5n-3 or TTA had been added was lower than that in lipids secreted from hepatocytes incubated with 18:1n-9 or 22:6n-3, suggesting that the last step in TAG synthesis was inhibited. Morphometric measurements revealed that hepatocytes incubated with 20:5n-3 accumulated significantly more cellular lipid than cells treated with 18:1n-9, 22:6n-3, TTA, or no treatment. The area occupied by mitochondria was also greater in these cells. The present study shows that dietary FO reduces TAG secretion from salmon hepatocytes and that 20:5n-3 mediates this effect.

Paper no. L9540 in *Lipids* 40, 477–486 (May 2005).

Fish oil (FO), which is particularly rich in the PUFA 20:5n-3 and 22:6n-3, has traditionally been used as the predominant lipid component of salmon feed. However, the uncertain supply and variable price of FO have led to an interest in using the more readily available plant oils rich in 18-carbon n-6 [soybean oil (SO) and sunflower oil] and n-9 (rapeseed oil) FA in salmon diets. Little information is available, however, concerning how these plant oils affect lipid deposition in salmon hepatocytes and how they affect the secretion of TAG-rich VLDL from these cells. There is considerable evidence that consumption of FO lowers plasma TAG concentrations in humans (1,2) and protects against coronary heart diseases (1,3,4). It is particularly important to study these processes in salmonids, since they are more predisposed to coronary arteriosclerosis than other fish species (5). Several mechanisms are probably involved in the inhibiting effect of FO on the secretion of TAG-rich VLDL particles in mammals, and the detailed mechanisms have not been completely elucidated. The effect has been attributed to the content of n-3 FA in the feed (6,7). Studies using primary hepatocytes from rats have shown that n-3 PUFA inhibit the secretion of TAG-rich VLDL (8–11). The PUFA inhibit diacylglycerol acyltransferase (DGAT, EC 2.3.1.20) (12–15), which is the rate-limiting enzyme in TAG synthesis, and they inhibit the assembly process of the VLDL particles (9,10,16). Furthermore, several studies in mammals have shown that the lipid-lowering effect of FO is mediated by 20:5n-3 and not by 22:6n-3 (13–15,17,18).

We have investigated the effects of several FA on lipid accumulation and on the secretion of glycerolipids in Atlantic salmon. We isolated hepatocytes from salmon fed diets supplemented with either FO or SO and then added the two main PUFA in FO (20:5n-3 and 22:6n-3) separately to the hepatocyte cultures. We incubated other cultures with 18:1n-9, which is a common FA in vegetable oils and which stimulates lipid secretion by cultivated rat hepatocytes (9,13,19). Finally, we compared the effects of these FA with the effects of a sulfur-substituted FA analog, tetradecylthioacetic acid (CH$_3$–(CH$_2$)$_{13}$–S–CH$_2$–COOH) (TTA), on glycerolipid secretion. TTA is unable to undergo β-oxidation (for review see Ref. 20), and it inhibits TAG secretion in mammals (14,21).

MATERIALS AND METHODS

Materials. TTA was produced at Dr. R. Berge's laboratory (Haukeland Hospital, University of Bergen, Norway). The radioactive isotope [1,2,3-³H]glycerol (30–60 Ci/mmol) was ob-

---

tained from American Radiolabeled Chemicals, Inc. (St. Louis, MO). Nonlabeled glycerol, Leibowitz-15 medium, FBS, antibiotics, HEPES, L-glutamine, collagenase, trypsin, FA, essential FA-free BSA, collagenase type 1, and 2′,7′-dichlorofluorescein were all supplied by Sigma-Aldrich (St. Louis, MO). Tissue culture plastic ware was obtained from NalgeNunc International (Naperville, IL). Acetic acid, chloroform, petroleum ether, diethyl ether, and methanol were purchased from Merck (Darmstadt, Germany). Benzene was obtained from Rathburn Chemicals, Ltd. (Walkerburn, Scotland). Methanolic HCl and 2,2-dimethoxypropane were purchased from Supelco Inc. (Bellefonte, PA). Glass-baked silica gel K6 plates were obtained from Whatman International, Ltd. (Maidstone, England). Glutaraldehyde, epon resin, copper grids, and lead citrate were supplied by Electron Microscopy Sciences (Fort Washington, PA).

Fish and experimental design. The feeding study was performed as described by Grisdale-Helland *et al.* (22). Briefly, Atlantic salmon in tanks containing seawater at 12°C were fed for approximately 950 day-degrees with one of two test diets. There were three tanks per diet. The diets, containing 30% fat, were based on fish meal and differed only in the type of supplementary oil that they contained [see Grisdale-Helland *et al.* (22) for a detailed description of the diets]. The fish were fed *ad libitum* using automatic band-feeders every 10 min, 24 h/d. Supplementary lipid in one diet, called "FO," came solely from fish oil (capelin oil), whereas the supplementary lipid in the other diet, called "SO," came solely from crude soybean oil. The salmon grew from an initial weight of 113 ± 5 g to a final weight of 338 ± 19 g.

Isolation of hepatocytes. Three fish from each tank were used for isolation of hepatocytes at the end of the growth period. The fish were anesthetized with metacain. The abdominal cavity was exposed and the vena porta cannulated. The liver was perfused following a two-step collagenase procedure developed by Seglen (23) and modified by Dannevig and Berg (24), to isolate hepatocytes. The hepatocytes were easily isolated after the collagenase digestion by gentle shaking of the digested liver in Leibowitz-15 medium. The suspension of parenchymal cells was filtered through a 100 μm nylon filter. Hepatocytes were isolated from this suspension by three sedimentations each of 2 min at $50 \times g$. The hepatocytes were resuspended in Leibowitz-15 culture medium containing 2% FBS, 2 mM L-glutamine, and 0.1 mg mL^{-1} gentamycin. Cell viability was assessed by staining with Trypan blue (0.4%). The protein content of the cell suspension was determined using the method described by Lowry *et al.* (25). Approximately 5×10^6 hepatocytes (approximately 8 mg of protein) were plated onto 75-mL Nunc flasks and left to attach overnight at 12°C.

Incubation with FA and [^{3}H]glycerol. The hepatocytes were thoroughly washed with Leibowitz-15 medium without serum supplementation, before the incubation with FA and [^{3}H]glycerol. Each cell flask with hepatocytes was incubated with 0.5 Ci/mmol [^{3}H]glycerol (final glycerol concentration 25 μM), 10 mM lactate, and either no FA (Ctr), 18:1n-9, 20:5n-3, 22:6n-3, or TTA in a total volume of 5 mL Leibowitz-15 medium. A

final FA concentration of 0.75 mM was used, a concentration often used in similar studies with mammalian cells (13,19). The FA were added to the medium in the form of their potassium salts bound to BSA (the molar ratio between an FA and BSA was 2.5). The cells were incubated for 1, 2, 6, or 24 h at 12°C, and then the medium from each culture flask was transferred to vials and centrifuged for 5 min at $50 \times g$. The supernatant (culture medium) from a flask was either immediately frozen at −70°C and stored until the analysis of radiolabeled lipids or directly used for the isolation of VLDL as described next. Hepatocytes were washed twice with 0.1 M PBS (pH 7.4), followed by preparation for electron microscopy.

Isolation and analysis of VLDL. To determine the most representative method for investigating the secretion of glycerolipids from cultivated hepatocytes, we compared the lipid analysis of secreted VLDL fractions with the analysis of total esterified lipids secreted to the culture media. Hepatocytes from SO-fed fish that had been incubated for 1, 2, 6, or 24 h in a medium without FA supplementation, but with [^{3}H]glycerol, were used for the comparison of the two methods. The culture media were divided in two halves at each time point; one for VLDL separation and one for determination of total secreted esterified lipids. A discontinuous NaCl/KBr gradient was formed by filling Bell-top Quick-Seal tubes with two layers with different densities, using a peristaltic pump. A layer of aqueous NaCl solution (10 mL, 0.9%) was pumped into the bottom of the tube, and then culture medium (5 mL), the density of which had been adjusted to 1.30 g mL^{-1} with KBr, was pumped underneath. The tubes were sealed with a cordless tube stopper and then ultracentrifuged (4 h, 4°C, average acceleration $167,153 \times g$) in a vertical rotor, using slow acceleration and deceleration below 160 rpm. The procedure was a modified version of the procedure developed by Chung *et al.* (26). Rotor shut-down added approximately 20 min to the total runtime. The top of the tube was gently sliced off using a scalpel, and the gradient was unloaded into 30 fractions (each of volume 0.5 mL) from the bottom of the tube using a peristaltic pump. The fractions covered the density range from 1.01 to 1.28 g mL^{-1}. The density of a fraction was determined by measuring its refractive index (n) in a refractometer, and calculating the density according to:

$$d = 3.298n - 3.396G \qquad [1]$$

where d is the density of the fraction and G is the density of the NaCl/KBr gradient at which this fraction was collected.

VLDL was recovered from the surface of the gradient with density lower than 1.015 g mL^{-1}. The VLDL fraction was frozen at −70°C and stored until the analysis of radiolabeled lipid classes and protein composition. Protein samples (0.5 μg protein) from the fraction associated with VLDL were added to a buffer containing SDS and boiled for 5 min. They were then loaded onto a 7% polyacrylamide gel for further analyses by SDS-PAGE as described by Burnette (27).

Lipid extraction and analysis of lipid classes and FA composition. Total lipids were extracted from culture media and

from VLDL by the method described by Folch *et al.* (28). The chloroform phase was dried under N_2, and the residual lipid extract was redissolved in hexane. Phospholipids (PL), mono- and diacylglycerols (MDG), and TAG were separated by TLC using a mixture of petroleum ether, diethyl ether, and acetic acid (113:20:2, by vol) as the mobile phase. The lipids were visualized by spraying the TLC plates with 0.2% (wt/vol) 2′,7′-dichlorofluorescein in methanol, and they were identified by comparison with known standards under UV light. The spots corresponding to PL, MDG, and TAG were scraped off into vials containing liquid scintillation fluid (InstaGel II Plus; Packard Instrument, Downers Grove, IL), and the radioactivity was measured in a liquid scintillation counter (TRI-CARB 1900 TR; Packard Instrument). There are certain limitations to the method used, and what is actually measured is the recovery of tritium (derived from tritiated glycerol) in the different lipid class fractions. The total FA profiles in the diets were determined by GC as described by Grisdale-Helland *et al.* (22). The total endogenous FA composition of hepatocytes was determined essentially as described by Ruyter *et al.* (29).

Preparation of hepatocytes for electron microscopy. After being washed in 0.1 M PBS, cells were scraped from the flask into 2 mL of 0.1 M PBS (pH 7.4), gently centrifuged, and then resuspended and fixed in 2% glutaraldehyde in 0.1 M cacodylate buffer (pH 7.4) at 4°C for 24 h. The cells were rinsed in the same buffer and post-fixed for 60 min in 2% OsO_4 containing 1.5% potassium ferrocyanide, followed by *en bloc* staining with 1.5% uranyl acetate. Cells were dehydrated in a series of ethanol solutions (70, 90, 96, and 100%) and propylene oxide, and then embedded in epon resin, which was polymerized at 60°C for 12 h. Ultrathin sections (approximately 50 nm) were cut on a Reichert Ultracut E ultramicrotome using a diamond knife. The sections were placed onto formvar/carbon-coated 75-mesh copper grids, post-stained for 2 min with 0.2% lead citrate solution in 0.1 M NaOH, and examined in a Philips CM 100 transmission electron microscope at an accelerating voltage of 80 kV.

Morphometry. Hepatocytes isolated from three fish in each feeding group were incubated for 24 h in medium containing either no FA (Ctr), 18:1n-9, 20:5n-3, 22:6n-3, or TTA. Lipid droplets and mitochondria in these samples were then analyzed by morphometry. Micrographs for morphometry were taken from 20 cells per treatment at a magnification of 2950×, at random positions in the sample. A square lattice grid was superimposed onto the micrographs, and the number of intersections falling on lipid droplets or on mitochondria was counted. We determined the total area of the mitochondria and of the lipid droplets in the cells relative to the total area of the cells (excluding the nuclei), as described by Hexeberg *et al.* (30). In brief, the percent area, A, of the cells constituting lipid droplets or mitochondria was calculated from:

$$A = (P_{lip}/P_{cell}) \times 100 \qquad [2]$$

where P_{lip} is the number of intersections falling on the lipid droplets and P_{cell} is the number of intersections falling on the cells (excluding the nuclei).

Statistical analysis. ANOVA was carried out using a model that included effects of diet, incubation time, and exogenous FA, and all interactions between these factors, to analyze the effect of endogenous FA composition on the secretion of total radiolabeled lipids. A reduced model in which only main effects were included was used where the interactions included in the full model gave nonsignificant results. Treatment differences were ranked using Duncan's multiple range test for the main effects. Pearson's correlation coefficient was calculated and used to analyze the correlation between the mitochondrial area and the lipid area.

One-way ANOVA (general linear model) was used to test the significance of the analysis of the level of [³H]glycerolipids secreted at different time points and at different additions of exogenous FA. Significant differences between means were analyzed using Duncan's test. Differences were considered to be significant at a 5% level. SAS computer software was used for all the statistical analyses (31).

RESULTS

FA composition. The SO diet contained more than eight times more n-6 FA (45.4%) than the FO diet (5.3%). The FO diet, on the other hand, contained almost twice as much n-3 FA (21.3%) as the SO diet (10.9%). The percentage of total monounsaturated FA was twice as high in the FO diet (49.3%) than in the SO diet (25.3%). The FA composition of hepatocytes isolated from fish fed either the SO or the FO diets was substantially affected by the dietary FA composition (Table 1). The percentage of n-3 FA in the hepatocyte lipids was 1.6 times greater in cells from fish fed the FO diet (39.3%) than in cells from fish fed the SO diet (24.5%). The percentage of n-6 FA was approximately seven times greater in cells from fish fed the SO diet (31%) than in cells from fish fed the FO diet (4.5%). There was an enrichment of 22:6 n-3 in hepatocytes isolated from both SO-fed (17%) and FO-fed fish (27%) compared with the corresponding percentages in the two diets (3 and 7%, respectively).

There were no major differences in the percentages of total saturated FA between cells in the two dietary groups.

[³H]Glycerolipids in the total extracted lipid fractions from culture media and from isolated VLDL particles. There was a lower recovery of secreted radiolabeled glycerolipids in the VLDL fraction than in the total culture media (Table 2). Lipid class analysis showed that whereas TAG dominated at all time points in the VLDL fractions, it constituted only 13% of the glycerolipid fraction in the total culture media at the early time points (1 and 2 h) and increased thereafter to 87% at the later time points (Table 2). The discrepancy between the results obtained by these two analytical methods can most probably be explained by the fact that exogenously added radiolabeled glycerol exhibits a natural time lag in its appearance in secreted glycerolipids. In addition, the procedure used for VLDL isolation (density gradient centrifugation) also may influence the results. In this method, the most TAG-rich VLDL particles will be more buoyant than the VLDL particles that are less TAG-rich. Only the TAG-rich VLDL particles will therefore be col-

TABLE 1
FA Composition of the Total Lipid Fraction of the Diets and Hepatocytes Isolated from Either Soybean Oil (SO)- or Fish Oil (FO)-Fed Fish[a]

	SO diet	FO diet	SO cells	FO cells
14:0	0.9	5.7	1.9 ± 0.22[a]	2.5 ± 0.01[a]
16:0	12.7	14.0	16.2 ± 1.18[a]	15.5 ± 0.22[a]
18:0	3.7	1.6	7.9 ± 0.31[b]	4.9 ± 0.02[a]
16:1n-7	1.3	7.5	1.1 ± 0.19[a]	3.8 ± 0.21[b]
18:1n-7	1.6	2.8	1.5 ± 0.18[a]	3.6 ± 0.13[b]
18:1n-9	20.3	10.3	15.9 ± 2.18[a]	13.9 ± 0.68[a]
20:1 (sum isomers)	1.1	12.8	3.2 ± 0.37[a]	5.0 ± 0.11[b]
22:1 (sum isomers)	1.0	15.9	0.4 ± 0.06[a]	0.9 ± 0.12[b]
18:2n-6	45.4	4.4	22.4 ± 0.99[b]	2.3 ± 0.18[a]
20:2n-6	ND	ND	2.4 ± 0.71[b]	0.5 ± 0.00[a]
18:3n-3	5.3	0.8	ND	ND
20:3n-6	ND	ND	3.2 ± 0.54[b]	0.2 ± 0.20[a]
18:4n-3	0.5	3.2	0.2 ± 0.23[a]	0.5 ± 0.11[b]
20:4n-3	ND	ND	2.9 ± 1.65[b]	0.8 ± 0.15[a]
20:4n-6	ND	ND	2.9 ± 0.15[b]	1.4 ± 0.22[a]
20:5n-3	2.1	9.0	3.3 ± 0.32[a]	8.5 ± 0.40[b]
22:5n-3	0.2	0.6	1.5 ± 0.22[a]	3.0 ± 0.25[b]
22:6n-3	2.8	7.0	16.6 ± 1.11[a]	26.5 ± 0.33[b]
ΣOthers	1.1	4.4	0.2 ± 4.76[a]	6.2 ± 0.60[b]
ΣSaturated	17.3	21.3	26.0 ± 0.22[b]	22.9 ± 0.08[b]
ΣMonoene	25.3	49.3	22.1 ± 0.37[b]	27.2 ± 0.21[b]
Σn-3	10.9	21.3	24.5 ± 5.21[b]	39.3 ± 0.31[b]
Σn-6	45.4	5.3	31.0 ± 4.76[b]	4.5 ± 0.60[b]

[a]The quantity of each FA is given as a percentage of the total FA. Data are means ± SEM ($n = 3$). ND, not detectable. Values with different roman superscripts are significantly different ($P \leq 0.05$; $n = 3$).

TABLE 2
Percentage Distributions of [³H]Glycerol in TAG, MDG, and PL of Isolated VLDL Particles and in Medium[a]

Incubation	VLDL fractions			Recovery VLDL	Total media		
time (h)	TAG	MDG	PL	(%)	TAG	MDG	PL
1	81.9 ± 4.68[a]	3.4 ± 1.54[a]	14.7 ± 3.19[b]	21.0	13.3 ± 6.05[a]	9.8 ± 3.78[a]	76.9 ± 10.32[b]
2	88.3 ± 0.71[a,b]	3.5 ± 0.83[a]	8.2 ± 0.16[a,b]	32.2	30.5 ± 5.75[b]	7.9 ± 1.59[a]	61.6 ± 5.10[b]
6	93.8 ± 1.86[b]	2.4 ± 0.09[a]	3.8 ± 1.93[a]	68.1	82.5 ± 3.33[c]	4.9 ± 0.53[a]	12.6 ± 2.79[a]
24	94.4 ± 0.1[b]	1.6 ± 0.68[a]	4.0 ± 0.68[a]	91.4	87.4 ± 1.13[c]	4.2 ± 0.09[a]	8.3 ± 1.05[a]

[a]Data are shown as means ± SEM ($n = 3$). Values marked with different roman letters indicate significant differences ($P \leq 0.05$) between lipid classes. VLDL recovery was calculated as the amounts of [³H]glycerolipids recovered in the isolated VLDL fraction as a percentage of the amounts of total [³H]glycerolipids recovered in the culture medium. Isolated VLDL and total media were from hepatocyte cultures isolated from SO-fed fish. MDG, mono- + diacylglycerols; PL, phospholipids; for other abbreviations see Table 1.

lected on the top of the gradient. Based on these results, the total recovery of glycerolipids in the culture media, and not the recovery of glycerolipids in isolated VLDL fraction, was used for the further analysis of glycerolipid secretion from hepatocytes.

Effect of endogenous FA composition on the secretion of total [³H]glycerolipids. The rate of secretion of total [³H]glycerolipids (the sum of PL, MDG, and TAG) was 36% lower in hepatocytes from fish fed the FO diet than in hepatocytes from fish fed the SO diet ($P = 0.003$) (Fig. 1).

Effects of time and exogenously added FA on the secretion of [³H]glycerolipids. Figure 2 shows the secretion of total [³H]glycerolipids (the sum of PL, MDG, and TAG) after 1-, 2-, 6-, and 24-h incubations with either no FA (Ctr), 18:1n-9, 20:5n-3, 22:6n-3, or TTA. Hepatocytes from SO-fed fish secreted more esterified lipids than cells from FO-fed fish at the early time-points (1 and 2 h) irrespective of FA supplementation. Incubation of the hepatocytes with a relatively high concentration (0.75
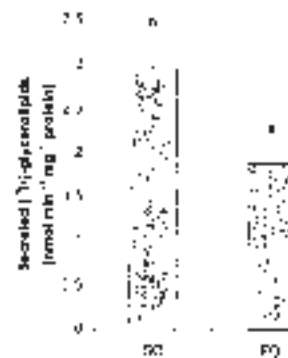
FIG. 1. Secretion rate of [³H]glycerolipids by hepatocytes from fish fed soybean oil (SO) or fish oil (FO) [the sum of TAG, mono- and diacylglyerols (MDG) and phospholipids (PL)]. The secretion rate is calculated as nmol [³H]glycerolipids secreted per min per mg protein. Data are means ± SEM ($n = 3$). The difference is significant at $P = 0.003$. Each data point (n) is the average of 20 individual measurements.
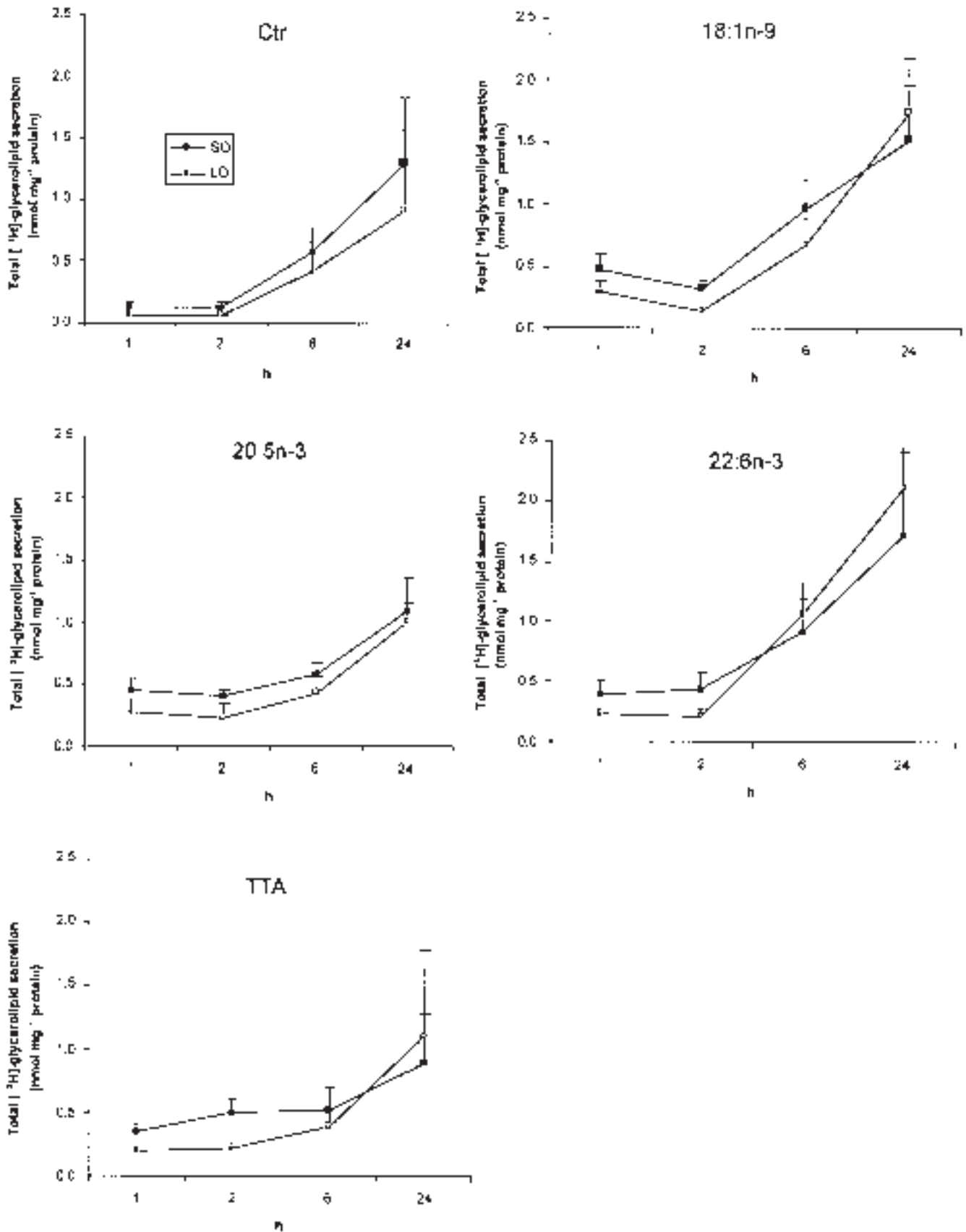
FIG. 2. Effect of exogenously added FA on the secretion of [³H]glycerolipids (the sum of TAG, MDG and PL) from fish fed SO or FO after incubations with an FA-free medium (Ctr) or media supplemented with 0.75 mM of either 18:1n-9, 20:5n-3, 22:6n-3, or tetradecylthioacetic acid (TTA) for 1, 2, 6, or 24 h. Data are means ± SEM (*n* = 3). For other abbreviations see Figure 1.
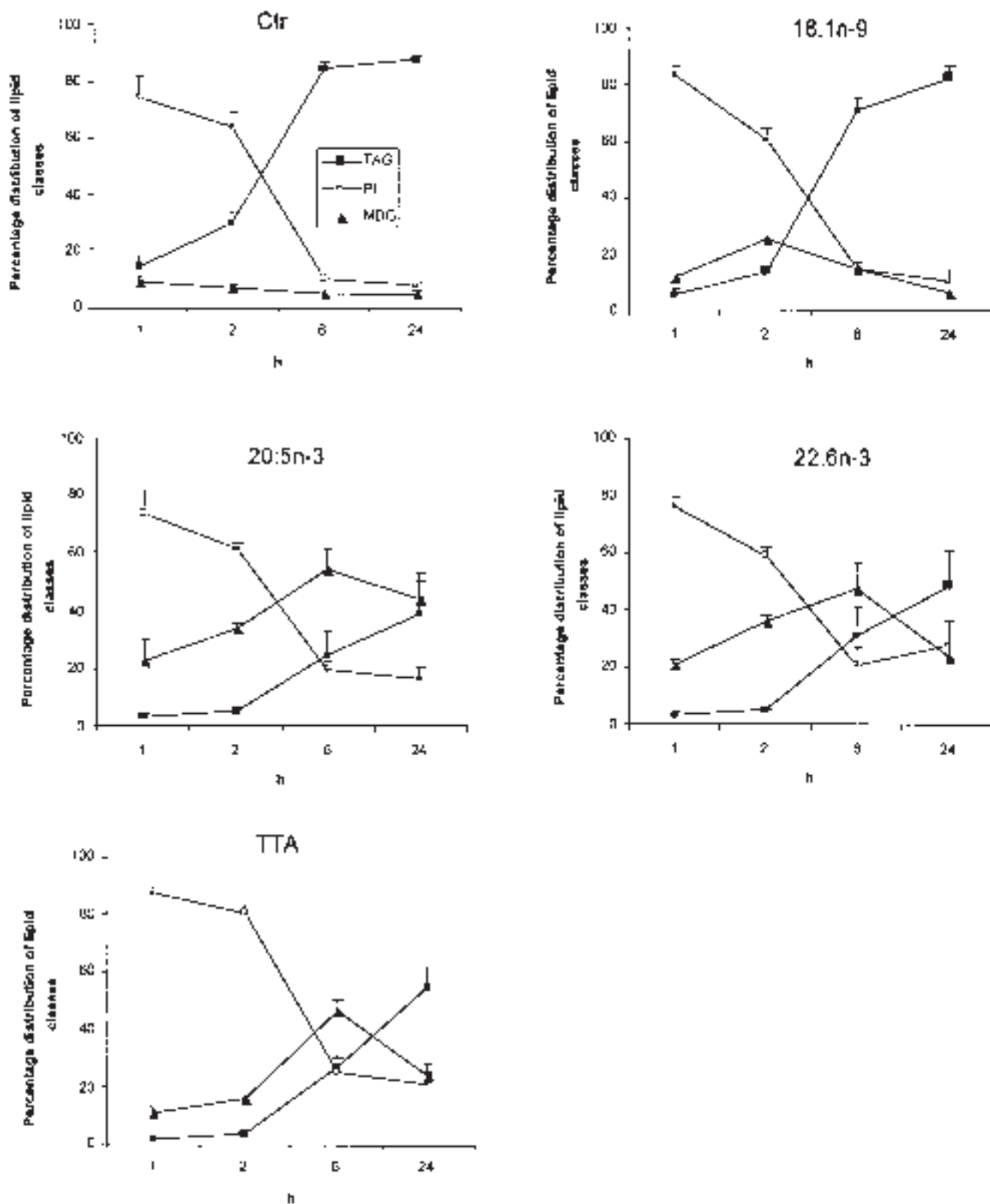
FIG. 3. Percentage distribution between the different [³H]glycerolipids (TAG, MDG, and PL) after incubations with an FA-free medium (Ctr) or media supplemented with 0.75 mM of either 18:1n-9, 20:5n-3, 22:6n-3, or TTA for 1, 2, 6, or 24 h. Each data point shown is a mean value of the two dietary groups ± SEM (*n* = 6). For abbreviations see Figures 1 and 2.

mM) of exogenously added FA for a longer period of time, however, reduced the effect of the feeding group that had been observed at 1 and 2 h. Approximately 6–7 times more [3H]glycerolipids were secreted at 24 h than at 1 h from hepatocytes incubated with 22:6n-3 or 18:1n-9, irrespective of dietary group. In comparison, there were only approximately 2–3 times more [3H]glycerolipids secreted at 24 h than at 1 h from control cells or cells incubated with 20:5n-3 or TTA. This shows that hepatocytes to which 18:1n-9 or 22:6n-3 had been added secreted [3H]glycerolipids more than twice as rapidly as control cells or cells to which 20:5n-3 or TTA had been added.

Figure 3 shows the effect of exogenously added FA on the secretion of different [3H]glycerolipid classes (TAG, MDG, and PL). No significant differences in percent distribution of glycerolipid classes were found between the two feeding groups at any time point. The results are therefore presented as mean values of the two feeding groups.

The majority of the [3H]glycerolipids secreted from all cell incubations after 24 h were in the form of TAG, except from hepatocytes incubated with 20:5n-3. The percentage of MDG secreted from the cells incubated with 20:5n-3 increased during the time period, giving a ratio of TAG to MDG of approximately 1 after 24 h of incubation. In comparison, this ratio was 23.5 in control cells after 24 h of incubation. The ratios of TAG to MDG after 24 h were approximately 10, 3, and 2.5, for cells incubated with 18:1n-9, 22:6n-3, and TTA, respectively. The secretion patterns for the different lipid classes from cells incubated with TTA were similar to those for cells incubated with 20:5n-3.

TAG secretion from 20:5n-3-treated cells was approximately 70% lower after 24 h of incubation than it was for control cells (Fig. 4). The FA 22:6n-3, in contrast to 20:5n-3, had

no major effect on the amount of TAG secreted. The only exogenously added FA that stimulated TAG secretion compared with control cells during the experiment was 18:1n-9. The amount of TAG secreted from cells incubated with TTA for 24 h was approximately 40% lower than that of control cells.

Morphometric quantification of lipid and mitochondrial area. The mitochondrial area of the hepatocytes was not affected by the composition of FA in the feed. There was a slightly higher intracellular lipid area in cells from the FO-fed fish than in cells from the SO-fed fish. Owing to a relatively high SD between the analyzed samples, the differences were, however, not significant. This allows us to present the morphometric results as mean values from all observed cells, irrespective of feeding group. The FA added to the cells in culture, on the other hand, affected the lipid area and the mitochondrial area more profoundly.

Figure 5 shows the percent area of lipid droplets and mitochondria after incubation with either no FA (Ctr), 18:1n-9, 20:5n-3, 22:6n-3, or TTA for 24 h, and Figure 6 shows representative micrographs of hepatocytes after each incubation. Lipid accumulations were observed as light and/or black droplets in the cytoplasm of hepatocytes. Cells incubated with 20:5n-3 had the largest lipid area (12.0%) (Figs. 5, 6C), whereas cells incubated with 18:1n-9 or 22:6n-3 had a significantly smaller lipid area: 4.8 and 6.7%, respectively (Figs. 5, 6B, 6D). Cells incubated with TTA had the lowest lipid area, 2%, a level similar to that of control cells (Figs. 5, 6A, 6E). The lipid area and the mitochondrial area were highly correlated (*P* = 0.002). The mitochondrial area was highest in cells incubated with 20:5n-3 (13.5%) and was significantly higher than in cells incubated with TTA (10.7%) and in control cells (9.7%), which had the lowest mitochondrial area.
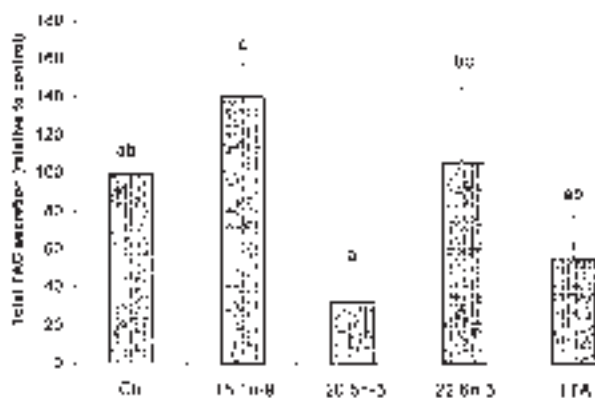
FIG. 4. Relative TAG secretion after incubations with an FA-free medium (Ctr) or media supplemented with 0.75 mM of either 18:1n-9, 20:5n-3, 22:6n-3, or TTA for 24 h. The control TAG levels are set to 100% in each incubation for both dietary groups, and the mean values of the two dietary groups are presented. The mean values of the TAG levels of the different FA incubations are presented relative to the control TAG levels. Data are means ± SEM (*n* = 6). Different letters indicate significant (*P* < 0.05) differences. For abbreviations see Figures 1 and 2.
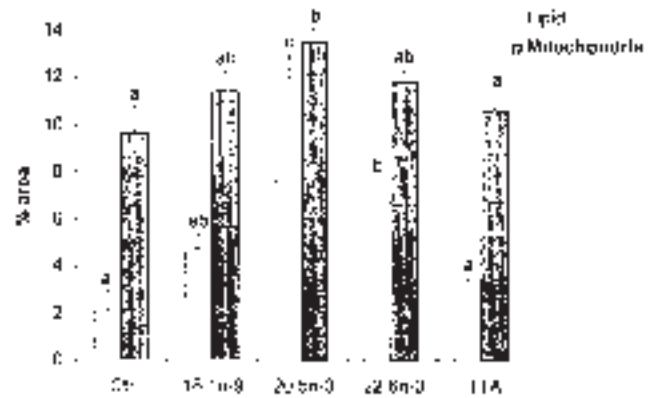
FIG. 5. Morphometrical estimates of lipid area and mitochondrial area of hepatocytes incubated for 24 h in an FA-free medium (Ctr) or media supplemented with 0.75 mM of either 18:1n-9, 20:5n-3, 22:6n-3, or TTA. Data are the relative areas of lipid droplets or mitochondria of total cell area (exclusive of the nuclei) and are shown as the mean values of the two dietary groups ± SEM (*n* = 6). Different letters indicate significant (*P* < 0.05) differences between the different FA-incubations. For abbreviation see Figure 2.
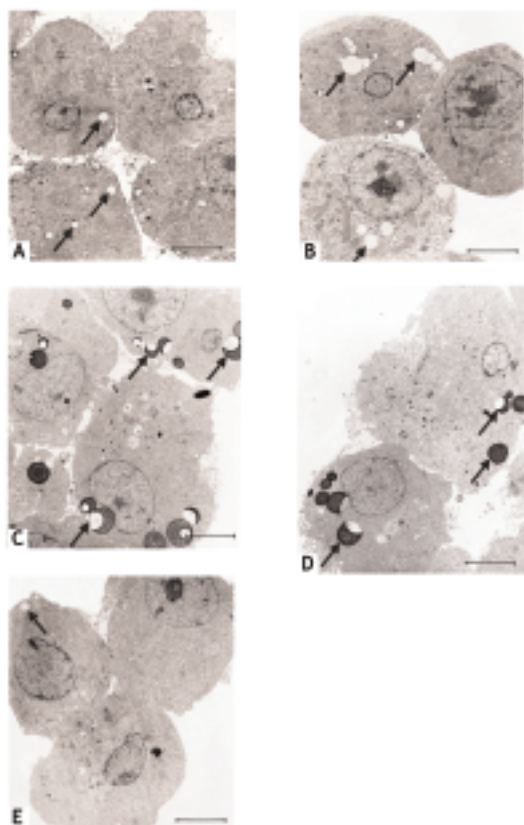
FIG. 6. Electron micrographs of hepatocytes incubated for 24 h in (A) an FA-free medium, or a medium supplemented with 0.75 mM of either (B) 18:1n-9, (C) 20:5n-3, (D) 22:6n-3, or (E) TTA. The micrographs shown are representative cells for each of the five treatments. Lipid accumulations (arrows) were observed as light and/or black droplets in the cytoplasm. The highest accumulation of lipid droplets was observed in hepatocytes incubated with 20:5n-3, whereas hepatocytes incubated with 18:1n-9 or 22:6n-3 showed a significantly lower lipid droplet area. No or only a few lipid droplets were observed in hepatocytes incubated with TTA or an FA-free medium. Bars = 5 μm. For abbreviation see Figure 2.

DISCUSSION

The endogenous FA composition of hepatocytes was influenced by the identity of the oil used as lipid source in the diet. This agrees with several studies using different types of vegetable oil in salmonid diets. Generally, the replacement of FO by SO results in higher levels of n-6 FA and lower levels of n-3 FA in the tissues of Atlantic salmon and rainbow trout (29,32–35). The marked differences in FA composition due to the diets had a pronounced effect on the secretion of glycerolipids. Lipid secretion from hepatocytes from fish fed the FO diet was 36% lower than the secretion from hepatocytes from fish fed the SO diet. A number of *in vivo* studies in mammals during the past few decades have shown that FO diets inhibit lipid secretion by hepatocytes (2,16,36). Our results from fish hepatocytes agree with the findings from mammals and show that an endogenous FA composition with a high n-6/n-3 ratio promotes lipid secretion to a level that is higher than that with a lower n-6/n-3 ratio. Other components in diets however,

may also influence the TAG-rich lipoprotein secretion from hepatocytes. SO may contain significant quantities of lecithin (37), whereas FO may contain relatively high levels of cholesterol (38), both of which are known to modify lipoprotein metabolism in mammals (39–41). We do not know whether dietary lecithin and cholesterol affect these processes in fish, but this topic will be important for further studies.

The mechanisms by which FO in the diet reduces TAG secretion in fish are not known, nor have they been completely elucidated in mammals. However, several mechanisms and regulatory sites may be involved. The present study demonstrates that 20:5n-3, and not 22:6n-3, inhibits TAG secretion in salmon hepatocytes, in accordance with the results of many studies in rat hepatocytes (13–15,17,19,42,43). Studies in mammals have shown that dietary FO interferes with the assembly of the initial VLDL precursor particles in hepatocytes and inhibits VLDL secretion in this way (9,10,16,44,45). Whether VLDL secretion in fish is regulated in the same manner is not known.

Several studies in mammals have shown that 20:5n-3 reduces the availability of intracellular TAG for incorporation into VLDL by inhibiting the activity of DGAT (13,14), that is, the enzyme catalyzing the conversion of 1,2DAG into TAG (13–15,19). In contrast, 22:6n-3 does not affect DGAT activity in rat hepatocytes (14). Although we did not measure the activity of DGAT, the reduced lipid secretion from hepatocytes incubated with 20:5 n-3 has led us to suggest that DGAT also may be a regulated step in fish. The inhibition of TAG synthesis should occur before or at the DGAT step, since the ratio of TAG to MDG secreted from these cells is lower than that secreted from control cells. The seemingly contradictory results of a reduced DGAT activity and the observed increase in intracellular lipid level in 20:5n-3 treated cells may be explained by an inhibiting effect of 20:5n-3 on the VLDL assembly step, leading to a net increase in cytosolic lipid droplets. Many factors seem to affect the different steps of the lipid secretion process and its regulation, and we cannot on the basis of our results draw conclusions about which regulatory mechanisms are most important for the lowering effect of 20:5n-3 on TAG secretion. However, lipid class composition of cellular lipids may give valuable additional information about the DGAT activity and TAG synthesis.

Furthermore, several studies in mammals have shown that 20:5n-3 reduces TAG secretion by stimulating mitochondrial β-oxidation, thus reducing the availability of FA for TAG synthesis (15,18,42), whereas 22:6n-3 is a poor substrate for mitochondrial β-oxidation in rats (14,15). Frøyland *et al.* (18) showed that the plasma TAG level decreased in rats fed 20:5n-3, but not in rats fed 22:6n-3. The decrease was caused by an increase in the number of mitochondria and an increase in the level of mitochondrial β-oxidation. We have not measured the activities of enzymes involved in β-oxidation. However, we have shown that incubation with 20:5n-3 leads to an increased mitochondrial area and that it reduces the secretion of glycerolipids. These results suggest that 20:5n-3 also stimulates the capacity of mitochondria to β-oxidize FA in salmon.

The microscopy study revealed only normal-sized mitochondria in all hepatocyte samples, without any observations of megamitochondria. Other investigators have found more dramatic effects on mitochondrial number and size after feeding trials in rats. It has been shown that EPA may initiate a signal for megamitochondria formation and subsequent proliferation (30,46). We suggest that a 24-h incubation is too short a time to achieve megamitochondria formation and high mitochondrial proliferative activity in our cell culture experiment. The observed increase in mitochondrial area in EPA-treated cells can therefore be a result of a moderate increase in the number of mitochondria.

The relative area of lipid droplets was highly correlated ($P = 0.002$) with the relative area of mitochondria, and both were significantly higher in cells incubated with 20:5n-3 than they were in control cells. It may be that the amount of accumulated lipid *per se* induces mitochondrial proliferation directly by an unknown mechanism, and that the potency of 20:5n-3 as a mitochondrial proliferator in salmon hepatocytes is related to the increased intracellular lipid level estimated in the cells through lipid droplet areas.

Although 22:6n-3 had no effect on TAG secretion, this FA resulted in the highest secretion of total glycerolipids. This was mainly due to a higher incorporation of 22:6n-3 into secreted PL. Previous results from salmon hepatocytes showed that 22:6n-3 was preferentially incorporated and conserved in PL (47,48).

Cells incubated with TTA secreted less TAG than control cells, in accordance with studies in mammals showing that TTA inhibits TAG secretion (14,21). This FA analog directs FA away from esterification and toward FA oxidation in rats (14,17,21) through regulations resulting in increased activities of enzymes involved in mitochondrial and peroxisomal β-oxidation (18,30), and by inhibiting DGAT (14).

We have shown that 18:1n-9 stimulates TAG secretion, which is in accordance with results from rat hepatocytes (13,19,43). However, the observed stimulating effect of SO and 18:1n-9 on lipid secretion, and the reported negative effects of some vegetable oils on fish heart histology (49,50), should be considered. These effects may give rise to problems that are similar to problems related to coronary heart diseases in humans. Such problems have been linked to a diet low in n-3 FA (1–4).

In conclusion, we have shown that lipids are secreted from cultivated salmon hepatocytes at a rate that is significantly lower in fish fed a diet containing FO as the only lipid source than in fish given a diet that has been supplemented with SO. Further, we have shown that 20:5n-3, and not 22:6n-3, somehow mediates this effect, whereas 18:1n-9 stimulates TAG secretion to levels that are higher than those in control cells. Our results indicate that in dietary FO, 20:5n-3 is the FA that reduces TAG secretion in fish and may be responsible for the hypotriglyceridemic effect of FO observed in fish and humans.

ACKNOWLEDGMENTS

REFERENCES

1. Harris, W.S., Connor, W.E., and McMurphy, M.P. (1983) The Comparative Reductions of the Plasma Lipids and Lipoproteins by Dietary Polyunsaturated Fats: Salmon Oil versus Vegetable Oils, *Metabolism 32*, 179–184.
2. Nestel, P.J. (1990) Effects of n-3 Fatty Acids on Lipid Metabolism, *Annu. Rev. Nutr. 10*, 149–167.
3. Bang, H.O., Dyerberg, J., and Nielsen, A.B. (1971) Plasma Lipid and Lipoprotein Pattern in Greenlandic West-Coast Eskimos, *Lancet 1*, 1143–1145.
4. Phillipson, B.E., Rothrock, D.W., Connor, W.E., Harris, W.S., and Illingworth, D.R. (1985) Reduction of Plasma Lipids, Lipoproteins and Apoproteins by Dietary Fish Oils in Patients with Hypertriglyceridemia, *N. Engl. J. Med. 312*, 1210–1216.
5. Farrell, A.P. (2002) Coronary Arteriosclerosis in Salmon: Growing Old or Growing Fast? *Comp. Biochem. Physiol. A Mol. Integr. Physiol. 132*, 723– 735.
6. Childs, M.T., King, I.B., and Knopp, R.H. (1990) Divergent Lipoprotein Responses to Fish Oils with Various Ratios of Eicosapentaenoic Acid and Docosahexaenoic Acid, *Am. J. Clin. Nutr. 52*, 632–639.
7. Rambjor, G.S., Walen, A.I., Windsor, S.L., and Harris, W.S. (1996) Eicosapentaenoic Acid Is Primarily Responsible for the Hypotriglyceridemic Effect of Fish Oil in Humans, *Lipids 31*, S45–S49.
8. Otto, D.A., Tsai, C.E., Baltzell, J.K., and Wooten, J.T. (1991) Apparent Inhibition of Hepatic Triacylglycerol Secretion, Independent of Synthesis, in High-Fat Fish Oil-Fed Rats: Role for Insulin, *Biochim. Biophys. Acta 1082*, 37–48.
9. Lang, C.A., and Davis, R.A. (1990) Fish Oil Fatty Acids Impair VLDL Assembly and/or Secretion by Cultured Rat Hepatocytes, *J. Lipid Res. 31*, 2079–2086.
10. Brown, A.M., Castle, J., Hebbachi, A.M., and Gibbons, G.F. (1999) Administration of n-3 Fatty Acids in the Diets of Rats or Directly to Hepatocyte Cultures Results in Different Effects on Hepatocellular ApoB Metabolism and Secretion, *Arterioscler. Thromb. Vasc. Biol. 19*, 106–114.
11. Zheng, X., Avella, M., and Botham, K.M. (2001) Comparison of the Effects of Dietary n-3 and n-6 Polyunsaturated Fatty Acids on Very Low-Density Lipoprotein Secretion When Delivered to Hepatocytes in Chylomicron Remnants, *Biochem. J. 357*, 481–487.
12. Haagsman, H.P, de Haas, C.G., Geelen, M.J., and van Golde, L.M. (1982) Regulation of Triacylglycerol Synthesis in the Liver. Modulation of Diacylglycerol Acyltransferase Activity *in vitro*, *J. Biol. Chem. 257*, 10593–10598.
13. Rustan, A.C., Nossen, J.Ø., Christiansen, E.N., and Drevon, C.A. (1988) Eicosapentaenoic Acid Reduces Hepatic Synthesis and Secretion of Triacylglycerol by Decreasing the Activity of Acyl-Coenzyme A:1,2-Diacylglycerol Acyltransferase, *J. Lipid Res. 29*, 1417–1426.
14. Berge, R.K., Madsen, L., Vaagenes, H., Tronstad, K.J., Göttlicher, M., and Rustan, A.C. (1999) In Contrast with Docosahexaenoic Acid, Eicosapentaenoic Acid and Hypolipidaemic Derivatives Decrease Hepatic Synthesis and Secretion of Triacylglycerol by Decreased Diacylglycerol Acyltransferase Activity and Stimulation of Fatty Acid Oxidation, *Biochem. J. 343*, 191–197.
15. Madsen, L., Rustan, A.C., Vaagenes, H., Berge, K., Dyrøy, E., and Berge, R.K. (1999) Eicosapentaenoic and Docosahexaenoic Acid Affect Mitochondrial and Peroxisomal Fatty Acid Oxidation in Relation to Substrate Preference, *Lipids 34*, 951–963.
16. Kendrick, J.S., and Higgins, J.A. (1999) Dietary Fish Oils Inhibit Early Events in the Assembly of Very Low Density Lipoproteins and Target ApoB for Degradation Within the Rough Endoplasmic Reticulum of Hamster Hepatocytes, *J. Lipid Res. 40*, 504–514.
17. Frøyland, L., Vaagenes, H., Asiedu, D.K., Garras, A., Lie, Ø., and Berge, R.K. (1996) Chronic Administration of Eicosapentaenoic Acid and Docosahexaenoic Acid as Ethyl Esters Reduced Plasma Cholesterol and Changed the Fatty Acid Composition in Rat Blood and Organs, *Lipids 31*, 169–178.

18. Frøyland, L., Madsen, L., Vaagenes, H., Totland, H., Auwerx, J., Kryvi, H., Staels, B., and Berge, R.K. (1997) Mitochondrion Is the Principal Target for Nutritional and Pharmacological Control of Triglyceride Metabolism, *J. Lipid Res. 38*, 1851–1858.

19. Nossen, J.Ø., Rustan, A.C., Gloppestad, S.H., Målbakken, S., and Drevon, C.A. (1986) Eicosapentaenoic Acid Inhibits Synthesis and Secretion of Triacylglycerols by Cultured Rat Hepatocytes, *Biochim. Biophys. Acta 879*, 56–65.

20. Berge, R.K., Skorve, J., Tronstad, K.J., Berge, K., Gudbrandsen, O.A., and Grav, H. (2002) Metabolic Effects of Thia Fatty Acids, *Curr. Opin. Lipidol. 13*, 295–304.

21. Skrede, S., Bremer, J., Berge, R.K., and Rustan, A.C. (1994) Stimulation of Fatty Acid Oxidation by a 3-Thia Fatty Acid Reduces Triacylglycerol Secretion in Cultured Rat Hepatocytes, *J. Lipid Res. 35*, 1395–1404.

22. Grisdale-Helland, B., Ruyter, B., Rosenlund, G., Obach, A., Helland, S.J., Sandberg, M.G., Standal, H., and Røsjø, C. (2002) Influence of High Contents of Dietary Soybean Oil on Growth, Feed Utilization, Tissue Fatty Acid Composition, Heart Histology and Standard Oxygen Consumption of Atlantic Salmon (*Salmo salar*) Raised at Two Temperatures, *Aquaculture 207*, 311–329.

23. Seglen, P.O. (1976) Preparation of Isolated Rat Liver Cells, *Methods Cell Biol. 1*, 29–59.

24. Dannevig, B.H., and Berg, T. (1985) Endocytosis of Galactose-Terminated Glycoproteins by Isolated Liver Cells of Rainbow Trout, *Comp. Biochem. Physiol. 82B*, 683–688.

25. Lowry, O.H., Rosebrough, N.J., Farr, A.L., and Randall, R.J. (1951) Protein Measurement with the Folin Phenol Reagent, *J. Biol. Chem. 193*, 265–275.

26. Chung, B.H., Wilkinson, T., Geer, J.C., and Segrest, J.P. (1980) Preparative and Quantitative Isolation of Plasma Lipoproteins: Rapid, Single Discontinuous Density Gradient Ultracentrifugation in a Vertical Rotor, *J. Lipid Res. 21*, 284–291.

27. Burnette, W.N. (1981) 'Western Blotting': Electrophoretic Transfer of Proteins from Sodium Dodecylsulfate–Polyacrylamide Gels to Unmodified Nitrocellulose and Radiographic Detection with Antibody and Radioiodinated Protein A, *Anal. Biochem. 112*, 195–203.

28. Folch, J., Lees, M., and Sloane-Stanley, G.M. (1957) A Simple Method for Isolation and Purification of Total Lipids from Animal Tissues, *J. Biol. Chem. 226*, 497–509.

29. Ruyter, B., Røsjø, C., Grisdale-Helland, B., Rosenlund, G., Obach, A., and Thomassen, M.S. (2003) Influence of Temperature and High Dietary Linoleic Acid Content on Esterification, Elongation, and Desaturation of PUFA in Atlantic Salmon Hepatocytes, *Lipids 38*, 833–840.

30. Hexeberg, S., Frøyland, L., Asiedu, D.K., Demoz, A., and Berge, R.K. (1995) Tetradecylthioacetic Acid Reduces the Amount of Lipid Droplets, Induces Megamitochondria Formation and Increases the Fatty Acid Oxidation in Rat Heart, *Mol. Cell. Cardiol. 27*, 1851–1857.

31. SAS (1990) *SAS/STAT User's Guide*, SAS Institute, Cary, NC, 1686 pp.

32. Hardy, R.W., Scott, T.M., and Harrell, L.W. (1987) Replacement of Herring Oil with Menhaden Oil, Soybean Oil, or Tallow in the Diets of Atlantic Salmon Raised in Marine Net-Pens, *Aquaculture 65*, 267–277.

33. Thomassen, M.S., and Røsjø, C. (1989) Different Fats in Feed for Salmon: Influence on Sensory Parameters, Growth Rate and Fatty Acids in Muscle and Heart, *Aquaculture 79*, 129–135.

34. Greene, D.H.S., and Selivonchick, D.P. (1990) Effects of Dietary Vegetable, Animal and Marine Lipids on Muscle Lipid and Hematology of Rainbow Trout (*Oncorhynchus mykiss*), *Aquaculture 89*, 165–182.

35. Finstad, B., and Thomassen, M.S. (1991) Does Dietary Lipid Composition Affect the Osmoregulatory Ability of Rainbow Trout (*Oncorhynchus mykiss*) at High and Low Temperatures? *Comp. Biochem. Physiol. 99A*, 463–471.

36. Willumsen, N., Vaagenes, H., Lie, Ø., Rustan, A.C., and Berge, R.K. (1996) Eicosapentaenoic Acid, but Not Docosahexaenoic Acid, Increases Mitochondrial Fatty Acid Oxidation and Upregulates 2,4-Dienol-CoA Reductase Gene Expression in Rats, *Lipids 31*, 579–592.

37. Chazan, J.B. (1996) Pharmacological and Dietetic Properties of Oils and Fats, in *Oils and Fats Manual*, (Karleskind, A., ed.), Vol. 1, pp. 675–702, Intercept Limited, Andover, Hants., United Kingdom.

38. Sébédio, J.L. (1996) Marine Oils, in *Oils and Fats Manual*, (Karleskind, A., ed.), Vol. 1, pp. 266–276, Intercept Limited, Andover, Hants., United Kingdom.

39. Mastellone, I., Polichetti, E., Gres, S., de la Maisonneuve, C., Domingo, N., Marin, V., Lorec, A.M., Farnarier, C., Portugal, H., Kaplanski, G., and Chanussot, F. (2000) Dietary Soybean Phosphatidylcholines Lower Lipidemia: Mechanisms at the Levels of Intestine, Endothelial Cell, and Hepato-biliary Axis, *J. Nutr. Biochem. 11*, 461–466.

40. LeBlanc, M.J., Brunet, S., Bouchard, G., Lamireau, T., Yousef, I.M., Gavino, V., Levy, E., and Tuchweber, B. (2003) Effects of Dietary Soybean Lecithin on Plasma Lipid Transport and Hepatic Cholesterol Metabolism in Rats, *J. Nutr. Biochem. 14*, 40–48.

41. Madani, S., Frenoux, J.M., Prost, J., and Belleville J. (2004) Changes in Serum Lipoprotein Lipids and Their Fatty Acid Compositions and Lipid Peroxidation in Growing Rats Fed Soybean Protein Versus Casein With or Without Cholesterol, *Nutrition 20*, 554–563.

42. Aarsland, A., Lundquist, M., Borretsen, B., and Berge, R.K. (1990) On the Effect of Peroxisomal β-Oxidation and Carnitine Palmitoyltransferase Activity by Eicosapentaenoic Acid in Liver and Heart from Rats, *Lipids 25*, 546–548.

43. Martin, L.J., Reaidi, G.B., Gavino, G.R., and Gavino, V.C. (1991) Effect of 4,7,10,13,16,19-Docosahexaenoic Acid on Triglyceride Accumulation and Secretion in Rat Hepatocytes in Culture, *Lipids 26*, 374–380.

44. Wang, H.X., Chen, X., and Fisher, E.A. (1993) n-3 Fatty Acids Stimulate Intracellular Degradation of Apoprotein B in Rat Hepatocytes, *J. Clin. Invest. 91*, 1380–1389.

45. Botham, K.M., Zheng, X., Napolitano, M., Avella, M., Cavallari, C., Rivabene, R., and Bravo, E. (2003) The Effects of Dietary n-3 Polyunsaturated Fatty Acids Delivered in Chylomicron Remnants on the Transcription of Genes Regulating Synthesis and Secretion of Very Low-Density Lipoprotein by the Liver: Modulation by Cellular Oxidative State, *Exp. Biol. Med. 228*, 143–151.

46. Totland, G.K., Madsen, L., Klementsen, B., Vaagenes, H., Kryvi, H., Frøyland, L., Hexeberg, S., and Berge, R. (2000) Proliferation of Mitochondria and Gene Expression of Carnitine Palmitoyltransferase and Fatty Acyl-CoA Oxidase in Rat Skeletal Muscle, Heart and Liver by Hypolipidemic Fatty Acids, *Biol. Cell 92*, 317–329.

47. Ruyter, B., and Thomassen, M.S. (1999) Metabolism of n-3 and n-6 Fatty Acids in Atlantic Salmon Liver: Stimulation by Essential Fatty Acid Deficiency, *Lipids 34*, 1167–1176.

48. Ruyter, B., Røsjø, C., Einen, O., and Thomassen, M.S. (2000) Essential Fatty Acids in Atlantic Salmon: Time Course of Changes in Fatty Acid Composition of Liver, Blood and Carcass Induced by a Diet Deficient in n-3 and n-6 Fatty Acids, *Aquacult. Nutr. 6*, 109–117.

49. Bell, J.G., McVicar, A.H., Park, M.T., and Sargent, J.R. (1991) High Dietary Linoleic Acid Affects the Fatty Acid Compositions of Individual Phospholipids from Tissues of Atlantic Salmon (*Salmo salar*): Association with Stress Susceptibility and Cardiac Lesion, *J. Nutr. 121*, 1163–1172.

50. Bell, J.G., Dick, J.R., McVicar, A.A., Sargent, J.R., and Thompson, K.D. (1993) Dietary Sunflower, Linseed and Fish Oils Affect Phospholipid Fatty Acid Composition, Development of Cardiac Lesions, Phospholipase Activity and Eicosanoid Production in Atlantic Salmon (*Salmo salar*), *Prostaglandins Leukotrienes Essent. Fatty Acids 49*, 665–673.

Changes in Phosphatidylcholine Molecular Species in the Shrimp *Macrobrachium borellii* in Response to a Water-Soluble Fraction of Petroleum

Sabrina Lavarías, Marcos S. Dreon, Ricardo J. Pollero, and Horacio Heras*

Instituto de Investigaciones Bioquímicas de La Plata (INIBIOLP), Consejo Nacional de Investigaciones Científicas y Técnicas (CONICET)–Cátedra de Bioquímica, Universidad Nacional de La Plata (UNLP), (1900) La Plata, Argentina

ABSTRACT: The effect of the water-soluble fraction (WSF) of crude oil on lipid contents, lipid classes, FA, and PC molecular species was studied in high-phospholipid (hepatopancreas) and low-phospholipid (egg) tissues of a freshwater crustacean. After a 21-d exposure to a sublethal concentration of WSF, a significant decrease in shrimp total lipids was observed, although no alterations could be detected in the hepatopancreas or egg lipid contents. TAG/phospholipid ratios increased in the hepatopancreas and decreased in the eggs, suggesting alterations either in the mobilization of TAG to phospholipid pools or in the energy balance. The FA composition of phosphoglycerides in the hepatopancreas and eggs was dominated by PUFA, whereas the n-3/n-6 ratio was not affected by WSF exposure, although there was a significant increase in hepatopancreas 18:1n-9. Analysis of the PC molecular species by HPLC-ELSD showed the presence of 15 species, with 16:0/18:1, 18:1/18:2, 16:0/20:5, and 16:1/20:5 being the major species in the hepatopancreas. The PC molecular species in the eggs showed a different pattern, dominated by 16:0/18:1 and 18:1/18:2. Of the PC molecular species, 10 contained 22:6n-3, 20:5n-3, and 20:4n-6. Small amounts of di-PUFA species were also found. Exposure to WSF altered the PC molecular species in both tissues. The four major hepatopancreas molecular species and most of the ones containing PUFA decreased. This was compensated for by an increase in 16:1/18:1 (152%) and 18:1/18:1 (50%). The two major egg PC molecular species decreased, whereas the PUFA-containing ones increased. The contrasting responses of both tissues to WSF contamination suggests the presence of different homeostatic mechanisms.

Paper no. L9587 in *Lipids 40*, 487–494 (May 2005).

The freshwater shrimp *Macrobrachium borellii* is a decapod crustacean widespread in South America that lives in turbid, tepid waters such as the ones in the Río de La Plata estuary (1,2). In several past studies the lipid composition and metabolism of *M. borellii* were investigated. Phospholipids (PL) and TAG were identified as the main lipid classes in adult tissues and eggs, respectively (3–5). Monounsaturated FA were the major group in egg TAG, whereas PUFA were the major group in PL after embryo organogenesis and in the total lipids of adult

tissues (4,5). PL classes and their FA composition play a key role in the structure and function of most cellular membranes, including *M. borellii* membranes, whose main PL class is PC (6,7). Knowledge of the molecular species of PL is important for understanding the membrane properties and functions (8). However, unlike vertebrates, few reports are available on the molecular species of PL in invertebrates (9–13), and none are available on the effect of the water-soluble fraction (WSF) of petroleum hydrocarbons (HC) on them.

When lipophilic contaminants such as petroleum HC are taken up by organisms, they partition at some equilibrium level between water and the lipids of the organism and become bioconcentrated in lipid compartments such as membranes, lipoproteins, and lipid storage tissues (14). Benthic organisms are known to accumulate HC directly from the water column or from the interstitial water in the sediment (15). Thus, *M. borellii* was chosen because it is a species with ecological relevance in the Río de La Plata estuary in which we had previously studied the bioaccumulation and biodepuration rates of WSF; we had observed that lipid compartments retain polyaromatic HC for long periods of time (16). Oil spills occur periodically in the Río de La Plata estuary, which has become the most contaminated region in the country in terms of HC (17). In the present study, we investigated the use of molecular species of PL as a potential biochemical marker for HC pollution. The effect of WSF on the lipid content and lipid class composition of *M. borellii* was examined. Changes in the pattern of PC molecular species after exposure to a sublethal concentration of HC are described.

EXPERIMENTAL PROCEDURES

Sample collection. Adult *M. borellii* were sampled during the spring and summer (October to February) in a watercourse free of petrogenic contamination close to the Rio de La Plata River in Argentina (20 km southwest of La Plata city), with temperatures ranging from 21 to 28°C. Ovigerous females with eggs were collected for the experiments in early summer, and adults were collected in the spring for another set of experiments. They were taken to the laboratory and kept in dechlorinated tap water at 24 ± 2°C and a 14-h light/10-h dark photoperiod for at least a week before the experiments (18). The eggs were removed from the pleopods of the ovigerous females and

*To whom correspondence should be addressed at INIBIOLP, Fac. Medicina, Universidad Nacional de La Plata, Calles 60 y 120, (1900) La Plata, Argentina. E-mail: h-heras@atlas.med.unlp.edu.ar

Abbreviations: HC, hydrocarbon(s); HP-TLC, high-performance thin-layer chromatography; PL, phospholipids; WSF, water-soluble fraction.

checked under a stereoscopic microscope to determine the stage of development (19).

Preparation of the WSF of crude oil. Light crude oil obtained from Punta Loyola (Santa Cruz, Argentina), stored at 4°C, was used to prepare the WSF. The oil was stirred in a 10-L stainless-steel mixing vessel equipped with a mechanical stirrer and a bottom drain, and was kept in a cold room at 4°C. Crude oil and fresh water in a ratio of 1:100 (vol/vol) were stirred at a low speed for 24 h and allowed to settle for an additional 48 h (shorter settling times produced a fraction with dispersed oil droplets). The WSF was collected daily using the bottom drain. During the experiments, fresh batches of WSF were prepared every 2 d, and a sample was extracted and analyzed by GLC following the method described by Lavarías *et al.* (16).

Exposure to WSF. Groups of 10 adults or 4 ovigerous females carrying eggs at developmental stage 3 (19) were placed into 750-mL glass flasks with air-tight screw-capped lids to avoid the loss of HC. The number of individuals per flask was selected to ensure the appropriate concentration of dissolved oxygen, which was checked daily. To evaluate the effect of WSF exposure on lipids in either the whole organism, hepatopancreas, or eggs, three groups were used as a control and another three were exposed to a sublethal concentration of WSF (0.6 ppm, chosen from the results of a previous study) (16). Shrimp were exposed for 21 d without being fed, and the WSF was replaced daily. After exposure, the eggs were removed from the female pleopods, the hepatopancreas was dissected from the adults, and the total weight of the samples was recorded. All animals per group were pooled at the end of the experiment. Individuals were dried on an absorbant tissue, weighed on a semi-analytical balance with 0.01-mg accuracy, and dissected; the size of the animals was homogeneous. Weight differences among the samples were minor, and mortality was always less than 10% of animals in the control and exposed groups.

Lipid extraction and analysis. Tissues were immediately homogenized in a Potter-type homogenizer (Thomas Scientific, Swedesboro, NJ) using 0.02 M Tris-HCl buffer, pH 7.5, and a subsample was taken for protein analysis for another experiment. For the analysis of whole organisms, homogenization was performed using an UltraTurrax tissue disrupter (Janke and Kunkel, Ika Werk, Germany). Lipids were extracted with a chloroform/methanol mixture following the method of Bligh and Dyer (20). Each group was analyzed separately.

The total lipid concentration was determined gravimetrically in an aliquot of chloroform, and the rest was kept in hexane under a nitrogen atmosphere at −70°C until further analysis.

A lipid class analysis was performed by TLC on silica gel Chromarods (type S-III) with quantification by FID using an Iatroscan TH-10, Mark III (Iatron Laboratories Inc., Tokyo, Japan), as described by Parrish and Ackman (21). The separation was conducted with a sequence of three different solvent systems according to Ackman *et al.* (22). The first development was carried out for 45 min in hexane/ethyl acetate/diethyl

ether/formic acid (91:6:3:1, by vol). The Chromarods were dried, partially scanned to analyze the neutral lipids, and then developed in acetone for 15 min to quantify the carotenoid peak. Finally, the Chromarods were developed in chloroform/methanol/formic acid/water (50:30:4:2, by vol) for 60 min and completely scanned to reveal the different PL. Tetracosanol was used as an internal standard, and quantification was performed using the calibration curves of authentic standards run under the same conditions. Carotenoids from the shrimp were purified for use as standards to avoid error caused by differing responses of the FID to different carotenoids. The lipids were identified as described previously (5).

FA analysis. Preparative high-performance TLC (HP-TLC) (Merck, Darmstadt, Germany) was used to isolate the neutral lipids from the polar lipids, as described previously (5). FAME from PL were prepared using a base-catalyzed transesterification microscale procedure according to Christie (23). Amidebound FA, like those in sphingomyelin, are not affected by alkaline transesterification; therefore, the PL FA analyzed came mainly from the PC and PE in this species. FAME were analyzed by GLC on an Omegawax 250 (30 m × 0.25 mm, 0.25 μm film; Supelco, Bellefonte, PA) capillary column in a Hewlett-Packard HP-6890 equipped with a FID. The column temperature was programmed for a linear increase of 3°C/min from 175 to 230°C. FA were identified by their characteristic retention times and by co-injecting the sample with authentic standards (Supelco, St. Louis, MO) or a FAME mixture of established composition run under the same conditions.

PC molecular species. PL fractions were isolated from lipid extracts by HPLC using a Merck-Hitachi L-6200 Intelligent pump (Hitachi Ltd., Tokyo, Japan). An Evaporative Light-Scattering Detector 500 (Alltech Associates Inc., Deerfield, IL) operating at a nitrogen flow rate of 2.2 mL/min and a drift tube temperature of 90°C was used for detection. To purify the PC, an Econosil Silica column (250 × 4.6 mm × 10 μm; Alltech Associates Inc.) and a guard column packed with the same material were used. Elution was performed as described elsewhere (24). PC was collected manually, the eluate was evaporated to dryness under a stream of nitrogen, and the PC was redissolved in chloroform/methanol (1:1, vol/vol).

Resolution of the PC molecular species was performed on two end-capped Lichrosphere 100 RP18 columns in series (250 × 4 mm; Merck, Darmstadt, Germany). Isocratic elution was applied with a mobile phase composed of acetonitrile/methanol/triethylamine (40:58:2, by vol) (25). Detection and quantification were done by ELSD using nitrogen as the nebulizer gas at a flow of 1.8 L/min and a temperature of 100°C (24).

The column eluate was collected every 30 s using an LKB 2212 Helirac fraction collector (Bromma, Sweden). The individual PC molecular species were identified by determining the FA composition of each peak by GLC as described, and its relative abundance was calculated from the areas of the peaks.

Statistical analyses. Data collected from all experiments were analyzed by ANOVA using Instat, v. 2.0 (GraphPad, San Diego, CA). Data were transformed prior to performing the statistical procedures. Results were considered significant at a level of 5%.

Total Lipid Concentration of Whole Organisms, Hepatopancreas, and Eggs of *Macrobrachium borellii* from Control and Water-Soluble Fraction (WSF)-Exposed Organisms[a]

	Control	WSF-exposed
Whole	11.2 ± 0.5	9.5 ± 0.2*
Hepatopancreas	11.3 ± 1.8	13.5 ± 4.2
Eggs	83.0 ± 5.1	90.3 ± 10.4

[a]Values are the means of triplicate analyses ± 1 SD and are expressed as mg/g wet weight. *$P < 0.05$.

RESULTS

Changes in lipid content and composition by WSF exposure. After a 21-d exposure to WSF, the total lipid concentrations of exposed animals decreased significantly compared with control organisms; however, the total lipid concentrations of the hepatopancreas and eggs did not vary significantly (Table 1).

To determine the effect of WSF on the lipids, each lipid class was studied separately in the adult hepatopancreas and eggs of control and exposed organisms. We also checked the muscle, but no changes were observed; therefore, it was not included in the present study. PL were the major lipids in the hepatopancreas, accounting for 74.4%, by weight of the total lipids, whereas egg lipids were dominated by TAG, representing 69.5% of the total lipids. This markedly different lipid composition provided us with two contrasting models within the same species to study the effect of HC contamination. After a 21-day exposure to WSF, both the hepatopancreas and eggs showed significant changes in their lipid class composition. The hepatopancreas showed a significant decrease in PL as well as a decrease in the carotenoid pigment (Table 2). PC in particular, representing the major lipid class in this tissue, showed a significant reduction from 62 to 53% by wet weight ($P < 0.05$) in WSF-exposed animals. However, the average sphingomyelin concentration in the WSF-exposed hepatopancreas was almost two times higher than the hepatopancreas control (Table 2). The eggs, in contrast, showed a significant decrease (more than 11%) in TAG reserves in WSF-exposed embryos compared with the percentage in controls. In addition, there was an overall increase in PL, whereas the carotenoid pig-

ment did not change significantly in WSF-exposed eggs (Table 2). The PL/TAG ratio decreased in the hepatopancreas of WSF-exposed animals because of the decrease in PL, whereas in the eggs the ratio increased from 0.4 to 0.6, reflecting both the decrease in TAG and the increase in PL (Table 2).

FA. Table 3 shows the FA profiles of phosphoglycerides from the hepatopancreas and eggs of control and WSF-exposed organisms. Regardless of treatment, EPA (20:5n-3) was the major FA in the hepatopancreas, followed by arachidonic (20:4n-6) and oleic acids (18:1n-9). The exposure of shrimp to WSF did not significantly change the FA profile of the PL, except for an increase in 18:1, which made it the second most important FA in the PL. The FA profile of the eggs was also dominated by 20:5n-3, followed by similar amounts of 18:1n-9, 16:0, and 18:0. After exposure to WSF, there were no statistically significant differences in the relative FA composition between the WSF and control groups. PUFA was the major group in the PL, regardless of the tissue or treatment analyzed.

PC molecular species. After studying the effect of WSF on total lipids, the lipid composition, and PL FA, we identified PC as the only PL whose concentration was significantly altered by the contaminant in both the hepatopancreas and eggs (Table 2). We therefore studied PC in detail, analyzing its molecular species. The eggs and hepatopancreas were chosen, as in preliminary experiments these tissues were found to be the ones most sensitive to HC pollution.

Using HPLC-ELSD, we were able to resolve 15 molecular species of PC in both the hepatopancreas and eggs of *M. borellii* (Fig. 1). The major molecular species of the hepatopancreas were 16:0/18:1, 18:1/18:2, 16:0/20:5, and 16:1/20:5, which represented more than 60% of the total (Fig. 2). Remarkably, 10 of the 15 PC species resolved contained 20-carbon PUFA, particularly 20:5n-3 and 20:4n-6, and some minor species were di-PUFA. On the other hand, PC molecular species in the eggs showed a different pattern, dominated by 16:0/18:1 and 18:1/18:2 (Fig. 3). These two species accounted for more than 55% of the total. When we exposed adult shrimp to WSF for 3 wk, the PC molecular species showed changes in both tissues. Except for 18:1/18:2, the major molecular species of the he-

TABLE 2
Lipid Class Composition[a] of the Hepatopancreas and Eggs of *M. borellii* from Control and WSF-Exposed Organisms

Class	Hp-control	Hp-WSF	Egg-control	Egg-WSF
ES	0.67 ± 0.38	0.33 ± 0.16	Trace	Trace
TAG	4.29 ± 1.69	7.20 ± 4.80	69.45 ± 1.99	61.76 ± 2.8*
FFA	Trace	Trace	0.50 ± 0.12	0.42 ± 0.26
ST	14.43 ± 2.01	11.95 ± 2.35	1.74 ± 0.22	1.35 ± 0.25
ASX	6.16 ± 0.69	4.54 ± 0.68*	1.54 ± 0.36	1.62 ± 0.08
PE	9.86 ± 1.76	10.13 ± 1.62	3.25 ± 0.22	4.61 ± 0.26**
PC	62.10 ± 2.15	53.29 ± 4.04*	23.84 ± 2.35	30.66 ± 3.19*
SM	2.84 ± 0.27	5.57 ± 1.08*	Trace	Trace
Σ PL	74.80 ± 1.32	68.99 ± 4.91	27.09 ± 2.42	35.27 ± 2.44
PL/TAG	17.43 ± 4.38	9.58 ± 4.07*	0.39 ± 0.04	0.57 ± 0.08**

[a]Values (mg lipid/100 mg tissue wet wt) are the means of triplicate analyses ± 1 SD. *Significant changes between control and exposed tissue ($P < 0.05$); **very significant ($P < 0.01$). Hp, hepatopancreas; ES, esterified sterols; ST, free sterols; ASX, carotenoids; SM, sphingomyelin; PL, phospholipids; for other abbreviation see Table 1.

TABLE 3
Major FA of the Phosphoglyceride Control and WSF-Exposed Hepatopancreas and Eggs of *M. borellii*[a]

	Hepatopancreas		Eggs	
FA	Control	WSF	Control	WSF
14:0	0.68 ± 0.10	0.74 ± 0.02	1.23 ± 0.29	1.55 ± 0.15
16:0	8.56 ± 0.86	7.91 ± 0.51	14.90 ± 1.64	15.61 ± 1.17
18:0	8.92 ± 0.54	9.15 ± 1.91	13.02 ± 2.42	12.88 ± 0.17
16:1n-7	5.22 ± 0.76	5.35 ± 0.39	4.85 ± 0.38	5.57 ± 1.02
18:1n-9	14.12 ± 2.16	18.46 ± 0.51*	13.89 ± 2.35	12.73 ± 1.55
18:1n-7	10.06 ± 1.99	7.35 ± 2.15	5.69 ± 1.40	6.69 ± 2.21
18:2n-6	6.18 ± 0.95	5.32 ± 0.68	6.80 ± 1.73	5.82 ± 1.02
18:3n-6	0.05 ± 0.04	0.02 ± 0.01	0.25 ± 0.36	0.02 ± 0.03
18:3n-3	1.48 ± 0.13	1.10 ± 0.04	3.59 ± 1.41	2.78 ± 0.51
20:3n-6	Trace	Trace	0.12 ± 0.15	0.11 ± 0.01
20:4n-6	15.25 ± 0.60	14.46 ± 1.01	8.68 ± 0.91	9.13 ± 1.45
20:5n-3	20.20 ± 1.47	21.25 ± 0.81	17.80 ± 3.23	16.02 ± 1.34
22:2n-6	Trace	Trace	0.40 ± 0.06	0.02 ± 0.03
22:6n-3	6.11 ± 1.27	6.27 ± 1.48	4.23 ± 1.12	6.87 ± 1.30
Σ Saturates	18.15 ± 0.84	17.84 ± 1.87	29.47 ± 4.41	28.34 ± 2.52
Σ Monounsaturates	29.42 ± 1.38	31.45 ± 3.13	23.58 ± 2.21	24.90 ± 0.68
Σ Polyunsaturates	51.59 ± 1.07	50.71 ± 1.17	46.95 ± 1.80	46.76 ± 2.30

[a]Values are the mean of triplicate analyses as % (w/w) ± SD; *$P < 0.05$. For abbreviation see Table 1.

patopancreas decreased significantly, together with most PUFA-containing molecular species. This was paralleled by an increase in molecular species containing monounsaturated FA

(mean increase 152% in 16:1/18:1 and 50% in 18:1/18:1) and increases in the minor species 18:0/18:2 and 18:0/20:4.

The two major egg PC molecular species showed a significant decrease after a 3-wk exposure to WSF, totaling 55% in the control and 45% in the exposed organisms. Unlike in the hepatopancreas, the proportions of several PUFA-containing molecular species in the exposed eggs (16:0/20:5, 16:0/22:6, 18:1/22:6, and 16:0/20:4) increased significantly.

FIG. 1. Typical chromatogram of the PC molecular species profile of the hepatopancreas of *Macrobrachium borellii*. Molecular species were analyzed by HPLC-ELSD identified by GLC as described in the Experimental Procedures section. 1, 20:5/20:4; 2, 20:5/22:6; 3, 18:3/20:5; 4, 16:1/20:5; 5, 16:0/20:5; 6, 16:0/22:6; 7, 18:1/22:6; 8, 16:0/20:4; 9, 16:1/20:4; 10, 16:1/18:1; 11, 18:1/18:2; 12, 18:0/18:2; 13, 18:0/20:4; 14, 18:1/18:1; 15, 16:0/18:1.
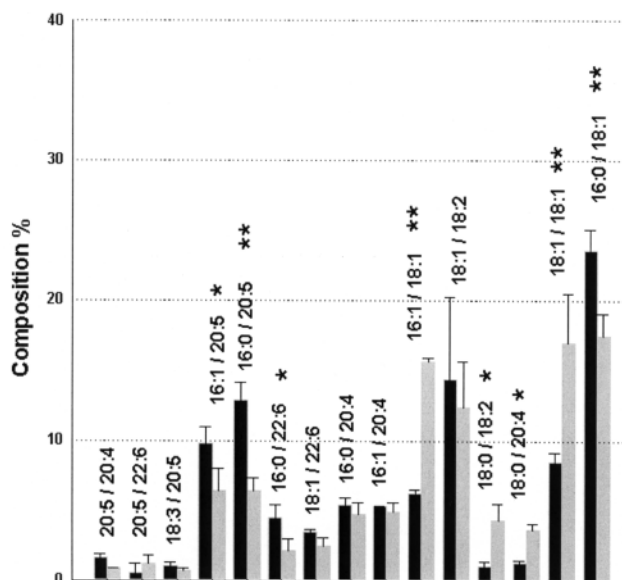
FIG. 2. Effect of the water-soluble fraction (WSF) on PC molecular species from the hepatopancreas of control and WSF-exposed *M. borellii* (by wt%). (■) Control; (▨) WSF-exposed. Molecular species were analyzed by HPLC-ELSD as described in the Experimental Procedures section. Results represent the average of three determinations ± 1 SD of the mean. *$P < 0.05$; **$P < 0.001$.
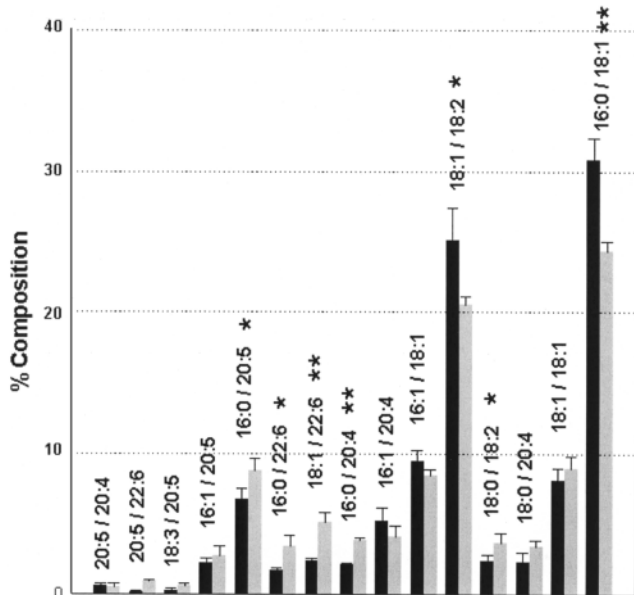
FIG. 3. Effect of WSF on PC molecular species from the eggs of control and WSF-exposed shrimp (by wt%). (■) Control; (▨) WSF-exposed. Molecular species were analyzed by HPLC-ELSD as described in the Experimental Procedures section. Results represent the average of three determinations ± 1 SD of the mean. *$P < 0.05$; **$P < 0.001$. For abbreviation see Figure 2.

DISCUSSION

Total lipid content as a pollution indicator. In this work, we analyzed the effect of a sublethal exposure to WSF on lipid contents, lipid classes, and the PL FA composition of adult *M. borellii* tissues and eggs and characterized the PC molecular species as well as the variations triggered by this contaminant.

When we analyzed the total lipid contents, we observed a significant decrease in the exposed adults, probably because the shrimp catabolized more of their lipid reserves to obtain energy for the detoxification processes triggered by the contaminant. Wang and Stickle (26), studying the crab *Callinectes sapidus*, also observed a decrease in the total lipid concentration after a 15-d exposure to crude oil. Nevertheless, when we determined total lipids in the hepatopancreas and eggs of *M. borellii*—tissues metabolically active in biosynthesis, degradation, and depuration—we found no differences between exposed and control organisms. Nowadays, it has become clear that the traditional use of total lipid content or lipid-normalized pollutant data as a pollution indicator is not always a safe approach because of variations in lipid extraction and analysis, differences in contaminant partitioning among lipid pools, and seasonal/physiological changes in the lipid concentration and composition (27). In addition, the homeostatic mechanisms of the organisms may not be overcome, thus avoiding the appearance of significant changes in lipid concentration. It is therefore important to consider the variations in lipid classes or, like the novel approach explored in the present study, changes in the PL molecular species induced by exposure to WSF.

Variations in lipid and FA classes in response to WSF. We

observed a significant decrease in PC concentration in the hepatopancreas of exposed shrimp, whereas the sphingomyelin increased significantly and the TAG showed an increasing trend. Similar changes in PC and TAG were also found in crabs (28) and mussels (29) in response to other pollutants. Those authors suggested this might result from membrane damage, a fact that could also be the case with *M. borellii*, whose membranes contain PC as the major component (30); PC changes could be affecting the structure and properties of *M. borellii* membranes (4). Moreover, there are indications that xenobiotics increase membrane lipid peroxidation (31), and because the hepatopancreas is in charge of xenobiotic detoxification in adult crustaceans (32), it was not surprising to observe that the concentration of astaxanthin, a very potent antioxidant, decreased in WSF-exposed organisms, suggesting its consumption to prevent oxidative damage.

The significant decrease in the PL/TAG ratio of the hepatopancreas of exposed organisms would also be reflective of a mechanism to raise TAG levels, either by increasing TAG synthesis or by decreasing TAG mobilization into PL pools, thereby raising the number of hydrophobic reservoirs for WSF and diminishing the contaminant bioavailability by dilution. This mechanism also has been observed in other aquatic organisms (29). Previous studies in *M. borellii* have shown that the bioconcentration of aromatic HC from the environment and their subsequent depuration rate is related to the lipid contents (16). Capuzzo and Lancaster (33) demonstrated the impairment of lipid utilization in lobsters exposed to oil and suggested that the disruption in energetics was caused by alterations in their lipid metabolism.

Macrobrachium borellii egg lipids are composed primarily of TAG, which serve as the main source of energy during development (5). In this model we observed a significant decrease of this reserve in embryos exposed to WSF. This contrasting effect, compared with the hepatopancreas, is probably related to the fact that, being a closed system, egg embryos are faced with a different pressure: They have no source of energy other than the vitellus and must expend more energy coping with the increase in free radicals and detoxification mechanisms induced by WSF, as shown by the highly significant increase in the PL/TAG ratio. Although the concentration of the antioxidant astaxanthin did not change, the enzymatic defense systems are well developed in these shrimp embryos (see ensuing discussion). We have previously shown that developing embryos have a high metabolic rate and an important consumption of lipids from the vitellus at later stages (5); thus, an alteration of the major energy source attributable to the presence of WSF was expected.

The FA profile of PL from the hepatopancreas of *M. borellii* did not differ much from the one previously reported for egg PL (5), the major FA being 20:5n-3, followed by 20:4n-6, the 18:1 isomers, 16:0, and 18:0. The n-3/n-6 ratio was below one, as is usual in freshwater environments. In both the hepatopancreas and eggs, this FA composition was not greatly affected by the WSF. Nevertheless, the significant increase in 18:1 in the hepatopancreas after WSF exposure is noteworthy, as it became the second most important FA in the tissue, and this in-

crease was coincident with the increase in PC molecular species containing this FA (see ensuing discussion). Embryos are enclosed in the eggshell, and as closed systems, they cannot afford to lose the PUFA they need for the active membrane synthesis that takes place during organogenesis. The embryos of the crustacean *Gammarus locusta* are known to have a more developed antioxidant defense system than that of adults (34). A study in progress shows that *M. borellii* embryos have background levels of antioxidant defense enzymes such as catalase and glutathion transferase over twice as high as levels in the adult hepatopancreas. This probably allows the embryos to reduce oxidative damage, thus accounting for the unchanged PUFA concentration in embryos caused by the stressor. In contrast to results for the hepatopancreas, the astaxanthin concentration did not change by WSF exposure, suggesting that this antioxidant pigment is conserved by the embryo, as was shown in a previous study (5).

Variations in PC molecular species in response to WSF. After studying the effect of WSF on total lipids, lipid classes, and the phosphoglyceride FA composition, we identified PC as the only lipid in both the hepatopancreas and eggs whose concentration was varied significantly by the contaminant. We therefore focused on this lipid class and analyzed its molecular species to investigate whether there was a remodeling of the PC molecular species in response to WSF. In the hepatopancreas and eggs, we were able to identify 15 PC molecular species, dominated by 16:0/18:1 (24 and 31% of the total, respectively). Currently, very few reports are available on the PC molecular species of aquatic arthropods. The PC molecular species of the amphipod *Gammarus* sp. were also dominated by this molecular species (12). Unlike those results and the ones reported for *Limulus polyphemus* amebocytes (13), no fully saturated species were detected in the caridean decapod *M. borellii* (present results), *Pandulus* sp., or *Parapandulus* sp. (9). Moreover, we found minor amounts of di-polyunsaturated molecular species. Nevertheless, the vast majority of PC molecular species in these species consisted of *sn*-1 saturated or monoenoic 16- or 18-carbon FA and *sn*-2 monoenoic and polyenoic PC molecular species. This was expected, as it is a feature also found in the composition of most PC molecular species of freshwater (35,36) and terrestrial (37–39) vertebrates. In general, the molecular species composition reflected the high level of PUFA found in the PL FA profile of *M. borellii*.

After 3 wk of exposure to WSF, the composition of the molecular species of hepatopancreatic PC was modified such that it probably compensated for any changes triggered by the stressor. Tissues with a lower TAG/PL ratio were more greatly affected by the WSF, as suggested by Bergen *et al.* (27) for mussels; with the hepatopancreas there was a significant decrease in most of the PUFA-containing PC molecular species, probably due to the high susceptibility of PUFA to lipoperoxidation induced by aromatic HC detoxification (32).

One inherent property of the cells in poikilothermic animals is their ability to adjust the physicochemical characteristics of their membranes to the prevailing temperatures. Saturated FA produce less fluid PL with increasing chain lengths (38), but PUFA make the membranes only slightly more fluid than do monounsaturated FA. Therefore, the decrease in the fluidizing highly PUFA-containing species triggered by WSF exposure could be compensated for by the increase in di-monounsaturated 18:1-containing PC species as well as the decrease in 16:0/18:1. Interestingly, these results are similar to those found for shrimp exposed to different temperatures in which changes in the PC molecular species were produced in such a way that the fluidity was roughly maintained (35). Reshuffling and restructuring of the molecular species might be an important factor in lipid membrane adaptation, minimizing alterations caused by exposure to the WSF, although the present data do not allow us to differentiate between an adaptation to the WSF or a direct effect of WSF on the membranes.

The lack of change caused by WSF in the FA composition of the eggs, together with significant changes in the PC molecular species (Fig. 2), indicates that the type and proportion of the FA at both the *sn*-1 and *sn*-2 positions had altered. This could be a consequence of the availability of different FA (for example, from the TAG pool), but also of changes found in the specific activity of enzymes involved in PC synthesis. A retailoring process was evidently induced, and a deacylation–reacylation at carbons *sn*-1 and *sn*-2 was also manifest, although not much information is available on these processes in crustaceans. The profile of the PC molecular species might also have been influenced by different types of pathways, such as PE N-methylation, which has been found to be very active in crustaceans (40), although this was not checked on these shrimp.

In contrast to the hepatopancreas, the eggs showed a significant decrease in molecular species containing oleic acid and an increase in the PUFA-containing molecular species in WSF-exposed embryos. The increase in PUFA-containing molecular species may be related to the fact that the embryos must conserve these EFA for proper development, and in this sense, we previously observed that developing time and hatching are not significantly altered in WSF-exposed embryos (16). Ongoing experiments are focusing on the changes in membrane properties, e.g., chemical reactivity, fluidity, and interaction with proteins, induced by WSF.

The PC species 16:0/18:1 was the most affected by exposure to WSF, and its marked decrease in the hepatopancreas or eggs could be used as a complementary early biochemical biomarker, indicating the presence of HC pollution. Nevertheless, work is needed to validate the suitability of PC species as biomarkers in the environment. The shift in molecular composition of PC is noteworthy since it illustrates that relatively small changes on a total scale (lipids and FA composition) are translated into major changes in the PUFA- and monounsaturated FA-containing PC fractions. The different responses observed in the adults and eggs of PC species reinforce the need to include different life history stages of species in toxicological tests, as well as an appropriate biomarker that integrates chemical data with biological responses, when aiming for a better evaluation of hazardous compounds.

REFERENCES

1. Boschi, E.E. (1981) Decapoda: Natantia, in *Fauna Argentina de agua dulce* (Boschi, E.E., ed.), Vol. 26, pp. 19–61, Fundación para la Educación, la ciencia y la cultura (FECIC), Buenos Aires, Argentina.
2. Morrone, J.J., and Lopretto, E.C. (1995) Distributional Patterns of Freshwater Decapoda (Crustacea: Malacostraca) in Southern South America: A Panbiogeographic Approach, *J. Biogeogr. 21*, 97–109.
3. González-Baró, M.R., and Pollero, R.J. (1998) Fatty Acid Metabolism of *Macrobrachium borellii*: Dietary Origin of Arachidonic and Eicosapentaenoic Acids, *Comp. Biochem. Physiol. 119*, 747–752.
4. González-Baró, M.R., and Pollero, R.J. (1988) Lipid Characterization and Distribution Among Tissues of the Freshwater Crustacean *Macrobrachium borellii* During an Annual Cycle, *Comp. Biochem. Physiol. 91*, 711–715.
5. Heras, H., González-Baró, M.R., and Pollero, R.J. (2000) Lipid and Fatty Acid Composition and Energy Partitioning During Embryo Development in the Shrimp *Macrobrachium borellii*, *Lipids 35*, 645–651.
6. González-Baró, M.R., Heras, H., and Pollero, R.J. (2000) Enzyme Activities Involved in Lipid Metabolism During Embryonic Development of *Macrobrachium borellii*, *J. Exp. Zool. 286*, 231–237.
7. Irazú, C.E., González Baró, M.R., and Pollero, R.J. (1992) Effect of Environmental Temperature on Mitochondrial β-Oxidation Activity in Gills and Hepatopancreas of the Freshwater Shrimp *Macrobrachium borellii*, *Comp. Biochem. Physiol. 102B*, 721–725.
8. Farkas, T., Fodor, E., Kitajka, K., and Halver, J.E. (2001) Response of Fish Membranes to Environmental Temperature, *Aquacult. Res. 32*, 645–655.
9. Farkas, T., Dey, I., Buda, C., and Halver, J.E. (1994) Role of Phospholipid Molecular Species in Maintaining Lipid Membrane Structure in Response to Temperature, *Biophys. Chem. 50*, 147–155.
10. Jeong, B.Y., Ohshima, T., and Koizumi, C. (1990) Molecular Species of 1-*O*-Alk-1′-enyl-2-acyl-, 1-*O*-Alkyl-2-acyl- and 1,2-Diacyl Glycerophospholipids in Japanese Oyster *Crassostrea gigas* (Thunberg), *Lipids 25*, 624–632.
11. Jeong, B.Y., Ohshima, T., and Koizumi, C. (1991) Changes in Molecular Species Compositions of Glycerophospholipids in Japanese Oyster *Crassostrea gigas* (Thunberg) During Frozen Storage, *Comp. Biochem. Physiol. 100B*, 99–105.
12. Lahdes, E., Balogh, G., Fodor, E., and Farkas, T. (2000) Adaptation of Composition and Biophysical Properties of Phospholipids to Temperature by the Crustacean, *Gammarus* spp., *Lipids 35*, 1093–1098.
13. MacPherson, E.J., Pavlovich, J.G., and Jacobs, R.S. (1998) Phospholipid Composition of the Granular Amebocyte from the Horseshoe Crab, *Limulus polyphemus*, *Lipids 33*, 931–940.
14. Di Toro, D.M., Allen, H.E., Bergman, H.L., Meyer, J.S., Paquin, P.R., and Santore, R.C. (2001) Biotic Ligand Model of the Acute Toxicity of Metals. 1. Technical Basis, *Environ. Toxicol. Chem. 20*, 2383–2396.
15. Bhattacharyya, S., Klerks, P.L., and Nyman, J.A. (2003) Toxic-

ity to Freshwater Organisms from Oils and Oil Spill Chemical Treatments in Laboratory Microcosms, *Environ. Pollut. 122*, 205–215.
16. Lavarías, S., Heras, H., and Pollero, R.J. (2004) Toxicity, Uptake and Release of the Water-Soluble Fraction of Crude Oil in Different Developing Stages of the Prawn *Macrobrachium borellii*, *Arch. Environ. Contam. Toxicol. 47*, 215–222.
17. Franja Costera Sur (FCS) (1994) *Calidad de las Aguas. Franja Costera Sur. Informe de avance*, p. 53, Servicio de Hidrografía Naval, Buenos Aires, Argentina.
18. Collins, P., and Petriella, A. (1999) Growth Pattern of Isolated Prawns of *Macrobrachium borellii* (Crustacea, Decapoda, Palaemonidae), *Invertebr. Reprod. Dev. 36*, 1–3.
19. Lavarías, S., Heras, H., Demichelis, S., Portiansky, E., and Pollero, R.J. (2002) Morphometric Study of Embryonic Development of *Macrobrachium borellii* (Arthropoda: Crustacea), *Invertebr. Reprod. Dev. 41*, 157–163.
20. Bligh, E.G., and Dyer, W.J. (1959) A Rapid Method of Total Lipid Extraction and Purification, *Can. J. Biochem. Physiol. 37*, 911–917.
21. Parrish, C.C., and Ackman, R.G. (1985) Calibration of the Iatroscan-Chromarod System for Marine Lipid Class Analyses, *Lipids 20*, 521–530.
22. Ackman, R.G., Heras, H., and Zhou, S. (1997) Improvements in Recovery of Petroleum Hydrocarbons from Marine Fish, Crabs and Mussels, in *New Techniques and Applications in Lipid Analysis* (McDonald, R.E., and Mossoba, M.M., eds.), pp. 380–394, AOCS Press, Champaign.
23. Christie, W.W. (1982) A Simple Procedure for Rapid Transmethylation of Glycerolipids and Cholesteryl Esters, *J. Lipid Res. 23*, 1072–1075.
24. Brenner, R.R., Ayala, S., and Garda, H.A. (2001) Effect of Dexamethasone on the Fatty Acid Composition of Total Liver Microsomal Lipids and Phosphatidylcholine Molecular Species, *Lipids 36*, 1337–1345.
25. Ves-Losada, A., Maté, S.M., and Brenner, R.R. (2001) Incorporation and Distribution of Saturated and Unsaturated Fatty Acids into Nuclear Lipids of Hepatic Cells, *Lipids 36*, 273–282.
26. Wang, S.Y., and Stickle, W.B. (1988) Biochemical Composition of the Blue Crab *Callinectes sapidus* Exposed to the Water Soluble Fraction of Crude Oil, *Mar. Biol. 98*, 23–30.
27. Bergen, B.J., Nelson, W.G., Quinn, J.G., and Jayaraman, S. (2001) Relationships Among Total Lipids, Lipid Classes, and Polychlorinated Biphenyl Concentrations in Two Indigenous Populations of Ribbed Mussels (*Geunkesia demissa*) over an Annual Cycle, *Environ. Toxicol. Chem. 20*, 575–581.
28. Capuzzo, J.M., and Leavitt, D.F. (1988) Lipid Composition of the Digestive Glands of *Mytilus edulis* and *Carcinus maenas* in Response to Pollutant Gradients, *Mar. Ecol. 46*, 139–145.
29. Capuzzo, J.M., Farrington, J.W., Rantamake, P., Clifford, C.H., Lancaster, B.A., Leavitt, D.F., and Jia, X. (1989) The Relationship Between Lipid Composition and Seasonal Differences in the Distribution of PCBs in *Mytilus edulis* L., *Mar. Environ. Res. 28*, 259–264.
30. González-Baró, M.R., Irazú, C.E., and Pollero, R.J. (1990) Palmitoyl-CoA Ligase Activity in Hepatopancreas and Gill Microsomes of the Freshwater Shrimp *Macrobrachium borellii*, *Comp. Biochem. Physiol. 97B*, 129–133.
31. Stegeman, J.J. (1985) Benzo(a)pyrene Oxidation and Microsomal Enzyme Activity in the Mussel (*Mytilus edulis*) and Other Bivalve Mollusc Species from the Western North Atlantic, *Mar. Biol. 89*, 21–30.
32. Livingstone, D.R. (1998) The Fate of Organic Xenobiotics in Aquatic Ecosystems: Quantitative and Qualitative Differences in Biotransformation by Invertebrates and Fish, *Comp. Biochem. Physiol. 120A*, 43–49.
33. Capuzzo, J.M., and Lancaster, B.A. (1982) Physiological Effects of Petroleum Hydrocarbons on Larval Lobsters (*Homarus*

americanus): Hydrocarbon Accumulation and Interference with Lipid Metabolism, in *Physiological Mechanisms of Marine Pollutant Toxicity* (Vernberg, W.B., Calabrese, A., Thurberg, F.P., and Vernberg, J.F., eds.), pp. 477–504, Academic Press, New York.

34. Correia, A.D., Costa, M.H., Luis, O.J., and Livingstone, D.R. (2003) Age-Related Changes in Antioxidant Enzyme Activities, Fatty Acid Composition and Lipid Peroxidation in Whole Body *Gammarus locusta* (Crustacea: Amphipoda), *J. Exp. Mar. Biol. Ecol. 289*, 83–101.

35. Dey, I., Buda, C., Wiik, T., Halver, J.E., and Farkas, T. (1993) Molecular and Structural Composition of Phospholipid Membranes in Livers of Marine and Freshwater Fish in Relation to Temperature, *Proc. Natl. Acad. Sci.* USA *90*, 7498–7502.

36. Farkas, T., Kitajka, K., Fodor, E., Csengeri, I., Lahdes, E., Yeo, Y.K., Krasznai, Z., and Halver, J.E. (2000) Docosahexaenoic Acid-Containing Phospholipid Molecular Species in Brains of Vertebrates, *Proc. Natl. Acad. Sci.* USA *97*, 6362–6366.

37. Delton-Vandenbroucke, I., Maude, M.B., Chen, H., Aguirre, G.D., Acland, G.M., and Anderson, R.E. (1998) Effect of Diet on the Fatty Acid and Molecular Species Composition of Dog Retina Phospholipids, *Lipids 33*, 1187–1193.

38. Garda, H.A., Bernasconi, A.M., Tricerri, M.A., and Brenner, R.R. (1997) Molecular Species of Phosphoglycerides in Liver Microsomes of Rats Fed a Fat-Free Diet, *Lipids 32*, 507–513.

39. Kurvinen, J.-P., Kuksis, A., Sinclair, A.J., Abedin, L., and Kallio, H. (2000) The Effect of Low α-Linolenic Acid Diet on Glycerophospholipid Molecular Species in Guinea Pig Brain, *Lipids 35*, 1001–1009.

40. Zwingelstein, G., Brichon, G., Bodennec, J., Chapelle, S., Abdul-Malak, N., and El-Babili, M. (1998) Formation of Phospholipid Nitrogenous Bases in Euryhaline Fish and Crustaceans. II. Phosphatidylethanolamine Methylation in Liver and Hepatopancreas, *Comp. Biochem. Physiol. 102B*, 475–482.

Lipid Composition Influences the Shape of Human Low Density Lipoprotein in Vitreous Ice

Andrea Coronado-Gray and Rik van Antwerpen*

Department of Biochemistry, Medical College of Virginia Campus,
Virginia Commonwealth University, Richmond, Virginia 23298

ABSTRACT: Earlier cryo-electron microscopic studies have indicated that the normal low density lipoprotein (N-LDL) has a discoid shape when its core is in the liquid-crystalline state. In the present study, we investigated whether the shape of LDL depends on the physical state and/or the lipid composition of the lipoprotein core. Using a custom-built freezing device, we vitrified N-LDL samples from either above or below the phase-transition temperature of the core (42 and 24°C, respectively). Cryo-electron microscopy revealed no differences between these samples and indicated a discoid shape of the N-LDL particle. In contrast, TG-enriched LDL (T-LDL) did not have discoid features and appeared to be quasi-spherical in preparations that were vitrified from either 42 or 24°C. These results suggest that the shape of N-LDL is discoid, regardless of the physical state of its core, whereas T-LDL is more spherical. Aspects that may influence the shape of LDL are discussed.

Paper no. L9583 in *Lipids 40*, 495–500 (May 2005).

Low density lipoprotein (LDL) transports cholesterol throughout the human body, and elevated levels of this lipoprotein in the blood correlate with increased risk of atherosclerosis and coronary heart disease. LDL is a quasi-spherical particle that contains a core of mainly cholesteryl esters and a surface monolayer of phospholipids, free cholesterol, and a single molecule of apolipoprotein B-100 (apoB; M_r ~550,000) (1,2). ApoB is a ligand for the apoB/E-receptor, allowing for receptor-mediated endocytosis of LDL by cells that express the receptor (3,4). In addition, apoB binds to proteoglycans in the vascular wall (5,6), which is one of the critical first steps in atherosclerosis (7,8). Thus, both the normal metabolism of LDL and the pathogenic properties of the lipoprotein particle depend on the structure of apoB.

Studies have shown that the lipid composition and size of the LDL core influence the conformation of apoB on the lipoprotein surface. Structural parameters, such as the relative amount of α-helical and β-sheet structure (9,10), the exposure of lysine amino groups on the LDL surface (11), the exposure of epitopes on the LDL surface (10–12), the susceptibility of apoB to protease digestion (9), and the affinity of apoB for the LDL receptor (9–14), all depend on the size of the LDL core. As a result, small, dense LDL particles appear to be more atherogenic than larger and more buoyant LDL (15,16).

Recent experiments have shown that the conformation of apoB on the LDL surface also depends on the physical state of the LDL core (17,18). The main components of the core, cholesteryl esters, are normally in a disordered liquid state at physiological temperature and in a more ordered liquid-crystalline state at room temperature (19–25). The temperature at which the transition between these two states occurs, i.e., the phase-transtion temperature, is usually around 30°C. However, animal studies have shown that diets with a high content of cholesterol and saturated fat can change the composition of the LDL core, and as a result elevate the phase-transition temperature to 40–45°C (26–28). Temperature-dependent IR spectroscopy and circular dichroism studies (17,18) indicate that these diet-induced changes in the physical state of the core may affect the conformation of apoB on the LDL surface, which in turn may influence the metabolic and pathogenic properties of the lipoprotein particle.

Recent cryo-electron microscopy (cryo-EM) studies have shown quite unexpectedly that LDL particles with a liquid-crystalline core may have an oblate ellipsoid or "discoid" shape (29–34). Low-resolution X-ray crystallography and high-performance gel-filtration chromatography appear to confirm the discoid nature of the LDL complex (35,36). Based on these observations, we have recently speculated that the liquid to liquid-crystalline transition of the LDL core may be associated with a spherical to discoid change in the shape of the lipoprotein particle, and that this shape change may be responsible for the observed change in the conformation of apoB on the LDL surface (18,33). A recent cryo-EM study seems to confirm this suggestion (34); however, high-performance gel-filtration chromatography indicates that LDL has a discoid shape regardless of the physical state of its core (36).

To address this issue further, we analyzed two LDL species with different core properties using cryo-EM. Our results suggest that the shape of normal LDL (N-LDL) is discoid, regardless of the physical state of its core, and that TG-rich LDL (T-LDL) is more spherical.

MATERIALS AND METHODS

LDL samples. N-LDL, $d = 1.019$–1.064 g/mL, was isolated from the blood of a healthy, nonsmoking, normolipidemic donor,

---

*To whom correspondence should be addressed at Department of Biochemistry, Medical College of Virginia Campus, Virginia Commonwealth University, P.O. Box 980614, Richmond, Virginia 23298.
E-mail: hgvanant@hsc.vcu.edu

Abbreviations: apoB, apolipoprotein B-100; cryo-EM, cryo-electron microscopy; DSC, differential scanning calorimetry; LDL, low density lipoprotein; N-LDL, normal low density lipoprotein; T-LDL, triglyceride-rich low density lipoprotein.

using sequential flotation ultracentrifugation as described earlier (18). T-LDL was produced by an *in vitro* lipid transfer procedure, using N-LDL, Intralipid (Sigma Chemical Company, St. Louis, MO), and lipoprotein-deficient plasma as a source for the cholesteryl ester transfer protein (18). The integrity of apoB in N-LDL and T-LDL was confirmed using SDS polyacrylamide gel electrophoresis according to Laemmli (37). Protein concentrations were determined with a modified Lowry assay, using BSA as a standard (38). Total cholesterol concentrations were determined using assay kit 439-17501 from Wako Chemicals (Richmond, VA). TG concentrations were determined using assay kit TR22421 from Thermo Trace (Melbourne, Australia).

Differential scanning calorimetry (DSC). DSC was performed using a Nano II Differential Scanning Calorimeter (Calorimetry Sciences Corporation, American Fork, UT). Before analysis, LDL samples were dialyzed into 10 mM sodium phosphate buffer (pH 7.4). Buffer and LDL samples were degassed under vacuum, after which 0.6 mL of each was loaded into the reference and sample cells of the calorimeter, respectively. LDL samples were analyzed at protein concentrations of 0.75–1.5 mg/mL. Thermograms were recorded over a temperature range of 0–45°C at heating and cooling rates of 60°C/h. Three sequential up-and-down scans were performed to verify reversibility of the phase transition.

Preparation of LDL for cryo-EM. Cryo-EM samples were prepared with a custom-built freezing device as described in Figure 1. Using this device, LDL samples were vitrified from either 24 or 42°C. Before loading samples into the freezing device, they were incubated for at least 15 min in a temperature-controlled water bath to bring the preparations to the desired temperature (either 24 or 42°C). Once the samples were loaded into the freezing device, they were equilibrated at the desired temperature for an additional 5 min before being plunge-frozen. These loading procedures assured that the LDL sample was at either 24 or 42°C immediately prior to vitrification.

Vitrification, i.e., freezing at rates that are high enough to prevent the formation of ice crystals, is commonly achieved when thin cryo-EM samples are plunged into liquid propane or ethane (29–31,39). Earlier studies have shown that the vitrification process is fast enough to capture membrane fusion intermediates and characteristic features of lipid phases that exist above the phase-transition temperature of the system (40–42). The present study, therefore, assumed that structural features related to the physical state of the LDL core were likewise preserved during vitrification.

Cryo-EM. N-LDL and T-LDL samples were analyzed under low-dose conditions, at 120 kV and –170°C, using a JEOL 1200EX electron microscope (JEOL, Ltd., Peabody, MA) and a Gatan model 626 cryo-transfer device (Gatan, Inc., Warrendale, PA) as described earlier (29–31). The following areas of the preparation were exluded from analysis: (i) Areas in which the ice was too thick for penetration of the electron beam. (ii) Areas with cubic or hexagonal ice crystals. These ice crystals, which prevent proper structural analysis, are easily recognized in electron diffraction patterns (in the electron microscope) and in the final cryo-EM image (photographic negative). (iii) Areas in
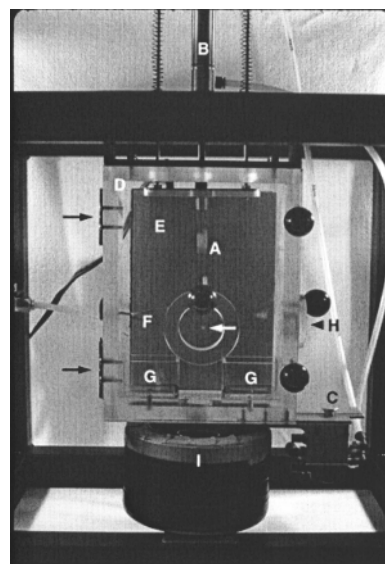
FIG. 1. Custom-built freezing device for the vitrification of samples of different temperatures. A pair of forceps (A), holding an electron microscopy (EM) grid with a lacy substrate (white arrow), is attached to a plunger (B). This plunger is connected to tubing that is pressurized with air. Air pressure in the tubing is adjusted with a control valve (not shown), usually set at 20 psi. Release of the pressure with a control switch (C) forces the plunger and the attached forceps down with high speed. The environment in the Plexiglas box (D) can be warmed by a heating pad in the back of the box (rectangle, E). The temperature near the EM sample is measured with a thermocouple (F) that is connected to a thermostat (not shown). In the bottom of the box are two small containers (G) that are filled with water. Filter paper soaked with water is guided from the water containers to the top of the heating pad to allow efficient distribution of water vapor throughout the box. The front panel of the box hinges on the left (black arrows) and can be opened to allow the forceps to be attached to the plunger and the sample to be applied to the EM grid (white arrow). After application of the sample, the front panel is closed and the environment is equilibrated at the desired temperature and high humidity. Subsequently, the bulk of the lipoprotein sample is blotted from the EM grid through a side entrance of the box (H), using a spatula covered with filter paper. Blotting of the sample results in the formation of thin films of lipoprotein solution in the holes of the lacy substrate on the EM grid. On formation of the thin films, the preparation is equilibrated at the set temperature for an additional 5 min. Subsequently, the control switch (C) pressurizes the plunger (B), which forces the attached forceps through the opened shutter into the container of liquid propane (I). Propane in the central compartment of the container (I) is kept in a liquid state by liquid nitrogen, present in the outer compartment of the container (I).

which the ice was too thin for random orientation of the LDL particles. These areas did not appear very often, and could be recognized by a steep gradient of background ice combined with an altered distribution of various projections (43). All other areas of the cryo-EM preparation were photographed and included in the analysis. At least 500 projections of each sample were measured. Images were recorded on Kodak 4489 film (Eastman Kodak Company, Rochester, NY) at a magnification of 30,000×. Photographic negatives were digitized at an optical resolution of 4800 dpi using a FlexTight Precision II Scanner (Imacon, Inc., Redmond, WA). Dimensions of the various LDL projections were determined using the measuring tool of Adobe Photoshop, software version 5.0 (Adobe Systems, Inc., San Jose, CA).
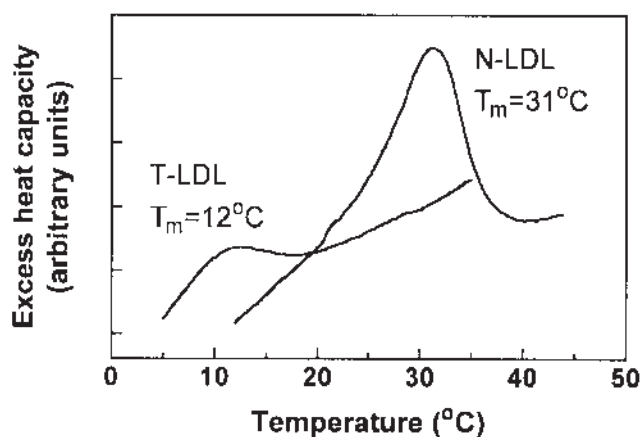
FIG. 2. DSC of normal low density lipoprotein (N-LDL) and TG-rich low density lipoprotein (T-LDL). Representative thermograms of N-LDL with a high phase-transition temperature (T_m = 31°C) and T-LDL with a low phase-transition temperature (T_m = 12°C) are shown.

RESULTS

The influence of the physical state and lipid composition of the LDL core on the overall shape and substructure of the lipoprotein particle was analyzed with two different LDL species: N-LDL, with a core phase-transition temperature of 31.1 ± 0.96°C, and *in-vitro*-produced T-LDL, with a core phase-transition temperature of 15.0 ± 1.79°C (Fig. 2, Table 1). The cholesterol and TG content, as well as some of the physical properties of these two LDL species, are shown in Table 1.

N-LDL samples vitrified from 24 or 42°C. Figure 3A shows a typical N-LDL preparation that was vitrified from 24°C (which is ~7°C below the phase-transition temperature of the N-LDL core). Various types of projections of the LDL structure were observed, including circular projections with a high-density ring and rectangular projections with two high-density bands. Earlier studies have shown that these projections represent face-on and edge-on views of a discoid structure, respectively (29–31). The projection most indicative of the discoid shape of N-LDL is the rectangular projection, resulting from an edge-on view of the structure. However, as the lipoprotein particles were free to rotate in solution immediately prior to vitrification, only a limited number of particles provided an edge-on view. In N-LDL preparations vitrified from 24°C, 12.8% of

all measured projections were unambiguously rectangular with two high-density bands (Fig. 4). This result is in good agreement with the number of rectangular projections observed in previous studies (29–31).

Figure 3B shows a typical N-LDL preparation that was vitrified from 42°C (which is ~11°C above the phase-transition temperature of the N-LDL core). As in preparations vitrified from 24°C, various types of projections of the LDL structure were observed, including circular projections with a high-density ring and rectangular projections with two high-density bands. The various projections observed in preparations frozen from 42°C were indistinguishable from those observed in preparations frozen from 24°C. In N-LDL preparations vitrified from 42°C, 10.2% of all measured projections were unambiguously rectangular with two high-density bands (Fig. 4). This percentage was not significantly different from the percentage of rectangular projections seen in N-LDL preparations frozen from 24°C (Fig. 4), indicating that, as at 24°C, N-LDL had a discoid shape at 42°C.

T-LDL samples vitrified from 24 or 42°C. T-LDL samples were vitrified from 24 and 42°C to further assess whether LDL particles with a liquid core have discoid features. Because the phase-transition temperature of the T-LDL core is ~15°C, T-LDL has a liquid core at both experimental temperatures. Figures 3C and 3D show typical cryo-EM preparations of T-LDL, vitrified from 24 and 42°C, respectively. In both types of T-LDL preparations, very few rectangular projections with two high-density bands were observed. In T-LDL preparations frozen from 24°C, only 0.8% of the measured projections were rectangular, whereas in preparations frozen from 42°C, 0.5% of the measured projections were rectangular (Fig. 4). These observations indicate that T-LDL particles are not discoid, but instead have a more spherical shape. The fact that N-LDL with a liquid core, vitrified from 42°C, had a discoid shape (see preceding discussion), suggests that the high TG content of the T-LDL core, and not the physical state of the core, is responsible for the quasi-spherical features of T-LDL (Table 2).

DISCUSSION

Molecular models of LDL generally depict the lipoprotein particle as a sphere. In these models, the liquid-crystalline LDL core is organized in concentric, spherical layers of cholesteryl

TABLE 1
Properties of Normal LDL (N-LDL) and TG-Rich LDL (T-LDL)[a]

	Chol/protein[b] (w/w)	TG/protein (w/w)	Chol/TG[b] (w/w)	T_m (°C)	Size (nm)
N-LDL	1.34 ± 0.08	0.15 ± 0.05	9.81 ± 2.57	31.1 ± 0.96	19.8 ± 1.85
T-LDL	1.08 ± 0.19	0.30 ± 0.08	3.81 ± 0.73	15.0 ± 1.79	18.5 ± 1.92

[a]Chol, total cholesterol; T_m, midpoint of the phase-transition of the low density lipoprotein (LDL) core, determined using differential scanning calorimetry (DSC). Size of the lipoprotein particles is indicated as the diameter of circular LDL projections in cryo-electron microscopy (cryo-EM) preparations frozen from 24°C. Values are the means of analyses on three different LDL preparations ± SE.
[b]Separate experiments showed that the *in vitro* conversion of N-LDL to T-LDL does not influence the free cholesterol and total phospholipid contents of the lipoprotein particle: The free cholesterol content of N-LDL and T-LDL was 0.35 ± 0.08 mg/mg protein (n = 5) and 0.30 ± 0.03 mg/mg protein (n = 5), respectively (P = 0.128), whereas the total phospholipid content of N-LDL and T-LDL was 0.82 ± 0.17 mg/mg protein (n = 5) and 0.75 ± 0.06 mg/mg protein (n = 5), respectively (P = 0.379).
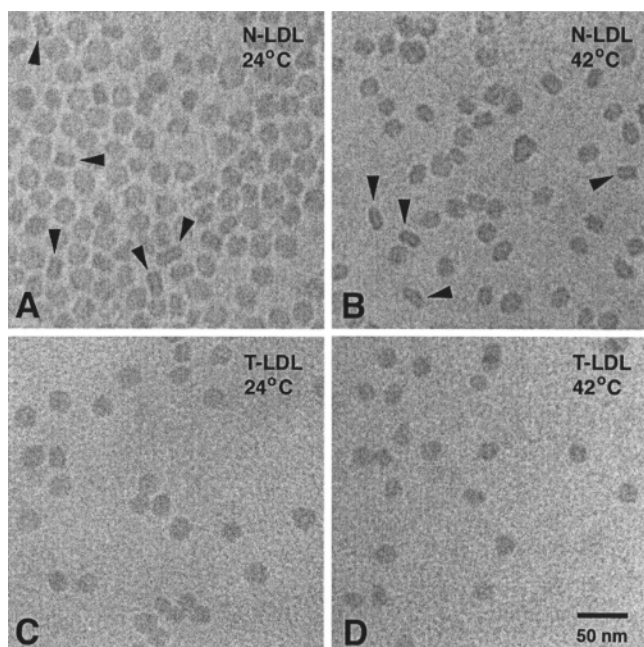
FIG. 3. Cryo-electron micrographs of N-LDL (A, B) and T-LDL (C, D), ultra-rapidly frozen from 24 (A, C) and 42°C (B, D). Arrowheads indicate rectangular projections with two high-density bands, representing edge-on views of the LDL disc (29–31). For abbreviations see Figure 2.

FIG. 4. Frequency distribution of rectangular projections with two high-density bands in cryo-EM preparations of N-LDL and T-LDL, vitrified from 24 or 42°C. The occurrence of rectangular projections in N-LDL preparations vitrified from 24 or 42°C is not significantly different (t-test; $P = 0.105$); n refers to the number of separate LDL preparations analyzed using cryo-EM. For abbreviations see Figure 2.

esters (19–25) (Fig. 5A). However, recent cryo-EM studies suggest that LDL has an oblate ellipsoid or discoid shape when its core is in the liquid-crystalline state (29–34). This suggestion has recently been supported by low-resolution X-ray crystallography (35) and high-performance gel-filtration chromatography (36). New LDL models therefore propose that the liquid-crystalline core is organized into flat layers of cholesteryl esters (32,35,36) (Fig. 5B), which is consistent with the crystallization of neat cholesteryl esters in flat sheets (44).

The present study was designed to test the hypothesis that the phase-transition of the LDL core is associated with a spherical to discoid change in the shape of the lipoprotein particle. Quite unexpectedly, projections of N-LDL in preparations vitrified from 42°C (i.e., ~11°C above the phase-transition of the LDL core) (Fig. 3B) were similar to those observed in preparations vitrified from 24°C (i.e., ~7°C below the phase-transition of the LDL core) (Fig. 3A). In addition, roughly equal numbers of rectangular projections, representing edge-on views of the discoid structure (29–31), were observed in preparations vitrified from 42 or 24°C (Fig. 4). These results suggest that the N-LDL particle has a discoid shape regardless of the physical state of its core.

Our present results are in agreement with a recent study by Teerlink *et al.* (36), who used compositional analyses in combination with high-performance gel-filtration chromatography to investigate the shape of LDL. Their results fit a discoid model of LDL better than a spherical model both at 24°C, when the core was liquid-crystalline, and at 37°C, when the core was liquid. Interestingly, however, our results seem to disagree with

a recent cryo-EM study by Sherman *et al.* (34) suggesting that LDL particles with a liquid core are spherical. The reason for this discrepancy is not clear. However, we have recently observed that discoid LDL particles may assume preferred face-on orientations in extremely thin aqueous films, resulting in a predominance of circular projections on the microscope screen (43). This predominance of circular projections may create the impression that the LDL particle has a spherical shape, while in fact only face-on orientations of a discoid structure are observed.

The present study shows that T-LDL does not have discoid features, indicating that the TG content of the LDL core plays a role in determining the shape of LDL. Consistent with this suggestion is the cryo-EM observation that TG-rich VLDL and intermediate density lipoproteins are spherical, whereas intermediate density lipoprotein particles with a lower TG content are discoid in preparations that are vitrified from room temperature (31). In addition, similar to T-LDL in the present study, TG-rich small, dense LDL from hypertriglyceridemic subjects lack discoid features (30). A possible explanation for the absence of discoid features in TG-rich lipoprotein particles may be found in a recent study by Pregetter *et al.* (45). The authors of this study propose that, below the phase transition temperature, the core of T-LDL contains two concentric compartments:

TABLE 2
Core Properties and Overall Shape of N-LDL and T-LDL[a]

	T_m (°C)	Physical state/shape at 24°C	Physical state/shape at 42°C
N-LDL	31.1 ± 0.96	Liquid crystalline/disc	Liquid/disc
T-LDL	15.0 ± 1.79	Liquid/sphere	Liquid/sphere

[a]Indicated are the physical state of the LDL core and the overall shape of the lipoprotein particle, as observed in cryo-electron micrographs. For abbreviations see Table 1.
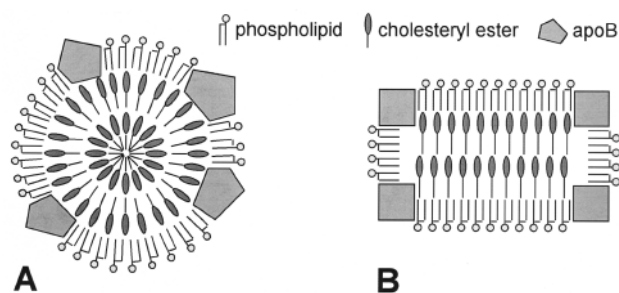
FIG. 5. Highly schematic representations of the liquid-crystalline LDL core (cross-sectional views). Free cholesterol and TG have been omitted from the drawings for clarity. (A) Generalized representation of earlier models (19–25). In these models, the LDL particle is spherical and the liquid-crystalline core is organized in concentric shells of cholesteryl esters. (B) Generalized representation of new models (32,35,36), in which the liquid-crystalline core contains flat layers of cholesteryl esters. For abbreviation see Figure 2.

a fluid inner core containing mostly TG, surrounded by a shell of cholesteryl esters in the liquid-crystalline state. Thus, the presence of a relatively large TG inner core may prevent the arrangement of cholesteryl esters in flat layers.

Presently, we cannot exclude the possibility that the discoid shape of normal LDL, observed with cryo-EM (29–34), X-ray crystallography (35), and high-performance gel-filtration chromatography (36), is generated during isolation or storage of the lipoprotein complex at nonphysiological temperatures, i.e., below the phase transition of the cholesteryl ester core. These conditions may irreversibly deform the shape of LDL, which, in the native state, may still be spherical. It will be important to resolve this issue while attempts are made to reconstruct the 3-D structure of LDL at a higher resolution.

ACKNOWLEDGMENTS

REFERENCES

1. Hevonoja, T., Pentikäinen, M.O., Hyvönen, M.T., Kovanen, P.T., and Ala-Korpela, M. (2000) Structure of Low Density Lipoprotein (LDL) Particles: Basis for Understanding Molecular Changes in Modified LDL, *Biochim. Biophys. Acta 1488,* 189–210.
2. Segrest, J.P., Jones, M.K., De Loof, H., and Dashti, N. (2001) Structure of Apolipoprotein B-100 in Low Density Lipoproteins, *J. Lipid Res. 42,* 1346–1367.
3. Borén, J., Lee, I., Zu, W., Arnold, K., Taylor, S., and Innerarity, T. (1998) Identification of the Low Density Lipoprotein Receptor-Binding Site in Apolipoprotein B100 and the Modulation of Its Binding Activity by the Carboxyl Terminus in Familial Defective Apo-B100, *J. Clin. Invest. 101,* 1084–1093.
4. Borén, J., Ekström, U., Ågren, B., Nilsson-Ehle, P., and Innerarity, T.L. (2001) The Molecular Mechanism for the Genetic Disorder Familial Defective Apolipoprotein B100, *J. Biol. Chem. 276,* 9214–9218.
5. Borén, J., Olin, K., Lee, I., Chait, A., Wight, T.N., and Innerarity, T.L. (1998) Identification of the Principal Proteoglycan Binding Site in LDL. A Single Point Mutation in Apo-B100 Severely Affects Proteoglycan Interaction Without Affecting LDL Receptor Binding, *J. Clin. Invest. 101,* 2658–2664.
6. Goldberg, I.J., Wagner, W.D., Pang, L., Paka, L., Curtiss, L.K., DeLozier, J.A., Shelness, G.S., Young, C.S.H., and Pillarisetti, S. (1998) The NH$_2$-terminal Region of Apolipoprotein B Is Sufficient for Lipoprotein Association with Glycosaminoglycans, *J. Biol. Chem. 273,* 35355–35361.
7. Camejo, G., Hurt-Camejo, E., Wiklund, O., and Bondjers, G. (1998) Association of Apo B Lipoproteins with Arterial Proteoglycans: Pathological Significance and Molecular Basis, *Atherosclerosis 139,* 205–222.
8. Boren, J., Gustafsson, M., Skalen, K., Flood, C., and Innerarity, T.L. (2000) Role of Extracellular Retention of Low Density Lipoproteins in Atherosclerosis, *Curr. Opinion Lipidol. 11,* 451–456.
9. Chen, G.C., Liu, W., Duchateau, P., Allaart, J., Hamilton, R.L., Mendel, C.M., Lau, K., Hardman, D.A., Frost, P.H., Malloy, M.J., and Kane, J.P. (1994) Conformational Differences in Human Apolipoprotein B-100 Among Subspecies of Low Density Lipoproteins (LDL). Association of Altered Proteolytic Accessibility with Decreased Receptor Binding of LDL Subspecies from Hypertriglyceridemic Subjects, *J. Biol. Chem. 269,* 29121–29128.
10. Galeano, N.F., Milne, R., Marcel, Y.L., Walsh, M.T., Levy, E., Ngu'yen, T.-D., Gleeson, A., Arad, Y., Witte, L., Al-Haideri, M., *et al.* (1994) Apoprotein B Structure and Receptor Recognition of Triglyceride-Rich Low Density Lipoprotein (LDL) Is Modified in Small LDL but Not in Triglyceride-Rich LDL of Normal Size, *J. Biol. Chem. 269,* 511–519.
11. Aviram, M., Lund-Katz, S., Phillips, M.C., and Chait, A. (1988) The Influence of the Triglyceride Content of Low Density Lipoprotein on the Interaction of Apolipoprotein B-100 with Cells, *J. Biol. Chem. 263,* 16842–16848.
12. McKeone, B.J., Patsch, J.R., and Pownall, H.J. (1993) Plasma Triglycerides Determine Low Density Lipoprotein Composition, Physical Properties, and Cell-Specific Binding in Cultured Cells, *J. Clin. Invest. 91,* 1926–1933.
13. De Graaf, J., Hendriks, J.C., Swinkels, D.W., Demacker, P.N., and Stalenhoef, A.F. (1993) Differences in LDL Receptor-Mediated Metabolism of Three Low Density Lipoprotein Subfractions by Human Monocyte-Derived Macrophages: Impact on the Risk of Atherosclerosis, *Artery 20,* 201–230.
14. Campos, H., Arnold, K.S., Balestra, M.E., Innerarity, T.L., and Krauss, R.M. (1996) Differences in Receptor Binding of LDL Subfractions, *Arterioscler. Thromb. Vasc. Biol. 16,* 794–801.
15. Austin, M.A., Breslow, J.L., Hennekens, C.H., Buring, J.E., Willet, W.C., and Krauss, R.M. (1988) Low-Density Lipoprotein Subclass Patterns and Risk for Myocardial Infarction. *JAMA 260,* 1917–1921.
16. Krauss, R.M. (1994) Heterogeneity of Plasma Low-Density Lipoproteins and Atherosclerosis Risk, *Curr. Opinion Lipidol. 5,* 339–349.
17. Bañuelos, S., Arrondo, J.L.R., Goñi, F.M., and Pifat, G. (1995) Surface-Core Relationships in Human Low Density Lipoprotein as Studied by Infrared Spectroscopy, *J. Biol. Chem. 270,* 9192–9196.
18. Coronado-Gray, A., and Van Antwerpen, R. (2003) The Physical State of the LDL Core Influences the Conformation of Apolipoprotein B-100 on the Lipoprotein Surface, *FEBS Lett. 533,* 21–24.
19. Deckelbaum, R.J., Shipley, G.G., Small, D.M., Lees, R.S., and

George, P.K. (1975) Thermal Transition in Human Plasma Low Density Lipoproteins, *Science 190,* 392.

20. Atkinson, D., Deckelbaum, R.J., Small, D.M., and Shipley, G.G. (1977) Structure of Human Plasma Low-Density Lipoproteins: Molecular Organization of the Central Core, *Proc. Natl. Acad. Sci. USA 74,* 1043–1046.

21. Deckelbaum, R.J., Shipley, G.G., and Small, D.M. (1977) Structure and Interactions of Lipids in Human Plasma Low Density Lipoproteins, *J. Biol. Chem. 252,* 744–754.

22. Müller, K., Laggner, P., Glatter, O., and Kostner, G. (1978) The Structure of Human-Plasma Low-Density Lipoprotein B. An X-Ray Small-Angle Scattering Study, *Eur. J. Biochem. 82,* 73–90.

23. Laggner, P., and Muller, K.W. (1978) The Structure of Serum Lipoproteins as Analysed by X-Ray Small-Angle Scattering, *Quart. Rev. Biophys. 11,* 371–425.

24. Atkinson, D., Small, D.M., and Shipley, G.G. (1980) X-ray and Neutron Scattering Studies of Plasma Lipoproteins, *Ann. N.Y. Acad. Sci. 348,* 284–298.

25. Laggner, P., Kostner, G.M., Degovics, G., and Worcester, D.L. (1984) Structure of the Cholesteryl Ester Core of Human Plasma Low Density Lipoproteins: Selective Deuteration and Neutron Small Angle Scattering, *Proc. Natl. Acad. Sci. USA 81,* 4389–4393.

26. Tall, A.R., Atkinson, D., Small, D.M., and Mahley, R.W. (1977) Characterization of the Lipoproteins of Atherosclerotic Swine, *J. Biol. Chem. 252,* 7288–7293.

27. Tall, A.R., Small, D.M., Atkinson, D., and Rudel, L. (1978) Studies on the Structure of Low Density Lipoproteins Isolated from *Macaca fascicularis* Fed an Atherogenic Diet, *J. Clin. Invest. 62,* 1354–1363.

28. Parks, J.S., and Bullock, B.C. (1987) Effect of Fish Oil Versus Lard Diets on the Chemical and Physical Properties of Low Density Lipoproteins of Nonhuman Primates, *J. Lipid Res. 28,* 173–182.

29. Van Antwerpen, R., and Gilkey, J.C. (1994) Cryo-Electron Microscopy Reveals Human Low Density Lipoprotein Substructure, *J. Lipid Res. 35,* 2223–2231.

30. Van Antwerpen, R., Chen, G.C., Pullinger, C.R., Kane, J.P., LaBelle, M., Krauss, R.M., Luna-Chavez, C., Forte, T.M., and Gilkey, J.C. (1997) Cryo-Electron Microscopy of Low Density Lipoprotein and Reconstituted Discoidal High Density Lipoprotein: Imaging of the Apolipoprotein Moiety, *J. Lipid Res. 38,* 659–669.

31. Van Antwerpen, R., La Belle, M., Navratilova, E., and Krauss, R.M. (1999) Structural Heterogeneity of Apolipoprotein B Containing Serum Lipoproteins Visualized Using Cryo-Electron Microscopy, *J. Lipid Res. 40,* 1827–1836.

32. Orlova, E.V., Sherman, M.B., Chiu, W., Mowri, H., Smith, L.C., and Gotto, A.M., Jr., (1999) Three-Dimensional Structure of Low Density Lipoproteins by Electron Cryomicroscopy, *Proc. Natl. Acad. Sci. USA 96,* 8420–8425.

33. Van Antwerpen, R. (2002) Structure of the Low-Density Lipoprotein, LDL. Workshop on Single Particle Reconstructions and Visualization, National Center for Macromolecular Imaging, University of Houston, Houston, TX, December 11–15, 2002.

34. Sherman, M.B., Orlova, E.V., Decker, G.L., Chiu, W., and Pownall, H.J. (2003) Structure of Triglyceride-Rich Human Low-Density Lipoproteins According to Cryo-Electron Microscopy, *Biochem. 42,* 14988–14993.

35. Lunin, V.Y., Lunina, N.L., Ritter, S., Frey, I., Berg, A., Diederichs, K., Padjarny, A.D., Urzhumtsev, A., and Baumstark, M.W. (2001) Low-Resolution Data Analysis for Low-Density Lipoprotein Particle, *Acta Cryst. D57,* 108–121.

36. Teerlink, T. , Scheffer, P.G., Bakker, S.J.L., and Heine, R.J. (2004) Combined Data from LDL Composition and Size Measurement Are Compatible with a Discoid Particle Shape, *J. Lipid Res. 45,* 954–966.

37. Laemmli, U.K. (1970) Cleavage of Structural Proteins During the Assembly of the Head of Bacteriophage T4, *Nature 227,* 680–685.

38. Peterson, G.L. (1983) Determination of Total Protein, *Methods Enzymol. 91,* 95–119.

39. Dubochet, J., Adrian, M., Chang, J.-J., Homo, J.-C., Lepault, J., McDowall, A.W., and Schultz, P. (1988) Cryo-Electron Microscopy of Vitrified Specimens, *Q. Rev. Biophys. 21,* 129–228.

40. Siegel, D.P., Burns, L., Chesnut, H., and Talmon, Y. (1989) Intermediates in Membrane Fusion and Bilayer/Non-bilayer Phase Transitions Imaged by Time-Resolved Cryo-Transmission Electron Microscopy, *Biophys. J. 56,* 161–169.

41. Frederik, P.M., Stuart, M.C.A., Bomans, P.H.H., Busing, W.M., Burger, K.N.J., and Verkleij, A.J. (1991) Perspective and Limitations of Cryo-Electron Microscopy. from Model Systems to Biological Specimens, *J. Microsc. 161,* 253–262.

42. Siegel, D.P., Green, W.J., and Talmon, Y. (1994) The Mechanism of Lamellar-to-Inverted Hexagonal Phase Transitions: A Study Using Temperature-Jump Cryo-Electron Microscopy, *Biophys. J. 66,* 402–414.

43. Van Antwerpen, R. (2004) Preferred Orientations of LDL in Vitreous Ice Indicate a Discoid Shape of the Lipoprotein Particle, *Arch. Biochem. Biophys. 432,* 122–127.

44. Ginsburg, G.S., Atkinson, D., and Small, D.M. (1984) Physical Properties of Cholesteryl Esters, *Prog. Lipid Res. 23,* 135–167.

45. Pregetter, M., Prassl, R., Schuster, B., Kriechbaum, M., Nigon, F., Chapman, J., and Laggner, P. (1999) Microphase Separation in Low Density Lipoproteins: Evidence for a Fluid Triglyceride Core Below the Lipid Melting Transition, *J. Biol. Chem. 274,* 1334–1341.

Effects of Droplet Size on the Oxidative Stability of Oil-in-Water Emulsions

Kyoko Nakaya[a], Hideki Ushio[a], Shingo Matsukawa[a],
Masataka Shimizu[b], and Toshiaki Ohshima[a,*]

[a]Department of Food Science and Technology, Tokyo University of Marine Science and Technology, Konan 4, Minato, Tokyo 108-8477, Japan, and [b]Miyazaki Prefectural Industrial Technology Center, Sadowara, Miyazaki 880-0303, Japan

ABSTRACT: The effects of droplet size and emulsifiers on oxidative stability of polyunsaturated TAG in oil-in-water (o/w) emulsions with droplet sizes of 0.806 ± 0.0690, 3.28 ± 0.0660, or 10.7 ± 0.106 μm (mean ± SD) were investigated. Hydroperoxide contents in the emulsion with a mean droplet size of 0.831 μm were significantly lower than those in the emulsion with a mean droplet size of 12.8 μm for up to 120 h of oxidation time. Residual oxygen contents in the headspace air of the vials containing an o/w emulsion with a mean droplet size of 0.831 μm were lower compared with those of the emulsion with a mean droplet size of 12.8 μm. Hexanal developed from soybean oil TAG o/w emulsions with smaller droplet size showed significantly lower residual oxygen contents than those of the larger droplet size emulsions. Consequently, oxidative stability of TAG in o/w emulsions could be controlled by the size of oil droplet even though the origins of TAG were different. Spin-spin relaxation time of protons of acyl residues on TAG in o/w emulsions measured by ^{1}H NMR suggested that motional frequency of some acyl residues was shorter in o/w emulsions with a smaller droplet size. The effect of the wedge associated with hydrophobic acyl residues of emulsifiers was proposed as a possible mechanism to explain differences in oxidative stability between o/w emulsions with different droplet sizes.

Paper no. L9705 in *Lipids 40*, 501–507 (May 2005).

Human epidemiological and experimental animal studies have suggested that regular consumption of fish oil reduces morbidity as well as mortality due to cardiovascular diseases (1). n-3 PUFA in marine oils are known to possess several kinds of physiological functions (2,3). Most foods contain oil droplets in a range of sizes varying from less than 0.2 μm to greater than 100 μm, depending on the product (4). The oxidation rate of PUFA-containing oils in a bulk system increases with their degree of unsaturation (5,6). Numerous factors influence the susceptibility of PUFA to lipid oxidation when it proceeds in a heterogeneous emulsion system consisting of an oil interior, interfacial region, and aqueous phase. With regard to the interfacial characteristics of emulsions, the electrical charge of the oil droplet deriving from surface-active components is one of the factors influencing the rate of lipid oxidation (7,8). In addition, the interfacial membrane may act as a physical barrier that separates lipid molecules from pro-oxidants in the aqueous phase (9). With regard to physical characteristics of droplets in emulsions, the physical state (10), concentration (11), and droplet size (12,13) influence the rate of lipid oxidation. Other factors influencing oxidative susceptibility of emulsions include transition metal ions (14), types of emulsifiers (15–18), pH (19,20), and pro-oxidative and antioxidative compounds (9,21–24).

The oxidative stability of PUFA in aqueous micelles decreases with increasing number of double bonds (1,25). Nevertheless, there have been few systematic studies on the influence of droplet size on the oxidative stability of oil-in-water (o/w) emulsions. Under fixed oil concentrations, the surface area of droplets increases with decreasing droplet diameter (26). Therefore, one would expect the rate of lipid oxidation to increase with decreasing droplet size. Recently, Lethuaut *et al.* (27) reported that the oxidative stability of a sunflower oil o/w emulsion became worse by increasing the diameter of the oil droplets. Coupland *et al.* (28) reported, however, that droplet size did not affect oxidation rate of o/w emulsions. In most previous studies on the influences of droplet sizes on oxidative stabilities of lipids in emulsion systems, the emulsions were prepared using traditional techniques such as ultrasonic agitation or high-speed mechanical blending. Those traditional techniques, however, usually provided undesirable oxidative stress to unsaturated lipids during preparation of emulsions prior to subjecting the emulsions to the oxidation process. An oxidative stress-free technique is therefore necessary when unsaturated oil emulsions are prepared for the purpose of evaluating the effects of droplet size on oxidative stability.

The present study was conducted to evaluate the effects of droplet sizes on the oxidative stability of cod liver oil and soybean oil TAG o/w emulsions prepared by an oxidative stress-free technique. To explain the differences in oxidative stabilities between o/w emulsions with different droplet sizes, the spin-spin relaxation times of protons (^{1}H T_2) of the acyl residues on TAG molecules in o/w emulsions were measured by ^{1}H NMR.

*To whom correspondence should be addressed at Department of Food Science and Technology, Tokyo University of Marine Science and Technology, Konan 4, Minato-ku, Tokyo 108-8477, Japan.
E-mail: tohshima@s.kaiyodai.ac.jp

Abbreviations: DPPP, diphenyl-1-pyrenylphosphine; EDTA·3K, EDTA tripotassium salt dihydrate; EPA, eicosapentaenoate; FIA, flow-injection analysis; HPO, hydroperoxide; NBD-labeled PC, 1-myristoyl-2[12-(7-nitro-2-1,3-benzoxadiazol-4-yl)amino dodecanoyl]-*sn*-glycero-3-phosphocholine; o/w emulsion, oil-in-water emulsion; SPG, Shirasu porous glasses; T_2, spin-spin relaxation time of proton.

MATERIALS AND METHODS

Materials and chemicals. Partially purified and refined cod liver oil and soybean oil were obtained from Toho Co., Ltd. (Tokyo, Japan) and Miyazawa Yakuhin Co. Ltd. (Tokyo, Japan), respectively. Sucrose lauryl ester and decaglycerol lauryl ester, both of which had HLB values of 16, were kindly donated by Mitsubishi-Kagaku Foods Co. (Tokyo, Japan). Diphenyl-1-pyrenylphosphine (DPPP) was purchased from Dojindo Laboratories Co. Ltd. (Kumamoto, Japan). 1-Myristoyl-2[12-(7-nitro-2-1,3-benzoxadiazol-4-yl)amino dodecanoyl]-*sn*-glycero-3-phosphocholine (NBD-labeled PC) was purchased from Avanti Polar Lipids, Inc. (Alabaster, AL). Shirasu porous glass (SPG) membranes were purchased from SPG Technology Co. Ltd. (Miyazaki, Japan).

Purification of cod liver oil and soybean TAG. Both cod liver oil and soybean oil were further purified by column chromatography on silica gel 60 (6 cm i.d. × 72 cm, Spherical, 40–50 µm; Kanto Chemical Co. Inc., Tokyo, Japan). Oils (35 g) were loaded on the top of the column, and the TAG fraction was eluted using *n*-hexane, followed by 5% (vol/vol) diethyl ether in *n*-hexane to remove polar compounds and tocopherol analogs.

Preparation of o/w emulsion. A solution containing 10% (w/w) TAG, 1% (w/w) sucrose lauryl ester or decaglycerol lauryl ester, 100 µM EDTA tripotassium salt dihydrate (EDTA·3K), and 25 mM citrate-phosphate buffer (pH 6.6) was prepared using ultrapure water. Components were pre-mixed gently in a glass beaker with a Teflon-coated magnetic stir bar. The singly dispersed o/w emulsions with different droplet sizes were prepared using a membrane filtration technique with an external pressure-type membrane emulsification instrument (SPG Technology Co. Ltd.) equipped with an SPG membrane with a mean pore size of 0.8, 1, 3, or 10 µm (29).

Measurement of droplet size. Droplet sizes of o/w emulsions were measured with a laser diffraction particle size analyzer model SALD-300V (Shimadzu Co., Kyoto, Japan).

Oxidation of o/w emulsions. To determine hydroperoxide (HPO) contents in the o/w emulsions, 50 mL of control or test emulsion was transferred into an Erlenmeyer flask. For determination of oxygen absorption, 10 mL of emulsion was placed in a glass vial of 61 mL in volume and subsequently sealed tightly with an aluminum cap with polytetrafluoroethylene/silicone liner (Supelco, Bellefonte, PA). Flasks and vials were shaken gently and horizontally in an oven at 40°C in the dark.

Determination of oxygen absorption. One-tenth of a milliliter of headspace air in the vial was withdrawn with a gas-tight microsyringe attached to a 24 G needle and immediately injected into a Shimadzu gas chromatograph model GC3BT equipped with a glass column (2.5 mm i.d. × 2.1 m) packed with molecular sieve 5A (80–100 mesh; Nihon Chromato Co. Ltd., Tokyo, Japan) and a thermal conductivity detector. The column oven, injection port, and detector temperatures were controlled at 67°C. Helium was used as a carrier gas at an inlet pressure of 1.2 kg/cm^2.

Determination of HPO. HPO content was determined by a flow-injection analysis (FIA) system with a DPPP fluorescent post-column detection system as reported previously (30). For the preparation of sample solution, 0.1 mL o/w emulsion was mixed with 1 mL DPPP solution (21.6 nmol/mL in methanol) in a 10 mL-volumetric flask, and then the mixture was made up to 10 mL using butanol. Next, 20 µL of the butanol solution was injected into the FIA system.

Determination of hexanal. Hexanal in headspace was determined following a method slightly modified from Frankel *et al.* (31). Volatiles were collected with a Hewlett-Packard model 19395A headspace sampler (Avondale, PA) and separated on a Shimadzu model GC-15A gas chromatograph (Kyoto, Japan) equipped with a Simplicity-5 capillary column (0.25 mm i.d. × 30 m, 0.25 µm in film thickness; Supelco), and the sample signals were integrated with a Shimadzu Chromatopac C-R4A. Sampling conditions of the headspace gas were as follows: sample loop and transfer line temperature of 100°C, sample temperature of 65°C, venting period of 10 s, and injection time of 1 min.

^{1}H NMR measurement. ^{1}H T_2 measurements for cod liver oil TAG molecules in the o/w emulsion were carried out with a Bruker Avance DRX-300 spectrometer operating at 300.15 MHz for ^{1}H. Acquisition time was 0.683 s, corresponding to 4048 points in the time domain. Dead time of the spectrometer was 4.5 µm. The temperature was continuously monitored with an optical fiber thermometer (Takaoka Electric Mfg. Co., Tokyo, Japan) placed in the sample tube and was maintained at 40 ± 0.5°C with a variable temperature unit (Bruker model VT-2000). The standard Carr–Purcell–Meiboom–Gill (CPMG) method with the pulse sequence of $\{\pi/2_x–(t–\pi_y–\tau– \text{echo}–)_n\}$ was used. The pulse spacing τ was 1 ms and the $\pi/2$ was 8.6 µs. Echo signals were measured varying the echo time $2\tau n$ from 4 to 1760 ms and Fourier-transformed to give spectra. Peak intensities were plotted against the echo time for each peak. ^{1}H T_2 was obtained from a least-squares fitting to the experimental data using Equation 1 for single-component decay and Equation 2 for two-component decay.

$$I/I_0 = \exp(- t/T_2) \qquad [1]$$
$$I/I_0 = f_1 \exp(- t/T_2,1) + f_2 \exp(- t/T_2,2) \qquad [2]$$

where I is peak intensity at echo time, I_0 is peak intensity at $t = 0$, and f_1 and f_2 are fractions of components 1 and 2, respectively.

Statistical analyses. Contents of HPO, residual oxygen, and hexanal were given as means ± SD. Student's *t*-test (32) was used to distinguish significant differences among the mean values. ANOVA was performed by a one-way procedure. Significant differences were determined at $P < 0.05$.

RESULTS

Droplet sizes of o/w emulsions. Droplet size distributions of cod liver oil TAG o/w emulsions stabilized by decaglycerol lauryl ester are shown in Figure 1A. The mean values of droplet sizes and SD of o/w emulsions prepared with an SPG membrane with a mean pore size of 0.8, 3.1, or 10 µm were 0.806 ±
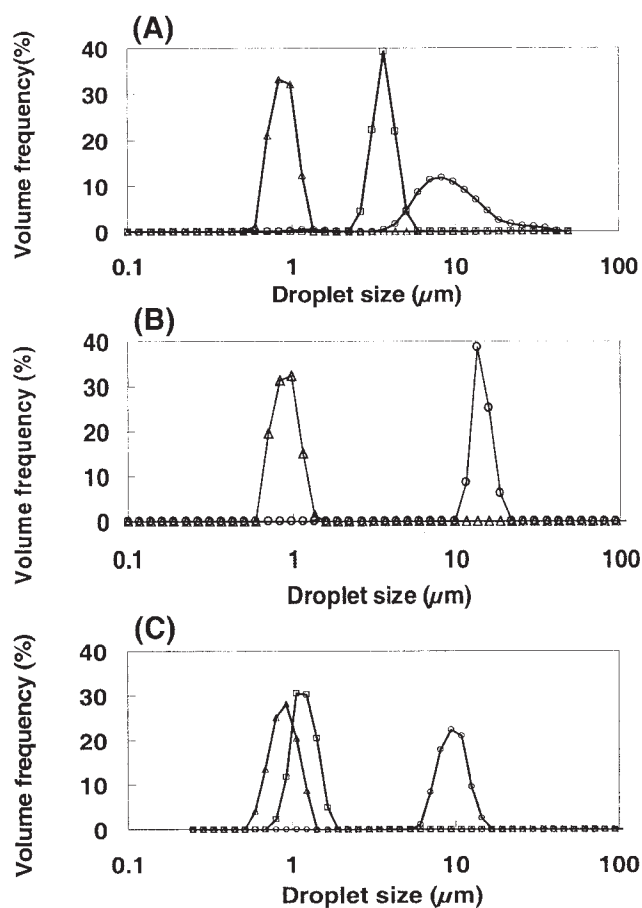
FIG. 1. Droplet size distributions of (A) cod liver oil-in-water emulsions (10% TAG in water) stabilized by 1% decaglycerol lauryl ester, (B) cod liver oil-in-water emulsions (10% TAG in water) stabilized by 1% sucrose lauryl ester, and (C) soybean oil TAG (10% oil-in-water emulsions) stabilized by 1% decaglycerol lauryl ester. The mean droplet sizes for (A) were: △, 0.806 μm; □, 3.28 μm; ○, 10.7 μm; for (B), △, 0.831 μm; ○, 12.8 μm; for (C), △, 0.828 μm; □, 1.09 μm; ○, 9.38 μm.

FIG. 2. Changes in total hydroperoxide contents (A) and in residual oxygen contents in the headspace air of vials (B) during oxidation of cod liver oil TAG 10% oil-in-water emulsions stabilized by 1% decaglycerol lauryl ester with mean droplet sizes of 0.806 (△), 3.28 (□), and 10.7 μm (○) at 40°C in the dark. Values represent the mean of replicate determinations ($n = 5$) ± SD at each time point. For each sample for the same oxidation period, values with different superscripts (a–c) are significantly different ($P < 0.05$).

0.0690, 3.28 ± 0.0660, and 10.7 ± 0.106 μm (mean ± SD), respectively. The use of sucrose lauryl ester as the emulsifier also provided single-dispersed emulsions with droplet sizes of 0.831 ± 0.0760 and 12.8 ± 0.0610 μm as shown in Figure 1B. When soybean oil TAG o/w emulsions were prepared by using decaglycerol lauryl ester as the emulsifier, the single-dispersed emulsions with mean droplet sizes of 0.828 ± 0.0850, 1.09 ± 0.0760, or 9.38 ± 0.276 μm were again obtained successfully as shown in Figure 1C.

Although the single-dispersed o/w emulsions were prepared successfully for TAG of both fish and vegetable oils as well as for both emulsifiers, emulsions with mean droplet sizes of over 3.28 μm showed creaming during standing without any shaking. Oil droplets of o/w emulsions were, however, physically stable over the period of oxidation, and droplet sizes of the emulsions remained unchanged at 40°C in the dark for up to 120 h of oxidation time (data not shown).

Oxidative stability of TAG in o/w emulsions. Changes in total HPO contents generated in cod liver oil TAG o/w emulsions

stabilized by decaglycerol lauryl ester are shown in Figure 2A. With decreasing droplet size of o/w emulsions from 10.7 to 0.806 μm, HPO contents in the vials became significantly less during oxidation for up to 120 h. Changes in residual oxygen contents in cod liver oil TAG o/w emulsions stabilized by 1% decaglycerol lauryl ester are shown in Figure 2B. Residual oxygen contents in the headspace air of the vials containing the o/w emulsion showed a trend similar to the case when sucrose lauryl ester was used as an emulsifier; with decreasing droplet sizes of the emulsions, the amount of absorbed oxygen became lower after 96 h of oxidation.

Changes in the contents of total HPO generated in cod liver oil TAG o/w emulsions stabilized by sucrose lauryl ester are shown in Figure 3A. Total HPO contents in emulsions with a mean droplet size of 0.831 μm were significantly lower than those in emulsions with a mean droplet size of 12.8 μm for 120 h of oxidation time. HPO contents in emulsions with a mean droplet size of 12.8 μm increased up to 58.1 mequiv/kg lipid. On the contrary, for the same oxidation period, the HPO contents in the emulsion with a mean droplet size of 0.831 μm was 14.3 mequiv/kg lipids. Decreases in residual oxygen contents in the headspace air of the vials containing the o/w emulsion that had a mean droplet size of 0.831 μm were significantly lower than that with the emulsion that had a mean droplet size
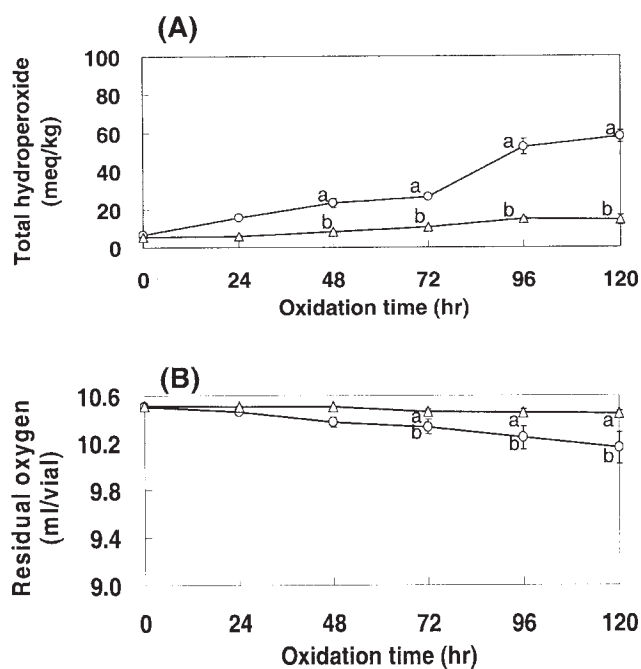
FIG. 3. Changes in total hydroperoxide contents (A) and in residual oxygen contents in the headspace air of vials (B) during oxidation of cod liver oil TAG 10% oil-in-water emulsions stabilized by 1% sucrose lauryl ester with mean droplet sizes of 0.831 (△) and 12.8 μm (○) at 40°C in the dark. Values represent the mean of replicate determinations (*n* = 5) ± SD at each time point. For each sample for the same oxidation period, values with different superscripts (a, b) are significantly different (*P* < 0.05).

of 12.8 μm after 72 h of oxidation as shown in Figure 3B. After 120 h oxidation, the residual oxygen content in the vial containing the emulsion with a mean droplet size of 0.831 μm amounted to 10.4 mL/vial; however, that in the vial containing the emulsion with a mean droplet size of 12.8 μm was significantly lower, amounting to 10.1 mL/vial.

Changes in total HPO contents of soybean oil TAG o/w emulsions stabilized by decaglycerol lauryl ester are shown in Figure 4A. With decreasing droplet size of o/w emulsions from 9.38 to 0.828 μm, HPO contents in the vials became significantly lower during oxidation for up to 72 h. Changes in residual oxygen contents in the o/w emulsion of the soybean oil TAG stabilized by 1% decaglycerol lauryl ester are shown in Figure 4B. Residual oxygen contents in the headspace air of the vials containing the emulsions showed a similar trend; with decreasing droplet size of the emulsions, the amount of absorbed oxygen became lower after 72 h of oxidation. The amounts of hexanal formed from the 9.38 μm emulsion were significantly higher than those of the 0.828 and 1.09 μm emulsions after 72 h of oxidation (Fig. 4C).

Spin–spin relaxation time of protons. ^{1}H NMR spectra of cod liver oil TAG o/w emulsions with a mean droplet size of 0.815 and 6.54 μm, which were stabilized by 1% decaglycerol lauryl ester, are summarized in Figure 5. Peaks at 0.94, 1.34, 1.63, 2.07, 2.29, and 2.87 ppm are assigned to methyl protons (a), alkyl protons (b), carboxyl terminal (c), olefin proton (d),
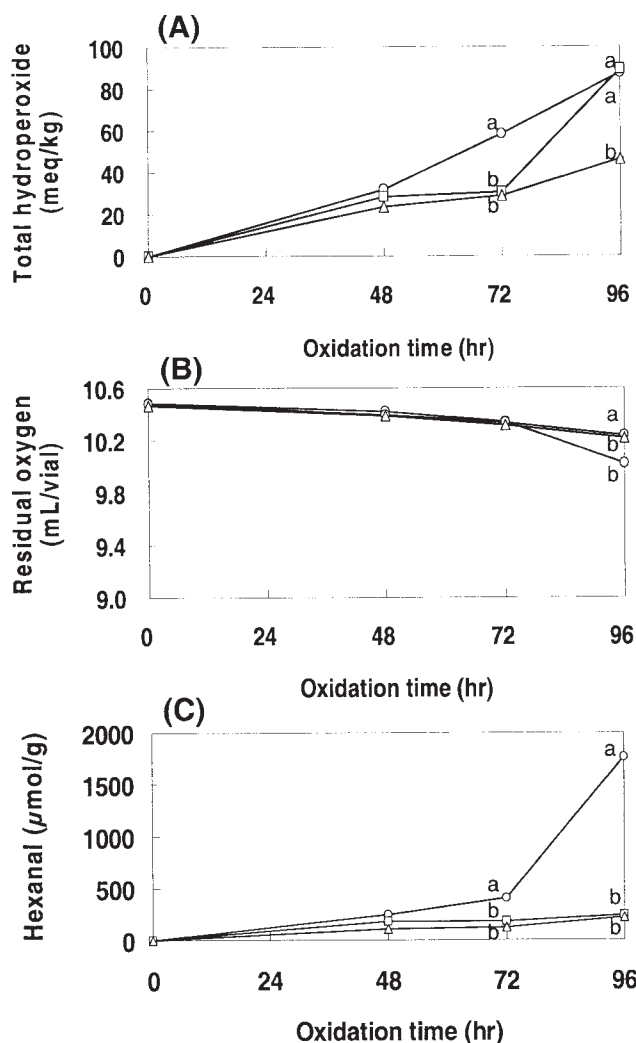
FIG. 4. Changes in total hydroperoxide contents (A), in residual oxygen contents in the headspace air of vials (B), and in hexanal contents in the headspace air of vials (C) during oxidation of soybean oil TAG 10% oil-in-water emulsions stabilized by 1% decaglycerol lauryl ester with mean droplet sizes of 0.828 (△), 1.09 (□), and 9.8 μm (○) at 50°C in the dark. Values represent the mean of replicated determinations (*n* = 5) ± SD at each time point. For each sample for the same oxidation period, values with different superscripts (a, b) are significantly different (*P* < 0.05).

and bisallylic proton (f), respectively. Figure 6A shows logarithmic plots of peak intensities against echo time. Plots for peaks at 0.94, 1.63, 2.07, 2.29, and 2.87 ppm regressed following a straight line, and ^{1}H T_2 values were calculated by using Equation 1. On the other hand, the plot for the peak at 1.34 ppm had a bend, indicating that each methylene proton has different ^{1}H T_2 depending on the position in the alkyl group. We assumed that these methylene protons can be divided into two groups with large and small ^{1}H T_2 and analyzed the decays by using Equation 2. The obtained ^{1}H T_2 values are summarized in Figure 6B.

For peaks at 0.94, 1.63, 2.07, 2.29, and 2.87 ppm, ^{1}H T_2 differed from peak to peak reflecting the chemical structure;
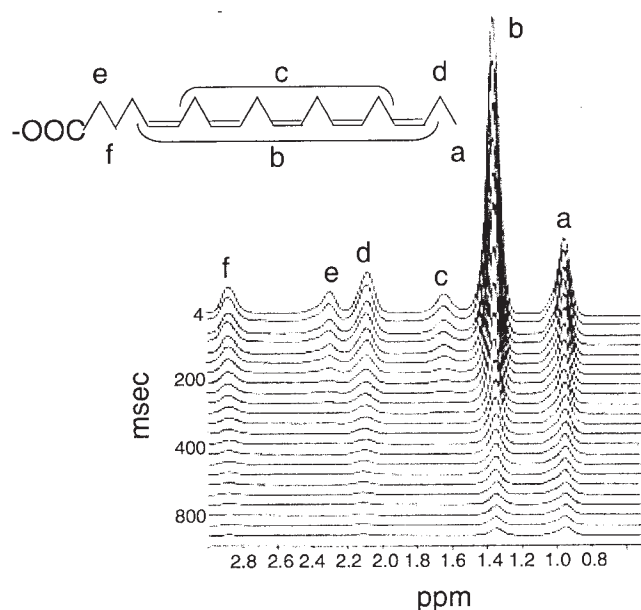
FIG. 5. Typical ^{1}H NMR spectra of cod liver oil TAG 10% oil-in-water emulsions stabilized by 1% decaglycerol lauryl ester with a mean droplet size of 0.815 μm.

however, it is difficult to discuss the small differences of ^{1}H T_2 between the o/w emulsions with different droplet sizes because small intensities for these peaks led to lower accuracy. For the large peak at 1.34 ppm, the ^{1}H T_2 of the slow decay component for the emulsion with smaller droplet size was smaller than that for the emulsion with larger droplet size.

DISCUSSION

The present study clearly showed that droplet size of an o/w emulsion influenced oxidative stability, and oxidative stability increased with decreasing droplet size. Additionally, differences between nonionic types of emulsifier were not an important factor in influencing the oxidative stability of the emulsions. Numerous reports have evaluated the effects of droplet size on oxidative stability of o/w emulsions. Gohtani *et al.* (13) compared the oxidative stability of free DHA o/w emulsions with droplet sizes of 3.4 and 6.4 μm and reported that the oxidative stability of the emulsion with the smaller droplet size was inferior to that of larger droplet size. They pointed out that the close-packed droplets gathered by creaming at the surface of emulsions and resulted in acccelerating a chain reaction in the oxidation step of DHA when the emulsion was kept standing without shaking. In the present study, however, emulsions were shaken gently and continuously during the oxidation process and therefore the density of droplets in the emulsion system should be similar between the emulsions with different droplet sizes.

As one possible mechanism to explain improvements in oxidative stability found in o/w emulsions with smaller droplet sizes, we propose the following hypothesis: The location of emulsifier molecules at the interface between oil and water phases may affect the mobility of TAG molecules existing at the surface of the oil phase and may participate in the improvement of oxidative stability of TAG. The ratio of the surface area of a sphere to its volume is inversely proportional to the radius. When the total interface areas as well as the total volumes of droplets of equal volume of two o/w emulsions differing in oil
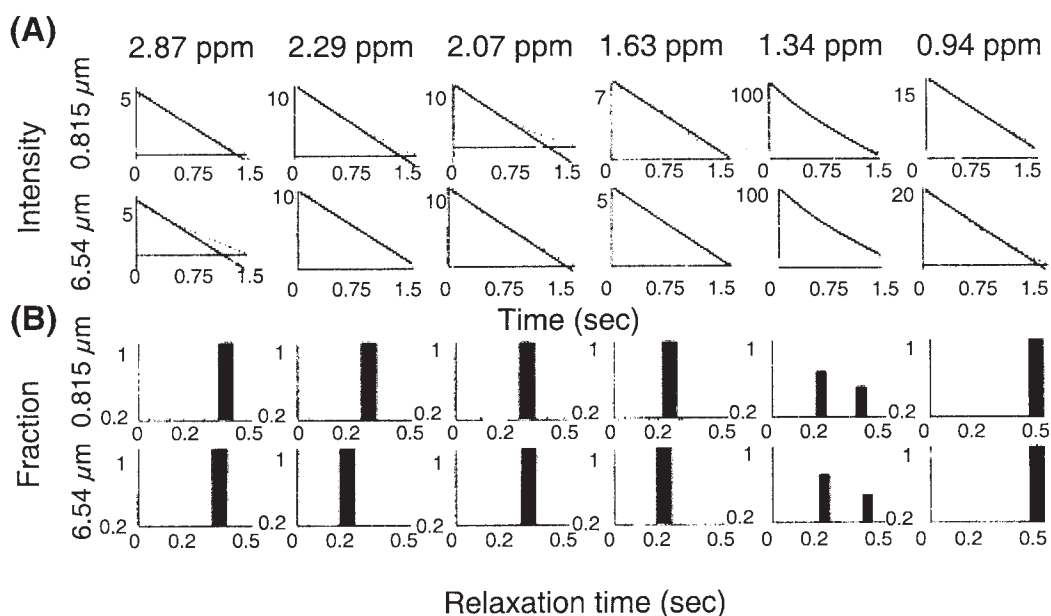
FIG. 6. ^{1}H NMR based on chemical shifts of cod liver oil TAG 10% oil-in-water emulsions stabilized by 1% decaglycerol lauryl ester with mean droplet sizes of 6.54 and of 0.815 μm. Logarithmic plots of peak intensities against echo time (A) and distributions of spin-spin relaxation times of protons (B).
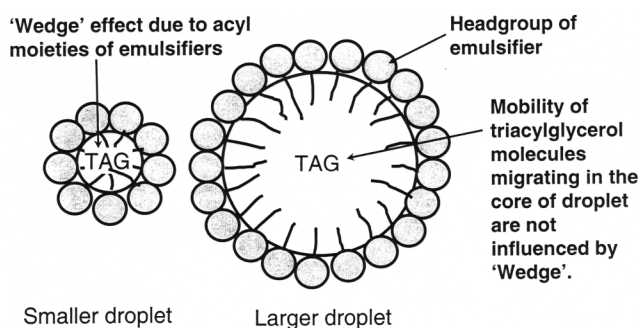
FIG. 7. Hypothesis on the effect of wedges due to hydrophobic acyl residues of sucrose lauryl ester or decaglycerol lauryl ester used as emulsifiers. The wedge driven in the oil phase of smaller-sized oil droplets suppresses the mobility of TAG molecules migrating in the oil phase of the droplet. In a larger droplet, however, the TAG molecules migrating in the core of the oil phase are not influenced by the wedge.

droplet diameter by 10 times from each other are compared, the relative concentration of the lauryl ester in the oil phase is inversely proportional to the radius of the oil droplet. Thus, the concentration of lauric acid residues of the emulsifier in the oil phase of the smaller droplet becomes 10 times higher than that of the larger droplet. On the other hand, the number of emulsifier molecules located at the interface of the smaller droplet is one-hundredth of that of the larger droplet, resulting in the actual concentration of lauric acid residues in smaller droplet becoming about 10 times higher than that in the larger droplet. Consequently, the concentration of unsaturated TAG in a smaller droplet becomes lower and thus lipids in the emulsion become more stable against oxidation.

Recently, Osborn and Akoh (11) investigated the oxidative stability of caprylic acid/canola oil o/w emulsion and reported that the droplet size of the emulsion did not affect oxidative stability. The emulsion system used in those studies contained no chelating agent, suggesting that HPO decompositions occurred easily to form secondary oxidation products in the early stages of the oxidation period. In our study, the added EDTA suppressed the decomposition of HPO and resulted in the differences in oxidative stabilities between emulsions with different droplet sizes.

As a possible mechanism to explain the different oxidative stabilities between o/w emulsions with different droplet sizes, another hypothesis on the wedge effect due to hydrophobic lauryl residues of a sugar ester or polyglycerol ester has been proposed and is illustrated in Figure 7. Emulsifier molecules located at the interface between the oil and water phases may influence the mobility of TAG molecules existing in the oil phase and may result in the improvement of oxidative stability of TAG. The wedge driven in the oil phase of a droplet with a small size suppresses the mobility of TAG molecules. In a larger droplet, however, the wedge does not influence TAG molecules located in the core of the droplet.

Yazu *et al.* (33,34) compared oxidation stabilities of methyl eicosapentaenoate (methyl EPA) and methyl linoleate in micelles and found that methyl EPA was more stable than methyl linoleate. They explained the mechanism of this phenomenon

as follows: HPO generated by oxidation of methyl EPA is polar, and HPO molecules located in the core of micelles move to the interface area. Consequently, the propagation rate of radicals becomes slower with increasing concentration of methyl EPA HPO at the surface compared with the micelle core. In the present study, oxidized TAG molecules with higher polarity distribute in the interface area of an oil droplet, and their mobility is restricted by wedges of emulsifier residues. The rate of radical propagation will therefore become slower and result in reduction of the oxidation rate. Since the distance from the core of the oil droplet to the interface is short in a small droplet, it will take less time to decrease the concentration of HPO molecules in the core of droplets compared with the case of larger droplets. Additionally, mobilities of polar HPO molecules moving to the interface will be restricted by the wedge effect of the emulsifier molecules.

The relaxation times of protons measured by ^{1}H NMR strongly support the foregoing hypothesis on wedge effect. The TAG has higher molecular mobility when located at the core than in the vicinity of the surface. When TAG migrates between the surface and the core of droplets in a shorter time than ^{1}H T_2, the observed ^{1}H T_2 ($T_{2,\mathrm{obs}}$) is expressed as follows:

$$1/T_{2,\mathrm{obs}} = F_{\mathrm{core}}/T_{2,\mathrm{core}} + F_{\mathrm{surf}}/T_{2,\mathrm{surf}} \qquad [3]$$

where F_{core} and F_{surf} are fractions of TAG migrating at the core of the droplet and in the vicinity of the surface, respectively, and $F_{\mathrm{core}} + F_{\mathrm{surf}} = 1$. $T_{2,\mathrm{core}}$ and $T_{2,\mathrm{surf}}$ are inherent T_2 values for TAG at the core and vicinity of the surface, respectively, and $T_{2,\mathrm{surf}} \ll T_{2,\mathrm{core}}$ because of the low molecular mobility at the vicinity of the surface. Smaller droplets have smaller F_{core}; therefore, $T_{2,\mathrm{obs}}$ becomes smaller. Thus, these observations support the preceding hypothesis on the wedge effect due to the hydrophobic residues of emulsifiers. The rates of chain oxidation reactions consequently become smaller in smaller droplet size emulsions due to the restriction of vibration frequency of the acyl chains of TAG molecules in the smaller oil droplet.

Our findings provide clear evidence that droplet size in o/w emulsions influences oxidative stability of oils. Decreasing emulsion droplet size directly improves oxidative stability of oils. These observations will provide useful knowledge in developing food with stable oxidative characteristics.

REFERENCES

1. Bruna, E., Petei, M., Beijean-Leymarie, M., Huynh, S., and Nouvelot, A. (1989) Specific Susceptibility of Docosahexaenoic Acid and Eicosapentaenoic Acid to Peroxidation in Aqueous Solution, *Lipids 24*, 970–975.
2. McLennan, P., Howe, P., Abeywardena, M., Muggli, R., Raederstorff, D., Mano, M., Rayner, T., and Head, R. (1996) The Cardiovascular Protective Role of Docosahexanoic Acid, *Eur. J. Pharmacol. 300*, 83–89.
3. Minami, M., Kimura, S., Endo, T., Hamaue, N., Hirafuji, M., Togashi, H., Matsumoto, M., Yoshioka, M., Saito, H., Watanabe, S., *et al.* (1997) Dietary Docosahexanoic Acid Increases Cerebral Acetylcholine Level and Improves Passive Avoidance

Performance in Stroke-Prone Spontaneously Hypertensive Rats, *Pharmacol. Biochem. Behav. 58*, 1123–1129.

4. McClements, D.J., and Decker, E.A. (2000) Lipid Oxidation in Oil-in-Water Emulsions: Impact of Molecular Environment on Chemical Reactions in Heterogeneous Food Systems, *J. Food Sci. 65*, 1270–1282.

5. Holman, R.T., and Elmer, O.C. (1947) The Rates of Oxidation of Unsaturated Fatty Acids and Esters, *J. Am. Oil Chem. Soc. 24*, 127–129.

6. Cosgrove, J.P., Church, D.F., and Pryor, W.A. (1987) The Kinetics of the Autoxidation of Polyunsaturated Fatty Acids, *Lipids 22*, 299–304.

7. Mei, L.Y., McClements, D.J., Wu, J.N., and Decker, E.A. (1998) Iron-Catalyzed Lipid Oxidation in Emulsions as Affected by Surfactant, pH and NaCl, *Food Chem. 61*, 307–312.

8. Mei, L.Y., McClements, D.J., and Decker, E.A. (1998) Evidence of Iron Association with Emulsion Droplets and Its Impact on Lipid Oxidation, *J. Agric. Food Chem. 46*, 5072–5077.

9. Silvestre, M.P.C., Chaiyasit, W., Brannnan, R.G., McClements, D.J., and Decker, E.A. (2000) Ability of Surfactant Head Group Size to Alter Lipid and Antioxidant in Oil-in-Water Emulsions, *J. Agric. Food Chem. 48*, 2057–2061.

10. Donnelly, J.L., Decker, E.A., and McClements, D.J. (1998) Iron-Catalyzed Oxidation of Menhaden Oils as Affected by Emulsifiers, *J. Food Sci. 63*, 997–1000.

11. Osborn, H.T., and Akoh, C. (2003) Effect of Emulsifier Type, Droplet Size, and Oil Concentration on Lipid Oxidation in Structured Lipid-Based Oil-in-Water Emulsions, *Food Chem. 84*, 451–456.

12. Shimada, K., Okada, H., Matsuo, M., and Yoshioka, S. (1996) Involvement of Chelating Action and Viscosity in the Antioxidative Effect of Xanthin in an Oil/Water Emulsion, *Biosci. Biotechnol. Biochem. 60*, 125–127.

13. Gohtani, S., Sirendi, M., Yamamoto, N., Kajikawa, K., and Yamamoto, Y. (1999) Effect of Droplet Size on Oxidation of Docosahexaenoic Acid in Emulsion System, *J. Dispersion Sci. Technol. 20*, 1319–1325.

14. Hegenauer, J., Saltman, P., Ludwig, D., Ripley, L., and Bajo, P. (1979) Effect of Supplemental Iron and Lipid Oxidation in Milk. 1. Comparison of Metal Complexes in Emulsified and Homogenized Milk, *J. Agric. Food Chem. 27*, 860–867.

15. Duh, P.-D., Yen, W.-J., and Yen, G.-C. (1999) Oxidative Stability of Polyunsaturated Fatty Acids and Soybean Oil in an Aqueous Solution with Emulsifiers, *J. Am. Oil Chem. Soc. 76*, 201–204.

16. Fomuso, L.B., Corredig, M., and Akoh, C.C. (2002) Effect of Emulsifier on Oxidation Properties of Fish Oil-Based Structured Lipid Emulsions, *J. Agric. Food Chem. 50*, 2957–2961.

17. Kubouchi, H., Kai, H., Miyashita, K., and Matsuda, K. (2002) Effect of Emulsifiers on the Oxidative Stability of Soybean Oil TAG in Emulsions, *J. Am. Oil Chem. Soc. 79*, 567–570.

18. Hu, M., McClements, D.J., and Decker, E.A. (2003) Impact of Whey Protein Emulsifiers on the Oxidative Stability of Salmon Oil-in-Water Emulsions, *J. Agric. Food Chem. 51*, 1435–1439.

19. Mancuso, J.R., McClements, D.J., and Decker, E.A. (1999) The Effects of Surfactant Type, pH, and Chelators on the Oxidation of Salmon Oil-in-Water Emulsions, *J. Agric. Food Chem. 47*, 4112–4116.

20. Kuwabara, K., Watanabe, Y., Adachi, S., Nakanishi, K., and Matsuno, R. (2003) Emulsifier Properties of Saturated Acyl L-Ascorbates for Preparation of O/W Emulsions, *Food Chem. 82*, 191–194.

21. Paiva-Martins, P., and Gordon, M.H. (2002) Effect of pH and Ferric Ions on the Antioxidant Activity of Olive Polyphenol in Oil-in-Water Emulsions, *J. Am. Oil Chem. Soc. 79*, 571–576.

22. Cho, Y.-J., McClements, D.J., and Decker, E. A. (2002) Ability of Surfactant Micelles to Alter the Physical Location and Reactivity of Iron in Oil-in-Water Emulsion, *J. Agric. Food Chem. 50*, 5704–5710.

23. Frankel, E.N. (1996) Antioxidants in Lipid Foods and Their Impact on Food Quality, *Food Chem. 57*, 51–55.

24. Abdalla, A.E., Tirzite, D., Tirzitis, G., and Roozen, J.P. (1999) Antioxidant Activity of 1,4-Dihydropyridine Derivatives in β-Carotene–Methyl Linoleate, Sunflower Oil and Emulsions, *Food Chem. 66*, 189–195.

25. Miyashita, K., Nara, E., and Ota, T. (1993) Oxidative Stability of Polyunsaturated Fatty Acids in an Aqueous Solution, *Biosci. Biotech. Biochem. 57*, 1638–1640.

26. Friberg, S.E. (1997) Emulsion Stability, in *Food Emulsions,* 3rd edn. (Friberg, S.E., and Larsson, K., eds.), pp. 1–55, Marcel Dekker, New York.

27. Lethuaut, L., Metro, F., and Genot, C. (2002) Effect of Droplet Size on Lipid Oxidation Rates of Oil-in-Water Emulsions Stabilized by Protein, *J. Am. Oil Chem. Soc. 79*, 425–430.

28. Coupland, J.N., Zhu, Z., McClements, D.J., Nawar, W.W., and Chinachoti, P. (1996) Droplet Composition Affects the Rate of Oxidation of Emulsified Ethyl Linoleate, *J. Am. Oil Chem. Soc. 73*, 795–801.

29. Nakashima, T., Shimizu, M., and Kukizaki, M. (2000) Particle Control of Emulsion by Membrane Emulsification and Its Applications, *Advanced Drug Delivery Rev. 45*, 47–56.

30. Sohn, J.-H., Taki, Y., Ushio, H., and Ohshima, T. (2005) Quantitative Determination of Total Lipid Hydroperoxides by a Flow Injection Analysis System, *Lipids 40*, 203–209.

31. Frankel, E.N., Hu, M.-L., and Tappel, A.L. (1989) Rapid Headspace Gas Chromatography of Hexanal as a Measure of Lipid Peroxidation in Biological Samples, *Lipids 24*, 976–981.

32. Box, G.E.P., Hunter, W.G., and Hunter, J.S. (1978) *Statistics for Experimenters*, pp. 21–56, John Wiley & Sons, New York.

33. Yazu, K., Yamamoto, Y., Ukegawa, K., and Niki, E. (1996) Mechanism of Lower Oxidizability of Eicosapentanoate Than Linoleate in Aqueous Micelles, *Lipids 31*, 337–340.

34. Yazu, K., Yamamoto, Y., Niki, E., Miki, K., and Ukegawa, K. (1998) Mechanism of Lower Oxidizability of Eicosapentanoate Than Linoleate in Aqueous Micelles. II. Effect of Antioxidants, *Lipids 33*, 597–600.

Relative Retention Order of All Isomers of *cis/trans* Conjugated Linoleic Acid FAME from the 6,8- to 13,15-Positions Using Silver Ion HPLC with Two Elution Systems

Pierluigi Delmonte[a], Ai Kataoka[a], B.A. Corl[b], D.E. Bauman[b], and Martin P. Yurawecz[a],*

[a]U.S. Food and Drug Administration, Center for Food Safety and Applied Nutrition, College Park, Maryland 20740, and [b]Department of Animal Science, Cornell University, Ithaca, New York

ABSTRACT: CLA, defined as one or more octadecadienoic acids (18:2) with conjugated double bonds, has been reported to be active in a number of biological systems. GC and silver ion HPLC (Ag⁺-HPLC) have been the primary techniques for identifying specific CLA isomers in both foods and biological extracts. Recently, GC relative retention times were reported for all *c,c, c/t* (*c,t* and *t,c*), and *t,t* CLA FAME from the 6,8- to the 13,15-positions in octadecadienoic acid (18:2). Presented here is the relative retention order of the same CLA FAME using Ag⁺-HPLC with two different elution systems. The first elution system, consisting of 0.1% acetonitrile/0.5% diethyl ether (DE) /hexane, has been used previously to monitor CLA composition in foods. Also presented here is the retention order of CLA FAME using 2% acetic acid/hexane elution solvent, which has advantages of more stable retention volumes and a complementary elution order of CLA FAME isomers. The data are reported using retention volumes (RV) adjusted for toluene, an estimator for dead volume, and relative to *c*9,*t*11-18:2. Measurement of relative RV in the analysis of 88 samples of cow plasma, milk, and rumen fluids using Ag⁺-HPLC is also presented here. The % CV ranged from 1.04 to 1.62 for *t,t* isomers and from 0 to 0.48 for *c/t* isomers.

Paper no. L9281 in *Lipids 40*, 509–514 (May 2005).

Conjugated linoleic acid and CLA are terms used to describe octadecadienoic (18:2) fatty acid(s) or ester(s) with two conjugated double bonds. Different double bond positions and geometric configurations can create a large set of compounds with similar structure but not necessarily similar chemical or biological properties. Twenty CLA isomers already have been reported in food (1). GC separation, using the best capillary columns that are currently available, typically elutes the CLA-18:2 FAME in a small interval, ~3.5 min, of a 70-min run. Insufficient resolution is obtained by GC to identify or quantify individual isomers. A typical Ag⁺-HPLC run of ~60 min will spread the area of elution for CLA isomers to >30 min. The two techniques, GC and Ag⁺-HPLC, are complementary and can be used successfully for separation of virtually all the isomers present in a test portion of a sample.

A major problem with Ag⁺-HPLC is the retention volume (RV) drift that occurs over time (2). This Ag⁺-HPLC technique, which provides a wide separation of CLA isomers, is gaining more acceptance but it is not yet in common use because the nonreproducibility of RV makes the identification of peaks difficult. To simplify the interpretation of Ag⁺-HPLC chromatograms, we present here the application of relative retention volumes (RRV) to the identification of CLA isomers. The mean (μ), standard deviation (σ), and % CV (100 × σ/μ) are presented for the RRV of 88 sample extracts from cow plasma, milk, and rumen fluid. Lack of knowledge concerning the chromatography of CLA FAME has been a point of concern in the accurate identification of specific isomers. In many reports, responses occurring at the retention time of *c*9,*t*11-CLA have been reported only as *c*9,*t*11-CLA even though, depending on the relative quantities present, the isomers *c*6,*t*8-, *t*7,*c*9-, and both *c/t* (*c,t* and *t,c*) 8,10-CLA give responses at this retention time (3). The use of relative retention times (GC) or RRV (HPLC), combined with the availability of reference materials for all CLA isomers from 6,8 to 13,15, allows the development of a basis for a more conservative approach to identification.

EXPERIMENTAL PROCEDURES

A mixture of CLA FFA, CLA FAME, γ-linolenic acid (*cis*-6, *cis*-9, *cis*-12-octadecatrienoic acid) and α-linolenic (*cis*-9, *cis*-12, *cis*-15-octadecatrienoic acid) FAME were purchased from Nu-Chek-Prep, Inc. (Elysian, MN). CLA isomers of known purity (*c*9,*t*11-, *t*10,*c*12-, *c*9,*c*11-, *c*11,*t*13-, and *t*9,*t*11-18:2) were obtained as FFA from Matreya, Inc. (Pleasant Gap, PA). The CLA isomers that were not commercially available were synthesized as previously reported (4). FAME were prepared from fat extracted from milk, plasma, and rumen fluid of dairy cows as previously described (5). Acetonitrile (MeCN) and hexane were UV grade. Diethyl ether (DE) was anhydrous. BF₃ in methanol was obtained from Supelco (Bellefonte, PA). Test portions of FAME were dissolved in 0.5% toluene/hexane (or isooctane) prior to chromatographic analysis. Normalization of the chromatograms shown in this work was accomplished using default functions of Microsoft® Excel (9.0 3821 SR-1) (Microsoft Corp., Redmond, WA). Chromatograms were ex-

ported from the acquisition software as the raw signals vs. time. HPLC data were exported from Millenium (Waters Associates, Milford, MA) as ASCII (ARW) files to Microsoft Excel. The new chromatograms, in the relative scale, were obtained as X-Y scatter plots of the signal vs. RRV. Column values were recalculated in the RRV scale using the following formula:

$$RRV_a = (RV_a - RV_{tol})/(RV_{c9,t11} - RV_{tol}) \qquad [1]$$

where RRV_a is the relative retention volume of a CLA isomer, RV_a is the retention volume of a CLA isomer, RV_{tol} is the retention volume of toluene, and $RV_{c9,t11}$ is the retention volume of the $c9,t11$-CLA.

Analytical Ag⁺-HPLC. Ag⁺-HPLC separation of the CLA FAME was carried out using a Waters 2960 chromatographic system (Waters Associates), equipped with a photodiode array detector (Waters 996) operating between 200 and 300 nm, and a Millenium 3.20 chromatography manager. Three Chrom-Spher 5 Lipids analytical silver-impregnated columns (each 4.6 mm i.d. × 250 mm stainless steel; 5 µm particle size; Chrompack, Bridgewater, NJ) were used in series. The temperature was maintained at 30°C. The first mobile phase, 0.1% MeCN/0.5% DE/hexane, was prepared fresh daily and introduced isocratically at a flow rate of 1.0 mL/min. The columns were conditioned with 1% MeCN/hexane then equilibrated with the elution solvent for 60 min each day prior to starting test portion analysis. Typical injections, 1–10 µL, for milk, plasma, or reference materials resulted in <100 µg FAME being loaded onto the columns. For test portions of rumen

FAME, column loads of >>100 µg were used. Single chromatograms of CLA isomers were extracted at 233 nm. To obtain the RRV values of all CLA isomers, iodine-isomerized mixtures of positional CLA isomers (4) were co-injected with a small amount of $c9,t11$-18:2 FAME and toluene. The second mobile phase used was 2% acetic acid/hexane eluted at 1 mL/min. HPLC chromatograms were obtained using the same three ChromSpher 5 Lipids analytical silver-impregnated columns described above. Responses were measured using UV detection at 233 nm.

RESULTS AND DISCUSSION

We recently completed an exhaustive analysis of CLA isomers in 88 samples of plasma, milk, and rumen fluid from dairy cows (5). Ag⁺-HPLC chromatograms from that study, from plasma, two samples of cow's milk and CLA reference material (Nu-Chek-Prep) are shown in Figure 1A–D, left side. As can be seen in the figure, the retention volumes (shown as retention times in the figures) shift for the elution of each isomer. The $c9,t11$ isomer elutes over a range of several minutes. In most of the cases, the rule that the $c9,t11$-isomer is the most abundant may be applied to CLA analysis by Ag⁺-HPLC, but in several other cases, as shown in Figure 1, this rule does not apply. Chromatogram A was obtained by injection of a plasma sample from a cow that had been fed a diet supplemented with $t10,c12$-CLA. Our original analysis of these samples involved many co-injections of standard with samples to verify the identities. We discovered that by using toluene as a reference to approximate the dead volume
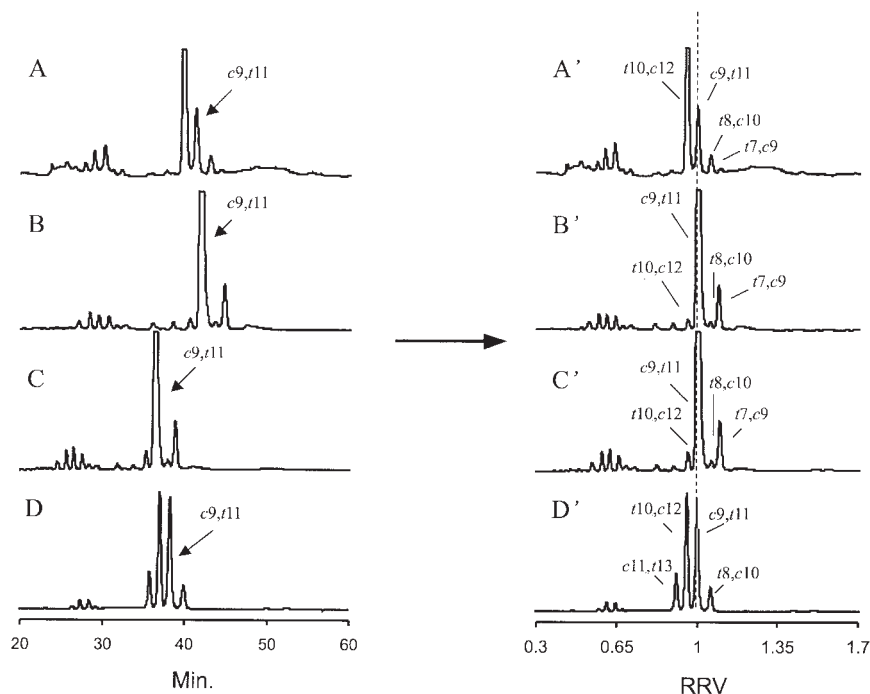
FIG. 1. Ag⁺-HPLC chromatograms. Time vs. response (233 nm) of FAME obtained from plasma (A), milk fat (B, C), and Nu-Chek-Prep CLA (D). The corresponding graphs A′–D′ of the same sample test portions plotting response vs. relative retention volumes (RRV) are shown on the right.

TABLE 1
Relative Retention Volumes for CLA FAME from Cow Milk, Plasma, and Rumen Fluids

	Milk			Plasma			Rumen			Total			
	n	μ	σ	n	μ	σ	n	μ	σ	n	μ	σ	% CV
*t*12,*t*14	48	0.533	0.008	24	0.538	0.005	16	0.544	0.010	88	0.536	0.009	1.62
*t*11,*t*13	48	0.574	0.007	24	0.579	0.005	16	0.586	0.010	88	0.578	0.008	1.46
*t*10,*t*12	48	0.609	0.007	24	0.612	0.005	16	0.620	0.010	88	0.611	0.008	1.34
*t*9,*t*11	48	0.649	0.007	24	0.655	0.007	16	0.658	0.010	88	0.653	0.008	1.27
*t*8,*t*10	48	0.680	0.007	21	0.686	0.006	9	0.681	0.007	78	0.682	0.007	1.04
*t*7,*t*9	48	0.716	0.009	22	0.719	0.006	0	NA[a]	NA	70	0.717	0.008	1.09
*c*11,*t*13	48	0.914	0.003	24	0.911	0.002	2	0.901	0.018	73	0.913	0.004	0.48
*t*11,*c*13	48	0.893	0.005	24	0.892	0.002	1	0.894	NA	73	0.893	0.004	0.44
*t*10,*c*12	48	0.957	0.003	24	0.956	0.001	16	0.958	0.003	88	0.957	0.003	0.27
*c*9,*t*11	48	1.000	0.000	24	1.000	0.000	16	1.000	0.000	88	1.000	0.000	0.00
*t*8,*c*10	48	1.059	0.002	24	1.060	0.003	0	NA	NA	72	1.059	0.002	0.22
*t*7,*c*9	48	1.095	0.003	24	1.094	0.002	7	1.094	0.017	79	1.094	0.005	0.47

[a]Not applicable.

in the HPLC system, and *c*9,*t*11 as a retention reference, the chromatographic data could be recalculated into a reproducible format using a formula derived from standard chromatography theory. The RRV was calculated as shown in the Experimental Procedures section. By using this format, the chromatograms were regenerated using Excel as shown in Figure 1A′–D′, but these chromatograms are plotted as response vs. RRV. This application of the RRV theory is based on the assumption that, for the small variation in MeCN in hexane concentration occurring during the analysis of a sample set, the change in composition of the mobile phase will affect the elution of all of the CLA isomers in the same way.

The reproducibility of RRV in sample data using a specific chromatography system was established as shown in Table 1. The % CV measured for the 88 samples was 1.04–1.62 for the *t,t* isomers, and 0–0.47 for the *c/t* isomers. The precision was

better for the plasma and milk samples, as is seen from the lower SD for these sample types in Table 1. A factor that leads to higher RRV SD of CLA isomers in rumen samples is related to critical (sample overload) chromatography conditions. CLA FAME isomers were present at trace levels in all the methylated rumen samples we analyzed, and test portions loaded onto the columns were increased to reach the detection limits of as many CLA isomers as possible. Co-eluting *cis* monoenoic FAME interfered with the CLA analysis of rumen test portions under these extreme conditions, requiring UV (232 nm) confirmation for every identification.

Ag^{+}-HPLC chromatograms, transformed using Equation 1, are presented in Figure 2. A small amount of *c*9,*t*11-CLA FAME was added to every sample shown in Figure 2 to aid in translating chromatograms to the RRV scale. A graphical representation in Figure 3 further elucidates the RRV pattern. The
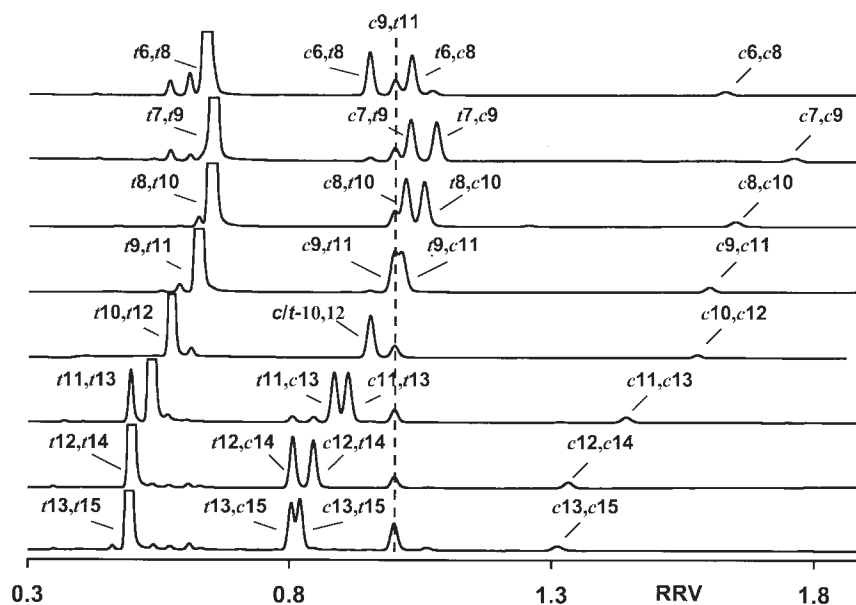
FIG. 2. Ag^{+}-HPLC chromatograms using 0.1% acetonitrile (MeCN)/0.5% diethyl ether (DE)/hexane elution, RRV vs. response (233 nm) of all geometric CLA isomers from the 6,8 to the 13,15 carbon–carbon double bond positions. A small quantity of *c*9,*t*11 was added to each positional mixture for reference.
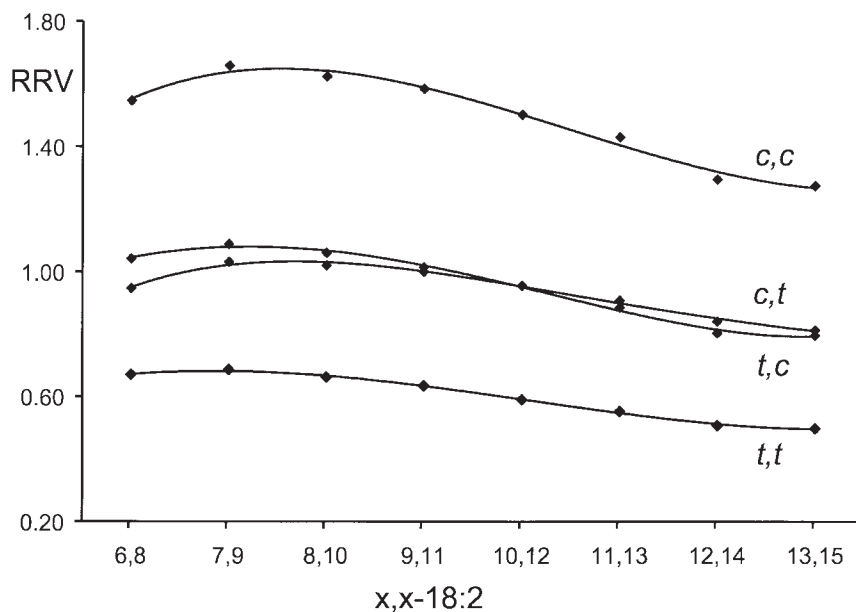
FIG. 3. Plot of RRV vs carbon-carbon double bond position for all geometric CLA isomers from the 6,8 to the 13,15 carbon–carbon double bond positions (using 0.1% MeCN/0.5% DE/hexane elution). For abbreviations see Figures 1 and 2.

RRV values of the *t,t*, *c,t*, and *t,c* isomers fit third-degree curves with R^2 greater than 0.99. The RRV values of the *c,c* isomers fit a third-degree equation with R^2 greater than 0.985. All four curves show a similar pattern, with a maximum corresponding to the 7,9 positional isomer, and an inflection point close to the 10,12 position. Isomers *c10,t12* and *t10,c12* have the same RRV, and the *c,t* and *t,c* curves intersect at the 10,12 position. For a given position, from 6,8 to 9,11 (all of these isomers elute

after the 10,12 *c/t* isomer), the RRV of the *t,c* isomer will be higher than that of the corresponding positional *c,t* isomer. For *c/t* isomers eluting before the *c/t* isomers of 10,12 (from 11,13 to 13,15), the *c,t* isomer will elute after the *t,c* isomer.

Chromatograms obtained using the second solvent system presented here are shown in Figure 4. The set of the iodine-isomerized solutions (4) containing all the positional isomers from 6,8- to 13,15-18:2 are presented. Under these operating
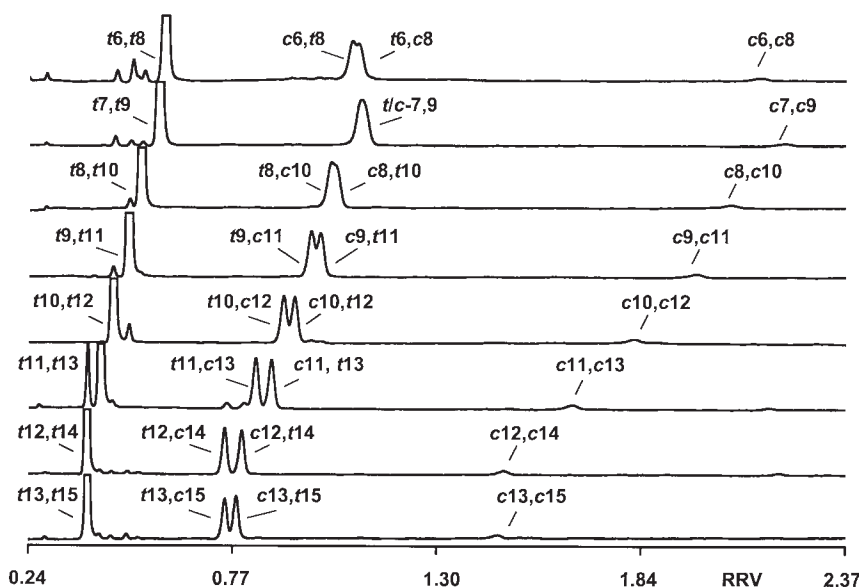
FIG. 4. Partial Ag$^+$-HPLC chromatograms (RRV) of the iodine-isomerized solutions from each CLA positional isomer from 6,8- to 13,15-18:2 as FAME. Chromatographic conditions: three ChromSpher 5 Lipids columns in series maintained at 25°C, 2% HOAc in hexane mobile phase at 1.0 mL/min, UV detection at 233 nm.
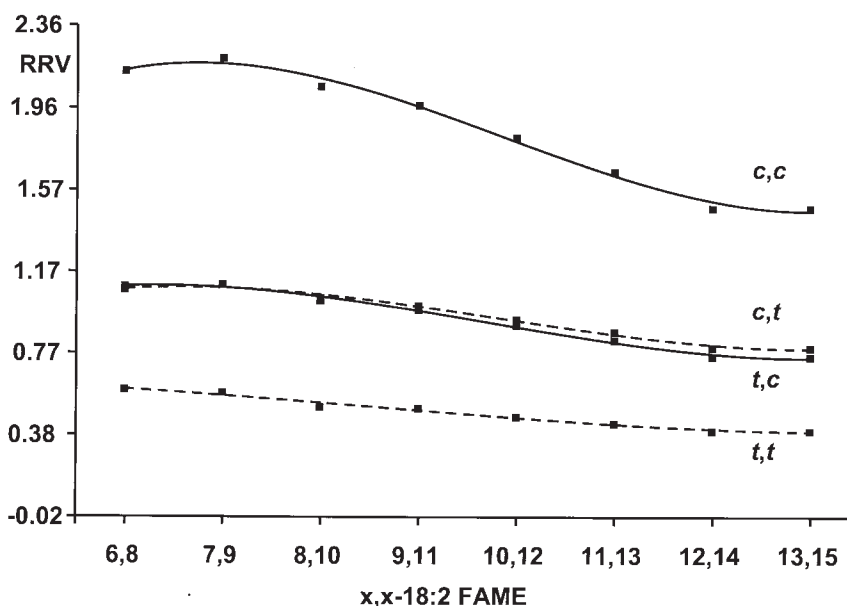
FIG. 5. Plot of RRV vs. double bond positions of CLA isomers. Three ChromSpher 5 Lipids columns maintained at 25°C were used in series, with 2% HOAc in the hexane mobile phase at 1.0 mL/min.

conditions there is no appreciable drift in RV, but the data are presented as RRV for a direct comparison of the retention order of CLA isomers eluted using either elution system. In Figure 5, the RRV of all the CLA isomers shown in Figure 4 are plotted as a function of double bond position. The plot in Figure 5 is similar to the plot in Figure 3 in that the *c,t* isomers of positional compounds near the carbonyl moiety elute before the corresponding *t,c* isomers. The plots differ in that for the 2% acetic acid/hexane mobile phase (Fig. 5) the position at which *c,t* and *t,c* isomers have the same RV is near the 7,9 position compared with the 10,12 position for the mobile phase containing MeCN (Fig. 3). The importance of this difference is emphasized by the separation of *t*10,*c*12- from *c*10,*t*12-18:2 and the partial separation of the *c*6,*t*8 from the *c/t* 7,9 isomers.

RRT are commonly used in GC analysis, but the use of RRV in HPLC analysis is less common. We believe that it is advantageous to use both in the instance of CLA analysis. The use of the *c*9,*t*11-CLA as a chromatographic reference in chromatographic analysis makes the identification of other peaks considerably easier, i.e., the analyst will know all the isomers that elute at a given RRV. The precision obtained, shown in Table 1, suggests that the drift in RV is only due to a loss of MeCN in the elution reservoir, and this is very consistent with the observation that adding more MeCN to the reservoir will re-establish the original RV. Column effects, particularly column temperature, age, and the amount of silver loaded, may, however, affect consistencies of RRV between different columns. Use of RRT (4) and RRV (presented herein) data also allows a substantially improved understanding of the GC and Ag⁺-HPLC chromatographic patterns of elution. The reproducibility of

RRV on a given column is excellent despite drifts in absolute RV.

The 2% acetic acid/hexane mobile phase produces a slightly different but complementary pattern of elution for CLA FAME. Its advantages include resolution of the two *c/t* 10,12 isomers and partial resolution for the *c*6,*t*8 isomer from the *t*7,*c*9 isomer. The disadvantages of this procedure are that it takes longer for a chromatographic run, 100 vs 60 min, and that in using this elution system it is not possible to use lower wavelengths, e.g., 205 nm, to monitor the chromatogram for interfering monoenoic (18:1) FAME that can interfere with CLA responses when present at a greatly elevated level.

The two Ag⁺-HPLC chromatographic techniques presented here, along with GC data (4), complement each other quite well, and these data demonstrate that use of relative retention parameters allows for a more rapid initial identification.

One observation that is clear from the Ag⁺-HPLC and GC (4) chromatographic patterns is that the identification of the *c*6,*t*8-18:2 CLA isomer, which is known (6) to be produced by the desaturation of *t*8-18:1 by Δ^6-desaturase, has been missed by every laboratory that depended on only GC (equipped with an FID) and Ag⁺-HPLC using an MeCN/hexane system for their analysis.

REFERENCES

1. Sehat, N., Kramer, J.K.G., Mossoba, M.M., Roach, J.A.G., Yurawecz, M.P., Eulitz, K., and Ku, Y. (1998) Identification of Conjugated Linoleic Acid (CLA) Isomers in Cheese by Gas Chromatography, Silver Ion High Performance Liquid Chromatography, and Mass Spectral Reconstructed Ion Profiles: Comparison of Chromatographic Elution Sequences, *Lipids 33*, 963–971.

2. Yurawecz, M.P., and Morehouse, K.M. (2001) Silver-Ion HPLC of Conjugated Linoleic Acid Isomers, *Eur. J. Lipid Sci. Technol. 103,* 609–613.
3. Yurawecz, M.P., Roach, J.A.G., Sehat, N., Mossoba, M.M., Kramer, J.K.G., Fritsche, J., and Steinhart, H. (1998) A New Conjugated Linoleic Acid (CLA) Isomer, 7-*trans,9-cis*-Octadeca-dienoic Acid, in Cow Milk, Cheese, Beef, and Human Milk and Adipose Tissue, *Lipids 33,* 803–809.
4. Delmonte, P., Roach, J.A.G., Mossoba, M.M., Losi, G., and Yu-rawecz, M.P. (2004) Synthesis, Isolation, and GC Analysis of All the 6,8- to 13,15-*cis/trans* Conjugated Linoleic Acid Isomers, *Lipids 39*, 185–191.
5. Corl, B., Baumgard, L.H., Griinari, J.M., Delmonte, P., More-house, K.M., Yurawecz, M.P., and Bauman, D.E. (2002) *Trans-*7,*cis*-9 CLA Is Synthesized Endogenously by Δ^9-Desaturase in Dairy Cows, *Lipids 37*, 681–688.
6. Pollard, M.R., Gunstone, F.D., James, A.T., and Morris, L.J. (1980) Desaturation of Positional and Geometric Isomers of Monoenoic Fatty Acids by Microsomal Preparations from Rat Liver, *Lipids 15*, 306–314.

Improved HPLC Assay for Lipid Peroxides in Human Plasma Using the Internal Standard of Hydroperoxide

Shu-Ping Hui[a,*], Tsuyoshi Murai[a], Teruki Yoshimura[a], Hitoshi Chiba[b],
Hironori Nagasaka[c], and Takao Kurosawa[a]

[a]Faculty of Pharmaceutical Sciences, Health Sciences University of Hokkaido, Hokkaido 061-0293, Japan,
[b]Department of Health Sciences, Hokkaido University School of Medicine, Sapporo 060-0812, Japan,
and [c]Division of Metabolism, Chiba Children's Hospital, Chiba 266-0007, Japan

ABSTRACT: We have developed a sensitive reversed-phase chemiluminescence HPLC approach for simultaneous quantitative and qualitative analyses of hydroperoxides of cholesteryl ester and TG in human plasma. Standard hydroperoxides of cholesteryl ester and TG and a novel internal standard (1-tetradecanyl 3-octadecenoyloxy-5β-cholan-24-oate monohydroperoxide) (I.S.) were chemically synthesized and the standard curves confirmed to be linear throughout the calibration range (1–1000 pmol). Within-day and between-day CV were less than 7%, and the recoveries were within the range of 84–93%. With sample size minimized to 0.1 mL of plasma for each run, plasma cholesteryl ester hydroperoxide levels were 189 ± 87 nM (mean ± SD) in healthy young (22–25 yr old; $n = 15$, male/female = 6:9) and 210 ± 69 nM in healthy elderly (39–60 yr old; $n = 6$, male/female = 3:3). TG hydroperoxide was not detected in healthy subjects. In patients with advanced liver failure (36–67 yr old; $n = 4$, male/female = 2:2), hydroperoxide levels of plasma cholesteryl ester and TG were 11,903 ± 9,553 nM and 3,318 ± 1,590 nM, respectively, indicating an involvement of lipid oxidation. Sensitive and specific monitoring of plasma lipid peroxides using the present chemiluminescence HPLC approach with the synthesized I.S. may help our understanding of chemical and pathophysiological aspects of lipid peroxidation.

Paper no. L9714 in *Lipids 40*, 515–522 (May 2005).

Lipid peroxidation has been linked to atherosclerosis (1), inflammation (2), carcinogenesis (3), diabetes (4,5), aging (6), and to a variety of other diseases, including nonalcoholic steatohepatitis (7) and alcoholic fatty liver (8). Several HPLC methods have been reported for the measurement of hydroperoxides of cholesteryl ester and TG in human plasma as lipid peroxidation products, generally using fluorimetry (9–11) or chemiluminescence methods with isoluminol (12–14). How-

ever, the cholesteryl ester hydroperoxide or TG hydroperoxide used as standards in previous chemiluminescence or fluorimetric methods was not well characterized in terms of their chemical structures (9–14). For instance, ^{1}H NMR or ^{13}C NMR spectra were not provided. Although previous studies reported the presence of cholesteryl ester hydroperoxides or TG hydroperoxides in plasma, only limited chemical information was given (9–14). Further, storage conditions for standard hydroperoxides and sample plasma were not optimized (9–11) or clearly described (12–14). We have in fact shown that a previously reported storage condition for standard monohydroperoxide cholesteryl linoleate at −25°C results in decomposition within a few months (9). Furthermore, a matter of the greatest importance is that previous measurements were performed without using any hydroperoxides as internal standard (12–14), and the wide discrepancies found in plasma lipid peroxide levels can be partly explained on this basis. It is widely recognized that lipid hydroperoxides are chemically unstable and consequently may be lost during analytical procedures. Moreover, detection that is based on chemiluminescence can gradually deteriorate during runs because of adhesion of unspecified plasma substances to the detector. The only solution for these problems is to use an internal standard, which must be similar to plasma lipid hydroperoxides in terms of not only extraction efficiency and retention time but also chemical stability and chemiluminescence efficiency.

Here we report sensitive and specific reversed-phase chemiluminescence HPLC with luminol for simultaneous measurement of hydroperoxides of cholesteryl ester and TG in human plasma. The internal standard of hydroperoxide was synthesized and its structure confirmed with reference to ^{1}H NMR and ^{13}C NMR spectra and elemental analysis as well as chromatographic behavior. Validation of the assay and its application to normal plasma and pathological plasma from patients with liver failure are also described here.

MATERIALS AND METHODS

Materials. Oleic acid was purchased from Tokyo Kasei Kogyo Co., Ltd. (Tokyo, Japan). N,N′-Dicyclohexylcarbodiimide (DCC), 4-dimethylaminopyridine (4-DMAP), lithocholic acid, oxalyl chloride, and cytochrome C (from horse heart) were from Wako Pure Chemical Industry, Ltd. (Osaka, Japan). Ethyl

acetate, *n*-hexane, and 2-propanol were also purchased from Wako Pure Chemical Industry, Ltd. (Osaka, Japan). Dehydrated dichloromethane (CH_2Cl_2), 2,6-di-*tert*-butyl-*p*-cresol (BHT), *tert*-butyl alcohol, methanol, ethanol, luminol, and sodium borohydride ($NaBH_4$) were from Kanto Chemical Co., Inc. (Tokyo, Japan). The solvents used for HPLC were all analytical grade. For column chromatography, Silica gel 60N (100–120 µm, Kanto Chemical Co.) was used, with aluminum sheets (Silica gel 60 F_{254}; Merck Co., Darmstadt, Germany) applied for TLC. ^{1}H NMR spectra were taken with a JEOL ECA 500 at 500 MHz with tetramethylsilane as an internal standard (abbreviations used are *s* for singlet, *d* for doublet, *dd* for doublets of doublet, *t* for triplet, *sext* for sextet, and *m* for multiplet).

Blood samples. For the measurements of hydroperoxides of cholesteryl ester and TG, blood was drawn into vacuum tubes containing disodium EDTA (1.5 mg/mL) after an overnight fast from healthy young subjects (22–25, 23 ± 1.0, yr old; *n* = 15, male/female = 6:9), healthy elderly (39–60, 50 ± 9.0, yr old; *n* = 6, male/female = 3:3), and patients (36–67, 54 ± 14, yr old; *n* = 4, male/female = 2:2) with liver failure due to cholangiocarcinoma (Cases 1 and 2), autoimmune liver cirrhosis (Case 3), and metastatic hepatoma (Case 4). Plasma was separated by centrifugation (2000 × *g*, 10 min, 4°C), and then stored at −80°C for no longer than 3 mon. Serum was also obtained from each blood sample and subjected to measurement of other lipids. These samples were used under the approval of the institute and after obtaining informed consent from the volunteers and patients.

HPLC analysis. A normal-phase HPLC was performed with the LC-10AD pump system equipped with an SCL-10A system controller (Shimadzu Co., Kyoto, Japan), including a CTO-10A injector and an SPD-10A UV-vis detector (Shimadzu Co.). The analytical column used for normal-phase HPLC was a Mightysil Si 60 (4.6 × 250 mm, 5 µm; Kanto Chemical Co.). The mobile phase was a mixture of *n*-hexane/2-propanol (250:1, vol/vol). The flow rate was 1 mL/min, and the temperature was ambient. The detection wavelength was 210 nm.

Reversed-phase HPLC with detection at 210 nm and with post-column chemiluminescence detection was also performed using a system equipped with an SCL-6A system controller (Shimadzu Co.), three LC-9A pumps (Shimadzu Co.), a CTO-10A injector, the SPD-10A UV-vis detector, and a CLD-10A chemiluminescence detector (Shimadzu Co.). The column used was an Inertsil ODS-2 (4.6 × 250 mm, 5 µm; GL Sciences Inc., Tokyo, Japan). The mobile phase was a mixture of ethanol/water (50:1, vol/vol), and the flow rate was 0.5 mL/min. The column eluant was mixed with luminescent reagent solution (0.5 mL/min) in a post-column mixing joint at 40°C.

Mobile solutions for both normal-phase HPLC and chemiluminescence HPLC were degassed by sonication under reduced pressure before use.The luminescent reagent consisted of cytochrome C (10 µg/mL) and luminol (2 µg/mL) in 50 mM borate buffer (H_3BO_3/KCl-Na_2CO_3, pH 10), and was also degassed (15). The solutions were prepared daily.

Preparation of standard hydroperoxides. (i) Monohydroperoxides of cholesteryl linoleate and cholesteryl oleate. Cholesteryl linoleate monohydroperoxide (CL-OOH) was chemically synthesized by our method as previously reported (16). Simply, cholesteryl linoleate (4 mmol) and hematoporphyrin (6 mg) were dissolved in pyridine (20 mL) and irradiated with a tungsten lamp (200 W) as O_2 gas was bubbled through a glass-ball filter for 1.0 h. The reaction mixture was extracted with diethyl ether and the extract was washed with cold water, 2 M HCl, and then dried over Na_2SO_4. The crude product was purified by a SiO_2 column chromatography (hexane/ethyl acetate, 10:1, vol/vol) to give pure CL-OOH as a colorless viscous liquid (a mixture of regioisomers). The structure of CL-OOH was elucidated by ^{1}H NMR, MS, and normal-phase HPLC (16).

With this method, cholesteryl oleate monohydroperoxide (CO-OOH) was also synthesized, and the structure was similarly elucidated.

(ii) TG monohydroperoxides. For measurement of TG hydroperoxides in human plasma, we synthesized three TG hydroperoxides: 1,2-dioleoyl-3-palmitoylglycerol monohydroperoxide (OOP-OOH), 2-linoleoyl-1-oleoyl-3-palmitoylglycerol monohydroperoxide (OLP-OOH), and triolein monohydroperoxide (OOO-OOH) by our previously described method (17). Briefly, the three TG were prepared by using a convenient, simple condensation of glycerol and corresponding acid chlorides in pyridine, then converting them into their monohydroperoxides by photosensitized peroxidation. The structures of these three TG hydroperoxides were confirmed by their ^{1}H NMR and ^{13}C NMR spectra and analyzed by normal and reversed-phase HPLC (17).

(iii) Synthesis of the internal standard (I.S.). Synthesis of the I.S. for the HPLC analysis of lipid peroxides was carried out as shown in Figure 1. DCC (24 mmol) was added to an ice-cooled, stirred solution of oleic acid (35 mmol) and 4-DMAP (40 mg) in dichloromethane (50 mL) at 0°C, and the whole was stirred for 10 min. Then lithocholic acid (**1**, 20 mmol) was added to the solution in several portions. The reaction mixture was stirred for 30 min at 0°C and then for 24 h at room temperature. Precipitates were filtered off, and the filtrate was concentrated in a vacuum evaporator. The crude products were subjected to SiO_2 column chromatography by eluting with *n*-hexane/ethyl acetate (8:1, vol/vol) to give 3-(9-*cis*-octadecenoyloxy)-5β-cholan-24-oic acid (**2**) at a yield of about 80%. The obtained compound (**2**) was used for the next reaction step without further purification. Compound **2** (10 mmol) was dissolved in dichloromethane (50 mL) containing 1-tetradecanol (10 mmol) and 4-DMAP (20 mg). Then DCC (12 mmol) was added to the ice-cooled, stirred solution followed by stirring for 30 min at 0°C and then for 24 h at room temperature. Precipitates were again filtered off, and the filtrate was concentrated by vacuum evaporation. The oily residue was then subjected to SiO_2 column chromatography by eluting with *n*-hexane/ethyl acetate (80:1, vol/vol) to give pure 1-tetradecanyl 3-(9-*cis*-octadecenoyloxy)-5β-cholan-24-oate (**3**) at a yield of 80%. ^{1}H NMR (CDC_3), δ: 0.64 (3H, *s*, 18-CH_3), 0.85 (3H, *d*, *J* = 6 Hz, 21-CH_3), 0.90 (6H, *t*, *J* = 6.4 Hz, –CH_2–CH_3),
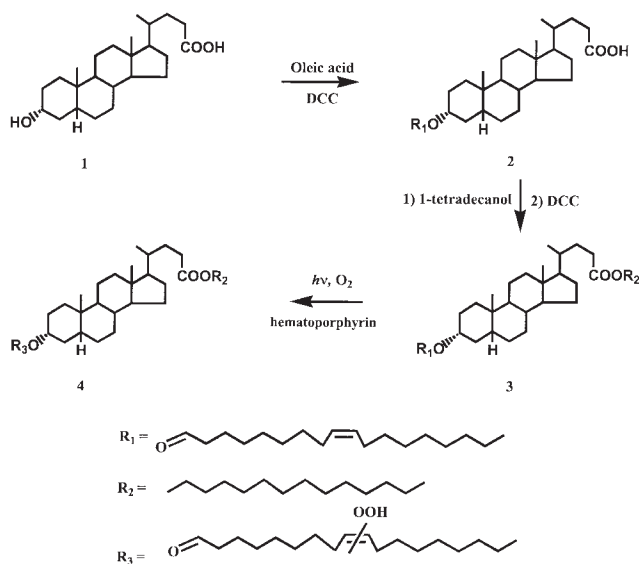
FIG. 1. Synthesis of internal standard (I.S.) (1-tetradecanyl 3-octade-cenoyloxy-5β-cholan-24-oate monohydroperoxide). DCC, *N,N′*-dicy-clohexylcarbodiimide.

0.93 (3H, *s*, 19-C*H*$_3$), 2.26 (4H, *m*, –C=C–C*H*$_2$–), 4.05, (4H, *t*, *J* = 6.7Hz, –OCO–C*H*$_2$–), 4.73 (1H, *m*, 3-*H*), 5.34 (2H, *m*, –C*H*=C*H*–). Then the solution of compound **3** (2 mmol) in pyridine (10 mL) containing hematoporphyrin (3 mg) was irradiated with a 200 W tungsten lamp for 1.5 h with bubbling of O$_2$ gas through a glass ball filter at 15°C. The reaction mixture was poured into ice-water, acidified with 2 mol/L HCl, and extracted with peroxide-free diethyl ether twice. The combined organic phase was washed with water and saturated sodium chloride solution and then dried over Na$_2$SO$_4$. After evaporating the solvent, the residue was subjected to SiO$_2$ column chromatography eluted with *n*-hexane/ethyl acetate (10:1, vol/vol) to give monohydroperoxide (**4**) as a colorless, viscous liquid at a yield of 30%. ^{1}H NMR (CDC$_3$), δ: 0.64 (3H, *s*, 18-C*H*$_3$), 0.85 (3H, *d*, *J* = 6.4Hz, 21-C*H*$_3$), 0.90 (6H, *t*, *J* = 6.4Hz, –CH$_2$–C*H*$_3$), 0.93 (3H, *s*, 19-C*H*$_3$), 2.26 (4H, *m*, –C=C–C*H*$_2$–), 4.05, (4H, *t*, *J* = 6.7Hz, –OCO–C*H*$_2$–), 4.26 (1H, *m*, –C=C–C*H*OOH), 4.73 (1H, *m*, 3-*H*), 5.36 (1H, *sext*, *J* = 15.6 and 6.4 Hz, –CH$_2$–C*H*=C–COOH), 5.76 (1H, *dd*, *J* = 15.6 and 8.4 Hz, –C=C*H*–CHOOH–). Anal. C: 77.37%, H: 11.60%; Found, C: 77.27%, H: 11.42%. The purity of the compound **4** was checked by TLC and HPLC. In the TLC, no contamination was detected after development with several solvent systems (*n*-hexane/ethyl acetate, 8:1; *n*-hexane/acetone, 6:1; benzene/acetone, 40:1, vol/vol), and spraying several color-producing reagents (20% sulfuric acid, 10% phosphomolybdic acid in ethanol, anisaldehyde-H$_2$SO$_4$ in acetic acid) and UV detection (254 and 365 nm). The three R_f values of TLC for these solvent systems were 0.375, 0.286. and 0.429, respectively.

Extraction of plasma. For extraction, 0.1 mL of plasma from a healthy human (0.01 mL plasma of subjects with liver failure) was mixed with 0.05 mL of I.S. solution (1 μM in ethanol), 0.2 mL of freshly prepared 0.2% BHT solution (as antioxidant, in methanol), and 2 mL of *n*-hexane. The mixture was

vigorously mixed with a vortex mixer for 1 min and then centrifuged at 2,000 × *g* for 1 min at 4°C. The methanol layer was discarded, while the upper phase (hexane layer) was collected and evaporated under vacuum in a rotary evaporator at room temperature. The residue was dissolved in 0.1mL of *n*-hexane/ethyl acetate (6:1, by vol) containing 2.2×10^{-3}% BHT and then subjected to short refining column (8 × 50 mm, 1.3 g of SiO$_2$) chromatography and eluted with *n*-hexane/ethyl acetate (6:1, vol/vol) containing 2.2×10^{-3}% BHT. The column was pre-washed with 20 mL of the above hexane/ethyl acetate before applying the sample solution. The first 0.8 mL of solution eluted from the column was thrown away, and the following 2.0 mL was collected and evaporated under vacuum. The residue was dissolved in 0.05 mL of CH$_2$Cl$_2$/ethanol (1:1, vol/vol), and the sample (0.02 mL) was injected into the chemiluminescence HPLC system. The chromatogram showed peak counts for the known quantities of I.S. and unknown initial plasma peroxides. In accordance with these data, the initial plasma peroxide concentrations were calculated.

Serum lipid measurements. Serum lipids were measured by automated enzymatic methods, using commercial kits: Determiner TC (Kyowa Medex Co., Tokyo, Japan) for total cholesterol (TC); AutoSera S TG-N (Daiichi Pure Chemicals, Tokyo, Japan) for TG; Determiner HDL-C (Kyowa Medex) for HDL-cholesterol; Cholestest LDL (Daiichi Pure Chemicals) for LDL-cholesterol.

Statistical analyses. All data are presented as means ± SD. Differences between groups, namely, liver failure vs. healthy elderly group (LF vs. Elder), liver failure vs. healthy young group (LF vs. Young), and healthy young group vs. healthy elderly group (Young vs. Elder) were assessed using the Mann–Whitney *U* test. Statistical significance was concluded at *P* < 0.05.

RESULTS

Synthesis of the I.S. To achieve a simultaneous quantitative determination of cholesteryl ester hydroperoxides and TG, a suitable I.S. is necessary. We synthesized 1-tetradecanyl 3-octadecenoyloxy-5β-cholan-24-oate monohydroperoxide as a convenient I.S. because of its stability and its desirable chromatographic behavior. Figure 1 shows the synthetic pathway. The ester, **3**, was prepared from lithocholic acid by the initial esterification of oleic acid and the subsequent esterification with tetradecanol using the well-known DCC method. The monohydroperoxide, **4**, was then derived by the method previously reported (16) and its chemical structure confirmed with reference to the ^{1}H NMR spectrum and elemental analysis.

Purity of the I.S. was checked by normal-phase HPLC, reversed-phase HPLC, and reversed-phase HPLC with chemiluminescence detection. All peaks observed with the three chromatograms for I.S. were single and symmetric, and no contamination was detected. The retention times were 7.9 min for normal-phase HPLC, 19.9 min for reversed-phase HPLC, and 20.4 min for reversed-HPLC with chemiluminescence detection (data not shown).
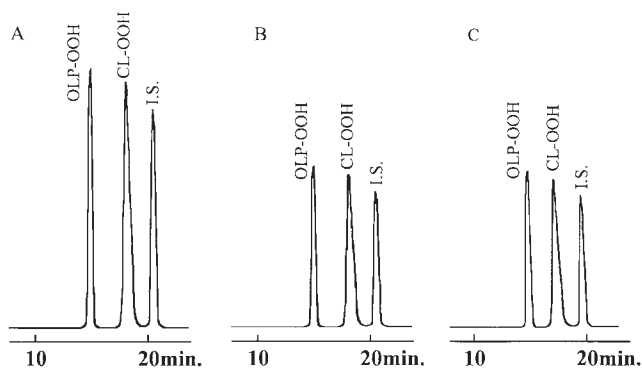
FIG. 2. Chromatograms of a mixture of OLP-OOH (50 pmol), CL-OOH (50 pmol), and I.S. (50 pmol) by reversed-phase HPLC with chemiluminescence detection. The mobile phase was ethanol/water (50:1, vol/vol) for (A), ethanol for (B), and *tert*-butyl alcohol/methanol (1:1, vol/vol) for (C). The mobile phase flow rate and the luminescent reagent rate were both 0.5 mL/min. OLP-OOH, 2-linoleoyl-1-oleoyl-3-palmitoylglycerol monohydroperoxide; CL-OOH, cholesteryl linoleate monohydroperoxide; for other abbreviation see Figure 1.

HPLC analysis of synthesized standard monohydroperoxides. Figure 2A shows a typical chromatogram in chemiluminescence HPLC detection for a mixture of chemically synthesized standard OLP-OOH, CL-OOH, and the I.S. (each 50 pmol). All peaks were symmetric and sufficiently resolved. The retention times were 15.5 min for OLP-OOH, 18.2 min for CL-OOH, and 20.9 min for the I.S. The peak areas for CL-OOH and OLP-OOH were larger than that for I.S. with the chemiluminescence system, although the same amounts (50 pmol) were injected. The relative sensitivities were 1.33 for CL-OOH to I.S., and 1.37 for the OLP-OOH to I.S., and these were used to calculate the amounts of CL-OOH and OLP-OOH in plasma.

Effects of the mobile phase. The effects of the solvent in the mobile phase on the peak area of synthesized CL-OOH, OLP-OOH, and I.S. (each 50 pmol) in the chemiluminescence HPLC system were investigated with the flow rate of the mobile phase set at 0.5 mL/min. Ethanol/water (50:1, vol/vol) gave the high-

est peak (Fig. 2A), but ethanol (Fig. 2B) and *tert*-butyl alcohol/methanol (1:1, vol/vol, Fig. 2C) gave 62 and 60% of the peaks in Figure 2A, respectively. Hence we selected ethanol/water (50:1, vol/vol) as the column eluant for the chemiluminescence HPLC system.

Effects of the flow rate of the mobile phase rate. The effects of flow rate of mobile phase (ethanol/water, 50:1, vol/vol) on the chemiluminescence counts for 50 pmol of chemically synthesized OLP-OOH, CL-OOH, and I.S. were studied. We set the reagent flow rate at 0.5 mL/min, and changed the flow rate of ethanol/water (50:1, vol/vol). The flow rates of mobile phase in the range 0.2–0.5 mL/min show gradually increasing chemiluminescence counts, but in the range 0.5–1.0 mL/min, show gradually decreasing chemiluminescence counts. At the flow rate of 0.5 mL/min, OLP-OOH, CL-OOH, and I.S. showed the maximum chemiluminescence response. Therefore, the flow rate of the mobile phase was set at 0.5 mL/min (data not shown).

Calibration curves of CL-OOH and OLP-OOH. Two calibration curves of CL-OOH and OLP-OOH were obtained by combination with the I.S. using the chemiluminescence HPLC system. They were plotted as the peak area ratios of CL-OOH and OLP-OOH to that of I.S. vs. the amounts of CL-OOH and OLP-OOH and showed good linearity throughout the range 1–1000 pmol (CL-OOH, $y = 0.1726x - 0.0958$, $r^2 = 0.999$; OLP-OOH, $y = 0.1778x - 0.0988$, $r^2 = 0.9995$; $x =$ amounts of hydroperoxide; $y =$ peak area ratio to I.S.). Each datum is the average of three determinations. These results allowed us to use the calibration curves of either CL-OOH or OLP-OOH in these ranges for the determination of hydroperoxides in human plasma. The detection limit for both CL-OOH and OLP-OOH was 0.5 pmol at a signal-to-noise ratio of 6 (calibration curves not shown).

Precision and relative recoveries for CL-OOH and OLP-OOH. For the determination of within-day and between-day precision, two defined, different amounts of CL-OOH and OLP-OOH (50 and 200 nM) were analyzed five times on the same day and once each on 10 different days, respectively. The results of the precision experiments are summarized in Table 1. All within-day and between-day CV were less than 7%. Table 1 also shows

TABLE 1
Precision and Recoveries of Hydroperoxides Determination in Plasma

Hydroperoxides	Found (nM)[a] (endogenous) Mean	SD	Added (nM)	Found (nM)[b] (total) Mean	SD	CV (%)	Recoveries (%)
CL-OOH							
Within-day	128.3	6.6	50	171.8	9.5	5.5	87
(n = 5)			200	314.3	18.5	5.9	93
Between-day	125.5	8.2	50	167.5	11.2	6.7	84
(n = 10)			200	307.5	21.2	6.9	91
OLP-OOH							
Within-day	ND[c]		50	45.5	2.2	4.8	91
(n = 5)			200	186.0	10.8	5.8	93
Between-day	ND		50	43.5	2.5	5.7	87
(n = 10)			200	172.0	10.2	5.9	86

[a]Endogenous concentration.
[b]Total concentration of endogenous and added standards.
[c]Not detected; values were estimated as being under the detection limit. CL-OOH, cholesteryl linoleate monohydroperoxide; OLP-OOH, 2-linoleoyl-1-oleoyl-3-palmitoylglycerol monohydroperoxide.
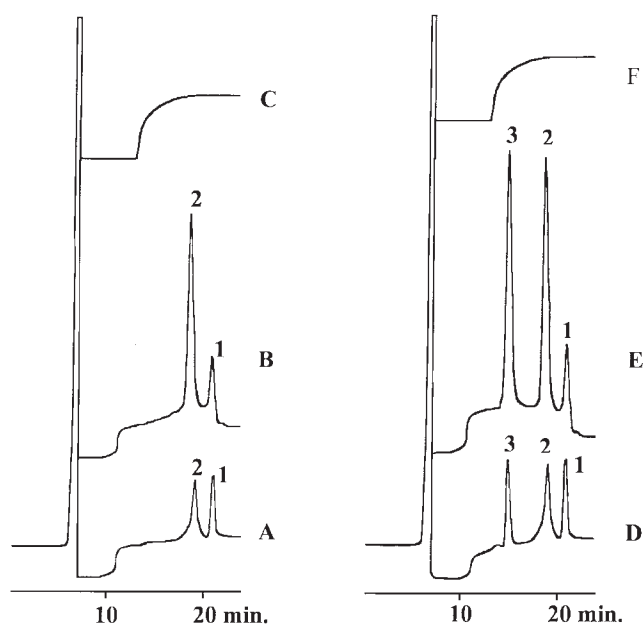
FIG. 3. Chromatograms of human plasma extracts with chemiluminescence detection. (A) From a healthy subject; (B) from a healthy subject, spiked with CL-OOH; (C) after reduction of the sample yielding (B) with NaBH$_4$; (D) from a case of liver failure; (E) from a case of liver failure, spiked with CL-OOH and OLP-OOH; (F) after reduction of the sample yielding (E) with NaBH$_4$. The mobile phase was a mixture of ethanol/water (50:1, vol/vol), and the flow rate was 0.5 mL/min. The luminescent reagent rate was also 0.5 mL/min. For other abbreviations, see Figure 2.

$-25°C$, which was reported for storage of standard monohydroperoxide cholesteryl linoleate in the literature (9). We confirmed by TLC and normal-phase HPLC that this condition resulted in decomposition, possibly owing to autoxidation, of the standard monohydroperoxides into unspecified substances within a few months (data not shown).

Qualitative analyses for hydroperoxides of cholesteryl ester and TG in human plasma. Figure 3A shows the typical chemiluminescence HPLC chromatogram of a plasma sample from a healthy volunteer, with two peaks observed. Peak 1 was assigned to the added I.S. and peak 2 was presumed to be CL-OOH from its retention time. Figure 3B shows the chemiluminescence HPLC chromatogram of the plasma sample from the same healthy volunteer spiked with synthesized CL-OOH. The height and area of peak 2 on Figure 3B were enhanced compared with that in Figure 3A, so peak 2 was assigned to CL-OOH. Furthermore, the above plasma sample was treated with NaBH$_4$ and reanalyzed by HPLC. As shown in Figure 3C, the peaks then completely disappeared, so that peak 2 in human plasma actually possesses a hydroperoxyl group in the molecule and can be identified as CL-OOH. We did not observe any peaks for TG hydroperoxide in the plasma from healthy subjects.

Figure 3D shows a chemiluminescence HPLC chromatogram of a plasma sample from a patient with liver failure, in which peaks 2 and 3 are evident. For their identification, we added synthetic CL-OOH and OLP-OOH to the sample. As shown in Figure 3E, the peaks 2 and 3 completely overlapped those of the added standards. These peaks also disappeared after treatment with NaBH$_4$ as above, as shown in Figure 3F. These results indicated that they were also the derivatives of hydroperoxide. Other lipid hydroperoxides, CO-OOH, OOP-OOH and OOO-OOH, that were synthesized in our laboratory were also added to the plasma sample from the patient with liver failure; however, the retention times of the peaks of these synthetic hydroperoxides did not agree with those of peaks 2 and 3.

Plasma lipid profiles of normal and liver failure subjects. As shown in Table 2, significantly lower TC and higher TG

recoveries relative to I.S. of CL-OOH and OLP-OOH added into 0.1 mL of plasma prior to extraction. At the concentrations of 50 and 200 nM of CL-OOH, they were within the range of 84–93%. The recoveries at the concentration of 50 and 200 nM of OLP-OOH were within the range of 86–93%.

Storage condition. The I.S. and standard hydroperoxides of cholesteryl ester and TG synthesized were found to be stable for at least 3 mon at $-80°C$. We tested a storage condition of

TABLE 2
Plasma Lipid Profile in Normal Subjects and Patients with Liver Failure[a]

Subjects	Age (yr)	TC (mg/dL)	TG (mg/dL)	LDL-C (mg/dL)	HDL-C (mg/dL)	CE-OOH (nM)	TG-OOH (nM)
Liver failure (LF)	54 ± 14	105 ± 48	138 ± 33	70 ± 43	7 ± 2	11,903 ± 9,553	3,318 ± 1,590
(n = 4)	(36–67)	(82–169)	(93–167)	(25–128)	(5–10)	(1,912–24,900)	(1,970–5,600)
Case 1 (male)	67	111	167	73	5	24,900	5,600
Case 2 (female)	61	58	134	25	6	1,912	1,970
Case 3 (female)	50	82	93	55	8	10,900	3,100
Case 4 (male)	36	169	157	128	10	9,900	2,600
Healthy elder	50 ± 9	201 ± 26	81 ± 32	105 ± 19	84 ± 18	210 ± 69	ND**
(n = 6, m:f = 3:3)	(39–60)	(162–236)	(48–138)	(86–139)	(61–112)	(107–289)	
Healthy young	23 ± 1	163 ± 27	62 ± 22	84 ± 21	70 ± 16	189 ± 87	ND**
(n = 15, m:f = 6:9)	(22–25)	(109–212)	(36–100)	(35–114)	(45–92)	(63–332)	
P (LF vs. elder)	0.5918	0.019*	0.033*	0.1356	0.0105*	0.0105*	0.0039*
P (LF vs. young)	0.0022*	0.0455*	0.0051*	0.2703	0.0027*	0.0027*	<0.0001
P (young vs. elder)	0.0004*	0.0114*	0.2126	0.0793	0.1605	0.5334	>0.9999

[a]Values are means ± SD. *$P < 0.05$; **ND: not detected, and the values were considered under detection limit. TC, total cholesterol; LDL-C, LDL-cholesterol; HDL-C, HDL-cholesterol; CE-OOH, cholesteryl ester monohydroperoxides; TG-OOH, triglyceride monohydroperoxides.

concentrations in serum were observed in the patients with liver failure in comparison with both healthy young and elderly groups. The very low HDL-cholesterol concentrations in the patients with liver failure well reflected their severe loss of liver functions. Serum TC concentrations in the healthy elderly group were significantly higher than those in the healthy young group. Serum LDL-cholesterol concentrations did not significantly differ among the three groups.

All four patients with liver failure showed a striking increase of cholesteryl ester monohydroperoxides in plasma (11,903 ± 9,553 nM, mean ± SD, range: 1,912–24,900 nM) in comparison with the two healthy groups (210 ± 69 nM, 107–289 nM for the elderly, and 189 ± 87 nM, 63–332 nM for the young). No statistically significant difference was observed in plasma concentrations of cholesteryl ester monohydroperoxide between the healthy elderly and young groups. TG monohydroperoxide was undetectable in plasma from all subjects in the healthy elder and healthy young groups. On the other hand, marked increase (3,318 ± 1,590 nM, 1,970–5,600 nM) was observed in all patients with liver failure.

DISCUSSION

In the present study we chemically synthesized CL-OOH and CO-OOH as standard cholesteryl ester hydroperoxides, since their precursors (CL, CO) are reported to be major cholesteryl esters in human plasma, accounting for 51 and 23%, respectively, of the total (18,19). In our previous report, synthetic CL-OOH was shown to be composed of regioisomers with the hydroperoxy group at 9-, 10-, 12-, and 13-positions of the FA chain, and these four isomers could be separated by normal-phase HPLC (16). However, in the present reversed-phase HPLC system with chemiluminescence detection, all four isomers eluted in a single peak, facilitating comparisons. Peak 2 in Figure 3A was assigned to CL-OOH, since its retention time was identical to that of the synthetic CL-OOH but not to that of the synthetic CO-OOH (16). This strongly suggests that CL-OOH is a predominant hydroperoxide of cholesteryl ester in human plasma.

For the measurement of plasma TG hydroperoxides, previous studies used trilinolein hydroperoxide as the standard (9,10,12). However, since trilinolein was reported to be absent in human plasma by Kuksis *et al.* (18,19) and by Ruíz-Gutiérrez *et al.* (20), the observed hydroperoxide peak by an HPLC study may not have been trilinolein hydroperoxide. To be able to assign each TG hydroperoxide in plasma, we need TG hydroperoxide standards and an HPLC system to separate them effectively. The major TG in human VLDL, which is the major plasma lipoprotein species containing TG as the preponderant lipid, are reported to be 1,2-dioleoyl-3-palmitoylglycerol (OOP, 32.8%), 2-linoleoyl-1-oleoyl-3-palmitoylglycerol (OLP, 22.3%,) and triolein (OOO, 12.2%) in healthy young men (20). Ruíz-Gutiérrez *et al.* (21) have reported a similar TG composition for human adipose tissue. From these studies, monohydroperoxides of the three major TG might be expected to be suitable standards and thus were initially synthesized in our

previous study (17) and their structures confirmed with reference to chromatographic behavior, ^{1}H NMR, ^{13}C NMR, and mass spectra. The results of normal-phase HPLC analysis showed the monohydroperoxides to be mixtures of regioisomers. Six peaks in the chromatogram of OLP-OOH corresponded to the isomers with a hydroperoxy group at 9-, 10-, 12-, or 13-position on the linoleoyl side chain and at 9- or 10-position on the oleoyl side chain. In the reversed-phase HPLC, however, the regioisomers of synthetic OLP-OOH eluted in a single peak, again advantageous for sensitive and simple measurement of TG hydroperoxides (17).

The presence of TG hydroperoxides in plasma has not been confirmed in previous studies. Akasaka *et al.* (9) reported detection in normal plasma stored at −30°C but not in fresh plasma, suggesting accumulation of TG hydroperoxides during storage. In a recent report of a structural analysis of oxidized TG in human and porcine lipoproteins by an HPLC-electrospray ionization-MS method, no hydroperoxides were detected, whereas the presence of ketones, epoxides, aldehydes, and hydroxides was confirmed (22,23).

In our present study, peak 3 (Fig. 3D) for a patient with liver failure was assigned to OLP-OOH based on the retention time. On the other hand, synthetic OOO-OOH and POO-OOH were confirmed to have retention times distinct from that for peak 3 (data not shown). Further, no peak comparable to the peak 3 was detectable in normal plasma (Fig. 3A), strongly suggesting that selective accumulation of OLP-OOH in plasma occurs with liver failure. OLP, reported to account for 22.3% of total TG in plasma, was lower than the 32.8% for OOP (20), which favors an interpretation of higher susceptibility to oxidation of linoleic acid than oleic acid. To our knowledge, this is the first report to identify TG hydroperoxides in human plasma as OLP-OOH.

Using the present method, we found plasma levels of cholesteryl ester hydroperoxide to be 210 ± 69 nM (mean ± SD, *n* = 6) in healthy elderly and 189 ± 87 (*n* = 15) in healthy young. In previous chemiluminescence HPLC methods, variable cholesteryl ester hydroperoxide levels were reported. For instance, Yamamoto *et al.* described the level of cholesteryl ester hydroperoxides in healthy human plasma to be 317 ± 2.0 (*n* = 3), 3.4 ± 2.0 (*n* = 23), and 8.0 ± 4.5 nM (*n* = 9) in their three different studies (12,14,24) with chemiluminescence assays. Although the reason for the discrepancy was not specified by the authors (24), it is likely that the lack of an I.S. contributed. We have observed significantly decreased detection counts during sequential sample injections in our HPLC system, which can be best explained by adhesion of unspecified substances in plasma to the flow cell, since the detection can be restored after washing the flow system.

Akasaka *et al.* (9) reported the level of cholesteryl ester hydroperoxides in fresh human plasma to be 24.5 ± 9.6 nM (*n* = 15) by a fluorometric HPLC method, a value lower than ours. They used a nonhydroperoxide compound as I.S. and then detected this and cholesteryl ester hydroperoxides, respectively, using UV and fluorimetric detectors. Here, we used a hydroperoxide, and detected both our I.S. and lipid hydroperoxides by

chemiluminescence. Moreover, as anticoagulant, they used heparin, which has no antioxidant action, whereas the EDTA used in our method is an effective antioxidant. Thus, the theoretical superiority of our method appears clear.

In the present study, we chemically synthesized the novel hydroperoxide of the ester composed of oleic acid, lithocholic acid, and tetradecanol, namely, 1-tetradecanyl 3-octadecenoyloxy-5β-cholan-24-oate monohydroperoxide for use as the I.S. for the first time. This compound has a number of virtues for the measurement of lipid hydroperoxides by chemiluminescence HPLC. First, it is relatively stable, which presumably is attributable to the stability of the monohydroperoxide of oleic acid, in line with our previous observation that CO-OOH is more stable than CL-OOH (16). Furthermore, the ratio of chemiluminescence intensities of the targeted lipid hydroperoxides and the I.S. is about 1.3 and constant throughout the range, which also contributes to good accuracy and precision with our HPLC system. Finally, two regioisomers (the 9- and 10-isomers) are included in the I.S., but they elute in a single peak on chemiluminescence HPLC, preventing interference with other substances and increasing sensitivity. The validation data showed good within-day and between-day reproducibility for the tested two hydroperoxides, with CV of less than 7% and recoveries between 84 and 93%. Thus, our chemiluminescence HPLC system allowed simultaneous measurements at picomolar to nanomolar levels of hydroperoxides of cholesteryl ester and TG in human plasma (Fig. 3A, B, D, E).

Since TG hydroperoxide was not detectable in plasma from normal persons, as previously reported by Yamamoto *et al*. (12), we tested whether any pathological condition might be associated with the appearance of TG hydroperoxide in plasma. For the first time, a striking increase of TG hydroperoxide was confirmed in all four patients with liver failure, without exception, whereas the compound was not detectable in any of 21 normal subjects (Table 2). Although the number of studied patients has not reached a statistically significant level, this finding not only indicates that our method for measuring lipid hydroperoxides is reliable but also suggests that a severe lipid oxidation process is involved in advanced liver disease. Accordingly, elevation of phospholipid hydroperoxides in plasma of patients with cirrhosis and hepatocellular carcinoma has been reported in the literature, suggesting the presence of increased oxidative stress in advanced liver disease (4). In our method, phospholipid hydroperoxides did not appear in the chromatogram, because they are more polar than the hydroperoxides of cholesteryl ester and TG and therefore should be extracted in the methanol phase to be discarded.

Additionally, cholesterol hydroperoxides have been reported to increase in lipid extracts from alcoholic fatty liver (8). In our previous study, we reported the occurrence of hydroperoxidation not only in the olefinic parts of FA chains but also in the sterol ring during the photosensitization of synthetic cholesteryl esters (16). The structures of the hydroperoxides were identified as 5-hydroperoxy- and 7-hydroperoxy-cholest-6-en-3-ol esters, according to their ^{1}H NMR spectra. In our reversed-phase system, these hydroperoxides showed retention times distinct from those of cholesteryl ester hydroperoxides carrying the hydroperoxy group in the FA chain (data not shown). Further, the formation of hydroperoxides at the sterol moiety was much slower than that at the FA chains, when synthetic cholesteryl esters were photosensitized (16). Hence, cholesteryl ester hydroperoxides carrying a hydroperoxy group only at the sterol ring are unlikely to occupy a major component in plasma.

As for a mechanism leading to the accumulation of oxidized lipids in plasma from patients with liver failure, some explanations seem possible. HDL is known to carry cholesteryl ester hydroperoxides to the liver where such oxidized lipids are detoxified effectively. Interestingly, LDL-associated cholesteryl ester hydroperoxides are neither removed nor detoxified in the liver (25). In this context, the extremely low levels of HDL in our patients might play a central role in the disruption of this salvaging system. Regarding the accumulation of TG hydroperoxides, Nagasaka *et al*. (26) have reported that in patients with progressive familial intrahepatic cholestasis, LDL particles were enriched with TG and were highly capable of transforming macrophages into foam cells, indicating the nature of this lipoprotein as an oxidized LDL species. Retarded hepatic clearance of LDL, predicted from both the suppressed LDL receptor expression and the modified physicochemical nature of LDL, has been proposed as a possible explanation by the authors. Further, we would like to stress a potential role of the failed bile excretion system in the accumulation of TG-rich oxidized LDL species in severe cholestasis. It is well known that free cholesterol and phospholipids are major components of bile. Supposing that oxidized lipids also are excreted into bile, the lack of bile formation and excretion commonly seen in the liver failure may result in the accumulation of oxidized lipids in the liver and blood. Additionally, ischemia, inflammation, and the loss of antioxidants in the failing liver could also be involved in this process.

Finally, the striking elevation of TG hydroperoxides in liver failure might suggest its potential as a specific clinical marker that could help in diagnosis, evaluation of severity, and monitoring of the effects of treatments in liver diseases.

ACKNOWLEDGMENTS

REFERENCES

1. Piotrowski, J.J., Hunter, G.C., Eskelson, C.D., Dubick, M.A., and Bernhard, V.M. (1990) Evidence for Lipid Peroxidation in Atherosclerosis, *Life Sci. 46,* 715–721.
2. Ramos, V.A., Ramos, P.A., and Dominguez, M.C. (2004) The Role of Oxidative Stress in Inflammation in Patients with Juvenile Rheumatoid Arthritis, *J. Pediatr. (Rio J.). 76 (2),* 125-132.
3. Sodum, R.S., and Chung, F.L. (1991) Stereoselective Formation of *in vitro* Nucleic Acid Adducts by 2,3-Epoxy-4-hydroxynonenal, *Cancer Res. 51,* 137–143.

4. Miyazawa, T. (1989) Determination of Phospholipid Hydroperoxides in Human Blood Plasma by a Chemiluminescence-HPLC Assay, *Free Radic. Biol. Med. 7,* 209–217.

5. Ziefler, D., Sohr, C.G., and Nourooz-Zadeh, J. (2004) Oxidative Stress and Antioxidant Defense in Relation to the Severity of Diabetic Polyneuropathy and Cardiovascular Autonomic Neuropathy, *Diabetes Care 27,* 2178–2183.

6. Cutler, R.G. (1991) Antioxidants and Aging, *Am. J. Clin. Nutr. 53,* 373–379.

7. Chalasani, N., Deeg, M.A., and Crabb, D.W. (2004) Systemic Levels of Lipid Peroxidation and Its Metabolic and Dietary Correlates in Patients with Nonalcoholic Steatohepatitis, *Am. J. Gastroenterol. 99,* 1497–1502.

8. Asano, M., Adachi, J., and Ueno, Y. (1999) Cholesterol-Derived Hydroperoxides in Alcoholic Liver Disease, *Lipids 34,* 557–561.

9. Akasaka, K., Ohrui, H., and Meguro, H. (1993) Determination of Triacylglycerol and Cholesterol Ester Hydroperoxides in Human Plasma by High-Performance Liquid Chromatography with a Fluorimetric Postcolumn Detection, *J. Chromatogr. 617,* 205-211.

10. Akasaka, K., Ohrui, H., and Meguro, H. (1993) Simultaneous Determination of Hydroperoxides of Phosphatidylcholine, Cholesterol Esters and Triacylglycerols by Column-Switching High-Performance Liquid Chromatography with a Post-Column System, *J. Chromatogr. 622,* 153–159.

11. Akasaka, K., Ohrui, H., and Meguro, H. (1994) Measurement of Cholesterol Ester Hydroperoxides of High and Combined Low and Very Low Density Lipoprotein in Human Plasma, *Biosci. Biotech.Biochem. 58,* 396–399.

12. Yamamoto, Y., Brodsky, M.H., Baker, J.C., and Ames, B.N. (1987) Detection and Characterization of Lipid Hydroperoxides at Picomole Levels by High-Performance Liquid Chromatography, *Anal. Biochem. 160,* 7–13.

13. Frei, B., Yamamoto, Y., Niclas, D., and Ames, B.N. (1988) Evaluation of Isoluminol Chemiluminescence Assay for the Detection of Hydroperoxides in Human Blood Plasma, *Anal. Biochem. 175,* 120–130.

14. Yamamoto, Y., and Niki, E. (1989) Presence of Cholesterylester Hydroperoxide in Human Blood Plasma, *Biochem. Biophys. Res. Commun. 165,* 988–993.

15. Miyazawa, T., Suzuki, T., Fujimoto, K., and Yasuda, K. (1992) Chemiluminescent Simultaneous Determination of Phosphatidylcholine Hydroperoxide and Phosphatidylethanolamine Hydroperoxide in Liver and Brain of the Rat, *J. Lipid Res. 23,* 1051–1058.

16. Hui, S-P., Yoshimura, T., Murai, T., Chiba, H., and Kurosawa, T. (2000) Determination of Regioisomeric Hydroperoxides of Fatty Acid Cholesterol Esters Produced by Photosensitized Peroxidation Using HPLC, *Anal. Sci. 16,* 1023–1028.

17. Hui, S-P., Murai, T., Yoshimura, T., Chiba, H., and Kurosawa, T. (2003) Simple Chemical Syntheses of Triacylglycerol Monohydroperoxides, *Lipids 38,* 1287–1292.

18. Kuksis, A., and Myher, J.J. (1990) Gas–Liquid Chromatographic Profiling of Plasma Lipids Using High-Temperature-Polarizable Capillary Columns, *J. Chromatogr. 500,* 427–441.

19. Kuksis, A., Myher, J.J., and Geher, K. (1993) Quantitation of Plasma Lipids by Gas–Liquid Chromatography on High Temperature Polarizable Capillary Columns, *J. Lipid Res. 34,* 1029–1038.

20. Ruíz-Gutiérrez, V., Prada, J.L., and Pérez-Jiménez, F. (1993) Determination of Fatty Acid and Triacylglycerol Composition of Human Very-Low-Density Lipoproteins, *J. Chromatogr. 622,* 117–124.

21. Ruíz-Gutiérrez, V., Montero, E., and Villar, J. (1992) Determination of Fatty Acid and Triacylglycerol Composition of Human Adipose Tissue, *J. Chromatogr. 581,* 171–178.

22. Suomela, J.P., Ahotupa, M., Sjövall, O., Kurvinen, J.P., and Kallio, H. (2004) New Approach to the Analysis of Oxidized Triacylglycerols in Lipoproteins, *Lipids 39,* 507–512.

23. Suomela, J.P., Ahotupa, M., Sjövall, O., Kurvinen, J.P., and Kallio, H. (2004) Diet and Lipoprotein Oxidation: Analysis of Oxidized Triacylglycerols in Pig Lipoproteins, *Lipids 39,* 639–647.

24. Mashima, R., Onodera, K., and Yamamoto, Y. (2000) Regioisomeric Distribution of Cholesteryl Linoleate Hydroperoxides and Hydroxides in Plasma from Healthy Humans Provides Evidence for Free Radical-Mediated Lipid Peroxidation *in vivo*, *J. Lipid Res. 41,* 109–115.

25. Christison, J., Karjalainen, A., Brauman, J., Bygrave, F., and Stocker, R. (1996) Rapid Reduction and Removal of HDL- but Not LDL-Associated Cholesteryl Ester Hydroperoxides by Rat Liver Perfused *in situ*, *Biochem. J. 314,* 739–742.

26. Nagasaka, H., Yorifuji, T., Egawa, H., Yanai, H., Fujisawa, T., Kosugiyama, K., Matsui, A., Hasegawa, M., Okada, T., Takayanagi, M., *et al.* (2005) Evaluation of Risk for Atherosclerosis in Alagille Syndrome and Progressive Familial Intrahepatic Cholestasis: Two Congenital Cholestatic Diseases with Different Lipoprotein Metabolisms, *J. Pediatr. 146,* 329–335.

Simultaneous Quantification of Free Fatty Acids, Free Sterols, Squalene, and Acylglycerol Molecular Species in Palm Oil by High-Temperature Gas Chromatography–Flame Ionization Detection

Harrison Lik Nang Lau[a,b], Chiew Wei Puah[a,b], Yuen May Choo[a],*, Ah Ngan Ma[a], and Cheng Hock Chuah[b]

[a]Malaysian Palm Oil Board (MPOB), Bandar Baru Bangi, 43000 Kajang, Selangor, Malaysia, and [b]University of Malaya, Lembah Pantai, 50603 Kuala Lumpur, Malaysia

ABSTRACT: This paper discusses a rapid GC-FID technique for the simultaneous quantitative analysis of FFA, MAG, DAG, TAG, sterols, and squalene in vegetable oils, with special reference to palm oil. The FFA content determined had a lower SE compared with a conventional titrimetric method. Squalene and individual sterols, consisting of β-sitosterol, stigmasterol, campesterol, and cholesterol, were accurately quantified without any losses. This was achieved through elimination of tedious conventional sample pretreatments, such as saponification and preparative TLC. With this technique, the separation of individual MAG, consisting of 16:0, 18:0, and 18:1 FA, and the DAG species, consisting of the 1,2(2,3)- and 1,3-positions, was sufficient to enable their quantification. This technique enabled the TAG to be determined according to their carbon numbers in the range of C_{44} to C_{56}. Comparisons were made with conventional methods, and the results were in good agreement with those reported in the literature.

Paper no. L9664 in *Lipids* **40**, 523–528 (May 2005).

Palm oil is one of the major oils consumed worldwide. Commercial palm oil is derived from the mesocarp of the *Elaeis guineensis*. Crude palm oil (CPO) consists of >90% TAG, 5.3–7.7% DAG, 0.21–0.34% MAG, 2.4–4.5% FFA, and 1% minor components such as carotenes, tocopherols and tocotrienols, sterols, and squalene (1,2). Analyzing these components using a single method is a challenging task as the components have a wide range of M.W., ranging from 200 to 1000 amu (e.g., FFA <300 amu, and TAG >800 amu). The analysis and quantification of these components generally require some pretreatment, which involves extensive work and the use of chemicals, as each component must be treated differently. A separate analytical method is required for each compound class.

The amount of FFA is an indicator of the quality of oils and fats. In practice, the FFA content in palm oil and its products is determined using an established method reported in *Palm Oil Research Institute of Malaysia* (*PORIM*) *Test Methods* (3). The method involves titration with the use of phenolphthalein as the indicator. However, CPO contains 500–700 ppm (2) of carotenes, which impart an orange-red color that obscures the color change of the indicator.

Sterols are the major portion of unsaponifiable matter in vegetable oils. The official method proposed by European Union legislation is based on the separation of the sterols fraction by silica gel chromatography (4). This method for the quantification of sterols also has been reported previously (5). The prevalent technique for quantifying squalene is also carried out using this method, followed by chromatographic separation. As reported by Moreda *et al.* (6), these methods are laborious and time-consuming, with a significant loss of squalene.

Partial acylglycerols (MAG and DAG) are important constituents in palm oil. They are the hydrolysis products of TAG in the oil, which will affect the physical properties of the oil. The presence of partial acylglycerols (MAG and DAG) in edible oils can cause cloudiness in the oil even though its total concentration is <10%. The DAG profile, i.e., the nature and concentration of DAG in the oil, enables the nucleation process in palm oil to be predicted (7). The nucleation process is the precursor to crystallization and the precipitation of DAG in the oil. Thus, the content of acylglycerols is an important determinant of oil quality.

The MAG, DAG, and TAG are typically determined using AOCS Recommended Practice Cd 11c–93 (8) with the extensive use of chemicals and solvents. The technique is time-consuming and requires a verification step using TLC. The only drawback to the method is the co-elution of FFA in the TAG and DAG fractions, which is not ideal for samples with a high FFA content. Other reported methods include the determination of TAG using GC-FID (9,10), silver-ion HPLC with FID (11), HPLC coupled with ELSD, UV-vis spectrophotometry, and refractive index detectors (12).

Three other AOCS Official Methods that use high-temperature GC to analyze MAG and DAG (Cd-11b-91) (13), tocopherols and sterols (Ce 3-74) (14), and TAG (Ce 5-86) (15) are widely accepted, with their own specificities of the targeted

compounds. Thus, efforts have been made to determine the acyglycerols that are normally present in bulk quantity and the minor components, such as sterols and squalene, simultaneously at the ppm level in a single GC injection.

In recent years, supercritical fluid chromatography (SFC) has been exploited in the analysis of lipids especially to quantify high-M.W. TAG (16–18). Although SFC has relatively few practical applications, this technique has unique advantages where relatively low column temperatures will prevent the degradation of heat-sensitive components and using carbon dioxide will permit the use of an FID.

This paper reports a rapid technique for the quantitative determination of a mixture of FFA, acylglycerols, sterols, and squalene in a single GC-FID injection of vegetable oils, with special reference to palm oil. It is a simplified method for analyzing sterols and squalene that has the possibility of replacing conventional sample preparation steps for routine sample analysis. This method has been tested for about 3 years in the Palm Diesel Quality Control Laboratory of the MPOB for numerous analyses of oil samples.

EXPERIMENTAL PROCEDURES

Materials. CPO was obtained from the MPOB Experimental Palm Oil Mill in Labu, Negeri Sembilan, Malaysia.

Standard and chemical reagents. Myristic acid (14:0), palmitic acid (16:0), stearic acid (18:0), and oleic acid (18:1); monopalmitin, monostearin, and monoolein; 1,2- and 1,3-dipalmitin, 1,2- and 1,3-distearin, and 1,2- and 1,3-diolein; tripalmitin and squalene, with a purity of 99%; and β-sitosterol (95%), campesterol (98%), stigmasterol (95%), and cholesterol (99%) were purchased from Sigma Aldrich Inc. (St. Louis, MO). The silylating reagent *N,O*-bis(trimethylsilyl) trifluoroacetamide with 1% trimethylchlorosilane (BSTFA) was purchased from Fluka Chemicals (Buchs, Switzerland). A TLC plate coated with silica gel 60 F_{254} (20 × 20 cm; Merck 1.05715.0001) was purchased from Merck (Darmstadt, Germany). All solvents were purchased from Merck and were of chromatographic or analytical grade.

FFA titration. The titration of FFA was carried out using a PORIM Test Method (3). A 5.0-g quantity of oil was weighed accurately into a 250-mL conical flask. Then 50 mL of neutralized 2-propanol was added. The flask was placed on a hot plate and the temperature was regulated to about 40°C. The sample was swirled gently while titrating with a standardized sodium hydroxide solution, using phenolphthalein as the indicator to the first permanent pink color. The color had to persist for 30 s.

Saponification (19). Oil (5.0 g) was saponified with 30 mL of absolute ethanol and 5 mL of aqueous potassium hydroxide (50%) for 1 h. The unsaponifiable matter was extracted five times with 30 mL of *n*-hexane. The combined extract was washed repeatedly with 100 mL of distilled water/ethanol (90:10, vol/vol) to neutralize the excess hydroxide. The solution was dried with anhydrous sodium sulfate. The solvent was removed by evaporation under reduced pressure.

TLC (20). The unsaponifiable fraction was subjected to preparative TLC with an eluting solvent system of chloro-

form/diethyl ether/acetic acid (99:5:1, by vol). After the plate was dried, the components were identified by iodine vapor using cholesterol and squalene as standard reference materials. The components were scraped off and extracted three times with 30 mL of *n*-hexane. The solvent was removed by evaporation under reduced pressure. The samples were injected into the gas chromatograph-FID (6).

GC. A 0.02 g quantity of sample was weighed accurately into a 2-mL GC vial. Then 1.2 mL of dichloromethane and 0.3 mL of the silylating reagent BSTFA were pipetted into the vial. The vial was capped tightly and heated at 60°C for 2 h. The instrument used was a Hewlett-Packard Series II gas chromatograph, model 5890 (Hewlett-Packard, Avondale, PA), equipped with an FID and an on-column injector. A BPX 5 fused-silica capillary column (15 m × 0.32 mm), coated with 5% phenyl/95% polysilphenyl-siloxane, with a film thickness of 0.25 μm (SGE, Austin, TX), was used. GC conditions were as follows: injector temperature, 45°C; detector temperature, 370°C; initial oven temperature, 100°C; initial holding time, 1 min; ramping rate, 10°C/min; final temperature, 360°C; final holding time, 16 min; carrier gas (He) flow rate, 2 cm^3/min; column pressure, 14.5 psi; injection volume, 1 mL. Quantification of the components was performed using a 5-point external standard calibration assay, with R^2 values of >0.9900.

RESULTS AND DISCUSSION

A typical gas chromatogram of derivatized CPO obtained using the rapid GC-FID technique is shown in Figure 1. The derivatization procedure prior to GC injection is an essential step in oils and fats analysis as it reduces the elution temperature of MAG, DAG, and especially TAG. It also enhances the response signal of the derivatized compound, which indirectly increases the sensitivity of the FID detector. The elution order of the components begins with FFA (9.0–15.0 min), MAG (15.5–17.0 min), squalene (17.2 min), free sterols (19.0–20.5 min), DAG (22.5–25.5 min), and TAG (28.0–38.0 min). Good resolutions of FFA, MAG, and DAG were achieved, as shown in enlargements of the chromatogram in Figure 2.

Determination of FFA. Table 1 depicts the percentage of FFA in CPO determined using the GC technique and the conventional titration method. Each determination was carried out in triplicate. We found that both techniques gave comparable results of about 4% FFA in the CPO samples. However, the SE of <1.0% calculated using this rapid technique was much smaller than that of the conventional titration technique of 3.0–5.0%. The smaller SE shows the increased precision in quantifying FFA in CPO. The GC technique overcomes the problem of determining the end point in the titration method, especially for palm oil, which has a high amount of red color pigments such as carotenes. In addition, this method provides a detailed analysis of individual FA.

Determination of sterols. With the use of the rapid GC technique, the individual sterols were separated and detected in the oil matrix without subjecting the oil to the conventional sample preparation method of (i) saponification of the sample (ii) isolation of the sterols fraction *via* TLC, (iii) derivatization of
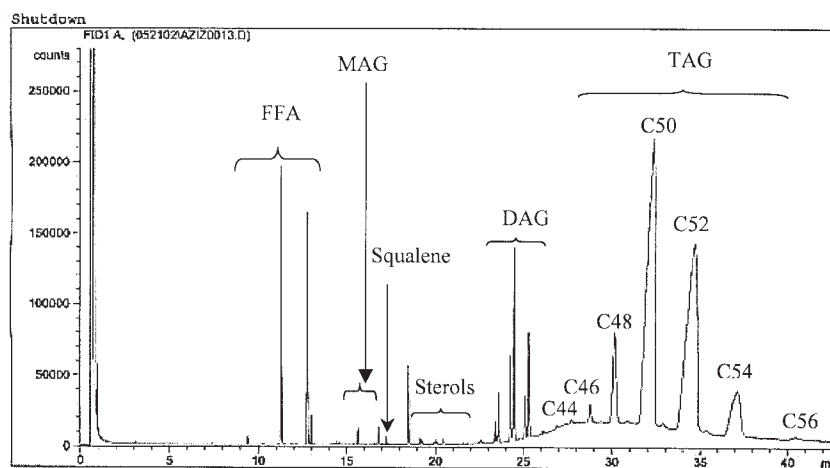
FIG. 1. A typical chromatogram of crude palm oil using the rapid GC-FID method.
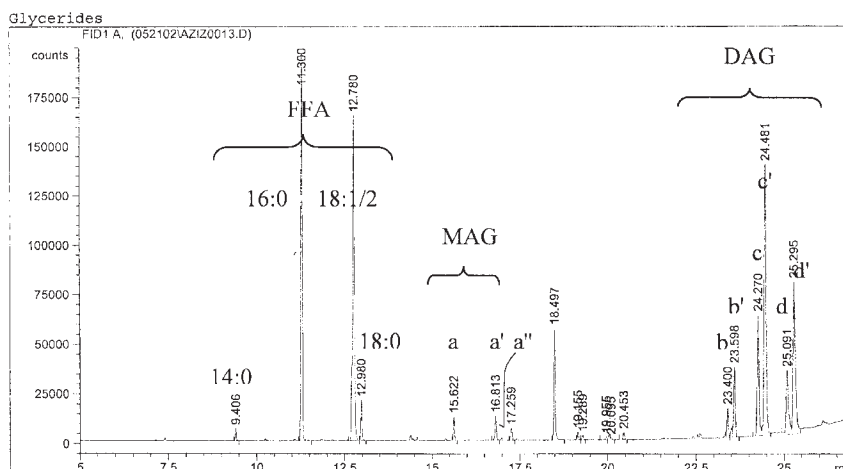
FIG. 2. Enlarged chromatogram of FFA, MAG, and DAG of Crude Palm Oil using the rapid GC-FID method. (a) Monopalmitin at the 1- or 2-position; (a′) monostearin at the 1- or 2-position; (a″) monoolein at the 1- or 2-position; (b) 1,2(2,3)-C_{32} DAG; (b′) 1,3-C_{32} DAG; (c) 1,2(2,3)-C_{34} DAG; (c′) 1,3-C_{34} DAG; (d) 1,2(2,3)-C_{36} DAG; (d′) 1,3-C_{36} DAG.

the recovered sterols, and (iv) GC analysis (20). The enlarged chromatogram (Fig. 3) shows a good separation of free sterols with little interference from the tocopherols and tocotrienols. However, a consistent repeatability of results was not obtained for the tocopherols and tocotrienols because these heat-sensitive compounds degraded during derivatization and because of the high-temperature oven programming. Other minor sterols such as Δ^5-avenasterol, Δ^7-stigmasterol, Δ^7-avenasterol, dimethylsterols, and methylsterols contributed to less than 10% of the total sterols (2). Table 2 shows the comparison of results obtained for selected individual sterols (%) in CPO using the rapid GC technique and the conventional method. The total concentration of sterols determined in the present study is consistent with the results reported by Tang (21). In addition, the percentage of individual sterols found is supported by data reported by Jalani and Rajanaidu (22). We observed that both techniques gave similar percentages of individual sterols. The absolute concentration of sterols found using the rapid GC-FID

method was slightly higher, which may be attributed to some losses during conventional sample preparation steps, such as saponification and TLC isolation.

Determination of squalene. The plant sources that contain squalene are palm oil and olive oil. Palm oil has been reported to contain 200–500 ppm squalene (2). The rapid GC technique was able to detect squalene in both crude and refined palm oil. The squalene content in CPO was determined to be 433 ± 3

TABLE 1
Comparison of FFA in Crude Palm Oil (CPO) by the Rapid GC and Conventional Titration Methods

Sample	FFA (%)	
	Rapid GC method	Conventional titration
CPO 1	4.47 ± 0.01	4.00 ± 0.12
CPO 2	4.32 ± 0.02	4.00 ± 0.17
CPO 3	4.29 ± 0.04	4.28 ± 0.12
CPO 4	4.49 ± 0.02	4.35 ± 0.22
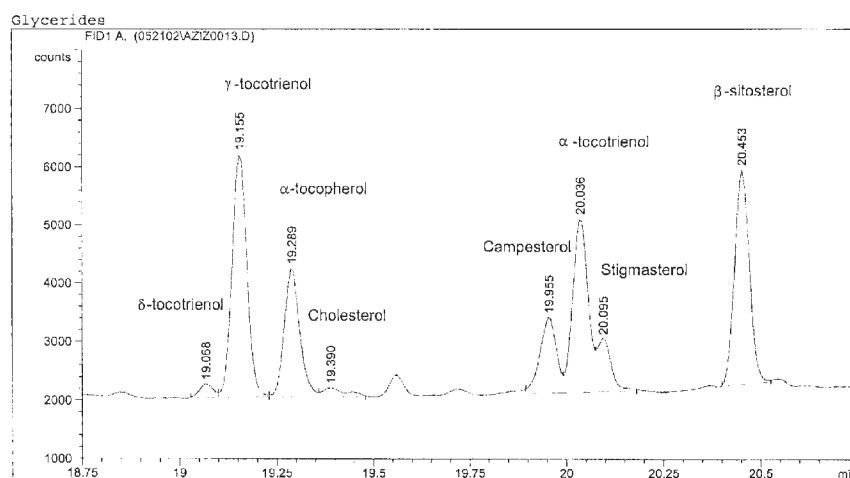
FIG. 3. Enlarged chromatogram of free sterols, tocopherols, and tocotrienols in crude palm oil using the rapid GC-FID method.

TABLE 2
Comparison of Selected Sterols in Crude Palm Oil by the Rapid GC and Conventional Methods

Component	Retention time (min)	Composition (%)	
		Rapid GC method	Conventional method
β-Sitosterol	20.453	60.93 ± 0.22	60.51 ± 0.78
Campesterol	20.095	24.50 ± 0.18	24.25 ± 0.33
Stigmasterol	19.955	12.56 ± 0.43	11.50 ± 0.55
Cholesterol	19.390	2.01 ± 0.13	3.74 ± 0.10

ppm using the rapid technique and 410 ± 4 ppm using the conventional method. The squalene content in refined, bleached, and deodorized palm olein was found to be 415 ± 5 ppm using the rapid technique and 395 ± 3 ppm using the conventional method. The results fell within the concentration range reported earlier (23). Squalene, a highly unsaturated hydrocarbon, may have been partially destroyed during the saponification step, and losses may have occurred during sample isolation by TLC, thus reducing the overall concentration of the compound as compared with the rapid GC technique. The higher recovery ensured greater accuracy in the analysis.

Determination of acylglycerols. The content of MAG was relatively low in CPO, <0.3% (1). However, the level of DAG is known to be exceptionally high in CPO compared with other oils (24). Table 3 shows the content of acylglycerols in CPO determined using the rapid GC-FID method. The content of

partial acylglycerols found in the present study is in agreement with that observed by Goh and Timms (1), with average concentrations of 0.10 and 3.90% for MAG and DAG, respectively. The FA composition of the MAG obtained in the present study showed a slight deviation for 18:0 as compared with that found by George and Arumughan (25) (Table 4). The ratio of saturated to unsaturated FA in MAG was 1:1, which was close to data reported previously (25). A detailed analysis of 1,2(2,3)- and 1,3-DAG could also be performed using the rapid method. We found from the present study that the 1,3-isomer predominated over the 1,2(2,3)-isomers at a ratio of 1.7:1 (Table 5). These results support those of Goh and Timms (1), who found a ratio of about 2:1, as well as those of Siew and Ng (7), who found a ratio of 2.3:1.

The successful separation and identification of the TAG composition in CPO by carbon number was demonstrated

TABLE 3
Composition of MAG, DAG, and TAG in Crude Palm Oil (CPO) by the Rapid GC Method

Sample	Composition (%)		
	MAG	DAG	TAG
CPO 1	0.10 ± 0.011	3.72 ± 0.13	91.72 ± 0.18
CPO 2	0.11 ± 0.007	3.95 ± 0.15	91.62 ± 0.22
CPO 3	0.08 ± 0.006	3.71 ± 0.11	91.92 ± 0.15
CPO 4	0.12 ± 0.010	4.20 ± 0.16	91.18 ± 0.19

TABLE 4
Composition of MAG in Crude Palm Oil (CPO) by the Rapid GC Method

MAG	Retention time (min)	Composition (%)			
		CPO 1	CPO 2	CPO 3	CPO 4
16:0	15.622	35.14 ± 0.21	34.37 ± 0.26	38.44 ± 0.13	38.59 ± 0.38
18:0	16.980	16.47 ± 0.19	14.44 ± 0.32	12.51 ± 0.23	10.64 ± 0.41
18:1/2	16.813	48.40 ± 0.19	51.19 ± 0.26	49.05 ± 0.31	50.77 ± 0.27

TABLE 5
Composition of DAG in Crude Palm Oil (CPO) by the Rapid GC Method

DAG	Retention time (min)	Composition (%)			
		CPO 1	CPO 2	CPO 3	CPO 4
$1,2(2,3)\text{-}C_{32}$	23.400	2.91 ± 0.06	2.60 ± 0.11	2.78 ± 0.09	3.11 ± 0.08
$1,3\text{-}C_{32}$	23.598	5.28 ± 0.10	5.49 ± 0.05	4.84 ± 0.16	5.44 ± 0.11
$1,2(2,3)\text{-}C_{34}$	24.270	20.83 ± 0.13	19.21 ± 0.12	20.17 ± 0.07	19.48 ± 0.07
$1,3\text{-}C_{34}$	24.481	34.12 ± 0.06	35.52 ± 0.11	34.31 ± 0.09	34.81 ± 0.16
$1,2(2,3)\text{-}C_{36}$	25.091	14.37 ± 0.13	13.01 ± 0.14	14.20 ± 0.09	13.25 ± 0.12
$1,3\text{-}C_{36}$	25.295	22.49 ± 0.16	24.17 ± 0.15	23.70 ± 0.16	23.92 ± 0.12

TABLE 6
Composition of TAG (by Carbon Number) in Crude Palm Oil (CPO) by the Rapid GC Method

TAG	Retention time (min)	Composition (%)			
		CPO 1	CPO 2	CPO 3	CPO 4
C_{44}	27.729	0.31 ± 0.006	0.21 ± 0.004	0.18 ± 0.008	0.23 ± 0.010
C_{46}	28.768	1.09 ± 0.06	1.16 ± 0.09	1.00 ± 0.10	1.06 ± 0.08
C_{48}	30.177	9.64 ± 0.12	9.38 ± 0.16	10.05 ± 0.17	9.98 ± 0.10
C_{50}	32.352	42.59 ± 0.19	42.70 ± 0.30	43.05 ± 0.28	43.02 ± 0.26
C_{52}	34.693	37.65 ± 0.25	37.81 ± 0.28	37.29 ± 0.20	37.23 ± 0.17
C_{54}	37.122	8.42 ± 0.24	8.53 ± 0.23	8.17 ± 0.16	8.36 ± 0.11
C_{56}	40.453	0.30 ± 0.001	0.20 ± 0.003	0.25 ± 0.016	0.11 ± 0.007

using the rapid GC method in the present study (Table 6). The composition of TAG in terms of carbon number is one of the important parameters that characterizes palm oil, with the major TAG being C_{50} and C_{52}. TAG defines some physical characteristics of palm oil such as its m.p. and crystallization properties. As can be seen, the data obtained in the present study are similar to those reported previously (21). The composition of TAG in palm olein and palm stearin obtained by dry fractionation was distinctive and differed significantly by the C_{48} TAG (26). With the rapid GC technique, compositional changes in TAG during the fractionation process can be monitored.

The rapid GC-FID method described in this report provided valuable information about the composition of oils; it required minimal analysis time and eliminated the need for saponification and TLC isolation of the minor components. The repeatability of the developed method for analyzing a mixture of FFA, sterols, squalene, and acylglycerols illustrates its use as a fast, quantitative technique for the analysis of vegetable oils.

ACKNOWLEDGMENTS

REFERENCES

1. Goh, E.M., and Timms, R.E. (1985) Determination of Mono- and Diglycerides in Palm Oil, Olein, and Stearin, *J. Am. Oil Chem. Soc. 62*, 730–734.
2. Goh, S.H., Choo, Y.M., and Ong, A.S.H. (1985) Minor Constituents of Palm Oil, *J. Am. Oil Chem. Soc. 62*, 237–240.
3. Palm Oil Research Institute of Malaysia (PORIM) (1995) Determination of Acidity, in *PORIM Test Methods*, pp. 40–42, PORIM, Selangor, Malaysia, Method No. P2.5.
4. de Blas, O.J., and del Valle González, A. (1996) Determination of Sterols by Capillary Column Gas Chromatography. Differentiation Among Different Types of Olive Oil: Virgin, Refined, and Solvent-Extracted, *J. Am. Oil Chem. Soc. 73*, 1685–1689.
5. Alonso, L., Fontecha, J., Lozada, L., and Juárez, M. (1997) Determination of Mixtures in Vegetable Oils and Milk Fat by Analysis of Sterol Fraction by Gas Chromatography, *J. Am. Oil Chem. Soc. 74*, 131–135.
6. Moreda, M., Perez-Camino, M.C., and Cert, A. (2001) Gas and Liquid Chromatography of Hydrocarbons in Edible Vegetable Oils, *J. Chromatogr. A*, 936, 159–171.
7. Siew, W.L., and Ng, W.L. (1999) Influence of Diglycerides on Crystallization of Palm Oil, *J. Sci. Food Agric. 79*, 722–726.
8. AOCS (1997) Quantitative Separation of Monoglycerides, Diglycerides, and Triglycerides by Silica Gel Column Chromatography,

in *Official Methods and Recommended Practices of the AOCS*, AOCS Press, Champaign, Recommended Practice Cd 11c-93.

9. Antoniosi Filho, N.R., Carrilho, E., and Lancas, F.M. (1993) Fast Quantitative Analysis of Soybean Oil in Olive Oil by High-Temperature Capillary Gas Chromatography, *J. Am. Oil Chem. Soc. 70*, 1051–1053.

10. Kuksis, A., Myher, J.J., and Geher, K. (1993) Quantification of Plasma Lipids by Gas–Liquid Chromatography on High Temperature Polarizable Capillary Columns, *J. Lipid Res. 34*, 1029–1038.

11. Neff, W.E., Adolf, R.O., List, G.R., and El Agaimy, M. (1994) Analyses of Vegetable Oil Triacylglycerols by Silver Ion High-Performance Liquid Chromatography with Flame Ionization Detection, *J. Liquid Chromatogr. 17*, 3951–3968.

12. Aparicio, R., and Aparicio-Ruiz, R. (2000) Authentication of Vegetable Oils by Chromatographic Techniques, *J. Chromatogr. A 881*, 93–104.

13. AOCS (1997) Determination of Mono- and Diglycerides by Capillary Gas Chromatography, in *Official Methods and Recommended Practices of the AOCS*, AOCS Press, Champaign, Official Method Cd 11b-91.

14. AOCS (1997) Determination of Tocopherols and Sterols in Soy Sludges and Residues by Gas–Liquid Chromatography, in *Official Methods and Recommended Practices of the AOCS*, AOCS Press, Champaign, Recommended Practice Ce 3-74.

15. AOCS (1997) Triglycerides by Gas Chromatography, in *Official Methods and Recommended Practices of the AOCS*, AOCS Press, Champaign, Official Method Ce 5-86.

16. Blomberg, L.G., Demirbuker, M., and Andersson, M. (1998) Characterization of Lipids by Supercritical Fluid Chromatography and Supercritical Fluid Extraction, in *Lipid Analysis in Oils and Fats* (Hamilton, R.J., ed.), pp. 34–58, Blackie, London.

17. King, J.W., and Snyder, J.M. (1997) Supercritical Fluid Chromatography: A Short-Cut in Lipid Analysis, in *New Techniques and Applications in Lipid Analysis* (McDonald, R.E., and Mossoba, M.M., eds.), pp. 139–162, AOCS Press, Champaign.

18. Hayes, D.G. (1997) Analysis of Unusual Triglycerides and Lipids Using Supercritical Fluid Chromatography, in *New Techniques and Applications in Lipid Analysis* (McDonald, R.E., and Mossoba, M.M., eds.), pp. 163–182, AOCS Press, Champaign.

19. Palm Oil Research Institute of Malaysia (PORIM) (1995) Determination of Unsaponifiable Matter, in *PORIM Test Methods*, pp. 45–47, PORIM, Selangor, Malaysia, Method No. P2.7.

20. Yap, S.C. (1995) Palm Oil Carotenes: Chemistry and Technology, pp. 201–202, Ph.D. Thesis, University of Malaya, Kuala Lumpur.

21. Tang, T.S. (2000) Composition and Properties of Palm Oil Products, in *Advances in Palm Oil Research, Volume II* (Yusof, B., Jalani, B.S., and Chan, K.W., eds.), pp. 845–894, Malaysian Palm Oil Board, Selangor, Malaysia.

22. Jalani, B.S., and Rajanaidu, N. (2000) Improvement in Oil Palm: Yield, Composition and Minor Components, *Lipid Technol. 12*, 5–8.

23. Ab. Gapor, M.T., and Hazrina, A.R. (2000) Squalene in Oils and Fats, *Palm Oil Dev. 32*, 36–40.

24. Tan, B.K., and Oh, F.C.H. (1981) Malaysian Palm Oil Chemical and Physical Characteristics, in *PORIM Technology Series No. 3*, Palm Oil Research Institute of Malaysia (PORIM), Selangor, Malaysia.

25. George, S., and Arumughan, C. (1992) Lipid Profile of Process Streams of Palm Oil Mill, *J. Am. Oil Chem. Soc. 69*, 283–287.

26. Pantzaris, T.P. (2000) *Pocketbook of Palm Oil Uses*, 5th edn., p. 14, Malaysian Palm Oil Board, Selangor, Malaysia.

COMMUNICATION

Fatty Acid Composition of Wild and Farmed Atlantic Salmon (*Salmo salar*) and Rainbow Trout (*Oncorhynchus mykiss*)

Carole Blanchet[a,b,]*, Michel Lucas[a], Pierre Julien[c],
Richard Morin[d], Suzanne Gingras[a], and Éric Dewailly[a,b]

[a]Public Health Research Unit, Centre Hospitalier Universitaire de Québec (CHUQ) and [b]Institut National
de Santé Publique du Québec, Québec G1V5B3 Canada, [c]Lipid Research Center, CHUQ, Québec G1V4G2 Canada,
and [d]Ministère de l'Agriculture, des Pêcheries et de l'Alimentation du Québec (MAPAQ), Québec G1R4X6 Canada

ABSTRACT: The goal of this study was to examine the FA composition of wild and farmed Atlantic salmon (AS) and rainbow trout (RT). FA profiles were obtained by GC/FID. Results showed that lipid and n-3 highly unsaturated FA contents of farmed and wild AS were similar. Total n-3 and n-6 PUFA were significantly higher in farmed AS than in wild AS. Farmed RT contained more fat and less n-3 PUFA than wild RT. Our results show that farmed salmonids provide high levels of n-3 HUFA to consumers.

Paper no. L9633 in *Lipids 40*, 529–531 (May 2005).

Public interest in the health benefits of long-chain n-3 FA is increasing because numerous studies report that a diet rich in fish protects against chronic diseases such as coronary heart disease (CHD) (1). Hence, it is recommended to consume at least two meals of fish, preferably oily, per week (1).

However, wild fish is a finite resource. The increase in demand for fish products over the past two decades has been met by aquaculture production. Given the increasing role of aquaculture in ensuring future per capita fish supplies as world population grows, farmed fish has a significant role to play in providing n-3 FA sources to consumers (2). Atlantic salmon (AS; *Salmo salar*) and rainbow trout (RT; *Oncorhynchus mykiss*) are the major farmed fish consumed by Quebecers, because of their great availability and accessibility in food markets. The goal of the present study was to examine and compare the FA composition of wild and farmed AS and RT.

MATERIAL AND METHODS

In 2003, Ministère de l'Agriculture, des Pêcheries et de l'Alimentation du Québec (MAPAQ) collected farmed AS ($n = 46$) and RT ($n = 37$) in Québec food markets. Wild AS samples ($n = 10$) were obtained from anglers of the Gaspésie area, the Centre Interuniversitaire de Recherche sur le Saumon Atlantique (CIRSA), and the Ministère des Ressources Naturelles, de la

Faune et des Parcs du Québec (FAPAQ). Wild RT samples ($n = 10$) were obtained from the Freshwater Fisheries Society of British Columbia and FAPAQ. Fish fillets were packaged in plastic bags and stored at $-20°C$ until laboratory analyses (within 2 months following sampling).

FA analyses. Analyses were conducted on raw, skinless fillets, excluding other types of fat such as subcutaneous or mesenteric fat. In the presence of PC containing 15:0 FA used as an internal standard, 300 mg of tissues was extracted three times with chloroform/methanol (2:1 vol/vol) (3). Lipid extract solvents were then evaporated under a stream of nitrogen, weighed, and methylated (4). FA profiles were obtained by capillary GC (Hewlett-Packard 5890 gas chromatograph, equipped with an automated injector 7673A and an FID injector). Injector and detector temperatures were 200 and 260°C, respectively. A capillary column (DB-23: 30 m × 0.25 mm i.d. × 0.25 µm film thickness; Agilent Technologies, Palo Alto, CA) was used with nitrogen as the carrier gas. The FA were identified with a standard mixture of 37 different FA (FAME 37; Supelco, Bellefonte, PA).

The arithmetic mean of total lipids and FA concentrations was calculated for each species. For each FA, comparison of the concentrations between the wild and farmed fish was assessed with the nonparametric Wilcoxon test. Statistical significance was set at $P < 0.05$.

RESULTS

Table 1 shows the FA compositions of wild and farmed AS and RT. The average total lipid contents of wild and farmed AS were similar. However, the range of lipid values was quite large for both types of AS, varying between 1.3 and 16.1 g/100 g of fish flesh. Total n-6 PUFA, n-6 HUFA (highly unsaturated FA), and linoleic acid in farmed AS were four-, two-, and sixfold higher, respectively, than in wild AS. Total n-3 PUFA, α-linolenic acid, and EPA were significantly higher in farmed AS than in wild AS, whereas concentrations of DHA and n-3 HUFA were similar. The ratio of n-3 to n-6 PUFA was 11.0 in wild AS compared with 3.6 in farmed AS. PUFA were the major FA in farmed AS compared with wild AS. Saturated FA (SFA) were 35% higher in farmed AS than in wild AS. In contrast, monounsaturated FA (MUFA) were 60% higher in wild AS than in farmed AS.

The total lipid content in farmed RT was 5.6-fold higher than that of wild RT. Total n-6 PUFA and n-6 HUFA in wild

*To whom correspondence should be addressed at the Institut National de Santé Publique du Québec, 945 Wolfe Ave., Sainte-Foy, Québec, Canada G1V 5B3. E-mail: carole.blanchet@inspq.qc.ca

Abbreviations: AS, Atlantic salmon; CIRSA, Centre interuniversitaire de Recherche sur le Saumon Atlantique; CHD, coronary heart disease; FAPAQ, Ministère des Ressources Naturelles, de la Faune et des Parcs du Québec; HUFA, highly unsaturated FA; MAPAQ, Ministère de l'Agriculture, des Pêcheries et de l'Alimentation du Québec; MUFA, monounsaturated FA; RT, rainbow trout; SFA, saturated FA.

TABLE 1
FA Composition[a] of Farmed and Wild Atlantic Salmon and Rainbow Trout

| | Atlantic salmon | | | | | Rainbow trout | | | | |
| | Farmed ($n = 46$) | | Wild ($n = 10$) | | | Farmed ($n = 37$) | | Wild ($n = 10$) | | |
	$\overline{X}$	SD	$\overline{X}$	SD	P	$\overline{X}$	SD	$\overline{X}$	SD	P
Lipids (g/100 g)	7.4	3.8	7.0	3.8		5.6	3.5	1.0	0.4	d
Total FA (g/100 g)	4.1	1.9	4.0	1.3		3.2	1.7	0.6	0.2	d
FA (wt% of total FA)										
Σn-6 PUFA	9.8	2.7	2.3	0.3	d	8.5	2.6	12.5	4.7	b
Σn-6 HUFA	1.7	0.4	0.8	0.1	d	1.7	0.3	7.9	4.1	c
18:2 (linoleic acid)	7.4	2.7	1.2	0.2	d	6.2	2.6	4.2	1.1	b
20:4 (arachidonic acid)	0.9	0.2	0.4	0.1	d	0.9	0.2	5.4	3.0	c
Σn-3 PUFA	31.1	7.5	25.0	3.9	b	32.2	8.6	46.2	6.4	c
Σn-3 HUFA	28.3	7.9	23.8	3.8		30.1	8.6	44.0	7.2	c
18:3 (α-linolenic acid)	1.6	0.7	0.5	0.1	d	1.0	0.4	1.7	0.8	b
20:5 (EPA)	7.9	1.8	6.6	1.1	b	7.3	2.2	8.1	1.1	
22:6 (DHA)	15.2	5.7	13.1	2.7		18.7	6.4	32.2	7.6	c
Σn-3/Σn-6 PUFA	3.6	1.8	11.0	2.7	d	4.4	2.4	4.8	3.3	
ΣPUFA	41.0	5.8	27.3	3.9	d	40.6	6.6	58.6	3.8	d
ΣMUFA	33.4	7.9	53.7	3.9	d	32.5	7.2	17.0	4.0	d
ΣSFA	25.6	2.9	19.0	1.0	d	26.9	2.2	24.4	1.4	c

[a]$\overline{X}$ = arithmetic mean; SD = standard deviation; HUFA, highly unsaturated FA; SFA, saturated FA; MUFA, monounsaturated FA. Σn-6 PUFA, (18:2 + 18:3 + 20:2 + 20:3 + 20:4 + 22:2 + 22:4 + 22:5); Σn-6 HUFA, (20:3 + 20:4 + 22:4 + 22:5); Σn-3 PUFA, (18:3 + 18:4 + 20:3 + 20:4 + 20:5 + 22:5 + 22:6); Σn-3 HUFA, (20:3 + 20:4 + 20:5 + 22:5 + 22:6); ΣMUFA, (14:1 + 18:1 + 20:1 + 22:1 + 24:1); ΣSFA: (14:0 + 15:0 + 16:0 + 18:0 + 20:0 + 22:0 + 24:0).
[b]$P < 0.05$.
[c]$P < 0.005$.
[d]$P < 0.0001$.

RT were significantly higher than in farmed RT, whereas linoleic acid was higher in farmed RT. Total n-3 PUFA, n-3 HUFA, α-linolenic acid, and DHA were higher in wild RT than in farmed RT whereas the ratio of n-3 to n-6 PUFA was similar in all trout samples. However, absolute concentrations showed that farmed RT provided threefold higher amounts of n-3 PUFA than wild RT (931 vs. 268 mg/100 g). PUFA were present in higher proportion in wild RT than in farmed RT. In contrast, SFA and MUFA were higher in farmed RT than in wild RT.

DISCUSSION

Although farmed salmonids generally display higher amount of lipids than wild fish (5,6), our results showed that the lipid content of farmed AS was lower than expected and similar to that of wild AS. Moreover, linoleic, α-linolenic, and arachidonic acids were, respectively, six-, three-, and twofold higher in farmed AS than in wild AS. The recent use of vegetable oils in feeds of farmed AS may explain these differences. It is well known that the FA composition of farmed fish greatly varies depending upon their diet (5,7). In the present study, the composition of the diets for the farmed fish was unknown, as they are mainly produced in Chile (Morin, R., unpublished data). Unexpectedly, the flesh of wild and farmed RT displayed a similar ratio of n-3/n-6 PUFA even though farmed RT contained

more lipid and less n-3 and n-6 PUFA than wild RT. Moreover, the concentration of arachidonic acid was sixfold higher in wild RT than in farmed RT, probably reflecting the greater consumption of terrestrial insects by wild RT (8).

In 2004, for primary prevention of CHD, nutrition experts of the International Society for the Study of Fatty Acids and Lipids recommended 500 mg of EPA + DHA per day (1). Fortunately, our results show that the consumption of farmed salmonids provides high levels of n-3 HUFA and consequently may have beneficial health effects for consumers.

ACKNOWLEDGMENTS

REFERENCES

1. Harris, W.S., and Von Schacky, C. (2004) The Omega-3 Index: A New Risk Factor for Sudden Cardiac Death? *Prev. Med. 39*, 212–220.
2. Delgado, C.L., Wada, N., Rosegrant, M.W., Meijer, S., and Ahmed, M. (2003) *Fish to 2020: Supply and Demand in Chang-*

ing Global Markets, ISBN 0-89629-725-X, International Food Policy Research Institute and WorldFish Center, Washington, DC.

3. Shaikh, N.A., and Downar, E. (1981) Time Course of Changes in Porcine Myocardial Phospholipid Levels During Ischemia. A Reassessment of the Lysolipid Hypothesis, *Circ. Res. 49*, 316–325.

4. Lepage, G., and Roy, C.C. (1986) Direct Transesterification of All Classes of Lipids in a One-Step Reaction, *J. Lipid Res. 127*, 114–120.

5. Cahu, C., Salen, P., and de Lorgeril, M. (2004) Farmed and Wild Fish in the Prevention of Cardiovascular Diseases: Assessing Possible Differences in Lipid Nutritional Values, *Nutr. Metab. Cardiovasc. Dis. 14*, 34–41.

6. Nettleton, J.A. (2000) Fatty Acids in Cultivated and Wild Fish, in *Proceedings of the International Institute of Fisheries Economics and Trade*, (July 10–14), II FET, Oregon State University, Corvallis.

7. Bell, J.G., McEvoy, J., Tocher, D.R., McGhee, F., Campbell, P.J., and Sargent, J.R. (2001) Replacement of Fish Oil with Rapeseed Oil in Diets of Atlantic Salmon (*Salmo salar*) Affects Tissue Lipid Compositions and Hepatocyte Fatty Acid Metabolism, *J. Nutr. 131*, 1535–1543.

8. Ackman, R.G., and Takeuchi, T. (1986) Comparison of Fatty Acids and Lipids of Smolting Hatchery-Fed and Wild Atlantic Salmon *Salmo salar*, *Lipids 21*, 117–120.

REVIEW

Astonishing Diversity of Natural Surfactants: 3. Carotenoid Glycosides and Isoprenoid Glycolipids

Valery M. Dembitsky*

Department of Organic Chemistry and School of Pharmacy, Hebrew University, Jerusalem, Israel

ABSTRACT: Carotenoid glycosides and isoprenoid glycolipids are of great interest, especially for the medicinal, pharmaceutical, food, cosmetic, flavor, and fragrance industries. These biologically active natural surfactants have good prospects for the future chemical preparation of compounds useful as antimicrobial, antibacterial, and antitumor agents, or in industry. More than 300 unusual natural surfactants are described in this review article, including their chemical structures and biological activities.

Paper no. L9708 in *Lipids 40*, 535–557 (June 2005).

Carotenoids and related compounds are an important group of natural pigments in both the prokaryote and eukaryote kingdoms, exhibiting colors from dark red to bright yellow. Carotenoids are important in human nutrition as a source of β-carotene (vitamin A) and possibly as preventive agents against cancer and heart disease. In addition, carotenoids add color to foods and beverages. Carotenoids are the precursors of many important chemicals responsible for the flavors of foods and the fragrances of flowers. Carotenoids are a class of isoprenoid hydrocarbons (carotenes) and their oxygenated derivatives (xanthophylls). About 700 carotenoids have been isolated from natural sources, and about 160 of these pigments contain a carbohydrate moiety and belong either to the carotenoid glycosides or to the carotenoid glycosyl esters. This article describes the basic principles of the structure, stereochemistry, and nomenclature of carotenoids. The relationships between the structure and the chemical and physical properties on which all the varied biological functions and actions of the carotenoids depend have been observed in some review articles and books (3–9). The conjugated polyene chromophore determines not only the light-absorption properties, and hence color, but also the photochemical properties of the molecule and consequent light-harvesting and photoprotective action. The polyene chain is also the feature mainly responsible for the chemical reactivity of carotenoids toward oxidizing agents and free radicals, and hence for any antioxidant role. *In vivo*, carotenoids are found in specific locations and orientations in subcellular structures, and their chemical and physical properties are strongly influenced by other molecules in their vicinity, especially proteins and membrane lipids. In turn, the carotenoids influence the properties of these subcellular structures. Structural features such as size, shape, and polarity are essential determinants of the ability of a carotenoid to fit correctly into its molecular environment to allow it to function. A role for carotenoids in modifying the structure, properties, and stability of cell membranes, and thus affecting the molecular processes associated with these membranes, may be an important aspect of their possible beneficial effects on human health (5–7,10).

Archaebacteria, the third primary kingdom of cells in addition to eukaryotes and eubacteria, are all characterized by unusual isoprenoid ether lipids (11–17). Archaebacteria, or Archaea, have been discovered in extreme environments such as hot springs and salt lakes (11–13). Lipids of these microorganisms always possess saturated C_{20}-, C_{25}-, and C_{40}-polyisoprenoid chains in the hydrophobic moiety. Many studies have indicated that the membranes of the polyisoprenoid lipids are stable at high temperatures and high salt concentrations. The prior reviews of membrane lipids in archaebacteria have revealed a remarkable variety of polar lipids classes, including phospholipids, glycolipids, phosphoglycolipids, and sulfolipids, all derived from the one basic core structure, diphytanylglycerol, and an equally remarkable set of novel pathways for their biosynthesis (15). These ether lipids normally account for 80–95% of the membrane lipids, with the remaining 5–20% being neutral squalenes and other isoprenoids. Specific combinations of various lipid core structures found in methanogens include diether-tetraether, diether-hydroxy diether, or diether-macrocyclic diether-tetraether lipid moieties (16). The unusual molecular architecture gives rise to substantial modifications in the organization of the lipidic layer of their membranes, which still retains the typical trilaminar structure (11–17).

CAROTENOID GLYCOSIDES

Acyclic Carotenoid Glycosides

The first carotenoid glycoside was isolated from saffron and described in 1818 (18). Crocin **1**, as the major carotenoid, was isolated from *Crocus sativus* by Karrer and Miki in 1929 (19), and was later isolated from *Nyctanthes arbortristis* (20). Saffron, the dried stigmas of *C. sativus* L. (Iridaceae), is a very expensive spice that is used mainly as an herbal medicine or food

---

*Address correspondence at Department of Organic Chemistry, P.O. Box 39231, Hebrew University, Jerusalem 91391, Israel.
E-mail: dvalery@cc.huji.ac.il

Abbreviations: DMPC, dimyristoylphosphatidycholine; ED_{50} (effective dose$_{50}$), the amount of material required to produce a specified effect in 50% of an animal population; InhA, a mycobacterial long-chain enoyl acyl carrier protein reductase (RV1484, EC 1.3.1.9); SQDG, sulfoquinovosyldiacylglycerol; TPA, 12-*O*-tetradecanoyl-phorbol-13-acetate.

coloring and flavoring agent in different parts of the world (21). Saffron originally grew in India, Iran, Spain, Greece, and other countries and has been successfully cultivated in various places in China, especially Tibet (21). It has historically been used in Chinese traditional medicine as an anti-anginal agent. Among the four crocins, crocin **1** is the most abundant in saffron and has been studied extensively for its pharmacological effects (22–24). The major biologically active ingredients of saffron (*C. sativus*) are crocin analogs, including crocins **1–4**, which are all glycosides of *trans*-crocetin **5–8**, a *cis*-carotenoid derivative **9** (25–27). The major yellow colorant, crocin **1**, has been isolated from the fruit of *Gardenia jasminoides* (28–31). Yellow colorants from *G. jasminoides* that are suitable for foodstuffs and natural dye preparations have been postulated to be crocetin glycosyl esters. The utility of carotenoid glycosyl esters as colorants for textiles (32) and food (33), as antioxidant quenchers for free radicals (34–36), and as antitumor agents (37) also has been reported. The unusual and adaptogenic xanthone carotenoid glycosidic conjugate termed mangicrocin **10** was isolated from Indian saffron *C. sativus* (38). A major new pigment isolated from *C. sativus* has been identified as the crocetin dineapolitanosyl ester **11** (39).
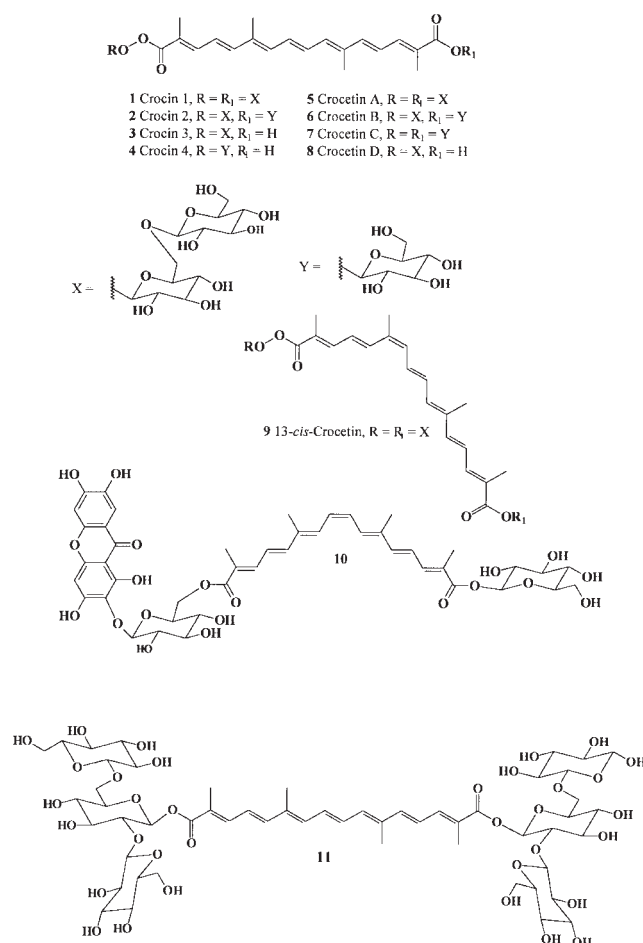
A series of dihydroxylycopene diglucoside diesters as a novel class of carotenoids, **12–18**, have been isolated from the phototrophic purple sulfur bacteria *Halorhodospira abdelmalekii* and *H. halochloris* (40). Diglucoside esters and diesters were esterified by two FA only: 12:0 (48% of total) and 14:1 (52%).

β-D-Glucosyl of the 4,4″-diapocarotene-6,6′-dioic acid **19** has been isolated from *Pseudomonas rhodos* and red-strain *Rhizobium lupini*, both isolated from *Lotononis bainesii* Baker (41–44). An apo-lycopenoate mannosyl ester, **20**, was found as a minor component in the yellow halophilic cocci strains H5B-2 and SE20-4 (45).

The carotenoid composition of the myxobacterium *Chondromyces apiculatus* was reported previously (46); a new acyclic carotenoid glucoside ester was isolated, and its structure was determined as the 1′-glucosyloxy-3′,4′-didehydro-1′,2′-dihydro-ψ,ψ-carotene monoesters **21–25**.
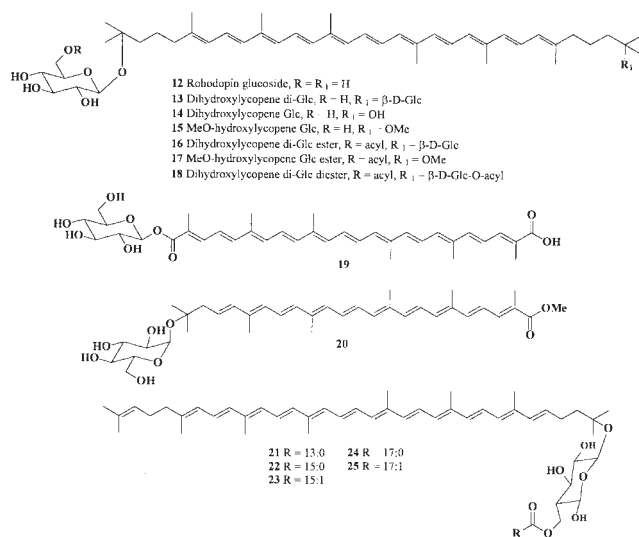
Staphylococcus aureus, a major human pathogen causing a wide spectrum of diseases, is able to survive under a variety of extreme conditions and produces staphyloxanthin **26** as a major pigment (47). Pigments of three species of alkaliphilic heliobacteria of the genus *Heliorestis*—*H. daurensis*, *H. baculata*, and an undescribed species, *Heliorestis* strain HH—produced two novel carotenoid glycosides, **27** and **28** (48). In these species, as in other heliobacteria, bacteriochlorophyll G esterified with farnesol was present. In addition, trace amounts of the biosynthetic intermediates OH-diaponeurosporene and OH-diaponeurosporene glucoside **29** were found. Trace amounts of a carotenoid with 20 carbon atoms, 8,8′-diapo-ζ-carotene, also were found in these species as well as in the non-alkaliphilic heliobacteria. The non-alkaliphilic species *Heliophilum fasciatum* also contained trace amounts of the two OH-diaponeurosporene glucoside esters. The results were used to predict the pathway of carotenoid biosynthesis in heliobacteria (47).

26

27 R = 16:0
28 R = 16:1
29 R = H
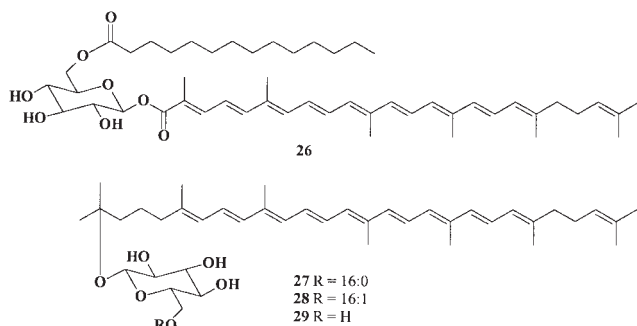
The carotenoid glycosides **30** and **31** were isolated from the myxobacteria *Chondromyces apiculatus* (46) and *Myxococcus fulvus* (49). Rhodopin β-D-glucoside **32** and rhodopinal β-D-glucoside **33** were isolated from photosynthetic non-sulfur bacteria of the Rhodospirillaceae: *Rhodopseudomona acidophila, Rhodospirillum tenue, Rhodocyclus purpureus*, and *Athiorhodaceae* species (50–52).

30

31 R = Glc

32 R = Glc

33 R = Glc
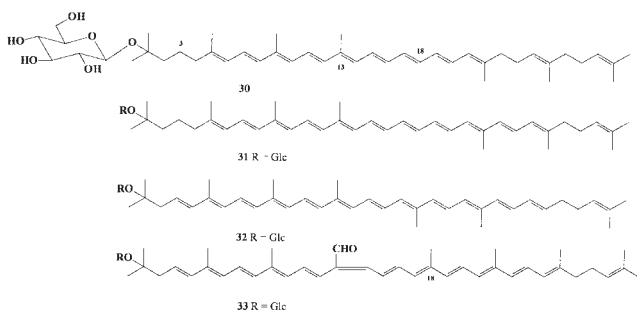
Mannosyl apo-lycopene alcohol **34** was a minor compound, as was apo-lycopenoate mannosyl **20** isolated from the yellow halophilic cocci strains H5B-2 and SE-20-4 (45). The mono-β-D-glucosyl ester **35** and the di-β-D-glucosyl ester **36** of 4,4′-diapocarotene-6,6′-dionic acid have been isolated both from a red strain of *Rhizobium* sp. isolated from the roots of *Lotononis bainesii* and from *Pseudomonas rhodos* (42,43,53–55). They represent the C$_{30}$ homologs of the glycosyl esters **1**–**8** and **11** occurring in *C. sativus* and *G. jasminoides*. Triterpenoid mono-β-D-glucosyl of 4,4′-diaponeurosporene **37** was produced by *Streptococcus faecium* UNH-564P (56). α-L-Rhamnopyranosyl, of the acyclic carotenoid named as oscillaxanthin **38**, is produced by the cyanobacterium *Oscillatoria rubescens* and represents the most important carotenoid glycoside in this group of cyanobacteria (57,58).

34 R = Man

35 R = Glc, R$_1$ = H
36 R = R$_1$ = Glc

37 R = Glc

38 R = R$_1$ = Rha
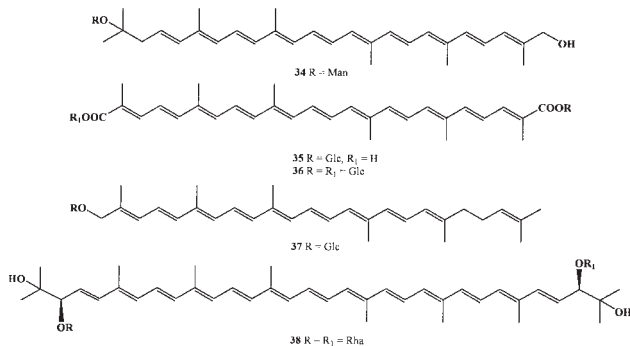
Neurosporene fucoside **39** and some other mono- and bicyclic carotenoid glycosides produced by the unicellular cyanobacterium *Synechocystis* sp. strain PCC 6803, which were isolated during myxoxanthophyll biosynthesis, have been studied (59).

Bacterioruberin mono- and diglycosides containing glycose **40** and **41** and mannose **42** and **43** sugars belonging to the C$_{50}$ carotenoid group have been isolated from the halophilic bacterial strain BOS 66 from glacial mud (60). The presence of C$_{50}$ carotenoids in halophilic bacteria is an interesting finding, and it has been suggested that the molecular length of C$_{50}$ carotenoids with two polar end groups is suitable in membrane architecture. It has been reported briefly that bacterioruberin reinforces the reconstituted lipid membrane of *Halobacterium* (61).

39

40 R = Glc, R$_1$ = H
41 R = R$_1$ = Glc
42 R = Man, R$_1$ = H
43 R = R$_1$ = Man
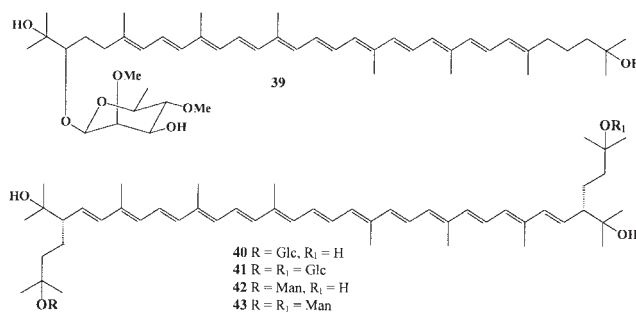
Monocyclic Carotenoid Glycosides

Monocyclic carotenoids are a large group of pigments that are produced by bacteria, lower fungi, and invertebrates (5,7,8,10). Some monocyclic carotenoids contain sugar moieties. Two carotenoid esters, salinixanthin **44** and **45**, have been isolated from the extremely halophilic eubacterium *Salinibacter ruber* (62). The same carotenoid glucoside in the acylated form in *Rhodothermus marinus* was isolated from marine hot springs (63). The FA ester of pheixanthophyll **46** was found in *Nocardia kirovani* (64). *Rhodococcus rhodochrous* RNMS1 (IAM 13988) contains a series of carotenoid glycoside esters with different FA residues, **47**–**55** (65). The same keto-myxoxanthin glycoside esters were isolated from a thermophilic filamentous photosynthetic bacterium *Roseiflexus castenholzii* (66). The FA composition was determined and included the acids 14:0 (24.1%), *iso*-15:0 (12.5%), 15:0 (6.2%), *iso*-16:0 (1%), 16:0 (29.8%), branched 17:0 (12.8%), *iso*-17:0 (10.3%), 17:0 (2.6%), and 18:0 (0.6%).

44 R = OH
45 R = H

46

47 R = 16:0
48 R = 17:0
49 R = 18:0
50 R = 19:0
51 R = 19:1

52 R = 18:1
53 R = 19:1
54 R = 20:1
55 R = 10-Me-18:0
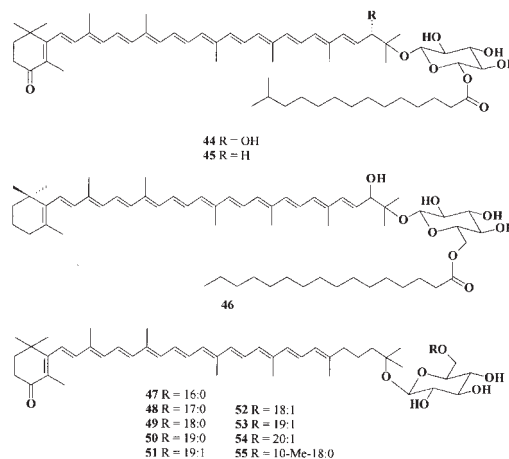
Dihydrochlorobactene glycoside laurate, **56**, was identified from the thermophilic green sulfur bacterium *Chlorobium tepidum* (67). Two new carotenoid glucoside mycolic acid esters, **57** and **58**, have been isolated from the nocardioform actinomycetes *R. rhodochrous* (68). Monocyclic carotenoid glucoside esters **59a–n**, which are major carotenoids, have been isolated from the green filamentous bacterium *Chloroflexus aurantiacus* (69). The major FA were hexadecanoic (16:0) and hexadecenoic (16:1) acids, whereas those of the cellular lipids were hexadecanoic, octadecanoic (18:0), and octadecenoic (18:1) acids. [Percentages included with **59a–n** represent the range of each FA in lipid extracts, calculated from total FA (100%)].

56

57 R = O   *n* = 1 and 3
58 R = H,H   *m* = 10 and 12

59a R = 14:0, 0.2 - 1.5%   **59h** R = 17:1, 4.6 - 26.3%
59b R = 14:1, 0.0 - 2.5%   **59i** R = 18:0, 0.9 - 20.7%
59c R = 15:0, 0.2 - 3.8%   **59j** R = 18:1, 3.8 - 21.9%
59d R = 15:1, 1.3 - 6.2%   **59k** R = 19:0, 0.0 - 0.8%
59e R = 16:0, 17.0 - 22.3%   **59l** R = 19:1, 0.5 - 12.5%
59f R = 16:1, 5.1 - 59.8%   **59m** R = 20:0, 0.0 - 0.3%
59g R = 17:0, 0.6 - 3.4%   **59n** R = 20:1, 0.0 - 3.8%
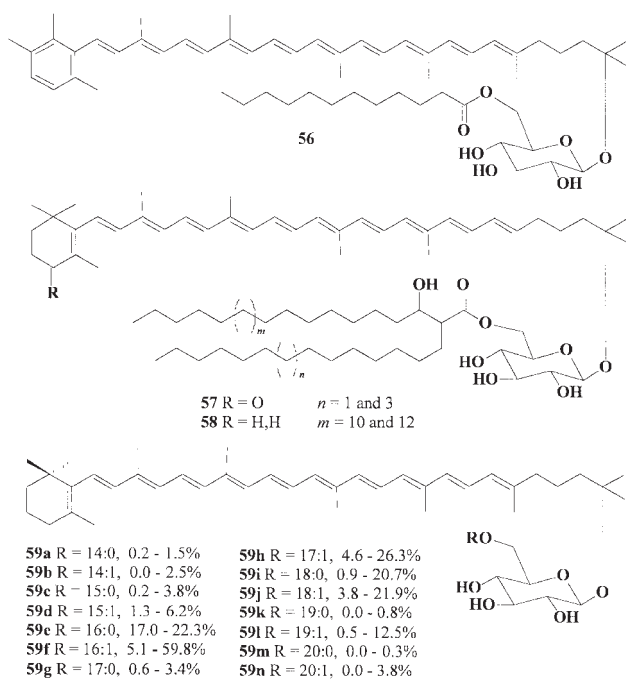
The nonacylated glycoside 4-keto-carotenoid **60a**, which is an analog of **44**, and phleixanthophyll **60b** were isolated from *Mycobacterium phlei* (70–72). Typical C_{40} carotenoids of the genus *Myxococcus* include myxobactone glycoside **61a** and their ester **61b**, and myxobactin glycosides and their esters **62a,b** and **63a,b**; both monocyclic carotenoid glucosides have been isolated from *Myxococcus fulvus, Stigmatella aurantiaca, Polyangium* sp., and from the gliding bacteria *Herpetosiphon giganteus, C. aurantiacus,* and other species (73–81). Four carotenoid glycosides with torulene derivatives, **64–67**, were isolated from the myxobacterium *Solanum compositum* (82) and from bacteriochlorophylls containing gliding bacterium species (79,80).

60a R = Glc, R₁,R₂ = O
60b R = Glc, R₁ = R₂ = H

61a R = Glc
61b R = Glc-6-O-Acyl

62a R = Glc
62b R = Glc-6-O-Acyl
63a R = Man
63b R = Man-O-6-Acyl

64 R = D-Glc, R₁ = H
65 R = D-Glc, R₁ = OH
66 R = L-Rha, R₁ = H
67 R = L-Rha, R₁ = OH
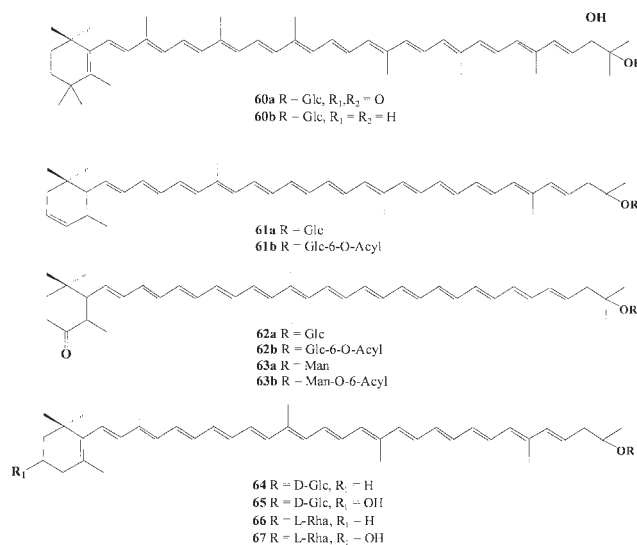
The thermophilic bacterium *Meiothermus ruber* produces a series of carotenoid glycoside esters. The major carotenoid has been identified as 1′-β-glucopyranosyl-3,4,3′,4′-tetradehydro-1′,2′-dihydro-β,ψ-caroten-2-one **68** (83). Acylated carotenoid glycoside esters at the 6″-position of the glucose unit contain a series of C_{10}–C_{17} FA **69–74**. Twelve FA from *M. ruber* carotenoids were characterized by GC–MS. The major component was a 10:1 FAME (37%). Other minor components were identified, ranging from 11 to 17 carbon atoms in length. Two branched-chain C_{15} FA esters also were identified. A similar substitution was found in the carotenoid glycosides of *Thermus thermophilus* (84). The major FA of the total cellular FA of *M. ruber* have been identified as branched-chain compounds, and 2-hydroxy FA were found to be produced in moderate amounts.

Some carotenoids, their glycosides **75** and **44** (with other FA residues), and their esters **76–91** have recently been detected in the thermophilic bacterium *Rhodothermus marinus* from submarine Icelandic hot springs (85). The FA profiles derived from the two acylated carotenoid glucosides **44** and **75** were found to be similar. The composition established with odd-carbon *iso*-13:0 (13%), *anteiso*-13:0 (16%), *iso*-15:0 (10%), and *anteiso*-15:0 (19%) as major FA in two carotenoid glucoside esters of **44** and **75** was reported. The minor even-carbon FA were found to be a mixture of the *n*- and *iso*-isomers, whereas the odd-carbon FA were a mixture of *iso*- and *anteiso*-isomers.

68 R = β-D-Glc

R	Glc-6-O-acyl:		R = Glc-6-O-acyl:
69	10:1	**75**	16:1
70	11:1	**76**	16:0
71	12:0	**71**	17:0
72	*iso*-15:0	**72**	18:1
73	*anteiso*-15:0	**73**	18:1
74	15:0	**74**	18:0

75 R = β-D-Glc

R = Glc-6-O-acyl:		R = Glc-6-O-acyl:	
76 *iso*-11:0		**84** *anteiso*-15:0	
77 *anteiso*-11:0		**85** 15:0	
78 *iso*-12:0		**86** *iso*-16:0	
79 *iso*-13:0		**87** 16:0	
80 *anteiso*-13:0		**88** *iso*-17:0	
81 *iso*-14:0		**89** *anteiso*-17:0	
82 14:0		**90** *iso*-18:0	
83 *iso*-15:0		**91** 18:0	
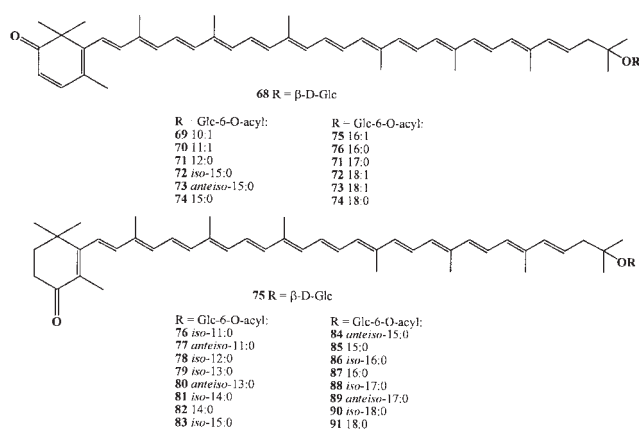
Three carotenoid glycosides, **92–94**, were isolated from the cyanobacterium *Synechocystis* sp. strain PCC 6803 (86); two compounds, **92** and **94**, contained the 2,4-*O*-Me sugar, α-L-fucose. *Curtobacterium flaccumfaciens* pvar. *poinsettiae* produced some acyclic, bicyclic, and monocyclic glycosides, **95** (87).

92 R - α-L-Fuc
93 R = α-L-Rha

94 R – Fuc

95 R = Glc
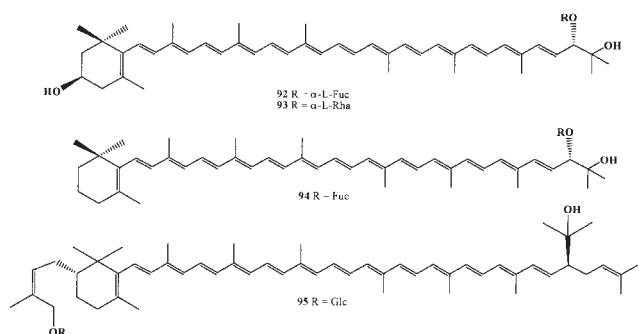
Interesting C$_{30}$ carotenoid derivative glycosides named iridalglycosides, **96–102**, have recently been isolated from the rhizomes of *Iris spuria* (Zeal), cultivated in Egypt (88). Some triterpenoid iridals (89) isolated from *I. germanica* showed high cytotoxic activity against the human tumor cell lines A2780 and K562 (90).

96 R = Glc(1->6)Glc, R$_1$ = Glc
97 R = R$_1$ = Glc

98 R = Glc(1->6)Glc, R$_1$ = Glc, R$_2$ = H
99 R = R$_1$ = Glc, R$_2$ = H
100 R = R1 = R$_2$ = Glc

101 R = R$_1$ = Glc

102 R = R$_1$ = Glc
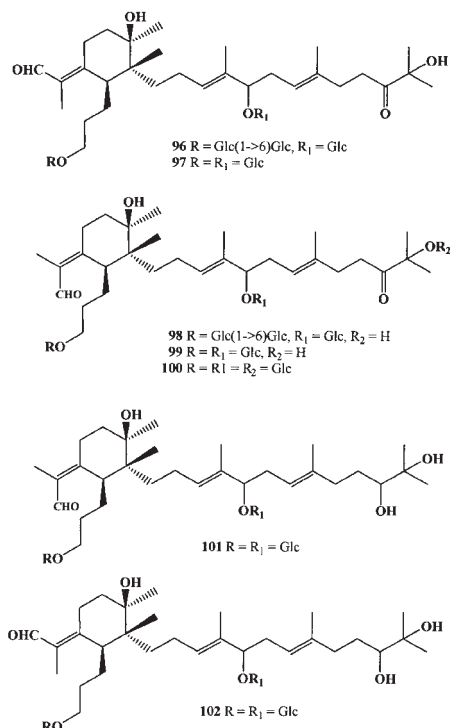
Lipophilic Vitamins

Among the lipophilic vitamins, which are derivatives of the carotenoids known as true retinoids, are retinyl-β-D-glucoside **103**, retinyl-β-D-glucuronide **104**, and retinoyl-β-D-glucuronide **105** (91; see Fig. 1). They are naturally occurring biologically active metabolites of vitamin A and are found in freshwater and marine fish and in mammals (92–94). Retinoyl-β-glucuronide **105** has been characterized as a metabolite of vitamin A in the plasma of humans (95) and in the plasma and tissues of several animals, such as the monkey (96), mouse (97), and rabbit (98).

Olson and co-workers (94,99,100) studied the metabolites of radioactive retinal and all-*trans* retinoic acid in the bile of bile-duct-cannulated rats and showed that the water-soluble metabolites were glucuronide derivatives of retinol and retinoic acid.
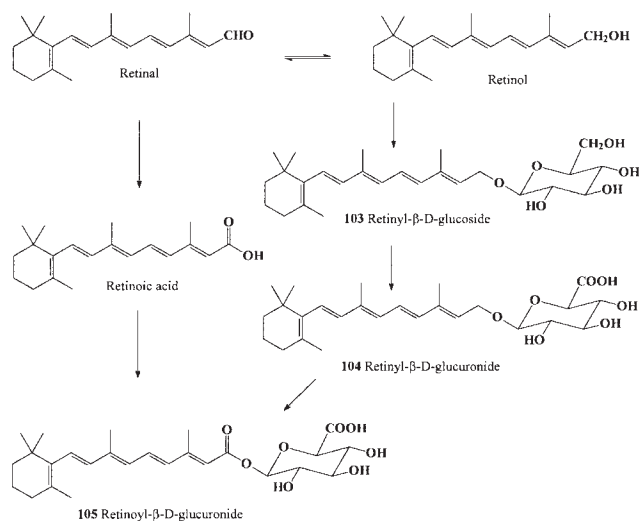
FIG. 1. Chemical structures of retinoid glucuronides and the pathways of their formation.

Thus, Olson's group discovered retinyl-β-glucuronide, the glucuronic acid derivative of retinol, and retinoyl-β-glucuronide, the glucuronic acid derivative of retinoic acid. Retinoyl-β-glucuronide was found to be an interesting retinoid that possessed the biological activity of retinoic acid but without pronounced toxicity. Retinoyl-β-glucuronide was also found to be as effective as retinoic acid in inhibiting LA-N-5 human neuroblastoma cell growth and might also serve as a less toxic alternative to 13-*cis* retinoic acid in the treatment of this tumor disease. Many reports have indicated that the biological activity of all-*trans* retinoyl-β-glucuronide is similar to that of all-*trans*-retinoic acid, but without the toxic side effects of retinoic acid (91,92).

The semisynthetic retinoyl-β-glucuronides **106–109**, as well as **105**, have been isolated from urine of the human, monkey, mouse, and rat (101–107).

106 9-*cis*-Retinoyl-β-glucuronide, R = H,H
107 4-Oxo-9-*cis*-retinoyl-β-glucuronide, R = O

108 13-*cis*-Retinoyl-β-glucuronide, R = H,H
109 4-Oxo-13-*cis*-retinoyl-β-glucuronide, R = O
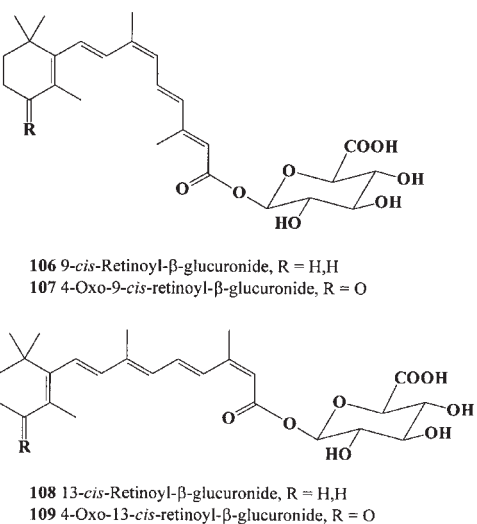
Bicyclic Carotenoid Glycosides

Zeaxanthin mono- and diglucosides and rhamnosides, **110–113**, represent an important group of natural pigments and occur

mostly in bacterial species (8–10,108). They are found in *Corynebacterium autrophicum* (109–111) and are produced by *Erwinia herbicola* and *Rhodobacter sphaeroides* (112). Seven zeaxanthin glycosides, **110–123**, including the Z-isomers **114–117**, have been isolated from the extreme thermoacidophilic archeabacterium *Sulfolobus shibatae* (113).

Zeaxanthin glucoside esters (called thermocryptoxanthins) with branched FA, **118–123**, were isolated from the thermophilic eubacterium *T. thermophilis* (114,115). The structures of the carotenoids were identified as symmetrical bis-FA esters of zeaxanthin-β-glucosides.

110 R = Glc, R₁ = H
111 R = R₁ = Glc
112 R = Rha, R₁ = H
113 R = R₁ = Rha
114 R = R₁ = 9Z-Rha
115 R = 9Z-Rha, R₁ = H
116 R = 13Z-Rha, R₁ = H
117 R =15Z-Rha, R₁ = H

118 R = X, R₁ = H, n = 6
119 R = X, R₁ = H, n = 8
120 R = X, R₁ = H, n = 10
121 R = R₁ = X, n = 6 and 6
122 R = R₁ = X, n = 6 and 8
123 R = R₁ = X, n = 8 and 8
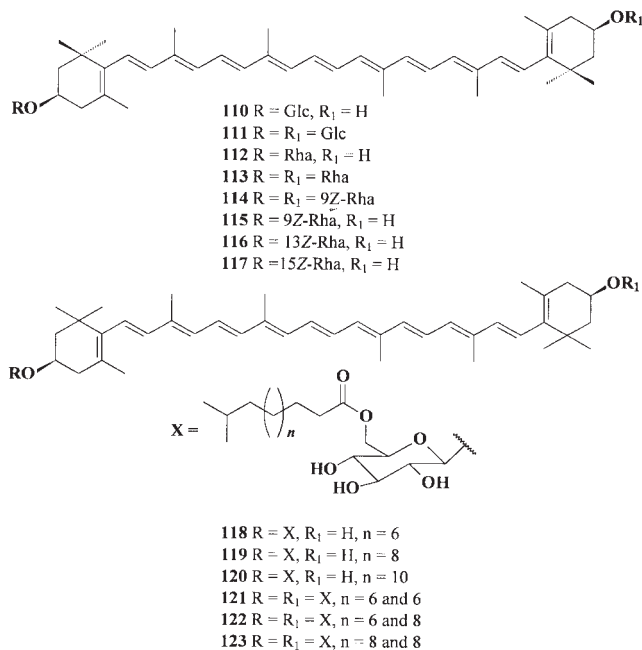
Carotenoid glycosides adonixanthin **124** and astaxanthin **125** were isolated from *T. thermophilus* and *Agrobacterium aurantiacum* (114–116). The mono- and dicarotenoid glucosides **124–129** are produced by *Escherichia coli* (117). The astaxanthin glycoside esters **130–144** have been isolated from the deep-water amphipod crustacean *Acanthogammarus (Branchyuropus) grewingkii* (118).

124 R = Glc, R₁ = H, X = O, Z = H,H
125 R = Glc, R₁ = H, X = Z = O
126 R = R₁ = Glc, X = O, Z = H,H
127 R = R₁ = Glc, X = Z = O
128 R = H, R₁ = Glc, X = O, Z = H,H
129 R = R₁ = Glc, X = Z = H,H

130 α-OH, R = 13:0, 4.2%
131 α-OH, R = 15:0, 14.7%
132 α-OH, R = 9-15:0, 2.9%
133 α-OH, R = 17:0, 11.2%
134 α-OH, R = 9-17:1, 10.0%
135 α-OH, R = 11-17:1, 12.6%
136 α-OH, R = 9,12-17:2, 14.3%

137 α-OH, R = 6,9,12-17:3, 10.3%
138 α-OH, R = 9,12,15-17:3, 7.1%
139 α-OH, R = 5,8,11,14-17:4, 1.5%
140 β-OH, R = 13:0, 4.3%
141 β-OH, R = 15:0, 1.7%
142 β-OH, R = 9-15:0, 2.9%
143 β-OH, R = 17:0, 1.7%
144 β-OH, R = 9-17:1, 2.2%
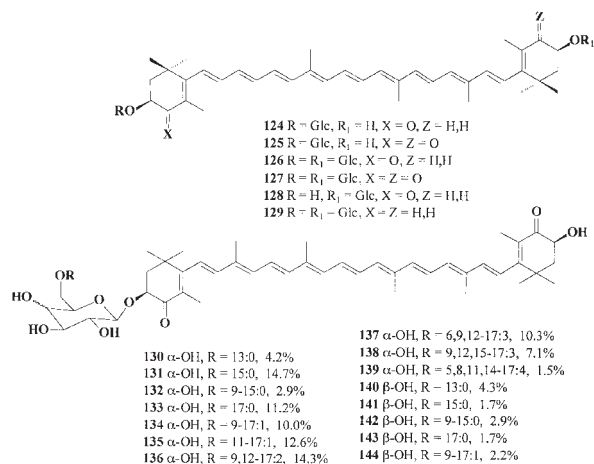
Five new triterpene galactosides, pouosides A–E **145–149**, have been isolated from a Pacific marine sponge, *Asteropus* sp. (119). The carbon skeleton of the pouoside aglycons is new for

naturally occurring triterpenes and parallels that of the C_{40} carotenoids. Glycoside **145** exhibits cytotoxicity against cancer cell P388, ED_{50} [effective dose$_{50}$; porcine stable (PS) kidney cell line] = 10 μM/mL (120).

The β-D-lactoside of 7′,8′-dihydroneoxanthin-20′-al **150** is produced by the toxic marine dinoflagellates *Thoracosphaera heimii* (121) and *Amphidinium carterae* (122).
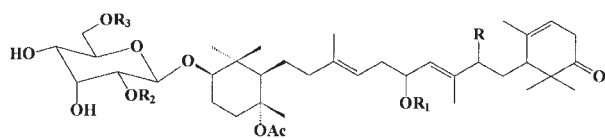
145 R = OAc, R_1 = Ac, R_2 = R_3 = H
146 R = OAc, R_1 = R_2 = R_3 = H
147 R = R_2 = R_3 = H, R_1 = Ac
148 R = OAc, R_1 = R_2 = Ac, R_3 = H
149 R = OAc, R_1 = R_3 = Ac, R_2 = H

150
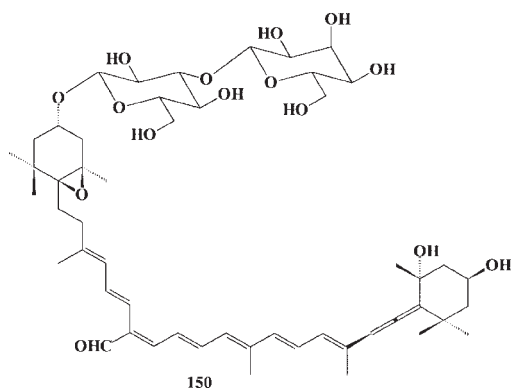
Among the C_{50} carotenoids produced exclusively by bacterial species, corynexanthin **151** was found in *Corynebacterium erythrogenes* (123), corynexanthin diglucoside **152** and monoglucoside **153** have been isolated from *Arthrobacter* sp. (124), and **154a** was recently discovered in *Curtobacterium flaccumfaciens* pvar. *poinsettiae* (87). Two mono- (**154a**) and di- (**154b**) glucosides of sarcinaxanthin were isolated from *Micrococcus luteus* (formerly *Sarcina lutea*) (125–128).
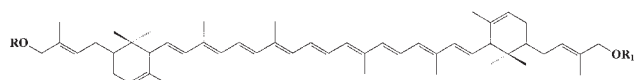
151 R = Glc, R_1 = H
152 R = R_1 = Glc
153 R Glc, R_1 = H, 7,8-dihydro
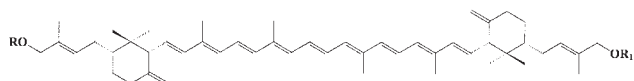
154a R = Glc, R_1 = H
154b R = R_1 = Glc

Two unusual squalene-derived triterpenoid glycosides, xestovanin A **155a** and secoxestovanin A **155b**, have been isolated from extracts of the Northeastern Pacific marine sponge *Xestospongia vanilla* (129). Xestovanin A **155a** showed antifungal activity against *Pythium ultimum* [>50 μg/DiSC (differential staining cytotoxicity) assay].

155a

155b
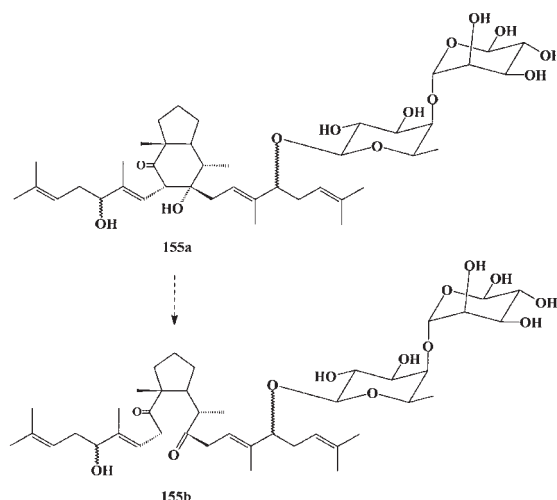
NORISOPRENOID GLYCOSIDES

Natural norisoprenoids structurally derived from carotenoids are widely distributed in the plant kingdom. Because they often have low flavor thresholds, many of them are highly potent aroma compounds and are thus of great interest for the flavor and fragrance industries (130,131). Norisoprenoids, as carotenoid degradation products (131), are the preferable cleavage of (6,7), (7,8), (8,9), and (9,10) bonds leading to flavor components with 9, 10, 11, and 13 carbon atoms, respectively. In the intact plant, carotenoid degradation is likely to be affected by oxygenase systems and by photo-oxygenation and other types of nonenzymatic oxidation (132). The sensory-active C_9-, C_{10}-, C_{11}-, and C_{13}-norisoprenoids naturally emerge from the oxidative cleavage of tetraterpenoid precursor carotenoids (130,133). Nonselective fission of the polyene chain induced by abiotic factors such as heat or light results in a broad spectrum of oxidized breakdown products (134,135). A smaller range of products, which often display biological activities, is released by enzymatic cleavage reactions. Enzymes catalyzing the centric or eccentric fission of specific carotenoids *in vivo* have been isolated from plants and characterized in recent years (136).

Recently, the chemical, photochemical, and oxidase-coupled degradation of carotenoids to norisoprenoids has been studied (137). The proposed biogenetic pathway in grapes that leads from carotenoids to C_{13}-norisoprenoids has been reported as involving the enzymatic degradation of carotenoids by regiospecific oxygenases (137). These findings include the preponderance of norisoprenoids possessing 13 carbon atoms, thereby indicating the specificity of cleavage; the configuration of the asymmetric centers and axes common to C_{13}-norisoprenoids and the corresponding carotenoids; the negative correlations observed between the levels of norisoprenoids and carotenoids during berry development; and the *in vivo* transfer of C_{13} markers from carotenoids to norisoprenoids in berries

between véraison (color change stage) and berry maturity. All of these findings are major arguments in favor of the hypothesis that glycosylated C_{13}-norisoprenoids are derived from carotenoids in the grapes. Carotenoids are mostly synthesized from the first stage of fruit formation until véraison, and then degrade between véraison and maturity to produce glycosylated C_{13}-norisoprenoids and other compounds. The formation of some norisoprenoid glycoside species is shown in Figure 2. Volatile C_{13}-norisoprenoids are thought to be the breakdown products of neoxanthin, a xanthophyll of the carotenoid group. In grapes, tobacco, tea, flower scents, and tropical fruits, norisoprenoids occur mainly as glycosidically bound precursors that can contribute considerably to the aroma. Carotenoid-derived aroma compounds are important carotenoid metabolites in the flavor and fragrance industries (138).

More than 50 filamentous fungi and yeasts, known for the *de novo* synthesis or biotransformation of mono-, sesqui-, tri-, or tetraterpenes, were screened for their ability to cleave β,β-carotene into flavor compounds, including norisoprenoids (139). Carotenoid-derived volatile products were detected in the media of *Ischnoderma benzoinum, Marasmius scorodonius*, and *Trametes versicolor*; β-ionone proved to be the main metabolite, whereas β-cyclocitral, dihydroactinidiolide, and 2-hydroxy-2,6,6-trimethylcyclohexanone were formed in minor quantities.

Many norisoprenoid glycosides, **156–253**, mostly belonging to megastigmane-type derivatives of cyclohexane (or cyclohexene), have been isolated from plant leaves (or roots) grown in different places, e.g., France, Italy, Turkey, China, Korea, Japan, Egypt, Thailand, Jordan, and other countries; and some of the glycosidic compounds isolated and tested have shown biological activities.

The norisoprenoid glycosides **156**, **157**, **228**, and **244–247** were isolated from the aerial parts of the Turkish medicinal plant *Salvia nemorosa* (140). Otsuka and co-workers (141–146) have studied Japanese plants belonging to several genera and have isolated many different norisoprenoid compounds. The megastigmane (ionol-type) glycosides **158–163**, **164–166**, **215**, **218–221**, **226–228**, and **252** were identified from the butanol-soluble fraction of the leaves of *Alangium platanifolium* var. *platanifolium* (Fukuoka Prefecture, Japan) (141,142). The leaves of *Alangium premnifolium* (Japanese name: Shima-urinoki) from Nakagami-gun (Okinawa Prefecture) were found to contain **191**, **194–196**, **241–243** (143), and **212–217** (144) glycosides. *Myrsine seguinii* (syn. *Rapanea neriifolia*), which is found in temperate and subtropical areas of Japan, contains the compounds **167–173** and **251** (145). The leaves of *Turpinia ternata* contains the glycosides **181–186** and **225–227** (146). Lasianthionosides A–C **236–238** were isolated from the leaves of *Lasianthus fordii* (147). Compounds of **175–177**, **231**, and **232** were isolated from the Turkish tree *Stachys byzantina* (Tokat, Turkey) (148), and **234** and **235** were isolated from the leaves of *Lonicera gracilipes* var. *glandulosa* (Sendai, Japan) (149).

The megastigmane glycosides **221–224**, **230**, and **244–247**
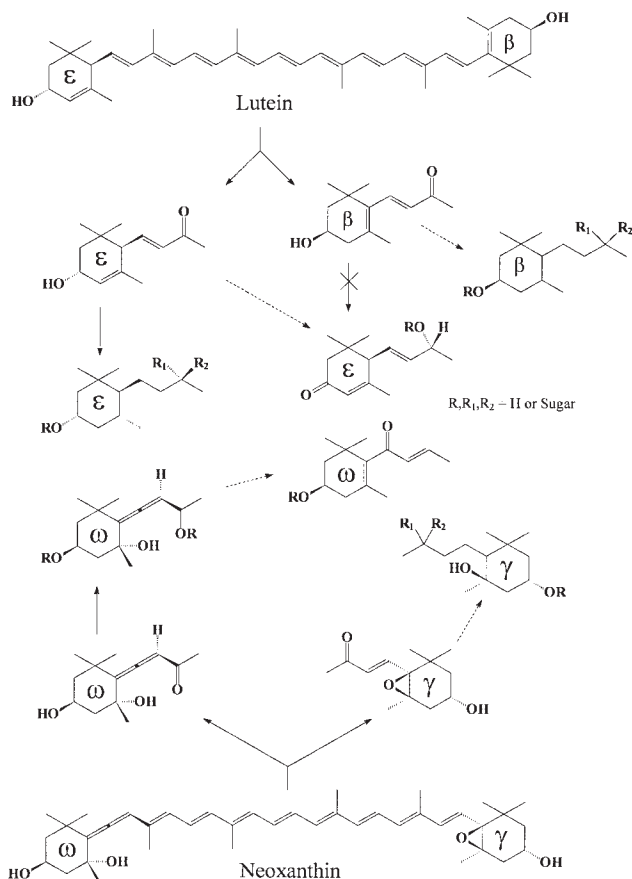
FIG. 2. Biodegradation of some carotenoid species and formation of C_{13}-norisoprenoids.

and their polyphenolic constituents isolated from the leaves of *Eriobotrya japonica* (Rosaceae) were found to inhibit the 12-*O*-tetradecanoyl-phorbol-13-acetate (TPA)-induced activation of the Epstein–Barr virus early antigen in Raji cells (150,151). Roseoside **230** significantly delayed carcinogenesis induced by peroxynitrite (the initiator) and TPA (the promoter), and its potency was comparable to that of a green tea polyphenol, (−)-epigallocatechin 3-*O*-gallate. The loquat, *E. japonica* (Rosaceae), is a small tree native to Japan and China that is widely cultivated for its succulent fruit. Its leaves have been used as a folk medicine for the treatment of chronic bronchitis, coughs, phlegm, high fever, and ulcers in Japan and other Asian countries (152). A traditional therapy using the leaves in a compress also has been used to treat cancers in Japan.

Five megastigmane glycosides, **230** and **244–247**, have been isolated from the seeds of *Trifolium alexandrinum* (153). The seeds of *T. alexandrinum* are popularly used in Egypt as an antidiabetic agent (154). Compounds of **172** and **191** were found in the glycosidic fraction of sloe tree *(Prunus spinosa)* leaves (155); **193**, **202**, **204**, and **228** were isolated from South American lulo (*Solanum quitoense*) leaves (156); **178** and **229** were isolated from *Caralluma negevensis* (157); an extract

from the tropical Chinese tree *Laggera alata* containing **179** is usually used for anti-inflammatory and antibacterial treatments (158); **180** was obtained from tea leaves (cv. Yabukita) (159); **187** and **188** were isolated from the aerial part of *Clerodendrum inerme* (160); **241**–**243** were isolated from *Acanthus ebracteatus* (161); **190** was isolated from the leaves of *Phlomis aurea* (162); and **198** was isolated from the leaves of *Carallia brachiata* (Rhizophoraceae), collected near Kuala Lumpur (Malaysia). The leaves of *C. brachiata* are used to prepare tea or, taken together with a mixture of turmeric, benzoin, and rice dust, are used for the treatment of gangrenous toxicity, whereas the bark is used to treat itching (163). **199** was isolated from grapevines (137); **195** and **237** were isolated from daylily (*Hemerocallis fulva*) leaves (164); **200** was isolated from the aerial part of *Taraxacum obovatum* (165); **156**, **174**, and **245** were isolated from barley (*Hordeum vulgare*) roots (166); and **229** and **230** were isolated from *Sauropus androgynus* (167).

Glycoside **194** was isolated from *Scurrula atropurpurea* (called "benalu teh" in Indonesia) belonging to the family Loranthaceae, a parasitic plant of the tea plant *Thea sinensis* (Theaceae). It showed 19.4% inhibitory activity against cancer cell invasion (inhibitory rate at 10 µg/mL) (168).

From the leaves of the poisonous perennial shrub *Breynia officinalis* (Euphorbiaceae), collected on Okinawa Island (Japan), were isolated the megastigmane glycosides **197**, **198**, **226**, and **248**–**251** (169); **194**, **201**, and **202** were isolated from the water-soluble fraction of the methanol extract of coriander (the fruit of *Coriandrum sativum*), which has historically been used as a spice and medicine (170).

Bay laurel (*Laurus nobilis*, Lauraceae) is a pyramid-shaped tree or large shrub with aromatic evergreen leaves and shiny gray bark; the popular culinary seasoning, bay leaf, is used extensively in French, Italian, Spanish, and Creole cooking and also in folk medicine. The extract of leaves from this shrub collected in Campania (Avellino, Italy) contained the megastigmane glycosides **199**, **202**, and **204**–**211** (171). An inhibitory effect was reported on nitric oxide production in lipopolysaccharide-activated murine macrophages. Compounds **227** and **228** and the acylated glycoside **253** were isolated from the aerial part of *Baccharis dracunculifolia* (Compositae) (172).

Biological activities of some C_{13}-norisoprenoids (not glycosides) have been reported. An inhibitory effect on mammary carcinoma cells induced by β-ionone was observed (173): β-ionone could inhibit the cell growth of MCF-7 cells (IC_{50} value, 104 µmol/L). Putative antiproliferative and cell-cycle inhibitory effects of β-ionone and geraniol were found on MCF-7 human breast cancer cells in a culture mediated by mevalonate depletion resulting from the inhibition of HMG-CoA activity (174). The effect of β-ionone on the proliferation of the human gastric adenocarcinoma cell line SGC-7901 and the inhibition of metalloproteinase was also studied (175). β-Ionone had an inhibitory effect on the growth of SGC-7901 cells; the IC_{50} value of β-ionone for SGC-7901 cells was estimated to be 89 µmol/L. Norisoprenoids that were isolated from

the leaves of *Cestrum parqui* (Solanaceae) showed phytotoxic effects on the germination and growth of *Lactuca sativa* (176).
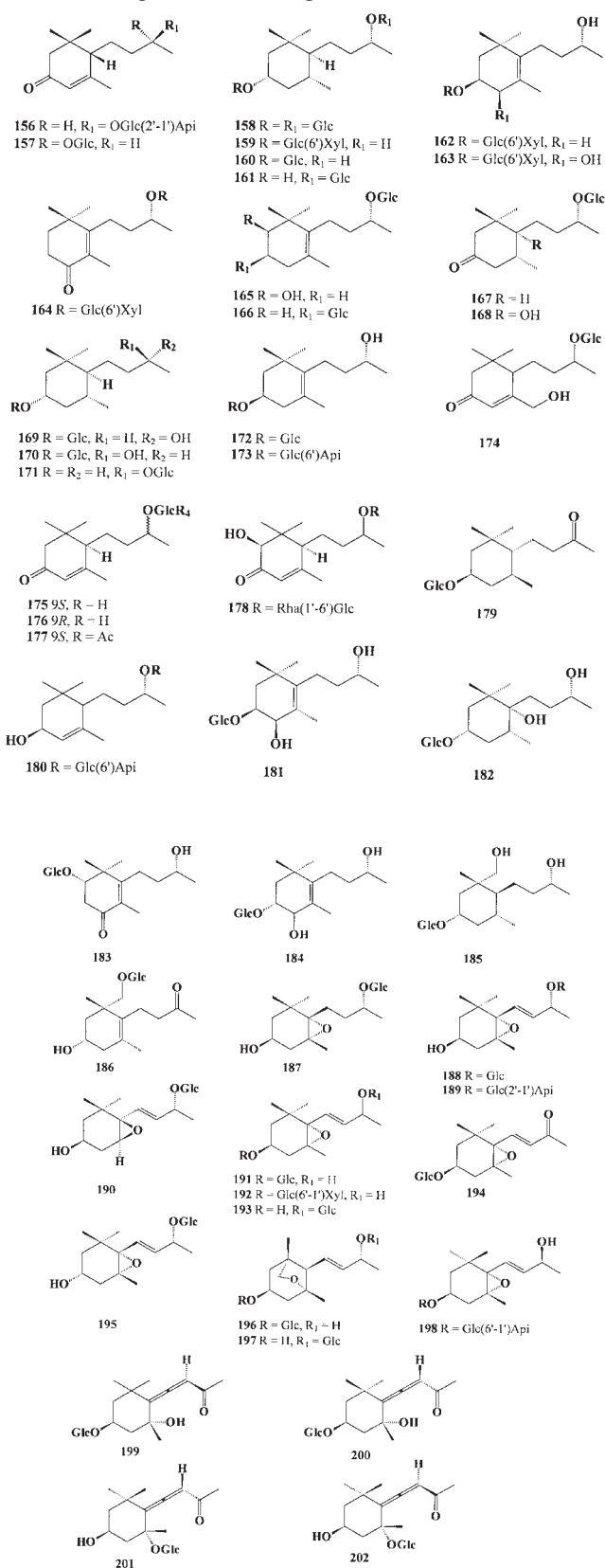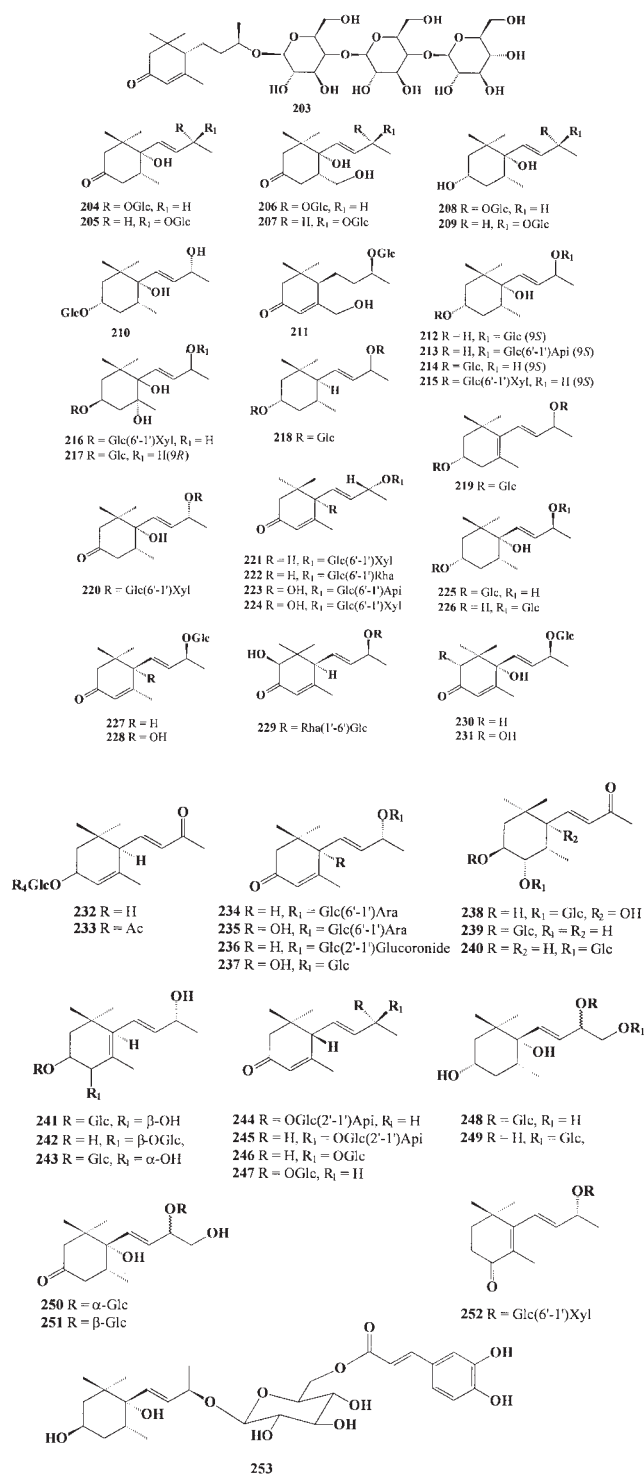
ISOPRENOID GLYCOLIPIDS

Organisms that are able to live in environments that exhibit extraordinary conditions, such as very high temperatures (50–110°C and/or up to 400°C in deep-sea thermal vents), very high salt conditions (20 to 25% of NaCl), or very low or very high pH values (from 1.0 to 5.5, and from 8.5 to 11.0), are extremophiles or Archaea (Archaebacteria) (177,178). Hyperthermophiles are found mainly in the water near places with volcanic activity. The magma of the volcanoes heats the water to very high temperatures (up to 400°C). Acidophiles and alkaliphiles are able to grow at low pH (below 5.5) and high pH (above 8.5). Barophiles can survive only at the high pressures (above 300 atm) mainly found in the deep sea. Halophiles live in salt lakes and cannot survive without these very high salt concentrations. Also, combinations of these features are possible, e.g., *Sulfolobus* is an acidophilic hyperthermophile. Extremophilic organisms are found in both the Bacteria and the Archaea.

Archaea and Bacteria are prokaryotes, and both are single-cell organisms. There are, however, distinct features that place Archaea and Bacteria each in their own domain. This distinction is mainly based on studies of 16sRNA. Also, the composition of the cytoplasmic membrane is different in Bacteria and Archaea. Bacteria have glycerol diester lipids with FA as the hydrophobic backbone (1,2-diacyl-*sn*-glycerol), whereas Archaea have glycerol diether and diglycerol tetraether lipids with a phytanoyl chain as the backbone (2,3-di-*O*-phytanyl-*sn*-glycerol, or 2,3,2′,3′-tetra-*O*-dibiphytanyl-di-*sn*-glycerol). The tetraether lipids do form a membrane-spanning monolayer, and diethers and diesters do form a bilayer. All Archaea, including the halotolerant species, are characterized by the presence of isopranyl glycerol ether lipids in their membranes, and more than 150 polar lipids from Archaea have now been structurally characterized (11–17,179,180).

DIETHER AND TETRAETHER GLYCOLIPIDS

The extremely halophilic bacteria classified as Archaea generally require saturated or nearly saturated (3.0–5.0 M) NaCl for optimal growth and survival, although some species are capable of growth in as low as 2.5 M NaCl (14). The diether glycolipids **254**–**260** have been isolated from halophilic bacteria (13). More than 40 years ago unusual lipids were found in an extreme halophile, *Halobacterium cutirubrum*, which differed considerably from moderate halophiles and nonhalophilic bacteria (181,182). The major glycolipid in *H. cutirubrum* is the sulfated triglycosylarchaeol S-TGA-1 **256** (183,184), but minor amounts of the sulfated tetraglycosylarchaeol S-TeGA **258** are also present, as are two unsulfated glycolipids, **257** and **259** (185). The lipids of an extremely halophilic bacterium, *Halobacterium marismortui*, isolated from the Dead Sea, were found to contain 86% polar lipids and 14% nonpolar lipids. The major glycolipid detected was **257** (186). Species of the genera *Haloarcula* and *Haloferax* contain **257** and **257a**, and **255**, respectively (186,187).

254 R = SO₂OH. R₁ = H

254a R = SO₃ (3')-β-Glc, R₁ – H

254b R = SO₃ (3')-β-Glc, R₁ = α-Glc

255 R = R₁ = H

256 R = SO₂OH

257 R = H, α-OH

257a R = H, β-OH

258 R = SO₃⁻ NH₄⁺

259 R = H
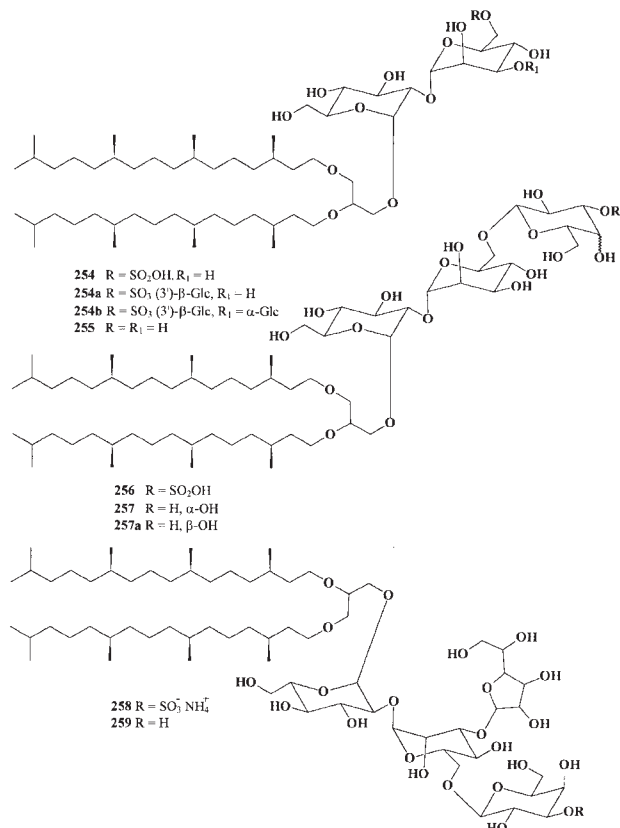
The lipids of the halophilic eubacteria *Planococcus* H8 (NRCC 14037) and *Haloferax volcanii* were studied and found to be remarkably simple in their polar lipid content, with 49% phosphatidylglycerol and cardiolipin, and surprisingly, 51% of the anionic lipid sulfoquinovosyldiacylglycerol (SQDG) (188). SQDG is a sulfonolipid associated with plants, algae, and other photosynthetic organisms (13). *Haloferax volcanii* and *Planococcus* H8 produce the same classes of polar lipids, consisting of phosphoglycerols, sulfoglycolipids, and cardiolipins. Because the glycolipids of both microbes contain sulfur, they may have the potential to exhibit the properties of certain other sulfoglyco ligands in inducing phagocytosis by binding to the mannose receptor (189). The new sulfated diglycosyl lipid S-

GL-1 **260** was isolated from *H. volcanii* (188). A novel bis-sulfated glycolipid, **261**, has been isolated in Japan from a nonalkaliphilic extremely halophilic Archaebacterium, strain 172 (190).

260

261
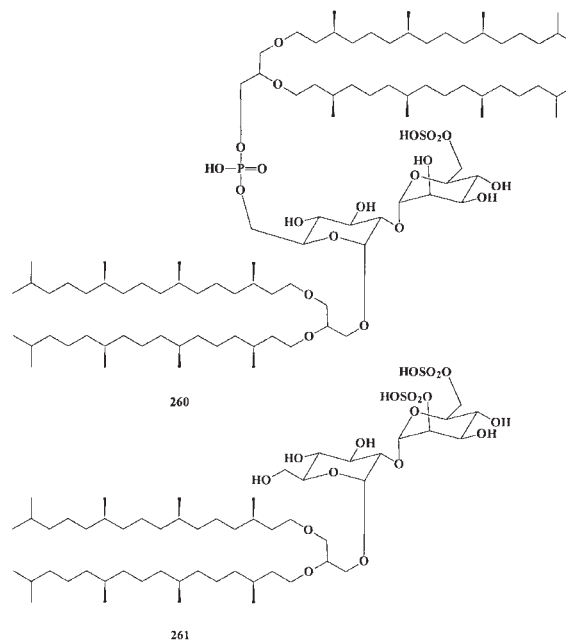
The lipids of methanogenic bacteria consist of di- and tetraether glycerol. More than 40 complete structures of ether polar lipids from seven methanogenic species have been determined to date. The isoprenoid glycolipids **262–281** have been isolated from methanogens and their structures have been elucidated. The glycolipid **262** is common to all methanogenic species (191,192). Compounds of **262**, **263**, and **268** are major lipids in *Methanococcus voltae* (193). The caldarchaeol core was predominant in the total lipids of *Methanobacterium thermoautotrophicum* (up to 83%), and the structures of 15 lipids from *M. thermoautotrophicum* have been determined in this species (193–196). Thirteen of the 15 lipids are as follows: a bare archaeol (type **262**), a bare caldarchaeol (tetraether type), two glycolipids [gentiobiosyl (β-Glc(1-6)-β-Glc), archaeol **263**, and gentiobiosyl caldarchaeol], six phospholipids, and three phosphoglycolipids.

262 R = Glc
263 R = Glc(6'-1')Glc
264 R = Gal
265 R = Man
266 R = A
267 R = B
268 R = C
269 R = D

270 R = Glc
271 R = Glc(6'-1')Glc
272 R = E
273 R = F

A =

B =

C =

D =

E =

F =

Glc(1')O

274 R = Glc
275 R = Gal
276 R = Man
277 R = Glc(6'-1')Glc
278 R = Glc(3'-1' and 6'-1')Glc

279 R = Glc
280 R = Gal
281 R = OPO₂(OH)(1')Glc
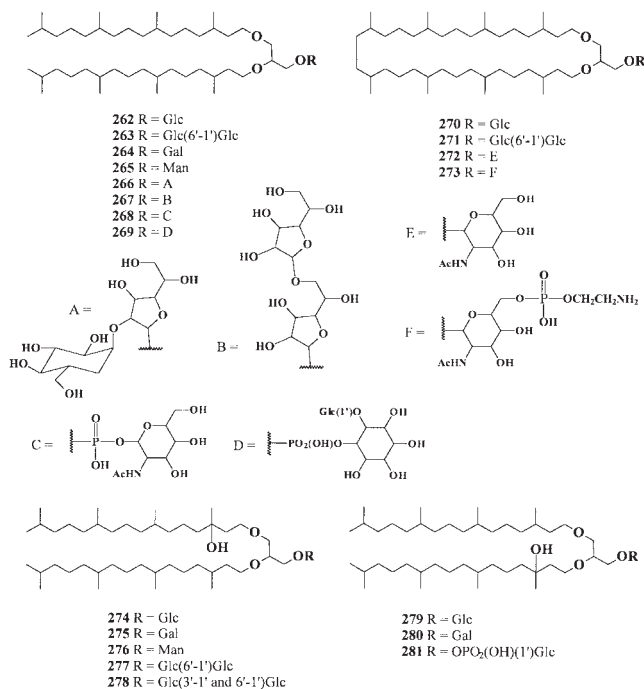
Methanococcus jannaschii is one of the extremely thermophilic methanogens that can grow at temperatures up to 86°C (197); it was isolated from the deep-sea hydrothermal vent in the East Pacific Rise (depth, 2,600 m). Because of the extreme thermophilicity of this bacterium, its lipids are very interesting. Besides the usual archaeol and caldarchaeol, a unique glycerol ether core lipid was identified in this organism. It was identified as a macrocyclic archaeol, in which a 40-carbon bifunctional 1,32-biphytanediyl (3,7,11,15,18,22,26,30-octamethyldotriacontamethylene) group was etherified at the *sn*-2 and *sn*-3 positions of the glycerol, forming a 36-member macrocyclic diether compound, **270**; lipids **271**–**274** also were isolated from this species (198).

282 R = A, R₁ = PO(OH)OCH₂CH(OH)CH₂OH
283 R = B, R₁ = PO(OH)OCH₂CH(OH)CH₂OH
284 R = A, R₁ = H
285 R = B, R₁ = H
286 R = A, R₁ = Gal

287 R = A, R₁ = C
288 R = B, R₁ = C
289 R = A, R₁ = D
290 R = B, R₁ = D

A =

B =

C =

D =
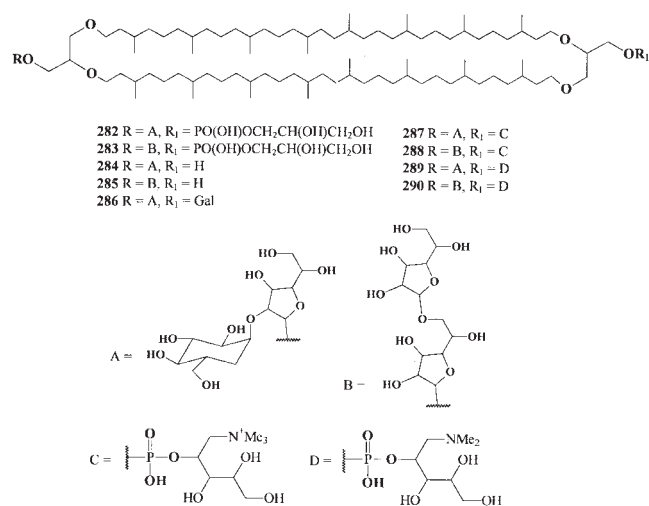
The lipids of GP1 *(Methanospirillum hungateii),* GP6 *(Methanothrix soehngenii = Methanosaeta concilii),* and MS *(Methanosarcina barkeri),* all bacteria belonging to the Methanomicrobiales, have been isolated and their structures deter-

mined by physical and chemical methods. Kates and co-workers (199) reported the structures of polar lipids from *M. hungateii* GP1 in 1981 as the first methanogenic polar lipids. These lipids consist of two phosphoglycolipids (both tetraether type) and four glycolipids (two tetraether and two diether types). The glycosyl residues of the six lipids comprise only two species: β-glucopyranosyl(1→2)β-galactofuranosyl **282** and β-galactofuranosyl-(1→6)β-galactofuranosyl **283**. The occurrence of galactofuranose residues in glycolipids is uncommon, and the phosphate ester group of the phosphoglycolipids is *sn*-glycerol-3-phosphate. More recently, Sprott and co-workers (200) isolated **266**, **267**, and **282**–**290** glycolipids from *M. hungatei*. A new acid-labile glycerol ether lipid, **274**, was identified in *M. soehngenii* GP6 (also known as *Methanothrix concilii* and *Methanosaeta concilii*) (201). The cause of the lability of the lipid is the presence of a hydroxyl group bound at the 3′ position of the phytanyl chain linked to the *sn*-3 position of the core glycerol moiety. The hydroxyarchaeol core made up 30% of the total lipids. The structures of eight polar lipids, **263** and **274**–**280**, of *M. soehngenii* were determined (202,203). The major lipids were two diglycosylated lipids, **263** and **274** (which made up 59% of the polar lipids), and archaetidylinositol (which made up 24%). Glycolipids of this organism contained three kinds of hexose residues: glucose, galactose, and mannose.

De Rosa and co-workers (17) reported that the lipid core of *M. barkeri* DSM800 consists of diphytanyltetritol, caldarchaeol with various numbers of cyclopentane rings, glyceroarchaeol with hydrocarbon chains with 20 and 25 carbons, and a typical archaeol. The hydroxyarchaeol of *M. barkeri* resembles the hydroxyarchaeol from *M. soehngenii* but differs in the position of glycerol on which the hydroxyphytanyl group is linked. The 3′-hydroxyphytanyl chain is etherified at the *sn*-2 position of glycerol in *M. barkeri* **274** and at the *sn*-3 position in *M. soehngenii* **279**. Six phospholipids, seven amino phospholipids, and one glycolipid of *M. barkeri* MS have been identified, including the unusual "hybrid lipid" **304** (204).

Several strains of extremely halophilic Archaebacteria, both nonalkaliphilic and alkaliphilic, including *Halobacterium*, *Haloferax*, and *Natronobacterium* species, were isolated from salt locales in India, and their lipids have been studied (205). The *Halobacterium* strains possessed the characteristic glycolipids, sulfated triglycosyl diether **254** and tetraglycosyl diether **254a**, and the unsulfated triglycosyl diether **257**; the *Haloferax* strains had the characteristic sulfated and unsulfated diglycosyl glycerol diethers **255** and **263**.

Lipid **293** and its analog, R₁ = PO₂(OH)-glycerol, have been isolated from cells of the acidophilic, autotrophic, mesophilic, ferrous compound-oxidizing archaeon *Ferroplasma acidiphilum* strain YT (206).

Thermoplasma acidophilum, a wall-less mycoplasma-like thermoacidophilic archaeon, grows at 59°C and pH 2.0 as its optimal conditions. The membrane lipids consist of derivatives of a tetra-*O*-di(biphytanyl) diglycerol and a 2,3-di-*O*-phytanyl-*sn*-glycerol similar to the usual archaea. Three types of polar ether lipids were found in *T. acidophilum* HO-62: phospholipids, glycolipids, and phosphoglycolipids (207). The seven glycolipids had different combinations of gulose, mannose, and

glucose, which formed the mono- or oligosaccharides **291a–e; 292a,b;** and **293–303.** Although gulose is an unusual sugar in nature, several glyco- and phosphoglycolipids in *T. acidophilum* contained gulose as one of the sugar moieties. All the ether lipids had isopranoid chains of C_{40} or C_{20} with zero to three cyclopentane rings (207). In *T. acidophilum,* the main polar lipid is phosphoglycolipid, composed of caldarchaeol, gulose, and *sn*-3 glycerophosphate at a molecular ratio of 1 to 1 to 1 and comprising about 46% of the total lipids. The structures of other neutral glycolipids, **291a**, **291d**, **292b**, and **294–296**, all of which contain gulose and/or glucose, have been detected by Uda and co-workers (208,209).

291a R = Glc, R_1 = H
291b R = Glc(6'-1')Glc, R_1 = H   291d R = Gal, R_1 = H
291c R = Glc(6'-1')Glc, R_1 = OP(OH)$_2$ 291e R = Man, R_1 = H

292a R = Glc(3'-1')Man, R_1 = H
292b R = Glc, R_1 = PO(OH)OCH$_2$CH(OH)CH$_2$OH

293 R = Glc, R_1 = H   297 R = Gul(3'-1')Man, R_1 = H
294 R = R_1 = Glc   298 R = Gul(3'-1')Man(3'-1')Man, R_1 = PO(OH)OCH$_2$CH(OH)CH$_2$OH
295 R = Glc, R_1 = Gul   299 R = Gul(3'-1')Man(3'-1')Man(3'-1')Man, R_1 = PO(OH)OCH$_2$CH(OH)CH$_2$OH
296 R = R_1 = Gul

300 R = Gul, R_1 = PO(OH)OCH$_2$CH(OH)CH$_2$OH
301 R = Gul(3'-1')Man, R_1 = Gul
302 R = Gul(3'-1')Man(3'-1')Man, R_1 = H

303 R = R_1 = Gul

All *Sulfolobus* are hyperthermophilic organisms and belong to the subkingdom of Crenarchaeotes. The first member of this group to be described was *Sulfolobus acidocaldarius* and was found by Brock and co-workers in 1972 in Yellowstone National Park (210). Many *Sulfolobus* strains have been found in terrestrial hydrothermal situations, mainly solfataric fields, in different parts of the world, for example, in the United States, Italy, Japan, Iceland, and New Zealand. They have been isolated from hot waters, mud pots, and the upper layers of soils with temperatures from 60 to 95°C and a pH of 1 to 5, and contain two major tetraether glycophospholipids, **305** and **306** (13,17,211,212).

Diglycerol tetraether lipids **306–312**, from thermoacidophilic Archaebacteria of the *Caldariella acidophila*, which grow in the temperature range of 75–89°C, with differently cyclized biphytanyl components have been detected (213–215).

304

305 R = PO$_2$(OH)-Inositol, R_1 = Glc

306 R = PO$_2$(OH)-Inositol, R_1 = Gal(3'-1')Glc
307 R = H, R_1 = Gal(3'-1')Glc
308 R = H, R_1 = Glc

309 R = H, R_1 = Glc
310 R = H, R_1 = Glc-SO$_4$
311 R = PO$_2$(OH)-Inositol, R_1 = Glc

312 R = H, R_1 = Glc
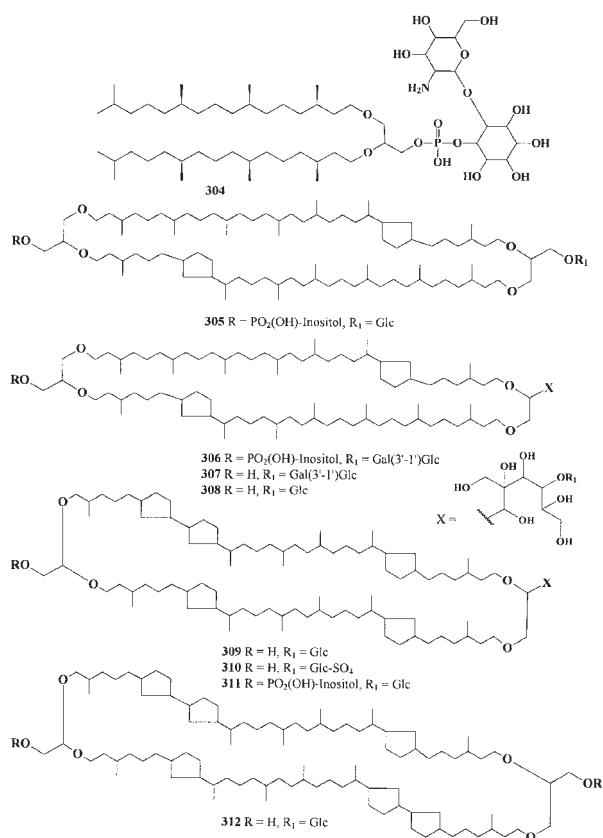
ISOPRENOID ETHER BOLAFORM AMPHIPHILES

Over the past several years, various archaebacterial symmetrical or asymmetrical, acyclic or macrocyclic bipolar lipid analogs have been synthesized to investigate, from well-defined molecules, the membrane organizing and packing properties of some new classes of amphiphiles and the results obtained have been reported and partly reviewed (15–17,216,217).

Archaeal natural tetraether bipolar lipids are thought to span the membrane to form monolayers and allow the microorganisms to maintain their membrane integrity in harsh environments (15,17,212). These bipolar membrane-spanning lipids give rise to several model systems with advantageous properties, such as mechanically and thermally stable monolayers, artificial black membranes, and highly thermostable liposomes (212,218). The archaeal 36-membered macrocyclic diether (e.g., type **270**) phospholipid was studied by measuring its membrane fluidity, liposomal proton permeability, and liposomal thermostability in comparison with its acyclic counterpart, diphytanyl-PC, its glycolipid derivatives, egg yolk lecithin, and a mixed lipid of dimyristoylphosphatidylcholine (DMPC)–cholesterol (220). Fluorescence anisotropy measurements indicated that the macrocyclic structure led to a greater decrease in the fluidity of the intermembrane hydrophobic part than in the membrane surface by limiting the motional freedom of the

alkyl chains. The proton permeability was also significantly reduced by introducing a macrocyclic structure. Liposomal thermostability measurements using 6-carboxyfluorescein suggested that the 36-membered diether formed liposomes with greater thermal stability than those of diphytanyl-PC. The data obtained suggested that the cyclic structure contributed to the formation of stable liposomes, especially at higher temperatures. These findings clearly demonstrate that the 36-membered macrocyclic lipid membrane plays an important role for the thermophilic Archaea in adapting to extreme environments.

Symmetrical and unsymmetrical archaeal tetraether glycolipid analogs **313–317** have been synthesized, and these compounds represent the first examples of tetraether-type analogs containing a phosphate unit and/or glycosyl moieties (221–223). The self-assembling properties of a new series of archaeal tetraether glycolipid analogs, **313–317**, were studied and were characterized by a bipolar architecture with two similar or different glycosidic and/or phosphate polar heads and a lipid core possessing a cyclopentane unit and/or branched chains (222). Supramolecular aggregates of the neutral glycolipids **313**, **314**, and **317** were found to depend on both the saccharidic polar heads and the chain composition. The presence of one glycosidic residue with rather marked hydrophilic properties, such as the lactosyl moiety, was required to allow the formation of multilamellar vesicles. Surprisingly, the introduction of a cyclopentane unit in the bridging chain was able to induce an apparent two-by-two membrane association; this unusual behavior might be the result of unsymmetrical interfacial properties of the lipid layer caused by the presence of the cyclopentane unit. Asymmetrical phosphate derivatives spontaneously formed thermostable monolayered vesicles, but neutral glycolipids **317**, which contain a cyclopentane ring in the middle of the bridging chain, did not form monolayer associations. Bipolar surfactants possessing a single polymethylene bridging chain were found to self-organize into bilayered or monolayered vesicles, disks, or fibers depending on the symmetrical or asymmetrical structure of the lipids, the bridging chain length, the nature of the polar groups and also the structure of the spacers (223).

Liposomes obtained from archaebacterial ether lipids (or synthetic analogs) named archaeosomes demonstrate relatively higher stabilities to oxidative stress, high temperature, alkaline pH, and the action of phospholipases, bile salts, and serum proteins. Some archaeosome formulations can be sterilized by autoclaving, without problems such as the fusion or aggregation of vesicles. The uptake of archaeosomes by phagocytic cells can be up to 50-fold greater than that of conventional liposome formulations. Studies in mice have indicated that systemic administration of several test antigens entrapped within certain archaeosome compositions gives humoral immune responses that are comparable to those obtained with the potent but toxic Freund's adjuvant. Archaeosome compositions can be selected to give a prolonged, sustained immune response and to generate a memory response. Tissue distribution studies of archaeosomes administered *via* various systemic and peroral routes indicate the potential for targeting specific organs. All *in vitro*

and *in vivo* studies performed to date have indicated that archaeosomes are safe and do not invoke any noticeable toxicity in mice. The stability, tissue distribution profiles, and adjuvant activity of archaeosome formulations indicate that they may offer a superior alternative to the use of conventional liposomes, at least for some biotechnology applications (224,225).

313 R = R₁ = A
314 R = B, R₁ = A
315 R = A, R₁ = C

316 R = A, R₁ = C
317 R = B, R₁ = A
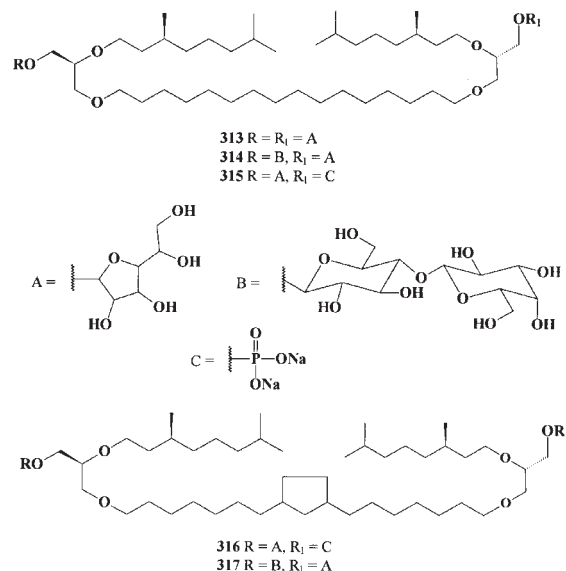
PHENOLIC GLYCOLIPIDS

Phenolic glycolipids were discovered more than 50 years ago (226) and exhibit a fascinating diversity in their structures and biological activities (227). Smith and co-workers (226) studied lipid extracts of bovine and human tubercle bacilli by IR spectrometry and found aromatic substituents, named glycolipids G. More recently, these aromatic glycolipids were detected in *Mycobacterium bovis* and *Mycobacterium kansasii*. These glycolipids attracted great interest at first for the unusual structure of their lipid part, and then as potential tools to detect infections by *Mycobacterium tuberculosis*. The structure of the lipid aglycone moiety (phenolphthiocerol) was studied by Gastambide-Odier and co-workers (228,229). It is unusual because of its terminal phenol moiety, derived biosynthetically from tyrosine, which bears a long chain with two hydroxyl groups acylated by multimethyl-branched FA. Although some phenolglycolipids bear only one methyl rhamnoside residue (in *M. bovis* and *M. marinum*), others have oligosaccharides, one of them with a labile dideoxyhexose at its nonreducing end (in *M. kansasii*) (230).

In 1961, MacLennan and co-workers (231) reported the occurrence of 2-*O*-Me-fucose, 2-*O*-Me-rhamnose, and 2,4-di-*O*-Me-rhamnose in a specific glycolipid from a photochromogenic atypical mycobacterium (now called *M. kansasii*). Structural reinvestigation in 1970 by Gastambide-Odier and co-workers (229,232) and in 1981 by Hunter and Brennan (233) confirmed the oligosaccharide composition; however, the presence of 3-*O*-Me-fucose and 3-*O*-Me-rhamnose was also noticed by the former group. Finally, in 1984 the following

trisaccharide was proposed (234) as the tentative structure for the oligosaccharide moiety of the phenolic glycolipid: 2,4-di-*O*-Me-L-Rha*p*(l→4)2-*O*-Me-L-Fuc*p*(l→4)2-*O*-Me-L-Rha*p*1-R. The aglycon R residue was identified by Gastambide-Odier and co-workers (229,232) as a phthiocerol molecule mainly esterified by mycocerosic FA. *Mycobacterium kansasii,* the "yellow" bacillus, is an important etiologic agent of chronic pulmonary infections indistinguishable from tuberculosis. This disease is the most important clinical problem arising from nontuberculous mycobacteria (235). A recent study has demonstrated that the species-specific phenolic glycolipid of *M. leprae* triggers uptake into Schwann cells by interaction with laminin-2 and the α-dystroglycan receptor. This finding emphasizes the importance of lipids in the biology of mycobacterial infections and suggests possible strategies to combat nerve damage in leprosy (236).

The major phenolic glycolipids **318–331**, with different aliphatic chains and sugar moieties, have been isolated from *M. kansasii* and *M. gastri* (**318–321**), *M. bovis* (**320**), *M. leprae* (**322–324**), *M. tuberculosis* (Canetti strain, **325–327**), *M. marium*, *M. ulcerans* (**328**), and *M. haemophilum* (**329–331**) (237,238).

318 R = 2,6-dideoxy-4-O-Me-Ara	**325** R = 2,3,4-tri-O-tri-Me-Fuc
319 R = 2-O-Me-Fuc	**326** R = Rha
320 R = 2-O-Me-Rha	**327** R = 2-O-Me-Rha
321 R = 2,4-O-di-Me-Rha	**328** R = 3-O-Me-Rha
322 R = 3,6-O-di-Me-Glc	**329** R = 2,3-O-di-Me-Rha
323 R = 2,3-O-di-Me-Rha	**330** R = 2-O-Me-Rha
324 R = 3-O-Me-Rha	**331** R = 2,3-O-di-Me-Rha
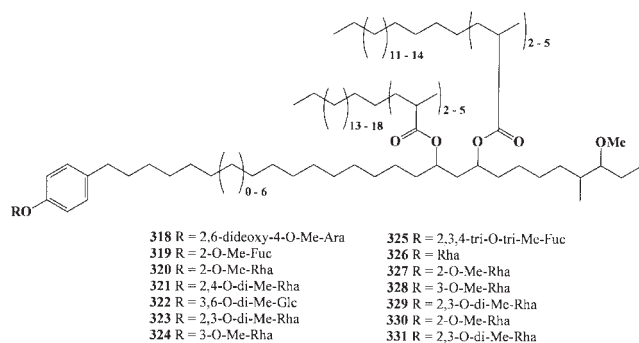
Phenolic glycolipids **332** and **333**, acylated in the 19 and 21 positions by multimethyl-branched FA, have been isolated from *M. kansasii*, and also found in *M. gastri* (239–241). The novel phenolic glycolipids **334–338** were isolated from *M. tuberculosis*, as were their deacylated analogs (242).

332 R = A. R₁ = B
333 R = A. R₁ = C

334 R = Me, R₁ = H
335 R = R₁ = H
336 R = R₁ = Me

337 R = Me
338 R = H
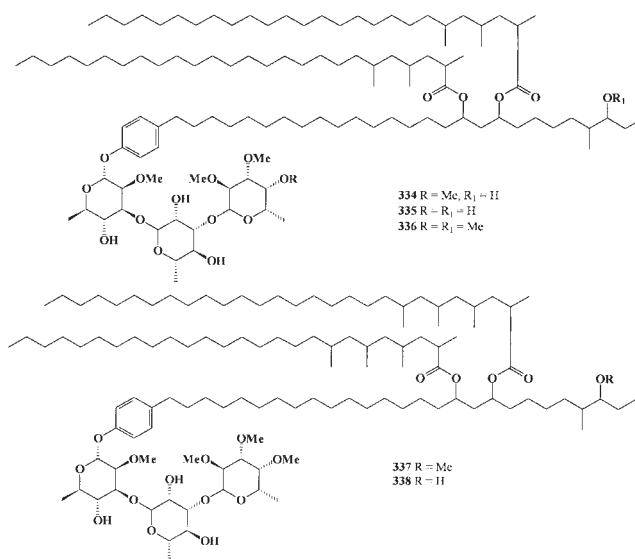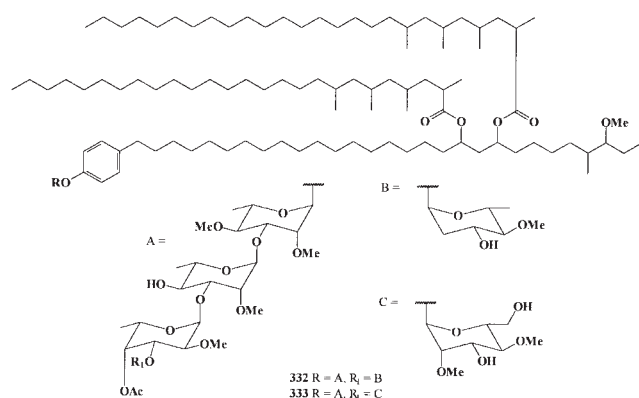
MYCOLIC GLYCOLIPIDS WITH MULTIMETHYL-BRANCHED FA

Mycolic acids of mycobacterial glycolipids are complex hydroxylated branched-chain FA with elevated (from 60 to 90) carbon numbers, and they may also contain diverse functional groups such as an epoxy ester group or keto, methoxy, and/or cyclopropane ring(s) (243). These FA were isolated and named by Stodola and co-workers in 1938 (244) from a waxy extract of the human tubercle bacillus (*M. tuberculosis*). Their common structure was elucidated in 1950 by Asselineau and co-workers (245,246) and was shown to be formed of a β-hydroxy-α-alkyl branched chain. Both *M. tuberculosis* and *M. leprae*, the causative agent of leprosy, have been shown to add unique cyclopropyl groups to their mycolic acids (243). Mutations that affect cyclopropane groups of mycolic acids have been shown to render *M. tuberculosis* unable both to core and to cause a persistent infection in mice. The cyclopropane lipids appear to represent a unique virulence factor that protects pathogenic mycobacteria against an effective immune response. Also, some glycolipids based on trehalose containing the multimethyl-branched FA **339** and **340** have been isolated from *M. tuberculosis* (247,248).

Mycobacterium tuberculosis, the tubercule bacillus, was originally described by Robert Koch (249) and, characterized by its unusual staining properties, was proved to be the causative agent of tuberculosis. These acid-fast staining properties have been found to result from the unique lipid surface, which is predominantly long-chain mycolic acids. These FA are common to the entire genus of *Mycobacterium*, thus providing a unique signature for the species. The tuberculosis-specific drugs isoniazid and ethionamide have been shown to target the synthesis of these mycolic acids. Using a combination of genetic, biochemical, and X-ray crystallographic analyses, the target, InhA (long-chain enoyl acyl carrier protein reductase, an enzyme involved in the biosynthesis of mycolic acids),

has been identified and characterized. Specific inhibition of InhA induces the lysis of mycobacterial cells, thus defining a key Achilles heel for the mycobacterial species that has led to novel drug development. Furthermore, it is noticeable that mycolic acids were the first known CD1-presented antigen (250); also, mammalian T-cells can recognize a foreign lipid structure by a CD1-dependent mechanism (251,252). It is now recognized that mycolic acids are localized in the inner leaflet of the mycobacterial cell wall, either covalently bound or loosely associated with arabino-galactan polymers (253). Mycolic acids have been involved in maintaining a rigid cell shape, but they also contribute to the resistance to chemical injury and to the protection of cells against hydrophobic antibiotics.

339 SL1

340 PAT
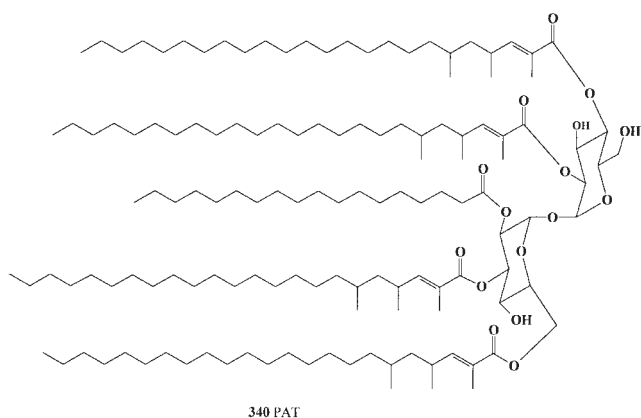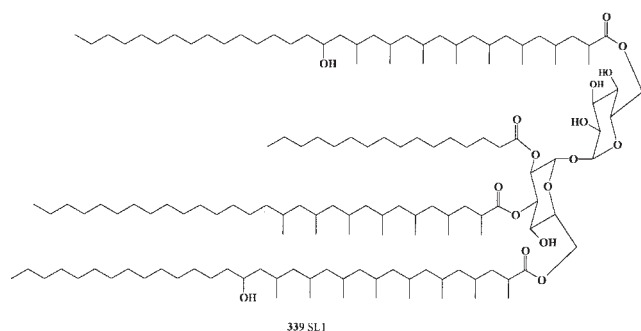
SUMMARY

Carotenoids and their glycosides are important factors in human health and are essential for vision. The role of β-carotene and other carotenoids as the main dietary source of vitamin A is well known. Protective effects of carotenoids and their glycosides against serious disorders such as cancer, heart disease, and degenerative eye disease have been recognized and have stimulated intensive research into the role of carotenoids as antioxidants and as regulators of the immune response system.

Archaeal lipids are based on ether links, and their aliphatic components are isoprenic in nature. These molecules are the structural components of a new model of biological membrane in which a monolayer of bipolar lipids replaces the conventional bilayer of monopolar lipids universally present in the biological membranes. Archaeal bolaform lipids can be obtained from the membranes of microorganisms grown at optimal temperature and pH conditions. Diether archaeal lipids and/or their synthetic analogs behave quite similarly to the ester analogs, whereas tetraether lipids behave in a more complex way. In fact, a bolaform lipid can have a U-shaped disposition, with both heads in contact with the aqueous subphase, or it may assume a stretched configuration, with only one polar interface in contact with water. Some interesting properties of these bolaform lipids make them attractive candidates as drug or antigen delivery systems and as stable S-layer supported lipid films for functional membrane protein reconstitutions or supported membrane biosensor devices.

Mycobacteria, members of which cause tuberculosis and leprosy, produce cell walls of unusually low permeability, which contribute to their resistance to therapeutic agents. Phenolic glycolipids are unusual surface-active lipid surfactants found only in pathogenic mycobacteria. They are extremely hydrophobic, having a high portion of long-chain moieties and relatively hydrophobic sugars. Most of the hydrocarbon chains of these lipids assemble to produce an asymmetrical bilayer of exceptional thickness. Structural considerations suggest that the fluidity is exceptionally low in the innermost part of the bilayer and that it gradually increases toward the outer surface. Differences in mycolic acid structure may affect the fluidity and permeability of the bilayer and may explain the different sensitivity levels of various mycobacterial species to lipophilic inhibitors. Phenolic glycolipids play an important key role as an antigenic probe for the serodiagnosis of some human pathogen mycobacterial infections.

REFERENCES

1. Dembitsky, V.M. (2004) Astonishing Diversity of Natural Surfactants. 1. Glycosides of Fatty Acids and Alcohols, *Lipids 39,* 933–953.
2. Dembitsky, V.M. (2005) Astonishing Diversity of Natural Surfactants. 2. Polyether Glycosidic Ionophores and Macrocyclic Glycosides, *Lipids 40*, 219–248.
3. Dembitsky, V.M. (2004) Chemistry and Biodiversity of Biologically Active Natural Glycosides, *Chem. Biodivers. 1*, 673–781.
4. Mercadante, A.Z. (1999) New Carotenoids: Recent Progress, *Pure Appl. Chem. 71*, 2263–2272.
5. Frank, H.A., Young, A.J., Britton, G., and Cogdell, R.J. (1999) *The Photochemistry of Carotenoids*, Advances in Photosynthesis 8, Kluwer Academic Publishers, Dordrecht, The Netherlands.
6. Higgli, U.A., and Pfander, H. (1999) Carotenoid Glycosides and Glycosyl Esters, in *Naturally Occurring Glycosides* (Ikan, R., ed.), pp. 125–145, John Wiley & Sons, New York.
7. Liaanen-Jensen, S., Pfander, H., and Britton, G. (1995) *Carotenoids: Isolation and Analysis*, Birkhäuser, Basel.
8. Britton, G., Liaanen-Jensen, S., and Pfander, H. (1995) *Carotenoids: Spectroscopy,* Birkhäuser, Basel.
9. Pfander, H. (1987) *Key to Carotenoids*, Birkhäuser, Basel.
10. Britton, G. (1995) Structure and Properties of Carotenoids in Relation to Function, *FASEB J. 9*, 1551–1558.
11. Kates, M. (1972) Ether-Linked Lipids in Extremely Halophilic

Bacteria, in *Ether Lipids, Chemistry and Biology* (Snyder, F., ed.), pp. 351–398, Academic Press, New York.

12. Kates, M. (1978) The Phytanyl Ether-Linked Polar Lipids and Isoprenoid Neutral Lipids of Extremely Halophilic Bacteria, *Prog. Chem. Fats Other Lipids 15*, 301–352.

13. Kates, M. (1993) Glyco-, Phosphoglyco-, and Sulfoglycoerolipids of Bacteria, in *Handbook of Lipid Research, Glycolipids, Phosphoglycolipids, and Sulfoglycolipids* (Kates, M., ed.), pp. 1–122, Plenum Press, New York.

14. Kamekura, M., and Kates, M. (1988) Lipids of Halophilic Archaebacteria, in *Halophilic Bacteria* (Rodriguez-Valera, R., ed.), pp. 25–54, CRC Press, Boca Raton, FL.

15. Kates, M. (1992) Archaebacterial Lipids: Structure, Biosynthesis and Function, *Biochem. Soc. Symp. 58*, 51–72.

16. Sprott, G.D. (1992) Structures of Archaebacterial Membrane Lipids, *J. Bioenerg. Biomembr. 24*, 555–566.

17. De Rosa, M., Gambacorta, A., and Gliozzi, A. (1986) Structure, Biosynthesis, and Physicochemical Properties of Archaebacterial Lipids, *Microbiol. Rev. 50*, 70–80.

18. Aschoff, S. (1818) Beiträge zur Kenntnis des Safrans, *Berl. Jb. Pharm. 19*, 142–157.

19. Karrer, P., and Miki, K. (1929) Pflanzenfarbstoffe XV. Der Zucker des α-Crocins, *Helv. Chim. Acta 12*, 985–986.

20. Karrer, P., and Salomon, H. (1933) Die Bruttoformel des Crocins, *Helv. Chim. Acta 16*, 643–651.

21. Bhat, J.V., and Broker, R. (1953) Riboflavine and Thiamine Contents of Saffron, *Crocus sativus* Linn, *Nature 172*, 544.

22. Koutroubakis, I.E., Malliaraki, N., Dimoulios, P.D., Karmiris, K., Castanas, E., and Kouroumalis, E.A. (2004) Decreased Total and Corrected Antioxidant Capacity in Patients with Inflammatory Bowel Disease, *Dig. Dis. Sci. 49*, 1433–1437.

23. Ochiai, T., Soeda, S., Ohno, S., Tanaka, H., Shoyama, Y., and Shimeno, H. (2004) Crocin Prevents the Death of PC-12 Cells Through Sphingomyelinase Ceramide Signaling by Increasing Glutathione Synthesis, *Neurochem. Int. 44*, 321–330.

24. Chen, X., Krakauer, T., Oppenheim, J.J., and Howard, O.M. (2004) Yin Zi Huang, an Injectable Multicomponent Chinese Herbal Medicine, Is a Potent Inhibitor of T-Cell Activation, *J. Altern. Complem. Med. 10*, 519–526.

25. Pfander, H., and Wittwer, F. (1975) Carotinoid-Glykoside 2. Mitteilung Untersuchungen zur Carotinoid-Zusammensetzung im Safran, *Helv. Chim. Acta 58*, 1608–1620.

26. Selim, K., Tsimidou, M., and Biliaderis, C.G. (2000) Kinetic Studies of Degradation of Saffron Carotenoids Encapsulated in Amorphous Polymer Matrices, *Food Chem. 71*, 199–206.

27. Li, C.-Y., and Wu, T.-W. (2002) Constituents of the Stigmas of *Crocus sativus* and Their Tyrosinase Inhibitory Activity, *J. Nat. Prod. 65*, 1452–1456.

28. Li, N., Lin, G., Kwan, Y.W., and Min, Z.D. (1999) Simultaneous Quantification of Five Major Biologically Active Ingredients of Saffron by High-Performance Liquid Chromatography, *J. Chromatogr. A 849*, 349–355.

29. Ozaki, A., Kitano, M., Furusawa, N., Yamaguchi, H., Kuroda, K., and Endo, G. (2002) Genotoxity of Gardenia Yellow and Its Components, *Food Chem. Toxicol. 40*, 1603–1610.

30. Choi, H.-J., Park, Y.S., Kim, M.G., Kim, T.K., Yoon, N.S., and Lim, Y.J. (2001) Isolation and Characterization of the Major Colorant in Gardenia Fruit, *Dyes Pigment. 49*, 15–20.

31. Sheu, S.-Y., and Hsin, W.-C. (1998) HPLC Separation of the Major Constituents of *Gardeniae fructus*, *J. High Resolut. Chromatogr. 21*, 523–526.

32. Liakopoulou-Kyriakides, M., Tsatsaroni, E., Laderos, P., and Georgiadou, K. (1998) Dyeing of Cotton and Wool Fibres with Pigments from *Crocus sativus*—Effect of Enzymatic Treatment, *Dyes Pigment. 36*, 215–221.

33. Dufresne, C., Cormier, F., Dorion, S., Niggli, U.A., Pfister, S., and Pfander, H. (1999) Glycosylation of Encapsulated Crocetin by a *Crocus sativus* L. Cell Culture, *Enzyme Microb.*

Technol. 24, 453–462.

34. Tubaro, F., Micossi, E., and Ursini, F. (1996) The Antioxidant Capacity of Complex Mixtures by Kinetic Analysis of Crocin Bleaching Inhibition, *J. Am. Oil Chem. Soc. 73*, 173–179.

35. Pham, T.Q., Cormier, F., Farnworth, E., Tong, V.H., and Van Calsteren, M.-R. (2000) Antioxidant Properties of Crocin from *Gardenia jasminoides* Ellis and Study of the Reactions of Crocin with Linoleic Acid and Crocin with Oxygen, *J. Agric. Food Chem. 48*, 1455–1461.

36. Manzocco, L., Calligaris, S., and Nicoli, M.C. (2002) Assessment of Pro-oxidant Activity of Foods by Kinetic Analysis of Crocin Bleaching, *J. Agric. Food Chem. 50*, 2767–2771.

37. Molnar, J., Szabo, D., Pusztai, R., Mucsi, I., Berek, L., Ocsovszki, I., Kawata, E., and Shoyama, Y. (2000) Membrane Associated Antitumor Effects of Crocine-, Ginsenoside- and Cannabinoid Derivates, *Anticancer Res. 20*, 861–867.

38. Ghosal, S., Singh, S.K., and Battacharya, S.K. (1989) Mangicrocin, an Adaptogenic Xanthone Carotenoid Glycosidic Conjugate from Saffron, *J. Chem. Res.–S 3*, 70–71.

39. Dufresne, C., Cormier, F., Dorion, S., Niggli, U.A., Pfister, S., and Pfander, H. (1999) Glycosylation of Encapsulated Crocetin by a *Crocus sativus* L. Cell Culture, *Enzyme Microb. Technol. 24*, 453–462.

40. Takaichi, S., Maoka, T., Hanada, S., and Imhoff, J.F. (2001) Dihydroxylycopene Diglucoside Diesters: A Novel Class of Carotenoids from the Phototrophic Purple Sulfur Bacteria *Halorhodospira abdelmalekii* and *Halorhodospira halochloris*, *Arch. Microbiol. 175*, 161–167.

41. Kleinig, H., Heumann, W., Meister W., and Englert G. (1977) Carotenoids of Rhizobia. I. New Carotenoids from *Rhizobium lupini*, *Helv. Chim. Acta 60*, 254–258.

42. Kleinig, H., and Broughton, W.J. (1982) Carotenoid Pigments in a Red Strain of *Rhizobium*, from *Lotononis bainesii* Baker, *Arch. Microbiol. 133*, 164–174.

43. Kleinig, H., and Schmitt, R. (1982) On the Biosynthesis of C_{30} Carotenoic Acid Glucosyl Esters in *Pseudomonas rhodos, Z. Naturforsch. 37C*, 758–760.

44. Liaaen-Jensen, S. (1969) Selected Examples of Structure Determination of Natural Carotenoids, *Pure Appl. Chem. 20*, 421–448.

45. Karrer, P., Benz, F., Morf, R., Raudnitz, H., Stoll, M., and Takahashi, H. (1932) Pflanzenfarbstoffe. 56. Konstitution des Crocetins und Bixins. Synthese des Perhydronorbixins, *Helv. Chim. Acta 15*, 1399–1419.

46. Kleinig, H., and Reichenbach, H. (1973) A New Carotenoid Glucoside Ester from *Chondromyces apiculatus*, *Phytochemistry 12*, 2483–2485.

47. Marshall, J.H., and Wilmoth, G.J. (1981) Pigments of *Staphylococcus aureus*, a Series of Triterpenoid Carotenoids, *J. Bacteriol. 147*, 900–913.

48. Takaichi, S., Oh-oka, H., Maoka, T., Jung, D.O., and Madigan, M.T. (2003) Novel Carotenoid Glucoside Esters from Alkaliphilic Heliobacteria, *Arch. Microbiol. 179*, 95–100.

49. Kleinig, H., and Reichenbach, H. (1973) Biosynthesis of Carotenoid Glucoside Esters in *Myxococcus vulvus* (Myxobacterales): Inhibition by Nicotine and Carotenoid Turnover, *Biochim. Biochim. Acta 306*, 249–256.

50. Schmidt, K. (1971) Carotenoids of Purple Nonsulfur Bacteria. Composition and Biosynthesis of the Carotenoids of Some Strains of *Rhodopseudomonas acidophila, Rhodospirillum tenue*, and *Rhodocyclus purpureus*, *Arch. Mikrobiol. 77*, 231–238.

51. Schmidt, K., Francis, G.W., and Liaaen-Jensen, S. (1971) Bacterial Carotenoids. 36. Remakble C_{43} Carotenoid Artefacts of Cross-Conjugated Carotenoids and New Carotenoid Glucosides from *Athiorhodaceae* spp., *Acta Chem. Scand. 25*, 2476–2486.

52. Heinemeyer, E.A., and Schmidt, K. (1983) Changes in

Carotenoid Biosynthesis Caused by Variations of Growth Conditions in Cultures of *Rhodopseudomonas acidophila* Strain 7050, *Arch. Mikrobiol. 134*, 217–221.

53. Kleinig, H., Meister, W., and Englert, G. (1978) Carotenoids of Rhizobia. II. The Effect of Nicotine on the Carotenoid Pattern of *Rhizobium lupine, Arch. Microbiol. 119*, 71–74.

54. Kleinig, H., Schmitt, R., Meister, W., Englert, G., and Thommen, H. (1979) New C_{30} Carotenoic Acid Glucosyl Esters from *Pseudomonas rhodos, Z. Naturforsch. 34C*, 181–185.

55. Naumov, G.N., and Bokhan, I.K. (1984) Carotenoid Pigments and the Enhanced Resistance of *Pseudomonas* to the Action of Ultraviolet Radiation, *Mikrobiologiia (USSR) 53*, 861–863.

56. Taylor, R.F., and Davies, B.H. (1974) Triterpenoid Carotenoids and Related Lipids. Triterpenoid Monohydroxy- and Monoglucosyloxy-Carotenoids from *Streptococcus faecium* UNH 564P, *Biochem. J. 139*, 761–769.

57. Heilbron, I.M., and Lythgoe, B. (1936) The Chemistry of the Algae. 2. The Carotenoid Pigments of *Oscillatoria rubescens*, *J. Chem. Soc.*, 1376–1380.

58. Hertzberg, S., and Liaaen-Jensen, S. (1966) The Carotenoids of Blue-Green Algae. 2. The Carotenoids of *Oscillatoria rubescens* and an *Athrospira* sp., *Phytochemistry 5*, 565–570.

59. Mohamed, H.E., and Vermaas, W. (2004) Slr1293 in *Synechocystis* sp. Strain PCC 6803 Is the C-3′,4′ Desaturase (CrtD) Involved in Myxoxanthophyll Biosynthesis, *J. Bacteriol. 186*, 5621–5628.

60. Arpin, N., Fiasson, J.-L., and Liaaen-Jensen, S. (1972) Bacterial Carotenoids XXXIX. C_{50} Carotenoids 10. Bacterioruberin Mono- and Diglycosides, *Acta Chem. Scand. 26*, 2526–2528.

61. Ourisson, G., and Nakatani, Y. (1989) Bacterial Carotenoids as Membrane Re-inforcers. A General Role for Polyterpenoids: Membrane Stabilization, in *Carotenoids, Chemistry and Biology* (Krinsky, N.I., Mathews-Roth, M.M., and Taylor, R.T., eds.), pp. 237–246, Plenum Press, New York.

62. Lutnaes, B.F., Oren, A., and Liaaen-Jensen, S. (2002) New $C_{(40)}$-Carotenoid Acyl Glycoside as Principal Carotenoid in *Salinibacter ruber*, an Extremely Halophilic Eubacterium, *J. Nat. Prod. 65*, 1340–1343.

63. Alfredsson, G.A., Kristjansson, J.K., Hjörleifsdóttir, S., and Stetter, K.O. (1988) *Rhodothermus marinus*, gen. nov., sp. nov., a Thermophilic, Halophilic Bacterium from Submarine Hot Springs in Iceland, *J. Gen. Microbiol. 134*, 299–306.

64. Guinand, M., Vacheron, M.J., and Michel, G. (1970) Structure des Parois Cellulaires des Nocardia. I—Isolement et Composition des Parois de *Nocardia kirovani, FEBS Lett. 6*, 37–39.

65. Takaichi, S., and Ishidsu, J.I. (1992) Carotenoid Glycoside Ester from *Rhodococcus rhodochrous*, *Methods Enzymol. 213*, 366–374.

66. Takaichi, S., Maoka, T., Yamada, M., Matsuura, K., Haikawa, Y., and Hanada, S. (2001) Absence of Carotenoids and Presence of a Tertiary Methoxy Group in a Carotenoid from a Thermophilic Filamentous Photosynthetic Bacterium *Roseiflexus castenholzii*, *Plant Cell Physiol. 42*, 1355–1362.

67. Takaichi, S., Wang, Z.Y., Umetsu, M., Nozawa, T., Shimada, M.T., and Madigan, M.T. (1997) New Carotenoids from the Thermophilic Green Sulfur Bacterium *Chlorobium tepidum*: 1′,2′-Dihydro-γ-carotene, 1′,2′-Dihydrochlorobactene, and OH-Chlorobactene Glucoside Ester, and the Carotenoid Composition of Different Strains, *Arch. Microbiol. 168*, 270–276.

68. Takaichi, S., Tamura, Y., Azegami, K., Yamamoto, Y., and Ishidsu, J.I. (1997) Carotenoid Glucoside Mycolic Acid Esters from the Nocardioform Actinomycetes, *Rhodococcus rhodochrous*, *Phytochemistry 45*, 505–508.

69. Takaichi, S., Tshuji, K., Matsuura, K., and Shimada, K. (1995) A Monocyclic Carotenoid Glucoside Ester Is a Major Carotenoid in the Green Filamentous Bacterium *Chloroflexus aurantiacus*, *Plant Cell Physiol. 36*, 773–778.

70. Hertzberg, S., and Liaaen-Jensen, S. (1966) Bacterial Carotenoids. 19. The Carotenoids of *Mycobacterium phlei* Strain Vera. 1. The Structures of the Minor Carotenoids, *Acta Chem. Scand. 20*, 1187–1194.

71. Hertzberg, S., and Liaaen-Jensen, S. (1967) 20. The Carotenoids of *Mycobacterium phlei* Strain Vera. 2. The Structures of Phleixanthophylls—Two Novel Tertiary Glycosides, *Acta Chem. Scand. 21*, 15–41.

72. Lederer, E. (1967) Glycolipids of Mycobacteria and Related Microorganisms, *Chem. Phys. Acta 1*, 294–315.

73. Kleinig, H., Reichenbach, H., and Achenbach, H. (1970) Carotenoid Pigments of *Stigmatella aurantiaca* (Myxobacterales). II. Acylated Carotenoid Glucosides, *Arch Mikrobiol. 74*, 223–234.

74. Kleinig, H., and Reichenbach, H. (1970) A New Type of Carotenoid Pigment Isolated from Myxobacteria, *Naturwissenschaften 57*, 92–93.

75. Reichenbach, H., and Kleinig, H. (1972) The Carotenoids of Myxobacteria, *Zentralbl. Bakteriol. A 220*, 458–463.

76. Kleinig H. (1972) Membranes from *Myxococcus fulvus* (Myxobacterales) Containing Carotenoid Glucosides. I. Isolation and Composition, *Biochim. Biophys. Acta 274*, 489–498.

77. Kleinig, H., and Reichenbach, H. (1977) Carotenoid Glucosides and Menaquinones from the Gliding Bacterium *Herpetosiphon giganteus* Hp A2, *Arch. Microbiol. 112*, 307–310.

78. Kleinig, H. (1975) On the Utilization *in vivo* of Lycopene and Phytoene as Precursors for the Formation of Carotenoid Glucoside Ester and on the Regulation of Carotenoid Biosynthesis in *Myxococcus fulvus*, *Eur. J. Biochem. 57*, 301–308.

79. Halfen, L.N., Pierson, B.K., and Francis, G.W. (1972) Carotenoids of a Gliding Organism Containing Bacteriochlorophylls, *Arch. Mikrobiol. 82*, 240–246.

80. Pierson, B.K., and Castenholz, R.W. (1974) A Phototrophic Gliding Filamentous Bacterium of Hot Springs, *Chloroflexus aurantiacus*, gen. and sp. nov., *Arch Microbiol. 100*, 5–24.

81. Pierson, B.K., and Castenholz, R.W. (1971) Bacteriochlorophylls in Gliding Filamentous Prokaryotes from Hot Springs, *Nat. New Biol. 233*, 25–27.

82. Kleinig, H., Reichenbach, H., Achenbach, H., and Stadler, J. (1971) Carotenoid Pigments of *Sorangium compositum* (Myxobacterales) Including Two New Carotenoid Glucoside Esters and Two New Carotenoid Rhamnosides, *Arch. Mikrobiol. 78*, 224–233.

83. Burgess, M.L., Barrow, K.D., Gao, C., Heard, G.M., and Glenn, D. (1999) Carotenoid Glycoside Esters from the Thermophilic Bacterium *Meiothermus ruber, J. Nat. Prod. 62*, 859–863.

84. Yokoyama, A., Sandmann, G., Hoshino, T., Adachi, K., Sakai, M., and Shizuri, Y. (1995) Thermozeaxanthins, New Carotenoid Glycoside Esters from Thermophilic Eubacterium *Thermus thermophilus*, *Tetrahedron Lett. 36*, 4901–4904.

85. Lutnaes, B.F., Strand, A., Petursdottir, S.K., and Liaaen-Jensen, S. (2004) Carotenoids of Thermophilic Bacteria *Rhodothermus marinus* from Submarine Icelandic Hot Springs, *Biochem. Syst. Ecol. 32*, 455–468.

86. Takaichi, S., Maoka, T., and Masamoto, K. (2001) Myxoxanthophyll in *Synechocystis* sp. PCC 6803 Is Myxol 2′-Dimethylfucoside, $(3R,2'S)$-Myxol 2′-(2,4-di-*O*-methyl-α-L-fucoside), not Rhamnoside, *Plant Cell Physiol. 42*, 756–762.

87. Haberli, A., Bircher, C., and Pfander, H. (2000) Isolation of a New Carotenoid and Two New Carotenoid Glycosides from *Curtobacterium flaccumfaciens* pvar. *poinsettiae*, *Helv. Chim. Acta 83*, 328–335.

88. Marner, F.J., Singab, A.N., Al-Azizi, M.M., El-Emary, N.A., and Schafer, M. (2002) Iridal Glycosides from *Iris spuria* (Zeal), Cultivated in Egypt, *Phytochemistry 60*, 301–307.

89. Marner, F.-J. (1997) Iridals and Cycloiridals, Products of an

Unusual Squalene Metabolism in Sword Lilies (Iridaceae), *Current Org. Chem. 1*, 153–186.

90. Bonfils, J.P., Pinguet, F., Culine, S., and Sauvaire, Y. (2001) Cytotoxicity of Iridals, Triterpenoids from Iris, on Human Tumor Cell Lines A2780 and K562, *Planta Med. 67*, 79–81.

91. Barua, A.B. (1997) Retinoyl β-Glucuronide: A Biologically Active Form of Vitamin A, *Nutr. Rev. 55*, 259–267.

92. Barua, A.B., and Sidell, N. (2004) Retinoyl β-Glucuronide: A Biologically Active Interesting Retinoid, *J. Nutr. 134*, 286S–289S.

93. Matsuno, T. (1991) Xanthophylls as Precursors of Retinoids, *Pure Appl. Chem. 63*, 81–88.

94. Dunagin, P.E., Meadows, E.H., and Olson, J.A. (1965) Retinoyl β-Glucuronic Acid: A Major Metabolite of Vitamin A in Rat Bile, *Science 148*, 86–87.

95. Barua, A.B., and Olson, J.A. (1986) Retinoyl β-Glucuronide: An Endogenous Compound of Human Blood, *Am. J. Clin. Nutr. 43*, 481–485.

96. Sandberg, J.A., Eckhoff, C., Nau, H., and Slikker, W., Jr. (1994) Pharmacokinetics of 13-*cis*-, all-*trans*-, 13-*cis*-4-Oxo-, and all-*trans*-4-Oxo Retinoic Acid After Intravenous Administration in the Cynomolgus Monkey, *Drug Metab. Dispos. 22*, 154–160.

97. Kraft, J.C., Eckhoff, C., Kochhar, D.M., Bochert, G., Chahoud, I., and Nau, H. (1991) Isotretinoin (13-*cis*-retinoic acid) Metabolism, *cis-trans* Isomerization, Glucuronidation, and Transfer to the Mouse Embryo—Consequences for Teratogenicity, *Teratogen. Carcinogen. Mutagen. 11*, 21–30.

98. Tzimas, G., Burgin, H., Collins, M.D., Hummler, H., and Nau, H. (1994) The High Sensitivity of the Rabbit to the Teratogenic Effects of 13-*cis*-Retinoic Acid (isotretinoin) Is a Consequence of Prolonged Exposure of the Embryo to 13-*cis* Retinoic Acid and 13-*cis*-4-Oxo Retinoic Acid, and Not of Isomerization to all-*trans*-Retinoic Acid, *Archiv. Toxicol. 68*, 119–128.

99. Zachman, R.D., and Olson, J.A. (1964) Formation and Enterohepatic Circulation of Water-Soluble Metabolite of Vitamin A and Vitamin A Acid, *Nature 203*, 410–412.

100. Lippell, K., and Olson, J.A. (1968) Biosynthesis of β-Glucuronides of Retinol and Retinoic Acid *in vivo* and *in vitro*, *J. Lipid Res. 9*, 168–175.

101. Sass, J.O., Tzimas, G., and Nau, H. (1994) 9-*cis*-Retinoyl-β-D-glucuronide Is a Major Metabolite of 9-*cis*-Retinoic Acid, *Life Sci. 54*, PL69–PL74.

102. Eckhoff, C., Wittfoht, W., Nau, H., and Slikker, W. (1990) Characterization of Oxidized and Glucuronidated Metabolites of Retinol in Monkey Plasma by Thermospray Liquid-Chromatography Mass-Spectrometry, *Biomed. Environm. Mass Spectrom. 19*, 428–433.

103. Li, S., Barua, A.B., and Huselton, C.A. (1996) Quantification of Retinyl-β-glucuronides in Rat Urine by Reversed-Phase High-Performance Liquid Chromatography with Ultraviolet Detection, *J. Chromatogr. B 683*, 155–162.

104. Sass, J.O., Masgrau, E., Saurat, J.H., and Nau, H. (1995) Metabolism of Oral 9-*cis* Retinoic Acid in the Human—Identification of 9-*cis*-Retinoyl-β-glucuronide and 9-*cis*-4-Oxo-retinoyl-β-glucuronide as Urinary Metabolites, *Drug Metab. Dispos. 23*, 887–891.

105. Blaner, W.S., and Olson, J.A. (1994) Retinol and Retinoic Acid Metabolism, in *The Retinoids* (Sporn, M.B., Roberts, A.B., and Goodman, D.S., eds.), pp. 229–256, Raven Press, New York.

106. Genchi, G., Wang, W., Barua, A., Bidlack, W.R., and Olson, J.A. (1996) Formation of β-Glucuronides and of β-Galacturonides of Various Retinoids Catalyzed by Induced and Noninduced Microsomal UDP-Glucuronosyltransferases of Rat Liver, *Biochim. Biophys. Acta 1289*, 284–290.

107. Nau, H. (1995) Chemical Structure–Teratogenicity Relationships, Toxicokinetics and Metabolism in Risk Assessment of Retinoids, *Toxicol. Lett. 82–83*, 975–979.

108. Pfander, H., and Hodler, M. (1974) Carotenoid Glycosides. Partial Synthesis and Characterization of Zeaxanthin Mono- and Diglucosides, *Helv. Chim. Acta 57*, 1641–1651.

109. Hertzberg, S., Borch, G., and Liaaen-Jensen, S. (1976) Bacterial Carotenoids. L. Absolute Configuration of Zeaxanthin Dirhamnoside, *Arch. Microbiol. 110*, 95–99.

110. Nybraaten, G., and Liaaen-Jensen, S. (1974) Bacterial Carotenoids. VLIV. Zeaxanthin Mono- and Dirhamnoside, *Acta Chem. Scand. B 28*, 1219–1224.

111. Misawa, N., Nakagawa, M., Kobayashi, K., Yamano, S., Izawa, Y., Nakamura, K., and Harashima, K. (1990) Elucidation of the *Erwinia uredovora* Carotenoid Biosynthetic Pathway by Functional Analysis of Gene Products Expressed in *Escherichia coli*, *J. Bacteriol. 172*, 6704–6712.

112. Hunter, C.N., Hundle, B.S., Hearst, J.E., Lang, H.P., Gardiner, A.T., Takaichi, S., and Cogdell, R.J. (1994) Introduction of New Carotenoids into the Bacterial Photosynthetic Apparatus by Combining the Carotenoid Biosynthetic Pathways of *Erwinia herbicola* and *Rhodobacter sphaeroides*, *J. Bacteriol. 176*, 3692–3697.

113. Kull, D.R., and Pfander, H. (1997) Isolation and Structure Elucidation of Carotenoid Glycosides from the Thermophilic Archaea *Sulfolobus shibatae*, *J. Nat. Prod. 60*, 371–374.

114. Yokoyama, A., Shizuri, Y., Hoshino, T., and Sandmann, G. (1996) Thermocryptoxanthins: Novel Intermediates in the Carotenoid Biosynthetic Pathway of *Thermus thermophilus*, *Arch. Microbiol. 165*, 342–345.

115. Yokoyama, A., Sandmann, G., Hoshino, T., Adachi, K., Sakai, M., and Shizuri, Y. (1995) Thermozeaxanthins, New Carotenoid Glycoside Esters from Thermophilic Eubacterium *Thermus thermophilus*, *Tetrahedron Lett. 36*, 4901–4904.

116. Yokoyama, A., Adachi, K., and Shizuri, Y. (1995) New Carotenoid Glucosides, Astaxanthin Glucoside and Adonixanthin Glucoside, Isolated from the Astaxanthin Producing Marine Bacterium, *Agrobacterium aurantiacum*, *J. Nat. Prod. 58*, 1929–1933.

117. Yokoyama, A., Shizuri, Y., and Misawa, N. (1998) Production of New Carotenoids, Astaxanthin Glucosides, by *Escherichia coli* Transformants Carrying Carotenoid Biosynthesis Genes, *Tetrahedron Lett. 39*, 3709–3712.

118. Dembitsky, V.M., and Rezanka, T. (1996) Comparative Study of the Endemic Freshwater Fauna of Lake Baikal—VII. Carotenoid Composition of the Deep-Water Amphipod Crustacean *Acanthogammarus* (*Brachyuropus*) *grewingkii*, *Comp. Biochem. Physiol. 114B*, 383–387.

119. Ksebati, M.B., Schmitz, F.J., and Gunasekera, S.P. (1988) Pouosides A–E, Novel Triterpene Galactosides from a Marine Sponge, *Asteropus* sp., *J. Org. Chem. 53*, 3917–3921.

120. Gueran, R.I., Greenberg, N.H., Macdonald, M.M., Schumacher, A.M., and Abbott, B.J. (1972) Protocols for Screening Chemical Agents and Natural Products Against Animal Tumors and Other Biological Systems, *Cancer Chemother. Rep. 3(2)* (Part 2), 103 pp.

121. Bjornland, T. (1990) Chromatographic Separation and Spectrometric Characterization of Native Carotenoids from the Marine Dinoflagellate *Thoracosphaera heimii*, *Biochem. Syst. Ecol. 18*, 307–316.

122. Aakermann, T., Guillard, R.R.L., and Liaaen-Jensen, S. (1993) Algal Carotenoids. 55. Structure Elucidation of (3*S*,5*R*,6*R*,3′*S*,5′*R*,6′*S*)-13′-*cis*-7′,8′-Dihydroneoxanthin-20′-al 3′-β-D-Lactoside (P457). 1. Re-isolation, Derivatization and Synthesis of Model Compounds, *Acta Chem. Scand. 47*, 1207–1213.

123. Weeks, O.B., and Andrewes, A.G. (1970) Structure of the Gly-

cosidic Carotenoid Corynexanthin, *Arch. Biochem. Biophys. 137*, 284–286.

124. Arpin, N., Liaaen-Jensen, S., and Trouilloud, M. (1972) Bacterial Carotenoids. 38. C_{50}-Carotenoids. 9. Isolation of Decaprenoxanthin Mono- and Diglucoside from an *Arthrobacter* sp., *Acta Chem. Scand. 26*, 2524–2526.

125. Norgard, S., Francis, G.W., Jensen, A., and Liaaen-Jensen, S. (1970) Bacterial Carotenoids. XXXIV. C_{50}-Carotenoids. 7. A C_{50}-Carotenyl-D-glucoside from *Sarcina lutea, Acta Chem. Scand. 24*, 1460–1462.

126. Hertzberg, S., and Liaaen-Jensen, S. (1977) Bacterial Carotenoids. LIII. C_{50}-Carotenoids. 19. Absolute Configuration of Sarcinaxanthin and Sarcinaxanthin Mono-β-D-glucoside. Isolation of Sarcinaxanthin Diglycoside, *Acta Chem. Scand. B 31*, 215–218.

127. Krubasik, P., Takaichi, S., Maoka, T., Kobayashi, M., Masamoto, K., and Sandmann, G. (2001) Detailed Biosynthetic Pathway to Decaprenoxanthin Diglucoside in *Corynebacterium glutamicum* and Identification of Novel Intermediates, *Arch Microbiol. 176*, 217–223.

128. Arpin, N., Norgard, S., Francis, G.W., and Liaaen-Jensen, S. (1973) Bacterial Carotenoids. XLI. C_{50}-Carotenoids. 11. C_{45}- and C_{50}-Carotenoids from *Sarcina lutea*–Sarcinaxanthin, *Acta Chem Scand. 27*, 2321–2334.

129. Northcote, P.T., Raymond J., and Andersen, R.J. (1989) Xestovanin **A** and Secoxestovanin **A**, Triterpenoid Glycosides with New Carbon Skeletons from the Sponge *Xestospongia vanilla, J. Am. Chem. Soc. 111*, 6276–6280.

130. Winterhalter, P., and Rouseff, R. (2002) Carotenoid Derived Aroma Compounds: An Introduction, in *Carotenoid Derived Aroma Compounds* (Winterhalter, P., and Rouseff, R.L., eds.), ACS Symposium Series, No. 802, pp. 1–17, American Chemical Society, Washington, DC.

131. Enzell, C. (1985) Biodegradation of Carotenoids—An Important Route to Aroma Compounds, *Pure Appl. Chem. 57*, 693–700.

132. Wahlberg, I., and Enzell, C.R. (1987) Tobacco Isoprenoids, *Nat. Prod. Rep. 4*, 237–276.

133. Schreier, P. (1995) Aromaforschung Aktuell, *Naturwissenschaften 82*, 21–27.

134. Beatriz, M., Gloria, A., Grulke, E.A., and Gray, J.I. (1993) Effect of Type of Oxidation on β-Carotene Loss and Volatile Products Formation in Model Systems, *Food Chem. 46*, 401–406.

135. Handelman, G.J., van Kuijk, G.M., Chatterjee, A., and Krinsky, N.I. (1991) Characterisation of Products Formed During the Autoxidation of β-Carotene, *Free Radical Biol. Med. 10*, 427–437.

136. Schwartz, S.H., Qin, X., and Zeevaart, J.A.D. (2001) Characterization of a Novel Carotenoid Cleavage Dioxygenase from Plants, *J. Biol. Chem. 276*, 25208–25211.

137. Baumes, R., Wirth, J., Bureau, S., Gunata, Y., and Razungles, A. (2002) Biogeneration of C_{13}-Norisoprenoid Compounds: Experiments Supportive for an apo-Carotenoid Pathway in Grapevines, *Anal. Chim. Acta 458*, 3–14.

138. Winterhalter, P., and Rouseff, R.L. (eds.) (2001) *Carotenoid Derived Aroma Compounds*, ACS Symposium Series, No. 802, 323 pp., American Chemical Society, Washington, DC.

139. Zorn, H., Langhoff, S., Scheibner, M., and Berger, R.G. (2003) Cleavage of β,β-Carotene to Flavor Compounds by Fungi, *Appl. Microbiol. Biotechnol. 62*, 331–336.

140. Takeda, Y., Zhang, H., Matsumoto, T., Otsuka, H., Oosio, Y., Honda, G., Tabata, M., Fujita, T., Sun, H., Sezik, E., and Yesilada, E. (1997) Megastigmane Glycosides from *Salvia nemorosa*, *Phytochemistry 44*, 117–120.

141. Otsuka, H., and Tamaki, A. (2002) Platanionosides D–J: Megastigmane Glycosides from the Leaves of *Alangium platanifolium* (Sieb. et Zucc.) Harms var. *platanifolium* Sieb. et Zucc., *Chem. Pharm. Bull. 50*, 390–394.

142. Tamaki, A., Otsuka, H., and Ide, T. (1999) Platanionosides A–C, Megastigmane Diglycosides from the Leaves of *Alangium platanifolium, J. Nat. Prod. 62*, 1074–1076.

143. Otsuka, H., Kamada, K., Yao, M., Yuasa, K., Kida, I., and Takeda, Y. (1995) Alangionosides C–F, Megastigmane Glycosides from *Alangium premnifolium*, *Phytochemistry 38*, 1431–1435.

144. Kijima, H., Otsuka, H., Ide, T., Ogimi, C., Hirata, E., Takushi, A., and Takeda, Y. (1996) Glycosides of Megastigmane and of the Simple Alcohols from *Alangium premnifolium*, *Phytochemistry 42*, 723–727.

145. Otsuka, H., Zhong, X.-N., Hirata, E., Shinzato, T., and Takeda, Y. (2001) Myrsinionosides A–E: Megastigmane Glycosides from the Leaves of *Myrsine seguinii* Lev., *Chem. Pharm. Bull. 49*, 1093–1097.

146. Yu, Q., Otsuka, H., Hirata E., Shinzato, T., and Takeda, Y. (2002) Turpinionosides A–E: Megastigmane Glycosides from the Leaves of *Turpinia ternata*, *Chem. Pharm. Bull. 50*, 640–644.

147. Takeda, Y., Shimizu, H., Masuda, T., Hirata, E., Shinzato, T., Bando, M., and Otsuka, H. (2004) Lasianthionosides A–C, Megastigmane Glucosides from Leaves of *Lasianthus fordii*, *Phytochemistry 65*, 485–489.

148. Takeda, Y., Zhang, H., Masuda, T., Honda, G., Otsuka, H., Sezik, E., Yesilada, E., and Sun, H. (1997) Megastigmane Glucosides from *Stachys byzantina*, *Phytochemistry 44*, 1335–1337.

149. Matsuda, N., Isawa, K., and Kikuchi, M. (1997) Megastigmane Glycosides from *Lonicera gracilipes* var. *glandulosa*, *Phytochemistry 45*, 777–779.

150. Ito, H., Kobayashi, E., Li, S.-H., Hatano, T., Sugita, D., Kubo, N., Shimura, S., Itoh, Y., and Yoshida, T. (2001) Megastigmane Glycosides and an Acylated Triterpenoid from *Eriobotrya japonica*, *J. Nat. Prod. 64*, 737–740.

151. Ito, H., Kobayashi, E., Li, S.-H., Hatano, T., Sugita, D., Kubo, N., Shimura, S., Itoh, Y., Tokuda, H., Nishino, H., and Yoshida, T. (2002) Antitumor Activity of Compounds Isolated from Leaves of *Eriobotrya japonica*, *J. Agric. Food Chem. 50*, 2400–2403.

152. Perry, L.M. (1980) *Medicinal Plants of East and Southeast Asia*, pp. 342–343, Massachusetts Institute of Technology Press, Cambridge.

153. Mohamed, K.M., Mohamed, M.H., Ohtani, K., Kasai, R., and Yamasaki, K. (1999) Megastigmane Glycosides from Seeds of *Trifolium alexandrinum*, *Phytochemistry 50*, 859–862.

154. Amer, M., El-Habibi, E.-S., and El-Gendy, A. (2004) Effects of *Trifolium alexandrinum* Extracts on Streptozotocin-Induced Diabetes in Male Rats, *Ann. Nutr. Metabol. 48*, 343–347.

155. Humpf, H.-U., and Schreier, P. (1992) 3-Hydroxy-5,6-epoxy-β-ionol β-D-Glucopyranoside and 3-Hydroxy-7,8-dihydro-β-ionol β-D-Glucopyranoside: New C_{13} Norisoprenoid Glucoconjugates from Sloe Tree *(Prunus spinosa* L.) Leaves, *J. Agric. Food Chem. 40*, 1898–1901.

156. Osorio, C., Duque, C., and Batista-Viera, F. (2003) Studies on Aroma Generation in Lulo (*Solanum quitoense*): Enzymatic Hydrolysis of Glycosides from Leaves, *Food Chem. 81*, 333–340.

157. Bader, A., Braca, A., De Tommasi, N., and Morelli, I. (2003) Further Constituents from *Caralluma negevensis*, *Phytochemistry 62*, 1277–1281.

158. Zheng, Q., Xu, Z., Sun, X., Yao, W., Sun, H., Cheng, C.H.K., and Zhao, Y. (2003) Eudesmane and Megastigmane Glucosides from *Laggera alata*, *Phytochemistry 63*, 835–839.

159. Ma, S.J., Watanabe, N., Yagi, A., and Sakata, K. (2001) The

(3*R*,9*R*)-3-Hydroxy-7,8-dihydro-β-ionol Disaccharide Glycoside Is an Aroma Precursor in Tea Leaves, *Phytochemistry 56*, 819–825.

160. Kanchanapoom, T., Kasai, R., Chumsri, P., Hiraga, Y., and Yamasaki, K. (2001) Megastigmane and Iridoid Glucosides from *Clerodendrum inerme, Phytochemistry 58*, 333–336.

161. Kanchanapoom, T., Kasai, R., Picheansoonthon, C., and Yamasaki, K. (2001) Megastigmane, Aliphatic Alcohol and Benzoxazinoid Glycosides from *Acanthus ebracteatus, Phytochemistry 58*, 811–817.

162. Kamel, M.S., Mohamed, K.M., Hassanean, H.A., Ohtani, K., Kasai, R., and Yamasaki, K. (2000) Iridoid and Megastigmane Glycosides from *Phlomis aurea*, *Phytochemistry 55*, 353–357.

163. Ling, S.-K., Takashima, T., Tanaka, T., Fujioka, T., Mihashi, K., and Kouno, I. (2004) A New Diglycosyl Megastigmane from *Carallia brachiata, Fitoterapia 75*, 785–788.

164. Zhang, Y., Cichewicz, R.H., and Nair, M.G. (2004) Lipid Peroxidation Inhibitory Compounds from Daylily (*Hemerocallis fulva*) Leaves, *Life Sci. 75*, 753–763.

165. Michalska, K., and Kisel, W. (2004) Taxonomically Significant Guaianolides from *Taraxacum obovatum*, *Biochem. Syst. Ecol. 32*, 765–768.

166. Peipp, H., Maier, W., Schmidt, J., Wray, V., and Strack, D. (1997) Arbuscular Mycorrhizal Fungus-Induced Changes in the Accumulation of Secondary Compounds in Barley Roots, *Phytochemistry 44*, 581–587.

167. Kanchanapoom, T., Chumsri, P., Kasai, R., Otsuka, H., and Yamasaki, K. (2003) Lignan and Megastigmane Glycosides from *Sauropus androgynus, Phytochemistry 63*, 985–988.

168. Ohashi, K., Winarno, H., Mukai, M., Inoue, M., Prana, M.S., Simanjuntak, P., and Shibuya, H. (2003) Indonesian Medicinal Plants. XXV. Cancer Cell Invasion Inhibitory Effects of Chemical Constituents in the Parasitic Plant *Scurrula atropurpurea* (Loranthaceae), *Chem. Pharm. Bull. 51*, 343–345.

169. Morikawa, H., Kasai, R., Otsuka, H., Hirata, E., Shinzato, T., Aramoto, M., and Takeda, Y. (2004) Terpenic and Phenolic Glycosides from Leaves of *Breynia officinalis* HEMSL, *Chem. Pharm. Bull. 52*, 1086–1090.

170. Ishikawa, T., Kondo, K., and Kitajima, J. (2003) Water Soluble Constituents of Coriander, *Chem. Pharm. Bull. 51,* 32–39.

171. De Marino, S., Borbone, N., Zollo, F., Ianaro, A., Di Meglio, P., and Iorizzi, M. (2004) Megastigmane and Phenolic Components from *Laurus nobilis* L. Leaves and Their Inhibitory Effects on Nitric Oxide Production, *J. Agric. Food Chem. 52*, 7525–7531.

172. Nagatani, Y., Warashina, T., and Noro, T. (2001) Studies on the Constituents from the Aerial Part of *Baccharis dracunculifolia* DC, *Chem. Pharm. Bull. 49,* 1388–1394.

173. Liu, J., Li, B., Ma, R., and Chen, B. (2004) Inhibitory Effect on Mammary Carcinoma Cells Induced by β-Ionone, *Wei Sheng Yan Jiu (in Chinese) 33*, 151–157.

174. Duncan, R.E., Lau, D., El-Sohemy, A., and Archer, M.C. (2004) Geraniol and β-Ionone Inhibit Proliferation, Cell Cycle Progression, and Cyclin-Dependent Kinase 2 Activity in MCF-7 Breast Cancer Cells Independent of Effects on HMG-CoA Reductase Activity, *Biochem. Pharmacol. 68*, 1739–1747.

175. Liu, J.R., Yang, B.F., Chen, B.Q., Yang, Y.M., Dong, H.W., and Song, Y.Q. (2004) Inhibition of β-Ionone on SGC-7901 Cell Proliferation and Upregulation of Metalloproteinases-1 and -2 Expression, *World J. Gastroenterol. 10*, 167–171.

176. D'Abrosca, B., DellaGreca, M., Fiorentino, A., Monaco, P., Oriano, P., and Temussi, F. (2004) Structure Elucidation and Phytotoxicity of C$_{13}$ Nor-isoprenoids from *Cestrum parqui*, *Phytochemistry 65*, 497–505.

177. Kandler, O. (1993) Archaea (Archaebacteria), *Prog. Bot. 54*, 1–24.

178. Herbert, R.A., and Sharp, R.J. (eds.) (1992) *Molecular Biology and Biotechnology of Extremophiles*, Blackie, Glasgow.

179. Boucher, Y., Kamekura, M., and Doolittle, W.F. (2004) Origins and Evolution of Isoprenoid Lipid Biosynthesis in Archaea, *Mol. Microbiol. 52*, 515–527.

180. Cubonova, L., and Smigan, P. (2004) Unique Lipids and Structures of Membranes in Archaebacteria, *Chem. Listy 98*, 75–79.

181. Sehgal, S.N., Kates, M., and Gibbons, N.E. (1962) Lipids of *Halobacterium cutirubrum*, *Can. J. Biochem. Physiol. 40*, 69–81.

182. Kates, M., Sastry, P.S., and Yengoyan, L.S. (1963) Isolation and Characterization of a Diether Analog of Phosphatidyl Glycerophosphate from *Halobacterium cutirubrum*, *Biochim. Biophys. Acta 70*, 705–707.

183. Kates, M., Palameta, B., Perry, M.P., and Adams, G.A. (1967) A New Glycolipid Sulfate Ester in *Halobacterium cutirubrum, Biochim. Biophys. Acta 137*, 213–216.

184. Kates, M., and Deroo, P.W. (1973) Structure Determination of the Glycolipid Sulfate from the Extreme Halophile *Halobacterium cutirubrum, J. Lipid Res. 14*, 438–445.

185. Smallbone, B.W., and Kates, M. (1981) Structural Identification of Minor Glycolipids in *Halobacterium cutirubrum, Biochim. Biophys. Acta 665*, 551–558.

186. Evans, R.W., Kushwaha, S.C., and Kates, M. (1980) The Lipids of *Halobacterium marismortui*, an Extremely Halophilic Bacterium in the Dead Sea, *Biochim. Biophys. Acta 619*, 533–544.

187. Kushwaha, S.C., Kates, M., Juez, G., Rodriguez-Valera, F., and Kushner, D.J. (1982) Polar Lipids of the Extremely Halophilic Bacterial Strain (R-4) Isolated from Salt Ponds in Spain, *Biochim. Biophys. Acta 711*, 19–27.

188. Sprott, G.D., Larocque, S., Cadotte, N., Dicaire, C.J., McGee, M., and Brisson, J.R. (2003) Novel Polar Lipids of Halophilic Eubacterium *Planococcus* H8 and Archaeon *Haloferax volcanii*, *Biochim. Biophys. Acta 1633,* 179–188.

189. Fiete, D.J., Beranek, M.C., and Baenziger, J.U. (1998) A Cysteine-rich Domain of the "Mannose" Receptor Mediates GalNAc-4-SO$_4$ Binding, *Proc. Natl. Acad. Sci. USA 95*, 2089–2093.

190. Matsubara, T., Iida-Tanaka, N., Kamekura, M., Moldoveanu, N., Ishizuka, I., Onishi, H., Hayashi, A., and Kates, M. (1994) Polar Lipids of a Non-alkaliphilic Extremely Halophilic Archaebacterium Atrain 172: A Novel Bis-sulfated Glycolipid, *Biochim. Biophys. Acta 1214*, 97–108.

191. Koga, Y., Nishihara, M., Morii, H., and Akagawa-Matsushita, M. (1993) Ether Polar Lipids of Methanogenic Bacteria: Structures, Comparative Aspects, and Biosyntheses, *Microbiol. Rev. 57*, 164–182.

192. Ferrante, G., Eldel, I., and Sprott, G.D. (1986) Structural Characterization of the Lipids of *Methanococcus voltae*, Including a Novel *N*-Acetylglucosamine 1-Phosphate Diether, *J. Biol. Chem. 261*, 17062–17066.

193. Nishihara, M., and Koga, Y. (1987) Extraction and Composition of Polar Lipids from the Archaebacterium, *Methanobacterium thermoautotrophicum*: Effective Extraction of Tetraether Lipids by an Acidified Solvent, *J. Biochem. 101*, 997–1005.

194. Nishihara, M., and Koga, Y. (1990) Natural Occurrence of Archaetidic Acid and Caldarchaetidic Acid (di- and tetraether analogues of phosphatidic acid) in the Archaebacterium *Methanobacterium thermoautotrophicum, Biochem. Cell Biol. 68*, 91–95.

195. Nishihara, M., Mori, H., and Koga, Y. (1987) Structure Determination of a Quartet of Novel Tetraether Lipids from *Methanobacterium thermoautotrophicum*, *J. Biochem. 101*, 1007–1015.

196. Nishihara, M., Mori, H., and Koga, Y. (1989) Heptads of Polar

Ether Lipids of an Archaebacterium, *Methanobacterium thermoautotrophicum*: Structure and Biosynthetic Relationship, *Biochemistry 28*, 95–102.

197. Jones, W.J., Leigh, J.A., Mayer, F., Woese, C.R., and Wolfe, R.S. (1983) *Methanococcus jannaschii* sp. nov., an Extremely Thermophilic Methanogen from a Submarine Hydrothermal Vent, *Arch. Microbiol. 136*, 254–261.
198. Comita, P.B., Gagosian, R.B., Pang, H., and Costello, C.E. (1984) Structural Elucidation of a Unique Macrocyclic Membrane Lipid from a New, Extremely Thermophilic, Deep Sea Hydrothermal Vent Archaebacterium, *Methanococcus jannaschii, J. Biol. Chem. 259*, 15234–15241.
199. Kushwaha, S.C., Kates, M., Sprott, G.D., and Smith, I.C.P. (1981) Novel Polar Lipids from the Methanogen *Methanospirillum hungatei* GP1, *Biochim. Biophys. Acta 664*, 156–173.
200. Sprott, G.D., Ferrante, G., and Ekiel, I. (1994) Tetraether Lipids of *Methanospirillum hungatei* with Head Groups Consisting of Phospho-*N,N*-dimethylaminopentanetetrol, Phospho-*N,N,N*-trimethylamino-pentanetetrol and Carbohydrates, *Biochim. Biophys. Acta 1214*, 234–242.
201. Ferrante, G., Ekiel, I., Patel, G.B., and Sprott, G.D. (1988) A Novel Core Lipid Isolated from the Aceticlastic Methanogen, *Methanothrix concilii* GP6, *Biochim. Biophys. Acta 963*, 173–182.
202. Ferrante, G., Brisson, J.-R., Patel, G.B., Eldel, I., and Sprott, G.D. (1989) Structures of Minor Ether Lipids Isolated from the Aceticlastic Methanogen, *Methanothrix concilii* GP6, *J. Lipid Res. 30*, 1601–1609.
203. Ferrante, G., Ekiel, I., Patel, G.B., and Sprott, G.D. (1988) Structure of the Major Polar Lipids Isolated from the Aceticlastic Methanogen, *Methanothrix concilii* GP6, *Biochim. Biophys. Acta 963*, 162–172.
204. Nishihara, M., and Koga, Y. (1991) Hydroxyarchaetidylserine and Hydroxyarchaetidyl-myo-inositol in *Methanosarcina barkeri*: Polar Lipids with a New Ether Core Portion, *Biochim. Biophys. Acta 1082*, 211–217.
205. Upasani, V.N., Desai, S.G., Moldoveanu, N., and Kates, M. (1994) Lipids of Extremely Halophilic Archaeobacteria from Saline Environments in India: A Novel Glycolipid in *Natronobacterium* Strains, *Microbiology 140*, 1959–1966.
206. Batrakov, S.G., Pivovarova, T.A., Esipov, S.E., Sheichenko, V.I., and Karavaiko, G.I. (2002) β-D-Glucopyranosyl Caldarchaetidylglycerol Is the Main Lipid of the Acidophilic, Mesophilic, Ferrous Iron-Oxidising Archaeon *Ferroplasma acidiphilum, Biochim. Biophys. Acta 1581*, 29–35.
207. Shimada, H., Nemoto, N., Shida, Y., Oshima, T., and Yamagishi, A. (2002) Complete Polar Lipid Composition of *Thermoplasma acidophilum* HO-62 Determined by High Performance Liquid Chromatography with Evaporative Light-Scattering Detection, *J. Bacteriol. 184*, 556–563.
208. Uda, I., Sugai, A., Kon, K., Ando, S., Itoh, Y.H., and Itoh, T. (1999) Isolation and Characterization of Novel Neutral Glycolipids from *Thermoplasma acidophilum, Biochim. Biophys. Acta 1439*, 363–370.
209. Uda, I., Sugai, A., Shimizu, A., Itoh, Y.H., and Itoh, T. (2000) Glucosylcaldarchaetidylglycerol, a Minor Phosphoglycolipid from *Thermoplasma acidophilum, Biochim. Biophys. Acta 1484*, 83–86.
210. Brock, T.D., Brock, K.M., Belly, R.T., and Weiss, R.L. (1972) *Sulfolobus*: A New Genus of Sulfur-Oxidizing Bacteria Living at Low pH and High Temperature, *Arch. Mikrobiol. 84*, 54–68.
211. Sugai, A., Sakuma, R., Fukuda, I., Kurosawa, N., Itoh, Y.H., Kon, K., Ando, S., and Itoh, T. (1995) The Structure of the Core Polyol of the Ether Lipids from *Sulfolobus acidocaldarius, Lipids 30*, 339–344.
212. Kates, M. (1992) Archaebacterial Lipids: Structure, Biosynthesis, and Function, in *The Archaebacteria: Biochemistry and*

Biotechnology (Dawson, M.J., Hough, D.W., and Lunt, G.G., eds.), pp. 51–72, Portland Press, London.
213. De Rosa, M., Esposito, E., Gambacorta, A., Nicolaus, B., and Bu'Lock, J.D. (1980) Complex Lipids of *Caldariella acidophila*, a Thermoacidophile Archaebacterium, *Phytochemistry 19*, 821–825.
214. De Rosa, M., Esposito, E., Gambacorta, A., Nicolaus, B., and Bu'Lock, J.D. (1980) Effects of Temperature on Ether Lipid Composition of *Caldariella acidophila, Phytochemistry 19*, 827–831.
215. De Rosa, M., Gambacorta, A., and Nicolaus, B. (1983) A New Type of Cell Membrane, in Thermophilic Archaebacteria, Based on Bipolar Ether Lipids, *J. Memb. Sci. 16*, 287–294.
216. Benvegnu, T., Brard, M., and Plusquellec, D. (2004) Archaeabacteria Bipolar Lipid Analogues: Structure, Synthesis and Lyotropic Properties, *Curr. Opin. Colloid Interface Sci. 8*, 469–479.
217. Lehn, J.M. (1990) Perspectives in Supramolecular Chemistry—From Molecular Recognition Towards Molecular Information Processing and Self-Organization, *Angew. Chem. Int. Edit. Engl. 29*, 1304–1319.
218. Gambacorta, A., Gliozzi, A., and De Rosa, M. (1995) Archaeal Lipids and Their Biotechnological Applications, *World J. Microbiol. Biotechnol. 11*, 115 –131.
219. Arakawa, K., Eguchi, T., and Kakinuma, K. (2001) Highly Thermostable Liposome from 72-Membered Macrocyclic Tetraether Lipid: Importance of 72-Membered Lipid for Archaea to Thrive Under Hyperthermal Environments, *Chem. Lett. 5*, 440–441.
220. Arakawa, K., Eguchi, T., and Kakinuma, K. (2001) 36-Membered Macrocyclic Diether Lipid Is Advantageous for Archaea to Thrive Under the Extreme Thermal Environments, *Bull. Chem. Soc. Jpn. 74*, 347–356.
221. Lecollinet, G., Auzely-Velty, R., Danel, M., Benvegnu, T., Mackenzie, G., Goodby, J.W., and Plusquellec, D. (1999) Synthetic Approaches to Novel Archaeal Tetraether Glycolipid Analogues, *J. Org. Chem. 64*, 3139–3150.
222. Lecollinet, G., Gulik, A., Mackenzie, G., Goodby, J.W., Benvegnu, T., and Plusquellec, D. (2002) Supramolecular Self-Assembling Properties of Membrane-Spanning Archaeal Tetraether Glycolipid Analogues, *Chem. Eur. J. 8*, 585–593.
223. Benvegnu, T., Lecollinet, G., Guilbot, J., Roussel, M., Brard, M., and Plusquellec, D. (2003) Novel Bolaamphiphiles with Saccharide Polar Headgroups: Synthesis and Supramolecular Self-Assemblies, *Polymer Internat. 52*, 500–506.
224. Sprott, G.D., Patel, G.B., and Krishnan, L. (2003) Archaeobacterial Ether Lipid Liposomes as Vaccine Adjuvants, *Methods Enzymol. 373*, 155–172.
225. Patel, G.B., and Sprott, G.D. (1999) Archaeobacterial Ether Lipid Liposomes (archaeosomes) as Novel Vaccine and Drug Delivery Systems, *Crit. Rev. Biotechnol. 19*, 317–357.
226. Smith, D.W., Harrell, W.K., and Randall, H.M. (1954) Correlation of Biologic Properties of Strains of *Mycobacterium* with Their Infrared Spectrums. III. Differentiation of Bovine and Human Varieties of *M. tuberculosis* by Means of Their Infrared Spectrums, *Am. Rev. Tuber. 66*, 505–510.
227. Goren, M.B. (1990) Mycobacterial Fatty Esters of Sugars and Sulfosugars, in *Handbook of Lipid Research: Glycolipids, Phospholipids and Sulfoglycolipids* (Kates, M., ed.), Vol. 6, pp. 363–461, Plenum Press, New York.
228. Gastambide-Odier, M., Sarda, P., and Lederer, E. (1965) Structure des Aglycones des Mycosides A et B, *Tetrahedron Lett. 35*, 3135–3143.
229. Gastambide-Odier, M., and Sarda, P. (1970) Contributions à l'étude de la Structure et de la Biosynthèse de Glycolipides Spécifiques Isolés de Mycobactéries. Les Mycosides A et B, *Pneumologie 142*, 241–255.

230. Fournié, J.J., Rivière, M., Papa, F., and Puzo, G. (1987) Structural Elucidation of the Major Phenolic Glycolipid from *Mycobacterium kansasii.* II. Presence of a Novel Dideoxyhexose, *J. Biol. Chem. 262*, 3180–3184.

231. MacLennan, A.P., Randall, H.M., and Smith, D.W. (1961) The Occurrence of Methyl Ethers of Rhamose and Fucose in Specific Glycolipids of Certain Mycobacteria, *Biochem. J. 80*, 309–318.

232. Gastambide-Odier, M., and Vilk, C. (1970) Deoxysugars Isolated from Mycoside A: Identification of Acetyl Derivatives of Methyl 2,4-Di-*O*-methyl-rhamnopyranoside, 2-*O*-Methyl-rhamnofuranoside, 3-*O*-Methyl-rhamnofuranoside, 2-*O*-Methyl-fucopyranoside and 3-*O*-Methyl-fucofuranoside, *Bull. Soc. Chim. Biol. (Paris) 52*, 679–693.

233. Hunter, S.W., and Brennan, P.J. (1981) A Novel Phenolic Glycolipid from *Mycobacterium leprae* Possibly Involved in Immunogenicity and Pathogenicity, *J. Bacteriol. 147*, 728–735.

234. Mehra, V., Brennan, P.J., Rada, E., Convit, J., and Bloom, B.R. (1984) Lymphocyte Suppression in Leprosy Induced by Unique *M. leprae* Glycolipid, *Nature 308*, 194–196.

235. Wolinsky, E. (1979) Nontuberculous Mycobacteria and Associated Diseases, *Am. Rev. Respir. Dis. 119*, 107–159.

236. Young, D.B. (2001) Leprosy Lipid Provides the Key to Schwann Cell Entry, *Trends Microbiol. 9*, 52–54.

237. Hartmann, S., and Minnikin, D.E. (1992) Mycobacterial Phenolic Glycolipids, in *Surfactants in Lipid Chemistry: Recent Synthetic, Physical, and Biodegradative Studies*, pp. 135–158, Royal Society of Chemistry, London.

238. Puzo, G. (1990) The Carbohydrate- and Lipid-Containing Cell Wall of Mycobacteria, Phenolic Glycolipids: Structure and Immunological Properties, *Crit. Rev. Microbiol. 17*, 305–327.

239. Watanabe, M., Aoyagi, Y., Ohta, A., and Minnikin, D.E. (1997) Structures of Phenolic Glycolipids from *Mycobacterium kansasii, Eur. J. Biochem. 248*, 93–98.

240. Riviere, M., Fournie, J.J., Vercellone, A., and Puzo, G. (1988) Particular Matrix for Fast Atom Bombardment Mass Spectrometric Analysis of Phenolic Glycolipid Antigens Isolated from Pathogen Mycobacteria, *Biomed. Environ. Mass Spectrom. 16*, 275–278.

241. Vercellone, A., Riviére, M., Fournié, J.-J., and Puzo, G. (1988) Structural Analogy Between the Major Phenolic Glycolipid Antigens from 2 *Mycobacteria* Species—*kansasii* and *gastri*, *Chem. Phys. Lipids 48*, 129–134.

242. Watanabe, M., Yamada, Y., Iguchi, K., and Minnikin, D.E. (1994) Structural Elucidation of New Phenolic Glycolipids from *Mycobacterium tuberculosis, Biochim Biophys Acta 1210*, 174–180.

243. Barry, C.E., III, Lee, R.E., Mdluli, K., Sampson, A.E., Schroeder, B.G., Slayden, R.A., and Yuan, Y. (1998) Mycolic Acids: Structure, Biosynthesis and Physiological Functions, *Prog. Lipid Res. 37*, 143–179.

244. Stodola, F.H., Lesuk, A., and Anderson, R.J. (1938) The Chemistry of the Lipids of Tubercle Bacilli. LIV. The Isolation and Properties of Mycolic Acid, *J. Biol. Chem. 126*, 505–513.

245. Asselineau, J., and Lederer, E. (1950) Structure of the Mycolic Acids of Mycobacteria, *Nature 166*, 782–783.

246. Asselineau, J., Ganz, E., and Lederer, E. (1951) The Chemical Structure of α- and β-Mycolic Acids from a Virulent Human Strain of *Mycobacterium tuberculosis*, *C.R. Hebd. Seances Acad. Sci. 232*, 2050–2052.

247. Besra, G.S., Bolton, R.C., McNeil, M.R., Ridell, M., Simpson, K.E., Glushka, J., van Halbeek, H., Brennan, P.J., and Minnikin, D.E. (1992) Structural Elucidation of a Novel Family of Acyltrehaloses from *Mycobacterium tuberculosis, Biochemistry 31*, 9832–9837.

248. Minnikin, D.E., Kremer, L., Dover, L.G., and Besra G.S. (2002) The Methyl-Branched Fortifications of *Mycobacterium tuberculosis, Chem. Biol. 9*, 545–553.

249. Koch, R. (1952) Tuberculosis Etiology, *Dtsch. Gesundheitsw. 7*, 457–465.

250. Beekman, E.M., Porcelli, S.A., Morita, C.T., Behar, S.M., Furlong, S.T., and Brenner, M.B. (1994) Recognition of a Lipid Antigen by CD1-Restricted α-β(+) T-Cells, *Nature 372*, 691–694.

251. Moody, D.B., Reinhold, B.R., Reinhold, V.N., Besra, G.S., and Porcelli, S.A. (1999) Uptake and Processing of Glycosylated Mycolates for Presentation to CD1b-Restricted T Cells, *Immunol. Lett. 65*, 85–91.

252. Jackman, R.M., Moody, D.B., and Porcelli, S.A. (1999) Mechanisms of Lipid Antigen Presentation by CD1, *Crit. Rev. Immunol. 19*, 49–63.

253. Watanabe, M., Aoyagi, Y., Mitome, H., Fujita, T., Naoki, H., Ridell, M., and Minnikin, D.E. (2002) Location of Functional Groups in Mycobacterial Meromycolate Chains: The Recognition of New Structural Principles in Mycolic Acids, *Microbiology 148*, 1881–1902.

Stability of Fatty Acyl-Coenzyme A Thioester Ligands of Hepatocyte Nuclear Factor-4α and Peroxisome Proliferator-Activated Receptor-α

Friedhelm Schroeder[a], Huan Huang[a], Heather A. Hostetler[a], Anca D. Petrescu[a],
Rachel Hertz[b], Jacob Bar-Tana[b], and Ann B. Kier[c],*

[a]Department of Physiology and Pharmacology, Texas A&M University, TVMC, College Station, Texas 77843-4467,
[b]Department of Human Nutrition and Metabolism, Hebrew University Medical School, Jerusalem 91120, Israel,
and [c]Department of Pathobiology, Texas A&M University, TVMC, College Station, Texas 77843-4467

ABSTRACT: Although long-chain fatty acyl-coenzyme A (LCFA-CoA) thioesters are specific high-affinity ligands for hepatocyte nuclear factor-4α (HNF-4α) and peroxisome proliferator-activated receptor-α (PPARα), X-ray crystals of the respective purified recombinant ligand-binding domains (LBD) do not contain LCFA-CoA, but instead exhibit bound LCFA or have lost all ligands during the purification process, respectively. As shown herein: (i) The acyl chain composition of LCFA bound to recombinant HNF-4α reflected that of the bacterial LCFA-CoA pool, rather than the bacterial LCFA pool. (ii) Bacteria used to produce the respective HNF-4α and PPARα contained nearly 100-fold less LCFA-CoA than LCFA. (iii) Under conditions used to crystallize LBD (at least 3 wk at room temperature in aqueous buffer), 16:1-CoA was very unstable in buffer alone. (iv) In the presence of the respective nuclear receptor (i.e., HNF-4α and PPARα), LBD 70–75% of 16:1-CoA was degraded after 1 d at room temperature in the crystallization buffer, whereas as much as 94–97% of 16:1-CoA was degraded by 3 wk. (v) Cytoplasmic LCFA-CoA binding proteins such as acyl-CoA binding protein, sterol carrier protein-2, and liver-FA binding protein slowed the process of 16:1-CoA degradation proportional to their respective affinities for this ligand. Taken together, these data for the first time indicated that the absence of LCFA-CoA in the crystallized HNF-4α and PPARα was due to the paucity of LCFA-CoA in bacteria as well as to the instability of LCFA-CoA in aqueous buffers and the conditions used for LBD crystallization. Furthermore, instead of protecting bound LCFA-CoA from autohydrolysis like several cytoplasmic LCFA-CoA binding proteins, these nuclear receptors facilitated LCFA-CoA degradation.

Paper no. L9730 in *Lipids 40*, 559–568 (June 2005).

Abbreviations: 16:1-CoA, palmitoleoyl-coenzyme A; 17:0-CoA, *n*-heptadecanoyl-coenzyme A; aa, amino acid; ACBP, acyl CoA-binding protein; CoA, coenzyme A; HNF-4α (aa 1–455), full-length hepatocyte nuclear factor 4α; HNF-4α-E (aa 132–370), N- and C-terminal truncation mutant of HNF-4α comprising aa 132–410 (i.e., ligand-binding domain E, but missing the negative regulatory domain F and the DNA-binding domain); HNF-4α-E-F (aa 132–455), N-terminal truncation mutant of HNF-4α comprising aa 132–455 (i.e., ligand-binding domain E and negative-regulatory domain F, but missing the DNA-binding domain); HNF-4α-E-0.5F (aa 132–410), N- and C-terminal truncation mutant of HNF-4α comprising aa 132–410 (i.e., ligand-binding domain E, but missing half of the negative-regulatory domain F and all of the DNA-binding domain); LBD, ligand-binding domain; LCFA, long-chain fatty acid; LCFA-CoA, long-chain fatty acyl CoA; L-FABP, liver fatty acid-binding protein; MPD, 2-methyl-2,4-pentanediol; PPARα, peroxisome proliferator-activated receptor-α, RARα, retinoic acid receptor-α; RXRα, retinoid X receptor α; SCP-2, sterol carrier protein-2.

Two members of the nuclear receptor superfamily, hepatocyte nuclear factor-4α (HNF-4α) and peroxisome proliferator-activated receptor-α (PPARα), bind coenzyme A (CoA) thioesters of long-chain FA (LCFA, C_{14}–C_{22}) in *in vitro* binding assays (1–7). Although early radioligand competition binding assays showed these proteins exhibiting only weak affinities (i.e., μM K_i) for LCFA-CoA (1,6), subsequent direct fluorescence binding assays demonstrated that both HNF-4α (2–4) and PPARα (7) exhibited high affinities (i.e., low nM K_d) for LCFA-CoA. Furthermore, in the case of HNF-4α this high affinity for LCFA-CoA was dependent on the presence of an intact F domain C-terminal to the ligand-binding domain (LBD). Deletion of the F domain abolished LCFA-CoA binding and enhanced that of LCFA (4). The molecular basis for the discrepancy reported in affinities obtained between radioligand competition and fluorescence binding assays is based on the fact that radioligand competition assays are known to significantly underestimate the affinities of ligand-binding proteins for LCFA-CoA and LCFA (8,9). For example, cytoplasmic LCFA-CoA-binding proteins such as acyl-CoA-binding protein (ACBP), sterol carrier protein-2 (SCP-2), and liver FA-binding protein (L-FABP) exhibit M K_d in radioligand binding assays (reviewed in Refs. 8 and 10), whereas those obtained with fluorescence and titration calorimetry binding assays display a 100- to 1000-fold stronger affinity (10–13).

Although PPARα is widely recognized as a ligand-inducible nuclear receptor that is activated only when specific ligands (e.g., peroxisome proliferators, LCFA, nonhydrolyzable LCFA-CoA, etc.) are present in cells (reviewed in Refs. 5, 7, 14, and 15), the transcriptional activity of HNF-4α in the liver, intestine, or pancreas as a function of specific ligands has been highly debated. For instance, some authors considered HNF-4α to be a constitutively active and ligand-independent nuclear receptor, even though its modular structure includes the LBD (16). In contrast, other groups demonstrated that various LCFA (C_{14}–C_{22}) were able to modulate the transcriptional activity of HNF-4α by reporter gene assays in transfected COS-7 cells in culture (1,3). In addition, overexpression of fatty acyl CoA synthase enhanced the ability of LCFA to modulate the transcriptional activity of HNF-4α, whereas overexpression of fatty acyl CoA hydrolase inhibited the ability of LCFA to modulate the transcriptional activity of HNF-4α (1). Furthermore, it was shown that purified full-length HNF-4α and truncation mutants

with an intact LBD and C-terminal F domain had an affinity for the CoA thioesters of LCFA several orders of magnitude higher than for the corresponding free LCFA *in vitro* (1–4).

Despite the above data indicating that both PPARα and HNF-4α bind LCFA-CoA with high affinity, the crystal structures of the LBD of PPARα (17) and HNF-4α (18,19) do not contain endogenously bound LCFA-CoA. Instead, these truncated proteins contain either no endogenously bound ligand, as for the PPARα LBD (17), or, in the case of the HNF-4α LBD, contain constitutively bound LCFA that do not influence the open vs. closed conformational state of the HNF-4α LBD. However, LCFA-CoA is known to alter PPARα conformation, as demonstrated by circular dichroism (7), and a nonhydrolyzable LCFA-CoA analog is known to alter PPAR LBD conformation, as evidenced by sensitivity to protease digestion and the ability to bind to co-activators (7,20). Likewise, LCFA-CoA and nonhydrolyzable LCFA-CoA analogs (but not LCFA) alter the conformation of full-length HNF-4α as well the HNF-4α LBD containing the C-terminal F domain (2,4,21). Such ligand-induced conformational changes are a hallmark of ligand-activated nuclear receptors (reviewed in Refs. 2 and 22–25).

Although the molecular basis for the above discrepancies is not yet known, at least three possibilities may be considered: First, the level of endogenous LCFA-CoA may be very small as compared with that of LCFA in the bacteria used to produce the recombinant truncated PPARα and HNF-4α constructs. Second, the FFA detected within the binding site of HNF-4α LBD by X-ray crystallography may arise from residual LCFA formed by degradation of CoA thioesters during the crystallization process. Third, truncation of the C-terminal F domain, especially long in HNF-4α, significantly alters the ligand specificity of the recombinant N- and C-terminal truncation proteins used for crystallography (4). The purpose of the present work was: (i) to examine the relative proportions of LCFA-CoA and LCFA in the recombinant bacteria, (ii) to show the stability of LCFA-CoA in the context of protein crystallization conditions; (iii) to show the effect of nuclear receptors that bind LCFA-CoA, i.e., HNF-4α and PPARα, on LCFA-CoA stability; and (iv) to determine the stability of LCFA-CoA in the context of the cytoplasmic LCFA-CoA-binding proteins ACBP, SCP-2, and L-FABP.

MATERIALS AND METHODS

Materials. Palmitoleoyl-CoA (16:1-CoA) and *n*-heptadecanoyl-CoA (17:0-CoA) were purchased from Sigma Chemical Co. (St. Louis, MO). Protease inhibitor cocktail, ultralow range color markers for SDS-PAGE, gel filtration M.W. markers (range 6,500–66,000 Da), alkaline phosphatase conjugated goat anti-rabbit IgG, alkaline phosphatase conjugated rabbit anti-goat IgG, and 5-bromo-4-chloro-3-indolyl-phosphate/nitroblue tetrazolium (BCIP/NBT) for Western analysis were purchased from Sigma-Aldrich (St. Louis, MO). Protein concentration was determined by the Bradford method using Protein Assay Dye Reagent Concentrate purchased from Bio-Rad Laboratories (Richmond, CA).

Rabbit polyclonal anti-rat HNF-4-LBD antisera were prepared according to Association for Assessment and Accreditation of Laboratory Animal Care (AAALAC) guidelines and further purified by affinity chromatography on protein-A-sepharose as described earlier (26). Rabbit polyclonal anti-mouse PPARα antibodies were from Affinity BioReagents (Golden, CO). Polyclonal antisera to murine recombinant L-FABP, human recombinant SCP-2 (12), and murine recombinant ACBP (28,29) were prepared as described (29) in the cited papers. The specificity of appropriate dilutions of the purified antibodies was determined as described earlier (30). None of the antisera cross-reacted with proteins other than the one against which the antisera were raised.

Expression and purification of recombinant full-length and deletion mutant forms of rat HNF-4α. The full-length rat HNF-4α [amino acids (aa) 1–455] and the N-terminal deletion mutant HNF-4α-E-F (aa 132–455) recombinant proteins were obtained as described previously (1,2). The cDNA of the rat C-terminal truncation mutant lacking the entire F domain, HNF-4α-E (aa 132–455) was obtained by PCR using the sense 5′-CATGC-CATGGGCAGCCATCATCATCATCATCACAGGTCAAGC-TACGAG and antisense 5′-GAAGATCTCTAGGCAGACC-CTCCAAG primers. Rat N-terminal His-tagged HNF-4α1 (aa 132–410) recombinant was prepared by PCR using the sense 5′-CATGCCATGGGCAGCCATCATCATCATCATCACAGGT-CAAGCTACGAG and antisense 5′-GAAGATCTCTAGGTG-GACATCTGTCC primers. The PCR products were cloned into pET11d plasmid. The recombinants plasmids were expressed in the *Escherichia coli* BL21(DE3)pLyS strain, and the His-tagged proteins were purified by affinity chromatography on nickel nitrilotriacetic resin (Qiagen, Chatsworth, CA) and stored at −70°C. Purity of the recombinant proteins was assessed by SDS-PAGE and Western blotting as described earlier (2–4).

Expression and purification of recombinant PPARα-ΔAB (aa 101–468). The cDNA encoding mouse PPARα with a deletion of the amino-terminal A/B domain (i.e., encoding PPARα aa 101–468) cloned into a $(His)_6$-tagged bacterial expression vector (pET-PPARα-ΔAB) was a gift from Dr. Noa Noy (Cornell University, Ithaca, NY) (31). Recombinant PPARα-ΔAB protein was expressed in BL21(DE3)pLysS strain of *E. coli* and purified by affinity chromatography with cobalt resin (BD Biosciences, Clontech, Palo Alto, CA) as described earlier (7). The purified recombinant PPARα-ΔAB protein eluting from the column was dialyzed against a buffer containing 10 mM Hepes (pH 8.0), 0.1 mM EDTA, 1 mM DTT, 400 mM KCl, and 10% glycerol, and stored in 25% glycerol at −80°C. Protein purity was assessed by SDS-PAGE and Western blotting as described earlier (7,31).

Expression and purification of recombinant ACBP, SCP-2, and L-FABP. Murine recombinant L-FABP (27), human recombinant SCP-2 (12), and murine recombinant ACBP (28,29) were purified as described in the cited papers. Protein purity was also determined by SDS-PAGE, silver staining, and Western blotting as described therein.

Analysis of LCFA-CoA content and distribution in purified recombinant HNF-4α and in E. coli cells expressing HNF-4α. After a known amount of 17:0-CoA internal standard was added

to each sample, total LCFA-CoA were extracted from purified full-length HNF-4α (aa 1–455), HNF-4α truncation mutants (i.e., HNF-4α-E, aa 132–370, and HNF-4α-E-F, aa 132–455), and cell homogenate of *E. coli* expressing full-length HNF-4α, by a solid-phase extraction procedure (32). The LCFA-CoA were then converted to fluorescent etheno CoA esters and resolved by HPLC with fluorescence detection (33). Comparison with the known standard LCFA-CoA in this procedure allowed determination of the total mass of LCFA-CoA/mg protein, mass of the individual LCFA-CoA species/mg protein, and relative percentage distribution of individual LCFA-CoA species basically as described earlier (34).

Analysis of free LCFA content of purified recombinant HNF-4α and E. coli expressing HNF-4. Purified full-length HNF-4α and bacterial cell homogenate were analyzed for total FFA using a Waco NEFA C test kit (Waco Chemicals USA, Inc., Richmond, VA) following the procedures provided by the manufacturer. A reagent blank, specimen blank, and standard curve with a known amount of FA were run as suggested.

Determination of HNF-4α protein concentration in E. coli expressing HNF-4α. *E. coli* cells expressing HNF-4α were lysed by sonication in the presence of protease inhibitor cocktail used for purification of His-tagged proteins from Sigma. The unbroken cells and debris were removed by centrifugation at $50,000 \times g$ for 10 min at 4°C. The supernatant was used to determine: (i) total protein by the BCA Protein Assay kit from Pierce (Rockford, IL) and (ii) HNF-4α protein by SDS-PAGE and Western blot analysis as described previously (2,26). Quantitative estimation of HNF-4α protein in Western blots was performed by densitometric analysis after image acquisition using a single-chip CCD (charge-coupled device) video camera and a computer workstation (IS-500 system; Alpha Innotech, San Leandro, CA). Image files were analyzed (mean 8-bit gray-scale density) using NIH Image (available by anonymous FTP). To obtain the HNF-4α protein concentration in the bacterial lysate supernatant samples, the HNF-4α pixel density in Western blots of bacterial lysate supernatant samples was compared with that of known amounts of pure recombinant His-tagged HNF-4α protein run as standards on the same blot.

Stability of LCFA-CoA under conditions used to crystallize N- and C-terminal truncation mutants of HNF-4α: Effect of ACBP. Equal concentrations of the three most prevalent cytosolic acyl-CoA binding proteins (ACBP, SCP-2, L-FABP), full-length HNF-4α (aa 1–455), HNF-4α-E-F (aa 132–455), HNF-4α-E-F (aa 132–410), and HNF-4α-E (aa 132–370) were individually incubated with 16:1-CoA (1:1 molar ratio of protein to 16:1-CoA) at room temperature in a buffer system previously described for HNF-4α-E (aa 132–382) crystallization [0.1 M sodium citrate, pH 8.0, 0.7 M ammonium acetate, 16% 2-methyl-2,4-pentanediol (MPD), and 10 mM DTT] (18). 16:1-CoA in buffer only was used as a blank for autohydrolysis in the absence of protein under the same conditions. After 1 d, 1 wk, and 3 wk, aliquots of the mixtures were taken and a known amount of 17:0-CoA internal standard was added to each sample as well as to a fresh aliquot of 16:1-CoA in buffer

without protein and without incubation. The amount of remaining 16:1-CoA was determined by extracting the 16:1-CoA using a solid-phase extraction procedure (32), converting the 16:1-CoA to fluorescent etheno CoA esters (33), and analyzing by HPLC with a fluorescence detector (33) as described earlier (34).

Stability of LCFA-CoA in the crystallization buffer used in PPARα LBD X-ray studies. PPARα-ΔAB or ACBP, both at 0.5 µM, were incubated with equimolar 16:1-CoA at room temperature in each of the following buffers previously used for PPARα LBD protein crystallization: (i) buffer 1 (5.5–9.6% PEG 35K, 50 mM di-ammonium hydrogen citrate, pH 4.9, 50 mM 1,3-bis-tris-propane (BTP), pH 7.0, 10% MPD (35); (ii) buffer 2 (10 mM Tris, pH 8.0, 75 mM sodium chloride, 5% glycerol, 0.5 mM tris-2-carboxyethyl)-phosphine hydrochloride, 1.6 M sodium formate, 50 mM Hepes, pH 7.5) (17). 16:1-CoA alone without added protein was used in each buffer for comparison. After 1 d, 1 wk, and 3 wk, aliquots of the mixtures were analyzed for remaining 16:1-CoA as compared with fresh 16:1-CoA controls and fresh 17:0-CoA that was added to each sample as an internal control. To determine the amount of each fatty acyl-CoA remaining, the fatty acyl-CoA were extracted by solid-phase extraction (33), converted to fluorescent etheno CoA esters, and analyzed by HPLC (33).

RESULTS

LCFA-CoA content of purified recombinant HNF-4α proteins. *In vitro* ligand-binding assays have clearly shown that recombinant full-length HNF-4α exhibits affinity for LCFA-CoA several orders of magnitude higher than LCFA in solution (1–4). Basically similar data are obtained with N-terminal truncation mutants containing the complete E and F domains (1–4). However, heretofore there have been no reports examining the presence of endogenously bound LCFA-CoA in purified recombinant full-length HNF-4α or in N-terminal truncation mutants of HNF-4α containing the complete E and F domains. Therefore, the content of LCFA-CoA in recombinant full-length HNF-4α (aa 1–455), as well as in its truncation mutants HNF-4α-EF (aa 132–455) and HNF-4α-E (aa 132–370), in solution was determined as described in the Materials and Methods section. However, no LCFA-CoA were detected in either the full-length HNF-4α (aa 1–455) or its truncation mutants containing the complete ligand-binding E and negative-regulatory F domains, i.e., HNF-4α-E-F (aa 132–455). Interestingly, the N-terminal and C-terminal truncation mutant HNF-4α-E (aa 132–370) also did not contain any detectable endogenously bound LCFA-CoA. The latter observation confirmed earlier data from X-ray crystals of such N- and C-terminal HNF-4α truncation mutants that contained bound LCFA, but not LCFA-CoA (18,19).

LCFA-CoA and free LCFA content of E. coli expressing the full-length HNF-4α. It is important to consider that not only the affinity for LCFA-CoA vs. LCFA but also the relative availability of the respective ligands in *E. coli* will contribute to the

TABLE 1
FFA and Long-Chain Fatty Acyl-Coenzyme A (LCFA-CoA) Content of *Escherichia coli* Cells Expressing Hepatocyte Nuclear Factor-4α (HNF-4α)[a]

Ligand	Ligand/total protein (nmol /mg)	Ligand/HNF-4α (nmol/mg)	Ligand/HNF-4α (mol/mol)
FFA	4.95 ± 0.62	396 ± 50	20
LCFA-CoA	0.055 ± 0.005	4.36 ± 0.36	0.22
FFA/LCFA-CoA	91:1	91:1	91:1

[a]Data presented are mean ± SE ($n = 5$).

type of endogenous ligand associated with HNF-4α and its mutants. Therefore, this possibility was examined in *E. coli* overexpressing the full-length HNF-4α. The contents of LCFA, LCFA-CoA, and HNF-4α were determined as described in the Materials and Methods section. As shown in Table 1, bacterial cells expressing the full-length HNF-4α contained 4.95 ± 0.62 nmol LCFA/mg total protein, equivalent to 396 ± 50 nmol LCFA/mg HNF-4α. When expressed on a molar basis, the molar ratio of LCFA/HNF-4α was 20:1. In contrast, *E. coli* contained much less LCFA-CoA, only 54.5 ± 4.5 pmol/mg total bacterial protein (Table 2). When expressed on the basis of HNF-4α content, this was equivalent to 4.36 ± 0.36 nmol LCFA-CoA/mg HNF-4α (Table 1). Thus, the molar ratio of LCFA-CoA/HNF-4α in bacterial extract was only 0.22:1.

LCFA-CoA composition of E. coli cells expressing HNF-4α. The acyl chain length and level of saturation of endogenous LCFA associated with HNF-4α constructs isolated from bacterial extracts differ substantially from that present in bacteria (3,18). For example, even though 16:0 and 18:1 are the most abundant LCFA present in *E. coli*, full-length HNF-4α (Hertz, R., personal communication), HNF-4α-E-F (aa 132–455) (3), or HNF-4α (aa 132–383) (19) contain 50–65% of 16:1, an LCFA barely detectable in bacteria (3,36). This finding cannot be explained simply on the basis of differences in affinities of the HNF-4α constructs (1–4). Instead, high endogenous 16:1 bound to HNF-4α constructs might reflect that in the bacterial LCFA-CoA pool, rather than in the LCFA pool. Hydrolysis of the bound LCFA-CoA during recombinant protein isolation could then account for the high endogenous 16:1 associated with the HNF-4α constructs. To examine this possibility, the acyl chain composition of bacterial LCFA-CoA was determined by HPLC analysis after solid-phase extraction of bacterial LCFA-CoA. The results showed that the most abundant LCFA-CoA was 16:1-CoA (34.9 ± 1.1%), followed by significantly less 16:0-CoA (13.8 ± 0.4%) and 18:1-CoA (25.8 ± 1.0%) (Table 2). Thus, the acyl chain composition of the bacterial LCFA-CoA pool, rather than that of the LCFA pool, re-

flected the acyl chain distribution of endogenously bound LCFA in recombinant HNF-4α constructs.

Stability of LCFA-CoA under protein crystallization conditions. Since X-ray crystallography detects only endogenous LCFA bound in N- and C-terminal truncation mutants of HNF-4α and HNF-4γ (19), it was concluded that only LCFA are endogenous ligands of HNF-4α and HNF-4γ (18,19). However, no data were provided supporting the assumption that LCFA-CoA were stable under the stringent crystallization conditions used therein. To begin to resolve this issue, the stability of 16:1-CoA under crystallization conditions (19) was tested, as described in the Materials and Methods section. In the crystallization buffer at 24°C, 16:1-CoA quickly decomposed. As quickly as 1 d at room temperature, 75% of the 16:1-CoA was degraded (Fig. 1A). Since crystals were typically formed over periods ranging in weeks, the stability was also examined after 1 and 3 wk. Only 13 and 6.6% of the 16:1-CoA remained intact after 1 and 3 wk, respectively (Fig. 1A). Thus, nearly 94% of 16:1-CoA was degraded by 3 wk, the time used for crystallizing the HNF-4α N- and C-terminal F domain truncation mutant (19). Thus, the instability of LCFA-CoA in solution, together with the lengthy isolation procedure required for isolating the recombinant proteins and, even more so, the 3 or more weeks at room temperature required for crystallization of such proteins, likely contributed to the lack of detectable endogenously bound LCFA-CoA therein.

Effect of HNF-4α (full-length and truncation mutants) on LCFA-CoA stability as compared with other LCFA-CoA-binding proteins under protein crystallization conditions. Although it has been hypothesized that cytosolic LCFA-CoA-binding proteins may protect LCFA-CoA from being hydrolyzed by intracellular esterases (reviewed in Refs. 8, 27, and 37), nothing is known regarding the effect of either cytosolic or nuclear LCFA-CoA-binding proteins on the autohydrolysis of LCFA-CoA in buffer alone, especially under protein crystallization conditions. To assess whether LCFA-CoA are protected from autodegradation in the buffer by association with a binding protein, the effects of several LCFA-CoA-binding proteins were examined.

First, the effect of intracellular LCFA-CoA-binding proteins such as ACBP, SCP-2, and L-FABP was examined. These cytosolic proteins bind LCFA-CoA with affinities in the order ACBP ≥ SCP-2 > L-FABP (reviewed in Refs. 8, 9, 11, and 12). When these proteins were individually incubated at 1:1 molar ratio with 16:1-CoA under conditions used to crystallize HNF-4α (i.e., crystallization buffer at room temperature), only the

TABLE 2
Composition of LCFA-CoA Thioesters of *E. coli* Cells Expressing Recombinant Rat HNF-4α[a]

LCFA-CoA	%	LCFA-CoA	%
16:0	13.8 ± 0.4	18:1	25.8 ± 1.0
16:1	34.9 ± 1.1	20:0	12.1 ± 1.4
18:0	5.8 ± 0.9		

[a]For abbreviations see Table 1.

highest-affinity proteins (ACBP, SCP-2) significantly reduced, but did not completely prevent, 16:1-CoA hydrolysis (Fig. 1B). The lower-affinity protein L-FABP was without effect (Fig. 1B). After 1 d in the presence of ACBP, SCP-2, or L-FABP, the majority of LCFA-CoA was degraded: 63, 65, and 80%, respectively (Fig. 1B). Thereafter, at longer incubation times only ACBP significantly protected 16:1-CoA from hydrolysis, albeit 81% of available 16:1-CoA was still hydrolyzed after 3 wk (Fig. 1B).

Second, the effects of the nuclear receptor HNF-4α (full-length) and HNF-4α deletion mutants on LCFA-CoA stability were similarly tested. Although full-length HNF-4α (aa 1–455) exhibits high affinity (i.e., nM K_d) for LCFA-CoA in *in vitro* binding assays (2–4), this did not protect LCFA-CoA from degradation. Instead, full-length HNF-4α (aa 1–455) enhanced hydrolysis as compared with incubation in the buffer alone: nearly 10-fold accelerated conversion of LCFA-CoA to free LCFA within 1 d of incubation and total degradation at longer incubation times (Fig. 1A). Similarly, the N-terminal DNA-binding domain deletion construct, i.e., HNF-4α-E-F (aa 132–455), also exhibits high affinity (i.e., nM K_d) for LCFA-CoA in *in vitro* binding assays (2–4), but it did not protect LCFA-CoA from degradation. Instead, 16:1-CoA hydrolysis was enhanced ninefold within 1 d of incubation, followed by total degradation at longer time points (Fig. 1A). Surprisingly, the N-terminal and partial C-terminal F domain deletion construct, HNF-4α-E-0.5F (aa 132–410), showed some protection against 16:1-CoA hydrolysis during the first day of incubation but not thereafter, since 16:1-CoA was degraded to the same high extent as in the crystallization buffer only at longer incubation times (Fig. 1A). The N-terminal and C-terminal F domain deletion construct, HNF-4α-E (aa 132–370), comprising only the LBD, only weakly binds LCFA-CoA in *in vitro* binding assays (4) and had no or little effect on LCFA-CoA degradation. At 1 d and 1 wk of incubation, 16:1-CoA hydrolysis was the same in the presence of HNF-4α-E (aa 132–370) as for buffer alone. Only at 3 wk incubation did HNF-4α-E (aa 132–370) slightly enhance 16:1-CoA hydrolysis as compared with buffer alone.

Stability of LCFA-CoA in the presence of PPARα vs. ACBP. To determine whether the unusual effect of HNF-4α to enhance LCFA-CoA degradation was a unique feature of this nuclear regulatory protein, the effect of another nuclear receptor that binds LCFA-CoA, i.e., PPARα (7,20), on LCFA-CoA stability was examined. Despite the high affinity (very low nM K_d) PPARα displays for LCFA-CoA, endogenously bound LCFA-CoA have also not been detected in X-ray crystal structures of PPARα LBD (17,35). To begin to address this issue, the possibility that LCFA-CoA are unstable under PPARα crystallization conditions was considered. To test the stability of LCFA-CoA under crystallization conditions, aliquots of 16:1-CoA were incubated in the absence or presence of added LCFA-CoA binding protein (i.e., PPARα or ACBP) in two types of buffers previously used to crystallize recombinant PPARα-LBD protein as described in the Materials and Methods section (17,35).
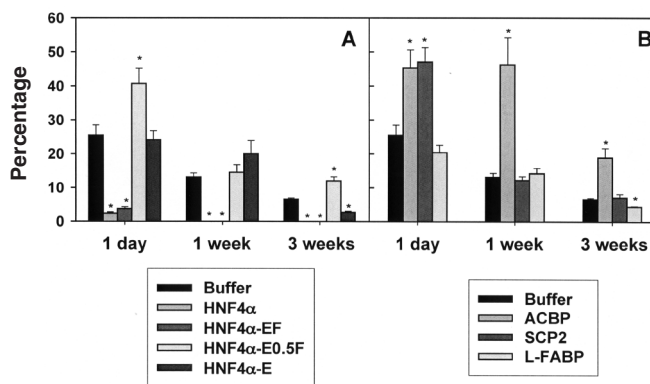
FIG. 1. Long-chain fatty acyl-coenzyme A (LCFA-CoA) stability under hepatocyte nuclear factor 4α (HNF-4α) crystallization conditions. 16:1-CoA was incubated in HNF-4α crystallization buffer (as described in the Materials and Methods section) in the absence or presence of proteins known to have affinity for LCFA-CoA, in a molar ratio of 1:1, for various time periods (1 d to 3 wk). (A) Percentage of 16:1-CoA recovered after incubation with full-length HNF-4α or truncated forms of HNF-4α, such as HNF-4α-E-F [amino acids (aa) 132–455; ligand-binding domain (LBD) E and negative-regulatory domain F, but missing the DNA-binding domain], HNF-4α-E-0.5F (aa 132–410; LBD E, but missing half of the negative-regulatory domain F and all of the DNA-binding domain), and HNF-4α-E (aa 132–370; LBD E, but missing the negative regulatory domain F and the DNA-binding domain). (B) Percentage 16:1-CoA recovered after incubation with acyl CoA-binding protein (ACBP), sterol carrier protein-2 (SCP-2), or liver FA-binding protein (L-FABP).

Solid-phase extraction was then used to determine the proportion of intact vs. hydrolyzed 16:1-CoA, as described in the Materials and Methods section.

In the absence of added LCFA-CoA binding protein (i.e., PPARα or ACBP), LCFA-CoA was very unstable in the incubation buffers and conditions (room temperature) used to crystallize PPARα LBD. Within 1 d of incubation, 70–75% of the 16:1-CoA was degraded (Figs. 2A,B). By 1 wk, 85–88% of the 16:1-CoA was degraded, and by 3 wk 86–97% was hydrolyzed (Fig. 2B). These data suggest that by the end of 3–6 wk, typical conditions used to crystallize the PPARα LBD protein, almost no LCFA-CoA would remain intact. However, it must be considered that protein-bound ligands are typically thought to be more stable in solution than free ligands. Therefore, the aforementioned experiments with the two crystallization buffers were repeated in the presence of LCFA-CoA binding proteins (i.e., PPARα or ACBP).

Recently, it was shown that PPAR is a nuclear receptor that binds LCFA-CoA (15) with very high affinity (low nM K_d) (7). However, the data indicate that in the presence of the LCFA-CoA binding protein PPARα, 16:1-CoA was not protected from degradation (Fig. 2). Instead, depending on the buffer used and the time period examined, PPAR enhanced 16:1-CoA degradation by 2- to 10-fold (Fig. 2). In any case, by 3 wk of incubation all of the 16:1-CoA was degraded in the presence of PPARα, regardless of the buffer used.

Although ACBP is primarily a cytosolic protein, low
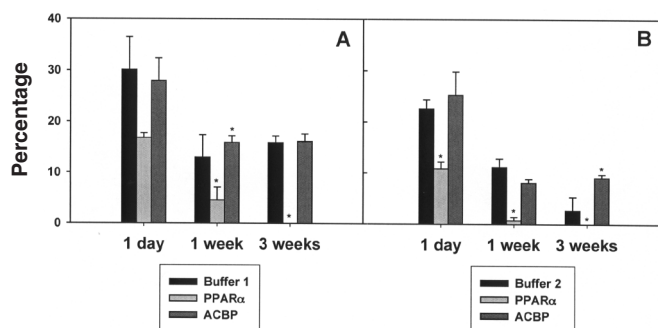
FIG. 2. LCFA-CoA stability under peroxisome proliferator-activated receptor-α (PPARα) crystallization conditions. 16:1-CoA was incubated in two different buffers that were previously used to crystallize the PPARα LBD (as described in the Materials and Methods section) in the absence or presence of PPARα and ACBP. (A) Buffer 1, as described in the Materials and Methods section. (B) Buffer 2, as described in the Materials and Methods section. For other abbreviations see Figure 1.

amounts of ACBP are detected in nuclei, where it interacts with nuclear receptors to influence transcriptional activity (26). Similar to PPARα, ACBP exhibits very high affinity (very low nM K_d) for LCFA-CoA (8,11,38). In contrast to PPARα, however, ACBP did not accelerate LCFA-CoA degradation but, depending on the buffer used, actually protected 16:1-CoA from hydrolysis. In buffer 2 (Fig. 2B), but not buffer 1 (Fig. 2A), ACBP protected 16:1-CoA from degradation at long time points, i.e., 3 wk, but not at short time points. As shown above, ACBP was even more protective of 16:1-CoA degradation in another buffer (i.e., 0.75 M ammonium phosphate, pH 5.0, and 10 mM DTT) used to crystallize HNF-4α truncation mutants (Fig. 1B).

DISCUSSION

Despite the importance of nuclear receptors such as HNF-4α and PPARα in glucose and FA metabolism, relatively little is known regarding the nature of the endogenous ligands, and in particular LCFA-CoA associated with these proteins.

A wide body of evidence is consistent with LCFA-CoA as putative endogenous, physiologically significant ligands of these nuclear receptors: (i) *In vitro* ligand-binding assays performed with the respective full-length proteins (or their N-terminal truncation constructs containing intact C-terminal F domains) clearly demonstrate that these nuclear receptors bind LCFA-CoA in aqueous buffers with equal (PPARα) (7,20) or considerably higher (HNF-4α) (2–4) affinities than exhibited for LCFA. (ii) The nM K_d obtained for LCFA-CoA binding by direct fluorescence binding assays (2–4,7) are in the same range as the concentration of LCFA-CoA in the nucleus of living cells (34). (iii) LCFA-CoA, but not LCFA, alter the conformation of HNF-4α (1–4,21) and PPARα (7,20). However, under other *in vitro* conditions only slight (39) or no (16) effects on conformation of HNF-4α were observed. (iv) Normal LCFA-CoA and nonhydrolyzable LCFA-CoA modulate the transactivation of HNF-4α in living cells (3,4,38). (v) Several investigators used purified recombinant HNF-4α to show that LCFA-CoA,

but not LCFA, regulate HNF-4α homodimer formation and DNA binding (gel mobility shift) *in vitro* (1,40). This action is analogous to LCFA-CoA regulating the binding of Fad-R (an *E. coli* DNA-binding protein) to its cognate DNA response element *in vitro* (41). However, the finding that LCFA-CoA regulates HNF-4α homodimer formation and DNA binding may depend on the exact conditions used for this *in vitro* assay (16,39). (vi) Recombinant purified PPARα has been used to show that LCFA-CoA or nonhydrolyzable LCFA-CoA analog binding increases PPARα co-activator recruitment (7). (vii) Manipulation of cellular LCFA-CoA levels affects HNF-4α transcriptional activity consistent with LCFA-CoA being endogenous HNF-4α ligands: Fatty acyl-CoA synthase overexpression enhances HNF-4α-mediated transactivation, whereas overexpression of fatty acyl-CoA hydrolase inhibits HNF-4α-mediated transactivation in living cells (1). Also, treatment with the fatty acyl-CoA synthase inhibitor triacsin C prevents suppression of HNF-4α transcriptional activity by inhibitory proligands (3).

In contrast to these findings, X-ray crystallographic analysis does not detect the presence of LCFA-CoA as endogenously bound ligands in HNF-4α and PPARα. Unfortunately, the X-ray crystallographic studies are limited by the inability to crystallize the full-length HNF-4α and PPARα. Thus, all available data were obtained with truncation mutants missing the DNA-binding domain and all or most of the C-terminal F domain. For example, X-ray analysis of crystalline recombinant LBD of both PPARα (17,35) and HNF-4α (18,19) does not contain any endogenously bound LCFA-CoA. In the case of PPARα, it is not yet completely clear whether the absence is due to the fact that the truncated nuclear receptors used for X-ray crystallography do not reflect the properties of the full-length PPARα or whether other factors contribute to the loss of LCFA-CoA. With regard to crystals of HNF-4α-E (i.e., the LBD) missing both the N-terminal DNA-binding domain and most of the C-terminal F negative regulatory domain, these crystals contain bound LCFA but not LCFA-CoA (18,19). *In vitro* binding assays performed in solution show that the truncated HNF-4α-E only binds LCFA with high affinity, but not LCFA-CoA (4), opposite to what was observed with the full-length HNF-4α or constructs containing the intact C-terminal F negative regulatory domain (2–4). In summary, the X-ray crystallographic findings with truncated proteins in the absence of water may not necessarily accurately reflect the endogenously bound ligand distribution of the respective full-length proteins in solution. As shown in the present investigation, several additional properties of LCFA-CoA and the nuclear receptors themselves also contribute to the inability to detect endogenously bound LCFA-CoA in these proteins.

First, the acyl chain distribution of the endogenously bound LCFA (3,18,19) reflected that of the bacterial LCFA-CoA pool (Table 2) rather than that of bacterial LCFA (3,18,19). Analysis of the LCFA associated with a variety of HNF-4α constructs revealed that 16:1 accounted for 50–65% of the total acyl chains of wild type HNF-4α (3,18,19). Although bacterial LCFA are enriched in 16:0 and 18:1, the level of 16:1 is barely

detectable in bacterial LCFA (3,18,19). In contrast, within the bacterial LCFA-CoA pool the 16:1-CoA was the single most prevalent LCFA-CoA (present data).

Second, the relative proportions of LCFA-CoA and LCFA in the recombinant bacteria heavily favored the availability of LCFA over LCFA-CoA for binding to the recombinant nuclear receptor proteins and their truncation mutants. The bacteria contained nearly 100-fold more LCFA than LCFA-CoA. Furthermore, the total concentration of LCFA-CoA was so low as to be sufficient for binding to only 20% of the available HNF-4α. Thus, even if the endogenous LCFA-CoA was not degraded during isolation of the respective recombinant proteins or by the nuclear receptors themselves, the vast majority of available nuclear receptor ligand-binding sites would be expected to be occupied by LCFA rather than LCFA-CoA.

Third, LCFA-CoA were unstable in the aqueous buffers used to isolate HNF-4α and PPARα or to crystallize the respective N- and C-terminal truncation mutants of HNF-4α and PPARα. Nearly 75–80% of LCFA-CoA was degraded by 1 d incubation in buffer alone. By 3 wk or longer, the incubation typically required to obtain crystalline protein, more than 97% of LCFA-CoA was degraded. Thus, the intrinsic instability of LCFA-CoA thioesters in aqueous buffers alone can significantly contribute to the inability to detect endogenously bound LCFA-CoA in the full-length nuclear receptors in solution or in crystals of truncation mutant proteins.

Fourth, although it is commonly assumed that bound ligands are more stable than in solution, this was the case for cytoplasmic LCFA-CoA binding proteins, but not the nuclear LCFA-CoA binding proteins. For example, the cytoplasmic LCFA-CoA-binding proteins ACBP, SCP-2, and L-FABP bound and protected LCFA-CoA from degradation directly in proportion to their relative affinities for this ligand. ACBP exhibits not only the highest affinity for LCFA-CoA in this group (reviewed in Refs. 8, 11, and 38), but was the most protective of LCFA-CoA hydrolysis. In fact, freshly isolated recombinant ACBP contains some detectable endogenously bound LCFA-CoA (42). In contrast, neither HNF-4α nor PPARα protected LCFA-CoA from degradation, but instead significantly accelerated LCFA-CoA hydrolysis by nearly 10- and 2-fold, respectively, within 1 d of incubation. Longer incubation periods reduced LCFA-CoA levels to almost nothing. Therefore, it is not surprising that despite the high affinities of full-length HNF-4α (aa 1–455) for LCFA-CoA, lipid extraction of full-length HNF-4α (aa 1–455) or HNF-4α truncation mutants and subsequent analysis did not detect the presence of endogenously bound LCFA-CoA (3,4,18,19). Instead, endogenously bound LCFA was detected even though LCFA is a much lower-affinity ligand for the respective proteins.

Together, the latter findings suggest that this enzymatic activity of nuclear receptors could operate to shut down LCFA-CoA-induced transcription activation/inhibition by LCFA-CoA processing such that it would not further affect the transcription activation function. Most models of molecular mechanisms underlying the ligand-induced activation function of nuclear receptors do not explain how the ligand effect is dimin-

ished and eliminated after the fact of modulation. Several possibilities could be considered: (i) The ligand is chemically modified (esterified, hydrolyzed, etc.) so that its binding in the LBD is reduced. In this case, the enzymatic activity required to modify the bound ligand could either be the nuclear receptor itself (as shown herein for HNF-4α and PPARα) or an entirely different protein proximal to it; (ii) complex formation of nuclear receptor molecules with co-activators/co-repressors may induce further conformational changes of the nuclear receptor, resulting in reduced affinity for the ligand and even its release from the binding site. Our data demonstrated that, like HNF-4α, PPARα hydrolyzed LCFA-CoA to free LCFA, and the effect of the catalytic activity of these nuclear receptors on the ligand-induced transcriptional activation function deserves further study. Taken together, these findings may help to explain the absence of endogenously bound LCFA-CoA, the presence of endogenously bound LCFA, and the acyl composition of the endogenously bound LCFA detected in a variety of recombinant HNF-4α proteins (3,19).

Finally, although the exact identity and structure of the esterase sites in HNF-4α and PPARα remain to be determined, comparisons with known long-chain acyl-CoA hydrolases/thioesterases may provide some insights. Long-chain acyl-CoA hydrolases/thioesterases are enzymes that catalyze the hydrolysis of fatty acyl-CoA to the corresponding FFA and CoA. Long-chain acyl-CoA hydrolases from rat liver microsomes (43,44), from rat liver and brain cytosol (45,46), and from rat liver mitochondria and peroxisomes (47,48) have been purified and characterized, demonstrating a wide variety of structures and mechanisms of catalysis. The long-chain acyl-CoA hydrolases from liver and brain cytosol are serine or cysteine-dependent esterases with a catalytic triad consisting of a nucleophile (serine or cysteine), an acidic group (aspartic or glutamic acid), and a histidine (43,46). Other forms of acyl-CoA hydrolases like those found in mitochondria and peroxisomes have an active site serine motif (Gly-X-Ser-X-Gly) common to carboxyl esterases and lipases in general (47,48). Although the existing X-ray crystal structures do not provide structural data on the F domain in HNF-4α (19,49) or in HNF-4γ (coded by a completely different gene and sharing only 37% sequence homology in the F domain with that of HNF-4α) (18), structural and sequence comparison with other long-chain acyl-CoA hydrolases/thioesterases suggests several possibilities comprising a potential hydrolytic/esterasic site. With regard to the catalytic motif of typical esterases containing a Gly-X-Ser-X-Gly motif, analysis of the full-length HNF-4α aa sequence indicated that there was no Gly-X-Ser-X-Gly motif within the LBD E (aa 132–370), the negative regulatory domain F (aa 371–455), or in any other parts of the protein. However, several residues of Ser, Cys, Glu/Gln, Asp/Asn, and His were present within the LBD E (aa 132–370) and the negative regulatory domain F (aa 371–455), suggesting that the acyl-CoA hydrolytic activity of HNF-4α may be explained by a coordinated action of Ser/Cys, Glu/Gln (or Asp/Asn), and His residues forming a 3-D triad positioned around the acyl-CoA thioester linkage. These aa can be separated by a variable number of aa, as long as the active

head groups are in the proper orientation to form a triad. The data presented herein demonstrated that only full-length HNF-4α (aa 1–455) and the truncation mutant containing the entire F domain (aa 132–455) exhibited acyl-CoA hydrolysis. In contrast, the truncation mutants containing a small part of the F domain (i.e., aa 132–410) or no F domain at all (i.e., aa 132–370) had no hydrolytic activity. Examination of the X-ray crystal structure of a truncated HNF-4α comprising the LBD (aa 132–382) (19,49) suggests that Cys246 and Glu184 are close to the carboxylic end of the FFA within the FA binding site. Only one histidine residue (His218) is present in the LBD (aa 132–382), but this residue is not close to the bound FA or FA carboxylate. Instead, the His involved in the catalytic activity could be provided by a histidine-rich sequence within the F domain (i.e., aa 371–455 containing His375, His377, His378, His381, His383, His388, and His402). The fact that the HNF-4α truncation mutant consisting of aa 132–410 did not exhibit acyl-CoA hydrolysis indicated that at least one of the three amino acids of the catalytic triad was missing. The HNF-4α F domain contains six serine residues (Ser427, Ser430, Ser432, Ser434, Ser436, and Ser452) and two Glu residues (Glu422 and Glu435) in the region between aa 411 to 455. These considerations would suggest that one or more of these Ser and/or His residues in the F domain, together with a Glu residue in the LBD E, could form a 3-D catalytic triad that accounts for the esterasic activity of HNF-4α.

Analysis of the PPARα aa sequence and structure (17) also suggests several possible esterasic motifs: (i) Analysis of the aa sequence of the LBD of PPARα reveals a potential SerX-HisXAsp motif (i.e., aa 414–418). However, as for the HNF-4α LBD, the crystal structure shows that these amino acids are not in the proper orientation/proximity to form an active esterase triad. (ii) Another potential esterase motif comprising Cys, Glu, His, and Asp is found at aa 191–194 of the PPARα (within the DNA-binding domain). However, since this region has not been crystallized, it is impossible to determine the orientation of the amino acids. Further, the presence of this region within the DNA-binding domain would suggest that it is not responsible for the acyl-CoA hydrolysis noted with the PPARα. (iii) Another potential esterase motif that may account for PPARα hydrolytic activity is composed of Gly, Ser, and Gly with one to two aa between them (50). Although a similar glycine- and serine-rich motif is present in the A/B domain of PPARα, comprising aa 42–50 (GlyXXSerSerGlySerXGly), this region is outside the area used for the crystallization studies and the recombinant protein used for the experiments described herein. Therefore, it is unlikely that this region was responsible for the acyl-CoA hydrolysis demonstrated in the Results section. (iv) Finally, a conserved motif of Cys, His, and Cys (formed by orientation rather than sequence order) has been suggested to serve as the catalytic site for thiolases (51). Examination of the X-ray crystal structure of PPARα reveals the presence of such a motif comprised of C278 folding in to interact with H274 and C275. The orientation of this motif and its location within the ligand-binding site suggests that this may represent an active thiolytic site. In summary, although the exact structure and location of the esterase sites in HNF-4α and PPARα are not known, examination of the respective aa sequences and available structures of truncation mutants of these proteins suggests several possible motifs consistent with those of known fatty acyl-CoA hydrolase/esterase enzymes.

REFERENCES

1. Hertz, R., Magenheim, J., Berman, I., and Bar-Tana, J. (1998) Fatty Acyl-CoA Thioesters Are Ligands of Hepatic Nuclear Factor-4α, Nature 392, 512–516.
2. Petrescu, A.D., Hertz, R., Bar-Tana, J., Schroeder, F., and Kier, A.B. (2002) Ligand Specificity and Conformational Dependence of the Hepatic Nuclear Factor-4α (HNF-4α), *J. Biol. Chem. 277*, 23988–23999.
3. Hertz, R., Ben-Haim, M., Petrescu, A., Kalderon, B., Berman, I., Eldad, N., Schroeder, F., and Bar-Tana, J. (2003) Rescue of MODY-1 by Agonist Ligands of HNF4α, *J. Biol. Chem. 278*, 22578–22585.
4. Petrescu, A., Huang, H., Hertz, R., Bar-Tana, J., Schroeder, F., and Kier, A.B. (2005) Role of Regulatory F-Domain in Hepatocyte Nuclear Factor-4α Ligand Specificity, *J. Biol. Chem. 280*, 16714–16727.
5. Elholm, M., Dam, I., Jorgenesen, C., Krogsdam, A.-M., Holst, D., Kratchamarova, I., Gottlicher, M., Gustafsson, J.A., Berge, R.K., Flatmark, T., Knudsen, J., Mandrup, S., and Kristiansen, K. (2001) Acyl CoA Esters Antagonize the Effects of Ligands on Peroxisome Proliferator Activated Receptor α Conformation, DNA Binding, and Interaction with Cofactors, *J. Biol. Chem. 276*, 21410–21416.
6. Murakami, K., Ide, T., Nakazawa, T., Okazaki, T., Mochizuki, T., and Kadowaki, T. (2001) Fatty Acyl CoA Thioesters Inhibit Recruitment of Steroid Receptor Co-activator 1 to α and γ Isoforms of Peroxisome Proliferator Activated Receptors by Competing with Agonists, *Biochem. J. 353*, 231–238.
7. Hostetler, H.A., Petrescu, A.D., Kier, A.B., and Schroeder, F. (2005) Peroxisome Proliferator Activated Receptor Alpha (PPARα) Interacts with High Affinity and Is Conformationally Responsive to Endogenous Ligands, *J. Biol. Chem. 280*, 18667–18682.
8. Gossett, R.E., Frolov, A.A., Roths, J.B., Behnke, W.D., Kier, A.B., and Schroeder, F. (1996) Acyl CoA Binding Proteins: Multiplicity and Function, *Lipids 31*, 895–918.
9. McArthur, M.J., Atshaves, B.P., Frolov, A., Foxworth, W.D., Kier, A.B., and Schroeder, F. (1999) Cellular Uptake and Intracellular Trafficking of Long Chain Fatty Acids, *J. Lipid Res. 40*, 1371–1383.
10. Knudsen, J., Jensen, M.V., Hansen, J.K., Faergeman, N.J., Neergard, T., and Gaigg, B. (1999) Role of Acyl CoA Binding Protein in Acyl CoA Transport, Metabolism, and Cell Signaling, *Mol. Cell. Biochem. 192*, 95–103.
11. Frolov, A.A., and Schroeder, F. (1998) Acyl Coenzyme A Binding Protein: Conformational Sensitivity to Long Chain Fatty Acyl-CoA, J. Biol. Chem. 273, 11049–11055.
12. Frolov, A., Cho, T.H., Billheimer, J.T., and Schroeder, F. (1996) Sterol Carrier Protein-2, a New Fatty Acyl Coenzyme A-Binding

Protein, *J. Biol. Chem. 271*, 31878–31884.

13. Frolov, A., Cho, T.H., Murphy, E.J., and Schroeder, F. (1997) Isoforms of Rat Liver Fatty Acid Binding Protein Differ in Structure and Affinity for Fatty Acids and Fatty Acyl CoAs, *Biochemistry 36*, 6545–6555.

14. Wahli, W., Devchand, P.R., Ijpenberg, A., and Desvergne, B. (1999) Fatty Acids, Eicosanoids, and Hypolipidemic Agents Regulate Gene Expression Through Direct Binding to Peroxisome Proliferator Activated Receptors, in *Lipoxygenases and Their Metabolites* (Nigam, S., and Pace-Asciak, C.R., eds.), pp. 199–209, Plenum Press, New York.

15. Ellinghaus, P., Wolfrum, C., Assmann, G., Spener, F., and Seedorf, U. (1999) Phytanic Acid Activates the Peroxisome Proliferator-Activated Receptor α (PPARα) in Sterol Carrier Protein-2-/Sterol Carrier Protein x-Deficient Mice, *J. Biol. Chem. 274*, 2766–2772.

16. Sladek, F.M., Ruse, M.D., Nepomuceno, L., Huang, S.-M., and Stallcup, M.R. (1999) Modulation of Transcriptional Activation and Coactivator Interaction by a Splicing Variation in the F Domain of Nuclear Receptor HNF4α, *Mol. Cell. Biol. 19*, 6509–6522.

17. Cronet, P., Peterson, J.F.W., Folmer, R., Blomberg, N., Sjoblom, K., Karlsson, U., Lindstedt, E.-L., and Bamberg, K. (2001) Structure of the PPARα and γ Ligand Binding Domain in Complex with AZ 242a: Ligand Selectivity and Agonist Activation in the PPAR Family, *Structure 9*, 699–706.

18. Wisely, G.B., Miller, A.B., Davis, R.G., Thornquest, A.D., Johnson, R., Spitzer, T., Sefler, A., Shearer, B., Moore, J.T., Miller, A.B., *et al.* (2002) Hepatocyte Nuclear Factor 4 Is a Transcription Factor That Constitutively Binds Fatty Acids, *Structure 10*, 1225–1234.

19. Dhe-Paganon, S., Duda, K., Iwamoto, M., Chi, Y.-I., and Shoelson, S.E. (2002) Crystal Structure of the HNF4α Ligand Binding Domain in Complex with Endogenous Fatty Acid Ligand, *J. Biol. Chem. 277*, 37973–37976.

20. Jorgensen, C., Krogsdam, A.-M., Kratchamarova, I., Willson, T.M., Knudsen, J., Mandrup, S., and Kristiansen, K. (2002) Opposing Effects of Fatty Acids and acyl-CoA Esters on Conformation and Cofactor Recruitment of Peroxisome Proliferator Activated Receptors, *Ann. N.Y. Acad. Sci. 967*, 431–439.

21. Hertz, R., Sheena, V., Kalderon, B., Berman, I., and Bar-Tana, J. (2001) Suppression of Hepatocyte Nuclear Factor 4α by Acyl-CoA Thioesters of Hypolipidemic Peroxisome Proliferators, *Biochem. Pharmacol. 61*, 1057–1062.

22. Francis, G.A., Fayard, E., Picard, F., and Auwerx, J. (2003) Nuclear Receptors and the Control of Metabolism, *Annu. Rev. Physiol. 65*, 261–311.

23. Xu, J., Nawaz, Z., Tsai, S.Y., Tsai, M.-J., and O'Malley, B.W. (1996) The Extreme C Terminus of the Progesterone Receptor Contains a Transcriptional Repressor Domain That Functions Through a Putative Corepressor, *Proc. Natl. Acad. Sci. USA 93*, 12195–12199.

24. Escher, P., and Wahli, W. (2000) Peroxisome Proliferator Activated Receptors: Insights into Multiple Cellular Functions, *Mutat. Res. 448*, 121–138.

25. Svensson, S., Osteberg, T., Jacobsson, M., Norstrom, C., Stefansson, K., Hallen, D., Johansson, I.C., Zachrisson, K., Ogg, D., and Jendeberg, L. (2003) Crystal Structure of the Heterodimeric Complex of LXRα and RXRβ Ligand Binding Domains in a Fully Agonistic Form, *EMBO J. 22*, 4625–4633.

26. Petrescu, A.D., Payne, H.R., Boedeker, A.L., Chao, H., Hertz, R., Bar-Tana, J., Schroeder, F., and Kier, A.B. (2003) Physical and Functional Interaction of Acyl CoA Binding Protein (ACBP) with Hepatocyte Nuclear Factor-4α (HNF4α), *J. Biol. Chem. 278*, 51813–51824.

27. Jolly, C.A., Wilton, D.A., and Schroeder, F. (2000) Microsomal Fatty Acyl CoA Transacylation and Hydrolysis: Fatty Acyl CoA Species Dependent Modulation by Liver Fatty Acyl CoA Binding Proteins, *Biochim. Biophys. Acta 1483*, 185–197.

28. Gossett, R.E., Edmondson, R.D., Jolly, C.A., Cho, T.H., Russell, D.H., Knudsen, J., Kier, A.B., and Schroeder, F. (1998) Structure and Function of Normal and Transformed Murine Acyl CoA Binding Proteins, *Arch. Biochem. Biophys. 350*, 201–213.

29. Chao, H., Martin, G., Russell, W.K., Waghela, S.D., Russell, D.H., Schroeder, F., and Kier, A. B. (2002) Membrane Charge and Curvature Determine Interaction with Acyl CoA Binding Protein (ACBP) and Fatty Acyl CoA Targeting, *Biochemistry 41*, 10540–10553.

30. Sambrook, J., Fritsch, E.F., and Maniatis, T. (1989) *Molecular Cloning: A Laboratory Manual*, 2nd edn., Cold Spring Harbor Laboratory, Cold Spring Harbor, NY.

31. Lin, Q., Ruuska, S.E., Shaw, N.S., Dong, D., and Noy, N. (1999) Ligand Selectivity of the Peroxisome Proliferator-Activated Receptor α, *Biochemistry 38*, 185–190.

32. Deutsch, J., Grange, E., Rapoport, S.I., and Purdon, A.D. (1994) Isolation and Quantitation of Long-Chain Acyl-Coenzyme A Esters in Brain Tissue by Solid-Phase Extraction, *Anal. Biochem. 220*, 321–323.

33. Larson, T.R., and Graham, I.A. (2001) A Novel Technique for the Sensitive Quantification of Fatty Acyl CoA Esters from Plant Tissues, *Plant J. 25*, 115–125.

34. Huang, H., Starodub, O., McIntosh, A., Atshaves, B.P., Woldegiorgis, G., Kier, A.B., and Schroeder, F. (2004) Liver Fatty Acid Binding Protein Colocalizes with Peroxisome Proliferator Receptor α and Enhances Ligand Distribution to Nuclei of Living Cells, *Biochemistry 43*, 2484–2500.

35. Xu, H.E., Stanley, T.B., Montana, V.G., Lambert, M.H., Shearer, B.G., Cobb, J.E., McKee, D.D., Galardi, C.M., Plunket, K.D., Nolte, R.T., *et al.* (2002) Structural Basis for Antagonist-Mediated Recruitment of Nuclear Co-repressors by PPARα, *Nature 415*, 813–817.

36. Cronan, J.E., Jr. (1975) Thermal Regulation of the Membrane Lipid Composition of *Escherichia coli*. Evidence for the Direct Control of Fatty Acid Synthesis, *J. Biol. Chem. 250*, 7074–7077.

37. Jolly, C.A., Chao, H., Kier, A.B., Billheimer, J.T., and Schroeder, F. (2000) Sterol Carrier Protein-2 Suppresses Microsomal Acyl CoA Hydrolysis, *Mol. Cell. Biochem. 205*, 83–90.

38. Faergeman, N.J., and Knudsen, J. (1997) Role of Long-Chain Fatty Acyl-CoA Esters in the Regulation of Metabolism and in Cell Signaling, *Biochem. J. 323*, 1–12.

39. Bogan, A.A., Dallas-Yang, Q., Ruse, M.D., Maeda, Y., Jiang, G., Nepomuceno, L., Scanlan, T.S., Cohen, F.E., and Sladek, F.M. (2000) Analysis of Protein Dimerization and Ligand Binding of Orphan Receptor HNF4α, *J. Mol. Biol. 302*, 831–851.

40. Rajas, F., Gautier, A., Bady, I., Montano, S., and Mithieux, G. (2002) Polyunsaturated Fatty Acyl CoA Suppress the Glucose-6-phosphate Promoter Activity by Modulating the DNA Binding of Hepatocyte Nuclear Factor 4α, *J. Biol. Chem. 277*, 15736–15744.

41. DiRusso, C.C., Heimert, T.L., and Metzger, A.K. (1992) Characterization of FadR, a Global Transcriptional Regulator of Fatty Acid Metabolism in *Escherichia coli*. Interaction with the fadB Promoter Is Prevented by Long Chain Fatty Acyl Coenzyme A, *J. Biol. Chem. 267*, 8685–8691 [published erratum appears in *J. Biol. Chem. 267*, 22693 (1992)].

42. van Aalten, D.M.F., Milne, K.G., Zou, J.Y., Kleywegt, G.J., Bergfors, T., Ferguson, M.A.J., Knudsen, J., and Jones, T.A. (2001) Binding Site Differences Revealed by Crystal Structures of *Plasmodium falciparum* and Bovine Acyl-CoA Binding Protein, *J. Mol. Biol. 309*, 181–192.

43. Berge, R.K. (1980) Physiochemical Properties of the Long Chain Acyl CoA Hydrolase from Rat Liver Microsomes, *Eur. J. Biochem. 111*, 67–72.

44. Mentlein, R., Suttorp, M., and Heymann, E. (1984) Specificity of Purified Monoacylglycerol Lipase, Palmitoyl-CoA Hydrolase,

Palmitoyl-Carnitine Hydrolase, and Nonspecific Carboxylesterase from Rat Liver Microsomes, *Arch. Biochem. Biophys. 228*, 230–246.

45. Yamada, J., Suga, K., Furihata, T., Kitahara, M., Watanabe, T., Hosokawa, M., Satoh, T., and Suga, T. (1998) cDNA Cloning and Genomic Organization of Peroxisome Proliferator-Inducible Long Chain Acyl CoA Hydrolase from Rat Liver Cytosol, *Biochem. Biophys. Res. Commun. 248*, 608–612.

46. Broustas, C.G., and Hajra, A.K. (1995) Purification, Properties, and Specificity of Rat Brain Cytosolic Fatty Acyl CoA Hydrolase, *J. Neurochem. 64*, 2345–2353.

47. Svensson, L.T., Enberg, S.T., Aoyama, T., Usuda, N., Alexson, S.E.H., and Hashimoto, T. (1998) Molecular Cloning and Characterization of a Mitochondrial Peroxisome Proliferator Induced Acyl CoA Thioesterase from Rat Liver, *Biochem. J. 329*, 608.

48. Westin, M.A.K., Alexson, S.E.H., and Hunt, M.C. (2004) Molecular Cloning and Characterization of Two Mouse Peroxisomal Proliferator Activated Receptor α (PPARα)-Regulated Peroxisomal Acyl CoA Thioesterases, *J. Biol. Chem. 279*, 21841–21848.

49. Duda, K., Chi, Y.-I., and Shoelson, S.E. (2004) Structural Basis for HNF4α Activation by Ligand and Coactivator Binding, *J. Biol. Chem. 279*, 23311–23316.

50. Brenner, S. (1988) The Molecular Evolution of Genes and Proteins: A Tale of Two Serines, *Nature 343*, 528–530.

51. Kursula, P., Ojala, J., Lambier, A.M., and Wieringa, R.K. (2002) The Catalytic Cycle of Biosynthetic Thiolase: A Conformational Journey of an Acetyl Group Through Four Binding Modes and Two Oxyanion Holes, *Biochemistry 41*, 15543–15556.

Fourier Transform Infrared Spectroscopy Evaluation of Low Density Lipoprotein Oxidation in the Presence of Quercetin, Catechin, and α-Tocopherol

Henry S. Lam[a], Andrew Proctor[a,*], John Nyalala[b],
Manford D. Morris[a,c], and W. Grady Smith[c]

[a]Department of Food Science, University of Arkansas, Fayetteville, Arkansas 72704, and Departments
of [b]Internal Medicine, Division of Endocrinology and [c]Biochemistry and Molecular Biology,
University of Arkansas for Medical Sciences, Little Rock, Arkansas 72205

ABSTRACT: We investigated the changes in human LDL primary and secondary lipid oxidation products and modification of the apolipoprotein B-100 (apoB-100) secondary structures during Cu^{2+}-mediated oxidation by FTIR spectroscopy in the presence of catechin, quercetin, and α-tocopherol at physiological concentrations. Catechin- and quercetin-containing samples had slower rates and longer lag phases for conjugated diene hydroperoxide (CD) formation than α-tocopherol-containing samples; however, all antioxidant-treated LDL samples generated similar CD levels ($P < 0.05$). A lower maximum (98.4 nmol/mg LDL protein) of carbonyl compounds was produced in the quercetin- and catechin-treated samples than in α-tocopherol samples. Modification of the apoB-100 secondary structures corresponded closely to the formation of carbonyls and was hampered by the presence of antioxidants. Physiological concentrations of catechin and quercetin offered similar levels of protection against modification by carbonyls of the apoB-100 at advanced stages (carbonyls ~96.0 nmol/mg LDL protein) but not at the intermediate stages (carbonyls ~58.0 nmol/mg LDL protein) of LDL oxidation probably owing to differences in the protein-binding mechanisms of catechin and quercetin. Relationships between peroxide formation, carbonyl products, and LDL protein denaturation were shown by the FTIR approach. The FTIR technique provided a simple new tool for a comprehensive evaluation of antioxidant performance in protecting LDL during *in vitro* oxidation.

Paper no. L9776 in *Lipids 40*, 569–574 (June 2005).

Oxidation of human LDL occurs *in vivo*, and oxidatively modified LDL seem to play a crucial role in several degenerative diseases, including atherosclerosis (1). One possible oxidative mechanism involves LDL PUFA peroxidation initiated by free radicals (2). The lipid hydroperoxides so formed cleave to form highly reactive aldehydes that react with lysine residues on the LDL apolipoprotein B-100 (apoB-100). These apoB-100 changes, and possibly other LDL oxidation-related changes, increase LDL recognition and uptake by the scavenger receptors on macrophages and decrease LDL uptake by the hepatic

apoB/E receptor (LDL receptor), which is primarily responsible for removing LDL from the circulation. These alterations are believed to be associated with the development of atherosclerosis (2).

Dietary intake of antioxidants such as vitamin E and flavonoids influences lipoprotein metabolism (3). Dietary flavonoids of significance include the flavonol quercetin, which is found in apples, onions, tea, and red wine, and the flavan-3-ol catechin, which is one of the most abundant flavonoids in foods especially in green tea and red wine (4). Epidemiological studies show an inverse relationship between dietary or plasma levels of naturally occurring antioxidants such as vitamin E (5), catechin, and quercetin (6) and the incidence of stroke or coronary artery disease. Vitamin E, catechin, and quercetin are chain-breaking free radical scavengers and prevent lipid peroxidation and modification of LDL proteins both *in vitro* and *in vivo* (7).

The progression of LDL oxidation and the influence of antioxidants on LDL oxidation have previously been followed by measuring the formation of either hydroperoxide or carbonyl groups. IR spectroscopy has also been used to investigate apoB-100 modifications during LDL oxidation and provide insight into the changes in the α-helix, β-sheet, and β-turn structures (8). This technique is rapid, requires only a small sample, and provides information on functional group composition. We have demonstrated that FTIR can be used to quantify LDL lipid primary and secondary oxidation products as well as changes in LDL protein conformations (9). Studies that simultaneously measure the primary and secondary oxidation products of lipoprotein lipids and of apoB-100 conformational changes and their interrelation are rare. Given that the apoproteins are recognition factors for LDL uptake, protection of their integrity may be of paramount concern in ameliorating arteriosclerosis. Therefore, the relative efficacy of a given antioxidant in protecting apoB conformation against lipid oxidation needs investigation. It is unknown how changes in LDL lipids and apoB-100 structural conformations proceed during LDL oxidation in the presence of antioxidants such as vitamin E and flavonoids.

In the present study, we used the FTIR techniques developed in our laboratories (9) in combination with band-fitting procedures to simultaneously evaluate the production of primary and

secondary oxidation products and apoB-100 modifications in the presence of the antioxidants quercetin, catechin, and α-tocopherol during LDL oxidation. Integrated intensities of the fitted component of LDL spectral bands were measured and analyzed to obtain the relative concentrations of the LDL lipid components and protein conformational structures.

The objective of this study was to measure by FTIR the formation of lipid hydroperoxides and carbonyls, the modification of apoB-100, and the effectiveness of α-tocopherol, quercetin, and catechin on the rate of *in vitro* LDL oxidation at reported physiologic concentrations.

EXPERIMENTAL PROCEDURES

Materials. Quercetin (3,3′,4′,5,7-pentahydroxyflavone) dihydrate, (+)-catechin hydrate, and (±)-α-tocopherol were obtained from Sigma-Aldrich (St. Louis, MO).

LDL isolation. Blood samples from five fasting human males were obtained in vacutainers containing 1 mg/mL EDTA and centrifuged for 10 min at $2000 \times g$ and 4°C to separate the plasma. Human LDL were isolated from the fresh human plasma by sequential floating ultracentrifugation, according to the method described by Lam *et al.* (9). The protein content of LDL was determined according to Lowry *et al.* (10) with BSA as a standard. LDL samples were desalted to remove EDTA using 3.5-mL PD-10 gel filtration columns (Supelco, Bellefonte, PA) pre-equilibrated with phosphate buffer (pH 7.4) immediately before the oxidation study.

In vitro LDL oxidation. Prior to oxidation, all LDL samples were diluted to a final concentration of 50 μg of protein/mL with EDTA-free phosphate buffer (pH 7.4). The *in vitro* oxidation of LDL was performed in the absence (control) or presence of 0.5 μM quercetin, 2.0 μM catechin, and 0.05 μM α-tocopherol (in ethanol) per mg LDL protein, as previously described (9). The concentrations of quercetin, catechin, and α-tocopherol used in this study corresponded to those reported in human plasma (4,11,12) and will from here on also be referred to as their physiological concentrations. Oxidation was initiated by adding freshly prepared $CuCl_2 \cdot 2H_2O$ solution (final concentration 5 μmol/L) in duplicate samples at 37°C. The LDL samples from the five donors were incubated individually.

IR spectroscopy. Duplicate 30-μL aliquots, taken every 5 min for 6 h from LDL incubated at 37°C, were evenly spread on one side of a multi-bounce attenuated total reflectance (ATR) window (Thermo Electron Corp., Madison, WI). The aliquots were allowed to dry under a steady stream of nitrogen to produce films (9). The spectra of the phosphate buffer containing the antioxidants were collected under the same conditions as the LDL sample spectra. FTIR spectra of the films were recorded at 22°C using a Nexus 670 spectrometer (Thermo Electron Corp.) equipped with a deuterated triglycine sulfate detector scanning over the frequency range of 4000–400 cm^{-1} at a resolution of 4 cm^{-1}. Spectra were collected by using rapid-scan software running under OMNIC (Nicolet, Madison, WI), and the spectrum for each sample was calculated from the average of 100 repetitive scans. The internal reflection element

was a Spectra-Tech ZnSe ATR trough plate crystal with an aperture angle of 45° generating seven bounces. A reference background absorbance spectrum was taken by scanning the clean and dry ATR crystal.

LDL conjugated diene and total carbonyls determinations. The primary and secondary products of LDL lipid oxidation were determined by predicting the conjugated diene hydroperoxide (CD) and total carbonyl contents from a calibration model obtained by partial least squares (PLS) regressions using the LDL spectral regions 1800–1500 cm^{-1} as described previously (9). Six LDL spectra from each of the four treatments (control, catechin, quercetin, and α-tocopherol) were selected to constitute a calibration set of 24 spectra of varying CD contents. The spectra (1800–1500 cm^{-1}) of the four LDL treatments at similar CD and total carbonyl contents were not significantly different (data not shown).

LDL protein secondary structures analysis. Quantitative information on the protein structure was obtained by decomposing the amide I band into its constituents. Spectral resolution enhancement was performed according to Byler and Susi (13) and the decomposition of amide I band conducted using the peak-fitting routine under Grams/AI (Thermo Galactic, Salem, NH). The frequencies of the overlapping amide I band components were obtained by calculating the second-derivative spectra. Band shapes were fitted with weighted sums of Gaussian-Lorentzian functions as described previously (14). The deconvolution parameters used for the amide I band were set with half-bandwidth at half-height at 10 cm^{-1} and a resolution enhancement factor, *K*, of 1.0. The intensities of the amide I band components were obtained and expressed as the area under the curve.

Data analysis and statistics. The area percentages of the amide I band components were reported as the mean of the duplicate samples. Differences between antioxidant experimental groups were determined by the Student's *t*-test.

RESULTS AND DISCUSSION

LDL CD. Figure 1 shows the FTIR/PLS-predicted primary LDL oxidation products expressed as CD content in the presence or absence of antioxidants at physiological antioxidant concentrations. The classic three phases of lipid oxidation, namely, the lag, propagation, and decomposition, were evident. However, a second propagation phase then developed after the decomposition phase, probably due to formation of unsaturated aldehyde oxidation products (15). The second propagation phase proceeded with similar patterns but attained higher levels in the control and α-tocopherol samples than in the quercetin and catechin samples, suggesting that the presence of flavonoids interfered with the release of the unsaturated aldehyde oxidation products.

Table 1 summarizes the effect of the presence of antioxidants on the formation of conjugated dienes as predicted by FTIR/PLS and shown in Figure 1. The presence of 0.5 μM quercetin, 2.0 μM catechin, and 0.05 μM α-tocopherol resulted in peak CD values of 8.0, 7.8, and 8.3 nM/mg LDL
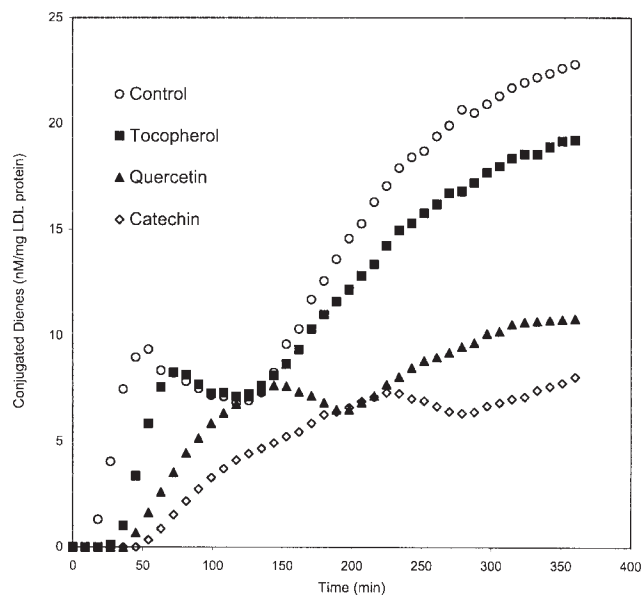
FIG. 1. Inhibition of production of lipoprotein lipids primary oxidation products by 2.0 µM catechin, 0.5 µM quercetin, and 0.05 µM α-tocopherol predicted by FTIR spectra as conjugated diene hydroperoxide content. Control has no antioxidant.

FIG. 2. Formation of lipoprotein lipids carbonyl oxidation products predicted by FTIR spectra in LDL incubated without (control) or with catechin, quercetin, and α-tocopherol.

protein, respectively, after the first propagation phase. The control samples produced higher contents of CD (9.8 nM/mg) than those produced in the presence of antioxidants. The decomposition phase, representing a decline in concentrations after the peak values, was longest in the control samples, followed by samples treated with 0.5 µM quercetin and 2.0 µM catechin, which had similar duration, and shorter in samples containing 0.05 µM α-tocopherol. The decomposition rates of the hydroperoxides were, however, similar probably owing to the fact that chain-breaking antioxidants influence the autocatalytic phase of lipid peroxidation rather than the peroxide decomposition phase (7).

LDL carbonyl compounds. Figure 2 presents the time course of FTIR/PLS-predicted generation of carbonyls as secondary oxidation compounds from the decomposition of lipoprotein lipid hydroperoxides. Carbonyl formation progressed through a gradual, exponential, and stabilized phase for all samples incubated with or without antioxidants. The carbonyls formed stabilized after the exponential phase even though CD was still

being produced, probably as a result of the binding of carbonyls to the lipoprotein residues (2). The period of gradual increase corresponded to the respective propagation phase of predicted CD formation whereas the exponential increase in carbonyls corresponded to the respective decomposition phase of the predicted CD formation profiles (Fig. 1). Predicted total carbonyl formation rates were slower and the gradual phase of carbonyl formation longer in the presence of the antioxidants as compared with those of the control. The predicted total levels of carbonyl compounds formed were similar in the 0.5 µM quercetin- and 2.0 µM catechin-treated samples but lower than those in the control and samples containing 0.05 µM α-tocopherol. This may be attributed to the inhibiting effect of the flavonoids on the hydroperoxide formation in LDL (16).

LDL protein secondary structures. Figure 3 is a typical FTIR spectrum of an LDL sample for the band region between 4000 and 800 cm^{-1}. The absorption bands include a 3280 cm^{-1} N–H stretch, 2930 and 2850 cm^{-1} methylene C–H stretches, and 1735 cm^{-1} C=O stretch. The band between 1700 and 1600

TABLE 1
Conjugated Diene Hydroperoxide (CD) Formation Rates and Profiles at the First Propagation and Decomposition Phases During LDL Incubation at 37°C With and Without Antioxidants[a] ($n = 10$)

Treatment	Lag time (min)	Propagation rate[b]	Maximum CD[c]	Decomposition rate[b]	Duration of decomposition phase (min)
Control	12[a]	0.24[c]	9.81[b]	0.04[a]	72[c]
α-Tocopherol (0.05 µM)	30[b]	0.18[b]	8.26[a]	0.03[a]	45[a]
Quercetin (0.5 µM)	42[c]	0.08[a]	7.94[a]	0.02[a]	51[b]
Catechin (2.0 µM)	54[d]	0.04[a]	7.83[a]	0.02[a]	54[b]

[a]Values followed by same letter in a column are not significantly different at $P < 0.05$.
[b]Rates expressed as nmol/mg LDL protein/min.
[c]CD concentration expressed as nmol/mg LDL protein.
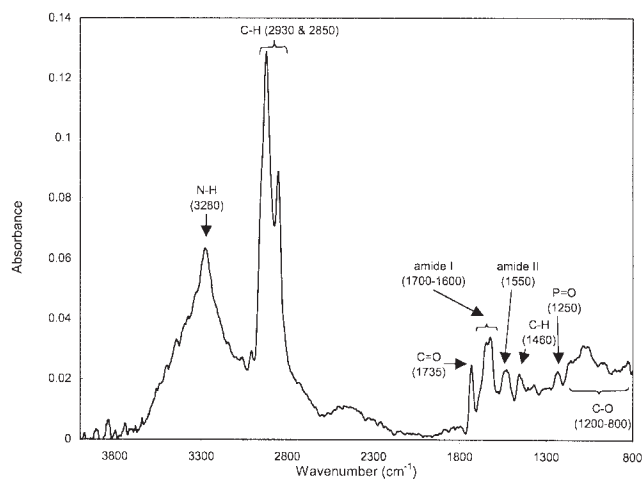
FIG. 3. Representative mid-IR spectrum of an LDL film showing the band assignment of observed bands including the amide I band (1700–1600 cm^{-1}) that was decomposed into its components.

FIG. 4. Percentage composition of the amide I band components (mean ± SD, $n = 2$), centered at different band frequencies, of LDL samples drawn at 10 min of incubation. Amide I band components at each wavenumber for LDL samples with or without antioxidants are not significantly different ($P < 0.05$).

cm^{-1} represents the amide I band arising mainly (>80%) from the stretching vibrations of the apoB-100 peptide bond C=O (8). The amide II band is centered at 1550 cm^{-1}, C–H scissoring at 1460 cm^{-1}, P=O stretching at 1250 cm^{-1}, and C–O vibrations in the bands between 1200 and 800 cm^{-1}. The protein of LDL accounts for the NH bands, the lipids mainly account for the methylene C–H and carbonyl bands, and the phospholipids are responsible for the band at 1250 cm^{-1}. The band at 1735 cm^{-1} increased in intensity with longer LDL incubation (data not shown), suggesting that it was due to the C=O groups from hydroperoxide decomposition.

Figure 4 shows a typical composition of the components of apoB-100 secondary structures obtained after amide I band decomposition for LDL samples with or without antioxidants. The compositions of the apoB-100 secondary structures were similar ($P < 0.05$) in LDL samples incubated in the presence or absence of antioxidants. This indicates that the presence of antioxidants or antioxidant type did not affect the quantification of the apoB-100 components. The apoB-100 secondary structures have previously been assigned (8,17,18). The band at 1616 cm^{-1} was assigned to β-strands, a structure that extends from the monolayer on the LDL outer shell to the inner core. Bands centered at 1680, 1670, and 1663 cm^{-1} arise from β-turns, and bands at 1697, 1631, and 1625 cm^{-1} are due to β-sheet. The band at 1643 cm^{-1} is due to the random (unordered) structure and that at 1651 cm^{-1} is due to the α-helix structure of the apoB-100.

Figure 5 represents a profile of changes in the ratio of random structure to α-helix structures of apoB-100 during LDL incubation with or without antioxidants, as an indicator of protein denaturation. The ratio of random to α-helical structures exhibited an initial gradual increase, followed by an exponential increase and a subsequent stabilization. The changes reflected the gradual, exponential, and stabilized phases of the carbonyl formation profile (Fig. 2). The similarity in pattern may be due to the modification of the amino acid residues of
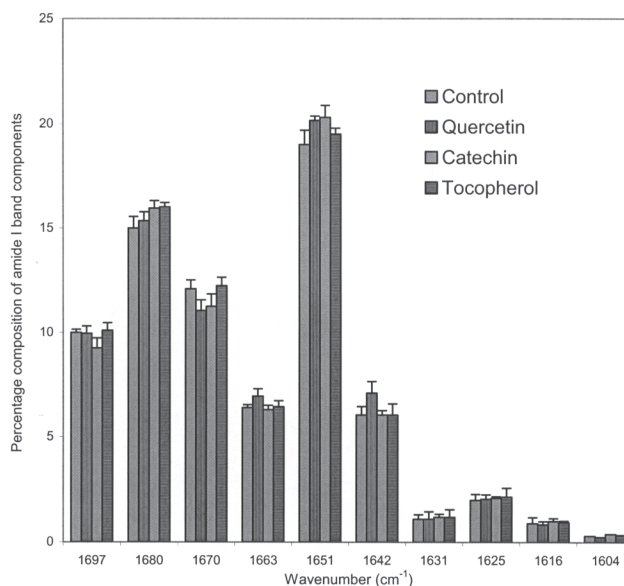
apoB-100 by the carbonyls generated during oxidation (19). The highest rate of apoB-100 denaturation corresponded to the exponential phase of carbonyl formation, reinforcing the fact that the random structures are formed during carbonyl modification of the apoB-100 α-helix structure (8). The control sample produced the highest ratios, followed by samples containing 0.05 µM
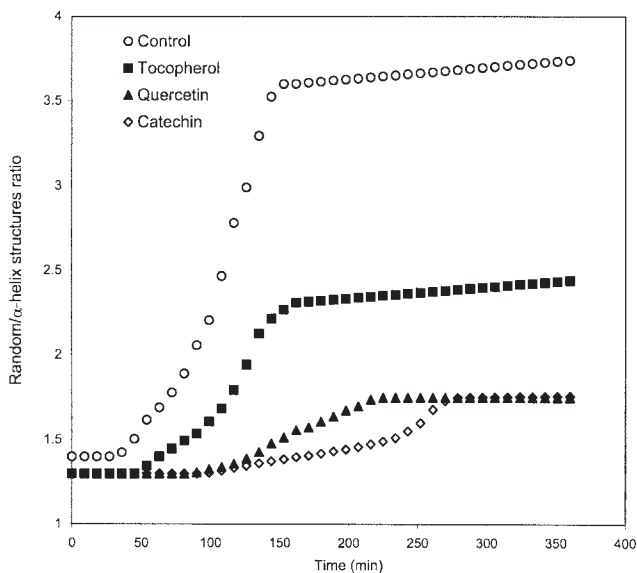
FIG. 5. The modification of apolipoprotein B-100 secondary structures, expressed as the ratio of random to α-helix structures during LDL oxidation, in the presence of catechin, quercetin, and α-tocopherol. Control has no antioxidant.

TABLE 2
Relative Intensity Ratios of Bands at 1735 (aldehydes C=O) to 1632 (β-sheet C=O) and 1735 to 1651 cm^{-1} (α-helix C=O) of Oxidized LDL in the Presence/Absence of Antioxidant

Total carbonyls		Intensity ratios[a]	
(nmol/mg protein)	Antioxidant	1735/1651	1735/1632
58	Control	0.79[d]	0.74[d]
	α-Tocopherol	0.62[c]	0.50[c]
	Quercetin	0.49[b]	0.42[b]
	Catechin	0.38[a]	0.33[a]
96	Control	1.13[c]	1.05[c]
	α-Tocopherol	0.92[b]	0.89[b]
	Quercetin	0.82[a]	0.70[a]
	Catechin	0.78[a]	0.68[a]

[a]Ratios in a column followed by same letter, at each total carbonyls concentration, are not significantly different at $P < 0.05$.

α-tocopherol, and samples with 0.5 μM quercetin and 2.0 μM catechin produced the lowest ratios. The pattern and rates of denaturation in the presence or absence of antioxidants reflected the pattern of carbonyl formation. However, differences observed between antioxidants, other than those due to concentration difference, probably reflected their solubilities and partitioning behavior between the aqueous and lipid phases in the LDL system and the α-helix structure location within the apoB-100 particle. The α-helix structures are located close to the surface of the apoB-100 particle, and the LDL molecule is surrounded by a monolayer of hydrophilic phospholipids (8). This implies that the more hydrophilic flavonoids would partition into the aqueous buffer layer surrounding the LDL molecule and provide better protection to the α-helix against carbonyl modification than the more lipophilic α-tocopherol as observed in this study. The α-tocopherol might also form micelles in the LDL-containing buffer solution that would render them less available for antioxidant activities on the LDL particles. It has previously been pointed out that the effectiveness of an antioxidant is influenced by its location within the system (20).

Effect of antioxidants on LDL protein secondary structure. Table 2 shows a comparison of the relationship between FTIR band intensities of carbonyls (1735 cm^{-1}) and of apoB-100 α-helix (1651 cm^{-1}) and β-sheet (1632 cm^{-1}) structures at the 58.0 and 96.0 nmol/mg total carbonyls stages of LDL oxidation in the presence or absence of antioxidants. The stages of carbonyl formation selected for each treatment were the intermediate carbonyl level (58.0 nmol/mg protein) and the high carbonyl level (96.0 nmol/mg protein). The band ratios 1735/1651 and 1735/1632 cm^{-1} may be considered as an indirect measurement of the amount of aldehydes C=O groups relative to α-helix and β-sheet structures, respectively, in oxidized LDL. These band ratios could therefore indirectly represent the extent of modification of the α-helix and β-sheet structures by the aldehydes.

The 1735/1651 and 1735/1632 cm^{-1} band ratios at the 58.0 nmol/mg LDL protein of total carbonyl stage were highest in the control samples, followed by samples containing α-tocopherol, quercetin, and catechin. At the total carbonyls of 96.0 nmol/mg LDL protein stage, the 1735/1651 and 1735/1632

cm^{-1} band ratios increased but remained highest in the control samples, followed by α-tocopherol-containing samples. The ratios were not significantly different between the quercetin- and catechin-containing samples but lower than those in α-tocopherol-treated samples. This may be attributed to the flavonoids binding to the apoB-100 and prohibiting LDL oxidative modification (21). It indicates that flavonoids, in addition to prohibiting the propagation phase of LDL oxidation, may also protect the apoB-100 protein from modification by the lipid secondary oxidation products.

This study included α-tocopherol, quercetin, and catechin only at physiological concentrations that represent the actual quantities reported *in vivo*; however, differences in concentrations may constrain the objective comparison of their activities *in vitro*. The concentrations of catechin in this study were 4 and 40 times higher than those of quercetin and α-tocopherol, respectively, and definitely contributed to the higher antioxidant activity of catechin observed. The mechanism of action of the flavonoids and α-tocopherol *in vivo* may not be just through direct action as implied in this study but probably through synergistic activities involving other LDL endogenous antioxidants such as carotenoids. Further studies would be needed with the antioxidants to clarify their possible effects on LDL oxidation *in vivo*. However, the findings of this study may be relevant and applicable to other flavonoids and lipophilic antioxidants owing to similarities in their structures and chemical properties.

In conclusion, the presence of antioxidants increased the induction period of hydroperoxide generation, and the presence of flavonoids significantly affected carbonyl formation more than α-tocopherol in oxidized LDL. The denaturation of apoB-100 was commensurate with the formation of carbonyls but alleviated by the presence of flavonoids. Our data showed that the presence of the antioxidants catechin, quercetin, and the α-tocopherol, at physiological concentrations, impeded the formation of primary and secondary oxidation products of lipoprotein lipids and the modification of apoB-100 *in vitro*. This suggests that levels of catechin and quercetin normally found in plasma may influence disease risks associated with LDL oxidation, as does α-tocopherol,

but their relative quantitative importance needs further study. The present study also demonstrated that FTIR in combination with chemometrics provided a comprehensive anaysis of LDL oxidation and antioxidant performance and is a potential tool for dynamic monitoring of LDL oxidation using multiple indicators such as CD, total carbonyls, and changes in the apoB-100 secondary structures.

ACKNOWLEDGMENTS

REFERENCES

1. Chisolm, G.M., and Steinberg, D. (2000) The Oxidation Modification Hypothesis of Atherogenesis: An Overview, *Free Radic. Biol. Med. 28*, 1815–1826.
2. Steinbrecher, U.P., Parthasarathy, S., Lee, D.C., Witztum, J.L., and Steinberg, D. (1984) Modification of Low Density Lipoprotein by Endothelial Cells Involves Lipid Peroxidation and Degradation of Low Density Lipoprotein Phospholipids, *Proc. Natl. Acad. Sci. USA 81*, 3883–3887.
3. Furhrman, B., and Aviram, M. (2001) Flavonoids Protect LDL from Oxidation and Attenuate Atherosclerosis, *Curr. Opin. Lipidol. 12*, 41–48.
4. Wiseman, H. (1999) The Bioavailability of Non-nutrient Plant Factors: Dietary Flavonoids and Phyto-oestrogens. *Proc. Nutr Soc. 58*, 139–146.
5. Rimm, E.H., Stampfer, M.J., Ascherio, A., Giovannucci, E.L., Colditz, G.A., and Willett, W.C. (1993) Vitamin E Consumption and the Risk of Coronary Disease in Men, *N. Engl. J. Med. 328*, 1450–1456.
6. Hertog, M.G.L., Feskens, E.J.M., Hollman, P.C.H., Katan, M.B., and Kromhout, D. (1993) Dietary Antioxidant Flavonoids and Risk of Coronary Heart Disease: The Zutphen Elderly Study, *Lancet 342*, 1007–1011.
7. Halliwell, B. (1995) Oxidation of Low-Density Lipoproteins: Questions of Initiation, Propagation, and the Effect of Antioxidants, *Am. J. Clin. Nutr. 61* (suppl.), 670S–677S.
8. Herzyk, E., Lee, D.C., Dunn, C., Bruckdorfer, K.R., and Chapman, D. (1987) Changes in the Secondary Structure of Apolipoprotein B-100 After Cu^{2+}-Catalyzed Oxidation of Human Low-Density Lipoproteins Monitored by Fourier Transform Infrared Spectroscopy, *Biochim. Biophys. Acta 922*, 145–154.
9. Lam, H.S., Proctor, A., Nyalala, J., Morris, M.D., and Smith, W.G. (2004) Quantitative Determination of Low Density Lipoprotein Oxidation by FTIR and Chemometric Analysis, *Lipids 39*, 687–692.
10. Lowry, O.H., Rosebrough, N., Farr, A.L., and Randall, R.J. (1951) Protein Measurement with the Folin Phenol Reagent, *J. Biol. Chem. 193*, 265–275.
11. Scalbert, A., and Williamson, G. (2000) Dietary Intake and Bioavailability of Polyphenols, *J. Nutr. 130* (suppl.), 2073S–2085S.
12. Princen, H.M., Van Duyvenvoorde, W., Buytenhek, R., Van de Laarse, A., Van Poppel, G., Gevers, L.J., and Van Hinsbergh, V. (1995) Supplementation with Low Doses of Vitamin E Protects LDL from Lipid Peroxidation in Men and Women, *Arterioscler. Thromb. Vasc. Biol. 15*, 325–333.
13. Byler, D.M., and Susi, H. (1986) Examination of the Secondary Structure of Proteins by Deconvolved FTIR Spectra, *Biopolymers 25*, 469–487.
14. Kaupinnenn, J.K., Moffat, D.J., Mantsch, H.H., and Cameron, D.G. (1981) Fourier Self-Deconvolution, *Appl. Spectrosc. 35*, 271–276.
15. Esterbauer, H., Jurgens, G., Quehenberger, O., and Koller, E. (1987) Autoxidation of Human Low Density Lipoprotein: Loss of Polyunsaturated Fatty Acids and Vitamin E and Generation of Aldehydes, *J. Lipid Res. 28*, 495–509.
16. Gugliucci, A., and Stahl, A.J.C. (1995) Low Density Lipoprotein Oxidation Is Inhibited by Extracts of *Ilex paraguariensis*, *Biochem. Mol. Biol. Int. 35*, 47–56.
17. Lee, D.C., Haris, P.I., Chapman, D., and Mitchell, R.C. (1990) Determination of Protein Secondary Structure Using Factor Analysis of Infrared Spectra, *Biochemistry 29*, 9185–9193.
18. Tanfani, F., Galeazzi, T., Curatola, G., Bertoli, E., and Ferreti, G. (1997) Reduced β-Strand Content in Apoprotein B-100 in Smaller and Denser Low-Density Lipoprotein Subclasses as Probed by Fourier Transform Infrared Spectroscopy, *Biochem. J. 322*, 765–769.
19. Steinbrecher, U.P. (1987) Oxidation of Human Low Density Lipoprotein Results in Derivatization of Lysine Residues of Apolipoprotein B by Lipid Peroxide Decomposition Products, *J. Biol. Chem. 262*, 3603–3608.
20. Frankel, E.N., and Meyer, A.S. (2000) The Problems of Using One-Dimensional Methods to Evaluate Multifunctional Food and Biological Antioxidants, *J. Sci. Food Agric. 80*, 1925–1941.
21. Ivanov, V., Carr, A.C., and Frei, B. (2001) Red Wine Antioxidants Bind to Human Lipoproteins and Protect Them from Metal Ion-Dependent and -Independent Oxidation, *J. Agric. Food Chem. 49*, 4442–4449.

Comparative Effects of Palm Vitamin E and α-Tocopherol on Healing and Wound Tissue Antioxidant Enzyme Levels in Diabetic Rats

M. Musalmah[a,*], M.Y. Nizrana[a], A.H. Fairuz[a], A.H. NoorAini[a],
A.L. Azian[b], M.T. Gapor[c], and W.Z. Wan Ngah[a]

Departments of [a]Biochemistry and [b]Anatomy, Faculty of Medicine, Universiti Kebangsaan Malaysia,
Kuala Lumpur, and [c]Department of Chemistry, Malaysian Palm Oil Board, Bangi, Malaysia

ABSTRACT: The effect of supplementing 200 mg/kg body weight palm vitamin E (PVE) and 200 mg/kg body weight α-tocopherol (α-Toc) on the healing of wounds in streptozotocin-induced diabetic rats was evaluated. The antioxidant potencies of these two preparations of vitamin E were also evaluated by determining the antioxidant enzyme activities, namely, glutathione peroxidase (GPx) and superoxide dismutase (SOD), and malondialdehyde (MDA) levels in the healing of dermal wounds. Healing was evaluated by measuring wound contractions and protein contents in the healing wounds. Cellular redistribution and collagen deposition were assessed morphologically using cross-sections of paraffin-embedded day-10 wounds stained according to the Van Gieson method. GPx and SOD activities as well as MDA levels were determined in homogenates of day-10 dermal wounds. Results showed that PVE had a greater potency to enhance wound repair and induce the increase in free radical-scavenging enzyme activities than α-Toc. Both PVE and α-Toc, however, were potent antioxidants and significantly reduced the lipid peroxidation levels in the wounds as measured by the reduction in MDA levels.

Paper no. L9408 in *Lipids 40*, 575–580 (June 2005).

Vitamin E consists of two subfamilies, namely, tocopherols and tocotrienols, each of which comprises four forms: α, β, γ, and δ (1). Although their structures are similar, the presence of three double bonds in the isoprenoid side chain of tocotrienols confers different potencies and biological activities between them (2–6). Some studies reported that tocotrienol possessed higher antioxidant activity than tocopherols (2,3). α-Tocotrienol was reported to exhibit greater peroxyl radical-scavenging potency than α-tocopherol (α-Toc) in liposomal membranes (2) and to possess greater anticancer activity (4). More recently, tocotrienols were reported to be more effective than α-Toc in preventing glutamate-induced neuronal cell death (5). On the other hand, the study by Suarna *et al.* (6) in 1993 did not show a significant difference in antioxidant activities between corresponding tocopherol and tocotrienol isomers.

Palm oil is the richest natural source of tocotrienols. Palm oil vitamin E extract consists largely of tocotrienols (70%) and only 30% tocopherols (7). In contrast, the vitamin E in most other vegetable oils consists of only tocopherols. In this study we compared the potency of palm vitamin E (PVE) extract and α-Toc, the most abundant form of vitamin E *in vivo*, on wound healing in diabetic rats. Delayed wound healing is one of the complications of diabetes, and free radicals have been postulated as one of the causes (8–10). In a clinical sense, delayed wound healing in persons with diabetes may lead to severe complications requiring extended hospitalization and amputation. Thus, it is of interest to determine the use of antioxidants in accelerating wound healing, not only in diabetes but also in other conditions of impaired healing.

The beneficial effects of antioxidant vitamins on the healing of wounds have mainly been studied using animal models. Only vitamin C has been shown to accelerate healing in human subjects (11). Oral and topical application of vitamin A has been shown to enhance healing in animals compromised by the administration of corticosteroids (12,13), the presence of a malignant tumor (14), and chemically induced diabetes mellitus (15). The benefit of vitamin E in wound healing has been reported by Martin (16) on guinea pigs. Vitamin E also was reported to accelerate the treatment of wounds resulting from exposure to radiation, including sunlight (17–19). Altavilla *et al*. (20) and Galeano *et al*. (21) have treated genetically diabetic rats with raxofelast, a hydrophilic vitamin E-like antioxidant compound and found accelerated healing of linear wounds. We have also studied the effects of oral vitamin E supplementation on 6-cm skin lesions in normal and chemically induced diabetic rats and found accelerated healing only in diabetic rats (22).

In this study, the effects of PVE and α-Toc on chemically induced diabetic rats were determined in an excision wound model. Full-skin punch biopsies were used, as they allow wound contraction, wound protein, lipid peroxidation, and antioxidant enzyme activities to be measured in the healing wounds.

MATERIALS AND METHODS

Materials. Streptozotocin was purchased from Sigma (St. Louis, MO). PVE and α-Toc were gifts from the Malaysian Palm Oil Board (Bangi, Malaysia).

Animals. This study was approved by the Universiti Ke-

---

bangsaan Malaysia Animal Ethics Committee. Male Sprague-Dawley rats weighing 250–300 g were used and were made diabetic with an intramuscular injection of streptozotocin (50 mg/kg body weight). Rats were considered diabetic when their fasting blood glucose levels were greater than 8 mmol/L using a glucose reagent strip and glucometer (Advantage, Boehringer Mannheim, Mannheim, Germany). The animals were allowed to rest for 10 d before the start of the experiment.

Diabetic rats were divided into groups of 6 animals each, according to the supplementation given: control, PVE, or α-Toc.

Study design. On the day of the experiment (day 1), the animals were anesthetized with Zoletil 50® (Virbac Labs, Carros Cedex, France). The back of each animal was then partially shaved, and the skin was cleaned with a 70% alcohol and iodine solution. Four 6-mm-diameter excision wounds were made to create full-thickness dorsal cutaneous wounds using a punch biopsy needle (Stiefel Laboratories, Dublin, Ireland). The animals were then force-fed (oral feeder; Popper and Sons Inc., New Hyde Park, NY) with either 200 mg/kg body weight PVE, 200 mg/kg body weight α-Toc, or an equal volume of olive oil (control). Animals were not fasted before being force-fed. The administration of olive oil or the vitamins was carried out daily by oral gavage until the animals were sacrificed on day 10. The animals were kept individually in separate cages and fed a standard diet (Gold Coin, Malaysia) and water *ad libitum.*

The progress of healing was monitored by determining the wound areas, total protein content in the full-skin punch biopsy wounds, and histological changes as examined after staining with Van Gieson stain.

Blood samples also were taken and were analyzed for fasting blood glucose (to ensure the diabetic status of the rats). Wound tissues were collected on day 10 for measurement of antioxidant enzyme activities, namely, glutathione peroxidase (GPx) and superoxide dismutase (SOD). Lipid peroxidation was determined as malondialdehyde (MDA) in the day-10 wound tissues.

Determination of wound closure. Wound areas were determined as the in-growth of epithelial cells by measuring wound areas on days 1, 6, and 10. Wound areas were traced onto a tracing paper and then calculated using an image analyzer (Axiovert S 100; Zeiss, Oberkochen, Germany) according to the method described by Baie and Sheikh (23).

Wound collection. Wounds were collected on day 10 after wounding. Briefly, the animals were anesthetized with Zoletil 50 (diethyl ether) before the procedure. The lesion and the surrounding areas were cut using a punch biopsy needle of the same diameter used earlier in the creation of wounds.

Protein determination. The total protein content was determined using one punch biopsy wound from each animal according to the method of Bradford (24). Briefly, wound tissues were homogenized in 1.15% calcium chloride at a ratio of 1:5 (wt/vol). A 0.1-mL quantity of the homogenate was added to 5 mL of Bradford reagent, mixed, and the absorbance read at 595 nm wavelength against a 0.1 M phosphate buffer, pH 7.4. Standards were treated similarly using BSA at concentrations of 0, 20, 40, 60, 80, and 100 μg/mL in 0.1 M phosphate buffer, pH 7.4.

Histological examination. Wound tissues were fixed by immersion in formalin for routine histology. The tissues were dehydrated in ascending concentrations of alcohol, cleaned in xylene, and impregnated in paraffin according to standard procedures. Just before staining, the lesions were sliced along a longitudinal plane and embedded on-edge. Sections of 5-μm thickness were treated with the Van Gieson stain (25).

GPx activity. For the determination of GPx activity in the wound tissue, day-10 wound tissues were prepared by homogenizing in 1.15% potassium chloride at a ratio of 1:5 (wt/vol). They were then centrifuged at 8,000 rpm for 20 min at 4°C. The resultant supernatant was again centrifuged at 35,000 rpm for 1 h at 4°C.

Erythrocyte GPx activity was determined according to the method described by Paglia and Valentine (26). The hemolysate was diluted with distilled water (1:5). A 0.5-mL quantity of Drabkin reagent (cyanmethemoglobin) was then added to 0.5 mL of the diluted hemolysate. Then 2.88 mL of substrate mixture was added to 0.02 mL of the resulting mixture. The substrate mixture consisted of 8.4 mM NADPH, 1.125 M sodium azide, 5 mM GSH, and 34.5 IU reduced GSH in 0.05 M phosphate buffer, pH 7.0. The reaction was started by adding 0.1 mL of hydrogen peroxide. The solutions in the test tubes were then mixed and the absorbance read at 340 nm wavelength for 5 min.

SOD activity. Hemolysates of the day-10 wound tissues were prepared as for GPx and were analyzed for SOD activity.

SOD was determined according to the method of Beyer and Fridovich (27). Hemolysate was mixed with a substrate mixture consisting of 50 mM phosphate buffer containing 0.1 mM EDTA, pH 7.8, prepared fresh on the day of analysis; L-methionine (0.03g/mL); nitroblue tetrazolium chloride (NBT·2HCl) (1.41 mg/mL); and 1% Triton X-100® (vol/vol). The reaction was started by adding 10 μL riboflavin (4.4 mg/100 mL). The mixtures were mixed, then left in an aluminum box illuminated with two fluorescent lamps of 20 W for 7 min, and the absorbance was read at 560 nm wavelength. The whole procedure was carried out in the dark because both riboflavin and NBT are sensitive to light.

MDA levels. MDA levels in the day-10 wound tissue homogenate were also determined to reflect the level of lipid peroxidation using the TBARS method, as described by Ledwozyw *et al.* (28). Briefly, the tissues were homogenized as just described in 1.15% potassium chloride and diluted 1:5 with distilled water before analysis. A 2.5-mL quantity of TCA solution was then added to the hemolysate and left at room temperature for 15 min. Thiobarbituric acid (1.5 mL) was then added to the mixture, mixed, and the solution incubated in a water bath at 100°C for 30 min. The tubes were then cooled and shaken vigorously for 30 min before adding 4 mL of *n*-butanol solution. The tubes were then centrifuged at 3000 rpm for 10 min at room temperature. The absorbance of the resulting upper layer was then read using a spectrofluorometer (Shimadzu, Kyoto, Japan).

Statistical calculation. The percent wound areas were calculated using ANOVA with repeated measures, followed by *post hoc* Student's *t*-test with correction for multiple comparisons. For the other parameters, ANOVA with multiple comparisons was used.

RESULTS

Wound healing was evaluated from the morphological changes observed with stained preparations of cross-sections of wounds taken on day 10 of healing using the Van Gieson techniques. We also measured the wound surface areas and total protein in the wounds during healing. The amount of protein in the wound reflects the synthesis of new cells and cellular redistribution (29).

Wound closure. Figure 1 shows that supplementation of PVE and α-Toc resulted in smaller wounds on day 10 postwounding compared with the control. Supplemented rats had significantly less wound area on day 10 of healing ($P < 0.05$) compared with the control, but the wound areas of rats supplemented with PVE were significantly smaller than those of the α-Toc-supplemented group.

Total protein content. Figure 2 shows the total protein (mean ± SEM) in the full-skin punch biopsy taken from each of the animals on day 10. Significant increases in the total protein content were observed in all supplemented groups compared with the control ($P < 0.01$). However, higher levels were observed with diabetic rats supplemented with PVE.

Morphological studies. Observations of stained paraffin sections of the wound sites on day 10 in full-skin punch biopsy wounds of diabetic rats showed little epidermal regeneration in the control rats (Fig. 3A). The underlying dermis showed an ill-formed granulation tissue and sparse collagen. PVE supplementation resulted in a well-formed and differentiated epidermis (Fig. 3B). There were complete re-epithelization and thick bundles of well-aligned collagen showing the advanced state of healing compared with the control. α-Toc supplementation resulted in a more dense infiltration of the wound bed and a
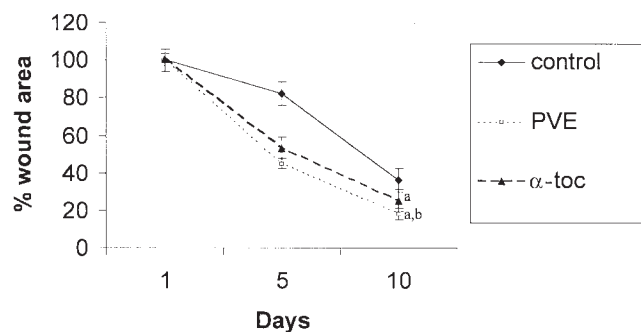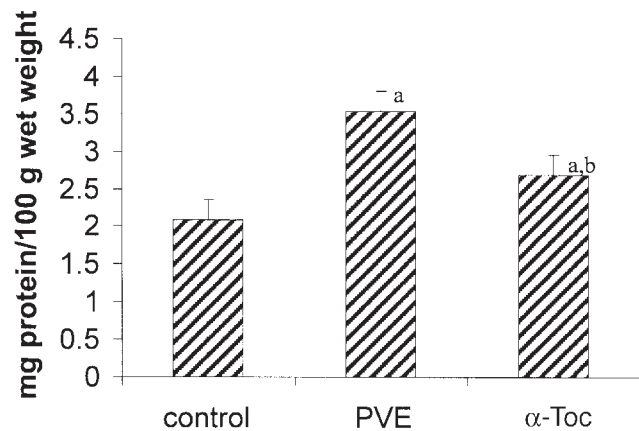
FIG. 2. Means ± SEM of total protein in day 10 full-skin punch biopsies of control, PVE-, and α-Toc-supplemented diabetic rats ($n = 6$). The letters a and b denote a significant difference from the control and α-Toc groups, respectively ($P < 0.01$). For abbreviations see Figure 1.

greater collagen content than the control (Fig. 3C) but at an earlier state of healing when compared with PVE supplementation.

Antioxidant enzymes and MDA levels in wound tissues. GPx and SOD activities and MDA levels were calculated, taking into account the amount of protein present in the healing wound, as this indicates the number of living cells present. Results showed that both enzymes were significantly elevated in rats receiving PVE ($P < 0.001$) compared with controls and the group treated with α-Toc (Table 1). There were significant reductions in MDA levels observed in the tissues taken from the rats supplemented with PVE and α-Toc ($P < 0.001$).

DISCUSSION

Wound healing is a complex but ordered process involving three overlapping phases: inflammation, granulation tissue formation, and remodeling of the extracellular matrix. These events include cellular migration, proliferation, adhesion, and phenotypic differentiation (30).

The present data demonstrate that PVE supplementation resulted in significantly smaller wound areas on day-10 postwounding compared with controls. Although α-Toc supplementation also resulted in smaller wound areas, the difference was not significant compared with controls. These data were further substantiated by the quantification of protein in the wounds. The amount of protein in wounds taken from the rats supplemented with PVE was significantly increased compared with controls and higher than those of α-Toc. Since the amount of wound protein reflects the rate of cellular proliferation, we deduced that PVE accelerates the synthesis and migration of new cells into the wound areas. Results of Van Gieson staining of cross-sections of paraffin-embedded day-10 wounds were also in agreement with these findings. There was a greater rate of proliferation and infiltration of cells at the wound sites taken from rats supplemented with PVE. These cells play an important role in matrix deposition and the restoration of tissue integrity, as shown

FIG. 1. Means ± SEM of percent wound areas during healing of excision dermal wounds of control, palm vitamin E (PVE)-, and α-tocopherol- (α-Toc-) supplemented diabetic rats ($n = 6$). The letters a and b denote a significant difference from the control and α-Toc groups, respectively ($P < 0.05$).
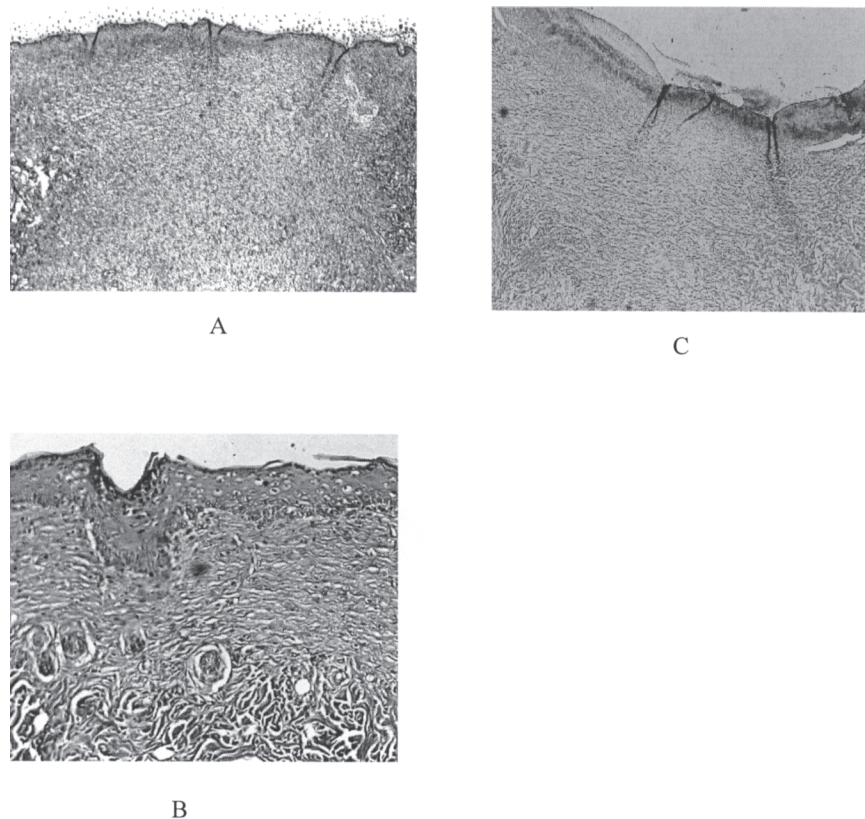
FIG. 3. Van Gieson stained paraffin sections of day-10 dermal wounds of control (A), PVE-supplemented (B), and α-Toc-supplemented (C) diabetic rats. Slides A and C are shown under 40× magnification, whereas slide B is shown under 100× magnification to better illustrate cellular growth and the formation of the different cell layers. Healing was most advanced in the PVE-supplemented group where there were complete re-epithelization, well-differentiated cells, and thick collagen bundles (B). α-Toc supplementation resulted in more epithelial cell migration to the wound bed with some collagen deposition (C). The wound bed of the control group (A) had a sparse number of epithelial cells with little collagen, showing that healing was at an earlier stage compared with the PVE- and α-Toc-supplemented groups. For abbreviations see Figure 1.

by the increased collagen content at the wound sites. Collagen is a major determinant of increased tensile strength of the healing wound (31).

We also performed a similar experiment on nondiabetic rats and found that supplementation with either PVE or α-Toc did not improve the rate of healing of excision wounds (results not shown). This result agrees with our earlier finding in which we used the linear incision model of wound healing and found no acceleration of wound closure with α-tocopherol supplementation (22).

In our earlier work, supplementation of the same dose of α-Toc resulted in significantly accelerated linear wound closure in diabetic rats, in contrast to what we observed here using the excision wound model (22). This probably reflects the complexity of healing in excision wounds compared with the incision model. Incision wounds cause only minimal damage to epithelial basement membrane continuity and the death of relatively few epithelial and connective tissue cells. The repair process involves primarily epithelial regeneration. The repair process for excision wounds, by contrast, is more complex, in-

volving the regeneration of parenchymal cells, extensive ingrowth of granulation tissue, and an accumulation of the extracellular matrix (32). Therefore, the dose of α-Toc needed to elicit a positive response may be much higher than that used in the present study.

The differences in the potencies of the vitamin preparations may be due to the fact that PVE is a mixture containing a high

TABLE 1

Means ± SEM of Glutathione Peroxidase (GPx) and Superoxide Dismutase (SOD) Activities and Malondialdehyde (MDA) Levels in Homogenates of Day-10 Dermal Wounds of Control, Palm Vitamin E (PVE), and α-Tocopherol- (α-Toc-) Supplemented Diabetic Rats ($n = 6$)

	Control	PVE	α-Toc
GPx (μactivity/g protein)	17.2 ± 0.3	26.4 ± 0.12[a,b]	17.3 ± 0.1
SOD (U/mg protein)	27.9 ± 0.3	38.2 ± 0.1[a,b]	25.6 ± 0.3
MDA (nmol/g protein)	81.5 ± 0.2	24.6 ± 0.2[a]	33.9 ± 0.1[a]

[a]The roman superscript letters [a] and [b] denote a significant difference from the control and α-Toc groups, respectively ($P < 0.001$).

percentage of tocotrienols, which in some conditions have been shown to be more potent antioxidants than tocopherols (2–4). Their effectiveness in wound healing may be because orally administered tocotrienols have been reported to accumulate in the skin (33). Traber *et al.* (33) reported that in mice, nearly 15% of tocotrienols given orally were distributed to the skin compared with only 1% of the tocopherols. This may be attributed to the unsaturated isoprenoid side chain of the tocotrienols, which had been suggested to provide higher mobility, allowing more efficient and uniform distribution into the bilayer cell membranes (34). This unique distribution of tocotrienols in the skin may give it superior properties in aiding wound repair. In contrast, topical application of a tocotrienol-rich fraction from palm oil on hairless mice was reported to result in a preferential increase in α-Toc in the skin, and no difference was observed in the potential to afford antioxidant protection against UV radiation or ozone (34). Weber *et al.* (36) suggested that the skin may have a specific mechanism for enrichment with α-Toc rather than tocotrienols.

Apart from the possible differences in distribution kinetics, studies have reported that tocotrienols exert a greater protective effect than tocopherols (37–41). Thus, Serbinova *et al.* (2) reported that α-tocotrienol was 40 to 60 times more potent in reducing lipid peroxidation in rat liver microsomal membrane and 6.5 times more potent against oxidative damage to cytochrome P-450 than was α-Toc (2). Tocotrienols showed a significant inhibition of human and mouse tumor cell growth compared with tocopherols (37–39). In a study on serum biliary enzyme, Ong *et al.* (41) reported that a higher concentration of α-Toc was needed to elicit the same level of reduction of hepatocyte γ-glutamyltranspeptidase release after rats were treated with a carcinogen. Perhaps in the case of wound healing in persons with diabetes, a higher dose of α-Toc is needed to elicit the same response as that of PVE, or perhaps the effect is best seen when a mixture of vitamin E (as in PVE) is supplemented, as was reported by Ong *et al.* (41) in their study on chemically induced hepatitis.

The present study also shows that rats supplemented with PVE had significantly higher levels of antioxidant enzyme activities than controls and those supplemented with α-Toc. SOD and GPx act as scavengers for free radicals: SOD turns superoxide radicals into hydrogen peroxide (42), and GPx neutralizes hydrogen peroxides to water (26). The reduction in free radical damage can be assessed by MDA as an index of lipid peroxidation. Results showed that both PVE and α-Toc were effective in significantly reducing the MDA levels. Although the present study was done on oral vitamin E supplementation, topical vitamin E also has been reported by other researchers to result in up-regulation of a network of enzymatic and nonenzymatic antioxidants such as SOD, reduced GSH, and ascorbate (35).

In conclusion, this study shows that PVE, a vitamin E mixture with a high tocotrienol content, was more potent at enhancing wound healing and inducing increased antioxidant enzyme levels in the wounds of diabetic rats than was α-Toc. However, both vitamins were able to reduce lipid peroxidation in the healing wounds.

REFERENCES

1. Pennock, J.F., Hemming, F.W., and Kerr, J.D. (1964) A Reassessment of Tocopherol in Chemistry, *Biochem. Biophys. Res. Commun. 17,* 542–548.
2. Serbinova, E., Kagan, V., Han, D., and Packer, L. (1991) Free Radical Recycling and Intramembrane Mobility in the Antioxidant Properties of α-Tocopherol and α-Tocotrienol, *Free Radic. Biol. Med. 10,* 263–275.
3. Suzuki, Y.J., Tsuchiya, M., Wassall, S.R., Choo, Y.M., Govil, G., Kagan, V.E., and Packer, L. (1993) Structural and Dynamic Membrane Properties of α-Tocopherol and α-Tocotrienol: Implication to the Molecular Mechanism of Their Antioxidant Potency, *Biochemistry 32,* 10692–10699.
4. Birt, D.F. (1986) Update on the Effect of Vitamins A, C and E and Selenium on Carcinogenesis, *Proc. Soc. Exp. Biol. Med. 138,* 311–315.
5. Sen, C.K., Khanna, S., Roy, S., and Packer, L. (2000) Tocotrienol Potently Inhibits Glutamate-Induced pp60[c-Src] Kinase Activity and Death of HT4 Neuronal Cells, *Biol. Chem. 275,* 13049–13055.
6. Suarna, C., Hood, R.L., Dean, R.T., and Stocker, R. (1993) Comparative Antioxidant Activity of Tocotrienols and Other Natural-Lipid Soluble Antioxidants in a Homogenous System, and in Rat and Human Lipoproteins, *Biochim. Biophys. Acta 1166,* 163–170.
7. Gapor, M.T., and Hashimoto, T. (1983) Effects of Processing on the Content and Composition of Tocopherols and Tocotrienols in Palm Oil, in *Palm Oil Product Technology in the Eighties: A Report of the Proceedings of the International Conference on Palm Oil Product Technology in the Eighties* (Pushparajah, E., and Rajagurai, M., eds.), pp. 145–156, Incorporated Society of Planters.
8. Hallberg, C.K., Troome, S.D., and Ansari, N.H. (1996) Acceleration of Corneal Wound Healing in Diabetic Rats by Antioxidant Trolox, *Res. Commun. Mol. Pathol. Pharmacol. 93,* 3–12.
9. Ceriello, A., Falleti, E., Moltz, E., Taboga, C., Tonutti, L., Ezsol, Z., Ganano, F., and Bartolli, E. (1998) Hyperglycaemia-Induced ICAM-1 Increase in Diabetes Mellitus: The Possible Role of Oxidative Stress, *Horm. Metab. Res. 30,* 146–149.
10. Maxwell, S.R., Thomason, H., Sandler, D., LeGuen C., Baxter, M.A., Thorpe, G.H., Jones, A.F., and Barnett, A.H. (1997) Poor Glycaemic Control Is Associated with Reduced Serum Free Radical Scavenging (antioxidant) Activity in NIDDM, *Ann. Clin. Biochem. 34* (pt 6), 638–644.
11. Ringsdorf, W.M., Jr., and Cheraskin, E. (1982) Vitamin C and Human Wound Healing, *Oral Surg. Oral Med. Oral Path. 53,* 231–236.
12. Haws, M., Brown, R.E., Suchy, H., and Roth, A. (1994) Vitamin-A Soaked Gelfoam Sponges and Wound Healing in Steroid-Treated Animals, *Ann. Plast. Surg. 194,* 42–50.
13. Trevisani, M.F., Ricci, M.A., Tolland, J.T., and Beck, W.C. (1987) Effect of Vitamin A and Zinc on Wound Healing in Steroid-Treated Mice, *Curr. Surg. 44,* 390–393.
14. Weinzweig, J., Levenson, S.M., Rettura, G., Weinzweig, N., Mendecki, J., Chang, T.H., and Seifter, E. (1990) Supplemental Vitamin A Prevents the Tumor-Induced Defect in Wound Healing, *Ann. Surg. 211,* 269–276.
15. Seifter, E., Retture, G., Padawer, J., Stratford, F., Kambosos, D., and Levenson, S.M. (1981). Impaired Wound Healing in Strep-

tozotocin Diabetes. Prevention by Supplemental Vitamin A, *Ann. Surg. 194,* 42–50.

16. Martin, A. (1996) The Use of Antioxiodants in Healing, *Dermatol. Surg. 22,* 156–160.

17. Nachbar, F., and Korting, H.C. (1995) The Role of Vitamin E in Normal and Damaged Skin, *J. Mol. Med. 73,* 7–17.

18. Fryer, M.J. (1993) Evidence for the Photoprotective Effects of Vitamin E, *Photochem. Photobiol. 58,* 304–312.

19. Taren, D.L., Chvapil, M., and Weber, C.M. (1987) Increasing the Breaking Strength of Wounds Exposed to Preoperative Radiation Using Vitamin E Supplementation, *Int. J. Vitam. Nutr. Res. 57,* 133–137.

20. Altavilla, D., Saitta, A., Cucinotta, D., Galeano, M., Deodato, B., Colonna, M., Torre, V., Russo, G., Sardella, A., Urna, G., *et al.* (2001) Inhibition of Lipid Peroxidation Restores Impaired Vascular Endothelial Growth Factor Expression and Stimulates Wound Healing and Angiogenesis in the Genetically Diabetic Mouse, *Diabetes 50,* 667–674.

21. Galeano, M., Torre, V., Deodato, B., Campo, G.M., Colonna, M., Sturiale, A., Squadrito, F., Cavallari, V., Cucinotta, D., Buemi, M., and Altavilla, D. (2001) Raxofelast, a Hydrophilic Vitamin E-like Antioxidant, Stimulates Wound Healing in Genetically Diabetic Mice, *Surgery 129,* 467–477.

22. Musalmah, M., Fairuz, A.H., Gapor, M.T., and Wan Ngah, W.Z. (2002) Effect of Vitamin E on Plasma Malondialdehyde, Antioxidant Enzyme Levels and the Rates of Wound Closures During Wound Healing in Normal and Diabetic Rats, *Asia Pac. J. Clin. Nutr. 11* (Suppl. 7), S448–S451.

23. Baei, S.H., and Sheikh, K.A. (2000) The Wound Healing Properties of *Channa striatus*-Cetrimide Cream—Wound Contraction and Glycosaminoglycan Measurement, *J. Ethnopharmacol. 73,* 15–30.

24. Bradford, M.M. (1976) A Rapid and Sensitive Method for the Quantitation of Microgram Quantities of Protein Utilizing the Principle of Protein-Dye Binding, *Anal. Biochem. 72,* 248–254.

25. Bancroft, J.D., and Cook, H.C. (1984) *Manual of Histological Techniques,* Churchill Livingstone, Edinburgh.

26. Paglia, D.E., and Valentine, W.N. (1984) Studies on the Quantitative and Qualitative Characterization of Erythrocyte Glutathione Peroxidase, *J. Lab. Clin. Med. 7,* 158–169.

27. Beyer, W.F., and Fridovich, I. (1987) Assaying for SOD Activity: Some Large Consequences in Minor Changes in Conditions, *Anal. Biochem. 161,* 559–566.

28. Ledwozyw, A., Michalak, J., Stepien , A., and Kadziolka, A. (1986) The Relationship Between Plasma Triglyceride, Cholesterol, Total Lipids and Lipid Peroxidation Products During Human Atheroclerosis, *Clin. Chim. Acta 155,* 275–284.

29. Chithra, P., Sajthlal, G.B., and Chandrakasan, G. (1998) Influence of Aloe Vera on Collagen Characteristics in Healing Dermal Wounds in Rats, *Mol. Cell. Biochem. 181,* 71–76.

30. Raghow, R. (1994) The Role of Extracellular Matrix Post-inflammatory Wound Healing and Fibrosis, *FASEB J. 8,* 823–831.

31. Bhartiya, D., Sklarsh, J.W., and Maheshwari, R.K. (1992) Enhanced Wound Healing in Animal Models by Interferon and on Interferon Inducer, *J. Cell. Physiol. 150,* 312–319.

32. Chandrasoma, P., and Taylor, C.R. (1995) Healing and Repair, in *Concise Pathology,* 2nd edn., pp. 78–88, Appleton & Lange, Norwalk, CT.

33. Traber, M.G., Podda, M., Weber, C., Yan, L.J., and Packer L. (1997) Diet Derived and Topically Applied Tocotrienols Accumulate in Skin and Protect the Tissue Against UV-Induced Oxidative Stress, *Asia Pac. J. Clin. Nutr. 6,* 63–67.

34. Kamat, J.P., and Devasagayam, T.P.A. (1995) Tocotrienols from Palm Oil as Potent Inhibitors of Lipid Peroxidation and Protein Oxidation in Rat Brain Mitochondria, *Neurosci. Lett. 195,* 179–182.

35. Lopez-Torres, M., Thiele, J.J., Shindo, Y., Han, D., and Packer, L. (1998) Topical Application of α-Tocopherol Modulates the Antioxidant Network and Diminishes Ultraviolet-Induced Oxidative Damage in Murine Skin, *Br. J. Derm. 138,* 207–215.

36. Weber, C., Podda, M., Rallis, M., Thiele, J.J., Traber, M.G., and Packer, L. (1997) Efficacy of Topically Applied Tocopherols and Tocotrienols in Protection of Murine Skin from Oxidative Damage Induced by UV-Irradiation, *Free Radic. Biol. Med. 22,* 761–769.

37. Komiyama, K., Lizuka, K., Yamaoka, M., Watanabe, H., Tsuchiya, H., Umezawa, I. (1989) Studies on the Biological Activity of Tocotrienols, *Chem. Pharm. Bull. 37,* 1369–1371.

38. Nesaretnam, K., Guthrie, N., Chambers, A.F., and Carroll, K.K. (1995) Effects of Tocotrienols on the Growth of a Human Breast Cancer Line in Culture, *Lipids 30,* 1139–1143.

39. Nesaretnam, K., Stephen, R., Dils, R., and Darbre, P. (1998) Tocotrienols Inhibit the Growth of Human Breast Cancer Lines Irrespective of Estrogen Receptor Status, *Lipids 33,* 461–469.

40. Qureshi, A.A., Qureshi, N., Wright, J.J.K., Shen, Z., Kramer, G., Gapor, A., and Chong, Y.H. (1991) Lowering of Serum Cholesterol in Hypercholesterolemic Humans by Tocotrienols (palm vitee), *Am. J. Clin. Nutr. 53,* 1021S–1026S.

41. Ong, F.B., Wan Ngah, W.Z., Top, A.G., Khalid, B.A., and Shamaan, N.A. (1994) Vitamin E, Glutathione S-Transferase and α-Glutamyl Transpeptidase Activities in Cultured Hepatocytes of Rats Treated with Carcinogens, *Int. J. Biochem. 26,* 397–402.

42. Vervaart, P., and Knight, K.R. (1996) Oxidative Stress and the Cell, *Clin. Biochem. Rev. 17,* 3–13.

Maternal Dietary Alpine Butter Intake Affects Human Milk: Fatty Acids and Conjugated Linoleic Acid Isomers

Isabelle Bertschi[a], Marius Collomb[b], Lukas Rist[c], Pius Eberhard[b], Robert Sieber[b], Ulrich Bütikofer[b], Daniel Wechsler[b], Gerd Folkers[d], and Ursula von Mandach[a,*]

[a]Department of Obstetrics, Zurich University Hospital, CH–8091 Zurich, [b]Agroscope Liebefeld-Posieux, Swiss Federal Research Station for Animal Production and Dairy Products (ALP), CH–3003 Berne, [c]Paracelsus Hospital, CH–8805 Richterswil, and [d]Institute of Pharmaceutical Sciences, Swiss Federal Institute of Technology Zurich, CH–8092 Zurich, Switzerland

ABSTRACT: Consumption of CLA by lactating women affects the composition of their milk, but the pattern of the different CLA isomers is still unknown. We determined the effects of short maternal supplementation with CLA-rich Alpine butter on the occurrence of FA and CLA isomers in human milk. In an open randomized controlled study with a two-period cross-over design, milk FA and CLA isomer concentrations were measured on postpartum days ≥20 in two parallel groups of lactating women before, during, and after consumption of defined quantities of Alpine butter or margarine with comparable fat content (10 d of butter followed by 10 d of margarine for one group, and vice versa in the other). In the 16 women who completed the study (8/group), Alpine butter supplementation increased the C_{16} and C_{18} FA, the sum of saturated FA, the 18:1 *trans* FA, and the *trans* FA with CLA. The CLA isomer 18:2 *c*9,*t*11 increased by 49.7%. Significant increases were also found for the isomers *t*9,*t*11, *t*7,*c*9, *t*11,*c*13, and *t*8,*c*10 18:2. The remaining nine of the total 14 detectable isomers showed no changes, and concentrations were <5 mg/100 g fat. A breastfeeding mother can therefore modulate the FA/CLA supply of her child by consuming Alpine butter. Further studies will show whether human milk containing this FA and CLA isomer pattern acts as a functional food for newborns.

Paper no. L9632 in *Lipids 40*, 581–587 (June 2005).

Human milk (from German women) contains more long-chain FA, with chain lengths of C_{20} to C_{24} including several double bonds, than bovine milk fat. It contains a high proportion of palmitic acid (16:0, 25.3%) and the isomeric groups of 18:1 and 18:2, their main components being oleic acid (*c*9, 29.0%) and linoleic acid (*c*9,*c*12, 9.5%) (8).

The major CLA isomer is *c*9,*t*11-octadecadienoic acid (*c*9,*t*11 18:2) (1), also called rumenic acid (2). Although linoleic acid is isomerized by the enzymatic conversion of the *c*12 to the *t*11 bond by the anaerobe *Butyrivibrio fibrisolvens* in the rumen (3), an estimated 64% of dairy milk fat CLA is of endogenous origin (4). Total CLA and isomer concentrations in dairy milk fat depend on feeding (i.e., pasture, oilseeds), the effects of altitude and season, as well as the age and breed of the cow (5–7). Total CLA and isomer concentrations in human milk depend on maternal diet, stage of lactation, and *de novo* synthesis (8–12). As humans do not synthesize PUFA, concentrations depend exclusively on dietary fat intake (13). A study reporting CLA concentrations (*c*9,*t*11 isomer) of 5.8 mg/g fat in milk from mothers on conventional diets vs. 11.2 mg/g fat in Hare Krishna mothers hypothesized that the difference was due to the large amounts of butter, ghee, and cheese consumed by the latter (9). Chronic dietary *c*9,*t*11 18:2 intake is thought to increase milk 18:2 *c*9,*t*11 concentrations (10). The proportions of partially hydrogenated oils and ruminant fats in the diet also determine *trans* 18:1 isomeric distribution (8), whereas maternal diet, i.e.. consumption of different products or amounts of milk and meat, has been shown to correlate with differences in the CLA content of human milk (11).

Several effects of a high-CLA diet in animals and humans have been described. However, for the effect of most interest to us, that on neonatal development, only animal data are available: in rats, increased milk CLA concentrations in dams on a high-CLA diet are associated with enhanced pup weight gain (14). Recent studies have also shown that individual isomers have different effects.

The aim of the present investigation as an essential preliminary to an efficacy study was to quantify CLA isomers and FA concentrations in human milk from mothers consuming defined quantities of CLA-rich Alpine butter.

SUBJECTS, MATERIALS, AND METHODS

Subjects. Following approval from the Institutional Review Board of the Departments of Obstetrics and Urology at Zurich University Hospital, healthy lactating women (*n* = 20) from the Obstetrics Department were recruited on day (D) 2–4 postpartum with their written informed consent. The noninclusion criteria were pre-existing disease, medication other than vitamins or minerals, HIV, mastitis, vegan or similar extreme diet, substance abuse (including alcohol), smoking, and inability to understand conversational German. Subjects started the study from D20 postpartum when at home and healthy in lactation stage III.

Protocol. Dietary treatment was randomized in sealed opaque envelopes according to an open controlled two-period cross-over design in two parallel groups. Group 1 followed a normal diet at home to day 20 postpartum (= study D1). From D1 through D10 (period 1), women were invited to supplement their diet with 40 g/d (4 packages of 10 g per 24 h) margarine (M) (Becel®;

www.unilever.com) containing 24 g fat and 16 g water. From D11 through D20 (period 2), the diet was supplemented with 30 g/d (3 packages of 10 g per 24 h) Alpine butter (AB) containing 25.7 g fat, 4.3 g water, and an average of 2.09 g CLA/100 g milk fat (equivalent to approximately 0.5 g CLA/d). The difference between the daily amount of M (30 g) and AB (40 g), respectively, should result in an equal daily fat intake from the study products. Group 2 women followed the same dietary schedule in reverse order (period 1: AB; period 2: M).

The Alpine butter originated from Alp Mutten (Graubünden, Switzerland, 2100 m altitude) and consisted of a blend of five 2-kg portions that was produced between July 1 and 25, 2003, and stored at −20°C until use. The 10-g portions of this blend contained 8.6 g fat, 1.4 g water, and 180.0 mg total CLA (corresponding to 2.09 g total CLA/100 g milk fat). The predominant CLA isomers were *c*9,*t*11, *t*11,*c*13, *t*7,*c*9, and *t*8,*c*10 18:2. The FA and CLA composition of the two supplements is shown in Table 1.

The women had to record the real daily intake of study products (weight). No additional Alpine milk or ruminant meat products were allowed during the study.

Dietary diary. The subjects documented potential additional sources of CLA by recording every day the estimated intake (volume or weight) of milk and dairy products (yogurt, sour cream, cream, cheese, etc.) and meat (type). The amount of a consumed product was given in the database of the EBIS program (15), which transforms the consumed volume or weight of a product in consumed grams fat by considering the product's specific percent fat. From the daily fat intake, the daily CLA intake (milligrams) was calculated using the values of Fritsche and Steinhart (16,17) for CLA amounts (grams CLA per gram fat) in different foods (German and others); for chicken or turkey the CLA values of Chin *et al.* (1) were used.

Milk sampling. On D1, D5, D10, D15, and D20, the subjects took milk samples at home according to a standardized procedure assisted by the principal investigator (IB): between 8:00 and 11:00 A.M. and 1–3 h after a continental breakfast, the breast that was not actually used for infant feeding at the last feed was emptied completely using an electric pump (Lactina™ Electric plus; Medela AG, Baar, Switzerland) and the volume measured; 2 × 10-mL aliquots were transferred to plastic tubes, cooled at +4°C (cold box), and stored at −20°C until analysis. The remainder was fed to the baby.

Lipid extraction and analysis of FA. (i) Lipid extraction. Milk fat was obtained gravimetrically using the Roese-Gottlieb method, i.e., the fat globule membranes were disrupted with ammonia and ethanol, the fat was extracted with diethyl ether and petroleum ether, and the pure fat was stored at −20°C until analysis (18).

(ii) FA. The milk fat was dissolved in hexane, and the glycerides were transesterified to the corresponding FAME using a solution of potassium hydroxide in methanol (2 mol/L) as per ISO standard 15885. FA composition was determined using a gas chromatograph (GC; Agilent 6890, www.agilent.com) equipped with an on-column injector and FID (19). Nearly 70 FA were separated on a capillary column (100 m × 0.25 mm ×

TABLE 1

Fatty Acids and CLA Isomers in Margarine and Alpine Butter Supplements[a,b] (per 100 g fat)[a]

FA	Unit	Margarine	Alpine butter
14:0	g	0.83	6.99
15:0	g	0.02	1.29
16:0	g	10.83	19.88
17:0	g	0.04	0.78
18:0	g	3.75	11.25
18:1 *c*9	g	24.24	20.55
18:1 *t*6-8	g	<0.01	0.16
18:1 *t*9	g	<0.01	0.28
18:1 *t*12	g	<0.01	0.18
18:1 *t*13-14 + *c*6-8	g	0.01	0.62
18:2 *c*9,*c*12	g	46.70	1.53
18:2 *t*7,*c*9 + *t*8,*c*10 + *c*9,*t*11	g	<0.01	1.85
18:2 *c*9,*c*11 + *t*9,*t*11 + *t*11,*c*13	g	<0.01	0.14
18:2 *t*12,*t*14	mg	ND	20.4
18:2 *t*11,*t*13	mg	ND	33.2
18:2 *t*10,*t*12	mg	ND	2.8
18:2 *t*9,*t*11	mg	ND	15.0
18:2 *t*8,*t*10	mg	ND	1.7
18:2 *t*7,*t*9	mg	ND	10.2
18:2 *t*6,*t*8	mg	ND	4.7
18:2 *c/t*12,14	mg	ND	5.3
18:2 *t*11,*c*13	mg	ND	148.2
18:2 *c*11,*t*13	mg	ND	3.4
18:2 *t*10,*c*12	mg	ND	1.6
18:2 *c*9,*t*11	mg	ND	1767.3
18:2 *t*8,*c*10	mg	ND	29.5
18:2 *t*7,*c*9	mg	ND	49.0
18:3 *c*9,*c*12,*c*15	g	0.12	1.24
Saturated FA[c]	g	18.97	51.80
Monounsaturated FA[d]	g	25.41	29.87
PUFA[e]	g	47.72	6.72
18:1 *trans*[f]	g	0.03	5.94
Σ18:2	g	47.34	5.03
18:2 *trans* without *trans* CLA[g]	g	0.08	1.45
18:2 *trans* with CLA[h]	g	0.09	3.31
trans FA without CLA[i]	g	0.11	7.72
trans FA with CLA[j]	g	0.12	9.59
n-3[k]	g	0.93	2.22
n-6[l]	g	46.79	2.38

[a]Values are means, *n* = 3.
[b]A selected summation of FA that addresses specific points to the discussion is presented. CLA isomers were analyzed by silver-ion HPLC and are ordered according to their retention time; ND, not detectable; *tt*NMID, *trans,trans* non-methylene interrupted diene; *cc*MID, *cis,cis* methylene interrupted diene.
[c]AB: 4:0, 5:0, 6:0, 7:0, 8:0, 10:0, 12:0, 12:0 iso, 12:0 aiso, 13:0 iso, 14:0, 14:0 iso, 14:0 aiso, 15:0, 15:0 iso, 16:0, 16:0 iso, 16:0 aiso, 17:0, 17:0 iso, 17:0 aiso, 18:0, 19:0, 20:0, 22:0; M: 8:0, 10:0, 12:0, 14:0, 15:0, 16:0, 16:0 aiso, 17:0, 17:0 aiso, 18:0, 20:0, 22:0, 24:0.
[d]AB: 10:1, 14:1 *ct*, 16:1 *ct*, 17:1 *ct*, 18:1 -*t*4, -*t*5, -*t*6-8, -*t*9, -*t*10-11, -*t*12, -(*t*13-14 + *c*6-8), 20:1 *t*, 20:1 *c*5, 20:1 *c*9, 20:1 *c*11; M: 16:1 *c*, 18:1 -*t*10, -*c*9, -*c*11, 20:1 *c*11.
[e]AB: 18:2 [Σ *tt*NMID, *t*9,*t*12, *c*9,*t*13 + (*t*8,*c*12), *c*9,*t*12 + (*cc*MID + *t*8,*c*13), *t*11,*c*15 + *t*9,*c*12), -*c*9,*c*12, -*c*9,*c*15, 18:3 -*c*6,*c*9,*c*12, -*c*9,*c*12,*c*15, 18:2-(*c*9,*t*11 + -*t*8,*c*10 + -*t*7,*c*9), -(*t*11,*c*13 + -*c*9,*c*11), -*t*9,*t*11, 20:2 *cc* n-6, 20:3n-6, 20:3n-3, 20:4n-6, 20:5n-3, 22:5n-3, 22:6n-3; M: 18:2 -(*c*9,*t*12 + *cc*MID + -*t*8,*c*13), -(*t*11,*c*15 + *t*9,*c*12], -*c*9,*c*12, -*c*9,*c*15, 18:3 *c*9,*c*12,*c*15, 20:3n-3, 20:4n-6, 20:5n-3.
[f]AB: 18:1 *t*4 to *t*13-14; M: 18:1 -*t*10.
[g]AB: 18:2 *trans* [Σ *tt*NMID, *t*9,*t*12, *c*9,*t*13 + (*t*8,*c*12), *c*9,*t*12 + (*cc*MID +,*t*8*c*13, *t*11,*c*15 + *t*9,*c*12]; M: 18:2 -(*c*9,*t*12 + *t*8,*c*13), -(*t*11,*c*15 + *t*9,*c*12).
[h]AB: 18:2 *t* + CLA *trans* (Σ C18:2 *t*7,*c*9, *t*8,*c*10, *c*9,*t*11, *t*9,*t*11, *t*11,*c*13); M: 18:2 -(*c*9,*t*12 + *t*8,*c*13), -(*t*11,*c*15 + *t*9,*c*12).
[i]AB: 14:1 *t*, 16:1 *t*, 17:1 *t*, 20:1 *t*, 18:1 *trans* and 18:2 *trans* (without CLA *trans*); M: 18:1 *t*10, 18:2 -(*c*9,*t*12 + *t*8,*c*13), -(*t*11,*c*15 + *t*9,*c*12).
[j]AB: 14:1 *t*, 16:1 *t*, 17:1 *t*, 20:1 *t*, 18:1 *trans*, 18:2 *trans* and CLA *trans*; M: 18:1 *t*10, 18:2 -(*c*9,*t*12 + *t*8,*c*13), -(*t*11,*c*15 + *t*9,*c*12).
[k]AB: 18:2 -*c*9,*c*15 + -*t*11,*c*15, 18:3 *c*9,*c*12,*c*15, 20:3, 20:5, 22:5, 22:6; M: 18:2 -*c*9,*c*15, -*t*11,*c*15, 18:3 *c*9,*c*12*c*15, 20:3, 20:5.
[l]AB: 18:1 -*t*12, -*c*12, 18:2 -*t*9,*t*12, -*c*9,*t*12, -*c*9,*c*12, 18:3 *c*6,*c*9,*c*12, 20:2*cc*, 20:3, 20:4; M: 18:2 -*c*9,*t*12, -*c*9,*c*12, 20:3, 20:4.
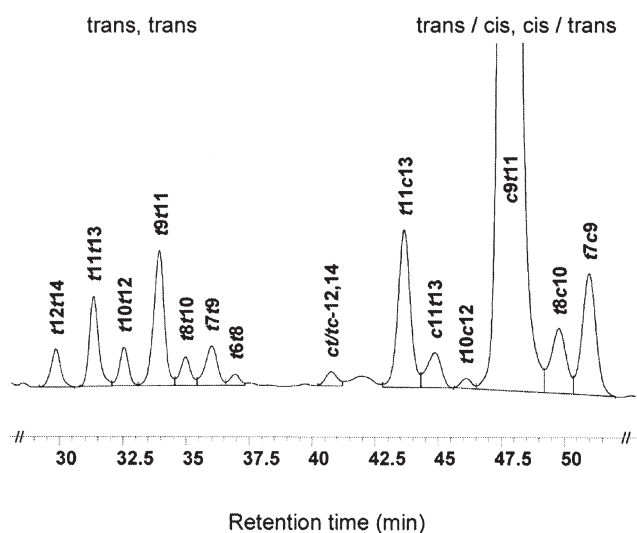
FIG. 1. Silver-ion HPLC (Ag⁺-HPLC) separation of CLA methyl esters of human milk using three columns in series (peak *t*6,*t*8 tentatively assigned according to Ref. 20).

0.20 μm, CP-Sil 88; www.varianinc.com) and quantified in absolute values (g FA/100 g fat) using nonanoic acid as internal standard.

(iii) CLA isomers. CLA isomers were analyzed by silver-ion (Ag⁺) HPLC according to Rickert *et al.* (20), modified by Kraft *et al.* (21). The analysis was performed on an Agilent LC series 1100 equipped with a photodiode array detector (234 nm) using three ChromSpher Lipids columns in series (stainless steel, 250 × 4.6 mm, 5 μm particle size; Chrompack, Middleburg, The Netherlands). The solvent consisted of UV-grade hexane with 0.1% acetonitrile and 0.5% ethyl ether (flow rate 1 mL min⁻¹), prepared fresh daily. Injection volumes were 10 μL, representing <250 μg lipid. The identification of CLA isomers was based on co-injection with commercial reference material and synthesized CLA. The methyl esters of *c*9,*t*11 (98%), *t*10,*c*12 (98%), and *c*9,*t*11 18:2 (75–78%) were obtained from Matreya Inc. (Pleasant Gap, PA). Other CLA isomers were synthesized by isomerization of the commercially available reference (technical grade) with I_2 (22). The results were expressed as absolute values in mg per 100 g fat. Fourteen different CLA isomers were separated by this HPLC method (Fig. 1).

Statistical analysis. A power calculation was performed based on an expected difference in CLA human milk content of 30% between the two phases, Alpine butter (AB) and margarine (M). The power was 80% for *n* = 8/group (α = 0.5).

Data were entered into Excel, analyzed in Systat for Windows, version 10.2 (www.uic.edu/depts/accc/software), and expressed as means ± SD. The Kolmogorov–Smirnov test was used for normality. Mean values were compared using the unpaired two-tailed *t*-test for cross-over design and a *P* value of <0.05. "Effect" refers to the differences between the two phases AB vs. M of group-pooled data, and "period" to the period effect, i.e., the differences between the two phases AB and M of group 1 vs. group 2.

RESULTS

Subjects. Three women withdrew because of lactation failure and one developed diarrhea in response to Alpine butter, leaving eight subjects per group. The groups did not differ statistically in age (27.8 ± 3.5 vs. 29.5 ± 5.6 yr, respectively), parity, gravidity, gestational age at delivery, or body mass index (BMI) during the study (Table 2).

Two group 2 women were excluded from the statistical analysis of the CLA isomers because of technical problems in the isomer analysis.

Study product intake and dietary diaries (Table 3). The mean daily intake of margarine was 29.75 g (group 1) and 30.25 g (group 2) and that of Alpine butter 22.0 g (group 1) and 23.75 g (group 2). Study product intake was thus below the requested level (margarine: up to 40.0 g; Alpine butter: up to 30.0 g). The higher intake of margarine than butter (*P* = 0.003) resulted in an equal daily fat intake in both groups (*P* = 0.25 differences between M and AB [effect] and differences between the groups [period]). Fat intake was calculated from 60 g fat/100 g (margarine) and 85.8 g fat/100 g (Alpine butter) as specified in the Subjects, Materials, and Methods section.

Dietary nonsupplement CLA intake, calculated from the daily dietary records, also did not differ statistically (*P* = 0.52) between phases or groups. Extremely small or zero amounts of ruminant meat (beef) were recorded in both groups, as requested (data not shown).

Human milk. (i) Fat content. In neither group did fat content of human milk differ significantly between margarine and butter phases (group 1: 3.3 ± 0.6 vs. 3.4 ± 1.6 g/100 mL milk; group 2: 2.9 ± 1.3 vs. 3.4 ± 1.1 g/100 mL milk) corresponding to a mean fat yield (g) per breast of 1.94 in the margarine and 1.90 in the butter phase (NS).

(ii) FA. The sum of saturated FA increased by 2.057 g/100 g fat during the pooled butter phases (*P* = 0.03), 18:1 *trans* FA by 0.428 g/100 g fat (*P* = 0.001), and *trans* FA with CLA by 0.178 g/100 g fat (*P* = 0.005) (all without period effects). There were significant pooled-group decreases in the butter phases in the sum of PUFA (3.502 g/100 g fat), 18:2 (3.252 g/100 g fat), n-6 FA (3.571 g/100 g fat) (all *P* = 0.001), and the sum of unsaturated FA (3.389 g/100 g fat; *P* = 0.02) (Table 4). The ratio of n-6/n-3 FA was lower in the butter than in the margarine phases (mean: 13.7 vs. 17.9, *P* < 0.01), but the dif-

TABLE 2
Population Demographic and Obstetric Data*a*

	Group 1 (*n* = 8)		Group 2 (*n* = 8)	
	Mean	SD	Mean	SD
Age (yr)	27.8	3.5	29.4	4.8
Parity (n)	1.6	0.5	1.8	0.7
Gravidity (n)	2.1	1.4	2.0	1.3
Gestational age (wk) at delivery	40.6	1.3	40.1	1.4
BMI*b* (kg/m²)	25.0	2.6	26.5	6.4
Days postpartum at study start	35.3	13.3	33.3	9.3

*a*Values between the groups do not differ.
*b*Mean of the five body weight values measured on the five sampling days. BMI, body mass index.

TABLE 3
Documented Intake of Study Products (and corresponding fat and CLA) and Dietary CLA (pooled study days)

| | Group 1 (*n* = 8) | | | | Group 2 (*n* = 8) | | | | P^a | |
| | M | | AB | | AB | | M | | | |
	Mean	SD	Mean	SD	Mean	SD	Mean	SD	Effect[b]	Period[c]
Study product intake										
Amount (g/d)	29.75	10.91	22.00	7.67	23.75	6.81	30.25	8.05	0.003	NS
Fat[d] (g/d)	17.85	6.55	18.88	6.58	20.38	5.85	18.15	4.83	NS	NS
CLA[e] (mg/d)	<2		379.4	132.3	409.6	117.6	<2		<0.001	NS
Dietary intake										
CLA[f] (mg/d)	81.1	79.7	64.9	52.3	109.7	104.2	70.9	63.4	NS	NS

[a]Unpaired two-tailed *t*-test for cross-over design: NS, nonsignificant.
[b]Effect: overall (both groups) AB (Alpine Butter) vs. M (Margarine).
[c]Period: AB vs. M of group 1 vs. group 2.
[d]Calculated from 85.8 g fat/100 g (AB) and 60 g fat/100 g (M).
[e]C18:2 *t*7,*c*9 + *t*8,*c*10 + *c*9,*t*11 and C18:2 *c*9, *c*11 + *t*9,*t*11 + *t*11,*c*13.
[f]C18:2 *c*9,*c*11 + *t*9,*t*11 + *t*11,*c*13 calculated by EBIS program (19) according to nutrition protocol.

ference was only minimal if we consider a ratio of 1 vs. 50 in the corresponding study products (see Table 1).

The butter phases showed highly significant pooled-group differences (g/100 g fat; all *P* < 0.001) vs. margarine in the following individual FA (Table 4): increases in C_{15} (0.116 g), C_{16} (1.507 g), C_{17} (0.072 g), C_{18} (0.960 g), and *t*9,*c*12 + *t*11,*c*15 18:2 (0.043 g); decreases in *c*9,*c*12 18:2 (3.632 g), *c*,*c*20:2n-6 (0.056 g), and 20:3n-6 (0.062 g) FA.

CLA isomers. (i) At baseline. The overall baseline concentration (D1, after normal nonstandardized diet, *n* = 14) showed a predominance of the *c*9,*t*11 (277 ± 195 mg/100 g fat, range 77–800), *t*9,*t*11 (13 ± 7 mg/100 g fat, range 4–31), and *t*11,*c*13 (12 ± 10 mg/100 g fat, range 2–37) 18:2 isomers, and a total CLA concentration of 352 ± 229 mg/100 g fat (range 103–956).

(ii) During the study. Analysis of the mean pooled study day values (D5 + D10 and D15 + D20, respectively), showed significant increases in *t*12,*t*14, *t*11,*t*13, *t*6,*t*8, *c*11,*t*13, *t*11,*c*13, *c*9,*t*11, and *t*8,*c*10 18:2 as well as in the sum of CLA isomers during Alpine butter intake of both groups (Table 4). There were no significant period effects. Pooled-group increases of the individual isomers, expressed per 100 g fat, are shown in Figure 2. The sum of CLA isomers increased by 129.4 mg (45.0%, *P* = 0.005) and the ratio of *t*11,*c*13 and *t*7,*c*9 18:2 isomers by 70.8% (*P* < 0.0001).

DISCUSSION

This study demonstrated that 10-d supplementation with Alpine butter, a natural CLA-rich product, affects the FA and CLA isomer content of human milk.

Butter significantly increased the concentrations of saturated FA. At study start (after a normal nonstandardized diet), 18 *c*9,*t*11 18:2 and total CLA concentrations in human milk were 277 ± 195 (range 7–800) and 352 ± 229 (range 103–956) mg/100 g fat, respectively. The isomers showing the highest increases in milk were *t*11,*c*13 (100.5%), *t*6,*t*8 (67.3 %), *t*12,*t*14 (61.3%), *c*9,*t*11 (49.7%), *c*11,*t*13 (39.6%), *t*11,*t*13 (34.0%), and *t*8,*c*10 (28.2%) (all *P* < 0.05).

Ethical limitations in standardization and compliance, which was not 100% in our study (Table 3), make human data inevitably more variable than their dairy counterparts. The women were allowed to consume their total supplement per 24 h in as many portions as they wished, and we could not control for the well-known differences in absorption relating to the amount of fat per portion (23). However, our study has certain advantages compared with others with human milk (9,10). The cross-over design excluded interindividual differences and differences due to lactation duration; all subjects consumed the same supplements with defined fat content and FA composition; milk sampling was standardized (volume, time of day) to minimize the effect of differential fat absorption (23) and milk volume (24); dietary intake of other dairy and beef products was recorded daily throughout the study; BMI was calculated throughout; milk analysis was longitudinal, with two time points per period. Since no significant differences were found in compliance, BMI, dietary (nonsupplement) CLA intake, or total milk fat content between periods or groups, these factors can be excluded as accounting for the differential milk content of FA or CLA isomers in response to butter supplementation.

Our basal value in human milk for the predominant isomer (*c*9,*t*11 18:2) (0.25 g/100 g fat) is similar to those reported by Jensen *et al.* (0.19 and 0.18 g/100 g fat) (25,26), Park *et al.* (0.21 g/100 g fat) (10), and Ritzenthaler *et al.* (0.28 g/100 g total FA) (12) in lactating American mothers during the low-dairy periods (10,25,26) or in baseline (12). However, McGuire *et al.* (27) and Innis and King (28) recorded higher basal values (0.4 g/100 g fat) in American mothers, matching those in German mothers (0.39 and 0.40 g/100 g fat) (29).

The increase in the predominant *c*9,*t*11 isomer in our study by 109.8 mg/100 g fat (49.7%) approximates that reported by Park *et al.* (10) (64.6%) from the low to the high CLA dairy period of their study and is higher than that reported by Ritzenthaler *et al.* (12) (29.0%) from baseline to 4 wk of consumption of high-CLA cheese. Unlike us, earlier investigators into human milk CLA content could identify, in addition to the predominant *c*9,*t*11 18:2 isomer, only *t*9,*t*11 (29), *t*10,*c*12 (12,27,29), *t*7,*c*9 (30), and *t*9,*t*11/*t*10,*t*12 18:2 (12). In milk

TABLE 4
FA and CLA Isomers in Human Milk (per 100 g human milk fat) During Maternal Supplementation with Margarine and Alpine Butter (pooled study days)

| | | Group 1 ($n = 8$) | | | | Group 2 ($n = 8^b$) | | | | P^c | |
| | | M | | AB | | AB | | M | | | |
FA[a]	Unit	Mean	SD	Mean	SD	Mean	SD	Mean	SD	Effect[d]	Period[e]
14:0	g	5.13	0.73	5.66	1.06	5.99	1.38	5.67	1.18	NS	NS
15:0	g	0.31	0.05	0.42	0.07	0.49	0.13	0.37	0.13	<0.001	NS
16:0	g	20.28	1.96	20.62	2.14	22.22	2.87	19.55	3.45	<0.001	<0.05
17:0	g	0.29	0.04	0.36	0.06	0.39	0.08	0.32	0.09	<0.001	NS
18:0	g	6.04	1.05	6.83	1.16	7.38	1.04	6.25	1.05	<0.001	NS
18:1 *c*9	g	26.38	3.19	26.16	3.75	26.91	3.54	27.02	3.50	NS	NS
18:1 *t*9	g	0.30	0.11	0.28	0.14	0.27	0.07	0.27	0.12	NS	NS
18:2 *c*9,*c*12	g	14.64	3.60	12.41	6.06	7.96	2.72	13.00	2.99	<0.001	NS
18:2 *t*12,*t*14	mg	1.46	0.62	2.90	1.56	2.77	1.90	2.06	0.92	0.007	NS
18:2 *t*11,*t*13	mg	4.18	1.57	6.83	2.24	6.43	4.07	5.72	1.90	0.03	NS
18:2 *t*10,*t*12	mg	2.49	0.99	3.71	1.63	2.40	0.78	3.17	0.34	NS	NS
18:2 *t*9,*t*11	mg	14.8	12.9	19.4	14.8	13.4	11.8	14.6	11.7	NS	NS
18:2 *t*8,*t*10	mg	3.21	0.61	3.21	1.27	2.96	1.50	2.88	0.72	NS	NS
18:2 *t*7,*t*9	mg	4.01	1.25	4.35	1.16	4.40	1.35	4.45	0.92	NS	NS
18:2 *t*6,*t*8	mg	0.46	0.16	0.90	0.34	0.83	0.23	0.58	0.22	0.002	NS
18:2 *ct/tc*12,14	mg	0.86	0.50	1.22	0.56	1.15	0.64	0.98	0.35	NS	NS
18:2 *t*11,*c*13	mg	6.2	3.1	15.6	6.1	17.1	10.9	10.1	5.0	0.001	NS
18:2 *c*11,*t*13	mg	3.26	1.19	5.14	2.16	5.99	3.13	4.71	1.69	0.02	NS
18:2 *t*10,*c*12	mg	1.31	1.07	1.94	1.58	0.90	0.27	1.44	0.59	NS	NS
18:2 *c*9,*t*11	mg	176.0	75.6	309.5	120.7	351.6	212.0	265.6	114.7	0.005	NS
18:2 *t*8,*c*10	mg	6.6	1.8	9.6	3.8	10.7	5.4	9.2	2.5	0.04	NS
18:2 *t*7,*c*9	mg	10.4	4.0	13.7	6.0	16.0	7.1	14.9	4.3	NS	NS
ΣCLA	mg	235.2	87.0	397.9	141.7	436.6	248.6	340.5	126.8	0.005	NS
18:3 *c*9,*c*12,*c*15	g	0.44	0.21	0.41	0.08	0.38	0.16	0.50	0.19	NS	NS
20:3n-6	g	0.31	0.09	0.26	0.09	0.21	0.12	0.29	0.11	<0.001	NS
20:4n-6	g	0.32	0.12	0.29	0.12	0.19	0.09	0.26	0.06	<0.01	NS
Saturated FA[f]	g	37.27	1.84	40.64	4.13	38.77	3.96	38.03	3.84	<0.05	NS
Monounsaturated FA[g]	g	30.11	4.17	31.57	5.01	30.17	6.49	31.36	4.17	NS	NS
PUFA[h]	g	16.28	4.17	14.77	6.30	9.35	3.64	14.84	3.43	<0.001	<0.05
18:1 *trans*[i]	g	1.31	0.21	1.85	0.49	1.72	0.56	1.40	0.52	<0.001	NS
Σ18:2	g	14.69	3.69	13.30	6.10	8.19	3.20	13.30	3.14	<0.001	<0.05
trans FA with CLA[j]	g	2.04	0.32	2.91	0.67	2.62	0.93	2.26	0.73	<0.001	NS
n-6[k]/n-3[l]		19.8	5.21	15.38	6.64	11.95	3.33	15.98	3.52	<0.01	NS

[a]CLA isomers and CLA were analyzed by silver-ion HPLC and are ordered according to their retention time.
[b]$n = 6$ for CLA isomers.
[c]Unpaired two-tailed *t*-test for cross-over design: NS, nonsignificant.
[d]Effect: overall (both groups) AB (Alpine Butter) vs. M (Margarine).
[e]Period: AB vs. M of group 1 vs. group 2.
[f]For footnote *f* see Table 1, footnote *c*.
[g]For footnote *g* see Table 1, footnote *d*.
[h]For footnote *h* see Table 1, footnote *e*.
[i]For footnote *i* see Table 1, footnote *f*.
[j]For footnote *j* see Table 1, footnote *j*.
[k]For footnote *k* see Table 1, footnote *l*.
[l]For footnote *l* see Table 1, footnote *k*.

from German women, *c*9,*t*11 18:2 accounted for no more than 0.39%, *t*9,*t*11 18:2 at most 0.04%, and *t*10,*c*12 18:2 at most 0.08% of total FA (29). For Yurawecz *et al.* (30), the *t*7,*c*9 18:2 isomer accounted for 5.5–9.9% of total CLA. In our study, the *c*9,*t*11, *t*9,*t*11, *t*7,*c*9, and *t*10,*c*12 isomers accounted for 0.380, 0.019, 0.018, and 0.002% of total FA and for 79, 3.9, 3.6, and 0.3% of total CLA; these values are consistent with those indicated above.

The distribution of other FA in milk during the study periods reflects some but not all of the differences between supplements (Table 1). The 18:1 *trans* FA other than *trans*10-11, which occur in low concentrations in both study products, also show low concentrations in human milk during both phases. This aspect could be of interest because in recent years attention has been given to the potential impairment of EFA metabolism to their long-chain metabolites by the *trans*-isomers in humans (31). It is therefore unlikely that the small amounts found in human milk in our study have any important negative effect on the newborn. The higher amounts of C_{15}, C_{16}, C_{17}, and C_{18} acids and the *trans* unsaturated octadecadienoic acids (*t*9,*c*12 + *t*11,*c*15 18:2) are likely to have resulted from their higher content in Alpine butter. C_{15} and C_{17} acids are synthe-
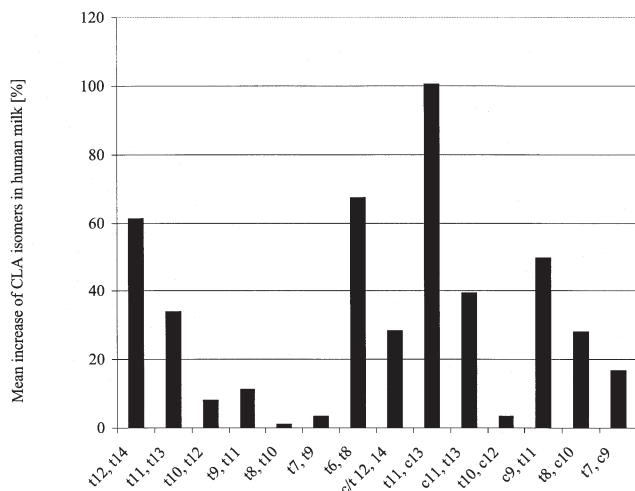
FIG. 2. Mean increase (%) of CLA isomers in human milk during pooled Alpine butter intake (*n* = 14).

sized by ruminant flora but not in humans owing to the uneven number of carbon atoms (32). They thus act as markers of a dairy fat diet (33,34). The highly significant decrease (3.63 g/100 g milk fat = 26.3%) in octadecadienoic acid (*c*9,*c*12 18:2) on butter vs. margarine is also probably due to its much lower content in butter than in margarine (1.53 g vs. 46.70 g/100 g fat). The n-6 FA that occur at high concentrations in margarine have an extremely low transfer into human milk.

Mothers can rapidly and easy modulate the fat composition of their milk by consuming Alpine butter (or related natural dairy products). This could have positive implications for the newborn. Several studies, most of them in animals, have indicated the potential impact of CLA-rich milk on the development of the newborn. One point could be the potential effect on body weight. In rats, the *c*9,*t*11 18:2 isomer increases body weight (14,35), whereas the *t*10,*c*12 18:2 isomer decreases it in both mice (35,36) and humans [loss of body fat in diabetics (37)]. Another point could be the protection of CLA-rich milk against development of atopy. In rats and mice, oral supplementation with 100 mg/kg CLA (isomer profile unknown) reduces allergic anaphylaxis (by decreasing blood pressure), vasodilatation, and scratching behavior in response to egg-white lysozyme (38). However, further studies in humans are necessary to confirm these effects and to show whether human milk with a special pattern of FA and CLA could be a functional food for newborns.

ACKNOWLEDGMENT

REFERENCES

1. Chin, S.F., Liu, W., Storkson, J.M., Ha, Y.L., and Pariza, M.W. (1992) Dietary Sources of Conjugated Dienoic Isomers of Linoleic Acid, a Newly Recognized Class of Anticarcinogens, *J. Food Comp. Anal. 5*, 185–197.
2. Kramer, J.K.G., Parodi, P.W., Jensen, R.G., Mossoba, M.M., Yurawecz, M.P., and Adlof, R.O. (1998) Rumenic Acid: A Proposed Common Name for the Major Conjugated Linoleic Acid Isomer Found in Natural Products, *Lipids 33*, 835.
3. Kepler, C.R., Hirons, K.P., McNeill, J.J., and Tove, S.B. (1966) Intermediates and Products of the Biohydrogenation of Linoleic Acid by *Butyrivibrio fibrisolvens*, *J. Biol. Chem. 241*, 1350–1354.
4. Griinari, J.M., Corl, B.A., Lacy, S.H., Chouinard, P.Y., Nurmela, K.V.V., and Bauman, D.E. (2000) Conjugated Linoleic Acid Is Synthesized Endogenously in Lactating Dairy Cows by Δ⁹-Desaturase, *J. Nutr. 130*, 2285–2291.
5. Lawless, F., Stanton, C., L'Escop, P., Devery, R., Dillon, P., and Murphy, J.J. (1999) Influence of Breed on Bovine Milk *c*9, *t*11-Conjugated Linoleic Acid Content, *Livestock Prod. Sci. 62*, 43–49.
6. Lawless, F., Murphy, J.J., Harrington, D., Devery, R., and Stanton, C. (1998) Elevation of Conjugated *cis*-9, *trans*-11-Octadecadienoic Acid in Bovine Milk Because of Dietary Supplementation, *J. Dairy Sci. 81*, 3259–3267.
7. Collomb, M., Bütikofer, U., Sieber, R., Jeangros, B., and Bosset, J.O. (2002) Composition of Fatty Acids in Cow's Milk Fat Produced in the Lowlands, Mountains and Highlands of Switzerland Using High-Resolution Gas Chromatography, *Int. Dairy J. 12*, 649–659.
8. Precht, D., and Molkentin, J. (1999) C18:1, C18:2 and C18:3 *trans* and *cis* Fatty Acid Isomers Including Conjugated *cis* Δ9,*trans* Δ11 Linoleic Acid (CLA) as Well as Total Fat Composition of German Human Milk Lipids, *Nahrung 43*, 233–244.
9. Fogerty, A.C., Ford, G.L., and Svoronos, D. (1988) Octadeca-9,11-dienoic Acid in Foodstuffs and in the Lipids of Human Blood and Breast Milk, *Nutr. Rep. Int. 38*, 937–944.
10. Park, Y., McGuire, M.K., Behr, R., McGuire, M.A., Evans, M.A., and Shultz, T.D. (1999) High-Fat Dairy Product Consumption Increases Δ9*c*,11*t*-18:2 (rumenic acid) and Total Lipid Concentrations of Human Milk, *Lipids 34*, 543–549.
11. Rist, L., Zweidler, R., and von Mandach, U. (2003) Biologische Ernährung und Gesundheit [Biological Diet and Health (German)], in *Ökologischer Landbau der Zukunft [Prospects in Organic Farming* (German)] (Freyer, B., ed.), pp. 237–240, Universität für Bodenkultur, Institut für Ökologischen Landbau/Institute for Organic Farming, Vienna,.
12. Ritzenthaler, K.L., McGuire, M.K., McGuire, M.A., Shultz, T.D., Koepp, A.E., Luedecke, L.O., Hanson, T.W., Dasgupta, N., and Chew, B.P. (2005) Consumption of Conjugated Linoleic Acid (CLA) from CLA-Enriched Cheese Does Not Alter Milk Fat or Immunity in Lactating Women, *J. Nutr. 135*, 422–430.
13. Francois, C.A., Connor, S.L., Wander, R.C., and Connor, W.E. (1998) Acute Effects of Dietary Fatty Acids on the Fatty Acids of Human Milk, *Am. J. Clin. Nutr. 67*, 301–308.
14. Chin, S.F., Storkson, J.M., Liu, W., Albright, K.J., and Pariza, M.W. (1994) Conjugated Linoleic Acid (9,11- and 10,12-octadecadienoic acid) Is Produced in Conventional but Not Germ-Free Rats Fed Linoleic Acid, *J. Nutr. 124*, 694–701.
15. Erhardt, J., and Bosch, R. (1995) Programm und Handbuch zur Ernährungsanamnese: EBIS; Ernährungsanamnese, Beratungs- und Informationssystem auf der Grundlage des Bundeslebensmittelschlüssels (BLS) [Dietary history programme and handbook: EBIS (Dietary History—Counselling and Information System Based on the German Food Code [BLS]). Stuttgart Hospital and University of Hohenheim.
16. Fritsche. J., and Steinhart, H. (1998) Amounts of Conjugated Linoleic Acid in German Foods and Evaluation of Daily Intake, *Z. Lebensm. Unters. Forsch. 201*, 77–82.
17. Fritsche, J., and Steinhart, H. (1998) Analysis, Occurrence and Physiological Properties of *trans* Fatty Acids with Particular Emphasis on Conjugated Linoleic Acid Isomers, *Fett/Lipid 100*, 190–210.

18. Collomb, M., Sieber, R., and Bütikofer, U. (2004) CLA Isomers in Milk Fat from Cows Fed Diets with High Levels of Unsaturated Fatty Acids, *Lipids 39*, 355–364.

19. Collomb, M., and Bühler, T. (2000) Analyse de la Composition en Acides Gras de la Graisse de Lait. I. Optimisation et Validation d'une Méthode Générale à Haute Résolution [Analysis of the Fatty Acid Composition of Milk Fat, I. Optimization and Validation of a General High Resolution Method (French)], *Trav. chim. aliment. hyg. 91*, 306–332.

20. Rickert, R., Steinhart, H., Fritsche, J., Sehat, N., Yurawecz, M.P., Mossoba, M.M., Roach, J.A.G., Eulitz, K., Ku,Y., and Kramer, J.K.G. (1999) Enhanced Resolution of Conjugated Linoleic Acid Isomers by Tandem-Column Silver-Ion High Performance Liquid Chromatography, *J. High Resolut. Chromatogr. 22*, 144–148.

21. Kraft, J., Collomb, M., Möckel, P., Sieber, R., and Jahreis, G. (2003) Differences in CLA Isomer Distribution of Cow's Milk Lipids, *Lipids 38*, 657–664.

22. Eulitz, K., Yurawecz, M.P., Sehat, N., Fritsche, J., Roach, J.A.G., Mossoba, M.M., Kramer, J.K.G., Adlof, R.O., and Ku, Y. (1999) Preparation, Separation, and Confirmation of the Eight Geometrical *cis/trans* Conjugated Linoleic Acid Isomers 8,10- through 11,13-18:2, *Lipids 34*, 873–877.

23. Ramirez, M., Amate, L., and Gil, A. (2001) Absorption and Distribution of Dietary Fatty Acids from Different Sources, *Early Hum. Dev. 65*, S95–S101.

24. Mitoulas, R.L., Gurrin, L.C., Doherty, D.A., Sheriff, J.L., and Hartmann, P.E. (2003) Infant Intake of Fatty Acids from Human Milk over the First Year of Lactation, *Br. J. Nutr. 90*, 979–986.

25. Jensen, R.G., Lammi-Keefe, C.J., Hill, D.W., Kind, A.J., and Henderson, R. (1998) The Anticarcinogenic Conjugated Fatty Acid, 9*c*, 11*t*-18:2, in Human Milk: Confirmation of Its Presence, *J. Hum. Lact. 14*, 23–27.

26. Jensen, R.G., and Lammi-Keefe, C. (2001) The Anticarcinogenic Conjugated Fatty Acid *c*9, *t*11-c18:2, or Rumenic Acid, in Human Milk: Amounts and Effects, *Adv. Exp. Med. Biol. 501*, 153–156.

27. McGuire, M.K., Park, Y., Behre, R.A., Harrison, L.Y., Shultz, T.D., and McGuire, M.A. (1997) Conjugated Linoleic Acid Concentrations of Human Milk and Infant Formula, *Nutr. Res. 17*, 1277–1283.

28. Innis, S.M., and King, D.J. (1999) *Trans* Fatty Acids in Human Milk Are Inversely Associated with Concentrations of Essential all-*cis* n-6 and n-3 Fatty Acids and Determine *trans*, but not n-6 and n-3, Fatty Acids in Plasma Lipids of Breast-Fed Infants, *Am. J. Clin. Nutr. 70*, 383–390.

29. Jahreis, G., Fritsche, J., Möckel, P., Schone, F., Möller, U., and Steinhart, H. (1999) The Potential Anticarcinogenic Conjugated Linoleic Acid, *cis*-9,*trans*-11 C18:2, in Milk of Different Species: Cow, Goat, Ewe, Sow, Mare, Woman, *Nutr. Res. 19*, 1541–1549.

30. Yurawecz, M.P., Roach, J.A.G., Sehat, N., Mossoba, M.M., Kramer, J.K.G., Fritsche, J., Steinhart, H., and Ku, Y. (1998) A New Conjugated Linoleic Acid Isomer, 7 *trans*, 9 *cis*-Octadecadienoic Acid, in Cow Milk, Cheese, Beef and Human Milk and Adipose Tissue, *Lipids 33*, 803–809.

31. Mojska, H. (2003) Influence of *trans* Fatty Acids on Infant and Fetus Development, *Acta Microbiol. Pol. 52, (Suppl.)*, 67–74.

32. Wu, Z., and Palmquist, D.L. (1991) Synthesis and Biohydrogenation of Fatty-Acids by Ruminal Microorganisms *in vitro*, *J. Dairy Sci. 74*, 3035–3046.

33. Smedman, A.E.M., Gustafsson, I.B., Berglund, G.T., and Vessby, B.O.H. (1999) Pentadecanoic Acid in Serum as a Marker for Intake of Milk Fat: Relations Between Intake of Milk Fat and Metabolic Risk Factors, *Am. J. Clin. Nutr. 69*, 22–29.

34. Wolk, A., Vessby, B., Ljung, H., and Barrefors, P. (1998) Evaluation of a Biological Marker of Dairy Fat Intake, *Am. J. Clin. Nutr. 68*, 291–295.

35. Pariza, M.W., Park, Y., and Cook, M.E. (2001) The Biologically Active Isomers of Conjugated Linoleic Acid, *Prog. Lipid Res. 40*, 283–298.

36. Loor, J.J., Lin, X.B., and Herbein, J.H. (2003) Effects of Dietary *cis* 9, *trans* 11-18:2, *trans* 10, *cis* 12-18:2 or Vaccenic Acid (*trans* 11-18:1) During Lactation on Body Composition, Tissue Fatty Acid Profiles, and Litter Growth in Mice, *Br. J. Nutr. 90*, 1039–1048.

37. Belury, M.A., Mahon, A., and Banni, S. (2003) The Conjugated Linoleic Acid (CLA) Isomer, *t*10*c*12-CLA, Is Inversely Associated with Changes in Body Weight and Serum Leptin in Subjects with Type 2 Diabetes Mellitus, *J. Nutr. 133*, 257S–260S.

38. Ishiguro, K., Oku, H., Suitani, A., and Yamamoto, Y. (2002) Effects of Conjugated Linoleic Acid on Anaphylaxis and Allergic Pruritus, *Biol. Pharm. Bull. 25*, 1655–1657.

Effect of Pasture vs. Concentrate Diet on CLA Isomer Distribution in Different Tissue Lipids of Beef Cattle

**Dirk Dannenberger[a], Karin Nuernberg[a],*, Gerd Nuernberg[b],
Nigel Scollan[c], Hans Steinhart[d], and Klaus Ender[a]**

Departments of [a]Muscle Biology and Growth and [b]Genetics and Biometry, Research Institute for Biology
of Farm Animals, D-18196 Dummerstorf, Germany [c]Institute of Grassland and Environmental Research,
Aberystwyth, SY23 3EB, United Kingdom, and [d]Institute of Biochemistry and Food Chemistry,
Department of Food Chemistry, University of Hamburg, D-20146 Hamburg, Germany

ABSTRACT: This study examined the effects of feeding pasture vs. concentrate on the distribution of CLA isomers in the lipids of *longissimus* and *semitendinosus* muscle, liver and heart muscle, and subcutaneous fat in beef bulls. Sixty-four German Holstein and German Simmental bulls were randomly allocated to either an indoor concentrate system or periods of pasture feeding followed by a finishing period on a concentrate containing linseed to enhance their beef content of n-3 PUFA and CLA. The concentrations of CLA isomers in the different tissues were determined by GC and silver ion HPLC. The diet affected the distribution of individual CLA isomers in the lipids of the different tissues. The concentration (mg/100 g fresh tissue) of the most prominent isomer, *cis*-9,*trans*-11 18:2, was increased up to 1.5 times in liver and heart tissue of bulls fed on pasture as compared with concentrate. However, no diet effect was observed for *cis*-9,*trans*-11 18:2 in the lipids of *longissimus* muscle and subcutaneous fat. In all tissues, the second-most abundant CLA isomer in concentrate-fed bulls was *trans*-7,*cis*-9 18:2. In contrast, *trans*-11,*cis*-13 18:2 was the second-most abundant CLA isomer in all investigated tissue lipids of pasture-fed bulls. The concentration of the *trans*-11,*cis*-13 18:2 isomer was up to 15 times higher in tissues of pasture-fed bulls as compared with concentrate-fed animals. Furthermore, diet affected the concentrations of the CLA *trans,trans* 18:2 isomers. Pasture feeding significantly increased the concentrations of some *trans,trans* 18:2 isomers as compared with concentrate, predominantly *trans*-12,*trans*-14 18:2 and *trans*-11,*trans*-13 18:2. Overall, pasture feeding resulted in significantly increased concentrations of the sum of CLA isomers in the lipids of *longissimus* muscle, subcutaneous fat, heart and liver muscle of German Holstein and German Simmental bulls, but not in *semitendinosus* muscle.

Paper no. L9674 in *Lipids* **40**, 589–598 (June 2005).

CLA consists of a collection of positional and geometric isomers of octadecadienoic acid, with conjugated double bonds ranging from positions 6,8- to 12,14-. For each positional isomer there are four possible geometric pairs of isomers (e.g., *cis,trans*; *trans,cis*; *trans,trans*; *cis,cis*). Ruminant meats and milk and their products are the main source of CLA in the human diet. CLA has been linked to a multitude of potential health benefits, including inhibition of carcinogenesis, reduced rate of fat deposition, altered immune response, reduced serum lipids, and antidiabetic and antiatherogenic effects (1–4). Most of the research has focused on two isomers: *cis*-9,*trans*-11 18:2 and *trans*-10,*cis*-12 18:2 (2–4). Studies on pure single isomers showed that they differ in biological activities as reported in recent reviews by Banni *et al.* (5), Khanal (6), and Martin and Valeille (7). In addition, current studies show that a mixture of *trans,trans* 18:2 isomers exhibited stronger cytotoxicity against NCI-N87 gastric cancer cells than *cis,trans/trans,cis* isomers (8). Therefore, the biological activities of all individual CLA isomers must be verified.

In ruminants, dietary PUFA undergo biohydrogenation in the rumen. *cis*-9,*trans*-11 18:2 is formed during biohydrogenation of linoleic acid in the rumen, and it was assumed that this was the source of *cis*-9,*trans*-11 18:2 in milk and intramuscular fat (9). Griinari *et al.* (10) and Palmquist (11) showed that the primary source of *cis*-9,*trans*-11 18:2 is the endogenous synthesis involving Δ^9-desaturase and *trans* vacccenic acid (18:1 *trans*-11), another intermediate in ruminal biohydrogenation. Recently, Kay *et al.* (12) demonstrated that a minimum estimate of 91% of *cis*-9,*trans*-11 18:2 in milk fat was produced endogenously in cows fed fresh pasture. The lipids in pasture are high in linolenic acid (18:3n-3), and in the rumen biohydrogenation of 18:3n-3 does not result in the production of *cis*-9,*trans*-11 18:2 as an intermediate. The processes of biosynthesis for the formation of CLA and its incorporation into ruminant products were described recently in reviews by Song and Kenelly (13) and Khanal and Dhiman (14). *cis*-9,*trans*-11 18:2 is the major CLA isomer in ruminant milk and meat products (15,16). *trans*-7,*cis*-9 CLA is the second-most abundant CLA isomer in ruminant fat and represents approximately 10% of total CLA in *longissimus* muscle of bulls (16). The CLA content of the ruminant fat can be increased by dietary modifications.

Several investigations demonstrated that feeding pasture to dairy cows doubles the CLA content of milk fat (17,18). Recently, Kraft *et al.* (19) and Collomb *et al.* (20) showed differences between the CLA isomer distribution in milk lipids of cows fed indoors with diets having high levels of unsaturated FA concentrate and of cows grazing in the Alps (Switzerland). The concentrations of many CLA isomers were highest in

the milk fat of cows fed on pasture in the Alps. In addition to the main isomer, *cis*-9,*trans*-11 18:2, there was a difference in the second-most abundant CLA isomer. *trans*-11,*cis*-13 18:2, in milk fat of pasture-fed cows CLA represented more than a fourth of the total CLA present in milk fat (19,20). However, overall there is only limited information about the effect of pasture on the concentration of individual CLA isomers in beef fat. Until now, the effects of pasture feeding on the CLA isomer distribution were predominantly investigated in milk products. Only a few publications deal with the CLA isomer distribution in different beef tissues. Nuernberg *et al.* (21) and Dannenberger *et al.* (22) described the effects of CLA isomer distribution in *longissimus* muscle of German Simmental and German Holstein bulls fed pasture compared with concentrates indoors. Pasture feeding compared with concentrate feeding decreased the proportion of *trans*-7,*cis*-9 18:2 to 4.1% of total CLA in the muscle and increased *trans*-11,*cis*-13 18:2 up to 18.5% of total CLA. Furthermore, pasture feeding resulted in significantly higher concentrations of *trans*-12,*trans*-14 18:2 and *trans*-11,*trans*-13 18:2 among the CLA *trans*,*trans* 18:2 isomers in the muscle lipids of both breeds (21,22).

In measuring CLA, it is important to separate the individual CLA isomers because of the different effects of some CLA isomers in biological systems. This is particularly important because the CLA distribution pattern in the tissue lipids will be affected by different diet systems. The silver-ion HPLC (Ag$^+$-HPLC) method has proven very useful for the separation of geometrical and positional CLA isomers (23–25).

A large study was established to investigate the effect of feeding pasture vs. concentrate to two different breeds (German Holstein and German Simmental) on the meat quality and the FA composition of intramuscular fat in muscles of bulls. The results regarding aspects of meat quality and FA composition in different lipid fractions (total lipids, TG, and phospholipids) have been reported recently by Nuernberg *et al.* (26) and Dannenberger *et al.* (22, 27). This paper reports the effects of pasture vs. concentrate diet on the concentration (mg/100 g fresh tissue) of individual CLA isomers in *longissimus* muscle, *semitendinosus* muscle, subcutaneous fat, and heart muscle and liver of German Holstein and German Simmental bulls.

EXPERIMENTAL PROCEDURES

Materials. Sixty-four bulls of two breeds (5–6 mon old), German Simmental (*n* = 31) and German Holstein (*n* = 33), were randomly assigned to two dietary treatments, concentrate or pasture. German Simmental (*n* = 16) and German Holstein bulls (*n* = 17) fed on concentrate were kept in a stable and fed using single-fodder workstations. The concentrate ration consisted of winter barley, molasses particles, soybean extraction particles, calcium carbonate, sodium chloride, and a mixture of minerals and vitamins. The forage component of the diet consisted of maize silage (13.8 kg/d), concentrated feed (3.2 kg/d), soybean extraction particles (0.15 kg/d), hay (0.1 kg/d), and straw (0.09 kg/d). German Simmental (*n*-15) and German Holstein bulls (*n*-16) were kept on pasture during two summer

periods (approximately 160 d) followed by indoor periods (approximately 190 d) when animals received semi-*ad libitum* a high-energy diet. The latter consisted of wilted silage (15 kg/d), hay (0.7 kg/d), a mixture of minerals and a mixture of vitamins, and a special concentrate diet containing 12% barley, 10% coarsely cracked linseed, and a mixture of minerals and vitamins. The chemical composition including the FA composition of the diets has been reported by Nuernberg *et al.* (26). All bulls were slaughtered at 620 kg live weight in the abattoir of the Research Institute for the Biology of Farm Animals Dummerstorf (Germany) and the carcasses were chilled (4°C) before muscle samples were removed. The heart and liver samples were taken immediately (35 min) after slaughter. Samples of the *longissimus* and *semitendinosus* muscles and of the subcutaneous fat were taken at the sixth rib of the left carcass side 24 h after slaughter and stored frozen at −70°C until lipid extraction and assessment of the FA composition of the muscle lipids.

A reference standard, Sigma-FAME mixture, and a mixture of methyl esters of CLA were obtained from Sigma-Aldrich (Deisenhofen, Germany). Individual isomers of CLA methyl esters (CLA-ME), *cis*-9,*trans*-11 18:2, *trans*-9,*trans*-11 18:2, *trans*-10,*cis*-12 18:2, and *cis*-9,*cis*-11 18:2, were purchased from Matreya (Pleasant Gap, PA). All solvents used were HPLC grade from Lab-Scan (Dublin, Ireland).

Methods. (i) Extraction of tissue lipids. The intramuscular fat from 1 to 2 g of tissue was extracted with chloroform/methanol (2:1, vol/vol) according to Folch *et al.* (28) by homogenization (UltraTurrax, 3 × 15 s, 12,000 rpm) at room temperature. The details of muscle lipid extraction were described previously (21). Nonadecanoic acid methyl ester, used as an internal standard, was added to the lipids prior to saponification and methylation.

(ii) GC analysis. The FA composition of tissue lipids was determined by capillary GC using a CP SIL 88 CB column (100 m × 0.25 mm; Chrompack-Varian, Bridgwater, NJ) installed in a PerkinElmer gas chromatograph Autosys XL with an FID and split injection (PerkinElmer Instruments, Shelton, CT). Initial oven temperature was 150°C, held for 5 min, subsequently increased to 175°C at a rate of 2°C min^{-1}, held for 15 min, then to 200°C at 7°C min^{-1}, held for 20 min, then to 220°C at 5°C min^{-1} and held for 25 min. Hydrogen was used as the carrier gas at a flow rate of 1 mL min^{-1}. The split ratio was 20:1, the injector was set at 260°C, and the detector at 280°C. The amounts were calculated using the internal standard method of Turbochrom workstation software. The calculation for the index of stearoyl CoA desaturase (Δ^9-desaturase) activity was calculated according Malau-Aduli *et al.* (29) [Δ^9-Desaturase index = 100 × (14:1 + 16:1 + 18:1)/(14:1 + 16:1 + 18:1 + 14:0 + 16:0 + 18:0)].

(iii) Ag$^+$-HPLC. The distribution of CLA isomers was determined using an HPLC system (LC10A; Shimadzu, Tokyo, Japan) equipped with a 50 μL injection loop, a photodiode array detector (SPD-M10Avp; Shimadzu) operated at 233 nm, and an operating system (Shimadzu CLASS-VP version 6.12 sp4). Two ChromSpher 5 Lipids silver-impregnated columns (4.6 mm i.d. × 250 mm stainless steel; 5 μm particle size; Varian, Palo Alto, CA) were used in series. The mobile phase (0.1% acetonitrile,

0.5% diethyl ether in *n*-hexane) was prepared fresh daily and pumped at a flow rate of 1.0 mL/min. The injection volume depended on the total amounts of CLA and ranged between 20 and 40 µL. The Ag⁺-HPLC quantification of CLA isomers is based on the measurement of the integrated area under the 233 nm peaks attributed to conjugated dienes. The identification of the CLA isomers was made by the retention times of the standard compounds (*cis*-9,*trans*-11 18:2, *trans*-9,*trans*-11 18:2, *trans*-10,*cis*-12 18:2, and *cis*-9,*cis*-11 18:2). Starting from these compounds, the other isomers were identified from the known elution order. The elution order of the CLA isomers in beef was reported previously by Fritsche *et al.* (16) and Rickert *et al.* (23) and recently reviewed by Cruz-Hernandez *et al.* (25). Additionally, the identity of each isomer was controlled by the typical UV spectra of CLA isomers from the photodiode array detector in the range from 190 to 360 nm. The external calibration plots of the standard solutions were adapted to the different concentration levels of the individual CLA isomers in the lipid extracts. The external calibration plot of area vs. µg *cis*-9,*trans*-11 18:2 was prepared for a standard mixture in a range of 9.0 to 700 µg/mL. The external calibration plots of area vs. µg *trans*-9,*trans*-11 18:2, µg *trans*-10,*cis*-12 18:2, and µg *cis*-9,*cis*-11 18:2 were made for a standard mixture in the range of 0.5 to 20 µg/mL. The calibration of *trans*-9,*trans*-11 18:2 was used for the other *trans,trans* 18:2 isomers; the calibration of *trans*-10,*cis*-12 18:2 for the *cis,trans– trans, cis* isomers; and the *cis*-9,*cis*-11 18:2 calibration for the other *cis,cis* 18:2 isomers. Fritsche *et al.* (16) already have described this procedure for quantification of CLA isomers, which is not commercially available, in beef fat. Because of possible formation of artifacts during the sample preparation procedure, the very low concentrations of CLA isomers (<0.02 mg/100 g fresh tissue) were indicated as ND (not detectable). The detection limit of CLA isomers was calculated from the fivefold signal/noise ratio.

Statistical analysis. All data were analyzed by the least-squares method using the GLM procedures of the Statistical Analysis System (SAS© Systems, Release 8.2, SAS Institute Inc., Cary, NC). All tables contain the least squares mean (LSM) and the standard error (SEM) of the LSM. All statistical tests of LSM were performed for a significance level of $P = 0.05$.

RESULTS

The distribution pattern of CLA isomers in the intramuscular fat of the *longissimus* muscle, *semitendinosus* muscle, heart, and liver were very similar to that in the subcutaneous fat of both breeds. The predominant CLA isomer in all samples was *cis*-9,*trans*-11 18:2. The concentration of *cis*-9,*trans*-11 18:2 (mg/100 g fresh muscle) was highest in subcutaneous fat, up to 325 mg/100 g muscle, followed by the intramuscular fat of the *longissimus* and liver muscle, 14.4 and 10.2 mg/100 g muscle, respectively. The lowest values of *cis*-9,*trans*-11 18:2 occurred in the intramuscular fat of *semitendinosus* and heart muscle, ranging from 1.7 to 4.8 mg/100 g fresh muscle (Tables 1 to 5). The concentration of *cis*-9,*trans*-11 18:2 in the lipids of heart, liver, and *semitendinosus* muscle of both breeds was significantly affected by the diet. Pasture feeding as compared with concentrate feeding significantly increased the concentration of *cis*-9,*trans*-11 18:2 in heart and liver muscle by a factor of

TABLE 1
Concentrations of CLA Isomers (mg/100 g fresh muscle) in Intramuscular Fat of *Longissimus* Muscle of German Holstein and German Simmental Bulls

	German Holstein[a]				German Simmental[a]				
	Concentrate		Pasture		Concentrate		Pasture		Significance[b]
	LSM	SEM	LSM	SEM	LSM	SEM	LSM	SEM	(*P* < 0.05)
	n = 14		*n* = 14		*n* = 13		*n* = 13		
I.m. fat (%)	2.7	0.2	2.3	0.2	2.6	0.2	1.5	0.3	D
trans,trans[c]									
trans-12,*trans*-14 18:2	0.07	0.04	0.5	0.04	0.03	0.05	0.1	0.04	D, B, D*B
trans-11,*trans*-13 18:2	0.1	0.08	0.8	0.07	0.05	0.08	0.2	0.08	D, B, D*B
trans-10,*trans*-12 18:2	0.1	0.02	0.2	0.02	0.07	0.03	0.06	0.03	B
trans-9,*trans*-11 18:2	0.2	0.04	0.4	0.04	0.1	0.04	0.1	0.04	B, D*B
trans-8,*trans*-10 18:2	0.07	0.02	0.1	0.02	0.04	0.02	0.02	0.02	B
trans-7,*trans*-9 18:2	0.06	0.02	0.2	0.02	0.04	0.02	0.05	0.02	D, B, D*B
cis,trans; trans,cis[c]									
cis-12,*trans*-14 18:2	0.1	0.03	0.3	0.03	0.07	0.03	0.08	0.03	D,B,D*B
trans-11,*cis*-13 18:2	0.2	0.02	2.9	0.23	0.1	0.2	1.0	0.2	D,B,D*B
trans-10,*cis*-12 18:2	0.2	0.03	0.4	0.03	0.1	0.04	0.2	0.04	D, B
cis-9,*trans*-11 18:2	11.7	1.5	14.4	1.5	6.5	1.5	8.0	1.5	B
trans-8,*cis*-10 18:2	0.4	0.1	0.4	0.09	0.2	0.1	0.2	0.1	B
trans-7,*cis*-9 18:2	1.4	0.2	1.6	0.2	0.7	0.2	0.5	0.2	B
Δ⁹-Desaturase index[d]	50.9	0.8	46.4	0.8	48.6	0.8	44.9	0.8	D, B

[a]LSM, least square means; SEM, standard error of LSM; I.m. fat, intramuscular fat.
[b]D, significant influence of diet; B, significant influence of breed; D*B, significant interaction of D*B.
[c]Geometric configuration of the double bond (*cis,trans; trans,cis* isomers are the sum of both geometrical isomers).
[d]Calculated according Malau-Aduli *et al.* (29).

TABLE 2
Concentrations of CLA Isomers (mg/100 g fresh muscle) in Intramuscular Fat of *Semitendinosus* Muscle of German Holstein and German Simmental Bulls[a]

	German Holstein[a]				German Simmental[a]				
	Concentrate		Pasture		Concentrate		Pasture		
	LSM	SEM	LSM	SEM	LSM	SEM	LSM	SEM	Significance[b]
	$n = 14$		$n = 13$		$n = 12$		$n = 10$		($P < 0.05$)
I.m. fat (%)	0.7	0.06	0.9	0.06	0.9	0.06	0.8	0.06	
trans,trans[c]									
trans-12,*trans*-14 18:2	ND	0.005	0.04	0.005	0.02	0.005	0.03	0.006	D
trans-11,*trans*-13 18:2	0.03	0.008	0.04	0.008	0.03	0.009	0.05	0.01	
trans-10,*trans*-12 18:2	ND		ND		ND		ND		
trans-9,*trans*-11 18:2	0.03	0.007	0.03	0.008	0.05	0.01	0.02	0.01	
trans-8,*trans*-10 18:2	0.03	0.008	ND	0.008	0.04	0.009	ND	0.009	D
trans-7,*trans*-9 18:2	ND		ND		ND		ND		
cis,trans; trans,cis[c]									
cis-12,*trans*-14 18:2	ND	0.003	0.02	0.003	ND	0.003	0.02	0.003	D
trans-11,*cis*-13 18:2	0.04	0.04	0.2	0.04	0.05	0.04	0.3	0.04	D
trans-10,*cis*-12 18:2	0.04	0.005	0.03	0.005	0.06	0.005	0.02	0.006	D, D*B
cis-9,*trans*-11 18:2	3.1	0.4	2.6	0.5	3.4	0.5	1.7	0.54	D
trans-8,*cis*-10 18:2	0.04	0.008	0.02	0.008	0.03	0.007	0.04	0.008	D*B
trans-7,*cis*-9 18:2	0.4	0.03	0.1	0.04	0.4	0.04	0.1	0.04	D
Δ^9-Desaturase index[d]	54.3	0.7	48.6	0.7	50.7	0.8	47.4	0.8	D, B

[a]LSM, least square means; SEM, standard error of LSM; I.m. fat, intramuscular fat; ND, not detected.
[b]D, significant influence of diet; B, significant influence of breed; D*B, significant interaction of D*B.
[c]Geometric configuration of the double bond (*cis,trans; trans,cis* isomers are the sum of both geometrical isomers).
[d]Calculated according Malau-Aduli *et al.* (29).

approximately 1.4. No diet effect was detected for the *cis*-9,*trans*-11 18:2 content in *longissimus* muscle and subcutaneous fat (Tables 1, 3). However, a pasture diet significantly decreased the *cis*-9,*trans*-11 18:2 concentration in *semitendinosus* muscle (Table 2).

No diet effect was observed for the *trans*-7,*cis*-9 18:2 isomer in the muscle lipids of tissues, except *semitendinosus* and heart muscle. This isomer was identified by Fritsche *et al.* (16) and Yurawecz *et al.* (30) and reported to be the second-most abundant CLA isomer in commercial milk fat and beef muscle. However, this study has found that the second-most abundant CLA isomer in muscle lipids and subcutaneous fat of pasture-fed bulls was *trans*-11,*cis*-13 18:2. The highest concentration of *trans*-11,*cis*-13 18:2 was measured in subcutaneous fat of pasture-fed German

TABLE 3
Concentrations of CLA Isomers (mg/100 g fresh tissue) in Subcutaneous Fat of German Holstein and German Simmental Bulls[a]

	German Holstein[a]				German Simmental[a]				
	Concentrate		Pasture		Concentrate		Pasture		
	LSM	SEM	LSM	SEM	LSM	SEM	LSM	SEM	Significance[b]
	$n = 12$		$n = 14$		$n = 14$		$n = 14$		($P < 0.05$)
I.m. fat (%)	47.6	2.2	39.9	2.3	42.2	2.4	37.8	2.2	D
trans,trans[c]									
trans-12,*trans*-14 18:2	1.0	0.8	5.6	0.8	2.8	0.8	13.4	0.8	D,B,D*B
trans-11,*trans*-13 18:2	1.8	1.0	7.9	1.0	2.8	1.0	16.9	0.9	D,B,D*B
trans-10,*trans*-12 18:2	1.2	0.3	1.8	0.2	2.4	0.2	2.2	0.2	B
trans-9,*trans*-11 18:2	5.9	0.5	7.5	0.5	7.1	0.5	9.5	0.5	D,B
trans-8,*trans*-10 18:2	1.3	0.3	2.0	0.3	2.7	0.3	2.4	0.3	B
trans-7,*trans*-9 18:2	1.4	0.4	2.7	0.4	2.7	0.4	3.4	0.4	D,B
cis,trans; trans,cis[c]									
cis-12,*trans*-14 18:2	1.3	0.7	4.0	0.6	2.3	0.6	8.6	0.6	D,B,D*B
trans-11,*cis*-13 18:2	4.8	5.2	44.9	4.8	7.4	4.8	110.6	4.8	D,B,D*B
trans-10,*cis*-12 18:2	2.3	0.4	1.6	0.4	3.4	0.4	1.5	0.4	D
cis-9,*trans*-11 18:2	324.6	23.1	299.9	21.4	285.9	21.4	295.1	21.4	
trans-8,*cis*-10 18:2	3.0	1.3	5.6	1.2	6.2	1.2	16.6	1.2	D,B,D*B
trans-7,*cis*-9 18:2	28.7	4.0	33.2	3.7	58.6	3.7	48.0	3.7	B
Δ^9-Desaturase index[d]	56.1	1.0	48.5	0.9	54.5	0.9	46.4	0.9	D

[a–d]For footnotes see Table 2.

TABLE 4
Concentrations of CLA Isomers (mg/100 g fresh muscle) in the Lipids of Liver Tissue of German Holstein and German Simmental Bulls[a]

	German Holstein[a]				German Simmental[a]				
	Concentrate		Pasture		Concentrate		Pasture		
	LSM	SEM	LSM	SEM	LSM	SEM	LSM	SEM	Significance[b]
	$n = 15$		$n = 13$		$n = 11$		$n = 8$		($P < 0.05$)
l.m. fat (%)	2.9	0.05	3.0	0.07	2.7	0.07	3.0	0.07	D,D*B
trans,trans[c]									
trans-12,trans-14 18:2	0.07	0.01	0.3	0.02	0.07	0.02	0.4	0.02	D
trans-11,trans-13 18:2	0.2	0.02	0.5	0.02	0.1	0.02	0.6	0.02	D,D*B
trans-10,trans-12 18:2	0.06	0.01	0.04	0.01	0.03	0.01	0.2	0.01	D,B,D*B
trans-9,trans-11 18:2	0.1	0.01	0.2	0.02	0.08	0.01	0.2	0.01	D
trans-8,trans-10 18:2	0.02	0.006	0.03	0.006	0.02	0.007	0.05	0.008	D
trans-7,trans-9 18:2	0.06	0.01	0.06	0.01	0.06	0.01	0.09	0.02	
cis,trans; trans,cis[c]									
cis-12,trans-14 18:2	0.07	0.01	0.1	0.02	0.07	0.02	0.2	0.02	D
trans-11,cis-13 18:2	0.1	0.1	1.3	0.1	0.1	0.11	1.8	0.1	D,B,D*B
trans-10,cis-12 18:2	0.07	0.02	0.2	0.01	0.09	0.01	0.2	0.02	D
cis-9,trans-11 18:2	7.4	0.7	9.9	0.7	7.0	0.8	10.2	0.9	D
trans-8,cis-10 18:2	0.2	0.05	0.6	0.05	0.3	0.06	0.4	0.06	D
trans-7,cis-9 18:2	0.6	0.08	0.7	0.08	0.6	0.09	0.7	0.1	
Δ^9-Desaturase index[d]	24.7	0.7	21.2	0.8	25.1	0.8	21.6	0.9	D

[a–d]For footnotes see Table 2.

Simmental bulls (110 mg/100 g muscle). A pasture diet resulted in a very high accumulation rate of trans-11,cis-13 18:2 up to a factor of 14.5 as well as in muscle tissues and subcutaneous fat as compared with concentrate fed bulls (Tables 1–5). Furthermore, the concentration of trans-11,cis-13 18:2 was significantly affected by breed. The intramuscular fat in the muscles and the subcutaneous fat of the German Simmental bulls had a significantly higher concentration of trans-11,cis-13 18:2 as compared with the German Holstein bulls, except for the longissimus muscle (Tables 1–5). The concentration of trans-10,cis-12 18:2 was affected by diet, except in the heart muscle. Pasture feeding increased the concentration of trans-10,cis-12 18:2 in the lipids of longissimus muscle and liver and decreased the values in semitendinosus muscle and subcutaneous fat. Overall, the level of trans-10,cis-12 18:2 was generally low in all samples and ranged between 0.02 and 0.35 mg/100 g fresh tissue (Tables 1–5). Among the trans,trans isomers of CLA, trans-12,trans-14 18:2 and trans-11,trans-13 18:2 were significantly affected by the diet in all tissues. Pasture feeding resulted in an increase in the concentration of trans-12,trans-14 18:2 by a factor of approximately 5 in the

TABLE 5
Concentrations of CLA Isomers (mg/100 g fresh muscle) in the Lipids of Heart Muscle of German Holstein and German Simmental Bulls[a]

	German Holstein[a]				German Simmental[a]				
	Concentrate		Pasture		Concentrate		Pasture		
	LSM	SEM	LSM	SEM	LSM	SEM	LSM	SEM	Significance[b]
	$n = 14$		$n = 14$		$n = 13$		$n = 13$		($P < 0.05$)
l.m. fat (%)	1.8	0.04	1.7	0.04	1.8	0.04	1.8	0.04	D,D*B
trans,trans[c]									
trans-12,trans-14 18:2	ND	0.003	0.02	0.003	ND	0.003	0.04	0.003	D,D*B
trans-11,trans-13 18:2	0.02	0.006	0.07	0.006	0.02	0.007	0.1	0.006	D,B,D*B
trans-10,trans-12 18:2	ND		ND		ND		ND		
trans-9,trans-11 18:2	ND		ND		ND		ND		
trans-8,trans-10 18:2	ND		ND		ND		ND		
trans-7,trans-9 18:2	ND		ND		ND		ND		
cis,trans; trans,cis[c]									
cis-12,trans-14 18:2	ND	0.003	0.02	0.003	ND	0.003	0.03	0.003	D,D*B
trans-11,cis-13 18:2	0.04	0.04	0.4	0.04	0.04	0.05	0.6	0.04	D,B,D*B
trans-10,cis-12 18:2	0.02	0.006	0.02	0.005	0.03	0.007	0.04	0.006	
cis-9,trans-11 18:2	2.2	0.3	4.0	0.3	2.1	0.3	4.8	0.3	D
trans-8,cis-10 18:2	0.03	0.005	0.04	0.005	0.03	0.006	0.02	0.005	
trans-7,cis-9 18:2	0.1	0.03	0.3	0.03	0.20	0.04	0.3	0.03	D
Δ^9-Desaturase index[d]	35.5	0.8	33.0	0.8	34.5	0.9	34.6	0.8	

[a–d]For footnote see Table 2.
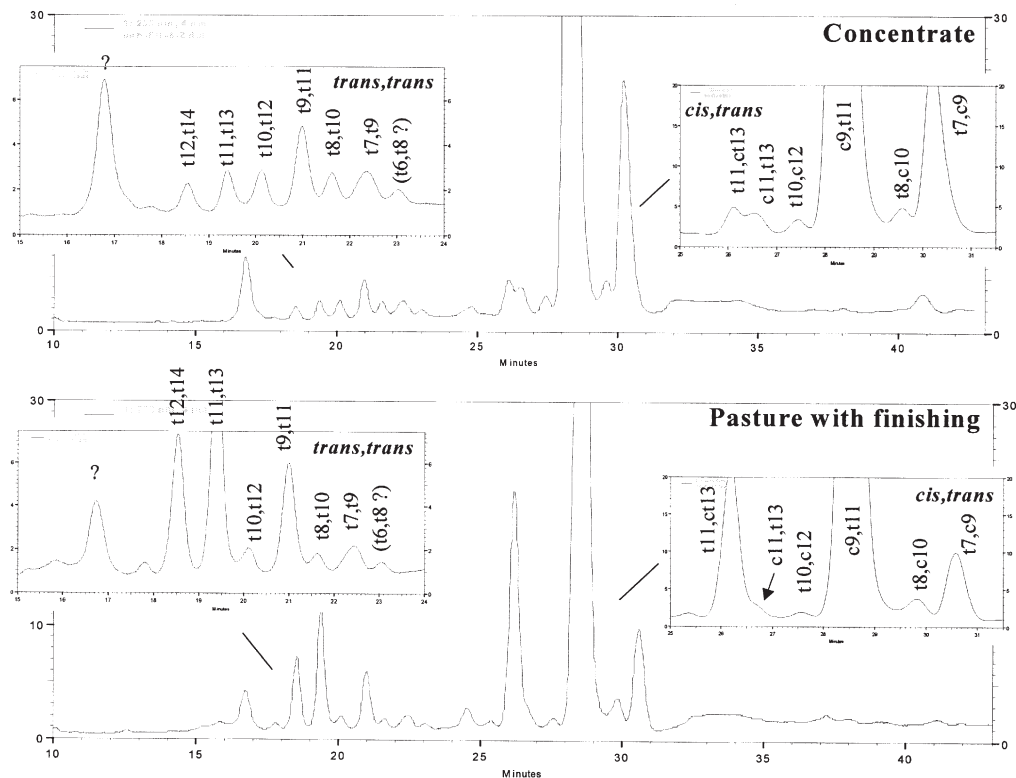
FIG. 1. Partial silver ion-HPLC chromatograms of subcutaneous fat of concentrate- and pasture-fed German Holstein bulls detected at 233 nm.

muscle tissues and subcutaneous fat (Tables 1–5). Furthermore, pasture feeding resulted in a significantly higher concentration of *trans*-11,*trans*-13 18:2 in all tissues. The concentrations of *trans*-10,*trans*-12 18:2, *trans*-9,*trans*-11 18:2, *trans*-8,*trans*-10 18:2, and *trans*-7,*trans*-9 18:2 were lower than the two other *trans,trans* isomers, described above. In the *semitendinosus* and heart muscles these *trans,trans* 18:2 isomers were mostly not detected. Additionally, the *cis,cis* 18:2 isomers were below the detection limit in all samples investigated. The peaks detected in the region of the CLA *cis,cis* isomers of the Ag⁺-HPLC chromatograms did not show UV spectra (photodiode array detector from 190 to 360 nm) typical of CLA isomers and were not identified as CLA *cis,cis* isomers. The geometrical isomer pairs of *cis,trans/trans,cis* 18:2 could not be separated by using a double-Ag⁺-HPLC column system. The concentrations of *cis,trans* or *trans,cis*18:2 in Tables 1 to 5 are the sum of both geometrical isomers. The use of six Ag⁺-HPLC columns in series clearly resolved (Fig. 1) the two 11,13 geometric isomers (32).

The total FA composition of the *longissimus* and *semitendinosus* muscle and subcutaneous fat was reported before (26,33). The total FA concentration (mg/100 g fresh muscle) of the heart muscle and liver is summarized in Tables 6 and 7.

Pasture feeding resulted in a significantly higher concentration of *cis*-9,*trans*-11 18:2 (determined by GC), up to 15.9 mg/100 g fresh muscle in the lipids of liver as compared with concentrate-fed bulls of both breeds (Tables 6, 7). The level of *cis*-9,*trans*-11 18:2 in the lipids of liver was approximately 2.5 times higher as compared with the concentration in the heart muscle (Tables 6, 7). Comparison of the *cis*-9,*trans*-11 18:2 concentration showed higher values measured by GC as compared with Ag⁺-HPLC. The values measured by GC included *cis*-9,*trans*-11 18:2, *trans*-7,*cis*-9 18:2, and *trans*-8,*cis*-10 18:2 (16). However, the sum of *cis*-9,*trans*-11 18:2, *trans*-7,*cis*-9 18:2, and *trans*-8,*cis*-10 18:2 values measured by Ag⁺-HPLC is lower than the concentration of *cis*-9,*trans*-11 18:2 measured by GC. One reason could be the occurrence of coeluting compounds detected with GC/FID, also described by Fritsche *et al.* (16) and Cruz-Hernandez *et al.* (25). Pasture-fed bulls had significantly increased total and individual n-3 FA concentrations in liver and heart muscle lipids of both breeds. The highest accumulation was detected for linolenic acid (18:3n-3) in the heart muscle of pasture-fed German Holstein bulls (concentrate: 13.2 mg/100 g vs. pasture: 59.4 mg/100 g, Table 7). In contrast, pasture feeding resulted in a significant decrease of total and individual n-6 FA concentrations in liver and heart muscle lipids of both breeds. Consequently, the n-6/n-3 ratio was beneficially low in pasture-fed bulls, ranging between 1.3 and 1.4 in the lipids of liver and 3.2 and 3.6 in the lipids of heart muscle (Tables 6, 7). However, no diet effect was detected for the concentration of saturated FA.

TABLE 6
Total FA Concentration (mg/100 g fresh muscle) in the Lipids of Liver Tissue of German Holstein and German Simmental Bulls[a]

	German Holstein[a]				German Simmental[a]				
	Concentrate		Pasture		Concentrate		Pasture		
	LSM	SEM	LSM	SEM	LSM	SEM	LSM	SEM	Significance
	$n = 17$		$n = 16$		$n = 16$		$n = 15$		$(P < 0.05)$
I.m. fat (%)	2.7	0.07	3.0	0.07	2.9	0.07	3.0	0.07	D,D*B
16:0	263.4	17.1	261.2	17.6	267.0	16.6	257.3	17.1	
18:0	721.7	19.4	750.7	20.0	747.6	18.8	769.9	19.4	
18:1 *cis*-9	300.0	15.7	278.6	16.2	300.8	15.3	261.0	15.7	
18:3n-3	23.1	4.1	62.0	4.2	21.2	4.0	82.8	4.1	D,B,D*B
cis-9 *trans*-11 18:2[b]	7.0	1.0	15.9	1.1	10.5	1.0	14.0	1.0	D,D*B
18:1-*trans*-11	28.0	1.9	50.2	2.0	27.8	1.8	36.3	1.9	D,B,D*B
Sum SFA	1017.3	31.7	1058.9	32.7	1052.7	30.7	1074.5	31.7	
Sum UFA	1413.6	34.6	1297.4	35.8	1348.1	33.6	1358.1	34.6	
Sum PUFA	957.4	22.8	809.0	23.6	886.5	22.1	923.4	22.8	D,D*B
Sum n-3 FA	154.3	10.3	346.8	10.7	151.4	10.0	372.3	10.3	D
Sum n-6 FA	735.7	16.1	422.0	16.6	684.0	15.6	509.2	16.1	D,D*B
n-6/n-3 ratio	4.9	0.1	1.3	0.1	4.6	0.1	1.4	0.1	D

[a]LSM, least square means; SEM, standard error of LSM; SFA, saturated FA; UFA, unsaturated FA; for other abbreviations see Table 2.
[b]Determined by GC, co-elution.

TABLE 7
Total FA Concentration (mg/100 g fresh muscle) in the Lipids of Heart Muscle of German Holstein and German Simmental Bulls[a]

	German Holstein[a]				German Simmental[a]				
	Concentrate		Pasture		Concentrate		Pasture		
	LSM	SEM	LSM	SEM	LSM	SEM	LSM	SEM	Significance
	$n = 17$		$n = 16$		$n = 16$		$n = 15$		$(P < 0.05)$
I.m. fat (%)	1.8	0.04	1.8	0.04	1.8	0.04	1.7	0.04	D,D*B
16:0	203.1	6.9	200.1	7.1	176.5	6.7	174.1	6.9	B
18:0	272.0	9.3	267.0	9.6	235.7	9.1	241.3	9.4	B
18:1 *cis*-9	243.0	13.0	227.8	13.4	214.5	12.6	193.1	13.0	B
18:2n-6	417.2	8.1	306.4	8.3	392.8	7.8	331.4	8.1	D,D*B
cis-9 *trans*-11 18:2[b]	3.2	0.2	6.5	0.2	2.9	0.2	5.3	0.2	D,B,D*B
18:3n-3	13.2	1.4	59.4	1.5	11.7	1.4	58.1	1.4	D
18:1*trans*-11	23.8	1.5	36.4	1.6	19.9	1.5	25.5	1.5	D,B,D*B
Sum SFA	503.4	17.0	500.4	17.5	436.3	16.5	443.5	17.0	B
Sum UFA	982.3	19.1	912.7	19.8	910.4	18.6	870.7	19.1	D,B
Sum PUFA	639.3	9.7	567.4	10.0	611.0	9.4	582.3	9.7	D,D*B
Sum n-3 FA	34.6	2.1	131.9	2.2	37.3	2.1	123.2	2.1	D,D*B
Sum n-6 FA	592.1	9.1	420.0	9.4	560.3	8.8	445.7	9.1	D,D*B
n-6/n-3 ratio	17.1	0.3	3.2	0.3	15.2	0.3	3.6	0.3	D,B,D*B

[a,b]For footnotes see Table 6.

DISCUSSION

The occurrence of the main CLA isomer, *cis*-9,*trans*-11 18:2, in the lipids of beef muscles as affected by feeding pasture compared with concentrate has been extensively investigated (34–39). Diets containing proportionally high levels of linolenic acid in the fat, such as fresh grass, grass silage, concentrates containing linseed, and pasture feeding with finishing periods, resulted in increased deposition of *cis*-9,*trans*-11 18:2 in the muscles (22,34,37,38). French *et al.* (34) reported a significant increase in *cis*-9,*trans*-11 18:2 in muscle of crossbred steers grazed for 85 d on pasture compared with concentrate, averag-

ing 1.08 and 0.37% of total FA, respectively. Steen and Porter (37) reported that the content of *cis*-9,*trans*-11 18:2 in muscle and subcutaneous fat from steers finished on pasture was three times higher than in those on concentrate. Similarly, Poulson *et al.* (38) observed a significant increase of *cis*-9,*trans*-11 18:2 in muscle of crossbred steers on forage and pasture without grain supplementation. Our results regarding CLA isomers analyzed by Ag^{+}-HPLC showed that the highest accumulation rates of the main isomer, *cis*-9,*trans*-11 18:2 (based on mg/100 g fresh tissue), occurred in the lipids of heart and liver tissue of pasture-fed bulls as compared with concentrate-fed bulls (Tables 4, 5). However, no effect of pasture feeding as compared

with concentrate was found for *cis*-9,*trans*-11 18:2 in the lipids of *longissimus* muscle and the subcutaneous fat as well as of German Holstein and German Simmental bulls. Furthermore, pasture feeding significantly decreased the *cis*-9,*trans*-11 18:2 concentration in the *semitendinosus* muscle (Table 2).

Most of the studies of biosynthetic formation of CLA, predominantly *cis*-9,*trans*-11, involving animals that were pasture-fed were carried out with milk fat (10–12,19,20). The lipids in pasture are high in linolenic acid (18:3n-3), and the biohydrogenation by rumen microorganisms does not include *cis*-9,*trans*-11 18:2 as an intermediate (9). *Trans* vaccenic acid (18:1 *trans*-11) is formed during the biohydrogenation of linolenic acid and linoleic acid to stearic acid, and therefore *trans* vaccenic acid is a common intermediate in the metabolic pathway of linoleic and linolenic acids (9). Griinari and Bauman (40) concluded that a relatively small proportion of the *cis*-9,*trans*-11 18:2 formed in the rumen escapes and is available for deposition in the muscles. Griinari *et al.* (10) showed that the primary source of *cis*-9,*trans*-11 18:2 was from the endogenous synthesis involving Δ^9-desaturase and *trans* vaccenic acid. Recently, Kay *et al.* (12) confirmed these results and demonstrated that approximately 90% of *cis*-9,*trans*-11 18:2 in milk fat was produced endogenously in cows fed fresh pasture. Furthermore, Piperova *et al.* (41) investigated duodenal samples and estimated that rumen synthesis of CLA was 4 to 7% and the rest derived through endogenous synthesis. No similar studies have been reported to investigate the importance of endogenous synthesis of CLA isomers in the adipose tissue of ruminant muscles. However, Δ^9-desaturase also occurs in the small intestine and adipose tissue of ruminants (42), suggesting some endogenous synthesis may occur in these tissues as well. Very recently, Khanal and Dhiman (14) speculated that the contribution from the endogenous synthesis in muscle tissues is similar to that reported for milk because *trans* vaccenic acid and Δ^9-desaturase are the two primary prerequisites for the synthesis of *cis*-9,*trans*-11 18:2. The Δ^9-desaturase enzyme is active in ruminant adipose tissue (43), and their mRNA is well expressed (44).

Pasture feeding increased the concentration of *cis*-9,*trans*-11 18:2 in the lipids of liver and heart muscle by a factor of approximately 2.0 as compared with concentrate feeding (Tables 4, 5). Also, the *trans* vaccenic acid concentrations were increased in the lipids of liver and heart muscle of pasture-fed bulls (Tables 6, 7). However, the other important parameter for the endogenous synthesis of *cis*-9,*trans*-11 18:2, the Δ^9-desaturase activity, calculated as a Δ^9-desaturase index according to Malau-Aduli (29), was significantly decreased by pasture feeding in the liver tissue (German Holstein bulls, concentrate: 24.7, pasture: 21.2, Table 4). No diet effect was found for the Δ^9-desaturase index in heart muscle (Table 5). The *cis*-9,*trans*-11 18:2 concentrations in the *longissimus* muscle tended to be higher in pasture compared with concentrate-fed bulls (significance at $P = 0.58$). The concentration of *cis*-9,*trans*-11 18:2 in the *longissimus* muscle was strongly correlated ($P < 0.001$) with *trans*-11 18:1 ($r = 0.80$, confidence interval 0.50–0.93) and also with *trans*-9 18:1 ($r = 0.75$, confidence interval 0.40–0.91), and *trans*-10 18:1 ($r = 0.86$, confidence interval

0.63–0.95) in pasture-fed compared with concentrate-fed bulls as described earlier (22).

Kay *et al.* (12) presented the first study to examine the importance of endogenous synthesis of *cis*-9,*trans*-11 18:2 in milk fat of pasture-fed cows. Pasture diets have a number of differences that are important considerations in the biology of *cis*-9,*trans*-11 18:2 in milk. First, pasture results in a milk fat with a higher content of *cis*-9,*trans*-11 18:2 than observed with typical totally mixed ration diets. Second, the FA present in concentrates and most plant oils that are used in dairy cow diets are high in linoleic acid (12). On the contrary, pasture lipids are high in linolenic acid, and its biohydrogenation produces *trans* vaccenic acid, but not *cis*-9,*trans*-11 18:2, as an intermediate (9). These differences suggest that endogenous synthesis may be a relatively more important source of CLA in milk from cows consuming pasture (12). Recently, different studies have shown the diet effect of pasture feeding on the distribution of all CLA isomers in lipids of milk fat analyzed by Ag$^+$-HPLC (19,20). However, the knowledge of the distribution of Ag$^+$-HPLC-analyzed CLA isomers in the lipids of beef products affected by pasture feeding is limited (21,22). Our study showed that, besides *cis*-9,*trans*-11 18:2, pasture feeding affected the concentration of *trans*-11,*cis*-13 18:2, *trans*-11,*trans*-13 18:2, and *trans*-12,*trans*-14 18:2 in the lipids of *longissimus*, liver, heart muscle and subcutaneous fat in German Holstein and German Simmental bulls, (Tables 1, 3, 4, 5). Pasture compared with concentrate feeding led to a very high accumulation of the isomer *trans*-11,*cis*-13 18:2, up to a factor of 14.5, as well as in muscle tissues and subcutaneous fat. The second- and third-highest accumulations in tissues and subcutaneous fat of pasture-fed bulls were observed for the *trans*-11,*trans*-13 and *trans*-12,*trans*-14 18:2 isomers, up to a factor of 7.1, respectively. These results confirmed the investigations of Kraft *et al.* (19) and Collomb *et al.* (20) in lipids of milk fat from cows fed high levels of unsaturated FA. The concentration of the *trans*-11,*cis*-13 18:2 isomer was about four times higher in milk fat from grazing cows in the Alps (Switzerland) as compared with indoor-fed cows (19,20). It is well known that the pathway for the biohydrogenation in the rumen of linolenic acid (*cis*-9,*cis*-12,*cis*-15 18:3), up to 65% in the lipids of pasture diets, involves an initial isomerization to a conjugated triene (*cis*-9,*trans*-11,*cis*-15 18:3). The next step is the hydrogenation to *trans*-11,*cis*-15 18:2, which undergoes further hydrogenation, depending on the bacteria involved, leaving *trans*-vaccenic acid. The final product is stearic acid (9). But the metabolic pathway from the intermediate *trans*-11,*cis*-15 18:2 to *trans*-11,*cis*-13 18:2 is unknown until now. Collomb *et al.* (20) inferred that the *trans*-11,*cis*-13 18:2 isomer could be a useful indicator of milk products of Alpine origin. Kraft *et al.* (19) hypothesized that linolenic acid is an indirect precursor of *trans*-11,*cis*-13 18:2 in milk fat. Furthermore, Kraft *et al.* (19) discussed that the *trans*-11 double bond seems to be the most stable *trans*-bond among the 18:1 and CLA isomers during the ruminal fermentation, and they observed the formation of larger amounts of CLA isomers with a *trans*-11 double bond—*cis*-9,*trans*-11, *trans*-11,*cis*-13, and *trans*-11,*trans*-13 18:2 isomers—in milk from grazing cows in the Alps. Also, we found that, among the CLA *trans*,*trans* isomers

in the lipids of muscle tissues and subcutaneous fat of both breeds, the *trans*-11,*trans*-13 18:2 was the most abundant compound, followed by the *trans*-12,*trans*-14 18:2 (Tables 1–5).

Previous studies showed that the *trans*-7,*cis*-9 18:2 isomer is the second-most abundant CLA isomer in beef meat and milk products (16,30,45–48). In the muscle lipids and subcutaneous fat of concentrate-fed German Holstein and German Simmental bulls, *trans*-7,*cis*-9 18:2 was also the second-most abundant CLA isomer. However, a pasture diet had no effect on the *trans*-7,*cis*-9 18:2 concentration in lipids of *longissimus* muscle, liver, and subcutaneous fat. The *trans*-7,*cis*-9 18:2 concentration in the lipids of heart and *semitendinosus* muscle was slightly increased and decreased, respectively, in pasture-fed bulls as compared with concentrate. Because of the significantly higher concentrations of *trans*-11,*cis*-13 18:2, *trans*-7,*cis*-9 18:2 is the third-most abundant isomer in the tissue lipids of pasture-fed bulls. Corl *et al.* (49) studied the metabolic pathway for the formation of *trans*-7,*cis*-9 18:2 in the rumen of dairy cows and showed that this CLA isomer is synthesized endogenously almost exclusively by Δ^9-desaturase using rumen-derived *trans*-7 18:1 as the substrate. Piperova *et al.* (46) also concluded that almost all *trans*-7,*cis*-9 18:2 present in milk fat was produced postruminally. The endogenous synthesis of *trans*-7,*cis*-9 18:2 in intramuscular and subcutaneous fat was not investigated until now, but it could be expected to be analogous to that of *cis*-9,*trans*-11 18:2 since both of them use the activity of the same enzyme. As mentioned earlier, in our study pasture feeding decreased the Δ^9-desaturase activity, calculated as a Δ^9-desaturase index according to Malau-Aduli (29). That could be one reason why the CLA *trans*-7,*cis*-9 were not affected by pasture compared with concentrate diet in most of the investigated tissues.

The concentration of *trans*-10,*cis*-12 18:2 was affected by diet, except in the heart muscle. Pasture feeding resulted in an increased *trans*-10,*cis*-12 18:2 concentration in the lipids of *longissimus* and liver muscle and in decreased concentration in the lipids of *semitendinosus* muscle and subcutaneous fat as compared with concentrate feeding. Though important physiologically, the proportion of *trans*-10,*cis*-12 18:2 to the sum of all isomers in the lipids of pasture- and concentrate-fed bulls was quite low (0.3–1.8%). Because mammals do not have Δ^{12}-desaturase, *trans*-10,*cis*-12 18:2 cannot be endogenously produced. *trans*-10,*cis*-12 18:2 reported in the lipids of milk and tissue originates from the absorption processes in the intestine (19).

Thus, pasture feeding resulted in a variation in the distribution pattern and concentration level of individual CLA isomers in all investigated tissues. Overall, pasture feeding enhanced the concentration of the sum of CLA isomers in the tissue lipids. Further studies will clarify the high accumulation rates and the metabolic pathways of CLA *trans*-11,*cis*-13 and some isomers of CLA *trans*, *trans* in the tissues of pasture-fed bulls.

ACKNOWLEDGMENT

REFERENCES

1. Bauman, D.E., Baumgard, L.H., Corl, B.A., and Griinari J.M. (1999) Biosynthesis of Conjugated Linolenic Acid in Ruminants, *Proc. Am. Soc. Anim. Sci.*, 1999. Available at: http://www.asas.org/jas/symposiua/proceedings/E30. Accessed (date to be supplied).
2. Belury, M.A. (2003) Conjugated Linoleic Acids in Type 2 Diabetes Mellitus: Implications and Potential Mechanisms, in *Advances in Conjugated Linoleic Acid Research* (Sebedio, J.L., Christie, W.W., and Adlof, R.O., eds.), Vol. 2, pp. 302–315, AOCS Press, Champaign.
3. Kritchevsky, D. (2003) Conjugated Linoleic Acids in Experimental Atherosclerosis, in *Advances in Conjugated Linoleic Acid Research* (Sebedio, J.L., Christie, W.W., and Adlof, R.O., eds.), Vol. 2, pp. 292–301, AOCS Press, Champaign.
4. Pariza, M.W., Park, Y., and Cook M.E. (2001) The Biologically Active Isomers of Conjugated Linoleic Acid, *Progr. Lipid Res. 40,* 283–298.
5. Banni, S., Heys, S.D., and Wahle, K.W.J (2003) Conjugated Linoleic Acids as Anticancer Nutrients: Studies *in vivo* and Cellular Mechanisms, in *Advances in Conjugated Linoleic Acid Research* (Sebedio, J.L., Christie, W.W., and Adlof, R.O., eds.), Vol. 2, pp. 267–282, AOCS Press, Champaign, Illinois.
6. Khanal, R.C. (2004) Potential Health Benefits of Conjugated Linoleic Acid (CLA): A Review, *Asian-Aust. J. Anim. Sci. 17*, 1315–1328.
7. Martin, C.J., and Valeille, K. (2002) Conjugated Linoleic Acids: All the Same or to Everyone Its Own Function? *Reprod. Nutr. Dev. 42,* 525–536.
8. Park, Y., Park, C.W., Kim, S.J., Kim, J.K., Kim, Y.R., Kim, Y.S., and Ha, Y.L. (2003) Divergent Cytotoxic Effects of Conjugated Linoleic Acid on NCI-N87 Cells, in *Food Factors in Health Promotion and Disease Prevention* (Shahidi, F., Ho, C.-T., Watanabe, S., and Osawa, T., eds.), pp. 113–118, ACS Symposium Series 851, American Chemical Society, Washington, DC.
9. Harfoot, C.G., and Hazelwood G.P. (1998) Lipid Metabolism in the Rumen, in *The Rumen Microbial Ecosystem* (Hobson, P.N., ed.), pp. 383–426, Elsevier Science Publishers, London.
10. Griinari, J.M., Corl, B.A., Lacy, S.H., Chouinard, P.Y., Nurmela, K.V., and Bauman, D.E. (2000) Conjugated Linoleic Acid Is Synthesized Endogenously in Lactating Dairy Cows by Δ^9–Desaturase, *J. Nutr. 130*, 2285–2291.
11. Palmquist, D.L. (2001) Ruminal and Endogenous Synthesis of CLA in Cows, *Aust. J. Dairy Technol. 56*, 134–137.
12. Kay, J.K., Mackle, T.R., Auldist, M.J., Thomson, N.A., and Bauman D.E. (2004) Endogenous Synthesis of *cis*-9,*trans*-11 Conjugated Linoleic Acid in Dairy Cows Fed Fresh Pasture, *J. Dairy Sci. 87*, 369–378.
13. Song, M.K., and Kenelly, J.K. (2003) Biosynthesis of Conjugated Linoleic Acid and Its Incorporation into Ruminant's Products, *Asian-Aust. J. Anim. Sci. 16*, 306–314.
14. Khanal, R.C., and Dhiman, T.R. (2004) Biosynthesis of Conjugated Linoleic Acid (CLA): A Review, *Pakistan J. Nutr. 3*, 72–81.
15. Parodi, P.W. (1977) Conjugated Octadecadienoic Acid of Milk Fat, *J. Dairy Sci. 60,* 1550–1553.
16. Fritsche, J., Fritsche, S., Solomon, M.B., Mossoba, M.M., Yurawecz, M.P., Morehouse, K., and Ku, Y. (2000) Quantitative Determination of Conjugated Linoleic Acid Isomers in Beef Fat, *Eur. J. Lipid Sci. Technol. 102*, 667–672.
17. Bauman, D.E., Corl, B.A., Baumgard, L.H., and Griinari, J.M. (2001) Conjugated Linoleic Acid (CLA) and the Dairy Cow, in *Recent Advances in Animal Nutrition* (Garnsworthy, P.C., and Wiseman, J., eds.), pp. 221–250, Nottingham University Press, Nottingham, United Kingdom.
18. Lock, A.L., and Garnsworthy, P.C.(2003) Seasonal Variations in Milk Conjugated Linoleic Acid and Δ^9-Desaturase Activity in Dairy Cows, *Livestock Prod. Sci. 79*, 47–59.

19. Kraft, J., Collomb, M., Möckel, P., Sieber, R., and Jahreis, G. (2003) Differences in CLA Isomer Distribution of Cow's Milk Lipids, *Lipids 38,* 657–664.

20. Collomb, M., Sieber, R., and Bütikofer, U. (2004) CLA Isomers in Milk Fat from Cows Fed Diets with High Levels of Unsaturated Fatty Acids, *Lipids, 39,* 355–364.

21. Nuernberg, K., Nuernberg, G., Ender, K., Lorenz, S., Winkler, K., Rickert, R., and Steinhart H. (2002) n-3 Fatty Acids and Conjugated Linoleic Acids of *Longissimus* Muscle in Beef Cattle, *Eur. J. Lipid Sci. Technol. 104,* 463–471.

22. Dannenberger, D., Nuernberg, G., Scollan, N., Schabbel, W., Steinhart, H., Ender, K., and Nuernberg, K. (2004) Effect of Diet on the Deposition of n-3 Fatty Acids, Conjugated Linoleic and C18:1*trans* Fatty Acid Isomers in Muscle Lipids of German Holstein Bulls, *J. Agric. Food Chem. 52,* 6607–6615.

23. Rickert, R., Steinhart, H., Fritsche, J., Sehat, N., Yurawecz, M.P., Mossoba, M.M., Roach, J.A.G., Eulitz, K., Ku, Y., and Kramer, J.K. (1999) Enhanced Resolution of Conjugated Linoleic Acid Isomers by Tandem-Column Silver-Ion High Performance Liquid Chromatography, *J. High Resolut. Chromatogr. 22,* 144–148.

24. Christie, W.W. (2003) Analysis of Conjugated Linoleic Acid: An Overview, in *Advances in Conjugated Linoleic Acid Research* (Sebedio, J.L., Christie, W.W., and Adlof, R.O., eds.) Vol. 2. pp. 1–12, AOCS Press, Champaign.

25. Cruz-Hernandez, C., Deng, Z., Zhou, J., Hill, A.R., Yurawecz, M.P., Delmonte, P., Mossoba, M., Dugan, M.E.R., and Kramer, J.K.G. (2004) Methods for Analysis of Conjugated Linoleic Acids and *trans* C18:1 Isomers in Dairy Fat by Using a Combination of Gas Chromatography, Silver-Ion Thin Layer Chromatography/Gas Chromatography, and Silver-Ion Liquid Chromatography, *J. AOAC Intl. 87,* 545–562.

26. Nuernberg, K., Dannenberger, D., Nuernberg, G., Ender, K., Voigt, J., Scollan, N., Wood, J., Nute, G., and Richardson I. (2005) Effect of a Grass-based and a Concentrate Feeding System on Meat Quality Characteristics and Fatty Acid Composition of *Longissimus* Muscle in Different Cattle Breeds, *Livestock Prod. Sci. 94,* 137–147.

27. Dannenberger, D., Nuernberg, K., Nuernberg, G., and Ender, K. (2003) Influence of Feeding on Meat Quality and Fatty Acid Composition in Beef, *Arch. Tierz. 46,* 162.

28. Folch, J., Lees, M., and Sloane-Stanley, G.H. (1957) A Simple Method for the Isolation and Purification of Total Lipids from Animal Tissue, *J. Biol. Chem. 226,* 497–509.

29. Malau-Aduli, A.E.O., Siebert, B.D., Bottema, C.D.K., and Pitchford, W.S. (1997) A Comparison of Fatty Acid Composition of Triacylglycerols in Adipose Tissue from Limousin and Jersey Cattle, *Aust. J. Agric. Res .48,* 715–722.

30. Yurawecz, M.P., Roach, J.A.G., Sehat, N., Mossoba, M.M., Kramer, J.K.G., Fritsche, J., and Steinhart, H. (1998) A New Conjugated Linoleic Acid Isomer, 7 *trans,*9 *cis*-Octadecadienoic Acid, in Cow Milk, Cheese, Beef, and Human Milk and Adipose Tissue, *Lipids 33*, 803–809.

31. Perfield, J.W., Sæbo, A., and Bauman, D.E. (2004) Use of Conjugated Linoleic Acid (CLA) Enrichments to Examine the Effects of *trans*-8, *cis*-10 CLA and *cis*-11, *trans*-13 CLA on Milk-Fat Synthesis, *J. Dairy Sci. 87,* 1196–1202.

32. Sehat, N., Rickert, R., Mossoba, M.M., Kramer, J.K.G., Yurawecz, M., Roach, P.J.A., Adlof, R.O., Morehouse, K.M., Fritsche, J., Eulitz, K.D., *et al.* (1999) Improved Separation of Conjugated Fatty Acid Methyl Esters by Silver Ion-High-Performance Liquid Chromatography, *Lipids 34,* 407–413.

33. Nuernberg, K., Dannenberger, D., and Ender, K. (2004) Fleisch wertvoller durch Anreicherung mit n-3 Fettsäuren (Meat more Valuable by Accumulation with n-3 Fatty Acids), *Ernährungsumschau, 51,* 409–413.

34. French, P., Stanton, C., Lawless, F., O'Riordan, O.G., Monahan, M.J., Caffrey, P.J., and Moloney, A.P. (2000) Fatty Acid Composition, Including Conjugated Linoleic Acid, of Intramuscular Fat from Steers Offered Grazed Grass, Grass Silage, or Concentrate-Based Diets, *J. Anim. Sci. 78,* 2849–2855.

35. Enser, M., Scollan, N.D., Choi, N.J., Kurt, E., Hallet, K., and Wood, J.D. (1999) Effect of Dietary Lipid on the Content of Conjugated Linoleic Acid (CLA) in Beef Muscle, *Anim. Sci. 69,* 143–146.

36. Scollan, N.D., Choi, N.J., Kurt, E., Fisher, A.V., Enser, M., and Wood, J.D. (2001) Manipulating the Fatty Acid Composition of Muscle and Adipose Tissue in Beef Cattle, *Br. J. Nutr. 85*, 115–124.

37. Steen, R.W.J., and Porter, M.G (2003) The Effects of High-Concentrate Diets and Pasture on the Concentration of Conjugated Linoleic Acid in Beef Muscle and Subcutaneous Fat, *Grass Forage Sci. 58,* 50–57.

38. Poulson, C.S., Dhiman, T.R., Cornforth, D., Olson, K.C., and Walters, J. (2001) Influence of Diet on Conjugated Linoleic Acid Content in Beef, *J. Anim. Sci. 79* (Suppl.) 1, 159.

39. Engle, T.E., and Spears, J.W. (2004) Effect of Finishing System (feedlot or pasture), High-Oil Maize, and Copper on Conjugated Linoleic Acid and Other Fatty Acids in Muscle of Finishing Steers, *Anim. Sci. 78,* 261–269.

40. Griinari, J.M., and Bauman, D.E. (1999) Biosynthesis of Conjugated Linoleic Acid and Its Incorporation into Meat and Milk in Ruminants, in *Advances in Conjugated Linoleic Acid Research* (Yurawecz, M.P., Mossoba, M.M., Kramer, J.K.G., Pariza, M.W., and Nelson, G.J., eds.) Vol. 1, pp. 180–200, AOCS Press, Champaign.

41. Piperova, L.S., Sampugna, J., Teter, B.B., Kalscheur, K.F., Yurawecz, M.P., Ku, Y., Morehouse, K.M., and Erdman, R.A. (2002) Duodenal and Milk *trans* Octadecenoic Acid and Conjugated Linoleic Acid (CLA) Isomers Indicate That Postabsorptive Synthesis Is the Predominant Source of *cis*-9-Containing CLA in Lactating Dairy Cows, *J. Nutr. 132,* 1235–1241.

42. Ward, R.J., Travers, M.T., Richards, S.E., Vernon, R.G., Salter, A.M., Buttery, P.J., and Barber, M.C. (1998) Stearoyl-CoA Desaturase mRNA Is Transcribed from a Single Gene in the Ovine Genome, *Biochim. Biophys. Acta 1391,* 145–156.

43. Porter, S.F. (2003) Conjugated Linoleic Acid in Tissues from Beef Cattle Fed Different Lipid Supplements, Master's Thesis, Utah State University, Logan.

44. Martin, G.S., Lunt, D.K., Britain, K.G., and Smith, S.B. (1999) Postnatal Development of Stearoyl Coenzyme A Desaturase Gene Expression and Adiposity in Bovine Subcutaneous Adipose Tissue, *J. Anim. Sci. 77,* 630–636.

45. Fritsche, S., Rumsey, T.S., Yurawecz, M.P., Yuoh, K., and Fritsche, J. (2001) Influence of Growth Promoting Implants on Fatty Acid Composition Including Conjugated Linoleic Acid Isomers in Beef Fat, *Eur. Food Res. Technol. 212*, 621–629.

46. Piperova, L., Teter, B.B., Bruckental, I., Sampugna, J., Mills, S.E., Yurawecz, M.P., Fritsche, J., Ku, K., and Erdman, R.A. (2000) Mammary Lipogenic Enzyme Activity, *trans* Fatty Acids and Conjugated Linoleic Acids Are Altered in Lactating Dairy Cows Fed a Milk Fat-Depressing Diet, *J. Nutr. 130,* 2568–2574.

47. Dhiman, T.R., Anand, G.R., Satter, L.D., and Pariza, M.W. (1999) Conjugated Linoleic Acid Content of Milk from Cows Fed Different Diets, *J. Dairy Sci. 82,* 2146–2156.

48. Chouinard, P.Y., Corneau, L., Butler, W.R., Chillard, Y., Drackley, J.K., and Bauman, D.E. (2001) Effect of Dietary Lipid Sources on Conjugated Linoleic Acid Concentrations in Milk Fat, *J. Dairy Sci. 84*, 680–690.

49. Corl, B.A., Baumgard, L.H., Griinari, J.M., Delmonte, P., Morehouse, K.M., Yurawecz, M.P., and Bauman, D.E. (2002) *Trans*-7,*cis*-9 CLA Is Synthesized Endogenously by Δ^9-Desaturase in Dairy Cows, *Lipids 37,* 681–688.

Daphnia magna Can Tolerate Short-Term Starvation Without Major Changes in Lipid Metabolism

E.A. Bychek[a], G.A. Dobson[b], J.L. Harwood[c],*, and I.A. Guschina[c]

[a]Institute of Ecology of the Volga River Basin RAS, Togliatti 445003, Russia, [b]Scottish Crop Research Institute, Invergowrie, Dundee DD2 5DA, United Kingdom, and [c]School of Biosciences, Cardiff University, Cardiff CF10 3US, United Kingdom

ABSTRACT: *Daphnia magna* is a common crustacean that is adapted to brief spells of fasting. Lipids are naturally a major component of their diet and are stored as energy reserves. However, there has been some controversy in the literature on the extent to which dietary lipids are used directly for complex lipid formation in *Daphnia*. We examined lipid metabolism in *D. magna* by labeling the animals using [1-^{14}C]acetate and then followed the turnover of radiolabeled lipids during a pulse chase. *Daphnia* were either fed or maintained without food during the chase period. The decrease in radioactivity during the chase was relatively unaffected by feeding, although there were some differences in the distribution of radioactivity between lipid classes or individual FA. The polar lipids, which were four times better labeled than nonpolar lipids, contained the most radioactivity in the zwitterionic phosphoglycerides, PE and PC. Under the experimental conditions, the turnover of the polar membrane lipids was unaffected by feeding. Within nonpolar lipids, TAG accounted for up to about 80% of the label, followed by DAG. Overall, our data show that *D. magna* is capable of high rates of lipid radiolabeling *de novo* and, in addition, is able to use—and indeed may be dependent on—some dietary components such as the PUFA linoleate and α-linolenate. The results also clearly show that *Daphnia* is able to tolerate brief spells of fasting (24 h) with very little change to its lipid metabolism.

Paper no. L9689 in *Lipids 40*, 599–608 (June 2005).

Crustaceans, like other animals, need a balanced supply of nutrients for development, growth, reproduction, and survival. Lipids, together with proteins and carbohydrates, are important dietary components for crustaceans, in which they function as both a general energy source and as essential nutrients. Crustaceans are considered to be unable to synthesize, and may consequently require an exogenous source of, linoleic (18:2n-6) and α-linolenic (18:3n-3) acids as examples of essential PUFA. However, it should be emphasized that an essential FA requirement has been unequivocally demonstrated only in mammals (1). In other organisms they may be better called essential nutrients, as defined by Lauritzen and Hansen (2). In addition, specific aspects of crus-

tacean lipid nutrition are the requirement for sterols (3) and possibly some phospholipids (4). Sterols are metabolic precursors of steroid hormones and molting hormones and cannot be synthesized by crustaceans *de novo* (5,6). Dietary phospholipids, such as PC and/or PI, have been suggested to accelerate the transport of dietary lipids, especially cholesterol, in some crustaceans (5). The major lipid classes of most aquatic animals are phosphoglycerides, TAG, wax esters, and sterols (7). The phosphoglycerides and sterols are structural and functional elements of cell membranes, whereas TAG and wax esters are storage biomolecules that provide metabolic energy through oxidative catabolic reactions. TAG contents are often highly variable and depend on the nutritional and physiological states of organisms. Moreover, they are influenced by environmental factors (8,9). In contrast, the phosphoglycerides of a given species are considered to be much less variable and essentially independent of their nutritional state (10).

Although lipids are important for zooplankton (11,12), little, in general, is known about lipid metabolic pathways in freshwater crustaceans. Nevertheless, it has been shown that zooplankton can accumulate large amounts of lipids (up to 40–70% of their dry body mass) (13,14), and Goulden and Place (15) were the first researchers who tried to answer the question "What proportion of accumulated lipids originate from the diet and how much is synthesized by animals *de novo*?" In a series of tracer experiments using ^{14}C-acetate or ^{3}H-water, incorporation of radioactivity into FA was studied and the rates of *de novo* FA synthesis were calculated in two species of daphniids, *Daphnia magna* and *D. pulicaria*. Goulden and Place (16) concluded that no more than 1.6 or 0.16% of the accumulated FA could be biosynthesized by either species under high-food and low-food conditions, respectively. According to their results, at least 98% of the total lipids, and virtually all of the storage lipids, were derived from the diet. Incorporated radioactivity was largely found in phosphoglycerides and was not present in storage lipids. In fact, they concluded that most of the incorporation was a result of the chain elongation of dietary acids. Thus, they suggested that storage lipid accumulation rates in daphniids were strongly regulated by the availability of dietary lipids (15,16).

In contrast, Farkas *et al*. (17) showed that some copepods, namely, *Cyclops strenuus* and *D. magna*, showed substantial FA synthesis rates. Their calculations indicated that 0.9% of

---

the total FA were renewed in 1 h in *D. magna*, and they suggested that the bulk of FA accumulated in both species could be synthesized by the animals. They also showed that incorporation of radioactivity from labeled acetate into total lipids was greatly affected by temperature, with large changes in the pattern of FA labeled in *D. magna* (17). Various other external (e.g., UV light, salinity, dissolved oxygen concentration, pH, water transparency, stressors) and internal (e.g., reproductive condition) factors may also influence zooplankton lipid composition and biosynthesis (13,18–20). *De novo* lipogenesis has also been measured in the euphausiids *Thysanoessa inermis* and *T. raschii,* where *de novo* lipogenesis was shown to be capable of accounting for much of the lipids accumulated by these animals in the field (21). Moreover, extensive lipid synthesis in the presence of a substantial input of dietary lipids has been noted when studying the importance of *de novo* lipid biosynthetic activity in the accumulation of wax esters by marine zooplankton (21). This finding is relatively unusual for animals, where the activity of FA synthase itself is often repressed by a substantial input of dietary FA (especially polyunsaturated ones) so that *de novo* FA biosynthesis no longer proceeds at significant rates (22,23). It is not known whether such repression takes place in freshwater copepods, which do not possess active wax ester synthesis and accumulation. Furthermore, according to Goulden and Place (15,16), in poorly fed daphniids, the rate of *de novo* synthesized FA was 10-fold slower than in well-fed animals. Thus, answers to the question, "How may food availability modify basic lipid metabolism in copepods?" are contradictory, and more experimental work is obviously needed to clarify the topic.

In the present work we studied lipid metabolism in the important freshwater crustacean *D. magna* by following the incorporation of radiolabel from [1-14C]acetate in pulse-chase experiments and its response to either starvation or feeding using the alga *Coccomyxa peltigeracea* as a food source. We used this radiolabeled precursor because it is regarded as a good compound with which to examine *de novo* FA biosynthesis and to allow comparison with the previous work referred to above (15–17). *Daphnia magna* represents freshwater cladocerans, which are important in the structure of the zooplankton community. *Daphnia* spp. are one of the most important live foods for fish, and *D. magna* is the largest of these species. Moreover, although this species has been widely used as a model animal in ecological, toxicological, and physiological studies (24,25), experimental data on changes in the lipid biochemistry of daphniids in response to altering feeding conditions are limited. Nevertheless, a number of publications have reported aspects of lipid composition (26,27), including those for other *Daphnia* species, which include examination of the possible physiological role of the diet (28–35). These provide a good background to our re-examination of the ability of *Daphnia* to synthesize FA *de novo* and incorporate them into lipids, and whether these processes are affected by their nutritional status.

EXPERIMENTAL PROCEDURES

Chemicals and reagents. FA standards were obtained from Nu-Chek-Prep. Inc. (Elysian, MN) and silica gel G plates were from Merck (Darmstadt, Germany). Complex lipid standards were from Sigma (Poole, Dorset, United Kingdom). [1-14C]Acetate, Na salt (sp. act. 1.85–2.29 GBq mmol^{-1}) was from Amersham Life Sciences Ltd. (Bucks, United Kingdom). Other reagents were of the best available grades and were from Sigma or from BDH (Poole).

Incubations. Stock cultures of *D. magna* Straus (Crustacea, Cladocera) were maintained in the laboratory in 0.45-μm filtered lake water at 24–25°C and fed with the green microalga *C. peltigeracea* grown in Bold's mineral medium (36). New hatchlings were used, and these were fed for 10 d prior to their use in the experiments. For pulse-chase experiments, immature parthenogenic females of *D. magna* with a body size of 1.7–2.0 mm were selected with a microscope, washed three times with 0.45-μm membrane filtered water, and 50 individuals transferred into 100-mL flasks containing 50 mL of filtered (0.45 μm) lake water at 24–25°C. This filter treatment of water is consistent with many previous studies using *Daphnia* spp. (28,32,34,35,37). For lipid labeling, 185 KBq of [1-14C]acetate was added to these flasks, and animals were incubated without algal food with radiolabel for 22 h (pulse period). At the end of the pulse period, the animals were rinsed three times with distilled water and transferred into the new 100-mL flasks containing 50 mL of filtered lake water. (This methodology did not impair the animal's ability for active movement or, in longer-term control experiments, to grow and reproduce. Furthermore, it did not result in any loss in detectable unlabeled or radiolabeled lipids compared with using filtered lake water.) Two feeding treatments were used. Animals in the first group were kept with no food until the end of the chase period, whereas the animals in the second group were fed with algae (1 mL, about 10 mg wet wt of the algal suspension to each flask). Sampling of the animals for lipid extraction was performed at 0, 4, 8, 12, and 24 h into the chase period. Experiments with each group were replicated at least three times.

Lipid analysis. Lipids were extracted by a modified method of Folch *et al.* (38) as described by Garbus *et al.* (39). FAME were prepared by transmethylation with 2.5% H_2SO_4 in dry methanol. Nonpolar lipids were separated by 1-D TLC on 20 × 20 cm silica gel G plates with double development, first with 140:60:1 (by vol) toluene/hexane/formic acid for the whole plate height, followed by 60:40:1 (by vol) hexane/diethyl ether/formic acid to half height. Polar lipids (PL) were separated by 2-D TLC on 10 × 10 cm silica gel G plates using 65:25:4 (by vol) chloroform/methanol/water in the first dimension and then 50:20:10:10:5 (by vol) chloroform/acetone/methanol/acetic acid/water in the second direction. Plates were sprayed with 0.05% (wt/vol) 8-anilino-4-naphthosulfonic acid in methanol and viewed under UV light to reveal lipids or were visualized under iodine vapor. Identification was made by reference to authentic standards and was confirmed using specific color reagents (40).

FA identification and analysis. Radiolabeled FAME were analyzed by radio-GLC using a Unicam GCD gas chromatograph connected *via* an effluent splitter to a LabLogic RAGA (LabLogic, Sheffield, United Kingdom) gas flow proportional counter. Glass columns (1.5 m × 4 mm i.d.) were packed with 10% SP-2330 on a 100/120 Supelcoport (Supelco, Bellefonte, PA). The SP-2330 column was run isothermally at 180°C. Routine identification was by reference to standards, and quantification (Rachel Software, LabLogic) was made by reference to an internal standard of pentadecanoate. Identification of FA was made by comparison with standards using GLC on a capillary column. GC of FAME was performed using a Hewlett-Packard model 5890 series II gas chromatograph equipped with a split/splitless injector, autosampler, and FID. A capillary column of fused silica coated with CP-Wax 52CB^{TM} (0.25 mm i.d. × 25 m in length, 0.2 µm film thickness; Chrompack UK Ltd., London, United Kingdom) was used, and hydrogen was the carrier gas at an initial flow rate of 1 mL min^{-1}. After holding the temperature at 170°C for 3 min, the column was temperature-programmed at 4°C min^{-1} to 220°C and then held at this point for an additional 15 min. In all analyses, the detector was set at 300°C, the injector at 230°C, and a split ratio of 50:1 was used. An HP 3365 Chemstation (Hewlett-Packard Ltd., Stockport, United Kingdom) was used for data acquisition.

Preparation of 4,4-dimethyloxazoline (DMOX) derivatives. The FAME were hydrolyzed with 0.1 mol L^{-1} KOH in 90% aqueous ethanol (0.25 mL per mg of sample) at 50°C for 3 h. After acidification with acetic acid and addition of water (2 mL), the FFA were extracted twice with 1:1 (vol/vol) diethyl ether/isohexane (6 mL, then 3 mL). The combined organic layers were passed through a short (3-cm) column of anhydrous sodium sulfate prepared in a Pasteur pipette, and were taken to dryness under nitrogen at 30°C on a heating block. The FFA were converted to DMOX derivatives by heating with 2-amino-2-methyl-1-propanol (0.25 mL) at 190°C for 16 h. These DMOX derivatives were made in order to have stable components for positional double-bond analysis without migration. On cooling, water (5 mL) was added and the DMOX derivatives were extracted with 1:1 (vol/vol) diethyl ether/isohexane (5 mL). The aqueous layer was re-extracted with fresh solvent (2 mL), and the combined solvent extracts were washed with water (3 mL) and dried over anhydrous sodium sulfate. Finally, the solvent extract was passed through a short (3-cm) column of anhydrous sodium sulfate prepared in a Pasteur pipette. The column was washed with isohexane and the sample containing the DMOX derivatives was taken to dryness under nitrogen at 30°C on a heating block. The DMOX derivatives were dissolved in isohexane containing BHT (50 ppm) and kept at −20°C until they were analyzed.

The positions of double bonds in the hexadecenoic and octadecenoic acid fractions were determined by GC–MS of their DMOX derivatives using a Hewlett-Packard 5890 Series II Plus gas chromatograph fitted with an on-column injector and a SUPELCOWAX^{TM} 10 (0.25 mm × 30 m, 0.25 µm film thickness; Supelco) capillary column, connected to a Hewlett-Packard 5989B MS Engine quadrupole mass spectrometer. The column temperature was held at 80°C for 3 min, temperature-programmed to 170°C at 20°C min^{-1}, then to 240°C at 2°C min^{-1} and to 280°C at 5°C min^{-1}, and was finally held at 280°C for 15 min. Helium was the carrier gas, at a flow rate of 1.4 mL min^{-1}, and pressure-programming was used in constant flow mode. The mass spectrometer was operated in EI mode at an ionization energy of 70 eV.

Radioactive counting was made using dried lipid or aqueous samples and Opti-Fluor (Packard Bioscience B.V., Groningen, The Netherlands) scintillant and a Beckman 1209 Rackbeta liquid scintillation counter. Quench correction was by the external standard channels ratio method.

Statistical analysis. Analysis was carried out using at least three independent samples in triplicate and a one-way ANOVA using Tukey's test comparing fed vs. starved animals.

RESULTS

Figure 1 shows the total lipid labeling in *D. magna* during a pulse-chase experiment. The label was significantly reduced (30–40%) in the first 4 h of chase, was relatively stable for the following 8 h of chase, and halved in the next 12 h of the chase period. The data also show that there were no statistically significant differences in the labeling of total lipids from [1-^{14}C]acetate in *D. magna* as a response to food supply during the chase period (Fig. 1). Among nonpolar lipids, DAG, sterols, nonesterified FA, TAG, waxes, and steryl esters were identified in *D. magna* (data not shown). TAG were the main labeled class, accounting for 50–80% of the total nonpolar lipid labeling.

For the nonpolar lipid fraction, some differences were noted in response to feeding (Fig. 2). Thus, the labeling in starved animals followed, to some extent, the labeling of total lipids noted above (Fig. 1) with a decrease in the first 4 h, less change in the next 8 h, and a decrease again in the period 12–24 h (Figs. 1,2). The final level of radiolabeling of total nonpolar lipids (Fig. 2) and its major component, TAG (Fig. 3), was significantly less for starved than for fed *Daphnia*. In contrast to the time-course of the total nonpolar lipid labeling in starved *Daphnia*, that of fed animals showed an increase between 4 and 12 h. As expected (given that TAG represented up to 80% of the labeling of the total nonpolar lipids), the time-courses of TAG labeling in fed vs. starved *Daphnia* were similar (Fig. 3B) to those for the total nonpolar lipids (Fig. 2). Thus, because of the increase in TAG labeling in the 4–12 h chase period for fed *Daphnia*, the amount of radioactivity in this lipid at the end of the chase period was about 75% of the starting value, whereas in starved animals the value was about 25%. Unexpectedly, DAG (which is a direct precursor of TAG) showed a different time-course of labeling (Fig. 3A). For both fed and starved *Daphnia*, there was a rapid decrease in labeling in the initial 4-h chase period, with the decrease more marked for fed animals. In the intermediate period
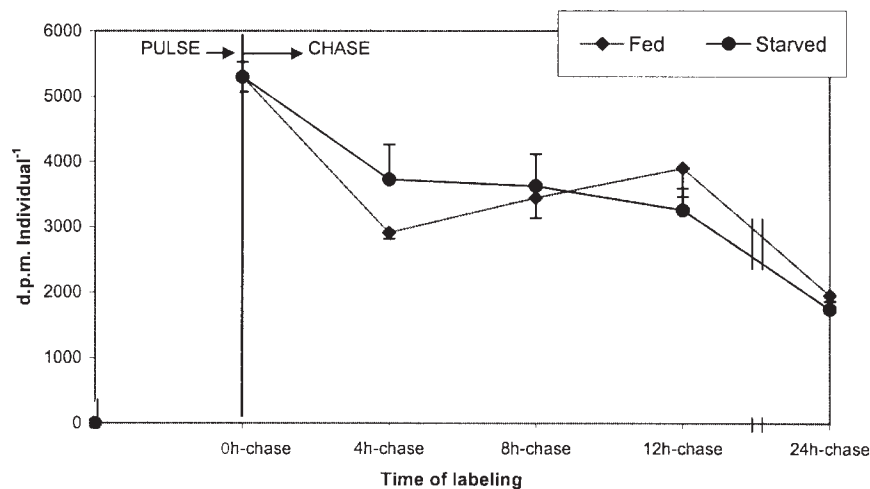
FIG. 1. Effect of starvation and feeding on the radiolabeling of total lipids in *Daphnia magna* from [1-^{14}C]acetate during a pulse-chase experiment. The radiolabel pulse was for 22 h. The results show means ± SD of three independent experiments. dpm, disintegration per minute.

(4–12 h), the alterations in fed *Daphnia* were less marked than for TAG and the decrease in the final 12–24 h period meant there was no significant difference between fed or starved animals in the radioactivity in DAG (Fig. 3A).

Our results showed that PL were much better labeled (3600 dpm individual^{-1}; 77% of total labeling) than nonpolar lipids (1030 dpm individual^{-1}). This agreed excellently with previous data for this species (15–17). The radiolabel in these polar membrane components decreased significantly for the first 4 h of chase and then decreased only slightly in the remainder of the chase period (Fig. 4). Essentially, there was little difference in the labeling of total PL between the fed or starved *Daphnia* (Fig. 4). Of course, since PL (mainly phos-

phoglycerides) represented over 75% of the total lipid labeling, the lack of effect of feeding was also reflected in the total labeling patterns (Fig. 1). In our study, PE was the best-labeled compound and accounted for about 50% of the total phospholipid labeling after the initial pulse, followed by PC (25%), PS, and PI (each about 10%). Phosphatidylglycerol (PG) was a minor labeled phosphoglyceride, representing only 5% of the total PL labeling (Fig. 5). Our results showed that the radiolabeled phospholipid patterns in *D. magna* were similar for both fed and starved animals (Figs. 5A, 5B). The labeling of PE and PS both reduced by about half or more within the first 4 h of chase. By 24 h, the radioactivity in these phosphoglycerides was of the order of one-fifth the starting
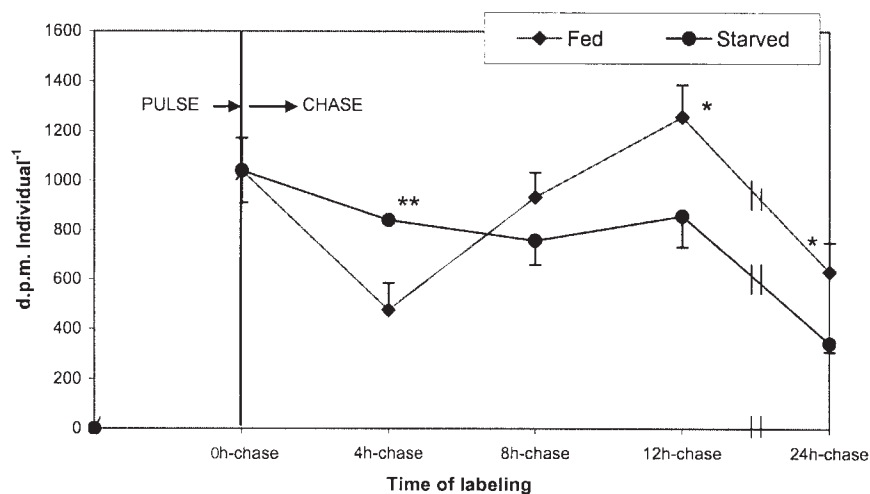
FIG. 2. Effect of starvation and feeding on the radiolabeling of total nonpolar lipids in *D. magna* during a pulse-chase experiment. The radiolabel pulse was for 22 h. The results show means ± SD of three independent experiments. Asterisks show statistically different values at $P < 0.005$ (**) and $P < 0.05$ (*) on statistical analysis by one-way ANOVA using a Tukey test for comparison of fed and starved *Daphnia*. For abbreviation see Figure 1.
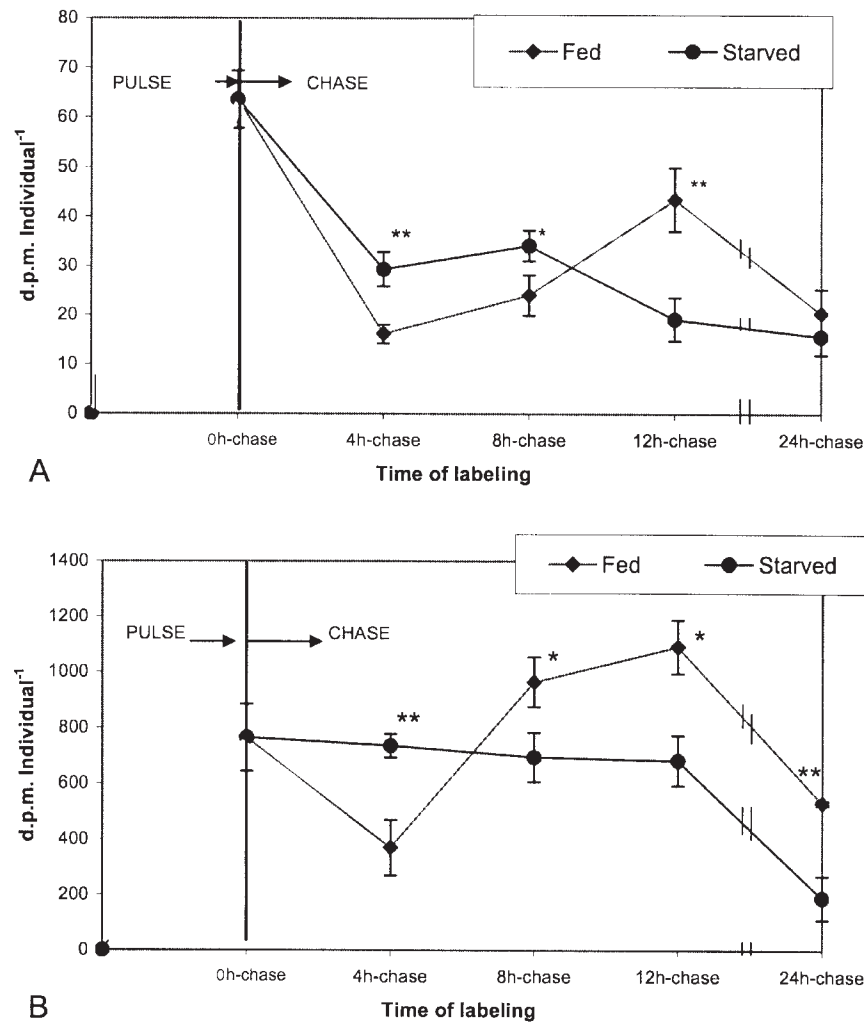
FIG. 3. Radiolabeling of DAG (A) and TAG (B) from [1-^{14}C]acetate in fed or starved *D. magna* during a pulse-chase experiment. The radiolabel pulse was for 22 h. The results show means ± SD of three independent experiments. Asterisks show statistically different values at $P < 0.005$ (**) and $P < 0.05$ (*) on statistical analysis by one-way ANOVA using a Tukey test comparing fed and starved animals. For abbreviation see Figure 1.

amount, regardless of the feeding regime. For the other phosphoglycerides (PC, PG, PI), the reductions were more gradual and caused about a halving in the starting radioactivity during the chase period (Fig. 5).

The main FA identified in *D. magna* were palmitic, linoleic, and α-linolenic acids. In addition, 16:1, 16:2, 16:3, and 18:1 were found in significant amounts. GC–MS was used to identify the double bond positions of the hexadecenoic and octodecenoic acid fractions, which were the main unsaturated FA radiolabeled during our experiments (see following discussion). There were two octadecenoic acid isomers, of which oleic acid (18:1n-9) represented 5.4% of the total FA and *cis*-vaccenic acid (18:1n-7) was 2.4%. Palmitoleic acid (16:1n-7) was a significant component (1.4% of total FA) but palmitvaccenic acid (16:1n-9) was not detected. The relative content of FA was consistent with data previously reported for *D. magna* (26,29) and was not changed sig-

nificantly during the experiment. Moreover, no significant differences were found in endogenous FA percentage compositions between starved and fed *Daphnia* (data not shown).

Figure 6 presents the data on FA labeling. The main FA labeled during the course of the experiment were palmitate (16:0), hexadecenoate (16:1), and octadecenoate (18:1). No radiolabel was detected in odd-chain or branched-chain FA, which are considered markers of bacterial FA (34). The proportional labeling of palmitate was stable and did not change during the chase under both food regimes, whereas the relative labeling of 16:1 and 18:1 was altered by the end of the chase, especially in fed animals (Fig. 6A). Thus, a significant increase in the percentage labeling of octadecenoate was seen at the expense of hexadecenoate between 12 and 24 h of chase. Because of the probability that palmitoleic acid is converted into the vaccenic acid by elongation, we also calculated the total amounts of radioactivity in the 16:0, 16:1, and 18:1 fractions
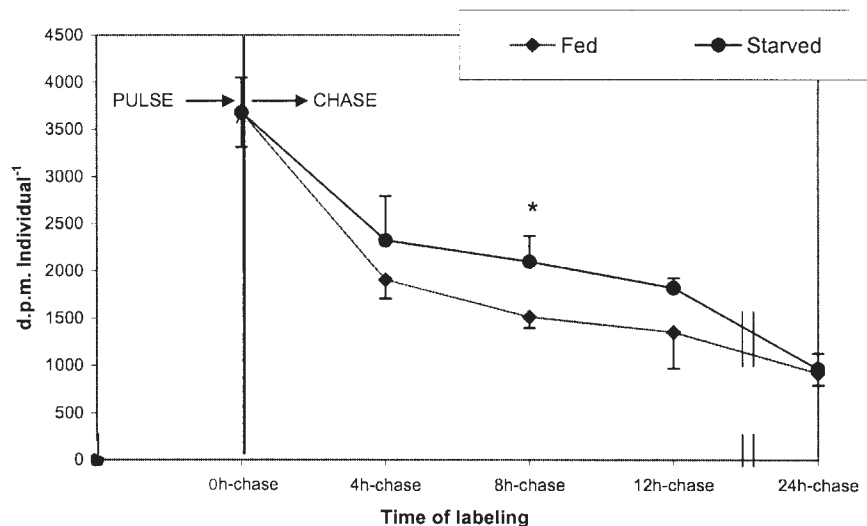
FIG. 4. Radiolabeling of total polar lipids from [1-^{14}C]acetate in fed or starved *D. magna* during a pulse-chase experiment. The results show means ± SD of three independent experiments. Asterisks show statistically different points at *P* < 0.05 on statistical analysis by one-way ANOVA using a Tukey test comparing fed and starved animals. For abbreviation see Figure 1.

during the total duration of the experiment. In both fed and starved *Daphnia*, there was a large decrease in the total amount of radioactivity during the first 4 h of chase (Fig. 1). However, because the percentage labeling of 18:1 increased (especially for starved animals), the total radioactivity in this fraction decreased less than, say, for palmitate. Between 4 and 12 h of chase, there was little change in total radioactivity (Fig. 1); therefore, all FA fractions remained labeled to a constant amount. Between 12 and 24 h of chase, there were significant losses of total radioactivity for both fed and starved animals (Fig. 1), and in the latter case, because of the altered percentage of labeling (Fig. 6), the loss in radioactivity was in the order 16:1 > 16:0 > 18:1.

DISCUSSION

It is well known that the ability of an animal to survive starvation depends on the amount of energy reserves and the way this energy is allocated to survival, growth, and reproduction (41). In a study of growth and mortality of fed and starved *D. magna* over 22 d, starved animals grew significantly less than fed animals (41). All animals survived at least 5 d of starvation. However, after a period of 3 d of starvation, energy reserves were not sufficient to allow further growth and reproduction (41). In fact, it appeared that lipid reserves were especially crucial because, although total carbohydrate and glycogen were reduced by 1 d of starvation, it was not until day 3 that the TAG stores were significantly depleted (41). In another daphnid, *D. galeata*, it was also shown that the animal was able to adapt quickly to short periods of starvation and to variations in food supply (42). Thus, it is perhaps not surprising that there were not large differences in the response of *D. magna* to feeding, rather than starva-

tion, during the time course of our experiments (Figs. 1–4).

Among individual phosphoglycerides, PE, PC, PS, PG, and PI were identified (see the Experimental Procedures section). A similar phospholipid composition with an abundance of PC (52.6% of total PL) and PE (31.9%) has been reported previously for *D. magna*, and their amounts are known to be significantly affected by growth temperature (43). The domination of PC and PE also has been found in three developmental stages of *D. magna*, with PC/PE ratios of 1.57, 2.22, and 1.26 from newborn, 3-d-old immature females, and mature females, respectively (44).

The preferential labeling of PL (mainly phosphoglycerides) compared with nonpolar lipids from ^{14}C-acetate (Figs. 2, 3) agrees with other studies with *D. magna* (17). In addition, these workers also found, as we did, that TAG was by far the highest labeled nonpolar lipid (Figs. 1, 2). The rapid decrease in total lipid radioactivity during the first 4 h of chase implies a rapid turnover of some acyl groups. In quantitative terms, this change is mainly located in the phospholipids, and indeed it is well known that many PL (including phosphoglycerides) show a rapid turnover of their acyl groups (23). After a 4-h chase, the decrease in both total lipid (Fig. 1) and PL (Fig. 4) radioactivity was slower but was approximately similar in both fed and starved animals. We interpret this to reflect the normal replacement of membrane phosphoglycerides that takes place in different organisms. Presumably, the replacement carbon in the starved *Daphnia* came from storage compounds, which could have been carbohydrates as well as TAG, whereas the fed animals could also have used dietary sources. Indeed, over the 24-h chase, the starved *Daphnia* appeared to turn over more of their TAG (Figs. 2, 3B), although they seemed to make some effort to conserve these reserves, as reflected in the constant amounts of radioactivity over the
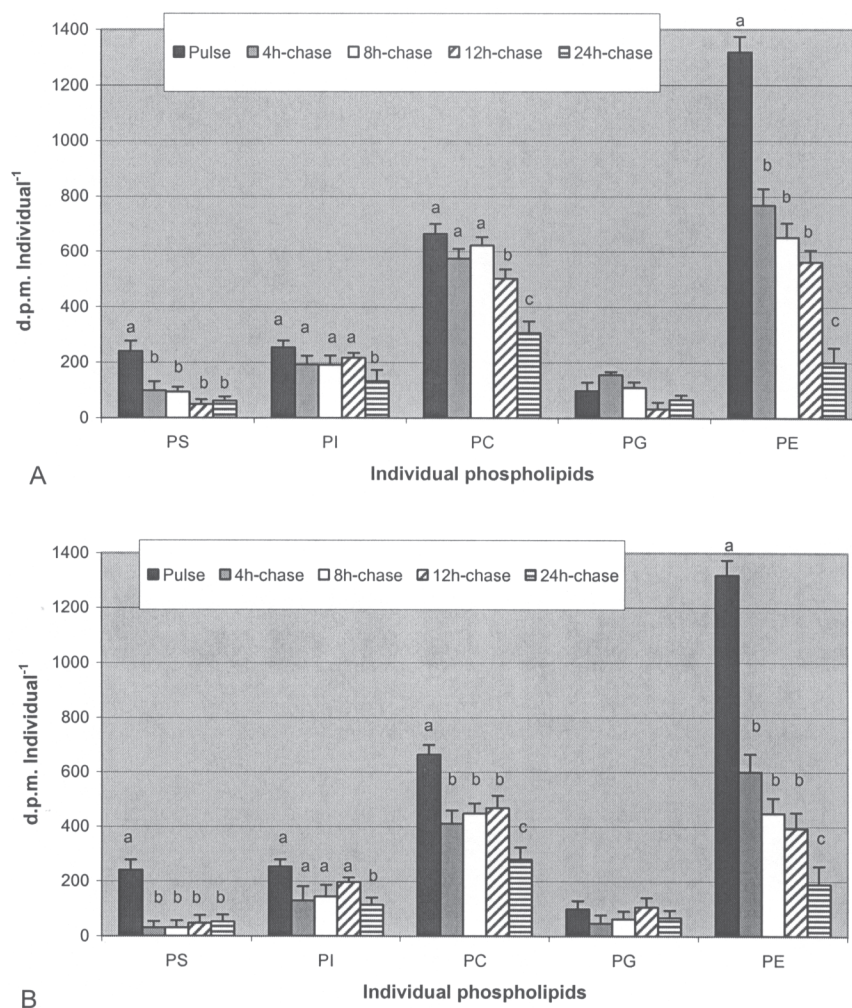
FIG. 5. Radiolabeling of individual phosphoglycerides from [1-^{14}C]acetate in fed (A) or starved (B) *D. magna* during a pulse-chase experiment. The results show means ± SD of three independent experiments. Different letters indicate statistically significant differences at $P < 0.01$ on statistical analysis by one-way ANOVA using a Tukey test comparing fed or starved animals with the initial pulse values. PG, phosphatidylglycerol; for other abbreviation see Figure 1.

first 12 h of chase (Fig. 3B). This would probably correspond to the period when carbohydrate reserves were being used (41). Fed *Daphnia* had no need to husband food reserves, so a dramatic drop in TAG radioactivity in the first 4 h of chase would not have been serious physiologically and TAG synthesis could continue to take place, with radiolabeled FA also possibly coming from membrane lipids, as these were replaced from food sources. The quicker labeling of TAG during the 4- to 12-h chase period compared with DAG (Fig. 3A) suggests that a major part of the DAG total pool may be formed from TAG during catabolism by the latter rather than *via* the role of DAG as an intermediate in the Kennedy pathway (23). In agreement with this, like Farkas *et al.* (17), we (data not shown) found 1,3-DAG to be more abundant than 1,2-DAG.

According to our results, both lipid fractions, PL and nonpolar lipids, were efficiently labeled from [1-^{14}C]acetate. About

25% of the label incorporated was found in nonpolar lipids, with TAG as their main constituent. In a previous study using *Daphnia*, Goulden and Place (15) found that "accumulation" of TAG was greater than that of phospholipids in fed *D. magna* and *D. pulex*. Even in *D. pulex* acclimated to a low food level (4,000 algal cells mL^{-1} d^{-1} vs. 100,000 algal cells mL^{-1} d^{-1} in control) for several generations (experiment for more than 20 d), the accumulation of TAG was still five times that of phospholipids. However, it is not clear from their results whether accumulation was really being measured, since no starting values were given. Moreover, although these authors also measured radiolabeling from both [U-^{14}C]acetate and [^{3}H]$_2$O, they did not separate labeling into different lipid classes. They did show, however, much less labeling of starved *D. pulex* from either radiolabeled precursor than of fed animals.

In general, the loss of label (30–40%) in total lipids in the first 4 h of chase may reflect the rapid turnover of some lipids
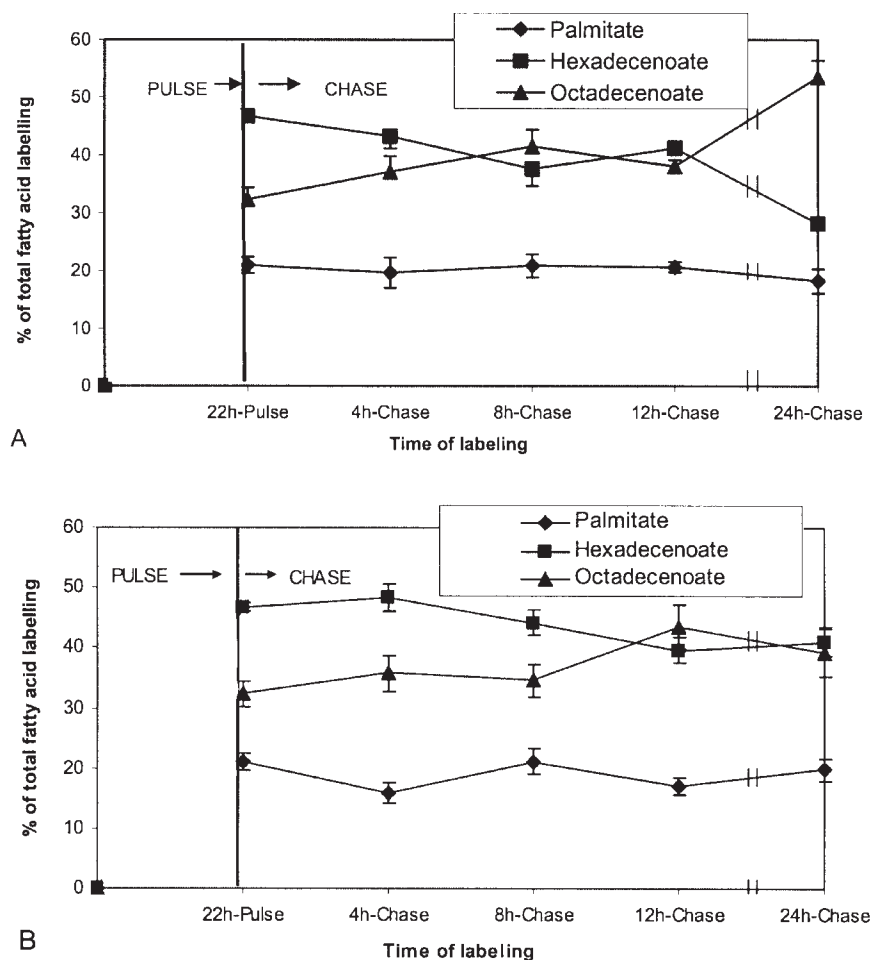
FIG. 6. Labeling of FA from the total lipids of *D. magna* that were fed (A) or starved (B) during a pulse-chase experiment. The results show means ± SD of three independent experiments. For abbreviation see Figure 1.

(e.g., PS, PE, DAG), whereas after 12 h, when the labeling of all lipids decreased, a general turnover was seen.

The labeling of phospholipids was not affected by food supply as much as that of nonpolar lipids, probably reflecting the relative independence of phospholipid synthesis on the nutritional state of the organisms (10). In contrast, Elendt (41) reported that the amount of these lipids diminished from about 6.3% of dry weight to 4.8% over a longer experimental period (6 d) of starvation in *D. magna*. We found that the turnover of the membrane compounds in *D. magna* was significant in that approximately 70% of the label previously incorporated into phosphoglycerides disappeared during the 24-h chase period. Although the experimental protocol is not directly comparable, Farkas *et al.* (17) also revealed a rapid turnover of lipids in *Daphnia*.

It was interesting that PE and PS lost half of their radioactivity in the first 4 h of the chase, whereas other phospholipids (PC, PI, and PG) lost half of their radioactivity only after 24 h (Fig. 5). This might indicate that PE and PS are important as (precursors of) signaling molecules or, alternately, that they play a significant role in metabolism.

Although the PUFA, linoleic and linolenic acids, accumulated in *D. magna* as two of the three main FA (a typical total FA composition was 23.2% palmitate, 23.2% linoleic, and 19.2% α-linolenic acids), no labeling of these molecules was noted during our experiments, probably indicating their dietary origin as suggested by various studies (28–33,35,37). This observation is in agreement with the accepted dogma that no animals (except a few insects, noninsect invertebrates, and protozoa) (45–48) can biosynthesize linoleic or α-linolenic acids. However, it must be borne in mind that sometimes the labeling of PUFA during radiolabeling experiments takes some time; therefore, the duration of the experiment is important. Nevertheless, we incubated *Daphnia* for 22 h, so we are confident that if there is any capacity for the synthesis of linoleic or α-linolenic acids, it is very small.

Because the radio-gas chromatograph used a packed column, we were unable to distinguish individual isomers of the two monoenoate peaks with any certainty. The endogenous octadecenoate contained oleate (5.4% total FA) and *cis*-vaccenate (2.4%), whereas the hexadecenoate fraction contained palmitoleate (1.4%) as a significant fraction. The presence of

vaccinate suggests that elongation of palmitoleate to this FA is a significant metabolic reaction (23). Indeed, the changes in total radioactivity that occurred during the chase period for the three FA fractions would be consistent with such elongation. Thus, for the starved *Daphnia* (Figs. 1, 6), the decrease in radioactivity in the 16:1 fraction was the highest (355 down to 100 dpm individual^{-1} between 12 and 24 h of chase), whereas that in 18:1 changed much less (327 to 197 dpm individual^{-1}). If elongation of palmitoleate to vaccinate was occurring, then that would explain the results.

One issue in interpreting the data that needs to be considered is how much bacterial contamination could affect the radiolabeling results. The filtered culture water was clearly not sterile, although the use of a 0.45-μm filter is a standard method in use for *Daphnia* (28,32,34,35,37). However, we took care in washing *D. magna* at the end of the experiment to exclude bacteria in the water, although consumption of radiolabeled organisms by the copepods cannot be excluded. Nevertheless, similar FA and acyl lipids were labeled by both fed and starved *Daphnia* (Figs. 5, 6), which would not be expected if (radiolabeled) bacteria were a major source of food for the starved *Daphnia*. Farkas *et al.* (17), in considering the question of bacterial contamination, thought that the gut was the main potential source but concluded that any contamination of radiolabeled products was negligible. Furthermore, the pattern of FA labeling in our experiments did not include significant amounts of typical "bacterial markers" (34) such as odd-chain or branched-chain acids; moreover, the pattern of labeling of the phospholipids (Fig. 5) was typical of a eukaryotic organism with high PC labeling and a low amount of PG. Therefore, we conclude that bacterial contribution to the overall lipid labeling in our experiments was not significant.

In summary, our data clearly show that *D. magna* is able to tolerate short-term starvation well and that the latter does not result in major changes in lipid metabolism. In addition, the results indicate that the animal is capable of good rates of lipid synthesis *de novo* in addition to being able to make direct use of dietary components, such as PUFA. Therefore, lipid metabolism can be said to be well-adapted to the normal lifestyle of *Daphnia*.

REFERENCES

1. Nakamura, M.T., and Nara, T.Y. (2003) Essential Fatty Acid Synthesis and Its Regulation in Mammals, *Prostaglandins, Leukotr. Essent. Fatty Acids 68,* 145–150.
2. Lauritzen, L., and Hansen, H.S. (2003) Which of the n-3 FA Should Be Called Essential? *Lipids 38,* 889–891.
3. Martin-Creuzburg, D., and Von Elert, E. (2004) Impact of 10 Dietary Sterols on Growth and Reproduction of *Daphnia galeata*, *J. Chem. Ecol. 30,* 483–500.
4. Teshima, S., Kanazava, W.A., and Koshio, S. (1993) Recent Developments in Nutrition and Microparticulate Diets of Larval Prawns, *Isr. J. Aquacult.–Bamidgen 45*, 175–184.
5. Teshima, S., and Kanazava., W.A. (1986) Nutritive Value of Sterols for the Juvenile Prawn, *Bull. Jpn. Soc. Sci. Fish. 52,* 1417–1422.
6. Kanazava, A. (2001) Sterols in Marine Invertebrates, *Fish. Sci. 67,* 997–1007.
7. Ackman, R.G. (1999) Comparison of Lipids in Marine and Freshwater Organisms, in *Lipids in Freshwater Ecosystems* (Arts, M.T., and Wainman, B.C., eds.), pp. 262–298, Springer, New York.
8. Arts, M.T., Evans, M.S., and Robarts, R.D. (1992) Seasonal Patterns of Total and Energy Reserve Lipids of Dominant Zooplanktonic Crustaceans from a Hyper-eutrophic Lake, *Oecologia 90*, 560–571.
9. Falk-Petersen, S., Sargent, J.R., Lonne, O.J., and Timofeev, S. (1999) Functional Biodiversity of Lipids in Antarctic Zooplankton: *Calanoides acutus, Calanus propinquus, Thysanoessa macrura* and *Euphausia crystallorophias*, *Polar Biol. 21*, 37–47.
10. Olsen, Y. (1999) Lipids and Essential Fatty Acids in Aquatic Food Webs: What Can Freshwater Ecologists Learn from Mariculture? in *Lipids in Freshwater Ecosystems* (Arts, M.T., and Wainman, B.C., eds.), pp. 161–203, Springer, New York.
11. Hagen, W. (1999) Reproductive Strategies and Energetic Adaptations of Polar Zooplankton, *Invertebr. Reprod. Dev. 36*, 25–34.
12. Hagen, W., and Auel, H. (2001) Seasonal Adaptations and the Role of Lipids in Oceanic Zooplankton, *Zool.-Anal. Complex Syst. 104*, 313–326.
13. Arts, M.T. (1999) Lipids in Freshwater Zooplankton: Selected Ecological and Physiological Aspects, in *Lipids in Freshwater Ecosystems* (Arts, M.T., and Wainman, B.C., eds.), pp. 71–90, Springer, New York.
14. Goulden, C.E., Moeller, R.E., McNair, J.N., and Place, A.R. (1999) Lipid Dietary Dependencies in Zooplankton, in *Lipids in Freshwater Ecosystems* (Arts, M.T., and Wainman, B.C., eds.), pp. 91–109, Springer, New York.
15. Goulden, C.E., and Place, A.R. (1990) Fatty Acid Synthesis and Accumulation Rates in Daphniids, *J. Exp. Zool. 256*, 168–178.
16. Goulden, C.E., and Place, A.R. (1993) Lipid Accumulation and Allocation in Daphniid Cladocera, *Bull. Mar. Sci. 53*, 106–114.
17. Farkas, T., Kariko, K., and Csengeri, I. (1981) Incorporation of [1-^{14}C]Acetate into Fatty Acids of the Crustaceans *Daphnia magna* and *Cyclops strenus* in Relation to Temperature, *Lipids 16*, 418–422.
18. Arts, M.T., Robarts, R.D., and Evans, M.S. (1993) Energy Reserve Lipids of Zooplanktonic Crustaceans from an Oligotrophic Saline Lake in Relation to Food Resources and Temperature, *Can. J. Fish. Aquat. Sci. 50*, 2404–2420.
19. Wainman, B.C., McQueen, D.J., and Lean, D.R.S. (1993) Seasonal Trends in Zooplankton Lipid Concentration and Class in Freshwater Lakes, *J. Plankton Res. 15*, 1319–1332.
20. Cauchie, H.M., Jasper-Versali, M.F., Hoffmann, L., and Thorne, J.P. (1999) Analysis of the Seasonal Variation in Biochemical Composition of *Daphnia magna* Straus (Crustacea: Branchiopoda: Anomopoda) from an Aerated Wastewater Stabilisation Pond, *Ann. Limnol./Intl. J. Limnol. 35,* 223–231.
21. Sargent, J.R., and Henderson, R.J. (1986) Lipids, in *The Biological Chemistry of Marine Copepods* (Corner, E.D.S., and O'Hara, S.C.M., eds.), pp. 59–108, Clarendon Press, Oxford.
22. Wakil, S.J., Stoops, J.K., and Joshi, V.C. (1983) Fatty Acid Synthesis and Its Regulation, *Annu. Rev. Biochem. 52*, 537–579.
23. Gurr, M.I., Harwood, J.L., and Frayn, K.N. (2002) *Lipid Biochemistry,* 5th edn. Blackwells, Oxford.
24. Knops, M., Altenburger, R., and Segner, H. (2001) Alterations of Physiological Energetics, Growth and Reproduction of *Daphnia magna* Under Toxicant Stress, *Aquat. Toxicol. 53*, 79–90.
25. Sakai, M. (2001) Chronic Toxicity Test with *Daphnia magna* for Examination of River Water Quality, *Food Contam. Agric. Wastes 36*, 67–74.
26. Barata, C., Carlos-Navarro, J., Varo, I., Carmen Riva, M., Arun, S., and Porte, C. (2005) Changes in Antioxidant Enzyme Activities, Fatty Acid Composition and Lipid Peroxidation in *Daphnia magna* During the Aging Process, *Compar. Biochem. Physiol. B: Biochem. Mol. Biol. 140B*, 81–90.

27. Ballantyne , A.P., Brett, M.T., and Schindler, D.E. (2003) The Importance of Dietary Phosphorus and Highly Unsaturated Fatty Acids for Sockeye (*Oncorhynchus nerka*) Growth in Lake Washington—A Bioenergetics Approach, *Can. J. Fish. Aquat. Sci. 60*, 12–22.

28. Von Elert, E. (2004) Food Quality Constraints in *Daphnia*: Interspecific Differences in the Response to the Absence of a Long Chain Polyunsaturated Fatty Acid in the Food Source, *Hydrobiologia 526*, 187–196.

29. Becker, C., Feuchtmayr, H., Brepohl, D., Santer, B., and Boersma, M. (2004) Differential Impacts of Copepods and Cladocerans on Lake Seston, and Resulting Effects on Zooplankton Growth, *Hydrobiologia 526*, 197–207.

30. Park, S., Müller-Navarra, D., and Goldman, C.R. (2003) Seston Essential Fatty Acids and Carbon to Phosphorus Ratios as Predictors for *Daphnia pulex* Dynamics in a Large Reservoir, Lake Berryessa, *Hydrobiologia 505*, 171–178.

31. Ravet, J.L., Brett, M.T., and Müller-Navarra, D.C. (2003) A Test of the Role of Polyunsaturated Fatty Acids in Phytoplankton Food Quality for *Daphnia* Using Liposome Supplementation, *Limnol. Oceanogr. 48*, 1938–1947.

32. Von Elert, E. (2002) Determination of Limiting Polyunsaturated Fatty Acids in *Daphnia galeata* Using a New Method to Enrich Food Algae with Single Fatty Acids, *Limnol. Oceanogr. 47*, 1764–1773.

33. Sundbom, M., and Vrede, T. (1997) Effects of Fatty Acid and Phosphorus Content of Food on the Growth, Survival and Reproduction of *Daphnia*, *Freshwater Biol. 38*, 665–674.

34. Kainz, M., and Mazumder, A. (2005) Effects of Algal and Bacterial Diet on Methyl Mercury Concentrations in Zooplankton, *Environ. Sci. Technol. 39*, 1666–1672.

35. Wacker, A., and Von Elert, E. (2001) Polyunsaturated Fatty Acids: Evidence for Non-substitutable Biochemical Resources in *Daphnia galeata*, *Ecology 82*, 2507–2520.

36. Ahmadjian, V. (1967) *The Lichen Symbiosis*, Blaisdell, Waltham, MA.

37. Kainz, M., Lucotte, M., and Parrish, C.C. (2002) Methyl Mercury in Zooplankton—The Role of Size, Habitat and Food Quality, *Can. J. Fish. Aquat. Sci. 59*, 1606–1615.

38. Folch, J., Lees, M., and Sloane Stanley, G.H. (1957) A Simple Method for the Isolation and Purification of Total Lipids from Animal Tissues, *J. Biol. Chem. 226*, 497–509.

39. Garbus, J., De Luca, H.F., Loomans, M.E., and Strong, F.M. (1963) The Rapid Incorporation of Phosphate into Mitochondrial Lipids, *J. Biol. Chem. 238*, 59–63.

40. Kates, M. (1986) *Techniques in Lipidology*, 2nd edn., Elsevier, Amsterdam.

41. Elendt, B.P. (1989) Effects of Starvation on Growth, Reproduction, Survival and Biochemical Composition of *Daphnia magna, Arch. Hydrobiol. 116*, 415–433.

42. Vrede, T., Persson, J., and Aronsen, G. (2002) The Influence of Food Quality (P:C Ratio) and Somatic Growth Rate of *Daphnia, Limnol. Oceanogr. 47*, 487–494.

43. Farkas, T., Nemecz, G.Y., and Csengeri, I. (1984) Differential Response of Lipid Metabolism and Membrane Physical State by an Actively and Passively Overwintering Planktonic Crustacean, *Lipids 19*, 436–442.

44. Bychek, E.A., and Gushchina, I.A. (1999) Age-Dependent Changes of Lipid Composition in *Daphnia magna*, *Biochemistry–Moscow 64*, 543–545.

45. Cripps, C., Blomquist, G.J., and Renobales, D.M. (1986) *De novo* Biosynthesis of Linoleic Acid in Insects, *Biochim. Biophys. Acta 876*, 572–580.

46. Blomquist, G.J., Borgeson, C.E., and Vundla, M. (1991) Polyunsaturated Fatty Acids and Eicosanoids in Insects, *Insect Biochem. 21*, 99–106.

47. Weinert, J., Blomquist, G.J., and Borgeson, C.E. (1993) *De novo* Biosynthesis of Linoleic Acid in 2 Non-insect Invertebrates—The Land Slug and the Garden Snail, *Experientia 49*, 919–921.

48. Avery, S.V., Lloyd, D., and Harwood, J.L. (1994) Changes in Membrane Fatty Acid Composition and Δ-12-Desaturase Activity During Growth of *Acanthamoeba castellanii* in Batch Culture, *J. Eukaryot. Microbiol. 41*, 396–401.

Dietary Phospholipids Are More Efficient Than Neutral Lipids for Long-Chain Polyunsaturated Fatty Acid Supply in European Sea Bass *Dicentrarchus labrax* Larval Development

E. Gisbert[a,*], L. Villeneuve[b], J.L. Zambonino-Infante[b], P. Quazuguel[b], and C.L. Cahu[b]

[a]Centre d'Aqüicultura, Institut de Recerca i Tecnologia Agroalimentaries (IRTA), Tarragona, Spain, and [b]Unité Mixte de Nutrition des Poissons, L'Institut Francais de Recherche pour l'Exploitation de la Mer (IFREMER)–Institut National de la Recherche Agronomique (INRA), IFREMER, 29280 Plouzané, France

ABSTRACT: We evaluated the effects of dietary lipid class (phospholipid vs. neutral lipid) and level of n-3 long-chain PUFA (LC-PUFA) on the growth, digestive enzymatic activity, and histological organization of the intestine and liver in European sea bass larvae. Fish were fed from the onset of exogenous feeding at 7 to 37 d post-hatch with five isoproteic and isolipidic compound diets with different levels of EPA and DHA. Diet names indicated the percentage of EPA and DHA contained in the phospholipids (PL) and neutral lipids (NL), as follows: PL5, PL3, PL1, NL1, and NL3. Histological observations showed different patterns of lipid absorption and accumulation in the intestinal mucosa depending on the level and nature of the dietary lipid fraction. Fish fed high levels of neutral lipids (11%, NL3 diet: 2.6% of EPA + DHA in the NL fraction) showed large intracellular and intercellular lipid deposits in the anterior intestine, but no such lipid accumulation was detected when larvae were fed with low and moderate levels of EPA and DHA in the phospholipid and neutral lipid fractions of the diet (PL and NL1 diets). PL were preferentially absorbed in the postvalvular intestine, and the accumulation of marine PL was inversely correlated to their dietary level. The postvalvular intestinal mucosa and liver showed signs of steatosis; large lipid vacuoles were observed in this region of the intestine and in the liver and were inversely correlated with the level of dietary neutral lipids. The best results in terms of growth, survival, and development (maturation of the digestive system and histological organization of the liver and intestinal mucosa) were obtained in the group fed with 2.3% of EPA and DHA in the PL fraction of the diet (PL3 diet), revealing that European sea bass larvae use the LC-PUFA contained in the PL fraction more efficiently than those from the NL fraction of the diet.

Paper no. L9685 in *Lipids 40*, 609–618 (June 2005).

Dietary lipids are the main energy source in developing fish larvae and serve as a source of the FA needed for the synthesis of new cellular structures that are required for normal larval growth and development (1). Lipid requirements of marine fish larvae have been extensively studied during the last two decades (1–3), and particular attention has been paid to long-

chain PUFA (LC-PUFA) and phospholipids (PL) (4–7). Like most marine fish, European sea bass is considered to have an absolute requirement for LC-PUFA, such as EPA (20:5n-3), DHA (22:6n-3), and arachidonic acid (20:4n-6), being unable to produce these FA from their precursors 18:3n-3 and 18:2n-6 (1). In this sense, the deficiency in LC-PUFA delays fish growth, induces mortality, reduces resistance to stress, and results in anatomical alterations associated with nutritional disorders (6). The EFA requirements of marine fish vary both qualitatively and quantitatively, and the optimal level of dietary components for marine fish is known to be around 3% of dry matter for EPA + DHA (1). However, most studies dealing with the determination of LC-PUFA requirements for first-feeding marine larvae were conducted using live prey to deliver different levels of LC-PUFA (3), but these studies did not evaluate the effect of the class of lipids [neutral lipids (NL) vs. PL] incorporated into the diet, since in most cases lipids and LC-PUFA are generally provided in the diet by fish oils, which are constituted mainly of neutral lipids (6,7).

Although it is generally accepted that there are beneficial effects from adding PL to microdiets (microparticulated diets having particle sizes of 200–400 µm) or live-prey enrichment emulsions on the larval growth, survival, stress tolerance, and larval quality (reduction of skeletal deformities) (2–4,6–8), their exact role in fish digestive physiology and development has not been completely characterized. Fish larvae are extremely sensitive to dietary PL deficiency and require higher levels of dietary PL than juveniles (see review in Ref. 8). Feeding gilthead sea bream larvae with microdiets containing marine PL instead of marine TAG resulted in better growth even if larvae were fed PL at lower levels than TAG (10). Recently, it has been shown that a diet containing 19% lipids including almost 9% PL induced good growth in European sea bass first-feeding larvae, demonstrating that the development of skeletal deformities in European sea bass during early development was more linked to the proportions of dietary PL and NL than to the total dietary lipid content (7). Dietary PL seem to have a marked effect on lipid absorption and transport (6,8,9,11,12). An accumulation of lipid droplets in enterocytes has been associated with PL deficiency (13–15) that may result in intestinal steatosis (16,17), suggesting that PL have a specific role in the synthesis and secretion of chylomicrons and VLDL from the intestinal mucosa into the circulatory system.

Different segments of the gastrointestinal tract in vertebrates have been shown to employ different cellular mechanisms in

---

*To whom correspondence should be addressed at Centre d'Aqüicultura, Institut de Recerca i Tecnologia Agroalimentaries (IRTA), Aptat. Correus 200, 43540 Sant Carles de la Ràpita, Tarragona, Spain.
E-mail: enric.gisbert@irta.es

Abbreviations: CCK, cholecystokinin; dph, days post-hatch; IFREMER, L'Institut Francais de Recherche pour l'Exploitation de la Mer; INRA, Institut National de la Recherche Agronomique; IS, intestinal segment; microdiet, microparticulated diet (particle size 200–400 µm; NL, neutral lipids; PL, phospholipids(s); PS, pancreatic segment.

response to diet quality (18). Thus, the use of the intestine and liver as indicator organs of the nutritional and physiological status in fish is well known (19–22). As the primary site of food digestion and nutrient uptake, the intestine is involved in important physiological digestive functions (23), whereas the liver is the central metabolic organ of the body, taking a predominant role in intermediary metabolism and having important functions in lipid storage and in digestive and detoxification processes (23). The optimal use of dietary nutrients ultimately depends on the effectiveness of functions in the intestine and liver (22). Consequently, the structural alteration of the histomorphological organization of the liver and intestine can provide useful information about the quality of the diet, the metabolism, and the nutritional status of the fish (18,20,21,24,25).

The present study evaluates the effect of the lipid class (PL vs. NL) and the level of n-3 LC-PUFA in the diet on the growth, the digestive enzymatic activities, and the histological organization of the intestine and liver in European sea bass larvae.

MATERIALS AND METHODS

Animals and diets. Three-day-old European sea bass (*Dicentrarchus labrax* L.) larvae were obtained from the Ecloserie

Marine de Gravelines (Gravelines, France) and shipped to the Fish Nutrition Laboratory at the IFREMER (Centre de Brest). Fish were acclimated and divided into fifteen 35-L cylindroconical fiberglass tanks (2100 larvae/tank) at an initial density of 60 larvae/L. Tanks were supplied with running sea water (35‰), which had previously been filtered through a sand filter, then passed successively through a tungsten heater and a degassing column packed with plastic rings. Throughout the experiment, the water temperature and salinity were 20°C and 35‰, respectively, and the oxygen level was maintained above 6 mg/L by setting the water exchange of the tank up to 30% per hour (flow rate: 0.18 L/min). Photoperiod was 24L:0D, and light intensity was 9 W/m^2 (900 lux) maximum at the water surface. All animal procedures and handling were conducted in compliance with the Guide for the Care and Use of Laboratory Animals (26).

At 4 d post-hatch (dph), European sea bass larvae were divided into 5 experimental groups (4 replicates per group) that were fed from the onset of exogenous feeding at 7 dph until 37 dph with experimental compounded microdiets. Five isonitrogenous and isolipidic diets (Table 1) were formulated to incorporate different levels of LC-PUFA (Table 2) and differed in their lipid class composition, PL vs. NL. Fish meal, normally

TABLE 1
Composition of the Experimental Compound Microdiets

Ingredients[a]	PL1	PL3	PL5	NL1	NL3
			Experimental diets		
			g/kg dry matter		
Defatted fish meal	510				
Hydrolyzed fish meal (CPSP)	140				
Cod liver oil	0	0	0	7	14
Marine lecithin[b]	7	14	21	0	0
Soy lecithin[c]	14	7	0	14	7
Vitamin mixture[d]	80				
Mineral mixture[e]	40				
Betaine	20				
Proximate composition (%)					
Proteins (N × 6.25)	59.9	61.6	60.4	58.7	59.6
Lipids	16.4	16.7	16.7	17.1	18.2
Phospholipids	13.2	13.0	12.1	11.1	8.1
EPA + DHA in PL	1.1	2.3	4.8	0.3	0.4
Neutral lipids	4.8	3.8	3.0	6.2	11.0
EPA + DHA in NL	0.3	0.3	0.3	1.3	2.6
Ash	17.4	17.0	16.8	15.6	15.6
Moisture	6.8	6.3	7.4	6.5	6.4
Energy (kJ/kg)[f]	1618	1658	1638	1624	1681

[a]All dietary ingredients were commercially available. Fish meal (La Lorientaise, Lorient, France), hydrolyzed fish meal (CPSP, Soluble Fish Protein Concentrate; Soropêche, Boulogne sur Mer, France), cod liver oil (La Lorientaise), marine lecithin (LC60, Phosphomins™; Phosphotech, Saint Herblain, France); and soy lecithin (Ets Louis François, St Maur des Fossés, France).
[b]Contains 60% phospholipids (with 45% PC, 20% ethanolamine, 16% PI), 5% TAG, 15% cholesterol, and 1 mg/g natural tocopherols as antioxidant.
[c]Contains 95% phospholipids (with 26% PC, 20% ethanolamine, and 14% PI).
[d]Per kg of vitamin mix: retinyl acetate 1 g; cholecalciferol 2.5 mg; all-*rac*-α-tocopherol acetate 10 g; menadione 1 g; thiamin 1 g; riboflavin 0.4 g; D-calcium pantothenate 2 g; pyridoxine HCl 0.3 g; cyanocobalamin 1 g; niacin 1 g; choline chloride 200 g; ascorbate polyphosphate 20 g; folic acid 0.1 g; biotin 1 g; meso-inositol 30 g; cellulose 732.1 g.
[e]Per kg of mineral mixture: KCl 90 g, KI$_4$O 40 mg, CaHPO$_4$·2H$_2$O 500 g, NaCl 40 g, CuSO$_4$·5H$_2$O 3 g, ZnSO$_4$·7H$_2$O 4 g, CoSO$_4$·7H$_2$O 20 mg, FeSO$_4$·7H$_2$O 20 g, MnSO$_4$·H$_2$O 3 g, CaCO$_3$ 215 g, MgSO$_4$·7H$_2$O 124 g, NaF 1g.
[f]Calculated as: fat × 37.7 J/kg; protein × 16.7 J/kg.

TABLE 2
Percentage of the Main FA in the Phospholipid and Neutral Lipid Fractions of Experimental Diets, Expressed in Percentage of Total FA in PL and NL

Diets	Phospholipids (PL)					Neutral lipids (NL)				
	PL1	PL3	PL5	NL1	NL3	PL1	PL3	PL5	NL1	NL3
14:0	0.6	1.4	2.0	0.6	1.6	3.8	4.3	4.7	6.0	6.2
16:0	19.2	23.4	25.6	18.0	18.4	15.7	16.3	17.2	15.8	16.2
18:0	3.9	3.5	2.6	4.4	4.1	4.0	3.8	3.8	2.8	2.8
ΣSaturated	24.0	28.5	30.1	23.5	24.4	23.9	24.6	25.9	24.8	25.4
16:1n-7	0.6	1.0	1.2	1.0	2.0	5.3	5.5	5.8	7.0	6.9
18:1n-7	0.0	0.0	0.2	0.0	0.0	0.5	0.5	0.5	1.1	1.1
18:1n-9	6.0	5.0	3.5	7.7	9.6	17.9	15.8	14.7	16.7	16.6
20:1n-9	1.1	2.3	3.7	0.8	1.6	6.3	6.9	8.1	5.0	5.4
18:1n-11	1.3	1.2	1.2	1.6	2.0	3.7	3.7	3.8	3.2	3.2
20:1n-11	0.0	0.0	0.4	0.0	0.0	1.1	1.1	1.4	0.8	0.8
22:1n-11	0.2	0.2	0.2	0.5	1.0	4.5	4.8	5.0	4.8	5.7
ΣMonosaturated	9.4	10.0	11.0	11.6	16.7	41.0	40.2	41.3	40.5	41.7
18:2n-6	44.2	25.8	0.3	51.3	42.0	12.8	6.8	1.8	4.8	3.5
20:4n-6	0.8	1.7	3.1	0.3	0.4	0.9	1.4	1.5	0.7	0.6
Σn-6 PUFA	45.4	28.3	4.2	52.1	42.8	14.6	9.4	4.3	6.5	5.1
18:3n-3	6.7	4.9	0.2	7.8	6.6	2.1	1.4	0.7	1.9	1.8
18:4n-3	0.1	0.2	0.2	0.2	0.6	1.4	1.5	1.5	2.6	2.5
20:4n-3	0.1	0.2	0.2	0.2	0.3	0.5	0.6	0.6	1.0	1.0
20:5n-3	3.8	7.5	13.7	1.5	3.0	6.5	8.3	9.3	9.6	9.5
22:6n-3	10.5	21.4	40.0	3.0	5.3	9.1	12.8	15.0	10.1	11.0
Σn-3 PUFA	21.2	33.2	54.6	12.8	16.1	20.4	25.7	28.3	28.2	27.8
n-3/n-6 ratio	0.47	1.17	13.06	0.25	0.38	1.39	2.75	6.63	4.34	5.45

containing 17% lipids, was rigorously defatted to control the experimental dietary lipid composition only by the addition of PL and NL. Lipid was extracted from fish meal using dichloromethane (5 mL/g fish meal) for 20 min at 40°C, rinsed, and dried until completely free of solvent. Diet names indicate the total percentage of EPA and DHA contained in the PL and NL fractions of the diet: PL5, PL3, PL1, NL1 and NL3 (Tables 1 and 2). The marine phospholipid fraction in PL diets varied in an inverse relation to soybean lecithin, whereas NL diets contained soybean lecithin in an inverse proportion to the marine TAG (cod liver oil). The composition of diet PL1 was close to the diet previously used (7) that had supported good growth and survival in European sea bass larvae; for comparative purposes it was considered in this study as the control diet. Microdiets were prepared as follows: fish meal, fish meal hydrolysate, betaine, and mineral mixture were first mixed. The oil, PL, and vitamin mixture were added as an emulsion to the dry mixture. Then water was added; and the mixture was thoroughly blended mechanically, pelleted, and dried at 50°C for 20 min (6). This procedure prevents undesirable reactions between ingredients (particularly between minerals and vitamins). The pellets were sieved to obtain two sizes of particles: 125–200 μm, used during the first 5 d, and 200—400 μm, used during the rest of the experiment. At this stage, a sample of each experimental diet was taken for analysis. Diets were then vacuum-packed and stored at 4°C until use. During the entire experimental period, larvae were continuously fed *ad libitum* 24 hours per day using an automatic belt feeder. Food inges-

tion was monitored by observing the larval digestive tract under a binocular microscope; dietary microparticles were visible by their transparency against tissue.

Sampling. To evaluate growth, 10 specimens were randomly sampled from each experimental tank (30 larvae per experimental diet) at 12, 16, 23, 30, and 37 dph and euthanized with an overdose of anesthetic (tricaine methanesulfonate, MS 222); their wet body weights were measured to the nearest 0.1 mg. To evaluate the level of maturation of the digestive system, larvae (20–50 larvae, depending on wet body weight) were sampled from each tank and kept at −20°C until analysis. Samples for measuring lipase (EC 3.1.1.3), and brush border intestinal enzymes (alkaline phosphatase, EC 3.1.3.1; and aminopeptidase N, EC 3.4.11.2) were taken at 30 and 37 dph, whereas trypsin (EC 3.4.21.4) and amylase (EC 3.2.1.1) secretions were only measured at 37 dph. For light microscopy purposes, 10 specimens were randomly sampled from rearing tanks at 30 and 37 dph, preserved in 10% buffered formalin (pH 7.2), and stored in the dark at 6–8°C. Repetitive sampling did not allow the determination of real survival (percentage of surviving individuals in relation to the initial number of larvae); however, relative survival, expressed as the percentage of surviving fish fed on a diet (i.e., NL1) in relation to the surviving specimens fed on the control diet (PL1), could be calculated.

Analytical methods. A minimum of 30 larvae per replicate and treatment were dissected on a glass cutting board kept on ice (0°C) under a binocular microscope. Individuals were cut into 4 parts: head, pancreatic segment (PS), intestinal segment

(IS), and tail, to limit the assay of enzymes to specific segments. This dissection inevitably produced a mixture of organs in each segment. Besides the pancreas, the pancreatic segment contained the liver, heart, muscle, and spine. The intestinal segment contained the intestine, muscle, and spine (27). Once dissected, pancreatic segments were homogenized in 5 vol (vol/wt) of ice-cold distilled water. Amylase and trypsin activities were measured using sodium benzoyl-DL-arginine-*p*-nitroaniline and starch as substrates (28,29), respectively, in both pancreatic and intestinal segments. Lipase was measured in the pancreatic segment using *p*-nitrophenyl myristate as substrate (30). Purified brush border membranes from the intestinal segment were obtained according to a method developed for intestinal scraping (31). The degree of purification of the brush border membrane, considering alkaline phosphatase and aminopeptidase N as markers of cell membrane fraction, was close to that reported in the literature (31), i.e., 11.0- and 10.8-fold, respectively. Alkaline phosphatase and aminopeptidase N, two enzymes of the intestinal brush border membrane, were quantified using *p*-nitrophenylphosphate (32) and L-leucine-*p*-nitroaniline (33) as substrates, respectively. Specific enzyme activities were expressed as mmol of substrate hydrolyzed per min and mg of protein (mU/mg protein), and protein was determined using the Bradford method (34). Secretions of trypsin and amylase were calculated as the ratio of the activity in the intestinal segment, related to total activity (PS + IS) considering that enzyme activity in PS can be used as an index of the synthesis function of pancreas and in IS as an index of pancreatic secretory function (35).

Dietary total lipid content was determined using a procedure slightly modified from Folch *et al.* (36), with chloroform being replaced by dichloromethane. The separation of NL and PL was carried out as described by Juaneda and Rocquelin (37). FA were saponified by a 2 M KOH/methanol solution, recovered, and then esterified in a 0.7 M HCl/methanol solution. FAME were separated by GC in an Auto-system PerkinElmer instrument with an FID on a BPX 70 capillary column (25 m × 0.22 mm i.d. × 0.25 μm film thickness; J&W Scientific, Folsom, CA), with a split-splitless injector and with helium as carrier gas (flow rate 1.4 mL/min). The injector and detector temperatures were, respectively, 220 and 260°C. The initial temperature of the oven was 50°C, increasing to 180°C by increments of 15°C/min, maintained for 5 min, and finally increased to 220°C by increments of 3°C/min. Data acquisition and handling were carried out by connecting the gas chromatograph to a Nelson computer. Each FAME was identified by comparison with the retention time of authentic standard mixtures of FAME, and the results of individual FA composition were expressed as area percentages of total identified FAME in the PL and NL fractions.

Light microscopy. Larvae were dehydrated in a graded series of aqueous ethanol mixtures, embedded in paraffin wax, and cut in serial longitudinal sections (5–7 μm thick). Slides were stained by hematoxylin and eosin for topographic observations of the liver, intestine (prevalvular and postvalvular regions), and swim bladder. The term steatosis was applied, without pathological connotation, when clear vacuoles with a diameter greater than 5 μm were observed in the enterocytes (13).

Statistical analyses. Results are given as mean ± SD. All data were checked for variance homogeneity using the Barlett's test (38). Growth, enzymatic specific activity, and arcsin ($x^{1/2}$)-transformed trypsin and amylase secretions were compared by means of a one-way ANOVA followed by Newman–Keuls multiple range test when significant differences were detected ($P < 0.05$).

RESULTS

Growth and survival. At the end of the rearing period (37 dph), statistically significant differences in larval growth were observed between experimental groups (ANOVA, $P < 0.05$, Fig. 1). Larvae fed PL3 exhibited the best growth performance. Larvae fed PL1 and PL5 were similar in weight, being 21 and 26% smaller than PL3 larvae, respectively. Larvae from the NL3 dietary group were smaller than all the other groups (e.g., 50% smaller than PL3 larvae). Because the NL3 group died before 37 dph, the larval body weight could not be compared with those of the other experimental groups, although it was significantly lower at early stages of development (23 and 30 dph).

The best survival, i.e., the largest number of fish at the end of the experiment, was observed in groups fed PL3 and NL 1 diets ($n = 710$ and 404, respectively). The relative survival of groups PL3, NL1, and PL5 was 226.1, 128.7, and 31.5% higher, respectively, than the control (PL1, $n = 314$).

Enzyme activities. At the end of the study, total EPA and DHA content in diets significantly affected trypsin and amylase secretion (ANOVA, $P < 0.05$; Fig. 2). Fish fed diets containing low levels of EPA and DHA (PL1 and NL1) exhibited
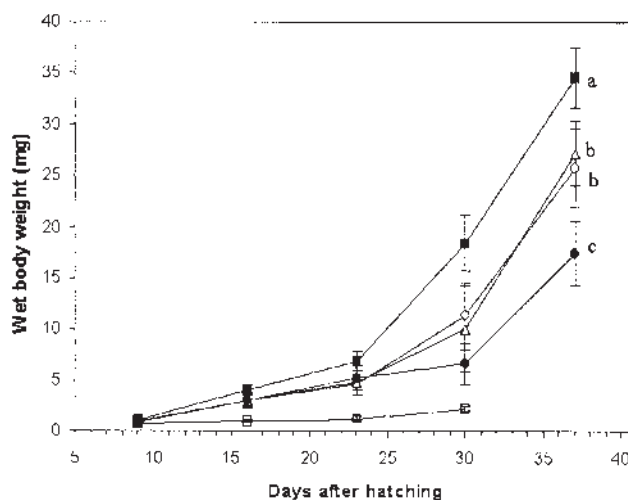
FIG. 1. Growth of European sea bass larvae fed isonitrogenous and isolipidic diets containing different levels of EPA and DHA. Diets are named according to the percentage of dietary EPA and DHA contained in the phospholipid (PL) and neutral lipid (NL) fraction of the diet: PL5 (○), PL3 (■), PL1 (△), NL1 (●), and NL3 (□). Results are shown as mean ± SD ($n = 4$). Different superscripts for the same day indicate significant differences ($P < 0.05$).
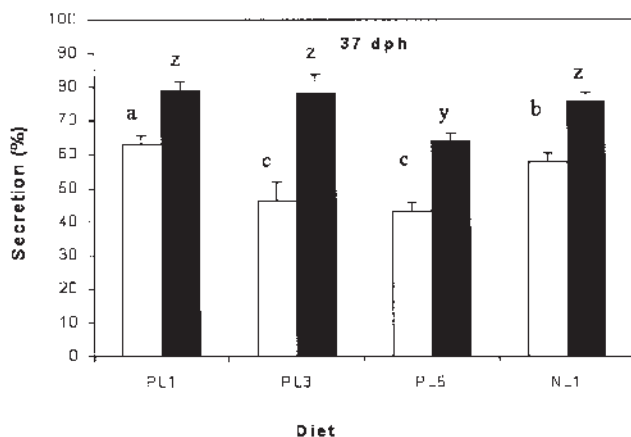
FIG. 2. Trypsin (□) and amylase (■) secretion in 37 days post-hatch (dph) European sea bass larvae fed isonitrogenous and isolipidic diets containing different levels of EPA and DHA. Means ± SD (*n* = 4) with different superscript letters were significantly different (*P* < 0.05). For other abbreviations see Figure 1.

the highest trypsin secretion rates, whereas those reared with PL3 and PL5 showed lower secretion values. Amylase secretion was negatively affected by a high dietary content of EPA and DHA (group PL5, Fig. 2), being 8.2% lower than in those groups fed low or medium levels of these two FA (PL3, PL1, and NL1 diets). Similarly, the specific activity of lipase was affected by the experimental diets (ANOVA, *P* < 0.05; Fig. 3). At 30 dph, lipase specific activity was two times higher in fish fed NL1 than in PL5 group. In 37-d-old larvae, the lipase activity in PL5 group was 55 and 45% higher than in fish fed PL3 and NL1, respectively.

The same effect was observed in the specific activities of brush border enzymes (ANOVA, *P* < 0.05; Fig. 4). At 30 dph, the highest alkaline phosphatase specific activity was observed in fish fed PL3; no differences in activity were observed between the other experimental groups (PL1, PL5, and NL1), which were significantly lower than in fish fed PL3. At day 37, the lowest alkaline phosphatase activity was detected in larvae
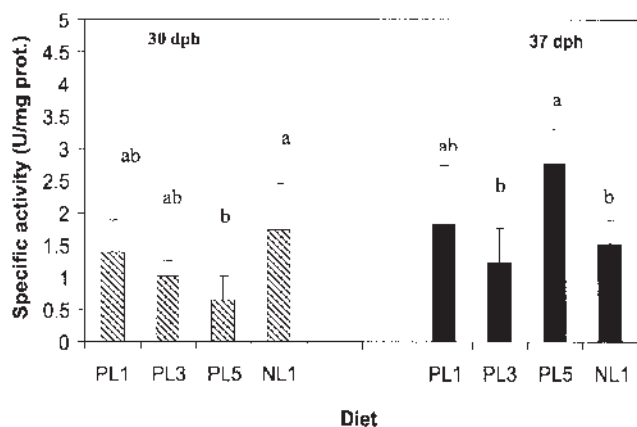
FIG. 3. Lipase specific activity in 30 and 37 dph European sea bass larvae fed isonitrogenous and isolipidic diets containing different levels of EPA and DHA. Means ± SD (*n* = 4) with different superscript letters were significantly different (*P* < 0.05). For abbreviations see Figures 1 and 2.
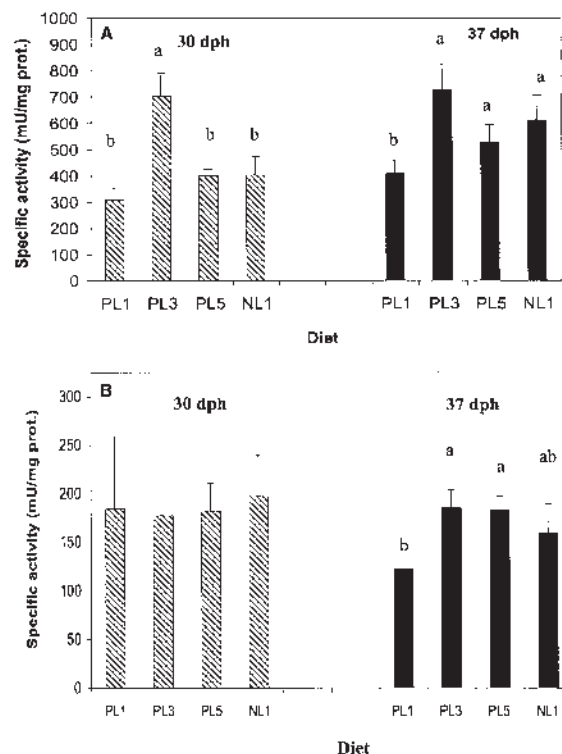
FIG. 4. Specific activity of alkaline phosphatase (A) and aminopeptidase N (B) of the intestinal brush border in European sea bass at 30 and 37 days dph fed isonitrogenous and isolipidic diets containing different levels of EPA and DHA. Means ± SD (*n* = 4) with different superscript letters were significantly different (*P* < 0.05). For abbreviations see Figures 1 and 2.

fed PL1, no differences being evidenced between the other dietary groups. No statistically significant differences at 30 dph were observed in aminopeptidase N specific activity of larvae fed different diets. At the end of the larval rearing period, aminopeptidase N specific activity was 30% lower in larvae fed PL1 (control group) compared with the rest of the dietary treatments.

Light microscopy. The liver of European sea bass larvae is organized in polygonal-shaped hepatocytes arranged along hepatic sinusoids. Nuclei position and lipid deposition depended on dietary levels of marine and vegetable PL (Fig. 5). Large central nuclei were observed in livers containing few lipid inclusions (PL1, PL3, PL5, and NL1), whereas peripheral nuclei were detected in livers of larvae showing high levels of lipid deposition (NL3).

The mucosa of the intestine (prevalvular and postvalvular regions) is lined by a simple columnar epithelium with prominent acidophilic brush borders and centrally located nuclei (Figs. 6a, 6b, 7). The only morphological differences observed between both regions are the number and size of mucosal folds, which are longer and more numerous in the anterior region. Changes in the histological organization of the prevalvular intestine were observed only in fish fed the NL3 diet, which showed a large accumulation of small lipid droplets, resulting in the displacement of nuclei to a basal position (Fig. 6c). Large intercellular lipid vacuoles were also observed (Fig. 6d). The mucosa of the postvalvular intestine exhibited remarkable signs
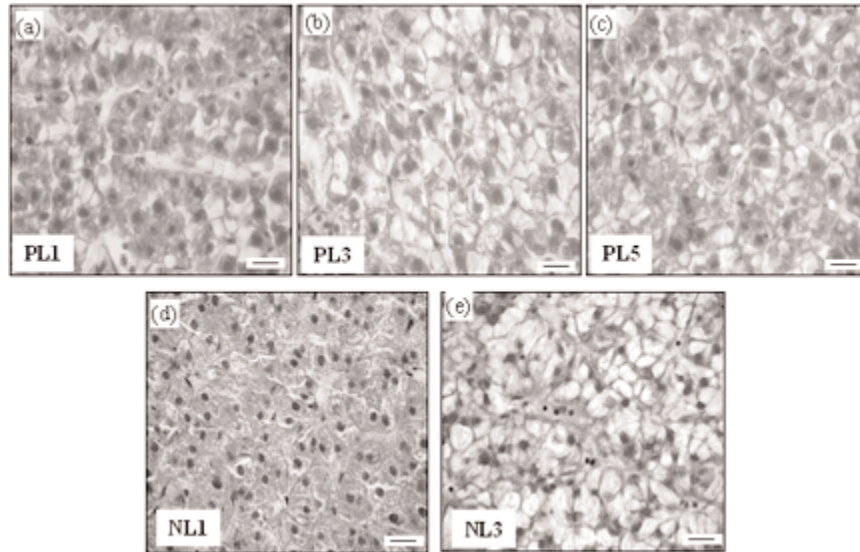
FIG. 5. Longitudinal paraffin sections of the liver in European sea bass larvae fed isonitrogenous and isolipidic diets containing different levels of EPA and DHA. Liver from fish fed control diet (PL1) and NL1 showing regular-shaped hepatocytes with very few lipid inclusions (a, d). Livers from fish fed PL3 and PL5 with a high (b) and intermediate (c) degree of cytoplasmatic lipid accumulation in hepatocytes. Liver from fish fed NL3 showing the displacement of the nucleus to the periphery of the hepatocytes and the presence of numerous varying-size cytoplasmatic lipid vacuoles (e). Histological sections from larvae fed PL and NL1 diets were from fish aged 37 dph, whereas those from the NL3 group were obtained from 30 dph. For abbreviations see Figures 1 and 2. Scale bar: 25 μm.

of steatosis in fish fed diets containing EPA and DHA derived mainly from the phospholipid fraction (PL diets) (Fig. 7a-d). Fish fed NL diets exhibited a lower lipid accumulation in this region than in the other experimental groups (Figs. 7e, 7f).

Fish fed on PL and NL1 diets had normally inflated swim bladders, which were organized in a stratified cuboidal epithelium and rete mirabile (Fig. 6e). Most of the larvae (90%) fed the NL3 diet did not inflate their swim bladders and showed hyperplasia of the gas gland cells, with hypertrophied cells occupying the swim bladder's lumen (Fig. 6f).

DISCUSSION

In a previous study, good growth and survival were obtained using a compound microdiet containing 11% phospholipids (7). We have used this PL dietary level in the current study to formulate experimental diets with an appropriate level of PL (PL5, PL3, PL1, and NL1 diets). However, even though the NL3 diet contained only 8% of PL, this content was acceptable in terms of growth and larval survival rates (7). In the present study, diets were efficiently ingested by European sea bass larvae. Thus, the differences observed in growth and survival rates in this study were not related to dietary PL level and/or larval food intake of compound diets.

In the present study, total DHA/EPA ratios in PL diets and in NL diets were close to 2 (i.e., higher than 1), which is considered as a suboptimal ratio for fish larvae, either by not providing sufficient DHA or by providing an undesirable excess of EPA (1). Therefore, the observed differences in growth and

survival of European sea bass in the present study could not be attributed to inappropriate DHA/EPA ratios. The tested diets, mainly differing by their LC-PUFA source included in the PL or NL fraction, induced large differences in growth and survival of European sea bass larvae. The diet containing a moderate level of EPA and DHA in the PL fraction (PL3) induced the best growth, survival, and intestinal maturation in comparison with the rest of the experimental diets, including the control (PL1), whereas the diet with a similar level of EPA and DHA in the neutral lipid fraction (NL3) was lethal for European sea bass larvae. A high content of EPA and DHA in the PL fraction (PL5) negatively affected growth, survival, and maturation of the digestive tract in larvae. The differences observed in growth between larvae feeding on a low dietary level of EPA and DHA depended on the form in which both EFA were supplied; if they were included in the PL fraction (PL1), good growth was observed, whereas it was significantly lower when they were included in the NL fraction. The more efficient use of EPA and DHA supplied in the PL class of the diet might be related to the ability of young larvae to better modulate phospholipase A2 expression than that of lipase, suggesting a more efficient capacity to use PL than TG (7).

PUFA, and especially DHA and EPA, which are vital constituents for cell membrane structure and function, are very susceptible to oxidation by oxygen and other radicals. The resultant PUFA oxidation of membrane PL can have dramatic consequences for cell membrane structure and fluidity, with a potential pathological effect on cells and tissues, and can result in a reduction in fish growth, loss of appetite, decreased feeding
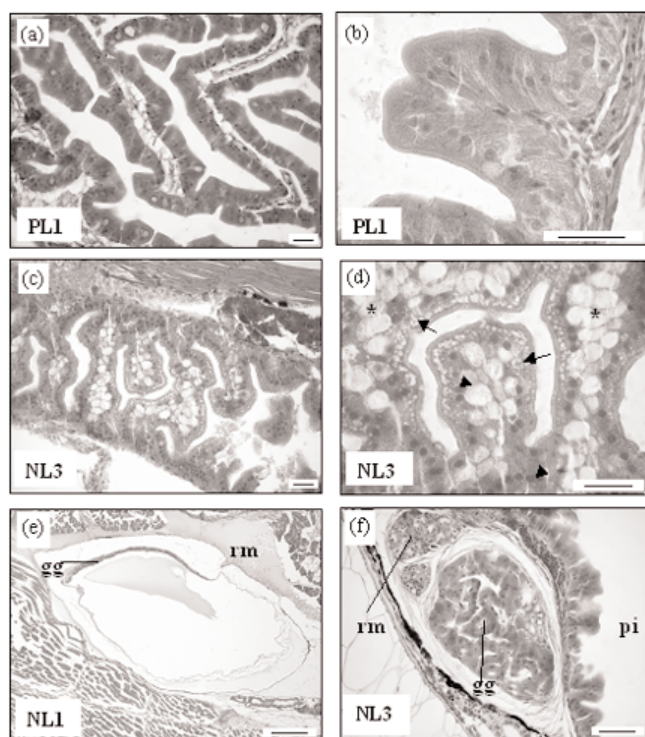
FIG. 6. Longitudinal paraffin sections of the prevalvular intestine and swim bladder in European sea bass larvae fed isonitrogenous and isolipidic diets containing different levels of EPA and DHA. Prevalvular intestine from 37-d-old larvae fed PL1 showing the mucosa lined by a simple columnar epithelium with centrally located nuclei and not containing lipid accumulations in cytoplasmatic vacuoles (a, b). Prevalvular intestinal mucosa from larvae aged 30 dph fed PL3 showing the presence of small apical lipid droplets (asterisk), the displacement of nuclei to a basal position (arrowhead), and large intercellular lipid vacuoles between enterocytes (arrow) (c, d). Normal inflated swim bladder from larvae fed PL1 (e). Noninflated swim bladder with hyperplasic gas gland cells (asterisk) from fish fed NL3 (f). gg, gas gland; pi, prevalvular intestine; rm, rete mirabile; for other abbreviations see Figures 1 and 2. Scale bar: 100 µm.

efficiency, and increased mortality (2). In the present study, differences in growth, survival, and histological organization of the intestine and liver in the European sea bass larvae were not attributed to *in vivo* lipid peroxidation, since any of the histological lesions commonly associated with this phenomenon, such as myopathy of skeletal muscle, lipoid liver degeneration, and accumulation of ceroid pigments (2), was not observed in the larvae fed high dietary levels of LC-PUFA. Moreover, diets were formulated using stable forms of vitamins, α-tocopherol acetate for vitamin E and ascorbate polyphosphate for vitamin C, at concentrations recommended by the National Research Council (26), to prevent the oxidation of unsaturated FA in the microparticles.

The level of secretion of the pancreatic enzymes (amylase, trypsin, and lipase) has been used as an indicator of intestinal maturation during European sea bass development (7,27,43). It is generally accepted that at a similar stage of development, pancreatic enzyme secretion is higher in fish exhibiting a good growth and normal development than in those showing a delay in these processes. In the present study, all the experimental
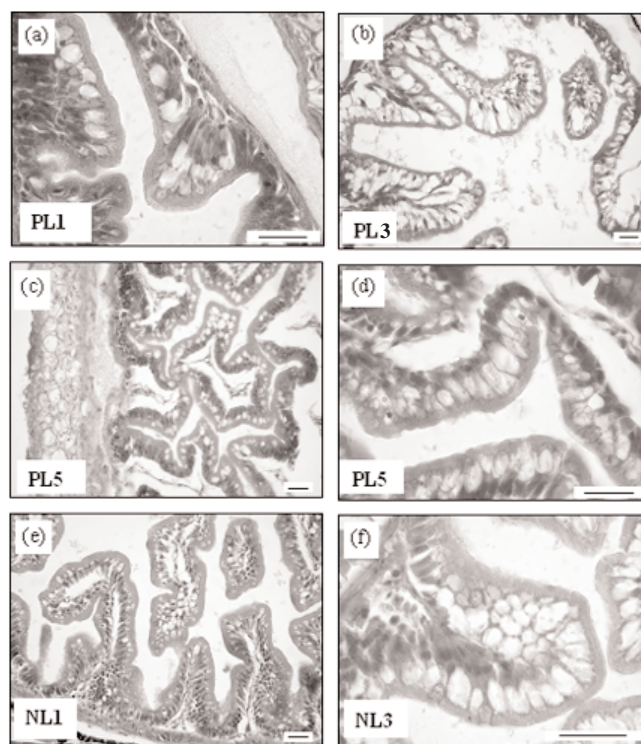
FIG. 7. Longitudinal paraffin sections of the postvalvular intestine in European sea bass larvae fed isonitrogenous and isolipidic diets containing different levels of EPA and DHA showing different levels of intestinal steatosis depending on the experimental diet [PL1 (a), PL3 (b), PL5 (c-d), NL1 (e) and NL3 (F)]. Note the lower accumulation of lipids in the enterocytes of fish fed NL3 in comparison with those fed PL3 diets (b, f). Scale bar: 100 µm.

groups exhibited a good level of trypsin secretion, but the fish fed the highest levels of EPA and DHA in the PL and NL fractions (PL5 and NL3 diets) showed lower values of amylase secretion than the rest of the experimental groups. It should be noted that although larvae fed PL1 and NL1 diets exhibited the highest values of trypsin and amylase secretion among all dietary treatments, these values should not be attributed to a major maturation of the digestive system and normal development of larvae, since the specific activity of intestinal brush border enzymes (particularly alkaline phosphatase) was lower in these groups in comparison with fish fed the PL3 diet. High secretion of pancreatic enzymes observed in the larvae fed PL1 and NL1 diets might be correlated with the high dietary content of linoleic acid, since C_{18} FA, such as linoleic and oleic acids, play an important role in the regulation of the pancreatic secretion (44). *In vitro* experiments have shown that these FA increased the intracellular calcium levels in enterocytes, stimulating the release of two gastrointestinal hormones, cholecystokinin (CCK) and secretin, which regulate the pancreatic secretion of amylase, trypsin, and lipase (12,44).

Despite major advances in our understanding of lipid digestion in juvenile or adult fish, knowledge of lipolytic enzymes in young larvae is scarce, particularly in terms of luminal digestion of dietary lipids (6). The capacity to digest fats is related to lipase secretion by the pancreas and the production of

bile salts in the liver, processes regulated by the levels of dietary TAG and the rate of intestinal absorption of lipids (12). In this sense, although it was not possible to determine the specific activity of pancreatic lipase in fish fed high levels of neutral lipids (NL3), since most of larvae died during the study, we observed that the specific activity of lipase in fish fed intermediate levels of neutral lipids (6.2%, NL1 diet) tended to be higher than that of fish fed PL diets at 30 dph. At the end of the experiment, this tendency in lipase activity was not observed. Such changes in specific activity might be related to the high accumulation of lipids observed in the enterocytes rather than to a lesser maturation of the digestive system, since lipids accumulated in the intestinal mucosa might have disrupted the metabolic capacity of the intestine to digest, absorb, and export lipids into the circulatory system. These observations strongly suggested that large quantities of accumulated lipids in the intestinal mucosa might have resulted in a reduction of the CCK secretion by intestinal endocrine cells in order to diminish lipase release by the pancreas and thus regulate lipid digestion and accumulation in enterocytes (44). The dramatic change in lipase activity in the PL5 group at day 37 compared with day 30 could not be attributed to a stimulation of lipase by its substrate, i.e., NL. This change probably reflected an indirect consequence of intraluminal FA concentration resulting from the hydrolysis of dietary PL, which in turn stimulated a hormonal mechanism involving secretin (45).

Generally, nutritional studies evaluating lipid digestion and absorption processes in fish are limited to the anterior region of the intestine, which is considered the region involved in the absorption of these nutrients (14,46). Nevertheless, lipid absorption still continues in the posterior and rectal regions of the intestine, particularly in carnivorous fish with short digestive tracts, such as European sea bass (47). The enterocytes of the pre- and postvalvular intestinal regions showed a larger degree of lipid accumulation than that observed by other authors (48). Such differences were due to the different level and nature of the lipid fraction contained in diets (compounded feeds vs. live preys). The results of the present study showed that European sea bass larvae have different patterns of lipid absorption and accumulation in the intestinal mucosa depending on the level and class of lipid used in the diet. Thus, we observed an important intracellular and intercellular accumulation of lipid in the anterior intestine of fish fed diets containing high levels of NL (11%, NL3 diet), whereas no such accumulation was detected when larvae were fed with low and moderate levels of NL (PL and NL1 diets). Similarly, the deposition of large lipid vacuoles in the postvalvular intestinal mucosa of larvae fed different experimental diets seemed to be inversely correlated with the level of dietary NL, since PL levels were almost the same among the diets, with the exception of NL3. The different n-6/n-3 ratio in the diets could have also influenced the accumulation of lipids in the enterocytes (14,49). Some authors have reported the use of unbalanced feeds in terms of lipid class composition as the cause of high, pathological level of intestinal accumulation of lipids (steato-

sis) (16,17). However, diet formulation and histological observations in the present study seemed to contradict this hypothesis; even though high levels of lipid deposition were observed in the postvalvular intestine of European sea bass larvae, they cannot be considered to be the cause of any pathological damage, since no signs of epithelial abrasion, cellular necrosis, and/or inflammatory reactions were detected along the intestinal mucosa.

The use of the liver as an indicator of the nutritional condition in fish is well known. Different studies have shown that structural alterations of the liver due to nutritional imbalances can provide useful information on diet quality and metabolism, complementing the information obtained with growth studies to evaluate the nutritional status of the fish. In the present study, levels of lipid accumulation in the liver of the larvae fed high levels of LC-PUFA in the neutral lipid fraction (NL3) were higher than those in fish fed similar or even higher levels of LC-PUFA contained in the diet as PPL (PL3 and PL5). These observations indicated that the form of dietary LC-PUFA supplied has a direct effect on fat storage in the liver, which could be related to a higher influx of chylomicrons and/or VLDL from the intestine due to the differences in lipid exportation capacities of the intestinal mucosa.

The comparative histological study carried out on 37-d-old larvae revealed the existence of a "dietary regime effect" on swim bladder inflation during early stages of development in European sea bass. The high frequency of occurrence of larvae without a functional swim bladder in the NL3 group (90%) contrasted with the rest of the experimental groups (PL and NL1). It is well recognized that inflation of the swim bladder is temporally limited and can only take place during a short window of larval morphogenesis, during which access to the air–water interface is critical for the normal inflation and development of the swim bladder (50). In the present study, the similar rearing conditions and procedures used for culturing larvae from different experimental groups, coupled with the low incidence of fish with non-inflated swim bladder in larvae fed PL and NL1 diets, suggested that anomalies in swim bladder inflation observed among larvae fed the NL3 diet might be related to diet quality rather than to problems of larvae in gulping air from the air–water interface. Thus, the high percentage of neutral lipids in the diet might be responsible for a disruption (retardation) of normal fish development, as growth results indicated, resulting in the failure to dilate the swim bladder lumen and the atrophy of this organ (51).

In conclusion, data on larval growth, survival, histological organization of the liver and intestine, and digestive enzyme activities showed that the quantity and form of EPA and DHA (NL or PL) supplied in the diet were determining for European sea bass larval development; fish used EPA and DHA more efficiently when these EFA were present in the PL rather than in the NL fraction of the diet. These results must be taken into account in the formulation of compound diet for larvae. Indeed, lipid and LC-PUFA are generally provided by fish oil, which is a neutral lipid, but marine PL would be a nutritionally better source of LC-PUFA.

ACKNOWLEDGMENTS

REFERENCES

1. Sargent, J.R., McEvoy, L., Estévez, A., Bell, G., Bell, M., Henderson, J., and Tocher, D. (1999) Lipid Nutrition in Marine Fish During Early Development: Current Status and Future Directions, *Aquaculture 79*, 217–230.
2. Sargent, J.R., Tocher, D.R., and Bell, J.B. (2002) The Lipids, in *Fish Nutrition*, 3rd edn. (Halver, J.E., and Hardy, R.W., eds.), pp. 182–257, Academic Press, San Diego.
3. Bell, J.G., McEvoy, L.A., Estévez, A., Shields, R.J., and Sargent, J.R. (2003). Optimizing Lipid Nutrition in First-Feeding Flatfish Larvae, *Aquaculture 227*, 211–220.
4. Kanazawa, A. (1993) Essential Phospholipids of Fish and Crustaceans, in *Fish Nutrition in Practice*, Les Colloques, No. 61 (Kaushik, S.J., and Luquet, P., eds.), pp. 519–530, INRA, Paris.
5. Geurden, I., Charlon, N., Marion, D., and Bergot, P. (1997) Influence of Purified Soybean Phospholipids on Early Development of Carp (*Cyprinus carpio* L.), *Aquacult. Int. 5*, 137–149.
6. Izquierdo, M.S., Socorro, J., Arantzamendi, L., and Hernández-Cruz, C.M. (2000) Recent Advances in Nutrition in Fish Larvae, *Fish Physiol. Biochem. 22*, 97–107.
7. Cahu, C.L., Zambonino Infante, J.L., and Barbosa, V. (2003) Effect of Dietary Phospholipid Level and Phospholipid:Neutral Lipid Value on the Development of Sea Bass (*Dicentrarchus labrax*) Larvae Fed a Compound Diet, *Br. J. Nutr. 90*, 21–28.
8. Coutteau, P., Geurden, I., Camara, M.R., Bergot, P., and Sorgeloos, P. (1997) Review of the Dietary Effects of Phospholipids in Fish and Crustacean Larviculture, *Aquaculture 155*, 14–164.
9. Kanazawa, A. (2003). Nutrition of Marine Fish Larvae, *J. Appl. Aquacult. 13*, 103–143.
10. Salhi, M., Izquierdo, M.S., Hernández-Cruz, C.M., Bessonart, M., and Fernández-Palacios, H. (1999) Effect of Different Dietary Polar Lipid Levels and Different n-3 HUFA Content in Polar Lipids on the Gut and Liver Histological Structure of Seabream (*Sparus aurata*) Larvae, *Aquaculture 179*, 253–264.
11. Koven., W.M., Kolkowski, S., Tandler, A., Kissil, G.W., and Sklan, D. (1993) The Effect of Dietary Lecithin and Lipase, as a Function of Age, on n-9 Fatty Acid Incorporation in the Tissue Lipids of *Sparus aurata* Larvae, *Fish Physiol. Biochem. 10*, 357–364.
12. Tso, P. (1994) Intestinal Lipid Absorption, in *Physiology of the Gastrointestinal Tract* (Johnson, L.R., ed.), pp. 1867–1907, Raven Press, New York.
13. Fontagné, S., Geurden, I., Escaffre, A.M., and Bergot, P. (1998) Histological Changes Induced by Dietary Phospholipids in Intestine and Liver of Common Carp (*Cyprinus carpio* L.) Larvae, *Aquaculture 161*, 213–223.
14. Olsen, R.E., Myklebust, R., Kaino, T., and Ringo, E. (1999) Lipid Digestibility and Ultrastructural Changes in the Enterocytes of Arctic Char (*Salvelinus alpinus* L.) Fed Linseed Oil and Soybean Lecithin, *Fish Physiol. Biochem. 21*, 35–44.
15. Olsen, R.E., Myklebust, R., Ringø, E., and Mayhew, T.M. (2000) The Influences of Dietary Linseed Oil and Saturated Fatty Acids on Caecal Enterocytes in Artic Char (*Salvelinus alpinus* L.): A Quantitative Ultrastructural Study, *Fish Physiol. Biochem. 22*, 207–216.
16. Deplano, M., Connes, R., Diaz, J.P., and Barnabé, G. (1991) Variation in the Absorption of Macromolecular Proteins in Larvae of the Sea Bass *Dicentrarchus labrax* During Transition to Exotrophic Phase, *Mar. Biol. 110*, 29–36.
17. Segner, H., Rösch, R., Verreth, J., and Witt, U. (1993) Larval Nutritional Physiology: Studies with *Clarias gariepinus, Coregonus lavaretus* and *Scophthalmus maximus*, *J. World Aquacult. Soc. 24*, 121–134.
18. Karasov, W.H., and Hume, I.D. (1997) Vertebrate Gastrointestinal System, in *Handbook of Physiology*, Section 13: Comparative Physiology (Dantzler, W.H., ed.), Vol. 1, pp. 409–480, Oxford University Press, New York.
19. Segner, H., and Juario, J.V. (1986) Histological Observations on the Rearing of Milkfish, *Chanos chanos*, Fry Using Different Diets, *J. Appl. Ichthyol. 4*, 162–173.
20. Deplano, M., Connes, R., Diaz, J.P., and Paris, J. (1989) Intestinal Steatosis in the Farm-Reared Sea-Bass, *Dicentrarchus labrax*, *Dis. Aquat. Org. 6*, 121–130.
21. Caballero, M.J., López-Calero, G., Socorro, J., Roo, F.J., Izquierdo, M.S., and Fernández, A.J. (1999) Combined Effect of Lipid Level and Fish Meal Quality on Liver Histology of Gilthead Seabream (*Sparus aurata*), *Aquaculture 179*, 277–290.
22. Caballero, M.J., Izquierdo, M.S., Kjorsvik, E., Montero, D., Socorro, J., Fernández, A.J., and Roselund, G. (2003) Morphological Aspects of Intestinal Cells from Gilthead Seabream (*Sparus aurata*) Fed Diets Containing Different Lipid Sources, *Aquaculture 225*, 325–340.
23. Dabrowski, K. and Guderley, H. (2002) Intermediary Metabolism, in *Fish Nutrition*, 3rd edn. (Halver, J.E., and Hardy, R.W., eds.), pp. 310–367, Academic Press, San Diego.
24. Hoehne-Reitan, K., and Kjorsvik, E. (2004) Functional Development of the Liver and Exocrine Pancreas, *Am. Fish. Soc. 40*, 9–36.
25. Storch, V., Stählin, W., and Juario, J.V. (1983) Effect of Different Diets on the Ultrastructure of Hepatocytes of *Chanos chanos* Fry (Chanidae: Teleostei): An Electron Microscopic and Morphometric Analysis, *Mar. Biol. 74*, 101–104.
26. National Research Council (1993) *Nutrient Requirements of Fish*, National Academy of Sciences, Washington, DC.
27. Zambonino-Infante, J.L., Cahu, C.L., and Péres, A. (1997) Partial Substitution of Di- and Tripeptides for Native Protein in Sea Bass Diet Improves *Dicentrarchus labrax* Larval Development, *J. Nutr. 127*, 604–614.
28. Metais, P., and Bieth, J. (1968). Détermination de l'α-amilase par une microtecnique (Determination of the α-Amylase by a Microtechnique), *Ann. Biol. Clin.* (Paris) *26*, 133–142.
29. Holm, H., Hanssen, L.E., Krogdahl, A., and Florholmen, J. (1988) High and Low Inhibitor Soybean Meals Affect Human Duodenal Proteinase Activity Differently: *In vivo* Comparison with Bovine Serum Albumin, *J. Nutr. 118*, 515–520.
30. Iijima, N., Tanaka, S., and Ota, Y. (1998) Purification and Characterization of Bile-Salt Activated Lipase from the Hepatopancreas of Red Sea Bream, *Pagrus major, Fish Physiol. Biochem. 18*, 59–69.
31. Crane, R.K., Boge, G., and Rigal, A. (1979) Isolation of Brush Border Membranes in Vesicular Form from the Intestinal Spiral Valve of the Small Dogfish (*Scyliorhinus canicula*), *Biochim. Biophys. Acta 554*, 264–267.
32. Bessey, O.A., Lowry, O.H., and Brock, M.J. (1946) A Method for the Rapid Determination of Alkaline Phosphatase with Five Cubic Millimeters of Serum, *J. Biol. Chem. 164*, 321–329.
33. Nicholson, J.A., and Kim, Y.S. (1975) A One-Step L-Amino Acid Oxidase Assay for Intestinal Peptide Hydrolase Activity, *Anal. Biochem. 63*, 110–117.
34. Bradford, M.M. (1976) A Rapid and Sensitive Method for the Quantification of Microgram Quantities of Protein Utilizing the Principle of Protein–Dye Binding, *Anal. Biochem. 72*, 248–254.
35. Péres, A., Zambonino-Infante, J.L., and Cahu, C.L. (1998)

Dietary Regulation of Activities and mRNA Levels of Trypsin and Amylase in Sea Bass (*Dicentrarchus labrax*) Larvae, *Fish Physiol. Biochem. 19*, 145–152.

36. Folch, J., Lees, M., and Sloane-Stanley, G.H. (1957) A Simple Method for the Isolation and Purification of Total Lipids from Animal Tissues, *J. Biol. Chem. 226*, 497–509.

37. Juaneda, P., and Rocquelin, G. (1985) Rapid and Convenient Separation of Phospholipids and Non Phosphorus Lipids from Rat Heart Using Silica Cartridges, *Lipids 20*, 40–41.

38. Dagnelie, P. (1975). Les méthodes de l'inférence statistique, in *Théorie et méthodes statistiques* (Ducolot, J., ed.), Vol. 2, pp. 1–463, Les Presses Agronomiques de Gembloux, Gembloux, Belgium.

39. Sargent, J.R., McEvoy, L.A., and Bell, J.G. (1997) Requirements, Presentation and Sources of Polyunsaturated Fatty Acids in Marine Larval Fish, *Aquaculture 155*, 117–127.

40. Rainuzzo, J.R., Farestveit, R., and Jorgensen, L. (1993) Fatty Acid and Aminoacid Composition During Embryonic and Larval Development in Plaice (*Pleuronectes platessa*), in *Physiological and Biochemical Aspects of Fish Development* (Walther, B.T., and Fhyn, H.J., eds.), pp. 290–295, Bergen University, Bergen, Norway.

41. Brinkmeyer, R., and Holt, G.J. (1998) Highly Unsaturated Fatty Acids in Diets for Red Drum (*Scianops ocellatus*) Larvae, *Aquaculture 161*, 253–268.

42. Rodriguez, C., Perez, J.A., Badia, P., Izquierdo, M.S., Fernández-Palacios, H., and Hernández, A.L. (1998) The n-3 Highly Unsaturated Fatty Acids Requirements of Gilthead Sea Bream (*Sparus aurata* L.) Larvae When Using an Appropriate Ratio in the Diet, *Aquaculture 169*, 9–23.

43. Zambonino Infante, J.L., and Cahu, C.L. (1999) High Dietary Lipids Levels Enhance Digestive Tract Maturation and Improve *Dicentrarchus labrax* Larval Development, *J. Nutr. 129*, 1195–1200.

44. Shintani, T., Takahashi, N., Fushiki, T., Kotera, J., and Sugimoto, E. (1995) Recognition System for Dietary Fatty Acids in the Rat Small Intestine, *Biosci. Biotech. Biochem. 59*, 1428–1432.

45. Sheele, G.A. (1993) Regulation of Pancreatic Gene Expression in Response to Hormones and Nutritional Substrates, in *The Pancreas: Biology, Pathobiology, and Disease* (Go, V.L.W., Gardner, J.D., Brooks, F.P., Lebenthal, E.P., Di Magno, E.P., and Sheele, G.A., eds.), pp. 103–120, Raven Press, New York.

46. Diaz, J.P., Guyot, E., Vigier, S., and Connes, R. (1997) First Events in Lipid Absorption During Post-Embryonic Development of the Anterior Intestine in Gilt-Head Sea Bream, *J. Fish Biol. 51*, 180–192.

47. Smith, L.S. (1989) Digestive Functions in Teleost Fishes, in *Fish Nutrition* (Harver, J.E., ed.), 2nd edn., pp. 331–421, Academic Press, San Diego.

48. García-Hernández, M.P., Lozano, M.T., Elbal, M.T., and Agulleiro, B. (2001) Development of the Digestive Tract of Sea Bass (*Dicentrarchus labrax* L.). Light and Electron Microscopic Studies, *Anat. Embryol. 204*, 39–57.

49. Caballero, M.J., Obach, A., Roselund, G., Montero, D., Gisvold, M., and Izquierdo, M.S. (2002) Impact of Different Dietary Lipid Sources on Growth, Lipid Digestibility, Tissue Fatty Acid Composition and Histology of Rainbow Trout, *Oncorhynchus mykiss*, *Aquaculture 214*, 253–271.

50. Chatain, B., and Ounais-Guschemann, N. (1990) Improved Rate of Initial Swim Bladder Inflation in Intensively Reared *Sparus auratus*, *Aquaculture 84*, 345–353.

51. Chatain, N. (1986) La vessie natatoire chez *Dicentrarchus labrax* et *Sparus auratus*. I. Aspects morphologiques du développement, *Aquaculture 53*, 303–311.

Docosahexaenoic Acid- and Eicosapentaenoic Acid-Enriched Cardiolipin in the Manila Clam *Ruditapes philippinarum*

Edouard Kraffe[a], Philippe Soudant[b], Yanic Marty[a],*, and Nelly Kervarec[c]

[a]Unité mixte Centre National de la Recherche Scientifique (CNRS) 6521, Université de Bretagne Occidentale, 29238 Brest cedex, France, [b]Unité mixte CNRS 6539, Institut Universitaire Européen de la Mer (IUEM), Université de Bretagne Occidentale, 29280 Plouzané, France, and [c]Laboratoire de Résonance Magnétique Nucléaire (RMN), Université de Bretagne Occidentale, 29285 Brest cedex, France

ABSTRACT: The FA composition of cardiolipin (CL) from the Manila clam *Ruditapes philippinarum* was investigated in whole body and individual organs. CL was isolated by HPLC and its chemical structure characterized using NMR spectroscopy. Two prominent FA, EPA and DHA, were found in approximately equal proportions, contributing together up to 73 mol% of the total FA. The FA composition of CL is presumed to reflect a specific synthesis pathway independent of diet and of total glycerophospholipid FA composition. To the best of our knowledge, this is the first time that a CL dominated by the two PUFA 22:6n-3 and 20:5n-3 has been characterized and described. This EPA + DHA specificity of the CL in the Manila clam is thought to reflect a functional and structural modification of mitochondrial membranes of this bivalve species compared with scallops, oysters, and mussels that possess a CL dominated by DHA. The FA composition and levels of CL differed little between separated organs, and the large pool of DHA and EPA was found fairly equally distributed in gills, mantle, foot, siphon, and muscle. However, whereas DHA and PUFA levels were most stable between organs, EPA and arachidonic acid were significantly more variable and seemed to be interrelated.

Paper no. L9694 in *Lipids 40*, 619–625 (June 2005).

Cardiolipin, a phospholipid carrying four acyl chains, is considered to occur exclusively in bacterial and mitochondrial membranes. It is recognized to be of great importance in the maintenance of optimal activity of a number of key mitochondrial membrane enzymes involved in cellular energy metabolism such as cytochrome *c* oxidase, ADP-ATP carrier, and the oligomycin-sensitive ATPase complex (1–5). Generally, the unique FA patterns of eukaryotic cardiolipins, particularly in the C_{18} chains, have been emphasized. In mammals these CL acyl chains are dominated by linoleic acid (18:2n-6), constituting up to 85 mol% of total FA of CL (2,4). This specific FA hydrophobic part appeared to be an important structural requirement for the high protein-binding affinity of CL (6). Dietary modification significantly affects the composition of FA in mammalian CL (2,7) and was shown to alter cytochrome *c* oxidase (8,9) and F_1F_0-ATP synthase activities (8). Thus, in addition to CL content, the molecular composition of CL may be critical for optimal mitochondrial respiratory performance.

Few studies have investigated whether the CL content and FA composition of CL vary between organs. CL content is assumed to reflect mitochondrial content and oxidative capacity of the organ (10,11). In terms of FA composition, the CL from rat kidney, heart, and liver are markedly enriched in linoleic acid (from 60 to 85%) whereas CL from rat brain, lung, and testis only contains from 8 to 15% linoleic acid (10,12,13). Nevertheless, mechanisms able to explain these variations of CL FA composition are still lacking (4).

In a previous study, we provided the first evidence for CL containing more than 80 mol% DHA (22:6n-3). This occurred in three marine bivalves, the scallop *Pecten maximus*, the mussel *Mytilus edulis,* and the oyster *Crassostrea gigas* (14). The predominance of 22:6n-3 acyl chains in CL of these bivalves goes against the concept that FA of eukaryotic CL are mostly constituted of C_{18} acyl chains with one or two double bonds. This may reflect the paucity of data about FA compositions of marine bivalve phospholipids (15) and in particular of minor phospholipid classes such as CL (16–18).

In the present study, a DHA–EPA-enriched CL found in the Manila clam *Ruditapes philippinarum* was isolated by HPLC and characterized by NMR. The potential of inter-organ variations in the CL content and its FA composition were also investigated. The possible functional significances of this CL structure composition are discussed.

MATERIALS AND METHODS

Materials. Boron trifluoride [BF_3, 10% (by wt) in methanol] was obtained from Supelco (St. Quentin Fallavier, France). Others reagents and solvents were purchased from Merck (Darmstadt, Germany).

Sample preparation and lipid extraction. Adult *R. philippinarum* Manila clams were collected from the Bay of Brest during spring and summer 2001. After removing the digestive

---

*To whom correspondence should be addressed at Unité mixte CNRS 6521, Université de Bretagne Occidentale, C.S. 93837, 29238 Brest cedex, France. E-mail: Yanic.Marty@univ-brest.fr

Abbreviations: CL, cardiolipin, common name of diphosphatidylglycerol; DQF-COSY, double-quantum filter correlated spectroscopy; GPL, glycerophospholipid(s); HMBC, heteronuclear multiple bond coherence HMQC, heteronuclear multiple quantum coherence; NL, neutral lipids; NMI, non-methylene interrupted..

tract, whole animals were pooled and homogenized with a Dangoumeau homogenizer at −180°C. Samples were taken in triplicate, each of three pooled individuals. Mantle, foot, siphon, gills, and adductor muscle of *R. philippinarum* clams were excised, pooled, weighed, and homogenized as above (triplicates of three pooled individuals). Lipids were extracted from tissue homogenates according to the method of Folch *et al.* (19). To ensure complete extraction of tissue lipids, a solvent-to-tissue ratio of 70:1 was used as described by Nelson (20). After removing the organic phase, the residue was washed with a mixture of $CHCl_3$/MeOH (2:1, vol/vol) to exclude any solvent retention. The final extract was stored at −20°C under nitrogen after 0.01 wt% BHT (antioxidant) was added.

Separation of polar lipids and CL by silica gel LC microcolumn. An aliquot of the lipid extracts was evaporated to dryness, and lipids were recovered with three washings of 500 µL of $CHCl_3$/MeOH (98:2, vol/vol) and deposited at the top of a silica gel microcolumn [30 × 5 mm i.d., packed with Kieselgel 60 (70–230 mesh; Merck)] previously heated at 450°C and deactivated with 6 wt% H_2O (21). Neutral lipids were eluted with 10 mL of $CHCl_3$/MeOH (98:2, vol/vol). CL was isolated from the rest of the glycerophospholipid (GPL) classes by rinsing the column with 15 mL of $CHCl_3$/MeOH (90:10, vol/vol) as described previously (14). An aliquot of the isolated fraction was taken for later confirmation of the presence of the CL class by HPLC. The rest of the polar lipids was recovered with 20 mL of MeOH and stored at −20°C for later GPL class separation by HPLC or FA composition analysis by GC. To obtain high quantities of CL for NMR analysis, the lipid extract of *R. philippinarum* was separated on a silica gel column [40 × 25 mm i.d, packed with Kieselgel 60 (70–230 mesh; Merck)] as described elsewhere (14).

Separation of phospholipid classes and FA analysis. Separation of the phospholipid classes followed the method previously described (14), using a Waters (Milford, MA) HPLC system (UV detection at 206 nm). Briefly, separation was performed on a Lichrosorb Diol column (OH-bound silica gel column, Lichrosorb Diol 5 µm, 250 × 4 mm i.d.; Merck) using a binary mobile phase. A linear gradient of 15 min was performed from 100% solvent A (acetonitrile) to an 8:2 ratio of solvent A and solvent B (acetonitrile/methanol/phosphoric acid, 93:5:1.5, by vol). This solvent ratio was maintained for 5 min, followed by a linear gradient to 100% solvent B in 10 min. Solvent B was maintained for another 30 min, and then switched to 100% solvent A for 15 min to reactivate the column. The solvent flow rate was 1 mL/min. The CL fraction as well as the other GPL classes was identified, collected, and analyzed for FA composition using GC after transesterification (MeOH/BF_3) (22).

NMR spectroscopy. All NMR spectra were recorded on Bruker DRX-500 Avance Spectrometers (Wissembourg, France) equipped with an indirect 5-mm TBI gradient $^1H/\{BB\}/^{13}C$ and an indirect 5-mm TXI gradient $^1H/^{13}C/^{31}P$ probeheads. The probe temperature was 25°C. Prior to analysis, lipid samples (CL from *R. philippinarum*) were dissolved into $CDCl_3$/CD_3OD (1:2.5, vol/vol). To promote solubilization

of the smallest lipid entities for a good resolution of resonances, samples were warmed and sonicated at about 30°C for about 5 min. 2-D NMR spectra were acquired with nonspinning samples with deuterium frequency locking. ^1H-^1H double-quantum filter correlated spectroscopy (DQF-COSY), heteronuclear multiple quantum coherence (HMQC), and heteronuclear multiple bond coherence (HMBC) were employed to assign signals. DQF-COSY and HMQC were performed according to standard pulse sequences, whereas HMBC was performed with 60 ms of delay. Measurements were recorded by collecting 1K (F2) × 200 (F1) data points zero filled to 1K (F1) using a spectral width of 500 Hz (500.13 MHz) with a repetition time of 2 s. ^1H and ^{13}C NMR chemical shifts were expressed in ppm by reference to tetramethylsilane as external standard.

Statistical analysis. To compare the differences between organs, *t*-tests and one-way ANOVA were performed using Statview (SAS Institute Inc., Cary, NC). Percentage data were transformed (arcsin of the square root) before ANOVA and *t*-test, but are presented in figure and table as untransformed percentage values. Differences were considered statistically significant if $P \le 0.05$.

RESULTS

FA composition of CL in whole animals. GC analysis of FAME derived from the isolated CL fraction of *R. philippinarum* showed a FA profile with 84.6 mol% of PUFA (Table 1). Interestingly, two predominant PUFA, 22:6n-3 and 20:5n-3, were found in similar proportions (34.9 and 37.9 mol% of the total FA of CL, respectively). The minor components included 20:4n-6, 16:0, and 18:0 (<6.8% individually). The CL class represented 0.9 mol% of the total GPL whereas 4.3 and 10.6 mol% of the total GPL content of DHA and EPA, respectively, were located in the CL fraction.

FA composition of GPL and neutral lipids (NL) in whole animals. The FA composition of GPL showed that DHA was found in higher proportions than EPA in *R. philippinarum* membranes (20.3 vs. 8.1%, respectively) (Table 1). On the contrary, NL (mainly TG) presented a higher level of EPA than DHA (12.7 vs. 6.5%, respectively).

NMR spectroscopy. Unsaturated acyl chains esterified to the glycerol backbone of a CL were characterized by the ^1H and ^{13}C resonances of olefinic –CH=CH–, bis-allylic methylene, allylic methylene, and $C_\alpha H_2$, $C_\beta H_2$ protons (where α and β positions are relative to the carbonyl group) (Fig. 1). The integral ratio of the characteristic multiplets at 0.85 (from 20:4n-6 and saturated acyl chains) and 0.95 ppm (from unsaturated n-3 acyl chains) confirmed that 75% of the FA are n-3 PUFA. As described in detail in an earlier study (14), the high-field single proton of C-2 outer glycerols resonated typically at 5.21 ppm whereas ^1H resonances between 3.7 and 4.5 ppm were characteristic of the glycerol protons of the two quasi-equivalent outer glycerols and of the central glycerol of a polyunsaturated CL.

From the HMBC spectrum it can be inferred that DHA chains are bound to the *sn*-2 position whereas EPA chains and others (mainly 20:4n-6 and saturated acyl chains) are bound to

TABLE 1
FA Composition of the Cardiolipin (CL), Total Glycerophospholipids (GPL), and Neutral Lipids (NL) from Whole Clam *Ruditapes philippinarum*[a]

	CL	GPL	NL
FA[b]			
16:0	4.3 ± 1.7	11.8 ± 0.7	12.4 ± 2.3
18:0	5.6 ± 0.7	9.9 ± 1.1	8.7 ± 4.2
18:1n-9	0.8 ± 0.1	3.4 ± 0.8	8.1 ± 2.3
18:1n-7	0.3 ± 0.1	1.5 ± 0.4	2.8 ± 0.4
20:1n-11	0.4 ± 0.2	2.9 ± 0.1	4.2 ± 1.2
20:1n-9	0.2 ± 0.1	1.5 ± 0.3	2.9 ± 0.7
20:1n-7	0.8 ± 0.3	2.1 ± 0.2	4.6 ± 1.3
18:2n-6	<0.1	0.2 ± 0.1	0.4 ± 0.2
18:3n-3	<0.1	0.4 ± 0.3	0.2 ± 0.2
20:4n-6	6.8 ± 0.6	6.4 ± 1.0	6.8 ± 0.8
20:5n-3	**34.9 ± 0.2**	**8.1 ± 0.9**	**6.5 ± 1.7**
21:5n-3	ND	1.0 ± 0.1	0.6 ± 0.1
NMI[c]	0.9 ± 0.2	9.0 ± 2.0	3.2 ± 1.1
22:4n-6	0.3 ± 0.1	3.4 ± 0.5	2.7 ± 1.6
22:5n-6	1.7 ± 0.1	1.6 ± 0.1	1.3 ± 0.4
22:5n-3	1.1 ± 0.2	4.6 ± 0.4	3.1 ± 1.0
22:6n-3	**37.9 ± 2.3**	**20.3 ± 0.8**	**12.7 ± 3.1**
Total SFA	12.3 ± 2.2	28.3 ± 1.0	25.4 ± 7.3
Total MUFA	3.1 ± 1.1	14.0 ± 1.4	29.7 ± 4.9
Total PUFA	**84.6 ± 3.3**	**58.3 ± 0.6**	**44.9 ± 7.4**
Proportion of total 22:6n-3 in CL (%)[d]	4.3 ± 0.6	ND	ND
Proportion of total 20:5n-3 in CL (%)	10.6 ± 2.3	ND	ND
CL (mol%)[e]	0.9 ± 0.2	ND	ND

[a]Results are expressed in mol% of the total FA of the fraction. Values are presented as mean ± SD (*n* = triplicate of three pooled individuals). SFA, saturated FA; MUFA, monounsaturated FA; ND, not detected.
[b]Main characteristic FA are represented. FA also detected but not represented are 14:0, 15:0, 17:0, 16:1n-7, 16:1n-5, 18:1n-5, 18:2n-4, 18:3n-6, 18:3n-4, 18:4n-3, 20:2n-6, 20:3n-6, 20:4n-3, 21:4n-6, none of which was more than 1.0 mol% (except for NL). "Totals" refer to all analyzed FA.
[c]22:2 non-methylene-interrupted (NMI) (7,15), 22:2 NMI (7,13), 20:2 NMI (5,13), 20:2 NMI (5,11), and 22:3 NMI (7,13,16) FA.
[d]Percentage of the total 22:6n-3 and 20:5n-3 of GPL located in the CL class.
[e]Percentage of the CL class relatively to other GPL classes.

FIG. 1. [1]H resonance spectrum of *Ruditapes philippinarum* cardiolipin. The insert shows the expanded ^{1}H glycerol backbone region. [a]$C_\alpha H_2$– protons of 20:5n-3, 20:4n-6, and saturated acyl chains. [b]$C_\beta H_2$– protons of 20:5n-3, 20:4n-6, and saturated acyl chains. Enlargement: [1]C-1 protons of the two outer glycerols (*sn*-1 *O*-acyl chain). [2,3]Outer glycerols C-3 (phosphate group) and central glycerol protons. For details of assignments see Reference 1.

the *sn*-1 position (Fig. 2). Indeed, when considering ^{13}C chemical shifts of the carbonyl carbon resonances in the 173–175 ppm region, the signal from *sn*-2 carbonyl carbons appeared at 173.45 ppm, typically shifted by about 0.85 ppm to a lower frequency than those of *sn*-1 carbonyls (174.3 ppm) (23). This is confirmed by the correlation between carbonyls at 174.3 ppm and part of the eight-line multiplet at 4.15 ppm assigned to the magnetically inequivalent methylene protons (C-1-H_1, C-1-H_1') of outer *sn*-1-glycerol. On the other hand, protons from both C_α and C_β carbons of DHA chains (multiplet at 2.37 ppm in relation with the Δ4 unsaturation) were clearly resolved from

those of C_α and C_β carbons of EPA chains, 20:4n-6, and saturated acyl chains (2.35 and 1.75 ppm, respectively). The former (DHA chains, multiplet at 2.37 ppm) appeared to be specifically correlated to *sn*-2 carbonyl carbons whereas the latter (mainly EPA chains, multiplet at 2.35 and 1.75 ppm) were correlated to *sn*-1 carbonyls (Fig. 2).

Content and FA composition of CL of different organs. In *R. philippinarum*, CL accounted for 0.6% of the total GPL in muscle, which was significantly different from the 1.3% in foot, while CL contents in mantle, siphon, and gills were very similar and were not significantly different from those in muscle and foot (Table 2). Although the same general FA composition as in the whole animals was observed in the different organs isolated from the Manila clam *R. philippinarum* with a predominant preference for 22:6n-3 and 20:5n-3, small but significant differences of EPA contents were observed between organs. In muscle and foot, 20:5n-3 was present at similar levels as 22:6n-3, but in gills, mantle, and siphon 20:5n-3 was less abundant than 22:6n-3. Interestingly, in these organs, significantly higher levels of 20:4n-6 (9.2, 7.8, and 7.4 mol% in gills, mantle, and
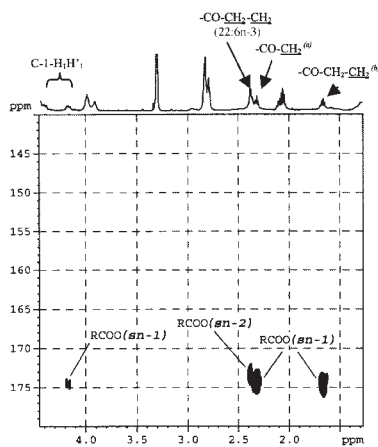
FIG. 2. Heteronuclear multiple bond coherence spectrum in the carbonyl carbon region of the unsaturated acyl chains of *Ruditapes philippinarum* cardiolipin. [a]C$_\alpha$H$_2$– protons of 20:5n-3, 20:4n-6, and saturated acyl chains. [b]C$_\beta$H$_2$– protons of 20:5n-3, 20:4n-6, and saturated acyl chains.

siphon, respectively) seemed to be interrelated to the lower levels of 20:5n-3 found.

FA composition of total GPL. The FA patterns of total GPL of gills, mantle, foot, siphon, and muscle from *R. philippinarum* are presented in Table 3. Major FA were 22:6n-3 > 16:0, 18:0 > 20:5n-3, non-methylene-interrupted (NMI) FA, and 20:4n-6. In each organ DHA was uniformly found in higher proportion than EPA.

DISCUSSION

A CL containing up to 73 mol% of EPA + DHA has been isolated from the Manila clam *R. philippinarum*. Interestingly, EPA and DHA were found in almost equimolar proportions. This polar lipid class showed the same HPLC retention time value as the DHA-enriched CL previously isolated and characterized in the three bivalves *P. maximus*, *M. edulis,* and *C. gigas* (14). The chemical structure of this EPA + DHA-enriched polar lipid class isolated from the clam *R. philippinarum* was analyzed using

TABLE 2

FA Composition of CL (expressed in mol% of the total FA of CL), Percentage of CL Relative to Other GPL Classes (in mol%), and Percentage of Total 22:6n-3 and 20:5n-3 of GPL Located in the CL Class in Individual Organs of the Manila clam *R. philippinarum*[a]

	Gills	Mantle	Siphon	Foot	Muscle
FA[b]					
16:0	5.3 ± 2.5[a]	2.9 ± 1.1[b]	4.1 ± 0.7[a,b]	3.1 ± 1.1[b]	5.5 ± 0.9[a]
18:0	7.2 ± 1.5[a]	4.0 ± 0.7[b]	6.4 ± 0.2[a]	4.1 ± 0.5[b]	5.1 ± 2.6[a,b]
18:1n-9	1.0 ± 0.2[a]	0.5 ± 0.1[b]	0.6 ± 0.1[b]	0.6 ± 0.2[b]	1.4 ± 0.4[a]
18:1n-7	0.8 ± 0.6	<0.1	0.4 ± 0.3	<0.1	ND
20:1n-11	0.3 ± 0.2	0.3 ± 0.2	0.4 ± 0.2	1.0 ± 0.9	ND
20:1n-9	0.7 ± 0.1	<0.1	0.2 ± 0.1	<0.1	ND
20:1n-7	1.3 ± 0.6[a]	0.4 ± 0.3[b]	0.9 ± 0.5[a]	0.7 ± 0.1[a]	0.9 ± 0.4[a]
18:2n-6	0.4 ± 0.3	ND	ND	ND	ND
18:3n-3	<0.1	ND	<0.1	<0.1	ND
20:4n-6	9.2 ± 2.3[a]	7.8 ± 1.4[a,b]	7.4 ± 0.3[b]	5.2 ± 0.7[c]	2.7 ± 0.4[d]
20:5n-3	**28.3 ± 0.1[a]**	**35.2 ± 0.7[b]**	**33.9 ± 0.6[b]**	**39.0 ± 1.2[c]**	**41.1 ± 2.3[c]**
21:5n-3	<0.1	ND	<0.1	ND	ND
NMI[c]	1.2 ± 0.1	1.3 ± 0.2	0.6 ± 0.2	1.0 ± 0.5	<0.1
22:4n-6	0.7 ± 0.1	0.7 ± 0.4	0.3 ± 0.2	0.3 ± 0.1	<0.1
22:5n-6	2.1 ± 1.2	1.9 ± 0.2	1.6 ± 0.1	1.7 ± 0.1	1.5 ± 0.5
22:5n-3	1.6 ± 0.6	1.0 ± 0.1	0.9 ± 0.1	0.9 ± 0.2	1.2 ± 0.8
22:6n-3	**35.8 ± 1.0[a]**	**40.7 ± 2.4[b]**	**38.0 ± 0.2[a,b]**	**39.4 ± 2.8[a,b]**	**36.8 ± 4.6[a,b]**
Total SFA	15.9 ± 2.1[a]	9.1 ± 2.3[b]	13.6 ± 0.7[a]	8.3 ± 0.7[b]	11.7 ± 3.4[a]
Total MUFA	4.5 ± 1.3[a]	1.4 ± 0.2[b]	2.8 ± 0.1[a]	3.1 ± 1.7[a]	3.6 ± 2.7[a]
Total PUFA	79.6 ± 3.1[a]	89.5 ± 2.5[b]	83.6 ± 0.8[a]	88.6 ± 2.4[b]	84.7 ± 6.1[a,b]
Proportion of total[d] in 22:6n-3 in CL (%)	5.2 ± 1.7[a]	5.3 ± 2.3[a]	4.7 ± 1.0[a]	6.1 ± 0.6[b]	2.5 ± 0.5[a]
Proportion of total 20:5n-3 in CL (%)	12.9 ± 2.6[a]	13.1 ± 5.7[a]	12.0 ± 1.6[a]	17.3 ± 0.3[a]	4.7 ± 0.9[b]
CL (mol%)[e]	0.9 ± 0.2[a,b]	1.0 ± 0.4[a,b]	1.0 ± 0.2[a,b]	1.3 ± 0.1[b]	0.6 ± 0.2[a]

[a]Different lowercase roman letters indicate significant difference between organs (ANOVA, $P < 0.05$). Values are presented as mean ± SD (n = triplicate of three pooled individuals). For abbreviations see Table 1.
[b]Main characteristic FA are represented. FA also detected but not represented are 14:0, 15:0, 17:0, 16:1n-7, 16:1n-5, 18:1n-5, 18:2n-4, 18:3n-6, 18:3n-4, 18:4n-3, 20:2n-6, 20:3n-6, 20:4n-3, 21:4n-6, none of which was more than 1.0 mol%. "Totals" refer to all analyzed FA.
[c]22:2 NMI (7,15), 22:2 NMI (7,13), 20:2 NMI (5,13), 20:2 NMI (5,11), and 22:3 NMI (7,13,16) FA.
[d]Percentage of the total 22:6n-3 and 20:5n-3 of GPL located in the CL class.
[e]Percentage of the CL class relatively to other GPL classes.

NMR in the 3.9–4.5 ppm (^{1}H) region (14,24) and was demonstrated to be exclusively constituted of CL molecules.

In mammals, it is well documented that CL molecules present the same marked enrichment in PUFA with low amounts of saturated FA. This apparent selectivity encountered in CL of most mammalian tissues is associated with linoleic acid, 18:2n-6 (2,4,25). In contrast, there is little knowledge concerning the FA composition of CL in marine animals. As reviewed in a previous study (14), although high amounts of both n-3 and n-6 PUFA were reported in some CL from marine animals, no specific PUFA was found to be predominant. Our demonstration of the existence of a DHA-dominant (22:6n-3 > 80 mol%) CL in the scallop *P. maximus*, the mussel *M. edulis,* and the oyster *C. gigas* (14) revealed the importance of long-chain PUFA in CL of mollusk bivalves. In the present study, the evidence of a CL enriched with EPA and DHA in almost equimolar proportions in the Manila clam *R. philippinarum* provided a new example of highly polyunsaturated CL.

The difference between Manila clam CL (DHA + EPA) and the DHA-enriched CL of the three bivalve species cited above can be hypothesized to reflect FA dietary variations between these species. Indeed, it was shown that diet significantly affects the composition of FA in mammalian CL (2). Then, it is conceivable that clam CL was not specifically enriched with DHA compared with the other bivalve species because of a DHA deficiency and/or an EPA enrichment of its diet. However, considering that the FA composition of *R. philippinarum* NL provided a good sig-

nature of the diet intake (26), the fact that NL contain 12.7% of DHA indicated that the diet was not deficient in DHA. Moreover, the fact that DHA represented up to 20.3% of the total FA of GPL (vs. 8.1% for EPA) showed that *R. philippinarum* is able to selectively incorporate and maintain DHA vs. EPA in its membranes. Obviously, these observations refute the possibility of a dietary imbalance for the Manila clam. Hence, the selective incorporation in equal amounts of EPA and DHA in *R. philippinarum* CL is likely to be metabolically controlled and to be involved in CL structural functions. CL, specifically located in mitochondria, was shown to be a key factor in the maintenance and modification of activity of major membrane proteins such as cytochrome *c* oxidase, ADP-ATP carrier, and pyruvate carrier or of other large complexes of oxidative phosphorylation including complex I (NADH-CoQ reductase), III (ubiquinol:ferricytochrome *c* oxidase), and V (F_0F_1-ATP synthase) (1–5,8,9,27,28). The FA hydrophobic part appeared to be an important structural requirement for this high protein-binding affinity of CL (6). Thus, the equal amounts of EPA and DHA in *R. philippinarum* CL may be critical for optimal mitochondrial respiratory performance of the Manila clam.

It was shown that increasing dietary levels of 22:6n-3 in the CL of rats reduced cytochrome *c* oxidase activity (8,9) and increased the activity of F_1F_0-ATP synthase (8). Although there are not enough literature data to support the idea that specific PUFA compositions (i.e., 18:2n-6 vs. 20:5n-3, or 20:5n-3 vs. 22:6n-3) have distinct effects on mitochondrial enzymes, it

TABLE 3
Compositions of the Main FA in GPL of *R. philippinarum* Organs[a]

	Gills	Mantle	Siphon	Foot	Muscle
FA[b]					
16:0	10.9 ± 0.7[a]	10.6 ± 0.1[a]	10.7 ± 0.3[a]	13.1 ± 0.2[b]	14.6 ± 0.2[c]
18:0	11.5 ± 1.0	10.5 ± 0.1	12.1 ± 0.5	10.2 ± 1.3	11.1 ± 0.2
18:1n-9	2.1 ± 0.4[a]	3.7 ± 0.4[b]	3.4 ± 0.3[b]	3.3 ± 0.3[b]	4.3 ± 0.3[b]
18:1n-7	1.1 ± 0.1[a]	1.1 ± 0.1[a]	1.0 ± 0.1[a]	1.1 ± 0.1[a]	1.7 ± 0.1[b]
20:1n-11	4.0 ± 0.3[a]	3.0 ± 0.6[b]	3.3 ± 0.4[b]	3.1 ± 0.3[b]	1.8 ± 0.1[c]
20:1n-9	2.1 ± 0.3[a]	1.6 ± 0.6[a]	1.5 ± 0.1[b]	1.4 ± 0.2[b]	1.8 ± 0.1[ab]
20:1n-7	2.1 ± 0.1[a]	1.9 ± 0.2[a]	2.1 ± 0.1[a]	2.3 ± 0.1[a]	3.1 ± 0.4[b]
18:2n-6	0.3 ± 0.1	0.2 ± 0.1	0.3 ± 0.2	0.3 ± 0.2	0.2 ± 0.1
18:3n-3	<0.1	0.2 ± 0.1	0.1 ± 0.1	0.3 ± 0.1	0.5 ± 0.1
20:4n-6	6.5 ± 1.0[a]	7.1 ± 0.1[a]	6.4 ± 0.4[a]	5.1 ± 0.2[b]	4.3 ± 0.1[b]
20:5n-3	**5.2 ± 0.1[a]**	**6.9 ± 0.3[b]**	**6.6 ± 0.9[b]**	**7.1 ± 0.7[b]**	**10.7 ± 0.5[c]**
21:5n-3	0.8 ± 0.1[a]	0.8 ± 0.1[a]	0.8 ± 0.1[a]	0.6 ± 0.3[a]	1.3 ± 0.1[b]
NMI[c]	13.1 ± 1.2[a]	9.5 ± 0.1[b]	8.8 ± 0.5[b]	10.3 ± 0.3[b]	3.9 ± 0.3[c]
22:4n-6	4.0 ± 0.3[a]	3.4 ± 0.5[b]	3.2 ± 0.4[b]	3.3 ± 0.1[b]	2.0 ± 0.3[b]
22:5n-6	1.8 ± 0.1[a]	1.7 ± 0.2[a]	1.6 ± 0.1[a]	1.6 ± 0.1[a]	1.2 ± 0.1[b]
22:5n-3	3.2 ± 0.1[a]	4.4 ± 0.6[b]	4.7 ± 0.2[a]	4.6 ± 0.3[a]	5.0 ± 0.3[a]
22:6n-3	**17.5 ± 0.5**	**20.1 ± 0.2**	**19.4 ± 1.6**	**20.2 ± 1.4**	**18.1 ± 1.4**
Total SFA	29.5 ± 1.5	28.1 ± 0.2	30.5 ± 1.6	29.6 ± 2.5	31.3 ± 1.3
Total MUFA	14.9 ± 0.7	14.2 ± 0.1	14.8 ± 1.0	13.9 ± 0.4	17.5 ± 2.0
Total PUFA	55.5 ± 0.8	57.7 ± 0.3	54.8 ± 2.7	56.5 ± 2.9	51.2 ± 3.3

[a]Results are expressed in mol% of the total FA of GPL. Different lowercase roman letters indicate significant difference between organs (ANOVA, *P* < 0.05). Values are presented as mean ± SD (*n* = triplicate of three pooled individuals). For abbreviations see Table 1.
[b]Main characteristic FA are represented. FA also detected but not represented are 14:0, 15:0, 17:0, 16:1n-7, 16:1n-5, 18:1n-5, 18:2n-4, 18:3n-6, 18:3n-4, 18:4n-3, 20:2n-6, 20:3n-6, 20:4n-3, 21:4n-6, none of which was more than 1.0 mol%. "Totals" refer to all analyzed FA.
[c]22:2 NMI (7,15), 22:2 NMI (7,13), 20:2 NMI (5,13), 20:2 NMI (5,11), and 22:3 NMI (7,13,16) FA.

could be supposed that the typical DHA + EPA-enriched CL (Manila clam) and the DHA-dominant CL (scallop, oyster, and mussel) may affect differentially the packing and the interaction of the CL with key metabolic enzymes. It can also be advanced that the specific positional distribution of EPA and DHA, respectively, on the *sn*-1 and *sn*-2 glycerol positions, deduced by the detailed examination of NMR data, would account in such functions.

Inter-organ variations. FA composition of CL varied little between separated organs, and the large pool of DHA and EPA was fairly equally distributed in gills, mantle, foot, siphon, and muscle. As for the whole body, the total GPL FA composition of each organ indicated that DHA is more efficiently incorporated and maintained than EPA in the membranes of *R. philippinarum*. In addition, although the CL represented less than 1.3% of total GPL classes, an important part of total EPA of GPL was located in the CL (up to 17 mol% in foot), indicating a specific incorporation of this FA into the CL class. Almost nothing is known about the inter-organ variability of bivalve CL. Only studies from Soudant *et al.* (16–18) have investigated the FA composition of male and female gonad CL from the scallop *P. maximus*. In both gonads, the composition of the DHA-dominant CL was unchanged. In mammals, CL FA composition can vary much more between organs. Indeed, even if linoleic acid is generally the predominant FA found in similar percentages in the CL from rat heart, liver, and kidney (up to 85% of total CL FA) (12,13), 18:2n-6 accounts for only 8–15% in rat brain, lung, testis, and spleen whereas 16:0 and 18:0 together represent 51–71% of total CL FA (10,13). In rabbit skeletal muscles, CL from the oxidative muscles contains less 18:2n-6 than CL from glycolytic muscles (76.3 and 84.5%, respectively) (29). The functional significance of such differences in mammals is not known. As CL contained almost equal amounts of DHA and EPA in the different organs of *R. philippinarum*, it can be inferred that the metabolic functions of CL requiring such a specific acyl composition are quite ubiquitous in these organs. However, in regard to mammals, the possibility of some variations between organs due to the small but significant differences of EPA contents, along with arachidonic acid, cannot be excluded.

The CL content differed little according to the organs of the clam *R. philippinarum*. In mammals, the organ concentration of CL is much more variable and is assumed to reflect mitochondrial content and oxidative capacity (10,11). CL constitutes 14.7, 12.6, and 9% of total GPL in rat, bovine, and human heart, respectively, whereas other muscle tissues that are not so highly specialized for oxidative phosphorylation have much smaller amounts of CL, ranging from 1.4–2.1% in the rat to 6.6 and 8.9% in human and bovine skeletal muscle, respectively. The CL content was also reported to be very low in the lung and spleen (less than 3%) (10). We hypothesize that the nearly constant proportions of CL in *R. philippinarum* may reflect the mitochondrial oxyconformity of marine bivalve invertebrates (30,31), contrary to mammals. which are oxyregulating organisms.

A DHA + EPA-enriched CL has been isolated from the Manila clam *R. philippinarum* that is different from the DHA-enriched CL found in the scallop *P. maximus*, the mussel *M. edulis,* and the oyster *C. gigas*. The differences were speculated to reflect means of modifications in oxidative phosphorylation between these species. It is unclear whether these differences could be related to the phylogeny of species. Further studies should investigate more bivalve species to determine whether other FA patterns of CL exist and the importance of these highly unsaturated PUFA CL differences in mitochondrial functioning.

REFERENCES

1. Robinson, N.C., Zborowski, J., and Talbert, L. H. (1990) Cardiolipin-Depleted Bovine Heart Cytochrome *c* Oxidase: Binding Stoichiometry and Affinity for Cardiolipin Derivatives, *Biochemistry 29*, 8962–8969.
2. Berger, A., German, J.B. and Gershwin, M.E. (1993) Biochemistry of CL: Sensitivity to Dietary Fatty Acids, in *Advances in Food and Nutrition Research* (Kissela, J.E., ed.), pp. 259–338, Academic Press, San Diego.
3. McAuley, K.E., Fyfe, P.K., Ridge, J.P., Isaacs, N.W., Cogdell, R.J., and Jones, M.R. (1999) Structural Details of an Interaction Between Cardiolipin and an Integral Membrane Protein, *Proc. Natl. Acad. Sci. USA 96*, 14706–14711.
4. Schlame, M., Rua, D., and Greenberg, M.L. (2000) The Biosynthesis and Functional Role of Cardiolipin, *Prog. Lipid Res. 39*, 257–288.
5. Zhang, M., Mileykovskaya, E., and Dowhan, W. (2002) Gluing the Respiratory Chain Together: Cardiolipin Is Required for Supercomplex Formation in the Inner Mitochondrial Membrane, *J. Biol. Chem. 277*, 43553–43556.
6. Ma, B.J., Taylor, W.A., Dolinsky, V.W., and Hatch, G.M. (1999) Acylation of Monolysocardiolipin in Rat Heart, *J. Lipid Res. 40*, 1837–1845.
7. Clandinin, M.T., Field, C.J., Hargraves, K., Morson, L., and Zsigmond, E. (1985) Role of Diet Fat in Subcellular Structure and Function, *Can. J. Physiol. Pharmacol. 63*, 546–556.
8. Yamaoka, S., Urade, R., and Kito, M. (1988) Mitochondrial Function in Rats Is Affected by Modification of Membrane Phospholipids with Dietary Sardine Oil, *J. Nutr. 118*, 290–296.
9. Watkins, S.M., Lin, T.Y., Davis, R.M., Ching, J.R., Depeters, E.J., Halpern, G.M., Walzem, R.L., and German, J.B. (2001) Unique Phospholipid Metabolism in Mouse Heart in Response to Dietary Docosahexaenoic or α-Linoleic Acids, *Lipids 36*, 247–254.
10. Hostetler, K. (1982) *Polyglycerophospholipids: Phosphatidylglycerol, Diphosphatidyl Glycerol, and Bis (Monoacylglycero)Phosphate*, Elsevier Biomedical Press, Amsterdam.
11. Schlame, M., Shanske, S., Doty, S., König, T., Sculco, T., Dimauro, S., and Blanck, T.J.J. (1999) Microanalysis of Cardiolipin in Small Biopsies Including Skeletal Muscle from Patients with Mitochondrial Disease, *J. Lipid Res. 40*, 1585–1592.
12. Wolff, R.L., Combe, N.A., and Entressangles, B. (1985) Positional Distribution of Fatty Acids in Cardiolipin of Mitochondria from 21-Day-Old Rats, *Lipids 20*, 908–914.
13. Berger, A., and German, J.B. (1990) Phospholipid Fatty Acid Composition of Various Mouse Tissues After Feeding α-Linolenate (18:3n-3) or Eicosatrienoate (20:3n-3), *Lipids 25*, 473–480.

14. Kraffe, E., Soudant, P., Marty, Y., Kervarec, N., and Jehan, P. (2002) Evidence of a Tetradocosahexaenoic Cardiolipin in Some Marine Bivalves, *Lipids 37*, 507–514.

15. Bell, M.V., and Sargent, J.R. (1985) Fatty Acid Analyses of Phosphoglycerides from Tissues of the Clam *Chlamys islandica* (Muller) and the Starfish *Ctenodiscus crispatus* (Retzius) from Balsfjorden, Northern Norway, *J. Exp. Mar. Biol. Ecol. 87*, 31–40.

16. Soudant, P., Moal, J., Marty, Y., and Samain, J.F. (1996) Impact of the Quality of Dietary Fatty Acids on Metabolism and the Composition of Polar Lipid Classes in Female Gonads of *Pecten maximus* (L.), *J. Exp. Mar. Biol. Ecol. 205*, 149–163.

17. Soudant, P., Moal, J., Marty, Y., and Samain, J.F. (1997) Composition of Polar Lipid Classes in Male Gonads of *Pecten maximus* (L.). Effect of Nutrition, *J. Exp. Mar. Biol. Ecol. 215*, 103–114.

18. Soudant, P., Van Ryckeghem, K., Marty, Y., Moal, J., Samain, J.F., and Sorgeloos, P. (1999) Comparison of the Lipid Class and Fatty Acid Composition Between a Reproductive Cycle in Nature and a Standard Hatchery Conditioning of the Pacific Oyster *Crassostrea gigas*, *Comp. Biochem. Phys. 123*, 209–222.

19. Folch, J., Lees, M., and Sloane-Stanley, G.H. (1957) A Simple Method for the Isolation and Purification of Total Lipids from Animal Tissues, *J. Biol. Chem. 226*, 497–509.

20. Nelson, G.J. (1993) Isolation and Purification of Lipids from Biological Matrices, in *Analysis of Fats, Oils and Derivatives* (Perkins, E.G., ed.), pp. 20–89, AOCS Press, Champaign.

21. Marty, Y., Delaunay, F., Moal, J., and Samain, J.F. (1992) Changes in the Fatty Acid Composition of the Scallop *Pecten maximus* (L.) During Larval Development, *J. Exp. Mar. Biol. Ecol. 163*, 221–234.

22. Soudant, P., Marty, Y., Moal, J., Masski, H., and Samain, J. F. (1998) Fatty Acid Composition of Polar Lipid Classes During Larval Development of Scallop *Pecten maximus* (L.), *Comp. Biochem. Physiol. A 121*, 279–288.

23. Vlahov, G. (1999) Application of NMR to the Study of Olive Oils, *Prog. Nucl. Magn. Reson. Spectrosc. 35*, 341–357.

24. Adosraku, R.K., Smith, J.D., Nicolaou, A., and Gibbons, W.A. (1996) *Tetrahymena thermophila*: Analysis of Phospholipids and Phosphonolipids by High-Field ^{1}H-NMR, *Biochim. Biophys. Acta 1299*, 167–174.

25. Schlame, M., Beyer, K., Hayer-Hartl, M., and Klingenberg, M. (1991) Molecular Species of Cardiolipin in Relation to Other Mitochondrial Phospholipids. Is There an Acyl Specificity of the Interaction Between Cardiolipin and the ADP/ATP Carrier? *Eur. J. Biochem. 199*, 459–466.

26. Ackman, R.G. (1983) Fatty Acid Metabolism of Bivalves, *Proc. 2nd Int. Conf. Aquac. Nutr. Spec. Publ. 2*, 358–375.

27. Paradies, G., and Ruggiero, F.M. (1990) Age-Related Changes in the Activity of the Pyruvate Carrier and in Lipid Composition in Rat-Heart Mitochondria, *Biochim. Biophys. Acta 1016*, 207–212.

28. Paradies, G., Ruggiero, F.M., Petrosillo, G., and Quagliariello, E. (1994) Enhanced Cytochrome Oxidase Activity and Modification of Lipids in Heart Mitochondria from Hyperthyroid Rats, *Biochim. Biophys. Acta 1225*, 165–170.

29. Alasnier, C., and Gandemer, G. (1998) Fatty Acid and Aldehyde Composition of Individual Phospholipid Classes of Rabbit Skeletal Muscles Is Related to the Metabolic Type of the Fibre, *Meat Sci. 48*, 225–235.

30. Tschischka, K., Abele, D., and Portner, H.O. (2000) Mitochondrial Oxyconformity and Cold Adaptation in the Polychaete *Nereis pelagica* and the Bivalve *Arctica islandica* from the Baltic and White Seas, *J. Exp. Biol. 203*, 3355–3368.

31. Abele, D., Heise, K., Portner, H.O., and Puntarulo, S. (2002) Temperature-Dependence of Mitochondrial Function and Production of Reactive Oxygen Species in the Intertidal Mud Clam *Mya arenaria*, *J. Exp. Biol. 205*, 1831–1841.

Unusual Minor Nonmethylene-Interrupted Di-, Tri-, and Tetraenoic Fatty Acids in Limpet Gonads

Hideki Kawashima

Bioscience Laboratory, Miyako College Division, Iwate Prefectural University, Iwate 027-0039, Japan

ABSTRACT: Unusual minor nonmethylene-interrupted (NMI) FA have been identified in the lipids of gonads from the limpets *Cellana grata* and *Collisella dorsuosa* by using GC–MS of the combination of their 4,4-dimethyloxazoline derivatives and picolinyl esters. Among 23 NMI unsaturated FA from C_{18} to C_{22} and C_{24} identified in this study, 5,11-nonadecadienoic (5,11-19:2), 7,16-heneicosadienoic (7,16-21:2), 9,15-tetracosadienoic (9,15-24:2), 5,9,15-docosatrienoic (5,9,15-22:3), and 5,9,15-tetracosatrienoic (5,9,15-24:3) acids may not have been reported previously from living organisms. The presence of 5,11,14,17-eicosatetraenonoic (5,11,14,17-20:4) and 7,13,16,19-docosatetraraenenoic (7,13,16,19-22:4) acids as FA components in marine mollusks may be reported here for the first time. In this study, the male and female gonads of both species showed distinct differences in both their composition and proportions of NMI FA. Most NMI FA identified were mainly present in the female gonads of both species, especially in TAG that contained 21 NMI FA.

Paper no. L9732 in *Lipids 40*, 627–630 (June 2005).

Although nonmethylene-interrupted (NMI) FA, especially C_{20} and C_{22} dienoic acids, are frequently present in small amounts in marine gastropods (1,2), only a few studies have been conducted on the occurrence of NMI FA in the gonads of marine gastropods, especially of both male and female gonad lipids, which are attracting increasing interest in the fields of cell development and the reproductive cycle. The FA composition has been compared in male and female gonads of the limpets *Cellana grata* and *Collisella dorsuosa*, which are widely distributed on tidal rocks (3), but the NMI FA were found in only small or trace amounts and so were not identified in the previous study. This paper describes the identification and occurrence of minor NMI FA, including unusual diene and triene isomers in the gonads of these limpets, which may not have been described previously.

EXPERIMENTAL PROCEDURES

Materials, lipid extraction, and preparation of FAME. Cellana grata (shell length = 30 mm) and *C. dorsuosa* (shell length = 30 mm) were obtained in August 2001 from Miyako Bay, Iwate

Prefecture, northern Japan, and were frozen at −20°C. These limpets were transported to our laboratory, where the gonads were immediately removed and placed on ice. The sex was determined by microscopic examination, and the gonads were distinguished as female or male. The gonads of males and females of each species were dissected, suspended in chloroform–methanol (2:1, vol/vol), and then homogenized for 30 s at $891 \times g$ by using an IKA UltraTurrax® T25 Basic (IKA Japan KK, Nara, Japan) to disrupt the cells. Lipids were extracted by using the method of Bligh and Dyer (4). The extracted total lipids were methylated in 14% BF_3/methanol (5).

Argentation TLC and preparation of 4,4-dimethyloxazoline (DMOX) derivatives and picolinyl esters. FAME were fractionated according to the degree of unsaturation by using argentation TLC on 5% (w/w) silver nitrate-impregnated layers of Kieselgel 60G. Derivatives of DMOX were prepared by adding 200 μL of 2-amino-2-methyl-1-propanol to the fractionated FAME in screw-capped tubes. The tubes were flushed for 1 min with N_2, capped, and heated at 185°C overnight. The reaction mixture was cooled and then dissolved in 2 mL of dichloromethane, which was washed three times with 2 mL of distilled water. After drying the organic phase with anhydrous Na_2SO_4, the dichloromethane phase was removed under a steam of N_2. The samples were dissolved in *n*-hexane for analysis by GC–MS. Picolinyl ester derivatives were prepared as described previously (6).

GLC and GC–MS. FAME, DMOX derivatives, and picolinyl esters were analyzed by using GLC with a Shimadzu GC-8A instrument (Shimadzu Seisakusho Co., Kyoto, Japan) equipped with an FID and a SUPELOWAX™-10 capillary column (30 m × 0.25 mm i.d., 0.25 μm film thickness; Supelco Inc., Bellefonte, PA). The column temperature was isothermal at 210°C or at 230°C. The injector and detector temperatures were 250 and 260°C, respectively. GC–MS analyses were recorded at an ionization energy of 70 eV (EI ionization) using a Hewlett-Packard Agilent 5973N MS ChemStation equipped with an OMEGAWAX™-320 capillary column (30 m × 0.32 mm i.d., 0.25 μm film thickness; Supelco Inc.). The carrier gas was helium at a flow rate of 1.5 mL/min. The column temperature was programmed as follows: isothermal at 200°C for 2 min, increased from 200 to 210°C (1°C/min), and maintained at 210°C for 30 min.

Statistical analysis. The procedures were repeated three times for three different male and female sets of gonads and samples for statistical analysis. All samples were analyzed in

triplicate. Data are means ± SD (n = 3). Statistical comparisons among NMI FA were made using Student's t-test. Differences were considered significant at $P < 0.05$.

RESULTS AND DISCUSSION

Table 1 lists 23 NMI FA of *C. grata* and *C. dorsuosa* gonads identified by using GC–MS of their DMOX derivatives. The most interesting characteristic was the presence of NMI dienes and trienes with a 5,9-double bond system; 5,11-nonadeca-dienoic (5,11-19:2), 7,16-heneicosadienoic (7,16-21:2), 9,15-tetracosadienoic (9,15-24:2), 5,9,15-docosatrienoic (5,9,15-22:3), and 5,9,15-tetracosatrienoic (5,9,15-24:3) acids may not have been reported previously from living organisms.

In the diene fraction, the mass spectrum (MS) of the DMOX derivative 5,11-19:2 had a molecular ion at m/z 347. The double bond positions at 5 and 11 were confirmed by a diagnostic ion at m/z 153, a gap of 12 amu between m/z 222 and 234. The structure of 5,11-19:2 was also confirmed by the MS of its picolinyl ester, which had a molecular ion at m/z 385, and the double bond positions were definitely assigned by a gap of 26 amu

between m/z 178 and 204 and between m/z 260 and 286. The MS of the DMOX derivative 7,16-21:2 had a molecular ion at m/z 375 and diagnostic peaks at m/z 168 and 180 for double bond 7, and 292 and 304 for double bond 16. The MS of the DMOX derivative 9,15-24:2 had a molecular ion at m/z 417 and diagnostic peaks at m/z 196 and 208 for double bond 9, and 278 and 290 for double bond 15. GC–MS data for the picolinyl esters confirmed the structure of 7,16-21:2 at m/z 413 [M$^+$] and 206, 232, 330, and 356, and of 9,15-24:2 at m/z 455 [M$^+$] and 234, 260, 316, and 342.

In the triene fraction (Table 1), the MS of DMOX derivatives 5,9,15-22:3 and 5,9,15-24:3 had diagnostic ions at m/z 153, 166, and 180 for a 5,9-double bond system and an interval of 12 amu between ions m/z 276 and 288, indicating a double bond at position 15. The mass spectra of the picolinyl esters 5,9,15-22:3 and 5,9,15-24:3 had a molecular ion at m/z 425 and 453, respectively, the ion at m/z 219 for a 5,9-double bond system, and a peak with a gap of 26 amu between m/z 314 and 340, confirming a double bond at position 15. Similarly, 5,9,17-24:3 was also characterized by using its DMOX derivative and picolinyl ester.

TABLE 1
Characteristic MS Fragments of 4,4-Dimethyloxazoline Derivatives of Nonmethylene-Interrupted FA in the Lipids from Gonads of the Limpets *Cellana grata* and *Collisella dorsuosa*

FA	RT^a (min)	Characteristic fragments (m/z, relative intensity)
Diene		
5,9-18:2	6.39	113 (100), 153 (5), 166 (3), 180 (95), 194 (0.8), 206 (1), 333 (M$^+$, 3)
5,11-18:2	6.54	113 (100), 153 (10), 222 (0.7), 234 (1), 333 (M$^+$, 2)
5,11-19:2^b	8.02	113 (100), 153 (11), 222 (0.5), 234 (1), 347 (M$^+$, 1.5)
5,13-19:2	8.19	113 (100), 153 (11), 250 (1), 262 (2), 347 (M$^+$, 3)
5,11-20:2	10.09	113 (100), 153 (11), 222 (1), 234 (1.5), 361 (M$^+$, 2)
5,13-20:2	10.21	113 (100), 153 (11), 250 (1), 262 (2), 361 (M$^+$, 4)
7,13-20:2	10.32	126 (100), 168 (11), 180 (52), 250 (7), 262 (6), 361 (M$^+$, 5)
7,13-21:2	12.82	126 (100), 168 (8), 180 (49), 250 (3), 262 (4), 375 (M$^+$, 6)
7,15-21:2	13.10	126 (100), 168 (11), 180 (21), 278 (2), 290 (4), 375 (M$^+$, 9)
7,16-21:2^c	13.28	126 (100), 168 (10), 180 (30), 292 (3), 304 (5), 375 (M$^+$, 11)
5,9-22:2	15.85	113 (100), 153 (4), 166 (3), 180 (96), 194 (1), 206 (2), 389 (M$^+$, 3)
7,13-22:2	15.99	126 (100), 168 (10), 180 (62), 250 (4), 262 (5), 389 (M$^+$, 7)
7,15-22:2	16.25	126 (100), 168 (9), 180 (28), 278 (2), 290 (3), 389 (M$^+$, 10)
9,15-22:2	16.45	126 (100), 196 (6), 208 (5), 278 (7), 290 (6), 389 (M$^+$, 13)
5,9-24:2	26.01	113 (100), 153 (6), 166 (5), 180 (85), 194 (1), 206 (2), 417 (M$^+$, 3)
9,15-24:2^d	26.48	126 (100), 196 (5), 208 (3), 278 (3), 290 (6), 417 (M$^+$, 11)
Triene		
5,11,14-20:3	11.24	126 (100), 153 (12), 222 (2), 234 (2), 262 (3), 274 (2), 359 (M$^+$, 3)
5,9,15-22:3^e	17.24	113 (87), 153 (6), 166 (4), 180 (100), 194 (2), 206 (2), 276 (1), 288 (1), 387 (M$^+$, 3)
7,13,16-22:3	18.02	126 (100), 168 (9), 180 (37), 250 (4), 262 (6), 290 (10), 302 (6), 387 (M$^+$, 10)
5,9,15-24:3^f	27.68	113 (91), 153 (5), 166 (4), 180 (100), 194 (1), 206 (2), 276 (1), 288 (1), 415 (M$^+$, 5)
5,9,17-24:3^g	28.11	113 (96), 153 (5), 166 (4), 180 (100), 194 (1), 206 (2), 304 (1), 316 (2), 415 (M$^+$, 4)
Tetraene		
5,11,14,17-20:4	13.02	113 (100), 153 (16), 222 (1), 234 (2), 262 (2), 274 (2), 302 (2), 314 (2), 357 (M$^+$, 3)
7,13,16,19-22:4	21.14	126 (100), 168 (9), 180 (27), 250 (3), 262 (4), 290 (9), 302 (6), 330 (7), 342 (9), 385 (M$^+$, 11)

^{a}Retention times: OMEGAWAX^{TM}-320 capillary column (Supelco, Bellefonte, PA); column temperature, isothermal at 200°C for 2 min, programmed at 1°C/min to 210°C and maintained for an additional 30 min.
^{b}Picolinyl ester: 93 (100), 164 (35), 178 (4), 204 (7), 260 (5), 286 (9), 385 (M$^+$, 22).
^{c}Picolinyl ester: 92 (100), 164 (70), 206 (7), 232 (5), 330 (4), 356 (6), 413 (M$^+$, 39).
^{d}Picolinyl ester: 92 (100), 164 (66), 234 (8), 260 (6), 316 (4), 342 (12), 455 (M$^+$, 30).
^{e}Picolinyl ester: 92 (100), 164 (35), 178 (4), 204 (2), 219 (49), 232 (7), 258 (4), 314 (6), 340 (4), 425 (M$^+$, 24).
^{f}Picolinyl ester: 92 (100), 164 (64), 178 (3), 204 (1), 219 (45), 232 (6), 258 (5), 314 (3), 340 (3), 453 (M$^+$, 20).
^{g}Picolinyl ester: 92 (100), 164 (44), 178 (4), 204 (2), 219 (41), 232 (4), 258 (6), 342 (5), 368 (4), 453 (M$^+$, 23).

In the tetraene fraction (Table 1), the MS of the DMOX derivatives 5,11,14,17-20:4 and 7,13,16,19-22:4 showed characteristic fragments; their spectra agreed with the data from other studies (7). Although 5,11,14,17-20:4 has usually been found in some marine bivalves (8) and seed oils from gymnosperms (9), 7,13,16,19-22:4 has been found only in mammalian cells (10,11).

To clarify the distribution of NMI FA in the male and female gonads of *C. grata* and *C. dorsuosa*, the FA and their positional isomers in TAG and polar lipids (PL) were analyzed to compare these gonads (Table 2). The positional isomers of NMI dienes C_{18} to C_{22} and trienes C_{22} and C_{24} were widely present in both species. Most NMI FA identified were mainly detected in the female gonads of both species, especially in the TAG of both species that contained 21 NMI FA. Among these NMI FA, the positional isomers of 24:3 were found only in the female gonads of both species. In this study the male and female gonads of both species showed distinct differences in both their composition and proportions of NMI FA. The proportions of 5,9-24:2 and 5,9,17-24:3 showed a statistically significant difference between the male and female gonads of both species. An interesting result was that the proportions of 5,9-18:2, 5,9-22:2, 5,9-24:2, 5,9,15-24:3, and 5,9,17-24:3 were higher in the PL of the female gonad of both species than in the female TAG,

and that both female gonads had the highest content of 5,9-22:2. These differences between the TAG and PL of female gonads of both species were statistical significant. The findings of this study suggest that the occurrence of 5,9-24:2 and 5,9,17-24:3 is a sexual difference and that female gonads have more specific NMI FA components of structural lipids (PL) than storage lipids (TAG). However, the NMI FA composition results in limpet gonads also might be related to the effects of seasonal variations or the reproductive cycle or both. Some NMI FA with a 5,9-double bond system could play an important role in female reproductive physiology because of their exclusive presence in the PL of female gonads and their unique structure. A clarification of the physiological role of NMI FA in limpet gonads will be the subject of future study.

Although both 5,9-24:2 and 5,9,17-24:3 are found in each of the two sponges *Hymeniacidon sanguinea* and *Dysidea fragilis* (12,13), the presence of 5,9,15-24:3 may not have been reported previously from any living organism. The NMI diene FA 5,9-18:2, 5,9-22:2, and 5,9-24:22 are found in the phospholipids of the Caribbean sponges *Plakortis halichondroides* and *Calyx podatypa* (14,15) and in the phospholipids of the anemone *Condylactis gigantea* and the zoanthid *Palythoa caribaeorum* (16). In contrast, 5,9-18:2 is also found in terrestrial seed lipids as well as in some marine sponge lipids

TABLE 2
Distribution of Nonmethylene-Interrupted (NMI) FA in Gonads of the Limpets *Cellana grata* and *Collisella dorsuosa*[a]

	Male gonad				Female gonad			
	TAG		Polar lipids		TAG		Polar lipids	
FA	*C. grata*	*C. dorsuosa*	*C. grata*	*C. dorsuosa*	*C. grata*	*C. dorsuosa*	*C. grata*	*C. dorsuosa*
5,9-18:2	Trace[a]	$0.07 \pm 0.01^{\alpha}$	—[b]	$0.03 \pm 0.01^{c,\alpha}$	$0.05 \pm 0.01^{a,A}$	0.06 ± 0.01^{B}	$0.38 \pm 0.03^{b,A}$	$0.18 \pm 0.02^{c,B}$
5,11-18:2	Trace[α]	Trace	$0.34 \pm 0.01^{\alpha}$	—	Trace	Trace	—	—
5,11-19:2	Trace	—	Trace	Trace	—	—	—	—
5,13-19:2	Trace	—	Trace	Trace	Trace	—	—	—
5,11-20:2	$0.22 \pm 0.01^{a,\alpha}$	$0.64 \pm 0.01^{b,\alpha}$	$0.37 \pm 0.01^{c,\alpha}$	$0.40 \pm 0.03^{\beta}$	$0.27 \pm 0.02^{a,A}$	$0.56 \pm 0.02^{b,B}$	$0.51 \pm 0.02^{c,A}$	0.45 ± 0.02^{B}
5,13-20:2	$0.09 \pm 0.02^{a,\alpha}$	$0.48 \pm 0.01^{b,\beta}$	Trace[c,α]	$0.32 \pm 0.01^{d,\beta}$	Trace[a,A]	$0.33 \pm 0.02^{b,B}$	$0.15 \pm 0.02^{c,A}$	$0.25 \pm 0.02^{d,B}$
7,13-20:2	$0.69 \pm 0.02^{a,\alpha}$	$0.73 \pm 0.02^{b,\beta}$	$0.48 \pm 0.02^{c,\alpha}$	$0.25 \pm 0.01^{d,\beta}$	$0.61 \pm 0.02^{a,A}$	$0.80 \pm 0.02^{b,B}$	$0.25 \pm 0.02^{c,A}$	$0.21 \pm 0.02^{d,B}$
7,13-21:2	—	$0.09 \pm 0.02^{a,\alpha}$	Trace	Trace[α]	Trace	Trace[a]	Trace	Trace
7,15-21:2	—	Trace	Trace	—	Trace	Trace	Trace	—
7,16-21:2	—	—	—	—	Trace	Trace	Trace	—
5,9-22:2	Trace[a]	Trace	—[b]	—[c]	$0.02 \pm 0.01^{a,A}$	0.02 ± 0.0^{B}	$2.30 \pm 0.05^{b,A}$	$2.16 \pm 0.02^{c,B}$
7,13-22:2	$0.35 \pm 0.01^{a,\alpha}$	$0.98 \pm 0.02^{b,\beta}$	$0.30 \pm 0.01^{c,\alpha}$	$0.74 \pm 0.03^{d,\beta}$	$1.37 \pm 0.03^{a,A}$	$1.11 \pm 0.04^{b,B}$	Trace[c,A]	Trace[d,B]
7,15-22:2	$0.06 \pm 0.01^{a,\alpha}$	$0.85 \pm 0.03^{b,\beta}$	$0.08 \pm 0.01^{c,\alpha}$	$0.36 \pm 0.03^{d,\beta}$	$0.47 \pm 0.01^{a,A}$	$1.03 \pm 0.02^{b,B}$	$0.25 \pm 0.02^{c,A}$	$0.65 \pm 0.02^{d,B}$
9,15-22:2	0.02 ± 0.0	0.02 ± 0.0	—	Trace	—	0.02 ± 0.0	—	—
5,9-24:2	Trace[a]	Trace[b]	Trace[c]	—[d]	$0.09 \pm 0.01^{a,A}$	$0.10 \pm 0.03^{b,B}$	$0.21 \pm 0.02^{c,A}$	$0.15 \pm 0.01^{d,B}$
9,15-24:2	—[a]	Trace[b]	—	—	$0.06 \pm 0.01^{a,A}$	$0.06 \pm 0.01^{b,B}$	—[A]	—[B]
5,11,14-20:3	$0.02 \pm 0.01^{a,\alpha}$	$0.50 \pm 0.02^{b,\beta}$	$0.15 \pm 0.01^{c,\alpha}$	$0.38 \pm 0.02^{d,\beta}$	$0.14 \pm 0.01^{a,A}$	$0.33 \pm 0.03^{b,B}$	$0.41 \pm 0.02^{c,A}$	$0.59 \pm 0.02^{d,B}$
5,9,15-22:3	—	$0.03 \pm 0.01^{a,\alpha}$	Trace[b]	—[c,α]	Trace[A]	$0.07 \pm 0.02^{a,B}$	$0.02 \pm 0.01^{b,A}$	$0.19 \pm 0.02^{c,B}$
7,13,16-22:3	$0.18 \pm 0.01^{a,\alpha}$	$0.92 \pm 0.03^{b,\beta}$	$0.23 \pm 0.02^{c,\alpha}$	$0.26 \pm 0.04^{\beta}$	$0.77 \pm 0.02^{a,A}$	$0.16 \pm 0.01^{b,B}$	$0.37 \pm 0.02^{c,A}$	0.30 ± 0.04^{B}
5,9,15-24:3	—	—[a]	—[b]	—[c]	0.03 ± 0.0^{A}	$0.14 \pm 0.02^{a,B}$	$0.74 \pm 0.02^{b,A}$	$0.80 \pm 0.02^{c,B}$
5,9,17-24:3	—[a]	—[b]	—[c]	—[d]	$0.04 \pm 0.01^{a,A}$	$0.06 \pm 0.01^{b,B}$	$0.25 \pm 0.01^{c,A}$	$0.49 \pm 0.01^{d,B}$
5,11,14,17-20:4	Trace[a,α]	0.02 ± 0.01^{b}	$0.59 \pm 0.01^{c,\alpha}$	0.02 ± 0.0	$1.00 \pm 0.06^{a,A}$	$1.07 \pm 0.02^{b,B}$	$0.30 \pm 0.03^{c,A}$	Trace[B]
7,13,16,19-22:4	Trace[a,α]	$0.40 \pm 0.01^{\beta}$	$0.52 \pm 0.02^{b,\alpha}$	$0.32 \pm 0.01^{c,\beta}$	$0.38 \pm 0.02^{a,A}$	0.43 ± 0.03^{B}	Trace[b,A]	$0.16 \pm 0.02^{c,B}$
Total NMI FA	1.63 ± 0.02	5.73 ± 0.02	3.06 ± 0.05	3.09 ± 0.03	5.30 ± 0.05	6.31 ± 0.10	6.11 ± 0.02	6.57 ± 0.05

[a]Values are expressed as mean ± SD ($n = 3$). For statistical analysis, "Trace" and "not detected" (—) were set as 0.01 and 0, respectively. Means with the same lowercase superscript letters are significantly different between sexes (Student's *t*-test, $P < 0.05$), those with the same capital letters are significantly different (Student's *t*-test, $P < 0.05$) between the TAG and polar lipid fractions of female gonads, and those with the same lowercase Greek superscript letters are significantly different (Student's *t*-test, $P < 0.05$) between the TAG and polar lipid fractions of male gonads. Trace, <0.01%; —, not detected.

(9,15,16). Therefore, the long-chain NMI FA 5,9-22:2, 5,9-24:2, 5,9,15-24:3, and 5,9,17-24:3 detected in this study might be biosynthesized by the limpet itself or by some of its symbiotic organisms. These dienes with 5,9 double bonds might be derived from the corresponding 9-monoenoic FA by $\Delta 5$ desaturation. On the other hand, the unusual isomers 5,9,15-24:3 and 5,9,17-24:3 might be derived from the typical NMI dienes 7,13-22:2 and 7,15-22:2, respectively, by chain elongation and subsequent $\Delta 5$ desaturation. In contrast, some NMI FA detected in these gonads might be derived from the diet or the result of marine food web effects, or both, because of their very small amounts. Thus, further research is needed to confirm whether the occurrence of NMI FA in limpet gonads is a consequence of intake from the marine food chain or *de novo* synthesis or both.

ACKNOWLEDGMENTS

REFERENCES

1. Paradis, M., and Ackman, R.G. (1975) Occurrence and Chemical Structure of Nonmethylene-Interrupted Dienoic Fatty Acids in American Oyster *Crassostrea virginica*, *Lipids 10*, 12–16.
2. Paradis, M., and Ackman, R.G. (1977) Potential for Employing the Distribution of Anomalous Non-Methylene-Interrupted Dienoic Fatty Acids in Several Marine Invertebrates as Part of Food Web Studies, *Lipids 12,* 170–176.
3. Kawashima, H., Ohnishi, M., and Uchiyama, H. (2002) Sexual Differences in Gonad Fatty Acid Compositions in Dominant Limpets Species from the Sanriku Coast in Northern Japan, *J. Oleo Sci. 51*, 503–508.
4. Bligh, E.G., and Dyer, A. (1959) A Rapid Method of Total Lipid Extraction and Purification, *Can. J. Biochem. Physiol. 37*, 911–917.
5. Morrison, W.R., and Smith, L.M. (1964) Preparation of Fatty Acid Methyl Esters and Dimethylacetals from Lipids with Boron Fluoride–Methanol, *J. Lipid Res. 5*, 600–608.
6. Kawashima, H., and Ohnishi, M. (2004) Identification of Minor Fatty Acids and Various Nonmethylene-Interrupted Diene Isomers in Mantle, Muscle, and Viscera of the Marine Bivalve *Megangulus zyonoensis*, *Lipids 39*, 256–271.
7. Scottish Crop Research Institute, http://www.lipidlibrary.co.uk/masspec.html (accessed March 2005).
8. Takagi, T., Itabashi, Y., and Kaneniwa, M. (1986) Fatty Acid Composition of Bivalves from Japanese Waters, *J. Jpn. Oil Chem. Soc. 35*, 517–521.
9. Takagi, T., and Itabashi, Y. (1982) *cis*-5-Olefinic Unusual Fatty Acids in Seed Lipids of Gymnospermae and Their Distribution in Triglycerols, *Lipids 17*, 716–723.
10. Schenck, P.A., Rakoff, H., and Emken, E. A. (1996) $\Delta 8$ Desaturation *in vivo* of Deuterated Eicosatrienoic Acid by Mouse Liver, *Lipids 31*, 593–600.
11. Dhopeshwarkar, G.A., and Subramanian, C. (1976) Biosynthesis of Polyunsaturated Fatty Acid in the Developing Brain: II. Metabolic Transformations of Intracranially Administered [3-^{14}C]-Eicosatrienoic Acid, Evidence for Lack of $\Delta 8$ Desaturase, *Lipids 11*, 689–692.
12. Nechev, J., Christie, W.W., Robaina, R., De Diego, R., Popov, S., and Stefanov, K. (2004) Chemical Composition of the Sponge *Hymeniacidon sanguinea* from the Canary Islands, *Comp. Biochem. Physiol. A 137*, 365–374.
13. Christie, W.W., Brechany, E.Y., Stefanov, K., and Popov, S. (1992) The Fatty Acids of the Sponge from *Dysidea fragilis* from the Black Sea, *Lipids 27*, 640–644.
14. Carballeira, N.M., and Shalabi, F. (1990) Identification of Naturally Occurring *trans*, *trans* $\Delta 5,9$ Fatty Acids from the Sponge *Plakortis halichondroides*, *Lipids 25*, 835–840.
15. Carballeria, N.M., Pagán, M., and Rodríguez, A.D. (1998) Identification and Total Synthesis of Novel Fatty Acids from the Caribbean Sponge *Calyx podatypa*, *J. Nat. Prod. 61*, 1049–1052.
16. Carballeria, N.M., and Morayma, R. (1995) Identification of a New 6-Bromo-5,9-eicosadienoic Acid from Anemone *Condylactis gigantea* and the Zoanthid *Palythoa caribaeorum*, *J. Nat. Prod. 58*, 1689–1694.

Dietary Nucleotides Do Not Alter Erythrocyte Long-Chain Polyunsaturated Fatty Acids in Formula-Fed Term Infants

Robert A. Gibson[a,b], Joanna S. Hawkes[a], and Maria Makrides[b,*]

[a]Child Health Research Institute, Flinders Medical Centre and Flinders University, Bedford Park, South Australia 5042, and [b]Child Health Research Institute and University of Adelaide Department of Paediatrics, Women's and Children's Hospital (WCH), North Adelaide, South Australia 5006, Australia

ABSTRACT: There have been conflicting reports regarding the effectiveness of dietary nucleotides (NT) to regulate tissue desaturases and hence stimulate accumulation of both n-6 and n-3 long-chain polyunsaturated fatty acids (LCPUFA). The aim of this study was to examine the effect of NT-supplemented cow's milk-based formula on erythrocyte phospholipid FA status in a large randomized controlled trial involving a well-nourished infant population born at term. Formula-fed infants were allocated to control formula with an innate level of NT at 10 mg/L ($n = 102$), or formula fortified with NT at 34 mg/L ($n = 98$). A parallel group of breastfed infants was included as a reference. Peripheral blood samples were collected by venipuncture at 7 mon of age and erythrocyte phospholipid FA determined by capillary GC. Erythrocyte LCPUFA levels did not differ between the NT-supplemented and control formula groups and were reduced in both groups compared with breastfed infants. We conclude that there is no induction of LCPUFA accumulation in erythrocyte phospholipids of term, formula-fed infants following 7 mon of NT supplementation.

Paper no. L9748 in *Lipids 40*, 631–634 (June 2005).

Human milk contains higher amounts of nonprotein nitrogen as nucleotides (NT), nucleosides, and nucleic acids compared with bovine milk from which most infant formulas are manufactured (1,2). NT in human milk are thought to play an important role in aspects of cellular function and metabolism, including growth and maturation of the gastrointestinal tract and the development of infant immunity (1,3). Recent changes in the composition of some infant formulas marketed throughout the world have resulted in the addition of NT in an attempt to mimic the typical composition of human milk. Some randomized controlled trials (RCT) involving formula-fed infants have reported beneficial effects of NT supplementation on various components of the immune system (4–6), the incidence of diarrhea (7), intestinal microflora (8), and growth in infants born small for gestational age (9). An area of controversy in NT nutrition relates to their ability to modulate the accumulation of long-chain PUFA (LCPUFA), such as DHA (22:6n-3) and arachidonic acid (20:4n-6) (10,11). Whereas reports from one laboratory suggest beneficial effects, subsequent studies involving preterm (12) or low-birth-weight infants (13) have been unable to confirm the LCPUFA-enhancing effects of supplemental NT compared with unsupplemented formula. In a more recent study designed primarily to examine the effect of added NT on iron status of term infants, there was also no significant difference between the NT-supplemented group and other formula groups in erythrocyte FA composition at both time points following commencement of feeding (4 and 6 mon of age) (14).

LCPUFA have been implicated as factors affecting growth and development of term infants (15). Healthy term infants randomly allocated to LCPUFA-supplemented formula have been shown to have better LCPUFA tissue status, and in some cases, improved indices of neural function compared with unsupplemented infants (16–18). Therefore, any interaction between NT and LCPUFA may be of importance in the nutrition of infants.

The purpose of this study was to investigate the effect of term infant formula supplemented with NT as marketed in Australia and Europe (33.5 mg/L 5'-monophosphates; 5 mg/100 kcal) on erythrocyte phospholipid LCPUFA status in comparison with unsupplemented formula. Infants were enrolled in a large RCT conducted with primary outcome measures focused on growth and biochemical indices of immune function (19). Secondary outcomes included erythrocyte phospholipid FA at 7 mon, which are reported here.

EXPERIMENTAL PROCEDURES

Subjects. Mothers with eligible infants were recruited from the postnatal ward at the Women's and Children's Hospital (WCH), Adelaide according to the protocol approved by the WCH Research Ethics Committee. Infants were eligible if they were born at term (≥37 wk gestation) and had a birth weight ≥2500 g and were excluded if they had major congenital deformities or illnesses, confirmed infection in the neonatal period requiring antibiotic therapy, or if their mother had diabetes requiring insulin during pregnancy. Infants allocated to the formula feeding groups had mothers who had decided

*To whom correspondence should be addressed at Child Health Research Institute, Women's and Children's Hospital, 72 King William Rd., North Adelaide, South Australia 5006. E-mail: makridesm@mail.wch.sa.gov.au

Abbreviations: ALA, α-linolenic acid; LA, linoleic acid; LCPUFA, long-chain PUFA; NT, nucleotide; RCT, randomized controlled trial.

to exclusively formula-feed from birth. Mothers who intended to breastfeed for at least 7 mon were approached for enrollment into the reference breastfed group.

Randomization and blinding. Formula-fed infants were randomly assigned to one of four masked formula codes corresponding to two different formulas. Assignment to the infant's feeding regimen was by sequentially numbered, opaque, sealed envelopes. Trial participants and study personnel had no knowledge of the next assignment prior to obtaining consent.

Treatments. Infants in the control group received standard whey-adapted, cow's-milk protein-based S26 (Wyeth Nutrition) in powder form to provide 67 kcal/100 mL and an innate level of NT at 10 mg/L (1.5 mg/100 kcal). Infants in the treatment group (NT+) received the same whey-adapted, cow's-milk protein-based S26 in powder form to provide 67 kcal/100 mL and fortified with cytidine monophosphate (CMP) at 17.3 mg/L (2.58 mg/100 kcal), uridine monophosphate (UMP) at 6.6 mg/L (0.99 mg/100 kcal), adenosine monophosphate (AMP) at 4.4 mg/L (0.66 mg/100 kcal), inosine monophosphate (IMP) at 3.1 mg/L (0.46 mg/100 kcal), and guanosine monophosphate (GMP) at 2.2 mg/L (0.33 mg/100 kcal). The composition of fat blends used to manufacture both the control and NT+ formulas was randomized palm olein (36% of total blend), high-oleic sunflower (21%), coconut (21%), soy (21%), and lecithin (0.98%). Both test formulas contained linoleic acid (LA, 16.2% of total FA) and α-linolenic acid (ALA, 1.5% of total FA) but no added LCPUFA (Wyeth Nutrition).

Mothers were asked to feed their infant their assigned study formula as the only milk source until 7 mon of age. For breastfed infants, breastfeeding was strongly encouraged for the entire 7-mon feeding period. The use of solid foods was strongly discouraged during the first 4 mon of the study. Intake of non-study milks, juice, or solid foods was recorded for all infants as part of monthly telephone contact throughout the study. Egg, meat, chicken, and fish were considered likely to contribute some LCPUFA to the diet.

Laboratory assessments. Blood samples were taken by venipuncture at 31.9 ± 1.6 wk of age for measurement of erythrocyte FA composition. Plasma and erythrocytes were separated by centrifugation at $690 \times g$ for 5 min at room temperature. Plasma samples were used for measurement of immune responses as reported elsewhere (19). Erythrocyte FAME were prepared, separated, and analyzed as described previously (20). Briefly, erythrocyte lipids were extracted with chloroform/propanol on the day of blood collection. The phospholipid fractions were separated by TLC, methylated, and quantified using a Hewlett-Packard 6890 gas chromatograph and identified based on the retention time of authentic lipid standards (Nu-Chek-Prep Inc., Elysian, MN).

Sample size and statistics. To cover all sample size estimates required for the primary outcome measures associated with this RCT, we aimed for 70 infants per group to complete the trial (19). We therefore enrolled approximately 100 infants per group. This allowed for 30% loss due to withdrawals, low compliance, and incomplete blood collections. Seventy infants per formula group enabled us to detect a minimum difference of 0.15% total phospholipid DHA (SD 0.3) between NT-supplemented and control formula-fed infants with 84% power and an α of 0.05. This level of difference is unlikely to be of any clinical relevance (21), and a statistical analysis supporting the null hypothesis would indicate equivalence of NT-supplemented and control formula in terms of LCPUFA status.

The effect of feeding formula with or without NT on erythrocyte FA composition was assessed on an intention-to-treat basis. Differences between the randomized dietary groups were analyzed by Independent Samples T Test. Secondary analyses included the comparison between the two formula-fed groups and the breastfed reference group using one-way ANOVA with *post hoc* analysis using Bonferroni corrections and analysis including only the infants who complied with the feeding protocol (≥80% of all milk feeds were study formula or breast milk). All analyses were completed using SPSS for Windows 10.0 (SPSS Inc., Chicago, IL).

RESULTS

Characteristics of trial participants. Two hundred mothers of formula-fed infants agreed to participate in the study and were allocated either to the control group ($n = 102$) or to the NT+ group ($n = 98$). Blood samples suitable for analysis of FA status were collected from 136 of 200 (68%) formula-fed infants at 7 mon of age. More than 90% (66 of 69 in the control group and 63 of 67 NT+ group) of all infants were receiving at least 80% of their milk feeds as study formula at the time of blood collection. One hundred twenty-five infants were enrolled in the breastfed reference group, and analysis of erythrocyte FA was completed on 96 (77%) infants at 7 mon of age. As expected, the number of infants receiving ≥80% of milk feeds as breast milk decreased throughout the study to 59% (57 of 96) at the end of the 7-mon feeding period.

Introduction of solids. Solids were introduced into the diet of 71% (97 of 136) of formula-fed infants by 4 mon of age. Only 6% of foods were likely to contribute to the LCPUFA intake of those infants receiving solids, and there was no difference in the rate of introduction of weaning foods or type of weaning foods between the treatment groups. Fewer infants in the breastfed reference group had received solids by 4 mon of age (56 of 96, 58%), and the proportion of foods likely to contribute some LCPUFA to the diet was 7% (7 of 96). By 7 mon of age, all infants in the study were receiving weaning foods and there was no difference between the groups regarding the proportion of foods likely to contribute LCPUFA to the diet (Control, 44 of 69; NT+, 41 of 67; breastfed, 62 of 96).

FA composition. Dietary NT had no effect on the LCPUFA status of erythrocyte membranes of formula-fed infants regardless of whether the comparison was on an intention-to-treat basis (Table 1) or only included the infants who were compliant with the feeding protocol (data not shown). The level of n-3 LCPUFA present in erythrocyte membrane phospholipids was higher in the breastfed group whereas monounsaturated FA and total n-6 FA were lower compared with both groups of infants receiving formula.

TABLE 1
Comparison of Erythrocyte Phospholipid FA from Control and NT-Supplemented Formula-Fed Infants at 7 mon of Age[a,b]

FA	Control formula (*n* = 69)	NT+ formula (*n* = 67)	Reference breastfed group[b] (*n* = 96)
Total saturates	42.0 ± 0.1	42.0 ± 0.1	42.4 ± 0.1
Total monounsaturates	18.2 ± 0.1	18.2 ± 0.1	17.2 ± 0.1
18:2n-6 (LA)	12.8 ± 0.1	12.8 ± 0.1	10.1 ± 0.2
20:3n-6 (DGLA)	1.9 ± 0.04	1.9 ± 0.1	1.6 ± 0.03
20:4n-6 (AA)	14.5 ± 0.1	14.4 ± 0.1	15.3 ± 0.1
22:4n-6	4.7 ± 0.04	4.7 ± 0.05	3.7 ± 0.06
Total n-6	35.4 ± 0.1	35.3 ± 0.2	31.8 ± 0.2
20:5n-3 (EPA)	0.2 ± 0.01	0.2 ± 0.01	0.4 ± 0.02
22:5n-3 (DPA)	1.6 ± 0.03	1.6 ± 0.03	2.2 ± 0.05
22:6n-3 (DHA)	2.1 ± 0.05	2.1 ± 0.04	4.9 ± 0.18
Total n-3	3.9 ± 0.07	4.0 ± 0.07	7.8 ± 0.2

[a]Mean ± SEM, % of total FA. LA, linoleic acid; DGLA, di-homo-γ-linoleic acid; AA, arachidonic acid; DPA, docosapentaenoic acid. Control, unsupplemented formula; NT+, nucleotide-supplemented formula.
[b]Differences between the randomized treatment groups were analyzed by Independent Samples T Test. There were no significant differences between the two randomized groups for any of the variables described. Data were also analyzed by ANOVA with *post hoc* analysis using Bonferroni corrections on an intention-to-treat basis. Breastfed infants were different from both formula-fed groups for all of the FA variables described ($P < 0.01$).

DISCUSSION

This is the largest RCT to rigorously test the effect of dietary NT on FA status in term infants. Our trial showed that supplementation of infant formula with 33.5 mg/L (5 mg/100 kcal) free NT did not influence the FA status of term infants at 7 mon of age. Our results support the findings of Hernell and Lönnerdal (14), Woltil *et al.* (13), and Axelsson *et al.* (12) but contrast with the frequently cited studies from Spain suggesting that dietary NT may play a role in enhancing enzymes involved in the conversion of 18-carbon PUFA precursors to their longer-chain derivatives (10,11,22). The Spanish studies report higher levels of LCPUFA in erythrocyte phospholipids, plasma lipids, and plasma phospholipids in the NT-supplemented group of infants compared with unsupplemented infants in the first months of life. In addition, DeLucchi *et al.* and Gil *et al.* reported that, in general, the pattern of LCPUFA in tissues from NT-supplemented infants was more like those of breastfed infants, as dietary NT appeared to stimulate accumulation of both n-6 and n-3 LCPUFA (10,11). Infants in our study were supplemented with a higher dose of NT (33.5 mg/L compared with 11.7 mg/L) for a longer period of time (7 mon compared with 1 mon), and group sizes were considerably larger (67–69 per group compared with 19 per group). Furthermore, the values seen in our current trial concur with those reported for formula-fed and breastfed infants in other studies (21,23). It would seem likely that the conditions under which our study was conducted would lead to measurable effects on LCPUFA status if dietary NT contribute to augmentation of LCPUFA synthesis.

There are no food composition tables that document NT content of Australian foods. Therefore, we have considered the age of introduction of solid foods and the proportion likely to contribute some LCPUFA and NT to the diet. There were no differences between the treatment groups in the timing or type of weaning foods introduced, thus it is unlikely that dietary intake of weaning foods is a confounding factor in this study. In fact, it appears that even against a background of increasing amounts of foods containing NT and LCPUFA, breastfed infants still maintain significantly higher levels of LCPUFA. Although we cannot exclude the possibility that NT supplementation may have an effect on the FA status of formula-fed infants at an earlier age, such an effect would be transitory in nature and may be of little clinical benefit.

We have shown in another study that infants in this age group have the capacity to alter their erythrocyte LCPUFA status in response to diet (21). In that study we showed that reducing the LA/ALA ratio from 10:1 to 5:1 (but keeping other constituents equal) resulted in an enhancement of EPA, docosapentaenoic acid, and DHA levels although not to the levels seen in breastfed infants. Thus, we are confident that we have the ability to detect small changes in erythrocyte LCPUFA status when they are present. The current study was larger than our earlier report (21).

In summary, in a pragmatic trial that considers usual and recommended feeding practices regarding the introduction of solids, the use of NT-supplemented formula does not change erythrocyte LCPUFA levels in late infancy.

Trust and a Senior Research Fellowship from the National Health and Medical Research Council of Australia.

REFERENCES

1. Carver, J.D. (1999) Dietary Nucleotides: Effects on the Immune and Gastrointestinal Systems, *Acta Paediatr. Suppl. 430*, 83–88.
2. Leach, J.L., Baxter, J.H., Molitor, B.E., Ramstack, M.B., and Masor, M.L. (1995) Total Potentially Available Nucleosides of Human Milk by Stage of Lactation, *Am. J. Clin. Nutr. 61*, 1224–1230.
3. Yu,V.Y. (2002) Scientific Rationale and Benefits of Nucleotide Supplementation of Infant Formula, *J. Paediatr. Child Health 38*, 543–549.
4. Carver, J.D., Pimentel, B., Cox, W.I., and Barness, L.A. (1991) Dietary Nucleotide Effects upon Immune Function in Infants, *Pediatrics 88*, 359–363.
5. Pickering, L.K., Granoff, D.M., Erickson, J.R., Masor, M.L., Cordle, C.T., Schaller, J.P., Winship, T.R., Paule, C.L., and Hilty, M.D. (1998) Modulation of the Immune System by Human Milk and Infant Formula Containing Nucleotides, *Pediatrics 101*, 242–249.
6. Schaller, J.P., Kuchan, M.J., Thomas, D.L., Cordle, C.T., Winship, T.R., Buck, R.H., Baggs, G.E., and Wheeler, J.G. (2004) Effect of Dietary Ribonucleotides on Infant Immune Status. Part 1: Humoral Responses, *Pediatr. Res. 56*, 883–890.
7. Yau, K.I., Huang, C.B., Chen, W., Chen, S.J., Chou, Y.H., Huang, F.Y., Kua, K.E., Chen, N., McCue, M., Alarcon, P.A., *et al.* (2003) Effect of Nucleotides on Diarrhea and Immune Responses in Healthy Term Infants in Taiwan, *J. Pediatr. Gastroenterol. Nutr. 36*, 37–43.
8. Gil, A., Corral, E., Martinez, A., and Molina, J.A. (1986) Effects of the Addition of Nucleotides to an Adapted Milk Formula on the Microbial Pattern of Faeces in At-Term Newborn Infants, *J. Clin. Nutr. Gastroenterol,* 127–132.
9. Cosgrove, M., Davies, D.P., and Jenkins, H.R. (1996) Nucleotide Supplementation and the Growth of Term Small for Gestational Age Infants, *Arch. Dis. Child. 74*, F122.
10. DeLucchi, C., Pita, M.L., Faus, M.J., Molina, J.A., Uauy, R., and Gil, A. (1987) Effects of Dietary Nucleotides on the Fatty Acid Composition of Erythrocyte Membrane Lipids in Term Infants, *J. Pediatr. Gastroenterol. Nutr. 6*, 568–574.
11. Gil, A., Lozano, E., De-Lucchi, C., Maldonado, J., Molina, J.A., and Pita, M. (1988) Changes in the Fatty Acid Profiles of Plasma Lipid Fractions Induced by Dietary Nucleotides in Infants Born at Term, *Eur. J. Clin. Nutr. 42*, 473–481.
12. Axelsson, I., Flodmark, C.E., Räihä, N., Tacconi, M., Visentin, M., Minoli, I., Moro, G., and Warm, A. (1997) The Influence of Dietary Nucleotides on Erythrocyte Membrane Fatty Acids and Plasma Lipids in Preterm Infants, *Acta Paediatr. 86*, 539–544.
13. Woltil, H.A., van Beusekom, C.M., Siemensma, A.D., Muskiet, F.A.J., and Okken, A. (1995) Erythrocyte and Plasma Cholesterol Ester Long Chain Polyunsaturated Fatty Acids of Low-Birth-Weight Babies Fed Preterm Formula With And Without Ribonucleotides: Comparison with Human Milk, *Am. J. Clin. Nutr. 62*, 943–949.
14. Hernell, O., and Lonnerdal, B. (2002) Iron Status of Infants Fed Low-Iron Formula: No Effect of Added Bovine Lactoferrin or Nucleotides, *Am. J. Clin. Nutr. 76*, 858–864.
15. Gibson, R.A., and Makrides, M. (2000) n-3 Polyunsaturated Fatty Acid Requirements of Term Infants, *Am. J. Clin. Nutr. 71*, 251S–255S.
16. Makrides, M., Neumann, M., Simmer, K., Pater, J., and Gibson, R.A. (1995) Are Long-Chain Polyunsaturated Fatty Acids Essential Nutrients in Infancy? *Lancet 345*, 1463–1468.
17. Willatts, P., Forsyth, J.S., DiModugno, M.K., Varma, S., and Colvin, M. (1998) Effect of Long-Chain Polyunsaturated Fatty Acids in Infant Formula on Problem Solving at 10 Months of Age, *Lancet 352*, 688–691.
18. Birch, E.E., Garfield, S., Hoffman, D.R., Uauy, R., and Birch, D.G. (2000) A Randomized Controlled Trial of Early Dietary Supply of Long-Chain Polyunsaturated Fatty Acids and Mental Development in Term Infants, *Dev. Med. Child Neurol. 42*, 174–181.
19. Makrides, M., Hawkes, J., Roberton, D., and Gibson, R. (2004) The Effect of Dietary Nucleotide Supplementation on Growth and Immune Function in Term Infants: A Randomised Controlled Trial, *Asia Pac. J. Clin. Nutr. 13*, S58.
20. Makrides, M., Neumann, M.A., and Gibson, R.A. (1996) Effect of Maternal Docosahexanoic Acid (DHA) Supplementation on Breast Milk Composition, *Eur. J. Clin. Nutr. 50*, 352–357.
21. Makrides, M., Neumann, M.A., Jeffrey, B., Lien, E.L., and Gibson, R.A. (2000) A Randomized Trial of Different Ratios of Linoleic to α-Linolenic Acid in the Diet of Term Infants: Effects on Visual Function and Growth, *Am. J. Clin. Nutr. 71*, 120–129.
22. Pita, M.L., Fernandez, M.R., De Lucchi, C., Medina, A., Martinez Valverde, A., Uauy, R., and Gil, A. (1988) Changes in the Fatty Acids Pattern of Red Blood Cell Phospholipids Induced by Type of Milk, Dietary Nucleotide Supplementation, and Postnatal Age in Preterm Infants, *J. Pediatr. Gastroenterol. Nutr. 7*, 740–747.
23. Makrides, M., Neumann, M.A., Simmer, K., and Gibson, R.A. (1999) Dietary Long Chain Polyunsaturated Fatty Acids (LC-PUFA) Do Not Influence Growth of Term Infants: A Randomized Clinical Trial, *Pediatrics 104*, 468–475.

Comparison of Effects of U18666A and Enantiomeric U18666A on Sterol Synthesis and Induction of Apoptosis

Richard J. Cenedella[a],*, Patricia S. Sexton[a],
Kathiresan Krishnan[b], and Douglas F. Covey[b]

[a]Department of Biochemistry, Kirksville College of Osteopathic Medicine, Kirksville, Missouri 63501 and [b]Department of
Molecular Biology and Pharmacology, Washington University School of Medicine, St. Louis, Missouri 63110

ABSTRACT: Treatment of animals or cells with the amphipathic tertiary amine U18666A {3β-[2-(diethylamino) ethoxy]androst-5-en-17-one} provides models for several human diseases (e.g., cataracts, Niemann–Pick disease, and epilepsy). Although U18666A can inhibit several enzymes in the cholesterol synthesis pathway, we hypothesized that induction of these varied conditions was due to physical effects of the amine rather than to inhibition of specific proteins. To test this possibility we compared the capacity of U18666A and its enantiomer, *ent*-U18666A, to inhibit net sterol synthesis and induce apoptosis in cultured bovine lens epithelial cells. Nonenantiospecific actions dependent on the physical properties of these mirror image molecules would be identical, but effects dependent upon enantiospecific interactions would be different for the enantiomers. At the same concentrations, both forms of the compound equally inhibited sterol synthesis and induced apoptosis. These observations supported a generalized mechanism of enzyme inhibition such as perturbation of the microenvironment of endoplasmic enzymes and alteration of membrane order, perhaps of the mitochondrial membrane, to explain induction of apoptosis.

Paper no. L9707 in *Lipids 40*, 635–640 (June 2005).

The steroid 3β-[2-(diethylamino) ethoxy]androst-5-en-17-one (U18666A) is a widely-studied inhibitor of sterol synthesis because, when given to intact animals or cells, it generates models of at least three human diseases: atypical absence (petit mal) epilepsy (1,2), cataracts (3,4), and Niemann–Pick type C disease (NPC) (5–7). U18666A has recently also been shown to induce apoptosis in cultured lens cells (4) and neurons (8). Understanding how a single inhibitor of sterol metabolism can induce such varied disorders is a long-term goal of these investigations. Although multiple mechanisms may underlie induction of these diverse conditions [U18666A can decrease the cholesterol content of membranes (1,3), alter sterol composition of cells (2,3), and increase cellular free cholesterol levels (8)], we hypothesized that its broad toxic actions are more related to general perturbation of membrane structure through direct intercalation of this molecule (4). Part of the complexity in understanding the effects of U18666A on cells may be due to its multiple effects on sterol biosynthesis.

Although U18666A is considered to be an inhibitor of oxidosqualene cyclase (OSC) (9), it can also inhibit sterol Δ8-isomerase (SI) (10) and desmosterol reductase (1l). The mechanism of enzyme inhibition is unclear. Catalysis by both OSC and SI proceeds through a high-energy carbocationic intermediate (12,13). Structural mimics of the intermediate that inhibit the enzyme include amphipathic molecules containing a suitable positive charge, often provided by an ammonium group. Examples of mimics include the azasqualene series of compounds (12), the 8-azadecalin series of compounds (13), as well as U18666A. Inhibition of OSC by the azasqualenes was shown to be noncompetitive (12), and both noncompetitive and competitive mechanisms of inhibition were seen for the azadecalins depending upon the specific compound (13).

U18666A and other Class 2 amphiphiles can also interfere with the intracellular movement of cholesterol and cause accumulation of unesterified cholesterol, mimicking NPC lipid storage disease (14), a genetic condition characterized by the deficiency of an integral membrane protein, NPC1 protein, which is important for the intracellular transport of cholesterol (15). The apoptosis induced in cultured neurons by U18666A was also believed due to intracellular accumulation of toxic levels of unesterified cholesterol (8). Although U18666A could directly interact with the NPC1 protein, the block in cholesterol trafficking could occur through a more general effect on membranes due to the structural diversity of the hydrophobic amines that induce NPC (6).

As part of our studies into the mechanism of the U18666A-induced cataract, we observed that the induction of apoptosis in cultured lens epithelial cells appeared unrelated to inhibition of cholesterol synthesis (4). In addition, because U18666A was shown to intercalate into lens lipid membranes and alter their structure, we hypothesized that the toxic actions of U18666A were due to direct perturbation of membrane structure. To further test this possibility in the current study, we compared the capacity of U18666A and its enantiomer (*ent*-U18666A) to inhibit sterol synthesis and induce apoptosis in cultured lens epithelial cells. U18666A and *ent*-U18666A differ in configuration at all stereocenters and are mirror images of one another (Fig. 1). Because enantiomers have the same chemical and physical properties, their effects on membrane structure should

---

*To whom correspondence should be addressed at Department of Biochemistry, Kirksville College of Osteopathic Medicine, 800 W. Jefferson St., Kirksville, MO 63501. E-mail: rcenedella@atsu.edu

Abbreviations: BLEC, bovine lens epithelial cells; DMEM, Dulbecco's modified Eagle's medium; ent, enantiomer; NPC, Niemann–Pick type C disease; NS, nonsaponifiable, nonsterol; OSC, oxidosqualene cyclase; SCH, squalene-hopene cyclase; SI, sterol Δ8-isomerase; U18666A, 3β-[2-(diethylamino) ethoxy]androst-5-en-17-one.
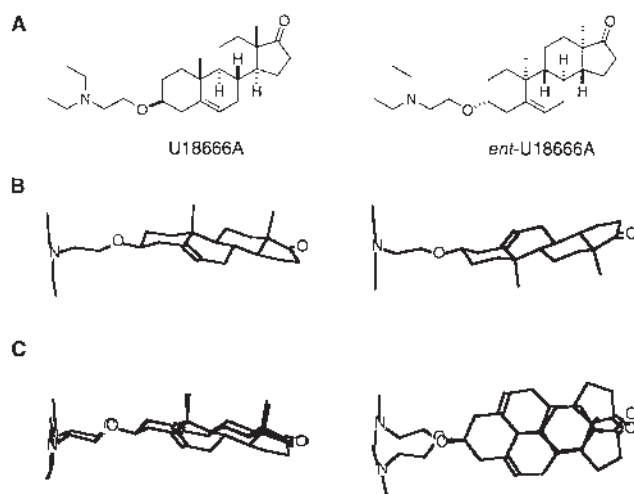
FIG. 1. (A) 2-D structures of the nonprotonated amine forms of U18666A {3β-[2-(diethylamino) ethoxy]androst-5-en-17-one} and the enantiomer of U18666A (*ent*-U18666A). (B) 3-D models of the two enantiomers (hydrogens not shown). Notice that the 3-substituent has the equatorial configuration in both enantiomers (see text for additional details). (C) An edge and top view of the superimposed enantiomers. The *ent*-U18666A has been turned upside down and the carbon atoms of the steroid A-rings have been superimposed.

be identical (16). On the other hand, enantiomers should demonstrate different actions on processes that are enantioselective, such as binding to an enzyme's active site (16). Thus, if U18666A inhibition of sterol synthesis and induction of apoptosis is due to interaction with specific proteins, the capacity of U18666A and *ent*-U18666A to cause these effects should markedly differ. Identical capacities would argue in favor of a more general mechanism, such as drug-induced changes in membrane structure. To conduct this study, we developed a method to synthesize the enantiomer of U18666A. This organic synthesis and the proof of structure are described.

MATERIALS AND METHODS

Synthesis of the ent-U18666A. The *ent*-U18666A was prepared by the same literature method used to prepare U18666A except that *ent*-dehydroepiandrosterone was used instead of dehydroepiandrosterone (17). A mixture of *ent*-dehydroepiandrosterone acetate (460 mg, 1.39 mmol) prepared according to the literature (18), ethylene glycol (1 mL), and *p*-toluenesulfonic acid (50 mg) in benzene (100 mL) was heated at reflux in a Dean–Stark distillation apparatus for 16 h. The reaction was cooled. The reaction mixture was made basic by adding a few drops of aqueous NaHCO₃ and stirred for a few minutes. Ethyl acetate (150 mL) was added, and the biphasic mixture was transferred to a separatory funnel and washed with aqueous saturated NaHCO₃ (3 × 100 mL), dried (anhydrous sodium sulfate), and concentrated to give a white solid, (500 mg). A mixture of the crude 17-ketal product (500 mg), methanolic KOH (85%, 200 mg dissolved in 25 mL), and THF (10 mL) was stirred at room temperature for 16 h to remove the 3-acetate

group. The solvents were removed to give a white solid that was partitioned between methylene chloride (100 mL) and water (100 mL). The methylene chloride layer was separated, and the aqueous layer was extracted with methylene chloride (40 mL × 3). The combined methylene chloride extracts were dried and concentrated to give the 17-ketal/3-alcohol as a colorless solid (290 mg, 63%) that was used in the next step without any further purification.

To a cold (0°C) solution of the 17-ketal/3-alcohol (280 mg, 0.84 mmol) in toluene (5 mL) was added 2.5 M butyl lithium in hexanes (0.37 mL, 0.92 mmol), and the resulting mixture was stirred at 0°C for 15 min. To that solution was added chloroethyldiethylamine (342 mg, 2.52 mmol, prepared by neutralization of the hydrochloride salt purchased from Aldrich Chemical Co., Milwaukee, WI) in toluene (2 mL), and the mixture was heated at reflux for 40 h under a nitrogen atmosphere. The reaction mixture was cooled, diethyl ether (200 mL) was added, and the organic layer was extracted with aqueous 1 N HCl (50 mL × 4). The organic layer was discarded. The combined aqueous extracts were further extracted with methylene chloride (50 mL × 4). The combined methylene chloride extracts were dried and concentrated to yield an oil, which was dried under high vacuum for 16 h. This material was purified by flash chromatography on 32–63 µm silica gel (Scientific Adsorbents, Atlanta, GA) using 10–25% methanol in ethyl acetate as eluents to give a solid. Ethereal HCl (5 mL, which was prepared by bubbling dry HCl into the cold ether solution) was added into a solution of the above-obtained solid (~200 mg) in anhydrous methylene chloride (6 mL), and the mixture was stirred for a few minutes. The solvents then were removed by distillation on a water bath to give an off-white solid. This material was dissolved in methanol to which was added 200 mg of decolorizing charcoal, and the resulting suspension was swirled at room temperature, then filtered through a J.T.Baker, Inc. (Phillipsburg. NJ) 6 mL Octadecyl (C₁₈) disposable extraction column (cat. # 7020-06). The filtrate was concentrated to give an off-white solid (180 mg, 51%) m.p. 200–202°C, [α]_D = −24 (methanol, c = 0.20); ¹³C NMR (CDCl₃) δ 220.99, 140.17, 121.44, 79.55, 62.47, 51.64, 51.21, 50.10, 47.45, 47.28 (2 × C), 38.70, 36.82 (2 × C), 35.77, 31.39, 31.34, 30.69, 28.06, 21.80, 20.78, 19.32, 13.48, 8.65 (2 × C). ¹H NMR (CDCl₃) δ 5.37 (1H, *b s*), 3.99 (2H, *b s*), 3.22 (*b s*, 7H), 2.60–0.90 (*m*, 19H), 1.42 (*t*, 6H, *J* = 7.1 Hz), 1.02 (*s*, 3H), 0.89 (*s*, 3H). Analysis calculated for C₂₅H₄₂ClNO₂: C, 70.81; H, 9.98; N, 3.30. Found: C, 70.60; H, 9.70; N, 3.34.

U18666A, prepared by the same procedure, had a m.p. of 196–199°C, identical ¹H and ¹³C NMR spectra, and [α]_D = +18.6 (methanol, c = 0.20). The reported literature values (17) for the m.p. and optical rotation of U18666A are 197–201°C and [α]_D = +17 (methanol).

Cell culture and measurement of sterol synthesis. Routine chemicals and reagents were from Sigma Chemical Co. (St. Louis, MO). Bovine lenses were obtained from cattle slaughtered for human food by local abattoirs. Bovine lens epithelial cells (BLEC) were cultured in 60-mm (diameter) dishes in Dulbecco's modified Eagle's medium (DMEM) containing 10%

calf serum as previously described in detail (19). Dishes of BLEC near confluence (about 1.3×10^6 cells and 1.0 mg protein/dish) were washed twice in serum-free DMEM and then incubated for 4 h at 37°C in 2.5 mL of serum-free DMEM containing 5.7 µCi/mL of sodium 1-^{14}C-acetate (56.5 mCi/mmol; PerkinElmer, Boston, MA). Media contained no compounds (controls) or U18666A or *ent*-U18666A at 0.1 or 1.0 µM, added in ethanol. The concentration of ethanol in all media was 0.14%. Simvastatin acid at 10 µM was examined as a positive control, i.e., an established inhibitor of HMG CoA reductase that should almost completely block the cholesterol synthesis pathway at this concentration. The magnitude of the ^{14}C-acetate incorporation into lens cell sterols may have been decreased due to adding the compounds in a metabolizable solvent vehicle, ethanol. However, since all incubations contained the same concentration of ethanol (0.14%, vol/vol), the relative effects of the compounds should be independent of a possible solvent effect.

Recovery of radiolabed sterols. Following incubation, cell layers were washed in ice cold PBS and PBS containing 15 mM sodium acetate and then dissolved in 1.6 mL of 1.0 M KOH, which was transferred to preweighed 125-mm screw-capped test tubes containing 100 µg of cholesterol added as carrier. The volume of KOH solution in each tube was determined by weighing and 40 µL was taken for protein assay. The mass of protein per tube (dish) was calculated. One milliliter of ethanol was added to each tube, the tubes were capped, and the samples saponified at 100°C for 1 h. Water (0.5 mL) was added, and the nonsaponifiable (NS) lipids were extracted into hexane (twice with 6 mL). The pooled hexane extracts were evaporated and the lipids separated by TLC on silica gel G plates using a solvent of hexane/diethyl ether/glacial acetic acid (73:25:2, by vol). The air-dried plates were briefly exposed to iodine vapor to locate the cholesterol (sterol) band. The R_f was about 0.25. The sterol band was recovered by scraping and transferred to a 20-mL scintillation counting vial. After adding 1.0 mL of methanol and 15 mL of scintillation solution, the dpm per sample were measured to generally 1% counting error. Results were expressed as dpm $\times 10^{-3}$ incorporated into sterols per mg of protein. Results were expressed as means of replicate dishes ± SEM, and differences from controls were statistically evaluated by the unpaired Student's *t*-test. We did not examine the media for labeled sterols potentially released from the cultured cells but assume that any release would have been proportional to that synthesized.

Apoptosis in lens epithelial cells treated with U18666A or ent-U19666A. BLEC grown to subconfluence on well-slides were incubated with either no inhibitors (controls) or 40 to 200 nM U18666A or *ent*-U18666A for 48 h at 37°C in an atmosphere of 6% carbon dioxide. Slides were washed twice with PBS and fixed for 25 min in 10% buffered formalin. Apoptosis was detected using the DeadEnd Colorimetric Apoptosis Detection System (Promega, Madison, WI) as done before (4). Briefly, cells were permeablized by exposure to Triton X-100, and biotinylated nucleotides were incorporated into the 3′OH ends of the DNA using terminal deoxynucleotidyl transferase.

Horseradish peroxidase-labeled streptavidin was then bound to the biotinylated nucleotides, and color development was detected using the substrate diaminobenzidine plus hydrogen peroxide. Positive control slides were exposed to DNase I to induce apoptosis.

RESULTS AND DISCUSSION

Comparison of the structure of U18666A and ent-U18666A. At first glance, the 2-D drawings of Figure 1A convey the impression that changing the configuration of the oxygen atom attached to C-3 changes an equatorial 3β-substituent to an axial 3α-substitutent. While it is true that the substituent is 3α, it is not true that the substituent has the axial configuration. Instead, the substituent remains in an equatorial configuration (see Fig. 1B). This results from the fact that the remaining chiral centers in the molecule (C-8, C-9, C-10, C-13, and C-14, i.e., the carbons at the ring fusions) are also inverted, thereby flipping the ring conformations in the molecule and placing the 3α-substituent back in an equatorial configuration. The inverted chair conformations for the steroid A ring are readily apparent in Figure 1B.

In Figure 1C, the A rings of U18666A and *ent*-U18666A have been superimposed to emphasize similarities and differences in the shapes of the enantiomers. The 3-substituents, steroid A and C rings, the 18- and 19-methyl groups, and the 17-keto groups can be placed in identical or nearly identical positions in 3-D space when the molecules are compared in this way. However, the steroid B rings, and the double bond contained therein, as well as the steroid D rings, lie in different positions. The different positions of these rings would form a steric basis for chiral discrimination by an enzyme if the molecules were aligned in this manner in the active site. However, the way that U18666A and *ent*-U18666A might be bound in the OSC active site is unknown, and it remains possible that each enantiomer might bind in a very different orientation to inhibit OCS activity.

Comparison of inhibition of sterol synthesis by U18666A and ent-U18666A. Sterols were separated by TLC from the NS fraction of BLEC incubated with 1-^{14}C-acetate. The sterol band would contain cholesterol and precursor sterols such as desmosterol and 7-dehydrocholesterol (11). Exposure of cells to 10 µM simvastatin acid decreased incorporation of ^{14}C-acetate into sterols by more than 98% (Table 1). Sterol synthesis by cells exposed to either 1 µM U18666A or *ent*-U18666A was decreased by 88–89%. U18666A and *ent*-U18666A at 0.1 µM similarly decreased sterol synthesis by 55–65% (Table 1). We did not examine the media for labeled sterols potentially released from the cultured cells but assume that any released would have been proportional to that synthesized.

The results of these incorporation studies clearly show that U18666A and *ent*-U18666A have essentially identical effects on total sterol synthesis and presumably OSC. Although this observation may suggest that the inhibition of OSC by U18666A is not competitive, the mechanism of catalysis by OSC and its interaction with inhibitors can be complex. Squa-

TABLE 1
Incorporation of ^{14}C-Acetate into Sterols by Cultured Bovine Lens Epithelial Cells

Sample	n dishes	μM	dpm $\times 10^{-3}$/mg protein[a]	$P(t)$ from control
Control	9	—	182.1 ± 9.8	—
Simvastatin acid	3	10.0	1.0 ± 0.1	<0.0001
U18666A	4	0.1	63.8 ± 7.0	<0.0001
U18666A	4	1.0	19.2 ± 0.2	<0.0001
Ent-U18666A	4	0.1	79.3 ± 9.1	<0.0001
Ent-U18666A	4	1.0	21.7 ± 1.8	<0.0001

[a]Values are mean incorporation by n dishes ± SEM. U18666A, 3β-[2-(diethylamino)ethoxy]androst-5-en-17-one.

lene-hopene cyclase (SHC) is the prokaryotic equivalent of eukaryotic OSC. Using X-ray diffraction analysis of recombinant SHC, Lenhart *et al.* (20,21) demonstrated that SHC, and presumably OSC, is a monotopic membrane protein with a deep hydrophobic pocket that extends from the protein surface to the plasma membrane surface from which the enzyme extracts its substrate. Kinetic analysis of OSC inhibition by Ro48-8071 (22) and similar compounds suggested noncompetitive or mixed noncompetitive mechanisms (20,21); however, binding of the inhibitors at the active site favors competitive inhibition. The inhibitors examined contained a tertiary amine cationic group at one end of the molecule and a ketone carbon separated from the amine by a hydrophobic domain at the other end of the molecule, as in U18666A and *ent*-U18666A. The inhibitor compounds insert into the active site cavity with the tertiary amine near the surface located close to Asp376, and the ketone carbon toward the membrane interface is near Phe601 and Phe606. The apparent paradox of noncompetitive inhibition kinetics and the OSC inhibitors binding at the active site is explained by "the inhibitors (being) kinetically captured in the sequestered cavity, feigning a noncompetitive case" (21).

Although we cannot exclude the possibility that U18666A and *ent*-U18666A could inhibit OSC equally well by binding in the active site of this enzyme, more generalized mechanisms of inhibition are also suggested by our results. Either inhibition resulting from perturbation of the microenvironment of the enzyme secondary to U18666A intercalation into membrane (4) or nonenantioselective binding of the inhibitor to sites other than the active site of the enzyme is a reasonable possibility. These more generalized mechanisms of inhibition may explain the capacity of U18666A to inhibit multiple endoplasmic late-stage enzymes of cholesterol biosynthesis (OSC, SI, and desmosterol reductase).

Comparison of induction of apoptosis by U18666A and ent-U18666A. U18666A and *ent*-U18666A both induced apoptosis in cultured BLEC in a highly concentration-dependent manner (Fig. 2). Neither induced apoptosis at 40 nM, but both did at 100 and 200 nM. At the lower concentrations (30–40 nM), U18666A can block proliferation of cultured BLEC due to inhibition of cholesterol synthesis, because adding cholesterol to the cholesterol-free media restored proliferation (4). However, adding cholesterol could not overcome the inhibition of cell proliferation or apoptosis caused by higher levels (100–200 nM) of U18666A

(4) (Fig. 2). These observations suggest that the induction of apoptosis in BLEC by U18666A and *ent*-U18666A is independent of cellular cholesterol levels. But Cheung *et al.* (8) reported that induction of apoptosis in cultured mouse neurons was related to accumulation of toxic levels of free cholesterol in U18666A-treated cells. The difference between the two sets of findings could be related to differences in the response of cell types to U18666A. Neither elevation of free cholesterol nor induction of significant apoptosis was seen in the neurons exposed to 236 nM U18666A (0.1 μg/mL media) (8), a concentration that was clearly apoptotic in the cultured lens epithelial cells. It is well documented that the sensitivity to induction of apoptosis by specific agents can greatly differ from one cell type to another (23). In fact, Cheung *et al.* (8) stated that U18666A did not induce apoptosis in other neuronal cell lines.

Although it appears unlikely that the apoptosis induced by U18666A and *ent*-U18666A in lens epithelial cells at the concentrations studied was due to raising intracellular cholesterol levels, the mechanism is unknown. Lovastatin, an inhibitor of the rate-limiting enzyme (HMG-CoA reductase) in the cholesterol synthesis pathway, can induce apoptosis in various tumor cell lines (24,25). The apoptosis was prevented by providing cells with geranylgeranyl pyrophosphate, an isoprene with anti-inflammatory roles formed prior to squalene, but not by providing squalene, sterol precursors of cholesterol, or cholesterol (25). U18666A does not appear to inhibit isoprene formation (26). The turnover of HMG-CoA reductase by proteolysis in BLEC is dependent on isoprene formation, and when HMG-CoA reductase is inhibited by lovastatin the half-life of this enzyme is prolonged by 10-fold (26). When mevalonic acid and U18666A were added to the lovastatin-exposed cells, the short half-life was restored. In light of these observations, it seems possible that the apoptotic activity of U18666A is unrelated to inhibition of the cholesterol synthesis pathway, i.e., it is independent of isoprene or cholesterol. The equivalent apoptotic activity of U18666A and *ent*-U18666A also argues against these molecules interacting with a specific apoptotic signaling protein. Rather, a more generalized mechanism of apoptosis dependent on the equal physical properties of the molecules is suggested. Radiolabeled U18666A became highly associated with mitochondria and membrane fractions when injected into rats (27). Mitochondrial destabilization precedes caspase activation in some types of apoptosis (28). Induction of apoptosis
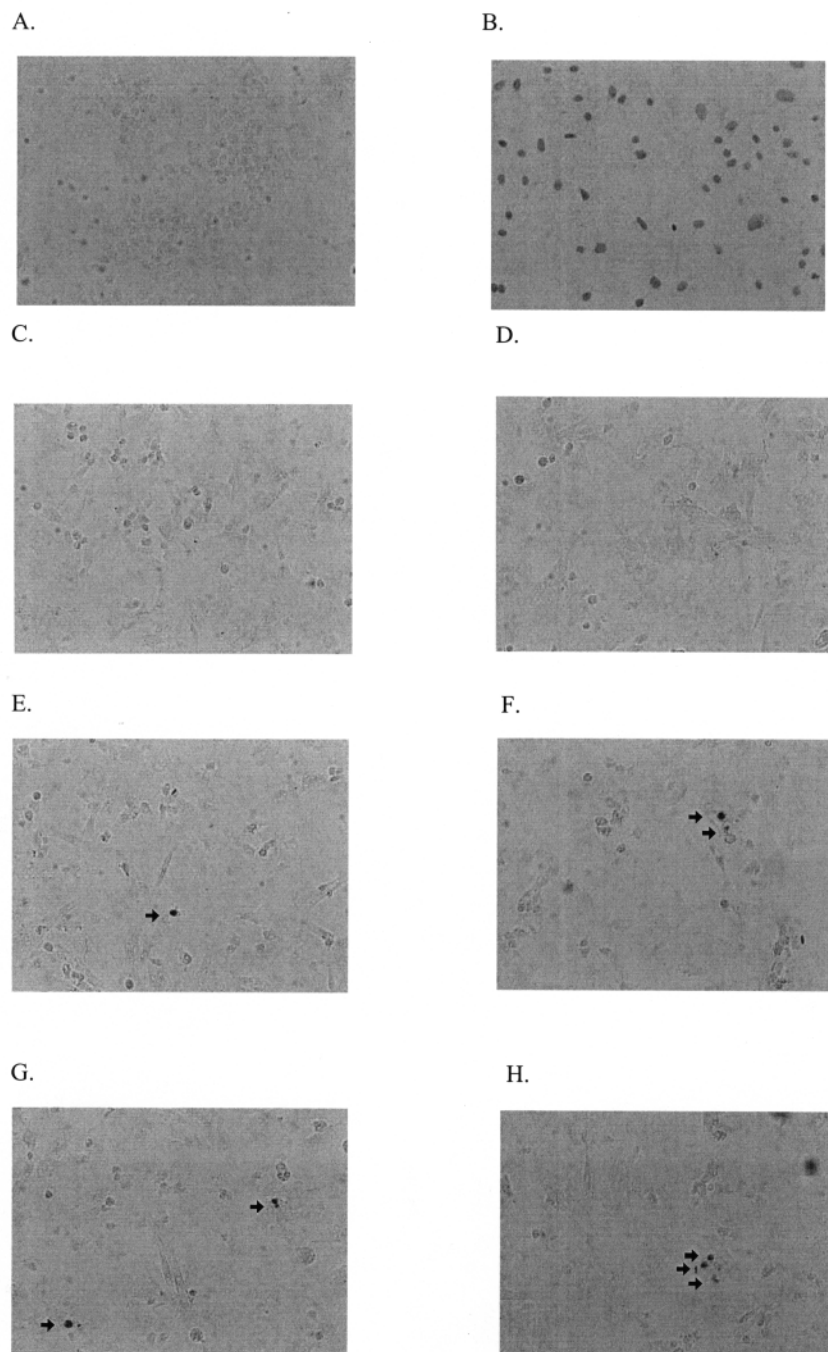
FIG. 2. Apoptosis in cultured bovine lens epithelial cells caused by U18666A and *ent*-U18666A. Bovine lens epithelial cells were cultured in Dulbecco's modified Eagle's medium plus 10% calf serum containing 40 (C), 100 (E), or 200 nM (G) of U18666A or 40 (D), 100 (F), or 200 nM (H) of *ent*-U18666A. Control (A) contained neither compound. Positive control (B) is a cell layer exposed to DNase I to induce DNA fragmentation. The arrows displayed in panels E, F, G, and H identify cells positive for DNA fragmentation as evaluated by the TUNEL assay. For full chemical name see Figure 1.

in cultured hepatocytes by hydrophobic bile salts was related to direct perturbation of mitochondrial structure as reflected by increased membrane lipid order (29). Such a mechanism might explain the induction of apoptosis by U18666A and *ent*-U18666A. Additionally, U18666A intercalated into lens membranes increased lipid order (4).

ACKNOWLEDGMENTS

REFERENCES

1. Bierkamper, G.G., and Cenedella, R.J. (1978) Induction of Chronic Epileptiform Activity in the Rat by an Inhibitor of Cholesterol Synthesis, U18666A, *Brain Res. 150*, 343–351.

2. Serbanescu, J., Ryan, M.A., Shukla, R., Cortez, M.A., Snead, O.C., III, and Cunnane, S.C. (2004) Lovastatin Exacerbates Atypical Absence Seizures with Only Minimal Effects on Brain Sterols, *J. Lipid Res. 45*, 2038–2043.

3. Cenedella, R.J., and Bierkamper, G.G. (1979) Mechanism of Cataract Production by 3-β(2-diethylaminoethoxy) Androst-5-en-17-one Hydrochloride, U18666A: An Inhibitor of Cholesterol Biosynthesis, *Exp. Eye Res. 28*, 673–688.

4. Cenedella, R.J., Jacob, R., Borchman, D., Tang, D., Neely, A.R., Samadi, A., Mason, R.P., and Sexton, P. (2004) Direct Perturbation of Lens Membrane Structure May Contribute to Cataracts Caused by U18666A, an Oxidosqualene Cyclase Inhibitor, *J. Lipid Res. 45*, 1232–1241.

5. Liscum, L., and Faust, J.R. (1989) The Intracellular Transport of Low Density Lipoprotein-Derived Cholesterol Is Inhibited in Chinese Hamster Ovary Cells Cultured with 3-β-[2-(diethylamino)ethoxy]androst-5-en-17-one, *J. Biol. Chem. 264*, 11796–11806.

6. Roff, C.F., Goldin, E., Comly, M.E., Cooney, A., Brown, A., Vanier, M.T., Miller, S.P., Brady, R.O., and Pentchev, P.G. (1991) Type C Niemann–Pick Disease: Use of Hydrophobic Amines to Study Defective Cholesterol Transport, *Dev. Neurosci. 13*, 315–319.

7. Mohammadi, A., Perry, R.J., Storey, M.K., Cook, H.W., Byers, D.M., and Ridgway, N.D. (2001) Golgi Localization and Phosphorylation of Oxysterol Binding Protein in Niemann–Pick C and U18666A-Treated Cells, *J. Lipid Res. 42*, 1062–1071.

8. Cheung, N.S., Koh, C.H., Bay, B.H., Qi, R.Z., Choy, M.S., Li, Q.T., Wong, K.P., and Whiteman, M. (2004) Chronic Exposure to U18666A Induces Apoptosis in Cultured Murine Cortical Neurons, *Biochem. Biophys. Res. Commun. 315*, 408–417.

9. Sexton, R.C., Panini, S.R., Azran, F., and Rudney, H. (1983) Effects of 3 β-[2-(diethylamino)ethoxy]androst-5-en-17-one on the Synthesis of Cholesterol and Ubiquinone in Rat Intestinal Epithelial Cell Cultures, *Biochemistry 22*, 5687–5692.

10. Bae, S., Seong, J., and Paik, Y. (2001) Cholesterol Biosynthesis from Lanosterol: Molecular Cloning, Chromosomal Localization, Functional Expression and Liver-Specific Gene Regulation of Rat Sterol Δ8-Isomerase, a Cholesterogenic Enzyme with Multiple Functions, *Biochem. J. 353*, 689–699.

11. Cenedella, R.J. (1980) Concentration-Dependent Effects of AY-9944 and U18666A on Sterol Synthesis in Brain. Variable Sensitivities of Metabolic Steps, *Biochem. Pharmacol. 29*, 2751–2754.

12. Duriatti, A., Bouvier-Nave, P., Benveniste, P., Schuber, F., Delprino, L., Balliano, G., and Cattel, L. (1985) *In vitro* Inhibition of Animal and Higher Plants 2,3-Oxidosqualene-Sterol Cyclases by 2-Aza-2,3-dihydrosqualene and Derivatives, and by Other Ammonium-Containing Molecules, *Biochem. Pharmacol. 34*, 2765–2777.

13. Hoshino, T., Kobayashi, N., Ishibashi, E., and Hashimoto, S. (1995) Inhibitory Activity of 8-Azadecalin Derivatives Towards 2,3-Oxidosqualene:Lanosterol Cyclases from Baker's Yeast and Pig's Liver, *Biosci. Biotechnol. Biochem. 59*, 602–609.

14. Lange, Y., Ye, J., Rigney, M., and Steck, T. (2000) Cholesterol Movement in Niemann–Pick Type C Cells and in Cells Treated with Amphiphiles, *J. Biol. Chem. 275*, 17468–17475.

15. Ory, D.S. (2000) Niemann–Pick Type C: A Disorder of Cellular Cholesterol Trafficking, *Biochim. Biophys. Acta 1529*, 331–339.

16. Westover, E.J., and Covey, D.F. (2004) The Enantiomer of Cholesterol, *J. Membrane Biol. 202*, 61–72.

17. Birkenmeyer, R.D., Lednicer, D., Kagan, F., and Magerlein, B.J. (1961) 17-Isonitrose-3-aminoethers of the Androstane Series. U.S. Patent 3,000,910.

18. Westover, E.J., and Covey, D.F. (2003) First Synthesis of *Ent*-Desmosterol and Its Conversion to *Ent*-Deuterocholesterol, *Steroids 68*, 159–166.

19. Hitchener, W.R., and Cenedella, R.J. (1985) Absolute Rates of Sterol Synthesis Estimated from [3H]Water for Bovine Lens Epithelial Cells in Culture, *J. Lipid Res. 26,* 1455–1463.

20. Lenhart, A., Weihofen, W.A., Pleschke, A.E., and Schulz, G.E. (2002) Crystal Structure of a Squalene Cyclase in Complex with the Potential Anticholesteremic Drug Ro48-8071, *Chem. Biol. 9*, 639–645.

21. Lenhart, A., Reinert, D.J., Aebi, J.D., Dehmlow, H., Morand, O.H., and Schulz, G.E. (2003) Binding Structures and Potencies of Oxidosqualene Cyclase Inhibitors with the Homologous Squalene-Hopene Cyclase, *J. Med. Chem. 46*, 2083–2092.

22. Morand, O.H., Aebi, J.D., Dehmlow, H., Ji, Y.H., Gains, N., Lengsfeld, H., and Himber, J. (1997) Ro 48-8.071, a New 2,3-Oxidosqualene:Lanosterol Cyclase Inhibitor Lowering Plasma Cholesterol in Hamsters, Squirrel Monkeys, and Minipigs: Comparison to Simvastatin, *J. Lipid Res. 38*, 373–390.

23. Strasser, A., O'Connor, L., and Dixit, V.M. (2000) Apoptosis Signaling, *Annu. Rev. Biochem. 69*, 217–245.

24. Macaulay, R.J., Wang, W., Dimitroulakos, J., Becker, L.E., and Yeger, H. (1999) Lovastatin-Induced Apoptosis of Human Medulloblastoma Cell Lines *in vitro, J. Neurooncol. 42*, 1–11.

25. Xia, Z., Tan, M.M., Wong, W.W., Dimitroulakos, J., Minden, M.D., and Penn, L.Z. (2001) Blocking Protein Geranylgeranylation Is Essential for Lovastatin-Induced Apoptosis of Human Acute Myeloid Leukemia Cells, *Leukemia 15*, 1398–1407.

26. Cenedella, R.J. (1997) Posttranslational Regulation of 3-Hydroxy-3-methylglutaryl Coenzyme A Reductase in Lens Epithelial Cells by Mevalonate-Derived Nonsterols, *Exp. Eye Res. 65*, 63–72.

27. Cenedella, R.J., Sarkar, C.P., and Towns, L. (1982) Studies on the Mechanism of the Epileptiform Activity Induced by U18666A. II. Concentration, Half-Life and Distribution of Radiolabeled U18666A in the Brain, *Epilepsia 23*, 257–268.

28. Mignotte, B., and Vayssiere, J.L. (1998) Mitochondria and Apoptosis, *Eur. J. Biochem. 252*, 1–15.

29. Sola, S., Brito, M.A., Brites, D., Moura, J.J., and Rodrigues, C.M. (2002) Membrane Structural Changes Support the Involvement of Mitochondria in the Bile Salt-Induced Apoptosis of Rat Hepatocytes, *Clin. Sci. 103*, 475–485.

REVIEW

Astonishing Diversity of Natural Surfactants: 4. Fatty Acid Amide Glycosides, Their Analogs and Derivatives

Valery M. Dembitsky*

Department of Organic Chemistry and School of Pharmacy, Hebrew University, Jerusalem, Israel

ABSTRACT: FA amide glycosides are of great interest, especially for the medicinal and pharmaceutical industries. These biologically active natural surfactants are good prospects for future chemical preparation of compounds useful as antibiotics, anticancer agents, or for industry. More than 200 unusual and interesting natural surfactants, including their chemical structures and biological activities, are described in this review article.

Paper no. L9744 in *Lipids 40*, 641–660 (July 2005).

Fatty (carboxylic) acid amides, their analogs and derivatives are widespread in nature, although the occurrence of their glycosides is more limited (2). They are incorporated into ceramides (3), glycosphingolipids (4,5), gangliosides (6,7), N-acylated lipids (8), bacterial lipoproteins (9), and other natural complex compounds. The best known FA amides, such as anandamide, oleamide, *N*-arachidonoyldopamine, and *N*-acylethanolamines, as well as aminoglycosides have a high biological activity. They and primary amines attracted attention as bioregulators for the first time in 1957 when Meisinger and co-workers (10) demonstrated that *N*-palmitoylethanolamine is an anti-inflammatory factor contained in the lipid fraction of soybean, peanut oil, and egg yolk. More interest in FA amides with primary amines was associated with the discovery of potent neuromodulatory effects of natural *N*-arachidonyl-ethanolamide (anandamide) (11) and oleoylamine (oleamide) (12).

Anandamide has attracted special interest because of its marked biological activities (11). Like the pharmacologically active compounds in marijuana (from *Cannabis sativa*), it exerts its effects through binding to and activation of specific cannabinoid receptors, designated CB1 and CB2, both of which are membrane-bound G-proteins. CB1 is found in the central nervous system and in some other organs, including the heart, uterus, testis, and small intestine, whereas the CB2 receptor is found in the periphery of the spleen and other cells as-

sociated with immunochemical functions, but not in brain (13). Recently, it has been shown that anandamide and presumably other polyunsaturated *N*-acylethanolamines bind to and activate both the central (CB1) and peripheral (CB2) cannabinoid receptors and elicit virtually all of the known effects of cannabis. Anandamide is believed to have important anti-inflammatory and anticarcinogenic properties, and it affects the cardiovascular system by inducing profound decreases in blood pressure and heart rate (14).

cis-9,10-Octadecenamide is a primary FA amide. It was first isolated from the cerebrospinal fluid of sleep-deprived cats, and has been characterized and identified as the signaling molecule responsible for causing sleep. It induces physiological sleep when injected directly into the brain of rats. Although other FA primary amides in addition to *cis*-9,10-octadecenamide are present naturally in the cerebrospinal fluid of animals, no others exhibit similar physiological activity (15). The biological effects of the other fatty acyl-ethanolamine derivatives are less clear, although they are by far the most abundant components of this lipid class.

FA amide glycosides such as ceramides, gangliosides, aminoglycosides, their analogs and derivatives also show high biological activity (3–7,16–18). FA (carboxylic) amides are produced synthetically in industry in large amounts (more than 400,000 tons per annum) for use as ingredients of detergents, lubricants, inks, and many other products (19–22). However, in this review article, we are concerned with those as simple, complex of fatty (carboxylic) acid amide glycosides, which are found in nature, and some of which have profound biological functions.

AMINOGLYCOSIDES AND DERIVATIVES

Since Florey and co-workers (23) reported in 1940 that penicillin, a microbial product, is active against pathogenic microorganisms, many investigations have focused on the screening of natural compounds with antibiotic properties (24). A great number of antibiotics, termed aminoglycosides, have been discovered from cultures of bacteria and actinomycetes such as *Bacillus, Nocardia, Micromonospora*, and *Streptomyces*. The aminoglycoside antibiotics show broad spectra against both Gram-positive and Gram-negative bacteria. The term "aminoglycoside" refers to their structural aspects. These compounds are a large and diverse class of antibiotics that characteristically contain two or more aminosugars linked by glycosidic bonds to an aminocyclitol component (24,25).

A few FA amide glycosides have been found. Amikacin **1** inhibits the growth of resistant bacteria producing APH(3′)-1

(3′-aminoglycoside phosphotransferase) and AAD(2′) (2′-amino acid decarboxylase). Amikacin **1** was biologically transformed from kanamycin by a mutant of butirosin-producing *Bacillus circulans* (26). Arbekacin **2** showed strong activity against resistant bacteria including *Pseudomonas*. It was launched into the clinical market in Japan in 1990 as a chemotherapeutic agent for the treatment of infections caused by methicillin-resistant *Staphylococcus aureus* (27). 2″-Amino-2″-deoxyarbekacin **3** demonstrated potent activity against *S. aureus* (28). Isepamicin **4** showed activity against resistant bacteria with lower toxicity than gentamicin B and has been useful in the clinical treatment of infection (24).

Fortimicins A **5** and B are bicyclic aminoglycoside antibiotics that contain a fortamine moiety instead of the deoxystreptamine; both are produced by strain *Micromonospora* sp. MK-7 (29,30), and fortimicin A also is produced by *M. olivoasterospora* KY 1151 (31). Fortimicin A showed excellent activity against 352 strains of Enterobacteriaceae (a concentration of 6.2 µg/mL inhibited the greatest number of strains, 92.6%) and other medically significant organisms, and weak activity against *Pseudomonas aeruginosa* strains (32,33). The marine bacterium *Streptomyces tenjimariensis* produced the antibiotics istamycin A **6** and B **7** under select laboratory culture conditions (34). Butirosin A **8** and B **9**, which are aminoglycosidic antibiotics produced by a mutant of *Bacillus circulans,* showed antibacterial activity *in vitro* in mice (35,36).

1 Amikacin, R,R₁,R₂ = OH
2 Arbekacin, R = NH₂, R₁,R₂ = H

3

5 Fortimicin A, R = NH₂, R₁,R₄ = H, R₂,R₃ = OH
6 Istamycin A, R = NH₂, R₁,R₂,R₃ = H, R₄ = Me
7 Istamycin B, R,R₂,R₃ = H, R₁ = NH₂, R₄ = Me

4 Isepamicin

8 Butirosin A, R = OH, R₁ = H
9 Butirosin B, R = H, R₁ = OH
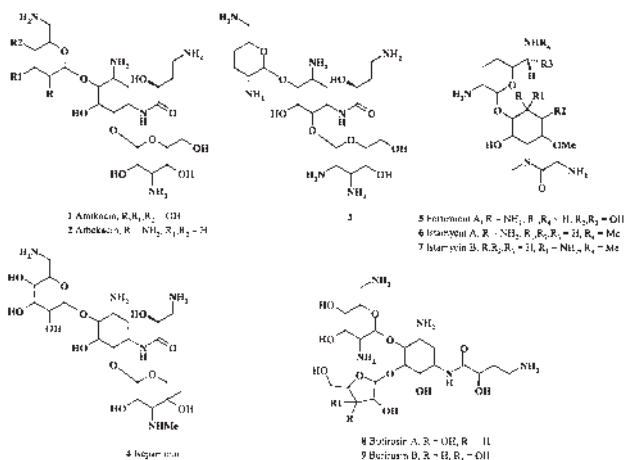
Simple amides of uronic acids **10–12** were isolated by mild acid degradation of the lipopolysaccharides of the marine bacterium *Shewanella fidelis* type strain KMM 3582T (37). Originally, this bacterial strain was isolated from a sipunculan (*Phascolosoma japonicum*), a common inhabitant of Troitsa Bay in the Gulf of Peter the Great (Sea of Japan, Russia) (38). Mycothiol **13** has been identified from the bacterial pathogen *Mycobacterium tuberculosis* and *M. bovis* (39).

10 α-OH

11 α-OH
12 β-OH

13 Mycothiol
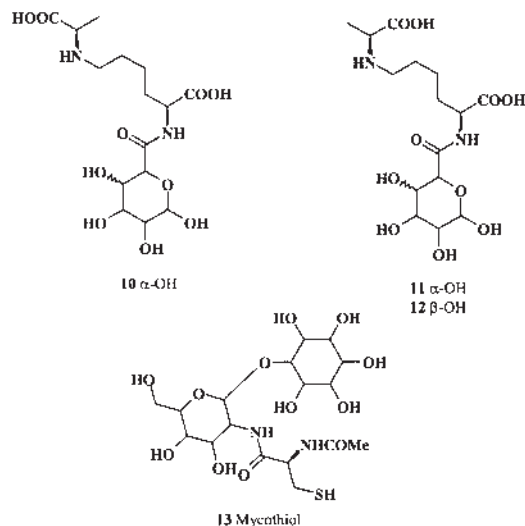
NUCLEOSIDE FATTY AMIDE GLYCOSIDES

Nucleosides are glycosylamines made by attaching a nucleobase to a ribose ring. Examples of these include cytidine, uridine, adenoside, guanosine, thymidine, and inosine. Nucleosides can be acylated and/or phosphorylated by specific kinases in the cell, producing bioactive compounds that are the molecular building blocks of DNA and RNA (40).

Many nucleosides are categorized as antibiotics and have nonspecific antibacterial activities (41–43). Three classes of nucleotide antibiotics are targeted against translocase I. The first class is represented by tunicamycin, which was identified from the fermentation broth of *Streptomyces lysosuperficus nov*. as having antiviral activity (44–46). Series of nucleoside fatty amide glycosides named tunicamycins I–X, **14–23**, respectively, containing uracil, have been isolated from *S. lysosuperficus nov.* (44–46). Tunicamycins showed antibacterial activities against Gram-positive bacteria, especially those of the genus *Bacillus* [minimal inhibitory concentration of antibiotic that inhibits a bacterium (MIC), from 0.1 to 20 µg/mL]. The related compounds of tunicamycins named streptovirudins (series II) **24–28** (47–49), corynetoxins **29–42** (50,51), and streptovirudins (series I, where uracil is replaced by dihydrouracil) **43–47** (52) have been isolated from *Streptomyces griseoflavus* subsp. *thuringiensis* (47–49), and from *Corynebacterium rathayi* (51), respectively. Streptovirudins (series II) **24–28** have potent antibacterial activities against the genus *Bacillus* (MIC, 0.31–10 µg/mL). All corynetoxins **29–42** exhibit toxicity against ryegrass (*Lolium rigidum*) (50). Sheep were very sensitive to corynetoxins (the lethal dose was about 35 µg/kg bodyweight) (53).
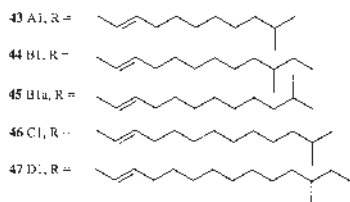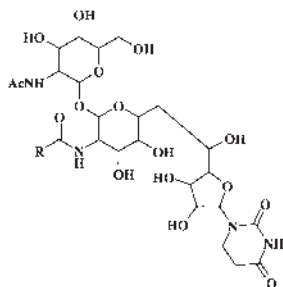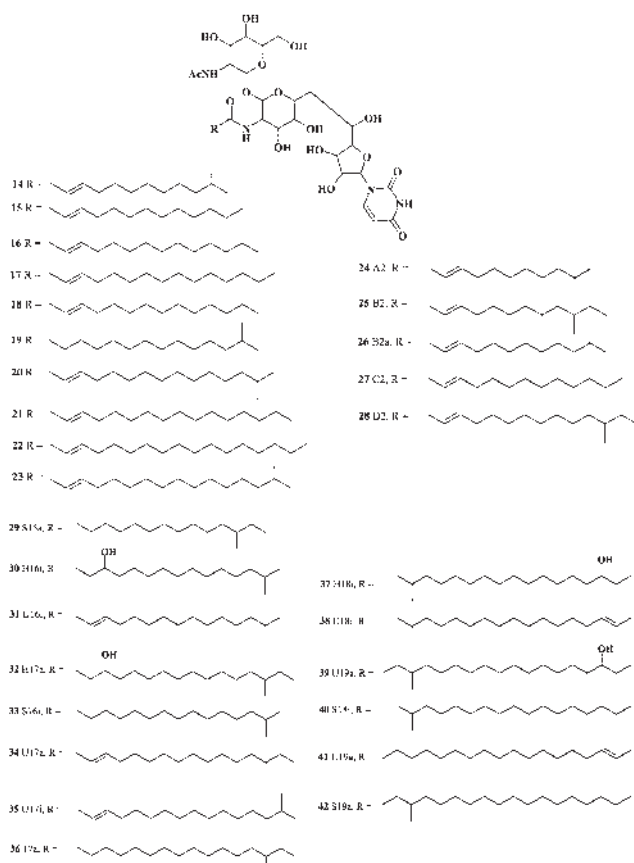
FATTY AMIDE OLIGOSACCHARIDES

Among natural surfactants there are some groups of high-molecular-mass bioemulsifiers, including amphipathic polysaccharides, proteins, lipopolysaccharides, lipoproteins, and complex mixtures of these biopolymers, that are more effective at stabilizing oil-in-water emulsions than the low-molecular-mass bioemulsifiers such as glycolipids, trehalose lipids, sophoro-

lipids, and rhamnolipids (2,54,55). Bioemulsifiers have several advantages over chemical surfactants, such as (i) low toxicity, (ii) biodegradability, (iii) high specificity and biocompatibility, (iv) molecular masses ranging from 500 to 1,500 Da, (v) solubility and surface-active properties that are dependent on the orientation of residues, and (vi) occurrence in a wide variety of microorganisms. These advantages should allow these compounds to become important in industrial and environmental applications. The potential commercial applications of bioemulsifiers include bioremediation of oil-polluted soil and water; enhanced oil recovery; replacement of chlorinated solvents used in cleaning up oil-contaminated pipes, vessels, and machinery; use in the detergent industry; formulations of herbicides and pesticides; and formation of stable oil-in-water emulsions for the food and cosmetic industries.

Bacterial lipopolysaccharides are the major components of the outer surface of Gram-negative bacteria (56). They are often of interest in medicine for their immunomodulatory properties. In small amounts they can be beneficial, but in larger amounts they may cause endotoxic shock. Although they share a common architecture (see structures **48**–**53**), their structural details exert a strong influence on their activity. These molecules comprise (i) a lipid moiety, called lipid A, which is considered to be the endotoxic component, (ii) a glycosidic part, consisting of a core of approximately 10 monosaccharides, and (iii) in "smooth-type" lipopolysaccharides, a third region, named O-chain, consisting of repetitive subunits of one to eight monosaccharides responsible for much of the immunospecificity of the bacterial cell.

The most common FA in lipid A have 10–16 carbon atoms although longer chains exist, i.e., C_{18} FA in *Helicobacter pylori* lipid A, and C_{18} and C_{21} in *Chlamydia trachomatis* (57–60). Hydroxylated FA are usually found in direct acylation of the sugar except in a few cases (see below) where they appear in secondary acylation. Some *Bordetella* strains have unhydroxylated FA at the C-3 position (61). In *Chlamydia* lipid A, hydroxylated FA occur only as amide-linked substituents whereas positions C-3 and C-3′ are both substituted by C_{14} FA (62,63). Another kind of FA, which has been described for a few species, is the 3-oxo FA, e.g., the 3-oxotetradecanoic acid found in *Rhodobacter capsulatus* and the 27-oxooctacosanoic and heptacosane-1,27-dioic acids found in *Legionella pneumophila* (64,65). The number of acyl groups present in a molecule has a direct effect on its toxicity: Six acyl groups constitute the optimum for many isolated lipopolysaccharides. FA chain length is also critical for lipid A toxicity since C_{12}, $C_{12}OH$, C_{14}, and $C_{14}OH$ FA are the moieties found in the most toxic lipids A (66). Unsaturated FA are rarely present in lipid A, but examples were found in *Rhodopseudomonas sphaeroides* and other species of this genus as well as in *Rhodobacter capsulatus* (67). Another kind of unusual FA, with a methyl branch at C_{n-1}, is found in some *Legionella* and *Porphyromonas* strains (68). Selected structures of lipid A isolated from bacteria are **48** (*Escherichia coli*), **49** (*Yersinia enterocolitica*, both species belonging to the Enterobacteriaceae; **50** isolated from *Bordetella pertussis*, **51** isolated from *Neisse-*

ria meningitidis, **52** from *Chlamydia trachomatis*, and **53** from *Rhizobium etli* (56).

48

49

50

51

52

53
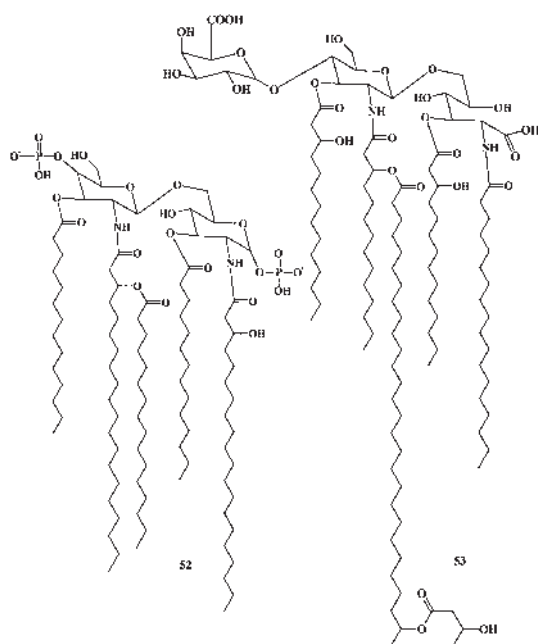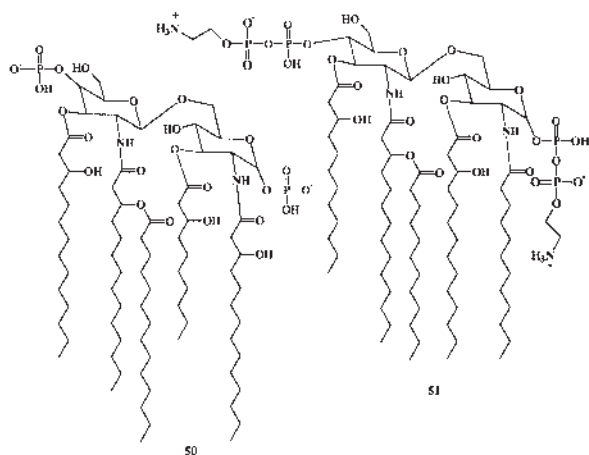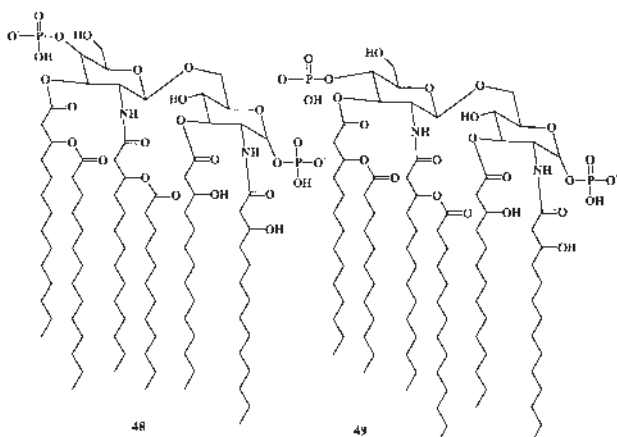
GUANIDINE GLYCOSIDE DERIVATIVES

A large number of biologically active molecules, including peptides, peptide mimetics, and guanidine-containing natural compounds, possess a guanidine group as an important structural element (69). Guanidine-containing bioactive molecules, particularly the analogs or derivatives of natural products, are notable targets for drug design and discovery (70–73). Because of the strongly basic character of the guanidine group, this group is protonated under physiological conditions. As a result of the positive charge thus imposed on the molecule, specific interactions between ligand and receptor or enzyme and substrate can be formed. With the current evolution in drug discovery whereby combinatorial chemistry plays an increasingly important role, the need for building blocks is rising as well (69).

Erylusamines A–E **54–58** are interleukin (IL)-6 receptor antagonists that were isolated from the Japanese sponge *Erylus placenta* (74,75). The cytotoxic glycolipids erylusamine TA **59**, erylusine **60**, and erylusidine **61,** similar to erylusamines, have been isolated from Red Sea sponge *Erylus cf. lendenfeldi* (76). Pachymoside A **62** has been isolated from crude extract of the North Sea marine sponge *Pachymatisma johnstonia* (77).
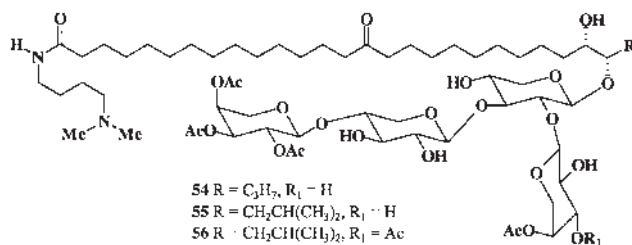
54 R = C$_3$H$_7$, R$_1$ = H
55 R = CH$_2$CH(CH$_3$)$_2$, R$_1$ = H
56 R = CH$_2$CH(CH$_3$)$_2$, R$_1$ = Ac
57 R = C$_4$H$_9$, R$_1$ = Ac
58 R = C$_5$H$_{11}$, R$_1$ = Ac

59 R = Me$_2$N—

60 R = Me$_2$N—

61

62 Pachymoside A
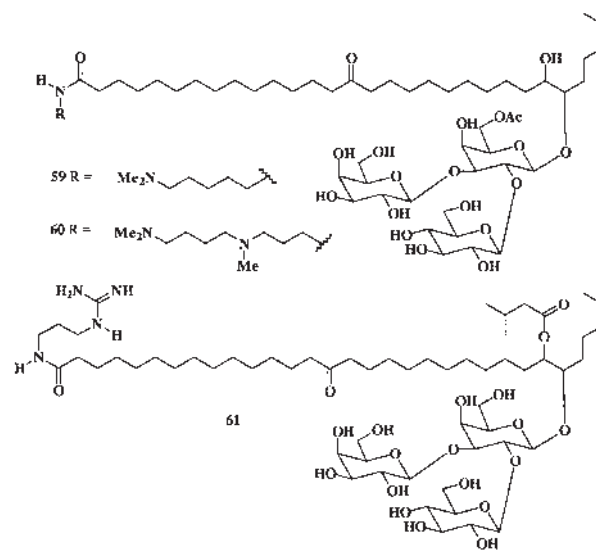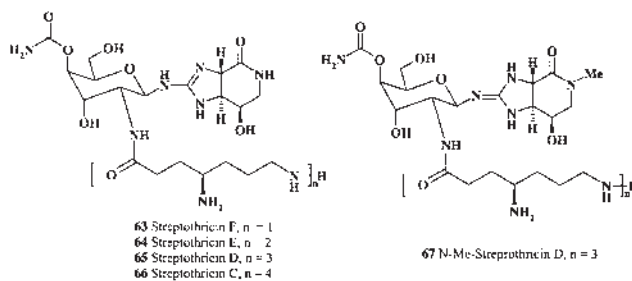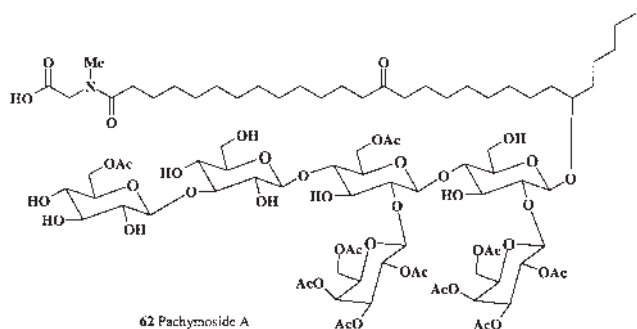
Streptothricins are a group of related basic antibiotics produced by a soil actinomycete (*Streptomyces* species) (78), and they show antibacterial, antimicrobial, antiviral, antiphage, and antifungal activities (79–81). Streptothricins F **63**, E **64**, D **65**, and C **66** have been isolated from *Streptomyces noursei* (78). A new member of the streptothricin family of antibiotics, *N*-methyl-streptothricin D **67**, has been isolated from an unidentified *Streptomyces* strain (82). This compound has a broad range of antimicrobial activity against fungi, Gram-positive and Gram-negative bacteria. Three streptothricin derivatives A-53930A **68**, A-53930B **69**, and A-53930C **70** (which was identical to streptothricin B) have been isolated from *Streptomyces vinausdrappus* SANK-62394 (83). These compounds showed inhibitory activity against N-type Ca^{2+} channels. Although A-53930C had antimicrobial activity against Gram-negative and Gram-positive bacteria and fungi, A-53930A and B showed weak activity only against Gram-negative bacteria. Streptothricins also are potent inhibitors of prokaryotic protein biosynthesis, but they are not used therapeutically because of their nephrotoxicity (84).
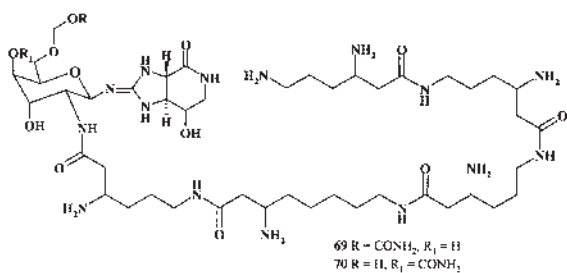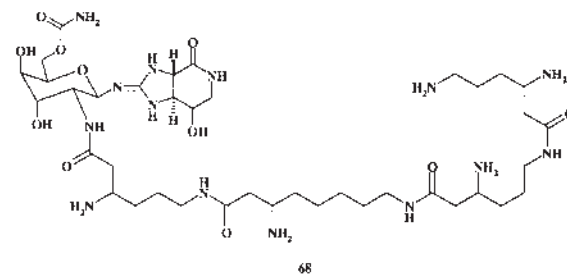
The nourseothricins **71**–**77** belong to the family of the streptothricin antibiotics that are produced by various streptomycete strains such as *Streptomyces noursei* (85). These compounds are nucleoside peptides containing a carbamido-D-gulosamine core, to which a poly-β-lysine chain and the unusual amino acid streptolydine are attached in amide and N-glycosidic linkages, respectively. The various members of the group differ in the length of their poly-β-lysine chains. Nourseothricin is currently being used under the name cloNAT (Werner Bioagents, Germany), and is an effective selective agent for molecular cloning technologies in fungi and plants (86–89).

63 Streptothricin F, n = 1
64 Streptothricin E, n = 2
65 Streptothricin D, n = 3
66 Streptothricin C, n = 4

67 N-Me-Streptothricin D, n = 3

68

69 R = CONH₂, R₁ = H
70 R = H, R₁ = CONH₂

71-77 n = 1-7
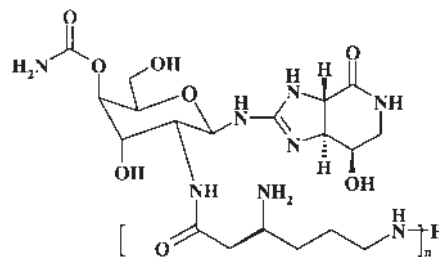
TETRAMIC ACID GLYCOSIDE DERIVATIVES

A culture of a marine strain of the fungus *Epicoccum purpurascens*, isolated from the inner tissue of the jellyfish *Aurelia aurita*, produced a novel tetramic acid derivative, epicoccamide **78** (90). Ancorinosides A **79**, B **80**, C **81**, and D **82**, inhibitors of membrane type 1 matrix metalloproteinase (MT1-MMP), were identified from the marine sponge *Penares sollasi* (91). Ancorinosides B–D inhibited MT1-MMP with IC$_{50}$ values of 180–500 µg/mL.
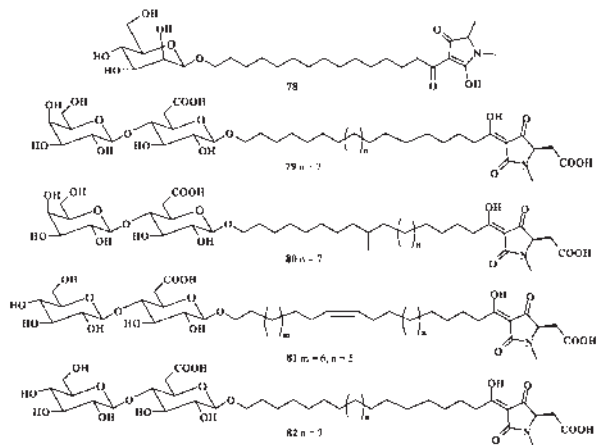
Aurantosides A **83** and B **84**, cytotoxic tetramic acid amine glycosides, have been isolated from the marine sponge *Theonella* sp. (92). The structures of these chlorinated metabolites were elucidated by chemical and physical methods. Aurantoside C **85,** which is lethal to brine shrimp, was found in the sponge *Homophymia conferta* (93). Other aurantosides D **86**, E **87** and F **88,** which exhibit potent antifungal activity against *Aspergillus fumigatus* and *Candida albicans,* were isolated from the marine sponge *Siliquariaspongia japonica* (94).
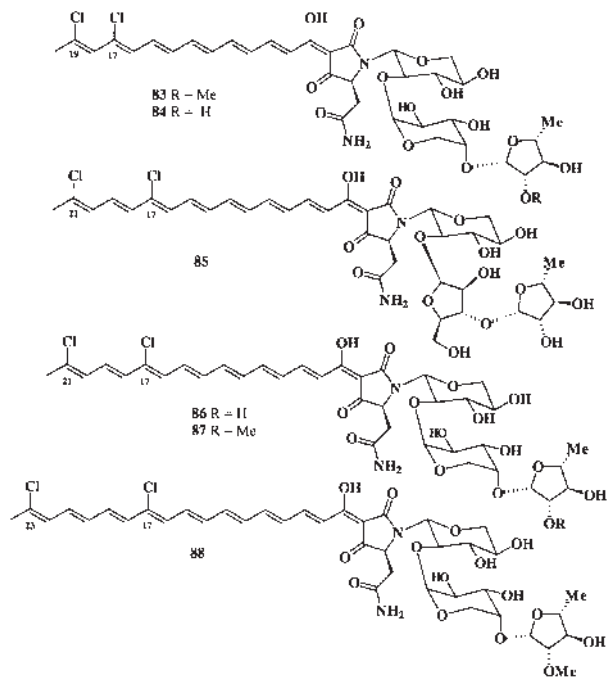
Rubroside A **89**, B **90**, C **93**, D **91**, G **92**, E **94**, F **95**, H **96**, and also hexadecahydrorubroside D **97**, aurantoside A **98**, and aurantoside B **99** have also been found in *Siliquariaspongia japonica* (95). The rubrosides induced numerous large intracellular vacuoles in 3Y1 rat fibroblasts at concentrations of 0.5–1.0 µg/mL, and rubrosides A, C, D, and E were cytotoxic against P388 murine leukemia cells with IC$_{50}$ (concentration at which growth or activity is inhibited by 50%) values of 0.046–0.21 µg/mL. Most rubrosides show antifungal activity against *Aspergillus fumigatus* and *Candida albicans.*
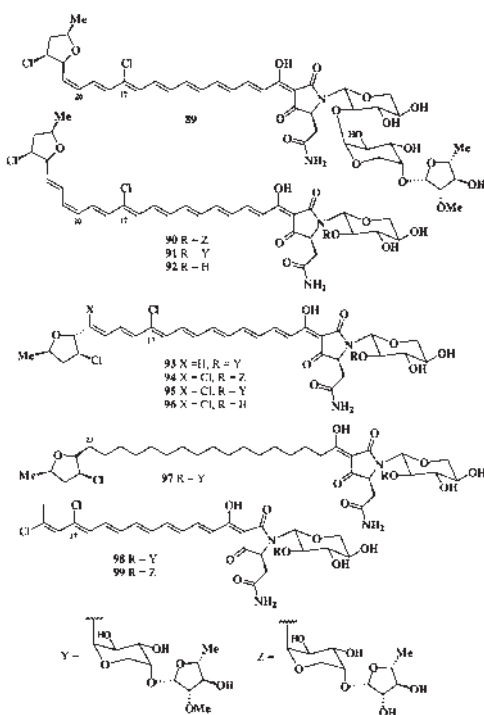
Aurantosides G–I **100**–**102** have been isolated from the lithistid sponge *Theonella swinhoei* from Papua New Guinea (96). Compounds **100**–**102** represent new monochloropentaenoyl tetramic acids with mono-, di-, and tri-N-saccharide substituents, respectively. Aurantosides G–I failed to show any significant cytotoxicity against the human colon tumor cell line HCT-116.
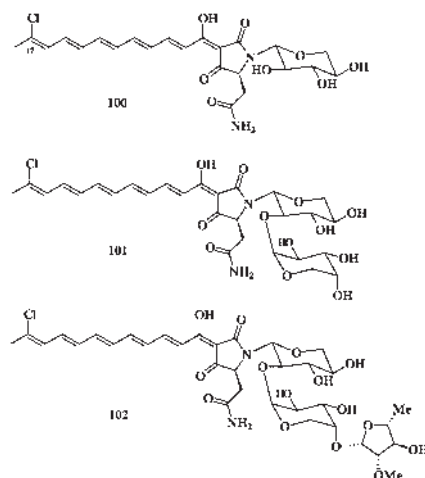
CEREBROSIDES

Cerebrosides are a group of glycosphingolipids composed of a hexose, a long-chain aminoalcohol (sphingoid), and an amide-linked long-chain FA. Galactocerebrosides were first isolated from brain tissue in the late 1800s (97). The "sphingosin" backbone of sphingolipids was so named by J.L.W. Thudichum in 1884 for its enigmatic ("Sphinx-like") properties. These mammalian cerebrosides include a mix of saturated and monoenoic *n*-alkyl and 2-hydroxy-FA, with sphingosine (4-*trans*-sphingenine, a 1,3-dihydroxy-2-aminoalcohol) as the major sphingoid (97). Over 30 years ago, glucocerebrosides were identified as a minor (<1%) lipid class in plant tissues (98). Perhaps because they constitute such a small portion of the total tissue lipids, plant glucocerebrosides received little attention prior to the recent finding (following development of the two-phase membrane partitioning method) that they can represent a major fraction of the total lipids in both the plasma membrane and tonoplast (99–102). Several reports have also implicated glucocerebrosides as playing a role in chilling injury (101) and in acclimation to cold and water-deficit stress in different plant species (99,103).

Many FA amides as well as their glycosides that have been isolated from marine microorganisms and invertebrates show high biological activity (104–106). Placosides A **103** and B **104** have been isolated from Bahamian sponge *Plakortis simplex* (107). These compounds exhibit immunosuppressive properties. Glycosyl ceramides **105**–**110** have been isolated from marine sponges *Agelas dispar* (108), *A. clathrodes* (109), *A. conifera* (110), and *A. longissima* (111,112). All the isolated compounds were tested using the mixed leucocyte reaction assay, and only **106**, **107**, and **110** were shown to be immunoactivating agents, suggesting a possible structure–activity relationship. It was also reported that glycosyl ceramides isolated from sponges belonging to the genus *Agelas* show antitumor activity (108,109).
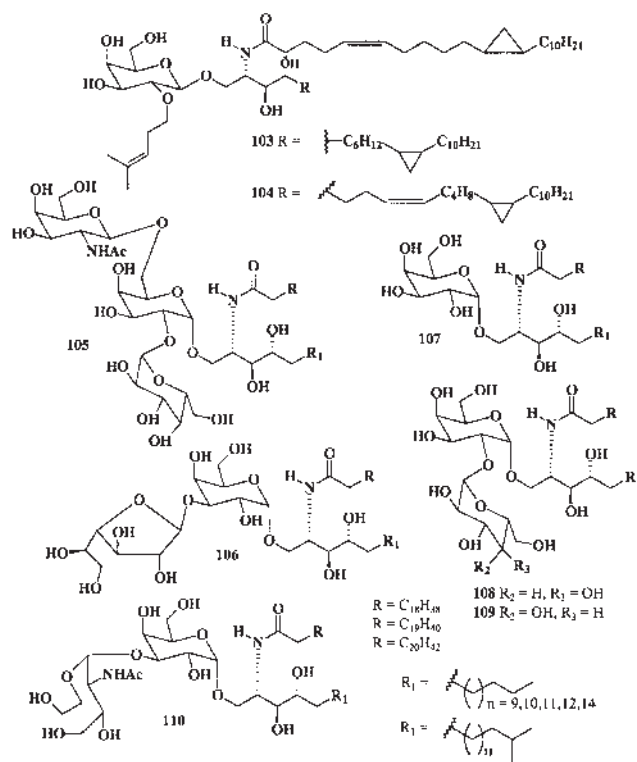
Another sponge species, *Agelas mauritianus*, from Okinawa Island contained a series of glycosphingolipids termed agelasphins: AGL-10 **111** and AGL-12 **112** (two major components), AGL-7A **113**, AGL-7B (mixture), AGL-9A **114**, AGL-9B **115**, AGL-11 **116**, and AGL-13 **117** (113). Three glycosphingolipids, regulosides A-C **118**–**120,** were obtained from extracts of the starfish *Pentaceraster regulus* (114), and two related compounds, temnosides A **121** and B **122**, were isolated from the sea urchin *Temnopleurus toreumaticus*; both specimens were collected from the Mandapam coast of India (115).

111 R = C$_{22}$H$_{45}$
112 R = C$_{23}$H$_{47}$

113 R$_1$ = C$_{22}$H$_{45}$, R$_2$ = C$_{12}$H$_{25}$
114 R$_1$ = C$_{22}$H$_{45}$, R$_2$ = C$_{13}$H$_{27}$
115 R$_1$ = C$_{22}$H$_{45}$, R$_2$ = (CH$_2$)$_3$CH(CH$_3$)$_2$
116 R$_1$ = C$_{22}$H$_{45}$, R$_2$ = (CH$_2$)$_{11}$CH(CH$_3$)C$_2$H$_5$
117 R$_1$ = C$_{23}$H$_{47}$, R$_2$ = (CH$_2$)$_{11}$CH(CH$_3$)C$_2$H$_5$

118 R = C$_{20}$H$_{41}$
119 R = C$_{21}$H$_{43}$
120 R = C$_{22}$H$_{45}$

121

122
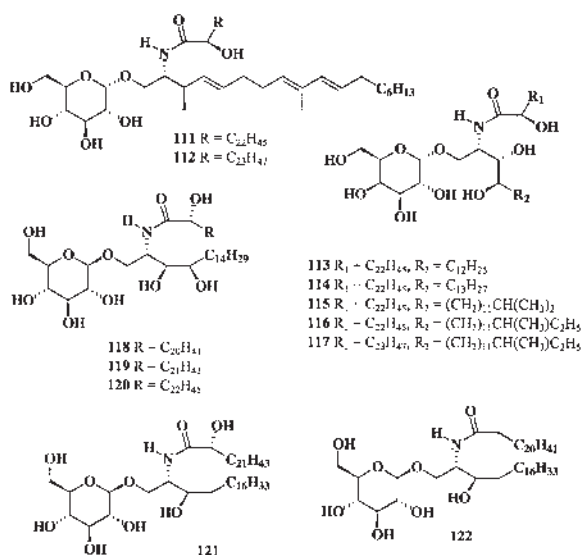
Six cerebrosides, acanthacerebrosides D–F **123**–**125** and A–C **126**–**128,** have been isolated from the starfish *Acanthaster planci* (116,117), along with two ceramide lactosides, acanthalactosides A **131** and B **132** (118). Ophidiacerebrosides A–F **133**–**137**, the cytotoxic cerebrosides, have been isolated from the Mediterranean starfish *Ophidiaster ophidiamus* (119). Cerebrosides CE-2b **138**, CE-2c **139,** and CE-2d **140** were found in the sea cucumber *Cucumaria echinata* (120); and cerebrosides PA-0–1 **129**, PA-0–5 **130**, PA-2–5 **141,** and PA-2–6 **142** were isolated from *Pentacta austalis* (121).

123 R = C$_{20}$H$_{41}$
124 R = C$_{21}$H$_{43}$
125 R = C$_{22}$H$_{45}$

126 R = C$_{12}$H$_{25}$, R$_1$ = C$_{22}$H$_{45}$
127 R = C$_{16}$H$_{37}$, R$_1$ = C$_{14}$H$_{29}$
128 R = (CH$_2$)$_8$CH=CHC$_8$H$_{17}$, R$_1$ = C$_{14}$H$_{29}$

129 R = C$_{17}$H$_{35}$, R$_1$ = CH$_2$CH=CHC$_9$H$_{19}$
130 R = C$_{21}$H$_{43}$, R$_1$ = C$_7$H$_{14}$CH(CH$_3$)C$_2$H$_5$

131 R = C$_{12}$H$_{25}$, R$_1$ = C$_{22}$H$_{45}$

132 R = (CH$_2$)$_8$CH=CHC$_8$H$_{17}$, R$_1$ = C$_{14}$H$_{29}$

133 R = C$_{20}$H$_{41}$
134 R = C$_{16}$H$_{37}$
135 R = C$_{19}$H$_{39}$
136 R = C$_{21}$H$_{43}$
137 R = C$_{22}$H$_{45}$

138 R = C$_{20}$H$_{41}$
139 R = C$_{21}$H$_{43}$
140 R = C$_{22}$H$_{45}$

141 R = C$_{20}$H$_{41}$
142 R = C$_{21}$H$_{43}$
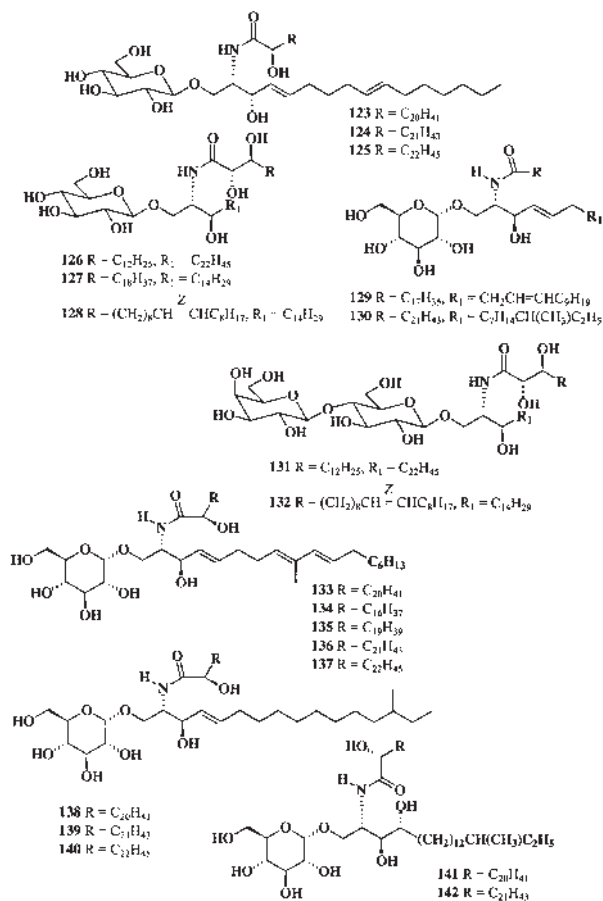
Axiceramides A **143** and B **144** were major components in a marine sponge belonging to the genus *Axinella* (122). Cerebroside **145**, which inhibits histidine decarboxylase, has been isolated from *Chondropsis* sp. (123). The ethanolic extract from the stem bark of *Dimocarpus fumatus* showed *in vitro* cytotoxic activity against KB cells. Fractionation of the extract gave compounds belonging to different classes, and one sphingolipid, soyacerebroside **146**, two glycosides of sitosterol, and FA were also identified (124).

143 R$_1$ = OH, R$_2$ = H
144 R$_1$ = H, R$_2$ = OH

145

146
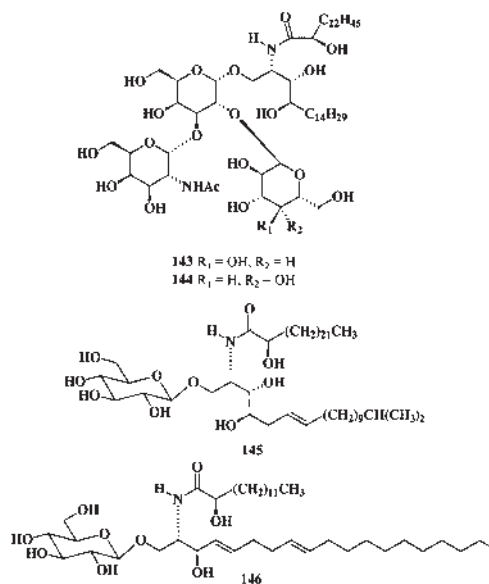
A series of neurogenic cerebrosides, termitomycesphins A–F **147**–**152**, have been isolated from the edible Chinese mushroom *Termitomyces albuminosus* (125,126). The isolated cerebrosides were shown to induce neuronal differentiation in rat PC12 cells. The marine fungus *Microsphaeropsis olivacea*, obtained from a sponge *Agelus* sp. (Florida), contains a cerebroside **153** (127). Common plant cerebrosides **154**–**157**, their structural diversity, biosynthesis, and functions have recently been reviewed (128). Also, a recent article reviewed the distribution, syntheses, and biological activities of the cerebrosides (129).

147 n = 2
148 n = 4

149 n = 2
150 n = 4

151 n = 2
152 n = 4

153

154 R = β-D-Man
155 R = β-D-Glc
156 R = [β-D-Man(1,4)]$_{1-5}$-β-D-Glc
157 R = β-D-Glc(1,4)-[β-D-Man(1,4)]$_{1,2}$-β-D-Glc
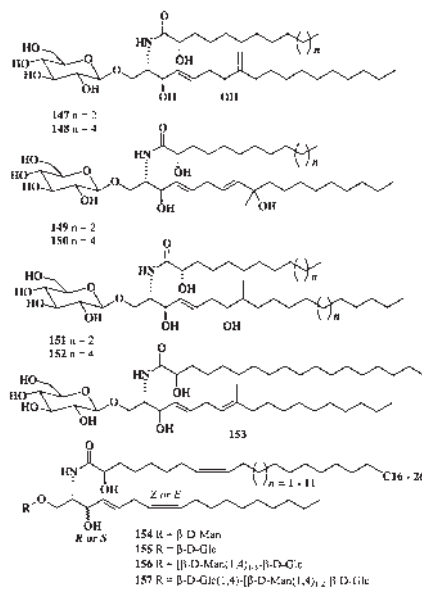
GANGLIOSIDES

Gangliosides are a family of glycosphingolipids containing one or more *N*-acetyl-neuraminic acid (sialic acid) residues in their structure. They are found in the plasma membrane of eukaryotic cells and confer a net negative charge on most animal cells. Localized mainly on the outer surface of cells, they are involved in various cellular functions including growth, differentiation, cell-to-cell interactions, and signal transduction (130). Gangliosides are also antigenic and participate in the pathogenesis of certain autoimmune diseases (131,132). The expression of gangliosides is tissue- and cell-specific and also development- and stage-specific. The species of animals is another determinant for ganglioside expression. Thus, it is suggested that gangliosides may carry a specific function(s) in a certain cell type of individual animal species (133).

The biological significance of the phylogenetic patterns of lenticular gangliosides is not known. Regarding brain gangliosides, it has been claimed that their remarkable changes in composition and concentration may be required for the development of brain structure and function and environmental adaptation during evolution (134–136). Lenticular gangliosides may perform specific function(s) in the formation and function of eye lenses (137).

According to the National Library of Medicine (Bethesda, MD), more than 11,000 original and review articles have been published on gangliosides since 1950. The structures of more than 500 gangliosides isolated from animals, invertebrates, and microorganisms have been elucidated, and many novel biologically active gangliosides were synthesized. This review article will cover the structures of only some novel gangliosides that were isolated from natural sources.

Two new ganglioside molecular species, named acanthaganglioside I **158** and acanthaganglioside J **159,** have been isolated from the whole body of the crown-of-thorns starfish *Acanthaster planci* (138). The *N*-acyl groups on residue are C22:0 and C24:0 FA, whereas the fatty alcohol is straight (C16:0) in both gangliosides. Two monomethylated GM3-type ganglioside molecular species, **160** and **161**, have been obtained from the polar lipid fraction of the chloroform/methanol extract of the starfish *Luidia maculata* (139). The ceramide moieties were composed of heterogeneous unsubstituted FA, 2-hydroxy FA, sphingosine, and phytosphingosine units. Compound **160**, designated as LMG-3, represented a new ganglioside molecular species, and compound **161** was a known ganglioside species.
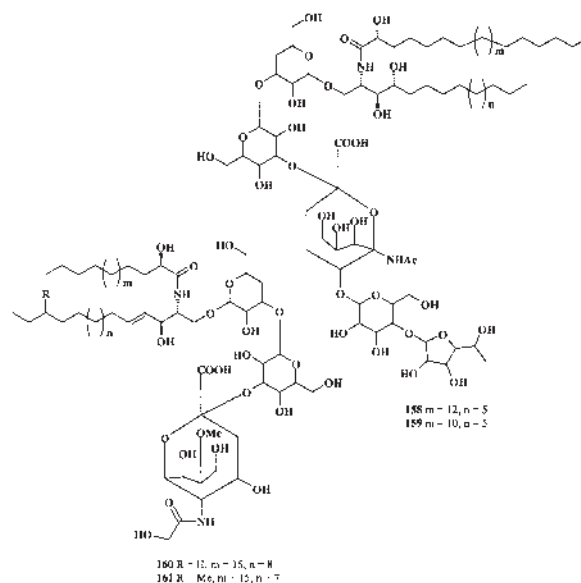
Three ganglioside molecular species, SCG-1 **162**, SCG-2 **163**, and SCG-3 **164**, were obtained from the lipid fraction of the sea cucumber *Stichopus chloronotus* (140). The ceramide moieties were composed of heterogeneous long-chain base and FA units. SCG-3 is the first type of ganglioside shown to contain a fucopyranose in the sialosyl trisaccharide moiety. Moreover, these three gangliosides exhibited neuritogenic activity toward the rat pheochromocytoma PC12 cells in the presence of nerve growth factor. The proportions of the neurite-bearing cells of SCG-1, SCG-2, and SCG-3 at a concentration of 3.3 mg/mL were 34.1, 24.4, and 24.5%, respectively. These effects were compared with that of the mammalian ganglioside GM1 (22.1% at a concentration of 3.3 mg/mL). Gangliosides with the same sugar moiety as that of SCG-1 have been identified from some marine invertebrates: *Cucumaria japonica* (141), *Holothuria atra*, *Telenota ananas* (142), *Stichopus japonicus* (143), *Holothuria leucospilota* (144), *Ophiura sarsi* (145), *Ophiocoma echinata*, *Ophiomastix annulosa* (146), *Ophiocoma scolopendrina* (147), and *Anthocidaris crassispina* (148). SCG-1 differs from them in the structure of the ceramide moiety. Gangliosides with the same sugar moiety as that of the major component of SCG-2 also have been obtained from *O. sarsi* (145), *O. scolopendrina* (147), and *Hemicentrotus pulcherrimus* (149), although the major component of SCG-2 is different from them in the ceramide structure.

162 n = 10

163 n = 4

164 n = 8

168 n = 3, m = 1
169 n = 5, m = 2
170 n = 7, m = 3
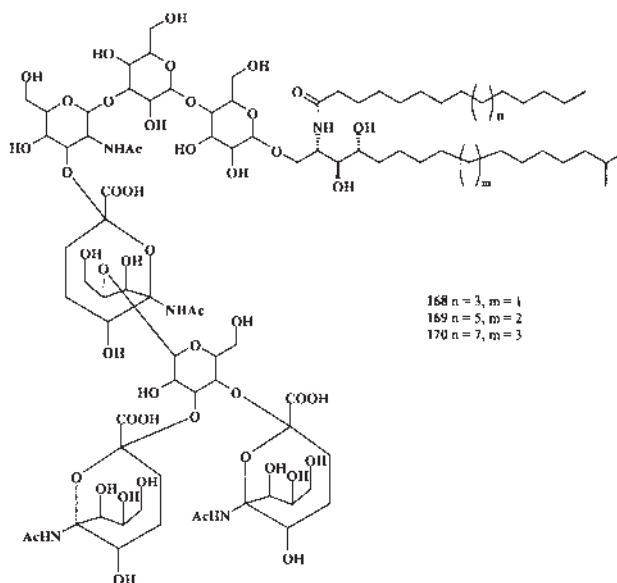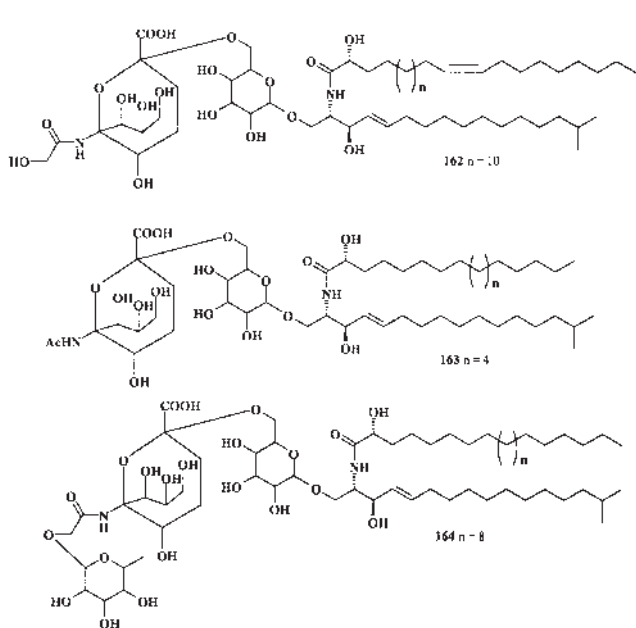
On the other hand, to the best of our knowledge, SCG-3 is a new ganglioside with a unique sialosyl trisaccharide moiety, **164**. The major species of gangliosides **165–167** were isolated from the Japanese sea cucumber *Stichopus chloronotus* (140). All three species displayed neuritogenic activity against PC12 cells in the presence of nerve growth factor. Structurally more complex ganglioside molecular species SJG-2 **168–170**, isolated from a Japanese collection of *S. japonicus*, also exhibited neuritogenic activity.

165 n = 6, m = 5

166 n = 12, m = 5

167 n = 11, m = 5
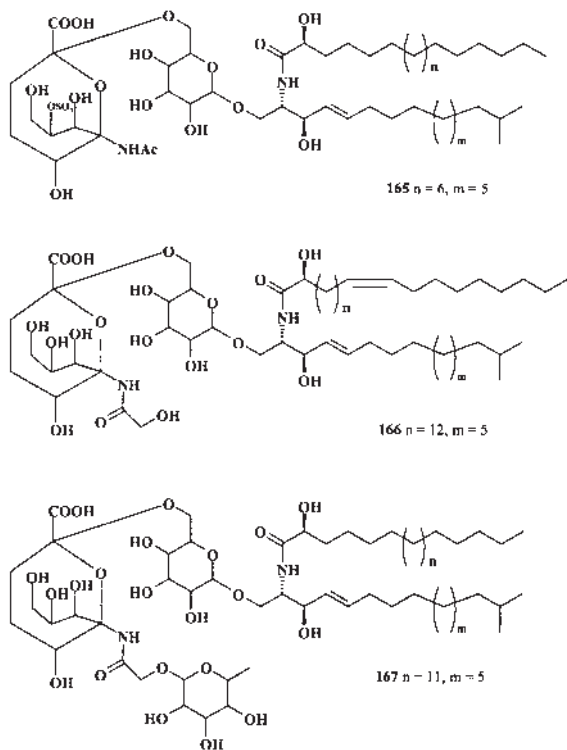
MACROLACTONE FATTY AMIDE GLYCOSIDES

Vicenistatin **171** is an antitumor antibiotic produced by *Streptomyces halstedii* HC-34. Its structure is unique in that it comprises a 20-membered lactam aglycon having an aminosugar vicenisamine. Its biological activity is also intriguing since antitumor activity has been particularly shown against xenographed models of certain human colon cancers. **171** and **172** have been isolated as minor congeners of vicenistatin **171** in the culture filtrate of the producing microorganism, and named as vicenistatin M **172**, because the minor congener is substituted by D-mycarose in place of vicenisamine of **171** (150,151). A novel ansamitocin amide N-glycoside, *N*-demethyl-*N*-β-D-glucopyranosyl ansamitocin P-2, named ansamitocinoside P-2 **173**, was isolated from *Actinosynnema pretiosum* (152).

171 R = NHMe
172 R = OH

173
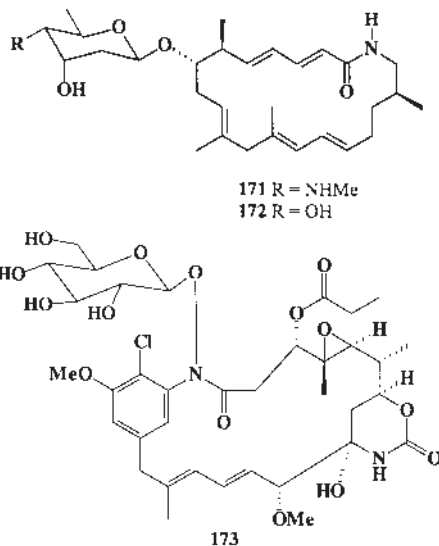
Fluvirucins A1 **174**, A2 **175**, B1 **176**, B2 **177**, and B3 **178** are macrolactam antibiotics produced by the actinomycete *Microtetraspora tyrrhenii* sp. nov. (*Actinomadura pusilla* group) strains Q464-31, L407-5, R-359-5, and R516-16 (153,154). All isolated compounds are active against the influenza A virus; B1 **176** is also active against *Candida* sp. (MIC, 0.91 µg/mL), and dermatophytes (MIC > 80.6 µg/mL) (154). Fluvirucin B2 **177** from the culture broth of *Streptomyces* inhibited PI-specific phospholipase C in cultured A431 cell cytosol with an IC$_{50}$ of 1.6 µg/mL (155).

174 R = Me
175 R = CH(OH)Me

176

177

178
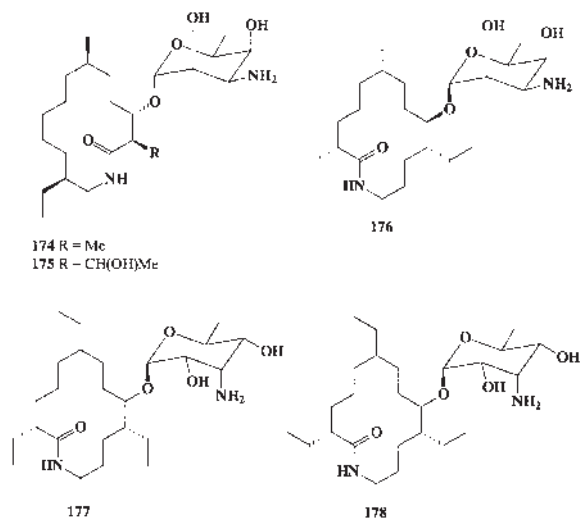
Semisynthetically produced 3-keto-substituted macrolide antibiotics (ketolides) **179** and **180** were compared for concentration-dependent inhibitory effects on growth rate, viable cell numbers, and protein synthesis rates in *Staphylococcus aureus* cells. Inhibitory effects on 50S ribosomal subunit formation were also examined, as this is a second target for these antibiotics. A concentration range of 0.01–0.1 µg/mL was tested. Compound **179** was the most effective from tested compounds with an IC$_{50}$ = 0.035 mg/mL. Telithromycin **180** had an IC$_{50}$ of 0.08 mg/mL (156). The authors concluded that these results indicate specific structural features of these antimicrobial agents contribute to defined inhibitory activities against susceptible organisms.

179

180
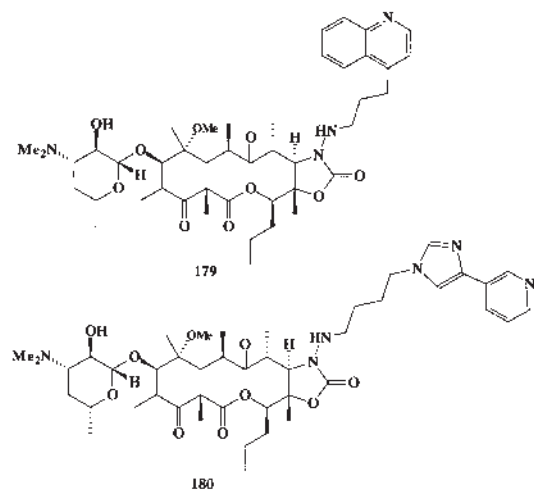
MISCELLANEOUS COMPOUNDS

A series of biologically active chlorinated metabolites that are derivatives of 7-methoxytetradec-4-enoic acid are produced by marine cyanobacteria belonging to the genus *Lyngbia* and by some marine invertebrates. The malyngamides, which are present in extracts of *L. majuscula*, consist typically of a FA side chain and a polar head group containing the unusual vinyl chloride functionality. The first malyngamide was isolated by Moore and co-workers in 1979 from Hawaiian *L. majuscula* (157). The (non-chlorine-containing) FA amide glycoside malyngamide J **181** isolated from Curaçao collections of *Lyngbia majuscula* (158) was toxic to both brine shrimp (LC$_{50}$ 18 µg/mL) and fish (goldfish LC$_{50}$ 40 µg/mL) (158). Malyngamide A **182** was found in a methanolic extract of *L. majuscula* (157) and isolated from the sea hare *Stylocheilus longicauda* (159). The sea hares (Opisthobranchia, Anaspidea) generally consume seaweeds that are chemically rich in secondary metabolites and concentrate these secondary metabolites in their digestive glands. The lipid extract of a Madagascan *L. majuscula* yielded malyngamides Q **183** and R **184** (160). Malyngamide R **184** was modestly toxic to brine shrimp (LD$_{50}$ 18 µg/mL). Isomalyngamides A (isomer **182**) and B **185** and the isomer of the latter, **186,** were isolated from *L. majuscula* collected from Hawaiian waters (161).

181

182

183 R = H
184 R = Me

185 Z
186 E
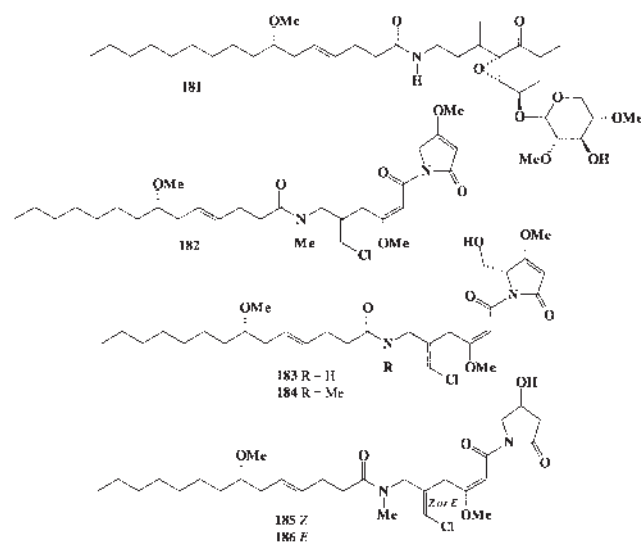
Three novel lipid nucleoside antibiotics named liposidomycins A **187**, B **188**, and C **189,** produced by *Streptomyces griseosporeus*, strongly inhibit bacterial peptidoglycan synthesis (162). The structure of the FA component of liposidomycin A **187** was a 3-hydroxy-7,10-hexadecadienoic acid, not previously found in nature.

187

R = dihydrouracil

188

189
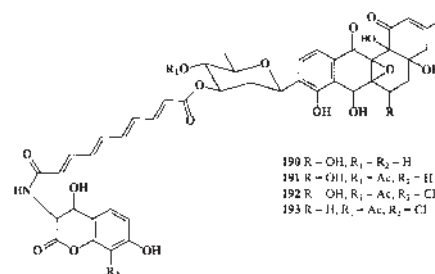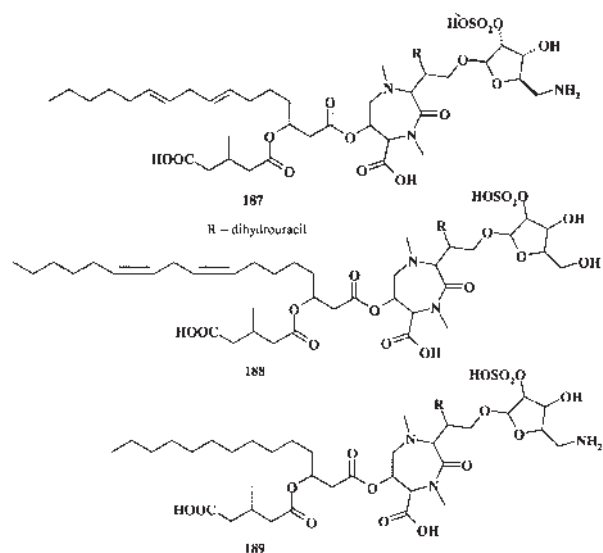
190 R = OH, R₁ = R₂ = H
191 R = OH, R₁ = Ac, R₂ = H
192 R = OH, R₁ = Ac, R₂ = Cl
193 R = H, R₁ = Ac, R₂ = Cl

194

195

196
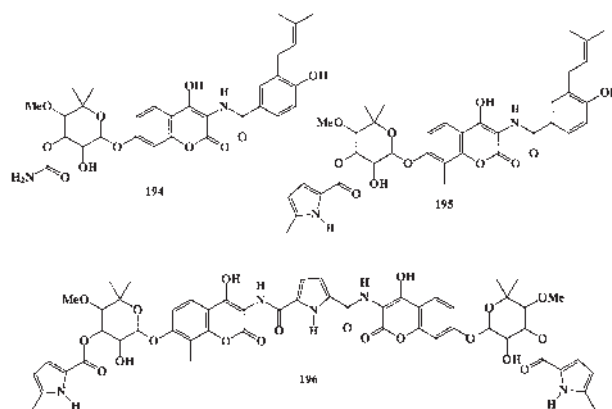
Simocyclinones are novel natural hybrid antibiotics isolated from the fermentation broth of *Streptomyces antibioticus* Tü 6040 that combine structural elements from various groups of known antibiotics such as aquayamycin, fumagillin, and novobiocin (163,164). So far, 14 different angucyclinone antibiotics have been isolated and classified in four series, A–D. The simocyclinones of the A-series consist solely of an angucycline ring. The components of series B are glycosylated. Compounds of the C-series have a tetraene side-chain, and those of the D-series **190–193** also have a coumarin ring system. A novel family of angucyclinone antibiotics demonstrated antibiotic activity against Gram-positive bacteria, as well as cytostatic effects against human tumor cell lines and antibacterial and antitumor activities (163–167). The 3-amino-4,7-dihydroxy-coumarin moiety is also found in the antibiotics novobiocin **194**, clorobiocin **195**, and coumermycin A1 **196**, which are very potent inhibitors of DNA gyrase (168). The aminocoumarin ring is of central importance for the binding of these compounds to the B subunit of gyrase (169–171). Recent experiments have suggested that simocyclinone D8 **193** is even more potent as a DNA gyrase inhibitor than novobiocin (171). The aminocoumarin antibiotics novobiocin **194**, clorobiocin **195,** and coumermycin A1 **196** are produced by different *Streptomyces* strains.

Ten different derivatives of glycine-containing glycolipids **197–206** have been isolated from a Gram-negative, biosurfactant-producing, *n*-alkane-degrading marine bacterium *Alcanivorax borkumensis* (172). This Gram-negative, aerobic, rod-shaped bacterium uses a limited number of organic compounds, including aliphatic hydrocarbons, volatile FA, and pyruvate and its methyl ether. During cultivation on *n*-alkanes as sole source of carbon and energy, all strains produced both extracellular and cell-bound surface-active glucose lipids **197–206** (173). This novel class of glucolipids was produced only by these strains, which were isolated from sediment samples collected near the Isle of Borkum (North Sea). The mixed active biosurfactants produced are characterized as glucose lipids, one of which consists of four 3-hydroxydecanoic acids linked together by ester bonds and coupled glycosidically with the C-1 of glucose. Other FA were found, namely, 16:0, 16:1, and 18:1, in the phospholipid fraction (173).
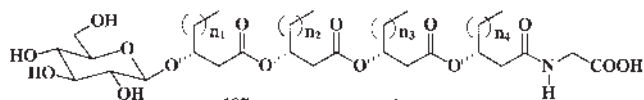
197 $n_1 = n_2 = n_3 = n_4 = 6$
198 $n_1 = n_2 = n_4 = 6, n_3 = 4$
199 $n_1 = n_2 = n_3 = 6, n_4 = 4$
200 $n_1 = n_3 = n_4 = 6, n_2 = 4$
201 $n_1 = 4, n_2 = n_3 = n_4 = 6$
202 $n_1 = n_4 = 4, n_2 = n_3 = 6$
203 $n_1 = n_3 = 6, n_2 = n_4 = 4$
204 $n_1 = n_4 = 6, n_2 = n_3 = 6$
205 $n_1 = n_2 = 6, n_3 = n_4 = 4$
206 $n_1 = 2, n_2 = n_3 = n_4 = 6$

The bengamides **207–225,** isolated from marine sponges belonging to the genus *Jaspidae*, comprise a large family of natural metabolites. In 1986, a group from the University of California–Santa Cruz reported the first examples of this class, (+) bengamide A **207** and (+) B **208**, as an easily separable mixture from a small sponge collection, subsequently identified as *Jaspis* cf. *coriacea* (Family Coppatiidae, Order Choristida) (174). These compounds display a wide and interesting range of biological activities, including antitumor, antibiotic, and antihelmintic properties. Bengamides A **207** and B **208** were more potent than bengamide P, with average IC_{50} values of 0.046, 0.011, and 2.70 fM, respectively (175). The *in vitro* antitumor activity against MDA-MB-435 human mammary carcinoma was also determined for natural bengamides A, B, E, F, P, M, O, and Z and for synthetic samples of B and O. The best activity was observed for the natural bengamides A (IC_{50} = 1 nM) and O (IC_{50} = 0.3 nM) (175).
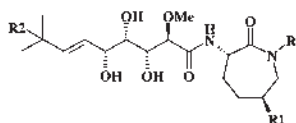
207 R, R_2 = H, R_1 = OCO(CH$_2$)$_{12}$CH$_3$
208 R = H, R_2 = Me, R_1 = OCO(CH$_2$)$_{12}$CH$_3$
209 R, R_1, R_2 = H
210 R = Me, R_1, R_2 = H
211 R = H, R_2 = Me, R_1 = OCOPh
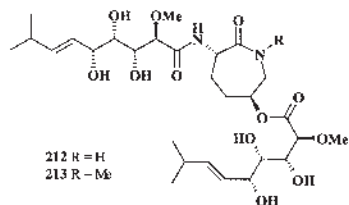
212 R = H
213 R = Me
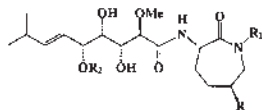
214 R = OCO(CH$_2$)$_{11}$CHMe$_2$, R_1,R_2 = H
215 R = OCO(CH$_2$)$_{11}$CHMe$_2$, R_1 = Me, R_2 = H
216 R = OCO(CH$_2$)$_{10}$CHMe$_2$, R_1,R_2 = H
217 R = OCO(CH$_2$)$_{10}$CHMe$_2$, R_1 = Me, R_2 = H
218 R = R,R_1 = H, R_2 = CO(CH$_2$)$_{12}$Me
219 R = H, R_1 = Me, R_2 = CO(CH$_2$)$_{13}$Me
220 R,R_1 = H, R_2 = CO(CH$_2$)$_{14}$Me
221 R = OH, R_1, R_2 = H
222 R = OH, R = Me, R_2 = H
223 R = OCO(CH$_2$)$_{11}$Me, R_1, R_2 = H
224 R = OCO(CH$_2$)$_{11}$Me, R_1 = Me, R_2 = H
225 R = OCO(CH$_2$)$_{13}$Me, R_1, R_2 = H

Pathogenic strains of the soilborne fungus *Periconia circinata* produce peritoxins **227–231** with host-selective toxicity against susceptible genotypes of sorghum at concentrations as low as 1.0 ng/mL (176,177). The peritoxins are low-M.W. hybrid molecules consisting of a peptide and a chlorinated polyketide **228–231**. Peritoxins A **228** and B **229** and periconins A **230** and B **231** have been isolated together with the known metabolite circinatin **226** from culture filtrates of the fungal pathogen *P. circinata*.
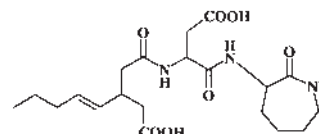
226
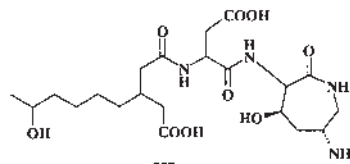
227
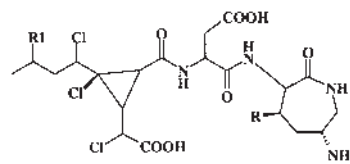
228 R, R_1 = OH
229 R = OH, R_1 = H
230 R = H, R_1 = OH
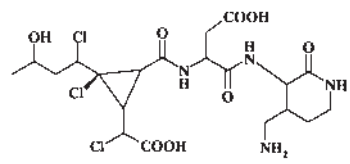
231

Several unusual α-glucosidase inhibitors **232–237** containing sulfated FA have been isolated from some marine sponge species. Penasulfate A **232**, a new α-glucosidase inhibitor, was isolated from a marine sponge *Penares* sp. (178); this compound included a novel sulfated FA (2-piperidine-carboxylic acid). Three similar α-glucosidase inhibitors named schulzeines A **233**, B **234**, and C **235** were isolated from the marine sponge *P. schulzei* (179). Schulzeines A–C showed inhibitory activity against α-glucosidase, with IC_{50} values of 48–170 nM. Unique 30- and 31-membered macrolides encompassing a proline residue and three sulfate groups, named penarolide sulfates A1 **236** and A2 **237**, have been isolated from a marine sponge *Penares* sp. (180). These metabolites inhibited α-glucosidase, with IC_{50} values of 1.2 and 1.5 mg/mL.

232

233

234 (S)-H
235 (R)-H

236

237
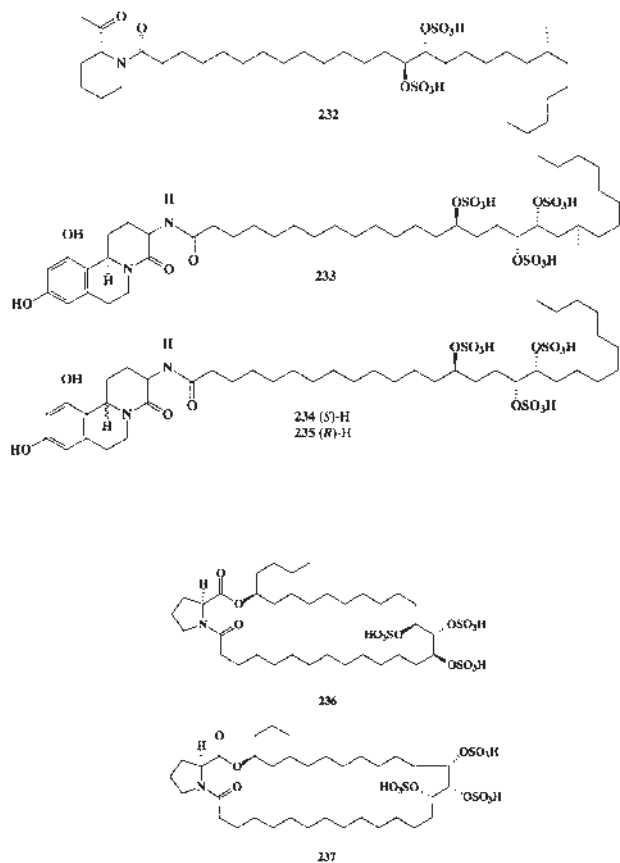
UNUSUAL AMIDE GLYCOSIDES

Amide surfactants are widely used as functional chemicals and are indispensable for various industrial fields (181–183). Synthetic detergents have molecular structures and properties that are similar to soap. Detergent molecular structures consist of a long hydrocarbon chain and a water-soluble ionic group. Most detergents have a negative ionic group and are called anionic detergents. Surfactants have a major impact on the performance of modern-day cleaning systems. In addition to performance, however, there is a growing appreciation for surfactants that are also environmentally friendly and produced from renewable resources. Sugar-based surfactants fit these requirements, and glucosamides (183–186) are one form that is experiencing rapid growth rates. In recent years, much attention has been paid from the ecologial and industrial viewpoints to sugar-based surfactants such as alkyl glucoside (187–189). Some interesting surfactants based on amide bond(s) that have biological activities have been synthesized (183).

Some diseases are initiated by the adherence of viruses, bacteria, or bacterial toxins to cell surface carbohydrates, a number of which are components of glycosphingolipids. Studies of the binding of lectins indicated that many adhered weakly to monomeric carbohydrate ligands (183,184). In addition to more completely defining ligand specificity of the carbohy-

drate-binding pathogen, identification of multivalent carbohydrate ligands has led to studies of their efficacy as pathogen inhibitors. This commentary focuses on pathogens that recognize the carbohydrate portion of glycosphingolipids. Because many glycosphingolipid-binding pathogens have been shown to bind multivalent saccharides, approaches for identifying and preparing them as well as methods for characterizing their effectiveness as ligands were reviewed (183,184). Several multivalent saccharide ligands were reported in the past 10 years.

Synthesis of amide glycoside derivatives of multivalent ligands that cross-link concanavalin A dimers of saccharides **238** and **239** and a biophysical evaluation of their interaction with the plant lectin concanavalin A have been reported (190). To the best of our knowledge, these structures are the first reported of their kind. Results obtained by Dimick *et al.* (190) indicate that hemagglutination assays evaluate the ability of ligands to inhibit the formation of cross-linked lattices, a process only tangentially related to reversible ligand binding. Cluster glycoside effects observed in agglutination assays must therefore be viewed with caution. Such effects may be relevant to the design of therapeutically useful amide saccharides.

238

239
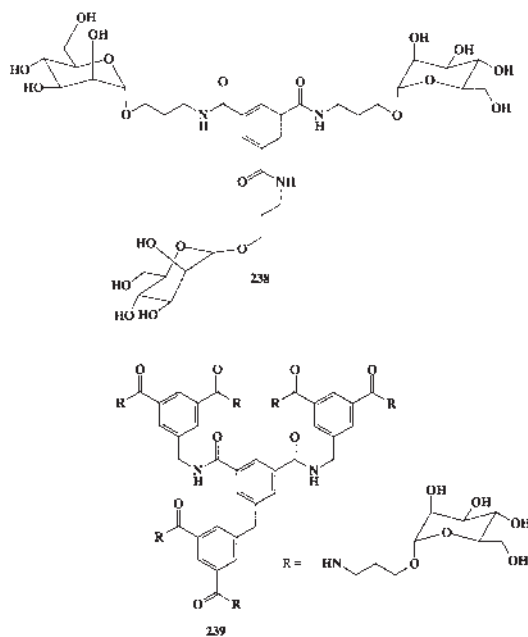
Several convergent glycodendrimer syntheses based on aromatic cores have been reported (183). Stoddart and co-workers reported convergent synthesis of polyvalent dendritic compound **240** (191). Thus, carbohydrate-centered ligands are terminated with a total of 12 glucose residues, although the microscopic environment of each is somewhat different. A related group of ligands, again derived from a convergent synthetic route and centered on an aromatic core, present terminal glucose residues in nominally equivalent microenvironments. Burke and co-workers synthesized three mannosyl residues around a macrocyclic core **241** to produce a rigid trivalent ligand (192).
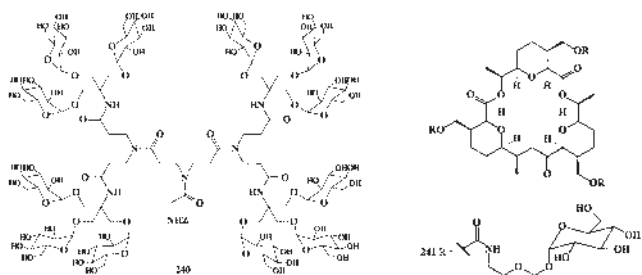
A group of so-called two-component toxins are responsible for the pathology of the world's most severe enterotoxic diseases; these toxins include the *Escherichia coli* heat-labile toxin, the shiga toxin, and the cholera toxin. The toxins are structurally and mechanistically related to the tetanus, diphtheria, and pertussis toxins and to the plant toxins abrin and ricin. Fan and co-workers (193) synthesized a pentavalent galactoside ligand for the *E. coli* heat-labile toxin based on a macrocyclic core **242–245**. Multivalent cyclo-oligosaccharides **246–250**, versatile carbohydrate clusters with dual roles as molecular receptors and lectin ligands, have recently been synthesized (194).

242 n = 1
243 n = 2
244 n = 3
245 n = 4

246 β-D-Glc
247 β-D-Gal
248 α-D-Man
249 β-D-Fuc
250 β-L-Fuc

n = 1,2,3,4,7
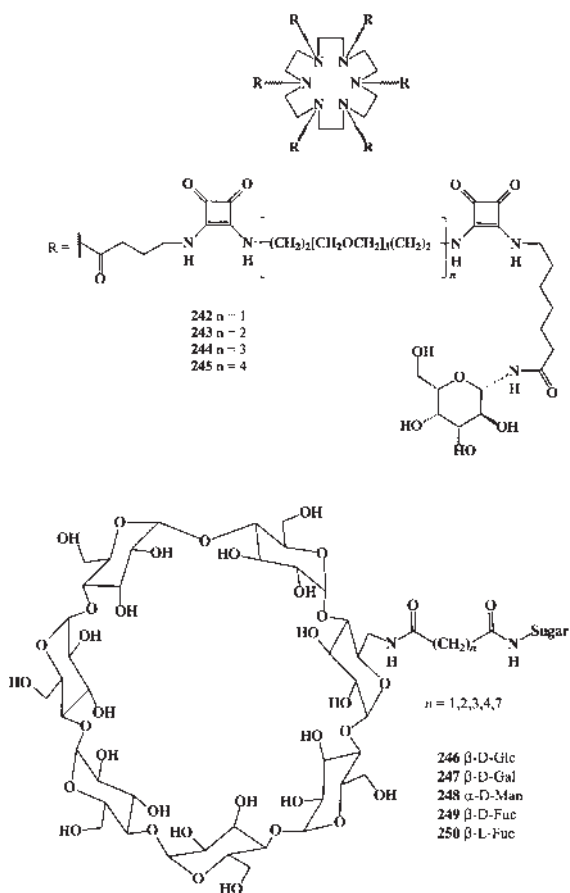
SUMMARY

FA amides are commonly used as foaming and wetting agents in hand dish-washing detergents, shampoos, and bar soaps, particu-larly the diethanollauryl amide. Amphoteric or zwitterionic surfactants have two functional group, one anionic and one cationic. In most cases it is the pH that determines which of the groups will dominate, by favoring one or the other ionization: anionic at alkaline pH and cationic at acid pH. Near the isoelectric point, these surfactants display both charges and are truly amphoteric, often with a minimum of interfacial activity and a concomitant maximum of water solubility. Amphoteric surfactants, particularly the amino acid ones, are quite biocompatible and are used in pharmaceuticals and cosmetics. Besides their excellent surfactant properties, i.e., wetting power, cleaning performance, foaming power, hard water tolerance, and lime soap dispersibility, particular emphasis is placed on the mildness of amphoteric surfactants and on their low toxicity toward the skin and eyes and, in particular, on the improvement in dermatological and mucous membrane compatibility in mixtures with anionic surfactants in shampoos. In addition, their zwitterionic character makes them compatible with both anionic and cationic surfactants. Amphoteric surfactants are a minor, but important ingredient of cosmetic products. Beside their activity as a surfactant, they contribute in combination with anionics toward the particular mildness and low toxicity of the products.

REFERENCES

1. Dembitsky, V.M. (2005) Astonishing Diversity of Natural Surfactants. 3. Carotenoid Glycosides and Isoprenoid Glycolipids, *Lipids 40*, 535–557.
2. Dembitsky, V.M. (2004) Chemistry and Biodiversity of Biologically Active Natural Glycosides, *Chem. Biodivers. 1*, 673–781.
3. Kester, M. (1997) Sphingolipid Metabolites and the Cellular Phenotype, *Trends Glycosci. Glycotechnol. 9*, 447–460.
4. Yowler, B.C., and Schengrund, C.L. (2004) Glycosphingolipids—Sweets for Botulinum Neurotoxin, *Glycoconj. J. 21*, 287–293.
5. Morales, A., Colell, A., Mari, M., Garcia-Ruiz, C., and Fernandez-Checa, J.C. (2003) Glycosphingolipids and Mitochondria: Role in Apoptosis and Disease, *Glycoconj. J. 20*, 579–588.
6. Tettamanti, G. (2003) Ganglioside/Glycosphingolipid Turnover: New Concepts, *Glycoconj. J. 20*, 301–317.
7. Malykh, Y.N., Schauer, R., and Shaw, L. (2001) *N*-Glycolylneuraminic Acid in Human Tumours, *Biochimie 83*, 623–634.
8. Schmid, H.H.O., Schmid, P.C., and Natarajan, V. (1990) N-Acylated Glycerophospholipids and Their Derivatives, *Prog. Lipid Res. 29*, 1–43.
9. Sutcliffe, I.C., and Harrington, D.J. (2004) Lipoproteins of *Mycobacterium tuberculosis*: An Abundant and Functionally Diverse Class of Cell Envelope Components, *FEMS Microbiol. Rev. 28*, 645–659.
10 Kuehl, F.A., Jr., Jacob, T.A., Ganley, O.H., Ormond, R.E., and Meisinger, M.A.P. (1957) The Identification of *n*-(2-Hydroxyethyl)-palmitamide as a Naturally Occurring Anti-inflammatory Agent, *J. Am. Chem. Soc. 79*, 5577–5578.
11. Devane, W.A., Hanus, L., Breuer, A., Pertwee, R.G., Stevenson, L.A., Griffin, G., Gibson, D., Mandelbaum, A., Etinger, A., and Mechoulam, R. (1992) Isolation and Structure of a Brain Constituent That Binds to the Cannabinoid Receptor, *Science 258*, 1946–1949.
12. Cravatt, B.F., Prospero-Garcia, O., Siuzdak, G., Gilula, N.B., Henriksen, J., Boger, D.L., and Lerner, R.A. (1995) Chemical Characterization of a Family of Brain Lipids That Induce Sleep, *Science 268*, 1506–1509.

13. Schuel, H., Burkman, L.J., Lippes, J., Crickard, K., Forester, E., Piomelli, D., and Giuffrida, A. (2002) *N*-Acylethanolamines in Human Reproductive Fluids, *Chem. Phys. Lipids 121*, 211–227.

14. Lambert, D.M., Vandevoorde, S., Jonsson, K.O., and Fowler, C.J. (2002) The Palmitoyl-ethanolamide Family: A New Class of Anti-inflammatory Agents? *Curr. Med. Chem. 9*, 663–674.

15. Fowler, C.J. (2004) Oleamide: A Member of the Endocannabinoid Family? *Br. J. Pharmacol. 141*, 195–196.

16. Touw, D.J., Neef, C., Thomson, A.H., and Vinks, A.A. (2005) Cost-effectiveness of Therapeutic Drug Monitoring—A Systematic Review, *Ther. Drug Monit. 27*, 10–17.

17. Carrasco, D.A., Vander, S.M., and Tyring, S.K. (2002) A Review of Antibiotics in Dermatology, *J. Cutan. Med. Surg. 6*, 128–150.

18. Begg, E.J., Barclay, M.L., and Kirkpatrick, C.M.J. (2001) The Therapeutic Monitoring of Antimicrobial Agents, *Br. J. Clin. Pharmacol. 52 (Suppl. 1)*, 35S–43S.

19. Fainerman, V.B., Mobius, D., and Miller, R., eds. (2001) *Surfactants: Chemistry, Interfacial Properties, Applications*, Elsevier, Amsterdam, The Netherlands, pp. 678.

20. Milton, J.R. (2004) *Surfactants and Interfacial Phenomena*, 3rd edn., 500 pp., John Wiley & Sons, New York.

21. Schramm, L.L., ed. (2000) *Surfactants: Fundamentals and Applications in the Petroleum Industry*, 630 pp., Cambridge University Press, Cambridge, United Kingdom.

22. Ash, M., and Ash, I. (1993) *Handbook of Industrial Surfactants: An International Guide to More Than 16,000 Products by Tradename, Application, Composition & Manufacturer*, 905 pp., Gower, Aldershot, Hants, England.

23. Chain, E., Florey, H.W., Gardner, A.D., Heatley, N.G., Jennings, M.A., Orr-Ewing, J., and Sanders, A.G. (1940) Penicillin as a Chemotherapeutic Agent, *Lancet 1*, 226–228.

24. Ikeda, D., and Umezawa, S. (1999) Aminoglycoside Antibiotics, in *Naturally Occurring Glycosides* (Ikan, R., ed.), pp. 13–42, Wiley & Sons, Chichester, England.

25. Umezawa, H., and Hooper, I.R., eds. (1982) *Aminoglycoside Antibiotics*, Springer–Verlag, Berlin.

26. Cappelletti, L.M., and Spagnoli, R. (1983) Biological Transformation of Kanamycin A to Amikacin (BBK-8), *J. Antibiot. (Tokyo) 36*, 328–330.

27. Yoshikawa, K., Suzuki, Y., Tanaka, M., Arihara, S., and Nigam, S.K. (1997) Three Acylated Saponins and a Related Compound from *Pithecellobium dulce*, *J. Nat. Prod. 60*, 1269–1274.

28. Kondo, S., and Hotta, K. (1999) Semisynthetic Aminoglycoside Antibiotics: Development and Enzymatic Modifications, *J. Infect. Chemother. 5*, 1–9.

29. Okachi, R., Takasawa, S., Sato, T., Sato, S., Yamamoto, M., Kawamoto, I., and Nara, T. (1977) Fortimicins A and B, New Aminoglycoside Antibiotics. II. Isolation, Physico-chemical and Chromatographic Properties, *J. Antibiot. (Tokyo) 30*, 541–551.

30. Egan, R.S., Stanaszek, R.S., Cirovic, M., Mueller, S.L., Tadanier, J., Martin, J.R., Collum, P., Goldstein, A.W., De Vault, R.L., Sinclair, A.C., *et al.* (1977) Fortimicins A and B, New Aminoglycoside Antibiotics. III. Structural Identification, *J. Antibiot. (Tokyo) 30*, 552–563.

31. Yamamoto, M., Okachi, R., Kawamoto, I., and Nara, T. (1977) Fortimicin A Production by *Micromonospora olivoasterospora* in a Chemically Defined Medium, *J. Antibiot. (Tokyo) 30*, 1064–1072.

32. Girolami, R.L., and Stamm, J.M. (1977) Fortimicins A and B, New Aminoglycoside Antibiotics. IV. *In vitro* Study of Fortimicin A Compared with Other Aminoglycosides, *J. Antibiot. (Tokyo) 30*, 564–570.

33. Yamashita, K., Kawabe, H., and Mitsuhashi, S. (1981) Synergistic Activities of Fortimicin A and β-Lactam Antibiotics Against *Pseudomonas aeruginosa*, *Antimicrob. Agents Chemother. 20*, 33–37.

34. Slattery, M., Rajbhandari, I., and Wesson, K. (2001) Competition-Mediated Antibiotic Induction in the Marine Bacterium *Streptomyces tenjimariensis*, *Microb. Ecol. 41*, 90–96.

35. Taylor, H.D., and Schmitz, H. (1976) Antibiotics Derived from a Mutant of *Bacillus circulans*, *J. Antibiot. (Tokyo) 29*, 532–535.

36. Umezawa, S. (1974) Structures and Syntheses of Aminoglycoside Antibiotics, *Adv. Carbohydr. Chem. Biochem. 30*, 111–182.

37. Kilcoyne, M., Perepelov, A., Shashkov, A.S., Nazarenko, E.L., Ivanova, E.P., Gorshkova, N.M., Gorshkova, R.P., and Savage, A.V. (2004) Structure of an Acidic O-Specific Polysaccharide from Marine Bacterium *Shewanella fidelis* KMM 3582^T Containing N$^\varepsilon$—[(*S*)-1-Carboxyethyl]-N$^\alpha$-(D-galacturonoyl)-L-Lysine, *Carbohydr. Res. 339*, 1655–1661.

38. Ivanova, E.P., Nedashkovskaya, O.I., Zhukova, N.V., Nicolau, D.V., Christen, R., and Mikhailov, V.V. (2003) *Shewanella waksmanii* sp. nov., Isolated from a Sipuncula (*Phascolosoma japonicum*), *Int. J. Syst. Evol. Microbiol. 53*, 1471–1477.

39. Spies, H.S.C., and Steenkamp, D.J. (1994) Thiols of Intracellular Pathogens—Identification of Ovothiol-A in *Leishmania donovani* and Structural Analysis of a Novel Thiol from *Mycobacterium bovis*, *Eur. J. Biochem. 224*, 203–213.

40. Gunaga, P., Moon, H.R., Choi, W.J., Shin, D.H., Park, J.G., and Jeong, L.S. (2004) Recent Advances in 4-Thionucleosides as Potential Antiviral and Antitumor Agents, *Curr. Med. Chem. 11*, 2585–2637.

41. Wrodnigg, T.M., and Sprenger, F.K. (2004) Bioactive Carbohydrates and Recently Discovered Analogues as Chemotherapeutics, *Mini Rev. Med. Chem. 4*, 437–459.

42. O'Riordan, T., and Faris, M. (1999) Inhaled Antimicrobial Therapy, *Respir. Care Clin. N. Am. 5*, 617–631.

43. Russell, A.D. (1969) The Mechanism of Action of Some Antibacterial Agents, *Prog. Med. Chem. 6*, 135–199.

44. Takatsuki, A., Arima, K., and Tamura, G. (1971) Tunicamycin, a New Antibiotic. I. Isolation and Characterization of Tunicamycin, *J. Antibiot. (Tokyo) 24*, 215–223.

45. Takatsuki, A., and Tamura, G. (1971) Tunicamycin, a New Antibiotic. II. Some Biological Properties of the Antiviral Activity of Tunicamycin, *J. Antibiot. (Tokyo) 24*, 224–231.

46. Takatsuki, A., and Tamura, G. (1971) Tunicamycin, a New Antibiotic. 3. Reversal of the Antiviral Activity of Tunicamycin by Aminosugars and Their Derivatives, *J. Antibiot. (Tokyo) 24*, 232–238.

47. Thrum, H., Eckardt, K., Bradler, G., Fugner, R., Tonew, E., and Tonew, M. (1975) Streptovirudins, New Antibiotics with Antibacterial and Antiviral Activity. I. Culture Taxonomy, Fermentation and Production of Streptovirudin Complex, *J. Antibiot. (Tokyo) 28*, 514–521.

48. Tonew, E., Tonew, M., Eckardt, K., Thrum, H., and Gumpert, B. (1975) Streptovirudins—New Antibiotics with Antiviral Activity. The Antiviral Spectrum and Inhibition of Newcastle Disease Virus in Cell Cultures, *Acta Virol. 19*, 311–317.

49. Elbein, A.D., Occolowitz, J.L., Hamill, R.L., and Eckardt, K. (1981) Streptovirudins of Series I and II: Chemical and Biological Properties, *Biochemistry 20*, 4210–4216.

50. Vogel, P., Petterson, D.S., Berry, P.H., Frahn, J.L., Anderton, N., Cockrum, P.A., Edgar, J.A., Jago, M.V., Lanigan, G.W., Payne, A.L., *et al.* (1981) Isolation of a Group of Glycolipid Toxins from Seedheads of Annual Ryegrass *Lolium rigidum* Gaud. Infected by *Corynebacterium rathayi*, *Aust. J. Exp. Biol. Med. Sci. 59*, 455–467.

51. Frahn, J.L., Edgar, J.A., Jones, A.J., Cockrum, P.A., Anderton, N., and Culvenor, C.C.J. (1984) Structure of the Corynetoxins, Metabolites of *Corynebacterium rathayi* Responsible for Toxicity of Annual Ryegrass (*Lolium rigidum*) Pastures, *Aust. J. Chem. 37*, 165–182.

52. Eckardt, K., Thrum, H., Bradler, G., Tonew, E., and Tonew, M. (1975) Streptovirudins, New Antibiotics with Antibacterial and

Antiviral Activity. II. Isolation, Chemical Characterization and Biological Activity of Streptovirudins A1, A2, B1, B2, C1, C2, D1, and D2, *J. Antibiot. (Tokyo) 28*, 274–279.

53. Jago, M.V., and Culvenor, C.C. (1987) Tunicamycin and Corynetoxin Poisoning in Sheep, *Aust. Vet. J. 64*, 232–235.

54. Rosenberg, E., and Ron, E.Z. (1999) High and Low Molecular Mass Microbial Surfactants, *Appl. Microbiol. Biotechnol. 52*, 154–162.

55. Lang, S., and Fischer, S. (1999) Design and Selection of Performance Surfactants in *Annual Surfactants Review*, (Karsa, D.R., ed.), Vol. 2 pp. 51–103, Academic Press, Sheffield.

56. Caroff, M., and Karibian, D. (2003) Structure of Bacterial Lipopolysaccharides, *Carbohydr. Res. 338*, 2431–2447.

57. Moran, A.P., Lindner, B., and Walsh, E.J. (1997) Structural Characterization of the Lipid A Component of *Helicobacter pylori* Rough- and Smooth-Form Lipopolysaccharides, *J. Bacteriol. 179*, 6453–6463.

58. Suda, Y., Ogawa, T., Kashihara, W., Oikawa, M., Shimoyama, T., Hayashi, T., Tamura, T., and Kusumoto, S. (1997) Chemical Structure of Lipid A from *Helicobacter pylori* Strain 206-1 Lipopolysaccharide, *J. Biochem. (Tokyo) 121*, 1129–1133.

59. Qureshi, N., Kaltashov, I., Walker, K., Doroshenko, V., Cotter, R.J., Takayama, K., Sievert, T.R., Rice, P.A., Lin, J.-S.L., and Golenbok, D.T. (1997) Structure of the Monophosphoryl Lipid A Moiety Obtained from the Lipopolysaccharide of *Chlamydia trachomatis*, *J. Biol. Chem. 272*, 10594–10600.

60. Heine, H., Müller-Loennies, S., Brade, L., and Brade, H. (2003) Endotoxic Activity and Chemical Structure of Lipopolysaccharides from *Chlamydia trachomatis* Serotypes E and L-2 and *Chlamydophila psittaci* 6BC, *Eur. J. Biochem. 270*, 440–450.

61. Zarrouk, H., Karibian, D., Bodie, S., Perry, M.B., Richards, J., and Caroff, M. (1997) Structural Characterization of the Lipids A of Three *Bordetella bronchiseptica* Strains: Variability of Fatty Acid Substitution, *J. Bacteriol. 179*, 3756–3760.

62. Rund, S., Lindner, B., Brade, H., and Holst, O. (1999) Structural Analysis of the Lipopolysaccharide from *Chlamydia trachomatis* Serotype L2, *J. Biol. Chem. 274*, 16819–16824.

63. Rund, S., Lindner, B., Brade, H., and Holst, O. (2000) Structural Analysis of the Lipopolysaccharide from *Chlamydophila psittaci* Strain 6BC, *Eur. J. Biochem. 267*, 5717–5726.

64. Krauss, J.H., Seydel, U., Weckesser, J., and Mayer, H. (1989) Structural Analysis of the Nontoxic Lipid-A of *Rhodobacter capsulatus* 37B4, *Eur. J. Biochem. 180*, 519–526.

65. Moll, H., Sonesson, A., Jantzen, E., Marre, R., and Zähringer, U. (1992) Identification of 27-Oxo-octacosanoic Acid and Heptacosane-1,27-dioic Acid in *Legionella pneumophila*, *FEMS Microbiol. Lett. 76*, 1–6.

66. Zähringer, U., Knirel, Y.A., Lindner, B., Helbig, J.H., Sonesson, A., Marre, R., and Rietschel, E.T. (1995) The Lipopolysaccharide of *Legionella pneumophila* Serogroup 1 (strain Philadelphia 1): Chemical Structure and Biological Significance, *Prog. Clin. Biol. Res. 392*, 113–139.

67. Mayer, H., Merkofer, T., Warth, C., and Weckesser, J. (1996) Position and Configuration of Double Bonds of Lipid A-Associated Monounsaturated Fatty Acids of Proteobacteria and *Rhodobacter capsulatus* 37B4, *J. Endotoxin Res. 3*, 345–352.

68. Kumada, H., Haishima, Y., Umemoto, T., and Tanamoto, K.I. (1995) Structural Study on the Free Lipid-A Isolated from Lipopolysaccharide of *Porphyromonas gingivalis*, *J. Bacteriol. 177*, 2098–2106.

69. Hannon, C.L., and Anslyn, E.V. (1993) The Guanidinium Group: Its Biological Role and Synthetic Analogs, in *Bioorganic Chemistry Frontiers*, (Dugas, H., ed.), Vol. 3, pp. 193–221, Springer-Verlag, Berlin.

70. Berlinck, R.G.S. (1999) Natural Guanidine Derivatives, *Nat. Prod. Rep. 16*, 339–365.

71. Berlinck, R.G.S. (2002) Natural Guanidine Derivatives, *Nat. Prod. Rep. 19*, 617–649.

72. Prandota, J. (2000) Unusual Distribution, Pharmacokinetics, and Metabolism of Some Drugs and Their Implications to Pharmacotherapy, *Am. J. Ther. 7*, 332–340.

73. Brown, T.D., Burris, H.A., Havlin, K.A., O'Rourke, T.J., Rodriguez, G.I., Wall, J.G., and Weiss, G.R. (1991) New Anticancer Agents, *Cancer Chemother. Biol. Response Modif. 12*, 111–146.

74. Sata, N., Asai, N., Matsunaga, S., and Fusetani, N. (1994) Erylusamines, IL-6 Receptor Antagonists, from the Marine Sponge, *Erylus placenta*, *Tetrahedron 50*, 1105–1110.

75. Fusetani, N., Sata, N., Asai, N., and Matsunaga, S. (1993) Isolation and Structure Elucidation of Erylusamine-B, a New Class of Marine Natural Products, Which Blocked an IL-6 Receptor, from the Marine Sponge *Erylus placenta* Thiele, *Tetrahedron Lett. 34*, 4067–4070.

76. Goobes, R., Rudi, A., and Kashman, Y. (1996) Three New Glycolipids from a Red Sea Sponge of the Genus *Erylus*, *Tetrahedron 52*, 7921–7928.

77. Warabi, K., Zimmerman, W.T., Shen, J.K., Gauthier, A., Robertson, M., Finlay, B.B., van Soest, R., and Andersen, R.J. (2004) Pachymoside A—A Novel Glycolipid Isolated from the Marine Sponge *Pachymatisma johnstonia*, *Can. J. Chem. 82*, 102–112.

78. Khokhlov, A.S., and Shutova, K.I. (1972) Chemical Structure of Streptothricins, *J. Antibiot. (Tokyo) 25*, 501–508.

79. Riabova, I.D., Reshetov, P.D., Zhdanov, G.L., and Khokhlov, A.S. (1965) Antimicrobial Activity of Streptothricins, *Antibiotiki (Moscow) 10*, 1066–1069 [in Russian].

80. Germanova, K.I., and Goncharskaia, T.I. (1969) Antiviral Properties of Streptothricins A, B, C, D, F, *Antibiotiki (Moscow) 14*, 48–51 [in Russian].

81. Germanova, K.I., and Goncharskaia, T.I. (1969) Antiphage Activity of Streptothricins A, B, C, D, F, *Antibiotiki (Moscow) 14*, 137–140 [in Russian].

82. Kim, B.T., Lee, J.Y., Lee, Y.Y., Kim, O.Y., Chu, J.H., and Goo, Y.M. (1994) *N*-Methyl-streptothricin D. A New Streptothricin Group Antibiotic from a *Streptomyces* spp., *J. Antibiot. (Tokyo) 47*, 1333–1336.

83. Hisamoto, M., Inaoka, Y., Sakaida, Y., Kagazaki, T., Enokida, R., Okazaki, T., Haruyama, H., Kinoshita, T., and Matsuda, K. (1998) A-53930A and B, Novel N-Type Ca^{2+} Channel Blockers, *J. Antibiot. (Tokyo) 51*, 607–617.

84. Hoffmann, H., Härtl, A., Bocker, H., Kahnel, H.-J., Hesse, G., and Flemming, J. (1986) Pharmacokinetics of Nourseothricin in Laboratory Animals, *Arch. Exp. Veterinarmed. 40*, 699–709 [in German].

85. Bocker, H., and Bergter, F. (1986) Nourseothricin: Properties, Biosynthesis, Production, *Arch. Exp. Veterinarmed. 40*, 646–657 [in German].

86. Haupt, I., Thrum, H., and Noack, D. (1986) Self-Resistance of the Nourseothricin Producing Strain *Streptomyces noursei*, *J. Basic Microbiol. 26*, 323–328.

87. Krügel, H., Fiedler, G., Gase, K., and Haupt, I. (1989) Streptothricin Resistance. in *Bioactive Metabolites from Microorganisms* (Bushell, M.E., and Gräfe, U., eds.), pp. 357–367, Elsevier, Amsterdam.

88. Krügel, H., Fiedler, G., Haupt, I., Sarfert, E., and Simon, H. (1988) Analysis of the Nourseothricin-Resistance Gene (*nat*) of *Streptomyces noursei*, *Gene 62*, 209–217.

89. Krügel, H., Fiedler, G., Smith, C., and Baumberg, S. (1993) Sequence and Transcriptional Analysis of the Nourseothricin Acetyltransferase-Encoding Gene *nat1* from *Streptomyces noursei*, *Gene 127*, 127–131.

90. Wright, A.D., Osterhage, C., and Konig, G.M. (2003) Epicoccamide, a Novel Secondary Metabolite from a Jellyfish Derived Culture of *Epicoccum purpurascens*, *Org. Biomolecul. Chem. 1*, 507–510.

91. Fujita, M., Nakao, Y., Matsunaga, S., Seiki, M., Itoh, Y., van

Soest, R.W.M., and Fusetani, N. (2001) Ancorinosides B–D, Inhibitors of Membrane Type 1 Matrix Metalloproteinase (MT1-MMP), from the Marine Sponge *Penares sollasi* Thiele, *Tetrahedron 57*, 1229–1234.

92. Matsunaga, S., Fusetani, N., Kato, Y., and Hiroda, H. (1991) Bioactive Marine Metabolites. 38. Aurantoside-A and Aurantoside-B—Cytotoxic Tetramic Acid Glycosides from the Marine Sponge *Theonella* sp., *J. Am. Chem. Soc. 113*, 9690–9692.

93. Wolf, D., Schmitz, F.J., Qiu, F., and Kelly-Borges, M. (1999) Aurantoside C, a New Tetramic Acid Glycoside from the Sponge *Homophymia conferta*, *J. Nat. Prod. 62*, 170–172.

94. Sata, N.U., Matsunaga, S., Fusetani, N., and van Soest, R.W.M. (1999) Aurantosides D, E, and F: New Antifungal Tetramic Acid Glycosides from the Marine Sponge *Siliquariaspongia japonica*, *J. Nat. Prod. 62*, 969–971.

95. Sata, N.U., Wada, S., Matsunaga, S., Watabe, S., van Soest, R.W.M., and Fusetani, N. (1999) Bioactive Marine Metabolites. Part 87. Rubrosides A–H, New Bioactive Tetramic Acid Glycosides from the Marine Sponge *Siliquariaspongia japonica*, *J. Org. Chem. 64*, 2331–2339.

96. Ratnayake, A.S., Davis, R.A., Harper, M.K., Veltri, C.A., Andjelic, C.D., Barrows, L.R., and Ireland, C.M. (2005) Aurantosides G, H, and I: Three New Tetramic Acid Glycosides from a Papua New Guinea *Theonella swinhoei*, *J. Nat. Prod. 68*, 104–107.

97. Hakomori, S. (1983) in *Handbook of Lipid Research,* Vol. 3, *Sphingolipid Biochemistry* (Kanfer, J.N., and Hakomori, S., eds.), pp. 1–37, Plenum Press, New York.

98. Sastry, P.S., and Kates, M. (1964) Lipid Components of Leaves. V. Galactolipids, Cerebrosides, and Lecithin of Runner Bean Leaves, *Biochemistry 3*, 1271–1280.

99. Lynch, D.V., and Steponkus, P.L. (1987) Plasma Membrane Lipid Alterations Associated with Cold-Acclimation of Winter Rye Seedlings (*Secale cereale* L-cv. *puma*), *Plant Physiol. 83*, 761–767.

100. Rochester, C.P., Kjellbom, P., Andersson, B., and Larsson, C. (1987) Lipid Composition of Plasma Membranes Isolated from Light-grown Barley (*Hordeum vulgare*) Leaves—Identification of Cerebroside as a Major Component, *Arch. Biochem. Biophys. 255*, 385–391.

101. Yoshida, S., Washio, K., Kenrick, J., and Orr, G. (1988) Thermotropic Properties of Lipids Extracted from Plasma Membrane and Tonoplast Isolated from Chilling-sensitive Mung Bean (*Vigna radiata* [L] Wilczek), *Plant Cell Physiol. 29*, 1411–1416.

102. Lynch, D.V. (1993) Sphingolipids, in *Lipid Metabolism in Plants* (Moore, T.S., Jr., ed.), pp. 285–308, CRC Press, Boca Raton, FL.

103. Norberg, P., and Liljenberg, C. (1991) Lipids of Plasma Membranes Prepared from Oat Root Cells—Effects of Induced Water Deficit Tolerance, *Plant Physiol. 96*, 1136–1141.

104. Burja, A.M., Banaigs, B., Abou-Mansour, E., Burgess, J.G., and Wright, P.C. (2001) Marine Cyanobacteria—A Prolific Source of Natural Products, *Tetrahedron 57*, 9347–9377.

105. Kobayashi, J., and Ishibashi, M. (1999) Marine Natural Products and Marine Chemical Ecology, in *Comprehensive Natural Products Chemistry* (Mori, K., ed.), Vol. 8, pp. 415–649, Elsevier, Amsterdam.

106. Dembitsky, V.M., and Srebnik, M. (2002) Natural Halogenated Fatty Acids: Their Analogues and Derivatives, *Prog. Lipid Res. 41*, 315–367.

107. Costantino, V., Fattorusso, E., Mangoni, A., Di Rosa, M., and Ianaro, A. (1997) Glycolipids from Sponges. 6. Plakoside A and B, Two Unique Prenylated Glycosphingolipids with Immunosuppressive Activity from the Marine Sponge *Plakortis simplex*, *J. Am. Chem. Soc. 119*, 12465–12470.

108. Costantino, V., Fattorusso, E., Mangoni, A., Di Rosa, M., Ia-

naro, A., and Maffia, P. (1996) Glycolipids from Sponges. IV. Immunomodulating Glycosyl Ceramides from the Marine Sponge *Agelas dispar*, *Tetrahedron 52*, 1573–1578.

109. Costantino, V., Fattorusso, E., and Mangoni, A. (1995) Glycolipids from Sponges. 3. Glycosyl Ceramides from the Marine Sponge *Agelas conifera*, *Liebigs Ann. Chem. 8*, 2133–2136.

110. Costantino, V., Fattorusso, E., and Mangoni, A. (1995) Glycolipids from Sponges. 1. Glycosyl Ceramide Composition of the Marine Sponge *Agelas clathrodes*, *Liebigs Ann. Chem. 8*, 1471–1475.

111. Cafieri, F., Fattorusso, E., Mahajnah, Y., and Mangoni, A. (1994) Longiside, a Novel Digalactosylceramide from the Caribbean Sponge *Agelas longissima*, *Liebigs Ann. Chem. 12*, 1187–1189.

112. Cafieri, F., Fattorusso, E., Mangoni, A., and Taglialatela-Scafati, O. (1995) Glycolipids from Sponges. 2. Glycosyl Ceramide Composition of the Marine Sponge *Agelas longissima*, *Liebigs Ann. Chem. 8*, 1477–1481.

113. Natori, T., Morita, M., Akimoto, K., and Koezuka, Y. (1994) Agelasphins, Novel Antitumor and Immunostimulatory Cerebrosides from the Marine Sponge *Agelas mauritianus*, *Tetrahedron 50*, 2771–2784.

114. Venkannababu, U., Bhandari, S.P.S., and Garg, H.S. (1997) Regulosides A–C: Glycosphingolipids from the Starfish *Pentaceraster regulus*, *Liebigs Ann. Chem. 6*, 1245–1247.

115. Babu, U.V., Bhandari, S.P.S., and Garg, H.S. (1997) Temnosides A and B, Two New Glycosphingolipids from the Sea Urchin *Temnopleurus toreumaticus* of the Indian Coast, *J. Nat. Prod. 60*, 732–734.

116. Kawano, Y., Higuchi, R., Isobe, R., and Komori, T. (1988) Biologically Active Glycosides from Asteroidea. 13. Glycosphingolipids from the Starfish *Acanthaster planci*. 2. Isolation and Structure of 6 New Cerebrosides, *Liebigs Ann. Chem. 1*, 19–24.

117. Sugiyama, S., Honda, M., and Komori, T. (1988) Biologically Active Glycosides from Asteroidea. 15. Asymmetric Synthesis of Phytosphingosine and Phytosphingosine Anhydro Base—Assignment of the Absolute Stereochemistry, *Liebigs Ann. Chem. 7*, 619–625.

118. Kawano, Y., Higuchi, R., Isobe, R., and Komori, T. (1988) Biologically Active Glycosides from Asteroidea. 17. Glycosphingolipids from the Starfish *Acanthaster planci*. 3. Isolation and Structure of 2 New Ceramide Lactosides, *Liebigs Ann. Chem. 12*, 1181–1183.

119. Jin, W., Rinehart, K.L., and Jares-Erijman, E.A. (1994) Ophidiacerebrosides—Cytotoxic Glycosphingolipids Containing a Novel Sphingosine from a Sea Star, *J. Org. Chem. 59*, 144–147.

120. Higuchi, R., Inagaki, K., Togawa, K., Miyamoto, T., and Komori, T. (1994) Constituents of Holothuroideae. 4. Isolation and Structure of 3 New Cerebrosides, Ce-2b, Ce-2c and Ce-2d, from the Sea Cucumber *Cucumaria echinata*, *Liebigs Ann. Chem. 1*, 79–84.

121. Higuchi, R., Inagaki, K., Togawa, K., Miyamoto, T., and Komori, T. (1994) Constituents of Holothuroideae. 5. Isolation and Structure of Cerebrosides from the Sea Cucumber *Pentacta australis*, *Liebigs Ann. Chem. 7*, 653–658.

122. Costantino, V., Fattorusso, E., Mangoni, A., Aknin, M., and Gaydou, E.M. (1994) Axiceramide-A and Axiceramide-B, 2 Novel Tri-α-glycosylceramides from the Marine Sponge *Axinella* sp., *Liebigs Ann. Chem. 12*, 1181–1185.

123. Endo, M., Nakagawa, M., Hamamoto, Y., and Ishihama, M. (1986) Pharmacologically Active Substances from Southern Pacific Marine Invertebrates, *Pure Appl. Chem. 58*, 387–394.

124. Voutquenne, L., Lavaud, C., Massiot, G., Sevenet, T., and Hadi, H.A. (1999) Cytotoxic Polyisoprenes and Glycosides of Longchain Fatty Alcohols from *Dimocarpus fumatus*, *Phytochemistry 50*, 63–69.

125. Qi, J., Ojika, M., and Sakagami, Y. (2000) Termitomycesphins

A–D, Novel Neuritogenic Cerebrosides from the Edible Chinese Mushroom *Termitomyces albuminosus*, *Tetrahedron 56*, 5835–5841.

126. Qi, J., Ojika, M., and Sakagami, Y. (2001) Neuritogenic Cerebrosides from an Edible Chinese Mushroom. Part 2: Structures of Two Additional Termitomycesphins and Activity Enhancement of an Inactive Cerebroside by Hydroxylation, *Bioorg. Med. Chem. 9*, 2171–2177.

127. Keusgen, M., Yu, C.M., Curtis, J.M., Brewer, D., and Ayer, S.W. (1996) A Cerebroside from the Marine Fungus *Microsphaeropsis olivacea* (Bonord.) Höhn, *Biochem. Syst. Ecol. 24*, 465–468.

128. Sperling, P., and E. Heinz, E. (2003) Plant Sphingolipids: Structural Diversity, Biosynthesis, First Genes and Functions, *Biochim. Biophys. Acta 1632*, 1–15.

129. Tan, R.X., and Chen, J.H. (2003) The Cerebrosides, *Nat. Prod. Rep. 20*, 509–534.

130. Colombaioni, L., and Garcia-Gil, M. (2004) Sphingolipid Metabolites in Neural Signalling and Function, *Brain Res. Brain Res. Rev. 46*, 328–355.

131. Paparounas, K. (2004) Anti-GQ1b Ganglioside Antibody in Peripheral Nervous System Disorders: Pathophysiologic Role and Clinical Relevance, *Arch. Neurol. 61*, 1013–1016.

132. Gleeson, A. (1994) Glycoconjugates in Autoimmunity, *Biochim. Biophys. Acta 1197*, 237–255.

133. Diatlovitskaia, E.V., and Kandyba, A.G. (2004) Bioeffector Sphingolipids as Stimulators of Cell Growth and Survival, *Bioorg. Khim. 30*, 227–233 [in Russian].

134. Avrova, N.F. (1985) Evolutionary Approach to the Analysis of Structure and Function of Gangliosides, *Neurochem. Res. 10*, 1547–1554.

135. Irwin, L.N. (1984) Phylogeny and Ontogeny of Vertebrate Brain Gangliosides, *Adv. Exp. Med. Biol. 174*, 319–329.

136. Kappel, T., Hilbig, R., and Rahmann, H. (1993) Variability in Brain Ganglioside Content and Composition of Endothermic Mammals, Heterothermic Hibernators and Ectothermic Fishes, *Neurochem. Int. 22*, 555–566.

137. Panzetta, P., and Allende, M.L. (2000) Ganglioside Expression During Differentiation of Chick Retinal Cells *in vitro*, *Neurochem. Res. 25*, 163–169.

138. Miyamoto, T., Yamamoto, A., Wakabayashi, M., Nagaregawa, Y., Inagaki, M., Higuchi, R., Iha, M., and Teruya, K. (2000) Biologically Active Glycosides from Asteroidea, Two New Gangliosides, Acanthagangliosides I and J from the Starfish *Acanthaster planci*, *Eur. J. Org. Chem.*, 2295–22301.

139. Kawatake, S., Inagaki, M., Isobe, R., Miyamoto, T., and Higuchi, R. (2002) Isolation and Structure of Monomethylated GM3-Type Ganglioside Molecular Species from the Starfish *Luidia maculate*, *Chem. Pharm. Bull. (Tokyo) 50*, 1386–1389.

140. Yamada, K., Hamada, A., Kisa, F., Miyamoto, T., and Higuchi, R. (2003) Constituents of Holothuroidea, 13. Structure of Neuritogenic Active Ganglioside Molecular Species from the Sea Cucumber *Stichopus chloronotus*, *Chem. Pharm. Bull. (Tokyo) 51*, 46–52.

141. Chekareva, N.V., Smirnova, G.P., and Kochetkov, N.K. (1991) Gangliosides of the Holothuria *Cucumaria japonica* Semper, *Bioorg. Khim. 17*, 398–402.

142. Smirnova, G.P. (1996) Gangliosides from *Holothuria atra* and *Telenota ananas*, *Bioorg. Khim. 22*, 134–139.

143. Kaneko, M., Kisa, F., Yamada, K., Miyamoto, T., and Higuchi, R. (2001) Constituents of Holothuroidea, 8. Structure of Neuritogenic Active Ganglioside from the Sea Cucumber *Stichopus japonicus*, *Eur. J. Org. Chem.* 3171–3174.

144. Yamada, K., Matsubara, R., Kaneko, M., Miyamoto, T., and Higuchi, R. (2001) Constituents of Holothuroidea, 10. Isolation and Structure of a Biologically Active Ganglioside Molecular Species from the Sea Cucumber *Holothuria leucospilota*, *Chem. Pharm. Bull. (Tokyo) 49*, 447–452.

145. Smirnova, G.P., Chekareva, N.V., and Kochetkov, N.K. (1986) Gangliosides of Ophiura, *Ophiura sarsi*, *Bioorg. Khim. 12*, 507–513.

146. Smirnova, G.P., Chekareva, N.V., and Kochetkov, N.K. (1991) Gangliosides from 2 Species of Ophiura, *Ophiocoma echinata* and *Ophiomastix annulosa* Clark, *Bioorg. Khim. 17*, 387–397.

147. Inagaki, M., Shibai, M., Isobe, R., and Higuchi, R. (2001) Constituents of Ophiuroidea. 1. Isolation and Structure of Three Ganglioside Molecular Species from the Brittle Star *Ophiocoma scolopendrina*, *Chem. Pharm. Bull. (Tokyo) 49*, 1521–1525.

148. Kubo, H., Irie, A., Inagaki, F., and Hoshi, M. (1990) Gangliosides from the Eggs of the Sea Urchin, *Anthocidaris crassispina*, *J. Biochem. (Tokyo) 108*, 185–192.

149. Ijuin, T., Kitajima, K., Song, Y., Kitazume, S., Inoue, S., Halsam, S.M., Morris, H.R., Dell, A., and Inoue, Y. (1996) Isolation and Identification of Novel Sulfated and Nonsulfated Oligosialyl Glycosphingolipids from Sea Urchin Sperm, *Glycoconj. J. 13*, 401–413.

150. Shindo, K., Kamishohara, M., Odagawa, A., Matsuoka, M., and Kawai, H. (1993) Vicenistatin, a Novel 20-Membered Macrocyclic Lactam Antitumor Antibiotic, *J. Antibiot. (Tokyo) 46*, 1076–1081.

151. Matsushima, Y., Nakayama, T., Fujita, M., Bhandari, R., Eguchi, T., Shindo, K., and Kakinuma, K. (2001) Isolation and Structure Elucidation of Vicenistatin M, and Importance of the Vicenisamine Aminosugar for Exerting Cytotoxicity of Vicenistatin, *J. Antibiot. (Tokyo) 54*, 211–219.

152. Lu, C., Bai, L., and Shen, Y. (2004) A Novel Amide N-Glycoside of Ansamitocins from *Actinosynnema pretiosum*, *J. Antibiot. (Tokyo) 57*, 348–350.

153. Naruse, N., Konishi, M., Oki, T., Inouye, Y., and Kakisawa, H. (1991) Fluvirucins A1, A2, B1, B2, B3, B4 and B5, New Antibiotics Active Against Influenza A Virus. III. The Stereochemistry and Absolute Configuration of Fluvirucin A1, *J. Antibiot. (Tokyo) 44*, 756–761.

154. Tomita, K., Oda, N., Hoshino, Y., Ohkusa, N., and Chikazawa, H. (1991) Fluvirucins A1, A2, B1, B2, B3, B4 and B5, New Antibiotics Active Against Influenza A Virus. IV. Taxonomy on the Producing Organisms, *J. Antibiot. (Tokyo) 44*, 940–948.

155. Ui, H., Imoto, M., and Umezawa, K. (1995) Inhibition of Phosphatidylinositol Specific Phospholipase C Activity by Fluvirucin B2, *J. Antibiot. (Tokyo) 48*, 387–390.

156. Champney, W.S., and Tober, C.L. (2001) Structure–Activity Relationships for Six Ketolide Antibiotics, *Curr. Microbiol. 42*, 203–210.

157. Cardellina, J.H., Marner, F.-J., and Moore, R.E. (1979) Malyngamide A, a Novel Chlorinated Metabolite of the Marine Cyanophyte *Lyngbya majuscula*, *J. Am. Chem. Soc. 101*, 240–242.

158. Wu, M., Milligan, K.E., and Gerwick, W.H. (1997) Three New Malyngamides from the Marine Cyanobacterium *Lyngbya majuscula*, *Tetrahedron 53*, 15983–15990.

159. Gallimore, W.A., and Scheuer, P.J. (2000) Malyngamides O and P from the Sea Hare *Stylocheilus longicauda*, *J. Nat. Prod. 63*, 1422–1424.

160. Milligan, K.E., Marquez, B., Williamson, R.T., Davies-Coleman, M., and Gerwick, W.H. (2000) Two New Malyngamides from a Madagascan *Lyngbya majuscula*, *J. Nat. Prod. 63*, 965–968.

161. Kan, Y., Sakamoto, B., Fujita, T., and Nagai, H. (2000) New Malyngamides from the Hawaiian Cyanobacterium *Lyngbya majuscula*, *J. Nat. Prod. 63*, 1599–1602.

162. Ubukata, M., Kimura, K., Isono, K., Nelson, C.C., Gregson, J.M., and McCloskey, J.A. (1992) Structure Elucidation of Liposidomycins, a Class of Complex Lipid Nucleoside Antibiotics, *J. Org. Chem. 57*, 6392–6403.

163. Schimana, J., Fiedler, H.P., Groth, I., Sussmuth, R., Beil, W., Walker, M., and Zeeck, A. (2000) Simocyclinones, Novel Cy-

tostatic Angucyclinone Antibiotics Produced by *Streptomyces antibioticus* Tü 6040 I. Taxonomy, Fermentation, Isolation and Biological Activities, *J. Antibiot. (Tokyo) 53*, 779–787.

164. Schimana, J., Walker, M., Zeeck, A., and Fiedler, H.P. (2001) Simocyclinones: Diversity of Metabolites Is Dependent on Fermentation Conditions, *J. Ind. Microbiol. Biotechnol. 27*, 144–148.

165. Eustaquio, A.S., Luft, T., Wang, Z.X., Gust, B., Chater, K.F., Li, S.M., and Heide, L. (2003) Novobiocin Biosynthesis: Inactivation of the Putative Regulatory Gene NovE and Heterologous Expression of Genes Involved in Aminocoumarin Ring Formation, *Arch. Microbiol. 180*, 25–32.

166. Galm, U., Schimana, J., Fiedler, H.P., Schmidt, J., Li, S.M., and Heide, L. (2002) Cloning and Analysis of the Simocyclinone Biosynthetic Gene Cluster of *Streptomyces antibioticus* TO 6040, *Arch. Microbiol. 178*, 102–114.

167. Holzenkampfer, M., and Zeeck, A. (2002) Biosynthesis of Simocyclinone D8 in an $^{18}O_2$-Rich Atmosphere, *J. Antibiot. (Tokyo) 55*, 341–342.

168. Li, S.M., and Heide, L. (2005) New Aminocoumarin Antibiotics from Genetically Engineered *Streptomyces* Strains, *Curr. Med. Chem. 12*, 419–427.

169. Lewis, R.J., Singh, O.M., Smith, C.V., Skarzynski, T., Maxwell, A., Wonacott, A.J., and Wigley, D.B. (1996) The Nature of Inhibition of DNA Gyrase by the Coumarins and the Cyclothialidines Revealed by X-Ray Crystallography, *EMBO J. 15*, 1412–1420.

170. Tsai, F.T., Singh, O.M., Skarzynski, T., Wonacott, A.J., Weston, S., Tucker, A., Pauptit, R.A., Breeze, A.L., Poyser, J.P., O'Brien, R., *et al.* (1997) The High-Resolution Crystal Structure of a 24-kDa Gyrase B Fragment from *E. coli* Complexed with One of the Most Potent Coumarin Inhibitors, Clorobiocin, *Proteins 28*, 41–52.

171. Flatman, R.H., Howells, A.J., Heide, L., Fiedler, H.P., and Maxwell, A. (2005) Simocyclinone D8, an Inhibitor of DNA Gyrase with a Novel Mode of Action, *Antimicrob. Agents Chemother. 49*, 1093–1100.

172. Abraham, W.R., Meyer, H., and Yakimov, M. (1998) Novel Glycine Containing Glucolipids from the Alkane Using Bacterium *Alcanivorax borkumensis*, *Biochim. Biophys. Acta 1393*, 57–62.

173. Yakimov, M.M., Golyshin, P.N., Lang, S., Moore, E.R., Abraham, W.R., Lunsdorf, H., and Timmis, K.N. (1998) *Alcanivorax borkumensis* gen. nov., sp. nov., a New, Hydrocarbon-Degrading and Surfactant-Producing Marine Bacterium, *Int. J. Syst. Bacteriol. 48*, 339–348.

174. Quinoa, E., Adamczeski, M., Crews, P., and Bakus, G.J. (1986) Bengamides, Heterocyclic Anthelmintics from a Jaspidae Marine Sponge, *J. Org. Chem. 51*, 4494–4497.

175. Thale, Z., Kinder, F.R., Bair, K.W., Bontempo, J., Czuchta, A.M., Versace, R.W., Phillips, P.E., Sanders, M.L., Wattanasin, S., and Crews, P. (2001) Bengamides Revisited: New Structures and Antitumor Studies, *J. Org. Chem. 66*, 1733–1741.

176. Macko, V., Stimmel, M.B., Wolpert, T.J., Dunkle, L.D., Acklin, W., Bänteli, R., Jaun, B., and Arigoni, D. (1992) Structure of the Host-specific Toxins Produced by the Fungal Pathogen *Periconia circinata*, *Proc. Natl. Acad. Sci. USA 89*, 9574–9578.

177. Churchill, A.C., Dunkle, L.D., Silbert, W., Kennedy, K.J., and Macko, V. (2001) Differential Synthesis of Peritoxins and Precursors by Pathogenic Strains of the Fungus *Periconia circinata*, *Appl. Environ. Microbiol. 67*, 5721–5728.

178. Nakao, Y., Maki, T., Matsunaga, S., van Soest, R.W.M., and Nobuhiro, F. (2004) Penasulfate A, a New α-Glucosidase Inhibitor from a Marine Sponge *Penares* sp., *J. Nat. Prod. 67*, 1346–1350.

179. Takada, K., Uehara, T., Nakao, Y., Matsunaga, S., van Soest, R.W.M., and Fusetani, N. (2004) Schulzeines A–C, New α-Glucosidase Inhibitors from the Marine Sponge *Penares schulzei*, *J. Am. Chem. Soc. 126*, 187–193.

180. Nakao, Y., Maki, T., Matsunaga, S., van Soest, R.W.M., and Fusetani, N. (2000) Penarolide Sulfates A1 and A2, New α-Glucosidase Inhibitors from a Marine Sponge *Penares* sp., *Tetrahedron 56*, 8977–8987.

181. Infante, M.R., Pérez, L., Pinazo, A., Clapés, P., Morán, M.C., Angelet, M., García, M.T., and Vinardell, M.P. (2004) Amino Acid-Based Surfactants, *C.R. Chimie 7*, 583–592.

182. Fernández-Pérez, M., and Otero, C. (2001) Enzymatic Synthesis of Amide Surfactants from Ethanolamine, *Enzyme Microb. Technol. 28*, 527–536.

183. Lundquist, J.J., and Toone, E.J. (2002) The Cluster Glycoside Effect, *Chem. Rev. 102*, 558–578.

184. Schengrund, C.-L. (2003) "Multivalent" Saccharides: Development of New Approaches for Inhibiting the Effects of Glycosphingolipid-Binding Pathogens, *Biochem. Pharmacol. 65*, 699–707.

185. Han, F., and Zhang, G. (2004) New Family of Gemini Surfactants with Glucosamide-Based Trisiloxane, *Colloid. Surf. A: Physicochem. Engineer. Aspects 237*, 79–85.

186. Turner, M.W. (2003) The Role of Mannose-Binding Lectin in Health and Disease, *Mol. Immunol. 40*, 423–429.

187. Abert, M., Mora, N., and Lacombe, J.M. (2002) Synthesis and Surface-Active Properties of a New Class of Surfactants Derived from D-Gluconic Acid, *Carbohydr. Res. 337*, 997–1006.

188. Larpent, C., Laplace, A., and Zemb, T. (2004) Macrocyclic Sugar-Based Surfactants: Block Molecules Combining Self-Aggregation and Complexation Properties, *Angew. Chem. Int. Ed. Engl. 43*, 3163–3167.

189. Kumpulainen, A.J., Persson, C.M., and Eriksson, J.C. (2004) Headgroup and Hydrocarbon Tail Effects on the Surface Tension of Sugar-Based Surfactant Solutions, *Langmuir 20*, 10935–10942.

190. Dimick, S.M., Powell, S.C., McMahon, S.A., Moothoo, D.N., Naismith, J.H., and Toone, E.J. (1999) On the Meaning of Affinity: Cluster Glycoside Effects and Concanavalin A, *J. Am. Chem. Soc. 121*, 10286–10296.

191. Colonna, B., Harding, V.D., Nepogodiev, S.A., Raymo, F.M., Spencer, N., and Stoddart, J.F. (1998) Synthetic Carbohydrate Dendrimers—Part 7—Synthesis of Oligosaccharide Dendrimers, *Chem. Eur. J. 4*, 1244–1254.

192. Burke, S.D., Zhao, Q., Schuster, M.C., and Kiessling, L.L. (2000) Synergistic Formation of Soluble Lectin Clusters by a Templated Multivalent Saccharide Ligand, *J. Am. Chem. Soc. 122*, 4518–4519.

193. Fan, E., Zhang, Z., Minke, W.E., Hou, Z., Verlinde, C.L.M.J., and Hol, W.G.J. (2000) High-Affinity Pentavalent Ligands of *Escherichia coli* Heat-Labile Enterotoxin by Modular Structure-Based Design, *J. Am. Chem. Soc. 122*, 2663–2664.

194. Mellet, C.O., Defaye, J., and Garcia-Fernandez, J.M. (2002) Multivalent Cyclooligosaccharides: Versatile Carbohydrate Clusters with Dual Role as Molecular Receptors and Lectin Ligands, *Chem. Eur. J. 8*, 1982–1990.

ARTICLES

Trans Fatty Acids and Atopic Eczema/Dermatitis Syndrome: The Relationship with a Free Radical *cis-trans* Isomerization of Membrane Lipids

Carla Ferreri[a,*], Federica Angelini[b], Chryssostomos Chatgilialoglu[a],
Sergio Dellonte[a], Viviana Moschese[b], Paolo Rossi[b], and Loredana Chini[b]

[a]Istituto per la Sintesi Organica e la Fotoreattività (ISOF), Consiglio Nazionale delle Ricerche, 40129 Bologna, Italy,
and [b]Dipartimento di Pediatria, Policlinico Tor Vergata, Università di Roma "Tor Vergata," 00133 Roma, Italy

ABSTRACT: The formation of *trans* FA residues in membrane phospholipids may be due to a free radical-catalyzed isomerization process occurring to the *cis* unsaturated FA moieties. Radical stress is well documented in inflammatory processes of atopic diseases, but no data are yet available about a possible association with *trans* FA detected in these patients. We investigated the presence of *trans* lipid isomers in the erythrocyte and T-lymphocyte membranes of 26 children affected by atopic eczema/dermatitis syndrome (AEDS). *Trans* lipid isomers were found in both cell membranes, up to a total content of 2.7 and 4.9% of the FA composition, respectively. By using the geometrical *trans* lipid library derived from *in vitro* models of thiyl radical-catalyzed isomerization, oleic and arachidonic acid isomers were detected. The statistical significance was evaluated by comparison with an age-matched control group. These results suggest the role of an endogenous free radical isomerization path occurring to membrane unsaturated lipids, complementary to the dietary contribution, which can be involved in the lipid impairment in AEDS. This study contributes to lipidomic research regarding the double bond structure and the influence of a geometrical change of membrane lipids in physiology and diseases.

Paper no. L9738 in *Lipids* 40, 661–667 (July 2005).

Several studies reviewed by Horrobin (1) have demonstrated abnormalities of EFA metabolism and altered PUFA profiles in atopic patients. This alteration can influence the physiological roles played by PUFA, as, for example, the T-cell receptor (TCR) signaling with suppression of the immune response (2). Moreover, the levels of PUFA and in particular of arachidonic acid can be correlated to functions other than structure, since they are precursors for a number of key mediators of inflammation, including prostaglandins, leukotrienes, and thromboxanes. These mediators alter T-helper (Th) lymphocyte activity by suppressing Th1-type (Th1) cytokine production and favoring a Th2-type (Th2) response characteristic of atopic disease.

Reports by us and other authors suggested using PUFA serum level as a potential marker for the risk of developing atopic disease, and considering the deficiency of a key enzyme, such as Δ^6-desaturase, as a favorable condition for developing allergy (3–5). However, in lipid analyses related to atopic diseases, attention was given only to FA with double bonds in the natural *cis* configuration.

As far as the geometry of the FA double bonds is concerned, several studies show the role of *trans* isomers in the perturbation of membrane properties (6,7), as well as in the functioning of embedded proteins and ion channels (8,9). Since humans do not synthesize *trans* FA (TFA), nutritional studies have focused on *trans* isomers contained in meat or milk and on partially hydrogenated fats (10). Dietary TFA are incorporated into both adult and, *via* placental transfer, fetal tissues (11–14). Although still debated, epidemiological studies have suggested the involvement of TFA intake in human diseases such as cardiovascular diseases (15) and allergy in children (16,17).

Studies on the *cis-trans* isomerization of unsaturated lipids catalyzed by free radicals that support the hypothesis of a different origin of TFA detected in tissues are now available (18). In fact, TFA can arise from the isomerization of natural *cis* lipids, a process studied under different conditions of radical stress (19–22), and recently also described during the normal incubation of human leukemia cell lines (THP-1) under physiological conditions (23). Interestingly, biomimetic models as well as *in vitro* studies showed that in the membranes the FA residue most affected by radical attack is arachidonic acid (18,20,22). It is worth recalling that the *trans* compounds formed by free radical processes are exclusively the geometrical isomers, that is, with the double bond in the same position of the naturally occurring *cis* FA but with the opposite configuration. This fact highlights the need for a more careful monitoring of lipid isomers during the analysis of biological samples, to distinguish between the isomers produced by a radical stress and the dietary *trans* isomers, which are mostly positional isomers with the *trans* double bond shifted to adjacent positions.

Atopic/eczema dermatitis syndrome (AEDS) is a disease in which radical stress and inflammatory conditions are realized (24). We hypothesized that the formation of *trans* phospholipids in cell membranes might occur by radical-based isomerizing species derived from chronic inflammation in AEDS, and

*To whom correspondnece should be addressed at ISOF, Consiglio Nazionale delle Ricerche, Via P. Gobetti 101, 40129 Bologna, Italy.
E-mail: cferreri@isof.cnr.it

Abbreviations: AEDS, atopic eczema/dermatitis syndrome; CD, cluster of differentiation; DGLA, dihomo-g-linolenic acid; MUFA, monounsaturated FA; PBMC, peripheral blood mononuclear cell; RAST, RadioAllergoSorbentTest; SCORAD, skin clinical score; SFA, saturated FA; TCR, T-cell receptor; TFA, trans FA; Th, T-helper; THP-1, a human leukemia cell line.

the effects could parallel those of dietary *trans* lipids. Indeed, the effect of TFA on lipid enzymatic pathways is well assessed (25–27).

Based on these premises, we approached the study of subjects affected by atopic diseases such as AEDS by investigating the alteration of membrane FA profiles due to the presence of TFA. To address specifically the presence of geometrical *trans* isomers in biological samples, TFA characterization was performed by comparison with a *trans* lipid library prepared by a radical-based protocol carried out on naturally occurring compounds (19–21,28). Examining all main FA residues, we could also address the interference of TFA with lipid enzymatic pathways.

Herein we report the results obtained for a group of children affected by AEDS. Red blood cell and T-lymphocyte membrane lipids were examined and, for the first time in the case of T-lymphocytes, TFA were detected. TFA levels were also correlated to other FA levels and to clinical data, such as the presence of IgE.

This study aims at contributing to lipidomic research regarding the double bond structure and the influence of FA geometrical change on cell membranes in physiological conditions and diseases.

MATERIALS AND METHODS

Subjects. Twenty-six Caucasian children, 18 females and 8 males, aged 6 mon–12 yr (mean age 5 yr), who were affected by AEDS were recruited in the Pediatric Department of the Policlinico Tor Vergata, Rome. The duration of the disease ranged from 3 mon to 7 yr. The skin clinical score (SCORAD) combines subjective and objective criteria, giving a global quantitative score that represents the intensity of the disease at a given time, and it was assessed according to the European task force on atopic dermatitis (29). The patients had SCORAD values ranging from 0 to 35. In 13 out of 26 AEDS patients, atopic dermatitis was not IgE-mediated [prick tests/RadioAllergoSorbent Test (RAST) negative]; 8 out of 13 IgE-mediated AEDS patients had prick tests/RAST positive for inhalants, and 8 out of 13 had positive prick tests and RAST for cow milk and were on a diet without milk proteins. None of the patients had a history of cardiovascular disease or a family history for hyperlipidemia and diabetes, and all of them had normal laboratory tests for liver and renal function. They were receiving antihistaminic treatment at the time of the investigation. A group of 10 age-matched normal subjects was included in the study as controls. Informed parental consent was obtained.

Cell isolation. Blood samples were taken by sterile venipuncture of the antecubital vein. Blood samples were collected with the addition of 1 mM EDTA and kept refrigerated at 4°C until processed for the separation. One aliquot was processed for the separation of erythrocytes and isolation of erythrocyte membranes (30). Another aliquot was used for separation of peripheral blood mononuclear cells (PBMC) and erythrocytes from whole blood by gradient centrifugation over Ficoll-Hypaque (Pharmacia Biotech, Uppsala, Sweden).

Monocytes and B-lymphocytes were isolated from PBMC by positive selection, using anti-CD14 and anti-CD19-conjugated magnetic Microbeads, respectively (MACS magnetic cell sorting system; Miltenyi Biotec, Belgish Gladbach, Germany), according to the manufacturer's instructions. T-lymphocytes were obtained by negative selection as a result of the above separation. Analysis of cell surface phenotype was performed by flow cytometry and routinely resulted in 95% purity of the three populations. Briefly, cells were stained for 20 min on ice, with monoclonal antibodies conjugated to fluorescein isothiocyanate or PE, specific for CD14, CD19, CD3, CD56, as well as with isotype controls (all from Pharmingen, San Diego, CA). A minimum of 1×10^4 events for each sample was acquired on a FACSCalibur (Becton Dickinson, San Jose, CA) using Cellquest software (Becton Dickinson).

Phospholipid extraction and analysis. Phospholipid extraction from cell membranes was performed according to Bligh and Dyer (31). The total phospholipid fraction was treated with 0.5 M KOH/MeOH (32) for 10 min at room temperature, and the corresponding FAME were formed and extracted with *n*-hexane. Geometrical TFA were recognized by comparison with a *trans* lipid library obtained by thiyl radical-catalyzed reaction of naturally occurring lipids, as already described (19,23,28). The GC protocol consisted of two injections of the same sample under previously described conditions (23): the first analysis gives the separation of C_{16} and C_{18} saturated FA (SFA) and unsaturated FA, and the second analysis gives separation of arachidonic acid and other eicosenoic FA. Representative GC runs performed under the two conditions are reported in Figures
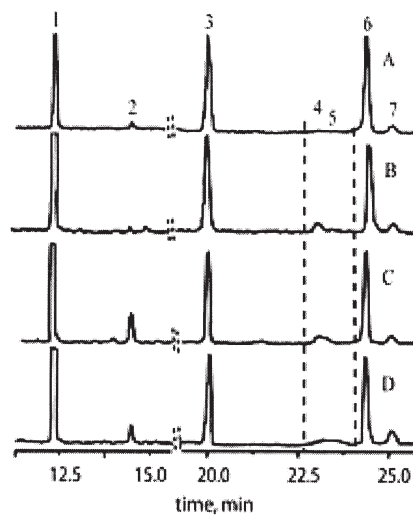
FIG. 1. Partial GC runs representing C_{16} and C_{18} FA residues of membrane phospholipids isolated from (A) erythrocyte of normal donor, (B) erythrocyte of normal donor treated under radical stress conditions, i.e., γ-irradiation in the presence of 2.8 μM mercaptoethanol (Ref. 20). (C) T-lymphocyte of atopic eczema/dermatitis syndrome (AEDS) children, and (D) erythrocyte of AEDS children. Peak labels: (1) methyl palmitate (16:0); (2) methyl palmitoleate (9*c*-16:1); (3) methyl stearate (18:0); (4) methyl elaidate (9*t*-18:1); (5) methyl *trans*-vaccenate (11*t*-18:1), (6) methyl oleate (9*c*-18:1), (7) methyl vaccenate (11*c*-18:1). Chromatograms are normalized to the methyl palmitate peak (100%).
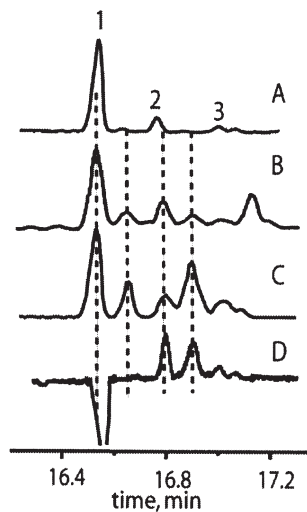
FIG. 2. Partial GC runs representing (A) C_{20} FA residues of erythrocyte membrane phospholipids isolated from normal donor, (B) C_{20} FA residues of erythrocyte membrane phospholipids isolated from AEDS children; (C) methyl arachidonate model isomerization, containing a mixture of *cis* and mono- and di-*trans* isomers (Ref. 20); (D) profile resulting from the subtraction of run A from the run obtained after treatment under radical stress conditions, i.e., γ-irradiation of the blood in the presence of 2.8 μM mercaptoethanol. The preferential formation of two isomers in the erythrocyte membrane is visible (Refs. 20,23). Peak labels: (1) methyl arachidonate (5*c*,8*c*,11*c*,14*c*-20:4); (2) methyl eicosatrienoate (8*c*,11*c*,14*c*-20:3); (3) methyl eicosenoate (11*c*-20:1). Chromatograms are normalized to methyl arachidonate (100%). For abbreviation see Figure 1.

1 and 2. In the separation of the arachidonate isomers of Figure 2, we could not completely resolve the peaks, and the 20:3 FA eluted together with other isomers (peak 2 in Fig. 2). In normal subjects (profile A) the most abundant C_{20} FA is arachidonic acid (peak 1), with 20:3 (peak 2) and 20:1 (peak 3) being the minor residues recognized by GC/MS analyses (*m/z* = 320 and 324, respectively). The isomer identity also was investigated by GC/MS analyses and, when the mass fragmentation was compatible with the structure of 20:4 isomers, the sum of the peak areas matching the isomer references was reported as *trans*-20:4 in Table 1. A more detailed description of the isomer analyses has been previously given (23).

Statistical analysis. FA levels are expressed as mean ± SD of the percentage of the total FA peak areas, as detected in the GC chromatograms. The results are listed in Table 1. Differences between the AEDS patients and controls were assessed by Kolmogorov–Smirnov test, and the statistical significance level *P* is given in the text for the relevant cases. A value of *P* < 0.05 was considered statistically significant for all analyses. All statistical analyses were performed using SPSS software (version 10 for PC; Chicago, IL).

RESULTS

GC analysis. In this study, erythrocyte and T-lymphocyte membrane phospholipids isolated from AEDS patients were analyzed by a protocol consisting of two parallel GC injections of

the same sample. Representative GC runs are shown in Figures 1 and 2, referred to the subjects and the reference isomeric mixtures obtained from the isomerization of naturally occurring lipids by thiyl radicals, as already described (19,23,28).

In particular, in Figure 1 the reference mixture of *cis/trans* isomers was obtained from erythrocyte membranes treated under radical stress condition (profile B), i.e., γ-irradiation in the presence of a certain amount of thiol (20). In this condition, geometrical C_{18} monounsaturated FA (MUFA) isomers can be formed, and they elute in a region of the GC chromatogram immediately before the corresponding *cis* isomers, which is indicated between two dashed lines in Figure 1 (peaks 4 and 5) (23). Profile A shows an example of erythrocyte membrane lipids from controls having <0.1% of *trans*- octadecenoic acid isomers. Profiles C and D show examples of T-lymphocyte and erythrocyte membranes from AEDS patients containing *trans* isomers as 0.7 and 0.3% of the total FA content, respectively.

In Figure 2, the regions of GC runs relative to eicosenoic FA residues of different samples are shown. In the atopic patients, arachidonic acid was still the most abundant residue, but the run was complicated by the presence of other components. The similarity of the altered FA in atopic patients, with the transformation of arachidonic acid under *in vitro* radical stress conditions, can be appreciated by comparison of profile B with profiles C and D (20,23). The analytical procedure and isomer analysis have been described in detail recently (23). It was gratifying to see that the components detected in atopic patients match the *trans* isomers of the references. In our cohort, different percentages of *trans* components were detected, and the alterations were reproduced similarly in erythrocyte and T-lymphocyte membranes of the same patient.

FA composition. Studies of FA composition have been reported in several cases of atopic dermatitis, one of the commonest chronic inflammatory diseases in childhood (33–35). In particular, disorders of EFA metabolism have been evidenced, with a possible inhibition of the enzymatic activity of desaturases (3,5,33–35). Although changes of less than 1% of the total FA were reported, they were considered to influence the normal prostaglandin production significantly (36).

In our study, we evaluated FA residues of erythrocyte and T-lymphocyte membrane phospholipids up to a total of 12 components, including geometric *cis* and *trans* isomers, identified as previously discussed in the GC analysis section. The values are reported in Table 1 and are expressed as percentages of the peak areas relative to the sum of the main FA residues detected by GC. Control values were obtained from a group of 10 children, age-matched with AEDS patients, and these were in agreement with data reported for normal subjects in the recent literature (37–40). It is known that lipid composition of erythrocytes and lymphocytes in the elderly can vary (41) whereas it does not change consistently in young subjects (42).

Examination of the naturally occurring FA led to the following results: (i) 16:0 values were significantly higher in AEDS patients compared with controls (*P* < 0.001), and this increase occurred both in erythrocyte and T-lymphocyte membranes. (ii) 18:0 levels were similar between patients and controls. (iii) The increase of 16:1 in both erythrocyte and T-lymphocyte

TABLE 1
Major FA and *trans* FA Isomers of Erythrocyte and T-Lymphocyte Membranes in AEDS Children and Comparison with Control Values

FAME[a]	Erythrocyte membrane[b] ($n = 26$)	Control[b] ($n = 10$)	T-cell membrane[b] ($n = 26$)	Control[b] ($n = 10$)
16:0	31.4 ± 5.3^c	21.8 ± 5.1	36.5 ± 7.1^c	24.1 ± 6.0
16:1	3.8 ± 2.9^c	0.3 ± 0.2	8.3 ± 6.5^c	0.3 ± 0.2
18:0	16.5 ± 4.8	16.5 ± 4.0	19.1 ± 5.9	21.0 ± 2.2
trans-18:1	0.5 ± 0.2^d	0.2 ± 0.1	0.5 ± 0.4^d	0.2 ± 0.1
9*c*-18:1	17.3 ± 3.5	13.5 ± 4.2	13.7 ± 4.8	16.0 ± 4.2
11*c*-18:1	1.1 ± 0.6	1.0 ± 0.4	1.1 ± 0.9	1.2 ± 0.3
9*c*,12*c*-18:2	11.0 ± 3.0^e	12.0 ± 4.5	5.6 ± 2.5^e	7.4 ± 2.6
5*c*,8*c*,11*c*,14*c*-20:4	11.7 ± 4.5^f	13.0 ± 2.9	5.9 ± 4.0^f	11.2 ± 4.9
trans-20:4	1.2 ± 1^c	0.3 ± 0.1	1.1 ± 0.6^c	0.4 ± 0.2
20:3[g]	2.1 ± 1.9	1.6 ± 0.5	4.6 ± 4.0	1.7 ± 0.2
20:5 (EPA)	2.7 ± 2.0	0.7 ± 0.2	1.2 ± 1.0	1.3 ± 0.2
22:6 (DHA)	2.8 ± 1.5^h	5.3 ± 1.1	1.1 ± 0.8^h	3.7 ± 1.9
SFA/MUFA	2.6 ± 0.5^c	1.9 ± 0.2	4.5 ± 3.0^c	2.2 ± 0.3
18:2n-6/18:0[i]	0.8 ± 0.2	0.4 ± 0.01	0.3 ± 0.2	0.32 ± 0.07
Total *trans*-FA	1.7 ± 1.1^c	$< 0.5^l$	1.7 ± 1.3^c	$< 0.6^l$

[a]FAME are obtained from total lipid extraction, derivatization, and GC analysis.
[b]These values are mean ± SD and are expressed as percentage of the peak areas as detected in the GC chromatogram.
[c]Values higher than normal in erythrocyte ($P < 0.001$) and lymphocyte ($P < 0.001$) membranes.
[d]Values higher than normal in erythrocyte ($P < 0.02$) and lymphocyte ($P < 0.01$) membranes.
[e]Values lower than normal in erythrocyte ($P < 0.493$) and lymphocyte ($P < 0.001$) membranes.
[f]Values lower than normal in erythrocyte ($P < 0.303$) and lymphocyte ($P < 0.001$) membranes.
[g]Detected in all samples and assigned to 8c,11c,14c-20:3 (dihomo-g-linolenic acid DGLA) by comparison with an authentic sample. In five samples of erythrocyte and lymphocyte membranes DGLA was > 10%.
[h]Values lower than normal in erythrocyte ($P < 0.001$) and lymphocyte ($P < 0.001$) membranes
[i]EFA deficiency index.
[l]Highest value detected in controls. AEDS, atopic eczema/dermatitis syndrome; SFA, saturated FA; MUFA, monounsaturated FA.

membranes was also significant ($P < 0.001$) compared with controls. (iv) No significant differences of linoleic and arachidonic acid levels were detected in erythrocytes compared with controls, whereas for lymphocytes low values of both FA were significant ($P < 0.001$). (v) The SFA/MUFA ratio was higher than in controls ($P < 0.001$).

Significant correlations were found in the case of palmitic acid, which had an inverse correlation with the levels of arachidonic acid ($r = -0.622$; $P = 0.001$) and a positive correlation with linoleic acid ($r = 0.432$; $P = 0.03$). For stearic acid, an inverse correlation was found with linoleic acid ($r = -0.555$; $P = 0.005$).

With respect to *trans* isomers, octadecenoic acid isomers were detected and, compared with controls belonging to the same geographical area, the values were significantly higher in AEDS patients both in erythrocyte ($P < 0.02$) and T-lymphocyte ($P < 0.01$) membranes. *Trans* isomers of arachidonic acid were found both in erythrocyte and T-lymphocyte membrane phospholipids of all patients (1.2 ± 1 and 1.1 ± 0.6, respectively), as well as in controls (0.3 ± 0.1 and 0.4 ± 0.2, respectively). Since the occurrence of these *trans* isomers is not yet well known even in control subjects, the statistical significance of the subjects compared with controls had a particular meaning, and it was found to be high ($P < 0.001$).

The sum of *trans* 18:1 and 20:4 isomers is reported in Table 1 as the total *trans*-FA (TFA) content. It is worth noting that the highest values of total TFA found in the erythrocyte and T-lymphocyte membranes were 2.7 and 4.9% of the FA composition, respectively, whereas controls did not exceed the value of 0.5–0.6%. Correlation between the total TFA contents and the other FA values in erythrocyte membranes was also evaluated. Significant correlations were found with SFA, such as palmitic acid ($r = 0.446$; $P = 0.03$) and inversely, stearic acid ($r = -0.618$; $P = 0.001$).

In five subjects, the arachidonic acid precursor, dihomo-γ-linolenic acid (DGLA; 8*c*,11*c*,14*c*-20:3), was found in high amounts compared with the normal values.

Generally, low levels of the long-chain PUFA 22:6n-3 (DHA) were found in almost all erythrocyte and T-lymphocyte membranes compared with controls ($P < 0.001$ in both cases).

Finally, we divided the 26 patients in two groups, based on the skin prick/RAST test for detecting the non-IgE-mediated dermatitis. Table 2 reports the total TFA levels found in erythrocyte and T-lymphocyte membranes of the two groups. The highest values were found in lymphocyte membranes from 10 out of the 13 patients with non-IgE-mediated dermatitis. However, the differences were not significant ($P = 0.169$).

TABLE 2
Comparison of Total *trans* FA Isomer Content in Erythrocyte and T-Lymphocyte Membrane Phospholipids of AEDS Patients

AEDS patients	Erythrocyte[a] (*n* = 13)	T-lymphocyte[a] (*n* = 13)
IgE-mediated	1.6 ± 1.1	1.3 ± 0.9
Not-IgE-mediated	1.5 ± 0.9	1.8 ± 0.9[b]

[a]Percentage of the peak areas as detected in the GC chromatograms expressed as mean ± SD.
[b]*P* = 0.169.

DISCUSSION

Although the results of different studies are not in agreement, the balance of evidence indicates that lipid metabolism is abnormal in atopic eczema (1). Data of the present study, as found in previous reports, show that in children affected by AEDS the FA membrane composition of red blood cells is altered. Control values obtained from a group of 10 children, age-matched with AEDS patients, were also found to be in agreement with data reported in the recent literature for normal subjects (36–40).

Moreover, here we report that the lipid composition in erythrocyte membranes had modifications that were reflected in membranes of T-lymphocytes, which are key effector cells in immunopathology of AEDS (compare with Table 1). The impairment consisted of an alteration of normal lipid ratios and, for the first time we report the presence of TFA isomers. In particular, with the help of a *trans* lipid library for GC analysis, not only octadecenoic acid isomers but also arachidonic acid isomers were detected in erythrocyte and T-lymphocyte membranes. The comparison of model radical-based isomerization of MUFA and PUFA, with the lipid trends of our patients shown in Figures 1 and 2, is gratifying.

In our model studies of arachidonate isomerization (20,21) and in the more recent work on the endogenous formation of TFA in THP-1 cells (23), we highlighted the relevance of the double bonds of arachidonic acid residues, which are the most affected by a radical-catalyzed isomerization process directly occurring in the biological membranes. Except for the presence of *trans* octadecenoic acids, which also can be expected from the diet, the *trans* 20:4n-6 isomers are not common in the diet, since their production from the *trans* 18:2 isomers is minimal. The four mono-*trans* isomers of arachidonic acid have been previously detected in human blood plasma and correlated to the presence of isomerizing radical species in smokers (22). Radical stress is also deeply involved in skin inflammation and atopic disease and, owing to a reduction of antioxidant defenses reported in these cases (24,43), it could affect membrane lipids, in particular polyunsaturated components. It must also be taken into account that lipid isomerization is inhibited by some antioxidants (44).

Considering other possible factors, in Europe TFA intake from the diet was correlated with childhood asthma and allergy (16). Our cohort had a diet balanced and normal for age as ascertained by the pediatrician, with no increased intakes of foods containing TFA isomers and olive oil as the main condiment, as ascertained during an interview with the parents. Eight children were on a diet free of cow's milk proteins and dairy prod-

ucts. Moreover, as discussed above, the presence of arachidonic acid isomers suggests that contributions from sources other than diet must be involved.

Once formed in the biological environment, TFA are active molecules known to inhibit desaturase and elongase enzymes and cause interruption of lipid pathways at different levels (25–27). The effects of *trans* arachidonic acid isomers are not yet fully disclosed, although some evidence for their interaction with lipid enzymes has been gathered (45–48).

In this study, significance was found for the correlation between total TFA levels and the high 16:0 and low 18:0 levels (*P* = 0.03 and *P* = 0.001, respectively). Together with the observation that high levels of 16:0 are inversely correlated with 20:4 levels (*P* = 0.001), a scenario results in which the inhibition of elongase enzyme can be suggested. Moreover, the reduced polyunsaturated content could couple with the high content of SFA and TFA, which are known to reduce the fluidity and permeability of cell membranes (6–9,44) as well as to affect membrane functions, including protein activities (7,8). The presence of higher amounts of palmitoleic acid residues could be explained from the activity of desaturase enzymes on the excess palmitic acid, and this MUFA residue could increase membrane fluidity. Therefore, activation of desaturase enzymes working with SFA could be a compensative mechanism in response to a general diminution of PUFA levels and lack of unsaturation observed in patients.

Cases of increased 20:3n-6 (DGLA), in particular in T-lymphocyte membranes, which is normally processed to arachidonic acid by Δ^5 desaturase activity, seem to indicate an inhibition of this pathway. It is also worth noting that a high amount of 20:3n-6 occurs in hematopoietic cells at an immature stage of development, which is also due to the absence of other cofactors (49). Generally, in our patients, low DHA contents were found in erythrocyte and lymphocyte membranes (*P* < 0.001, respectively). The low levels of arachidonic and linoleic acids compared with controls were significant only in T-lymphocytes (*P* < 0.001), thus showing some differences between the two cell populations in the same group of subjects. More recently, defects of PUFA have been related to a lack in the gene expression for FA enzymes (50).

The above-described correlation between the high content of 16:0 and the low content of 20:4 in erythrocytes could also indicate a possible relationship with desaturase enzymatic inhibition given by TFA. A clear correlation between high 18:1 *trans* isomers with low amounts of arachidonic acid and DHA in infant development has been described (51) although in our patients this correlation was not statistically significant.

Finally, we examined the relationship between TFA levels in erythrocyte and T-lymphocyte membranes and the presence of IgE (Table 2). In 13 out of 26 children where atopic disease was not IgE-mediated, the highest levels of TFA were detected in lymphocytes (1.8 ± 0.9%). However, the statistical significance of this parameter between the two groups appears not to be meaningful (*P* = 0.169), and a larger survey of patients is needed to address this point properly.

These data point out the need for a more comprehensive

picture of diseases involving lipid impairment, which has to include *cis* and *trans* isomer detection along with elucidation of their exogenous or endogenous origin. Indeed, the connection of diseases based on inflammation and free radical production with an *in vivo cis-trans* isomerization is an interesting hypothesis that is also connected with the concomitant unbalance of antioxidant defenses reported in these cases. In view of the radical-based mechanism of lipid alteration, the suggested supplementation of PUFA in skin disorders should be combined with compounds having a radical-repair activity (52).

Owing to the types and amounts of TFA detected in our AEDS patients, the contribution of radical-based isomerization to the presence of FA isomers in skin inflammatory diseases is proposed here for the first time. We speculate that the formation of TFA isomers in T-cell membranes of AEDS patients might affect membrane fluidity and produce consequences on the location and behavior of membrane-bound receptors and therefore might alter the activities of T cell signaling.

ACKNOWLEDGMENTS

REFERENCES

1. Horrobin, D.F. (2000) Essential Fatty Acid Metabolism and Its Modification in Atopic Eczema, *Am. J. Clin. Nutr. 71*, 367S–372S.
2. Zeyda, M., Szekeres, A.B., Saemann, M.D., Geyeregger, R., Stockinger, H., Zlabinger, G.J., Waldhausl, W., and Stulnig, T.M. (2003) Suppression of T Cell Signaling by Polyunsaturated Fatty Acids: Selectivity in Inhibition of Mitogen-Activated Protein Kinase and Nuclear Factor Activation, *J. Immunol. 170*, 6033–6039.
3. Galli, E., Picardo, M., Chini, L., Passi, S., Moschese, V., Terminali, O., Paone, F., Fraioli, G., and Rossi, P. (1994) Analysis of Polyunsaturated Fatty Acids in Newborn Sera: A Screening Tool for Atopic Disease? *Br. J. Dermatol. 130*, 752–756.
4. Yu, G., and Bjorksten, B. (1998) Serum Levels of Phospholipid Fatty Acids in Mothers and Their Babies in Relation to Allergic Disease, *Eur. J. Pediatr. 157*, 298–303.
5. Calder, P.C., and Miles, E.A. (2000) Fatty Acids and Atopic Disease, *Pediatr. Allergy Immunol. 11* (*Suppl. 13*), 29–36.
6. Roach, C., Feller, S.E., Ward, J.A., Raza Shaikh, S., Zerouga, M., and Stillwell, W. (2004) Comparison of *cis* and *trans* Fatty Acid Containing Phosphatidylcholines on Membrane Properties, *Biochemistry 43*, 6344–6351.
7. Niu, S.-L., Mitchell, D.C., and Litman, B.J. (2005) *Trans* Fatty Acid Derived Phospholipids Show Increased Membrane Cholesterol and Reduced Receptor Activation as Compared to Their *cis* Analogs, *Biochemistry 44*, 4458–4465.
8. Helmkamp, G.M., Jr. (1980) Effects of Phospholipid Fatty Acid Composition and Membrane Fluidity on the Activity of Bovine Brain Phospholipid Exchange Protein, *Biochemistry 19*, 2050–2056.
9. Kummerow, F.A., Zhou, Q., and Mahfouz, M. (1999) Effect of *trans* Fatty Acids on Calcium Influx into Human Arterial Endothelial Cells, *Am. J. Clin. Nutr. 70*, 832–838.
10. Sébédio, J.L., and Christie, W.W., (eds.) (1998) *Trans* Fatty Acids in Human Nutrition*, The Oily Press, Dundee.
11. Larque, E., Zamora, S., and Gil, A. (2001) Dietary *trans* Fatty Acids in Early Life: A Review, *Early Hum. Dev. 65*, S31–S41.
12. Wolff, R.I., and Entressangles, B. (1994) Steady-state Fluorescence Polarization Study of Structurally Defined Phospholipids from Liver Mitochondria of Rats Fed Elaidic Acid, *Biochim. Biophys. Acta 1211*, 198–206.
13. Acar, N., Chardigny, J.M., Darbois, M., Pasquis, B., and Sébédio, J.L. (2003) Modification of the Dopaminergic Neurotransmitters in Striatum, Frontal Cortex and Hippocampus of Rats Fed for 21 Months with *trans* Isomers of α-Linolenic Acid, *Neurosci. Res. 45*, 375–382.
14. Sébédio, J.L., Vermunt, S.H.F., Chardigny, J.M., Beaufrere, B., Mensink, R.P., Armstrong, R.A., Christie, W.W., Niemela, J., Henon, G., and Riemersma, R.A. (2000) The Effects of Dietary *trans* α-Linolenic Acid on Plasma Lipids and Platelet Fatty Acid Composition: The *Trans*LinE Study, *Eur. J. Clin. Nutr. 54*, 104–113.
15. Lemaitre, R.N., King, I.B., Raghunathan, T.E., Pearce, R.M., Weinmann, S., Knopp, R.H., Copass, M.K., Cobb, L.A., and Siscovick, D.S. (2002) Cell Membrane *trans*-Fatty Acids and the Risk of Primary Cardiac Arrest, *Circulation 105*, 697–701.
16. Weiland, S.K., von Mutius, E., Husing, A., and Asher, M.I. (1999) Intake of *trans* Fatty Acids and Prevalence of Childhood Asthma and Allergies in Europe, ISAAC Steering Committee, *Lancet 353*, 2040–2041.
17. Nagel, G., and Linseisen, J. (2005) Dietary Intake of Fatty Acids, Antioxidants and Selected Food Groups and Asthma in Adults, *Eur. J. Clin. Nutr. 59*, 8–15.
18. Chatgilialoglu, C., and Ferreri, C. (2005) *Trans* Lipids: The Free Radical Path, *Acc. Chem. Res. 38*, 441–448.
19. Ferreri, C., Costantino, C., Perrotta, L., Landi, L., Mulazzani, Q.G., and Chatgilialoglu, C. (2001) *Cis-trans* Isomerization of Polyunsaturated Fatty Acid Residues in Phospholipids Catalyzed by Thiyl Radicals, *J. Am. Chem. Soc. 123*, 4459–4468.
20. Ferreri, C., Faraone-Mennella, M.R., Formisano, C., Landi, L., and Chatgilialoglu, C. (2002) Arachidonate Geometrical Isomers Generated by Thiyl Radicals: The Relationship with *trans* Lipids Detected in Biological Samples, *Free Radic. Biol. Med. 33*, 1516–1526.
21. Ferreri, C., Samadi, A., Sassatelli, F., Landi, L., and Chatgilialoglu, C. (2004) Regioselective *cis-trans* Isomerization of Arachidonic Double Bonds by Thiyl Radicals: The Influence of Phospholipid Supramolecular Organization, *J. Am. Chem. Soc. 126*, 1063–1072.
22. Zghibeh, C.M., Gopal, V.R., Poff, C.D., Falck, J.R., and Balazy, M. (2004) Determination of *trans*-Arachidonic Acid Isomers in Human Blood Plasma, *Anal. Biochem. 332*, 137–144.
23. Ferreri, C., Kratzsch, S., Brede, O., Marciniak, B., and Chatgilialoglu, C. (2005) *Trans* Lipids Formation Induced by Thiols in Human Monocytic Cells, *Free Radic. Biol. Med. 38*, 1180–1187.
24. Tsukahara, H., Shibata, R., Ohshima, Y., Todoroki, Y., Sato, S., Ohta, N., Hiraoka, M., Yoshida, A., Nishima, S., and Mayumi, M. (2003) Oxidative Stress and Altered Antioxidant Defenses in Children with Acute Exacerbation of Atopic Dermatitis, *Life Sci. 72*, 2509–2516.
25. Berdeaux, O., Blond, J.P., Bretillon, L., Chardigny, J.M., Mairot, T., Vatele, J.M., Poullain, D., and Sébédio, J.L. (1998) *In vitro* Desaturation or Elongation of Monotrans Isomers of Linoleic Acid by Rat Liver Microsomes, *Mol. Cell. Biochem. 185*, 17–25.
26. Rosenthal, M.D., and Doloresco, M.A. (1984) The Effects of *trans* Fatty Acids on Fatty Acyl Δ5 Desaturation by Human Skin Fibroblast, *Lipids 19*, 869–874.
27. O'Keefe, S.F., Lagarde, M., Grandgirard, A., and Sébédio, J.L. (1990) *Trans* n-3 Eicosapentaenoic and Docosahexaenoic Acid

Isomers Exhibit Different Inhibitory Effects on Arachidonic Acid Metabolism in Human Platelets Compared to the Respective *cis* Fatty Acids, *J. Lipid Res. 31*, 1241–1246.

28. Samadi, A., Andreu, I., Ferreri, C., Dellonte, S., and Chatgilialoglu, C. (2004) Thiyl Radical Catalyzed Isomerization of Oils: An Entry to the *trans* Lipid Library, *J. Am. Oil Chem. Soc. 81*, 753–758.

29. (1993) Severity Scoring of Atopic Dermatitis: The SCORAD Index. Consensus Report of the European Task Force on Atopic Dermatitis, *Dermatology 186*, 23–31.

30. Baldwin, S.A., and Lienhard, G.E. (1989) Purification and Reconstitution of Glucose Transporter from Human Erythrocytes, *Methods Enzymol. 174*, 39–45.

31. Bligh, E.G., and Dyer, W.J. (1959) A Rapid Method of Total Lipid Extraction and Purification, *Can. J. Biochem. Physiol. 37*, 911–917.

32. Kramer, J.K.G., Fellner, V., Dugan, M.E.R., Sauer, F.D., Mossoba, M.M., and Yurawecz, M.P. (1997) Evaluating Acid and Base Catalysts in the Methylation of Milk and Rumen Fatty Acids with Special Emphasis on Conjugated Dienes and Total *trans* Fatty Acids, *Lipids 32*, 1219–1228.

33. Wright, S. (1985) Atopic Dermatitis and Essential Fatty Acids. A Biochemical Basis for Atopy, *Acta Derm. Venereol. 114 (suppl.)*, 143–145.

34. Oliwiecki, S., Burton, J.L., Elles, K., and Horrobin, D.F. (1991) Levels of Essential and Other Fatty Acids in Plasma and Red Cell Phospholipids from Normal Controls and Patients with Atopic Eczema, *Acta Derm. Venereol. 71*, 224–228.

35. Duchén, K., and Björktén, B. (2001) Polyunsaturated n-3 Fatty Acids and the Development of Atopic Disease, *Lipids 36*, 1033–1042.

36. Biagi, P.L., Hrelia, S., Celadon, M., Turchetto, E., Masi, M., Ricci, G., Specchia, F., Cannella, M.V., Horrobin, D.F., and Bordoni, A. (1993) Erythrocyte Membrane Fatty Acid Composition in Children with Atopic Dermatitis Compared to Age-Matched Controls, *Acta Paediatr. 82*, 789–790.

37. Agatha, G., Hafer, R., and Zintl, F. (2001) Fatty Acid Composition of Lymphocyte Membrane Phospholipids in Children with Acute Leukemia, *Cancer Lett. 173*, 139–144.

38. Paganelli, F., Maixent, J.M., Duran, M.J., Parhizgar, R., Pieroni, G., and Sennoune, S. (2001) Altered Erythrocyte n-3 Fatty Acids in Mediterranean Patients with Coronary Artery Disease, *Int. J. Cardiol. 78*, 27–32.

39. Barò, L., Hermoso, J.C., Nuñez, M.C., Jimenez-Rios, J.A., and Gil, A. (1998) Abnormalities in Plasma and Red Blood Cell Fatty Acid Profiles of Patients with Colorectal Cancer, *Br. J. Cancer 77*, 1978–1983.

40. Ponnappan, V., Holley, D.H., and Lipschitz, D.A. (1996) Effect of Age on the Fatty Acid Composition of Phospholipids in Human Lymphocytes, *Exp. Gerontol. 31*, 125–133.

41. Caprari, P., Scuteri, A., Salvati, A.M., Banco, C., Cantafora, A., Masella, R., Modesti, D., Tarzia, A., and Marigliano, V. (1999) Aging and Red Blood Cell Membranes: A Study of Centenarians, *Exp. Gerontol. 34*, 47–57.

42. Decsi, T., and Koletzko, B. (1994) Fatty Acid Composition of Plasma Lipid Classes in Healthy Subjects from Birth to Young Adulthood, *Eur. J. Pediatr. 153*, 520–525.

43. Fuchs, J., Zollner, T.M., Kaufmann, R., and Podda, M. (2001) Redox-Modulated Pathways in Inflammatory Skin Diseases, *Free Radic. Biol. Med. 30*, 337–353.

44. Chatgilialoglu, C., Zambonin, L., Altieri, A., Ferreri, C., Mulazzani, Q.G., and Landi, L. (2002) Geometrical Isomerism of Monounsaturated Fatty Acids. Thiyl Radical Catalysis and Influence of Antioxidant Vitamins, *Free Radic. Biol. Med. 33*, 1681–1692.

45. Egmond, G.J.N., Pabon, H.J.J., and van Dorp, D.A. (1977) Total Synthesis of Methyl *t*-5,*c*-8,*c*-11,*c*-14-Eicosatetraenoate and of *t*-2,*c*-5,*c*-8,*c*-11,*c*-14-Eicosapentaenoic Acid, *Rec. Trav. Chim, Pays-Bas 96*, 172–175.

46. Berdeaux, O., Vatèle, J.-M., Eynard, T., Nour, M., Poullain, D., Noël, J.P., and Sébédio, J.L. (1995) Synthesis of (9*Z*,12*E*)- and (9*E*,12*Z*)-[1-^{14}C]Linoleic Acid and (5*Z*,8*Z*,11*Z*,14*E*)-[1-^{14}C]Arachidonic Acid, *Chem. Phys. Lipids 78*, 71–80.

47. Berdeaux, O., Chardigny, J.M., Sébédio, J.L., Mairot, T., Poullain, D., Vatèle, J.M., and Noël, J.P. (1996) Effects of a *trans* Isomer of Arachidonic Acid on Rat Platelet Aggregation and Eicosanoid Production, *J. Lipid Res. 37*, 2244–2250.

48. Roy, U., Loreau, O., and Balazy, M. (2004) Cytochrome P450/NADPH-Dependent Formation of *trans* Epoxides from *trans*-Arachidonic Acids, *Bioorg. Med. Chem. Lett. 14*, 1019–1022.

49. Marzo, I., Martinez-Lorenzo, M.J., Anel, A., Desportes, P., Alava, M.A., Naval, J., and Piñeiro, A. (1995) Biosynthesis of Unsaturated Fatty Acids in the Main Cell Lineages of Human Leukemia and Lymphoma, *Biochim. Biophys. Acta 1257*, 140–148.

50. Williard, D.E., Nwankwo, J.O., Kaduce, T.L., Harmon, S.D., Irons, M., Moser, H.W., Raymond, G.V., and Spector, A.A. (2001) Identification of a Fatty Acid Δ^6-Desaturase Deficiency in Human Skin Fibroblasts, *J. Lipid Res. 42*, 501–508.

51. Decsi, T., Boehm, G., Ria Tjoonk, H.M., Molnár, S., Dijck-Brouwer, D.A.J., Hadders-Algra, M., Martini, I.A., Muskiet, F.A.I., and Boersma, E.R. (2002) *Trans* Isomeric Octadecenoic Acids Are Related Inversely to Arachidonic Acid and DHA and Positively Related to Mead Acid in Umbilical Vessel Wall Lipids, *Lipids 37*, 954–965.

52. Graham-Brown, R. (2000) Atopic Dermatitis: Unapproved Treatments or Indications, *Clin. Dermatol. 18*, 153–158.

Fish Oil Supplementation of Lactating Mothers Affects Cytokine Production in 2½-Year-Old Children

Lotte Lauritzen[a,*], **Tanja M.R. Kjær**[b], **Maj-Britt Fruekilde**[b], **Kim F. Michaelsen**[a], **and Hanne Frøkiær**[b]

[a]Center for Advanced Food Studies, Department of Human Nutrition, The Royal Veterinary & Agricultural University, 1958 Frederiksberg, Denmark, and [b]BioCentrum, Biochemistry & Nutrition Group, Technical University of Denmark, 2800 Lyngby, Denmark

ABSTRACT: n-3 PUFA influence immune functioning and may affect the cytokine phenotype during development. To examine whether maternal fish oil supplementation during lactation could modify later immune responses in children, 122 lactating Danish mothers with a fish intake below the population median were randomized to groups supplemented for the first 4 mon of lactation with 4.5 g/d of fish oil (equivalent to 1.5 g/d of n-3 long-chain PUFA) or olive oil. Fifty-three mothers with a fish intake in the highest quartile of the population were also included. The FA composition of erythrocyte membranes was measured at 4 mon and at 2½ yr. Plasma immunoglobulin E (IgE) levels and cytokine production in lipopolysaccharide-stimulated whole-blood cultures were determined at 2½ yr. Erythrocyte n-3 PUFA at 4 mon were higher in infants from the fish oil group compared with the olive oil group ($P < 0.001$) but were no longer different at 2½ yr. The median production of lipopolysaccharide-induced interferon γ (IFN-γ) in the fish oil group was fourfold higher than that in the olive oil group ($P = 0.034$), whereas interleukin-10 (IL-10) production was similar. The IFN-γ/IL-10 ratio was twofold higher in the fish oil group ($P = 0.019$) and was positively correlated with 20:5n-3/20:4n-6 in erythrocytes at 4 mon ($P = 0.050$). The percentages of atopic children and plasma IgE were not different in the two groups, but the study was not designed to look at atopy. Cytokine responses and erythrocyte FA composition in children of mothers with a high fish intake were intermediate in comparison with those in the randomized groups. Fish oil supplementation during lactation resulted in increased *in vitro* IFN-γ production in the children 2 yr after the supplementation was given, which may reflect a faster maturation of the immune system.

Paper no. L9666 in *Lipids 40,* 669–676 (July 2005).

Because of the immunosuppressive action of n-3 PUFA, there has been some concern about the safety of an increased intake of n-3 long-chain PUFA (LCPUFA) in infancy (1). However, it has also been hypothesized that an increased intake of n-3 PUFA may protect against atopy (2). There has been an in-crease in the prevalence of atopic diseases in the last decades, which could be due to environmental factors. Atopic sensitization occurs early in life and may therefore be specifically sensitive to environmental factors, e.g., diet, that are introduced in this period. It is therefore possible that some "nutritional programming" of the immune system may occur.

Infants are born with an immature immune system characterized by a polarization of T helper lymphocytes (Th) toward a proallergic Th2-type response. The capacity to induce protective Th1 immune responses is impaired in early childhood, and immune maturation in childhood is characterized by a Th1 polarization. Breast milk contains numerous components that may promote the development of the infant's immune system (3), including PUFA. The maternal diet is the most important determinant of infant PUFA accretion in membranes of breast-fed children (4). Thus, variations in maternal intake of PUFA may influence the maturation and polarization of the infant immune system.

Immune maturation occurs faster in breast-fed than in formula-fed infants and is enhanced by the addition of LCPUFA to infant formula (1,5). Fish oil (FO) supplementation of pregnant women has been shown to affect immune function in the neonate and atopic sensitization during early life (6,7). Some longitudinal studies found that a higher n-3 PUFA content in breast milk was associated with a decreased likelihood of atopy in infants (8–10), whereas another study found contrasting results (11). Supplementation with n-3 PUFA during lactation has been found to reduce the prevalence of wheezing during the first 18 mon of life (12). The effect of maternal FO supplementation during lactation on later immune function in the offspring has not been investigated.

We performed a randomized trial in which the n-3 LCPUFA intake of breast-fed infants was raised *via* FO supplementation to the mother during the first 4 mon of lactation. The trial was designed to investigate the effects on breast-milk FA composition, n-3 PUFA levels in infant erythrocytes (RBC), and development during the first year of life (13). The long-term effect on immune function was investigated at a follow-up visit, when the children were 2½ yr old. The aim of this study was to see whether maternal FO supplementation during lactation would affect later immune function, determined by the cytokine phenotype and assessed by the *in vitro* production of interferon γ (IFN-γ) and interleukin 10 (IL-10) and plasma immunoglobulin E (IgE). The study did not have the power to look at atopic sensitization.

SUBJECTS AND METHODS

The study hypothesis was tested in a parallel-group randomized trial. A diagram of the trial profile, with special focus on the present follow-up study, is shown in Figure 1. The details of the study design, recruitment procedure, and subjects, which have been reported elsewhere (13), are described briefly here.

During 1999, participants were selected from among pregnant women recruited for the Danish National Birth Cohort (14) based on their intake of n-3 LCPUFA. Women with a fish intake below the population median (<0.4 g n-3 LCPUFA/d) were recruited for the randomized intervention trial, and women with a fish intake in the upper quartile (>0.8 g n-3 LC-PUFA/d) as a high-fish-intake reference group (HFI group). The inclusion criteria were: an uncomplicated pregnancy, pre-pregnancy body mass index < 30 kg/m^2, no metabolic disorders, and the intention to breast-feed for at least 4 mon. Furthermore, the newborns had to be healthy, term, singleton infants with normal weight for gestation (15) and an Apgar score > 7, and the mothers were to begin taking the supplements within 2 wk after birth. One hundred twenty-two and 53 of the women with a low and high fish intake, respectively, fulfilled all criteria.

The protocols for the intervention trial and follow-up study were approved by the local scientific ethical committee (KF 01-300/98 and KF 01-183/01). Both parents of all participating children gave written consent to participate after the study had been explained to them orally as well as in writing.

Trial and supplements. After birth, women with a fish intake below the median were randomly allocated to daily supplementation for the first 4 mon of lactation with microencapsulated FO or olive oil (OO) given in müesli bars (Halo Foods Ltd., Tywyn Gwynedd, Wales, United Kingdom). The FO supplement (Dry n-3^{TM}; BASF Health and Nutrition A/S, Ballerup, Denmark) provided 1.5 g/d of n-3 LCPUFA (equivalent to 4.5 g/d of fish oil). As an alternative, the supplements were offered in homemade cookies or oil capsules (a gift from Lupe/ProNova Biocare, Lysaker, Norway). The overall self-reported compliance in both groups was, on average, 91% (range 67–100%, n = 64). Investigators and families were blinded to the randomization throughout the first year of life.

One hundred seven mothers complied with the criterion for exclusive breast-feeding for 4 mon. Mothers who did not fulfill this criterion were not excluded from the trial, but we estimated to which extent breast milk covered the energy needs of the infants from their intake of formula and complementary food. Breast milk was estimated to be the dominant source in all but 15 of the infants, most of whom were from the FO group [but the overall degree of breast-feeding did not differ between the two randomized groups (P = 0.059)]. The typical infant formulas on the Danish market at the time had an n-6/n-3 PUFA ratio of around 10 and contained no LCPUFA. One hundred mothers completed the intervention, and 50 mothers from the HFI group remained in the study for the initial 4-mon period. The biochemical effect of the intervention was assessed from the FA composition of breast milk and RBC from mothers and infants at the end of the intervention (13).

Follow-up study. When the children were 2½ yr old, all 150 families were invited to participate in the follow-up examination
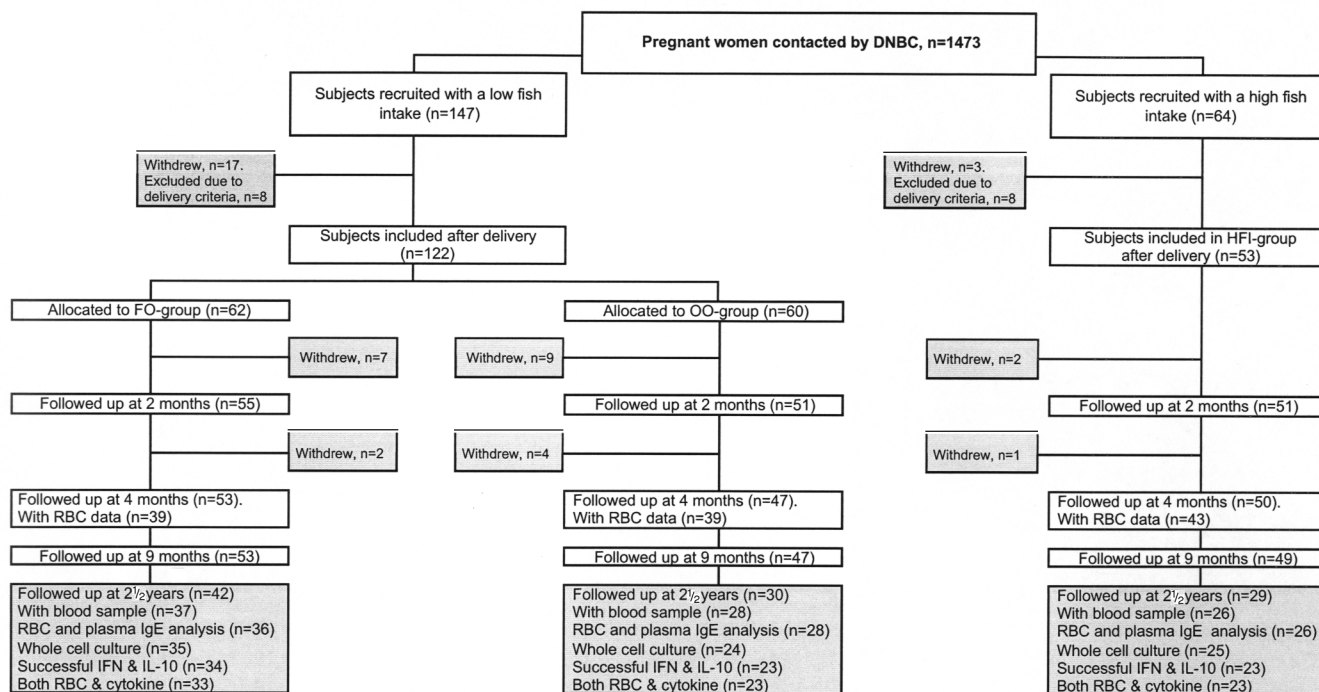
FIG. 1. Trial profile summarizing participant flow, number of randomization assignments, and follow-up examinations for all groups, with special focus on the assessment of immune function at 2½ years of age. DNBC, Danish National Birth Cohort; FO, fish oil; IFN, interferon; IL, interleukin; OO, olive oil; HFI-group, group of mothers with a high fish intake; RBC, red blood cell.

TABLE 1
Characteristics of the 91 Children in the Follow-up Study on Immune Function[a]

	HFI	Olive oil	Fish oil
n	26	28	37
Sex (% boys)	61.5	57.1	62.2
Parity (% with no siblings)	50	39	59
Birth weight (kg)	3.64 ± 0.08	3.56 ± 0.08	3.68 ± 0.07
Mean duration of breast-feeding (mon)	10.0 ± 0.9	9.9 ± 0.9	8.2 ± 0.8
Degree of breast-feeding (% 100 and <50)[b]	80.8 & 7.7	78.6 & 3.6	59.5 & 24.3
Age at follow-up (mon)	31.7 ± 0.2	31.9 ± 0.2	31.7 ± 0.1
Height at $2\frac{1}{2}$ yr (cm)	93.4 ± 0.6	92.6 ± 0.6	92.8 ± 0.5
Weight at $2\frac{1}{2}$ yr (kg)	14.0 ± 0.3	13.7 ± 0.2	14.2 ± 0.2
Family history of atopy (% with 1 and >1)[c]	36.0 & 20.0	42.9 & 21.4	33.3 & 16.7
Children with no signs, of eczema, wheezing, and food allergy (%)[d]	64, 20, 16, 4	64, 14, 21, 4	64, 14, 31, 9
Plasma IgE (titer-value)	8.7 (8.2--9.1)	8.8 (7.3--9.2)	8.9 (8.0--9.2)

[a]Data given as mean ± SE or percentage of all children of mothers with a habitual high fish intake (HFI) or mothers supplemented during lactation with olive oil or fish oil. There were no statistically significant differences between groups. IgE, immunoglobulin E.
[b]Children exclusively breast-fed in the first 4 mon of lactation and those estimated to have had less than 50% of their energy intake covered by breast milk.
[c]1 and >1 atopic family members (parents or siblings).
[d]Only children with an atopic diagnosis made by a physician.

at the Department of Human Nutrition, as previously described (16). The follow-up rates in the randomized groups and in the HFI group were 72 and 58%, respectively. At the time of the follow-up study, the children were healthy, i.e., they were not given continuous medication and did not suffer from chronic disease (except for some having allergies). The parents were interviewed about allergy diagnoses in the child, signs of allergic tendencies, and family history of allergy using questions that has been validated with respect to atopic dermatitis (17). Only allergic tendencies (itchy rash, wheezing, or food allergy) reported that had been verified by a doctor were used for categorization.

At the end of the follow-up examination, a 1-mL blood sample was collected from the children in ice-cold heparin-conditioned tubes by venipuncture. The study group in the present study consisted only of children with successful blood sampling; their characteristics are shown in Table 1.

Within 30 min after sampling, 30-μL aliquots of heparinized whole blood were cultured with lipopolysaccharide (LPS) for measurement of cytokine production. Within 1 h after sampling, RBC were separated from plasma and leukocytes by centrifugation and washed three times in physiological saline. The plasma samples were frozen at −80°C. The isolated, packed RBC were reconstituted 1:1 in physiological saline with 1 mM EDTA and 0.005% BHT (Sigma, St. Louis, MO) and kept at −80°C until the FA composition was determined (maximum storage time 8 mon).

Measurement of cytokine production by whole-blood cultures. Heparinized blood was diluted 1 in 7 with RPMI 1640 medium supplemented with 0.1% FCS and 30 IU/mL Na-heparin. Diluted whole-blood cultures were set up in 96-well culture plates, with 8 wells for each child. In 4 wells, LPS (from *Escherichia coli* O26:B6; Sigma) was added to give a final concentration of 1 μg/mL, and 4 wells with control cultures were the added medium alone. Cultures were incubated at 37°C in a 5% CO_2 atmosphere for 22.5 ± 1.5 h, the supernatant was carefully removed, and aliquots were frozen at −20°C.

Cytokine concentrations in the culture supernatants were measured by ELISA. IFN-γ, IL-12 p70, and IL-4 were measured with commercial kits (Duosets DY285, DY1270, and DY204; R&D Systems Europe, Abington, United Kingdom) in accordance with the manufacturer's instructions. The IL-10 concentration was determined with paired antibodies (BD Pharmingen, San Diego, CA) using anti-human IL-10 (clone JES3-19F1, 2 μg/mL) as the coating antibody and biotinylated anti-human IL-10 (clone JES3-12G8, 1 μg/mL) as the detector antibody. Cytokine concentrations were quantified relative to standard curves representing a range of dilutions of recombinant cytokine using a four-parameter curve-fit analysis (KinetiCalc software, version KC4 Rev 29; Bio-Tek Instruments). Limits of detection for these assays were 62 pg/mL (IFN-γ), 33 pg/mL (IL-10), 33 pg/mL (IL-12), and 31 pg/mL (IL-4). Nondetected values were set to 0.5× the limit of detection in calculating the ratios of IFN-γ to IL-10. IFN-γ IL-10, and IL-12 were determined in most of the children, whereas the IL-4 analysis was carried out only with the supernatants from 10 of the children. The were no correlations between the determined levels of cytokines in the supernatants and storage time (data not shown).

Measurement of IgE in plasma. IgE was measured in plasma from heparinized blood samples with paired antibodies (BD Pharmingen) in a sandwich ELISA. It was performed as described above, but with antibodies against human IgE. Anti-human IgE (clone G7-18) was used as the capture antibody at 2 μg/mL, and biotin-coupled anti-human IgE (clone G7-26) at 2 μg/mL was used as the detector antibody. Plasma from high-IgE producers (a kind gift from ALK-Abello, Hørsholm, Denmark) was used as a reference to control for plate-to-plate variation. Samples were serially diluted and antibody titers were expressed as $\log_2$ titers and defined as the dilution (four-parameter analysis, KinetiCalc software; Bio-Tek Instruments) of a blood sample leading to an absorbance at 0.2 above background.

RBC FA analysis. Thawed RBC from the heparin blood samples were hemolyzed in redistilled water, and the lipids were extracted by the procedure of Folch *et al.* (18). Lipids were methylated with BF_3 in methanolic NaOH (19), and the

resulting FAME were extracted and separated by GLC as previously described (13). All peaks from lauric acid (12:0) to docosahexaenoic acid (22:6n-3) were identified from the retention times of commercial standards (Nu-Chek-Prep Inc., Elysian, MN) as previously described (20). On average, 96.9 ± 0.1% (mean ± SE) of the chromatogram areas were identified (excluding BHT). The FA compositions of all RBC samples were determined in duplicate. Results are expressed as the area percentage of each FA relative to that of all FA peaks together.

Statistical analysis. The results are given as average ± SE for normally distributed variables (RBC FA composition) and as the median (10th and 90th percentiles) for other variables (all immune variables). RBC FA composition and immune responses in the two randomized groups and in atopic and nonatopic children were compared by Student's *t*-test and the Mann–Whitney U-test, respectively. The distribution of LPS-induced IL-10 production in the two randomized groups was performed by Levene's test for equal variances. Paired comparisons of the LPS stimulation in cytokine production were performed using a Wilcoxon signed ranks test. Associations between immune variables and between RBC FA composition and cytokine production were calculated by Kendall ι. A Pearson correlation analysis was used to analyze the correlation between RBC FA compositions in mothers and children. All data were analyzed using SPSS for Windows 11.0 (Chicago, IL).

RESULTS

FO supplementation had a pronounced effect on the FA composition of breast milk (13) and on that of RBC from infants in month 4 of lactation (Table 2). The ratio of 20:5n-3 to 20:4n-6

in the RBC of infants was significantly higher in the FO group than in the OO-group at the end of the 4-mon intervention period. The 91 children with follow-up blood samples at $2\frac{1}{2}$ yr of age were similar to the children with no follow-up blood sample with respect to gestational age, weight, length at birth, degree of breast-feeding, dietary group, and RBC FA composition at 4 mon (data not shown). However, the follow-up group had significantly better compliance in the intervention trial (89 vs. 85%), and the follow-up rate for boys was higher ($P = 0.020$). At $2\frac{1}{2}$ yr of age, no differences were apparent in RBC FA compositions between children from the two randomized groups (Table 2).

At $2\frac{1}{2}$ yr of age, no group difference was observed in plasma IgE levels (Table 1). Cytokine production was not detectable in the supernatants of unstimulated cultures, except in a few children (Fig. 2). LPS induced a marked increase in IL-10 production to levels approximately 18 times above the detection limit (Fig. 2). Median LPS-induced IL-10 level did not differ between the FO and OO groups ($P = 0.367$), but the distribution of IL-10 in the two groups did ($P = 0.003$). LPS-induced IFN-γ production was significantly increased compared with the control in both the OO and FO groups ($P = 0.008$ and $P < 0.001$, respectively). LPS induced detectable levels of IFN-γ in 62% of the children in the FO group and 39% in the OO group (chi-square, $P = 0.093$). The median IFN-γ production was still undetectable in the OO group, but was 2.2 times above the limit of detection in the FO group and significantly higher than in the OO group ($P = 0.034$, Fig. 2). This difference was also significant when the child with detectable control levels of IFN-γ was excluded ($P = 0.049$), and there was a trend in the same direction when all children who were breast-fed <50% during the

TABLE 2

FA Composition of Erythrocytes at 4 mon and $2\frac{1}{2}$ yr of Age from Offspring of Mothers Randomized to Groups Supplemented with Olive Oil or Fish Oil During the First 4 mon of Lactation or Mothers with a High Habitual Fish Intake (HFI)[a]

	4 mon			$2\frac{1}{2}$ yr		
	HFI	Olive oil	Fish oil	HFI	Olive oil	Fish oil
n	20	25	27	26	28	36
SFA	43.3 ± 0.7	42.4 ± 0.6	41.9 ± 0.4	41.2 ± 0.1	41.4 ± 0.2	41.7 ± 0.2[d]
MUFA	17.6 ± 0.5	17.9 ± 0.5	17.2 ± 0.5	16.7 ± 0.1	16.8 ± 0.2	16.8 ± 0.1
20:3n-9	0.05 ± 0.01	0.07 ± 0.01	0.05 ± 0.01	0.10 ± 0.01	0.10 ± 0.01	0.10 ± 0.005
18:2n-6	7.9 ± 0.2	8.6 ± 0.2[e]	8.6 ± 0.2[d]	10.2 ± 0.1	10.2 ± 0.2	10.5 ± 0.1
20:2n-6	0.29 ± 0.01	0.31 ± 0.01	0.30 ± 0.01	0.25 ± 0.01	0.24 ± 0.005	0.25 ± 0.01
20:3n-6	1.8 ± 0.1	1.9 ± 0.1	1.8 ± 0.1	1.7 ± 0.1	1.7 ± 0.1	1.7 ± 0.1
20:4n-6	15.1 ± 0.5	15.8 ± 0.5	14.8 ± 0.3	16.3 ± 0.2	16.2 ± 0.2	16.0 ± 0.2
22:4n-6	2.4 ± 0.1	2.8 ± 0.1[d]	2.4 ± 0.1[a]	2.9 ± 0.1	3.0 ± 0.1	3.0 ± 0.1
22:5n-6	0.41 ± 0.03	0.55 ± 0.03[e]	0.54 ± 0.02[f]	0.54 ± 0.02	0.58 ± 0.03	0.54 ± 0.02
n-6 PUFA	27.9 ± 0.7	29.9 ± 0.6[d]	28.4 ± 0.4[a]	31.9 ± 0.2	31.9 ± 0.3	31.9 ± 0.2
18:3n-3	0.10 ± 0.01	0.09 ± 0.01	0.09 ± 0.01	0.14 ± 0.01	0.14 ± 0.01	0.15 ± 0.01
20:5n-3	0.95 ± 0.10	0.56 ± 0.06[e]	1.21 ± 0.12[c]	0.79 ± 0.04	0.75 ± 0.06[d]	0.78 ± 0.04
22:5n-3	2.0 ± 0.1	2.1 ± 0.1	1.9 ± 0.1	2.6 ± 0.1	2.5 ± 0.1	2.5 ± 0.1
22:6n-3	7.3 ± 0.4	6.3 ± 0.4	8.5 ± 0.5[c]	5.9 ± 0.2	5.5 ± 0.2	5.4 ± 0.2
n-3 PUFA	10.4 ± 0.6	9.0 ± 0.5	11.7 ± 0.6[b]	9.4 ± 0.2	9.0 ± 0.3	8.9 ± 0.2
n-3/n-6	2.8 ± 0.2	3.6 ± 0.2[d]	2.8 ± 0.3[a]	3.5 ± 0.1	3.7 ± 0.2	3.7 ± 0.1
20:5n-3/20:4n-6	0.063 ± 0.007	0.035 ± 0.003[f]	0.082 ± 0.009[c]	0.049 ± 0.003	0.047 ± 0.004	0.049 ± 0.003

[a]The values are given as area% of all FA in the chromatogram − mean ± SE. Individual FA are named by the number of carbon atoms:number of double bonds and the position of the last double bond. SFA, saturated FA; MUFA, monounsaturated FA. Statistical differences between groups are indicated by superscript letters: [a]$P < 0.05$, [b]$P < 0.01$, and [c]$P < 0.001$ compared with the olive oil group, and [d]$P < 0.05$, [e]$P < 0.01$, and [f]$P < 0.001$ compared with the HFI group.
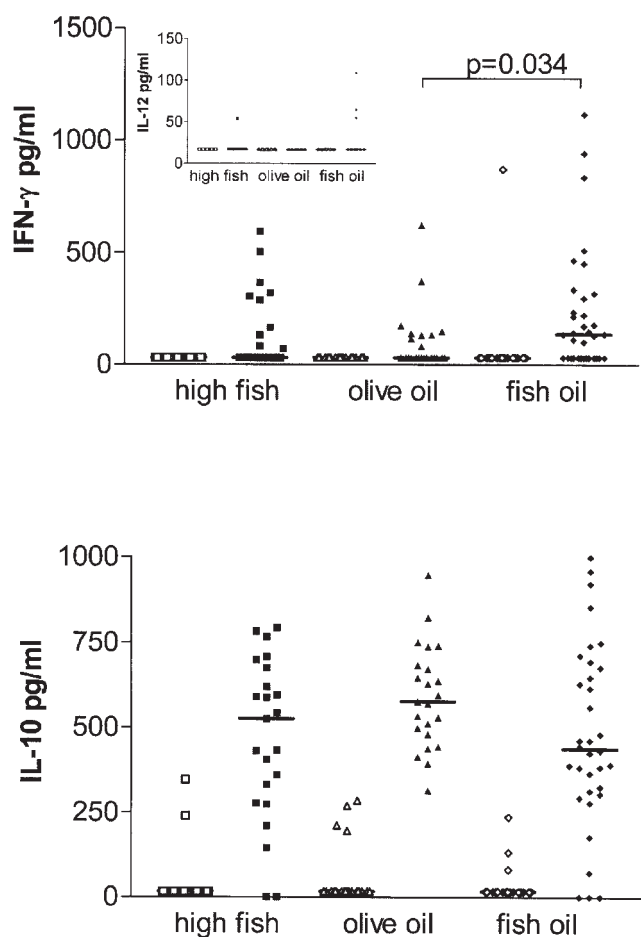
FIG. 2. *In vitro* lipopolysaccharide-stimulated cytokine production in 2½-year-old children in the maternal dietary groups (high fish intake and olive oil- or fish oil-supplemented). Cytokine production (pg/mL) for each child is given as the mean of three to four values. Open and filled symbols give control and lipopolysaccharide-stimulated values, respectively. The solid lines indicate median values in each group (*n* = 23 in the high fish intake group, 23 in the olive oil group, and 34 in the fish oil group).

intervention were excluded from this analysis (*P* = 0.063). The HFI group was intermediate with respect to LPS-induced IFN-γ production, which was detectable in 44% of the children. LPS-induced IL-12 production was detectable in only three children from the FO group and one from the HFI group (Fig. 2, insert). LPS stimulation did not result in detectable levels of IL-4 (data not shown). The ratio of IFN-γ/IL-10 was significantly higher in the FO group compared with that in the OO group [being 0.27 (0.04–1.11) and 0.07 (0.04–0.56), respectively (*P* = 0.019)]. The ratio was also significantly different in the two randomized groups when those children who were breast-fed <50% during the intervention period were excluded from the analysis (*P* = 0.033, *n* = 47). The HFI group had an intermediate ratio (data not shown).

Thirty-six percent of the children were reported to have a diagnosis of eczema, wheezing, or food allergy, and these children were equally distributed between the three groups (Table 1). Total plasma IgE was not significantly higher in children

with a diagnosis of eczema, wheezing, or food allergy compared with nondiagnosed children, although there was a trend in that direction (*P* = 0.071). LPS induced detectable levels of IFN-γ in 37% of the whole-blood cultures from diagnosed children and 58% from nondiagnosed children (*P* = 0.084). There was no significant difference between atopic and nonatopic children with respect to LPS-stimulated production of IFN-γ (*P* = 0.378), IL-10 (*P* = 0.782), or IFN-γ/IL-10 (*P* = 0.435). Also, there was no significant association between plasma IgE and LPS-induced IFN-γ or IL-10 production (*r* = 0.011, *P* = 0.895 and *r* = 0.142, *P* = 0.075, respectively). No differences were observed in the FA composition of RBC from atopic and nonatopic children at either 4 mon or 2½ yr of age (data not shown).

In children from the randomized groups, LPS-induced IFN-γ production and the ratio of IFN-γ to IL-10 correlated with the ratio of 20:5n-3 to 20:4n-6 in infant RBC (*r* = 0.220 and *r* = 0.205, respectively; *P* = 0.050 and *n* = 44 for both). The correlations between LPS-induced IFN-γ production and IFN-γ/IL-10 and maternal RBC 20:5n-3/20:4n-6 were more prominent, probably due to the higher power (*n* = 56; *r* = 0.249, *P* = 0.011 and *r* = 0.222, *P* = 0.016, respectively). IFN-γ/IL-10 was also correlated with the levels of 22:6n-3 in the RBC of mothers at the end of the intervention and of the randomized children at 2½ yr of age (data not shown). However, these correlations were weaker (lower *r*-values and less significant), and the RBC 22:6n-3 of both mothers and 2½-yr-old children was associated with RBC 20:5n-3/20:4n-6 at the end of the intervention (data not shown). No correlation was observed between LPS-induced IL-10 production and any PUFA in the RBC of the mother, infant, or child.

DISCUSSION

FO is known to be immunosuppressive and to suppress the production of inflammatory cytokines (2). Because of such immunomodulatory actions of n-3 PUFA, several FO intervention studies have been conducted in atopic patients. Atopy is characterized by increased B-lymphocyte IgE-production, which is regulated by cytokines produced by Th cells according to the Th1/Th2 hypothesis (21). FO-supplementation studies show conflicting results regarding the effect on Th1/Th2 cytokines and tend to show a limited efficacy once the allergic immune responses are established (2). However, atopic sensitization occurs early in life; therefore, perinatal n-3 PUFA exposure may affect immune maturation in infants and the risk of subsequent disease. Several studies indicate that the development of allergies may be associated with breast-milk PUFA (8–10). FO-supplementation of lactating atopic mothers has been found to reduce the prevalence of wheezing in the child (12). To our knowledge, no other studies have assessed the potential immunomodulatory function of FO supplementation in breast-feeding mothers.

Maturation of the immune system during infancy is characterized by an increase in IFN-γ production and a shift from Th2 to Th1 polarization in the immune response (1). In the present

study, maternal FO supplementation increased LPS-induced IFN-γ production. Furthermore, IL-12 was found only in children of FO-supplemented mothers or mothers with a high fish intake, which strengthens the IFN-γ result. No effect of FO was observed on IL-10 production, although this had a significantly broader distribution, but the IFN-γ to IL-10 ratio was higher after maternal FO supplementation during lactation. Our data indicate that an increased n-3 LCPUFA intake early in life gives rise to faster immune maturation and is able to polarize the immune response later in childhood toward Th1. These results are in agreement with other observations. Field *et al.* (5) observed a slower maturation of the immune response in formula-fed infants compared with breast-fed infants, which disappeared with the addition of LCPUFA (22:6n-3 and 20:4n-6) to the formula. Maternal FO supplementation during pregnancy has been shown to reduce levels of IL-13 in cord plasma (6) and to reduce the allergen-induced production of IL-10 (7).

In vitro cytokine production in whole-blood cultures of the children in the present study was on the limit of detection, which is a general problem in studies of young children (6,22). We were able to detect only IL-12 in a few of the children, although this may have been improved if we had primed the cells with IFN-γ. Instead, we measured the concentration of IFN-γ, as we had demonstrated that IFN-γ production in stimulated whole-blood could be inhibited by the addition of anti-IL-12 antibodies (Jensen, M., Christensen, H.R., and Frøkiær, H., unpublished manuscript). Moreover, we used only one toll-like receptor ligand to stimulate cytokine production; hence, we explored only a small potential of the immune response, and LPS is primarily a Th1 polarizing agent. We were not able to detect IL-4 in LPS-stimulated whole-blood samples and therefore used IL-10, which was detectable in almost all samples, as a Th2 marker. However, IL-10 is secreted by a wide variety of cell types, including Th cells, monocytes, macrophages, dendritic cells, and mast cells. IL-10 possesses potent immune-suppressive functions and is currently believed to drive the differentiation of regulatory T cells. However, we found that IL-10 tended to correlate positively with plasma IgE, which, although not significant, may indicate that IL-10 in young children may be a marker of Th2 response. The LPS-induced responses in IL-10 and IFN-γ production were variable. This variability could be due to differences in cell counts of mononuclear cells between samples, as we did not assess this. However, it is not likely to give rise to a bias between the groups that could explain the observations. Unfortunately, the power of the study was not sufficient to show any difference in the number of high and low responders between the groups, although there was a trend. To overcome the differences in response level, we focused on the ratio between the production of IFN-γ and IL-10. In the study we used OO as a control supplement. However, OO also has been suggested to have some immunomodulatory actions and anti-inflammatory effects, and many of the effects observed for FO are also shown for OO (23). Accordingly, the difference between the FO group and the control group may have been larger if we had used a more neutral control oil.

A fast immune maturation and Th1 polarization could result in better immune functioning and a decreased risk of atopic sensitization. The study was not powered to look at atopic sensitization, and no differences in atopy and plasma IgE were observed between the groups. The children were not selected to have a high risk of atopy, but the prevalence of self-reported eczema, wheezing, or food allergy was high. Furthermore, the study is limited by a low rate of follow-up (around 70%). Plasma IgE is a very crude measure of atopy and does not give an indication of allergen sensitization. Allergen-specific immune responses provide information on cytokine production by allergen-reactive cells influenced by prior antigen exposure, whereas cytokine production after polyclonal stimulation, as in the present study, examines the underlying predisposition of cytokine production. This is especially important in light of the findings that both Th1 and Th2 allergen-induced cytokine responses are increased in children with atopic disease concomitant with a reduced polyclonal Th1 response (22). No association was found between *in vitro* cytokine production and plasma IgE levels; also, there was no association between IgE and eczema, wheezing, or food allergy, although both associations tended to be positive. A weak association may not be surprising considering the self-reported diagnosis and the low power of the study with respect to atopy. Supplementation with n-3 PUFA during pregnancy and in the first year of life has been shown to reduce the prevalence of self-reported wheeze symptoms, which were not associated with a decrease in serum IgE or atopy (12). Allergic diseases may be related to a dysfunction of various IL-10-producing regulatory cells, and allergen-specific IL-10 is known to be down-regulated in atopic children (24). Low levels of IL-12 in cord blood have been associated with later IgE sensitization (25), and high-risk children who developed clinical allergy tended to have lower neonatal Th1 responses (26,27). It has been suggested that a relative absence of IL-12 favors the development of a default Th2 cytokine profile (28). Maturation of antigen-presenting cells, and thus increased IL-12 production, is a key rate-limiting step in the postnatal development of Th1 function.

The present data show that n-3 LCPUFA intake in early infancy appears to be able to increase the polyclonal Th1 response. The FO-induced changes in RBC FA composition during the intervention were no longer evident at $2\frac{1}{2}$ yr of age. RBC were used as a proxy for the FA composition of body tissue membranes in general. Therefore, the effect of FO supplements on immune function during lactation does not appear to be mediated *via* membrane n-3 LCPUFA in whole-blood cultures. We speculate that a long-term effect may be caused by a shift in immune polarization during infancy, which, because of a mutual inhibition between the Th1 and Th2 responses, is maintained or even attenuated throughout early childhood. The mechanism behind the immune-modulating effect of n-3 PUFA could be mediated through changes in prostaglandin E_2 (PGE_2) synthesis (2), but other mechanisms cannot be excluded. PGE_2 enhances Th2 differentiation and suppresses the differentiation of Th1 cells. *In vitro* studies have shown that all PGE subtypes equipotently inhibit Th1 cytokine production (29,30), but they

may influence the ratio of Th1 to Th2 cytokines and T cell proliferation differently (29). We found an association between IFN-γ/IL-10 and RBC 20:5n-3/20:4n-6 in RBC, thus suggesting that n-3 PUFA may exert the effect on cytokine production by competition in eicosanoid synthesis and action.

In summary, we found an increased LPS-induced *in vitro* IFN-γ production and higher IFN-γ to IL-10 ratio in 2$\frac{1}{2}$-year-old children after maternal FO supplementation in lactation. These results indicate that early n-3 PUFA intake may result in faster maturation of the immune system and/or a TH1 polarization. An important finding of this present study is the observation that the immunomodulating effect is present 2 yr after the supplements were given.

ACKNOWLEDGMENTS

REFERENCES

1. Field, C.J., Clandinin, M.T., and van Aerde, J.E. (2001) Polyunsaturated Fatty Acids and T-Cell Function: Implications for the Neonate, *Lipids 36*, 1025–1032.
2. Prescott, S.L., and Calder, P.C. (2004) n-3 Polyunsaturated Fatty Acids and Allergic Disease, *Curr. Opin. Clin. Nutr. Metab. Care 7*, 123–129.
3. Hanson, L.A., Korotkova, M., Haversen, L., Mattsby-Baltzer, I., Hahn-Zoric, M., Silfverdal, S.A., Strandvik, B., and Telemo, E. (2002) Breast-feeding, a Complex Support System for the Offspring, *Pediatr. Int. 44*, 347–352.
4. Lauritzen, L., Hansen, H.S., Jørgensen, M.H., and Michaelsen, K.F. (2001) The Essentiality of Long-Chain n-3 Fatty Acids in Relation to Development and Function of the Brain and Retina, *Prog. Lipid Res. 40*, 1–94.
5. Field, C.J., Thomson, C.A., van Aerde, J.E., Parrott, A., Euler, A., Lien, E., and Clandinin, M.T. (2000) Lower Proportion of CD45R0(+) Cells and Deficient Interleukin-10 Production by Formula-fed Infants, Compared with Human-fed, Is Corrected with Supplementation of Long-Chain Polyunsaturated Fatty Acids, *J. Pediatr. Gastroenterol. Nutr. 31*, 291–299.
6. Dunstan, J.A., Mori, T.A., Barden, A., Beilin, L.J., Taylor, A.L., Holt, P.G., and Prescott, S.L. (2003) Maternal Fish Oil Supplementation in Pregnancy Reduces Interleukin-13 Levels in Cord Blood of Infants at High Risk of Atopy, *Clin. Exp. Allergy 33*, 442–448.
7. Dunstan, J.A., Mori, T.A., Barden, A., Beilin, L.J., Taylor, A.L., Holt, P.G., and Prescott, S.L. (2003) Fish Oil Supplementation in Pregnancy Modifies Neonatal Allergen-Specific Immune Responses and Clinical Outcomes in Infants at High Risk of Atopy: A Randomized, Controlled Trial, *J. Allergy Clin. Immunol. 112*, 1178–1184.
8. Reichardt, P., Muller, D., Posselt, U., Vorberg, B., Diez, U., Schlink, U., Reuter, W., and Borte, M. (2004) Fatty Acids in Colostrum from Mothers of Children at High Risk of Atopy in Relation to Clinical and Laboratory Signs of Allergy in the First Year of Life, *Allergy 59*, 394–400.
9. Duchén, K., Yu, G., and Björksten, B. (1998) Atopic Sensitization During the First Year of Life in Relation to Long Chain Polyunsaturated Fatty Acid Levels in Human Milk, *Pediatr. Res. 44*, 478–484.
10. Duchén, K., Casas, R., Fageras-Bottcher, M., Yu, G., and Björksten, B. (2000) Human Milk Polyunsaturated Long-Chain Fatty Acids and Secretory Immunoglobulin A Antibodies and Early Childhood Allergy, *Pediatr. Allergy Immunol. 11*, 29–39.
11. Stoney, R.M., Woods, R.K., Hosking, C.S., Hill, D.J., Abramson, M.J., and Thien, F.C.K. (2004) Maternal Breast Milk Long-Chain n-3 Fatty Acids Are Associated with Increased Risk of Atopy in Breastfed Infants, *Clin. Exp. Allergy 34*, 194–200.
12. Mihrshahi, S., Peat, J.K., Marks, G.B., Mellis, C.M., Tovey, E.R., Webb, K., Britton, W.J., and Leeder, S.R. (2003) Eighteen-Month Outcomes of House Dust Mite Avoidance and Dietary Fatty Acid Modification in the Childhood Asthma Prevention Study (CAPS), *J. Allergy Clin. Immunol. 111*, 162–168.
13. Lauritzen, L., Jørgensen, M.H., Mikkelsen, T.B., Skovgaard, I.M., Straarup, E.M., Olsen, S.F., Høy, C.-E., and Michaelsen, K.F. (2004) Maternal Fish Oil Supplementation in Lactation: Effect on Visual Acuity and n-3 Fatty Acid Content of Infant Erythrocytes, *Lipids 39*, 195–206.
14. Olsen, J., Melby, M., Olsen, S.F., Sørensen, T.I.A., Aaby, P., Andersen, A.M.N., Taxbøl, D., Hansen, K.D., Juhl, M., Schow, T.B., *et al.* (2001) The Danish National Birth Cohort—Its Background, Structure and Aim, *Scand. J. Public Health 29*, 300–307.
15. Greisen, G., and Michaelsen, K.F. (1989) Perinatal Vækst, *Ugeskr. Laeger 151*, 1813–1816.
16. Ulbak, J., Lauritzen, L., Hansen, H.S., and Michaelsen, K.F. (2004) Diet and Blood Pressure in 2.5 Year-Old Danish Children, *Am. J. Clin. Nutr. 79*, 1095–1102.
17. Benn, C.S., Benfeldt, E., Andersen, P.K., Olesen, A.B., Melbye, M., and Björksten, B. (2003) Atopic Dermatitis in Young Children: Diagnostic Criteria for Use in Epidemiological Studies Based on Telephone Interviews, *Acta Derm. Venereol. 83*, 347–350.
18. Folch, J., Lees, M., and Sloane Stanley, G.H. (1957) A Simple Method for the Isolation and Purification of Total Lipids from Animal Tissues, *J. Biol. Chem. 226*, 497–509.
19. Hamilton, S., Hamilton, R.J., and Sewell, P.A. (1992) Extraction of Lipids and Derivative Formation, in *Lipid Analysis: A Practical Approach* (Hamilton, R.J., and Hamilton, S., eds.), pp. 13–64, IRL Press, Oxford.
20. Lauritzen, L., Jørgensen, M.H., Hansen, H.S., and Michaelsen, K.F. (2002) Fluctuations in Human Milk Long-Chain PUFA Levels in Relation to Dietary Fish Intake, *Lipids 37*, 237–244.
21. Romagnani, S. (2001) T Cells in Allergy and Asthma, *Curr. Opin. Allergy Clin. Immunol. 1*, 73–78.
22. Smart, J.M., and Kemp, A.S. (2002) Increased Th1 and Th2 Allergen-Induced Cytokine Responses in Children with Atopic Disease, *Clin. Exp. Allergy 32*, 796–802.
23. Harwood, J.L., and Yaqoob, P. (2002) Nutritional and Health Aspects of Olive Oil, *Eur. J. Lipid Sci. Technol. 104*, 685–697.
24. van der Velden, V.H.J., Laan, M.P., Baert, M.R.M., Malefyt, R.D., Neijens, H.J., and Savelkoul, H.F.J. (2001) Selective Development of a Strong Th2 Cytokine Profile in High-Risk Children Who Develop Atopy: Risk Factors and Regulatory Role of IFN-γ, IL-4 and IL-10, *Clin. Exp. Allergy 31*, 997–1006.
25. Nilsson, C., Larsson, A.K., Hoglind, A., Gabrielsson, S., Blomberg, M.T., and Lilja, G. (2004) Low Numbers of Interleukin-12-Producing Cord Blood Mononuclear Cells and Immunoglobulin E Sensitization in Early Childhood, *Clin. Exp. Allergy 34*, 373–380.

26. Prescott, S.L., Taylor, A., King, B., Dunstan, J., Upham, J.W., Thornton, C.A., and Holt, P.G. (2003) Neonatal Interleukin-12 Capacity Is Associated with Variations in Allergen-Specific Immune Responses in the Neonatal and Postnatal Periods, *Clin. Exp. Allergy 33*, 566–572.

27. Prescott, S.L., King, B., Strong, T.L., and Holt, P.G. (2003) The Value of Perinatal Immune Responses in Predicting Allergic Disease at 6 Years of Age, *Allergy 58*, 1187–1194.

28. Jankovic, D., Kullberg, M.C., Hieny, S., Caspar, P., Collazo, C.M., and Sher, A. (2002) In the Absence of IL-12, CD4(+) T Cell Responses to Intracellular Pathogens Fail to Default to a Th2 Pattern and Are Host Protective in an IL-10(−/−) Setting, *Immunity 16*, 429–439.

29. Miles, E.A., Aston, L., and Calder, P.C. (2003) *In vitro* Effects of Eicosanoids Derived from Different 20-Carbon Fatty Acids on T Helper Type 1 and T Helper Type 2 Cytokine Production in Human Whole-Blood Cultures, *Clin. Exp. Allergy 33*, 624–632.

30. Dooper, M.M.B.W., Wassink, L., M'Rabet, L., and Graus, Y.M.F. (2002) The Modulatory Effects of Prostaglandin-E on Cytokine Production by Human Peripheral Blood Mononuclear Cells Are Independent of the Prostaglandin Subtype, *Immunology 107*, 152–159.

Lymphatic Transport in Rats of Interesterified Oils Containing Conjugated Linoleic Acids

Ellen Marie Straarup, Trine Porsgaard*, Huiling Mu,
Christina H. Hansen, and Carl-Erik Høy[†]

Biochemistry and Nutrition Group, BioCentrum-DTU, Technical University of Denmark, DK-2800 Lyngby, Denmark

ABSTRACT: In this study we examined the lymphatic transport in rats of FA after administration of interesterified oils containing CLA, with emphasis on the location of CLA and octanoic acid in the TAG. The oils were produced by enzymatic interesterification. Eight oils with different structures or FA profiles were examined in this study: MCM, CMC, OCO, and COC, where M was expected to be octanoic acid and O oleic acid. In group 1, C was CLA as a mixture of the two CLA isomers $c9,t11$ or $t10,c12$, and in group 2, C was mainly the isomer $t10,c12$. Rats were subjected to cannulation of the mesenteric lymph duct, and the following day they were intragastrically administered one of the oils and lymph samples were collected for 24 h. The lymphatic transport of total FA from 0 to 8 h in group 1 was significantly ($P < 0.05$) higher for the OCO-1 and the COC-1 oils than for the CMC-1 oil. Similarly, in group 2 the transport was higher for the OCO-2 oil than for the CMC-2 oil. The recovery of both of the CLA isomers examined was similar (50–70%) and independent of the isomer, oil structure, and FA profile, whereas more octanoic acid was recovered from the CMC oils than from the MCM oils. The results indicated that the FA profiles and the position of octanoic acid had only a minor influence on the absorption of CLA.

Paper no. L9717 in *Lipids 40*, 677–684 (July 2005).

CLA is a collective term for several conjugated isomers of linoleic acid that differ in the geometry and position of the double bonds. The CLA isomer $c9,t11$ is the major isomer occurring naturally in food, mainly in milk fat and meat from ruminants (1), whereas the $t10,c12$ isomer is naturally present in much lower amounts in food products. Furthermore, CLA is produced by alkaline isomerization of linoleic acid (e.g., safflower, sunflower, or soybean oil). The resulting oil contains 60–80% CLA, dominated by the two isomers $c9,t11$ and

$t10,c12$ (50:50) (2). These isomers have been reported to have various health-related benefits (3), including anticarcinogenic, antiatherosclerotic, lean body mass enhancing-, and immune function-enhancing effects, while also reducing inflammation and reducing body fat and diabetic symptoms in some animal models (4).

Dietary TAG are hydrolyzed in humans by gastric (5) and pancreatic lipases (6) in the stomach and duodenum, respectively, by specific hydrolysis of the sn-1/3 ester bonds. The hydrolysis results in the formation of sn-2-MAG and FFA. The nature of the FA in the TAG molecule determines the hydrolysis rate, and some experiments have shown that medium-chain FA (MCFA) are hydrolyzed faster than highly unsaturated long-chain FA (LCFA) (7–9). The sn-2-MAG is absorbed intact into the enterocytes (10,11), whereas the FFA are absorbed either directly into the portal blood (mostly short-chain FA and MCFA) or, together with the sn-2-MAG, into the enterocytes. In the enterocytes, sn-2-MAG are reesterified with exogenous as well as endogenous FA to form a new pool of TAG, packed into chylomicrons, and secreted into the lymphatic duct (12). Therefore, the intramolecular TAG structures play important roles in the absorption of fat. Studies have shown that CLA $c9,t11$ is absorbed better from the sn-1/3-positions than from the sn-2-position of the TAG molecules (13). In milk (14) and meat from ruminants (15,16), CLA $c9,t11$ is primarily located in the outer positions, indicating that the CLA in these products is well absorbed.

Structured lipids are synthesized either by chemical or enzymatic interesterification (17). The advantage of enzymatic interesterification is the specificity of the enzyme to generate TAG molecules with a well-defined structure. Structured TAG containing MCFA in the outer positions and LCFA in the sn-2-position combine the advantages of rapid intestinal hydrolysis of MCFA as well as being a source of LCFA. Oils with this kind of structure were shown to be absorbed faster and to a higher degree than oils containing only LCFA in normal-, but especially in malabsorbing, rats (18–20). Furthermore, the absorption of the FA located in the sn-2-position of the structured oil was also increased. This may be explained by a faster hydrolysis in the intestine of MCFA when located in the sn-1/3-positions compared with LCFA (7,9). The advantage of specific structured oils with MCFA in the sn-1/3-positions was used to improve the fat uptake, and thereby energy intake, and to increase nitrogen digestibility in weaning piglets (21).

Because of the reported health-related benefits of CLA, it is

---

of major interest to maximize the uptake of the CLA ingested. We examined the possibility of enhancing the absorption by incorporating CLA into oils with different structures and FA profiles, including MCFA. The study was carried out in rats with normal absorption, mainly with emphasis on investigating the absorption of the two CLA isomers *c*9,*t*11 and *t*10,*c*12, but also that of other FA. Dietary fats were produced by enzymatic interesterification of either an oil containing a mixture of the two isomers *c*9,*t*11 and *t*10,*c*12 or one with *t*10,*c*12 as the major CLA isomer.

MATERIALS AND METHODS

Interesterified oils. The conjugated trilinoleylglycerol (CLA), a mix of *c*9,*t*11 and *t*10,*c*12 (75% TAG), and *t*10,*c*12 (75% TAG), as well as a mix of *c*9,*t*11 and *t*10,*c*12 (80% FFA) and a product enriched with *t*10,*c*12 (80% FFA) were kindly donated by Natural Lipids Ltd. A/S (Hovdebygda, Ålesund, Norway). Octanoic acid (8:0) was purchased from Brøste A/S (Lyngby, Denmark), trioctanoin (Myritol 888) was from Cognis Japan Ltd. (Shinagawaku, Tokyo, Japan), oleic acid (95%) was from AppliChem GmbH (Darmstadt, Germany), and high-oleic sunflower oil was from Aarhus United A/S (Aarhus, Denmark). Novo Nordisk A/S (Bagsværd, Denmark) donated the Lipozyme IM, in which an *sn*-1/3-specific lipase from *Rhizomucor miehei* was immobilized on a macroporous ion resin.

For the survey, eight dietary groups were divided into two groups: group 1—MCM-1, CMC-1, OCO-1, COC-1; and group 2—MCM-2, CMC-2, OCO-2, and COC-2. C was CLA, O was oleic acid (18:1n-9), and M was 8:0. Group 1 contained both the CLA isomers *c*9,*t*11 and *t*10,*c*12, whereas the CLA in group 2 was primarily the *t*10,*c*12 isomer.

The four different oils containing CLA as a mix of *c*9,*t*11 and *t*10,*c*12 were produced by enzymatic interesterification in a packed-bed reactor (22). The substrate mixture had a molar ratio of 6:1 (FFA/TAG) and a water content adjusted to 0.09%. A constant reactor temperature of 60°C was maintained by circulating water between the inner and outer tube of the reactor. CLA, as a mix of *c*9,*t*11 and *t*10,*c*12, was used as a substrate in the production of the MCM-1 and OCO-1 oils. Trioctanoin and sunflower oil were used to produce the CMC and COC oils (O was 18:1n-9), respectively. The FFA, either as the CLA mix, 8:0, or 18:1n-9, was spontaneously esterified in the *sn*-1/3-positions because of their abundance in the reaction mixture. A two-step short-path distillation process was used to separate FFA from TAG in the interesterification products.

The four different oils containing CLA as *t*10,*c*12 were produced by enzymatic interesterification in a batch reactor (23). CLA *t*10,*c*12, as TAG and FFA, was not available in quantities necessary for packed-bed reactor interesterification. The substrate molar ratio and water content were as described for the packed-bed reactor interesterification. The enzyme Lipozyme IM was added to the reaction flask as 15% (wt) on a total substrate basis. The reaction proceeded for 10 h with magnetic stirring in a 55°C water bath. The enzyme resin was removed by filtration through sterile, degreased cotton wool, and the prod-

ucts were sparged with nitrogen and stored at −20°C until distillation.

The interesterified products were distilled to separate the FFA from the TAG. Interesterification products with a mixture of 8:0, CLA, and 18:1n-9 FFA were distilled by a two-step short-path distillation process. The 8:0 evaporated at 90–100°C and the LCFA at 190°C under vacuum (10^{-3} mbar).

Lipid analysis. FAME were prepared from oil dissolved in heptane by transesterification catalyzed by KOH in methanol (24). To determine the FA profiles, lipids from lymph samples were extracted according to the method of Folch *et al.* (25) and transmethylated to FAME as described above. FAME were analyzed by GLC using a Hewlett-Packard 5890 series II chromatograph with an FID (Hewlett-Packard GmbH, Ingelsheim, Germany), and a fused-silica capillary column (SP-2380, 60 m, i.d. 0.25 mm, 0.2 µm film thickness; Supelco Inc., Bellefonte, PA). The temperature of the injector and FID was 270°C. A split (1:11) injection mode was used. The carrier gas was helium with a column flow of 1.2 mL/min. The initial oven temperature was 70°C for 0.5 min, and the temperature programming was as follows: a rate of 15°C/min to 160°C; 1.5°C/min to 200°C, which was maintained for 15 min; and finally 30°C/min to 225°C, which was maintained for 5 min.

Regiospecific analysis of the structured oils was performed by degradation with allylmagnesium bromide as Grignard reagent (26). The *sn*-2-MAG fraction was isolated by TLC on boric acid-impregnated plates developed twice (2 × 60 min) in chloroform/acetone (90:10 vol/vol), transesterified into FAME, and analyzed by GLC as described above. The FA profiles of TAG and *sn*-2-MAG are listed in Table 1.

TAG species of the oils were analyzed by RP-HPLC. A high-performance liquid chromatograph (JASCO Corporation, Tokyo, Japan) was used with two pumps, a solvent-mixing module, an autosampler, and an ELSD (Sedere, Alfortville, France) operated at 40°C at a gas pressure of 2.2 bar. The separation was performed on a Supelcosil LC-C$_{18}$ column (l = 25 cm, i.d. = 4.6 mm, particle size = 5 µm; Supelco Inc., Bellefonte, PA) with a binary solvent system of acetonitrile (solvent A) and isopropanol/hexane (solvent B, 2:1 vol/vol) (27). A linear gradient of solvent B from 25 to 40% for 15 min, followed by an increase to 45% for another 25 min was applied at a flow rate of 1 mL/min. The structured lipid samples were dissolved in chloroform, and 10-µL aliquots were injected for analysis. The TAG species were expressed in terms of relative percentages of the total TAG after normalization to 100.

TAG species were identified by their equivalent carbon numbers (ECN) and confirmed by LC-MS (HP 1100 Series LC/MSD system; Hewlett-Packard, Waldbronn, Germany) as described by Mu and Høy (28). The column and solvents were as described above. Separation occurred according to chain length and saturation of the acyl chains; for example, it was impossible to distinguish between linoleic acid and CLA. However, only a small amount of linoleic acid was present in the substrates and products as determined by GLC (Table 1). The TAG species are listed in Table 2.

Animals. The experiment was performed with male Wistar

TABLE 1
FA Profiles (in mol%) of TAG and 2-MAG of Structured Oils Containing CLA[a]

FA	Group 1				Group 2			
	MCM-1	CMC-1	OCO-1	COC-1	MCM-2	CMC-2	OCO-2	COC-2
				mol%				
TAG								
8:0	23.5	44.2	—[b]	—	28.1	35.9	—	0.2
16:0	3.2	2.1	4.4	3.3	0.0	0.2	2.0	1.6
18:0	1.1	0.6	1.7	2.6	0.0	0.1	0.9	2.2
18:1n-9	10.2	7.1	36.6	52.0	0.7	1.5	33.8	47.4
18:2n-6	1.0	0.7	7.0	4.1	0.0	0.4	7.3	3.6
CLA c9,t11	28.3	22.1	22.4	18.0	2.1	2.1	1.6	1.4
CLA t10,c12	29.4	20.9	23.0	17.0	68.2	58.4	51.1	41.9
Others	3.3	2.3	4.9	3.0	0.8	1.5	3.3	1.7
Total CLA	57.7	43.0	45.4	35.0	70.3	60.5	52.7	43.3
sn-2-MAG								
8:0	1.6	89.6	0.1	0.2	1.2	87.1	—	—
16:0	4.4	0.5	5.8	0.5	0.1	0.2	0.6	0.4
18:0	1.8	0.2	1.8	0.3	0.0	0.1	0.3	0.4
18:1n-9	15.4	2.0	18.4	87.7	1.2	2.1	9.2	88.1
18:2n-6	1.4	0.2	2.0	6.4	0.0	1.3	1.7	6.3
CLA c9,t11	34.9	3.8	33.4	2.1	3.0	0.3	2.7	0.2
CLA t10,c12	35.5	3.1	33.9	2.0	93.0	7.7	83.8	4.6
Others	5.0	0.6	4.6	0.8	1.5	1.2	1.7	0.1
Total CLA	70.4	6.9	67.3	4.1	96.0	8.0	86.5	4.8

[a]FA profiles of total TAG and sn-2-MAG of enzymatically interesterified oils: C in group 1 is a mixture of CLA c9,t11 and CLA t10,c12, and C in group 2 is mainly CLA t10,c12; M is 8:0 and O is 18:1n-9.
[b]A dash (—) indicates "not detected."

rats (Taconic M&B, Ll. Skensved, Denmark). The animals were acclimatized for a minimum of 10 d. They were housed in polyethylene cages, each with 2 rats, and fed a commercial pelleted rat diet (Altromin no. 1324; Chr. Petersen A/S, Ringsted, Denmark) containing approximately 4 wt% fat. The feed was removed just prior to surgery. The room was illuminated to give a cycle of 12 h light and 12 h darkness, and the temperature control was $21 \pm 3°C$ and RH $55 \pm 15\%$. At the time of surgery, the rats weighed 292 ± 2.3 g (mean ± SEM).

Collection of lymph. The Danish National Committee for Animal Experiments approved the experiment.

Rats were anesthetized intramuscularly with a combination of zolazepam, xylaxin, and butorphanol (Zoletil solution 0.06 mL/100 g; Royal Veterinary and Agricultural University, Frederiksberg, Denmark), and were subjected to cannulation of the main mesenteric lymph duct (29) with clear vinyl tubing (i.d. 0.5 mm, o.d. 0.8 mm; Dural Plastics and Engineering, Crictley Electrical Products Pty. Ltd., NSW, Australia). A gastrostomy tube (silicone tubing i.d. 1.0 mm, o.d. 3.0 mm; Polystan, Værløse, Denmark) was inserted 2 cm into the fundus region of the stomach and fixed with a purse-string suture. After surgery the rats were placed in individual restraining cages (30) and given 0.05 mL of a 5 mg/mL atipamezol solution (Antisedan, Orion, Espoo, Finland). They were kept hydrated by infusion of 2 mL/h of a saline–glucose solution (0.15 M NaCl + 4 mM KCl + 0.28 M glucose) administered through the gastrostomy tube and with free access to drinking water. Six hours after surgery and during the experiment, the rats received 0.3 mL of a 5 mg/mL carprofen solution (Rimadyl® Vet; Vericore Ltd, Dundee, Scotland) and 0.2 mL of a 5 mg/mL diazepam solu-

tion (Stesolid; Dumex-Alpharma A/S, Copenhagen, Denmark) to reduce pain and stress.

The rats recovered from surgery overnight. The following day, 270 mg of test oil was administered as a bolus through the gastrostomy tube followed by 0.5 mL of saline. One-hour lymph samples were collected from –1 h (i.e., 1 h prior to fat administration) to 8 h, one sample was collected from 8 to 23 h, and a 23- to 24-h sample was collected. The lymph was collected at room temperature in nontransparent tubes containing 100 μL (700 μL for overnight fractions) 10% (wt/vol) $Na_2EDTA \cdot 2H_2O$ solution. The samples were stored at $-20°C$ until analyzed.

Statistical analysis. Results are expressed as mean ± SEM. The incremental area under the curve from 0 to 8 h [IAUC, using the trapezoidal rule (31)] was used to compare lymphatic transport among the groups.

Recoveries of total and individual FA were calculated using an internal standard (TAG 15:0, added to lymph samples before extraction). The recovery was calculated as the amount of a FA found in lymph divided by the amount of the same FA in the oil, multiplied by 100. By doing this, differences in CLA and 8:0 contents between the oils were eliminated. The recovery calculations included a contribution of endogenous FA transported in the lymph; thus, recoveries could exceed 100%. Significant differences among groups of IAUC and recoveries were determined using one-way ANOVA. A Newmann–Keuls multiple comparison test was used to determine the exact nature of the differences. The computer program, GraphPad PRISM (version 3.02; GraphPad Software, San Diego, CA) was used for all calculations. The level of statistical significance was $P < 0.05$.

TABLE 2
TAG Species of the Enzymatically Interesterified Oils Containing CLA[a]

		Group 1				Group 2			
ECN	TAG species	MCM-1	CMC-1	OCO-1	COC-1	MCM-2	CMC-2	OCO-2	COC-2
				area%					
24	8:0/8:0/8:0	0.1	0.8	—[b]	—	0.8	0.2	—	—
30	8:0/8:0/18:2	12.0	26.4	—	—	24.0	38.6	—	—
32	8:0/8:0/18:1	1.4	13.2	—	—	—	0.2	—	—
34	8:0/16:0/8:0	0.3	3.1	—	—	—	—	—	—
36	8:0/18:2/18:2	25.3	33.0	—	—	40.2	51.0	—	—
38	8:0/18:2/18:1	15.9	17.3	—	—	0.5	1.5	—	—
38	8:0/18:2/16:0	3.5	3.0	—	—	0.1	0.2	—	—
40	8:0/16:0/18:1	0.7	0.5	—	—	—	0.5	—	—
42	18:2/18:2/18:2	24.4	1.0	13.2	2.3	33.1	5.9	7.9	27.3
44	18:2/18:2/18:1	11.2	0.4	38.8	31.0	—	—	29.7	34.5
44	16:0/18:2/18:2	2.4	—	3.7	0.8	—	0.2	—	3.8
46	18:2/18:1/18:1	1.2	—	31.2	30.8	—	—	27.7	26.3
46	16:0/18:2/18:1	0.3	—	6.0	5.7	—	—	4.9	3.4
48	18:1/18:1/18:1	—	—	4.3	17.3	—	—	14.4	2.9
48	16:0/18:1/18:1	—	—	1.3	—	—	0.2	7.0	0.3
48	16:0/16:0/18:1	—	—	—	3.5	—	—	1.2	—
50	18:0/18:1/18:1	—	—	—	2.1	—	—	1.6	—
50	16:0/18:0/18:1	—	—	—	2.1	—	—	—	—
52	18:0/18:0/18:1	—	—	—	1.6	—	—	2.7	—
52	16:0/18:0/18:0	—	—	—	1.3	—	—	1.4	—

[a]TAG species of the eight enzymatically interesterified oils: C in group 1 is a mixture of CLA c9,t11 and CLA t10,c12, and C in group 2 is mainly CLA t10,c12; M is 8:0 and O, 18:1n-9. ECN, equivalent carbon number.
[b]A dash (—) indicates "not detected."

RESULTS

FA profiles of interesterified oils. FA compositions of TAG and *sn*-2-MAG of the interesterified oils are shown in Table 1. CLA in four of the oils was a mixture of the two isomers *c*9,*t*11 and *t*10,*c*12 (MCM-1, CMC-1, OCO-1, and COC-1; group 1), whereas in the other four oils CLA was primarily the isomer *t*10,*c*12 (MCM-2, CMC-2, OCO-2, and COC-2; group 2). The total content of CLA in the oils containing both CLA and MCFA was 57.7, 43.0, 70.3, and 60.5 mol% in MCM-1, CMC-1, MCM-2, and CMC-2, respectively, and the content of CLA in the *sn*-2 position was 70.4, 6.9, 96.0, and 8.0 mol%, respectively. Similarly, for the oils containing CLA and 18:1n-9, total CLA was 45.4, 35.0, 52.7, and 43.3 mol% for OCO-1, COC-1, OCO-2, and COC-2, respectively, and in the *sn*-2-position the content was 67.3, 4.1, 86.5, and 4.8 mol%, respectively. These were not the expected results for the oils, but the compositions of the *sn*-2-FA show that a large part of the CLA in the MCM and OCO oils was located in this position, whereas this was 8 mol% or less in the CMC and COC oils. However, owing to a high (MCM and OCO oils) and respectively low (CMC and COC oils) total CLA incorporation, the content of CLA in the outer positions of the MCM and OCO oils was higher and those of CMC and COC were lower than expected.

TAG species. The TAG species of the oils are listed in Table 2, and a chromatogram of the TAG species in the CMC-2 oil is shown in Figure 1. The original TAG, which was CCC for the OCO-1 and OCO-2 oils and OOO for the COC-1 and COC-2 oils, represented 3–17% of the product highest in COC-1 and lowest in COC-2, whereas MMM, the original TAG of the CMC

oils, constituted only 0.8%. In the OCO-1 oil, 31% was the desired TAG species (COO), and 38% was the CCO species. Similarly, for the COC-1 oil 30% was the desired product (CCO) and 30% was the COO species. The MCM-1 production resulted in a wide range of TAG species, with 12% MMC. The analyses of
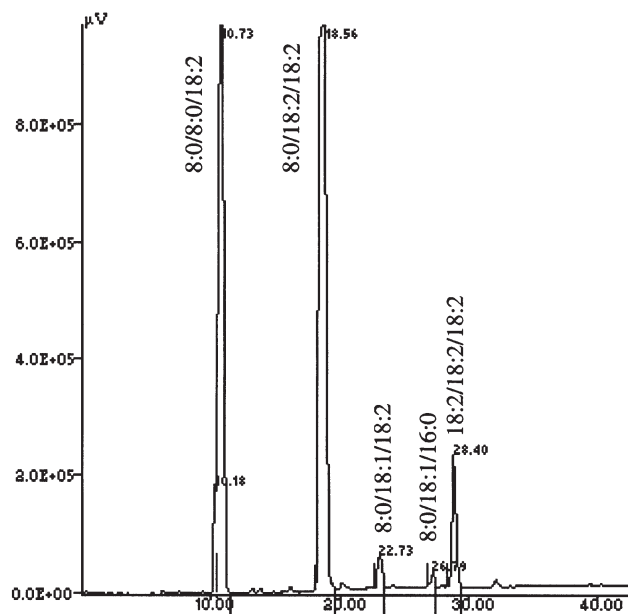
FIG. 1. Chromatogram of TAG species of the CMC-2 oil analyzed by reversed-phase HPLC. CMC, structured TAG with CLA primarily in the *sn*-1/3-positions and 8:0 in the *sn*-2-position.

the oils in group 2 showed that the desired TAG species in the MCM-2, CMC-2, OCO-2, and COC-2 oils constituted, respectively, 24 (MMC), 51 (MCC), 27 (COO), and 34% (CCO) of the total species.

Lymphatic transport. The lymphatic transport of total FA showed a slow increase from the time of oil administration to 1 h after oil administration (Fig. 2). The increase continued at a higher rate from 1–2 h, with the maximum transport appearing between 2 and 6 h for group 1 and between 2 and 3 h for group 2, followed by a slower decrease toward baseline in both groups. The lymphatic transport of total FA measured as the IAUC in group 1 was significantly higher in rats fed OCO-1 and COC-1 compared with rats fed CMC-1 ($P < 0.05$), and tended to be higher in rats fed MCM-1 than rats fed CMC-1 ($P = 0.08$, Fig. 2A). In group 2 the total FA transport was similar except for OCO-2, which had a higher transport of total FA than CMC-2 ($P < 0.05$, Fig. 2B). After 24 h,

the lymphatic transport of total FA in all groups had returned to baseline.

Recoveries. In group 1 the recovery of total FA tended to be lower in the lymph fractions after 6 and 7 h ($P < 0.1$) and was significantly lower at 8 h ($P < 0.05$) in the CMC-1 group than in the OCO-1 and COC-1 groups. In the other lymph fractions and among the other groups, the recoveries of total FA were similar (Fig. 3A). The recoveries of the individual CLA isomers ($c9,t11$ and $t10,c12$) were similar in all groups at 24 h. At 8 h, however, the recovery of each of the two isomers tended to be lower in the CMC-1 than in the COC-1 ($P < 0.1$).

In group 2 the recoveries of total FA were significantly different from 4 to 8 h ($P < 0.05$) between the CMC-2 and OCO-2 groups, whereas the recoveries of both CLA $c9,t11$ and CLA $t10,c12$ tended to be different between the CMC-2 and OCO-2 groups ($P < 0.09$) after 4 h. At 24 h the recoveries of CLA $c9,t11$, CLA $t10,c12$, and total FA were similar both in group 1 and group 2—between 50 and 70% for CLA and 70 and 115% for total FA (Fig. 3).

The recovery of 8:0 differed among groups depending on the TAG structure (Fig. 4). The recovery of 8:0 was similar in all four groups until 5 h after oil administration, after which the curves diverged; CMC-1 and CMC-2 continued to increase slowly, whereas the curves for MCM-1 and MCM-2 did not increase further from 4 h after oil administration. The highest recovery was observed when CMC was administered to the rats, which was about 12–13% compared with only about 4–5% in the MCM groups after 24 h. Already after 6 h, significant differences appeared among groups fed the two oil types ($P < 0.05$).

FIG. 2. Lymphatic transport of total FA over 24 h in rats administered enzymatically interesterified oils: MCM, CMC, OCO, and COC, with M as 8:0 and O as 18:1n-9. In group 1, C was CLA as a mixture of the two CLA isomers $c9,t11$ or $t10,c12$, and in group 2, C was mainly the isomer $t10,c12$. (A) Incremental area under the curve (IAUC) for 0–8 h was significantly higher in the OCO-1 and COC-1 groups than in the CMC-1 group ($P < 0.05$), $n = 4$–5. (B) IAUC for 0–8 h was significantly higher in the OCO-2 group compared with the CMC-2 group ($P < 0.05$), $n = 5$–6. MCM, structured TAG with the major proportion of CLA in the sn-2-position and 8:0 in the sn-1/3-positions; OCO, structured TAG with CLA primarily in the sn-2-position and 18:1n-9 in the sn-1/3-positions; COC, structured TAG with the major proportion of CLA in the sn-1/3-positions and 18:1n-9 in the sn-2-position; for other abbreviation see Figure 1.

DISCUSSION

The recoveries of the two CLA isomers, $c9,t11$ and $t10,c12$, were similar during 24 h, independent of the FA profile of the TAG, demonstrating that TAG containing CLA were well hydrolyzed and absorbed in the intestines of rats with normal absorption. However, there was a tendency for CLA from an oil containing MCFA primarily in the sn-2-position (CMC oils) to be transported more slowly than CLA from an oil containing only LCFA (OCO-1, COC-1, and OCO-2 oils). This difference in the recovery of FA was significant for total FA, especially after 4 h, as observed in group 2, and was probably not due to the hydrolysis rate of the TAG, because the difference did not occur until after 4 h. In the intestine, the TAG are hydrolyzed to sn-2-MAG and FFA. In LML oils (where L is LCFA) the MCFA in the sn-2-position tends to migrate to the sn-1/3 positions of the TAG (32,33) and then is substrate for the pancreatic lipase. The products of hydrolysis will be three FFA and glycerol instead of 2-MAG and two FFA. This results in a lack of 2-MAG for the resynthesis of TAG in the enterocytes and a delayed or lower absorption of the fat, a tendency we saw in our study for the CMC oils both in lymphatic transport and recoveries. Jensen *et al.* (34) reported that the conservation of MCFA in the sn-2-MAG after absorption was about 40%, whereas Åkesson *et al.* (35) reported that this was 75% for
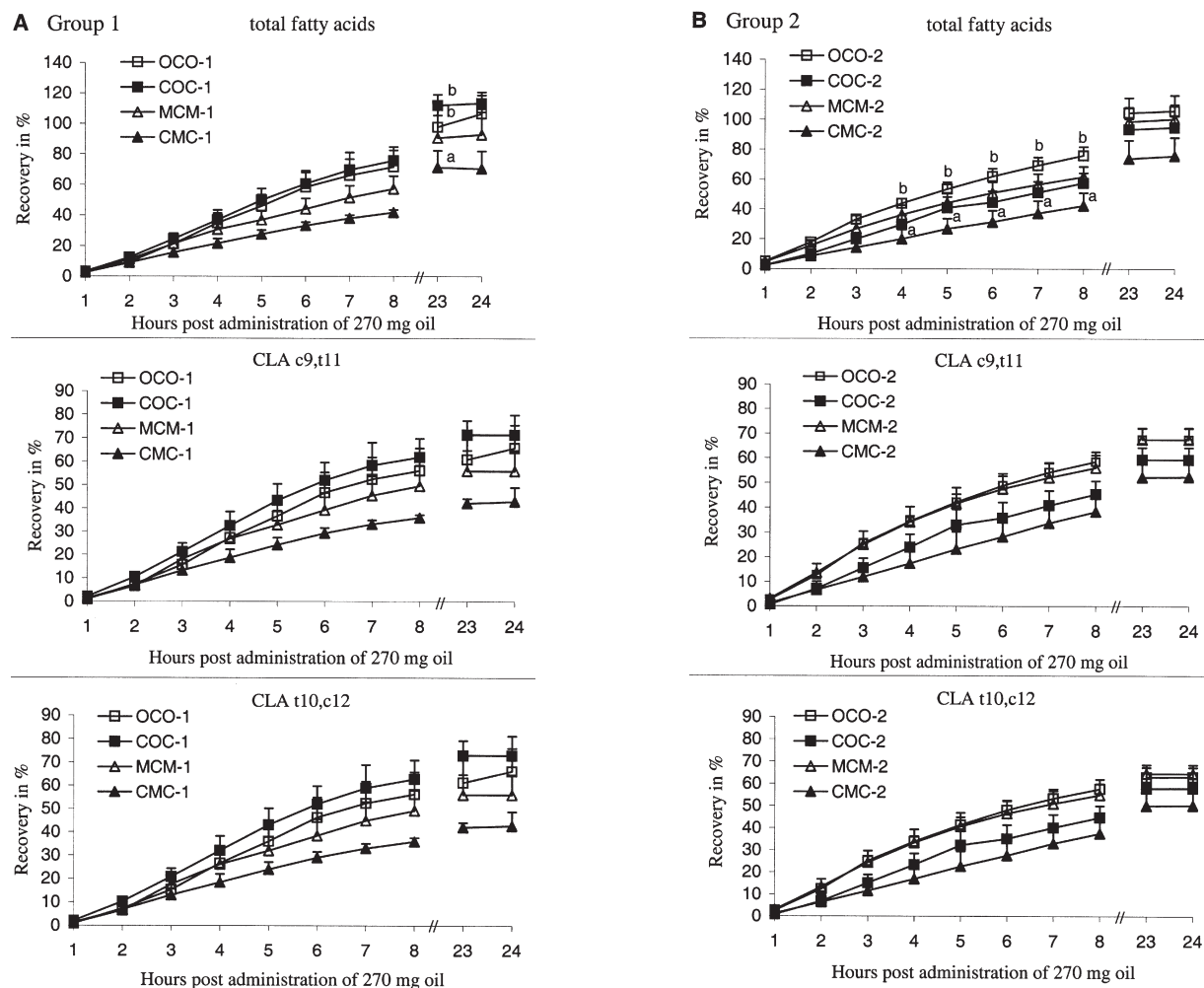
FIG. 3. Lymphatic recovery of total FA, CLA *c*9,*t*11, and CLA *t*10,*c*12 from oils containing M as 8:0 and O as 18:1n-9. (A) C was a mixture of CLA *c*9,*t*11 and CLA *t*10,*c*12, and (B) C was primarily CLA *t*10,*c*12. Curves with different letters at similar time points are significantly different ($P < 0.05$), and curves without letters are similar to the other curves. $n = 4$–6. For abbreviations see Figures 1 and 2.

LCFA. Jensen *et al.* (34) used a mixture of MCFA containing twice as much 8:0 as 10:0, and Mu and Høy showed that 10:0 was transported by the lymph in rats to a higher degree than 8:0 (36). In the present study the conservation of the *sn*-2-MAG FA from CMC oils may therefore be less than 40%. This was supported by the 12% recovery of 8:0 in the lymph after 24 h. When *sn*-2-MAG is lacking for the resynthesis of TAG, the pathway shifts from the *sn*-2-MAG pathway to the glycero-3-phosphate pathway, which uses glycerol and three FFA to synthesize TAG in the intestine (37). This pathway, however, has to be up-regulated before resynthesis can occur, resulting in slower formation of TAG and therefore a slower secretion of chylomicrons into the bloodstream.

In agreement with our results, Ikeda *et al.* (20) observed a higher lymphatic transport of 8:0 when it was present in the *sn*-2-position of the TAG than when it was located in the outer positions. Furthermore, they observed a similar absorption of linoleic acid following administration of MLM, LML, or LLL oils to rats with normal absorption.

Because MCFA (as 8:0 and 10:0) as FFA are transported pri-

marily *via* the portal vein (38) to the liver, structured fats containing MCFA in the outer positions of the TAG molecules will be short of FFA for TAG resynthesis after hydrolysis. This results in an increased utilization of endogenous FA for TAG resynthesis in the enterocytes, and may delay the lymphatic transport of exogenous fat (18). These observations were emphasized by the present study, since we recovered only 4–5% 8:0 in the lymph after administration of the MCM oil. A recent study by Porsgaard *et al.* (39) showed a faster *in vitro* pancreatic lipase hydrolysis of fish oil compared with MLM and LML oils containing n-3 long-chain PUFA. This correlated well with a faster absorption of the fish oil compared with the two structured oils, and the authors concluded that the absorption was highly influenced by the lipase hydrolysis rate. These results are partly in agreement with the present results; however, we observed similar recovery of the different oils after 4 and 8 h, with a tendency toward lower recovery of the CMC oil. These discrepancies may be due to all our oils being interesterified, whereas the LLL oil in the experiment by Porsgaard *et al.* used natural fish oil.
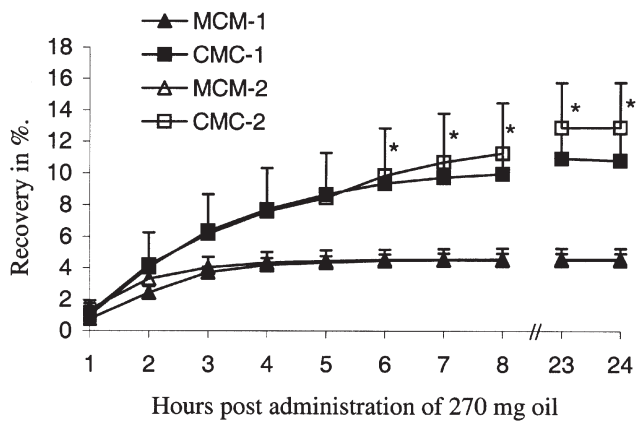
FIG. 4. Lymphatic recovery of 8:0 from the enzymatically interesterified oils MCM-1, MCM-2, CMC-1, and CMC-2, with M as 8:00 and C as a CLA mix in group 1 and as CLA $t10,c12$ in group 2. Recoveries of 8:0 were calculated as 8:0 gained in the lymph relative to that in the oil. An asterisk (*) shows significant differences ($P < 0.05$) between the curves for the MCM groups and those for the CMC groups, $n = 4–6$. For abbreviations see Figures 1 and 2.

A previous study (13) showed that CLA $c9,t11$ is absorbed better from the sn-1/3-positions than from the sn-2-position. Our results cannot confirm these observations, probably because our oils with the majority of CLA in the sn-2-position had a relatively high content of CLA in the sn-1/3-positions compared with CLA in the sn-2-position. However, the oils with CLA located in the sn-1/3-positions (CMC and COC oils) contained only small amounts of CLA in the sn-2-position. Furthermore, in the study by Chardigny *et al.* (13), absorption and excretion were measured as radioactivity, which is a very sensitive method.

We observed recoveries of CLA of 50–70%, which is lower than the recovery of oleic acid (86.5%) observed by Yanagita *et al.* (40) in thoracic lymph duct-cannulated rats. However, the recovery of 50–70% of the two CLA isomers after 24 h was similar to the recovery of linoleic acid (41,42) and was similar in all groups. Therefore, the FA and the position of CLA in the TAG did not seem to influence the absorption and transport of CLA on a long-term basis (24 h) in rats with normal absorption. Furthermore, these results showed no discrimination in the absorption of the two CLA isomers. The incorporation of the two CLA isomers into tissues has been shown to be selective, with a preference for the incorporation of CLA $c9,t11$ compared with CLA $t10,c12$, but this discrimination was not observed in enterocytes of rats fed a butter-rich diet and therefore probably did not appear before the absorption was finished and when FA had reached the blood circulation (Lund, P., Sejrsen, K. and Straarup, E.M., unpublished results). Our observation is in accordance with that of Martin *et al.* (40), who found that the two main CLA isomers ($c9,t11$ and $t10,c12$) were equally well transported through the lymphatic pathway when administered as TAG.

On the other hand, the position of 8:0 in the TAG influenced the lymphatic transport of 8:0, as shown by the higher recovery of this FA when administered as CMC oils compared with

MCM oils. In agreement with the foregoing discussion, this shows that the sn-2-MAG MCFA was preserved to some extent and not fully hydrolyzed in the CMC oils.

A specific structure of the TAG with MCFA in the outer positions and LCFA in the sn-2-position has previously been shown to improve the absorption of fat in malabsorbing and, to some degree, in normal rats (18,19). However, the specificity of the oil is very important for absorption; the best results were obtained with most of, or preferably all, the MCFA located in the sn-1/3-positions and the LCFA in the sn-2-position. Furthermore, the effect of structure was mainly observed in malabsorption, where the sn-3-specific gastric lipase with a preference for short and MCFA may play an important role (5). As previous studies (20,43) show, the structure of TAG is almost without importance for the absorption of specific FA (e.g., CLA, n-3) under normal absorption conditions when MCFA are present in the outer positions of the TAG molecules, whereas when they are present in the sn-2-position, the tendency was for the absorption to be slowed or even decreased. We observed no differences in the absorption of CLA from our oils, although the CMC and COC, compared with the OCO, had different structures regarding the position of CLA in the TAG, with very little CLA in the sn-2-position of the former oils. However, structured TAG containing MCFA in the outer position may increase the uptake of FA, e.g., as in LCFA as EFA, in malabsorption conditions, and could therefore be of great importance in the clinical treatment of these patients.

REFERENCES

1. Griinari, J.M., and Bauman, D.E. (1999) Biosynthesis of Conjugated Linoleic Acid and Its Incorporation into Meat and Milk in Ruminants, in *Advances in Conjugated Linoleic Acid Research, Volume 1* (Yurawecz, M.P., Mossoba, M.M., Kramer, J.K.G., Pariza, M.W., and Nelson, G.J., eds.), pp. 180–200, AOCS Press, Champaign.
2. Gaullier, J.-M., Berven, G., Blankson, H., and Gudmundsen, O. (2002) Clinical Trial Results Support a Preference for Using CLA Preparations Enriched with Two Isomers Rather than Four Isomers in Human Studies, *Lipids 37*, 1019–1025.
3. Belury, M.A. (2002) Dietary Conjugated Linoleic Acid in Health: Physiolgical Effects and Mechanisms of Action, *Annu. Rev. Nutr. 22*, 505–531.
4. Pariza, M.W. (2004) Perspective on the Safety and Effectiveness of Conjugated Linoleic Acid, *Am. J. Clin. Nutr. 79* (Suppl.), 1132S–1136S.
5. Hamosh, M. (1994) Gastric and Lingual Lipases, in *Physiology of the Gastrointestinal Tract* (Johnson, L.R., ed.), pp. 1239–1253, Raven Press, New York.
6. Mattson, F.H., and Lutton, E.S. (1958) The Specific Distribution of Fatty Acids in the Glycerides of Animal and Vegetable Fats, *J. Biol. Chem. 233*, 868–871.
7. Bottino, N.R., Vandenburg, G.A., and Reiser, R. (1967) Resistance of Certain Long-Chain Polyunsaturated Fatty Acids of Marine Oils to Pancreatic Lipase Hydrolysis, *Lipids 2*, 489–493.

8. Chen, Q., Sternby, B., and Nilsson, B. (1989) Hydrolysis of Triacylglycerol Arachidonic and Linoleic Acid Ester Bonds by Human Pancreatic Lipase and Carboxyl Ester Lipase, *Biochim. Biophys. Acta 1004*, 372–385.

9. Jandacek, R.J., Whiteside, J.A., Holcombe, B.N., Volpenhein, R.A., and Taulbee, J.D. (1987) The Rapid Hydrolysis and Efficient Absorption of Triglycerides with Octanoic Acid in the 1 and 3 Positions and Long-Chain Fatty Acid in the 2 Position, *Am. J. Clin. Nutr. 45*, 940–945.

10. Tomarelli, R.M., Meyer, B.J., Weaber, J.R., and Bernhart, F.W. (1968) Effect of Positional Distribution on the Absorption of the Fatty Acids of Human Milk and Infant Formulas, *J. Nutr. 95*, 583–590.

11. Innis, S.M., and Dyer, R. (1997) Dietary Triacylglycerols with Palmitic Acid (16:0) in the 2-Position Increase 16:0 in the 2-Position of Plasma and Chylomicron Triacylglycerols, but Reduce Phospholipid Arachidonic and Docosahexaenoic Acids, and Alter Cholesteryl Ester Metabolism in Formula-Fed Piglets, *J. Nutr. 127*, 1311–1319.

12. Mattson, F.H., and Volpenhein, R.A. (1964) The Digestion and Absorption of Triglycerides, *J. Biol. Chem. 239*, 2772–2777.

13. Chardigny, J.M., Masson, E., Sergiel, J.P., Darbois, M., Loreau, O., Noël, J.P., and Sébédio, J.-L. (2003) The Position of Rumenic Acid on Triacylglycerols Alters Its Bioavailability in Rats, *J. Nutr. 133*, 4212–4214.

14. Valeille, K., and Martin, J.C. (2004) Complete Stereospecific Determination of Conjugated Linoleic Acids in Triacylglycerol of Milk-Fat, *Reprod. Nutr. Dev. 44*, 459–464.

15. King, D.A., Behrends, J.M., Jenschke, B.E., Rhoades, R.D., and Smith, S.B. (2004) Positional Distribution of Fatty Acids in Triacylglycerols from Subcutaneous Adipose Tissue of Pigs Fed Diets Enriched with Conjugated Linoleic Acid, Corn Oil, or Beef Tallow, *Meat Sci. 67*, 675–681.

16. Paterson, L.J., Weselake, R.J., Mir, P.S., and Mir, Z. (2002) Positional Distribution of CLA in TAG of Lamb Tissues, *Lipids 37*, 605–611.

17. Høy, C.-E., and Xu, X. (2001) Structured Triacylglycerols, in *Structured and Modified Lipids* (Gunstone, F.D., ed.), 209–239, Marcel Dekker, New York.

18. Straarup, E.M., and Høy, C.-E. (2000) Structured Lipids Improve Fat Absorption in Normal and Malabsorbing Rats, *J. Nutr. 130*, 2802–2808.

19. Christensen, M.S., Müllertz, A., and Høy, C. (1995) Absorption of Triglycerides with Defined or Random Structure by Rats with Biliary and Pancreatic Diversion, *Lipids 30*, 521–526.

20. Ikeda, I., Tomari, Y., Watanabe, S., and Nagata, J. (1991) Lymphatic Absorption of Structured Glycerolipids Containing Medium-Chain Fatty Acids and Linoleic Acid, and Their Effect on Cholesterol Absorption in Rats, *Lipids 26*, 369–373.

21. Straarup, E.M., Danielsen, V., Jakobsen, K., and Høy, C.-E. (2003) Fat Digestibility, Nitrogen Retention, and Fatty Acid Profiles in Blood and Tissues of Post-weaning Piglets Fed Interesterified Fats, *J. Anim. Feed Sci. 12*, 539–559.

22. Xu, X., Balchen, S., Høy, C.-E., and Adler-Nissen, J. (1998) Production of Specific-Structured Lipids by Enzymatic Interesterification in a Pilot Continuous Enzyme Bed Reactor, *JAOCS 75*, 1573–1579.

23. Xu, X., Balchen, S., Høy, C.-E., and Adler-Nissen, J. (1998) Pilot Batch Production of Specific-Structured Lipids by Lipase-Catalyzed Interesterification: Preliminary Study on Incorporation and Acyl Migration, *JAOCS 75*, 301–308.

24. Christopherson, S.W., and Glass, R.L. (1969) Preparation of Milk Fat Methyl Esters by Alcoholysis in an Essential Nonalcoholic Solution, *J. Dairy Sci. 52*, 1289–1290.

25. Folch, J., Lees, M., and Sloane Stanley, G.H. (1957) A Simple Method for the Isolation and Purification of Total Lipids from Animal Tissue, *J. Biol. Chem. 226*, 497–509.

26. Becker, C.C., Rosenquist, A., and Hølmer, G. (1993) Regiospecific Analysis of Triacylglycerols Using Allyl Magnesium Bromide, *Lipids 28*, 147–149.

27. Mu, H., Kalo, P., Xu, X., and Høy, C.-E. (2000) Chromatographic Methods in the Monitoring of Lipase-Catalyzed Interesterification, *Eur. J. Lipid Sci. Technol. 2000*, 202–211.

28. Mu, H., and Høy, C.-E. (2000) Application of Atmospheric Pressure Chemical Ionization Liquid Chromatography–Mass Spectroscopy in Identification of Lymph Triacylglycerols, *J. Chromatography B 748*, 425–437.

29. Bollman, J.L., Cain, J.C., and Grindlay, J.H. (1948) Techniques for the Collection of Lymph from the Liver, Small Intestine, or Thoracic Duct of the Rat, *J. Lab. Clin. Med. 33*, 1349–1352.

30. Bollman, J.L. (1948) A Cage Which Limits the Activity of Rats, *J. Lab. Clin. Med. 33*, 1348.

31. Matthews, J.N.S., Altman, D.G., Campbell, M.J., and Royston, P. (1990) Analysis of Serial Measurements in Medical Research, *BMJ 300*, 230–235.

32. Xu, X., Skands, A.R.H., Høy, C.-E., Mu, H., Balchen, S., and Adler-Nissen, J. (1998) Production of Specific-Structured Lipids by Enzymatic Interesterification: Elucidation of Acyl Migration by Response Surface Design, *JAOCS 75*, 1179–1186.

33. Boswinkel, G., Derksen, J.T.P., van't Riet, K., and Cuperus, F.P. (1996) Kinetics of Acyl Migration in Monoglycerides and Dependence on Acyl Chainlength, *JAOCS 73*, 707–711.

34. Jensen, M.M., Christensen, M.S., and Høy, C. (1994) Intestinal Absorption of Octanoic, Decanoic, and Linoleic Acids: Effect of Triglyceride Structure, *Ann. Nutr. Metab. 38*, 104–116.

35. Åkesson, B., Gronowitz, S., Herslof, B., and Ohlson, R. (1978) Absorption of Synthetic, Stereochemically Defined Acylglycerols in the Rat, *Lipids 13*, 338–343.

36. Mu, H., and Høy, C.-E. (2000) Effects of Different Medium-Chain Fatty Acids on Intestinal Absorption of Structured Triacylglycerols, *Lipids 35*, 83–89.

37. Lehner, R., and Kuksis, A. (1996) Biosynthesis of Triacylglycerols, *Prog. Lipid Res. 35*, 169–201.

38. Bernard, A., and Carlier, H. (1991) Absorption and Intestinal Catabolism of Fatty Acids in the Rat: Effect of Chain-Length and Unsaturation, *Exp. Physiol. 76*, 445–455.

39. Porsgaard, T., Xu, X., Göttsche, J., and Mu, H. (2005) Differences in the Intramolecular Structured Oils Do Not Affect Pancreatic Lipase Activity *in vitro* or Absorption by Rats of (n-3) Fatty Acids, *J. Nutr. 135*, 1705–1711.

40. Yanagita, T., Ikeda, I., Wang, Y.-m., and Nakagiri, H. (2004) Comparison of the Lymphatic Transport of Radiolabeled 1,3-Dioleoyglycerol and Trioleoylglycerol in Rats, *Lipids 39*, 827–832.

41. Martin, J.-C., Sébédio, J.-L., Caselli, C., Pimont, C., Martine, L., and Bernard, A. (2000) Lymphatic Delivery and *in vitro* Pancreatic Lipase Hydrolysis of Glycerol Esters of Conjugated Linoleic Acids in Rats, *J. Nutr. 130*, 1108–1114.

42. Vistisen, B., Mu, H., and Høy, C.-E. (2003) Recoveries of Rat Lymph FA After Administration of Specific Structured ^{13}C-TAG, *Lipids 38*, 903–911.

43. Straarup, E.M., and Høy, C.-E. (2001) Lymphatic Transport of Fat in Rats with Normal- and Malabsorption Following Intake of Fats Made from Fish Oil and Decanoic Acid. Effects of Triacylglycerol Structure, *Nutr. Res. 21*, 1001–1013.

Preferential Effect of Lead Exposure During Lactation on Non-Essential Fatty Acids in Maternal Organs

Sun-Young Lim[a], James Loewke[b], John D. Doherty[c], and Norman Salem, Jr.[b,*]

[a]Division of Marine Environment & Bioscience, Korea Maritime University, Busan, Republic of Korea, [b]Laboratory of Membrane Biochemistry and Biophysics, National Institute on Alcohol Abuse and Alcoholism (NIAAA), National Institutes of Health (NIH), Rockville, Maryland, and [c]U.S. Environmental Protection Agency, Office of Pesticide Programs, Health Effects Division, Washington, D.C.

ABSTRACT: This study determined the effects of lead exposure during the lactational period on maternal organ FA compositions in rat dams that were fed either an n-3 adequate (n-3 Adq) or deficient (n-3 Def) diet prior to conception. On giving birth, dams were subdivided into four groups in a 2×2 design with n-3 FA supply and Pb exposure as the dependent variables. Pb acetate (0.2 wt%) was administered in the drinking water from the time they gave birth to weaning 3 wk later. Following weaning, the dams were decapitated. and the liver, plasma, kidney, brain, and retina analyzed for FA composition. The n-3 deficient diets markedly decreased the percentages of total n-3 FA, including docosahexaenoic acid (DHA), and increased total n-6 FA including both arachidonic (AA) and n-6 docosapentaenoic acids in all tissues ($P < 0.05$). The principal effects of Pb occurred in the liver and plasma, where 20–32% losses in total FA concentration concurrent with increased relative percentages of AA ($P < 0.05$) were observed. In kidney, the percentages of AA and DHA also increased after Pb exposure ($P < 0.05$) with lesser effects in the nervous system. There was a diet × Pb interaction for liver, plasma, and retinal 20-C n-6 PUFA ($P < 0.05$). Generally, shorter-chain saturated and monounsaturated FA concentrations were decreased after Pb exposure. An analysis of the changes in the tissue concentrations induced by Pb indicated that the increases in the percentages of PUFA likely reflected a preferential loss of non-EFA. The mechanisms by which Pb affects saturated and monounsaturated FA concentration are unknown.

Paper no. L9720 in *Lipids 40*, 685–693 (July 2005).

Recent experiments from our laboratory have tested the hypothesis that dietary deficiency in n-3 FA may worsen the impact of other developmental challenges. More specifically, the hypothesis tested was that low dietary intakes of n-3 FA during fetal and postnatal growth would worsen performance on behavioral tasks in animals exposed to high levels of lead (Pb)

*To whom correspondence should be addressed at 5625 Fishers Ln., Room 3N-07, MSC 9410, Bethesda, MD 20892-9410
E-mail: nsalem@niaaa.nih.gov

Abbreviations: AA, arachidonic acid, 20:4n-6; DGLA, dihomo-γ-linolenic acid, 20:3n-6; DHA, docosahexaenoic acid, 22:6n-3; DMA, dimethyl acetal derivative; DPAn-3, n-3 docosapentaenoic acid, 22:5n-3; DPAn-6, n-6 docosapentaenoic acid, 22:5n-6; DTA, docosatetraenoic acid, 22:4n-6; EFA, essential fatty acid; EPA, eicosapentaenoic acid, 20:5n-3; FA, fatty acid, GLA, γ-linolenic acid, 18:3n-6; LA, linoleic acid, 18:2n-6; LNA, α-linolenic acid, 18:3n-3; n-3 Adq-Na, n-3 adequate and Na control group; n-3 Adq-Pb, n-3 adequate and Pb exposure group; n-3 Def-Na, n-3 deficient and Na control group; n-3 Def-Pb, n-3 deficient and Pb exposure group; NIAAA, National Institute on Alcohol Abuse and Alcoholism; NIH, National Institutes of Health.

via lactation (1). Both Pb exposure (2) and a lower n-3 intake (3,4) are developmental risks that frequently occur together in lower income, urban populations, and so a lower n-3 FA status may exacerbate adverse effects of Pb. Or, from a different perspective, higher n-3 status may serve to counteract some of the adverse effects of Pb on neurodevelopment. A deficit in n-3 FA intake during the fetal or early postnatal period leads to a loss of brain DHA and suboptimal nervous system development as reflected by poorer performance in a variety of behavioral tasks (5–7). Similarly, Pb exposure during early development leads to a variety of neurodevelopmental abnormalities (8–10).

In the experiments of Lim and colleagues, rat pups lactating to dams receiving Pb in their drinking water were examined both for performance on spatial tasks and olfactory discriminations (1) and for the FA compositions of various organs (11). Although both Pb exposure and DHA deficiency led to poorer performance in the probe trial of the Morris water maze and in the olfactory reversal task, no protective effect of higher n-3 FA intake was apparent. It was also observed, in the acquisition of two-odor olfactory discriminations, that Pb exposure and n-3 FA deficiency led to behavioral deficits and produced additive effects. Even though Pb exposure was discontinued at 3 wk of age, some of the effects on organ FA compositions noted at weaning persisted until adulthood. At weaning, the liver was the most affected organ: total FA concentrations were decreased by 56% after Pb exposure. The percentages of liver arachidonic acid (AA, 20:4n-6) and DHA (22:6n-3) were increased but the tissue concentrations were not different after Pb exposure as non-EFA were lost.

In these previous experiments, pups were exposed to Pb indirectly, as Pb was administered to the dams in drinking water during the lactational period. In the present study, our aim is to examine the direct effects of both dietary deficiency in n-3 FA and Pb exposure on the dam tissues with respect to their FA compositions. A 2×2 study design was implemented with Pb and n-3 FA as the dependent variables and with FA analyses performed for plasma, brain, retina, liver, and kidney.

MATERIALS AND METHODS

Animals and study design. Animals were bred and raised as previously described (1). Briefly, 120 Long-Evans female rats (F1) were raised from 3 wk of age on either an n-3 FA adequate (n-3 Adq) or n-3 FA deficient (n-3 Def) diet (see the following

TABLE 1
Diet Composition and FA Content of Diet

Ingredient	n-3 Deficient	n-3 Adequate
	g/100 g diet	
Casein, vitamin-free[a]	20	20
Cornstarch	15	15
Sucrose	10	10
Dextrose	19.9	19.9
Maltose-dextrin	15	15
Cellulose	5	5
Mineral salt mix[b]	3.5	3.5
Vitamin mix[c]	1	1
L-Cystine	0.3	0.3
Choline bitartrate	0.25	0.25
TBHQ	0.002	0.002
Fat	10	10
Hydrogenated coconut oil	8.1	7.45
Safflower oil	1.9	1.77
Flaxseed oil	None	0.48
DHASCO[d]	None	0.3
FA composition[e]	% of total FA weight	
Saturates	78.1	72.7
Monounsaturates	4.5	5.7
18:2n-6	15.1	14.8
18:3n-3	0.09	3.0
22:6n-3	ND	1.45
n-6/n-3	168	3.3

[a]Dyets Inc. (Bethlehem, PA) catalog #400625.
[b]Dyets Inc. catalog #210025.
[c]Dyets Inc. catalog #310025.
[d]DHASCO is a trademark of Martek Biosciences Corp. (Columbia, MD) and contains approximately 45% of FA as DHA.
[e]Only trace quantities of long-chain polyunsaturates including 20:4n-6, 20:5n-3, and 22:5n-3 were detected (ND), i.e., less than 0.01%. Other minor peaks were not included.

section). At birth, half of the dams (F1) in each dietary group were given either a 0.2% by weight lead acetate trihydrate solution or a 0.2% by weight solution of sodium acetate (Aldrich Chemical Company, Milwaukee, WI) for their drinking water. This dose was similar to that given in previous studies (12–14). These solutions were maintained for their drinking water until the pups (F2) were weaned at postnatal day 21. The four groups of dams were designated as n-3 Adq-Na, n-3 Adq-Pb, n-3 Def-Na, and n-3 Def-Pb to identify the n-3 FA intake in the diet (n-3 Adq or n-3 Def) and treatment with either Pb acetate (Pb) or sodium acetate (Na). Pb exposure was discontinued after weaning (day 21), and the dams were sacrificed 4 d later on postnatal day 25. Generally, 6 dams were used per group. This experimental protocol was approved by the Animal Care and Use Committee of the NIAAA, NIH.

Experimental diet. The experimental diets (Table 1), n-3 Adq and n-3 Def, were based on the AIN-93G formulation (15) with several modifications to obtain the extremely low n-3 FA level required in this study. Custom pelleted diets were commercially prepared using a cold-pressing process to preserve PUFA (Dyets, Bethlehem, PA). The critical difference between the n-3 Adq and n-3 Def diets was the presence of the n-3 FA, α-linolenic acid (LNA) and DHA. The total fat content in both

diets was 10 wt%, and the amount of LNA in the n-3 Def and n-3 Adq diets was 0.09 and 3.0% of total FA, respectively, with the n-3 Adq diet also containing 1.45% DHA. There was no difference in linoleic acid (LA) content between the two diets.

Lipid composition. Shortly after weaning, the dams (now 18 wk of age) were decapitated, and their organs (brain, liver, and kidney) were weighed and quickly frozen (−80°C) for subsequent analyses for lipid composition. Blood was collected into centrifuge tubes containing EDTA (10.8 mg/tube) and immediately centrifuged at $1000 \times g$ at 4°C, and the plasma was removed for analysis. The Pb concentration was measured by a commercial laboratory (Antech Diagnostics, Farmingdale, NY), using atomic absorption spectrometry on whole blood samples. Lipid extraction (16), FA transmethylation (17), and GC analysis (18) of FA profiles were performed as previously described.

Statistical analysis All data were expressed as the mean percentage or concentration of total FA ± SEM, and significance was determined by two-way ANOVA with interactions for diet and Pb exposure effects using Statistica (StatSoft, Tulsa, OK). When the *F*-test was significant ($P < 0.05$), comparisons among groups were performed using Tukey's HSD (Honest Significant Difference) test.

RESULTS

Body and organ weight. Lead exposure affected the dam body, brain, and liver but not kidney weights (Table 2). After weaning, dams fed either the n-3 Adq-Pb or n-3 Def-Pb diets were 17 or 18% smaller based on body weight, respectively ($P < 0.05$), with 18 or 14% lower liver weights, respectively ($P < 0.05$), in comparison with those in the respective Na groups. There was a main effect of Pb on brain weight with the mean values showing a 5% difference between the two n-3 Adq groups and a 14% difference between the two n-3 Def groups ($P < 0.05$). Pb exposure led to a significantly increased ratio of kidney to body weight particularly in the n-3 Adq group ($P < 0.05$). The kidney weights were similar in the Pb-exposed groups to the control groups in spite of the decrease in body weight in those exposed to Pb. There was also a main effect of diet on body and liver weight, but not brain and kidney weight. Body and liver weights in the n-3 Def groups were lower than in the n-3 Adq groups ($P < 0.05$).

At weaning (3 wk), the brains of pups exposed to Pb during lactation exhibited Pb concentrations of 7.17 ± 0.47 in the n-3 Adq and 6.49 ± 0.63 nmol Pb/g wet weight in the n-3 Def diets, and Pb was at background levels in the Na groups. Brain Pb concentrations were not available for the dams; however, the mean whole blood Pb concentration for dams was 14.9 ± 2.7 μmol/L for the two Pb groups combined and the Na groups were at the background level of 0.005 μmol/L.

Effects of diet on FA compositions. The total FA concentrations of the liver, plasma, kidney, or retina did not differ between the n-3 Def and the n-3 Adq groups, but the brain total FA concentrations were significantly greater in the n-3 Adq groups. As expected, the percentages of total and many individual n-3 FA were reduced in all tissues studied for both groups given the n-3

TABLE 2
Effect of Pb Exposure and n-3 FA Deficiency on Body and Organ Weights in 18-wk-old Dams[a]

	n-3 Adequate		n-3 Deficient	
	Na control	Pb-exposed	Na control	Pb-exposed
Body weight, g	378.1 ± 9.63*	310.5 ± 13.3*,[†]	337.6 ± 17.2	281.3 ± 20.9[†]
Brain weight, g	1.92 ± 0.04	1.82 ± 0.05[†]	2.05 ± 0.11	1.77 ± 0.06[†]
Ratio of brain to body weight	0.005 ± 0.0001	0.006 ± 0.0004	0.006 ± 0.001	0.006 ± 0.0003
Liver weight, g	16.8 ± 0.58*	13.7 ± 0.95*,[†]	14.4 ± 0.46	12.1 ± 0.72[†]
Ratio of liver to body weight	0.045 ± 0.002	0.044 ± 0.002	0.043 ± 0.001	0.043 ± 0.002
Kidney weight, g	3.50 ± 0.25	3.43 ± 0.13	2.98 ± 0.25	3.13 ± 0.10
Ratio of kidney to body weight	0.009 ± 0.001	0.043 ± 0.002[†]	0.009 ± 0.001	0.012 ± 0.001[†]

[a]Values are means ± SEM, n = 6. *Significant effect of diet, $P < 0.05$; [†]significant effect of Pb exposure, $P < 0.05$.

TABLE 3
Effect of Pb Exposure and n-3 FA Deficiency on Liver FA Composition[a]

	n-3 Adequate		n-3 Deficient	
	Na control	Pb-exposed	Na control	Pb-exposed
	g/100 g FA[b]			
Total saturated	49.6 ± 4.01*	41.1 ± 1.01*	51.2 ± 2.69	52.2 ± 3.45
Total monounsaturated	20.8 ± 2.53	20.9 ± 2.34	24.5 ± 2.33	17.1 ± 1.18
18:2n-6	6.91 ± 0.71*	10.0 ± 1.29*	5.25 ± 0.56	5.14 ± 0.28
18:3n-6	0.13 ± 0.01	0.23 ± 0.03[†]	0.16 ± 0.01	0.28 ± 0.04[†]
20:2n-6	0.10 ± 0.02	0.13 ± 0.02	0.12 ± 0.04	0.07 ± 0.01
20:3n-6	0.89 ± 0.13[a]	0.94 ± 0.06[a]	0.92 ± 0.07[a]	0.56 ± 0.07[b]
20:4n-6	7.71 ± 1.36*	10.6 ± 0.94*,[†]	14.8 ± 1.55	20.4 ± 1.72[†]
22:4n-6	0.10 ± 0.01*	0.21 ± 0.04*,[†]	0.50 ± 0.05	0.65 ± 0.06[†]
22:5n-6	0.12 ± 0.02[d]	0.23 ± 0.03[c]	4.92 ± 0.57[b]	6.95 ± 0.67[a]
Total n-6	16.0 ± 2.03*	22.3 ± 1.24*,[†]	26.7 ± 2.49	34.1 ± 2.42[†]
18:3n-3	0.31 ± 0.05*	0.37 ± 0.10*	ND	ND
20:5n-3	0.86 ± 0.15*	1.15 ± 0.14*	0.02 ± 0.002	0.01 ± 0.004
22:5n-3	0.27 ± 0.04[b]	0.49 ± 0.07[a]	0.04 ± 0.01[c]	0.04 ± 0.01[c]
22:6n-3	7.72 ± 1.16*	10.6 ± 1.01*,[†]	0.82 ± 0.17	1.25 ± 0.28[†]
Total n-3	9.16 ± 1.35*	12.7 ± 1.10*,[†]	0.87 ± 0.18	1.30 ± 0.28[†]
	µg/mg tissue[c]			
Total saturated	20.4 ± 3.26	11.3 ± 0.34[†]	17.6 ± 1.08	11.8 ± 0.53[†]
Total monounsaturated	8.08 ± 0.78	5.73 ± 0.59[†]	9.95 ± 1.49	4.75 ± 0.46[†]
18:2n-6	2.74 ± 0.26*	2.80 ± 0.41*	2.05 ± 0.16	1.41 ± 0.08
18:3n-6	0.05 ± 0.01	0.06 ± 0.01	0.07 ± 0.01	0.08 ± 0.01
20:2n-6	0.04 ± 0.01	0.04 ± 0.01	0.05 ± 0.01	0.02 ± 0.002
20:3n-6	0.35 ± 0.05	0.26 ± 0.02[†]	0.37 ± 0.04	0.15 ± 0.02[†]
20:4n-6	2.97 ± 0.41*	2.92 ± 0.27*	5.76 ± 0.52	5.62 ± 0.50
22:4n-6	0.04 ± 0.004*	0.06 ± 0.01*[†]	0.20 ± 0.02	0.18 ± 0.01[†]
22:5n-6	0.05 ± 0.01[c]	0.06 ± 0.01[b]	1.90 ± 0.16[a]	1.90 ± 0.17[a]
Total n-6	6.23 ± 0.62*	6.20 ± 0.47*	10.4 ± 0.75	9.37 ± 0.66
18:3n-3	0.12 ± 0.02*	0.10 ± 0.03*	ND	ND
20:5n-3	0.33 ± 0.05*	0.32 ± 0.04*	0.006 ± 0.002	0.003 ± 0.001
22:5n-3	0.11 ± 0.02[b]	0.14 ± 0.02[a]	0.02 ± 0.003[c]	0.01 ± 0.002[c]
22:6n-3	3.02 ± 0.41*	2.94 ± 0.28*	0.32 ± 0.08	0.34 ± 0.08
Total n-3	3.58 ± 0.48*	3.50 ± 0.32*	0.34 ± 0.08	0.36 ± 0.08
Total FA (µg/mg tissue)	40.4 ± 2.85	27.6 ± 0.79[†]	39.7 ± 2.22	27.7 ± 1.11[†]

[a]Values are mean ± SEM, n = 6. *Significant effect of diet, $P < 0.05$; [†]significant effect of Pb exposure, $P < 0.05$; significant diet × Pb exposure interaction and means with different alphabetical superscripts are significantly different by Tukey HSD test at $P < 0.05$.
[b]Percentage of FA.
[c]Concentration of FA. ND, not detected, i.e., less than 0.01%.

TABLE 4
Effect of Pb Exposure and n-3 FA Deficiency on Plasma FA Composition[a]

	n-3 Adequate		n-3 Deficient	
	Na control	Pb-exposed	Na control	Pb-exposed
	g/100 g FA[b]			
Total saturated	38.7 ± 0.34	36.9 ± 0.54	38.5 ± 1.16	39.0 ± 1.65
Total monounsaturated	20.8 ± 2.49	14.1 ± 0.38[†]	21.7 ± 1.26	17.1 ± 0.96[†]
18:2n-6	13.2 ± 0.74*	16.0 ± 1.09*,[†]	10.3 ± 0.52	10.8 ± 0.37[†]
18:3n-6	0.21 ± 0.05	0.27 ± 0.02	0.27 ± 0.03	0.35 ± 0.04
20:2n-6	0.10 ± 0.03*	0.09 ± 0.01*	0.07 ± 0.01	0.05 ± 0.003
20:3n-6	1.02 ± 0.23*	0.84 ± 0.07*,[†]	0.83 ± 0.15	0.39 ± 0.09[†]
20:4n-6	10.9 ± 0.67*	14.6 ± 0.96*,[†]	17.5 ± 0.91	20.2 ± 2.12[†]
22:4n-6	0.12 ± 0.01*	0.13 ± 0.02*	0.32 ± 0.02	0.31 ± 0.03
22:5n-6	0.11 ± 0.02*	0.14 ± 0.01*	2.39 ± 0.12	2.66 ± 0.24
Total n-6	25.6 ± 1.17*	32.0 ± 0.57*,[†]	31.4 ± 1.18	34.8 ± 2.02[†]
18:3n-3	0.78 ± 0.09*	0.63 ± 0.11*	0.01 ± 0.001	0.01 ± 0.001
20:5n-3	1.47 ± 0.28*	1.49 ± 0.14*	0.03 ± 0.004	0.02 ± 0.003
22:5n-3	0.29 ± 0.03*	0.26 ± 0.03*	0.02 ± 0.002	0.02 ± 0.001
22:6n-3	5.20 ± 0.23*	5.39 ± 0.18*	0.34 ± 0.05	0.41 ± 0.08
Total n-3	7.74 ± 0.36*	7.77 ± 0.25*	0.40 ± 0.05	0.46 ± 0.08
	μg/mg tissue[c]			
Total saturated	5.60 ± 0.61	3.81 ± 0.08	6.24 ± 1.16	5.02 ± 0.47
Total monounsaturated	3.10 ± 0.63	1.46 ± 0.04[†]	3.59 ± 0.68	2.20 ± 0.23[†]
18:2n-6	1.92 ± 0.26*	1.66 ± 0.14*,[†]	1.56 ± 0.19	1.39 ± 0.11[†]
18:3n-6	0.03 ± 0.01	0.03 ± 0.003	0.04 ± 0.01	0.04 ± 0.01
20:2n-6	0.02 ± 0.01	0.01 ± 0.001	0.01 ± 0.002	0.01 ± 0.001
20:3n-6	0.14 ± 0.02	0.09 ± 0.01[†]	0.14 ± 0.04	0.05 ± 0.01[†]
20:4n-6	1.55 ± 0.11*	1.50 ± 0.09*	2.69 ± 0.32	2.53 ± 0.20
22:4n-6	0.02 ± 0.003*	0.01 ± 0.002*	0.05 ± 0.01	0.04 ± 0.01
22:5n-6	0.02 ± 0.003*	0.02 ± 0.001*	0.39 ± 0.07	0.33 ± 0.03
Total n-6	3.68 ± 0.34*	3.31 ± 0.13*	4.88 ± 0.60	4.39 ± 0.23
18:3n-3	0.12 ± 0.04[a]	0.07 ± 0.01[b]	0.001 ± 0.001[c]	0.001 ± 0.001[c]
20:5n-3	0.21 ± 0.04*	0.15 ± 0.02*,[†]	0.005 ± 0.001	0.003 ± 0.001[†]
22:5n-3	0.04 ± 0.01*	0.03 ± 0.003*	0.003 ± 0.001	0.003 ± 0.001
22:6n-3	0.76 ± 0.11[a]	0.56 ± 0.02[b]	0.05 ± 0.01[c]	0.05 ± 0.01[c]
Total n-3	1.13 ± 0.15[a]	0.80 ± 0.03[b]	0.06 ± 0.01[c]	0.06 ± 0.01[c]
Total FA (μg/mg tissue)	14.5 ± 1.65	10.3 ± 0.24[†]	16.0 ± 2.53	12.8 ± 0.85[†]

[a]Values are mean ± SEM, $n = 6$. *Significant effect of diet, $P < 0.05$; [†]significant effect of Pb exposure, $P < 0.05$; Significant diet × Pb exposure interaction. Means with different alphabetical superscripts are significantly different by Tukey's HSD test at $P < 0.05$.
[b]Percentage of FA
[c]Concentration of FA.

Def diets (Tables 3–7). In the n-3 Def groups, a very marked effect was observed with much lower percentages of total n-3 FA in the livers (≥90%, Tables 3), plasma (≥94%, Table 4), or kidney (≥91%, Table 5) relative to the n-3 Adq groups ($P < 0.05$). However, although the brain (Table 6) and retina (Table 7) also showed significantly lower percentages of total n-3 FA in the n-3 Def groups (18–26% lower for brain and 31–39% lower for retina, $P < 0.05$), these effects were of a lower magnitude than the peripheral tissues. Most of the decrease in total n-3 FA percentages could be accounted for by a lower percentage of DHA. In liver, plasma, and kidney, LNA, EPA (20:5n-3), and n-3 docosapentaenoic acid (DPAn-3, 22:5n-3) were also markedly lower in the n-3 Def group ($P < 0.05$).

Replacing the n-3 FA in the n-3 Def group was a higher percentage of n-6 FA. Within the n-6 FA family, there were large increases in the n-6 docosapentaenoic acid (DPAn-6, 22:5n-6) percentage in all tissues in the n-3 Def group ($P < 0.05$). For example, the DPAn-6 content was 3.47 and 9.08% in brain and retina, respectively, in the n-3 Def-Na group but was 0.28% for brain (Table 6) and 0.18% for retina (Table 7) in the n-3 Adq-Na group. A 38-fold difference between the n-3 Adq and n-3 Def groups in the concentration of DPAn-6 was evident in the liver (Table 3). Also, there were several significant changes in the major n-6 species AA and LA ($P < 0.05$). The AA percentages were higher in the liver (92%), plasma (61%), kidney (38%), brain (18%), and retina (30%) in the n-3 Def groups.

TABLE 5
Effect of Pb Exposure and n-3 FA Deficiency on Kidney FA Composition[a]

	n-3 Adequate		n-3 Deficient	
	Na control	Pb-exposed	Na control	Pb-exposed
	g/100 g FA[b]			
Total saturated	43.7 ± 0.78	43.5 ± 0.52	44.9 ± 0.32	43.6 ± 0.71
Total monounsaturated	31.4 ± 1.21	28.5 ± 0.86[†]	29.6 ± 1.41	26.0 ± 1.90[†]
18:2n-6	8.64 ± 0.25*	9.46 ± 0.46*,[†]	6.98 ± 0.29	7.93 ± 0.29[†]
18:3n-6	0.05 ± 0.003*	0.05 ± 0.002*	0.07 ± 0.004	0.08 ± 0.01
20:2n-6	0.12 ± 0.01	0.15 ± 0.01[†]	0.11 ± 0.01	0.15 ± 0.02[†]
20:3n-6	0.58 ± 0.09*	0.53 ± 0.05*	0.48 ± 0.03	0.34 ± 0.05
20:4n-6	9.97 ± 0.71*	11.7 ± 0.61*,[†]	13.8 ± 1.16	17.2 ± 1.50[†]
22:4n-6	0.23 ± 0.04*	0.30 ± 0.02*	0.66 ± 0.13	0.85 ± 0.12
22:5n-6	0.05 ± 0.01[c]	0.08 ± 0.002[c]	1.31 ± 0.13[b]	1.85 ± 0.19[a]
Total n-6	19.6 ± 0.56*	22.3 ± 0.73*,[†]	23.5 ± 1.56	28.4 ± 1.61[†]
18:3n-3	0.50 ± 0.06*	0.45 ± 0.03*	ND	ND
20:5n-3	0.68 ± 0.10*	0.58 ± 0.10*	ND	ND
22:5n-3	0.24 ± 0.02*	0.26 ± 0.01*	0.02 ± 0.002	0.02 ± 0.003
22:6n-3	2.33 ± 0.16*	2.83 ± 0.15*,[†]	0.24 ± 0.04	0.36 ± 0.06[†]
Total n-3	3.76 ± 0.17*	4.11 ± 0.24*	0.26 ± 0.04	0.38 ± 0.06
	µg/mg tissue[c]			
Total saturated	17.1 ± 0.82	16.5 ± 0.62	18.5 ± 1.40	14.6 ± 1.39
Total monounsaturated	12.4 ± 1.04	10.9 ± 0.77[†]	12.3 ± 1.29	9.07 ± 1.69[†]
18:2n-6	3.40 ± 0.26*	3.60 ± 0.22*	2.85 ± 0.20	2.68 ± 0.33
18:3n-6	0.02 ± 0.001*	0.02 ± 0.001*	0.03 ± 0.003	0.03 ± 0.002
20:2n-6	0.05 ± 0.003	0.06 ± 0.004[†]	0.05 ± 0.002	0.05 ± 0.004[†]
20:3n-6	0.23 ± 0.04*	0.20 ± 0.01*,[†]	0.20 ± 0.02	0.11 ± 0.01[†]
20:4n-6	3.85 ± 019*	4.42 ± 0.16*	5.53 ± 0.22	5.61 ± 0.36
22:4n-6	0.09 ± 0.01*	0.12 ± 0.01*	0.25 ± 0.03	0.27 ± 0.01
22:5n-6	0.02 ± 0.002*	0.03 ± 0.001*	0.52 ± 0.04	0.60 ± 0.04
Total n-6	7.64 ± 0.26*	8.44 ± 0.26*	9.42 ± 0.36	9.34 ± 0.54
18:3n-3	0.20 ± 0.04*	0.17 ± 0.01*	ND	ND
20:5n-3	0.26 ± 0.04*	0.21 ± 0.03*	ND	ND
22:5n-3	0.09 ± 0.004*	0.10 ± 0.01*	0.01 ± 0.001	0.01 ± 0.001
22:6n-3	0.90 ± 0.04[b]	1.07 ± 0.04[a]	0.10 ± 0.02[c]	0.12 ± 0.02[c]
Total n-3	1.46 ± 0.06*	1.55 ± 0.05*	0.11 ± 0.02	0.13 ± 0.02
Total FA (µg/mg tissue)	39.1 ± 0.17	38.1 ± 1.59	41.1 ± 2.96	33.7 ± 3.55

[a]Values are mean ± SEM, $n = 6$. *Significant effect of diet, $P < 0.05$; [†]significant effect of Pb exposure, $P < 0.05$; significant diet × Pb exposure interaction. Means with different alphabetical superscripts are significantly different by Tukey's HSD test at $P < 0.05$.
[b]Percentage of FA.
[c]Concentration of FA. ND, not detected.

The docosatetraenoic acid (DTA, 22:4n-6) percentage was also higher in all tissues in the n-3 Def group, with the brain exhibiting a 38% and retina an 87% higher content ($P < 0.05$). However, an exception to the generally higher tissue percentage of n-6 FA in the n-3 Def groups was LA, for which a lower percentage was found in the liver (24%), plasma (22%), kidney (19%), and brain (27%) ($P < 0.05$). In most cases, with the exception of liver and retina, there was also a lower concentration of dihomo-γ-linolenic acid (DGLA, 20:3n-6) in the n-3 Def group ($P < 0.05$). In general, there were no main effects of diet on the tissue concentrations of saturated and monounsaturated FA. However, the percentages of liver total saturated FA

for the n-3 Adq groups were lower than those of the n-3 Def groups ($P < 0.05$).

Pb effects on liver FA composition. The effects of Pb on the FA composition were most pronounced in the liver (Table 3) where Pb exposure resulted in increased percentages of total n-6 (67% in the n-3 Adq-Pb and 28% in the n-3 Def-Pb group) and total n-3 (39% in the n-3 Adq-Pb and 49% in the n-3 Def-Pb group) FA ($P < 0.05$). Within the n-6 FA family, γ-linolenic acid (GLA, 18:3n-6), AA, and DTA were increased by Pb exposure. Liver DHA was 37% higher in the n-3 Adq-Pb and 52% higher in the n-3 Def-Pb relative to their respective Na-control groups. A significant decline in saturated FA after Pb

TABLE 6
Effect of Pb Exposure and n-3 FA Deficiency on Brain FA Composition[a]

	n-3 Adequate		n-3 Deficient	
	Na control	Pb-exposed	Na control	Pb-exposed
	g/100 g FA[b]			
Total saturated	37.3 ± 0.69^{c}	36.3 ± 0.31^{b}	38.1 ± 0.62^{a}	38.9 ± 0.26^{a}
Total monounsaturated	27.7 ± 0.64	27.1 ± 0.71	27.4 ± 0.64	27.4 ± 0.48
18:2n-6	$0.60 \pm 0.03^{*}$	$0.64 \pm 0.02^{*}$	0.44 ± 0.01	0.44 ± 0.01
20:2n-6	0.14 ± 0.01	0.12 ± 0.004	0.13 ± 0.01	0.11 ± 0.004
20:3n-6	$0.44 \pm 0.27^{*}$	$0.41 \pm 0.02^{*,\dagger}$	0.34 ± 0.01	$0.27 \pm 0.01^{\dagger}$
20:4n-6	$7.56 \pm 0.67^{*}$	$7.56 \pm 0.14^{*}$	8.92 ± 0.23	9.62 ± 0.15
22:4n-6	$2.47 \pm 0.07^{*}$	$2.38 \pm 0.05^{*}$	3.42 ± 0.09	3.44 ± 0.03
22:5n-6	$0.28 \pm 0.14^{*}$	$0.15 \pm 0.01^{*}$	3.47 ± 0.31	3.56 ± 0.31
Total n-6	$11.5 \pm 0.29^{*}$	$11.3 \pm 0.19^{*}$	16.7 ± 0.45	17.4 ± 0.34
22:5n-3	$0.19 \pm 0.01^{*}$	$0.18 \pm 0.004^{*}$	0.03 ± 0.004	0.04 ± 0.004
22:6n-3	$12.9 \pm 0.42^{*}$	$12.6 \pm 0.27^{*}$	9.22 ± 0.32	9.96 ± 0.38
Total n-3	$14.2 \pm 0.45^{*}$	$13.8 \pm 0.33^{*}$	10.5 ± 0.34	11.3 ± 0.42
	µg/mg tissue[c]			
Total saturated	13.9 ± 0.40	14.8 ± 1.13	12.4 ± 0.62	13.7 ± 0.94
Total monounsaturated	10.4 ± 0.51	11.2 ± 1.21	8.90 ± 0.47	9.70 ± 0.86
18:2n-6	$0.22 \pm 0.02^{*}$	$0.26 \pm 0.03^{*}$	0.14 ± 0.01	0.15 ± 0.01
20:2n-6	$0.05 \pm 0.01^{*}$	$0.05 \pm 0.01^{*}$	0.04 ± 0.002	0.04 ± 0.004
20:3n-6	$0.17 \pm 0.01^{*}$	$0.17 \pm 0.02^{*}$	0.11 ± 0.01	0.10 ± 0.01
20:4n-6	2.81 ± 0.04	$3.07 \pm 0.20^{\dagger}$	2.90 ± 0.16	$3.37 \pm 0.21^{\dagger}$
22:4n-6	$0.92 \pm 0.02^{*}$	$0.97 \pm 0.07^{*}$	1.11 ± 0.06	1.21 ± 0.10
22:5n-6	$0.11 \pm 0.06^{*}$	$0.06 \pm 0.003^{*}$	1.14 ± 0.13	1.27 ± 0.17
Total n-6	$4.28 \pm 0.13^{*}$	$4.58 \pm 0.32^{*}$	5.44 ± 0.34	6.14 ± 0.48
22:5n-3	0.07 ± 0.01	$0.07 \pm 0.01^{*}$	0.01 ± 0.001	0.01 ± 0.002
22:6n-3	$4.81 \pm 0.13^{*}$	$5.09 \pm 0.30^{*,\dagger}$	2.97 ± 0.10	$3.47 \pm 0.19^{\dagger}$
Total n-3	$5.29 \pm 0.14^{*}$	$5.60 \pm 0.32^{*}$	3.38 ± 0.11	3.93 ± 0.20
Total FA (µg/mg tissue)	$37.4 \pm 1.68^{*}$	$40.9 \pm 3.30^{*}$	32.6 ± 1.91	35.2 ± 2.62

[a]Values are mean $\pm$ SEM, $n = 6$. *Significant effect of diet, $P < 0.05$; [†]significant effect of Pb exposure, $P < 0.05$; Significant diet $\times$ Pb exposure interaction. Means with different alphabetical superscripts are significantly different by Tukey's HSD test at $P < 0.05$.
[b]Percentage of FA.
[c]Concentration of FA.

exposure occurred for 12:0, 14:0, and 16:0, however, the percentages of 20:0, 22:0 and 24:0 were increased by Pb exposure ($P < 0.05$). Among monounsaturated FA, Pb exposure resulted in a significant decline in the percentages of 14:1 and 16:1 but increases in 24:1n-9 ($P < 0.05$). There were interactions between Pb $\times$ diet for several n-6 and n-3 FA in the liver with significant interactions of Pb $\times$ diet for DGLA, DPAn-6, and DPAn-3 ($P < 0.05$).

The concentration of total FA was significantly decreased by 32% in the livers of the n-3 Adq-Pb group in comparison with the n-3 Adq-Na group and, in the n-3 Def groups, Pb exposure led to a 30% loss in total FA concentration ($P < 0.05$). When the data were expressed in terms of concentration, there were significant losses of total saturates, monounsaturates, and DGLA in the Pb-exposed groups. As for the percentage data, there were Pb $\times$ diet interactions for the DPAn-3 and DPAn-6 FA. In addition, there was an interaction for the DGLA as Pb exposure led to a decrease in the n-3 Def group but an increase in the n-3 Adq group. Besides those just noted, no other polyunsaturate concentration was significantly altered by Pb exposure.

Pb effects on plasma FA composition. There were no main effects of Pb in the plasma on either the total saturated or the total n-3 FA in plasma (Tables 4). However, Pb exposure decreased total monounsaturated (32% decline for n-3 Adq-Pb and 21% decline for n-3 Def-Pb) and total FA concentrations (29% decline for n-3 Adq-Pb and 20% decline for n-3 Def-Pb) but increased total n-6 FA (25% for n-3 Adq-Pb and 11% for n-3 Def-Pb) ($P < 0.05$). Within the n-6 FA family, GLA and AA were increased by Pb exposure but DGLA was decreased. Plasma AA was 34% higher in n-3 Adq-Pb and 15% higher in n-3 Def-Pb relative to the Na-control groups. With respect to the saturated FA after Pb exposure, the 16:0 percentage was decreased but 20:0, 22:0 and 24:0 were increased ($P < 0.05$). Among monounsaturated FA, Pb exposure decreased the percentages of 16:1,

TABLE 7
Effect of Pb Exposure and n-3 FA Deficiency on Retina FA Composition[a]

	n-3 Adequate		n-3 Deficient	
	Na control	Pb-exposed	Na control	Pb-exposed
	g/100 g FA[b]			
Total saturated	40.9 ± 0.29	40.9 ± 0.53	41.6 ± 0.20	40.7 ± 0.39
Total monounsaturated	10.3 ± 0.18*	10.6 ± 0.33*	11.1 ± 0.47	11.4 ± 0.29
18:2n-6	0.54 ± 0.06	0.71 ± 0.13	0.53 ± 0.03	0.51 ± 0.05
18:3n-6	0.02 ± 0.002	0.03 ± 0.002	0.03 ± 0.002	0.04 ± 0.002
20:2n-6	0.10 ± 0.01[a,b]	0.09 ± 0.004[b]	0.11 ± 0.003[a]	0.07 ± 0.01[c]
20:3n-6	0.23 ± 0.02[a]	0.17 ± 0.01[b]	0.24 ± 0.02[a]	0.11 ± 0.01[c]
20:4n-6	6.77 ± 0.16[c]	7.56 ± 0.36[b]	8.77 ± 0.26[a]	8.42 ± 0.27[a]
22:4n-6	1.12 ± 0.02[c]	1.20 ± 0.03[c]	2.09 ± 0.07[a]	1.84 ± 0.07[b]
22:5n-6	0.18 ± 0.01*	0.22 ± 0.01*	9.08 ± 0.79	8.29 ± 0.65
Total n-6	8.95 ± 0.24*	9.98 ± 0.50*	20.9 ± 1.08	19.3 ± 0.85
22:5n-3	0.48 ± 0.03*	0.45 ± 0.02*	0.12 ± 0.02	0.13 ± 0.01
22:6n-3	35.1 ± 0.39*	33.0 ± 0.60*	21.8 ± 1.12	23.1 ± 1.20
Total n-3	35.7 ± 0.39*	33.6 ± 0.59*	21.9 ± 1.13	23.3 ± 1.22
	µg/mg tissue[c]			
Total saturated	4.12 ± 0.29	6.43 ± 1.88	4.79 ± 0.44	5.38 ± 0.19
Total monounsaturated	1.04 ± 0.01	1.63 ± 0.43	1.26 ± 0.08	1.51 ± 0.07
18:2n-6	0.06 ± 0.01	0.11 ± 0.03	0.06 ± 0.01	0.07 ± 0.01
18:3n-6	0.002 ± 0.001	0.004 ± 0.001	0.004 ± 0.001	0.01 ± 0.001
20:2n-6	0.01 ± 0.001	0.01 ± 0.004	0.01 ± 0.001	0.01 ± 0.001
20:3n-6	0.02 ± 0.003	0.03 ± 0.01	0.03 ± 0.003	0.02 ± 0.001
20:4n-6	0.68 ± 0.06	1.17 ± 0.32	1.02 ± 0.11	1.11 ± 0.05
22:4n-6	0.11 ± 0.01*	0.20 ± 0.06*	0.24 ± 0.03	0.24 ± 0.01
22:5n-6	0.02 ± 0.001*	0.04 ± 0.01*	1.06 ± 0.15	1.08 ± 0.06
Total n-6	0.91 ± 0.08*	1.56 ± 0.43*	2.42 ± 0.29	2.53 ± 0.08
22:5n-3	0.05 ± 0.01*	0.07 ± 0.02*	0.01 ± 0.002	0.02 ± 0.002
22:6n-3	3.52 ± 0.23*	5.26 ± 1.64*,[†]	2.52 ± 0.27	3.08 ± 0.27[†]
Total n-3	3.57 ± 0.21*	5.33 ± 1.67*,[†]	2.53 ± 0.27	3.10 ± 0.28[†]
Total FA				
(µg/mg tissue)	10.1 ± 0.65	15.9 ± 4.88	11.5 ± 1.04	13.2 ± 0.56

[a]Values are mean ± SEM, $n = 6$. *Significant effect of diet, $P < 0.05$; [†]significant effect of Pb exposure, $P < 0.05$; significant diet × Pb exposure interaction. Means with different alphabetical superscripts are significantly different by Tukey's HSD test at $P < 0.05$.
[b]Percentage of FA.
[c]Concentration of FA.

18:1n-9, 18:1n-7, and 20:1n-9 but increased the level of 24:1n-9 ($P < 0.05$).

When examined in terms of concentration, Pb exposure led to decreases in monounsaturates and total FA, but the decreased levels of saturates did not reach statistical significance. There were also significant decreases in LA, DGLA, and EPA concentrations due to Pb. There were interactive effects of Pb × diet for LNA and DHA.

Pb effects on kidney FA composition. In the kidney, there were main effects of Pb on total monounsaturated (9% decline for n-3 Adq-Pb and 12% decline for n-3 Def-Pb) and total n-6 (14% increase for n-3 Adq-Pb and 21% increase for n-3 Def-Pb) FA ($P < 0.05$) (Table 5). Pb exposure resulted in increased percentages of LA, docosadienoic acid (20:2n-6), and AA. For the monounsaturated FA, Pb exposure decreased the percentage of 16:1 but increased the percentage of 18:1-DMA (dimethyl acetal derivative) and 20:1n-9 ($P < 0.05$). Pb exposure

did not affect the percentages of total saturated or total n-3 FA or the total FA concentration. However, kidney DHA was increased by 21% in the n-3 Adq-Pb group and by 50% in the n-3 Def-Pb after Pb exposure ($P < 0.05$). Among the saturated FA, the percentages of 16:0-DMA, 18:0-DMA, 18:0, 20:0, and 22:0 after Pb exposure were increased, but the percentages of 10:0 and 16:0 were decreased by Pb exposure ($P < 0.05$). There was significant interaction between Pb × diet for the percentage of DPAn-6 in the kidney ($P < 0.05$).

When expressed in terms of concentration, Pb exposure led to a significant loss of monounsaturates, docosadienoic acid, and DGLA. The lower levels of saturates and total FA did not reach significance.

Pb effects on brain FA composition. There were no main effects of Pb exposure on total FA concentration, or the percentages of total monounsaturated, total n-6, or total n-3 FA in brain (Table 6). However, there was a diet × Pb exposure interaction for total

saturated FA and for 24:1n-9 ($P < 0.05$). The percentages of 12:0 and DGLA were decreased by Pb exposure, but 16:1 was increased ($P < 0.05$). In terms of concentration, both AA and DHA were increased by Pb exposure. In contrast to the responses observed in peripheral tissues, both saturated and monounsaturated FA concentration increased in Pb-exposed groups, but not significantly so.

Pb effects on retina FA composition. There were no main effects of Pb exposure on total FA, total saturated, total monounsaturated, or total n-6 FA in the retina either when expressed as a percentage or as a concentration (Table 7). However, there was a diet × Pb exposure interaction for 12:0 and several n-6 FA including 20:2n-6, DGLA, AA, and DTA ($P < 0.05$). The percentage of 20:1n-9 was decreased by Pb exposure ($P < 0.05$). As was observed in the brain, the DHA concentration was significantly increased after Pb exposure, and this led to a significant increase in total n-3 FA as well.

DISCUSSION

Lead exposure solely during the lactational period significantly altered the dam liver, plasma, and kidney FA composition but produced weaker effects on the nervous system tissues. In particular, the percentages of 20-C PUFA were increased by Pb exposure, with AA being most affected. As expected, the n-3 Def diets markedly decreased the percentages of total n-3 FA including DHA, and increased total n-6 FA including both arachidonic (AA) and DPAn-6 in all tissues.

It has been known that Pb exposure resulted in increased percentages of AA in rats (19), chickens (12,13,20,21), and humans (22). However, in a previous study of lactational Pb exposure (11), Lim *et al.* observed that pup liver AA and DHA at weaning were increased in terms of the percentages but that the organ concentrations of AA and DHA were not in fact different. In many of the previous studies of FA composition after Pb exposure, although only the percentage of FA was measured and no internal standard was used, the data are often discussed in terms of concentration (12,13,20–22), leading to much confusion. This is an especially unfortunate error since there are in fact both percentage changes in many FA subsequent to Pb exposure and changes in total FA absolute concentrations. Our tables are constructed to facilitate the comparisons of various PUFA expressed in both manners. Since Pb generally decreases the tissue total FA concentration, even those FA that appear to be increased when expressed as a percentage may in fact exhibit little or no change when the organ concentration is determined. The large increases in the percentages of polyunsaturates may then simply reflect a preferential decrease in non-EFA concentration.

In fact, when the concentration data are examined, our results show that there is no significant difference in AA concentration in maternal liver and plasma. More specifically, the percentage of liver AA was increased by 37% in the n-3 Adq-Pb group compared with the n-3 Adq-Na group, but the actual concentrations were 2.92 and 2.97 µg/mg, respectively. Similarly, the liver DHA concentrations in the two n-3 Adq groups were

unchanged, as they were 3.02 (Na) and 2.94 µg/mg (Pb). However, the concentrations of 16:0 and 18:0 fell rather precipitously in liver as did the monounsaturates 16:1 and 18:1 in the Pb-exposed groups. Qualitatively similar results were observed in the plasma and kidney. The nervous system was an exception to this. In both the brain and retina, DHA concentration was significantly increased by Pb exposure. Pb-induced increases in AA were also observed in both retina and brain, but only those in the brain were statistically significant. The nervous system was also distinct from the peripheral tissues in that non-EFA were not decreased and even rose somewhat subsequent to Pb exposure. It is apparent that Pb alters the FA profile in the nervous system in a different manner from that for peripheral tissues.

The mechanisms underlying these changes in essential and non-EFA composition are unclear. Previous discussions of Pb effects on FA have centered on lipid peroxidation as a result of the observation that high levels of Pb exposure in chicks led to increased production of malondialdehyde (20). However, peroxidative reactions would be expected to selectively remove PUFA species in preference to saturates and monounsaturates. In general, the opposite pattern is observed here in the dams and to an even greater extent in pups exposed to Pb through lactation (11), as non-EFA are lost in Pb-exposed animals in preference to EFA. Such a FA profile is also inconsistent with a hypothesis that Pb alters FA desaturation. A more straightforward interpretation of these results would be that the increased percentages of the highly unsaturated FA reflect preferential sparing of these lipids with respect to non-essential species. The loss of body weight in the Pb-exposed groups indicates that there may have been a decrease in food intake (although not measured here) associated with the high level of Pb in the drinking water. It is likely that non-EFA were then preferentially metabolized for energy as a consequence of Pb exposure.

One hypothesis to be tested was to determine whether an n-3 Def diet would lead to greater effects of Pb exposure on FA composition, or, alternatively, whether an n-3 Adq diet would lead to "protective" effects on FA composition of various tissues. Several interactions of the two key variables of this study, diet and Pb exposure, occurred mainly in the 20- and 22-carbon PUFA. For example, Pb exposure increased liver DPAn-6 and 22:5n-3 and kidney DHA concentrations in the n-3 Adq group, but not in the n-3 Def group. In plasma, Pb exposure reduced 18:3n-3, DHA, and total n-3 FA concentrations only in the n-3 Adq group. There were interactions between diet and Pb exposure for several of the n-6 PUFA in the retina including DGLA, AA, and 22:4n-6.

Another manner in which to examine protective effects of diet is to compare the magnitude of the principal changes in FA concentrations with or without Pb for the two diets (i.e., compare the FA concentrations for the groups as follows: $100 - $ [(Adq-Pb)/(Adq-Na) × 100] vs. $100 - $ [(Def-Pb/Def-Na) × 100]). In the dam liver, Pb exposure in the n-3 Def groups led to significant decreases in saturates, monounsaturates, DGLA, and total FA. The n-3 Adq diet led to a smaller Pb-induced loss for the monounsaturates and DGLA. Similarly, in the plasma,

the n-3 Adq diet led to a smaller Pb-induced loss of DGLA and EPA concentrations. Also, in the kidney, the n-3 Adq diet led to a smaller Pb-induced loss in monounsaturates and DGLA.

It is of interest to compare responses of the dam exposed to Pb through drinking water to that of her pups exposed *via* lactation (11). The main effect of Pb in the weanling pup liver was losses in saturates, monounsaturates, and total FA concentrations. In all three cases, the losses in the n-3 Adq group were considerably greater than those in the n-3 Def group. In the pups given the n-3 Adq diet, there was a significant interaction with Pb exposure for liver DHA and a 37% loss in the n-3 Adq group but a 60% increase in the n-3 Def group. In the dams, there was no effect of Pb exposure on DHA concentrations in either dietary group. Thus, the protective effects noted above for the n-3 Adq diet in the dam appeared to be lost for the pups exposed to Pb during lactation.

ACKNOWLEDGMENT

REFERENCES

1. Lim, S.-Y., Doherty, J., McBride, K., Miller-Ihli, N., Carmona, G., Stark, K., and Salem, N., Jr. (2005) Lead Exposure and (n-3) Fatty Acid Deficiency During Neonatal Development Affect Subsequent Spatial Task Performance and Olfactory Discrimination, *J. Nutr. 135*, 1019–1026.
2. Bernard, S.M., and McGeehin, M.A. (2003) Prevalence of Blood Lead Levels > or = 5 µg/dL Among US Children 1 to 5 Years of Age and Socioeconomic and Demograpic Factors Associated with Blood Levels 5 to 10 µg/dL, Third National Health and Nutrition Examination Survey, 1988–1994, *Pediatrics 112*, 1308–1313.
3. Lewis, N.M., Widga, A.C., Buck, J.S., and Frederick, A.M. (1995) Survey of Omega-3 Fatty Acids in Diets of Midwest Low-Income Pregnant Women, *J. Agromed. 2*, 49–57.
4. Stark, K.D., Beblo, S., Murthy, M., Buda-Abela, M., Janisse, J., Rockett, H., Whitty, J.E., Martier, S.S., Sokol, R.J., Hannigan, J.H., and Salem, N., Jr.. (2004) Comparison of Bloodstream Fatty Acid Composition from African-American Women at Gestation, Delivery and Postpartum, *J. Lipid Res. 46*, 516–525.
5. Okuyama, H., Kobayashi, T., and Watanabe, S. (1996) Dietary Fatty Acids—The n-6/n-3 Balance and Chronic Elderly Diseases. Excess Linoleic Acid and Relative n-3 Deficiency Syndrome Seen in Japan, *Prog. Lipid Res. 35*, 409–457.
6. Salem, N., Jr., Litman, B., Kim, H.Y., and Gawrisch, K. (2001) Mechanisms of Action of Docosahexaenoic Acid in the Nervous System, *Lipids 36*, 945–959.
7. Uauy, R., Hoffman, D.R., Mena, P., Llanos, A., and Birch, E.E. (2003) Term Infant Studies of DHA and ARA Supplementation on Neurodevelopment: Results of Randomized Controlled Trials, *J. Pediatr. 143*, S17–S25.
8. Banks, E.C., Ferretti, L.E., and Shucard, D.W. (1997) Effects of Low Level Lead Exposure on Cognitive Function in Children: A Review of Behavioral, Neuropsychological and Biological Evidence, *Neurotoxicology 18*, 237–281.
9. Goyer, R.A. (1996) Results of Lead Research: Prenatal Exposure and Neurological Consequences, *Environ. Health Perspect. 104*, 1050–1054.
10. Rice, D.C. (1996) Behavioral Effects of Lead: Commonalities Between Experimental and Epidemiologic Data, *Environ. Health Perspect. 104 (Suppl. 2)*, 337–351.
11. Lim, S.-Y., Doherty, J., and Salem, N., Jr. (2005) Lead Exposure and (n-3) Fatty Acid Deficiency During Rat Neonatal Development Alter Liver, Plasma and Brain Polyunsaturated Fatty Acid Composition, *J. Nutr. 135*, 1027–1033.
12. Donaldson, W.E., and Leeming, T.K. (1984) Dietary Lead: Effects on Hepatic Fatty Acid Composition in Chicks, *Toxicol. Appl. Pharmacol. 73*, 119–123.
13. Lawton, L.J., and Donaldson, W.E. (1991) Lead-Induced Tissue Fatty Acid Alterations and Lipid Peroxidation, *Biol. Trace Elem. Res. 28*, 83–97.
14. Lasley, S.M., Green, M.C., and Gilbert, M.E. (1999) Influence of Exposure Period on *in vivo* Hippocampal Glutamate and GABA Release in Rats Chronically Exposed to Lead, *Neurotoxicology 20*, 619–629.
15. Reeves, P.G., Nielsen, F.H., and Fahey, G.C., Jr. (1993) AIN-93 Purified Diets for Laboratory Rodents: Final Report of the American Institute of Nutrition *ad hoc* Writing Committee on the Reformulation of the AIN-76A Rodent Diet, *J. Nutr. 123*, 1939–1951.
16. Folch, J., Lees, M., and Sloane Stanley, G.H. (1957) A Simple Method for the Isolation and Purification of Total Lipids from Animal Tissues, *J. Biol. Chem. 226*, 497–509.
17. Morrison, W.R., and Smith, L.M. (1964) Preparation of Fatty Acid Methyl Esters and Dimethylacetals from Lipids with Boron Fluoride–Methanol, *J. Lipid Res. 53*, 600–608.
18. Salem, N., Jr., Reyzer, M., and Karanian, J. (1996) Losses of Arachidonic Acid in Rat Liver After Alcohol Inhalation, *Lipids 31 (Suppl.)*, S153–S156.
19. Zimmermann, L., Pages, N., Antebi, H., Hafi, A., Boudene, C., and Alcindor, L.G. (1993) Lead Effect on the Oxidation Resistance of Erythrocyte Membrane in Rat Triton-Induced Hyperlipidemia, *Biol. Trace Elem. Res. 38*, 311–318.
20. Knowles, S.O., and Donaldson, W.E. (1996) Dietary Lead Alters Fatty Acid Composition and Membrane Peroxidation in Chick Liver Microsomes, *Poult. Sci. 75*, 1498–1500.
21. Knowles, S.O., Donaldson, W.E., and Andrews, J.E. (1998) Changes in Fatty Acid Composition of Lipids from Birds, Rodents, and Preschool Children Exposed to Lead, *Biol. Trace Elem. Res. 61*, 113–125.
22. Osterode, W., and Ulberth, F. (2000) Increased Concentration of Arachidonic Acid in Erythrocyte Membranes in Chronically Lead-Exposed Men, *J. Toxicol. Environ. Health A 59*, 87–95.

Fish Oil Fatty Acid Esters of Phytosterols Alter Plasma Lipids but Not Red Blood Cell Fragility in Hamsters

Isabelle Demonty, Naoyuki Ebine, Xiaoming Jia, and Peter J.H. Jones*

School of Dietetics and Human Nutrition, McGill University, Sainte-Anne-de-Bellevue, Québec, Canada, H9X 3V9

ABSTRACT: In an attempt to combine the hypocholesterolemic properties of plant sterols with the hypotriglyceridemic action of fish oil FA, plant sterols have recently been esterified to fish oil n-3 PUFA. The objective of this study was to determine the effects of plant sterols esterified to n-3 PUFA on plasma lipid levels and erythrocyte fragility. For 5 wk, male Golden Syrian hamsters were fed diets varying in cholesterol and plant sterol content: (i) Non-cholesterol (semipurified diet with no added cholesterol or plant sterols) (ii), Cholesterol (0.25% cholesterol) (iii), Sterols (0.25% cholesterol plus 1% nonesterified plant sterols), or (iv) Fish oil esters of plant sterols (0.25% cholesterol plus 1.76% EPA and DHA sterol esters, providing 1% plant sterols). The addition of fish oil esters of plant sterols to the cholesterol diet decreased ($P = 0.001$) plasma total cholesterol levels by 20%, but nonesterified plant sterols did not have such a beneficial impact. In addition, non-HDL cholesterol concentrations were 29% lower in hamsters fed fish oil esters of plant sterols than in hamsters fed nonesterified plant sterols ($P < 0.0001$). Despite higher ($P < 0.0001$) plant sterol levels in whole erythrocytes of hamsters fed nonesterified plant sterols and fish oil esters of plant sterols compared with hamsters fed no plant sterols, no difference was observed in erythrocyte fragility. The present results show that EPA and DHA esters of plant sterols have a hypocholesterolemic effect in hamsters, and that these new esters of plant sterols exert no detrimental effect on erythrocyte fragility.

Paper no. L9712 in *Lipids 40*, 695–702 (July 2005).

Elevated blood lipid concentrations, including increased levels of total and LDL cholesterol, as well as high TG concentrations, are among the major risk factors for cardiovascular disease (CVD) (1). In patients who do not respond to dietary changes by a significant decrease in cholesterolemia, an alternative approach to pharmaceutical intervention is supplementation with plant sterols. Recently, the National Cholesterol Education Program included the consumption of 2 g of plant sterols/stanols in its recommendations to lower elevated LDL cholesterol levels (2). Indeed, the lowering effect of plant sterols on plasma total and LDL cholesterol in humans is well documented (3). However, plant sterols do not have any beneficial impact on circulating TG levels (3,4). Thus, in patients presenting both elevated cholesterol and TG concentrations, plant sterols do not offer an optimal reduction in CVD risk.

Dietary components that do have a hypotriglyceridemic effect in humans and animal models are n-3 PUFA from fish oil (5,6). In an attempt to combine the hypocholesterolemic proper-

ties of plant sterols with the hypotriglyceridemic action of fish oil FA, plant sterols have recently been esterified to fish oil n-3 PUFA. Plant sterols are usually esterified to unsaturated FA from vegetable oils, which increases their solubility and allows their incorporation into fat-containing foods such as margarines. Whether the esterification of plant sterols with FA improves their hypocholesterolemic effect is still unclear (7). Preliminary studies in guinea pigs (8) and obese, insulin-resistant rats (9) suggest that fish oil–plant sterol esters may decrease both plasma cholesterol and TG concentrations. In those experiments, however, plant sterol esters were not compared with free forms of plant sterols, and the possible contribution of esterification to the lowering effect on cholesterolemia could not be evaluated.

Plant sterols are considered to be relatively safe for human health (3). However, results obtained in spontaneously hypertensive rats, showing that plant sterols may decrease red blood cell deformability and life span in these animals (10), have raised the question of the effects of plant sterols on blood rheological properties. Whether the detrimental effects of plant sterols on spontaneously hypertensive rats can be extrapolated to healthy animals and other animal species still remains to be determined. On the other hand, fish oil FA, *via* their incorporation in red blood cell membrane phospholipids, may improve erythrocyte lipid fluidity and deformability, and consequently reduce their fragility (11–15). It can be hypothesized that the esterification of plant sterols to fish oil FA may protect red blood cells against the increased fragility potentially associated with plant sterol consumption.

Our working hypothesis was that fish oil esters of phytosterols would have a beneficial impact on both plasma cholesterol and TG concentrations, as well as on red blood cell fragility. The present study was therefore undertaken to compare the effects of nonesterified plant sterols and fish oil FA esters of plant sterols on plasma lipids and red blood cell fragility. The Golden Syrian hamster was chosen as an animal model because of its well-established similarities with human cholesterol and bile metabolism (16–18).

MATERIALS AND METHODS

Animals. Male Golden Syrian hamsters (Charles River Laboratories, Montreal, Quebec, Canada) initially weighing 80–100 g and 35–45 d old were housed individually in stainless-steel wire-bottomed mesh cages. The temperature ($20 \pm 1°C$) of the animal room was constant and the hamsters were kept under a 12-h light–dark cycle (light: 7:00–19:00). During an adaptation period of 2 wk, hamsters were fed a plain, pelleted chow diet (Charles River Laboratories). They were then randomly assigned to one of four dietary groups ($n = 10$ per group). Semi-

TABLE 1
Composition of the Experimental Diets Fed to Golden Syrian Hamsters (*n* = 10 per group) for 5 wk

Ingredients	Noncholesterol	Cholesterol	Sterols	Fish oil esters of plant sterols
		(g/kg)		
Casein[a]	200.0	200.0	197.7	196.1
Cornstarch[a]	280.0	280.0	276.7	274.5
Sucrose	363.0	360.0	356.1	353.2
Beef tallow[a]/safflower oil[b]	50.0	50.0	50.0	50.0
Cellulose[a]	50.0	50.0	49.4	49.0
DL-Methionine[a]	5.0	5.0	5.0	5.0
Mineral mixture[a,c]	40.0	40.0	40.0	40.0
Vitamin mixture[a,c]	10.0	10.0	10.0	10.0
Choline bitartrate[a]	2.0	2.2	2.0	2.0
BHT[a]	0.2	0.2	0.2	0.2
Cholesterol[a]	—	2.5	2.5	2.5
Phytosterols[d]	—	—	10.0	—
EPA/DHA esters of phytosterols[d]	—	—	—	17.6

[a]Purchased from ICN Biomedicals (Aurora, OH).
[b]Purchased from a local supermarket.
[c]AIN-93 purified diets for laboratory rodents (48).
[d]Provided by Forbes Medi-Tech Inc. (Vancouver, BC, Canada).

purified diets and water were provided on an *ad libitum* basis for 5 wk. Records of food intake were taken every 3 d, with corrections made for spillage. Body weight was monitored once a week. The protocol was approved by the Animal Care and Research Ethics Committee of McGill University according to the guidelines of the Canadian Council on Animal Care.

Experimental diets. The semipurified diets were prepared every 2 wk and stored at –20°C. Diets were similar except for the cholesterol and phytosterol content (Table 1), consisting of either (i) no added cholesterol or plant sterols (Noncholesterol diet), (ii) 0.25% cholesterol and no added plant sterols (Cholesterol diet), (iii) 0.25% cholesterol plus 1% nonesterified plant sterols (Sterols diet), or (iv) 0.25% cholesterol plus 1.76% EPA and DHA sterol esters furnishing 1% of plant sterols (Fish oil esters of plant sterols diet). All diets contained 5% fat provided by a mix of beef tallow and safflower oil yielding a polyunsaturated-to-saturated FA ratio of 0.4. Nonesterified plant sterols (Forbes Medi-Tech Inc., Vancouver, British Columbia, Canada) consisted mostly of β-sitosterol (37.9% w/w), campesterol, (23.1% w/w), stigmasterol (17.5% w/w), and brassicasterol (5.12% w/w). Traces of sitostanol (2.78% w/w) were detected. Other minor phytosterols were present at a concentration of 9.82% (w/w), and minor chemical components represented 0.23%. For the preparation of fish oil esters of plant sterols, free plant sterols from the same batch as those used for the plant sterol diet were esterified to fish oil FA. The fish oil used for esterification to plant sterols was stabilized with ascorbylpalmitate, citric acid, and mixed tocopherols. The resulting fish oil FA esters of plant sterols (Forbes Medi-Tech Inc.) contained 37.4% (w/w) β-sitosterol and a total of 62.5% (w/w) plant sterols. The remaining components (37.5% w/w) consisted in 41.1% (w/w) EPA and 19.8% (w/w) DHA. The energy content of the diets was measured in an automatic adiabatic calorimeter (Model 1241; Parr Instruments, Moline, IL) and the diets were found to be isoenergetic, with values ranging from 18.7 to 19.1 kJ/g. After 5 wk of feeding with the semipurified diets, hamsters were deprived of food overnight. Animals

were then anesthetized with halothane and decapitated, and blood samples were collected immediately.

Plasma lipid analyses. Blood samples were collected in vacutainer tubes containing EDTA (Becton Dickinson, Missisauga, Ontario, Canada) and centrifuged at 1,300 rpm for 15 min to isolate plasma. Plasma samples were stored at –80°C until lipid determination. Part of the whole red blood cell samples, collected from the bottom of the vacutainer tubes after centrifugation, was stored at –80°C for plant sterol determination, and the remainder was used immediately at room temperature for red cell fragility determination. Analyses were done in duplicate. Plasma total cholesterol and HDL cholesterol concentrations were measured by an enzymatic method using the CHOD-PAP kit from Roche Diagnostics (Laval, Québec, Canada). HDL cholesterol concentrations were measured after the precipitation of apoB-containing lipoproteins with phosphotungstic acid and magnesium ions as described by Burstein *et al.* (19). Because the Friedewald *et al.* equation (20) may not be applicable in hamsters, results are expressed as non-HDL cholesterol levels. Non-HDL cholesterol was determined by subtracting HDL cholesterol from total cholesterol. Plasma total TG were determined enzymatically (21) using Triglyceride/GB kits from Roche Diagnostics. The procedure includes a preliminary step to eliminate free glycerol prior to the enzymatic dosage of TG.

Plant sterol measurement in red blood cells. Plant sterols (campesterol and β-sitosterol) and a cholesterol precursor (lathosterol), as well as cholesterol concentrations in whole red blood cells, were determined by GLC as reported previously (22). Briefly, an internal standard of 5α-cholestane (Sigma-Aldrich Canada Ltd., Oakville, Ontario, Canada) was added to each sample of red blood cells (100 μg/0.5 g red blood cells). Samples were saponified for 2 h at 100°C with 0.5 M methanolic KOH. Nonsaponified materials were then extracted two times with petroleum ether and dried under nitrogen flux. The extracts were derivatized using 1.5 mL of TMS reagent (pyridine-hexamethyldisilazane-trimethylchlorosilane 9:3:1, by vol) (Sigma-Aldrich Canada Ltd.) (23). After evaporation under nitrogen, the samples were dissolved

in 750 μL of hexane and injected into a gas–liquid chromatograph (HP 5890 Series II; Hewlett-Packard, Palo Alto, CA) equipped with an FID and an auto-injector system. Separation was achieved on a 30-m capillary column with an i.d. of 0.25 mm and film thickness of 0.25 μm (SAC-5; Supelco, Sigma-Aldrich Canada Ltd.). A 2-μL quantity of sample was used for a split injection. The carrier gas (helium) flow rate was 7.5 psi. Samples were injected at 300°C. The oven temperature remained at 160°C for 1 min after injection, was increased to 245°C at a rate of 15°C/min, and was then kept constant for 5 min. This was followed by a rise to 285°C at a rate of 15°C/min. Afterward, the temperature was kept constant at 285°C for 20 min. The detector was set at 310°C. Plant sterols (campesterol, β-sitosterol) and lathosterol were identified using authentic standards (Sigma-Aldrich Canada Ltd.).

Red blood cell fragility determination. Red cell fragility was assessed on fresh red blood cells by an osmolar tolerance test. Red blood cells were collected at the bottom of vacutainer tubes containing EDTA after centrifugation and the collection of plasma. The intermediate layer, containing white blood cells, was discarded. A 0.2-mL sample of red cells was added to 2 mL of unbuffered saline containing graded concentrations of sodium chloride (0.2–0.6%). Samples were mixed gently for 30 s. After 1 h, the cells were centrifuged at $1000 \times g$ for 5 min and the supernatant O.D. was read at 520 nm (24–27). Data are presented as O.D. readings. The saline concentration required to obtain 50% hemolysis was determined using O.D. readings adjusted as a percentage of the maximal density obtained and assuming a linear response between 0.55 and 0.4% sodium chloride.

Statistical analyses. Results are expressed as mean ± SEM, and a *P* value of 0.05 was considered significant. Data were subjected to ANOVA procedures using the general linear model approach of the Statistical Analysis System (SAS Institute, Cary, NC) to determine the main diet effects. When statistically significant effects were detected, a *post hoc* Tukey test was performed to identify differences among the diet groups.

RESULTS

Food consumption and body weight gain. Food consumption, initial and final weight, and body weight gain of hamsters fed the various diets are presented in Table 2. Average food consumption did not differ among the treatment groups. Initial body weights were similar in all diet groups. All animals gained weight during the experiment. After 5 wk of experimental feeding, diets had no significant effect on final body weight or weight gain.

Plasma lipids and lipoproteins. Effects of the experimental diets on plasma total cholesterol, HDL cholesterol, non-HDL cholesterol, and the HDL cholesterol/total cholesterol ratio are shown in Figure 1. Plasma total cholesterol concentrations were higher ($P < 0.005$) in hamsters fed various cholesterol-containing diets than in hamsters fed the noncholesterol diet. The addition of fish oil esters of plant sterols to the cholesterol diet partially prevented the increase in total cholesterolemia ($P = 0.001$). However, such a beneficial impact on total cholesterolemia was not observed when hamsters were fed the nonesterified plant sterols. Consequently, plasma total cholesterol concentrations were lower ($P < 0.0001$) in hamsters fed fish oil esters of plant sterols than in hamsters fed nonesterified sterols. Similar to plasma total cholesterol levels, HDL cholesterol concentrations were lower ($P = 0.002$) in fish oil ester-fed hamsters than in cholesterol-fed animals. However, the HDL cholesterol/total cholesterol ratio remained unchanged in hamsters fed fish oil esters of plant sterols. Nonesterified plant sterols resulted in HDL cholesterol levels intermediate to, and not significantly different from, those observed with cholesterol and fish oil FA esters of plant sterols. In hamsters fed the fish oil ester diet, non-HDL cholesterol levels were not significantly decreased compared with hamsters fed the cholesterol diet. When compared with the nonesterified sterol diet, however, plant sterols esterified with fish oil FA significantly decreased ($P = 0.0016$) the non-HDL cholesterol concentrations.

Plasma total TG concentrations in hamsters fed the experimental diets are presented in Figure 2. TG levels were higher in cholesterol-fed hamsters than in hamsters fed the cholesterol-free diet, but the difference was significant only between sterol- and noncholesterol-fed animals ($P = 0.03$). Fish oil esters of plant sterols did not significantly lower plasma TG levels in comparison with nonesterified sterols and diets containing no plant sterols.

Plant sterol concentrations in whole red blood cells. No significant impact of diets was observed on the cholesterol content in whole red blood cells, with values of 5.56 ± 0.14, 6.38 ± 0.14, 6.00 ± 0.32, and 6.41 ± 0.42 mmol/g in hamsters fed the noncholesterol, cholesterol, sterols, and fish oil esters of plant sterols diets, respectively. The concentrations of lathosterol, campesterol, and β-sitosterol, as well as the phytosterol/cholesterol ratios in whole red blood cells are displayed in Figure 3. No significant effect of diet was observed on cholesterol and lathosterol concentrations. There was a trend toward lower lathosterol/cholesterol ratios in the red blood cells of hamsters fed cholesterol-containing diets compared with hamsters fed the noncholesterol diet, but this was statistically significant only in comparison with the fish oil ester group ($P = 0.0468$). Compared with the cholesterol diet, nonesterified plant sterols and fish oil esters of plant sterols did not affect the lathosterol/cholesterol ratios in red

TABLE 2
Food Consumption and Body Weight of Golden Syrian Hamsters (*n* = 10 per group) Fed Experimental Diets Varying in Cholesterol and Plant Sterol Content

Dietary group	Food consumption (g/d)	Initial body weight (g)	Final body weight (g)	Body weight gain (g/35 d)
Noncholesterol	7.15 ± 0.16	117.97 ± 2.28	134.67 ± 2.19	16.70 ± 1.86
Cholesterol	6.92 ± 0.19	118.05 ± 2.39	130.92 ± 3.41	12.87 ± 2.30
Sterols	7.11 ± 0.14	118.20 ± 2.40	131.69 ± 2.35	13.49 ± 2.06
Fish oil esters of plant sterols	7.09 ± 0.21	118.30 ± 2.43	134.34 ± 3.31	16.04 ± 1.40
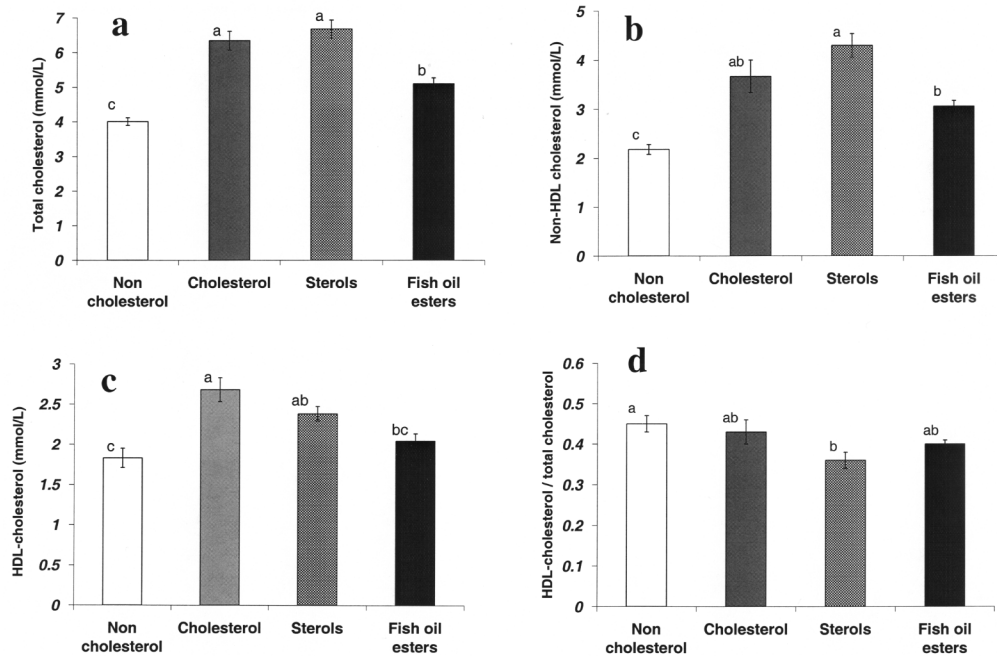
FIG. 1. Total plasma cholesterol (a), non-HDL cholesterol (b), HDL-cholesterol (c), and HDL cholesterol/total cholesterol ratio (d) in Golden Syrian hamsters ($n = 10$ per group) fed experimental diets varying in cholesterol and plant sterol content for 5 wk. Values are means ± SEM. Noncholesterol, semipurified diet with no added cholesterol or plant sterols; Cholesterol, diet with 0.25% cholesterol; Sterols, diet with 0.25% cholesterol plus 1% nonesterified plant sterols; Fish oil esters, diet with 0.25% cholesterol plus 1.76% EPA and DHA sterol esters, providing 1% plant sterols. Different letters represent significant differences between treatment groups ($P < 0.05$). For details on diet composition, see Table 1.

blood cells. Animals fed nonesterified sterols and fish oil esters of plant sterols had higher campesterol concentrations and campesterol/cholesterol ratios in red blood cells than animals fed diets containing no added sterols ($P < 0.0001$). Sitosterol and sitosterol/cholesterol ratios were higher ($P < 0.0001$) in the red blood cells of hamsters fed fish oil esters of plant sterols than in hamsters fed nonesterified sterols or no plant sterols.

Red blood cell fragility. O.D. did not differ between groups after the red blood cells of hamsters fed the various diets were added to eight different saline concentrations (data not shown). Mean saline concentrations associated with 50% hemolysis were similar among the dietary groups (0.48 ± 0.01%, 0.49 ± 0.01%, 0.49 ± 0.01%, and 0.48 ± 0.01% in hamsters fed the noncholesterol, cholesterol, nonesterified sterols, and fish oil esters of plant sterols diets, respectively).

DISCUSSION

In the present study, plant sterols esterified to fish oil FA lowered plasma total cholesterol concentrations in hamsters, whereas nonesterified plant sterols did not have such a beneficial impact. No detrimental effect of plant sterols was observed on red blood cell fragility, whether they were esterified with n-3 PUFA or not.

A lowering effect of plant sterols on total and LDL cholesterol levels is a common observation in humans (3). Plant sterols are thought to interfere with the intestinal absorption of cholesterol by displacing cholesterol from micelles (4,28). An

up-regulation of the expression of ATP-binding cassette transporters in intestinal cells, resulting in an increased excretion of cholesterol by the enterocyte back into the lumen, may also be implicated (29). Cholesterol metabolism in the hamster model presents many similarities with that in humans, such as a low rate of hepatic cholesterol synthesis (30) and a significant proportion of cholesterol associated with the LDL fraction (31,32). However, the impact of plant sterols on plasma cholesterol concentrations in hamsters is less consistent than in humans. In a
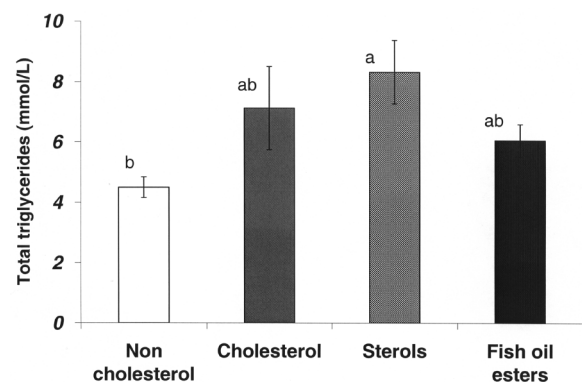
FIG. 2. Plasma total TG concentrations in Golden Syrian hamsters ($n = 10$ per group) fed experimental diets varying in cholesterol and plant sterol content for 5 wk. Values are means ± SEM. Different letters represent significant differences between treatment groups ($P < 0.05$). For diet descriptions see Figure 1; for details on diet composition see Table 1.
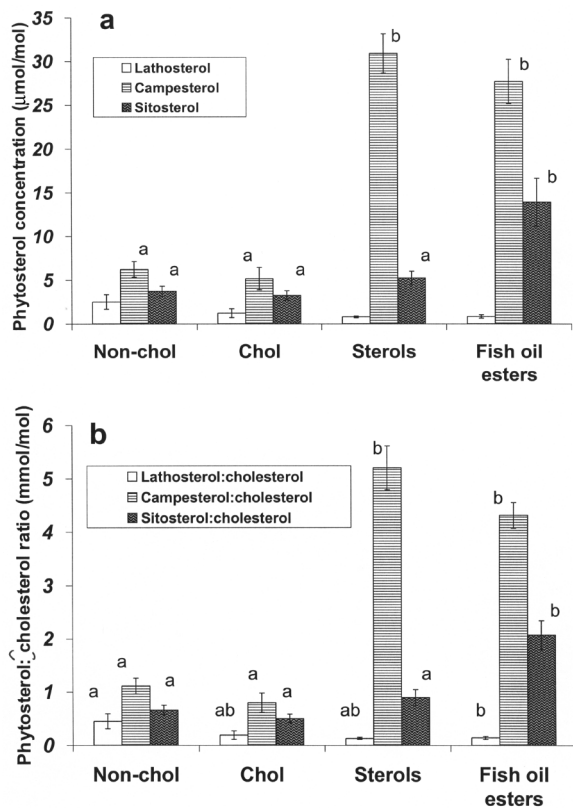
FIG. 3. Plant sterol concentrations (a) and plant sterol/cholesterol ratios (b) in whole red blood cells of Golden Syrian hamsters (*n* = 10 per group) fed experimental diets varying in cholesterol and plant sterol content for 5 wk. Values are means ± SEM. Non-chol, noncholesterol diet; Chol, cholesterol diet; Sterols, nonesterified plant sterol diet; Fish oil esters, diet with fish oil esters of plant sterols. Different letters represent significant differences between treatment groups (*P* < 0.05). For diet descriptions see Figure 1; for details on diet composition see Table 1.

few studies, nonesterified plant sterols have been shown to decrease plasma cholesterol (33,34) and cholesterol absorption (34). In other studies in hamsters, feeding plant sterol esters has resulted in decreased total cholesterol concentrations (34–36). However, in most of these studies showing a beneficial impact of free or esterified plant sterols in hamsters, the amount of cholesterol in the diet was lower (0.08–0.09%) (34,35) than in the present experiment (0.25%). It is therefore possible that the hypercholesterolemic impact of a greater intake of cholesterol in the present study may not have been counteracted completely by plant sterol consumption. Other results are in accordance with the absence of a beneficial impact of nonesterified plant sterols, as observed in the present study (22,37,38). Indeed, feeding a diet containing 1% of a plant sterol mixture supplying almost no sitostanol for 45 d did not affect plasma cholesterol concentrations in hamsters (22). In rats, a sitostanol-free phytosterol mixture had no significant effect on total and LDL cholesterol concentrations (37). However, when the rats were fed a phytosterol mixture containing sitostanol, total and LDL cholesterol levels were decreased (37). Similar results have been obtained in rabbits fed increasing amounts of sitostanol (38). A diet supplemented with a 1% phytosterol mixture furnishing 0.01% sitostanol had no impact on total cholesterol

concentrations, whereas a higher concentration (0.8%) of sitostanol was associated with a significant decrease in plasma cholesterol levels (38). These data, along with those observed in rats by Ling and Jones (37) and in hamsters by Ntanios and Jones (22) as well as in the present study, suggest that plant stanols may be more efficient in lowering cholesterolemia in rodents than plant sterols.

In the present study, plasma total cholesterol concentrations were significantly decreased in animals fed fish oil esters of plant sterols compared with animals fed no plant sterols or nonesterified plant sterols. Lower plasma cholesterol concentrations have been reported previously in guinea pigs after consumption of a phytosterol–fish oil conjugate (8). Phytosterols esterified with EPA and DHA also have been shown to decrease total plasma cholesterol in obese, insulin-resistant rats (9). In those studies in guinea pigs and obese rats, however, the control diets did not contain nonesterified plant sterols. The results of the present study, where fish oil–phytosterol esters were compared with nonesterified plant sterols, suggest that plant sterols esterified with EPA and DHA may result in lower plasma cholesterol concentrations than free sterols. On the other hand, the hypocholesterolemic impact of fish oil esters of plant sterols was accompanied by a decrease in HDL cholesterol levels, but the HDL cholesterol/total cholesterol ratio remained unchanged. This may be due in part to the fact that in hamsters, HDL transport a larger proportion of cholesterol than other lipoproteins (39). It is difficult to determine to which extent the decrease in total cholesterol in hamsters fed fish oil–plant sterols in the present experiment may be due to a possible reducing effect of fish oil on total and HDL cholesterol. Studies on the effect of fish oil on lipoprotein metabolism in hamsters have led to inconsistent results, probably because of the great variability in diet composition from one study to another. Whereas decreased total and HDL cholesterol have been reported in hamsters fed relatively high amounts of fish oil (40–42), some studies have shown no lowering effect on total and HDL cholesterol (41,43,44). Other results suggest that a small amount of fish oil, similar to the one supplemented in the present study, may not result in decreased total and HDL cholesterol concentrations in cholesterol-fed hamsters. Indeed, Surette *et al.* (45) reported no impact on total cholesterol with doses of n-3 PUFA ranging from 0–1.9% (w/w diet), and no lowering effect on HDL cholesterol levels with doses of 1.5% or less. It is therefore possible that the improvement in plasma total cholesterol concentrations in hamsters fed plant sterols esterified to fish oil FA is related to another mechanism. It could be hypothesized that a higher bioavailability of esterified sterols compared with nonesterified sterols might be implicated. Indeed, sitosterol concentrations in red blood cells were higher in hamsters fed fish oil esters of plant sterols compared with hamsters fed nonesterified sterols, suggesting that sitosterol may be more bioavailable when supplied as fish oil FA esters than in a free form. However, plasma campesterol concentrations were not increased after supplementation in an esterified form compared with a free form. The absorption of campesterol is known to be higher (10–15%) than that of sitosterol (4–7%) (3). The increased concentrations of sitosterol, but

not campesterol, when supplemented in esterified form may suggest that esterification may increase the bioavailability of plant sterols that are usually absorbed in small proportions, such as sitosterol, and that no further increase may be obtained for plant sterols that are already absorbed in high proportions, such as campesterol. Further investigation is required to determine the impact of the esterification of different plant sterols on their bioavailability.

The decrease in plasma total cholesterol concentrations observed with fish oil esters of plant sterols in the present study was reflected in non-HDL cholesterol concentrations, but this effect was significant only in comparison with nonesterified sterols. In guinea pigs, however, fish oil esters of plant sterols resulted in lower non-HDL cholesterol concentrations than the control diet (8). An increase in LDL cholesterol concentrations attributable to fish oil supplementation has been documented in humans (46,47) and hamsters (33,40,41). It is therefore possible that in the present study, the lowering effect of plant sterols may have been counteracted in part by an increasing effect of fish oil on non-HDL cholesterol. Species differences in cholesterol metabolism may therefore be responsible for the discrepancies between the present study in hamsters and results obtained in guinea pigs and hypertensive rats (8,9). Whether fish oil esters of plant sterols may be efficient in decreasing not only total cholesterol but also LDL cholesterol, without affecting HDL cholesterol concentrations in humans, remains to be determined.

The idea behind the esterification of plant sterols with fish oil FA was to maximize their lipid-lowering effects by combining the hypocholesterolemic properties of plant sterols with the hypotriglyceridemic action of fish oil FA. In the present study, plasma TG concentrations were not significantly decreased in hamsters fed fish oil esters of plant sterols compared with hamsters fed nonesterified sterols. These results may appear to be inconsistent with the significant hypotriglyceridemic effect reported in guinea pigs (8) and insulin-resistant rats (9) fed fish oil–phytosterol conjugates. However, a decrease in triglyceridemia following fish oil supplementation has not been consistently observed in hamsters. Although some studies showed decreased plasma TG concentrations following fish oil feeding (33,41,48,49), other reports did not show a beneficial impact on TG levels (40,42–44). Variations in diet composition may be responsible for some of the discrepancies observed between studies in hamsters. It appears that cholesterol feeding may somewhat counteract the beneficial impact of fish oil on plasma TG concentrations in hamsters. In fact, Kubow *et al.* (44) observed higher plasma TG levels in hamsters fed a fish oil rich in cholesterol compared with a low-cholesterol fish oil, as well as in hamsters fed a low-cholesterol fish oil to which cholesterol was added compared with a low-cholesterol fish oil without added cholesterol. In the present study, hamsters were fed 0.25% cholesterol, whereas guinea pigs supplemented with fish oil–plant sterol esters in the study of Ewart *et al.* (8) and insulin-resistant rats in the study of Russel *et al.* (9) were fed regular low-cholesterol rodent diets. The proportion of fish oil esters of plant sterols in the diets and the quantity of EPA and DHA supplemented may also explain in part the discrepancies between the results obtained in the present study in hamsters and the beneficial effects

observed previously in guinea pigs and insulin-resistant rats (8,9). Indeed, increasing the amount of n-3 FA in the diet of hamsters gradually lowered plasma TG concentrations (50). In the study by Ewart *et al.* (8), the diets fed to guinea pigs contained 25 g/kg of phytosterol–fish oil conjugate, whereas the proportion of fish oil esters in the diet fed to hamsters in the present study was only 17.6 g/kg. It is therefore possible that the quantity of EPA and DHA supplied to hamsters in the present study may have been less than the amount of fish oil FA provided to guinea pigs. Interestingly, Russell *et al.* (9) reported a diminution of plasma TG concentrations in obese, insulin-resistant rats fed 2.6 g/kg body weight of phytosterol–fish oil esters, but no effect was observed on blood lipids when the rats were fed 0.5 g/kg of fish oil esters. Since the fish oil ester preparation contained 55% of EPA and DHA, the dose of fish oil FA supplied to the rats by 2.6 and 0.5 g/kg body weight of fish oil–plant sterol conjugate was 0.28 and 1.43 g/kg body weight, respectively (9). In the present study, hamsters were fed approximately 0.23 g EPA and DHA/kg body weight, given an approximate proportion of EPA and DHA in the fish oil–plant sterol conjugate of 23%, an average daily food consumption of 7 g/d, and an average body weight of 125 g. Therefore, the absence of a significant effect of fish oil esters of plant sterols on plasma TG concentrations in the present experiment is in accordance with the absence of a beneficial impact of the lowest dose of phytosterol–fish oil conjugates (0.28 g EPA and DHA/kg body weight) given to obese rats (9). Although the lipid metabolism in hamsters and obese, insulin-resistant rats may differ, results from these studies suggest that more than 0.2 g of fish oil FA/kg body weight is necessary to induce a hypotriglyceridemic effect in rodents when EPA and DHA are supplied in the form of plant sterol esters.

Compared with cholesterol, which is absorbed in the intestine at 35–70%, plant sterols are poorly absorbed (10–15% for campesterol and campestanol, 4–7% for sitosterol, and 1% for sitostanol) (3). Nevertheless, in humans (51) and rodents (37,52,53), an increased consumption of plant sterols leads to higher levels of plant sterols in plasma. When present in the blood circulation, plant sterols are partly incorporated in red blood cell membranes (10,54). In the present study, campesterol and β-sitosterol concentrations were increased in whole red blood cells of hamsters fed nonesterified sterols and fish oil esters of plant sterols compared with hamsters fed diets containing no added plant sterols. The increase in campesterol concentrations was more pronounced than the increase in β-sitosterol levels, reflecting a higher absorption of campesterol (55). Results from a previous study suggested that the replacement of a part of the cholesterol by plant sterols in red cell membranes may decrease red blood cell deformability and life span in stroke-prone spontaneously hypertensive rats (10). In the present experiment, the amount of plant sterols fed to hamsters (1 g/100 g diet) was higher than the quantity supplemented to hypertensive rats (0.2 g/100 g) (10), and no detrimental effect was observed on red blood cell fragility. A possible explanation might be that spontaneously hypertensive rats suffer from a deficiency of cholesterol in the blood and in cell membranes (10). In these rats, plant sterol supplementation leads to lower cholesterol concentrations in erythrocytes, possibly as a conse-

quence of a higher absorption and incorporation of plant sterols in tissues as a substitute for cholesterol (10). Although plant sterol concentrations were increased in hamsters fed the plant sterols in the present study, the cholesterol content in red blood cells was not affected, suggesting that plant sterols replaced only a very small proportion of cholesterol in the cell membranes. In humans, consumption of a diet rich in plant sterols (1 g/1000 kcal) (25,27) and supplementation of plant sterol esters (54) did not affect red cell fragility. These data, along with the findings of the present experiment, suggest that the results obtained in spontaneously hypertensive rats fed plant sterols cannot be extrapolated to other species or to hyperlipidemic, otherwise healthy humans.

Some studies in rats (11,12) and humans (13–15) have suggested that fish oil FA may decrease CVD risk in part by decreasing osmolar fragility and increasing the deformability of red blood cells. In the present study, we tested for the first time the impact on red cell fragility of fish oil FA in the form of plant sterol esters. The fish oil–plant sterol conjugates did not modify the osmolar fragility of erythrocytes in hamsters. This is in accordance with the results obtained from a previous study in guinea pigs showing no effect of fish oil on red blood cell deformability (56). Another study in humans also has shown no effect of supplementation with up to 6 g/d of EPA and DHA ethyl esters (57). Some species differences may explain the discrepancies between the effects observed in different studies, as well as the form and quantity of n-3 PUFA supplemented.

Hence, EPA and DHA esters of plant sterols decreased plasma total cholesterol concentrations in hamsters, whereas nonesterified sterols did not have such a beneficial impact. No significant hypotriglyceridemic effect was observed after fish oil–plant sterol feeding, maybe because of the low dose of EPA and DHA supplemented and the distinctive characteristics of lipid metabolism in the hamster model. The present data show that these new esters of plant sterols have no detrimental effect on red blood cell fragility. Clinical trials are needed to evaluate the impact of these conjugates on the lipoprotein profile and other health risk parameters in humans.

ACKNOWLEDGMENTS

REFERENCES

1. Fruchart, J.-C., Nierman, M.C., Stroes, E.S.G., Kastelein, J.J.P., and Duriez, P. (2004) New Risk Factors for Atherosclerosis and Patient Risk Assessment, *Circulation 109* (Suppl. III), III15–III19.

2. Stone, N.J., and Van Horn, L. (2002) Therapeutic Lifestyle Change and Adult Treatment Panel III: Evidence Then and Now, *Curr. Atheroscler. Rep. 4*, 433–443.

3. Katan, M.B., Grundy, S.M., Jones, P., Law, M., Miettinen, T., and Paoletti, R. (2003) Efficacy and Safety of Plant Stanols and Sterols in the Management of Blood Cholesterol Levels, *Mayo Clin. Proc. 78*, 965–978.

4. Ostlund, R.E. (2002) Phytosterols in Human Nutrition, *Annu. Rev. Nutr. 22*, 533–549.

5. Harris, W.S. (1997) n-3 Fatty Acids and Serum Lipoproteins: Human Studies, *Am. J. Clin. Nutr. 65* (Suppl.), 1645S–1654S.

6. Harris, W.S. (1997) n-3 Fatty Acids and Serum Lipoproteins: Animal Studies, *Am. J. Clin. Nutr. 65* (Suppl.), 1611S–1616S.

7. Moreau, R.A., Whitaker, B.D., and Hicks, K.B. (2002) Phytosterols, Phytostanols, and Their Conjugates in Foods: Structural Diversity, Quantitative Analysis, and Health-Promoting Uses, *Prog. Lipid Res. 41*, 457–500.

8. Ewart, S.H., Cole, L.K., Kralovec, J., Layton, H., Curtis, J.M., Wright, J.L.C., and Murphy, M.G. (2002) Fish Oil Containing Phytosterol Esters Alters Blood Lipid Profiles and Left Ventricle Generation of Thromboxane A$_2$ in Adult Guinea Pigs, *J. Nutr. 132*, 1149–1152.

9. Russell, J.C., Ewart, S.H., Kelly, S.E., Kralovec, J., Wright, J.L.C., and Dolphin, P.J. (2002) Improvement of Vascular Dysfunction and Blood Lipids of Insulin-Resistant Rats by a Marine Oil-Based Phytosterol Compound, *Lipids 37*, 147–152.

10. Ratnayake, W.M.N., L'Abbé, M.R., Mueller, R., Hayward, S., Plouffe, L., Hollywood, R., and Trick, K. (2000) Vegetable Oils High in Phytosterols Make Erythrocytes Less Deformable and Shorten the Life Span of Stroke-Prone Spontaneously Hypertensive Rats, *J. Nutr. 130*, 1166–1178.

11. Rabbani, P.I., Alam, H.Z., Chirtel, S.J., Duvall, R.E., Jackson, R.C., and Ruffin, G. (2001) Subchronic Toxicity of Fish Oil Concentrates in Male and Female Rats, *J. Nutr. Sci. Vitaminol. (Tokyo) 47*, 201–212.

12. Pöschl, J.M.B., Leray, C., Groscolas, R., Ruef, P., and Linderkamp, O. (1996) Dietary Docosahexaenoic Acid Improves Red Blood Cell Deformability in Rats, *Thromb. Res. 81*, 283–288.

13. Gans, R.O., Bilo, H.J., Weersink, E.G., Rauwerda, J.A., Fonk, T., Popp-Snidjers, C., and Donker, A.J. (1990) Fish Oil Supplementations in Patients with Stable Claudication, *Am. J. Surg. 160*, 490–495.

14. Cartwright, I.J., Pockley, A.G., Galloway, J.H., Greaves, M., and Preston, F.E. (1985) The Effects of Dietary Omega-3 Polyunsaturated Fatty Acids on Erythrocyte Membrane Phospholipids, Erythrocyte Deformability and Blood Viscosity in Healthy Volunteers, *Atherosclerosis 55*, 267–281.

15. Terano, T., Hirai, A., Hamazaki, T., Kobayashi, S., Fujita, T., Tanura, Y., and Kumagai, A. (1983) Effect of Oral Administration of Highly Purified Eicosapentaenoic Acid on Platelet Function, Blood Viscosity and Red Cell Deformability in Healthy Human Subjects, *Atherosclerosis 46*, 321–331.

16. Kris-Etherton, P.M., and Dietschy, J. (1997) Design Criteria for Studies Examining Individual Fatty Acid Effects on Cardiovascular Disease Risk Factors: Human and Animal Studies, *Am. J. Clin. Nutr. 65*, 1590S–1596S.

17. Spady, D.K., Stange, E.F., Bilhartz, L.E., and Dietschy, J.M. (1986) Bile Acids Regulate Hepatic Low-Density Lipoprotein Receptor Activity in the Hamster by Altering Cholesterol Flux Across the Liver, *Proc. Natl. Acad. Sci. USA 83*, 1916–1920.

18. Spady, D.K., Turley, S.D., and Dietschy, J.M. (1985) Rates of Low-Density Lipoprotein Uptake and Cholesterol Synthesis Are Regulated Independently in the Liver, *J. Lipid Res. 26*, 465–472.

19. Burstein, M., Scholnick, H.R., and Morfin, R.V. (1970) Rapid Method for the Isolation of Lipoproteins from Human Serum by Precipitation with Polyanions, *J. Lipid Res. 11*, 583–595.

20. Friedewald, W.T., Levy, R.I., and Fredrickson, D.S. (1972) Estimation of the Concentration of Low-Density Lipoprotein Cholesterol in Plasma, Without Use of the Preparative Ultracentrifuge, *Clin. Chem. 18*, 499–502.

21. Kohlmeier, M. (1986) Direct Enzymic Measurement of Glycerides in Serum and in Lipoprotein Fractions, *Clin. Chem. 32* (1, Pt. 1), 63–66.

22. Ntanios, F.Y., and Jones, P.J.H. (1998) Effects of Variable Dietary Sitostanol Concentrations on Plasma Lipid Profile and Phytosterol Metabolism in Hamsters, *Biochim. Biophys. Acta 1390*, 237–244.

23. Lütjohann, D., Meese, C.O., Crouse, J.R., III, and von Bergmann,

K. (1993) Evaluation of Deuterated Cholesterol and Deuterated Sitostanol for Measurement of Cholesterol Absorption in Humans, *J. Lipid Res. 34*, 1039–1046.

24. Naito, Y., Konishi, C., and Ohara, N. (2000) Blood Coagulation and Osmolar Tolerance of Erythrocytes in Stroke-Prone Spontaneously Hypertensive Rats Given Rapeseed Oil or Soybean Oil as the Only Dietary Fat, *Toxicol. Lett. 117*, 209–215.

25. Jenkins, D.J.A., Kendall, C.W.C., Faulkner, D., Vidgen, E., Trautwein, E.A., Parker, T.L., Marchie, A., Koumbridis, G., Lapsley, K.G., Josse, R.G., *et al.* (2002) A Dietary Portfolio Approach to Cholesterol Reduction: Combined Effects of Plant Sterols, Vegetable Proteins, and Viscous Fibers in Hypercholesterolemia, *Metabolism 51*, 1596–1604.

26. Jenkins, D.J., Kendall, C.W., Marchie, A., Faulkner, D., Vidgen, E., Lapsley, K.G., Trautwein, E.A., Parker, T.L., Josse, R.G., Leiter, L.A., *et al.* (2003) The Effect of Combining Plant Sterols, Soy Protein, Viscous Fibers, and Almonds in Treating Hypercholesterolemia, *Metabolism 52*, 1478–1483.

27. Jones, P.J., Raeini-Sarjaz, M., Jenkins, D.J.A., Kendall, C.W., Vidgen, E., Trautwein, E.A., Lapsley, K.G., Marchie, A., Cunnane, S.C., and Connelly, P.W. (2005) Effects of a Diet High in Plant Sterols, Vegetable Proteins and Viscous Fibers (dietary portfolio) on Circulating Sterol Levels and Red Cell Fragility in Hypercholesterolemic Subjects, *Lipids 40*, 169–174.

28. De Jong, A., Plat, J., and Mensink, R.P. (2003) Metabolic Effects of Plant Sterols and Stanols (review), *J. Nutr. Biochem. 14*, 362–369.

29. Plat, J., and Mensink, R.P. (2002) Increased Intestinal ABCA1 Expression Contributes to the Decrease in Cholesterol Absorption After Plant Stanol Consumption, *FASEB J. 16*, 1248–1253.

30. Dietschy, J.M., Turley, S.D., and Spady, D.K. (1993) Role of Liver in the Maintenance of Cholesterol and Low Density Lipoprotein Homeostasis in Different Animal Species, Including Humans, *J. Lipid Res. 34*, 1637–1659.

31. Goulinet, S., and Chapman, M.J. (1993) Plasma Lipoproteins in the Golden Syrian Hamster (*Mesocricetus auratus*): Heterogeneity of ApoB- and ApoA-I-Containing Partcles, *J. Lipid Res. 34*, 943–959.

32. Sicart, R., Sable-Amplis, R., and Guiro, A. (1984) Comparative Studies of the Circulating Lipoproteins in Hamster (*Mesocricetus auratus*) with a Normal or Spontaneous High Level of Cholesterol in the Plasma, *Comp. Biochem. Physiol. 78A*, 511–514.

33. Ntanios, F.Y., MacDougall, D.E., and Jones, P.J.H. (1998) Gender Effects of Tall Oil Versus Soybean Phytosterols as Cholesterol-Lowering Agents in Hamsters, *Can. J. Physiol. Pharmacol. 76*, 780–787.

34. Meijer, G.W., Bressers, M.A., de Groot, W.A., and Rudrum, M. (2003) Effect of Structure and Form on the Ability of Plant Sterols to Inhibit Cholesterol Absorption in Hamsters, *Lipids 38*, 713–721.

35. Trautwein, E.A., Schulz, C., Rieckhoff, D., Kunath-Rau, A., Erbersdobler, H.F., de Groot, W.A., and Meijer, G.W. (2002) Effect of Esterified 4-Desmethylsterols and -Stanols or 4′,4′-Dimethylsterols on Cholesterol and Bile Acid Metabolism in Hamsters, *Br. J. Nutr. 87*, 227–237.

36. Wang, Y.W., Jones, P.J.H., Pischel, I., and Fairow, C. (2003) Effects of Policosanols and Phytosterols on Lipid Levels and Cholesterol Biosynthesis in Hamsters, *Lipids 38*, 165–170.

37. Ling, W.H., and Jones, P.J.H. (1995) Enhanced Efficacy of Sitostanol-Containing Versus Sitostanol-Free Phytosterol Mixtures in Altering Lipoprotein Cholesterol Levels and Synthesis in Rats, *Atherosclerosis 118*, 319–331.

38. Ntanios, F.Y., Jones, P.J.H., and Frohlich, J.J. (1998) Dietary Sitostanol Reduces Plaque Formation but Not Lecithin Cholesterol Acyl Transferase Activity in Rabbits, *Atherosclerosis 138*, 101–110.

39. Sessions, V.A., and Salter, A.M. (1994) The Effects of Different Dietary Fats and Cholesterol on Serum Lipoprotein Concentrations in Hamsters, *Biochim. Biophys. Acta 1211*, 207–214.

40. de Silva, P.P., Agarwal-Mawal, A., Davis, P.J., and Cheema, S.K. (2005) The Levels of Plasma Low Density Lipoprotein Are Independent of Cholesterol Ester Transfer Protein in Fish-Oil Fed FIB

Hamsters, *Nutr. Metab. 2*, 8.

41. Lu, S.-C., Lin, M.-H., and Huang, P.-C. (1996) A High Cholesterol, (n-3) Polyunsaturated Fatty Acid Diet Induces Hypercholesterolemia More Than a High Cholesterol, (n-6) Polyunsaturated Fatty Acid Diet in Hamsters, *J. Nutr. 126*, 1759–1765.

42. Spady, D.K., Horton, J.D., and Cuthbert, J.A. (1995) Regulatory Effects of n-3 Polyunsaturated Fatty Acids on Hepatic LDL Uptake in the Hamster and Rat, *J. Lipid Res. 36*, 1009–1020.

43. Valeille, K., Gripois, D., Blouquit, M.-F., Souidi, M., Riottot, M., Bouthegourd, J.-C., Sérougne, C., and Marint, J.-C. (2004) Lipid Atherogenic Risk Markers Can Be More Favourably Influenced by the *cis*-9,*trans*-11-Octadecadienoate Isomer Than a Conjugated Linoleic Acid Mixture or Fish Oil in Hamsters, *Br. J. Nutr. 91*, 191–199.

44. Kubow, S., Goyette, N., Kermasha, S., Stewart-Phillip, J., and Koski, K.G. (1996) Vitamin E Inhibits Fish Oil-Induced Hyperlipidemia and Tissue Lipid Peroxidation in Hamsters, *Lipids 31*, 839–847.

45. Surette, M.E., Whelan, J., Broughton, K.S., and Kinsella, J.E. (1992) Evidence for Mechanisms of the Hypotriglyceridemic Effect of n-3 Polyunsaturated Fatty Acids, *J. Lipid Res. 33*, 263–271.

46. Rivellese, A.A., Maffettone, A., Vessby, B., Uusitupa, M., Hermansen, K., Berglund, L., Louheranta, A., Meyer, B.J., and Riccardi, G. (2003) Effects of Dietary Saturated, Monounsaturated and n-3 Fatty Acids on Fasting Lipoproteins, LDL Size and Postprandial Lipid Metabolism in Healthy Subjects, *Atherosclerosis 167*, 149–158.

47. Harris, W.S. (1996) n-3 Fatty Acids and Lipoproteins: Comparisons of Results from Human and Animal Studies, *Lipids 31*, 243–252.

48. Field, F.J., Born, E., and Mathur, S.N. (2003) Fatty Acid Flux Suppresses Fatty Acid Synthesis in Hamster Intestine Independently of SREBP-1 Expression, *J. Lipid Res. 44*, 1199–1208.

49. Berr, F., Goetz, A., Schreiber, E., and Paumgartner, G. (1993) Effect of Dietary n-3 Versus n-6 Polyunsaturated Fatty Acids on Hepatic Excretion of Cholesterol in the Hamster, *J. Lipid Res. 34*, 1275–1284.

50. Surette, M.E., Whelan, J., Broughton, K.S., and Kinsella, J.E. (1992) Evidence for Mechanisms of the Hypotriglyceridemic Effect of n-3 Polyunsaturated Fatty Acids, *Biochim. Biophys. Acta 1126*, 199–205.

51. Weststrate, J.A., and Meijer, G.W. (1998) Plant Sterol-Enriched Margarines and Reduction of Plasma Total- and LDL-Cholesterol Concentrations in Normocholesterolaemic and Mildly Hypercholesterolaemic Subjects, *Eur. J. Clin. Nutr. 52*, 334–343.

52. Hassan, A.S., and Rampone, A.J. (1979) Intestinal Absorption and Lymphatic Transport of Cholesterol and β-Sitostanol in the Rat, *J. Lipid Res. 20*, 646–653.

53. Ntanios, F.Y., van de Kooij, A.J., de Deckere, E.A.M., Duchateau, G.S.M.J.E., and Trautwein, E.A. (2003) Effects of Various Amounts of Dietary Plant Sterol Esters on Plasma and Hepatic Sterol Concentration and Aortic Foam Cell Formation of Cholesterol-Fed Hamsters, *Atherosclerosis 169*, 41–50.

54. Hendriks, H.F.J., Brink, E.J., Meijer, G.W., Princen, H.M.G., and Ntanios, F.Y. (2003) Safety of Long-Term Consumption of Plant Sterol Esters-Enriched Spread, *Eur. J. Clin. Nutr. 57*, 681–692.

55. Heinemann, T., Axtmann, G., and von Bergmann, K. (1993) Comparison of Intestinal Absorption of Cholesterol with Different Plant Sterols in Man, *Eur. J. Clin. Invest. 23*, 827–831.

56. Pöschl, J.M.B., Paul, K., Leischenring, M., Han, S.R., Pfisterer, M., Bremer, H.J., and Linderkamp, O. (1999) Effects of Dietary Supplementation of Saturated Fatty Acids and n-6 or n-3 Polyunsaturated Fatty Acids on Plasma and Red Blood Cell Membrane Phospholipids and Deformability in Weanling Guinea Pigs, *Lipids 34*, 467–473.

57. Blonk, M.C., Bilo, H.J., Nauta, J.J., Popp-Snijders, C., Mulder, C., and Donker, A.J. (1990) Dose–Response Effects of Fish-Oil Supplementation in Healthy Volunteers, *Am. J. Clin. Nutr. 52*, 120–127.

Distribution of 22:6n-3 Newly Synthesized from 18:3n-3 into Glycerolipid Classes from Tissues of Rainbow Trout (*Oncorhynchus mykiss*)

Michael V. Bell* and James R. Dick

Institute of Aquaculture, Faculty of Natural Sciences, University of Stirling, Stirling FK9 4LA, Scotland, United Kingdom

ABSTRACT: The distribution of D_5-22:6n-3 following ingestion of a pulse of D_5-18:3n-3 was measured quantitatively by GC–negative chemical ionization MS in lipid classes from liver, cecal mucosa, and brain from rainbow trout to further our understanding of the processes determining accretion and turnover of 22:6n-3 in fish. The accretion of D_5-22:6n-3 was expressed in two ways, as percent enrichment and as ng D_5-22:6n-3/µg 22:6n-3/mg D_5-18:3n-3 eaten. In cecal mucosa at 2 d post-dose, PC was the most enriched lipid class followed by PE and then TAG. Enrichment fell in all lipid classes in cecal mucosa from 2 to 7 d post-dose of D_5-18:3n-3. In liver, PC was also the most enriched lipid class at 2 d, but in this tissue all lipid classes were more enriched in D_5-22:6n-3 by 7 d. When expressed in terms of the 22:6n-3 content of the different lipid classes, TAG became relatively less important in cecal mucosa and more important in liver. Over a time course of 3 to 35 d, the percent enrichment of D_5-22:6n-3 in liver peaked at 7 d in PC, PE, PS, and PI and fell rapidly in TAG from 3 d. PC from liver was the most enriched lipid class at 3 and 7 d, and thereafter PE was the most enriched lipid class. However, TAG had the highest specific activity at all times except 7 d. In brain, the enrichment of D_5-22:6n-3 was very low in all lipid classes at 3 d and increased progressively to 35 d with PC and PE similarly enriched. TAG from brain had the highest specific activity at all times. This study is the first to present quantitative information on rates of accretion and depletion of newly synthesized 22:6n-3 into the main lipid classes of fish tissues.

Paper no. L9486 in *Lipids 40*, 703–708 (July 2005).

There is little information in the literature describing quantitatively the metabolism of PUFA at the whole-animal level, including the partitioning of newly synthesized or ingested PUFA between different tissues and lipid classes. Consequently, it is not possible to model the fate of dietary PUFA, which is a major problem in our understanding of the metabolic interactions between n-3 and n-6 PUFA and the importance of dietary C_{18} vs. C_{20} and C_{22} PUFA. Stable isotope studies are now beginning to address these issues.

We have previously described a method for measuring quantitatively the conversion of 18:3n-3 to 22:6n-3 in fish using a deuterated tracer and GC–negative chemical ionization (CI) MS (1). In rainbow trout fed a diet containing 18:3n-3 as the only n-3 PUFA, conversion of 18:3n-3 to 22:6n-3 was slow, and whole-body accumulation of newly synthesized 22:6n-3 peaked at 4.3 µg/g fish/mg 18:3n-3 eaten after 14 d (1). The amount of newly synthesized 22:6n-3 peaked in liver at 7 d and in brain and eyes at 24 d; in visceral and eye socket adipose tissue it plateaued after 14 d (1). The capacity to synthesize 22:6n-3 from 18:3n-3 changed rapidly during early development in trout (2). First-feeding trout of *ca.* 0.2 g weight gave an initial rate of 5.4 µg 22:6n-3/g fish/mg 18:3n-3 eaten/7 d, which increased rapidly to *ca.* 50 µg 22:6n-3/g fish/mg 18:3n-3 eaten/7 d at around 1 g weight, then declined rapidly to *ca.* 12 µg 22:6n-3/g fish/mg 18:3n-3 eaten/7 d at 2 g weight and continued to fall thereafter (2). Using the same methodology, we showed that, at 2 d post-dose of D_5-18:3n-3, pyloric ceca contained a higher concentration of newly synthesized D_5-22:6n-3 than liver, indicating that pyloric ceca was capable of PUFA synthesis (3). This has since been confirmed directly using fish enterocytes (4).

Few studies have examined the deposition of 22:6n-3 newly synthesized from 18:3n-3 in different phospholipid classes from different tissues. In trout hepatocytes incubated with 1-[14]C-18:3n-3 or 1-[14]C-20:5n-3 for 3 h, 22:6n-3 was the major product PUFA from both substrates and TAG was the major labeled lipid class followed by PC (5). Turbot injected with 1-[14]C 22:6n-3 showed the greatest accumulation of label in PC after 48 h, followed by PE, TAG, and sterol ester (6). Turbot brain cells incubated with 1-[14]C-22:6n-3 for 6 h accumulated 22:6n-3 mainly in PC, followed by PE, with very little in PS or PI (7).

This study was undertaken to obtain quantitative information on the partitioning of newly synthesized 22:6n-3 into lipid classes from three tissues in juvenile rainbow trout after feeding a pulse of D_5-18:3n-3. Liver and cecal mucosa were chosen as tissues synthesizing 22:6n-3 and, over a longer time period, liver was compared with brain, a tissue with a high requirement for 22:6n-3.

MATERIALS AND METHODS

Chemicals. Chloroform, methanol, ethanol, acetic acid, isohexane, and diethyl ether were HPLC grade from Fisher (Loughborough, Leicestershire, United Kingdom). Diisopropylamine, anhydrous acetonitrile, and pentafluorobenzyl (PFB) bromide were obtained from Aldrich (Gillingham, Dorset, United King-

dom). D$_5$(17,17,18,18,18)-linolenic acid was purchased from Cambridge Isotope Laboratories (Andover, MA) as the fatty acid ethyl ester (FAEE). Heneicosatetraenoic acid (Δ6,9,12,15-21:4) ethyl ester was prepared by a one-carbon addition to 20:4n-6 FA (8). All other chemicals were from Sigma (Poole, Dorset, United Kingdom). TLC plates were from Merck (VWR International Ltd., Poole, Dorset, United Kingdom).

Fish and diets. Rainbow trout were obtained from a commercial hatchery and kept in a running freshwater aquarium at ambient temperature (3.5 to 16.5°C) on a 14 h/10 h light/dark cycle. Fish were fed a diet based on casein and a blend of vegetable oil containing predominantly oleic acid with 18:2n-6 and 18:3n-3 at approximately 1% each, this to maximize 22:6n-3 synthesis and satisfy the fishes' EFA requirements. The full composition of the diet was described previously (1). The final diet provided 50% crude protein and 11% oil blended to give, as a percentage of the final diet, 0.99% 18:2n-6, 1.02% 18:3n-3, and 0.12% highly unsaturated FA (20:5n-3 and 22:6n-3) from the fish meal, which was added to make the diet palatable and readily accepted by the fish. The remaining FA were predominantly 16:0 (1.02%) and 18:1n-9 (7.18%). Fish from the longer time course (up to 35 d) weighed 5.6 ± 1.0 g at the start of the experiment and had been reared on the experimental diet for 8 wk before feeding tracer (1). Fish from the shorter time course had been on the experimental diet for 34 wk and weighed 60.1 ± 11.3 g (3).

Preparation of labeled diet. A small portion of diet containing D$_5$-18:3n-3 FAEE and 21:4n-6 FAEE was prepared as follows. An oil sample containing 10 mg D$_5$-18:3n-3 FAEE, 2.5 mg 21:4n-6 FAEE, 153 mg of high oleic acid sunflower oil, and 61 μg antioxidant was dissolved in 0.82 mL of isohexane, and 1.335 g of dry diet mix was added. The isohexane was then removed at 37°C under nitrogen and the diet desiccated *in vacuo* for 18 h. The diet was mixed thoroughly, then 0.95 mL water added and mixed to a stiff paste. This was extruded through a 1-mL disposable syringe, dried at room temperature for 2–3 h and cut into 3–4 mm lengths. The diet was stored under argon at −20°C and was used within 3 d. The 21:4n-6 FAEE was added to diets as a marker since it is much less readily catabolized than 18:3n-3 and therefore gives a higher recovery, enabling more precise determination of the amount of labeled diet eaten by individual fish (1).

Experimental protocol. Groups of fish were acclimated in a 100-L circular tank with running water for at least 4 d before starting an experiment. They were then fed the labeled diet, all of which was observed to be eaten, and fed the normal unlabeled diet daily until sampled. The temperature ranged from 9.0 to 16.0°C during the experiments.

The fish were weighed and individual tissues dissected for analysis as described earlier (1,3). Samples were homogenized in chloroform/methanol 2:1 (vol/vol) using a Potter or Ultra-Turrax homogenizer and an extract was prepared according to Folch *et al.* (9). Tritricosanoyl glycerol (tri23:0) standard was added to each tissue sample before homogenization. Samples were kept on ice under nitrogen during workup and were stored at −20°C under argon.

Preparation of lipid classes. PC, PS, PI, PE, and TAG were prepared from 1 mg of total lipid by TLC (20 × 20 cm, silica gel 60, Merck no. 5721 plates) in methyl acetate/chloroform/propan-2-ol/methanol/0.25% (by wt) KCl (25:25:25:10:9, by vol). The plates were dried *in vacuo* for 30 min and redeveloped in isohexane/diethyl ether/acetic acid (80:20:1, by vol) to separate TAG. The dried plates were then sprayed with 0.1% (wt/vol) 2,7-dichlorofluorescein in 97% (by vol) methanol and the lipid bands visualized under UV light. Bands were scraped from the plates into stoppered test tubes and the lipids saponified *in situ*.

Quantification of FA. Lipid samples were saponified with 2 mL of 0.1 M KOH in 95% (by vol) ethanol under argon for 1 h at 78°C in the presence of 17:0 internal standard to quantify unlabeled FA. Tri23:0 was added to the phospholipid classes to quantify D$_5$-FA. Saponified samples were then diluted with 5 mL of water, acidified, and the FFA extracted with diethyl ether. PFB esters were then prepared using acetonitrile/diisopropylamine/PFB bromide (1000:10:1, by vol) at 60°C for 30 min under nitrogen (12). Excess reagent and solvent were removed under nitrogen and samples dissolved in isohexane and stored at −20°C under argon until analyzed.

Calibration standards of individual FA (18:3n-3, 21:4n-6, and 22:6n-3) with 23:0 were prepared by varying the amount of each FA while keeping the 23:0 constant and plotting the peak area ratio against the mass ratio of the different FA. Sample volumes for analysis were adjusted such that the amount of 23:0 injected onto the gas chromatograph–mass spectrometer (GC–MS) was constant. PFB esters were chromatographed and quantified on a Fisons MD 800 GC–MS fitted with an on-column injector and a ZB wax column (60 m × 0.32 mm i.d., 0.25 μm film thickness; Phenomenex, Macclesfield, Cheshire, United Kingdom), using helium as carrier gas (column head pressure 20 psi) and running in negative CI mode with methane as reagent gas (pressure 7 psi). The temperature program was 80–240°C at 40°C/min, then 240°C for 50 min. FA were identified by selective ion scanning for the required masses using a dwell time of 80 ms and cycle time of 20 ms, and quantified by reference to the appropriate FA calibration curve. Calibration curves were run before and after each batch of samples to check the performance of the electron source.

FA analysis of PFB esters was performed on a Thermo Finnigan Trace GC fitted with an electron capture detector, a split injector (1:10 split ratio) (Thermo Finnigan, Hemel Hempstead, Herts, United Kingdom), and a ZB Wax column (30 m × 0.25 mm i.d., 0.25 μm film thickness) (Phenomenex) using helium as carrier gas at a constant flow rate of 2 mL/min. The temperature was programmed from 110 to 240°C at 20°C/min then held at 240°C for 25 min.

Quantification of lipid classes. Lipid classes were resolved by double-development high-performance TLC (HPTLC; 10 × 10 cm, silica gel 60, Merck no. 5633 plates) using the two solvent systems given earlier (10). After chromatography, plates were dried, sprayed with 3% (wt/vol) cupric acetate in 8% (by vol) phosphoric acid (11), and charred at 160°C for 15 min. Quantification was performed using a Camag TLC scanner 3 (VWR International Ltd.).

Statistical analysis. Sample means were compared using either one-way ANOVA or a paired *t*-test using GraphPad Prism® (San Diego, CA).

RESULTS

PC was the most enriched lipid class in cecal mucosa at all times, with a peak enrichment of 0.1922% at 2 d falling to half this level by 7 d (Fig. 1A). PE was the next most enriched lipid class in cecal mucosa (0.0682% enrichment at 5 d) with low enrichments in TAG, PI, and PS (Fig. 1A). Liver showed the opposite pattern of D_5-22:6n-3 accretion. Enrichments were higher at 7 d than 2 d in all lipid classes from liver (Fig. 1B). In liver, PC was again the most enriched lipid class at all times, but levels increased more than fivefold between 2 and 7 d (0.4053% enrichment at 7 d) (Fig. 1B). Liver PE and TAG showed a large increase between 2 and 7 d (6- and 12-fold, respectively). Amounts of D_5-22:6n-3 in PS and PI, although increasing from 2 to 7 d, were low (Fig. 1B).

When the results are expressed as the amount of D_5-22:6n-3 relative to the content of 22:6n-3 in each lipid class, the pattern of distribution within the different lipid classes changes owing to the contribution of each lipid class to the total lipid class pool and the concentration of 22:6n-3 in that lipid class. The unit ng D_5-22:6n-3/µg 22:6n-3/mg D_5-18:3n-3 eaten is analogous to the term *specific activity* used with radioisotopes, with a correction to account for the different amounts of tracer eaten by individual fish. When expressed in terms of 22:6n-3 content, the differences between phospholipid classes were less marked in cecal mucosa (Fig. 2A). The contribution of TAG also becomes less important because this is the major lipid class in cecal mucosa. PC showed the highest specific activity (5.57 ng D_5-22:6n-3/µg 22:6n-3/mg D_5-18:3n-3 eaten at 2 d), PE and PI were similar, and PS and TAG much lower (Fig.2A). The low content of 22:6n-3 in TAG from liver meant that the specific activity of TAG was higher than that of the four phospholipid classes at all times (Fig. 2B).

Over the longer time course to 35 d, PC was again the main site of deposition of newly synthesized D_5-22:6n-3 in liver with the percent enrichment increasing rapidly from 3 to 7 d to peak

FIG. 1. The percent enrichment of D_5–22:6n-3 in lipid classes from cecal mucosa (A) and liver (B) 2 to 7 d post-feeding D_5-18:3n-3. Bars represent mean ± SD, *n* = 4 for day 2 and *n* = 3 for days 5 and 7. Comparison of day 2 liver vs. day 2 cecal mucosa gave *P* = 0.0253 for PS and *P* = 0.0065 for PI (paired Student *t*-test).
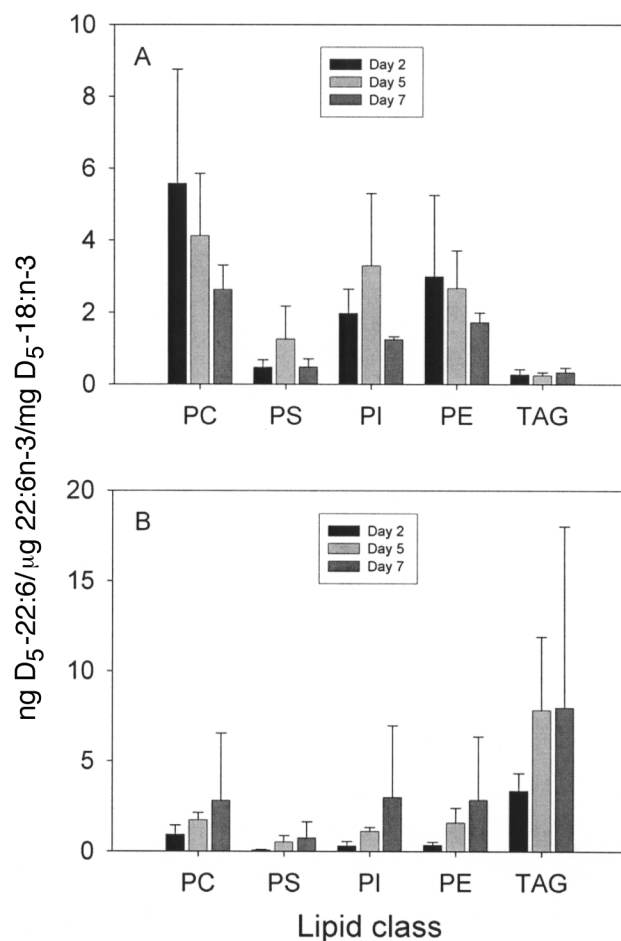
FIG. 2. The distribution of D_5-22:6n-3 in lipid classes from cecal mucosa (A) and liver (B) 2 to 7 d post-feeding D_5-18:3n-3 expressed as ng D_5-22:6n-3/µg 22:6n-3/mg D_5-18:3n-3 eaten. Bars represent mean ± SD, *n* = 4 for day 2 and *n* = 3 for days 5 and 7. Comparison of day 2 cecal mucosa vs. day 2 liver gave *P* = 0.0495 for PC, *P* = 0.0265 for PS, *P* = 0.0232 for PI, and *P* = 0.0082 for TAG (paired Student *t* test).

at 0.2047% then falling steadily to 35 d (Fig. 3A). PE was the next most enriched lipid class in liver, plateauing at 0.061–0.077% enrichment between 7 and 24 d (Fig. 3A). Very little D_5-22:6n-3 was found in PS and PI from liver (<0.0087 and <0.0049%, respectively), but the pattern of accumulation was similar to PE, peaking between 7 and 24 d (Fig. 3A). In TAG, peak enrichment in D_5-22:6n-3 was at 3 d (0.0212%), about one-third the level in PC at that time, and fell steadily to 35 d (Fig. 3A). By 35 d the percent enrichments in PC and PE were very similar and those in PS, PI, and TAG about tenfold lower (Fig. 3A).

In brain, very little D_5-22:6n-3 was present at 3 d in any lipid class (Fig. 3B). D_5-22:6n-3 accumulated in PC and PS up to 35 d (0.0204 and 0.0060% enrichment, respectively) and plateaued in PE and TAG around 14 to 35 d (peaks of 0.0210 and 0.0072% enrichment, respectively) (Fig. 3B). Thus, PC and PE were equally enriched by 35 d, with much lower amounts of D_5-22:6n-3 in PS and TAG. Very little D_5-22:6n-3

was found in PI throughout the time course, peaking at 0.0008% enrichment at 35 d (Fig. 3B).

TAG had the highest specific activity of incorporated D_5-22:6n-3 in liver (24.0 ng D_5-22:6n-3/μg 22:6n-3/mg D_5-18:3n-3 eaten at 3 d) owing to the low content of 22:6n-3 (2.9 mol%) (Fig. 4A). PC and PE, with the highest 22:6n-3 contents (23.0 and 27.3 mol%, respectively), become relatively less important with peaks of 21.5 and 12.8 ng D_5-22:6n-3/μg 22:6n-3/mg D_5-18:3n-3 eaten, respectively, at 7 d (Fig. 4A). PS and PI also become more important relative to PC and PE owing to their smaller contributions to the lipid class pool and lower 22:6n-3 content (6.3% in the case of PI). The low amount of 22:6n-3 in TAG from brain (5.5 mol%) compared with PC, PS, and PE (22.7, 34.2, and 32.2 mol%, respectively) gave TAG the highest specific activity at all time points in brain, and markedly so from 14 d onward (Fig. 4B). Within the phospholipid classes
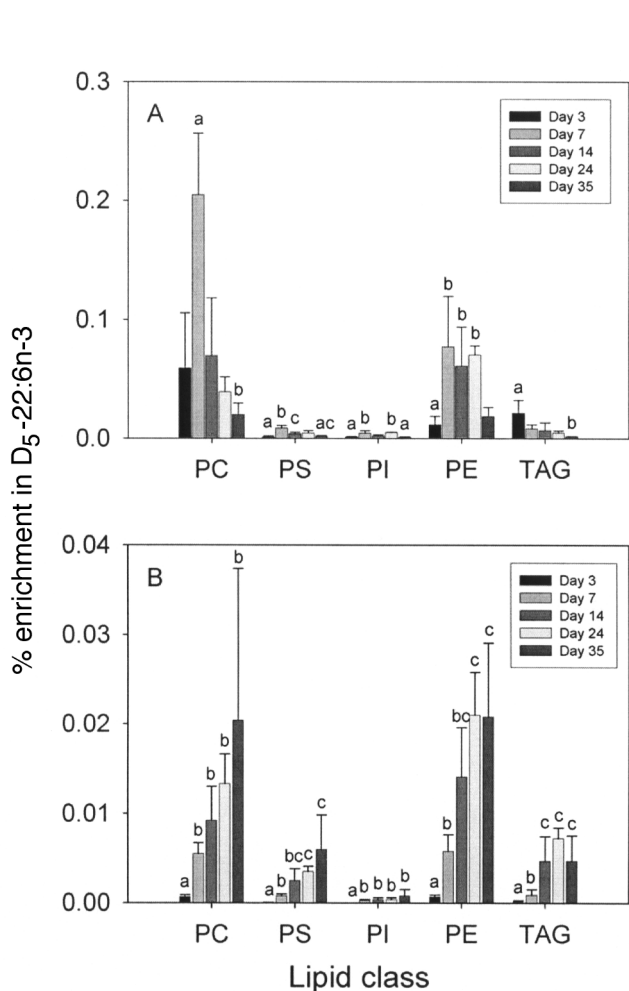
FIG. 3. The percent enrichment of D_5-22:6n-3 in lipid classes from liver (A) and brain (B) 3 to 35 d post-feeding D_5-18:3n-3. Mean ± SD, $n = 5$ for day 3, $n = 4$ for day 7, $n = 5$ for day 14, $n = 3$ for day 24, and $n = 4$ for day 35. One-way ANOVA gave differences for liver of $P = 0.0038$ for PC, $P < 0.0001$ for PS and PI, $P = 0.0002$ for PE, and $P < 0.0007$ for TAG, and for brain of $P < 0.0001$ for PC, PS, PI, PE, and TAG. Different superscripts within classes represent differences significant at $P < 0.01$.
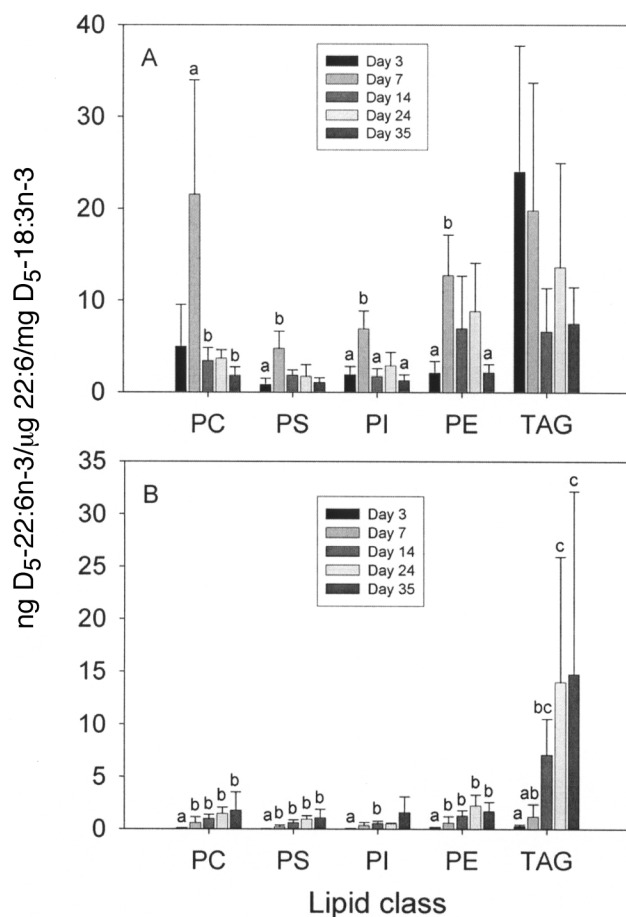
FIG. 4. The distribution of D_5-22:6n-3 in lipid classes from liver (A) and brain (B) 3, 7, 14, 24, and 35 d post-dose of D_5-18:3n-3 presented as ng D_5-22:6n-3/μg 22:6n-3/mg D_5-18:3n-3 eaten. Mean ± SD, $n = 5$ for day 3, $n = 4$ for day 7, $n = 5$ for day 14, $n = 3$ for day 24, and $n = 4$ for day 35. One-way ANOVA gave differences for liver of $P < 0.0007$ for PC, $P = 0.0036$ for PS, $P = 0.0017$ for PI, $P = 0.0010$ for PE, and $P = 0.1757$ for TAG, and for brain of $P < 0.0001$ for PC, PS, PE, and TAG and $P = 0.0098$ for PI. Different superscripts within classes represent differences significant at $P < 0.01$.

from brain, the specific activities of D_5-22:6n-3 were similar throughout the time course (Fig. 4B).

DISCUSSION

In the present study, we examined the distribution of D_5-22:6n-3 in the main lipid classes from three tissues of juvenile trout following ingestion of a pulse of D_5-18:3n-3. The FA compositions of the rearing diet and the diet containing the D_5-18:3n-3 tracer were identical, so the fish were under steady-state conditions with respect to dietary FA intake throughout the pre-experimental and experimental periods. Liver and ceca were examined as tissues involved in 22:6n-3 synthesis, and brain as a tissue with a high requirement for this PUFA (13). A number of factors influence the kinetics of PUFA metabolism and distribution of PUFA within tissues and lipid classes, including the lipid form in which FA tracer is supplied, the route of uptake (ingestion or injection), the nutrient and physiological status of the organism, and developmental stage. The substrate for the desaturases and elongases may be esterified FA, which could influence accretion in different lipid classes. In plants it is well established that FA esterified to PC is the main substrate rather than acyl CoA (14), and a Δ-5 desaturase from rat liver uses *sn*-2 esterified PUFA of lecithin (15). When comparing studies on fish and mammals, other factors are also significant, including slower metabolic processes in poikilotherms, different absolute and relative requirements for n-3 and n-6 PUFA, and gut as well as liver being an important site of 22:6n-3 synthesis in salmonid fish.

Over a short time course of up to 7 d, the distributions of D_5-22:6n-3 in lipid classes from cecal mucosa and liver were very different. Peak accretion of D_5-22:6n-3 was at 2 d in all lipid classes in cecal mucosa whereas, in liver, D_5-22:6n-3 increased in all lipid classes from 2 to 7 d. PC was much more enriched than TAG in cecal mucosa. The amount of D_5-22:6n-3 in PI from cecal mucosa was unexpected since this PUFA is not accumulated in PI to any great extent (e.g., Ref. 16) but it was turned over at a similar rate to PE. In liver, PC was the predominant site of D_5-22:6n-3 accretion, with TAG becoming increasingly important by 7 d, though the large scatter in day 7 data makes interpretation difficult. In trout hepatocytes incubated with ^{14}C-18:3n-3, TAG was the major labeled lipid class at 3 h followed by PC (5).

Liver and cecal mucosa therefore appear to be processing 22:6n-3 in different ways. Gut cells have a high turnover, and therefore substantially more PUFA may be required for local use in this tissue than in liver, which has a major role in the synthesis of PUFA for the whole organism. The increase in D_5-22:6n-3 in liver TAG is suggestive of 22:6n-3 for export, but it is possible that 22:6n-3 is exported from liver, and especially from ceca, as PC or is converted to lysophosphatidylcholine (LPC) (17). Rat liver can secrete large amounts of LPC, which is bound to albumin in the blood, and LPC is often the second most abundant phospholipid in plasma (18). A major proportion of the FA in rat LPC was PUFA (18). It was concluded that LPC may be an important delivery system for PUFA and choline to other tissues (18).

The percent enrichment of D_5-22:6n-3 up to 7 d in the four phospholipid classes from liver was similar over the short and long time courses. The amount of D_5-22:6n-3 fell in all lipid classes from liver from 7 d onward, the decrease being most marked in PC indicating a more rapid turnover of this lipid class. The main differences between the two time courses was that the D_5-22:6n-3 content of TAG fell from 3 d over the long time course whereas it increased from 2 to 7 d over the short time course. This difference may be due to the size of the fish in the two experiments (5.6 g increasing to 10.4 g, long time course, *ca*. 60 g, short time course) with the former group growing rapidly with an increasing lipid pool.

PC and PE from brain were similarly enriched in D_5-22:6n-3 throughout the time course, and by 35 d the specific activity of all four phospholipid classes from brain was similar. TAG from brain showed by far the highest specific activity of D_5-22:6n-3 and therefore turnover of 22:6n-3. The phospholipids in liver were more enriched than their counterparts in brain at 7 d by 10- to 20-fold. A study by Lagarde *et al.* (19) concluded that LPC may be the preferred physiological carrier of 22:6n-3 to the brain. If the blood–brain barrier in fish is similar to that in mammals with respect to FA transport, then 22:6n-3 is probably entering as FFA or LPC and is then incorporated into brain phospholipids, either by deacylation-reacylation reactions or by synthesis of the entire phospholipid *de novo*. The rapid accretion of newly synthesized 22:6n-3 in TAG from brain is therefore rather surprising and underlines our lack of knowledge of these processes in fish brain.

The essentiality of 22:6n-3 in neural tissues is largely imparted by DHA-enriched aminophospholipids, and the brain of rainbow trout contains large amounts of 22:6n-3, much of it as di22:6n-3 molecular species of phospholipids (20). However, despite the crucial importance of 22:6n-3 in neural tissue, the uptake of 22:6n-3 in brain appears to be a slow process. After 7 d, the percent enrichment in PC from liver was 37 times higher than in PC from brain, which was the most enriched lipid class in brain by some margin. In whole trout, the turnover of 22:6n-3 was estimated to be 0.17%/d (1). The data here showed that the accumulation of newly synthesized 22:6n-3 was slow in PE and PS from brain even though this was the most abundant FA in these lipid classes. Several dietary repletion studies in mammals have shown that recovery of 22:6n-3 levels in neural tissues is slow. In rhesus monkeys recovering from an n-3-deficient diet, the half-life of 22:6n-3 in brain PE was estimated to be 21 d (21). n-3-Deficient rats fed a repletion diet replaced 22:6n-3 in serum and liver within 2 wk, but full recovery in brain and retina took 8 wk, suggesting that a slow exchange with 22:5n-6 limited 22:6n-3 repletion in neural tissues (22). Rapoport *et al.* (23) found that after intra-arterial injection of tracer in rats, 2–8% of esterified brain 22:6n-3 was replaced daily by unesterified PUFA in plasma, indicating a half-life of 1–2 wk for plasma–brain exchange of 22:6n-3 in the order PE > PC > TAG > PI > PS. Though the concentration of FFA in plasma was very low, the plasma–brain exchange was very rapid and the rate was thought to be sufficient to supply the brain without the need for exchange of lipoproteins. Slow FA turnover seems to be an inherent property of brain lipids.

In humans, studies on PUFA turnover have concentrated, of necessity, on plasma lipids. Following ingestion of [13]C-22:6n-3 as PC, labeled FA first appeared in plasma as nonesterified FA and TAG, then as LPC and finally as PC and PE (24). This study concluded that the form of ingested 22:6n-3 affected the kinetics and metabolic fate of this FA. In human females, [13]C-22:6n-3 was sevenfold higher in plasma PC than in TAG following ingestion of [13]C-18:3n-3 as FFA (25).

The present study has shown that there are substantial differences in the rates of accretion of newly synthesized 22:6n-3 in lipid classes from different tissues in rainbow trout. Generally, PC, PE, and TAG had higher accretion rates than PS or PI. These differences probably reflect varied functions between tissues and lipid classes. Phospholipid from cecal mucosa contained the great majority of newly synthesized 22:6n-3 in that tissue, whereas in liver TAG was relatively more important. If cecal mucosa exports 22:6n-3, it is likely to be as PC or perhaps LPC and not as TAG. Brain accumulated a surprising amount of D_5-22:6n-3 in TAG, given the abundance and functional significance of 22:6n-3 in phospholipid from this tissue. Much remains to be elucidated regarding the transport of EFA between and within cellular compartments in fish.

ACKNOWLEDGMENTS

REFERENCES

1. Bell, M.V., Dick, J.R., and Porter, A.E.A. (2001) Biosynthesis and Tissue Deposition of Docosahexaenoic Acid (22:6n-3) in Rainbow Trout (*Oncorhynchus mykiss*), *Lipids 36*, 1153–1159.
2. Bell, M.V., and Dick, J.R. (2004) Changes in Capacity to Synthesise 22:6n-3 During Early Development in Rainbow Trout (*Oncorhynchus mykiss*). *Aquaculture, 235*, 393–409.
3. Bell, M.V., Dick, J.R., and Porter, A.E.A. (2003) Pyloric Ceca Are Significant Sites of Newly Synthesized 22:6n-3 in Rainbow Trout (*Oncorhynchus mykiss*), *Lipids 38*, 39–44.
4. Tocher, D.R., Fonseca-Madrigal, J., Bell, J.G., Dick, J.R., Henderson, R.J., and Sargent, J.R. (2002) Effects of Diets Containing Linseed Oil on Fatty Acid Desaturation and Oxidation in Hepatocytes and Intestinal Enterocytes in Atlantic Salmon (*Salmo salar*), *Fish Physiol. Biochem. 26*, 157–170.
5. Buzzi, M., Henderson, R.J., and Sargent, J.R. (1996) The Desaturation and Elongation of Linolenic Acid and Eicosapentaenoic Acid by Hepatocytes and Liver Microsomes from Rainbow Trout (*Oncorhynchus mykiss*) Fed Diets Containing Fish Oil or Olive Oil, *Biochim. Biophys. Acta 1299*, 235–244.
6. Linares, F., and Henderson, R.J. (1991) Incorporation of ^{14}C-Labelled Polyunsaturated Fatty Acids by Juvenile Turbot, *Scophthalmus maximus* (L.) *in vivo*, *J. Fish Biol. 38*, 335–347.
7. Tocher, D.R., Mourente, G., and Sargent, J.R. (1992) Metabolism of [1-^{14}C] Docosahexaenoate (22:6n-3), [1-^{14}C] Eicosapentaenoate (20:5n-3) and [1-^{14}C] Linolenate (18:3n-3) in Brain Cells from Juvenile Turbot *Scophthalmus maximus*, *Lipids 27*, 494–499.
8. Rodriguez, C., Henderson, R..J., Porter, A.E.A., and Dick, J.R. (1997) Modification of Odd-Chain Length Unsaturated Fatty Acids by Hepatocytes of Rainbow Trout (*Oncorhynchus mykiss*) Fed Diets Containing Fish Oil or Olive Oil, *Lipids 32*, 611–619.
9. Folch, J., Lees, M., and Sloan-Stanley, G.H. (1957) A Simple Method for the Isolation and Purification of Total Lipids from Animal Tissues, *J. Biol. Chem. 226*, 497–509.
10. Olsen, R.E., and Henderson, R.J. (1989) The Rapid Analysis of Neutral and Polar Marine Lipids Using Double-Development HPTLC and Scanning Densitometry, *J. Exp. Mar. Biol. Ecol. 129*, 189–197.
11. Fewster, M.E., Burns, B.J., and Mead, J.F. (1969) Quantitative Densitometric Thin-Layer Chromatography of Lipids Using Copper Acetate Reagent, *J. Chromatogr. 43*, 120–126.
12. Pawlosky, R.J., Sprecher, H.W., and Salem, N. (1992) High-Sensitivity Negative Ion GC–MS Method for the Detection of Desaturated and Chain-Elongated Products of Deuterated Linoleic and Linolenic Acids, *J. Lipid Res. 33*, 1711–1717.
13. Lauritzen, L., Hansen, H.S., Jorgensen, M.H., and Michaelson, K.F. (2001) The Essentiality of Long-Chain n-3 Fatty Acids in Relation to Development and Function of the Brain and Retina, *Prog. Lipid Res. 40*, 1–94.
14. Gurr, M.I., and Harwood, J.L. (1991) *Lipid Biochemistry*. 4th edn., pp. 65–69, Chapman & Hall, London.
15. Pugh, E.L., and Kates, M. (1979) Membrane-Bound Phospholipid Desaturases, *Lipids 14*, 159–165.
16. Bell, M.V., Simpson, C.M.F., and Sargent, J.R. (1983) (n-3) and (n-6) Polyunsaturated Fatty Acids in the Phosphoglycerides of Salt-Secreting Epithelia from Two Marine Fish Species, *Lipids 18*, 720–726.
17. Scott, B.L., and Bazan, N.G. (1989) Membrane Docosahexaenoate Is Supplied to the Developing Brain and Retina by the Liver, *Proc. Natl. Acad. Sci. USA 86*, 2903–2907.
18. Brindley, D.N. (1993) Hepatic Secretion of Lysophosphatidylcholine: A Novel Transport System for Polyunsaturated Fatty Acids and Choline, *J. Nutr. Biochem. 4*, 442–449.
19. Lagarde, M., Bernoud, N., Brossard, N., Lemaitre-Delaunay, D., Thies, F., Croset, M., and Lecerf, J. (2001) Lysophosphatidylcholine as a Preferred Carrier Form of Docosahexaenoic Acid to the Brain, *J. Mol. Neurosci. 16*, 201–204.
20. Bell, M.V., and Tocher, D.R. (1989) Molecular Species Composition of the Major Phospholipids in Brain and Retina from Rainbow Trout (*Salmo gairdneri*), *Biochem. J. 264*, 909–915.
21. Connor, W.E., Neuringer, M., and Lin, D.S. (1990) Dietary Effects on Brain Fatty Acid Composition: The Reversibility of n-3 Fatty Acid Deficiency and Turnover of Docosahexaenoic Acid in the Brain, Erythrocytes and Plasma of Rhesus Monkeys, *J. Lipid Res. 31*, 237–247.
22. Moriguchi, T., Loewke, J., Garrison, M., Catalan, J.N., and Salem, N. (2001) Reversal of Docosahexaenoic Acid Deficiency in the Rat Brain, Retina, Liver and Serum, *J. Lipid Res. 42*, 419–427.
23. Rapoport, S.I., Chang, M.C.J., and Spector, A.A. (2001) Delivery and Turnover of Plasma-Derived Essential PUFAs in Mammalian Brain, *J. Lipid Res. 42*, 678–685.
24. Lemaitre-Delauney, D., Pachiaudi, C., Laville, M., Pousin, J., Armstrong, M., and Lagarde, M. (1999) Blood Compartmental Metabolism of Docosahexaenoic Acid (DHA) in Humans After Ingestion of a Single Dose of [^{13}C]DHA in Phosphatidylcholine, *J. Lipid Res. 40*, 1867–1874.
25. Burdge, G.C., and Wootton, S.A. (2002) Conversion of α-Linolenic Acid to Eicosapentaenoic, Docosapentaenoic and Docosahexaenoic Acids in Young Women, *Br. J. Nutr. 88*, 411–420.

Effects of Dietary Supplementation of Rapeseed Oil on Metabolism of [1-^{14}C]18:1n-9, [1-^{14}C]20:3n-6, and [1-^{14}C]20:4n-3 in Atlantic Salmon Hepatocytes

C. Moya-Falcón[a,*], M.S. Thomassen[a,b], J.V. Jakobsen[c], and B. Ruyter[a]

[a]AKVAFORSK, Institute of Aquaculture Research, NO-1432 Ås, Norway, [b]Department of Animal and Aquacultural Sciences, Norwegian University of Life Sciences, NO-1432 Ås, Norway, and [c]EWOS Innovation AS, NO-4335 Dirdal, Norway

ABSTRACT: Atlantic salmon were fed fish meal-based diets supplemented with either 100% fish oil (FO) or 100% rapeseed oil (RO) from an initial weight of 85 g to a final average weight of 280 g. The effects of these diets on the capacity of Atlantic salmon hepatocytes to elongate, desaturate, and esterify [1-^{14}C]18:1n-9 and the immediate substrates for the Δ^5 desaturase, [1-^{14}C]20:3 n-6 and [1-^{14}C]20:4n-3, were investigated. Radiolabeled 18:1n-9 was mainly esterified into cellular TAG, whereas the more polyunsaturated FA, [1-^{14}C]20:3n-6 and [1-^{14}C]20:4n-3, were primarily esterified into cellular PL. More of the elongation product, [1-^{14}C]20:1n-9, was produced from 18:1n-9 and more of the desaturation and elongation products, 22:5n-6 and 22:6n-3, were produced from [1-^{14}C]20:3n-6 and [1-^{14}C]20:4n-3, respectively, in RO hepatocytes than in FO hepatocytes. Further, we studied whether increased addition of [1-^{14}C]18:1n-9 to the hepatocyte culture media would affect the capacity of hepatocytes to oxidize 18:1n-9 to acid-soluble products and CO_2. An increase in exogenous concentration of 18:1n-9 from 7 to 100 µM resulted in a nearly twofold increase in the amount of 18:1n-9 that was oxidized. The conversion of 20:4n-3 and 20:3n-6 to the longer-chain 22:6n-3 and 22:5n-6 was enhanced by RO feeding in Atlantic salmon hepatocytes. The increased capacity of RO hepatocytes to produce 22:6n-3 was, however, not enough to achieve the levels found in FO hepatocytes. Our data further showed that there were no differences in the hepatocyte FA oxidation capacity and the lipid deposition of carcass and liver between the two groups.

Paper no. L9624 in *Lipids 40*, 709–717 (July 2005).

The use of vegetable oils as a substitute for fish oil (FO) in high-energy diets of farmed fish has increased in recent years owing to the limited availability of FO (1–10). A major reason for adding dietary marine oils to salmon feed is to provide adequate amounts of PUFA of the n-3 series in the fish muscle so as to secure the nutritional quality of the fish for human consumption. Many studies in the last decade have shown that salmonids can use vegetable oils in seawater without negative effects on fish growth (1,2,5,7) provided the diets contain enough n-3 PUFA to satisfy EFA requirements (3,4,6,8,11). Rapeseed oil (RO) is a

good supplement for FO in salmon feeds as it has moderate levels of 18:3n-3, is relatively rich in 18:2n-6, and is very rich in 18:1n-9 (7). Culture of salmonids on diets containing high levels of vegetable oils does, however, considerably alter the FA composition of the fish muscle, giving high levels of C_{18} FA and much lower levels of the PUFA 20:5n-3 and 22:6n-3, which are known to have several positive health effects in humans (2,7). The level of these healthful PUFA in fish muscle may be of major importance for the human acceptance of the salmon product. For this reason, there is currently considerable interest in creating diets with FA compositions that can enhance the ability of the fish to produce 20:5n-3 and 22:6n-3 from 18:3n-3, by stimulation of the Δ^5 and Δ^6 desaturases and the elongases involved in the conversion (10). Atlantic salmon can elongate and desaturate C_{18} FA of the n-3 and n-6 series to C_{20} and C_{22} PUFA (8,11–13). The composition of lipids in the diet may, however, modulate the ability of the fish to desaturate and to elongate these FA (11,13–16). Ruyter *et al.* (11) showed that the rates of conversion of 18:3n-3 and 18:2n-6 to 22:6n-3 and 22:5n-6, respectively, are higher in hepatocytes from Atlantic salmon fed an EFA-deficient diet than they are in hepatocytes from fish fed a FO diet. The activity of the Δ^5 desaturase in Atlantic salmon is also found to be higher in hepatocytes from fish fed a diet containing a 1:1 blend of linseed oil and RO than it is in fish fed a diet containing FO (12). This is also the case for fish fed soybean oil diets (17). C_{18} FA were used as radiolabeled substrates for all these studies of desaturation and elongation capacities. It is known, however, that high levels of C_{18} FA may inhibit the conversion of 18:3n-3 to 22:6n-3 in Atlantic salmon, owing to the competition between C_{18} FA and C_{22} FA for the same Δ^6 desaturase (18). In this trial, we incubated with the longer-chain radiolabeled specific Δ^5 desaturase substrates, 20:4n-3 and 20:3n-6, to test whether RO feeding affected the production of 22:6n-3 and 22:5n-6 from C_{20} FA in Atlantic salmon hepatocytes.

To avoid increased lipid deposition, it is important that the FA of the dietary oil is easily oxidized by the fish. *In vitro* studies of mitochondrial β-oxidation in fish suggest that saturated and monounsaturated FA are preferred over PUFA as FA substrates (reviewed by Henderson, 19), but it is not yet known whether RO feeding affects the capacity of salmon liver to oxidize 18:1n-9, which is the dominant FA of RO. Another aim of this study was to investigate whether a dietary supplementation of RO to Atlantic salmon affects the capacity of hepatocytes to oxidize

*To whom correspondence should be addressed at AKVAFORSK, Institute of Aquaculture Research, P.O. Box 5010, NO-1432 Ås, Norway.
E-mail: corina.moya-falcon@akvaforsk.no

Abbreviations: ASP, acid-soluble products; DM, dry matter; FER, feed efficiency ratio; FO, fish oil; L-15, Leibowitz-15 medium; LT, low temperature MS-222, Metacaine; MDG, MAG and DAG; PL, phospholipids; RO, rapeseed oil; SGR, specific growth rate.

18:1n-9 and, further, whether it affects lipid deposition in the carcass and the liver.

MATERIALS AND METHODS

Chemicals. The radiolabeled FA [1-^{14}C]18:1n-9, [1-^{14}C]20:3n-6, and [1-^{14}C]20:4n-3 were obtained from American Radiolabeled Chemicals (St. Louis, MO); and nonlabeled FA, BSA that was essentially free of FA, HEPES, 2′,7′-dichlorofluorescein, and collagenase type 1 were obtained from Sigma Chemical Co. (St. Louis, MO). Metacaine (MS-222) was obtained from Norsk Medisinaldepot (Oslo, Norway). Acetic acid, chloroform, petroleum ether, and methanol were all obtained from Merck (Darmstadt, Germany). Benzene was obtained from Rathburn Chemicals Ltd. (Walkerburn, Scotland). Methanolic HCl and 2,2-dimethoxypropane were purchased from Supelco Inc. (Bellefonte, PA). Silica gel K6-coated glass plates were obtained from Whatman International Ltd. (Maidstone, England).

Fish, facilities, and experimental design. The trial was conducted at the AKVAFORSK Research Station, Sunndalsøra, Norway. Atlantic salmon (*Salmo salar*) with a mean initial weight of approximately 85 g were placed into six cylindrical-conical tanks (0.85 m diameter) with 40 fish per tank. The tanks were supplied with seawater at a constant temperature of 12°C. The fish were fed commercial diets before the start of the experiment. The growth trial consisted of one period of 8 wk. Two diets were randomly assigned to triplicate tanks. The feed was distributed by electrically driven disc-feeders (Akvaprodukter AS, Sunndalsøra, Norway). The tanks were designed such that waste feed could be collected from the effluent water in wire mesh boxes. Uneaten feed was collected to monitor daily feed intake in each tank (20).

Diets. The experimental fishmeal-based diets were provided by EWOS Innovation SA (Dirdal, Norway) in the form of 3-mm pellets. The feed contained 0.1% yttrium oxide (Y_2O_3) as an inert marker for determining digestibility (21). The experimental diets, FO and RO, were produced from one common feed mix. The two diets were obtained by coating the common feed pellet with the different oils. The diets contained either 100% FO (capelin oil) or 100% RO. Table 1 shows the formulations and chemical compositions of the diets.

Initial and final sampling. The fish were fasted for 2 d before the initial sampling. The fish from each tank were anesthetized in MS-222, weighed, and measured at the beginning and at the end of the experiment. The fish were not fasted before the final sampling, because of the collection of feces. Five fish from each tank were stripped to collect fecal samples following the procedure described by Austreng (22). Fecal samples from each tank were pooled. The samples were stored at −20°C prior to analyses. A further five fish per tank were anesthetized, killed by a blow to the head, and used for determination of whole body chemical composition.

Chemical analysis. Fish sampled at the beginning and at the end of the experiment were analyzed for dry matter (DM), fat, protein, ash, and energy. DM was determined by drying the fish homogenate to constant weight at 105°C. All diets and fecal samples were analyzed for DM, fat, protein, ash, energy, and yttrium. The amount of protein was determined using a Kjeltec Autoanalyser-N*6.25, whereas the amount of ash was determined by heating to 550°C until constant weight was reached. The amount of fat was determined by ethyl-acetate extraction [NS 9402, 1994 (Atlantic Salmon—Fat Measurement, Norwegian Standards Association, Oslo)], and the amount of yttrium by using inductively coupled plasma-atomic emission spectroscopy at Jordforsk, Ås, Norway, after wet-ashing the samples. Energy in the diets, feces, and whole fish homogenates was analyzed by adiabatic bomb calorimetry using a Parr 1271 bomb calorimeter.

Preparation of salmon hepatocytes. Hepatocytes were isolated from three fish from each tank. The fish were anesthetized in MS-222. The abdominal cavity was exposed and the vena porta cannulated. The liver was perfused, and parenchymal cells were isolated using a two-step collagenase perfusion procedure as described by Seglen *et al.* (23) and modified by Danneving and Berg (24). After collagenase perfusion, the parenchymal cells were easily isolated by gently shaking the liver in Leibowitz-15 medium (L-15). The suspension of parenchymal cells was filtered through a nylon filter with 100-μm mesh. Hepatocytes were isolated from the filtrate by centrifuging it three times, each time for 2 min at $50 \times g$. The hepatocytes were resuspended in L-15 culture medium containing 2% FBS, 2 mM L-glutamine, and 0.1 mg/mL gentamycin. Cell viability was assessed by staining with Trypan blue (0.4%). The protein content of the cell suspension was determined using the method described by Lowry *et al.* (25). Approximately 9×10^6 cells (9–10 mg of protein) were plated onto 75 mL Nunc flasks and left to attach overnight at 12°C.

Incubations with radiolabeled FA. The hepatocytes were thoroughly washed with L-15 medium without additional serum and then incubated at 12°C before the incubation with

TABLE 1
Formulations and Chemical Compositions of the Diets[a]

	Diets	
	FO	RO
Formulation (% of total)		
Fish meal, LT	67.8	67.8
Capelin oil[b]	21.3	
Rapeseed oil[c]		21.3
Wheat	10.4	10.4
Astax[d]-Cantax[e]	0.06	0.06
Mineral/vitamin premix	0.49	0.49
Yttrium oxide	0.01	0.01
Chemical composition		
Dry matter (%)	97.1	97.3
Protein (%)	51.9	51.8
Fat (%)	26.9	28.0
Ash (%)	10.8	10.7
Energy (MJ/kg)	23.8	23.9

[a]Diets: FO (100% fish oil diet), RO (100% rapeseed oil diet).
[b]Capeline oil, Norsildmel, Bergen, Norway.
[c]Rapeseed oil, Ohlmuhle, Germany.
[d]Asta, BASF, lucanthin red.
[e]Canta, lucanthin pink.

radiolabeled FA. We analyzed the desaturation and elongation of FA in hepatocytes incubated for 24 h with 35 nmol [1-^{14}C]18:1n-9, [1-^{14}C]20:3n-6, or [1-^{14}C]20:4n-3 (final concentration 7 µM), and 10 mM lactate in a total volume of 5 mL L-15 medium. The specific radioactivity of the FA was 55 mCi/mmol (1.9 µCi of radioactive FA substrate was added to each cell flask). Hepatocytes were incubated, in a parallel experiment, with 500 nmol of [1-^{14}C]18:1n-9 in a total volume of 5 mL L-15 medium (final concentration 100 µM). The specific radioactivity of the FA was 10 mCi/mmol (5 µCi of radioactive FA substrate was added to each cell flask). The radiolabeled FA were added to the medium in the form of their potassium salts bound to BSA. Control incubations were performed for each radiolabeled FA substrate, and they were treated in the same way as the samples, except that the cell protein was denatured by heating to 80°C prior to the incubations. Samples were incubated for 24 h, and then the culture medium was transferred to vials and centrifuged for 5 min at $50 \times g$. The supernatants were immediately frozen at −40°C and stored until the analysis of radiolabeled lipids. Hepatocytes remaining in the culture flask were washed twice in PBS. The cells were then harvested in PBS, frozen at −40°C, and stored until the analysis of radiolabeled lipids.

Lipid extraction, analysis of lipid classes, and FA composition. Total lipids were extracted from culture media and cells using the method described by Folch *et al.* (26). The chloroform phase produced by the method of Folch *et al.* was then divided in two. One part of the lipid extract was dried under nitrogen gas, and the residual lipid extract was redissolved in hexane. FFA, phospholipids (PL), MAG and DAG (MDG), and TAG were separated by TLC using a mixture of petroleum ether, diethyl ether, and acetic acid (113:20:2 by vol) as the mobile phase. The TLC plates were sprayed with 0.2% (wt/vol) 2′,7′-dichlorofluorescein in methanol and viewed in UV light. Then the lipids classes were identified by comparison with known standards. The spots corresponding to PL, FFA, MDG, and TAG were scraped off into vials containing liquid scintillation fluid (InstaGel II Plus; Packard Instrument, Downers Grove, IL), and radioactivity was measured using a liquid scintillation counter (Tri-Carb 1900TR; Packard Instrument).

The remaining lipid extract was placed into glass tubes and transmethylated overnight with 2,2-dimethoxypropane, methanolic HCl, and benzene at room temperature, as described by Mason and Waller (27). The compositions of the radioactive FA of the total lipid fraction were determined by reversed-phase HPLC as described by Narce *et al.* (28) The mobile phase was acetonitrile/H$_2$O (80:20 vol/vol, isocratic elution) at a flow rate of 1 mL/min at 30°C. A reversed-phase Symmetry 3.5 µm C-18 HPLC column from Waters was used. The levels of radioactivity from FA were measured in a radioactive flow detector A100 (Tri-Carb 1900TR; Packard Instuments). The absorbance of nonradioactive FA was measured in a UV detector (SPD-6AV UV-visible spectrophotometric detector; Shimadzu) at 215 nm. The FA were identified by comparing the sample retention times with the retention times of FA standards.

The total FA compositions of hepatocytes were determined essentially as described by Ruyter *et al.* (17). Lipids were extracted and then transmethylated as described above. The methyl esters of FA thus formed were separated in a gas chromatograph (GC) using a Perkin-Elmer Auto system GC equipped with an injector, programmable split/splitless injector with a CP Wax 52 column (length 25 m, internal diameter 0.25 mm, and film thickness 0.2 µm), FID. The carrier gas was He, and the injector and detector temperatures were 280°C. The oven temperature was raised from 50 to 180°C at the rate of 10°C min^{-1}, and then raised to 240°C at the rate of 0.7°C min^{-1}. The relative quantity of each FA present was determined by measuring the area under the peak corresponding to the particular FA.

Measurement of [1-^{14}C]ASP (acid-soluble products) and [1-^{14}C]CO$_2$. FA oxidation was measured essentially as described by Christiansen *et al.* (29). The amount of gaseous [1-^{14}C]CO$_2$ produced during the incubation was determined by transferring 1.5 mL of medium to a glass vial, which was then sealed. The glass vial had a central well containing Whatman filter paper moistened with 0.3 mL of phenylethylamine/methanol (1:1, vol/vol). The medium was acidified with 0.3 mL 1 M HClO$_4$. The samples were incubated for 1 h, and then the wells, containing the filter papers, were placed into vials for scintillation counting. The quantities of [1-^{14}C]

ASP present were determined by acidifying 1 mL of the medium with 0.5 mL ice-cold 2 M HClO$_4$ and incubating the sample for 60 min at 4°C. The medium was then centrifuged, and an aliquot of the supernatant was collected for scintillation counting.

Calculations. Apparent digestibility coefficients were calculated as described by Austreng *et al.* (21). Hepatosomatic index (HSI), specific growth rate (SGR), and thermal growth coefficient (TGC) were calculated as follows, based on individual recordings of weights and lengths:

$$\text{HSI} = 100 \times \text{liver weight} \times W_f^{-1} \qquad [1]$$

$$\text{SGR} = \{\exp\,[(\ln W_f - \ln W_i)/\text{days}] - 1\} \times 100 \qquad [2]$$

$$\text{TGC} = (W_f^{1/3} - W_i^{1/3}) \times 1000/(\text{d} \times °\text{C}) \qquad [3]$$

where W_i is the initial weight and W_f is the final weight, and

$$\text{recovery} = \text{total nmol of }^{14}\text{C}_{\text{whole incubation}} \qquad [4]$$

where the radioactivity recovered in the whole incubation was the radioactivity recovered in hepatocytes lipid + the radioactivity recovered in the culture media.

Statistical analysis. All data were subjected to two-way ANOVA for the factors "FA" and "diet," and differences were ranked by Duncan's multiple range test. The significance level was set at 5%. Data that were identified as nonhomogeneous by Bartlett's test were subjected to arcsine transformation before analysis.

TABLE 2
Effect of Dietary Supplementation of RO on Growth, Nutrient Digestibility, and Chemical Composition in the Carcass in Atlantic Salmon

		Diets[a]	
		FO	RO
Growth[a]			
Initial weight, g		85 ± 2	85 ± 1
Final weight, g		278 ± 7	285 ± 3
Hepatosomatic index		1.1 ± 0.01	1.0 ± 0.03
Thermal growth coefficient		2.6 ± 0.44	2.7 ± 0.01
Specific growth rate		1.8 ± 0.02	1.8 ± 0.01
Relative feed intake body weight × d^{-1})		1.45 ± 0.04[a]	1.29 ± 0.04[b]
Total feed efficiency ratio			
(weight gain/dry feed intake)		1.23 ± 0.05[b]	1.41 ± 0.04[a]
Mortality (*n*)		0.7 ± 0.32	0.7 ± 0.004
Nutrient digestibility[a]			
Protein		87.7 ± 0.15	88.6 ± 0.05
Energy		89.5 ± 0.08	90.4 ± 0.13
Fat		97.3 ± 0.58	97.5 ± 0.20
ΣSaturated FA		93.2 ± 1.54	93.4 ± 0.63
ΣMonounsaturated FA		97.6 ± 0.49	97.5 ± 0.08
ΣPUFA		98.3 ± 0.37	96.6 ± 0.17
Chemical composition of the carcass[b]	Start		
Crude lipid (%)	8.3	10.6 ± 0.01	10.9 ± 0.29
Crude protein (%)	16.8	18.1 ± 0.06	18.2 ± 0.24
Dry matter (%)	27.6	31.1 ± 0.12	31.4 ± 0.24
Ash (%)	2.3	2.0 ± 0.05	1.9 ± 0.05
Energy (MJ/kg)	7.1	8.5 ± 0.03	8.5 ± 0.07
Liver lipid content (%)	—	4.9 ± 0.27	5.2 ± 0.18

[a]Values are means ± SEM (*n* = 3). [a,b]Differences between mean values within a given row are significant (*P* ≤ 0.05), as indicated by different superscript letters.
[b]Values are g/100 g wet tissue Atlantic salmon sampled at the beginning (start) and at the end (means ± SEM. *n* = 3) of the experiment were analyzed for dry matter, fat, protein, ash, and energy content. For abbreviations see Table 1.

RESULTS

Growth, feed intake. and nutrient digestibilities. The fish in both dietary groups grew from an initial weight of approximately 85 g to a final weight of approximately 280 g, a three-fold increase. The two groups had the same SGR, 1.8 (Table 2). The feed efficiency ratio (FER) was significantly higher for the fish fed the RO diet (FER = 1.41) than it was for the fish fed the FO diet (FER = 1.23) (Table 2). The total digestibility of FA in both dietary groups was high, approximately 97%. There were no significant differences in nutrient digestibility between the two groups in this trial (Table 2).

Body composition and liver lipid content. Dietary RO did not affect the gross chemical composition of the carcass (Table 2). The total liver lipid content in fish fed the RO and the FO diet was approximately 5%, and there was no statistical difference between the two groups.

FA compositions of diets and hepatocytes. The FA compositions of the diets clearly reflected that of added oils (Table 3). The levels of the n-3 FA, however, were higher in the diets than in the added oils, since the feed contained significant amounts of fish meal. The FO diet was characterized by relatively high levels of the long-chain n-3 FA 20:5n-3 and 22:6n-3, and low

levels of FA with 18-carbon chains. The RO diet, on the other hand, contained approximately 40% 18:1n-9.

Table 3 also shows the endogenous FA composition of the total lipid fraction of hepatocytes. The percentages of 18:1n-9 were 22 and 12 for fish fed the RO and FO diet, respectively. The percentage of 18:2n-6 in the total lipids from hepatocytes was almost five times greater in fish fed the RO diet than in fish fed the FO diet. RO hepatocytes also had significantly higher percentages of the desaturation product of 18:2n-6, 18:3n-6, than FO hepatocytes. The percentage of 20:4n-6 was, however, approximately the same for the FO hepatocytes as it was for the RO hepatocytes. The percentage of the longer-chain n-3 PUFA, 20:5n-3 and 22:6n-3, in the total lipid fraction of hepatocytes was 41% in the FO group, whereas it was 31% in the RO group. The percentage of saturated FA was approximately 22% in the FO hepatocytes and 18% in the RO hepatocytes.

Figure 1 shows the relative distribution of 18:1n-9, 18:2n-6, 20:5n-3, and 22:6n-3 within the lipid classes TAG, PL, and FFA. The percentage of 18:1n-9 found as FFA in RO hepatocytes was significantly higher (about 40% of the total endogenous FFA pool) than in FO hepatocytes (about 12%). RO hepatocytes also had a higher percentage of 18:2n-6 in the PL and FFA fractions than FO hepatocytes. The 22:6n-3 was primarily

TABLE 3
FA Compositions of the Diets and of the Total Lipid Fractions of Hepatocytes[a]

FA	Diet		Hepatocytes	
(% of total)	FO	RO	FO	RO
14:0	6.7	1.7	2.0 ± 0.19[a]	0.9 ± 0.02[b]
16:0	11.8	8.0	15.6 ± 0.27[a]	12.8 ± 0.23[b]
18:0	1.4	1.9	3.8 ± 0.37	4.4 ± 0.26
22:0	0.2	0.2	0.1 ± 0.07	0.2 ± 0.03
ΣSaturated[b]	20.7	12.4	21.9 ± 0.11[a]	18.3 ± 0.44[b]
16:1n-7	7.1	2.0	2.4 ± 0.18	1.2 ± 0.02
18:1n-7	3.1	3.5	2.7 ± 0.04	2.5 ± 0.10
18:1n-9	11.5	40.4	12.0 ± 0.14[b]	22.0 ± 1.06[a]
20:1n-9	0.5	0.2	0.3 ± 0.008	0.10 ± 0.05
20:1n-11	17.9	4.9	4.8 ± 0.13[a]	3.4 ± 0.16[b]
22:1n-9	1.9	0.7	0.9 ± 0.03	0.5 ± 0.04
ΣMonounsaturated[c]	56.9	55.9	24.8 ± 0.23[b]	30.5 ± 1.52[a]
18:2n-6	2.7	15.1	1.4 ± 0.09[b]	6.9 ± 0.16[a]
18:3n-6	0.1	0.0	0.2 ± 0.09[b]	2.1 ± 0.06[a]
18:3n-3	0.7	7.1	0.1 ± 0.06[b]	1.3 ± 0.05[a]
20:5n-3	5.9	2.9	9.2 ± 0.34[a]	5.5 ± 0.51[b]
20:3n-6	ND	ND	0.4 ± 0.02[b]	1.7 ± 0.09[a]
20:4n-6	0.3	0.2	2.4 ± 0.23	2.3 ± 0.03
22:5n-3	0.5	0.2	5.6 ± 0.18	1.4 ± 0.19
22:6n-3	6.4	3.8	31.7 ± 0.05[a]	25.2 ± 0.31[b]
ΣPolyunsaturated[d]	19.8	30.4	49.9 ± 0.32	48.3 ± 0.74
EPA + DHA	12.5	6.7	40.9 ± 0.36[a]	30.7 ± 0.82[b]

[a]The quantity of each FA is given as percentage (mean ± SEM) of the total FA. Values within the same row with different superscripts are significantly different. $P \le 0.05$. $n = 3$; ND = not detected; for other abbreviations see Table 1.
[b]Includes 12:0; 15:0; 17:0; 20:0.
[c]Includes 16:1n-9; 18:1n-6; 22:1n-11.
[d]Includes 16:3n-4; 20:4n-3; 20:2n-6; 20:3n-3.

esterified into PL and there were only minor differences in the percentage of this FA in the PL between the two dietary groups. The percentage of 22:6n-3 was, however, about fivefold higher in the FFA fraction of the FO hepatocytes than in RO hepatocytes.

Recovery of [1-^{14}C]FA in lipid classes, extracellular lipids, and oxidation products. Hepatocytes were incubated for 24 h with 7 μM [1-^{14}C]18:1n-9, [1-^{14}C]20:3n-6, or [1-^{14}C]20:4n-3 to study FA uptake, oxidation, and esterification. Table 4 shows the amounts of radioactivity that were incorporated into each fraction during the 24-h incubation as percentages of the total radioactivity recovered from the whole incubation. No significant differences were observed between the FO and RO hepatocytes. In both groups, significantly more radioactivity from the [1-^{14}C]20:3n-6 and [1-^{14}C]20:4n-3 substrates (approximately 70%) was present in hepatocytes than from the [1-^{14}C]18:1n-9 substrate (50–55%). Radiolabeled 18:1n-9 was mainly esterified in the TAG fraction of hepatocytes, where it constituted approximately 30% of the total radioactivity, whereas approximately 15% was esterified in the PL. In contrast, the radiolabeled n-3 and n-6 FA were esterified to a greater extent in the PL fraction, where they constituted 52–56% of the total radioactivity. Esterified n-3 and n-6 FA constituted 6–10% in the TAG and 2–4% in the pooled MAG and DAG (MDG) fraction. Between 4 and 6% of the total radioactivity from the three radioactive substrates was not esterified but recovered as FFA. Table 5 shows also the recovery of

radiolabeled lipids in the culture media. Significantly higher percentages of radiolabeled lipids were recovered from the culture media for cells incubated with [1-^{14}C]18:1n-9 than for cells incubated with [1-^{14}C]20:3n-6 and [1-^{14}C]20:4n-3, which was primarily in the form of FFA (23–25%). More of the substrates [1-^{14}C]18:1n-9 and [1-^{14}C]20:3n-6 was oxidized (approximately 13%) than of the [1-^{14}C]20:4n-3 substrate (10%).

Figure 2 shows the oxidation of [1-^{14}C]18:1n-9 to ASP and CO_2 when the hepatocytes were incubated with either 7 or 100 μM [1-^{14}C]18:1n-9 substrate for 24 h. The higher exogenous
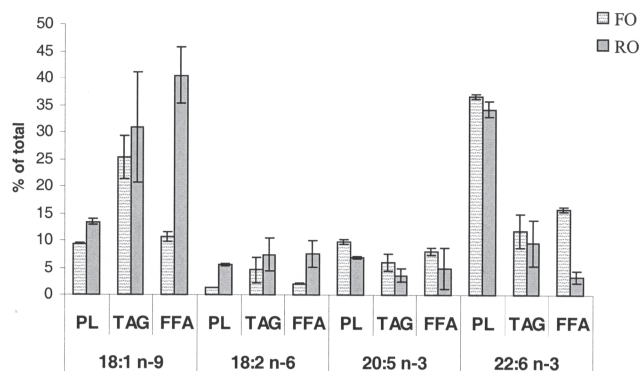
FIG. 1. Relative distribution of some FA in the different lipid classes of hepatocytes. Diets: FO (100% fish oil diet); RO (100% rapeseed oil diet). Values are means ± SEM ($n = 3$).

TABLE 4
Proportional Distribution of Radioactivity in Lipids of Hepatocytes and Culture Media and Oxidation Products[a]

	FO			RO		
	[1-^{14}C]18:1n-9	[1-^{14}C]20:3n-6	[1-^{14}C]20:4n-3	[1-^{14}C]18:1n-9	[1-^{14}C]20:3n-6	[1-^{14}C]20:4n-3
Recovery[b] (nmol)	24.7 ± 1.68	33.6 ± 2.49	28.2 ± 7.18	26.1 ± 0.85	32.4 ± 3.43	25.4 ± 0.72
Hepatocyte lipids (%)						
PL	15.0 ± 3.47[b]	53.0 ± 3.47[a]	54.7 ± 4.34[a]	15.4 ± 1.96[b]	52.6 ± 3.50[a]	52.4 ± 4.71[a]
MDG	3.9 ± 0.43[a]	2.2 ± 0.62[b]	2.3 ± 0.89[a,b]	3.5 ± 0.47[a]	1.5 ± 0.74[b]	3.2 ± 0.29[a,b]
FFA	3.8 ± 0.59	5.6 ± 1.65	5.2 ± 2.15	3.6 ± 0.45	3.8 ± 0.58	4.1 ± 1.73
TAG	27.7 ± 3.85[a]	8.4 ± 1.31[b]	6.4 ± 3.22[b]	32.2 ± 4.53[a]	8.0 ± 2.18[b]	10.4 ± 0.51[b]
Total	50.4 ± 4.57[b]	69.2 ± 0.002[a]	68.6 ± 4.97[a]	54.7 ± 7.01[b]	65.9 ± 0.01[a]	70.1 ± 4.91[a]
Culture media (%)						
PL	1.6 ± 0.37[b]	1.9 ± 0.32[b]	3.5 ± 0.90[a]	1.5 ± 0.32[b]	2.2 ± 0.24[a,b]	2.7 ± 0.95[a]
MDG	0.7 ± 0.12	0.4 ± 0.08	0.7 ± 0.22	0.6 ± 0.16	0.6 ± 0.07	0.5 ± 0.19
FFA	23.3 ± 1.57[a]	11.1 ± 1.59[b]	12.8 ± 3.66[b]	24.8 ± 2.71[a]	15.2 ± 0.95[b]	13.5 ± 0.79[b]
TAG *	8.2 ± 2.48[a]	1.6 ± 0.45[b]	4.7 ± 1.74[a,b]	6.2 ± 2.70[a]	1.7 ± 0.79[b]	2.4 ± 1.42[b]
Total	33.9 ± 4.49[a]	15.5 ± 1.10[c]	21.8 ± 3.12[b]	33.2 ± 4.9[a]	20.1 ± 0.50[b]	19.1 ± 3.22[b]
Oxidation products (%)						
(CO$_2$ + ASP)	15.8 ± 3.02[a]	15.3 ± 1.09[a]	10.1 ± 2.34[b]	12.1 ± 2.12[a]	14.0 ± 0.5[a]	9.4 ± 1.82[b]

[a]Hepatocytes from fish fed the FO and RO diets were incubated with 7 μM [1-^{14}C] FA. Data are means ± SEM ($n = 3$). [a,b] Differences between mean values within a given row are significant ($P ≤ 0.05$) except for (*) where $P ≤ 0.01$. Data that were identified as nonhomogeneous by Bartlett's test were subjected to arcsine transformation before analysis.
[b]Recovery = total nmol of radioactivity recovered in the whole incubation calculated as the sum of radioactivity recovered in (PL + MDG + FFA + TAG)$_{hepatocytes lipids}$ + (PL + MDG + FFA + TAG)$_{culture media}$ + oxidation products after 24 h incubation. PL, phospholipids; MDG, MAG + DAG; ASP, acid-soluble products; for other abbreviations see Table 1.

TABLE 5
Percentage Distributions of Radioactivity from [1-^{14}C]18:1n-9, [1-^{14}C]20:3n-6, and [1-^{14}C]20:4n-3 into Their Desaturation and Elongation Products in Total Lipid Fraction of Hepatocytes[a]

	FO	RO
[1-^{14}C]18:1n-9		
Recovery (nmol)	12.5 ± 1.65	14.2 ± 1.65
18:1n-9	91.5 ± 0.78[b]	86.6 ± 0.47[a]
20:1n-9	8.5 ± 0.78[a]	13.4 ± 0.47[b]
[1-^{14}C]20:3n-6		
Recovery (nmol)	23.2 ± 1.73	21.4 ± 2.26
20:3n-6	71.9 ± 3.87	64.6 ± 3.71
20:4n-6	17.0 ± 2.51	20.4 ± 3.41
22:4n-6	2.1 ± 0.33	2.7 ± 0.05
22:5n-6*	2.0 ± 0.25[b]	3.1 ± 0.64[a]
24:5n-6	4.5 ± 0.52	3.9 ± 0.34
DI $_{20:3 n-6}$ (%)	30 ± 4.0	40 ± 5.0
[1-^{14}C]20:4n-3		
Recovery (nmol)	20.1 ± 6.67	17.9 ± 1.76
20:4n-3	48.5 ± 4.53	43.7 ± 3.95
20:5n-3**	22.9 ± 2.79[a]	17.1 ± 0.53[b]
22:5n-3	10.3 ± 0.43	9.0 ± 0.97
22:6n-3	12.5 ± 3.80[b]	23.5 ± 5.29[a]
24:5n-3	2.5 ± 0.46	3.4 ± 0.42
24:6n-3	0.6 ± 0.19	1.0 ± 0.18
DI$_{20:4n-3}$ (%)	50 ± 5.0	60 ± 4.0

[a]Hepatocytes from fish fed the FO and RO diets were incubated with 7 μM [1-^{14}C] FA. DI = desaturation index; DI$_{20:3n-6}$ was calculated as: (20:4 + 22:4 + 22:5 + 24:5n-6/20:3 +20:4 +22:4 + 22:5 + 24:5) × 100 and DI$_{20:4n-3}$ as: (20:5 + 22:5 + 22:6 + 24:5 + 24:6/20:4 +20:5 + 22:5 + 22:6 + 24:5 + 24:6) × 100. Data are means ± SEM ($n = 3$). [a,b]Differences between mean values within a given row are significant ($P ≤ 0.05$) except for (*) and (**) where $P ≤ 0.01$. Data that were identified as nonhomogeneous by Bartlett's test were subjected to arcsine transformation before analysis. Recovery = nmol of [1-^{14}C]FA recovered in lipid total fractions of hepatocytes after 24 h incubation. The total recoveries of radioactivity of the incubations are shown in Table 4. For other abbreviations see Table 1.
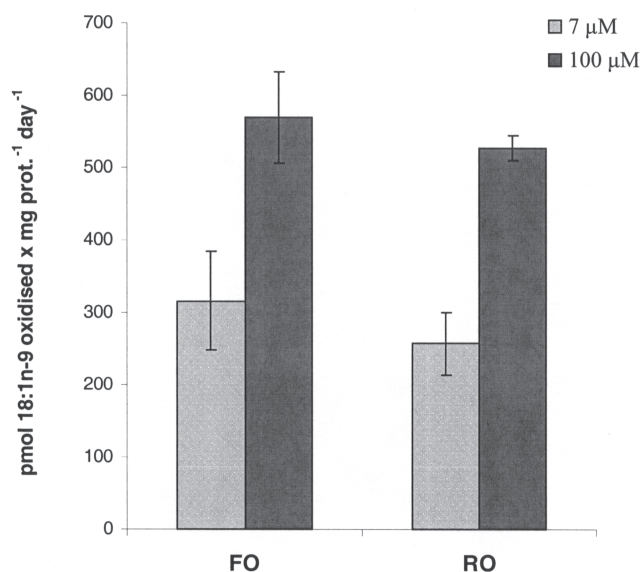
FIG. 2. The effects of different exogenous levels (7 and 100 µM) of [1-^{14}C]18:1n-9 on the capacity of hepatocytes to oxidize [1-^{14}C]18:1n-9. The values are given as means of pmol [1-^{14}C]18:1n-9 oxidized per mg protein per day.

concentration of 18:1n-9 led to a twofold increase in the amount of oxidation products formed compared with the lower concentration. There were no significant differences in the amount of oxidation products formed between the two dietary groups.

Desaturation and elongation of [1-^{14}C]18:1n-9, [1-^{14}C]20:3n-6, and [1-^{14}C]20:4n-3. Table 5 shows the desaturation and chain-elongation of [1-^{14}C]FA in the total lipids of hepatocytes. The main radiolabeled FA recovered from [1-^{14}C]18:1n-9 were the unchanged substrate 18:1n-9 and its elongated product 20:1n-9. The production of 20:1n-9 was significantly higher in RO hepatocytes (13%) than in FO hepatocytes (9%). The main metabolites from [1-^{14}C]20:3n-6 were the unchanged substrate and 20:4n-6. The only significant difference in results between the groups was in the final product, 22:5n-6, which was higher for the RO hepatocytes than it was for the FO hepatocytes. The main metabolites in the lipid fraction from [1-^{14}C]20:4n-3 were the unchanged substrate, 20:5n-3, and 22:6n-3. Further, the percentage of the Δ^5 desaturase product, 20:5n-3, was significantly lower for the RO hepatocytes than it was for the FO hepatocytes. Interestingly, the production of the final elongation product, 22:6n-3, was higher for the RO hepatocytes than it was for the FO hepatocytes.

DISCUSSION

This work shows that RO is an effective substitute for FO in Atlantic salmon diets, giving similar growth rates and having no apparent ill effects on fish health, which is also in agreement with what we have previously shown (2), and which has also been confirmed by more recent studies (7). The endogenous FA composition of hepatocyte lipids was, as expected, influenced by the dietary oils. The RO diet considerably increased the per-

centages of 18:1n-9, 18:2n-6, 18:3n-3, and 20:3n-6 in hepatocyte lipids. These results agree with those of Bell *et al.* (7), who found that the level of 18:1n-9 in the Atlantic salmon liver was well correlated to the dietary level of RO. Further, Ruyter *et al.* (8) found higher levels of total n-6 FA in salmon hepatocytes fed diets supplemented with soybean oil. In our results, these increases were accompanied by decreases in the percentages of 20:5n-3, 22:6n-3, and saturated FA in the total lipids of hepatocytes. The FA 18:3n-6 and 20:3n-6 were detected in RO hepatocytes, although they were not present in the RO diet. Both the appearance of these FA in the hepatocyte lipids and the reduced percentage of hepatocyte 18:2n-6 relative to the diet suggest a substantial desaturation and elongation of 18:2n-6 in the RO hepatocytes. The percentage of 20:4n-6 was, however, not higher in RO hepatocytes than in FO hepatocytes. Similarly, a reduced percentage of 18:3n-3 and increased percentages of 20:5n-3, 22:5n-3, and 22:6n-3 in RO hepatocytes relative to the RO diet may suggest an active desaturation and elongation of 18:3n-3, although not enough to keep the levels of these important FA as high as observed for the FO hepatocytes. This reduction in the very long n-3 FA with vegetable oil feeding has been repeatedly observed, in total salmon lipids as well as in PL and TAG fractions of muscle and organs such as liver and heart (2–4,7–10).

We found that higher percentages of radioactive n-3 and n-6 PUFA (20:3n-6 and 20:4n-3) were incorporated into hepatocyte lipids than the monounsaturated 18:1n-9, indicating that the longer n-3 and n-6 PUFA are more rapidly taken up by the cell than 18:1n-9 during 24 h of incubation. It has recently been reported (30) that salmon muscle cells have a higher capacity for incorporating n-3 FA than they have for n-9 FA. Further, we recovered more than twice as much radioactivity from the [1-^{14}C]18:1n-9 substrate as extracellular FFA and also as secreted radiolabeled TAG in the culture media than we recovered from any of the n-3 and n-6 substrates. The extracellular radiolabeled FFA are probably unmetabolized FA substrates, since FA that are taken up by the cells and then further secreted to the medium are primarily in an esterified form (31).

The distribution of radioactivity among different lipid classes differed for the different [1-^{14}C]FA substrates added to the hepatocytes but was not affected by dietary oil. For both dietary groups, radiolabeled 18:1n-9 was preferentially incorporated into TAG, whereas the longer-chain n-3 and n-6 PUFA were preferentially incorporated into cellular PL. *In vivo* experiments have previously shown that dietary 18:1n-9 is preferentially incorporated into TAG in Atlantic salmon (32), and *in vitro* experiments with [1-^{14}C]18:1n-9 in mammals (33) have shown the same. In contrast, longer-chain n-3 and n-6 PUFA are primarily incorporated into PL (32,34). This is probably due to specificity of the esterification enzymes involved in the formation of PL and TAG (35).

The rate of elongation of 18:1n-9 is reflected in the ratio of 20:1/18:1. This ratio was significantly higher in RO hepatocytes than it was in hepatocytes from fish fed the FO diet. The mechanism behind the increased elongation of 18:1n-9 to 20:1n-9 in the hepatocytes from RO-fed fish is not clear.

Substrate induction due to the high level of 18:1n-9 in the FFA fraction of RO hepatocytes is possible. An elongase of broad substrate specificity is described in the liver of salmon, and its expression may be induced by vegetable oil feeding (36). To what extent this elongase is responsible for the elongation of 18:1n-9 is, however, at present not clarified.

The reason why 18:1n-9 was elongated mainly to 20:1 (dead-end elongated product) rather than desaturated and elongated through the n-9 pathway is explained by competition between 18:1n-9, 18:2n-6, and 18:3n-3 for the Δ^6 desaturase (37). The presence of C_{18} FA of the n-3 and n-6 families prevents formation and accumulation of more unsaturated n-9 FA. Thus, 18:1n-9 is further desaturated and elongated to 20:3n-9 only in the absence of both EFA 18:2n-6 and 18:3n-3 (11,38).

The production of the end-product [1-^{14}C]22:5n-6 from 20:3n-6 was significantly higher in RO than it was in FO hepatocytes. Similarly, in the n-3 series, [1-^{14}C]22:6n-3 also was produced from 20:4n-3 to a greater extent in RO hepatocytes, strongly suggesting that the Δ^5 desaturase activity was higher in these cells. To our knowledge the present study is the first one to use the immediate substrates for the Δ^5 desaturase, and our results agree with studies where C_{18} FA was used (7,10,13,39), showing that the hepatic FA desaturation and elongation activities were increased with dietary inclusion of vegetable oils. The mechanism(s) behind the increased Δ^5 desaturase activity are still being debated. In a recent study (36), dietary linseed oil led to increased mRNA expression of a Δ^5 desaturase in salmon liver. However, in the same study, the apparent Δ^5 desaturase activity, calculated from results after incubation of hepatocytes with radiolabeled 18:3n-3, showed no clear relationship to the level of dietary linseed oil. Feedback inhibition of both Δ^5 and Δ^6 desaturase activities by high levels of 22:6n-3 also has been suggested. This may explain the lower 22:6n-3 production in FO hepatocytes, which contained a relatively higher percentage of 22:6n-3 in the FFA fractions than comparable RO hepatocytes.

Hepatocytes incubated with 100 µM 18:1n-9 had twice as high a capacity to β-oxidize radiolabeled 18:1n-9 than hepatocytes incubated with 7 µM 18:1n-9. However, the higher endogenous percentage of 18:1n-9 in RO hepatocytes (22%) than in FO hepatocytes (12) did not significantly affect the β-oxidation of 18:1n-9. Addition of radiolabeled FA into pools of potentially different FA compositions, as in the present study, may lead to some interpretation problems. The significantly higher percentage of unlabeled 18:1n-9 observed in the FFA fraction of the RO hepatocytes may thus be expected to lead to a higher dilution of the radiolabeled substrate, resulting in an underestimation of the oxidation capacity. If we assume that the endogenous pool of nonlabeled 18:1n-9 FFA would oxidize to the same extent as the exogenously added radiolabeled 18:1n-9, then the actual amount of 18:1n-9 oxidized would be higher in the RO group than in the FO group. Another unlabeled FFA that differs in endogeneous concentration between the two dietary groups and might also influence the oxidation capacity is 22:6n-3. It is known that 22:6n-3 may induce peroxisomal FA oxidation (40).

In conclusion, supplementing the diet of Atlantic salmon with RO changes the endogenous FA composition of hepatocytes and leads to higher endogenous percentages of 18:1n-9, 18:2n-6, 18:3n-3, and 20:3n-6. Our results strongly suggest an increased elongase and Δ^5 desaturase activity, since higher percentages of 20:1n-9, 22:5n-6, and 22:6n-3 were formed from their radiolabeled precursors. The increased capacity of RO hepatocytes to produce 22:6n-3 was, however, not enough to keep the level of this important FA as high as observed in the FO hepatocytes. Further, lipid deposition in the carcass and liver did not differ between the two dietary groups. Increased addition of [1-^{14}C]18:1n-9 to the hepatocyte culture media, however, resulted in an increase in the amount of 18:1n-9 that was oxidized.

REFERENCES

1. Dosanjh, B.S., Higgs, D.A., Plotnikoff, M.D., Markert, J.R., and Buckley, J.T. (1988) Preliminary Evaluation of Canola Oil, Pork Lard and Marine Lipids Singly and in Combination as Supplemental Dietary Lipid Sources for Juvenile Fall Chinook Salmon (*Oncorhynchus tshawytscha*), *Aquaculture 68*, 325–343.
2. Thomassen, M.S., and Røsjø, C. (1989) Different Fats in Feed for Salmon: Influence on Sensory Parameters, Growth Rate and Fatty Acids in Muscle and Heart, *Aquaculture 79*, 129–135.
3. Polvi, S.M., and Ackman, R.G. (1992) Atlantic Salmon (*Salmo salar*) Muscle Lipids and Their Response to Alternative Dietary Fatty Acid Sources, *J. Agric. Food Chem. 40*, 1001–1007.
4. Bell, J.C., Dick, J.R., McVicar, A.H., Sargent, J.R., and Thompson, K.D. (1993) Dietary Sunflower, Linseed and Fish Oils Affect Phospholipid FA Composition, Development of Cardiac Lesions, Phospholipase Activity and Eicosanoid Production in Atlantic Salmon, *Salmo salar*, *Prostaglandins Leukot. Essent. Fatty Acids 49*, 665–673.
5. Røsjø, C., Berg, T., Manum, K., Gjøen, T., Magnusson, S., and Thomassen, M.S. (1994) Effects of Temperature and Dietary n-3 and n-6 Fatty Acids on Endocytic Processes in Isolated Rainbow Trout (*Oncorhynchus mykiss*, Walbaum) Hepatocytes, *Fish Physiol. Biochem. 13*, 119–132.
6. Guillou, A., Soucy, P., Khalil, M., and Adambounou, L. (1995) Effects of Dietary Vegetable and Marine Lipid on Growth, Muscle Fatty Acid Composition and Organoleptic Quality of Flesh of Brook Charr (*Salvelinus fontinalis*). *Aquaculture 136*, 351–362.
7. Bell, J.C., McEvoy, J., Tocher, D.R., McGhee, F., Campbell, P.J., and Sargent, J.R. (2001) Replacement of Fish Oil with Rapeseed Oil in Diets of Atlantic Salmon *(Salmo salar)* Affects Tissue Lipid Compositions and Hepatocyte Fatty Acid Metabolism, *J. Nutr. 131*, 1535–1543.
8. Ruyter, B., Røsjø, C., Einen, O., and Thomassen, M.S. (2000) Essential Fatty Acids in Atlantic Salmon: Effects of Increasing Dietary Doses of n-6 and n-3 Fatty Acids on Growth, Survival and Fatty Acid Composition of Liver, Blood and Carcass. *Aquaculture Nutr. 6*, 119–127.
9. Grisdale-Helland, B., Ruyter, B., Rosenlund, G., Obach, A., Helland, S.J., Sandberg, M.G., Standal, H., and Røsjø, C. (2002) Influence of High Contents of Dietary Soybean Oil on Growth, Feed Utilization, Tissue Fatty Acid Composition, Heart Histology and Standard Oxygen Consumption of Atlantic Salmon

(*Salmo salar*) Raised at Two Temperatures, *Aquaculture 207*, 3–4, 311–329.

10. Tocher, D.R., Bell, J.G., Dick, J.R., and Crampton, V.O. (2003) Effects of Dietary Vegetable Oil on Atlantic Salmon Hepatocyte Fatty Acid Desaturation and Liver Fatty Acids Compositions, *Lipids 38*, 723–732.

11. Ruyter, B., and Thomassen, M.S. (1999) Metabolism of n-3 and n-6 Fatty Acids in Atlantic Salmon Liver: Stimulation by Essential Fatty Acid Deficiency, *Lipids 34*, 1167–1176.

12. Bell, J.G., Tocher, D.R., Farndale, B.M., Cox, D.I., McKinney, R.W., and Sargent, J.R. (1997) The Effect of Dietary Lipid on Polyunsaturated Fatty Acid Metabolism in Atlantic Salmon (*Salmo salar*) Undergoing Parr-Smolt Transformation, *Lipids 32*, 515–525.

13. Tocher, D.R., Bell, J.G., Dick, J.R., and Sargent, J.R. (1997) Fatty Acyl Desaturation in Isolated Hepatocytes from Atlantic Salmon (*Salmo salar*): Stimulation by Dietary Borage Oil Containig γ-Linolenic Acid, *Lipids 32*, 1237–1247.

14. Brenner, R.R. (1981) Early Effects of Essential Fatty Acid Deficiency on the Structure and Enzymatic Activity of Rat Liver Microsomes, *Progr. Lipid Res. 20*, 41–47.

15. Cinti, D.L., Cook, L., Nagi, M.N., and Suneja, S.K. (1992) The Fatty Acid Chain Elongation System of Mammalian Endoplasmatic Reticulum. *Prog. Lipid Res. 31*, 1–51.

16. Buzzi, M., Henderson, R.J., and Sargent, J.R. (1996) The Desaturation and Elongation of Linolenic Acid and Eicosapentanoic Acid by Hepatocytes and Liver Microsomes from Rainbow Trout (*Oncorhynchus mykiss*) Fed Diets Containing Fish Oil or Olive Oil, *Biochim. Biophys. Acta 1299*, 235–244.

17. Ruyter, B., Røsjø, C., Grisdale-Helland, B., Rosenlund, G., Obach, A., and Thomassen, M.S. (2003) Influence of Temperature and High Dietary Linoleic Acid Content on Esterification, Elongation, and Desaturation of PUFA in Atlantic Salmon Hepatocytes, *Lipids 38,* 833–840.

18. Leger, C., and Fremont, L. (1981) Fatty Acid Composition of Lipids in the Trout (*Salmo gairdneri*)—I. Influence of Dietary Fatty Acids on the Triglyceride Fatty Acid Desaturation in Serum, Adipose Tissue, Liver, White and Red Muscle, *Comp. Biochem. Physiol.. 69B* 99–105.

19. Henderson, R.J. (1996) Fatty Acid Metabolism in Freshwater Fish with Particular Reference to Polyunsaturated Fatty Acids in Liver of Rainbow Trout, *Comp. Biochem. Physiol. 82B*, 79–85.

20. Helland, S.J., Grisdale-Helland, B., and Nerland, S. (1996) A Simple Method for the Measurement of Daily Feed Intake of Groups of Fish in Tanks, *Aquaculture 139*, 157–163.

21. Austreng, E., Storebakken, T., Thomassen, M.S., Refstie, S., and Thomassen, Y. (2000) Evaluation of Selected Trivalent Metal Oxides as Inert Markers Used to Estimate Apparent Digestibility in Salmonids, *Aquaculture 188*, 65–78.

22. Austreng, E. (1978) Digestibility Determination in Fish Using Chromic Oxide Marking Analysis of Contents from Different Segments of the Gastrointestinal Tract, *Aquaculture 13*, 265–272.

23. Seglen, P.O. (1976) Preparation of Isolated Rat Liver Cells, *Methods Cell Biol. 13*, 29–59.

24. Dannevig, B.H., and Berg, T. (1985) Endocytosis of Galactose-Terminated Glycoproteins by Isolated Liver Cells of Rainbow Trout, *Comp. Biochem. Physiol. 82B*, 683–688.

25. Lowry, O.H., Rosebrough, N.J., Farr, A.L., and Randall, R.J. (1951) Protein Measurement with the Folin Phenol Reagent, *J. Biol. Chem. 193*, 265–275.

26. Folch, A.C., Lees, M., and Sloane-Stanley, G.M. (1957) A Simple Method for Isolation and Purification of Total Lipids from Animal Tissues, *J. Biol. Chem. 226*, 497–509.

27. Mason, M.E., and Walter, G.R. (1964) Dimethoxypropane Induces Transesterification of Fats and Oils in Preparations of Methylesthers for Gas Chromatographic Analysis, *Anal. Chem. 36*, 583–586.

28. Narce, M., Gresti, J., and Bezard, J. (1988) Method for Evaluating the Bioconversion of Radioactive Polyunsaturated Fatty Acids by Use of Reversed-Phase Liquid Chromatography, *J. Chromatogr. 448*, 249–264.

29. Christiansen, R., Borrebæk, B., and Bremer, J. (1976) The Effect of (−) Carnitine on the Metabolism of Palmitate in Liver Cells Isolated from Fasted and Re-fed Rats, *FEBS Lett. 62*, 313–317.

30. Vegusdal, A., Gjøen, T., Berge, R.K., Thomassen, M.S., and Ruyter, B. (2004) Effect of 18:1n-9, 20:5n-3, and 22:6n-3 on Lipid Accumulation and Secretion by Atlantic Salmon Hepatocytes, *Lipids 39*, 649–658.

31. Vegusdal, A., Østbye, T.K., Tran, T.N., Gjøen, T., and Ruyter, B. (2004) β-Oxidation, Esterification and Secretion of Radiolabeled Fatty Acids in Cultivated Atlantic Salmon Skeletal Muscle Cells, *Lipids 40,* 477–486.

32. Moya-Falcón, C., Hvattum, E., Dyrøy, E., Skorve, J., Stefansson, S.O., Thomassen, M.S., Jakobsen, J.V., Berge, R.K., and Ruyter, B. (2004) Effects of 3-Thia Fatty Acids on Feed Intake, Growth, Tissue Fatty Acid Composition, β-Oxidation and Na$^+$, K$^+$-ATPase Activity in Atlantic Salmon, *Comp. Biochem. Physiol. B Biochem Mol Biol. 139*, 657–668.33. Bruce, J.S., and Salter, A.M. (1996) Metabolic Fate of Oleic Acid, Palmitic Acid and Stearic Acid in Cultured Hamster Hepatocytes, *Biochem. J. 316*, 847–852.

33. Bruce, J.S., and Salter, A.M. (1996) Metabolic Fate of Oleic Acid, Palmitic Acid and Stearic Acid in Cultured Hamster Hepatocytes, *Biochem. J. 316*, 847–852.

34. Xia, T., Mostafa, N., Ganesh Bhat, B., Florant, G.L., and Coleman, R.A. (1993) Selective Retention of Essential Fatty Acids; The Role of Hepatic Monoacylglycerol Acyltransferase, *Am. J. Physiol. 265*, 414–419.

35. Henderson, R.J., and Tocher, D.R. (1987) The Lipid Composition and Biochemistry of Freshwater Fish, *Prog. Lipid Res. 26*, 281–347.

36. Zheng, X., Tocher, D.R., Dickson, A.A., Bell, J.G., and Teale, A.J. (2004) Effects of Diets Containing Vegetable Oil on Expression of Genes Involved in Liver of Atlantic Salmon (*Salmo salar*), *Aquaculture 236*, 467–483.

37. Leger, C., and Fremont, L. (1981) Fatty Acid Composition of Lipids in the Trout (*Salmo gairdneri*), *Comp. Biochem. Biophys. B Biochem Mol. Biol. 69B*, 99–105.

38. Castell, J.D., Sinnhuber, R.O., Lee, D.J., and Wales, S.H. (1972) Essential Fatty Acids in the Diet of Rainbow Trout (*Salmo gairdneri*): Physiological Symptons of EFA Deficiency, *J. Nutr. 102*, 87–92.

39. Ghioni, C., Tocher, D.R., Bell, M.V., Dick, J.R., and Sargent, J.R. (1999) Low C$_{18}$ to C$_{20}$ Fatty Acid Elongase Activity and Limited Conversion of Stearidonic Acid, 18:4(n-3), to Eicosapentaenoic Acid, 20:5(n-3), in a Cell Line from the Turbot, *Scophthalmus maximus*, *Biochim. Biophys. Acta 1437*, 170–181.

40. Frøyland, L., Madsen, L., Vaagenes, H., Totland, G.K., Auwerx, J., Kryvi, H., Staels, B., and Berge, R.K. (1997) Mitochondrion Is the Principal Target for Nutritional and Pharmacological Control of Triglyceride Metabolism, *J. Lipid Res. 38*, 1851–1856.

Changes of the Transcriptional and Fatty Acid Profiles in Response to n-3 Fatty Acids in SH-SY5Y Neuroblastoma Cells

Bénédicte Langelier, Jean-Marc Alessandri*, Marie-Hélène Perruchot, Philippe Guesnet, and Monique Lavialle

Nutrition & Food Safety, Neurobiology of Lipids, INRA (l'Institut National de la Recherche Agronomique), Jouy-en-Josas, France

ABSTRACT: Synthesis of docosahexaenoic acid (DHA) from its metabolic precursors contributes to membrane incorporation of this FA within the central nervous system. Although cultured neural cells are able to produce DHA, the membrane DHA contents resulting from metabolic conversion do not match the high values of those resulting from supplementation with preformed DHA. We have examined whether the DHA precursors downregulate the incorporation of newly formed DHA within human neuroblastoma cells. SH-SY5Y cells were incubated with gradual doses of α-linolenic acid (α-LNA), EPA, or docosapentaenoic acid (DPA), and the incorporation of DHA into ethanolamine glycerophospholipids was analyzed as a reflection of synthesizing activity. The incorporation of EPA, DPA, and preformed DHA followed a dose–response saturating curve, whereas that of DHA synthesized either from α-LNA, EPA, or DPA peaked at concentrations of precursors below 15–30 μM and sharply decreased with higher doses. The mRNA encoding for six FA metabolism genes were quantified using real-time PCR. Two enzymes of the peroxisomal β-oxidation, L-bifunctional protein and peroxisomal acyl-CoA oxidase, were expressed at lower levels than fatty acyl-CoA ligase 3 (FACL3) and Δ6-desaturase (Δ6-D). The Δ6-D mRNA slightly increased between 16 and 48 h of culture, and this effect was abolished in the presence of 70 μM EPA. In contrast, the EPA treatment resulted in a time-dependent increase of FACL3 mRNA. The terminal step of DHA synthesis seems to form a "metabolic bottleneck," resulting in accretion of EPA and DPA when the precursor concentration exceeds a specific threshold value. We conclude that the critical precursor- concentration window of responsiveness may originate from the low basal expression level of peroxisomal enzymes.

Paper no. L9735 in *Lipids 40,* 719–728 (June 2005).

---

*To whom correspondence should be addressed at LNSA, INRA, 78352 Jouy-en-Josas, France. E-mail: Jean-Marc.Alessandri@jouy.inra.fr

Abbreviations: α-LNA, α-linolenic acid; AOX, peroxisomal acyl-CoA oxidase; ChoGpl, choline glycerophospholipids; Ct, threshold cycle number; DBP, D-bifunctional protein; Δ6-D, Δ6-desaturase; DHA, docosahexaenoic acid (22:6n-3); DMA, dimethylacetals; DPA, docosapentaenoic acid (22:5n-3); ELOVL4, brain fatty acid elongase-4; EPA, eicosapentaenoic acid (20:5n-3); ER, endoplasmic reticulum; EtnGpl, ethanolamine-glycerophospholipids; FACL3, fatty acyl-CoA ligase 3; GAPDH, glyceraldehyde-3-phosphate dehydrogenase; LBP, L-bifunctional protein; PlsEtn, 1-*O*-alkyl-1'-enyl-2-acyl-*sn*-glycero-3-phosphoethanolamine; PPAR, peroxisome proliferator-activated receptors; PtdEtn, phosphatidylethanolamine; PtdSer, phosphatidylserine; RT-PCR, reverse-transcription polymerase chain reaction; THA, tetracosahexaenoic acid (24:6n-3).

The incorporation of docosahexaenoic acid (DHA, 22:6n-3) in the nerve membranes during perinatal development is essential to the development of cerebral and retinal functions (reviewed in Refs. 1 and 2). DHA may be taken up through blood vessels by the brain (3) and retina (4), or synthesized by the brain and retinal cells from its dietary precursors, mainly α-linolenic acid (α-LNA, 18:3n-3) and eicosapentaenoic acid (EPA, 20:5n-3). The conversion of α-LNA, the essential precursor, into EPA, docosapentaenoic acid (DPA, 22:5n-3), and tetracosahexaenoic acid (THA, 24:6n-3) occurs in the endoplasmic reticulum (ER) through successive desaturations and elongations. THA is then transferred to the peroxisomes, where it is β-oxidized to give DHA (5,6). The essentiality of this peroxisomal step has been demonstrated in studies on human fibroblasts, in which gene mutations of peroxisomal acyl-CoA oxidase (AOX) or of D-bifunctional protein (DBP) were associated with the loss of DHA synthesis capacity (7,8).

Increasing the α-LNA intakes in humans has been considered as a possible way of increasing DHA synthesis. However, α-LNA dietary intakes do not appear to support DHA levels in the neonate brain as high as those in preformed DHA intake (9–11). Actually, studies in newborn infants fed milk replacers (12–14) and clinical studies in adults (15,16) have shown that the α-LNA nutritional strategy mainly induces the DHA upstream precursors, EPA and DPA, to increase in the blood lipids, not DHA. Clinical studies using stable isotope tracers in adults have demonstrated that the conversion of plasma α-LNA to DHA accounts for much less than 1% (16–20). This could result from the preferential β-oxidation of α-LNA, reducing its entry into the pathway of long-chain synthesis (21–25). It is also proposed that a feedback control mechanism responsive to the plasma concentration of DHA regulates its own synthesis, thereby maintaining DHA homeostasis during dietary changes in n-3 FA (19).

The mechanisms responsible for the low conversion rate at the cellular and molecular levels remain hypothetical. The peroxisomal pathway could be the limiting step, as it requires complex movements of very long chain derivatives between the ER and the peroxisomes (26). On the other hand, α-LNA itself may down-regulate its conversion (23), possibly by competing with 24:5n-3 for Δ6-desaturation. *In vitro* studies have shown that rat astrocytes (27–30), retinal cells in primary cul-

ture (31), and established cell lines from human retinoblastoma (32–34) all have the enzyme activities needed for DHA synthesis. Nevertheless, it has never been shown that the incorporation of precursor-derived DHA into phospholipids can reach levels as high as those resulting from the incubation of cells with equivalent concentrations of preformed DHA. In previous works, we demonstrated that the phospholipid incorporation of preformed DHA in the cells from human neuroblastoma and retinoblastoma lines can reach the high physiological plateau value that is characteristic of the retina and brain (35), whereas the major FA to increase in phospholipids upon incubation with the DHA upstream precursors are EPA and DPA, not DHA (36,37). A possible hypothesis explaining why the incorporation of the newly formed DHA into phospholipids is strongly limited in spite of its actual synthesis may be that the gene expression of some enzymes of the ER and/or peroxisomal pathways is readily down-regulated. We previously found that the mRNA expression of AOX in Y79 retinoblastoma cells was depressed as the α-LNA dose in the medium increased (37), raising the question of whether this effect was induced by α-LNA itself or by one of its downstream products. In the present study, we have considered the hypothesis that transcription of genes involved in DHA synthesis could be modulated in the neuroblastoma cells by EPA, the main long-chain product of α-LNA. We have quantified, in human neuroblastoma cells (SH-SY5Y), the mRNA levels of genes encoding for several key enzymes of both the ER and peroxisomal steps of FA metabolism, i.e., the FA-CoA ligase 3 (FACL3), Δ6-desaturase (Δ6-D), brain FA elongase-4 (ELOVL4), and peroxisomal enzymes of β-oxidation, AOX, DBP, and L-bifunctional protein (LBP). Concurrently, we analyzed, as reflecting n-3 metabolism, the incorporation into cell phospholipids of EPA itself and of the newly formed DPA and DHA. We then examined whether the mRNA profile responded to a dose of EPA found to be inhibiting toward DHA incorporation.

MATERIALS AND METHODS

Cell culture. Human SH-SY5Y neuroblastoma cells, obtained from the European Collection of Animal Cell Culture (Porton Down, Salisbury, United Kingdom), were cultured as a suspension in DMEM supplemented with 10% heat-inactivated FBS, 50 IU/mL penicillin, 50 μg/mL streptomycin, and 2 mM glutamine (Gibco BRL, Cergy-Pontoise, France). The cells were grown in Falcon 75-cm^2 tissue culture flasks in an incubator maintained at 37°C with 5% CO_2 in humidified air as the gas phase. In all experiments, the cells were seeded at a density of 5×10^6 cells/flask and left to adhere to the plastic flask for 24 h before being incubated with FA. The DNA contents were measured using the bisbenzimide fluorescence assay (38) on cells cultured for 16 or 48 h (postadhesion) with 70 μM EPA.

FA analysis. Cells were transferred to media supplemented with gradual concentrations (7 to 70 μM) of α-LNA, EPA, DPA, or DHA that did not exceed their maximum capacity of phospholipid incorporation, for the reason that these concentrations should be considered as bordering on physiological

values (35). FA sodium salts (Nu-Chek-Prep, Elysian, MN) were directly dissolved in the 10% FCS medium to give a concentration of 7, 15, 30, or 70 μM. After 16, 48, or 72 h (postadhesion) of incubation, the cells were trypsinized and harvested by centrifugation, washed with PBS containing 50 μM FA-free albumin (Sigma-Aldrich Chimie, Saint Quentin Fallavier, France) to remove any FA adsorbed onto the cell surface. The total lipids were extracted from 1 vol of cell homogenate with 4 vol of chloroform/methanol (2:1, vol/vol) in the presence of 0.005% (by wt) BHT. The lipid bottom phase was washed, dried, solubilized in chloroform, and stored at −80°C until separation of the ethanolamine-glycerophospholipids including plasmenylethanol-amines (total EtnGpl). The EtnGpl fraction was purified by solid-phase extraction on a 500-mg prepacked aminopropyl cartridge (J.T.Baker, Deventer, The Netherlands) (36). The cartridges were equilibrated beforehand with eluent 1 (isopropanol/chloroform, 1:2, vol/vol). Each sample of total lipids was dried under nitrogen, resolubilized in 250 μL of eluent 1 and deposited onto a single cartridge, which was immediately eluted successively with 3 mL of eluent 1, 3 mL of diethyl ether/acetic acid (98:2, vol/vol), 1 mL of acetonitrile, and 8 mL of acetonitrile/*n*-propanol (3:1, vol/vol) to recover the choline glycerophospholipids (ChoGpl) fraction, and then with 2 mL of acetonitrile/*n*-propanol (1:1, vol/vol) and 3 mL of methanol to recover the EtnGpl fraction consisting of a mixture of phosphatidylethanolamine (PtdEtn) and 1-*O*-alkyl-1′-enyl-2-acyl-*sn*-glycero-3-phosphoethanolamine (PlsEtn). The phosphatidylserine (PtdSer) fraction was recovered by eluting with isopropanol/methanolic HCl (4:1, vol/vol). All fractions were dried under a nitrogen flux and transmethylated by methanol at 90°C in the presence of BF_3. The methyl esters were extracted, washed, and injected through the on-column injector of a 9000 gas chromatograph (Chrompack, Middelburg, The Netherlands) equipped with a retention gap and a CP-WAX 52 CB bonded fused-silica capillary column of 0.25 mm i.d. and 60 m length (Varian, Les Ullis, France). The oven temperature was programmed for 79–212°C at a heating rate of 4°C/min. The instrument responses attributable to FAME and to dimethylacetals (DMA, issuing from transmethylation of the alkenyl-acyl phospholipids) were automatically integrated, and their factor response and ECL were compared with standard compounds. All compositions were expressed as a percentage by weight of total FA.

Quantification of mRNA expression by real-time reverse transcription (RT)-PCR. RNA extraction and cDNA synthesis. Total cellular RNA was prepared from cells cultured for 16 or 48 h with 70 μM of EPA by using an RNeasy Lipid Tissue Midi Kit according to the manufacturer's instructions (Qiagen S.A., Courtaboeuf, France). Total RNA concentrations were determined by absorbance measurements at 260 nm using a Biophotometer (Eppendorf SARL, Le Pecq, France). Subsequently, 6 μg total RNA was reverse-transcribed using the High Capacity cDNA Archive Kit (Applied Biosystems, Foster City, CA) according to the manufacturer's instructions.

Primers. Primers for the target were designed with the assistance of Primer Express 2.0 (Applied Biosystems). Glycer-

TABLE 1
Real Time PCR Primer Characteristics for cDNA Amplification

Gene	GenBank acc. no.	Oligonucleotide[a]	Sequence
AOX	NM-004035 (human)	Fwd primer (1384–1403)	5′-CAG GAA AGT TGG TGT GTG GC-3′
		Rev primer (1533–1515)	5′-AAT CTG GCT GCA CGG AGT TT-3′
ELOVL4	AF277094 (human)	Fwd primer (759–779)	5′-TGG CCC ATG GAT TCA GAA AT-3′
		Rev primer (902–881)	5′-TTA GAG CCC AGT GCA TCC ATT-3′
FACL3	NM-004457 (human)	Fwd primer (889–910)	5′-AGG GCA TCA TTG TGC ATA CCA-3′
		Rev primer (990–969)	5′-TGC AAT ATC TGA GGG CAA TGG-3′
GAPDH	X01677 (human)	Fwd primer (246–265)	5′-TGA GAA CGG GAA GCT TGT CA-3′
		Rev primer (366–347)	5′-GAA GAC GCC AGT GGA CTC CA-3′
DBP	BC003098 (human)	Fwd primer (544–565)	5′-TTGGCCAGGCCAATTATAGTG-3′
		Rev primer (669–649)	5′-CATCCGTGATCCCGCATTAG-3′
LBP	NM-001966 (human)	Fwd primer (687–708)	5′-TGTCTTGCACAGGAGGCTTGT-3′
		Rev primer (808–788)	5′-CTCTAGCCTGCCCTGATTGC-3′

[a]Coordinates according to GenBank. AOX, peroxisomal acyl-CoA oxidase; ELOVL4, brain FA elongase-4; FACL3, fatty acyl-CoA ligase 3; GAPDH, glyceraldehyde-3-phosphate dehydrogenase; DBP, D-bifunctional protein; LBP, L-bifunctional protein.

aldehyde-3-phosphate dehydrogenase (GAPDH) was used as a housekeeping gene to normalize the mRNA abundance of each target gene. We conducted BLASTN searches against Gen-Bank to check the total gene specificity of the nucleotide sequences chosen for the primers (Tables 1, 2). The expression of Δ6-D was evalutated using quantitative RT-PCR based on a specific set of primers and probes (Assays-on-Demand, gene expression products; Applied Biosystems). Quantitative values for cDNA amplification were obtained (using Sequence Detector) from the threshold cycle number (Ct) at which the increase in the signal associated with exponential growth of PCR products begins to be detected.

Real-time quantitative PCR amplification. PCR reactions were performed using the ABI Prism 7000 Sequence Detection Systems (Applied Biosystems). Each cDNA was amplified in a 25-μL volume containing 12.5 μL of 2× SYBR Green master mix (Applied Biosystems) and 300-nM concentrations of gene-specific primers (Table 1). Melting curves were used to determine the temperature at which only the amplicon, and not primer dimers, accounted for the SYBR Green-bound fluorescence. For Δ6-D cDNA amplification, the 25-μL reaction volume contained 10 μL of 2× TaqMan Universal Master Mix (Applied Biosys-

tems) and 1 μL of 20× Assays-on-Demand (Hs00188654-m1 and Hs99999905-m1 for Δ6-D and GAPDH, respectively). Thermal cycling conditions comprised an initial denaturation step at 95°C for 10 min and 45 cycles at 95°C for 15 s and 60°C for 1 min. Amplification of cDNA was performed in triplicate for each data point, with each condition (culture duration, incubation with EPA) also being reproduced in triplicate.

Standard curves. To establish the calibration curves, a cDNA fragment of each gene was amplified using conventional PCR (Table 2). These fragments were purified using the Qiaquick Gel Extraction and PCR Purification kits (Qiagen), quantified spectrophotometrically, and sequenced (Genome Express, Meylan, France). PCR amplification was performed with template dilutions ranging from 101 to 106 copies. Overall efficiencies (*E*) of PCR were calculated from the slopes of the standard curves according to the equation

$$E = [10^{-1/\text{slope}}] - 1 \qquad [1]$$

Normalization. All cDNA were amplified with an efficiency above 98%, indicating that GAPDH and target genes were amplified with the same efficiency. Therefore, we used the ΔCt

TABLE 2
Conventional PCR Primer Characteristics for Establishing the cDNA-Amplification Standard Curves

Gene	GenBank acc. no.	Oligonucleotide[a]	Sequence	Amplicon size (bp)
AOX	NM-004035 (human)	Fwd primer (1211–1231)	5′-CAC TGG CAT TGA AGC ATG TC-3′	530
		Rev primer (1740–1720)	5′-AAT ACA GCA GAC ATA AAC TC-3′	
ELOVL4	AF277094 (human)	Fwd primer (254–274)	5′-GTG TGG AAA ATT GGC CTC TG-3′	743
		Rev primer (996–977)	5′-CAT GGC TGT TTT TCC AGC TT-3′	
FACL3	NM-004457 (human)	Fwd primer (727–747)	5′-TCC AGC CAT TGT TCA TGC AT-3′	413
		Rev primer (1139–1057)	5′-CAT GGG CCA GAG GCA AAT A-3′	
GAPDH	X01677 (human)	Fwd primer (244–263)	5′-GCT GAG AAC GGG AAG CTT G-3′	358
		Rev primer (602–582)	5′-ATG GCA TGG ACT GTG GTC AT-3′	
DBP	BC003098 (human)	Fwd primer (353–375)	5′-GTGGTCAACAATGCTGGAATTC-3′	401
		Rev primer (753–732)	5′-CTCTCGTGACAAAGCCAAAGG-3′	
LBP	NM-001966 (human)	Fwd primer (437–458)	5′-GGAGTTCCTGCTGCACTTGAC-3′	405
		Rev primer (841–820)	5′-TGCTTTCCTTTCAGCGAAGAA-3′	

[a]Coordinates according to GenBank. For abbreviations see Table 1.

method to quantify the PCR products. Triplicate measurements of Ct were performed in each sample (intra-assay variation), and the average of three values was used to determine the ΔCt ($Ct_{GAPDH} - Ct_{gene}$). In theory, when the PCR efficiency is equal to 100%, a gap of 3.3 cycles of amplification between the target gene and the housekeeping gene corresponds to a 10-fold difference in the respective amounts of amplicon. From the ΔCt value, the abundance of each mRNA was thus reported relative to the GAPDH abundance according to the following equation:

$$\text{mRNA relative abundance} = 100/[(\Delta Ct \times 10)/3.3] = 33/\Delta Ct \quad [2]$$
(expressed in percentage of GAPDH)

Statistical analysis. The data were analyzed using StatView+ Graphics software (Abacus Concepts Inc., Berkeley, CA) by one-way ANOVA (time factor or treatment factor) followed by the multiple-comparison Fisher test. The differences due to culture duration in mean values (± SD) for FA within the EtnGpl fraction were compared after 16 and 72 h of culture without n-3 supplementation (time factor) at three levels of significance: $P < 0.02$, $P < 0.01$, or $P < 0.001$. Differences in the relative abundance of mRNA produced by a given target gene after 16 or 48 h of incubation with EPA were compared considering four treatments: 16 h/EPA 0 µM, 48 h/EPA 0 µM, 16 h/EPA 70 µM, and 48 h/EPA 70 µM. The differences in mRNA abundances due to the EPA treatment were considered significant at $P < 0.01$ or $P < 0.001$.

RESULTS

Effect of EPA on cell growth. Supraphysiological concentrations (500 µM) of PUFA in the culture medium have genotoxic effects on hepatocytes, especially in cells cultured without serum or antioxidants (39). Although we used EPA only at physiological concentrations, we checked to ensure that EPA did not reduce the growth rate of SH-SY5Y cells. A 70-µM quantity of EPA had no significant impact on cell growth, even after 48 h in culture (Table 3).

FA composition of cell phospholipids in standard conditions. The FA composition in EtnGpl from cells cultured for 16, 48, and 72 h in 10% FCS medium, and the ChoGpl and PtdSer FA compositions at 72 h are reported in Table 4. The data at 72 h show that the concentration of total n-3 FA was higher in EtnGpl (9.1% of total FA) than in PtdSer (4.4%) and ChoGpl (1.9%). Owing to this specific FA composition, we focused on the impact of the n-3 treatment within the EtnGpl fraction.

The time-dependent changes in the EtnGpl FA composition mainly consisted of a 44% increase in n-3 FA ($P < 0.01$), which compensated for a 55% decrease in n-6 FA ($P < 0.001$). In the absence of supplemental n-3 FA, this change in the FA composition within growing neural cells may reflect the increasing use of n-3 FA from the FCS lipids for membrane biogenesis. Nevertheless, even after 72 h of culture, the n-6 content in the three classes was two times higher than that of n-3 FA, finally reflecting the relative proportions of n-6 and n-3 FA in the

TABLE 3
Effect of EPA (70 µM) on Cell Proliferation

| | | EPA µM | |
		0	70
16 h	DNA (µg/flask)	2.96 ± 0.17	2.92 ± 0.05
	Growth rate	1.4 ± 0.08	1.38 ± 0.03
48 h	DNA (µg/flask)	5.11 ± 0.33	4.68 ± 0.32
	Growth rate	2.42 ± 0.16	2.22 ± 0.15

medium (36). It is noteworthy that, at the same time, cells increased their content of trienoic FA, 20:3n-9 and 22:3n-9 ($P < 0.001$), which is indicative of their metabolic ability to compensate for their low content of very long chain PUFA. This "spontaneous" synthesis of trienoic FA suggests that the desaturases are constitutively active in SH-SY5Y cells. Nevertheless, neuroblastoma cells cultured with 10% FCS must be considered as being specifically deficient in DHA, more particularly if their high "avidity" for the preformed DHA is taken into account (35). Actually, the basal DHA content in SH-SY5Y cells (around 5% in EtnGpl) is equivalent to that found in the cortex of rats chronically deprived of dietary n-3 FA (35). However, it has been shown previously in cultured astrocytes that preloading the cells with exogenous DHA reduces their ability to produce new DHA from radiolabeled α-LNA (28). Therefore, the state of spontaneous DHA deficiency within cultured cells seems particularly appropriate for determining their ability to synthesize DHA.

Incorporation of preformed DHA. The dose–response study was performed to determine whether SH-SY5Y cells have the capacity to synthesize DHA from each of its upstream precursors, α-LNA, EPA, or DPA, and especially whether the newly formed DHA was actually incorporated into cell phospholipids. The incorporation of the precursor-derived DHA was compared with that resulting from the incubation of cells with increasing amounts of preformed DHA. The changes of the main n-3 and n-6 FA in EtnGpl, the fraction having the highest content of FA from both series, are presented in Figure 1. The maximum preformed DHA incorporated into the EtnGpl (around 32% of total FA) (Fig. 1A) reached the physiological plateau of brain cells (35), indicating that the uptake, trafficking, and acylation of supplemental DHA are not limiting in SH-SY5Y cells.

Biphasic pattern of neoformed DHA incorporation. Cells incubated with increasing doses of α-LNA (Fig. 1B), EPA (Fig. 1C), or DPA (Fig. 1D) showed an initial increase in DHA incorporation, corresponding to the lower range of concentration of the precursors, and a second phase of decreased incorporation at higher concentrations. The incorporation of newly formed DHA peaked at 9–10% in the EtnGpl of cells incubated with α-LNA (Fig. 1B) and at 8–9% in cells incubated with EPA (Fig. 1C). Cells incubated with DPA showed a maximum of 12% DHA incorporation in EtnGpl (Fig. 1D), equal to only one-third of the maximum incorporation resulting from incubation with DHA itself (see Fig. 1A). In the ChoGpl fraction, the newly formed DHA peaked at only 2.3% of total FA (data not shown).

TABLE 4
FA Composition in the EtnGpl, ChoGpl, and PtdSer Fractions of SH-SY5Y Cells[a]

	EtnGpl			ChoGpl	PtdSer
	16 h (n = 3)	48 h (n = 3)	72 h (n = 13)	72 h (n = 14)	72 h (n = 3)
14:0	0.6 ± 0.1	0.6 ± 0.1	0.6 ± 0.2	3.9 ± 0.4	1.1 ± 0.1
16:0	7.2 ± 0.3	8.5 ± 1.1	7.6 ± 0.4	30.3 ± 1.2	9.8 ± 0.1
18:0	16.6 ± 0.9	13.9 ± 0.5	15.6 ± 0.8	5.3 ± 0.6	26.7 ± 0.6
20:0	0.3 ± 0.03	< 0.1	0.2 ± 0.03	0.1 ± 0.05	0.5 ± 0.02
Total SFA	25.8 ± 1.0	23.9 ± 1.2	25.1 ± 0.6	39.5 ± 1.2	40.6 ± 0.6
16:1n-9	1.0 ± 0.3	1.0 ± 0.3	1.6 ± 0.3	8.8 ± 0.9	1.9 ± 0.1
16:1n-7	1.4 ± 0.01	2.2 ± 0.3	1.3 ± 0.3	3.7 ± 0.4	1.9 ± 0.2
18:1n-9	12.6 ± 0.3	13.9 ± 0.2	12.7 ± 0.3	25.9 ± 0.6	16.4 ± 0.5
18:1n-7	4.1 ± 0.1	3.6 ± 0.1	3.3 ± 0.3	9.4 ± 0.6	8.1 ± 0.1
20:1n-9	<0.1	<0.1	0.4 ± 0.06	0.5 ± 0.1	0.7 ± 0.01
Total MUFA	22.9 ± 0.4	24.6 ± 0.9	24.2 ± 0.7	48.5 ± 1.1	32.4 ± 0.7
20:3n-9	0.9 ± 0.07	1.2 ± 0.1	3.1 ± 0.2[a]	1.5 ± 0.2	6.0 ± 0.2
22:3n-9	1.3 ± 0.08	1.9 ± 0.03	5.3 ± 0.3[a]	0.9 ± 0.2	4.7 ± 0.1
18:2n-6	0.8 ± 0.01	0.9 ± 0.3	0.3 ± 0.03	0.4 ± 0.1	1.1 ± 0.2
20:3n-6	0.4 ± 0.1	0.4 ± 0.1	0.3 ± 0.1	0.5 ± 0.1	0.7 ± 0.03
20:4n-6	17.2 ± 0.9	16.7 ± 1.6	13.3 ± 0.6[c]	3.2 ± 0.2	5.0 ± 0.3
22:4n-6	10.8 ± 0.4	8.5 ± 0.4	6.1 ± 0.4[a]	0.8 ± 0.1	1.9 ± 0.1
22:5n-6	2.5 ± 0.1	2.7 ± 0.2	1.9 ± 0.1[c]	0.3 ± 0.04	0.8 ± 0.1
Total n-6 PUFA	31.7 ± 1.0	29.0 ± 1.8	21.9 ± 0.8[a]	5.2 ± 0.5	9.9 ± 0.8
18:3n-3	<0.1	<0.1	<0.1	0.1 ± 0.02	0.3 ± 0.1
20:4n-3	<0.1	<0.1	<0.1	0.1 ± 0.03	0.1 ± 0.05
20:5n-3	0.2 ± 0.1	0.2 ± 0.1	1.0 ± 0.1[c]	0.3 ± 0.04	1.2 ± 0.04
22:5n-3	2.9 ± 0.2	2.2 ± 0.2	2.6 ± 0.2	0.5 ± 0.1	1.1 ± 0.2
22:6n-3	3.3 ± 0.2	5.3 ± 0.9	5.4 ± 0.3[b]	0.9 ± 0.1	1.5 ± 0.1
Total n-3 PUFA	6.4 ± 0.5	7.6 ± 0.8	9.1 ± 0.5[b]	1.9 ± 0.3	4.4 ± 0.5
Total DMA	8.5 ± 0.2	9.2 ± 0.6	10.4 ± 0.3[c]	0.1 ± 0.03	1.2 ± 0.2
Other	2.5 ± 0.2	2.6 ± 0.2	0.9 ± 0.1	2.4 ± 0.2	0.8 ± 0.1

[a]Cells were cultured in 10% FCS (without n-3 supplementation) for 16, 48, or 72 h. [a]$P < 0.001$; [b]$P < 0.01$; [c]$P < 0.02$; significant changes in EtnGpl (72 vs. 16 h). EtnGpl, ethanolamine-glycerophospholipids; ChoGpl, choline glycerophospholipids; PtdSer, phosphatidylserine; SFA, saturated FA; MUFA, monounsaturated FA; DMA, dimethylacetals.

The value of the precursor concentration that produced the reversion of the neoformed DHA incorporation in EtnGpl, the so-called concentration of reversion, was graphically calculated by using the double reciprocal plot method (35). As shown in Figure 2, the coordinate of the intersection point of the broken line (issuing from the biphasic pattern) is the inverse value of the concentration of reversion. This method led to the values of each concentration of reversion, equal to 15 μM α-LNA, 26 μM EPA, and 30 μM DPA, respectively, thereby indicating that α-LNA, with the lower concentration of reversion, was the least efficient precursor regarding the incorporation of newly formed DHA into cell phospholipids. Moreover, the concentration of reversion of α-LNA (15 μM) is also the concentration at which this FA began to increase in ChoGpl and EtnGpl (Fig. 3). The increase in α-LNA may be the hallmark of a saturating effect on the capacity of cells to metabolize this precursor, which is normally present in very low amounts within the brain phospholipids. However, in cells dosed with 70 μM of α-LNA, the increase of α-LNA in Et-

nGpl (plus 1% by weight of total FA) did not compensate for the decreased incorporation of α-LNA-derived DHA (minus 7%). Actually, the supplemental α-LNA was more rapidly and more efficiently incorporated into ChoGpl than into EtnGpl (Fig. 3). Therefore, the increased incorporation of α-LNA into EtnGpl cannot explain the biphasic pattern of DHA incorporation. Thus, SH-SY5Y cells can synthesize DHA from α-LNA, EPA, or DPA and can incorporate the newly formed DHA into phospholipids, but only imperfectly. In contrast, the incorporation of EPA resulting from incubations with α-LNA (Fig. 1B) or DPA (Fig. 1D), and the incorporation of DPA resulting from α-LNA (Fig. 1B) or EPA (Fig. 1C) increased regularly with the concentration of precursor in the medium. The decrease in DHA and the increase in EPA occurred concurrently. However, the increase in EPA was very gradual, in contrast to the biphasic incorporation of newly formed DHA. Moreover, EPA incorporation clearly did not counteract the incorporation of DPA. These data raised the question of whether the increase in EPA was the secondary hallmark of a primary down-regula-
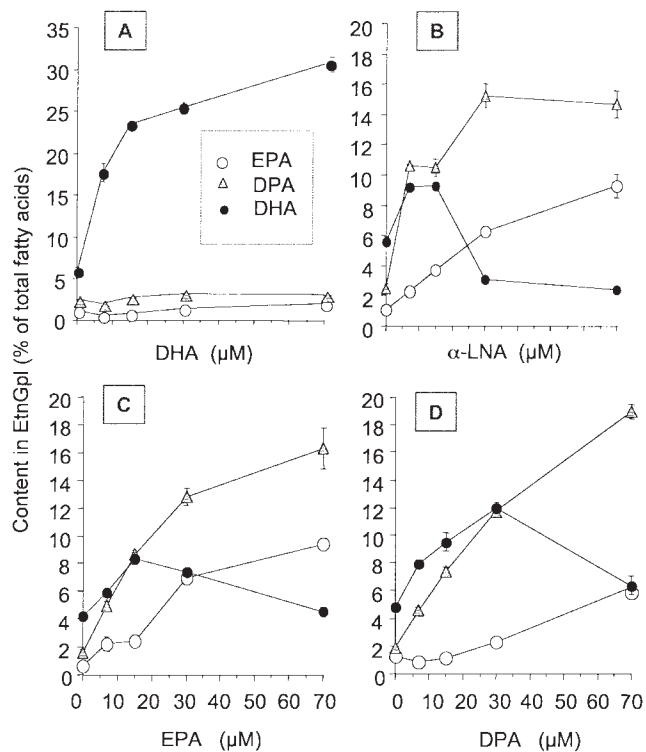
FIG. 1. Distributions of eicosapentaenoic acid (EPA, 20:5n-3), docosapentaenoic acid (DPA, 22:5n-3), and docosahexaenoic acid (DHA, 22:6n-3) in the ethanolamine-glycerophospholipid (EtnGpl) fraction from SH-SY5Y cells cultured with a range of concentrations of (A) DHA, (B) α-linolenic acid (α-LNA, 18:3n-3), (C) EPA, or (D) DPA. Cells were incubated in medium supplemented with 7 to 70 μM unesterified FA. Each value is the mean ± SD of three separate cultures, expressed in percentage by weight of total FA in EtnGpl. Note that the *y*-axis in panel A is different from those in panels B–D.

FIG. 2. Double reciprocal plot drawn from the inverted data (see Ref. 35 for details) of the biphasic incorporation of newly formed DHA (Fig. 1B–D). The intersection point of the V-shaped lines defines the inverse value of the precursor concentration at which the incorporation of newly formed DHA peaked (concentration of reversion). The double reciprocal plot drawn from the incorporation of preformed DHA (not shown) produces a straight line (35). For abbreviations see Figure 1.

tion that led to the decrease in DHA synthesis and/or incorporation. To address this question, we analyzed the effect of 70 μM EPA on the mRNA encoded by genes involved in FA conversion.

Effect of the n-3 FA on endogenous n-6 FA. The incorporation of the main long-chain n-6 FA, 20:4n-6 (arachidonic acid), 22:4n-6 (adrenic acid), and 22:5n-6 (n-6 docosapentaenoic acid), either provided by the serum or synthesized from serum linoleic acid, decreased when the cells were incubated with increasing concentrations of each supplemental n-3 FA, DHA, α-LNA, EPA, or DPA (Fig. 4). The EtnGpl contents of n-6 PUFA decreased to about 50% in cells incubated with 70 μM of each n-3 FA. These patterns indicate that the acylation of the preformed and newly formed n-3 FA counteracts that of the "endogenous" n-6 FA.

Quantification of mRNA encoding for lipid metabolism genes. The mRNA relative abundances show that various lipid metabolism genes produce concentrations of mRNA varying from 3 to 9% that of GAPDH (Fig. 5). This is the first report, to our knowledge, that SH-SY5Y human neuroblastoma cells express the main enzymes of PUFA metabolism. We quantified the mRNA after 16 and 48 h of culture in the presence of 70 μM EPA to determine whether the transcription levels in the EPA-treated cells

depended on the same duration of treatment as that producing changes in the FA composition. The data clearly show that the mRNA levels depended more on the culture duration than on the presence of EPA. There was a general trend (although not statistically significant regarding each gene) for a transcriptional increase between 16 and 48 h of culture, with the exception of the LBP mRNA abundance, which remained at the same low level throughout experiment. Actually, the relative abundance of Δ6-D mRNA increased by one point between 16 and 48 h in the absence of EPA ($P < 0.001$), but not in the presence of 70 μM EPA, showing that the time-dependent increase in Δ6-D mRNA was lost. On the other hand, incubation with EPA produced a significant time-dependent increase in the relative abundance of FACL3 mRNA ($P < 0.01$). Therefore, EPA had opposing effects on the time-dependent changes in mRNA, attenuating the weak increase in Δ6-D mRNA and slightly amplifying the change in FACL3 mRNA. The EPA treatment had no impact on the mRNA levels of LBP, ELOVL4, AOX, and DBP.

DISCUSSION

The incorporation of newly formed DHA into cell phospholipids results from synthesis, acylation, phospholipid metabolism, and turnover, with the relative content of DHA within membrane phospholipids giving a final reflection of the whole process. Our data show that the FA compositional changes in-
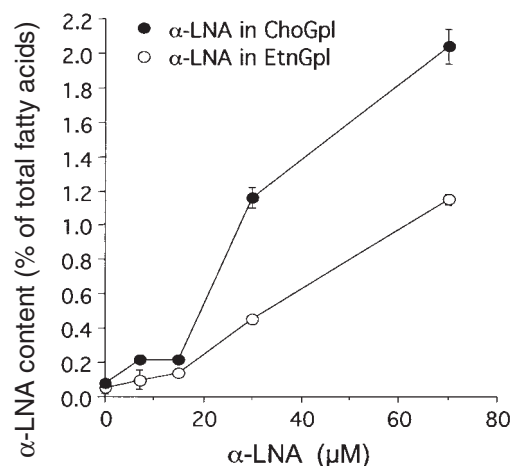
FIG. 3. Incorporation of α-LNA (18:3n-3) in the choline glycerophospholipid (ChoGpl) and EtnGpl fractions from SH-SY5Y cells cultured with a range of concentrations of α-LNA. All conditions are identical to those described in Figure 1B. For other abbreviations see Figure 1.

FIG. 4. Distribution of 20:4n-6 (arachidonic acid), 22:4n-6 (adrenic acid), and 22:5n-6 (n-6 DPA) in the EtnGpl fraction from SH-SY5Y cells cultured with 7 to 70 μM (A) DHA, (B) α-LNA, (C) EPA, or (D) DPA. Cells were incubated in medium containing unesterified FA. Each value is the mean ± SD of three culture flasks, expressed in percentage by weight of total FA in EtnGpl. For abbreviations see Figure 1.

duced by graded doses of the n-3 precursors follow a dose–response effect in EtnGpl, which is representative of the global metabolic capacities of cells. In particular, EtnGpl appeared to be the preferential class for the phospholipid incorporation of DHA in SH-SY5Y cells. This specificity of neuroblastoma cells may have a physiological significance, since it has been shown that DHA is more concentrated in the EtnGpl fraction from rat brain phospholipids than in the other classes (40). (According to that study, rat brain EtnGpl contains around 67 mol% of the total amount of brain DHA, compared with 22 mol% in PtdSer and 10 mol% in ChoGpl.)

The incorporation of n-3 FA into EtnGpl indicates that the synthesis of DPA from α-LNA or from EPA is an active process in SH-SY5Y cells, with the incorporation of DPA responding to the concentration of each precursor in a saturable manner. The increases in DHA and DPA at low precursor concentrations were concurrent, suggesting that newly synthesized DHA (from α-LNA, EPA, or DPA) and DPA did not compete for phospholipid acylation. Therefore, SH-SY5Y cells have the capacity to complete the metabolic chain of n-3 FA conversion through the ER and peroxisomal pathways, leading to DHA synthesis and to its effective incorporation into the membrane phospholipids. However, several features of the FA profile indicate that the peroxisomal step is limited in these cells. First, the DHA level was particularly low in basal conditions of culture despite the influx of n-3 PUFA from the medium. Animal studies of n-3 PUFA deficiency have shown that 22:5n-6 is formed through the action of desaturases and elongases on n-6 precursors, to compensate for the reduced input of n-3 PUFA. Thus, in physiological conditions, 24:5n-6 is formed within the ER and β-oxidized in the peroxisomes to produce 22:5n-6. However, in SH-SY5Y cells, the 22:5n-6 level remained low throughout 72 h of culture, whereas the total n-6 FA accounted for 22% of FA in EtnGpl, suggesting that the formation of the n-6 end product is limited. An impairment of the peroxisomal
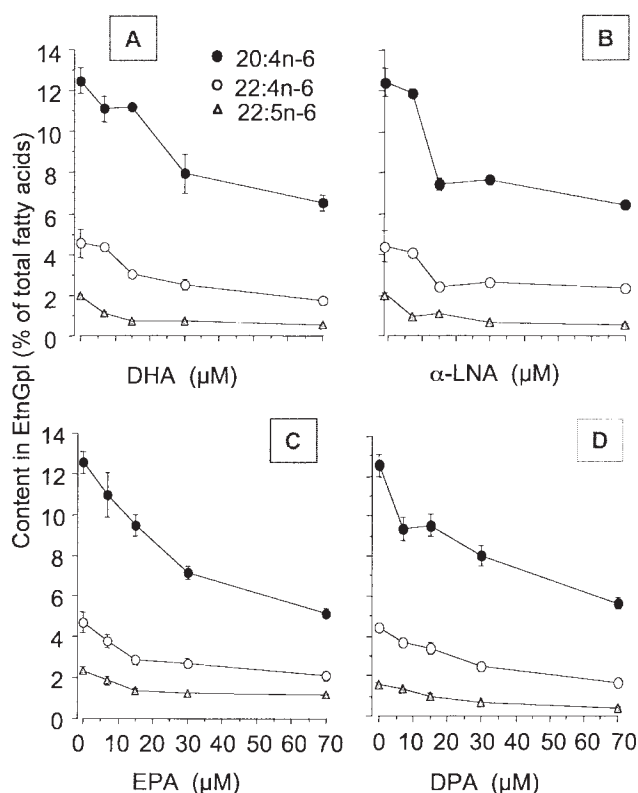
synthesis of 22-carbon PUFA from both the n-6 and n-3 series may explain the compensating rise in trienoic FA (20:3n-9 and 22:3n-9), whose synthesis is circumscribed to the ER, contrary to that of 22:5n-6 and DHA, which both require peroxisomal oxidation.

The second observation of our study was that increasing the doses of one n-3 precursor, α-LNA, DPA, or EPA, resulted in a sharp decrease in the incorporation of newly formed DHA, with the concentration of reversion being proportional to the precursor chain length. Hence, the most effective way to increase the DHA incorporation into cell phospholipids (apart from using preformed DHA) is to provide the cells with a 22-carbon precursor (DPA), not 18- or 20-carbon (α-LNA or EPA). Our finding that the concentration of reversion by α-LNA was two times lower than with DPA suggests that α-LNA is, paradoxically, the most potent down-regulator of DHA synthesis and/or incorporation among the DHA precursors. We previously showed that the DHA content of Y79 retinoblastoma cells peaked in the EtnGpl fraction from cells incubated with 7 μM α-LNA, and that it decreased on incubation with higher concentrations (37). The precursor-induced reversion of newly formed DHA incorporation seems to be a common feature of all neural cells in culture. This specific down-regulation
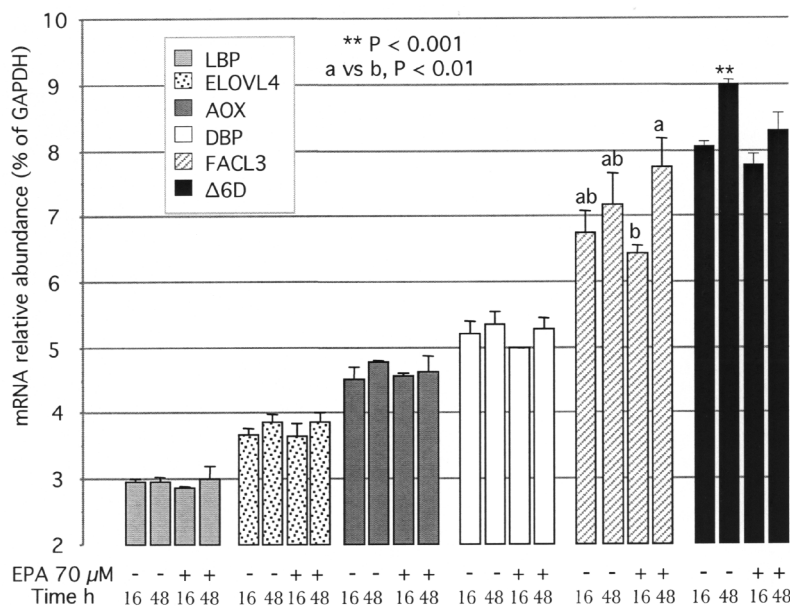
FIG. 5. Relative abundance of mRNA encoding target genes in SH-SY5Y cells incubated for 16 or 48 h with 0 or 70 μM EPA. Each value is the mean ± SD of three culture flasks (one flask value being the mean of three real-time PCR), expressed in percentage of glyceraldehyde-3-phosphate dehydrogenase (GAPDH) abundance. Levels of mRNA with distinct superscripts on histograms [a, b for fatty acyl-CoA ligase 3 (FACL3) or ** for Δ6-desaturase (Δ6-D)] are significantly different at $P < 0.01$ (FACL3) or $P < 0.001$ (Δ6-D). LBP, L-bifunctional protein; ELOVL4, brain FA elongase-4; AOX, peroxisomal acyl-CoA oxidase; DBP, D-bifunctional protein; for other abbreviation see Figure 1.

of DHA incorporation is likely due to competition for phospholipid acylation, as previously shown in CaCo-2 intestinal cells, with the acylation of the newly formed DHA being progressively replaced by that of its major upstream precursor, EPA (41). It was also reported that treatment of CaCo-2 cells with the dose of 100 μM EPA increases the EPA and DPA contents in EtnGpl (without modifying that of DHA) and decreases by 2.5 times the Δ6- and Δ5-D activities, showing that EPA at 100 μM inhibits enzymes of DHA synthesis (42). However, it was not determined in that study whether the desaturase-specific activities decreased through enzyme inhibition by excess substrate or through down-regulation of desaturase gene expression.

Some aspects of DHA incorporation suggest that the biphasic pattern results from mechanisms that are more complex than a simple molecular competition between EPA and DHA. First, the incorporation of α-LNA-derived DHA at low external α-LNA concentrations predominated over the incorporation of newly formed EPA (Fig. 1B), even though the synthesis of EPA necessarily precedes that of DHA. The incorporation of EPA-derived DHA also predominated over that of EPA in cells incubated with low concentrations of preformed EPA (Fig. 1C). Last, the EtnGpl fraction more avidly incorporated preformed DHA than preformed EPA. Therefore, the high specificity and "suddenness" of the reversion process are difficult to explain by the competition of EPA and DHA for acylation alone. In the second part of this study, we examined whether the EPA-induced decrease in DHA incorporation

could also result from transcriptional down-regulation of enzymes involved in DHA synthesis.

The mRNA profile shows that several key genes of the FA metabolism are expressed at relatively low levels, accounting for less than 10% of the housekeeping gene-mRNA abundance. However, Δ6-D mRNA appears to be 1.8 and 2.7 times more abundant than the mRNA of LBP, ELOVL4, and AOX. Moreover, Δ6-D mRNA was the only one whose concentration increased significantly throughout the 48 h in culture, which suggests that the growing neuroblastoma cells increase their capacity to desaturate FA. Therefore, the precursor-induced rise in EPA, DPA, and DHA and the mRNA profile both indicate that Δ6-desaturation is probably not a limiting step in the FA metabolism of SH-SY5Y cells. In comparison, the LBP gene produces the lower amount of mRNA, suggesting that peroxisomal β-oxidation may be rate limiting.

With the notable exception of Δ6-D, the mRNA levels were remarkably stable throughout the 48 h of culture. There was a trend toward increased mRNA abundance between 16 and 48 h, but this was significant only for Δ6-D in the absence of EPA, and only for FACL3 in the presence of EPA. The low amplitude of these transcriptional changes does not seem to support our hypothesis that a depression of mRNA encoding for FA metabolism genes may account for the biphasic pattern of newly formed DHA, at least in the presence of preformed EPA. However, since it has been demonstrated that (i) compounds acting as peroxisome proliferators activate the transcription of β-oxidation enzymes (43), (ii) AOX and LBP genes are direct

targets of peroxisome proliferator-activated receptor-α (PPAR-α) (44–47), and (iii) EPA is able to activate the PPAR-α-mediated transcription of a reporter gene in transfected cells (48,49), the hypothesis is plausible that EPA may be a modulator of mRNA encoding peroxisomal enzymes through the activation of cognate nuclear receptors. It should be noted that EPA exhibited its transcriptional effect (49) within a range of concentrations (250–1000 µM), which should be considered as being supraphysiological, especially regarding the cell capacity for phospholipid incorporation.

It cannot be excluded that transcriptional regulation of other genes (or isotypes), perhaps those involved in the peroxisomal assembly and/or in the functioning of peroxisomal membrane transporters, are key events in the down-regulation of phospholipid incorporation of the newly formed DHA. Alternatively, the biphasic pattern may also directly result from inhibition of enzyme activity(ies) without implicating transcriptional effects. The phospholipid incorporation of newly formed DPA being saturable and not submitted to down-regulation in the SH-SY5Y cells, we can suppose that the enzyme activities taking place in the ER are fully operant, at least until the step of DPA synthesis, whereas the final synthesis of THA and/or the peroxisomal enzyme activities would be inhibited. From this point of view, α-LNA should be the most potent inhibitor among the DHA precursors.

We conclude that, under conditions mimicking an n-3 physiological influx, the incorporation of newly formed DHA into phospholipids is strongly inhibited in SH-SY5Y cells, in spite of their ability to desaturate FA and produce DHA from each of the upstream precursors. The incorporation of newly formed DHA reveals a critical precursor-concentration window of responsiveness that may be related to the low basal transcription level of LBP and AOX without implicating further alterations in the mRNA profile. The biphasic incorporation of DHA probably sets in motion competition with EPA for phospholipid acylation, and possibly impairment of enzyme activities and/or of acyl-CoA carriers that are involved in the peroxisomal step of DHA synthesis. This combination of events results in a much lower incorporation of newly formed DHA into phospholipids than that resulting from an influx of preformed DHA, thereby reproducing in cultured neural cells the bloodstream FA composition of humans receiving the DHA precursors.

REFERENCES

1. Lauritzen, L., Hansen, H.S., Jùrgensen, M.H., and Michaelsen, K.F. (2001) The Essentiality of Long Chain n-3 Fatty Acids in Relation to Development and Function of the Brain and Retina, *Prog. Lipid Res. 40*, 1–94.
2. Alessandri, J.M., Guesnet, P., Vancassel, S., Astorg, P., Denis, I., Langelier, B., Aïd, S., Poumès-Ballihaut, C., Champeil-Potokar, G., and Lavialle, M. (2004) Polyunsaturated Fatty Acids in the Nervous System: Evolution of Concepts and Nutritional Implications Throughout Life, *Reprod. Nutr. Dev. 44*, 509–538.
3. Thies, F., Pillon, C., Moliere, P., Lagarde, M., and Lecerf, J. (1994) Preferential Incorporation of *sn*-2 LysoPC DHA over Unesterified DHA in the Young Rat Brain, *Am. J. Physiol. 36*, R1273–R1279.
4. Bazan, N.G., Gordon, W.C., and Rodriguez de Turco, E.B. (1992) Docosahexaenoic Acid Uptake and Metabolism in Photoreceptors: Retinal Conservation by an Efficient Retinal Pigment Epithelial Cell-Mediated Recycling Process, *Adv. Exp. Med. Biol. 318*, 295–306.
5. Voss, A., Reinhart, M., Sankarappa, S., and Sprecher, H. (1991) The Metabolism of 7,10,13,16,19-Docosapentaenoic Acid to 4,7,10,13,16,19-Docosahexaenoic Acid in Rat Liver Is Independent of a Δ4-Desaturase, *J. Biol. Chem. 266*, 19995–20000.
6. Sprecher, H., Luthria, D.L., Mohammed, B.S., and Baykousheva, S.P. (1995) Reevaluation of the Pathways for the Biosynthesis of Polyunsaturated Fatty Acids, *J. Lipid Res. 36*, 2471–2477.
7. Ferdinandusse, S., Denis, S., Mooijer, P.A.W., Zhang, Z., Reddy, J.K., Spector, A.A., and Wanders, R.J.A. (2001) Identification of the Peroxisomal β-Oxidation Enzymes Involved in the Biosynthesis of Docosahexaenoic Acid, *J. Lipid Res. 42*, 1987–1995.
8. Su, H.M., Moser, A.B., Moser, H.W., and Watkins, P.A. (2001) Peroxisomal Straight-Chain Acyl-CoA Oxidase and D-Bifunctional Protein Are Essential for the Retroconversion Step in Docosahexaenoic Acid Synthesis, *J. Biol. Chem. 276*, 38115–38120.
9. Makrides, M., Neumann, M.A., Byard, R.W., Simmer, K., and Gibson, R.A. (1994) Fatty Acid Composition of Brain, Retina, and Erythrocytes in Breast- and Formula-Fed Infants, *Am. J. Clin. Nutr. 60*, 189–194.
10. Su, H.M., Bernardo, L., Mirmiran, M., Ma, X.H., Corso, T.N., Nathanielsz, P.W., and Brenna, J.T. (1999) Bioequivalence of Dietary α-Linolenic and Docosahexaenoic Acids as Sources of Docosahexaenoate Accretion in Brain and Associated Organs of Neonatal Baboons, *Pediatr Res. 45*, 87–93.
11. Cunnane, S.C., Francescutti, V., Brenna, J.T., and Crawford, M.A. (2000) Breast-Fed Infants Achieve a Higher Rate of Brain and Whole Body Docosahexaenoate Accumulation Than Formula-Fed Infants Not Consuming Dietary Docosahexaenoate, *Lipids 35*, 105–111.
12. Putnam, J.C., Carlson, S.E., DeVoe, P.W., and Barness, L.A. (1982) The Effect of Variations in Dietary Fatty Acids on the Fatty Acid Composition of Erythrocyte Phosphatidylcholine and Phosphatidylethanolamine in Human Infants, *Am. J. Clin. Nutr. 36*, 106–114.
13. Jensen, C.L., Chen, H., Fraley, J.K., Anderson, R.E., and Heird, W.C. (1996) Biochemical Effects of Dietary Linoleic/α-Linolenic Acid Ratio in Term Infants, *Lipids 31*, 107–113.
14. Ponder, D.L., Innis, S.M., Benson, J.D., and Siegman, J.S. (1992) Docosahexaenoic Acid Status of Term Infants Fed Breast Milk or Infant Formula Containing Soy Oil or Corn Oil, *Pediatr. Res. 32*, 683–688.
15. Burdge, G.C., Jones, A.E., and Wootton, S.A. (2002) Eicosapentaenoic and Docosapentaenoic Acids Are the Principal Products of α-Linolenic Acid Metabolism in Young Men, *Br. J. Nutr. 88*, 355–363.
16. Burdge, G.C. (2004) α-Linolenic Acid Metabolism in Men and Women: Nutritional and Biological Implications, *Curr. Opin. Clin. Nutr. Metab. Care 7*, 137–144.
17. Pawlosky, R.J., Hibbeln, J.R., Novotny, J.A., and Salem, N., Jr. (2001) Physiological Compartmental Analysis of {α}-Linolenic Acid Metabolism in Adult Humans, *J. Lipid Res. 42*, 1257–1265.
18. Hoffman, D.R., DeMar, J.C., Heird, W.C., Birch, D.G., and Anderson, R.E. (2001) Impaired Synthesis of DHA in Patients with X-Linked Retinitis Pigmentosa, *J. Lipid Res. 42*, 1395–1401.
19. Pawlosky, R.J., Hibbeln, J.R., Lin, Y., Goodson, S., Riggs, P., Sebring, N., Brown, G.L., and Salem, N., Jr. (2003) Effects of Beef- and Fish-based Diets on the Kinetics of n-3 Fatty Acid Metabolism in Human Subjects, *Am. J. Clin. Nutr. 77*, 565–572.

20. Salem, N., Jr., Lin, Y., Brenna, T.J., and Pawlosky, R.J. (2003) α-Linolenic Acid Conversion Revisited, *PUFA Newslett.*, http://www.fatsoflife.com/article.asp?i=a&id=162 (accessed January 2005).

21. Poumes-Ballihaut, C., Langelier, B., Houlier, F., Alessandri, J.M., Durand G., Latge, C., and Guesnet, P. (2001) Comparative Bioavailability of Dietary α-Linolenic and Docosahexaenoic Acids in the Growing Rat, *Lipids 36,* 793–800.

22. Burdge, G.C., and Wootton, S.A. (2003) Conversion of α-Linolenic Acid to Palmitic, Palmitoleic, Stearic and Oleic Acids in Men and Women, *Prostaglandins Leukot. Essent. Fatty Acids 69*, 283–290.

23. Burdge, G.C., Finnegan, Y.E., Minihane, A.M., Williams, C.M., and Wootton, S.A. (2003) Effect of Altered Dietary n-3 Fatty Acid Intake upon Plasma Lipid Fatty Acid Composition, Conversion of [^{13}C]α-Linolenic Acid to Longer-Chain Fatty Acids and Partitioning Towards β-Oxidation in Older Men, *Br. J. Nutr. 90*, 311–321.

24. Cunnane, S.C. (2001) New Developments in α-Linolenate Metabolism with Emphasis on the Importance of β-Oxidation and Carbon Recycling, *World Rev. Nutr. Diet. 88,* 178–183.

25. Sinclair, A.J., Attar-Bashi, N.M., and Li, D. (2002) What Is the Role of α-Linolenic Acid for Mammals? *Lipids 37,* 1113–1123.

26. Ferdinandusse, S., Denis, S., Dacremont, G., and Wanders, R.J.A. (2003) Studies on the Metabolic Fate of n-3 Polyunsaturated Fatty Acids, *J. Lipid Res. 44*, 1992–1997.

27. Moore, S.A., Yoder, E., Murphy, S., Dutton, G.R., and Spector, A.A. (1991) Astrocytes, Not Neurons, Produce Docosahexaenoic Acid (22:6n-3) and Arachidonic Acid, *J. Neurochem. 56*, 518–524.

28. Williard, D.E., Harmon, S.D., Kaduce, T.L., Preuss, M., Moore, S.A., Robbins, M.E.C., and Spector, A.A. (2001) Docosahexaenoic Acid Synthesis from n-3 Polyunsaturated Fatty Acids in Differentiated Rat Brain Astrocytes, *J. Lipid Res. 42,* 1368–1376.

29. Williard, D.E., Harmon, S.D., Kaduce, T.L., and Spector, A.A. (2002) Comparison of 20-, 22-, and 24-Carbon n-3 and n-6 Polyunsaturated Fatty Acid Utilization in Differentiated Rat Brain Astrocytes, *Prostaglandins Leukot. Essent. Fatty Acids 67*, 99–104.

30. Innis, S.M., and Dyer, R.A. (2002). Brain Astrocyte Synthesis of Docosahexaenoic Acid from n-3 Fatty Acids Is Limited at the Elongation of Docosapentaenoic Acid, *J. Lipid Res. 43*, 1529–1536.

31. Chen, H., Ray, J., Scarpino, V., Acland, G.M., Aguirre, G.D., and Anderson, R.E. (1999) Synthesis and Release of Docosahexaenoic Acid by the RPE Cells of prcd-Affected Dogs, *Invest. Ophthalmol. Vis. Sci. 40*, 2418–2422.

32. Hyman, B.T., and Spector, A.A. (1981) Accumulation of n-3 Polyunsaturated Fatty Acids Cultured Human Y79 Retinoblastoma Cells, *J. Neurochem. 37*, 60–69.

33. Yorek, M.A., Bohnker, R.R., Dudley, D.T., and Spector, A.A. (1984) Comparative Utilization of n-3 Polyunsaturated Fatty Acids by Cultured Human Y-79 Retinoblastoma Cells, *Biochim. Biophys. Acta 795*, 277–285.

34. Marzo, I., Alava, M.A., Pineiro, A., and Naval, J. (1996) Biosynthesis of Docosahexaenoic Acid in Human Cells: Evidence That Two Different Δ6-Desaturase Activities May Exist, *Biochim Biophys Acta 1301*, 263–272.

35. Alessandri, J.M., Poumès-Ballihaut, C., Langelier, B., Perruchot, M.H., Raguénez, G., Lavialle, M., and Guesnet, P. (2003) Incorporation of Docosahexaenoic Acid into Nerve Membrane Phospholipids: Bridging the Gap Between Animals and Cultured Cells, *Am. J. Clin. Nutr. 78,* 702–710.

36. Goustard-Langelier, B., Alessandri, J.M., Raguenez, G., Durand, G., and Courtois, Y. (2000) Phospholipid Incorporation and Metabolic Conversion of n-3 Polyunsaturated Fatty Acids in the Y79 Retinoblastoma Cell Line, *J. Neurosci. Res. 60*, 678–685.

37. Langelier, B., Furet, J.P., Perruchot, M.H, and Alessandri, J.M. (2003) Docosahexaenoic Acid Membrane Content and mRNA Expression of acyl-CoA Oxidase and of Peroxisome Proliferator-Activated Receptor-δ Are Modulated in Y79 Retinoblastoma Cells Differently by Low and High Doses of α-Linolenic Acid, *J. Neurosci. Res. 74*, 134–141.

38. Labarca, C., and Paigen, K. (1980) A Simple, Rapid, and Sensitive DNA Assay Procedure, *Anal. Biochem. 102*, 344–352.

39. Foretz, M., Foufelle, F., and Ferre, P. (1999) Polyunsaturated Fatty Acids Inhibit Fatty Acid Synthase and Spot-14-Protein Gene Expression in Cultured Rat Hepatocytes by a Peroxidative Mechanism, *Biochem. J. 341*, 371–376.

40. Chang, M.C., Bell, J.M., Purdon, A.D., Chikhale, E.G., and Grange, E. (1999). Dynamics of Docosahexaenoic Acid Metabolism in the Central Nervous System: Lack of Effect of Chronic Lithium Treatment, *Neurochem. Res.* 24, 399–406.

41. Chen, Q., and Nilsson, A. (1993) Desaturation and Chain Elongation of n-3 and n-6 Polyunsaturated Fatty Acids in the Human CaCo-2 Cell Line, *Biochim. Biophys. Acta 1166*, 193–201.

42. Dias, V.C., and Parsons, H.G. (1995) Modulation in Δ9, Δ6 and Δ5 Fatty Acid Desaturase Activity in the Human Intestinal Caco-2 Cell Line, *J. Lipid Res. 36*, 552–563.

43. Reddy, J.K., Goel, S.K., Nemali, M.R., Carrino, J.J., Laffler, T.G., Reddy, M.K., Sperbeck, S.J., Osumi, T., Hashimoto, T., Lalwani, N.D., Rao, M.S. (1986) Transcription Regulation of Peroxisomal Fatty Acyl-CoA Oxidase and Enoyl-CoA Hydratase/3-Hydroxyacyl-CoA Dehydrogenase in Rat Liver by Peroxisome Proliferators, *Proc. Natl. Acad. Sci. U.S.A. 83*, 1747–1751.

44. Dreyer, C., Krey, G., Keller, H., Givel, F., Helftenbein, G., and Wahli, W. (1992) Control of the Peroxisomal β-Oxidation Pathway by a Novel Family of Nuclear Hormone Receptors, *Cell 68*, 879–887.

45. Tugwood, J.D., Issemann, I., Anderson, R.G., Bundell, K.R., McPheat, W.L., and Green, S. (1992) The Mouse Peroxisome Proliferator Activated Receptor Recognizes a Response Element in the 5′ Flanking Sequence of the Rat Acyl CoA Oxidase Gene, *EMBO J. 11*, 433–439.

46. Zhang, B., Marcus, S.L., Sajjadi, F.G., Alvares, K., Reddy, J.K., Subramani, S., Rachubinski, R.A., and Capone, J.P. (1992) Identification of a Peroxisome Proliferator-Responsive Element Upstream of the Gene Encoding Rat Peroxisomal Enoyl-CoA Hydratase/3-Hydroxyacyl-CoA Dehydrogenase, *Proc. Natl. Acad. Sci. U.S.A. 89*, 7541–7545.

47. Marcus, S.L., Miyata, K.S., Zhang, B., Subramani, S., Rachubinski, R.A., and Capone, J.P. (1993) Diverse Peroxisome Proliferator-Activated Receptors Bind to the Peroxisome Proliferator-Responsive Elements of the Rat Hydratase/Dehydrogenase and Fatty Acyl-CoA Oxidase Genes but Differentially Induce Expression, *Proc. Natl. Acad. Sci. U.S.A. 90*, 5723–5727.

48. Forman, B.M., Chen, J., and Evans, R.M. (1997) Hypolipidemic Drugs, Polyunsaturated Fatty Acids, and Eicosanoids Are Ligands for Peroxisome Proliferator-Activated Receptors α and δ, *Proc. Natl. Acad. Sci. U.S.A. 94*, 4312–4317.

49. Pawar, A., and Jump, D.B. (2003) Unsaturated Fatty Acid Regulation of Peroxisome Proliferator-Activated Receptor α Activity in Rat Primary Hepatocytes, *J. Biol. Chem. 278*, 35931–35939.

Synthesis and Biological Activity of New Iodoacetamide Derivatives on Mutants of Squalene-Hopene Cyclase

Maurizio Ceruti[a], Gianni Balliano[a], Flavio Rocco[a], Alexander Lenhart[b],
Georg E. Schulz[b], Francesco Castelli[c], and Paola Milla[a,*]

[a]Dipartimento di Scienza e Tecnologia del Farmaco, Università degli Studi di Torino, 10125 Torino, Italy,
[b]Institut für Organische Chemie und Biochemie, Universität Freiburg, D-79104 Freiburg im Breisgau, Germany,
and [c]Dipartimento di Scienze Chimiche, Università degli Studi di Catania, 95125 Catania, Italy

ABSTRACT: New iodoacetamide derivatives, containing a dodecyl or a squalenyl moiety, were synthesized. The effect of these new thiol-reacting molecules was studied on two mutants of *Alicyclobacillus acidocaldarius* squalene-hopene cyclase constructed especially for this purpose. In the quintuple mutant, all five cysteine residues of the enzyme are substituted with serine; in the sextuple mutant, this quintuple substitution is accompanied by the substitution of aspartate D376, located at the enzyme's active site, with a cysteine. *N*-Dodecyliodoacetamide had little activity toward either mutant, whereas *N*-squalenyliodoacetamide showed a stronger effect on the sextuple than on the quintuple mutant, as expected.

Paper no. L9759 in *Lipids* 40, 729–735 (July 2005).

Prokaryotic squalene-hopene cyclase (SHC) (EC 5.4.99.17) and eukaryotic 2,3-oxidosqualene-lanosterol cyclase (OSC) (EC 5.4.99.7) are two enzymes that catalyze the conversion of linear isoprenoid precursors to penta- and tetracyclic triterpenes (1–4) (Scheme 1). Bacterial SHC cyclizes squalene to hopene and other pentacyclic triterpenes, whereas OSC cyclizes (3*S*)-2,3-oxidosqualene (OS) to lanosterol in mammals and fungi, and to cycloartenol and other tetra- and pentacyclic triterpenes in plants. The enzymatic cyclization of squalene and OS is a complex and fascinating biochemical reaction, and many studies have been carried out over the last 50 yr in the attempt to elucidate at the atomic level the mechanism that transforms a conformationally flexible substrate, squalene or OS, into a cyclized product, with precise structural and stereochemical control.

OSC and, more recently, SHC have been the targets of inhibition studies. Initially, effective inhibitors that mimicked the carbocationic intermediates formed during the cyclization of OS were obtained by designing squalene-derived structures in which the positively charged carbocation is replaced by a nitrogen (5–7). Different series of cyclized aza derivatives (8) and sulfur-containing OS derivatives (9–11) have been developed. Among the substrate mimics, 2,3;18,19-dioxidosqualene shows strong inhibitory potency (12). Finally, a strategy that has been successfully adopted is to intercept the enzyme's active-site nucleophiles with a stable allylic cation, resulting in an irreversible covalent modification of OSC. Following this strategy, Prestwich and colleagues (13,14), Corey *et al.* (3,15), and our group (16) have synthesized various 2,3-oxidosqualenoid dienes, some of which have proved to be selective and time-dependent inhibitors of yeast or animal OSC. Few specific SHC inhibitors have been developed; the most potent ones include amidrazone and amidoxime derivatives (17), whereas some inhibitors of OSC have been studied for their inhibitory activity on SHC (11,18,19).

Determination of the 3-D crystal structure of SHC from *Alicyclobacillus acidocaldarius* (20,21) and, very recently, of human OSC (22) has been a very important step in determining the aminoacidic residues locating at the active site but has provided little information about the role of the residues directly involved in the cyclization process. The 3-D crystal structure of SHC from *A. acidocaldarius* in the presence of a reversible inhibitor similar to squalene, 2-aza-2,3-dihydrosqualene, has only very recently been described (23).

In a previous paper (24), we reported a new approach to study the arrangement of squalene in the active site cavity of SHC. By exploiting site-directed mutagenesis, this strategy inserts a critically located cysteine residue in the active site, which can act as a "sticking point" for thiol-reacting squalene-like molecules. The goal of this strategy, which may be applicable to many other enzymes different from cyclases, is to covalently bind a structure similar to the natural substrate to the active site so as to facilitate the study of interactions between substrate and residues at the active site by X-ray analysis. Using this approach, we have already studied the interactions of a series of thiol-reacting squalene-like inhibitors with the D376C/C435S mutant of SHC for the purpose of identifying an irreversibly binding molecule that mimics the folding of squalene at the active site of the enzyme (24).

Here we report the results obtained with a pair of new thiol-reacting molecules, *N*-dodecyliodoacetamide **3** and *N*-squalenyliodoacetamide **9** (Scheme 2, Fig. 1) on the C25S/C50S/D376C/C435S/C455S/C537S mutant of SHC (sextuple mutant). In this mutant, all five cysteine residues are substituted with a serine and one of three aspartates at the top of the active

SCHEME 1

site (D376) is substituted with a cysteine. The SHC mutant C25S/C50S/C435S/C455S/C537S (quintuple mutant) was used as control. In this mutant, all the cysteine residues are substituted with a serine to create an enzyme without any suitable points for covalent binding of thiol-reacting molecules.

MATERIALS AND METHODS

Chemicals. ^{1}H NMR spectra were recorded on a Bruker AC 200 instrument (Karlsruhe, Germany) for samples in CDCl$_3$ solution at room temperature, with Me$_4$Si (tetramethylsilane) as internal standard. Coupling constants (*J*) are given in Hz. IR spectra were recorded on a PE 781 (PerkinElmer, Palo Alto, CA) spectrophotometer. Mass spectra were recorded on a Finnigan MAT TSQ 700 spectrometer (San Jose, CA). Microanalyses were determined on an elemental analyzer 1106 (Carlo Erba Strumentazione, Milano, Italy) and were within

±0.3% of the theoretical values. The reactions were monitored by TLC on F$_{254}$ silica gel precoated sheets (Merck, Darmstadt, Germany); after development, the sheets were exposed to iodine vapor. Flash-column chromatography was performed on 230–400 mesh silica gel. Diethyl ether and toluene were dried over sodium benzophenone ketyl. All solvents were distilled prior to flash chromatography.

Squalene, lanosterol, and polyoxyethylene 9 lauryl ether were from Sigma Chemical Co. (St. Louis, MO). 1,1′,2-Tris-nor-squalene aldehyde **4** was obtained as described elsewhere (6). 1,1′,2-Tris-nor-squalene alcohol **5** was obtained as described elsewhere (25), starting from **4** (Fig. 1).

N-Dodecylchloroacetamide (2, Scheme 2). In a two-necked flask containing a solution of chloroacetyl chloride (1 equiv, 244 mg, 2.16 mmol) in ethyl acetate (5 mL), a solution of dodecylamine **1** (2 equiv, 800 mg, 4.32 mmol) in ethyl acetate (2 mL) was added within 10 min. The addition was performed,
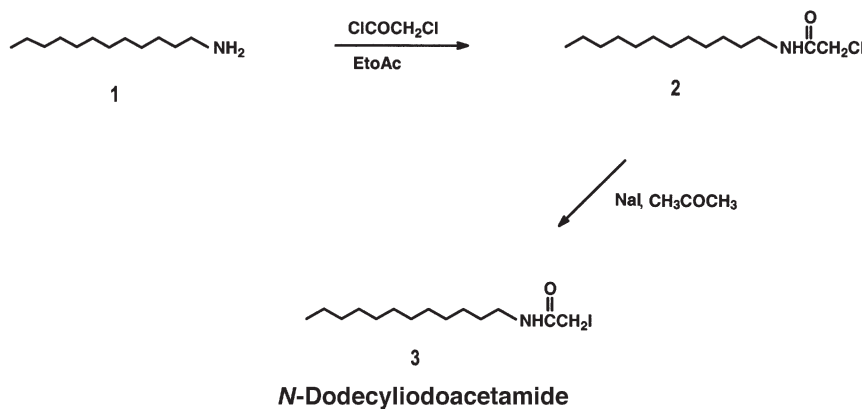
SCHEME 2
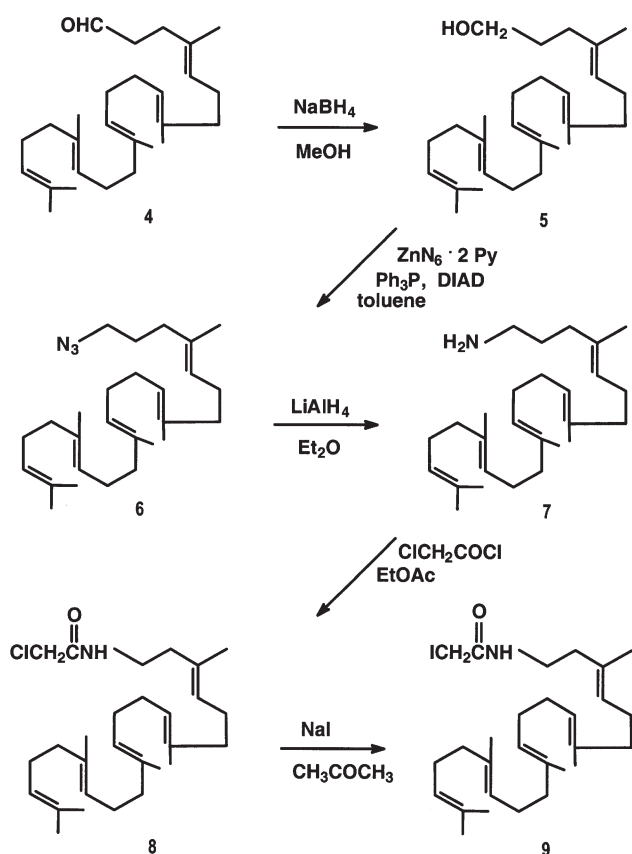
FIG. 1. Synthesis of *N*-squalenyliodoacetamide **9** starting from 1,1′,2-tris-nor-squalene aldehyde **4**. ZnN$_6$·2Py, zinc azide/bis-pyridine comlex; DIAD, diisopropylazodicarboxylate; **5**, 1,1′,2-tris-nor squalene alcohol; **6**, squalene azide; **7**, squalene amine; **8**, *N*-squalenylchloroacetamide.

under a flux of dry nitrogen, in an ice bath. After the addition was complete, the flask was heated under reflux for 12 h. The reaction mixture was then cooled, diluted with ethyl acetate (20 mL), and washed with water (3 × 20 mL), dried with anhydrous sodium sulfate, and evaporated to dryness. The crude product was purified with silica gel flash chromatography in a gradient elution of petroleum ether/diethyl ether = 95:5, 90:10, 85:15, 80:20, and finally 70:30, vol/vol. *N*-Dodecylchloroacetamide **2** (26,27) (487 mg, 1.86 mmol) was obtained in 43% yield (86% yield referred to chloroacetyl chloride). ^{1}H NMR (CDCl$_3$): δ, 0.84–0.88 (*t*, 3H, CH$_3$), 1.24–1.28 [*m*, 20H, (CH$_2$)$_{10}$CH$_2$N], 3.24–3.34 (*m*, 2H, CH$_2$NH), 4.04 (*s*, 2H, CH$_2$Cl), 6.78 (*m*, 1H, NH). MS (EI): *m/z* 261 (M$^+$, 0.5), 226 (68), 212 (100), 184 (5), 170 (3); MS (CI): *m/z* 262 (100), 228 (16), 226 (0.5), 212 (0.5). Analyzed for C$_{14}$H$_{28}$NOCl (261.84); calcd.: C, 64.22; H, 10.78; N, 5.35; Cl, 13.54; found: C, 64.20; H, 10.77; N, 5.34; Cl, 13.52.

N-Dodecyliodoacetamide (3, Scheme 2). *N*-Dodecylchloroacetamide **2** (1 equiv, 94.3 mg, 0.360 mmol) was dissolved in anhydrous acetone (1 mL) under a flux of dry nitrogen, with stirring. Sodium iodide (1.1 equiv, 59.1 mg, 0.396 mmol) was added, allowed to react for 3 h at room temperature, and then heated under reflux for 2 h. The reaction mixture

was cooled, filtered to remove precipitated sodium chloride, and evaporated to dryness; it was extracted with ethyl acetate (3 × 20 mL) after addition of water (20 mL); the combined extracts were dried over anhydrous sodium sulfate and evaporated to dryness. The crude product was purified with silica gel flash chromatography in a gradient elution of petroleum ether/diethyl ether = 90:10, 85:15, 80:20, 75:25, and finally 70:30, vol/vol. *N*-Dodecyliodoacetamide **3** (80 mg, 0.227 mmol) was obtained in 63% yield. ^{1}H NMR (CDCl$_3$): δ, 0.84–0.90 (*t*, 3H, CH$_3$), 1.24–1.29 [*m*, 20H, (CH$_2$)$_{10}$CH$_2$N], 3.21–3.31 (*m*, 2H, CH$_2$NH), 3.70 (*s*, 2H, CH$_2$I), 6.23 (*m*, 1H, NH). MS (EI): *m/z* 352 (M$^+$, 0.1), 226 (100), 212 (20), 184 (15), 169 (10). MS (CI): *m/z* 354 (100), 352 (34), 339 (0.5), 338 (5), 324 (3), 310 (0.5). Analyzed for C$_{14}$H$_{28}$NOI (352.67); calcd.: C, 47.68; H, 8.00; N, 3.97; I, 35.98; found: C, 47.66; H, 8.01; N, 3.97; I, 35.95.

*Squalene azide: (4E,8E,12E,16E)-4,8,13,17,21-pentamethyl-4,8,12,16,20-docosapentaenyl azide (**6**, Fig. 1)*. Zinc azide/bis-pyridine complex (ZnN$_6$·2Py) was obtained as described elsewhere (28,29). ZnN$_6$·2Py (0.75 equiv, 1.91 g, 6.22 mmol) was added to a solution of 1,1′,2-tris-nor-squalene alcohol **5** (1 equiv, 3.21 g, 8.3 mmol) and triphenylphosphine (2 equiv, 4.35 g, 16.6 mmol) in anhydrous toluene (50 mL) under a flux of dry nitrogen, with stirring. The reaction mixture was cooled in an ice bath, and diisopropylazodicarboxylate (2 equiv, 3.36 g, 2.78 mL, 16.6 mmol) was added dropwise and left to react for 2 h at room temperature. The solvent was evaporated *in vacuo*, and the crude product was purified with silica gel flash chromatography in a gradient elution of petroleum ether/diethyl ether = 99.5:0.5 and 99:1, vol/vol. Squalene azide **6** (3.08 g, 7.47 mmol) was obtained in 90% yield. ^{1}H NMR (CDCl$_3$): δ, 1.61–1.71 (*m*, 18H, allylic CH$_3$), 2.00–2.08 (*m*, 20H, allylic CH$_2$ and NCH$_2$CH$_2$), 3.23 (*t*, 2H, CH$_2$N$_3$), 5.12–5.18 (*m*, 5H, vinylic CH). MS (EI): *m/z* 411 (M$^+$, 3), 384 (4), 368 (9), 314 (18), 300 (5), 246 (18), 192 (10), 178 (20), 137 (30), 110 (61), 95 (30), 81 (74), 69 (100). IR (liquid film): cm^{-1} 3400, 2960, 2920, 2840, 2100, 1650, 1450. Analyzed for C$_{27}$H$_{45}$N$_3$ (411.36); calcd.: C, 78.84; H, 11.03; N, 10.21; found: C, 78.80; H, 11.01; N, 10.22.

*Squalene amine: (4E,8E,12E,16E)-4,8,13,17,21-pentamethyl-4,8,12,16,20-docosapentaenylamine (**7**, Fig. 1)*. Squalene azide **6** (1 equiv, 2.53 g, 6.15 mmol) was dissolved in anhydrous diethyl ether (40 mL) and cooled in an ice bath under a flux of dry argon, with stirring. LiAlH$_4$ (1.13 equiv, 263.5 mg, 6.94 mmol) was added in portions and left at room temperature for 12 h, with stirring. The reaction mixture was then cooled in an ice bath, water was added to destroy unreacted LiAlH$_4$, and the mixture was extracted with diethyl ether (3 × 30 mL). The combined extracts were washed with saturated brine (3 × 30 mL), dried over anhydrous sodium sulfate, and evaporated to dryness. Crude squalene amine **7** (1.71 g, 4.43 mmol, 72% yield) was sufficiently pure for the following step. An analytical sample was obtained by preparative TLC [eluent: CH$_2$Cl$_2$/MeOH/NH$_3$ (32%), 96:1:3]. ^{1}H NMR (CDCl$_3$): δ, 1.61–1.71 (*m*, 18H, allylic CH$_3$), 2.00–2.08 (*m*, 20H, allylic CH$_2$, and NCH$_2$CH$_2$), 3.23 (*t*, 2H, CH$_2$N), 5.12–5.18 (*m*, 5H,

vinylic CH). MS (EI): *m/z* 385 (M$^+$, 3), 356 (10), 288 (18), 248 (13), 220 (32), 180 (10), 152 (100), 138 (11), 112 (58), 95 (74), 69 (93). IR (liquid film): cm^{-1} 3380, 2960, 2920, 2850, 1660, 1570, 1450. Analyzed for C$_{27}$H$_{47}$N (385.68); calcd.: C, 84.08; H, 12.28; N, 3.63; found: C, 84.01; H, 12.27; N, 3.61.

N-Squalenylchloroacetamide: N-[(4E,8E,12E,16E)-4,8,13, 17,21-pentamethyl-4,8,12,16,20-docosapentaenyl]chloro-acetamide (8, Fig. 1). Squalene amine **7** (2 equiv, 733 mg, 1.90 mmol) was added within 10 min to a solution of chloroacetyl chloride (1 equiv, 0.95 mmol, 107 mg, 76 mL) in ethyl acetate (5 mL), in an ice bath, under a flux of dry nitrogen, with stirring. The mixture was heated under reflux in an oil bath for 12 h. After cooling, ethyl acetate (20 mL) was added, and the organic phase was washed with water (3 × 20 mL), dried over anhydrous sodium sulfate, and evaporated to dryness. The crude product was purified with silica gel flash chromatography in a gradient elution of *n*-hexane/dichloromethane = 80:20, 70:30, 60:40, 55:45, 50:50, and finally 45:55, vol/vol. *N*-Squalenylchloroacetamide **8** (351 mg, 0.76 mmol) was obtained in 40% yield (80% yield referred to chloroacetyl chloride), as a pale yellow oil. ^{1}H NMR (CDCl$_3$): δ, 1.67–1.72 (*m*, 18H, allylic CH$_3$), 1.99–2.07 (*m*, 20H, allylic CH$_2$ and N-CH$_2$-*CH$_2$*), 3.22–3.26 (*m*, 2H, CH$_2$-N), 4.03 (*s*, 2H, CH$_2$Cl), 5.12–5.17 (*m*, 5H, vinylic CH), 6.66 (*m*, 1H, NH). MS (EI): *m/z* 461 (M$^+$, 5), 418 (2), 324 (2), 299 (3), 269 (5), 231 (6), 203 (5), 188 (10), 176 (20), 163 (30), 149 (24), 107 (21), 95 (100), 69 (82). MS (CI): *m/z* 462 (100), 428 (2), 413 (2). Analyzed for C$_{29}$H$_{48}$NOCl (461.45); calcd.: C, 75.48; H, 10.48; N, 3.04; Cl, 7.68; found: C, 75.50; H, 10.50; N, 3.03; Cl, 7.66.

N-Squalenyliodoacetamide: N-[(4E,8E,12E,16E)-4,8,13,17, 21-pentamethyl-4,8,12,16,20-docosapentaenyl]iodoacetamide (9, Fig. 1). NaI (1.1 equiv, 35.8 mg, 0.240 mmol) was added to a solution of *N*-squalenylchloroacetamide **8** (1 equiv, 100.6 mg, 0.218 mmol) in anhydrous acetone (2 mL), under a flux of dry argon, with stirring, at room temperature for 4 h. The reaction mixture was filtered to remove NaCl and evaporated to dryness. Ethyl acetate (20 mL) was then added, and the solution was washed with water (2 × 10 mL), dried over anhydrous sodium sulfate, and evaporated to dryness. The crude product was purified with silica gel flash chromatography with petroleum ether/diethyl ether = 80:20, vol/vol. *N*-Squalenyliodoacetamide **9** (73.5 mg, 0.133 mmol) was obtained in 61% yield as a pale yellow oil. ^{1}H NMR (CDCl$_3$): δ 1.60–1.66 (*m*, 18H, allylic CH$_3$), 1.99–2.06 (*m*, 20H, allylic CH$_2$ and NCH$_2$C*H$_2$*), 3.21–3.25 (*m*, 2H, CH$_2$N), 3.69 (*s*, 2H, CH$_2$I), 5.12–5.15 (*m*, 5H, vinylic CH), 6.66 (*m*, 1H, NH). MS (EI): *m/z* 553 (M$^+$, 0.5), 510 (0.5), 484 (1.5), 470 (0.2) 426 (25), 356 (5), 302 (2), 234 (9), 198 (20), 163 (41), 107 (22), 95 (100), 69 (88). MS (EI): *m/z* 554 (100), 514 (0.1), 500 (0.1). IR (liquid film): cm^{-1} 3300, 2940, 2860, 1650, 1555, 1450, 1385, 1305, 1255, 1170, 1120, 985. Analyzed for C$_{29}$H$_{48}$NOI (553.00); calc.: C, 62.99; H, 8.75; N, 2.53; I, 22.95; found: C, 63.00; H, 8.74; N, 2.53; I, 22.91.

Radiochemicals. [2-^{14}C]Mevalonate (50 mCi/mmol) was from NEN (Boston, MA). [^{14}C]-(3*S*)-2,3-Oxidosqualene was prepared as described elsewhere (24). Briefly, 25 mg of pro-

teins of S$_{10}$ supernatant from a pig's liver homogenate was incubated with 1 µCi of [^{14}C]mevalonate in the presence of the OSC inhibitor U14266A 200 µM [U14266A: 3β-(2,2-dimethyl-aminoethoxy)-androst-5-en-17-one] (30), as described by Popjak (31). The nonsaponifiable lipids were separated by two-step TLC on silica gel plates (Merck; 20 × 20 cm, 0.5 mm layer). The plates were first developed for about 10 cm above the origin in light petroleum, then dried and developed to 15 cm above the origin with *n*-hexane/ethyl acetate (90:10; vol/vol). The radioactive area corresponding to OS, was scraped off and eluted with dichloromethane. The solvent was dried under N$_2$, and [^{14}C]-(3*S*)-2,3-oxidosqualene was dissolved in benzene. The radiochemical purity of the product was evaluated by scanning TLC plates with a System 2000 Imaging Scanner (Hewlett-Packard, Palo Alto, CA). Radioactivity was measured by liquid scintillation counting (Beckman LS500 TD; Beckman Instruments, Fullerton, CA). The radiolabeled compound was compared chromatographically with authentic radio-inert samples. Determination of the radioactive substance, as well as isotope counting, was carried out as described elsewhere (25,32).

Generation of mutants. Quintuple and sextuple mutants C25S/C50S/C435S/C455S/C537S and C25S/C50S/D376C/C435S/C455S/C537S were generated using existing plasmids coding for mutants D376C, C435S, and for the quadruple mutant C25S/C50S/C455S/C537S described elsewhere (21,24) and derived from pKK223-3 (Pharmacia, Uppsala, Sweden). The quintuple mutant was obtained by exchanging a *Xho* I–*Xho* I restriction fragment of the quadruple mutant with that of mutant C435S. Both plasmids were digested with *Xho* I, and the restriction fragments were purified by agarose gel electrophoresis and gel extraction. The fragments of interest were ligated using Ready-to-Go ligase (Amersham Bioscience, Buckinghamshire, United Kingdom), and the resulting plasmids were transformed into *Escherichia coli* JM 105 cells following standard protocols (33). The quintuple mutant sequence was validated by DNA sequencing (SeqLab, Göttingen, Germany). In an analogous approach, the sextuple mutant was obtained by exchanging an *Apa* I–*Sac* I restriction fragment of the quintuple mutant plasmid with that of mutant D376C.

Expression and purification. Escherichia coli JM105, transformed with plasmids coding for quintuple and sextuple mutants of SHC, were used for expression and solubilization of the mutant SHC. Cells were grown in LB medium containing 100 µg/mL of ampicillin at 37°C until OD$_{578}$ = 0.6 and then induced for 6 h with 1 mM isopropyl-thio-β-D-galactoside. Cells were sedimented; resuspended in a buffer containing 200 mM Tris, pH 8.00, 0.5 M sucrose, 2.5 mM EDTA, 5 U/mL DNase, 0.1 U/mL RNase, 100 µg/mL PMSF, and 0.1 mg/mL lysozyme; vortexed vigorously, and frozen overnight at −20°C. Cells were then thawed at room temperature, vortexed vigorously, incubated for 15 min at 30°C, and diluted 1:1 with cold deionized water. Cells were disintegrated by indirect sonication (60 W for 2 min, 30-s pulse and 30-s pause) at 4°C. Membranes were sedimented by centrifugation (40,000 × *g*, 60 min at 4°C), resuspended in 0.1 M Na citrate buffer pH 6.00, 1

mg/mL polidocanol, 10% (wt/vol) glycerol, and centrifuged ($40,000 \times g$, 60 min at 4°C). The supernatant contained solubilized enzyme of a good degree of purity (about 90% as estimated by SDS-PAGE).

Enzyme assays. Solubilized SHC (0.3–0.6 mg protein) was incubated at 50°C for 30 min in 1 mL 0.1 M Na citrate buffer pH 6.00, 1 mg/mL polidocanol, 10% (wt/vol), glycerol, and 10 µM [^{14}C]-(3S)-2,3-oxidosqualene (1200 cpm). The reaction was stopped by adding 1 mL 10% KOH in MeOH, and nonsaponifiable lipids were extracted twice with 1 mL petroleum ether and chromatographed on silica gel plates developed in CH_2Cl_2. The radioactivity of chromatographic bands [OS and hop-22(29)-en-3-ol] [34] was evaluated using a System 2000 Imaging Scanner (Packard). IC$_{50}$ values (the concentration of inhibitor that reduced the enzymatic activity by 50%) were determined by adding the inhibitors to the mixture of radiolabeled and nonradiolabeled substrates and by incubating with SHC as described.

Time-dependent inactivation of SHC was determined as described in Reference 35. Briefly, solubilized SHC (0.3–0.6 mg protein) was incubated at 50°C for different times in 1 mL 0.1 M Na citrate buffer, pH 6.00, 1 mg/mL polidocanol, 10% (wt/vol) glycerol, and 10 µM [^{14}C]-(3S)-2,3-oxidosqualene (1200 cpm) in the presence of different concentrations of inhibitor. The reaction was stopped by adding 1 mL 10% KOH in MeOH, and the nonsaponifiable lipids were extracted and analyzed as described.

RESULTS AND DISCUSSION

Chemistry. N-Dodecyliodoacetamide **3** was obtained in two steps (Scheme 2). Condensation between chloroacetyl chloride and a twofold excess of dodecylamine in ethyl acetate under reflux afforded *N*-dodecylchloroacetamide **2** in 86% yield (referred to chloroacetyl chloride). Compound **2** was then reacted with sodium iodide in anhydrous acetone, under reflux, to afford *N*-dodecyliodoacetamide **3** in 63% yield. Initially, we tried a one-pot synthesis, by reacting dodecylamine directly with iodoacetyl chloride, but the yield was very poor.

The synthesis of *N*-squalenyliodoacetamide **9** was then developed (Fig. 1). 1,1′,2-Tris-nor-squalene aldehyde **4**, obtained as described elsewhere (6,11,36), was reduced to 1,1′,2-tris-nor-squalene alcohol **5** with sodium borohydride in methanol and submitted to the Mitsunobu reaction (28,29) to give squalene azide **6** in 90% yield. 1,1′,2-Tris-nor-squalene alcohol **5** and

triphenylphosphine in toluene and then diisopropylazodicarboxylate were added. Squalene azide **6** was reduced to squalene amine **7** with lithium aluminum hydride in 72% yield, and amine **7** was reacted with chloroacetyl chloride in ethyl acetate, to give *N*-squalenylchloroacetamide **8** in 80% yield (referred to as chloroacetyl chloride). Finally, reaction with sodium hydride in acetone gave *N*-squalenyliodoacetamide **9** in 61% yield.

Biological activity. The effect of the new thiol-reacting molecules, *N*-dodecyliodoacetamide **3** and *N*-squalenyliodoacetamide **9**, was studied on two mutants of *A. acidocaldarius* SHC to identify the first irreversible inhibitor able to bind covalently to the active site and mimic the folding of the natural substrate. The squalenic or dodecylic structure of these inhibitors was expected to allow them to reach the lipophilic cavity of the active site, whereas the iodoacetamide moiety should specifically react with critically located cysteine residues (37,38). The mutants used, expressly designed for this study, were a C25S/C50S/C435S/C455S/C537S (quintuple mutant), in which all five cysteine residues are substituted with a serine, and a C25S/C50S/D376C/C435S/C455S/C537S (sextuple mutant), in which all the cysteine residues are substituted, and in addition aspartate D376, located at the top of the active site, is substituted with a cysteine. Because the quintuple mutant lacks all the cysteine residues, we expected thiol-reacting inhibitors to be inactive or poorly active (and reversible, of course) against this mutant, whereas the inhibitors should irreversibly inactivate the sextuple mutant, bearing a cysteine at the active site.

The SHC sextuple mutant lost its ability to cyclize squalene, due to the absence of one of the two critical aspartate residues in the DDTA (a highly conserved aspartate-rich motif) sequence (39), but was still able to cyclize OS, although less efficiently than the wild-type. The inhibitory effect of the two thiol reagents was thus assayed toward OSC activity. Furthermore, SHC quintuple and sextuple mutants are less stable than the wild-type enzyme if incubated at 60°C, which is the optimal temperature for SHC (40); for this reason the SHC activity was determined at 50°C. K_M values for the cyclization of OS are 1.5 µM for the wild-type, 1.0 µM for the quintuple mutant, and 2.3 µM for the sextuple mutant; K_M values for the cyclization of squalene are 13.2 µM for the wild-type and 10.0 µM for the quintuple mutant, whereas the sextuple mutant is totally inactive.

IC$_{50}$ values for the two thiol-reacting molecules (Table 1) show that *N*-dodecyliodoacetamide **3** has little effect against either mutant (IC$_{50}$ > 200 µM), and *N*-squalenyliodoacetamide

TABLE 1
Inhibition Values (IC$_{50}$) of Thiol-Modifying Inhibitor on Oxidosqualene Cyclizing Activity of Squalene-Hopene Cyclase (SHC) Wild-Type, Quintuple Mutant, and Sextuple Mutant

	IC$_{50}$[a] (µM)		
Compound[b]	SHC wild-type[c]	C25S/C50S/C435S/C455S/C537S SHC quintuple mutant[c]	C25S/C50S/D376C/C435S/C455S/C537S SHC sextuple mutant[c]
3	>200	>200	>200
9	>200	>200	50

[a]IC$_{50}$, inhibitor concentration reducing enzymatic conversion by 50%.
[b]For compound structures, see Scheme 2 and Figure 1.
[c]Data are mean values from three independent experiments with a mean deviation of ±10%.
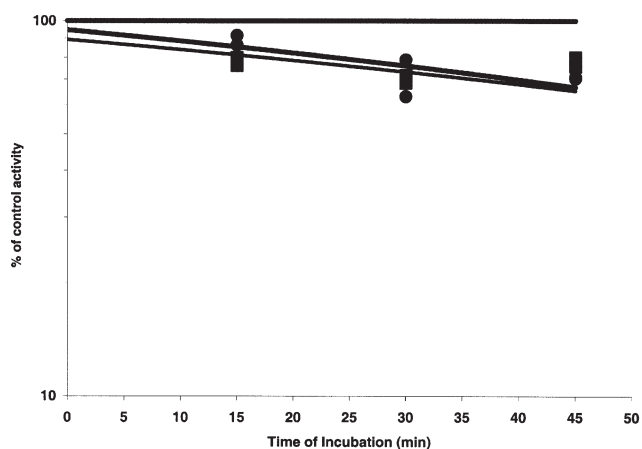
FIG. 2. Inhibition of squalene-hopene cyclase (SHC) quintuple mutant by *N*-dodecyliodoacetamide **3** 200 µM (●) and by *N*-squalenyliodo-acetamide **9** 200 µM (■).

FIG. 3. Inhibition of SHC sextuple mutant by *N*-dodecyliodoacetamide **3** 50 µM (△) and 200 µM (▲), and by *N*-squalenyliodoacetamide **9** 50 µM (□) and 200 µM (■). For abbreviation see Figure 2.

9 has a stronger inhibitory effect on the sextuple than on the quintuple mutant (IC$_{50}$ = 50 µM and >200 µM, respectively). The two molecules are almost inactive on wild-type SHC. A first attempt to clarify the type of inhibition, reversible or irreversible, was made with a classical preincubation and dilution protocol that entails preincubation of SHC mutants for different times in the presence of inhibitors at different concentrations, dilution of the preincubation mixture by almost 1:20 to decrease the concentration of the inhibitor, and finally determination of residual SHC activity. Unfortunately, this protocol could not be applied with the sextuple mutant, as SHC activity of this enzyme is very slight compared with that of the quintuple mutant, and the enzyme was rapidly denatured during incubation; for this reason, it was not possible to determine the residual activity after preincubation and dilution.

To demonstrate the irreversibility of the inactivation of the sextuple mutant by *N*-squalenyliodoacetamide **9**, we used a protocol that does not require the dilution step (35): SHC mutants were incubated for different times in the presence of inhibitors at different concentrations, and the residual activity was compared with the activity of a control incubated without the inhibitor. All the inhibitors proved to have very little effect on the SHC quintuple mutant (Fig. 2), whereas on the sextuple mutant the good activity of *N*-squalenyliodoacetamide **9** was confirmed (Fig. 3). The slopes did not clearly indicate the type of inhibition (reversible or irreversible) of the inhibitors tested. A possible reason could be the complexity of the biphasic system required for the determination of enzymatic activity (i.e., the presence of detergent and hydrophobic compounds) that might influence the availability of substrate and inhibitor.

The novel thiol-reacting molecule, *N*-squalenyliodoacetamide, should in the near future prove itself to be a useful tool to study the exact geometry of the cyclization reaction in eukaryotic OSC. Very recently, human OSC was crystallized and the 3-D structure of this enzyme determined (22). According to the crystallographic data, three critically located cysteine residues are present in human OSC: Cys456, Cys533, and
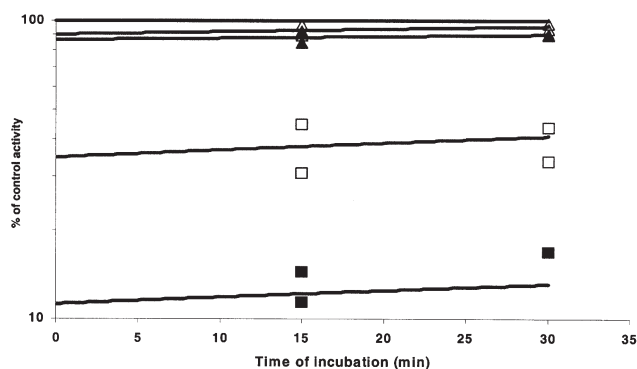
Cys233 (22). Our approach of labeling a critical cysteine residue with a substrate analog such as *N*-squalenyliodo-acetamide could be profitably applied to human OSC with the goal of preparing a stable covalent enzyme–squalenic molecule complex for structural analysis. The crystallization and 3-D structure determination of this complex will be of great value to elucidate the mechanism whereby a squalenic molecule folds into the OSC active site.

ACKNOWLEDGMENTS

REFERENCES

1. Abe, I., Rohmer, M., and Prestwich, G.D. (1993) Enzymatic Cyclization of Squalene and Oxidosqualene to Sterols and Triterpenes, *Chem. Rev. 93*, 2189–2206.
2. Wendt, K.U., Schulz, G.E., Corey, E.J., and Liu, D.R. (2000) Enzyme Mechanisms for Polycyclic Triterpene Formation, *Angew. Chem. Int. Ed. Engl. 39*, 2812–2833.
3. Corey, E.J., Virgil, S.C., Cheng, H., Hunter Baker, C., Matsuda, S.P.T., Singh, V., and Sarshar, S. (1995) New Insights Regarding the Cyclization Pathway for Sterol Biosynthesis from (*S*)-2,3-Oxidosqualene, *J. Am. Chem. Soc. 117*, 11819–11820.
4. Nes, W.D., Koike, K., Jia, Z., Sakamoto, Y., Satou, T., Nikaido, T., and Griffin, J.F. (1998) Cycloartenol Analysis by ^{1}H and ^{13}C NMR, Crystallographic Observations, and Molecular Mechanics Calculations, *J. Am. Chem. Soc. 120*, 5970–5980.
5. Cattel, L., Ceruti, M., Viola, F., Delprino, L., Balliano, G., Duriatti, A., and Bouvier-Navé, P. (1986) The Squalene-2,3-epoxide Cyclase as a Model for the Development of New Drugs, *Lipids 21*, 31–38.
6. Ceruti, M., Balliano, G., Viola, F., Cattel, L., Gerst, N., and Schuber, F. (1987) Synthesis and Biological Activity of Azasqualenes, Bis-azasqualenes and Derivatives, *Eur. J. Med. Chem. 22*, 199–208.
7. Ceruti, M., Balliano, G., Viola, F., Grosa, G., Rocco, F., and Cattel, L. (1992) 2,3-Epoxy-10-aza-10,11-dihydrosqualene, a High-Energy Intermediate Analogue Inhibitor of 2,3-Oxidosqualene Cyclase, *J. Med. Chem. 35*, 3050–3058.
8. Taton, M., Benveniste, P., Rahier, A., Johnson, W.S., Liu,

H.-T., and Sudhakar, A.R. (1992) Inhibition of 2,3-Oxidosqualene Cyclases, *Biochemistry 31*, 7892–7898.

9. Stach, D., Zheng, Y.F., Perez, A.L., Oehlschlager, A.C., Abe, I., Prestwich, G.D., and Hartman, P.G. (1997) Synthesis and Inhibition Studies of Sulfur-Substituted Squalene Oxide Analogues as Mechanism-Based Inhibitors of 2,3-Oxidosqualene Lanosterol Cyclase, *J. Med. Chem. 40*, 201–209.

10. Abe, I., Liu, W., Oehlschlager, A.C., and Prestwich, G.D. (1996) Mechanism-Based Active Site Modification of Oxidosqualene Cyclase by Tritium-Labeled 18-Thia-2,3-oxidosqualene, *J. Am. Chem. Soc. 118*, 9180–9181.

11. Rocco, F., Oliaro Bosso, S., Viola, F., Milla, P., Roma, G., Grossi, G., and Ceruti, M. (2003) Conjugated Methyl Sulfide and Phenyl Sulfide Derivatives of Oxidosqualene as Inhibitors of Oxidosqualene and Squalene-Hopene Cyclases, *Lipids 38*, 201–207.

12. Abad, J.L., Guardiola, M., Casas, J., Sanchez-Baeza, F., and Messeguer, A. (1996) 2,3;18,19-Dioxidosqualene Stereoisomers: Characterization and Activity as Inhibitors of Purified Pig Liver 2,3-Oxidosqualene-Lanosterol Cyclase, *J. Org. Chem. 61*, 7603–7607.

13. Xiao, X., and Prestwich, G.D. (1991) 29-Methylidene-2,3-oxidosqualene: A Potent Mechanism-Based Inactivator of Oxidosqualene Cyclase, *J. Am. Chem. Soc. 113*, 9673–9674.

14. Abe, I., Bai, M., Xiao, X.-Y., and Prestwich, G.D. (1992) Affinity Labeling of Vertebrate Oxidosqualene Cyclases with a Tritiated Suicide Substrate, *Biochem. Biophys. Res. Commun. 187*, 32–38.

15. Corey, E.J., Cheng, H., Hunter Baker, C., Matsuda, S.P.T., Li, D., and Song, X. (1997) Studies on the Substrate Binding Segments and Catalytic Action of Lanosterol Synthase. Affinity Labeling with Carbocations Derived from Mechanism-Based Analogs of 2,3-Oxidosqualene and Site-Directed Mutagenesis Probes, *J. Am. Chem. Soc. 119*, 1289–1296.

16. Ceruti, M., Rocco, F., Viola, F., Balliano, G., Milla, P., Arpicco, S., and Cattel, L. (1998) 29-Methylidene-2,3-oxidosqualene Derivatives as Stereospecific Mechanism-Based Inhibitors of Liver and Yeast Oxidosqualene Cyclase, *J. Med. Chem. 41*, 540–554.

17. Ganem, B., Dong, Y.H., Zheng, Y.F., and Prestwich, G.D. (1999) Amidrazone and Amidoxime Inhibitors of Squalene Hopene Cyclase, *J. Org. Chem. 64*, 5441–5446.

18. Viola, F., Ceruti, M., Cattel, L., Milla, P., Poralla, K., and Balliano, G. (2000) Rationally Designed Inhibitors as Tools for Comparing the Mechanism of Squalene-Hopene Cyclase with Oxidosqualene Cyclase, *Lipids 35*, 297–303.

19. Ceruti, M., Balliano, G., Rocco, F., Milla, P., Arpicco, S., Cattel, L., and Viola, F. (2001) Vinyl Sulfide Derivatives of Truncated Oxidosqualene as Selective Inhibitors of Oxidosqualene and Squalene-Hopene Cyclases, *Lipids 36*, 629–636.

20. Wendt, K.U., Poralla, K., and Schulz, G.E. (1997) Structure and Function of Squalene Cyclase, *Science 277*, 1811–1815.

21. Wendt, K.U., Feil, C., Lenhart, A., Poralla, K., and Schulz, G.E. (1997) Crystallization and Preliminary X-ray Crystallographic Analysis of Squalene-Hopene Cyclase from *Alicyclobacillus acidocaldarius*, *Protein Sci. 6*, 722–724.

22. Thoma, R., Schulz-Gasch, T., D'Arcy, B., Benz, J., Aebi, J., Dehmlow, H., Hennig, M., Stihle, M., and Ruf, A. (2004) Insight into Steroid Scaffold Formation from the Structure of Human Oxidosqualene Cyclase, *Nature 432*, 118–122.

23. Reinert, D.J., Balliano, G., and Schulz, G.E. (2004) Conversion of Squalene to the Pentacarbocyclic Hopene, *Chem. Biol. 11*, 121–126.

24. Milla, P., Lenhart, A., Grosa, G., Viola, F., Weihofen, W.A., Schulz, G.E., and Balliano, G. (2002) Thiol-Modifying Inhibitors for Understanding Squalene Cyclase Function, *Eur. J. Biochem. 269*, 2108–2116.

25. Ceruti, M., Grosa, G., Rocco, F., Dosio, F., and Cattel, L. (1994) A Convenient Synthesis of [3-3H]Squalene and [3-3H]-2,3-Oxidosqualene, *J. Labelled Comp. Radiopharm. 34*, 577–585.

26. Van Esch, J.H., Hoffmann, M.A.M., and Nolte, R.J.M. (1995) Reduction of Nicotinamides, Flavins, and Manganese Porphyrins by Formate, Catalyzed by Membrane-Bound Rhodium Complexes, *J. Org. Chem. 60*, 1599–1610.

27. Tam-Chang, S.-W., Biebuyck, H.A., Whitesides, G.M., Jeon, N., and Nuzzo, R.G. (1995) Self-Assembled Monolayers on Gold Generated from Alkanethiols with the Structure RNHCOCH₂SH, *Langmuir 11*, 4371–4382.

28. Viaud, M.C., and Rollin, P. (1990) Zinc Azide Mediated Mitsunobu Substitution. An Expedient Method for the One-Pot Azidation of Alcohols, *Synthesis,* 130–132.

29. Grosa, G., Viola, F., Ceruti, M., Brusa, P., Delprino, L., Dosio, F., and Cattel, L. (1994) Synthesis and Biological Activity of a Squalenoid Maleimide and Other Classes of Squalene Derivatives as Irreversible Inhibitors of 2,3-Oxidosqualene Cyclase, *Eur. J. Med. Chem. 29*, 17–23.

30. Field, R.B., Holmlund, C.E., and Whittaker, N.F. (1979) The Effects of the Hypocholesteremic Compound 3β-(2,2-dimethylaminoethoxy)-Androst-5-en-17-one on the Sterol and Steryl Ester Composition of *Saccharomyces cerevisiae*, *Lipids 14*, 741–747.

31. Popjak, G. (1969) Enzymes of Sterol Biosynthesis in Liver and Intermediates of Sterol Biosynthesis, in *Methods in Enzymology Vol. 15*, pp. 393–454, Elsevier, New York.

32. Balliano, G., Viola, F., Ceruti, M., and Cattel, L. (1992) Characterization and Partial Purification of Squalene-2,3-oxide Cyclase from *Saccharomyces cerevisiae*, *Arch. Biochem. Biophys. 293*, 122–129.

33. Sambrook, J., Frisch, E.F., and Maniatis, T. (1989) *Molecular Cloning: A Laboratory Manual*, 2nd edn., Cold Spring Harbor Laboratory Press, Cold Spring Harbor, NY.

34. Dang, T.Y., and Prestwich, G.D. (2000) Site-Directed Mutagenesis of Squalene-Hopene Cyclase: Altered Substrate Specificity and Product Distribution, *Chem. Biol. 7*, 643–649.

35. Lindsey, S., and Harwood, H.J. (1995) Inhibition of Mammalian Squalene Synthetase Activity by Zaragozic Acid A Is a Result of Competitive Inhibition Followed by Mechanism-Based Irreversible Inactivation, *J. Biol. Chem. 16*, 9083–9096.

36. Ceruti, M., Viola, F., Dosio, F., Cattel, L., Bouvier-Navé, P., and Ugliengo, P. (1988) Stereospecific Synthesis of Squalenoid Epoxide Vinyl Ethers as Inhibitors of 2,3-Oxidosqualene Cyclase, *J. Chem. Soc., Perkin Trans. 1*, 461–469.

37. Wawrzynow, A., and Collins, J.H. (1993) Chemical Modification of the Ca²⁺-ATPase of Rabbit Skeletal-Muscle Sarcoplasmic-Reticulum—Identification of Sites Labeled with Aryl-Isothiocyanates and Thiol-Directed Conformational Probes, *Biochim. Biophys. Acta 1203*, 60–70.

38. Wan, L., Chen, Y.H., and Chang, T.W. (2003) Improving Pharmacokinetic Properties of Adrenocorticotropin by Site-Specific Lipid Modification, *J. Pharm. Sci. 92*, 1882–1892.

39. Feil, C., Süssmuth, R., Jung, G., and Poralla, K. (1996) Site-Directed Mutagenesis of Putative Active-Site Residues in Squalene-Hopene Cyclase, *Eur. J. Biochem. 242*, 51–55.

40. Seckler, B., and Poralla, K. (1986) Characterization and Partial Purification of Squalene-Hopene Cyclase from *Bacillus acidocaldarius*, *Biochim. Biophys. Acta 881*, 356–363.

COMMUNICATIONS

Plasma Kinetics of Free and Esterified Cholesterol in Familial Hypercholesterolemia: Effects of Simvastatin

Raul D. Santos[a], Ana P.M. Chacra[a], Aleksandra Morikawa[a], Carmen C. Vinagre[a], and Raul C. Maranhão[a,b],*

[a]Lipid Metabolism Laboratory and Lipid Clinic, The Heart Institute (InCor), University of São Paulo, Medical School Hospital (InCor–HCFMUSP), and [b]Faculty of Pharmaceutical Sciences, University of São Paulo, São Paulo, Brazil

ABSTRACT: The objective of this study was to evaluate the kinetics of both free and esterified forms of cholesterol contained in a emulsion that binds to LDL receptors (LDE) in subjects with heterozygous familial hypercholesterolemia (FH), and the same subjects under the effects of high-dose simvastatin treatment, as compared with a control normolipidemic group (NL). Twenty-one FH patients (44.0 ± 13.0 yr, 12 females, LDL cholesterol levels 6.93 ± 1.60 mmol/L) and 22 normolipidemic patients (44.0 ± 15.0, 10 females, LDL cholesterol levels 3.15 ± 0.62 mmol/L) were injected intravenously with ^{14}C-cholesteryl ester and ^{3}H-cholesterol. FH patients were also evaluated after 2 mon of 40 or 80 mg/d simvastatin treatment, and plasma samples were collected over 24 h to determine the residence time (RT, in h) of both LDE labels, expressed as the median (25%; 75%). The RT of both ^{14}C-cholesteryl ester and ^{3}H-cholesterol were greater in FH than in NL [FH: 36.0 (20.5; 1191.0), NL: 17.0 (12.0–62.5), $P = 0.015$; and FH: 52.0 (30.0; 1515.0); NL 20.5 (14.0–30.0) $P < 0.0001$]. Treatment reduced LDL cholesterol by 36% ($P < 0.0001$), RT of ^{14}C-cholesteryl ester by 49% ($P = 0.0029$ vs. baseline), and ^{3}H-cholesterol RT by 44% ($P = 0.019$ vs. baseline). After treatment, the RT values of ^{14}C-cholesteryl ester in the FH group approached the NL values ($P = 0.58$), but the RT of ^{3}H-cholesterol was still greater than those for the NL group ($P = 0.01$). The removal of LDE cholesteryl esters and free cholesterol was delayed in FH patients. Treatment with a high dose of simvastatin normalized the removal of cholesterol esters but not the removal of free cholesterol.

Paper no. L9724 in *Lipids* 40, 737–743 (July 2005).

Emulsions of defined composition resembling the lipidic structure of plasma lipoproteins have been used as a tool to investigate lipid intravascular metabolism (1–6). Emulsion models of lymph chylomicrons facilitate the study of chylomicron metabolism in several disease states and under the action of antilipidemic drugs (6–10). It is also feasible to use artificial emulsions as probes to explore the metabolism of LDL instead of using the native lipoprotein. In this regard, we have studied the metabolic behavior of a cholesterol-rich emulsion termed LDE that roughly resembles the lipidic structure of LDL. LDE is made without protein, but when injected into the bloodstream it acquires several apolipoproteins, including apo E (2,3). Apo E endows LDE with particles that bind to the LDL receptors, since those receptors recognize not only the apo B present in LDL, but also apo E, which is not found in the LDL fraction (11). Apo E binds to the LDL receptors with a greater affinity than apo B-100 and, as previously shown, is therefore removed more rapidly than the natural lipoprotein (5). The fact that LDE is removed from the plasma faster than native LDL is a methodological advantage because it shortens the period required to perform the plasma kinetics test. Among other advantages of this model is the possibility of using the same preparation to test several subjects. Because of the risk of contamination, this procedure cannot be done with the natural lipoprotein, which requires use of the autologous lipoprotein. Furthermore, LDE is a standard preparation compared with native lipoproteins, which show great variation among individuals; this facilitates labeling by radioactive or other means. All these operational advantages greatly facilitate performing systematic studies on the plasma kinetics of lipids.

The kinetics of LDL in the plasma is traced by labeling apo B, which is virtually the only apolipoprotein present in the LDL particles (12,13). Because apo B is not an exchangeable protein, the kinetics of apo B plasma reflects the kinetics of LDL particles (11). However, lipoproteins are constantly being remodeled, and each lipid component may have a distinct metabolic fate in health and in disease. Tracing the intravascular metabolism of the lipidic components of lipoprotein may be important and is greatly facilitated by the use of artificial probes such as LDE. Indeed, we recently (14) showed that after intravenous injection of LDE doubly labeled with radioactive cholesteryl esters and unesterified cholesterol, the two forms of cholesterol showed different plasma kinetic behaviors in normolipidemic (NL) subjects with coronary artery disease (CAD) and in non-CAD subjects, which can eventually shed new light on the mechanisms of arterial lipid deposition. In fact, comparative investigations of the plasma kinetic behaviors of the two forms of cholesterol have scarcely been explored in the literature (15,16).

Familial hypercholesterolemia (FH) is a dominant autosomic disease wherein the removal from plasma of LDL particles is reduced because of defects in the expression and function of LDL receptors (17). FH is characterized by an

*To whom correspondence should be addressed at Instituto do Coração do HC-FMUSP, Laboratório de Metabolismo Lipídico, Av. Dr. Eneas de Carvalho Aguiar 44, CEP 05403-000, São Paulo, SP, Brazil.
E-mail: ramarans@usp.br

Abbreviations: apo, apolipoprotein; CAD, coronary artery disease; FCR, fractional catabolic rates; FH, familial hypercholesterolemia; LDE, cholesterol-rich emulsion; NL, normolipidemic; PLTP, phospholipid transfer proteins; RT, residence time.

early onset of atherosclerosis caused by an accumulation of LDL and an increase in the cholesterol plasma pool. However, the removal of free cholesterol, which accounts for around 30% of the plasmatic cholesterol pool, was not established in this disease (18).

HMG-CoA reductase inhibitors, such as simvastatin, have been used to reduce LDL cholesterol levels, and consequently the risk of coronary heart disease, in hypercholesterolemia (19). Because of the increased risk of coronary heart disease associated with FH, statins are now a mandatory treatment in adults with this disease (20).

In this study using LDE to model LDL in plasma kinetics, we hypothesized that the LDL receptor defects that cause FH would differently affect the removal of free and esterified forms of cholesterol, i.e., that the decrease in the removal of the esterified cholesterol would be greater than that of the free form in the presence of FH. Furthermore, we were interested in evaluating whether statin treatment, which is universally used, would be more effective in accelerating the removal of one cholesterol form than the other. To address those issues, LDE labeled with free and esterified cholesterol was injected into patients with FH and into control subjects without the disease. Kinetic studies were repeated in FH patients after 8 wk of simvastatin treatment.

MATERIALS AND METHODS

Study subjects. The participants in the study were selected from among outpatients of the Lipid Clinic of the Heart Institute of the São Paulo University Medical School Hospital. Twenty-one recently diagnosed FH patients were studied. All patients were first-degree relatives of subjects that already had the diagnosis of FH and were being followed in our clinic. FH was diagnosed using the U.S. MED PED (Make Early Diagnosis Prevent Early Disease) group criteria (20).They were compared with 22 healthy normolipidemic volunteer subjects (LDL cholesterol < 4.1 mmol/L, plasma TG < 2.2 mmol/L, HDL cholesterol > 1.0 mmol/L). Clinical data for the studied subjects are shown in Table 1. None of the patients were addicted to alcohol consumption or had diabetes, liver, renal, thyroid, or other metabolic diseases. They had not used lipid-lowering drugs for at least the last 2 months prior to the study. There were no differences between the groups regarding age, sex, body mass index, hypertension, and smoking habits. One FH patient had had a myocardial infarction episode 1 yr before enrolling in the study.

Plasma lipids and apolipoproteins. Blood samples for the determination of plasma lipids were collected after a 12-h fast on the same day the kinetic studies were performed. Commercial enzymatic methods were used to determine total cholesterol (Boehringer-Mannheim, Penzberg, Germany) and TG (Abbott Laboratories, Abbott Park, IL). HDL cholesterol was determined by the same method used for total cholesterol after lipoprotein precipitation with magnesium phosphotungstate. VLDL cholesterol and LDL cholesterol were calculated by the formula of Friedewald *et al.* (21).

LDE preparation. LDE was prepared from a lipid mixture

TABLE 1
Clinical Characteristics of Familial Hypercholesterolemia (FH) and Normolipidemic (NL) Subjects

	NL ($n = 22$)	FH ($n = 21$)	P
Age (yr)	44.0 ± 15.0	44.0 ± 14.0	0.9
Female sex, n (%)	10 (47.6)	12 (57)	0.54
Body mass index (kg/m^2)	27.6 ± 5.0	25.3 ± 2.8	0.07
Arterial hypertension, n (%)	2 (9)	4 (19)	0.4
Smokers, n (%)	1 (4.5)	4 (19)	0.18
Coronary heart disease, n (%)	0 (0)	1 (4.7)	0.47

composed of 40 mg cholesteryl oleate, 20 mg egg PC, 1 mg triolein, and 0.5 mg cholesterol, purchased from Nu-Chek-Prep (Elysian, MN). ^{14}C-Cholesteryl ester (cholesteryl oleate) and ^{3}H-cholesterol, purchased from Amersham International (Amersham, United Kingdom), were added to the mixture. The procedures for emulsifying the lipids, i.e., by prolonged ultrasonic irradiation in aqueous media and two-step ultracentrifugation of the crude emulsion with density adjustment by addition of KBr, to obtain the LDE microemulsion were carried out using the method of Ginsburg *et al.* (1), modified by Maranhão *et al.* (2). LDE was dialyzed against saline solution and passed through a 0.22-μm filter for injection into the patients.

LDE plasma kinetics. The participants fasted for 12 h at the beginning of the test, at approximately 9 AM, but they were allowed two standard meals during the study, at approximately 12:30 and 7 PM. LDE containing 37 kBq of ^{14}C-cholesteryl ester and 74 kBq of ^{3}H-cholesterol, for a total of 5–6 mg in a volume of 500 μL, was injected intravenously in a bolus. Plasma samples were collected for 24 h in intervals of 5 min and at 1, 2, 4, 6, and 24 h after the injection. Aliquots (1.5 mL) of blood plasma were extracted with chloroform/methanol/water (2:1:1, by vol) overnight at 4°C (13). The organic phase was transferred to a test tube and dried under nitrogen flux. Lipids were resuspended with 5 mL of the solution described by Folch *et al.* (22) (chloroform/methanol 2:1) and transferred to counting vials containing 7.0 mL of scintillation solution [2,5 diphenyloxazole scintillation grade (PPO)/dimethyl POPOP (1,4-bis[2-(5-phenyl)-oxazolyl]benzene)/Triton X-100/toluene, 5 g/0.5 g/333 mL/667 mL (Merck, Darmstadt, Germany). Radioactivity was counted using a Beckman LS100C spectrometer.

Estimation of plasma residence times (RT) of the radioisotopes. The plasma decay curves for both radioisotopes were determined. The fractional catabolic rates (FCR) of the LDE ^{14}C-cholesteryl ester and ^{3}H-cholesterol were calculated according to the method described by Matthews (23) as FCR, where a_1, a_2, b_1, and b_2 were estimated from biexponential curves obtained from the remaining radioactivity found in plasma after injection, fitted by a least squares procedure, as

$$y = (a_1 \cdot e^{-b_1 t}) + (a_2 \cdot e^{-b_2 t}) \quad [1]$$

where y represents the plasma radioactivity decay as a function of time (t), and a and b indicate the linear coefficient and the angular coefficient, respectively, which represent the FCR in h^{-1}. The FCR were estimated from parameters a_1, b_1, and b_2

by the following equation: RT = $(a_1/b_1 + a_2/b_2)^{-1}$. Calculations were performed using ANACOMP software (24). The RT represent the inverse of the FCR (25).

Simvastatin treatment. After performing the LDE kinetic study, a 30-d treatment with 40 mg simvastatin (Zocor; Merck, Sharpe & Dohme, São Paulo, Brazil) was started in all patients. The dosage was doubled to 80 mg/d for the next 4 wk. Plasma lipids and kinetic studies were repeated in all 21 subjects after the treatment period.

Statistical analysis. Data are expressed as mean ± SD except for the RT of the radioisotopes and plasma TG, which are expressed as medians (25%; 75%). Because of the non-Gaussian distribution of these parameters, they were evaluated by the Kolmogorov–Smirnov procedure. Categorical data were compared between FH and NL by Fisher's exact test. The comparison of parametric and nonparametric data between FH and NL was performed, respectively, by Student's *t*-test and the Mann–Whitney test. The effects of simvastatin treatment on plasma lipids and emulsion kinetics were evaluated by paired *t*-tests or the Wilcoxon signed rank test when necessary. The correlation between the RT of ^{3}H-cholesterol and ^{14}C-cholesterol ester, and of these parameters with plasma lipids in the entire population studied (*n* = 43) were performed by Spearman's rho. In all analyses, a difference in the two-tailed tests of *P* < 0.05 was considered statistically significant.

Informed consent and radiological safety. The experimental protocol was approved by the Ethical Committee of the Heart Institute, and written informed consent was given by all participants. All women of reproductive age were using contraceptive methods, and pregnancy was excluded before beginning the kinetic studies and simvastatin treatment.

The safety of the radioactive dose intravenously injected into the patients was ensured according to the regulations of the International Commission on Radiological Protection (26). The injected dose in each experiment was 0.03 mSv and was well below the annual limit for intake of radionuclides (50 mSv).

RESULTS

Table 2 shows the plasma lipids of FH and NL subjects. Total plasma and LDL cholesterol of the FH subjects were roughly twice the values of the NL. Also, plasma TG were higher in FH than in NL. No significant differences were found in HDL cholesterol between the two groups. Table 2 also shows the effects of simvastatin treatment on the plasma lipids and the RT of the LDE radioisotopic labels. The reduction in LDL cholesterol concentration under simvastatin treatment was 36% (*P* < 0.0001).

Figures 1A and 1B show the plasma decay curves of ^{3}H-cholesterol and ^{14}C-cholesteryl ester in FH patients before and after simvastatin treatment and in controls. Both radioisotopes presented a slower decay in FH than in NL. Accordingly, Table 2 shows that the RT of ^{14}C-cholesteryl ester and ^{3}H-cholesterol in FH subjects were 2.5 and 1.7 times the values of NL subjects (*P* = 0.015 and *P* < 0.0001, respectively). Simvastatin treatment accelerated the plasma decay of both radioisotopes, as shown in Figures 1A and 1B. This trend was seen for both radioisotopes at the 4-, 6-, and 24-h points and was marked at the 24-h point of ^{14}C-cholesteryl ester radioactivity after simvastatin treatment. As shown in Table 2, the reductions in the RT of ^{14}C-cholesteryl ester and ^{3}H-cholesterol were, respectively, 49% (*P* = 0.0029 vs. baseline) and 44% (*P* = 0.019 vs. baseline). Before simvastatin treatment, no differences were found between the RT of both radioisotopes (*P* = 0.17); however, after treatment the RT of ^{14}C-cholesteryl ester became shorter than those of ^{3}H-cholesterol (*P* = 0.011; Table 2). Also, after treatment the RT of ^{14}C-cholesteryl ester in FH subjects were no longer different from those of NL subjects (*P* = 0.84), but the RT of ^{3}H-cholesterol was still increased when compared with NL values (*P* = 0.0084; Table 2).

The RT of ^{3}H-cholesterol, but not that of the ^{14}C-cholesteryl ester, was positively correlated with total and LDL cholesterol levels, respectively (*r* = 0.42, *P* = 0.005 and *r* = 0.39, *P* = 0.009). No correlation was found between the RT of both labels and the other plasma lipids (data not shown). The RT of ^{14}C-cholesteryl ester were not correlated with the plasma lipids. The RT of ^{3}H-cholesterol and ^{14}C-cholesteryl ester presented a positive but weak correlation (*r* = 0.39, *P* = 0.01).

DISCUSSION

Our current results show that the LDE cholesteryl ester was removed slowly in patients with FH, in whom LDL receptors are

TABLE 2
Plasma Lipids (mmol/L) and Residence Times (RT) of the Radioisotopes of LDE (in h) in Normolipidemics (NL) and Familial Hypercholesterolemia (FH) Subjects Before and After Simvastatin Treatment[a]

	NL (*n* = 22)	FH baseline (*n* = 21)	FH simvastatin (*n* = 21)	*P*, FH vs. baseline
Total cholesterol[b]	4.96 ± 0.88	9.26 ± 1.68[a]	6.52 ± 1.8[b]	<0.0001
LDL cholesterol[b]	3.15 ± 0.62	6.93 ± 1.60[a]	4.48 ± 1.8[c]	<0.0001
HDL cholesterol[b]	1.19 ± 0.28	1.32 ± 0.36	1.36 ± 0.54	0.54
VLDL cholesterol[c]	0.60 (0.48; 0.74)	0.70 (0.47; 1.11)	0.63 (0.46; 0.7)	0.01
TG[c]	1.31 (0.83; 1.63)	1.55 (1.03; 2.43)	1.39 (1.00; 1.53)	0.01
RT of ^{3}H-cholesterol[c]	20.5 (14.0; 30.0)	52.0 (30.0; 1515)[a]	35.0 (22.0; 70.0)[c]	0.019
RT of ^{14}C-cholesteryl ester[c]	17.0 (12.0; 62.5)	36.0 (20.5; 1191)[d]	24.5 (16.5; 29.0)[e]	0.0029

[a]LDE, cholesterol-rich emulsion. Lowercase roman letters indicate: [a]*P* < 0.0001 vs. NL ; [b]*P* < 0.001 vs. NL; [c]*P* < 0.01 vs NL; [d]*P* = 0.015 vs. NL; [e]*P* = 0.01 vs. RT of ^{14}C-cholesteryl ester after simvastatin treatment.
[b]Expressed as mean ± SD.
[c]Expressed as medians (25%; 75%).
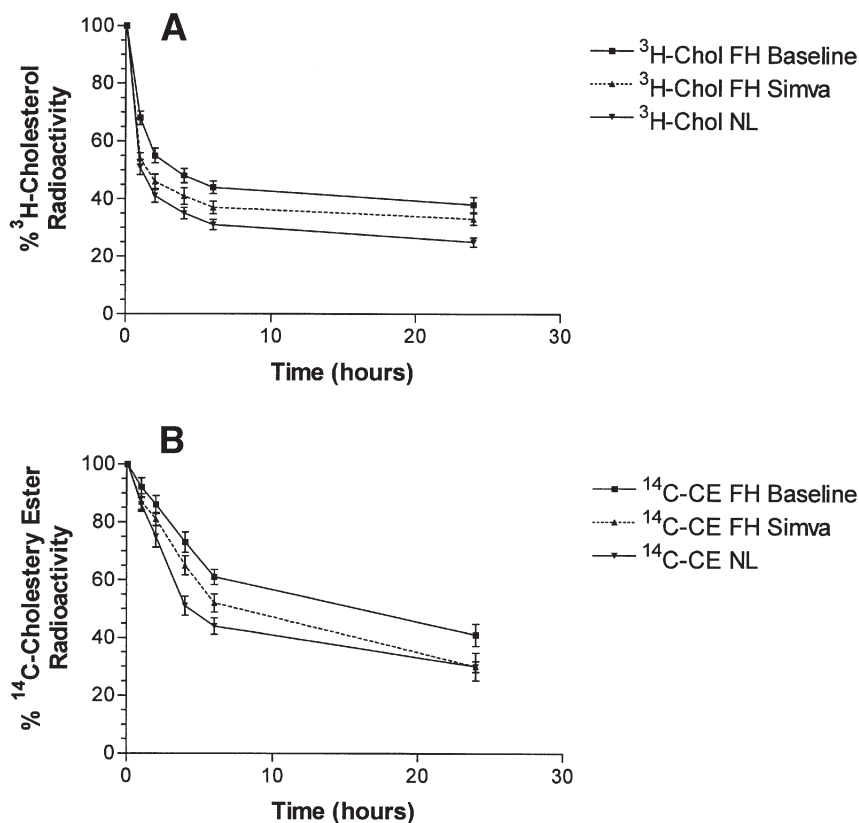
FIG. 1. Decay curves of the emulsion ^{3}H-cholesterol (A) and ^{14}C-cholesteryl ester (B) obtained from subjects with familial hypercholesterolemia (FH) (*n* = 21) at baseline and after simvastatin treatment (Simva), and from normolipidemic (NL) subjects (*n* = 22). Data expressed as mean ± SEM.

defective (17,20). In several studies, we have shown that the radioactively labeled cholesteryl ester moiety of LDE behaves like the labeled apo B of native LDL, although it is removed faster from the plasma than apo B (2,4,5,27). In this respect, as expected from apo B-labeled native LDL (13), the removal of LDE cholesteryl esters was slower in patients with hypercholesterolemia (4) and was accelerated in untreated patients with acute myeloid leukemia (3) because of the LDL receptor up-regulation existing in the neoplastic cells (28). Conversely, after the disease remission achieved by chemotherapy, LDE removal decreased because of destruction of the neoplastic cells with receptor up-regulation (3). The LDE FCR negatively correlates with age (27), which is expected for the native LDL particles, because LDL receptor expression indeed diminishes with aging (29).

In FH, the removal of LDL from the plasma is slow, as had been demonstrated by labeling LDL apo B with radioactive iodine or with stable isotopes (30,31). The slowed removal of LDE cholesteryl ester had not yet been documented in heterozygous hypercholesterolemia, but we expect from our preceding studies with LDE that the impaired clearance of the lipoprotein particles would lead to this effect (3,4,27).

There are substantial and well-known differences between free and esterified cholesterol regarding the stability of the two cholesterol forms in the lipoprotein structure (32,33). Free cholesterol, which originates from both tissue and plasma lipoproteins, can be esterified in the lipoprotein surface monolayer, mainly in HDL but to a lesser extent in β-lipoproteins, by the action of LCAT. Cholesteryl esters are generally incorporated into the lipoprotein core or transferred to other lipoproteins by CETP but also by phospholipid transfer proteins (PLTP). Cholesteryl esters can then be removed by the liver either directly by VLDL and LDL binding to hepatic receptors or indirectly by HDL in the reverse cholesterol transport. The esterification of free cholesterol creates a concentration gradient that permits the efflux of unesterified cholesterol from cells to HDL particles (34,35). Studies have shown that plasma cholesterol esterification is augmented by increased TG levels and increased LDL/HDL ratios (36,37). This concentration gradient seems to be important even when actively mediated transport, such as the one mediated by ATP-binding cassette transporter A1, predominate (38). Despite this evidence, only a few studies have evaluated the plasma cholesterol kinetics in human subjects (15,16). A recent *in vivo* study showed that 70% of cholesteryl esters are generated from free cholesterol in HDL and 30% in LDL, IDL, and VLDL (16).

Similar to native lipoproteins, esterified cholesterol makes up the lipoprotein LDE core and shifts to other lipoprotein

classes by means of the transfer proteins CETP and PLTP (2,33,34). In contrast, unesterified cholesterol, which is slightly polar and is located in the lipoprotein surface monolayer, constitutes a much more unstable plasma cholesterol pool (32). It may freely diffuse from the lipoprotein or the microemulsion to the plasma without the assistance of transfer proteins and may eventually precipitate on the arterial wall. There is evidence that not only cholesteryl esters but also unesterified cholesterol are associated with atherosclerosis. Free cholesterol is found in atherosclerotic plaques in both experimental animals (39,40) and humans (41). Free cholesterol accumulation is a potent inducer of macrophage apoptosis and secondary necrosis, a fact associated with plaque rupture and acute coronary events (41). Also, free cholesterol in modified lipoproteins has been associated with the inflammatory process of atherosclerosis (42). In fact, an increase in the content of unesterified cholesterol of lipoproteins, expressed as an increased free cholesterol/phospholipid ratio, has been found in subjects prone to atherosclerosis (43), such as in persons with diabetes and patients with hyperbetalipoproteinemia, as well as in subjects with CAD in a population study (44). An increase in unesterified cholesterol reduces the extent of cholesteryl ester transfer from VLDL and LDL particles in a concentration-dependent mechanism. Also, it stimulates the transfer of cholesteryl esters out of the HDL particles, thus changing the reverse cholesterol transport unfavorably. In these subjects, it was demonstrated an increase in the influx of unesterified cholesterol from plasma to cells (45,46).

In our recent study (14), we have shown that in CAD non-hypercholesterolemic patients, the free cholesterol of LDE is removed faster than in non-CAD subjects, whereas there is no difference between CAD and non-CAD patients regarding the removal of the LDE cholesteryl esters. This clearly indicates that the two cholesterol forms initially contained in the same lipoprotein or microemulsion particles can have distinct metabolic behaviors in the intravascular compartment and be separately involved in pathophysiological events. Indeed, the weak correlation found in our study subjects between the RT of ^{3}H-cholesterol and ^{14}C-cholesteryl ester supports the assumption that after injection, both labels are metabolized through different metabolic pathways. It is interesting that in hypercholesterolemic patients, the LDE free cholesterol tended to be removed even slower than the cholesteryl esters, although the difference between the two labels was not statistically significant. It is possible that the accumulation of LDL in patients facilitates the transfer of free cholesterol from LDE to the plasma lipoproteins rather than that of the cholesteryl esters, which also depend on transfer proteins (33). Because native circulating lipoproteins are removed slower than LDE, transfer to the lipoprotein fractions is implied in delayed clearance (4,5).

Only very few studies have addressed the issue of *in vivo* kinetics of the free and esterified forms of cholesterol contained in LDL (15,16). Recently, the *in vivo* kinetics of both free and esterified cholesterol contained in the LDL and HDL of bile fistula, and in NL subjects as well as in one homozygous FH subject were evaluated (16). The output of cholesteryl esters from the plasma was similar to that of previous studies that evaluated apo B kinetics, showing that cholesteryl esters are removed from the plasma within the lipoprotein holoparticle. This finding strengthens the validity of labeling LDE with cholesteryl esters to trace the clearance of the microemulsion particles. Specifically, in the sole homozygous FH patient, the output from the plasma of both free and esterified cholesterol in LDL was reduced when compared with the NL and bile fistula subjects. The results from this single patient with the most severe presentation of the disease is in accordance with our present data from heterozygous FH and contribute to other studies in which LDL metabolism was evaluated by LDE kinetics (3,4,27,47).

The introduction of more potent statins, such as atorvastatin, has increased interest in using higher doses of the previous generation of statins—of which simvastatin has been the most widely used—as well as interest in the mechanism of action of these drugs in FH (48). Two mechanisms have been proposed for the effects of statins on plasma lipids: (i) an increase in the removal from the plasma of LDL and its precursors, and (ii) a reduction of the hepatic production of VLDL. The first mechanism has been demonstrated in kinetic studies with the labeling of apo B-containing lipoproteins (12,49) and is reinforced by the results of our study showing a faster removal of LDE after high-dose simvastatin treatment in heterozygous FH patients. The second mechanism was shown in studies with homozygous and compound heterozygous FH patients, in whom receptors are absent or nonfunctional and who presented reductions of about 25% in LDL cholesterol levels with 80–160 mg of simvastatin and 80 mg of atorvastatin (50,51). Treatment with statins increases the removal from plasma of LDL particles, as traced by labeled LDL apo B. Because LDE cholesteryl esters behave like LDL apo B (2–4), the acceleration of removal from plasma of this cholesterol form, as observed in this study, would then be expected. Similar to the effects on LDE kinetics found in this study, statin treatment increased the removal from plasma of chylomicron-like emulsions in subjects with CAD (9). A reduction in the plasma RT of LDL as well as chylomicrons, as shown by the artificial emulsions, implies that these lipoproteins might become less prone to oxidation and therefore would become less atherogenic.

It is noteworthy that the effects of statin treatment on LDE free cholesterol were less marked than in LDE cholesteryl esters. This is probably because of the diminution of CETP that occurs with statin use (52). LDE cholesteryl esters would be less prone to transfer to the plasma native lipoproteins, which are removed slowly in comparison with LDE, whereas the free cholesterol would not be affected by the changes in CETP action, since CETP does not influence free cholesterol shifts among the lipoprotein particles (33). Another issue worth noting in our results is the fact that we found a correlation between the RT of the LDE free cholesterol and total and LDL cholesterol, a correlation that did not exist regarding LDE cholesteryl esters. In fact, this supports the assumption that the two forms of cholesterol composing the structure of the same lipoprotein particles may have different metabolic fates.

One of the limitations of this and previous studies with LDE (3,4,14,27,47) is that our analysis concentrated mainly on the early and fast phase of radioisotope decay. This protocol design aimed to ensure patient comfort in view of the long blood collection period. However, in this study there was an important fall in the radioactivity of ^{14}C-cholesteryl ester remaining in the plasma at the 24-h point after simvastatin treatment. At any rate, in future studies a greater number of blood samples should be taken in the interval between 6 and 24 h to achieve a better description of the late phase of the decay curve.

ACKNOWLEDGMENTS

REFERENCES

1. Ginsburg, G.S., Small, D.M., and Atkinson, D. (1982) Microemulsions of Phospholipids and Cholesterol Esters. Protein-free Models of Low Density Lipoprotein, *J. Biol. Chem. 257*, 8216–8227.

2. Maranhão, R.C., Cesar, T.B., Pedroso-Mariani, S.R., Hirata, M.H., and Mesquita, C.H. (1993) Metabolic Behavior in Rats of a Nonprotein Microemulsion Resembling Low Density Lipoprotein, *Lipids 28*, 691–696.

3. Maranhão, R.C., Garicochea, B., Silva, E.L., Dorlhiac-Llacer, P., Cadena, S.M., Coelho, I.J., Meneghetti, J.C., Pileggi, F.J., and Chamone, D.A. (1994) Plasma Kinetics and Biodistribution of a Lipid Emulsion Resembling Low-Density Lipoprotein in Patients with Acute Leukemia, *Cancer Res. 54*, 4660–4666.

4. Maranhão, R.C., Roland, I.A., Toffoletto, O., Ramires, J.A., Goncalves, R.P., Mesquita, C.H., and Pileggi, F. (1997) Plasma Kinetic Behavior in Hyperlipidemic Subjects of a Lipidic Microemulsion That Binds to Low Density Lipoprotein Receptors, *Lipids 32*, 627–633.

5. Hirata, R.D.C., Hirata, M.H., Mesquita, C.H., Cesar, T.B., and Maranhão, R.C. (1999) Effects of Apolipoprotein B-100 on the Metabolism of a Lipid Microemulsion Model in Rats, *Biochim. Biophys. Acta 1437*, 53–62.

6. Maranhão, R.C., Feres, M.C., Martins, M.T., Mesquita, C.H., Toffoletto, O., Vinagre, C.G., Gianinni, S.D., and Pileggi, F. (1996) Plasma Kinetics of a Chylomicron-like Emulsion in Patients with Coronary Artery Disease, *Atherosclerosis 126*, 15–25.

7. Borba, E.F., Bonfa, E., Vinagre, C.G., Ramires, J.A., and Maranhão, R.C. (2000) Chylomicron Metabolism Is Markedly Altered in Systemic Lupus Erythematosus, *Arthritis Rheum. 43*, 1033–1040.

8. Vinagre, C.G., Stolf, N.A., Bocchi, E., and Maranhão, R.C. (2000) Chylomicron Metabolism in Patients Submitted to Cardiac Transplantation, *Transplantation 69*, 532–537.

9. Santos, R.D., Sposito, A.C., Ventura, L.I., Cesar, L.A., Ramires, J.A., and Maranhão, R.C. (2000) Effect of Pravastatin on Plasma Removal of a Chylomicron-like Emulsion in Men with Coronary Artery Disease, *Am. J. Cardiol. 85*, 1163–1166.

10. Santos, R.D., Ventura, L.I., Sposito, A.C., Schreiber, R., Ramires, J.A., and Maranhão, R.C. (2001) The Effects of Gemfibrozil upon the Metabolism of Chylomicron-like Emulsions in Patients with Endogenous Hypertriglyceridemia, *Cardiovasc. Res. 49*, 456–465.

11. Mahley, R.W., and Innerarity, T.L. (1983) Lipoprotein Receptors and Cholesterol Homeostasis, *Biochim. Biophys. Acta 737*, 197–222.

12. Gaw, A., Packard, C.J., Lindsay, G.M., Murray, E.F., Griffin, B.A., Caslake, M.J., Colquhoun, I., Wheatley, D.J., Lorimer, A.R., and Shepherd, J. (1996) Effects of Colestipol Alone and in Combination with Simvastatin on Apolipoprotein B Metabolism, *Arterioscl. Thromb. Vasc. Biol. 16*, 236–249.

13. Vega, G.L., and Grundy, S.M. (1986) *In vivo* Evidence for Reduced Binding of Low Density Lipoproteins to Receptors as a Cause of Primary Moderate Hypercholesterolemia, *J. Clin. Invest. 78*, 1410–1414.

14. Santos, R.D., Hueb, W., Oliveira, A.A., Ramires, J.A., and Maranhão, R.C. (2003) Plasma Kinetics of a Cholesterol-rich Emulsion in Subjects With or Without Coronary Artery Disease, *J. Lipid Res. 44*, 464–469.

15. Schwartz, C.S., Zech, L.A., VandenBroek, J.M., and Cooper, P.S. (1993) Cholesterol Kinetics in Subjects with Bile Fistula, *J. Clin. Invest. 91*, 923–938.

16. Schwartz, C.S., VandenBroek, J.M., and Cooper, P.S. (2004) Lipoprotein Cholesteryl Ester Production, Transfer and Output *in vivo* in Humans, *J. Lipid Res. 45*, 1594–1607.

17. Austin, M.A., Hutter, C.M., Zimmern, R.L., and Humphries, S.E. (2004) Familial Hypercholesterolemia and Coronary Heart Disease: A HuGE Association Review, *Am. J. Epidemiol. 160*, 421–429.

18. Glomset, J.A., and Norum, K.R. (1973) The Metabolic Role of Lecithin:Cholesterol Acyltransferase: Perspectives from Pathology, *Adv. Lipid Res. 11*, 1–65.

19. The Scandinavian Simvastatin Survival Study Group (1994) Randomised Trial of Cholesterol Lowering in 4444 Patients with Coronary Heart Disease: The Scandinavian Simvastatin Survival Study (4S), *Lancet 344*, 1383–1389.

20. Civeira, F. (2004) International Panel on Management of Familial Hypercholesterolemia. Guidelines for the Diagnosis and Management of Heterozygous Familial Hypercholesterolemia, *Atherosclerosis 173*, 55–68.

21. Friedewald, W.T., Levy, R.I., and Fredrickson, D.D. (1972) Estimation of the Concentration of Low Density Lipoprotein Cholesterol in Plasma, Without Use of the Preparative Ultracentrifuge, *Clin. Chem. 18*, 499–502.

22. Folch, J., Lees, M., and Sloane Stanley, G.H. (1957) A Simple Method for the Isolation and Purification of Total Lipids from Animal Tissues, *J. Biol. Chem. 226*, 497–509.

23. Matthews, C.M.E. (1957) The Theory of Tracer Experiments with ^{131}I-Labelled Plasma Proteins, *Phys. Med. Biol. 2*, 36–53.

24. Marchese, S.R.M., Mesquita, C.H., and Cunha I.I.L. (1998) ANACOMP Program Application to Calculate ^{137}Cs Transfer Rates in Marine Organisms and Dose in Man, *J. Radioanal. Nucl. Chem. 232*, 233–236.

25. Vélez-Carrasco, W., Lichtenstein, A.H., Barrett, P.H.R, Sun, Z., Dolnikowski, G.G., Welty, F.K., and Schaefer, E.J. (1999) Human Apolipoprotein A-I Kinetics Within Triglyceride-rich Lipoproteins and High Density Lipoproteins, *J. Lipid Res. 40*, 1695–1700.

26. International Commission on Radiological Protection (ICRP) (1979) Radiation Protection, in *Part I. Limits for Intakes of Radionuclides by Workers* (Sowby, F.S., ed.), ICRP Publication 30, pp. 1–73, Pergamon, Oxford, England.

27. Pinto, L.B., Wajngarten, M., Silva, E.L., Vinagre, C.C., and Maranhão, R.C. (2001) Plasma Kinetics of a Cholesterol-rich Emulsion in Young, Middle-Aged, and Elderly Subjects, *Lipids 36*, 1307–1311.

28. Ho, Y.K., Smith, R.G., Brown, M.S., and Goldstein, J.L. (1978) Low-Density Lipoprotein (LDL) Receptor Activity in Human Acute Myelogenous Leukemia Cells, *Blood 52*, 1099–1114.

29. Millar, J.S., Lichtenstein, A.H., Cuchel, M., Dolnikowski, G.G., Hachey, D.L., Cohn, J.S., and Schaefer, E.J. (1995) Impact of Age on the Metabolism of VLDL, IDL, and LDL Apolipoprotein B-100 in Men, *J. Lipid Res. 36*, 1155–1167.

30. Barret, P.H.R., and Watts, G.F. (2002) Shifting the LDL-Receptor Paradigm in Familial Hypercholesterolemia: Novel Insights from Recent Kinetic Studies of Apolipoprotein B-100 Metabolism, *Atherosclerosis Suppl. 2*, 1–4.

31. Gaffney, D., Forster, L., Caslake, M.J., Bedford, D., Stewart, J.P., Stewart, G., Wieringa, G., Dominiczak, M., Miller, J.P., and Packard, C.J. (2002) Comparison of Apolipoprotein B Metabolism in Familial Defective Apolipoprotein B and Heterogeneous Familial Hypercholesterolemia, *Atherosclerosis 162*, 33–43.

32. Yen, F.T., and Nishida, T. (1990) Rapid Labeling of Lipoproteins in Plasma with Radioactive Cholesterol. Application for Measurement of Plasma Cholesterol Esterification, *J. Lipid Res. 31*, 349–353.

33. Morton, R.E. (1999) Cholesteryl Ester Transfer Protein and Its Plasma Regulator: Lipid Transfer Inhibitor Protein, *Curr. Opin. Lipidol. 10*, 321–327.

34. Fielding, C.J., and Fielding, P.E. (1995) Molecular Physiology of Reverse Cholesterol Transport, *J. Lipid Res. 36*, 211–228.

35. Fielding, C.J. (1984) The Origin and Properties of Free Cholesterol Potential Gradients in Plasma, and Their Relation to Atherogenesis, *J. Lipid Res. 25*, 1624–1628.

36. Dobiasova, M., and Frohlich, J. (1998) Understanding the Mechanism of LCAT Reaction May Help to Explain the High Predictive Value of LDL/HDL Cholesterol Ratio, *Physiol. Res. 47*, 387–397.

37. Dobiasova, M., and Frohlich, J. (2001) The Plasma Parameter Log (TG/HDL-C) as an Atherogenic Index: Correlation with Lipoprotein Particle Size and Esterification Rate in apoB-Lipoprotein-Depleted Plasma (FER(HDL)), *Clin. Biochem. 34*, 583–588.

38. Rothblat, G.H., de la Llera-Moya, M., Atger, V., Kellner-Weibel, G., Williams, D.L., and Phillips, M.C. (1999) Cell Cholesterol Efflux: Integration of Old and New Observations Provides New Insights, *J. Lipid Res. 40*, 781–796.

39. Rosenfeld, M.E., Chait, A., Bierman, E.L., King, W., Goodwin, P., Walden, C.E., and Ross, R. (1988) Lipid Composition of Aorta of Watanabe Heritable Hyperlipemic and Comparably Hypercholesterolemic Fat-Fed Rabbits. Plasma Lipid Composition Determines Aortic Lipid Composition of Hypercholesterolemic Rabbits, *Arteriosclerosis 8*, 338–347.

40. Bates, S.R., and Wissler, W. (1976) Effects of Hyperlipidemic Serum on Cholesterol Accumulation in Monkey Aortic Medial Cells, *Biochim. Biophys. Acta 450*, 78–88.

41. Tabas, I. (2002) Consequences of Cellular Cholesterol Accumulation: Basic Concepts and Physiological Implications, *J. Clin. Invest. 110*, 905–911.

42. Taskinen, S., Kovanen, P.T., Jarva, H., Meri, S., and Pentikainen, M.O. (2002) Binding of C-Reactive Protein to Modified Low-Density-Lipoprotein Particles: Identification of Cholesterol as a Novel Ligand for C-Reactive Protein, *Biochem. J. 367*, 403–412.

43. Morton, R.E. (1988) Free Cholesterol Is a Potent Regulator of Lipid Transfer Protein Function, *J. Biol. Chem. 263*, 12235–12241.

44. Kuksis, A., Myher, J.J., Geher, K., Jones, G.J., Breckenridge, W.C., Feather, T., Hewitt, D., and Little, J.A. (1982) Decreased Plasma Phosphatidylcholine/Free Cholesterol Ratio as an Indicator of Risk for Ischemic Vascular Disease, *Arteriosclerosis 2*, 296–302.

45. Fielding, C.J., Reaven, G.M., and Fielding, P.E. (1982) Human Noninsulin-Dependent Diabetes: Identification of a Defect in Plasma Cholesterol Transport Normalized *in vivo* by Insulin and *in vitro* by Selective Immunoadsorption of Apolipoprotein E, *Proc. Natl. Acad. Sci. USA 79*, 6365–6369.

46. Fielding, P.E., Fielding, C.J., Havel, R.J., Kane, J.P., and Tun, P. (1983) Cholesterol Net Transport, Esterification, and Transfer in Human Hyperlipidemic Plasma, *J. Clin. Invest. 71*, 449–460.

47. Melo, N.R., Latrilha, M.C., Santos, R.D., Pompei, L.M., and Maranhão, R.C. (2005) Effects in Post-menopausal Women of Transdermal Estrogen Associated with Progestin upon the Removal from the Plasma of a Microemulsion That Resembles Low-Density Lipoprotein (LDL), *Maturitas 50*, 275–281.

48. Aguilar Salinas, C.A., Barrett, H., and Schonfeld, G. (1998) Metabolic Modes of Action of the Statins in Hyperlipoproteinemias, *Atherosclerosis 141*, 203–207.

49. Bilheimer, D.W., Grundy, S.M., Brown, M.S., and Goldstein, J.L. (1983) Mevinolin and Colestipol Stimulate Receptor-Mediated Clearance of Low Density Lipoprotein from Plasma in Familial Hypercholesterolemia Heterozygotes, *Proc. Natl. Acad. Sci. USA 80*, 4124–4128.

50. Raal, F.J., Pilcher, G.J., Illingworth, D.R., Pappu, A.S., Stein, E.A., Laskarzewski, P., Mitchel, Y.B., and Melino, M.R. (1997) Expanded-Dose Simvastatin Is Effective in Homozygous Familial Hypercholesterolaemia, *Atherosclerosis 135*, 249–256.

51. Marais, A.D., Naoumova, R.P., Firth, J.C., Penny, C., Neuwirth, C.K., and Thompson, G.R. (1997) Decreased Production of Low Density Lipoprotein by Atorvastatin After Apheresis in Homozygous Familial Hypercholesterolemia, *J. Lipid Res. 38*, 2071–2078.

52. Homma, Y., Ozawa, H., Kobayashi, T., Yamaguchi, H., Sakane, H., and Nakamura, H.R. (1995) Effects of Simvastatin on Plasma Lipoprotein Subfractions, Cholesterol Esterification Rate, and Cholesteryl Ester Transfer Protein in Type II Hyperlipoproteinemia, *Atherosclerosis 114*, 223–234.

REVIEW

Furan Fatty Acids: Occurrence, Synthesis, and Reactions. Are Furan Fatty Acids Responsible for the Cardioprotective Effects of a Fish Diet?

Gerhard Spiteller*

Lehrstuhl für Organische Chemie I, University of Bayreuth, D 95440 Bayreuth, Germany

ABSTRACT: Furan FA (F-acids) are tri- or tetrasubstituted furan derivatives characterized by either a propyl or pentyl side chain in one of the α-positions; the other is substituted by a straight long-chain saturated acid with a carboxylic group at its end. F-acids are generated in large amounts in algae, but they are also produced by plants and microorganisms. Fish and other marine organisms as well as mammals consume F-acids in their food and incorporate them into phospholipids and cholesterol esters. F-acids are catabolized to dibasic urofuran acids, which are excreted in the urine. The biogenetic precursor of the most abundant F-acid, F_6, is linoleic acid. Methyl groups in the β-position are derived from adenosylmethionine. Owing to the different alkyl substituents, synthesis of F-acids requires multistep reactions. F-acids react readily with peroxyl radicals to generate dioxoenes. The radical-scavenging ability of F-acids may contribute to the protective properties of fish and fish oil diets against mortality from heart disease.

Atherosclerosis (1,2) is a disease of the Western life style: Cardiovascular diseases account for half of the mortality in countries where people live with a surplus of food, but atherosclerosis is rare where people suffer from starvation. Moreover, a great number of animal and human experiments have revealed that consumption of food rich in cholesterol and fat induces atherosclerosis after a prolonged feeding period (3–8).

Nevertheless, despite their high consumption of fat and cholesterol, atherosclerosis is less common in Greenlanders (9–11), whose traditional diet is rich in fish and marine organisms. Compared with other foods, the content of lipids in fish is generally low, and the composition of the FA in the different lipid classes is somewhat different from other animal-derived food. Lipids of fish (12,13) and fish oils (14) are characterized by a high content of n-3 PUFA, especially of EPA and DHA (12). The connection between consumption of fish or ingestion of fish oils and protection against coronary heart disease mortality has been confirmed in several studies (15,16). Based on the fact that fish and fish oils are rich in n-3 PUFA, it has been deduced that ingestion of n-3 PUFA reduces the risk of death from cardiovascular diseases and their consequences (17–21) although some believe that an adequate explanation of this phenomenon is missing (22).

Fish accumulate dietary-derived n-3 PUFA in large amounts in their tissues as well as furan FA (F-acids) (23); the latter have been shown to be scavengers of hydroxyl (24) and peroxyl radicals (25).

In this paper the occurrence, isolation, biosynthesis, synthesis, and reactions of F-acids are reviewed, and deductions about the possible protective properties of the presence of F-acids in mammalian tissue and blood are presented. How the low amounts of linoleic acid (LA) in fish fat may influence the level of oxidized LDL in humans after fish consumption and how they may contribute to the protective properties of a fish diet against cardiovascular diseases are discussed.

STRUCTURES OF F-ACIDS

F-acids (furanoid FA) (23) are a large group of FA characterized by a furan ring, which carries in one α-position an unbranched FA chain with 9, 11, or 13 carbon atoms and in the other α-position a short straight-chain alkyl group with 3 or 5 carbon atoms. Either both β-positions of the furan ring are substituted by a methyl residue or else there is only a methyl group in the β-position adjacent to the long aliphatic chain (Table 1). The F-acids are numbered by indices according to increasing GC elution times of their dimethyl esters (26) and the letter F. The most common F-acid is F_6, or **6** (see Fig. 4 below), a furan

TABLE 1
Structures of the Most Abundant Furan FA

Number	Compound	m	n	R
1	F_1	2	8	CH_3
2	F_2	4	8	H
3	F_3	4	8	CH_3
4	F_4	2	10	CH_3
5	F_5	4	10	H
6	F_6	4	10	CH_3
7	F_7	4	12	H
8	F_8	4	12	CH_3
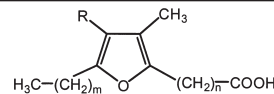
*E-mail: gerhard.spiteller@uni-bayreuth.de

Abbreviations: AA, arachidonic acid; CLE, cholesterol ester; F-acid, furan FA; LA, linoleic acid; LOOH, lipid hydroperoxide; LOX, lipoxygenase; LPO, lipid peroxidation; OA, oleic acid; PL, phospholipids; TX, thromboxane.

FA with methyl groups in both β-positions, a pentyl residue in one α-position, and a –(CH$_2$)$_{10}$–COOH residue in the other.

OCCURRENCE

F-acids were detected by Glass *et al*. (26) in the Northern pike (*Esox lucius*). Shortly before, Kluytmans and Zandee (27) had reported on an investigation of the lipids in the same fish, but overlooked the high content of F-acids. In contrast to Glass *et al*. (23), Kluytmans and Zandee (27) had determined only GC retention times. Since F-acids and unsaturated FA with several double bonds of the same chain length have similar retention indices (26) this method is not adequate to distinguish between these two groups of compounds. Thus, Kluytmans and Zandee apparently attributed the peak of the most abundant F-acid, **6,** to 22:3n-3. In contrast, Glass *et al*. (26) used EI mass spectra, which allow unequivocal distinction between F-acids and n-3 PUFA, for compound characterization in addition to determination of retention indices. Measuring retention indices is often used as the only identification method, and this may be the reason why most authors have overlooked the presence of F-acids.

F-acids were found in a great number of freshwater (28,29) and marine fish (29–35) (see Table 2), and some minor compounds with variations in the chain length have been detected (36). Morover, F-acids were found as constituents of cod liver oil (29,36,37). F acids have been detected in invertebrates (38), such as crustaceans (crayfish) (39–41), amphibians (bullfrog) (40), and reptiles (turtle) (40).

F-acids with unusual highly unsaturated chains in α-positions were isolated from marine sponges (42). F-acids were also found in marine bacteria (43–45), algae (46,47), plants (48–50), yeast (49) and fungi (49), food fats such as butter (51) and virgin olive oil (52), mammalian tissue (53), and blood in-

cluding that of humans (54–56). Thus, F-acids seem to be widely distributed in all living matter.

The variations in the content of F-acids in the northern pike during the year and their accumulation in large amounts in testes and the liver of males in spawning times seemed to indicate a correlation between F-acids and the fertilization process (28). Subsequently, these increases in F-acids were correlated with starvation (30). F-acids were detected in all fish tissues examined (28) and in their blood (35). The best source for F-acids was the liver (23,24).

F-acids occur in living cells, like all other FA, as esters, but not in the free form. They are esterified to cholesterol in fish liver, and are found in TG and phospholipids in lower concentration (28). During starvation, the liver cholesterol esters become especially enriched in F-acids (29,30). In contrast, F-acids occur in fish testes nearly exclusively in the TG fraction (28,32). They are also predominantly esterified to glycerol in salmon roe (31). In the flesh of fish they are enriched in the phospholipids fraction (34) where they occur mainly in PC (31). Enrichment of F-acids was also reported in the PC derived from muscle tissue of crustaceae, such as crayfish (41) (see Table 2).

In liver tissue of mammals, F-acids are enriched in the cholesterol ester and in the TG fraction (53), but in mammalian (54) and human blood plasma (54) they are found mainly in the choline and ethanolamine phospholipids (55). Thus, F-acids are not equally distributed in the different organs in either fish or mammals.

F-acids of plant origin occur mainly in phospholipids, where they are predominantly localized in position 2 of the phospholipids. They constitute about 7% of LA, the most abundant FA in sugar cane cell cultures (50).

The reported F-acids that lack methyl substituents (57) are at least in part artifacts originating from lipid peroxidation

TABLE 2
Occurrence of Furan FA in Different Organs and Blood of Lipid Fractions in Animals[a]

Organism	Organ/blood	PL	CLE	TG	References
Fish	Liver	—	++++	++	26,28–34
Fish	Testes	++	++	++++	23,26,28–34
Fish	Ovaries	—	++++	—	35
Fish	Sperm	—	—	—	35
Fish	Egg	—	—	—	35
Fish	Roe	++	+	—	31
Fish	Muscle	+	++++	—	26,33,34
Fish	Blood	—	++++	—	26
Crayfish	Hepatopancreas	+	+++	+	39,40
Crayfish	Muscle	+++	+	—	41
Sponges		—	++	—	42
Beef	Liver	—	+	+	53
Beef	Blood	+++	+	+	53
Humans	Blood	++	+	+	54–56
Plants	Grasses, dandelion, olive				48–50,52
Plants	Cell culture	+++	+	+	50
Algae					46,47

[a]PL, phospholipid, CLE, cholesterol ester. The symbols +, ++, +++, and ++++ indicate relative abundances of furan FA (F-acids) in the different species. PL containing F-acids readily undergo oxidative decomposition during chromatographic separation on silica gel columns. Therefore, the absence of F-acids in the PL fraction may be due to complete decomposition (31).

products of PUFA, such as epoxyoxoenes, which are generated by grinding of tissue (see below) (58,59). These products will not be discussed in this review, nor will the disubstituted F-acids obtained by singlet oxygen oxidation of conjugated FA (for a review see Ref. 60).

ISOLATION

As outlined later, F-acids—especially those with two β-methyl substituents—can scavenge peroxyl radicals. These react with F-acids to form dioxoenes (*c.f.*, Fig. 10) (53,61) and further degradation products thereof (62,63). Therefore, F-acids are quantitatively degraded during homogenization of tissue in aqueous solution and escape detection if biological material is processed in buffer solutions. Thus, F-acids were found only occasionally when fish tissue was homogenized in organic solvents (26). After isolation of the lipid fraction according to Folch *et al.* (64) or Bligh and Dyer (65), lipids were separated by TLC into a cholesteryl ester fraction, TG, and phospholipids. The esters were transesterified with methanolic sodium methoxide solution to form FAME (23,26) and investigated by GC–MS. Alternatively, the lipid fraction was saponified with HCl or pancreatic lipase and then methylated (26). To enrich the F-acid methyl esters and to separate them from those of the straight-chain PUFA, the methyl ester fraction was hydrogenated, leaving the F-acids unchanged. The obtained saturated FAME were precipitated by addition of urea (66). The supernatant containing F-acid methyl esters (26,29) was separated from the crystals of the urea complexes of the saturated FAME and subjected to separation by GC in combination with MS (23). Since side reactions are inevitable during hydrogenation with platinum as catalyst (23), hydrogenation is sometimes avoided by subjecting the mixture of methyl esters to urea precipitation followed by silver ion chromatography, which allows separation of methyl esters of unsaturated FA from F-acid methyl esters (23,29). These additional separation steps are especially useful for detection of minor compounds in the F-acid methyl ester fraction (30). F-acid methyl esters show very characteristic mass spectra, which give complete structural information (23). Similar isolation methods are applied to obtain F-acids from mammalian tissue (61). To avoid the time-consuming separation by urea precipitation, enrichment of F-acid methyl esters can be achieved by hydrogenation of the furan rings with a rhodium catalyst on alumina (67) to THF derivatives (54). The latter can easily be separated from saturated and unsaturated FAME owing to their high polarity. Application of multidimensional GC (trapping fractions and analyzing these by using a second gas chromatograph combined with a mass spectrometer registering characteristic ions) is nowadays applied for direct identification of F-acid methyl esters without prior separation from straight-chain fatty acid methyl esters (56).

CATABOLISM OF F-ACIDS

In an investigation of FA excreted in human urine, a previously unknown group of tetra-substituted dicarboxylic acids with a furan ring was detected (68). The structures of the main representatives of this group of compounds were recognized to be 3-carboxy-4-methyl-5-propyl-2-furopropanoic acid, **9**, and 3-carboxy-4-methyl-5-pentyl-2-furopropanoic acid, **10** (Fig. 1) (69). These acids were also found in human blood (70). Later, furan acids lacking the methyl substituent in position 4 of the furan ring were detected in traces in human urine, too (71). Excretion of **10** was enriched three- to sixfold after consumption of a fish diet (72).

Interestingly, the metabolism of F-acids differs considerably in various mammals. The long carboxylic acid α-side chain is degraded stepwise in all mammals to 3 carbon atoms. Additionally, in humans (73) the methyl group adjacent to this side chain is transformed to a carboxylic acid group, whereas in rats (74) and cattle (75) both α-side chains are preferentially oxidized (Fig. 1). An F-acid with a short carboxylic acid side chain, detected in soft corals, probably represents a degradation product of larger molecules (76).

Compounds **9** and **10** are enriched in plasma of patients with chronic renal failure (77). Although F-acids with a pentyl side chain usually are more abundant in the liver, the concentration of the degradation product with a propyl side chain, **9**, greatly exceeds that with a pentyl side chain, **10**, in plasma of subjects
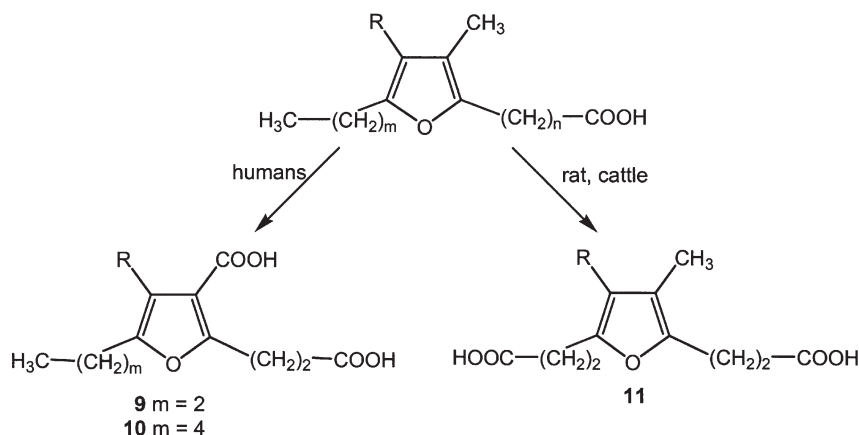
FIG. 1. Catabolism of F-acids.

suffering from chronic renal failure. Since **9** inhibits the hepatic glutathione S-transferase, its enrichment in uremic serum has been connected to the toxic properties of uremic plasma (78). Removal of **9** by conventional hemodialysis is difficult owing to its strong binding to plasma protein (78–80). This property also interferes with the binding of drugs to albumin (81,82). The competitive binding of **9** alters the excretion of various drugs, drug conjugates, and other organic acids (83). Further investigations revealed that only free **9** is ultrafiltered in the glomeruli and then excreted in the urine (84); **9** is an inhibitor of mitochondrial respiration (85) and erythropoiesis and thus may contribute to anemia in renal failure (86). It also decreases the bilirubin-binding capacity (87) and has been hypothesized to be related to neurological abnormalities in uremia (88). Moreover, **9** inhibits proliferation of cultured human T-lymphocytes (89). Efforts to reduce **9** in serum by continuous ambulatory peritoneal analysis were partly successful (86). Several procedures were elaborated to determine **9** by HPLC methods (82,90–92) or by immunoassay (93). By applying these sensitive methods, **9** can be determined even in hair and sweat (94).

BIOSYNTHESIS

Originally, it was believed that F-acids are generated in fish (23). Feeding ^{14}C-labeled acetate to fish revealed that the acetate is incorporated into the carboxylic side chain by chain elongation. Chain shortening of the carboxylic side chain also was observed, but acetate was incorporated neither into the furan ring nor into the alkyl side chain (95), an indication that fish synthesize neither the alkyl side chain nor the furan ring of F-acids.

It is much easier to perform feeding experiments with rats to collect urine samples than with fish. Analysis of the rats' livers indicated the presence of F-acids. In order to prove the hypothesis that F-acids are derived from linoleic acid, a homolog of linoleic acid was fed to rats, but no homologous F-acids could be detected in their livers. As a consequence it was assumed that F-acids may be derived from rat food (96). This assumption was confirmed later by an investigation of plants (49). All investigated plants and algae (the final source of fish food) contained F-acids. In contrast, early hints that 2,5-disubstituted alkylfurans are transformed by incubation with liver homogenates (97) could not be reproduced. The observation that F-acids are generated in plants allowed further studies in cell cultures by feeding labeled compounds. It was thus recognized that plants synthesize the basic skeleton of F-acids from acetate (98). The methyl groups in the β-position of the furan ring originate from methionine (99,100), and the furan oxygen is derived from air (101). Originally, it was assumed that LA (**12**) was the precursor of the carbon skeleton of F-acids having a pentyl side chain by generation of a hydroperoxide in position 13, whereas F-acids with a propyl side chain were hypothesized to be derived from a hydroperoxide in position 12 of linolenic acid (47). Investigation of algal cell cultures proved that F-acids with a pentyl side chain originate from **12** but that F-acids with a propyl side chain are not derived from linolenic acid. Instead, they are generated from 9,12-hexadecadienoic

acid **13** (47). The peroxidation is initiated apparently by an unusual lipoxygenase (LOX) that counts—in contrast to most others—starting from the carboxylic end of the unsaturated FA (47) (Fig. 2).

The F-acids that primarily are generated are elongated by acetate units to higher homologs.

On the basis of the intermediates that were isolated—but without labeling experiments—it was proposed that in marine bacteria living in fish, F-acids are generated in a different way, starting by introduction of a methyl group into *cis*-vaccenic acid, **20**, followed by incorporation of a second double bond. The generated diunsaturated FA is assumed to react with oxygen, followed by ring closure to an F-acid (44) (Fig. 3).

CHEMICAL SYNTHESIS OF F-ACIDS

F-acids represent tri- or tetra-substituted furan derivatives. Their synthesis therefore requires several steps. Originally, **6** was prepared by starting from 3,4-bis(acetoxymethyl)furan, **23**, which was condensed with pentanoic acid anhydride to its
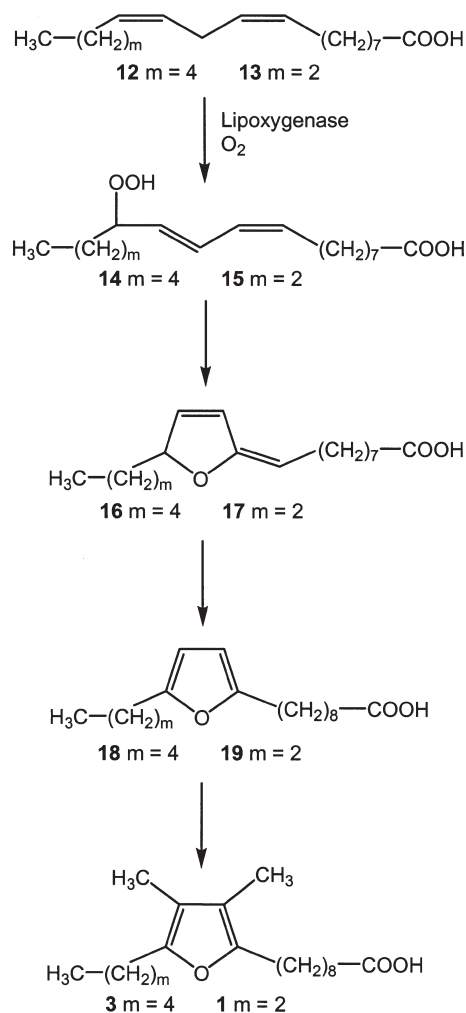
FIG. 2. Biosynthesis of F-acids.
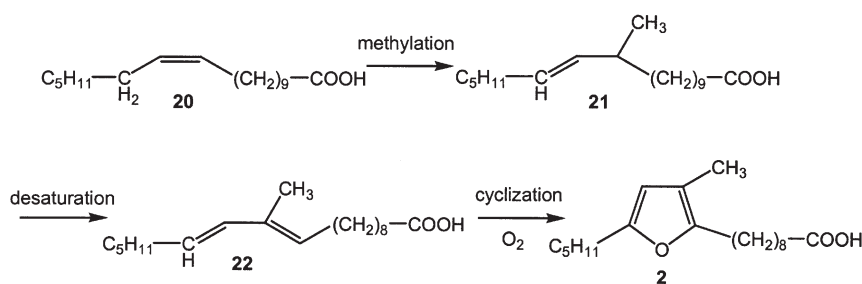
FIG. 3. Proposed biosynthesis of F-acids in marine bacteria.

butylketone **24**, which was then transformed by reduction with hydrazine to the pentylfuran derivative **25**. The hydroxy groups of the latter were exchanged by chlorine. The resultant dichloro derivative **26** was subsequently reduced with $LiAlH_4$ to 3,4-dimethyl-2-pentylfuran, **27**. Introduction of the fourth substituent was achieved after treatment with BuLi by reaction with 1-chloro-10-iododecane. The resulting product **28** was finally converted by exchange of the chlorine to the Li-compound that was reacted with CO_2 to the F-acid **6** (102) (Fig. 4).

The difficult introduction and conversion of the carboxylic acid side chain is facilitated by using the acid chloride of the half ester derived from undecanedioic acid for condensation with 3,4-dimethy-2-pentylfuran, **27,** by catalysis with $SnCl_4$ to

29, followed by removal of the carbonyl function in a Wolff–Kishner reaction leading to **6** (61) (Fig. 5).

The key intermediate, 3,4-dimethyl-2-pentylfuran, **27**, is synthesized (103) by starting from 2,3-dimethyl-2-buten-4-olide **30**, which is reacted with pentylmagnesium bromide in ether to form the condensation product **31**. The latter is readily transformed without isolation by treatment with 2 N sulfuric acid to 3,4-dimethyl-2-pentylfuran, **27** (Fig. 6).

The lactone **30** is obtained by $LiAlH_4$ reduction of 2,3-dimethylmaleic acid anhydride, prepared by methylation of maleic acid anhydride by thermal decomposition of acetic acid (providing methyl radicals) in the presence of 2-aminopyridine (104) or by cyclization of 4-chloro-3-hydroxy-2,3-dimethylbutanoic acid
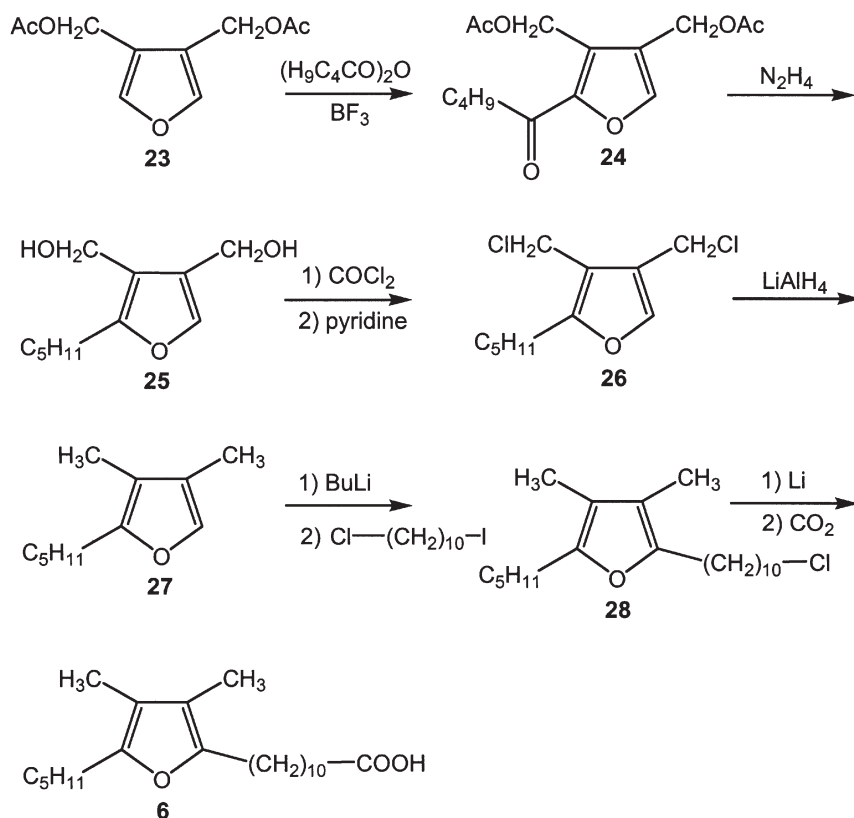
FIG. 4. Synthesis of F_6, **6**.
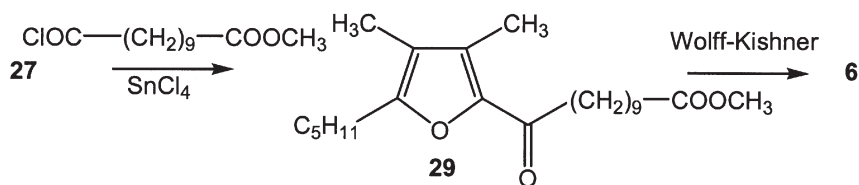
FIG. 5. Alternative route from 3,4-dimethyl-2-pentylfuran **27** to F$_6$, **6**.
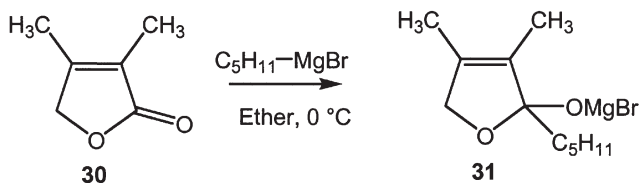
FIG. 6. Generation of the starting material for the synthesis of 3,4-di-methyl-2-pentylfuran **27**.

methyl ester in presence of methoxide (103). The trisubstituted F-acid **5** was prepared by starting from 3-methyl 2-methylfuroate **32**. The pentyl side chain in position 5 of the furan ring was introduced in a manner similar to the route presented in Figure 5 by reaction with valeric acid anhydride and reduction of the resulting ketone, **33**, with hydrazine. The obtained acid, **34**, was decarboxylated to 4-methyl-2-pentylfuran, **35**. The introduction of the second α-side chain to **5** was performed as outlined for F$_6$ (102) (Fig. 7).

F$_6$ labeled in the carboxylic group with ^{14}C, **6a**, was prepared, starting from 3,4-dimethyl-5-pentylfuran, **27**, by introduction of an aldehydic group into the second α-position by a Vilsmeyer reaction to **37**, followed by a Wittig reaction to **38**, hydrogenation of the double bond in the side chain to **6a**, and an Arndt–Eistert reaction with ^{14}CH$_2$N$_2$ (Fig. 8) (105).

The rather moderate yield from these multistep reactions is considerably improved by a synthesis that takes advantage of

the different reactivities of bromine substituents at the furan ring. 4,5-Dibromofurfural, **39**, reacts in a Pd(0)-catalyzed reaction with 10-undecynoic acid benzyl ester by selective coupling in position 2 to **40**. The aldehydic group in **40** is subjected to a Wittig reaction. The bromine atom of the obtained product **41** is then exchanged by a methyl group by treatment with MeZnCl under catalysis of PdCl$_2$(PPh$_3$)$_2$ to the unsaturated benzyl ester **42**, which is transformed in one step by reduction with Pd(OH)$_2$ to **5** (106) (Fig. 9).

The 3,4-unsubstituted F-acids are available by epoxidation of both double bonds in LA, followed by treatment with NaI and propyliodide in dimethylsulfoxide (107).

3,4-Dimethyl-substituted F-acid esters are available starting from 3-methyl F-acids (present in latex rubber plants) by opening of the furan ring with acid to a dioxo ester, followed by methylation with methyl iodide/KOH in dimethylsulfoxide and cyclodehydration with BF$_3$ in methanol (107).

REACTIONS OF F-ACIDS

Like α,α-aryl-substituted furans, α,α-alkyl-substituted F-acids **3** undergo oxidation by ring opening (61,62) to form dioxoenes **43** (Fig. 10), which have been shown to inhibit blood platelet aggregation *in vitro*, albeit at high concentrations (108).

Investigation of the mechanism of this reaction showed that the oxidation is not restricted, as assumed originally, to singlet oxygen (109) but is common to radical-generating agents, such
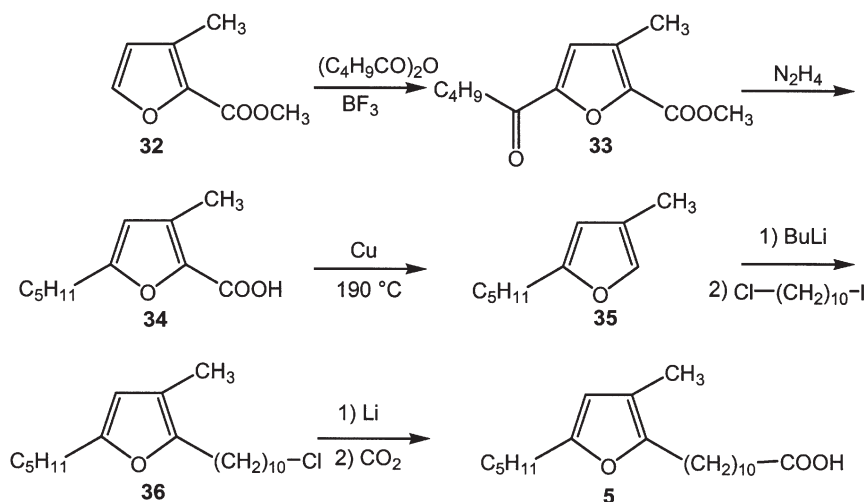
FIG. 7. Synthesis of F$_5$, **5**.
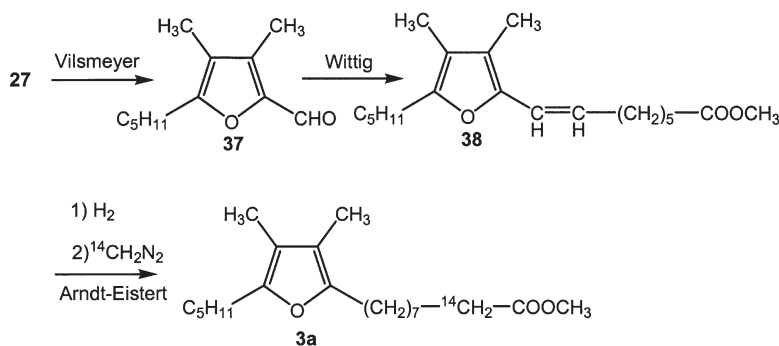
FIG. 8. Synthesis of ^{14}C labelled F_3 **3a**. Reagents for the Vilsmeyer reaction: $POCl_3$, dimethylformamide, reagents for the Wittig reaction: triphenylphosphine, 7-iodoheptanoic acid methyl ester.
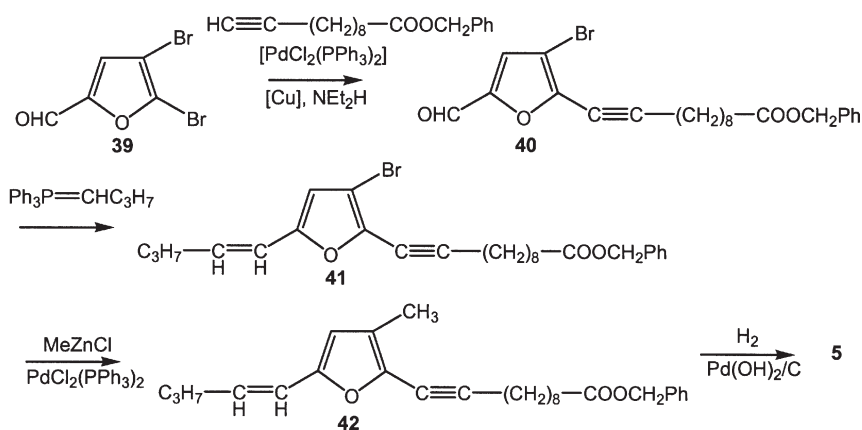
FIG. 9. Alternative synthesis of F_5, **5**.

as the Fenton reagent (Fe^{2+} + LO-OH → Fe^{3+} +OH^- +LO•), hypochlorous acid, or lipid hydroperoxides (110). It was therefore unexpected that this reaction was induced not only by radical-producing oxidizing chemical reagents but also by LOX. This reaction required the presence of LA as co-substrate. Free iron ions react extremely easily with lipid hydroperoxide (LOOH) molecules in the Fenton reaction. Nevertheless, iron ions are used extensively as catalysts for enzymatic redox reactions in nature, for instance in LOX. In order to avoid the Fenton reaction, metal ions are shielded in redox enzymes by complexation. Thus in LOX any contact with released LOOH molecules is prevented. It was therefore suspected (112) from the experiment illustrated in Figure 10 that iron ions were made

available for catalysis by alteration of LOX to induce nonenzymatic lipid peroxidation (LPO) reactions. This was clarified by model reactions using plant LOX (112): When soybean LOX-1 (requiring free PUFA for generation of LOOH molecules) was added to F-acid esters, these remained unchanged. Likewise no oxidation products of F-acids were generated if F-acid esters were incubated with pure LA, but if LA was added to the solution of soybean LOX-1, and F-acid esters, dioxoenes were produced (Fig. 10). This demonstrates involvement of radicals. Radicals are formed in a Fenton reaction requiring bivalent metal ions (113). The only available metal ions in this experiment are those in LOX. Moreover, it has been demonstrated that LOX is inactivated if it is exposed to high amounts of substrate
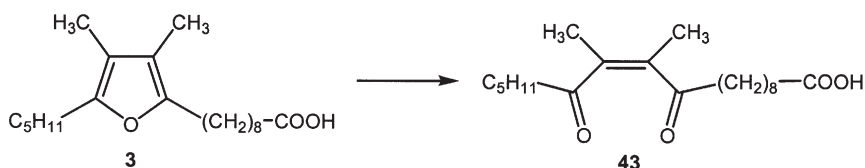
FIG. 10. Transformation of F-acids to dioxoenes 43.
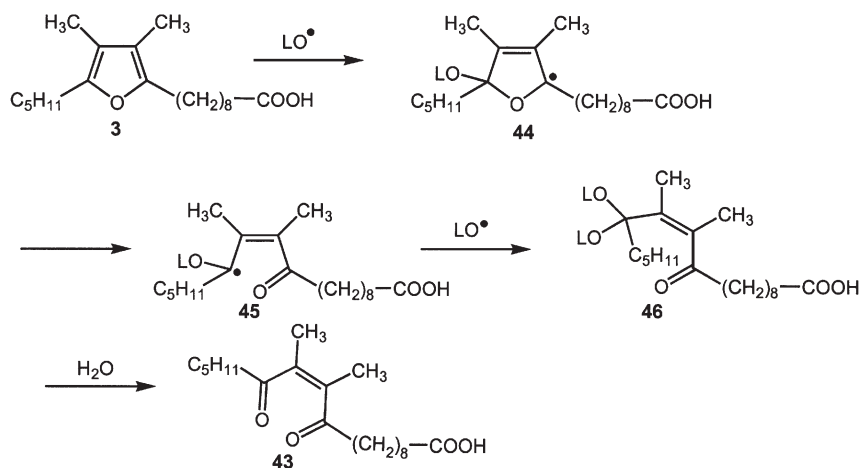
FIG. 11. F-acids act as scavengers of radicals.

(114,115), which is certainly present if free LA is used as starting material as in the experiment just described. Thus, LOOH molecules were cleaved in the course of the reaction to alkoxyl radicals (116). These added to either position 2 or 5 of the furan ring of an F-acid, forming an intermediate, **44**, that undergoes ring opening to a mesomeric radical **45** of high stability. Consequently, it is much less reactive than a peroxyl or alkoxy radical. This property enhances its lifetime and enables it to trap a second radical, such as an alkoxy radical, generating a ketal, **46**. Thus, a stable molecule is generated and two radicals are removed in the course of the reaction (Fig. 11).

Ultimately, the ketal **46** undergoes hydrolysis to a dioxoene **43**. The catalytic availability of iron ions after alteration of LOX, which has not been taken into account previously, represents an alternative route to the well-known biological sources of iron ions, such as the heme present in blood or ferritin, as discussed by Welch *et al.* (117). The generation of free radicals by LOX iron ions could take place in tissues in which LOX enzymes have been expressed.

The idea that iron ions derived from inactivated oxygenase enzymes might be involved in the induction of radical reactions is further supported by considering that a single iron ion theoretically is able to start a radical chain reaction. In addition, the iron ion now made available to catalyze radical formation should be close to the generated LOOH molecule so as to avoid interruption of the Fenton reaction, for instance by reduction of LOOH to LOH molecules.

Alkoxy radicals attack double allylic activated hydrogens not only of free PUFA, as most LOX do (113), but also of PUFA bound to phospholipids **47** (118) or to cholesterol (118). Alkyl radicals **48** thus generated react with oxygen to form peroxyl radicals **49** (Fig. 12).

The reactivity of peroxyl radicals considerably exceeds that of LOOH or H_2O_2. For instance, LOO• radicals react with secondary alcohol groups by oxidation to carbonyl compounds, as exemplified by oxidation of hydroxy acids to oxo acids (118); with thioethers, such as methionine, to sulfoxides (118); with

amino acids containing a primary amino group, such as lysine, by oxidation to an aldehydic group (118); and with compounds containing double bonds, such as cholesterol (118) and linoleic acid, linolenic acid (119), or oleic acid (OA) (120) to their epoxides. Many of these products are toxic (121,122) or undergo transformation to toxic products (123). Thus, peroxyl radicals, generated in the reaction path outlined in Fig. 12, are a major source of cell-damaging processes.

Preferred substrates for the attack of peroxyl radicals are apparently F-acids, as reflected, for instance, by the observation that F-acids are not detectable after tissue has been homogenized, whereas they are found in plants (40) and tissues of animals (61) if homogenization is carried out after samples have been boiled or worked up with an organic solvent. Since boiling destroys enzymes, and workup in organic solvents usually prevents enzyme activity, as demonstrated long ago in the processing of plant tissues (124), the oxidation reaction is concluded to be induced by an enzymatic reaction (125). Apparently any change in membrane structure, inevitably caused by cell-damaging processes (homogenization), alters also proteins of cell channels combined with influx of Ca^{2+}ions into the cell (126); Ca^{2+} ions activate many phospholipases. These generate free PUFA from phospholipids, which serve as substrates for oxygenases. Inactivation of such enzymes by an accumulation of large amounts of free PUFA may be associated with altered binding activities of iron ions (114,115) and switches the controlled enzymatic LPO to uncontrolled nonenzymatic LPO, resulting in production of peroxyl radicals as already discussed.

Peroxyl radicals attack F-acids by ring opening to dioxoenes **43** (61,62,127) (Fig. 10). F-acids occur in some tissues in form of phospholipids (54). These naturally occurring tetra-alkyl-substituted furan derivatives are prone to oxidation (25,128) by peroxyl radicals, as already mentioned (127). Therefore, F-acids may serve in nature as antioxidants (128) as also suggested by electron spin resonance investigations (24).

Diet-derived F-acids are incorporated into the tissue and blood of mammals, especially into phospholipids (54, 55)
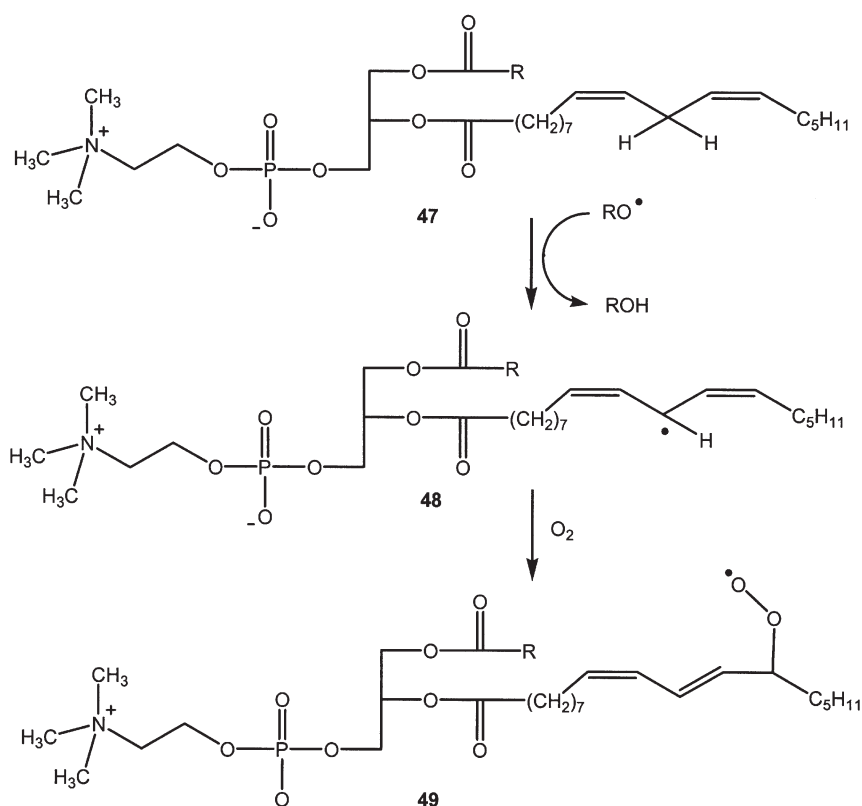
FIG. 12. Generation of peroxyl radicals, exemplified with a phospholipid containing a PUFA.

where they partly substitute for PUFA. As a consequence, they are localized exactly at sites where LPO reactions occur in atherosclerosis and where they are needed to trap radicals. This might increase their value as radical scavengers in comparison with other radical-scavenging compounds, such as tocopherols.

The ring-opening reaction of F-acids to dioxoenes different in α,α,β,β-tetra-alkyl-substituted furans compared with α,α-di-alkyl-substituted furans. The latter are rearranged to rather stable *trans* dioxoenes. This rearrangement is inhibited in tetra-alkyl-substituted furans such as **3**; the products **43** remain in the *cis* form (127). In alkaline solution this isomer undergoes an intramolecular aldol condensation to the cyclopentenolones **50** and **51** (61) (Fig. 13).

Cyclopentenolones **50** and **51** are detectable after homogenation of tissue in aqueous solvents (61,129). Dioxoenes generated as intermediates, such as **52**, add nucleophiles (62) such as water or thiols (62), e.g., glutathione. The addition products are able to react further by ring closure forming a-substituted F-acids (Fig. 14). These can either undergo a second oxidative ring opening, followed by addition of a second nucleophile and a second ring closure reaction (62), or react by loss of the substituent by formation of derivatives with an α,β-double bond (Fig. 14). As a consequence, all of these different artifacts, such as **53–56**, are detectable after processing biological materials.

The preferential oxidation of F-acids by peroxyl radicals, compared with attack on PUFA, becomes evident following investigation of plant (124) or animal tissue samples (130,131). After homogenization in aqueous solution, F-acids are completely missing, whereas the content of PUFA remains largely unchanged (61).

The great tendency of F-acids to undergo oxidation suggests that plants and algae can use these compounds as radical scavengers to defend against the deleterious effect of UV radiation. To remove radiation-induced radicals, plants and algae are assumed to generate F-acids and incorporate them into PC (50). Thus, for instance, antioxidant activity in soybean PC liposomes is recognized (128). The potency of F-acids as scavengers of, for example, hydroxyl radicals (24) is further exemplified by the findings that they suppress hemolysis better than other quenchers of singlet oxygen, such as dimethylfuran, α-tocopherol, ascorbic acid, or uric acid (24).

All these deductions are corroborated by the observation that the content of F-acids in plants increases from nearly zero at the beginning of leaf growth to maximal values in July in the Northern Hemisphere and then remains constant till the end of the vegetation period (Schulz, D., and Spiteller, G. unpublished data).

Phospholipids represent the outermost layer of cells and are therefore exposed first to the attack of microorganisms. This mechanical injury induces a reaction cascade, leading to generation of radicals as already outlined. The defence processes should end once the invader is destroyed. F-acids incorporated in cell membranes seem to contribute to stop the progress of LPO reactions after a successful defense against the invaders.
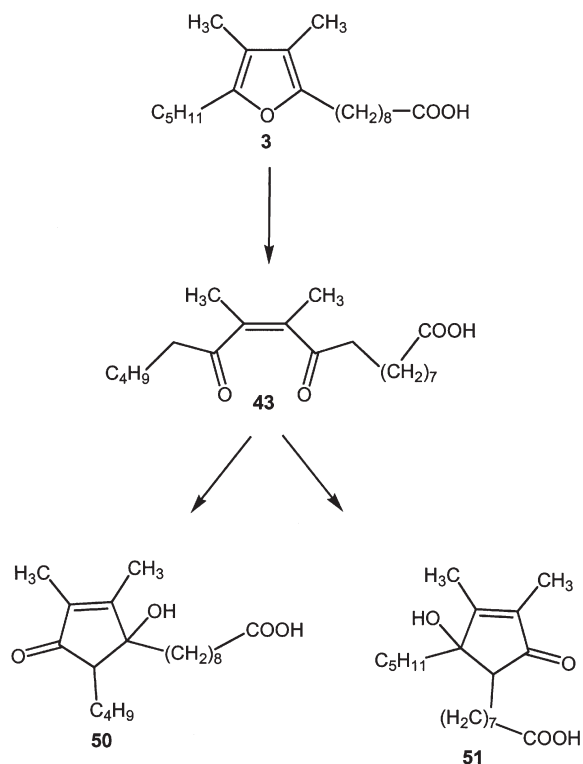
FIG. 13. Generation of cyclopentenolones **50** and **51** by reaction of dioxoenes with alkali.

Drying of plant material is connected with LPO processes (132) that generate peroxyl radicals that oxidize F-acids. Some of the oxidative degradation products of F-acids generated by plant injury are characterized by a typical smell. For instance, 3-methyl-2,4-nonanedione is responsible for the hay-like scent of dried spinach (133).

In contrast to F-acids, urofuran acids, their biological oxidation products, are rather stable to further oxidation. Nevertheless, they also undergo oxidative ring opening when treated with powerful oxidizing agents, such as hypochlorous acid (134).

ARE F-ACIDS INVOLVED IN PROTECTION AGAINST CARDIOVASCULAR DISEASES?

As pointed out in the introduction, a diet rich in marine food (9,10,15) or fish oil (16, 135–138) was protective against cardiovascular diseases. It lowers the amount of TG in LDL (135,139,140) and—most importantly—decreases the risk of sudden heart death in patients (136,137) apparently closely related with a reduction of Ca^{2+} ion release from cell stores (137,141). Fish oils are thought to increase slightly the HDL level (135,142) and to reduce the level of the VLDL. Since fish are rich in n-3 PUFA, the protective properties of fish consumption have been ascribed to these n-3 PUFA (17,18). These deductions do not consider the possibility that minor natural products might have much greater physiological effects than the major constituents and that n-3 PUFA, like all other PUFA, readily undergo lipid peroxidation, while saturated and mononounsaturated FA remain unaffected.

The increase in susceptibility of LDL to oxidation by an exchange of saturated FA and OA vs. more highly unsaturated PUFA has been experimentally confirmed (143–145). In confirmation, an increase in LPO products was found after n-3 FA were incorporated into plasma and tissue (146). Thus, a fish diet is expected to produce an increase in atherogenic effects, not a decrease, as observed. In fact, some reports claim an increase in the oxidizability of LDL after consumption of fish oil (147).

These controversial observations and deductions require a
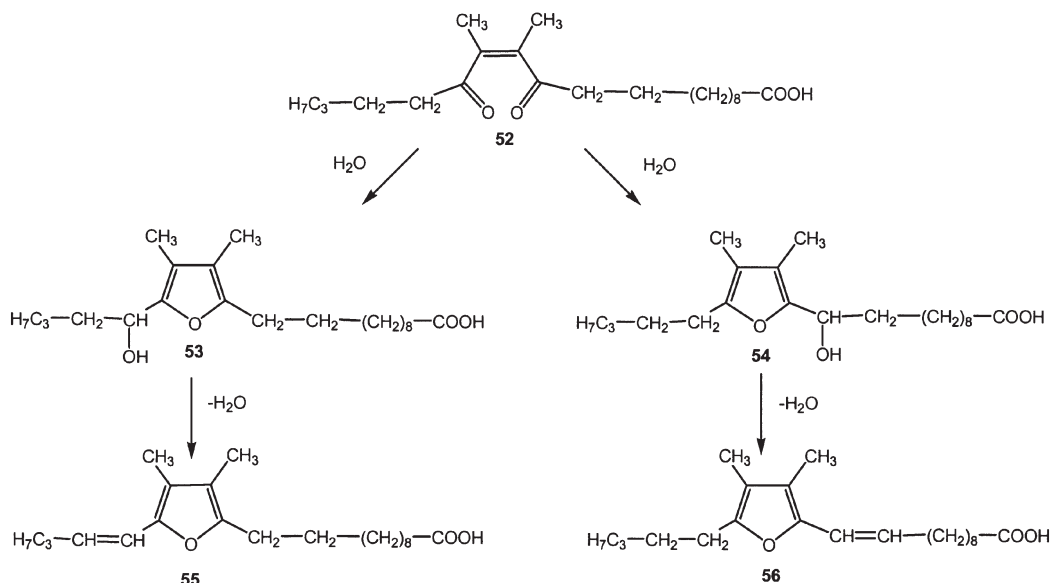
FIG. 14. Generation of α-substituted F-acids and their dehydration products.

short discussion about the present knowledge about atherogenesis.

Atherosclerosis (1,2,148) is related to the oxidation of LDL (149–151). Oxidized LDL induces apoptosis of cells (152,153), raising the question of which oxidation products might cause these effects.

LDL is a macromolecule composed of a core of cholesterol esters and a phospholipid membrane in which a protein is embedded (148). The latter is recognized by the LDL receptor of the endothelium (148).

PUFA are incorporated into the phospholipid membrane of LDL and into its cholesterol ester-containing core. Compared with all other constituents of LDL, PUFA show the highest sensitivity to oxidation by molecular oxygen. This sensitivity becomes evident by storage of fat that contains PUFA, resulting in rancidity (154), or by storage of blood plasma that develops atherogenic modifications (155). Likewise, wounding of plant (124) and animal (130,131) tissue is associated with LPO. Therefore, partly oxidized phospholipids are detected after artificial oxidation of LDL (156), after addition of activated human monocytes (157) (corresponding interactions influence the membrane structure), or after storage (155,158). Hydrolysis of such oxidized LDL allows quantification of the different oxidized PUFA products by flow injection electrospray ionization MS (158) or, after saponification, by GC–MS. The latter method revealed that the main oxidation products are derived from LA (159–161), which represents the most abundant PUFA in LDL of people consuming a Western-type diet (148). Compared with LA, arachidonic acid (AA) is present in LDL in much smaller amounts (AA/LA = 1:5). The content of n-3 PUFA is much lower. The most abundant n-6 PUFA in people consuming a Western diet is LA, representing about 20–30% of the total amount of FA in LDL (159).

The content of FA in LDL is strongly dependent on the FA composition of the food consumed, as exemplified by feeding an OA-rich diet to rabbits (162) or humans (144), which changed the LDL fatty composition in favor of OA. Likewise, the content of FA in wild-living fish varies with season and with living conditions. For instance, in starving fish, the content of F-acids increases in the liver cholesterol ester fraction (29).

FA of fish tissue can be distinguished from those of mammalian tissue by the presence of larger amounts of long-chain highly unsaturated n-3 PUFA. EPA amounts in fish are between 7 and 10%, and DHA is between 20 and 40% of the total FA content, depending on the kind of fish and the investigated organ (12–14).

Since the nutritional sources of fats strongly influence the composition of blood fats, it is not surprising that the contents of EPA and DHA in the blood plasma of Greenlanders (9), whose main nutritional source is marine organisms, are much higher than those of people consuming a Western diet, although they are still not a major fraction: EPA is present on the average in the phospholipid and TG fraction to a maximum of 8%, whereas it accumulates in the cholesterol ester fraction to 15% of the total FA content. DHA amounts to values not exceeding

3–4% in all three lipid classes (phospholipids, TG, and cholesterol esters) (10) although DHA is more abundant in most fish than EPA. The presence of relatively large amounts of n-3 FA was assumed to be responsible to the beneficial properties of a fish diet (10).

n-3 PUFA, like n-6 PUFA, possess one or more –CH=CH-CH_2-CH=CH– groups, the prerequisite to undergo a nonenzymatically induced LPO process. Therefore, n-3 PUFA are not distinguished in their capacity to be attacked by radicals, and both classes of PUFA are subjected equally to radical induced LPO reactions. Consequently, the reason for the beneficial properties of a fish diet cannot be a suppresion of LPO reactions.

Owing to the low content of n-3 PUFA in LDL of people living on a Western-style diet (the most abundant n-3 FA, linolenic acid, is present in an amount less than 2%), the contribution of n-3 PUFA to oxidation products of LDL is extremely low. In contrast, the relatively high level of n-3 PUFA in the blood of Greenlanders should contribute to their LPO. Degradation of LPO products of AA and LA produces nearly identical toxic products, such as 2,4-decadienal (123), 4-hydroxynonenal (163,166), or epoxyenoic acids (122). Because LA is much more abundant than AA in LDL, more toxic products are derived by LPO of LA than by AA.

Since n-3 PUFA (164) decompose in nonenzymatic LPO reactions in an analogous manner to n-6 PUFA (165), no change in the production of toxic compounds (166) in bulk-phase reactions is expected by exchange of n-6 PUFA with n-3 PUFA. Nevertheless, consumption of fish or fish oil does decrease the rate of LDL oxidation (147,167). This observation was corroborated by feeding volunteers a fish oil supplement, which caused enrichment of their LDL with EPA and DHA. This LDL proved more stable against *ex vivo* oxidation and less able to induce apoptosis in U 937 cells (168) (a characteristic behavior of atherosclerotic cells) than LDL enriched with LA (169).

This puzzling effect has been explained by arguing that the beneficial effects of food rich in EPA and DHA, which are incorporated in increased amounts into phospholipids with respect to AA, decrease the generation of thromboxane (TX) A_2, which causes platelet aggregation and increases prostacyclin activity (170), thus reducing the risk of atherogenesis. The hypothesis that altering the AA/EPA/DHA relation by consumption of a fish diet reduces the AA amount and therefore TX production does not consider that production of TX is an enzymatic and therefore a physiological process. In contrast, the reactions devastating cells in cardiovascular diseases seem to be induced by radicals. The change in the AA/EPA/DHA relation does not necessarily influence the generation of radicals, since all PUFA are equally able to induce generation of radicals. A decrease in radicals can be achieved only by radical scavengers. Therefore, it seems reasonable to assume that the presence of other components in a diet rich in fish or fish oil, or other factors not taken into account previously, might be responsible for the observed reduction of LDL oxidation, as has been already suggested (171). This assumption is further corroborated by the observation that the amount of propylurofu-

ran acids increased by a factor of 3–6 after consumption of a fish oil diet (72). Since urofuran acids are degradation products of F-acids, this indicates that fish oils are abundant sources of F-acids.

Although F-acids occur in fish only in amounts of around 1% (29,36) they might reduce the oxidation of LDL to a considerable extent because they serve as potential radical scavengers (24) and inhibit progression of nonenzymatic lipid peroxidation reactions (172). And because radicals induce a chain reaction, the amount of F-acids may be sufficient to suppress LDL oxidation.

Although the content of F-acids in fish and fish oils could explain the positive effects of a fish diet, similar effects were reported from fish oils in which n-3 PUFA were enriched. During n-3 PUFA enrichment, at least a reduction in F-acid contents might be expected. But separation of F-acids from other FA is very difficult and requires special workup procedures (66). Such procedures are not used in preparing fish oil supplements. Therefore, F-acids might remain during the enrichment procedure (36).

F-acids are mainly incorporated into phospholipids of blood plasma (54), which is in intimate contact with the surface of endothelial cells where oxidation of LDL occurs (172). Thus, the scavenger molecules (F-acids) are incorporated exactly at the sites where they can prevent lipid oxidation most effectively. Consequently, F-acids may contribute to the protective properties of a fish or fish oil diet. The suggestion that F-acids are effective antioxidants is further corroborated by the observation that phospholipids of eggs from marine salmon withstand lipid peroxidation induced by copper ions much better than do phospholipids of chicken eggs (174). Moreover, it can be assumed that the polar F-acids are more easily in contact with the polar hydroperoxides than with less polar FA esters, as shown by investigations of oil-in-water emulsions (174–176).

DOES THE REDUCTION IN TOTAL PUFA CONTRIBUTE TO THE PROTECTIVE PROPERTIES OF A FISH DIET?

As pointed out earlier, Dyerberg *et al*. (10) compared plasma samples obtained from Greenlanders living nearly exclusively on a marine diet with those of Danes living on a typical Western diet. They noted a substantial increase of EPA and DHA in LDL of Greenlanders compared with LDL of Danes. But the reported FA content also indicates a considerably increased PUFA concentration in all three lipid classes (phospholipids, cholesterol esters, and TG) in Danes compared with Greenlanders. In the phospholipids located at the outer surface of the LDL particle, where lipids are especially exposed to oxidation, the PUFA content exceeds that of saturated and monounsaturated FA by more than twofold; in the cholesterol esters representing the core compounds by one-third; and in the less important class of TG by about 20% (10). Considering that only PUFA are subjected to lipid peroxidation, this means a reduction in the overall likelihood of generating toxic LPO products

in LDL of Greenlanders compared with people living on a Western-style diet.

As shown in many experiments, the plasma FA content reflects with few exceptions (one is the content of DHA) the content of FA consumed in the diet (144,162). Apparently, AA may be substituted by EPA, as recognized from the fact that the amount of AA in the phospholipids of Danes corresponds nearly exactly to the amount of EPA in that of Greenlanders (10).

Although it has been assumed that EPA and DHA are more prone to oxidation compared with n-6 PUFA, which have a lower number of double bonds (161), this deduction may not relate to biological processes because it is based on model reactions with mixtures of pure PUFA carried out by adding an excess of catalytic bivalent metal ions (177). In biological material, such an excess of metal ions is never produced, since decomposition of iron-containing proteins—which allows iron ions to become available for peroxidation catalysis—is a relatively rare event, except if massive mechanical destruction of tissue is performed, for instance by homogenization (131). As a consequence, the total amount of PUFA in LDL combined with the ability to remove generated peroxyl radicals may determine their transformation rate to toxic compounds.

The increase in saturated and monounsaturated FA in plasma of Greenlanders compared with Danes and their decreased incidence of atherogenesis is in contradiction to the statement that ingestion of food rich in saturated FA increases the atherogenic risk (3,7,8). Saturated and monounsaturated FA withstand oxidation; thus these acids are not attacked by LPO, as shown by artificial oxidation of LDL or during storage (159). Although monounsaturated FA are less stable to LPO than saturated ones, they are much less prone to undergo LPO compared with PUFA, as proven experimentally by LDL oxidation (159). Therefore, only PUFA are significantly subjected to LPO in LDL, at least *in vitro*.

The comparison of the nutrition of Greenlanders and Danes on the basis of their blood concentrations of FA indicates that there are more than twice as many PUFA molecules in the phospholipid fraction of Danes compared with that of Greenlanders (10) and perhaps this—besides the content of F-acids—could be responsible for the fact that Greenlanders were less affected in the past to atheroclerosis.

CONCLUSION

F-acids seem to be distributed in all mammals, plants, and algae, where they apparently play an important role in scavenging radicals and contribute to inhibiting the progression of nonenzymatic LPO reactions. F-acids are accumulated in fish, fish products, and other marine organisms. F-acids are also present in plants, although in lower amounts. F-acids are introduced into the body through the diet. This may be one reason why fish consumption reduces the risk of atherogenesis and its eventual complications.

A fish diet has an additional effect: Although it increases the content of n-3 PUFA in tissue and blood, it reduces the total

amount of PUFA in the phospholipid fraction of plasma in favor of saturated and monounsaturated FA in LDL, which withstand oxidation. Since all PUFA are susceptible to LPO, the reduction of the total amount of PUFA in LDL—besides the content of F-acids—might be a second reason for the protective properties of a fish diet.

ACKNOWLEDGMENTS

REFERENCES

1. Ross, R. (1993) The Pathogenesis of Atherosclerosis. A Perspective for the 1990s, *Nature 362*, 801–809.

2. Lusis, A.J. (2000) Atherosclerosis, *Nature, 407*, 233–241.

3. National Cholesterol Education Program (1993) *Second Report of the Expert Panel on Detection, Evolution, and Treatment of High Blood Cholesterol in Adults,* National Institutes of Health, NIH Publication No. 93-3095.

4. Gerrity, R.G., Naito, H.K., Richardson, M., and Schwartz, C.J. (1979) Dietary Induced Atherogenesis in Swine, *Am. J. Pathol. 95*, 775–792.

5. Mott, G.E., Jackson, E.M., McMahan, C.A., and McGill, H.C., Jr. (1992) Dietary Cholesterol and Type of Fat Differentially Affect Cholesterol Metabolism and Atherosclerosis in Baboons, *J. Nutr. 122*, 1397–1406.

6. Keys, A. (1979) *Coronary Heart Disease in Seven Countries*, Monograph 29, American Heart Association, New York.

7. Grundy, S.M. (1997) What Is the Desirable Ratio of Saturated, Polyunsaturated, and Monounsaturated Fatty Acids in the Diet? *Am. J. Nutr. 66 (Suppl.)*, 988S–990S.

8. Grundy, S.M., and Denke, M.A. (1990) Dietary Influences on Serum Lipids and Lipoproteins, *J. Lipid Res. 31*, 1149–1172.

9. Bang, H.O., and Dyerberg, J. (1980) Lipid Metabolism and Ischemic Heart Disease in Greenland Eskimos, *Adv. Nutr. Res. 3*, 1–22.

10. Dyerberg, J., Bang, H.O., and Hjørne, N. (1975) Fatty Acid Composition of the Plasma Lipids in Greenland Eskimos, *Am. J. Clin. Nutr. 28*, 958–966.

11. Dewailly, É., Blanchet, C., Lemieux, S., Sauvé, L., Gingras, S., Ayotte, P., and Holub, B.J. (2001) n-3 Fatty Acids and Cardiovascular Disease Risk Factors Among the Inuit of Nunavik, *Am. J. Clin. Nutr. 74*, 464–473.

12. Saito, H., Watanabe, T., and Murase, T. (1995) The Fatty Acid Composition of a Highly Migratory Fish, with Seasonal Variation of Docosahexaenoic Acid Content in Lipid of Bonito (*Euthynnus pelamis*), *Biosci. Biotechnol. Biochem. 59*, 2186–2188.

13. Saito, H., and Ishihara, K. (1996) Docosahexaenoic Acid Content of Fatty Acids in the Lipid of Two Species of Frigate Mackerel, *Auxis rocheri* and *Auxis thazard*, *Biosci. Biotechnol. Biochem. 60*, 1014–1016.

14. Ando, Y., Satake M., and Takahashi, Y. (2000) Reinvestigation of Positional Distribution of Fatty Acids in Docosahexaenoic Acid-Rich Fish Oil Triacyl-*sn*-glycerols, *Lipids 35*, 579–582.

15. Burr, M.L., Fehily, A.M., Gilbert, J.F., Rogers, S., Holliday, R.M., Sweetman, P.M., Elwood, P.C., and Deadman, N.M. (1989) Effects of Changes in Fat, Fish, and Fibre Intakes on Death and Myocardial Infarction: Diet and Re-infarction Trial (DART) *Lancet 2*, 757–761.

16. GISSI-Prevenzione Investigators (Gruppo Italiano per lo Studio della Sopravivenza nell'Infarto Miocardico), Dietary Supplementation with n-3 Polyunsaturated Fatty Acids and Vitamin E After Myocardial Infarction: Results of the GISSI- Prevenzione Trial (1999) *Lancet 354*, 447–455.

17. Leaf, A., and Weber, P.C. (1988) Medical Progress: Cardiovascular Effects of n-3 Fatty Acids, *New Engl. J. Med. 318*, 549–557.

18. Endres, S., De Caterina, R., Schmidt, E.B., and Kristensen, S.D. (1995) n-3 Polyunsaturated Fatty Acids: Update 1995, *Eur. J. Clin. Invest. 25*, 629–638.

19. Siscovick, D.S., Raghunathan, T.E., King, I., Weinmann, S., Wicklund, K.G., Albright, J., Bovbjerg, V., Arbogast, P., Smith, H., Kushi, L.H., *et al.* (1995) Dietary Intake and Cell Membrane Levels of Long Chain n-3 Polyunsaturated Fatty Acids and the Risk of Primary Cardiac Arrest, *J. Am. Med. Assoc. 274*, 1363–1367.

20. Connor, W.E. (2001) n-3 Fatty Acids from Fish Oil: Panacea or Nostrum? *Am. J. Clin. Nutr. 74*, 415–416.

21. Madsen, T., Skou, H.A., Hansen, V.E., Fog, L., Christensen, J.H., Toft, E., and Schmidt, E.B. (2001) C-Reactive Protein, Dietary n-3 Fatty Acids, and the Extent of Coronary Artery Disease, *Am. J. Cardiol. 88*, 1139–1142.

22. Das, U.N. (2000) Beneficial Effect(s) of n-3 Fatty Acids in Cardiovascular Diseases: but, Why and How?, *Prostaglandins, Leukotrienes Essent. Fatty Acids 63*, 351–362.

23. Glass, R.L., Krick, T.P., Sand, D.M., Rahn, C.H., and Schlenk, H. (1975) Furanoid Fatty Acids from Fish Lipids, *Lipids 10*, 695–702.

24. Okada, Y., Kaneko, M. and Okajima, H. (1996) Hydroxy Radical Scavenging Activity of Naturally Occurring Furan Fatty Acids, *Biol. Pharm. Bull. 19*, 1607–1610.

25. Okada, Y., Okajima, H., Konishi, H., Terauchi, M., Ishii, K., Liu, I.M., and Watanabe, H. (1990), Antioxidant Effect of Naturally Occurring Furan Fatty Acids on Oxidation of Linoleic Acid in Aqueous Dispersion. *J. Am. Oil Chem. Soc. 67*, 858–862.

26. Glass, R.L., Krick, T.P., and Eckhardt, A.E. (1974) New Series of Fatty Acids in Northern Pike (*Esox lucius*), *Lipids 9*, 1004–1008.

27. Kluytmans, J.H.F.M., and Zandee, D.I. (1973) Lipid Metabolism in the Northern Pike (*Esox lucius* L.)—II. The Composition of the Total Lipids and of the Fatty Acids Isolated from Lipid Classes and Some Tissues of the Northern Pike, *Comp. Biochem. Physiol. 44B*, 459–466.

28. Glass, R.L., Krick, T.P., Olson, D.L., and Thorson, R.L. (1977) The Occurrence and Distribution of Furan Fatty Acids in Spawning Male Freshwater Fish, *Lipids 12*, 828–836.

29. Gunstone, F.D., Wijesundera, R.C., and Scrimgeour, C.M. (1978) The Component Acids of Lipids from Marine and Freshwater Species with Special Reference to Furan-Containing Acids, *J. Sci. Food Agric. 29*, 539–550.

30. Gunstone, F.D., Wijesundera, R.C., Love, R.M., and Ross, D. (1976) Relative Enrichment of Furan Containing Fatty Acids in the Liver of Starving Cod, *J. Chem. Soc. Chem. Commun.*, 630–631.

31. Ishii, K., Okajima, H., Okada, Y., and Watanabe, H. (1988) Studies on Furan Fatty Acids of Salmon Roe Phospholipids, *J. Biochem. (Tokyo) 103*, 836–839.

32. Ota, T., and Takagi, T. (1990) Changes in Furan Fatty Acids of Testis Lipids of Chum Salmon *Oncorhynchus keta* at Spawning Season, *Nippon Suisan Gakkaishi 56*, 153–157.

33. Sasaki, S., Ota, T., and Takagi, T. (1989) Composition of Fatty Acids in the Lipids of Chum Salmon During Spawning Migra-

tion, *Nippon Suisan Gakkaishi 55*, 2191–2197.

34. Ota, T., and Takagi, T., (1992) Furan Fatty Acids in the Lipids of the Cresthead Flounder, *Nippon Suisan Gakkaishi 58*, 721–725.

35. Ota, T., and Takagi, T. (1991) Furan Fatty Acids of Lipids from Serum and Sexual Organs of Chum Salmon, *Nippon Suisan Gakkaishi 57*, 1565–1571.

36. Wahl, H.G., Liebich, H.M., and Hoffmann, A. (1994) Identification of Fatty Acid Methyl Esters as Minor Components of Fish Oil by Multidimensional GC–MSD: New Furan Fatty Acids, *J. High Resolut. Chromatogr. 17*, 308–311.

37. Scrimgeour, C.M. (1977) Quantitative Analysis of Furanoid Fatty Acids in Crude and Refined Cod Liver Oil, *J. Am. Oil Chem. Soc. 54*, 210–211.

38. Dembitsky, V.M., and Rezanka, T. (1996) Furan Fatty Acids of Some Brackish Invertebrates from the Caspian Sea, *Comp. Biochem. Physiol. 114 B*, 317–320.

39. Okajima, H., Ishii, K., and Watanabe, H., (1984) Studies in Lipids of Crayfish, *Procambarus clarkii* I. Furanoid Fatty Acids, *Chem. Pharm. Bull. 32*, 3281–3286.

40. Ishii, K., Okajima, H., Koyamatsu, T., Okada, Y., and Watanabe, H. (1988) The Composition of Furan Fatty Acids in the Crayfish, *Lipids 23*, 694–700.

41. Ishii, K., Okajima, H., Okada, Y., Konishi, H., and Watanabe, H. (1989) Fatty Chain Composition of Phospholipids from Muscle of Crayfish, *Procambarus clarkii*, *Chem. Pharm. Bull. 37*, 1564–1567.

42. Ciminiello, P., Fattorusso, E., Magno, S., Mangoni, A., Ialenti, A., and Di Rosa, M. (1991) Furan Fatty Acid Steryl Esters from the Marine Sponge *Dictyonella incisa* Which Show Inflammatory Activity, *Experientia 47*, 739–743.

43. Shirasaka, N., Nishi, K., and Shimizu, S. (1995) Occurrence of Furan Fatty Acids in Marine Bacteria, *Biochim. Biophys. Acta 1258*, 225–227.

44. Shirasaka, N., Nishi, K., and Shimizu, S. (1997) Biosynthesis of Furan Fatty Acids (F-acids) by a Marine Bacterium, *Shewanella putrefaciens, Biochim. Biophys. Acta 1346*, 253–260.

45. Carballeira, N.M., Guzmán, A., Nechev, J.T., Lahtchev, K., Ivanova, A., and Stefanov, K. (2000) Unusual Lipid Composition of a *Bacillus* sp. Isolated from Lake Pomorie in Bulgaria, *Lipids 35*, 1371–1375.

46. Kazlauskas, R., Murphy, P.T., Wells, R.J., and Gregson, R.P. (1982) Two New Furans from the Brown Alga *Acrocarpia paniculata*: The Use of 4-Phenyl-4H-1,2,4-triazoline-3,5-dione to Determine the Substitution Pattern of a Furan, *Austral. J. Chem. 35*, 165–170.

47. Batna, A., Scheinkönig, J., and Spiteller, G. (1993) The Occurrence of Furan Fatty Acids in *Isochrysis* sp. and *Phaeodactylum tricornutum*, *Biochim. Biophys. Acta 1166*, 171–176.

48. Hasma, H., and Subramaniam, A. (1978) The Occurrence of a Furanoid Fatty Acid in *Hevea brasiliensis* Latex, *Lipids 13*, 905–907

49. Hannemann, K., Puchta, V., Simon, E., Ziegler, H., Ziegler, G., and Spiteller, G. (1989) The Common Occurrence of Furan Fatty Acids in Plants, *Lipids 24*, 296–298.

50. Scheinkönig, J., and Spiteller, G. (1993) F-Säure-haltige Phospholipidmoleküle in Zuckerrohrzellen, *Liebigs Ann. Chem.*, 121–124.

51. Guth, H., and Grosch, W. (1992) Furan Fatty Acids in Butter and Butter Oil, *Lebensm. Unters. Forsch. 194*, 360–362.

52. Boselli, E., Grob, K., and Lercker, G. (2000) Determination of Furan Fatty Acids in Extra Virgin Olive Oil, *J. Agric. Food Chem. 48*, 2868–2873.

53. Schödel, R., and Spiteller, G. (1987) Über das Vorkommen von F-Säuren in Rinderleber und deren enzymatischen Abbau bei Gewebeverletzung, *Liebigs Ann. Chem.*, 459–462.

54. Puchta, V., Spiteller, G., and Weidinger, H. (1988) F-Säuren: Eine bisher unbekannte Komponente der Phospholipide des

55. Puchta, V., and Spiteller, G. (1988) Struktur der F-Säuren enthaltenden Plasmalipide, *Liebigs Ann. Chem.*, 1145–1147.

56. Wahl, H.G., Chrzanowski, A., Müller, C., Liebich, H.M., and Hoffmann, A. (1995) Identification of Furan Fatty Acids in Human Blood Cells and Plasma by Multi-dimensional Gas Chromatography–Mass Spectrometry, *J. Chromatogr. A 697*, 453–459.

57. Morris, L.J., Marshall, M.O., and Kelly, W. (1966) A Unique Furanoid Fatty Acid from *Exocarpus* Seed Oil, *Tetrahedron Lett. 16*, 4249–4253.

58. Gunstone, F.D., and Wijesundera, R.C. (1979) Fatty Acids, Part 54. Some Reactions of Long-Chain Oxygenated Acids with Special Reference to Those Furnishing Furanoid Acids, *Chem. Phys. Lipids 24*, 193–208.

59. Hidalgo, F.J., and Zamora, R. (1995) Epoxyoxoene Fatty Esters: Key Intermediates for the Synthesis of Long-chain Pyrrole and Furan Fatty Esters, *Chem. Phys. Lipids 77*, 1–11.

60. Yurawecz, M.P., Sehat, N., Mossoba, M.M., Roach, J.A.G., and Ku, Y. (1997) Oxidation Products of Conjugated Linoleic Acid and Furan Fatty Acids, in *New Techniques and Applications in Lipid Analysis*, edited by R.E. McDonald and M.M. Mossoba, pp. 183–215, AOCS Press, Champaign.

61. Schödel, R., and Spiteller, G. (1985) Über die Strukturaufklärung von (Hydroxy-oxo-cyclopentenyl)alkansäuren, den Aldolkondensationsprodukten von Dioxoencarbonsäuren aus Rinderleber, *Helv. Chim. Acta 68*, 1624–1634.

62. Jandke, J., Schmidt, J., and Spiteller G. (1988) Über das Verhalten von F-Säuren bei der Oxidation mit Lipoxydase in Anwesenheit von SH-haltigen Verbindungen, *Liebigs Ann. Chem.*, 29–34.

63. Jandke, J., and Spiteller, G. (1988) (Dimethylamino)ethylester von Fettsäuren: bisher unbekannte Naturstoffe, *Liebigs Ann. Chem.*, 1057–1060.

64. Folch, J., Lees, M., and Sloane Stanley, G.H. (1957) A Simple Method for the Isolation and Purification of Total Lipids from Animal Tissues, *J. Biol. Chem. 226*, 497–509.

65. Bligh, E.G., and Dyer, W.J. (1959) A Rapid Method for Total Lipid Extraction and Purification, *Can. J. Biochem. Physiol. 37*, 911–917.

66. Schlenk, H. (1961) Crystallization of Fatty Acids, *J. Am. Oil Chem. Soc. 38*, 728–736.

67. Gerlach, H., and Wetter, H. (1974) Synthesen der Nonactinsäure, *Helv. Chim. Acta 57*, 2306–2321.

68. Spiteller, M., and Spiteller, G. (1979) Trennung und Charakterisierung saurer Harnbestandteile, *J. Chromatogr. 164*, 253–317.

69. Spiteller, M., Spiteller, G., and Hoyer, G.-A. (1980) Urofuransäureneine bisher unbekannte Klasse von Stoffwechselprodukten, *Chem. Ber. 113*, 699–709.

70. Pfordt, J., Thoma, H., and Spiteller, G. (1981) Identifizierung, Strukturableitung und Synthese bisher unbekannter Urofuransäuren im menschlichen Blut, *Liebigs Ann. Chem.*, 2298–2308.

71. Bauer, S., and Spiteller, G. (1985) Strukturaufklärung und Synthese bisher unbekannter Furancarbonsäuren aus Humanurin, *Liebigs Ann. Chem.*, 813–821.

72. Wahl, H.G., Tetschner, B., and Liebich, H.M. (1992) The Effect of Dietary Fish Oil Supplementation on the Concentration of 3-Carboxy-4-methyl-5-propyl-2-furanpropionic Acid in Human Blood and Urine, *J. High Resolut. Chromatogr. 15*, 815–818.

73. Schödel, R., Dietel, P., and Spiteller, G. (1986) F-Säuren als Vorstufen der Urofuransäuren, *Liebigs Ann. Chem.*, 127–131.

74. Sand, D.M., Schlenk, H., Thoma, H., and Spiteller, G. (1983) Catabolism of Fish Furan Fatty Acids to Urofuran Acids in the Rat , *Biochim. Biophys. Acta 751*, 455–461.

75. Bauer, S., and Spiteller, G. (1985) Furancarbonsäuren aus Rinderharn, *Helv. Chim. Acta 68,* 1635–1638.

76. Groweiss, A., and Kashman, Y. (1978) A New Furanoid Fatty Acid from the Soft Corals *Sarcophyton glaucum* and *gemmatum*, *Experientia 33*, 299.

77. Liebich, H.M., Pickert, A., and Tetschner, B. (1984) Gas Chromatographic and Gas Chromatographic–Mass Spectrometric Analysis of Organic Acids in Plasma of Patients with Chronic Renal Failure, *J. Chromatogr. 289*, 259–266.

78. Mabuchi, H., and Nakahashi, H. (1988) Inhibition of Hepatic Glutathione S-Transferase by a Major Endogenous Ligand Substance Present in Uremic Serum, *Nephron 49*, 281–283.

79. Henderson, S.J., and Lindup, W.E. (1990) Interaction of 3-Carboxy-4-methyl-5-propyl-2-furanpropanoic Acid, an Inhibitor of Plasma Protein Binding in Uraemia, with Human Albumin, *Biochem. Pharmacol. 40*, 2543–2548.

80. Costigan, M.G., and Lindup, W.E. (1996) Plasma Clearance in the Rat of Furan Dicarboxylic Acid Which Accumulates in Uremia, *Kidney Int. 49*, 634–638.

81. Niwa, T., Takeda, N., Maeda, K., Shibata, M., and Tatematsu, A. (1988) Accumulation of Furancarboxylic Acids in Uremic Serum as Inhibitors of Drug Binding, *Clin. Chim. Acta 173*, 127–138.

82. Liebich, H.M., Bubeck, J.I., Pickert, A., Wahl, G., and Scheiter, A. (1990) Hippuric Acid and 3-Carboxy-4-methyl-5-propyl-2-furanpropionic Acid in Serum and Urine, Analytical Approaches and Clinical Relevance in Kidney Diseases, *J. Chromatogr. 500*, 615–627.

83. Henderson, S.J., and Lindup, E. (1992) Renal Organic Acid Transport: Uptake by Rat Kidney Slices of a Furan Dicarboxylic Acid Which Inhibits Plasma Protein Binding of Acidic Ligands in Uremia, *J. Pharmacol. Exp. Ther. 263*, 54–60.

84. Sato, M., Koyama, M., Miyazaki, T., and Niwa, T. (1996) Reduced Renal Clearance of Furancarboxylic Acid, a Major Albumin-Bound Organic Acid, in Undialyzed Uremic Patients, *Nephron 74*, 419–421.

85. Niwa, T., Aiuchi, T., Nakaya, K., Emoto, Y., Miyazaki, T., and Maeda, K. (1993) Inhibition of Mitochondrial Respiration by Furancarboxylic Acid Accumulated in Uremic Serum in Its Albumin-Bound and Non-dialyzable Form, *Clin. Nephrol. 39*, 92–96.

86. Niwa, T., Yazawa, T., Kodama, T., Uehara, Y., Maeda, K., and Yamada, K. (1990) Efficient Removal of Albumin-Bound Furancarboxylic Acid, an Inhibitor of Erythropoiesis, by Continuous Ambulatory Peritoneal Dialysis, *Nephron, 56*, 241–245.

87. Tsutsumi, Y., Maruyama, T., Takadate, A., Shimada, H., and Otagiri, M. (2000) Decreased Bilirubin-Binding Capacity in Uremic Serum Caused by an Accumulation of Furan Dicarboxylic Acid, *Nephron 85*, 60–64.

88. Costigan, M.G., O'Callaghan, C.A., and Lindup, W.E. (1996) Hypothesis: Is Accumulation of a Furan Dicarboxylic Acid (3-carboxy-4-methyl-5-propyl-2-furanpropanoic acid) Related to the Neurological Abnormalities in Patients with Renal Failure? *Nephron 73*, 169–173.

89. Koval'chuk, L.V., Pavlyuk, A.S., Shchiglenko, N.A., Sinyukhin, V.N., Kharlamova, L.A., and Chirun, N.V. (1999) Polyfurancarbonic Acid Inhibits Proliferation and Induces Apoptosis of Cultured Human T Lymphocytes *in vitro*, *Bull. Exp. Biol. Med. 6*, 613–614.

90. Mabuchi, H., and Nakahashi, H. (1987) Determination of 3-Carboxy-4-methyl-5-propyl-2-furanpropanoic Acid, a Major Endogenous Ligand Substance in Uremic Serum, by High-Performance Liquid Chromatography with Ultraviolet Detection, *J. Chromatogr. 415*, 110–117.

91. Pickert, A., Bäuerle, A., and Liebich, H.M. (1989) Determination of Hippuric Acid and Furanic Acid in Serum of Dialysis Patients and Control Persons by High-Performance Liquid Chromatography, *J. Chromatogr. 495*, 95–104.

92. Niwa, T., Kawagishi, I., and Ohya, N. (1994) Rapid Assay for Furancarboxylic Acid Accumulated in Uremic Serum Using High-Performance Liquid Chromatography and On-line Mass Spectrometry, *Clin. Chim. Acta 226*, 89–94.

93. Tanaka, T., Ikebuchi, H., Sawada, J.-I., and Tanaka, Y. (1998) Production of Antiserum for Sensitive Enzyme-Linked Immunosorbent Assay of 3-Carboxy-4-methyl-5-propyl-2-furanpropanoic Acid by Chemiluminescence, *Lipids 33*, 733–736.

94. Sassa, T., Matsuno, H., Niwa, M., Kozawa, O., Takeda, N., Niwa, T., Kumada, T., and Uematsu, T. (2000) Measurement of Furancarboxylic Acid, a Candidate for Uremic Toxin, in Human Serum, Hair, and Sweat, and Analysis of Pharmacological Actions *in vitro*, *Arch. Toxicol. 73*, 649–654.

95. Sand, D.M., Glass, R.L., Olson, D.L., Pike, H.M., and Schlenk, H. (1984) Metabolism of Furan Fatty Acids in Fish, *Biochim. Biophys. Acta 793*, 429–436.

96. Gorst-Allman, C.P., Puchta, V., and Spiteller, G. (1988) Investigations of the Origin of the Furan Fatty Acids (F-acids), *Lipids 23*, 1032–1036.

97. Dietel, P., and Spiteller, G. (1988) Inkubation von 2,5-disubstituierten F-Säuren mit Rinderleberhomogenisat, *Liebigs Ann. Chem.*, 397–403.

98. Scheinkönig, J., and Spiteller, G. (1993) Herkunft des Kohlenstoff-Grundskeletts von F-Säuren, *Liebigs Ann. Chem.*, 251–253.

99. Scheinkönig, J., and Spiteller, G. (1991) Herkunft der Methylsubstituenten in F-Säuren, *Liebigs Ann. Chem.,* 451–453.

100. Scheinkönig, J., Hannemann, K., and Spiteller, G. (1995) Methylation of the β-Positions of the Furan Ring in F-Acids, *Biochim. Biophys. Acta 1254*, 73–76.

101. Batna, A., and Spiteller, G. (1991) Herkunft des Sauerstoffatoms im Furanring von F-Säuren, *Liebigs Ann. Chem.*, 861–863.

102. Rahn, C.H., Sand, D.M., Wedmid, Y., Schlenk H., Krick, T.P., and Glass R.L. (1979) Synthesis of Naturally Occurring Furan Fatty Acids, *J. Org. Chem. 44*, 3420–3424.

103. Prasselsberger, G. (1985) Synthese von tetrasubstituierten Furan Fettsäuren, Diploma Thesis, pp. 11–18, University of Bayreuth, Germany.

104. Baumann, M.E., and Bosshard, H. (1978) Decarboxylative Dimerization of Maleic Acid Anhydride to Dimethyl Maleic Anhydride, *Helv. Chim. Acta 61*, 2751–2753.

105. Rahn, C.H., Sand, D.M., Krick, T.P., Glass, R.L., and Schlenk, H. (1981) Synthesis of Radioactive Furan Fatty Acids, *Lipids 16*, 360–364.

106. Bach, T., and Krüger, L. (1998) Sequential Pd(0)-Catalyzed Reactions for the Construction of Multiple Substituted Furans. A Short Synthesis of the F_5 Furan Fatty Acid, *Tetrahedron Lett. 39*, 1729–1732.

107. Lie Ken Jie, M.S.F., and Ahmad, F. (1981) Conversion of Linoleic and Latex Furanoid Acid to Fish C_{18} Dimethyl Furanoid Isomeres, *J. Chem. Soc. Chem. Commun.*, 1110–1111.

108. Graff, G., Gellerman, J.L., Sand, D.M., and Schlenk, H. (1984) Inhibition of Blood Platelet Aggregation by Dioxo-ene Compounds, *Biochim. Biophys. Acta 799*, 143–150.

109. Boyer, R.F., Lindstrom, C.G., Darby, B., and Hylarides, M. (1975) The Peracid Oxidation of Singlet Oxygen Acceptors, *Tetrahedron Lett. 16*, 4111–4114.

110. Takayama, K., Noguchi, T., and Nakano, M. (1977) Reactivities of Diphenylfuran (a singlet oxygen trap) with Singlet Oxygen and Hydroxyl Radical in Aqueous Systems, *Biochem. Biophys. Res. Commun. 75*, 1052–1058.

111. Boyer, R.F., Litts, D., Kostishak, J., Wijesundera, R.C., and Gunstone, F.D. (1979) The Action of Lipoxygenase-1 on Furan Derivatives, *Chem. Phys. Lipids 25*, 237–246.

112. Batna, A., and Spiteller, G. (1994) Oxidation of Furan Fatty Acids by Soybean Lipoxygenase-1 in the Presence of Linoleic Acid, *Chem. Phys. Lipids 70*, 179–185.

113. Halliwell, B., and Gutteridge, J.M.C. (1990) Role of Free Radicals and Catalytic Metal Ions in Human Disease: An Overview,

Methods Enzymol. 186, 1–85.

114. Gan, Q.-F., Witkop, G.L., Sloane, D.L., Straub, K.M., and Sigal, E. (1995) Identification of a Specific Methionine in Mammalian 15-Lipoxygenase Which Is Oxygenated by the Enzyme-Product 13-HPODE: Dissociation of Sulfoxide Formation from Self-Inactivation, *Biochemistry 34*, 7069–7079.

115. Fuchs, C., and Spiteller, G. (2000) Iron Release from the Active Site of Lipoxygenase, *Z. Naturforsch. 55c*, 643–648.

116. Marnett, L.J. (1987) Peroxyl Free Radicals: Potential Mediators of Tumor Initiation and Promotion, *Carcinogenesis 8*, 1365–1373.

117. Welch, K.D., Davis, T.Z., Van Eden, M.E., and Aust, S.D. (2002) Deleterious Iron-Mediated Oxidation of Biomolecules, *Free Radic. Biol. Med. 32*, 577–583.

118. Spiteller, G. (1998) Linoleic Acid Peroxidation—The Dominant Lipid Peroxidation Process in Low Density Lipoprotein— and Its Relationship to Chronic Diseases, *Chem. Phys. Lipids 95*, 105–162.

119. Ozawa, T., Sugiyama, S., Hayakawa, M., Satake, T., Taki, F., Iwata, M., and Taki, K. (1988) Existence of Leukotoxin 9,10-Epoxy-12-octadecenoate in Lung Lavages from Rats Breathing Pure Oxygen and from Patients with the Adult Respiratory Distress Syndrome, *Am. Rev. Respir. Dis. 137*, 535–540.

120. Walther, U., and Spiteller, G. (1993) Zur Bildung von Ölsäureepoxid bei der Lagerung technischer Ölsäure, *Fett Wiss. Technol. 95*, 472–474.

121. Bordoni, A., Hrelia, S., Caboni, M.F., Lercker, G., and Biagi, P.L. (1995) Incorporation of Cholesterol Oxidation Products into Cell Lipids and Their Influence on the Proliferation of Cultured Cardiomyocytes, *Cardiosciences 6*, 107–113.

122. Sugiyama, S., Hayakawa, M., Nagai, S., Ajioka, M., and Ozawa T. (1987) Leukotoxin, 9,10-Epoxy-12-octadecenoate, Causes Cardiac Failure in Dogs, *Life Sci. 40*, 225–231.

123. Nappez, C., Battu, S., and Beneytout, J.L. (1996) *trans,trans*-2,4-Decadienal: Cytotoxicity and Effect on Glutathione Level in Human Erythroleukemia (HEL) Cells, *Cancer Lett. 99*, 115–119.

124. Galliard, T. (1975) Degradation of Plant Lipids by Hydrolytic and Oxidative Enzymes, *Annu. Proc. Phytochem. Soc. 12*, 319–357.

125. Spiteller, G. (1996) Enzymic Lipid Peroxidation—A Consequence of Cell Injury? *Free Radic. Biol. Med. 21*, 1003–1009.

126. Siddiqui, R.A., Labarrere, C.A., and Kovacs, R.J. (2000) Prevention of Cardiac Hypertrophy with Omega 3-Fatty Acids: Potential Cell Signaling Targets, *Curr. Org. Chem. 4*, 1145–1157.

127. Batna, A., and Spiteller, G. (1994) Effects of Soybean Lipoxygenase-1 on Phosphatidylcholines Containing Furan Fatty Acids, *Lipids 29*, 397–403.

128. Ishii, K., Okajima, H., Okada, Y., and Watanabe, H. (1989) Effects of Phosphatidylcholines Containing Furan Fatty Acid on Oxidation in Multilamellar Liposomes, *Chem. Pharm. Bull. 37*, 1396–1398.

129. Spreitzer, H., Schmidt, J., and Spiteller, G. (1989) Vergleichende Untersuchungen der Fettsäureoxidation in Gemüse in Abhängigkeit von der Vorbehandlung, *Fat Sci. Technol. 91*, 108–113.

130. Wills, E.D. (1966) Mechanisms of Lipid Peroxide Formation in Animal Tissues, *Biochem. J. 99*, 667–676.

131. Kießling, U., and Spiteller, G. (1998) The Course of Enzymatically Induced Lipid Peroxidation in Homogenized Porcine Kidney Tissue, *Z. Naturforsch. 53c*, 431–437.

132. Imbusch, R., and Mueller, M.J. (2000) Formation of Isoprostane F_2-Like Compounds (phytoprostanes F_1) from a-Linolenic Acid in Plants, *Free Radic. Biol. Med 28*, 720–726.

133. Masanatz, C., Guth, H., and Grosch, W. (1998) Fishy and Hay-Like Off-Flavours of Dry Spinach, *Lebensm. Unters. Forsch. A 206*, 108–113.

134. Ohki, T., Maeda, K., Sakakibara, J., Suzuki, E., and Yamanaka, N. (1993) Structural Analysis of Oxidation Products of Urofuran Acids by Hypochlorous Acid, *Lipids 28*, 35–41.

135. Harris, W.S. (1989) Fish Oils and Plasma Lipid and Lipoprotein Metabolism in Humans: A Critical Review *J. Lipid Res. 30*, 785–807.

136. Marchioli, R., Schweiger, C., Tavazzi, L., and Valagussa, F. (2001) Efficacy of n-3 Polyunsaturated Fatty Acids After Myocardial Infarction: Results of GISSI-Prevenzione Trial, *Lipids 36 (Suppl.)* S119–S126.

137. Pepe, S., and McLennan, P.L. (2002) Cardiac Membrane Fatty Acid Composition Modulates Myocardial Oxygen Consumption and Postischemic Recovery of Contractile Function, *Circulation 105*, 2303–2308.

138. Yaqoob, P., and Calder, P.C. (2003) n-3 Polyunsaturated Fatty Acids and Inflammation in the Arterial Wall, *J. Med. Res. 8*, 337–354.

139. Roche, H.M., and Gibney, M.J. (1999) Long-chain n-3 Polyunsaturated Fatty Acids and Triacylglycerol Metabolism in the Postprandial State, *Lipids 34 (Suppl.)*, S259–S265.

140. Harris, W.S. (1999) n-3 Fatty Acids and Human Lipoprotein Metabolism: An Update, *Lipids 34 (Suppl.)*, S257–S258.

141. Leifert, W.R., Dorian, C.L., Jahangiri, A., and McMurchie, E.J. (2001) Dietary Fish Oil Prevents Asynchronous Contractility and Alters Ca^{2+} Handling in Adult Rat Cardiomyocytes, *J. Nutr. Biochem. 12*, 365–376.

142. Bjerregaard, P., Pedersen, H.S., and Mulvad, G. (2000) The Associations of a Marine Diet with Plasma Lipids, Blood Glucose, Blood Pressure and Obesity Among the Inuit in Greenland, *Eur. J. Clin. Nutr. 54*, 732–737.

143. Abbey, M., Belling, B., Noakes, M., Hirata, F., and Nestel, P.J. (1993) Oxidation of Low-Density Lipoproteins: Intraindividual Variety and the Effect of Dietary Linoleate Supplementation, *Am. J. Clin. Nutr. 57*, 391–398.

144. Reaven, P.D., Grasse, B.J., and Tribble, D.L. (1994) Effects of Linoleate-Enriched and Oleate-Enriched Diets in Combination with a-Tocopherol on the Susceptibility of LDL and LDL Subfractions on Oxidative Modification in Humans, *Arterioscler. Thromb. 14*, 557–566.

145. Leigh-Firbank, E.C., Minihane, A.M., Leake, D.S., Wright, J.W., Murphy, M.C., Griffin, B.A., and Williams, C.M. (2002) Eicosapentaenoic Acid and Docosahexaenoic Acid from Fish Oils: Differential Associations with Lipid Responses, *Br. J. Nutr. 87*, 435–445.

146. Song, J.H., Fujimoto, K., and Miyazawa, T.(2000) Polyunsaturated (n-3) Fatty Acids Susceptible to Peroxidation Are Increased in Plasma and Tissue Lipids of Rats Fed Docosahexaenoic Acid-Containing Oils, *J. Nutr. 130*, 3028–3033.

147. Suzukawa, M., Abbey, M., Howe, P.R.C., and Nestel, P.J. (1995) Effect of Fish Oil Fatty Acids on Low Density Lipoprotein Size, Oxidizability, and Uptake by Macrophages, *J. Lipid Res. 36*, 473–484.

148. Goldstein, J.L., and Brown, M. (1977) The Low Density Lipoprotein Pathway and Its Relation to Atherosclerosis, *Annu. Rev. Biochem. 46*, 897–930.

149. Steinbrecher, U.P., Parthasarathy, S., Leake, D.S., Witztum, J.L., and Steinberg, D. (1984) Modification of Low Density Lipoprotein by Endothelial Cells Involves Lipid Peroxidation and Degradation of Low Density Lipoprotein Phospholipids, *Proc. Natl. Acad. Sci. USA 81*, 3883–3887.

150. Cathcart, M.K., Morel, D.W., and Chisholm, G.M., III (1985) Monocytes and Neutrophiles Oxidize Low Density Lipoprotein Making It Cytotoxic, *J. Leucocyte Biol. 38*, 341–350.

151. Iuliano, L. (2001) The Oxidant Hypothesis of Atherogenesis, *Lipids 36 (Suppl.)*, S41–S44.

152. Hardwick, S.J., Hegyi, L., Clare, K., Law, N.S., Keri, L.H., Carpenter, L.H., Mitchinson, M.J., and Skepper, J.N. (1996)

Apoptosis in Human Monocyte-Macrophages Exposed to Oxidized Low Density Lipoprotein, *J. Pathol. 179*, 294– 302.

153. Wintergerst, E.S., Jelk, J., Rahner, C., and Asmis, R. (2000) Apoptosis Induced by Oxidized Low Density Lipoprotein in Human Monocyte-Derived Macrophages Involves CD36 and Activation of Caspase-3, *Eur. J. Biochem. 267*, 6050–6058.

154. Frankel, E.N. (1998) *Lipid Oxidation,* The Oily Press, Dundee.

155. Berliner, J.A., Territo, M.C., Sevanian, A., Ramin, S., Kim, J.A., Bamshad, B., Esterson, M., and Fogelman, A.M. (1990) Minimally Modified Low Density Lipoprotein Stimulates Monocyte Endothelial Interactions, *J. Clin. Invest. 85*, 1260–1266.

156. Podrez, E.A., Poliakov, E., Shen, Z., Zhang, R., Deng, Y., Sun, M., Finton, P.J., Shan, L., Gugiu, B., Fox, P.L.,*et al.* (2002) Identification of a Novel Family of Oxidized Phospholipids That Serve as Ligands for the Macrophage Scavenger Receptor CD36, *J. Biol. Chem. 277*, 38503–38516.

157. Folcik, V.A., and Cathcart, M.K. (1994) Predominance of Esterified Hydroperoxy-Linoleic Acid in Human Monocyte-Oxidized LDL, *J. Lipid Res. 35*, 1570–1582.

158. Watson, A.D., Leitinger, N., Navab, M., Faull, K.F., Hörkkö, S., Witzum, J.L., Palinski, W., Schwenke, D., Salomon, R.G., Sha, W., *et al.* (1997) Structural Identification by Mass Spectrometry of Oxidized Phospholipids in Minimally Oxidized Low Density Lipoprotein That Induce Monocyte/Endothelial Interactions and Evidence for Their Presence *in vivo, J. Biol. Chem. 272*, 13597–13607.

159. Spiteller, D., and Spiteller, G. (2000) Oxidation of Linoleic Acid in Low-Density Lipoprotein: An Important Event in Atherogenesis, *Angew. Chem. Int. Ed. 39*, 585–589.

160. Wang, T., and Powell W.S: (1991) Increased Levels of Monohydroxy Metabolites of Arachidonic Acid and Linoleic Acid in LDL and Aorta from Atherosclerotic Rabbits, *Biochim. Biophys. Acta 1084*, 129–138.

161. Wander, R.C., Du, S.-H., and Thomas, D.R. (1998) Influence of Long-Chain Polyunsaturated Fatty Acids on Oxidation of Low Density Lipoprotein, *Prosaglandins. Leukotrienes, Essent. Fatty Acids 59*, 143–151.

162. Parthasarathy, S., Khoo, J.C., Miller, E., Barnett, J., Witztum, J.L., and Steinberg, D. (1990) Low Density Lipoprotein Rich in Oleic Acid Is Protected Against Oxidative Modification: Implications for Dietary Prevention of Atherosclerosis, *Proc. Natl. Acad. Sci. USA 87*, 3894–3898.

163. Esterbauer, H., Jürgens, G., Quehenberger, O., and Koller, E. (1987) Autoxidation of Human Low Density Lipoprotein: Loss of Polyunsaturated Fatty Acids and Vitamin E and Generation of Aldehydes. *J. Lipid Res. 28*, 495–509.

164. Mlakar, A., and Spiteller, G. (1994) Reinvestigation of Lipid Peroxidation of Linolenic Acid, *Biochim. Biophys. Acta 1214*, 209–220.

165. Spiteller, P., Kern, W., Reiner, J., and Spiteller, G. (2001) Aldehydic Lipid Peroxidation Products Derived from Linoleic Acid, *Biochim. Biophys. Acta 1531*, 188–208.

166. Poli, G., and Schaur, R.J. (2000) 4-Hydroxynonenal in the Pathomechanisms of Oxidative Stress, *Life 50*, 315–321.

167. Thomas, M.J., Thornburg, T., Manning, J., Hooper, K., and Ruddel, L.L. (1994) Fatty Acid Composition of Low-Density Lipoprotein Influences Its Susceptibility to Autoxidation, *Biochemistry 33*, 1828–1834.

168. Wu, T., Geigerman, C., Lee, Y.-S., and Wander, R.C. (2002) Enrichment of LDL with EPA and DHA Decreased Oxidized LDL-Induced Apoptosis in U937 Cells, *Lipids 37*, 789–796.

169. Higdon, J.V., Du, S.H., Lee, Y.S., Wu, T., and Wander, R.C. (2001) Supplementation of Postmenopausal Women with Fish Oil Does Not Increase Overall Oxidation of LDL *ex vivo* Compared to Dietary Oils Rich in Oleate and Linoleate. *J. Lipid Res. 42*, 407–418.

170. Fischer, S., Weber, P.C., and Dyerberg, J. (1986) The Prostacyclin/Thromboxane Balance Is Favourably Shifted in Greenland Eskimos, *Prostaglandins 32*, 235–241.

171. Sanders, T.A.B., and Hinds, A. (1992) The Influence of a Fish Oil High in Docosahexaenoic Acid on Plasma Lipoprotein and Vitamin E Concentrations and Haemostatic Function in Healthy Male Volunteers, *Br. J. Nutr. 68*, 163–173.

172. Fuchs, C.T., and Spiteller, G. (1999) 9-(3,4-Dimethyl-5-pentyl-furan-2-yl)nonanoic Acid and 9-(3,4-Dimethyl-5-propyl-furan-2-yl)nonanoic Acid: New Naturally Occurring Peroxidase Inhibitors, *Z. Naturforsch. 54c*, 932–936.

173. Steinberg, D. (1997) Low Density Lipoprotein Oxidation and Its Pathobiological Significance, *J. Biol. Chem. 272*, 20963–20966.

174. Nara, E., Miyashita, K., and Ota, T. (1997) Oxidative Stability of Liposomes Prepared from Soybean PC, Chicken Egg PC, and Salmon Egg PC, *Biosci. Biotech. Biochem. 61,* 1736–1738.

175. McClements, D.J., and Decker, E.A. (2000) Lipid Oxidation in Oil-in-Water Emulsions: Impact of Molecular Environment on Chemical Reactions in Heterogeneous Food Systems, *J. Food Sci. 65*, 1270–1282.

176. Nuchi, C.D., Hernandez, P., McClements, D.J., and Decker, E.A. (2002) Ability of Lipid Hydroperoxides to Partition into Surfactant Micelles and Alter Lipid Oxidation Rates in Emulsions, *J. Agric. Food Chem. 50*, 5445–5449.

177. Cosgrove, J.P., Church, D.F., and Pryor, W.A. (1987) The Kinetics of the Autoxidation of Polyunsaturated Fatty Acids, *Lipids 22*, 299–304.

Identification and Quantification of Glycerolipids in Cotton Fibers: Reconciliation with Metabolic Pathway Predictions from DNA Databases

Sylvia W. Wanjie[a], Ruth Welti[b], Robert A. Moreau[c], and Kent D. Chapman[a],*

[a]University of North Texas, Department of Biological Sciences, Center for Plant Lipid Research, Denton, Texas 76203-5220,
[b]Kansas State University, Division of Biology, Kansas Lipidomics Research Center, Manhattan, Kansas 66506-4901,
and [c]USDA, ARS, Eastern Regional Research Center, Wyndmoor, Pennsylvania 19038

ABSTRACT: The lipid profiles of cotton fiber cells were determined from total lipid extracts of elongating and maturing cotton fiber cells to see whether the membrane lipid composition changed during the phases of rapid cell elongation or secondary cell wall thickening. Total FA content was highest or increased during elongation and was lower or decreased thereafter, likely reflecting the assembly of the expanding cell membranes during elongation and the shift to membrane maintenance (and increase in secondary cell wall content) in maturing fibers. Analysis of lipid extracts by electrospray ionization and tandem MS (ESI-MS/MS) revealed that in elongating fiber cells (7–10 d post-anthesis), the polar lipids—PC, PE, PI, PA, phosphatidylglycerol, monogalactosyldiacylglycerol, digalactosyldiacylglycerol, and phosphatidylglycerol—were most abundant. These same glycerolipids were found in similar proportions in maturing fiber cells (21 dpa). Detailed molecular species profiles were determined by ESI-MS/MS for all glycerolipid classes, and ESI-MS/MS results were consistent with lipid profiles determined by HPLC and ELSD. The predominant molecular species of PC, PE, PI, and PA was 34:3 (16:0, 18:3), but 36:6 (18:3,18:3) also was prevalent. Total FA analysis of cotton lipids confirmed that indeed linolenic (18:3) and palmitic (16:0) acids were the most abundant FA in these cell types. Bioinformatics data were mined from cotton fiber expressed sequence tag databases in an attempt to reconcile expression of lipid metabolic enzymes with lipid metabolite data. Together, these data form a foundation for future studies of the functional contribution of lipid metabolism to the development of this unusual and economically important cell type.

Paper no. L9784 in *Lipids 40*, 773–785 (August 2005).

Cotton fibers are trichomes that arise from the differentiation of ovular epidermal cells near or on the day of anthesis (1). Development of these cells progresses through stages of elongation and secondary wall deposition forming extremely long single cells, over an inch (2.5 cm) long (2), during a period of about 25 d. This period of rapid cellular elongation requires substantial synthesis of macromolecules, including lipids necessary for the developing vacuoles and plasma membranes. The major research focus on cotton fiber development historically has been on cellulose synthesis, which accounts for the bulk of the mass of mature fiber cells; however lipid metabolism is likely to be an important factor in the development of cotton fibers, and this subject has received little attention.

Electron microscopy studies have shown that fiber initiation occurs near or on the day of anthesis, as fibers emerge as protrusions from the epidermal layer of cotton ovules (3,4). This is followed by elongation, in which the cells undergo rapid expansion with increases in length and diameter, and concurrent primary cell wall formation. On average, this continues for 15–27 d (3). Secondary cell wall synthesis begins around 16–19 d post-anthesis (dpa) and is thought to overlap with elongation (5). This process consists of the deposition of successive layers of cellulose microfibrils in a helical pattern around fiber cells (2,6). Maturation of fibers ends about 45–60 dpa, and it includes seed capsule dehiscion, dehydration, and collapse of fiber cells (2).

Synthesis of cellular constituents, including lipids for incorporation into the vacuole and plasma membranes, must be necessary during the period of rapid cell expansion in cotton fiber cells. In plants, FA biosynthesis occurs *de novo* in plastids. The newly synthesized FA can be either incorporated into plastidial glycerolipids or transported to the endoplasmic reticulum (ER) for incorporation into extraplastidial complex lipids (7) such as those destined for vacuole and plasma membranes. Developing fiber cells, undergoing rapid elongation, have a higher lipid content and were shown to incorporate the majority of ^{14}C-labeled acetate into polar lipids at a rate that declines as cell elongation ceases [from 10 to 20 dpa (2)]. As polar lipids are the major constituents of lipid bilayers, these results suggest that fiber cells are involved in active membrane synthesis during early stages of development.

Recent technical advances now make it possible to perform rapid, detailed glycerolipid profiling (8). Electrospray ionization

(ESI) and tandemmass spectrometry (MS/MS) are currently used to determine the classes, molecular species, and amount of lipids in plant cells (8). Here we have applied this technique to identify and quantify the classes and molecular species of polar lipids in developing cotton fiber cells. These data provide a critical knowledge base of information for how lipid composition changes with fiber development. The results were compared with those from other approaches, including GC-FID, to determine total FA composition, and HPLC analysis combined with ELSD or MS to profile polar lipids as well as sterols, sterol esters, and sterol glycosides (SG) (9,10). SG and their acylated components in cotton fiber cells have been implicated as primers for elongation of β1–4 glucan chains that form cellulose microfibrils during secondary cell wall development (11); hence the sterol composition of cotton fiber cells may be important to understanding more about cell wall formation in these fiber cells.

Several genes that are preferentially expressed in cotton fibers during the rapid elongation process have been identified, including some that are involved in lipid metabolism, such as those encoding a putative acyltransferase and a putative 24-sterol-C methyltransferase (12). Transcripts for a gene encoding a fiber-specific acyl carrier protein (ACP) were highly expressed during the stage of elongation, and this ACP was proposed to play a role in synthesis of membrane lipids (13). Cotton fiber-specific cDNA encoding lipid transfer proteins have been isolated and shown to have a temporal expression pattern, accumulating from 6 to 14 dpa (14,15); transcript levels for one isoform, lipid transfer protein-3, reached a maximum at 15 dpa (16). The results of these studies indicate that transcription of genes involved in lipid metabolism in cotton fiber occurs in a developmentally regulated manner. However, a more global examination of gene expression in cotton fiber cells during the stage of rapid elongation might provide more insights into the mechanisms responsible for the development of these cells.

More than 50,000 expressed sequence tags (EST) from *Gossypium* sp. fiber cells have been sequenced by several laboratories [predominantly Brookhaven National Laboratory (Brookhaven, NY) and Clemson University Genomics Institute (Clemson, SC)] and compiled by The Institute for Genomic Research (TIGR; Rockville, MD) at their web site at http://www.tigr.org. Most all of these EST are derived from cotton fibers at 6 or 7 to 10 dpa, during the stage of rapid cell elongation, and most likely include expressed genes of lipid metabolism important for this development stage. The occurrence of EST for enzymes involved in lipid metabolism can be used to begin to predict which metabolic pathways are operating during this stage of rapid cell elongation, as was done recently for oil biosynthesis in *Arabidopsis* seeds (17). The combination of metabolic profiles and DNA database information provides a unique perspective on membrane biogenesis for fiber cell elongation and will serve as a basis for the development of hypotheses regarding the regulation of membrane biogenesis in this important agricultural plant.

The main objective of this research was to characterize the glyceroplipid metabolites in cotton fiber cells at different stages of development and estimate a gene expression profile for lipid metabolism genes in elongating cotton fibers. Toward this end we compiled a list of EST for enzymes involved in lipid metabolism in developing cotton fibers, using EST data annotated and assembled into tentative consensus (TC) sequences by The Institute for Genomic Research. Unique TC sequences are estimates of individual transcripts in cases such as cotton where the genome has not yet been sequenced. The data on EST profiles were viewed, compared, and correlated with the levels of various lipids (including both lipid classes and their individual molecular species) and were used to predict lipid metabolic pathways in developing cotton fiber cells.

MATERIALS AND METHODS

Plant material. Cotton (*Gossypium hirsutum* L. cv. Coker 312) plants were greenhouse grown in April to October in Denton, Texas, with day/night temperatures of 95/80°F (35/27°C) and an approximate 16 h photoperiod (day length extended with sodium vapor lamps when necessary). Flowering plants were tagged on the day of anthesis, and bolls were harvested at 7–10, 14, 21, and 28 dpa. Material in locules (fiber and ovules) was excised and immediately placed in boiling isopropanol, since experiments in which samples were kept on ice or stored at –20 or –80°C resulted in large amounts of post-harvest-generated PA. Replicate fiber samples were dried overnight at 50°C to determine dry weight of fiber samples. Dry weights ranged from 45 to 100 mg. Total FA profiles also were determined for cv. Stoneville 474 (SG474), grown in Stoneville, Mississippi, over the same period for comparison. In this case, bolls were provided by Dr. Jodi Scheffler, USDA-ARS, Cotton Physiology and Genetics (Stoneville, MS).

Chemicals. Diheptadecanoyl (17:0) L-α-PC, L-α-PC (Type II) from soybean, cabbage phospholipase D (PLD) (Type V), and BSA were obtained from Sigma Chemical Co. (St. Louis, MO). [1-^{14}C]Dipalmitoyl-L-α-PC was purchased from NEN Life Sciences (Boston, MA). All other chemicals were from Fisher Scientific unless otherwise stated. Phospholipid and galactolipid standards for ESI-MS/MS were obtained and quantified as previously described (8).

Lipid extraction and analysis. Total lipid extraction of cotton tissues was by a modified version of the Bligh/Dyer method using isopropanol and chloroform (as described in Ref.18). Approximately, 0.5 g of fiber samples was placed in 2 mL boiling isopropanol (70°C). L-α-Diheptadecanoyl (17:0) PC (1–5 mg) was added to some samples as a quantitative standard, and the tubes were incubated at 70°C for 30 min. The samples were allowed to cool to room temperature, 1 mL of chloroform was added, and the samples were extracted overnight at 4°C. Following overnight extraction, phase separation was achieved by addition of 2 mL of KCl and 1 mL of chloroform, and facilitated by centrifugation at 480 −× *g* for 10 min in a Beckman TJ-6 benchtop centrifuge. The upper, aqueous phase was aspirated, and the remaining organic layer was washed two times with 2 mL 1 M KCl and finally with 1 mL ultrapure water

(Milli-Q). The chloroform was evaporated using a Multivap118 nitrogen evaporator (Organomation Associates, Berlin, MA), and 2 mL of fresh chloroform was added to the remaining lipid extract. The lipid samples were stored under nitrogen at –20°C for subsequent FA analysis, or evaporated to dryness and shipped overnight under nitrogen to the Kansas Lipidomics Research Center (KLRC) Analytical Laboratory for ESI-MS/MS analysis, or to the Eastern Regional Research Laboratory, USDA, for HPLC-ELSD analysis.

For total FA analysis, the lipid extracts were evaporated to dryness with nitrogen gas and transesterified in 1 mL acidic (1% H_2SO_4) methanol for 30 min at 65°C. FAME were extracted into hexanes, washed with 5% (wt/vol) NaCl, and dried over Na_2SO_4 columns. FAME in hexanes were analyzed by GC-FID using a Hewlett-Packard Series II plus 5890 gas chromatograph. Samples were separated over a 30 m SUPELCOW-AX^{TM}-10 fused-silica capillary column (Supelco, Bellefonte, PA) at an oven temperature of 200°C, with nitrogen as the carrier gas, and FID was used to quantify FAME. Injector and detector temperatures were 250°C. Identification of FA in samples was achieved by comparison with lipid standards (FAME Mix GLC–10; Supelco), and the amount of each FA was calculated based on the amount of the internal heptadecanoyl standard (from the transesterification of diheptadecanoyl PC).

The polar lipid classes and molecular species in cotton fiber lipids were determined by direct infusion ESI and MS/MS at the KLRC Analytical Laboratory. The samples were dissolved in chloroform. Two aliquots were taken for MS analysis, one sample of 10 µL for phospholipid analysis and one of 10 µL for galactolipid analysis. For phospholipid analysis, cotton lipid extract in chloroform was combined with solvents and internal standards, such that the ratio of chloroform/methanol/300 mM ammonium acetate in water was 300:665:35, the final volume was 1 mL, and the sample contained 0.66 nmol di14:0-PC, 0.66 nmol di24:1-PC, 0.66 nmol 13:0-lysoPC, 0.66 nmol 19:0-lysoPC, 0.36 nmol di14:0-PE, 0.36 nmol di24:1-PE, 0.36 nmol 14:0-lysoPE, 0.36 nmol 18:0-lysoPE, 0.36 nmol di14:0-phosphatidylglycerol (PG), 0.36 nmol di24:1-PG, 0.36 nmol 14:0-lysoPG, 0.36 nmol 18:0-lysoPG, 0.36 nmol di14:0-PA, 0.36 nmol di20:0(phytanoyl)-PA, 0.24 nmol di14:0-PS, 0.24 nmol di20:0(phytanoyl)-PS, 0.20 nmol 16:0–18:0-PI, and 0.16 nmol di18:0-PI. For galactolipid analysis, plant lipid extract in chloroform was combined with solvent and internal standards, such that the ratio of chloroform/methanol/50 mM sodium acetate in water was 300:665:35, the final volume was 1 mL and the sample contained 2.01 nmol 16:0–18:0-monogalactosyldiacylglycerol (MGDG), 0.39 nmol di18:0-MGDG, 0.49 nmol 16:0–18:0-digalactosyldiacylglycerol (DGDG), and 0.71 nmol di18:0-DGDG.

The samples were analyzed on a triple quadrupole tandem mass spectrometer (API 4000; Applied Biosystems, Foster City, CA) equipped for ESI. The source temperature (heated nebulizer) was 100°C, and -4.5 or +5.5 kV was applied to the electrospray capillary. The two ion source gases were each set at 45 arbitrary units; the curtain gas was set at 20 arbitrary units; the declustering potential was ±100 V for phospholipids,

+150 V for MGDG, and +215V for DGDG; and the entrance potential was ±10 to ±15 V. With the interface heater on, the sample was introduced using an autosampler (LC Mini PAL; CTC Analytics AG, Zwingen, Switzerland) and presented to the ESI needle at 30 µL/min. Precursors of lipid head-group-derived fragments were detected, using the scans previously described (8,19,20). The collision energies, with nitrogen in the collision cell, were 28 V for PE, 40 V for PC, −58 V for PI, −57 V for PA and PG, −34 V for PS, 50 V for monogalactosyldiacylglycerol (MGDG), and 84 V for digalactosyldiacylglyerol (DGDG). The mass analyzers were adjusted to a resolution of 0.7 amu full width at half height. For each spectrum, 9–150 continuum scans were averaged in multiple channel analyzer mode.

Data processing was performed using Analyst software (Applied Biosystems) with a custom script written by Anna Lisyansky of Applied Biosystems. In each spectrum, the background was subtracted, the data were smoothed, and then peak area was determined. Identification of the peaks of interest and calculation of lipid species amounts were performed using Microsoft Excel. Corrections for overlap of isotopic variants (A + 2 peaks) in higher mass lipids were applied. The lipids in each class were quantified in comparison with the two internal standards of that class as described (8).

For the quantitative analysis of the polar and nonpolar lipid classes, the total lipid extract was dissolved in chloroform/methanol (10 mg/mL in 85:15, vol/vol) and injected in an HPLC system equipped with ELSD. The method used an Agilent 1100 HPLC system, a Sedex Model 55 ELSD, and a DIOL column, as previously described (10). Lipid classes were identified by cochromatography with commercial standards and by MS (LC-MS with atmospheric pressure chemical ionization in the positive ion mode).

Bioinformatics and data mining. Cotton EST from different tissues in cotton have been assembled into TC sequences at The Institute for Genomic Research web site at http://www.tigr.org. These include EST from two libraries for cotton fibers at 7–10 dpa and at 6 dpa, which is the stage of rapid cell expansion. We queried these databases to catalog EST to identify the major enzymes involved in lipid metabolism in elongating cotton fiber. At the time of our analysis 38,814 EST were annotated from the 7–10 dpa library, and 8,003 from the 6 dpa library. Hence, the number of EST and TC sequences discussed here are almost exclusively those of the larger (7–10 dpa) library, with certain noted exceptions. Some EST were already annotated, whereas others were identified using the WU-BLAST program with cDNA and protein sequences from other plants as queries. Many of these plant sequences were obtained from a lipid gene database for *Arabidopsis thaliana* housed at http://www.plantbiology.msu.edu/lipids/genesurvey/index.htm (17). In addition, protein motif identification, domain organization analysis, and subcellular location predictions were accomplished with web-based bioinformatics tools (interpro, BLOCKS, NCBI-DART, PSORT, TargetP) where possible. Sequences of lipid metabolism genes in cotton were placed in the context of known lipid metabolism pathways and used to predict

the metabolic capacity for cotton fibers to produce various lipid metabolites. Actual metabolite data were compared with these metabolic schemes to provide an overall view of lipid metabolism in elongating cotton fiber cells.

All experiments were repeated at least three times and the data presented are the means ± SD.

RESULTS

FA composition of cotton fiber cells. Total lipid extracts were obtained from cotton fiber cells (*G. hirsutum*, L., cv. SG474 and Coker 312) harvested at different ages (7, 14, 21, and 28 dpa) representative of different stages of fiber development. Total FA composition was determined by GC-FID using heptadecanoic acid (17:0) as a quantitative internal standard. The percentage by weight of each of the common FA, palmitic (16:0), stearic (18:0), oleic (18:1), linoleic (18:2) and linolenic (18:3), remained relatively constant over the entire period of fiber development (Fig. 1). Linolenic was found to be the most abundant FA, accounting for about 40 to over 50% by weight of total FA. Palmitic was the second-most abundant FA, representing 25–35% by weight of total FA. Linoleic acid constituted

10–15% by weight of FA present, whereas low levels of oleic and even lower levels of stearic acid were observed in all stages of development. A slight increase in the ratio of saturated to unsaturated FA was observed in the later stages of fiber development.

The total amounts of individual FA increased (or were highest) during the elongation stage and decreased thereafter (Fig. 2), despite a relative increase in the size of bolls and fiber content during fruit development. During the early stages of fiber development, cells are undergoing rapid elongation (2) and are engaged in lipid synthesis for membrane development; hence, an increase in fiber mass in bolls is associated with a concomitant increase in lipid content. In maturing fibers, cells are involved in secondary cell wall synthesis, which begins around 16–19 dpa and continues up to 25 dpa (2). During this stage of development, cellulose accumulates and accounts for the bulk of the mass in fiber cells. As a result, the proportion of lipids relative to the overall weight of fiber is lower in maturing fibers. The slight difference in the time course of lipid accumulation between the two cultivars may be genetic or may be environmental; however, the trends are the same, with lipid accumulating early to support cell elongation, and then tapering off as fiber cell wall thickening proceeds. Cotton embryos begin to synthesize seed oil at around 20–25 dpa. Hence, membrane lipid synthesis in fiber cells may decline prior to this period of TAG accumulation during cottonseed development.
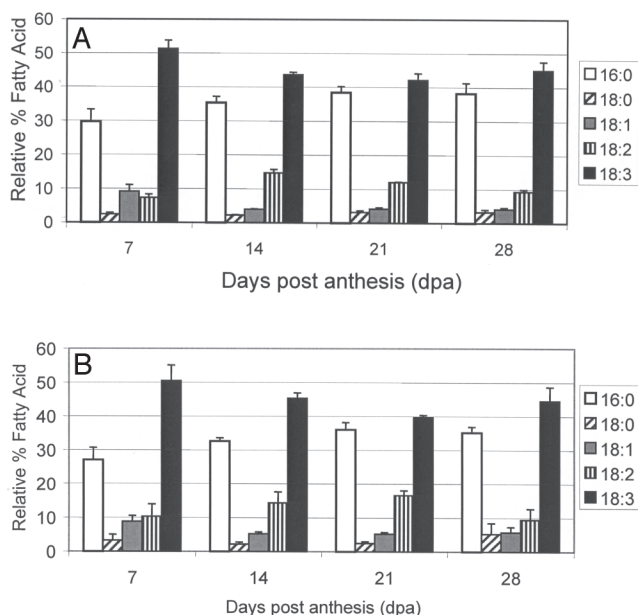
FIG. 1. The FA composition of cotton fiber cells at different stages of development [7, 14, 21, and 28 d post-anthesis (dpa)] was determined for two different cultivars–*Gossypium hirsutum* L. cv. Stoneville SG474, upper panel, and cv. Coker 312, lower panel. Total lipids were extracted from fiber cells with addition of diheptadecanoyl (di17:0) PC as an internal standard. Following acid-catalyzed transesterification, total FAME were analyzed by GC-FID and quantified based on the amount of methyl heptadecanoate (17:0) from the internal standard. The relative proportions (wt %) of the common FA present in SG474 fibers and Coker 312 fiber cells were compared. The overall composition was similar for both cultivars throughout the entire period of fiber growth and maturation, and 18:3 and 16:0 were the most abundant FA at each stage of development. Bars represent the means and SD of three (SG474) or four (Coker 312) independent extractions.
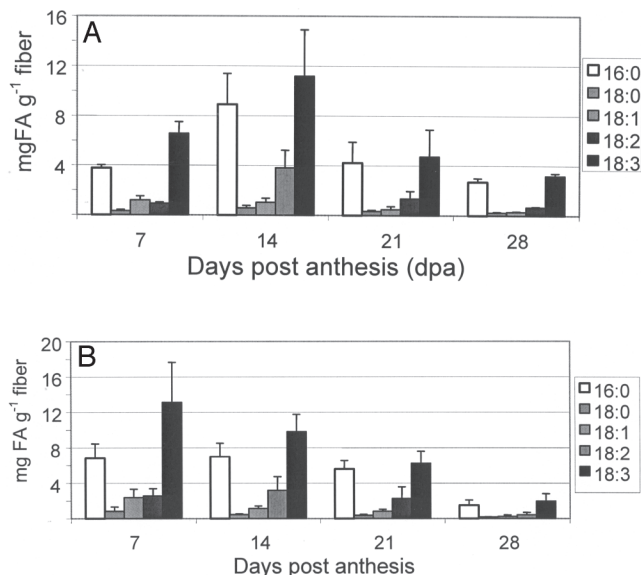
FIG. 2. Individual FA content was quantified (mg per dry weight of fiber) at the different stages of fiber development. In SG474 (A), an increase in 16:0, 18:2, and 18:3 content occurred from 7 to 14 dpa (during cell elongation), with levels declining on a cell dry weight basis thereafter (during maturation). For Coker 312 (B), the levels of individual FA were highest at 7 and 14 dpa (during cell elongation), and similar to SG474. All FA decreased on a cell dry weight basis at 21 and 28 dpa (during maturation). Bars represent the means and SD of three (SG474) or four (Coker 312) independent extractions.
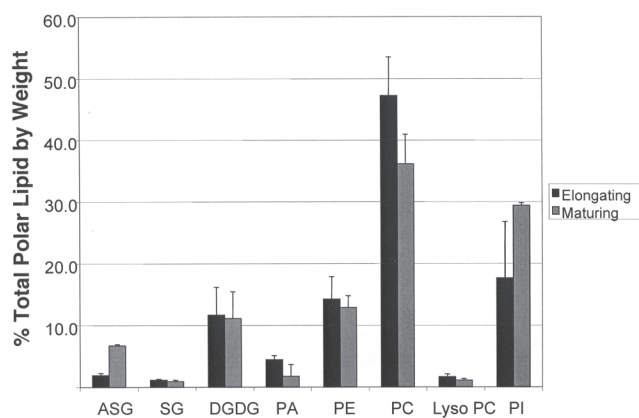
FIG. 3. Comparison of polar lipid classes of elongating (8–10 dpa) and maturing (21 dpa) fiber cells (from cv. Coker 312) determined by HPLC-ELSD and expressed as weight percentage of the total polar lipid (10). Lipids were quantified based on standard curves developed for each lipid class. ASG, acylated sterol glycoside; SG, sterol glycoside; DGDG, digalactosyldiacylglycerol (may include MGDG, monogalactosyldiacylglycerol); PA, phosphatidic acid; LPC, lysophosphatidylcholine. Bars represent the means and SD of three independent extractions.

Polar lipid profiles in cotton fiber cells. The polar lipid classes of elongating and maturing cotton fiber cells were quantitatively analyzed by HPLC-ELSD analysis (Fig. 3). PC was the most abundant lipid class, constituting 47% of elongating and 36% of maturing cell total lipids by weight. PI also was a prevalent polar lipid in cotton fiber cells. Although values were variable when quantified by HPLC-ELSD, PI consistently was more abundant in maturing fibers, averaging 29% of total polar lipids, than in elongating fibers, where PI levels averaged 18% by weight of total polar lipids. PE and DGDG were present in similar proportions in elongating and maturing fibers from 11 to 14% by weight of total polar lipids. Relatively low levels of PA were observed, with only 2 and 4% (by weight) of total polar lipids in elongating and maturing fiber cells, respectively. The levels of acylated sterol glycoside (ASG) were higher in maturing fiber cells (7%) than in elongating fiber cells (2%), whereas similar levels of SG were observed at both developmental stages.

Recent advances MS methods have facilitated detailed class and molecular species analyses of plant glycerolipids (21). The classes and molecular species of polar lipids in elongating and maturing cotton fibers were determined by direct infusion ESI followed by tandem MS. This method does not incorporate HPLC or any other chromatographic separation. Instead, the species in each headgroup class are detected, as they produce a common headgroup fragment following collisionally activated dissociation. Classes are detected by sequential scans during continuous infusion, and quantification is in comparison with two internal standards of each headgroup class (21). The composition and relative proportions of the different glycerolipid classes were similar in elongating and maturing fiber cells (Fig. 4). The only major difference observed was in the relative amounts of lipid per dry weight (Fig. 4B), which was two times higher in elongating than in maturing fiber cells. This was con-
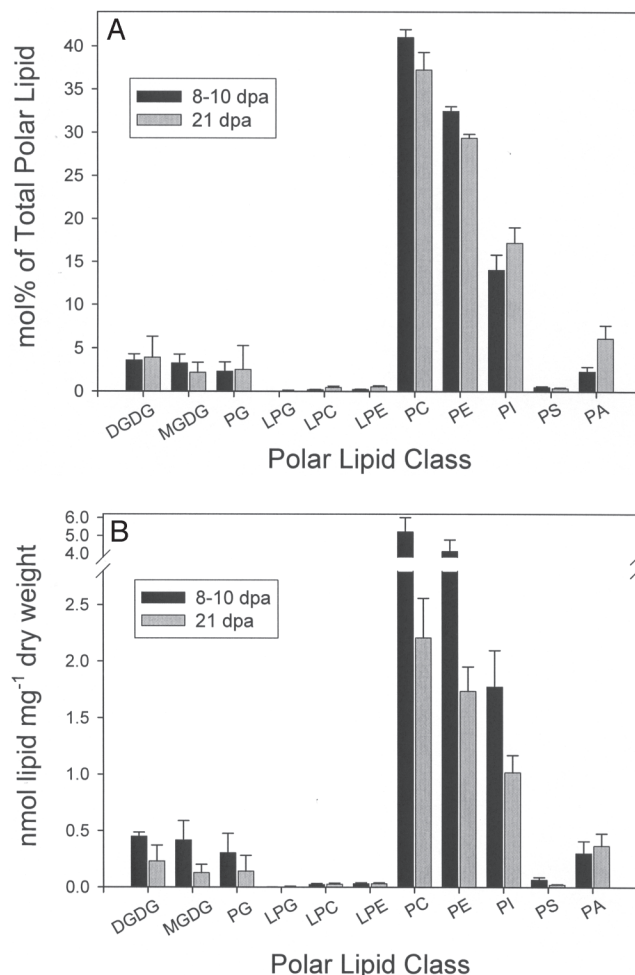
FIG. 4. Comparison of glycerolipid content of elongating (8–10 dpa) and maturing (21 dpa) fiber cells (from cv. Coker 312) determined by ESI-MS/MS. In panel A lipid quantities are presented as mol% of total glycerolipid, and in panel B lipids are quantified on nmol mg^{-1} dry weight basis. Lipid quantities were calculated based on internal standards included for each class (see methods) and the amount for each class represents the sum of individual molecular species for that class. PG; phosphatidylglycerol; LPG, lysophosphatidylglycerol; LPC, lysophosphatidylcholine; LPE, lysophosphatidylethanolamine; PA, phosphatidic acid. Bars represent the means and SD of five independent extractions.

sistent with results from total FA content measured above (Fig. 2) and is likely due to the increase in relative cellulose content at the later stages of fiber maturation. PC, PE, and PI were the predominant phospholipids in cotton fiber cells at both stages, and, consistent with data from HPLC-ELSD, the relative percentage of PI was somewhat higher in maturing than in elongating fiber cells (Fig. 4A).

PE constituted a considerably higher proportion of total polar lipid when measured by ESI-MS/MS (compared with HPLC-ELSD), about 30% of total polar lipid. It is possible that the lower levels of PE measured *via* HPLC-ELSD vs. *via* ESI-MS/MS may occur because PE (a basic lipid) is not accurately separated (chromatographed) by this system (even though the PE standard is used to determine the retention time and the PE

S.W. WANJIE *ET AL.*
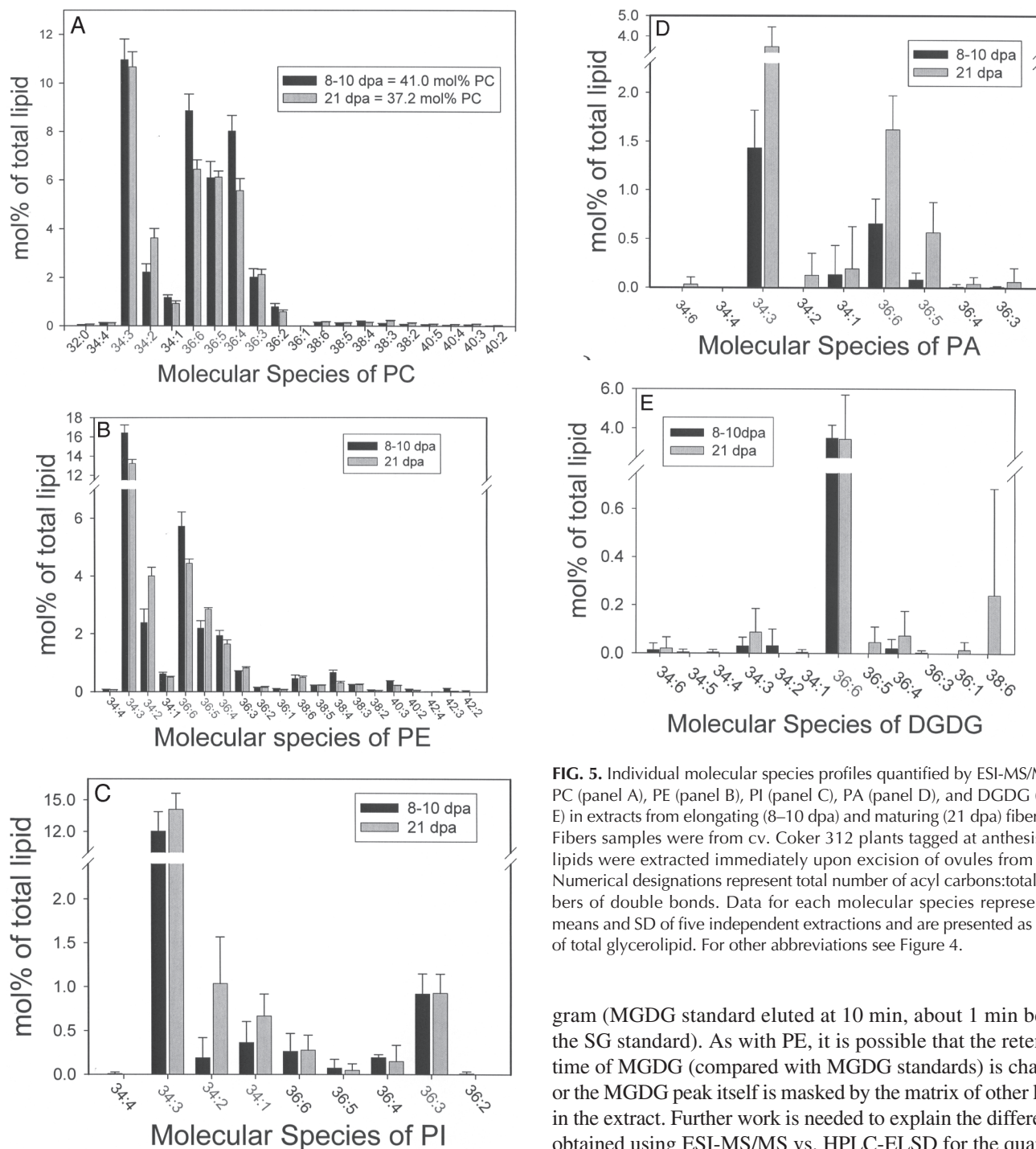
FIG. 5. Individual molecular species profiles quantified by ESI-MS/MS for PC (panel A), PE (panel B), PI (panel C), PA (panel D), and DGDG (panel E) in extracts from elongating (8–10 dpa) and maturing (21 dpa) fiber cells. Fibers samples were from cv. Coker 312 plants tagged at anthesis, and lipids were extracted immediately upon excision of ovules from bolls. Numerical designations represent total number of acyl carbons:total numbers of double bonds. Data for each molecular species represent the means and SD of five independent extractions and are presented as mol% of total glycerolipid. For other abbreviations see Figure 4.

standard is used to construct a calibration curve of PE mass vs. PE peak area. A possible explanation is that the retention time of PE (compared with PE standard, which elutes at 23 min) may be changed by the matrix of other lipids (or ions) in the extract, perhaps causing it to bind to another lipid and elute as part of a peak of another lipid class or to bind irreversibly to the column. It should similarly be noted that although MGDG is detected at significant levels *via* ESI-MS/MS (Fig. 4), no peak of MDGD was detected in the HPLC-ELSD chromato-

gram (MGDG standard eluted at 10 min, about 1 min before the SG standard). As with PE, it is possible that the retention time of MGDG (compared with MGDG standards) is changed or the MGDG peak itself is masked by the matrix of other lipids in the extract. Further work is needed to explain the differences obtained using ESI-MS/MS vs. HPLC-ELSD for the quantitative analysis of lipid classes. Although there were differences in the analytical results obtained by these two very different methods, overall trends and amounts of polar lipids quantified were similar.

The detailed molecular species profiles of the major glycerolipid classes were determined (Fig. 5). There were some similarities and differences in the profiles of glycerolipid molecular species, which are presented as the combined acyl composition. Major molecular species of PC and PE were quite similar (Fig. 5A, B), including 34:3 (16:0, 18:3), 34:2 (16:0,

18:2 or 16:1, 18:1), 34:1 (16:0, 18:1), 36:6 (18:3, 18:3), 36:5 (18:2, 18:3), 36:4 (18:1, 18:3 or 18:2, 18:2), and 36:3 (18:0, 18:3 or 18:1, 18:2). Relatively speaking, PE had more minor long-chain species (series of PE38, PE40, and PE42) than PC. PI molecular species profiles were much less complex than profiles of PC or PE (compare Fig. 5A–C), and were almost entirely dominated by PI 34:3 in fiber cells at both stages of development. The most abundant molecular species for PC, PE, PI, and PA was 34:3 (18:3,16:0). In addition, 36:6 (18:3,18:3) also was prevalent in PC, PE and PA, but not in PI (compare Fig. 5A–D). The composition and relative proportions of molecular species found in PA were similar to those found in PC and PE, suggesting that these PA species are indeed metabolites (precursors or products) of the two major phospholipids. The precise identity of the acyl groups is tentative in some of molecular species because multiple combinations of FA at the *sn*-1 and *sn*-2 positions of the glycerolipids can make up the reported total number of acyl carbons and double bonds. However, it should be noted that the prevalence of 18:3- and 16:0-containing molecular species is entirely reasonable, given total FA composition of the lipids in these cells (Fig. 1).

Relatively low levels of PS, PG, MGDG, and DGDG were present in cotton fiber lipid extracts analyzed by ESI and tandem MS (Fig. 4). Longer-chain FA were found to comprise the major molecular species in PS, with PS 40:3 being the most prevalent, and lower levels of PS 38:3 and PS 34:3 were detected (not shown). For PG, the most abundant molecular species were PG 32:0 (16:0, 16:0) and PG 32:1 (16:0,16:1); some PG 34:3 (18:3,16:0) was detected in fiber lipid samples as well (not shown). The major molecular species present in MGDG and DGDG were 36:6 (18:3, 18:3) (Fig. 5E).

Overall, there were subtle but significant differences in molecular species profiles between elongating and maturing fiber cells. The higher relative levels of 34:2 (16:0, 18:2) PC, PE, PI, and PA in the maturing as compared with the elongating cells are consistent with the higher levels of palmitic and linoleic acids in the maturing cells (Fig. 1). Higher levels of PE 36:5 (18:2, 18:3) may also reflect higher 18:2 levels, but higher levels in maturing fiber cells of PA 34:3, 36:5, and 36:6 than in elongating cells probably just reflect the higher total levels of PA in the maturing cells, as determined by ESI-MS/MS. On the other hand, PC 36:6, PC 36:4, PE 34:3, and PE 36:6 were higher on a mol% basis in elongating cells than in maturing fiber cells. It should be emphasized that polar lipid profiles were dramatically different when fiber samples were frozen prior to analysis; considerably higher amounts of PA (up to 40 mol%) were measured by both ESI-MS/MS and HPLC-ELSD in extracts from frozen fiber samples, and several pilot experiments determined that this could be attributed to the post-harvest hydrolytic activity of PLD. This was not observed with other cotton tissues (e.g., leaves) and indicates a considerable capacity for PLD hydrolysis in fiber cells. Caution should be exercised when handling and processing cotton fibers for polar lipid profiles.

Profile of EST in developing cotton fibers. Expressed genes in cotton fibers have been identified through several EST pro-

jects, and these publicly available sequences have been assembled into contigs by the efforts of researchers at The Institute for Genomic Research (http://www.tigr.org). These include EST from two libraries for cotton fibers at 7–10 dpa and 6 dpa, which is the stage of rapid elongation. We used these data to catalog EST for the major enzymes involved in lipid metabolism in elongating cotton fiber cells (Table 1). Approximately 39,000 EST have been derived from the 7–10 dpa library, as compared with only 8,000 from the 6 dpa library. Hence, the number of EST and TC sequences discussed here are mostly representative of the 7–10 dpa library, with certain noted exceptions. In some cases, the EST were already annotated, whereas in other instances homologs were tentatively identified by WU-BLAST with cDNA and/or protein sequences from other plants as queries. Many of these plant sequences were obtained from a lipid gene database for *A. thaliana* housed at http://www.plantbiology.msu.edu/lipids/genesurvey/index.htm (17) which also provides detailed reactions and metabolic pathway(s) for plant lipid metabolism. Hence, we also compared the total number of lipid enzyme EST from all tissues in *A. thaliana* to those in cotton fiber cells. The abundances of EST were used only as an indicator of the potential capacity for fiber cells to produce the different gene products and respective lipid metabolites.

EST for enzymes and proteins of *de novo* FA biosynthesis were prevalent in elongating cotton fiber cDNA libraries, including those encoding subunits of acetyl-CoA carboxylase, ACP, β-ketoacyl-ASP synthase I (KAS I), and stearoyl-ACP desaturase. Several EST were predicted to encode for different isoforms of ACP, including a fiber-specific ACP (13). No EST were annotated as encoding KAS II and KAS III enzymes, but KAS II shares high homology with KAS I, and some of the EST predicted to encode for KAS I could in fact encode for other enzymes. These results support metabolic data that cotton fiber cells at this stage of development have a high capacity for the *de novo* biosynthesis of FA and identify candidate cotton sequences that can be targeted for future functional studies.

The FA synthesized in the plastids can either be transferred from acyl-ACP into plastidial glycerolipids, or cleaved by a thioesterase to form free acyl chains that are exported to the ER for extraplastidial glycerolipid assembly (7). Three EST for FatA, the thioesterase that acts preferentially on unsaturated FA (22), and 11 EST for Fat B, which exhibits a preference for saturated acyl-ACP (23), were identified. Eleven EST were annotated as encoding for acyl-CoA synthetase, which esterifies the free acyl chains to CoA forming acyl-CoA (7), the precursors for ER glycerolipids.

Glycerolipid synthesis initiated by the transfer of acyl chains (from acyl-ACP in plastids or acyl-CoA in the ER) to glycerol-3-phosphate (G3P) forming lysophosphatidic acid (LPA) in a reaction is catalyzed by a G3P acyltransferase (7). Several EST were annotated as acyltransferases. Only a single EST from the 6 dpa library could be annotated as encoding an acyl-ACP acyltransferase. Nine EST, representing one TC, exhibited high identity with sequences of known acyl-CoA acyltransferases. In *A. thaliana*, only two EST for each of these enzymes have been

TABLE 1

Catalog of Expressed Sequence Tags (EST) Predicted to Encode for Enzymes and Other Proteins Involved in Lipid Metabolism in Two Cotton Fiber Libraries[a] (7–10 and 6 dpa)

	Enzyme or protein	Cotton fiber			*Arabidopsis* (all tissues)	
		EST	EST	TC	EST	Genes
EC #	FA biosynthesis	7–10 dpa	6 dpa	7–10 dpa		
6.4.1.2	Acetyl-CoA carboxylase subunits	47	8	6	68	1
	Fiber-specific ACP	7	2	1		
	ACP plastidial isoform 1	12	0	1	42	5
	ACP plastidial isoform 2	5	1	1		
	ACP mitochondrial isoform	9	1	3	12	3
2.3.1.39	ACP S-malonyltransferase	9	0	1	3	3
2.3.1.41	Ketoacyl-ACP synthase 1	40	18	5	39	1
2.3.1.41	Ketoacyl-ACP synthase II	0	0	0	2	1
2.3.1.41	Ketoacyl-ACP synthase III	0	0	0	6	1
1.1.1.100	β-Ketoacyl-ACP reductase	3	2	1	35	5
4.2.1.*	β-Hydroxyl-ACP dehydratase	2	3	1	7	2
1.3.1.9	Enoyl-ACP reductase	5	2	2	11	1
1.14.19.2	Stearoyl-ACP desaturase	22	4	5	43	7
3.1.2.14	Palmitoyl-ACP thioester (FatB)	11	1	3	35	1
3.1.2.14	Oleoyl-ACP hydrolase (FatA)	3	0	1	5	2
	Glycerolipid synthesis					
	Acyltransferase	66	17	3		
2.3.1.15	Acyl-ACP G3P acyltransferase	1	0	0	2	1
2.3.1.15	Acyl-CoA G3P acyltransferase	9	0	1	2	2
2.3.1.51	LPA Acyltransferase-plastidial	13	0	1	7	1
2.3.1.51	LPA Acyltransferase-ER	7	3	1	5	11
2.7.7.41	Phosphatidic acid phosphatase	1	2	0	2	1
2.7.1.107	DAG kinase-like protein	4	1	2	33	8
2.3.1.20	DAG transferase	0	0	0	7	2
2.7.7.41	CDP:DAG synthetase	0	0	0	4	3
2.7.8.5	PGP synthase (CDP:DAG G3P phosphotransferase)	2	0	1	3	1
2.7.8.5	ER PGP synthase	0	1	1	7	1
3.1.3.27	PGP phosphatase	0	0	0	0	0
2.7.8.11	PI synthase	0	0	0	6	2
2.7.1.32	Choline/ethanolamine kinase	0	3	1	13	4
2.7.7.15	Phospholipid cytidyltransferase	4	0	1	8	2
2.7.8.2	Aminoalcoholphosphotransferase	2	0	1	11	1
1.14.99.*	ω-6 FAD ER (FAD2)	10	10	2	131	1
1.14.99.*	Plastidial FAD 6	1	0	1	9	1
1.14.99.*	ω-3-FAD ER (FAD3)	5	4	1	31	4
1.14.99.*	Plastidial (FAD7/FAD8)	8	1	1	18	2
2.7.1.46	MGDG synthase	0	0	0	5	3
2.4.1.184	DGDG synthase	2	0	1	8	2
	Sphingolipid biosynthesis					
2.3.1.50	Serine palmitoyltransferase	4	2	2	13	3
1.1.1.102	3-Ketosphinganine reductase	29	2	2	18	2
	Acyl-CoA independent ceramide synthase	1	1	1	0	0
2.3.1.24	Sphinganine acyltransferase	0	0	0	0	0
	Δ 8 Sphingolipid desaturase	1	0	1	36	2
	FA elongation/wax synthesis					
6.2.1.3	Long-chain acyl-CoA synthetase	11	4	2	63	9
	β-Ketoacyl-CoA synthase	150	43	16	183	20
	β-Ketoacyl reductase	15	7	2	47	2
4.2.1.17	3-Hydroxyl-CoA dehydrase	0	0	0	0	0
1.3.1.44	Enoyl-CoA reductase	0	0	0	31	1
	CER1-aldehyde decarboxylase	24	5	1	36	5
	CER2	0	1	1	28	3
	CER3	0	5	1	7	1
	Lipid transfer protein precursor	151	254	4	362	14
	Lipid transfer protein 3 precursor	67	125	4	28	8
	Palmitoyl-protein thioester- like protein	2	2	1	44	7

(Continued)

TABLE 1 (*Continued*)

	Enzyme or protein	Cotton fiber			*Arabidopsis* (all tissues)	
		EST	EST	TC	EST	Genes
EC #	FA biosynthesis	7–10 dpa	6 dpa	7–10 dpa		
	Sterol biosynthesis					
1.1.1.34	HMG-CoA reductase	21	0	3	N/A	N/A
	24-Sterol C-methyltransferase	14	11	1	N/A	N/A
	Sterol C14 reductase FACKEL	2	0	1	N/A	N/A
	Δ 8 Δ 7 Isomerase	2	0	1	N/A	N/A
	Sterol-C4-α methyl oxidase	5	2	1	N/A	N/A
	UDP:glucose sterol glucosyl transferase	6	2	2	N/A	N/A
	Sterol methyltransferase	8	0	1	N/A	N/A
	Lipases					
3.1.4.4	Phospholipase D (α)	25	3	1	35	4
3.1.4.4	Phospholipase D (β1)	2	0	1	4	2
3.1.4.4	Phospholipase D (δ)	1	0	1	13	3
3.1.1.32	Putative phospholipase A1	2	0	1	2	1
3.1.1.4	Putative phospholipase A2	7	0	1	6	2
3.1.1.5	Lysophospholipase homolog	84	11	18	28	9
3.1.4.11	Phospholipase C	1	3	0	11	6
3.1.4.11	PI-specific phospholipase C	12	1	3	24	9
	FA amide hydrolase	16	7	5	5	2
	β-Oxidation					
1.3.3.6	Acyl-Co A oxidase	4	1	2	61	6
4.2.1.17	EnoylCoA hydratase	7	1	1	6	2
1.1.1.35	3-Hydroxybutyryl-CoA dehydrogenase	3	0	1	10	1
2.3.1.16	3-KetoacylCoA thiolase	5	0	1	65	3
	AcylCoA synthase	8	0	2	0	0

[a]The number of tentative consensus sequences (TCs) in the 7–10 dpa library is noted and may indicate the potential number of genes for each protein. The EST data were obtained from The Institute for Genomic Research (TIGR) through the web site at http://www.tigr.org. Comparisons were made to EST involved in lipid metabolism in *Arabidopsis thaliana*, using data compiled in the *Arabidopsis* lipid gene database housed at www.plantbiology.msu.edu/lipids/genesurvey/index.htm (17). Lipid metabolic genes for which no EST have been annotated in this database are marked as N/A. ACP, acyl carrier protein; G3P, glycerol-3-phosphate; LPA, lysophosphatidic acid; ER, endoplasmic reticulum; PGP, phosphatidylglycerol phosphate; MGDG, monogalactosyldiacylglycerol; DGDG, digalactosyldiacylglycerol.

identified. Transfer of a second acyl chain to the *sn*-2 position of LPA forms PA, and several EST were identified for the plastidial and ER isoforms of LPA acyltransferase. The occurrence of these EST suggests that the synthesis of PA occurs in both the plastid and ER of fiber cells. Of interest, 66 cotton fiber EST appeared to encode acyltransferases of unidentified function.

PA serves as the precursor to most glycerolipids and is converted to DAG or cytidine diphosphate:diacylglycerol (CDP:DAG) for complex glycerolipid assembly (24). PA may be dephosphorylated by PA phosphatase, forming DAG, and a single EST predicted to encode this enzyme was present, whereas four EST (two TC) for DAG kinase (which catalyzes the reverse reaction) were identified. DAG also is used as a substrate in the synthesis of plastidial galactolipids, MGDG and DGDG. Only EST corresponding to DGDG synthase were identified. DAG may also be acylated by DAG acyltransferase to form TAG, but no EST were identified for this protein, nor were any EST identified as encoding a phospholipid diacylglycerol acytransferase, which catalyzes the transfer of an acyl group from a phospholipid to DAG forming a TAG and a lysophospholipid. These results might be expected since elongating fiber cells are not primary sites for TAG biosynthesis, but rather likely are more involved in the synthesis of membrane glycerolipids.

In the ER, DAG acts as a direct precursor for synthesis of PC

and PE in the ER *via* the action of a phosphotransferase, displacing cytidine monophosphate (CMP) from the nucleotide-activated amino alcohols, CDP-choline or CDP ethanolamine. The amino alcohols are themselves produced in a series of reactions in which they are first phosphorylated, and then reacted with CTP to produce the CDP derivatives (24). Three cotton EST were identified as candidate choline/ethanolamine kinase homologs. Four EST were annotated as encoding the cytidyltransferase enzyme, while 2 EST were predicted to encode an aminoalcohol phosphotransferase. A single aminoalcohol phosphotransferase catalyzes the final step, producing PC or PE (25).

PA may be converted to CDP:DAG by action of CDP:DAG synthase, but surprisingly no EST encoding for this enzyme were identified. CDP:DAG is the precursor for PG, PI, and PS (26). Phosphatidylglycerol phosphate (PGP) synthase uses CDP:DAG and G3P to form PGP, which is the precursor to PG, and 2 EST were predicted to encode for the plastidial isoform of PGP synthase, while a single EST in the 6 dpa library was annotated as encoding for the ER isoform. However, no EST were identified as encoding for PGP phosphatase, which produces PG from PGP. Additionally, no EST were predicted to encode for PI synthase or PS synthase, which both use CDP:DAG as a precursor.

Desaturation of glycerolipid acyl chains occurs in both the plastid and ER and is catalyzed by different proteins in these

organelles. Ten EST predicted to encode for the ER δ-12 desat-urase [fatty acid desaturase 2 (FAD2)] were identified, while only a single EST was annotated as encoding the plastidial iso-form, FAD6. Five EST were identified as an ER Δ-15 desat-urase (FAD3), while eight EST were predicted to encode the plastidial isoforms FAD7/FAD8.

The large number of EST predicted to code for enzymes in-volved in FA elongation and wax biosynthesis suggests that elongating fiber cells are actively engaged in these processes. The FA elongase system, which adds two carbons per cycle to C_{18}-acyl-CoA, consists of four components; β-ketoacyl-CoA synthase, β-ketoacyl -CoA reductase, β-hydroxylacyl-CoA de-hydratase, and enoyl-CoA reductase (23). A large number of EST (150) were identified as encoding for β-ketoacyl-CoA synthase, while15 EST were annotated as encoding for the re-ductase, but no EST were identified for the latter two compo-nents of the pathway. A surprisingly high number of EST were identified for lipid transfer protein precursors, but this is a fea-ture of many cDNA libraries. A total of 218 EST in the 7–10 dpa library and 379 EST in the 6 dpa library were annotated as encoding for this type of protein. Lipid transfer proteins are thought to have a role in cutin/wax deposition (27), and fiber-specific transcripts of this enzyme that were highly expressed during the stage of rapid elongation have been identified in cot-ton (14,16).

Sphingolipids are constituents of membranes (particularly, plasma membranes), and several EST for enzymes involved in their biosynthesis were identified in the cotton fiber databases. Four EST were annotated as encoding a serine palmitoyltrans-ferase, which catalyzes the condensation reaction between ser-ine and palmitoyl-CoA forming 3-ketosphinganine in the first step of the pathway (28). Several EST were identified for 3-ke-tosphinganine reductase, which forms sphinganine. Ceramide synthesis is thought to occur either by acylation of sphinganine with a free FFA or an acyl-Co A donor (28). Ceramide synthase catalyzes the former reaction, and a single EST was identified for this enzyme, while no EST were annotated as encoding for sphinganine acyltransferase, which catalyzes the latter reac-tion. A single EST predicted to encode a sphingolipid desat-urase was identified.

Sterols are minor components of cotton fiber (29), and sev-eral EST encoding enzymes involved in sterol biosynthesis were identified in the cotton fiber databases. These include 21 EST for HMG-CoA reductase, a major precursor in sterol biosynthesis, 14 EST for 24 sterol methytransferase, 2 EST for sterol C_{14} reductase, 2 EST for the Δ 8, Δ 7 isomerase, 5 EST for sterol 4-α methyl oxidase, 6 EST for UDP-glucose: sterol glucosyltransferase, and 8 EST annotated as a *S*-adenosyl-methionine-sterol methyltransferase.

Plant lipids undergo membrane remodeling during growth and development, as well as in response to various environ-mental conditions, and lipases are involved in these processes (30). PLD is known to hydrolyze phospholids producing PA and a headgroup, and multiple isoforms of this enzyme have been identified in plants (31). In the cotton fiber libraries, the most abundant PLD EST were those for PLDβ, for which 25 EST were identified, while only 2 EST were identified as en-coding for PLDβ and a single EST was identified for the PLD δ isoform. Eighty-four EST were grouped as homologs of lysophospholipases. Two EST were specifically annotated as encoding phospholipase A1, which cleaves phospholipids at the *sn*-1 position, while 7 EST were predicted to encode phos-pholipase A2, which cleaves phospholipids at the *sn*-2 posi-tion. Additionally, 12 EST were annotated as encoding PI-spe-cific phospholipase C, suggesting that PI-mediated signaling may be a feature of cotton fiber cell elongation. Orthologs of the recently discovered plant FA amide hydrolase (32) also were expressed in developing cotton fibers.

FA are turned over in plant cells by the peroxisomal β-oxi-dation pathway (33). Several EST for each of the enzymes in-volved in this process were present in the cotton fiber data-bases. These included 8 EST for acyl-CoA synthase, 4 EST for acyl-CoA oxidase, 7 EST for enoyl-CoA hydratase, 3 EST for 3-hydroxybutyryl-CoA dehydrogenase, and 5 EST for 3-keto-cyl-CoA thiolase. The expression of these genes in elongating cotton fiber cells suggests that FA degradation occurs even at the early stages of fiber development.

DISCUSSION

Cotton fibers are single cells that develop relatively synchro-nously, forming extremely long cells in a period of a few days; hence, they represent a good system for studying plant cell ex-pansion (6). The rapid elongation of these cells requires sub-stantial lipid synthesis to support the developing organelle and membranes, and this was supported by estimates of acyl lipid content at several stages of fiber development (Fig. 2). The presence of several EST for enzymes involved in FA biosyn-thesis indicated that this pathway is quite active at the early stage of fiber development (Table 1). A large number of EST were predicted to encode for subunits of acetyl-CoA carboxy-lase, which is considered to be the major regulatory enzyme in the pathway (34). Several EST were identified for ACP, which carry the FA through the assembly process, as well as for KAS I, which participates in fatty acyl chain elongation. Glyc-erolipid synthesis usually begins with incorporation of 16:0 and 18:1 acyl chains onto a glycerol-3-phosphate backbone. KAS II is responsible for the elongation of 16:0 to stearate (18:0), and we hypothesize that some of the EST annotated as encod-ing for KAS I may in fact be KAS II EST, owing to the high sequence homology. Several EST for stearoyl-ACP desaturase, which introduces a double bond in stearate (18:0) to form oleate (18:1), were prevalent as well. These EST profiles indi-cate that cotton fiber cells are capable of producing a substan-tial amount of 16:0 and 18:1, and these FA are then incorpo-rated into complex lipids during plastidial and extraplastidial glycerolipid synthesis and modification. It should be empha-sized that additional quantitative proteomics data (or western blotting) will be required to provide information about actual abundance of proteins in these pathways. Nonetheless, lipid

and EST profiles do confirm the metabolic capacity of cotton fiber cells for these pathways.

The molecular species composition of glycerolipids can be used to gain information as to how these lipids might be synthesized in cells. For example, glycerolipids are usually synthesized in plants from a PA precursor *via* two pathways, the prokaryotic and the eukaryotic pathway (35). In the prokaryotic pathway, 16-carbon FA are found predominantly in the *sn*-2 position. In the eukaryotic pathway, 16-carbon FA, when present, are found at the *sn*-1 position, and 18-carbon FA can be esterified to either position (36). Although acyl positions have only been tentatively assigned to the species identified by ESI-MS/MS, some conclusions can nonetheless be drawn from results such as those presented in Figure 5. DGDG (and MGDG) contained 36:6 (18:3,18:3) as the most abundant molecular species (Fig. 5E); this points to the DAG moieties of these lipids being synthesized *via* the eukaryotic pathway, since this is the only mechanism by which 18-carbon acyl chains are placed at both *sn*-1 and *sn*-2 positions. On the other hand, most of the PG is likely to be synthesized by the prokaryotic pathway, since the major molecular species of PG were 32:0 (16:0, 16:0) and 32:1 (16:0,16:1) (not shown).

In this same context, it is possible to deduce the scheme by which the major phospholipid species are synthesized in cotton fibers, and the EST occurrence supports the metabolic compartmentation scheme for PC (and PE) biosynthesis shown in Figure 6. As in most plant cell types, 16:0 and 18:1 FA are the major FA synthesized in and exported from plastids to the ER for complex lipid formation. These FA are incorporated *via* CoA esters into the *sn*-1 and -2 position of G3P by G3P acyltransferase and LPA acyltransferase, respectively, to form PA. Although not shown, 18:1 (or 18:0) could be incorporated into either acyl position of PA. PA is dephosphorylated to yield DAG, which is used for the synthesis of PC (and PE) *via* the membrane-bound aminoalcohol phosphotransferase enzyme with the appropriate CDP donor. The 18:1 acyl chains are modified by the Δ-12 (FAD2) and the Δ-15 (FAD3) desaturases to yield 18:2 and 18:3 FA.

The principal molecular species of PC (16:0, 18:3) and PE (16:0, 18:3) together were about 25 mol% of the total polar lipid fraction (Figs. 5A and 5B). These two lipids are likely to be the principal phospholipid components of both vacuole and plasma membranes of expanding cotton fiber cells, and they are most likely synthesized by cooperation between the plastidial and ER compartments *via* the scheme shown in Figure 6. Additional molecular species for these two lipid classes wherein 18-carbon FA are at both positions (36:6, 36:5, 36:4, 36:3) together were the majority of the remaining molecular species of both PC and PE, and these metabolites are likely to be synthesized by the same machinery. EST for all of these enzymatic steps were identified, so the molecular informatics and metabolite profiles are consistent for the major phospholipid biosynthetic pathways in elongating cotton fiber cells.

The major molecular species of PI was 34:3, and the acylglycerol backbone could be synthesized using the same machinery for the major PC species described above. Less clear is
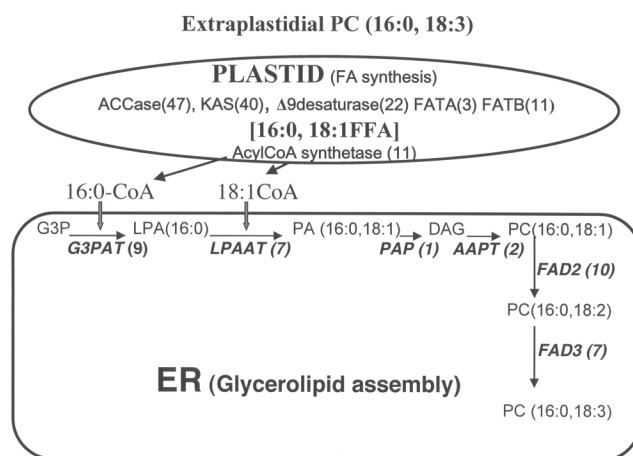
FIG. 6. Summary scheme for the cellular compartmentation and proposed pathway leading to the synthesis of PC 34:3 (16:0, 18:3), a major glycerolipid molecular species in both elongating and maturing fiber cells. The diagram is based on both metabolite profiles (Figs. 1–5) and expressed sequence tag (EST) occurrences (numbers in parentheses) for enzymes in these pathways (Table 1), and is consistent with the synthetic pathways described for extraplastidial PC in other types of plant cells (35). The FA are assembled *de novo* in the plastids of fiber cells and exported to the endoplasmic reticulum (ER) for glycerolipid assembly and subsequent modification (e.g., introduction of additional double bonds). The acylglycerol base for other phospholipids, such as PE and PI, can be synthesized using the same machinery. ACCase, acetyl-CoA carboxylase; KAS, ketoacyl ACP synthase; FatA, FA thioesterase A; FatB, FA thioesterase B; G3P, glycerol-3-phosphate; G3PAT, G3P acyltransferase; LPA, lysophosphatidic acid; LPAAT, LPA acyltransferase; PAP, PA phosphatase; AAPT, aminoalcohol phosphotransferase; FAD, FA desaturase. Numerical designations for FA represent total number of acyl carbons:total numbers of double bonds.

how the headgroup of PI is incorporated into this glycerolipid class. No EST were predicted to encode for PI synthase (or PS synthase), which uses CDP:DAG as a precursor. The DAG base could be derived from the PC or PE pathway, but the headgroup metabolism is unclear since no CDP:DAG transferase EST were identified. This is somewhat surprising given the particular abundance of PI in fiber cells, and may indicate that these enzymes have rare or substantially diverged messages not yet identified in these libraries, or that PI, PS, and perhaps even PG are produced *via* alternative pathways in cotton fiber cells.

From the lipid metabolite data, it is possible to make some predictions about how lipid metabolism may be directed in fiber cells as they shift from the rapid elongation phase to the maturation phase. For example, there was a significant reduction in PE 34:3 and PE 34:6, whereas there was an increase in PE 34:2 and a slight increase in PE 34:5. A similar increase was noted in PC 34:2 with a decrease in PC 36:6. These results suggest a reduction in FAD3 activity during the maturation phase and could impart a subtle change in membrane fluidity to fiber cells.

By combining lipid metabolite data with EST profiles it may be possible to identify lipid metabolic pathways important in fiber cells that have not been appreciated previously. For example, saturated FA such as 16:0 and 18:0 are important for

membrane stability, but they also may be elongated to very long-chain FA that serve as precursors for the biosynthesis of surface components such as waxes (27,37). A major amount of 16:0 FA was detected in fibers at all stages of elongation and maturation (Fig. 1). Moreover, an abundance of EST for FA elongation and wax biosynthesis enzymes indicated that elongating fibers may be actively involved in these processes and would certainly require the necessary acyl chain precursors.

Lipid profiling and EST data suggest that sterol metabolism may be important to cotton fiber development, as has been suggested by others (11). ASG levels were higher in maturing fiber cells than in elongating fiber cells (Fig. 3), and ASG is mostly associated with plasma membranes (10,38,39). Others have implicated SG in the biosynthesis of cellulose (11). EST were identified for several sterol/SG enzymes in the elongating fibers, and these represent excellent targets to test the importance of sterol-containing lipids in the shift of fiber cells from the synthesis of primary to secondary cell walls.

Likewise, lipid profiling and EST data may suggest that PLD plays a role in cotton fiber development. PLD EST were quite prevalent in elongating fiber libraries, and the rapid, albeit artifactual, production of PA in frozen fiber cell extracts suggests that there is a substantial capacity for PLD-mediated phospholipid metabolism in fiber cells. It is possible that this signifies that PLD has an important function in the normal development of cotton fiber cells. PLD are thought to interact with cytoskeletal filaments and to influence cell expansion (40–42), and their role in membrane trafficking in mammalian systems is well documented (43). Perhaps the results gleaned from these lipidomics approaches will prompt additional molecular and biochemical experiments to characterize the impact of surface lipids, sterol metabolism, lipid hydrolases, and the like on the development of cotton fibers.

To our knowledge these studies represent the first attempt to reconcile detailed lipid metabolite profiles and EST profiles from DNA databases for this unusual and economically important cell type. It is anticipated that these results will provide the basis for continued efforts to understand the coordinated regulation of cotton fiber development at the molecular, biochemical and physiological levels, and that this approach, originally applied to *Arabidopsis* seeds (17), will encourage additional efforts to integrate metabolic and genomics information to improve our understanding of the importance of lipid metabolism to plant cell growth and development.

ACKNOWLEDGMENTS

REFERENCES

1. Lang, A.G. (1938) Origin of Lint and Fuzz Hairs in Cotton, *J. Agric. Res. 56*, 507–521.
2. Basra, A.S., and Malik, P. (1984) Development of Cotton Fiber, *Int. Rev. Cytol. 89*, 65–109.
3. Ramsey, J.C., and Berlin, J.D. (1976) Ultrastructural Aspects of Early Stages in Cotton Fiber Elongation, *Am. J. Bot. 63*, 868–876.
4. Stewart, J.D. (1975) Fiber Initiation on the Cotton Ovule (*Gossypium hirsutum*), *Am. J. Bot. 62*, 723–730.
5. Schubert, A.M., Benedict, J.D., Berlin, J.D., and Kohel, R.J. (1973) Kinetics of Cell Elongation and Secondary Cell Wall Thickening, *Crop Sci. 13*, 704–709.
6. Kim, H.J., and Triplett, B.A. (2001) Cotton Fiber Growth *in planta* and *in vitro*. Models for Plant Cell Elongation and Cell Wall Biogenesis, *Plant Physiol. 127*, 1361–1366.
7. Somerville, C., Browse, J., Jaworski, J.G., and Ohlrogge, J.B. (2000) Lipids, in *Biochemistry & Molecular Biology of Plants* (Buchanan, B., Gruissem, W., and Jones, R., eds.), pp. 456–527, American Society of Plant Physiologists, Rockville, MD.
8. Welti, R., Li, M., Li, W., Sang, Y., Biesiada, H., Zhou, H.-E., Rajashekar, C., Williams, T., and Wang, X. (2002) Profiling Membrane Lipids in Plant Stress Response, *J. Biol. Chem. 277*, 31994–32002.
9. Christie, W.W. (1992) Detectors for High-Performance Liquid Chromatography of Lipids with Special Reference to Evaporative Light-Scattering Detection, in *Advances in Lipid Methodology—One*, pp. 239–271, The Oily Press, Ayr, Scotland.
10. Moreau, R.A., Powell, M.J., and Singh, V. (2003) Pressurized Liquid Extraction of Polar and Nonpolar Lipids in Corn and Oats with Hexane, Methylene Chloride, Isopropanol, and Ethanol, *J. Am. Oil Chem. Soc. 80*, 1063–1067.
11. Peng, L., Kawagoe, Y., Hogan, P., and Delmer, D. (2002) Sitosterol-β-glucoside as a Primer for Cellulose Synthesis in Plants, *Science 295*, 147–149.
12. Ji, S.J., Lu, Y.C., Feng, J.X., Wei, G., Li, J., Shi, Y.H., Fu, Q., Liu, D., Luo, J.C., and Zhu, Y.X. (2003) Isolation and Analyses of Genes Preferentially Expressed During Early Cotton Fiber Development by Subtractive PCR and cDNA Array, *Nucleic Acids Res. 31*, 2534–2543.
13. Song, P., and Allen, R. (1997) Identification of a Cotton Fiber Specific Acyl Carrier Protein cDNA by Differential Display, *Biochim. Biophys. Acta 1351*, 305–312.
14. Orford, S.J., and Timmis, J.N. (2000) Expression of a Lipid Transfer Protein Gene Family During Cotton Fiber Development, *Biochim. Biophys. Acta 1483*, 275–284.
15. Orford, S.J., and Timmis, J.N. (1997) Abundant mRNAs Specific to the Developing Cotton Fibre, *Theor. Appl. Genet. 94*, 909–918.
16. Ma, D.P., Tan, H., Si, Y., Creech, R.G., and Jenkins, J.N. (1995) Differential Expression of a Lipid Transfer Protein Gene in Cotton Fiber, *Biochim. Biophys. Acta 1257*, 81–84.
17. Beisson, F., Koo, A.J., Ruuska, S., Schwender, J., Pollard, M., Thelen, J.J., Paddock, T., Salas, J.J., Savage, L., Milcamps, A., *et al.* (2003) Arabidopsis Genes Involved in Acyl Lipid Metabolism. A 2003 Census of the Candidates, a Study of the Distribution of Expressed Sequence Tags in Organs, and a Web-Based Database, *Plant Physiol. 132*, 681–697.
18. Chapman, K.D., and Moore, T.S., Jr. (1993) *N*-Acylphosphatidylethanolamine Synthesis in Plants: Occurrence, Molecular Composition, and Phospholipid Origin, *Arch. Biochem. Biophys. 301*, 21–33.
19. Brugger, B., Erben, G., Sandhoff, R., Wieland, F.T., and Lehmann, W.D. (1997) Quantitative Analysis of Biological Membrane Lipids at the Low Picomole Level by Nano-Electrospray Ionization Tandem Mass Spectrometry, *Proc. Natl. Acad. Sci. USA 94*, 2339–2344.

20. Kim, Y.H., Choi, J.S., Yoo, J.S., Park, Y.M., and Kim, M.S. (1999) Structural Identification of Glycerolipid Molecular Species Isolated from Cyanobacterium *Synechocystis* sp. PCC 6803 Using Fast Atom Bombardment Tandem Mass Spectrometry, *Anal. Biochem. 267*, 260–270.

21. Welti, R., and Wang, X. (2004) Lipid Species Profiling: A High Throughput Approach to Identify Lipid Compositional Changes and Determine the Function of Genes Involved in Lipid Metabolism and Signaling, *Curr. Opin. Plant Biol. 7*, 337–344.

22. Salas, J.J., and Ohlrogge, J.B. (2002) Characterization of Substrate Specificity of Plant FatA and FatB Acyl-ACP Thioesterases, *Arch. Biochem. Biophys. 403*, 25–34.

23. Huynh, T.T., Pirtle, P.R., and Chapman, K.D. (2002) Expression of a *Gossypium hirsutum* cDNA Encoding a FatB Palmitoyl-Acyl Carrier Protein Thioesterase in *Eschericia coli, Plant Physiol. Biochem.* 40, 1–10.

24. Kinney, A. (1993) Phospholipid Head Groups, in *Lipid Metabolism in Plants* (Moore, T.S., ed.), pp. 259–284, CRC Press, Boca Raton, FL.

25. Goode, J.H., and Dewey, R.E. (1999) Characterization of Aminoalcoholphosphotransferases from *Arabidopsis thaliana* and Soybean, *Plant Physiol. Biochem. 37*, 445–457.

26. Joyard, J. (1993) Origin and Synthesis of Galactolipid and Sulfolipid Head Groups, in *Lipid Metabolism in Plants* (Moore, T.S., ed.), pp. 231–258, CRC Press, Boca Raton, FL.

27. Kunst, L., and Samuels, A.L. (2003) Biosynthesis and Secretion of Plant Cuticular Wax, *Prog. Lipid Res. 42*, 51–80.

28. Lynch, D.V. (1993) Sphingolipids, in *Lipid Metabolism in Plants* (Moore, T.S., ed.), pp. 285–308, CRC Press, Boca Raton, FL.

29. Amin, S.A., and Truter, E.V. (1972) Cotton Lipids: A Preliminary Survey, *J. Sci. Food Agric. 23*, 39–44.

30. Chapman, K.D. (1998) Phospholipase Activity During Plant Growth and Development and in Response to Environmental Stress, *Trends Plant Sci. 3*, 419–426.

31. Wang, X. (2000) Multiple Isoforms of Phospholipase D in Plants: The Gene Family, Catalytic and Regulatory Properties and Cellular Functions, *Prog. Lipid Res. 39*, 109–149.

32. Chapman, K.D. (2004) Occurrence, Metabolism, and Prospective Functions of *N*-Acylethanolamines in Plants, *Prog. Lipid Res. 43*, 302–327.

33. Graham, I.A., and Eastmond, P.J. (2002) Pathways of Straight and Branched Chain Fatty Acid Catabolism in Higher Plants, *Prog. Lipid Res. 41*, 156–181.

34. Ohlrogge, J.B., Jaworski, J.G., and Post-Beittenmiller, D. (1993) *De Novo Fatty Acid Biosynthesis*, CRC Press, Boca Raton, FL.

35. Ohlrogge, J.B., and Browse, J. (1995) Lipid Biosynthesis, *Plant Cell 7*, 957–970.

36. Frentzen, M. (1993) Acyltransferases and Triacylglycerols, in *Lipid Metabolism in Plants* (Moore, T.S., ed.), pp. 195–230, CRC Press, Boca Raton, FL.

37. Post-Beittenmiller, D. (1996) Biochemistry and Molecular Biology of Wax Production in Plants, *Annu. Rev. Plant Physiol. Plant Mol. Biol. 47*, 405–430.

38. Moreau, R.A., Powell, M.J., Whitaker, B.D., Bailey, B.A., and Anderson, J.D. (1994) Xylanase Treatment of Plant Cells Induces Glycosylation and Fatty Acylation of Phytosterols, *Physiol. Plant. 91*, 575–580.

39. Moreau, R., Whitaker, B.D., and Hicks, K.B. (2002) Phytosterols, Phytostanols, and Their Conjugates in Foods: Structural Diversity, Quantitative Analysis, and Health-Promoting Uses, *Prog. Lipid Res. 41*, 457–500.

40. Dhonukshe, P., Laxalt, A.M., Goedhart, J., Gadella, T.W., and Munnik, T. (2003) Phospholipase D Activation Correlates with Microtubule Reorganization in Living Plant Cells, *Plant Cell 15*, 2666–2679.

41. Gardiner, J., Collings, D.A., Harper, J.D., and Marc, J. (2003) The Effects of the Phospholipase D-Antagonist 1-Butanol on Seedling Development and Microtubule Organisation in *Arabidopsis*, *Plant Cell Physiol. 44*, 687–696.

42. Gardiner, J.C., Harper, J.D., Weerakoon, N.D., Collings, D.A., Ritchie, S., Gilroy, S., Cyr, R.J., and Marc, J. (2001) A 90-Kd Phospholipase D from Tobacco Binds to Microtubules and the Plasma Membrane, *Plant Cell 13*, 2143–2158.

43. Cockcroft, S. (2001) Signalling Roles of Mammalian Phospholipase D1 and D2, *Cell. Mol. Life Sci. 58*, 1674–1687.

Dietary α-Linolenic Acid Increases Brain but Not Heart and Liver Docosahexaenoic Acid Levels

**Gwendolyn Barceló-Coblijn[a], Lauren W. Collison[b],
Christopher A. Jolly[b], and Eric J. Murphy[a,c,*]**

[a]Department of Pharmacology, Physiology, and Therapeutics, University of North Dakota, Grand Forks,
North Dakota 58202-9037, [b]Division of Nutritional Science, University of Texas, Austin, Texas 78712,
and [c]Department of Chemistry, University of North Dakota, Grand Forks, North Dakota 58202-9037

ABSTRACT: Fish oil-enriched diets increase n-3 FA in tissue phospholipids; however, a similar effect by plant-derived n-3 FA is poorly defined. To address this question, we determined mass changes in phospholipid FA, individual phospholipid classes, and cholesterol in the liver, heart, and brain of rats fed diets enriched in flax oil (rich in 18:3n-3), fish oil (rich in 22:6n-3 and 20:5n-3), or safflower oil (rich in 18:2n-6) for 8 wk. In the heart and liver phospholipids, 22:6n-3 levels increased only in the fish oil group, although rats fed flax oil accumulated 20:5n-3 and 22:5n-3. However, in the brain, the flax and fish oil diets increased the phospholipid 22:6n-3 mass. In all tissues, these diets decreased the 20:4n-6 mass, although the effect was more marked in the fish oil than in the flax oil group. Although these data do not provide direct evidence for 18:3n-3 elongation and desaturation by the brain, they demonstrate that 18:3n-3-enriched diets reduced tissue 20:4n-6 levels and increased cellular n-3 levels in a tissue-dependent manner. We hypothesize, based on the lack of increased 22:6n-3 but increased 18:3n-3 in the liver and heart, that the flax oil diet increased circulating 18:3n-3, thereby presenting tissue with this EFA for further elongation and desaturation.

Paper no. L9709 in *Lipids 40*, 787–798 (August 2005).

In recent years, many health benefits of n-3 FA have been demonstrated (1,2). These benefits range from improved patient responsiveness to Li$^+$ treatment (3) to improvement in cardiovascular function (4). The premise that the n-3 FA EPA (20:5-n-3) and DHA (22:6n-3) are beneficial stems from two general lines of thought. (i) First, that n-3 FA esterified in membrane phospholipids modulate the biophysical environment of the membrane in such a way as to positively alter physiological function. The membrane order regulates very important processes such as signal transduction (5–7), release of synaptic

vesicles during synaptic transmission (8,9), and heart contraction (10). (ii) Second, that n-3 FA replace n-6 FA, arachidonic acid (20:4n-6) in particular, thereby reducing the potential release of 20:4n-6 under basal conditions and during pathophysiological insult. Mechanistically, this would effectively reduce the basal levels of proinflammatory eicosanoids as well as reduce levels released upon pathophysiological insult or during inflammatory conditions (11). To elevate n-3 cellular levels, it is necessary to increase n-3 dietary intake because mammals are not able to synthesize α-linolenic acid (18:3n-3), the precursor of the n-3 family. The accretion of higher-chain n-3 in tissue phospholipids may be dependent on the particular n-3 FA that is provided in the diet, e.g., 18:3n-3 or 20:5n-3/22:6n-3.

Two metabolic pathways for 18:3n-3 have been demonstrated. The β-oxidation pathway is considered the major catabolic route, as 60–85% of 18:3n-3 goes through this pathway (12,13). However, it is important to note that similar levels of β-oxidation occur with dietary 22:6n-3 (65%) and n-6 FA (50%) (13). Thus, the current idea that dietary 18:3n-3 is β-oxidized to a much greater extent than other dietary FA should be reexamined.

The second fate is the elongation and desaturation of 18:3-n-3 to 20:5n-3, 22:5n-3 (docosapentaenoic acid), and 22:6n-3. A number of studies in mammals demonstrate the effective conversion of 18:3n-3 into 20:5n-3 and 22:5n-3, including studies in rats (14,15), hamsters (16), guinea pigs (17), piglets (18), baboons (19), and humans (20,21). More controversial is the effectiveness of the conversion and accumulation of 22:6n-3 from dietary 18:3n-3 (22). Rats fed diets enriched in 18:3n-3 have a significant accumulation of 22:6n-3 in the brain compared with controls (17,23). Other studies with similar diets did not demonstrate an accumulation of 22:6n-3 in different rat body compartments (14) or in human plasma (21). Because a number of variables can modulate the efficiency of 18:3n-3 conversion to 22:6n-3, including the amount of 18:3n-3 ingested (16), the n-3 to n-6 ratio in the diet (23), and the dietary background of the animals prior to the study (15), it is important to compare, in a single study, the effects flax oil and fish oil diets on tissue n-3 accretion.

Western diets have considerably reduced the consumption of n-3 PUFA in favor of n-6 PUFA (24,25). There have been great efforts to promote fish oil incorporation into the Western diets, since it is considered the best source of 20:5n-3 and

22:6n-3. However, because there is a geographical restriction on the availability of marine sources of n-3 FA, plant-derived n-3 sources (rich in 18:3n-3) have wider availability. Hence, it is critical to have a more complete understanding of 18:3n-3 metabolism and the effectiveness of 18:3n-3 to enhance tissue 20:5n-3 and 22:6n-3 levels as compared with the effects of fish oil on the accretion of these same FA.

To address this question, we determined the effect of flax oil (rich in 18:3n-3) and fish oil (rich in 20:5n-3 and 22:6n-3) on the liver, heart, and brain phospholipid mass and phospholipid acyl chain mass using standard lipid analytical techniques. In both groups, 20:4n-6 mass was decreased in each tissue, although the magnitude of the reduction was less in the flax group than in the fish group. These results clearly indicate that 18:3n-3 was elongated, desaturated, and accumulated and that these processes were highly tissue dependent.

MATERIALS AND METHODS

Animals. Four-month-old male, Sprague-Dawley rats, previously maintained on an n-3 FA-sufficient diet (18:3n-3, 7.0% total FA), were randomly assigned to diets containing either safflower oil (*n* = 5/group), flax oil (*n* = 5/group), or fish oil (*n* = 5/group). Rats were housed under a 12-h light–dark cycle and had free access to diets and water. Following 8 wk of feeding, the rats were euthanized with CO_2, and the brains, hearts, and livers were rapidly removed and frozen in liquid nitrogen. All procedures were approved by the University of Texas Animal Use and Care Committee.

Diets. Diet ingredients were purchased from Dyets, Inc. (Bethlehem, PA), prepared fresh each week and maintained at 4°C. Isocaloric diets were designed to meet the nutritional requirements of rats as determined by the American Institute of Nutrition (26). Diets contained 200 g/kg soy protein, 300 g/kg dextrose, 310 g/kg cornstarch, 35 g/kg cellulose, 100 g/kg lipid, 2 g/kg choline, 1.5 g/kg DL-methionine, 1.5 g/kg L-cysteine, 1.3 g/kg α-tocopherol, 1.2 g/kg γ-tocopherol, 1 g/kg TBHQ, 35 g/kg mineral mix (AIN-93M-MX), and 15 g/kg vitamin mix (AIN-93-VX). The composition of the vitamin and mineral mix has been reported in detail elsewhere (26). Rats were fed one of three semipurified diets differing only in lipid content: (i) 10% w/w safflower oil (safflower) enriched in linoleic acid, (ii) 3% safflower plus 7% flaxseed oil (flax) enriched in 18:3n-3, and (iii) 3% safflower plus 7% fish oil (fish) enriched in 20:5n-3 and 22:6n-3 (Table 1).

Lipid extraction. Tissues were pulverized under liquid nitrogen temperatures to a fine homogeneous powder, and lipids were extracted using *n*-hexane/2-propanol (3:2 vol/vol) (27,28). Tissue extracts were centrifuged at $1,000 \times g$ to pellet debris. The lipid containing the liquid phase was decanted and stored under nitrogen at −80°C until analysis.

TLC. Individual phospholipid classes and neutral lipids were separated by TLC. Whatman silica gel-60 plates (20 × 20 cm, 250 μm) were heat-activated at 110°C for 1 h, and samples were streaked onto the plates. Phospholipids were separated using chloroform/methanol/acetic acid/water (55:37.5:3:2 by

TABLE 1
FA Composition of the Experimental Diets[a]

	% Total FA		
FA	Safflower oil	Flax oil	Fish oil
14:0	—	—	12.43
16:0	—	4.89	20.03
16:1n-7	ND	ND	13.77
18:0	1.56	1.65	2.04
18:1n-9	13.19	14.46	8.71
18:2n-6	78.95	22.29	17.53
18:3n-3	Trace	56.71	ND
20:5n-3	—	—	13.63
22:6n-3	—	—	11.85

[a]The three experimental groups were 10% (w/w) safflower oil, 7% flax oil plus 3% safflower oil, and 7% fish oil plus 3% safflower oil. Safflower was added to the flax and fish oil diets as a source of linoleic acid to prevent EFA deficiency. ND, not detected. Additional information regarding the composition of these diets is provided in the Materials and Methods section.

vol) (29). This method separates all the major phospholipids. Neutral lipids were separated in petroleum ether/diethyl ether/acetic acid (75:25:1.3 by vol) (30). This solvent system resolves cholesteryl esters, DAG, nonesterified FA, and TAG. Lipid fractions were identified using authentic standards (Doosan-Serday, Englewood Cliffs, NJ, and Nu-Chek-Prep, Elysian, MN).

Plasmalogen analysis. The plasmalogen mass was determined following separation of individual phospholipid classes in the heart and brain lipid extracts by HPLC (31). One-half of the choline glycerophospholipid (ChoGpl) and ethanolamine glycerophospholipid (EtnGpl) fractions were dried under nitrogen and subjected to mild acidic hydrolysis followed by separation using HPLC (32). The proportion of plasmalogen determined following this separation was used to calculate the plasmalogen mass using the EtnGpl and ChoGpl masses determined following separation by TLC, as reported above.

Phosphorus and cholesterol assay. The phospholipid mass was determined by assaying for the lipid phosphorus content of individual lipid classes separated by TLC as described above (33). The cholesterol and cholesteryl ester masses were assayed using an iron-binding assay after separation by TLC as described previously (34).

FA analysis. The ChoGpl, EtnGpl, phosphatidylinositol (PtdIns), and phosphatidylserine (PtdSer) fractions were subjected to base-catalyzed transesterification, converting the phospholipid acyl chains to FAME. To each fraction, 2 mL of 0.5 M KOH dissolved in anhydrous methanol was added (35). FAME were extracted from the methanol using 2 mL of *n*-hexane, and the *n*-hexane phase containing the FAME was removed. The lower phase was reextracted two more times with 3 mL of *n*-hexane, and these washes were combined with the original aliquot.

Individual FA were separated by GLC using an SP-2330 column (0.32 mm i.d. × 30 m length) and a Trace GLC (ThermoElectron, Austin, TX) equipped with dual autosamplers and dual FID. FA were quantified using a standard curve from commercially purchased standards (Nu-Chek-Prep) and 17:0 was used as the internal standard.

Statistics. Statistical analysis was done using Instat2 from GraphPad (San Diego, CA). Statistical significance was assessed using one-way ANOVA and the Student–Newman–Keuls post-test, with $P < 0.05$ considered to be statistically significant.

RESULTS

Effect of n-3 dietary PUFA on individual phospholipid masses. The total phospholipid mass was not altered as a function of diet in any of the three tissues analyzed; however, some individual phospholipid classes were changed (Table 2). In rats fed fish oil, the liver EtnGpl mass was decreased 23% and the sphingomyelin (CerPCho) mass was increased 1.1-fold as compared with the control (see the Materials and Methods section). In hearts, the EtnGpl mass was decreased 19% in the fish oil group, whereas in this same group the CerPCho and phosphatidic acid (PtdOH) masses were increased 1.3- and 1.6-fold, respectively, as compared with the control (safflower oil). In the flax oil group, the heart PtdSer mass was decreased 23% as compared with the control. In the brain, the Ptd$_2$Gro and PtdIns masses were decreased 33 and 10%, respectively, in the flax oil group, whereas the PtdOH and PtdIns masses were increased

1.5- and 1.1-fold, respectively, in the fish oil group. Hence, there were subtle changes in individual phospholipid masses induced by flax oil or fish oil feeding that differed depending on the tissue analyzed.

Effect of n-3 dietary PUFA on phospholipid subclasses. The brain and heart have considerable amounts of ethanolamine (PlsEtn) and choline plasmalogens (PlsCho) (36–39), and fish oil diets may increase the plasmalogen mass (40). We did not find any significant difference in brain plasmalogens between groups (Table 3); however, the heart PlsEtn mass was decreased by 25% in the fish oil group, but PlsCho was unchanged. These results indicate a moderate effect of dietary n-3 FA on modulating the heart plasmalogen mass.

Effect of n-3 dietary PUFA on cholesterol levels. Cholesterol is an important component of the membranes, and its content may be affected by changes in dietary FA (41). In the liver, the cholesterol mass was not affected in the flax oil group, whereas it was decreased by 21% in the fish oil group (Table 4). This change in cholesterol mass caused a significant 25% decrease in the cholesterol-to-phospholipid ratio. In the fish oil group, the heart cholesterol mass was decreased by 10%, but this change did not alter the cholesterol-to-phospholipid ratio. In

TABLE 2
Phospholipid Mass Changes in Brain, Heart, and Liver Tissues[a]

	Safflower oil (nmol/g ww)		Flax oil (nmol/g ww)		Fish oil (nmol/g ww)	
	Mean	SD	Mean	SD	Mean	SD
Liver						
CerPCho	3032	265	3,084	185	3,390	169*,**
ChoGpl	13,788	1,075	14,050	1,312	14,530	711
PtdSer	800	71	830	68	807	100
PtdIns	2,010	177	2,200	220	2,278	317
EtnGpl	4,285	548	3,809	351	3,300	385*
PtdOH	536	31	463	67	594	129
Ptd$_2$Gro	1,473	121	1,641	161	1,639	53
Total	25,428	1,592	26,120	2,245	26,537	1,348
Heart						
CerPCho	2,326	195	2,221	178	3,032	279*,**
ChoGpl	9,439	211	9,063	511	8,984	559
PtdSer	737	49	564	56*	745	66**
PtdIns	1,023	51	955	93	1,029	87
EtnGpl	6,089	513	6,322	314	4,930	699*,**
PtdOH	276	21	296	32	432	36*,**
Ptd$_2$Gro	1,639	71	1,623	110	1,649	265
Total	20,614	1,131	20,704	1,609	20,542	1,293
Brain						
CerPCho	7,049	326	7,545	263	7,062	381
ChoGpl	20,048	1,038	20,253	753	20,850	579
PtdSer	6,046	985	5,977	424	6,390	416
PtdIns	2,340	160	2,086	167*	2,577	131*,**
EtnGpl	16,479	3,568	16,596	647	16,424	1,893
PtdOH	1,722	243	1,689	102	2,606	160*,**
Ptd$_2$Gro	1,430	106	956	102*	1,373	53**
Total	55,000	4,868	55,351	2,695	57,131	3,092

[a]Values are expressed as mass (nmol/g ww) and represent mean ± SD, $n = 4$–5. The asterisk (*) indicates a significant effect of the experimental oils (flax and fish) as compared with the control ($P < 0.05$), and the double asterisk (**) indicates a significant effect of the fish oil vs. flax oil. CerPCho, sphingomyelin; ChoGpl, choline glycerophospholipids; PtdSer, phosphatidylserine; PtdIns: phosphatidylinositol; EtnGpl, ethanolamine glycerophospholipids; PtdOH, phosphatidic acid; Ptd$_2$Gro, cardiolipin.

TABLE 3
Plasmalogen Mass Changes in Heart and Brain Tissues[a]

	Safflower oil (nmol/g ww)		Flax oil (nmol/g ww)		Fish oil (nmol/g ww)	
	Mean	SD	Mean	SD	Mean	SD
Heart						
PakEtn + PtdEtn	4,246	382	5,083	489*	3,329	572*,**
PlsEtn	1,664	244	1,409	107	1,249	267*
PakCho + PtdCho	8,408	663	7,764	1,131	8,364	424
PlsCho	717	158	642	148	7,35	135
Brain						
PakEtn + PtdEtn	7,452	1,501	7,777	491	7,818	798
PlsEtn	9,027	2,077	8,818	427	8,605	1,118
PakCho + PtdCho	18,250	1,864	18,091	277	18,741	364
PlsCho	1,797	993	2,162	665	2,109	394

[a]Values are expressed as mass (nmol/g ww) and represent mean ± SD, $n = 4$–5, for each experimental oil. The asterisk (*) indicates a significant effect of the experimental oils (flax and fish) as compared with the control ($P < 0.05$), and the double asterisk (**) indicates a significant effect of the fish oil vs. flax oil. PakEtn, 1-*O*-alkyl-2-acyl-*sn*-glycero-3-phospho-ethanolamine; PtdEtn, phosphatidylethanolamine; PlsEtn, 1-*O*-alkyl-1′-enyl-2-acyl-*sn*-glycero-3-phosphoethanolamine; PakCho, 1-*O*-alkyl-2-acyl-*sn*-glycero-3-phosphocholine; PtdCho, phosphatidylcholine; PlsCho, 1-*O*-alkyl-1′-enyl-2-acyl-*sn*-glycero-3-phosphocholine.

the flax oil group, the brain cholesterol mass was decreased by 17%; consequently, the cholesterol-to-phospholipid ratio was decreased by 17%. In the fish oil group, the brain cholesterol and the cholesterol-to-phospholipid ratio were unchanged.

Effect of n-3 dietary PUFA on the FA mass. The dietary FA content markedly affected the FA mass of EtnGpl, ChoGpl, PtdSer, and PtdIns from the brain, heart, and liver. However, dietary modulation can enhance the formation of other FA not normally found in tissues. For instance, an increase in the 22:5n-6 (docosapentaenoic acid n-6) mass is indicative of n-3 FA-deficient diets (42,43). In the safflower oil group (control), the total brain phospholipids contained a minor amount of 22:5n-6 (0.7% of total FA), similar to that reported for the n-3-sufficient control diets, where 22:5n-6 comprised 0.5 to 0.9% of the total brain phospholipid FA (42,43). Thus, using this parameter, our control group was considered adequate in n-3 FA. Similarly, the absence of 20:3n-9 (Mead acid) indicates that these diets did not produce n-6-deficient rats.

Liver FA changes. The flax oil group accumulated 22:6n-3 only in PtdSer (1.8-fold), but accumulated 20:5n-3 and 22:5n-3 at levels similar to or even higher than those in the fish oil group in the four phospholipid classes (Table 5). In addition, 18:3n-3 was accumulated in EtnGpl and ChoGpl. The arachidonic acid (20:4n-6) mass was decreased by 48% in EtnGpl, 51% in ChoGpl, and 27% in PtdSer but was unaltered in PtdIns. In the fish oil group, 22:6n-3 accumulated in the four individual phospholipid classes (Table 5). The DHA mass was increased 3.0-fold in EtnGpl, 4.4-fold in ChoGpl, 5.0-fold in PtdSer, and 2.2-fold in PtdIns. Consequently, there was a large reduction in 20:4n-6 in each of these phospholipids. In EtnGpl, the reduction was significantly larger than that observed in the flax oil group, 74% vs. 48%. The decrease was lower but still considerable in ChoGpl (56%), PtdSer (49%), and PtdIns (32%). In EtnGpl, the linoleic acid (18:2n-6) mass was decreased by 50%, which is important because it is the precursor for 20:4n-6. In summary, the flax oil diet increased the 18:3n-3,

TABLE 4
Cholesterol Mass Changes in Liver, Heart, and Brain Tissues[a]

	Safflower oil		Flax oil		Fish oil	
	Mean	SD	Mean	SD	Mean	SD
	Cholesterol mass (nmol cholesterol/g ww)					
Liver	5,147	357	4,867	334	4,075	332*,**
Heart	4,308	334	4,053	152	3,849	122*
Brain	42,159	3,584	35,262	807*	45,655	3,545**
	Cholesterol/phospholipid ratio					
Liver	0.20	0.02	0.19	0.01	0.15	0.01*,**
Heart	0.21	0.01	0.20	0.02	0.19	0.02
Brain	0.80	0.03	0.66	0.02*	0.79	0.03**

[a]Values are expressed as mass (nmol/g ww) and represent mean ± SD, $n = 4$–5, for each experimental oil. The asterisk (*) indicates a significant effect of the experimental oils (flax and fish) as compared with the control ($P < 0.05$), and the double asterisk (**) indicates a significant effect of the fish oil vs. flax oil.

TABLE 5
Effects of Diets on n-3 FA Masses in Individual Phospholipid Classes in Rat Liver Tissue[a]

FA	Safflower oil Mean	SD	Flax oil Mean	SD	Fish oil Mean	SD
	EtnGpl (nmol/g ww)					
16:0	1,871	287	1,378	97*	1,576	199*
18:0	2,167	215	1,989	148	1,552	229*,**
Total saturated	4,038	490	3,367	232*	3,128	420*
18:1n-9	287	50	355	78	127	20*,**
18:1n-7	310	59	196	47*	149	25*
Total MUFA	597	90	551	125	276	40*,**
18:2n-6	784	130	837	171	380	84*,**
20:4n-6	2,401	358	1,255	185*	611	112*,**
22:5n-6	138	18	6	1*	20	2*
Total n-6 PUFA	3,443	483	2,098	343*	1,011	192*,**
18:3n-3	ND	—	146	23*	ND	—
20:5n-3	ND	—	502	64*	453	102*
22:5n-3	126	33	455	19*	299	65*,**
22:6n-3	493	116	504	18	1,453	60*,**
Total n-3 PUFA	619	124	1,607	100*	2,205	152*,**
n-3/n-6 ratio	0.18	0.03	0.77	0.07*	2.18	0.38*,**
	ChoGpl (nmol/g ww)					
16:0	8,031	679	7,912	643	9,933	540*,**
18:0	4,372	325	4,747	593	4,082	308
Total saturated	12,403	941	12,659	1,116	14,015	775*,**
16:1	392	53	300	67*	619	30*,**
18:1n-9	836	107	1,306	156*	961	74**
18:1n-7	944	115	669	131*	730	70*
Total MUFA	2,172	142	2,275	341	2,310	41
18:2n-6	4,180	323	6,198	793*	3,869	253**
20:3n-6	175	29	227	24	241	22
20:4n-6	7,654	590	3718	557*	3,337	231*
22:5n-6	151	16	6	2*	33	2*
Total n-6 PUFA	12,160	822	10,149	1,324*	7,480	477*,**
18:3n-3	ND	—	517	53*	ND	—
20:5n-3	ND	—	1,315	220*	2,100	151*,**
22:5n-3	79	14	449	35*	427	80*
22:6n-3	627	47	771	116	2,789	320*,**
Total n-3 PUFA	706	61	3,052	393*	5,316	321*,**
n-3/n-6 ratio	0.06	0.01	0.30	0.04*	0.71	0.06*,**
	PtdSer (nmol/g ww)					
16:0	276	26	222	41*	251	21
18:0	877	93	868	68	786	95
Total saturated	1,153	112	1,090	102	1,037	97
18:2n-6	88	10	98	18	78	10
20:4n-6	314	80	230	37*	159	47*
22:5n-6	16	6	3	0*	7	2*,**
Total n-6 PUFA	418	86	331	47	244	56*,**
20:5n-3	ND	—	60	17*	45	6*,**
22:5n-3	ND	—	99	33*	71	22*
22:6n-3	45	15	82	20*	224	33*,**
Total n-3 PUFA	45	15	241	49*	340	54*,**
n-3/n-6 ratio	0.11	0.03	0.73	0.09*	1.39	0.17*,**
	PtdIns (nmol/g ww)					
16:0	474	77	529	68	469	100
18:0	1,746	195	2,378	455*	1,690	362**
Total saturated	2,220	226	2,907	517*	2,159	460**
18:1n-7	62	15	119	25*	48	11**
Total MUFA	62	15	119	25*	48	11**
18:2n-6	146	30	218	40*	107	25**
20:3n-6	60	30	135	24*	91	27**
20:4n-6	1,385	138	1,625	449	945	196*,**
Total n-6 PUFA	1,591	164	1,978	501	1,143	240**
20:5n-3	ND	—	98	27*	71	17*,**
22:5n-3	ND	—	164	41*	128	37*
22:6n-3	146	79	182	38	327	108*,**
Total n-3 PUFA	146	79	444	80*	526	156*
n-3/n-6 ratio	0.10	0.06	0.22	0.01*	0.46	0.06*,**

[a]Values are expressed as mass (nmol/g ww) and represent mean ± SD, $n = 4–5$, for each experimental oil. The asterisk (*) indicates a significant effect of the experimental oils (flax and fish) as compared with the control ($P < 0.05$), and the double asterisk (**) indicates a significant effect of the fish oil vs. flax oil. For abbreviations see Tables 1 and 2.

20:5n-3, and 22:5n-3 masses, whereas the fish oil diet increased the 20:5n-3, 22:5n-3, and 22:6n-3 masses; both lowered 20:4-n-6, although the effect was more marked in the fish oil group than in the flax oil group.

Although large changes were not found in saturated FA in ChoGpl, PtdSer, and PtdIns, the total saturated mass was decreased by 20% in EtnGpl in both experimental diets. In the fish oil group, the total MUFA mass decreased by 54% in Etn-Gpl, whereas in the flax oil group, it was increased 1.9-fold in PtdIns. Although the total PUFA mass (i.e., n-3 plus n-6 FA mass) was not altered by the diet, there were robust changes in the n-3 to n-6 ratio in all the individual phospholipid classes. The increase was higher in the fish oil than in the flax oil group, particularly in EtnGpl (12-fold vs. 4.3-fold), ChoGpl (12-fold vs. 5-fold), and PtdSer (12.6-fold vs. 6.6-fold) and to a lesser degree in PtdIns (4.6-fold vs. 2.2-fold).

Heart FA changes. The pattern of changes in the FA mass of heart tissue was similar to those observed in the liver tissue (Table 6). In the flax oil group, the 22:6n-3 mass was not increased in any of the phospholipid classes analyzed. Nonetheless, the 20:4n-6 mass was decreased by 33% in ChoGpl and 55% in PtdSer in the flax oil group. Interestingly, this group had increased the 22:5n-3 and 20:5n-3 masses above those observed in the fish oil group. Similar to the liver, 18:3n-3 was accumulated in EtnGpl and ChoGpl in the flax oil group. In the fish oil group, the 22:6n-3 mass was increased in all the phospholipid classes, 2.4-fold in EtnGpl, 5.4-fold in ChoGpl, 2.1-fold in PtdSer, and 3.7-fold in PtdIns. Consistent with this increase in the 22:6n-3 mass, the 20:4n-6 mass was dramatically decreased by 73% in EtnGpl, 31% in ChoGpl, and 46% in PtdSer. In addition, the 18:2n-6 mass was decreased by 71% in EtnGpl and 44% in ChoGpl. Therefore, in the heart tissue, the flax oil diet increased the 18:3n-3, 20:5n-3, and 22:5n-3 masses, whereas the fish oil diet increased the 20:5n-3, 22:5n-3, and 22:6n-3 masses. Thus, both experimental diets provoked an increase in the total n-3 FA mass. Conversely, the fish oil diet, and to a lesser extent the flax oil diet, reduced the total n-6 FA mass.

There were no significant changes in the saturated and monounsaturated FA masses in any of the individual phospholipid classes as a function of diet, except in the fish oil group, where the EtnGpl 18:1n-9 (oleic acid) mass was reduced by 45%. The total PUFA mass was not altered by the experimental diets, although very important changes occurred in the n-3 to n-6 ratio. Similar to the liver, these changes were more profound in the fish oil than in the flax oil group. The flax oil diet increased the n-3 to n-6 ratio in the four phospholipid classes between 2- and 3-fold, whereas it was increased 5- to 10-fold in the fish oil group.

Brain FA changes. Both experimental diets increased the mass of n-3 FA (Table 7), with a marked increase in 22:6n-3. In the flax oil group, the 22:6n-3 mass in EtnGpl and ChoGpl was increased 1.2-fold, and 22:5n-3 was accumulated in Etn-Gpl, ChoGpl, and PtdSer. In the same group, the 20:4n-6 mass was reduced by 12% in ChoGpl but was not affected in the rest of the individual phospholipid classes analyzed. In the fish oil group, the 22:6n-3 mass was increased 1.4-fold in EtnGpl and

ChoGpl, 1.3-fold in PtdSer, and 1.5-fold in PtdIns. There was an accumulation of 22:5n-3 similar to that observed in the flax oil group. The 20:4n-6 mass was reduced by 25% in EtnGpl and 17% in ChoGpl. Interestingly, the 20:4n-6 mass in PtdIns was increased 1.2-fold in the fish oil group. Thus, the flax oil and fish oil diets increased the 22:5n-5 and 22:6n-3 masses, increasing the total n-3 FA in brain tissue. The total mass of n-6 FA was reduced in both experimental groups, but to a greater extent in the fish oil group than in the flax oil group.

No major changes occurred in the total saturated and unsaturated FA masses in any of the four phospholipid classes analyzed. The total PUFA mass was not altered, although the n-3-to-n-6 ratio was increased 1.5- to 2.0-fold by either diet in EtnGpl, ChoGpl, and PtdSer.

DISCUSSION

At present, at least four possible mechanisms for the positive effects of n-3 FA on health have been proposed, including: (i) alteration of the membrane order; (ii) substitution of n-3 FA for n-6 FA and, consequently, a decrease in the production of proinflammatory derivatives; (iii) alteration of the gene expression; and (iv) direct generation of second messengers (44–47). None of these provides a mechanism of action for a particular FA that would exclude the rest. Hence, the accumulation of 18:3n-3 or any of its conversion products, 20:5n-3, 22:5n-3, and 22:6n-3, might have potentially beneficial effects on health.

In human trials, plant-derived n-3 FA have demonstrated beneficial effects on health. Diets enriched in 18:3n-3 reduce cardiovascular risk factors (48), decrease the estimated risk of ischemic heart disease (49), and lower plasma TAG concentrations (50). However, these diets do not increase 22:6n-3 content in the plasma (21,51), membrane erythrocytes (21), and neutrophils (20). This lack of 22:6n-3 accumulation and the high estimated percentage lost in β-oxidation (12,52) are the main arguments used to challenge the health benefits of 18:3n-3-enriched diets. However, it is important to note that dietary FA, including 22:6n-3, are oxidized to a similar extent as 18:3n-3 (13).

In this study, we showed that increased dietary 18:3n-3 intake leads to a significant accumulation of the 18:3n-3, 20:5n-3, and 22:5n-3 masses in heart and liver phospholipids, but 22:6n-3 was not increased. Depending on the tissue and phospholipid class, the accumulation of 18:3n-3, 20:5n-3, and 22:5n-3 was higher in the flax group than in rats fed fish oil. These results are in agreement with other studies in different mammals fed 18:3n-3-enriched diets in which 18:3n-3 is efficiently converted to 22:5n-3, but none of them show an accumulation of 22:6n-3 (14–18). In our study, 22:6n-3 was accumulated in the liver and heart only in the fish oil diet group, where the phospholipid 22:6n-3 mass was dramatically increased (Tables 5, 6). Because 18:3n-3 is not converted to 22:6n-3 in the plasma, but rather is found as 18:3n-3, 20:5n-3, and 22:5n-3 (15, 16,21,48,51), our findings suggest that the FA compositions of the liver and heart more closely reflect the FA composition of the plasma compartment.

TABLE 6
Effects of Diets on n-3 FA Masses in Individual Phospholipid Classes in Rat Heart Tissue[a]

	Safflower oil		Flax oil		Fish oil	
	Mean	SD	Mean	SD	Mean	SD
EtnGpl (nmol/g ww)						
16:0	661	50	806	125	661	134
18:0	3,123	298	3,678	392*	2,460	403*,**
Total saturated	3,784	317	4,484	511*	3,121	534*,**
18:1n-9	381	26	614	46*	169	43*,**
18:1n-7	240	8	225	18	174	33
Total MUFA	621	32	839	63*	343	75*,**
18:2n-6	1,361	183	1,297	152	395	90*,**
20:4n-6	2,728	308	2,574	95	742	181*,**
22:5n-6	271	55	18	5*	58	13*
Total n-6 PUFA	4,360	476	3,889	216	1,195	282*,**
18:3n-3	ND	—	159	20*	ND	—
20:5n-3	ND	—	115	7*	180	36*,**
22:5n-3	212	25	774	204*	274	83**
22:6n-3	1,252	201	1,332	191	2,987	467*,**
Total n-3 PUFA	1464	219	2,380	312*	3,441	557*,**
n-3/n-6 ratio	0.34	0.04	0.61	0.06*	2.87	0.26*,**
ChoGpl (nmol/g ww)						
16:0	3,603	309	3,075	534	4,168	360**
18:0	4,190	389	4,551	626	4,333	530
Total saturated	7,793	600	7,626	1,138	8,501	858
16:1	69	16	36	7*	138	18*,**
18:1n-9	679	87	865	133*	535	61*,**
18:1n-7	833	75	624	91*	895	129**
Total MUFA	1,581	173	1,525	221	1,568	183
18:2n-6	3,568	592	3,402	539	1,984	325*,**
20:4n-6	4,049	380	2,701	332*	2,807	330*
22:5n-6	66	14	8	2*	40	6*,**
Total n-6 PUFA	7,683	611	6,111	840*	4,831	652*,**
18:3n-3	ND	—	253	41*	ND	—
20:5n-3	ND	—	102	14*	441	81*,**
22:5n-3	101	17	523	144*	392	47*,**
22:6n-3	442	84	413	75	2,401	212*,**
Total n-3 PUFA	543	99	1,290	203*	3,249	327*,**
n-3/n-6 ratio	0.07	0.01	0.21	0.03*	0.67	0.06*,**
PtdSer (nmol/g ww)						
16:0	73	19	69	14	136	39*,**
18:0	803	56	623	59	756	171
Total saturated	876	55	692	80	892	190
18:1n-7	73	6	75	6	78	18
Total MUFA	73	6	75	6	78	18
18:2n-6	115	16	78	10*	92	31
20:4n-6	214	28	97	18*	116	24*
22:5n-6	63	17	ND	—	14	1*,**
Total n-6 PUFA	392	46	175	18*	222	55*
22:5n-3	ND	—	86	6*	117	45*
22:6n-3	170	21	95	28	355	97*,**
Total n-3 PUFA	170	21	181	26	472	129*,**
n-3/n-6 ratio	0.43	0.05	1.03	0.06*	2.13	0.26*,**
Ptdlns (nmol/g ww)						
16:0	280	33	223	35*	293	53**
18:0	660	81	655	101	701	76
Total saturated	940	75	878	123	994	80
18:1n-9	87	17	118	10*	84	10**
18:1n-7	125	11	91	19*	143	10**
Total MUFA	212	23	209	28	231	7
18:2n-6	224	39	174	28*	173	10*
20:4n-6	492	33	446	56	410	70
22:2n-6	101	37	96	49	55	3
Total n-6 PUFA	817	55	716	68	721	154
18:3n-3	ND	—	23	4*	ND	—
22:5n-3	ND	—	44	12*	36	11*
22:6n-3	29	9	39	12	1,039	251*,**
Total n-3 PUFA	29	9	106	23*	158	41*,**
n-3/n-6 ratio	0.04	0.01	0.15	0.02*	0.22	0.03*,**

[a]Values are expressed as mass (nmol/g ww) and represent mean ± SD, n = 4–5, for each experimental oil. The asterisk (*) indicates a significant effect of the experimental oils (flax and fish) as compared with the control ($P < 0.05$), and the double asterisk (**) indicates a significant effect of the fish oil vs. flax oil. For abbreviations see Tables 1 and 2.

TABLE 7
Effects of Diets on n-3 FA Masses in Individual Phospholipid Classes in Rat Brain Tissue[a]

	Safflower oil		Flax oil		Fish oil	
	Mean	SD	Mean	SD	Mean	SD
			EtnGpl (nmol/g ww)			
16:0	1,464	275	1,512	63	1,333	152
18:0	5,254	941	5,156	211	4,906	376
20:0	92	38	64	10	68	23
Total saturated	6,810	1,224	6,732	214	6,307	496
18:1n-9	5,003	1,345	5,304	298	5,546	1,326
18:1n-7	1,902	587	1,909	120	1,728	396
20:1n-9	1,039	389	993	169	898	206
Total MUFA	7,944	2,317	8,206	445	8,172	1,839
18:2n-6	113	26	132	6	94	15**
20:3n-6	112	29	109	11	119	16
20:4n-6	3,465	608	3,030	172	2,608	254*
22:4n-6	1,418	303	1,161	88	989	128*
22:5n-6	314	62	115	8*	109	19*
Total n-6 PUFA	5,422	1,010	4,547	244	3,919	401*
20:5n-3	ND	—	ND	—	ND	—
22:5n-3	ND	—	190	10*	214	24*,**
22:6n-3	4,073	628	4,778	402*	5,574	298*,**
Total n-3 PUFA	4,073	628	4,968	408*	5,788	319*,**
n-3/n-6	0.75	0.04	1.09	0.06*	1.47	0.08*,**
			ChoGpl (nmol/g ww)			
16:0	17,471	1,350	17,314	867	18,086	1,100
18:0	5,238	393	5,309	259	5,407	168
Total saturated	22,709	1297	22,623	747	23,493	949
16:1	170	22	161	12	214	15*,**
18:1n-9	8,159	691	8,270	321	8,958	374**
18:1n-7	2,501	210	2,480	82	2,596	169
20:1n-9	423	78	432	43	438	104
Total MUFA	11,253	982	11,343	437	12,206	626
18:2n-6	407	22	493	34*	360	14*,**
20:4n-6	2,458	238	2,157	59*	2,041	80*
22:4n-6	243	27	199	16*	152	15*,**
22:5n-6	91	11	21	4*	21	5*
Total n-6 PUFA	3,199	290	2,870	108	2,574	215*,**
22:5n-3	ND	—	102	51*	106	79*
22:6n-3	1,157	108	1,351	89*	1,673	79*,**
Total n-3 PUFA	1,157	108	1,453	134*	1,779	131*,**
n-3/n-6	0.36	0.04	0.51	0.03*	0.70	0.06*,**
			PtdSer (nmol/g ww)			
16:0	177	37	165	37	147	17
18:0	5,656	860	5,216	268	5,499	291
20:0	62	17	51	4	65	18
22:0	93	21	70	9	93	26
Total saturated	5,988	951	5,502	284	5,804	317
18:1n-9	2,270	512	2,338	180	2,578	445
18:1n-7	310	77	300	21	330	77
20:1n-9	371	135	328	48	314	64
22:1n-9	71	23	43	24	71	21
Total MUFA	3,022	754	3,009	224	3,293	699
20:4n-6	408	108	354	29	332	33
22:4n-6	361	64	297	17*	251	30*
22:5n-6	238	44	95	14*	98	12*
Total n-6 PUFA	1,007	205	746	33*	681	70*
20:5n-3	ND	—	ND	—	ND	—
22:5n-3	ND	—	69	8*	72	11*
22:6n-3	2,149	288	2,437	184	2,826	326*
Total n-3 PUFA	2,149	288	2,506	190*	2,898	335*
n-3/n-6	2.13	0.25	3.36	0.67*	4.26	0.62*
			PtdIns (nmol/g ww)			
16:0	418	101	423	96	478	36
18:0	1,781	270	1,517	137*	1,904	83**
Total saturated	2,199	317	1,940	169	2,382	117**
18:1n-9	204	38	216	11	262	26*,**
18:1n-7	90	18	91	7	113	14**
Total MUFA	294	55	307	17	375	40*,**
20:4n-6	1,730	252	1,726	167	2,134	115*,**
Total n-6 PUFA	1,730	252	1,726	167	2,134	115*,**
22:6n-3	171	44	199	52	263	74
Total n-3 PUFA	171	44	199	52	263	74
n-3/n-6	0.10	0.02	0.12	0.03	0.12	0.04

[a]Values are expressed as mass (nmol/g ww) and represent mean ± SD, n = 4–5, for each experimental oil. The asterisk (*) indicates a significant effect of the experimental oils (flax and fish) as compared with the control ($P < 0.05$), and the double asterisk (**) indicates a significant effect of the fish oil vs. flax oil. For abbreviations see Tables 1 and 2.

TABLE 8
Changes in Brain DHA Content in Studies Using ALA- or DHA-Enriched Diets

Study	Species	Sex	Age diet initiated	Duration	Diet	Brain
Arbuckle and Innis, 1992 (72)	Yorkshire piglets	Male	At parturition[a]	15 d	Low ALA diet: 0.7% ALA[b]; high ALA diet: 3.9% ALA; low ALA + DHA diet: 0.6% ALA + 0.3% DHA	The 22:6n-3 in synaptic plasma membrane EtnGpl increased significantly only in the low ALA + DHA diet
Abedin et al., 1999 (17)	Pigmented guinea pigs	Female	3 wk old	12 wk	ALA diet: 7.1%; ALA DHA diet: 1.0% ALA + 1.8% DHA	ALA diet: 22:6n-3 EtnGpl 11.5% total FA (1.3-fold increase vs. control); DHA diet: 22:6n-3 EtnGpl 15.0% total FA (1.7-fold increase vs. control)
Valenzuela et al., 2004 (73)	Wistar rats	Female	Since conception; mothers received experimental diets 40 d before mating	21 d	DHA diet: diet supplemented with 6 mg/kg of DHA-EE; ALA diet: diet supplemented with 60 mg/kg ALA-EE	DHA and ALA diets significantly increased the frontal cortex, cerebellum, and hippocampus DHA mass to similar levels
Lefkowitz et al., 2005 (74)	Long-Evans rats	Both	8 d old[a]	28 d	ALA diet: 1% ALA; DHA diet: 1.1% ALA + 2% DHA	ALA diet: total DHA 5.6 mg/whole brain; DHA diet: total DHA 7.0 mg/whole brain

[a]At this point the pups were raised artificially.
[b]Expressed as percent of total FA. The abbreviations are as follows: ALA, α-linolenic acid (18:3n-3); ALA-EE, AAA ethyl ester; DHA, 22:6n-3; DHA-EE, DHA ethyl ester.

This is important because the elongation and desaturation of 18:2n-6 and 18:3n-3 are thought to occur in the liver, with subsequent distribution of the conversion products to other tissues through the plasma. Our results demonstrated a significant increase in the 22:6n-3 mass in the brains of rats fed flax oil as well as those fed fish oil. Others have shown that rats fed 18:3-n-3 have an increased 22:6n-3 mass in brain EtnGpl (17,23) and in synaptic plasma membrane phospholipids (14). The results obtained from other studies on the effect of 18:3n-3- and 22:6n-3-enriched diets on brain 22:6n-3 accumulation are summarized in Table 8. Our study is important because, unlike these other studies, it was done in adult animals following myelination and because it clearly demonstrates an accretion of 22:6n-3 in the brains of rats fed a diet enriched in 18:3n-3. The intriguing question is the origin of this 22:6n-3 in the rats fed a diet enriched in 18:3n-3—that is, whether it was imported from the blood as preformed 22:6n-3 or synthesized in the brain from plasma-derived 18:3n-3. Although we did not analyze the plasma FA mass, a number of studies demonstrate minimal elongation and desaturation of 18:3n-3 in the plasma, with conversion limited to 20:5n-3 and 22:5n-3 (15,16,21,48,51). Therefore, it is reasonable to conclude that animals fed flax oil would have increased 18:3n-3, 20:5n-3, and 22:5n-3 levels, but not 22:6n-3 levels, in their plasma. Thus, it is unlikely that an increase in the plasma 22:6n-3 mass is responsible for the increased 22:6n-3 in the brain; rather, it suggests that 18:3n-3, 20:5n-3, and 22:5n-3 are taken up by the brain and converted to 22:6n-3.

This is not without precedence, as during postnatal development the rat brain takes up, elongates, and desaturates 18:3n-3 (53,54). The conversion of 18:3n-3 into 20:5n-3, 22:5n-3, and

22:6n-3 is possible because Δ5- and Δ6-desaturase are present in the brain (55,56). In fact, the Δ6-desaturase mRNA content is several times greater in the brain than in other tissues (55,56). Increasing evidence supports the hypothesis that 22:6n-3 can be constitutively synthesized in the brain from its precursors (57). Cultured astrocytes can synthesize 22:6n-3 from 18:3n-3, and this may be a major source of 22:6n-3 in the brain (58). Recently, strong evidence was presented indicating that neurons themselves can elongate 18:3n-3 to 22:6n-3 (Spector, A., personal communication), suggesting a robust ability of the brain to elongate 18:3n-3 to maintain the brain 22:6n-3 mass.

Thus, we hypothesize, based on the lack of increased 22:6n-3 but increased 18:3n-3 in the liver and heart, that the flax oil diet increased plasma 18:3n-3, thereby presenting tissue with this EFA for further elongation and desaturation. The ability to elongate and desaturate 18:3n-3 to 22:6n-3 appears to be highly tissue dependent, suggesting that the brain is uniquely positioned to carry out this process.

In the present study, we showed that the flax oil diet had a lesser effect than the fish oil diet on decreasing EtnGpl 20:4n-6 levels. It is well established that an increase in n-3 dietary PUFA leads to a decrease in n-6 PUFA tissue content, because these two families of EFA compete for the same set of enzymes (59). Decreased n-6 levels are considered beneficial because 20:4n-6 and its cyclooxygenase metabolites are related to the onset of different diseases, such as atherosclerosis (60) and inflammation (61–63), and the promotion of tumor proliferation (64). Nevertheless, all the beneficial effects associated with 22:6n-3- and 20:5n-3-enriched diets have overshadowed the importance of 20:4n-6 in general physiological functioning. A severe decrease in 20:4n-6, such as that observed with a high 22:6n-3 consumption, may compromise the

biosynthesis of prostaglandins, thereby affecting many normal metabolic processes.

Although the total phospholipid mass was not affected by these diets, some of the individual phospholipid class masses were changed. The most remarkable change was the 20% decrease in the EtnGpl mass in heart and liver tissues in rats fed fish oil, including a 25% reduction in the heart PlsEtn (Table 3). Changes in the mass of these phospholipids were not observed in the brain; however, in the liver the EtnGpl mass was significantly reduced, by 23%, in the fish oil group. This result differs from that of a previous study showing an accumulation of EtnGpl in the brain tissue of animals fed fish oil (40). Other studies have demonstrated an effect of saturated vs. unsaturated FA on the phospholipid composition, although there is no consensus regarding these effects on the phospholipid mass (65,66). Rats fed a diet enriched in 20:5n-3 did not have altered EtnGpl and ChoGpl masses in the erythrocytes (67). On the other hand, a soybean oil-enriched diet increased the ChoGpl and decreased the EtnGpl content in macrophages (68). In addition, the liver and heart CerPCho masses were increased in the fish oil group as compared with the other two groups. The increase in the PtdOH mass in the heart and brain suggest a potential reduction in PtdOH utilization for phospholipid biosynthesis, although an alternative hypothesis would be increased formation from a catabolic route. Thus, we demonstrate a profound effect of fish oil-based diets on the liver and heart EtnGpl mass, suggesting that diets enriched in this FA are capable of modulating phospholipid synthesis and degradation to a greater degree than those based on flax oil.

Because the cholesterol-to-phospholipid ratio and the phospholipid acyl chain composition are important factors in determining the biophysical properties of the membrane (41,69–71), it was also important to determine whether changes in n-3 intake would affect the cholesterol content in brain, liver, and heart tissues. In fish oil-fed rats, there was a slight decrease in the cholesterol mass in heart and liver tissues, but the brain was unaffected. In the flax oil-fed rats, the brain cholesterol mass was decreased by 17% as compared with the control, but the liver and heart cholesterol masses were unaffected. These changes resulted in a 17% decrease in the brain cholesterol-to-phospholipid ratio in the flax oil group and a 25% reduction in this ratio in the heart from the fish oil-fed group. These changes, in addition to changes in the phospholipid acyl chain composition, may result in altered brain and heart membrane biophysical parameters that may alter the physiological functioning of these tissues.

In summary, we demonstrated that 18:3n-3-enriched diets significantly increased the n-3 FA mass and decreased the n-6 FA levels, especially 20:4n-6, in the brain, heart, and liver. However, this decrease was of a lesser magnitude in the flax oil group than in the fish oil group. The apparent elongation and desaturation of 18:3n-3 to 22:6n-3 in the brain compared with the limited conversion in the heart and liver may reflect a distinct need by the brain for 22:6n-3. Although these data do not provide direct evidence for 18:3n-3 elongation by the brain, they do demonstrate that the 18:3n-3-enriched diet reduced tissue levels of 20:4n-6 and increased tissue levels of 22:6n-3 in a highly tissue-dependent manner. The accumulation of n-3 PUFA, together with the decrease in n-6 PUFA, might account for the beneficial health effects associated with 18:3n-3-enriched diets.

REFERENCES

1. Lauritzen, L., Hansen, H.S., Jørgensen, M.H., and Michaelsen, K.F. (2001) The Essentiality of Long-Chain n-3 Fatty Acids in Relation to Development and Function of the Brain and Retina, *Prog. Lipid Res. 40*, 1–94.
2. Leaf, A., Kang, J.X., Xiao, Y.-F., and Billman, G.E. (2003) Clinical Prevention of Sudden Cardiac Death by n-3 Polyunsaturated Fatty Acids and Mechanism of Prevention of Arrhythmias by n-3 Fish Oils, *Circulation 107*, 2646–2652.
3. Stoll, A.L., Severus, W.E., Freeman, M.P., Rueters, S., Zboyan, H.A., Diamond, E., Cress, K.K., and Marangell, L.B. (1999) Omega 3 Fatty Acids in Bipolar Disorder: A Preliminary Double-Blind, Placebo-Controlled Trial, *Arch. Gen. Psychiatry 56*, 407–412.
4. Wijendran, V., and Hayes, K.C. (2004) Dietary n-6 and n-3 Fatty Acid Balance and Cardiovascular Health, *Annu. Rev. Nutr. 24*, 597–615.
5. Sunshine, C., and McNamee, M.G. (1994) Lipid Modulation of Nicotinic Acetylcholine Receptor Function: The Role of Membrane Lipid Composition and Fluidity, *Biochim. Biophys. Acta 1191*, 59–64.
6. Gerbi, A., Maixent, J.-M., Barbey, O., Jamme, I., Pierlovisi, M., Coste, T., Pieroni, G., Novelot, A., Vague, P., and Raccah, D. (1998) Alterations of Na,K-ATPase Isoenzymes in the Rat Diabetic Neuropathy: Protective Effect of Dietary Supplementation with n-3 Fatty Acids, *J. Neurochem. 71*, 732–740.
7. Cannon, B., Hermansson, M., Györke, S., Somerharju, P., Virtanen, J.A., and Cheng, K.H. (2003) Regulation of Calcium Channel Activity by Lipid Domain Formation in Planar Lipid Bilayers, *Biophys. J. 85*, 933–942.
8. Lesa, G.M., Palfreyman, M., Hall, D.H., Clandinin, M.T., Rudolph, C., Jorgensen, E.M., and Schiavo, G. (2003) Long Chain Polyunsaturated Fatty Acids Are Required for Efficient Neurotransmission in *C. elegans*, *J. Cell Sci. 116*, 4965–4975.
9. Kodas, E., Galineau, L., Bodard, S., Vancassel, S., Guilloteau, D., Besnard, J.-C., and Chalon, S. (2004) Sertoninergic Neurotransmission Is Affected by n-3 Polyunsaturated Fatty Acids in the Rat, *J. Neurochem. 89*, 695–702.
10. Pepe, S., and McLennan, P.L. (2002) Cardiac Membrane Fatty Acid Composition Modulates Myocardial Oxygen Consumption and Postischemic Recovery of Contractile Function, *Circulation 105*, 2303–2308.
11. Gilroy, D.W., Newson, J., Sawmynaden, P., Willoughby, D.A., and Croxtall, J.D. (2004) A Novel Role for Phospholipase A_2 Isoforms in the Checkpoint Control of Acute Inflammation, *FASEB J. 18*, 489–498.
12. Cunnane, S.C., and Anderson, M.J. (1997) The Majority of Dietary Linoleate in Growing Rats Is β-Oxidized or Stored in Visceral Fat, *J. Nutr. 127*, 146–152.

13. Poumès-Ballihaut, C., Langelier, B., Houlier, F., Alessandri, J.-M., Durand, G., Latge, C., and Guesnet, P. (2001) Comparative Bioavailability of Dietary α-Linolenic and Docosahexaenoic Acids in the Growing Rat, *Lipids 36*, 793–800.

14. Bowen, R.A.R., and Clandinin, M.T. (2000) High Dietary 18:3n-3 Increases in the 18:3n-3 but Not the 22:6n-3 Content in the Whole Body, Brain, Skin, Epididymal Fat Pads, and Muscles of Suckling Rat Pups, *Lipids 35*, 389–394.

15. MacDonald-Wicks, L.K., and Garg, M.L. (2004) Incorporation of n-3 Fatty Acids into Plasma and Liver Lipids of Rats: Importance of Background Dietary Fat, *Lipids 39*, 545–551.

16. Morise, A., Combe, N., Boué, C., Legrand, P., Catheline, D., Delplanque, B., Fénart, E., Weill, P., and Hermier, D. (2004) Dose Effect of α-Linolenic Acid on PUFA Conversion, Bioavailability, and Storage in the Hamster, *Lipids 39*, 325–334.

17. Abedin, L., Lien, E.L., Vingrys, A.J., and Sinclair, A.J. (1999) The Effects of Dietary α-Linolenic Acid Compared with Docosahexaenoic Acid on Brain, Retina, Liver, and Heart in the Guinea Pig, *Lipids 34*, 475–482.

18. Bazinet, R.P., McMillan, E.G., and Cunnane, S.C. (2003) Dietary α-Linolenic Acid Increases the n-3 PUFA Content of Sow's Milk and the Tissues of the Suckling Piglet, *Lipids 38*, 1045–1049.

19. Su, H.M., Huang, M.C., Saad, N.M., Nathanielsz, P.W., and Brenna, J.T. (2001) Fetal Baboons Convert 18:3n-3 to 22:6n-3 *in vivo*. A Stable Isotope Tracer Study, *J. Lipid Res. 42*, 581–586.

20. Mantzioris, E., James, M.J., Gibson, R.A., and Cleland, L.G. (1994) Dietary Substitution with an α-Linolenic Acid-rich Vegetable Oil Increases Eicosapentaenoic Acid Concentrations in Tissues, *Am. J. Clin. Nutr. 59*, 1304–1309.

21. Burdge, G.C., Jones, A.E., and Wooton, S.A. (2002) Eicosapentaenoic and Docosapentaenoic Acids Are the Principal Products of α-Linolenic Acid Metabolism in Young Men, *Br. J. Nutr. 88*, 355–363.

22. Burdge, G. (2004) α-Linolenic Acid Metabolism in Men and Women: Nutritional and Biological Implications, *Curr. Opin. Clin. Nutr. Metab. Care 7*, 137–144.

23. Barcelo-Coblijn, G., Kitajka, K., Puskas, L.G., Hogyes, E., Zvara, A., Hackler, L., Jr., and Farkas, T. (2003) Gene Expression and Molecular Composition of Phospholipids in Rat Brain in Relation to Dietary n-6 and n-3 Fatty Acid Ratio, *Biochim. Biophys. Acta 1632*, 72–79.

24. Meyer, B.J., Mann, N.J., Lewis, J.L., Milligan, G.C., Sinclair, A.J., and Howe, P.R. (2003) Dietary Intakes and Food Sources of Omega-6 and Omega-3 Polyunsaturated Fatty Acids, *Lipids 38*, 391–398.

25. Astorg, P., Arnault, N., Czernichow, S., Noisette, N., Galan, P., and Hercberg, S. (2004) Dietary Intakes and Food Sources of n-6 and n-3 PUFA in French Adult Men and Women, *Lipids 39*, 527–535.

26. Reeves, P.G., Nielsen, F.H., and Fahey, C.G., Jr. (1993) AIN-93 Purified Diets for Laboratory Rodents: Final Report of the American Institute of Nutrition *ad hoc* Writing Committee on the Reformation of the AIN-76A Rodent Diet, *J. Nutr. 123*, 1939–1951.

27. Hara, A., and Radin, N.S. (1978) Lipid Extraction of Tissues with a Low-Toxicity Solvent, *Anal. Biochem. 90*, 420–426.

28. Radin, N.S. (1988) Lipid Extraction, in *Neuromethods, Vol. 7, Lipids and Related Compounds* (Boulton, A.A., Baker, G.B., and Horrocks, L.A., eds.), pp. 1–61, Humana Press, Clifton, NJ.

29. Jolly, C.A., Hubbell, T., Behnke, W.D., and Schroeder, F. (1997) Fatty Acid Binding Protein: Stimulation of Microsomal Phosphatidic Acid Formation, *Arch. Biochem. Biophys. 341*, 112–121.

30. Marcheselli, V.L., Scott, B.L., Reddy, T.S., and Bazan, N.G. (1988) Quantitative Analysis of Acyl Group Composition of Brain Phospholipids, Neutral Lipids, and Free Fatty Acids, in *Neuromethods, Vol. 7, Lipids and Related Compounds* (Boulton, A.A., Baker, G.B., and Horrocks, L.A., eds.), pp. 83–110, Humana Press, Clifton, NJ.

31. Dugan, L.L., Demediuk, P., Pendley, C.E., II, and Horrocks, L.A. (1986) Separation of Phospholipids by High Pressure Liquid Chromatography: All Major Classes Including Ethanolamine and Choline Plasmalogens, and Most Minor Classes, Including Lysophosphatidylethanolamine, *J. Chromatogr. 378*, 317–327.

32. Murphy, E.J., Stephens, R., Jurkowitz-Alexander, M., and Horrocks, L.A. (1993) Acidic Hydrolysis of Plasmalogens Followed by High-Performance Liquid Chromatography, *Lipids 28*, 565–568.

33. Rouser, G., Siakotos, A., and Fleischer, S. (1969) Quantitative Analysis of Phospholipids by Thin Layer Chromatography and Phosphorus Analysis of Spots, *Lipids 1*, 85–86.

34. Bowman, R.E., and Wolf, R.C. (1962) A Rapid and Specific Ultramicro Method for Total Serum Cholesterol, *Clin. Chem. 8*, 302–309.

35. Brockerhoff, H. (1975) Determination of the Positional Distribution of Fatty Acids in Glycerolipids, *Methods Enzymol. 35*, 315–325.

36. Gross, R.W. (1985) Identification of Plasmalogen as the Major Phospholipid Constituent of Cardiac Sarcoplasmic Reticulum, *Biochemistry 24*, 1662–1668.

37. Gross, R.W. (1984) High Plasmalogen and Arachidonic Acid Content of Canine Myocardial Sarcolemma: A Fast Atom Bombardment Mass Spectroscopic and Gas Chromatography–Mass Spectroscopic Characterization, *Biochemistry 23*, 158–165.

38. Horrocks, L.A. (1967) Composition of Myelin from Peripheral and Central Nervous System of the Squirrel Monkey, *J. Lipid Res. 8*, 569–576.

39. Horrocks, L.A., and Sun, G.Y. (1972) Ethanolamine Plasmalogens, in *Research Methods in Neurochemistry, Vol. 1* (Rodnight, R., and Marks, N., eds.), pp. 223–231, Plenum Press, New York.

40. Lin, D.S., Connor, W.E., Anderson, G.J., and Neuringer, M. (1990) Effects of Dietary n-3 Fatty Acids on the Phospholipid Molecular Species of Monkey Brain, *J. Neurochem. 55*, 1200–1207.

41. Heemskerk, J.W., Feijge, M.A., Simonis, M.A., and Hornstra, G. (1995) Effects of Dietary Fatty Acids on Signal Transduction and Membrane Cholesterol Content in Rat Platelets, *Biochim. Biophys. Acta 1255*, 87–97.

42. Greiner, R.S., Catalan, J.N., Moriguchi, T., and Salem, N., Jr. (2003) Docosapentaenoic Acid Does Not Completely Replace DHA in n-3 FA-Deficient Rats During Early Development, *Lipids 38*, 431–435.

43. Bourre, J.M., Dumont, O., Pascal, G., and Durand, G. (1993) Dietary α-Linolenic Acid at 1.3 g/kg Maintains Maximal Docosahexaenoic Acid Concentration in Brain, Heart and Liver of Adult Rats, *J. Nutr. 123*, 1313–1319.

44. Stubbs, C.D., and Smith, A.D. (1984) The Modification of Mammalian Membrane Polyunsaturated Fatty Acid Composition in Relation to Membrane Fluidity and Function, *Biochim. Biophys. Acta 779*, 89–137.

45. Clamp, A.G., Ladha, S., Clark, D.C., Grimble, R.F., and Lund, E.K. (1997) The Influence of Dietary Lipids on the Composition and Membrane Fluidity of Rat Hepatocyte Plasma Membrane, *Lipids 32*, 179–184.

46. Jump, D.B. (2002) The Biochemistry of n-3 Polyunsaturated Fatty Acids, *J. Biol. Chem. 277*, 8755–8758.

47. Marcheselli, V.L., Hong, S., Lukiw, W.J., Tian, X.H., Gronert, K., Musto, A., Hardy, M., Giminez, J.M., Chiang, N., Serhan, C.N., *et al.* (2003) Novel Docosanoids Inhibit Brain Ischemia-Reperfusion-Mediated Leukocyte Infiltration and Pro-inflammatory Gene Expression, *J. Biol. Chem. 278*, 43807–43817.

48. Zhao, G., Etherton, T.D., Martin, K.R., West, S.G., Gillies, P.J., and Kris-Etherton, P.M. (2004) Dietary α-Linolenic Acid Reduces Inflammatory and Lipid Cardiovascular Risk Factors in Hypercholesterolemic Men and Women, *J. Nutr. 134*, 2991–2997.

49. Bemelmans, W.J.E., Broer, J., Feskens, E.J.M., Smit, A.J., Muskiet, F.A.J., Lefrandt, J.D., Bom, V.J.J., May, J.F., and Meyboom-de Jong, B. (2002) Effect of an Increased Intake of α-Linolenic Acid and Group Nutritional Education on Cardiovascular Risk Factors: The Mediterranean α-Linolenic Enriched Groningen Dietary Intervention (MARGARIN) Study, *Am. J. Clin. Nutr. 75*, 221–227.

50. Djoussé, L., Pankow, J.S., Eckfeldt, J.H., Folsom, A.R., Hopkins, P.N., Province, M.A., Hong, Y., and Ellison, R.C. (2001) Relation Between Dietary Linolenic Acid and Coronary Artery Disease in the National Heart, Lung, and Blood Institute Family Heart Study, *Am. J. Clin. Nutr. 74*, 612–619.

51. de Groot, R.H.M., Hornstra, G., van Houwelingen, A.C., and Roumen, F. (2004) Effect of α-Linolenic Acid Supplementation During Pregnancy on Maternal and Neonatal Polyunsaturated Fatty Acid Status and Pregnancy Outcome, *Am. J. Clin. Nutr. 79*, 251–260.

52. Pawlosky, R.J., Hibbeln, J.R., Novotny, J.A., and Salem, N., Jr. (2001) Physiological Compartmental Analysis of α-Linolenic Acid Metabolism in Adult Humans, *J. Lipid Res. 42*, 1257–1265.

53. Pawlosky, R.J., Ward, G., and Salem, N., Jr. (1996) Essential Fatty Acid Uptake and Metabolism in the Developing Rodent Brain, *Lipids 31*, S103–S107.

54. Dhopeshwarkar, G.A., and Subramanian, C. (1976) Biosynthesis of Polyunsaturated Fatty Acids in the Developing Brain: I. Metabolic Transformations of Intracranially Administered $^{1\text{-}14}$C Linolenic Acid, *Lipids 11*, 67–71.

55. Cho, H.P., Nakamura, M., and Clarke, S.D. (1999) Cloning, Expression, and Fatty Acid Regulation of the Human Δ-5 Desaturase, *J. Biol. Chem. 274*, 37335–37339.

56. Cho, H.P., Nakamura, M.T., and Clarke, S.D. (1999) Cloning, Expression, and Nutritional Regulation of the Mammalian Δ-6 Desaturase, *J. Biol. Chem. 274*, 471–477.

57. Williard, D.E., Harmon, S.D., Kaduce, T.L., Preuss, M., Moore, S.A., Robbins, M.E.C., and Spector, A.A. (2001) Docosahexaenoic Acid Synthesis from n-3 Polyunsaturated Fatty Acids in Differentiated Rat Brain Astrocytes, *J. Lipid Res. 42*, 1368–1376.

58. Bernoud, N., Fenart, L., Bénistant, C., Pageaux, J.F., Dehouck, M.P., Molière, P., Lagarde, M., Cecchelli, R., and Lecerf, J. (1998) Astrocytes Are Mainly Responsible for the Polyunsaturated Fatty Acid Enrichment in Blood–Brain Barrier Endothelial Cells *in vitro*, *J. Lipid Res. 39*, 1816–1824.

59. Mohrmauer, H., Christiansen, K., Gan, M.V., Deubig, M., and Holman, R.T. (1967) Chain Elongation of Linoleic Acid and Its Inhibition by Other Fatty Acids *in vitro*, *J. Biol. Chem. 242*, 4507–4514.

60. Watson, A.D., Leitinger, N., Navab, M., Faull, K.F., Hörkkö, S., Witztum, J.L., Palinski, W., Schwenke, D., Salomon, R.G., Sha, W., *et al.* (1997) Structural Identification by Mass Spectrometry of Oxidized Phospholipids in Minimally Oxidized Low Density Lipoprotein That Induce Monocyte/Endothelial Interactions and Evidence for Their Presence *in vivo*, *J. Biol. Chem. 272*, 13597–13607.

61. Calder, P.C. (2001) Polyunsaturated Fatty Acids, Inflammation, and Immunity, *Lipids 36*, 1007–1024.

62. Rosenberger, T.A., Villacreses, N.E., Hovda, J.T., Boestti, F., Weerasinghe, G., Wine, R.N., Harry, G.J., and Rapoport, S.I. (2004) Rat Brain Arachidonic Acid Metabolism Is Increased by a 6-Day Intracerebral Ventricular Infusion of Bacterial Lipopolysaccharide, *J. Neurochem. 88*, 1168–1178.

63. Lee, H., Villacreses, N.E., Rapoport, S.I., and Rosenberger, T.A. (2004) *In vivo* Imaging Detects a Transient Increase in Brain Arachidonic Acid Metabolism: A Potential Marker of Neuroinflammation, *J. Neurochem. 91*, 936–945.

64. Avis, I., Hong, S.H., Martinez, A., Moody, T., Choi, Y.H., Trepel, J., Das, R., Jett, M., and Mulshine, J.L. (2001) Five-Lipoxygenase Inhibitors Can Mediate Apoptosis in Human Breast Cancer Cell Lines Through Complex Eicosanoid Interactions, *FASEB J. 15*, 2007–2009.

65. Khuu Thi-Dinh, K.L., Demarne, Y., Nicolas, C., and Lhuillery, C. (1990) Effect of Dietary Fat on Phospholipid Class Distribution and Fatty Acid Composition in Rat Fat Cell Plasma Membrane, *Lipids 25*, 278–283.

66. Turini, M.E., Thomson, A.B., and Clandinin, M.T. (1991) Lipid Composition and Peroxide Levels of Mucosal Cells in the Rat Large Intestine in Relation to Dietary Fat, *Lipids 26*, 431–440.

67. Gibson, R.A., Neumann, M.A., Burnard, S.L., Rinaldi, J.A., Patten, G.S., and McMurchie, E.J. (1992) The Effect of Dietary Supplementation with Eicosapentaenoic Acid on the Phospholipid and Fatty Acid Composition of Erythrocytes of Marmoset, *Lipids 27*, 169–176.

68. Oliveros, L.B., Videla, A.M., Ramirez, D.C., and Gimenez, M.S. (2003) Dietary Fat Saturation Produces Lipid Modifications in Peritoneal Macrophages of Mouse, *J. Nutr. Biochem. 14*, 370–377.

69. Jefferson, J.R., Powell, D.M., Rymaszewski, Z., Kukowska-Latallo, J., Lowe, J.B., and Schroeder, F. (1990) Altered Membrane Structure in Transfected Mouse L-Cell Fibroblasts Expressing Rat Liver Fatty Acid Binding Protein, *J. Biol. Chem. 265*, 11062–11068.

70. Woodford, J.K., Jefferson, J.R., Wood, W.G., Hubbell, T., and Schroeder, F. (1993) Expression of Liver Fatty Acid Binding Protein Alters Membrane Lipid Composition and Structure in Transfected L-Cell Fibroblasts, *Biochim. Biophys. Acta 1145*, 257–265.

71. Murphy, E.J., Prows, D., Stiles, T., and Schroeder, F. (2000) Phospholipid and Phospholipid Fatty Acid Composition of L-Cell Fibroblast: Effect of Intestinal and Liver Fatty Acid Binding Protein, *Lipids 35*, 729–738.

72. Arbuckle, L.D., and Innis, S.M. (1992) Docosahexaenoic Acid in Developing Brain and Retina of Piglets Fed High or Low α-Linolenate Formula With and Without Fish Oil, *Lipids 27*, 89–93.

73. Valenzuela, A., von Bernhardi, R., Valenzuela, V., Ramírez, G., Alarcón, R., Sanjueza, J., and Nieto, S. (2004) Supplementation of Female Rats with α-Linolenic Acid or Docosahexaenoic Acid Leads to the Same Omega-6/Omega-3 LC-PUFA Accretion in Mother Tissues and in Fetal and Newborn Brains, *Ann. Nutr. Metab. 48*, 28–35.

74. Lefkowitz, W., Lim, S.-Y., Lin, Y., and Salem, N., Jr. (2005) Where Does the Developing Brain Obtain Its Docosahexaenoic Acid? Relative Contributions of Dietary α-Linolenic Acid, Docosahexaenoic Acid, and Body Stores in the Developing Rat, *Pediatr. Res. 57*, 157–165.

Effects of Aging and Dietary n-3 Fatty Acids on Rat Brain Phospholipids: Focus on Plasmalogens

A. André[a], P. Juanéda[a], J.L. Sébédio[b], and J.M. Chardigny[a],*

[a]Unité Mixte de Recherche Institut National de la Recherche Agronomique–Etablissement National d'Enseignement Superieur Agronomique de Dijon Flaveur, Vision et Comportement du consommateur, 21065 Dijon Cedex, France, and
[b]Unité du Métabolisme Protéinoénergétique, 63001 Clermont-Ferrand Cedex, France

ABSTRACT: The aging brain undergoes modifications in the lipid composition of cell membranes and especially in plasmalogens. These phospholipids represent between one-half and two-thirds of the ethanolamine phospholipids in the brain. They are known to facilitate membrane fusion and act as endogenous antioxidants. During normal aging and in some pathological conditions, plasmalogen and DHA levels fall. In this context, we aimed to evaluate the influence of n-3 FA intake on plasmalogens in the brain during aging. Littermates from two generations of n-3-deficient rats were fed an n-3-deficient diet or an equilibrated diet containing either α-linolenic acid alone (α-LNA) or with two doses of DHA (0.3 or 0.6% w/w). After weaning, 9 mon of diet, or 21 mon of diet, plasmalogen levels were assessed, and the *sn*-2 substitutions of plasmenylethanolamines were analyzed in the cortex, striatum, and hippocampus. Our results showed that plasmalogen contents were not influenced by the diet. Plasmalogen levels were significantly decreased in aged rats compared with adults, whereas DHA levels increased in the hippocampus and remained stable in the cortex and striatum. DHA levels were significantly and similarly increased in total phospholipids and especially in plasmenylethanolamines after 9 mon of diet containing α-LNA alone or combined with DHA. This study showed that each structure sustained specific age-induced modifications. Dietary n-3 FA may not oppose the physiological decrease in brain plasmalogen levels during aging. Moreover, α-LNA appears to be equally as potent as preformed DHA at replacing DHA in the brain of our rat model.

Paper no. L9756 in *Lipids* **40**, 799–806 (August 2005).

The aging brain is characterized by morphological and neurochemical changes involving numerous biochemical alterations of the neural components, such as modifications in the lipid composition of cell membranes (1). The hippocampus, which is a structure of the limbic system involved in memory storage and retrieval (2), is particularly vulnerable to alterations due to aging. Biomedical research has played an important role in finding ways at least to slow the process of aging. Genetic, environmental, and dietary factors affecting the process of aging have been identified and widely studied. However, few works have considered the fate of plasmalogens, phospholipids distinguished by their vinyl-ether bond at the *sn*-1 position of the glycerol backbone. They are ubiquitous and are found in considerable amounts as a constituent of mammalian cell membranes (3) and represent the major subclass of ethanolamine glycerophospholipids in the brain (between one-half and two-thirds of the ethanolamine phospholipids) (4). Their high content suggests that they play an important role in the structure and function of biological membranes. Plasmenylethanolamines (PlsEtn) are concentrated in several subcellular fractions, which undergo rapid membrane fusion and may thus facilitate synaptic transmission (5). Plasmalogens are also known to be reservoirs of PUFA, as they predominantly contain arachidonic acid or DHA at their *sn*-2 position (6). The involvement of oxidative stress during aging has been postulated by many investigators (7). In this context, plasmalogens are more susceptible to oxidative reactions, as compared with their FA ester analogs, because of the reactivity of their vinyl-ether bond (8). Plasmalogens may act as endogenous antioxidants (9), protecting PUFA at the *sn*-2 position from oxidation. A decline of plasmalogen concentrations has been observed in the brain during normal aging (10) and in some pathological conditions such as Alzheimer's disease (AD) (11). Moreover, patients with AD have extremely low levels of DHA in their brains (12). One of the factors that makes studies in aging difficult is the tight, almost inseparable connection between aging and age-related disease. In this context, n-3-deficient animals constitute an interesting model. Indeed, in a dietary α-linolenic acid(α-LNA)-deficiency model, cognitive processes, learning, and memory were altered in the same way as during aging (13). An n-3-deficiency in the brain is a means to mimic what happens during physiological aging without the impact of age-related diseases. We specifically investigated the effect of DHA because the brain contains high levels of this FA, which is essential in nervous system function (14). Moreover, supplementation with DHA has been shown to correct the modification in PUFA composition with increasing age (15).

In this work, we studied whether dietary α-LNA alone or combined with DHA may prevent biochemical alterations due to aging. We focused on PlsEtn in the brain of rats from two generations of n-3-deficient animals.

MATERIALS AND METHODS

Animals and diets. Animals were housed in animal quarters under controlled temperature (21°C ± 1°C) and light conditions (12-h light/12-h dark cycle). Two generations of Wistar rats (Janvier, Le Genest-St-Isle, France) were fed an α-LNA-deficient diet (diet Def). At weaning, male littermates (average weight, 90 g) were randomly allocated to four experimental

---

groups, which received one of the following diets: diet Def, diet D0 containing 2.5% of α-LNA (w/w) as the only source of n-3 FA, diet D3 containing 1.2% of α-LNA acid and 0.3% of DHA (w/w), or diet D6 containing 1.1% of α-LNA and 0.6% of DHA. The detailed composition of the diets and the dietary lipids is presented in Tables 1 and 2 respectively. Diets were prepared as pellets by UPAE (INRA, Jouy en Josas, France) and were given *ad libitum.* The protocol was carried out according to the current French regulation regarding animal experiments (authorization A 21200 for the animal housing and personal authorization 21 CAE 056 for experimentation on animals).

Tissue collection and lipid analysis. After weaning, 9 mon of diet, or 21 mon of diet, three animals per group were sacrificed by decapitation. Brains were rapidly dissected to remove the frontal cortex, the striatum, and the hippocampus. Each structure was weighed and kept at −80°C in chloroform/methanol (2:1 vol/vol) until the analysis.

Total lipids were extracted according to the procedure of Folch *et al.* (16). Total phospholipids were separated from neutral lipids according to Juanéda and Rocquelin (17) and were transesterified with boron trifluoride (BF_3) in methanol (7 g/L) following the method of Morrison and Smith (18). This reaction yielded mixtures of FAME and plasmalogen-derived dimethylacetals (DMA). They were analyzed on a Hewlett-Packard (Palo Alto, CA) 5890 series II gas chromatograph equipped with a split/splitless injector, an FID, and a BPX 70-silica capillary column (120 m × 0.25 mm i.d.; film thickness 0.25 µm; SGE, Melbourne, Australia). The injector and the detector were maintained at 250 and 280°C, respectively. Hydrogen was used as the carrier gas (inlet pressure 300 kPa). The oven temperature was fixed at 60°C for 1 min, increased to 170°C at a rate of 20°C/min, held at this temperature for 60 min, then increased to 210°C at a rate of 5°C/min and kept at this temperature until the end of the analysis. DMA were identified by comparison of their retention times with those of synthetic standards. They were quantified using nonadecanoic acid methyl ester as internal standard and the Diamir software (JMBS Inc., Portage, MI).

Plasmalogen analysis. Total phospholipids were fractionated by TLC on silica gel plates. Phospholipid standards were

TABLE 1
Composition of the Diets

Ingredient	Amount (g/kg diet)	Ingredient	Amount (g/kg diet)
Casein	180	Fat[a]	50
Cornstarch	460	Mineral mix[b]	50
Sucrose	230	Vitamin mix[c]	10
Cellulose	20		

[a]Represented by oil mixtures (Table 2).
[b]Composition (g/kg): sucrose, 110.7; $CaCO_3$, 240; K_2HPO_4, 215; $CaHPO_4$, 215; $MgSO_4\cdot7H_2O$, 100; NaCl, 60; MgO, 40; $FeSO_4\cdot7H_2O$, 8; $ZnSO_4\cdot7H_2O$, 7; $MnSO_4\cdot H_2O$, 2; $CuSO_4\cdot5H_2O$, 1; $Na_2SiO_7\cdot3H_2O$, 0.5; $AlK(SO_4)_2\cdot12H_2O$, 0.2; K_2CrO_4, 0.15; NaF, 0.1; $NiSO_4\cdot6H_2O$, 0.1; H_3BO_3, 0.1; $CoSO_4\cdot7H_2O$, 0.05; KIO_3, 0.04; $(NH_4)^6Mo_7O_{24}\cdot4H_2O$, 0.02; LiCl, 0.015; Na_2SeO_3, 0.015; NH_4VO_3, 0.01.
[c]Composition (g/kg): sucrose, 549.45; retinyl acetate, 1; cholecalciferol, 0.25; DL-α-tocopheryl acetate, 20; phylloquinone, 0.1; thiamine HCl, 1; riboflavin, 1; nicotinic acid, 5; calcium pantothenate, 2.5; pyridoxine HCl, 1; biotin, 1; folic acid, 0.2; cyanobalamin, 2.5; choline HCl, 200; DL-methionine, 200; *p*-aminobenzoic acid, 5; inositol, 10.

TABLE 2
FA Composition of Dietary Lipids (% of total FA)

	Experimental groups			
	Def	D0	D3	D6
14:0	0.4	0.5	0.6	0.6
15:0	0.0	0.0	0.1	0.1
16:0	7.7	19.7	22.7	21.7
17:0	0.1	0.1	0.1	0.1
18:0	4.3	3.0	3.3	3.4
20:0	0.4	0.4	0.3	0.3
22:0	0.7	0.4	0.4	0.4
SFA	13.6	24.1	27.6	26.6
16:1	0.2	0.2	0.3	0.4
18:1	24.9	60.6	59.7	60.2
20:1	0.2	0.6	0.4	0.4
MUFA	25.3	61.4	60.4	61.0
18:2n-6	60.0	11.5	9.8	9.4
18:3n-6	0.0	0.1	0.1	0.0
n-6	60.0	11.6	9.9	9.4
18:3n-3	0.0	2.5	1.2	1.1
20:5n-3	0.0	0.0	0.1	0.2
22:6n-3	0.0	0.0	0.3	0.6
n-3	0.0	2.5	1.6	1.9
PUFA	60.0	14.1	11.5	11.3

also spotted on a TLC plate to determine migration characteristics of the researched compounds. The plate was developed in a mixture of chloroform/methanol/water (65:25:4, by vol). The band corresponding to phosphoethanolamines ($R_f = 0.45$) was scraped off and extracted two times with a mixture of chloroform and methanol (2:1 vol/vol). Dried phospholipids were exposed to HCl fumes for 5 min to hydrolyze the vinyl-ether bonds of plasmalogens. Hydrolysis products were resuspended in a small volume of chloroform/methanol and spotted on another TLC plate developed with the same solvent system. The standard of lysophosphatidylethanolamine ($R_f = 0.27$) was visualized by placing the plate in iodine vapor. The corresponding band was scraped off, and the phospholipids were transesterified with sodium methanolate. The *sn*-2 position of PlsEtn was analyzed in the same way as total phospholipids.

Separation of phospholipid classes. Phospholipid classes were separated by HPLC (19) and quantified using cholesterol as the external standard. The HPLC instrument was a Varian model 9010 liquid chromatograph using a ternary solvent mixture equipped with a 100-µL Valco compressed-air injector fitted with a loop. The detector was a Cunow light-scattering detector Model 10, connected to filtered compressed air. The column was a Lichrosorb Si60 silica, 5 µm, 250 × 7.5 mm i.d. (Merck, Darmstadt, Germany). The nebulized air pressure was set at 2.1 psi and the additional air at 0.5 psi. The solvents used for the mobile phase gradient were hexane (A), 2-propanol/chloroform (4:1) (B), and 2-propanol/water (1:1) (C). The mobile phase was changed from 42% A/52% B/6% C to 41% A/52% B/7% C in 5 min and then to 32% A/52% B/16% C in 20 min. The heated pipe temperature was 40°C. The flow rate was 2.5 mL/min. Chloroform/methanol (2:1 vol/vol) was used as the injector solvent.

Statistical analysis. Results are presented as mean values with their SE. The data were submitted to a one-way ANOVA with diet or age as factors. Means were compared using Dunnett's test at 9 and 21 mon, independently, to determine the effect of diet (diet Def was chosen as the control group). The effect of age was analyzed by a Kruskal–Wallis test comparing values at 9 and 21 mon independently of the diet. The criterion for statistical significance was $P < 0.05$. All the calculations were performed with NCSS 6.01 software (Alsyd, Meylan, France).

RESULTS AND DISCUSSION

In this report, we present the combined effects of aging and n-3 dietary FA intake on phospholipids and specifically on plasmalogens from the hippocampus, striatum, and cortex of n-3-deficient rats.

The relative content of the major phospholipid classes in the cortex (Fig. 1), the hippocampus, and the striatum (data not shown) was assessed at weaning and after 9 or 21 mon of diet. This parameter was not significantly influenced by the nature and the level of n-3 dietary FA, either after 9 or after 21 mon of diet. However, we can underline the same significant age-induced changes in the three structures studied. After 21 mon, choline glycerophospholipids (ChoGpl) significantly decreased whatever the diet (by 23, 24, 31, and 12% between 9 and 21 mon in the cortex, for diets Def, D0, D3, and D6, respectively). This decrease was balanced by a strong significant increase of phosphatidylinositol (PtdIns) and phosphatidylserine (PtdSer) (a threefold increase in the cortex and hippocampus whatever the diet, a lesser increase in the striatum) and a less important increase of ethanolamine glycerophospholipids (EtnGpl) (by 18% in the striatum and cortex and by 25% in the hippocampus). In previous studies, a decrease in the content in major phospholipid classes, i.e., EtnGpl and ChoGpl, was already observed in the hippocampus of 12-mon-old rats (20) and in the cortex of 24-mon-old rats (21) fed an α-LNA-deficient diet. At the same time, the content of minor phospholipid classes, i.e., PtdIns and PtdSer, was markedly increased. From our results, we can say that n-3 FA intake (α-LNA or DHA) may not prevent the effect of physiologic aging in our experimental model. It has been well established that PtdIns and PtdSer are involved in signal transduction pathways (22). On this basis, one can speculate that the aging brain tries to regulate the programmed cognitive decline by increasing PtdIns and PtdSer levels.

The impact of dietary n-3 FA intake on the FA composition of total phospholipids from the hippocampus (Table 3), cortex (Table 4), and striatum (Table 5) was investigated. At weaning, we observed a classical balance of the n-3 deficiency by high levels of 22:5n-6 and, to a lesser extent, of 22:4n-6 (23). We can notice that the n-3 deficiency affected the acyl composition of phospholipids differently according to the brain regions. The percentage of total PUFA was higher in the frontal cortex than in the hippocampus or striatum (29.0 vs. 19.6 and 26.6%, respectively, see Tables 3–5). Our results are in concordance with previous studies showing a specific composition of each structure of the brain (24). After 9 mon of diet, numerous and similar changes were observed for diets D0, D3, and D6 in the three structures. The 22:5n-6 levels were significantly decreased and the 22:6n-3 levels significantly increased compared with diet Def. The same recovery of DHA in brain phospholipids was observed for diets D0, D3, or D6. This was due to preformed or *in vivo* biosynthesized DHA. It has previously been shown that DHA-deficient animals recovered from losses of 22:6n-3 in the brain when switched to an n-3 FA-adequate diet (25). The recovery of DHA in brain phospholipids was quicker in the cortex and in the striatum than in the hippocampus, whose DHA levels increased again from 9 to 21 mon. Our results clearly demonstrate that α-LNA is equally as potent at replacing DHA and reducing 22:5n-6 levels as is preformed DHA in our n-3-deficient rat model. In addition, such results are consistent with the work of Spector (26). The brain seems to have the capacity to elongate and desaturate α-LNA. Indeed, the cerebral endothelium synthesizes DHA from dietary metabolic precursors, such as α-LNA, *via* Δ6-desaturation and retroconversion
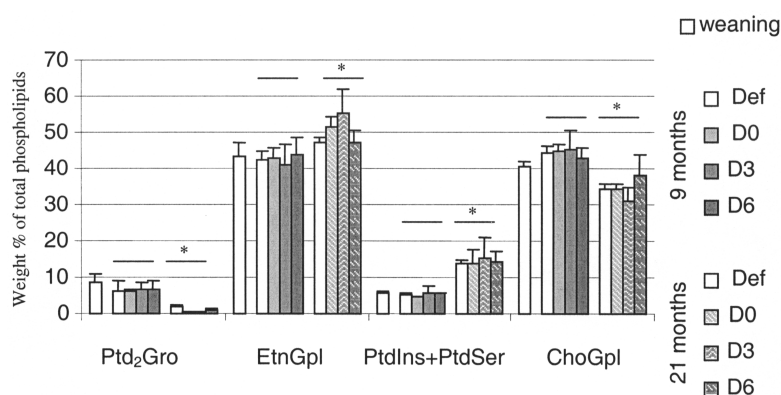
FIG. 1. Percentage of major phospholipid classes of rat cortex at weaning and after having been fed diet Def, D0, D3, or D6 for 9 or 21 mon. Values are mean ± SD, $n = 3$. Values with an asterisk (*) are significantly different from 9 mon at the $P < 0.05$ level as determined by ANOVA followed by a Kruskal–Wallis test. Ptd$_2$Gro, cardiolipin; ChoGpl, choline glycerophospholipids; EtnGpl, ethanolamine glycerophospholipids; PtdIns, phosphatidylinositol; PtdSer, phosphatidylserine.

TABLE 3
FA Composition[a] (as wt% of total identified FA) of Rat Hippocampus Phospholipids at Weaning or After Having Been Fed Diet Def, D0, D3, or D6[b] for 9 or 21 mon

		SFA			MUFA				PUFA							
		16:0	18:0	Σ SFA	18:1n-9	18:1n-7	20:1n-9	Σ MUFA	18:2n-6	20:4n-6	22:4n-6	22:5n-6	22:6n-3	Σ PUFA	n-3/n-6
Weaning		17.2 ± 0.7	21.7 ± 1.0	42.6 ± 1.7	19.4 ± 0.7	3.1 ± 0.1	0.9 ± 0.0	25.3 ± 1.0	1.1 ± 0.1	11.2 ± 0.6	2.3 ± 0.4	4.3 ± 1.4	0.1 ± 0.0	19.6 ± 1.8	0.01 ± 0.0
9 mon	Def	19.0 ± 0.1	19.5 ± 0.4	40.9 ± 0.6	18.3 ± 0.7	4.6 ± 0.1	1.8 ± 0.6	26.0 ± 1.4	0.5 ± 0.1	8.5 ± 1.5	3.0 ± 0.5	5.8 ± 1.4	1.3 ± 0.2	22.5 ± 1.6	0.1 ± 0.0
	D0	13.9 ± 0.9*	15.7 ± 1.5*	33.0 ± 1.8*	28.6 ± 2.8*	4.2 ± 0.1	2.5 ± 0.2*	37.7 ± 2.6*	1.9 ± 0.4*	6.1 ± 0.1*	2.6 ± 0.1*	0.1 ± 0.0*	3.7 ± 0.7*	17.0 ± 0.8*	0.4 ± 0.1*
	D3	14.1 ± 2.2*	17.4 ± 0.4	35.5 ± 3.4	26.6 ± 4.3	4.2 ± 0.3	2.7 ± 0.2*	36.3 ± 4.3*	1.1 ± 0.3	6.7 ± 0.9*	2.7 ± 0.2*	0.1 ± 0.0*	3.5 ± 0.4*	16.6 ± 1.3*	0.4 ± 0.0*
	D6	13.6 ± 0.5*	16.7 ± 0.8*	34.1 ± 1.0*	27.1 ± 3.0*	4.2 ± 0.1	2.6 ± 0.3*	36.9 ± 2.8*	1.1 ± 0.2	6.4 ± 0.5*	2.6 ± 0.4*	0.2 ± 0.0*	3.0 ± 0.2	16.1 ± 1.2*	0.3 ± 0.0*
21 mon	Def	9.4 ± 0.9	20.2 ± 0.6	31.7 ± 0.6	13.5 ± 0.7	3.8 ± 0.1	1.3 ± 0.2	19.3 ± 1.1	0.4 ± 0.1	14.4 ± 0.4	4.8 ± 0.4	11.0 ± 1.1	6.3 ± 0.8	38.9 ± 2.1	0.2 ± 0.0
	D0	20.8 ± 1.3*	19.5 ± 0.3	41.9 ± 1.5*	17.6 ± 1.2*	4.4 ± 0.3*	1.3 ± 0.3	24.2 ± 1.9*	0.3 ± 0.1	9.2 ± 1.2*	2.3 ± 0.2*	0.7 ± 0.1*	9.6 ± 1.6	23.7 ± 2.0*	0.8 ± 0.1*
	D3	20.5 ± 0.5*	18.8 ± 0.7	42.0 ± 0.4*	16.7 ± 0.8*	4.3 ± 0.1	1.0 ± 0.2	25.6 ± 0.9*	0.2 ± 0.1	9.5 ± 0.4*	1.8 ± 0.2*	0.7 ± 0.1*	9.0 ± 0.7	22.9 ± 0.2*	0.7 ± 0.1*
	D6	22.2 ± 2.2*	20.0 ± 1.6	43.8 ± 3.7*	18.0 ± 1.0*	4.5 ± 0.3*	1.2 ± 0.4	24.7 ± 1.5*	0.2 ± 0.0	8.3 ± 1.8*	1.7 ± 0.2*	0.5 ± 0.2*	8.8 ± 2.9	21.3 ± 5.0*	0.8 ± 0.1*

[a]Values are mean ± SD, n = 3. Values with an asterisk (*) are significantly different from diet Def (control group) at the $P < 0.05$ level as determined by ANOVA analysis followed by Dunnett's test.
[b]For composition of the Def, D0, D3, and D6 diets, see Tables 1 and 2. SFA, saturated FA; MUFA, monounsaturated FA.

TABLE 4
FA Composition[a] (as wt% of total identified FA) of Rat Cortex Phospholipids at Weaning or After Having Been Fed Diet Def, D0, D3, or D6[b] for 9 or 21 mon

		SFA			MUFA				PUFA							
		16:0	18:0	Σ SFA	18:1n-9	18:1n-7	20:1n-9	Σ MUFA	18:2n-6	20:4n-6	22:4n-6	22:5n-6	22:6n-3	Σ PUFA	n-3/n-6
Weaning		23.4 ± 0.7	20.6 ± 0.2	45.5 ± 1.2	12.4 ± 0.1	3.2 ± 0.1	0.4 ± 0.1	17.0 ± 0.1	1.0 ± 0.1	11.6 ± 0.2	3.0 ± 0.3	11.8 ± 0.6	1.2 ± 0.0	29.0 ± 1.2	0.04 ± 0.01
9 mon	Def	24.4 ± 2.2	21.3 ± 1.5	45.7 ± 3.7	14.1 ± 0.8	4.2 ± 0.2	0.6 ± 0.0	19.7 ± 0.8	0.5 ± 0.0	9.2 ± 1.4	2.7 ± 0.6	8.5 ± 1.5	2.7 ± 0.4	25.6 ± 3.9	0.1 ± 0.0
	D0	23.0 ± 0.4	16.5 ± 0.5*	41.5 ± 0.3	16.9 ± 0.5*	4.5 ± 0.0	1.3 ± 0.1*	24.4 ± 0.6*	0.6 ± 0.0	9.7 ± 0.3	2.4 ± 0.0	0.5 ± 0.1*	9.6 ± 0.4*	24.3 ± 0.7	0.7 ± 0.0*
	D3	23.7 ± 0.7	16.6 ± 0.3*	42.0 ± 1.0	16.9 ± 0.6*	4.4 ± 0.2	1.0 ± 0.1*	23.7 ± 0.7*	0.6 ± 0.1	10.1 ± 0.2	2.4 ± 0.1	0.4 ± 0.0*	10.4 ± 0.2*	25.1 ± 0.2	0.8 ± 0.0*
	D6	23.2 ± 1.5	16.6 ± 0.2*	41.7 ± 1.2	16.0 ± 0.3*	4.4 ± 0.0	1.1 ± 0.2*	23.0 ± 0.4*	0.6 ± 0.1	10.1 ± 0.2	2.5 ± 0.1	0.4 ± 0.0*	10.7 ± 0.3*	25.8 ± 0.3	0.8 ± 0.0*
21 mon	Def	9.7 ± 0.7	20.8 ± 0.7	34.3 ± 2.4	13.0 ± 0.6	3.7 ± 0.3	1.5 ± 0.3	18.9 ± 1.2	0.4 ± 0.1	13.1 ± 1.0	5.1 ± 0.3	11.7 ± 1.6	5.3 ± 1.1	37.6 ± 3.5	0.2 ± 0.0
	D0	21.1 ± 1.0*	20.3 ± 0.7	45.3 ± 3.0*	12.5 ± 2.4	3.0 ± 1.0	0.7 ± 0.2	23.6 ± 2.1	0.3 ± 0.1	8.5 ± 1.0*	1.7 ± 0.8*	0.6 ± 0.1*	10.6 ± 1.8*	23.1 ± 3.3*	0.9 ± 0.1*
	D3	23.6 ± 1.1*	21.0 ± 1.0	45.9 ± 2.3*	16.1 ± 2.0	4.2 ± 0.5	1.0 ± 0.2	23.6 ± 3.4	0.3 ± 0.0	9.0 ± 1.4*	2.0 ± 0.5*	0.5 ± 0.1*	10.3 ± 1.9*	22.3 ± 2.8*	0.8 ± 0.0*
	D6	22.1 ± 0.3*	19.3 ± 0.6	43.4 ± 0.9*	15.4 ± 1.1	4.2 ± 0.1	1.0 ± 0.1	23.9 ± 2.1	0.2 ± 0.0	9.0 ± 0.8*	1.9 ± 0.7*	0.4 ± 0.1*	11.3 ± 0.3*	24.0 ± 1.8*	1.0 ± 0.0*

[a]Values are mean ± SD, n = 3. Values with an asterisk (*) are significantly different from diet Def (control group) at the $P < 0.05$ level as determined by ANOVA analysis followed by Dunnett's test.
[b]For composition of the Def, D0, D3, and D6 diets, see Tables 1 and 2. For other abbreviations, see Table 3.

TABLE 5
FA Composition[a] (as wt% of total identified FA) of Rat Striatum Phospholipids at Weaning or After Having Been Fed Diet Def, D0, D3, or D6[b] for 9 or 21 mon

		SFA			MUFA				PUFA						
		16:0	18:0	Σ SFA	18:1n-9	18:1n-7	20:1n-9	Σ MUFA	18:2n-6	20:4n-6	22:4n-6	22:5n-6	22:6n-3	Σ PUFA	n-3/n-6
Weaning		20.7 ± 1.1	19.1 ± 0.3	41.2 ± 1.6	14.7 ± 1.6	3.9 ± 0.1	0.8 ± 0.1	21.2 ± 1.1	0.8 ± 0.0	10.3 ± 0.6	3.2 ± 0.1	10.7 ± 0.6	1.0 ± 0.2	26.6 ± 1.1	0.04 ± 0.0
9 mon	Def	20.9 ± 2.4	20.0 ± 0.6	45.3 ± 3.0	13.5 ± 2.0	4.1 ± 0.7	1.2 ± 0.3	19.7 ± 3.4	0.6 ± 0.2	9.1 ± 1.3	2.7 ± 0.4	7.2 ± 1.3	2.8 ± 0.4	25.7 ± 1.5	0.1 ± 0.0
	D0	18.5 ± 1.3	17.6 ± 0.7	38.5 ± 1.1	18.5 ± 2.1*	4.8 ± 0.2	1.8 ± 0.2*	26.8 ± 1.7*	1.1 ± 0.6	7.8 ± 2.0	2.1 ± 0.7	0.3 ± 0.2*	10.4 ± 0.1*	24.3 ± 1.1	0.8 ± 0.1*
	D3	16.9 ± 1.0	17.6 ± 0.7	37.1 ± 1.6	18.8 ± 1.2*	4.7 ± 0.2	1.9 ± 0.3*	24.5 ± 0.6*	0.7 ± 0.1	9.2 ± 0.3	2.3 ± 0.1	0.2 ± 0.1*	10.3 ± 0.7*	24.5 ± 0.4	0.8 ± 0.0*
	D6	17.3 ± 0.6	17.6 ± 0.5	36.8 ± 1.0	18.0 ± 0.8	4.8 ± 0.1	2.0 ± 0.1*	24.2 ± 0.3*	0.7 ± 0.1	9.3 ± 0.2	2.3 ± 0.1	0.3 ± 0.0*	9.7 ± 0.3*	24.2 ± 0.2	0.8 ± 0.0*
21 mon	Def	10.6 ± 0.5	19.5 ± 0.4	30.2 ± 0.6	14.3 ± 0.3	4.2 ± 0.1	2.4 ± 0.3	22.0 ± 0.8	0.5 ± 0.1	12.2 ± 0.5	4.7 ± 0.3	9.4 ± 1.3	5.4 ± 0.4	31.3 ± 0.7	0.2 ± 0.0
	D0	18.9 ± 0.5*	19.5 ± 0.2	40.0 ± 0.5*	17.4 ± 0.1	4.7 ± 0.1*	1.6 ± 0.3	24.5 ± 0.3*	0.2 ± 0.0*	9.1 ± 0.2*	2.4 ± 0.2*	0.5 ± 0.1*	11.1 ± 0.7*	25.0 ± 0.8*	0.9 ± 0.1*
	D3	18.9 ± 0.9*	19.3 ± 0.3	39.9 ± 0.8*	17.4 ± 0.6	4.8 ± 0.1*	1.6 ± 0.1	24.9 ± 0.9*	0.2 ± 0.0*	8.9 ± 0.3*	2.1 ± 0.0*	0.4 ± 0.1*	10.5 ± 0.8*	24.1 ± 0.7*	0.9 ± 0.1*
	D6	18.5 ± 0.7*	18.9 ± 0.5	40.1 ± 0.3*	17.1 ± 1.1	4.7 ± 0.1*	1.9 ± 0.2	26.8 ± 1.6*	0.1 ± 0.1*	8.4 ± 0.6*	1.6 ± 0.2*	0.3 ± 0.0*	9.9 ± 0.5*	22.0 ± 1.0*	0.9 ± 0.0*

[a]Values are mean ± SD, n = 3. Values with an asterisk (*) are significantly different from diet Def (control group) at the $P < 0.05$ level as determined by ANOVA analysis followed by Dunnett's test.
[b]For composition of the Def, D0, D3, and D6 diets, see Tables 1 and 2. For other abbreviations, see Table 3.

steps, whereas astrocytes are able to synthesize DHA either from 18-, 20-, and 22-carbon n-3 precursors (*via* desaturation and elongation steps) or from 24-carbon precursors (27). In contrast, neurons may be unable to carry out FA desaturation and thus may be dependent on preformed long-chain PUFA released from endothelial cells or astrocytes. In addition, almost all 22:6n-3 is recycled from phospholipid breakdown (28,29), and this recycling ensures a well-regulated level in brain membranes (30).

The impact of aging and dietary n-3 FA intake on plasmalogen levels was assessed by the quantification of DMA (Table 6). The alkenyl chains of plasmalogens are mainly saturated. The most abundant DMA were hexadecanal dimethylacetal and octadecanal dimethylacetal. Minor amounts of monounsaturated species are present. At weaning, plasmalogen levels represented 25% of total phospholipids in the hippocampus, 21% in the striatum, and 17% in the cortex. The diet had no effect on DMA levels in the three structures whatever the age. Our results can be related to previous reports. Indeed, it has been shown that dietary supplementation with DHA-ethyl ester to Zellweger patients whose tissues and cells are strongly deficient in DHA and plasmalogens (31) increased plasmalogen concentrations in erythrocytes after DHA concentrations were normalized (32). In our study, the plasmalogen contents were not different between the four experimental groups, whereas DHA levels were quite different. First, we can suppose that DHA is not the only parameter to influence plasmalogen levels. Second, Zellweger patients received 0.1 g DHA/kg of body mass/d (pharmacological approach), whereas rats in the present study were fed 0.007 or 0.014 g DHA/kg of body mass/d (nutritional approach). Animals were not in a pathological situation, which may explain why the plasmalogen content was not influenced by the DHA level. Between 9 and 21 mon of diet, the plasmalogen levels fell significantly in the hippocampus and cortex. This decrease supports the free radical theory of aging and the potential physiological antioxidant function of plasmalogens. A decline of plasmalogen levels in neuronal tissue has already been observed in normal aging in human beings (10) and in old cattle (33). Moreover, the loss of myelin, a membrane very rich in plasmalogens, is a normal phenomenon in aging brains (34), which may explain the decrease in plasmalogen content in aged rats. Whereas plasmalogen levels decreased after 21 mon of diet, DHA levels increased in the hippocampus and remained stable in the cortex and striatum. Other studies showed a decrease in DHA levels during aging (35). Such a difference may be explained by the experimental model of n-3-deficient animals. We may assume that the intake of α-LNA alone or combined with DHA at nutritional levels may not be sufficient in aged animals to oppose the physiological decrease in plasmalogen levels.

Finally, the impact of dietary FA intake on the *sn*-2 substitution of PlsEtn in the hippocampus (Table 7), cortex (Table 8), and striatum (Table 9) was assessed. PlsEtn were specifically considered because of their high content in the brain. The FA composition of PlsEtn was different in the three brain regions of weaned rats. The *sn*-2 substitutions were mainly saturated FA in the hippocampus and the striatum (45.9% and 43.8%, respectively) whereas monounsaturated FA (40%) and PUFA

TABLE 6
Dimethylacetal Levels[a] (μg/g wet brain) in the Rat Hippocampus, Cortex, and Striatum at Weaning and After Having Been Fed Diet Def, D0, D3, or D6[b] for 9 or 21 mon

		Hippocampus	Cortex	Striatum
Weaning		3.45 (± 0.11)	1.83 (± 0.16)	2.43 (± 0.52)
9 mon	Def	4.58 (± 1.11)	1.62 (± 0.79)	2.64 (± 1.26)
	D0	6.69 (± 2.36)	2.27 (± 0.33)	4.38 (± 2.87)
	D3	8.44 (± 1.08)	2.61 (± 0.03)	5.31 (± 0.68)
	D6	7.88 (± 1.01)	2.57 (± 0.37)	5.14 (± 1.15)
21 mon	Def	2.45 (± 0.83)	1.60 (± 0.14)	2.83 (± 0.63)
	D0	2.89 (± 0.86)	1.86 (± 0.52)	3.26 (± 0.13)
	D3	2.43 (± 0.38)	1.86 (± 0.20)*	3.68 (± 0.45)
	D6	2.62 (± 0.47)	1.94 (± 0.45)*	3.49 (± 0.35)*

[a]Values are mean ± SD, $n = 3$. Values with an asterisk (*) are significantly different from 9 mon at the $P < 0.05$ level as determined by ANOVA analysis followed by a Kruskal–Wallis test.
[b]For composition of the Def, D0, D3, and D6 diets, see Tables 1 and 2. For other abbreviations, see Table 3.

(38%) were more abundant in the cortex. The main changes in the FA composition of PlsEtn were similar for diets D0, D3, and D6. After 9 mon of diet, in our animal model, the n-3 repletion with α-LNA alone or combined with DHA led to the same high and significant increase in DHA levels. Our results are controversial with regard to previous ones showing that DHA is more efficient at restoring DHA levels in the brain than is α-LNA (36–38). These findings indicate that 18:3n–3 supplementation at 0.12 g/100 g of diet may be sufficient to support recovery of the 22:6n-3 concentration in PlsEtn. After 21 mon of diet, PUFA represented more than 40% of the *sn*-2 substitutions in PlsEtn whatever the structure. PUFA levels were the highest in the cortex where they reached 55, 57, and 57% for diets D0, D3, and D6, respectively. DHA was the first major PUFA and arachidonic acid the second. These FA are incorporated selectively in PlsEtn, which represent a reservoir of PUFA. They are released from plasmalogens by the plasmalogen-selective phospholipase A$_2$ (39) to be metabolized into eicosanoids and docosanoids. The rapid turnover of brain plasmalogens (40) may suggest that their antioxidant properties are not their only physiological functions. It is thought that they may function as signaling molecules in the brain, as they do in the heart (41–42).

ACKNOWLEDGMENTS

REFERENCES

1. Svennerholm, L., Bostrom, K., Helander, C.G., and Jungbjer, B. (1991) Membrane Lipids in the Aging Human Brain, *J. Neurochem. 56*, 2051–2059.
2. Eichenbaum, H., Otto, T., and Cohen, N.J. (1992) The Hippocampus—What Does It Do? *Behav. Neurol. Biol. 57*, 2–36.
3. Horrocks, L.A. (1972) Content, Composition, and Metabolism of Mammalian and Avian Lipids that Contain Ether Groups, in *Ether Lipids: Chemistry and Biology* (Snyder, F., ed.), pp. 177–272, Academic Press, New York.

TABLE 7
FA Composition[a] (as wt% of total identified FA) of Ethanolamine Plasmalogens of Rat Hippocampus at Weaning and After Having Been Fed Diet Def, D0, D3, or D6b for 9 or 21 mon

		SFA			MUFA				PUFA				
		16:0	18:0	Σ SFA	18:1n-9	18:1n-7	20:1n-9	Σ MUFA	18:2n-6	20:4n-6	22:4n-6	22:6n-3	Σ PUFA
Weaning		22.6 ± 4.8	23.2 ± 16.2	45.9 ± 17.8	18.9 ± 10.8	1.8 ± 1.1	1.6 ± 0.8	22.3 ± 11.4	8.6 ± 7.3	7.5 ± 6.9	4.0 ± 3.5	1.1 ± 1.0	21.2 ± 8.8
9 mon	Def	24.8 ± 3.0	22.5 ± 4.7	47.4 ± 7.7	18.6 ± 3.9	3.3 ± 0.5	4.0 ± 0.1	25.9 ± 4.1	6.5 ± 3.5	6.8 ± 2.6	4.5 ± 1.7	1.9 ± 0.8	19.8 ± 1.6
	D0	15.8 ± 5.4	17.2 ± 3.8	33.1 ± 3.1	16.1 ± 1.2	1.7 ± 0.4*	3.1 ± 1.4	20.9 ± 1.8	9.8 ± 3.6	1.8 ± 1.1	3.2 ± 2.4	22.2 ± 1.1*	37.1 ± 4.0*
	D3	16.9 ± 8.5	15.2 ± 2.8	32.1 ± 8.4	24.1 ± 4.6	2.9 ± 0.6	6.6 ± 3.4	33.6 ± 5.8	4.1 ± 1.9	5.0 ± 2.7	5.9 ± 3.9	25.0 ± 1.0*	39.1 ± 6.1*
	D6	17.4 ± 7.8	20.2 ± 4.4	37.8 ± 6.9	18.7 ± 5.9	2.1 ± 0.6	2.9 ± 1.0	23.7 ± 7.3	6.4 ± 1.6	2.8 ± 2.3	3.0 ± 1.5	22.6 ± 1.7*	34.9 ± 3.4*
21 mon	Def	9.1 ± 3.4	7.1 ± 2.8	16.2 ± 6.1	21.3 ± 3.4	3.2 ± 0.2	4.1 ± 1.4	28.7 ± 4.6	1.0 ± 0.3	19.9 ± 0.2	11.1 ± 1.6	8.2 ± 0.4	40.2 ± 1.1
	D0	2.8 ± 1.7*	4.2 ± 1.7	7.0 ± 3.4*	23.0 ± 5.6	3.2 ± 1.0	8.5 ± 0.4*	34.7 ± 7.0	0.5 ± 0.1	14.3 ± 1.8*	12.0 ± 2.6	27.4 ± 5.1*	54.2 ± 9.4
	D3	4.3 ± 0.6*	7.5 ± 0.7	11.8 ± 1.3	25.2 ± 0.9	3.9 ± 0.3	8.1 ± 0.9*	37.2 ± 0.2	1.3 ± 0.3	12.8 ± 0.2*	8.9 ± 0.1	24.2 ± 0.5*	47.1 ± 1.1
	D6	3.2 ± 0.3*	4.1 ± 0.6	7.3 ± 0.5*	24.6 ± 2.7	2.6 ± 1.4	8.8 ± 1.1*	36.1 ± 4.6	1.1 ± 0.4	14.9 ± 0.7*	11.1 ± 0.9	24.0 ± 2.8*	51.1 ± 3.7

[a]Values are mean ± SD, $n = 3$. Values with an asterisk (*) are significantly different from diet Def (control group) at the $P < 0.05$ level as determined by ANOVA analysis followed by Dunnett's test.
[b]For composition of the Def, D0, D3, and D6 diets, see Tables 1 and 2. For other abbreviations, see Table 3.

TABLE 8
FA Composition[a] (as wt% of total identified FA) of Ethanolamine Plasmalogens of Rat Cortex at Weaning and After Having Been Fed Diet Def, D0, D3, or D6b for 9 or 21 mon

		SFA			MUFA				PUFA				
		16:0	18:0	Σ SFA	18:1n-9	18:1n-7	20:1n-9	Σ MUFA	18:2n-6	20:4n-6	22:4n-6	22:6n-3	Σ PUFA
Weaning		13.0 ± 3.0	4.6 ± 1.4	17.5 ± 3.4	28.8 ± 2.5	4.4 ± 0.3	7.0 ± 1.3	40.3 ± 3.4	1.8 ± 0.4	19.3 ± 1.2	11.6 ± 1.9	5.5 ± 1.4	38.1 ± 3.4
9 mon	Def	14.9 ± 1.0	5.0 ± 1.4	20.0 ±2.2	29.4 ± 3.2	3.1 ± 0.8	5.7 ± 2.3	38.2 ± 6.1	0.5 ± 0.3	21.1 ± 2.3	10.1 ± 2.5	4.8 ± 0.6	36.7 ± 5.6
	D0	10.6 ± 3.1	6.1 ± 1.3	16.6 ± 4.4	24.6 ± 5.7	3.2 ± 0.8	5.6 ± 0.6	33.4 ± 7.0	0.8 ± 0.4	15.8 ± 2.1	7.6 ± 2.2	17.5 ± 2.0*	41.8 ± 5.2
	D3	9.1 ± 3.4	7.9 ± 2.8	17.0 ± 5.6	23.1 ± 2.5	3.3 ± 0.3	5.1 ± 0.5	31.7 ± 3.1	0.6 ± 0.2	16.7 ± 2.1	8.7 ± 1.3	21.8 ± 1.9*	47.7 ± 5.1
	D6	4.4 ± 0.7*	5.7 ± 3.1	10.1 ± 3.8	25.9 ± 4.5	3.4 ± 0.8	7.3 ± 2.9	36.7 ± 8.1	0.4 ± 0.3	14.0 ± 2.8*	8.9 ± 2.2	24.1 ± 2.6*	47.4 ± 7.2
21 mon	Def	7.5 ± 2.1	6.9 ± 0.1	14.4 ± 2.3	20.3 ± 0.2	2.8 ± 0.3	4.6 ± 0.8	27.7 ± 0.9	0.4 ± 0.2	21.4 ± 1.1	11.9 ± 0.1	7.8 ± 1.1	41.5 ± 0.1
	D0	3.8 ± 0.1*	4.2 ± 0.3*	8.0 ± 0.1*	24.2 ± 0.6*	3.2 ± 0.1	6.1 ± 0.4	33.5 ± 1.1	0.5 ± 0.0	18.5 ± 0.3	10.9 ± 0.1	25.4 ± 0.9*	55.3 ± 1.3*
	D3	3.4 ± 0.8*	3.0 ± 0.1*	6.4 ± 0.8*	23.6 ± 1.0	3.0 ± 0.2	6.7 ± 1.7	33.2 ± 2.8	0.4 ± 0.1	19.2 ± 1.2	11.1 ± 0.4	26.2 ± 1.1*	56.9 ± 2.9*
	D6	2.7 ± 1.4*	2.5 ± 0.3*	5.2 ± 1.8*	23.7 ± 1.6	3.3 ± 0.1	7.6 ± 0.1	34.5 ± 1.5*	0.4 ± 0.1	17.6 ± 1.1*	11.3 ± 0.5	27.4 ± 1.5*	56.7 ± 2.7*

[a]Values are mean ± SD, n = 3. Values with an asterisk (*) are significantly different from diet Def (control group) at the $P < 0.05$ level as determined by ANOVA analysis followed by Dunnett's test.
[b]For composition of the Def, D0, D3, and D6 diets, see Tables 1 and 2. For other abbreviations, see Table 3.

TABLE 9
FA Composition[a] (as wt% of total identified FA) of Ethanolamine Plasmalogens of Rat Striatum at Weaning and After Having Been Fed Diet Def, D0, D3, or D6b for 9 or 21 mon

		SFA			MUFA				PUFA				
		16:0	18:0	Σ SFA	18:1n-9	18:1n-7	20:1n-9	Σ MUFA	18:2n-6	20:4n-6	22:4n-6	22:6n-3	Σ PUFA
Weaning		31.5 ± 5.1	12.3 ± 2.2	43.8 ± 7.3	20.6 ± 1.8	2.5 ± 0.3	1.9 ± 0.9	25.0 ± 3.0	5.4 ± 0.4	8.3 ± 1.9	2.5 ± 1.0	1.9 ± 0.7	18.0 ± 4.0
9 mon	Def	23.6 ± 0.6	16.5 ± 0.9	40.1 ± 1.6	24.3 ± 4.3	4.0 ± 0.8	2.1 ± 0.1	30.5 ± 5.0	2.4 ± 0.5	12.5 ± 1.3	6.1 ± 0.6	2.7 ± 0.5	28.4 ± 0.5
	D0	19.3 ± 3.7	19.1 ± 3.1	38.4 ± 0.6	19.3 ± 5.4	1.9 ± 0.4*	1.7 ± 0.4	23.3 ± 8.2	5.1 ± 0.2*	2.0 ± 0.7*	2.1 ± 1.5*	20.8 ± 1.6*	36.0 ± 3.6
	D3	18.3 ± 5.1	13.2 ± 2.7	31.5 ± 7.1	21.0 ± 3.1	2.8 ± 0.7	3.9 ± 2.2	27.6 ± 5.6	3.8 ± 2.0	7.5 ± 3.2*	4.4 ± 2.3	18.8 ± 4.5*	33.8 ± 7.9
	D6	17.1 ± 3.1	14.1 ± 2.9	31.2 ± 5.7	27.8 ± 6.2	2.9 ± 0.8	2.8 ± 1.6	33.5 ± 3.4	4.2 ± 1.0	5.1 ± 3.3*	2.4 ± 1.8*	18.6 ± 5.0*	30.3 ± 8.9
21 mon	Def	18.7 ± 5.8	14.8 ± 5.8	33.5 ± 6.5	24.6 ± 3.6	2.9 ± 1.9	4.3 ± 1.4	31.8 ± 4.3	3.5 ± 0.8	9.9 ± 3.1	6.8 ± 2.6	4.4 ± 2.1	24.7 ± 3.9
	D0	3.8 ± 1.2*	4.0 ± 0.4*	7.7 ± 0.8*	28.5 ± 5.6	4.3 ± 0.6	9.6 ± 0.7*	42.4 ± 5.4	0.8 ± 0.2	16.8 ± 1.2*	9.2 ± 1.5	19.1 ± 2.6*	45.9 ± 5.2*
	D3	4.5 ± 2.1*	7.0 ± 4.5	11.4 ± 6.6*	26.1 ± 3.9	3.9 ± 0.7	8.5 ± 0.7*	38.6 ± 5.0	0.7 ± 0.1	15.9 ± 3.6*	9.0 ± 1.7	21.3 ± 4.3*	46.9 ± 9.6*
	D6	3.8 ± 1.1*	4.6 ± 1.2*	8.3 ± 2.3*	31.7 ± 3.6	5.0 ± 0.7	9.9 ± 0.6*	46.7 ± 3.6*	0.4 ± 0.2	13.7 ± 1.0	8.0 ± 1.4	18.9 ± 3.2*	41.3 ± 5.7

[a]Values are mean ± SD, n = 3. Values with an asterisk (*) are significantly different from diet Def (control group) at the $P < 0.05$ level as determined by ANOVA analysis followed by Dunnett's test.
[b]For composition of the Def, D0, D3, and D6 diets, see Tables 1 and 2. For other abbreviations, see Table 3.

4. Nagan, N., and Zoeller, R.A. (2001) Plasmalogens: Biosynthesis and Functions, *Prog. Lipid Res. 40*, 199–229.

5. Glaser, P.E., and Gross, R.W. (1994) Plasmenylethanolamine Facilitates Rapid Membrane Fusion: A Stopped-Flow Kinetic Investigation Correlating the Propensity of a Major Plasma Membrane Constituent to Adopt an HII Phase with Its Ability to Promote Membrane Fusion, *Biochemistry. 33*, 5805–5812.

6. Farooqui, A.A., and Horrocks, L.A. (2001) Plasmalogens, Phospholipase A$_2$, and Docosahexaenoic Acid Turnover in Brain Tissue, *J. Mol. Neurosci. 16*, 263–284.

7. Harman, D. (1992) Free Radical Theory of Aging, *Mutat. Res. 275*, 257–266.

8. Mangold, H.K., and Weber, N. (1987) Biosynthesis and Biotransformation of Ether Lipids, *Lipids 22*, 789–799.

9. Zoeller, R.A., Lake, A.C., Nagan, N., Gaposchkin, D.P., Legner, M.A., and Lieberthal, W. (1999) Plasmalogens as Endogenous Antioxidants: Somatic Cell Mutants Reveal the Importance of the Vinyl Ether, *Biochem. J. 338*, 769–776.

10. Weisser, M., Vieth, M., Stolte, M., Riederer, P., Pfeuffer, R., Leblhuber, F., and Spiteller, G. (1997) Dramatic Increase of α-Hydroxyaldehydes Derived from Plasmalogens in the Aged Human Brain, *Chem. Phys. Lipids 90*, 135–142.

11. Han, X., Holtzman, D.M., and McKeel, D.W. (2001) Plasmalogen Deficiency in Early Alzheimer's Disease Subjects and in Animal Models: Molecular Characterization Using Electrospray Ionization Mass Spectrometry, *J. Neurochem. 77*, 1168–1180.

12. Soderberg, M., Edlund, C., Kristensson, K., and Dallner, G. (1991) Fatty Acid Composition of Brain Phospholipids in Aging and in Alzheimer's Disease, *Lipids 26*, 421–425.

13. Frances, H., Coudereau, J.P., Sandouk, P., Clement, M., Monier, C., and Bourre, J.M. (1996) Influence of a Dietary α-Linolenic Acid Deficiency on Learning in the Morris Water Maze and on the Effects of Morphine, *Eur. J. Pharmacol. 298*, 217–225.

14. Mitchell, D.C., Gawrisch, K., Litman, B.J., and Salem, N. (1998) Why Is Docosahexaenoic Acid Essential for Nervous System Function? *Biochem. Soc. Trans. 26*, 365–370.

15. Favrelière, S., Perault, M.C., Huguet, F., De Javel, D., Bertrand, N., Piriou, A., and Durand, G. (2003) DHA-Enriched Phospholipid Diets Modulate Age-Related Alterations in Rat Hippocampus, *Neurobiol. Aging 24*, 233–243.

16. Folch, J., Lees, M., and Sloane Stanley, G.H. (1957) A Simple Method for the Isolation and Purification of Total Lipids from Animal Tissues, *J. Biol. Chem. 226*, 497–509.

17. Juanéda, P., and Rocquelin, G. (1985) Rapid and Convenient Separation of Phospholipids and Non Phosphorus Lipids from Rat Heart Using Silica Cartridges, *Lipids 20*, 40–41.

18. Morrison, W.R., and Smith, L.M. (1964) Preparation of Fatty Acid Methyl Esters and Dimethylacetals from Lipids with Boron Fluoride–Methanol, *J. Lipid Res. 5*, 600–608.

19. Juanéda, P., Rocquelin, G., and Astorg, P.O. (1990) Separation and Quantification of Heart and Liver Phospholipid Classes by High-Performance Liquid Chromatography Using a New Light-Scattering Detector, *Lipids 25*, 756–759.

20. Delion, S., Chalon, S., Guilloteau, D., Lejeune, B., Besnard, J.C., and Durand, G. (1997) Age-Related Changes in Phospholipid Fatty Acid Composition and Monoaminergic Neurotransmission in the Hippocampus of Rats Fed a Balanced or an n-3 Polyunsaturated Fatty Acid-Deficient Diet, *J. Lipid Res. 38*, 680–689.

21. Delion, S., Chalon, S., Guilloteau, D., Besnard, J.C., and Durand, G. (1996) α-Linolenic Acid Dietary Deficiency Alters Age-Related Changes of Dopaminergic and Serotoninergic Neurotransmission in the Rat Frontal Cortex, *J. Neurochem. 66*, 1582–1591.

22. Nishizuka, Y. (1984) The Role of Protein Kinase C in Cell Surface Signal Transduction and Tumour Promotion, *Nature 308*, 693–698.

23. Bourre, J.M., Pascal, G., Durand, G., Masson, M., Dumont, O., and Piciotti, M. (1984) Alterations in the Fatty Acid Composition of Rat Brain Cells (neurons, astrocytes, and oligodendrocytes) and of Subcellular Fractions (myelin and synaptosomes) Induced by a Diet Devoid of n-3 Fatty Acids, *J. Neurochem. 43*, 342–348.

24. Favrelière, S., Barrier, L., Durand, G., Chalon, S., and Tallineau, C. (1998) Chronic Dietary n-3 Polyunsaturated Fatty Acid Deficiency Affects the Fatty Acid Composition of Plasmenylethanolamine and Phosphatidylethanolamine Differently in Rat Frontal Cortex, Striatum, and Cerebellum, *Lipids 33*, 401–407.

25. Moriguchi, T., Loewke, J., Garrison, M., Catalan, J.N., and Salem, N. (2001) Reversal of Docosahexaenoic Acid Deficiency in the Rat Brain, Retina, Liver, and Serum, *J. Lipid Res. 42*, 419–427.

26. Spector, A.A. (2001) Plasma Free Fatty Acid and Lipoproteins as Sources of Polyunsaturated Fatty Acid for the Brain, *J. Mol. Neurosci. 16*, 159–165.

27. Moore, S.A. (2001) Polyunsaturated Fatty Acid Synthesis and Release by Brain-Derived Cells *in vitro*, *J. Mol. Neurosci. 16*, 195–221.

28. Rapoport, S.I. (1996) *In vivo* Labeling of Brain Phospholipids by Long-Chain Fatty Acids: Relation to Turnover and Function, *Lipids 31*, S97–S101.

29. Rapoport, S.I., Chang, M.C., and Spector, A.A. (2001) Delivery and Turnover of Plasma-Derived Essential PUFAs in Mammalian Brain, *J. Lipid Res. 42*, 678–685.

30. Gazzah, N., Gharib, A., Bobillier, P., Lagarde, M., and Sarda, N. (1994) Evidence for Brain Docosahexaenoate Recycling in the Free-Moving Adult Rat: Implications for Measurement of Phospholipid Synthesis, *Neurosci. Lett. 177*, 103–106.

31. Martinez, M. (1992) Abnormal Profiles of Polyunsaturated Fatty Acids in the Brain, Liver, Kidney and Retina of Patients with Peroxisomal Disorders, *Brain Res. 583*, 171–182.

32. Martinez, M. (2001) Restoring the DHA Levels in the Brains of Zellweger Patients, *J. Mol. Neurosci. 16*, 309–316.

33. Weisser, M., and Spiteller, G. (1996) Increase of Aldehydic Compounds Derived from Plasmalogens in the Brain of Aged Cattle, *Chem. Phys. Lipids 82*, 173–178.

34. Guttmann, C.R., Jolesz, F.A., Kikinis, R., Killiany, R.J., Moss, M.B., Sandor, T., and Albert, M.S. (1998) White Matter Changes with Normal Aging, *Neurology 50*, 972–978.

35. Favrelière, S., Stadelmann-Ingrand, S., Huguet, F., De Javel, D., Piriou, A., Tallineau, C., and Durand, G. (2000) Age-Related Changes in Ethanolamine Glycerophospholipid Fatty Acid Levels in Rat Frontal Cortex and Hippocampus, *Neurobiol. Aging 21*, 653–660.

36. Menard, C.R., Goodman, K.J., Corso, T.N., Brenna, J.T., and Cunnane, S.C. (1998) Recycling of Carbon into Lipids Synthesized *de novo* Is a Quantitatively Important Pathway of α-[U-^{13}C]Linolenate Utilization in the Developing Rat Brain, *J. Neurochem. 71*, 2151–2158.

37. Sinclair, A.J., Attar-Bashi, N.M., and Li, D. (2002) What Is the Role of α-Linolenic Acid for Mammals? *Lipids 37*, 1113–1123.

38. Su, H.M., Bernardo, L., Mirmiran, M., Ma, X.H., Nathanielsz, P.W., and Brenna, J.T. (1999) Dietary 18:3n-3 and 22:6n-3 as Sources of 22:6n-3 Accretion in Neonatal Baboon Brain and Associated Organs, *Lipids 34*, S347–S350.

39. Hirashima, Y., Farooqui, A.A., Mills, J.S., and Horrocks, L.A. (1992) Identification and Purification of Calcium-Independent Phospholipase A$_2$ from Bovine Brain Cytosol, *J. Neurochem. 59*, 708–714.

40. Rosenberger, T.A., Oki, J., Purdon, A.D., Rapoport, S.I., and Murphy, E.J. (2002) Rapid Synthesis and Turnover of Brain Microsomal Ether Phospholipids in the Adult Rat, *J. Lipid Res. 43*, 59–68.

41. Hazen, S.L., Ford, D.A., and Gross, R.W. (1991) Activation of a Membrane-Associated Phospholipase A$_2$ During Rabbit Myocardial Ischemia Which Is Highly Selective for Plasmalogen Substrate, *J. Biol. Chem. 266*, 5629–5633.

42. McHowat, J., Liu, S., and Creer, M.H. (1998) Selective Hydrolysis of Plasmalogen Phospholipids by Ca^{2+}-Independent PLA$_2$ in Hypoxic Ventricular Myocytes, *Am. J. Physiol. 274*, C1727–C1737.

Docosahexaenoic Acid Supplementation in Vegetarians Effectively Increases Omega-3 Index: A Randomized Trial

Julia Geppert, Veronika Kraft, Hans Demmelmair, and Berthold Koletzko*

Division of Metabolic Diseases and Nutrition, Dr. von Hauner Children's Hospital,
Ludwig Maximilians University of Munich, D-80337 Munich, Germany

ABSTRACT: Low red blood cell (RBC) membrane content of EPA + DHA (hereafter called omega-3 index) has recently been described as an indicator for increased risk of death from coronary heart disease. The relationship between plasma and RBC FA, focusing on omega-3 index, and the response to DHA supplementation were investigated in a double-blind, randomized, placebo-controlled, intervention study. Healthy vegetarians (87 f, 17 m) consumed daily a microalgae oil from *Ulkenia* sp. (0.94 g DHA/d) or olive oil (placebo) for 8 wk. DHA supplementation significantly increased DHA in RBC total lipids (7.9 vs. 4.4 wt%), in RBC PE (12.1 vs. 6.5 wt%), in RBC PC (3.8 vs. 1.4 wt%), and in plasma phospholipids (PL) (7.4 vs. 2.8 wt%), whereas EPA levels rose to a much lesser extent. Microalgae oil supplementation increased the omega-3 index from 4.8 to 8.4 wt%. After intervention, 69% of DHA-supplemented subjects (but no subject of the placebo group) reached an omega-3 index above the desirable value of 8 wt%. Omega-3 index and EPA + DHA levels in RBC PE, RBC PC, and plasma PL were closely correlated (*r* always > 0.9). We conclude that an 8-wk supplementation with 0.94 g DHA/d from microalgae oil achieves a beneficial omega-3 index of ≥8% in most subjects with low basal EPA + DHA status. RBC total FA analyses can be used instead of RBC lipid fraction analyses for assessing essential FA status, e.g., in clinical studies.

Paper no. L9761 in *Lipids 40*, 807-814 (August 2005)

The risk for many chronic diseases, including coronary heart disease (CHD), is influenced by dietary FA intake (1–3). A higher degree of incorporation of n-3 long-chain PUFA (n-3 LCPUFA) into myocardial membranes reduces deaths following myocardial ischemia (4). Harris *et al.* (5) showed that n-3 LCPUFA content in red blood cell (RBC) membranes reflects that of cardiac membranes. A low RBC EPA + DHA percentage content (hereafter called omega-3 index) has recently been identified as a risk indicator for death from CHD (6). The relationship between the omega-3 index and the risk for CHD

death, especially sudden cardiac death, was evaluated using the data from several published primary and secondary prevention studies. An omega-3 index of ≥8% was associated with the greatest cardioprotection, whereas an index of ≤4% was associated with the highest risk. For clinical studies it is of interest to know whether RBC total lipid FA correspond to values found in other lipid classes [plasma phospholipids (PL), RBC PC, RBC PE] in subjects whose FA composition is in a steady state. Harris and von Schacky (6) observed significant increases of the omega-3 index after EPA and DHA supplementation (1 g/d) for 5 mon, ranging after intervention from 5 to 13%. These different levels in people consuming the same amount of EPA + DHA were caused by individual differences in baseline values of the omega-3 index, digestion, absorption, transport, uptake in target tissues, metabolism from storage sites, and *in vivo* conversion of α-linolenic acid (ALA) to LCPUFA derivatives. Consequently, a subject with low baseline omega-3 index may require a larger dose than a person with a high baseline value. Further studies investigating the dose–response relationship between EPA + DHA intake and the omega-3 index in subjects with different background diets are needed.

Ovolacto vegetarians consume minimal amounts of EPA and varying amounts of DHA from eggs, milk, and dairy products (average intakes < 33 mg/d) (7). Vegans consume negligible amounts of n-3 LCPUFA and rely entirely on *in vivo* biosynthesis of n-3 LCPUFA from the precursor ALA, but conversion via desaturation and elongation, especially to DHA, is not efficient (8). Previous studies with stable isotopically labeled ALA have shown conversion of ALA to EPA varying from 6–21% (9–11) to much lower values (0.1–0.2%) (12–14). Reports on the conversion of ALA to DHA range from 4–9% (9,11) to 0.04% (15), or undetectable DHA synthesis (10). Lack of EPA and DHA in vegetarian diets is reflected in reduced amounts of these FA in platelets, RBC, and plasma (16–21). Thus, uptake of preformed DHA from the diet may be critical for maintaining adequate membrane DHA concentrations.

The aim of the present study was to investigate the effects of a supplementation with a single-cell oil derived from microalgae *Ulkenia* sp. (Nutrinova DHA, Nutrinova GmbH, Frankfurt/Main, Germany) on plasma and RBC FA composition in subjects with a low habitual n-3 LCPUFA intake. In addition, the relationship between FA of various lipid fractions, focusing on omega-3 index, was determined.

MATERIALS AND METHODS

Study design and subjects. A randomized, double-blind, placebo-controlled, parallel-intervention study was performed. One hundred fourteen free-living and healthy vegetarians aged from 18–43 yr were recruited in the Munich area *via* posters displayed in health food shops and on the university campus, as well as through personal contacts. For inclusion in the study, volunteers were required to have been on a vegetarian diet for at least 1 yr. A vegetarian was defined as someone who ate no meat and not more than one fish meal a month. Inclusion criteria were age ≥ 18 yr and a body mass index (BMI) between 18 and 25 kg/m^2. Exclusion criteria were intake of medication with known influence on the lipid metabolism during the last 3 mon; intake of supplements with n-3 FA; metabolic, cardiovascular, renal, or neurological diseases; and pregnancy or lactation. The study received ethical approval by the Bavarian Board of Physicians. All subjects provided their written, informed consent before study entry and received financial compensation (200 Euro each) for their participation in the study.

The study was conducted between June and November 2003. The subjects consumed either four capsules per day containing a total of 2.28 g DHA-rich oil from microalgae *Ulkenia* sp., providing 0.94 g DHA/d, or olive oil as placebo for 8 wk. They were randomly assigned to the two intervention groups with stratification for gender. The FA composition of the two study oils is given in Table 1. To ensure that the treatments had the same antioxidant content, each oil contained 1000 ppm mixed natural tocopherols (equals 2.2–2.3 mg mixed natural tocopherols per day).

Before the first visit, subjects had to complete a questionnaire that included a survey on medications, metabolic and cardiovascular diseases, dietary supplements, frequency of fish and egg consumption, and a 3-d dietary record (two weekdays and one weekend day). At the end of the intervention period, they recorded their diet again for 3 d. Subjects were weighed before and after the intervention; height was measured at study entry. Compliance was assessed by counting leftover capsules and by the plausibility of the DHA increase in RBC PE. Subject characteristics ($n = 114$) at entry were age (25.9 ± 5.6 yr;

mean ± SD), BMI (21.3 ± 1.9 kg/m^2), years on a vegetarian diet (9.3 ± 5.2 yr), gender ratio (87 f, 27 m), and proportion of non-smokers (77%) with no significant differences in these parameters between the two groups ($P > 0.05$).

Dietary evaluation. Three-day dietary records were evaluated with the Prodi version 4.5 LE 2003 software (Wissenschaftliche Verlagsgesellschaft mbH, Stuttgart, Germany). Nutrient intake was calculated based on the German Nutrient database BLS, version II.3 (BgVV, Berlin, Germany).

Sample collection procedures. At day 0 (prior to supplementation) and after 56–60 d of capsule intake, blood samples were collected from an antecubital vein of the forearm into EDTA-containing tubes (Sarstedt, Nümbrecht, Germany) after an overnight fast. Blood was centrifuged at $1000 \times g$ for 7 min at room temperature within 2 h. Subsamples of plasma were stored at −80°C and analyzed within 12 mon of storage. Blood cells were washed 3 times with 0.9% NaCl (Baxter, Lessines, Belgium) and the buffy coat was removed. After lysis with distilled water (at least 200 μL/0.5 mL RBC sediment) (B.Braun, Melsungen, Germany), isopropanol (Merck, Darmstadt, Germany) with BHT (50 mg/l) (Fluka, Neu-Ulm, Germany) was added to prevent oxidation, and the tubes were frozen at −80°C. For each lipid fraction, FA analyses of a given subject were performed within the same analytical run.

FA analysis in study oils, plasma, and RBC. Unless otherwise indicated, all reagents used were obtained from Merck. FAME from microalgae and olive oil TG were obtained by reaction with 1.5 M methanolic hydrochloric acid (Supelco, Bellefonte, PA) in *n*-hexane at 90°C for 60 min in closed glass tubes. After adding distilled water and *n*-hexane with BHT (2 g/L), the samples were vortexed and centrifuged. The upper *n*-hexane phase containing the FAME was analyzed by capillary GLC (Hewlett-Packard 5890 Series II gas chromatograph, equipped with a 60 m × 0.32 mm BPX-70 column from SGE, Weiterstadt, Germany). FID signals were evaluated with the software EZ-Chrom Elite version 2.61 (Scientific Software, Pleasanton, CA). FAME peaks were identified by comparison with commercial standards (Nu-Chek-Prep, Elysian, MN). Values were calculated as weight percentages of all FA determined (14–24 C atoms).

Lipids from plasma were extracted three times; initially with *n*-hexane/isopropanol (3:2 vol/vol), then twice with *n*-hexane. PL, free cholesterol, nonesterified FA, TG, and cholesterol ester were separated using TLC (Merck) with *n*-heptane, diisopropylether, and glacial acetic acid (60:40:3, by vol) as mobile phase (22).

Lipids from RBC samples were extracted twice; initially by using 10 mL isopropanol/chloroform (3:2 vol/vol), then by using 4 mL chloroform. TLC with chloroform, methanol, and 25% ammonia solution (73:27:5, by vol) as mobile phase was used for separating RBC PE and PC. For the analysis of RBC total lipids, instead of deposition of the lipids on the TLC plate, they were directly transferred into glass tubes and taken to dryness under nitrogen.

FAME from individual fractions and from total lipids were obtained by reaction with 3 M methanolic hydrochloric acid at 85°C for 45 min in closed glass tubes. Derivatives were extracted into *n*-hexane and stored until GC analysis at −20°C.

TABLE 1
Major FA of Microalgae and Placebo Oils (wt%)[a]

	Microalgae oil ($n = 12$)	Placebo oil ($n = 12$)
SFA	39.99 ± 0.25	14.62 ± 0.98
18:1n-9	0.52 ± 0.03	75.86 ± 0.76
18:1n-7	0.08 ± 0.01	2.37 ± 0.04
18:2n-6	1.21 ± 0.08	5.32 ± 0.14
18:3n-6	0.22 ± 0.01	ND
20:4n-6	0.09 ± 0.01	ND
22:5n-6	9.70 ± 0.14	ND
18:3n-3	0.11 ± 0.01	0.68 ± 0.02
20:5n-3	0.29 ± 0.01	ND
22:5n-3	0.09 ± 0.01	ND
22:6n-3	46.13 ± 0.20	ND

[a]Values are reported as mean ± SD. ND, not detected; SFA, saturated fatty acids.

Analysis of FAME was performed by capillary GLC as described for the microalgae and olive oil. CV (intra- and interassay) were below 10% for all presented FA.

Statistical methods. All statistical analyses were done using the Statistical Package for the Social Sciences, version 12.0 (SPSS Inc., Chicago, IL). After checking for the normal distribution of the data, group differences were tested for significance using Student's unpaired *t*-test for normally distributed variables or the Mann–Whitney U-test for variables not normally distributed. Within-group comparisons were performed by Student's *t*-test for dependent samples or the Wilcoxon nonparametric test, respectively. Correlations between parameters were estimated by computing the Spearman ρ correlation coefficient. For bivariate tabular analysis the χ^2 test was used. In cases of expected values smaller than 5, a Fisher exact test was used instead. Unless otherwise stated, all values are given as mean ± SEM; values of $P < 5\%$ were considered significant.

RESULTS

Two of the 114 subjects recruited in the study dropped out during the intervention period. One subject in the placebo group came down with a renal colic, which was considered unrelated to the dietary supplement, and the contact to one subject of the DHA group was lost. Four subjects were excluded from the analyses. The reasons for exclusions were poor compliance with study protocol ($n = 2$; both from the DHA group) and diarrhea/vomitus for more than 6 d of the intervention period ($n = 2$; one subject from each group). Thus, 108 subjects (94.7%) are included in the analysis.

Body weight, BMI, and dietary intake. Body weight and BMI did not differ between DHA and placebo group at week 0 and week 8. An examination of within-group changes demonstrated a slight but significant increase of body weight (from 61.4 ± 8.6 to 61.9 ± 8.6 kg, mean ± SD, $P = 0.005$) in the placebo group, but no changes in the DHA group.

The proportion of macronutrients and the intakes of energy, alcohol, cholesterol, and n-3 LCPUFA with the background diet (not including supplements for placebo and DHA group) were not different between the two groups before the intervention and did not change (with the exception of energy intake in the DHA group) in both groups during intervention (Table 2). Energy intake in the DHA group was significantly lower during intervention compared with baseline and also tended to be reduced compared with placebo ($P = 0.069$). Dietary fiber intake was comparable between both groups before intervention; during intervention, it was significantly lower in the DHA than in the placebo group. Baseline intakes of EPA + DHA (median, 5th and 95th percentile in parentheses) were 23 mg/d (0, 121 mg/d) in the DHA group and 23 mg/d (3, 118 mg/d) in the placebo group. Before intervention, DHA and placebo group differed in dietary linoleic acid (LA) intake (% of energy) (median: 3.3 vs. 5.0) and LA/ALA ratios (median: 6.6:1 vs. 7.9:1). Dietary LA and LA/ALA ratio decreased in the placebo group during the study, resulting in values comparable to the DHA group at study end. The Spearman ρ correlation coefficients between dietary LA intake (g/d) and LA (wt%) in RBC total lipids, RBC PE, RBC PC, and plasma PL were 0.454, 0.470, 0.391, and 0.318, respectively (P always < 0.01).

FA response to DHA supplementation. FA composition of RBC and plasma lipids was not different between groups at baseline and changed negligibly in the placebo group (Tables 3, 4). After DHA supplementation, no changes or slight increases were observed in saturated FA (16:0 and 18:0). The monounsaturated FA 16:1n-7 and 18:1n-9 decreased significantly in all measured fractions relative to baseline. Microalgae oil supplementation resulted in significant increases of 22:5n-6 [n-6 docosapentaenoic

TABLE 2
Daily Dietary Intakes (not including supplements for DHA and placebo group) Before and During Intervention[a]

	DHA group		Placebo group	
	Before intervention	During intervention	Before intervention	During intervention
	$n = 55$		$n = 53$	
Energy (kJ)	9142 ± 392	8099 ± 314[c]	8835 ± 332	8996 ± 375
Protein (% of energy)	13.4 ± 0.4	13.2 ± 0.4	13.0 ± 0.4	12.7 ± 0.3
Total fat (% of energy)	28.7 ± 1.0	28.4 ± 0.8	31.4 ± 1.2	30.5 ± 1.2
Carbohydrate (% of energy)	54.2 ± 1.1	54.3 ± 1.0	51.6 ± 1.2	52.9 ± 1.1
Fiber (g)	32.1 ± 2.2	29.8 ± 2.0[e]	34.8 ± 2.1	35.8 ± 2.8
Alcohol (g)	7.3 ± 1.5	6.4 ± 1.3	7.0 ± 1.3	6.8 ± 1.1
Cholesterol (mg)	167 ± 15	160 ± 13	148 ± 13	168 ± 15
LA (% of energy)	4.4 ± 0.4[f]	4.5 ± 0.4	5.8 ± 0.5	5.1 ± 0.6[b]
ALA (% of energy)	0.63 ± 0.04	0.61 ± 0.04	0.73 ± 0.06	0.65 ± 0.04
LA/ALA ratio	6.9 ± 0.4[e]	7.5 ± 0.6	8.4 ± 0.5	7.9 ± 0.7[b]
EPA (mg)	1.7 ± 0.5	2.5 ± 0.7	2.8 ± 1.0	2.5 ± 0.7
DHA (mg)	37.0 ± 5.3	30.6 ± 4.7	29.7 ± 4.5	32.6 ± 5.3

[a]Values are reported as mean ± SEM.
[b,c,d]Significant difference between week 0 and week 8 ([b]$P < 0.05$, [c]$P < 0.01$, [d]$P < 0.001$).
[e,f,g]Significant difference between DHA and placebo group at the same time point ([e]$P < 0.05$, [f]$P < 0.01$, [g]$P < 0.001$); ALA, α-linolenic acid; LA, linoleic acid.

TABLE 3
FA Composition (wt%) of Plasma PL and RBC Total Lipids at Week 0 and Week 8[a]

	Plasma PL				RBC total lipids			
	DHA group ($n = 55$)		Placebo group ($n = 53$)		DHA group ($n = 52$)		Placebo group ($n = 51$)	
	Week 0	Week 8	Week 0	Week 8	Week 0	Week 8	Week 0	Week 8
16:0	28.3 ± 0.3	28.5 ± 0.2[e]	28.0 ± 0.3	27.8 ± 0.3	21.5 ± 0.1	21.7 ± 0.1[d,f]	21.4 ± 0.1	21.2 ± 0.1[b]
18:0	12.0 ± 0.2	12.0 ± 0.2	12.1 ± 0.2	12.1 ± 0.2	13.9 ± 0.1	14.0 ± 0.1[b]	13.9 ± 0.1	14.0 ± 0.1[c]
16:1n-7	0.68 ± 0.04	0.49 ± 0.02[d]	0.64 ± 0.04	0.62 ± 0.04	0.37 ± 0.02	0.30 ± 0.01[d]	0.36 ± 0.03	0.35 ± 0.02
18:1n-9	10.3 ± 0.2	9.1 ± 0.2[d,g]	10.3 ± 0.2	10.5 ± 0.2	12.2 ± 0.1	12.0 ± 0.1[b,f]	12.3 ± 0.1	12.5 ± 0.1
20:3n-9	0.17 ± 0.02	0.09 ± 0.01[d,g]	0.15 ± 0.01	0.15 ± 0.01	0.08 ± 0.00	0.05 ± 0.00[d,g]	0.07 ± 0.00	0.08 ± 0.00
18:2n-6	22.0 ± 0.4	20.6 ± 0.4[d,g]	23.0 ± 0.4	22.9 ± 0.4	10.2 ± 0.2	9.7 ± 0.2[d,f]	10.5 ± 0.2	10.6 ± 0.2
18:3n-6	0.12 ± 0.01	0.06 ± 0.00[d,g]	0.11 ± 0.01	0.10 ± 0.01	0.05 ± 0.00	0.03 ± 0.00[d,g]	0.05 ± 0.00	0.04 ± 0.00
20:3n-6	3.5 ± 0.1	2.6 ± 0.1[d,g]	3.3 ± 0.1	3.3 ± 0.1	1.92 ± 0.06	1.59 ± 0.05[d,g]	1.89 ± 0.06	1.91 ± 0.07
20:4n-6	8.9 ± 0.2	8.1 ± 0.2[d,g]	8.9 ± 0.2	9.0 ± 0.2	13.9 ± 0.1	12.7 ± 0.1[d,g]	14.0 ± 0.1	14.0 ± 0.1
22:4n-6	0.43 ± 0.01	0.25 ± 0.01[d,g]	0.40 ± 0.01	0.40 ± 0.01	3.4 ± 0.1	2.6 ± 0.1[d,g]	3.3 ± 0.1	3.3 ± 0.1
22:5n-6	0.37 ± 0.02	0.66 ± 0.02[d,g]	0.34 ± 0.02	0.34 ± 0.02	0.78 ± 0.03	1.07 ± 0.02[d,g]	0.72 ± 0.03	0.72 ± 0.03
18:3n-3	0.20 ± 0.01	0.18 ± 0.01	0.22 ± 0.02	0.20 ± 0.01	0.13 ± 0.01	0.11 ± 0.00[d,f]	0.14 ± 0.01	0.13 ± 0.00
20:5n-3	0.58 ± 0.03	0.77 ± 0.03[d,g]	0.57 ± 0.04	0.52 ± 0.03[b]	0.41 ± 0.02	0.48 ± 0.02[d,f]	0.42 ± 0.02	0.40 ± 0.02
22:5n-3	0.90 ± 0.04	0.55 ± 0.02[d,g]	0.85 ± 0.04	0.85 ± 0.04	2.3 ± 0.1	1.7 ± 0.1[d,g]	2.3 ± 0.1	2.3 ± 0.1
22:6n-3	2.8 ± 0.1	7.4 ± 0.2[d,g]	2.6 ± 0.1	2.5 ± 0.1	4.4 ± 0.2	7.9 ± 0.2[d,g]	4.2 ± 0.1	4.0 ± 0.1[c]
EPA + DHA	3.4 ± 0.1	8.1 ± 0.2[d,g]	3.1 ± 0.1	3.0 ± 0.1	4.8 ± 0.2	8.4 ± 0.2[d,g]	4.6 ± 0.1	4.4 ± 0.1[c]

[a]Values are reported as mean ± SEM.
[b,c,d]Significant difference between week 0 and week 8 ([b]$P < 0.05$, [c]$P < 0.01$, [d]$P < 0.001$).
[e,f,g]Significant difference between DHA and placebo group at the same time point ([e]$P < 0.05$, [f]$P < 0.01$, [g]$P < 0.001$). PL, phospholipids; RBC, red blood cells.

acid (DPA)], EPA, and DHA levels and significant decreases of 20:3n-9, 18:2n-6, 18:3n-6, 20:3n-6, 20:4n-6 [arachidonic acid (AA)], 22:4n-6, and 22:5n-3 (n-3 DPA) levels in all measured fractions relative to baseline. Relative to placebo, DHA supplementation resulted in significantly higher contents of 16:0, n-6 DPA, EPA (not significant in RBC PE), and DHA, and lower contents of 16:1n-7 (not significant in plasma PL and RBC total lipids), 18:1n-9 (not significant in RBC PE), 20:3n-9, 18:2n-6, 18:3n-6, 20:3n-6, AA, 22:4n-6, 18:3n-3 (not significant in

plasma PL and RBC PC), and n-3 DPA (Tables 3, 4). After DHA supplementation, the highest relative FA changes were observed in DHA, n-6 DPA, and EPA in all measured lipid classes (Fig. 1). The degree of these changes was different in the various lipid classes, with higher percentage changes in RBC PC and plasma PL than in RBC total lipids and RBC PE for DHA, n-6 DPA, and EPA.

Statistically significant increases in EPA + DHA levels vs. baseline values were observed after 8 wk of microalgae oil

TABLE 4
FA Composition (wt%) of RBC PE and RBC PC at Week 0 and Week 8[a]

	RBC PE				RBC PC			
	DHA group ($n = 55$)		Placebo group ($n = 52$)		DHA group ($n = 55$)		Placebo group ($n = 52$)	
	Week 0	Week 8	Week 0	Week 8	Week 0	Week 8	Week 0	Week 8
16:0	16.0 ± 0.2	16.5 ± 0.2[d,f]	15.9 ± 0.2	15.8 ± 0.2	35.7 ± 0.2	36.1 ± 0.2[c,e]	35.6 ± 0.3	35.4 ± 0.3[b]
18:0	7.6 ± 0.1	7.6 ± 0.1	7.6 ± 0.1	7.7 ± 0.1[d]	9.9 ± 0.2	10.1 ± 0.2[b]	9.8 ± 0.2	10.0 ± 0.2
16:1n-7	0.27 ± 0.01	0.19 ± 0.01[d,f]	0.27 ± 0.02	0.26 ± 0.02	0.64 ± 0.03	0.48 ± 0.02[d,e]	0.63 ± 0.05	0.59 ± 0.04
18:1n-9	16.4 ± 0.2	16.1 ± 0.2[c]	16.7 ± 0.2	16.7 ± 0.2	15.9 ± 0.2	15.5 ± 0.2[d,f]	16.0 ± 0.2	16.2 ± 0.2
20:3n-9	0.10 ± 0.01	0.08 ± 0.00[d,f]	0.10 ± 0.00	0.11 ± 0.00[c]	0.09 ± 0.01	0.05 ± 0.00[d,g]	0.08 ± 0.01	0.09 ± 0.01
18:2n-6	6.5 ± 0.2	5.8 ± 0.2[d,g]	6.9 ± 0.2	6.9 ± 0.2	21.1 ± 0.3	20.2 ± 0.3[d,f]	21.6 ± 0.3	21.4 ± 0.3
18:3n-6	0.11 ± 0.00	0.09 ± 0.00[d,g]	0.11 ± 0.00	0.11 ± 0.00	0.08 ± 0.01	0.05 ± 0.00[d,g]	0.08 ± 0.00	0.07 ± 0.00
20:3n-6	1.70 ± 0.06	1.52 ± 0.05[d,f]	1.69 ± 0.06	1.71 ± 0.06	2.50 ± 0.07	1.96 ± 0.06[d,g]	2.45 ± 0.09	2.45 ± 0.09
20:4n-6	25.6 ± 0.2	23.8 ± 0.3[d,g]	25.5 ± 0.2	25.6 ± 0.2	6.0 ± 0.1	5.5 ± 0.1[d,f]	6.0 ± 0.1	6.0 ± 0.2
22:4n-6	8.5 ± 0.2	6.6 ± 0.2[d,g]	8.4 ± 0.2	8.5 ± 0.2	0.33 ± 0.02	0.24 ± 0.01[d,g]	0.30 ± 0.01	0.32 ± 0.01[c]
22:5n-6	1.15 ± 0.04	1.67 ± 0.04[d,g]	1.07 ± 0.05	1.07 ± 0.04	0.18 ± 0.01	0.32 ± 0.01[d,g]	0.16 ± 0.01	0.16 ± 0.01
18:3n-3	0.14 ± 0.01	0.11 ± 0.01[d,g]	0.16 ± 0.02	0.15 ± 0.01	0.20 ± 0.01	0.18 ± 0.01[c]	0.20 ± 0.02	0.19 ± 0.01
20:5n-3	0.77 ± 0.04	0.85 ± 0.04[d]	0.76 ± 0.04	0.78 ± 0.04	0.34 ± 0.02	0.45 ± 0.02[d,g]	0.34 ± 0.02	0.31 ± 0.02
22:5n-3	5.1 ± 0.1	3.6 ± 0.1[d,g]	5.1 ± 0.1	5.1 ± 0.1	0.52 ± 0.02	0.37 ± 0.01[d,g]	0.51 ± 0.02	0.51 ± 0.02
22:6n-3	6.5 ± 0.3	12.1 ± 0.3[d,g]	6.0 ± 0.3	5.8 ± 0.3[c]	1.38 ± 0.07	3.78 ± 0.13[d,g]	1.25 ± 0.06	1.23 ± 0.06
EPA + DHA	7.3 ± 0.3	12.9 ± 0.3[d,g]	6.8 ± 0.3	6.6 ± 0.3[b]	1.72 ± 0.08	4.22 ± 0.14[d,g]	1.58 ± 0.06	1.54 ± 0.06

[a]Values are reported as mean ± SEM.
[b,c,d]Significant difference between week 0 and week 8 ([b]$P < 0.05$, [c]$P < 0.01$, [d]$P < 0.001$).
[e,f,g]Significant difference between DHA and placebo group at the same time point ([e]$P < 0.05$, [f]$P < 0.01$, [g]$P < 0.001$). For abbreviation see Table 3.
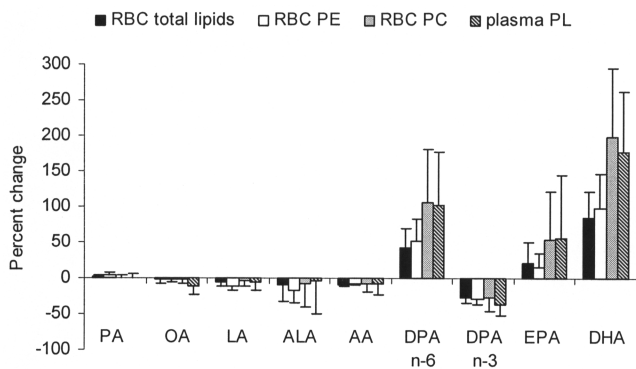
FIG. 1. Relative changes of selected FA in RBC total lipids, RBC PE, RBC PC, and plasma PL in the DHA group compared with baseline values (*n* = 52 in RBC total lipids, otherwise *n* = 55). Values were calculated as individual's percent change in each lipid fraction and are reported as mean + SD. PA, 16:0; OA, 18:1n-9; LA, 18:2n-6; ALA, 18:3n-3; AA, 20:4n-6; DPA n-6, 22:5n-6; DPA n-3, 22:5n-3; EPA, 20:5n-3; DHA, 22:6n-3; PL, phospholipids; RBC, red blood cells.

supplementation in all investigated lipid fractions (Tables 3, 4). The omega-3 index rose significantly from 4.8 ± 0.2 wt% to 8.4 ± 0.2 wt% in the DHA-supplemented group, ranging after 8 wk from 4.7 to 11.0 wt%. Relative to placebo application, supplementation with DHA-rich microalgae oil resulted in significantly higher contents of EPA + DHA in all tested lipid fractions. At baseline, 29% of the DHA group and 33% of the placebo group volunteers had an omega-3 index of ≤4%, and no one reached an omega-3 index of ≥8%. After 8 wk of intervention, an omega-3 index of ≤4% did not occur anymore in the DHA group, but remained in 39% of the placebo group subjects ($P < 0.001$). Sixty-nine percent of the DHA-supplemented subjects had an omega-3 index of ≥8%, while no subject of the placebo group showed an omega-3 index above 8% ($P < 0.001$).

Correlations between FA of RBC total lipids and other lipid fractions. Spearman ρ correlation coefficients were computed

between the relative levels of FA in RBC total lipids and FA percentages in RBC PE, RBC PC, and plasma PL for all subjects at both time points (Table 5). Relative FA content in RBC total lipids correlated significantly with the corresponding FA content in the other lipid classes (plasma PL, RBC PC, and RBC PE) (*r* always > 0.49). RBC total lipid DHA and RBC total lipid EPA + DHA consistently showed the strongest correlations with the other lipid fractions at both time points (*r* always > 0.90).

At baseline, correlation coefficients between omega-3 index and EPA + DHA from RBC PE, RBC PC, and plasma PL were almost identical in DHA and placebo groups (Fig. 2). After the intervention, correlation coefficients remained similar to baseline in the placebo group but were lower in the DHA group. The correlations between EPA + DHA at week 0 and EPA + DHA at week 8 were also lower in the DHA group in all tested lipid fractions (in the placebo group *r* = 0.841–0.970; in the DHA group *r* = 0.464–0.856, *P* always < 0.001).

In the DHA group, Spearman ρ correlations were computed between RBC total lipid or plasma PL relative FA changes and percentage changes in the other lipid fractions for LA, AA, n-6 DPA, ALA, EPA, n-3 DPA, DHA, and EPA + DHA. Relative changes in RBC total lipid n-6 and n-3 FA correlated significantly and positively with changes in the other lipid classes (*r* always > 0.48); here, the correlations were highest for n-6 DPA, EPA, DHA, and the omega-3 index (*r* always > 0.75). Relative changes in RBC PE correlated better with RBC total lipid than with plasma PL changes for all tested FA (data not shown). Relative changes in plasma PL correlated best with RBC PC for all tested n-6 and n-3 FA with exception of ALA.

DISCUSSION

A daily intake of 0.94 g DHA from Ulkenia oil markedly increased the DHA content of plasma and RBC phospholipids. Previous studies reported a two- to threefold increase of the DHA content of serum and platelet PL after supplementation

TABLE 5
Spearman ρ Correlations Between RBC Total Lipid FA (wt%) and FA from RBC PE, RBC PC, and Plasma PL at Week 0 and Week 8 in All Subjects (*n* = 103)

	RBC PE		RBC PC		Plasma PL	
	Week 0	Week 8	Week 0	Week 8	Week 0	Week 8
16:0	0.491[a]	0.521[a]	0.785[a]	0.705[a]	0.745[a]	0.753[a]
18:1n-9	0.711[a]	0.664[a]	0.782[a]	0.704[a]	0.528[a]	0.515[a]
18:2n-6	0.896[a]	0.887[a]	0.858[a]	0.930[a]	0.759[a]	0.802[a]
20:3n-6	0.798[a]	0.791[a]	0.777[a]	0.757[a]	0.790[a]	0.781[a]
20:4n-6	0.700[a]	0.826[a]	0.615[a]	0.700[a]	0.581[a]	0.661[a]
22:4n-6	0.946[a]	0.965[a]	0.668[a]	0.821[a]	0.604[a]	0.758[a]
22:5n-6	0.973[a]	0.969[a]	0.905[a]	0.910[a]	0.899[a]	0.895[a]
18:3n-3	0.612[a]	0.672[a]	0.815[a]	0.827[a]	0.747[a]	0.743[a]
20:5n-3	0.939[a]	0.913[a]	0.857[a]	0.856[a]	0.830[a]	0.817[a]
22:5n-3	0.947[a]	0.961[a]	0.691[a]	0.755[a]	0.762[a]	0.851[a]
22:6n-3	0.954[a]	0.971[a]	0.921[a]	0.955[a]	0.921[a]	0.944[a]
EPA + DHA	0.956[a]	0.972[a]	0.900[a]	0.959[a]	0.911[a]	0.944[a]

[a]Significant correlations between RBC total lipid FA and FA of the other lipid fractions (*P* < 0.001). For abbreviations see Table 3.
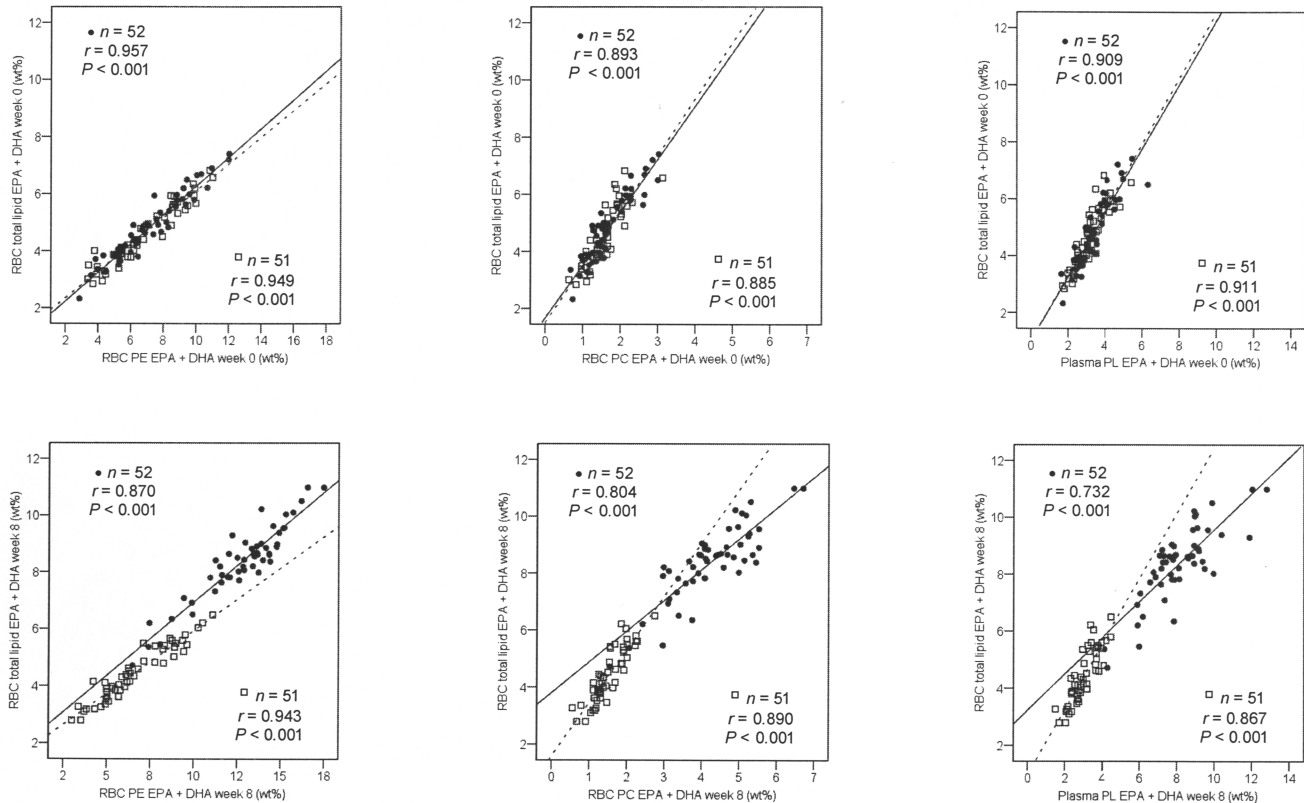
FIG. 2. Correlations between EPA + DHA in RBC total lipids (wt%) vs. EPA + DHA in RBC PE, PC, and plasma PL (Spearman ρ correlation coefficient). □ and dashed line, placebo group; • and solid line, DHA group. For abbreviations see Figure 1.

with 0.75, 1.50, or 1.62 g DHA/d for 6 wk (23–25) and a rise of DHA levels in plasma PL by 76% and in RBC phosphoglycerides by 58%, respectively, after 3 mon of supplementation with 0.7 g DHA/d (26). The observed increase of EPA in RBC and plasma lipids after DHA supplementation in our study appears to reflect retroconversion of DHA, as suggested also by other observations (23,24,27,28). We found a decrease in n-6 LCPUFA (20:3n-6, 20:4n-6, 22:4n-6), accompanied by a decrease in n-3 DPA, consistent with other findings (23–25,27). In contrast, n-3 DPA shows considerable enrichment in serum and platelet phospholipids when fish or seal oils (providing EPA, DHA, and some n-3 DPA) are fed (29,30). Thus, dietary DHA and possibly also n-6 DPA appear to partially replace n-3 DPA in circulating and cellular phospholipids in human subjects. In contrast to other studies using DHA-rich oils from an algal source, which reported significant decreases in n-6 DPA (23,24,27), we observed an increase of n-6 DPA in plasma and RBC PL, which is explained by the significant n-6 DPA content in the tested oil derived from microalgae *Ulkenia* sp. (9.7 wt%).

The omega-3 index rose significantly from 4.8 ± 1.2 (mean ± SD) to 8.4 ± 1.3 wt% in the DHA-supplemented group. A similar increase of the omega-3 index was reported by Harris *et al.* (6) after EPA and DHA supplementation (1 g/d) for 5 mon. We found the relative and absolute changes in omega-3

index to be inversely correlated to baseline levels ($r = -0.760$, $P < 0.001$ and $r = -0.311$, $P = 0.025$, respectively), indicating that the (relative and absolute) increase of the omega-3 index is higher in subjects with lower baseline levels. At baseline, no subject reached a desirable omega-3 index of ≥8 wt%, although more than 50% of the subjects reached or exceeded recommended intakes for LA (2.5% of energy) and ALA (0.5% of energy) and 26% had a dietary LA/ALA ratio below 5:1 as considered desirable (31). These results suggest that the *in vivo* conversion of ALA to n-3 LCPUFA is not adequate to reach a desirable EPA + DHA status even with a low dietary LA/ALA ratio. Thus, a dietary intake of preformed n-3 LCPUFA seems to be necessary to enhance the omega-3 index.

Relative changes of n-6 DPA, EPA, and DHA were greater in plasma PL and RBC PC (Fig. 1) than in RBC total lipids or RBC PE, with strong correlations between RBC PC and plasma PL FA changes. RBC PE and plasma PL FA changes were less closely related. Plasma PL FA change relatively fast and reflect dietary intakes over the past few days (32). RBC PL are asymmetrically distributed between the outer and the inner layer of the membrane (33): the major part of PE is located at the inner layer, whereas PC occurs predominantly on the outer layer and can exchange more easily with plasma lipids. Thus, PC reflects more directly the FA composition of PL of the plasma (34), whereas the FA composition of PE

appears to be more independent from the plasma FA and depends on selective incorporation of PUFA and LCPUFA into PE (35).

Relative changes in RBC total lipid n-6 DPA, EPA, and DHA were lower than their average changes in RBC PE and RBC PC (Fig. 1), indicating that these FA were preferentially incorporated into PE and PC, which constitute about 23 and 22% of total membrane lipids (modified from Ref. 36, calculated without cholesterol), but less in the other lipids of the RBC membrane such as sphingomyelin, PS, glycolipids, and other lipids, constituting about 23, 9, 4, and 18% of total membrane lipids, respectively.

Even though each lipid fraction revealed a distinct and characteristic FA pattern, RBC total lipid FA were significantly correlated with FA from RBC PC, RBC PE, and plasma PL (Table 5) at both time points. In agreement, Vlaardingerbroek and Hornstra (37) and Harris *et al.* (6) also reported strong correlations between RBC and plasma PL LCPUFA. In contrast, a study by Leichsenring *et al.* (38) did not find any relation of RBC DHA (PE, PC, and total lipids) values to DHA levels in plasma PL, which might be due to a greater heterogeneity of their subjects with respect to age and diet.

After supplementation, correlation coefficients between omega-3 index and RBC PE, RBC PC, and plasma PL, EPA + DHA were higher in the placebo than in the DHA group (Fig. 2), and additionally, correlations between omega-3 index from weeks 0 and 8 were stronger for the placebo group. These findings may indicate that EPA + DHA contents in plasma and RBC lipid fractions are not in a steady state after 8 wk of DHA supplementation. Another explanation may be that the supplemented FA show individual differences in digestion, absorption, and preferential incorporation into the different lipid fractions.

Reported energy intake in the DHA group was significantly lower during intervention compared with baseline (−11%), but remained unchanged in the placebo group (Table 2). We observed no changes in body weight over the study period of 8 wk in the DHA group, but a slight weight gain in the placebo group (+0.5 kg). An explanation for the reduced energy intake without weight loss in the DHA group and the weight gain without increased energy intake in the placebo group could be that the energy requirements decreased in both groups during the intervention period, e.g., because of less physical activity related to seasonal influences. The participation in a nutritional study and the intake of oil-containing capsules might have caused larger reductions in dietary intakes and/or a greater "underreporting" of consumed foods than before the intervention in both groups at the days of the dietary record. Since we observed a trend toward lower energy intakes in the DHA group relative to placebo, the tested microalgae oil might have had a different effect on appetite or regulation of food intake than olive oil in the vegetarian subjects studied. As 8-wk supplementation with 0.94 g DHA/d from microalgae oil (*Ulkenia* sp.) achieves a desirable omega-3 index of ≥8% in subjects with low basal n-3 LCPUFA status, microalgae oil might be a valuable alternative to fish/fish oil for vegetarians.

REFERENCES

1. Bucher, H.C., Hengstler, P., Schindler, C., and Meier, G. (2002) n-3 Polyunsaturated Fatty Acids in Coronary Heart Disease: A Meta-Analysis of Randomized Controlled Trials, *Am. J. Med. 112*, 298–304.
2. Kris-Etherton, P.M., Harris, W.S., and Appel, L.J. (2002) Fish Consumption, Fish Oil, Omega-3 Fatty Acids, and Cardiovascular Disease, *Circulation 106*, 2747–2757.
3. Whelton, S.P., He, J., Whelton, P.K., and Muntner, P. (2004) Meta-analysis of Observational Studies on Fish Intake and Coronary Heart Disease, *Am. J. Cardiol. 93*, 1119–1123.
4. Leaf, A., Kang, J.X., Xiao, Y., and Billman, G.E. (2003) Clinical Prevention of Sudden Cardiac Death by n-3 Polyunsaturated Fatty Acids and Mechanism of Prevention of Arrhythmias by n-3 Fish Oils, *Circulation 107*, 2646–2652.
5. Harris, W.S., Sands, S.A., Windsor, S.L., Ali, H.A., Stevens, T.L., Magalski, A., Porter, C.B., and Borkon, A.M. (2004) Omega-3 Fatty Acids in Cardiac Biopsies from Heart Transplantation Patients: Correlation with Erythrocytes and Response to Supplementation, *Circulation 110*, 1645–1649.
6. Harris, W.S., and von Schacky, C. (2004) The Omega-3 Index: A New Risk Factor for Death from Coronary Heart Disease? *Prev. Med. 39*, 212–220.
7. Conquer, J.A., and Holub, B.J. (1997) Docosahexaenoic Acid (omega-3) and Vegetarian Nutrition, *Veg. Nutr. Int. J. 1/2*, 42–49.
8. Li, D., Sinclair, A.J., Wilson, A., Nakkote, S., Kelly, F., Abedin, L., Mann, N.J., and Turner, A. (1999) Effect of Dietary α-Linolenic Acid on Thrombotic Risk Factors in Vegetarian Men, *Am. J. Clin. Nutr. 69*, 872–882.
9. Burdge, G.C., and Wootton, S.A. (2002) Conversion of α-Linolenic Acid to Eicosapentaenoic, Docosapentaenoic and Docosahexaenoic Acids in Young Women, *Br. J. Nutr. 88*, 411–420.
10. Burdge, G.C., Jones, A.E., and Wootton, S.A. (2002) Eicosapentaenoic and Docosapentaenoic Acids Are the Principal Products of α-Linolenic Acid Metabolism in Young Men, *Br. J. Nutr. 88*, 355–363.
11. Emken, E.A., Adlof, R.O., and Gulley, R.M. (1994) Dietary Linoleic Acid Influences Desaturation and Acylation of Deuterium-Labeled Linoleic and Linolenic Acids in Young Adult Males, *Biochim. Biophys. Acta 1213*, 277–288.
12. Hussein, N., Ah-Sing, E., Wilkinson, P., Leach, C., Griffin, B.A., and Millward, D.J. (2005) Long-Chain Conversion of [13C]Linoleic Acid and α-Linolenic Acid in Response to Marked Changes in Their Dietary Intake in Men, *J. Lipid Res. 46*, 269–280.
13. Pawlosky, R.J., Hibbeln, J.R., Novotny, J.A., and Salem, N., Jr. (2001) Physiological Compartmental Analysis of α-Linolenic Acid Metabolism in Adult Humans, *J. Lipid Res. 42*, 1257–1265.
14. Pawlosky, R.J., Hibbeln, J.R., Lin, Y., Goodson, S., Riggs, P., Sebring, N., Brown, G.L., and Salem, N., Jr. (2003) Effects of Beef- and Fish-Based Diets on the Kinetics of n-3 Fatty Acid Metabolism in Human Subjects, *Am. J. Clin. Nutr. 77*, 565–572.
15. Burdge, G.C., Finnegan, Y.E., Minihane, A.M., Williams, C.M., and Wootton, S.A. (2003) Effect of Altered Dietary n-3 Fatty Acid Intake upon Plasma Lipid Fatty Acid Composition, Conversion of [13C]α-Linolenic Acid to Longer-Chain Fatty Acids

and Partitioning Towards β-Oxidation in Older Men, *Br. J. Nutr. 90*, 311–321.

16. Sanders, T.A.B., and Roshanai, F. (1992) Platelet Phospholipid Fatty Acid Composition and Function in Vegans Compared with Age- and Sex-Matched Omnivore Controls, *Eur. J. Clin. Nutr. 46*, 823–831.

17. Agren, J.J., Törmälä, M.L., Nenonen, M.T., and Hänninen, O.O. (1995) Fatty Acid Composition of Erythrocyte, Platelet, and Serum Lipids in Strict Vegans, *Lipids 30*, 365–369.

18. Krajcovicova-Kudlackova, M., Simoncic, R., Bederova, A., and Klvanova, J. (1997) Plasma Fatty Acid Profile and Alternative Nutrition, *Ann. Nutr. Metab. 41*, 365–370.

19. Li, D., Ball, M., Bartlett, M., and Sinclair, A.J. (1999) Lipoprotein(a), Essential Fatty Acid Status and Lipoprotein Lipids in Female Australian Vegetarians, *Clin. Sci. 97*, 175–181.

20. Lee, H.Y., Woo, J., Chen, Z.Y., Leung, S.F., and Peng, X.H. (2000) Serum Fatty Acid, Lipid Profile and Dietary Intake of Hong Kong Chinese Omnivores and Vegetarians, *Eur. J. Clin. Nutr. 54*, 768–773.

21. Manjari, V., Suresh, Y., Sailaja Devi, M.M., and Das, U.N. (2001) Oxidant Stress, Anti-oxidants and Essential Fatty Acids in South Indian Vegetarians and Non-vegetarians, *Prostaglandins Leukotrienes Essent. Fatty Acids 64*, 53–59.

22. Carnielli, V.P., Pederzini, F., Vittorangeli, R., Luijendijk, I.H., Boomaars, W.E., Pedrotti, D., and Sauer, P.J. (1996) Plasma and Red Blood Cell Fatty Acid of Very Low Birth Weight Infants Fed Exclusively with Expressed Preterm Human Milk, *Pediatr. Res. 39*, 671–679.

23. Conquer, J.A., and Holub, B.J. (1996) Supplementation with an Algae Source of Docosahexaenoic Acid Increases (n-3) Fatty Acid Status and Alters Selected Risk Factors for Heart Disease in Vegetarian Subjects, *J. Nutr. 126*, 3032–3039.

24. Conquer, J.A., and Holub, B.J. (1997) Dietary Docosahexaenoic Acid as a Source of Eicosapentaenoic Acid in Vegetarians and Omnivores, *Lipids 32*, 341–345.

25. Conquer, J.A., and Holub, B.J. (1998) Effect of Supplementation with Different Doses of DHA on the Levels of Circulating DHA as Non-esterified Fatty Acid in Subjects of Asian Indian Background, *J. Lipid Res. 39*, 286–292.

26. Theobald, H.E., Chowienczyk, P.J., Whittall, R., Humphries, S.E., and Sanders, T.A.B. (2004) LDL Cholesterol-Raising Effect of Low-Dose Docosahexaenoic Acid in Middle-Aged Men and Women, *Am. J. Clin. Nutr. 79*, 558–563.

27. Stark, K.D., and Holub, B.J. (2004) Differential Eicosapentaenoic Acid Elevations and Altered Cardiovascular Disease Risk Factor Responses After Supplementation with Docosahexaenoic Acid in Postmenopausal Women Receiving and Not Receiving Hormone Replacement Therapy, *Am. J. Clin. Nutr. 79*, 765–773.

28. Buckley, R., Shewring, B., Turner, R., Yaqoob, P., and Minihane, A.M. (2004) Circulating Triacylglycerol and ApoE Levels in Response to EPA and Docosahexaenoic Acid Supplementation in Adult Human Subjects, *Br. J. Nutr. 92*, 477–483.

29. Conquer, J.A., Cheryk, L.A., Chan, E., Gentry, P.A., and Holub, B.J. (1999) Effect of Supplementation with Dietary Seal Oil on Selected Cardiovascular Risk Factors and Hemostatic Variables in Healthy Male Subjects, *Thromb. Res. 96*, 239–250.

30. Laidlaw, M., and Holub, B.J. (2003) Effects of Supplementation with Fish Oil-Derived n-3 Fatty Acids and γ-Linolenic Acid on Circulating Plasma Lipids and Fatty Acid Profiles in Women, *Am. J. Clin. Nutr. 77*, 37–42.

31. German Nutrition Society (2002) *Reference Values for Nutrient Intake*, 1st edn., pp. 45–49, Umschau Braus GmbH, Frankfurt am Main, Germany.

32. Arab, L. (2003) Biomarkers of Fat and Fatty Acid Intake, *J. Nutr. 133*, 925S–993S.

33. Verkleij, A.J., Zwaal, R.F.A., Roelofsen, B., Comfurius, P., Kastelijn, D., and Van Deenen, L.L.M. (1973) The Asymmetric Distribution of Phospholipids in the Human Red Cell Membrane. A Combined Study Using Phospholipases and Freeze-Etch Electron Microscopy, *Biochim. Biophys. Acta 323*, 178–193.

34. Renooij, W., and Van Golde, L.M.G. (1977) The Transposition of Molecular Classes of Phosphatidylcholine Across the Rat Erythrocyte Membrane and Their Exchange Between the Red Cell Membrane and Plasma Lipoproteins, *Biochim. Biophys. Acta 470*, 465–474.

35. Renooij, W., Van Golde, L.M.G., Zwaal, R.F.A., Roelofsen, B., and Van Deenen, L.L.M. (1974) Preferential Incorporation of Fatty Acids at the Inside of Human Erythrocyte Membranes, *Biochim. Biophys. Acta 363*, 287–292.

36. Alberts, B., Johnson, A., Lewis, J., Raff, M., Roberts, K., and Walter, P. (1995) *Molekularbiologie der Zelle*, 3rd edn., pp. 675–685, Wiley-VCH, Weinheim.

37. Vlaardingerbroek, H., and Hornstra, G. (2004) Essential Fatty Acids in Erythrocyte Phospholipids During Pregnancy and at Delivery in Mothers and Their Neonates: Comparison with Plasma Phospholipids, *Prostaglandins Leukotrienes Essent. Fatty Acids 71*, 363–374.

38. Leichsenring, M., Hardenack, M., and Laryea, M.D. (1992) Relationship Among the Fatty Acid Composition of Various Lipid Fractions in Normally Nourished German Adults, *Int. J. Vitam. Nutr. Res. 62*, 181–185.

Eicosapentaenoic Acid, but Not Oleic Acid, Stimulates β-Oxidation in Adipocytes

Wen Guo*, Weisheng Xie, TianGuang Lei, and James A. Hamilton

Obesity Research Center, Boston University School of Medicine, Boston, Massachusetts 02118

ABSTRACT: The beneficial roles of dietary fish oil in lowering serum TAG levels in animals and humans have been attributed in part to the high content of two n-3 polyunsaturated very long-chain FA, EPA, and DHA. Recent studies show that EPA induces mitochondrial β-oxidation in hepatocytes, which might contribute to the systemic lipid-lowering effect. Whether EPA affects FA storage or oxidation in adipocytes is not clear. To investigate this possibility, 3T3-L1 adipocytes incubated with EPA (100 µM) for 24 h were assayed for β-oxidation, carnitine palmitoyl transferase 1 (CPT-1) activity, protein, and mRNA expression of CPT-1. For comparison, cells treated with oleic acid, octanoic acid, and clofibrate, a synthetic ligand for peroxisome proliferator-activated receptor α were also analyzed. Mitochondria were isolated by differential centrifugation, and the mitochondrial membrane acyl chain composition was measured by GLC. EPA increased the oxidation of endogenous FA but did not inhibit lipogenesis. Oleic acid and clofibrate did not affect FA oxidation or lipogenesis, whereas octanoic acid suppressed the oxidation of endogenous FA and inhibited lipogenesis. Increased β-oxidation by EPA was associated with increased CPT-1 activity but without changes in its mRNA and protein expression. EPA treatment increased the percentage of this FA in the mitochondrial membrane lipids. We suggest that EPA increased the activity of CPT-1 and β-oxidation in adipocytes by altering the structure or dynamics of the mitochondrial membranes.

Paper no. L9788 in *Lipids 40*, 815–821 (August 2005).

The beneficial roles of dietary fish oil in the human diet have been attributed to the high content of two n-3 polyunsaturated very long-chain FA, EPA, and DHA (1–4). Animal studies as well as *in vitro* cell studies have provided some insights into possible mechanisms for these effects (5–10). Both EPA and DHA activate peroxisome proliferator-activated receptor α (PPARα), the nuclear transcription factor that regulates the expression of key enzymes in the control of FA β-oxidation in mitochondria and peroxisomes (6). EPA has been shown to induce mitochondrial FA oxidation and contribute to lipid-lowering effects (7), whereas the effects of DHA are still debatable (7,11). In hepatocytes, EPA increases the expression of carnitine palmitoyl transferase 1 (CPT-1), which increases the flux of FA toward mitochondrial β-oxidation and reduces the sub-

strates for lipid synthesis and lipoprotein secretion. In hepatocytes EPA directly reduces TAG synthesis by direct inhibition of DAG acyltransferase activity (6). EPA also inhibits apolipoprotein secretion in both enterocytes and hepatocytes (12,13). Any one or a combination of these mechanisms could contribute to the systemic lipid-lowering effects of fish oil or EPA dietary supplements.

Several previous reports have shown that fish oil reduces adipocyte cell size and fat pad mass, and that it increases the cellular response to insulin and β-agonist-stimulated lipolysis (1,5,8,14,15). It is not clear whether these effects are caused by n-3 FA acting on adipocytes or are secondary to the changes in hepatic or systemic metabolism. In this work, we studied the effects of EPA on FA oxidation and lipid synthesis in 3T3-L1 adipocytes. We found that EPA significantly increased the β-oxidation of endogenous FA with a concomitant increase in CPT-1 enzyme activity, consistent with the prior studies on hepatocytes. In contrast, treatment with oleic acid or octanoic acid did not affect CPT-1 activity in adipocytes. On the other hand, EPA did not appear to inhibit either *de novo* FA synthesis or TAG synthesis in adipocytes, implying that the mechanisms by which EPA modulated lipid metabolism in hepatocytes (6) might not be directly extrapolated to adipocytes, although both cell types share many of their lipid metabolic pathways.

MATERIALS AND METHODS

Cell culture and FA treatment. 3T3-L1 adipocytes were prepared as described previously (16). For each experiment, cells were incubated with serum-free DMEM for 14 h before the test reagents were added. EPA (100 µM in a complex with 40 µM BSA), oleic acid (100 µM in a complex with 40 µM BSA), octanoic acid (1.0 mM, with 40 µM BSA), and clofibrate (300 µM, with 40 µM BSA) were added to the cells maintained in DMEM. The higher concentration of octanoic acid was required because of the much lower partitioning of this medium-chain FA into the plasma membrane (17). Control cells were maintained in DMEM with 40 µM BSA. All concentrations are given as final concentrations in the incubation medium.

FA oxidation. Adipocytes grown in six-well plates were preincubated with [9,10-^{3}H] oleic acid (0.5 µCi/mL) for 4 d in DMEM with 10% FBS. To enhance the enrichment of isotope in the endogenous pool, fresh isotope tracer was added every day. The absolute amount of oleic acid added by this procedure was very low (<10 nM), and its perturbation of cellular metabolism

*To whom correspondence should be addressed at Department of Medicine, Room 805, 650 Albany St., Boston, MA 02118.
E-mail: wguo@bu.edu

Abbreviations: CPT, carnitine palmitoyl transferase; PPARα, peroxisome proliferator-activated receptor α.

was considered to be negligible. Cells were then washed three times with warm PBS and added to 2 mL of phenol red-free DMEM containing the test reagents described above. After 24 h, 1.2 mL of the medium from each incubation was removed into three small plastic vials (0.4 mL/vial), which in turn were placed in one large screw-capped glass vial surrounded with 1.2 mL of unlabeled water and sealed with paraffin. This closed system was placed in an incubator at 58°C for 24 h to allow equilibrium to be reached between the labeled and unlabeled water phases. The small vial containing the original medium was then removed, and the radioactivity absorbed into the bulk water phase through vapor exchange was used for quantification by scintillation counting as described previously (18).

Incorporation of ^3H_2O and [U-^{14}C]glucose into cellular lipids. Adipocytes treated in parallel under the above conditions (except without preincubation of the isotope-labeled FA) were incubated with ^3H_2O (100 μCi/mL) or [U-^{14}C]glucose (0.5 μCi/mL). After 24 h, the cellular lipids were harvested and hydrolyzed as described previously (16). The amount of tritium accumulated in the FA fraction was quantified by β-counting and was used to calculate the amount of FA synthesized *de novo*. The amount of ^{14}C recovered from the glycerol fraction was quantified by β-counting and was used to calculate the amount of TAG synthesized in this period of time.

Mitochondrial isolation and CPT-1 activity. Mitochondria were isolated using a standard protocol (19) with slight modifications. Cultured adipocytes were harvested into 5 mL of homogenization buffer (250 mM sucrose, 10 mM Tris-HCl, 1.0 mM EDTA, 1 mM PMSF, pH 7.0). Cells were homogenized using 10 strokes of a Potter–Elvehjem tissue grinder at the maximum power setting. The homogenate was centrifuged at $600 \times g$ for 10 min. The supernatant was then centrifuged at $16,000 \times g$ for 10 min at 4°C. The pellet was resuspended in 10 mL of sucrose cushion (3 g sucrose dissolved in the same homogenization buffer) and centrifuged at $25,000 \times g$ for 10 min at 4°C. The final mitochondrial pellet was resuspended in CPT assay buffer (150 mM KCl, 5 mM Tris-HCl, 4 mM MgCl$_2$, pH 7.2). CPT activity was measured using a published protocol (20).

The assay mix (100 μL per reaction) was prepared with the assay buffer added with l-[methyl-^{3}H]carnitine (0.5 mM, 10 μCi/mL), 100 μM palmitoyl-CoA, 4 mM ATP, 0.25 mM glutathione, 2 mM KCN, 40 mg/L rotenone, and 0.5% FA-free BSA. The reaction was started by adding 20 μg of mitochondrial protein, and the assay mix was incubated at room temperature for 6 min. The reaction was stopped by adding 100 μL of 1 N HCl, followed by the extraction of palmitoyl-[^{3}H]carnitine using 1-butanol. For each measurement, the CPT activity was measured in the absence (CPT-1 and partial CPT-2) and in the presence of 100 μM malonyl-CoA (CPT-1 inhibited). The CPT-1 activity was calculated as the difference between these two measurements.

Western blot analysis. A cell lysate was prepared using a mammalian cell lysis kit according to the manufacturer's instructions. The proteins were separated by SDS-PAGE with protein loading of 15 μg/lane. The primary antibody for CPT-1

(rabbit-anti-mouse) was from Alpha Diagnostic Inc. (San Antonio, TX). The secondary antibody (goat-anti-rabbit) was from Pierce (Rockford, IL).

Mitochondrial phospholipid FA composition analysis. After measuring the CPT-1 activity, the residual mitochondrial fraction was extracted by the method of Folch *et al.* (21). The lipid mixture was separated by TLC (hexane/ether/acetic acid, 80:20:1). The phospholipid fraction was eluted from the silica gel with CHCl$_3$/CH$_3$OH/NH$_4$OH (1:1:0.07), dried under a stream of N$_2$, and methylated using a BF$_3$/CH$_3$OH kit from Supelco (St. Louis, MO) according to the manufacturer's instructions. The acyl chain composition was analyzed using a GLC method as described previously (16).

RNA analysis. Total RNA was prepared and analyzed as described previously (22). The primer sequence used for CPT-1 was from the literature (23).

Other biochemical assays. Concentrations of cellular TAG, DNA, protein, and glycerol release were measured using commercial kits from Sigma as described previously (16).

Materials. Unless otherwise indicated, all regular cell culture supplies were from Fisher (Agawa, MA); all radioactive isotope-labeled chemicals were from NEN (Boston, MA); and all other reagents and organic solvents were from Sigma.

Statistics. Data are expressed as means ± SE. Comparisons between two groups of data were made using Student's *t*-test. For others, the results were analyzed using one-way ANOVA and Duncan's multiple comparison tests. Differences were considered statistically significant when $P < 0.05$.

RESULTS

EPA increased FA oxidation in adipocytes. To provide a pool of endogenous FA that could be monitored during the experiments with EPA and other additives, cells were prelabeled with [9,10-^{3}H]oleic acid (>95% of the labeled oleic acid was found in TAG after lipid fractionation analysis, data not shown). β-Oxidation was measured by quantifying the release of ^3H_2O from the endogenous esterified [9,10-^{3}H]oleic acid. As shown in Figure 1A, EPA increased β-oxidation of endogenous oleic acid in adipocytes by about 40% ($P < 0.05$, $n = 5$). Incubation with octanoic acid decreased the oxidation of [9,10-^{3}H]oleic acid, probably caused by substrate competition between octanoic acid and oleic acid, which favors octanoic acid because it can be β-oxidized independently of CPT-1 (24). Incubation with oleic acid and clofibrate slightly increased the oxidation of endogenous oleic acid, but the difference was not statistically significant ($P = 0.5$ and 0.7, respectively). The amount of glycerol released from cells treated under these five conditions was similar in all cases (250 ± 10 nmol/24 h/10^{6}cells), implying that the release of endogenous FA did not account for the difference in β-oxidation.

EPA increases in vitro CPT-1 activity of adipocytes. Since CPT-1 is the only known enzyme that transports activated long-chain FA into the mitochondria for β-oxidation (19), we then determined whether the observed changes in β-oxidation were associated with corresponding changes in CPT-1 activity. To
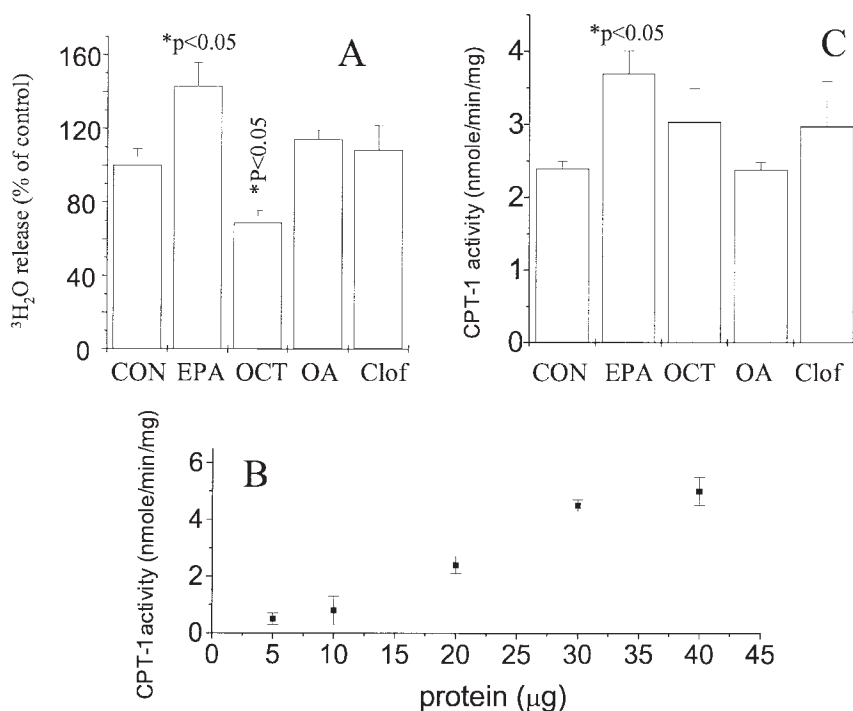
FIG. 1. Effects of EPA on β-oxidation and carnitine palmitoyl transferase 1 (CPT-1) activity. (A) Adipocytes were preincubated with [9,10-^{3}H]oleic acid for 4 d, and then treated with EPA (100 µM), oleic acid (OA, 100 µM), octanoic acid (OCT, 1 mM), or clofibrate (Clof, 300 µM) in serum-free DMEM with 0.5% BSA for 24 h. The amount of ^{3}H$_2$O liberated in this period was measured as the index for β-oxidation of endogenous FA. Data are means ± SE, n = 4; *t-test vs. control (CON). (B) CPT-1 activity was measured with different amounts of mitochondrial crude proteins from the control cells to determine the linear range of measurement. Data are means ± SE, n = 3, for each data point. (C) Cells were treated with EPA and other additives for 24 h, the same as those shown above. The mitochondrial fraction was isolated by sequential centrifugation, and the CPT-1 activity was assayed as described in the Materials and Methods section. Data are means ± SE, n = 5. *P < 0.05, vs. control.

determine the optimal mitochondrial protein concentration for the enzyme activity assay, we first measured the CPT-1 activity using different amounts of proteins prepared from the control cells, which showed a linear range from 5 to 30 µg (Fig. 1B). The final enzyme activity was measured using 20 µg of mitochondrial crude proteins. As shown in Figure 1C, CPT-1 activity in the isolated mitochondria was increased by ~40% after cells were treated with EPA. Under otherwise identical conditions, octanoic acid, oleic acid, and clofibrate did not significantly affect CPT-1 activity (P = 0.2, 0.5, 0.8, respectively). These findings show that the CPT-1 activity assayed from isolated mitochondria was proportional to the rate of β-oxidation in intact cells.

EPA did not change the expression level of CPT-1. To determine whether the changes in CPT-1 activity were associated with increased expression levels of this enzyme, the relative abundance of mRNA and protein of CPT-1 were analyzed by semiquantitative reverse-transcription (RT)-PCR. As shown in Figure 2A, EPA, as well as octanoic acid and oleic acid, did cause detectable effects on CPT-1 mRNA. There was a trend of increased CPT-1 expression in cells treated with clofibrate (Fig. 2A, 2B), but the difference did not reach statistical significance (P = 0.2 and 0.5 for mRNA and protein, respectively, n = 3 for each). The results of these measurements were validated

by PCR measurements using different cycle conditions and by Western blot analysis with different protein loadings to ensure that the results were within the linear range of comparison (data not shown). As an independent verification of our methods, we also measured the mRNA in human hepatoma cells (HepG2) treated in parallel. We found that EPA, oleic acid, and clofibrate increased the expression of CPT-1 by 50, 38, and 72%, respectively (n = 3, P < 0.05 compared with control). whereas octanoic acid had no effect, consistent with previous reports (6).

Alteration in the fatty acyl composition of mitochondrial membrane lipids. Since EPA has been shown to displace proteins from membrane rafts by altering the membrane lipid composition (25), we next investigated whether the changes in CPT-1 enzyme activity were associated with a change in the mitochondrial membrane lipid composition. As shown in Figure 3, EPA typically constitutes a very small fraction of the FA in mitochondrial phospholipids. Incubation with exogenous EPA increased the percentage of EPA in the mitochondrial membrane lipids by about fivefold. This was accompanied by a reduction of 16:1 in the mitochondrial membrane lipids as compared with the control cells. The net change caused an increase in the degree of unsaturation. Incubation with either octanoic acid or clofibrate did not cause detectable changes in the mitochondrial membrane lipid composition (Fig. 3). Adding

RT-PCR analysis   Western analysis
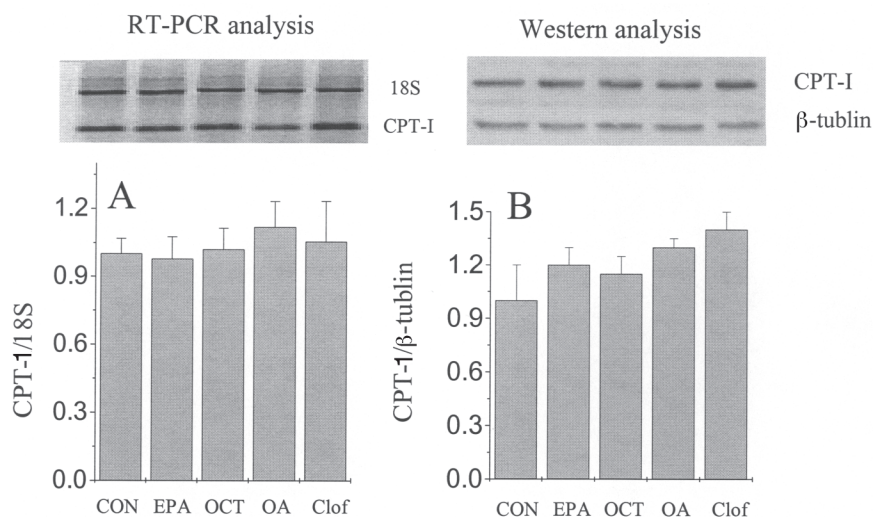
FIG. 2. Effects of EPA on mRNA (A) and protein (B) expression of CPT-1. Cells were prepared the same as those in Figure 1. RNA and protein were isolated after 24 h of incubation and analyzed as described in the Materials and Methods section (mean ± SE, *n* = 3). RT-PCR, reverse-transcription polymerase chain reaction; for other abbreviations see Figure 1.

oleic acid to the exogenous medium slightly increased the percentage of 18:1 in the membrane lipids, accompanied by a similar decrease of 16:1. Therefore, the overall acyl chain unsaturation remained unchanged.

Lipogenesis in adipocytes treated with EPA and other additives. Since lipid synthesis is one of the major metabolic events that directly affects the storage of fat in adipocytes, we investigated how treatment with EPA would affect this process, in comparison with cells treated with other additives. We found that EPA treatment did not affect *de novo* FA synthesis but increased TAG synthesis, as measured by the incorporation of glucose into the glycerol backbone (Table 1). Treatment with

oleic acid caused a similar result, suggesting this might be a common effect of adding exogenous long-chain FA to cell cultures. Octanoic acid inhibited *de novo* FA synthesis but did not affect TAG synthesis, as reported previously (26). Clofibrate affected neither *de novo* FA synthesis nor TAG synthesis.

Despite the difference in β-oxidation and lipid synthesis, total TAG stores did not differ significantly in adipocytes treated as described in the Materials and Methods section, possibly because most of the stored fat was acquired before the treatments. These results also indicate that it was easier to detect the changes in a smaller pool of FA undergoing β-oxidation than in the much larger pool of FA stored in TAG.
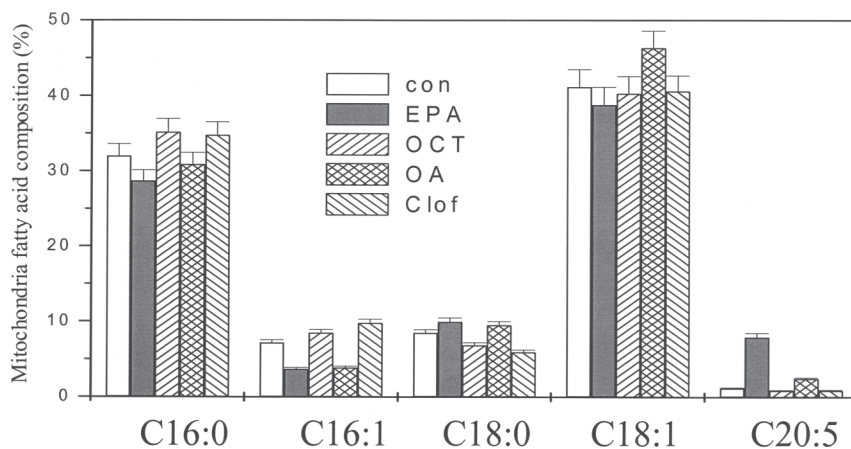
FIG. 3. Effects of EPA on mitochondrial membrane lipid FA composition. Cells were prepared the same as those in Figure 1. Mitochondrial phospholipids were isolated as described in the Materials and Methods section. The fatty acyl methyl esters were analyzed by GLC (*n* = 3). The assignment was done by reference to known fatty acyl methyl ester standards. Small amounts of other acyl chains were also detected (<3%, not shown). For abbreviations see Figures 1 and 2.

TABLE 1
The Effects of EPA on *de novo* FA Synthesis from $^3H_2O^a$, TAG-Glycerol Synthesis[b], and Total Cellular TAG Content[c]

Additives	Control	EPA	Octanoic acid	Oleic acid	Clofibrate
De novo synthesized FA	5.9 ± 0.5	7.0 ± 0.8	1.9 ± 0.2*	5.0 ± 1.0	5.8 ± 0.6
Newly synthesized TAG-[U-^{14}C]glycerol	15.9 ± 0.5	22.8 ± 1.1**	16.1 ± 0.4	25.5 ± 0.7**	16.1 ± 1.1
Cellular TAG	465 ± 31	421 ± 15	441 ± 15	476 ± 21	443 ± 25

[a]Measured as pmol/h/10^6 cells.
[b]Measured as pmol/h/10^6 cells, as TAG-derived [U-^{14}C]glycerol.
[c]Measured as mg/10^6 cells, as total TAG-derived glycerol. Cells were treated as in Figure 1 (mean ± SE, *n* = 4); *$P < 0.05$ significantly reduced; **$P < 0.05$, significantly increased compared with the control.

DISCUSSION

That dietary FA activate FA β-oxidation in hepatocytes has been well established (27–29), but such a direct effect in adipocytes had not been determined in a controlled setting *in vitro*. Our results demonstrate that the β-oxidation of endogenous FA in adipocytes was increased by treatment with EPA but was not affected by oleic acid (Fig. 1A). This is consistent with a previous study showing that feeding rats with n-3 FA, but not monounsaturated FA, stimulated mitochondrial oxidation in adipose tissue (30). Clofibrate, the activating ligand for PPARα, also did not affect FA oxidation. Octanoic acid, on the other hand, inhibited the oxidation of endogenous FA (Fig. 1A). EPA also increased adipocyte mitochondrial CPT-1 activity, whereas oleic acid, octanoic acid, and clofibrate did not (Fig. 1B). EPA, as well as oleic acid and clofibrate, did not affect *de novo* FA synthesis (Table 1). Both EPA and oleic acid increased net TAG synthesis (Table 1). Octanoic acid, on the other hand, inhibited *de novo* FA synthesis but did not affect basal TAG synthesis (Table 1). However, within the 24-h incubation period, none of these changes had a significant effect on total cellular TAG contents.

EPA is known to be an activating ligand for PPARα, the nuclear transcription factor that regulates the expression of FA catabolic genes, including CPT-1 (31–35). An EPA-induced increase in CPT-1 expression is considered to be one of the main mechanisms for increased CPT-1 activity in hepatocytes (6). One would expect that EPA-induced CPT-1 activity in adipocytes might also be a result of ligand activation of PPARα, leading to increased transcription of this enzyme (36). However, we did not detect significant effects of EPA on CPT-1 at either the mRNA or the protein level (Fig. 2). The mRNA levels of PPARα and a few of its downstream targets, including acyl-CoA oxidase and acyl-CoA synthase, were also unchanged by the treatment with EPA or other additives used in this work (data not shown). Therefore, we conclude that under our experiment conditions, EPA-induced CPT-1 activity is not likely mediated through the PPARα pathway. The low abundance of PPARα expressed in adipocytes as compared with its high abundance in hepatocytes might partly explain the discrepancy in the effects of EPA on CPT-1 expression between these two cell types. Even clofibrate, a synthetic PPARα-specific ligand, failed to induce significant changes in CPT-1 expression (Fig. 2), consistent with findings that fenofibrate, another synthetic PPARα-specific ligand, had minimal effects on

the expression of PPARα target genes in either rat adipose tissue or 3T3-L1 adipocytes (37).

On the other hand, although expressed to a limited extent, PPARα has been demonstrated to be functional in adipocytes (23,36,38), and might be regulated by supra-high dosages of synthetic ligands (39). Therefore, the lack of effects of EPA, or oleic acid and clofibrate, on CPT-1 mRNA in adipocytes might not be entirely due to the low expression levels of PPARα in these cells. An alternative possibility is that ligand stimulation of PPARα might already have been saturated in adipocytes because of its constant exposure to high levels of endogenous FA. Most of these FA can also be activating ligands of PPARα (34). In this regard, moderate variations in exogenous FA within a short period of time might not be sufficient to alter the transcriptional activity of PPARα in adipocytes. Hence, an alternative mechanism needs to be considered to interpret the EPA-mediated increase in CPT-1 activity and the associated increase in FA oxidation.

Mitochondrial CPT-1 activity can be modified by the fluidity of the membranes in which it resides, as shown by an earlier study (40). Because mitochondrial lipids contain a low proportion of cholesterol, membrane fluidity is largely controlled by the acyl chain unsaturation of the phospholipids. As shown in Figure 3, exogenous EPA was incorporated into mitochondrial membrane lipids with a simultaneous decrease in palmitoleic acid (16:1). These changes in the mitochondrial membrane lipids are expected to alter membrane structure and cell functions (2,11), as we also confirmed (Fig. 1A, 1B). The direct cause(s) of changes in CPT-1 activity, however, merit further investigation.

In addition to its effects on β-oxidation and CPT-1 activity, EPA has been shown to inhibit lipogenesis and reduce TAG synthesis in hepatocytes (41). In contrast, we found that EPA did not inhibit *de novo* FA synthesis and even increased TAG synthesis in adipocytes, as evidenced by the increased synthesis of the TAG-glycerol moiety (Table 1). Similar results were found when cells were treated with oleic acid but not octanoic acid (26). Such an increase in TAG synthesis is likely caused by an increased availability of exogenous substrates, which implies that EPA can be used for lipid synthesis in adipocyte analogs to oleic acid.

A quantitative comparison of the results in Table 1 shows that the amount of FA or TAG synthesized *de novo* during the 24-h incubation period accounted for only a small fraction of the total storage of TAG, implying that the majority of cellular

TAG was preformed before the incubation was initiated. Hence, although EPA and oleic acid both increased TAG synthesis, they did not substantially change the total TAG storage. In addition, since *de novo* FA synthesis occurred at a slower rate than net TAG synthesis, most of the FA substrate used for TAG synthesis in these cells might come from intracellular FA recycling or from exogenously added FA.

In summary, we showed that EPA increases CPT-1 activity and β-oxidation in adipocytes. Since FA oxidation normally accounts for only a very small part of the fat disposition in adipocytes (18), we did not detect an acute effect of EPA on lipid synthesis and storage in adipocytes, as previously established in hepatocytes. Our results support the hypothesis that the hypolipidemic effect of EPA or fish oil found *in vivo* might be primarily a liver-mediated systemic effect. However, a small but steady increase in β-oxidation might gradually modulate fat storage in adipocytes on a long-term basis.

ACKNOWLEDGMENTS

REFERENCES

1. Parrish, C.C., Pathy, D.A., Parkes, J.G., and Angel, A. (1991) Dietary Fish Oils Modify Adipocyte Structure and Function, *J. Cell. Physiol. 148*, 493–502.
2. Seo, T., Blaner, W.S., and Deckelbaum, R.J. (2005) Omega-3 Fatty Acids: Molecular Approaches to Optimal Biological Outcomes, *Curr. Opin. Lipidol. 16*, 11–18.
3. Belayev, L., Marcheselli, V.L., Khoutorova, L., de Turco, E.B.R., Busto, R., Ginsberg, M.D., and Bazan, N.G. (2005) Docosahexaenoic Acid Complexed to Albumin Elicits High-Grade Ischemic Neuroprotection, *Stroke 36*, 118–123.
4. Buckley, R., Shewring, B., Turner, R., Yaqoob, P., and Minihane, A.M. (2004) Circulating Triacylglycerol and apoE Levels in Response to EPA and Docosahexaenoic Acid Supplementation in Adult Human Subjects, *Br. J. Nutr. 92*, 477–483.
5. Ezaki, O., Tsuji, E., Momomura, K., Kasuga, M., Itakura, H., and Momoura, K. (1992) Effects of Fish and Safflower Oil Feeding on Subcellular Glucose Transporter Distributions in Rat Adipocytes, *Am. J. Physiol. 263*, E94–E101.
6. Berge, R.K., Madsen, L., Vaagenes, H., Tronstad, K.J., Gottlicher, M., and Rustan, A.C. (1999) In Contrast with Docosahexaenoic Acid, Eicosapentaenoic Acid and Hypolipidaemic Derivatives Decrease Hepatic Synthesis and Secretion of Triacylglycerol by Decreased Diacylglycerol Acyltransferase Activity and Stimulation of Fatty Acid Oxidation, *Biochem. J. 343*, 191–197.
7. Froyland, L., Madsen, L., Vaagenes, H., Totland, G.K., Auwerx, J., Kryvi, H., Staels, B., and Berge, R.K. (1997) Mitochondrion Is the Principal Target for Nutritional and Pharmacological Control of Triglyceride Metabolism, *J. Lipid Res. 38*, 1851–1858.
8. Luo, J., Rizkalla, S.W., Boillot, J., Alamowitch, C., Chaib, H., Bruzzo, F., Desplanque, N., Dalix, A.M., Durand, G., Slama, G., *et al.* (1996) Dietary (n-3) Polyunsaturated Fatty Acids Improve Adipocyte Insulin Action and Glucose Metabolism in Insulin-Resistant Rats: Relation to Membrane Fatty Acids, *J. Nutr. 126*, 1951–1958.
9. Hong, D.D., Takahashi, Y., Kushiro, M., and Ide, T. (2003) Divergent Effects of Eicosapentaenoic and Docosahexaenoic Acid Ethyl Esters, and Fish Oil on Hepatic Fatty Acid Oxidation in the Rat, *Biochim. Biophys. Acta 1635*, 29–36.
10. Lee, J.Y., Plakidas, A., Lee, W.H., Heikkinen, A., Chanmugam, P., Bray, G., and Hwang, D.H. (2003) Differential Modulation of Toll-like Receptors by Fatty Acids: Preferential Inhibition by n-3 Polyunsaturated Fatty Acids, *J. Lipid Res. 44*, 479–486.
11. Ovide-Bordeaux, S., and Grynberg, A. (2004) Docosahexaenoic Acid Affects Insulin Deficiency- and Insulin Resistance-Induced Alterations in Cardiac Mitochondria, *Am. J. Physiol. Regul. Integr. Comp. Physiol. 286*, R516–R527.
12. Wang, H., Lu, S., Du, J., Yao, Y., Berschneider, H.M., and Black, D.D. (2001) Regulation of Apolipoprotein Secretion by Long-Chain Polyunsaturated Fatty Acids in Newborn Swine Enterocytes, *Am. J. Physiol. Gastrointest. Liver Physiol. 280*, G1137–G1144.
13. Brown, A.-M., Castle, J., Hebbachi, A.-M., and Gibbons, G.F. (1999) Administration of n-3 Fatty Acids in the Diets of Rats or Directly to Hepatocyte Cultures Results in Different Effects on Hepatocellular ApoB Metabolism and Secretion, *Arterioscler. Thromb. Vasc. Biol. 19*, 106–114.
14. Parrish, C.C., Pathy, D.A., and Angel, A. (1990) Dietary Fish Oils Limit Adipose Tissue Hypertrophy in Rats, *Metabolism 39*, 217–219.
15. Fickova, M., Hubert, P., Cremel, G., and Leray, C. (1998) Dietary (n-3) and (n-6) Polyunsaturated Fatty Acids Rapidly Modify Fatty Acid Composition and Insulin Effects in Rat Adipocytes, *J. Nutr. 128*, 512–519.
16. Guo, W., Choi, J.K., Kirkland, J.L., Corkey, B.E., and Hamilton, J.A. (2000) Esterification of Free Fatty Acids in Adipocytes: A Comparison Between Octanoic Acid and Oleic Acid, *Biochem. J. 349*, 463–471.
17. Kamp, F., and Hamilton, J.A. (1993) Movement of Fatty Acids, Fatty Acid Analogues, and Bile Acids Across Phospholipid Bilayers, *Biochemistry 32*, 11074–11086, and appendix therein.
18. Wang, T., Zang, Y., Ling, W., Corkey, B.E., and Guo, W. (2003) Metabolic Partitioning of Endogenous Fatty Acid in Adipocytes, *Obes. Res. 11*, 880–887.
19. McGarry, J.D., Mills, S.E., Long, C.S., and Foster, D.W. (1983) Observation on the Affinity for Carnitine, and Malonyl-CoA Sensitivity, of Carnitine Palmitoyl-Transferase-1 in Animal and Human Tissues, *Biochem. J. 214*, 21–28.
20. Esser, V., Brown, N.F., Cowan, A.T., Foster, D.W., and McGarry, J.D. (1996) Expression of a cDNA Isolated from Rat Brown Adipose Tissue and Heart Identifies the Product as the Muscle Isoform of Carnitine Palmitoyltransferase 1 (M-CPT-1), *J. Biol. Chem. 271*, 6972–6977.
21. Folch, J., Lees, M., and Sloane Stanley, G.H. (1957) A Simple Method for the Isolation and Purification of Total Lipids from Animal Tissues, *J. Biol. Chem. 226*, 497–509.
22. Han, J., Farmer, S.R., Kirkland, J.L., Corkey, B.E., Yoon, R., Pirtskhalava, T., Ido, Y., and Guo, W. (2002) Octanoic Acid Attenuates Adipogenesis in 3T3-L1 Preadipocytes, *J. Nutr. 132*, 904–910.
23. Lee, Y., Yu, X., Gonzales, F., Mangelsdorf, D.J., Wang, M.Y., Richardson, C., Witters, L.A., and Unger, R.H. (2002) PPARα Is Necessary for the Lipopenic Action of Hyperleptinemia on White Adipose and Liver Tissue, *Proc. Natl. Acad. Sci. USA 99*, 11848–11853.
24. Bach, A.C., Ingenbleek, Y., and Frey, A. (1996) The Usefulness of Dietary Medium Chain Triglycerides in Body Weight Control: Fact or Fancy? *J. Lipid Res. 37*, 708–726.
25. Stulnig, T.M., Huber, J., Leitinger, N., Imre, E., Angelisova, P., Nowotny, P., and Waldhausl, W. (2001) Polyunsaturated Eicosapentaenoic Acid Displaces Proteins from Membrane Rafts by

Altering Raft Lipid Composition, *J. Biol. Chem. 276*, 37335–37340.

26. Guo, W., Lei, T., Wang, T., Corkey, B.E., and Han, J. (2003) Octanoic Acid Inhibits Triglyceride Synthesis in 3T3-L1 and Human Adipocytes, *J. Nutr. 133*, 2512–2518.

27. Halvorsen, B., Rustan, A.C., Madsen, L., Reseland, J., Berge, R.K., Sletnes, P., and Christiansen, E.N. (2001) Effects of Long-Chain Monounsaturated and n-3 Fatty Acids on Fatty Acid Oxidation and Lipid Composition in Rats, *Ann. Nutr. Metab. 45*, 30–37.

28. Madsen, L., Froyland, L., Kryvi, H., Auwerx, J., Staels, B., and Berge, R.K. (1999) The Mitochondrion Is the Principal Target for Nutritional and Pharmacological Control of Plasma Triglyceride, *Lipids 34* (Suppl.), S167.

29. Totland, G.K., Madsen, L., Klementsen, B., Vaagenes, H., Kryvi, H., Froyland, L., Hexeberg, S., and Berge, R.K. (2000) Proliferation of Mitochondria and Gene Expression of Carnitine Palmitoyltransferase and Fatty Acyl-CoA Oxidase in Rat Skeletal Muscle, Heart and Liver by Hypolipidemic Fatty Acids, *Biol. Cell. 92*, 317–329.

30. Halvorsen, B., Rustan, A.C., Madsen, L., Reseland, J., Berge, R.K., Sletnes, P., and Christiansen, E.N. (2001) Effects of Long Chain Monounsaturated and n-3 Fatty Acids on Fatty Acid Oxidation and Lipid Accumulation in Rats, *Ann. Nutr. Metab. 45*, 30–37.

31. Johnson, T.E., and Ledwith, B.J. (2001) Peroxisome Proliferators and Fatty Acids Negatively Regulate Liver X Receptor-Mediated Activity and Sterol Biosynthesis, *J. Steroid Biochem. Mol. Biol. 77*, 59–71.

32. Armstrong, M.B., and Towle, H.C. (2001) Polyunsaturated Fatty Acids Stimulate Hepatic UCP-2 Expression *via* a PPARα-Mediated Pathway, *Am. J. Physiol. Endocrinol. Metab. 281*, E1197–E1204.

33. Braissant, O., Foufelle, F., Scotto, C., Dauca, M., and Wahli, W. (1996) Differential Expression of Peroxisome Proliferator-Activated Receptors (PPARs): Tissue Distribution of PPAR-α, -β, and -γ in the Adult Rat, *Endocrinology 137*, 354–366.

34. Desvergne, B., and Wahli, W. (1999) Peroxisome Proliferator-Activated Receptors: Nuclear Control of Metabolism, *Endocr. Rev. 20*, 649–688.

35. Wahli, W., Devchand, P.R., IJpenberg, A., and Desvergne, B. (1999) Fatty Acids, Eicosanoids, and Hypolipidemic Agents Regulate Gene Expression Through Direct Binding to Peroxisome Proliferator-Activated Receptors, *Adv. Exp. Med. Biol. 447*, 199–209.

36. Wang, M.Y., Lee, Y., and Unger, R.H. (1999) Novel Form of Lipolysis Induced by Leptin. *J. Biol. Chem. 274*, 17541–17544.

37. Martin, G., Schoonjans, K., Lefebvre, A.M., Staels, B., and Auwerx, J. (1997) Coordinate Regulation of the Expression of the Fatty Acid Transport Protein and Acyl-CoA Synthetase Genes by PPARα and PPARγ Activators, *J. Biol. Chem. 272*, 28210–28217.

38. Ding, S.T., Schinckel, A.P., and Weber, T.E. (2000) Expression of Porcine Transcription Factors and Genes Related to Fatty Acid Metabolism in Different Tissues and Genetic Populations, *J. Anim. Sci. 78*, 2127–2134.

39. Cabrero, A., Alegret, M., Sanchez, R.M., Adzet, T., Laguna, J.C., and Vazquez, M. (2001) Bezafibrate Reduces mRNA Levels of Adipocyte Markers and Increases Fatty Acid Oxidation in Primary Culture of Adipocytes, *Diabetes 50*, 1883–1890.

40. Power, G.W., Yaqoob, P., and Harvey, D.J. (1994) The Effect of Dietary Lipid Manipulation on Hepatic Mitochondrial Phospholipid Fatty Acid Composition and Carnitine Palmitoyltransferase I Activity, *Biochem. Mol. Biol. Int. 34*, 671–684.

41. Willumsen, N., Skorve, J., Hexeberg, S., Rustan, A.C., and Berge, R.K. (1993) The Hypotriglyceridemic Effect of Eicosapentaenoic Acid in Rats Is Reflected in Increased Mitochondrial Fatty Acid Oxidation Followed by Diminished Lipogenesis, *Lipids 28*, 683–690.

Effect of Abomasal Infusions of Geometric Isomers of 10,12 Conjugated Linoleic Acid on Milk Fat Synthesis in Dairy Cows

Asgeir Sæbø[a], Per-Christian Sæbø[a], J. Mikko Griinari[b], and Kevin J. Shingfield[c,*]

[a]Natural ASA, N-6160, Hovdebygda, Norway, [b]Department of Animal Science, University of Helsinki, Helsinki, Finland, and [c]Centre for Dairy Research, Department of Animal Science, The University of Reading, Reading, RG6 6AT, United Kingdom

ABSTRACT: The *trans*-10,*cis*-12 isomer of conjugated linoleic acid (CLA) decreases TAG accumulation in 3T3-L1 adipocytes, reduces lipid accretion in growing animals, and inhibits milk fat synthesis in lactating mammals. However, there is evidence to suggest that other FA may also exert antilipogenic effects. In the current experiment, the effects of geometric isomers of 10,12 CLA on milk fat synthesis were examined using four Holstein-British Friesian cows in a 4×4 Latin Square experiment with 14-d periods. Treatments consisted of abomasal infusions of skim milk, or skim milk containing *trans*-10,*cis*-12 CLA (T1), *trans*-10,*trans*-12 CLA (T2), or a mixture of predominantly 10,12 isomers containing (g/100 g) *trans*-10,*cis*-12 (35.0), *cis*-10,*trans*-12 (23.2), *trans*-10,*trans*-12 (14.9), and *cis*-10,*cis*-12 (5.1). CLA supplements were prepared from purified ethyl linoleate and infused as nonesterified FA. Infusions were conducted over a 4-d period with a 10-d interval between treatments and targeted to deliver 4.5 g/d of 10,12 CLA isomers. Compared with the control, *trans*-10, *trans*-12 CLA had no effect ($P > 0.05$) on milk fat yield, whereas treatments T1 and T3 depressed ($P < 0.05$) milk fat content (19.8 and 22.9%, respectively) and decreased milk fat output (20.8 and 21.3%, respectively). Comparable reductions in milk fat synthesis to 4.14 and 1.80 g *trans*-10,*cis*-12/d supplied by treatments T1 and T3 indicate that other 10,12 geometric isomers of CLA have the potential to exert antilipogenic effects. The relative abundance of *cis*-10,*trans*-12 CLA in treatment T3 and the low transfer efficiency of this isomer into milk suggest that *cis*-10,*trans*-12 CLA was the active component..

Paper no. L9762 in *Lipids 40*, 823–832 (August 2005).

It is well established that isomers of CLA are involved in the regulation of lipid metabolism. Supplements of a mixture of CLA isomers containing *trans*-8,*cis*-10; *cis*-9,*trans*-11; *trans*-10,*cis*-12; and *cis*-11,*trans*-13 have been shown to reduce body fat in growing animals and decrease milk fat content in several species including the pig, cow, and human (1). Investigations with pure isomers in the 3T3-L1 adipocyte cell culture model (2), mice (3), and lactating dairy cows (4) have revealed that the antilipogenic effects are attributable to the *trans*-10,*cis*-12 isomer. In addition, studies in dairy cows have also shown that *cis*-9,*trans*-11 (4) or a mixture of CLA isomers containing *trans*-8,*cis*-10 or *cis*-11,*trans*-13 (5) has no effect on milk fat content. Thus far, *trans*-10,*cis*-12 is the only isomer of CLA shown unequivocally to reduce milk fat synthesis in lactating dairy cows.

Formation of *trans*-10,*cis*-12 CLA in the rumen is enhanced when high concentrate–low fiber diets are fed, with an increase in ruminal formation of this isomer being related to decreases in milk fat secretion (6,7). However, during diet-induced milk fat depression, concentrations of *trans*-10,*cis*-12 CLA in milk fat are less than half those when comparable reductions in milk fat secretion are induced with postruminal *trans*-10,*cis*-12 CLA infusions (8). Furthermore, small or negligible increases in *trans*-10,*cis*-12 CLA have been reported during milk fat depression when diets containing marine oils are fed (9,10). Overall, these findings tend to suggest that other biohydrogenation intermediates formed in the rumen also may have a role in the regulation of milk fat synthesis, but the identity of these FA remains unclear.

Park and Pariza (11) reported that a mixture of conjugated nonadecadienoic acid (CNA) isomers, containing *cis*-10,*trans*-12 CNA and *trans*-11,*cis*-13 CNA as major components, decreased fat deposition in mice to a greater extent than *trans*-10,*cis*-12 CLA. Since the CNA supplement contained comparable amounts of *cis*-10,*trans*-12 CNA and *trans*-11,*cis*-13 CNA, isomer-specific effects could not be determined. Owing to the structural analogy with *trans*-10,*cis*-12 CLA, the antilipogenic effects were attributed to the *trans*-11,*cis*-13 isomer of CNA (11). However, it is possible that the antilipogenic effects of *trans*-10,*cis*-12 CLA relate to the position of the 10,12 conjugated double bond structure relative to the carboxyl rather than the methyl group of the FA moiety, with the implication that the reduction in tissue lipid accretion of CNA isomers in mice could be a direct response to *cis*-10,*trans*-12 CNA.

To test this hypothesis, the effects of a mixture of 10,12 CLA isomers containing a structural 18-carbon analog (*cis*-10,*trans*-12 CLA) as a major component on milk fat synthesis in the lactating dairy cow were examined in the current study, relative to *trans*-10,*trans*-12 CLA and the known inhibitor *trans*-10,*cis*-12 CLA.

MATERIALS AND METHODS

Experimental animals and diet. Four multiparous lactating Holstein-British Friesian cows (679 ± 10.3 kg live weight and 303 ± 25.9 d in lactation; mean ± SE) fitted with rumen fistula (100 mm i.d.; Bar Diamond, Parma, ID) were used in the present experiment lasting 56 d. All procedures used were licensed, regulated, and inspected by the United Kingdom Home Office under the Animals (Scientific Procedures) Act of 1986.

*To whom correspondence should be addressed at Animal Production Research, MTT Agrifood Research Finland, FIN 31600, Jokioinen, Finland. E-mail: kevin.shingfield@mtt.fi

Abbreviations: CNA, conjugated nonadecadienoic acid; T1, treatment with *trans*-10,*cis*-12 CLA; T2, treatment with *trans*-10,*trans*-12 CLA; T3, treatment with a mixture of 10,12 geometric isomers of CLA.

The animals were housed in individual stalls within the Metabolism Unit of the Centre for Dairy Research, University of Reading, United Kingdom. Cows were offered a total mixed ration formulated (Table 1) to meet or exceed nutrient requirements according to the Agricultural and Food Research Council (12). Diets were offered *ad libitum* and fed as equal meals at 0800 and 1600. Cows had continuous access to water and trace-mineralized salt blocks (Baby Red Rockies, Winsford, Cheshire, United Kingdom) and were milked at approximately 0600 and 1630.

Experimental design and treatments. Cows were randomly assigned treatments in a 4 × 4 Latin Square design. Treatments consisted of abomasal infusions targeted to provide 0 (control) or 4.5 g/d of *trans*-10,*cis*-12 CLA (T1), *trans*-10,*trans*-12 CLA (T2), or a mixture of 10,12 geometric isomers of CLA (T3). Infusions started at 1630 and lasted for 4 d with a 10-d interval between infusion periods to minimize treatment carry-over effects. Postruminal infusion was used as a convenient means of delivering FA to the small intestine, avoiding ruminal biohydrogenation and possible effects on the microbial population in the rumen and enabling the amount of FA supplied by each treatment to be accurately determined. Infusion lines were established using Nalgene tubing that passed through the rumen fistula and reticulo-omasal orifice and a peristaltic pump

TABLE 1
Diet Formulation and Chemical Composition

Composition	
Ingredient (g/100 g dry matter)	
Grass silage	10.0
Corn silage	30.0
Cracked wheat	16.7
Ground barley	9.2
Rapeseed meal[a]	4.1
Soybean meal	6.1
Molassed sugarbeet pulp[b]	9.2
Wheat feed (middlings)	8.2
Blended cane molasses and urea[c]	4.0
High protein corn gluten meal (Prairie meal)	1.0
Minerals and vitamins[d]	1.5
Chemical composition (g/100 g dry matter)	
Dry matter[e]	50.7
Organic matter	93.0
Crude protein	17.8
Neutral detergent fiber	26.0
Starch	31.5
Water-soluble carbohydrate	2.9
Metabolizable energy (MJ/kg dry matter)	11.8

[a]Solvent-extracted rapeseed meal of low glucosinolate content.
[b]By-product of the manufacture of sugar comprised of dried shredded sugarbeet pulp, to which molasses has been added.
[c]Regumaize 44 (SvG Intermol Limited, Bootle, Merseyside, United Kingdom). Declared composition (g/100 g dry matter) crude protein (44.0), water-soluble carbohydrate (55.0), and metabolizable energy content (11.8 MJ/kg dry matter).
[d]Proprietary mineral and vitamin supplement (Dairy Direct, Bury St. Edmonds, United Kingdom) contained (g/kg) calcium (270), magnesium (60), sodium (40), phosphorus (40), zinc (5.0), manganese (4.0), copper (1.5); (mg/kg), iodine (500), cobalt (50), selenium (15); (IU/g) retinyl acetate (500), cholecalciferol (100), dl-α-tocopheryl acetate (0.5).
[e]Oven dry matter content corrected for volatile losses (16).

(Model 202; Watson-Marlow, High Wycombe, United Kingdom) calibrated to deliver 3 kg of infusate/d. Infusions were conducted over a period of 23 h/d at a rate of 130 g/h to allow time for daily line flushing to prevent deterioration of infusion rates. Four-day infusions were used, since earlier studies showed that reductions in milk fat synthesis due to *trans*-10,*cis*-12 CLA reach a nadir after this period of infusion (4,13).

The CLA treatments in the form of nonesterified FA preparations were infused as an emulsion with skim milk. Three separate skim milk and CLA emulsions (13.5 L/treatment) were prepared in the morning before each infusion period by mixing the appropriate amount of CLA material and skim milk (85°C) with a high-shear mixer (Model L4RT; Silverson Machines, Chesham, United Kingdom) and passing each mixture through a single-stage pressure homogenizer (APV; Rannie, Copenhagen, Denmark). Two passes were performed at pressures of 200 and 50 bar, respectively, to ensure uniform dispersion of the CLA supplements in skim milk. Once prepared, emulsions were stored at 4°C before infusion.

Measurements and sampling. Individual cow intakes were measured daily during each infusion period. Representative samples of fresh diets and feed refusals were composited daily and stored at −20°C. Dry matter contents were determined after drying at 100°C for 24 h. Frozen feed samples were analyzed for volatile components or dried at 60°C, ground, and submitted for the determination of chemical composition using accredited and Parliament-approved procedures for feedstuff analysis (14,15) by a commercial laboratory (Natural Resources Management, Bracknell, United Kingdom). Dry matter content of silage was corrected for volatile losses according to Porter *et al.* (16).

Milk yields were recorded daily. Samples of milk for the determination of fat, protein, and lactose were collected from each cow at each milking 24 h before and during the 96-h infusion period. Milk samples were treated with potassium dichromate preservative (1 mg/mL; Lactabs; Thompson & Capper, Runcorn, United Kingdom) and stored at 4°C prior to analysis. Milk fat, crude protein, and lactose were determined using a Milko-Scan 133B analyzer (Foss Electric Ltd., York, United Kingdom). FA composition was determined in untreated samples of milk collected during the last 24 h of each infusion period and bulked according to yield. Milk samples for FA determinations were stored at −20°C until submitted for analysis.

Synthesis of CLA supplements. The CLA supplements were synthesized by Natural ASA (Hovdebygda, Norway) using a FA ethyl ester distillate prepared from safflower oil (Cognis GmbH, Düsseldorf, Germany) as the starting material. After dissolving in acetone and cooling to −60°C, precipitated oleic acid was removed by filtration, and the ethyl ester contained approximately 95% ethyl linoleate after solvent removal. The purified ethyl linoleate concentrate was heated at 120°C for 3 h with catalytic amounts of potassium ethoxide and ethanol (17) to yield a mixture of *cis*-9,*trans*-11 and *trans*-10,*cis*-12 ethyl esters, which contained less than 3 g/100 g of other CLA isomers. Thereafter, the mixture of conjugated ethyl esters was distilled in a molecular distillation plant, and a concentrate of *trans*-10,*cis*-12 was obtained by low-temperature crystallization at −60°C.

Precipitated material was removed and dried under vacuum. Analysis by GC confirmed the composition of the precipitate as containing (g/100 g total CLA) primarily *trans*-10,*cis*-12 (93.8) and small amounts of *cis*-9,*trans*-11 (4.0).

Part of the *trans*-10,*cis*-12 ethyl ester-enriched fraction was retained, and the remainder was isomerized by heating at 85°C under a nitrogen atmosphere and strong agitation for 9 h with 2% (by weight) concentrated nitric acid (85%) to yield a mixture of 10,12 conjugated ethyl esters. After numerous washes with hot water, oil was dried under vacuum and subjected to repeated low-temperature crystallizations, yielding two fractions containing *trans*-10,*trans*-12 or a mixture of isomers enriched with *cis*-10,*trans*-12. All conjugated ethyl ester fractions synthesized were converted to nonesterified CLA by reaction with aqueous potassium hydroxide and methanol. Reaction mixtures were neutralized with citric acid (18), and the oil obtained was washed with distilled water, dried under vacuum, and stored under nitrogen until infused.

Lipid extraction and preparation of FAME. Before extraction, milk samples were thawed, heated to 40°C, cooled to 20°C, and mixed (IKA-Ultraturrax T50; Janke & Kunkel, Staufen, Germany) for few seconds. Lipid in 1 mL of milk was extracted in duplicate using diethylether/hexane (5:4, vol/vol) according to reference procedures (IDF 1C:1987; IDF 16C:1987; International Dairy Federation, Brussels, Belgium). Extracts were combined and evaporated to dryness at 60°C under nitrogen for 1 h. Samples were dissolved in hexane and methyl acetate and transesterified to FAME using freshly prepared methanolic sodium methoxide (19). The mixture was neutralized with oxalic acid (1 g oxalic acid in 30 mL diethyl ether), centrifuged, and dried using calcium chloride (20). Lipid in samples of infused emulsified CLA treatments was extracted using the same procedures used for milk. FA in CLA supplements and infusion samples were converted to FAME using 1% (vol/vol) sulfuric acid in methanol at 50°C for 30 min (21), and the amount of CLA isomers provided by each infu-

sion treatment was determined using methyl pentacosanoate (Sigma, St. Louis, MO) as an internal standard.

GC analysis of FAME. The FAME prepared from CLA supplements, infused treatments, and milk samples were separated and quantified using a gas chromatograph (Model 6890; Hewlett-Packard, Wilmington, DE) equipped with an FID, quadrupole mass selective detector (Model 5973N; Agilent Technologies Inc.), automatic injector, split injection port, and a 100-m fused-silica capillary column (i.d., 0.25 mm) coated with a 0.2-μm film of cyanopropyl polysiloxane (CP-SIL 88; Chrompack 7489, Middelburg, The Netherlands) using hydrogen as the carrier gas operated at constant pressure (20 psi) and flow rate of 0.5 mL/min. Injector and detector temperatures were maintained at 255°C. The total FAME profile in a 2-μL sample at a split ratio of 1:50 was determined using a temperature gradient program (22). Peaks were identified using authentic FAME standards (GLC #463 and GLC #606; Nu-Chek-Prep, Elysian, MN) and comparison of EI ionization spectra of each peak with that of known standards and an online reference library (http://www.lipids.co.uk/infores/masspec.html; Christie, W.W., personal communication). Individual isomers of 18:1, 18:2, and CLA methyl esters were further resolved in a separate analysis under isothermal conditions at 170°C (22). Under these conditions, it was possible to resolve the *cis*-10,*trans*-12, *cis*-10,*cis*-12, and *trans*-10,*cis*-12 isomers, but *trans*-10,*trans*-12 CLA could not be separated from *trans*-7,*trans*-9 CLA, *trans*-8,*trans*-10 CLA, and *trans*-9,*trans*-11 CLA, which co-elute as a single GC peak (Fig. 1).

Ag⁺-HPLC analysis of FAME. The distribution of isomers in CLA supplements was determined using an HPLC system (Model 1090; Hewlett-Packard), equipped with autosampler, photodiode array detector, 20-μL injection loop, heated column compartment, and four silver-impregnated silica columns (ChromSpher 5 Lipids, 250 × 4.6 mm, 5 μm particle size; Varian Ltd., Walton-on-Thames, United Kingdom) coupled in series. Methyl esters of CLA were separated under isocratic conditions at 22°C using 0.1% (by vol) of acetonitrile (Rathburn
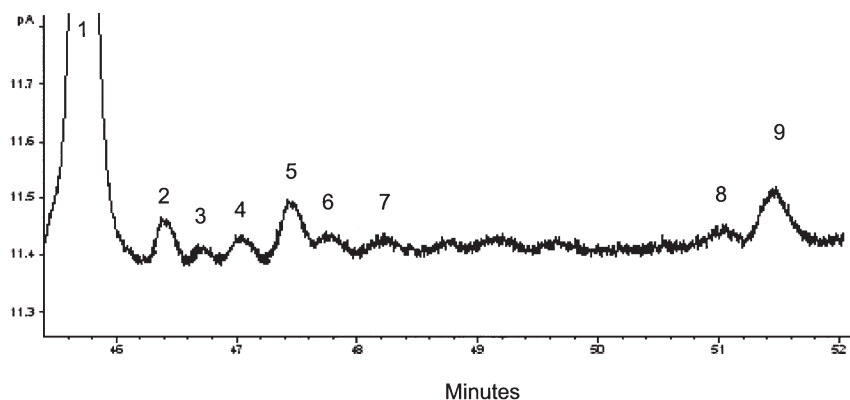
FIG.1. Partial gas chromatogram indicating typical separation of methyl esters of CLA prepared from milk from cows receiving postruminal infusions of a mixture of geometric 10,12 CLA isomers (treatment T3) using a 100-m fused-silica capillary column (CP-SIL 88) under isothermal conditions at 170°C. Peak identification: (1) unresolved *cis*-9,*trans*-11 CLA, *trans*-7,*cis*-9 CLA, and *trans*-8,*cis*-10 CLA, (2) *cis*-10,*trans*-12 CLA, (3) *trans*-9,*cis*-11 CLA, (4) 21:0, (5) *trans*-10,*cis*-12 CLA, (6) unresolved *cis*-9,*cis*-11 CLA and *trans*-11,*cis*-13 CLA, (7) *cis*-10,*cis*-12 CLA, (8) *trans*-11,*trans*-13 CLA, and (9) unresolved *trans*-7,*trans*-9 CLA, *trans*-8,*trans*-10 CLA, *trans*-9,*trans*-11 CLA, and *trans*-10,*trans*-12 CLA
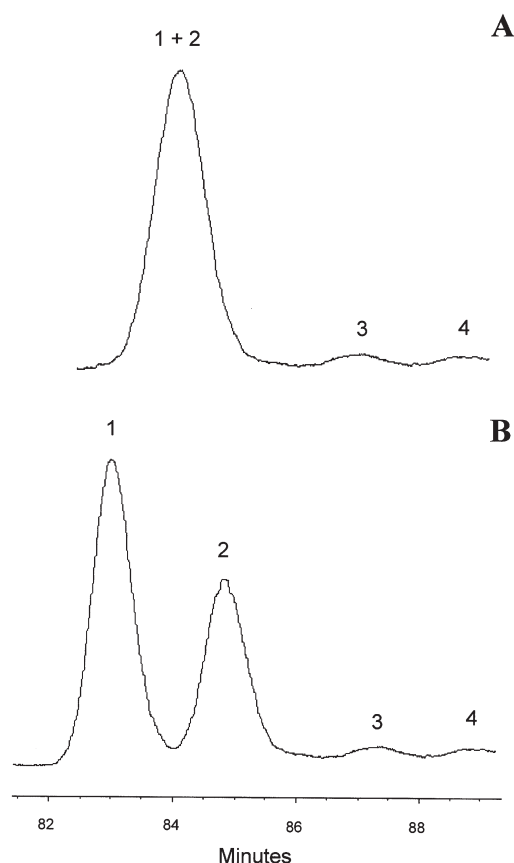
FIG. 2. Partial silver ion-high performance liquid chromatograms indicating the separation of *cis-trans* and *trans-cis* 9,11 and 10,12 isomers of CLA methyl esters prepared from treatment T3 attained using four silver impregnated silica columns coupled in series and a mobile phase containing (A) 0.1% (vol/vol) acetonitrile in heptane (22), or (B) 2.0% (vol/vol) acetic acid (23) under isocratic conditions at 22°C. Peak identification: (1) *trans*-10,*cis*-12 CLA, (2) *cis*-10,*trans*-12 CLA, (3) *cis*-9,*trans*-11 CLA, and (4) *trans*-9,*cis*-11 CLA

Chemicals Limited, Walkerburn, United Kingdom) in heptane at a flow rate of 1 mL/min (total run time 100 min) and monitoring column effluent at 233 and 210 (reference wavelength) nm (22). Even though most isomers were well-resolved, *cis*-10,*trans*-12 and *trans*-10,*cis*-12 CLA co-elute under these conditions (Fig. 2). To achieve baseline separation of these isomers, Ag+-HPLC analysis was repeated under isocratic conditions at 22°C using 2.0% (vol/vol) of acetic acid in heptane as the mobile phase (23) at a flow rate of 1 mL/min (total run time 100 min) and monitoring column effluent at 233 and 210 (reference wavelength) nm. Typical injection volumes were 10–20 μL, representing <250 μg lipid. Identification of CLA isomers was performed using commercially available CLA methyl ester standards (Matreya Incorporated, Pleasant Gap, PA; Sigma), comparison of the elution order reported in the literature (23), and cross-referencing the GC analysis of CLA supplements with reference milk samples for which the distribution of CLA isomers had previously been determined by Ag+-HPLC (22,24). Only the isomer profile in CLA supplements was determined by Ag+-HPLC, since most of the isomers of interest

in milk samples, other than *cis*-9,*cis*-11 CLA and *trans*-10,*trans*-12 CLA, could be determined by GC analysis.

Calculations and statistical analysis. Milk FA composition was expressed as a weight percentage of total FA using response factors determined by analysis of butter oil of known FA composition (CRM 164 milk fat reference standard, Community Bureau of Reference, Brussels, Belgium). Yields of individual FA were determined using tritridecanoin (Nu-Chek-Prep) as an internal standard. Concentrations of specific conjugated isomers in CLA supplements were calculated based on proportionate peak area responses determined by both Ag+-HPLC methods and total CLA weight percentage determined by GC. Apparent transfer efficiencies of infused 10,12 CLA isomers from the abomasum into milk were calculated as: [(amount of isomer secreted in milk during CLA infusion − amount of isomer secreted during the control infusion)/amount of isomer infused]. The apparent transfer of *cis*-9,*trans*-11 CLA and total CLA were not determined, since postruminal infusions of *trans*-10,*cis*-12 CLA inhibit the conversion of *trans*-11 18:1 and reduce endogenous synthesis of *cis*-9,*trans*-11 (4,13).

Nutrient intake, milk production, and milk FA composition data measured on the last day of infusion were evaluated by ANOVA for a 4×4 Latin Square design using the mixed procedure of SAS (25). The statistical model included the random effects of cow and the fixed effects of period and experimental treatment. Treatment effects were considered significant at $P < 0.05$.

RESULTS

Supplements of nonesterified FA preparations used to supply *trans*-10,*cis*-12 CLA or *trans*-10,*trans*-12 CLA were relatively pure, whereas the mixture of geometric 10,12 isomers also contained several other positional isomers of CLA (Table 2). Preparation of CLA supplements as emulsions in skim milk supplied the targeted amounts of total CLA for treatment T2, but the amounts of *trans*-10,*cis*-12 CLA and total 10,12 CLA isomers infused for treatments T1 and T3, respectively, were marginally lower than originally intended (Table 3).

Relative to the control treatment, infusions of *trans*-10,*trans*-12 CLA had no effect on dry matter intake or milk production, whereas treatments T1 and T3 reduced ($P < 0.05$) milk fat content and output (Table 4). Infusion of treatments T1 and T3 resulted in a progressive reduction in milk fat content and secretion (Fig. 3). With the exception of reduced concentrations of lactose ($P < 0.05$) for T3 compared with T2, treatments had no effect.

Treatments caused significant increases in the concentration of specific 10,12 isomers corresponding to those contained in the infused CLA supplement (Table 5). In addition, CLA supplements also resulted in significant ($P < 0.05$) reductions in the *cis*-9 14:1/14:0, *cis*-9 16:1/16:0, *cis*-9 18:1/18:0, and *cis*-9,*trans*-11 CLA/*trans*-11 18:1 desaturase ratios, with relatively minor, but often significant, effects on the concentration of other FA in milk (Table 5). Compared with the control, treatment T2 had no effect on milk FA yield other than increasing ($P < 0.05$) the output of *trans*-10,*trans*-12 CLA in milk, but treatments T1 and T3 decreased the secretion of FA in milk

TABLE 2
FA Composition of CLA Supplements

FA[a] (g/100 g)	Treatment		
	T1	T2	T3
cis-9 18:1	0.89	0.00	2.76
trans-10 18:1	0.17	0.00	0.00
trans-11 18:1	0.19	0.00	0.00
cis-9,cis-11 CLA	0.05	0.02	3.08
cis-9,trans-11 CLA	5.89	0.29	2.80
trans-9,cis-11 CLA	0.00	0.06	2.12
trans-9,trans-11 CLA	1.08	1.30	9.40
cis-10,cis-12 CLA	0.09	0.31	5.13
cis-10,trans-12 CLA	0.00	0.00	23.18
trans-10, cis-12 CLA	90.22	2.09	35.00
trans-10,trans-12 CLA	1.14	95.67	14.93
Other CLA	0.00	0.25	1.23
Total CLA	98.46	100.00	96.87

[a]FA composition determined in duplicate based on a combination of GC and Ag+-HPLC analysis of methyl esters. Separation of CLA methyl esters by Ag+-HPLC analysis was conducted under isocratic conditions at 22°C using both 0.1% (vol/vol) acetonitrile in heptane (22) and 2.0% acetic acid (vol/vol) in heptane (23) as the mobile phase.

(Table 6). Reductions in the secretion of C_{4-14}, C_{16}, and C_{18-24} FA accounted for proportionately 0.33, 0.42, and 0.17, and 0.34, 0.40, and 0.22 of the total decrease in milk FA output during abomasal infusions of *trans*-10,*cis*-12 CLA and the mixture of 10,12 geometric CLA isomers, respectively.

Apparent transfer of infused *trans*-10,*cis*-12 and *cis*-10,*trans*-12 at the abomasum was similar, but *trans*-10,*trans*-12 and *cis*-10,*cis*-12 were transferred at a higher efficiency (Table 7).

DISCUSSION

Although *trans*-10,*cis*-12 is the only CLA isomer shown unequivocally to reduce milk fat synthesis in the dairy cow, there is indirect evidence that other FA produced during ruminal biohydrogenation of dietary PUFA also may elicit antilipogenic effects that are similar to or even more potent than those of *trans*-10,*cis*-12 CLA. This comes in part from examination of milk FA composition, which indicates little or no change in *trans*-10,*cis*-12 CLA during diet- induced milk fat depression

TABLE 3
Mean Amounts of CLA Isomers Delivered to the Abomasum During 4-d Infusion Periods

Amount infused[a] (g/d)	Treatment		
	T1	T2	T3
cis-9,cis-11 CLA	0.002 ± <0.001	0.001 ± <0.001	0.159 ± 0.006
cis-9,trans-11 CLA	0.270 ± 0.037	0.014 ± 0.001	0.144 ± 0.005
trans-9,cis-11 CLA	ND	0.003 ± <0.001	0.109 ± 0.004
trans-9,trans-11 CLA	0.049 ± 0.007	0.063 ± 0.003	0.484 ± 0.018
cis-10,cis-12 CLA	0.004 ± 0.0003	0.015 ± 0.001	0.264 ± 0.010
cis-10,trans-12 CLA	ND	ND	1.194 ± 0.044
trans-10,cis-12 CLA	4.137 ± 0.564	0.101 ± 0.005	1.802 ± 0.067
trans-10,trans-12 CLA	0.052 ± 0.007	4.615 ± 0.216	0.769 ± 0.029
ΣCLA	4.52 ± 0.62	4.82 ± 0.23	4.99 ± 0.19

[a]Values represent the amount (mean ± SD) of CLA isomers supplied during 4-d infusions to four cows for each treatment. ND, isomers not detected.

TABLE 4
Intake and Milk Production of Dairy Cows During Abomasal Infusions of CLA Supplements

Variable[c]	Treatment[a]				SEM[b]
	Control	T1	T2	T3	
Intake (kg dry matter/d)	19.7	20.4	19.7	20.4	0.38
Yield					
Milk (kg/d)	19.7	21.0	19.9	20.2	1.92
Fat (g/d)	677[x]	536[y]	694[x]	533[y]	41.5
Protein (g/d)	734	754	712	753	52.5
Lactose (g/d)	866	931	895	870	81.1
Concentration					
Fat (g/kg)	36.3[x]	29.1[y]	37.2[x]	28.0[y]	1.66
Protein (g/kg)	37.9	36.8	36.6	37.9	1.34
Lactose (g/kg)	43.1[x,y]	43.6[x,y]	44.6[x]	42.1[y]	0.59

[a]Cows received 4-d abomasal infusions (3 kg/d) of skim milk (control), or skim milk containing emulsified supplements of *trans*-10,*cis*-12 CLA (T1), *trans*-10,*trans*-12 CLA (T2), or a mixture of geometric isomers of 10,12 CLA (T3). See Table 2 for the FA composition of CLA supplements.
[b]Error DF, 6.
[c]Values represent the mean for day 4 of infusion for four cows. Means within row not sharing common roman superscripts differ significantly (*P* < 0.05).
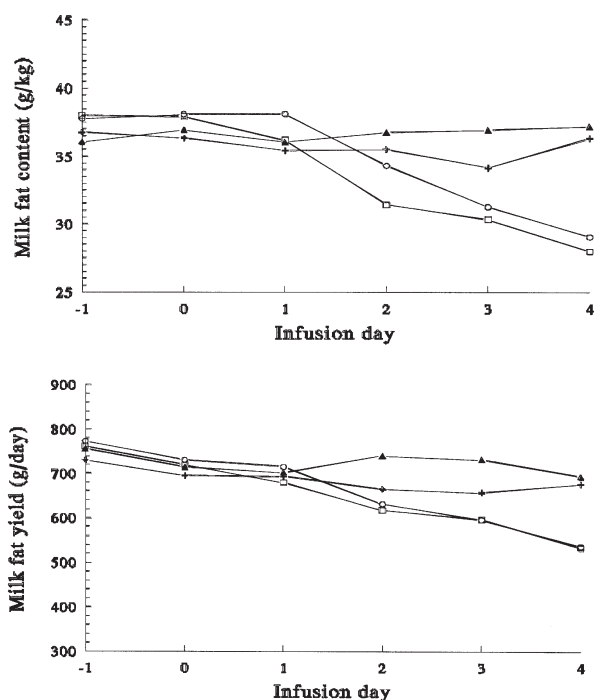
FIG.3. Temporal changes in milk fat content and milk fat yield during abomasal infusion of mixtures of CLA supplements. Infusions were continuously infused during a 4-d period. Values represent means from four animals. SEM for milk fat content and milk fat yield was 1.66 g/kg and 53.8 g/d, respectively. The mean amounts of CLA isomers infused for each treatment are listed in Table 3. (+) Control, (○) T1, (▲) T2, (□) T3. For treatment descriptions see Figure 1.

when marine oils are fed and from the observation that supplements of rumen-protected CLA isomers cause larger decreases in milk fat secretion than would be expected based on milk fat *trans*-10,*cis*-12 CLA content (8,26). Reductions in milk fat yield have been reported in response to postruminal infusions of a mixture of CLA isomers devoid of *trans*-10,*cis*-12 CLA (27), and more recent studies have established that *cis*-9,*trans*-11 (4), *trans*-8,*cis*-10, and *cis*-11,*trans*-13 CLA (5) are not involved in the regulation of milk fat synthesis in the dairy cow.

The unique antilipogenic effect of *trans*-10,*cis*-12 CLA also has been demonstrated in growing mice (3) and cultured 3T3-L1 adipocytes (2), indicating a consistency in the response to *trans*-10,*cis*-12 CLA between these experimental models and the inhibitory effects on milk fat synthesis in the lactating bovine (4,13). The lactating dairy cow represents a convenient and robust means for examining potential antilipogenic effects, since changes in milk fat output can be readily quantified over a short period of time (4,13,27), occur in a predictable manner, and are sufficiently sensitive to respond to small amounts of infused FA with antilipogenic activity (28,29). Furthermore, administering CLA treatments by postruminal infusions enables the amount of FA supplied by each treatment to be accurately determined, while avoiding possible effects on the microbial population in the rumen.

It was not possible to produce *cis*-10,*trans*-12 CLA in sufficient quantities for the present experiment, and therefore a mix-

ture of CLA isomers had to be used. The *cis*-10,*trans*-12-enriched CLA supplement was composed of three main positional 10,12 isomers that accounted for proportionately 0.755 of total CLA content, but it also contained positional 9,11 isomers. The occurrence of 9,11 isomers can be attributed to the small amounts of *cis*-9,*trans*-11 ethyl esters in the *trans*-10,*cis*-12 fraction used to synthesize other positional 10,12 CLA isomers, which during isomerization were converted to ethyl esters of *trans*-9,*trans*-11 CLA, *trans*-9,*cis*-11 CLA, and *cis*-9,*cis*-11 CLA.

To account for the contribution of the major 10,12 isomers other than *cis*-10,*trans*-12 to the overall response to the mixture of CLA isomers in treatment T3, the effect of relatively pure preparations of *trans*-10,*cis*-12 CLA and *trans*-10,*trans*-12 CLA on milk fat synthesis also were evaluated. Treatments T1, T2, and T3 supplied 4.19, 4.73, and 4.03 g of geometric 10,12 CLA isomers/d, respectively. Postruminal infusions of 4.62 g *trans*-10,*trans*-12 CLA/d (treatment T2) had no effect on milk fat synthesis but decreased the ratios of *cis*-9 14:1/14:0, *cis*-9 16:1/16:0, *cis*-9 18:1/18:0, and *cis*-9,*trans*-11 CLA/*trans*-11 18:1, which serve as a proxy for Δ-9 stearoyl CoA desaturase in the mammary gland (1). Reductions in desaturase ratios in the absence of changes in milk fat yield are consistent with earlier observations (30) and underline the lack of a direct involvement of Δ-9 stearoyl CoA desaturase in the inhibition of mammary lipid metabolism.

Since postruminal *trans*-10,*trans*-12 CLA infusion had no effect on milk fat yield, the contribution of this isomer to the overall reduction in milk fat yield to treatment T3 can be discounted. Treatments T1 and T3 supplied 4.14 and 3.00 g/d of the other major 10,12 isomers, *trans*-10,*cis*-12 CLA and *cis*-10,*trans*-12 CLA, but resulted in similar decreases in milk fat secretion compared with the control (20.8 and 21.3%, respectively). The reduction in milk fat yield in response to postruminal infusions of *trans*-10,*cis*-12 CLA from treatment T1 is in line with a predicted decrease of 24.8% based on the relationship developed using data from several experiments (28). However, comparable decreases in milk fat output in response to infusions of 4.14 and 1.80 g *trans*-10,*cis*-12 CLA/d supplied by treatments T1 and T3 indicate that other conjugated isomers in the T3 supplement also inhibit milk fat synthesis.

Treatment T3 supplied small amounts of *cis*-10,*cis*-12 CLA (0.26 g/d). The possible involvement of this isomer in the decrease in milk fat synthesis can be examined by comparing the apparent transfer efficiencies of the major CLA isomers from the abomasum into milk fat. Apparent transfer of the known inhibitor *trans*-10,*cis*-12 CLA is typically lower than that of other CLA isomers that are not involved in the regulation of milk fat synthesis (5,27). These observations point toward a relatively low apparent transfer efficiency being a characteristic of conjugated FA that exert antilipogenic effects. It is interesting to note that the transfer of *trans*-10,*cis*-12 CLA and *cis*-10,*trans*-12 CLA from treatment T3 into milk were virtually identical, whereas the transfer efficiency for *cis*-10,*cis*-12 CLA was substantially higher, leading to the overall conclusion that *cis*-10,*cis*-12 CLA is unlikely to have been a causal factor underlying the reduction in milk fat yield to treatment T3 in the

TABLE 5
Milk FA Composition During Abomasal Infusions of CLA Supplements (g/100 g FA)

FA[c]	Treatment[a]				SEM[b]
	Control	T1	T2	T3	
4:0	2.49[x]	3.17[y]	3.00[y,z]	2.73[x,z]	0.116
6:0	1.97[x]	1.85[x]	2.31[y]	1.63[z]	0.066
8:0	1.35[x]	1.12[y]	1.59[z]	1.07[y]	0.049
10:0	3.47[x]	2.71[y]	4.02[z]	2.88[y]	0.134
12:0	4.55[x]	3.54[y]	5.04[z]	3.95[w]	0.110
14:0	12.03[x]	12.88[y]	13.05[y]	13.01[y]	0.218
cis-9 14:1	1.60[x]	1.48[x,y]	1.47[x,y]	1.33[y]	0.052
15:0	1.93[x]	1.24[y]	1.53[z]	1.52[z]	0.049
16:0	33.42[x]	32.21[y]	33.73[x]	32.07[y]	0.363
cis-9 16:1	2.68[x]	2.24[y]	2.34[x,y]	2.24[y]	0.111
17:0	0.94[x]	0.73[y]	0.82[z]	0.83[z]	0.009
18:0	6.30[x]	9.73[y]	6.92[x]	9.45[y]	0.364
18:1					
cis-9	14.67[x,y]	15.60[x]	13.14[y]	14.53[x,y]	0.470
cis-11	0.69[x]	0.69[x]	0.51[y]	0.71[x]	0.029
cis-12	0.21[x]	0.20[x]	0.19[x]	0.24[y]	0.006
cis-13	0.072	0.067	0.061	0.073	0.004
cis-15	0.11[x]	0.12[x,y]	0.11[x]	0.14[y]	0.005
cis-16	0.053	0.055	0.058	0.061	0.0032
trans-4	0.012[x]	0.014[y]	0.010[z]	0.014[y]	0.0004
trans-5	0.013	0.015	0.013	0.014	0.0014
trans-6+7+8	0.23[x]	0.25[x]	0.19[y]	0.27[x]	0.010
trans-9	0.19[x]	0.17[x,y]	0.15[y]	0.19[x]	0.007
trans-10	0.47[x]	0.42[x,z]	0.32[y]	0.40[z]	0.018
trans-11	0.95[x,y]	0.87[x,y]	0.70[x]	1.09[y]	0.078
trans-12	0.29[x,y]	0.26[x]	0.24[x]	0.32[y]	0.014
trans-13 + 14	0.36[x]	0.43[y]	0.30[z]	0.52[w]	0.015
trans-15	0.18	0.21	0.16	0.23	0.020
trans-16 + cis-14	0.24[x]	0.25[x,y]	0.21[x]	0.29[y]	0.013
Σcis	15.80[x]	16.73[x]	14.07[y]	15.75[x,y]	0.499
Σtrans	2.94[x]	2.89[x]	2.31[y]	3.34[x]	0.139
Σ18:1	18.74[x]	19.61[x]	16.37[y]	19.08[x]	0.628
cis-9,cis-12 18:2	2.20[x]	1.89[y]	1.90[y]	2.29[x]	0.080
Σ18:2[d]	2.81[x]	2.39[y]	2.46[y]	2.90[x]	0.091
cis-10,cis-12 CLA	0.000[x]	0.000[x]	0.000[x]	0.023[y]	0.0008
cis-9,trans-11 CLA[e]	0.57[x]	0.40[x,y]	0.39[y]	0.44[x,y]	0.050
cis-10,trans-12 CLA	0.00[x]	0.00[x]	0.00[x]	0.05[y]	0.003
trans-11,cis-13 + cis-9,cis-11 CLA	0.013	0.011	0.010	0.013	0.0010
trans-9,cis-11 CLA	0.015[x]	0.009[y]	0.009[y]	0.011[y]	0.0009
trans-10,cis-12 CLA	0.012[x]	0.181[y]	0.007[x]	0.074[z]	0.0040
trans-11,trans-13	0.037	0.038	0.023	0.037	0.0045
trans,trans CLA[f]	0.023[x]	0.036[y]	0.200[z]	0.093[w]	0.0024
ΣCLA	0.67	0.68	0.64	0.74	0.043
18:3n-3	0.35[x]	0.33[x,y]	0.30[y]	0.37[x]	0.014
20:0	0.12[x]	0.14[y]	0.11[x]	0.15[y]	0.005
21:0	0.023	0.019	0.024	0.021	0.0033
Ratio					
cis-9 14:1/14:0	0.132[x]	0.114[y]	0.114[y]	0.101[y]	0.0049
cis-9 16:1/16:0	0.080	0.070	0.070	0.070	0.0033
cis-9 18:1/18:0	2.36[x]	1.61[y]	1.88[z]	1.64[y]	0.066
cis-9, trans-11 CLA/trans-11 18:1	0.627[x]	0.456[y]	0.532[z]	0.449[y]	0.0134

[a]Cows received 4-d abomasal infusions (3 kg/d) of skim milk (control), or skim milk containing emulsified supplements of trans-10,cis-12 CLA (T1), trans-10,trans-12 CLA (T2), or a mixture of geometric isomers of 10,12 CLA (T3). See Table 2 for the FA composition of CLA supplements.
[b]Error DF, 6. Means within row not sharing common roman superscripts differ significantly ($P < 0.05$).
[c]Values represent the mean for day 4 of infusion for four cows. FA composition was determined by GC using both a temperature gradient and isothermal conditions for the separation of 18:1, 18:2, and CLA isomers.
[d]Sum of 18:2 excluding isomers of CLA.
[e]Refers to unresolved trans-7,cis-9 CLA, trans-8,cis-10 CLA, and cis-9,trans-11 CLA.
[f]Refers to unresolved trans-7,trans-9 CLA, trans-8,trans-10 CLA, trans-9,trans-11 CLA, and trans-10,trans-12 CLA.

current experiment. However, further studies would be required to confirm the assertion that cis-10,cis-12 CLA is not a potent inhibitor of milk fat synthesis in the dairy cow.

In addition to the 10,12 CLA isomers, the T3 supplement also contained four positional 9,11 isomers that accounted for proportionately 0.180 of total CLA content, and as such treatment T3 supplied 0.48 g trans-9,trans-11 CLA, 0.16 g cis-9,cis-11 CLA, 0.14 g cis-9,trans-11 CLA, and 0.11 g trans-

TABLE 6
Output of FA in Milk During Abomasal Infusions of CLA Supplements (g/d)

FA[c]	Control	T1	T2	T3	SEM[b]
		Treatment[a]			
4:0	12.2[x]	13.1[x]	16.4[y]	11.0[x]	0.93
6:0	10.4[x]	8.0[x,z]	13.1[y]	6.8[z]	0.92
8:0	7.4[x]	5.0[x,y]	9.3[x]	4.6[y]	0.73
10:0	20.0[x]	12.4[y]	24.0[x]	12.9[y]	2.02
12:0	27.2[x]	16.5[y]	30.3[x]	18.3[y]	2.31
14:0	73.4[x,y]	61.2[x]	80.6[y]	62.3[x]	5.11
cis-9 14:1	9.8[x]	7.1[y]	8.8[x,y]	6.7[y]	0.77
15:0	11.7[x]	5.7[y]	9.0[x,y]	7.5[y]	1.08
16:0	200[x]	153[y]	208[x]	155[y]	13.0
cis-9 16:1	15.6[x]	10.6[y]	13.8[x]	10.7[y]	0.83
17:0	5.8[x]	3.5[y]	5.0[x,y]	4.0[y]	0.48
18:0	37.0[x]	45.4[y]	42.1[x,y]	42.1[x,y]	2.35
Σ*cis* 18:1	96.7	80.4	85.5	74.1	6.73
Σ*trans* 18:1	17.0[x]	14.1[y]	14.1[y]	15.1[x,y]	0.70
Σ18:1	110.0	92.5	106.1	82.5	10.62
Σ18:2 [d]	16.8[x]	11.7 [y]	15.0[x,z]	13.5[y,z]	0.65
cis-10,*cis*-12 CLA	0.00[x]	0.00[x]	0.00[x]	0.11[y]	0.009
cis-9,*trans*-11 CLA[e]	3.27[x]	2.02[y]	2.36[y]	2.08[y]	0.149
cis-10,*trans*-12 CLA	0.00[x]	0.00[x]	0.00[x]	0.20[y]	0.007
trans-9,*cis*-11 CLA	0.09[x]	0.04[y]	0.06[z]	0.05[y,z]	0.003
trans-10,*cis*-12 CLA	0.06[x]	0.86[y]	0.04[x]	0.33[z]	0.055
trans,*trans* CLA[f]	0.13[x]	0.16[x]	1.20[y]	0.42[z]	0.068
ΣCLA	3.90[x]	3.31[y]	3.85[x]	3.44[x,y]	0.135
18:3n-3	2.07[x]	1.58[y]	1.86[x,z]	1.66[y,z]	0.068
20:0	0.68	0.66	0.68	0.65	0.040
ΣFA	593[x]	470[y]	606[x]	468[y]	36.4
Summary					
Σ ≤C14	168[x]	127[y]	189[x]	126[y]	12.4
Σ C16	216[x]	164[y]	224[x]	166[y]	13.6
Σ ≥C18	188	167	177	161	10.4

[a]Cows received 4-d abomasal infusions (3 kg/d) of skim milk (control), or skim milk containing emulsified supplements of *trans*-10,*cis*-12 CLA (T1), *trans*-10,*trans*-12 CLA (T2), or a mixture geometric isomers of 10,12 CLA (T3). See Table 2 for the FA composition of CLA supplements.
[b]Error DF, 6. Means within a row not sharing common roman superscripts differ significantly (*P* < 0.05).
[c]Values represent the mean for day 4 of infusion for four cows. FA composition was determined by GC using both a temperature gradient and isothermal conditions for the separation of 18:1 and 18:2 isomers.
[d]Sum of 18:2 excluding isomers of CLA.
[e]Refers to unresolved *trans*-7,*cis*-9 CLA, *trans*-8,*cis*-10 CLA, and *cis*-9,*trans*-11 CLA.
[f]Refers to unresolved *trans*-7,*trans*-9 CLA, *trans*-8,*trans*-10 CLA, *trans*-9,*trans*-11 CLA, and *trans*-10,*trans*-12 CLA.

9,*cis*-11 CLA/d. Postruminal infusions of *cis*-9,*trans*-11 CLA (4) or *trans*-9,*trans*-11 CLA (31), the predominant 9,11 isomer in treatment T3, are known to have no effects on milk fat synthesis in the dairy cow. Although there is evidence in the literature that *trans*-9,*cis*-11 CLA concentrations are increased in milk from cows fed diets causing milk fat depression (10,24) and may contribute to the reduction in milk fat synthesis when infused postruminally (31), the amount of this isomer supplied by the T3 infusion is very small. Furthermore, a lack of increase in the concentration of *trans*-9,*cis*-11 CLA in milk, which is known to be efficiently transferred in response to postruminal infusions (31), suggests that the amounts of *trans*-9,*cis*-11 CLA available to the mammary gland were extremely small and therefore unlikely to have had a significant role in the regulation of milk fat synthesis in the current experiment. Under the GC conditions used in this study, *cis*-9,*cis*-11 CLA and *trans*-11,*cis*-13 CLA are not resolved and elute as a single peak (22). However, there was no change in the concentration of these co-eluting isomers in milk fat from cows infused with treatment T3, suggesting that the concentration of *cis*-9,*cis*-11 CLA was not substantially increased. In light of the nonsignificant changes in milk fat *cis*-9,*cis*-11 and *trans*-11,*cis*-13 concentrations, it is probable that the amounts of *cis*-9,*cis*-11 CLA available to the mammary gland were not sufficiently large to contribute significantly to the decrease in milk fat yield in response to treatment T3.

It is evident that the decreases in milk fat synthesis in response to treatment T3 are not explained by the amounts of *trans*-10,*cis*-12 CLA supplied by this infusion. *Cis*-10,*trans*-12 was the second-most abundant CLA isomer in treatment T3, and was transferred from the abomasum into milk at a similar efficiency as the known inhibitor *trans*-10,*cis*-12 CLA. In view of the amount of *cis*-10,*trans*-12 CLA supplied by treatment T3 (1.19 g/d), comparable transfer characteristics to the known inhibitor *trans*-10,*cis*-12 CLA, and the relative amounts of other CLA isomers, effects of which can largely be accounted for, leads to the overall conclusion that *cis*-10,*trans*-12 CLA contributed to the reduction in milk fat synthesis in response to treatment T3.

TABLE 7
Apparent Transfer of CLA Isomers from the Abomasum into Milk Fat for Different CLA Supplements

Transfer efficiency[b] (%)	Treatment[a]		
	T1	T2	T3
cis-10,cis-12 CLA	—		39.6 ± 11.52
cis-10,trans-12 CLA	—		16.7 ± 1.69
trans-10,cis-12 CLA	19.2 ± 4.88		14.9 ± 2.03
trans,trans CLA[c]	—	23.0 ± 5.19[d]	

[a]Cows received 4-d abomasal infusions (3 kg/d) of skim milk (control) or skim milk containing emulsified supplements of trans-10,cis-12 CLA (T1), trans-10,trans-12 CLA (T2), or a mixture of 10,12 geometric isomers of CLA (T3). See Table 2 for the FA composition of CLA supplements.
[b]Values represent the apparent transfer efficiency (mean ± SD) from the abomasum into milk for four cows on day 4 of infusion.
[c]Transfer of trans-10,trans-12 CLA was unable to be calculated for treatment T3 owing to the contribution of trans-9,trans-11 in the infused CLA supplement and co-elution of trans-9,trans-11 with trans-10,trans-12 CLA under the GC conditions used to determine milk FA composition.
[d]Infused CLA supplement delivered only small amounts of trans-9,trans-11 CLA (Table 3), and therefore the increase in trans-7,trans-9 CLA, trans-8,trans-10 CLA, trans-9,trans-11 CLA, and trans-10,trans-12 CLA content in milk determined by GC was assumed to be trans-10,trans-12 CLA.

Park and Pariza (11) reported a dramatic reduction in the fat content of growing mice fed supplements containing a mixture of CNA isomers enriched with cis-10,trans-12 19:2 and trans-11,cis-13 19:2. Data from the present experiment suggest that, by structural analogy with cis-10,trans-12 CLA, the cis-10,trans-12 19:2 rather than trans-11,cis-13 19:2 was the isomer of CNA with antilipogenic properties. Furthermore, the effect of CNA on body fat in growing mice was significantly greater than a mixture of CLA isomers containing cis-9,trans-11 CLA and trans-10,cis-12 CLA. Milk fat responses observed in the current study tend to support an increased potency of 10,12 conjugated FA when the trans-10,cis-12 arrangement of double bonds is substituted for the cis-10,trans-12 structure. However, it is important to recognize that the difference in potency between the two 10,12 CLA isomers infused in this experiment was less dramatic in terms of milk fat synthesis compared with the differences in lipid accretion of growing mice fed a mixture of cis-10,trans-12 CNA and trans-11,cis-13 CNA relative to trans-10,cis-12 CLA (11).

Evaluation of several CLA cognates on glycerol release and TAG accumulation in cultured 3T3-L1 adipocytes has pointed toward a trans-10,cis-12 double bond arrangement in conjunction with a free carboxyl group on the first carbon atom as being an integral structural component for antilipogenic effects, with the implication that either a trans-10 or cis-12 double bond is an essential feature (2). Data from the present experiment tend to suggest that the antilipogenic effects of 10,12 geometric isomers of CLA containing both a cis and trans double bond are more pronounced when the double bond closest to the carboxyl group. In support of this, TAG accumulation in fully differentiated 3T3-L1 adipocytes has recently been shown to be reduced during incubation with cis-10 17:1 or cis-10 19:1, albeit to a lesser extent than trans-10,cis-12 CLA, whereas trans-10 17:1 and trans-10 19:1 have no effect (2). Overall these findings are consistent with the position and orientation of the double bond relative to the carboxyl group of the FA moiety being fundamental to the inhibitory effects on lipid accretion in cultured adipocytes or milk fat synthesis in lactating dairy cows.

Further support for the importance of an uninterrupted carbon chain between the trans-10,cis-12 double bond structure and the carboxyl group is provided by studies that have examined the effects of calendic acid (trans-8,trans-10,cis-12 18:3) on body composition of growing mice (32), conjugated 18:3 (cis-6,trans-10,cis-12 18:3) on milk fat synthesis in dairy cows (33), and methyl-branched CLA (α-methyl trans-10,cis-12 18:2) on fat accumulation in adipocytes and hepatocytes (34). In all experimental models the addition of the double bond or a methyl group between the terminal carboxyl group and the trans-10,cis-12 conjugated bond system abolished or markedly reduced the inhibitory effects on lipid synthesis associated with the trans-10,cis-12 carbon–carbon double bond structure.

A complex mixture of CLA isomers was used to examine the role of cis-10,trans-12 CLA in the regulation of milk fat synthesis in the current study. Even though the data suggest that cis-10,trans-12 CLA is a potent inhibitor of milk fat synthesis, these findings need to be confirmed in studies using higher-purity cis-10,trans-12 CLA preparations. Since the unique inhibitory effects of trans-10,cis-12 CLA on lipid synthesis have been demonstrated both in the lactating dairy cow (4,13) and the 3T3-L1 adipocyte cell culture model (2,34), a small amount of cis-10,trans-12 CLA was purified from the isomer mixture infused in this study (treatment T3) and used to examine the effects of this isomer on lipid accumulation of murine 3T3-L1 adipocytes. Adipocyte cells were cultured with cis-10,trans-12 CLA, trans-10,cis-12 CLA, cis-9,trans-11 CLA, or a control medium. Both cis-10,trans-12 CLA and trans-10,cis-12 CLA markedly reduced lipid accumulation (0.27 and 0.24 mg TAG/mg protein, respectively) compared with the control or cis-9,trans-11 CLA treatments (corresponding values 1.00 and 1.20, respectively) (35).

In conclusion, postruminal infusions of a mixture of 10,12 CLA isomers were found to result in similar decreases in milk fat output as relatively pure preparations of trans-10,cis-12 CLA. Comparable reductions in milk fat synthesis in response to 1.80 and 4.14 g trans-10,cis-12/d, supplied by treatments T3 and T1, indicate that other isomers of CLA have the potential to exert antilipogenic effects. Trans-10,trans-12 CLA had no effect on mammary lipid metabolism, and the evidence from this experiment points toward cis-10,trans-12 exerting at least as potent antilipogenic effects as the known inhibitor trans-10,cis-12 CLA.

ACKNOWLEDGMENTS

REFERENCES

1. Bauman, D.E., Corl, B.A., and Peterson, D.G. (2003) The Biology of Conjugated Linoleic Acid in Ruminants, in *Advances in Conjugated Linoleic Acid Research*, (Sébédio, J.-L., Christie,

W.W., and Adlof, R.O., eds.), Vol. 2, pp. 146–173, AOCS Press, Champaign.

2. Park, Y., Storkson, J.M., Liu, W., Albright, K.J., Cook, M.E., and Pariza, M.W. (2004) Structure–Activity Relationship of Conjugated Linoleic Acid and Its Cognates in Inhibiting Heparin-Releasable Lipoprotein Lipase and Glycerol Release from Fully Differentiated 3T3-L1 Adipocytes, *J. Nutr. Biochem. 15*, 561–569.

3. Park, Y., Albright, K.J., Storkson, J.M., Liu, W., and Pariza, M.W. (1999) Evidence That the *trans*-10,*cis*-12 Isomer of Conjugated Linoleic Acid Induces Body Composition Changes in Mice, *Lipids 34*, 235–241.

4. Baumgard, L.H., Corl, B.A., Dwyer, D.A., Sæbø, A., and Bauman, D.E. (2000) Identification of the Conjugated Linoleic Acid Isomer That Inhibits Milk Fat Synthesis, *Am. J. Physiol. 278*, R179–R184.

5. Perfield, J.W., Sæbø, A., and Bauman, D.E. (2004) Use of Conjugated Linoleic Acid (CLA) Enrichments to Examine the Effects of *trans*-8,*cis*-10 CLA, and *cis*-11,*trans*-13 CLA on Milk Fat Synthesis, *J. Dairy Sci. 87*, 1196–1202.

6. Griinari, J.M., and Bauman, D.E. (1999) Biosynthesis of Conjugated Linoleic Acid and Its Incorporation into Meat and Milk in Ruminants, in *Advances in Conjugated Linoleic Acid Research* (Yurawecz, M.P., Mossoba, M.M., Kramer, J.K.G., Pariza, M.W., and Nelson, G.J., eds.), Vol. 1. pp. 180–200, AOCS Press, Champaign.

7. Piperova, L.S., Teter, B.B., Bruckental, I., Sampugna, J., Mills, S.E., Yurawecz, M.P., Fritsche, J., Ku, K., and Erdman, R.A. (2000) Mammary Lipogenic Enzyme Activity, *Trans* Fatty Acids and Conjugated Linoleic Acids Are Altered in Lactating Dairy Cows Fed a Milk Fat-Depressing Diet, *J. Nutr. 130*, 2568–2574.

8. Bauman, D.E., and Griinari, J.M. (2003) Nutritional Regulation of Milk Fat Synthesis, *Annu. Rev. Nutr. 23*, 203–227.

9. Offer, N.W., Marsden, M., and Phipps, R.H. (2001) Effect of Oil Supplementation of a Diet Containing a High Concentration of Starch on Levels of *Trans* Fatty Acids and Conjugated Linoleic Acids in Bovine Milk, *Anim. Sci. 73*, 533–540.

10. Ärölä, A., Shingfield, K.J., Vanhatalo, A., Toivonen, V., Huhtanen, P., and Griinari, J.M. (2002) Biohydrogenation Shift and Milk Fat Depression in Lactating Dairy Cows Fed Increasing Levels of Fish Oil, *J. Dairy Sci. 85* (Suppl. 1), 143.

11. Park, Y., and Pariza, M.W. (2001) The Effects of Dietary Conjugated Nonadecadienoic Acid on Body Composition in Mice, *Biochim. Biophys. Acta 1533*, 171–174.

12. Agricultural and Food Research Council (1993) *Energy and Protein Requirements of Ruminants*, An Advisory Manual Prepared by the AFRC Technical Committee on Responses to Nutrients. CAB International, Wallingford, United Kingdom.

13. Baumgard, L.H., Sangster, J.K., and Bauman, D.E. (2001) Milk Fat Synthesis in Dairy Cows Is Progressively Reduced by Increasing Supplemental Amounts of *trans*-10,*cis*-12 Conjugated Linoleic Acid (CLA), *J. Nutr. 131*, 1764–1769.

14. Statutory Instruments (1982) Number 1144. Agriculture. The Feeding Stuffs (Sampling and Analysis) Regulations. Her Majesty's Stationery Office, London.

15. Statutory Instruments (1985) Number 1119. Agriculture. The Feeding Stuffs (Sampling and Analysis Amendment) Regulations. Her Majesty's Stationery Office, London.

16. Porter, M.G., Patterson, D.C., Steen, R.W.J., and Gordon, F.J. (1984) Determination of Dry Matter and Gross Energy of Grass Silage, in *Proceedings of the Seventh Silage Conference*, The Queen's University, Belfast.

17. Sæbø, A., Skarie, C., Jerome, D., and Haroldsson, G. (2003) Conjugated Linoleic Acid Compositions and Methods of Making Same, U.S. Patent 6,610,868.

18. Sæbø, A., and Sæbø, P.C. (2004) Conjugated Linoleic Acid Compositions, U.S. Patent Application 20040225142 A1.

19. Christie, W.W. (1982) A Simple Procedure for Rapid Trans-methylation of Glycerolipids and Cholesteryl Esters, *J. Lipid Res. 23*, 1072–1075.

20. Griinari, J.M., Dwyer, D.A., McGuire, M.A., Bauman, D.E., Palmquist, D.L., and Nurmela, K.V.V. (1998) *Trans*-Octadecenoic Acids and Milk Fat Depression in Lactating Dairy Cows, *J. Dairy Sci. 81*, 1251–1261.

21. Christie, W.W. (1989) *Gas Chromatography and Lipids: A Practical Guide*, p. 68, The Oily Press, Ayr, Scotland.

22. Shingfield, K.J., Ahvenjärvi, S., Toivonen, V., Ärölä, A., Nurmela, K.V.V., Huhtanen, P., and Griinari, J.M. (2003) Effect of Fish Oil on Biohydrogenation of Fatty Acids and Milk Fatty Acid Content in Cows, *Anim. Sci. 77*, 165–179.

23. Delmonte, P., Kataoka, A., Corl, B.A., Bauman, D.E., and Yurawecz, M.P. (2005) Relative Retention Order of All Isomers of *cis/trans* Conjugated Linoleic Acid FAME from the 6,8- to 13,15-Positions Using Silver Ion HPLC with Two Elution Systems, *Lipids 40*, 509–514.

24. Shingfield, K.J., Reynolds, C.K., Lupoli, B., Toivonen, V., Yurawecz, M.P., Delmonte, P., Griinari, J.M., Grandison, A.S., and Beever, D.E. (2005) Effect of Forage Type and Proportion of Concentrate in the Diet on Milk Fatty Acid Composition in Cows Fed Sunflower Oil and Fish Oil, *Anim. Sci. 80*, 225–238.

25. SAS (2001) *SAS/STAT Users Guide* (release 8.0), SAS Institute Inc., Cary, NC.

26. Bauman, D.E., and Griinari, J.M. (2001) Regulation and Nutritional Manipulation of Milk Fat: Low-Fat Milk Syndrome, *Livest. Prod. Sci. 70*, 15–29.

27. Chouinard, P.Y., Corneau, L., Sæbø, A., and Bauman, D.E. (1999) Milk Yield and Composition During Abomasal Infusion of Conjugated Linoleic Acids in Dairy Cows, *J. Dairy Sci. 82*, 2737–2745.

28. Peterson, D.G., Baumgard, L.H., and Bauman, D.E. (2002) Short Communication: Milk Fat Response to Low Doses of *trans*-10,*cis*-12 Conjugated Linoleic Acid (CLA), *J. Dairy Sci. 85*, 1764–1766.

29. deVeth, M.J., Griinari, J.M., Pfeiffer, A.M., and Bauman, D.E. (2004) Effect of CLA on Milk Fat Synthesis in Dairy Cows: Comparison of Inhibition by Methyl Esters and Free Fatty Acids, and Relationships Among Studies, *Lipids 39*, 365–372.

30. Perfield, J.W., Delmonte, P., Lock, A.L., Yurawecz, M.P., and Bauman, D.E. (2004) *Trans*-10,*trans*-12 Conjugated Linoleic Acid (CLA) Reduces the Δ^9-Desaturase Index Without Affecting Milk Fat Yield in Lactating Cows, *J. Dairy Sci. 87* (Suppl. 1), 128.

31. Perfield, J.W., II, Lock, A.L., Sæbø, A., Griinari, J.M., and Bauman, D.E. (2005) *Trans*-9,*cis*-11 Conjugated Linoleic Acid (CLA) Reduces Milk Fat Synthesis in Lactating Dairy Cows, *J. Dairy Sci. 88* (Suppl. 1), 211.

32. Chardigny, J.M., Hasselwander, O., Genty, M., Kraemer, K., Ptock, A., and Sébédio, J.L. (2003) Effect of Conjugated FA on Feed Intake, Body Composition, and Liver FA in Mice, *Lipids 38*, 895–902.

33. Sæbø, A., Perfield, J.W., Delmonte, P., Yurawecz, M.P., Lawrence, P., Brenna, J.T., and Bauman, D.E. (2005) Milk Fat Synthesis Is Unaffected by Abomasal Infusion of the Conjugated Diene 18:3 Isomers *cis*-6,*trans*-10,*cis*-12 and *cis*-6,*trans*-8,*cis*-12, *Lipids 40*, 89–95.

34. Granlund, L., Larsen, L.N., Nebb, H.I., and Pedersen, J.I. (2005) Effects of Structural Changes of Fatty Acids on Lipid Accumulation in Adipocytes and Primary Hepatocytes, *Biochim. Biophys. Acta 1687*, 23–30.

35. Griinari, J.M., Granlund, L., Pedersen, J.I., Delmonte, P., Shingfield, K., and Sæbø, A. (2005) *Cis*-10,*trans*-12 Conjugated Linoleic Acid Inhibits Lipid Accumulation During Adipocyte Differentiation in *Proceedings of the International Society of Fat Research*, September 25–28, 2005, Prague, Czech Republic.

Isolation and Characterization of Some Hydroxy Fatty and Phosphoric Acid Esters of 10-Hydroxy-2-decenoic Acid from the Royal Jelly of Honeybees (*Apis mellifera*)

Naoki Noda[a],*, Kazue Umebayashi[a], Takafumi Nakatani[a], Kazumoto Miyahara[a], and Kaori Ishiyama[b]

[a]Faculty of Pharmaceutical Sciences, Setsunan University, Osaka 573-0101, Japan , and
[b]Institute for Health Science, Yamada Apiculture Center, Inc., Okayama 708-0393, Japan

ABSTRACT: The present work characterizes novel FA in the royal jelly of honeybees (*Apis mellifera*). TLC analysis showed that the chloroform/methanol extract obtained from royal jelly consists mainly of FA. The FABMS spectrum of this extract gave several ion peaks due to compounds with higher M.W. than those of the FA so far reported. The methanol extract was found to contain unknown phospholipids. By means of reversed-phase HPLC with various solvent systems, 13 compounds were obtained in pure state. Their structures including absolute configurations were determined by chemical, NMR, and MS spectral analysis. Six compounds were identified as novel mono- or diesters of 10-hydroxy-2*E*-decenoic acid in which the hydroxyl group was esterified by another FA unit, and one was hydroxy-2*E*-decenoic acid 10-phosphate. In addition, we demonstrated that 9-hydroxy-2*E*-decenoic acid exists as a mixture of optical isomers.

Paper no. L9758 in *Lipids 40*, 833–838 (August 2005).

Royal jelly is a thick, milky substance secreted from the hypopharyngeal and mandibular glands of young worker honeybees. Royal jelly is the sole food of queen bees for all their lives; it is also a popular traditional health food all over the world. Many studies of its biological activities as well as chemical composition have been conducted (1–4).

Up to now, various compounds such as proteins, sugars, lipids, vitamins, minerals, and free amino acids have been identified as its constituents (5,6). In particular, FA are regarded as unique and chemically interesting constituents of royal jelly. Unlike organic acids of most animal and plant materials, the FA of royal jelly have 8–10 carbon atoms, and they are usually either hydroxy FA or dicarboxylic acids (7).

Among them, a major FA was characterized as 10-hydroxy-2*E*-decenoic acid (10-HDA); it constitutes approximately 70% of the diethyl ether-soluble fraction (8–11).

This FA is considered to be one of the active ingredients in royal jelly, and it has been found to have some pharmacological activities (12–14).

Recently we found that the chloroform/methanol extract obtained from royal jelly contains several acids with higher M.W. than those of the FA so far reported. The methanol extract gave, unlike the dark blue spots of the usual glycerophospholipids, a pale blue spot with Dittmer–Lester's reagent (15) on TLC, indicating the presence of new compounds possessing a phosphorus atom.

This study was undertaken to analyze these components in the lipid fraction of royal jelly. By application of a preparative HPLC technique for the isolation of intact compounds in the pure state, 12 FA and one phosphate were obtained from the chloroform/methanol and methanol extracts, respectively. From chemical and NMR and MS spectral data, it was proven that six compounds were novel mono- or diesters of 10-HDA in which the hydroxyl group was esterified by another FA unit, and one was HDA 10-phosphate. Furthermore, we found that 9-HDA exists in royal jelly as an enantio-mixture (*R/S*) in a ratio of *ca* 2:1.

MATERIALS AND METHODS

Materials. Lyophilized royal jelly powder (from China, lot no. 030411B) was supplied by Yamada Apiculture Center Inc. (Okayama, Japan). A voucher specimen was deposited in the Faculty of Pharmaceutical Sciences, Setsunan University.

Instrumentation. Optical rotations were measured at 25°C with a JASCO DIP-140 polarimeter (JASCO, Tokyo, Japan). ^{1}H and ^{13}C NMR spectra were recorded on a JEOL JMN GX400 or ECA 600SN spectrometer (JEOL, Tokyo, Japan), using tetramethylsilane as an internal reference. ^{31}P NMR spectra were recorded on JEOL ECA 600SN using 85% phosphoric acid as an external reference. All samples were measured at a probe temperature of 35°C. The 2-D heteronuclear multiple-bond correlation (HMBC) spectrum was recorded at 600 MHz with 64 scans ($^{2,3}J_{CH}$ = 8 Hz). EI-MS and FABMS, including high-resolution MS, were recorded on a JEOL JMS-700T spectrometer. (EI-MS: ionization voltage, 30 eV; accelerating voltage, 10 kV; FABMS: accelerating voltage, 5 kV; matrix, glycerin or triethanolamine; collision gas, He). TLC was carried out on silica-gel precoated Al sheets (Merck, Darmstadt, Germany). Spots were visualized with 5% sulfuric acid in methanol (by heating) or Dittmer–Lester's reagent. Column

---

chromatography was carried out on Diaion HP-20 (Mitsubishi Chemical Co., Tokyo, Japan), Sephadex LH-20 (Amersham Pharmacia Biotech AB, Uppsala, Sweden), silica gel (Kieselgel 60; Merck), and Cosmosil 75C$_{18}$-OPN (Nacalai Tesque, Inc., Tokyo, Japan). Preparative HPLC was conducted over Mightysil RP-18 GP (5 µm, 20 × 250 mm; Kanto Chemical Co. Inc., Tokyo, Japan), and Mightysil RP-18 GP Aqua (5 µm, 10 × 250 mm; Kanto Chemical Co., Inc.) columns with a JASCO 980-PU (JASCO). The elution profile was monitored by a refractive index detector, RI504R (GL Sciences Inc., Tokyo, Japan).

Isolation of compounds, 1–13. Lyophilized royal jelly powder (1.5 kg) was percolated with 3 L of chloroform, 3 L of chloroform/methanol (2:1, vol/vol), and then 5 L of methanol, successively, each for 7 d at room temperature. Each of the extracts was concentrated *in vacuo* to give chloroform (121.7 g), chloroform/methanol (45.4 g), and methanol (192.3 g) extracts. The chloroform/methanol extract (25.0 g) was chromatographed on a Cosmosil 75C$_{18}$-OPN column using 80% methanol to give two fractions, fr. I (20.7 g) and fr. II (4.0 g). Fr. I (1.5 g) was separated by a Cosmosil 75C$_{18}$-OPN column using 50% methanol to give a mixture of FA. It was further separated on a reversed-phase column (Mightysil RP-18 GP Aqua column) using 70% acetonitrile to give compounds **1** (56.1 mg), **2** (36.7 mg), **3** (3.2 mg), **4** (25.4 mg), **5** (6.7 mg), and **6** (3.7 mg), together with a less polar fraction. The latter fraction (110 mg) was separated by a Mightysil RP-18 GP column using 30% acetonitrile to give compounds **7** (8.7 mg), **8** (14.7 mg), and **9** (15.4 mg). Fr. II (128 mg) was subjected to preparative HPLC with a Mightysil RP-18 GP Aqua column using 80% acetonitrile to give compounds **10** (22.2 mg), **11** (20.3 mg), and **12** (4.2 mg) (Scheme 1). The methanol extract (1.8 g) was placed on a Diaion HP-20 ion exchange resin, washed with excess water, and then eluted with methanol. The methanol layer was concentrated *in vacuo* and chromatographed on silica gel (chloroform/methanol/water, 7:3:0.5 by vol). The eluates were monitored by TLC using chloroform/methanol/water (6:4:1, by vol). Those eluates showing a positive spot on spraying with Dittmer–Lester's reagent (15) were combined and concentrated *in vacuo* to give compound **13** (53.0 mg) (Scheme 1). **1**: FABMS *m/z*: 185 [M − H]⁻. **5**: [α]$_D$ +6.45° at 0.3 g/100 mL in methanol. **7**: High-resolution FABMS *m/z*: 327.2171 (calcd. for C$_{18}$H$_{31}$O$_5$: 327.2172) [M − H]⁻. FABMS *m/z*: 327 [M − H]⁻ (100%), 185 (30%), 159 (38%). **8**: m.p. 35.5–37.0°C. *m/z*: 355 [M − H]⁻ (100%), 187 (26%), 185 (21%), 169 (7%). **9**: m.p. 55.5–58.0°C. *m/z*: 369 [M − H]⁻ (100%), 201 (13%), 185 (20%)). **10**: m.p. 33.0–35.0°C. [α]$_D$ −7.89° at 0.9 g in chloroform. *m/z*: 355 [M − H]⁻ (100%), 187 (38%), 185 (47%). **11**: m.p. 35.0–40.0°C. *m/z*: 497 [M − H]⁻ (100%), 355 (10%), 329 (10%), 185 (19%), 159 (27%). **12**: m.p. 43.0–45.0°C. *m/z*: 525 [M − H]⁻ (100%), 357 (7%), 355 (7%), 187 (28%), 185 (18%), 169 (10%). **13**: Powder, m.p. 260.0–290.0°C (dec.). High-resolution FABMS *m/z*: 265.0843 (calcd. for C$_{10}$H$_{18}$O$_6$P: 265.0841) [M − H]⁻. *m/z*: 265 [M − H]⁻ (100%), 185 (8%). ¹H and ¹³C NMR (600 Mz) spectral data of **1** and **7–13** are shown in Tables 1 and 2.

Methanolysis of 7–12. Compounds **7** through **12** (*ca.* 1.0 mg) were each heated with 3% methanolic hydrogen chloride (0.3 mL) at 90°C for 1 h. The reaction mixture was shaken with 2 mL of chloroform/water (1:1, vol/vol), and the lower layer was analyzed by GC on a Hitachi G-3000 SLF (Hitachi, Tokyo, Japan) using a fused-silica Capillary Column Bonded MPS-50 (OV-17; 0.25 mm × 50 m; column temperature, 230°C; carrier gas, He 33.4 mol; GL Sciences Inc., Tokyo). Retention time (min): 4.6 (methyl 8-hydroxy-octanoate) and 6.0 (methyl 10-hydroxy-2-decenoate) from **7**, 5.4 (methyl 10-hydroxy-decanoate) and 6.0
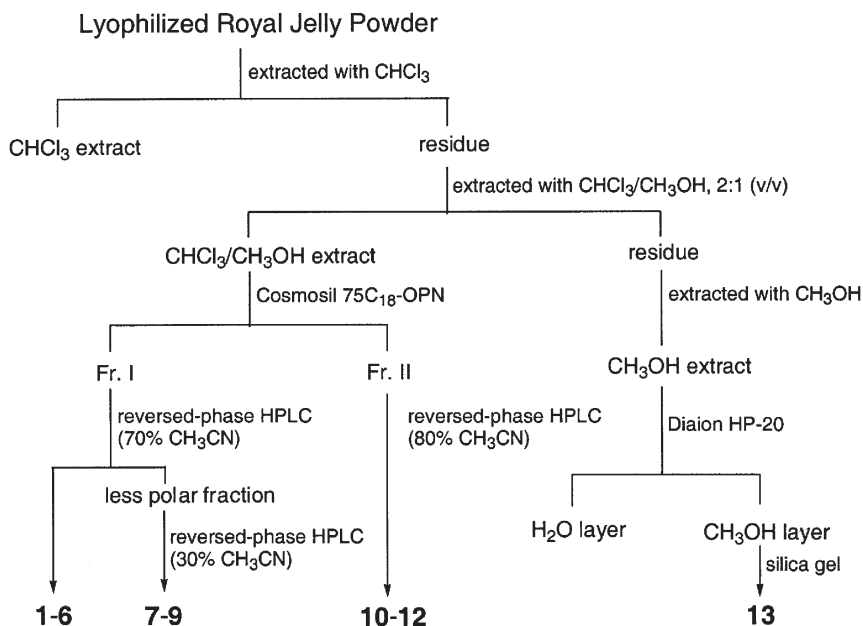
SCHEME 1

TABLE 1
^{1}H NMR Chemical Shifts^a of Compounds 1 and 7–13

	1	7	8	9
2-H$_2$	5.79 (dt, 1.6, 15.6)	5.82 (dt, 1.5, 15.6)	5.82 (d, 15.6)	5.82 (d, 15.6)
3-H$_2$	6.95 (dt, 6.8, 15.6)	7.06 (dt, 7.1, 15.6)	7.06 (dt, 7.1, 15.6)	7.07 (dt, 6.9, 15.6)
4-H$_2$	2.22 (dt, 6.8, 6.9)	2.23 (ddt, 1.5, 6.9, 7.1)	2.23 (ddt, 1.5, 7.1, 7.3)	2.23 (dt, 6.9, 7.0)
10-H$_2$	3.54 (t, 6.8)	4.06 (t, 6.8)	4.06 (t, 6.6)	4.06 (t, 6.6)
2'-H$_2$		2.30 (t, 7.2)	2.30 (t, 7.6)	2.29 (t, 7.4)
8'-H$_2$		3.64 (t, 6.8)		
9'-H$_2$				2.34 (t, 7.5)
10'-H$_2$			3.64 (t, 6.6)	

	10	11	12	13
2-H$_2$	5.82 (d, 15.6)	5.82 (dt, 1.2, 16.0)	5.82 (dt, 1.2, 16.0)	5.80 (d, 12.8)
3-H$_2$	7.06 (dt, 7.2, 15.6)	7.06 (dt, 7.0, 16.0)	7.05 (dt, 7.0, 16.0)	6.95 (dt, 7.2, 12.8)
4-H$_2$	2.23 (dt, 6.5, 7.2)	2.23 (ddd, 1.2, 7.2, 8.4)	2.22 (ddd, 1.2, 7.2, 8.4)	2.32 (m)
9-H$_2$				1.62 (m)
10-H$_2$	4.11 (dt, 2.4, 4.4)	4.05 (t, 6.6)	4.05 (t, 6.6)	3.87 (m)
2'-H$_2$		2.29 (t, 7.8)	2.28 (t, 7.8)	
2'-Ha	2.41 (dd, 9.0, 16.5)			
2'-Hb	2.51 (dd, 3.6, 16.5)			
3'-H	4.00 (m)			
10'-H$_2$		4.06 (t, 6.6)	4.06 (t, 6.6)	
10'-H$_3$	0.88 (t, 7.1)			
2''-H$_2$		2.29 (t, 7.8)	2.28 (t, 7.8)	
8''-H$_2$		3.64 (t, 6.6)		
10''-H$_2$			3.64 (t, 6.6)	

^{a}δ in ppm from tetramethylsilane (TMS) (splitting patterns and coupling constants, J, in Hz). **1** and **13** were dissolved in CD$_3$OD and **7**–**12** were dissolved in CDCl$_3$.

(methyl 10-hydroxy-2-decenoate) from **8**, 5.6 (dimethyl decane-dioate) and 6.0 (methyl 10-hydroxy-2-decenoate) from **9**, 4.7 (methyl 9-hydroxy-2-decenoate) and 6.0 (methyl 10-hydroxy-2-decenoate) from **10**, 4.6 (methyl 8-hydroxyoctanoate), 5.4 (methyl 10-hydroxydecanoate), and 6.0 (methyl 10-hydroxy-2-decenoate) from **11**, 5.4 (methyl 10-hydroxydecanoate) and 6.0 (methyl 10-hydroxy-2-decenoate) from **12**.

Each peak substance was identified as the corresponding

methyl ester by retention time and EI-MS comparison with an authentic sample.

Preparation of (−)- and (+)-2-methoxy-2-trifluoromethyl-phenylacetate (MTPA) ester derivatives. Compounds **5, 6,** and **10** (2–5 mg) were each treated with diazomethane in diethyl ether. (−)- and (+)-MTPA chlorides (Tokyo Kasei Kogyo Co. Ltd., 20.0 mg) were separately added to a solution of the above product (1–3 mg) in CCl$_4$ (0.2 mL) and pyridine (1.0 mL), and

TABLE 2
^{13}C NMR Chemical Shifts^a of 1 and 7–13

Carbon	1	7	8	9	10	11	12	13
1	169.9	171.2	171.3	171.5	171.5	171.0	170.0	170.1
2	122.3	120.7	120.7	120.4	120.8	120.7	120.4	122.3
3	151.0	152.1	152.0	152.0	152.0	151.9	151.9	151.0
4	33.1	32.2	32.2	32.2	32.2	32.2	32.2	33.1
9								31.8 (d, 8.3)
10	62.9	64.3	64.3	64.2	64.8	64.3	64.2	66.3 (d, 4.9)
1'		174.0	174.1	179.6	173.2	174.0	173.9	
2'		34.4	34.4	34.4	41.3	34.3	34.3	
3'					68.1			
8'		63.0						
9'				34.0				
10'			63.0	173.7	14.1	64.4	64.4	
1''						174.1	174.0	
2''						34.3	34.3	
8''						62.9		
10''							63.0	

^{a}δ in ppm from TMS (splitting patterns and coupling constants, J, in Hz). **1** and **13** were dissolved in CD$_3$OD and **7**–**12** were dissolved in CDCl$_3$. For abbreviation see Table 1.

the mixture was left to stand at room temperature overnight. After removal of the solvent under a nitrogen stream, the reaction mixture was subjected to silica gel column chromatography (*n*-hexane/ethylacetate, 5:1, vol/vol) to give a MTPA derivative. **(–)-MTPA ester of methyl ester of 5**: ^{1}H NMR (400 MHz, CDCl$_3$) δ: 1.28–1.70 (12H, *m*, CH$_2$ × 6), 2.56 (1H, *dd*, *J* = 4.8, 16.0 Hz, Ha-2), 2.64 (1H, *dd*, *J* = 8.0, 16.0 Hz, Hb-2), 3.52 (3H, *s*, OCH$_3$), 3.55 (3H, *s*, OCH$_3$), 3.59 (3H, *s*, CO$_2$CH$_3$), 4.30 (2H, *m*, H$_2$-10), 5.46 (1H, *m*, H-3), 7.40 (6H, *m*, Ph), 7.52 (4H, *m*, Ph). **(+)-MTPA ester of methyl ester of 5**: ^{1}H NMR (400 MHz, CDCl$_3$) δ: 1.20–1.68 (12H, *m*, CH$_2$ × 6), 2.59 (1H, *dd*, *J* = 4.8, 16.0 Hz, Ha-2), 2.69 (1H, *dd*, *J* = 8.4, 16.0 Hz, Hb-2), 3.54 (3H, *s*, OCH$_3$), 3.55 (3H, *s*, OCH$_3$), 3.66 (3H, *s*, CO$_2$CH$_3$), 4.30 (2H, *m*, H$_2$-10), 5.46 (1H, *m*, H-3), 7.40 (6H, *m*, Ph), 7.52 (4H, *m*, Ph). **(–)-MTPA ester of methyl ester of 6**: ^{1}H NMR (400 MHz, CDCl$_3$) δ: 1.16–1.66 (8H, *m*, CH$_2$ × 4), 1.26 (0.96H, *d*, *J* = 6.4 Hz, H$_3$-10 of *S*-form), 1.33 (2.04H, *d*, *J* = 6.4 Hz, H$_3$-10 of *R*-form), 2.15 (2H, *m*, H$_2$-4), 3.53 (0.94H, *m*, OCH$_3$ of *S*-form), 3.56 (2.04H, *m*, OCH$_3$ of *R*-form), 3.73 (3H, *s*, CO$_2$CH$_3$), 5.13 (1H, *m*, H-9), 5.80 (0.68H, *dt*, *J* = 1.6, 15.6 Hz, H-2 of *R*-form), 5.82 (0.32H, *dt*, *J* = 1.6, 15.6 Hz, H-2 of *S*-form), 6.94 (1H, *m*, H-3), 7.38–7.42 (3H, *m*, Ph), 7.52–7.55 (2H, *m*, Ph). **(+)-MTPA ester of methyl ester of 6**: ^{1}H NMR (400 MHz, CDCl$_3$) δ: 1.16–1.66 (8H, *m*, CH$_2$ × 4), 1.26 (2.04H, *d*, *J* = 6.4 Hz, H$_3$-10 of *R*-form), 1.33 (0.96H, *d*, *J* = 6.4 Hz, H$_3$-10 of *S*-form), 2.15 (2H, *m*, H$_2$-4), 3.53 (2.04H, *m*, OCH$_3$ of *R*-form), 3.56 (0.96H, *m*, OCH$_3$ of *S*-form), 3.73 (3H, *s*, CO$_2$CH$_3$), 5.13 (1H, *m*, H-9), 5.80 (0.32H, *dt*, *J* = 1.6, 15.6 Hz, H-2 of *S*-form), 5.81 (0.68H, *dt*, *J* = 1.6, 15.6 Hz, H-2 of *R*-form), 6.94 (1H, *m*, H-3), 7.38–7.42 (3H, *m*, Ph), 7.52–7.55 (2H, *m*, Ph). **(–)-MTPA ester of methyl ester of 10**: ^{1}H NMR (400 MHz, CDCl$_3$) δ: 0.88 (3H, *J* = 7.2 Hz, H$_3$-10′), 1.20–1.68 (22H, *m*, CH$_2$ × 11), 2.20 (1H, *ddt*, *J* = 1.2, 6.5, 6.8 Hz, H$_2$-4), 2.56 (1H, *dd*, *J* = 4.8, 16.0 Hz, Ha-2′), 2.65 (1H, *dd*, *J* = 8.4, 16.0 Hz, Hb-2′), 3.53 (3H, *s*, OCH$_3$), 3.73 (3H, *s*, CO$_2$CH$_3$), 3.98 (2H, *t*, *J* = 6.8 Hz, H$_2$-10), 5.48 (1H, *m*, H-3′), 5.81 (1H, *dt*, *J* = 1.2, 15.6 Hz, H-2), 6.97 (1H, *dt*, *J* = 6.8, 15.6 Hz, H-3), 7.26–7.41 (3H, *m*, Ph), 7.52–7.54 (2H, *m*, Ph). **(+)-MTPA ester of methyl ester of 10**: ^{1}H NMR (400 MHz, CDCl$_3$) δ: 0.87 (3H, *J* = 7.2 Hz, H$_3$-10′), 1.20–1.68 (22H, *m*, CH$_2$ × 11), 2.19 (1H, *ddt*, *J* = 1.2, 6.5, 6.8 Hz, H$_2$-4), 2.60 (1H, *dd*, *J* = 4.8, 16.0 Hz, Ha-2′), 2.70 (1H, *dd*, *J* = 8.4, 16.0 Hz, Hb-2′), 3.54 (3H, *s*, OCH$_3$), 3.73 (3H, *s*, CO$_2$CH$_3$), 4.08 (2H, *t*, *J* = 6.4 Hz, H$_2$-10), 5.48 (1H, *m*, H-3′), 5.82 (1H, *dt*, *J* = 1.2, 15.6 Hz, H-2), 6.97 (1H, *dt*, *J* = 6.8, 15.6 Hz, H-3), 7.26–7.42 (3H, *m*, Ph), 7.52–7.55 (2H, *m*, Ph). The ratio of *R* to *S* of **6** was determined by the intensity of the signals arising from both enantiomers.

RESULTS AND DISCUSSION

Isolation of compounds 1–13. Lyophilized royal jelly powder was extracted successively with chloroform, chloroform/methanol, and methanol. TLC analysis showed that the chloroform and chloroform/methanol extracts consisted mainly of FA.

As described in the Materials and Methods section, we applied a preparative HPLC technique to separate the components of the chloroform/methanol extract and isolated 12 FA (**1–12**) in a pure state (Scheme 1).

On thin-layer plates, the methanol extract gave a pale blue spot with Dittmer–Lester's reagent (15). Its color and R_f value differed from those of common glycerophospholipids, suggesting that the extract contained unknown phospholipids. Separation with a Diaion HP-20 followed by purification by silica gel column chromatography yielded considerable amounts of compound **13**.

Structures of FA, 1–6. Compounds **1–6** were identified, respectively, as 10-HDA (**1**); 8-hydroxy-octanoic (**2**), 10-hydroxy-decanoic (**3**), 9-carboxy-2*E*-nonenoic (**4**), and 3,10-di-hydroxy-decanoic (**5**) acids; and 9-HDA (**6**), based on their NMR and MS spectral data.

The absolute configurations of compounds **5** and **6** were determined by a modified Mosher's method (16,17).

The methyl ester of **5** was converted into its (–)- and (+)-MTPA esters. The ^{1}H NMR spectra of the (±)-MTPA esters showed that the Δδ values [the chemical shift differences, Δδ: δ(–)-MTPA ester − δ(+)-MTPA ester] with regard to the respective Ha-2, Hb-2, and ester methyl proton signals were −0.03, −0.05, and −0.07 ppm. These observations confirmed the configuration of C-3 in **5** to be *R*.

The ^{1}H NMR spectrum of the (–)-MTPA derivative derived from the methyl ester of 9-HDA (**6**) exhibited two sets of signals in the ratio of *ca*. 2:1. Major signals at δ 1.33 and 5.80 were assigned, respectively, as H$_3$-10 and H-2 of a derivative having the *R* configuration, whereas minor signals at δ 1.26 and 5.82 were assigned as those of *S*. The ^{1}H NMR spectrum of the (+)-MTPA derivative also gave two sets of signals similar to those of the (–)-MTPA ester. These findings showed that 9-HDA was a mixture of optical isomers (*R/S*) in a ratio of *ca* 2:1. Scheme 2 shows their structures.

Structures of monoesters of 10-HDA, 7–10. The molecular formula, C$_{18}$H$_{32}$O$_5$, of **7** was established by high-resolution FABMS. The ^{1}H NMR spectrum of **7** showed two *trans* olefinic (δ 5.82, 7.06), hydroxy methyl (δ 3.64), and allylic (δ 2.23) proton signals that were quite similar to those of 10-HDA. In addition, together with approximately 20 aliphatic proton signals, two hydroxy methyl proton signals appeared at δ 4.06 and 2.30. The ^{13}C NMR spectrum exhibited two olefinic (δ 120.7, 152.1) and two carbonyl carbon signals (δ 171.2, 174.0) (Tables 1 and 2). These findings indicated that **7** was a monoester of 10-HDA in which the hydroxyl group was esterified by another FA unit.

Methanolysis of **7** with 3% methanolic hydrogen chloride liberated two FAME. They were identified as methyl esters of 10-HDA and **2** by GC and EI-MS analysis. In the HMBC spectrum of **7**, one carboxyl carbon (δ 171.2, C-1) showed correlation with two olefinic protons (H-2 and H-3), and the other (δ 174.0) showed cross peaks with three protons (H-10, H-2′, and H-3′). The preceding information, combined with the observation of fragment peaks at *m/z* 159 and 185 in its FABMS spectrum, showed that the structure of compound **7** was 10-(8′-hydroxyoctanoyloxy)-2*E*-decenoic acid (Fig. 1).
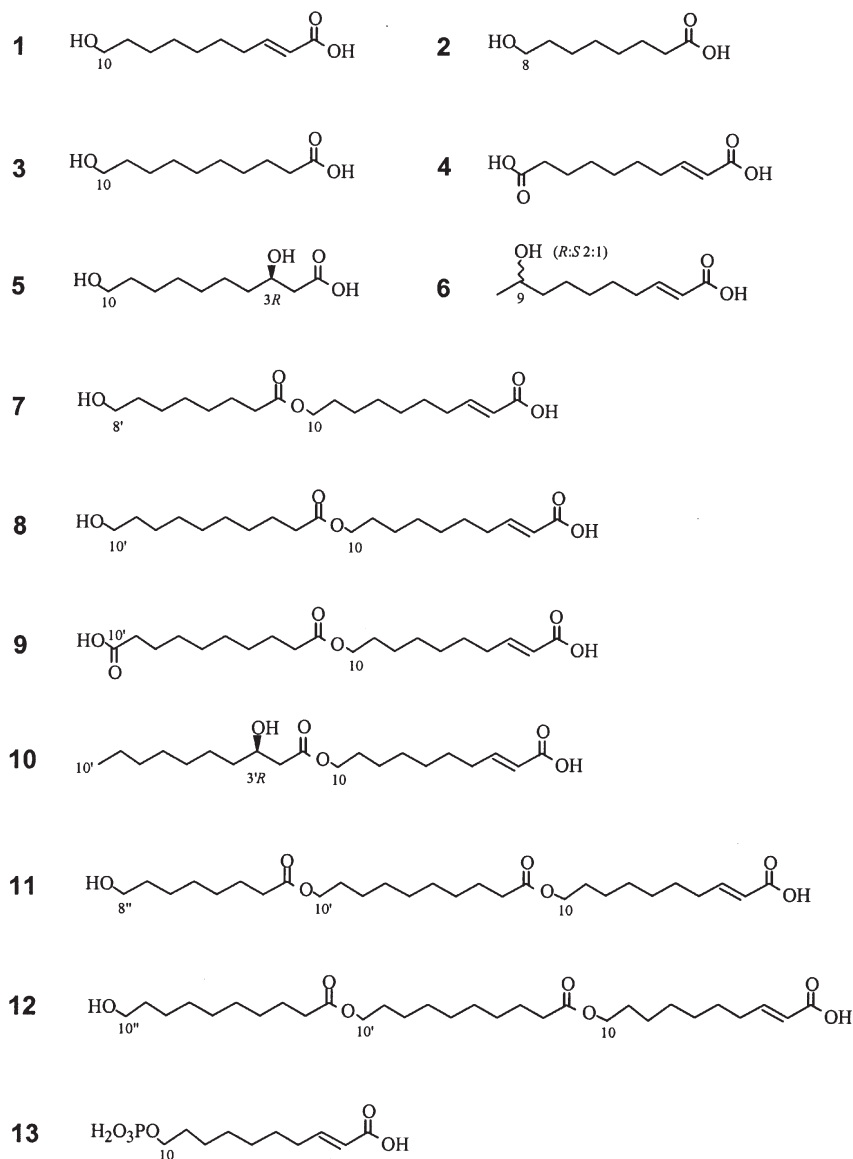
SCHEME 2

The structures of **8**, **9**, and **10** were elucidated in the same manner as described for **7**. Their chemical and spectral data revealed that they were also monoesters of 10-HDA differing in the FA residue. The configuration of the chiral center in **10** was proven to be *R*.

*Structures of diesters of 10-HDA, **11** and **12**.* The FABMS spectrum of **11** exhibited a [M − H]⁻ ion peak at *m/z* 497, and its mass was approximately three times more than those of known FA in royal jelly. From its ^{1}H and ^{13}C NMR spectral data, **11** was considered to be a diester composed of three FA units involving a 10-HDA residue.

Methanolysis of **11** gave three products, which were identified as methyl esters of compounds **1**, **2**, and **3**. The HMBC spectral data together with diagnostically important fragment ion peaks observed at *m/z* 159 and 329 in its FABMS revealed the sequence of the three FA units; therefore, the structure of **11** was characterized as shown in Figure 2.

Compound **12** was identified in the same manner as described for **11**; it was found to be another diester of 10-HDA that differed from **11** in the FA residue. The terminal 8-hydroxy-octanoyl unit in **11** was replaced by a 10-hydroxy-decanoyl group.

*Structure of 10-HDA phosphate (**13**).* The molecular formula of **13** was determined to be $C_{10}H_{18}O_6P$ by high-resolution FABMS. The presence of one phosphate was further substantiated by a signal at δ 25.6 ppm in the ^{31}P NMR spectrum. Its ^{1}H NMR spectrum showed, on comparison with that of 10-HDA, the signals ascribable to H_2-10 shifted downfield (0.33 ppm). Furthermore, in the ^{13}C NMR spectrum, the signals due to C-9 (*J* = 8.3 Hz) and C-10 (*J* = 4.9 Hz) appeared as doublets owing to coupling with ^{31}P (18). Accordingly, the phosphate group was located at the C-10 position, and the structure of **13** was thus characterized as shown in Scheme 2.
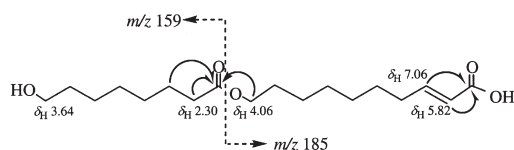
FIG. 1. Heteronuclear multiple-bond correlation of **7**.
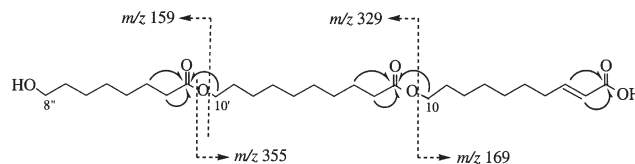
FIG. 2. Heteronuclear multiple-bond correlation of **11**.

We isolated seven novel FA esters along with six known FA from the lipid fraction of royal jelly.

In a study of the activity of 10-HDA on tumor cells, Robinson (19) presumed that polyesters were formed from 10-HDA. Later, Pain and coworkers (20) predicted the existence of di- or oligoesters of 10-HDA in the lipid fraction of queen larvae. However, no report on their isolation has so far appeared. We demonstrated that esters of 10-HDA are present in royal jelly.

We also found that royal jelly contains significant amounts of HDA 10-phosphate. In addition, it should be noted that, among the FA having the secondary hydroxyl group isolated in this study, only 9-HDA exists in royal jelly as a mixture of enantiomers.

REFERENCES

1. Tamura, T., Fuji, A., and Kubota, N. (1987) Anti-tumor Effects of Royal Jelly (RJ), *Folia Pharmacol. Jpn. 89*, 73–80 (in Japanese).
2. Sauerwald, N., Polster, J., Bengsch, E., Niessen, L., and Vogel, R.F. (1998) Combined Antibacterial and Antifungal Properties of Water-soluble Fraction of Royal Jelly, *Adv. Food Sci. 20*, 46–52.
3. Kamakura, M., Mitani, N., Fukuda, T., and Fukushima, M. (2001) Anti-fatigue Effect of Fresh Royal Jelly in Mice, *J. Nutr. Sci. Vitaminol. (Tokyo) 47*, 394–401.
4. Tokunaga, K., Yoshida, C., Suzuki, K., Maruyama, H., Futamura, Y., Araki, Y., and Mishima, S. (2004) Antihypertensive Effect of Peptides from Royal Jelly in Spontaneously Hypertensive Rats, *Biol. Pharm. Bull. 27*, 189–192.
5. Takenaka, T. (1982) Chemical Composition of Royal Jelly, *Honeybee Sci. 3*, 69–74.
6. Svoboda, J.A., Herbert, E.W., Jr., Thompson, M.J., and Feldlaufer, M.F. (1986) Selective Sterol Transfer in the Honey Bee: Its Significance and Relationship to Other Hymenoptera, *Lipids 21*, 97–101.
7. Lercker, G., Capella, P., Conte, L.S., Ruini, F., and Giordani, G. (1981) Components of Royal Jelly: I. Identification of the Organic Acids, *Lipids 16*, 912–919.
8. Antinelli, J.-F., Davico, R., Rognone, C., Faucon, J.-P., and Lizzani-Cuvelier, L. (2002) Application of Solid/Liquid Extraction for the Gravimetric Determination of Lipids in Royal Jelly, *J. Agric. Food Chem. 50*, 2227–2230.
9. Barker, S.A., Foster, A.B., Lamb, D.C., and Hodgson, N. (1959) Identification of 10-Hydroxy-Δ^2-Decenoic Acid in Royal Jelly, *Nature 183*, 996–997.
10. Butenandt, A., and Rembold, H. (1957) Über den Weiselzellenfuttersaft der Honigbiene I. Isolierung, Konstitutionsermittlung und Vorkommen der 10-Hydroxy-Δ^2-decensäure, *Z. Physiol. Chem. 308*, 284–289.
11. Brown, W.H., and Freure, R.J. (1959) Some Carboxylic Acids Present in Royal Jelly, *Can. J. Chem. 37*, 2042–2046.
12. Townsend, G.F., Morgan, J.F., and Hazlett, B. (1959) Activity of 10-Hydroxydecenoic Acid from Royal Jelly Against Experimental Leukaemia and Ascitic Tumours, *Nature 183*, 1270–1271.
13. Pollet, S., Bottex-Gauthier, C., Li, M., Potier, P., Favier, A., and Vidal, D. (2002) Insight into Some of the Signaling Pathways Triggered by a Lipid Immunomodulator, *Immunopharmacol. Immunotoxicol. 24*, 527–546.
14. Koya-Miyata, S., Okamoto, I., Ushio, S., Iwaki, K., Ikeda, M., and Kurimoto, M. (2004) Identification of a Collagen Production-promoting Factor from an Extract of Royal Jelly and Its Possible Mechanism, *Biosci. Biotechnol. Biochem. 68*, 767–773.
15. Dittmer, J.C., and Lester, R.L. (1964) Specific Spray for the Detection of Phospholipids on Thin-layer Chromatograms, *J. Lipid Res. 5*, 126–127.
16. Kusumi, T., Ohtani, I., Inoue, Y., and Kakisawa, H. (1988) Absolute Configurations of Cytotoxic Marine Cembranolides; Consideration of Mosher's Method, *Tetrahedron Lett. 29*, 4731–4734.
17. Ono, M., Yamada, F., Noda, N., Kawasaki, T., and Miyahara, K. (1993) Determination by Mosher's Method of the Absolute Configurations of Mono- and Dihydroxyfatty Acids Originated from Resin Glycosides, *Chem. Pharm. Bull. (Tokyo) 41*, 1023–1026.
18. Breitmaier, E., and Voelter, W. (1987) *Carbon-13 NMR Spectroscopy*, 3rd edn., pp. 250–254, VCH Verlagsgesellschaft, Weinheim.
19. Robinson, S.R. (1960) The Biological Activity and Synthesis of Royal Jelly Acid, *Croat. Chem. Acta 32*, 119–122.
20. Pain, J., Barbier, M., Bogdanovsky, D., and Lederer, E. (1962) Some Carboxylic Acids Present in Royal Jelly, *Comp. Biochem. Physiol. 6*, 233–241.

Synthesis and Characterization of a Series of Carbamate-Linked Cationic Lipids for Gene Delivery

Dongliang Liu[a],*, Jianjun Hu[a], Weihong Qiao[a], Zongshi Li[a], Shubiao Zhan[b], and Lvbo Cheng[a]

[a]State Key Laboratory of Fine Chemicals, Dalian University of Technology, Dalian, 116012, China, and
[b]Department of Chemical Engineering, Dalian Nationalities University, Dalian, 116600, China

ABSTRACT: A series of pH-sensitive lipids, **1a–h** [(2,3-bis-alkyl-carbamoyloxy-propyl)-trialkylammonium halide] and **2a–d** (1-dimethylamino-2,3-bis-alkylcarbamoyloxy-propane), with carbamate linkages between the hydrocarbon chains and an ammonium or tertiary amine head, were synthesized for liposome-mediated gene delivery. The variable length of the carbon chains and the quaternary ammonium or neutral tertiary amine heads allowed us to identify the structure–function relationship showing how these factors would affect cationic lipids in gene delivery performance.

Paper no. L9790 in *Lipids 40*, 839–848 (August 2005).

In 1987, Felgner and coworkers (1) first reported the utilization of an unnatural diether-linked cationic lipid as a synthetic carrier to deliver genes to cells. Since then, a number of published reports have described strategies for synthesizing versatile cationic lipids for gene delivery (for reviews of cationic lipid synthesis, see Refs. 2 and 3). These studies cover diverse kinds of cationic lipids, such as glycerol backbone-based, cholesterol-based, cationic peptide-based, poly(ethylenimine)-based, and poly(L-lysine)-based structures (4–18). Cationic lipids, with their prominent nonimmunogenic character and low cellular toxicity in delivering genes, have engendered considerable interest among researchers in the gene therapy community (19,20). It is generally believed that electrostatic interaction brings cationic lipids and polyanionic DNA together to form DNA/liposome complexes. These complexes, once exposed to cells, are then taken up by the cells and the inserted gene is expressed. Most of the spacers in the aforementioned synthesized lipids are ether, ester, or amide bonds, which are either too stable to be biodegraded and thus cause cytotoxicity (e.g., ether linkers) or liable to decompose in the circulation system (e.g., ester linkers). In contrast with these strategies, in a previous paper (21) we developed six carbamate-linked lipids (**1a**, **1d**, **1e**, **1h**, **2a**, and **2d)** having either quaternary ammonium or neutral tertiary amine heads for the purpose of taking advantage of the pH sensitivity of the carbamate bond (Scheme 1).

In our previous work, the dodecyl and octadecyl length of the carbon chain were selected because they represented the two extremes of short and long; however, a series of cationic lipids covering the carbon chain lengths C_{12}, C_{14}, C_{16}, and C_{18} were needed to discuss the gene-delivery properties of these kinds of lipids. In this paper, we introduce the synthesis of the aforementioned lipids **1a–h** and **2a–d**.

Compounds that include a carbamate bond are known to be stable in neutral circumstances and prone to acid-catalyzed hydrolysis. For example, di-*tert*-butyl dicarbonate $[O(boc)_2]$ is usually used as an excellent amino-protective reagent because the carbamate formed can remain stable in the foregoing reaction and can be acid-hydrolyzed in acidic conditions (22). As is well known, the pH value within the cell is 1~2 pH units lower than that in the circulation system; thus, these carbamate-linked lipids are expected to remain stable within the circulation system but decompose to release DNA after entering the cell because of the decrease in pH from outside to inside the cell. Our idea coincides somewhat with those of Boomer and Thompson (23) and Boomer *et al.* (24), who adopted a vinyl ether bond as the linkage in their lipids. Quaternary ammonium heads with or without an ethyl group were used to determine whether different cationic heads would influence their binding with DNA phosphates. Iodide ions rather than chloride ions were adopted here as the counterions to investigate the gene-delivery properties of these kinds of ions; we expected that they would be unlikely to have significantly different gene-delivery properties since the DNA phosphates would exchange with these counterions during the complexation step preceding transfection.

To acquire the aforementioned eight cationic lipids, four intermediates were synthesized, **2a–d**. Compound **2** was then converted to **1** through quaternization with suitable halogenated hydrocarbons. Cationic lipids are known to combine well with the anionic DNA through electrostatic attraction to form DNA/liposome complexes, yet cationic liposomes may also cause cytotoxicity. Here we used the neutral intermediates **2a** and **2b** as a kind of lipid vector and found that liposomes could be formed through the Bangham method (1,25). These lipids are expected to reduce the cytotoxicity caused by their cationic counterparts.

EXPERIMENTAL PROCEDURES

Reagents and apparatus. 3-Chloro-1,2-propanediol, a 33% aqueous dimethylamine solution, laurylamine, tetradecylamine,

---

*To whom correspondence should be addressed at State Key Laboratory of Fine Chemicals, Dalian University of Technology, Zhongshan Rd. 158th, Dalian, 116012, China. E-mail: dut-liu@163.com

Abbreviations: APCI, atmospheric pressure chemical ionization; API-ES, atmospheric pressure ionization-electrospray; BTC, bis(trichloromethyl)carbonate; DODAB, dioctadecyldimethylammonium bromide; DODAC, dioctadecyldimethylammonium chloride; HRMS, high-resolution mass spectrometry; TEM, transmission electron microscopy.

SCHEME 1

hexadecylamine, bis(trichloromethyl)carbonate (BTC), triethyl-amine, and sodium hydroxide (all analytically pure) were from Sinopharm Chemical Reagent Co. Ltd. (Shanghai, China). Octadecanamine (analytically pure) was from Acros Organics (Fairlawn, NJ). All solvents (analytically pure) were from Sinopharm Chemical Reagent Co. Ltd.

A model HP6890 gas chromatograph–HP5973 mass spectrometer, a model HP1100 electrospray ionization mass spectrometer, a Micromass LC/Q-TOF high-resolution mass spectrometer, and a Varian INOVA 400-MHz nuclear magnetic resonance spectrometer were used to analyze the products. A model JEM-2000EX transmission electron microscope (JEOL, Tokyo, Japan) was used for transmission electron microscopy (TEM). A KQ218 ultrasonic instrument (Kunshan Ultrasonic Instrument Co. Ltd., Kunshan, China) was used to prepare the liposomes.

Preparation of 1-dimethylamino-2,3-propanediol. Sodium hydroxide (11 g, 0.275 mol) was dissolved in the 33% aqueous dimethylamine solution (74.2 mL, 0.537 mol); 3-chloro-1,2-propanediol (45.4 g, 0.413 mol) was then added dropwise and the mixture was stirred at 30°C for 24 h. The mixture was then gradually heated to 105°C, with the unreacted dimethylamine distilled therefrom being absorbed in water. The water was distilled from the remaining mixture under reduced pressure. The residue from the distillation was cooled to 40°C and mixed with 40 mL of methanol, whereupon sodium chloride precipitated from the mixture. The precipitate was removed by filtration, and the filter cake was washed with another 20 mL of methanol. The methanol in the combined filtrate was recovered by distillation at reduced pressure, and the desired compound was then recovered. Fractional distillation yielded 1-dimethyl-amino-2,3-propanediol [29.5 g, 60% yield, b.p. 102–104°C/2 mmHg; Lit. 111°C/15 mmHg (26)]. ^{1}H NMR (Bruker Avance; 400 MHz, CDCl$_3$): δ 4.56 (*s*, 2H, 2 × OH); 3.78 (*m*, 1H, CH$_2$C*H*CH$_2$N); [3.63 (tetra, *J* = 3.6, 8.0, 3.6, 1H), 3.48 (tetra, *J* = 6.0, 5.6, 5.6, 1H), C*H$_2$*CHCH$_2$N]; [2.49 (tetra, *J* = 9.2, 3.2, 9.2, 1H), 2.23 (tetra, *J* = 4.0, 8.8, 4.0, 1H), CH$_2$CHC*H$_2$*N]; 2.28 [*s*, 6H, N(CH$_3$)$_2$]. MS *m/z*: 42 (10.0%), 58 [100%, (CH$_3$)$_2$N$^+$=CH$_2$], 72 (1.3%), 88 (19.7%), 102 (0.4%), 119 (5.2%); Lit. *m/z*: 42 (5.3%), 58 (100%), 88 (13%), 119 (2.9%) (27).

Preparation of isocyanates. Alkyl amine (30 mmol) in CH$_2$Cl$_2$ solution (150 mL) was added to a three-necked flask, and then a saturated aqueous solution of Na$_2$CO$_3$ (60 mL) was added. After stirring for 5 min, BTC (22 g, 74 mmol) in

CH$_2$Cl$_2$ solution (1 N) was added in batch and the mixture was stirred vigorously at room temperature for 2 h. The organic phase was then separated and the aqueous phase was extracted with CH$_2$Cl$_2$. The combined organic phases were dried (CaCl$_2$) and concentrated with a rotary evaporator to afford the alkyl isocyanates, which were used for the next step without further purification.

Lauryl isocyanate: Yield 63%. ^{1}H NMR (400 M, CDCl$_3$): δ 3.28 (*t*, *J* = 6.8, 6.4, 2H, NCH$_2$), 1.60 (*m*, 2H, NCH$_2$CH$_2$), 1.26 [*s*, 18H, (CH$_2$)$_9$], 0.88 (*t*, *J* = 5.2, 6.8, 3H, CH$_3$). MS *m/z*: 30 (1.9%), 41 (24.3%), 55 (27.2%), 69 (15.5%), 85 (12.6%), 99 (100%, [C$_5$H$_9$NO]$^+$), 112 (48.5%), 126 (25.2%), 140 (9.7%), 154 (5.8%), 168 (4.9%), 182 (3.9%), 196 (1.0%), 210 (1.9%). Tetradecyl isocyanate: Yield 61%. ^{1}H NMR (400 M, CDCl$_3$): δ 3.28 (*t*, *J* = 6.4, 6.8, 2H, NCH$_2$), 1.61 (*m*, 2H, NCH$_2$CH$_2$), 1.26 [*s*, 22H, (CH$_2$)$_{11}$], 0.88 (*t*, *J* = 6.4, 7.2, 3H, CH$_3$). MS *m/z*: 39 (3.3%), 55 (26.9%), 84 (13.2%), 99 (100%, [C$_5$H$_9$NO]$^+$), 126 (25.3%), 154 (6.6%), 169 (3.8%), 196 (4.4%), 222 (1.1%), 238 (1.6%). Hexadecyl isocyanate: Yield 60%. ^{1}H NMR (400 M, CDCl$_3$): δ 3.28 (*t*, *J* = 6.4, 6.8, 2H, NCH$_2$), 1.61 (*m*, 2H, NCH$_2$CH$_2$), 1.26 [*s*, 26H, (CH$_2$)$_{13}$], 0.88 (*t*, *J* = 6.4, 7.2, 3H, CH$_3$); MS *m/z*: 43 (28.4%), 69 (16.2%), 99 (100%, [C$_5$H$_9$NO]$^+$), 126 (22.5%), 154 (5.4%), 180 (3.4%), 196 (3.9%), 224 (6.4%), 250 (1.0%), 266 (2.0%). Octadecyl isocyanate: Yield 58%. ^{1}H NMR (400 M, CDCl$_3$): δ 3.27 (*t*, *J* = 6.0, 6.0, 2H, NCH$_2$), 1.60 (*t*, *J* = 6.4, 6.8, 2H, NCH$_2$CH$_2$), 1.26 [*s*, 30H, (CH$_2$)$_{15}$], 0.88 (*t*, *J* = 6.0, 6.4, 3H, CH$_3$). MS *m/z*: 43 (31.6%), 69 (18.9%), 84 (10.5%), 99 (100%, [C$_5$H$_9$NO]$^+$), 126 (23.7%), 154 (5.3%), 182 (3.9%), 210 (5.2%), 238 (6.1%), 253 (4.8%), 281 (2.6%). Lit. *m/z*: 43 (100%), 69 (21.0%), 84 (9.0%), 99 (67%), 126 (6.0%), 154 (0.6%) (28).

Preparation of carbamates. 1-Dimethylamino-2,3-propane-diol (1 g, 8.4 mmol) and alkyl isocyanate (33 mmol) in toluene solution were added to a three-necked flask. Et$_3$N (0.85 g, 8.4 mmol) was then added as the catalyst and the mixture was stirred at 60–70°C for 4 h. The reaction mixture was then concentrated with a rotary evaporator. The white solid formed was dissolved in chloroform, applied to a gel column, and eluted with chloroform/methanol (4:1 vol/vol) to afford the desired compounds.

Compound **2a**: Yield 45%. IR (KBr) ν$_{max}$: 3324 (ν$_{NH}$), 1717 (ν$_{CO}$), 1697 (ν$_{CO}$), 1265–1254 (ν$_{COC}$, ν$_{CN}$). ^{1}H NMR (400 M, CDCl$_3$): δ [5.82, 5.17, 5.07 (OCH, 2 × NH)], [4.29 (*d*, *J* = 11.2, 1H), 4.22 (*d*, *J* = 11.2, 1H), OCH$_2$], [3.24, 3.13, 2.94, (2 × NHCH$_2$, NCH$_2$)], 2.72 [*s*, 6H, N(CH$_3$)$_2$], 1.48 (*m*, 4H, 2 ×

NHCH$_2$CH$_2$), 1.23 [s, 36H, 2 × (CH$_2$)$_9$], 0.86 (t, J = 5.6, 6.8, 6H, 2 × CH$_3$). ^{13}C NMR (400 M, CDCl$_3$): δ 155.98 (C=O), 67.22 (OCH), 63.92 (OCH$_2$), 58.03 (NCH$_2$), 44.23 (NHCH$_2$), 41.44 [N(CH$_3$)$_2$], 32.11–22.88 [(CH$_2$)$_{10}$], 14.32 (CH$_3$). High-resolution mass spectrometry (HRMS) m/z: Found [M + H]$^+$ 542.4888, C$_{31}$H$_{63}$N$_3$O$_4$ calcd. for [M + H]$^+$ 542.4897. Compound **2b**: Yield 44%. IR (KBr) ν$_{max}$: 3318 (ν$_{NH}$), 1691 (ν$_{CO}$), 1275–1258 (ν$_{COC}$, ν$_{CN}$). ^{1}H NMR (400 M, CDCl$_3$): δ [5.05, 4.82, 4.75 (OCH, 2 × NH)], [4.25 (d, J = 11.0, 1H), 4.14 (m, 1H), OCH$_2$], [3.15, 2.55, 2.44, (2 × NHCH$_2$, NCH$_2$)], 2.29 [s, 6H, N(CH$_3$)$_2$], 1.48 (m, 4H, 2 × NHCH$_2$CH$_2$), 1.26 [s, 44H, 2 × (CH$_2$)$_{11}$], 0.88 (t, J = 6.4, 7.2, 6H, 2 × CH$_3$). ^{13}C NMR (400 M, CDCl$_3$): δ 156.36, 156.03 (2 × C=O), 70.16 (OCH), 65.02 (OCH$_2$), 59.66 (NCH$_2$), 46.08 (NHCH$_2$), 41.30 [N(CH$_3$)$_2$], 32.10–22.87 [(CH$_2$)$_{12}$], 14.30 (CH$_3$). HRMS m/z: Found [M + H]$^+$ 598.5516, C$_{35}$H$_{71}$N$_3$O$_4$ calcd. for [M + H]$^+$ 598.5523. Compound **2c**: Yield 43%. IR (KBr) ν$_{max}$: 3316 (ν$_{NH}$), 1690 (ν$_{CO}$), 1267–1255 (ν$_{COC}$, ν$_{CN}$). ^{1}H NMR (400 M, CDCl$_3$): δ [5.05, 4.94, 4.83 (OCH, 2 × NH)], [4.26 (d, J = 12.0, 1H), 4.15 (m, 1H), OCH$_2$], [3.15, 2.63, 2.45, (2 × NHCH$_2$, NCH$_2$)], 2.32 [s, 6H, N(CH$_3$)$_2$], 1.48 (m, 4H, 2 × NHCH$_2$CH$_2$), 1.25 [s, 52H, 2 × (CH$_2$)$_{13}$], 0.88 (t, J = 6.4, 7.2, 6H, 2 × CH$_3$). ^{13}C NMR (400 M, CDCl$_3$): δ 156.32, 155.98 (2 × C=O), 69.94 (OCH), 64.93 (OCH$_2$), 59.54 (NCH$_2$), 45.92 (NHCH$_2$), 41.29 [N(CH$_3$)$_2$], 32.09–22.86 [(CH$_2$)$_{14}$], 14.29 (CH$_3$). HRMS m/z: Found [M + H]$^+$ 654.6156, C$_{39}$H$_{79}$N$_3$O$_4$ calcd. for [M + H]$^+$ 654.6149. Compound **2d**: Yield 41%. IR (KBr) ν$_{max}$: 3320 (ν$_{NH}$), 1691 (ν$_{CO}$), 1271–1257 (ν$_{COC}$, ν$_{CN}$). ^{1}H NMR (400 M, CDCl$_3$): δ [5.10, 4.87 (OCH, 2 × NH)], 3.83 (d, J = 9.6, 2H, OCH$_2$), [3.15, 2.84, 2.76 (2 × NHCH$_2$, NCH$_2$)], 2.45 [s, 6H, N(CH$_3$)$_2$], 1.49 (m, 4H, 2 × NHCH$_2$CH$_2$), 1.25 [s, 60H, 2 × (CH$_2$)$_{15}$], 0.86 (t, J = 4.6, 6.4, 6H, 2 × CH$_3$). ^{13}C NMR (400 M, CDCl$_3$): δ 155.98 (C=O), 70.73 (OCH), 64.86 (OCH$_2$), 60.74 (NCH$_2$), 45.96 (NHCH$_2$), 41.34 [N(CH$_3$)$_2$], 32.12–22.89 [(CH$_2$)$_{16}$], 14.33 (CH$_3$). HRMS m/z: found [M + H]$^+$ 710.6770, C$_{43}$H$_{87}$N$_3$O$_4$ calcd. for [M + H]$^+$ 710.6775.

Alkylation of carbamates. A suitable halogenated hydrocarbon (108 mmol) was condensed in a pressure apparatus containing a suitable carbamate **2** (1.8 mmol) with or without a petroleum ether solution. The sealed vessel was stirred behind a safety shield at 70°C for 48 h. After cooling to 0°C, the reaction vessel was opened and the reaction mixture was filtered to eliminate the excess halogenated hydrocarbon/petroleum ether solution. The remaining halogenated hydrocarbons in the filter cake were allowed to evaporate and were then evaporated under reduced pressure. The crude residue was recrystallized from acetonitrile to afford **1**.

Compound **1a**: Yield 97%. IR (KBr) ν$_{max}$: 3461 (ν$_{NH}$), 1728 (ν$_{CO}$), 1711 (ν$_{CO}$), 1267–1248 (ν$_{COC}$, ν$_{CN}$). ^{1}H NMR (400 M, CDCl$_3$): δ [5.98, 5.47, 5.39 (OCH, 2 × NH)], 4.30–4.17 (OCH$_2$, NCH$_2$), 3.50 [s, 9H, N(CH$_3$)$_3$], 3.15 (d, J = 6.8, 4H, 2 × NHCH$_2$), 1.51 (d, J = 6.4, 4H, 2 × NHCH$_2$CH$_2$), 1.26 [s, 36H, 2 × (CH$_2$)$_9$], 0.88 (t, J = 6.4, 6.4, 6H, 2 × CH$_3$). ^{13}C NMR (400 M, CDCl$_3$): δ 155.78 (C=O), 66.76 (OCH), [63.27, 61.28 (OCH$_2$, NCH$_2$)], 55.08 [N(CH$_3$)$_3$], [41.58, 41.38 (2 × NHCH$_2$)], 32.09–22.86 [(CH$_2$)$_{10}$], 14.30 (CH$_3$). HRMS m/z:

Found [M − I]$^+$ 556.5062, C$_{32}$H$_{66}$IN$_3$O$_4$ calcd. for [M − I]$^+$ 556.5053. Compound **1b**: Yield 96%. IR (KBr) ν$_{max}$: 3460 (ν$_{NH}$), 1728 (ν$_{CO}$), 1712 (ν$_{CO}$), 1268–1255 (ν$_{COC}$, ν$_{CN}$). ^{1}H NMR (400 M, CDCl$_3$): δ [5.97, 5.48, 5.40 (OCH, 2 × NH)], 4.21, 4.19 (OCH$_2$, NCH$_2$), 3.50 [s, 9H, N(CH$_3$)$_3$], 3.14 (s, 4H, 2 × NHCH$_2$), 1.51 (s, 4H, 2 × NHCH$_2$CH$_2$), 1.26 [s, 44H, 2 × (CH$_2$)$_{11}$], 0.88 (t, J = 6.4, 6.4, 6H, 2 × CH$_3$). ^{13}C NMR (400 M, CDCl$_3$): δ 155.80, 154.72 (2 × C=O), 66.73 (OCH), [66.57, 63.32 (OCH$_2$, NCH$_2$)], 55.08 [N(CH$_3$)$_3$], [41.55, 41.36 (2 × NHCH$_2$)], 32.07–22.84 [(CH$_2$)$_{12}$], 14.27 (CH$_3$). HRMS m/z: Found [M − I]$^+$ 612.5682, C$_{36}$H$_{74}$IN$_3$O$_4$ calcd. for [M − I]$^+$ 612.5679. Compound **1c**: Yield 95%. IR (KBr) ν$_{max}$: 3461 (ν$_{NH}$), 1728 (ν$_{CO}$), 1712 (ν$_{CO}$), 1264–1247 (ν$_{COC}$, ν$_{CN}$). ^{1}H NMR (400 M, CDCl$_3$): δ [5.86, 5.46, 5.27 (OCH, 2 × NH)], 4.30, 4.22 (OCH$_2$, NCH$_2$), 3.50 [s, 9H, N(CH$_3$)$_3$], 3.15 (s, 4H, 2 × NHCH$_2$), 1.52 (s, 4H, 2 × NHCH$_2$CH$_2$), 1.26 [s, 52H, 2 × (CH$_2$)$_{13}$], 0.88 (t, J = 6.0, 6.8, 6H, 2 × CH$_3$). ^{13}C NMR (400 M, CDCl$_3$): δ 155.86, 154.84 (2 × C=O), 67.03 (OCH), [64.80, 61.75 (OCH$_2$, NCH$_2$)], 55.43 [N(CH$_3$)$_3$], 41.71 (NHCH$_2$), 32.12–22.65 [(CH$_2$)$_{14}$], 14.20 (CH$_3$). HRMS m/z: Found [M − I]$^+$ 668.6302, C$_{40}$H$_{82}$IN$_3$O$_4$ calcd. for [M − I]$^+$ 668.6305. Compound **1d**: Yield 93%. IR (KBr) ν$_{max}$: 3461 (ν$_{NH}$), 1727 (ν$_{CO}$), 1697 (ν$_{CO}$), 1266–1256 (ν$_{COC}$, ν$_{CN}$). ^{1}H NMR (400 M, CDCl$_3$): δ [5.86, 5.48, 5.32 (OCH, 2 × NH)], [4.24, 3.79 (OCH$_2$, NCH$_2$)], 3.46 [s, 9H, N(CH$_3$)$_3$], 3.15 (d, J = 4.8, 4H, 2 × NHCH$_2$), 1.51 (d, J = 6.4, 4H, 2 × NHCH$_2$CH$_2$), 1.26 [s, 60H, 2 × (CH$_2$)$_{15}$], 0.88 (t, J = 6.4, 6.8, 6H, 2 × CH$_3$). ^{13}C NMR (400 M, CDCl$_3$): δ 155.89, 154.87 (2 × C=O), 66.98 (OCH), [65.84, 61.38 (OCH$_2$, NCH$_2$)], 55.36 [N(CH$_3$)$_3$], 41.69 (NHCH$_2$), 32.10–22.84 [(CH$_2$)$_{14}$], 14.19 (CH$_3$). HRMS m/z: Found [M − I]$^+$ 724.6961, C$_{44}$H$_{90}$IN$_3$O$_4$ calcd. for [M − I]$^+$ 724.6931. Compound **1e**: Yield 95%. IR (KBr) ν$_{max}$: 3339 (ν$_{NH}$), 1697 (ν$_{CO}$), 1266–1243 (ν$_{COC}$, ν$_{CN}$). ^{1}H NMR (400 M, CDCl$_3$): δ [5.90, 5.52, 5.45 (OCH, 2 × NH)], 4.23, 4.14 (OCH$_2$, NCH$_2$), 3.73 (m, 2H, NCH$_2$CH$_3$), 3.39 (s, 6H, N(CH$_3$)$_2$), 3.13 [d, J = 4.4, 4H, 2 × NHCH$_2$], 1.58 (m, 4H, 2 × NHCH$_2$CH$_2$), 1.46 (m, 3H, NCH$_2$CH$_3$), 1.26 (s, 44H, 2 × (CH$_2$)$_{11}$], 0.88 (t, J = 5.6, 6.4, 6H, 2 × CH$_3$). ^{13}C NMR (400 M, CDCl$_3$): δ 155.85, 154.84 (C=O), 66.63 (OCH), [64.50, 63.30 (OCH$_2$, NCH$_2$)], 61.62 (NCH$_2$CH$_3$), 51.96, 51.79 [N(CH$_3$)$_2$], 41.60, 40.83 (NHCH$_2$), 32.03–22.77 [(CH$_2$)$_{10}$], 14.12 (CH$_3$), 9.02 (NCH$_2$CH$_3$). HRMS m/z: Found [M − I]$^+$ 570.5208, C$_{33}$H$_{68}$IN$_3$O$_4$ calcd. for [M − I]$^+$ 570.5210. Compound **1f**: Yield 94%. IR (KBr) ν$_{max}$: 3337 (ν$_{NH}$), 1696 (ν$_{CO}$), 1267–1243 (ν$_{COC}$, ν$_{CN}$). ^{1}H NMR (400 M, CDCl$_3$): δ [5.89, 5.48, 5.28 (OCH, 2 × NH)], 4.23, 4.16 (OCH$_2$, NCH$_2$), 3.71 (m, 2H, NCH$_2$CH$_3$), 3.37 [s, 6H, N(CH$_3$)$_2$], 3.16 (m, 4H, 2 × NHCH$_2$), 1.59 (s, 4H, 2 × NHCH$_2$CH$_2$), 1.46 (m, 3H, NCH$_2$CH$_3$), 1.26 [s, 44H, 2 × (CH$_2$)$_{11}$], 0.88 (t, J = 6.0, 7.2, 6H, 2 × CH$_3$). ^{13}C NMR (400 M, CDCl$_3$): δ 154.73 (C=O), 66.45 (OCH), [64.65, 63.40 (OCH$_2$, NCH$_2$)], 61.75 (NCH$_2$CH$_3$), 51.69 [N(CH$_3$)$_2$], 41.43 (NHCH$_2$), 32.11–22.88 [(CH$_2$)$_{12}$], 14.31 (CH$_3$), 8.92 (NCH$_2$CH$_3$). HRMS m/z: Found [M − I]$^+$ 626.5828, C$_{37}$H$_{76}$IN$_3$O$_4$ calcd. for [M − I]$^+$ 626.5836. Compound **1g**: Yield 93%. IR (KBr) ν$_{max}$: 3341 (ν$_{NH}$), 1712 (ν$_{CO}$), 1265–1242 (ν$_{COC}$, ν$_{CN}$). ^{1}H NMR (400 M, CDCl$_3$): δ [5.75, 5.49, 5.32

TABLE 1
$L_{4,3}$ Orthogonal Test of Reaction Conditions[a]

Test no.	Temperature (°C)	Time (h)	Ratio	Concentration of $NH(CH_3)_2$ (%)	Yield (%)
1	**1** 50	**1** 24	**1** 1:1.3	**1** 33	51.75
2	**2** 40	**1** 24	**2** 1:1.328	**2** 24.5	50.11
3	**3** 30	**1** 24	**3** 1:1.4	**3** 30	51.75
4	**1** 50	**2** 36	**3** 1:1.4	**2** 24.5	20.66
5	**2** 40	**2** 36	**2** 1:1.328	**3** 30	20.04
6	**3** 30	**2** 36	**1** 1:1.3	**1** 33	32.73
7	**1** 50	**3** 18	**2** 1:1.328	**3** 30	37.64
8	**2** 40	**3** 18	**3** 1:1.4	**1** 33	29.04
9	**3** 30	**3** 18	**1** 1:1.3	**2** 24.5	42.75
I (yield sum of **1**)	110.05	153.61	107.79	113.52	Total = **I** + **II** + **III** = 336.47
II (yield sum of **2**)	99.19	73.43	101.45	113.52	
III (yield sum of **3**)	127.23	109.43	127.23	109.43	
R (range of **1**, **2**, and **3**)	28.04	80.18	25.78	4.09	

[a]The boldfaced numbers **1**, **2**, and **3** represent three different values for each factor.

(OCH, 2 × NH)], 4.20, 4.10 (OCH$_2$, NCH$_2$), 3.68 (*m*, 2H, NC*H*$_2$CH$_3$), 3.36 [*s*, 6H, N(CH$_3$)$_2$], 3.18 (*m*, 4H, 2 × NHCH$_2$), 1.58 (*s*, 4H, 2 × NHCH$_2$CH$_2$), 1.47 (*m*, 3H, NCH$_2$C*H*$_3$), 1.26 [*s*, 52H, 2 × (CH$_2$)$_{13}$], 0.88 (*t*, *J* = 6.2, 7.2, 6H, 2 × C*H*$_3$). ^{13}C NMR (400 M, CDCl$_3$): δ 155.86, 154.85 (C = O), 66.66 (OCH), [64.69, 63.20 (OCH$_2$, NCH$_2$)], 61.81 (NCH$_2$CH$_3$), 52.13, 51.94 [N(CH$_3$)$_2$], 41.66, 41.52 (NHCH$_2$), 32.08–22.80 [(CH$_2$)$_{14}$], 14.17 (CH$_3$), 9.12 (NCH$_2$CH$_3$). HRMS *m/z*: Found [M − I]$^+$ 682.6454, C$_{41}$H$_{84}$IN$_3$O$_4$ calcd. for [M − I]$^+$ 682.6462. Compound **1h**: Yield 91%. IR (KBr) ν$_{max}$: 3343 (ν$_{NH}$), 1709 (ν$_{CO}$), 1267–1255 (ν$_{COC}$, ν$_{CN}$). ^{1}H NMR (400 M, CDCl$_3$): δ [5.88, 5.46, 5.36 (OCH, 2 × NH)], 4.25, 4.15 (OCH$_2$, NCH$_2$), 3.70 (*m*, 2H, NC*H*$_2$CH$_3$), 3.37 [*s*, 6H, N(CH$_3$)$_2$], 1.60 (*s*, 4H, 2 × NHCH$_2$CH$_2$), 1.48 (*m*, 3H, NCH$_2$C*H*$_3$), 1.25 [*s*, 60H, 2 × (CH$_2$)$_{15}$], 0.88 (*t*, *J* = 5.6, 6.8, 6H, 2 × C*H*$_3$). ^{13}C NMR (400 M, CDCl$_3$): δ 154.76 (C=O), 66.47 (OCH), [64.48, 63.10 (OCH$_2$, NCH$_2$)], 61.62 (NCH$_2$CH$_3$), 51.70 [N(CH$_3$)$_2$], 41.44 (NHCH$_2$), 32.12–22.88 [(CH$_2$)$_{16}$], 14.31 (CH$_3$), 8.92 (NCH$_2$CH$_3$). HRMS *m/z*: Found [M − I]$^+$ 738.7076, C$_{45}$H$_{92}$IN$_3$O$_4$ calcd. for [M − I]$^+$ 738.7088.

Liposome preparation. A solution of lipid (20 mg) in chloroform/methanol (1 mL) was evaporated to dryness under a stream of nitrogen, and the residual solvent was removed under vacuum overnight. Liposomes were prepared by resuspending the lipids in deionized water (2 mL) at 45°C and sonicating them to clarity at this temperature for 2 h in a closed vial.

RESULTS AND DISCUSSION

Preparation of 1-dimethylamino-2,3-propanediol. Alquist and Slagh (29) previously prepared 1-dimethylamino-2,3-propanediol with dimethylamine and glycerol monochlorhydrin under pressure. To prepare 1-dimethylamino-2,3-propanediol in a small quantity, our process used a normal-atmosphere reactor. Glycerol monochlorhydrin was titrated into a mixture of dimethylamine and an aqueous sodium hydroxide solution, and the mixture was heated to 25°C and maintained for 24 h. But after purification, the yield was only 30–40% of the theoretical amount. To obtain a better yield, an $L_{4,3}$ orthogonal test was

used; the four factors were reaction temperature, reaction time, ratio of glycerol monochlorhydrin to dimethylamine, and dimethylamine concentration (30). The results are shown in Table 1. The boldfaced numbers **1**, **2**, and **3** represent three different values for each factor, and **I**, **II**, and **III** represent the sums of yields for **1**, **2**, and **3**, respectively.

As shown in the above data, the reaction time had the greatest range, at 80.18 [max. (**I**, **II**, **III**)–min. (**I**, **II**, **III**) = 153.61–73.43]; the ranges for reaction temperature, monochlorhydrin/dimethylamine ratio, and dimethylamine concentration were 28.04, 25.78, and 4.09, respectively. This meant that reaction time had the greatest influence on the reaction yield. With regard to reaction time, the sum of three yields at 24 h was 153.61, which was the greatest among the yield sums at the three different reaction times of 18, 24, and 36 h. The 24-h reaction time was the best of these three reaction times, so the optimal reaction time was chosen as 24 h. In this way, other optimal factors such as reaction temperature, monochlorhydrin/dimethylamine ratio, and dimethylamine concentration also could be decided. We finally chose the optimal reaction conditions of a 33% dimethylamine concentration, a chloropropanediol/dimethylamine ratio of 1:1.3, 30°C, and 24 h. A 60% yield was finally attained under these conditions (Scheme 2).

1-Dimethylamino-2,3-propanediol was characterized correctly by ^{1}H NMR and MS. The formula weight of 1-dimethylamino-2,3-propanediol was 119, and the highest peak in the fragments, *m/z* 58, was obtained as shown in Scheme 3 (31).

Reagents and conditions: 1.3 equiv dimethylamine in aqueous solution, 1.5 equiv sodium hydroxide, 24 h, 33°C, 60%..

SCHEME 2

SCHEME 3

SCHEME 4

Reagents and conditions: 5 equiv bis(trichloromethyl)carbonate (BTC) in CH_2Cl_2 solution, saturated $NaCO_3$ aqueous solution, 2 h, room temperature, 60%. R = $C_{12}H_{25}$, $C_{14}H_{29}$, $C_{16}H_{33}$, $C_{18}H_{37}$.
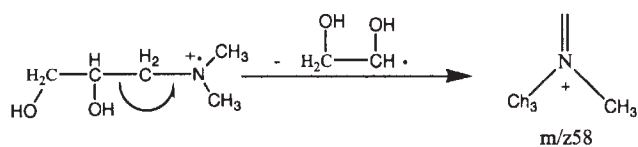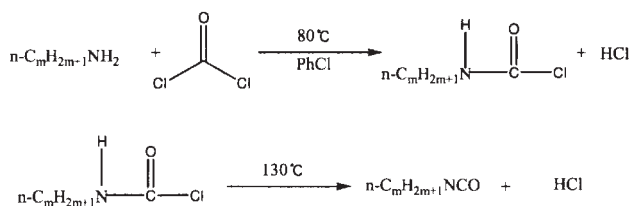
SCHEME 6

Preparation of isocyanates. Alkyl isocyanate is commonly prepared by the phosgene route in industrial production (Scheme 4).

As is well known, phosgene is an excellent acylation reagent with high activity, but its strong toxicity limits its application. In our work, BTC was tentatively substituted for phosgene to avoid the strong toxicity of the latter (32). BTC, which is much less toxic than phosgene, can release triple phosgene under nucleophilic catalysis (Scheme 5).

For lauryl isocyanate, for example, for the first time BTC was substituted for triphosgene and reacted with laurylamine under the same conditions as phosgene. BTC was 100% in excess. The amount of pyridine catalyst was 7.1% of the laurylamine mass. A BTC/chlorobenzene solution was titrated into a mixture of laurylamine and a pyridine/chlorobenzene solution, and the mixture was heated to 130°C for 3 h. When the reaction mixture was cooled to room temperature, a large amount of unreacted laurylamine separated out.

A considerable amount of laurylamine in the reaction was unreacted; one reason may be that the organic base pyridine caused BTC to release phosgene so fast that the rapidly created phosgene escaped quickly from the reaction system. To reduce the release rate of phosgene from BTC under these conditions, the catalyst was tentatively substituted with an inorganic base, a saturated aqueous solution of Na_2CO_3 (33). The saturated aqueous solution of Na_2CO_3 was added to an alkyl amine CH_2Cl_2 solution; after stirring for 5 min, a solution of BTC (1 N) in CH_2Cl_2 was added and the mixture was stirred vigorously at room temperature for 2 h (Scheme 6).

Under these conditions, BTC was catalyzed to slowly release phosgene. A little 100% pure lauryl isocyanate was obtained by reduced-pressure distillation and was characterized correctly by GC–MS and ^{1}H NMR. The highest peak in the alkyl isocyanate MS fragments, *m/z* 99, was obtained as shown in Scheme 7 (28,31).

In 1966 Ruth and Philippe (28) researched the mass spectra of short-chain isocyanates (<C_8) and some aromatic isocyanates as well as one long-chain isocyanate (octadecyl isocyanate); they also reached the conclusion that the $[C_5H_9NO]^+$ peak, *m/z* 99, is an important ion when the alkyl chain is long enough. However, the base peak of their octadecyl isocyanate was *m/z* 43, and our conclusion did not agree with theirs, perhaps because the ion source wall of octadecyl isocyanate in their experiment was 74°C.

In the same way, tetradecyl, hexadecyl, and octadecyl isocyanate were also prepared and used for the next step without further purification.

Preparation of carbamates. For **2a**, for example, because isocyanate could react easily with active hydrogen, 1-dimethylamino-2,3-propanediol and lauryl isocyanate were first reacted at room temperature. The catalyst triethylamine also played a role as a solvent because it had no active hydrogen. The product was filtered and recrystallized from chloroform after 15 h. From the IR spectrum of the product, in addition to the vibrations of –C=O at 1583 and 1617 cm^{-1}, an –NH group could be seen in the molecule at 3300 cm^{-1}, which indicated the isocyanate had reacted with the hydroxyl of 1-dimethylamino-2,3-propanediol. However, the detected M.W. of the acquisition was 396, which was not the expected substance. The substance acquired was speculated to be dilauryl urea because in the strongly polar solvent triethylamine there may inevitably be a little water. Under the conditions with triethylamine, isocyanate will be hydrolyzed into alkylamine; thus, the alkylamine generated will react with isocyanate to afford urea. The reaction may take place according to Scheme 8.

SCHEME 5

SCHEME 7

n=6, 8, 10, 12.
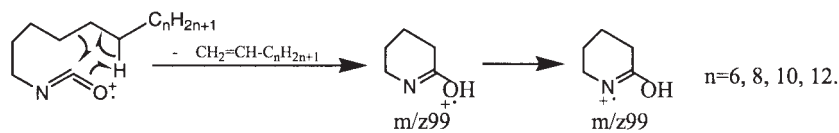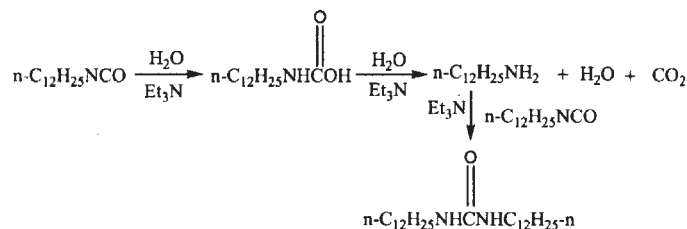
SCHEME 8

The speculation was confirmed by ^{1}H NMR data for dilauryl urea as follows: (CDCl$_3$): δ 4.36 (*s*, 2H, 2 × NH), 3.14 (tetra, *J* = 6.0, 6.4, 6.4, 4H, 2 × NHCH$_2$), 1.48 (*s*, 4H, 2 × NHCH$_2$CH$_2$), 1.26 [*s*, 36H, 2 × (CH$_2$)$_9$], 0.88 (*t*, *J* = 5.6, 6.8, 6H, 2 × CH$_3$).

To ensure anhydrous conditions, the solvent was substituted for anhydrous toluene and the amount of triethylamine was reduced to 1 equiv of 1-dimethylamino-2,3-propanediol. The reaction was undertaken at 60–70°C for 4 h (Scheme 9) (34). The reaction mixture was then concentrated and recrystallized from chloroform to afford crude **2a**.

In the atmospheric pressure chemical ionization (APCI)-MS spectrum of crude **2a** under these conditions, in addition to the main [M + H]$^+$ peak at 542.5, we concluded that the M.W. of the product was 541, which was in accordance with **2a**. Another peak at 331.3 referred to a substance with a M.W. of 330, which showed there was a little single-substitution product in the acquisition (Scheme 10).

To acquire pure **2a**, the crude product was applied to a silica gel column and eluted with chloroform/methanol (4:1, vol/vol). Compound **2a** was thus acquired and characterized by IR, atmospheric pressure ionization-electrospray (API-ES) MS, and NMR. The [M + H]$^+$ peak of the single-substitution product in the MS spectrum was eliminated this time. IR, MS, and NMR

data showed that the structure of **2a** was correct and that the purity of **2a** with this method was satisfactory.

Proceeding in a similar manner, **2b**, **2c**, and **2d** were prepared.

Alkylation of carbamates. The four carbamates were reacted with methyl iodide in the petroleum ether solution in a pressure reactor (1). After 48 h at 70°C, the reactions were cooled to room temperature and the pressure reactor was opened. Crude salts were afforded *via* filtration and were purified through recrystallization from an acetonitrile solution (Scheme 11).

Using **1c** as an example, the API-ES MS of **1c** in the positive mode was 668, and it was 127 in the negative mode. The M.W. of **1c**, which was an iodide salt, was 795. Subtracting 127, the atomic weight of iodine, from 795 amounted to 668, which agreed with the data shown in the spectrum.

In ^{1}H NMR, chemical shifts of 5.86 (1H), 5.46 (1H), and 5.27 (1H) referred to protons in OCH and 2 × NH; 4.30 (2H) and 4.22 (2H) were the proton chemical shifts of OCH$_2$ and NCH$_2$. To acquire proof of the assignments of the above signals, 2-D homonuclear correlation spectroscopy, heteronuclear single quantum correlation, and heteronuclear multiple-bond correlation analyses were carried out, which confirmed the

2a R=C$_{12}$H$_{25}$
2b R=C$_{14}$H$_{29}$
2c R=C$_{16}$H$_{33}$
2d R=C$_{18}$H$_{37}$
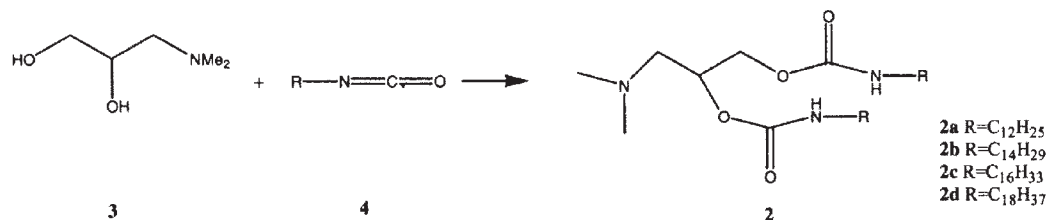
Reagents and conditions: 4 equiv **4**, 1 equiv Et$_3$N in toluene solution, 4 h, 60–70°C, 43%.

SCHEME 9

SCHEME 10

1a: R=C$_{12}$H$_{25}$
1b: R=C$_{14}$H$_{29}$
1c: R=C$_{16}$H$_{33}$
1d: R=C$_{18}$H$_{37}$
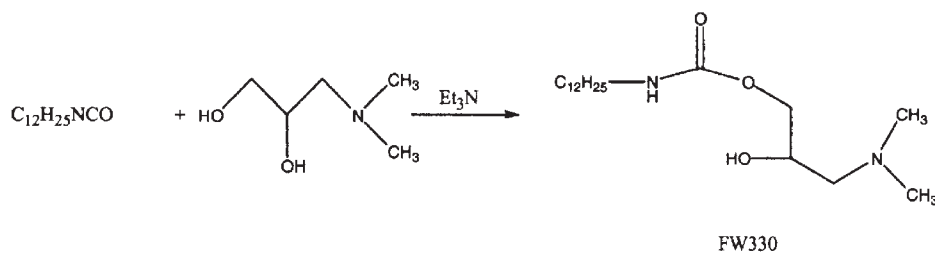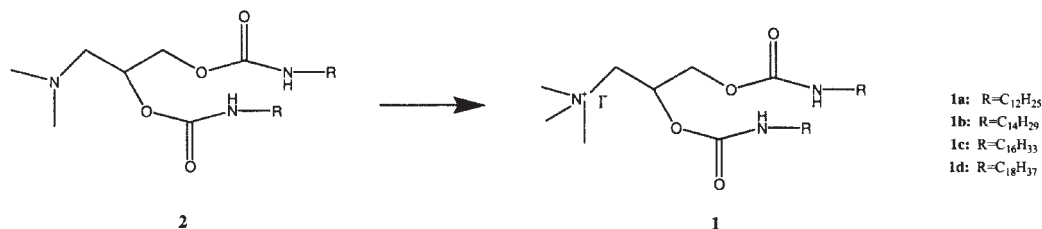
Reagents and conditions: 60 equiv CH$_3$I, petroleum ether solution, 48 h, 70°C, 95%.

SCHEME 11

assignments were correct. However, distinguishing the various absolute peaks was difficult because the proton chemical shifts in these two groups were too near to be differentiated or were even mixed together. The chemical shift 3.50 (9H) represented protons in N(CH$_3$)$_3$. The chemical shift 3.15 (4H) referred to protons in CH$_2$ connected to NH, and the chemical shift 1.52 (4H) represented protons in CH$_2$ next to NH. The chemical shift 0.88 (6H) referred to protons of the end CH$_3$ in the lipid chains, and 1.26 (52H) referred to protons in the remaining lipid carbon chains. IR, MS, and NMR data (see the Experimental Procedures section) confirmed that the structure of **1c** was correct.

Proceeding in a similar manner, **1a**, **1b**, and **1d** were prepared.

With regard to reactions between the carbamates and iodoethane, for **1g**, for example, the carbamate was reacted first under the same conditions as methyl iodide. But after reacting

for 48 h followed by purification, we observed almost half of the carbamate in the salts by ^{1}H NMR.

Because the reactivity of iodoethane was lower than that of methyl iodide, some measures had to be taken to increase the reaction velocity. As is well known, the products in these reactions were iodide salts whose polarities were strong, whereas the petroleum ether solvent, with a weak polarity in the reaction system, may have retarded the formation of salts. Hence, in the subsequent reaction, the petroleum ether solvent was abandoned, and the carbamates were submerged directly into the iodoethane liquid. In this manner, after 48 h at 70°C, the reactions were cooled to room temperature and the pressure reactor was opened. Crude salts were afforded *via* filtration and were purified through recrystallization from the acetonitrile solution (Scheme 12).

The API-ES MS of **1g** in the positive mode was 682, and it was 127 in the negative mode. The M.W. of **1g** was 809, which was an iodide salt. Subtracting 127, the atomic weight of

1e: R=C$_{12}$H$_{25}$
1f: R=C$_{14}$H$_{29}$
1g: R=C$_{16}$H$_{33}$
1h: R=C$_{18}$H$_{37}$
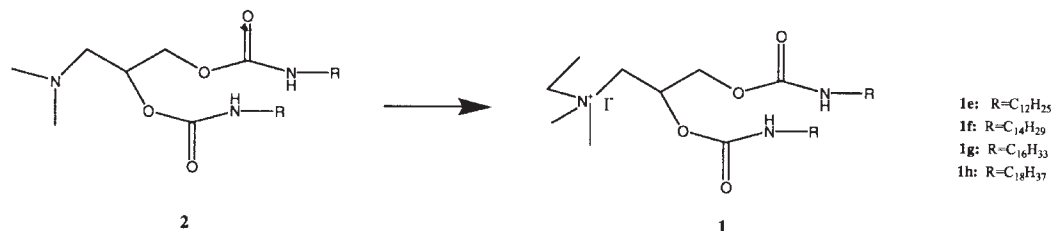
Reagents and conditions: 60 equiv CH$_3$CH$_2$I, 48 h, 70°C, 93%.

SCHEME 12

iodine, from 809 amounted to 682, which was in accord with the data shown in the spectrum. From the ¹H NMR data, one can see that no remaining carbamate was detected in this way. IR, MS, and NMR data (see the Experimental Procedures section) showed that the structure was correct.

Proceeding in a similar manner, **1e**, **1f**, and **1h** were prepared.

Liposome preparation. Commonly, liposomes are prepared through the Bangham method (25), nonultrasonic stirring (35), the ultrasonic method (36), the injection method (37), or the extrusion method (37). For a particular sample, specific factors must be taken into account.

Dispersant selection. Chloroform is usually used as the solvent in preparing lecithin liposomes, but sometimes if the lipid molecules contain a radical of strong polarity, which decreases its solubility in chloroform and leads to poor dispersibility in the solvent, it is usually necessary to add some methanol. Here, through solution tests, we found that chloroform alone dissolved the lipids well enough, and we finally obtained good dispersibility on the flask wall.

Contrasting lipids selection. Lecithin is a natural lipid that is widely used in controlled-release medicines, and the preparation of lecithin liposomes is classical. Dioctadecyldimethylammonium bromide (DODAB) is also a lipid usually applied in liposome/DNA complex (lipolex) research. Here, the counterpart to DODAB, dioctadecyldimethylammonium chloride (DODAC), as well as lecithin were selected as contrasting lipids for liposome research.

Liposome preparation and negative-stained TEM. Cationic lipids can combined well with anionic DNA through electrostatic attraction to form a DNA/liposome complex, yet cationic liposomes may also cause cytotoxicity. Here we took the neutral intermediates **2a**–**d** also as kinds of lipids to see whether they were able to form liposomes through the Bangham method.

For lecithin, DODAC, **2a,** and **1a,** for example, liposomes were prepared by the Bangham method, and ultrasonication was applied to half of each solution. Both ultrasonicated and nonultrasonicated samples were observed by TEM.

The hydrating temperatures used to make liposomes should usually be above the gel-to-liquid phase-transition temperature of the system (38). Lecithin, DODAC, **2a**, and **1a** are considered to have different transition temperatures; thus, it was convincing that the Bangham method gave no liposome structure if the flask did not warm when the lipid films were mixed with water. Basu *et al.* (39) and Hata *et al.* (40) both concluded that the phase transition temperature of phospholipids, which were similar in structure to the lipids discussed here, was around 40°C. In addition, in studies by Uchegbu *et al.* (41) and Uchegbu and Florence (42), polymers also had a phase transition temperature of around 40°C. For the moment, we used 40°C as the phase transition temperatures of the lipids discussed here, and we hydrated and sonicated them at 45°C to see whether they could form liposomes. Finally, the liposome structure was observed by negative-stained TEM, which in reverse showed that the phase transition temperatures of all the lipids discussed here were under 45°C.
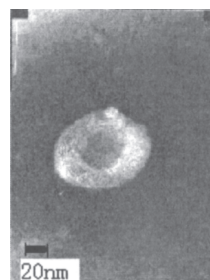
FIG. 1. Lecithin liposomes without sonication.
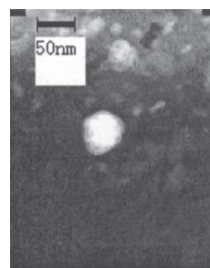
FIG. 2. Sonicated lecithin liposome.
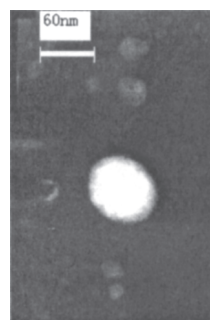
FIG. 3. Sonicated dioctadecyldimethylammonium chloride liposome.

Commonly, electron microscopy can be divided into freeze-fracture scanning electron microscopy and negative-stained TEM. The latter can clearly indicate the inner structure of the samples (43), which was what we were concerned with. By this means, we could identify the layers and diameters of the liposomes. Negative-stained transmission electron micrographs of the aforementioned liposomes are shown in Figures 1–5.

As one can see from these figures, the unsonicated lecithin liposomes had a multilayered structure, the diameter of which was about 100 nm; this was reduced to 50 nm after sonication. In the unsonicated DODAC, **2a**, and **1a** solutions, no liposome structures were observed. In contrast, single-layered liposomes with a diameter of about 60 nm appeared in the DODAC solution when sonication was applied. Compound **2a** formed multilayered liposomes, the diameters of which were about 40 nm, whereas **1a** formed 50-nm single-layered liposomes after sonication.

One can see that ultrasonication helped smaller liposomes to form. Lecithin could form both multilayered and single-layered liposomes because of the different preparation conditions (Figs. 1, 2). Furthermore, sonication sometimes plays a important role
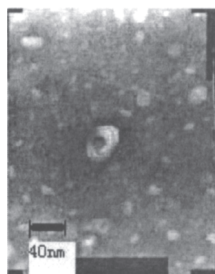
FIG. 4. Sonicated liposome of **2a**.
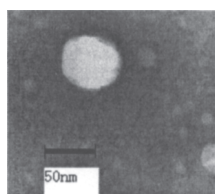
FIG. 5. Sonicated liposome of **1a**.

in liposome formation, because the latter three lipids could not form liposomes without sonication. The neutral lipid **2a** easily formed multilayered liposomes (Fig. 4), whereas the cationic lipids **1a** and DODAC preferentially formed single-layered liposomes (Figs. 3, 5). This may be due to the different structures among them. Neutral lipids may be more likely to form multilayered liposomes compared with their cationic counterparts. As gene vectors, multilayered liposomes would probably carry more DNA, whereas single-layered liposomes would probably enter into cells more easily because of their small size. Factors affecting the formation of multilayered or single-layered liposomes and the applications of these liposomes as DNA carriers *in vitro* and *in vivo* need to be discussed further.

A series of carbamate-linked lipids were prepared, and IR, GC–MS, HRMS, and NMR data were used to confirm their structures. Negative-stained TEM showed that these lipids could form single- or multilayered liposomes with a diameter of around 50 nm through an ordinary method. Application of these carbamate-linked cationic lipids as DNA carriers to deliver genes to cells *in vitro* and *in vivo* requires further research.

ACKNOWLEDGMENTS

REFERENCES

1. Felgner, P.L., Gadek, T.R., Holm, M., Roman, R., Chan, H.W., Wenz, M., Northrop, J.P., Ringold, G.M., and Danielsen, M. (1987) Lipofection: A Highly Efficient, Lipid-Mediated DNA-Transfection Procedure, *Proc. Natl. Acad. Sci. USA 84*, 7413–7417.
2. Miller, A.D. (1998) Cationic Liposomes for Gene Therapy, *Angew. Chem. Int. Ed. 37*, 1768–1785.
3. Zhang, S.B., Xu, Y.M., Wang, B., Qiao, W.H., Liu, D.L., and Li, Z.S. (2004) Cationic Compounds Used in Lipoplexes and Polyplexes for Gene Delivery, *J. Controlled Release 100*, 165–180.
4. Leventis, R., and Silvius, J.R. (1990) Interactions of Mammalian Cells with Lipid Dispersions Containing Novel Metabolizable Cationic Amphiphiles, *Biochim. Biophys. Acta 1023*, 124–132.
5. Bennett, M.J., Malone, R.W., and Nantz, M.H. (1995) A Flexible Approach to Synthetic Lipid Ammonium Salts for Polynucleotide Transfection, *Tetrahedron Lett. 36*, 2207–2210.
6. Kikuchi, I.S., and Carmona-Ribeiro, A.M. (2000) Interactions Between DNA and Synthetic Cationic Liposomes, *J. Phys. Chem. B 104*, 2829–2835.
7. Kim, A., Lee, E.H., Choi, S.H., and Kim, C.K. (2004) *In vitro* and *in vivo* Transfection Efficiency of a Novel Ultradeformable Cationic Liposome, *Biomaterials 25*, 305–313.
8. Gao, X., and Huang, L. (1991) A Novel Cationic Liposome Reagent for Efficient Transfection of Mammalian Cells, *Biochem. Biophys. Res. Commun. 179*, 280–285.
9. Bottega, R., and Epand. R.M. (1992) Inhibition of Protein Kinase C by Cationic Amphiphiles, *Biochemistry 31*, 9025–9030.
10. Walker, S., Sofia, M.J., Kakarla, R., Kogan, N.A., Wierichs, L., Longley, C.B., Bruker, K., Axelrod, H.R., Midha, S., Babu, S., and Kahne, D. (1996) Cationic Facial Amphiphiles: A Promising Class of Transfection Agents, *Proc. Natl. Acad. Sci. USA 93*, 1585–1590.
11. Smith, A.E. (1995) Viral Vectors in Gene Therapy, *Annu. Rev. Microbiol. 4*, 807–838.
12. Smith, L.C., Duguid, J., Wadhwa, M.S., Logan, M.J., Tung, C.H., Edwards, V., and Sparrow, J.T. (1998) Synthetic Peptide-based DNA Complexes for Nonviral Gene Delivery, *Adv. Drug Deliv. Rev. 30*, 115–131.
13. Rittner, K., Benavente, A., Bompard-Sorlet, A., Heitz, F., Divita, G., Brasseur, R., and Jacobs, E. (2002) New Basic, Membrane-Destabilizing Peptides for Plasmid-based Gene Delivery *in vitro* and *in vivo*, *Mol. Ther. 5*, 104–114.
14. El-Aneed, A. (2004) An Overview of Current Delivery Systems in Cancer Gene Therapy, *J. Controlled Release 94*, 1–14.
15. Boussif, O., Lezoualc'h, F., Zanta, M.A., Mergny, M.D., Scherman, D., Demeneix, B., and Behr, J.P. (1995) A Novel, Versatile Vector for Gene and Oligonucleotide Transfer into Cells in Culture and *in vivo*: Polyethylenimine, *Proc. Natl. Acad. Sci. USA 92*, 7297–7301.
16. Lampela, P., Elomaa, M., Ruponen, M., Urtti, A., Männistö, P.T., and Raasmaja, A. (2003) Different Synergistic Roles of Small Polyethylenimine and Dosper in Gene Delivery, *J. Controlled Release 88*, 173–183.
17. Wu, G.Y., and Wu, C.H. (1987) Receptor Mediated *in vitro* Gene Transformation by a Soluble DNA Carrier System, *J. Biol. Chem. 262*, 4429–4432.
18. Ward, C.M., Pechar, M., Oupicky, D., Ulbrich, K., and Seymour, L.W. (2002) Modification of pLL/DNA Complexes with a Multivalent Hydrophilic Polymer Permits Folate-Mediated Targeting *in vitro* and Prolonged Plasma Circulation *in vivo*, *J. Gene Med. 4*, 536–547.
19. Hood, J.D., Bednarski, M., Frausto, R., Guccione, S., Reisfeld, R.A., Xiang, R., and Cheresh, D.A. (2002) Tumor Regression by Targeted Gene Delivery to the Neovasculature, *Science 296*, 2404–2407.
20. Cavazzana-Calvo, M., Thrasher, A., and Mavilio, F. (2004) The Future of Gene Therapy, *Nature 427*, 779–781.
21. Liu, D.L., Hu, J.J., Qiao, W.H., Li, Z.S., Zhang, S.B., and Cheng, L.B. (2005) Synthesis of Carbamate-Linked Lipids for Gene Delivery, *Bioorg. Med. Chem. Lett. 15*, 3147–3150.
22. Kokotos, G., Verger, R., and Chiou, A. (2000) Synthesis of 2-Oxo Amide Triacylglycerol Analogues and Study of Their Inhibition Effect on Pancreatic and Gastric Lipases, *Chem. Eur. J. 6*, 4211–4217.

23. Boomer, J.A., and Thompson, D.H. (1999) Synthesis of Acid-Labile Diplasmenyl Lipids for Drug and Gene Delivery Applications, *Chem. Phys. Lipids 99*, 145–153.

24. Boomer, J.A., Thompson, D.H., and Sullivan, S.M. (2002) Formation of Plasmid-based Transfection Complexes with an Acid-Labile Cationic Lipid: Characterization of *in vitro* and *in vivo* Gene Transfer, *Pharm. Res. 19*, 1292–1301.

25. Bangham, A.D., Standish, M.M., and Watkins, J.C. (1965) Diffusion of Univalent Ions Across the Lamellae of Swollen Phospholipids, *J. Mol. Biol. 13*, 238–253.

26. Rider, T.H., and Hill, A.J. (1930) Studies of Glycidol. I. Preparation from Glycerol Monochlorohydrin, *J. Am. Chem. Soc. 52*, 1521–1527.

27. National Institute of Advanced Industrial Science and Technology (AIST), Spectral Database for Organic Compounds, SDBS, http://www.aist.go.jp/RIODB/SDBS/cgi-bin/direct_frame_top.cgi?lang=eng (accessed July, 2005).

28. Ruth, J.M., and Philippe, R.J. (1966) Mass Spectra of Isocyanates, *Anal. Chem. 38*, 720–723.

29. Alquist, F.N., and Slagh, H.R. (1939) Manufacture of 1-Dimethylamino-2,3-propanediol, U.S. Patent 2,147,226.

30. Chinese Statistics Society (1985) *Orthogonal Test and Thrice Design,* pp. 1–100, Science Press, Beijing (in Chinese).

31. Chen, Y. (1981) *Organic Analysis,* pp. 713–716, Higher Education Press, Beijing (in Chinese).

32. Cotarca, L., Delogu, P., Nardelli, A., and Šunjić, V. (1996) Bis(trichloromethyl) Carbonate in Organic Synthesis, *Synthesis 5*, 553–576.

33. Wang, X.Z., Li, X.Q., Shao, X.B., Zhao, X., Deng, P., Jiang, X.K., Li, Z.T., and Chen, Y.Q. (2003) Selective Rearrangements of Quadruply Hydrogen-Bonded Dimer Driven by Donor–Acceptor Interaction, *Chem. Eur. J. 9*, 2904–2913.

34. Moniruzzaman, M., Goodbrand, B., and Sundararajan, P.R. (2003) Morphology and Thermal Behavior of Self-Assembling Carbamates, *J. Phys. Chem. B 107*, 8416–8423.

35. Feitosa, E., Barreleiro, P.C.A., and Olofsson, G. (2000) Phase Transition in Dioctadecyldimethylammonium Bromide and Chloride Vesicles Prepared by Different Methods, *Chem. Phys. Lipids 105*, 201–213.

36. Feitosa, E., and Brown, W. (1997) Fragment and Vesicle Structures in Sonicated Dispersions of Dioctadecyldimethylammonium Bromide, *Langmuir 13*, 4810–4816.

37. Cuccovia, I.M., Sesso, A., Abuin, E.B., Okino, P.F., Tavares, P.G., Campos, J.F.S., Florenzano, F.H., and Chaimovich, H. (1997) Characterization of Dioctadecyldimethylammonium Chloride Vesicles Prepared by Membrane Extrusion and Dichloromethane Injection, *J. Mol. Liq. 72*, 323–336.

38. Uchegbu, I.F., and Vyas, S.P. (1998) Non-ionic Surfactant Based Vesicles (niosomes) in Drug Delivery, *Int. J. Pharm. 172*, 33–70.

39. Basu, R., De, S., and Nandy, P. (1998) Effect of *n*-Decane on Lecithin Phase Transition Temperatures: A Microscopic Study, *Colloids Surf. B: Biointerfaces 11*, 29–31.

40. Hata, T., Matsuki, H., and Kaneshina, S. (2000) Effect of Local Anesthetics on the Phase Transition Temperatures of Ether- and Ester-Linked Phospholipid Bilayer Membranes, *Colloids Surf. B: Biointerfaces 18*, 41–50.

41. Uchegbu, I.F., Schätzlein, A., and Florence, A.T. (1996) Non-ionic Surfactant Vesicle (niosome) Phase Transitions, *Eur. J. Pharm. Sci. 4* (Suppl. 1), S138.

42. Uchegbu, I.F., and Florence, A.T. (1995) Non-ionic Surfactant Vesicles (niosomes): Physical and Pharmaceutical Chemistry, *Adv. Colloid Interface Sci. 58*, 1–55.

43. Harris, J.R., Roos, C., Djalali, R., Rheingans, O., Maskos, M., and Schmidt, M. (1999) *Micron 30*, 289–298.

Antioxidant Activity of Various Teas Against Free Radicals and LDL Oxidation

Reiko Ohmori[a,*], **Tamami Iwamoto**[b], **Motomi Tago**[b], **Tadakazu Takeo**[c],
Tomonori Unno[c], **Hiroshige Itakura**[d], **and Kazuo Kondo**[b]

[a]First Department of Internal Medicine, National Defense Medical College, Tokorozawa, Saitama 359-8513,
[b]Institute of Environmental Science for Human Life, Ochanomizu University, Bunkyo-ku, Tokyo 112-0012,
[c]Center Research Institute, Itoen Ltd., Haibara-gun, Shizuoka 421-0516, and
[d]Department of Life Sciences, Ibaraki Christian University, Hitachi-shi, Ibaraki 319-1221, Japan.

ABSTRACT: Tea is a widely consumed beverage throughout the world. We assessed the antioxidant activity of six teas, including the aqueous extracts of green tea and oolong tea (*Camellia sinensis*), tochu (*Eucommia ulmoides*), *Gymnema sylvestre*, Japanese mugwort (*Artemisia princeps*), and barley (*Hordeum vulgare*), against 1,1-diphenyl-2-picrylhydrazyl (DPPH) radicals and LDL oxidation, and examined the association of LDL oxidizability with the plasma catechin levels in 10 healthy volunteers with a single dose of 5 g green tea powder. *In vitro*, the inhibitory effects of DPPH radicals and LDL oxidation were found to be strongest in the extract of green tea and weakest in that of barley. After the ingestion of green tea powder, the lag time increased from basal 52.2 ± 4.1 to 60.3 ± 4.2 min at 1 h and 59.5 ± 4.1 min at 2 h, and then returned to the baseline lag time (51.9 ± 1.4 at 4 h and 52.1 ± 4.7 min at 6 h). Regarding the plasma catechin levels, epigallocatechingallate and epicatechingallate significantly increased from basal 3.7 ± 1.3 and 0.8 ± 0.8 ng/mL to 65.7 ± 11.6 and 54.6 ± 12.6 ng/mL at 1 h, and 74.4 ± 18.6 and 49.4 ± 7.1 ng/mL at 2 h, respectively. Green tea therefore showed the strongest antioxidant activity among the six different teas, and the inhibitory effects of green tea on LDL oxidation depended on the plasma catechin levels.

Paper no. L9601 in *Lipids 40,* 849–853 (August 2005).

Oxidized LDL is considered to be an important factor in the atherogenic progression of coronary artery disease (CAD) (1). Oxidized LDL can attract monocytes into the arterial wall where they can be transformed into macrophages—the precursors of foam cells—thus leading to the formation of early atherosclerotic lesions (2,3). As a result, protecting LDL against oxidation is assumed to be a useful therapy for the prevention of atherogenic disease.

Regnstrom *et al.* (4) suggested that LDL oxidizability was associated with the severity of coronary atherosclerosis. *In vitro*, LDL oxidation occurs in three phases: a lag phase, a propagation phase, and a decomposition phase. During the lag phase, endogenous LDL antioxidants are consumed (5). The

consumption of antioxidant foods such as flavonoids and soyfoods has been reported to be associated with either an elevated resistance of LDL to oxidation or a reduced CAD mortality (6,7).

Green tea and oolong tea, which inhibit LDL oxidation *in vitro* (8,9), are manufactured from the same plant species, *Camellia sinensis*. However, the antioxidant effects of the extracts from other plants on LDL oxidation have not yet been investigated. We assessed the antioxidant activity of six teas, consisting of the aqueous extracts of green tea and oolong tea (*C. sinensis*), tochu (*Eucommia ulmoides*), *Gymnema sylvestre*, Japanese mugwort (*Artemisia princeps*), and barley (*Hordeum vulgare* L.), against 1,1-diphenyl-2-picrylhydrazyl (DPPH) radicals; their effects on LDL oxidizability; and the inhibitory effect of green tea on LDL oxidation in 10 healthy volunteers.

MATERIALS AND METHODS

Tea preparations. Six teas, including aqueous extracts of green tea and oolong tea (*C. sinensis*), tochu (*E. ulmoides*), *G. sylvestre*, Japanese mugwort (*A. princeps*) and barley (*H. vulgare*), were prepared by infusing either 6 g (DPPH radicals test) or 1 g (LDL oxidizability test) of each commercially available tea for 1 min at 80°C in 100 mL of water.

Free radical-scavenging activity. The free radical-scavenging activity was determined using DPPH (Wako Pure Chemical Industries, Osaka, Japan). An aliquot of each tea was mixed with 2 mL of 0.1 mM DPPH in ethanol. Following incubation for 20 min at 37°C, the absorbance was measured at 516 nm with a Beckman Model DU 650 spectrophotometer. The volume of each tea required to cause a 50% decrease in the absorbance at 516 nm relative to the control was then calculated.

Isolation and preparation of LDL. Blood samples were collected in sodium EDTA-containing tubes from fasting normolipidemic volunteers after obtaining their informed consent. Plasma samples were immediately prepared by centrifugation at $2,000 \times g$ for 10 min at 4°C. The LDL was separated by single-spin density gradient ultracentrifugation ($417,000 \times g$, 40 min, 4°C) using a TLA-100.4 fixed angle-rotor (Beckman Instruments, Fullerton, CA) (10). The LDL protein concentration was determined using a Micro BCA Protein Assay Kit (Pierce Laboratories, Rockford, IL). Before the start of the oxidation

---

experiments, the LDL samples were diluted with PBS to give a final concentration of 70 µg/mL LDL protein.

Measurement of LDL oxidizability. The LDL oxidizability was measured according to the method described in our previous report (11). The prepared LDL samples were oxidized with or without 5 µL of each tea or 50–400 ng/mL of green tea extract by 400 µM 2,2′-azobis(4-methoxy-2,4-dimethylvaleronitrile) (AMVN-CH$_3$O; Wako Pure Chemical Industries), which was an oxidative inducer. The kinetics of LDL oxidation were obtained by monitoring the absorbance of conjugated dienes at 234 nm with a Beckman Model DU 650 spectrophotometer at 4 min intervals at 37°C. The lag time of lipid peroxidation is defined as the time interval between the initiation and the intercept of the two tangents drawn to the lag and propagation phase of the absorbance curve at 234 nm, and it was expressed in minutes. All steps in the experiments investigating LDL oxidation were quickly performed on ice by the same laboratory assistant to minimize the loss of antioxidants in LDL.

Clinical study. Our study subjects were 5 male and 5 female healthy volunteers, ranging from 20 to 22 yr of age, whose body mass index was 20 ± 2 (kg/m^2); none of them took any medications, vitamin supplements, or special dietary additives. This study was approved by our ethics committee. All subjects gave their informed consent to participate in the study. We asked all the subjects not to consume any kinds of tea, wine, citrus fruit juices, or supplements for 3 d before the experimental day. After over 12 h of fasting, blood samples were collected between 8:00 and 9:00 A.M. Subjects then ingested 5 g of green tea powder dissolved in 150 mL of hot water over a period of 10 min. The green tea powder contained 3.20 wt% of epigallocatechingallate (EGCg), 0.96 wt% of epicatechingallate (ECg), 0.49 wt% of epicatechin (EC), and 3.81 wt% of caffeine. Plasma samples were taken at baseline, and 1, 2, 4, and 6 h after the green tea powder had been consumed; they were then either analyzed immediately or stored at −20°C until analysis. Of the 10 healthy volunteers, blood samples obtained from the five males were used for an analysis of the plasma catechin levels, because the five females did not agree to give blood samples for the catechin analysis. The analysis of plasma catechin levels was the same as that described in our previous report (12). Briefly, chloroform with ethyl gallate was added to plasma

samples as an internal standard, and sample fractions containing catechins were purified by solid-phase extraction using Bond Elut cartridges (Varian, Harbor City, CA). An analysis of the catechin levels was performed by HPLC with an electrochemical detector.

Statistical analysis. The results are expressed as the mean values ± SEM. The precision of the DPPH radical test and LDL oxidizability was tested before the start of this study. In the DPPH test, the mean ± SD (µL) of 0.9 mg/mL catechin required to cause a 50% decrease in the absorbance at 516 nm relative to the control ($n = 5$) was 7.49 ± 0.66. The CV was 8.8%. In the analysis of LDL oxidizability, the mean ± SD (min) of plasma samples A ($n = 4$) and B ($n = 5$), collected from subjects A and B, respectively, was 41.8 ± 1.6 and 87.8 ± 1.6, respectively. The CV for samples A and B was 3.8 and 1.8%, respectively. The mean ± SD (min) of the lag time for plasma samples C and D (collected from subjects A and B, respectively, and stored at 4°C until analysis), which was measured once a day for 3 d, was 51.4 ± 1.4 and 84.5 ± 1.4, respectively. The CV for samples C and D was 2.8 and 1.6% in an interassay, respectively. Any significant differences in the clinical study were evaluated by a repeated-measures ANOVA and the *post hoc* test (Scheffe test), and a *P* value of <0.05 was considered to be statistically significant.

RESULTS AND DISCUSSION

Antioxidant activity of various teas and green tea extracts. A number of studies on the antioxidant effects of green tea and oolong tea have been reported (8,9,13,14), although the antioxidant effects of teas brewed from other plants have not yet been sufficiently investigated. The present study elucidated the antioxidant activity of various teas regarding DPPH radicals and LDL oxidation. The results of the DPPH radical scavenging activity of various teas are shown in Table 1. Green tea and oolong tea required 1.9 and 5.1 µL, respectively, for scavenging 50% of the DPPH radicals. These teas showed a remarkably higher scavenging activity than the extracts of other plants. Among the teas tested, barley tea was the weakest scavenger and required 119.8 µL, which was several dozen times higher than for green tea and oolong tea.

TABLE 1
Antioxidant Activity of Various Teas

	DPPH test (µL)	LDL oxidizability	
		Lag time (min)[a,b]	Oxidation rate (nmol conjugated diene/ min/mg LDL protein)[a]
Control		21.2 (1.0)	10.3
Green tea	1.9	201.8 (9.9)	3.7
Oolong tea	5.1	62.3 (2.8)	8.4
Tochu tea	21.2	62.4 (2.8)	8.3
Gymnema sylvestre tea	32.1	40.2 (1.8)	11.1
Japanese mugwort tea	35.6	38.7 (1.8)	11.8
Barley tea	119.8	23.5 (1.1)	12.9

[a]Five microliters of each tea was added to the LDL solution (70 µg/mL of LDL protein).
[b]The prolongation rate of the lag time relative to the control is shown in parentheses.

TABLE 2
Dose–Response Effect of Green Tea Components on LDL Oxidizability[a]

Amount added	EC		ECg		EGCg	
(ng/mL)	Lag time (min)	μM	Lag time (min)	μM	Lag time (min)	μM
0	47.2 ± 1.2	0	36.7 ± 0.9	0	32.1 ± 0.8	0
50	78.9 ± 2.0	0.17	39.5 ± 1.0	0.11	37.9 ± 0.9	0.11
100	102.4 ± 2.6	0.34	46.7 ± 1.2	0.23	42.6 ± 1.1	0.22
200	161.8 ± 4.0	0.68	78.7 ± 2.0	0.45	58.2 ± 1.5	0.44
400	186.6 ± 4.7	1.38	118.7 ± 3.0	0.90	88.1 ± 2.2	0.87

[a]The results are expressed as the mean ± SEM ($n = 3$). The M.W. of epicatechin (EC), epicatechingallate (ECg), and epigallocatechin-3-gallate (EGCg) are 290.3, 442.4, and 458.4, respectively.

The inhibitory effects of various teas for LDL oxidation induced by $AMVN\text{-}CH_3O$ are also shown in Table 1. Compared with the control, green tea was the most effective for both the prolongation rate of the lag time (9.9-fold) and the oxidation rate (3.7 nmol conjugated diene/min/mg LDL protein). The inhibitory effects of LDL oxidation were similar for oolong tea and tochu tea as well as for *G. sylvestre* tea and Japanese mugwort tea. Barley tea had the weakest antioxidant activity for LDL oxidation among all the teas used in this experiment. The antioxidant effects of green tea extract components, which are EC, ECg, and EGCg, on LDL oxidation are shown in Table 2. Each catechin prolonged the lag time of LDL oxidation in a dose-dependent manner *in vitro*.

Green tea showed the strongest antioxidant activity among the six teas in both experiments. Herbs such as tochu, *G. sylvestre*, and Japanese mugwort have been widely used as folk medicines for several diseases. Tochu has been considered to have antimutagenicity (15,16), a preventive effect against oxidative gastric injury (17), and an antihypertensive action (18). Tochu tea has an inhibitory effect against LDL oxidation, which was as strong as that for oolong tea in the present study. The scavenging activity of tochu tea on reactive oxygen species correlated with its protocatechuic acid content (19). This substance was not evaluated in our study, but it might also help prevent LDL oxidation. *G. sylvestre* has been used in Indian traditional medicine and as a health food in tea bags and beverages in Japan. Several reports on its pharmacological action showed antihyperglycemic (20) and antidiabetic (21) effects, and these actions might be due to its ability to suppress glucose absorption from the intestinal tract (22). Japanese mugwort is associated with anticoagulation (23), the proliferation of endothelial cells (24), and the inhibition of protein fragmentation damage (25). The antioxidant effects of *G. sylvestre* and Japanese mugwort were moderately strong among the six teas analyzed for this paper. Our study is the first report on the antioxidant ability of *G. sylvestre* and Japanese mugwort. We measured the polyphenol and EGCg content of green and oolong teas, which had the strongest antioxidant activity among all the tested teas. The polyphenol contents of green and oolong tea were 1.4 ± 0.1 and 0.4 ± 0.03 mg/mL, respectively, whereas the EGCg contents of green and oolong tea were 317 ± 29 and 57 ± 6 μg/mL, respectively. Our previous reports showed a positive correlation between the polyphenol content and the antioxidant activities, which are the DPPH radical scavenging activity or the prolongation rate of LDL oxidation-lag time, in vegetables (26).

Clinical trial. Ten subjects consumed green tea, which had the strongest antioxidant activity among the six teas. After ingesting 5 g of green tea powder, the lag time increased from a basal time of 52.2 ± 4.1 to 60.3 ± 4.2 min at 1 h and 59.5 ± 4.1 min at 2 h, and then returned to the baseline lag time (51.9 ± 1.4 min at 4 h and 52.1 ± 4.7 min at 6 h) but these changes did not reach statistical significance (Fig. 1). Of 10 subjects, 5 subjects had the longest lag time at 1 h after the ingestion; the lag time of the other 5 subjects showed a peak at 2 h (Table 3).

Regarding the plasma catechin levels after the consumption of green tea powder, EGCg and ECg significantly increased from a basal value of 3.7 ± 1.3 and 0.8 ± 0.8 ng/mL to 65.7 ± 11.6 and 54.6 ± 12.6 ng/mL at 1 h, and 74.4 ± 18.6 and 49.4 ± 7.1 ng/mL at 2 h, respectively (Fig. 2). Green tea increased the lag time of LDL oxidation after 1 and 2 h, which was related to an increase in the plasma catechin levels. However, we could not find any significant correlation within each individual person between the plasma catechin levels and the lag time of LDL oxidation at different times. No significant increase was seen in the plasma levels of β-carotene, vitamin E, vitamin C, and uric acid. Regarding the effects of small increases in flavonoids on LDL oxidation, Nakagawa *et al.* (27) reported results similar to ours. Plasma EGCg levels slightly increased
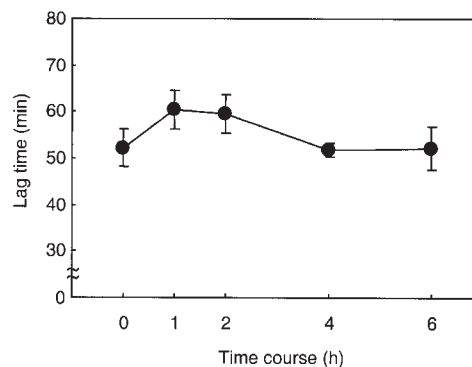
FIG. 1. The lag time in 2,2′-azobis(4-methoxy-2,4-dimethylvaleronitrile)-induced LDL oxidation after the consumption of green tea powder in 10 healthy volunteers.

TABLE 3
The LDL Oxidation-Lag Time (min) After the Consumption of Green Tea Powder in 10 Subjects[a]

Subjects	0 h	1 h	2 h	4 h	6 h
1	44.5	56.1	47.7	50.5	52.8
2	55.9	53.6	56.8	52.6	54.2
3	54.8	58.9	52.3	47.8	52.8
4	50.3	54.8	51.7	50.7	42.1
5	53.7	57.5	58.2	54.6	−
6	82.4	94.8	90.8	−	81.6
7	45.0	48.6	46.4	43.7	38.1
8	43.7	53.4	61.5	57.7	48.4
9	58.0	68.5	69.0	56.3	−
10	33.5	56.7	60.9	53.0	47.1

[a]Subjects 1–5 are male and 6–10 are female.

to 267 pmol/mL, although the plasma PC hydroperoxide levels decreased by half after 60 min with a single oral intake of green tea extract tablet containing 254 mg catechins. In our study, the plasma EGCg levels increased to 74.4 ng/mL (162 pmol/mL) 2 h after the intake of green tea containing 160 mg catechins. In an *in vitro* study, we showed that 50 and 100 ng/mL of EGCg prolonged the lag time by 5.8 and 10.5 min, respectively, and 50 ng/mL of ECg prolonged the lag time by 2.8 min (Table 2). The catechin level found in plasma clearly prolonged the LDL oxidation lag time *in vitro*. It is important to elucidate the fact that catechins are responsible for the increase in the measured lag times. However, we did not measure the catechins in the LDL fraction. An additional experiment is thus called for to clarify the correlation between catechins and LDL fractions. Green tea is well known to be a strong antioxidant beverage (8), due to its catechin content (28). Unno *et al.* (12) showed that the serum catechin level reaches its highest level at approximately 2 h after the ingestion of green tea. Our results for the peak catechin level were thus compatible with theirs. The physiological function of green tea has been studied in animals and in humans (13,14), although few studies determined the plasma catechin level. The plasma or serum catechin level as well as the serum antioxidants such as vitamin E and vitamin C should be analyzed in a future study of green tea intake. Such a study

will allow us to estimate more exactly the physiological and pharmacological action of the green tea component. Regarding the limitations of this study, it was not a placebo-controlled study. To clarify the effects of green tea on LDL oxidation, a further study should be done using a placebo-controlled study in a larger population.

The findings of previous studies confirmed that the French paradox, which is a high intake of dietary fat but low mortality from CAD, may be attributable in part to high wine consumption (29–31). The smoking rate of Japanese males (52.8%) is very high in comparison with that of other industrialized countries such as the United Kingdom (27%) and the United States of America (25.7%) (32), although the mortality rate from CAD is much lower in Japan than in the United States and the United Kingdom (33). We therefore hypothesize that the daily consumption of green tea by Japanese might be an important clue to help elucidate the reason for the "Japanese paradox" regarding CAD.

ACKNOWLEDGMENT

REFERENCES

1. Steinberg, D., Parthasarathy, S., Carew, T.E., Khoo, J.C., and Witztum, J.L. (1989) Beyond Cholesterol. Modifications of Low-Density Lipoprotein That Increase Its Atherogenicity, *N. Engl. J. Med. 320*, 915–924.
2. Fogelman, A.M., Shechter, I., Seager, J., Hokom, M., Child, J.S., and Edwards, P.A. (1980) Malondialdehyde Alteration of Low Density Lipoproteins Leads to Cholesteryl Ester Accumulation in Human Monocyte-Macrophages, *Proc. Natl. Acad. Sci. USA 77*, 2214–2218.
3. Rosenfeld, M.E., Khoo, J.C., Miller, E., Parthasarathy, S., Palinski, W., and Witztum, J.L. (1991) Macrophage-Derived Foam Cells Freshly Isolated from Rabbit Atherosclerotic Lesions Degrade Modified Lipoproteins, Promote Oxidation of Low-Density Lipoproteins, and Contain Oxidation-Specific Lipid-Protein Adducts, *J. Clin. Invest. 87*, 90–99.
4. Regnstrom, J., Nilsson, J., Tornvall, P., Landou, C., and Hamsten, A. (1992) Susceptibility to Low-Density Lipoprotein Oxidation and Coronary Atherosclerosis in Man, *Lancet 339*, 1183–1186.
5. Esterbauer, H., Jurgens, G., Quehenberger, O., and Koller, E. (1987) Autoxidation of Human Low Density Lipoprotein: Loss
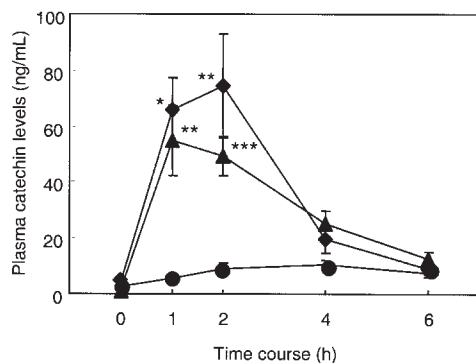
FIG. 2. Plasma catechin levels in five subjects after the consumption of green tea powder. ***, $P < 0.001$; **, $P < 0.005$; *, $P < 0.05$ based on the findings of the Scheffe test compared with the control. ◆, Epigallocatechingallate (EGCg); ▲, epicatechingallate (ECg); ●, epicatechin (EC).

of Polyunsaturated Fatty Acids and Vitamin E and Generation of Aldehydes, *J. Lipid Res. 28*, 495–509.

6. Hertog, M.G., Feskens, E.J., Hollman, P.C., Katan, M.B., and Kromhout, D. (1993) Dietary Antioxidant Flavonoids and Risk of Coronary Heart Disease: The Zutphen Elderly Study, *Lancet 342*, 1007–1011.

7. Tikkanen, M.J., Wahala, K., Ojala, S., Vihma, V., and Adlercreutz, H. (1998) Effect of Soybean Phytoestrogen Intake on Low Density Lipoprotein Oxidation Resistance, *Proc. Natl. Acad. Sci. USA 95*, 3106–3110.

8. Luo, M., Kannar, K., Wahlqvist, M.L., and O'Brien, R.C. (1997) Inhibition of LDL Oxidation by Green Tea Extract, *Lancet 349*, 360–361.

9. Kurihara, H., Fukami, H., Toyoda, Y., Kageyama, N., Tsuruoka, N., Shibata, H., Kiso, Y., and Tanaka, T. (2003) Inhibitory Effect of Oolong Tea on the Oxidative State of Low Density Lipoprotein (LDL), *Biol. Pharm. Bull. 26*, 739–742.

10. Chung, B.H., Segrest, J.P., Ray, M.J., Brunzell, J.D., Hokanson, J.E., Krauss, R.M., Beaudrie, K., and Cone, J.T. (1986) Single Vertical Spin Density Gradient Ultracentrifugation, *Methods Enzymol. 128*, 181–209.

11. Hirano, R., Kondo, K., Iwamoto, T., Igarashi, O., and Itakura, H. (1997) Effects of Antioxidants on the Oxidative Susceptibility of Low-Density Lipoprotein, *J. Nutr. Sci. Vitaminol. (Tokyo) 43*, 435–444.

12. Unno, T., Kondo, K., Itakura, H., and Takeo, T. (1996) Analysis of (−)-Epigallocatechin Gallate in Human Serum Obtained Ffter Ingesting Green Tea, *Biosci. Biotechnol. Biochem. 60*, 2066–2068.

13. Tijburg, L.B., Wiseman, S.A., Meijer, G.W., and Weststrate, J.A. (1997) Effects of Green Tea, Black Tea and Dietary Lipophilic Antioxidants on LDL Oxidizability and Atherosclerosis in Hypercholesterolaemic Rabbits, *Atherosclerosis 135*, 37–47.

14. Princen, H.M., van Duyvenvoorde, W., Buytenhek, R., Blonk, C., Tijburg, L.B., Langius, J.A., Meinders, A.E., and Pijl, H. (1998) No Effect of Consumption of Green and Black Tea on Plasma Lipid and Antioxidant Levels and on LDL Oxidation in Smokers, *Arterioscler. Thromb. Vasc. Biol. 18*, 833–841.

15. Nakamura, T., Nakazawa, Y., Onizuka, S., Satoh, S., Chiba, A., Sekihashi, K., Miura, A., Yasugahira, N., and Sasaki, Y.F. (1997) Antimutagenicity of Tochu Tea (an Aqueous Extract of *Eucommia* ulmoides Leaves): 1. The Clastogen-Suppressing Effects of Tochu Tea in CHO Cells and Mice, *Mutat. Res. 388*, 7–20.

16. Li, Y., Metori, K., Koike, K., Kita, F., Che, Q.M., Sato, T., Shirai, W., and Takahashi, S. (2000) Granuloma Maturation in the Rat is Advanced by the Oral Administration of *Eucommia ulmoides* Oliver Leaf, *Biol. Pharm. Bull. 23*, 60–65.

17. Yang, J., Kato, K., Noguchi, K., Dairaku, N., Koike, T., Iijima, K., Imatani, A., Sekine, H., Ohara, S., Sasano, H., *et al.* (2003) Tochu (*Eucommia lmoides*) Leaf Extract Prevents Ammonia and Vitamin C Deficiency Induced Gastric Mucosal Injury, *Life Sci. 73*, 3245–3256.

18. Kwan, C.Y., Chen, C.X., Deyama, T., and Nishibe, S. (2003) Endothelium-Dependent Vasorelaxant Effects of the Aqueous Extracts of the *Eucommia ulmoides* Oliv. Leaf and Bark: Implications on Their Antihypertensive Action, *Vascul. Pharmacol. 40*, 229–235.

19. Yen, G.C., and Hsieh, C.L. (2000) Reactive Oxygen Species Scavenging Activity of Du-Zhong (*Eucommia ulmoides* Oliv.) and Its Active Compounds, *J. Agric. Food Chem. 48*, 3431–3436.

20. Sugihara, Y., Nojima, H., Matsuda, H., Murakami, T., Yoshikawa, M., and Kimura, I. (2000) Antihyperglycemic Effects of Gymnemic Acid IV, a Compound Derived from *Gymnema sylvestre* Leaves in Streptozotocin-Diabetic Mice, *J. Asian Nat. Prod. Res. 2*, 321–327.

21. Baskaran, K., Kizar Ahamath, B., Radha Shanmugasundaram, K., and Shanmugasundaram, E.R. (1990) Antidiabetic Effect of a Leaf Extract from *Gymnema sylvestre* in Non-Insulin-Dependent Diabetes Mellitus Patients, *J. Ethnopharmacol. 30*, 295–300.

22. Shimizu, K., Iino, A., Nakajima, J., Tanaka, K., Nakajyo, S., Urakawa, N., Atsuchi, M., Wada, T., and Yamashita, C. (1997) Suppression of Glucose Absorption by Some Fractions Extracted from *Gymnema sylvestre* Leaves, *J. Vet. Med. Sci. 59*, 245–251.

23. Hayashi, T., Hayakawa, Y., Hayashi, T., Sasaki, H., and Sakuragawa, N. (1997) Sulfated Polysaccharide from the Leaves of *Artemisia princeps* Activates Heparin Cofactor II Independently of the Lys173 and Arg189 Residues of Heparin Cofactor II, *Thromb. Res. 87*, 105–112.

24. Kaji, T., Kaga, K., Miezi, N., Ejiri, N., and Sakuragawa, N. (1990) A Stimulatory Effect of Artemisia Leaf Extract on the Proliferation of Cultured Endothelial Cells, *Chem. Pharm. Bull. (Tokyo) 38*, 538–540.

25. Toda, S. (2004) Inhibitory Effects of Polyphenols in Leaves of *Artemisia princeps* PAMP on Protein Fragmentation by Cu(II)-H_2O_2 *in vitro*, *J. Med. Food 7*, 52–54.

26. Thu, N.N., Sakurai, C., Uto, H., Van Chuyen, N., Lien Do, T.K., Yamamoto, S., Ohmori, R., and Kondo, K. (2004) The Polyphenol Content and Antioxidant Activities of the Main Edible Vegetables in Northern Vietnam, *J. Nutr. Sci. Vitaminol. 50*, 203–210.

27. Nakagawa, K., Ninomiya, M., Okubo, T., Aoi, N., Juneja, L.R., Kim, M., Yamanaka, K., and Miyazawa, T. (1999) Tea Catechin Supplementation Increases Antioxidant Capacity and Prevents Phospholipid Hydroperoxidation in Plasma if Humans, *J. Agric. Food Chem. 47*, 3967–3973.

28. Miura, S., Watanabe, J., Tomita, T., Sano, M., and Tomita, I. (1994) The Inhibitory Effects of Tea Polyphenols (flavan-3-ol derivatives) on Cu^{2+} Mediated Oxidative Modification of Low Density Lipoprotein, *Biol. Pharm. Bull. 17*, 1567–1572.

29. Renaud, S., and de Lorgeril, M. (1992) Wine, Alcohol, Platelets, and the French Paradox for Coronary Heart Disease, *Lancet 339*, 1523–1526.

30. Frankel, E.N., Kanner, J., German, J.B., Parks, E., and Kinsella, J.E. (1993) Inhibition of Oxidation of Human Low-Density Lipoprotein by Phenolic Substances in Red Wine, *Lancet 341*, 454–457.

31. Criqui, M.H., and Ringel, B.L. (1994) Does Diet or Alcohol Explain the French Paradox? *Lancet 344*, 1719–1723.

32. World Health Organization (2002) *The Tobacco Atlas* (netlink: www.who.int/tobacco/statistics/tobacco_atlas/en/).

33. World Health Organization. (1989) *World Health Statistics Annual*, WHO, Geneva.

METHOD

A Rapid Method for the Quantification of Fatty Acids in Fats and Oils with Emphasis on *trans* Fatty Acids Using Fourier Transform Near Infrared Spectroscopy (FT-NIR)

Hormoz Azizian[a],* and John K.G. Kramer[b]

[a]NIR Technologies Inc., Oakville, Ontario, Canada, and [b]Food Research Program,
Agriculture and Agri-Food Canada, Guelph, Ontario, Canada

ABSTRACT: A rapid method was developed for classifying and quantifying the FA composition of edible oils and fats using Fourier Transform near infrared spectroscopy (FT-NIR). The FT-NIR spectra showed unique fingerprints for saturated FA, *cis* and *trans* monounsaturated FA, and all n-6 and n-3 PUFA within TAG to permit qualitative and quantitative comparisons of fats and oils. The quantitative models were based on incorporating accurate GC data of the different fats and oils and FT-NIR spectral information into the calibration model using chemometric analysis. FT-NIR classification models were developed based on chemometric analyses of 55 fats, oils, and fat/oil mixtures that were used in the identification of similar materials. This database was used to prepare three calibration models—one suitable for the analysis of common fats and oils with low levels of *trans* FA, and the other two for fats and oils with intermediate and high levels of *trans* FA. The FT-NIR method showed great potential to provide the complete FA composition of unknown fats and oils in minutes. Compared with the official GC method, the FT-NIR method analyzed fats and oils directly in their neat form and required no derivatization of the fats to volatile FAME, followed by time-consuming GC separations and analyses. The FT-NIR method also compared well with the official FTIR method using an attenuated total reflectance (ATR) cell; the latter provided only quantification of specific functional groups, such as the total *trans* FA content, whereas FT-NIR provided the complete FA profile. The FT-NIR method has the potential to be used for rapid screening and/or monitoring of fat products, *trans* FA determinations for regulatory labeling purposes, and detection of contaminants. The quantitative FT-NIR results for various edible oils and fats and their mixtures are presented based on the FT-NIR models developed.

Paper no. L9743 in *Lipids 40*, 855–867 (August 2005).

The intake of *trans* FA is known to be associated with higher risk factors for cardiovascular disease (1–3) and biomarkers of inflammation (4). The main sources of *trans* FA are industrially produced partially hydrogenated vegetable oils (PHVO) as well as milk and meat fats from ruminants. Minor amounts of

trans FA are thermally produced during commercial refining of vegetable oils (specifically deodorization) or domestic frying (5,6). Trace amounts of *trans* FA are found naturally in plant lipids (7). The *trans* FA isomers present in PHVO, heated vegetable oils, and ruminant fats consist mainly of mono-*trans* monoenoic, dienoic, and trienoic FA. Di-*trans* isomers of these FA are present in trace amounts. Industrial and ruminant fats generally contain the same *trans* FA isomers but differ mainly in their amounts and relative proportions (8–12). Differences in the *trans* FA isomer distribution among industrially produced fats depend on the catalyst and conditions used, whereas differences in ruminant fats depend on which supplements, if any, are fed and the amount of supplements fed, as well as on feeding practices. Since the *trans* FA isomers responsible for the negative effects have not been identified, it is difficult to assess whether the *trans* FA from PHVO and ruminant fats present similar risk factors (13,14). Therefore, it is becoming increasing important to analyze fat products using methods that provide the composition of all the different *trans* FA isomers.

In an effort to reduce the total *trans* FA content of food products, the governments of Canada (15,16), the United Sates (11,17), Argentina, Brazil, Paraguay, and Uruguay (18) have introduced, or are in the process of introducing, mandatory labeling of total isolated *trans* FA in commercially prepared food products; conjugated linoleic acids (CLA) are excluded from the total *trans* content. On the other hand, the government of Denmark has restricted the sale of all industrially produced fats and oils with more than 2% total *trans* FA, but has placed no restriction on the *trans* FA content from ruminant fats (19). For a more comprehensive review of *trans* regulations see Ratnayake and Zehaluk (16). The exclusion of CLA from mandatory labeling appears to be based on the evidence that CLA protects against cancer (20,21). However, by not specifying the CLA isomer, CLA isomers other than 9*cis*,11*trans*-CLA could be included, with undesirable health effects (22). In addition, 11*trans*-18:1 was not excluded from mandatory *trans* FA labeling even though it is the metabolic precursor to 9*cis*,11*trans*-CLA (23). Future regulation of *trans* FA may exclude both 9*cis*,11*trans*-CLA and 11*trans*-18:1 from mandatory labeling, as well as any other beneficial *trans* FA isomer. The availability of accurate and rapid methods to quantify the different CLA and *trans* FA isomers will be most helpful for implementing such new regulations.

At the present time, official methods are available for determining the total *trans* FA content based on chromatographic

---

and spectroscopic techniques (24–26). The official GC methods involve acid or base digestion of the test portion, extraction of the lipids with organic solvents, addition of an internal standard, acid- or base-catalyzed methylation to prepare FAME for GC analysis, and GC separation using 100-m highly polar fused-silica capillary columns [AOAC 994.15 (27); AOCS Ce 1f-96 (28)]. Despite the use of the highly efficient GC columns, there are still extensive overlaps of many *cis* and *trans* FA isomers, which require prior separation of the geometric FAME isomers by silver-ion TLC and GC analyses at low isothermal temperature conditions for their complete and unequivocal analysis (10,29,30).

The official IR methods for the quantification of *trans* FA involve FTIR spectroscopy in conjunction with an attenuated total reflectance (ATR) cell (24,31), i.e., method Cd 14d-99 from the AOCS (32) and method 2000.10 from the AOAC (33). The FTIR instruments have many advantages over the dispersive-based IR instruments outlined by Mossoba *et al.* (24) and more recently by Setiowaty and Che Man (34). The advantages include a better signal-to-noise ratio and better wavelength precision provided by an internal reference laser. Compared with the GC methods, the ATR-FTIR methods for oils and fats are rapid and require no prior derivatization or organic solvents, but the information is limited to measuring the total *trans* FA content greater than 5%, and no information is available on individual *trans* FA or other FA in the test portion. Furthermore, ATR-FTIR is not applicable if the test sample contains substances with absorption frequencies near that of the C–H deformation of isolated *trans* at 966 cm^{-1}. Conjugated FA with absorption frequencies near 986 and 950 cm^{-1} as well as FFA near 935 cm^{-1} pose a unique challenge for the analysis of total *trans* by ATR-FTIR (24,35). By contrast, GC easily resolves most of these *trans*-containing FA. Christy *et al.* (36) recently attempted to quantify isolated *trans* FA in the presence of CLA using the ATR-FTIR method by preparing calibration models for each of these two FA and using chemometrics. Despite obtaining rather reasonable results, the authors concluded that the resolution of *trans* FA and CLA might be too difficult using this approach. Milosevic *et al.* (37) reported better resolution of the closely associated IR absorption bands of *trans* FA by evaluating the second derivative of ATR-FTIR spectra.

There is an urgent need to develop a more versatile method that combines the speed of the ATR-FTIR method with the greater information available from the GC technique. It is not surprising that, to date, the GC method remains the method of choice despite its rather lengthy procedure.

The Fourier transform near infrared spectroscopy (FT-NIR) technique has many of the same advantages as ATR-FTIR, being rapid, nondestructive, performed directly on the fat or oil (neat), and requiring no chemical preparations. In addition, FT-NIR has the same advantages as FTIR over their respective dispersive-based spectrometries (24,34). Although it is not an official method of *trans* FA determination, FT-NIR has been evaluated for determination of the total *cis* and *trans* contents, iodine values, and saponification numbers of several fats and oils (38,39). Chemometric analysis was used because the FT-NIR absorption

spectra consist of broad and overlapping overtones of fundamental FTIR bands that cannot be resolved by means of traditional univariate analysis techniques. Chemometric techniques, such as partial least squares (PLS), have been applied to the NIR and FT-NIR spectra of products from the food, agricultural, pharmaceutical, medical, and plastics industries for quality control and assurance measurements (40). Two recent papers (41,42) have shown the application of NIR dispersive instruments in predicting the FA composition of olive oil and goose fatty liver with limited success. FT-NIR also has been used to measure oxidative changes in different food products (43). However, to our knowledge, the FT-NIR method has not been applied for determination of the FA composition of an oil or fat, including *trans* FA and CLA. Such an approach had not been attempted because of the assumption that the FT-NIR spectral information of FA present at low concentrations in a fat or oil is below the detection limit of that technique.

In the present communication we describe the development of FT-NIR models based on incorporating the FA composition of selected fats and oils obtained by GC and analyzing the data using chemometrics. The results are presented to show that the complete FA composition of a product can then be determined based on its FT-NIR spectrum and by applying appropriate FT-NIR models that were derived from accurate GC data obtained using 100-m highly polar fused-silica capillary columns. This new FT-NIR method would appear to be applicable for the rapid determination of individual *trans* FA and CLA isomers for regulatory purposes, for ensuring the quality of fats and oils during production, and for simultaneously providing the complete FA profile of fat and oil products. A patent application for this method was recently submitted (44).

MATERIALS AND METHODS

Several commercial vegetable oils (three canola oils, corn oil, two flax oils, olive oil, three soybean oils, five sunflower oils, and two walnut oils), seven margarines, two shortenings, lard, and two types of partially hydrogenated oil fractions (five from canola oil, and five from soybean oil) were used in the development of the reference model. Eighteen mixtures were gravimetrically prepared by combining specific fats and oils in different ratios. Triolein (glycerol tri9*cis*-octadecenoate), trielaidin (glycerol tri9*trans*-octadecenoate), trilinolein (glycerol tri9*cis*12*cis*-octadecadienoate), and trilinolenin (glycerol tri9*cis*12*cis*15*cis*-octadecatrienoate) were purchased from Nu-Chek-Prep Inc. (Elysian, MN). All chemicals and solvents were of analytical grade.

GC analysis. All fat and oil products and their mixtures (about 20 mg each) were methylated separately using anhydrous 5% HCl/methanol (w/w) for 1 h at 80°C, and a 0.5% solution of NaOCH$_3$ in methanol (#33080; Supelco Inc., Bellefonte, PA) for 15 min at 50°C. In each case, the resultant FAME were extracted with hexane after addition of water (5% by vol). Hexane was removed and the FAME were purified by TLC on silica gel G plates (Fisher Scientific, Ottawa, Ontario, Canada) using the developing solvent hexane/diethyl ether/acetic acid (85:15:1). The

FAME band on TLC was identified after spraying the plates with 2′7′-dichlorofluorescein in methanol, and the band was visualized under UV light. The FAME band on TLC was scraped off, transferred into a Pasteur pipette (5.75 in.) containing a previously cleaned glass wool plug (using chloroform/methanol, 1:1), and the FAME were eluted with hexane. For GC analysis, appropriate concentrations of FAME (1–2 µg/µL) in hexane were prepared.

All the FAME preparations were analyzed by GC (Model 5890 Series II; Hewlett-Packard, Palo Alto, CA) equipped with a splitless injection port flushed after 0.3 min, an FID, an autosampler (Model 7673; Hewlett-Packard), a 100-m CP-Sil 88 fused-silica capillary column (100 m × 0.25 mm i.d. × 0.2 µm film thickness; Varian Inc., Mississauga, Ontario, Canada), and a Hewlett-Packard ChemStation software program (version A.09). The operating conditions were as follows: injector and detector temperatures both at 250°C; H_2 as the carrier gas (1 mL/min) and for the FID (30 mL/min), N_2 as the makeup gas (30 mL/min), and air (300 mL/min). All gases were of the highest purity. The following temperature program was used: initial temperature of 45°C and held for 4 min, programmed at 13°C/min to 175°C and held for 27 min, then programmed at 4°C/min to 215°C and held for 35 min (29,45,46). FAME were identified by comparison with a GC reference FAME standard (#463) spiked with the four-positional CLA isomer mixture (#UC-59M), and the long-chain saturated FAME 21:0, 23:0, and 26:0 (all samples obtained from Nu-Chek-Prep Inc.). The *trans* isomers of linoleic and linolenic acids were prepared as described previously (46). All GC results are presented as relative percentages of the total FAME based on the flame ionization response.

Depending on the FA profile of the sample, higher or lower concentrations of the FAME mixtures were analyzed by GC to give maximum resolution of the *cis*- and *trans*-18:1 isomers at a low sample load and clearly identifiable peaks of all the minor FAME at a high sample load. The overlap of the *cis*-20:1 and *cis/cis/trans*-18:3 isomers using this type of 100-m capillary column and temperature program was resolved by conducting the GC separation at isothermal conditions of 150°C (47). Under these GC conditions, the *cis*-20:1 isomers from 8*cis*- to 11*cis*-20:1 eluted after linolenic acid, whereas any *trans*-containing 18:3 isomer eluted before it.

The GC results of the FAME prepared by the acid- and base-catalyzed procedures were compared. The results of the two methylation procedures were generally similar except for differences in the CLA isomer composition; acid conditions resulted in a higher content of the *trans,trans*-CLA isomers because of the acid-catalyzed isomerization (48). The final FA composition was obtained by averaging the results of both methylation procedures, but the CLA isomer distribution was taken from the results of the base-catalyzed methylation. Identification of the CLA isomers was confirmed using silver-ion HPLC separation (29,45).

FT-NIR measurements. The FT-NIR spectra of a number of edible oils, shortening, lard, and partially hydrogenated soybean and canola oils were acquired over the range of 10,000–4,000 cm^{-1} (1000–2500 nm) using a Bruker Optics Matrix F spectrometer equipped with a temperature-stabilized InGaAs detector and a solid transflectance fiber-optic probe with a liquid attachment and/or a Vector 22/N spectrometer equipped with a Ge Diode detector and the same type of solid transflectance fiber-optic probe with a liquid attachment. The spectral resolution was set at 8 cm^{-1} and the path length setting was 2 mm. The resolution setting of 4 cm^{-1} gave high background noise, whereas the setting of 16 cm^{-1} provided inadequate resolution. The OPUS software tools from Bruker Optics were used to collect and handle the data using chemometric analysis.

The following procedure was used in the development of a classification or quantification spectral reference model. The FT-NIR spectral measurements consisted of five scans obtained of the neat sample in liquid form and using the liquid attachment tool available from the instrument supplier. The actual scan required only 25 s. All samples were scanned at 22 ± 2°C except semisolid fat samples, which were melted and scanned at 30 ± 2°C. An average absorption file for each fat and oil sample was created and used in the development of a classification reference model or quantification model. These models were then used to classify fats and oils having a similar FA composition at a 99% confidence interval or to quantify for FA composition. In the quantification model, the FA composition results obtained by GC were incorporated into PLS1 model development to determine the FA composition of edible oils and fats, including *trans* FA. The quantitative model for FA analysis by FT-NIR required both internal (cross-validation) and external validation by using different oils with similar FA compositions. The complete analysis of all major FA in the edible oil sample was performed on the average spectrum obtained following the scanning and averaging process.

The complete analysis, including scanning, cleaning of the probe, and analysis, was achieved in a few minutes. The present method is limited to neat fats and oils and does not apply to fat/water mixtures such as those found in butter or margarine. To analyze such samples will require the development of a new FT-NIR model or a prior separation of the fat portion from the product.

Chemometric analysis. The classification process involved a spectral comparison of the test sample with those in the classification reference model. The result of a comparison between two spectra is expressed in terms of the Euclidean distance $D_{\text{test sample}}$:

$$D_{\text{test sample}} = \sqrt{\Sigma[A_{\text{test sample}}(k) - A_{\text{reference}}(k)]^2} \qquad [1]$$

where $A_{\text{test sample}}(k)$ is the absorption of the test sample spectrum at wavelength k, and $A_{\text{reference}}(k)$ is the absorption of the reference spectrum at wavelength k. Based on the equation, the more similar a spectrum is to the reference spectrum, the smaller is the Euclidean distance $D_{\text{test sample}}$. For any two test samples with identical spectra, $A_{\text{test sample}}(k) = A_{\text{reference}}(k)$, for every (k), and the value of $D_{\text{test sample}}$ will be zero.

The second parameter used in the classification process was the threshold distance (D_T), which defines the tolerance of the

classification model. In this case, a 99% confidence interval was applied in calculating the threshold value. The optimal setting for the threshold depended on the reference samples incorporated in the classification model. If the value for D_T was set too high, the model incorrectly identified samples as identical, when in fact they were different. On the other hand, if the D_T was set too low, the model rejected samples that should have been accepted.

In a typical classification analysis, the average spectrum of a test sample was compared with all references and/or to a single reference. In the latter case, there were three possible outcomes: (i) The hit quality (a measure of the similarity of the test sample to each reference sample) for the test sample was lower than the threshold value of the reference sample, and no other hits were found to meet this criterion. The result was reported as "IDENTICAL," i.e., the test sample was identical to the reference. (ii) The hit quality of one or more of the test samples was smaller than the threshold of the reference. The identity test was reported as "CAN BE CONFUSED WITH <N> OTHER HITS." This outcome was possible only if the classification reference library contained very similar materials, such as two soybean oils from two different sources with very similar FA compositions or the same soybean oil analyzed using two separate FT-NIR instruments. (iii) The hit quality was greater than the threshold, and no match was found of the test sample to any reference in the spectral library. In this case the sample was reported as "NOT IDENTICAL." This situation could also arise if the sample was not scanned properly, contained impurities, the batch-to-batch variations were too large, or the test sample had a FA composition outside the range of any reference sample in the library.

The quantitative analysis was performed using the OPUS "Quant 2" program provided with the instrument. The data incorporated into this program included the FA composition obtained by GC (independent variables) and the FT-NIR spectra. A combination of processing parameters was then selected, such as first or second derivatives, vector normalization, spectral regions, and validation type (i.e., cross-validation), all of which were then analyzed by PLS1 procedures. Once a reasonable calibration model was established (first derivative plus vector normalization and the specific spectral regions 4547–4794, 5423–6013, and 6974–7290 cm^{-1}), it was applied to determine the FA concentration in selected samples from within the calibration set, as well as external samples that were not part of the model. The final FT-NIR predicted values were then compared with GC data for the same sample.

RESULTS AND DISCUSSION

A review of the differences between FTIR and FT-NIR and their respective uses is beyond the scope of this paper; however, Workman (49) has provided a concise description of FT-NIR and how it can be applied. It is sufficient to say that band assignments in the NIR region are difficult since a single band may be attributed to several possible combinations of fundamental and overtone vibrations. However, in the last decade advances in instrumentation and computing power combined with ones in chemometric analysis have made it possible to analyze FT-NIR spectral features based on characteristic overtones and combination bands of any given chemical compound. The FT-NIR spectral fingerprints of a material or a mixture are unique, and unless the chemical structure of the molecules is altered or the recording temperature is very different, the FT-NIR spectrum would remain constant. In simple terms, chemometric analysis involves storing FT-NIR spectral information as references and comparing these spectra with those of a test sample.

Figure 1 shows broad peaks in the FT-NIR spectra for triolein and trielaidin, which are the result of overtones and combinations of the fundamental bands in the FTIR region. Using the chemometric functions available through the OPUS software, we obtained second-derivative spectra that showed significantly different patterns among various materials. Figure 2 shows the second derivative of triolein and trielaidin with marked differences in the 4500–4750 cm^{-1} and 5600–5900 cm^{-1} regions. Figure 3 shows the differences in second-derivative spectra among triolein, trilinolein, and trilinolenin. In the second derivative, the intensity of the peaks at 5830 and 5870 cm^{-1} increased, whereas the intensity of the peaks at 5768 and 5680 cm^{-1} decreased, as the number of double bonds in the TAG molecule increased from 3 to 9. These spectral features are physical characteristic of each material or mixture and do not change unless the material or mixture has been chemically altered. As described above, these were the spectral features used to produce a reliable quantitative data analysis.

FT-NIR classification of fats and oils. Either the standard or factorization method available with OPUS software can be used to classify the FT-NIR spectra of fats or oils. In this study the factorization method was used because it provided additional information for the components of each sample. In the factorized analysis, each average spectrum was assessed with
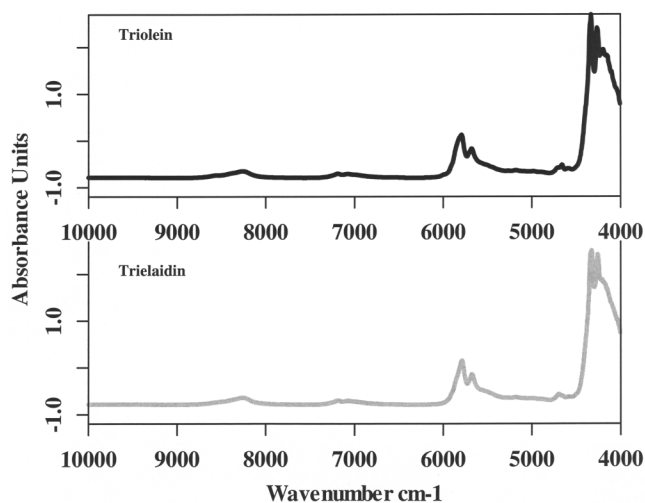
FIG. 1. Fourier transform NIR (FT-NIR) absorption spectra of triolein (black line) and trielaidin (gray line) in the spectral region from 4,000 to 10,000 cm^{-1}.
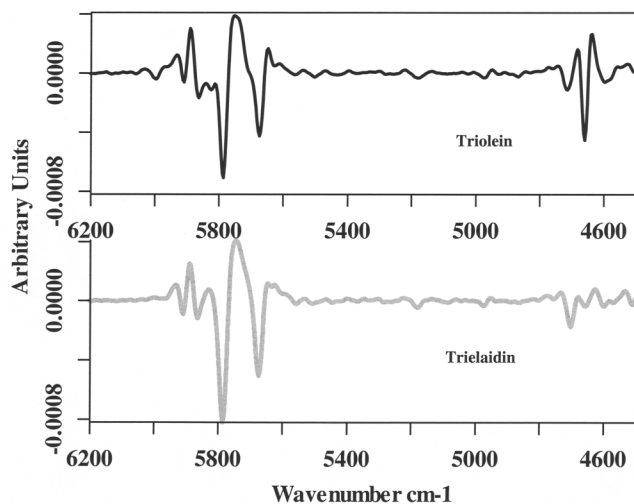
FIG. 2. Second-derivative FT-NIR spectra of triolein (black line) and trielaidin (gray line) in the spectral region from 4,500 to 6,200 cm^{-1}. For abbreviation see Figure 1.

respect to different components (known as vectors) present within the sample. Once the average spectrum of any given fat or oil was collected and stored, chemometric analysis was performed to generate a classification reference model. This classification model was generated by collecting spectral fingerprints for all the edible oils studied and has been used to classify unknown edible oils by comparing their spectra with reference fats and oils. As mentioned above, the spectra for liquid oils were obtained at 22 ± 2°C and the semisolid fat samples were first melted and scanned at 30 ± 2°C because there was a temperature effect. A sample scanned at 30 ± 2°C would have a different response than that scanned at 22 ± 2°C. This effect was more noticeable in the hit quality value than was the type of fat or oil. Therefore, separate models were prepared for the liquid (low-*trans*) and semisolid (medium- and high-*trans*)
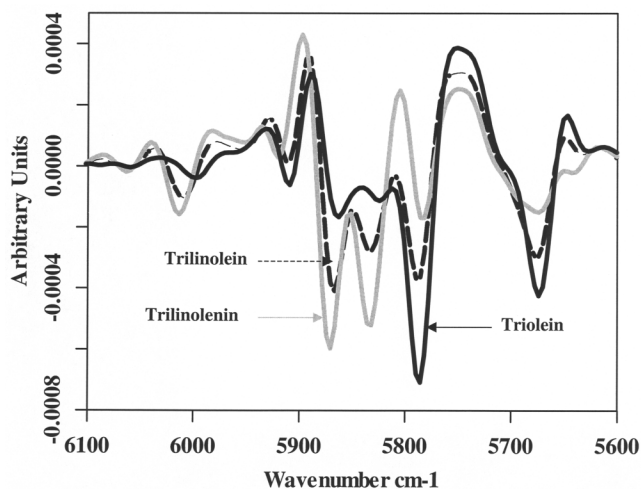
FIG. 3. Overlaid second-derivative FT-NIR spectra of triolein, trilinolein, and trilinolenin in the spectral region from 5,600 to 6,100 cm^{-1}. For abbreviation see Figure 1.
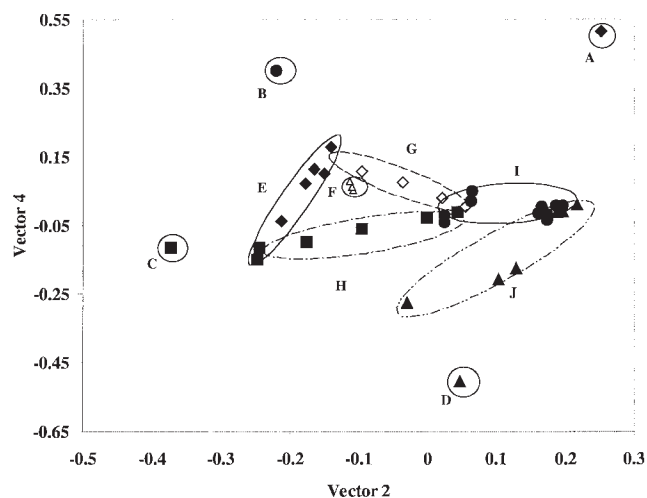
FIG. 4. Vectors 2 and 4 of a factor analysis of triolein, trielaidin, trilinolein, trilinolenin, and several vegetable oils, fats, and fat/oil mixtures. (A) trielaidin; (B) trilinolein; (C), trilinolenin; (D) triolein; (E) flax oil and walnut oil mixtures; (F) different soybean oils; (G) walnut oil and commercial shortening mixtures; (H) flax oil and commercial shortening mixtures; (I) partially hydrogenated soybean oil fractions (supplier A); and (J) partially hydrogenated canola oil fractions (supplier B).

samples. Plots of the vector components were used to reveal similarities or differences between individual materials and/or groups of materials.

Figure 4 shows the plot of two of the vectors (2 and 4) identified in the analysis of the different fats, oils, and their mixtures. Generally, many vectors combine together to form a classification model, depending on the complexity of the model. As shown in Figure 4, vectors 2 and 4 were selected to illustrate the large spectral differences among triolein, trielaidin, trilinolein, and trilinolenin and how oils consisting of mixtures of these FA relate to the extremes in which TAG consist of single FA. Vectors are mathematical expressions used to quantify changes and differences between data sets and should not be confused with specific FA, since they appear to include general chemical and physical characteristics of lipids such as fluidity, unsaturation, and structural packing. A number of conclusions were evident from a qualitative inspection of Figure 4. TAG consisting of different single FA were distinctly separated. Soybean and canola oils were different, but their respective hydrogenated fractions converged with increasing hydrogenation, i.e., their respective fractions highest in *trans* and saturated FA were similar. Flax, walnut, and canola oils showed characteristic similarities to trilinolenin, trilinolein, and triolein, respectively, because these oils contained significant amounts of the corresponding FA. Mixtures of walnut or soybean oil with commercial shortening (a partially hydrogenated soybean oil product) altered the cluster from one predominant in unsaturated FA toward increased *trans* and saturated FA (vector 2). Cluster F showed limited variation, as expected, since it represented two different samples of soybean oil with slightly different FA compositions, scanned using two different FT-NIR spectrometers manufactured by Bruker Optics (Matrix-F and

TABLE 1
Classification of Various Oils and Fats

Sample name[a]	Hit quality	Threshold	Total *trans* content (%)
Oils high in linoleic acid (9*c*,12*c*-18:2)			
Soybean oil A	0.000001	0.013260	0.41
Soybean oil B	0.030700	0.020194	2.08
Walnut oil A	0.075013	0.016251	3.97
Walnut oil B	0.075306	0.027301	1.99
Sunflower oil	0.134202	0.005296	1.10
Oils high in oleic acid (9*c*-18:1)			
Triolein	0.000001	0.012354	0
Canola oil (high-oleic canola)	0.172119	0.047503	2.92
Olive oil	0.213459	0.028742	0.52
Canola oil A	0.234829	0.024741	3.60
Canola oil B	0.274546	0.009170	1.88
Fats high in *trans* FA			
PH canola oil D[b]	0.000001	0.054277	59.49
PH soybean oil D[b]	0.098692	0.019102	50.25
PH canola oil C[b]	0.171336	0.026738	53.06
PH soybean oil C[b]	0.204038	0.013046	43.60
Commercial shortening[c]	0.292006	0.025527	20.09

[a]All oils and fats were locally purchased products.
[b]Partially hydrogenated (PH) soybean and canola oils were provided by two separate suppliers.
[c]The commercial shortening was purchased locally.

Vector 22/N). It should be noted that in a simple classification model made by mixing two materials, one would expect two different vectors representing the respective concentrations of the two materials in question. However, in a complex classification model, such as the one presented in Figure 4, a single vector may represent more than one component. For example, an increase in vectors 2 and 4 represents higher concentrations of *trans* in the samples, whereas a decrease in these two vectors represents increased unsaturation, as evidenced by higher levels of linolenic acid.

Once the classification reference model was established, scanning and classification of new unknown fats or oils were achieved rapidly and easily without the necessity of time-consuming preparations of volatile FAME derivatives and GC analysis. Typical classification reports of oils high in linoleic acid, oleic acid, and partially hydrogenated fractions high in *trans* FA (up to 60% total *trans*) are shown in Table 1. Each classification report includes the hit quality, the threshold value (a value based on the SD at a 99% confidence interval), and the total *trans* content. In each case, the test samples were first compared with themselves, which accounted for a hit quality (or an Euclidean distance $D_{\text{test sample}}$) of or near zero.

Oils high in linoleic acid, including two different soybean (A and B) and walnut (A and B) oils that were scanned on the same FT-NIR spectrometer using the conditions specified in the Materials and Methods section, showed significantly different hit quality values. Both duplicate oils showed minor differences in their respective hit quality values (soybean oil A, 0.0000, and soybean oil B, 0.0307; walnut oil A, 0.0750, and walnut oil B, 0.0753) and significant differences between the two oils attributable to differences in their FA composition. The linoleic acid (9*cis*,12*cis*-18:2) contents of the soybean and walnut oils were 49 and 56%, respectively, with additional differences in their

oleic acid (9*cis*-18:1) and linolenic acid (9*cis*,12*cis*,15*cis*-18:3) contents. Other oils, such as sunflower oil, showed an even greater hit quality value of 0.13. In the second analysis, triolein was compared with itself, and it showed a hit quality value near zero. By comparison, olive and canola oils, known to contain high levels of 9*cis*-18:1, showed higher hit quality values, demonstrating their dissimilarity to triolein. However, it is interesting to note that the closest match to triolein was a high-oleic canola oil followed by olive oil and not any of the two normal canola oils (canola oil A or canola oil B). All oils other than olive and canola in the classification model had significantly higher hit quality values (data not shown).

Partially hydrogenated canola oil containing about 60% total *trans* FA was compared with other partially hydrogenated soybean and canola oil fractions. The hit quality values increased as the *trans* content decreased in the partially hydrogenated soybean or canola fractions, indicating that the lower-*trans*-containing samples were dissimilar to the test sample. It is interesting to note that the closest match to partially hydrogenated canola oil D was partially hydrogenated soybean oil D and not the other partially hydrogenated canola oil sample (canola oil C). The results suggest that the composition of the material is a more important parameter in determining the hit quality in this comparison than the origin of the oil. These results were in agreement with the FA composition of these fractions determined independently by GC (data not presented).

FT-NIR quantification of FA. FT-NIR is a nondestructive method applied directly to fats or oils (neat) and has been used to a limited extent in measurements of fats and oils, primarily to quantify selective FA or groups of FA, such as *trans* and unsaturated FA (38–43). The limited application appears to be based on the general assumption that the FT-NIR signals were too weak and broad, and lacked the sensitivity required for a

detailed FA determination. However, chemometric analysis was shown to overcome these concerns. To quantify the FT-NIR spectra, it was necessary to determine response factors for each FA by preparing appropriate calibration curves. There was a further concern that the sample matrix might have an effect on quantification, since in the FT-NIR method the whole sample was scanned without isolating each TAG component. This matrix dependence was recently demonstrated when traces of residual solvent affected the outcome (50).

FA generally occur in the form of mixed TAG in fats and oils. To prepare response factors for every FA in a mixed TAG was for all purposes considered impossible. Several single-FA TAG such as triolein, trielaidin, trilinolein, and trilinolenin that were available (Nu-Chek-Prep Inc.) were used as qualitative references. Many more pure and mixed TAG would be necessary to prepare all the references and validation curves required to cover the complete range of FA present in all the fats and oils in order to make FT-NIR the primary method of analysis and still establish a relatively universal calibration model. Therefore, we decided to rely on the GC results as the primary reference of FA composition and on FT-NIR as the secondary method of analysis. Furthermore, by including a variety of fingerprints from fats and oils that varied in saturation, *cis* (up to three double bonds) unsaturation , and *trans* unsaturation (low, medium, high), a relatively universal calibration model could be developed that would be applicable to most of the common fats and oils. With this approach, the accuracy of the GC results was critical, since any errors would be directly passed onto the FT-NIR models.

The accuracy of the GC results was ensured by purifying all FAME preparations by TLC prior to GC analysis. This was done to remove any non-FA components that coextracted or any artifacts produced during the methylation procedure, since such organic substances would also result in a GC-FID signal. (The added benefit of TLC purification of FAME was a longer life expectancy of the GC columns.) Furthermore, it was essential to maximize the resolution of FAME isomers by using highly polar, 100-m fused-silica capillary GC columns, such as CP Sil 88 (Varian Inc.) or SP 2560 (Supelco Inc.). Additional separations were achieved by manipulating the temperature of the GC program, such as by lowering the oven temperature to resolve the 20:1 and 18:3 isomers (47). Silver-ion TLC was used effectively to complement the GC separation of the *trans*- and *cis*-18:1 isomers by isolating the FAME based on their geometric (*cis* from *trans*) configuration and number of double bonds (10,29,30,45). These isolated *trans*- and *cis*- TLC bands were then resolved by GC at an oven temperature of 120°C, which separated most of the *trans*- and *cis*-18:1 isomers (10,29,30,45,51). The GC–MS and GC-FTIR techniques were also used to identify the FAME (51,52).

In total, 55 different edible oils and various mixtures thereof were included in the development of the FT-NIR model. All the fats and oils, and several of the mixtures were analyzed by GC. Some of the fat/oil mixtures were only scanned by FT-NIR to develop a robust model for the determination of unknown fats and oils with different FA concentrations. To enhance the accuracy of the model for the analysis of *trans*-containing samples, we developed three separate models for low (<2%), medium (2–20%), and high (20–60%) *trans* contents. Table 2

TABLE 2
Error Predictions Obtained from Cross-Validation for Low (<2%), Medium (<20%), and High (<60%)
***trans* Contents**

FA	Rank	$R^{2\ a}$	RMSECV[b]	Range
Low *trans*				
16:0	4	0.85	2.05	3.58–24.21
18:0	4	0.85	1.25	1.97–14.64
9c-18:1	8	0.99	2.28	15.74–69.74
9c,12c-18:2	7	0.98	2.61	10.68–71.15
9c,12c,15c-18:3	7	0.96	2.28	0.15–51.83
Medium *trans*				
16:0	6	0.88	1.75	3.58–24.21
18:0	5	0.84	1.23	1.97–14.64
10t-18:1	7	0.93	0.35	0.02–4.95
11t-18:1	5	0.87	0.41	0.01–3.79
9c-18:1	7	0.99	2.21	15.75–69.74
9c,12c-18:2	8	0.98	2.73	10.68–71.15
9c,12c,15c-18:3	8	0.96	2.12	0.15–51.83
High *trans*				
16:0	7	0.67	1.76	4.04–16.01
18:0	5	0.93	1.05	3.18–16.25
10t-18:1	7	0.91	0.91	0.46–10.26
11t-18:1	7	0.74	1.13	0.37–8.35
9c-18:1	7	0.98	2.1	6.26–51.93
9c,12c-18:2	5	0.99	0.88	0.02–50.08
9c,12c,15c-18:3	8	0.97	0.37	0–8.17

[a]Values below 0.85 should be used with caution. We are currently investigating potential improvements to calibration curves with $R^2 \leq 0.85$.
[b]RMSECV, root mean square error of cross-validation.
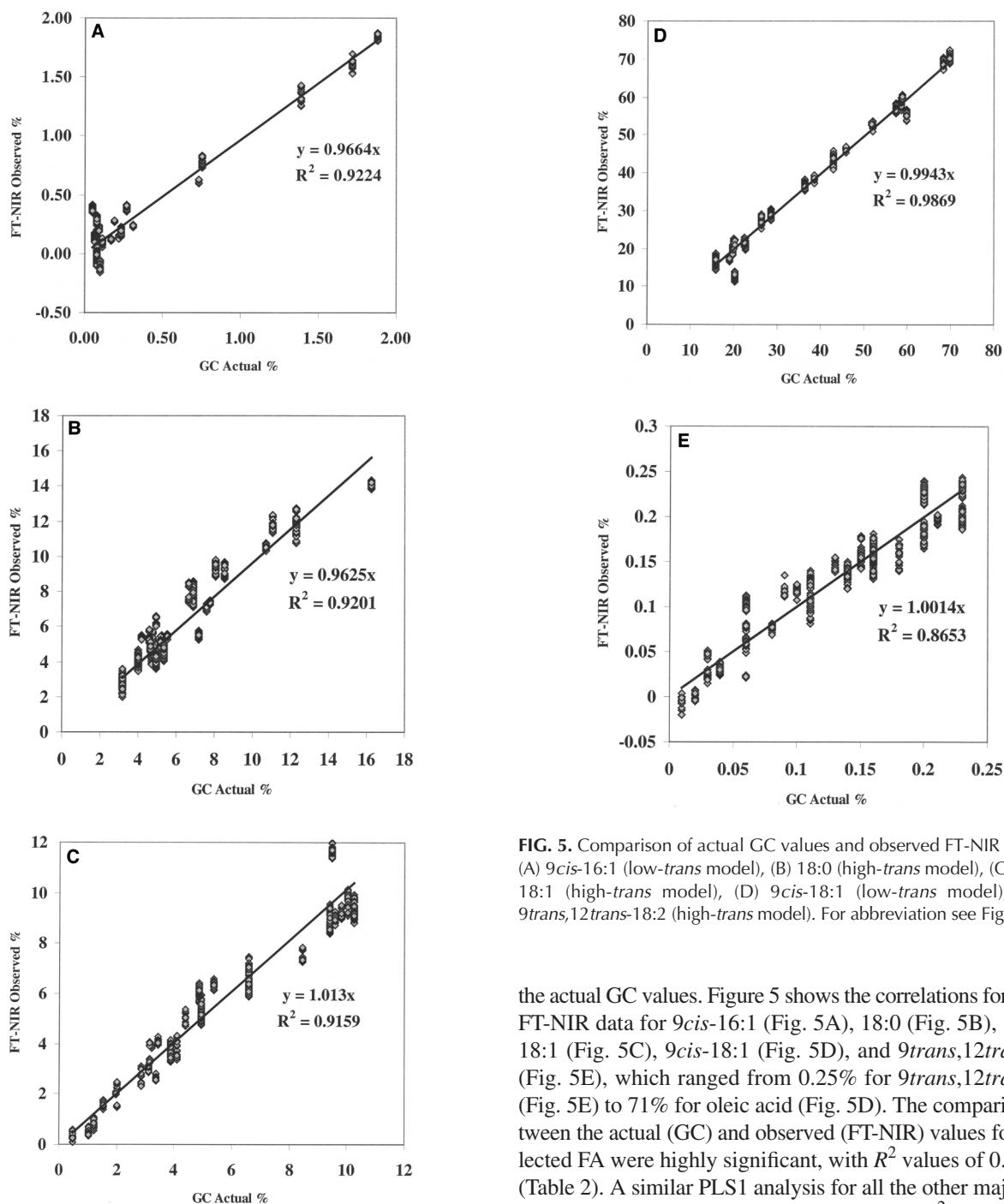
FIG. 5. Comparison of actual GC values and observed FT-NIR values for (A) 9*cis*-16:1 (low-*trans* model), (B) 18:0 (high-*trans* model), (C) 10*trans*-18:1 (high-*trans* model), (D) 9*cis*-18:1 (low-*trans* model), and (E) 9*trans*,12*trans*-18:2 (high-*trans* model). For abbreviation see Figure 1.

shows cross-validation error predictions for the low, medium, and high *trans* models, respectively. Furthermore, the root mean square error of cross-validation (RMSECV) values depended on the relative concentration of the FA in the sample, being lower at low concentrations. For example, the RMSECV for 10*trans*-18:1 was 0.91 when present in the range of 0.46–10.26% and was 0.35 in the range of 0.02–4.95%.

All three models proved to be highly successful in predicting the content of the major FA in these fats and oils, as demonstrated by comparing the FT-NIR obtained by PLS1 analysis and the actual GC values. Figure 5 shows the correlations for GC and FT-NIR data for 9*cis*-16:1 (Fig. 5A), 18:0 (Fig. 5B), 10*trans*-18:1 (Fig. 5C), 9*cis*-18:1 (Fig. 5D), and 9*trans*,12*trans*-18:2 (Fig. 5E), which ranged from 0.25% for 9*trans*,12*trans*-18:2 (Fig. 5E) to 71% for oleic acid (Fig. 5D). The comparisons between the actual (GC) and observed (FT-NIR) values for the selected FA were highly significant, with R^2 values of 0.86–0.98 (Table 2). A similar PLS1 analysis for all the other major FA in the fats and oils provided equally significant R^2 values (values not included). The RMSECV for several of the FA are shown in Table 2 using the low-, medium-, and high-*trans* calibration models. Further improvements to the calibration model should be possible, especially for those with lower R^2 values, by studying all FA individually and including samples having a wider range in each of the FA.

The quantitative FT-NIR models developed were used to measure the FA composition of unknown fats or oils using the OPUS software supplied with the instrument, provided the FA ranges in the unknown fats or oils were similar to those existing in the reference library. Table 3 presents the results for three

TABLE 3
Comparison of GC and FT-NIR Results for Different Oils[a]

FA	Soybean oil		Olive oil		Flaxseed oil	
	GC (%)	FT-NIR (%)	GC (%)	FT-NIR (%)	GC (%)	FT-NIR (%)
14:0	0.09	0.10	0.41	0.42	0.43	0.42
16:0	10.44	10.56	11.49	11.50	4.93	4.78
9c-16:1	0.08	0.08	0.75	0.75	0.05	0.05
17:0	0.11	0.11	0.06	0.06	0.06	0.06
9c-17:1	0.00	0.00	0.09	0.09	0.04	0.04
18:0	4.49	4.48	2.76	2.77	4.31	4.26
6t–8t-18:1	0.01	0.03	0.05	0.03	0.01	0.02
9t-18:1	0.05	0.02	0.15	0.16	0.01	0.07
10t-18:1	0.08	0.07	0.06	0.03	0.02	0.03
11t-18:1	0.04	0.06	0.01	−0.02	0.01	0.01
12t-18:1	0.02	0.01	0.01	−0.01	0.01	0.02
13t/14t-18:1	0.04	0.04	0.01	−0.02	0.00	0.01
15t-18:1	0.00	−0.01	0.00	−0.01	0.00	0.01
9c-18:1	19.86	19.61	68.34	68.55	20.20	20.04
11c-18:1	1.40	1.40	2.05	2.07	0.66	0.64
12c-18:1	0.04	0.10	0.00	−0.02	0.01	−0.01
13c-18:1	0.05	0.05	0.00	0.00	0.01	0.01
14c/16t-18:1	0.00	0.00	0.00	0.00	0.00	0.00
15c-18:1	0.00	0.00	0.00	0.00	0.00	0.00
19:0	0.01	0.01	0.00	0.00	0.00	0.00
9c,12t-18:2	0.06	0.09	0.06	0.06	0.06	0.06
9t,12c-18:2	0.01	0.03	0.04	0.04	0.01	0.01
9c,12c-18:2	52.70	52.78	10.68	10.55	15.40	15.68
20:0	0.36	0.35	0.52	0.52	0.17	0.16
c,c,t-18:3	0.04	0.05	0.03	0.04	0.23	0.21
9c-20:1	0.02	0.02	0.02	0.02	0.02	0.02
t,c,c-18:3	0.02	0.02	0.04	0.03	0.03	0.04
11c-20:1	0.17	0.16	0.36	0.37	0.18	0.18
9c,12c,15c-18:3	8.85	8.83	0.64	0.68	51.83	51.88
Σ CLA	0.04	0.07	0.06	0.06	0.02	0.02
22:0	0.36	0.36	0.24	0.24	0.14	0.14
24:0	0.10	0.10	0.10	0.10	0.09	0.09
Σ Sat	16.04	16.17	15.64	15.67	10.20	9.96
Σ MUFA	21.52	21.32	70.84	70.99	21.11	20.92
Σ PUFA	61.59	61.65	11.32	11.31	67.27	67.60
Σ trans MUFA	0.27	0.16	0.30	0.14	0.05	0.14
Σ trans DUFA	0.13	0.24	0.16	0.16	0.09	0.09
Σ trans TUFA	0.08	0.09	0.07	0.09	0.29	0.26
Σ trans	0.47	0.47	0.52	0.39	0.44	0.51

[a]The calibration curves for some very minor FA were lower than zero, with the intercept giving negative values. Several minor FA were not included. FT-NIR, Fourier transform NIR spectroscopy; Sat, saturated FA; MUFA, monounsaturated FA; DUFA, diunsaturated FA; TUFA, triunsaturated FA.

different oils (soybean, olive, and flax) in which the GC and FT-NIR values are compared. The data showed a good correlation between the GC and FT-NIR results based on the low-*trans* model. The FT-NIR technique was able to predict the FA composition of these oils, including the minor *trans* FA isomers of 18:1, 18:2, and 18:3 as low as 0.2% as well as total CLA. Since these three oils were among the 55 samples used to develop the FT-NIR model, it could be argued that this good fit was predictable.

A more critical evaluation of the model is presented in Table 4, which reports the GC and FT-NIR results of two unknown samples prepared by mixing shortening and lard. These samples were not among the 55 samples. The consistency of the FT-NIR and GC data in Table 4 demonstrates the potential of the FT-NIR technique to recognize the fingerprints of and similarity between

these two fat samples. It related these two fats correctly to their family of products, and quantitatively determined the FA composition, including most of the minor *cis/trans* and *cis/cis/trans* FA and CLA isomers, many at about 0.2%. The gas chromatogram of the 21:79 mixture of shortening and lard is shown in Figure 6. From our experience, the absolute need to provide accurate GC data for the development of the FT-NIR models should be stressed, since poor correlations between GC and FT-NIR results were often attributed to misidentified and coeluting GC peaks. It should be noted that GC analysis depends on the analyst's interpretation, whereas FT-NIR is based strictly on the physical characteristics of the FA.

None of the fats or oils investigated in this study contained ruminant fats; therefore, the CLA isomers present were those produced during catalytic or heating processes. The total CLA

TABLE 4
Validation of the FT-NIR Method for Mixtures of Shortening and Lard with GC Results for Comparison[a]

FA	GC (%) 80% shortening/20% lard	FT-NIR (%) 80% shortening/20% lard	GC (%) 21% shortening/79% lard	FT-NIR (%) 21% shortening/79% lard
10:0	0.06	0.05	0.06	0.05
12:0	0.04	0.05	0.04	0.00
14:0	0.23	0.69	0.32	1.05
16:0	17.01	17.97	22.03	22.61
9c-16:1	0.45	0.82	1.57	1.55
17:0	0.18	0.22	0.35	0.32
9c-17:1	0.10	0.13	0.25	0.21
18:0	10.63	10.54	13.09	13.18
6t–8t-18:1	1.32	1.32	0.47	0.67
9t-18:1	1.56	1.84	0.62	1.04
10t-18:1	3.35	3.06	1.08	1.38
11t-18:1	2.50	2.45	0.82	1.15
12t-18:1	1.12	1.14	0.38	0.48
13t/14t-18:1	1.11	1.43	0.45	0.67
15t-18:1	0.30	0.37	0.20	0.14
9c-18:1	27.10	26.82	34.53	32.25
11c-18:1	1.85	2.11	2.38	2.25
12c-18:1	3.40	2.67	1.04	1.08
13c-18:1	0.22	0.24	0.15	0.16
14c/16t-18:1	0.22	0.28	0.10	0.13
19:0	0.28	0.24	0.14	0.09
9t,12t-18:2	0.10	0.08	0.03	0.04
9c,13t-/8t12c-18:2	0.77	0.85	0.25	0.33
9c,12t 18:2	1.26	0.73	0.50	0.40
9t,12c-18:2	1.04	0.66	0.41	0.30
11t,15c-18:2	0.26	0.32	0.06	0.10
9c,12c-18:2	19.36	17.40	14.94	16.13
20:0	0.38	0.32	0.28	0.24
c,c,t-18:3	0.24	0.18	0.13	0.18
9c-20:1	0.13	0.05	0.09	0.05
t,c,c-18:3	0.18	0.17	0.14	0.18
11c-20:1	0.31	0.32	0.65	0.40
9c,12c,15c-18:3	1.00	1.50	0.73	0.17
Σ CLA	0.14	0.07	0.08	0.08
11c,14c-20:2	0.12	0.14	0.43	0.35
22:0	0.27	0.17	0.09	0.13
24:0	0.09	0.06	0.02	0.04
Σ Sat	29.17	30.30	36.41	37.81
Σ cis MUFA	33.08	33.79	39.05	38.19
Σ cis PUFA	20.48	20.06	16.10	17.04
Σ trans MUFA	11.40	11.97	4.07	5.48
Σ trans DUFA	3.57	2.69	1.33	1.21
Σ trans TUFA	0.55	0.42	0.36	0.42
Σ trans	15.51	15.15	5.76	6.94

[a]The calibration curve for some very minor FA was lower than zero, with the intercept giving negative values. Several minor FA were not included. For abbreviations see Table 3.

content in these fats and oils ranged from 0.1 to 0.2% of total FAME and consisted of a random array of all positional and geometric isomers from 8,10- to 12,14-CLA (see the CLA profile in Fig. 7 of the same shortening and lard mixture shown in Fig. 6). The CLA profile in commercial fats is unlike that present in ruminant fats, in which the 9cis,11trans-CLA isomer (rumenic acid) predominates. The difference is that the CLA isomers formed during catalytic or heating processes are randomly formed by a combination of free-radical chain reactions and sigmatropic rearrangements (6), whereas the CLA isomers in ruminants are produced enzymatically by a combination of isomerization and reduction (23). It would not be prudent to exclude the CLA content produced during partial hydrogenation of vegetable oils from total trans, as specified in the trans labeling act (15–19), since this CLA mixture contains many CLA isomers with unknown physiological and biological effects. Fortunately, the CLA content of industrial fats is generally not high (<0.2%), although we have observed some PHVO with as much as 2% total CLA (unpublished data).

This new FT-NIR method, based on models developed for quantifying FA by low-, medium-, and high-trans FA content, will need to be evaluated in a collaborative study before it can be recommended as an official FT-NIR method. Efforts are in progress to conduct a collaborative study. Factors that will need
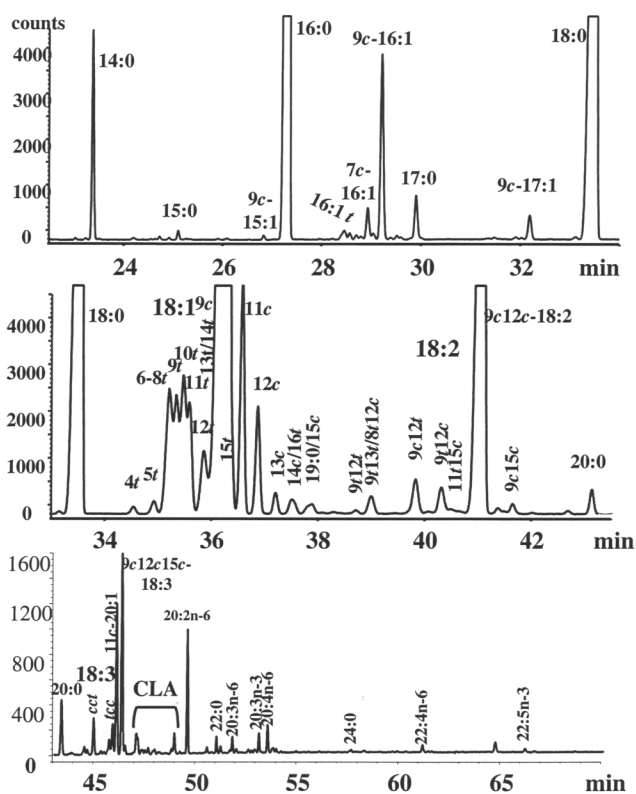
FIG. 6. GC chromatogram of the 21:79 mixture of commercial shortening and lard using a 100-m CP Sil 88 capillary column and temperature program described in the Materials and Methods section.

to be addressed are the accuracy and reproducibility of the FT-NIR method for determining the FA composition of a fat or oil product, the limits of FA detection, the effect of positional isomers of mixed TAG, the effect of trace levels of non-TAG components such as plant sterols (or cholesterol) and tocopherols, and any parameters that will need to be controlled, such as the

temperature of analysis. The present study involved over 55 samples covering a variety of edible oils and their mixtures, and the results suggest that the FT-NIR method has great potential for complementing the GC technique when routine analysis of many samples is required. It should be emphasized that this is a relatively universal model for edible oils, and it cannot be applied to other products such as salad dressings and margarines. To analyze these products directly, a separate unique model needs to be developed.

An FT-NIR calibration reference model was developed based on chemometric analyses of the FT-NIR absorptions and accurate FA compositions obtained by GC. Three separate models were developed based on scanning 55 fats, oils, and fat/oil mixtures to serve as low-, medium-, and high-*trans*-containing samples. These calibration models were designed to rapidly screen and/or monitor the *trans* content for regulatory labeling purposes. The results showed that the FT-NIR method was rapid, comprehensive, and accurate. It compared well with the current certified methods of *trans* fat analysis by ATR-FTIR by providing the complete FA composition of the fat or oil instead of only the total *trans* content, as in the FT-IR method. Special modifications were required for both methods to melt semisolid fats before measurements were taken. On the other hand, the FT-NIR and the GC methods complemented each other. Even though the GC method remains essential to establish reliable FA compositional data to develop the FT-NIR models, subsequent labor- and time-consuming GC analyses of routine fat and oil samples will not be necessary. A large number of analyses can be performed rapidly and just as comprehensively by FT-NIR as by GC. We recommend that product-specific quantitative FT-NIR models be developed for greater accuracy. Whereas the FT-NIR model needs to be developed only once, GC analyses need to be performed on every sample, including the conversion to FAME followed by GC separation and interpretation of the data. This provides obvious time and cost savings in routine quality control when many samples are
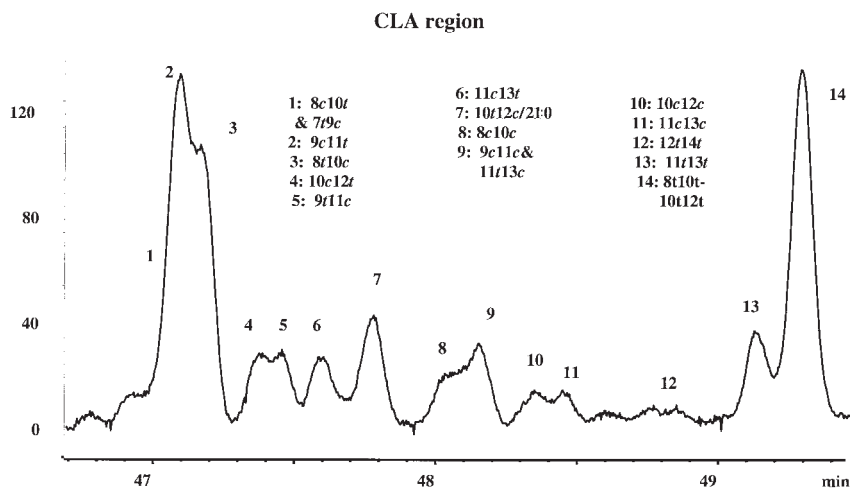
FIG. 7. Partial GC chromatogram of the CLA region from the sample presented in Figure 6.

involved. However, if only a few samples are involved, the FT-NIR technique provides no advantage.

ACKNOWLEDGMENTS

REFERENCES

1. Mensink, R.P., and Katan, M.B. (1990) Effects of Dietary *trans* Fatty Acids on High-Density and Low-Density Lipoprotein Cholesterol Levels in Healthy Subjects, *N. Engl. J. Med. 323*, 439–445.

2. Ascherio, A., Katan, M.B., Zock, P.L., Stampfer, M.J., and Willett, W.C. (1999) *Trans* Fatty Acids and Coronary Heart Disease, *N. Engl. J. Med. 340*, 1994–1998.

3. Mensink, R.P., Zock, P.L., Kester, A.D.M., and Katan, M.B. (2003) Effects of Dietary Fatty Acids and Carbohydrates on the Ratio of Serum Total to HDL Cholesterol and on Serum Lipids and Apolipoproteins: A Meta-analysis of 60 Controlled Trials, *Am. J. Clin. Nutr. 77*, 1146–1155.

4. Lopez-Garcia, E., Schulze, M.B., Meigs, J.B., Manson, J.E., Rifai, N., Stampfer, M.J., Willett, W.C., and Hu, F.B. (2005) Consumption of *trans* Fatty Acids Is Related to Plasma Biomarkers of Inflammation and Endothelial Dysfunction, *J. Nutr. 135*, 562–566.

5. Sébédio, J.L., Catte, M., Boudier, M.A., Prevost, J., and Grandgirard, A. (1996) Formation of Fatty Acid Geometric Isomers and Cyclic Fatty Acid Monomers During the Finish Frying of Frozen Prefried Potatoes, *Food Res. Internat. 29*, 109–116.

6. Destaillats, F., and Angers, P. (2005) Thermally Induced Formation of Conjugated Isomers of Linoleic Acid, *Eur. J. Lipid Sci. Technol. 107*, 167–172.

7. Ohnishi, M., and Thompson, G.A., Jr. (1991) Biosynthesis of the Unique *trans* Δ³-Hexadecenoic Acid Component of Chloroplast Phosphatidylglycerol: Evidence Concerning Its Site and Mechanism of Formation, *Arch. Biochem. Biophys. 288*, 591–599.

8. Precht, D., and Molkentin, J. (1997) *Trans*-Geometrical and Positional Isomers of Linoleic Acid Including Conjugated Linoleic Acid (CLA) in German Milk and Vegetable Fats, *Fett/Lipid 99*, 319–326.

9. Ratnayake, W.M.N., Pelletier, G., Hollywood, R., Bacler, S., and Leyte, D. (1998) *Trans* Fatty Acids in Canadian Margrines: Recent Trends, *J. Am. Oil Chem. Soc. 75*, 1587–1594.

10. Precht, D., and Molkentin, J. (2000) Recent Trends in the Fatty Acid Composition of German Sunflower Margarines, Shortenings and Cooking Fats with Emphasis on Individual C16:1, C18:1, C18:2, C18:3 and 20:1 *trans* Isomers, *Nahrung 44*, 222–228.

11. Satchithanandam, S., Oles, C.J., Spease, C.J., Brandt, M.M., Yurawecz, M.P., and Rader, J.I. (2004) *Trans*, Saturated, and Unsaturated Fat in Foods in the United States Prior to Mandatory *trans*-Fat Labeling, *Lipids 39*, 11–18.

12. Kraft, J., Collomb, M., Möckel, P., Sieber, R., and Jahreis, G. (2003) Differences in CLA Isomer Distribution of Cow's Milk Lipids, *Lipids 38*, 657–664.

13. Parodi, P.W. (2004) Milk Fat in Human Nutrition, *Austr. J. Dairy Technol. 59*, 3–59.

14. Weggemans, R.M., Rudrum, M., and Trautwein, E.A. (2004) Intake of Ruminant Versus Industrial *trans* Fatty Acids and Risk of Coronary Heart Disease B: What Is the Evidence? *Eur. J. Lipid Sci. Technol. 106*, 390–397.

15. Department of Health (2003, Jan. 1) Regulations Amending the Food and Drug Regulations (Nutritional Labelling, Nutrient Content Claims and Health Claims), *Canada Gazette, Part II (Ottawa, Canada) 137*, 154–409.

16. Ratnayake, W.M.N., and Zehaluk, C. (2005) *Trans* Fatty Acids in Foods and Their Labeling Regulations, in *Healthful Lipids* (Akoh, C.C., and Lai, O.-M., eds.), pp. 1–32, AOCS Press, Champaign, IL.

17. Department of Health and Human Services, Food and Drug Administration (2003) Food Labeling: *Trans* Fatty Acids in Nutrition Labeling: Nutrient Content Claims, and Health Claims. Final Rule, July 11, 2003, *Fed. Regist. 68*, 41434–41506.

18. ANVISA, National Agency of Sanitary Monitoring Brazil (2003, Dec. 23) Mercusul Regulamento Técico Sobre Rotulagem Nutricional de Alimentos Embalados, RDC No 360.

19. Stender, S., and Dyerberg, J. (2004) Influence of *trans* Fatty Acids on Health, *Ann. Nutr. Metab. 48*, 61–66.

20. Aro, A., Männistö, S., Salminen, I., Ovaskainen, M.-L., Kataja, V., and Uusitupa, M. (2000) Inverse Association Between Dietary and Serum Conjugated Linoleic Acid and Risk of Breast Cancer in Postmenopausal Women, *Nutr. Cancer 38*, 151–157.

21. Corl, B.A., Barbano, D.M., Bauman, D.E., and Ip, C. (2003) *Cis*-9,*trans*-11 CLA Derived Endogenously from *trans*-11 18:1 Reduces Cancer Risk in Rats, *J. Nutr. 133*, 2893–2900.

22. Kramer, J.K.G., Cruz-Hernandez, C., Or-Rashid, M., and Dugan, M.E.R. (2004) The Use of Total *trans*-11 Containing FA, Rather than Total An-7″ FA, Is Recommended to Assess the Content of FA with a Positive Health Image in Ruminant Fats, *Lipids 39*, 693–695.

23. Bauman, D.E., and Griinari, J.M. (2003) Nutritional Regulation of Milk Fat Synthesis, *Annu. Rev. Nutr. 23*, 203–227.

24. Mossoba, M.M., Kramer, J.K.G., Delmonte, P., Yurawecz, M.P., and Rader, J.I. (2003) *Official Methods for the Determination of* trans *Fat*, AOCS Press, Champaign, IL.

25. Ratnayake, W.M.N. (2004) Overview of Methods for the Determination of *trans* Fatty Acids by Gas Chromatography, Silver-Ion Thin-Layer Chromatography, Silver-Ion Liquid Chromatography, and Gas Chromatography/Mass Spectrometry, *J. AOAC Int. 87*, 523–539.

26. Mossoba, M.M., Yurawecz, M.P., Delmonte, P., and Kramer, J.K.G. (2004) Overview of Infrared Methodologies for *trans* Fat Determination, *J. AOAC Int. 87*, 540–544.

27. AOAC (2000) Total *cis*- and *trans*-Octadecenoic Isomers and General Fatty Acid Composition in Hydrogenated Vegetable Oils and Animal Fats (41.1.35A), in *Official Methods of Analysis*, 17th edn., pp. 32–36, AOAC International, Gaithersburg, MD, Official Method 994.15.

28. AOCS (2002) Determination of *cis*- and *trans*-Fatty Acids in Hydrogenated and Refined Oils and Fats by Capillary GLC, in *Official Methods and Recommended Practices*, 5th edn. (D. Firestone, ed.), AOCS Press, Champaign, IL, Official Method Ce 1f-96.

29. Cruz-Hernandez, C., Deng, Z., Zhou, J., Hill, A.R., Yurawecz, M.P., Delmonte, P., Mossoba, M.M., Dugan, M.E.R., and Kramer, J.K.G. (2004) Methods for Analysis of Conjugated Linoleic Acids and *trans*-18:1 Isomers in Dairy Fats Using a Combination of Gas Chromatography, Silver-Ion Thin-Layer Chromatography/Gas Chromatography, and Silver-Ion Liquid Chromatography, *J. AOAC Intl. 87*, 545–562.

30. Precht, D., and Molkentin, J. (1999) C18:1, C18:2, and C18:3 *trans* and *cis* Fatty Acid Isomers Including Conjugated *cis* Δ9,

trans Δ11 Linoleic Acid (CLA) as Well as Total Fat Composition of German Human Milk Lipids, *Nahrung 43*, 233–244.

31. Adam, M., Chew, M., Wasserman, S., McCollum, A., McDonald, R.E., and Mossoba, M.M. (1998) Determination of *trans* Fatty Acids in Hydrogenated Vegetable Oils by Attenuated Total Reflection Infrared Spectroscopy: Two Limited Collaborative Studies, *J. Am. Oil Chem. Soc. 75*, 353–358.

32. AOCS (1999) Rapid Determination of Isolated *trans* Geometric Isomers in Fats and Oils by Attenuated Total Reflection Infrared Spectroscopic, 5th edn. (D. Firestone, ed.), AOCS Press, Champaign, IL, Official Method Cd 14d.99.

33. AOAC (2002) Determination of Isolated *trans* Unsaturated Fatty Acids in Fats and Oils, in *Official Methods of Analysis*, 17th edn., 41.1.37A, AOAC International, Gaithersburg, MD, Official Method 2000.10.

34. Setiowaty, G., and Che Man, Y.B. (2004) Multivariate Determination of Cloud Point in Palm Oil Using Partial Least Squares and Principal Component Regression Based FTIR Spectroscopy, *J. Am. Oil Chem. Soc. 81*, 7–11.

35. Mossoba, M.M., McDonald, R.E., Armstrong, D.J., and Page, S.W. (1991) Identification of Minor C_{18} Triene and Conjugated Diene Isomers in Hydrogenated Soybean Oil and Margarine by GC-MI-FT-IR Spectroscopy, *J. Chromatogr. Sci. 29*, 324–330.

36. Christy, A.A., Egeberg, P.K., and Østensen, E.T. (2003) Simultaneous Quantitative Determination of Isolated *trans* Fatty Acids and Conjugated Linoleic Acids in Oils and Fats by Chemometric Analysis of the Infrared Profiles, *Vib. Spectrosc. 33*, 37–48.

37. Milosevic, M., Milosevic, V., Kramer, J.K.G., Azizian, H., and Mossoba, M.M. (2004) Determining Low Levels of *trans* Fatty Acids in Foods Using an Improved ATR-FTIR Procedure, *Lipid Technol. 16*, 252–255.

38. Li, H., van de Voort, F.R., Sedman, J., and Ismail, A.A. (1999) Rapid Determination of *cis* and *trans* Content, Iodine Value, and Saponification Number of Edible Oils by Fourier Transform Near-Infrared Spectroscopy, *J. Am. Oil Chem. Soc. 76*, 491–497.

39. Li, H., van de Voort, F.R., Ismail, A.A., Sedman, J., and Cox, R. (2000) *Trans* Determination of Edible Oils by Fourier Transform Near-Infrared Spectroscopy, *J. Am. Oil Chem. Soc. 77*, 1061–1067.

40. Davies, A.M.C., and Garrido-Varo, A. (eds.) (2003) *Near Infrared Spectroscopy*: *Proceedings of the 11th International Conference*, (Cordoba, Spain, 6–11 April 2003), NIR Publications, Chichester, United Kingdom, www.nirpublications.com/nir03.html.

41. Mailer, R.J. (2004) Rapid Evaluation of Olive Oil Quality by NIR Reflectance Spectroscopy, *J. Am. Oil Chem. Soc. 81*, 823–827.

42. Molette, C., Berzaghi, P., Dalle Zotte, A., Remignon, H., and Babile, R. (2001) The Use of Near-Infrared Reflectance Spectroscopy in the Prediction of the Chemical Composition of Goose Fatty Liver, *Poult. Sci. 80*, 1625–1629.

43. Jensen, P.N., Christiansen, J., and Engelsen, S.B. (2004) Oxidative Changes in Pork Scratchings, Peanuts, Oatmeal and Muesli Viewed by Fluorescence, Near-Infrared and Infrared Spectroscopy, *Eur. Food Res. Technol. 219*, 294–304.

44. Azizian, H. (2004) FT-NIR Fatty Acid Determination Method, U.S. Patent Application 10/840277.

45. Kramer, J.K.G., Cruz-Hernandez, C., and Zhou, J. (2001) Conjugated Linoleic Acids and Octadecenoic Acids: Analysis by GC, *Eur. J. Lipid Sci. Technol. 103*, 600–609.

46. Kramer, J.K.G., Blackadar, C.B., and Zhou, J. (2002) Evaluation of Two GC Columns (60-m SUPELCOWAX 10 and 100-m CP Sil 88) for Analysis of Milkfat with Emphasis on CLA, 18:1, 18:2, and 18:3 Isomers, and Short- and Long-Chain FA, *Lipids 37*, 823–835.

47. Wolff, R.L. (1994) Analysis of α-Linolenic Acid Geometrical Isomers in Deodorized Oils by Capillary Gas–Liquid Chromatography on Cyanoalkyl Polysiloxane Phases: A Note of Caution, *J. Am. Oil Chem. Soc. 71*, 907–909.

48. Kramer, J.K.G., Fellner, V., Dugan, M.E.R., Sauer, F.D., Mossoba, M.M., and Yurawecz, M.P. (1997) Evaluating Acid and Base Catalysts in the Methylation of Milk and Rumen Fatty Acids with Special Emphasis on Conjugated Dienes and Total *trans* Fatty Acids, *Lipids 32*, 1219–1228.

49. Workman, J.J. (1995) Interpretive Spectroscopy for Near Infrared, in *Near Infrared Spectroscopy: The Future Waves, Proceedings of the 7th International Conference on Near Infrared Spectroscopy* (Davies, A.M.C., and Williams, P., eds.), pp. 6–13 (Montreal, Canada, 6–11 August 1995), NIR Publications, Chichester, United Kingdom.

50. Azizian, H., Kramer, J.K.G., Kamalian, A.R., Hernandez, M., Mossoba, M.M., and Winsborough, S.L. (2004) Quantification of *trans* Fatty Acids in Food Products by GC, ATR-FTIR and FT-NIR Methods, *Lipid Technol. 16*, 229–231.

51. Precht, D., and Molkentin, J. (1996) Rapid Analysis of the Isomers of *trans*-Octadecenoic Acid in Milk Fat, *Int. Dairy J. 6*, 791–809.

52. Roach, J.A.G., Mossoba, M.M., Yurawecz, M.P., and Kramer, J.K.G. (2002) Chromatographic Separation and Identification of Conjugated Linoleic Acid Isomers, *Anal. Chim. Acta 465*, 207–226.

REVIEW

Astonishing Diversity of Natural Surfactants: 5. Biologically Active Glycosides of Aromatic Metabolites

Valery M. Dembitsky*

Department of Organic Chemistry and School of Pharmacy, Hebrew University, Jerusalem, Israel

ABSTRACT: This review article presents 342 aromatic glycosides, isolated from and identified in plants and microorganisms, that demonstrate different biological activities. They are of great interest, especially for the medicinal and/or pharmaceutical industries. These biologically active natural surfactants are good prospects for the future chemical preparation of compounds useful as antioxidant, anticancer, antimicrobial, and antibacterial agents. These glycosidic compounds have been classified into several groups, including simple aromatic compounds, stilbenes, phenylethanoids, phenylpropanoids, naphthalene derivatives, and anthracene derivatives.

Paper no. L9814 in *Lipids 40*, 869–900 (September 2005).

The father of modern medicine was Hippocrates, who lived sometime between 460 and 377 BC. Hippocrates left historical records of pain-relief treatments, including the use of a powder made from the bark and leaves of the willow tree to help heal headaches, pains, and fevers. Since the time of Hippocrates, people have chewed on willow leaves and bark to alleviate pain. About 2,000 years later, aspirin began being manufactured from a compound extracted from the tree. As it turns out, that family of compounds, called phenolic glycosides, also plays a key role in plant health, making many plants tough and disease resistant.

Aromatic compounds, including phenolic compounds, are widely distributed in the plant kingdom (2). These compounds are essential for the growth and reproduction of plants and are produced as a response to defend injured plants against pathogens. In recent years, interest has been growing in aromatic compounds and their presumed role in the prevention of various degenerative diseases, such as cancer and cardiovascular diseases (3–5). The antioxidant activities of aromatic compounds and their possible use in processed foods as natural antioxidants have gained considerable recognition in recent years (3,6,7). Terrestrial vascular plants and their aquatic counterparts contain several types of phenylpropanoid metabolites. In vascular plants, this pathway provides major classes of organic compounds of specialized function and structure. These include neolignans and lignans, structural cell wall polymers (lignins and the aromatic portion of suberins), proanthocyanidins (condensed tannins, i.e., the phenylalanine-derived portion), and related compounds. Without this pathway, the normal growth, development, and survival of both woody and nonwoody plants would not be possible. Indeed, since approximately 10–45% of all vascular plant material is of phenylpropanoid origin, these metabolites constitute a major sink of organic carbon. Many of these molecules can occur in plants in the form of glycosides, which means they have one or more simple sugars, such as glucose, galactose, mannose, xylose, or another sugar attached to them. Not only are thousands of aromatic compounds known, but some of the smaller molecules also can polymerize, or join together to form larger and more complex molecules. Different kinds of molecules might be found in one polymer (8–11).

Phenolic compounds (a molecule containing an aromatic ring that bears one or more hydroxyl groups is referred to as "phenolic") can also be bound to certain proteins, polysaccharides, or lipids (12–18), and as if this were not complex enough, some molecules can have multiple isomers, forms in which their atoms are arranged slightly differently.

Simple and polyphenolic compounds and/or their glycosides of fruits and vegetables may play an important role in physiological functions related to human health (19–26). Different polyphenolics may have varied biological activities, such as having anticancer, anti-inflammatory, cytostatic, cytotoxic, antimitotic, neurotoxic, antiplatelet, antibacterial, antifungal, aggregational, or antiradical activities, as well as antioxidant or cardioprotective activities (3,20,22,24,27–29).

Aromatic glycosides, representative of a large group of natural compounds mainly originating from plant species that can be separated on several groups, including simple aromatic glycosides, stilbene glycosides, phenylethanoid and phenylpropanoid glycosides, naphthalene glycosides, and glycosides of anthracene derivatives (anthraquinones, angucyclines, oxanthrones, and anthrones), as considered in this review article.

*Address correspondence at Department of Organic Chemistry, P.O. Box 39231, Hebrew University, Jerusalem 91391, Israel.
E-mail: dvalery@cc.huji.ac.il

Abbreviations: D-GalN, D-galactosamine; EC_{50}, the median effect concentration, being a statistsically derived concentration of a substance that can be expected to cause (i) an adverse reaction in 50% of organisms or (ii) a 50% reduction in growth or in the growth rate of organisms; GI_{50}, the concentration needed to reduce the growth of treated cells to half that of untreated (i.e., control) cells; HUVEC, human umbilical vein endothelial cells; IC_{50}, concentration at which growth or activity is inhibited by 50% (applies to ligand and growth inhibition); K_i, prolyl hydroxylase activity, expressed as mol/mg protein; LLC, Lewis lung carcinoma; LPS, lipopolysaccharide; MIC, minimum inhibitory concentration of an antibiotic that inhibits a bacterium; MPP^+, 1-methyl-4-phenylpyridinium ion; OLE, olive leaf extract; SDG, secoisolariciresinol diglycoside **245**; TNF-α, tumor necrosis factor α.

SIMPLE AROMATIC GLYCOSIDES

Simple aromatic (including phenolic) glycosides have been isolated mainly from plants, although a few compounds have been isolated from microorganisms. Compounds in this group often also possess alcoholic, aldehydic, and carboxylic acid groups. Medicinal herbs constitute an important source of biologically active compounds, and they have given us a number of important drugs that are mainstays of treatment in synthetic systems of medicine (30–32).

The Egyptians (*ca.* 1500 BC) recorded a collection of recipes for medicines that included a recipe using an infusion of dried myrtle leaves (which contain salicylic acid) to relieve back pain. The effects of aspirin-like substances have been known since the ancient Romans recorded the use of willow bark as a fever fighter. The leaves and bark of the willow tree contain a substance called salicin, **1**, a naturally occurring compound similar to acetylsalicylic acid (aspirin) (33). Aspirin is probably the most successful medicine of all time, and new uses for it continue to be discovered (34–37).

In 1828, Johann Buchner, a professor at Munich University, isolated pure salicin from willow bark (*Salix alba*). Two Italians, Luigi Brugnatelli and Carlo Fontana, had in fact already obtained salicin in 1826, but in a highly impure form. By 1829, Henri Leroux, a French chemist, had improved the extraction procedure to obtain about 30 g from *S. alba* bark. In 1838, Raffaele Piria, an Italian chemist then working at the Sorbonne in Paris, split salicin into a sugar and an aromatic component (salicylaldehyde) and converted the latter, by hydrolysis and oxidation, to an acid of crystallized colorless needles, which he named salicylic acid (38–43). The name salicin was derived from *salix*, which is the Latin word for willow tree. Many well-known drugs have come from studying natural plant compounds such as salicin, the active constituent found in white willow bark. This herb has been used for centuries to ease discomfort associated with the joints and muscles. Occurring as white crystals or powder, salicin has analgesic, antipyretic, disinfectant, and antiseptic properties, and it has been found in a number of plant species: *S. alba, Salix tetresperma, Salix fragilis, Populus nigra, Populus alba, Populus tremula*, and *Filipendula ulmaria* (39–44).

Salicin-related compounds, such as gaultherin **2** (formerly known as monotropitoside or monotropitin), monotropin, and spiraein are some of the known compounds present in plant flora having activity similar to salicin. Gaultherin **2** is a glycoside of methyl salicylate that is present in *Gaultheria procumbens* (wintergreen); it is also known as monotropitoside and is used as a source for the manufacture of salicylic acid (44). Salicin is found in most Salicaceae species, together with other much less abundant glycosides such as populin, tremuloidin, fragilin, glycosmin, picein, salireposide, grandidentatin, triandrin, salicylpopulin (salicyloylpopulin), and salidroside (salicyloylpopulin) (45). Salicylates have long been known as water-soluble compounds derived from a number of plants, particularly willow (*Salix* spp.), meadowsweet (*Spirea* spp. and *F. ulmaria*), sweet birch (*Betula lenta*), white birch (*Betula pendula*), wintergreen (*G. procumbens*), balsam poplar (*Populus balsamifera*), black poplar (*P. nigra*), balm of Gilead (*Populus candicans*), black haw (*Viburnum prunifolium*), and sweet violet (*Viola odorata*), with analgesic, antipyretic and anti-inflammatory properties (46–48). In 1953, Paris and Pointet (49) reported the presence of gaultherin **2** in the bark of *Ostryopsis davidiana*. More recently, Towers *et al.* (50) studied leaf extracts of 22 species of *Gaultheria* after acid or alkali hydrolysis, yielding *p*-hydroxybenzoic, *o*-pyrocatechuic, protocatechuic, gentisic, vanillic, *p*-coumaric, caffeic, and ferulic acids, and found that 13 species contained derivatives of salicylic acid as well; the glycoside gaultherin **2** was isolated from *G. procumbens* and *Gaultheria hispidula*. Gaultheria oil (or wintergreen oil), which consists almost solely of methyl salicylate, was formerly distilled on a commercial scale from the leaves of this species. *Gaultheria procumbens*, also known as teaberry, wintergreen, Canada tea, partridge berry, checkerberry, boxberry, wax cluster, spice berry, mountain tea, deerberry, spicy wintergreen, aromatic wintergreen, chink, ground berry, grouse berry, red pollom, redberry tea, hillberry, and ivory plum, is related to the Northwest native evergreen groundcover *Gaultheria shallon*, which was used by Quinault and Klallum Indians for its medicinal properties as a stimulant, antiseptic, astringent, diuretic, emmenagogue, and aromatic, and was also useful in chronic inflammatory rheumatism, rheumatic fever, sciatica, diabetes, all bladder troubles, scrofula, and skin diseases (51). Spiraein **3**, which contains salicylaldehyde, xylose, and glucose, was first isolated from *F. ulmaria* (52) and was later was found in other plant species, i.e., *Populus tremuloides*, *Salix purpurea*, *S. fragilis, Salix nigricans*, and *Salix rosmarinifolia* (53). Leonuriside A **4** and erigeside C **5** were isolated from the aerial parts of *Acanthus ilicifolius* (54). Two new salicin derivative glucosides, 7-*O*-methyl-salicin **6** and 7-*O*-(2,6-dihydroxy-benzoyl)salicin **7**, were isolated from the leaves of *Alangium platanifolium* var. *trilobum* (55). Salicin **1** and populin **8** were isolated from hot-water bark extracts of *Populus tomentosa, Populus davidiana, Populus euphratica*, and *Populus simonii* (56).
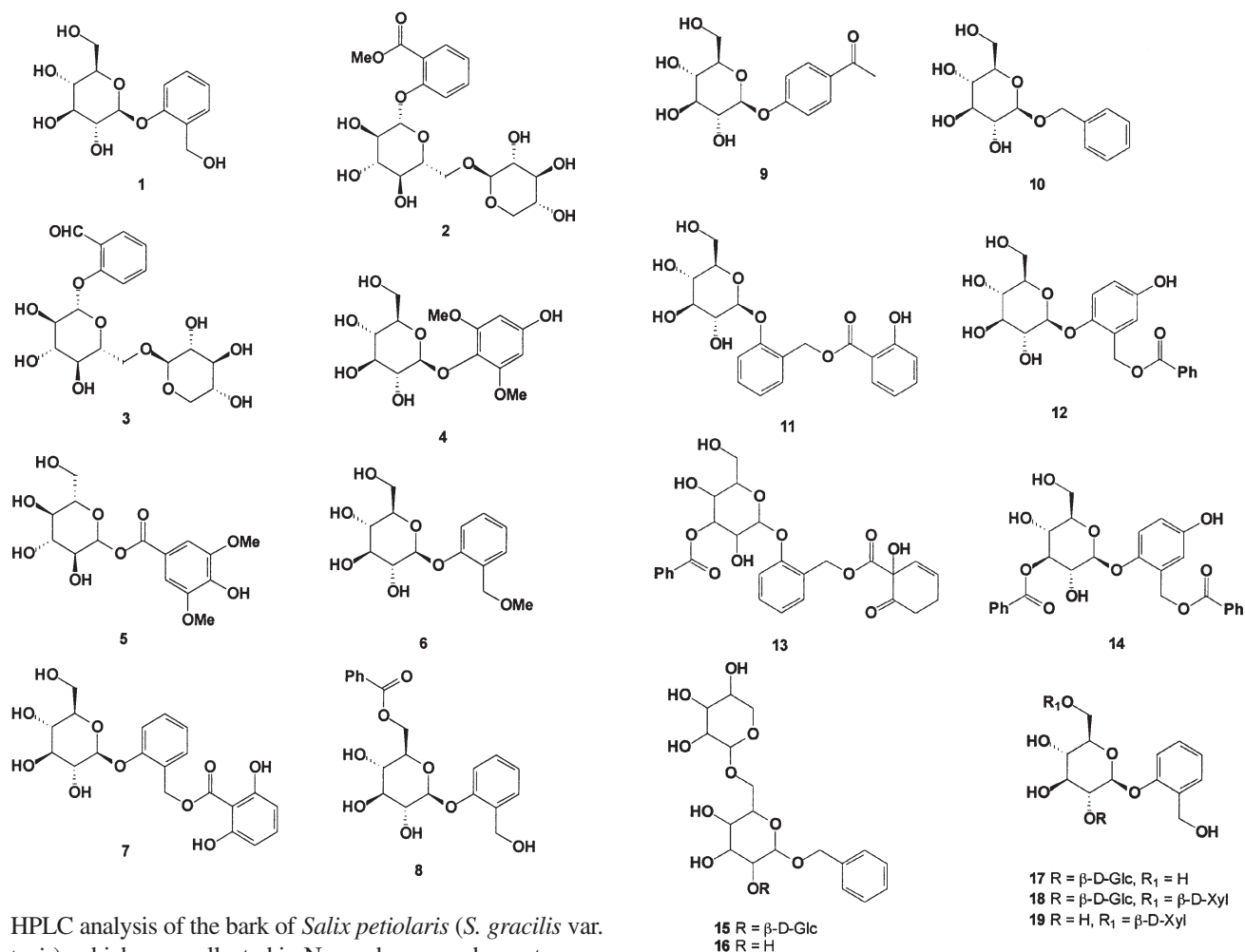
HPLC analysis of the bark of *Salix petiolaris* (*S. gracilis* var. *textoris*), which was collected in November, was shown to contain salicin **1**, populin **8**, picein **9**, salicyloylsalicin **11**, salireposide **12**, grandidentatin, vimalin, tremulacin **13**, and salicyloyl-salicin-2-*O*-benzoate **14** (57). Golden root (*Rhodiola rosea*) has been used for many years as an adaptogen in Chinese traditional medicine and was reported by Tolonen *et al.* (58) to have many pharmacological properties; its known phenylpropanoid metabolites, picein **9** and benzyl-*O*-β-glucopyranoside **10**, were recently isolated. Three new glycosides, benzyl alcohol β-D-glucopyranosyl-(1→2)-[β-D-xylopyranosyl-(1→6)]-β-D-glucopyranoside **15**, 2′-*O*-β-D-glucopyranosylsalicin **17**, and 2′-*O*-β-D-glucopyranosyl-6′-*O*-β-D-xylopyranosylsalicin **18**, along with the known benzyl alcohol β-D-xylopyranosyl-(1→6)-β-D-glucopyranoside **16** and 6′-*O*-β-D-xylopyranosyl-salicin **19**, were isolated from the water-soluble fraction of the dried leaves of *Alangium chinense* (59).

Dill (*Anethum graveolens*) has been cultivated in Europe since antiquity and is popular aromatic herb and spice. Its seed also has been used for medicinal purposes to relieve digestive problems and to stimulate milk for nursing mothers. Dill water was believed to have a soothing effect on the digestive system and was given to babies to relieve hiccups and colic, and essential oils from dill have antimicrobial (60,61), antihyperlipidemic, and antihypercholesterolemic activities (62). From the water-soluble fraction of an ethanol extract of dill seed, which has been used as a spice and medicine, 33 compounds were obtained, including the known compound **10** and the new aromatic glucosides **20**–**25** (63).

20

21

26 R = H
27 R = Api
28 R = Glc

29

22

23

30

31

24

25

32

33 R = H
34 R = Api
35 R = Rha

36 R = Rha

37
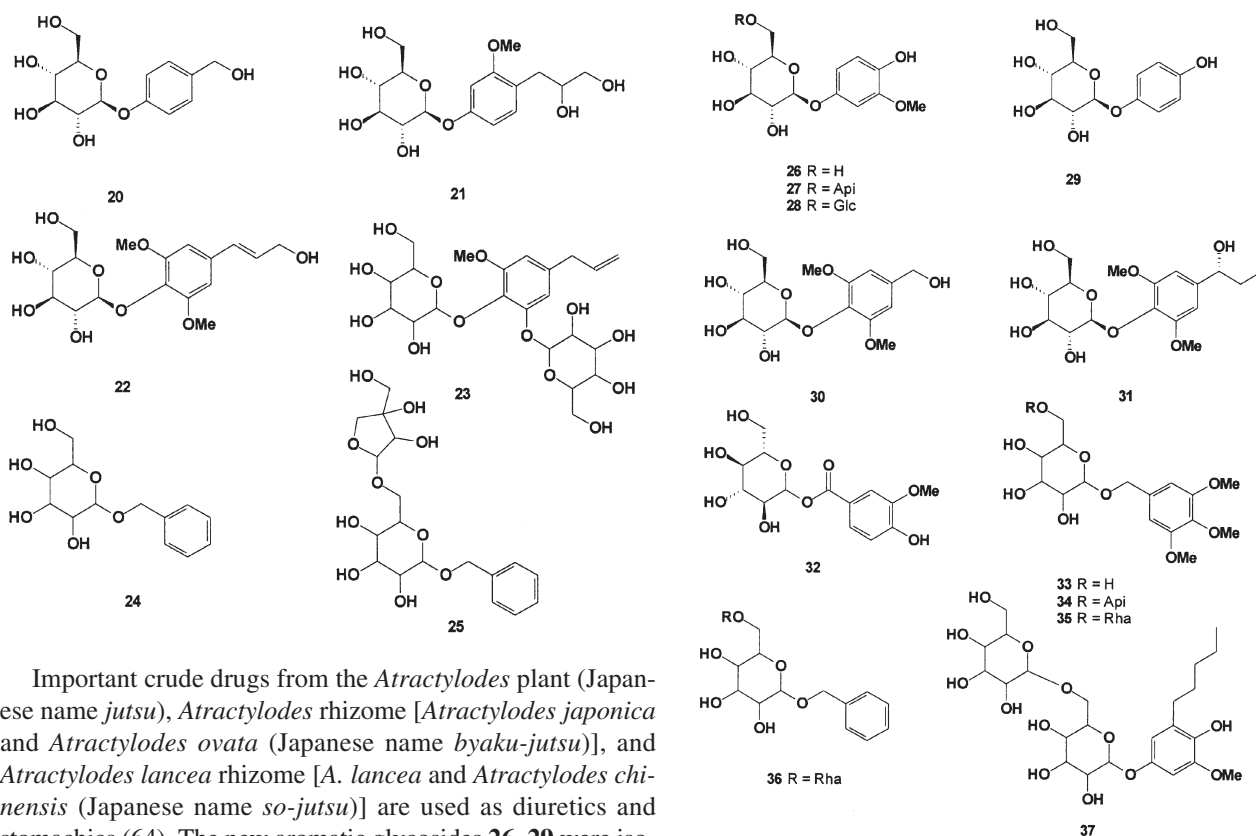
Important crude drugs from the *Atractylodes* plant (Japanese name *jutsu*), *Atractylodes* rhizome [*Atractylodes japonica* and *Atractylodes ovata* (Japanese name *byaku-jutsu*)], and *Atractylodes lancea* rhizome [*A. lancea* and *Atractylodes chinensis* (Japanese name *so-jutsu*)] are used as diuretics and stomachics (64). The new aromatic glycosides **26–29** were isolated together with 10 known compounds, including **25**, from the water-soluble fraction of the fresh rhizome of *A. japonica* (65).

Coriander (*Coriandrum sativum*) has one of the longest recorded histories of any of the spices. There is evidence that this native of the Mediterranean and Near East has been in use since 5000 BC. Its seeds have been found in Bronze Age ruins on the Aegean Islands and in the tombs of the pharaohs. Coriander is mentioned in the Ebers Papyrus and in the books of Moses. It was grown in Assyria and Babylon and was used in minced meat dishes, sausages, and stews. The seeds have been used as a drug for indigestion, against worms, and as a component of embrocations for rheumatism and pains in the joints. From the water-soluble portion of a methanol extract of coriander fruits, two new aromatic glycosides, **30** and **31**, were isolated together with the known compounds **4**, **24**, and **25** (66).

The seed of the *Amomum* plant is one of the most ancient and highly valued spices in the world. The seed of *Amomum xanthioides* (Zingiberaceae) also has been used for medicinal purposes; it is prescribed in traditional medicines for stomachic and digestive disorders and contains the simple aromatic glycosides **24** and **32** (67).

The Aceraceae plant *Acer nikoense* is indigenous to Japan (Japanese name, *megusurinoki*), and its stem bark has been used as a folk medicine for the treatment of hepatic disorders and eye diseases. The new aromatic glycoside nikoenoside **33** and also kelampayoside A **34**, **35**, and **36** were isolated from the stem bark of *A. nikoense* (68).

Plants of the genus *Eugenia* showed antidiabetic (69), hypoglycemic (70), and also antibacterial and antifungal activities against gram-positive bacteria (*Bacillus subtilis*, *Staphylococcus aureus*), gram-negative bacteria (*Salmonella typhimurium, Pseudomonas aeruginosa, Klebsiella pneumoniae*, and *Escherichia coli*), and fungal strains (*Candida albicans, Cryptococcus neoformans, Aspergillus flavus, Aspergillus fumigatus, Aspergillus niger, Rhizopus* sp., *Trichophyton rubrum, Trichophyton mentagrophytes*, and *Microsporum gypseum*) (71). Lambertianoside **37**, a novel phenylglycoside with anti-HIV activity, has been isolated from the aqueous extract of leaves from *Eugenia lambertiana* [HIV EC_{50} (i.e., median effect concentration causing an adverse reaction in 50% of organisms or a 50% reduction in the growth or growth rate of an organism), 3 µg/mL; HIV IC_{50} (i.e., 50% inhibition concentration), 25 µg/mL] (72).

Pumpkin, the fruit of *Cucurbita moschata* (Cucurbitaceae), has been a popular vegetable in cooking since antiquity, and salted, roasted pumpkin seeds are used in several countries as snacks; pumpkin seeds are also an important traditional Chinese medicine used in the treatment of cestodiasis, ascariasis, and schistosomiasis. Pharmacological studies on the seeds have demonstrated hepatoprotective (73) and antitumor activities (74). The new phenolic glycosides cucurbitosides A–E, **38–42**, were isolated from the seeds of *C. moschata* (75). The dried stem bark of *Albizzia julibrissin* (Leguminosae) has been used in Chinese herbal medicine to treat insomnia, diuresis, asthenia, ascaricide, and confusion. From the stem bark of *A.*

julibrissin, two new phenolic glycosides were isolated, albibrissinosides A **43** and B **44**. Albibrissinoside B **44** showed a strong 1,1-diphenyl-2-picrylhydrazyl radical-scavenging activity, with an IC_{50} value of 10.2 μM (positive control, L-ascorbic acid IC_{50} 10.4 mM), whereas albibrissinoside A **43** showed a weak scavenging activity, with an IC_{50} value of 253 μM (76).

38 R = H
39 R = OH

40 R = H
41 R = OH

42

43 R = Me, R₁ = OMe
44 R = R₁ = H
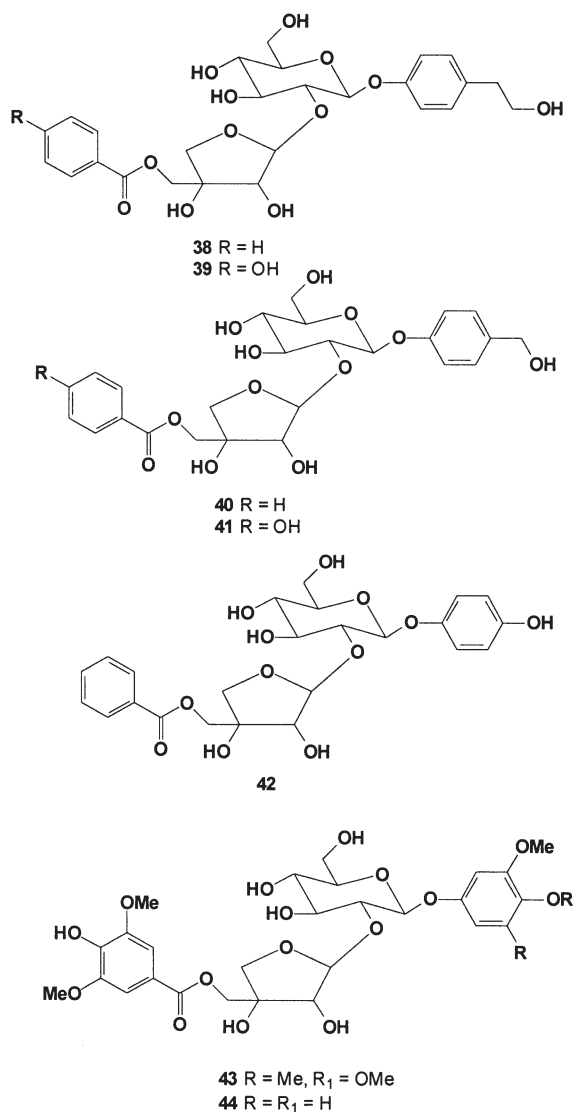
Three new phenolic compounds, 2-methoxy-5-(1′2′3′-trihydroxypropyl)-phenyl-1-*O*-(6″-galloyl)-β-D-glucopyranoside **45**, 2-methoxy-5-hydroxymethyl-phenyl-1-*O*-(6″-galloyl)-β-D-glucopyranoside **46**, and 1-galloyl-β-D-glucopyranosyl-(1→4)-β-D-galactopyranoside **47**, were isolated from the leaves of *Baseonema acuminatum* (Asclepiadaceae) (77). The antimicrobial activity of all compounds was evaluated *in vitro* against the bacteria *S. aureus* (two strains), *Bacillus cereus*, *B. subtilis*, *E. coli*, and *Salmonella typhimurium* and against three strains of *C. albicans*. The new compounds **45** and **46** showed antifungal activity against two clinically isolated *C. albicans* strains and against *C. albicans* ATCC 2091 [minimum inhibitory concentration (MIC) values in the range of 25–100 μg/mL]. Compound

47 inhibited only one strain of *C. albicans* at the maximum concentration used. Melilotoside **48** was isolated from *Ephedra nebrodensis* (78). The new phenolic glycosides quercetin β-D-glucopyranosyl 4-*O*-β-D-glucopyranosylcaffeate **49**, methyl 3-*O*-β-D-glucopyranosyl-5-hydroxycinnamate **50**, and β-D-glucopyranosyl 4-*O*-β-D-glucopyranosylbenzoate **51** were isolated from the flowers of *Moricandia arvensis* (79). Compounds **49**–**51** showed antioxidant activity, and **49** proved to possess the most potent radical-scavenging activity.

45

46

48

47

49

50

51
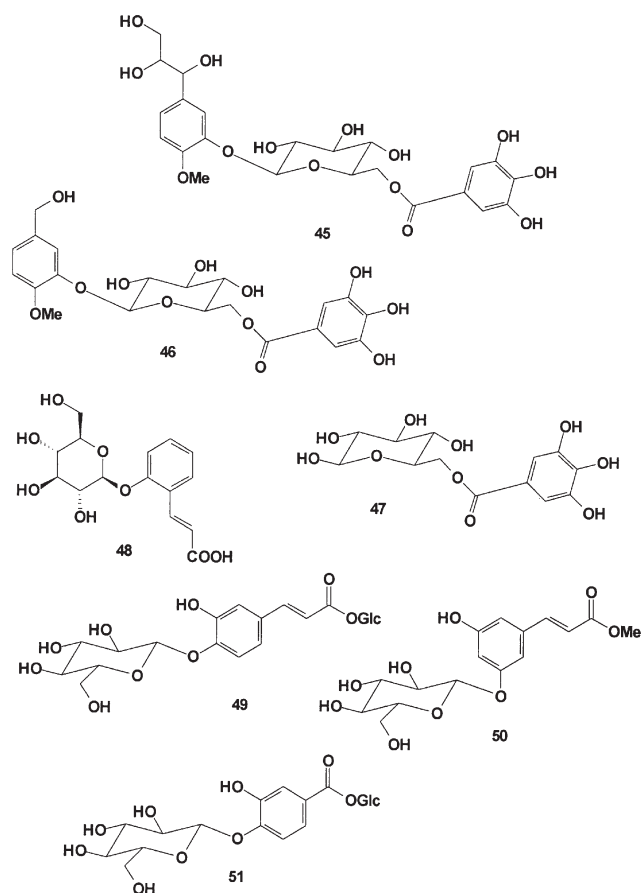
Curculigo orchioides (Amaryllidaceae) is a tiny herbal plant widely distributed in China, India, Malaysia, Japan, and Australia. Its rhizomes have the properties of warming the kidneys, invigorating yang, expelling cold, and eliminating dampness, and are used as the traditional Chinese medicine *xian mao* to cure impotence, enuresis, cold sperm, cold pain of the back and knee, and numbness of the limbs (80). In India, the tuberous roots of this plant are considered to be a tonic, alterative, demulcent, diuretic, and restorative, and are used as a poultice for itching and skin diseases (81). Three phenolic glycosides, curculigosides **52**, B **53**, and C **54**; orcinol glycoside **55**; and anacardoside **56** have been isolated from the rhizomes of *C. orchioides* and have been described in some recently published papers (81–88).

Three rare new chlorophenyl glycosides, curculigin A **57**, B **58**, and C **59**, have been isolated from *C. orchioides* (82,86). A new chlorine-containing phenoloid named capitulatin A **60** has been isolated from the rhizomes of *Curculigo capitulata* (89).

52 R = Me, R₁ = H
53 R = R₁ = H
54 R = Me, R₁ = OH

55 R = H
56 R = Glc

57

58

59

60

61 R = H
62 R = Malonic acid
63 R = Api
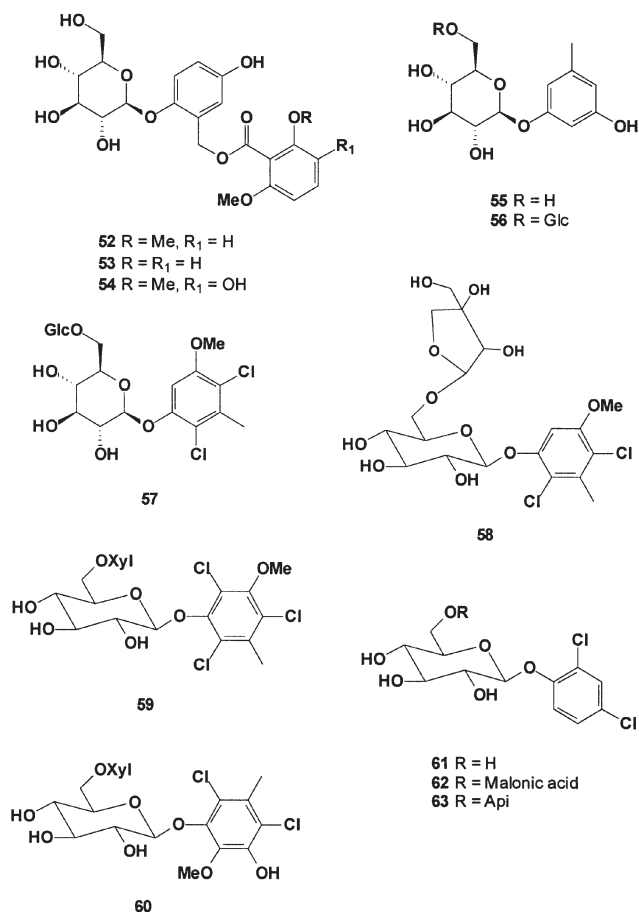
Three chlorophenyl glycosides **61–63** were extracted from the tissues of *Lemna minor* exposed to 2,4-dichlorophenol (90). Chlorophenols are an important class of xenobiotics used in a variety of biocides and have been shown to be resistant to microbial degradation. Enzyme-catalyzed hydrolysis with β-glucosidase was found to be ineffective in releasing the β-glucosides with chemical modifications at C-6. The presence of these

glucoconjugates confirmed that *L. minor* was capable of xenobiotic uptake and transformation. The products identified suggested that chlorophenols were incorporated into the vacuoles and cell walls of *L. minor* (90). The chlorophenol glucuronides **64** and **65** were isolated from human urine (91). β-(2-Chloroethyl)-D-glucoside **66** was isolated from the green plant *Taraxacum officinale* (92). Chlorophenol glycosides with the common structure **67** can be synthesized by aquatic plants and have been isolated from aquatic environments (93).

64

65

66

67
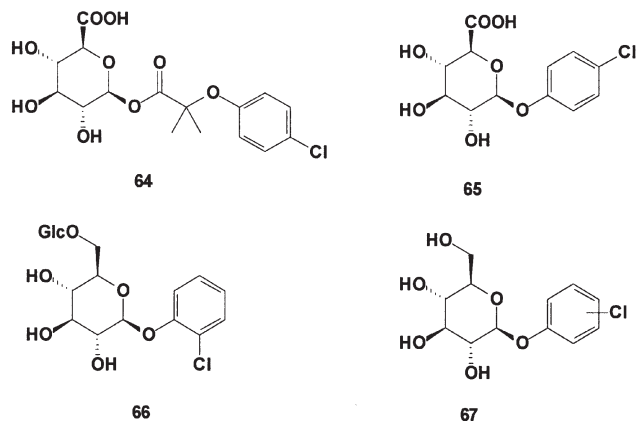
From the rhizomes of *Curculigo pilosa*, two benzylbenzoate diglucosides, piloside A **68** and B **69**; the *O*-methyl derivative **70**; nyasicoside **71**; and a glucosyl-fused norlignan, pilosidine **72**, previously obtained only as the tetra-*O*-methyl derivative **73**, were isolated. Pilosidine **72** showed a facilitating effect on adrenaline-evoked contractions in rabbit aorta (85). Nyasicoside **71** also was found in the rhizomes of *C. capitulata* (94). A monoglucoside, shipamanine **77**, and the related compounds obtuside A **74**, obtuside B **75**, and hypoxoside **76** were isolated from the rhizomes of *Hypoxis obtusa* (95,96). Shipamanine **77** and hypoxoside **76** showed antiviral, antitumoral, and analgesic activities.

68 R = H
69 R = OH
70 R = OMe

71

72 R = R₁ = H
73 R = Me, R₁ = H

74

75 R = H
76 R = Glc

77

78 R = p-Cou, R₁ = H
79 R = Bz, R₁ = H
80 R = p-OHBz, R₁ = H
81 R = Bz, R₁ = Api
82 R = H, R₁ = Api

83 R = H

84 R =

85 R =

86 R =

87 R =

88

89

90

91
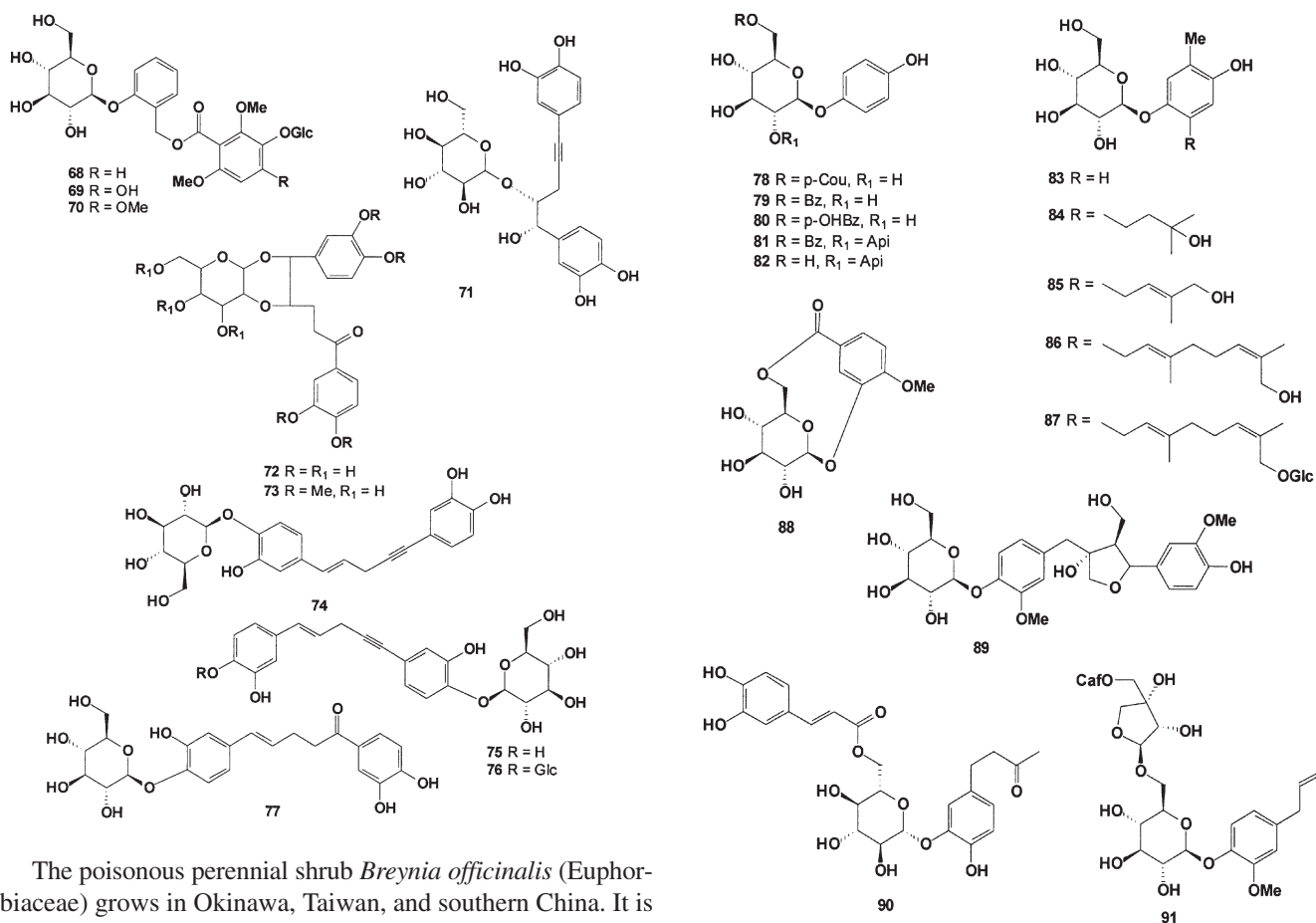
The poisonous perennial shrub *Breynia officinalis* (Euphorbiaceae) grows in Okinawa, Taiwan, and southern China. It is administered orally as a remedy for healing wounds and edema, as an ointment, for syphilis, and for intestinal hemorrhage due to overwork (97). The novel phenolic glycosides **78–82** have been isolated from the leaves of *B. officinalis* collected on Okinawa Island (98).

The herbaceous plant *Pyrola japonica* (Pyrolaceae) is widespread in Korea, Japan, and China; the leaves are used as a detoxicant for the bites of snakes, insects, and dogs, and as a drug to cure yellowish and bloody sputum (99). Five new phenolic glycosides, **83–87**, were isolated from the whole plants of *P. japonica* (100), and a new cyclic compound, jujuphenoside **88**, was isolated from the seeds of *Ziziphus jujuba* var. *spinosa* (101).

Three active glycosides (including sinenoside 1 **89**), which afford protection to red blood cell membranes to resist hemolysis induced by the peroxyl radical initiator 2,2′-azo-bis-(2-amidinopropane) dihydrochloride, were isolated from *Ligustrum sinense* (102). Dracunculifoside K **90** and N **91**, and 10

other glycosides were isolated from the aerial part of *Baccharis dracunculifolia* (Compositae); these compounds have an (*E*)-caffeoyl group like dracunculifosides A–J, which were reported previously (103).

Syringic acid 4-β-D-glucoside **92** was isolated from the aerial part of *Erigeron breviscapus* (104), and a lignan, glycoside (−)-secoisolariciresinol-*O*-α-L-rhamnopyranoside **93**, was isolated from the aerial parts of *Rubus amabilis* (105). Dictamnoside A **94** was isolated from the whole herb of *E. breviscapus* (106).

Four erythro-anethole glycol monoglucosides, **95–98**, and two new glycosides of *p*-hydroxyphenylpropylene glycol were isolated from the methanolic extract of the seed of *Foeniculum vulgare* (Umbelliferae). This is the first report of the isolation of all four *O*-β-D-glucopyranosides, which have the glucosyl unit attached to the hydroxy group of the erythro-glycol function of individual stereoisomeric aglycons (107).

92

94

93

95

96

97

98
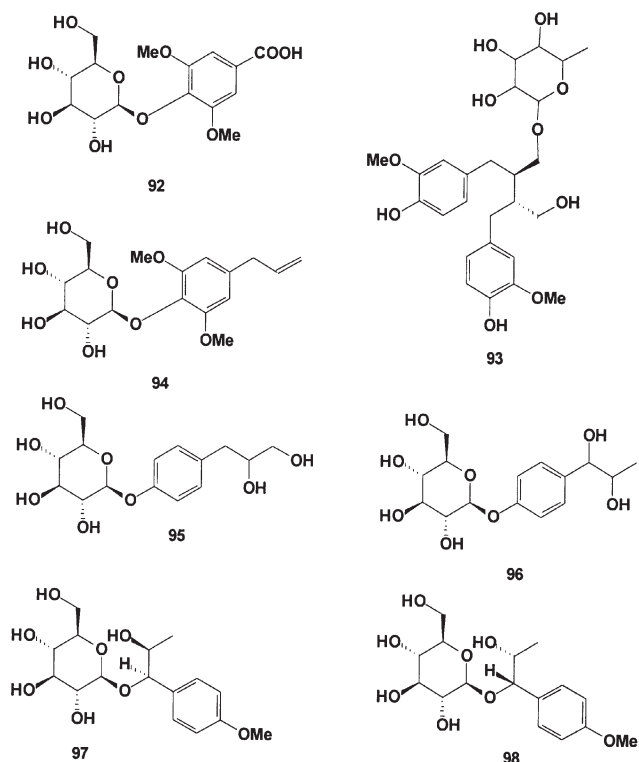
Aromatic glycosides, named hovetrichoside G **99** and F **100**, shashenoside I **101**, arillanin F **102**, and kelampayoside A **103**, have been isolated from the bark of *Hovenia trichocarea* (108).

The HIV-inhibitory activity of the extract was traced to polymeric tannins, whereas 2-hydroxy-3-*O*-β-D-glucopyranosyl-benzoic acid **104** was inactive in the National Cancer Institute's primary anti-HIV screening. This glycoside was isolated from *Geniostoma antherotrichum* (109).

The unusual compound (7*S*,8*S*)-3,5,8-trihydroxy-7-(4-hydroxyphenyl)-bicyclo[4.2.0]-octa-1,3,5-trien-2-yl-β-D-glucopyranoside **105** was isolated from an aqueous extract of *Polygonum multiflorum* (110).

99

100

101

102 R = Xyl
103 R = Api

104

105
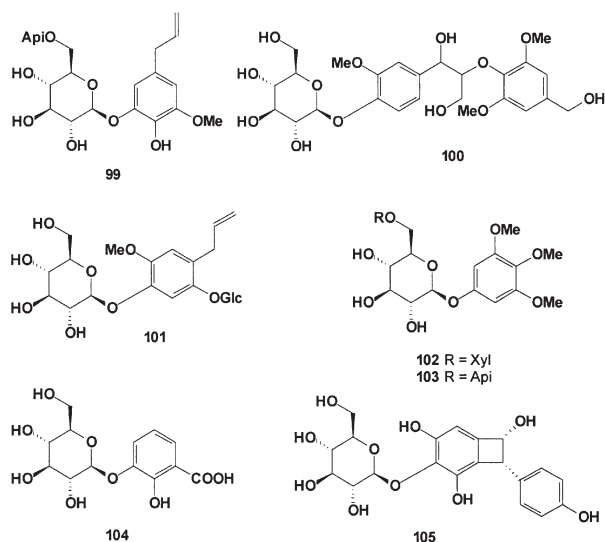
Many other simple aromatic glycosides with biological activities have been isolated from plant species, and readers of *Lipids* can find additional interesting information in a number of review articles (111–122).

STILBENES

Stilbenes—or 1,2-diphenylethylenes, of which more than 300 are known—are biologically active compounds that have shown different activities, such as nitric oxide production inhibition and antibacterial, antifungal, antioxidant, anti-inflammatory, anticancer, and antimalarial activities (123–128). These compounds and/or their glycosides also have attracted much attention for their biological effects, including antioxidant cyclooxygenase-I and -II inhibitory (129), antiplatelet-aggregation (130), antifungal (131), tyrosinase-inhibitory (132), anti-HIV-1, and cytotoxic effects (133), which play an important role in photochemical reactions (134,135). They have been found in many families of higher plants but mainly in Vitaceae, Gnetaceae, Polygonaceae, Liliaceae, Moraceae, and Cyperaceae. According to the National Library of Medicine (National Center for Biotechnology Information, Bethesda, MD), more than 28,000 research papers have been published on the activities of stilbenes and related compounds.

Two novel bibenzyl glucosides, together with their known aglycons batatasin III **106** and 3′-*O*-methylbatatasin III **107**, were isolated from the tubers of *Pleione bulbocodioides* (136); icariside A6 **108** also was isolated from the aerial parts of *Epimedium grandiflorum* var. *thunbergianum* as a minor constituent (137).

The tree *Acer mono* (*A. truncatum* subsp. *mono,* Aceraceae), known as *gorosoe* in Korean, is widely distributed in Korea, China, and Japan. The leaves of *A. mono* have been used in Korean folk medicine for hemostasis, and the roots have been used for the treatment of arthralgia and cataclasis. The sap of *A. mono* has been used to treat difficulty in urination, constipation, other gastroenteric disorders, gout, and neuralgia (138). Two new stilbene glycosides, **109** and **110**, were isolated from the leaves of *A. mono* along with seven known compounds. Compounds **109** and **110** showed significant hepatoprotective activities (97.3% protection against toxicity induced by H_2O_2 at 50 µg/mL) in primary cultures of rat hepatocytes (139). Compounds **109** and **111**, isolated from the stem bark extract of *Boswellia papyrifera* (140), exhibited significant inhibition of phosphodiesterase I and xanthine oxidase (140).

Resveratroloside **112**, a well-known stilbene glycoside, is widely distributed in grapes and wines (141). The highest contents of resveratrol and resveratrol glycoside **112** were observed in wines made with the mourvedre, pinot, and cabernet sauvignon varieties; the lowest were in those made with gamay, cabernet franc, or grenache (141). It has also been found in many other plant species (142). Resveratroloside **112** exhibited relatively higher cytotoxic activities against human oral squamous cell carcinoma and salivary gland tumor cell lines than against normal human gingival fibroblasts (143). Other pharmacological activities of resveratrol and their glycosides have

recently been reviewed (144). 4′-*O*-β-D-(6″-*O*-Galloyl)-glucopyranoside **113** was isolated from the Japanese rhubarb, *shinshu daio* (145). *Trans*-piceid **114**, *trans*-astringin **115**, isorhapontigenin 3-*O*-β-D-glucoside **116**, and pinostilbenoside **117** were isolated from the bark of some *Pinaceae* species (146). Compounds **115** and **116** also were found in the Colorado blue spruce (*Picea pungens*) and Engelmann spruce (*Picea engelmannii*) (147). Resveratroloside **112** and pinostilbenoside **117** were found in the inner bark of *Pinus sibirica* (148). Hydroxystilbene glycoside **111** was isolated from the roots of the Italian tree *Terminalia sericea* (149), and **118** was isolated from the Australian *Eucalyptus sideroxylon* (149). Deoxyrhaponticin **119**, rhaponticoside **120**, piceatannol 3′-*O*-β-D-glucopyranoside **121**, and compound **117** were obtained from an extract of the rhizomes of *Rheum rhaponticum* (150).

trans-Piceid **114** and compound **122** were found in grapes and wine (151). Kimura and Okuda (151) studied the effects of stilbene glucosides, which were isolated from medicinal plants and grapes, on tumor growth and lung metastasis in mice bearing highly metastatic Lewis lung carcinoma (LLC) tumors, and also the inhibitory effects of stilbene glucosides on the differentiation of human umbilical vein endothelial cells (HUVEC). Piceid **114** inhibited the DNA synthesis in LLC cells at a concentration of 1000 μM, but not at lower concentrations (10–100 μM). 2,3,5,4′-Tetrahydroxystilbene-2-*O*-D-glucoside **122** also inhibited DNA synthesis in LLC cells (IC$_{50}$, 81 μM). In addition, both stilbene glucosides inhibited the formation of capillary-like tube networks (angiogenesis) of HUVEC at concentrations of 100–1000 μM. It was suggested that the antitumor and antimetastatic activities of the stilbene glucosides piceid and 2,3,5,4′-tetrahydroxystilbene-2-*O*-D-glucoside **122** might be due to the inhibition of DNA synthesis in LLC cells and angiogenesis of HUVEC. The pharmacological effect of stilbene glycoside **122** on two kinds of cell models of amentia imitation was observed; the protective mechanism of stilbene glycoside, the main effective component of the tuber fleeceflower root on nerve cells, was explored; and a basis was provided for clarification of the efficacy of a Chinese drug compound from the tuber fleeceflower root (152). The results indicated that stilbene glycoside **122** significantly promoted cell viability and reduced cell membrane damage in β-amyloid 25–35 and H$_2$O$_2$, treating nerve cells. This drug may antagonize the cell damage initially induced by hydrogen peroxide and prevent subsequent toxicity of the amyloid β-protein in nerve cells. This nerve protection of the drug will be the basis for treating Alzheimer's disease and other neurodegenerative diseases.
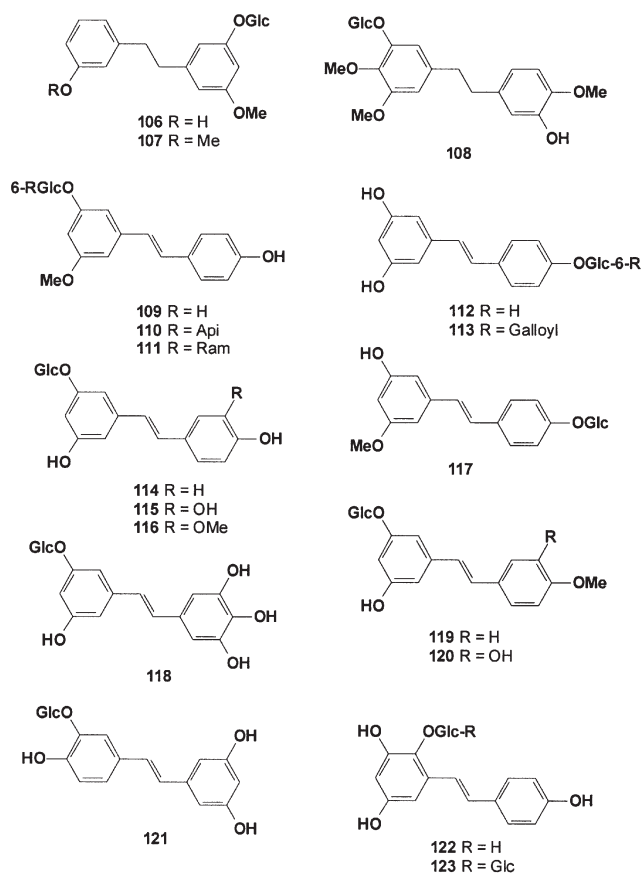
The tetrahydroxystilbene glycosides **122**–**125** were isolated from *P. multiflorum* (153). These isolated tetrahydroxystilbene glucosides are used to prepare drug and/or health-care foods for the prevention and treatment of cerebrovascular and cardiovascular diseases.

Stilbenes isolated from the rhizomes of the Korean rhubarb *Rheum undulatum* and related compounds were investigated for their antiallergenic activities (154). Thus, the effects of substitutes on the aromatic rings of stilbenes have indicated that stilbenes substituted with methoxyl groups at the 3-, 5-, and 40-positions exhibit higher activity than those with hydroxyl groups. Moreover, the activity is dramatically decreased when there is no substitute on aromatic rings. Substitution of the glycoside moiety on the ring dramatically decreases the activity, which can be observed from the inhibitory activities of rhaponticin [**126**, IC$_{50}$ > 100 (9.4) μM], and rhaponticin 2-*O*-gallate (**127**, 45.6 μM), isorhapontin (**128**, 23.5 μM), and piceatannol 30-*O*-β-D-glucopyranoside (**131**, −7.1 μM) compared with

nonglycosidic compounds such as rhapontigenin (11 μM), isorhapontigenin (12 μM), and piceatannol (24 μM). The results revealed that 3,5,40-trimethylpiceatannol exhibited the most potent inhibition against β-hexosaminidase release as a marker of degranulation in RBL-2H3 cells (IC$_{50}$ 2.1 μM), followed by trimethylresveratrol (IC$_{50}$ 5.1 μM). Glycosides **128**–**130** also were found in extracts from the root bark of *Picea abies* (155). The stilbenes rutinoside **132** and dihydrochalcone glucoside **133** were isolated from *Guibourtia tessmanii* (156).

Species of the Dipterocarpaceae family are a rich source of polyphenols, particularly resveratrol oligomers, and they show various biological activities such as being cytotoxic, antiviral, and anti-inflammatory (157). Resveratrol glycosides **134**–**136**, together with known compounds, were isolated from the acetone-soluble part of the stem of *Upuna borneensis* (Dipterocarpaceae) (157).

124 R = OMe
125 R = H

126 R = H
127 R = 2-Galloyl

128 R = OMe
129 R = OH
130 R = H

131

132 R = Ram

133

134 R = p-OH-Benzoyl
135 R = E-Feruloyl
136 R = E-Coumaroyl
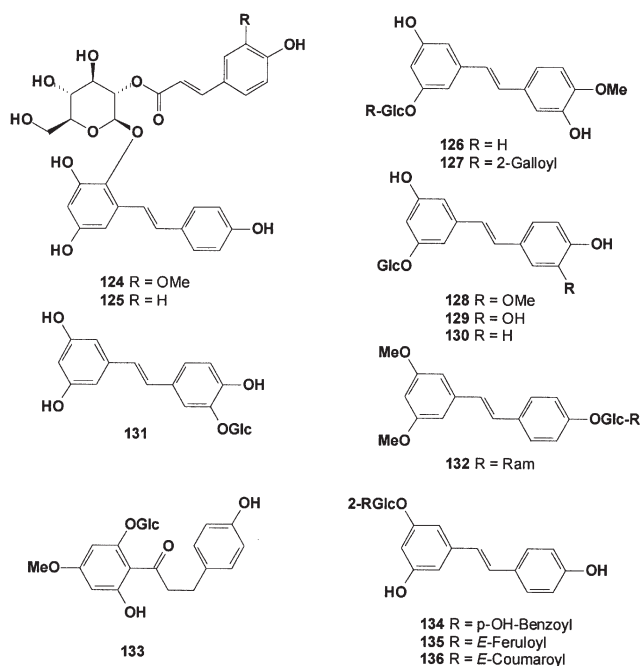
Two new stilbene dimer glucosides, resveratrol (*E*)-dehydrodimer 11-*O*-β-D-glucopyranoside **137** and resveratrol (*E*)-dehydrodimer 11′-*O*-β-D-glucopyranoside **138**, were isolated from grape *Vitis vinifera* cell cultures (158). The structures and stereochemistry of the new compounds were determined on the basis of spectroscopic data analysis. Compounds **137** and **138** are dimers that belong to a new type of oligostilbene formed from a resveratrol unit and a resveratrol glucoside unit. Compound **137** exhibited nonspecific inhibitory activity against cyclooxygenase-I and -II, with an IC$_{50}$ value of 5 μM.

The genus *Gnetum* (Gnetaceae) is known to contain abundant stilbene derivatives that have interesting biological activities, such as inducing apoptosis in colon cancer (159) and reducing blood sugar (160), revealing the importance of plants

containing stilbenoids as resources for the development of new drugs. The new stilbene glucosides gnemonosides F **139**, G **140**, H **141**, I **142**, and J **143** were isolated from the liana stems of *Gnetum gnemonoides* and *Gnetum africanum*, along with nine known stilbenoids (161). Other stilbene derivatives, gnemonols K and L (resveratrol trimers), M (isorhapontigenin dimer), and gnemonoside K (glucoside of resveratrol trimer, *cis*-**144** and *trans*-**145** isomers), together with known stilbenoids and a lignan, were isolated from the methanol-soluble parts of the root of *Gnetum gnemon* (Gnetaceae). The antioxidant activity of the nonglycoside stilbenoids on lipid peroxide inhibition and superoxide scavenging activity were reported previously (162).

137 R = Glc, R$_1$ = H
138 R = H, R$_1$ = Glc

139 R = Glc
140 R = H

141 R = Glc
142 R = H

143

144 7,8-*cis*
145 7,8-*trans*
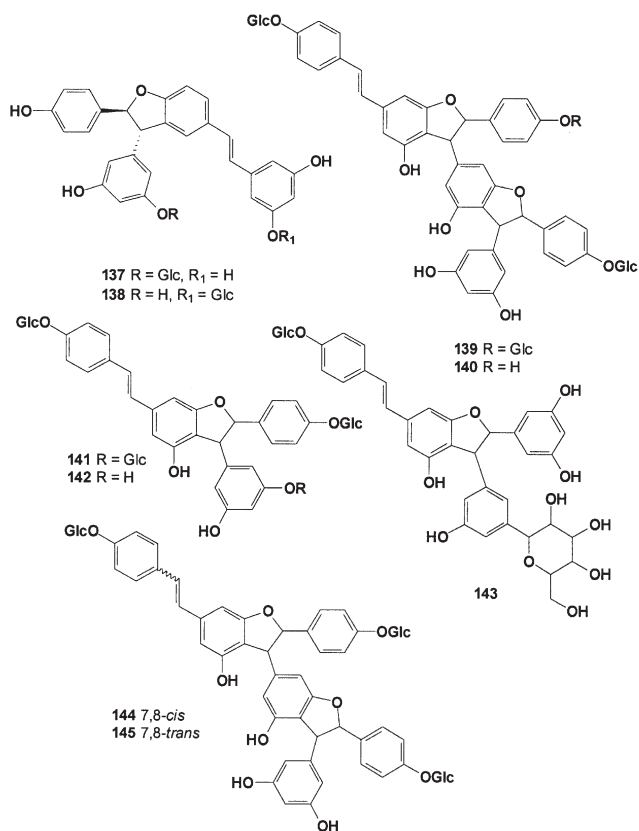
Two dimeric stilbene glycosides, **146** and **147**, were isolated from the root of *Polygonum cuspidatum* (163). One of these glycosides **147**, possesses a novel four-membered ring. Both compounds exhibited strong inhibition of lipid peroxidation but showed no cytotoxic DNA-cleavage activities and no inhibition of protein tyrosine phosphatase 1B.

New glycosides of the stilbene trimers foeniculosides I **148**, II **149**, III **150**, and IV **151** were isolated from *Foeniculum fructus* (seed of *F. vulgare*), along with the known stilbene trimers miyabenol C and *cis*-miyabenol C (164).

The rare, naturally occurring stilbene glycoside sulfates **152**–**161** were isolated from an aquatic extract of the root of *P. cuspidatum* (165).

146

147

152 R = SO₃M, R₁,R₂,R₃,R₄ = H
153 R,R₂,R₃,R₄ = H, R₁ = SO₃M
154 R,R₁,R₃,R₄ = H, R₂ = SO₃M
155 R,R₁,R₂,R₄ = H, R₃ = SO₃M
156 R,R₁,R₂,R₃ = H, R₄ = SO₃M

M = Na⁺ or K⁺

148 R = Glc, R₁ = R₂ = H
149 R = R₂ = H, R₁ = Glc
150 R = H, R₁ = R₂ = Glc
151 R = R₁ = Glc, R₂ = H

157 R = SO₃M, R₁,R₂,R₃,R₄ = H
158 R,R₂,R₃,R₄ = H, R₁ = SO₃M
159 R,R₁,R₃,R₄ = H, R₂ = SO₃M
160 R,R₁,R₂,R₄ = H, R₃ = SO₃M
161 R,R₁,R₂,R₃ = H, R₄ = SO₃M
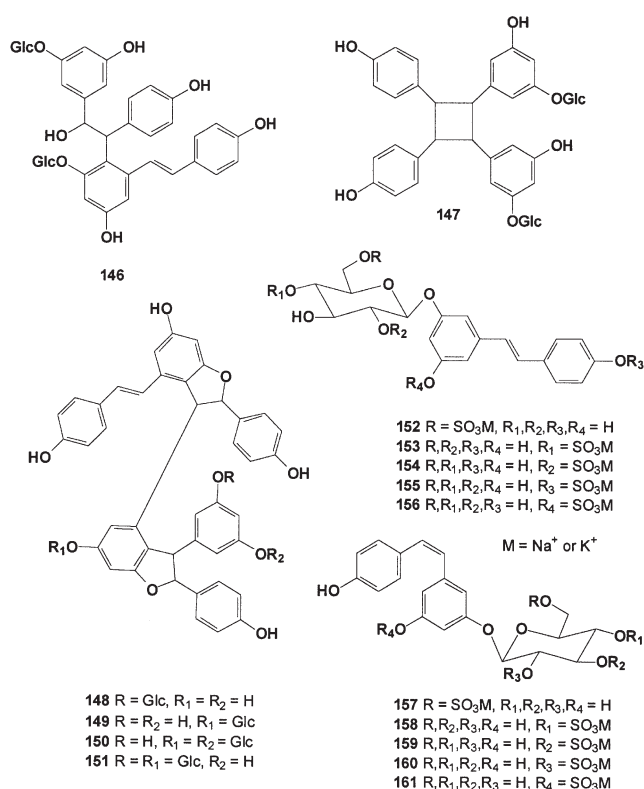
A lowland forest tree, *Upuna borneensis* (Dipterocarpaceae), is a monotypic genus distributed in Malaysia (Borneo, including Sabah, Sarawak, and Brunei) (166). Four new stilbene glucosides, upunosides A **162**, B **165**, C **166**, and D **167**, were isolated from the stem of *U. borneensis* (Dipterocarpaceae), together with three known glucosides, vaticaside B **163,** vaticaside C **164**, and paucifloroside A **168**. Upunoside A **162** is the first natural instance of a glucoside of a resveratrol pentamer, and its aglycone has a dibenzo-fused bicyclo[5.3.0]octadiene and two dihydrobenzofuran moieties (167).

162

165

166

163 R = H, R₁ = Glc
164 R = Glc, R₁ = H

167 7,8 (*Z*)
168 7,8 (*E*)
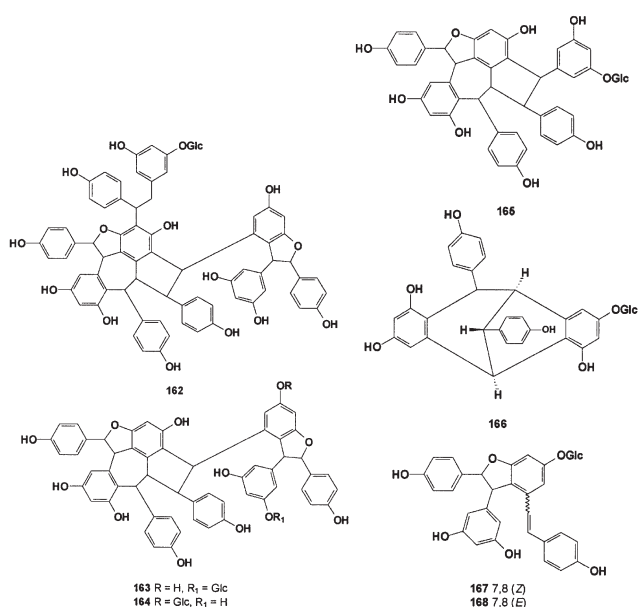
PHENYLETHANOID GLYCOSIDES

Phenylethanoid glycosides are a group of water-soluble natural compounds widely distributed in medicinal plants but also found in other plant species (168–170). Structurally, these metabolites are characterized by benzoic acid derivatives and phenylethyl moieties attached to a β-glucopyranose (apiose, galactose, rhamnose, or xylose) through ester and glycosidic linkages, respectively. More recently, phenylethanoid derivatives attached by an ether and/or ester bond to iridoid glucosides have been found. Phenylethanoid glycosides have been isolated from the aerial parts, leaves, stems, fruit, flowers, roots, and bark of plants or the whole plant; they have been found in the plant families Acanthaceae, Alangiaceae, Asteraceae, Berberidaceae, Bignoniaceae, Buddejaceae, Crassulaceae, Lamiaceae, Magnoliaceae, Oleaceae, Orobanchaceae, Plantaginaceae, Scrophulariaceae, and Verbenaceae (170).

Phenethyl β-D-glucopyranoside **169** and phenethyl β-D-galactopyranoside **170** are simple among the identified phenylethanoid glycosides. Phenethyl β-D-glucopyranoside **169** was found in the flowers of *Rosa gallica* (171), and **170** was obtained by fermentation of phenethyl alcohol and the β-galactosidase of *E. coli* (172). Calceolarioside A **171** and B **172** were isolated from the aerial parts of *Calceolaria hypericina* (173). Calceolarioside B **172** and osmanthuside E **173** were isolated from the aerial parts of *Scutellaria galericulata* (Lamiaceae) and showed antimicrobial activity against two gram-positive bacteria, two gram-negative bacteria, and three yeast-like fungi. Among the glycosides, only calceolarioside B **172** and martynoside seemed to possess antifungal activity; both had high MIC values except against the *C. albicans* strain (174). Plantainosides A–F **174**–**179** were isolated from an aqueous extract of the whole plant *Plantago asiatica*, together with eight known phenylethanoid glycosides (175), and the phenylethanoid glycosides **174** and **175** showed antioxidant activity. Calceolarioside A **171**, plantainoside A **174**, and forsythoside A **180** were isolated from *Forsythia suspense* (176). Compounds **171** and **174** were isolated from the genus for the first time, and compound **180** showed immune-enhancing activity in mice (176). Scroside D **181** was isolated from the roots of *Picrorhiza scrophulariiflora* (Scrophulariaceae) (177) and also showed antioxidant activity.

Acteoside **182** (also known as kusaginin, NSC 603831, TJC 160, and verbascoside) is a very active phenylethanoid glycoside that has been isolated from many plant species (170). Acteoside **182** and isoacteoside **183** (isoverbascoside) were isolated from the southwestern Indian paintbrush, *Castilleja linariaefolia* (178). The extracts displayed *in vivo* activity against murine P-388 lymphocytic leukemia (178), and the pure glycosides acteoside **182** (ED₅₀ 2.6 µg/mL) and isoacteoside **183** (ED₅₀ 10 µg/mL) showed high cytotoxic activity against the murine P-388 cell line. Acteoside **182** and angoroside A **184** showed strong anti-inflammatory activity *in vitro* (179). Acteoside **182** reduced the risk of atherosclerosis, not only by protecting LDL from oxidative modification but also by its free radical-scavenging properties (180); it also inhibited

human leukocyte elastase (181) and lipopolysaccharide-inducible nitric oxide synthase *in vitro* (182). Acteoside **182** inhibited the telomerase activity (12.5–27 mg/mL) of the human gastric adenocarcinoma cell MKN45 (183). Acteoside **182** and isoacteoside **183** showed antiproliferative activities against B16F10 cells [acteoside, GI$_{50}$ (concentration needed to reduce the growth of treated cells to half that of untreated cells) 8 μM; isoacteoside, GI$_{50}$ 8 μM] and their methanolysis products (methyl caffeate GI$_{50}$ 26 μM; 3,4-dihydroxyphenethyl alcohol GI$_{50}$ 8 μM; 3,4-dihydroxyphenethyl glucoside GI$_{50}$ 10 μM; desrhamnosyl acteoside GI$_{50}$ 6 μM; and desrhamnosyl isoacteoside GI$_{50}$ 6 μM), suggesting that the 3,4-dihydroxyphenethyl alcohol group might be more responsible for the activities of acteoside and isoacteoside than the caffeoyl group (184). Acteoside showed no apparent effect on the marked elevation of serum tumor necrosis factor α (TNF-α), but it partially prevented *in vitro* TNF-α-induced cell death (100 ng/mL) in D-galactoseamine (D-GalN)-sensitized hepatocytes (0.5 mM) at concentrations of 50, 100, and 200 μM. These results indicated that D-GalN/lipopolysaccharide (LPS)-induced hepatic apoptosis can be blocked by an exogenous antioxidant, suggesting the involvement of reactive oxygen intermediates in TNF-α-dependent hepatic apoptosis (185). Acteosides also showed an inhibitory effect on histamine- and bradykinin-induced contractions of guinea pig ileum (186). Campneoside I **185** and II **186** were isolated from a butanol extract of *Paulownia tomentosa* stems and showed antibacterial activity against *S. aureus* (SG511, 285, and 503), *Streptococcus pyogenes* (A308 and A77), and *Streptococcus faecium* MD8b (187). The most active compound of the extract was identified as campneoside I **185**, which had an MIC value of 150 μg/mL against *Streptococcus* and *Staphylococcus* species. From such antibacterial activity, the methoxy group of campneoside I was postulated to be the essential element for the antibacterial activity (187). The protective effect of campneoside II **185**, isolated from *Cistanche tubulosa*, on the apoptosis of neurons induced by the neurotoxin 1-methyl-4-phenylpyridinium ion (MPP$^+$) was reported (188).

169 α-OH
170 β-OH

171 R = Caffeoyl, R$_1$ = H
172 R = H, R$_1$ = Caffeoyl
173 R = H, R$_1$ = *trans*-Feruloyl

174 R,R$_1$,R$_3$,R$_4$ = H, R$_2$ = Caffeoyl
175 R,R$_2$,R$_3$,R$_4$ = H, R$_1$ = Caffeoyl
176 R,R$_1$,R$_3$ = H, R$_2$ = Ram, R$_4$ = Feruloyl
177 R,R$_1$,R$_3$ = H, R$_2$ = Glc, R$_4$ = Caffeoyl
178 R = Me, R$_1$,R$_3$ = H, R$_2$ = Glc, R$_4$ = Feruloyl
179 R = Me, R$_1$,R$_3$ = H, R$_2$ = All, R$_4$ = Feruloyl
180 R,R$_1$,R$_2$,R$_3$ = H, R$_4$ = Feruloyl
181 R,R$_1$,R$_2$,R$_3$ = H, R$_4$ = Glc

182

183 R = Caffeoyl
184 R = Glc

185 R = Me
186 R = H
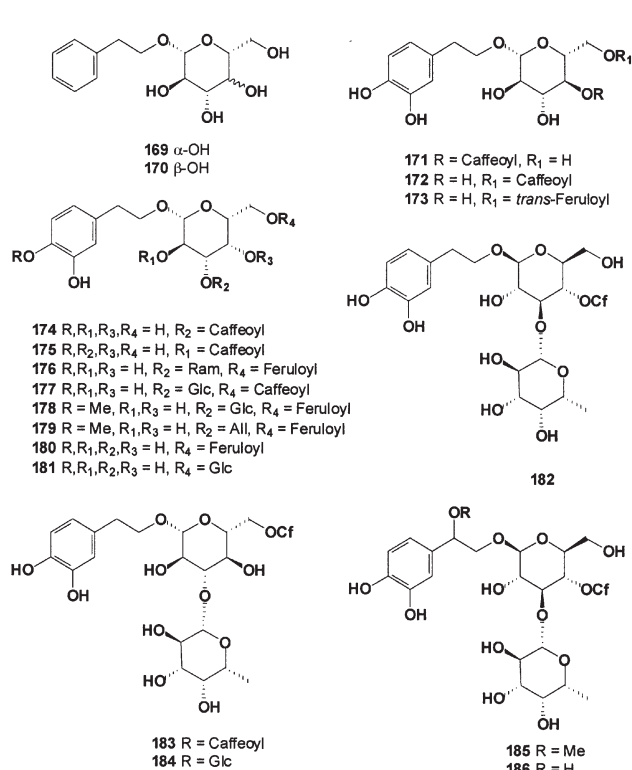
A series of biologically active phenylethanoid trisaccharides with α-L-rhamnose attached to the C-6′ of glucose **187**–**197** have been isolated from some *Mussatia* species (189–192). Mussatiosides I **188**, II **190**, and III **193** showed inhibitory action on ADP-induced rat platelet aggregation (192). The order of activity was: **188** > **190** > **193**. This antiplatelet effect is likely related to the reported inhibition of cAMP-phosphodiesterase.

Two new phenylethanoid glycosides with cytotoxic activity, 1-*O*-3,4-dimethoxy-phenylethyl-4-*O*-3,4-dimethoxy cinnamoyl-6-*O*-cinnamoyl-β-D-glucopyranose **198** and 1-*O*-3,4-dimethoxyphenylethyl-4-*O*-3,4-dimethoxy cinnamoyl-β-D-glucopyranose **199**, have been isolated from the acetone extract of

Psidium guaijava seeds (193). The biological assay of an acetone extract and two isolated compounds showed that the extract had moderate inhibitory activity against both Ehrlich ascites carcinoma (EAC) cells and leukemia P-388 (180% and ED_{50} 1/4 14:6), whereas the two new isolated compounds **198** and **199** showed high inhibitory activity against EAC (220 and 240%) and low activity against leukemia P-388 (ED_{50} 1/4 17:3 and 16:1).
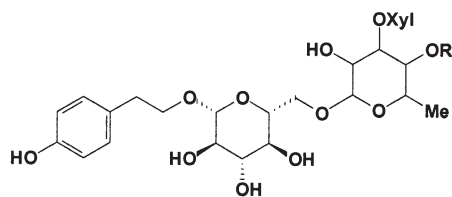
187 R = H
188 R = Cinnamoyl
189 R = Coumaroyl
190 R = Di-Me-Caffeonyl
191 R = Feruloyl
192 R = Coumaroyl
193 R = Me-Coumaroyl
194 R = Vanilloyl
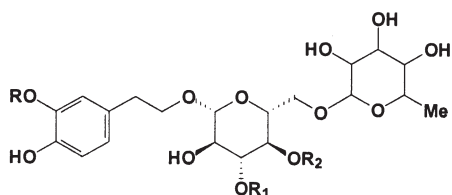
195 R = H, R_1 = Api, R_2 = Cf
196 R = Me, R_1 = Api, R_2 = Fr
197 R = H, R_1 = Glc, R_2 = Cf
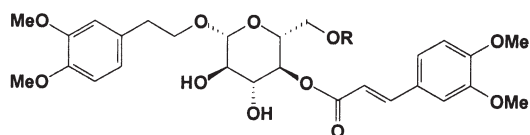
198 R = Cinnamoyl
199 R = H

Types of phenylethanoid glycosides linked with iridoids or secoiridoid glucosides have been isolated from plants. Oleoacteoside **200** was isolated from *Syringa reticulata* (194,195), *Jasminum polyanthum* (196,197), and *Picconia excelsa* (198). Oleoechinacoside **201** was isolated from *S. reticulata* (194), and nuzhenide **202** was isolated from the leaves of *S. reticulata* (199). The esterglucoside **203** was found in *Ligustrum japonicum* (200). The unusual polyglucosidic metabolite **204** was isolated from embryos of the American ash (*Fraxinus americana*) (201).

200 R = H
201 R = Glc

202 R = H
203 R = Oleosyl

204
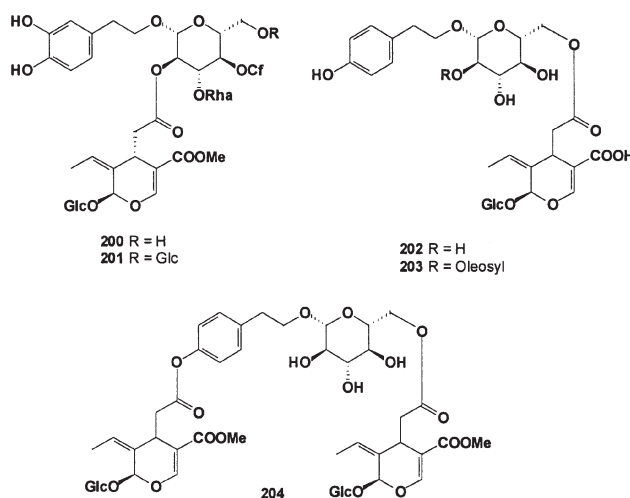
Phenylethanoid derivatives attached by ether and/or ester bonds with iridoid and/or secoiridoid glucosides have been isolated from the Oleaceae family (202). A new secoiridoid glycoside named hiiragilide **205** was isolated from the leaves of *Osmanthus ilicifolius* (203). Oleuroside **206** was isolated from *Olea europaea* (204) and from tissues of the novel olive cultivar Hardy's Mammoth (205,206). The antiviral activity of olive leaf extract (OLE), containing oleuroside **206**, hydroxytyrosol, oleuropein, and verbascoside, was reported recently (207). Also, OLE was shown to inhibit acute infection and cell-to-cell transmission of HIV-1, as assayed by syncytia formation using uninfected MT2 cells co-cultured with HIV-1-infected H9 T-lymphocytes. OLE also inhibited HIV-1 replication, as assayed by the expression of p24 in infected H9 cells. These anti-HIV effects of OLE are dose dependent, with an EC_{50} of 0.2 µg/mL (207). 10-Acetoxyligstroside **207** and 10-acetoxy-oleuropein **208** were found in an extract of the bark of *Osmanthus asiaticus* (208). Ligustaloside A **209** and ligustaloside B **210** were isolated from the leaves of *Ligustrum lucidum* (Oleaceae) (209) and *Ligustrum vulgare* (210). Kikuchi and Yamauchi (211) found a corresponding pair of compounds, ligstrosidic acid **211** and oleuropeinic acid **212**, in the fruit of *Ligustrum japonica* and *L. lucidum.* Ligstroside **213** and the cytotoxic compound oleuropein **214** were isolated from the stem bark of *Syringa velutina* (212). Oleuropein **214** showed the most potent cytotoxic effect on several tumor cell lines (P-388, L-1210, SNU-5, and HL-60) among eight isolated compounds. Three new secoiridoid glucosides, jasamplexosides A **215**, B **216**, and C (like B, but with the additional part of a secoiridoid glucoside; structure not shown), were isolated from the crude drug *niu du teng*, the leaves and stems of *Jasminum amplexicaule* (213). An unusual cyclic secoiridoid glucoside, insularoside **217**, was isolated

from *Fraxinus insularis* (214), and fraxuhdoside **218** was isolated from the bark of *Fraxinus uhdei* (215).

205

206

207 R = H
208 R = OH

209 R = OH
210 R = H

211 R = H
212 R = OH

213 R = H
214 R = OH

215 R = H
216 R = OH

217 R = H
218 R = Glc

219

220

221 R = H
222 R = OH

223

224 R = H
225 R = OH

226

227 R = H
228 R = OH
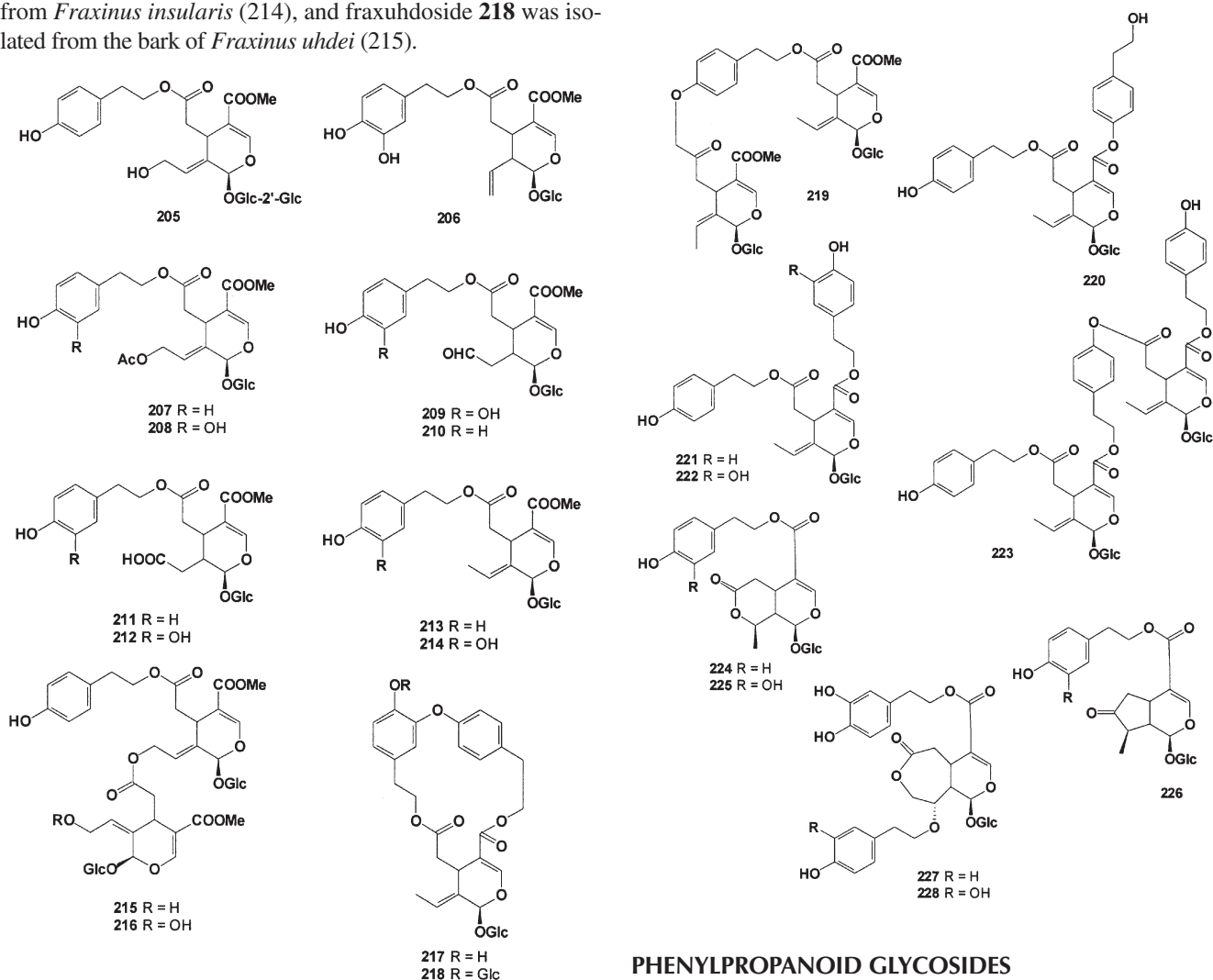
A minor iridoid named austromoside **219** was found in *Osmanthus austrocaledonica* (216), and fraxiformoside **220** was isolated from *Fraxinus formosana* (217) and *Fraxinus malacophylla* (218). Framoside **221**, which has anti-inflammatory activity, was isolated from *Fraxinus* species (219); neooleuropein **222** was isolated from *Fraxinus chinensis* (220); and fraximalacoside **223** was isolated from *F. malacophylla* (218). Lilacoside **224** and fliederoside **225** were isolated from *Syringa vulgaris* (221). In 1970, syringopicroside **226** was isolated from *S. vulgaris* (222) and more recently was found in many *Syringa* species (223). A unique series of seven-membered lactones exemplified by jasmolactone C **227** and D **228** were isolated from the aerial part of *Jasminum multiflorum* (224,225). The structures of these compounds, which contain a novel bicyclic 2-oxo-oxepano[4,5-c]pyran ring system, were tested for pharmacological activity, and **227** and **228** were found to possess coronary vasodilating and cardiotropic activities (224).

PHENYLPROPANOID GLYCOSIDES

Phenylpropanoids and phenylethanoid glycosides are a large class of water-soluble natural metabolites widely distributed in plant species (226–231). Phenylpropanoids can conveniently be treated as a group of aromatic compounds consisting of the derivatives of phenylpropanols and/or benzoic acids (caffeic, cinnamic, coumaric, ferulic, sinapic, and others), including their glycosides (see also the Simple Aromatic Glycosides section). More complex phenylpropanoid glycosides are compounds based on phenylethanes (see the Phenylethanoid Glycosides section). Phenylpropanoid compounds have a wide array of important functions in plants. They serve in the interaction of plants with their biotic and abiotic environments, mediate certain aspects of plant growth and development, and are important structural components of the secondary cell wall. Phenylethanoid glycosides have been isolated from the aerial parts of plants, leaves, stems, fruit, flowers, roots, bark, and/or whole plant; they are found in the plant families Araliaceae,

Bignoniaceae, Crassulaceae, Labiatae, Lamiaceae, Oleaceae, Polygonaceae, Scrophulariaceae, Smilacaceae, Verbenaceae, and several others.

The natural phenylpropanoid glycosides isolated from plants showed activities such as being antitumoral, antiviral, anti-inflammatory, antibacterial, antiatherosclerotic, antiplatelet aggregational, antihypertensive, antifatigue, analgesic, hepatoprotective, immunosuppressive, protective of sex and learning behavior, protective of neurodegeneration, reverse transformative of tumor cells, inhibitive of telomerase and capable of shortening the telomere length in tumor cells, having effects on enzymes and cytokines, antioxidative, free radical scavenging, and quickly repairing oxidatively damaged DNA, among others (227).

Simple phenylpropanoid glycosides such as rosin **229**, rosavin **230**, rosarin **231**, triandrin **232**, and vimalin **233** have been isolated from different plant species belonging to the Crassulacea, Liliaceae, and Salicaceae families (226,227). The biologically active substances rosin **229**, rosavin **230**, rosarin **231**, and tyrosol, which are mainly found in plant rhizomes, have demonstrated therapeutic effects (232). These active components affected the central nervous system by increasing the ability to concentrate and mental and physical power; they were efficient in improving asthenic states and the general resistance of the cells and the organism against harmful outer influences. They also prevented the heart system from stress and arrhythmias, and they possessed some antioxidant activities. Some data confirm that the *Rhodiola rosea* preparations stopped the growth of malignant tumors and metastases in the liver (232). Rosin **229**, rosarin **231**, rosavin **231**, and rosiridin isolated from *R. rosea* showed neurotropic activity in mice (233). Citrusin A **234**, B **235**, C **236**, D **237**, E **238**, and F **239** have been isolated from citrus fruit peels, e.g., from the lemon, unshiu, and kinkan (234,235), and after *in vivo* injection of the compounds indicated above into stroke-prone spontaneously hypotensive rats, they were found to lower the blood pressure (236,237).
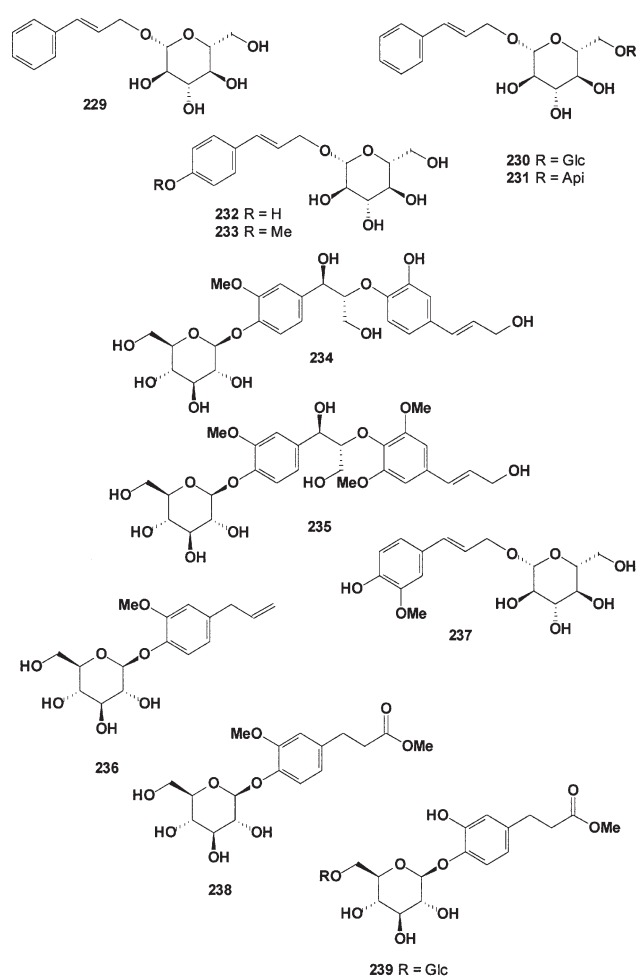
A new phenylpropanoid glycoside, crenatoside **240**, as well as the known phenylpropanoid, acteoside **182**, have been isolated from the aerial parts of *Orobanche crenata* (238). Two new phenylpropanoid glycosides, junipercomnoside E **241** and F **242**, were isolated from the aerial parts of *Juniperus communis* var.

depressa (239); betuloside **243** was isolated from *Betula alba* (240); and cistanoside F **244** was isolated from the stem bark of *Acanthopanax trifoliatus* (241).

240

241

243

242

244
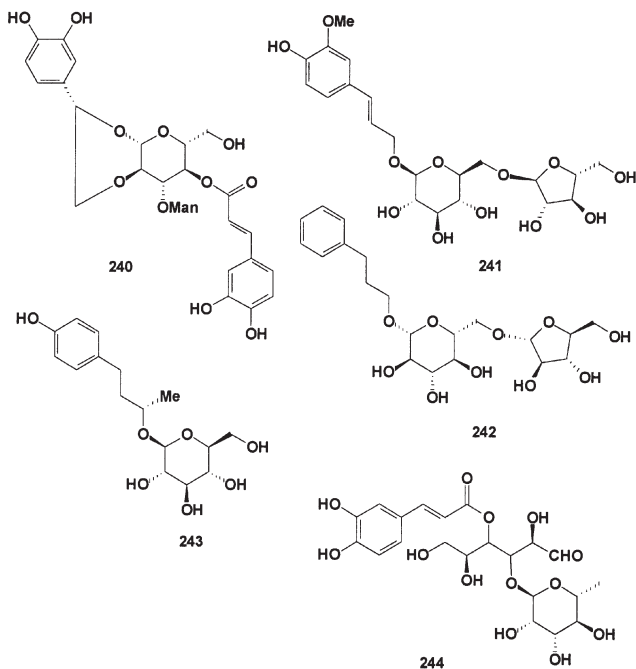
LIGNAN GLYCOSIDES

Lignans are natural bis-phenylpropanoids having a large spectrum of biological activities, and they are widely distributed in the plant kingdom. They are present in small amounts in most unrefined grains such as barley, buckwheat, millet, and oats; legumes such as soybeans; and some vegetables (242–244). Sometimes lignans are referred to as phytoestrogens. However, this term is misleading, as it suggests that lignans may act just like the hormone estrogen in the body. The richest source of lignans is flaxseed, which contains high levels of the lignan precursor secoisolariciresinol diglycoside **245** (SDG). Plant lignans are polyphenolic substances derived from phenylalanine *via* the dimerization of substituted cinnamic alcohols (242). Mammalian lignans are lignans derived from plant lignans. For example, following ingestion, SDG is converted to the aglycone secoisolariciresinol, which is then metabolized to the mammalian lignans enterolactone and enterodiol (245). Most of the effects of oral SDG are mediated by enterolactone and enterodiol (246). SDG has estrogenic and antioxidant activities, and also has antitumor, antiestrogenic, anticarcinogenic, antiatherogenic, and antidiabetic activities (247–249). Similar structures have the glycosides (−)-secoisolariciresinol-*O*-α-L-rhamnopyranoside **93** (105) and (+)-secoisolariciresinol 9-*O*-β-D-xylopyranoside **246** (isolated from the leaves of *Laurus nobilis*) (250). The underground parts of *Glehnia littoralis* (Umbelliferae) contain two new lignan glycosides named glehlinosides A **247** and B **248** (251).

Styraxlignolides C **249**, D **250**, E **251**, and F **252**, butyrolactone lignan glucosides with antioxidant activity, were isolated

from the stem bark of *Styrax japonica* (252). Styraxlignolides C **249**, D **250**, and E **251** exhibited weak radical-scavenging activity in the 1,1-diphenyl-2-picrylhydrazyl assay, with IC_{50} values of 380, 278, and 194 μM, respectively.

Lignans having a diarylhydroxybutyrolactone skeleton, i.e., nortrachelogenin 8′-*O*-β-D-glucopyranoside **253**, nortrachelogenin 5′-*C*-β-D-glucopyranoside **254**, and nortracheloside **255**, were found in a water-soluble extract of the leaves and stems of *Trachelospermum jasminoides* (253).

The root of *Strobilanthes cusia* (Acanthaceae), popularly known as *da-ching-yeh*, has commonly been used in traditional Chinese medicine. It is used to treat influenza, epidemic cerebrospinal meningitis, encephalitis B, viral pneumonia, mumps, and severe acute respiratory syndrome. A new lignan glycoside, **256**, and the known (+)-9-*O*-β-D-glucopyranosyl lyoniresinol **257** were found in *S. cusia* roots. The isolated compounds **256** and **257** were examined for anti-herpes simplex virus type-1 activity and showed moderate activity (253a).

245

246

247 R = Vaniloyl, R₁ = H
248 R = Vaniloyl, R₁ = OMe

249 R,R₃ = Me, R₁ = Glc, R₂ = H
250 R,R₂ = Me, R₁ = Glc, R₃ = H
251 R,R₂ = Me, R₁ = H, R₃ = Glc
252 R,R₂,R₃ = Me, R₁ = Glc

253 R₁,R₂ = H, R = Glc
254 R,R₁ = H, R₂ = Glc
255 R,R₂ = Me, R₁ = Glc

256 R = Api
257 R = H
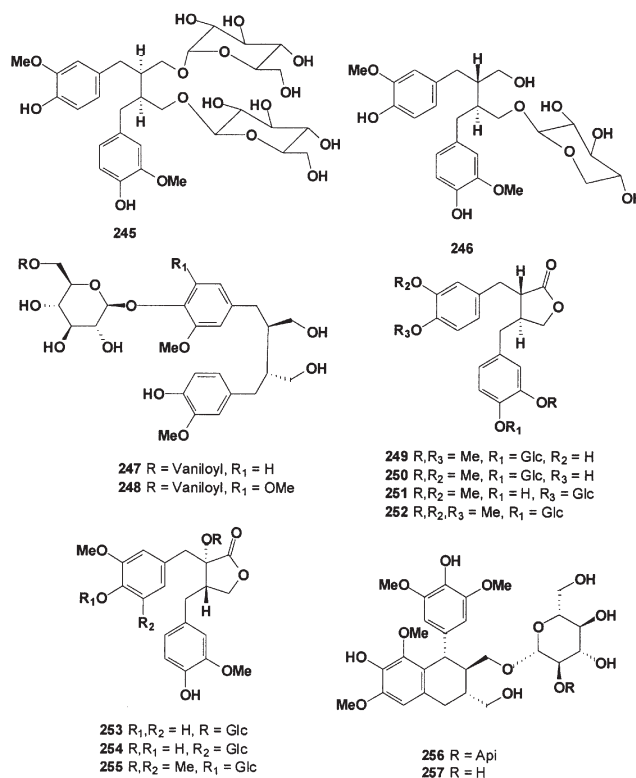
Bonaspectin C **258** and bonaspectin D **259**, isolated from the aerial parts of *Bonamia spectabilis* (Convolvulaceae), led to the isolation of four minor THF-type sesquilignans (254). Bonaspectin C 4″-*O*-glucoside **258**, its aglycon, and bonaspectin D 4″-*O*-glucoside **259** revealed the highest antiplasmodial activities against *Plasmodium falciparum* [IC_{50} values of 0.98 and 5.1 μM/mL (chloroquine-sensitive strain of *P. falciparum*), and 1.3 and 2.9 μM/mL (chloroquine-resistant clone of *P. falciparum*), respectively]. The cytotoxicity of **258** was estimated by a proliferation assay using the tetrazolium salt 3-(4,5-dimethylthiazol-2-yl)-2,5-diphenyltetrazolium bromide assay against human endothelial cells (ECV-304). A new lignan glucoside, the first 7,9′-monoepoxytetrahydrofuran-type

lignan, named tibeticoside **260**, was isolated from the medicinal plant (roots, stems, and leaves) *Lancea tibetica* (255). Two lignan diglucosides, **261** and **262**, were identified from extracts of germinated sesame seeds (256). The lignan glycoside arctiin **263** is widely distributed in the Compositae family and is used as a chemotaxonomic marker for this family (257). This lignan showed neuroprotective activity against glutamate-induced toxicity in primary cultures of rat cortical cells (258).

release of β-hexosaminidase (IC$_{50}$ 64 μM) as well as TNF-α and interleukin-4 (IC$_{50}$ 16, 34 μM) in RBL-2H3 cells.

258

259

260

261 R = Glc, R$_1$ = H
262 R = H, R$_1$ = Glc

263

264

265

266

267 R = H
268 R = OMe

269

270 R = H, R$_1$ = n-Bu
271 R = n-Bu, R$_1$ = H
272 R, R1 = n-Bu
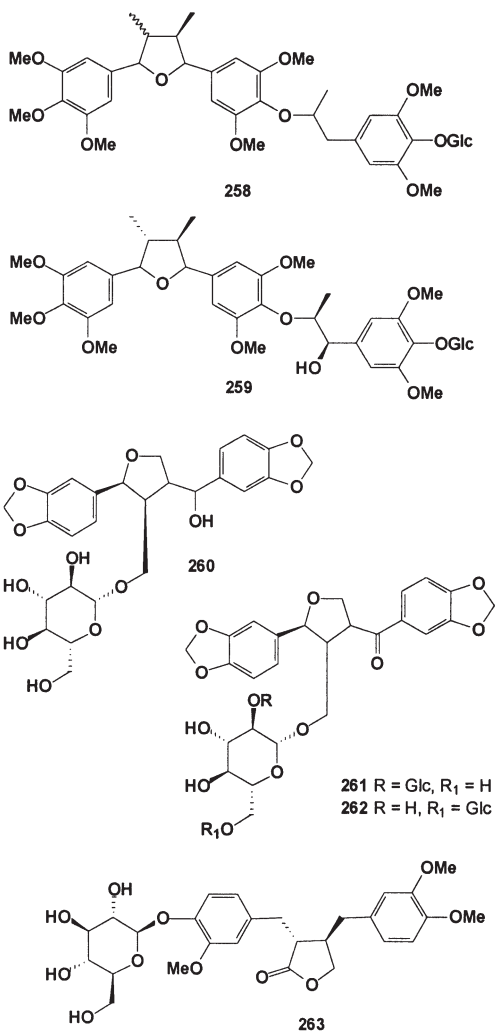
The neolignan glucosides tortosides B **264**, D **265**, and E **266** were isolated from *Pedicularis torta* (259,260). The new lariciresinol-based lignan bis-glucosides, 7*S*,8*R*,8′*R*-(−)-lariciresinol-4,4′-bis-*O*-β-D-glucopyranoside **267** and 7*S*,8*R*,8′*R*-(−)-5-methoxylariciresinol-4,4′-bis-*O*-β-D-glucopyranoside **268** were isolated from the *n*-butanol extract of *Galium sinaicum* roots (261). The two lignan glucosides **267** and **268** were subjected to a cytotoxicity bioassay against the P-388 leukemia cell line, and the tested compounds exhibited weak *in vitro* cytotoxic activity, with IC$_{50}$ values of 100 and 42.0 μg/mL, respectively.

The new neolignan glycosides named dichotomosides A **269**, B **270**, C **271**, and D **272** were isolated from a Chinese natural medicine, the roots of *Stellaria dichotoma* var. *lanceolata* (262). Among them, dichotomoside D **272** inhibited the

A novel lignan glycoside, hibiscuside **273**, which exhibited good antioxidant activity and strongly inhibited lipid peroxidation in rat liver microsomes, was isolated from the roots of *Hibiscus* species (263). Also, a new lignan named eleutheroside E **274** was extracted from the stem bark of *Acanthopanax trifoliatus* (241). A water-soluble natural antioxidant, pinoresinol glycoside **275**, was isolated from sesame seeds (264). Pinoresinol glycoside **275** prevented the oxidation of linoleic acid *in vitro* in an aqeous solution and that of rabbit red cell ghost membranes by *tert*-butyl hydroperoxide (264). A new lignan, triglucoside **276**, was isolated from sesame seeds; this compound had branched (1→2)- and (1→6)-glucosidic linkages and showed antioxidative activity (265). A new furofuran lignan from *Lactuca indica*, lactucaside **277**, showed significant antidiabetic activity (266). *Coptis japonica* (Ranunculaceae) is known to possess several biological activities, such as anti-inflammatory effects. Pinoresinol glycoside **275** and syringaresinol glycoside **278**, which were isolated from the rhizomes of *C. japonica*, were tested to evaluate their *in vitro* anti-inflammatory effects. Pinoresinol glycoside **275** and isolariciresinol showed higher inhibitory effects on TNF-α production than syringaresinol glycoside **278**, whereas syringaresinol glycoside **278** strongly suppressed lymphocyte proliferation (267). For more information on lignans, neolignans, and related compounds, readers are referred to several review articles (242–244,268).
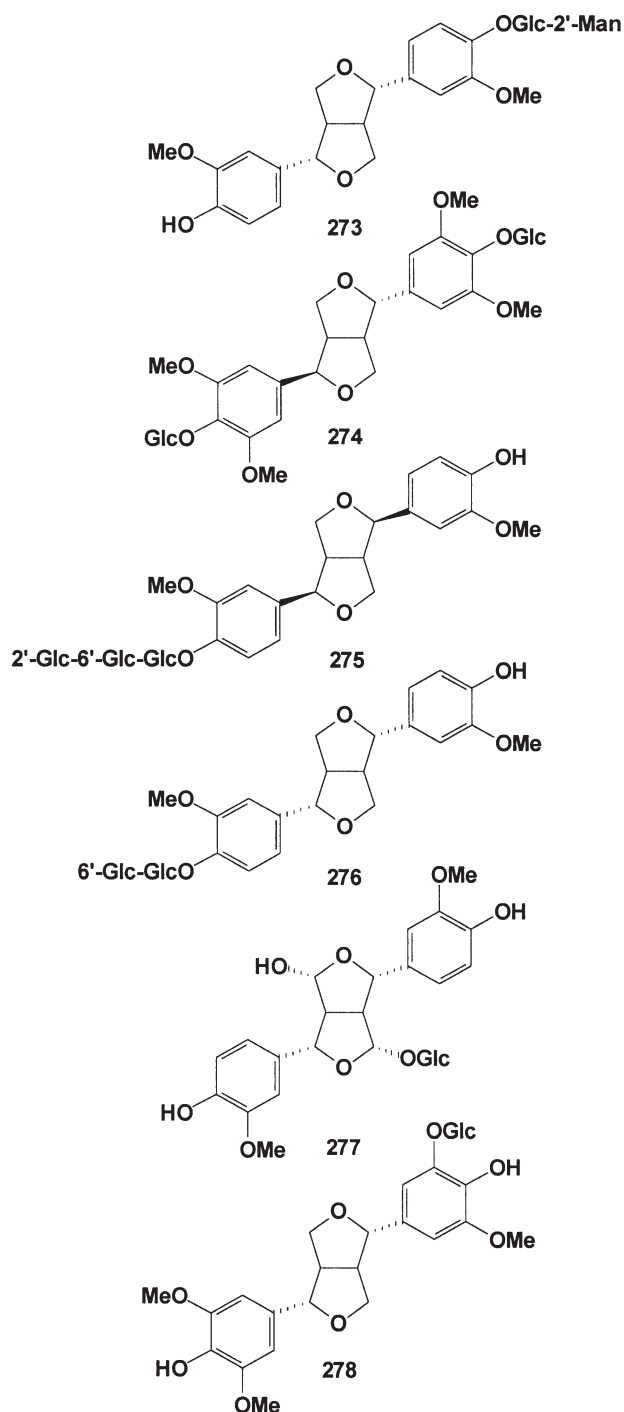
GLYCOSIDES OF NAPHTHALENE DERIVATIVES

Naphthalene, the fused-ring aromatic hydrocarbon, was first isolated by crystallization from the naphthalene fraction of coal tar, which still remains its major source (269,270). It was also found in combustion processes, including the combustion of refuse, tobacco smoke, coal tar pitch fumes, and oil spills. Most of the naphthalene derivatives found in nature are naphtho-quinones, which may arise through the polyketide, terpenoid, or shikimate pathways or a mixture of these (271,272).

The genus *Rumex* (Polygonaceae) is represented by 25 species in the flora of Turkey (273). The roots of *R. patientia* are used as a purgative and tonic in traditional medicine, and its leaves are commonly used as a green vegetable called *labada* or *develik*. Nine *Rumex* species, including *R. patientia*, have been attributed to the Chinese herbal medicine *yangti*, which has been used as a hemostatic and antifungal agent. Two new chlorinated naphthalene derivatives, patientosides A **279** and B **280**, were isolated from the roots of *R. patientia* (274). Daylily flowers are used as an important ingredient in tradi-tional Asian cuisine and are also valued for their reputed medi-cinal effects. A new naphthalene glycoside, stelladerol **281**, has been isolated from edible daylily (*Hemerocallis*) flowers (275). This isolated compound was tested for antioxidant and cy-clooxygenase inhibitory activities and was found to possess strong antioxidant properties, inhibiting lipid oxidation by 94.6% (10 μM) in an *in vitro* assay. Also from this plant, three new naphthalene glycosides, rumexoside **282**, rumexoside **283**, and labadoside **284** were identified (276). A new naphthalene glycoside, cassitoroside **285**, was isolated from the seeds of *Cassia tora* (277). One new naphthalene glycoside, 5-hydroxy-dianellin **286**, and a known naphthalene glycoside, dianellin **287**, were isolated from roots of the daylily *Hemerocallis fulva* 'Kwanzo' Kaempfer (278). Diospyrosonaphthoside **288** was isolated from an ethanolic extract of the stem bark of *Diospy-ros angustifolia* (279), and plicataloside **289**, an *O,O*-diglyco-sylated naphthalene derivative, was isolated from *Aloe pli-catilis* (280).
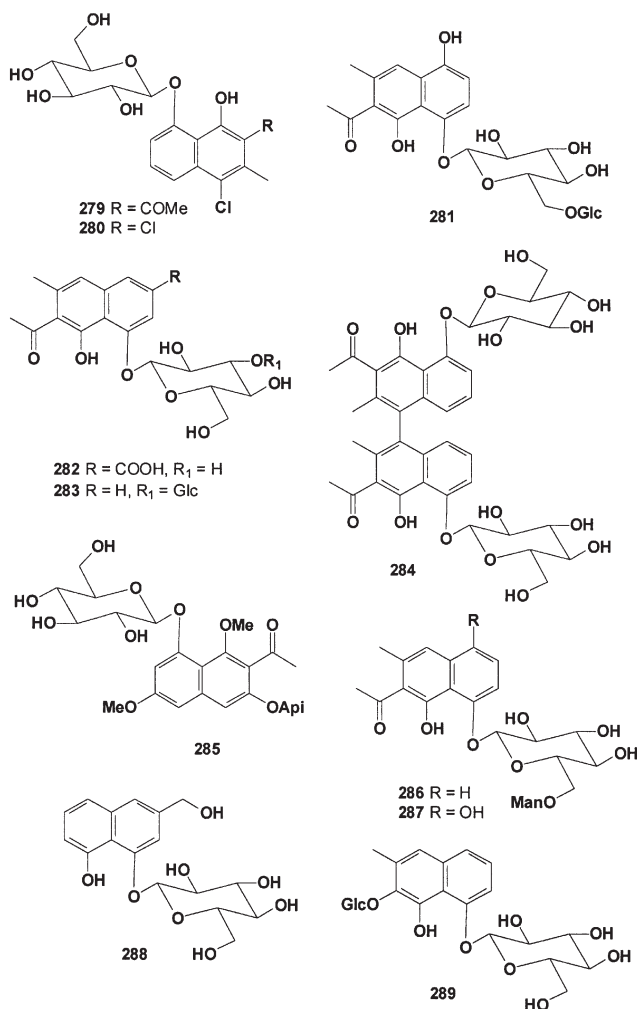
The twigs of *Diospyros lycioides*, a plant commonly known as muthala, are frequently used as chewing sticks by the rural and urban people in Namibia for cleaning the teeth. Studies showed that a methanol extract of *D. lycioides* inhibited the growth of selected oral pathogens. Subsequent bioassay-guided

fractionation led to the isolation of four novel bioactive naphthalene glycosides, diospyrosides A **290**, B **291**, C **292**, and D **293** (281). These compounds inhibited the growth of oral cariogenic bacteria (*Streptococcus mutans* and *Streptococcus sanguis*) and periodontal pathogens (*Porphyromonas gingivalis* and *Prevotella intermedia*) at MIC values ranging from 0.019 to 1.25 mg/mL.

Lactonic 6-methoxysorigenin 8-*O*-β-D-glucopyranoside **294** was isolated from the cortex of *Rhamnus catharticus* (282), and **295** was isolated from *Rhamnus nakaharai* (283). From the leaves and pods of *Cassia senna* and *C. angustifolia*, the new tinnevellin glucoside **296** was isolated (284). The monoglucoside **297** and diglucoside **298** of 2-naphthalenecarboxylic acid were isolated and characterized from the roots of *Rubia ustulata* (285).
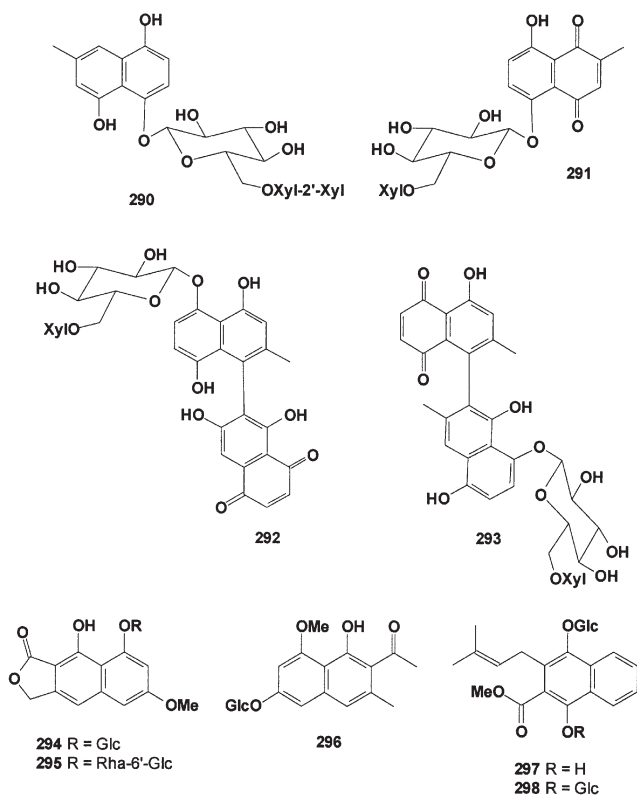
GLYCOSIDES OF ANTHRACENE DERIVATIVES

Glycosides of anthracene derivatives are widely distributed in the plant kingdom, and many of them have shown anticancer, antiviral, antimicrobial, and other biological activities (286–290). Different anthracene glycosides have been isolated from an aromatic bark called cassia (also known as cinnamon, bastard cinnamon, Chinese cinnamon, *Cassia lignea*, cassia bark, *Cassia aromaticum*, or Canton cassia). Over 400 species of cassia are known. Most are indigenous to North, Central, and South America and Africa, but they are now also found in the tropical and subtropical regions of all continents except Europe. Some are native to South Asia, particularly India and Ceylon, and are now widely cultivated in the tropics; others are considered ornamental trees in southern Florida, the West Indies, and Central and South America. The dried unripe fruit, or Chinese cassia buds, have the odor and taste of the bark and are rather like small cloves in appearance. They have been known as a spice in Europe since the Middle Ages and were probably used in preparing a spiced wine called hippocras. Now they are used in confectionery and in making potpourris.

Emodin is perhaps the most nearly ubiquitous natural anthraquinone, occurring in several higher plants, in fungi, and in lichens. In higher plants, it is chiefly present in glycoconjugates. Emodin and chrysophanol frequently occur together in plants such as *Cassia tora, Rumex japonicus, Rhamnus purshiana, Polygonum multiflorum,* and *P. cuspidatum* (291). Emodins 1-*O*-**299** and 3-*O*-**300** were isolated from the Chinese cassia species (292); 8-*O*-β-glucopyranoside **301** was isolated from *C. tora, R. japonicus, R. purshiana, P. multiflorum,* and *P. cuspidatum*; and chrysophanol-8-*O*-β-glucoside **302** was found in *R. japonicus* (291). Emodin (IC$_{50}$ 3.3 μM) is an inhibitor of the growth factor-signaling enzyme phosphatidylinositol-3-kinase (293). A rare sulfated emodin glucoside, emodin 8-*O*-β-D-glucopyranosyl-6-*O*-sulfate **303**, was isolated from the roots of the Nepalese medicinal plant *Rheum emodi* (294). Aloe-emodin diglucoside **304** and aloe-emodin ω-*O*-β-D-glucopyranoside **305** were isolated from Chinese cassia species (292). Emodin 8-*O*-β-glucopyranoside **301**, chrysophanol-8-*O*-β-glucoside **302**, and rhein-8-β-D-glucoside **306**, as well as sennoside A **307**, were isolated from *Rheum palmatum* and *R. tanguticum* (295). Sennoside A **307**, sennoside C **308**, and sennoside E **309** were isolated from *R. palmatum* and *R. tanguticum* species (295).

290

291

292

293

294 R = Glc
295 R = Rha-6'-Glc

296

297 R = H
298 R = Glc

299 and barbaloin **314** showed antiviral activity, but only emodin was a virucidal agent (301). A new cytotoxic 10-epi-uveoside, **318**, was isolated from the root bark of *Picramnia antidesma* (302), along with picramnioside E **319** and mayoside B **320**. One new anthraquinone glycoside, *M*-4′-demethylknipholone-2′-*O*-β-D-glucopyranoside **321**, was found in the methanolic extract of the Australian medicinal plant *Bulbine capitata* (303).
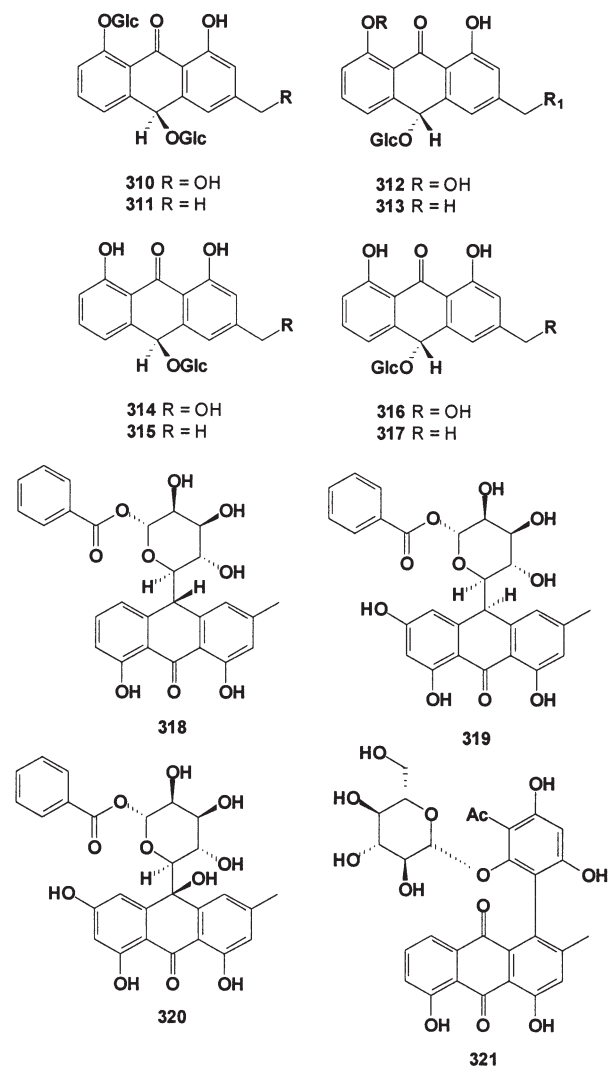
Doxorubicin **322**, an anthraquinone glycoside, is currently one of the clinically most important antineoplastic drugs. In pharmacokinetic studies of doxorubicin **322**, capillary blood sampling was recommended, especially for pediatric patients, to avoid the sometimes traumatic venous blood sampling procedure (304). A new anthraquinone glycoside, emodin-6-*O*-β-D-glucopyranoside **323**, and the earlier isolated chrysophanol-8-*O*-β-glucoside **302**, together with seven known phenolic compounds, have been isolated from the roots of *Rumex patientia*. The cytotoxic effects and radical-scavenging properties of the isolated compounds have been demonstrated (305). The medicinal plant *Bulbine narcissifolia* is used by the Basotho, Griqua, and Whites of southern Africa for wound healing and as a mild purgative. Extraction of the powered root has yielded acetosyringone, chrysophanol,

Cascara sagrada is the common name for *Rhamnus purshiana* (family Rhamnaceae), a short shrubby tree native to the Pacific Northwest in the United States. The dried bark of this tree, also called cascara sagrada, is the source of several anthraquinone laxative drugs, a class of laxatives used by many people throughout the world (296). Dried cascara sagrada bark contains approximately 7–10% hydroxyanthraquinone glycosides (297,298). Hydroxyanthraquinone glycosides are hydroxyanthracene derivatives with hydroxyl groups at the C-1 and C-8 positions and sugar groups at the hydroxyl groups (*O*-glycosides) or at the C-10 position (*C*-glycosides) (296,299). Not less than 60% of this 7–10% consists of cascarosides, expressed as cascaroside A **310**. There are four forms of cascarosides: A **310**, B **312**, C **311**, and D **313**. Cascarosides A **310** and B **312** are diastereoisomers, as are cascarosides C **311** and D **313**. Additional constituents of the dried cascara sagrada bark are the diasteroisomers of barbaloin **314** and **316** and chrysaloin **315** and **317**. Barbaloin stimulates the growth of *Eubacterium* species strain BAR (300). The anthraquinones emodin

knipholone, isoknipholone, 10,7′-bichrysophanol, and chrysalodin in addition to two new anthraquinone glycosides, knipholone-8-*O*-β-D-gentiobioside **324** and chrysalodin-10-β-D-gentiobioside **325**. NMR spectroscopy was used to elucidate the structures of **324** and **325** and to show that **324** binds weakly to DNA (306).

Frangulin A **326** (also known as emodin-L-rhamnoside, franguloside, or rhamnoxanthin) was discovered in 1907 by Tunman (307) in the bark of *Rhamnus frangula* (alder buckthorn); later, in 1909 the German chemist Schmidt (308), and again in 1913 the Russian scientist Krasovskii (309) found the compound in other *Rhamnus* species. More recently, biologically active frangulin A **326**, frangulin B **327**, glucofrangulin A **328**, and glucofrangulin B **329** have been isolated from *Rhamnus* and *Hypericum* species (310–312). Emodin **299** and frangulin B **326** showed significant antiplatelet effects (313); frangulin B **326** also showed potent inhibitory effects on TNF-α formation in LPS/interferon-γ-stimulated murine microglial cell line N9 (314).

comprising an ureido group at one of the four sugar units (315). Compound **330** exhibited inhibitory activity against pentagastrin-stimulated acid secretion as well as protective activities against HCl/ethanol- and indomethacin-induced gastric lesions.

The colored urdamycins A **331**, B **332**, C **333**, D **334**, E **335**, and F **336** are six new angucycline antibiotics produced from the *Streptomyces fradiae* strain Tu 2717 (316,317). They are biologically active against gram-positive bacteria and stem cells of murine L1210 leukemia. The urdamycins are glycosides and differ in their aglycones, which can be liberated by acidic hydrolysis in addition to the sugars D-olivose and L-rhodinose.

An angucycline series compound, P371 A1 **330**, from *Streptomyces* sp. P371, was established as having a novel structure

333

334

335

336
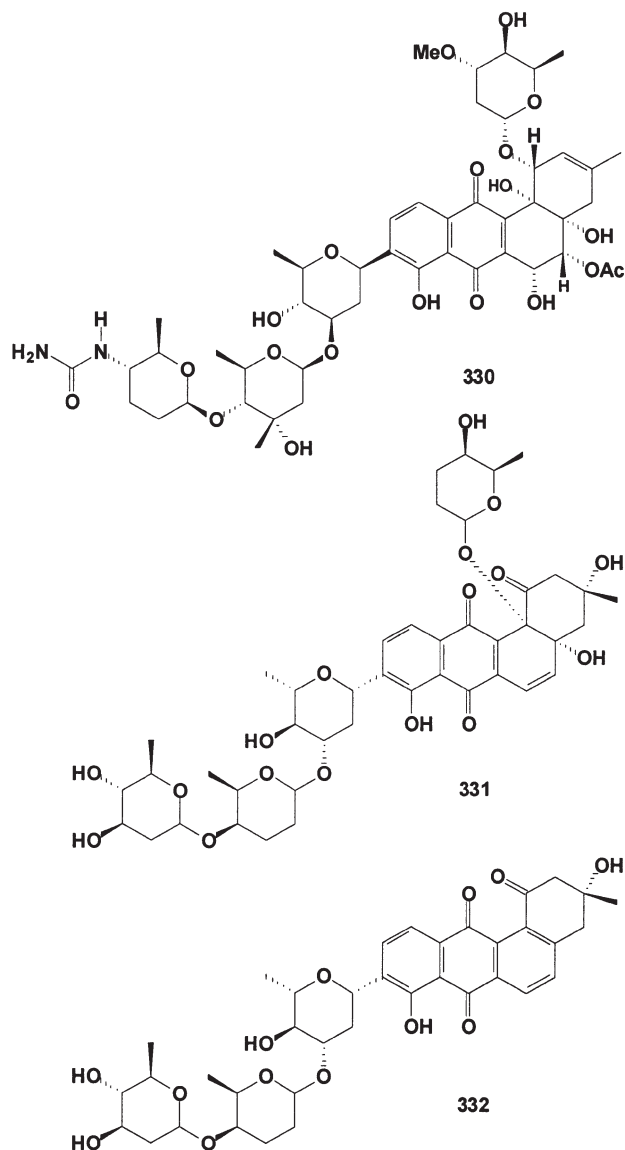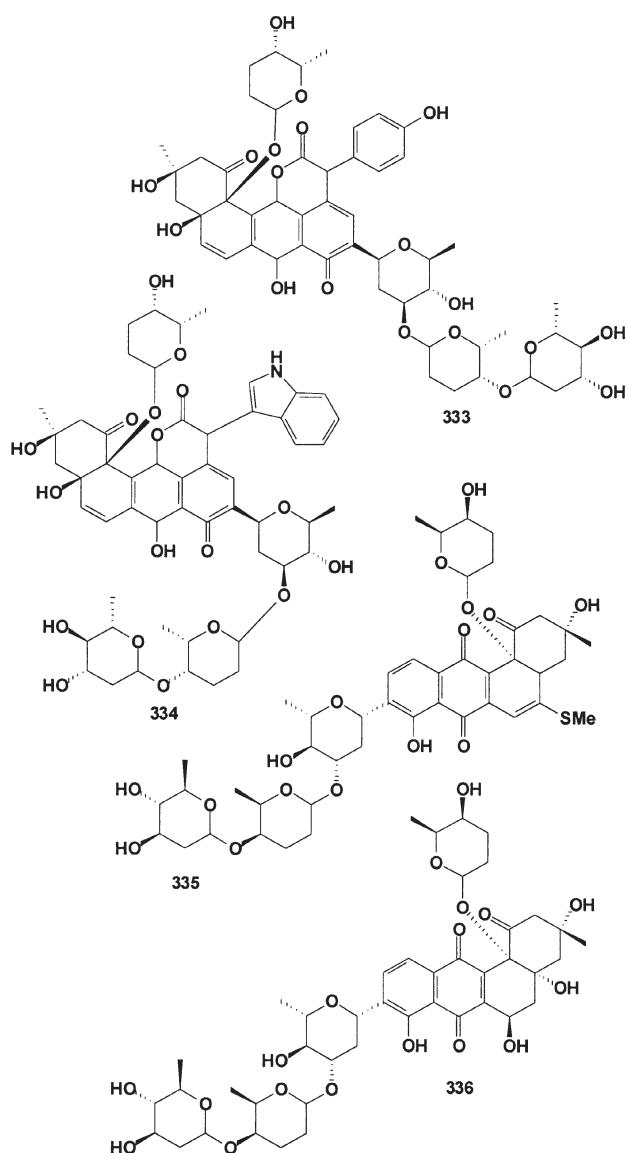
The antibiotic landomycins A **337**, B **338**, C **339**, D **340**, and E **341** are produced by species of streptomycetes (318–320). Streptomycetes, which are the producers of different polyketide antibiotics, can be divided into four groups based on their sensitivity to landomycins A and E: (i) *Streptomyces glaucescens* Tu49, producer of tetracenomycin, and *Streptomyces aureofaciens* 019, producer of chlortetracycline, belong to the most landomycin-sensitive strains. (ii) *Streptomyces cyanogenus* S136, producer of landomycin A, and *Streptomyces lividans* TK24, producer of actinorhodin, are sensitive to mean and high doses of landomycin E (more than 60–80 µg/mL). (iii) *Streptomyces globisporus* 1912 (producer of landomycin E), *S. cyanogenus* S136, *S. fradiae* Tu2717 (producer of urdamycins), and *Streptomyces coelicolor* A3(2) (producer of actinorhodin) have moderate sensitivity to all doses of both antibiotics, but strain S136 is sensitive only to low doses. (iv)

Resistance to landomycins A and E was observed in strain *Streptomyces olivaceus* Tu2353, producer of elloramycin. In all these experiments, landomycin E showed lethal activity one to two orders higher than landomycin A, whose molecule is composed of the same aglycon landomycenone A but a longer polysaccharide chain, which probably hampers the penetration of the antibiotic through the cell membrane (319).

A derivative of anthraquinone glycoside, P-1894B **342**, is a potent prolyl hydroxylase inhibitor produced by *Streptomyces albogriseolus* subspecies no. 1894; it inhibited 50% of the activity of purified chick embryo prolyl hydroxylase at a concentration of 2.2×10^{-6} M (321). The inhibition was noncompetitive with respect to Pro-Pro-Gly, with a K_i (prolyl hydroxylase activity, expressed in mol/mg protein) of 1.8×10^{-6} M. When excess amounts of Fe^{2+} or ascorbate were added to the reaction mixture, the inhibition was slightly reversed. Compound **342**, at a dose of 0.15 mg/kg, reduced the hydroxylation of peptidyl-proline and caused a significant inhibition of collagen biosynthesis in the uterus of the immature rat when stimulated by the administration of 17-β-estradiol.

Biological activities, structures, and other information about glycosides of the anthracene derivatives anthraquinones, angucyclines, oxanthrones, anthranols, and anthrones can be found in several review articles (322–326).

337 R =

338 R =

339

340

341
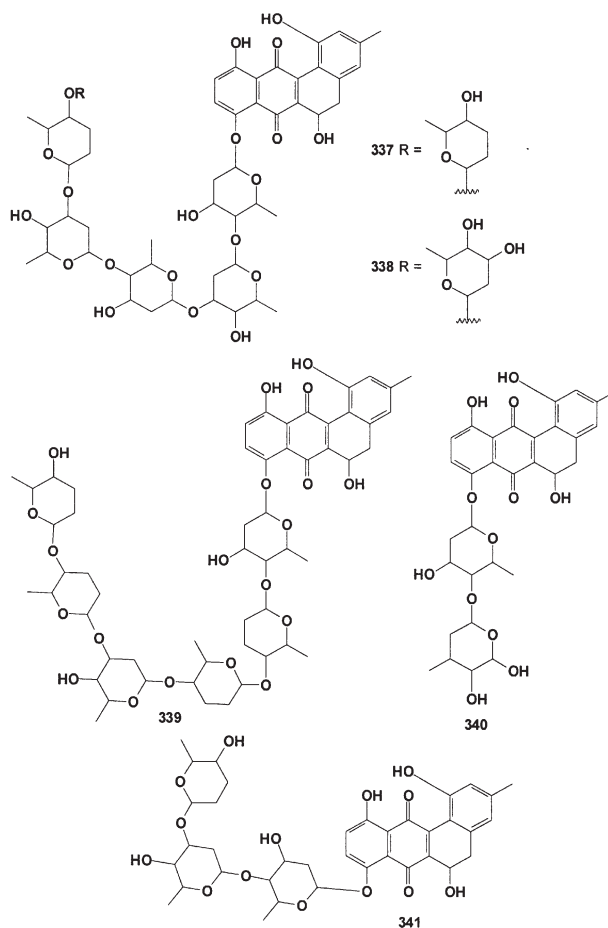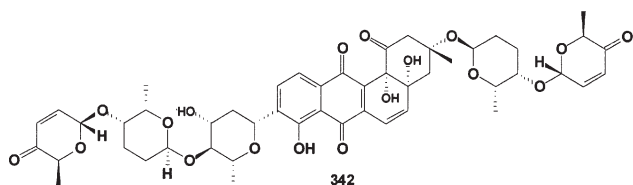
SUMMARY

Aromatic natural products have been used for thousands of years, and they are the basis of modern medicines. However, the same yardstick used for modern medicines should not be used to compare natural materials. Modern medicines work very quickly, they are concentrated, they are single components, the results are dramatic, and the risks of side effects are very real. The last couple of decades has seen a tremendous increase in interest in the biological properties of aromatic products as a means of identifying novel small compounds that could have potential in clinical medicine. To that end, stilbenes, lignans, naphthalene-like compounds, and anthracene-like compounds have been of particular interest because of their presence in diet constituents and because of the reported beneficial effects on diverse biological processes and disease conditions. The human diet contains an array of aromatic compounds (phytochemicals) with antioxidant activities capable of coping with reactive oxygen species, thus preventing oxidative stress. Of all the different phenolics, lignans, which are alkylphenolic compounds, constitute the largest class of polyphenols; they have proved to be one of the most powerful antioxidants present in the diet. The latest research has focused on understanding the role played by these dietary metabolites in disease prevention, suggesting a new role for "ancient" food items such as tea, cocoa, grapes (wine), and natural oils as functional foods.

   As far as the economic importance of plant aromatic compounds is concerned, different types of medicinal plants are used to treat various ailments pertaining to the nervous system, circulatory system, neuromuscular system, skeletal system, skin, and gastrointestinal system, and are used as immunosuppressives, in oral hygiene, and for the reproductive system. Plant aromatics also find a use as antiviral agents, as metabolic probes, in taxonomy, in genetics, in biotechnology, and in commerce.

REFERENCES

1. Dembitsky, V.M. (2005) Astonishing Diversity of Natural Surfactants. 4. Fatty Acid Amide Glycosides, Their Analogs and Derivatives, *Lipids 40*, 641–660.
2. Dey, P.M., and Harborne, J.B. (1997) *Plant Biochemistry*, Academic Press, 554 pp.
3. Karakaya, S. (2004) Bioavailability of Phenolic Compounds, *Crit. Rev. Food Sci. Nutr. 44*, 453–464.
4. Dell'Agli, M., Busciala, A., and Bosisio, E. (2004) Vascular Effects of Wine Polyphenols, *Cardiovasc. Res. 63*, 593–602.
5. Kris-Etherton, P.M., Hecker, K.D., Bonanome, A., Coval, S.M., Binkoski, A.E., Hilpert, K.F., Griel, A.E., and Etherton, T.D. (2002) Bioactive Compounds in Foods: Their Role in the Prevention of Cardiovascular Disease and Cancer, *Am. J. Med. 113* (Suppl. 9B), 71S–88S.
6. Cai, Y., Luo, Q., Sun, M., and Corke, H. (2004) Antioxidant Activity and Phenolic Compounds of 112 Traditional Chinese Medicinal Plants Associated with Anticancer, *Life Sci. 74*, 2157–2184.
7. Duthie, G., and Crozier, A. (2000) Plant-Derived Phenolic Antioxidants, *Curr. Opin. Clin. Nutr. Metab. Care 3*, 447–451.
8. Bravo, L. (1998) Polyphenols: Chemistry, Dietary Sources, Metabolism, and Nutritional Significance, *Nutr. Rev. 56*, 317–333.
9. Gubitz, G.M., and Paulo, A.C. (2003) New Substrates for Reliable Enzymes: Enzymatic Modification of Polymers, *Curr. Opin. Biotechnol. 14*, 577–582.
10. King, A., and Young, G. (1999) Characteristics and Occurrence of Phenolic Phytochemicals, *J. Am. Diet. Assoc. 99*, 213–218.
11. Plomion, C., Leprovost, G., and Stokes, A. (2001) Wood Formation in Trees, *Plant Physiol. 127*, 1513–1523.
12. Rabinovich, M.L., Bolobova, A.V., and Vasil'chenko, L.G. (2004) Decomposition of Natural Aromatic Structures and Xenobiotics by Fungi, *Prikl. Biokhim. Mikrobiol. 40*, 5–23.
13. Ros Barcelo, A. (1997) Lignification in Plant Cell Walls, *Int. Rev. Cytol. 176*, 87–132.
14. Wallace, G., and Fry, S.C. (1994) Phenolic Components of the Plant Cell Wall, *Int. Rev. Cytol. 151*, 229–267.
15. Brennan, P.J. (1989) Structure of Mycobacteria: Recent Developments in Defining Cell Wall Carbohydrates and Proteins, *Rev. Infect. Dis.* (Suppl. 2), S420–S430.
16. Dembitsky, V.M. (2004) Chemistry and Biodiversity of Biologically Active Natural Glycosides, *Chem. Biodivers. 1*, 673–781.
17. Dembitsky, V.M. (2005) Astonishing Diversity of Natural Surfactants. 2. Polyether Glycosidic Ionophores and Macrocyclic Glycosides, *Lipids 40*, 219–248.
18. Figueroa-Espinoza, M.C., and Villeneuve, P. (2005) Phenolic Acids Enzymatic Lipophilization, *J. Agric. Food Chem. 53*, 2779–2787.
19. Oak, M.H., El Bedoui, J., and Schini-Kerth, V.B. (2005) Antiangiogenic Properties of Natural Polyphenols from Red Wine and Green Tea, *J. Nutr. Biochem. 16*, 1–8.
20. De la Lastra, C.A., and Villegas, I. (2005) Resveratrol as an Anti-inflammatory and Anti-aging Agent: Mechanisms and Clinical Implications, *Mol. Nutr. Food Res. 49*, 405–430.
21. Pervaiz, S. (2004) Chemotherapeutic Potential of the Chemopreventive Phytoalexin Resveratrol, *Drug Resist. Updat. 7*, 333–344.
22. Gescher, A. (2004) Polyphenolic Phytochemicals Versus Nonsteroidal Anti-inflammatory Drugs: Which Are Better Cancer Chemopreventive Agents? *J. Chemother.* (Suppl. 4), 3–6.
23. Lambert, J.D., and Yang, C.S. (2003) Cancer Chemopreventive Activity and Bioavailability of Tea and Tea Polyphenols, *Mutat. Res. 523–524*, 201–208.
24. Lopez-Velez, M., Martinez-Martinez, F., and Del Valle-Ribes, C. (2003) The Study of Phenolic Compounds as Natural Antioxidants in Wine, *Crit. Rev. Food Sci. Nutr. 43*, 233–244.
25. Stark, A.H., and Madar, Z. (2002) Olive Oil as a Functional Food: Epidemiology and Nutritional Approaches, *Nutr. Rev. 60*, 170–176.
26. Hollman, P.C., and Katan, M.B. (1999) Health Effects and Bioavailability of Dietary Flavonols, *Free Radic. Res. 31* (Suppl.), S75–S80.
27. Orsini, F., Pelizzoni, F., Bellini, B., and Miglierini, G. (1997) Synthesis of Biologically Active Polyphenolic Glycosides (combretastatin and resveratrol series), *Carbohydr. Res. 301*, 95–109.
28. Cheynier, V. (2005) Polyphenols in Foods Are More Complex Than Often Thought, *Am. J. Clin. Nutr. 81* (Suppl. 1), 223S–229S.

29. Lee, K.H. (1999) Novel Antitumor Agents from Higher Plants, *Med. Res. Rev. 19*, 569–596.

30. Tan, B.K.H., and Vanitha, J. (2004) Immunomodulatory and Antimicrobial Effects of Some Traditional Chinese Medicinal Herbs: A Review, *Curr. Med. Chem. 11*, 1423–1430.

31. Wojcikowski, K., Johnson, D.W., and Gobe, G. (2004) Medicinal Herbal Extracts—Renal Friend or Foe? Part One: The Toxicities of Medicinal Herbs, *Nephrology 9*, 313–318.

32. Pittler, M.H., and Ernst, E. (2003) Systematic Review: Hepatotoxic Events Associated with Herbal Medicinal Products, *Aliment. Pharmacol. Therapeut. 18*, 451–471.

33. Parojcic, D. (2003) A Historical Overview of the Discovery of Aspirin with Some New Aspects on Its Development, *Arh. Farm. (Belgr.) 53*, 51–70.

34. Weissmann, G. (1991) Aspirin, *Sci. Am. 264*, 84–90.

35. Alstaedter, R. (ed.) (1984) *Aspirin, the Medicine of the Century*, Bayer AG, Leverkusen, Germany.

36. Rainsford, K.D. (1984) *Aspirin and the Salicylates*, Butterworths, London.

37. Gross, M., and Greenburg, L.A. (1948) *The Salicylates: A Critical Bibliographical Review*, Hillhouse, New Haven, CT.

38. Brewer, S. (2000) The Relationship Between Natural Products and Synthetic Chemistry in the Discovery Process, *Spec. Pub. Royal Soc. Chem. 257*, 59–65.

39. Malterud, K.E. (2000) Medicines from Nature, *Kjemi 60*, 10–15.

40. Nahrstedt, A. (1990) Use of Plant Secondary Metabolites by Animals and Humans, *Dtsch. Apoth. Ztg. 130*, 2155–2161.

41. Lukic, P. (1967) Natural Sources of Analgesics, *Arh. Farm. (Belgr.) 17*, 261–270.

42. Bridel, M. (1919) Application of the Biochemical Method to the Branches and Barks of Various Species of the Genus *Populus*, *J. Pharma. Chim. (France) 19*, 429–434.

43. Bridel, M., and Picard, P. (1928) Primeveroside of Salicylic Acid, *Bull. Soc. Chim. Biol. 10*, 381–385.

44. Vane, J.R. (1971) Salicylates, *Nature 231*, 232.

45. Thieme, H. (1963) The Phenolic Glycosides of the Salicaceae. I. General Review (discovery, elucidation of structure, synthesis, occurrence), *Pharmazie 18*, 770–774.

46. Yunes, R.A., Filho, V.C., Ferreira, J., and Calixto, J.B. (2005) The Use of Natural Products as Sources of New Analgesic Drugs, *Stud. Nat. Prod. Chem. Bioact. Nat. Prod. 30*, 191–212.

47. Brubacher, J.R., and Hoffman, R.S. (1996) Salicylism from Topical Salicylates: Review of the Literature, *J. Toxicol. Clin. Toxicol. 34*, 431–436.

48. Smith, M.J.H., and Smith, P.K. (eds.) (1966) *The Salicylates: A Critical Bibliographical Review*, Wiley Interscience, New York, 313 pp.

49. Paris, R.A., and Pointet, M. (1953) Presence of a Monotroposide in the Bark of *Ostryopsis davidiana*, *Ann. Pharm. Fr. 11*, 346–348.

50. Towers, G.H.N., Tse, A., and Maass, W.S.G. (1966) Phenolic Acids and Phenolic Glycosides of *Gaultheria* Species, *Phytochemistry 5*, 677–681.

51. Boas, F. (1966) *Kwakiutl Ethnobotany*, (Codere, H., ed.) The University of Chicago Press, Chicago.

52. Thieme, H. (1965) Isolation and Structural Clarification of Spiraein, a Phenol Glycoside from *Filipendula ulmaria*, *Pharmazie 20*, 113–114.

53. Meier, B., Lehmann, D., and Sticher, O. (1987) Salicylate in Medicinal Plants. Screening Methods (HPLC, TLC) for Detection, *Dtsch. Apoth. Zeit. (Germany) 127*, 2401–2417.

54. Kanchanapoom, T., Kamel, M.S., Kasai, R., Picheansoonthon, C., Hiraga, Y., and Yamasaki, K. (2001) Benzoxazinoid Glucosides from *Acanthus ilicifolius*, *Phytochemistry 58*, 637–640.

55. Itoh, A., Tanahashi, T., and Nagakura, N. (1993) Two Phenolic Glucosides and an Iridoid Glucoside from *Alangium platani-folium* var. *trilobum*, *Phytochemistry 33*, 161–164.

56. Wei, S., Zhou, Y., and Chang, Y. (1985) Phenolic Glucosides and Phenolic Acids from the Bark of Several Poplar Species, *Linchan Huaxue Yu Gongye 5*, 1–8.

57. Steele, J.W., Weitzel, P.F., and Audette, R.C.S. (1972) Phytochemistry of the Salicaceae. IV. Bark of *Salix petiolaris* (*S. gracilis* var. *textoris*), *J. Chromatogr. 71*, 435–441.

58. Tolonen, A., Pakonen, M., Hohtola, A., and Jalonen, J. (2003) Phenylpropanoid Glycosides from *Rhodiola rosea*, *Chem. Pharm. Bull. (Tokyo) 51*, 467–470.

59. Itoh, A., Tanahashi, T., Nagakura, N., Inoue, K., Kuwajima, H., and Wu, H.X. (2001) Glycosides of Benzyl and Salicyl Alcohols from *Alangium chinense*, *Chem. Pharm. Bull. (Tokyo) 49*, 1343–1345.

60. Delaquis, P.J., Stanich, K., Girard, B., and Mazza, G. (2002) Antimicrobial Activity of Individual and Mixed Fractions of Dill, Cilantro, Coriander and Eucalyptus Essential Oils, *Int. J. Food Microbiol. 74*, 101–109.

61. Singh, G., Kapoor, I.P., Pandey, S.K., Singh, U.K., and Singh, R.K. (2002) Studies on Essential Oils: Part 10: Antibacterial Activity of Volatile Oils of Some Species, *Phytother. Res. 16*, 680–682.

62. Yazdanparast, R., and Alavi, M. (2001) Antihyperlipidaemic and Antihypercholesterolaemic Effects of *Anethum graveolens* Leaves After the Removal of Furocoumarins, *Cytobios 105*, 185–191.

63. Ishikawa, T., Kudo, M., and Kitajima, J. (2002) Water-Soluble Constituents of Dill, *Chem. Pharm. Bull. (Tokyo) 50*, 501–507.

64. Society of Japanese Pharmacopoeia (2001) *Japanese Pharmacopoeia*, 14th edn., pp. 2708–2709, 2869–2871, Hirokawa Publishing, Tokyo.

65. Kitajima, J., Kamoshita, A., Ishikawa, T., Takano, A., Fukuda, T., Isoda, S., and Ida, Y. (2003) Glycosides of *Atractylodes japonica*, *Chem. Pharm. Bull. (Tokyo) 51*, 152–157.

66. Ishikawa, T., Kondo, K., and Kitajima, J. (2003) Water-Soluble Constituents of Coriander, *Chem. Pharm. Bull. (Tokyo) 51*, 32–39.

67. Kitajima, J., and Ishikawa, T. (2003) Water-Soluble Constituents of Amomum Seed, *Chem. Pharm. Bull. (Tokyo) 51*, 890–893.

68. Morikawa, T., Tao, J., Ueda, K., Matsuda, H., and Yoshikawa, M. (2003) Medicinal Foodstuffs. XXXI. 1). Structures of New Aromatic Constituents and Inhibitors of Degranulation in RBL-2H3 Cells from a Japanese Folk Medicine, the Stem Bark of *Acer nikoense*, *Chem. Pharm. Bull. (Tokyo) 51*, 62–67.

69. Ravi, K., Sivagnanam, K., and Subramanian, S. (2004) Antidiabetic Activity of *Eugenia jambolana* Seed Kernels on Streptozotocin-Induced Diabetic Rats, *J. Med. Food 7*, 187–191.

70. Ravi, K., Sekar, D.S., and Subramanian, S. (2004) Hypoglycemic Activity of Inorganic Constituents in *Eugenia jambolana* Seed on Streptozotocin-Induced Diabetes in Rats, *Biol. Trace Elem. Res. 99*, 145–155.

71. Chandrasekaran, M., and Venkatesalu, V. (2004) Antibacterial and Antifungal Activity of *Syzygium jambolanum* Seeds, *J. Ethnopharmacol. 91*, 105–108.

72. Bokesch, H.R., Young, S.M., McKee, T.C., Blunt, J.W., and Boyd, M.R. (1998) Lambertianoside, a Novel Phenylglycoside from *Eugenia lambertiana*, *Nat. Prod. Lett. 11*, 211–216.

73. Hase, K., Kadota, S., Basnet, P., Namba, T., and Takahashi, T. (1996) Hepatoprotective Effects of Traditional Medicines. Isolation of the Active Constituent from Seeds of *Celosia argentea*, *Phytother. Res. 10*, 387–392.

74. Xia, H.C., Li, F., Li, Z., and Zhang, Z.C. (2003) Purification and Characterization of Moschatin, a Novel Type I Ribosome-inactivating Protein from the Mature Seeds of Pumpkin (*Cucurbita moschata*), and Preparation of Its Immunotoxin Against Human Melanoma Cells, *Cell Res. 13*, 369–374.

75. Koike, K., Li, W., Liu, L., Hata, E., and Nikaido, T. (2005) New Phenolic Glycosides from the Seeds of *Cucurbita moschata*, *Chem. Pharm. Bull. (Tokyo) 53*, 225–228.

76. Jung, M.J., Kang, S.S., Jung, Y.J., and Choi, J.S. (2004) Phenolic Glycosides from the Stem Bark of *Albizzia julibrissin*, *Chem. Pharm. Bull. (Tokyo) 52*, 1501–1503.

77. De Leo, M., Braca, A., De Tommasi, N., Norscia, I., Morelli, I., Battinelli, L., and Mazzanti, G. (2004) Phenolic Compounds from *Baseonema acuminatum* Leaves: Isolation and Antimicrobial Activity, *Planta Med. 70*, 841–846.

78. Cottiglia, F., Bonsignore, L., Casu, L., Deidda, D., Pompei, R., Casu, M., and Floris, C. (2005) Phenolic Constituents from *Ephedra nebrodensis*, *Nat. Prod. Res. 19*, 117–123.

79. Braham, H., Mighri, Z., Jannet, H.B., Matthew, S., and Abreu, P.M. (2005) Antioxidant Phenolic Glycosides from *Moricandia arvensis*, *J. Nat. Prod. 68*, 517–522.

80. Liu, G.-W. (2001) *Chinese Herbal Medicine*, HuaXia Publishing House, Beijing (in Chinese).

81. Shri, N.G., Laxmi, N.M., and Shantosh, K.A. (1989) Corchioiside A, an Orcinol Glycoside from *Curculigo orchioides, Phytochemistry 28*, 1771–1772.

82. Xu, J.P., and Xu, R.S. (1992) Phenyl Glycosides from *Curculigo orchioides*, *Yao Xue Xue Bao 27*, 353–357.

83. Li, N., Zhao, Y., Jia, A., Liu, Y., and Zhou, J. (2003) Study on the Chemical Constituents of *Curculigo orchioides*, *Tianran Chanwu Yanjiu Yu Kaifa 15*, 208–211.

84. Lu, H., Zhu, B., and Liang, Y. (2002) Determination of Curculigoside in *Curculigo orchioides* by HPLC, *Zhongguo Zhongyao Zazhi 27*, 192–194.

85. Palazzino, G., Galeffi, C., Federici, E., Delle Monache, F., Francesca Cometa, M., and Palmery, M. (2000) Benzylbenzoate and Norlignan Glucosides from *Curculigo pilosa*: Structural Analysis and *in vitro* Vascular Activity, *Phytochemistry 55*, 411–417.

86. Chen, C., Ni, W., and Mei, W. (1999) Glycosides from *Curculigo orchioides*, *Yunnan Zhi Wu Yan Jiu 21*, 521–524.

87. Fu, D.-X., Lei, G.-Q., Cheng, X.-W., Chen, J.-K., and Zhou, T.-S. (2004) Curculigoside C, a New Phenolic Glucoside from Rhizomes of *Curculigo orchioides*, *Acta Bot. Sin. 46*, 621–624.

88. Wu, H., Liu, Y., and Chen, Y. (1999) Determination of Curculigoside in Rhizomes of *Curculigo orchioides* Gaertn. by HPLC, *Yaowu Fenxi Zazhi 19*, 105–107.

89. Li, N., Tan, N.-H., and Zhou, J. (2004) New Chlorine-Containing Phenoloid from *Curculigo capitulate*, *J. Asian Nat. Prod. Res. 6*, 7–10.

90. Day, J.A., and Saunders, E. (2004) Glycosidation of Chlorophenols by *Lemna minor*, *Environ. Toxicol. Chem. 23*, 613–620.

91. Rothley, D., and Oelschlaeger, H. (1982) Unequivocal Determination of Glucuronides, in Particular of Clofibric β-Glucuronide, *Arch. Pharm. (Weinheim) 315*, 457–462.

92. Miller, L.P. (1957) Monosaccharide Components of an Induced Glycoside of Trichloroethyl Alcohol from Dandelion Tops, *Contrib. Boyce Thompson Inst. 19*, 113–115.

93. Day, J.A., III (2002) Formation and Fate of Chlorophenol Glycosides in an Aquatic Plant Environment, Georgia Institute of Technology, Atlanta, 255 pp. [abstracted in *Diss. Abstr. Int. B 63*, 5435 (2003)].

94. Chang, W.-L., Chen, C.-H., and Lee, S.-S. (1999) Three Novel Constituents from *Curculigo capitulata* and Revision of C-2 Stereochemistry in Nyasicoside, *J. Nat. Prod. 62*, 734–739.

95. Galeffi, C., Federici, E., Palazzino, G., and Nicoletti, M. (1997) Research on African Medicinal Plants. XXXVIII. Further Norlignans from *Hypoxis obtusa* Burch, *Gazz. Chim. Ital. 127*, 501–504.

96. Marini Bettolo, G.B., Patamia, M., Nicoletti, M., Galeffi, C., and Messana, I. (1982) Research on African Medicinal Plants. II. Hypoxoside, a New Glycoside of Uncommon Structure from *Hypoxis obtusa* Busch, *Tetrahedron 38*, 1683–1687.

97. Chang, P.C., and Wu, C.C. (1979) *Herbs of Taiwan in Color*, Vol. 1, Nan Cun (South Villa) Trade Co., Taipei, Republic of China, p. 99.

98. Morikawa, H., Kasai, R., Otsuka, H., Hirata, E., Shinzato, T., Aramoto, M., and Takeda, Y. (2004) Terpenic and Phenolic Glycosides from Leaves of *Breynia officinalis* HEMSL, *Chem. Pharm. Bull. (Tokyo) 52*, 1086–1090.

99. Perry, L.M. (1980) *Medicinal Plants of East and Southeast Asia: Attributed Properties and Uses*, The MIT Press, Cambridge.

100. Kim, J.S., Shim, S.H., Xu, Y.N., Kang, S.S., Son, K.H., Chang, H.W., Kim, H.P., and Bae, K. (2004) Phenolic Glycosides from *Pyrola japonica*, *Chem. Pharm. Bull. (Tokyo) 52*, 714–717.

101. Li, L.M., Liao, X., Peng, S.L., and Ding, L.S. (2005) Chemical Constituents from the Seeds of *Ziziphus jujube* var. *spinosa* (Bunge) Hu, *J. Integrative Plant Biol. (*formerly *Acta Bot. Sin.) 47*, 494–498.

102. Ouyang, M.-A., He, Z.-D., and Wu, C.-L. (2003) Anti-oxidative Activity of Glycosides from *Ligustrum sinense*, *Nat. Prod. Res. 17*, 381–387.

103. Nagatani, Y., Warashina, T., and Noro, T. (2002) Studies on the Constituents from the Aerial Part of *Baccharis dracunculifolia* DC. II, *Chem. Pharm. Bull. (Tokyo) 50*, 583–589.

104. Zhang, W., Chen, W., Wang, Y., Liu, W., Kong, D., and Li, H. (2001) Two New Glycosides from *Erigeron breviscapus* (Vant.) Hand.–Mazz, *Zhongguo Zhongyao Zazhi 26*, 689–690.

105. Chen, X.C., and Jia, Z.J. (2000) Two New Glycosides from *Rubus amabilis*, *Chin. Chem. Lett. 11*, 897–900.

106. Zhang, W., Tam, H.A., Thi, B., Chen, W., Kong, D., Li, H., Wang, Y., and Fouraste, I. (2000) Two New Glycosides from *Erigeron breviscapus*, *J. Chinese Pharmaceut. Sci. 9*, 122–124.

107. Kitajima, J., Ishikawa, T., and Tanaka, Y. (1998) Water-Soluble Constituents of Fennel. II. Four *erythro*-Anethole Glycol Glycosides and Two *p*-Hydroxyphenylpropylene Glycol Glycosides, *Chem. Pharm. Bull. (Tokyo) 46*, 1591–1594.

108. Yoshikawa, K., Eiko, K., Mimura, N., Kondo, Y., and Arihara, S. (1998) Hovetrichosides C–G, Five New Glycosides of Two Auronols, Two Neolignans, and a Phenylpropanoid from the Bark of *Hovenia trichocarea*, *J. Nat. Prod. 61*, 786–790.

109. Rashid, M.A., Gustafson, K.R., Cardellina, J.H., II, and Boyd, M.R. (1996) A Benzoic Acid Glycoside from *Geniostoma antherotrichum*, *Phytochemistry 41*, 1205–1207.

110. Xiao, K., Xuan, L., Xu, Y., and Bai, D. (2002) Novel Stilbene Glycosides from *Polygonum multiflorum*, *Acta Bot. Sin. 44*, 1491–1494.

111. Heitzman, M.E., Neto, C.C., Winiarz, E., Vaisberg, A.J., and Hammond, G.B. (2005) Ethnobotany, Phytochemistry and Pharmacology of *Uncaria* (Rubiaceae), *Phytochemistry 66*, 5–29.

112. Kong, J.M., Goh, N.K., Chia, L.S., and Chia, T.F. (2003) Recent Advances in Traditional Plant Drugs and Orchids, *Acta Pharmacol. Sin. 24*, 7–21.

113. Lu, Y.R., and Foo, L.Y. (2002) Polyphenolics of *Salvia*—A Review, *Phytochemistry 59*, 117–140.

114. Lovkova, M.Ya., Buzuk, G.N., Sokolova, S.M., and Kliment'eva, N.I. (2001) Chemical Features of Medicinal Plants (review), *Appl. Biochem. Microbiol. 37*, 229–237.

115. Agarwal, S.K., Singh, S.S., Lakshmi, V., Vermam, S., and Kumar, S. (2001) Chemistry and Pharmacology of Rhubarb (*Rheum* species)—A Review, *J. Scient. Indust. Res. 60*, 1–9.

116. Von Kruedener, S., Schneider, W., and Elstner, E. (1995) A Combination of *Populus tremula*, *Solidago virgaurea* and *Fraxinus excelsior* as an Antiinflammatory and Antirheumatic Drug—A Short Review, *Arzneim. Forsch./Drug Res. 45*, 169–171.

117. Ahmad, Y.U., and Rahman, A. (1994) *Handbook of Natural Products Data*, Vol. 2, Elsevier, Amsterdam, The Netherlands.

118. Bandyukova, V.A. (1983) Plant Phenol Acids, Their Esters and Glycosides, *Khim. Prirod. Soed. (USSR) 3*, 263–273.

119. Miller, L.P. (1973) Glycosides, *Phytochemistry 1*, 297–375.

120. Hopkinson, S.M. (1969) Chemistry and Biochemistry of Phenolic Glycosides, *Quart. Rev. Chem. Soc. 23*, 98–124.

121. Kompantsev, V.A. (1969) Phenolic Glycosides from *Salix pentandroides*, *Khim. Prirod. Soed. (USSR) 5*, 183–201.

122. Psenak, M. (1967) Phenol Glycosides: Their Significance and Structure, *Biologia (Bratislava) 22*, 704–714.

123. Kondratyuk, T.P., and Pezzuto, J.M. (2004) Natural Product Polyphenols of Relevance to Human Health, *Pharmaceut. Biol. 42* (Suppl. S.), 46–63,

124. Matsuda, H., Kageura, T., Morikawa, T., Toguchida, I., Harima, S., and Yoshikawa, M. (2000) Effects of Stilbene Constituents from Rhubarb on Nitric Oxide Production in Lipopolysaccharide-Activated Macrophages, *Bioorg. Med. Chem. Lett. 10*, 323–327.

125. Nicolaou, K.C., Roecker, A.J., Barluenga, S., Pfefferkorn, J.A., and Cao, G.-Q. (2001) Discovery of Novel Antibacterial Agents Active Against Methicillin-Resistant *Staphylococcus aureus* from Combinatorial Benzopyran Libraries, *ChemBioChem 2*, 460–465.

126. Schultz, T.P., Hubbard, T.F., Jr., Jin, L., Fisher, T.H., and Nicholas, D.D. (1990) Role of Stilbenes in the Natural Durability of Wood—Fungicidal Structure–Activity Relationships, *Phytochemistry 29*, 1501–1507.

127. Shen, F., Chen, S.-J., Dong, X.-J., Zhong, H., Li, Y.-T., and Cheng, G.-F. (2003) Suppression of IL-8 Gene Transcription by Resveratrol in Phorbol Ester Treated Human Monocytic Cells, *J. Asian Nat. Prod. Res. 5*, 151–157.

128. Boonlaksiri, C., Oonanant, W., Kongsaeree, P., Kittakoop, P., Tanticharoen, M., and Thebtaranonth, Y. (2000) An Antimalarial Stilbene from *Artocarpus integer*, *Phytochemistry 54*, 415–417.

129. Banwell, M.G., Bezos, A., Chand, S., Dannhardt, G., Kiefer, W., Nowe, U., Parish, C.R., Savage, G.P., and Ulbrich, H. (2003) Convergent Synthesis and Preliminary Biological Evaluations of the Stilbenolignan (+/−)-Aiphanol and Various Congeners, *Org. Biomol. Chem. 1*, 2427–2429.

130. Orsini, F., Pelizzoni, F., Verotta, L., Aburjai, T., and Roger, C.B. (1997) Isolation, Synthesis, and Antiplatelet Aggregation Activity of Resveratrol 3-*O*-β-D-Glucopyranoside and Related Compounds, *J. Nat. Prod. 60*, 1082–1087.

131. Pacher, T., Seger, C., Engelmeier, D., Vajrodaya, S., Hofer, O., and Greger, H. (2002) Antifungal Stilbenoids from *Stemona collinsae*, *J. Nat. Prod. 65*, 820–827.

132. Likhitwitayawuid, K., and Sritularak, B. (2001) A New Dimeric Stilbene with Tyrosinase Inhibitiory Activity from *Artocarpus gomezianus*, *J. Nat. Prod. 64*, 1457–1459.

133. Dai, J.R., Hallock, Y.F., Cardellina, J.H., and Boyd, M.R. (1998) HIV-Inhibitory and Cytotoxic Oligostilbenes from the Leaves of *Hopea malibato*, *J. Nat. Prod. 61*, 351–353.

134. Hazai, L., and Hornyak, G. (1998) Photochemical Reactions of Stilbenes and Their Heterocyclic Derivatives—A Review, *Ach.-Model, Chem. 135*, 493–514.

135. Hagen, S., and Hopf, H. (1998) Modern Routes to Extended Aromatic Compounds, Carbon Rich Compounds I, *Topic. Curr. Chem. 196*, 45–89.

136. Bai, L., Masukawa, N., Yamaki, M., and Takagi, S. (1997) Two Bibenzyl Glucosides from *Pleione bulbocodioides*, *Phytochemistry 44*, 1565–1567.

137. Toshio, M., and Akira, U. (1991) Ionone and Bibenzyl Glycosides from *Epimedium grandiflorum* var. *thunbergianum*, *Phytochemistry 30*, 1727–1728.

138. Bae, K.H. (2002) *Medicinal Plants of Korea*, Kyo-Hak Publishing Co., Seoul, pp. 302.

139. Yang, H., Sung, S.H., and Kim, Y.C. (2005) Two New Hepatoprotective Stilbene Glycosides from *Acer mono* Leaves, *J. Nat. Prod. 68*, 101–103.

140. Rahman, A., Naz, H., Fadimatou, Makhmoor, T., Yasin, A., Fatima, N., Ngounou, F.N., Kimbu, S.F., Sondengam, B. L., and Choudhary, M.I. (2005) Bioactive Constituents from *Boswellia papyrifera*, *J. Nat. Prod. 68,* 189–193.

141. Roggero, J.P., and Archier, P. (1994) Quantitative Determination of Resveratrol and of One of Its Glycosides in Wines, *Sci. Aliments 14*, 99–107.

142. Vastano, B.C., Chen, Y., Zhu, N., Ho, C.T., Zhou, Z., and Rosen, R.T. (2000) Isolation and Identification of Stilbenes in Two Varieties of *Polygonum cuspidatum*, *J. Agric. Food Chem. 48*, 253–256.

143. Shi, Y.Q., Fukai, T., Sakagami, H., Kuroda, J., Miyaoka, R., Tamura, M., Yoshida, N., and Nomura, T. (2001) Cytotoxic and DNA Damage-Inducing Activities of Low Molecular Weight Phenols from Rhubarb, *Anticancer Res. 21*, 2847–2853.

144. Kimura, Y. (2003) Pharmacological Studies on Resveratrol, *Methods Find. Exp. Clin. Pharmacol. 25*, 297–310.

145. Nonaka, G., Minami, M., and Nishioka, I. (1977) Studies on Rhubarb (*Rhei rhizoma*). III. Stilbene Glycosides, *Chem. Pharm. Bull. (Tokyo) 25*, 2300–2305.

146. Gromova, A.S., Lutskii, V.I., and Tyukavkina, N.A. (1979) Stilbenes from the Bark of Some *Pinaceae* Species, *Koksnes Kimija 3*, 103–109.

147. Pearson, T.W., Kriz, G.S., Jr., and Taylor, R.J. (1977) Absolute Identification of Hydroxystilbenes, Chemical Markers in Engelmann *spruce*, *Wood Sci. 10*, 93–98.

148. Gromova, A.S., Tyukavkina, N.A., Lutskii, V.I., Kalabin, G.A., and Kushnarev, D.F. (1975) Hydroxystilbenes of the Inner Bark of *Pinus sibirica*, *Khim. Prirod. Soed. (USSR) 11*, 677–682.

149. Bombardelli, E., Martinelli, E.M., and Mustich, G. (1975) Plants of Mozambique. IX. New Hydroxystilbene Glycoside from *Terminalia sericea*, *Fitoterapia 46*, 199–200.

150. Nkiliza, J. (2003) Rhubarb Extract, Compositions Obtained from This Extract, Procedure for Obtaining, and Uses, French Patent: FR 2835185, 20 pp.

151. Kimura, Y., and Okuda, H. (2000) Effects of Naturally Occurring Stilbene Glucosides from Medicinal Plants and Wine, on Tumor Growth and Lung Metastasis in Lewis Lung Carcinoma-Bearing Mice, *J. Pharm. Pharmacol. 52*, 1287–1295.

152. Zhang, L., Li, L., and Li, Y. (2004) Mechanism of the Protection of Effective Component of Tuber Fleeceflower Root Stilbene Glycoside on Nerve Cells, *Zhongguo Linchuang Kangfu 8*, 118–120.

153. Chen, W., Li, L., Yin, X., Yang, G., Qiao, C., Zhang, W., and Chen, H. (2001) Tetrahydroxy-diphenylethylene Glycosides for Preventing and Treating Cardiovascular and Cerebrovascular Diseases, Chinese Patent: CN 1303858, 11 pp.

154. Matsuda, H., Tewtrakul, S., Morikawa, T., and Yoshikawa, M. (2004) Anti-allergic Activity of Stilbenes from Korean Rhubarb (*Rheum undulatum* L.): Structure Requirements for Inhibition of Antigen-Induced Degranulation and Their Effects on the Release of TNF-α and IL-4 in RBL-2H3 Cells, *Bioorg. Med. Chem. 12*, 4871–4876.

155. Pan, H., and Lundgren, L.N. (1995) Phenolic Extractives from Root Bark of *Picea abies*, *Phytochemistry 39*, 1423–1428.

156. Fuendjiep, V., Wandji, J., Tillequin, F., Mulholland, D.A., Budzikiewicz, H., Fomum, Z.T., Nyemba, A.M., and Koch, M. (2002) Chalconoid and Stilbenoid Glycosides from *Guibourtia tessmanii, Phytochemistry 60*, 803–806.

157. Ali, Z., Ito, T., Tanaka, T., Nakaya, K.I., Murata, J., Darnaedi, D., and Iinuma, M. (2004) Acetophenone *C*-Glucosides and Stilbene *O*-Glucosides in *Upuna borneensis*, *Phytochemistry 65*, 2141–2146.

158. Waffo-Teguo, P., Lee, D., Cuendet, M., Merillon, J.-M., Pezzuto, J.M., and Kinghorn, A.D. (2001) Two New Stilbene

Dimer Glucosides from Grape (*Vitis vinifera*) Cell Cultures, *J. Nat. Prod. 64*, 136–138.

159. Ito, T., Akao, Y., Tanaka, T., Iinuma, M., and Nozawa, Y. (2002) Vaticanol C, a Novel Resveratrol Tetramer, Inhibits Cell Growth Through Induction of Apoptosis in Colon Cancer Cell Lines, *Biol. Pharm. Bull. 25*, 147–148.

160. Iliya, I., Tanaka, T., Furusawa, M., Ali, Z., Nakaya, K., Iinuma, M., Shirataki, Y., Murata, J., and Darnaedi, D. (2001) Four New Glucosides of Stilbene Oligomers from the Stem of *Gnetum gnemonoides*, *Heterocycles 55*, 2123–2130.

161. Iliya, I., Tanaka, T., Iinuma, M., Furusawa, M., Ali, Z., Nakaya, K.I., Murata, J., and Darnaedi, D. (2002) Five Stilbene Glucosides from *Gnetum gnemonoides* and *Gnetum africanum*, *Helv. Chim. Acta 85*, 2394–2402.

162. Iliya, I., Ali, Z., Tanaka, T., Iinuma, M., Furusawa, M., Nakaya, K., Murata, J., Darnaedi, D., Matsuura, N., and Ubukata, M. (2003) Stilbene Derivatives from *Gnetum gnemon* Linn, *Phytochemistry 62*, 601–606.

163. Xiao, K., Xuan, L., Xu, Y., Bai, D., Zhong, D., Wu, H., Wang, Z., and Zhang, N. (2002) Dimeric Stilbene Glycosides from *Polygonum cuspidatum*, *Eur. J. Org. Chem. 3*, 564–568.

164. Ono, M., Ito, Y., Kinjo, J., Yahara, S., Nohara, T., and Niiho, Y. (1995) Four New Glycosides of Stilbene Trimer from *Foeniculi fructus* (fruit of *Foeniculum vulgare* Miller), *Chem. Pharm. Bull. (Tokyo) 43*, 868–871.

165. Xiao, K., Xuan, L., Xu, Y., and Bai, D. (2000) Stilbene Glycoside Sulfates from *Polygonum cuspidatum*, *J. Nat. Prod. 63*, 1373–1376.

166. Ashton, P.S. (1982) Flora Malesiana, in *Spermatophyta*, Series 1, Vol. 9 (Steenis C.G.G.J., ed.), Martivus Nijhoff Publishers, Leiden, The Netherlands, pp. 337–340.

167. Ito, T., Ali, Z., Iliya, I., Furusawa, M., Tanaka, T., Nakaya, K.C., Takahashi, Y., Sawa, R., Murata, J., Darnaedi, D., *et al.* (2005) Occurrence of Stilbene Glucosides in *Upuna borneensis*, *Helv. Chim. Acta 88*, 23–34.

168. Taskova, R.M., Gotfredsen, C.H., and Jensen, S.R. (2005) Chemotaxonomic Markers in Digitalideae (Plantaginaceae), *Phytochemistry 66*, 1440–1447.

169. Li, Y., and Ohizumi, Y. (2004) Search for Constituents with Neurotrophic Factor-Potentiating Activity from the Medicinal Plants of Paraguay and Thailand, *Yakugaku Zasshi 124*, 417–424.

170. Jimenez, C., and Riguera, R. (1994) Phenylethanoid Glycosides in Plants: Structure and Biological Activity, *Nat. Prod. Rep. 11*, 591–606.

171. Mel'nikov, V.N., Bugorskii, P.S., and Medvedkova, V.V. (1975) β-Phenethyl-β-D-glucopyranoside from the Flowers of *Rosa gallica*, *Khim. Prirod. Soed. (USSR) 11*, 807–809.

172. Kimura, T., Utida, M., Nakajima, H., and Dombou, M. (2000) Enzymatic Synthesis of Phenethyl Glycoside and Its Application, *J. Appl. Glycosci. 47*, 55–59.

173. Nicoletti, M., Galeffi, C., Messana, I., Garbarino, J.A., Gambaro, V., Nyandat, E., and Marini-Bettolo, G.B. (1986) New Phenylpropanoid Glucosides from *Calceolaria hypericina*, *Gazz. Chim. Ital. 116*, 431–433.

174. Ersoz, T., Ozalp, M., Ekizoglu, M., and Calis, I. (2002) Antimicrobial Activities of the Phenylethanoid Glycosides from *Scutellaria galericulata*, *Hacettepe Univ. Eczacilik Fak. Derg. (Turkey) 22*, 1–8.

175. Miyase, T., Ishino, M., Akahori, C., Ueno, A., Ohkawa, Y., and Tanizawa, H. (1991) Phenylethanoid Glycosides from *Plantago asiatica*, *Phytochemistry 30*, 2015–2018.

176. Liu, D.-L., Zhang, Y., Xu, S.-X., Xu, Y., and Wang, Z.-X. (1998) Phenylethanoid Glycosides from *Forsythia suspensa* Vahl, *J. Chinese Pharmaceut. Sci. 7*, 103–105.

177. Wang, H., Sun, Y., Ye, W.-C., Xiong, F., Wu, J.-J., Yang, C.-H., and Zhao, S.-X. (2004) Antioxidative Phenylethanoid and Phenolic Glycosides from *Picrorhiza scrophulariiflora*, *Chem. Pharm. Bull. (Tokyo) 52*, 615–617.

178. Pettit, G.R., Numata, A., Takemura, T., Ode, R.H., Narula, A.S., Schmidt, J.M., Cragg, G.M., and Pase, C.P. (1990) Antineoplastic Agents, 107. Isolation of Acteoside and Isoacteoside from *Castilleja linariaefolia*, *J. Nat. Prod. 53*, 456–458.

179. Diaz, A.M., Abad, M.J., Fernandez, L., Silvan, A.M., De Santos, J., and Bermejo, P. (2004) Phenylpropanoid Glycosides from *Scrophularia scorodonia*: *In vitro* Anti-inflammatory Activity, *Life Sci. 74*, 2515–2526.

180. Chiou, W.-F., Lin, L.-C., and Chen, C.-F. (2003) The Antioxidant and Free Radical Scavenging Properties of Acteoside, *Chin. Pharm. J. (Taipei) 55*, 347–353.

181. Boje, K., Lechtenberg, M., and Nahrstedt, A. (2003) New and Known Iridoid- and Phenylethanoid Glycosides from *Harpagophytum procumbens* and Their *in vitro* Inhibition of Human Leukocyte Elastase, *Planta Med. 69*, 820–825.

182. Lee, J.Y., Woo, E.-R., and Kang, K.W. (2005) Inhibition of Lipopolysaccharide-Inducible Nitric Oxide Synthase Expression by Acteoside Through Blocking of AP-1 Activation, *J. Ethnopharmacol. 97*, 561–566.

183. Zhang, F., Jia, Z., Deng, Z., Fan, J., Chen, J., Wu, H., Zhao, C., and Wei, Y. (2002) Inhibition of Verbascoside on the Telomerase Activity of Human Gastric Adenocarcinoma Cell MKN45, *Shijie Huaren Xiaohua Zazhi 10*, 366–367.

184. Nagao, T., Abe, F., and Okabe, H. (2001) Antiproliferative Constituents in the Plants. 7. Leaves of *Clerodendron bungei* and Leaves and Bark of *C. trichotomum*, *Biol. Pharm. Bull. 24*, 1338–1341.

185. Xiong, Q., Hase, K., Tezuka, Y., Namba, T., and Kadota, S. (1999) Acteoside Inhibits Apoptosis in D-Galactosamine and Lipopolysaccharide-Induced Liver Injury, *Life Sci. 65*, 421–430.

186. Schapoval, E.E.S., Winter de Vargas, M.R., Chaves, C.E.G., Bridi, R., Zuanazzi, J.A., and Henriques, A.T. (1998) Antiinflammatory and Antinociceptive Activities of Extracts and Isolated Compounds from *Stachytarpheta cayennensis*, *J. Ethnopharmacol. 60*, 53–59.

187. Kang, K.H., Jang, S.K., Kim, B.K., and Park, M.K. (1994) Antibacterial Phenylpropanoid Glycosides from *Paulownia tomentosa* Steud., *Arch. Pharm. Res. 17*, 470–475.

188. Pu, X., Li, X., Li, H., Tu, P., Song, Z., and Li, C. (2001) Campneoside II of *Cistanche tubulosa* (Schenk) R. Wight Protects Neurons from Apoptosis Induced by Neurotoxin 1-Methyl-4-phenylpyridinium (MPP+), *Beijing Daxue Xuebao, Yixueban 33*, 217–220.

189. Jimenez, C., Villaverde, M.C., Riguera, R., Castedo, L., and Stermitz, F.R. (1987) Three Phenylpropanoid Glycosides from *Mussatia*, *Phytochemistry 26*, 1805–1810.

190. Jimenez, C., Villaverde, M.C., Riguera, R., Castedo, L., and Stermitz, F.R. (1988) Five Phenylpropanoid Glycosides from *Mussatia*, *Phytochemistry 27*, 2947–2951.

191. Jimenez, C., Villaverde, M.C., Riguera, R., Castedo, L., and Stermitz, F. (1989) Phenylpropanoid Glycosides from *Mussatia hyacinthine*, *J. Nat. Prod. 52*, 408–410.

192. Cano, E., Veiga, M., Jimenez, C., and Riguera, R. (1990) Pharmacological Effects of Three Phenylpropanoid Glycosides from *Mussatia*, *Planta Med. 56*, 24–26.

193. Salib, J.Y., and Michael, H.N. (2004) Cytotoxic Phenylethanol Glycosides from *Psidium guaijava* Seeds, *Phytochemistry 65*, 2091–2093.

194. Kikuchi, M., and Yamauchi, Y. (1986) Structural Analysis on the Constituents of *Syringa* Species. II. Structures of Components from the Leaves of *Syringa reticulata* (Blume) Hara, *Ann. Rep. Tohoku Coll. Pharm. 33*, 63–68.

195. Kikuchi, M., Yamauchi, Y., Takahashi, Y., and Sugiyama, M. (1989) Studies on the Constituents of *Syringa* Species. VIII.

Isolation and Structures of Phenylpropanoid Glycosides from the Leaves of *Syringa reticulata* (Blume) Hara, *Yakugaku Zasshi 109*, 366–371.

196. Shen, Y.-C., Lin, S.-L., Hsieh, P.-W., and Chein, C.-C. (1996) Secoiridoid Glycosides from *Jasminum polyanthum*, *J. Chinese Chem. Soc. (Taipei) 43*, 171–176.

197. Shen, Y.-C., Lin, S.-L., and Chein, C.-C. (1996) Jaspolyside, a Secoiridoid Glycoside from *Jasminum polyanthum*, *Phytochemistry 42*, 1629–1631.

198. Damtoft, S., Franzyk, H., and Jensen, S.R. (1997) Iridoid Glucosides from *Picconia excelsa*, *Phytochemistry 45*, 743–750.

199. Machida, K., Kaneko, A., Hosogai, T., Kakuda, R., Yaoita, Y., and Kikuchi, M. (2002) Studies on the Constituents of *Syringa* Species. X. Five New Iridoid Glycosides from the Leaves of *Syringa reticulata* (Blume) Hara, *Chem. Pharm. Bull. (Tokyo) 50*, 493–497.

200. Fukuyama, Y., Koshino, K., Hasegawa, T., Yamada, T., and Nakagawa, K. (1987) New Secoiridoid Glucosides from *Ligustrum japonicum*, *Planta Med. 53*, 427–431.

201. LaLonde, R.T., Wong, C., and Tsai, A.I.-M. (1976) Polyglucosidic Metabolites of Oleaceae. The Chain Sequence of Oleoside Aglucon, Tyrosol, and Glucose Units in Three Metabolites from *Fraxinus americana*, *J. Am. Chem. Soc. 98*, 3007–3013.

202. Jensen, S.R., Franzyk, H., and Wallander, E. (2002) Chemotaxonomy of the Oleaceae: Iridoids as Taxonomic Markers, *Phytochemistry 60*, 213–231.

203. Kikuchi, M., and Yamauchi, Y. (1985) Studies on the Constituents of Osmanthus Species. III. On the Components of the Leaves of *Osmanthus ilicifolius* (Hassk.) Mouillefert, *Yakugaku Zasshi 105*, 442–448.

204. Kuwajima, H., Uemura, T., Takaishi, K., Inoue, K., and Inouye, H. (1988) Monoterpene Glucosides and Related Natural Products. Part 60. A Secoiridoid Glucoside from *Olea europaea*, *Phytochemistry 27*, 1757–1759.

205. Ryan, D., Antolovich, M., Herlt, T., Prenzler, P.D., Lavee, S., and Robards, K. (2002) Identification of Phenolic Compounds in Tissues of the Novel Olive Cultivar Hardy's Mammoth, *J. Agric. Food Chem. 50*, 6716–6724.

206. Ryan, D., Prenzler, P.D., Lavee, S., Antolovich, M., and Robards, K. (2003) Quantitative Changes in Phenolic Content During Physiological Development of the Olive (*Olea europaea*) Cultivar Hardy's Mammoth, *J. Agric. Food Chem. 51*, 2532–2538.

207. Lee-Huang, S., Zhang, L., Huang, P.L., Chang, Y.-T., and Huang, P.L. (2003) Anti-HIV Activity of Olive Leaf Extract (OLE) and Modulation of Host Cell Gene Expression by HIV-1 Infection and OLE Treatment, *Biochem. Biophys. Res. Commun. 307*, 1029–1037.

208. Sugiyama, M., Machida, K., Matsuda, N., and Kikuchi, M. (1993) Studies on the Constituents of *Osmanthus* Species. Part 15. A Secoiridoid Glycoside from *Osmanthus asiaticus*, *Phytochemistry 34*, 1169–1170.

209. Kikuchi, M., and Kakuda, R. (1999) Studies on the Constituents of *Ligustrum* species. XIX. Structures of Iridoid Glucosides from the Leaves of *Ligustrum lucidum* AIT, *Yakugaku Zasshi (J. Pharm. Soc. Japan) 119*, 444–450.

210. Tattini, M., Galardi, C., Pinelli, P., Massai, R., Remorini, D., and Agati, G. (2004) Differential Accumulation of Flavonoids and Hydroxycinnamates in Leaves of *Ligustrum vulgare* Under Excess Light and Drought Stress, *New Phytol. 163*, 547–561.

211. Kikuchi, M., and Yamauchi, Y. (1985) Studies on the Constituents of *Ligustrum* Species. XI. On the Secoiridoids of the Fruits of *Ligustrum japonica* Thunb. and *L. lucidum* Ait, *Yakugaku Zasshi 105*, 142–147.

212. Park, H.J., Lee, M.S., Lee, K.T., Sohn, I.C., Han, Y.N., and Miyamoto, K. (1999) Studies on Constituents with Cytotoxic Activity from the Stem Bark of *Syringa velutina*, *Chem. Pharm. Bull. (Tokyo) 47*, 1029–1031.

213. Tanahashi, T., Shimada, A., Nagakura, N., and Nayeshiro, H. (1992) Jasamplexosides A, B and C: Novel Dimeric and Trimeric Secoiridoid Glucosides from *Jasminum amplexicaule*, *Planta Med. 58*, 552–555.

214. Tanahashi, T., Shimada, A., Nagakura, N., Inoue, K., Kuwajima, H., Takashi, K., and Chen, C.C. (1993) A Secoiridoid Glucoside from *Fraxinus insularis, Phytochemistry 33*, 397–400.

215. Iossifova, T., Mikhova, B., and Kostova, I. (1995) A Secoiridoid Dilactone from *Fraxinus ornus* Bark, *Monatsh. Chem. 126*, 1257–1264.

216. Benkrief, R., Ranarivelo, Y., Skaltsounis, A.-L., Tillequin, F., Koch, M., Pusset, J., and Sevenet, T. (1998) Monoterpene Alkaloids, Iridoids and Phenylpropanoid Glycosides from *Osmanthus austrocaledonica*, *Phytochemistry 47*, 825–832.

217. Tanahashi, T., Watanabe, H., Itoh, A., Nagakura, N., Inoue, K., Ono, M., Fujita, T., and Chen, C.C. (1992) A Secoiridoid Glucoside from *Fraxinus formosana*, *Phytochemistry 31*, 2143–2145.

218. He, Z.D., Ueda, S., Inoue, K., Akaji, M., Fujita, T., and Yang, C. (1994) Secoiridoid Glucosides from *Fraxinus malacophylla*, *Phytochemistry 35*, 177–181.

219. Ivanovska, N., Iossifova, T., and Kostova, I. (1996) Complement-Mediated Anti-inflammatory Action of Extracts and Pure Secoiridoids Isolated from *Fraxinus* species, *Phytotherapy Res. 10*, 555–558.

220. Kuwajima, H., Morita, M., Takaishi, K., Inoue, K., Fujita, T., He, Z.D., and Yang, C.R. (1992) Secoiridoid, Coumarin and Secoiridoid-Coumarin Glucosides from *Fraxinus chinensis*, *Phytochemistry 31*, 1277–1280.

221. Damtoft, S., Franzyk, H., and Jensen, S.R. (1995) Biosynthesis of Iridoids in *Syringa* and *Fraxinus*: Carbocyclic Iridoid Precursors, *Phytochemistry 40*, 785–792.

222. Asaka, Y., Kamikawa, T., Tokoroyama, T., and Kubota, T. (1970) The Structure and Absolute Configuration of Syringopicroside. A New Iridoid Glucoside from *Syringa vulgaris* L., *Tetrahedron 26*, 2365–2370.

223. Kikuchi, M., Yamauchi, Y., and Sugiyama, M. (1989) The Constituents of *Syringa* species. IX. Structure of Oxidative Products from Syringopicroside with Perbenzoic Acid, *Ann. Rep. Tohoku Coll. Pharm. 36*, 97–104.

224. Shen, Y.C., and Chen, C.H. (1989) Novel Secoiridoid Lactones from *Jasminum multiflorum*, *J. Nat. Prod. 52*, 1060–1070.

225. Shen, Y.-C., and Chen, C.-H. (1994) A New Secoiridoid Lactone from *Jasminum multiflorum*, *J. Chin. Chem. Soc. 41*, 473–476.

226. Kurkin, V.A. (2003) Phenylpropanoids from Medicinal Plants: Distribution, Classification, Structural Analysis, and Biological Activity, *Chem. Nat. Comp. 39*, 123–153.

227. Pan, J., Yuan, C., Lin, C., Jia, Z., and Zheng, R. (2003) Pharmacological Activities and Mechanisms of Natural Phenylpropanoid Glycosides, *Pharmazie 58*, 767–775.

228. Milkowska-Leyck, K., Borkowski, B., and Strzelecka, H. (2001) Selected Polyphenol Compounds. Part IV. Characteristics and Occurrence of Phenylpropanoid Glycosides, *Herba Polonica 47*, 225–244.

229. Sawabe, A., Kumamoto, H., and Matsubara, Y. (1998) Bioactive Glycosides in Citrus Fruit Peels, *Kinki Daigaku Nogaku Sogo Kenkyusho Hokoku 6*, 57–67.

230. Cometa, F., Tomassini, L., Nicoletti, M., and Pieretti, S. (1993) Phenylpropanoid Glycosides. Distribution and Pharmacological Activity, *Fitoterapia 64*, 195–217.

231. He, Z., and Yang, C. (1989) The Advances of Phenylpropanoid Glycosides in Plants, *Tianran Chanwu Yanjiu Yu Kaifa 1*, 29–41.

232. Kucinskaite, A., Briedis, V., and Savickas, A. (2004) Experimental Analysis of Therapeutic Properties of *Rhodiola rosea* L. and Its Possible Application in Medicine, *Medicina (Kaunas) 40*, 614–619.

233. Sokolov, S.Ya., Ivashin, V.M., Zapesochnaya, G.G., Kurkin, V.A., and Shchavlinskii, A.N. (1985) Studies of Neurotropic Activity of New Compounds Isolated from *Rhodiola rosea*, *Khim. Farmatsev. Z. (USSR) 19*, 1367–1371.

234. Sawabe, A., Matsubara, Y., Iizuka, Y., and Okamoto, K. (1988) Physiologically Active Substances in Citrus Fruit Peels. XIII. Structure and Physiological Activity of Phenyl Propanoid Glycosides in the Lemon (*Citrus limon* Burm. f.), Unshiu (*Citrus unshiu*), and Kinkan (*Fortunella japonica*), *Nippon Nogeikagaku Kaishi 62*, 1067–1071.

235. Matsubara, Y., Kumamoto, H., Sawabe, A., Iizuka, Y., and Okamoto, K. (1985) Structure and Physiological Activity of Phenyl Propanoid Glycosides in Lemon, Unshiu and Orange Peelings, *Kinki Daigaku Igaku Zasshi 10*, 51–58.

236. Sawabe, A. (1996) Bioactive Compounds in Citrus Fruit Peels, *Foods Food Ingred. J. Japan 169*, 37–44.

237. Matsubara, Y., Yusa, T., Sawabe, A., Iizuka, Y., and Okamoto, K. (1991) Studies on Physiologically Active Substances in Citrus Fruit Peel. Part XX. Structure and Physiological Activity of Phenyl Propanoid Glycosides in Lemon (*Citrus limon* Burm. f.) Peel, *Agric. Biol. Chem. 55*, 647–650.

238. Afifi, M.S., Lahloub, M.B., El-Khayaat, S.A., Anklin, C.G., Ruegger, H., and Sticher, O. (1993) Crenatoside: A Novel Phenylpropanoid Glycoside from *Orobanche crenata*, *Planta Med. 59*, 359–362.

239. Nakanishi, T., Iida, N., Inatomi, Y., Murata, H., Inada, A., Murata, J., Lang, F.A., Iinuma, M., and Tanaka, T. (2004) New Neolignan and Phenylpropanoid Glycosides in *Juniperus communis* var. *depressa*, *Heterocycles 63*, 2573–2580.

240. Sosa, A. (1934) Biochemical Study of *Betula alba* L. A New Heteroside: Betuloside, and Its Prosthetic Group, Betuligenol, *Rev. Acad. Cienc. (Madrid) 31*, 81–100.

241. Kiem, P.V., Minh, C.V., Dat, N.T., Cai, X.F., Lee, J.J., and Kim, Y.H. (2003) Two New Phenylpropanoid Glycosides from the Stem Bark of *Acanthopanax trifoliatus*, *Arch. Pharm. Res. 26*, 1014–1017.

242. Miyazawa, M. (2001) Biotransformation of Lignans and Neolignans, *Curr. Org. Chem. 5*, 975–986.

243. Ramos, A.C., De Clairac, R.P.L., and Medarde, M. (1999) Heterolignans, *Heterocycles 51*, 1443–1469.

244. Damayanthi, Y., and Lown, J.W. (1998) Podophyllotoxins: Current Status and Recent Developments, *Curr. Med. Chem. 5*, 205–252.

245. Begum, A.N., Nicolle, C., Mila, I., Lapierre, C., Nagano, K., Fukushima, K., Heinonen, S., Adlercreutz, H., Remesy, C., and Scalbert, A. (2004) Dietary Lignins Are Precursors of Mammalian Lignans in Rats, *J. Nutr. 134*, 120–127.

246. Wang, L.Q. (2002) Mammalian Phytoestrogens: Enterodiol and Enterolactone, *J. Chromatogr. B 777*, 289–309.

247. Qu, H.Y., Madl, R.L., Takemoto, D.J., Baybutt, R.C., and Wang, W.Q. (2005) Lignans Are Involved in the Antitumor Activity of Wheat Bran in Colon Cancer SW480 Cells, *J. Nutr. 135*, 598–602.

248. Ranich, T., Bhathena, S.J., and Velasquez, M.T. (2001) Protective Effects of Dietary Phytoestrogens in Chronic Renal Disease, *J. Ren. Nutr. 11*, 183–193.

249. Kitts, D.D., Yuan, Y.V., Wijewickreme, A.N., and Thompson, L.U. (1999) Antioxidant Activity of the Flaxseed Lignan Secoisolariciresinol Diglycoside and Its Mammalian Lignan Metabolites Enterodiol and Enterolactone, *Mol. Cell. Biochem. 202*, 91–100.

250. Yahara, S., Nakazono, M., Tutumi, H., and Nohara, T. (1992) Lignans from Leaves of *Laurus nobilis* L, *Shoyakugaku Zasshi 46*, 184–186.

251. Yuan, Z., Tezuka, Y., Fan, W., Kadota, S., and Li, X. (2002) Constituents of the Underground Parts of *Glehnia littoralis*, *Chem. Pharm. Bull. (Tokyo) 50*, 73–77.

252. Min, B.-S., Na, M.-K., Oh, S.-R., Ahn, K.-S., Jeong, G.-S., Li, G., Lee, S.-K., Joung, H., and Lee, H.-K. (2004) New Furofuran and Butyrolactone Lignans with Antioxidant Activity from the Stem Bark of *Styrax japonica*, *J. Nat. Prod. 67*, 1980–1984.

253. Tan, X.Q., Chen, H.-S., Liu, R.-H., Tan, C.-H., Xu, C.-L., Xuan, W.-D., and Zhang, W.-D. (2005) Lignans from *Trachelospermum jasminoides*, *Planta Med. 71*, 93–95.

253a. Tanaka, T., Ikeda, T., Kaku, M., Zhu, X.-H., Okawa, M., Yokomizo, K., Uyeda, M., and Nohara, T. (2004) A New Lignan Glycoside and Phenylethanoid Glycosides from *Strobilanthes cusia* Bremek, *Chem. Pharm. Bull. 52*, 1242–1245.

254. Kraft, C., Jenett-Siems, K., Kohler, I., Tofern-Reblin, B., Siems, K., Bienzle, U., and Eich, E. (2002) Antiplasmodial Activity of Sesquilignans and Sesquineolignans from *Bonamia spectabilis*, *Phytochemistry 60*, 167–173.

255. Su, B., Zhu, Q., Gao, K., Yuan, C., and Jia, Z. (1999) Lignan and Phenylpropanoid Glycosides from *Lancea tibetica* and Their Antitumor Activity, *Planta Med. 65*, 558–561.

256. Kuriyama, K., Tsuchiya, K., and Murui, T. (1995) Generation of New Lignan Glucosides During Germination of Sesame Seeds, *Nippon Nogeikagaku Kaishi 69*, 685–693.

257. Haensel, R., Schulz, H., and Leuckert, C. (1964) The Lignane Glycoside Arctiin as a Chemotaxonomic Characteristic in the Compositae Family, *Z. Naturforsch B 19*, 727–734.

258. Jang, Y.P., Kim, S.R., and Kim, Y.C. (2001) Neuroprotective Dibenzylbutyrolactone Lignans of *Torreya nucifera*, *Planta Med. 67*, 470–472.

259. Wang, C.Z., and Jia, Z.J. (1996) Neolignan Glucosides from *Pedicularis torta*, *Chin. Chem. Lett. 7*, 145–148.

260. Wang, C., and Jia, Z. (1997) Lignan, Phenylpropanoid and Iridoid Glycosides from *Pedicularis torta*, *Phytochemistry 45*, 159–166.

261. El Gamal, A.A., Takeya, K., Itokawa, H., Halim, A.F., Amer, M.M., and Saad, H.-E.A. (1997) Lignan Bis-glucosides from *Galium sinaicum*, *Phytochemistry 45*, 597–600.

262. Morikawa, T., Sun, B., Matsuda, H., Wu, L.J., Harima, S., and Yoshikawa, M. (2004) Bioactive Constituents from Chinese Natural Medicines. XIV. New Glycosides of β-Carboline-Type Alkaloid, Neolignan, and Phenylpropanoid from *Stellaria dichotoma* L. var. *lanceolata* and Their Antiallergic Activities, *Chem. Pharm. Bull. (Tokyo) 52*, 1194–1199.

263. Lee, I.G., Lee, S.J., Yoo, I.D., Yoo, I.J., and Yoon, B.S. (2001) Novel Lignan Glycoside Having Inhibition Activity of Lipid Peroxidation, Korean Patent KR 2001002647.

264. Kawagishi, S., Oosawa, T., and Katsuzaki, H. (1994) Pinoresinol Glycoside, Sesame Seed Extract Containing the Glycoside, and Its Use for Preventing Oxidation of Lipids, Japanese Patent JP 06116282, 5 pp.

265. Katsuzaki, H., Kawakishi, S., and Osawa, T. (1993) Structure of Novel Antioxidative Lignan Triglucoside Isolated from Sesame Seed, *Heterocycles 36*, 933–936.

266. Hou, C.C., Lin, S.J., Cheng, J.T., and Hsu, F.L. (2003) Antidiabetic Dimeric Guianolides and a Lignan Glycoside from *Lactuca indica*, *J. Nat. Prod. 66*, 625–629.

267. Cho, J.Y., Kim, A.R., and Park, M.H. (2001) Lignans from the Rhizomes of *Coptis japonica* Differentially Act as Anti-inflammatory Principles, *Planta Med. 67*, 312–316.

268. Ward, R.S. (1999) Lignans, Neolignans and Related Compounds, *Nat. Prod. Rep. 16*, 75–96.

269. Zainullin, R.A., Kukovinets, O.S., Kunakova, R.V., and Tolstikov, G.A. (2001) Naphthalene Oxidation and Reduction Reactions: A Review, *Petroleum Chem. (Russia) 41*, 143–158.

270. Simon, M.A., Bonner, J.S., McDonald, T.J., and Autenrieth, R.L. (1999) Bioaugmentation for the Enhanced Bioremediation of Petroleum in a Wetland, *Polycyc. Aromat. Comp. 14*, 231–239.

271. Bode, H.B., Wegner, B., and Zeeck, A. (2000) Biosynthesis of

Cladospirone Bisepoxide, a Member of the Spirobisnaphthalene Family, *J. Antibiot. 53*, 153–157.

272. Watanabe, A., and Ebizuka, Y. (2002) A Novel Hexaketide Naphthalene Synthesized by a Chimeric Polyketide Synthase Composed of Fungal Pentaketide and Heptaketide Synthases, *Tetrahedron Lett. 43*, 843–846.

273. Davis, P.H. (1988) *Flora of Turkey and the East Aegean Islands*, University Press, Edinburgh, United Kingdom.

274. Kuruüzüm, A., Demirezer, L.Ö., Bergère, I., and Zeeck, A. (2001) Two New Chlorinated Naphthalene Glycosides from *Rumex patentia*, *J. Nat. Prod. 64*, 688–690.

275. Cichewicz, R.H., and Nair, M.G. (2002) Isolation and Characterization of Stelladerol, a New Antioxidant Naphthalene Glycoside, and Other Antioxidant Glycosides from Edible Daylily (*Hemerocallis*) Flowers, *J. Agric. Food Chem. 50*, 87–91.

276. Demirezer, Ö., Kuruüzüm, A., Bergere, I., Schiewe, H.J., and Zeeck, A. (2001) Five Naphthalene Glycosides from the Roots of *Rumex patentia*, *Phytochemistry 56*, 399–402.

277. Choi, J.S., Jung, J.H., Lee, H.J., Lee, J.H., and Kang, S.S. (1995) A Naphthalene Glycoside from *Cassia tora*, *Phytochemistry 40*, 997–999.

278. Cichewicz, R.H., Lim, K.C., McKerrow, J.H., and Nair, M.G. (2002) Kwanzoquinones A–G and Other Constituents of *Hemerocallis fulva* 'Kwanzo' Roots and Their Activity Against the Human Pathogenic Trematode *Schistosoma mansoni*, *Tetrahedron 58*, 8597–8606.

279. Pathak, A., Kulshreshtha, D.K., and Maurya, R. (2004) Coumaroyl Triterpene Lactone, Phenolic and Naphthalene Glycoside from Stem Bark of *Diospyros angustifolia*, *Phytochemistry 65*, 2153–2158.

280. Wessels, P.L., Holzapfel, C.W., van Wyk, B.-E., and Marais, W. (1996) Plicataloside, an *O,O*-Diglycosylated Naphthalene Derivative from *Aloe plicatilis*, *Phytochemistry 41*, 1547–1551.

281. Cai, L., Wei, G.-X., Van der Bijl, P., and Wu, C.D. (2000) Namibian Chewing Stick, *Diospyros lycioides*, Contains Antibacterial Compounds Against Oral Pathogens, *J. Agric. Food Chem. 48*, 909–914.

282. Rauwald, H.W., and Just, H.D. (1983) Study of the Constituents of Buckthorn Cortex. III. A New Lactonic Naphthalene Glycoside from the Cortex of *Rhamnus catharticus* L, *Arch. Pharm. (Weinheim) 316*, 409–412.

283. Lin, C.N., and Wei, B.L. (1994) The Constituents of Formosan Rhamnus Species. 8. Flavonol and Naphthalene Glycosides from *Rhamnus nakaharai*, *J. Nat. Prod. 57*, 294–297.

284. Lemli, J., Toppet, S., Cuveele, J., and Janssen, G. (1981) Naphthalene Glycosides in *Cassia senna* and *Cassia angustifolia*. Studies in the Field of Drugs Containing Anthracene Derivatives. XXXII, *Planta Med. 43*, 11–17.

285. Liou, M.-J., Teng, C.-M., and Wu, T.-S. (2002) Constituents from *Rubia ustulata* Diels and *R. yunnanensis* Diels and Their Antiplatelet Aggregation Activity, *J. Chin. Chem. Soc. (Taipei) 49*, 1025–1030.

286. Auvray, P., Bichat, F., and Genne, P. (2000) Preclinical Evaluation of Aromatase Inhibitors Antitumor Activity, *Bull. Cancer 87*, 7–22.

287. Sendelbach, L.E. (1989) A Review of the Toxicity and Carcinogenicity of Anthraquinone Derivatives, *Toxicology 57*, 227–240.

288. Sissi, C., and Palumbo, M. (2004) Antitumor Potential of Azabioisosterism in Anthracenedione-Based Drugs, *Curr. Top. Med. Chem. 4*, 219–230.

289. De Witte, P. (1993) Metabolism and Pharmacokinetics of Anthranoids, *Pharmacology 47* (Suppl. 1), 86–97.

290. Franz, G. (1993) The Senna Drug and Its Chemistry, *Pharmacology 47* (Suppl. 1), 2–6.

291. Koyama, J., Morita, I., Kawanishi, K., Tagahara, K., and Kobayashi, N. (2003) Capillary Electrophoresis for Simultaneous Determination of Emodin, Chrysophanol, and Their 8-β-D-Glucosides, *Chem. Pharm. Bull. (Tokyo) 51*, 418–420.

292. Yin, J., and Guo, L. (1993) *Modern Study of Chinese Drugs and Clinical Applications*, Xueyuan Press, Beijing, China (in Chinese).

293. Frew, T., Powis, G., Berggren, M., Abraham, R.T., Ashendel, C.L., Zalkow, L.H., Hudson, C., Qazia, S., Gruszecka-Kowalik, E., and Merriman, R. (1994) A Multiwell Assay for Inhibitors of Phosphatidylinositol-3-kinase and the Identification of Natural Product Inhibitors, *Anticancer Res. 14*, 2425–2458.

294. Krenn, L., Presser, A., Pradhan, R., Bahr, B., Paper, D.H., Mayer, K.K., and Kopp, B. (2003) Sulfemodin 8-*O*-β-D-Glucoside, a New Sulfated Anthraquinone Glycoside, and Antioxidant Phenolic Compounds from *Rheum emodi*, *J. Nat. Prod. 66*, 1107–1109.

295. Koyama, J., Morita, I., Fujiyoshi, H., and Kobayashi, N. (2005) Simultaneous Determination of Anthraquinones, Their 8-β-D-Glucosides, and Sennosides of *Rhei rhizoma* by Capillary Electrophoresis, *Chem. Pharm. Bull. (Tokyo) 53*, 573–575.

296. Van Gorkom, B.A.P., Vries, E.G.E., Karrenbeld, A., and Kleibeuker, J.H. (1999) Review Article: Anthranoid Laxatives and Their Potential Carcinogenic Effects, *Aliment. Pharmacol. Therapeut. 13*, 443–452.

297. Newall, C.A., Anderson, L.A., and Phillipson, J.D. (1996) *Herbal Medicines*: *A Guide for Health Care Professionals*, The Pharmaceutical Press, London.

298. Wichtl, M., and Bisset, N.G. (eds., English transl. by Bisset, N.G.) (1994) *Rhamni purshiani* Cortex—Cascara Bark, in *Herbal Drugs and Phytopharmaceuticals*, pp. 90–91, CRC Press, Stuttgart.

299. Van Os, F.H. (1976) Anthraquinone Derivatives in Vegetable Laxatives, *Pharmacology 14* (Suppl. 1), 7–17.

300. Che, Q.M., Akao, T., Hattori, M., Tsuda, Y., Namba, T., and Kobashi, K. (1991) Barbaloin Stimulates Growth of *Eubacterium* sp. Strain BAR, a Barbaloin-Metabolizing Bacterium from Human Feces, *Chem. Pharm. Bull. (Tokyo) 39*, 757–760.

301. Alves, D.S., Perez-Fons, L., Estepa, A., and Micol, V. (2004) Membrane-Related Effects Underlying the Biological Activity of the Anthraquinones Emodin and Barbaloin, *Biochem. Pharmacol. 68*, 549–561.

302. Hernandez-Medel, M.R., and Pereda-Miranda, R. (2002) Cytotoxic Anthraquinone Derivatives from *Picramnia antidesma*, *Planta Med. 68*, 556–558.

303. Qhotsokoane-Lusunzi, M.A., and Karuso, P. (2001) Secondary Metabolites from Basotho Medicinal Plants. II. *Bulbine capitata*, *Aust. J. Chem. 54*, 427–430.

304. Palm, C., Bjork, O., Bjorkholm, M., and Eksborg, S. (2001) Quantification of Doxorubicin in Plasma—A Comparative Study of Capillary and Venous Blood Sampling, *Anticancer Drugs 12*, 859–864.

305. Demirezer, L.O., Kuruuzum-Uz, A., Bergere, I., Schiewe, H.-J., and Zeeck, A. (2001) The Structures of Antioxidant and Cytotoxic Agents from Natural Source: Anthraquinones and Tannins from Roots of *Rumex patientia*, *Phytochemistry 58*, 1213–1217.

306. Qhotsokoane-Lusunzi, M.A., and Karuso, P. (2001) Secondary Metabolites from Basotho Medicinal Plants. I. *Bulbine narcissifolia*, *J. Nat. Prod. 64*, 1368–1372.

307. Tunman, T. (1907) Alder Buckthorn Bark and Its Glucoside, *Chem. Zentralbl. (Germany) 48*, 99–103.

308. Schmidt, E. (1909) Contributions on the Rhamnosides, *Arch. Pharm. (Germany) 246*, 214–224.

309. Krasovskii, N. (1913) Rhamnoxanthin from *Rhamnus cathartica* and Frangulin from *Rhamnus frangula, Zh. Russ. Fiziko-Khim, Obshchest. (Russia) 45*, 188–193.

310. Koch, W. (2001) Studies on Biologically Active Substances of *Hypericum* L. Species, *Farmatsevt. Zh. (Kiev) 4*, 50–55.

311. Muhlemann, H. (1955) Anthraquinone and Anthraquinine Glycosides. XVII, *Pharm. Acta Helv. 30*, 350–355.

312. Francis, G.W., Aksnes, D.W., and Holt, O. (1998) Assignment of the ^{1}H and ^{13}C NMR Spectra of Anthraquinone Glycosides from *Rhamnus frangula*, *Magnet. Reson. Chem. 36*, 769–772.

313. Chung, M.I., Gan, K.H., Lin, C.N., Ko, F.N., and Teng, C.M. (1993) Antiplatelet Effects and Vasorelaxing Action of Some Constituents of Formosan Plants, *J. Nat. Prod. 56*, 929–934.

314. Wei, B.L., Lu, C.M., Tsao, L.T., Wang, J.P., and Lin, C.N. (2001) *In vitro* Anti-inflammatory Effects of Quercetin 3-*O*-Methyl Ether and Other Constituents from *Rhamnus* Species, *Planta Med. 67*, 745–747.

315. Uesato, S., Tokunaga, T., and Takeuchi, K. (1998) Novel Angucycline Compound with Both Antigastrin and Gastric Mucosal Protective Activities, *Bioorg. Med. Chem. Lett. 8*, 1969–1972.

316. Drautz, H., Zahner, H., Rohr, J., and Zeeck, A. (1986) Metabolic Products of Microorganisms. 234. Urdamycins, New Angucycline Antibiotics from *Streptomyces fradiae*. I. Isolation, Characterization and Biological Properties, *J. Antibiot. 39*, 1657–1669.

317. Rohr, J., and Zeeck, A. (1987) Metabolic Products of Microorganisms. 240. Urdamycins, New Angucycline Antibiotics from *Streptomyces fradiae*. II. Structural Studies of Urdamycins B to F, *J. Antibiot. 40*, 459–467.

318. Henkel, T., Rohr, J., Beale, J.M., and Schwenen, L. (1990) Landomycins, New Angucycline Antibiotics from *Streptomyces* sp. I. Structural Studies on Landomycins A–D, *J. Antibiot. 43*, 492–503.

319. Matseliukh, B.P., Konovalova, T.A., Polishchuk, L.V., and Bambura, O.I. (1998) The Sensitivity to Landomycins A and E of Streptomycetes, Producers of Polyketide Antibiotics, *Mikrobiol. Zh. (Kiev) 60*, 31–36.

320. Liu, H.-W., Sherman, D.H., and Zhao, L. (2002) Recombinant Bacteria Producing Substances with Altered Sugar Moieties and Their Use for Production of These Substances, U.S. Patent Application A2 20020411, 174 pp.

321. Ishimaru, T., Kanamaru, T., Takahashi, T., Ohta, K., and Okazaki, H. (1982) Inhibition of Prolyl Hydroxylase Activity and Collagen Biosynthesis by the Anthraquinone Glycoside, P-1894B, an Inhibitor Produced by *Streptomyces albogriseolus*, *Biochem. Pharmacol. 31*, 915–919.

322. Bechthold, A., Domann, S., Faust, B., Hoffmeister, D., Stockert, S., Trefzer, A., Weitnauer, G., and Westrich, L. (1999) Glycosylated Natural Products: Perspectives for Combinatorial Biosynthesis, *Chemother. J. 8*, 130–135.

323. Singh R, Geetanjali, Chauhan SMS. (2004) 9,10-Anthraquinones and Other Biologically Active Compounds from the Genus *Rubia*, *Chem. Biodiver. 1*, 1241–1264.

324. Krenn, L., Pradhan, R., Presser, A., Reznicek, G., and Kopp, B. (2004) Anthrone *C*-Glucosides from *Rheum emodi*, *Chem. Pharm. Bull. (Tokyo) 52*, 391–393.

325. Muhlemann, H. (1949) Anthraquinone and Anthraquinone Glycoside. VI. Anthrone and Anthranol Glycosides, *Pharm. Acta Helv. 24*, 343–351.

326. Fairbairn, J.W. (1949) Active Constituents of Vegetable Purgatives Containing Anthracene Derivatives. I. Glycosides and Aglycones, *J. Pharm. Pharmacol. 1*, 683–692.

Molecular Cloning, Expression, and Characterization of Secretory Phospholipase A$_2$ in Tobacco

Ritsuko Fujikawa, Yukichi Fujikawa, Noriaki Iijima, and Muneharu Esaka*

Graduate School of Biosphere Sciences, Hiroshima University, Higashi-Hiroshima, 739-8528, Japan

ABSTRACT: Phospholipase A$_2$ (PLA$_2$) activity was investigated in various tissues of tobacco (*Nicotiana tabacum*). PLA$_2$ activity in the flower was 15 times higher than that in the leaf, stem, and root. PLA$_2$ activity in the flower appears to have originated from both Ca^{2+}-dependent and -independent PLA$_2$. A cDNA clone for protein with homology to animal secretory PLA$_2$ (sPLA$_2$), denoted as Nt PLA$_2$, was isolated from the tobacco flower. The cDNA of Nt PLA$_2$ encoded a mature protein of 127 amino acid residues with a putative signal peptide of 30 residues. The amino acid sequence for mature Nt PLA$_2$ contains 12 cysteines, a Ca^{2+} binding loop, and a catalytic domain that are commonly conserved in animal sPLA$_2$. The Nt PLA$_2$ mRNA was mainly expressed in the root and stem of tobacco. The recombinant Nt PLA$_2$ was expressed as a fusion protein with thioredoxin in *Escherichia coli*. From the bacterial cell lysate, the fusion protein was recovered in soluble form and cleaved by Factor Xa proteinase. Then the recombinant mature Nt PLA$_2$ was purified by ion exchange chromatography. It was discovered that the purified Nt PLA$_2$ essentially requires Ca^{2+}, for the enzyme activity when the activity was determined using mixed-micellar phospholipid substrates with sodium cholate. The optimal activity of Nt PLA$_2$ was at pH 8–10 when PC was used as a substrate.

Paper no. L9753 in *Lipids 40,* 901–908 (September 2005).

Phospholipase A$_2$ (phosphatide 2-acylhydrolase, EC 3.1.1.4) catalyzes the hydrolysis of a fatty acyl ester bond at the *sn*-2 position of glycerophospholipids to liberate FFA and lysophospholipids. In animals, PLA$_2$ are recognized as a large superfamily of distinct enzymes, based on MW, primary structure, Ca^{2+}-dependency, and cellular localization (1–5). Secretory PLA$_2$ (sPLA$_2$) are known to be low molecular mass enzymes (13–18 kDa) with five to eight disulfide bridges, Ca^{2+}-dependency, and a broad specificity for the phospholipid head group and FA (1). Animal sPLA$_2$ are classified into eight groups—I, II, III, V, IX, X, XII, and XV—based on their primary structures (1,4,6–8). sPLA$_2$ are reportedly involved in various physiological and pathological functions including lipid digestion, cell proliferation, and antibacterial defense (1,2,9). Two types of high-MW PLA$_2$ exist in

animals. One is termed cytosolic PLA$_2$ (cPLA$_2$), based on its distribution in the cytosol of cells (9,10). cPLA$_2$ respond to various hormonal stimuli and are activated by submicromolar Ca^{2+} and phosphorylation by mitogen-activated protein kinase. The other does not require Ca^{2+} for its enzymatic activity. This Ca^{2+}-independent PLA$_2$, referred to as iPLA$_2$, has a function in the remodeling of FA composition of phospholipids and can also be activated by stimuli (11).

In plants, several studies on PLA$_2$ have been reported using the crude preparations (12–14). The products generated by PLA$_2$ have also been shown to stimulate several plasma membrane enzymes, such as H$^+$-ATPase and protein kinase. These enzymes have been proposed to be involved in signal transduction. It has been suggested that the PLA$_2$ is associated with signal transduction involved in cell growth, wounding response, cell elongation, and shoot gravitropism *via* auxin-related signal transduction, as well as lipid metabolism (15–19). Recently, a putative sPLA$_2$, which is similar to animal sPLA$_2$, has been purified from elm (*Ulmus glabra*) (20). Rice (*Oryza sativa*) sPLA$_2$ also has been partially purified (21). The cDNA for putative sPLA$_2$ have been cloned from rice, carnation (*Dianthus caryophyllus* L. cv. Degio*)* and *Arabidopsis* (*A. thaliana*) (19,21–23). The analysis of silenced or overexpressed sPLA$_2$ from transgenic *Arabidopsis* suggested that sPLA$_2$ is related to cell elongation and shoot gravitropism (19). At present, plant sPLA$_2$ have been classified into groups XIA and XIB, based on their primary structures (1). However, little is known about the physiological role of plant sPLA$_2$, in contrast to many reports on the functions of animal sPLA$_2$ (24,25).

In this study, we investigated the distribution of PLA$_2$ activity in various tissues of tobacco and found a high PLA$_2$ activity in the flower. We also isolated a full-length cDNA clone for sPLA$_2$, named Nt PLA$_2$, and examined its expression in tobacco tissues. Furthermore, we characterized the enzymatic properties of the recombinant Nt PLA$_2$.

MATERIALS AND METHODS

Materials. 1-Palmitoyl-2-oleoyl-*sn*-glycero-3-phosphocholine (POPC), 1-palmitoyl-2-oleoyl-*sn*-glycero-3-phosphoethanolamine (POPE), and 1-palmitoyl-2-oleoyl-*sn*-glycero-3-phosphoglycerol (POPG) were purchased from Avanti Polar Lipids, Inc (Birmingham, AL). Sodium cholate was obtained from Funakoshi Co., Ltd (Tokyo, Japan). The POROS HS/M cation-exchange column and Cosmosil 5C18 column were from PerSeptive Biosystems (Framingham, MA) and Nacalai Tesque (Kyoto,

*To whom correspondence should be addressed at Graduate School of Biosphere Sciences, Hiroshima University, 1-4-4, Kagamiyama, Higashi-Hiroshima, 739-8528 Japan. E-mail: mesaka@hiroshima-u.ac.jp

Abbreviations: AGPC, acid guanidinium thiocyanate-phenol-chloroform; bp, base pair; cPLA$_2$, cytosolic PLA$_2$; iPLA$_2$, Ca^{2+}-independent PLA$_2$; IPTG, isopropyl-1-thio-β-D-galactopyranoside; PLA$_2$, phospholipase A$_2$; POPC, 1-palmitoyl-2-oleoyl-*sn*-glycero-3-phosphocholine; POPE, 1-palmitoyl-2-oleoyl-*sn*-glycero-3-phosphoethanolamine; POPG, 1-palmitoyl-2-oleoyl-*sn*-glycero-3-phosphoglycerol; RACE, rapid amplification of cDNA ends; RT, reverse transcription; sPLA$_2$, secretory PLA$_2$.

Japan), respectively. Isopropyl-1-thio-β-D-galactopyranoside (IPTG) and ampicillin were purchased from Wako Pure Chemicals (Osaka, Japan), Factor Xa proteinase was from Promega (Madison, WI), and pET32a and BL21(DE3) were from Novagen (Madison, WI). The DC Protein assay kit was obtained from Bio-Rad Laboratories (Hercules, CA)

Plant materials. Tobacco (*Nicotiana tabacum* L. cv. SR-1) plants were grown at 28°C in light/dark (16 h/8 h) in the green house.

Preparation of crude extract from tobacco tissues. Tobacco tissues were homogenized in extraction buffer (20 mM Tris-HCl, pH 8.0, 1 M KCl, and 2 mM EDTA) and centrifuged at $10,000 \times g$ for 5 min. The resulting supernatant was used as a crude extract for determination of PLA_2 activity.

Standard assay for PLA_2 activity. PLA_2 activity was determined as described previously (26–29). The standard incubation systems (100 μL) for the assay of PLA_2 activity contain 2 mM POPC, 8 mM sodium cholate, 100 mM NaCl, 10 mM $CaCl_2$, and 50 mM Tris-HCl (pH 8.0). The reaction was carried out at 37°C for 60 min. Oleic acid released by PLA_2 action was labeled with 9-anthryldiazomethane, and the derivatized FA was separated by RP-HPLC using a Cosmosil 5C18 column (4.6×100 mm) with acetonitrile as solvent at a flow rate of 1 mL per min. The oleic acid was quantified by monitoring with a spectrofluorometer using heptadecanoic acid as an internal standard. One unit (U) was defined as the liberation of 1 μmol FFA (oleic acid) per min. Each experiment was performed two times and the results presented are the means.

RT (reverse transcription)-PCR. Total RNA was isolated from tobacco flowers with acid guanidinium thiocyanate-phenol-chloroform (AGPC) method (30). Total RNA (3 μg) was reverse-transcribed by using PowerScript Reverse Transcriptase (BD Biosciences Clontech, Tokyo, Japan) and oligo-dT primer, 5′-ATGACGAATTCGCACGGGCTTCCTCGAGTTTT-TTTTTTT-TTTTTT-3′. PCR was carried out for 40 cycles of 30 s at 95°C for denaturation, 30 s at 60°C for annealing, and 60 s at 72°C for polymerization, using a forward primer, T2 (5′-AA-GAATGCAGTAGAACATGTGAATC-3′), designed according to a partial amino acid sequence (Phe12–Arg20) of potato putative $sPLA_2$ (GeneBank Accession No. BM406320), and a reverse primer, 5′-ATGACGAATTCGCACGGG-3′. An aliquot of the primary PCR product was used in secondary PCR with T2 and a reverse primer, 5′-CGCACGGGCTTCCTCGAG-3′. The secondary PCR was carried out under the same conditions as the primary PCR, except for annealing at 55°C. The PCR product was subcloned into pGEM-T Easy vector (Promega) and transformed into XL-1 Blue cell, and the positive clone was selected according to the manufacturer's protocol. Plasmid DNA was purified from the positive clone with QIAprep Spin Miniprep Kit (Qiagen, Tokyo, Japan) and sequenced by ABI 373A sequencer (Applied Biosystems, Foster City, CA) using the DYEnamic ET Terminator Cycle Sequencing Kit (Amersham Biosciences, Piscataway, NJ), according to the manufacturer's protocol. A protein encoded by the cDNA was named as Nt PLA_2.

RACE (rapid amplification of cDNA ends)-PCR. Adaptor-ligated double-stranded cDNA were synthesized using Marathon cDNA Amplification Kit (BD Biosciences Clontech) according to the manufacturer's instruction. For the 5′-end of Nt PLA_2 cDNA, PCR was carried out for 40 cycles of 30 s at 95°C, 30 s at 63°C, and 60 s at 72°C with a reverse gene-specific primer, 5′-GAGCTCCTGATTTCGTGAACGTAG-3′ and a forward primer, 5′-CCATCCTAATACGACTCACTATAGG-GC-3′. An aliquot of the primary PCR product was used in secondary PCR with a reverse gene-specific primer, 5′-CCCTGGACATC-CACTGTATAGAAC-3′and a forward primer, 5′-ACTCAC-TATAGGGCTCGAGCGGC-3′. The PCR was performed under the same conditions as the primary PCR. A unique band obtained by the RACE was subcloned into pGEM-T Easy vector as described above.

RNA extraction and RT-PCR. Total RNA was isolated from the flower, leaf, stem, and root of tobacco with the AGPC method as described above and treated with DNase I (Takara, Tokyo, Japan). Total RNA (500 ng) was reverse-transcribed by using ReverTraAce (Toyobo, Osaka, Japan) and oligo-dT primer. PCR was carried out for 40 cycles of 60 s at 95°C for denaturation, 30 s at 60°C for annealing, and at 72°C for polymerization, using gene-specific primers. A pair of primers (5′-CGGAAT-TCTTTTGTGCAGTTCCTCCATTC-3′ and 5′-CGGGATCCTCAGCCAGAATGACAATGGTA-3′) for Nt PLA_2 was used to amplify a 461 bp fragment. The primers for the actin gene (Acc. No. AB158612) as an internal control were 5′-TGCAGATCGTATGAGCAAGG-3′ and 5′-GTGGA-CAATGGAAGGACCAG-3′ for amplifying the 181 bp fragment. The reaction products were electrophoresed on a 1% agarose gel.

Expression and purification of recombinant Nt PLA_2. The cDNA encoding mature protein of Nt PLA_2 was subcloned into an expression vector pET32a, and *Escherichia coli* BL21 (DE3) was transformed with the chimera plasmid. Four hundred milliliters of LB medium containing 1% tryptone peptone, 0.5% yeast extract, 0.5% NaCl, and 50 μg/mL ampicillin were inoculated with 4 mL of overnight culture from a transformed single colony. The cells were grown at 30°C. When the absorbance of the culture at 600 nm reached 0.5, the recombinant protein was expressed by induction with 0.1 mM IPTG for 3 h at 30°C. Cells were harvested at $3000 \times g$ for 5 min and frozen at −20°C. The cells were resuspended in 15 mL of a buffer containing 20 mM Tris-HCl (pH 8.0) and 2 mM EDTA. The cells were lysed by adding 6 mL of 1 N NaOH and neutralized with 1 N HCl. The lysate was centrifuged at $8000 \times g$ for 30 min at 4°C, and the resulting cell extract was dialyzed against 2 L of 20 mM Tris-HCl (pH 7.0). The dialysate was digested with Factor Xa proteinase for 90 min at 37°C (the ratio of Factor Xa proteinase to protein was 1:1000), and loaded on a POROS HS/M cation-exchange column (4.6×100 mm; PerSeptive Biosystems) at a flow rate of 2 mL/min, which was equilibrated with 20 mM MES-NaOH (pH 6.0). The protein was eluted with a linear gradient of NaCl. The active fractions were pooled and stored at −40°C.

SDS-PAGE. SDS-PAGE was carried out by using a 16% polyacrylamide gel in the presence of 2-mercaptoethanol, and the proteins were visualized with Coomassie brilliant blue staining.

TABLE 1
Distribution of Phospholipase A₂ (PLA₂) Activity in the Various Tissues of Tobacco[a]

| | | PLA₂ activity (mU/mg tissue) | | |
| | | | EDTA | |
Tissues	10 mM CaCl₂	1 mM	10 mM	20 mM
Flower	0.328	0.158	0.096	0.105
Leaf	0.004	ND	NT	NT
Stem	0.002	ND	NT	NT
Root	0.022	0.002	NT	NT

[a]The reaction mixture consisted of 50 mM Tris-HCl (pH 8.0), 2 mM 1-palmitoyl-2-oleoyl-*sn*-glycero-3-phosphocholine, 8 mM sodium cholate, 10 mM CaCl₂, and 0.1 M NaCl in a final volume of 0.1 mL. Data were obtain in duplicate. EDTA was added to remove the effect of Ca²⁺. ND, not detected; NT, not tested.

RESULTS AND DISCUSSION

Distribution of PLA₂ activity in the various tissues of tobacco. The crude extracts were prepared from the various tissues of tobacco, and PLA₂ activity in the extract was measured using the mixed-micellar POPC substrate with sodium cholate. As shown in Table 1, PLA₂ activity was extremely high in the flower, followed by the root, but it was hardly detected in the leaf and stem. Animal PLA₂ are divided into two types, based on their Ca²⁺ dependency (1–5). Thus, we next investigated the effect of EDTA on the PLA₂ activity in the various tissues. The PLA₂ activities in the root, leaf, and stem were almost completely inhibited by the addition of 1 mM EDTA. However, approximately one-third of the PLA₂ activity in the flower still remained even in the presence of 20 mM EDTA. The results suggest that two types of PLA₂, Ca²⁺-dependent and -independent PLA₂, exist in the tobacco flower. It has been reported that the expression of AtPLA IVC, which is a member of patatin-like PLA₂ in *Arabidopsis,* was observed in the flower (31). The patatin-like PLA₂ is homologous to animal Ca²⁺-independent PLA₂. Therefore, the Ca²⁺-independent PLA₂ activity in the tobacco flower may be derived from patatin-like PLA₂. In elm,

sPLA₂ has been purified from developing seed and requires Ca²⁺ for the enzyme activity (20). Furthermore, a cDNA clone of sPLA₂ with homology to elm sPLA₂ has been isolated from the carnation flower (22). Accordingly, almost two-thirds of the PLA₂ activity in the flower appears to be derived from the sPLA₂ that needs Ca²⁺ for the enzyme activity.

Isolation of the cDNA clone for Nt PLA₂. Since high Ca²⁺-dependent PLA₂ activity was detected in the tobacco flower, we tried to isolate cDNA for sPLA₂ from the flower. The primer for PCR was designed based on the amino acid sequence of potato sPLA₂. RT-PCR was performed with total RNA prepared from the tobacco flower. A partial cDNA fragment that encodes putative sPLA₂ in tobacco was isolated. Based on the sequence information, a gene-specific primer for 5′-RACE was designed to yield a full-length cDNA. Sequence analysis indicates that the nucleotide sequence of Nt PLA₂ cDNA includes a 471 bp open reading frame (Accession No. AB190178). The calculated molecular mass and pI value of Nt PLA₂ were 17,054 Da and 8.57, respectively. The hydropathy profile suggests that the N-terminal amino acid sequence of Nt PLA₂ includes the signal sequence. As shown in Figure 1, SignalP computer analysis (32) for the potential cleavage positions
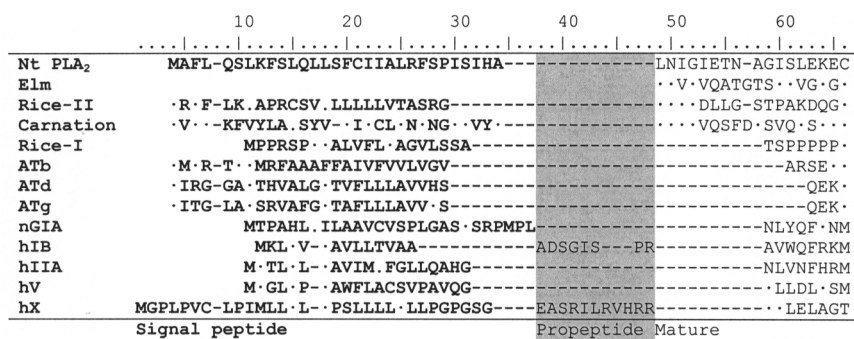
FIG. 1. Alignment of amino acid sequences in signal sequences of tobacco Nt PLA₂ with other plant and animal sPLA₂. The N-terminal signal sequences predicted by the SignalP program are indicated by bold. Propeptide is shown in shadow. Dots indicate the conserved amino acid residues identical to those of Nt PLA₂. Nt PLA₂, tobacco [*Nicotiana tabacum*] PLA₂ (this study, Acc. No. AB190178); Elm, elm PLA₂ (20); Rice-II, rice Rice-II PLA₂ (Acc. No. AJ238117); Carnation, carnation PLA₂ (Acc. No. AF064732); Rice-I, rice Rice-I PLA₂ (Acc. No. AJ238116); Rice2, ATb, *Arabidopsis* PLA₂ beta (Acc. No. AF541915); ATd, *Arabidopsis* PLA₂ delta (Acc. No. AY148347); ATg, *Arabidopsis* PLA₂ gamma (Acc. No. AY148346); nGIA, *Naja naja atra* group IA sPLA₂ (Acc. No. CAA54802); hIB, human group IB sPLA₂ (Acc. No. NP_000928); hIIA, human group IIA sPLA₂ (Acc. No. NP_000291); hV, human group V sPLA₂ (Acc. No. NP_000920); hX, human group X sPLA₂ (Acc. No. NP_003552). PLA₂, phospholipase A₂.

```
                    10        20        30        40        50        60        70        80        90       100
              ....|....|....|....|....|....|....|....|....|....|....|....|....|....|....|....|....|....|....|....|
T2 PLA2       LNIGIETN-AGISLEKECSRTCESKFCVPPLLRYGKYCGVLYSGCPGEQPCDGLDACOMKHDICIQRKGN------------NYLNLECNQSFLNCVA
Elm           ··V·VQATGTS··VG-G··K··E··S···F····L····K··
Rice-II       ····DLLG-STPAKDQG····Q··TIA····I·····R··A····V·HCVDTHND------------D··TM·CENL·SCID
Carnation     ····VQSFD·SVQ·S····K··E·SL····L·····M····S··V·S··D------------D··SQ·SNKLISCME
Rice-I        TSPPPPPP··SCAALNCDSVG-I·····GW··D··E··D··RD·HCVDK·-------------LMSVKCHEK·K··MR
ATb           ARSE··T··CIAQNCDTLS-I·····IGH····E··D··KI··HCVELN·------------MT·ISCHKK·QRC·N
ATd           QEKC·K··CIAQKCN-LG-I·····IG·F···P··D··T··NCVDL·------------MTYVDCHKQ·QRC·N
ATg           QEKC·N··CIAQNCNSLG-V·····IG·F···P··D··T··NCVDL·------------MTYVNCHKQ·KRC·N
nGIA          NLYQF·NMICCTVP-SRSWWDFAD··C··RGG··T-----V·D··HCYNEAEKISGC-----WPYSKTYSY·CS·GT·TCKG
hIB           AVWQFRKMIKCVIPGSDPFLEYNN··C··LGG··T-----V·E··KCQT··NCYDQAKKLDSCKFLLDNPYTHTYSYSCSG·AITCSS
hIIA          NLVNFHRMIKLTTG-KEAALSYGF··CHC··GGR··S-----K··TCWCYK·LEKRG·C-----GTKFLSYKFSNSG·RITCAK
hV            ·LLDL·SMIEKVTG-KNALTNYGF··C··WGGR··T-----K··TCWCWA··HCYG·LEEKG·C-----NIRTQSYKYRFAWGVVTCEP
hX            ··LELAGTVGC-VG-PRTPIAYMK··CFC·LGGH·Q-----R·AI··WCHG··CCYT·AEEAG·C-----SPKTERYSWQCVNQSVLCGP
                                      Ca2+ binding loop    Catalytic domain
```

```
                    110       120       130       140       150       160       170       180       190   Identity
              ....|....|....|....|....|....|....|....|....|....|....|....|....|....|....|....|....|....|....|      (%)
T2 PLA2       TFTKSGA-----PSFKGNTCLVGTVVRVITDVIDAAVVAGKIFKKP                                                 100
Elm                                                                                                         68
Rice-II       RVSG--------AT·P··KCN··QTAS··RG··ET··F····LH·RDDGQ                                             51
Carnation     N·KAH·------HT···S·CQADD·IQ··KF·ME··IL··RVLH                                                   58
Rice-I        KVK·A·------KIGFSRKCPYEMAMATM·SGM·M·IMLSQLGTQ-KLEL                                              31
ATb           RLS·AIKQSKNKKVGFSTKCPYSV·IPTVNQGM·IGILFSQLGNDMKTEL                                             29
ATd           ELKQ·IQESNNQKVGFSKECPYS··IPTVYRGMNYGIFFSG·GNIIIPKKPASAGPVVEVDLARSKADTKDGLGTNQGPQTKDGSKVSVPMNPSPS  23
ATg           KLS··IKHSNGEKIGFSTQCPYSI·IPTVFNGM·YGIFFSG·GNIFNPP-VLGSVPVVEVDLARSKVDTKDGLGTKLGLQTKEGSKVSASLNI---  24
nGIA          GNNACA·A--------VCDCDRLAAICFAG-APYNNNNYNIDL·ARCQ                                               18
hIB           KNKECE·F--------IONCDRNAAICFSK-APYNKAHKNLDT··YCQS                                               16
hIIA          QD-SCRSQ--------ILECDKAAATCFARNKTTYNKKYQYYSN·HCRGSTPRC                                          13
hV            GP-FCHVN--------ICACDRKL·YCLKRNLRSYNPQYQYFPNILCS                                               15
hX            AEN·CQEL--------LCKCDQEIANCLAQ--TEYNLKYLFYPQFLCEPDSPKCD                                         14
```

FIG. 2. Alignment of the amino acid sequences of tobacco Nt PLA$_2$ with other plant and animal sPLA$_2$. Sequences of mature sPLA$_2$ protein are shown. Dots indicate the conserved amino acid residues identical to those of Nt PLA$_2$. Residues identical among plant and animal sPLA$_2$ are indicated by gray boxes. The Cys residues are indicated by black boxes. The sequences corresponding to the Ca^{2+} binding loop and the catalytic domain of animal sPLA$_2$ are underlined. Sequence identity (%) of mature Nt PLA$_2$ with plant and animal sPLA$_2$ is indicated in the lower far right of the table. sPLA$_2$, secretory PLA$_2$; for other abbreviations and accession numbers see Figure 1.

in the signal sequence suggests that Nt PLA$_2$ contains 30 residues of signal sequence preceding the N-terminal amino acid (Leu of position 49) of mature enzyme. The N-terminal amino acid sequence between Leu49 and Cys66 of Nt PLA$_2$ shows high similarity (68%) with that of mature elm sPLA$_2$ protein purified and determined with protein sequencer (20). Thus, the N-terminal amino acid (Leu49) of mature Nt PLA$_2$ is also predicted by comparison with the N-terminal amino acid sequences of elm sPLA$_2$. An alignment of the amino acid sequence of mature Nt PLA$_2$ with mature sPLA$_2$ of various plants and animals is shown in Figure 2. Animal sPLA$_2$ contain six absolutely conserved disulfide bonds (37–147, 39–59, 58–127, 65–120, 75–105, and 98–118, in Fig. 2), which play an important role in the structural stability for the enzymatic activity (1,4). They commonly contain the Ca^{2+}-binding loop (Tyr35–Gly45) and the catalytic domain (Asp56–Tyr66) required for the catalytic reaction. Furthermore, there are several other conserved residues, Tyr66, Tyr87, and Asp121 among animal sPLA$_2$ (Fig. 2), which may be involved in hydrogen-bonding network (9,33,34). Nt PLA$_2$ contains 12 Cys residues, which are well conserved among plant sPLA$_2$. Only 7 of these 12 Cys residues in plant sPLA$_2$ agree with those of animal sPLA$_2$. Thus, a folding of the plant sPLA$_2$ may have a considerable difference from that of animal sPLA$_2$. However, the number and position of Cys residues in plant sPLA$_2$ are well conserved among plant sPLA$_2$. Thus, the Cys residues contribute to the structural enzyme stability for the activity as well as in animal sPLA$_2$. In addition, the Ca^{2+}-binding loop (Tyr35–Gly45) and catalytic domain (Asp56–Ile/Val66) are also highly conserved among plant sPLA$_2$. A comparison of the sequences of plant and animal sPLA$_2$ shows that plant

sPLA$_2$ have an insertion of four residues (position 47–50 in Fig. 2) between the Ca^{2+}-binding loop and the catalytic domain. Since the 4 amino acid residues among plant sPLA$_2$ were not found in animal sPLA$_2$, the residues may be a unique sequence characteristic of plant sPLA$_2$. Identities of amino acid sequences among plant sPLA$_2$ show that Nt PLA$_2$ is highly similar to elm, carnation, and rice (Rice-II) sPLA$_2$ (51–68%) and has a lower similarity to rice (Rice-I) and *Arabidopsis* PLA$_2$ (23–31%, Fig. 2). A phylogenetic tree was derived from an alignment of the amino acid sequences between plant and animal sPLA$_2$, using the CLUSTAL W program (35) and Tree view (36) (Fig. 3). This tree shows that plant sPLA$_2$ are separated into two subgroups, XIA PLA$_2$ and XIB PLA$_2$, according to the classification of sPLA$_2$ by Six and Dennis (1). Nt PLA$_2$ is considered to belong to group XIB, which contains elm, carnation, and rice (Rice-II) sPLA$_2$, while three *Arabidopsis* and rice (Rice-I) sPLA$_2$ are classified to group XIA PLA$_2$.

The mRNA expression of Nt PLA$_2$ in tobacco tissues. It was difficult to detect the transcripts by northern blotting. The amount of the transcripts appears to be small in the tobacco tissues. Thus, the expression of Nt PLA$_2$ transcripts in various tissues of tobacco was analyzed by RT-PCR. As shown in Figure 4, amplification of tobacco actin mRNA produced a band of 187 bp, providing a positive control. The intense signals of Nt PLA$_2$ transcripts were detected in root and stem, while there was a low signal in the flower. As described above, high PLA$_2$ activity was detected in the tobacco flower, but the expression level of Nt PLA$_2$ mRNA was low. This may indicate that Nt PLA$_2$ protein accumulates in the flower under normal conditions. There is also another possibility that highly Ca^{2+}-dependent PLA$_2$ activity in the flower, which is almost two-thirds of
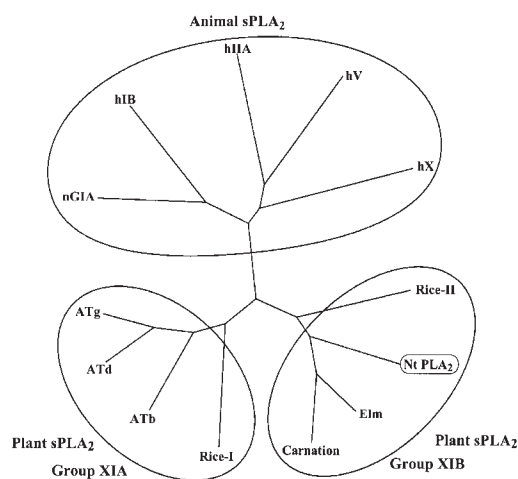
FIG. 3. A phylogenetic tree of various plant and animal sPLA$_2$. For abbreviations and accession numbers see Figures 1 and 2. Nt PLA$_2$ is boxed.

FIG. 4. Reverse transcription-PCR (RT-PCR) analysis for the tissue distribution of Nt PLA$_2$. Five hundred nanograms of total RNA from leaf, root, stem, and flower of tobacco were used as template for RT-PCR. The PCR product was analyzed on a 1% agarose gel. The RT-PCR product for actin was also analyzed as a control. For other abbreviation see Figure 1.

the PLA$_2$ activity, is due to the coexistence of Nt PLA$_2$ and other PLA$_2$ isozymes. In fact, both group XIA PLA$_2$ (ATd in Fig. 3) and group XIB PLA$_2$ (ATb and ATg in Fig. 3) are coexpressed in the *Arabidopsis* flower (19,23). Furthermore, we isolated a second tobacco PLA$_2$ cDNA with homology to NtPLA$_2$ cDNA (data not shown). We are now characterizing the properties of the second tobacco PLA$_2$. It is necessary to investigate the presence of Nt PLA$_2$ protein and other PLA$_2$ isozymes in the flower to answer the above question.

Expression and purification of recombinant Nt PLA$_2$. To characterize the enzymatic properties of Nt PLA$_2$, a cDNA region encoding the mature protein of Nt PLA$_2$ was fused with a sequence coding thioredoxin by a linker of a Factor Xa cleavage site (Ile-Glu-Gly-Arg). To obtain a recombinant Nt PLA$_2$ in bacteria, the chimera plasmid was used to transform *E. coli* BL21 cells for protein expression. When the expression of the recombinant Nt PLA$_2$ in the transformed *E. coli* BL21 cells was induced by IPTG, a band derived from a fusion protein was detected in whole-cell lysates on SDS-PAGE analysis. The fusion protein of the recombinant Nt PLA$_2$ was recovered in soluble form, and the cell extract was dialyzed against 20 mM Tris-HCl (pH 7.0). The recombinant Nt PLA$_2$ was expressed as a fusion protein with thioredoxin having the Factor Xa protease cleavage site adjacent to the N-terminal residue of the mature Nt PLA$_2$. Thus, the fusion protein can be cleaved by Factor Xa protease. The fusion protein digested with Factor Xa protease was applied to a POROS HS/M cation-exchange column. As the PLA$_2$ activity was detected only in the peak indicated by an inverted triangle in Figure 5A, the peak was pooled
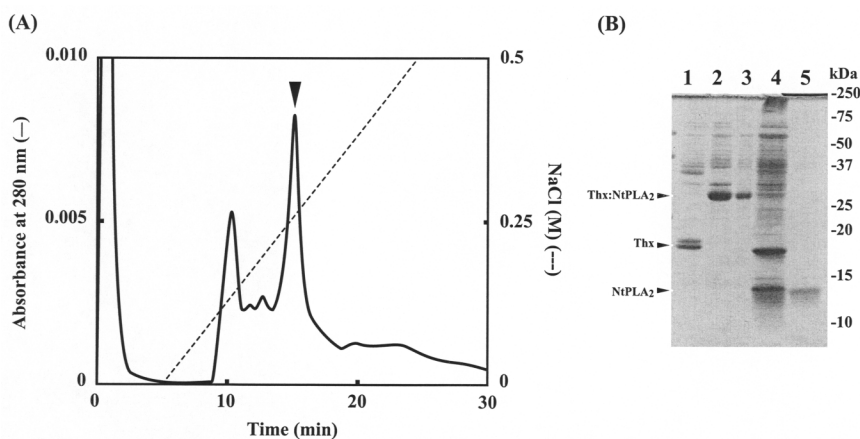
FIG. 5. Elution profile of recombinant Nt PLA$_2$ on ion exchange HPLC (A) and SDS-PAGE of recombinant Nt PLA$_2$ (B). The factor Xa digested mixture was applied to a POROS HS/M column (4.6 × 100 mm; PerSeptive Biosystems, Framingham, MA), which was pre-equilibrated with 20 mM MES-NaOH (pH 6.0). The elution of protein was followed by monitoring the absorbance at 280 nm (—). The dashed line indicates the linear gradient of NaCl. The flow rate was 2 mL/min. The pooled fraction is indicated by an inverted triangle. (B) Molecular mass of marker proteins, from top to bottom: 250, 75, 50, 37, 25, 20, 15, and 10 kDa. The protein was stained with Coomassie brilliant blue. Lane 1, *Escherichia coli* cells expressing thioredoxin; lane 2, *E. coli* cells expressing thioredoxin fusion Nt PLA$_2$; lane 3, the crude extract of *E. coli* expressing thioredoxin fusion Nt PLA$_2$; lane 4, the crude extract after treating with Factor Xa proteinase; lane 5, the purified Nt PLA$_2$. The recombinant protein is indicated by the triangle. Thx, thioredoxin; Thx:NtPLA2, thioredoxin fusion NtPLA$_2$; for other abbreviations see Figure 1.
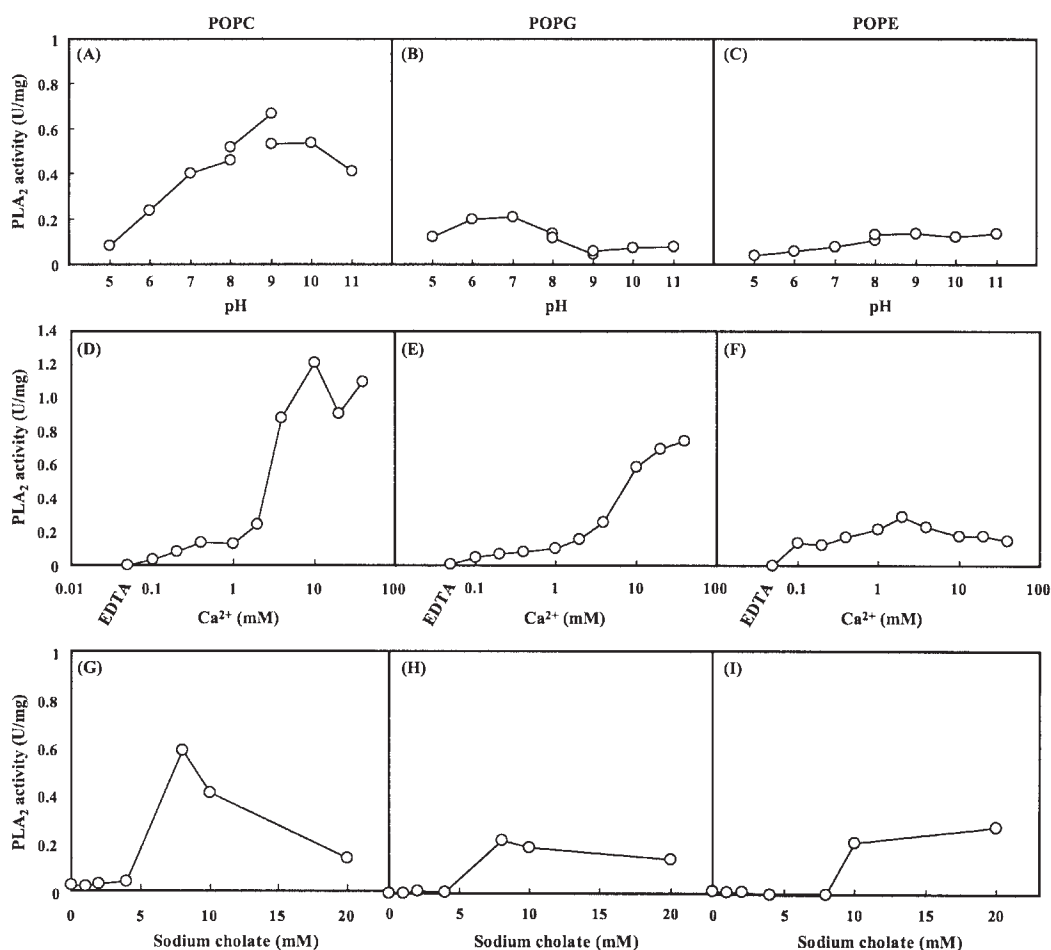
FIG. 6. Effects of pH (A, B, C), Ca^{2+} (D, E, F), and sodium cholate (G, H, I) on the activities of purified recombinant tobacco Nt PLA_2 for the phospholipids palmitoyl-2-oleoyl-*sn*-glycero-3-phosphocholine (POPC) (A, D, G), 1-palmitoyl-2-oleoyl-*sn*-glycero-3-phosphoglycerol (POPG) (B, E, H), and 1-palmitoyl-2-oleoyl-*sn*-glycero-3-phosphoethanolamine (POPE) (C, F, I). (A, B, C) The reaction mixtures containing purified Nt PLA_2, 2 mM phospholipid, 6 mM sodium cholate, 100 mM NaCl, and 5 mM $CaCl_2$ were incubated for 60 min at 37°C in a total volume of 100 µL. The buffers used were 50 mM Tris-maleate buffer at pH 5–8, 50 mM Tris-HCl at pH 8 and 9, and 50 mM glycine-NaOH at pH 9–11. (D, E, F) The reaction mixtures containing purified Nt PLA_2, 2 mM phospholipid, 6 mM sodium cholate, 100 mM NaCl, 50 mM Tris-HCl (pH 8.0), and 1 mM EDTA or 0–40 mM $CaCl_2$ were incubated. (G, H, I) The reaction mixtures containing purified Nt PLA_2, 2 mM phospholipid, 100 mM NaCl, 50 mM Tris-HCl (pH 8.0), and various concentrations of sodium cholate. PLA_2 activity was measured as described in the Materials and Methods section. For other abbreviations see Figure 1.

as the purified recombinant Nt PLA_2 to yield a final enzyme preparation (arrowhead in lane 5 of Fig. 5B).

Characterization of recombinant Nt PLA_2. The effects of pH and the concentrations of Ca^{2+} and sodium cholate on the activities of the purified recombinant Nt PLA_2 toward phospholipids containing three head groups (POPC, POPE, and POPG) are shown in Figure 6. Nt PLA_2 could hydrolyze efficiently mixed-micellar POPC with sodium cholate in the pH 8–10 region and POPG at pH 6–7 (Fig. 6A and B). On the other hand, the activity of Nt PLA_2 toward POPE was low (Fig. 6C). There are only a few studies on the enzymatic properties of plant $sPLA_2$. Elm $sPLA_2$ hydrolyzes mixed-micellar 1,2-dipalmitoyl-*sn*-glycero-3-phosphocholine with lubrol PX in pH 8–9 (20). However, the head group specificity of elm $sPLA_2$ has not

been investigated yet. *Arabidopsis* $sPLA_2$ gamma (ATg shown in Fig. 3), showed a head group specificity to PE rather than to PC (23). On the other hand, the low-MW *Vicia faba* PLA_2, whose primary structure has not been determined yet, hydrolyzed both PC and PE at similar rates (13). As a result of the few enzymatic studies of plant $sPLA_2$, it is still difficult to explain the differences in substrate specificity and pH optima for enzyme activity among plant $sPLA_2$.

The activity of Nt PLA_2 was totally abolished by EDTA (1 mM), indicating a requirement for Ca^{2+}. Although the activity of Nt PLA_2 toward POPC and POPG was extremely low in the presence of less than 2 mM Ca^{2+}, it was sufficiently high at 10–40 mM Ca^{2+} (Fig. 6D–F). Thus, Nt $sPLA_2$ requires essentially millimolar concentration of Ca^{2+} for the optimal enzyme activity.

Although the activities of Nt PLA$_2$ toward the phospholipids were not detected in the absence of sodium cholate, they were greately increased by the addition of sodium cholate. The optimal activity of Nt PLA$_2$ was found in the presence of 8 mM sodium cholate (cholate/phospholipids molar ratio of 4) toward POPC and POPG, and in the presence of 20 mM sodium cholate toward POPE (cholate/phospholipids molar ratio of 10, Fig. 6G–I).

In the present study, we isolated a cDNA encoding tobacco NtPLA$_2$, and it is predicted to have a putative signal sequence for secreting extracellularly. In *Arabidopsis,* AtsPLA$_2$-γ also has a putative signal sequence and is localized in the intercellular space (23). Therefore, Nt PLA$_2$ should be secreted into the intercellular space. It still remains unclear why high PLA$_2$ activity was detected in the flower, in which the mRNA expression of Nt PLA$_2$ was low. In order to answer the above questions, it is necessary to investigate the distribution of Nt PLA$_2$ protein in the tobacco flower.

ACKNOWLEDGMENT

REFERENCES

1. Six, D.A., and Dennis, E.A. (2000) The Expanding Superfamily of Phospholipase A$_2$ Enzymes: Classification and Characterization, *Biochim. Biophys. Acta 1488*, 1–19.
2. Murakami, M., and Kudo, I. (2002) Phospholipase A$_2$, *J. Biochem. (Tokyo) 131*, 285–292.
3. Tischfield, J.A. (1997) A Reassessment of the Low Molecular Weight Phospholipase A$_2$ Gene Family in Mammals, *J. Biol. Chem. 272*, 17247–17250.
4. Valentin, E., and Lambeau, G. (2000) Increasing Molecular Diversity of Secreted Phospholipases A$_2$ and Their Receptors and Binding Proteins, *Biochim. Biophys. Acta 1488*, 59–70.
5. Balsinde, J., Balboa, M.A., Insel, P.A., and Dennis, E.A. (1999) Regulation and Inhibition of Phospholipase A$_2$, *Annu. Rev. Pharmacol. Toxicol. 39*, 175–189.
6. Kishimura, H., Ojima, T., Hayashi, K., and Nishita, K. (2000) cDNA Cloning and Sequencing of Phospholipase A$_2$ from the Pyloric Ceca of the Starfish *Asterina pectinifera*, *Comp. Biochem. Physiol. B Biochem. Mol. Biol. 126*, 579–586.
7. Talvinen, K.A., and Nevalainen, T.J. (2002) Cloning of a Novel Phospholipase A$_2$ from the Cnidarian *Adamsia carciniopados*, *Comp. Biochem. Physiol. B Biochem. Mol. Biol. 132*, 571–578.
8. Gelb, M.H., Valentin, E., Ghomashchi, F., Lazdunski, M., and Lambeau, G. (2000) Cloning and Recombinant Expression of a Structurally Novel Human Secreted Phospholipase A$_2$, *J. Biol. Chem. 275*, 39823–39826.
9. Kudo, I., and Murakami, M. (2002) Phospholipase A$_2$ Enzymes, *Prostaglandins Other Lipid Mediat. 68–69*, 3–58.
10. Dessen, A. (2000) Structure and Mechanism of Human Cytosolic Phospholipase A$_2$, *Biochim. Biophys. Acta 1488*, 40–47.
11. Winstead, M.V., Balsinde, J., and Dennis, E.A. (2000) Calcium-Independent Phospholipase A$_2$: Structure and Function, *Biochim. Biophys. Acta 1488*, 28–39.
12. Kawakita, K., Senda, K., and Doke, N. (1993) Factors Affecting *in vitro* Activation of Potato Phospholipase A$_2$, *Plant Sci. 92*, 183–190.
13. Kim, D.K., Lee, H.J., and Lee, Y. (1994) Detection of Two Phospholipase A$_2$ (PLA$_2$) Activities in Leaves of Higher Plant *Vicia faba* and Comparison with Mammalian PLA$_2$'s, *FEBS Lett. 343*, 213–218.
14. Roy, S., Pouénat, M., Caumont, C., Cariven, C., Prévost, M., and Esquerré-Tugayé, M. (1995) Phospholipase Activity and Phospholipid Patterns in Tobacco Cells Treated with Fungal Elicitor, *Plant Sci. 107*, 17–25.
15. Creelman, R.A., and Mullet, J.E. (1997) Biosynthesis and Action of Jasmonates in Plants, *Annu. Rev. Plant Physiol. Plant Mol. Biol. 48*, 355–381.
16. Chapman, K.D. (1998) Phospholipase Activity During Plant Growth and Development and in Response to Environmental Stress, *Trends Plant Sci. 3*, 419–426.
17. Narvaez-Vasquez, J., Florin-Christensen, J., and Ryan, C.A. (1999) Positional Specificity of a Phospholipase A Activity Induced by Wounding, Systemin, and Oligosaccharide Elicitors in Tomato Leaves, *Plant Cell 11*, 2249–2260.
18. Scherer, G.F. (2002) Secondary Messengers and Phospholipase A$_2$ in Auxin Signal Transduction, *Plant Mol. Biol. 49*, 357–372.
19. Lee, H.Y., Bahn, S.C., Kang, Y.M., Lee, K.H., Kim, H.J., Noh, E.K., Palta, J.P., Shin, J.S., and Ryu, S.B. (2003) Secretory Low Molecular Weight Phospholipase A$_2$ Plays Important Roles in Cell Elongation and Shoot Gravitropism in *Arabidopsis*, *Plant Cell 15*, 1990–2002.
20. Ståhl, U., Ek, B., and Stymne, S. (1998) Purification and Characterization of a Low-Molecular-Weight Phospholipase A$_2$ from Developing Seeds of Elm, *Plant Physiol. 117*, 197–205.
21. Ståhl, U., Lee, M., Sjodahl, S., Archer, D., Cellini, F., Ek, B., Iannacone, R., MacKenzie, D., Semeraro, L., Tramontano, E., *et al.* (1999) Plant Low-Molecular-Weight Phospholipase A$_2$s (PLA$_2$s) Are Structurally Related to the Animal Secretory PLA$_2$s and Are Present as a Family of Isoforms in Rice (*Oryza sativa*), *Plant Mol. Biol. 41*, 481–490.
22. Kim, J.Y., Chung, Y.S., Ok, S.H., Lee, S.G., Chung, W.I., Kim, I.Y., and Shin, J.S. (1999) Characterization of the Full-Length Sequences of Phospholipase A$_2$ Induced During Flower Development, *Biochim. Biophys. Acta 1489*, 389–392.
23. Bahn, S.C., Lee, H.Y., Kim, H.J., Ryu, S.B., and Shin, J.S. (2003) Characterization of *Arabidopsis* Secretory Phospholipase A$_2$-γ cDNA and Its Enzymatic Properties, *FEBS Lett. 553*, 113–118.
24. Laxalt, A.M., and Munnik, T. (2002) Phospholipid Signalling in Plant Defence, *Curr. Opin. Plant Biol. 5*, 332–338.
25. Ryu, S.B. (2004) Phospholipid-Derived Signaling Mediated by Phospholipase A in Plants, *Trends Plant Sci. 9*, 229–235.
26. Tojo, H., Ono, T., and Okamoto, M. (1991) Spleen Phospholipases A$_2$, *Methods Enzymol. 197*, 390–399.
27. Tojo, H., Ono, T., and Okamoto, M. (1993) Reverse-Phase High-Performance Liquid Chromatographic Assay of Phospholipases: Application of Spectrophotometric Detection to Rat Phospholipase A$_2$ Isozymes, *J. Lipid Res. 34*, 837–844.
28. Iijima, N., Chosa, S., Uematsu, K., Goto, T., Hoshita, T., and Kayama, M. (1997) Purification and Characterization of Phospholipase A$_2$ from the Pyloric Caeca of Red Sea Bream, *Pagrus major*, *Fish Physiol. Biochem. 16*, 487–498.
29. Iijima, N., and Ono, H. (1998) Purification and Characterization of Phospholipase A$_2$ Isoforms from the Hepatopancreas of Red Sea Bream, *Pagrus major*, *Fish Physiol. Biochem. 18*, 135–147.
30. Chomczynski, P., and Sacchi, N. (1987) Single-Step Method of RNA Isolation by Acid Guanidinium Thiocyanate-Phenol-Chloroform Extraction, *Anal. Biochem. 162*, 156–159.
31. Holk, A., Rietz, S., Zahn, M., Quader, H., and Scherer, G.F. (2002) Molecular Identification of Cytosolic, Patatin-Related Phospholipases A from *Arabidopsis* with Potential Functions in Plant Signal Transduction, *Plant Physiol. 130*, 90–101.
32. Nielsen, H., Brunak, S., and von Heijne, G. (1999) Machine Learning Approaches for the Prediction of Signal Peptides and Other Protein Sorting Signals, *Protein Eng. 12*, 3–9.
33. Scott, D.L., White, S.P., Otwinowski, Z., Yuan, W., Gelb, M.H.,

and Sigler, P.B. (1990) Interfacial Catalysis: The Mechanism of Phospholipase A$_2$, *Science 250*, 1541–1546.

34. White, S.P., Scott, D.L., Otwinowski, Z., Gelb, M.H., and Sigler, P.B. (1990) Crystal Structure of Cobra-Venom Phospholipase A$_2$ in a Complex with a Transition-State Analogue, *Science 250*, 1560–1563.

35. Thompson, J.D., Higgins, D.G., and Gibson, T.J. (1994) CLUSTAL W: Improving the Sensitivity of Progressive Multiple Sequence Alignment Through Sequence Weighting, Position-Specific Gap Penalties and Weight Matrix Choice, *Nucleic Acids Res. 22*, 4673–4680.

36. Page, R.D. (1996) TreeView: An Application to Display Phylogenetic Trees on Personal Computers, *Comput. Appl. Biosci. 12*, 357–358.

Effects of the Individual Isomers *cis*-9,*trans*-11 vs. *trans*-10,*cis*-12 of Conjugated Linoleic Acid (CLA) on Inflammation Parameters in Moderately Overweight Subjects with LDL-Phenotype B

Julian D. Ramakers[a], Jogchum Plat[a], Jean-Louis Sébédio[b], and Ronald P. Mensink[a],*

[a]Department of Human Biology, Nutrition and Toxicology Research Institute Maastricht, Maastricht University, Maastricht, The Netherlands, and [b]Institut National de la Recherche Agronomique (INRA), Unité de Nutrition Lipidique, Dijon, France

ABSTRACT: Immune-modulating effects of CLA have been reported in animals, but results are inconsistent. In humans, CLA has shown no effects or only minor effects on immune function. The objective of this study was to evaluate the immune-modulating effects of 3 g *cis*-9,*trans*-11 (*c*9,*t*11) vs. *trans*-10,*cis*-12 (*t*10,*c*12) CLA isomers in a population with a high risk of coronary heart disease characterized by moderate overweight (body-mass index, 25–32.5 kg/m^2) in combination with LDL-phenotype B (≥35% small LDL cholesterol, density ≥ 1.040 g/mL). After a run-in period of 1 wk, 42 men and women were randomly allocated to the *c*9,*t*11 CLA group, the *t*10,*c*12 CLA group, or the placebo group. Effects of 13 wk of consumption of 3 g of CLA isomers on cytokine production by *ex vivo* lipopolysaccharide (LPS)-stimulated peripheral blood mononuclear cells (PBMC) and whole blood, and on plasma C-reactive protein (CRP) concentrations were evaluated. To generate hypotheses for future studies, protein expression patterns of 42 cytokines, chemokines, and growth factors were evaluated with an antibody array in pooled, nonstimulated, fasting plasma samples. LPS induced interleukin (IL)-6, IL-8, and tumor necrosis factor-α production by PBMC, and whole blood as well as plasma CRP concentrations were not significantly changed by the *c*9,*t*11 and the *t*10,*c*12 CLA isomers. The cytokine expression profile in nonstimulated plasma suggested that both CLA isomers induced a specific inflammatory signature, in which the *c*9,*t*11 CLA group showed more activity in terms of numbers of proteins regulated. We conclude that daily consumption of 3 g of *c*9,*t*11 or *t*10,*c*12 CLA isomer did not affect LPS-stimulated cytokine production by PBMC or whole blood and plasma CRP levels. Inflammatory signatures in fasting, nonstimulated plasma as determined by an antibody array may indicate enhanced immune function by both CLA isomers.

Paper no. L9763 in *Lipids* 40, 909–918 (September 2005).

*To whom correspondence should be addressed at the Department of Human Biology, Nutrition and Toxicology Research Institute Maastricht, Maastricht University, P.O. Box 616, 6200 MD Maastricht, The Netherlands.
E-mail: r.mensink@hb.unimaas.nl
Present address of the third author: INRA, Unité du Métabolisme Protéino-Énergétique, Clermont Ferrand, France.

Abbreviations: ANCOVA, analysis of covariance; BMI, body-mass index; CHD, coronary heart disease; CRP, C-reactive protein; CSF, colony-stimulating factor; *c*9,*t*11, *cis*-9,*trans*-11; GRO, growth-regulated protein; IL, interleukin; LPS, lipopolysaccharide; MCP-1, monocyte chemotactic protein-1; MCSF, macrophage colony-stimulating factor; PBMC, peripheral blood mononuclear cells; TMB, tetramethylbenzidine; TNF-α, tumor necrosis factor-α; *t*10,*c*12, *trans*-10,*cis*-12.

CLA is a mixture of positional (e.g., 9,11; 10,12) and geometrical (*cis* or *trans*) conjugated isomers of linoleic acid (18:2n-6). It is a natural food component, predominantly found in the lipid fraction of meat, milk, and other dairy products. Many health effects have been ascribed to CLA. The earlier studies mainly focused on its anticarcinogenic properties (1,2), but later studies also examined additional health benefits such as antidiabetic, antiobesity, and antiatherosclerotic effects (3). Most of these effects were, however, found in laboratory animals. CLA also has been reported to have immunomodulatory properties in animals, but results are inconsistent (3,4).

Data from human studies are limited and—if anything—only minor effects of mixtures of CLA isomers on immune functions have been shown (3,4). Effects may, however, be isomer-specific (4). Tricon *et al.* (5) therefore compared side-by-side *cis*-9,*trans*-11 (*c*9,*t*11) and *trans*-10,*cis*-12 (*t*10,*c*12) CLA. Both isomers decreased mitogen-induced lymphocyte activation but had no effects on lymphocyte subpopulations, *ex vivo* cytokine production, and serum C-reactive protein (CRP) concentration. The absence of clear effects may be related to the healthy population in that study. It is very well possible that effects are more apparent if the immune system is already triggered. In the present placebo-controlled study we therefore evaluated the effects on inflammation parameters of consumption of 3 g of the individual *c*9,*t*11 CLA or *t*10,*c*12 CLA isomers in moderately overweight subjects. It is known that overweight and obese persons are at increased risk for coronary heart diseases (CHD), which may be related to their proinflammatory serum profiles (6). In addition, subjects were characterized by LDL-phenotype B, which is typified by the presence of increased proportions of the highly atherogenic, small, dense LDL particles (7,8). Subjects with LDL-phenotype B have an increased risk for CHD that might be explained by the increased oxidative susceptibility of the small, dense LDL particles (9). Since leukocytes are easily triggered by oxidized LDL particles (10,11), potential positive effects on leukocyte immunoreactivity may be more evident in this population. Leukocyte function was determined *ex vivo* by measurement of interleukin (IL)-6, IL-8, and tumor necrosis factor (TNF)-α production after lipopolysaccharide (LPS) stimulation of isolated peripheral blood mononuclear cells (PBMC) and of whole blood. However, plasma concentrations of inflammation markers such as CRP, IL-6, and monocyte chemotactic protein-1

(MCP-1) are also strong predictors of future CHD risk (12–14). Therefore, we also measured plasma concentrations of CRP and of 42 different cytokines, chemokines, and growth factors in pooled plasma samples using an antibody array.

SUBJECTS AND METHODS

Subjects. Forty-two apparently healthy, moderately overweight (body-mass index (BMI) 25–32.5 kg/m^2), middle-aged (35–65 yr), men ($n = 22$) and women ($n = 20$), classified as having LDL-phenotype B ($\geq$35% small LDL cholesterol, density $\geq$ 1.040 g/mL), were included in the study. Volunteers were recruited through announcements in local newspapers. Eligible subjects completed a standard blood test and filled in a medical questionnaire. All subjects were nonhypercholesterolemic (mean serum total cholesterol < 7.0 mmol/L and mean serum TAG < 3.0 mmol/L), as measured on two separate occasions with at least a 3-d interval after an overnight fast. Exclusion criteria were diastolic blood pressure > 85 mmHg or systolic blood pressure > 150 mmHg; unstable body weight or attempts to lose weight during the previous 3 mon; presence of proteinuria or glucosuria; use of medication, a diet or a clinical condition known to affect lipid or glucose metabolism; drug or alcohol abuse; history of CHD, decompensatio cordis (Class III or IV), cardiomyopathy or kidney, liver and pancreatic disease or malignancies < 5yr ago; pregnancy or breastfeeding; and participation in another biochemical trial < 30 d ago. The subjects were requested not to change their usual diets, levels of physical exercise, smoking habits, or use of alcohol during the study. The Ethical Committee had approved the study protocol, and all subjects signed informed consent forms before entering the study.

Study design. This study was part of a larger project on the health effects of CLA in overweight middle-aged Europeans (Fifth European Commission framework program QLK1–1999–00076). Of this larger multicenter study, 42 participants from Maastricht were used to measure the immune-modulating effects of CLA. The study was designed as a placebo-controlled, double-blind parallel design. During the first week of the study (run-in period), subjects consumed 100 mL of a drinkable dairy product enriched with 3 g of a high-oleic acid sunflower oil (placebo) each day. Thereafter, the volunteers were randomly allocated to one of three treatment groups. Randomization was balanced for males and females, BMI, and LDL-phenotype. For the next 13 wk of the study (intervention period), the first group continued to consume the placebo drinkable yogurt-like dairy product enriched with 3 g of a high-oleic acid sunflower oil (100 mL/d). The second group consumed the same product enriched with 3 g of *c*9,*t*11 CLA instead of the oleic acid, while the third group consumed this product enriched with 3 g of *t*10,*c*12 CLA. No extra antioxidants were added to the experimental products.

The two CLA isomers were given as a TAG and were produced by Natural Lipids Ltd. (Hovdebygda, Norway), as described (15). The CLA was incorporated into a yogurt-like dairy product (by Danone; Palaiseau, France), which contained (wt/wt) 67% water, 20% milk [3.2% proteins, 5% lactose, 0.7% minerals (1250 ppm Ca) and 0.05% fat], 4.1% oils, 8% saccharose, 0.4% pectin, 0.35% citric acid, and 0.12% flavorings. The

*c*9,*t*11 CLA concentrate contained >80% *c*9,*t*11 CLA, <5% *t*10,*c*12 CLA, and other isomers in minor amounts. The *t*10,*c*12 CLA concentrate contained > 80% *t*10,*c*12 CLA, <5% *c*9,*t*11 CLA, and other isomers in minor amounts.

During the study, subjects recorded in diaries any signs of illness or any side effects experienced. Food intake was measured at the end of the run-in and the intervention period, using 3-d dietary records. Energy and nutrient intakes were calculated using the Dutch Food Composition Table (NEVO-tabel) (16).

Both at the end of the run-in period (week 1) and the end of the intervention period (week 14) blood was sampled after an overnight fast of at least 10 h. Subjects were not allowed to consume alcohol 24 h before blood sampling and were not allowed to smoke the morning before blood sampling. Blood was sampled in EDTA tubes and serum tubes (Becton Dickinson Vacutainer Systems, Franklin Lakes, NJ). Plasma was obtained by centrifugation at 2,000 × *g* for 30 min and used for CRP analysis and antibody arrays. Serum was obtained by centrifugation at 2,000 × *g* for 30 min and was used for lipid and lipoprotein analysis. Plasma and serum samples were stored at –80°C until analysis. In addition, blood was sampled in endotoxin-free heparinized tubes (Becton Dickinson Vacutainer Systems; final heparin concentration 10 U/mL) for PBMC and whole blood stimulation.

PBMC and whole blood stimulation. To examine *ex vivo* cytokine production by PBMC, cells were isolated from whole blood using Lymphoprep (Nycomed Pharma, Oslo, Norway) under sterile conditions. After isolation, PBMC were immediately plated in 24-well flat-bottom culture plates (2.5 × 10^6 cells/mL per well; 200–600 μL per well), and mixed with LPS (*Escherichia coli* 055:B5, Sigma, St Louis, MO; final concentrations 1 and 10 ng/mL in endotoxin-free buffered saline) or 20 μL polymixin B (Sigma; final concentration 1 mg/mL in endotoxin-free buffered saline). RPMI-1640 was used as the culture medium, containing 1% penicillin/streptomycin, 1% sodium pyruvate, and 1% of a heat-inactivated human serum pool. The cells were incubated for 6 h at 37°C. After incubation, the culture media were aspirated. The aspirated media were centrifuged at 1,000 × *g* for 30 min to obtain cell-free media, which were stored at –80°C until analysis.

To examine *ex vivo* cytokine production by PBMC in whole blood, 2 mL of whole blood was immediately mixed with 20 μL LPS (final concentrations 1 and 10 ng/mL) or polymixin B (final concentration 1 mg/mL). The blood samples were incubated for 6 h at 37°C. After incubation, samples were centrifuged at 1,000 × *g* for 30 min and platelet-poor plasma was stored at –80°C until analysis.

Cytokine and CRP analysis. IL-6, IL-8, and TNF-α concentrations in platelet-poor plasma of stimulated whole blood and cell-free media of stimulated PBMC were assessed by sandwich ELISA as previously described (17–20). Briefly, plates (Greiner Bio-one, Frickenhausen, Germany) were coated with monoclonal murine antihuman IL-6, IL-8, or TNF-α antibodies. Recombinant human IL-6, IL-8, and TNF-α were used for their respective standard titration curves. Immobilized IL-6 or IL-8 was detected using a specific biotinylated rabbit-anti-human IL-6 or IL-8 polyclonal antibody, followed by the addition of peroxidase-

conjugated streptavidin (Zymed Laboratories, San Francisco, CA) and tetramethylbenzidine (TMB) substrate (Kirkegaard & Perry Laboratories, Gaithersburg, MD). Immobilized TNF-α was detected using a specific rabbit-anti-human TNF-α antibody, followed by the addition of goat-anti-rabbit peroxidase (Jackson ImmunoResearch, West Grove, PA) and TMB substrate.

Plasma CRP concentrations were measured with a highly sensitive immunoturbidimetric assay (Kamiya Biomedical Company, Seattle, USA) (21).

Cytokine expression profiles. To generate hypotheses for future studies, expression patterns of multiple cytokines, chemokines, and growth factors were detected simultaneously with the human cytokine antibody array III (RayBiotech Inc., Norcross, GA) according to the manufacturer's instructions. We therefore evaluated changes in protein expression profiles, or patterns of protein clusters to be able to define possible differential immune-modulating effects of the two CLA isomers. For this, fasting EDTA plasma samples from all participants of each group were pooled at the end of the run-in period and at the end of the intervention period. This means that six arrays (placebo group, $c9,t11$ CLA group, and $t10,c12$ CLA group at the end of the run-in period and at the end of the intervention period) were analyzed. In brief, 1 mL of the pooled plasma samples was added to the array membranes. After incubating and washing, the cytokine-bound membrane was incubated with a cocktail of biotin-labeled antibodies, followed by adding horseradish peroxidase-conjugated streptavidin. Array spot intensity was detected by using a LAS-3000 Lite Image reader (Raytest GmbH, Straubenhart, Germany) based on chemiluminescence imaging. Finally, intensity of the spots was quantified by densitometry using Aida software version 3.50 (Raytest GmbH), thereby correcting for background staining of the gel. Comparison of protein expression profiles was possible after normalization of each spot on an array using the positive controls provided by the manufacturer. For each group, responses to the dietary supplements were calculated as the percent change between values at the end of the run-in period (week 1) and those at the end of the intervention period (week 14). Next,

for each cytokine the change in the control group was subtracted from the change in the intervention groups.

Lipids, apolipoproteins, and LDL-phenotype. Total, LDL, HDL cholesterol and TAG concentrations were determined as described (22). LDL-phenotype was determined by Y.A. Carpentier from L. Deloyers Laboratory for Experimental Surgery of the Université Libre de Bruxelles (Brussels, Belgium) as described (23).

FA composition of plasma phospholipids. FA composition of plasma phospholipids was measured in EDTA plasma as described by Sébédio *et al.* (24).

Statistics. For each subject, responses to the dietary supplements were calculated as the change between values at the end of the run-in period (week 1) and those at the end of the intervention period (week 14). Since the concentrations of IL-6, IL-8, and TNF-α as well as FA compositions were not normally distributed, the differences in changes were evaluated with the nonparametric Kruskal–Wallis test, followed by the Mann–Whitney test if the Kruskal–Wallis test showed a significant difference between the groups. The differences in changes of CRP were evaluated by ANOVA. CRP concentrations at the end of the run-in period (week 1) were different between the three groups. Therefore, an analysis of covariance (ANCOVA) with week 1 concentrations as covariate also was carried out. Correlation analyses were performed using the Spearman correlation test.

All statistical analyses were performed using SPSS for Macintosh 10.0 (SPSS, Chicago, IL). Normally distributed values are presented as means ± SD, nonnormally distributed values as medians (ranges). A *P*-value for the diet-effect of <0.05 was considered as statistically significant. If a Tukey or Mann–Whitney test was performed, a *P*-value of <0.017 was considered as statistically significant.

RESULTS

Baseline characteristics of the 38 subjects that completed the study are presented in Table 1. Three subjects dropped out during the intervention period, because of appearance of rashes

TABLE 1
Baseline Characteristics of Subjects Before Start of the Study[a]

	Control (*n* = 12)	*c*9,*t*11 CLA (*n* = 14)	*t*10,*c*12 CLA (*n* = 12)
Age (y)	58 ± 5	53 ± 7	56 ± 6
Sex, M:F	6:6	7:7	6:6
BMI (kg/m²)	29 ± 2	29 ± 2	29 ± 3
Visceral adiposity (waist/hip ratio)	0.95 ± 0.08	0.94 ± 0.08	0.94 ± 0.07
Systolic blood pressure (mmHg)	138 ± 14	140 ± 20	136 ± 13
Diastolic blood pressure (mmHg)	86 ± 9	88 ± 9	88 ± 5
Total cholesterol (mmol/L)[b]	6.22 ± 1.15	6.17 ± 0.79	5.80 ± 0.92
LDL cholesterol (mmol/L)[b]	4.19 ± 1.12	4.02 ± 0.92	3.95 ± 0.92
HDL cholesterol (mmol/L)[b]	1.54 ± 0.79	1.31 ± 0.74	1.18 ± 0.35
TAG (mmol/L)[b,c]	1.08 ± 0.39	1.82 ± 0.90	1.45 ± 0.65
LDL-phenotype (%)[d]	40.9 (34.5–60.7)	41.2 (33.2–58.1)	41.3 (33.9–55.1)

[a]Values are means ± SD except for LDL-phenotype medians (ranges).
[b]Fasting serum concentrations of total cholesterol, LDL cholesterol, HDL cholesterol, and TAG were measured during the first and second screening visit, with an interval of at least 3 d.
[c]Significant difference between the groups (*P* = 0.043)
[d]LDL-phenotype is expressed as the proportion of LDL cholesterol in LDL particles with a density ≥ 1.040 g/mL.

TABLE 2
Proportions of FA in Phospholipids [% of total FA (w/w)][a]

	Control (n = 12)	c9,t11 CLA (n = 14)	t10,c12 CLA (n = 12)	P-value
CLA c9,t11				
Run-in period	0.126	0.145	0.108	
	(0.000–0.224)	(0.094–0.731)	(0.091–0.185)	
Intervention period	0.136	0.694	0.183	
	(0.081–0.290)	(0.078–1.280)	(0.145–0.196)	
Change	−0.013	0.579[b,c]	0.077	0.001
	(−0.042–0.196)	(−0.126–1.135)	(−0.010–0.139)	
CLA t10,c12				
Run-in period	0.000	0.000	0.000	
	(0.000–0.000)	(0.000–0.098)	(0.000–0.557)	
Intervention period	0.000	0.088	0.505	
	(0.000–0.208)	(0.000–0.183)	(0.000–0.755)	
Change	0.000	0.088[c]	0.489[d]	< 0.001
	(0.000–0.208)	(−0.053–0.183)	(0.000–0.755)	

[a]During the run-in period of 1 wk subjects consumed a drinkable dairy product enriched with 3 g of a high-oleic acid sunflower oil (placebo) per day. During the intervention period of 13 wk the control group continued to consume the placebo product, the c9,t11 CLA group consumed 3 g of c9,t11 CLA, while the c10,t12 CLA group consumed 3 g of t10,c12 CLA. Values are medians (ranges).
[b]c9,t11 CLA group vs. control group $P < 0.01$.
[c]c9,t11 CLA group vs. t10,c12 CLA group $P < 0.01$.
[d]t10,c12 CLA group vs. control group $P < 0.001$.

(n = 1, control group), because of participation in another clinical trial (n = 1, t10,c12 CLA group), or because of a lung infection (n = 1, t10,c12 CLA group). After the study, one man from the control group was excluded from the analysis, because of a nonfasting blood sample at the end of the intervention period. Seven subjects were smokers (1 subject from the control group and 3 subjects from each CLA group). One woman from the c9,t11 CLA group and 2 women from the t10,c12 CLA group used oral contraception. Five women from the control group, 5 women from the c9,t11 CLA group, and 4 women from the t10,c12 CLA group were postmenopausal. At baseline, there were no significant differences between the three groups, except for serum TAG concentrations (Table 1).

Compliance to the drinks was confirmed by the incorporation of the CLA isomers into plasma phospholipids (Table 2). For the c9,t11 CLA group, the change in the proportion of c9,t11 CLA was significantly higher as compared with the changes in the control ($P < 0.01$) and the t10,c12 CLA groups ($P < 0.01$). The t10,c12 CLA group had significantly higher increases in the proportions of the t10,c12 CLA as compared with those in the control ($P < 0.001$) and the c9,t11 CLA groups ($P < 0.01$).

Daily intakes of energy, and the percentages of energy from fat, saturated FA, monounsaturated FA, PUFA, protein, and carbohydrates as well as daily intake of cholesterol, fiber, and alcohol did not differ during the run-in and intervention period (data not shown).

PBMC and whole blood stimulation at the end of the run-in period. Stimulation of PBMC and whole blood with 1 and 10 ng/mL LPS resulted in dose-dependent increases in IL-6, IL-8, and TNF-α production. Conclusions, however, did not depend on the dose of LPS used and therefore only the 10 ng/mL LPS results are presented. All polymixin B controls were negative (data not shown).

IL-6, IL-8, and TNF-α productions by PBMC at the end of the run-in period varied between the groups, but differences did not reach statistical significance (Table 3).

At the end of the run-in period, the IL-6 and IL-8 production in whole blood was about 20 ng/mL, whereas the TNF-α production was much lower (about 4 ng/mL). There were no statistically significant differences between the three groups at the end of the run-in period (Table 4).

As shown in Table 5, Spearman correlations between the different cytokine concentrations produced by stimulated PBMC at the end of the run-in period were high ($P < 0.0001$). Spearman correlations between the cytokines in whole blood were weaker than those of PBMC but still reached statistical significance ($P < 0.05$).

Effects of c9,t11 or t10,c12 CLA on PBMC and whole blood stimulation. Effects of the dietary interventions on IL-6, IL-8, and TNF-α production in PBMC and whole blood after LPS stimulation are shown in Tables 3 and 4. In PBMC, IL-6, IL-8, and TNF-α, production increased in both intervention groups and in the control group. Although the increase in the three cytokines was the highest in the t10,c12 CLA group, the differences between the groups did not reach significance (P-values for diet effects: IL-6, $P = 0.439$; IL-8, $P = 0.427$; TNF-α, $P = 0.175$; Table 3). In whole blood, IL-6, IL-8, and TNF-α, production decreased in both intervention groups and in the control group. The decrease in the three cytokines was less in the t10,c12 CLA group, but again the differences between the groups did not reach significance (P-values for diet effects: IL-6, $P = 0.121$; IL-8, $P = 0.506$; TNF-α, $P = 0.659$; Table 4).

CRP. Two subjects of the control group and two subjects of the c10,t12 CLA group with CRP values higher than 8 mg/mL were excluded from the analysis. At the end of the run-in period, CRP concentrations were significantly different between the

TABLE 3
Effects of *c9,t*11 CLA or *t*10,*c*12 CLA on *ex vivo* Cytokine Production by Isolated PBMC in Response to Stimulation with LPS[a]

	Control	*c9,t*11 CLA	*t*10,*c*12 CLA	*P*-value
IL-6 (ng/ml)				
n	11	13	9	
Run-in period	4.71	15.01	3.74	
	(0.89–41.65)	(0.53–65.21)	(0.63–32.21)	
Intervention period	6.96	9.42	11.76	
	(1.12–52.23)	(2.19–7.15)	(1.21–50.86)	
Change	0.59	1.66	4.40	0.439
	(−9.05–46.17)	(−40.34–38.26)	(−9.74–48.26)	
IL-8 (ng/ml)				
n	10	12	9	
Run-in period	8.29	18.62	7.97	
	(1.89–46.83)	(1.10–42.91)	(3.12–42.00)	
Intervention period	17.37	16.08	21.38	
	(3.53–53.80)	(4.15–51.97)	(7.07–35.80)	
Change	2.61	1.84	4.90	0.427
	(−7.48–46.23)	(−14.27–30.20)	(−6.20–22.03)	
TNF-α (ng/ml)				
n	11	13	9	
Run-in period	1.06	1.31	0.61	
	(0.16–2.74)	(0.10–4.77)	(0.28–2.44)	
Intervention period	1.60	1.56	2.44	
	(0.24–4.75)	(0.47–6.65)	(0.34–5.39)	
Change	0.12	0.48	1.30	0.175
	(−0.39–2.01)	(−3.33–4.10)	(−0.08–4.78)	

[a]For experimental details, see Table 2. Peripheral blood mononuclear cells (PBMC) were isolated from whole blood and stimulated for 6 h with 10 ng/mL lipopolysaccharide (LPS) from *Escherichia coli* 055:B5. Values are medians (ranges). The results of five subjects (one of the control, one of the *c9,t*11 and three of the *t*10,*c*12 CLA group) were missing, because PBMC isolation from the blood was not successful. The results of the interleukin (IL)-8 production by PBMC of one subject of the control group and one subject of the *c9,t*11 CLA group were missing, because the amount of the samples was limited. TNF, tumor necrosis factor.

TABLE 4
Effects of *c9,t*11 CLA or *t*10,*c*12 CLA on *ex vivo* Cytokine Production by PBMC in Whole Blood in Response to Stimulation with LPS[a]

	Control (*n* = 12)	*c9,t*11 CLA (*n* = 13)	*t*10,*c*12 CLA (*n* = 12)	*P*-value
IL-6 (ng/ml)				
Run-in period	25.28	20.14	20.65	
	(5.63–63.61)	(10.14–43.40)	(4.54–32.89)	
Intervention period	16.42	17.60	16.84	
	(3.19–41.24)	(3.58–33.64)	(3.16–27.33)	
Change	−8.82	−6.06	−2.10	0.121
	(−22.37–5.84)	(−20.08–17.35)	(−14.57–6.07)	
IL-8 (ng/ml)				
Run-in period	21.28	20.09	19.28	
	(14.80–43.30)	(9.72–49.71)	(6.74–40.12)	
Intervention period	8.86	8.68	9.40	
	(3.16–17.51)	(3.32–39.50)	(2.65–20.56)	
Change	−14.60	−10.21	−8.83	0.506
	(−25.79–0.85)	(−23.89–4.87)	(−32.82–4.77)	
TNF-α (ng/ml)				
Run-in period	4.12	4.51	4.00	
	(1.57–14.89)	(0.70–7.03)	(1.60–8.88)	
Intervention period	2.53	3.42	2.38	
	(0.77–7.56)	(0.99–4.50)	(1.50–7.32)	
Change	−1.61	−1.37	−0.86	0.659
	(−9.53–2.95)	(−5.13–3.07)	(−4.84–2.11)	

[a]For experimental details, see Table 2. Values are medians (ranges). Whole blood was stimulated for 6 h with 10 ng/mL LPS from *E. coli* 055:B5. Values are medians (ranges). The results of one subject of the *c9,t*11 CLA group were missing, because not enough blood was drawn. For abbreviations see Table 3.

TABLE 5
Spearman Rank Correlations at the End of the Run-in Period Between Different Cytokine Concentrations After Stimulation of PBMC or Whole Blood and Between Cytokine Concentrations After Stimulation of PBMC vs. Whole Blood[a]

PBMC	r	P-value
IL-6 vs. IL-8	0.91	<0.0001
IL-6 vs. TNF-α	0.81	<0.0001
IL-8 vs. TNF-α	0.74	<0.0001
Whole blood		
IL-6 vs. IL-8	0.51	0.002
IL-6 vs. TNF-α	0.47	0.005
IL-8 vs. TNF-α	0.33	0.048
PBMC vs. whole blood		
IL-6	0.29	0.113
IL-8	0.31	0.094
TNF-α	0.17	0.340

[a]PBMC and whole blood were stimulated for 6 h with 10 ng/mL LPS from *E. coli* 055:B5. For abbreviations see Table 3

groups ($P = 0.042$; Table 6). Changes between groups, however, were not significantly different ($P = 0.557$; Table 6). Also ANCOVA analysis with week 1 concentrations as covariate resulted in the same conclusion.

Cytokine profiles. In the pooled plasma samples, 27 cytokines, chemokines, or growth factors of the 42 different spots on the antibody arrays were detectable and could be semiquantified. Figure 1 shows the absolute values (in arbitrary units) of the control group at the end of the run in period. Figure 2 shows that the number as well as the extent of the changes was more pronounced in the $c9,t11$ CLA group as compared with those in the $t10,c12$ CLA group. The observed changes were mostly increases, but decreases were also found.

Consumption of the $c9,t11$ and $t10,c12$ CLA isomers caused changes in the same directions [e.g., thymus and activation-regulated chemokine (TARC) and IL-1α], as well as into opposite directions [e.g., epidermal growth factor (EGF) and TNF-β]. Further, some cytokines showed only a change in the $c9,t11$ CLA group (e.g., stromal cell-derived factor (SDF-1), IL-1β, and IL-2] or in the $t10,c12$ CLA group [e.g., growth-regulated protein (GRO)]. The increases of the three MCP values in the $c9,t11$ CLA group were very consistent, whereas some IL showed changes into different directions (e.g., IL-1α and IL-1β). When the cytokines were divided into different classes [chemokines, colony-stimulating factors (CSF), growth factors, and stimulating and suppressive cytokines], the profile remained complex.

However, in both CLA groups the concentrations of chemokines that attract granulocytes (neutrophils, eosinophils, and basophils) (except GRO in the $t10,c12$ CLA group) increased, while concentrations of chemokines that mainly attract monocytes, macrophages, and T-lymphocytes decreased [except MIP (macrophage inflammatory protein)-1δ and Rantes (regulated upon activation normal T-cell expressed and secreted) in the $c9,t11$ CLA group]. Furthermore, concentrations of macrophage colony-stimulating factor (MCSF) and thrombopoietin (Tpo), two CSF, were clearly elevated in both CLA groups, but in a more pronounced fashion in the $c9,t11$ CLA group. Also concentrations of IL-10, an example of a suppressive cytokine, were increased, an effect that was stronger in the $t10,c12$ CLA group. Effects on growth factors and stimulating cytokines were less uniform. Leptin plasma concentrations were decreased in both CLA groups.

Correlations. At the end of the run-in period, no significant correlations were found between the proportions of $c9,t11$ and $t10,c12$ CLA in plasma phospholipids with cytokine production. Body weight, however, correlated positively with TNF-α production in whole blood ($r = 0.359$, $P = 0.029$), as well as with IL-6 or IL-8 production by PBMC ($r = 0.423$, $P = 0.014$ and $r = 0.406$, $P = 0.023$). In line with this, TNF-α production by PBMC correlated with BMI ($r = 0.395$, $P = 0.023$), and IL-6 production by whole blood and PBMC with visceral adiposity ($r = 0.438$, $P = 0.007$ and $r = 0.436$, $P = 0.011$, respectively). Also BMI correlated with plasma CRP concentrations ($r = 0.568$, $P = 0.001$). At

TABLE 6
Effects of $c9,t11$ CLA or $t10,c12$ CLA on Plasma C-Reactive Protein (CRP) Concentrations[a]

	Control (n = 9)	c9,t11 CLA (n = 14)	t10,c12 CLA (n = 10)	P-value
CRP (mg/L)				
Run-in period[b]	0.90 ± 0.50	2.77 ± 2.21	1.68 ± 1.50	
Intervention period	0.75 ± 0.55	2.97 ± 2.40	2.01 ± 1.39	
Change	−0.15 ± 0.36	0.19 ± 0.99	0.33 ± 1.32	0.557

[a]For experimental details, see Table 2. Values are means ± SD. Two subjects of the control group and two subjects of the $t10,c12$ group with values higher than 8 mg/L were excluded for analysis. For one subject of the control group no CRP analysis was performed, because of lack of samples.
[b]Significant difference between the groups at the end of the run-in period ($P = 0.042$).
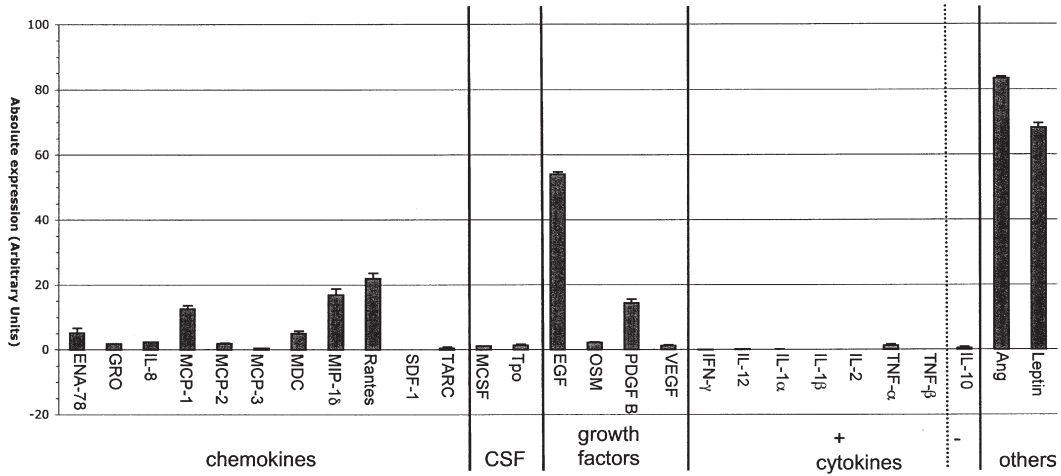
FIG. 1. The absolute protein expression (in Arbitrary Units) of different cytokines, chemokines, and growth factors of the control group at the end of the run-in period as measured by an antibody array. The sensitivity of the array is not the same for the different proteins, therefore the heights of the bars do not represent concentrations. For experimental details see the Subjects and Methods section. The proteins are divided into different classes, i.e., chemokines, colony stimulating factors (CSF), growth factors, and stimulating (+) and suppressive (−) cytokines. ENA, epithelial-derived neutrophil-activating protein; GRO, growth-regulated protein; IL, interleukin; MCP, monocyte chemotactic protein; MDC, macrophage-derived chemokine; MIP, macrophage inflammatory protein; Rantes, regulated upon activation normal T-cell expressed and secreted; SDF, stromal cell-derived factor; TARC, thymus- and activation-regulated chemokine; MCSF, macrophage colony-stimulating factor; Tpo, thrombopoietin; EGF, epidermal growth factor; OSM, oncostatin M; PDGF, platelet-derived growth factor; VEGF, vascular endothelial growth factor; IFN, interferon; TNF, tumor necrosis factor; Ang, angiogenin.
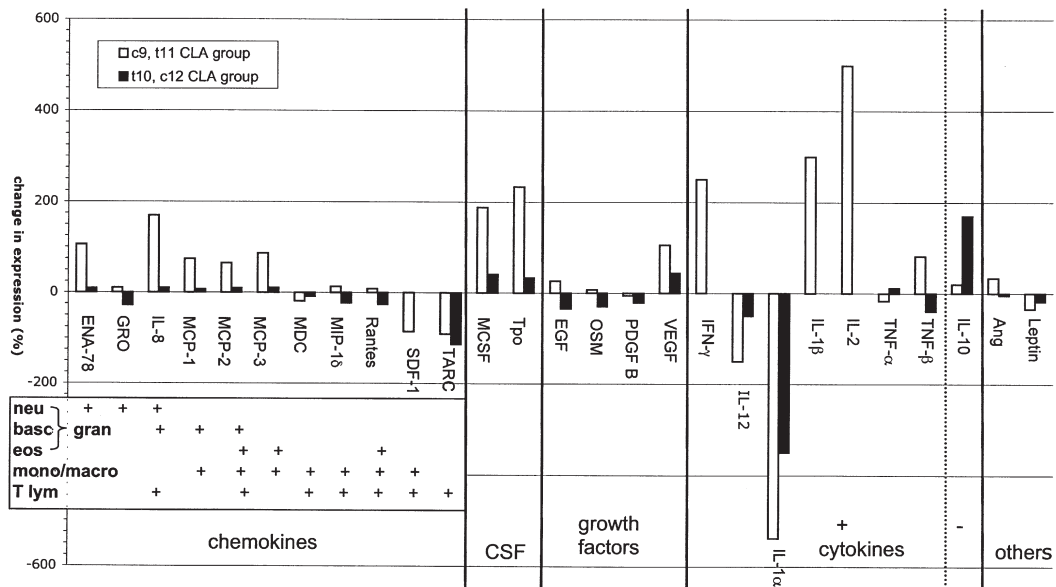
FIG. 2. Effects of 13 wk of *c*9,*t*11 CLA or *t*10,*c*12 CLA consumption on plasma concentrations of different cytokines, chemokines, and growth factors as measured by an antibody array. The percent changes for each protein in the intervention groups were calculated compared with the control group. For experimental details see the Subjects and Methods section. The proteins are divided into different classes, i.e., chemokines, CSF, growth factors, and stimulating (+) and suppressive (−) cytokines. The chemokines are further subdivided into chemokines that attract granulocytes (gran) [neutrophils (neu), basophils (baso), ,and eosinophils (eos)], monocytes/macrophages (mono/macro), and T-lymphocytes (T lym). For other abbreviations see Figure 1.

the end of the intervention period, we found a significant correlation of 0.698 ($P = 0.008$) only between the changes in the proportions of $c9,t11$ CLA in plasma phospholipids and the changes in TNF-α production in whole blood in the $c9,t11$ CLA group.

DISCUSSION

In animals, inconsistent effects of CLA on immune parameters have been reported, whereas in most humans no effects of CLA mixtures could be shown at all (3,4). It has been suggested that these inconsistencies might be due to opposite effects of the two most common CLA isomers (4). Recently, however, Tricon *et al.* (5) showed no effects of the $c9,t11$ or $t10,c12$ CLA isomers on *ex vivo* cytokine production by LPS and concanavalin A-stimulated PBMC. It is possible that this lack of effect is related to the fact that the study population consisted of young, healthy subjects. Another explanation might be the absence of effects on cytokine production by stimulated PBMC, whereas CLA may affect plasma cytokine concentrations in nonstimulated conditions. In our study we have therefore evaluated the effects of the two individual CLA isomers side-by-side in moderately overweight subjects at increased risk for CHD, which are expected to have a proinflammatory profile based on their BMI, both after LPS stimulation and in nonstimulated plasma. We found positive correlations between different indices of obesity (weight, BMI, visceral adiposity) and LPS-stimulated production of different cytokines (IL-6, IL-8, and TNF-α) by PBMC and in whole blood. It is thus conceivable that our study population is more responsive to interventions with potential effects on inflammation parameters. However, in the present study we also found no effects of a daily consumption of 3 g of $c9,t11$ or $t10,c12$ CLA for 13 wk on *ex vivo* cytokine production by isolated PBMC or by PBMC present in whole blood after stimulation with LPS. Our results agree not only with those of Tricon *et al.* (5) but also with earlier studies in which mixtures of the various CLA isomers did not alter the *ex vivo* cytokine production by LPS-stimulated PBMC in healthy men and women (25,26). Taken together, however, studies in various population groups do not suggest that consumption of the purified CLA isomers or mixtures of CLA isomers affects *ex vivo* cytokine production by stimulated PBMC or whole blood.

Effects of CLA on immune cell functions also have been studied in various animal models. Results were equivocal and varied from stimulation to inhibition, depending on the parameter examined. In fact, conflicting results for the same parameter have even been found within the same animal species, for which there is no clear explanation (3). It is possible, however, that effects may depend on the composition of the background diet. When rats were fed a soybean oil-based diet supplemented with a CLA mixture, *ex vivo* basal and LPS-stimulated secretions of IL-6 by resident peritoneal macrophages were reduced (27). These effects were not observed when the CLA mixture was added to a menhaden and safflower oil-based diet (27). In the same study, CLA feeding also decreased basal, but not LPS-stimulated, secretion of TNF-α, but in this case effects did not depend on the background diet (27). When mice were fed a diet

supplemented with purified $c9,t11$ or $t10,c12$ CLA, increases in TNF-α and IL-6 secretion were found by *ex vivo* cultured splenocytes after LPS stimulation. Effects were comparable for both CLA groups (28). These two animal studies examined immune function in a comparable manner as we did and found both immune-stimulating and -suppressing effects. Many other animal studies have examined other aspects of the immune system, such as lymphocyte proliferation and antibody responses, and also reported both immune stimulation and suppression (3,4).

The reason that we observed no significant effects of each isomer cannot be explained by noncompliance, as shown by the significant changes in FA composition of plasma phospholipids. Further, it has been demonstrated that both $c9,t11$ and $t10,c12$ CLA are incorporated into PBMC lipids, although less efficiently than into plasma PC and cholesteryl esters (29). In our study CLA was given to the volunteers with a dairy product and not by capsules, as in many other studies. This, however, did not affect the bioavailability of the CLA, as we have recently reported that the proportion of CLA incorporated into plasma phospholipids was in good agreement with studies that have used capsules (30). In our study, plasma CRP concentrations increased slightly, in particular in the $t10,c12$ CLA group. Differences between the groups did not, however, reach statistical significance. This agrees with the findings of Tricon *et al.* (5), who also showed no effects of a daily intake of 2.5 g of the individual CLA isomers on serum CRP concentrations in healthy subjects. Risérus *et al.* (31), however, observed that 12 wk supplementation with 3.4 g of the purified $t10,c12$ CLA isomer increased plasma CRP concentrations of obese men with metabolic syndrome. It is possible that these inconsistencies can be explained by differences in intakes, which was the highest in the study of Risérus *et al.* As BMI is a major determinant of CRP concentrations, another explanation is that $t10,c12$ CLA may affect CRP concentrations in subjects with increased CRP concentrations. Again, the mean BMI of the subjects in the study of Risérus *et al.* was the highest (30 kg/m^2) and in the study of the Tricon *et al.* the lowest (25 kg/m^2).

Besides cytokine production of LPS-stimulated PBMC, effects of CLA consumption on plasma concentrations of cytokines were also evaluated. To our opinion, in this way two different processes are measured. When stimulating PBMC with LPS, the potency of leukocytes to respond to a bacterial infection is simulated. Plasma cytokines do not originate only from leukocytes, and they may also be secreted from other cells, such as adipocytes (32,33). In particular, fasting levels of various cytokines, acute phase proteins, and/or chemokines are valuable predictors of future coronary risk (12–14). Risérus *et al.* (31) measured fasting plasma concentrations of TNF-α and IL-6 but showed no changes after intake of the CLA mixture (containing 35.4% $c9,t11$ and 35.9% $t10,c12$ CLA) and the purified $t10,c12$ CLA isomer. We extended these observations by measuring an inflammatory signature consisting of 27 different cytokines, chemokines, or growth factors in pooled plasma with an antibody array. Our array data, however, suggested slight changes in fasting plasma TNF-α concentrations, which increased in the $t10,c12$ CLA group and decreased in the $c9,t11$ CLA group.

Since these signatures were analyzed in pooled material, we cannot draw any conclusions based on statistical analysis. However, as already indicated, this array was intended to generate hypotheses on possible differential immune-modulating effects of the two CLA isomers, which will be discussed below.

When expression profiles of different cytokines, chemokines, and growth factors in pooled plasma samples were evaluated, we found that the $c9,t11$ and $t10,c12$ CLA isomers induced different protein expression profiles, whereas changes in the $c9,t11$ CLA group were more pronounced. It has indeed been suggested that the two CLA isomers have different effects on immune functions (4). Furthermore, in general, both isomers induced more increases in protein concentrations than decreases, which indicates an enhanced immune function. This observation was particularly apparent for the $c9,t11$ CLA isomer. When looking in more detail at the protein expression profiles, we observed that plasma concentrations of chemokines that attract granulocytes, which are important in the first phase of an acute inflammation caused by microorganisms (neutrophils) or parasites (eosinophils and basophils), were increased by mainly the $c9,t11$ CLA isomer. On the other hand, concentrations of chemokines more related to monocyte and lymphocyte migration were hardly affected and even tended to be lowered. Therefore, the expression profiles of both CLA isomers, and particularly that of $c9,t11$ CLA, suggested improved resistance against pathogens. Animal studies have indeed reported that CLA increased resistance to infections (4). Also in humans, 12 wk of consumption of 1.7 g/d of a 50:50 mixture of $c9,t11/t10,c12$ CLA isomers beneficially affected the initiation of a specific antibody response toward hepatitis B vaccination, indicating enhanced immune function (25). However, a similar approach to test the effects of consumption of 3.9 g/d of a CLA mixture for 9 wk on antibody response toward an influenza vaccine was not successful (34). The lack of effect in this study could be due to the wide range of CLA isomers in the mixture ($t10,c12$, 22.6%; $c11,t13$, 23.6%; $c9,t11$, 17.6%; $t8,c10$, 16.6%; other isomers 19.6%). The effects on growth factors and cytokines cannot easily be interpreted. Again, effects of the $c9,t11$ CLA on each of the detectable proteins were more pronounced. The concentrations of the colony-stimulating factor MCSF (also called CSF-1) and of interferon-γ, which both stimulate monocyte/macrophage cells, were increased. The cytokine IL-1α, which is produced by macrophages, was, however, decreased. The increase in IL-2 expression in the $c9,t11$ CLA group has also been reported in mice (4). Whether our findings are favorable or not is difficult to conclude. On one hand, the changes in the inflammation parameters could result in increased resistance against pathogens. On the other hand, increased plasma concentrations of inflammatory markers (e.g., MCP-1) may be related to increased cardiovascular risk, especially in a high CHD risk population (12–14).

The antibody array did suggest modest decreases in leptin concentrations in both CLA groups. Decreases in leptin levels were also shown in mice models and a similar tendency was seen in rats (35). In humans, effects on leptin are contradictory. Medina *et al.* (36) showed a significant decrease only after 7 wk, which returned to baseline after 9 wk of intervention with a CLA mixture. Two other studies showed no effects on leptin levels after 12 wk and after 1 yr (37,38).

Thus, there are no effects of a daily consumption of 3 g of the $c9,t11$ or $t10,c12$ CLA isomer on *ex vivo* LPS-stimulated cytokine production by PBMC and by whole blood in moderately overweight subjects with a high risk for CHD. Also, plasma CRP concentrations did not change. However, inflammatory signatures in nonstimulated fasting plasma raised the hypothesis that both CLA isomers enhanced immune function—in particular an increased resistance against pathogens—with more pronounced effects of the $c9,t11$ CLA isomer. These effects, however, should be confirmed in future studies for the individual cytokines, chemokines, and growth factors.

ACKNOWLEDGMENTS

REFERENCES

1. Pariza, M.W., and Ha, Y.L. (1990) Conjugated Dienoic Derivatives of Linoleic Acid: A New Class of Anticarcinogens, *Med. Oncol. Tumor Pharmacother. 7*, 169–171.
2. Pariza, M.W., and Ha, Y.L. (1990) Conjugated Dienoic Derivatives of Linoleic Acid: Mechanism of Anticarcinogenic Effect, *Prog. Clin. Biol. Res. 347*, 217–221.
3. Kelley, D.S., and Erickson, K.L. (2003) Modulation of Body Composition and Immune Cell Functions by Conjugated Linoleic Acid in Humans and Animal Models: Benefits vs. Risks, *Lipids 38*, 377–386.
4. O'Shea, M., Bassaganya-Riera, J., and Mohede, I.C. (2004) Immunomodulatory Properties of Conjugated Linoleic Acid, *Am. J. Clin. Nutr. 79*, 1199S–1206S.
5. Tricon, S., Burdge, G.C., Kew, S., Banerjee, T., Russell, J.J., Grimble, R.F., Williams, C.M., Calder, P.C., and Yaqoob, P. (2004) Effects of *cis*-9,*trans*-11 and *trans*-10,*cis*-12 Conjugated Linoleic Acid on Immune Cell Function in Healthy Humans, *Am. J. Clin. Nutr. 80*, 1626–1633.
6. Yudkin, J.S., Kumari, M., Humphries, S.E., and Mohamed-Ali, V. (2000) Inflammation, Obesity, Stress and Coronary Heart Disease: Is Interleukin-6 the Link? *Atherosclerosis 148*, 209–214.
7. Austin, M.A., Breslow, J.L., Hennekens, C.H., Buring, J.E., Willett, W.C., and Krauss, R.M. (1988) Low-density Lipoprotein Subclass Patterns and Risk of Myocardial Infarction, *JAMA 260*, 1917–1921.
8. Berneis, K.K., and Krauss, R.M. (2002) Metabolic Origins and Clinical Significance of LDL Heterogeneity, *J. Lipid Res. 43*, 1363–1379.
9. Krauss, R.M. (1995) Dense Low Density Lipoproteins and Coronary Artery Disease, *Am. J. Cardiol. 75*, 53B–57B.
10. Hansson, G.K. (2001) Immune Mechanisms in Atherosclerosis, *Arterioscler. Thromb. Vasc. Biol. 21*, 1876–1890.
11. Ross, R. (1999) Atherosclerosis—An Inflammatory Disease, *N. Engl. J. Med. 340*, 115–126.
12. Ridker, P.M., Rifai, N., Stampfer, M.J., and Hennekens, C.H.

(2000) Plasma Concentration of Interleukin-6 and the Risk of Future Myocardial Infarction Among Apparently Healthy Men, *Circulation 101*, 1767–1772.

13. Ridker, P.M., Hennekens, C.H., Buring, J.E., and Rifai, N. (2000) C-Reactive Protein and Other Markers of Inflammation in the Prediction of Cardiovascular Disease in Women, *N. Engl. J. Med. 342*, 836–843.

14. de Lemos, J.A., Morrow, D.A., Sabatine, M.S., Murphy, S.A., Gibson, C.M., Antman, E.M., McCabe, C.H., Cannon, C.P., and Braunwald, E. (2003) Association Between Plasma Levels of Monocyte Chemoattractant Protein-1 and Long-Term Clinical Outcomes in Patients with Acute Coronary Syndromes, *Circulation 107*, 690–695.

15. Malpuech-Brugere, C., Verboeket-Van De Venne, W.P., Mensink, R.P., Arnal, M.A., Morio, B., Brandolini, M., Saebo, A., Lassel, T.S., Chardigny, J.M., Sébédio, J.L., *et al.* (2004) Effects of Two Conjugated Linoleic Acid Isomers on Body Fat Mass in Overweight Humans, *Obes. Res. 12*, 591–598.

16. NEVO, S. (2001) NEVO Food Composition Table, The Netherlands Nutrient Databank 2001, The Hagne, NEVO Foundation.

17. Dentener, M.A., Bazil, V., Von Asmuth, E.J., Ceska, M., and Buurman, W.A. (1993) Involvement of CD14 in Lipopolysaccharide-Induced Tumor Necrosis Factor-Alpha, IL-6 and IL-8 Release by Human Monocytes and Alveolar Macrophages, *J. Immunol. 150*, 2885–2891.

18. Bouma, M.G., Stad, R.K., van den Wildenberg, F.A., and Buurman, W.A. (1994) Differential Regulatory Effects of Adenosine on Cytokine Release by Activated Human Monocytes, *J. Immunol. 153*, 4159–4168.

19. Engelberts, I., Moller, A., Schoen, G.J., van der Linden, C.J., and Buurman, W.A. (1991) Evaluation of Measurement of Human TNF in Plasma by ELISA, *Lymphokine Cytokine Res. 10*, 69–76.

20. Engelberts, I., Stephens, S., Francot, G.J., van der Linden, C.J., and Buurman, W.A. (1991) Evidence for Different Effects of Soluble TNF-Receptors on Various TNF Measurements in Human Biological Fluids, *Lancet 338*, 515–516.

21. Huddleston, D.J., Deitrick, C.L., Budrean, S.A., and Katholi, R.E. (2001) Performance Characteristics of an Automated Method for High-Sensitivity CRP on the Roche Cobas Mira Analyzer, *Journal of the Association for Laboratory Automation 6*, 32–33.

22. Plat, J., and Mensink, R.P. (2000) Vegetable Oil Based Versus Wood Based Stanol Ester Mixtures: Effects on Serum Lipids and Hemostatic Factors in Non-hypercholesterolemic Subjects, *Atherosclerosis 148*, 101–112.

23. Lins, R.L., Matthys, K.E., Billiouw, J.M., Dratwa, M., Dupont, P., Lameire, N.H., Peeters, P.C., Stolear, J.C., Tielemans, C., Maes, B., *et al.* (2004) Lipid and Apoprotein Changes During Atorvastatin Up-titration in Hemodialysis Patients with Hypercholesterolemia: A Placebo-Controlled Study, *Clin. Nephrol. 62*, 287–294.

24. Sébédio, J.L., Juaneda, P., Dobson, G., Ramilison, I., Martin, J.C., Chardigny, J.M., and Christie, W.W. (1997) Metabolites of Conjugated Isomers of Linoleic Acid (CLA) in the Rat, *Biochim. Biophys. Acta 1345*, 5–10.

25. Albers, R., van der Wielen, R.P., Brink, E.J., Hendriks, H.F., Dorovska-Taran, V.N., and Mohede, I.C. (2003) Effects of *cis*-9,*trans*-11 and *trans*-10,*cis*-12 Conjugated Linoleic Acid (CLA) isomers on Immune Function in Healthy Men, *Eur. J. Clin. Nutr. 57*, 595–603.

26. Kelley, D.S., Simon, V.A., Taylor, P.C., Rudolph, I.L., Benito, P., Nelson, G.J., Mackey, B.E., and Erickson, K.L. (2001) Dietary Supplementation with Conjugated Linoleic Acid Increased Its Concentration in Human Peripheral Blood Mononuclear Cells, but Did Not Alter Their Function, *Lipids 36*, 669–674.

27. Turek, J.J., Li, Y., Schoenlein, I.A., Allen, K.G.D., and Watkins, B.A. (1998) Modulation of Macrophage Cytokine Production by Conjugated Linoleic Acids Is Influenced by the Dietary n-6:n-3 Fatty Acid Ratio, *J. Nutr. Biochem. 9*, 258–266.

28. Kelley, D.S., Warren, J.M., Simon, V.A., Bartolini, G., Mackey, B.E., and Erickson, K.L. (2002) Similar Effects of *c*9,*t*11-CLA and *t*10,*c*12-CLA on Immune Cell Functions in Mice, *Lipids 37*, 725–728.

29. Burdge, G.C., Lupoli, B., Russell, J.J., Tricon, S., Kew, S., Banerjee, T., Shingfield, K.J., Beever, D.E., Grimble, R.F., Williams, C.M., *et al.* (2004) Incorporation of *cis*-9,*trans*-11 or *trans*-10,*cis*-12 Conjugated Linoleic Acid into Plasma and Cellular Lipids in Healthy Men, *J. Lipid Res. 45*, 736–741.

30. Thijssen, M.A., Malpuech-Brugere, C., Gregoire, S., Chardigny, J.M., Sebedio, J.L., and Mensink, R.P. (2005) Effects of Specific CLA isomers on Plasma Fatty Acid Profile and Expression of Desaturases in Humans, *Lipids 40*, 137–145.

31. Risérus, U., Basu, S., Jovinge, S., Fredrikson, G.N., Ärnlöv, J., and Vessby, B. (2002) Supplementation with Conjugated Linoleic Acid Causes Isomer-Dependent Oxidative Stress and Elevated C-Reactive Protein: A Potential Link to Fatty Acid-Induced Insulin Resistance, *Circulation 106*, 1925–1929.

32. Christiansen, T., Richelsen, B., and Bruun, J.M. (2005) Monocyte Chemoattractant Protein-1 Is Produced in Isolated Adipocytes, Associated with Adiposity and Reduced After Weight Loss in Morbid Obese Subjects, *Int. J. Obes. Relat. Metab. Disord. 29*, 146–150.

33. Bruun, J.M., Pedersen, S.B., and Richelsen, B. (2001) Regulation of Interleukin 8 Production and Gene Expression in Human Adipose Tissue *in vitro*, *J. Clin. Endocrinol. Metab. 86*, 1267–1273.

34. Kelley, D.S., Taylor, P.C., Rudolph, I.L., Benito, P., Nelson, G.J., Mackey, B.E., and Erickson, K.L. (2000) Dietary Conjugated Linoleic Acid Did Not Alter Immune Status in Young Healthy Women, *Lipids 35*, 1065–1071.

35. Terpstra, A.H. (2004) Effect of Conjugated Linoleic Acid on Body Composition and Plasma Lipids in Humans: An Overview of the Literature, *Am. J. Clin. Nutr. 79*, 352–361.

36. Medina, E.A., Horn, W.F., Keim, N.L., Havel, P.J., Benito, P., Kelley, D.S., Nelson, G.J., and Erickson, K.L. (2000) Conjugated Linoleic Acid Supplementation in Humans: Effects on Circulating Leptin Concentrations and Appetite, *Lipids 35*, 783–788.

37. Risérus, U., Arner, P., Brismar, K., and Vessby, B. (2002) Treatment with Dietary *trans*10*cis*12 Conjugated Linoleic Acid Causes Isomer-Specific Insulin Resistance in Obese Men with the Metabolic Syndrome, *Diabetes Care 25*, 1516–1521.

38. Gaullier, J.M., Halse, J., Hoye, K., Kristiansen, K., Fagertun, H., Vik, H., and Gudmundsen, O. (2004) Conjugated Linoleic Acid Supplementation for 1 y Reduces Body Fat Mass in Healthy Overweight Humans, *Am. J. Clin. Nutr. 79*, 1118–1125.

Dietary Sitostanol and Campestanol: Accumulation in the Blood of Humans with Sitosterolemia and Xanthomatosis and in Rat Tissues

William E. Connor[a],*, **Don S. Lin[a]**, **Anuradha S. Pappu[a]**,
Jiri Frohlich[b], and **Glenn Gerhard[a]**

[a]Division of Endocrinology, Diabetes and Clinical Nutrition, Department of Medicine,
Oregon Health & Science University, Portland, Oregon, and [b]Healthy Heart Program,
St. Paul's Hospital, The University of British Columbia, Vancouver, British Columbia, Canada

ABSTRACT: Dietary sitostanol has a hypocholesterolemic effect because it decreases the absorption of cholesterol. However, its effects on the sitostanol concentrations in the blood and tissues are relatively unknown, especially in patients with sitosterolemia and xanthomatosis. These patients hyperabsorb all sterols and fail to excrete ingested sitosterol and other plant sterols as normal people do. The goal of the present study was to examine the absorbability of dietary sitostanol in humans and animals and its potential long-term effect. Two patients with sitosterolemia were fed the margarine Benecol (McNeill Nutritionals, Ft. Washington, PA), which is enriched in sitostanol and campestanol, for 7–18 wk. Their plasma cholesterol levels decreased from 180 to 167 mg/dL and 153 to 113 mg/dL, respectively. Campesterol and sitosterol also decreased. However, their plasma sitostanol levels increased from 1.6 to 10.1 mg/dL and from 2.8 to 7.9 mg/dL, respectively. Plasma campestanol also increased. After Benecol withdrawal, the decline in plasma of both sitostanol and campestanol was very sluggish. In an animal study, two groups of rats were fed high-cholesterol diets with and without sitostanol for 4 wk. As expected, plasma and liver cholesterol levels decreased 18 and 53%, respectively. The sitostanol in plasma increased fourfold, and sitostanol increased threefold in skeletal muscle and twofold in heart muscle. Campestanol also increased significantly in both plasma and tissues. Our data indicate that dietary sitostanol and campestanol are absorbed by patients with sitosterolemia and xanthomatosis and also by rats. The absorbed plant stanols were deposited in rat tissues. Once absorbed by sitosterolemic patients, the prolonged retention of sitostanol and campestanol in plasma might increase their atherogenic potential.

Paper no. L9750 in *Lipids 40*, 919–923 (September 2005).

In the 1950s, Peterson demonstrated that plant sterols had a plasma cholesterol-lowering effect in chickens fed cholesterol (1). Further studies in other animals, and later in humans, documented that the decreased plasma cholesterol levels occurred because of decreased cholesterol absorption (2,3). Sitosterol, the most common plant sterol, was later marketed as a choles-terol-lowering drug, but its effect was mild and it fell into disuse. Excellent reviews of this subject are found in Kritchevsky and others (2,3).

Recently, there has been interest in both sitosterol when esterified and a saturated sterol derived from sitosterol, sitostanol. Like sitosterol, sitostanol interferes with cholesterol absorption (4–6). When consumed in margarine, sitostanol produced, on average, a 10% reduction of plasma cholesterol and a 12% LDL cholesterol-lowering effect (7). Sitostanol may be helpful in the therapy of hypercholesterolemic patients and in sitosterolemia in which hyperabsorption of all sterols occurs (8,9).

Sitosterolemia with xanthomatosis was first described in 1974 by Bhattacharyya and Connor (10). High levels of plant sterols were found in the patients' blood and tissues. The cause was twofold: (i) hyperabsorption of all sterols, including the usually poorly absorbed plant sterols, and (ii) poor excretion of sterols by the liver (10–13). The major clinical manifestations included tendon xanthomas of the extensor tendons, and tuberous xanthomas of the skin of the elbows and knees, premature atherosclerosis and coronary heart disease (11–14). Recent studies indicated that this Niemann-Pick C1 like 1 (NPC1L1) gene is critical for cholesterol absorption (15) and also suggested that this disorder is caused by mutations in either of two genes that encode the ATP binding cassette (ABC) half transporters, ABCG5 and ABCG8 (16,17).

In 1995, Lutjohann *et al.* (4) treated two sitosterolemic patients with sitostanol for 4 wk. They observed decreased plasma cholesterol and sitosterol levels in these patients. These authors reported that sitostanol was not absorbed to a significant degree in patients with sitosterolemia. They therefore concluded that oral administration of sitostanol was a new approach for the treatment of these patients. However, after feeding 2063 mg a day of a plant sterol mixture as a spread for 10–12 weeks to heterozygotes for sitosterolemia, Kwiterovich *et al.* (18) recently found significant increases in both campesterol and sitosterol levels in the plasma of these relatives. No sitostanol was fed. The authors discussed their concern about implications for development of coronary heart disease when plasma plant sterol levels were elevated.

In the present study, we examined the changes of plasma sitostanol and campestanol of two patients with sitosterolemia

---

and xanthomatosis after consuming a diet rich in sitostanol and campestanol. In a parallel study, we determined the effects of dietary sitostanol and campestanol on the levels of these stanols in both blood and tissues of a rat model.

METHODS

Human study. (i) Description of patients. The first patient was a 70-yr-old Japanese–Canadian woman with sitosterolemia and xanthomatosis, diagnosed in 1994. She weighed 44 kg and was 1.5 m in height. Her plasma cholesterol was 180 mg/dL, and her plasma plant sterol/stanol levels totaled 25.2 mg/dL (12% of the total sterol/stanol levels). The second patient was a 14-yr-old Hispanic girl diagnosed with sitosterolemia in 1994 at the age of five. She weighed 34 kg and was 1.46 m in height. Her plasma cholesterol level was 153 mg/dL, and her plasma total plant sterol/stanol levels were 36.5 mg/dL (19% of the total sterol/stanol levels).

(ii) Diet and Benecol margarine supplement. Throughout the study period, patients were instructed to maintain a sterol-free diet. Counseling with General Clinical Research Centers (GCRC) dietitians and obtaining special sterol-free diet recipes designed by the GCRC dietitians achieved this. Each patient was given three packages of Benecol margarine (McNeill Nutritionals, Ft. Washington, PA) a day. Benecol margarine contained mainly stanols (campestanol and sitostanol). Each package of Benecol contained 744 mg sitostanol, 281 mg campestanol, and 14 mg sitosterol. The dietitians recorded the actual consumption.

On average, patient #1 consumed 2.7 packets of Benecol margarine per day, containing a total of 2009 mg/d of sitostanol, for 7 wk. Blood samples were collected at baseline and at 7 wk during the Benecol supplement, and 12 wk after Benecol was withdrawn from the diet.

Patient #2 consumed 2.3 packages of Benecol margarine per day (1713 mg/d sitostanol) for 18 wk. Blood samples were taken at baseline and at 3 and 10 wk during Benecol feeding. Because of logistic difficulty, the 18-wk sample was not obtained. Blood was analyzed 43 wk after Benecol was withdrawn from the diet.

The design of the rat study of dietary sitostanol and campestanol. Eighteen young male Wistar rats (weight 130–150 g) were divided into two groups. The experimental group was fed

standard rat chow containing 5% lard, 0.5% cholesterol, and 0.5% stanols (sitostanol/campestanol comparable to Benecol provided by B.C. Chemicals, Vancouver, Canada). The control group was fed the same diet without stanols. The sterol composition of the control and experimental diet is presented in Table 1. After consuming the respective diets for 4 wk, these rats were killed; and the plasma, liver, heart, and skeletal muscle were collected for analysis.

Biochemical analyses. The sterols and stanols of plasma were analyzed by a method reported previously (19). Plasma samples were saponified with alcoholic KOH, and the sterols were extracted with hexane. Trimethylsilyl ether derivatives of these sterols were subjected to analysis by a gas–liquid chromatograph equipped with a hydrogen FID (Model 8500; PerkinElmer, Norwalk, CT) and containing a nonpolar 30-m SE-30 capillary column (Alltech, Deerfield, IL) with 0.25-mm i.d. and 0.25-µm film thicknesses. Cholestane was used as the internal standard. The temperatures of column, detector, and injection port were 240, 280, and 280°C, respectively. Helium was used as the carrier gas. The relative retention time (related to cholestane) was 2.07 for cholesterol, 2.65 for campesterol, 2.86 for stigmasterol, 3.28 for sitosterol, and 3.39 for sitostanol.

The lipids of the Benecol margarine supplement and rat tissues were extracted by the method of Folch, Lees, and Sloane Stanley (20). The lipid extracts were saponified with alcoholic KOH. The recovered sterols and stanols were analyzed by the GLC system just described. To avoid blood contamination, tissues were washed three times with saline and blotted dry before lipid extractions..

Statistical analysis. Statistical analysis was performed using the SPSS statistical software package 10 (SPSS, Chicago, IL) (21). All results were expressed as a mean ± SD.

RESULTS

Human studies in the sitosterolemic patients. After consuming Benecol in the diet, there were uniform decreases in plasma sterols and increases in the plasma stanols of these patients (Table 2, Fig. 1). After 7 wk of Benecol feeding, the plasma cholesterol level in patient #1 decreased from 180 to 167 mg/dL and rebounded to 179 mg/dL 12 wk after Benecol was withdrawn from the diet. The plasma campesterol level decreased from 8.4 mg/dL at baseline to 6.0 mg/dL after 7 wk of Benecol feeding, and it did not change at 12 wk after the subsequent Benecol-free diet. Sitosterol decreased from 14.7 mg/dL at baseline to 10.1 mg/dL at 7 wk and increased slightly after withdrawing Benecol from the diet. In contrast, the plasma campestanol level of this patient increased from 0.5 to 5.2 mg/dL at 7 wk and had only decreased to 3.6 mg/dL after 12 wk of the Benecol-free diet (Fig. 1). Sitostanol increased from 1.6 mg/dL at baseline to 10.1 mg/dL at 7 wk and only dropped to 6.2 mg/dL after 12 wk on the Benecol-free diet.

Similar results occurred in patient #2 (Table 2, Fig. 1). Her plasma cholesterol decreased from 153 mg/dL at baseline to 146 mg/dL at 3 wk and to 113 mg/dL at 10 wk after Benecol feeding. The cholesterol level returned to 137 mg/dL after

TABLE 1
Sterol and Stanol Content of the Control and Experimental Diets in Rat Studies (mg/kg chow)

Sterols	Control	Experimental
Cholesterol	5,280	5,278
Campesterol	38	38
Stigmasterol	16	16
Sitosterol	178	177
Campestanol	6	1,006
Sitostanol	27	4,027
Total	5,545	10,542

TABLE 2
Changes of Plasma Sterols and Stanols of Sitosterolemic Patients Before, During, and After the Administration of Benecol Margarine

	Plasma sterols and stanols (mg/dL)						
	Patient 1			Patient 2			
	Baseline	Benecol (+)	Benecol (−)	Baseline	Benecol (+)		Benecol (−)
Sterols and stanols		7^a	12^b		3^a	10^a	43^b
Cholesterol	180	167	179	153	146	113	137
Campesterol	8.4	6.0	6.0	12.4	6.2	7.9	9.2
Stigmasterol	—	—	—	0.6	—	—	0.9
Sitosterol	14.7	10.1	11.6	20.1	17.2	16.3	17.0
Campestanol	0.5	5.2	3.6	0.6	0.7	2.0	2.0
Sitostanol	1.6	10.1	6.2	2.8	3.7	7.9	5.6
Total sterols plus stanols	205	198	206	190	174	147	172

[a]Weeks after Benecol feeding.
[b]Weeks after withdrawing Benecol.

Benecol was removed from her diet for 43 wk. Campesterol dropped from 12.4 to 6.2 mg/dL at 3 wk and was 7.9 mg/dL at 10 wk. It increased to 9.2 mg/dL after the Benecol-free diet. Plasma sitosterol decreased from 20.1 mg/dL at baseline to 17.2 mg/dL at 3 wk and 16.3 mg/dL at 10 wk. It remained at 17 mg/dL without Benecol in the diet. Opposite changes were seen in the plasma stanols (Fig. 1). The plasma campestanol increased from 0.6 mg/dL at baseline to 0.7 mg/dL at 3 wk and 2.0 mg/dL at 10 wk. After withdrawing Benecol from the diet for 43 wk, its level remained at 2.0 mg/dL. The plasma sitostanol rose from 2.8 to 3.7 mg/dL at 3 wk and 7.9 mg/dL at 10 wk. Plasma sitostanol remained high at 5.6 mg/dL after the patient had consumed a Benecol-free diet for 43 wk.

The effects of dietary sitostanol and campestanol in the rat. Dietary sitostanol and campestanol significantly increased the plasma stanols in the rats consuming the diet containing stanols (Table 3, Fig. 2). The plasma sitostanol increased from 0.05 to 0.2 mg/dL. Campestanol increased from zero to 0.3 mg/dL. These stanols were subsequently deposited into various tissues (Table 3, Fig. 2). In the liver, campestanol increased from zero to 19.0 µg/g while the sitostanol concentration remained the same. In skeletal muscle, campestanol increased from 1.1 to 3.7 µg/g and sitostanol increased from 2.6 to 8.4 µg/g. In heart muscle, campestanol increased from 8.7 to 18.1 µg/g and sitostanol increased from 6.0 to 14.6 µg/g. Thus, these two stanols not only were absorbed but also were deposited in the tissues.

DISCUSSION

It was not too surprising that dietary sitostanol decreased plasma cholesterol levels in both the sitosterolemic patients and the animals. Several studies had already demonstrated that dietary sitostanol decreases plasma cholesterol by reducing cholesterol absorption in normal subjects as well as in sitosterolemic patients (4–6). It was, however, unexpected to find the sharp increases of plasma stanols after Benecol feeding because we had assumed that these dietary stanols would not be absorbed. For our two patients, who consumed 2009 and 1713

mg of sitostanol per day for 7 and 10 wk, their plasma sitostanol level increased 531 and 182%, respectively. These results are quite different from the results of Lutjohann *et al.* (4). They fed 1500 mg sitostanol per day to two sitosterolemic patients for 4 wk. They observed decreased plasma cholesterol levels and reduced cholesterol absorption, with little to no change in plasma stanol concentrations. Because the recovery of deuterated sitostanol was similar to that of Cr_2O_3, a nonabsorbable marker, these authors concluded that sitostanol was not absorbed to a significant degree in patients with sitosterolemia. The reason for these divergent results may be that the sitostanol in gelatin capsules was poorly absorbed in contrast to our study in which the sitostanol was incorporated in a margarine as a sitostanol ester and given with other foods. Micellar formation of sterols is enhanced by the concurrent presence of dietary fat. Further, in contrast to only 4 wk of sitostanol feeding, we fed Benecol to our patients for 7 and 10 wk, respectively.
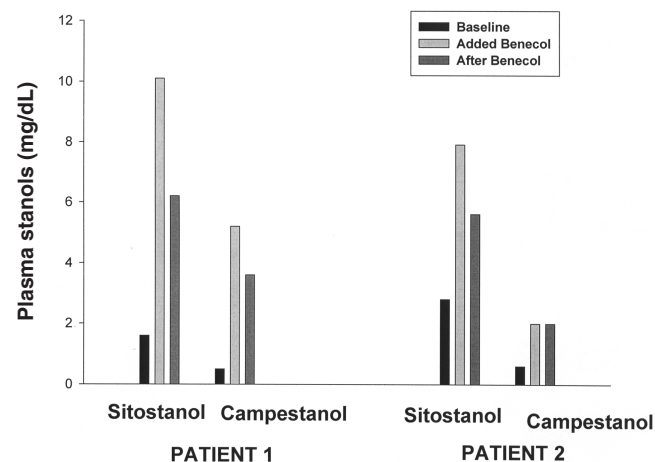
FIG. 1. The changes of plasma campestanol and sitostanol of two sitosterolemic patients consuming diets with and without Benecol (patient #1 after 7 wk Benecol and 12 wk after its withdrawal; patient #2 after 10 wk Benecol and 43 wk after its withdrawal).

TABLE 3
Effects of Dietary Sitostanol/Campestanol on the Sterol and Stanol Composition of Plasma (mg/dL plasma) and Tissues (mg/g dried wt) in Control (n = 9) and Experimental Rats (n = 9)

Sterols and Stanols	Plasma		Liver		Skeletal muscle		Heart muscle	
	Control	Expl.[a]	Control	Expl.[a]	Control	Expl.[a]	Control	Expl.[a]
Cholesterol	98.6‡ ± 7.1	80.7± 5.2	16,109 ± 3,154	7,579[+] ± 1,944	948 ± 359	891 ± 513	2,407 ± 1,043	2,781 ± 1,035
Campesterol	0.8 ± 0.2	0.5*** ± 0.1	91 ± 25	37[+] ± 16	6.1 ± 2.4	5.9 ± 2.8	22.0 ± 9.4	19.4 ± 8.0
Stigmasterol	0.1 ± 0.05	0.03*** ± 0.02	35 ± 17	13*** ± 9	2.4 ± 1.3	5.5 ± 5.4	15.1 ± 10.4	10.9 ± 7.2
Sitosterol	0.6 ± 0.01	0.4*** ± 0.08	37 ± 17	24 ± 14	8.0 ± 4.0	21.3* ± 18.4	24.7 ± 12.1	30.8 ± 12.1
Campestanol	—[b]	0.3[+] ± 0.07	—[b]	19 ± 6.6	1.1 ± 0.05	3.7* ± 3.3	8.7 ± 2.2	18.1*** ± 7.7
Sitostanol	0.05 ± 0.02	0.2[+] ± 0.06	7.3 ± 4.1	8.7 ± 5.6	2.6 ± 1.7	8.4* ± 7.7	6.0 ± 3.5	14.6* ± 9.2

[a]Experimental vs. control group: *$P < 0.05$; **$P < 0.01$; ***$P < 0.005$; [+]$P < 0.001$; ‡ mean ± SD.
[b]Not detectable.

In the rat study, the feeding of the stanol mixture (comparable to Benecol) for 4 wk resulted in significant increases in the concentrations of plasma campestanol and sitostanol, a result similar to the increased plasma stanols observed in our two sitosterolemic patients. Concurrently, there was a significant increase of these two stanols in the liver, skeletal muscle, and heart muscle of these rats. Based on these observations, we hypothesize that the increase of stanols in the plasma after sitostanol feeding probably would result in higher tissue stanol content in these sitosterolemic patients. Incidentally, previous studies showed that plasma sterols were deposited in all the tissues in these patients (except brain) in the same proportion as theywere present in plasma (10,11).

Sitosterolemic patients may have normal plasma cholesterol levels and elevated plasma plant sterols, although their plasma total sterols levels are usually much lower than in hypercholesterolemic patients. Yet, premature atherosclerosis with death has been observed in these patients (11–13). Thus, dietary sitosterol is pathologic in the patients with sitosterolemia (12). Dietary sitosterol might even be more atherogenic than dietary cholesterol. In a cross-sectional study, Glueck and coworkers (22) reported such modestly elevated levels of plant sterols in probands and relatives from families with premature coronary heart disease. Sitostanol may be similar to sitosterol in this aspect. Recently, we found that sitosterol and sitostanol were much less esterified by the ACAT enzyme than was cholesterol (Connor, W.E., and Lin, D.S., unpublished data). This may result in more of the free form of these sterols in the tissues. Free sterols are more toxic than esterified sterols (23). Furthermore, in the current study, the turnover of plasma sitostanol was very sluggish (Fig. 1). It has already been documented that the turnover of sitosterol in these patients was very slow (12,24). Therefore, the increased plasma stanols from sitostanol and campestanol feeding to these patients could result in undesirable consequences. It is noteworthy that in a recent report, ezetimibe, a compound known to reduce cholesterol absorption, reduced both plasma cholesterol and plant sterols (25).

Our data indicate that the rat is capable of absorbing stanols from the diet and develops increased sitostanol and campestanol levels in both plasma and tissues after sitostanol feeding. As rats and humans absorb dietary cholesterol similarly (26,27), the rat seems a good model for sterol metabolism in the human intestinal tract.

Sitostanol and campestanol have been incorporated into a margarine, Benecol, which is recommended to the public for daily use to decrease plasma cholesterol levels. From our study, sitostanol and campestanol are absorbed by rats and by humans as well. The consequences of long-term daily consumption of Benecol and the possible accumulation of these stanols in the tissues should be considered. Similar considerations would apply to the use of another margarine, Take Control (Lipton, Englewood Cliffs, NJ), which contains a sitosterol ester. Clearly, neither of these margarines would be recommended for sitosterolemic patients. However, even their use in other patients would present the human intestinal tract with enormous quantities of plant sterols and stanols, up to 10 times or more the usual intake of plant sterols in the United States (28).

Thus, margarines containing sitostanol (Benecol) or sitosterol itself (Take Control) could be hazardous to patients with sitosterolemia and xanthomatosis, and we recommend that they be strictly avoided just as other margarines and liquid vegetable oils containing other plant sterols should be. Medium-chain TG oil would be an exception since it is virtually sterol-free (29). Furthermore, the balance of benefit and possible drawbacks of the long-term feeding of pharmacological amounts of sitostanol and sitosterol in the human diet needs to be evaluated.
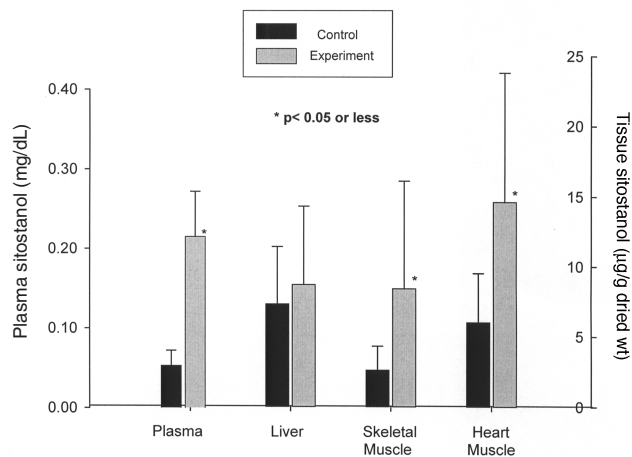
FIG. 2. Sitostanol content in plasma and tissues of control and experimental rats (n = 9 each).

ACKNOWLEDGMENTS

REFERENCES

1. Peterson, D.N. (1951) Effects of Soybean Sterols in the Diet on Plasma and Liver Cholesterol in Chicks, *Proc. Soc. Exp. Biol. Med. 78*, 143–147.
2. Pollak, O.J., and Kritchevsky, D. (1981) Sitosterol, in *Monographs on Atherosclerosis* (Clarkson, T.B., Kritchevsky, D., and Pollak, O.J., eds.) Vol. 10, S. Karger, Basal.
3. Lees, A.M., Mok, H.Y., Lees, R.S., McCluskey, M.A., and Grundy, S.M. (1977) Plant Sterols As Cholesterol-Lowering Agents: Clinical Trials in Patients with Hypercholesterolemia and Studies of Sterol Balance, *Atherosclerosis 28*, 325–338.
4. Lutjohann, D., Bjorkhem, I., Beil, U.F., and von Bergmann, K. (1995) Sterol Absorption and Sterol Balance in Phytosterolemia Evaluated by Deuterium-Labeled Sterols: Effect of Sitostanol Treatment, *J. Lipid Res. 36*, 1763–1773.
5. Vanhaven, H.T., Kajander, J., Lehtovirta, H., and Miettinen, T.A. (1994) Serum Levels, Absorption Efficiency, Fecal Elimination and Synthesis of Cholesterol During Increasing Doses of Dietary Sitostanol Esters in Hypercholesterolemic Subjects, *Clin. Sci. 87*, 61–67.
6. Heinemann, I.G., Kullak-Ublick, A., Pietruck, B., and von Bergmann, K. (1991) Mechanisms of Action of Plant Sterols on Inhibition of Cholesterol Absorption, *Eur. J. Clin. Pharmacol. 40* (*Suppl. 1*), 559–563.
7. Miettinen, T.A., Puska, P., Gylling, H., Vanhanen, H., and Vartiainen, E. (1995) Reduction of Serum Cholesterol with Sitostanol Ester Margarine in a Mildly Hypercholesterolemic Population, *N. Engl. J. Med. 333*, 1308–1312.
8. Becker, M., Staab, D., and Von Bergmann, K. (1993) Treatment of Severe Familial Hypercholesterolemia in Children with Sitosterol and Sitostanol, *J. Pediatr. 122*, 292–296.
9. Jones, P.J., Rasini-Sarjaz, M., Ntarios, F.Y., Vanstone, C.A., Feng, J.G., and Parsons, W.E. (2000) Modulation of Plasma Lipid Levels and Cholesterol Kinetics by Phytosterol Versus Phytostanol Esters, *J. Lipid Res. 41*, 697–705.
10. Bhattacharyya, A.K., and Connor, W.E. (1974) Sitosterolemia and Xanthomatosis: A Newly Described Lipid Disease in Two Sisters, *J. Clin. Invest. 53*, 1033–1043.
11. Salen, G., Horak, I., Rothkopf, M., Cohen, J.L., Speck, J., Tint, G.S., Shore, V., Dayal, B., Chen, T., and Shefer, S. (1985) Lethal Atherosclerosis Associated with Abnormal Plasma and Tissue Sterol Composition in Sitosterolemia with Xanthomatosis, *J. Lipid Res. 26*, 1126–1132.
12. Miettinen, T.A. (1980) Phytositosterolemia, Xanthomatosis and Pre Mature Atherosclerotic Arterial Disease, a Case with High Plant Sterol Absorption, Impaired Sterol Elimination and Low Cholesterol Synthesis, *Eur. J. Clin. Invest. 10*, 27–35.
13. Salen, G., Kwiterovich, P.O., Jr., Shefer, S., Tint, G.S., Horak, I., Shore, V., Dayal, B., and Horak, E. (1985) Increased Plasma Cholestanol and 5 Alpha-Saturated Plant Sterol Derivatives in Subjects with Sitosterolemia and Xanthomatosis, *J. Lipid Res. 26*, 203–209.
14. Wang, E., Lin, H.J., Chan, T.K., Salen, G., Chan, W.C., and Tse, T.F. (1981) A Unique Patient with Coexisting Cerebrotendinous Xanthomatosis and β-Sitosterolemia, *Am. J. Med. 71*, 313–319.
15. Altmann, S.W., Davis, H.R., Jr., Zhu, L.J., Yao, X., Hoos, L.M., Tetzloff, G., Iyer, S.P., Maguire, M., Golovko, A., Zeng, M., *et al*. (2004) Niemann-Pick C1 Like 1 Protein Is Critical for Intestinal Cholesterol Absorption, *Science 303*, 1201–1202.
16. Berge, K.E., Tian, H., Graf, G.A., Yu, L., Grishin, N.V., Schultz, J., Kwiterovich, P., Shan, B., Barnes, R., and Hobbs, H.H. (2000) Accumulation of Dietary Cholesterol in Sitosterolemia Caused by Mutations in Adjacent ABC Transporters, *Science 290*, 1771–1775.
17. Lee, M.H., Lu, K., Hazard, S., Yu, H., Shulenin, S., Hidaka, H., Kojima, H., Allikmets, R., Sakuma, N., Sakuma, N., *et al*. (2001) Identification of a Gene, ABCG5, Important in the Regulation of Dietary Cholesterol Absorption, *Nat. Genet. 27*, 79–83.
18. Kwiterovich, P.O., Chen, S.C., Virgil, D.G., Schweitzer, A., Arnold, D.R., and Kratz, L.E. (2003) Response of Obligate Heterozygotes for Phytosterolemia to a Low-Fat Diet and to a Plant Sterol Ester Dietary Challenge, *J. Lipid Res. 44*, 1143–1155.
19. Connor, W.E., Lin, D.S., Wolf, D.P., and Alexander, M. (1998) Unique Distribution of Desmosterol and Docosahexaenoic Acid in the Heads and Tails of Monkey Sperm, *J. Lipid Res. 39*, 1404–1411.
20. Folch, J., Lees, M.B., and Sloane Stanley, G.H. (1957) Method for the Isolation and Purification of Total Lipids from Animal Tissues, *J. Biol. Chem. 226*, 497–509.
21. *SPSS Statistical Version 10.* SPSS Inc., Chicago,.
22. Glueck, C.T., Speirs, J., Streicher, P., Illig, E., and Vandegroft, J. (1991) Relationships of Serum Plant Sterols (phytosterols) and Cholesterol in 595 Hypercholesterolemic Subjects and Familial Aggregation of Phytosterols, Cholesterol and Premature Coronary Heart Decrease in Hypercholesterolemic Probands and Their First Degree Relatives, *Metabolism 40*, 842–848.
23. Small, D.M., and Shipley, G.G. (1974) Physical-chemical Basis of Lipid Deposition in Atherosclerosis. The Physical State of the Lipids Helps to Explain Lipid Deposition and Lesion Reversal in Atherosclerosis, *Science 185*, 222–229.
24. Bhattacharyya, A.K., Connor, W.E., Lin, D.S., McMurry, M.M., and Shulman, R.S. (1991) Sluggish Sitosterol Turnover and Hepatic Failure to Excrete Sitosterol into Bile Cause Expansion of Body Pool of Sitosterol in Patients with Sitosterolemia and Xanthomatosis, *Arterioscler. Thromb. 11*, 1287–1294.
25. Salen, G., von Bergmann, K., Lutjohann, D., Kwiterovich, P., Kane, J., Patel, S.B., Musliner, T., Stein, P., Musser, B., and Multicenter Sitosterolemia Study Group (2004) Ezetimibe Effectively Reduces Plasma Plant Sterols in Patients with Sitosterolemia, *Circulation 109*, 966–971.
26. Borgström, B. (1968) Quantitative Aspects of the Intestinal Absorption and Metabolism of Cholesterol and β-Sitosterol in the Rat, *J. Lipid Res. 9*, 473–481.
27. Connor, W.E., and Lin, D.S. (1974) The Intestinal Absorption of Dietary Cholesterol by Hypercholesterolemic (Type II) and Normocholesterolemic Humans, *J. Clin. Invest. 53*, 1062–1070.
28. Connor, W.E., Dietary Sterols: Their Relationship to Atherosclerosis, (1968) *J. Am. Diet. Assoc. 52*, 202–208.
29. Bhattacharyya, A.K., and Connor, W.E. (1997) Familial Diseases with Storage of Sterols Other Than Cholesterol, Cerebrotendinous Xanthomatosis, Sitosterolemia and Xanthomatosis, in *The Metabolic Basis of Inherited Disease* (Standbury, J.B., Wyngaarden, J.D., and Fredrickson, D.S., eds.), 4th edn., pp. 656–669, McGraw-Hill, New York.

Dietary Fish Oil Dose–Response Effects on Ileal Phospholipid Fatty Acids and Contractility

Glen S. Patten*, Michael J. Adams, Julie A. Dallimore, and Mahinda Y. Abeywardena

CSIRO Human Nutrition, Adelaide, South Australia 5000, Australia

ABSTRACT: We have reported that dietary fish oil (FO) leads to the incorporation of long-chain n-3 PUFA into the gut tissue of small animal models, affecting contractility, particularly of rat ileum. This study examined the FO dose response for the incorporation of n-3 PUFA into ileal tissue and how this correlated with *in vitro* contractility. Groups of ten to twelve 13-wk-old Wistar-Kyoto rats were fed 0, 1, 2.5, and 5% FO-supplemented diets balanced with sunflower seed oil for 4 wk, after which ileal total phospholipid FA were determined and *in vitro* contractility assessed. For the total phospholipid fraction, increasing the dietary FO levels led to a significant increase first evident at 1% FO, with a stepwise, nonsaturating six-fold increase in n-3 PUFA as EPA (20:5n-3), DPA (docosapentaenoic acid, 22:5n-3), and DHA, but mainly as DHA (22:6n-3), replacing the n-6 PUFA linoleic acid (18:2n-6) and arachidonic acid (20:4n-6) over the dosage range. There was no difference in KCl-induced depolarization-driven contractility. However, a significant increase in receptor-dependent maximal contractility occurred at 1% FO for carbachol and at 2.5% FO for prostaglandin E_2, with a concomitant increase in sensitivity for prostaglandin E_2 at 2.5 and 5% FO. These results demonstrate that significant increases in ileal membrane n-3 PUFA occurred at relatively low doses of dietary FO, with differential receptor-dependent increases in contractility observed for muscarinic and prostanoid agonists.

Paper no. L9760 in *Lipids 40*, 925–929 (September 2005).

Recent studies in our laboratory have revealed that dietary fish oil (FO) rich in n-3 PUFA as EPA (20:5n-3) and DHA (22:6n-3) can modulate gut contractility in isolated tissue from small animal models (1,2). In healthy Sprague-Dawley (SD) rats fed FO, there was an increase in the maximal contraction of ileum to muscarinic and eicosanoid agonists that was not evident for colon (2). Further studies with spontaneously hypertensive rats (SHR) demonstrated diminished ileal and colonic responses to prostaglandins (PG) E_2 and $F_{2\alpha}$ (3) that were restored in ileum, but not colon, with 5% FO feeding (4). This PG-induced increase in ileal contractility was not evident for α-linolenic acid-rich (18:3n-3) canola oil (4). For SHR, FO feeding also led to a significant increase in acetylcholine-driven maximal contraction in colonic tissue that was not manifest in normotensive SD rats (2). These changes in functionality for SHR were corre-

lated with an increase in ileal tissue total phospholipid FA with DHA as the active agent, but not EPA (4).

It is yet to be established at what lower dosage the dietary n-3 PUFA from FO can affect gut contractility. To date, relatively high concentrations of 5–10% dietary FO have been used in our laboratory (2,4) for periods of between 4 and 12 wk. This resulted in increased total phospholipid n-3 PUFA incorporation into gut tissue that was dependent on the ratio of EPA to DHA in the FO (2,4). A recently published time and dose study has demonstrated that erythrocyte and cardiac membrane n-3 PUFA concentrations derived from dietary FO were maximal at 4 wk (5), with significant increases in tissue total phospholipid n-3 PUFA evident at 1.25% dietary FO. Until recently, little attention has been paid to the role of dietary FO in gut membrane FA profiles and how this may relate to the physiology of contraction (2,4). Therefore, the aims of this study were to evaluate a dosage range for dietary FO rich in DHA fed to Wistar-Kyoto (WKY) rats for 4 wk on ileal n-3 PUFA levels and to assess how this correlated with nonreceptor- and receptor-induced ileal contractility.

MATERIALS AND METHODS

Animals and diets. Male WKY rats were purchased from the Animal Resource Centre (Canning Vale, Western Australia, Australia) at 12 wk of age and housed in the small animal colony of CSIRO Human Nutrition. The rats were fed a standard commercial laboratory rat chow containing approximately 5% fat with a low n-3 PUFA content (Glen Forrest Stockfeeders, Glen Forrest, Western Australia, Australia) and water *ad libitum* for 1 wk to acclimatize them. They were subjected to a 12-h light/dark cycle at 23°C. The rats were housed and the experiment conducted with the approval of the CSIRO Human Nutrition animal ethics committee.

At 13 wk of age, the rats were separated into 4 dietary groups of 10–12, housed 3–5 per cage, and fed synthetic diets *ad libitum* for 4 wk. To avoid oxidation, diets were stored at −20°C and changed daily. The isoenergetic semipurified diets were based on the AIN-93M diet (6) and contained (g/kg): casein, 180; mineral mix, 35; vitamin mix, 10; α-cellulose, 50; cornstarch, 580.7; L-cysteine, 1.8; choline chloride, 2.5; and sucrose, 90. In addition, the diets contained 0, 1, 2.5, and 5% FO high in DHA (0, 10, 25, and 50 g/kg) at 41% n-3 PUFA with a DHA/EPA ratio of 30.3:8.4 by GLC analysis (HiDHA®; Clover Corporation Ltd., Altona North, Victoria, Australia),

*To whom correspondence should be addressed at CSIRO Human Nutrition, P.O. Box 10041, Adelaide BC, 5000, Australia. E-mail: glen.patten@csiro.au
Abbreviations: DPA, docosapentaenoic acid; FO, fish oil; PG, prostaglandin; SD, Sprague-Dawley; SHR, spontaneously hypertensive rat; WKY, Wistar-Kyoto.

balanced with 5, 4, 2.5, and 0% sunflower seed oil (50, 40, 25, and 0 g/kg) rich in linoleic acid (18:2n-6) (61%) (Goodman Fielder Pty. Ltd., North Ryde, Sydney, New South Wales, Australia). The FA compositions of the diets are shown in Table 1.

Diet FA content. Increasing the FO content of the synthetic diets from 0 to 5% progressively increased the content of n-3 PUFA as EPA, docosapentaenoic acid (DPA), and DHA, but mainly as DHA (Table 1). At 5% FO in the diet, the total n-3 PUFA content of the diet FA pool was 28%. There was also a concomitant increase in saturated fat from the FO with a decrease in PUFA mainly as linoleic acid (18:2n-6), with minimal change in the level of monounsaturated FA (Table 1).

Tissue collection. At the completion of the 4-wk feeding experiment, the rats were anesthetized with Nembutal (sodium pentobarbitone, 60 mg/kg intraperitoneal) and killed by exsanguination. The small intestine was removed and prepared for physiological recordings as described previously (1,2,4,7). Tissue samples of distal ileum were snap-frozen in liquid nitrogen at −80°C for later tissue total phospholipid FA analysis.

Total phospholipid FA analysis of tissue. Small frozen sections (150 mg) of ileal tissue were ground in a glass homogenizer, the total lipids were extracted in methanol/chloroform/water (2:4:1) and separated by TLC, and the FA were methylated and analyzed by GLC as described previously (1,2).

Physiological recording of ileal contractility. Sections of the distal ileum (approximately 4 cm) were secured by suture cotton, at the proximal end of the tissue, to a small plastic plug connected to a glass plug *via* a plastic sleeve at the bottom of a water-jacketed glass chamber. The distal end of the tissue was connected to the free end of a 15-cm arm of an isotonic transducer (catalog #60–3001; Harvard Bio-science, South Nattick, MA) by a short length of suture cotton. The transducer was sustaining 0.5 g of tension at the other end. A 15° rotation of the torsion arm was equivalent to 2 V. Results are given as volts per gram of ileal tissue (V/g). The buffer conditions and con-

traction properties were determined as described previously (1–4,7). Initially, tissue was elicited to contract receptor-independently by KCl-induced depolarization stepwise at 10, 20, and finally 30 mmol/L, which gave the maximal contraction in this system, and was then washed out. After 15 min to stabilize, the tissue was contracted sequentially by the receptor-dependent agonists carbachol and PGE_2. Dose–response curves were generated by the cumulative addition of the agents added as a small bolus to the incubating tissue (2–4). The weights of the ileal tissue for the 0, 1, 2.5, and 5% FO treatments (g ± SEM) used in the organ chambers were 0.138 ± 0.003, 0.139 ± 0.002, 0.144 ± 0.004, and 0.148 ± 0.005, respectively, and they were not significantly different.

Pharmacologic agents and suppliers. Carbamylcholine chloride (carbachol) and fine chemicals, including KCl, were from Sigma Chemical (Sydney, New South Wales, Australia). PGE_2 was from Sapphire Bioscience (Crows Nest, New South Wales, Australia).

Data analysis. Data are shown as means ± SEM. A statistical evaluation was performed by ANOVA, with a Bonferroni post test when $P < 0.05$, or by using Dunnett's multiple comparison post test with 0% FO as the control, performed to generate a q value and to determine when $P < 0.05$. The EC_{50} (nmol/L) and maximal ileal contraction values (V/g of tissue) were determined from concentration dose curves using graph fits in GraphPad Prism 4.0 (GraphPad Software, San Diego, CA) with R^2 values > 0.99.

RESULTS

Ileal membrane lipid composition. With a diet containing 5% fat as a combination of sunflower seed oil and increasing FO rich in DHA, there was no change in ileal membrane total saturated or polyunsaturated fat, and only a modest increase in total monounsaturated at 5% FO. However, there was a significant incremental increase in total n-3 PUFA as EPA, DPA, and DHA (Fig. 1), with a concomitant decrease in n-6 PUFA as linoleic and arachidonic acid (Table 2).

TABLE 1
FA Composition of Experimental FO-Supplemented Diets[a]

FA	0% FO[b]	1% FO	2.5% FO	5% FO
		g/100 g FA		
14:0	0.5	1.2	2.1	3.8
16:0	7.6	10.8	15.3	23.4
18:0	4.1	3.6	5.7	6.6
18:1n-9	25.0	23.9	22.2	19.0
18:2n-6	60.9	51.7	35.4	7.0
20:5n-3	0.0	1.0	2.5	5.4
22:5n-3	0.0	0.2	0.5	1.1
22:6n-3	0.0	3.9	9.7	21.1
Σ Saturated	13.1	16.2	23.8	35.2
Σ Monounsaturated	25.5	26.0	26.7	27.7
Σ Polyunsaturated	61.4	57.8	49.6	37.1
Σ n-6	60.9	52.2	36.2	9.0
Σ n-3	0.5	5.6	13.3	28.1
n-6/n-3	120.7	9.3	2.7	0.3

[a]Values are means of two samples performed in duplicate. Percentages were derived from the full FA set.
[b]Diets were complemented with sunflower seed oil to include 5 g fat/100 g total per diet. FO, fish oil.
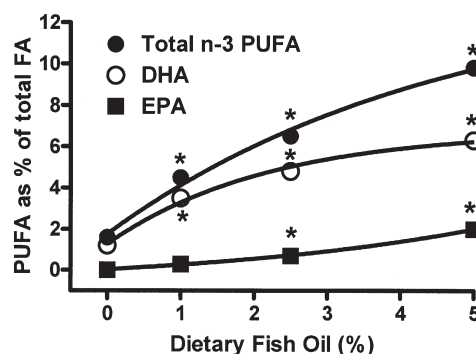
FIG. 1. Dose–response of dietary fish oil (FO) on the n-3 PUFA composition of the ileal total phospholipid fraction from Wistar-Kyoto (WKY) rats. Values are mean ± SEM for *n* = 5 rats. *Denotes a significant difference from the control (0% FO) diet by ANOVA, $P < 0.05$.

TABLE 2
FA Levels of the Total Phospholipid Fraction of Ileum from WKY Rats Fed FO-Supplemented Diets for 4 wk[a]

FA	0% FO	1% FO	2.5% FO	5% FO
		g/100 g FA		
16:0	26.8 ± 0.5^a	27.2 ± 0.6^a	$28.6 \pm 0.3^{a,b}$	29.3 ± 0.3^b
18:0	29.1 ± 0.3^a	$28.3 \pm 0.2^{a,b}$	27.9 ± 0.1^b	27.4 ± 0.2^b
24:0	4.9 ± 0.2^a	3.5 ± 0.1^b	2.6 ± 0.1^c	2.0 ± 0.1^d
18:1n-9	9.7 ± 0.1^a	9.9 ± 0.1^a	10.1 ± 0.2^a	11.7 ± 0.2^b
18:2n-6	8.7 ± 0.9^a	7.8 ± 0.5^a	7.4 ± 0.2^a	3.7 ± 0.2^b
20:4n-6	12.2 ± 0.3^a	11.4 ± 0.5^a	9.5 ± 0.4^b	8.7 ± 0.2^b
20:5n-3	0.1 ± 0.0^a	0.3 ± 0.0^b	0.7 ± 0.0^c	2.0 ± 0.3^d
22:5n-3	0.3 ± 0.0^a	0.8 ± 0.0^b	1.1 ± 0.0^c	1.4 ± 0.1^d
22:6n-3	1.2 ± 0.2^a	3.5 ± 0.2^b	4.8 ± 0.2^c	6.3 ± 0.2^d
Σ Saturated	64.4 ± 0.9^a	62.5 ± 1.0^a	62.6 ± 0.5^a	62.1 ± 0.5^a
Σ Monounsaturated	11.4 ± 0.2^a	$12.0 \pm 0.2^{a,b}$	12.6 ± 0.2^b	14.9 ± 0.4^c
Σ Polyunsaturated	24.2 ± 0.8^a	25.4 ± 0.8^a	24.9 ± 0.4^a	23.0 ± 0.4^a
Σ n-6	22.6 ± 0.9^a	$20.9 \pm 0.9^{a,b}$	18.4 ± 0.6^b	13.2 ± 0.3^c
Σ n-3	1.6 ± 0.2^a	4.5 ± 0.2^b	6.5 ± 0.2^c	9.8 ± 0.4^d
n-6/n-3	16.4 ± 0.9^a	4.7 ± 0.3^b	2.8 ± 0.2^c	1.4 ± 0.1^c

[a]Values are means ± SEM for $n = 5$, derived from the full FA set. Means in a row without a common roman superscript letter differ by ANOVA; $P < 0.05$. WKY, Wistar-Kyoto; for other abbreviation see Table 1.

Receptor-independent-induced ileal contraction. There were no significant differences for 10 (results not shown), 20, or 30 mmol/L KCl-induced ileal contractility for the 0, 1, 2.5, and 5% FO treatments. Contraction values (V/g) at 20 mmol/L KCl were 10.8 ± 1.1, 10.2 ± 0.6, 10.4 ± 1.1, and 10.8 ± 1.0, and the maximal contraction values at 30 mmol/L KCl were 11.8 ± 1.4, 11.9 ± 0.9, 11.8 ± 1.3, and 11.9 ± 1.0 for 0, 1, 2.5, and 5% FO treatments, respectively, for $n = 10$–12 rats, performed in duplicate (Fig. 2).

Receptor-induced ileal contraction. Significant increases in ileal receptor-mediated maximal contraction (V/g) occurred at 1 and 5% FO diets for carbachol compared with the 0% FO control (Fig. 3). There was also a trend for increased contraction at 2.5% FO that did not quite reach significance. There were no changes in sensitivity (EC_{50}) values across the FO diets for carbachol. For PGE_2, there was a significant increase

in maximal contractility at 2.5 and 5% FO, with a concomitant increase in sensitivity (lower EC_{50}) compared with the 0% FO control (Fig. 4). The EC_{50} (nmol/L) and maximal contraction values (V/g) derived from Figures 3 and 4 are given in Table 3.

DISCUSSION

A recent time-course study with rats (5) has indicated that tissue n-3 PUFA incorporation plateaued at 4 wk in erythrocyte and cardiac tissue. We have previously determined that dietary FO doses of 5–10% fed for 4–12 wk maximally increased the
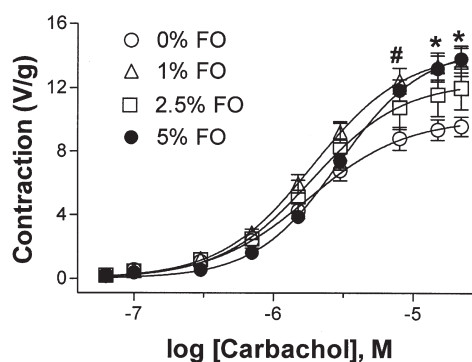
FIG. 3. Effect of carbachol dose on the contraction of ileum from WKY rats fed 0, 1, 2.5, and 5% FO-supplemented diets. The results are plotted as means ± SEM generated from pooled data for contractions from $n = 10$–12 rats performed in duplicate determined as V/g tissue. Significant differences for individual concentrations determined by one-way ANOVA with Dunnett's multiple comparison post tests, with 0% FO as control, are indicated as follows: at 8 mmol/L, [#]$P < 0.05$ for control vs. 1% FO; at 15 and 22 mmol/L, *$P < 0.05$ for control vs. 1 and 5% FO diets. The calculated EC_{50} (nmol/L) and maximal contraction (V/g tissue) for carbachol are shown in Table 3. For abbreviations see Figure 1.

FIG. 2. Effect of 30 mmol/L added KCl on contraction of the ileum from WKY rats fed 0, 1, 2.5, or 5% FO-supplemented diets. The results are plotted at means ± SEM for $n = 10$–12 WKY rats performed in duplicate, determined as voltage per gram of tissue (V/g). No significant difference was found between groups. For abbreviations see Figure 1.
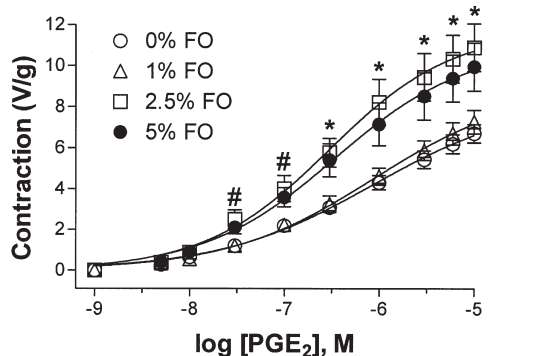
FIG. 4. Effect of prostaglandin E$_2$ (PGE$_2$) dose on the contraction of ileum from WKY rats fed 0, 1, 2.5, and 5% FO-supplemented diets. The results are plotted as means ± SEM generated from pooled data for contractions from n = 10–12 rats performed in duplicate determined as V/g tissue. Significant differences for individual concentrations determined by one-way ANOVA with Dunnett's multiple comparison post tests, with 0% FO as control, are indicated as follows: at 30 nmol/L and 100 nmol/L, $^\#P < 0.05$ for control vs. 2.5% FO; at 300–10,000 nmol/L, $^*P < 0.05$ for control vs. 2.5 and 5% FO diets. The calculated EC$_{50}$ (nmol/L) and maximal contraction (V/g tissue) for PGE$_2$ are shown in Table 3. For abbreviations see Figures 1 and 3.

receptor-induced contractility of ileum from normotensive SD and SHR (2,4). The aims of the present study were to investigate the effect of dietary FO dose on ileal n-3 PUFA incorporation and to correlate this with receptor-independent (KCl-induced depolarization) or receptor-dependent (muscarinic and PG) effects on *in vitro* contractility after 4 wk of feeding.

Increasing the dietary FO dose led to an increase in total saturated FA levels in the diet that did not translate to an increase in saturated FA in the total phospholipid fraction of ileum. We previously showed that the level of dietary saturated fat had little effect on the contractility of WKY or SHR gut tissue, although there was a modest increase in n-3 PUFA content (3); however, it was profoundly affected by n-3 PUFA as EPA and DHA but not by α-linolenic acid as canola oil at 5% (2,4). Rats fed diets low in n-3 PUFA had low levels of endogenous gut n-3 PUFA of around 1–2%. Feeding WKY rats 5% FO high in DHA for 4 wk resulted in 9.8% total n-3 PUFA (2% EPA, 1.4% DPA, and 6.3% DHA). We have also fed SD rats similar FO at 10% and achieved 11.9% total ileal n-3 PUFA (2.8% EPA, 1.4% DPA, 7.8% DHA) (8). These experiments suggested that

tissue n-3 PUFA saturates of between 5 and 10% dietary FO contain high DHA. However, when the diet containing 10% FO rich in EPA (EPA/DHA, 17:11) with 7% Sunola™ oil was fed to SD rats for 4 wk (2), the total n-3 PUFA level increased to 17.4% (9% EPA, 2.2% DPA, and 7.1% DHA). This implied that while DHA may be saturating, EPA can still be incorporated into gut smooth muscle membranes and further increase the n-3 PUFA pool. We have found that in contrast to gut tissue, rat myocardium preferentially accumulated DHA to approximately 25% with minimal EPA incorporation (< 2%) even when rats were fed FO high in EPA (9,10). Further experiments are needed to delineate between the two major n-3 PUFA in dietary studies and gut membrane FA incorporation profiles.

It is important to note that in this study, dietary supplementation of up to 5% FO did not lead to significantly higher ileal tissue weights when approximately the same experimental tissue lengths were used. This was also observed in our previous studies in which using 5 and 10% dietary FO did not affect the experimental weight of rat ileal tissue pieces over tissues of comparable lengths relative to other fats or dietary elements (2,4,8). Indeed the calculated densities of the whole small intestine with or without FO in the diets were almost identical (8). This implies that density considerations in contractility have not been an issue in our studies thus far but are critical when inflammatory damage is induced by genetic or chemical means that alters tissue thickness and density (11).

In this study, receptor-independent KCl-induced contractility (12) in the ileum was not affected by the level of dietary FO. However, a significant increase in receptor-mediated maximal contraction (V/g) occurred at 1 and 5% FO for the muscarinic agonist carbachol and at 2.5 and 5% FO for PGE$_2$, with a concomitant increase in sensitivity (lower EC$_{50}$). This extends previous studies from our laboratory, which demonstrated a trend toward increased sensitivity to PGE$_2$ in SD rats in a 10% FO-treated group (2) that was significant in a larger study for the SHR strain at 5% FO (4) compared with saturated fat diets. Although dietary saturated fat led to a small increase in total ileal n-3 PUFA, it did not profoundly influence contractility (2–4). The threshold for increased receptor-dependent gut contraction appears to be around 4.5% total tissue n-3 PUFA. It has yet to be determined whether muscarinic contraction can be influenced with diets lower than 1% FO. We previously showed that dietary FO does not lead to changes in total muscarinic binding

TABLE 3
Dose–Response Effect of Dietary FO on EC$_{50}$ (nmol/L) and Maximal Contraction (V/g tissue) Values Derived from Concentration-Response Curves for Carbachol and PGE$_2$ Applied to Ileum from WKY Rats Fed for 4 wk

Agonist		0% FO	1% FO	2.5% FO	5% FO
Carbachol	EC$_{50}$	2,081 ± 260[a]	2,137 ± 353[a]	2,051 ± 247[a]	2,925 ± 230[a]
	V/g	10.2 ± 0.6[a]	14.4 ± 1.0[b]	13.4 ± 1.4[a,b]	14.4 ± 0.9[b]
PGE$_2$	EC$_{50}$	1,211 ± 248[a]	1,293 ± 270[a]	370 ± 73[b]	350 ± 83[b]
	V/g	8.2 ± 0.5[a]	9.1 ± 0.8[a]	12.0 ± 1.1[b]	11.4 ± 1.1[b]

[a]Values are means ± SEM for n = 10–12 ileal tissues performed in duplicate. Means in a row without a common roman superscript letter differ by ANOVA; $P < 0.05$. PGE$_2$, prostaglandin E$_2$; for other abbreviations see Tables 1 and 2.

in the ileum of adult rats (4). It is worth noting that tissue PGE_2 receptor-binding studies were not investigated in this study. It is likely, however, that dietary FO and the incorporation of n-3 PUFA into gut membranes influences the postreceptor mechanisms that modulate ion channels and/or Ca^{2+} handling linked to electrical coupling and contraction in gut smooth muscle in a manner analogous to cardiac and vascular smooth muscle systems (12–16).

The subtle differential in muscarinic and PG sensitivity to membrane phospholipid n-3 PUFA content and contractility is yet to be elucidated but may also relate to calcium handling. However, other intrinsic mechanisms involving the cytosolic FA-binding proteins described in rat skeletal and cardiac muscle (17) or nuclear proteins such as farnesoid X receptors, which are antagonized by PUFA (18), may be acting in gut smooth muscle cells to alter contractility *via* calcium handling or *via* alteration of specific biochemical mediators or signaling mechanisms as a result of dietary FA composition.

Here we have demonstrated that rat ileal tissue increased n-3 PUFA content over the range of FO dose used (0–5%) after 4 wk of feeding. The incorporation of n-3 PUFA into the total phospholipid fraction was significant at 1% FO, at the expense of n-6 PUFA, and appears to saturate between 5 and 10% FO when high in DHA. There were no effects on receptor-independent (KCl) gut contractility. However, there were significant increases in muscarinic-induced maximal contraction apparent at 1% FO as well as increased PG-induced (PGE_2) maximal contraction and sensitivity commencing at 2.5% FO by mechanisms yet to be elucidated but which may involve postreceptor calcium handling.

REFERENCES

1. Patten, G.S., Bird, A.R., Topping, D.L., and Abeywardena, M.Y. (2002) Dietary Fish Oil Alters the Sensitivity of Guinea Pig Ileum to Electrically Driven Contractions and 8-*iso*-PGE_2, *Nutr. Res. 22*, 1413–1426.
2. Patten, G.S., Abeywardena, M.Y., McMurchie, E.J., and Jahangiri, A. (2002) Dietary Fish Oil Increases Acetylcholine- and Eicosanoid-Induced Contractility of Isolated Ileum, *J. Nutr. 132*, 2506–2513.
3. Patten, G.S., Adams, M.J., Dallimore, J.A., and Abeywardena, M.Y. (2004) Depressed Prostanoid-Induced Contractility of Gut in Spontaneously Hypertensive Rat (SHR) is Not Affected by Level of Dietary Fat, *J. Nutr. 134*, 2924–2929.
4. Patten, G.S., Adams, M.J., Dallimore, J.A., Rogers, P.F., Topping, D.L., and Abeywardena, M.Y. (2005) Restoration of Depressed Prostanoid-Induced Ileal Contraction in Spontaneously Hypertensive Rats by Dietary Fish Oil, *Lipids 40*, 69–79.
5. Owen, A.J., Peter-Przyborowska, B.A., Hoy, A.J., and McLennan, P.L. (2004) Dietary Fish Oil Dose- and Time-Response Effects on Cardiac Phospholipid Fatty Acid Composition, *Lipids 39*, 955–961.
6. Reeves, P.G., Nielsen, F.H., and Fahey, G.C., Jr. (1993) AIN-93 Diets for Laboratory Rodents: Final Report of the American Institute of Nutrition *ad hoc* Writing Committee on the Reformulation of the AIN-76A Rodent Diet, *J. Nutr. 123*, 1939–1951.
7. Patten, G.S., Head, R.J., Abeywardena, M.Y., and McMurchie, E.J. (2001) An Apparatus to Assay Opioid Activity in the Infused Lumen of the Intact Isolated Guinea Pig Ileum, *J. Pharmacol. Toxicol. Methods 45*, 39–46.
8. Patten, G.S., Conlon, M.A., Bird, A.R., Adams, M.J., Topping, D.L., and Abeywardena, M.Y. (2005) Interactive Effects of Dietary Resistant Starch and Fish Oil on SCFA Production and Agonist-Induced Contractility in Ileum of Young Rats, *Dig. Dis. Sci. 50*, in press.
9. Abeywardena, M.Y., and Charnock, J.S. (1995) Dietary Lipid Modification of Myocardial Eicosanoids Following Ischemia and Reperfusion in the Rat, *Lipids 30*, 1151–1156.
10. Charnock, J.S., Abeywardena, M.Y., and McLennan, P.L. (1986) Comparative Changes in the Fatty-Acid Composition of Rat Cardiac Phospholipids After Long-Term Feeding of Sunflower Seed Oil- or Tuna Fish Oil-Supplemented Diets, *Ann. Nutr. Metab. 30*, 393–406.
11. Moreels, T.G., Nieuwendijk, R.J., De Man, J.G., De Winter, B.Y., Herman, A.G., Van Marck, E.A., and Pelckmans, P.A. (2004) Concurrent Infection with *Schistosoma mansini* Attenuates Inflammation Induced by Changes in Colonic Morphology, Cytokine Levels, and Smooth Muscle Contractility of Trinitrobenzene Sulphonic Acid Induced Colitis in Rats, *Gut 53*, 99–107.
12. Huddart, H., and Syson, A.J. (1975) The Effect of Caffeine on Calcium Efflux and Calcium Translocation in Skeletal and Visceral Muscle, *J. Exp. Biol. 63*, 131–142.
13. Skuladottir, G.V., and Johannsson, M. (1997) Inotropic Responses of Rat Heart Papillary Muscle to α-1 and β-Adrenoceptor Stimulation in Relation to Dietary n-6 and n-3 Polyunsaturated Fatty Acids (PUFA) and Age, *Pharmacol. Toxicol. 80*, 85–90.
14. Leifert, W.R., Jahangiri, A., Saint, D.A., and McMurchie, E.J. (2000) Effects of Dietary n-3 Fatty Acids on Contractility, Na^+ and K^+ Currents in a Rat Cardiomyocytes Model of Arrhythmia, *J. Nutr. Biochem. 11*, 382–392.
15. Hirafuji, M., Ebihara, T., Kawahara, F., Hamaue, N., Endo, T., and Minami, M. (2001) Inhibition by Docosahexaenoic Acid of Receptor-Mediated Ca^{2+} Influx in Rat Vascular Smooth Muscle Cells Stimulated by 5-Hydroytryptamine, *Eur. J. Pharmacol. 427*, 195–201.
16. Nyby, M.D., Hori, M.T., Ormsby, B., Gabrielian, A., and Tuck, M.L. (2003) Eicosapentaenoic Acid Inhibits Ca^{2+} Mobilization and PKC Activity in Vascular Smooth Muscle Cells, *Am. J. Hypertens. 16*, 708–714.
17. Clavel, S., Farout, L., Briand, M., and Briand, Y. (2002) Effect of Endurance Training and/or Fish Oil Supplemented Diet on Cytoplasmic Fatty Acid Binding Protein in Rat Skeletal Muscles and Heart, *Eur. J. Appl. Physiol. 87*, 193–201.
18. Zhao, A., Yu, J., Lew, J.L., Huang, L., Wright, S.D., and Cui, J. (2004) Polyunsaturated Fatty Acids are FXR Ligands and Differentially Regulate Expression of FXR Targets, *DNA Cell Biol. 23*, 519–526.

Techniques for Delivery of Arachidonic Acid to Pacific Oyster, *Crassostrea gigas*, Spat

C. Seguineau[a], P. Soudant[b,*], J. Moal[a], M. Delaporte[a], P. Miner[a], C. Quéré[a], and J.-F. Samain[a]

[a]Laboratoire de Physiologie des Invertébrés, Institut Français de Recherché pour l'Exploitation de la Mer (IFREMER) de Brest, 29280 Plouzané, France, and [b]Unité Mixte de Recherche Centre National de la Recherche Scientifique-6539, Institut Universitaire Européen de la Mer (IUEM), Université de Bretagne Occidentale, 29280 Plouzané, France

ABSTRACT: The present study tested two techniques for dietary supplementation of *Crassostrea gigas* spat with PUFA, such as arachidonic acid (AA). The first technique consisted of a preliminary enrichment and growth of an algal concentrate (T-ISO, *Isochrysis* sp.) with AA dissolved in an ethanol solution, the whole culture then being fed to the spat. This enrichment increased the AA weight percentage in T-ISO neutral and polar lipids from 0.6 to 22.4% and from 0.4 to 6.8%, respectively. The second delivery technique was direct addition separately of free AA dissolved in ethanol solution and algal concentrate (T-ISO + AA) to the spat-rearing tank. To test the efficiency of these delivery techniques, oyster spat were supplemented with AA-enriched T-ISO, T-ISO + AA, and T-ISO alone. The possible biological impacts of these dietary treatments were assessed by measuring growth, condition index, and TAG content of oyster spat. Dry weight and condition index of spat fed AA-enriched T-ISO decreased by 24 and 49%, respectively, after 26 d of feeding; basically, TAG content declined 88% after 34 d of conditioning. When AA was added directly to seawater, spat growth and condition index were comparable with those of oysters fed T-ISO alone. AA incorporation in oyster tissues was assessed by analysis of the FA compositions in both neutral and polar lipid fractions. After 34 d, AA content in neutral lipids reached 7 and 11.7% in the spat fed, respectively, AA-enriched T-ISO and T-ISO + AA, as compared with 1.1% in spat fed only T-ISO. AA incorporation was greater in polar lipids than in neutral lipids, reaching 7.8 and 12.5% in spat fed AA-enriched T-ISO and T-ISO + AA, respectively. A direct addition of PUFA along with the food supply represents an effective and promising means to supplement PUFA to oyster spat.

Paper no. L9701 in *Lipids 40*, 931–939 (September 2005).

In bivalve hatcheries and nurseries, live microalgae are traditionally used as the primary food source. The development of artificial diets, whose nutritional composition can be precisely manipulated, would facilitate studies of bivalve nutrition. The use of artificial diets for bivalve aquaculture has been reviewed by Robert

and Trintignac (1) and Knauer and Southgate (2). Microcapsules of the cross-linked, protein-walled type were used to examine aspects of protein (3,4) and carbohydrate (5) metabolism in bivalves. Further efforts were devoted to lipid nutrition, as it was established that bivalves have limited ability to synthesize essential PUFA (6–9), such as DHA (22:6n-3), EPA (20:5n-3), and cholesterol (10–12). Lipids were first successfully supplied to bivalves using gelatin-acacia microcapsules (GAM) (13–16) and lipid microspheres (17–19). Emulsions were subsequently demonstrated to be an alternative way to deliver EFA (20–23) and sterols (24). Liposomes also have been used to deliver essential lipids and water-soluble compounds to oysters (25–28). Nutritional values of these artificial diets were generally tested as a supplement to deficient microalgae. Encapsulation of PUFA in GAM to supplement algal diets lacking essential PUFA, such as EPA or DHA, improved growth of *Crassostrea gigas* spat (15,29–31). GAM-containing microalgal lipid was also shown to successfully support the metamorphosis of *C. virginica* larvae (16). Supplementation of *Dunaliella tertiolecta* (which lacks both EPA and DHA) with an EPA- and DHA-rich emulsion improved the reproductive output of *C. gigas* broodstock, as measured by hatching rate (21). These biological effects resulting from modifications in dietary lipid composition were generally accompanied by changes in FA composition of the oysters themselves (21,30,31).

To investigate the incorporation efficiency of microencapsulated lipids, different strategies/techniques have been applied, including radiolabeled ^{14}C lipids (31), natural lipid biomarkers (24), and deuterated lipids (32). In most cases, the incorporation of microencapsulated essential lipids was found to be low. Thus, it appeared important to develop more effective techniques of PUFA delivery that would be easy to apply in the hatchery.

Recently, a method to supplement freshwater filter feeders with a single FFA was developed, using the microalgal cell itself as a transfer vehicle; this allowed successful supplementation of *Daphnia galatea* with individual essential PUFA (33). Also, feeding rotifers with DHA-enriched *Euglena gracilis* resulted in an increase in DHA in neutral and polar lipids of rotifers, a feed animal commonly used for rearing fish larvae (34,35).

The present study was conducted to test the efficiency of individual PUFA delivery to *C. gigas* spat with (i) an artificially AA-enriched T-ISO (*Isochrysis* sp. clone Tahiti) culture, and (ii) a direct supply of AA into the tank water, along

---

*To whom correspondence should be addressed at Unité Mixte de Recherche Centre National de la Recherche Scientifique-6539, Institut Universitaire Européen de la Mer (IUEM), Université de Bretagne Occidentale, 29280 Plouzané, France.
E-mail: Philippe.Soudant@univ-brest.fr

Abbreviations: CI, condition index; FAO, free alcohol; FS, free sterol; GAM, gelatin-acacia microcapsules; HPTLC, high-performance TLC; SE, steryl ester; T-ISO, *Isochrysis* sp. clone Tahiti.

with addition of a normal T-ISO culture. AA was selected as the PUFA model because its proportion is generally low in oyster spat, which makes incorporation easier to monitor. The biological impacts of the experimental dietary treatments were assessed by measuring the growth and the condition index (CI) of spat. TAG content of spat was used to assess the physiological status, as it is an indicator of energy reserves. Incorporation and assimilation of arachidonic acid (AA) was determined by analyzing the FA composition of neutral and polar lipids of the spat.

MATERIALS AND METHODS

AA enrichment of T-ISO. T-ISO was cultivated continuously in the exponential phase in a 6-L glass container filled with 1 µm-filtered, steam-sterilized, 35‰ seawater enriched with Conway medium (36) at 1 mL per liter of seawater. The algal culture was maintained at $20 \pm 1°C$ with continuous irradiance from cool-white fluorescence lights (378 µEinstein units/m^2/s) and aeration (air/CO$_2$, 98.5%/1.5%, 500 mL·min^{-1}). Cultures were supplied continuously with fresh medium by a peristaltic pump (30% renewal per day). T-ISO cells were harvested by collecting them in a secondary glass container using a glass pipe welded to the top of the primary glass container containing the algal culture. The AA enrichment was performed on the collected cells. The concentration of the collected cells ranged from $2.3·10^7$ to $2.7·10^7$ cells/mL.

The microalgal enrichment technique was modified from Von Elert (33). AA from Sigma-Aldrich (St Quentin Fallavier, France) was dissolved in absolute ethanol at 2.5 mg/mL. The harvested algae were first diluted to 5×10^6 cells/mL in 1500 mL, and then the AA solution (3 mL) was added directly to the algal culture to obtain a ratio of 1 µg AA for 10^6 cells of T-ISO. To determine the optimal time of contact, the FA compositions of T-ISO and AA-enriched T-ISO after 0.1, 1, 2, and 4 h of incubation were analyzed twice in triplicate.

For lipid extraction, samples (5–15 mL of culture) were filtered onto GF/F glass fiber filters (0.7 µm), previously heat-treated at 450°C. Filters were then rinsed with 15 mL of seawater and transferred into a glass vial containing 6 mL of a mixture of CHCl$_3$/MeOH (2:1, vol/vol). Samples were then stored under nitrogen at –20°C prior to lipid class and FA analyses.

Spat culture. Crassostrea gigas spat were provided by a commercial hatchery (SATMAR, Barfleur, France). Spat weighed approximately 50 mg on arrival; they were acclimated at 18°C for 14 d with T-ISO as a monospecific diet prior to the dietary experiment. Two hundred spat for each experimental group were maintained in a closed system, using a 20 L tank equipped with airlifts and filled with 1 µm-filtered seawater. The tanks and animals were cleaned daily. T-ISO feeding rations, calculated as equivalent dry weight of algae, were provided daily to spat at 0.75% of spat wet weight (including shell). The algal ration was applied for the entire duration of the dietary experiment (34 d). A peristaltic pump was adjusted to distribute the algal ration over a 4-h period twice a day.

Three dietary treatments were tested: (i) T-ISO, (ii) AA-enriched T-ISO (after 1 h of incubation of algae and AA together), and (iii) T-ISO and AA added directly into the tank (T-ISO + AA). For the latter treatment, AA was added into the tank at the same final concentration as the AA-enriched T-ISO treatment (1 µg AA per 10^6 cells of T-ISO). After 11, 18, 26, and 34 d, oyster spat were sampled randomly, rinsed, and weighed. Dry meat and shell weights were measured on 20 individual oysters. Condition index was then calculated as CI = (dry weight meat/dry weight shell) × 100 (37). Three pools of 10 individuals were also sampled after 18, 26, and 34 d of treatment for lipid analysis. Animals removed for lipid analyses were starved for 48 h to avoid artifacts of nonassimilated FA from microalgae and any supplemented free AA, which could still be present in the digestive tract at the time of the sampling.

Lipid class analysis. Total lipids were extracted according to Folch *et al.* (38) and stored at −20°C under nitrogen until use. Neutral lipid classes were analyzed using a CAMAG HPTLC (high performance TLC) system (CAMAG Automatic TLC sampler 4 and scanner 3; Muttenz, Switzerland). A preliminary run was carried out to remove possible impurities using hexane/diethyl ether (1:1), then the plates were activated for 30 min at 120°C. Lipid samples (0.5–5 µg) were directly spotted on the plate by the CAMAG automatic sampler. A double development was performed using two solvent systems: hexane/diethyl ether/acetic acid, 20:5:0.5 (by vol), then hexane/diethyl ether, 97:3 (vol/vol). Lipid classes appeared as black spots after dipping plates in a cupric sulfate phosphoric acid solution and heating for 20 min at 160°C (charring). Black spots were quantified by Wincats software (CAMAG), based upon a plate scanning at 370 nm.

The different lipid classes were identified according to authentic standards. To quantify the oyster lipid classes, a standard mixture was run on each HPTLC plate. This standard mixture was prepared in proportions similar to those found in oyster neutral lipids: 1.1 µg·mL^{-1} menhaden oil for TAG, 0.33 µg·mL^{-1} cholesterol, 59.1 µg·mL^{-1} oleyl alcohol, 38.8 µg·mL^{-1} cholesterol oleate, and 26.7 µg·mL^{-1} oleic acid. Results were expressed as µg of each identified neutral lipid class per oyster.

FA analysis. Total lipid extracts were evaporated to dryness under vacuum and were recovered with three washings of 500 µL each of CHCl$_3$/MeOH (98:2, vol/vol). The neutral and polar lipids were separated on a silica gel microcolumn (30 × 5 mm, 70–230 mesh, Kieselgel; Merck, Darmstadt, Germany) using CHCl$_3$/MeOH (98:2, vol/vol) and MeOH, respectively. The fractions were collected in tapering vials containing 2.3 µg of 23:0 (internal standard) and transesterified with 12% BF$_3$ (w/w) in methanol for 15 min at 100°C (39). After cooling, the FAME were extracted with hexane. Separation of FAME was carried out on a gas chromatograph (HP 6890), equipped with an FID, an on-column injector, and a J&W (Folsom, CA) DB-WAX capillary column (30 m × 0.25 mm; 0.25 µm film thickness). The column was temperature-programmed from 60 to 150°C at 30°C/min and 150 to 220°C

at 2°C/min. Hydrogen was used as the carrier gas at 2.0 mL·min^{-1}. Identification of FAME was based on comparison of retention times with those of authentic standards. Non-methylene-interrupted PUFA 22:2Δ7,13 and 22:2Δ7,15 were designated 22:2i and 22:2j, respectively. FA peaks were integrated and analyzed using HP Chemstation software. Results were expressed as µg FA/oyster or as weight percent FA composition for each fraction.

RESULTS

FA composition of spat fed with T-ISO. After 14 d of feeding with T-ISO for acclimation, several FA increased in both neutral and polar lipids of spat. The 18:1n-9, 18:2n-6, 18:3n-3, and 22:6n-3 weight percentages increased, while the 20:5n-3 weight percentage decreased (Table 1).

AA enrichment of T-ISO (Table 2). FA compositions of T-ISO and T-ISO incubated with AA for 0.1, 1, 2, and 4 h were analyzed in this experiment. Results for neutral lipids and polar lipids are reported in Table 2. The mean AA percent-

ages in oysters fed T-ISO were 0.6 and 0.4% in neutral and polar lipids, respectively. At 0.1 h after the addition of AA to the algae (i.e., after the lipid extraction procedure), a significant increase in AA percentage in the microalgae was observed in both neutral (22.4%) and polar (3.4%) lipids. Then, after 4 h of incubation, the AA weight percentage decreased from 22.4 to 16.7% in the neutral lipids, but it increased from 3.4 to 6.8% in polar lipids. Accordingly, the 22:6n-3 weight percentage decreased from 3.9 to 2.4% in neutral lipids, and from 9.5 to 2.3% in polar lipids. As a consequence, the n-3/n-6 ratio declined from 2.9 to 0.5 in neutral lipids and from 3.1 to 0.9 in polar lipids after 4 h of AA incubation.

Growth and performance of spat under different dietary treatments (Table 3). Growth and performance parameters, as measured by dry weight and CI of spat fed T-ISO, AA-enriched T-ISO, T-ISO + AA were monitored for 34 d.

For the spat fed T-ISO, dry weight increased steadily until 26 d. The CI was maintained between 4.6 and 5.1 from 11 to 26 d. But after 34 d, dry weight dropped to 2.7 mg and CI to 4.1. The AA-enriched T-ISO dietary treatment clearly impaired spat

TABLE 1
FA Composition of Neutral and Polar Lipids of *Crassostrea gigas* Spat Prior to and 14 d After Acclimation to T-ISO Diet[a]

	Spat prior to acclimation				Spat after acclimation			
	Neutral lipids		Polar lipids		Neutral lipids		Polar lipids	
	Mean	SD	Mean	SD	Mean	SD	Mean	SD
14:0	6.0	0.2	2.2	0.1	10.7	0.5	3.1	0.2
16:0	9.4	0.2	13.2	0.5	9.1	0.1	10.9	0.6
18:0	2.3	0.14	4.3	0.1	1.3	0.1	2.8	0.2
16:1n-7	7.6	0.1	2.5	0.1	3.6	0.1	1.5	0.2
18:1n-9	2.9	0.4	1.3	0.3	20.4	0.4	4.4	0.2
18:1n-7	10.5	0.2	7.1	0.4	4.9	0.3	5.2	0.3
20:1n-9	0.0	0.1	0.1	0.1	0.9	0.0	1.3	0.0
20:1n-7	2.7	0.0	4.4	0.3	2.4	0.2	4.1	0.2
18:2n-6	0.9	0.1	0.6	0.1	10.0	0.2	3.8	0.2
18:3n-3	0.4	0.0	0.3	0.0	5.7	0.2	1.9	0.1
18:4n-3	3.4	0.1	1.5	0.1	5.4	0.1	1.7	0.1
20:2n-6	0.1	0.0	0.1	0.0	0.5	0.0	0.5	0.1
20:3n-6	0.1	0.0	0.1	0.0	0.2	0.0	0.1	0.0
20:4n-6	0.5	0.0	1.1	0.1	0.5	0.0	1.5	0.5
20:4n-3	0.2	0.0	0.1	0.0	0.2	0.0	0.2	0.0
20:5n-3	24.6	0.5	21.2	1.2	3.2	0.4	8.7	0.3
22:2i	0.1	0.0	1.4	0.1	0.3	0.0	1.2	0.1
22:2j	1.3	0.1	0.2	0.0	1.3	0.2	5.1	0.2
22:4n-6	0.0	0.0	5.5	0.3	0.1	0.0	0.2	0.0
22:5n-6	0.1	0.0	0.1	0.0	1.5	0.0	2.5	0.1
22:5n-3	0.3	0.0	0.3	0.0	0.2	0.0	0.7	0.0
22:6n-3	3.0	0.3	8.6	0.3	9.4	0.9	15.3	0.3
Total FA (µg/oyster)	57.1	4.1	16.9	7.6	47.3	3.1	12.3	3.8

[a]Results are expressed as weight percentage of total FA and as total µg per oyster of neutral or polar lipids (mean and SD, *n* = 3). T-ISO, *Isochrysis* sp. clone Tahiti; 22:2i, 22:2Δ7,13; 22:2j, 22:2Δ7,15.

TABLE 2
FA Composition of Neutral and Polar Lipids of T-ISO and T-ISO Incubated 0.1, 1, 2, and 4 h with AA at a Ratio of 1 µg per 10^6 Cells[a]

Incubation time	T-ISO 0 h		AA-enriched T-ISO 0.1 h		1 h		2 h		4 h	
	Mean	SD	Mean	SD	Mean	SD	Mean	SD	Mean	SD
Neutral lipid										
20:4n-6	0.6[a]	0.2	22.4[b]	5.0	19.2[b,c]	4.1	18.3[b,c]	4.7	16.7[c]	5.1
20:5n-3	0.4[a]	0.2	0.2[a,b]	0.1	0.2[b]	0.1	0.2[a,b]	0.1	0.2[a,b]	0.0
22:6n-3	3.9[a]	0.9	2.6[b]	0.9	2.6[b]	0.5	2.5[b]	0.6	2.4[b]	0.4
n-3/n-6	2.9[a]	0.5	0.5[b]	0.2	0.5[b]	0.1	0.6[b]	0.1	0.5[b]	0.0
Total FA (ng/cell)	1.2[a,b]	0.3	1.5[a,b]	0.3	1.2[a]	0.3	1.6[b]	0.4	1.3[a,b]	0.3
Polar lipid										
20:4n-6	0.4[a]	0.2	3.4[b]	0.90	6.2[c]	1.2	6.0[c]	2.1	6.8[c]	1.1
20:5n-3	0.8[a]	0.3	0.7[a,b]	0.1	0.5[b,c]	0.1	0.4[b,c]	0.1	0.2[c]	0.0
22:6n-3	9.5[a]	3.3	5.2[b]	1.4	3.7[b,c]	0.3	3.0[b,c]	0.5	2.3[c]	0.3
n-3/n-6	3.1[a]	0.8	2.1[b]	0.1	1.5[c]	0.2	1.4[c]	0.1	0.9[c]	0.2
Total FA (ng/cell)	1.2[a]	0.2	1.3[a]	0.7	0.7[b]	0.1	0.6[b]	0.2	0.5[b]	0.1

[a]Results are expressed as percentage of total FA and as total ng FA per algal cell in neutral and polar lipids (mean and SD, $n = 6$). Different letters denote significant differences between conditions (ANOVA, $P < 0.05$). AA, arachidonic acid; for other abbreviation see Table 1.

growth and condition. Mean dry weight of the spat fed AA-enriched T-ISO was significantly lower than that of spat fed T-ISO from 18 to 34 d of conditioning. Similarly, CI was lowest in spat fed AA-enriched T-ISO at all sampling dates. In contrast, when AA was added directly to the tank, no such negative effects were observed. Some slight reductions (statistically significant) in dry weight and CI were observed in this treatment, compared with T-ISO alone after 26 days of dietary conditioning. However, these differences were not seen after 34 d.

Lipid class composition of spat under different dietary treatments (Table 4). HPTLC analysis identified and quantified five lipid classes in the neutral lipids of oyster spat: steryl ester (SE), TAG, free sterol (FS), free alcohol (FAO), and FFA. As SE and FAO were found in small amounts, occasion-

ally below the detection threshold, only the results obtained for the TAG, FS, and FFA are presented here. TAG was the major storage lipid class detected in spat. The TAG, FS, and FFA contents in spat at the beginning of the experiment (after the acclimation period) were, respectively, 65.4, 18.2, and 1.6 µg/oyster. The TAG content increased from 65.4 to 148.9 µg/oyster in spat fed T-ISO, and to 130.6 µg/oyster in spat fed T-ISO + AA. There was no significant difference in TAG between these two dietary treatments during the experiment. In contrast, feeding spat with AA-enriched T-ISO resulted in a drastic decrease of TAG content after 18 d, when it dropped below 22 µg/oyster at the end of the experiment.

The FFA content (Table 4) ranged from 0.3 to 1.9 µg/oyster, regardless of treatment or sampling time, and maximal percent-

TABLE 3
Impact of Dietary Conditioning [T-ISO alone, AA-enriched T-ISO, and T-ISO and AA added directly into the tank (T-ISO + AA)] on the Dry Weight (mg/oyster) and Condition Index (CI) of *C. gigas* Spat[a] (mean and SD, $n = 20$)

Diets Dry weight	T-ISO		AA-enriched T-ISO		T-ISO + AA	
	Mean	SD	Mean	SD	Mean	SD
T0	2.1	0.5				
11 d	2.3[a]	0.8	1.8[a]	0.8	2.2[a]	1.1
18 d	3.1[a]	1.4	1.8[b]	0.8	2.8[a]	1.1
26 d	4.1[a]	2.3	1.8[b]	0.5	2.9[c]	0.8
34 d	2.7[a]	0.7	1.6[b]	0.4	2.6[a]	1.2
CI						
T0	5.6	1.5				
11 d	4.6[a]	1.1	3.6[b]	0.8	4.0[b]	0.7
18 d	4.6[a]	1.1	2.8[b]	0.6	4.1[a]	1.4
26 d	5.1[a]	0.9	2.6[b]	0.7	3.6[c]	0.9
34 d	4.1[a]	0.8	2.7[b]	0.4	4.0[a]	1.3

[a]Different letters denote significant differences between conditions (ANOVA, $P < 0.05$). CI = (dry weight meat/dry weight shell) × 100. For abbreviations see Table 1.

TABLE 4
Impact of Dietary Conditioning on the TAG, FFA, and Sterol Contents[a] of *C. gigas* Spat
(mean and SD, *n* = 3)

Diets	T-ISO		AA-enriched T-ISO		T-ISO + AA	
FFA	Mean	SD	Mean	SD	Mean	SD
T0	1.6	0.4				
18 d	1.3[a]	0.2	0.3[b]	0.0	0.6[c]	0.1
26 d	1.5[a]	0.2	0.5[b]	0.1	1.4[a]	0.3
34 d	1.9[a]	0.8	0.7[b]	0.3	1.5[a,b]	0.1
TAG						
T0	65.4	8.1				
18 d	114.3[a]	32.2	21.6[b]	6.3	85.3[a]	9.6
26 d	131.2[a]	28.7	22.0[b]	3.4	135.2[a]	29.8
34 d	148.9[a]	29.8	18.3[b]	6.1	130.6[a]	25.5
Sterols						
T0	18.2	2.7				
18 d	22.5	3.2	12.7	2.8	19.6	3.0
26 d	22.9	3.4	13.4	0.8	23.9	6.0
34 d	27.9	1.6	14.2	2.1	23.2	0.4

[a]Results are expressed in µg of lipid class/oyster. Different letters denote significant differences between conditions (ANOVA, $P < 0.05$). For abbreviations see Tables 1 and 3.

ages in neutral lipids were 1.7, 3.5, and 1.4% in spat fed T-ISO, AA-enriched T-ISO, and T-ISO + AA, respectively.

FA composition of spat under different dietary treatments. Proportions of saturated, monounsaturated, and polyunsaturated FA were not affected by the dietary treatments and were stable in both neutral and polar lipids for the entire duration of the experiment (data not shown). After 18 d of conditioning, and when compared with spat fed T-ISO alone, the 20:4n-6 weight-percentage in spat fed the AA-enriched T-ISO diet increased by approximately fourfold in neutral lipids (Table 5) and by twofold in polar lipids (Table 5). The 20:4n-6 weight percentage increased nine times in neutral lipids (Table 5) and three times in polar lipids (Table 5) in spat fed T-ISO + AA added separately. The 20:4n-6 weight percentage in both polar and neutral lipids of spat AA-supplemented diets continued to increase between 18 and 26 d and reached a plateau between 26 and 34 d (Table 5). After 26 d of feeding with the T-ISO + AA diet, 20:4n-6 reached approximately 12% of the PUFA content in both neutral and polar lipids. The 22:4n-6 weight percentage in neutral and polar lipids followed the same pattern as the 20:4n-6 percentage, according to dietary treatment (Table 5). The weight percentage increases in 20:4n-6 and 22:4n-6 observed with AA-supplemented diets were partially compensated by a decrease of 22:6n-3 in polar lipids (Table 5). Finally, after 34 d of conditioning, the n-3/n-6 ratio of spat fed T-ISO + AA decreased to 1.1 in both neutral and polar lipids and was much lower than in spat fed T-ISO alone, which had an n-3/n-6 ratio at 2.0 and 2.2 in neutral and polar lipids, respectively.

DISCUSSION

AA algal enrichment. The present study demonstrated that AA was immediately incorporated into both algal neutral and polar lipids. This quick AA association with neutral lipids,

rather than polar lipids alone, suggested that most of the AA probably was absorbed as FFA on the surface of T-ISO cells and that this enrichment was probably the result of an algal coating by adsorption. HPTLC analysis showed that FFA increased in the AA-treated algal samples (15.8%) in comparison with nontreated T-ISO (5.5%). Von Elert (33) made similar observations when enriching *Scenedesmus obliquus* and *Stephanodiscus hantzschii* with various unsaturated FA (18:1n-7, 18:3n-3, 20:4n-6, 20:5n-3, and 22:6n-3) and was uncertain whether these PUFA were only adsorbed on cell surfaces or were truly incorporated within the cells.

The rapid increase in AA within polar lipids cannot be explained by the above mechanism, but this percentage increased steadily during incubation and may indicate that some of the adsorbed AA may have been incorporated in membrane phospholipids thereafter by deacylation–acylation processes (40). Our results are in agreement with those obtained with *Chlorella vulgaris* and *Euglena gracilis* PUFA enrichments (34,35). When *E. gracilis* was enriched with 0.5% of 22:6n-3 (DHA) for 24 h, exogenous DHA was mainly accumulated in neutral lipids and, to a lesser extent, in the three major phospholipids of *E. gracilis:* namely PC, PE, and PI. Because of the rapid incorporation of AA within the algae, a significant reduction in DHA percentage from 3.9 to 2.4% in neutral lipids and from 9.5 to 2.3% in polar lipids was observed after 4 h of incubation, as well as a decrease in n-3/n-6 ratio from 2.9 to 0.5 in neutral lipids and from 3.1 to 0.9 in polar lipids. These changes may affect the functional metabolism of the enriched algae when ingested by the spat, since DHA is well established to be an essential PUFA for bivalve growth and reproduction (6–9).

AA absorption by spat. Ingestion and assimilation of AA were estimated by analyzing the FA composition changes of neutral and polar lipids in spat during the experiment. Oyster spat represent a good model target organism for dietary experiments because the FA compositions of polar lipids, and

TABLE 5
FA Composition[a] of Neutral and Polar Lipids in Oyster Spat After 18, 26, and 34 d of Feeding with T-ISO, AA-Enriched T-ISO, and T-ISO and AA Added Directly into the Tank

| | Initial | | 18 d | | | | | | 26 d | | | | | | 34 d | | | | | |
| | | | T-ISO | | AA-enriched T-ISO | | T-ISO + AA | | T-ISO | | AA-enriched T-ISO | | T-ISO + AA | | T-ISO | | AA-enriched T-ISO | | T-ISO + AA | |
	Mean	SD	Mean	SD	Mean	SD	Mean	SD	Mean	SD	Mean	SD	Mean	SD	Mean	SD	Mean	SD	Mean	SD
Neutral lipid																				
20:4n-6	0.5	0.0	0.9	0.2	4.3	0.3	9.4	1.4	1.0	0.1	6.2	0.9	12.1	0.5	1.1	0.1	7.0	0.2	11.7	0.3
20:5n-3	3.2	0.4	1.8	0.2	3.3	0.9	2.4	0.4	1.9	0.0	3.7	0.7	2.3	0.0	1.9	0.3	3.3	0.4	2.0	0.1
22:4n-6	0.1	0.0	0.1	0.0	0.2	0.0	0.4	0.0	0.1	0.0	0.3	0.0	0.7	0.3	0.1	0.0	0.4	0.1	0.5	0.0
22:5n-6	1.5	0.0	2.1	0.1	1.5	0.3	2.0	0.3	2.3	0.0	1.7	0.3	2.3	0.1	2.4	0.2	1.7	0.2	2.4	0.0
22:5n-3	0.2	0.0	0.3	0.0	0.3	0.1	0.2	0.0	0.3	0.0	0.4	0.1	0.3	0.0	0.3	0.0	0.4	0.3	0.2	0.0
22:6n-3	9.4	0.9	10.1	0.7	9.3	3.1	9.3	0.6	11.8	0.3	9.2	1.8	9.6	0.1	12.0	0.7	8.5	1.2	9.4	0.2
n-3/n-6	1.9	0.1	2.5	0.1	1.8	0.2	1.3	0.1	2.3	0.1	1.5	0.2	1.1	0.1	2.0	0.1	1.3	0.1	1.1	0.0
Total FA (µg/oyster)	47.3	3.1	57.8	15.5	19.4	3.1	43.4	29.5	116.8	7.2	25.4	0.9	102.3	34.2	109.5	26.8	19.6	6.8	107.8	14.0
Polar lipid																				
20:4n-6	1.5	0.5	2.8	0.2	5.9	0.3	10.1	0.1	3.4	0.4	7.7	1.4	12.3	0.7	3.7	0.2	7.8	0.7	12.5	0.6
20:5n-3	8.7	0.3	5.6	0.5	7.4	0.4	5.5	0.3	5.0	0.2	6.3	0.5	4.0	0.1	4.8	0.2	5.0	0.3	3.7	0.0
22:4n-6	0.2	0.0	0.3	0.0	0.4	0.0	0.8	0.0	0.3	0.0	0.5	0.0	1.3	0.0	0.3	0.0	0.9	0.1	1.3	0.1
22:5n-6	2.5	0.1	3.9	0.1	2.9	0.1	3.0	0.1	4.1	0.1	2.7	0.2	3.3	0.2	4.5	0.1	3.1	0.2	3.1	0.2
22:5n-3	0.7	0.0	0.7	0.1	0.8	0.0	0.7	0.0	0.6	0.0	0.8	0.0	0.6	0.0	0.6	0.0	0.9	0.1	0.5	0.0
22:6n-3	15.3	0.3	18.2	1.0	16.1	1.5	14.7	0.4	18.3	0.5	15.0	0.8	14.2	0.6	18.8	0.4	15.7	0.8	12.6	0.3
n-3/n-6	3.4	0.2	2.7	0.1	2.2	0.1	1.5	0.0	2.3	0.1	1.9	0.2	1.2	0.1	2.2	0.1	1.9	0.1	1.1	0.1
Total FA (µg/oyster)	12.3	3.8	25.4	2.8	28.6	1.2	33.3	4.5	54.6	7.4	32.0	2.5	31.6	7.0	54.3	4.9	21.2	3.1	30.8	4.6

[a]Results are expressed as percentage of total FA of polar and neutral lipids (mean and SD, $n = 3$). For abbreviations see Tables 1 and 3.

especially neutral lipids, are rapidly affected by dietary modifications. Fourteen days of feeding acclimation with T-ISO was enough to change the proportions of the PUFA, such as 20:5n-3 and 22:6n-3, appreciably. The dietary imprint of T-ISO was observed consistently when this was used as a monospecific diet for various species of bivalves: oysters, clams, and scallops (41–44). This prior knowledge facilitated the distinction of FA composition modifications atributable to AA supplementation, without confounding effects of the monospecific diet imprint.

After 18 d of feeding with AA-enriched T-ISO, a clear increase in the AA weight percentage in spat neutral and polar lipids, up to 4.3 and 5.9%, respectively, was obtained, and a plateau was reached at 7.0% in neutral lipids and 7.8% in polar lipids after 34 d of feeding, respectively, i.e., seven and two times the values of the T-ISO alone dietary treatment. These results demonstrate the high efficiency of AA incorporation within spat. We considered the possibility that the AA-enriched T-ISO condition could have been detrimental/toxic for the microalgae, modifying their morphological and/or motility characteristics. Indeed, T-ISO was observed to lose its motility after 4 h of contact with AA at 0.01 mg·mL^{-1} in the AA-enriched T-ISO condition (Miner, P., personal communication). The loss of motility of T-ISO could possibly affect feeding behavior of the spat and thus could explain a lower AA incorporation compared with the T-ISO + AA condition.

Indeed, the direct addition of AA to the tank, simultaneously with the microalgae (T-ISO + AA), permitted the highest incorporation of AA in both neutral and polar lipids of spat, reaching approximately 12% in neutral and polar lipids after 26 and 34 d of feeding. This higher incorporation efficiency, compared with the AA-enriched T-ISO feeding, is possibly related to a higher algal ingestion rate or direct AA absorption by spat. Some papers showed that marine invertebrates can absorb dissolved organic matter (45,46). More specifically, bivalves can absorb free amino acids from seawater and use them as a nutritional supplement (47,48). Jaeckle and Manahan (49) demonstrated that addition of 1 μM glucose and of a mixture of 16 amino acids enhanced the metabolic rate of oyster larvae and concluded that the organic chemistry of seawater can affect the growth and metabolism of oyster larvae. However, there is only one paper demonstrating such direct absorption for dissolved lipids or, more specifically, for FFA (50).

Biological effects. The possible biological impacts of these dietary treatments (T-ISO, AA-enriched T-ISO, and T-ISO + AA diets) were assessed by measuring growth, CI, and lipid storage indicators of the conditioned spat.

Results of the present study demonstrated that the AA-enriched T-ISO diet had an unexpected but very clearly negative effect on spat growth compared with the T-ISO diet. Specifically, dry weight and CI of spat fed AA-enriched T-ISO showed a decrease of 24 and 49%, respectively, after 26 d of feeding, and the content of TAG (a storage lipid) was reduced by 88% after 34 d, as compared with spat fed the unsupplemented T-ISO diet.

Thus, one possible explanation for such a biological effect could be that the enrichment of T-ISO with AA resulted in drastic morphological and/or biochemical changes in T-ISO cells, making the microalgae toxic or unsuitable for filtration/ingestion by spat. Moreover, this biological effect is unlikely to be the result of spat FA composition changes by the AA-enriched T-ISO diet, because the T-ISO + AA diet, which affected the spat FA composition more, or at least to the same extent, had similar growth performance and lipid storage content as the unsupplemented T-ISO diet. Nevertheless, the absence of significant effects of the high AA enrichment (12% in polar and neutral lipids) obtained with the T-ISO + AA diet on spat performance is quite surprising. These modifications of FA composition may, however, have other important biological functions, such as defense mechanisms, as previously reported by Delaporte *et al.* (44) and Sargent *et al.* (51). Finally, it must be noted that, according to previous field and laboratory experiments, the highest values of AA measured in oyster neutral or polar lipids always remained below a 10% threshold. For instance, AA weight percentage ranged from 0.9 to 2% in NL and from 1.5 to 4.3% in PL of *C. gigas* natural spat (52). The AA weight percentage reached 6% of total FA of *C. virginica* gills (in which lipids are mostly in polar lipids) after 56 d of feeding with a microalgae mixture containing in equal proportions: *Tetraselmis maculata, Thalassiosira weissflogi, Chaetoceros calcitrans,* and *Isochrysis galbana* (53). Delaporte *et al.* (44) measured up to 7.5% of AA in hemocyte polar lipids of *C. gigas* fed for 8 wk *C. calcitrans,* which contained 2% AA. Thus, the 12% value measured in polar lipids of spat feed the T-ISO + AA diet in our experiment is above values reported previously.

ACKNOWLEDGMENTS

REFERENCES

1. Robert, R., and Trintignac, P. (1997) Substitutes for Live Microalgae in Mariculture: A Review, *Aquat. Living Resour. 10*, 315–327.
2. Knauer, J., and Southgate, P.C. (1999) A Review of the Nutritional Requirements of Bivalves and the Development of Alternative and Artificial Diets for Bivalve Aquaculture, *Rev. Fish. Sci. 7*, 241–280.
3. Langdon, C.J., and Siegfried, C.A. (1984) Progress in the Development of Artificial Diets for Bivalve Filter Feeders, *Aquaculture 39*, 135–153.
4. Kreeger, D.A., and Langdon, C.J. (1994) Digestion and Assimilation of Protein by *Mytilus trossulus* (Bivalvia; Mollusca) Fed Mixed Carbohydrate/Protein Microcapsules, *Mar. Biol. 118*, 479–488.
5. Kreeger, D.A. (1996) Use of Dual-Labeled Microcapsules to Discern the Physiological Fates of Assimilated Carbohydrate,

Protein Carbon, and Protein Nitrogen in Suspension-Feeding Organisms, *Limnol. Oceanogr. 41*, 208–215.

6. Chu, F.-L.E., and Greaves, J. (1991) Metabolism of Palmitic, Linoleic, and Linolenic Acids in Adult Oysters, *Crassostrea virginica*, *Mar. Biol. 110*, 229–236.

7. De Moreno, J.E.A., Moreno, V.J., and Brenner, R.R. (1976) Lipid Metabolism of the Yellow Clam, *Mesodesma mactroïdes*: 2-Polyunsaturated Fatty Acid Metabolism, *Lipids 11*, 561–566.

8. De Moreno, J.E.A., Moreno, V.J., and Brenner, R.R. (1977) Lipid Metabolism of the Yellow Clam, *Mesodesma mactroïdes*: 3 Saturated Fatty Acids and Acetate Metabolism, *Lipids 12*, 804–808.

9. Waldock, M.J., and Holland, D.L. (1984) Fatty Acid Metabolism in Young Oysters, *Crassostrea gigas*: Polyunsaturated Fatty Acids, *Lipids 19*, 332–336.

10. Teshima, S. (1983) Sterol Metabolism, in *Biological and Physiological Approaches to Shellfish Nutrition, Proceedings of the 2nd Conference of Aquaculture Nutrition* (Pruder, G.D., Langdon, C., and Conklin, C., eds.), pp. 205–216, Louisiana State University, Baton Rouge.

11. Holden, M.J., and Patterson, G.W. (1991) Absence of Sterol Biosynthesis in Oyster Tissue Culture, *Lipids 26*, 81–82.

12. Knauer, J., Russel, G.K., Lindley, D., and Southgate, P.C. (1998) Sterol Metabolism of Pacific Oyster (*Crassostrea gigas*) Spat, *Comp. Biochem. Physiol. 119B*, 81–84.

13. Numaguchi, K., and Nell, J.A. (1991) Effects of Gelatin-Acacia Microcapsule and Algal Meal Supplementation of Algal Diets on Growth Rates of Sydney Rock Oyster, *Saccostrea commercialis* (Iredale & Roughley), Larvae, *Aquaculture 94*, 65–78.

14. Southgate, P.C. (1988) Use of Microencapsulated Diets in the Culture of Giant Clam Larvae, in *Giant Clams in Asia and the Pacific* (Copland, J.W., and Lucas, J.S., eds.), pp. 155–160, Australia Centre for International Agricultural Research, Canberra.

15. Langdon, C.J., and Waldock, M.J. (1981) The Effect of Algal and Artificial Diets on the Growth and Fatty Acid Composition of *Crassostrea gigas* Spat, *J. Mar. Biol. Ass. UK 61*, 431–448.

16. Chu, F.L.E., Webb, K.L., Hepworth, D.A., and Casey, B.B. (1987) Metamorphosis of Larvae of *Crassostrea virginica* Fed Microencapsulated Diets, *Aquaculture 64*, 185–197.

17. Robinson, A. (1992) Dietary Supplements for the Reproductive Conditioning of *Crassostrea gigas* Kumamoto (Thunberg): I Effects on Gonadal Development, Quality of Ova and Larvae Through Metamorphosis, *J. Shellfish Res. 11*, 437–441.

18. Robinson, A. (1992) Dietary Supplements for the Reproductive Conditioning of *Crassostrea gigas* Kumamoto (Thunberg): II Effects of Glycogen; Lipid and Fatty Acid Content of Broodstock Oysters and Eggs, *J. Shellfish Res. 11*, 443–447.

19. Heras, H., Kean-Howie, J., and Ackman, R.G. (1994) The Potential Use of Lipid Microspheres as Nutritional Supplements for Adult *Ostrea edulis*, *Aquaculture 123*, 309–322.

20. Caers, M., Coutteau, P., Sorgeloos, P., and Gajardo, G. (2003) Impact of Algal Diets and Emulsions on the Fatty Acid Composition and Content of Selected Tissues of Adult Broodstock of the Chilean Scallop *Argopecten pupuratus* (Lamarck, 1819), *Aquaculture 217*, 437–452.

21. Caers, M., Utting, S.D., Coutteau, P., Millican, P.F., and Sorgeloos, P. (2002) Impact of the Supplementation of a Docosahexaenoic Acid-Rich Emulsion on the Reproductive Output of Oyster Broodstock, *Crassostrea gigas*, *Mar. Biol. 140*, 1157–1166.

22. Caers, M., Coutteau, P., and Sorgelos, P. (1999) Dietary Impact of Algal and Artificial Diets, Fed at Different Feeding Rations, on the Growth and Fatty Acid Composition of *Tapes philippinarum* (L.) Spat, *Aquaculture 170*, 307–322.

23. Coutteau, P., and Sorgelos, P. (1993) Substitute Diets for Live Algae in the Intensive Rearing of Bivalve Mollusks—A State of the Art Report, *World Aquacult. 24*, 45–50.

24. Soudant, P., Val Sanles, M., Quéré, C., Le Coz, J.R., Marty, Y., Moal, J., Samain, J.F., and Sorgeloos, P. (2000) The Use of Lipid Emulsions for Sterol Supplementation of Spat of the Pacific Oyster, *Crassostrea gigas*, *Aquaculture 184*, 315–326.

25. Parker, R.S., and Selivonchik, D.P. (1986) Uptake and Metabolism of Lipid Vesicles from Seawater by Juvenile Pacific Oysters (*Crassostrea gigas*), *Aquaculture 53*, 215–228.

26. Caers, M., Coutteau, P., and Sorgeloos, P. (2000) Incorporation of Different Fatty Acids, Supplied as Emulsions or Liposomes, in the Polar and Neutral Lipids of *Crassostrea gigas* Spat, *Aquaculture 186*, 157–171.

27. Moal, J., Seguineau, C., Samain, J.F., Soudant, P., Cansell, M., Le Coz, J.R., Migaud, H., Sanles, M., Ponce, B., and Langdon, C. (1999) How to Provide Essential Nutriments to Bivalves in Hatchery, *J. Shellfish Res. 18,* 332, abstract.

28. Cansell, M., Bailhache, E., Samain, J.F., Moal, J., Gouyou, J.P., and Entresangles, B. (1998) Potential Water Soluble Vitamin Delivery Using Liposomes Based on Marine Lipids, in *Marine Lipids. Proceedings of the Symposium Held in Brest, 19–20 November 1998* (Baudimant, G., Guezennec, J., Roy, P., and Samain, J.F., eds.), pp. 212–220, IFREMER, Brest.

29. Langdon, C.J., and De Bevoise, A.E. (1990) Effect of Microcapsule Type on Dietary Delivery of Protein to a Marine Suspension-Feeder, the Oyster *Crassostrea gigas*, *Mar. Biol. 105*, 437–443.

30. Knauer, J., and Southgate, P.C. (1997) Growth and Fatty Acid Composition of Pacific Oyster (*Crassostrea gigas*) Spat Fed a Spray-Dried Freshwater Microalga (*Spongiococcum excentricum*) and Microencapsulated Lipids, *Aquaculture 154*, 293–303.

31. Knauer, J., and Southgate, P.C. (1997) Assimilation of Gelatin-Acacia Microencapsulated Lipid by Pacific Oyster (*Crassostrea gigas*) Spat, *Aquaculture 153*, 291–300.

32. Novoa, S., Martinez, D., Ojea, J., Soudant, P., Samain, J.F., Le Coz, J.R., and Rodriguez, J.L. (2002) Ingestion, Digestion and Assimilation of Gelatin Acacia Microcapsules Incorporating Deuterium-Labeled Arachidonic Acid by Larvae of the Clam *Venerupis pullastra*, *J. Shellfish Res. 21*, 649–658.

33. Von Elert, E. (2002) Determination of Limiting Polyunsaturated Fatty Acids in *Daphnia galeata* Using a New Method to Enrich Food Algae with Single Fatty Acids, *Limnol. Oceanogr. 47*, 1764–1773.

34. Hayashi, M., Yukino, T., Maruyama, I., Kido, S., and Kitaoka, S. (2001) Uptake and Accumulation of Exogenous Docosahexanoic Acid by *Chlorella*, *Biosci. Biotechnol. Biochem. 65*, 202–204.

35. Hayashi, M., Yukino, T., and Park, B.S., Distribution of Docosahexanoic Acid in DHA-Enriched *Euglena gracilis* in *Proceedings of International Commemorative Symposium,* edited by K. Namba, Tokyo, Japan, 2002, pp. 1002–1003.

36. Walne, P.R. (1970) Studies on the Food Value of Nineteen Genera of Algae to Juvenile Bivalves of the Genera *Ostrea, Crassostrea, Mercenaria* and *Mytilus*, *Fish Invest. 26*, 1–61.

37. Mann, R., and Glomb, S.J. (1978) The Effect of Temperature on Growth and Gametogenesis in the Manila Clam *Tapes japonica*, *Est. Coast. Mar. Sci. 6*, 335–339.

38. Folch, J., Lees, M., and Sloane-Stanley, G.H. (1957) A Simple Method for the Isolation and Purification of Total Lipids from Animal Tissues, *J. Biol. Chem. 266*, 497–509.

39. Metcalfe, L.D., and Schmitz, A.A. (1961) The Rapid Preparation of Fatty Acid Esters for Gas Chromatographic Analysis, *Anal. Chem. 33*, 363–364.

40. Béréziat, G., Chambaz, J., Colard, O., and Polonovski, J. (1988) *Biologie des Lipides chez l'Homme*, pp. 81–89, Editions médicales internationales, E.M., Paris.

41. Soudant, P., Marty, Y., Moal, J., Masski, H., and Samain, J.F. (1998) Fatty Acid Composition of Polar Lipid Classes During Larval Development of Scallop *Pecten maximus* (L.), *Comp. Biochem. Physiol. A 121*, 279–288.

42. Soudant, P., Moal, J., Marty, Y., and Samain, J.F. (1996) Impact of the Quality of Dietary Fatty Acids on Metabolism and the Composition of Polar Lipid Classes in Female Gonads of *Pecten maximus* (L.), *J. Exp. Mar. Biol. Ecol. 205*, 149–163.

43. Soudant, P., Marty, Y., Moal, J., Robert, R., Quéré, C., Le Coz, J.-R., and Samain, J.F. (1996) Effect of Food Fatty Acid and Sterol Quality on *Pecten maximus* Gonad Composition and Reproduction Process, *Aquaculture 143*, 361–378.

44. Delaporte, M., Soudant, P., Moal, J., Lambert, C., Quéré, C., Miner, P., Choquet, G., Paillard, C., and Samain, J.-F. (2003) Effect of a Mono-specific Algal Diet on Immune Functions in Two Bivalves Species *Crassostrea gigas* and *Ruditapes philippinarum*, *J. Exp. Biol. 206*, 3053–3064.

45. Sorokin, Y.I., and Wyshkwarzev, D.I. (1973) Feeding on Dissolved Organic Matter by Some Marine Animals, *Aquaculture 2*, 141–148.

46. Fankboner, P.V., and De Burgh, M.E. (1978) Comparative Rates of Dissolved Organic Carbon Accumulation by Juveniles and Pediveligers of the Japanese Oyster *Crassostrea gigas* Thunberg, *Aquaculture 13*, 205–212.

47. Manahan, D.T., and Crisp, D.J. (1983) Autoradiographic Studies on the Uptake of Dissolved Aminoacids from Sea Water by Bivalve Larvae *J*, *Mar. Biol. Assoc. UK 63*, 673–682.

48. Manahan, D.T., and Stephens, G.C. (1983) The Use of High Performance Liquid Chromatography to Measure Dissolved Organic Compounds in Bivalve Aquaculture Systems, *Aquaculture 32*, 339–346.

49. Jaeckle, W.B., and Manahan, D.T. (1992) Experimental Manipulations of the Organic Compositions of Seawater: Implications for Studies of Energy Budgets in Marine Invertebrate Larvae, *J. Exp. Mar. Biol. Ecol. 156*, 273–284.

50. Bünde, T.A., and Fried, M. (1978) The Uptake of Dissolved Free Fatty Acids from Seawater by a Marine Filter Feeder, *Crassostrea virginica*, *Comp. Biochem. Physiol. 60*, 139–144.

51. Sargent, J., Bell, G., McEvoy, L., Tocher, D., and Estevez, A. (1999) Recent Developments in the Essential Fatty Acid Nutrition of Fish, *Aquaculture 177*, 191–199.

52. Pazos, A.J., Ruíz, C., Garcia-Martin, O., Abad, M., and Sanchez, J.L. (1996) Seasonal Variations of the Lipid Content and Fatty Acid Composition of *Crassostrea gigas* Cultured in El Grove, Galicia, N.W. Spain, *Comp. Biochem. Physiol. B 114*, 171–179.

53. Chu, F.-L.E., Soudant, P., and Hale, R.C. (2003) Relationship Between PCB Accumulation and Reproductive Output in Conditioned Oysters *Crassostrea virginica* Fed a Contaminated Algal Diet, *Aquat. Toxicol. 65*, 293–307.

High Docosahexaenoic Acid Levels in Both Neutral and Polar Lipids of a Highly Migratory Fish: *Thunnus tonggol* (Bleeker)

Hiroaki Saito*, Yutaka Seike, Hisashi Ioka, Kazufumi Osako, Mikiko Tanaka, Akihito Takashima, Joseph M. Keriko, Sevim Kose, and Juan C. Rodriguez Souza

National Research Institute of Fisheries Science, Fisheries Research Agency, Yokohama-shi 236-8648, Japan

ABSTRACT: The lipid and FA compositions of various organs (light muscle, dark muscle, liver, pyloric cecum, and the orbital region) and of the stomach contents of a highly migratory fish species *Thunnus tonggol* (Bleeker) were analyzed. TAG and phospholipids (PE and PC) were the major lipid classes in the total lipids of *T. tonggol*. DHA was characteristically the major FA of all the major classes of all its organs except for only one case of liver TAG. The mean DHA contents of the various organs accounted for more than 20% of the total FA (TFA), even though it is a neutral depot lipid. However, DHA in the stomach contents, originating from their prey, fluctuated and was generally low. DHA levels were generally higher in a year (2000) when water temperatures were colder than in one when it was warmer (1998). Furthermore, DHA levels in muscle TAG were consistently high in spite of the fluctuation of those in the visceral TAG, which might be directly influenced by the prey lipids. This phenomenon suggests the physiological selective accumulation of DHA in the muscle, after the migration of the digested FA in the vascular system and absorption of the prey lipids in the intestine. In contrast, the FA composition of other species is generally variable and their DHA contents of TAG are usually less than 20% of TFA.

Paper no. L9485 in *Lipids 40*, 941–953 (September 2005).

Comparatively high DHA levels in the lipids of tissues of all species of highly migratory tuna species, such as the genera *Thunnus*, *Euthynnus*, and *Auxis* belonging to the tribe Thunnini, have been reported—specifically, for *T. thynnus* (1), *T. alalunga* (2,3), *T. albacares* (4), *E. pelamis* (1,5,6), *E. affinis* (7), *A. rochei*, and *A. thazard* (1,8)—and confirmed (9). In particular, markedly high DHA levels have been found in tuna phospholipids, similar to those of other fish phospholipids (10). The cause of the high DHA levels of tuna species might be the accumulation of DHA during long-distance migrations (7), because it is the most important EFA for marine fish (11,12) and is a less effective fat as an energy source (13–15).

Although high DHA levels in total lipids (TL) of these fish species have been reported, it is not clear which lipid class contains the major portion of DHA. It is well known that DHA levels in fish tissue phospholipids are high, whereas n-3 PUFA are present in comparatively low levels in neutral depot lipid TAG. In many cases, the FA compositions of neutral lipids vary with environmental conditions, such as the stage of fish maturation, seawater temperature, prey lipids, and so on (16,17). Moreover, in marine fishes, the DHA contents in neutral lipids are generally less than 20% of the total FA (TFA), but saturated FA (SFA) and monounsaturated FA (MUFA), such as 16:0, 18:0, and 18:1n-9, are major components. High levels of DHA in the neutral lipids characteristic of tuna species, such as the orbital fats and head oils [for *T. obesus* and *E. pelamis* (18); for *Thunnus* spp. and *E. pelamis* (19)], have been described in only a few papers. There are no other reports for high DHA contents in neutral lipids except for the lipids of these tuna species.

Neither ecology nor lipid physiology of the tuna fish species *T. tonggol* (Bleeker), which is considered to migrate in the northern Pacific Ocean, has yet been thoroughly investigated. To determine the DHA levels in the various lipid classes of this species, and to estimate how they relate to its ecology and physiology, the lipid classes and the FA composition of its muscles and other internal organs including the stomach contents were analyzed in the present study.

MATERIALS AND METHODS

Materials. Specimens of *T. tonggol* were caught in the Japan Sea (35°00′N, 132°15′E and 34°55′N, 132°10′E) by using the same set-net in August 1998 (sample 1) and in June 2000 (sample 2), respectively (see Table 1). The biological data of 49 specimens (body length: 506 ± 7 mm, body weight: 2458 ± 149 g) for sample 1 and 24 specimens (body length: 480 ± 3 mm) for sample 2 were measured. Then 5 animals from sample 1 and 6 from sample 2 were selected at random, immediately frozen, and stored at –40°C for 2 wk to 1 mon prior to lipid extraction.

Lipid extraction and the analysis of lipid classes. Each sample was homogenized in a mixture of chloroform and methanol (2:1, vol/vol), and a portion of each homogenized sample was extracted according to the procedure of Folch *et al.* (20). The

*To whom correspondence should be addressed at National Research Institute of Fisheries Science, Fisheries Research Agency, 2-12-4, Fuku-ura, Kanazawa-ku, Yokohama-shi 236-8648, Japan.
E-mail address: hiroakis@affrc.go.jp

Present addresses: (second author) Industrial Technology Institute of Tottori Prefecture, Tottori 684-0041, Japan; (third author) Shimane Prefectural Fisheries Institute, Shimane Prefecture, Shimane 697-0061, Japan; (fourth author) Nagasaki Prefectural Institute of Fisheries, Taira, Nagasaki 851-2213, Japan.

Abbreviations: DMOX, 4,4-dimethyloxazoline; GE, diacylglyceryl ethers; MUFA, monounsaturated FA (monounsaturates); ST, sterols; SE, steryl esters; SFA, saturated FA (saturates); TFA, total FA; TL, total lipids; WE, wax esters.

TABLE 1
Locality of Capture and Biological Data of *Thunnus tonggol* Examined

Scientific name *Thunnus tonggol*	Sample no.	Date	Locality	Temperature	Replicate animals (*n*)	Length[a] (mm)	Weight[a] (g)
	1	August 2, 1998	35°00′N, 132°15′E	28°C	5	477 ± 9	2028 ± 133
	2	June 28, 2000	34°55′N, 132°10′E	22°C	6	513 ± 6	2902 ± 92

[a]Results are expressed as mean ± SE (*n* = 5–6).

crude TL were separated into classes on silicic acid columns (Kieselgel 60, 70–230 mesh; Merck and Co. Ltd., Darmstadt, Germany), and a quantitative analysis of the lipid constituents was performed using gravimetric analysis of fractions collected from column chromatography. The first eluate (dichloro-methane/*n*-hexane, 2:3, vol/vol) contained the steryl esters (SE), wax esters (WE), and diacyl glyceryl ethers (GE). This was followed by: dichloro-methane eluting the TAG; dichloromethane/ether (35:1, vol/vol), sterols (ST); dichloro-methane/ether (9:1, vol/vol), DAG; dichloromethane/methanol (9:1, vol/vol), FFA; dichloro-methane/methanol (1:1, vol/vol), PE; dichloromethane/methanol (1:5, vol/vol), the other minor phospholipids; and dichloromethane/methanol (1:20, vol/vol), PC fractions (21). Individual lipids from each lipid class were identified by comparison of R_f values from authentic samples using TLC (Kieselgel 60, thickness of 0.25 mm for analysis; Merck & Co. Ltd.) and characteristic peaks using NMR spectrometry (22). All sample lipids were dried under argon at room temperature and stored at −40°C.

NMR spectrometry. Spectra were recorded on a GSX-270 NMR spectrometer (JEOL Co. Ltd., Tokyo, Japan) in the pulsed Fourier transform mode at 270 MHz in deuterochloroform solution using tetramethylsilane as an internal standard (22).

The preparation of methyl esters and GLC of the esters. The TAG, PE, and PC fractions were directly transesterified with boiling methanol containing 1% concentrated hydrochloric acid under reflux for 1.5 h to produce FAME, as previously reported (23). The methyl esters were purified using silica gel column chromatography by elution with a mixture of *n*-hexane and dichloromethane (1/2, vol/vol).

Analysis of the FAME was performed on an HP-5890 (Hewlett-Packard Co., Yokogawa Electric Corporation, Tokyo, Japan) gas chromatograph equipped with an Omegawax®-250 fused-silica capillary column (30 m × 0.25 μm i.d.; 0.25 μm film; Supelco Japan Co. Ltd., Tokyo, Japan). The temperatures of the injector and the column were held at 250 and 210°C, respectively, and the split ratio was 1:76. Helium was used as the carrier gas at a constant inlet rate of 0.7 mL/min.

Quantification of individual components was performed by means of Shimadzu Model C-R3A (Shimadzu Seisakusho Co. Ltd., Kyoto, Japan) and HP ChemStation System (A. 06 revision, Yokogawa HP Co. Ltd., Tokyo, Japan) electronic integrators.

Preparation of 4,4-dimethyloxazoline (DMOX) derivatives and analysis of DMOX derivatives by GC–MS. The DMOX derivatives were prepared by adding an excess amount of 2-amino-2-methyl-propanol to a small amount of the FAME in a test tube under an argon atmosphere. The mixture was heated at 180°C for 36 h and the usual workup was carried out (24). Analysis of the DMOX derivatives was performed on a GC-MCD 1800 (Hewlett-Packard Co., Yokogawa Electric Corporation) gas chromatograph–mass spectrometer equipped with the same capillary GC column. The temperatures of the injector and the column were held at 240 and 210°C, respectively. The split ratio was 1:76, and the ionization voltage was 70 eV. Helium was used as the carrier gas at a constant inlet rate of 0.7 mL/min.

FAME were identified by using marine lipid methyl esters as standards (Omegawax® test mixture No. 4-8476; Supelco Japan Ltd.) and by comparing mass spectral data obtained by GC–MS.

Statistical analyses. For all samples of the FA determination by GLC, more than five replications (*n* = 5–10) were made. The significant differences in the data of the total SFA, total MUFA, total n-6 PUFA, and total n-3 PUFA of the classes (TAG, PE, and PC) of samples 1 and 2 were determined using Student's *t*-test at a significance level of *P* < 0.05.

RESULTS

Lipid content and biological data. The biological data from the specimens examined and their TL content are given in Tables 1 and 2. Although the fish size and the environmental conditions differed between samples 1 and 2, taken in 1998 and 2000 (Table 1), respectively, the TL contents of the light muscle were similar (0.7 ± 0.1 and 0.7 ± 0.2%). Both the visceral and orbital lipids were comparatively high (2.8–4.4% for liver, 2.0–3.1% for pyloric cecum, and 12.9–19.9% for the orbital lipids).

Lipid classes of the respective organs of T. tonggol. Table 2 shows the various lipid classes of the respective organs separated by silicic acid column chromatography. In all the organs, the neutral lipids contained mainly TAG, ST, and FFA, and the polar lipids contained PE and PC, with small amounts of SE (0.3–1.2%), WE (0.0–0.6%), GE (0.8–2.5%), and DAG (0.2–6.1%). Phospholipids were mainly PC and PE, which were identified by comparing with R_f values of authentic samples on TLC.

The highest levels of TAG (82.7–87.0%) were found in the orbital lipids, for which the lipid contents (12.5–19.0%) were much higher than those of the other organs. In the visceral lipids, comparatively high FFA levels were found, particularly in the pyloric cecum and the liver of sample 1. Sterols were present at moderate levels (4.0–19.4%) in all samples. The purified sterols were immediately crystallized after isolation, and cholesterol

TABLE 2
The Lipid Contents and Lipid Classes of *T. tonggol* Examined[a]

Sample no.	Lipid contents[b]	WE[c]	SE[c]	GE[c]	TAG[c]	ST[c]	DAG[c]	FFA[c]	PE[c]	OPL[c]	PC[c]
Sample 1 (1998)[d]											
Ordinary muscle	0.7 ± 0.1	0.1 ± 0.0	1.4 ± 0.3		34.0 ± 3.8	12.5 ± 1.8	2.0 ± 2.0	5.0 ± 0.6	12.7 ± 0.5	8.3 ± 2.5	24.3 ± 3.2
Dark muscle	2.5 ± 0.1	0.0 ± 0.0	1.0 ± 0.1		33.2 ± 4.4	6.9 ± 1.0	0.9 ± 0.9	11.1 ± 1.5	14.9 ± 2.4	8.0 ± 1.3	24.1 ± 2.9
Liver	4.4 ± 0.3	0.2 ± 0.1	4.7 ± 1.1		39.3 ± 6.0	9.8 ± 1.3	2.0 ± 1.2	20.1 ± 1.9	7.1 ± 0.6	6.5 ± 1.1	10.5 ± 2.9
Pyloric cecum	2.0 ± 0.3	0.1 ± 0.0	2.3 ± 0.4		22.2 ± 7.2	12.8 ± 3.8	6.1 ± 3.1	35.7 ± 4.6	7.4 ± 1.4	5.5 ± 1.2	7.9 ± 3.4
Orbital	12.9 ± 2.5	0.0 ± 0.0	1.1 ± 0.6		87.0 ± 2.9	4.2 ± 0.8	0.2 ± 0.2	2.9 ± 1.3	2.1 ± 0.6	1.3 ± 0.5	1.1 ± 0.5
Stomach contents	2.7 ± 0.1		2.4 ± 0.1		6.1 ± 1.4	22.6 ± 2.5	3.3 ± 3.3	17.1 ± 2.1	22.2 ± 2.2	20.6 ± 3.0	5.8 ± 1.3
Sample 2 (2000)[e]											
Ordinary muscle	0.7 ± 0.2	0.1 ± 0.0	0.4 ± 0.1	0.8 ± 0.2	46.1 ± 8.9	10.8 ± 1.7	1.0 ± 0.1	5.8 ± 1.1	9.4 ± 1.6	2.9 ± 1.1	22.8 ± 4.1
Dark muscle	3.2 ± 0.6	0.0 ± 0.0	0.5 ± 0.1	0.8 ± 0.2	42.9 ± 3.7	5.3 ± 0.4	2.2 ± 0.1	16.0 ± 2.5	10.9 ± 0.6	4.6 ± 1.4	16.5 ± 1.2
Liver	2.8 ± 0.5	0.2 ± 0.1	1.1 ± 0.6	2.3 ± 0.9	9.1 ± 6.1	19.4 ± 1.7	2.0 ± 1.3	10.5 ± 2.3	25.0 ± 5.0	8.7 ± 2.6	21.7 ± 4.1
Pyloric cecum	3.1 ± 0.4	0.1 ± 0.0	1.0 ± 0.2	2.4 ± 0.8	37.0 ± 11.5	14.1 ± 1.7	1.6 ± 0.4	13.0 ± 2.9	10.1 ± 1.9	6.9 ± 2.3	13.9 ± 3.4
Orbital	19.9 ± 1.7	0.0 ± 0.0	0.3 ± 0.0	0.1 ± 0.1	89.5 ± 1.1	2.1 ± 0.5	0.4 ± 0.1	1.1 ± 0.1	2.6 ± 0.7	1.5 ± 0.9	2.4 ± 0.5
Stomach contents	2.8 ± 0.8	0.0 ± 0.0	0.8 ± 0.4	0.8 ± 0.6	45.9 ± 6.3	10.5 ± 4.8	3.3 ± 1.9	13.0 ± 4.0	8.8 ± 1.8	3.6 ± 0.1	13.2 ± 4.7

[a]Data are mean ± SE (*n* = 4–6) except for the stomach contents, because the contents of sample 2 in 2000 were obtained from only two specimens.
[b]Results are expressed as weight percentage of wet tissues.
[c]Results are expressed as weight percentage of total lipids. WE, SE, GE, and ST refer to mean wax esters, steryl esters, glyceryl ethers, and sterols, respectively. OPL means other phospholipids.
[d]The SE fraction of sample 1 contained small amounts of WE and GE.
[e]The NMR method was used only on sample 2 in 2000 for quantitative determination of lipid classes fraction 1 to 4 (WE, SE, GE, and TAG).

was found to be predominant in the sterol fraction by identification with authentic cholesterol by TLC and NMR.

FA composition of TAG. The FA composition of the TAG from the various organs of *T. tonggol* are shown in Table 3. At least 50 FA compounds were detected and identified, of which about 40 occurred at a level of 0.1% or more of TFA. On the contrary, only four components were found as major acids in the TAG of all the organs: SFA, 16:0 (16.2–25.2%) and 18:0 (5.6–10.4%); MUFA, 18:1n-9 (8.7–23.2%); and n-3 PUFA, DHA (9.0–29.5%) as shown in Table 3. These main FA were detected at levels of 5% or more in almost all of the organs. Noticeable amounts (mean >2%) of several other FA were found in both samples 1 and 2, including 14:0 (0.9–3.4%), 16:1n-7 (2.6–5.2%), 18:1n-7 (2.5–3.8%), 20:1-n-9 (1.3–2.7%), 22:1n-11 (0.9–3.5%), and 20:5n-3 (EPA, 2.5–7.7%). However, DHA levels in the liver of the sample 1 were extremely low (9.0 ± 0.8%).

FA composition in tissue phospholipids. Similar to the FA composition of the tissue TAG, the high levels of n-3 PUFA (25.0–51.3% for PE and 35.2–58.6% for PC) were found in the tissue phospholipids of both samples 1 and 2 (Tables 4 and 5). Four major FA were also found in the PE of all specimens at levels of about 5% or more of the TFA: SFA 16:0 (3.0–15.0%) and 18:0 (14.1–27.6%); MUFA 18:1n-9 (2.5–20.6%); and the n-3 PUFA DHA (20.6–43.8%). The same FA were also major components in the PC: SFA 16:0 (11.2–22.9%) and 18:0 (3.4–13.9%); MUFA 18:1n-9 (4.7–12.0%); and the n-3 PUFA EPA (4.0–11.1%) and DHA (26.4–49.5%). Measurable amounts (>2%) of other FA— MUFA 18:1n-7 (1.6–3.5% for PE and 1.1–2.5% for PC); n-6 PUFA 20:4n-6 (2.3–6.6% for PE and 3.0–4.4% for PC); n-3 PUFA EPA (1.8–4.8% for PE)—were also found in these phospholipids. Although the major components of the PE were similar to those of the PC, slightly higher n-3 PUFA levels were found in PC in all the organs than in PE. EPA was a major component of PC (4.0–11.3%).

Lipid and FA compositions of the stomach contents of T. tonggol under two different conditions. Partly digested and undigested fish, such as horse mackerel, were observed in the stomachs of the *T. tonggol* examined. The lipid classes in stomach contents varied slightly in comparison with those in the organs, whereas the lipid classes of the stomach contents were similar to those of the organs. The stomach contents (Table 6) contained various levels of DHA; for example, the DHA levels in the stomach contents of samples 1 and 2 were notably different, and only three shorter-chain and lower unsaturated components (at levels of 5% or more) were found as major acids in sample 1: SFA, 16:0 (25.2 ± 0.6%) and 18:0 (9.9 ± 0.3%); and MUFA, 18:1n-9 (13.0 ± 0.4%) (Table 6).

DISCUSSION

Lipid content and biological data. The TL contents of the wet tissues of *T. tonggol* light muscle were similar to each other and were also similar to those of other tuna species, such as *T. obesus* [0.8 ± 0.3%, (1)], *T. albacares* [0.6 ± 0.0% (1); 0.5

TABLE 3
The FA Composition of the TAG in the Respective Organs of *T. tonggol*[a,b]

Sample no.	Light muscle[c] 1 Mean SE	Light muscle[c] 2 Mean SE	Dark muscle[c] 1 Mean SE	Dark muscle[c] 2 Mean SE	Liver[d] 1 Mean SE	Liver[d] 2 Mean SE	Pyloric cecum[d] 1 Mean SE	Pyloric cecum[d] 2 Mean SE	Orbital[e] 1 Mean SE	Orbital[e] 2 Mean SE
Total saturated	32.8 ± 1.7	33.0 ± 1.1	38.7 ± 1.9	32.7 ± 0.5	40.5 ± 1.6	31.2 ± 2.4	36.9 ± 4.1	30.7 ± 1.4	34.5 ± 3.6	29.7 ± 1.0
14:0	2.7 ± 0.2	2.3 ± 0.2	2.1 ± 0.1	2.0 ± 0.2	0.9 ± 0.2	1.5 ± 0.2	2.1 ± 0.5	1.7 ± 0.3	3.4 ± 0.4	2.7 ± 0.2
15:0	0.7 ± 0.0	0.7 ± 0.0	0.6 ± 0.0	0.6 ± 0.0	0.5 ± 0.1	0.6 ± 0.1	0.5 ± 0.2	0.6 ± 0.1	0.8 ± 0.1	0.7 ± 0.0
15:0 i	0.2 ± 0.0	0.1 ± 0.0	0.1 ± 0.0	0.1 ± 0.0	0.2 ± 0.1	0.1 ± 0.0	0.1 ± 0.0	0.1 ± 0.0	0.2 ± 0.1	0.2 ± 0.0
16:0	17.7 ± 0.6	16.7 ± 0.8	19.1 ± 1.2	16.2 ± 0.9	25.2 ± 2.5	18.2 ± 1.8	19.3 ± 3.3	15.9 ± 0.8	19.7 ± 1.7	17.4 ± 0.8
16:0 i	0.1 ± 0.0	0.1 ± 0.0	0.2 ± 0.1	0.1 ± 0.0	0.1 ± 0.0	0.1 ± 0.0	0.5 ± 0.4	0.1 ± 0.0	0.1 ± 0.0	0.1 ± 0.0
17:0	1.1 ± 0.1	1.1 ± 0.1	1.2 ± 0.1	1.2 ± 0.0	1.4 ± 0.1	1.2 ± 0.1	1.1 ± 0.3	1.2 ± 0.1	1.1 ± 0.1	1.0 ± 0.0
17:0 i	0.4 ± 0.0	0.5 ± 0.0	0.4 ± 0.0	0.5 ± 0.0	0.5 ± 0.0	0.5 ± 0.1	0.5 ± 0.1	0.4 ± 0.0	0.4 ± 0.0	0.4 ± 0.0
18:0	7.1 ± 0.7	8.5 ± 0.4	9.2 ± 0.7	9.2 ± 0.3	9.8 ± 0.9	7.4 ± 0.6	10.4 ± 1.4	8.4 ± 0.5	6.4 ± 0.8	5.6 ± 0.4
18:0 i	0.6 ± 0.1	0.4 ± 0.0	0.6 ± 0.1	0.4 ± 0.0	0.4 ± 0.0	0.3 ± 0.0	0.3 ± 0.1	0.3 ± 0.0	0.5 ± 0.1	0.3 ± 0.0
19:0	0.5 ± 0.0	0.6 ± 0.1	0.6 ± 0.0	0.5 ± 0.0	0.3 ± 0.1	0.3 ± 0.0	0.4 ± 0.0	0.4 ± 0.0	0.4 ± 0.0	0.3 ± 0.0
20:0	1.0 ± 0.1	1.0 ± 0.1	1.3 ± 0.0	0.9 ± 0.1	0.5 ± 0.1	0.4 ± 0.1	0.6 ± 0.1	0.8 ± 0.1	0.9 ± 0.2	0.5 ± 0.0
22:0	0.5 ± 0.1	0.4 ± 0.1	1.0 ± 0.1	0.5 ± 0.1	0.3 ± 0.1	0.2 ± 0.1	0.5 ± 0.1	0.4 ± 0.1	0.4 ± 0.0	0.3 ± 0.0
24:0	0.3 ± 0.2	0.6 ± 0.1	2.4 ± 0.4	0.5 ± 0.2	0.5 ± 0.1	0.3 ± 0.1	0.6 ± 0.3	0.5 ± 0.1	0.1 ± 0.1	0.1 ± 0.1
Total monoenoic	29.5 ± 2.0	27.4 ± 0.4	29.0 ± 2.6	24.0 ± 0.5	37.1 ± 1.2	28.3 ± 3.2	20.6 ± 3.7	24.2 ± 1.6	30.8 ± 3.1	29.0 ± 1.4
14:1n-9	0.1 ± 0.0	0.0 ± 0.0	0.0 ± 0.0	0.0 ± 0.0	0.0 ± 0.0	0.0 ± 0.0	0.2 ± 0.2	0.0 ± 0.0	0.0 ± 0.0	0.0 ± 0.0
15:1n-6	0.0 ± 0.0	0.0 ± 0.0	0.0 ± 0.0	0.0 ± 0.0	0.0 ± 0.0	0.0 ± 0.0	0.0 ± 0.0	0.0 ± 0.0	0.0 ± 0.0	0.0 ± 0.0
16:1n-11	0.0 ± 0.0	0.5 ± 0.1	0.1 ± 0.1	0.3 ± 0.1	0.0 ± 0.0	0.4 ± 0.1	0.0 ± 0.0	0.4 ± 0.1	0.0 ± 0.0	0.2 ± 0.1
16:1n-7	4.1 ± 0.3	2.9 ± 0.3	3.1 ± 0.1	2.6 ± 0.3	3.4 ± 0.3	3.0 ± 0.1	3.0 ± 0.7	2.6 ± 0.3	5.2 ± 0.1	4.9 ± 0.5
16:1n-5	0.1 ± 0.0	0.2 ± 0.1	0.1 ± 0.0	0.1 ± 0.0	0.1 ± 0.0	0.1 ± 0.0	0.4 ± 0.2	0.1 ± 0.0	0.2 ± 0.0	0.1 ± 0.0
17:1n-8	0.6 ± 0.0	0.5 ± 0.0	0.5 ± 0.0	0.5 ± 0.0	0.8 ± 0.1	0.7 ± 0.1	0.5 ± 0.0	0.5 ± 0.0	0.6 ± 0.1	0.8 ± 0.1
18:1n-13	0.0 ± 0.0	0.0 ± 0.0	0.0 ± 0.0	0.0 ± 0.0	0.0 ± 0.0	0.0 ± 0.0	0.0 ± 0.0	0.1 ± 0.0	0.0 ± 0.0	0.0 ± 0.0
18:1n-9	12.5 ± 0.7	12.3 ± 0.5	11.1 ± 1.0	10.8 ± 0.6	23.2 ± 1.9	16.1 ± 3.0	8.7 ± 1.7	12.6 ± 1.4	13.4 ± 0.8	14.9 ± 0.8
18:1n-7	2.8 ± 0.1	2.8 ± 0.1	2.7 ± 0.1	2.5 ± 0.1	3.8 ± 1.0	3.3 ± 1.0	2.8 ± 0.3	3.0 ± 0.2	3.0 ± 0.2	2.5 ± 0.1
18:1n-5	0.1 ± 0.0	0.2 ± 0.0	0.2 ± 0.0	0.1 ± 0.0	0.3 ± 0.0	0.2 ± 0.0	0.2 ± 0.0	0.1 ± 0.0	0.2 ± 0.0	0.2 ± 0.0
19:1n-11	0.1 ± 0.0	0.1 ± 0.0	0.1 ± 0.0	0.1 ± 0.0	0.1 ± 0.0	0.1 ± 0.0	0.1 ± 0.0	0.1 ± 0.0	0.1 ± 0.0	0.1 ± 0.0
19:1n-9	0.1 ± 0.0	0.1 ± 0.0	0.1 ± 0.0	0.1 ± 0.0	0.3 ± 0.0	0.2 ± 0.0	0.1 ± 0.0	0.2 ± 0.0	0.1 ± 0.0	0.1 ± 0.0
20:1n-11	0.6 ± 0.1	0.7 ± 0.2	1.2 ± 0.5	0.3 ± 0.1	0.4 ± 0.1	0.3 ± 0.1	0.3 ± 0.1	0.3 ± 0.1	0.4 ± 0.1	0.2 ± 0.1
20:1n-9	2.5 ± 0.5	2.2 ± 0.1	2.2 ± 0.7	2.0 ± 0.1	2.0 ± 0.2	1.7 ± 0.2	1.3 ± 0.4	1.6 ± 0.1	2.7 ± 0.7	2.1 ± 0.1
20:1n-7	0.3 ± 0.0	0.3 ± 0.0	0.3 ± 0.1	0.3 ± 0.0	0.3 ± 0.0	0.3 ± 0.1	0.3 ± 0.0	0.3 ± 0.0	0.3 ± 0.0	0.3 ± 0.0
20:1n-5	0.0 ± 0.0	0.1 ± 0.0	0.0 ± 0.0	0.0 ± 0.0	0.0 ± 0.0	0.0 ± 0.0	0.0 ± 0.0	0.0 ± 0.0	0.0 ± 0.0	0.1 ± 0.0
22:1n-11	3.3 ± 0.9	2.4 ± 0.3	3.5 ± 1.0	2.0 ± 0.2	0.9 ± 0.5	0.9 ± 0.2	1.0 ± 0.5	1.1 ± 0.1	2.9 ± 1.0	1.6 ± 0.1
22:1n-9	0.5 ± 0.1	0.4 ± 0.0	0.6 ± 0.1	0.4 ± 0.0	0.3 ± 0.1	0.2 ± 0.0	0.2 ± 0.1	0.3 ± 0.0	0.4 ± 0.1	0.2 ± 0.0
22:1n-7	0.2 ± 0.0	0.2 ± 0.0	0.3 ± 0.0	0.2 ± 0.0	0.1 ± 0.0	0.1 ± 0.0	0.1 ± 0.0	0.2 ± 0.0	0.2 ± 0.0	0.1 ± 0.0
24:1n-9	1.5 ± 0.2	1.6 ± 0.2	2.9 ± 0.2	1.5 ± 0.2	1.0 ± 0.2	0.5 ± 0.1	1.6 ± 0.5	0.8 ± 0.1	1.2 ± 0.2	0.5 ± 0.1

(continued)

TABLE 3 (continued)
The FA Composition of the TAG in the Respective Organs of *T. tonggol*[a,b]

Sample no.	Light muscle[c]		Dark muscle[c]		Liver[d]		Pyloric cecum[d]		Orbital[e]	
	1	2	1	2	1	2	1	2	1	2
	Mean SE	Mean SE	Mean SE	Mean SE	Mean SE	Mean SE	Mean SE	Mean SE	Mean SE	Mean SE
Total polyenoic	34.7 ± 3.6	37.2 ± 1.2	29.1 ± 2.9	40.7 ± 0.8	19.0 ± 1.9	37.2 ± 4.9	33.2 ± 5.8	42.6 ± 2.3	32.4 ± 6.7	39.2 ± 2.4
n-6 series	4.4 ± 0.3	4.7 ± 0.1	4.0 ± 0.4	4.5 ± 0.1	4.3 ± 0.5	7.1 ± 0.9	6.4 ± 1.4	6.7 ± 0.9	4.9 ± 0.3	4.8 ± 0.1
18:2n-6	1.4 ± 0.1	1.0 ± 0.1	1.0 ± 0.1	1.0 ± 0.1	0.9 ± 0.1	1.2 ± 0.1	1.0 ± 0.2	1.1 ± 0.1	1.5 ± 0.1	1.2 ± 0.0
20:2n-6	0.3 ± 0.0	0.3 ± 0.0	0.3 ± 0.0	0.3 ± 0.0	0.4 ± 0.1	0.4 ± 0.0	0.2 ± 0.0	0.3 ± 0.0	0.3 ± 0.0	0.3 ± 0.0
20:3n-6	0.2 ± 0.0	0.3 ± 0.0	0.2 ± 0.1	0.2 ± 0.0	0.1 ± 0.0	0.2 ± 0.0	0.1 ± 0.0	0.2 ± 0.0	0.3 ± 0.2	0.2 ± 0.0
20:4n-6	1.4 ± 0.1	1.5 ± 0.0	1.3 ± 0.1	1.3 ± 0.0	1.5 ± 0.2	3.7 ± 0.7	3.5 ± 1.2	3.4 ± 0.9	1.3 ± 0.2	1.5 ± 0.0
22:3n-6	0.2 ± 0.0	0.2 ± 0.0	0.1 ± 0.0	0.2 ± 0.0	0.1 ± 0.0	0.1 ± 0.0	0.1 ± 0.0	0.2 ± 0.0	0.2 ± 0.1	0.2 ± 0.0
22:4n-6	0.4 ± 0.0	0.3 ± 0.0	0.4 ± 0.0	0.3 ± 0.0	0.8 ± 0.2	0.6 ± 0.1	0.4 ± 0.1	0.4 ± 0.1	0.3 ± 0.0	0.3 ± 0.0
22:5n-6	1.0 ± 0.1	1.2 ± 0.1	1.0 ± 0.1	1.1 ± 0.1	0.5 ± 0.1	0.8 ± 0.2	1.3 ± 0.3	1.0 ± 0.1	0.9 ± 0.1	1.1 ± 0.1
n-3 series	30.3 ± 3.7	32.5 ± 1.2	25.1 ± 2.6	36.2 ± 0.6	14.7 ± 1.5	30.2 ± 4.1	26.9 ± 4.5	35.9 ± 1.5	27.5 ± 6.4	34.4 ± 2.3
18:3n-3	0.5 ± 0.1	0.4 ± 0.0	0.2 ± 0.0	0.4 ± 0.0	0.2 ± 0.0	0.5 ± 0.1	0.3 ± 0.1	0.4 ± 0.0	0.5 ± 0.0	0.5 ± 0.0
18:4n-3	1.0 ± 0.2	0.4 ± 0.1	0.4 ± 0.1	0.5 ± 0.1	0.1 ± 0.0	0.5 ± 0.1	0.4 ± 0.2	0.5 ± 0.1	0.8 ± 0.2	0.6 ± 0.1
20:3n-3	0.1 ± 0.0	0.1 ± 0.0	0.1 ± 0.0	0.1 ± 0.0	0.2 ± 0.0	0.2 ± 0.0	0.2 ± 0.0	0.1 ± 0.0	0.2 ± 0.0	0.2 ± 0.0
20:4n-3	0.4 ± 0.1	0.3 ± 0.0	0.3 ± 0.0	0.3 ± 0.0	0.5 ± 0.1	0.5 ± 0.1	0.2 ± 0.0	0.3 ± 0.0	0.4 ± 0.1	0.4 ± 0.0
20:5n-3	4.5 ± 0.7	3.8 ± 0.4	2.7 ± 0.4	3.7 ± 0.3	2.5 ± 0.4	7.7 ± 1.3	4.2 ± 0.6	6.6 ± 1.1	4.4 ± 1.4	4.8 ± 0.3
22:4n-3	0.0 ± 0.0	0.0 ± 0.0	0.0 ± 0.0	0.0 ± 0.0	0.0 ± 0.0	0.2 ± 0.1	0.0 ± 0.0	0.0 ± 0.0	0.0 ± 0.0	0.1 ± 0.0
22:5n-3	1.6 ± 0.2	1.4 ± 0.1	1.8 ± 0.2	1.7 ± 0.1	2.2 ± 0.3	3.3 ± 0.3	1.2 ± 0.1	2.0 ± 0.3	1.4 ± 0.4	1.6 ± 0.0
22:6n-3	22.2 ± 2.9	26.0 ± 1.1	19.6 ± 2.0	29.5 ± 1.1	9.0 ± 0.8	17.3 ± 2.9	20.4 ± 4.0	25.9 ± 0.6	19.8 ± 4.4	26.2 ± 2.0
Total FA	97.0 ± 0.2	97.7 ± 0.1	96.8 ± 0.1	97.3 ± 0.1	96.5 ± 0.3	96.7 ± 0.3	90.7 ± 4.9	97.5 ± 0.2	97.6 ± 0.3	97.8 ± 0.1

[a]Results are expressed as weight percentage of total FA. Data are mean ± SE for several samples ($n = 5$).
[b]In Tables 3–5, the major FA are selected if at least one mean datum was detected at a level of 0.5% or more of total FA.
[c]As for the TAG in the muscle lipids, significant differences between samples 1 and 2 are found in the case of total saturates (38.7 and 32.7%) and total n-3 PUFA (25.1 and 36.2%) of the dark muscle, respectively. There is no significant difference for the other FA (total saturates, total monoenes, total n-6 PUFA, and total n-3 PUFA) of the light muscles, respectively.
[d]As for the TAG in the visceral lipids, there is no significant difference between samples 1 and 2 in the case of total saturates, total monoenes, and total n-6 PUFA of the pyloric cecum, respectively. All the FA (total saturates, total monoenes, total n-6 PUFA, and total n-3 PUFA) of the liver lipids between samples 1 and 2 are significantly different, respectively.
[e]In the orbital lipids, there is no significant difference for all the FA (total saturates, total monoenes, total n-6 PUFA, and total n-3 PUFA).

TABLE 4
The FA Composition of the PE in the Respective Organs of *T. tonggol*[a,b]

Sample no.	Light muscle[c] 1 Mean SE	Light muscle[c] 2 Mean SE	Dark muscle[c] 1 Mean SE	Dark muscle[c] 2 Mean SE	Liver[c,d] 1 Mean SE	Liver[c,d] 2 Mean SE	Pyloric cecum[c,d] 1 Mean SE	Pyloric cecum[c,d] 2 Mean SE	Orbital[e] 1 Mean SE	Orbital[e] 2 Mean SE
Total saturated	38.2 ± 5.3	35.5 ± 3.9	34.7 ± 4.4	31.8 ± 0.7	36.4 ± 5.0	30.0 ± 1.1	38.6 ± 4.3	33.7 ± 1.8	33.7 ± 2.7	31.9 ± 4.7
14:0	0.2 ± 0.0	0.1 ± 0.0	0.1 ± 0.0	0.1 ± 0.0	1.0 ± 0.8	0.1 ± 0.0	0.8 ± 0.1	0.2 ± 0.0	1.4 ± 0.3	0.8 ± 0.2
15:0	0.1 ± 0.0	0.2 ± 0.0	0.1 ± 0.0	0.1 ± 0.0	0.5 ± 0.1	0.1 ± 0.0	0.4 ± 0.0	0.2 ± 0.0	0.5 ± 0.1	0.6 ± 0.2
15:0i	0.0 ± 0.0	0.0 ± 0.0	0.0 ± 0.0	0.0 ± 0.0	0.1 ± 0.0	0.0 ± 0.0	0.0 ± 0.0	0.0 ± 0.0	0.2 ± 0.1	0.0 ± 0.0
16:0	9.0 ± 0.8	7.1 ± 0.7	3.7 ± 0.6	2.8 ± 0.1	13.6 ± 2.0	12.2 ± 1.0	15.0 ± 1.3	12.0 ± 0.8	11.5 ± 2.0	8.5 ± 1.1
16:0i	0.1 ± 0.0	0.0 ± 0.0	0.3 ± 0.1	0.0 ± 0.0	0.1 ± 0.0	0.3 ± 0.1	0.6 ± 0.3	0.0 ± 0.0	0.2 ± 0.1	0.0 ± 0.0
17:0	1.1 ± 0.1	1.0 ± 0.1	0.9 ± 0.1	0.8 ± 0.0	1.2 ± 0.3	1.3 ± 0.1	1.6 ± 0.2	1.5 ± 0.1	1.1 ± 0.1	0.8 ± 0.1
17:0i	0.3 ± 0.0	0.4 ± 0.0	0.1 ± 0.0	0.1 ± 0.0	0.3 ± 0.1	0.4 ± 0.1	0.3 ± 0.1	0.4 ± 0.0	0.4 ± 0.0	0.5 ± 0.0
18:0	24.6 ± 4.0	24.6 ± 2.8	27.2 ± 3.5	26.1 ± 0.6	17.5 ± 4.5	14.1 ± 0.7	18.0 ± 3.2	17.6 ± 0.8	16.1 ± 2.4	17.9 ± 3.2
18:0i	1.1 ± 0.2	0.6 ± 0.1	0.5 ± 0.1	0.2 ± 0.0	0.7 ± 0.1	0.5 ± 0.0	0.4 ± 0.0	0.5 ± 0.0	0.4 ± 0.1	0.2 ± 0.1
19:0	0.9 ± 0.2	0.8 ± 0.1	1.1 ± 0.1	1.0 ± 0.0	0.7 ± 0.1	0.6 ± 0.0	0.5 ± 0.1	0.6 ± 0.0	0.5 ± 0.1	0.5 ± 0.1
20:0	0.5 ± 0.1	0.4 ± 0.1	0.6 ± 0.1	0.4 ± 0.0	0.4 ± 0.1	0.3 ± 0.0	0.4 ± 0.0	0.4 ± 0.0	0.5 ± 0.1	0.4 ± 0.1
22:0	0.1 ± 0.0	0.1 ± 0.0	0.0 ± 0.0	0.0 ± 0.0	0.2 ± 0.1	0.0 ± 0.0	0.2 ± 0.1	0.1 ± 0.0	0.3 ± 0.0	0.4 ± 0.1
24:0	0.1 ± 0.1	0.2 ± 0.1	0.1 ± 0.0	0.1 ± 0.0	0.2 ± 0.1	0.0 ± 0.0	0.4 ± 0.1	0.1 ± 0.0	0.8 ± 0.2	1.3 ± 0.2
Total monoenoic	14.3 ± 1.5	10.7 ± 0.4	12.9 ± 1.8	7.1 ± 0.5	14.4 ± 3.4	6.7 ± 0.3	13.2 ± 2.2	6.6 ± 0.5	28.6 ± 3.0	30.6 ± 1.7
14:1n-9	0.0 ± 0.0	0.0 ± 0.0	0.0 ± 0.0	0.0 ± 0.0	0.0 ± 0.0	0.0 ± 0.0	0.0 ± 0.0	0.0 ± 0.0	0.0 ± 0.0	0.0 ± 0.0
15:1n-6	0.0 ± 0.0	0.0 ± 0.0	0.0 ± 0.0	0.0 ± 0.0	0.0 ± 0.0	0.0 ± 0.0	0.2 ± 0.0	0.0 ± 0.0	0.1 ± 0.1	0.1 ± 0.0
16:1n-11	0.0 ± 0.0	0.2 ± 0.0	0.0 ± 0.0	0.0 ± 0.0	0.0 ± 0.0	0.1 ± 0.0	0.1 ± 0.0	0.1 ± 0.0	0.0 ± 0.0	0.4 ± 0.1
16:1n-7	1.2 ± 0.1	1.2 ± 0.5	1.1 ± 0.1	0.4 ± 0.0	2.3 ± 0.9	0.3 ± 0.1	1.6 ± 0.2	0.4 ± 0.1	2.7 ± 0.6	1.7 ± 0.2
16:1n-5	0.1 ± 0.0	0.1 ± 0.0	0.0 ± 0.0	0.0 ± 0.0	0.2 ± 0.1	0.1 ± 0.0	0.3 ± 0.1	0.1 ± 0.0	0.2 ± 0.1	0.0 ± 0.0
17:1n-8	0.3 ± 0.0	0.3 ± 0.1	0.2 ± 0.0	0.1 ± 0.0	0.4 ± 0.1	0.2 ± 0.0	0.4 ± 0.0	0.2 ± 0.0	0.6 ± 0.3	0.6 ± 0.1
18:1n-13	0.0 ± 0.0	0.0 ± 0.0	0.0 ± 0.0	0.0 ± 0.0	0.0 ± 0.0	0.0 ± 0.0	0.0 ± 0.0	0.0 ± 0.0	0.0 ± 0.0	0.0 ± 0.0
18:1n-9	6.9 ± 0.6	4.7 ± 0.4	6.6 ± 0.9	3.5 ± 0.3	5.5 ± 1.8	2.7 ± 0.2	5.0 ± 1.5	2.4 ± 0.2	15.6 ± 2.4	20.6 ± 1.9
18:1n-7	3.5 ± 0.5	2.3 ± 0.2	2.9 ± 0.5	1.8 ± 0.1	3.3 ± 0.5	1.6 ± 0.1	2.7 ± 0.2	1.9 ± 0.1	3.4 ± 0.1	2.6 ± 0.3
18:1n-5	0.1 ± 0.0	0.1 ± 0.0	0.1 ± 0.0	0.1 ± 0.0	0.1 ± 0.0	0.1 ± 0.0	0.1 ± 0.0	0.1 ± 0.0	0.1 ± 0.0	0.0 ± 0.0
19:1n-11	0.1 ± 0.0	0.0 ± 0.0	0.0 ± 0.0	0.0 ± 0.0	0.0 ± 0.0	0.0 ± 0.0	0.0 ± 0.0	0.0 ± 0.0	0.0 ± 0.0	0.1 ± 0.0
19:1n-9	0.1 ± 0.0	0.1 ± 0.0	0.1 ± 0.0	0.1 ± 0.0	0.2 ± 0.0	0.1 ± 0.0	0.1 ± 0.0	0.2 ± 0.0	0.1 ± 0.0	0.1 ± 0.0
20:1n-11	0.4 ± 0.3	0.1 ± 0.0	0.1 ± 0.0	0.0 ± 0.0	0.6 ± 0.3	0.0 ± 0.0	0.2 ± 0.1	0.0 ± 0.0	0.1 ± 0.0	0.1 ± 0.0
20:1n-9	0.8 ± 0.2	0.8 ± 0.1	0.9 ± 0.2	0.6 ± 0.1	0.6 ± 0.2	0.8 ± 0.0	0.7 ± 0.2	0.6 ± 0.0	0.8 ± 0.1	0.7 ± 0.1
20:1n-7	0.1 ± 0.0	0.1 ± 0.0	0.1 ± 0.0	0.1 ± 0.0	0.1 ± 0.0	0.1 ± 0.0	0.2 ± 0.0	0.1 ± 0.0	0.5 ± 0.3	0.1 ± 0.0
20:1n-5	0.0 ± 0.0	0.0 ± 0.0	0.0 ± 0.0	0.0 ± 0.0	0.0 ± 0.0	0.0 ± 0.0	0.0 ± 0.0	0.0 ± 0.0	0.0 ± 0.0	0.0 ± 0.0
22:1n-11	0.1 ± 0.1	0.1 ± 0.0	0.1 ± 0.0	0.1 ± 0.0	0.2 ± 0.2	0.2 ± 0.0	0.1 ± 0.1	0.1 ± 0.0	0.6 ± 0.2	0.3 ± 0.0
22:1n-9	0.1 ± 0.1	0.0 ± 0.0	0.2 ± 0.1	0.0 ± 0.0	0.2 ± 0.1	0.0 ± 0.0	0.2 ± 0.1	0.0 ± 0.0	0.1 ± 0.0	0.1 ± 0.0
22:1n-7	0.0 ± 0.0	0.0 ± 0.0	0.0 ± 0.0	0.0 ± 0.0	0.0 ± 0.0	0.0 ± 0.0	0.0 ± 0.0	0.0 ± 0.0	0.2 ± 0.0	0.2 ± 0.0
24:1n-9	0.5 ± 0.1	0.5 ± 0.1	0.4 ± 0.1	0.1 ± 0.0	0.6 ± 0.2	0.1 ± 0.0	1.4 ± 0.3	0.2 ± 0.1	3.3 ± 1.1	3.0 ± 0.7

(continued)

TABLE 4 (continued)
The FA Composition of the PE in the Respective Organs of *T. tonggol*[a,b]

Sample no.	Light muscle[c] 1 Mean SE	Light muscle[c] 2 Mean SE	Dark muscle[c] 1 Mean SE	Dark muscle[c] 2 Mean SE	Liver[c,d] 1 Mean SE	Liver[c,d] 2 Mean SE	Pyloric cecum[c,d] 1 Mean SE	Pyloric cecum[c,d] 2 Mean SE	Orbital[e] 1 Mean SE	Orbital[e] 2 Mean SE
Total polyenoic	43.1 ± 6.2	49.2 ± 3.1	50.9 ± 6.1	59.2 ± 1.2	46.3 ± 7.1	59.8 ± 1.8	42.1 ± 3.0	56.7 ± 1.7	31.6 ± 4.8	32.2 ± 3.4
n-6 series	8.3 ± 0.9	8.7 ± 0.3	8.7 ± 0.7	8.3 ± 0.3	9.7 ± 1.0	8.5 ± 0.4	10.0 ± 0.6	9.6 ± 0.2	6.0 ± 0.7	7.2 ± 0.3
18:2n-6	1.6 ± 0.2	0.9 ± 0.1	3.2 ± 0.3	1.4 ± 0.1	1.2 ± 0.1	0.4 ± 0.0	0.8 ± 0.1	0.5 ± 0.0	1.2 ± 0.1	0.9 ± 0.2
20:2n-6	0.4 ± 0.0	0.2 ± 0.0	0.7 ± 0.1	0.3 ± 0.0	0.5 ± 0.1	0.2 ± 0.0	0.2 ± 0.0	0.2 ± 0.0	0.3 ± 0.0	0.2 ± 0.0
20:3n-6	0.1 ± 0.0	0.1 ± 0.0	0.5 ± 0.0	0.2 ± 0.0	0.2 ± 0.0	0.1 ± 0.0	0.1 ± 0.0	0.1 ± 0.0	0.1 ± 0.0	0.1 ± 0.0
20:4n-6	3.4 ± 0.5	4.3 ± 0.2	2.3 ± 0.2	2.7 ± 0.1	5.6 ± 1.0	4.6 ± 0.1	6.6 ± 0.4	6.5 ± 0.2	3.0 ± 0.4	3.6 ± 0.3
22:3n-6	0.0 ± 0.0	0.0 ± 0.0	0.0 ± 0.0	0.0 ± 0.0	0.0 ± 0.0	0.0 ± 0.0	0.0 ± 0.0	0.0 ± 0.0	0.0 ± 0.0	0.0 ± 0.0
22:4n-6	0.3 ± 0.0	0.5 ± 0.0	0.5 ± 0.1	0.7 ± 0.0	0.3 ± 0.1	0.6 ± 0.1	0.4 ± 0.1	0.4 ± 0.0	0.5 ± 0.1	0.8 ± 0.1
22:5n-6	2.4 ± 0.5	2.6 ± 0.1	2.7 ± 0.1	3.0 ± 0.2	1.8 ± 0.2	2.5 ± 0.2	1.8 ± 0.2	1.8 ± 0.1	1.1 ± 0.1	1.5 ± 0.1
n-3 series	34.8 ± 5.5	40.5 ± 2.9	42.2 ± 6.3	50.9 ± 1.1	36.5 ± 6.6	51.3 ± 1.5	32.1 ± 2.4	47.1 ± 1.7	25.6 ± 4.3	25.0 ± 3.3
18:3n-3	0.2 ± 0.0	0.1 ± 0.0	0.4 ± 0.1	0.3 ± 0.0	0.3 ± 0.1	0.1 ± 0.0	0.2 ± 0.0	0.2 ± 0.0	0.4 ± 0.1	0.5 ± 0.1
18:4n-3	0.2 ± 0.0	0.1 ± 0.0	0.2 ± 0.0	0.1 ± 0.0	0.3 ± 0.2	0.1 ± 0.0	0.2 ± 0.1	0.1 ± 0.0	0.4 ± 0.1	0.3 ± 0.1
20:3n-3	0.1 ± 0.0	0.1 ± 0.0	0.2 ± 0.0	0.2 ± 0.0	0.2 ± 0.0	0.1 ± 0.0	0.1 ± 0.0	0.1 ± 0.0	0.1 ± 0.0	0.1 ± 0.0
20:4n-3	0.2 ± 0.0	0.1 ± 0.0	0.5 ± 0.1	0.3 ± 0.0	0.4 ± 0.1	0.1 ± 0.0	0.2 ± 0.1	0.2 ± 0.0	0.3 ± 0.0	0.2 ± 0.0
20:5n-3	2.0 ± 0.4	2.6 ± 0.3	1.8 ± 0.4	2.6 ± 0.1	3.2 ± 0.8	4.4 ± 0.1	4.8 ± 1.2	4.7 ± 0.1	2.1 ± 0.4	2.0 ± 0.4
22:4n-3	0.0 ± 0.0	0.0 ± 0.0	0.0 ± 0.0	0.0 ± 0.0	0.0 ± 0.0	0.0 ± 0.0	0.0 ± 0.0	0.0 ± 0.0	0.0 ± 0.0	0.0 ± 0.0
22:5n-3	0.5 ± 0.1	1.0 ± 0.1	1.5 ± 0.3	2.1 ± 0.1	1.2 ± 0.2	3.0 ± 0.3	1.4 ± 0.6	1.2 ± 0.1	1.1 ± 0.2	1.3 ± 0.2
22:6n-3	31.6 ± 5.0	36.3 ± 2.5	37.5 ± 5.6	45.4 ± 1.1	31.0 ± 6.4	43.4 ± 1.3	25.1 ± 2.2	40.6 ± 1.5	21.4 ± 3.7	20.6 ± 2.6
Total FA	95.6 ± 1.6	95.4 ± 1.0	98.5 ± 0.1	98.1 ± 0.6	97.1 ± 0.5	96.5 ± 0.6	93.9 ± 1.6	97.0 ± 0.7	93.9 ± 1.7	94.7 ± 0.7

[a]Results are expressed as weight percentage of total FA. Data are mean ± SE for several samples ($n = 5$).
[b]In Tables 3–5, the major FA are selected if at least one mean datum was detected at a level of 0.5% or more of total FA.
[c]As for the PE, the significant differences between samples 1 and 2 are found in the total monoenes of all the organ lipids except for the orbital lipids.
[d]There are significant differences between samples 1 and 2 at the total n-3 PUFA of the liver and pyloric cecum.
[e]In the orbital lipids, there are no significant differences for all the FA (total saturates, total monoenes, total n-6 PUFA, and total n-3 PUFA).

TABLE 5
The FA Composition of the PC in the Respective Organs of *T. tonggol*[a,b]

Sample no.	Light muscle 1 Mean SE	Light muscle 2 Mean SE	Dark muscle 1 Mean SE	Dark muscle 2 Mean SE	Liver[c] 1 Mean SE	Liver[c] 2 Mean SE	Pyloric cecum[c] 1 Mean SE	Pyloric cecum[c] 2 Mean SE	Orbital[c] 1 Mean SE	Orbital[c] 2 Mean SE
Total saturated	24.9 ± 2.0	28.6 ± 2.0	21.0 ± 1.3	25.6 ± 2.2	38.1 ± 4.4	35.0 ± 1.8	40.7 ± 3.4	30.5 ± 2.9	35.1 ± 2.8	27.3 ± 0.4
14:0	0.2 ± 0.2	0.1 ± 0.0	0.2 ± 0.0	0.3 ± 0.0	0.2 ± 0.0	0.3 ± 0.0	0.6 ± 0.1	0.6 ± 0.1	0.3 ± 0.1	0.3 ± 0.0
15:0	0.2 ± 0.0	0.2 ± 0.0	0.1 ± 0.0	0.3 ± 0.0	0.4 ± 0.1	0.4 ± 0.1	0.5 ± 0.1	0.5 ± 0.1	0.2 ± 0.0	0.2 ± 0.0
15:0 i	0.0 ± 0.0	0.0 ± 0.0	0.1 ± 0.0	0.1 ± 0.0	0.0 ± 0.0	0.0 ± 0.0	0.1 ± 0.0	0.0 ± 0.0	0.1 ± 0.0	0.0 ± 0.0
16:0	19.8 ± 1.8	22.9 ± 1.7	11.2 ± 1.6	15.5 ± 1.5	23.9 ± 2.1	20.2 ± 2.0	22.0 ± 3.7	20.4 ± 2.0	17.7 ± 2.7	16.2 ± 0.8
16:0 i	0.1 ± 0.0	0.1 ± 0.0	0.2 ± 0.1	0.0 ± 0.0	0.0 ± 0.0	0.1 ± 0.0	0.2 ± 0.1	0.1 ± 0.0	0.1 ± 0.0	0.0 ± 0.0
17:0	0.5 ± 0.1	0.6 ± 0.0	0.7 ± 0.0	0.9 ± 0.1	1.0 ± 0.2	1.1 ± 0.1	1.3 ± 0.1	0.9 ± 0.1	0.9 ± 0.1	0.5 ± 0.0
17:0 i	0.2 ± 0.0	0.2 ± 0.0	0.1 ± 0.0	0.2 ± 0.0	0.2 ± 0.0	0.3 ± 0.0	0.3 ± 0.0	0.3 ± 0.0	0.2 ± 0.0	0.2 ± 0.0
18:0	3.4 ± 0.3	3.9 ± 0.2	7.5 ± 0.5	7.2 ± 0.5	11.1 ± 1.9	10.8 ± 1.7	13.9 ± 2.0	6.8 ± 0.6	11.4 ± 1.4	6.7 ± 0.3
18:0 i	0.2 ± 0.0	0.1 ± 0.0	0.2 ± 0.0	0.3 ± 0.0	0.3 ± 0.1	0.4 ± 0.1	0.3 ± 0.0	0.2 ± 0.0	0.3 ± 0.1	0.2 ± 0.1
19:0	0.2 ± 0.0	0.2 ± 0.0	0.3 ± 0.0	0.3 ± 0.0	0.5 ± 0.1	0.6 ± 0.1	0.5 ± 0.1	0.3 ± 0.0	0.5 ± 0.1	0.2 ± 0.0
20:0	0.1 ± 0.0	0.1 ± 0.0	0.2 ± 0.0	0.2 ± 0.0	0.3 ± 0.1	0.5 ± 0.1	0.4 ± 0.1	0.2 ± 0.0	0.4 ± 0.1	0.4 ± 0.1
22:0	0.0 ± 0.0	0.0 ± 0.0	0.1 ± 0.0	0.1 ± 0.0	0.1 ± 0.0	0.1 ± 0.0	0.3 ± 0.0	0.1 ± 0.0	0.5 ± 0.3	0.5 ± 0.1
24:0	0.0 ± 0.0	0.1 ± 0.0	0.1 ± 0.1	0.3 ± 0.0	0.1 ± 0.0	0.2 ± 0.0	0.3 ± 0.1	0.1 ± 0.0	2.4 ± 1.5	1.9 ± 0.4
Total monoenoic	11.5 ± 1.0	12.4 ± 0.8	9.7 ± 0.9	10.3 ± 0.5	9.2 ± 0.8	15.1 ± 1.6	12.0 ± 1.2	10.6 ± 0.7	18.3 ± 3.6	18.1 ± 2.1
14:1n-9	0.0 ± 0.0	0.0 ± 0.0	0.0 ± 0.0	0.0 ± 0.0	0.0 ± 0.0	0.0 ± 0.0	0.0 ± 0.0	0.0 ± 0.0	0.1 ± 0.0	0.0 ± 0.0
15:1n-6	0.0 ± 0.0	0.0 ± 0.0	0.0 ± 0.0	0.0 ± 0.0	0.0 ± 0.0	0.0 ± 0.0	0.0 ± 0.0	0.0 ± 0.0	0.0 ± 0.0	0.0 ± 0.0
16:1n-11	0.0 ± 0.0	0.2 ± 0.0	0.0 ± 0.0	0.2 ± 0.0	0.0 ± 0.0	0.4 ± 0.0	0.2 ± 0.1	0.5 ± 0.1	0.1 ± 0.1	0.3 ± 0.0
16:1n-7	0.7 ± 0.0	0.6 ± 0.1	0.4 ± 0.1	0.6 ± 0.1	0.6 ± 0.1	0.6 ± 0.1	0.8 ± 0.2	0.9 ± 0.1	0.7 ± 0.2	1.0 ± 0.1
16:1n-5	0.1 ± 0.0	0.1 ± 0.0	0.2 ± 0.1	0.1 ± 0.0	0.5 ± 0.1	0.1 ± 0.0	0.3 ± 0.1	0.1 ± 0.0	0.3 ± 0.2	0.1 ± 0.0
17:1n-8	0.2 ± 0.0	0.2 ± 0.0	0.1 ± 0.0	0.2 ± 0.0	0.2 ± 0.0	0.3 ± 0.0	0.2 ± 0.0	0.3 ± 0.0	0.3 ± 0.0	0.2 ± 0.0
18:1n-13	0.0 ± 0.0	0.0 ± 0.0	0.0 ± 0.0	0.0 ± 0.0	0.0 ± 0.0	0.0 ± 0.0	0.0 ± 0.0	0.0 ± 0.0	0.0 ± 0.0	0.0 ± 0.0
18:1n-9	7.6 ± 0.7	8.4 ± 0.6	5.6 ± 0.6	5.9 ± 0.3	4.7 ± 0.5	9.0 ± 1.3	5.2 ± 0.7	5.3 ± 0.2	10.0 ± 3.0	12.0 ± 1.8
18:1n-7	1.1 ± 0.1	1.3 ± 0.1	1.6 ± 0.2	1.6 ± 0.1	1.6 ± 0.2	2.4 ± 0.2	2.4 ± 0.3	2.1 ± 0.2	2.5 ± 0.6	1.7 ± 0.1
18:1n-5	0.1 ± 0.0	0.1 ± 0.0	0.1 ± 0.0	0.1 ± 0.0	0.1 ± 0.0	0.1 ± 0.0	0.1 ± 0.0	0.1 ± 0.0	0.3 ± 0.3	0.1 ± 0.1
19:1n-11	0.2 ± 0.1	0.1 ± 0.0	0.0 ± 0.0	0.0 ± 0.0	0.0 ± 0.0	0.0 ± 0.0	0.0 ± 0.0	0.0 ± 0.0	0.0 ± 0.0	0.1 ± 0.1
19:1n-9	0.1 ± 0.0	0.0 ± 0.0	0.1 ± 0.0	0.1 ± 0.0	0.1 ± 0.0	0.1 ± 0.0	0.1 ± 0.0	0.1 ± 0.0	0.1 ± 0.0	0.1 ± 0.0
20:1n-11	0.2 ± 0.0	0.1 ± 0.0	0.1 ± 0.0	0.0 ± 0.0	0.1 ± 0.0	0.1 ± 0.0	0.1 ± 0.0	0.0 ± 0.0	0.2 ± 0.1	0.1 ± 0.0
20:1n-9	0.4 ± 0.0	0.5 ± 0.1	0.6 ± 0.0	0.7 ± 0.0	0.5 ± 0.1	1.0 ± 0.1	0.5 ± 0.1	0.5 ± 0.0	0.7 ± 0.1	0.6 ± 0.0
20:1n-7	0.1 ± 0.0	0.1 ± 0.0	0.1 ± 0.0	0.1 ± 0.0	0.1 ± 0.0	0.2 ± 0.0	0.1 ± 0.0	0.1 ± 0.0	0.2 ± 0.1	0.1 ± 0.0
20:1n-5	0.0 ± 0.0	0.0 ± 0.0	0.0 ± 0.0	0.0 ± 0.0	0.0 ± 0.0	0.0 ± 0.0	0.0 ± 0.0	0.0 ± 0.0	0.0 ± 0.0	0.0 ± 0.0
22:1n-11	0.1 ± 0.1	0.2 ± 0.0	0.0 ± 0.0	0.1 ± 0.0	0.1 ± 0.0	0.3 ± 0.0	0.1 ± 0.1	0.2 ± 0.0	0.3 ± 0.1	0.2 ± 0.0
22:1n-9	0.1 ± 0.0	0.0 ± 0.0	0.2 ± 0.0	0.0 ± 0.0	0.1 ± 0.0	0.0 ± 0.0	0.2 ± 0.0	0.0 ± 0.0	0.2 ± 0.0	0.2 ± 0.0
22:1n-7	0.0 ± 0.0	0.0 ± 0.0	0.0 ± 0.0	0.0 ± 0.0	0.0 ± 0.0	0.0 ± 0.0	0.0 ± 0.0	0.0 ± 0.0	0.1 ± 0.0	0.1 ± 0.0
24:1n-9	0.5 ± 0.1	0.4 ± 0.1	0.7 ± 0.1	0.4 ± 0.1	0.6 ± 0.1	0.3 ± 0.1	1.3 ± 0.2	0.5 ± 0.2	2.2 ± 0.8	1.4 ± 0.3

(continued)

TABLE 5 (continued)
The FA Composition of the PC in the Respective Organs of *T. tonggol*[a,b]

Sample No.	Light muscle		Dark muscle		Liver[c]		Pyloric cecum[c]		Orbital[c]	
	1	2	1	2	1	2	1	2	1	2
	Mean SE	Mean SE	Mean SE	Mean SE	Mean SE	Mean SE	Mean SE	Mean SE	Mean SE	Mean SE
Total polyenoic	62.6 ± 2.9	57.9 ± 2.8	67.8 ± 2.1	62.2 ± 2.1	51.1 ± 5.1	48.4 ± 2.9	45.3 ± 4.5	57.1 ± 3.4	44.1 ± 5.6	53.1 ± 2.3
n-6 series	8.3 ± 0.7	7.9 ± 0.2	9.2 ± 0.6	8.5 ± 0.1	7.6 ± 0.8	6.8 ± 0.4	10.2 ± 0.4	8.2 ± 0.1	8.0 ± 1.4	6.1 ± 0.1
18:2n-6	0.6 ± 0.0	0.6 ± 0.0	0.7 ± 0.0	0.6 ± 0.0	0.6 ± 0.1	0.5 ± 0.0	0.6 ± 0.0	0.9 ± 0.1	0.9 ± 0.3	0.5 ± 0.0
20:2n-6	0.2 ± 0.0	0.2 ± 0.0	0.2 ± 0.0	0.2 ± 0.0	0.2 ± 0.0	0.3 ± 0.0	0.2 ± 0.0	0.2 ± 0.0	0.8 ± 0.6	0.2 ± 0.0
20:3n-6	0.1 ± 0.0	0.2 ± 0.0	0.1 ± 0.0	0.1 ± 0.0	0.1 ± 0.0	0.1 ± 0.0	0.1 ± 0.0	0.2 ± 0.0	0.1 ± 0.0	0.1 ± 0.0
20:4n-6	3.8 ± 0.3	3.5 ± 0.1	5.0 ± 0.3	4.7 ± 0.1	5.1 ± 0.4	3.3 ± 0.2	6.4 ± 0.4	5.0 ± 0.2	3.6 ± 0.7	3.0 ± 0.0
22:3n-6	0.0 ± 0.0	0.1 ± 0.0	0.1 ± 0.0	0.1 ± 0.0	0.0 ± 0.0	0.0 ± 0.0	0.0 ± 0.0	0.1 ± 0.0	0.0 ± 0.0	0.1 ± 0.0
22:4n-6	0.3 ± 0.0	0.4 ± 0.0	0.5 ± 0.0	0.4 ± 0.0	0.5 ± 0.1	0.6 ± 0.1	0.5 ± 0.0	0.5 ± 0.0	0.8 ± 0.2	0.5 ± 0.0
22:5n-6	3.3 ± 0.4	2.9 ± 0.1	3.3 ± 0.3	2.4 ± 0.0	1.8 ± 0.0	1.9 ± 0.2	2.2 ± 0.2	1.4 ± 0.2	2.3 ± 0.4	1.7 ± 0.1
n-3 series	54.3 ± 3.5	50.0 ± 2.8	58.6 ± 2.3	53.8 ± 2.2	43.5 ± 5.0	41.6 ± 3.0	35.2 ± 4.2	48.9 ± 3.5	36.1 ± 5.4	46.9 ± 2.1
18:3n-3	0.1 ± 0.0	0.1 ± 0.0	0.1 ± 0.0	0.1 ± 0.0	0.1 ± 0.0	0.1 ± 0.0	0.1 ± 0.0	0.2 ± 0.0	0.1 ± 0.1	0.1 ± 0.0
18:4n-3	0.1 ± 0.0	0.1 ± 0.0	0.1 ± 0.0	0.1 ± 0.0	0.2 ± 0.1	0.2 ± 0.1	0.1 ± 0.0	0.2 ± 0.0	0.0 ± 0.0	0.3 ± 0.2
20:3n-3	0.0 ± 0.0	0.1 ± 0.0	0.1 ± 0.0	0.1 ± 0.0	0.1 ± 0.0	0.1 ± 0.0	0.1 ± 0.0	0.1 ± 0.0	0.1 ± 0.0	0.1 ± 0.0
20:4n-3	0.2 ± 0.0	0.3 ± 0.0	0.2 ± 0.0	0.2 ± 0.0	0.2 ± 0.0	0.2 ± 0.0	0.2 ± 0.0	0.3 ± 0.0	0.2 ± 0.0	0.2 ± 0.0
20:5n-3	5.2 ± 0.4	4.7 ± 0.3	6.8 ± 0.5	7.5 ± 0.4	7.4 ± 1.2	6.3 ± 0.6	7.0 ± 1.2	11.3 ± 0.6	4.0 ± 1.1	5.5 ± 0.2
22:4n-3	0.0 ± 0.0	0.0 ± 0.0	0.0 ± 0.0	0.0 ± 0.0	0.0 ± 0.0	0.0 ± 0.0	0.0 ± 0.0	0.0 ± 0.0	0.0 ± 0.0	0.0 ± 0.0
22:5n-3	1.0 ± 0.1	1.5 ± 0.1	1.9 ± 0.1	1.7 ± 0.1	1.6 ± 0.2	2.6 ± 0.2	1.3 ± 0.1	1.6 ± 0.2	1.6 ± 0.3	1.5 ± 0.0
22:6n-3	47.5 ± 3.0	43.2 ± 2.4	49.5 ± 2.7	44.1 ± 1.7	34.0 ± 3.7	32.1 ± 3.0	26.4 ± 3.1	35.1 ± 3.7	30.0 ± 4.4	39.3 ± 2.0
Total FA	99.1 ± 0.3	98.9 ± 0.1	98.5 ± 0.1	98.1 ± 0.5	98.3 ± 0.2	98.6 ± 0.1	98.0 ± 0.1	98.2 ± 0.1	97.5 ± 0.5	98.5 ± 0.2

[a]Results are expressed as weight percentages of total FA. Data are mean ± SE for several samples (*n* = 5).
[b]In Tables 3–5, the major FA are selected if at least one mean datum was detected at a level of 0.5% or more of total FA.
[c]Significant differences for PC between samples 1 and 2 are found only in the case of total monoenes of the liver and total n-6 and total n-6 PUFA of the pyloric cecum, and total saturates of the orbital lipids.

TABLE 6
FA Composition of the Respective Classes in the Stomach Contents of *T. tonggol*[a,b]

Sample No.	TAG		PE		PC	
	1	2	1	2	1	2
	Mean SE	Mean SE	Mean SE	Mean SE	Mean SE	Mean SE
Total saturated	49.8 ± 0.6	36.9 ± 1.1	52.1 ± 1.8	34.6 ± 3.0	52.3 ± 4.7	32.9 ± 2.3
14:0	2.4 ± 0.6	4.1 ± 0.0	1.4 ± 0.6	1.1 ± 0.5	1.2 ± 0.4	0.8 ± 0.1
15:0	1.0 ± 0.2	0.8 ± 0.0	0.6 ± 0.1	0.3 ± 0.1	0.7 ± 0.1	0.6 ± 0.0
15:0 i	0.6 ± 0.3	0.2 ± 0.0	0.3 ± 0.1	0.1 ± 0.0	0.4 ± 0.2	0.0 ± 0.0
16:0	25.1 ± 1.2	18.4 ± 1.0	22.8 ± 2.3	11.2 ± 2.0	29.6 ± 2.0	23.1 ± 1.8
16:0 i	0.6 ± 0.4	0.1 ± 0.0	0.3 ± 0.2	0.0 ± 0.0	0.2 ± 0.0	0.1 ± 0.0
17:0	1.5 ± 0.1	1.2 ± 0.0	2.1 ± 0.1	1.3 ± 0.1	1.6 ± 0.2	0.8 ± 0.0
17:0 i	0.5 ± 0.1	0.4 ± 0.0	0.4 ± 0.1	0.4 ± 0.1	0.7 ± 0.2	0.3 ± 0.0
18:0	9.9 ± 0.6	9.2 ± 0.3	21.0 ± 3.2	18.0 ± 0.3	14.5 ± 2.6	5.4 ± 0.2
18:0 i	1.3 ± 0.7	0.4 ± 0.0	0.5 ± 0.1	0.4 ± 0.0	0.6 ± 0.1	0.2 ± 0.0
19:0	0.4 ± 0.1	0.4 ± 0.0	0.5 ± 0.1	0.4 ± 0.2	0.4 ± 0.1	0.2 ± 0.0
20:0	0.9 ± 0.3	1.0 ± 0.1	0.6 ± 0.2	0.6 ± 0.0	0.7 ± 0.3	0.2 ± 0.0
22:0	1.0 ± 0.1	0.4 ± 0.0	0.5 ± 0.2	0.3 ± 0.0	0.6 ± 0.2	0.3 ± 0.0
24:0	4.8 ± 2.6	0.3 ± 0.1	1.2 ± 0.4	0.4 ± 0.1	1.2 ± 0.4	1.1 ± 0.0
Total monoenoic	31.3 ± 1.7	28.4 ± 0.2	23.9 ± 0.7	13.8 ± 1.1	25.8 ± 3.0	15.6 ± 0.6
14:1n-9	0.4 ± 0.2	0.0 ± 0.0	0.0 ± 0.0	0.0 ± 0.0	0.1 ± 0.1	0.0 ± 0.0
15:1n-6	0.2 ± 0.1	0.0 ± 0.0	0.0 ± 0.0	0.1 ± 0.0	0.1 ± 0.1	0.0 ± 0.0
16:1n-11	0.5 ± 0.5	0.3 ± 0.2	0.0 ± 0.0	0.3 ± 0.1	0.4 ± 0.2	0.4 ± 0.0
16:1n-7	3.7 ± 0.9	5.1 ± 0.5	2.5 ± 0.5	1.4 ± 0.4	1.7 ± 0.7	1.6 ± 0.1
16:1n-5	0.4 ± 0.2	0.2 ± 0.0	0.3 ± 0.1	0.2 ± 0.1	0.4 ± 0.3	0.1 ± 0.0
17:1n-8	0.7 ± 0.1	0.8 ± 0.0	0.3 ± 0.1	0.4 ± 0.1	0.6 ± 0.1	0.4 ± 0.0
18:1n-13	0.0 ± 0.0	0.0 ± 0.0	0.0 ± 0.0	0.1 ± 0.1	0.0 ± 0.0	0.0 ± 0.0
18:1n-9	13.0 ± 0.9	13.3 ± 0.8	11.7 ± 0.9	5.9 ± 0.5	14.8 ± 1.5	9.4 ± 0.4
18:1n-7	3.8 ± 0.5	2.4 ± 0.1	5.7 ± 0.9	2.7 ± 0.2	2.7 ± 0.8	1.9 ± 0.1
18:1n-5	0.1 ± 0.0	0.2 ± 0.0	0.1 ± 0.0	0.1 ± 0.0	0.1 ± 0.0	0.1 ± 0.0
19:1n-11	0.0 ± 0.0	0.2 ± 0.0	0.0 ± 0.0	0.3 ± 0.2	0.1 ± 0.1	0.1 ± 0.0
19:1n-9	0.0 ± 0.0	0.1 ± 0.0	0.1 ± 0.0	0.2 ± 0.0	0.1 ± 0.0	0.1 ± 0.0
20:1n-11	0.5 ± 0.1	0.2 ± 0.1	0.2 ± 0.1	0.2 ± 0.1	0.4 ± 0.1	0.1 ± 0.0
20:1n-9	1.5 ± 0.5	1.3 ± 0.2	0.9 ± 0.2	0.5 ± 0.0	0.8 ± 0.4	0.3 ± 0.0
20:1n-7	0.3 ± 0.1	0.3 ± 0.0	0.2 ± 0.0	0.2 ± 0.0	0.3 ± 0.1	0.1 ± 0.0
20:1n-5	0.0 ± 0.0	0.0 ± 0.0	0.0 ± 0.0	0.1 ± 0.0	0.0 ± 0.0	0.0 ± 0.0
22:1n-11	1.6 ± 1.1	2.1 ± 0.6	0.3 ± 0.1	0.2 ± 0.0	0.7 ± 0.6	0.2 ± 0.0
22:1n-9	0.3 ± 0.2	0.3 ± 0.1	0.1 ± 0.1	0.1 ± 0.0	0.2 ± 0.1	0.1 ± 0.0
22:1n-7	0.2 ± 0.1	0.2 ± 0.0	0.1 ± 0.1	0.0 ± 0.0	0.2 ± 0.1	0.1 ± 0.0
24:1n-9	3.8 ± 0.9	1.4 ± 0.3	1.2 ± 0.4	0.9 ± 0.1	2.1 ± 0.6	0.8 ± 0.0
Total polyenoic	9.1 ± 2.5	32.4 ± 1.0	17.3 ± 2.6	46.3 ± 2.5	18.1 ± 6.8	50.2 ± 2.8
n-6 series	4.1 ± 1.1	4.2 ± 0.3	9.9 ± 0.9	5.0 ± 0.1	7.7 ± 2.2	4.9 ± 0.1
18:2n-6	0.7 ± 0.1	1.4 ± 0.0	1.9 ± 0.3	0.8 ± 0.0	0.9 ± 0.1	0.8 ± 0.0
20:2n-6	1.0 ± 0.8	0.3 ± 0.0	0.4 ± 0.1	0.2 ± 0.0	1.7 ± 1.4	0.2 ± 0.0
20:3n-6	0.1 ± 0.1	0.2 ± 0.1	0.3 ± 0.1	0.1 ± 0.0	0.2 ± 0.1	0.1 ± 0.0
20:4n-6	1.0 ± 0.4	1.2 ± 0.1	4.8 ± 0.9	2.4 ± 0.0	2.6 ± 1.2	2.5 ± 0.1
22:3n-6	0.2 ± 0.1	0.2 ± 0.0	0.0 ± 0.0	0.1 ± 0.0	0.0 ± 0.0	0.1 ± 0.0
22:4n-6	0.4 ± 0.3	0.2 ± 0.0	1.1 ± 0.1	0.4 ± 0.0	1.2 ± 0.6	0.2 ± 0.0
22:5n-6	0.8 ± 0.5	0.5 ± 0.1	1.6 ± 0.5	1.0 ± 0.0	1.5 ± 0.9	0.8 ± 0.1
n-3 series	5.1 ± 1.7	28.2 ± 0.7	7.4 ± 1.8	41.4 ± 2.4	10.4 ± 5.0	45.3 ± 2.6
18:3n-3	0.2 ± 0.0	0.5 ± 0.0	0.4 ± 0.2	0.2 ± 0.0	0.2 ± 0.0	0.2 ± 0.0
18:4n-3	0.1 ± 0.1	0.6 ± 0.1	0.1 ± 0.1	0.1 ± 0.0	0.0 ± 0.0	0.2 ± 0.0
20:3n-3	0.1 ± 0.1	0.1 ± 0.0	0.2 ± 0.0	0.1 ± 0.0	0.1 ± 0.0	0.0 ± 0.0
20:4n-3	0.1 ± 0.1	0.4 ± 0.0	0.3 ± 0.1	0.2 ± 0.0	0.1 ± 0.1	0.3 ± 0.0
20:5n-3	0.6 ± 0.3	5.8 ± 0.5	1.0 ± 0.4	3.9 ± 0.0	1.5 ± 0.8	9.4 ± 0.0
22:4n-3	0.0 ± 0.0	0.0 ± 0.0	0.0 ± 0.0	0.0 ± 0.0	0.0 ± 0.0	0.0 ± 0.0
22:5n-3	0.4 ± 0.1	1.6 ± 0.0	0.6 ± 0.2	2.1 ± 0.1	1.1 ± 0.6	1.7 ± 0.0
22:6n-3	3.5 ± 1.3	19.2 ± 1.3	4.8 ± 1.5	34.7 ± 2.3	7.3 ± 3.5	33.4 ± 2.6
Total FA	90.2 ± 3.0	97.7 ± 0.0	93.4 ± 1.8	94.7 ± 1.7	96.2 ± 0.5	98.7 ± 0.1

[a]Results are expressed as weight percentage of total FA. Data are mean ± SE for several samples (*n* = 5).
[b]In Tables 3–5, the major FA are selected if at least one mean datum was detected at a level of 0.5% or more of total FA.

± 0.3% (4)], and *T. thynnus* [1.0 ± 0.5% (1); 1.4 ± 0.6% (25)]. On the other hand, both its visceral and orbital lipids were comparatively high, and this paralleled that of other tuna species (8). The comparatively low lipid levels of the muscles (light and dark muscle) are a characteristic of this species and are a general tendency of all the tuna species.

Since the lipid compositions of its stomach contents were at the same levels (2.7–2.8%) in samplings in both 1998 and 2000 (the samples 1 and 2), and since partly digested small horse mackerel were found in the stomachs, these small fish may be its main prey.

Lipid classes. The lipids of all specimens consistently contained high levels of TAG, PE, and PC, amounting to more than 50% (78.9–81.3% for the muscles, 49.1–66.5% for the viscera, and 91.2–91.7% for the orbital lipids) of TL in all of its organs. These high levels of glycerol derivatives might be typical of marine fish, similar to those in other fish species.

The high level of TAG in the orbital lipids is a characteristic of this organ, similar to other tuna species. Moderate levels of FFA (10.5–35.7%) were found in the pyloric cecum and liver; this may be a result of the degradation of TAG and phospholipids by enzymatic metabolism. There have not been many papers reporting the detailed lipid classes of tuna species.

FA composition of TAG and the influence of the prey lipids on the visceral TAG. The lipids of marine pelagic fish species generally contain many kinds of FA that originate from phytoplankton through zooplankton and micronekton in the marine food chain. Similar to lipids of other marine fish, such as its prey fish (26), more than 50 FA compounds were detected and identified in *T. tonggol* lipids; this wide range in the kinds of FA detected in this species results from its high dietary intake. Although various kinds of FA, such as SFA, monoenes, and PUFA, were found in its lipids, the total number of the major FA in its TAG was limited to only several components, whereas all other fish species generally have a less selective accumulation of FA at significant levels. For example, the particularly high DHA levels in all classes (TAG, PE, and PC) of all its organs differed from those of other marine fish species. DHA was the only major PUFA in its muscle TAG, while low DHA levels were found in its stomach contents TAG.

On the other hand, the visceral lipids contained lower DHA levels compared with those in muscle lipids. In particular, the DHA levels in the livers of sample 1 were low (9.0 ± 0.8%), which appeared to be related to the low DHA levels in the prey lipids (3.5 ± 1.3%) originating from other marine fish species (Table 6). Furthermore, the DHA levels (17.3 ± 2.9%) of the liver TAG of sample 2 might also be influenced by the lipids in the stomach contents (19.2 ± 1.3%). In addition, compared with the high DHA levels in the muscle TAG, the lower DHA levels in the visceral TAG might be directly due to the prey lipids. Similarly, high levels of SFA, such as 16:0 and 18:0 (25.2 ± 2.5 and 9.8 ± 0.9%, respectively), were found in the livers of sample 1, in accordance with those (25.1 ± 1.2 and 9.9 ± 0.6%, respectively) in its prey lipids. The differences in DHA levels in the visceral TAG (Table 4) between

samples 1 and 2 might reflect different climate conditions between 1998 and 2000, because the average seawater temperature at the site sampled in 1998 was higher than that in 2000 (28 vs. 22°C), and the lower DHA levels of sample 1 might be attributed to the high seawater temperature, similar to that of stomach of prey fish.

As for the differences in DHA contents among the respective organs, the DHA levels of muscle (light and dark) TAG were higher than that of visceral TAG such as liver and orbital TAG. The higher DHA levels in muscle compared with internal organs suggest the selective accumulation of DHA from the visceral depot lipids to the muscle TAG. The digestion of lipid nutrients from prey organisms may be immediately related to the visceral lipid composition, such as liver lipids, after absorption in the gastrointestinal tract of the fish. Although prey lipids directly influenced the visceral ones, the small fluctuation and higher DHA levels in the visceral lipids compared with the large fluctuation and lower DHA levels of the prey lipids suggest an accumulation of DHA during lipid absorption. In sample 2, a great similarity in the FA composition of liver TAG lipid and stomach contents was found, and a similar tendency was also seen in the liver of prey lipid TAG in sample 1; therefore, the liver lipids seem greatly influenced by the prey lipids.

In contrast, the difference in the FA composition of the orbital TAG between the two samples was very small, similar to that of the light muscle (see footnotes in Table 3); therefore, some concentration mechanism might be supposed in the orbital lipids.

FA composition of tissue phospholipids. High levels of n-3 PUFA are generally found in the tissue phospholipids in all marine fish (1,10), because cell phospholipids serve many membrane functions in the cells and are believed to be rich in n-3 PUFA for membrane fluidity at marine temperatures. Almost all DHA levels in the phospholipids (PE and PC) in the *T. tonggol* lipids exceeded 20% of TFA, similar to other tuna species (1,10). The major FA components in PE were similar to those in PC, with higher n-3 PUFA levels in PC; this is a general tendency of all marine fish species. Consequently, EPA was another major component of PC, coinciding with high levels of DHA.

Characteristics of the FA composition in T. tonggol muscle lipids. Consistently high DHA levels were observed in both depot TAG and tissue phospholipids of muscle lipids. Although there were different conditions for samples 1 and 2, such as seawater temperature, body size, and season, the FA compositions of the muscles in samples from both 1998 and 2000 were very similar. A high correlation between the respective TFA of samples 1 and 2 both in the light muscle and in the dark muscle were found; almost all of the types of FA (TSA, total monoenes, total n-6 PUFA, and total n-3 PUFA in TAG, PE, and PC) in sample 1 were the same as those in sample 2 according to *t*-test (11 similar in 12 cases of TFA in the light muscle and 9 similar in 12 cases in the dark muscle). This is a characteristic lipid pattern in *T. tonggol*, and it suggests physiological control of the transfer of FA.

Difference in FA composition between muscle and visceral lipids and estimation of accumulation mechanism. The high DHA levels in both TAG and phospholipids of both light and dark muscle lipids characteristically differ from those in many other fish species. The same tendency is seen in other highly migratory fish. Note that *T. tonggol* belongs to the genus *Thunnus* in the tribe Thunnini, and is similar to other tuna species (18,19). According to the consistently high levels of DHA in all muscle lipids including TAG, the muscle lipids are less directly influenced by the prey lipid composition, and this suggests a selective accumulation in muscle.

Characteristics of orbital lipids. The orbital lipids might also have the same accumulation mechanism as muscle lipids, but different from that of visceral organs, such as liver. The lipid and FA compositions of the orbital lipids in both samples 1 and 2 are very similar to each other, as seen with the FA composition of the muscle lipids. A great similarity in the respective TFA between samples 1 and 2 in the orbital was found. Almost all the types of FA in TFA (TSA, total monoenes, total n-6 PUFA, and total n-3 PUFA in TAG, PE, and PC) in sample 1 were the same as those in the sample 2 according to the *t*-test (11 similar of 12 FA in the orbital lipid). This same tendency is seen in muscle lipids of *T. tonggol*, and it suggests the same accumulation mechanism occurs in the orbital region; therefore, the consistency of the FA composition of the orbital lipids might indicate an important role in the physiological homeostasis of the eyes.

Generality of high DHA levels in tuna species. The DHA in the lipids of tuna species, such as *T. tonggol*, is derived from the prey organisms and is accumulated; marine fish are almost incapable of synthesizing DHA from shorter carbon chains and lower unsaturated FA (11,12) and have a requirement for DHA as an essential nutrient. On the other hand, Tocher (13) and Sidell *et al.* (14) suggested that MUFA are preferentially oxidized for energy compared with DHA. Although tuna species, including *T. tonggol*, absorb various FA from their prey during their long migrations, they save only DHA, while using SFA, monoenes, and shorter-chain and lower unsaturated FA as an energy source. Tuna species therefore may accumulate DHA as a result of both its physiological essentiality and metabolic stability. We conclude that all tuna species may have a mechanism for concentrating DHA in both their depot TAG and tissue phospholipids, resulting in the highest DHA levels in their muscles. Moreover, it is suggested from its lipid profile that the migratory ecology of *T. tonggol* is similar to that of other tuna species, whose migration areas generally include the whole northwestern Pacific Ocean. The close relationship between the lipid and DHA compositions of this species and those of other tuna species might be due to their similar metabolic adaptations to long-distance migration; the high DHA levels in both neutral and polar lipids among all the highly migratory fish species have been discussed (7).

REFERENCES

1. Medina, I., Santiago, P., Aubourg, P., and Martin, R.P. (1995) Composition of Phospholipids of White Muscle of Six Tuna Species, *Lipids 30*, 1127–1135.
2. García-Arias, M.T., Sánchez-Muniz, F.J., Castrillón, A.M., and Navarro, M.P. (1994) White Tuna Canning, Total Fat, and Fatty Acid Changes During Processing and Storage, *J. Food Comp. Anal. 7*, 119–130.
3. Murase, T., and Saito, H. (1996) The Docosahexaenoic Acid Content in the Lipid of Albacore, *Thunnus alalunga* Caught in Two Separate Localities, *Fish. Sci. 62*, 634–638.
4. Saito, H., Ishihara, K., and Murase, T. (1996) Effect of Prey Fish Lipids on the Docosahexaenoic Acid Content of Total Fatty Acids in the Lipid of *Thunnus albacares* Yellowfin Tuna, *Biosci. Biotechnol. Biochem. 60*, 962–965.
5. Saito, H., Watanabe, T., and Murase, T. (1995) The Fatty Acid Composition Characteristic of a Highly Migratory Fish, with Seasonal Variation of Docosahexaenoic Acid Content in Lipid of Bonito (*Euthynnus pelamis*), *Biosci. Biotechnol. Biochem. 59*, 2186–2188.
6. Tanabe, T., Suzuki, T., Ogura, M., and Watanabe, Y. (1999) High Proportion of Docosahexaenoic Acid in the Lipid of Juvenile and Young Skipjack Tuna, *Katsuwonus pelamis* from the Tropical Western Pacific, *Fish. Sci. 65*, 806–807.
7. Saito, H., Yamashiro, R., Ishihara, K., and Xue, C. (1999) Lipids of Three Different Highly Migratory Species: Subfamily Scombrinae (*Euthynnus affinis* and *Sarda orientalis*), and Family Carangidae (*Elagatis bipinnulata*), *Biosci. Biotechnol. Biochem. 63*, 2028–2030.
8. Saito, H., and Ishihara, K. (1996) Docosahexaenoic Acid Content of Fatty Acids in the Lipids of Two Species of Frigate Mackerels, *Auxis rocheri* and *Auxis thazard*, *Biosci. Biotechnol. Biochem. 60*, 1014–1016.
9. Saito, H., Ishihara, K., and Murase, T. (1997) The Fatty Acids Composition in Tuna (bonito, *Euthynnus pelamis*) Caught at Three Different Localities from Tropics to Temperate, *J. Sci. Food Agric. 63*, 53–59.
10. Takama, K., Suzuki, T., Yoshida, K., Arai, H., and Anma, H. (1994) Lipid Content and Fatty Acid Composition of Phospholipids in White-Flesh Fish Species, *Fish. Sci. 60*, 177–184.
11. Owen, J.M., Adron, J.W., Middleton, C., and Cowey, C.B. (1975) Elongation and Desaturation of Dietary Fatty Acids in Turbot *Scophthalmus maximus* L., and Rainbow Trout *Salmo gairdnerii* Rich, *Lipids 10*, 528–531.
12. Kanazawa, A., Teshima, S.-I., and Ono, K. (1979) Relationship Between Essential Fatty Acid Requirements of Aquatic Animals and the Capacity for Bioconversion of Linolenic Acid to Highly Unsaturated Fatty Acids, *Comp. Biochem. Physiol. 63B*, 295–298.
13. Tocher, D.R. (2003) Metabolism and Functions of Lipids and Fatty Acids in Teleost Fish, *Rev. Fish. Sci. 11*, 107–184.
14. Sidell, B.D., Crockett, E.L., and Driedzic, W.R. (1995) Antarctic Fish Tissues Preferentially Catabolize Monoenoic Fatty Acids, *J. Exp. Zool. 271*, 73–81.

15. Cancio, I., and Cajaraville, M.P. (2000) Cell Biology of Peroxisomes and Their Characteristics in Aquatic Organisms, *Int. Rev. Cytol. 199*, 201–293.
16. Bell, M.V., Henderson, R.J., and Sargent, J.R. (1986) The Role of Polyunsaturated Fatty Acids in Fish, *Comp. Biochem. Physiol. 83B*, 711–719.
17. Morris, R.J., and Culkin, F. (1989) Fish, in *Marine Biogenic Lipids, Fats, and Oils* (Ackman, R.G., ed.), Vol. 2, CRC Press, Boca Raton, pp. 145–178.
18. Sawada, T., Takahashi, K., and Hatano, M. (1993) Triglyceride Composition of Tuna and Bonito Orbital Fats, *Nippon Suisan Gakkaishi* (in Japanese) *59*, 285–290.
19. Ando, Y., Satake, M., and Takahashi, Y. (2000) Reinvestigation of Positional Distribution of Fatty Acids in Docosahexaenoic Acid-Rich Fish Oil Triacyl-*sn*-glycerols, *Lipids 35*, 579–582.
20. Folch, J., Lees, M., and Sloane Stanley, G.H. (1957) A Simple Method for the Isolation and Purification of Total Lipids from Animal Tissues, *J. Biol. Chem. 226*, 497–509.
21. Saito, H., Yamashiro, R., Alasalvar, C., and Konno, T. (1999) Influence of Diet on Fatty Acids of Three Subtropical Fish, Subfamily Caesioninae (*Caesio diagramma* and *C. tile*) and Family Siganidae (*Siganus canaliculatus*), *Lipids 34*, 1073–1082.
22. Saito, H. (2004) Lipid and Fatty Acid Composition of Pearl Oyster *Pinctada fucata martensii*: Relationship with the Prey Phytoplankton Lipids, *Lipids 39*, 997–1005.
23. Saito, H., and Kotani, Y. (2000) Lipids of Four Boreal Species of Calanoid Copepods: Origin of the Monoene Fats of Marine Animals at Higher Trophic Levels in the Grazing Food Chain in the Subarctic Ocean Ecosystem, *Mar. Chem. 71*, 69–82.
24. Saito, H., Kotani, Y., Keriko, J.M., Xue, C., Taki, K., Ishihara, K., Ueda, T., and Miyata, S. (2002) High Levels of n-3 Polyunsaturated Fatty Acids in *Euphausia pacifica* and Its Role as a Source of Docosahexaenoic and Icosapentaenoic Acids for Higher Trophic Levels, *Mar. Chem. 78*, 9–28.
25. Ishihara, K., and Saito, H. (1996) The Docosahexaenoic Acid Content in the Lipid of Juvenile Bluefin Tuna (*Thunnus thynnus*) Caught in the Sea off Japanese Coast, *Fish. Sci. 62*, 840–841.
26. Osako, K., Yamaguchi, A., Kurokawa, T., Kuwahara, K., Saito, H., and Nozaki, Y. (2003) The Fatty Acid Composition of Horse Mackerel Caught at Different Localities, *Fish. Sci. 69*, 589–596.

Sesamol Induces Nitric Oxide Release from Human Umbilical Vein Endothelial Cells

Pey-Rong Chen[a,b], Chingmin E. Tsai[c], Hang Chang[d], Tsuei-Ling Liu[a,b], and Chun-Chung Lee[d,e,*]

[a]Department of Nutrition and Food Science, Fu Jen Catholic University, Taipei, Taiwan, [b]Department of Dietetics, National Taiwan University Hospital and National Taiwan University College of Medicine, Taipei, Taiwan, [c]Department of Bioscience Technology, Chung Yuan University, Taoyan, Taiwan, [d]Department of Medical Education and Research, Shin Kong Wu Ho-Su Memorial Hospital, Taipei, Taiwan, and [e]Department of Pharmacy, Chia Nan University of Pharmacy and Science, Tainan, Taiwan.

ABSTRACT: Sesamol, which is derived from sesame seed lignans, is reportedly an antioxidant. Nitric oxide (NO), the most important vascular relaxing factor, is regulated in the endothelium. In addition, NO is involved in protecting endothelium and has antiatherosclerotic and antithrombotic activities. The endothelium produces NO through the regulation of both endothelial NO synthase (eNOS) expression and activity in endothelial cells. This study sought to investigate the effect of sesamol on NO released from human umbilical vein endothelial cells (HUVEC) and to examine the expression and activity of eNOS. Sesamol induced NO release from endothelial cells in a dose-dependent manner (from 1 to 10 µM), as measured 24 h after treatment; the expression of the eNOS gene at both transcription and translation levels; and NOS activity in endothelial cells. The content of cGMP was also increased by sesamol through NO signaling. The transcription of eNOS induced by sesamol was confirmed through the activation of PI-3 kinase-Akt (protein kinase B) signaling. The results demonstrate that sesamol induces NOS signaling pathways in HUVEC and suggest a role for sesamol in cardiovascular reactivity *in vivo*.

Paper no. L9718 in *Lipids 40*, 955–961 (September 2005).

Sesame, an important oilseed derived from *Sesamum indicum*, is one of the oldest oilseeds known to humans and is considered to have nutritional value as well as medicinal effects. The seed contains the minor components sesamin and sesamolin, which are lignan compounds. After roasting sesame seeds, their sesamolin content is lost, and the content of their derivative compound sesamol increases (1,2) (Scheme 1). Extensive studies of sesamin have identified its antihypertensive effects (3–8),

SCHEME 1

antioxidative effects (9), and its ability to inhibit desaturation in PUFA biosynthesis (10) and cholesterol absorption (11). Sesamol has been found to have antioxidative effects (12) and to induce growth arrest and apoptosis in cancer and cardiovascular cells (13). Our previous study suggested that sesamol might enhance vascular fibrinolytic capacity by its ability to up-regulate the expression of plasminogen activators (PA), such as urokinase PA (uPA) and tissue PA (tPA), in endothelial cells (EC) (14).

The endothelium plays a primary regulatory role by secreting substances that control both vascular tone and structure. The most widely studied endothelium-derived relaxing factor (EDRF) is nitric oxide (NO) (15,16); it is also considered to be the most important EDRF. NO is derived from the transformation of the amino acid L-arginine to citrulline by NO synthase (NOS) (17,18). Endothelial NOS (eNOS, or NOS3) is the main type of NOS that is constitutively expressed in endothelium. NO activates soluble guanylyl cyclase, which stimulates the production of cGMP. Increased intracellular cGMP content in vascular smooth muscle cells (VSMC) facilitates the extrusion of intracellular calcium and leads to vascular relaxation (19). In addition to stimulating vascular relaxation, NO plays a role in antiatherosclerosis (20), antithrombosis (21), protection of EC from damage by reactive oxygen species (ROS) (22), and the survival of endothelium attacked by proinflammatory molecules (23).

In this study, we report that sesamol induces NO release from EC and increases the levels of the product of NO signaling, cGMP, in EC. The sesamol-induced increase in NO produced

from EC is derived from both the induction of eNOS gene expression and the increase in NOS activity. Sesamol-induced eNOS gene expression is confirmed to be mediated through the PI-3 kinase (PI-3K)-Akt (protein kinase B) pathway.

MATERIALS AND METHODS

Chemicals and reagents. A nitrate/nitrite colorimetric assay kit and cyclic GMP enzyme-linked immunosorbent assay (EIA) kit were purchased from Cayman Chemical Co. Inc. (Ann Arbor, MI). Collagenase and Taq DNA polymerase were obtained from Roche Applied Science (Indianapolis, IN). M-199 medium, penicillin-streptomycin-glutamine (100×), FBS, and SuperScript II Reverse Transcriptase were bought from Invitrogen Corporation (Carlsbad, CA). The $[^3H]$-L-arginine-^{32}P-dCTP, polyvinylidene difluoride (PVDF) membrane, nylon membrane (Hybond-N +), enhanced chemiluminescence (ECL) detection system, random prime labeling system (Rediprime), and hybridization buffer (Rapid-hyb buffer) were sourced from Amersham Pharmacia Biotech (Arlington Heights, IL). Sesamol, wortmannin, Nω-nitro-L-arginine methyl ester (L-NAME), and DMSO were purchased from Sigma-Aldrich Corporation (St. Louis, MO). EGM (EC medium) was purchased from Clonetics (San Diego, CA). A nitric oxide synthase assay kit was bought from Calbiochem, EMD Biosciences, Inc. (Darmstadt, Germany). The Coomassie blue protein assay was procured from Bio-Rad Laboratories, Inc. (Richmond, CA). eNOS polyclonal antibody and Akt 1/2 polyclonal antibody were bought from Santa Cruz Biotechnology (Santa Cruz, CA). GAPDH (glyceraldehyde-3-phosphate dehydrogenase) monoclonal antibody was obtained from Biogenesis (Dorset, United Kingdom). The deoxy oligonucleotides were synthesized from Mission Biotech (Taipei, Taiwan). QIAquick Gel Extraction kit was obtained from Qiagen Inc. (Germantown, MD). Tri-Reagent was bought from Molecular Research Center, Inc. (Cincinnati, OH). Phospho-Akt (Ser473) monoclonal antibody was gotten from Cell Signaling Technology (Beverly, MA).

Primary human umbilical vein endothelial cells (HUVEC) culture. Human umbilical cords from normal deliveries or cesarean sections were collected. In a tissue culture hood, both ends of each cord (1 cm long) were excised with a sterile scalpel to expose a sterile surface. The umbilical vein was perfused with 1× PBS and then with 0.2% collagenase in PBS solution until the vein was distended. The two ends of the cord were clamped with sterile clamps and incubated for 30 min at 37°C. Then, the cords were gently massaged to facilitate EC detachment from the vessel wall. The solution was flushed out, and the lumen of the vein was washed with M199 medium (containing 1% penicillin-streptomycin). The cell suspension was collected and centrifuged at about $100 \times g$ for 5 min at 4°C. The pellet was resuspended in M199 medium (containing 10% serum and 1% penicillin-streptomycin). The cells were plated on 10-cm culture plates and incubated in 37°C and 5% CO_2 overnight. After attaching overnight, the cells were washed with 1× PBS and grown in EGM supplemented with 12% FBS.

After full growth was completed, HUVEC were divided or stored in liquid nitrogen (medium containing 20% DMSO when stored). HUVEC between passages 3 and 7 were used for experiment.

Treatment of cells. Before treatment, 1×10^6 cells were seeded in each 10-cm dish in the medium containing 2% FBS and incubated at 37°C under 5% CO_2 overnight. The cells were treated with sesamol (dissolved in DMSO) at various doses. For the control group only DMSO was added. After treatment, the cells were scraped from the dish, and medium and cells were separated by centrifugation. The media and cell pellets were stored at −70°C for the next step in the analysis.

Nitrate/nitrite measurement. Since the final products of NO are nitrite (NO_2^-) and nitrate (NO_3^-), and the relative proportion of NO_2^- and NO_3^- is variable and cannot be predicted with certainty, the best index of total NO production is the sum of NO_2^- plus NO_3^-. The Cayman Chemical Nitrate/Nitrite Colorimetric Assay kit provides a method for measurement of total nitrate/nitrite (the final products of NO); it was used to determine the NO concentration in the cultured medium of cells. The EC were treated with various doses of sesamol, after which the medium was quickly collected. Nitrate in the sample was first converted to nitrite with the addition of nitrate reductase. The presence of nitrite in the samples or standards was detected by the addition of Griess reagents and was quantitatively measured by spectrophotometer at 550 nm as described in the manual of the Cayman Chemical Nitrate/Nitrite Colorimetric Assay kit.

Northern blot analysis. The eNOS and GAPDH probes for Northern blot analysis were synthesized by RT-PCR. The reverse transcription (RT) was performed as described in the SuperScript II Reverse Transcriptase manual. The PCR was performed as described below. The primer used for eNOS was forward, 5′-tccagtaacacagacagtgca-3′; reverse, 5′-caggaagtaagtgagagc-3′. GAPDH: forward, 5′-tggtatcgtggaaggactca-3′; reverse, 5′-agtgggtgtcgctgttgaag-3′. The PCR mixture contained 1× PCR buffer (50 mM Tris/HCl, 10 mM KCl, 5 mM $(NH_4)_2SO_4$, and 2 mM $MgCl_2$), 0.2 mM dNTP, 0.4 μM of each primer, and 2.5 unit of Fast Start Taq DNA polymerase. The PCR condition for eNOS probe was as follows: The initial denaturing phase lasted 5 min at 94°C and was followed by a 40-cycle amplification phase consisting of denaturation at 94°C for 1min, annealing at 63°C for 1 min, and elongation at 72°C for 1 min. Amplification was terminated at 72°C for 7 min. The GAPDH probe synthesis was as previously described (24). The size of PCR product for eNOS and GAPDH was 693 and 370 bp, respectively. The PCR product was purified with the QIAquick Gel Extraction kit. Twenty nanograms of DNA fragment was labeled with ^{32}P-dCTP by the random prime labeling system for Northern blot assay. Total RNA was isolated from cells cultured in 10-cm dishes by the method that was described in the Tri-Reagent's protocol. Ten to 20 μg of total RNA was loaded and run in 1% agarose/formaldehyde gel electrophoresis as described previously (25) and then was transferred onto a nylon membrane. Hybridization took place at 65°C for 16 h as described in the hybridization buffer manual. The membrane was then washed once with solution A [5× saline-sodium citrate (SSC), 0.1% SDS] at

65°C for 20 min, and twice with solution B (0.1× SSC, 0.1% SDS) at 65°C for 20 min. Finally, the membrane was analyzed by autoradiography.

Western blot analysis. Western blot was used to detect the protein level of the eNOS. Cell lysate was prepared in cell lysis buffer [150 mM NaCl, 1% NP-40, 0.5% deoxycholate, 0.1% SDS, 50 mM Tris (pH 7.5), 1 µM Na orthovanadate, 2 mM sodium pyrophosphate, 1 mM PMSF, and 0.7 µg/mL leupeptin], and the protein content of the lysate was determined using the Coomassie blue protein assay. Forty micrograms of protein was loaded and run in 10% SDS-PAGE and transferred to PVDF membranes in a semidry apparatus. The membranes were blocked in 20 mM Tris (pH 7.6), 137 mM NaCl, 0.1% Tween-20 (Tris-buffered saline Tween-20; TBST), and 4% nonfat dry milk for 90 min at room temperature. Membranes were first incubated overnight at 4°C in TBST containing nonfat milk and primary antibody, then washed three times for 15-min intervals at 22°C in TBST, and finally incubated for 90 min at room temperature in TBST containing nonfat milk and secondary antibody (1:7,500 dilution). Following three washes in TBST, immunoreactive bands were detected using the ECL detection system from Amersham Pharmacia Biotech according to the manufacturer's instructions.

Total NO synthase activity (L-citrulline assay). Total NO synthase activity was quantified by measuring conversion of [^{3}H]-L-arginine to [^{3}H]-L-citrulline by the Nitric Oxide Synthase Assay Kit. Cells were first lysed with 1× homogenization buffer as described in kit protocol materials. Cell membranes were isolated from the pellet fraction after centrifugation at $15,000 \times g$. The pellet was then suspended in 100 µL of 1× homogenization buffer. The protein concentration of the homogenized sample was first quantified; each sample was assayed as described in the manual of the kit. The NOS activity was determined by detecting the radioactivity of [^{3}H]-L-citrulline and normalized according to the radioactivity of [^{3}H]-L-arginine applied and the protein concentration of the lysate of HUVEC.

Cyclic GMP assay. A cyclic GMP EIA kit was used to quantify the level of cGMP in the cells. All the procedures were carried out according to the method described in the kit.

Statistical tests. All values are given as the mean ± SD of triplicates. All the data were subjected to statistical analysis before normalization according to the control. Statistical analysis of Northern blot, Western blot, or NOS assays was performed after normalization according to the internal control. Differences between the groups were calculated by ANOVA with *post hoc* analysis (LSD). A value of $P < 0.05$ was considered significant.

RESULTS

Sesamol induces NO release from HUVEC. Since the medicinal effects of sesamol are not clear, and NO plays a role in vasorelaxation and endothelium protection, we are interested in whether sesamol will induce NO release from EC. HUVEC were treated with different concentrations (1, 5, and 10 µM) of sesamol for 8 and 24 h; and the concentration of nitrate and ni-
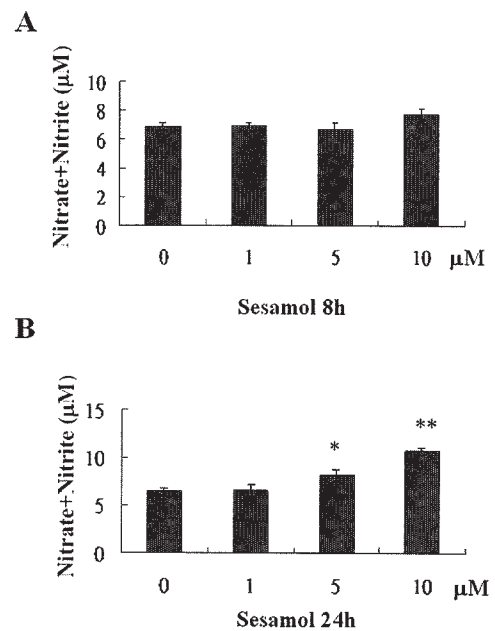
FIG. 1. Nitric oxide (NO) level in the medium of human umbilical vein endothelial cells (HUVEC) treated with sesamol. The NO concentration was determined by detection of total nitrate and nitrite in the medium of HUVEC treated with sesamol for 8 h (A) and 24 h (B). *$P < 0.05$, **$P < 0.01$ vs. control, $n = 3$ per group by ANOVA test with *post hoc* analysis (LSD). The control levels of nitrate and nitrite after 8 and 24 h of treatments are 6.89 ± 0.24 and 6.44 ± 0.39 µM, respectively.

trite, the end products of NO, in the culture medium of cells was determined. After 8 h, we did not find any variation in the NO concentration in the medium for the three sesamol treatments (Fig. 1A). However, after 24 h, the NO concentration had increased in a dose-dependent manner. The highest induction of NO concentration was an approximately 1.6-fold increase with treatment by 10 µM of sesamol (Fig. 1B).

Sesamol increases cGMP content in HUVEC through NO signaling. Since cGMP is the subsequent signal induced by NO, we checked the content of cGMP in the sesamol-treated HUVEC. After 24 h of treatment, sesamol increased the cGMP content in EC in a dose-depent manner (Fig. 2A). We further checked the cGMP level when sesamol was coincubated with the inhibitor of NOS, L-NAME. The induction of cGMP level by sesamol (10 µM)-treated EC was inhibited by 3 mM of L-NAME (Fig. 2B). Our results indicated that the cGMP induced by sesamol was through NO signaling.

Sesamol induces eNOS mRNA expression in HUVEC. Since sesamol induced NO release from EC after 24 h, we first determined the eNOS mRNA expression in EC treated with sesamol. From the Northern blot (Fig. 2A), the eNOS mRNA expression was found to be induced about twofold by sesamol with 5 and 10 µM in HUVEC after 24 h of cell treatment (Fig. 3A). We further checked the time intervals of eNOS mRNA expression in HUVEC treated with 10 µM of sesamol. As shown in Figure 3B, the eNOS mRNA expression of the cells treated with 10 µM of sesamol was more than the control group at each interval from 8 to 48 h.

A

B
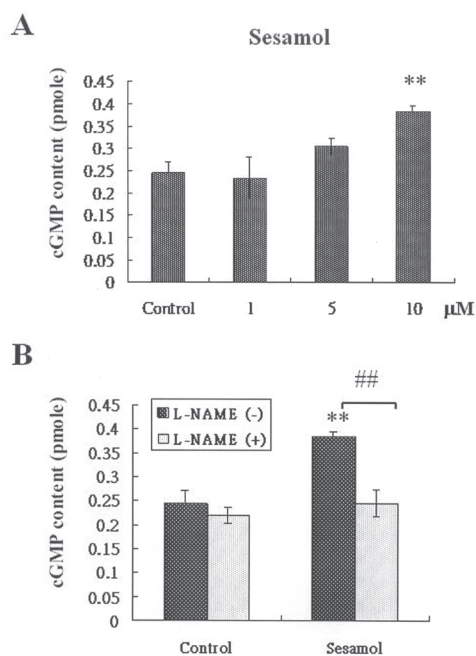
FIG. 2. cGMP content in HUVEC treated with sesamol. (A) The content of cGMP in HUVEC treated with different doses of sesamol (shown) for 24 h. **$P < 0.01$ vs. control, $n = 3$ per group by ANOVA test with *post hoc* analysis (LSD). (B) The cGMP content in HUVEC treated with sesamol (10 μM) or sesamol (10 μM) combined with Nω-nitro-L-arginine methyl ester (L-NAME) (3 mM) for 24 h. **$P < 0.01$ vs. control, ##$P < 0.01$ sesamol alone vs. sesamol combined with L-NAME, $n = 3$ per group by *t* test. The control level of cGMP is 0.24 ± 0.025 pmol per plate. For other abbreviation see Figure 1.

Sesamol induces eNOS protein expression and NOS activity in HUVEC. From previous results indicating that sesamol induced eNOS mRNA expression in the EC, we further checked the protein expression and enzyme activity of eNOS when EC were treated with sesamol. Western blot showed that the expression of eNOS protein was induced by sesamol in a concentration-dependent manner (from 1 to 10 μM) after 24 h of treatment (Fig. 4A). The induction of eNOS protein by 5 or 10 μM of sesamol treatment was about 2- to 2.5-fold. We further analyzed the NOS activity of the EC treated with sesamol. The NOS activity of EC was significantly induced by 5 and 10 μM sesamol to about 1.5- and 1.6–fold, respectively, after 24 h of treatment (Fig. 4B). Thus, we confirmed that the induction of NO release from EC by sesamol was due to the induction of eNOS expression and activity by sesamol.

PI-3K/Akt pathway is involved in sesamol-induced eNOS gene expression. eNOS expression and activity are reported to be regulated by PI-3K/Akt (26–29). To determine whether sesamol-induced eNOS gene expression was through PI-3K/Akt, we used the PI-3K inhibitor, wortmannin. The Northern blot results indicated that the eNOS gene expression was induced 1.4-fold by 10 μM of sesamol after 24 h of treatment; however, the induction of eNOS gene expression by sesamol was down-regulated to the range as control by wortmannin (50 nM)(Fig. 5A). Furthermore, we checked whether the phosphorylation of Akt (Ser 473) would be induced in EC by sesamol.

A

B
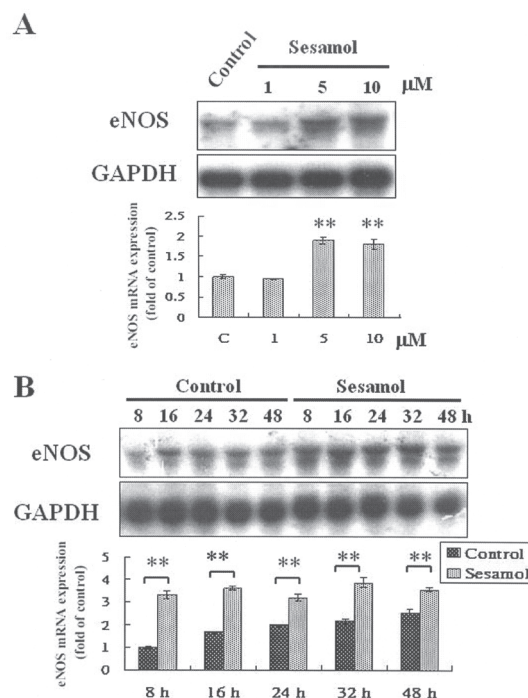
FIG. 3. The endothelial NO synthase (eNOS) mRNA expression in HUVEC treated with sesamol. (A) The Northern blot of eNOS mRNA expression in HUVEC treated with a control (C) (DMSO) and different doses of sesamol (shown) for 24 h. The signals were quantified by densitometer, and the comparative eNOS mRNA expression was calculated by normalization to glyceraldehyde-3-phosphate dehydrogenase (GAPDH) and control. **$P < 0.01$ vs. control, $n = 3$ per group by ANOVA test with *post hoc* analysis (LSD). (B) The Northern blot of eNOS mRNA expression in HUVEC treated with DMSO (control) and sesamol (10 μM) with different time intervals. The signals were quantified by densitometer, and the comparative eNOS mRNA expression was calculated by normalization to GAPDH and control 8 h. **$P < 0.01$ sesamol vs. each time interval of control by *t* test, $n = 3$ per group. For other abbreviation see Figure 1.

From Western blot, we found that the Akt phosphorylation (Ser 473) was induced by sesamol in a concentration-dependent manner after 24 h of sesamol treatment (5 and 10 μM with 1.4- and 2.3-fold respectively) (Fig. 5B).

DISCUSSION

The EC serves several functions in the vascular milieu, one of the most important being the regulation of vascular tone. A major determinant of vascular tone is the endothelial product, EDRF, which is NO or a related molecule. In sesame lignans, many *in vivo* studies suggest that sesamin has a role in the antihypertensive response (3–8), but the role of sesamol has never been elucidated. In our previous investigation, we found that sesamin (10 μM) not only enhanced NO release but also decreased endothelin-1 (ET-1), a potent vasoconstrictor produced from EC. Furthermore, we found that sesamin (10 μM) could induce eNOS but inhibit endothelin-converting enzyme-1 (ECE-1) mRNA and protein expressions. We suggested that the induction of NO and the inhibition of ET-1 by sesamin was
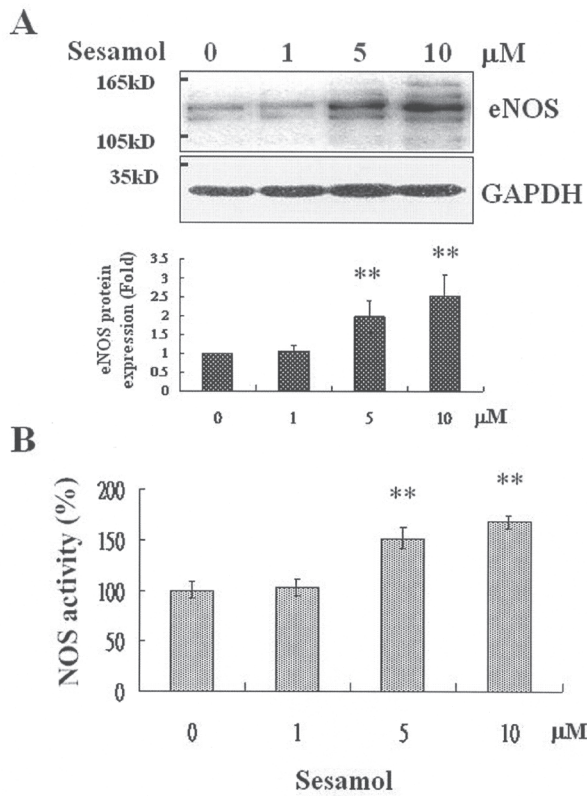
FIG. 4. The eNOS protein expression and nitric oxide synthase (NOS) activity in HUVEC treated with sesamol. (A) The Western blot of eNOS protein expression in HUVEC treated with different doses of sesamol for 24 h. The signals were quantified by densitometer, and the comparative eNOS protein expression was calculated by normalization to GAPDH and control. **$P < 0.01$ vs. control, $n = 3$ per group by ANOVA test with *post hoc* analysis (LSD). (B) The NOS activity was determined by detecting the radioactivity in [³H]-L-citrulline that was converted from [³H]-L-arginine by the lysate of HUVEC after 24 h of sesamol treatment. After the radioactivity of [³H]-L-citrulline had been determined, the comparative activity was performed by normalization to the radioactivity of [³H]-L-arginine applied, concentration of protein. *$P < 0.01$ vs. control, $n = 3$ per group by ANOVA test with *post hoc* analysis (LSD). The control value of [³H]-L-citrulline/[³H]-L-arginine/protein concentration is 2.54 ± 0.2. For other abbreviations see Figures 1 and 3.

FIG. 5. The effect of eNOS mRNA induced by sesamol through PI-3K and the sesamol on the activation of Akt in HUVEC. (A) The Northern blot of eNOS mRNA expression in HUVEC treated with DMSO (control) or treated with sesamol (10 µM) in the presence or absence of wortmannin (50 nM) for 24 h. The signals were quantified by densitometer, and the comparative eNOS mRNA expression was calculated by normalization to GAPDH and control. **$P < 0.01$ vs. control, $n = 3$ per group by t test. ##$P < 0.01$ sesamol combined with wortmannin vs. sesamol alone, $n = 3$ per group by t test. (B) The Western blot of phospho-Akt (Ser 473) expression in HUVEC treated with sesamol for 24 h. The signals were quantified by densitometer, and the comparative phospho-Akt (Ser 473) expression was calculated by normalization to total Akt and control. *$P < 0.05$, **$P < 0.01$ vs. control, $n = 3$ per group by ANOVA test with *post hoc* analysis (LSD). Akt, protein kinase B; PI-3K, PI-3 kinase; for other abbreviations see Figures 1 and 3.

implicated in its antihypertensive effects (30). In this study, we investigated the other sesame lignan, sesamol, and found that sesamol (10 µM) could also induce NO release from EC through inducing the expression of eNOS and through the enhancement of NOS activity in the HUVEC. Furthermore, we also demonstrated that sesamol could increase the levels of NO and cGMP, the latter of which is induced by NO signaling and is responsible for the relaxation of the VSMC. However, we did not obtain the same result when using sesamin (10 µM) to inhibit ET-1 as when we treated the HUVEC with 10 µM of sesamol (data not shown). We did, however, observe that the ET-1 and ECE-1 expression could be inhibited by 100 µM of sesamol (data not shown). Whether sesamol has an antihypertensive effect by vasorelaxation in the hypertensive rat model needs to be determined.

The physiological function of NO derived from endothelium is not just in inducing vasodilation. NO also plays a role

in inhibiting the expression of adhesion molecules on EC; thus NO helps prevent the adherence of cellular elements to the vascular wall. NO has also antithrombotic effects by inhibiting platelet aggregation and inhibiting synthesis of different factors involved in the coagulation cascade (31). Moreover, NO plays a role in protecting EC from the cellular or the DNA injury induced by ROS or other cytotoxic agents (22,32–35). The deficiency of vascular endothelium in the generation of bioactive NO correlates with the aging of the EC (36). NO also promotes EC survival by inhibiting the cysteine protease activity of caspases *via* S-nitrosylation of the reactive cysteine residue (37). In this study, the finding that sesamol induced NO and eNOS gene expression in EC prompts us to recognize the value of role of sesamol in the prevention of the aging process of EC and the repair capacity of injured vascular EC, as well as in the prevention of atherosclerosis and thrombosis in vessels. In addition, our previous study showed that sesamol increased the

production of uPA and tPA significantly and also up-regulated the mRNA expressions of these proteins. The induction of uPA and tPA suggests that the overall vascular fibrinolytic capacity may be enhanced by the treatment with sesamol (14). These results demonstrate that sesamol induces NOS signaling pathways in HUVEC and suggest it has a role in cardiovascular reactivity *in vivo*. Perhaps sesamol has positive effects in preventing the processes of atherosclerosis and thrombosis, the major problems evident in cardiovascular disease.

The enhancement of EC survival by NO is derived from the activation of eNOS, which is phosphorylated and activated through PI-3K/Akt signaling activation (26,27). The expression of the eNOS gene, regulated through a PI-3K-dependent pathway, has also been investigated (28,29). Our results—that sesamol-induced eNOS mRNA expression was blocked by PI-3K inhibitor and that Akt phosphorylation was induced by sesamol in EC—suggest that one of the mechanisms of sesamol in inducing eNOS gene expression is through PI-3K/Akt activation. Since the role of PI-3K/Akt activation and NO is strongly correlated with EC survival and angiogenesis (38), the effect of sesamol on EC deserves further investigation. The concentration of NO in the cell medium was not altered by sesamol treatment at less than 8 h of exposure to the compound, but was concentration-dependently influenced after 24 h of treatment. From the Northern blots, we found that sesamol induced the expression of eNOS mRNA before 8 h. The reason for the time delay of NO may be due to the process of NO synthesis and the conversion to nitrate and nitrite. In addition, nitrate and nitrite are trace elements that require time to accumulate to a significant level.

REFERENCES

1. Fukuda, Y., Nagata, M., Osawa, T., and Namiki, M. (1986) Chemical Aspects of the Antioxidative Activity of Roasted Sesame Seed Oil and the Effect of Using the Oil for Frying, *Agric. Biol. Chem. 50*, 857–862.
2. Fukuda, Y., Nagata, M., Osawa, T., and Namiki, M. (1986) Contribution of Lignan Analogues to Antioxidative Activity of Refined Unroasted Sesame Seed Oil, *J. Am. Oil Chem. Soc. 63*, 1027–1031.
3. Kita, S., Matsumura, Y., Morimoto, S., Akimoto, K., Furuya, M., Oka, N., and Tanaka, T. (1995) Antihypertensive Effect of Sesamin. II. Protection Against Two-Kidney, One-Clip Renal Hypertension and Cardiovascular Hypertrophy, *Biol. Pharm. Bull. 18*, 1283–1285.
4. Matsumura, Y., Kita, S., Morimoto, S., Akimoto, K., Furuya, M., Oka, N., and Tanaka, T. (1995) Antihypertensive Effect of Sesamin. Protection Against Deoxycorticosterone Acetate-Salt-Induced Hypertension and Cardiovascular Hypertrophy, *Biol. Pharm. Bull. 18*, 1016–1019.
5. Matsumura, Y., Kita, S., Ohgushi, R., and Okui, T. (2000) Effects of Sesamin on Altered Vascular Reactivity in Aortic Rings of Deoxycorticosterone Acetate-Salt-Induced Hypertensive Rat, *Biol. Pharm. Bull. 23*, 1041–1045.
6. Matsumura, Y., Kita, S., Tanida, Y., Taguchi, Y., Morimoto, S., Akimoto, K., and Tanaka, T. (1998) Antihypertensive Effect of Sesamin. III. Protection Against Development and Maintenance of Hypertension in Stroke-Prone Spontaneously Hypertensive Rats, *Biol. Pharm. Bull. 21*, 469–473.
7. Nakano, D., Itoh, C., Takaoka, M., Kiso, Y., Tanaka, T., and Matsumura, Y. (2002) Antihypertensive Effect of Sesamin. IV. Inhibition of Vascular Superoxide Production by Sesamin, *Biol. Pharm. Bull. 25*, 1247–1249.
8. Noguchi, T., Ikeda, K., Sasaki, Y., Yamamoto, J., Seki, J., Yamagata, K., Nara, Y., Hara, H., Kakuta, H., and Yamori, Y. (2001) Effects of Vitamin E and Sesamin on Hypertension and Cerebral Thrombogenesis in Stroke-Prone Spontaneously Hypertensive Rats, *Hypertens. Res. 24*, 735–742.
9. Nakai, M., Harada, M., Nakahara, K., Akimoto, K., Shibata, H., Miki, W., and Kiso, Y. (2003) Novel Antioxidative Metabolites in Rat Liver with Ingested Sesamin, *J. Agric. Food Chem. 51*, 1666–1670.
10. Shimizu, S., Akimoto, K., Shinmen, Y., Kawashima, H., Sugano, M., and Yamada, H. (1991) Sesamin Is a Potent and Specific Inhibitor of Δ5 Desaturase in Polyunsaturated Fatty Acid Biosynthesis, *Lipids 26*, 512–516.
11. Hirose, N., Inoue, T., Nishihara, K., Sugano, M., Akimoto, K., Shimizu, S., and Yamada, H. (1991) Inhibition of Cholesterol Absorption and Synthesis in Rats by Sesamin, *J. Lipid Res. 32*, 629–638.
12. Uchida, M., Nakajin, S., Toyoshima, S., and Shinoda, M. (1996) Antioxidative Effect of Sesamol and Related Compounds on Lipid Peroxidation, *Biol. Pharm. Bull. 19*, 623–626.
13. Jacklin, A., Ratledge, C., Welham, K., Bilko, D., and Newton, C.J. (2003) The Sesame Seed Oil Constituent, Sesamol, Induces Growth Arrest and Apoptosis of Cancer and Cardiovascular Cells, *Ann. N.Y. Acad. Sci. 1010*, 374–380.
14. Chen, P.R., Lee, C.C., Chang, H., and Tsai, C.E. (2005) Sesamol Regulates Plasminogen Activator Gene Expression in Cultured Endothelial Cells: A Potential Effect on Fibrinolytic System, *J. Nutr. Biochem. 16*, 59–64.
15. Furchgott, R.F., and Zawadzky, J.V. (1980) The Obligatory Role of Endothelial Cells in the Relaxation of Arterial Smooth Muscle by Acetylcholine, *Nature 288*, 373–376.
16. Palmer, R.M.J., Ferrige, A.G., and Moncada, S. (1987) Nitric Oxide Release Accounts for the Biological Activity of Endothelium-Derived Relaxing Factor, *Nature 327*, 524–526.
17. Palmer, R.M.J., Ashton, D.S., and Moncada, S. (1988) Vascular Endothelial Cells Synthesize Nitric Oxide from L-Arginine, *Nature 333*, 664–666.
18. Bredt, D.S., Hwang, P.M., Glatt, C.E., Lowenstein, C., Reed, R.R., and Snyder, S.H. (1991) Cloned and Expressed Nitric Oxide Synthase Structurally Resembles Cytochrome P-450 Reductase, *Nature 351*, 714–718.
19. Denninger, J.W., and Marletta, M.A. (1999) Guanylate Cyclase and NO/cGMP Signaling Pathway, *Biochim. Biophys. Acta 1441*, 334–350.
20. Cooke, J.P., Singer, A.H., Tsao, P., Zera, P., Rowan, R.A., and Billingham, M.E. (1992) Antiatherogenic Effects of L-Arginine in the Hypercholesterolemic Rabbit, *J. Clin. Invest. 90*, 1168–1172.
21. Shultz, P.J., and Raij, L. (1992) Endogenously Synthesized Nitric Oxide Prevents Endotoxin-Induced Glomerular Thrombosis, *J. Clin. Invest. 90*, 1718–1725.
22. Wink, D.A., Hanbauer, I., Krishna, M.C., DeGraff, W., Gamson, J., and Mitchell, J.B. (1993) Nitric Oxide Protects Against Cellular Damage and Cytotoxicity from Reactive Oxygen Species, *Proc. Natl. Acad. Sci. USA 90*, 9813–9817.
23. Dimmeler, S., and Zeiher, A.M. (1999) Nitric Oxide—An Endothelial Cell Survival Factor, *Cell Death Differ. 6*, 964–968.
24. Lee, C.C., Shyu, K.G., Lin, S., Wang, B.W., Liu, Y.C., and Chang, H. (2002) Cell Adhesion Regulates the Plasminogen Activator Inhibitor-1 Gene Expression in Anchorage-Dependent Cells, *Biochem. Biophys. Res. Commun. 291*, 185–190.
25. Maniatis, T., Fritsch, E.F., and Sambrook, J. (1989) Extraction, Purification, and Analysis of Messenger RNA from Eukaryotic Cells, in *Molecular Cloning, A Laboratory Manual*, pp.

7.1–7.87, Cold Spring Harbor Laboratory Press, Cold Spring Harbor, New York.

26. Dimmeler, S., Fisslthaler, B., Fleming, I., Hermann, C., Busse, R., and Zeiher, A.M. (1999) Activation of Nitric Oxide Synthase in Endothelial Cells *via* Akt-Dependent Phosphorylation, *Nature 399*, 601–605.

27. Fulton, D., Gratton, J.P., McCabe, T.J., Fontana, J., Fujio, Y., Walsh, K., Franke, T.F., Papapetropoulos, A., and Sessa, W.C. (1999) Regulation of Endothelium-Derived Nitric Oxide Production by the Protein Kinase Akt, *Nature 399*, 597–601.

28. Hashiguchi, A., Yano, S., Morioka, M., Hamada, J., Ushio, Y., Takeuchi, Y., and Fukunaga, K. (2004) Up-regulation of Endothelial Nitric Oxide Synthase *via* Phosphatidylinositol 3-Kinase Pathway Contributes to Ischemic Tolerance in the CA1 Subfield of Gerbil Hippocampus, *J. Cereb. Blood Flow Metab. 24*, 271–279.

29. Cieslik, K., Abrams, C.S., and Wu, K.K. (2001) Up-regulation of Endothelial Nitric-Oxide Synthase Promoter by the Phosphatidylinositol 3-Kinase γ/Janus Kinase 2/MEK-1-Dependent Pathway, *J. Biol. Chem. 276*, 1211–1219.

30. Lee, C.C., Chen, P.R., Lin, S., Tsai, S.C., Wang, B.W., Chen, W.W., Tsai, C.E., and Shyu, K.G. (2004) Sesamin Induces Nitric Oxide and Decreases Endothelin-1 Production in HUVECs: Possible Implications for Its Antihypertensive Effect, *J. Hypertens. 22*, 2329–2338.

31. Tiefenbacher, C.P., and Kreuzer, J. (2003) Nitric Oxide-Mediated Endothelial Dysfunction—Is There Need to Treat? *Curr. Vasc. Pharmacol. 1*, 123–133.

32. Chang, J., Rao, N.V., Markewitz, B.A., Hoidal, J.R., and Michael, J.R. (1996) Nitric Oxide Donor Prevents Hydrogen Peroxide-Mediated Endothelial Cell Injury, *Am. J. Physiol. 270*, L931–L940.

33. Grosser, N., and Schroder, H. (2003) Aspirin Protects Endothelial Cells from Oxidant Damage *via* the Nitric Oxide-cGMP Pathway, *Arterioscler. Thromb. Vasc. Biol. 23*, 1345–1351.

34. Polte, T., Oberle, S., and Schröder, H. (1997) Nitric Oxide Protects Endothelial Cells from Tumor Necrosis Factor-Mediated Cytotoxicity: Possible Involvement of Cyclic GMP, *FEBS Lett. 409*, 46–48.

35. Wink, D.A., Cook, J.A., Pacelli, R., DeGraff, W., Gamson, J., Liebmann, J., Krishna, M.C., and Mitchell, J.B. (1996) The Effect of Various Nitric Oxide-Donor Agents on Hydrogen Peroxide-Mediated Toxicity: A Direct Correlation Between Nitric Oxide Formation and Protection, *Arch. Biochem. Biophys. 331*, 241–248.

36. McCarty, M.F. (2004) Optimizing Endothelial Nitric Oxide Activity May Slow Endothelial Aging, *Med. Hypotheses 63*, 719–723.

37. Dimmeler, S., Haendeler, J., Nehls, M., and Zeiher, A.M. (1997) Suppression of Apoptosis by Nitric Oxide *via* Inhibition of ICE-like and CPP32-like Proteases, *J. Exp. Med. 185*, 601–608.

38. Shiojima, I., and Walsh, K. (2002) Role of Akt Signaling in Vascular Homeostasis and Angiogenesis, *Circ. Res. 90*, 1243–1250.

Trans and Positional Ethylenic Bonds in Two Dominant Isomers of Eicosapentaenoic Acid from the Freshwater Sponge *Baicalospongia bacillifera*

Andrey B. Imbs* and Svetlana A. Rodkina

Institute of Marine Biology, Far Eastern Branch of the Russian Academy of Sciences, 690041 Vladivostok, Russian Federation

ABSTRACT: Reinvestigation of the current FA composition of the regional freshwater sponge *Baicalospongia bacillifera* showed that the main measured isomer of EPA (14% of the total FA now detected) is, in fact, an unusual 5*Z*,8*Z*,11*Z*,14*Z*,18*E*-EPA. Two other isomers of this acid also present were identified as a novel 5*Z*,8*Z*,11*Z*,15*Z*,18*E*-EPA and the common methylene-interrupted 5*Z*,8*Z*,11*Z*,14*Z*,17*Z*-EPA (usually written simply as EPA). Isolation of these acids as their methyl ester derivatives was accomplished with the use of a combination of silver-ion column chromatography and HPLC. The structure of the two new compounds was deduced from GC–MS and detailed NMR data. Partial hydrazine reduction of all three isolated EPA esters followed by separation of *cis/trans* isomers of the resulting monoenoic acids and GC–MS analysis of their dimethyl disulfide adducts were used for determination of the configuration and position of the double bonds. We may assume that the sponge *B. bacillifera* cannot receive these unusual EPA isomers directly from food sources (e.g., algal diatoms), and accordingly restructuring of ordinary EPA to novel acids may take place in the sponge tissue.

Paper no. L9786 in *Lipids 40*, 963–968 (September 2005).

Freshwater and marine sponges are very primitive multicellular animals characterized by the presence of several groups of symbiotic organisms and an extremely wide diversity in their FA compositions (1). Unique sponge biomembranes contain a high proportion of unusual FA (2,3) (i.e., very long chain C_{24}–C_{32} constituents named demospongic acids), some of which show a high biological activity (4–7). Among more than 5000 known sponges, about 150 species live in freshwater. Three regional genera, *Baicalospongia*, *Lubomirskia,* and *Swartschewskia,* occur in Lake Baikal (Russia); these sponges are leading species of biological bottom communities of the lake. The FA composition of Baikal sponges was reported for the first time by Dembitsky in 1981 (8,9). Further investigation of lipids of these sponges led to description of 185 FA in *B. bacillifera* (10) and of 183 FA in *L. baicalensis* (11). Unfortunately, individual FA have not been isolated from sponge lipids and have been identified solely using GC or GC–MS methods; NMR data have also not been reported. As with other sponge species, a careful analysis of FA chemical structures in the Lake Baikal sponges was performed for demospongic acids with very long chains.

In 1998, during our investigation of medium- and long-chain Δ^5 and Δ^4 FA in the Baikal sponge *B. bacillifera,* we showed the presence of a few minor isomers of EPA in the total FA (12). One of them was identified as 5*Z*,8*Z*,11*E*,14*Z*,17*Z*-EPA (0.7% of total FA), but, following other researchers, we determined the main EPA isomer (<7% of total FA) to be normal methylene-interrupted 5*Z*,8*Z*,11*Z*,14*Z*,17*Z*-EPA on the basis of its GC and MS data only (12). To monitor the food relationship between the main symbiotic groups of the Lake Baikal sponges, we have now paid more attention to some isomeric FA in the species under study. This work describes the results of our attempts to isolate and determine the chemical structures of all of the EPA isomers from the freshwater sponge *B. bacillifera.*

EXPERIMENTAL PROCEDURES

Materials. All solvents, acetyl chloride, dimethyl disulfide (DMDS), iodine, platinum oxide, pyrrolidine, silver nitrate, sodium thiosulfate, and sodium sulfate were purchased from Merck (Darmstadt, Germany). All reagents and solvents were of analytical or HPLC grade. The methyl ester of 5*Z*,8*Z*,11*Z*,14*Z*,17*Z*-EPA (EPA) and the saturated FA (14:0, 16:0, 20:0) used as GC standards were obtained from Sigma Chemical Co. (St Quentin-Fallavier, France). Methyl esters of 9*Z*-octadecenoic and 9*E*-octadecenoic acids were purchased from Sigma (St. Louis, MO). TLC was carried out on precoated Merck Kieselgel 60 G plates (10 × 10 cm). Aldrich (Steinheim, Germany) silica gel, Merck grade 9385, 60 Å was used for column chromatography. Evaporation was carried out under reduced pressure at 35°C.

Preparation of total FAME. Baicalospongia bacillifera specimens were collected in May 2003 on the western coast of Lake Baikal at 15 m depth using scuba equipment. Extraction of total lipids was conducted according to Bligh and Dyer (13) immediately after sampling. The extract was stored at –18°C.

On an analytical scale, total FAME were obtained by a sequential treatment of the total lipids with 1% MeONa/MeOH (30 min, 60°C) and 5% HCl/MeOH (30 min, 60°C) according to Carreau and Dubacq (14). The crude FAME were extracted with hexane and purified on a preparative TLC plate that was eluted with benzene.

On a preparative scale, about 1 g of total lipids was suspended in 1% MeONa/MeOH (30 mL) and heated with peri-

---

*To whom correspondence should be addressed at Laboratory of Comparative Biochemistry, Institute of Marine Biology, Far Eastern Branch of the Russian Academy of Sciences, Palchevskogo str.-17, 690041 Vladivostok, Russian Federation. E-mail: andreyimbs@hotmail.com
Abbreviations: DMDS, dimethyl disulfide.

odic shaking during 1 h at 65°C in a capped vial. After cooling, water (1 mL) was added, and crude FAME were extracted with hexane (3 × 10 mL). The combined extracts were evaporated, and the residue (0.6 g) was redissolved in a small amount of hexane and placed on a column (25 × 2 cm i.d.) with 50 g of silica gel in hexane. The column was eluted (3 mL/min) by a step gradient of hexane/benzene [9:1 (100 mL), 7:3 (100 mL), 4:6 (100 mL), and 1:9 (200 mL), vol/vol]. Fractions of 20 mL were collected and their compositions checked by TLC plates developed in benzene. Fractions with pure FAME were combined, and 0.5 g of pure FAME was obtained after evaporation.

Isolation of EPA isomers. About 0.5 g of pure FAME was placed onto a column (25 × 2 cm i.d.) with 50 g of silica gel impregnated with 5 g of AgNO$_3$ in hexane and eluted (3 mL/min) by a step gradient of hexane/benzene [9:1 (100 mL), 2:8 (200 mL), vol/vol], and pure benzene (500 mL). Fractions (15 mL) were collected and their compositions checked by silver-ion TLC plates developed in hexane/benzene (4:6, vol/vol). The fractions containing polyunsaturated FAME were combined to give 50 mg of a light yellow oil. This oil was subjected to HPLC on a Zorbax (Chadds Ford, PA) ODS column (25 cm × 9.4 mm i.d., 5 μm), eluted with acetonitrile at 4 mL/min, using a Laboratorni pristroje (Prague, Czech Republic) HPP-5001 pump equipped with a Rheodyne (Rohnert Park, CA) Model 7125i injector and a differential refractometer RIDK-102 (Laboratory Instruments, Prague, Czech Republic). The peaks were collected manually and their compositions determined by GC. The fraction containing a mixture of EPA methyl esters was repeatedly separated by HPLC, using acetonitrile/water (75:25, vol/vol) as the eluting solvent, to obtain 1.5 mg of ester **l**, 15 mg of ester **2**, and 2 mg of ester **3** with a purity of more than 90% each, shown by GC data (Scheme 1)**.**

Reduction of EPA esters to monoenoic FAME. Hydrazine reduction of methyl esters **1–3** (1 mg of each) was performed at 60°C in the mixture of 1.5 mL MeOH, 80 μL H$_2$O$_2$, and 120 μL hydrazine hydrate. After 90 min, the reaction was terminated by addition of 1.5 mL 2 N HCl. FAME were extracted with 3 mL hexane, and monoenoic *cis* and *trans* isomers were isolated by silver-ion TLC in benzene/hexane (6:4, vol/vol). Methyl esters of 9Z-18:1 and 9E-18:1 were used as the authentic control standards. The monoenoic FAME obtained were analyzed by GC and additionally converted to DMDS adducts as
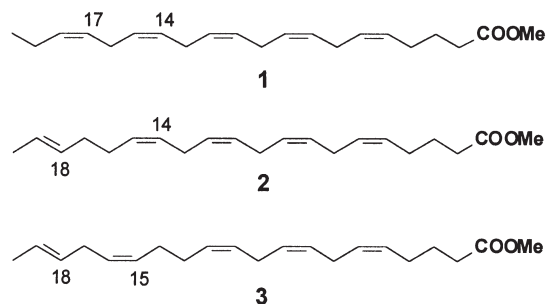
follows (15): The monoenoic FAME (0.3 mg) were dissolved in DMDS (0.2 mL), and a solution (0.05 mL) of iodine in diethyl ether (60 mg/mL) was added. After 24 h, hexane (5 mL) was added; the mixture was washed with dilute sodium thiosulfate solution, dried over anhydrous sodium sulfate, and evaporated to dryness. The DMDS adducts of monoenoic FAME obtained were analyzed by GC–MS.

FAME derivatization. N-Acyl pyrrolidide derivatives were prepared by direct treatment of the FAME with pyrrolidine/acetic acid (10:1, vol/vol) in a capped vial (24 h, 25°C) followed by ethereal extraction from the acidified solution and purification by preparative TLC developed in ethyl acetate. Hydrogenation of FAME was carried out in methanol solution in the presence of catalytic amounts of PtO$_2$.

Chromatographic and instrumental methods. Preparative Ag$^+$-TLC of FAME was carried out on plates impregnated with AgNO$_3$ by immersion in a 10% (wt/vol) solution of AgNO$_3$ in MeOH according to current practice (16). The plates were developed twice with hexane/ether/AcOH (94:3:3, by vol). After development, plate edges (0.5 cm) were sprayed with 10% H$_2$SO$_4$/MeOH and heated at 110°C. Bands corresponding to the FAME identified were scraped from the plate, eluted with chloroform/methanol (9:1, vol/vol), evaporated, and stored at −18°C in hexane solution.

GC analysis of FAME was carried out on a Shimadzu GC-17A gas chromatograph (Kyoto, Japan) with an FID on a SU-PELCOWAX 10 (Supelco, Bellefonte, PA) capillary column (30 m × 0.25 mm i.d.) at 210°C. Helium was used as the carrier gas at a linear velocity 30 cm/s. FAME were identified by comparison with authentic standards and suggestions using the table of ECL (17).

GC–MS of FAME from *B. bacillifera* was performed with a Shimadzu GCMS-QP5050A instrument using GS-MS Solution software for data analysis. A Supelco MDN-5S capillary column (5% diphenyl/95% dimethylsiloxane; 30 m × 0.25 mm) was used in the split (1:25) injection mode. The injector temperature was 250°C, and the oven temperature was 160°C with a 2°C/min temperature ramp to a final temperature of 240°C that was then held for 20 min (detector temperature 250°C). Helium was used as the carrier gas at a linear velocity 30 cm/s. GC–MS of *N*-acyl pyrrolidide and DMDS derivatives was performed on the same instrument; injector and detector temperatures were 300°C. For analysis of pyrrolidide, the oven temperature was 210°C with a 3°C/min temperature ramp to a final temperature of 270°C that was held for 40 min. For DMDS adducts analysis, the oven temperature was 220°C with a 1.5°C/min temperature ramp to a final temperature of 290°C that was held for 40 min.

^{1}H and ^{13}C NMR of the FAME were recorded using a Bruker DPX-500 spectrometer (Karlsruhe, Germany) at 500 and 125 MHz, respectively, in CDCl$_3$ with tetramethylsilane as an internal standard.

RESULTS AND DISCUSSION

The GC–MS chromatogram of total FAME from *B. bacillifera* indicated the presence of several peaks with molecular ions

SCHEME 1

(M+) at *m/z* 316 each that were preliminarily assumed to be the methyl esters of EPA isomers (20:5). We earlier determined one of these isomers as the methyl ester of 5Z,8Z,11E,14Z,17Z-EPA (12). To investigate the chemical structure of the other EPA isomers, a polyunsaturated fraction of FAME was separated by low-pressure Ag+ column chromatography. The total fraction of EPA methyl esters was isolated from the fraction obtained by fast RP-HPLC using acetonitrile, and then individual EPA ester isomers were separated by RP-HPLC using a mixture of acetonitrile/water to give the three main compounds A, B, and C (1:10:1.3, by weight) of <90% purity according to GC.

Compounds A–C were transformed into the saturated derivatives by catalytic hydrogenation. The latter compounds coeluted with authentic methyl eicosanoate (20:0) on GC analysis, and their mass spectra gave a molecular ion peak at *m/z* 326 (M+), confirming the presence of five double bonds and a straight C_{20} chain in the original FAME. Our attempt to determine the position of double bonds in compounds A–C by GC–MS analysis of their *N*-acyl pyrrolidide derivatives was unsuccessful. A molecular ion peak of the derivatives at *m/z* 355 (M+) corresponded to the pyrrolidide of EPA, but we could not detect a significant difference between the pyrrolidide mass spectra of authentic EPA and compounds A–C, and also we could not determine the exact positions of double bonds because of a low intensity of distinctive fragmentation ions in a high mass range.

To solve this new problem, the generally accepted method of hydrazine reduction used to determine the position and geometry of double bonds in the carbon chain of PUFA (18) was initially applied to the whole A–C fraction. After nonselective partial reduction of double bonds in the EPA molecules, we obtained a mixture of C_{20} acids of varying degrees of unsaturation, containing about 30% of monoenoic acids. These monoenoic acids must contain a mixture of five *cis* isomeric 20:1 acids, each corresponding to one of the five double bonds in the carbon chain of the normal EPA molecule and describing the position and geometry of these double bonds. However, the monoenoic acids from A–C could be separated by preparative Ag-TLC into two fractions: *cis* and *trans* isomers possessing R_f 0.31–0.53 and R_f 0.53–0.73, respectively. It has been demonstrated that in GC analysis the peaks of *cis* and *trans* isomers do not overlap in the vast majority of cases (19). The double bond positions were then determined by GC–MS of the corresponding DMDS adducts of the respective fractions of monoenoic FAME.

All five monoenoic FAME obtained by reduction of component A were found in the fraction of *cis* isomers. The mass spectra of the DMDS adducts of these five monoenoic FAME gave molecular ion peaks at *m/z* 418 (M+) and five pairs of abundant fragments at *m/z* 161 ($C_7H_{13}SO_2^+$) and 257 ($C_{16}H_{33}S^+$), *m/z* 203 ($C_{10}H_{19}SO_2^+$) and 215 ($C_{13}H_{27}S^+$), *m/z* 245 ($C_{13}H_{25}SO_2^+$) and 173 ($C_{10}H_{21}S^+$), *m/z* 287 ($C_{16}H_{31}SO_2^+$) and 131 ($C_7H_{15}S^+$), and *m/z* 329 ($C_{19}H_{37}SO_2^+$) and 89 ($C_4H_9S^+$), indicating that the double bonds were localized at 5, 8, 11, 14 and 17 carbon atoms of the original compound A, correspondingly. These fragments reflect the cleavages exempli-

fied by Figure 1B,D,E. We also observed characteristic peaks at *m/z* 129, 171, 213, 255, and 297, which are due to the loss of methanol from the corresponding fragment ion peaks ($C_nH_{2n-1}SO_2$ – MeOH)+. From these data, the structure of compound A was determined as the methyl ester of the commonly occurring EPA, 5Z,8Z,11Z,14Z,17Z-EPA **1**.

Four of five monoenoic FAME (20:1) obtained by reduction of component B belonged to the fraction of *cis* isomers. The mass spectra of their DMDS adducts afforded the same molecular ion and fragment peaks as the DMDS adducts synthesized from compound A (see above), indicating that four double bonds were localized at 5, 8, 11, and 14 carbon atoms of the original compound B (Fig. 1D,E). The last monoenoic 20:1 ester was found in the Ag-TLC fraction of *trans* isomers. The MS of the DMDS adduct of this ester showed a molecular ion peak at *m/z* 418 (M+, 5%). The double bond was localized between carbons 18 and 19 based on the abundant fragmentations at *m/z* 343 ($C_{20}H_{39}SO_2^+$, 100%) and *m/z* 75 ($C_3H_7S^+$, 91%) (Fig. 1A). We could also observe a characteristic peak at *m/z* 311 ($C_{20}H_{39}SO_2^+$ – MeOH, 90%). From these data, the structure of the compound B was determined as the methyl ester of the unusual 5Z,8Z,11Z,14Z,18E-EPA **2**.

Four of five monoenoic FAME obtained by reduction of component C were 5Z-20:1, 8Z-20:1, 11Z-20:1, and 18E-20:1 acid methyl esters. The structures of these monoenoic FAME were determined using preparative Ag-TLC and GC–MS of DMDS adducts (Fig. 1A,E) as described above for components A and B. The fifth 20:1 methyl ester was present in the *cis* isomer fraction. The MS of the DMDS adduct of this ester showed a molecular ion peak at *m/z* 418 (M+, 5%). The double bond was located between carbons 15 and 16 based on the fragmentations at *m/z* 301 ($C_{17}H_{33}SO_2^+$, 100%), 117 ($C_6H_{13}S^+$, 99%), and 269 ($C_{17}H_{33}SO_2^+$ – MeOH, 96%) (Fig. 1C). From these data, the structure of compound B was determined to be the methyl ester of the unusual 5Z,8Z,11Z,15Z,18E-EPA **3**.

It should be noted that only DMDS adducts of 14Z-20:1, 15Z-20:1, 17Z-20:1, and 18E-20:1 methyl esters completely separated during GC–MS analysis using the MDN-5S column. Partially resolved DMDS adducts of other monoenoic acid methyl esters (5Z-20:1, 8Z-20:1, and 11Z-20:1) containing a double bond in the middle of a chain were eluted as one broad peak, but the determination of individual components in this peak is very simple because of clear and unambiguous interpretation (15) of the fragmentation of DMDS adduct (Fig. 1E).

The NMR data for the methyl ester of the novel EPA isomer **2** are shown in Table 1. The 1H NMR (500 MHz) in CDCl3 showed the presence of two olefinic methines (δ 5.41–5.48) separated from another eight olefinic methines (δ 5.33–5.41), one methoxycarbonyl group (δ 3.67), three aliphatic methylenes located between double bonds (= CH–CH2–CH=) (δ 2.79–2.84), one aliphatic methylene in an β-position to the carboxyl group (δ 2.32), three allylic methylenes (–CH2–CH=) (δ 2.01–2.15), one aliphatic methylene in a β-position to the carboxyl group (δ 1.71), and one methyl group (δ 1.65). Owing to the influence of the nearest Δ^{18} double bond, the chemical shift of the terminal methyl group in ester **2** was noticeably higher
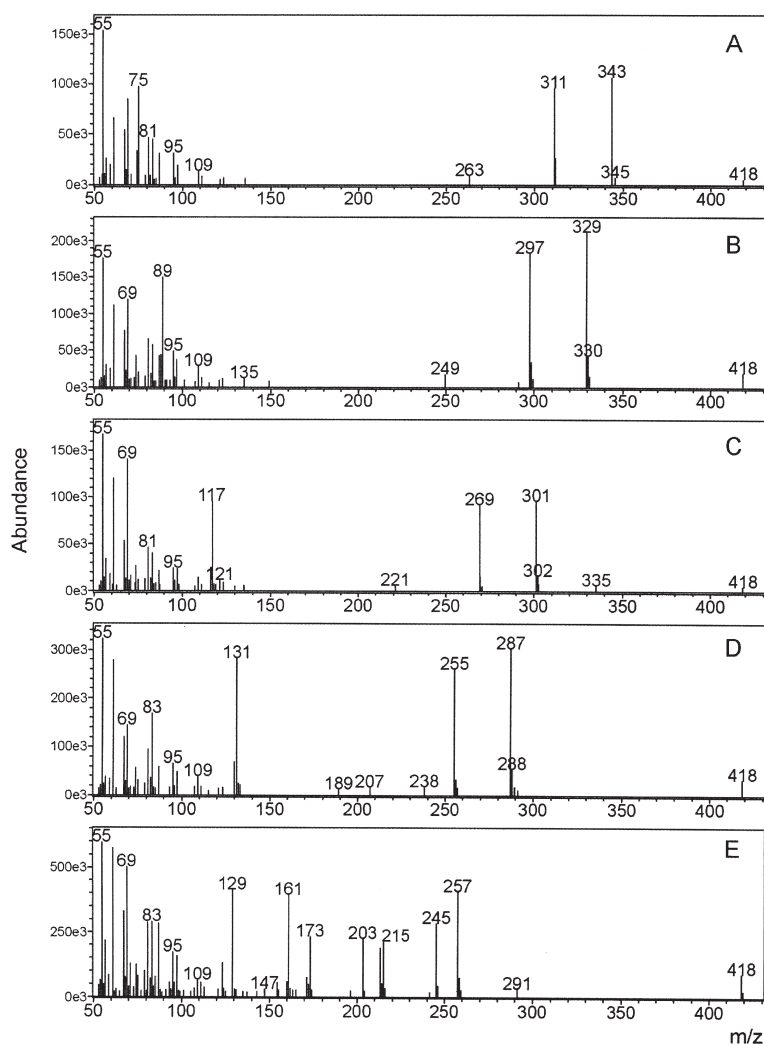
FIG. 1. EI mass spectra of dimethyl disulfide adducts of methyl esters of 18*E*-20:1 (A), 17*Z*-20:1 (B), 15*Z*-20:1 (C); 14*Z*-20:1 (D), and a mixture of 5*Z*-20:1, 8*Z*-20:1, and 11*Z*-20:1 (E) eicosenoic acids obtained by a partial hydrazine reduction of the methyl eicosapentaenoate isomers (**1–3**). MS conditions are described in the Experimental Procedures section.

than the shift of the same group (δ 0.89) in most aliphatic FAME. The attribution of the proton signals was mainly obtained from a ^{1}H-^{1}H chemical shift correlation spectroscopy (COSY-45) experiment (Fig. 2). On the one hand, the amount, chemical shifts, and interactions of protons at the range from C-2 to C-15 were typical for Δ^5 polyunsaturated methylene-interrupted FAME (20). The signal of $\Delta^{5,8,11,14}$ protons in the range of 5.33–5.41 correlated with the multiplets at δ 2.79–2.84 (2H-7, 2H-10, 2H-13) and at δ 2.09–2.15 (2H-4, 2H-16). On the other hand, the COSY experiment showed characteristic coupling from the n-1 protons (3H, δ 1.65, doublet) to the separated olefinic signal at δ 5.41–5.48 (H-19, H-17) that in turn indicated coupling with the methylene group at δ 2.04 (2H-17).

The ^{13}C NMR (125 MHz) spectrum in CDCl$_3$ confirmed the presence of 21 carbon atoms in a molecule of the main EPA isomer ester **2** (12 peaks of primary and tertiary atoms and 8 peaks of secondary atoms, as was shown in the distortionless enhancement by polarization transfer-135 experiment). It was clear from

our data (Table 1) that there were one carbonyl carbon (δ 173.98), ten olefinic methines (=CH–) (δ 125–131), one methoxycarbonyl group (δ 51.38), eight aliphatic methylenes (δ 24–34), and one methyl group (δ 17.81) shifted to a low field in comparison with a terminal methyl group of hydrocarbons (δ 14.07). The attribution of the carbon signals was mainly obtained from ^{1}H-^{13}C heteronuclear single quantum connectivity and heteronuclear multiple bond coherence experiments. A long-range coupling was shown from 2H-2 and the OMe protons to a quaternary carbon (carbonyl) at δ 173.98, and assignments of C-4, C-16, C-17, and C-19 also were confirmed. The signals of C-14 and C-15 olefinic atoms were shifted to the low-field region in comparison with that of methyl 5Z,8Z,11Z,14Z,17Z-eicosapentaenoate (21). The value of the chemical shift of the C-18 olefinic atom (δ 130.79) was similar to that of polyunsaturated FAME with an n-3 *trans* double bound (22). The signal of the C-19 atom (δ 125.14) was instead shifted down because of a neighboring terminal methyl group. The assignment of the five olefinic atoms

TABLE 1
NMR Data for Methyl 5Z,8Z,11Z,14Z,18E-Eicosapentaenoate (2)[a]

Position	¹H NMR δ (ppm)	m, J (Hz)	¹³C NMR δ (ppm)
1			173.98
2	2.32	t, 7.5	33.43
3	1.71	p, 7.5	24.77
4	2.09–2.15[b]	m	26.54
5	5.33–5.41[b]	m	128.90
6	5.33–5.41[b]	m	128.86
7, 10, 13	2.79–2.84[b]	m	25.59–25.66[b]
8	5.33–5.41[b]	m	128.16
9	5.33–5.41[b]	m	127.92
11	5.33–5.41[b]	m	127.88
12	5.33–5.41[b]	m	128.17
14	5.33–5.41[b]	m	128.45
15	5.33–5.41[b]	m	129.70
16	2.09–2.15[b]	m	27.33
17	2.04	m	32.51
18	5.41–5.48[b]	m	130.79
19	5.41–5.48[b]	m	125.14
20	1.65	dt, 4.5, 1.5	17.81
–OCH₃	3.67	s	51.38

[a]In CDCl₃ with tetramethylsilane as internal standard.
[b]Overlapped signals were not assigned.
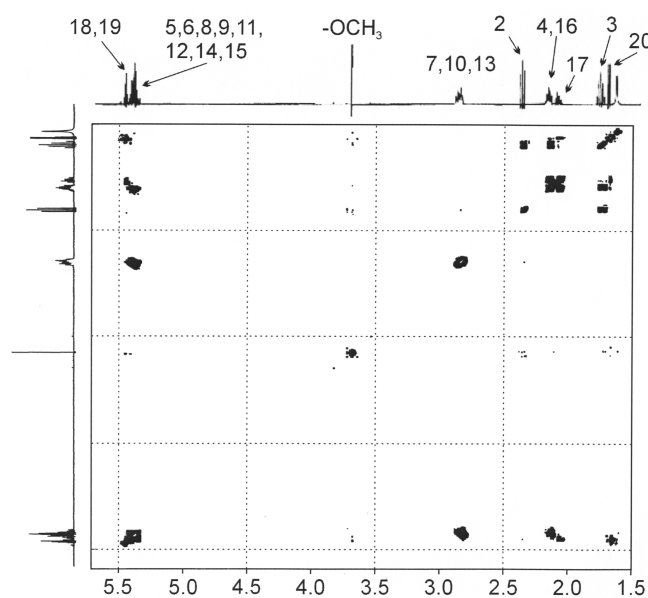
FIG. 2. ¹H-¹H NMR correlation spectroscopy (COSY-45) of methyl 5Z,8Z,11Z,14Z,18E-eicosapentaenoate (**2**).

(C-6, C-8, C-9, C-11, C-12) was based on a high degree of comparability between the low-field region of the ¹H NMR spectrum (20) and the ¹³C NMR spectrum (21) for methyl 5Z,8Z,11Z,14Z,17Z-eicosapentaenoate with that of methyl ester **2**. The geometry of the double bonds was confirmed by analysis of the ¹³C NMR chemical shifts of the neighboring carbons of the double bonds (23). It is known that carbons adjacent to *trans* double bonds have chemical shifts in the δ 29.5–38.0 range, whereas those adjacent to *cis* double bonds have values of δ 26.0–28.5. The five signals of the ester **2** were in the δ 25.59–27.33 range (C-4, C-7, C-10, C-13, and C-16) (Table 1), confirming the *cis* configuration of Δ⁵,⁸,¹¹,¹⁴ double bonds, and one signal at δ 32.51 (C-17) corresponded to the *trans* configuration of the Δ¹⁸ double bond. Thus, the NMR data just discussed confirmed the structure of the ester of the main EPA isomer **2,** which was determined by GC–MS analysis of its derivatives.

In the present investigation, identified isomeric esters **1**, **2**, and **3** found in total lipids of the Baikal sponge *B. bacillifera* accounted, respectively, for 1.9, 14.0, and 2.5% of total FAME. In our previous experiments, the value of EPA content in the total FAME of *B. bacillifera* varied from 7.6 (12) to 12.2% (24). Since methylene- and nonmethylene-interrupted EPA isomers (**1**, **2**) were earlier determined together, we do not know whether the difference observed in the total EPA content depends on variations in the content of one isomer or whether the ratio of EPA isomers is relatively constant and variations in the total EPA content depend on effects of the environment and food sources.

The parazoans are classed as animals but are extremely dependent on auxiliary and simpler life forms. These animals or their symbionts may be heavily influenced by the current climate changes in northern latitudes, perhaps especially severe after air masses have crossed Europe and most of Asia. It is not surprising that there are different EPA isomers in *B. bacillifera*

complexes collected from Lake Baikal in May 2003 compared with those reported in 1998 (12).

Unsaturated FA in plants and animals typically have a *cis* configuration, but the presence of a *trans* double bond is actually not rare in living organisms (25). As examples of EPA *trans* isomers isolated from aquatic sources, two acids (5Z,7E,9E,14Z,17Z-20:5 and 5E,7E,9E,14Z,17Z-20:5) were obtained from the red seaweed *Ptilota filicina* (26), and 5Z,8Z,10E,12E,14Z-20:5 was obtained from the from red alga *Bossiella orbigniana* (27). However, natural *trans* isomers of EPA were found in very small amounts. Therefore, our discovery of a non-methylene-interrupted *trans* isomer of EPA (as one of the principal components in a total FA composition) seems important.

Except in our earlier report (12), *trans* isomers of EPA have not yet been reported in sponge lipids, although several mono-, di-, and trienoic acids with *trans* double bonds have been detected (28,29). As a rule, the presence of *trans* polyunsaturated FAME was attributed either to special diets containing *trans* unsaturated acids, to the elongation/desaturation of *trans* monoenoic acids of bacterial origin, or to the enzymatic isomerization of *cis* polyunsaturated FAME (25).

A biosynthetic origin of *trans* EPA **2** and **3** from *trans* bacterial FA does not seem to be the case for *B. bacillifera* since the n-2 *trans* unsaturated FA were not detected in sponge symbiotic bacteria. We suggest that enzymatic isomerization of all-*cis*-EPA or specific desaturation of arachidonic acid would be possible ways of synthesizing the identified isomeric *trans* EPA **2** and **3**. We showed earlier that the Baikal sponges receive EPA predominantly from food sources, which can be diatoms and peridineans enriched in EPA (24). It is possible that some of the dietary EPA undergoes isomerization by a unique enzyme complex of sponge cells or sponge symbionts. We also detected

a small amount of FAME with conjugated double bounds in the total EPA fraction (Imbs, A.B., and Rodkina, S.A., unpublished data). Therefore, we believe that the mechanism of formation of the novel *trans* EPA isomers in *B. bacillifera* is, to some extent, similar to that in the marine alga *P. filicina* (30).

REFERENCES

1. Bergquist, P.R., Lawson, M.P., Lavis, A., and Cambie, R.C. (1984) Fatty Acid Composition and the Classification of the Porifera, *Biochem. Syst. Ecol. 12*, 63–84.
2. Litchfield, C., and Morales, R.W. (1976) Are Demospongiae Membranes Unique Among Living Organisms? in *Aspects of Sponge Biology* (Harrison, F.W., and Cowden, R.K., eds.), pp. 183–200, Academic Press, New York.
3. Djerassi, C., and Lam, W.K. (1991) Sponge Phospholipids, *Acc. Chem. Res. 24*, 69–75.
4. Ichiba, T., Scheuer, P.J., and Kellyborges, M. (1995) Two Cytotoxic 3,6-Epidioxy Fatty Acids from an Indonesian Sponge, *Plakotris* sp. 1, *Tetrahedron 51*, 12195–12202.
5. Fatope, M.O., Adoum, O.A., and Takeda, Y. (2000) C-18 Acetylenic Fatty Acids of *Ximenia americana* with Potential Pesticidal Activity, *J. Agric. Food Chem. 48*, 1872–1874.
6. Makarieva, T.N., Santalova, E.A., Gorshkova, I.A., Dmitrenok, A.S., Guzii, A.G., Gorbach, V.I., Svetashev, V.I., and Stonik, V.A. (2002) A New Cytotoxic Fatty Acid (5Z,9Z)-22-Methyl-5,9-tetracosadienoic Acid and the Sterols from the Far Eastern Sponge *Geodinella robusta*, *Lipids 37*, 75–80.
7. Meyer, M., and Guyot, M. (2002) 5,9,23-Triacontatrienoic Methyl Ester, an Elastase Inhibitor from the Marine Sponge *Chondrilla nucula*, *Lipids 37*, 1109–1111.
8. Dembitsky, V.M. (1981) Fatty Acids Composition of Class Demospongiae Freshwater Sponges. I. Genus *Lubomirskia*, *Khim. Prirod. Soed. (USSR) 4*, 511–513, *Chem. Abst. 96*, 31906m.
9. Dembitsky, V.M. (1981) Fatty Acids Composition of Class Demospongia Freshwater Sponges. II. Genera *Swartchewskia* and *Baicalospongia*, *Khim. Prirod. Soed. (USSR) 4*, 513–515, *Chem. Abst. 96*, 17249t.
10. Dembitsky, V.M., Rezanka, T., and Kashin, A.G. (1993) Comparative Study of the Endemic Freshwater Fauna of Lake Baikal. 2. Unusual Lipid Composition of Two Sponges *Baicalospongia bacillifera* and *B. intermedia* (Family Lubomirskiidae, Class Demospongia), *Comp. Biochem. Physiol. 106B*, 825–831.
11. Dembitsky, V.M., Rezanka, T., and Kashin, A.G. (1994) Comparative Study of the Endemic Freshwater Fauna of Lake Baikal—VI. Unusual Fatty Acid and Lipid Composition of the Endemic Sponge *Lubomirskia baicalensis* and Its Amphipod Crustacean Parasite *Brandtia (Spinacantus) parasitica*, *Comp. Biochem. Physiol. 109B*, 415–426.
12. Imbs, A.B., and Latyshev, N.A. (1998) New Δ5 and Δ4 Unsaturated Medium- and Long-Chain Fatty Acids in the Freshwater Sponge *Baicalospongia bacillifera*, *Chem. Phys. Lipids 92*, 117–125.
13. Bligh, E.G., and Dyer, W.J. (1959) A Rapid Method of Total Lipid Extraction and Purification, *Can. J. Biochem. Physiol. 37*, 911–918.
14. Carreau, J.P., and Dubacq, J.P. (1979) Adaptation of Macro-scale Method to the Micro-scale for Fatty Acid Methyl Transesterification of Biological Lipid Extracts, *J. Chromatogr. 151*, 384–390.
15. Christie, W.W. (1997) Structural Analysis of Fatty Acids, in *Advances in Lipid Methodology* (Christie, W.W., ed.), Vol. 4, pp. 119–169, Oily Press, Dundee.
16. Kaneniwa, M., Itabashi, Y., and Takagi, T. (1987) Unusual 5-Olefinic Acids in the Lipids of Algae from Japanese Waters, *Bull. Jpn. Soc. Sci. Fish. 53*, 861–866.
17. Christie, W.W. (1988) Equivalent Chain Lengths of Methyl Ester Derivatives of Fatty Acids on Gas Chromatography—A Reappraisal, *J. Chromatogr. 447*, 305–314.
18. Ratnayake, W.M.N., Grossert, J.S., and Ackman, R.G. (1990) Studies on the Mechanism of the Hydrazine Reduction Reaction—Applications to Selected Monoethylenic, Diethylenic and Triethylenic Fatty Acids of *cis* Configurations, *J. Am. Oil Chem. Soc. 67*, 940–946.
19. Toschi, T.G., Capella, P., Holt, C., and Christie, W.W. (1993) A Comparison of Silver Ion HPLC Plus GC with Fourier-Transform IR Spectroscopy for the Determination of *trans*-Double Bonds in Unsaturated Fatty Acids, *J. Sci. Food Agric. 61*, 261–266.
20. Aursand, M., Rainuzzo, J.R., and Grasdalen, H. (1993) Quantitative High-Resolution ^{13}C and ^{1}H Nuclear Magnetic Resonance of ω3 Fatty Acids from White Muscle of Atlantic Salmon (*Salmo salar*), *J. Am. Oil Chem. Soc. 70*, 971–981.
21. Sacchi, R., Medina, I., Paolillo, L., and Addeo, F. (1994) High-Resolution ^{13}C-NMR Olefinic Spectra of DHA and EPA Acids, Methyl Esters and Triacylglycerols, *Chem. Phys. Lipids 69*, 65–73.
22. Vatele, J.M., Doan, H.D., Chardigny, J.M., Sebedio, J.L., and Grandgirard, A. (1994) Synthesis of Methyl (5Z,8Z,11Z, 14Z,17E)-Eicosapentaenoate and Methyl (4Z,7Z,10Z,13Z, 16Z,19E)-Docosahexaenoate, *Chem. Phys. Lipids 74*, 185–193.
23. Choudhury, S.R., Traquair, J.P., and Jarvis, W.R. (1995) New Extracellular Fatty Acids in Culture Filtrates of *Sporothrix flocculosa* and *S. rugulosa*, *Can. J. Chem. 73*, 84–87.
24. Latyshev, N.A., Zhukova, N.V., Efremova, S.M., Imbs, A.B., and Glysyna, O.I. (1992) Effect of Habitat on Participation of Symbionts in Formation of the Fatty Acid Pool of Fresh-Water Sponges of Lake Baikal, *Comp. Biochem. Physiol. 102B*, 961–965.
25. Ackman, R.G. (1997) Has Evolution and Long-Term Coexistence Adapted Us to Cope with *trans* Fatty Acids? *J. Food Lipids 4*, 295–318.
26. Lopez, A., and Gerwick, W.H. (1987) 2 New Icosapentaenoic Acids from the Temperate Red Seaweed *Ptilota filicina* J. Agardh, *Lipids 22*, 190–194.
27. Burgess, J.R., Delarosa, R.I., Jacobs, R.S., and Butler, A. (1991) A New Eicosapentaenoic Acid Formed from Arachidonic Acid in the Coralline Red Algae *Bossiella orbigniana*, *Lipids 26*, 162–165.
28. Carballeira, N.M., and Shalabi, F. (1990) Identification of Naturally-Occurring *trans, trans* Δ-5,9 Fatty Acids from the Sponge *Plakortis halichondroides*, *Lipids 25*, 835–840.
29. Vysotskii, M.V., Imbs, A.B., Popkov, A.A., Latyshev, N.A., and Svetashev, V.I. (1990) *Trans*-Olefinic Very-Long-Chain Fatty Acid (26:3-Δ-5c,9c,19t) in Lipids of Fresh Water Sponges of Lake Baikal, *Tetrahedron Lett. 31*, 4367–4370.
30. Zheng, W., Wise, M.L., Wyrick, A., Metz, J.G., Yuan, L., and Gerwick, W.H. (2002) Polyenoic Fatty Acid Isomerase from the Marine Alga *Ptilota filicina*: Protein Characterization and Functional Expression of the Cloned cDNA, *Arch. Biochem. Biophys. 401*, 11–20.

Monitoring the Oxidation of Docosahexaenoic Acid in Lipids

Ann-Marie Lyberg*, Ezio Fasoli, and Patrick Adlercreutz

Department of Biotechnology, Center for Chemistry and Chemical Engineering, Lund University, Lund, S-221 00 Lund, Sweden

ABSTRACT: The oxidation of free DHA, DHA mixed with PC, and DHA incorporated into PC, PE, or TG was evaluated to determine which lipid provided DHA with the best protection against oxidation. DHA was either situated at the *sn*-1 position, *sn*-2 position, or both positions of the phospholipid, whereas the TG contained DHA at all positions. All lipids were incubated as bulk lipids, in chloroform, or as an emulsion in contact with air at 25–30°C for 28 d. Since DHA, which is highly sensitive to oxidation, has a great impact on our health and is desired as a food additive, the stability of this FA is of great importance. This study was mainly focused on the primary oxidation products, which were monitored as eight monohydroperoxy-DHA isomer groups, the total amount of polyhydroperoxides, and the PV. However, a measure of secondary oxidation products, the carbonyl value, was also monitored. We found that DHA was most protected against hydroperoxide formation when it was incorporated at one position of either PC or PE. In these lipids, hydroperoxide formation at carbon atoms 4, 7, 8, and 11 was completely prevented. DHA mixed with PC was also protected, although to a lesser extent, and all hydroperoxide isomers were detected. In contrast, PC and TG containing DHA at all positions should be avoided, since they were highly oxidized.

Paper no. L9795 in *Lipids 40*, 969–979 (September 2005).

The n-3 FA DHA has a considerable impact on health. DHA is required in the development of the brain and eyesight of both the fetus and infant (1). In adults, DHA is required to maintain the normal functioning of the brain and nervous system (2). A DHA deficiency has been found in several disorders such as Alzheimer's disease, schizophrenia, dyslexia, and some cases of attention-deficit/hyperactivity disorder (3–6). The human body can obtain DHA from the diet either directly or by converting α-linolenic acid to DHA. If the n-6 to n-3 ratio within the diet is high, which is usual in the Western world today, both the conversion to DHA and the incorporation of n-3 FA into the phospholipid membranes are low (7). However, a reduction of the n-6 to n-3 ratio will increase both conversion and incorporation. The eicosanoids derived from the n-3 FA EPA will thereby increase, which suppresses the synthesis of eicosanoids derived from the n-6 FA arachidonic acid (AA). The former eicosanoids have anti-inflammatory effects, whereas the latter eicosanoids can cause both inflammation and cancer (7). Among the n-3 FA obtained from the diet, EPA and DHA have a larger suppressive effect on the synthesis of eicosanoids derived from AA than does α-linolenic acid. Furthermore, there are indications that the consumption of fish containing EPA and DHA reduces the risk of death from coronary heart disease (8).

DHA is, however, highly sensitive to oxidation, and toxic oxidation products such as hydroperoxides and aldehydes can be formed (9,10). High amounts of oxidation products in the human body cause oxidative stress. This condition can induce various kinds of diseases such as cancer, diabetes, and rheumatoid arthritis (9).

PUFA, DHA in particular, need to be protected, and different strategies have been used to avoid oxidation. A common way to reduce oxidation is to use a synthetic or natural antioxidant (9). Since there is a desire to reduce the amount of synthetic material in food, natural antioxidants are more attractive. One group of natural compounds that has shown antioxidant activity is the phospholipids. Synergistic effects have been observed in the protection of fish oil by combinations of tocopherol, phospholipids (lecithin), and ascorbic acid (11). Another approach is to incorporate DHA into a lipid. DHA incorporated into phospholipids has been found to be more resistant to oxidation than both TG and ethyl esters containing DHA (12). Phospholipids are therefore highly interesting as food additives to stabilize DHA. However, there is a large variety of phospholipids, and it is necessary to evaluate which phospholipid structures containing DHA give the best protection against oxidation.

In this study, the oxidation of eight DHA lipids stored at 25–30°C was investigated. Free DHA was compared with DHA that was either mixed with PC or incorporated into PC, PE, or TG. DHA was either situated at the *sn*-1 position, the *sn*-2 position, or both positions of the phospholipid, whereas the TG contained DHA at all positions. These DHA lipids were incubated as bulk lipids, in chloroform, or as an emulsion. These model systems were selected, since DHA is most often stored in bulk or in a water system, such as an emulsion, when added to food. The solvent system was of interest, since DHA appears as isolated molecules in this system, which is not possible in an aqueous system. The oxidation profile of the DHA lipids was obtained by monitoring eight monohydroperoxy-DHA isomer groups, the total amount of polyhydroperoxides, the PV, and the carbonyl value (CV).

MATERIALS AND METHODS

Materials. Dipalmitoyl L-α-PC, 1-palmitoyl lysophosphatidylcholine (LPC), tridocosahexaenoin (purity 99%), and 4,7,10,13,16,19-DHA (purity 95%) were bought from Larodan Fine Chemicals AB (Malmö, Sweden). 1,2-Didocosahexaenoyl-*sn*-glycero-3-phosphocholine (purity 99%) was purchased from Avanti Polar Lipids, Inc. (Alabaster, AL). Lipases from *Rhizomucor miehei* (Lipozyme IM) and *Candida antarctica* (Novozym 435) were obtained from Novozymes A/S (Bagsvaerd, Denmark). The lipase *Chromobacterium viscosum* was obtained from Biocatalysts Ltd. (Cardiff, United Kingdom). Phospholipase D (PLD) from *Streptomyces* was a gift from Chemi SpA (Patrica, Italy). 4-Dimethylaminopyridine (DMAP, >99%) and 1-(3-dimethylaminopropyl)-3-ethylcarbodiimide hydrochloride (EDCI, >98%) were purchased from the Aldrich Chemical Company (St. Louis, MO). Ethanolamine was bought from Sigma (St. Louis, MO). Ethanol (95%) was bought from Kemityl (Haninge, Sweden), and all other solvents and chemicals were of at least analytical grade.

Enzymatic synthesis of 2-palmitoyl LPC. 2-Palmitoyl LPC from PC was synthesized using a procedure based on a previously described method (13). Lipozyme IM (9.3 g) catalyzed the reaction between 4.6 g of 1,2-dipalmitoyl-*sn*-glycero-3-PC and 93 mL of ethanol (95%). The reaction was performed with shaking at 25°C until 2 mol% PC was left in the mixture. The reaction was then stopped by filtering off the enzyme, and the ethanol was evaporated. The residue was washed with diethyl ether (464 mL) to dissolve the FFA and FA ethyl esters. The dispersion was centrifuged (13,500 × *g*, 20 min) and the supernatant was discarded. The washing procedure was performed four times. The substance was then dried with respect to the diethyl ether under reduced pressure for 30 min. The 2-palmitoyl-LPC was then dissolved in 46 mL of water, followed by lyophilization.

Esterification of 2-palmitoyl LPC catalyzed with lipase. The esterification of 2-palmitoyl LPC with DHA was carried out as described previously (14). The synthesis of PC was performed at a water activity of 0.22 obtained by gas-phase equilibrium in a simple reactor containing a saturated aqueous solution of KAc. The substrates DHA (1 M in toluene, bubbled with argon) and LPC were first separately equilibrated at a water activity of 0.22 for at least 15 h. They were

TABLE 1
The DHA-Containing Lipids Studied

Formulation	Abbreviation	Molar ratio
DHA	DHA	
DHA + 1,2-palmitoyl-PC	DHA + PC	1:1
1,2-diDHA-PC + 1,2-dipalmitoyl-PC	1,2-DHA-PC	1:1
1-DHA-2-palmitoyl-PC	1-DHA-PC	
1-palmitoyl-2-DHA-PC	2-DHA-PC	
1-DHA-2-palmitoyl-PE	1-DHA-PE	
1-palmitoyl-2-DHA-PE	2-DHA-PE	
1,2,3-triDHA-TG	DHA-TG	

then combined and vortexed until the LPC (0.1 M) had dissolved, and the immobilized lipase *C. antarctica* (0.1 g/mL) was added to the solution. To prevent the oxidation of DHA, argon gas was added to both the solution and the reactor at the beginning of the reaction, which was performed at 25°C. Two batches of PC were synthesized, with reaction volumes of 26 and 31 mL. The reaction was monitored with respect to phospholipid (PC + LPC) content by HPLC using the method described in the following section. The two batches obtained 42 mol% of PC after 24- and 28-h reaction times. The enzyme was then filtered off. After rinsing the enzyme with toluene, the solvent was evaporated.

Chemical synthesis of PC with DHA at the sn-2 position. The chemical synthesis of PC with DHA at the *sn*-2 position was carried out as described previously (14). The substrates DHA (3.83 g, 11.7 mmol) and 1-palmitoyl LPC (1.06 g, 2.14 mmol) were dissolved in 12.2 mL of dichloromethane. The coupling agent EDCI (2.66 g, 13.84 mmol) and the catalyst DMAP (0.71 g, 5.79 mmol) were then dissolved in the reaction medium. To minimize the oxidation of DHA, the reaction medium was bubbled with argon. This solution was stirred on a magnetic stirrer for 1 h, by which time all the 1-palmitoyl LPC had been transformed into PC. The reaction was terminated by adding 33 mL of dichloromethane and 15.2 mL of 0.5 M HCl to extract the catalyst into the aqueous phase. The organic phase containing PC was washed three times with 0.5 M of HCl, whereas the HCl phase was washed with dichloromethane. Separation was enhanced by centrifugation, since the emulsion phase formed by the surfactant PC was reduced. Finally, the dichloromethane phases were combined.

Purification by flash chromatography. To separate PC from LPC and FA, the product was purified by flash chromatography (14). The flash column was packed with 60 g silica. FFA were first eluted with cyclohexane/isopropanol (1:1, 260 mL), and LPC was then separated from PC with the solvent system chloroform/methanol/H$_2$O (65:35:5, 500 mL). Fractions of 30 mL were collected. The fractions were preliminarily analyzed by TLC, and the PC-containing fractions were then analyzed by HPLC. The fractions containing PC were pooled and the solvent was evaporated, followed by lyophilization. The yields for DHA incorporated at the *sn*-1 position (two batches) or *sn*-2 were 24, 22, and 70 mol%, respectively. The yield was defined as the molar ratio between the PC obtained after lyophilization and the LPC substrate. The purity of PC was at least 95%, whereas the DHA content of PC was at least 40% (14).

Synthesis of PE from PC (15). PLD from *Streptomyces* was obtained in a Celite-adsorbed form. Before use, the PLD powder (3200 U/g) was suspended in water containing NaOAc (0.1 M) and CaCl$_2$ (0.1 M). The suspension was then filtered with a Celite filter to obtain a clear solution.

PC (0.4 g, 0.521 mmol) was dissolved in 6 mL of dichloromethane and mixed with 12 mL of the aqueous enzyme solution (enzyme activity 10 U/mL). Ethanolamine (0.72 mL, 0.012 mol) was added to the enzyme–water phase

to obtain a 1 M concentration, and the water phase pH was adjusted to 5.5 with acetic acid. The reaction mixture was stirred for 2 h, at the end of which the HPLC analysis showed that the PC had been completely transformed into PE. The emulsion so formed was allowed to stand in a separatory funnel for a few minutes to facilitate phase separation. The organic phase was then washed three times with 4 mL of water. After treatment with anhydrous sodium sulfate, the organic phase was evaporated under reduced pressure, and the resulting yellow powder was lyophilized for 24 h. PE was obtained at a yield of 85% and at least 95% purity.

HPLC analysis of the lipid concentration. An HPLC analysis was performed with a Beckman System Gold Instrument (Beckman Instruments, Palo Alto, CA) equipped with a 156 refractive index detector (attenuation 16×) (16). The column was a Waters Spherisorb amino phase column from Hichrom (Reading, United Kingdom). A precolumn from the same manufacturer was fitted between the injector and the column. Phospholipids were eluted with a mobile phase composed of ethanol (95%) and a 10 mM aqueous solution of oxalic acid (92:8 vol/vol). The flow rate was 1 mL/min at room temperature.

Oxidation stability. Eight formulations containing DHA were investigated with respect to their ability to withstand oxidation when in contact with air at 25°C, which is the normal storage temperature for oils (Table 1). The different formulations were incubated at 25°C and shielded from UV light, either as bulk lipids, in chloroform, or in an emulsion, for 2.5 wk. The temperature was then increased to 30°C and maintained for a further 1.5 wk. Samples were removed after 0, 1, 3, 7, 14, and 28 d. All samples were analyzed with respect to CV and PV. The formulations kept as bulk lipids or dissolved in chloroform were also analyzed with respect to monohydroperoxides and polyhydroperoxides. Since the formulations were kept in vials or bottles with caps, fresh air was let in when the samples were removed. All vials and bottles were also opened for a 3-min period on days 10, 18, 21, and 25 to let in more air.

The bulk lipids were kept in 10-mL vials with caps. Each vial contained 0.1–0.2 g of DHA. The mixture of DHA and PC was obtained by dissolving the substances at a molar ratio of 1:1 in chloroform and then evaporating the solvent. The same procedure was performed to obtain a mixture of 1,2-diDHA-PC and 1,2-dipalmitoyl-PC.

The formulation dissolved in chloroform was kept in 50-mL bottles with caps. Each vial contained 13–23 mL of solution. The concentration of DHA, either free or incorporated into a lipid, was maintained at 12.5 mM. Formulations containing a phospholipid also had a total phospholipid concentration of 12.5 mM.

The oil-in-water emulsions were prepared from one part oil (g), 9 parts (mL) water, and Tween 20 (0.1 g/g oil) (17). The oil part contained the DHA formulation (Table 1), palmitic acid, and trioctyl glycerol. The latter was used to make up the oil part. The concentration of DHA (12 mM), either free or incorporated, was kept constant in all emulsions.

The total concentration of phospholipid and FFA was also kept constant (12 mM). The former was possible by adding 1,2-dipalmitoyl-PC when the formulation was 1,2-DHA-PC. The latter was achieved by adding palmitic acid to the formulation with DHA incorporated into the lipid. (Estimation of the concentration was simplified by assuming that the density of the emulsion was 1.0 g/mL.) The oil part, a portion of water, and Tween 20 were sonicated in a tube with a UP400S instrument (Dr. Hielscher GmbH, Stuttgart, Germany) at maximum power for 1 min at room temperature. The tube was then placed in an ice bath, and sonication was continued for 4.5 min, adding water in four portions every half minute. The average droplet size of the emulsion containing trioctyl glycerol, water, and Tween 20 was around 0.5 µm. During the stability study, the emulsions containing the formulation were stored in 10-mL vials and contained 3–4.5 mL of emulsion.

Analysis of mono- and polyhydroperoxy-DHA. The HPLC analysis of mono- and polyhydroperoxy-DHA was carried out according to a recently developed method (Lyberg, A.-M. and Adlercreutz, P., unpublished manuscript). The samples contained about 15 µmol DHA. The solvent was evaporated from the samples in chloroform. The lipids with DHA incorporated were hydrolyzed as described below, whereas 1 mL of acetonitrile was added to the other samples. When necessary, the samples were filtered prior to analysis. The HPLC analysis was performed on a LaChrom system (Hitachi High Technologies America, Schaumburg, IL) consisting of a D-7000 interface, an L-7100 pump, an L-7250 autosampler (20 µL injection loop), and an L-7400 UV detector, detecting at a wavelength of 234 nm. The separation of different monohydroperoxides in DHA was performed on a Lichrospher® 100 RP-18 (5 µm) column (Merck, Darmstadt, Germany) with a 1 mL/min flow rate of mobile phase consisting of an acetonitrile/aqueous solution of acetic acid (1%) at a ratio of 55:45 (vol/vol). To prevent DHA from accumulating in the column, each analysis was concluded by increasing the acetonitrile concentration to 90% for 1 min, after which the concentration was maintained for 9 min. The acetonitrile concentration was then decreased for 1 min to 55% to equilibrate the column before the next analysis. This concentration was maintained for 14 min.

The monohydroperoxy-DHA eluted within 19–36 min, whereas the polyhydroperoxides eluted between 1 and 10 min. To obtain the total amount of polyhydroperoxides, the sum of the peaks between 1 and 10 min was calculated for all the formulations except those containing DHA incorporated into a phospholipid. In this case, the polyhydroperoxides were obtained from the sum of the peaks between 1 and 5 min. Since there was not a significant amount of polyhydroperoxides in the phospholipids with a retention time above 5 min, this simplification was acceptable. In this way, interference from peaks from the hydrolyzed phospholipids with retention times above 5 min could be neglected.

Hydrolysis of phospholipids. The hydrolysis of PC prior to the HPLC analysis of hydroperoxides was performed in 1 mL of water-saturated toluene, whereas PE was hydrolyzed in 1

TABLE 2
Amount of Hydroperoxides, PV, and Carbonyl Value (CV) of 2-DHA-PC after 14 d of Storage[a]

Method	Bulk (mol%)	Solvent (mol%)	Emulsion (mol%)
Total amount of monohydroperoxides	0.25 ± 0.07	0.19 ± 0.04	—
Total amount of polyhydroperoxides	3.33 ± 0.20	5.22 ± 0.07	—
PV	6.3 ± 1.3	8.4 ± 1.2	9.9 ± 0.4
CV	1.45 ± 0.09	1.63 ± 0.37	1.32 ± 0.13

[a]Data are presented as the average of three sample measurements ± the SD.

mL of toluene and 0.1 mL of 50 mM Tris buffer, pH 8. Both reactions were catalyzed with 100 mg of Novozym 435 (immobilized *C. antarctica* lipase B) with shaking at 25°C. To prevent further oxidation, argon gas was added at the beginning of the reaction. The PC and PE reactions were terminated after 20 and 24 h, respectively, when the hydrolysis was complete. To remove the enzyme from the sample, the solution was withdrawn using a syringe. The enzyme was washed with 1 mL of toluene, which was also withdrawn using the syringe. The pooled toluene phases were evaporated. Then 1 mL of acetonitrile was added and the solutions were filtered prior to analysis.

Hydrolysis of TG. The hydrolysis of TG was performed in 0.5 mL of 50 mM Tris buffer, pH 8. The reaction was catalyzed by nonimmobilized *C. viscosum* lipase (50 mg) with shaking at 25°C. To prevent further oxidation, argon gas was added at the beginning of the reaction. After a 20-h reaction period, 0.6 mL of acetonitrile was added. The solution was filtered prior to analysis only if it contained polymerized TG.

PV. The PV was determined with an iodometric method as described previously (18,19). Minor changes were made in the standard protocol in that chloroform was used instead of hexane in sample analysis because of the better solubility of phospholipids in chloroform. A 0.2-mL sample (2–10 mg of bulk lipids dissolved in chloroform to a concentration of 10 mg lipid/mL, lipids in chloroform, or lipids in emulsion) was mixed with 0.5 mL of a 2% potassium iodide ethanol solution, 0.5 mL of 2% water-free $AlCl_3$ + 0.02% *o*-phenantroline ethanol solution, and 1 mL of chloroform in a centrifuge tube. The mixture was incubated for 15 min at 37°C in a water bath. Then 10 mL of HCl (10 mM) was added to the mixture to quench the reaction. The reaction mixture was centrifuged at $600 \times g$ for 3 min, and the absorbance of the water phase and a blank of 10 mM HCl was measured at 360 nm using a UV-1650PC spectrophotometer (Shimadzu Corporation, Kyoto, Japan).

CV. The CV was determined as described previously (20). Before use, isopropyl alcohol was refluxed with a suitable amount of sodium borohydride ($NaBH_4$) to reduce the acetone, which is normally contained in the commercial solvent, to isopropanol. After refluxing for 1 h, isopropanol was distilled to separate it from the $NaBH_4$. Because peroxides also show an absorbance at 420 nm in the CV method, they must be reduced. This was done by adding triphenyl phosphine (0.4 mg/mL) to the solvent for the sample.

The samples contained 2–10 mg of bulk lipids, 100 μL of lipid solution dissolved in chloroform, or 50 μL of emulsion. The bulk sample was dissolved in isopropanol to a concentration of 10 mg lipid/mL, of which 100 μL was used. The chloroform in the solvent sample was evaporated and replaced by isopropanol, whereas 50 μL of isopropanol was added to the emulsion. The sample was then mixed in an Eppendorf tube with 0.1 mL of a reactant, which consisted of 50 mg of 2,4-dinitrophenylhydrazine in 3.5 mL of concentrated HCl diluted to 100 mL with isopropyl alcohol. The solution was heated for 20 min at 40°C in a water bath. Then 0.8 mL of KOH solution (2%) in isopropyl alcohol was added. The Eppendorf tube was centrifuged at $11,500 \times g$ for 3 min. The liquid phase was analyzed with the UV-1650PC spectrophotometer at 420 nm.

Units. The unit used for mono- and polyhydroperoxides was mol% hydroperoxides, and that used for PV and CV was mol% peroxides. These units correspond to mol hydroperoxides and mol peroxides, respectively, divided by the amount of pure DHA (mol) expected in an unoxidized sample. The free DHA was assumed to be totally pure and lipids with DHA in a certain position were assumed to contain only DHA in that position. These assumptions were simplifications that would cause only a small discrepancy in the true values.

Reproducibility. The reproducibility of the analysis methods is presented in Table 2. The reproducibility of the measurements was obtained by analyzing 3 samples with each analysis method at the same time, for 2-DHA-PC in all systems. The analysis was performed on day 14.

RESULTS

Oxidation stability of DHA. Eight formulations containing DHA were evaluated with respect to their ability to withstand the oxidation of DHA. The formulations were incubated at 25–30°C in three different systems, i.e., bulk lipids, a solvent (chloroform), and an emulsion. Samples were taken out at six times over a period of 28 d. These samples were analyzed with respect to eight monohydroperoxy-DHA isomer groups, polyhydroperoxy-DHA, PV, and CV, except those kept in the emulsion, which were analyzed only for PV and CV. The CV quantified secondary oxidation products, whereas the other measurements quantified primary oxidation products. The mild storage conditions mainly induced primary oxidation products in the eight formulations; thus, the CV remained at
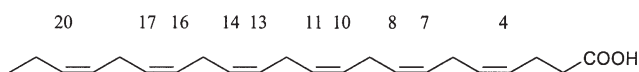
FIG. 1. The DHA molecule. Each number corresponds to and is placed above a carbon atom in the DHA molecule. The monohydroperoxides incorporated at any of the indicated carbon atoms were measured with our HPLC method. The isomer with a hydroperoxide group incorporated on carbon 20 is referred to as C20-monohydroperoxy-DHA and so forth.

0–2 mol% throughout the entire stability test. Therefore, attention is directed toward the primary oxidation products in this paper.

Monohydroperoxides. The monohydroperoxides are presented below, either as the total amount of monohydroperoxy-DHA or as eight groups of monohydroperoxy-DHA isomers containing one to two isomers. The hydroperoxides that contained a conjugated diene were measured with our HPLC method. The locations of these hydroperoxide groups within the molecule are presented in Figure 1. Since C5-, C19-, C21- and C3-monohydroperoxy-DHA did not contain conjugated diene groups, they were not detected with this HPLC method.

Monohydroperoxides in bulk lipids. The total amount of monohydroperoxy-DHA in the eight bulk lipids is presented in Figure 2A. The monohydroperoxides increased most rapidly in free DHA and the highest level, i.e., 8 mol%, of DHA was obtained after 1 d. Thereafter, the monohydroperoxides decreased with time. When PC was added to DHA, the monohydroperoxides increased to a lesser extent, and the highest level of monohydroperoxides in DHA was 2 mol%. Thus, the addition of PC had a protective effect on DHA. The amount of monohydroperoxides in PC with DHA at either the *sn*-1 or *sn*-2 position was more or less constant at a level below 0.4 mol%. PE with DHA at the *sn*-1 and *sn*-2 position showed an initial value of 0.6–0.7 mol% monohydroperoxides in DHA, which decreased with time to 0.1–0.2 mol% after 28 d. The monohydroperoxides in DHA-TG and 1,2-DHA-PC were more or less constant at around 0.3 mol%.

Monohydroperoxides of lipids in chloroform. The total amount of monohydroperoxy-DHA in the eight DHA-containing lipids in chloroform is shown in Figure 2B. Both free DHA and DHA mixed with PC showed lower amounts of monohydroperoxides in solvent than in bulk. Nevertheless, free DHA was the lipid in solvent that showed the most rapid increase in monohydroperoxides, and a peak of nearly 3 mol% was observed after 1 d. Two days later, the value had fallen to the initial level. We also observed that the monohydroperoxides in 1,2-DHA-PC increased from 0.1 to 0.5 mol% over the 28 d. Otherwise no clear trends were observed, and the level of monohydroperoxides was below 0.7 mol% in the other DHA-containing lipids, i.e., PC and PE with DHA at one position, DHA-TG, and DHA + PC.

Monohydroperoxide isomers. Both free DHA and DHA + PC were oxidized to all of the monohydroperoxy-DHA isomers measured with our HPLC method when incubated either in bulk or in the solvent phase. In these lipids the C20-mono-

hydroperoxide was the most abundant on day 1 (Tables 3, 4). The second highest level of a single isomer was exhibited by the C4-monohydroperoxy-DHA. The formation of a hydroperoxide on only carbon atoms 16, 17, 13, 14, 10, 11, 7, or 8 was less extensive, assuming that peaks containing two isomers had the same contribution from each isomer. Thus, this part of the DHA was more resistant to oxidation. These findings indicated that when the DHA molecule was oxidized rapidly, a major part arose from the C20- and C4-monohydroperoxy-DHA (Fig. 3). When oxidation progressed further, the isomers were rapidly oxidized even more, forming polyhydroperoxy-DHA, and the contribution from the C4-monohydroperoxy-DHA to the total amount of monohydroperoxy-DHA isomers then decreased (Fig. 3).

All the DHA-containing phospholipids exhibited monohydroperoxides only at carbon atoms 20, 16 + 17, 13 + 14, and 10, whereas DHA-TG showed all eight monohydroperoxy-DHA isomers measured with our HPLC method (Table 3). Thus, the two double bonds nearest the ester group of the phospholipid and carbon 11 on the third double bond were totally protected under these mild storage conditions (Fig. 1). PC with one DHA exhibited the four isomer groups at similar levels. However, PE containing one DHA showed the lowest contribution from the C20-monohydroperoxy-DHA. Thus, the phospholipid molecule with one DHA prevented the major incorporation of a hydroperoxide at carbon 20, which was vulnerable to oxidation in free DHA.

Polyhydroperoxides in bulk lipids. The total amount of polyhydroperoxides obtained in the eight bulk formulations is shown in Figure 4. The initial values of free DHA, DHA-PC/PE, and DHA-TG were 0, 0–4, and 5 mol%, respectively. The polyhydroperoxides in free DHA increased during the first 3 d, reaching 12 mol%, and then decreased slowly with time. Thus, the monohydroperoxides that showed a peak on day 1 were transformed into polyhydroperoxides. The polyhydroperoxides probably did not increase throughout the entire study because of polymerization of the DHA molecules. This was visually noted as the liquid DHA became more viscous with time. Mixing DHA with PC reduced the oxidation with respect to polyhydroperoxides, which increased during the first day and was then maintained at 1–3 mol% throughout the study.

DHA-TG was highly oxidized to polyhydroperoxides in the bulk phase (Fig. 4). This formulation also showed the highest amount of polyhydroperoxides, 14 mol%, after 3 d. Since the amount of monohydroperoxides was always maintained at a low level, the monohydroperoxides formed must have been transformed quickly into polyhydroperoxides. After 3 d, the polyhydroperoxides decreased rapidly, probably due to polymerization of the molecules; this was visually noted by the liquid formulation becoming more viscous with time.

For all the bulk formulations with DHA incorporated into either PC or PE, the level of polyhydroperoxides was quite stable, in the range 2–5 mol% (Fig. 4). Thus, these lipids provided a means of protecting DHA against oxidation under these conditions.
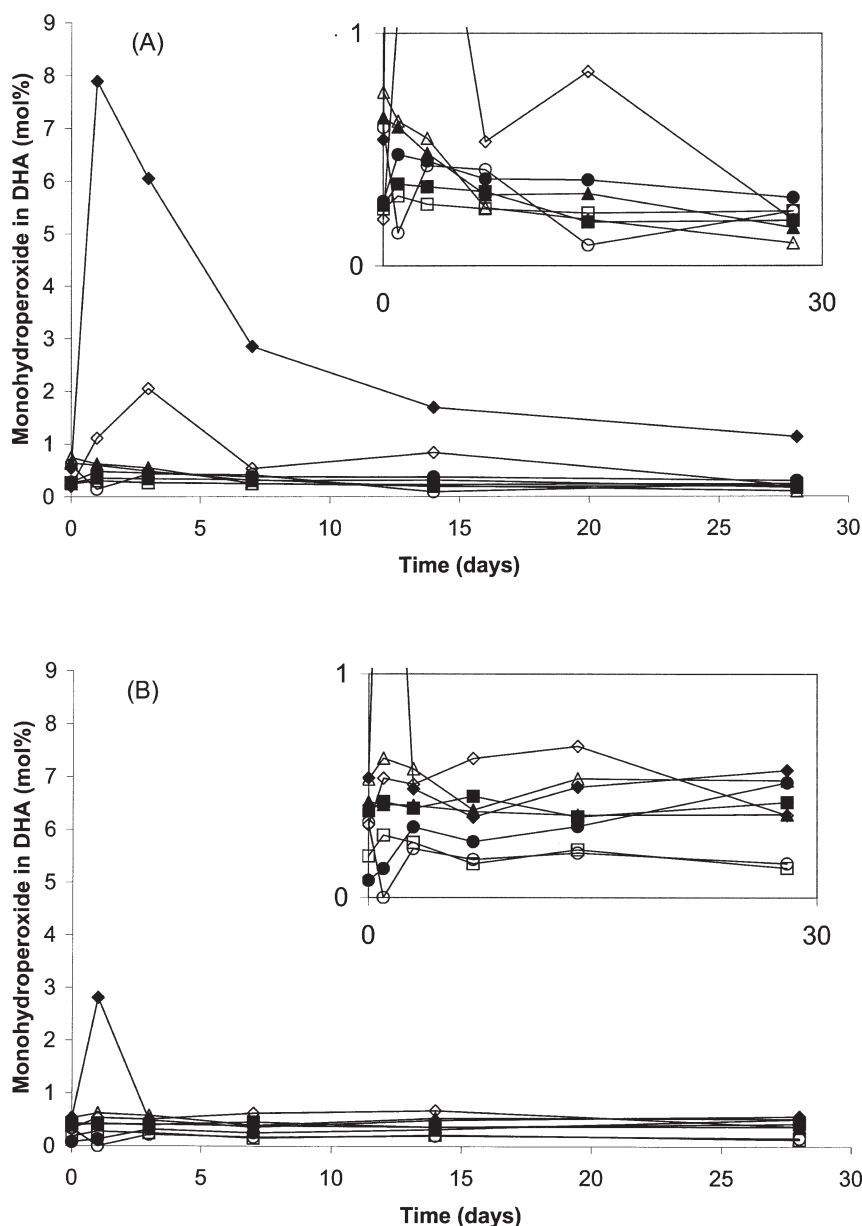
FIG. 2. (A) Total amount of monohydroperoxides in bulk; (B) total amount of monohydroperoxides in chloroform. 1-DHA-PC (■), 2-DHA-PC (□), 1-DHA-PE (▲), 2-DHA-PE (△), DHA-TG (○), DHA (◆), 1,2-DHA-PC (●), DHA + PC (◇).

Polyhydroperoxides in lipids in chloroform. The polyhydroperoxides increased with time in both DHA and DHA + PC when dissolved in chloroform. The free DHA, which initially showed no polyhydroperoxides, exhibited 16 mol% hydroperoxides after 4 wk. The oxidation rate was considerably lower for DHA + PC, which contained 6 mol% after the same time.

DHA-TG formed a large amount of polyhydroperoxides in the solvent system. During the first week, the polyhydroperoxide level was constant at 5 mol%, after which the hydroperoxides increased considerably and reached 17 mol%

after 4 wk. Thus, the oxidation of the formulation started later in the solvent than in the bulk lipids.

The phospholipids exhibited initial values of 2–5 mol%, and those with only one DHA were quite stable in this system (Fig. 4). However, rapid formation of polyhydroperoxides was observed for 1,2-DHA-PC (in contrast with its stability in the bulk system), and after 4 wk 17 mol% was reached. This formulation not only formed considerable amounts of polyhydroperoxides with time, but polymerization also occurred to such large extent that a polymer film was

TABLE 3
Ratios Between Different Monohydroperoxy-DHA Isomers for All DHA Bulk Lipids on Day 1[a]

	Monohydroperoxides (%)							
	C20	C16 + C17	C13 + C14	C10	C11	C7	C8	C4
DHA	25	15	16	8	6	9	7	14
DHA + PC	30	14	13	6	4	7	8	18
1-DHA-PC	19	24	23	34	0	0	0	0
2-DHA-PC	19	25	29	26	0	0	0	0
1-DHA-PE	13	33	27	27	0	0	0	0
2-DHA-PE	13	31	28	28	0	0	0	0
1,2-DHA-PC	17	36	20	27	0	0	0	0
DHA-TG	10	25	9	12	8	7	18	12

[a]For abbreviations see Table 1.

TABLE 4
Ratios Between Different Monohydroperoxy-DHA Isomers for Four DHA Lipids in Solvent on Day 1[a]

	Monohydroperoxides (%)							
	C20	C16 + C17	C13 + C14	C10	C11	C7	C8	C4
DHA	24	16	17	10	5	9	6	12
DHA + PC	24	19	19	11	3	6	7	10
1-DHA-PC	19	36	21	23	0	0	0	0
2-DHA-PC	20	32	12	36	0	0	0	0

[a]For abbreviations see Table 1.

seen floating on the surface of the solvent after only 2 wk.

PV. It is common to measure oxidation in oil in terms of the PV, which can be determined by different procedures (9). The PV obtained depends on the procedure used. The procedure used here was based on an iodometric method, but chloroform was used instead of *n*-hexane because the PC was difficult to dissolve in *n*-hexane. The measurement can be affected by light, oxygen in the air, and the reaction between iodine and unsaturated FA. Thus, the PV of the DHA-containing lipids should only be compared with each other and not with the hydroperoxide data obtained with our HPLC method.

PV of bulk lipids. The PV supported the findings that free DHA as bulk lipids formed the highest amount of peroxides, which was reached after 3 d (Fig. 5). DHA + PC was oxidized less, but the peak was observed after the same time, whereas DHA-TG reached a maximal PV after 7 d.

A high initial PV was observed for the phospholipids in bulk (Fig. 5). PC with DHA in both positions, and PC and PE with DHA at the *sn*-1 position showed 22, 24, and 26 mol%, respectively. Lower initial values, i.e., 11 and 13 mol%, were observed for PC and PE with DHA at the *sn*-2 position, respectively. This difference in initial values was not noted with our HPLC method. One explanation for this could be that PV measures all peroxides, whereas the HPLC method measures only hydroperoxides containing conjugated dienes. According to these findings, the preparation of DHA-PC induced more peroxides with DHA at the *sn*-1 position than at the *sn*-2 position. This indicated that the enzymatic esterification of 2-palmitoyl LPC with DHA induced more oxidation than the chemical esterification

of 1-palmitoyl LPC with DHA. It should be remembered that the chemical reaction lasted no longer than an hour, whereas the enzymatic reaction lasted 15 h (for preincubation) plus 28 h (for the reaction). Thus, in this enzymatic procedure a higher degree of oxygen protection would be beneficial. Only minor oxidation was induced when PC was transformed into PE.

The PV of all DHA-containing phospholipids decreased with time except 1,2-DHA-PC, which showed a peak on day 3 (28 mol%) and then decreased with time (Fig. 5). After 2 wk, the PV of PC and PE with one DHA had decreased to 5–8 mol%, whereas 1,2-DHA-PC contained 14 mol%.

PV of lipids dissolved in chloroform. The system itself, i.e., solvent or bulk, induced considerable variation in the initial PV. This was especially true for DHA mixed with or incorporated into phospholipids, which in most cases showed a much higher value in chloroform. Therefore, there is reason to believe that part of the PV might be an artifact produced by the combination of the solvent and phospholipid. Direct comparisons of the values obtained for bulk and chloroform samples are thus unreliable. However, comparisons can be made between values within these two groups.

Free DHA with and without the addition of PC exhibited different PV profiles in chloroform (Fig. 5). The PV of the free DHA in solvent was quite stable during the first 3 d. It then started to increase, and after 2 wk a peak of 33 mol% was observed. The PV of DHA + PC increased during the first day, showing a peak of 28 mol%. During the following days, the PV fell, and during the last 3 wk, the PV was stable at 12–14 mol%. These data do not support our finding (HPLC method) that PC
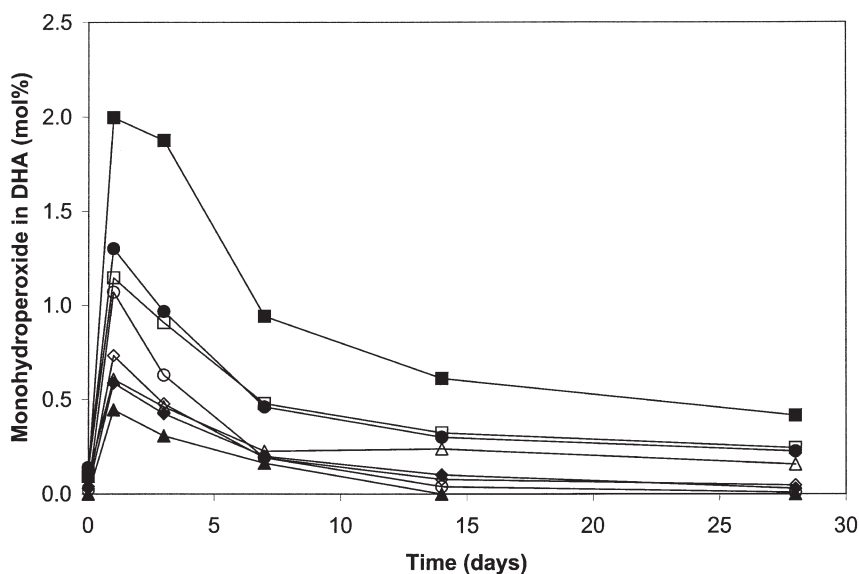
FIG. 3. The isomer profile of bulk DHA. C20 (■), C16 + C17 (□), C13 + C14 (●), C10 (△), C11 (▲), C7 (◇), C8 (◆), C4 (○).

provides considerable protection against the oxidation of DHA in solvent. However, the PV of DHA + PC was probably overestimated because of the combination of chloroform and phospholipid.

DHA-TG was the most unstable formulation in the solvent system according to the PV measurements (Fig. 5). The PV increased with time, and on day 14 a peak of 69 mol% was observed.

All of the phospholipids showed a lower PV after 28 d (Fig. 5). The PV decreased with time for all the phospholipids with one DHA except PC with DHA at the *sn*-2 position, which first exhibited a peak on day 1 and then decreased with time. The PV of 1,2-DHA-PC initially increased, showing a peak on day 7 of 30 mol%, which then decreased with time.

PV of lipids in emulsion. According to the PV, the emulsion system reduced the oxidation rate of the free DHA considerably (Fig. 6). A peak of 12 mol% was observed after 14 d. A different PV profile was exhibited by DHA + PC. In this case, the peak of 12 mol% was observed already after 1 d. Thus, the addition of PC affected the system but did not provide protection, according to these results. The TG was found to be the most unstable formulation in the emulsion system. The same trend was observed in the solvent system using the PV method. However, the peak after 2 wk was about half that observed in the solvent system. Thus, the emulsion also provided protection against TG formulation, although it was less stable than other lipids in this system. For all the DHA-containing phospholipids in emulsion, we noted that the initial value was always higher than the PV obtained after 4 wk of incubation.

DISCUSSION

The formation of hydroperoxides in DHA incubated at 25–30°C was almost completely prevented by incorporating one DHA into either PC or PE. No significant difference was observed between lipids with DHA at position *sn*-1 or *sn*-2 of the phospholipid. Thus, these four DHA lipids protected DHA against oxidation to hydroperoxides equally well under the mild conditions studied. According to our findings, the phospholipid completely prevented oxidation of carbon atoms 4, 7, 8, and 11 of the DHA molecule. Furthermore, the oxidation of carbon atom 20, which was most vulnerable to oxidation in free DHA, was reduced considerably.

Phospholipids have been shown to be efficient antioxidants. The mechanism of their antioxidative effect has not yet been elucidated in detail, but the polar group clearly plays a key role, and the nitrogen-containing phospholipids PC and PE are the most efficient antioxidants under most conditions (21). It is likely that the best protection is afforded to those parts of the DHA that are closest to the polar group, i.e., the parts closest to the carboxyl group. Furthermore, carbon atom 20 seemed to be near the polar group because of the reduced oxidation of this carbon. This is possible because the DHA chain contains several bonds that make the chain highly curved.

DHA mixed with PC was also protected against the formation of hydroperoxides, although the degree of protection was less than when DHA was incorporated into a phospholipid. All of the hydroperoxy-DHA isomers studied were formed in the DHA-PC mixture, although the levels were low. This might be because the distance between DHA and the polar group in PC was greater than when DHA was incorporated into PC.
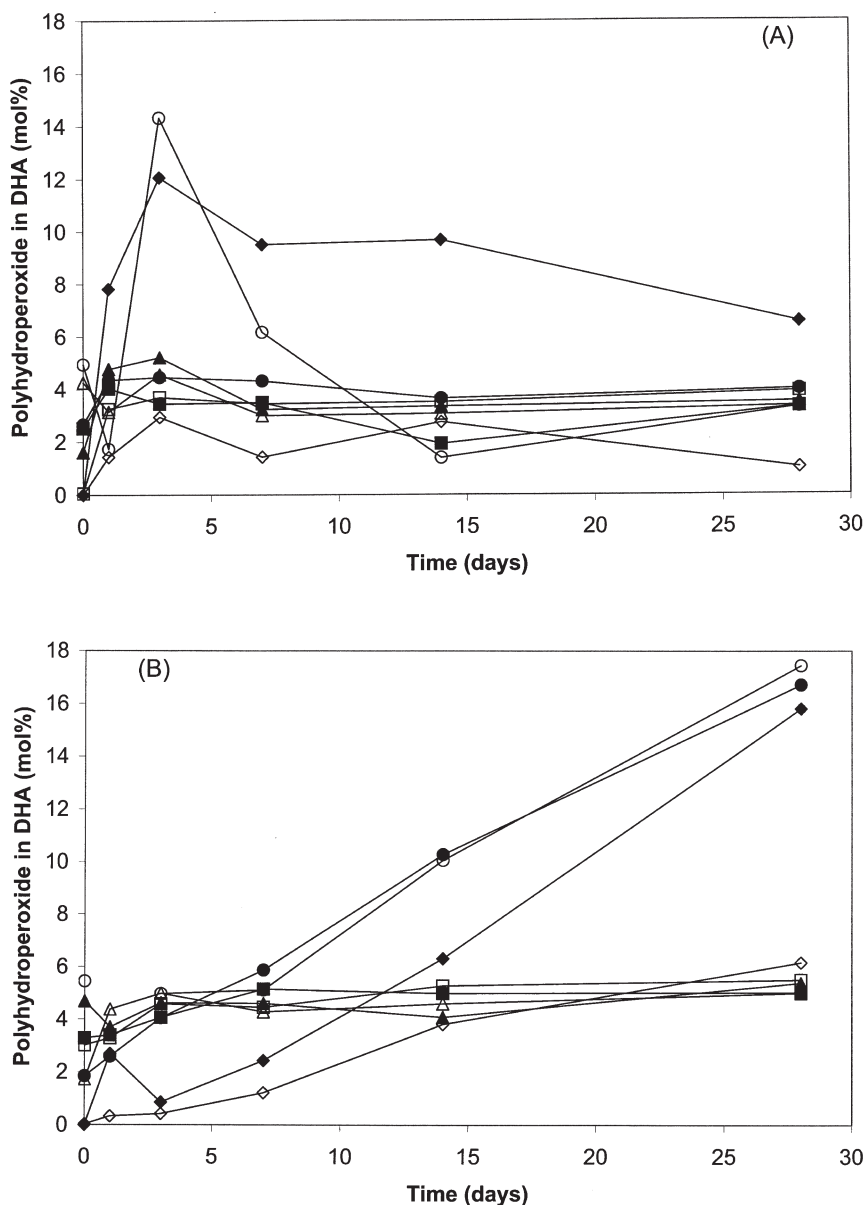
FIG. 4. (A) Polyhydroperoxides in bulk; (B) polyhydroperoxides in solvent. 1-DHA-PC (■), 2-DHA-PC (□), 1-DHA-PE (▲), 2-DHA-PE (△), DHA-TG (○), DHA (◆), 1,2-DHA-PC (●), DHA + PC (◇).

In contrast, 1,2-DHA-PC mixed with 1,2-palmitoyl-PC exhibited extensive hydroperoxide formation in the solvent system, whereas it was protected against hydroperoxide formation in the bulk system. This type of formulation is thus not recommended for protecting DHA. The vulnerability of this lipid in the solvent may be because the two DHA chains in the lipid were close to each other, whereas the distance to other lipids was greater. This may have led to pronounced oxidation to hydroperoxides and to polymerization. Another study showed similar results in that 1-palmitoyl-2-arachidonoyl-PC was found to be more stable than 1,2-diarachi-donoyl-PC mixed with 1,2-dipalmitoyl-PC at the ratio of 1:1 when incubated at 37°C (22).

Incorporation of DHA at all positions of a TG is not an appropriate solution for protecting DHA, since a considerable amount of hydroperoxides was formed. Furthermore, all the monohydroperoxy-DHA isomers were formed in this lipid, although the levels were low, which indicates that the isomers formed were quickly transformed into polyhydroperoxides. Earlier findings have shown that the oxidation stability differs between a TG containing one or three eicosapentaenoic acids (23). The former was more stable than the latter. Therefore,
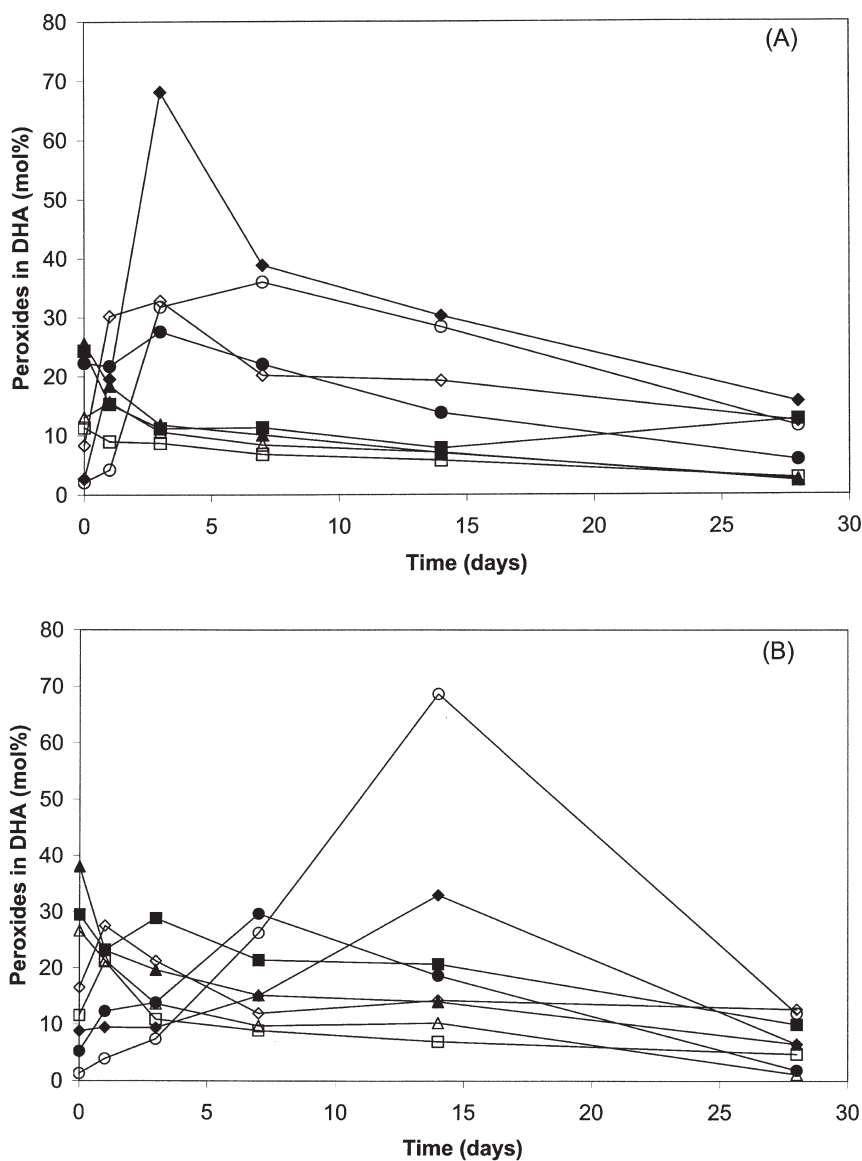
FIG. 5. PV for formulations in the two systems. (A) Bulk; (B) solvent. 1-DHA-PC (■), 2-DHA-PC (□), 1-DHA-PE (▲), 2-DHA-PE (△), DHA-TG (○), DHA (◆), 1,2-DHA-PC (●), DHA + PC (◇).

DHA is probably oxidized less when only one DHA residue is incorporated into each TG molecule than the tested TG with three DHA.

The fact that DHA-containing phospholipids provide better protection of DHA than TG is supported by earlier findings in studies on phospholipids, TG, and ethyl esters containing 11 mol% DHA, each in a bulk lipid system at 25°C (12). When 1-palmitoyl-2-DHA-PC was incubated at a higher temperature, 37°C, pronounced oxidation occurred on the first day; thus, this temperature is not suitable for this formulation (22).

The bulk lipids were generally more prone to oxidization than the lipids incubated in the solvent or emulsion. The bulk lipids exposed a larger surface to the air, whereas fewer lipid molecules were in contact with the air at the liquid surface of both the solvent and the emulsion. Since the nonionic emulsifier (Tween 20) provided a barrier that inhibited the diffusion and penetration of radicals or trace metals, the lipids in the emulsion system were protected against oxidation (9).

Our investigation showed that incorporating DHA into PC and PE at one position can offer protection of DHA against peroxidation under mild storage conditions. Earlier findings have shown that the combination of tocopherol, ascorbic acid, and lecithin has a higher protective effect on PUFA than tocopherol, ascorbic acid, or lecithin alone (11). To achieve maximal protection of DHA, we therefore recommend that it be incorporated into PC or PE (one DHA molecule per lipid molecule) and that both tocopherol and ascorbic acid be added.
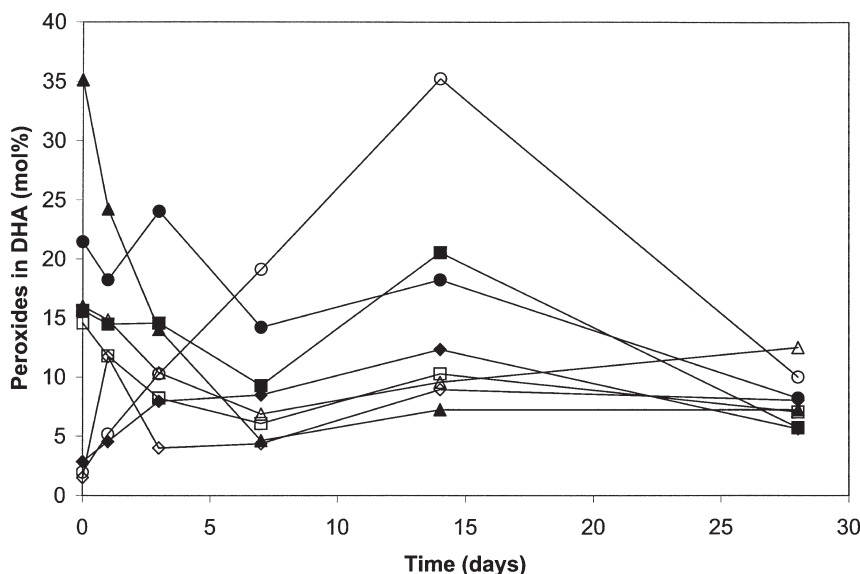
FIG. 6. The PV for formulations in the emulsion. 1-DHA-PC (■), 2-DHA-PC (□), 1-DHA-PE (▲), 2-DHA-PE (△), DHA-TG (○), DHA (◆), 1,2-DHA-PC (●), DHA + PC (◇).

REFERENCES

1. Birch, E.E., and O'Connor, A.R. (2001) Preterm Birth and Visual Development, *Semin. Neonatol. 6*, 487–497.
2. Horrocks, L.A., and Yeo, Y.K. (1999) Health Benefits of Docosahexaenoic Acid (DHA), *Pharmacol. Res. 40*, 211–225.
3. Lim, G.P., Calon, F., Morihara, T., Yang, F., Teter, B., Ubeda, O., Salem, N., Jr., Frautschy, S.A., and Cole, G.M. (2005) A Diet Enriched with the Omega-3 Fatty Acid Docosahexaenoic Acid Reduces Amyloid Burden in an Aged Alzheimer Mouse Model, *J. Neurosci. 25*, 3032–3040.
4. Horrobin, D.F. (1998) The Membrane Phospholipid Hypothesis as a Biochemical Basis for the Neurodevelopmental Concept of Schizophrenia, *Schizophr. Res. 30*, 193–208.
5. Stordy, B.J. (2000) Dark Adaptation, Motor Skills, Docosahexaenoic Acid, and Dyslexia, *Am. J. Clin. Nutr. 71*, 323S–326S.
6. Richardson, A.J., and Puri, B.K. (2000) The Potential Role of Fatty Acids in Attention-Deficit/Hyperactivity Disorder, *Prostaglandins Leukot. Essent. Fatty Acids 63*, 79–87.
7. Larsson, S.C., Kumlin, M., Ingelman-Sundberg, M., and Wolk, A. (2004) Dietary Long-Chain n-3 Fatty Acids for the Prevention of Cancer: A Review of Potential Mechanisms, *Am. J. Clin. Nutr. 79*, 935–945.
8. Holub, D.J., and Holub, B.J. (2004) Omega-3 Fatty Acids from Fish Oils and Cardiovascular Disease, *Mol. Cell. Biochem. 263*, 217–225.
9. Frankel, E. (1998) *Lipid Oxidation*. The Oily Press, Dundee, Scotland.
10. Kamal-Eldin, A., and Yanishlieva, N.V. (2002) n-3 Fatty Acids for Human Nutrition: Stability Considerations, *Eur. J. Lipid Sci. Technol. 104*, 825–836.
11. Yanishlieva, N.V., and Marinova, E.M. (2001) Stabilisation of Edible Oils with Natural Antioxidants, *Eur. J. Lipid Sci. Technol. 103*, 752–767.
12. Song, J.H., Inoue, Y., and Miyazawa, T. (1997) Oxidative Stability of Docosahexaenoic Acid-Containing Oils in the Form of Phospholipids, Triacylglycerols, and Ethyl Esters, *Biosci. Biotechnol.*

Biochem. 61, 2085–2088.
13. Sarney, D.B., Fregapane, G., and Vulfson, E.N. (1994) Lipase-Catalyzed Synthesis of Lysophospholipids in a Continuous Bioreactor, *J. Am. Oil Chem. Soc. 71*, 93–96.
14. Lyberg, A.-M., Adlercreutz, D., and Adlercreutz, P. (2005) Enzymatic and Chemical Synthesis of Phosphatidylcholine Regioisomers Containing Eicosapentaenoic Acid or Docosahexaenoic Acid, *Eur J Lipid Sci Tech. 107*, 279–290.
15. D'Arrigo, P., de Ferra, L., Piergianni, V., Selva, A., Servi, S., and Strini, A. (1996) Preparative Transformation of Natural Phospholipids Catalyzed by Phospholipase D from *Streptomyces*, *J. Chem. Soc., Perkin Trans. 1*2651–2656.
16. Adlercreutz, D., Budde, H., and Wehtje, E. (2001) Synthesis of Phosphatidylcholine with Defined Fatty Acid in the *sn*-1 Position by Lipase-Catalyzed Esterification and Transesterification Reaction, *Biotechnol. Bioeng. 78*, 403–411.
17. Huang, S.-W., Hopia, A., Schwarz, K., Frankel, E.N., and German, J.B. (1996) Antioxidant Activity of α-Tocopherol and Trolox in Different Lipid Substrates: Bulk Oils vs. Oil-in-Water Emulsions, *J. Agric. Food Chem. 44*, 444–452.
18. Asakawa, T., and Matsushita, S. (1980) A Colorimetric Microdetermination of Peroxide Values Utilizing Aluminum Chloride as the Catalyst, *Lipids 15*, 965–967.
19. Jessup, W., Dean, R.T., and Gebicki, J.M. (1994) Iodometric Determination of Hydroperoxides in Lipids and Proteins, *Methods Enzymol. 233*, 289–303.
20. Endo, Y., Li, C.M., Tagiri-Endo, M., and Fujimoto, K. (2001) A Modified Method for the Estimation of Total Carbonyl Compounds in Heated and Frying Oils Using 2-Propanol as a Solvent, *J. Am. Oil Chem. Soc. 78*, 1021–1024.
21. King, M.F., Boyd, L.C., and Sheldon, B.W. (1992) Antioxidant Properties of Individual Phospholipids in a Salmon Oil Model System, *J. Am. Oil Chem. Soc. 69*, 545–551.
22. Araseki, M., Yamamoto, K., and Miyashita, K. (2002) Oxidative Stability of Polyunsaturated Fatty Acid in Phosphatidylcholine Liposomes, *Biosci. Biotechnol. Biochem. 66*, 2573–2577.
23. Endo, Y., Hoshizaki, S., and Fujimoto, K. (1997) Oxidation of Synthetic Triacylglycerols Containing Eicosapentaenoic and Docosahexaenoic Acids: Effect of Oxidation System and Triacylglycerol Structure, *J. Am. Oil Chem. Soc. 74*, 1041–1045.

COMMUNICATION

New Fatty Acid Derivatives
from *Homaxinella* sp., a Marine Sponge

Tayyab A. Mansoor[a], Bok Hee Bae[a], Jongki Hong[b],
Chong-O. Lee[c], Kwang Sik Im[a], and Jee H. Jung[a,*]

[a]College of Pharmacy, Pusan National University, Busan 609-735, Korea, [b]Kyung Hee University,
Seoul 130-701, Korea, and [c]Korea Research Institute of Chemical Technology, Daejon 305-343, Korea

ABSTRACT: Fractionation of the MeOH extract of *Homaxinella* sp., a marine sponge, led to the isolation of a sodium salt of a new brominated FA (**1**), two new MG (**2** and **4**), and a new lysoPC (**6**). The geometry of the double bonds in **1** and **2** was defined by comparison of the NMR chemical shifts of the allylic carbons, nuclear Overhauser effect spectroscopy correlations of the allylic protons, and coupling constants of the vinylic protons with those reported. Evidence mainly from NMR and MS analyses established the planar structures of the compounds. Compounds **1**, **2**, **4**, and **6** were evaluated for cytotoxicity against a panel of five human solid tumor cell lines. Only compound **1** showed moderate activity.

Paper no. L9802 in *Lipids* 40, 981–985 (September 2005).

Marine sponges of the genus *Homaxinella* (family Axinellidae, order Halichondrida) are reported to contain various unusual sterols (1), bromopyrrole alkaloids (2), and aromatic antimicrobial compounds (3).

In the course of our study on cytotoxic compounds from the marine sponge *Homaxinella* sp., we have isolated butenolides (4), a cyclopentenone derivative (4), and degraded sterols (5). In a continuing study on the same sponge we have isolated a sodium salt of a new brominated FA (**1**), two MG (**2** and **4**), and a 3′-methylated lysoPC (**6**), along with their known analogs (**3**, **5**, and **7**–**9**), from the MeOH extract of the sponge (Scheme 1).

Brominated FA (6–14), lysoPC derivatives (15–17), and glycerol derivatives (18,19) with various chain length, substitution, and unsaturation patterns were reported from several sponges. Both brominated FA derivatives and lysoPC derivatives have shown interesting biological activities such as cytotoxicity to tumor cell lines and inhibition of cholesterol biosynthesis (12,15–17).

EXPERIMENTAL PROCEDURES

General experimental procedures. Optical rotations were measured using a JASCO DIP-370 digital polarimeter. ^{1}H and 2D [COSY, HMBC (heteronuclear multiple bond correlation),

HSQC (heteronuclear single quantum correlation), and NOESY (nuclear Overhauser effect spectroscopy)] NMR data were collected on a Varian INOVA 500 spectrometer. Chemical shifts were reported with reference to the respective residual solvent or deuterated solvent peaks (δ_H 3.30 and δ_C 49.0 for CD$_3$OD). FABMS data were obtained on a JEOL JMS SX-102A mass spectrometer. High-resolution FABMS (HRFABMS) data were obtained on a JEOL JMS SX-101A mass spectrometer. HPLC was performed with a YMC (Kyoto, Japan) packed ODS column (250 × 10 mm, 5 μm, 120 Å) and a C18–5E Shodex (Showa Denko K.K., Tokyo, Japan) packed column (250 × 10 mm, 5 μm, 100 Å) using a Gilson 133-RI (refractive index) detector.

SCHEME 1

Animal material. The sponge was collected in August 1998 at a depth of 20 m off Jeju Island, Korea. The specimen was identified as *Homaxinella* sp. by Prof. Chung Ja Sim, Hannam University. A voucher specimen (J98J–1) of this sponge (registry No. Spo. 39) was deposited in the Natural History Museum, Hannam University, Daejon, Korea, and has been described elsewhere (4).

Extraction and isolation procedure. The frozen sponge (7 kg) was extracted with MeOH at room temperature. The MeOH extract showed toxicity (LD_{50} 57 µg/mL) against brine shrimp larvae (20). The MeOH extract was partitioned between CH_2Cl_2 and water. The CH_2Cl_2 layer was further partitioned between aqueous MeOH and *n*-hexane. The aqueous MeOH fraction was subjected to a step gradient reversed-phase flash column chromatography (YMC Gel ODS-A, 60 Å, 400–500 mesh) with a solvent system of 60–100% $MeOH/H_2O$ to afford 22 fractions. The bioactive fraction 13 was subjected to successive RP-HPLC (C18–5E Shodex packed) by eluting with 97% MeOH followed by another RP-HPLC (YMC-Pack ODS) with elution by 91% MeOH to afford compounds **1** (1.2 mg), **2** (1.0 mg), and **6** (0.7 mg). Fraction 11 (506.8 mg), one of the bioactive fractions (LD_{50} 10 µg/mL), was subjected to reversed-phase medium-pressure LC (RP-MPLC) (YMC ODS-A, 120 Å, 30–50 µm), eluting with a stepped-gradient solvent system of 60–100% $MeOH/H_2O$ to afford 10 subfractions. Compounds **5** (1.3 mg) and **8** (21.2 mg) were obtained by separation of subfractions 8 (52.2 mg) and 7 (65.9 mg) by RP-HPLC (YMC-Pack ODS) eluting with 90 and 92% MeOH, respectively. Fraction 12 (1.2 g), another bioactive fraction (LD_{50} 27 µg/mL), was also subjected to a RP-MPLC (YMC ODS-A,

120 Å, 30–50 µm) with elution by a stepped-gradient solvent system of 65–100% $MeOH/H_2O$ to afford 10 subfractions. Compounds **3** (2.1 mg), **4** (1.0 mg), **7** (1.2 mg), and **9** (3.5 mg) were obtained by separation and purification of subfraction 4 (225.1 mg) by RP-HPLC (C18–5E Shodex packed), eluting with 90% MeOH.

*(i) Compound **1**.* Colorless oil; ^{1}H NMR (CD_3OD, 500 MHz) δ 5.86 (1H, *t*, *J* = 8.0 Hz, H-5), 5.41 (1H, *dt*, *J* = 10.5, 7.5 Hz, H-10), 5.34 (1H, *dt*, *J* = 10.5, 7.5 Hz, H-9), 2.48 (4H, *t*, *J* = 7.5 Hz, H-2,7), 2.28 (2H, *m*, H-8), 2.08 (2H, *m*, H-4), 2.05 (2H, *m*, H-11), 1.66 (2H, *quint*, *J* = 7.5 Hz, H-3), 1.52 (1H, *m*, H-21), 1.20–1.35 (16H, *m*, H-12–H-19), 1.15 (2H, *q*, *J* = 6.5 Hz, H-20), 0.87 (6H, *d*, *J* = 7.0 Hz, H-22,23); ^{13}C NMR (based on HSQC and HMBC assignments, CD_3OD, 500 MHz) δ 177.2 (C-1), 34.8 (C-2), 25.9 (C-3), 29.2 (C-4), 133.1 (C-5), 126.9 (C-6), 36.8 (C-7), 26.8 (C-8), 132.8 (C-9), 126.9 (C-10), 27.5 (C-11), 29.1–30.3 (C-12–C-19), 39.0 (C-20), 29.0 (C-21), 22.8 (C-22,23); FABMS *m/z* 451/453 [M + H]+, 473/475 [M + Na]+ HRFABMS *m/z* 473.2041/475.1959 ([M + Na]+, calculated for $C_{23}H_{40}O_2$-[79]$BrNa_2/C_{23}H_{40}O_2$[81]$BrNa_2$, 473.2007/475.1990).

*(ii) Compound **2**.* Colorless oil; $[\alpha]^{25}_D$ +6° (*c* 0.03, MeOH); ^{1}H and ^{13}C NMR data (see Table 1); FABMS *m/z* 485/487 [M – H_2O + H]+.

*(iii) Compound **4**.* White amorphous powder; $[\alpha]^{25}_D$ +7° (*c* 0.08, MeOH); ^{1}H NMR (CD_3OD, 500 MHz) δ 4.14 (1H, *dd*, *J* = 11.5, 4.5 Hz, H-1$_a$), 4.05 (1H, *dd*, *J* = 11.5, 6.5 Hz, H-1$_b$), 3.80 (1H, *m*, H-2), 3.53 (2H, *m*, H-3), 2.35 (2H, *t*, *J* = 7.5, H-2′), 1.61 (2H, *m*, H-3′), 1.25–1.35 (6H, *m*, H-4′–6′), 1.38 (2H, *m*, H-7′), 0.67 (2H, *m*, H-8′, 9′), 1.18 (2H, *m*, H-10′), 1.20–1.35 (10H, *m*, H-11′–H-15′), 0.90 (3H, *t*, *J* = 7.0 Hz, H-16′), 0.59

TABLE 1
^{1}H and ^{13}C NMR Data of Compounds 2 and 6

| | **2** | | | **6** | |
Position	[1]H[a]	[13]C[b]	Position	[1]H[a]	[13]C[b]
1$_a$	4.15 (1H, *dd*, 11.5, 5.0)	66.3	1	4.18 (1H, *dd*, 11.5, 5.0)	65.9
1$_b$	4.06 (1H, *dd*, 11.5, 5.0)			4.11 (1H, *dd*, 11.5, 5.0)	
2	3.81 (1H, *m*)	70.0	2	3.96 (1H, *m*)	69.5
3	3.64 (2H, *m*)	63.9	3	3.89 (2H, *m*)	67.7
1′		174.7	1′		174.3
2′	2.36 (2H, *t*, 8.0)	33.9	2′	2.36 (1H, *dd*, 14.5, 5.0)	42.3
3′	1.69 (2H, *quint*, 8.0)	25.5		2.15 (1H, *dd*, 14.5, 5.0)	
4′	2.09 (2H, *q*, 8.0)	29.6	3′	1.93 (1H, *m*)	31.1
5′	5.85 (1H, *t*, 8.0)	132.4	4′	1.17 (2H, *m*)	40.0
6′		126.9	5′-15′	1.22-1.32 (22H, *m*)	30.0-33.3
7′	2.47 (2H, *t*, 7.5)	36.4	16′	1.07 (2H, *m*)	38.0
8′	2.29 (2H, *q*, 7.0)	26.5	17′	1.53 (1H, *m*)	28.8
9′	5.42 (1H, *dt*, 10.5, 7.5)	132.6	18′	0.88 (3H, *d*, 6.5)[c]	19.9[c]
10′	5.34 (1H, *dt*, 10.5, 7.5)	128.4	19′	0.88 (3H, *d*, 6.5)[c]	19.9[c]
11′	2.07 (2H, *m*)	27.8	20′	0.94 (3H, *d*, 7.0)	19.2
12′-19′	1.20-1.35 (14H, *m*)	29.8-33.3	1″	4.28 (2H, *m*)	60.1
20′	1.17 (2H, *q*, 7.0)	39.8	2″	3.63 (2H, *m*)	67.2
21′	1.52 (1H, *m*)	29.2	N-CH$_3$	3.21 (9H, *s*)	54.4
22′	0.87 (3H, *d*, 7.0)[c]	22.5			
23′	0.87 (3H, *d*, 7.0)[c]	22.5			

[a]Measured at 500 MHz in CD_3OD.
[b]The assignments are based on the heteronuclear single quantum correlation and heteronuclear multiple bond correlation data.
[c]Assignment with the same superscript in the same column may be interchanged.

(1H, *td*, *J* = 7.8, 3.6, H-17a′), −0.33 (1H, *td*, *J* = 5.4, 3.6, H-17$_b$′); ^{13}C NMR (based on HSQC and HMBC assignments, CD$_3$OD, 500 MHz) δ 66.1 (C-1), 77.0 (C-2), 63.8 (C-3), 175.3 (C-1′), 34.6 (C-2′), 25.3 (C-3′), 31.2–29.1 (C-4′–6′), 30.1 (C-7′), 16.7 (C-8′, 9′), 30.1 (C-10′), 31.2–29.1 (C-11′–C-15′), 14.1 (C-16′), 12.2 (C-17′); FABMS *m/z* 365 [M + Na]$^+$, HRFABMS *m/z* 365.2659 ([M + Na]$^+$, calculated for C$_{20}$H$_{38}$O$_4$Na, 365.2668), FAB-collision-induced dissociation-tandem mass spectroscopy *m/z* 365 [M + Na]$^+$ (100), 349 (0.2), 335 (0.2), 321 (0.4), 307 (0.3), 293 (0.4), 279 (0.4), 265 (0.4), 251 (0.2), 239 (0.2), 225 (0.4), 211 (0.5), 197 (0.2), 183 (0.5), 169 (2.4), 155 (0.9), 113 (1.4), 97 (0.8), 55 (0.5), 23 (2.6).

(iv) Compound 6. White amorphous powder; [α]$^{22}_D$ −4° (*c* 0.06, MeOH), ^{1}H and ^{13}C NMR data (see Table 1); FABMS *m/z* 552 [M + H]$^+$, 574 [M + Na]$^+$ HRFABMS *m/z* 552.4040 ([M + H]$^+$, calculated for C$_{28}$H$_{59}$NO$_7$P, 552.4029).

Cell lines and culture conditions. The SK-MEL-2 human melanoma, A549 nonsmall cell lung, SKOV-3 ovarian, HCT-15 colon, and XF-498 central nervous system tumor cell lines were maintained as stocks in RPMI 1640 (Gibco, Gaithersburg, MD) supplemented with 10% FBS (Gibco). Cell cultures were passaged once or twice weekly using trypsin–*trans*-1,2-diaminocyclohexanetetraacetate to detach the cells from their culture flasks.

Bioassay. The sulforhodamine B (SRB) assay, developed for measuring the cellular protein content of the cultures, is applied for the measurement of the cytotoxicity of the compounds against tumor cells. The rapidly growing cells were harvested, counted, and inoculated at the appropriate concentrations (1–2 × 10^4 cells/well) into 96-well microtiter plates. After incubation for 24 h, the compounds dissolved in culture medium were applied to the culture wells in triplicate, followed by incubating for 48 h at 37°C under a 5% CO$_2$ atmosphere. The cultures fixed with cold TCA were stained by 0.4% SRB dissolved in 1% acetic acid. After solubilizing the bound dye with 10 mM unbuffered Tris base by gyratory shaker, the absorbance at 520 nm was measured with a microplate reader (Dynatech Model MR 700). Fifty percent inhibitory concentration (ED$_{50}$) was defined as the concentration that reduced absorbance by 50% of untreated wells compared with the control in the SRB assay.

RESULTS AND DISCUSSION

Compound 1, a sodium salt of a FA, was isolated as a colorless oil. Its molecular formula was established as C$_{23}$H$_{40}$O$_2$BrNa on the basis of MS and NMR spectral data. The FABMS showed [M + H]$^+$ and [M + Na]$^+$ ion clusters at *m/z* 451/453 and *m/z* 473/475, respectively. The exact mass of the [M + Na]$^+$ ions at *m/z* 473.2041 and 475.1959 matched well with the expected molecular formula of C$_{23}$H$_{40}$O$_2$^{79}BrNa$_2$ (Δ +3.4 mmu), and C$_{23}$H$_{40}$O$_2$^{81}BrNa$_2$ (Δ +3.1 mmu), respectively. The ^{1}H NMR spectrum showed the presence of two multiplets at δ 5.32 and 5.41, corresponding to vicinal olefinic protons. An additional triplet at δ 5.84 (*J* = 7.8 Hz) suggested the presence of a trisubstituted double bond. The connectivities from H-2 to H-11 were resolved by COSY spectrum. The H-9 proton was cou-
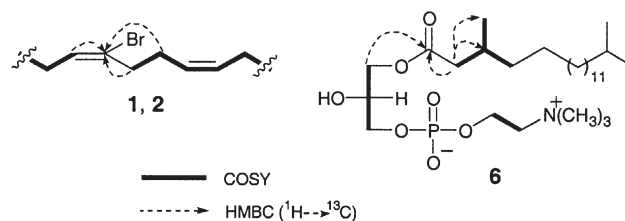
FIG. 1. Key COSY and heteronuclear multiple bond correlations of compounds **1**, **2**, and **6**.

pled to the H-8 methylene protons, which were in turn coupled to those at C-7, while the H-10 proton was coupled to the H-11 methylene protons. The H-5 proton, however, was coupled only to the H-4 methylene, which suggested that the trisubstituted and disubstituted double bonds were located at C-5 and C-9, respectively. The bromine atom had to be attached to the C-6 position, and the connection between C-6 and C-7 was revealed by HMBC correlations for H-5/C-6, H-7/C-6, and H-8/C-6 (Fig. 1). The geometry of Δ^9 was defined as *cis* on the basis of chemical shifts of the allylic carbons (δ 26.8 and 27.5) (15–17), which was further corroborated by the characteristic coupling constant of the olefinic protons (*J*$_{9,10}$ = 10.5 Hz). The configuration of Δ^5 was deduced to be *trans* by comparison of ^{13}C NMR data of the allylic carbons C-4 (δ 29.2) and C-7 (δ 36.8) with those of the similarly bromo-substituted olefinic compounds (7,10,12). Furthermore, the NOESY correlations H$_2$-4/H$_2$-7 and H$_2$-8/H$_2$-11 also supported the 5*E*,9*Z* configuration. Thus, the structure of **1** was established as a sodium salt of (5*E*,9*Z*)-6-bromo-21-methyldocosa-5,9-dienoic acid, and the free acid was named homaxinolic acid A. The 6-Br-iso-25:2 (Δ^{5,9}), 6-Br-iso-27:2 (Δ^{5,9}), and 6-Br-iso-29:2 (Δ^{5,9}) acids were previously reported (6–14). The isolation of compound **1** expanded this series to the 6-Br-iso-23:2 (Δ^{5,9}) acid, and hence expanded our present knowledge of iso odd-chain 6-Br-iso-(Δ^{5,9}) FA.

Homaxinolin A (**2**) was isolated as a colorless oil. Its molecular formula was established as C$_{26}$H$_{47}$O$_4$Br on the basis of MS and NMR spectral data. The FABMS showed [M – H$_2$O + H]$^+$ peaks at *m/z* 485 and 487. The presence of a glycerol moiety in **2** was deduced by the characteristic oxygenated proton signals at δ 4.15 (H-1$_a$), 4.06 (H-1$_b$), 3.81 (H-2), and 3.64 (H$_2$-3). Furthermore, the HMBC correlations from H-1$_a$ and H-1$_b$ to the carbonyl carbon at δ 174.7 (C-1′) confirmed the ester linkage in the molecule. The 5′*E*,9′*Z*-geometry was similarly defined as in the case of **1**. The stereochemistry at C-2 of the glycerol moiety was defined as *S* on the basis of the positive optical rotation (21). Thus, the structure of **2** was established as 1-*O*-[(5*E*,9*Z*)-6-bromo-21-methyldocosa-5,9-dienoyl]-*sn*-glycerol. The isolation of compound **2** showed that this type of brominated FA could occupy the C-1 position of a MG.

Homaxinolin B (**4**) was isolated as a white amorphous powder. Its molecular formula was established as C$_{20}$H$_{38}$O$_4$ on the basis of HRFABMS and ^{13}C NMR spectral data. The exact mass of the [M + Na]$^+$ ion (*m/z* 365.2669) matched well with the expected molecular formula of C$_{20}$H$_{38}$O$_4$Na (Δ −0.9 mmu).
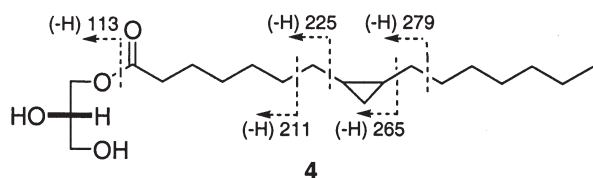
FIG. 2. Key fragmentations of the [M + Na]⁺ ion of **4** in fast atom bombardment–collision-induced dissociation–tandem mass spectroscopy.

TABLE 2
Cytotoxicity Data of Compounds 1, 2, 4, and 6[a]

Compound	A549	SK-OV-3	SK-MEL-2	XF498	HCT15
1	15.6	8.50	12.9	18.5	9.30
2	>30.0	>30.0	>30.0	>30.0	>30.0
4	>30.0	>30.0	>30.0	> 30.0	>30.0
6	>30.0	>30.0	>30.0	>30.0	>30.0
Doxorubicin	0.09	0.16	0.07	0.04	0.13

[a]Data expressed in ED_{50} values (μg/mL). A549, human lung cancer; SK-OV-3, human ovarian cancer; SK-MEL-2, human skin cancer; XF498, human central nervous system cancer; HCT15, human colon cancer.

The ¹H NMR spectrum showed characteristic oxygenated proton signals of the glycerol moiety at δ 4.14 (H-1$_a$), 4.05 (H-1$_b$), 3.80 (H-2), and 3.53 (H$_2$-3). The HMBC correlation from H-1$_a$ and H-1$_b$ to the carbonyl carbon signal (δ 175.3) indicated the presence of an ester linkage. The characteristic ¹H NMR signals for a cyclopropane moiety (δ 0.67, 0.59, and −0.33) were observed. The position of the cyclopropane moiety in the acyl chain was deduced from the prominent fragment ions at *m/z* 279 and 211, produced by β-cleavages of the three-membered ring (Fig. 2). Suppressed fragment ions between *m/z* 265 and 225 also indicated the position of the cyclopropane moiety. The J_{cis} (~8.0 Hz) between the ring methylene and methine protons in the cyclopropane is generally larger than the J_{trans} (~5.0 Hz) (15,22). The large coupling constant (J_{cis} = 7.8 Hz) between H-17′ and H-8′/H-9′ supported the *cis* ring substitution pattern. Furthermore, the larger difference in the chemical shifts of the ring geminal methylene protons (Δδ 0.9) also supported the *cis*-disubstituted ring orientation (15,23). In case of *trans*-disubstituted cyclopropanes, the geminal methylene protons are reported to appear side by side (Δδ 0.1) (23,24). The configuration at C-2 was established to be *S* on the basis of the positive optical rotation (21). Based on these data, the structure of **4** was established as 1-*O*-(*cis*-8,9-methylenehexadecanoyl)-*sn*-glycerol. There are several reports on FA containing a cyclopropane group (25–27), including a *cis*-methylenehexadecanoic acid (cy-16:0) isolated from a bacterium with the position of the cyclopropane moiety undetermined (28) and another report from an industrial source (29). To the best of our knowledge, this is the first report on the isolation of *cis*-(8,9)-methylenehexadecanoic acid from any natural source, as a FA derivative in general and as a C-1 substituent of a MG in particular.

Homaxicholine A (**6**) was isolated as a white amorphous solid. Its molecular formula was established as $C_{28}H_{58}NO_7P$ on the basis of MS and NMR spectral data. The FABMS showed a [M + H]⁺ peak at *m/z* 552 and a [M + Na]⁺ peak at *m/z* 574. The exact mass of the [M + H]⁺ ion (*m/z* 552.4040) matched well with the expected molecular formula of $C_{28}H_{58}NO_7P$ (Δ +1.1 mmu). The ¹H NMR spectrum featured a characteristic pattern of the PC skeleton. The doublet at δ 0.94 (H$_3$-20′) showed correlation to a multiplet at δ 1.93 (H-3′) in the COSY spectrum, which was further correlated to two doublets of doublets centered at δ 2.36 and 2.15 (H$_2$-2′) and a multiplet at δ 1.17 (H$_2$-4′). In the HMBC spectrum, correlations were observed from H-2′ to C-1′, 3′, 4′, from H-20′ to C-2′, 3′, 4′, and from H$_2$-1 of the glycerol moiety to C-1′ (Fig. 1). These correlations revealed that the methyl group was present at C-3′. The configuration of the C-3′ methyl remains to be determined. The stereochemistry at

C-2 was defined as *R* on the basis of the negative optical rotation data (17). Thus, the structure of **6** was determined to be 1-*O*-(3,17-dimethyloctadecanoyl)-*sn*-glycero-3-phosphocholine.

The isolation of acyl moieties containing a methyl group at C-3 in guanidine alkaloids and spermidine derivatives has been reported from sponge and soft coral, respectively (30,31). To the best of our knowledge, this acyl moiety, 3,17-dimethyloctadecanoic acid, is unprecedented in the literature.

The known compounds (**3**, **5**, and **7–9**) were identified by comparison of their NMR/MS data with those reported (15–17). The stereochemistry at C-2 of the glycerol moiety of **3**, **5**, and **7–9** was presumed to be the same as those of reported from sponges (15–17).

Compounds **1**, **2**, **4**, and **6** were evaluated for cytotoxicity against a panel of five human tumor cell lines (Table 2). Of the compounds tested, only **1** showed a moderately cytotoxic profile to most of the tumor cell lines tested. Compounds **2**, **4**, and **6** were virtually inactive.

REFERENCES

1. Eggersdorfer, M.L., Kokke, W.C.M.C., Crandell, C.W., Hochlowski, J.E., and Djerassi, C. (1982) Sterols in Marine Invertebrates. 32. Isolation of 3β-(Hydroxymethyl)-*A*-nor-5α-cholest-15-ene, the First Naturally Occurring Sterol with 15α16 Double Bond, *J. Org. Chem. 47*, 5304–5309.
2. Umeyama, A., Ito, S., Yuasa, E., Arihara, S., and Yamada, T. (1998) A New Bromopyrrole Alkaloid and the Optical Resolution of the Racemate from the Marine Sponge *Homaxinella* sp., *J. Nat. Prod. 61*, 1433–1433.
3. Sharma, G.M., Vig, B., and Burkholder, P.R. (1968) Antimicrobial Substances of Sponges. 3. Chemical Properties of Some Antibacterial Compounds from Marine Sponges, *Drugs Sea Trans. Symp.*, 119–126.
4. Mansoor, T.A., Hong, J., Lee, C., Sim, C.J., Im, K.S., Lee, D.S., and Jung, J.H. (2004) New Cytotoxic Metabolites from a Marine Sponge *Homaxinella* sp., *J. Nat. Prod. 67*, 721–724.
5. Mansoor, T.A., Hong, J., Lee, C., Bae, S., Im, K.S., Lee, D.S., and Jung, J.H. (2005) Cytotoxic Sterol Derivatives from a Marine Sponge *Homaxinella* sp., *J. Nat. Prod. 68*, 331–336.
6. Wijekoon, W.M.D., Ayanoglu, E., and Djerassi, C. (1984) Phospholipid Studies of Marine Organisms 9. New Brominated Demospongic Acids from the Phospholipids of Two *Petrosia* species,

Tetrahedron Lett. 25, 3285–3288.

7. Lam, W., Hahn, S., Ayanoglu, E., and Djerassi, C. (1989) Phospholipid Studies of Marine Organisms. 22. Structure and Biosynthesis of a Novel Brominated Fatty Acid from a Hymeniacidonid Sponge, *J. Org. Chem. 54*, 3428–3432.

8. Carballeira, N.M., and Shalabi, F. (1993) Novel Brominated Phospholipid Fatty Acids from the Caribbean Sponge *Petrosia* sp., *J. Nat. Prod. 56*, 739–746.

9. Carballeira, N.M., and Emiliano, A. (1993) Novel Brominated Fatty Acids from the Caribbean Sponge *Agelas* sp., *Lipids 28*, 763–766.

10. Garson, M.J., Zimmermann, M.P., Hoberg, M., Larsen, R.M., Battershill, C.N., and Murphy, P.T. (1993) Isolation of Brominated Long-Chain Fatty Acids from the Phospholipids of the Tropical Marine Sponge *Amphimedon terpenensis, Lipids 28*, 1011–1014.

11. Garson, M.J., Zimmermann, M.P., Battershill, C.N., Holden, J.L., and Murphy, P.T. (1994) The Distribution of Brominated Long-Chain Fatty Acids in Sponge and Symbiont Cell Types from the Tropical Marine Sponge *Amphimedon terpenensis, Lipids 29*, 509–516.

12. Li, Y., Ishibashi, M., Sasaki, T., and Kobayashi, J. (1995) New Bromine-Containing Unsaturated Fatty Acid Derivatives from the Okinawan Marine Sponge *Xestospongia* sp., *J. Chem. Res.*, 901–923.

13. Brantley, S.E., Molinski, T.F., Preston, C.M., and DeLong, E.F. (1995) Brominated Acetylenic Fatty Acids from *Xestospongia* sp., a Marine Sponge–Bacteria Association, *Tetrahedron 51*, 7667–7672.

14. Carballeira, N.M. (1997) The Brominated Fatty Acids in the Phospholipids of Marine Invertebrates, in *Recent Research Developments in Lipids Research* (Pandalai, S.G., ed.), Vol. 1, pp. 9–17, Transworld Research Network, Trivandrum, India.

15. Shin, B.A., Kim, R.Y., Lee, I., Sung, C.K., Hong, J., Sim, C.J., Im, K.S., and Jung, J.H. (1999) Lyso-PAF Analogues and Lysophosphatidylcholines from the Marine Sponge *Spirastrella abata* as Inhibitors of Cholesterol Biosynthesis, *J. Nat. Prod. 62*, 1554–1557.

16. Alam, N., Bae, B.H., Hong, J., Lee, C., Shin, B.A., Im, K.S., and Jung, J.H. (2001) Additional Bioactive Lyso-PAF Congeners from the Sponge *Spirastrella abata, J. Nat. Prod. 64*, 533–535.

17. Zhao, Q., Mansoor, T.A., Hong, J., Lee, C., Im, K.S., Lee, D.S., and Jung, J.H. (2003) New Lysophosphatidylcholines and Monoglycerides from the Marine Sponge *Stelletta* sp., *J. Nat. Prod. 66*, 725–728.

18. Myers, B.L., and Crews, P. (1983) Chiral Ether Glycerides from a Marine Sponge, *J. Org. Chem. 48*, 3583–3585.

19. Lee, S., Zhao, Q., Choi, K., Hong, J., Lee, D.S., Lee, C., and Jung, J.H. (2003) A New Glycerol Ether from a Marine Sponge *Stelletta* sp., *Nat. Prod. Sci. 9*, 232–234.

20. Meyer, B.N., Ferrigni, N.R., Putnam, J.E., Jacobsen, L.B., Nichols, D.E., and McLaughlin, J.L. (1982) Brine Shrimp: A Convenient General Bioassay for Active Plant Constituents, *J. Med. Plant Res. 45*, 31–34.

21. Ungur, N., Gavagnin, M., Fontana, A., and Cimino, G. (1999) Absolute Stereochemistry of Natural Sesquiterpenoid Diacylglycerols, *Tetrahedron*: *Assymetry 10*, 1263–1273.

22. Murakami-Murofushi, K., Shioda, M., Kaji, K., Yoshida, S., and Murofushi, H. (1992) Inhibition of Eukaryotic DNA Polymerase α with a Novel Lysophosphatidic Acid (PHYLPA) Isolated from Myxoamoebae of *Physarum polycephalum, J. Biol. Chem. 267*, 21512–21517.

23. Iguchi, K., Fujita, M., Nagaoka, H., Mitome, H., and Yamada, Y. (1993) Aragusterol A: A Potent Antitumor Marine Steroid from the Okinawan Sponge of the Genus *Xestospongia, Tetrahedron Lett. 34*, 6277–6280.

24. Iguchi, K., Shimura, H., Taira, S., Yokoo, C., Matsumoto, K., and Yamada, Y. (1994) Argusterol B and D, New 26,27-Cyclosterols from the Okinawan Marine Sponge of the Genus *Xestospongia, J. Org. Chem. 59*, 7499–7502.

25. Fenical, W., Sleeper, H.L., Paul, V.J., Stallard, M.O., and Sun, H.H. (1979) Defensive Chemistry of Navanax and Related Opisthobranch Mollusks, *Pure Appl. Chem. 51*, 1865–1874.

26. Nemoto, T., Ojika, M., and Sakagami, Y. (1997) Amphimic Acid, Novel Unsaturated C28 Fatty Acids as DNA Topoisomerase I Inhibitors from an Australian Sponge *Amphimedon* sp., *Tetrahedron Lett. 38*, 5667–5670.

27. Nemoto, T., Ojika, M., and Sakagami, Y. (1997) Amphimic Acid and Related Long-chain Fatty Acids as DNA Topoisomerase I Inhibitors from an Australian Sponge, *Amphimedon* sp.: Isolation, Structure, Synthesis, and Biological Evaluation, *Tetrahedron 49*, 16699–16710.

28. Joyeux, C., Fouchard, S., Llopiz, P., and Neunlist, S. (2004) Influence of the Temperature and the Growth Phase on the Hopanoids and Fatty Acids Content of *Frateuria aurantia* (DSMZ 6220), *FEMS Microbiol. Ecol. 47*, 371–379.

29. Bianchini, J.P., Ralaimanarivo, A., and Gaydou, E.M. (1982) Reversed-Phase High-Performance Liquid Chromatography of Fatty Acid Methyl Esters with Particular Reference to Cyclopropenoic and Cyclopropanoic Acids, *J. High Resolut. Chromatogr. 5*, 199–204.

30. Honma, K., Tsuda, M., Mikami, Y., and Kobayashi, J. (1995) Aplysillamides A and B, New Antimicrobial Guanidine Alkaloids from the Okinawan Marine Sponge *Psammmaplysilla purea, Tetrahedron 51*, 3745–3748.

31. Choi, Y., and Schmitz, F. (1997) Cytotoxic Acylated Spermidine from a Soft Coral, *Sinularia* sp., *J. Nat. Prod. 60*, 495–496.

REVIEW

Recent Advances in the Biochemistry and Clinical Relevance of the Isoprostane Pathway

Erik S. Musiek, Huiyong Yin, Ginger L. Milne, and Jason D. Morrow*

Division of Clinical Pharmacology, Departments of Pharmacology and Medicine,
Vanderbilt University School of Medicine, Nashville, Tennessee 37232

ABSTRACT: Isoprostanes (IsoPs), lipid peroxidation products formed *via* the free radical-mediated oxidation of arachidonic acid, have become the "gold standard" biomarker of oxidative stress *in vivo* over the past 15 yr. Significant advances have been made in understanding this important pathway of lipid peroxidation. Recent studies from our laboratory are discussed that have provided insights into the mechanism of formation and regioisomeric distribution of these compounds and that have identified novel products of the IsoP pathway such as cyclized dioxolane IsoPs, IsoP-derived racemic prostaglandins, and reactive cyclopentenone IsoP, the latter of which possess potent biological actions. Furthermore, new independent studies have demonstrated that IsoPs are the most reliable available marker of lipid peroxidation *in vivo*, and recent work examining IsoP formation has provided valuable information about the pathogenesis of numerous human diseases. Thus, the complexity of the IsoP pathway has expanded, providing novel insights into mechanisms of lipid peroxidation *in vivo* and allowing investigators to explore the role of oxidative stress in human disease.

Paper no. L9822 in *Lipids 40*, 987–994 (October 2005).

First described by Morrow and Roberts in 1990, the isoprostanes (IsoPs) are lipid peroxidation products derived from the oxidation of the ubiquitous PUFA arachidonic acid (AA) (1). IsoPs are so named because they are isomeric to enzymatically derived prostaglandins (PG), potent lipid mediators produced from free arachidonate *via* the action of cyclooxygenase (COX) enzymes. Unlike PG, however, IsoPs are formed nonenzymatically as a result of free radical-mediated peroxidation of AA. Over the past 15 yr, IsoPs have emerged as an excellent biomarker of oxidative damage *in vivo*, and considerable effort has been focused on the elucidation of this important lipid peroxidation pathway. Work by our group and many others has yielded novel insights into the biochemistry of this pathway, has generated improved analytical techniques for the analysis of these compounds, and has expanded the ever-growing list of human disease states and biological processes in

which both IsoP formation and oxidative stress have been implicated.

ADVANCES IN IsoP BIOCHEMISTRY

The mechanism of IsoP formation, which has been the source of some controversy and is discussed more thoroughly later, is outlined in Figure 1. Following abstraction of a bisallylic hydrogen atom and the addition of a molecule of oxygen to AA to form a peroxyl radical, *exo*-cyclization occurs and an additional molecule of oxygen is added to form prostaglandin (PG)G$_2$-like compounds. These unstable bicycloendoperoxide intermediates then spontaneously form parent IsoP. Based on this mechanism of formation, four IsoP regioisomers are generated, each with 16 stereoisomers, resulting in a total of 64 IsoP isomers (1–3). IsoP regioisomers are denoted as either 5-, 12-, 8-, or 15-series compounds depending on the carbon atom to which the side chain hydroxyl is attached (4). IsoPs that contain the F-type prostane ring are isomeric to PGF$_{2\alpha}$ and are thus referred to as F$_2$-IsoPs. It should be noted that IsoPs containing alternative PG ring structures (such as those containing E/D and A/J rings) can also be formed by this mechanism; these will be discussed later (5,6). F$_2$-IsoPs, however, have been the most studied class of IsoP and, because of their stability, afford the most accurate measure of oxidant stress (7). An alternative nomenclature system for the IsoPs has been proposed by FitzGerald and colleagues in which the abbreviation iP is used for isoprostane, and regioisomers are denoted as III–VI based on the number of carbons between the omega carbon and the first double bond (8,9). This nomenclature system can also be applied to IsoP-like compounds derived from other FA, such as EPA and DHA.

There are several key distinctions between IsoPs and COX-derived PG. First, PG are generated with side chains that are predominantly oriented *trans* to the prostane ring whereas IsoP are formed almost exclusively with *cis* side chains, a more thermodynamically favorable configuration (1–3). A second important difference between these two classes of molecules is that IsoPs are formed *in situ* esterified to phospholipids and are subsequently released by a phospholipase(s) (5), whereas PG are generated only from free AA (10). Thus, IsoPs can be quantified both in membrane-esterified or free fractions. Furthermore, membrane-esterifed IsoPs can potentially affect the integrity and fluidity of membranes, owing to their contorted 3-D structure (5).

*To whom correspondence should be addressed at Division of Clinical Pharmacology, Departments of Pharmacology and Medicine, Vanderbilt University School of Medicine, 526 RRB, 23rd and Pierce Aves., Nashville, TN 37232-6602. E-mail: jason.morrow@vanderbilt.edu

Abbreviations: AA, arachidonic acid; AD, Alzheimer's disease; APCI, atmospheric pressure chemical ionization; COX, cyclooxygenase; ESI, electrospray ionization; GSH, glutathione; IsoPs, isoprostane; LPS, lipopolysaccharide; MDA, malondialdehyde; NICI, negative ion chemical ionization; PG, prostaglandin; PPARγ, peroxisome proliferator-activated receptor-gamma; ROS, reactive oxygen species.

FIG. 1. Mechanism of formation of the F_2-isoprostanes (IsoPs). Four regioisomers are formed, each consisting of 8 racemic diastereomers. The 15- and 5-series regioisomers are more abundant than the 12- and 8-series, as the hydroperoxyl radicals that give rise to 12- and 8-series IsoPs can also undergo further cyclization to form 12- and 8-series dioxolane IsoPs. Stereochemistry is not indicated.

Mechanism of IsoP formation. The exact chemical mechanism by which IsoPs are formed has been the topic of some debate. The mechanism depicted in Figure 1 was first proposed by our group (1,2,11). Under this scheme, the initial arachidonyl peroxyl radical undergoes successive 5-*exo* cyclizations in a process similar to that proposed for enzymatic PG biosynthesis (Fig. 1). A second mechanism was subsequently proposed involving 4-*exo* cyclization of the peroxyl radical and leading to a dioxetane intermediate (12), based on an alternative mechanism proposed for PG formation originally put forward by Corey and Wang (13). For a diagram depicting both mechanisms, see Ref-

erence 8. To determine the primary mechanism of IsoP formation, we isolated optically pure cholesteryl-15- hydroperoxye-icosatetraenoic acid (Ch-15-HpETE), one of the arachidonyl hydroperoxides that give rise to IsoP, and oxidized this compound *in vitro*, giving rise to the 15-peroxyl radical depicted in Figure 1 (14). According to the 5-*exo* mechanism, oxidation of this optically pure reactant should give rise to a racemic mixture of IsoP products, whereas the 4-*exo* "dioxetane mechanism" would yield optically pure compounds. Analysis of the products of this reaction using atmospheric pressure CI-MS (APCI/MS) coupled with chiral HPLC revealed that the IsoP formed were a mixture
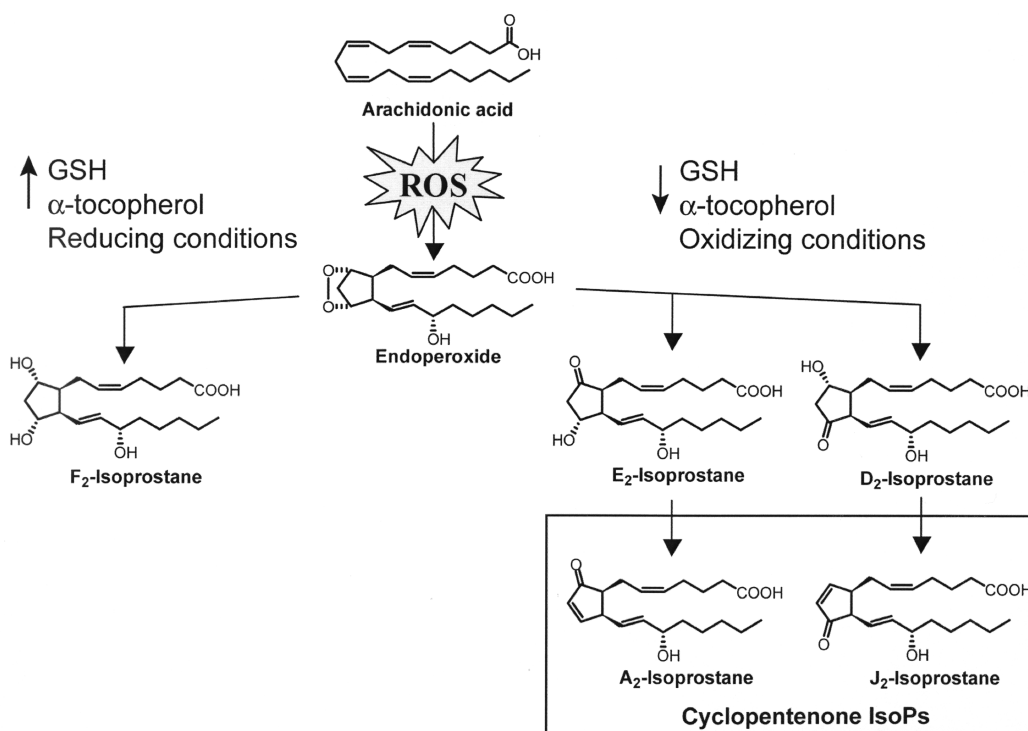
FIG. 2. Formation of cyclopentenone IsoP. The arachidonate endoperoxide intermediate can undergo reduction [facilitated by high local concentrations of glutathione (GSH) or α-tocopherol] to form stable F_2-IsoP. Alternatively, when the reducing conditions of the cell are depleted, the endoperoxide can undergo isomerization to form E_2- and D_2-IsoP, which spontaneously dehydrate to yield electrophilic A_2- and J_2-IsoP, also known as cyclopentenone IsoP. All compounds depicted are 15-series, but IsoP of all regioisomer series can be formed with each of these ring structures. ROS, reactive oxygen species; for other abbreviation see Figure 1.

of racemic diastereomers, a finding consistent with the original 5-*exo* mechanism (Fig. 1) and providing evidence against the formation of dioxetane intermediates (14).

Distribution of IsoP regioisomers. Although the initial abstraction of any of the bisallylic hydrogen atoms of arachidonate is equally likely, the four classes of IsoP regioisomers are not formed in equivalent proportions. Waugh *et al.* (15) demonstrated that 5- and 15-series regioisomers (also known as types II and III regioisomers, respectively) are significantly more abundant than 8- and 12-series compounds (also termed types I and IV regioisomers, respectively). An explanation for this difference was elucidated by Yin *et al.* (16,17), who demonstrated that the arachidonyl hydroperoxides that give rise to 8- and 12-series regioisomers, the less abundant species, readily undergo further oxidation to yield bicyclic and serial cyclic endoperoxides, which go on to form bi or serial-cyclic IsoPs (see Fig. 1). The 5- and 15-series regioisomers, which are the more abundant species, arise from endoperoxides, which cannot undergo further oxidation or cyclization and thus accumulate in tissues and fluids. These bicyclic endoperoxides, as well as further cyclized IsoPs (termed dioxolane-IsoPs), were identified both in oxidized arachidonate and LDL.

Analytical methods allowing separation and quantification of each of the four classes of IsoP regioisomers, as well as their individual stereoisomers, have recently been developed in our laboratory. These techniques, which include chiral LC coupled to tandem MS (MS/MS) with electrospray ionization (ESI) or APCI, allow for more thorough examination of IsoP formation *in vivo* (18).

Formation of E_2/D_2-IsoP. Although IsoPs are formed as four different regioisomers, they are also generated with different prostane ring structures. The arachidonyl endoperoxide intermediate depicted in Figure 2 can undergo reduction to yield F-ring IsoP, which resemble $PGF_{2\alpha}$, or isomerization to form E- and D-ring IsoPs, which are isomeric to PGE_2 and PGD_2, respectively. F_2-IsoPs are extremely stable, nonreactive compounds that have been thoroughly studied over the past 15 yr and have proven to be exceptional biomarkers of oxidative stress *in vivo* (*vide infra*). However, recent advances in the study of IsoPs with alternative ring types are beginning to yield important insights into this lipid peroxidation pathway. E_2/D_2-IsoPs are formed competitively with F_2-IsoPs (19), and recent studies have demonstrated that the depletion of cellular reducing agents, such as glutathione (GSH) or α-tocopherol, favors the formation of E_2/D_2-IsoPs over that of reduced F_2-IsoPs (20). Importantly, depletion of GSH and α-tocopherol occurs in various human tissues under conditions of oxidant injury, including the brains of patients with Alzheimer's disease (AD) (21). Thus, Reich *et al.* (22,23) examined the ratio of F-ring to E/D-ring IsoPs in postmortem brain tissues from patients with AD and found not only

that levels of both E_2/D_2- and F_2-IsoPs were significantly elevated but also that E_2/D_2-IsoPs were the favored products of the IsoP pathway in affected brain regions. This increased ratio of E_2/D_2-IsoPs to F_2-IsoPs provides information not only about lipid peroxidation in a given tissue but also about the reducing environment in that tissue.

Cyclopentenone IsoPs. E_2/D_2-IsoPs, however, are not terminal products of the IsoP pathway. These compounds readily dehydrate *in vivo* to yield A_2/J_2-IsoPs, which are also known as cyclopentenone IsoPs because they contain an α,β-unsaturated cyclopentenone ring structure (see Fig. 2) (24,25). A_2/J_2-IsoPs are highly reactive electrophiles that readily form Michael adducts with cellular thiols, including those found on cysteine residues in proteins and GSH (6,24). These cyclopentenone IsoPs are rapidly metabolized *in vivo* by GSH transferase enzymes to water-soluble modified GSH conjugates (25–27). The major urinary cyclopentenone IsoP metabolite in rats, a $15-A_{2t}$-IsoP mercapturic acid sulfoxide conjugate, was recently identified in our laboratory (28). This metabolite can be readily quantified in urine by LC/MS/MS and was found to accumulate significantly over 24 h following induction of lipid peroxidation with CCl_4, providing evidence that A_2/J_2-IsoPs are formed, released from membrane phospholipids, and metabolized *in vivo* (28). This assay allows integrated measurement of whole-body cyclopentenone IsoP production over a given time and should be a valuable tool in elucidating the role of these compounds in various models of disease.

A_2/J_2-IsoPs also can be directly quantified in rat liver tissue by GC/MS, and were found to increase 24-fold following hepatic oxidative injury with CCl_4 (6). Recently, our group has developed a novel LC/MS/MS-ESI method to quantify cyclopentenone IsoPs *in vivo* and have found that they are highly abundant in both rodent and human brain tissue and are found in higher concentrations than F_2-IsoPs (29). Following oxidative injury, A_2/J_2-IsoP levels in brain homogenate increase 12-fold, reaching concentrations roughly equal to 560 nM. Thus, our measurements of both A_2/J_2-IsoPs and their precursors, E_2/D_2-IsoPs, in brain tissue suggest that reduction of the arachidonyl endoperoxide to F_2-IsoPs is the less favored side of the pathway.

The observation that A_2/J_2-IsoPs are preferred products of the IsoP pathway in brain has important implications. The chemical reactivity of cyclopentenone IsoP suggested that these compounds might be biologically active. The recent synthesis of two cyclopentenone IsoPs regioisomers, $15-A_2$-IsoP and $15-J_2$-IsoP, has allowed us to examine their bioactivity (30,31). Studies using primary cortical neuronal cultures demonstrated that $15-A_2$-IsoPs, one of the most abundant cyclopentenone IsoP regioisomers *in vivo*, potently induces neuronal apoptosis and exacerbates neurodegeneration caused by other insults at concentrations as low as 100 nM (29). $15-A_2$-IsoP elicits neuronal apoptosis *via* a discrete signaling pathway that overlaps extensively with cell death signaling cascades triggered by other oxidative insults. A second cyclopentenone

IsoP, $15-J_2$-IsoP, is also highly neurotoxic, suggesting that all A_2/J_2-IsoPs share this characteristic (24). Thus, A_2/J_2-IsoPs, or the downstream signaling pathways activated by these compounds, might represent novel neuroprotective therapeutic targets. These findings are reinforced by studies demonstrating that inhibition of lipid peroxidation, or overexpression of GST enzymes (which scavenge reactive lipid peroxidation products including cyclopentenone IsoPs) protects neuronal cells from oxidative injury (32–35)

Cyclopentenone IsoPs also exert biological effects in nonneural tissue. Recent studies using macrophages revealed that $15-A_2$-IsoPs potently suppress lipopolysaccharide (LPS)-induced inflammatory signaling *via* inhibition of the nuclear factor κ-B pathway (36). $15-A_2$-IsoPs abrogate inducible nitric oxide synthase and COX-2 expression in response to LPS, as well as the elaboration of several proinflammatory cytokines (25,36). Similar anti-inflammatory effects were seen with $15-J_2$-IsoPs. However, $15-J_2$-IsoPs also activate the peroxisome proliferator-activated receptor-γ (PPARγ) with an effective concentration required to elicit 50% maximal response (EC_{50}) of approximately 3 μM. This receptor modulates a wide variety of biological processes, including inflammatory signaling and FA metabolism. $15-J_2$-IsoPs also induce macrophage apoptosis at low micromolar concentrations in a PPARγ-independent manner (36). Thus, there is a diversity of actions among cyclopentenone IsoP isomers. It appears that these compounds could act as negative-feedback regulators of the inflammatory response, as oxidative stress and lipid peroxidation often occur under conditions of chronic inflammation (36,37).

Generation of PG via the IsoP pathway. As previously described, IsoPs are so named because they are isomers of PG, lipid mediators produced by the enzymatic oxidation of arachidonate by COX. PG can easily be distinguished from IsoPs chromatographically because of their exclusive *trans* side-chain stereochemistry and lack of regio- or stereoisomers. However, recent work from our laboratory has revealed significant overlap between the two pathways. Gao *et al.* (38) demonstrated that $15-E_{2t}$-IsoPs can undergo keto-enol tautomerization in aqueous buffer to yield PGE_2, thus establishing a COX-independent mechanism for PG formation. Because this process is nonenzymatic, the PGE_2 formed *via* the IsoP pathway is expected to be a racemic mixture of stereoisomers, unlike the optically pure (single stereoisomer) PGE_2 generated by COX. Accordingly, phospholipid-esterified racemic PGE_2 and PGD_2, which cannot be generated by COX, were identified in rat liver tissue and increased 35-fold following oxidant injury, even in the presence of COX inhibitors (38). These data suggest that cross-talk exists between the COX-PG pathway, usually associated with inflammation, and the IsoP pathway, associated with oxidative stress. An implication of these findings is that COX inhibitors should be unable to suppress PG formation fully under conditions of oxidative injury, a hypothesis in keeping with clinical observations (39).

F_2-IsoPs AS BIOMARKERS OF OXIDATIVE STRESS *IN VIVO*

Since their discovery in 1990, F_2-IsoPs have emerged as the gold standard marker of lipid peroxidation *in vivo*. Increased levels of F_2-IsoPs have been detected in tissue and fluids from human patients with a vast array of acute and chronic diseases, including atherosclerosis, cancer, rheumatoid arthritis, AD, HIV infection, and many others (for review, see Refs. 8, 40). We have defined normal levels of F_2-IsoPs in human biological fluids such as plasma and urine and have found that significant quantities of IsoPs are generated at all times in normal, healthy subjects, suggesting that humans are subject to incompletely suppressed oxidative stress at all times (1–3). It is important to note that quantities of these compounds exceed those of COX-derived PG by at least an order of magnitude in most tissue and fluids, suggesting that IsoPs are a major pathway of AA disposition. Further, levels of F_2-IsoPs are sufficient to be detected in every normal biological tissue and fluid that has been assayed including plasma, urine, bronchoalveolar lavage fluid, cerebrospinal fluid, and bile (3).

Quantification of IsoPs by GC/MS. To analyze F_2-IsoPs, our laboratory uses a GC/negative ion CI mass spectrometric (GC/NICI-MS) approach with stable isotope dilution (3,40). For quantification purposes, we measure the F_2-IsoPs, 15-F_{2t}-IsoP, and other F_2-IsoPs that coelute with this compound. Several internal standards are available from commercial sources to quantify the IsoP. These include $[^2H_4]15$-F_{2t}-IsoP ($[^2H_4]$ 8-iso-PGF$_{2\alpha}$) and $[^2H_4]$-PGF$_{2\alpha}$. Other investigators, including FitzGerald and colleagues (12,41), use similar methods that require solid phase extraction using a C18 column, TLC purification, and chemical derivatization. By this method, IsoP are also quantified using GC/NICI-MS but the assay measures F_2-IsoP isomers other than 15-F_2-IsoP. This method appears to be comparable to ours in terms of utility. The advantages of MS over other approaches include its high sensitivity and specificity, which yield quantitative results in the low picogram range. Its drawbacks are that it is labor intensive and requires considerable expenditures on equipment.

The measurement of F_2-IsoP accumulation in urine is particularly attractive, as this capability would potentially provide an index of systemic oxidant stress integrated over time. However, the measurement of free F_2-IsoPs in urine is confounded by the potential contribution of local IsoP production in the kidney (42). In light of this issue, we previously identified the primary urinary metabolite of 15-F_{2t}-IsoP to be 2,3-dinor-5,6-dihydro-15-F_{2t}-IsoP, and developed a highly sensitive and accurate MS assay to quantify this molecule (43–45). Thus, the quantification of 2,3-dinor-5,6-dihydro-15-F_{2t}-IsoP may represent a truly noninvasive, time-integrated measurement of systemic oxidation status that can be applied to living subjects.

Recent studies confirm IsoP as an excellent biomarker of oxidative stress in vivo. Recently, an extensive multilaboratory effort termed the Biomarkers of Oxidative Stress Study was coordinated by the National Institutes of Health to evaluate and compare several indices of oxidative stress in a head-to-head manner (46). Rats were treated with increasing concentrations

of CCl$_4$, a compound known to induce severe lipid peroxidation in the liver. Lipid peroxidation was evaluated at several time points by quantifying multiple markers in plasma and urine, including F_2-IsoP (by GC/MS), lipid hydroperoxides, TBARS, malondialdehyde (MDA), protein carbonyls, methionine sulfoxidation, tyrosine products, 8-hydroxy-2′-deoxyguanosine, leukocyte DNA–MDA adducts, and DNA-strand breaks. Only F_2-IsoPs were elevated in both plasma and urine in both a dose- and time-dependent manner (46). A final phase of the study examined the effect of the nonselective COX inhibitor indomethicin on several of these biomarkers (47). The study found that all markers tested could be partially suppressed by indomethicin, suggesting not that these compounds are catalytic products of COX, but rather that COX-dependent proinflammatory signaling contributes to nonenzymatic lipid peroxidation in CCl$_4$ poisoning. These collaborative multicenter studies further demonstrate that the quantification of F_2-IsoPs by GC/MS is indeed the most reliable method of assessing lipid peroxidation *in vivo*.

Other methods to measure F_2-IsoP. Although the measurement of F_2-IsoPs by GC/MS is considered the gold standard, a number of alternative assay methodologies have been developed. ELISA methods to quantify 15-F_{2t}-IsoP (8-iso-PGF$_{2\alpha}$) and of 2,3-dinor-5,6-dihydro-15-F_{2t}-IsoP, the major urinary F_2-IsoP metabolite, are commercially available from several vendors and are commonly used owing to their low cost and minimal equipment requirements. However, concerns remain about the cross-reactivity of the antibodies used in these assays, the variability of these kits between manufacturers, as well as their accuracy and precision across various sample preparations. Indeed, a recent study comparing the measurement of 2,3-dinor-5,6-dihydro-15-F_{2t}-IsoP by ELISA and GC/MS demonstrated a poor correlation and found the ELISA method to be unreliable (48). Furthermore, these ELISA methods require similar off-line purification as GC/MS assays and thus do not save processing time. Further study is required to determine exactly what compounds are quantified by these immunoassays in various types of tissue and fluids before they can be considered equivalent to GC/MS.

An emerging methodology for IsoP measurement is LC/MS/MS. Several groups have reported novel LC/MS/MS methods for detecting F_2-IsoPs in urine and plasma that require minimal offline purification and appear to be quite sensitive and specific (49–52). Although LC/MS/MS is very promising, many of these methods have not been compared with the established GC/MS method [the methods of Li *et al.* (49) and Liang *et al.* (52) are notable exceptions], and their reliability and specificity across sample preparation types remains to be confirmed.

Quantification of IsoP in animal models of disease and human disorders. The measurement of F_2-IsoPs by GC/MS has been thoroughly validated by numerous *in vitro* methods and has been found to correlate extremely well with other indices of lipid peroxidation (for review, see Ref. 7). The true utility of F_2-IsoP, however, is in the quantification of lipid peroxidation *in vivo*. F_2-IsoPs have provided important information concerning the role

of oxidative stress in a vast array of animal models and human diseases, including atherosclerosis (53,54), neurodegenerative diseases (21,55), hypercholesterolemia (56,57), diabetes (58), obesity (59,60), rheumatoid arthritis (37), myocardial ischemia/reperfusion (61), and many others (for a more comprehensive list see Ref. 40). F_2-IsoPs have also provided a means of assessing the efficacy of various therapeutic interventions in affecting oxidative stress in these patients (56,62). Thus, the clinical utility of F_2-IsoP has been great and continues to grow.

As an example, considerable recent efforts have focused on F_2-IsoPs in the study of atherosclerosis, the leading cause of death in the United States. Increased oxidative stress has been associated with the development of atherosclerosis, and elevated quantities of F_2-IsoPs were detected as markers of oxidative damage in atherosclerotic plaques from human patients (53,63). F_2-IsoPs are also increased in several human disease states that are associated with increased risk of atherosclerosis, including diabetes (58), hypercholesterolemia (56), and cigarette smoking (64). However, Schwedhelm *et al.* (65) recently tested the hypothesis that increased F_2-IsoPs are an independent risk factor for atherosclerosis. Ninety-three patients with established coronary artery disease were matched with 93 control subjects without disease. Several indices were found to be elevated in diseased subjects, including C-reactive protein and urinary F_2-IsoP levels, the latter of which were elevated by a mean of 1.9-fold in diseased patients. All of these characteristics predicted coronary atherosclerosis in a univariate analysis. In a multivariate analysis, however, the odds ratios of atherosclerosis were increased only for urinary F_2-IsoPs (≥ 131 pmol/mmol; $P < 0.001$) and C-reactive protein (>3 mg/L; $P < 0.01$) by 30.8 and 7.2, respectively. The authors concluded that the F_2-IsoPs represent a novel marker in addition to known risk factors of coronary heart disease and that urinary excretion of the compounds correlates with the number of risk factors for all subjects ($P < 0.001$ for trend). Recent data from the CARDIA study also showed that increased F_2-IsoP levels are associated with increased risk of coronary artery calcification, a sign of advanced atherosclerosis (66). A third study by Vassalle *et al.* (67) suggests that elevated F_2-IsoP formation also predicts the extent and severity of coronary artery disease. Despite the strong association between oxidative injury and atherosclerosis, several attempts to prevent atherosclerotic disease with dietary antioxidants, particularly vitamin E, have been unsuccessful (68–70). This is perhaps due to the limited efficacy of vitamin E as an antioxidant *in vivo*, or to inadequate dosage and duration of vitamin E supplementation. Indeed, work by Fitzgerald and colleagues (71) demonstrated that vitamin E supplementation up to 2000 IU per day for 5 wk failed to lower plasma IsoP levels in human subjects, suggesting that this antioxidant regimen does not fully suppress oxidative damage *in vivo*. Data from our laboratory have further shown that high doses and longer durations of vitamin E supplementation than those used in most studies, including the high profile negative studies, are required to suppress IsoP production in humans (Morrow, J., and Roberts, L.J., unpublished data). Thus, it is possible that more effective antioxidant therapies might demonstrate increased success in combating atherosclerosis and that the suppression of F_2-IsoP formation might serve as an indicator of antioxidant efficacy for future studies. Thus, the study of F_2-IsoPs continues to yield important clinical insight into a variety of human diseases, including atherosclerosis, and provides a potential pharmacological end point for the development of future antioxidant therapies.

CONCLUSIONS

The discovery of F_2-IsoPs as products of nonenzymatic lipid peroxidation has opened up new areas of investigation regarding the role of free radicals in human physiology and pathophysiology and appears to be the most useful tool currently available to explore the role of free radicals in the pathogenesis of human disease. Our understanding of the IsoP pathway continues to expand, providing new insights into the nature of lipid peroxidation *in vivo* and revealing new molecules that exert potent biological actions and might serve as unique indices of disease. Basic research into the biochemistry and pharmacology of this pathway, coupled with clinical studies using these molecules as biomarkers, should continue to provide important insights into the role of oxidative stress in human disease.

REFERENCES

1. Morrow, J.D., Hill, K.E., Burk, R.F., Nammour, T.M., Badr, K.F., and Roberts, L.J., II (1990) A Series of Prostaglandin F_2-like Compounds Are Produced *in vivo* in Humans by a Non-cyclooxygenase, Free Radical-Catalyzed Mechanism, *Proc. Natl. Acad. Sci. USA 87*, 9383–9387.
2. Morrow, J.D., Harris, T.M., and Roberts, L.J., II (1990) Noncyclooxygenase Oxidative Formation of a Series of Novel Prostaglandins: Analytical Ramifications for Measurement of Eicosanoids, *Anal. Biochem. 184*, 1–10.
3. Morrow, J.D., and Roberts, L.J., II (1999) Mass Spectrometric Quantification of F_2-Isoprostanes in Biological Fluids and Tissues as Measure of Oxidant Stress, *Methods Enzymol. 300*, 3–12.
4. Taber, D.F., Morrow, J.D., and Roberts, L.J., II (1997) A Nomenclature System for the Isoprostanes, *Prostaglandins 53*, 63–67.
5. Morrow, J.D., Awad, J.A., Boss, H.J., Blair, I.A., and Roberts, L.J., II (1992) Non-cyclooxygenase-Derived Prostanoids (F_2-isoprostanes) Are Formed *in situ* on Phospholipids, *Proc. Natl. Acad. Sci. USA 89*, 10721–10725.
6. Chen, Y., Morrow, J.D., and Roberts, L.J., II (1999) Formation of Reactive Cyclopentenone Compounds *in vivo* as Products of the Isoprostane Pathway, *J. Biol. Chem. 274*, 10863–10868.
7. Fam, S.S., and Morrow, J.D. (2003) The Isoprostanes: Unique Products of Arachidonic Acid Oxidation—A Review, *Curr. Med. Chem. 10*, 1723–1740.
8. Lawson, J.A., Rokach, J., and FitzGerald, G.A. (1999) Isoprostanes: Formation, Analysis and Use as Indices of Lipid Peroxidation *in vivo*, *J. Biol. Chem. 274*, 24441–24444.
9. Rokach, J., Khanapure, S.P., Hwang, S.W., Adiyaman, M., Lawson, J.A., and FitzGerald, G.A. (1997) Nomenclature of Isoprostanes: A Proposal, *Prostaglandins 54*, 853–873.

10. Morrow, J.D., and Roberts, L.J., II (2001) Lipid-Derived Autocoids: Eicosanoids and Platelet Activating Factor, in *Goodman and Gilman's The Pharmcological Basis of Therapeutics* (Hardman, J.G., and Limbird, L.E., eds.), pp. 669–687, McGraw-Hill, New York.

11. Roberts, L.J., II, and Morrow, J.D. (2002) Products of the Isoprostane Pathway: Unique Bioactive Compounds and Markers of Lipid Peroxidation, *Cell. Mol. Life Sci. 59*, 808–820.

12. Rokach, J., Khanapure, S.P., Hwang, S.W., Adiyaman, M., Lawson, J.A., and FitzGerald, G.A. (1997) The Isoprostanes: A Perspective, *Prostaglandins 54*, 823–851.

13. Corey, E.J., and Wang, Z. (1994) Conversion of Arachidonic Acid to the Prostaglandin Endoperoxide PGG_2, a Chemical Analog of the Biosynthetic Pathway, *Tetrahedron Lett. 35*, 539–542.

14. Yin, H., Havrilla, C.M., Gao, L., Morrow, J.D., and Porter, N.A. (2003) Mechanisms for the Formation of Isoprostane Endoperoxides from Arachidonic Acid. "Dioxetane" Intermediate Versus β-Fragmentation of Peroxyl Radicals, *J. Biol. Chem. 278*, 16720–16725.

15. Waugh, R.J., Morrow, J.D., Roberts, L.J., II, and Murphy, R.C. (1997) Identification and Relative Quantitation of F_2-Isoprostane Regioisomers Formed *in vivo* in the Rat, *Free Radic. Biol. Med. 23*, 943–954.

16. Yin, H., Morrow, J.D., and Porter, N.A. (2004) Identification of a Novel Class of Endoperoxides from Arachidonate Autoxidation, *J. Biol. Chem. 279*, 3766–3776.

17. Yin, H., Havrilla, C.M., Morrow, J.D., and Porter, N.A. (2002) Formation of Isoprostane Bicyclic Endoperoxides from the Autoxidation of Cholesteryl Arachidonate, *J. Am. Chem. Soc. 124*, 7745–7754.

18. Yin, H., Porter, N.A.,, and Morrow, J.D. (2005) Separation and Identification of F(2)-Isoprostane Regioisomers and Diastereomers by Novel Liquid Chromatographic/Mass Spectrometric Methods, *J. Chromatogr. B,* epub ahead of print.

19. Morrow, J.D., Minton, T.A., Mukundan, C.R., Campbell, M.D., Zackert, W.E., Daniel, V.C., Badr, K.F., Blair, I.A., and Roberts, L.J., II (1994) Free Radical-Induced Generation of Isoprostanes *in vivo*. Evidence for the Formation of D-Ring and E-Ring Isoprostanes, *J. Biol. Chem. 269*, 4317–4326.

20. Montine, T.J., Montine, K.S., Reich, E.E., Terry, E.S., Porter, N.A., and Morrow, J.D. (2003) Antioxidants Significantly Affect the Formation of Different Classes of Isoprostanes and Neuroprostanes in Rat Cerebral Synaptosomes, *Biochem. Pharmacol. 65*, 611–617.

21. Montine, T.J., Neely, M.D., Quinn, J.F., Beal, M.F., Markesbery, W.R., Roberts, L.J., and Morrow, J.D. (2002) Lipid Peroxidation in Aging Brain and Alzheimer's Disease, *Free Radic. Biol. Med. 33*, 620–626.

22. Reich, E.E., Markesbery, W.R., Roberts, L.J., II, Swift, L.L., Morrow, J.D., and Montine, T.J. (2001) Brain Regional Quantification of F-Ring and D-/E-Ring Isoprostanes and Neuroprostanes in Alzheimer's Disease, *Am. J. Pathol. 158*, 293–297.

23. Reich, E.E., Markesbery, W.R., Roberts, L.J., II, Swift, L.L., Morrow, J.D., and Montine, T.J. (2001) Quantification of F-Ring and D-/E-Ring Isoprostanes and Neuroprostanes in Alzheimer's Disease, *Adv. Exp. Med. Biol. 500*, 253–256.

24. Musiek, E.S., Milne, G.L., McLaughlin, B., and Morrow, J.D. (2005) Cyclopentenone Eicosanoids as Mediators of Neurodegeneration: A Pathogenic Mechanism of Oxidative Stress-Mediated and Cyclooxygenase-Mediated Neurotoxicity, *Brain Pathol. 15*, 149–158.

25. Milne, G.L., Musiek, E.S., and Morrow, J.D. (2005) The Cyclopentenone (A_2/J_2) Isoprostanes—Unique, Highly Reactive Products of Arachidonate Peroxidation, *Antioxid. Redox Signal. 7*, 210–220.

26. Milne, G.L., Zanoni, G., Porta, A., Sasi, S., Vidari, G., Musiek, E.S., Freeman, M.L., and Morrow, J.D. (2004) The Cyclopentenone Product of Lipid Peroxidation, 15-A_{2t}-Isoprostane, Is Efficiently Metabolized by HepG2 Cells *via* Conjugation with Glutathione, *Chem. Res. Toxicol. 17*, 17–25.

27. Hubatsch, I., Mannervik, B., Gao, L., Roberts, L.J., Chen, Y., and Morrow, J.D. (2002) The Cyclopentenone Product of Lipid Peroxidation, 15-A_{2t}-Isoprostane (8-isoprostaglandin A_2), Is Efficiently Conjugated with Glutathione by Human and Rat Glutathione Transferase A4-4, *Chem. Res. Toxicol. 15*, 1114–1118.

28. Milne, G.L., Gao, L., Zanoni, G., Vidari, G., and Morrow, J.D. (2005) Identification of the Major Urinary Metabolite of the Highly Reactive Cyclopentenone Isoprostane 15-A_{2t}-Isoprostane *in vivo*, *J. Biol. Chem. 280*, 25178–25184.

29. Musiek, E.S., Milne, G.L., Breeding, R.L., Morrow, J.D., and McLaughlin, B. (2005) Cyclopentenone Isoprostanes, Novel Bioactive Products of Lipid Oxidation, Enhance Neurodegeneration, *J. Neurochem.*, in press.

30. Zanoni, G., Porta, A., and Vidari, G. (2002) First Total Synthesis of A_2 Isoprostane, *J. Org. Chem. 67*, 4346–4351.

31. Zanoni, G., Porta, A., Castronovo, F., and Vidari, G. (2003) First Total Synthesis of J_2 Isoprostane, *J. Org. Chem. 68*, 6005–6010.

32. Xie, C., Lovell, M.A., Xiong, S., Kindy, M.S., Guo, J., Xie, J., Amaranth, V., Montine, T.J., and Markesbery, W.R. (2001) Expression of Glutathione-S-Transferase Isozyme in the SY5Y Neuroblastoma Cell Line Increases Resistance to Oxidative Stress, *Free Radic. Biol. Med. 31*, 73–81.

33. Zimniak, L., Awasthi, S., Srivastava, S.K., and Zimniak, P. (1997) Increased Resistance to Oxidative Stress in Transfected Cultured Cells Overexpressing Glutathione S-Transferase mGSTA4-4, *Toxicol. Appl. Pharmacol. 143*, 221–229.

34. Beal, M.F. (1995) Aging, Energy, and Oxidative Stress in Neurodegenerative Diseases, *Ann. Neurol. 38*, 357–366.

35. Keller, J.N., and Mattson, M.P. (1998) Roles of Lipid Peroxidation in Modulation of Cellular Signaling Pathways, Cell Dysfunction, and Death in the Nervous System, *Rev. Neurosci. 9*, 105–116.

36. Musiek, E.S., Gao, L., Milne, G.L., Han, W., Everhart, M.B., Wang, D., Backlund, M.G., Dubois, R.N., Zanoni, G., Vidari, G., Blackwell, T.S., and Morrow, J.D. (2005) Cyclopentenone isoprostanes inhibit the inflammatory response in macrophages, *J. Biol. Chem.* doi:10.1074jbc.M504785200.

37. Basu, S., Whiteman, M., Mattey, D.L., and Halliwell, B. (2001) Raised Levels of F_2-Isoprostanes and Prostaglandin $F_{2\alpha}$ in Different Rheumatic Diseases, *Ann. Rheum. Dis. 60*, 627–631.

38. Gao, L., Zackert, W.E., Hasford, J.J., Danekis, M.E., Milne, G.L., Remmert, C., Reese, J., Yin, H., Tai, H.H., Dey, S.K., *et al.* (2003) Formation of Prostaglandins E_2 and D_2 *via* the Isoprostane Pathway: A Mechanism for the Generation of Bioactive Prostaglandins Independent of Cyclooxygenase, *J. Biol. Chem. 278*, 28479–28489.

39. Murphey, L.J., Williams, M.K., Sanchez, S.C., Byrne, L.M., Csiki, I., Oates, J.A., Johnson, D.H., and Morrow, J.D. (2004) Quantification of the Major Urinary Metabolite of PGE_2 by a Liquid Chromatographic/Mass Spectrometric Assay: Determination Of Cyclooxygenase-Specific PGE_2 Synthesis in Healthy Humans and Those with Lung Cancer, *Anal. Biochem. 334*, 266–275.

40. Musiek, E.S., and Morrow, J.D. (2005) F_2-Isoprostanes as Markers of Oxidant Stress: An Overview, in *Current Protocols in Toxicology* (Costa, L.G., Hodgson, E., Lawrence, D. and Reed, D.J., eds.), *Supp. 24, 17.5–17.6,* John Wiley & Sons, New York

41. Praticò, D., Barry, O.P., Lawson, J.A., Adiyaman, M., Hwang, S.W., Khanapure, S.P., Iuliano, L., Rokach, J., and FitzGerald, G.A. (1998) $IPF_{2\alpha}$-I: An Index of Lipid Peroxidation in Humans, *Proc. Natl. Acad. Sci. USA 95*, 3449–3454.

42. Morrow, J.D., and Roberts, J., II (1997) The Isoprostanes: Unique Bioactive Products of Lipid Peroxidation, *Prog. Lipid Res. 36*, 1–21.

43. Roberts, J., II, Moore, K.P., Zackert, W.E., Oates, J.A., and Mor-

row, J.D. (1996) Identification of the Major Urinary Metabolite of the F_2-Isoprostane 8-Iso-prostaglandin $F_{2\alpha}$ in Humans, *J. Biol. Chem. 271*, 20617–20620.

44. Morrow, J.D., Zackert, W.E., Yang, J.P., Kurhts, E.H., Callewaert, D., Dworski, R., Kanai, K., Taber, D., Moore, K., Oates, J.A., and Roberts, L.J. (1999) Quantification of the Major Urinary Metabolite of 15-F_{2t}-Isoprostane (8-iso-PGF$_{2\alpha}$) by a Stable Isotope Dilution Mass Spectrometric Assay, *Anal. Biochem. 269*, 326–331.

45. Morales, C.R., Terry, E.S., Zackert, W.E., Montine, T.J., and Morrow, J.D. (2001) Improved Assay for the Quantification of the Major Urinary Metabolite of the Isoprostane 15-F_{2t}-Isoprostane (8-iso-PGF$_{2\alpha}$) by a Stable Isotope Dilution Mass Spectrometric Assay, *Clin. Chim. Acta 314*, 93–99.

46. Kadiiska, M.B., Gladen, B.C., Baird, D.D., Germolec, D., Graham, L.B., Parker, C.E., Nyska, A., Wachsman, J.T., Ames, B.N., Basu, S., *et al*. (2005) Biomarkers of Oxidative Stress Study II. Are Oxidation Products of Lipids, Proteins, and DNA Markers of CCl_4 Poisoning? *Free Radic. Biol. Med. 38*, 698–710.

47. Kadiiska, M.B., Gladen, B.C., Baird, D.D., Graham, L.B., Parker, C.E., Ames, B.N., Basu, S., FitzGerald, G.A., Lawson, J.A., Marnett, L.J., *et al*. (2005) Biomarkers of Oxidative Stress Study III. Effects of the Nonsteroidal Anti-Inflammatory Agents Indomethacin and Meclofenamic Acid on Measurements of Oxidative Products of Lipids in CCl_4 Poisoning, *Free Radic. Biol. Med. 38*, 711–718.

48. Il'yasova, D., Morrow, J.D., Ivanova, A., and Wagenknecht, L.E. (2004) Epidemiological Marker for Oxidant Status: Comparison of the ELISA and the Gas Chromatography/Mass Spectrometry Assay for Urine 2,3-Dinor-5,6-dihydro-15-F_{2t}-isoprostane, *Ann. Epidemiol. 14*, 793–797.

49. Li, H., Lawson, J.A., Reilly, M., Adiyaman, M., Hwang, S.W., Rokach, J., and FitzGerald, G.A. (1999) Quantitative High Performance Liquid Chromatography/Tandem Mass Spectrometric Analysis of the Four Classes of F_2-Isoprostanes in Human Urine, *Proc. Natl. Acad. Sci. USA 96*, 13381–13386.

50. Bohnstedt, K.C., Karlberg, B., Wahlund, L.O., Jonhagen, M.E., Basun, H., and Schmidt, S. (2003) Determination of Isoprostanes in Urine Samples from Alzheimer Patients Using Porous Graphitic Carbon Liquid Chromatography–Tandem Mass Spectrometry, *J. Chromatogr. B 796*, 11–19.

51. Ohashi, N., and Yoshikawa, M. (2000) Rapid and Sensitive Quantification of 8-Isoprostaglandin $F_{2\alpha}$ in Human Plasma and Urine by Liquid Chromatography–Electrospray Ionization Mass Spectrometry, *J. Chromatogr. B 746*, 17–24.

52. Liang, Y., Wei, P., Duke, R.W., Reaven, P.D., Harman, S.M., Cutler, R.G., and Heward, C.B. (2003) Quantification of 8-Isoprostaglandin-$F_{2\alpha}$ and 2,3-Dinor-8-iso-prostaglandin-$F_{2\alpha}$ in Human Urine Using Liquid Chromatography–Tandem Mass Spectrometry, *Free Radic. Biol. Med. 34*, 409–418.

53. Morrow, J.D. (2005) Quantification of Isoprostanes as Indices of Oxidant Stress and the Risk of Atherosclerosis in Humans, *Arterioscler. Thromb. Vasc. Biol. 25*, 279–286.

54. Praticò, D., Tangirala, R.K., Rader, D.J., Rokach, J., and FitzGerald, G.A. (1998) Vitamin E Suppresses Isoprostane Generation *in vivo* and Reduces Atherosclerosis in ApoE-Deficient Mice, *Nat. Med. 4*, 1189–1192.

55. Praticò, D., Uryu, K., Leight, S., Trojanoswki, J.Q., and Lee, V.M. (2001) Increased Lipid Peroxidation Precedes Amyloid Plaque Formation in an Animal Model of Alzheimer Amyloidosis, *J. Neurosci. 21*, 4183–4187.

56. Kaikkonen, J., Porkkala-Sarataho, E., Morrow, J.D., Roberts, L.J., II, Nyyssonen, K., Salonen, R., Tuomainen, T.P., Ristonmaa, U., Poulsen, H.E., and Salonen, J.T. (2001) Supplementation with Vitamin E but Not with Vitamin C Lowers Lipid Peroxidation *in vivo* in Mildly Hypercholesterolemic Men, *Free Radic. Res. 35*, 967–978.

57. Patrono, C., and FitzGerald, G.A. (1997) Isoprostanes: Potential Markers of Oxidant Stress in Atherothrombotic Disease, *Arterioscler. Thromb. Vasc. Biol. 17*, 2309–2315.

58. Davì, G., Ciabattoni, G., Consoli, A., Mezzetti, A., Falco, A., Santarone, S., Pennese, E., Vitacolonna, E., Bucciarelli, T., Costantini, F., *et al*. (1999) *In vivo* Formation of 8-Iso-Prostaglandin $F_{2\alpha}$ and Platelet Activation in Diabetes Mellitus: Effects of Improved Metabolic Control and Vitamin E Supplementation, *Circulation 99*, 224–229.

59. Hansel, B., Giral, P., Nobecourt, E., Chantepie, S., Bruckert, E., Chapman, M.J., and Kontush, A. (2004) Metabolic Syndrome Is Associated with Elevated Oxidative Stress and Dysfunctional Dense High-Density Lipoprotein Particles Displaying Impaired Antioxidative Activity, *J. Clin. Endocrin. Metab. 89*, 4963–4971.

60. Morrow, J.D. (2003) Is Oxidant Stress a Connection Between Obesity and Atherosclerosis? *Arterioscler. Thromb. Vasc. Biol. 23*, 368–370.

61. Delanty, N., Reilly, M.P., Praticò, D., Lawson, J.A., McCarthy, J.F., Wood, A.E., Ohnishi, S.T., Fitzgerald, D.J., and FitzGerald, G.A. (1997) 8-Epi PGF$_{2\alpha}$ Generation During Coronary Reperfusion. A Potential Quantitative Marker of Oxidant Stress *in vivo*, *Circulation 95*, 2492–2499.

62. Quinn, J.F., Montine, K.S., Moore, M., Morrow, J.D., Kaye, J.A., and Montine, T.J. (2004) Suppression of Longitudinal Increase in CSF F_2-Isoprostanes in Alzheimer's Disease, *J. Alzheimer's Dis. 6*, 93–97.

63. Gniwotta, C., Morrow, J.D., Roberts, L.J., II, and Kühn, H. (1997) Prostaglandin F_2-like compounds, F_2-Isoprostanes, Are Present in Increased Amounts in Human Atherosclerotic Lesions, *Arterioscler. Thromb. Vasc. Biol. 17*, 3236–3241.

64. Morrow, J.D., Frei, B., Longmire, A.W., Gaziano, J.M., Lynch, S.M., Shyr, Y., Strauss, W.E., Oates, J.A., and Roberts, L.J., II. (1995) Increase in Circulating Products of Lipid Peroxidation (F_2-isoprostanes) in Smokers. Smoking as a Cause of Oxidative Damage, *N. Engl. J. Med. 332*, 1198–1203.

65. Schwedhelm, E., Bartling, A., Lenzen, H., Tsikas, D., Maas, R., Brümmer, J., Gutzki, F.M., Berger, J., Frölich, J.C., and Böger, R.H. (2004) Urinary 8-Iso-Prostaglandin $F_{2\alpha}$ as a Risk Marker in Patients with Coronary Heart Disease: A Matched Case-Control Study, *Circulation 109*, 843–848.

66. Gross, M., Steffes, M., Jacobs, D.R., Jr., Yu, X., Lewis, L., Lewis, C.E., and Loria, C.M. (2005) Plasma F_2-Isoprostanes and Coronary Artery Calcification: The CARDIA Study, *Clin. Chem. 51*, 125–131.

67. Vassalle, C., Petrozzi, L., Botto, N., Andreassi, M.G., and Zucchelli, G.C. (2004) Oxidative Stress and Its Association with Coronary Artery Disease and Different Atherogenic Risk Factors, *J. Int. Med. 256*, 308–315.

68. The Alpha-Tocopherol Beta Carotene Cancer Prevention Study Group. (1994) The Effect of Vitamin E and Beta Carotene on the Incidence of Lung Cancer and Other Cancers in Male Smokers, *N. Engl. J. Med. 330*, 1029–1035.

69. Gruppo Italiano per lo Studio della Sopravvivenza nell'Infarto miocardico (1999) Dietary Supplementation with n-3 Polyunsaturated Fatty Acids and Vitamin E After Myocardial Infarction: Results of the GISSI-Prevenzione Trial, *Lancet 354*, 447–455.

70. Yusuf, S., Dagenais, G., Pogue, J., Bosch, J., and Sleight, P. (2000) Vitamin E Supplementation and Cardiovascular Events in High-Risk Patients: The Heart Outcomes Prevention Evaluation Study Investigators, *New Engl. J. Med. 342*, 154–160.

71. Meagher, E.A., Barry, O.P., Lawson, J.A., Rokach, J., and FitzGerald, G.A. (2001) Effects of Vitamin E on Lipid Peroxidation in Healthy Persons, *JAMA 285*, 1178–1182.

ARTICLES

Paradoxical Effect of n-3-Containing Vegetable Oils on Long-Chain n-3 Fatty Acids in Rat Heart

Leslie G. Cleland[a,b], Robert A. Gibson[c], Janet Pedler[a], and Michael J. James[a,b,*]

[a]Hanson Institute and Rheumatology Unit, Royal Adelaide Hospital and [b]Department of Medicine, University of Adelaide, SA, Australia; and [c]Child Nutrition Research Centre, Child Health Research Institute, and Department of Paediatrics, University of Adelaide, Women's & Children's Hospital, North Adelaide, SA, Australia

ABSTRACT: Flaxseed, echium, and canola oils contain α-linolenic acid (18:3n-3, ALA) in a range of concentrations. To examine their effect on elevating cardiac levels of long-chain n-3 FA, diets based on these n-3-containing vegetable oils were fed to rats for 4 wk. Sunflower oil, which contains little ALA, was a comparator. Despite canola oil having the lowest ALA content of the three n-3-containing vegetable oils, it was the most potent for elevating DHA (22:6n-3) levels in rat hearts and plasma. However, the relative potencies of the dietary oils for elevation of EPA (20:5n-3) in heart and plasma followed the same rank order as their ALA content, i.e., flaxseed > echium > canola > sunflower oil. This paradox may be explained by lower ALA intake leading to decreased competition for $\Delta 6$ desaturase activity between ALA and the 24:5n-3 FA precursor to DHA formation.

Paper no. L9796 in *Lipids 40*, 995–998 (October 2005).

A substantial body of evidence exists regarding the cardiovascular benefits of dietary n-3 FA (1). Marine foods are an important source of long-chain (LC) n-3 FA that have cardioprotective and anti-inflammatory effects. However, stocks of many edible marine organisms are already stressed and marine sources could not sustain a generalized application of advice to increase dietary n-3 FA (2,3). For this reason, attention must be directed toward terrestrial food sources of dietary n-3 FA.

Edible oils such as flaxseed oil, and to a lesser extent canola oil, contain α-linolenic acid (18:3n-3, ALA), which can act as a metabolic precursor for the LC n-3 FA, EPA (20:5n-3) and DHA (22:6n-3) (4). In a study with piglets, we observed that ALA intake had a direct relationship to erythrocyte, liver, and brain EPA levels, but not to DHA levels in the same tissues. DHA levels were depressed with both low and high ALA intakes relative to intermediate intakes (5). Although the latter situation appeared paradoxical, we proposed that higher ALA intakes led to excessive ALA competition with the FA, 24:5n-3, for $\Delta 6$ desaturase metabolism to DHA (5).

If this proposal is correct, it can be hypothesized that canola oil with low ALA content may be disproportionately effective in elevating tissue DHA levels when compared with flaxseed oil with high ALA content. This is important when one considers the debate on whether cardioprotection from dietary n-3 fats

requires fish oil or whether ALA is beneficial also. For example, the conclusion in a recent article that fish or fish oil should remain the recommended source of n-3 FA for prevention of heart disease (6) was challenged in a response from the authors of the Lyon Diet Heart Study where the intervention involved, among other things, dietary ALA from rapeseed products (7).

Another approach to efficient elevation of cardiac LC n-3 FA with a vegetable oil is to use one that contains stearidonic acid (18:4n-3, SDA) because we demonstrated that dietary supplementation with purified SDA in healthy humans was approximately fourfold more effective in elevating tissue EPA than an equivalent dose of purified ALA (8).

An understanding of these issues of FA metabolism is pertinent to the pursuit of land-based sources of n-3 FA for their ability to elevate cardiac LC n-3 FA and to the understanding of current literature on dietary n-3 intake and adverse cardiac outcomes. This study involves a comparison of three n-3 FA-containing vegetable oils with regard to their ability to elevate EPA and DHA in rat heart. For context, the n-3-containing vegetable oils were compared with sunflower oil, which is rich in the 18-carbon n-6 FA, linoleic acid (18:2n-6, LA) and poor in n-3 FA.

MATERIALS AND METHODS

Animals. Six-week-old female Dark Agouti rats were obtained from the Institute of Medical and Veterinary Science Animal House. The study was approved by the Animal Ethics Committee of the Institute of Medical and Veterinary Science. Rats (4 per group) were provided with chow and water *ad libitum*. The diets were prepared by addition of various oils to previously described fat-free rat chow to achieve 5% w/w fat (9). The oils and their sources were: sunflower (Sunbeam, FloraFoods, Sydney, Australia), canola (Gold'n Canola, Meadow Lea Ltd., Sydney, Australia), echium (Grow Omega, Bridgewater, SA, Australia), and flaxseed (Melrose Laboratories, Mitcham, Victoria, Australia). The FA compositions of the oils are detailed in Table 1. There was no statistically significant difference in weights between the groups either at baseline or after the 4-wk dietary intervention. The average baseline weight was 112.6 ± 4.5 g (mean ± SD) and the average weight gain during the trial was 51 ± 3.3 g.

Procedures. After 4 wk of consumption of the test diets, blood was obtained by cardiac puncture under fluothane anesthesia, and the heart was then removed. Plasma or diced heart

TABLE 1
FA Composition of Test Diets

FA	Sunflower	Canola	Echium	Flaxseed
			% of total FA	
16:0	5.7	4.1	7.0	5.5
18:0	4.2	1.9	3.1	4.2
Total saturates	11.3	7.3	10.4	10.3
18:1n-9	31.6	57.9	13.9	16.1
Total monounsaturates	32.6	63.1	16.0	17.1
18:2n-6 (linoleic acid)	55.6	19.6	15.5	15.9
18:3n-6 (γ-linolenic acid)	<0.1	0.1	10.0	<0.1
Total n-6	55.6	19.8	25.6	16.0
18:3n-3 (α-linolenic acid)	0.4	9.7	35.4	56.5
18:4n-3 (stearidonic acid)	<0.1	<0.1	12.5	<0.1
20:5n-3 (EPA)	<0.1	<0.1	<0.1	<0.1
22:5n-3 (docosapentaenoic acid)	<0.1	<0.1	<0.1	<0.1
22:6n-3 (DHA)	<0.1	<0.1	<0.1	<0.1
Total n-3	0.4	9.7	48.0	56.6

was then subjected to lipid extraction in chloroform/methanol (10). Cardiac FA are known to have reached steady state by 4 wk of dietary intervention in rats (11).

FA analysis. Phospholipids from all extracts were separated from other lipid classes by TLC and transesterified by methanolysis to form the FAME. These were separated and quantified by GLC as described (10).

RESULTS

Dietary FA. This study used four vegetable oils containing 18-carbon n-3 FA. Sunflower oil contained little measurable ALA, canola had a low content of ALA, and echium and flaxseed had increasingly higher amounts. In addition, echium oil contained 12.5% SDA (Table 1). Canola, echium, and flaxseed oils all had similar amounts of LA, and these were much lower than the LA content of sunflower oil (Table 1).

LC n-3 FA in the heart and plasma phospholipids. The relative potencies of the three n-3-containing vegetable oils in raising cardiac EPA was flaxseed > echium > canola > sunflower, which reflected the rank order of their ALA content (Fig. 1). For elevation of cardiac docosapentaenoic acid (22:5n-3; DPA), the echium and flaxseed diets were similar to each other and both were approximately twice as effective as canola oil (Fig. 1).

Regardless of diet, DHA was the major n-3 PUFA in the heart. Importantly, the DHA level achieved with the canola diet (15.5% total FA) was significantly greater than that achieved with the echium (12.7%) and flaxseed (12.3%) diets even though echium and flaxseed had ALA contents 3.6- and 5.8-fold greater than that of canola (Fig. 1, Table 1). In addition, echium contained SDA.

The relative efficacy of each of the n-3-containing vegetable oils in elevating plasma phospholipid LC n-3 FA was the same as that for the cardiac FA. Of the three n-3-containing vegetable oils, canola oil was the least effective for elevating EPA and DPA but the most effective for elevating DHA (Fig. 1).

n-6 FA in the heart and plasma phospholipids. In both the

heart and plasma phospholipids, AA and the total n-6 FA were highest in the sunflower oil group and lowest in the flaxseed oil group (Table 2).

DISCUSSION

A central purpose of this study was to examine the relative efficacy of vegetable oils containing differing amounts of ALA and SDA in elevating cardiac LC n-3 PUFA. This is considered relevant because of the known cardioprotective benefits of fish oil that contains LC n-3 PUFA, particularly DHA (1). One of
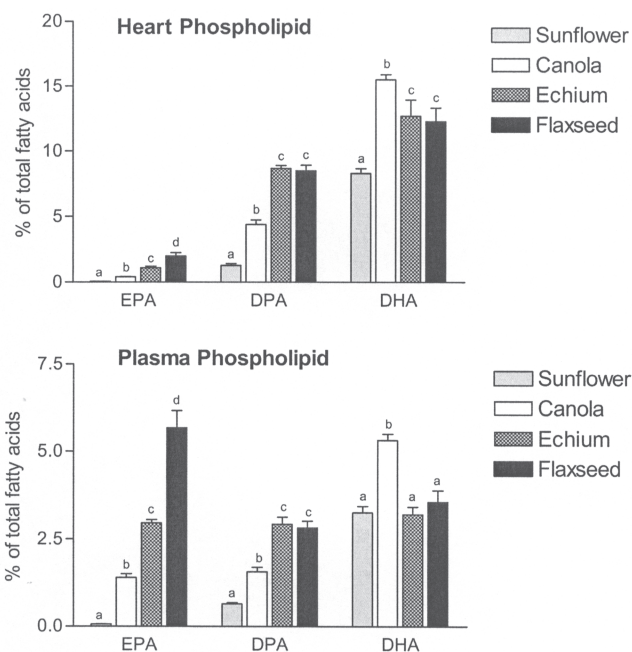
FIG. 1. Effect of vegetable oil diets on long-chain n-3 FA content of heart and plasma phopholipids. Bars and vertical lines represent means + SD. For each FA, bars with different letters are significantly different from each other ($P < 0.05$; ANOVA followed by Newman–Keuls multiple comparison test). DPA, docosapentaenoic acid.

TABLE 2
Heart and Plasma Phospholipid n-6 FA Content

FA		Sunflower	Canola	Echium	Flaxseed
		% of total FA[a]			
20:4n-6 (arachidonic acid)	Heart	23.9 ± 1.0^a	20.3 ± 0.6^b	21.0 ± 0.8^b	15.3 ± 0.6^c
	Plasma	23.8 ± 0.8^a	15.9 ± 0.9^b	17.5 ± 0.6^c	8.8 ± 1.3^d
Total n-6	Heart	47.8 ± 1.1^a	35.9 ± 1.2^b	$34.3 \pm 1.1^{b,c}$	33.0 ± 1.7^c
	Plasma	38.2 ± 1.1^a	28.0 ± 1.4^b	28.6 ± 0.4^b	23.9 ± 1.9^c

[a]Within each row, different letters indicate statistically significant difference from each other ($P < 0.05$, ANOVA followed by Newman–Keuls multiple comparison test).

the most striking cardioprotective effects of fish oil is that for sudden death as reported in the GISSI Prevenzione trial (12). The possibility that the benefit of fish oil is due to a direct antiarrhythmic effect of cardiac LC n-3 PUFA elevated by dietary intervention is supported by antiarrhythmic effects of dietary n-3 FA observed in rats and marmosets (13,14).

The relative potencies of the vegetable oils in elevating EPA appear to be proportional to their ALA contents. Because echium also contains 12.5% SDA, a FA that in purified form was fourfold more effective than ALA at elevating tissue EPA in human volunteers (8), it might be expected that echium oil would be at least as effective as flaxseed oil in elevating EPA. This was not the case. It is possible that the 10% γ-linolenic acid (GLA, 18:3n-6) contained in echium oil competed with SDA for enzymic metabolism to EPA. However, if this were the case for EPA, it was not reflected in cardiac DPA levels where echium had a comparable effect to flaxseed oil and both were superior to canola oil. The equivalent effects of echium and flaxseed oils in elevating cardiac DPA levels, despite echium having lower levels of ALA than flaxseed oil, suggest that the SDA contained in echium contributed to the elevation in cardiac DPA.

In each of the dietary groups, myocardial content of DHA was higher than that of DPA and EPA. Preferential accumulation of cardiac DHA in rats has been reported previously (15). However, the finding that canola oil was superior to flaxseed and echium oil in raising cardiac DHA levels appears surprising since canola oil has a much lower content of ALA and SDA than either flaxseed or echium oils. It has been reported that DHA levels in piglet plasma, red blood cells, liver, and brain had a bimodal relationship with dietary ALA. In fact, tissue

DHA increased as ALA intake decreased to a certain level (5). The authors attributed this phenomenon to decreased competition from ALA for 24:5n-3 metabolism by Δ6 desaturase to DHA (5) (Fig. 2). The results of the present study provide support for this proposition. LA also is a substrate for the Δ6 desaturase. However, it is unlikely to be a confounder of the proposed ALA/24:5n-3 competition for the Δ6 desaturase because the three n-3-containing vegetable oils had similar LA contents, with canola having the highest value (Table 1).

The observed effect of the canola diet in raising cardiac DHA is noteworthy since DHA is regarded as the key n-3 FA for cardiomyocyte membrane stability (15). These data are pertinent to the findings of the Lyon Diet Heart Study in which canola-based products were used in the treatment group, along with advice on other dietary changes. The comparator group received the standard advice from their doctor, which was presumed to follow the American Heart Association prudent diet. The dietary intervention in the Lyon Diet Heart Study showed a protective effect against cardiac death to an extent leading to premature termination for the trial after the planned interim analysis (16). The only plasma FA associated with the positive outcome was ALA (17). The results of the present study suggest that the ALA intake from canola oil use may have been very effective in elevating cardiac DHA content in the Lyon Diet Heart Study. This adds considerably to the debate on whether fish oil n-3 fats should be the first-line or only recommended source of n-3 FA for prevention of heart disease (6,7).

Overall, this study provides a basis for the use of ALA-containing oils in human diets for cardioprotection. Echium may prove to be a useful oil for elevating EPA and DPA and for providing GLA. This may be especially useful for anti-inflammatory
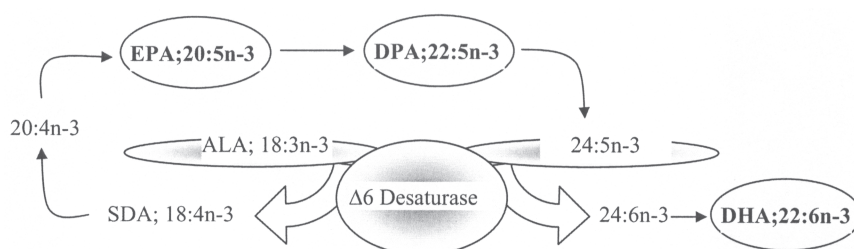
FIG. 2. Scheme illustrating the potential for α-linolenic acid (ALA) to influence DHA formation in two ways; one as a progenitor and one as a competitor (adapted from Ref. 5). SDA, stearidonic acid; for other abbreviation see Figure 1.

applications. Whereas all three oils increased cardiac DHA content and therefore may provide protection against cardiac death in at-risk populations, canola oil was the most effective in elevating DHA. Thus, these oils may provide useful alternatives and/or adjuncts to fish in elevating tissue LC n-3 PUFA for various health benefits.

ACKNOWLEDGMENT

REFERENCES

1. Kris-Etherton, P.M., Harris, W.S., and Appel, L.J. (2002) Fish Consumption, Fish Oil, Omega-3 Fatty Acids, and Cardiovascular Disease, *Circulation 106*, 2747–2757.
2. Naylor, R.L., Goldburg, R.J., Primavera, J.H., Kautsky, N., Beveridge, M.C.M., Clay, J., Folke, C., Lubchenco, J., Mooney, H., and Troell, M. (2000) Effect of Aquaculture on World Fish Supplies, *Nature 405*, 1017–1024.
3. Pauly, D., Christensen, V., Guenette, S., Pitcher, T.J., Sumaila, U.R., Walters, C.J., Watson, R., and Zeller, D. (2002) Towards Sustainability in World Fisheries, *Nature 418*, 689–695.
4. Uauy, R., Mena, P., Wegher, B., Nieto, S., and Salem, N., Jr. (2000) Long Chain Polyunsaturated Fatty Acid Formation in Neonates: Effect of Gestational Age and Intrauterine Growth, *Pediatr. Res. 47*, 127–135.
5. Blank, C., Neumann, M.A., Makrides, M., and Gibson, R.A. (2002) Optimizing DHA Levels in Piglets by Lowering the Linoleic Acid to α-Linolenic Acid Ratio, *J. Lipid Res. 43*, 1537–1543.
6. Brouwer, I.A., Katan, M.B., and Zock, P.L. (2004) Dietary α-Linolenic Acid Is Associated with Reduced Risk of Fatal Coronary Heart Disease, but Increased Prostate Cancer Risk: A Meta-analysis, *J. Nutr. 134*, 919–922.
7. de Lorgeril, M., and Salen, P. (2004) α-Linolenic Acid, Coronary Heart Disease, and Prostate Cancer, *J. Nutr. 134*, 3385–3386.
8. James, M.J., Ursin, V.M., and Cleland, L.G. (2003) Metabolism of Stearidonic Acid in Human Subjects: Comparison with the Metabolism of Other n-3 Fatty Acids, *Am. J. Clin. Nutr. 77*, 1140–1145.
9. James, M.J., Cleland, L.G., Gibson, R.A., and Hawkes, J.S. (1991) Interaction Between Fish and Vegetable Oils in Relation to Rat Leucocyte Leukotriene Production, *J. Nutr. 121*, 631–637.
10. Mantzioris, E., James, M.J., Gibson, R.A., and Cleland, L.G. (1994) Dietary Substitution with an α-Linolenic Acid-Rich Vegetable Oil Increases Eicosapentaenoic Acid Concentrations in Tissues, *Am. J. Clin. Nutr. 59*, 1304–1309.
11. Owen, A.J., Peter-Przyborowska, B.A., Hoy, A.J., and McLennan, P.L. (2004) Dietary Fish Oil Dose- and Time-Response Effects on Cardiac Phospholipid Fatty Acid Composition, *Lipids 39*, 955–961.
12. GISSI Prevenzione Investigators (1999) Dietary Supplementation with n-3 Polyunsaturated Fatty Acids and Vitamin E After Myocardial Infarction: Results of the GISSI-Prevenzione Trial, *Lancet 354*, 447–455.
13. McLennan, P.L. (1993) Relative Effects of Dietary Saturated, Monounsaturated, and Polyunsaturated Fatty Acids on Cardiac Arrhythmias in Rats, *Am. J. Clin. Nutr. 57*, 207–212.
14. McLennan, P.L., Bridle, T.M., Abeywardena, M.Y., and Charnock, J.S. (1992) Dietary Lipid Modulation of Ventricular Fibrillation Threshold in the Marmoset Monkey, *Am. Heart J. 123*, 1555–1561.
15. McLennan, P.L. (2001) Myocardial Membrane Fatty Acids and the Antiarrhythmic Actions of Dietary Fish Oil in Animal Models, *Lipids 36*, S111–S114.
16. de Lorgeril, M., Renaud, S., Mamelle, N., Salen, P., Martin, J.L., Monjaud, I., Guidollet, J., Touboul, P., and Delaye, J. (1994) Mediterranean α-Linolenic Acid-Rich Diet in Secondary Prevention of Coronary Heart Disease, *Lancet 343*, 1454–1459.
17. de Lorgeril, M., Salen, P., Martin, J.L., Monjaud, I., Delaye, J., and Mamelle, N. (1999) Mediterranean Diet, Traditional Risk Factors, and the Rate of Cardiovascular Complications After Myocardial Infarction: Final Report of the Lyon Diet Heart Study, *Circulation 99*, 779–785.

Microtubular Integrity Differentially Modifies the Saturated and Unsaturated Fatty Acid Metabolism in Cultured Hep G2 Human Hepatoma Cells

Carlos A. Marra* and María J.T. de Alaniz

INIBIOLP (Instituto de Investigaciones Bioquímicas de La Plata), Consejo Nacional de Investigaciones Científicas y Técnicas (CONICET)-UNLP, Facultad de Ciencias Médicas, Universidad Nacional de La Plata, La Plata, Argentina

ABSTRACT: The influence of cytoskeleton integrity on the metabolism of saturated and unsaturated FA was studied in surface cultures and cell suspensions of human Hep G2 hepatoma cells. We found that colchicine (COL), nocodazol, and vinblastin produced a significant inhibition in the incorporation of labeled saturated FA, whereas incorporation of the unsaturated FA remained unaltered. These microtubule-disrupting drugs also diminished Δ9-, Δ5-, and Δ6-desaturase capacities. The effects produced by COL were dose (0–50 μM) and time (0–300 min) dependent, and were antagonized by stabilizing agents (phalloidin and DMSO). Dihydrocytochalasin B (20 μM) was tested as a microfilament-disrupting drug and produced no changes in either the incorporation of [14C]FA or the desaturase conversion of the substrates. We hypothesized that the interactions between cytoskeleton and membrane proteins such as FA desaturases may explain the functional organization, facilitating both substrate channeling and regulation of unsaturated FA biosynthesis.

Paper no. L9767 in *Lipids 40*, 999–1006 (October 2005).

The specialized functions of differentiated mammalian cells require the utilization of FA. These FA, particularly PUFA from the linoleic and α-linolenic families, are essential structural components of the membranes that determine their physical and chemical characteristics (1–4). Within the cells, the endoplasmic reticulum membrane is the site of residence of the elongating FA enzymes and the Δ9-, Δ6-, and Δ5-desaturases (5) that evoke monounsaturated FA biosynthesis and polyunsaturation, on which the structure and fluidity of the membranes depend. Moreover, PUFA and their CoA derivatives either directly or indirectly regulate the activity of many cellular processes, including membrane receptors, enzymes, ion channels, cell differentiation, cellular development, and gene expression (6–9), and by means of their metabolites, they also serve as intracellular signaling molecules (10–12). Because of these crucial functional roles, it is important to understand the mechanism(s) in which cells are involved in the selective incorporation and conversion of FA.

Cellular uptake of FA may be a multistep process that involves a variety of membrane-associated events (13–19). On the other hand, reorganization of the cytoskeleton in response to intra- or extracellular stimuli has been recognized as critical to a variety of biological effects. However, little information is available concerning the relationship between the cellular metabolism of FA and the integrity of the cytoskeleton. In this regard, several recent investigations have described the role that phospholipids may play in the organization of the cytoskeletal network (20,21); however, much less attention has been given to the influence of cytoskeleton integrity on FA metabolism. Taking these considerations into account, we studied the influence of cytoskeleton integrity on the metabolism (elongation–desaturation) of saturated and unsaturated FA in a human hepatoblastoma cell line under controlled incubation conditions.

MATERIALS AND METHODS

Chemicals. [1-14C]FA [palmitic, stearic, linoleic, α-linolenic, and dihomo-γ-linolenic (DGLA) acids, 98–99% pure, 50–60 mCi/mmol] were obtained from Amersham Biosciences (Buckinghamshire, United Kingdom). Colchicine (COL) [ring C, methoxy-3H] (87 mCi/mmol) was from NEN Research Products (DuPont, Boston, MA). Unlabeled FA were provided by Nu-Chek-Prep (Elysian, MN). All acids were stored in benzene under a nitrogen atmosphere at −20°C. The concentrations and purities were routinely checked by both gas–liquid radiochromatography and liquid-scintilliation counting. Mass determinations were performed by GLC of FAME prepared in the presence of internal standards. FAME mixtures, HEPES, delipidated serum albumin (BSA; fraction V from bovine), minimum essential Eagle's medium (MEM) with Earle's salts, L-glutamine, unlabeled COL, β-lumicolchicine, vinblastin (sulfate) (VBS), nocodazole (methyl-(5-[2-thienylcarbony]-1-H-benzimidazole-2-yl)-carbamate) (NCD), dihydrocytochalasin-B (DHCB), DMSO, phalloidin (from *Amanita phalloides*; PHAL), FBS, Earle's balanced salts, and improved MEM-zinc option (IMEM-Zo) were from Sigma Chemical Co. (St. Louis,

*To whom correspondence should be addressed at Facultad de Medicina, Universidad Nacional de La Plata, 60 y 120 (1900) La Plata, Argentina. Phone number: +54-221-482-4894/423-6967; FAX: +54-221-258988 E-mail: camarra@atlas.med.unlp.edu.ar

Abbreviations: ACS, acyl-CoA synthetase; COL, colchicine; DGLA, dihomo-γ-linolenic acid; DHCB, dihydrocytochalasin B; IMEM-Zo, improved minimal essential medium-zinc option; MEM, minimal essential medium; NCD, nocodazole; PHAL, phalloidin; VBS, vinblastin (sulfate).

MO). All solvents were of HPLC grade and were provided by Carlo Erba (Milano, Italy).

Cell culture and general experimental procedure with labeled FA. Hep G2 hepatoblastoma cells were grown in surface cultures using 70-cm^2 flasks at 37°C with 20 mL MEM supplemented with 10% (vol/vol) FBS, 0.30 g/L glutamine, and 25 mM HEPES. One type of experiment was performed using Hep G2 cells in surface cultures. When the cells were at the logarithmic phase of growth (approx. 72 h after seeding), the culture medium was replaced by IMEM-Zo minus linoleic acid and containing HEPES (25 mM final concentration). After a short period of adaptation (incubation for 30 min at 37°C under slow agitation in a metabolic incubator), considered arbitrarily as "zero time," the medium was aspirated and replaced by fresh medium at 37°C supplemented with [1-^{14}C]palmitate, [1-^{14}C]stearate, [1-^{14}C]linoleate, [1-^{14}C]α-linolenate, or [1-^{14}C]DGLA (1 μM final concentration). FA were added as sodium salt bound to delipidated albumin (0.33 μM final concentration) according to Spector *et al.* (22) and treated, or not, with different cytoskeletal-disrupting drugs as described in the following section. The incubation was stopped at different times (0 to 300 min) following the method of Samuel *et al.* (23). After separation of the incubation medium (5 min in the cold at 2000 × *g*), the cells were washed twice with 5 mL of cold Earle's balanced salt solution (pH 7.40) containing 0.5% BSA. An aliquot of each cellular suspension was taken for protein measurements following the method of Lowry *et al.* (24). Control flasks were supplemented with defatted BSA at the same concentration used in the experimental flasks. Radioactivity recovered from the last wash routinely represented less than 6% of the total radioactivity remaining bound to the cells (radioactivity incorporated). Other incubations were done in suspended Hep G2 cells. The cells were mechanically detached using a conventional sterile procedure and suspended (5 × 10^6 cells/25-mL siliconized flask) in IMEM-Zo (5 mL final volume) following a method described previously (25). The cells were supplemented with BSA-complexed FA and/or cytoskeletal-modifying drugs, as mentioned.

Incubations with cytoskeletal-disrupting agents. To study the effect of cytoskeleton integrity on the incorporation and conversion of labeled [1-^{14}C]FA, surface cultures of Hep G2 cells at the logarithmic phase of growth were treated with either COL (10 μM) or DHCB (20 μM), which was added at zero time. After a day, the medium was changed to fresh medium supplemented with the same drug together with labeled BSA-complexed FA at a 1-μM final concentration. The surface cultures were incubated for another 16 h, then processed for lipid analyses as already described. Other experiments were performed with suspensions of Hep G2 cells (5 × 10^6 cells/5 mL of IMEM-Zo) that were treated with microtubule-depolymerizing (inhibitors of the microtubule-tubulin assembly) or microfilament-disrupting agents using the following experimental approaches. In one set of experiments, COL (10 μM) was added at zero time together with either [1-^{14}C]palmitate (1 μM) or [1-^{14}C]DGLA (1 μM). After different periods of incubation (0 to 300 min), samples were taken and analyzed for incorporation and metabolic conversion of the labeled FA. Other incubations were done by adding COL (10 μM) at zero time and supplementing the media 5 h later with 1 μM [1-^{14}C]FA (palmitate or DGLA). Simultaneous incubation with COL and FA was prolonged for another hour, and the incorporation and metabolic conversion of [^{14}C]FA were then studied. This scheme was also used to study the effect of VBS (50 μM) or NCD (50 μM) as a microtubule-disrupting drug, DMSO (50 mM) as a microtubule-stabilizing agent, PHAL (1 μM) as an actin-stabilizing drug, DHCB (20 μM) as a microfilament (actin)-disrupting drug, and β-lumicolchicine (10 μM) as an inactive isomer of COL. Some of the agents mentioned were also used in competition experiments in which the first drug with a stabilizing effect (DMSO 50 mM) was added at zero time, and after 60 min the second drug with microtubule-disrupting activity (COL, 10 μM; VBS, 50 μM; or NCD, 50 μM) was added. The incubations were continued in the presence of both types of drugs for 5 h, and the [1-^{14}C]FA (palmitate or DGLA) was then added at a 1 μM concentration and incubated for another 60 min.

Lipid analyses. Washed cell pellets (5 min at 2,000 × *g*) from either surface cultures or suspended cells were immediately treated with 4 mL of Folch reagent (26) and shaken vigorously. The resulting emulsions were transferred to ice-cold tubes and processed to obtain cellular lipid extracts (27). After dissolving the lipid residues in an exact volume of 2 mL Folch reagent, the appropriate aliquots (20–100 μL) were transferred directly into scintillation vials containing 10 mL of AQS II$^®$ Scintillation Cocktail from Amersham Pharmacia Biotech (Buckinghamshire, United Kingdom) for radioactivity measurements. A Beckman LS-5801 liquid scintillation counter with 95% efficiency for ^{14}C was used. Differences in the incorporation of ^{14}C values of flasks from the same experimental group did not exceed 6%. Aliquots of the lipid extracts were methylated with BF$_3$/MeOH according to the method of Morrison and Smith (28). To determine the metabolic elongation–desaturation of the FA incubated, the distribution of radioactivity among the obtained FAME was analyzed using a radiochromatograph (Varian Star 3400 CX) in tandem with a proportional gas detector (GC-Ram; Inus System Inc.), following the method described in a previous paper (29).

Other analytical procedures. Cell viability (>96%) was assessed by the exclusion tests of trypan blue (30) or erythrosine B (31). To quantify the amount of polymerized and depolymerized forms of tubulin in Hep G2 cells under different incubation conditions, the radiochemical method of Pipeleers *et al.* (32) was performed with the modifications described by Rajan and Menon (33). Cellular protein was measured by the method of Lowry *et al.* (24).

Software and calculations. Data are reported as the mean and SEM calculated from four independent analyses. Systat software (version 8.0 for Windows; SPSS Science, Chicago, IL) was used for statistical studies (correlation coefficients for nonlinear curve fitting, linear regressions, Student's *t*-test, and ANOVA). Data were also plotted and analyzed using Sigma Scientific Graphing Software (version 8.0) from Sigma Chemical Co.

TABLE 1
Content of Free and Polymerized Tubulin in Hep G2 Cells
Treated with Cytoskeleton-Disrupting or -Stabilizing Agents[a]

| Enzyme | pmol tubulin/10^6 cells | | |
	Free	Polymerized	Total
Control	15 ± 2	59 ± 3	74 ± 5
Colchicine (10 µM)	99 ± 4*	Trace*	99 ± 4
Vinblastin (50 µM)	102 ± 6*	8 ± 1*	110 ± 7*
Nocodazol (50 µM)	94 ± 5*	3 ± 0.4*	97 ± 6
DMSO (50 mM)	4 ± 1*	83 ± 5*	87 ± 7
Dihydrocytochalasin B (20 µM)	18 ± 3	54 ± 4	72 ± 6
Phalloidin (1 µM)	10 ± 2	61 ± 7	71 ± 5

[a]Free and polymerized tubulins were determined radiochemically as described in the Materials and Methods section. Suspensions of Hep G2 cells were incubated for 6 h with the drugs indicated. Results are expressed as pmol tubulin/10^6 cells and are the mean ± 1 SEM of four independent assays. *Significantly different from control data; $P < 0.01$. "Trace" means <1%.

RESULTS

Cytoskeleton integrity and cell viability. The experimental conditions provoked significant alterations in cytoskeleton integrity (Table 1). COL (10 µM), VBS (50 µM), and NCD (50 µM) produced increases of 660, 680, and 627%, respectively, in the content of free tubulin compared with control cells. The amount of polymerized tubulin in COL-, VBS-, or NCD-treated Hep G2 cells was concomitantly reduced, whereas the total tubulin was increased in the three treatments by 18, 31, and 16% compared with control cells, although only in the case of VBS-treated cells was the increase statistically significant. DMSO (50 mM) increased the content of polymerized tubulin by 41%, whereas PHAL (1 µM) or DHCB (20 µM) produced no significant change in the amount of free or polymerized tubulin. None of the drugs assayed produced significant modifications in cell viability as judged by the criterion of the trypan blue or erythrosine B exclusion test (data not shown).

Incorporation and conversion of labeled FA and cytoskeleton integrity. The effect of cytoskeletal-disrupting agents on the incorporation and metabolic conversion of [^{14}C]FA was studied in surface (Tables 2, 3) and suspension (Table 4) cultures of Hep G2 cells. The amount of [^{14}C]FA incorporated by cultured Hep G2 cells after a 16-h period of incubation with 1 µM FA was equivalent to that incorporated after a 5-h period of incubation in suspension experiments. This fact may be ascribed to differences in both the surface of the membrane exposed to the incubation medium and to the diffusional characteristics of the experimental models. In surface Hep G2 cultures, the COL, VBS, or NCD treatment produced decreases of 34 to 40% in the incorporation of ^{14}C from saturated FA, whereas the labeling in cells incubated with unsaturated FA remained unchanged compared with control experiments (data not shown). DHCB did not modify the cellular-associated labeling of any of the FA studied. Saturated FA (palmitate and stearate) were transformed into the corresponding monoenoates (Δ9-desaturase activities) with a high efficiency of conversion (19.8 and 28.6% of palmitoleate and oleate, respectively) (Table 2). The COL, VBS, or NCD treatments produced a significant reduction in the formation of both monoenoates (−33 to −49% change compared with control incubations), whereas perturbation of the microfilament assembly by incubating the cells with DHCB produced no significant changes (Table 2). The other FA desaturase activities were also affected by microtubule depolymerization (Table 3). The conversion of linoleate to γ-linolenate and the formation of 18:4n-3 at the expense of α-linolenate (Δ6-desaturase activities) were reduced by COL, VBS, or NCD treatments, as suggested by the increases observed in the elongation routes that yielded C-20 and C-22 metabolites generated from these precursors (20:2n-6 plus 22:2n-6, and 20:3n-3 plus 22:3n-3, respectively). A substantial decrease in the formation of higher n-3 metabolites of the desaturation pathway (20:5n-3 and 22:5n-3) was also noticeable. Production of arachidonate (Δ5-desaturase activity)

TABLE 2
Metabolic Conversion of Saturated [1-^{14}C]FA in Surface Cultures of Hep G2 Cells Treated with Cytoskeleton-Disrupting Agents[a]

| Labeled metabolites | [1-^{14}C]Palmitate | | | | | [1-^{14}C]Stearate | | | | |
	C	COL	VBS	NCD	DHCB	C	COL	VBS	NCD	DHCB
16:0	56.4 ± 2.7	72.8 ± 3.4*	74.5 ± 3.0*	75.1 ± 2.6*	58.2 ± 1.8	3.0 ± 0.2	2.9 ± 0.2	3.1 ± 0.3	2.7 ± 0.2	3.5 ± 0.2
16:1	19.8 ± 1.1	10.1 ± 0.8*	10.4 ± 0.9*	7.7 ± 0.6*	16.5 ± 1.0	Trace	Trace	0.1 ± 0.02	Trace	0.2 ± 0.0
18:0	18.5 ± 2.7	14.9 ± 3.4	13.0 ± 2.8*	15.5 ± 3.0*	19.2 ± 1.6	68.4 ± 3.4	77.6 ± 2.7*	79.2 ± 2.9*	78.6 ± 2.8*	68.3 ± 3.1
18:1	5.3 ± 1.1	2.2 ± 0.5*	2.1 ± 0.3*	1.7 ± 0.4*	6.1 ± 0.8	28.6 ± 2.0	19.5 ± 1.4*	17.6 ± 2.0*	18.7 ± 1.5*	28.0 ± 2.3

[a]Surface cultures of Hep G2 cells were incubated (24 h) in the presence of colchicine (COL) (10 µM), vinblastin (sulfate) (VBS) (50 µM), nocodazole (NCD) (50 µM), or dihydrocytochalasin B (DHCB) (20 µM). [^{14}C]FA (1 µM concentration) complexed to delipidated BSA (1:3 BSA/FA; 0.33 µM final concentration of BSA) were added and the incorporation was continued for another 16 h. Control bottles (C) received only complexed FA. Results are expressed as the percentage conversion of the corresponding substrate and are the mean of four independent incubations ± 1 SEM. *Significantly different with respect to C; $P < 0.01$.

TABLE 3
Metabolic Conversion of Unsaturated [1-^{14}C]FA in Surface Cultures of Hep G2 Cells Treated with Cytoskeleton-Disrupting Agents[a]

Labeled metabolites	[1-^{14}C]Linoleate					[1-^{14}C]α-Linolenate					[1-^{14}C]DGLA				
	C	COL	VBS	NCD	DHCB	C	COL	VBS	NCD	DHCB	C	COL	VBS	NCD	DHCB
16:0	2.0 ± 0.1	2.5 ± 0.2	2.7 ± 0.2	2.5 ± 0.3	1.8 ± 0.1	1.5 ± 0.1	2.0 ± 0.1	1.8 ± 0.1	2.1 ± 0.2	1.3 ± 0.1	1.0 ± 0.2	1.3 ± 0.1	0.9 ± 0.1	1.5 ± 0.2	1.1 ± 0.2
16:1	1.0 ± 0.1	Trace*	0.1 ± 0.01*	Trace*	0.6 ± 0.1	1.0 ± 0.2	Trace*	0.1 ± 0.02*	Trace*	0.1 ± 0.0*	Trace	Trace	Trace	Trace	0.1 ± 0.0
18:0	2.0 ± 0.1	2.0 ± 0.2	1.9 ± 0.2	2.0 ± 0.3	1.7 ± 0.0	2.0 ± 0.2	2.5 ± 0.2	2.2 ± 0.1	2.4 ± 0.2	2.2 ± 0.2					
18:1	2.0 ± 0.2	Trace*	Trace*	0.1 ± 0.02*	2.2 ± 0.1	1.5 ± 0.1	Trace*	Trace*	0.1 ± 0.03*	1.6 ± 0.1					
18:2n-6	78.6 ± 4.0	83.8 ± 3.1	83.1 ± 3.5	83.5 ± 4.5	78.2 ± 3.5										
18:3n-3						48.7 ± 3.0	48.3 ± 4.1	48.9 ± 3.3	45.3 ± 4.0	49.3 ± 2.8					
18:4n-3						Trace	Trace	Trace	Trace	Trace					
20:2n-6	4.8 ± 0.3	6.4 ± 0.3*	7.0 ± 0.3*	6.8 ± 0.3*	5.0 ± 0.3										
20:3n-3						9.5 ± 0.9	14.0 ± 1.1*	13.7 ± 0.8*	15.3 ± 0.7*	8.9 ± 0.8					
20:3n-6	4.1 ± 0.1	1.5 ± 0.2*	1.1 ± 0.1*	1.4 ± 0.1*	4.4 ± 0.1						73.1 ± 2.0	82.2 ± 3.1*	83.3 ± 2.9*	82.5 ± 3.3*	71.7 ± 2.4
20:4n-6	3.0 ± 0.3	Trace*	0.1 ± 0.2*	Trace*	3.1 ± 0.2						25.9 ± 1.0	16.5 ± 1.7*	15.8 ± 1.5*	16.0 ± 2.0*	27.1 ± 1.3
Σ 20:4n-3						22.8 ± 2.0	24.0 ± 2.2	23.7 ± 2.1	25.0 ± 3.0	23.6 ± 1.5					
20:5n-3						11.0 ± 1.3	7.0 ± 0.8*	6.8 ± 0.5*	7.2 ± 0.7*	12.2 ± 1.2					
22:2n-6	2.5 ± 0.2	3.8 ± 0.2*	4.0 ± 0.2*	3.7 ± 0.2*	3.0 ± 0.3										
22:3n-3						1.0 ± 0.1	2.2 ± 0.2*	2.8 ± 0.2*	2.5 ± 0.2*	0.8 ± 0.1					
22:4n-6	Trace		Trace		Trace										
22:5n-3						1.0 ± 0.2	Trace*		0.1 ± 0.02*	Trace					

[a]Surface cultures of Hep G2 cells were incubated (24 h) in the presence of COL (10 µM), VBS (50 µM), NCD (50 µM), or DHCB (20 µM). [1-^{14}C]FA (1 µM concentration) complexed to delipidated BSA (1:3 BSA/FA; 0.33 µM final concentration of BSA) were added and the incubation was continued for another 16 h. Control bottles (C) received only complexed FA. Results are expressed as the percentage conversion of the corresponding substrate and are the mean of four independent incubations ± 1 SEM. *Significantly different with respect to C; $P < 0.01$. DGLA, dihomo-γ-linolenic acid; for other abbreviations see Table 2.

from its direct precursor (DGLA) under microtubule-disrupting conditions (COL, VBS, or NCD) decreased by 36 to 39% compared with control incubations (Table 3). Again, no significant changes were observed in the conversion of either n-3 or n-6 substrates under DHCB treatment (Table 3). Suspensions of Hep G2 cells reacted in a similar way, as did surface cultures under COL, VBS, NCD, or DHCB treatments (Table 4). Microtubule-disrupting drugs such as COL (10 µM), VBS (50 µM), or NCD (50 µM) produced 43, 47, and 39% reductions, respectively, in the cellular-associated labeling from palmitate compared with control incubations. Under equivalent incubation conditions, the ^{14}C incorporation from DGLA was not significantly affected (Table 4). The addition of either the microfilament-disrupting agent DHCB or the microtubule-stabilizing drug DMSO (50 µM) to Hep G2 suspensions produced no significant changes in the incorporation of labeled palmitate or DGLA (Table 4). The Δ9-desaturase capacity was reduced by 41, 43, and 33% under COL, VBS, or NCD treatment, respectively. Δ5-Desaturase activity decreased by 30 to 35% under similar experimental conditions (Table 4). The other drugs tested (DHCB and DMSO) were unable to modify the conversion of the substrates.

To study whether the effects observed under microtubule-depolymerizing conditions may be attributed to any other (unknown) mechanism of action, we carried out competition experiments between disrupting and stabilizing agents (Table 4). In these experiments, the depolymerizing activities of COL, VBS, or NCD were antagonized with the stabilizing agent (DMSO) added to the incubation medium before the disrupting drug. Results indicated that the inhibitory action of COL, VBS, or NCD on both the incorporation of ^{14}C and the conversion of palmitate to palmitoleate was completely neutralized when the microtubule system had previously been stabilized. A similar conclusion was obtained for the inhibitory effect of disrupting agents on the conversion of DGLA (Table 4). Moreover, treatment of the cells with an inactive isomer of COL (β-lumicolchicine, 10 µM) showed no effect either in the retention of labeling or in the conversion of palmitic or DGLA acids (Table 4).

Time-course and dose-response curves for the effect of COL on [^{14}C] FA incorporation and conversion. The concentration of COL used in the preceding experiments could be insufficient to produce the maximum inhibitory response on both the incorporation of [^{14}C]FA and the conversion of palmitate. In addition, this concentration may not be high enough to develop a noticeable effect on [^{14}C]DGLA incorporation. For these reasons, we studied the biological effect–inhibition of the cellular-associated labeling and conversion of FA under increasing COL concentrations, maintaining the incubation time constant at 5 h (Fig. 1). COL was able to decrease the conversion of both palmitate and DGLA in a dose-dependent manner. It produced a significant effect at a concentration as low as 2 µM. The maximum effect was observed at a 10-µM concentration. Incorporation of [^{14}C]palmitate was inhibited by approximately 20% at 2 µM, whereas [^{14}C]DGLA incorporation remained approximately constant within the range of concentrations studied (0–50 µM). The time course of the effects of COL (10 µM) on

TABLE 4
Uptake and Conversion of [^{14}C]FA in Suspensions of Hep G2 Cells Treated with Cytoskeleton-Modifying Drugs[a]

Treatment	^{14}C incorporation		Conversion	
	[1-^{14}C]16:0	[1-^{14}C]DGLA	[1-^{14}C]16:0 to 16:1	[1-^{14}C]DGLA to 20:4n-6
Control	334 ± 11	304 ± 15	47 ± 3	77 ± 4
Colchicine (10 μM)	195 ± 12*	275 ± 13	28 ± 4*	53 ± 6*
Vinblastin (50 μM)	182 ± 13*	315 ± 10	27 ± 5*	51 ± 7*
Nocodazole (50 μM)	203 ± 10*	282 ± 17	31 ± 4*	50 ± 5*
Dihydrocytochalasine B (20 μM)	293 ± 16	334 ± 11	55 ± 5	80 ± 5
DMSO (50 mM)	365 ± 11	313 ± 12	53 ± 4	80 ± 7
DMSO → colchicine	243 ± 13	281 ± 7	36 ± 5	65 ± 5
DMSO → vinblastin	233 ± 14	296 ± 10	37 ± 3	66 ± 6
DMSO → nocodazole	308 ± 9	299 ± 7	38 ± 5	71 ± 6
β-Lumicolchicine (10 μM)	347 ± 14	283 ± 12	46 ± 4	79 ± 5

[a]Suspensions of Hep G2 cells [5 · 10^6 cells/5 mL of improved minimal essential medium-zinc option (IMEM-Zo)] were incubated for 5 h with the agents indicated, then supplemented with the [^{14}C]FA complexed with BSA for another hour. In competition experiments, DMSO was added at zero time, and the second drug was added 60 min later. The incubation proceeded for 5 h and was then supplemented with the radioactive acid as indicated for the single-drug experiments. Incorporation of [^{14}C]FA and their conversion was performed as indicated in the text. Results are expressed as pmol/mg cellular protein and are the mean ± 1 SEM of five independent incubations. *Significantly different with respect to control flasks; $P < 0.01$.

the ^{14}C incorporation and conversion of palmitate and DGLA are given in Figures 2A and 2C. The depolymerization of microtubules produced a significant inhibition in the incorporation of palmitate (Fig. 2A) after 90 min of incubation, whereas the conversion to palmitoleate (Fig. 2C) was decreased after only 30 min of incubation. Similar experiments performed with DHCB (20 μM) (Figs. 2B, 2D) did not demonstrate any significant change in the incorporation of labeling or conversion of palmitate within the time studied (0–300 min). Incorporation of [^{14}C]DGLA was not affected by COL (Fig. 2A) or DHCB (Fig. 2B) treatments, whereas the production of arachidonate was significantly depressed after 90 min of COL treatment (Fig. 2C). DHCB showed no inhibitory effect on the Δ5-desaturase capacity (Fig. 2C).

DISCUSSION

Involvement of the cytoskeleton in the transmembrane transport of lipids has been studied using microscopic, biochemical, and radiochemical methods. These experimental studies were focused on the transepithelial transport of lipoproteins (33–37) rather than on the uptake and subsequent conversion of FA. In this paper we demonstrated that depolymerization of the microtubular system reduced the cellular-associated ^{14}C labeling of saturated FA (palmitate and stearate) in both surface cultures and suspended Hep G2 cells. This inhibitory effect was time

COL   DHCB
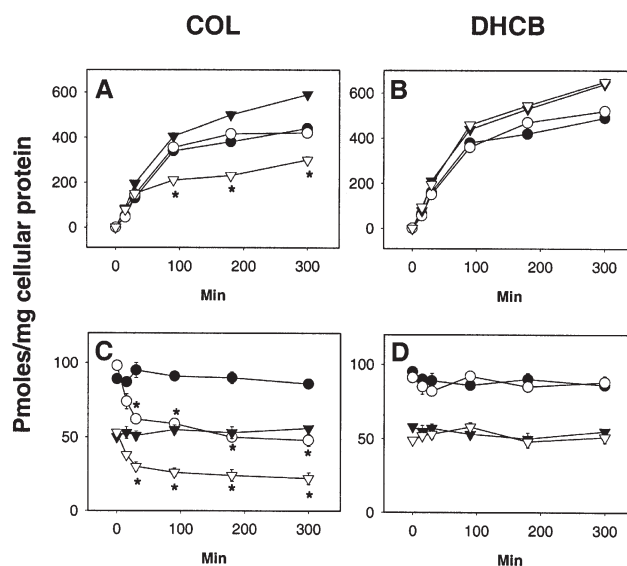
FIG. 2. Time course of ^{14}C incorporation (A, B) and conversion (C, D) of [1-^{14}C]palmitate (▼,▽) or [1-^{14}C]DGLA (●,○) in suspensions of Hep G2 cells treated with cytoskeleton-modifying agents. Filled symbols, control incubations; open symbols, colchicine (COL) (10 μM)-treated cells (A, C) or dihydrocytochalasin B (DHCB) (20 μM)-treated cells (B, D). Results are the mean ± 1 SEM of four independent incubations. *Significantly different from the corresponding control assay; $P < 0.01$.

FIG. 1. Dose-response curve for the ^{14}C incorporation (●,▼) and conversion (○,▽) of [1-^{14}C]palmitate (triangles) or [1-^{14}C]dihomo-γ-linolenic acid (DGLA) (circles) in suspensions of Hep G2 cells treated with colchicine (0–50 μM). Results were expressed as the percentage change with respect to the corresponding control incubations and are the mean of four independent assays ± 1 SEM. Control values were 292 ± 9 and 286 ± 11 pmol of [^{14}C]FA incorporated/mg of cellular protein for [^{14}C]palmitate and [^{14}C]DGLA, respectively; 46 ± 3 and 78 ± 5 pmol of FA converted/mg of cellular protein for [^{14}C]palmitate and [^{14}C]DGLA, respectively. *Significantly different from the corresponding control data; $P < 0.01$.

and dose dependent, and was specific to microtubular-disrupting drugs, since microfilament perturbation had no significant effects. Interestingly, the cell-associated labeling from unsaturated FA was independent of the microtubular and/or microfilamental state. Other authors (31) have demonstrated that certain aspects of lipid metabolism may be disturbed by the state of polymerization of one of the two major components (microtubules or microfilaments) of the cytoskeletal structure. This fact suggests a specific regulatory effect exerted by cytoskeleton integrity on the FA metabolism. In a previous work using L6 myoblastoma cells in culture, we demonstrated that the uptake of FA is a complex mechanism that can distinguish between saturated and unsaturated FA, and that it depends on one (or more) protein structures present in the plasma membrane. The uptake could be studied by analyzing the overall process as the sum of facilitated (modified hyperbolic) and unsaturable (linear) submechanisms (18). Previous experimental evidence has shown a relationship between the cytoskeleton and membrane proteins that are responsible for the uptake of different types of substrates, such as amino acids (38,39), neurotransmitters (40), or cations (41,42). Moreover, COL was used to differentiate the membrane transport systems involved in thyroid hormone uptake (43), which in fact, have very similar chemical structures. In our experimental conditions, we measured the metabolic handling of the FA studied rather than their rates of uptake. Despite the fact that there is some experimental evidence regarding the role of microtubules in membrane structure and functions (44) and that the cortical cytoskeleton modifies lipid rafts and several membrane transport processes (45–50), we assumed that the differences observed in the incorporation of labeling from saturated and unsaturated FA could be the consequence of a metabolic perturbation rather than an alteration in the transmembrane process of FA permeation.

In conclusion, we assumed that the depolymerization of microtubules differentially inhibited FA utilization, directly affecting one or more proteins involved in their intracellular transport and utilization. In fact, the metabolism of the FA must be the force that drives additional quantities of FA into the cell from the large reserve on the FA/BSA complex. One of the proteins involved in the intracellular transport may be of the FABP family (51) and among the acyl-CoA-synthetases, the first type of enzymes involved in FA utilization. From a physiological point of view, the cellular availability of saturated FA could be related to the different roles this type of FA plays in metabolic regulation. Recent investigations have demonstrated that cytoskeletal and related genes are controlled by unsaturated FA (mainly arachidonate, which is derived from DGLA by $\Delta 5$-desaturation), whereas saturated and monounsaturated FA do not markedly affect gene expression for the cytoskeleton protein family (52). As we demonstrated, microtubule disruption produced an inhibition in the $\Delta 5$-desaturase capacity that may have led to a decrease in the availability of arachidonate. Suppression of the arachidonate signal by a simultaneous inhibition of $\Delta 5$ activity and the uptake of its direct precursor could then have resulted in a complete failure of cytoskeleton integrity, whereas decreased levels of saturated and monoenoic FA could be harmless for normal cell physiology. Another explanation, by the differential impact of microtubule disruption on saturated and unsaturated FA handling, may be related to their different affinities for the acyl-CoA synthetase (ACS) isoforms. Saturated FA are mainly activated by plasma membrane-associated ACS1, whereas PUFA are activated by ACS4. Possibly, disruption of the microtubule structure modifies the plasma membrane molecular architecture. As a result, ACS1 could be inhibited with no significant effect on ACS4, which in turn, limits the transport and metabolic utilization of saturated FA.

In relation to FA conversion, the metabolic elongation–desaturation of FA is known to be one of the major factors regulating the quality and quantity of the acyl chains present in complex lipid moieties. This study demonstrated that FA conversion by oxidative desaturation is inhibited by cytoskeletal disruption. Our findings are in agreement with those of Kasturi *et al.* (53), who documented an inhibitory effect of COL on lipogenic enzymes such as FA synthetase and $\Delta 9$-desaturase. This effect was attributed to the depolymerizing action of COL since, as observed in our experiments, β-lumicolchicine was completely inactive. In addition, we demonstrated that stabilizing the cytoskeletal structure before treatment with the disrupting agent completely antagonized the inhibitory effect observed in both the incorporation of labeled FA and the desaturase conversion of the substrates. As suggested by others for soluble or membrane-anchored enzymes (54), we think that adsorption of enzymes (and other proteins) to the microtrabecular lattice formed by cytoskeletal components, and the interaction between cytoskeletal and membrane proteins such as FA desaturases, is a likely explanation for the functional organization, facilitating both substrate channeling and metabolic regulation. The role of motor proteins and cytoskeleton integrity in metabolic regulation remains poorly understood (20,49). It is also possible that the cytoskeleton could be essential in lipid metabolism for maintaining certain enzyme activities within their physiological ranges. Under conditions of microtubule or microfilament disruption, the activities of these enzymes may be modified, causing a significant alteration in the metabolism of substrates and their derived metabolites that would be channeled further. One of these putative proteins may be ACS1, since its inhibition may reduce the availability of activated substrates for $\Delta 9$- and $\Delta 5$-desaturases. However, this possibility would not be in agreement with previous experimental evidence pointing out that acylation of substrates is not the limiting step for FA desaturation (55). In spite of that, inhibition of the ACS1 isoform may be responsible for any other metabolic alteration in FA handling, such as the proportion of fatty-acyl derivatives available for transesterification. ACS activity also could be influenced by ATP generation that is partially inhibited by cytoskeletal disrupters. In this context, PUFA activate mitochondrial β-oxidation and might compensate for the drug effects, whereas saturated FA are unable to do so.

In conclusion, we demonstrated that microtubules are involved in the processing of saturated and unsaturated FA, and

in the subsequent metabolism of these precursors, causing alterations in the elongation–desaturation pathway. These effects had differential characteristics depending on the degree of unsaturation of the FA studied. The relationship between FA metabolism and cytoskeleton integrity is relevant not only from a physiological point of view (20,56), but also when considering the increasing experimental evidence suggesting different roles of such interaction in the etiology and/or evolution of human illnesses, for example, Alzheimer's disease (57,58), inflammatory intestinal damage (59), and redox-associated injuries such as toxic bile acid damage, chronic alcohol intake, and hypoxia-reperfusion, among others (60).

ACKNOWLEDGMENTS

REFERENCES

1. Stubbs, C.D., and Smith, A.D. (1984) The Modification of Mammalian Membrane Polyunsaturated Fatty Acid Composition in Relation to Membrane Fluidity and Functions, *Biochim. Biophys. Acta 779*, 89–137.
2. Spector, A.A., and Yorek, M.A. (1985) Membrane Lipid Composition and Cellular Function, *J. Lipid Res. 26*, 1015–1035.
3. Brenner, R.R. (1984) Effect of Unsaturated Acids on Membrane Structure and Enzyme Kinetics, *Prog. Lipid Res. 23*, 69–96.
4. Leger, C.L. (1993) Physicochemical Approach of the Function of the Fatty Acid Incorporation in Biological Membranes, *Prostaglandins Leukot. Essent. Fatty Acids 48*, 17–21.
5. Brenner, R.R. (1974) The Oxidative Desaturation of Unsaturated Fatty Acids in Animals, *Mol. Cell. Biochem. 3*, 41–52.
6. Ek, B.A., Cistola, D.P., Hamilton, J.A., Kaduce, T.L., and Spector, A.A. (1997) Fatty Acid Binding Proteins Reduce 15-Lipoxygenase-Induced Oxygenation of Linoleic Acid and Arachidonic Acid, *Biochim. Biophys. Acta 1346*, 75–85.
7. Glatz, J.F., Borchers, T., Spener, F., and van der Vusse, G.J. (1995) Fatty Acids in Cell Signaling: Modulation by Lipid Binding Proteins, *Prostaglandins Leukot. Essent. Fatty Acids 52*, 121–127.
8. Hertz, R., Mangenheim, J., Berman, I., and Bar-Tana, J. (1998) Fatty Acyl-CoA Thioesters Are Ligands of Hepatic Nuclear Factor-4α, *Nature 392*, 512–516.
9. Price, P.T., Nelson, C.M., and Clarke, S.D. (2000) Omega-3 Polyunsaturated Fatty Acid Regulation of Gene Expression, *Curr. Opin. Lipidol. 11*, 3–7.
10. Wood, J.N. (1990) Essential Fatty Acids and Their Metabolites in Signal Transduction, *Biochem. Soc. Trans. 18*, 785–786.
11. Stuhlmeier, K.M., Kao, J.J., and Bach, F.H. (1997) Arachidonic Acid Influences Proinflammatory Gene Induction by Stabilizing the Inhibitor-κB α/Nuclear Factor κB (NF-κB) Complex, thus Suppressing the Nuclear Translocation of NF-κB, *J. Biol. Chem. 272*, 24679–24683.
12. Lim, H., Gupta, R.A., Ma, W.G., Paria, B.C., Moller, D.E., Morrow, J.D., DuBois, R.N., Trzaskos, J.M., and Dey, S.K. (1999) Cyclo-oxygenase-2-Derived Prostacyclin Mediates Embryo Implantation in the Mouse *via* PPARδ, *Genes Dev. 13*, 1561–1574.
13. Sorrentino, D., Stump, D., Potter, B.J., Robinson, R.B., White, R., Kiang, C.L., and Berk, P.D. (1988) Oleate Uptake by Cardiac Myocytes Is Carrier Mediated and Involves a 40-kD Plasma Membrane Fatty Acid Binding Protein Similar to That in Liver, Adipose Tissue and Gut, *J. Clin. Invest. 82*, 928–935.
14. Potter, B.J., Sorrentino, D., and Berk, P.D. (1989) Mechanisms of Cellular Uptake of Free Fatty Acids, *Annu. Rev. Nutr. 9*, 253–270.
15. Glatz, J.F., Luiken, J.J., van Nieuwenhoven, F.A., and van der Vusse, G.J. (1997) Molecular Mechanism of Cellular Uptake and Intracellular Translocation of Fatty Acids, *Prostaglandins Leukot. Essent. Fatty Acids 57*, 3–9.
16. Hamilton, J.A. (1998) Fatty Acid Transport: Difficult or Easy? *J. Lipid Res. 39*, 467–481.
17. Stump, D.D., Fan, X., and Berk, P.D. (2001) Oleic Acid Uptake and Binding by Rat Adipocytes Define Dual Pathways for Cellular Fatty Acid Uptake, *J. Lipid Res. 42*, 509–520.
18. Marra, C.A., Girón González, M.D., and Suárez Ortega, M.D. (2002) Evidence in Favor of a Facilitated Transport System for Fatty Acid Uptake in Cultured L6 Cells, *Lipids 37*, 273–283.
19. Luiken, J.J., Bonen, A., and Glatz, J.F. (2002) Cellular Fatty Acid Uptake Is Acutely Regulated by Membrane-Associated Fatty Acid-Binding Proteins, *Prostaglandins Leukot. Essent. Fatty Acids 67*, 73–78.
20. Murray, J.W., and Wolkoff, A.W. (2003) Roles of the Cytoskeleton and Motor Proteins in Endocytic Sorting, *Adv. Drug Deliv. Rev. 55*, 1385–1403.
21. Takenawa, T., and Itoh, T. (2001) Phosphoinositides, Key Molecules for Regulation of Actin Cytoskeletal Organization and Membrane Traffic from the Plasma Membrane, *Biochim. Biophys. Acta 1533*, 190–206.
22. Spector, A.A., Steinberg, D., and Tanaka, A. (1965) Uptake of Free Fatty Acids by Ehrlich Ascites Tumor Cells, *J. Biol. Chem. 240*, 1032–1041.
23. Samuel, D., Paris, S., and Ailhaud, G. (1976) Uptake and Metabolism of Fatty Acids and Analogues by Cultured Cardiac Cells from Chick Embryo, *Eur. J. Biochem. 64*, 583–595.
24. Lowry, O.H., Rosebrough, M.J., Farr, A.L., and Randall, R.J. (1951) Protein Measurement with the Folin Phenol Reagent, *J. Biol. Chem. 193*, 265–275.
25. Marra, C.A., de Alaniz, M.J.T., and Brenner, R.R. (1986) Dexamethasone Blocks Arachidonate Biosynthesis in Isolated Hepatocytes and Cultured Hepatoma Cells, *Lipids 21*, 212–219.
26. Folch, J., Lees, M., and Sloane Stanley, G.H. (1957) A Simple Method for the Isolation and Purification of Total Lipids from Animal Tissues, *J. Biol. Chem. 226*, 497–509.
27. Marra, C.A., and de Alaniz, M.J.T. (1992) Incorporation and Metabolic Conversion of Saturated and Unsaturated Fatty Acids in SK-Hep1 Human Hepatoma Cells in Culture, *Mol. Cell. Biochem. 117*, 107–118.
28. Morrison, W.R., and Smith, L.M. (1964) Preparation of Fatty Acid Methyl Esters and Dimethylacetals from Lipids with Boron Fluoride–Methanol, *J. Lipid Res. 53*, 600–608.
29. Albino, L., Polo, M.P., Bravo, M.G., and de Alaniz, M.J.T. (2001) Uptake and Metabolic Conversion of Saturated and Unsaturated Fatty Acids in Hep2 Human Larynx Tumor Cells, *Prostaglandins Leukot. Essent. Fatty Acids 65*, 295–300.
30. Jauregui, H.O., Hayner, N.T., Driscoll, J.L., Williams-Holland, R., Lipsky, M.H., and Galletti, P.M. (1981) Trypan Blue Dye Uptake and Lactate Dehydrogenase in Adult Rat Hepatocytes—Freshly Isolated Cells, Cell Suspensions, and Primary Monolayer Cultures, *In Vitro 17*, 1100–1110.
31. George, T.P., Cook, H.W., Byers, D.M., Palmer, F.B., and Spence, M.W. (1991) Inhibition of Phosphatidylcholine and Phosphatidylethanolamine Biosynthesis by Cytochalasin B in Cultured Glioma Cells: Potential Regulation of Biosynthesis by Ca^{++}-Dependent Mechanisms, *Biochim. Biophys. Acta 1084*, 185–193.
32. Pipeleers, D.G., Pipeleers-Marichal, M.A., Sherline, P., and Kipnis, D.M. (1977) A Sensitive Method for Measuring Polymerized and Depolymerized Forms of Tubulin in Tissues, *J. Cell Biol. 74*, 341–350.

33. Rajan, V.P., and Menon, K.M. (1985) Involvement of Microtubules in Lipoprotein Degradation and Utilization for Steroidogenesis in Cultured Rat Luteal Cells, *Endocrinology 117*, 2408–2416.

34. Pavelka, M., and Gangl, A. (1983) Effects of Colchicine on the Intestinal Transport of Endogenous Lipid. Ultrastructural, Biochemical, and Radiochemical Studies in Fasting Rats, *Gastroenterology 84*, 544–555.

35. Nishikawa, M., Seki, K., Matsuzawa, Y., Minami, Y., Kawata, S., Miyoshi, S., Imai, Y., Saitoh, R., Noda, S., Tamura, S., *et al.* (1984) Effect of High Doses of Synthetic Estrogen on Lipid Metabolism in Castrated Male Rats, *Lipids 19*, 777–783.

36. Dijkstra, J., van Galen, M., and Scherphof, G. (1985) Effects of (Dihydro)cytochalasin-B, Colchicine, Monensin, and Trifluoperazine on Uptake and Processing of Liposomes by Kupffer Cells in Culture, *Biochim. Biophys. Acta 845*, 34–42.

37. Dashti, N., and Wolfbauer, G. (1986) Studies on the Binding and Degradation of Human Very-Low-Density Lipoproteins by Human Hepatoma Cell Line Hep G2, *Biochim. Biophys. Acta 875*, 473–486.

38. Nassar, C.F., Jurjus, A.R., Haddad, M.E., and Sarru, E. (1984) Cytoskeletal Control of Alanine Transport Across the Rat and Turtle Small Intestine, *Comp. Biochem. Physiol. A 79*, 161–164.

39. Takadera, T., and Mohri, T. (1985) Effect of Intracellular Free Ca^{++} on Leucine Transport in Chang Liver Cells, *Cell Struct. Funct. 10*, 349–359.

40. O'Leary, M.E., and Suszkiw, J.B., (1983) Effect of Colchicine on ^{45}Ca and Choline Uptake, and Acetylcholine Release in Rat Brain Synaptosomes, *J. Neurochem. 40*, 1192-1195.

41. Tsunoda, Y., and Mizuno, T. (1985) Participation of the Microtubular–System on Intracellular Ca^{++} Transport and Acid Secretion in Dispersed Parietal Cells, *Biochim. Biophys. Acta 820*, 189–198.

42. Johnson, G., Jacobs, P., and Purves, L.R. (1985) The Effects of Cytoskeletal Inhibitors on Intestinal Iron Absorption in the Rat, *Biochim. Biophys. Acta 843*, 83–91.

43. Riley, W.W., and Eales, J.G. (1994) Characterization of 3,5,3′-Triiodo-L-thyronine Transport into Hepatocytes Isolated from Juvenile Rainbow Trout (*Oncorhynchus mykiss*), and Comparison with L-Thyroxine Transport, *Gen. Comp. Endocrinol. 95*, 301–309.

44. Aszalos, A., Yang, G.C., and Gottesman, M.M. (1985) Depolymerization of Microtubules Increases the Motional Freedom of Molecular Probes in Cellular Plasma Membranes, *J. Cell Biol. 100*, 1357–1362.

45. Ikonen, E. (2001) Roles of Lipid Rafts in Membrane Transport, *Curr. Opin. Cell Biol. 13*, 470–477.

46. Jacobson, K., and Dietrich, C. (1999) Looking at Lipid Rafts? *Trends Cell Biol. 9*, 87–91.

47. Holowka, D., Sheets, E.D., and Baird, B. (2000) Interactions Between Fc(ε)RI and Lipid Raft Components Are Regulated by the Actin Cytoskeleton, *J. Cell Sci. 113*, 1009–1019.

48. Umeda, M., and Emoto, K. (1999) Membrane Phospholipid Dynamics During Cytokinesis: Regulation of Actin Filament Assembly by Redistribution of Membrane Surface Phopsholipid, *Chem. Phys. Lipids 101*, 81–91.

49. Bevers, E.M., Comfurius, P., Dekkers, D.W., and Zwaal, R.F. (1999) Lipid Translocation Across the Plasma Membrane of Mammalian Cells, *Biochim. Biophys. Acta 1439*, 317–330.

50. Bevers, E.M., Comfurius, P., and Zwaal, R.F. (2004) Membrane Phospholipid Asymmetry: Biochemical and Pathophysiological Perspectives, *Adv. Mol. Cell Biol. 33*, 389–422.

51. Glatz, J.F., van Nieuwenhoven, F.A., Luiken, J.J., Schaap, F.G., and van der Vusse, G.J. (1997) Role of Membrane-Associated and Cytoplasmic Fatty Acid-Binding Proteins in Cellular Fatty Acid Metabolism, *Prostaglandins Leukot. Essent. Fatty Acids 57*, 373–378.

52. Verlengia, R., Gorjao, R., Kanunfre, C.C., Bordin, S., de Lima, T.M., and Curi, R. (2003) Effect of Arachidonic Acid on Proliferation, Cytokine Production, and Pleiotropic Gene Expression in Jurkat Cells. A Comparison with Oleic Acid, *Life Sci. 73*, 2939–2951.

53. Kasturi, R., Joshi, V.C., and Wakil, S.J. (1984) Colchicine Inhibition of Insulin Induction of Stearoyl-CoA Desaturase and Fatty Acid Synthetase in Cultured Avian Liver Explants, *Arch. Biochem. Biophys. 233*, 530–539.

54. Walsh, J.L., and Knull, H.R. (1988) Heteromerous Interactions Among Glycolytic Enzymes and of Glycolytic Enzymes with F-Actin: Effects of Poly(ethylene glycol), *Biochim. Biophys. Acta 952*, 83–91.

55. Brenner, R.R. (1981) Nutritional and Hormonal Factors Influencing Desaturation of Essential Fatty Acids, *Prog. Lipid Res. 20*, 41–47.

56. Pedersen, S.F., Hoffmann, E.K., and Mills, J.W. (2001) The Cytoskeleton and Cell Volume Regulation, *Comp. Biochem. Physiol. A 130*, 385–399.

57. Scheff, S.W., and Price, D.A. (2003) Synaptic Pathology in Alzheimer's Disease: A Review of Ultrastructural Studies, *Neurobiol. Aging 24*, 1029–1046.

58. Yao, P.J., Zhu, M., Pyun, E.I., Brooks, A.I., Therianos, S., Meyers, V.E., and Coleman, P.D. (2003) Defects in Expression of Genes Related to Synaptic Vesicle Trafficking in Frontal Cortex of Alzheimer's Disease, *Neurobiol. Dis. 12*, 97–109.

59. Sturm, A., and Dignass, A.U. (2002) Modulation of Gastrointestinal Wound Repair and Inflammation by Phospholipids, *Biochim. Biophys. Acta 1582*, 282–288.

60. Fernández-Checa, J.C. (2003) Redox Regulation and Signalling Lipids in Mitochondrial Apoptosis, *Biochim. Biophys, Res. Commun. 304*, 471–479.

Modulation of Respiratory Syncytial Virus-Induced Prostaglandin E₂ Production by n-3 Long-Chain Polyunsaturated Fatty Acids in Human Respiratory Epithelium

Dani-Louise Bryan[a], Prue Hart[b], Kevin Forsyth[a], and Robert Gibson[c],*

Departments of [a]Paediatrics and Child Health and [b]Microbiology and Infectious Diseases, Flinders University, and
[c]Child Nutrition Research Centre, Child Health Research Institute, Flinders Medical Centre
and Women's and Children's Hospital, Adelaide, South Australia, 5042, Australia

ABSTRACT: Infection with respiratory syncytial virus (RSV) results in substantial infant morbidity and has been associated with the subsequent development of childhood asthma. Inflammatory mediators produced by both the epithelium and tissue leukocytes during RSV infection stimulate the release of chemotactic factors by the respiratory epithelium and the subsequent influx of inflammatory cells, predominantly neutrophils. We investigated the production of inflammatory mediators [prostaglandin E₂ (PGE₂), interleukin (IL)-1β, tumor necrosis factor α] and chemokines [IL-8, RANTES (regulation on activation, normal T cell expressed and secreted)] by alveolar epithelial cells in response to RSV infection. Infection of a human alveolar epithelial transformed cell line (A549 cells) with live RSV substantially increased production of PGE₂, IL-8, and RANTES. By altering cell membrane FA through incorporation of the long-chain PUFA (LCPUFA) arachidonic acid, EPA, and DHA, we were subsequently able to significantly modulate PGE₂ production by the infected epithelium. Because of the dynamic nature of the effects of PGE₂ on lung function, regulation of this prostaglandin during RSV infection by n-3 LCPUFA has the potential to significantly alter the disease process.

Paper no. L9769 in *Lipids 40*, 1007–1011 (October 2005).

Respiratory syncytial virus (RSV) is the most common childhood respiratory pathogen infecting nearly all infants in the first 12–24 mon of life. Of those infected, a significant number require hospitalization because of bronchiolitis, and of these infants, at least 50% will go on to develop childhood asthma (1,2), making RSV infection one of the most important causal factors for infant and child morbidity in the developed world.

The means by which RSV predisposes infants to the development of asthma is unclear. However, the extensive damage caused to the respiratory airways by the virus through acute inflammation is a probable causative factor. Initial exposure to RSV in the airways induces the production of inflammatory mediators such as interleukin (IL) 1β and tumor necrosis factor (TNF) α by alveolar macrophages and epithelial cells. This production of inflammatory cytokines is exacerbated *via* upregulation of chemotactic factors such as IL-8 and RANTES (regulation on activation, normal T cell expressed and secreted) by the respiratory epithelium, resulting in an influx of leukocytes into the airways. These migratory leukocytes include a large population of polymorphonuclear granulocytes, particularly neutrophils and eosinophils (3,4). Degranulation of these cells leads to airway edema, sensory nerve stimulation, and triggering of reflex bronchoconstriction, resulting in airway hyperresponsiveness and persistent wheezing (5), as well as increased permeability of the airway mucosa to allergens (6). The influx of activated inflammatory cells such as monocytes/macrophages and lymphocytes also contributes to a positive feedback of cytokine production, further enhancing the secretion of both inflammatory and chemotactic mediators by airway cells (7).

The role of prostaglandin production by the respiratory epithelium in RSV-mediated bronchiolitis and the effects on the subsequent development of asthma have not been investigated. However, a significant increase in both prostaglandin E₂ (PGE₂) and prostaglandin F₂α production in response to RSV infection in alveolar macrophages has been reported (8,9). Prostaglandins play a substantial role in the regulation of lung function through their complementary function in the dilation and constriction of both the blood vessels and bronchioles (10) *via* neural pathways and through direct effects on airway smooth muscle. In addition to the role of PGE₂ in the inflammatory mediator cascade, these often contradictory effects on the primary structures of the lung make the regulation of this prostaglandin a potentially important aspect of RSV infection that requires elucidation.

This study investigated the production of inflammatory mediators (prostaglandin and cytokines) and chemokines by the respiratory epithelium in response to infection by RSV. Production of PGE₂, IL-1β, TNF-α, IL-8, and RANTES in response to infection with RSV was examined *in vitro* using a human transformed alveolar epithelial cell line (A549).

EXPERIMENTAL PROCEDURES

Cell line. A549 cells were used throughout these experiments. The cells were maintained in a continuous culture prior to each

---

experiment. The culture medium (DMEM; JRH Biosciences, Lenexa, KS) contained 2 mM L-glutamine, 50 U/mL penicillin, 37.5 U/mL streptomycin, and 5% heat-inactivated FBS (CSL Biosciences, Victoria, Australia) unless otherwise indicated. All media components were purchased presterilized and endotoxin free.

Virus propagation. The RSV used for this study was characterized as the long strain of RSV (88:RS4; Dr. P. Young, Sir Albert Sakzewski Virus Research Centre, Queensland, Australia). The virus was grown in confluent monolayers of A549 cells for 24 h. The cells were then harvested using a sterile cell scraper, centrifuged ($890 \times g$, 5 min), aliquoted, and preserved in liquid nitrogen. Prior to use, virus aliquots were sonicated at 20 kHz for 10 s (Ultrasonics W375 sonicator; Heat Systems, Plainview, NY) to release the intracellular virus. The titer of the stock virus measured between 1 and 3×10^8 fluorescent focus units (ffu)/mL. Aliquots of this stock were rendered noninfective by UV inactivation through exposure to an intense UVC germicidal light source for 20 min at <10 cm distance, after which they were aliquoted and stored in liquid-phase liquid nitrogen. Uninfected A549 cells were also processed similarly for use as a control for the A549 cell contribution to the viral medium.

RSV infection of respiratory epithelial cells. A549 cells (4×10^5 cells/mL) were cultured in 24-well cell culture plates (Greiner Labortechnik GmbH, Frickenhausen, Germany). At confluence (24 h), the supernatants were removed and cells were cultured for 3 h with or without either live RSV at a multiplicity of infection (MOI) of 3, an equivalent aliquot of UV-inactivated virus, or A549-conditioned medium, in 150 μL DMEM (as above) supplemented with 2% FBS. The cells were then washed with 1 mL/well serum-free DMEM to remove the unbound virus before a final culture in 625 μL/well serum-free DMEM. Aliquots of the cell culture supernatant were harvested at 6, 24, and 48 h post infection and stored at −80°C.

Prostaglandin assay. Cell culture supernatants were assayed for PGE_2 by a competitive enzyme immunoassay (EIA) (Prostaglandin E_2 EIA Kit–Monoclonal; Cayman Chemical Company, Ann Arbor, MI). Samples were diluted 1:10 in the EIA buffer supplied according to the manufacturer's instructions.

Cytokine assays. Cell culture supernatants were assayed for IL-1β, TNF-α (Endogen, Woburn, MA), IL-8 (BD Pharmingen, San Diego, CA), and RANTES (R&D Systems Inc., Minneapolis, MN) using a double-antibody sandwich ELISA as described previously (11). The limits of detection for each ELISA were 8, 10, 20, and 4 pg/mL, respectively. Samples were diluted 1:10 and 1:20 in PBS/0.05% Tween 20/1% BSA for the measurement of IL-8 and RANTES, respectively.

RSV infection of long-chain PUFA (LCPUFA)-supplemented cells. A549 cells were cultured in the presence or absence of 10 μg/mL EPA (20:5n-3), arachidonic acid (AA, 20:4n-6), or DHA (22:6n-3) (Nu-Check-Prep Inc., Elysian, MN) as FFA. At confluence (24 h), the supernatants were removed, the cells were cultured with RSV, and the supernatants were harvested as described above.

The incorporation of FFA was determined in separate tripli-

cate experiments whereby A549 cells were cultured in the presence or absence of 5–50 μg/mL EPA, AA, or DHA (Nu-Check-Prep). Cellular lipids were extracted using the method described by Broekhuyse (12). The phospholipid fraction was separated *via* TLC, the lipids were transesterified, and the FAME were separated and quantified as described previously (13).

Statistical analysis. Data are presented as mean ± SEM. Differences between virus and FA treatments, as well as culture times, were examined using one-way ANOVA followed by a Student–Newman–Keuls *post hoc* analysis. All analyses were performed using SPSS for Windows, v. 10.0 (SPSS Inc., Chicago, IL).

RESULTS

RSV infection of A549 cells. A549 cells infected with live RSV at an MOI of 3 showed visible cytopathic effects of viral replication by 48 h post infection. Wells incubated with UV-inactivated virus, A549-conditioned medium, or medium alone demonstrated none of these visible effects beyond 72 h post infection, confirming their inability to infect the cells.

Production of PGE_2 and cytokines in response to infection with RSV. Infection with live RSV significantly increased the production of PGE_2, IL-8, and RANTES by A549 cells when
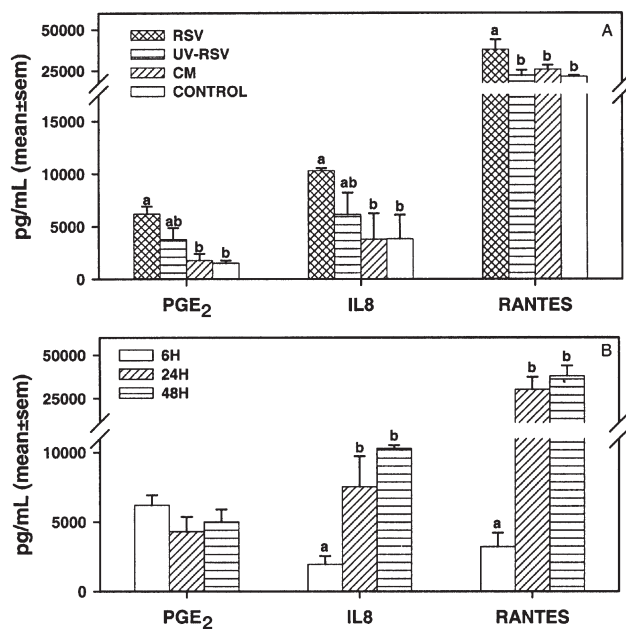
FIG. 1. (A) Production of PGE_2, IL-8, and RANTES by A549 cells in response to incubation with live RSV, UV-inactivated RSV, A549-conditioned medium, or medium alone at 48 h post infection. (B) Production of PGE_2, IL-8, and RANTES by A549 cells in response to incubation with live RSV at 6, 24, and 48 h post infection. Results from three separate experiments are expressed as mean ± SEM. Bars with different superscripts indicate significant differences ($P < 0.05$). PGE_2, prostaglandin E_2; IL-8, interleukin-8; RANTES, regulation on activation, normal T cell expressed and secreted; A549, human transformed alveolar epithelial cell line; RSV, respiratory syncytial virus; CM, A549-conditioned media.
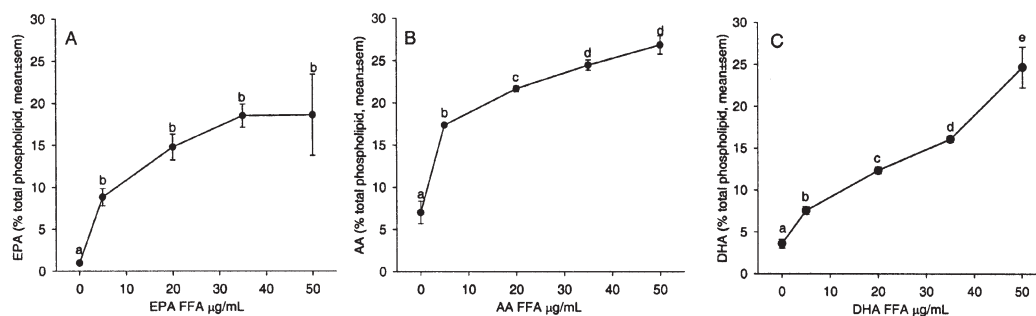
FIG. 2. Cell membrane phospholipid (A) EPA, (B) arachidonic acid (AA), and (C) DHA from respiratory epithelial cells incubated with EPA, AA, or DHA as FFA to confluence (24 h). Results from three to four experiments are expressed as a relative percentage of the total FA (mean ± SEM). Points with different superscripts indicate significant differences ($P < 0.05$).

compared with the conditioned medium and the medium alone. Stimulation of the cells with the UV-inactivated virus also resulted in an increase in IL-8 and PGE$_2$ that was not found with RANTES. However, greater variability between experiments using the UV-inactivated RSV did not allow for a statistical distinction from that induced by the live virus, nor from the controls (Fig. 1A). This demonstrates some degree of stimulation of A549 cells to produce IL-8 and PGE$_2$, but not RANTES, by RSV proteins independent of an active infection.

The time course for stimulation of the chemokines by RSV demonstrated an increase from 6 h post infection to a maximum production by 24 h post infection for both IL-8 and RANTES. The maximal production of PGE$_2$, however, was observed at 6 h post infection (Fig. 1B).

Although there was constitutive production of the inflammatory cytokine IL-1β (913 ± 99 pg/mL, mean ± SEM) at all sample times, there was little to no spontaneous production of TNF-α at any time (13 ± 3 pg/mL, mean ± SEM). No difference was found in the production of either IL-1β or TNF-α between those cells treated with live RSV and any of the study controls (UV-inactivated virus, A549-conditioned medium, and medium alone) at any of the culture times tested (data not shown).

Effect of LCPUFA incorporation into A549 cells on PGE$_2$ production. Cell membrane EPA, AA, and DHA were increased dose dependently up to a maximal level of incorporation (Fig. 2A–C). The change in membrane composition resulting from the incorporation of each FA into the cells was offset by a decrease in the monounsaturated FA levels, largely owing to a loss of oleic acid (18:1n-9). In addition, the incorporation of each of the n-3 FA, EPA and DHA, resulted in a decrease in membrane AA from 7 to 3% total phospholipids in the control and 50 μg/mL-supplemented cells, respectively. Similarly, incorporation of AA resulted in a decrease in total membrane n-3 from 5 to 1.5% total phospholipids in the control and 50 μg/mL-supplemented cells, respectively (data not shown).

The incorporation of each of the n-3 LCPUFA, EPA and DHA, into the membranes of A549 cells at 10 μg/mL resulted in a significant decrease in the production of PGE$_2$ in response to RSV infection when compared with the control (no FFA). In

contrast, the incorporation of a similar amount of the n-6 LCPUFA, AA, into these cells resulted in a significant increase in PGE$_2$ production compared with that of the control cells (Fig. 3). However, the incorporation of each of the LCPUFA into these cells and the subsequent changes in PGE$_2$ production appeared to neither hasten nor delay the appearance of visible cytopathic effects of infection with live RSV.

In addition, incorporation of LCPUFA into the cells had no measurable effect on the production of the chemokines IL-8 or RANTES in response to infection with RSV (data not shown).

DISCUSSION

RSV was shown here to elicit an increase in PGE$_2$ production in the absence of lipopolysaccharide, and also to upregulate production of this prostaglandin by RSV in human airway epithelial cells. These findings are supported by a recent paper by Richardson and colleagues (14). Furthermore, the upregulation of PGE$_2$ production in response to RSV infection established in our study occurred in the absence of any increase in production of the proinflammatory cytokines IL-1β or TNF-α. In previous studies, IL-1β and TNF-α in the absence of RSV increased PGE$_2$ production by A549 cells *via* enhanced cyclooxygenase (COX)-2 expression (15,16). We have shown
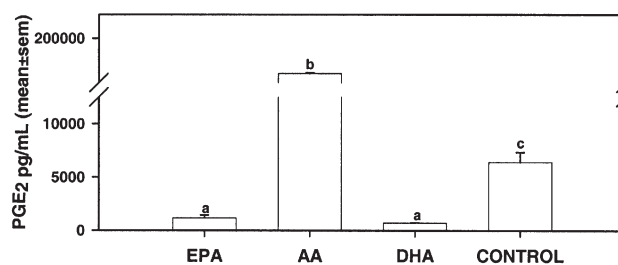
FIG. 3. Production of PGE$_2$ in response to incubation with live RSV by A549 cells treated with long-chain PUFA (10 μg/mL) compared with the control (no FFA). Results from three separate experiments are expressed as mean ± SEM. Bars with different superscripts indicate significant differences ($P < 0.05$). For abbreviations see Figure 1.

that the infection of epithelial cells by RSV will increase airway PGE_2 independently of the production of proinflammatory cytokines released in the airways during RSV disease. This apparent anomaly may be due to the stimulation caused by the release of AA from the cell membrane in response to RSV infection. This supposition is supported by the demonstrated suppressive effects of the n-3 PUFA, EPA and DHA, on RSV-induced PGE_2 production because of the competitive relationship of these n-3 and n-6 FA for release and metabolism (17). These LCPUFA-mediated changes in PGE_2 production may be regulated *via* COX-2, as AA supplementation was previously shown to upregulate PGE_2 production in A549 cells *via* increased expression of this enzyme (18). Because the level of n-3 PUFA accumulated in our cells was similar to levels seen in erythrocytes of infants fed breast milk with high n-3 PUFA levels (19), it is conceivable that this might lead to a potential treatment for bronchiolitis.

In this study we also corroborated the upregulation of IL-8 and RANTES production by respiratory epithelial cells in response to RSV infection (4). In addition, production of both IL-8 and PGE_2 in response to incubation with the UV-inactivated virus was found to lie between that of the live virus and non-RSV controls. IL-8 gene expression and protein release occur as early as 2 h following RSV infection and are not dependent on viral replication (20). UV inactivation disables the ability of RSV to replicate but not to bind to receptors, so although the presence of RSV has some limited effect, the lack of a new productive infection limits the total effect of RSV. In previous studies we found that UV inactivation gives some limited stimulation by RSV to epithelial cells, but full stimulation occurs only if the RSV is dividing and giving a new productive infection (21).

Previous studies examining the effect of live infection with RSV on cytokine production by A549 respiratory epithelial cells also have found increased production of IL-1β and TNF-α (22,23). The levels of cytokines seen in these studies were low, at 20 and 75 pg/mL for IL-1β and TNF-α, respectively. Although the previously reported concentration of TNF-α exceeded that seen in this study, the amount of IL1-β was considerably less than the constitutive expression measured here. This increase in baseline production of IL-1β may have masked the small increases observed on RSV infection in former studies and may have been due to variability in the detection of IL-1β isoforms with the antibodies used in each study.

Very few published studies have examined PGE_2-induced responses in RSV disease. An increase in plasma PGE_2 was observed 3 d after primary infection in a bovine model of RSV (24). However, PGE_2 effects in asthma have been rigorously examined because of the dichotomous nature of its actions in regulating the dilation and constriction of both the bronchioles and resident blood vessels. Murine studies have attempted to elucidate the opposing effects of PGE_2 and, through the use of receptor knockout models, have delineated the different effects on airway tone caused by the expression patterns and subsequent binding to each of the four PGE_2 receptors—E-prostanoid 1–4 (25). Differences in the expression of these receptors, both between different cell types and between individuals, may contribute to explaining the contradictory results obtained in clinical trials of aerosolized PGE_2 for the treatment of asthma. Whereas, for the majority of asthma patients, inhaled PGE_2 acted as a bronchodilator, in a substantial proportion of test subjects, treatment resulted in profound bronchoconstriction, requiring β agonist rescue (26). It may therefore be postulated that the dilatory and constricting effects of PGE_2 in RSV disease and its possible contribution to the development of asthma in these infants may be equally tissue and individual specific.

Although prostaglandins are implicit in regulating bronchiolar and vascular constriction and dilation, they also can aid in the regulation of cytokine production. PGE_2 derived from stimulating A549 cells with IL-1β can increase IL-10 and decrease IL-12 production by alveolar macrophages (27). These cytokines perform many functions in the immune system. However, one of their well-defined roles is as regulators of T helper (Th) lymphocyte maturation and activation, with IL-10-promoting Th2 and IL-12-promoting Th1 cell development, respectively. Altering the balance of these cells, and their cytokine products, to a predominant Th2 environment has been implicated in the development of atopy (28). High levels of IL-10 during RSV bronchiolitis have been associated with the development of recurrent wheezing and asthma during the months following recovery (29). Equally, the duration of respiratory failure and acute bronchiolitis as a result of infection with RSV has been associated with a decreased ability to produce IL-12 (30,31). Regulation of prostaglandin production may aid in alleviating the imbalances found in IL-10 and IL-12 at a crucial time of early immune activation, which may prevent skewing of the developing immune system toward inappropriate immune responses such as asthma.

Downregulation of PGE_2 production by dietary n-3 LCPUFA consumption in infants during infection with RSV may therefore be beneficial owing to the variety of mechanisms through which this prostaglandin contributes to immune function in the airways. A decrease in PGE_2 induced by the incorporation of dietary n-3 LCPUFA into respiratory epithelial cells may reduce both the short- and long-term effects of RSV infection *via* regulation of cytokine production. Modulation of the production of PGE_2 with variations to the n-6 to n-3 ratio may help regulate bronchiolar and vascular constriction and dilation and thereby decrease the long-term detrimental effects of RSV infection on the lung. Although COX inhibitors may be used to diminish the production of PGE_2 by the respiratory epithelium in this airway disease, as suggested in the recent paper by Richardson and colleagues (14), from our study it may be hypothesized that PGE_2 production could be regulated *via* an intake of n-3 LCPUFA, either maternally derived through human milk feeding or by addition to infant formula. Further work is required to elucidate the role of PGE_2 in infant airways during RSV disease and to determine the extent to which dietary LCPUFA may modulate these effects *in vivo*.

ACKNOWLEDGMENTS

REFERENCES

1. Sigurs, N., Bjarnason, R., Sigurbergsson, F., Kjellman, B., and Bjorksten, B. (1995) Asthma and Immunoglobulin E Antibodies After Respiratory Syncytial Virus Bronchiolitis: A Prospective Cohort Study with Matched Controls, *Pediatrics 95*, 500–505.

2. Phelan, P.D. (1994) The Epidemiology of Acute Respiratory Infections, in *Practical Paediatrics* (Robinson, M.J., and Roberton, D.M., eds.), p. 341, Churchill Livingstone, Melbourne.

3. Smith, P.K., Wang, S.Z., Dowling, K.D., and Forsyth, K.D. (2001) Leucocyte Populations in Respiratory Syncytial Virus-Induced Bronchiolitis, *J. Paediatr. Child Health 37*, 146–151.

4. Harrison, A.M., Bonville, C.A., Rosenberg, H.F., and Domachowske, J.B. (1999) Respiratory Syncytical Virus-Induced Chemokine Expression in the Lower Airways: Eosinophil Recruitment and Degranulation, *Am. J. Respir. Crit. Care Med. 159*, 1918–1924.

5. Schwarze, J., Hamelmann, E., Bradley, K.L., Takeda, K., and Gelfand, E.W. (1997) Respiratory Syncytial Virus Infection Results in Airway Hyperresponsiveness and Enhanced Airway Sensitization to Allergen, *J. Clin. Invest. 100*, 226–233.

6. Schwarze, J., and Gelfand, E.W. (2002) Respiratory Viral Infections as Promoters of Allergic Sensitization and Asthma in Animal Models, *Eur. Respir. J. 19*, 341–349.

7. Thomas, L.H., Wickremasinghe, M.I., Sharland, M., and Friedland, J.S. (2000) Synergistic Upregulation of Interleukin-8 Secretion from Pulmonary Epithelial Cells by Direct and Monocyte-Dependent Effects of Respiratory Syncytial Virus Infection, *J. Virol. 74*, 8425–8433.

8. Skoner, D.P., Fireman, P., Caliguiri, L., and Davis, H. (1990) Plasma Elevations of Histamine and a Prostaglandin Metabolite in Acute Bronchiolitis, *Am. Rev. Respir. Dis. 142*, 359–364.

9. Panuska, J.R., Midulla, F., Cirino, N.M., Villani, A., Gilbert, I.A., McFadden, E.R., Jr., and Huang, Y.T. (1990) Virus-Induced Alterations in Macrophage Production of Tumor Necrosis Factor and Prostaglandin E$_2$, *Am. J. Physiol. 259*, L396–L402.

10. Vancheri, C., Mastruzzo, C., Sortino, M.A., and Crimi, N. (2004) The Lung as a Privileged Site for the Beneficial Actions of PGE$_2$, *Trends Immunol. 25*, 40–46.

11. Hawkes, J.S., Bryan, D.-L., James, M.J., and Gibson, R.A. (1999) Cytokines (IL-1β, IL-6, TNFα, TGFβ$_1$ and TGFβ$_2$) and Prostaglandin E$_2$ in Human Milk During the First Three Months Postpartum, *Pediatr. Res. 46*, 194–199.

12. Broekhuyse, R.M. (1974) Improved Lipid Extraction of Erythrocytes, *Clin. Chim. Acta 51*, 341–343.

13. Bryan, D.-L., Hart, P., Forsyth, K., and Gibson R. (2001) Incorporation of α-Linolenic Acid and Linoleic Acid into Human Respiratory Cell Lines, *Lipids 36*, 713–717.

14. Richardson, J.Y., Ottolini, M.G., Pletneva, L., Boukhvalova, M., Zhang, S., Vogel, S.N., Prince, G.A., and Blanco, J.C.G. (2005) Respiratory Syncytial Virus (RSV) Infection Induces Cyclooxygenase 2: A Potential Target for RSV Therapy, *J. Immunol. 174*, 4356–4364.

15. Newman, S.P., Flower, R.J., and Croxtall, J.D. (1994) Dexamethasone Suppression of IL-1 β-Induced Cyclooxygenase 2 Expression Is not Mediated by Lipocortin-1 in A549 Cells, *Biochem. Biophys. Res. Commun. 202*, 931–939.

16. Newton, R., Kuitert, L.M., Slater, D.M., Adcock, I.M., and Barnes, P.J. (1997) Cytokine Induction of Cytosolic Phospholipase A$_2$ and Cyclooxygenase-2 mRNA Is Suppressed by Glucocorticoids in Human Epithelial Cells, *Life Sci. 60*, 67–78.

17. Trebble, T.M., Wootton, S.A., Miles, E.A., Mullee, M., Arden, N.K., Ballinger, A.B., Stroud, M.A., and Beattie, R.M. (2003) Prostaglandin E$_2$ Production and T Cell Function After Fish-Oil Supplementation: Response to Antioxidant Cosupplementation, *Am. J. Clin. Nutr. 78*, 376–382.

18. Saunders, M.A., Belvisi, M.G., Cirino, G., Barnes, P.J., Warner, T.D., and Mitchell, J.A. (1999) Mechanisms of Prostaglandin E$_2$ Release by Intact Cells Expressing Cyclooxygenase-2: Evidence for a "Two-Component" Model, *J. Pharmacol. Exp. Ther. 288*, 1101–1106.

19. Gibson, R.A., Neumann, M.A., and Makrides, M. (1997) Effect of Increasing Breast Milk Docosahexaenoic Acid on Plasma and Erythrocyte Phospholipid Fatty Acids and Neural Indices of Exclusively Breast Fed Infants, *Eur. J. Clin. Nutr. 51*, 578–584.

20. Fiedler, M.A., Wernke-Dollries, K., and Stark, J.M. (1996) Mechanism of RSV-Induced IL-8 Gene Expression in A549 Cells Before Viral Replication, *Am. J. Physiol. 271*, L963–L971.

21. Wang, S.Z., Xu, H., Wraith, A., Bowden, J.J., Alpers, J.H., and Forsyth, K.D. (1998) Neutrophils Induce Damage to Respiratory Epithelial Cells Infected with Respiratory Syncytial Virus, *Eur. Respir. J. 12*, 612–618.

22. Jiang, Z., Kunimoto, M., and Patel, J.A. (1998) Autocrine Regulation and Experimental Modulation of Interleukin-6 Expression by Human Pulmonary Epithelial Cells Infected with Respiratory Syncytial Virus, *J. Virol. 72*, 2496–2499.

23. Patel, J.A., Kunimoto, M., Sim, T.C., Garofalo, R., Eliott, T., Baron, S., Ruuskanen, O., Chonmaitree, T., Ogra, P.L., and Schmalstieg, F. (1995) Interleukin-1 α Mediates the Enhanced Expression of Intercellular Adhesion Molecule-1 in Pulmonary Epithelial Cells Infected with Respiratory Syncytial Virus, *Am. J. Respir. Cell Mol. Biol. 13*, 602–609.

24. Gershwin, L.J., Giri, S.N., Stewart, R.S., and Chen, J. (1989) Prostaglandin and Thromboxane Concentrations in Plasma and Lung Lavage Fluids During Sequential Infection of Vaccinated and Nonvaccinated Calves with Bovine Respiratory Syncytial Virus, *Am. J. Vet. Res. 50*, 1254–1262.

25. Tilley, S.L., Hartney, J.M., Erikson, C.J., Jania, C., Nguyen, M., Stock, J., McNeisch, J., Valancius, C., Panettieri, R.A., Jr., Penn, R.B., and Koller, B.H. (2003) Receptors and Pathways Mediating the Effects of Prostaglandin E$_2$ on Airway Tone, *Am. J. Physiol. Lung Cell. Mol. Physiol. 284*, L599–L606.

26. Mathe, A.A., and Hedqvist, P. (1975) Effect of Prostaglandin F$_2$α and E$_2$ on Airway Conductance in Healthy Subjects and Asthmatic Patients, *Am. Rev. Respir. Dis. 111*, 313–320.

27. Huang, M., Stolina, M., Sharma, S., Mao, J.T., Zhu, L., Miller, P.W., Wollman, J., Herschman, H., and Dubinett, S.M. (1998) Non-Small Cell Lung Cancer Cyclooxygenase-2-Dependent Regulation of Cytokine Balance in Lymphocytes and Macrophages: Up-regulation of Interleukin 10 and Down-regulation of Interleukin 12 Production, *Cancer Res. 58*, 1208–1216.

28. Romagnani, S., Maggi, E., Parronchi, P., Macchia, D., Piccinni, M.P., and Ricci, M. (1991) Increased Numbers of Th2-like CD4+ T Cells in Target Organs and in the Allergen-Specific Repertoire of Allergic Patients. Possible Role of IL-4 Produced by Non-T Cells, *Int. Arch. Allergy Appl. Immunol. 94*, 133–136.

29. Bont, L., Heijnen, C.J., Kavelaars, A., van Aalderen, W.M., Brus, F., Draaisma, J.T., Geelen, S.M., and Kimpen, J.L. (2000) Monocyte IL-10 Production During Respiratory Syncytial Virus Bronchiolitis Is Associated with Recurrent Wheezing in a One-Year Follow-up Study, *Am. J. Respir. Crit. Care Med. 161*, 1518–1523.

30. Bont, L., Kavelaars, A., Heijnen, C.J., van Vught, A.J., and Kimpen, J.L. (2000) Monocyte Interleukin-12 Production Is Inversely Related to Duration of Respiratory Failure in Respiratory Syncytial Virus Bronchiolitis, *J. Infect. Dis. 181*, 1772–1775.

31. Blanco-Quiros, A., Gonzalez, H., Arranz, E., and Lapena, S. (1999) Decreased Interleukin-12 Levels in Umbilical Cord Blood in Children Who Developed Acute Bronchiolitis, *Pediatr. Pulmonol. 28*, 175–180.

Use of a ^{13}C Tracer to Investigate Lutein as a Ligand for Plasma Transthyretin in Humans

Liwei Chen[a], Xixuan Hu Collins[a], Louisa B. Tabatabai[b], and Wendy S. White[a],*

[a]Center for Designing Foods to Improve Nutrition, Iowa State University, Ames, Iowa 50011,
and [b]National Animal Disease Center, ARS, USDA, Ames, Iowa 50010

ABSTRACT: The selective accumulation of lutein in the macula of the human retina is likely to be mediated by specific transport and/or binding proteins. Our objective was to determine whether transthyretin (TTR) is a plasma transport protein for lutein. We used a biosynthetic ^{13}C-lutein tracer and GC–combustion interfaced–isotope ratio MS to gain the requisite sensitivity to detect the minute amounts of lutein expected as a physiological ligand for TTR. Subjects ($n = 4$) each ingested 1 mg of ^{13}C-lutein daily for 3 d and donated blood 24 h after the final dose. For three subjects, the plasma TTR–retinol-binding protein (RBP) complex was partially purified by anion-exchange (diethylaminoethyl, DEAE) chromatography and then dissociated by hydrophobic-interaction chromatography to yield the TTR component. For subject 4, the initial DEAE purification step was omitted and total plasma TTR (RBP-bound and free) was isolated by hydrophobic-interaction chromatography. In each case, the crude TTR fractions were then purified to homogeneity by RBP–Sepharose affinity chromatography. Pure TTR was extracted with chloroform, and unlabeled lutein was added to the extract as a carrier. The mean ^{13}C/^{12}C ratio (expressed in delta notation, δ^{13}C) of the lutein fraction isolated from the plasma TTR extracts of the four subjects was -30.53 ± 3.29‰. The δ^{13}C value of the unlabeled lutein carrier was -30.97 ± 0.27‰. Thus, no ^{13}C enrichment was detected in association with TTR. We conclude that lutein is not associated with TTR in human plasma after being ingested in physiological amounts.

Paper no. L9713 in *Lipids 40*, 1013–1022 (October 2005).

Age-related macular degeneration (AMD) is the leading cause of blindness among Caucasians in the United States, accounting for 54.4% of cases (1). AMD is a progressive disease involving degeneration of the retinal pigment epithelium and photoreceptors in the small central region of the retina known as the macula. Lutein and zeaxanthin are dietary carotenoids that circulate in plasma and accumulate in the macula (2,3). A protective role for these macular pigments is suggested by associations of higher plasma lutein concentrations and/or higher macular pigment densities with lower risk of AMD (4–6). Increased consumption of foods or supplements rich in lutein and zeaxanthin raises serum concentrations of these carotenoids and, in many cases, increases macular pigment density (7–10). In small clinical studies, there were improvements in visual acuity in AMD patients after lutein supplementation (11,12).

The active accumulation of lutein and zeaxanthin in the macula is almost certainly mediated by transport and/or binding proteins. The macular pigment concentration approaches a remarkable 1 mM in the central macula (13). This concentration exceeds typical lutein concentrations in serum (0.1–1.23 μM) by a factor of 10^3 to 10^4 (14). The uptake of lutein and zeaxanthin by the macula is highly selective; other prominent serum carotenoids such as α-carotene, β-carotene, and lycopene are not present (13). Lutein and zeaxanthin are constitutional isomers that have hydroxyl groups on the cyclic end rings; the only structural distinction is the placement of one double bond in one of the rings (Fig. 1). The systematic spatial distribution of zeaxanthin in the macula and the presence of a unique steroisomer, *meso*-zeaxanthin (3*R*,3′*S*-zeaxanthin), strongly point to the existence of a biochemical pathway for the conversion of lutein to zeaxanthin (3). Recently, retinal *meso*-zeaxanthin was shown to be derived from dietary lutein in rhesus monkeys (15). According to this model, lutein is transported to strategic sites within the retina where it is converted to *meso*-zeaxanthin.

One candidate lutein transport protein is transthyretin (TTR). TTR is a multifunctional protein that associates with
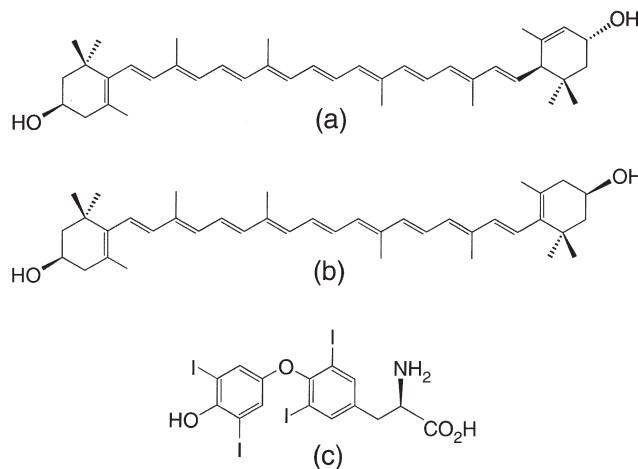
FIG. 1. Structures of (a) lutein, (b) zeaxanthin, and (c) thyroxine.

several molecules of biological importance (16). The two well-established functions of human TTR are the transport of thyroxine (17) and the transport of retinol *via* the retinol-binding protein (RBP)–TTR complex (18). Also associated with TTR in human plasma are various small biomolecules, including fatty acids (19), amino acids, glutathione, and a yellow hydrophobic compound (16). In chicken serum, the yellow component was shown to be lutein, which is transported in specific association with TTR to the exclusion of other carotenoids (20). Chickens are fed rations supplemented with lutein as a source of broiler and yolk pigmentation (21), which results in serum lutein concentrations 15- to 40-fold higher than those in humans (22). In human plasma, the major yellow component associated with TTR was not lutein and was tentatively identified as a yellow pterin derivative, 7,8-dihydropterin-6-carboxaldehyde (23). However, the presence of carotenoid-derived components could not be excluded (20).

In the mammalian eye, TTR has widespread distribution in cells of the retinal pigment epithelium, retinal ganglion, ciliary and iris epithelium, corneal endothelium, and lens capsule (24,25). However, TTR mRNA is found only in the retinal pigment epithelium (26). Both TTR and RBP are synthesized and secreted by retinal pigment epithelial cells (27–29). Since TTR is present in both plasma and retina, an additional biological function of TTR could be selective lutein transport in the plasma and selective deposition in the central retina. The photoreceptors of the retina require retinol for the synthesis of rhodopsin. Retinol is delivered to the retinal pigment epithelium *via* membrane receptors that bind the holo–RBP–TTR complex (30). This model would allow specific and coordinated delivery of both retinol and lutein to the retina. Although lutein is remarkably concentrated in the central retina, the absolute amounts deposited are small. The macula contains only 5–40 ng of lutein concentrated within a 4–5 mm radius (31). When lutein is ingested in physiological amounts, the minute amounts of lutein present as a ligand to transport or binding proteins could escape detection by conventional means such as HPLC with UV/vis detection. Our objective was to use physiological doses of a uniformly labeled ^{13}C-lutein tracer and high-precision GC–combustion interfaced–isotope ratio MS (GC–C–IRMS) as a high-sensitivity approach to investigate lutein as a potential physiological ligand for TTR in human plasma.

MATERIALS AND METHODS

Materials. The source of RBP and TTR for preparation of the RBP– and TTR–Sepharose affinity columns, respectively, was outdated human plasma donated by the Blood Bank of Mary Greeley Hospital, Ames, Iowa. All-*trans*-retinol, phenyl-Sepharose CL-4B, Coomassie Brilliant Blue G, and Bradford reagent were purchased from Sigma (St. Louis, MO). The anion-exchange resin DE 52 was obtained from Whatman International Ltd. (Maidstone, Kent, United Kingdom). The CNBr-activated Sepharose 4B affinity medium was supplied by Amersham Pharmacia Biotech (Piscataway, NJ). Solvents

used for HPLC analysis were HPLC grade and purchased from Fisher Scientific (Pittsburgh, PA).

Subjects. Informed consent was obtained from all subjects, and study protocols were approved by the Iowa State University Human Subjects Review Committee. Four healthy women 19–38 years of age were enrolled in the study. Subjects were screened initially by interview using a standardized questionnaire that addressed health and lifestyle factors. Exclusion criteria were current or recent (previous 12 mon) cigarette smoking, frequent consumption of alcoholic beverages (>1 drink/d), current or planned pregnancy, current or recent (previous 6 mon) use of oral contraceptive agents or contraceptive implants, current or recent (previous 1 mon) use of medications that may affect lipid absorption or transport (including antibiotics), and current or recent (previous 3 mon) use of multivitamin, β-carotene, lutein, or other carotenoid supplements. Also excluded were those who had a history of anemia or excessive bleeding, psychological aversion to phlebotomy, whole blood donation within an 8-wk period preceding scheduled blood donation for the study, chronic disease, macular degeneration or other eye diseases, lipid malabsorption or gastrointestinal disorders, lactose intolerance, abnormal thyroid status, photosensitivity, vegetarian diet, obesity (body mass index ≥ 30) and recent change in body weight (>4.5 kg in previous month). The final exclusion criteria were a blood hemoglobin concentration < 125 g/L or abnormal hematocrit or red cell indices as measured at the Iowa State University Thielen Student Health Center within the 7-d period preceding the scheduled blood donation for the study.

^{13}*C-Lutein tracer.* The ^{13}C-lutein tracer was isolated from the nonsaponifiable fraction of a crude lipid extract of *Chlorella* sp. (Martek Bioscience Corp, Columbia, MD) by using a modification of our published method (32). The algae were grown under an environment of ^{13}C-labeled CO_2 so that all biomolecules, including lutein, were uniformly labeled with ^{13}C. The purified crystalline ^{13}C-lutein was stored under argon in the dark at −80°C. Confirmatory mass spectra of the purified ^{13}C-lutein tracer were obtained using a Finnegan (currently Thermoquest, San Jose, CA) TSQ 700 triple quadrupole mass spectrometer in electron ionization mode (70 eV). The sample was introduced into the ion source by direct insertion probe at 200°C. Mass spectra were acquired over the range *m/z* 100–800 in 0.75 s.

Study protocol. Subjects were instructed to avoid fruits, vegetables, and dietary supplements with a high lutein content for a 3-wk period preceding dosing with ^{13}C-lutein. The intent was to deplete serum TTR of lutein originating from the diet to maximize saturation of TTR with lutein originating from the ^{13}C-lutein doses. Subjects ingested an emulsion prepared with banana (30 g), fat-free milk (70 mL), and high-oleic sunflower oil (28 g; Abitec Corporation, Janesville, WI) that contained 1.0 mg of ^{13}C-labeled lutein (32). Each subject ingested the ^{13}C-lutein-containing emulsion on each day of the 3-d treatment period. The emulsion was ingested at 24-h intervals under observation in the Human Metabolic Unit in the Center for Designing Food to Improve Nutrition at Iowa State University.
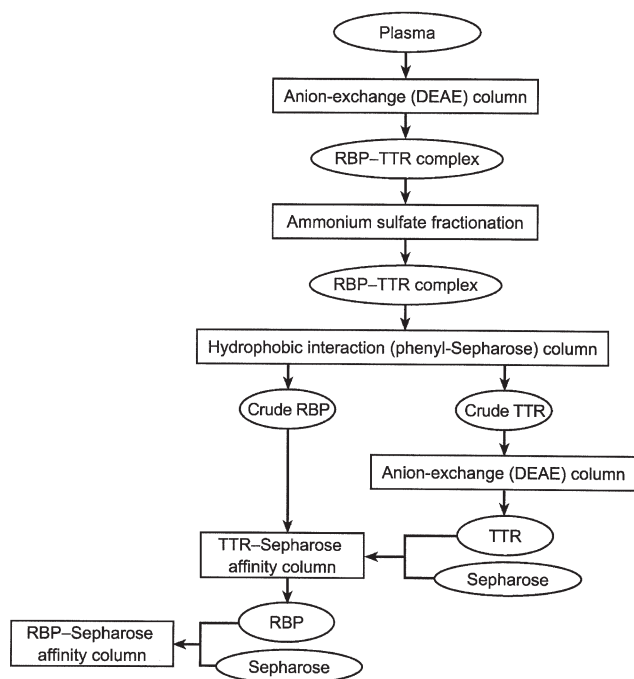
FIG. 2. Protocol for preparation of the retinol-binding protein (RBP)–Sepharose affinity column used in the final purification of plasma transthyretin (TTR) from subjects who ingested a ^{13}C-lutein tracer. DEAE, diethylaminoethyl.

The 1.0-mg daily dose of lutein is within the range of typical daily intakes of lutein in the U.S. population (22).

Each subject donated 500 mL of blood for isolation of TTR 24 h after ingestion of the third and final dose of ^{13}C-labeled lutein. Blood was collected in the Human Metabolic Unit by a registered nurse used as a phlebotomist at a local blood bank. Plasma was separated by using a plasma extractor (Baxter Healthcare Corp., Round Lake, IL). The individual plasma samples were stored at −70°C until used for isolation of TTR.

Preparation of affinity columns. An RBP–Sepharose affinity column was used in the final purification step to isolate TTR from the plasma of our subjects who were dosed with ^{13}C-lutein. To prepare the RBP–Sepharose affinity column, a TTR–Sepharose affinity column was first prepared and used to purify the plasma RBP fraction to homogeneity (Fig. 2). The purified RBP was then used to prepare the RBP–Sepharose affinity column. The source of the RBP and TTR used to prepare the affinity columns was outdated human plasma. All procedures were carried out at 4°C.

(i) Purification of TTR from outdated human plasma. The outdated plasma (1 L) was filtered though a 0.25-in. bed of Celite to remove lipids. The filtrate was then dialyzed for 16 h against 5 L of 0.05 M phosphate buffer, pH 7.4, containing 0.05 M NaCl. The presence of retinol bound to RBP is essential for the formation of a stable complex with TTR (33). To ensure saturation of the RBP with retinol, the dialyzed plasma was incubated with a 5×10^{-4} M solution of all-*trans*-retinol in DMSO. An equimolar amount of retinol to RBP was used. The mixture was incubated for 30 min at room temperature in the

dark. The plasma was then centrifuged at $10,000 \times g$ for 30 min to remove any precipitate.

Anion-exchange (diethylaminoethyl, DEAE) chromatography was used to partially purify the holo-RBP–TTR complex. The dialyzed plasma was applied to a DE 52 column (2.5×22 cm), which was previously equilibrated in the dialysis buffer, and washed with 0.05 M phosphate buffer, pH 7.4, containing 0.05 M NaCl until there was no absorbance at 280 nm. The column was eluted with a 500-mL linear gradient of NaCl from 0.05 to 0.5 M in 0.05 M phosphate buffer, pH 7.4, at a flow rate of 70 mL/h. Fractions of 5 mL were collected and scanned for absorbance at 280 nm, 330 nm (resulting from bound retinol), and 450 nm (for detection of yellow pigment). The elution of the RBP–TTR complex was also monitored by following the fluorescence of the bound retinol (335 nm excitation, 460 nm emission). Fractions with both fluorescence and UV absorbance contained the RBP–TTR complex.

The RBP–TTR complex was further purified by ammonium sulfate fractionation. The sample was concentrated under nitrogen pressure to a volume of 100 mL in an Amicon ultrafiltration cell (Amicon, Inc., Beverly, MA) with a YM-3 filter (Millipore Corporation, Bedford, MA). Ammonium sulfate was added to a final concentration of 1.5 M, the pH was adjusted to 6.0 by 2 M citric acid, and the solution was allowed to stand overnight. The precipitate was removed by centrifugation at $10,000 \times g$ for 10 min.

The RBP–TTR complex was then dissociated by using hydrophobic-interaction chromatography (34). The clear supernatant from the ammonium sulfate precipitation was applied to a phenyl-Sepharose CL-4B column (2.5×33 cm) previously equilibrated with 0.05 M citrate buffer, pH 6.0, containing 1.5 M ammonium sulfate. The column was immediately eluted with a linear gradient from the starting buffer to 0.03 M phosphate buffer, pH 7.0 (1500 mL). The flow rate was 120 mL/h; 10-mL fractions were collected and tested for absorbance at 280, 330, and 400 nm. Fractions 50–120 contained TTR. The RBP eluted before fraction 150. The pooled TTR fractions (about 150 mL) were dialyzed overnight against 0.05 M Tris-acetate buffer, pH 8.3.

The crude TTR fraction was further purified using a second DEAE column (2.5×30 cm), which was previously equilibrated in the dialysis buffer. Elution was carried out with a 500-mL linear gradient from 0.05 M Tris-acetate buffer, pH 8.3, to 0.33 M Tris-acetate buffer containing 0.2 M NaCl at a flow rate of 60 mL/h. Fractions of 5 mL were collected and scanned for protein absorbance. The major peak, which contained TTR, was concentrated by ultrafiltration and stored at −80°C until used for packing the TTR–Sepharose affinity column.

(ii) Preparation of the TTR–Sepharose affinity column. To prepare the TTR–Sepharose affinity column, the purified TTR was concentrated and dialyzed using a Micro ProDiCon CE membrane (Spectrum, Houston, TX) in a Micro-ConFilt Vacuum Dialysis Unit (Bio-Molecular Dynamics, Beaverton, OR). The concentrated TTR was then coupled with the CNBr-activated Sepharose 4B affinity medium according to the instructions provided by the supplier. A total of 35 mg of purified TTR was used to pack a 5-mL (1.5×3.0 cm) column.

(iii) Purification of RBP by TTR–Sepharose affinity chromatography. The crude RBP fraction previously eluted from the phenyl-Sepharose column was then purified to homogeneity by using the TTR–Sepharose affinity column. The RBP fraction was first dialyzed against 0.01 M PBS buffer containing 0.5 M NaCl, pH 7.4, using a Slide-A-Lyzer Dialysis Cassette (Pierce, Rockford, IL). The dialyzed sample was then applied to the TTR–Sepharose affinity column, which had been equilibrated with the dialysis buffer. Fractions of 2 mL were collected and the flow rate was adjusted to 1.0 mL/min. After the sample was loaded onto the column, followed by 1 mL of starting buffer, the flow was stopped for 20 min to ensure binding of the RBP to the gel matrix. The column was then washed with 3 bed volumes of starting buffer followed by 3 bed volumes of 0.01 M PBS (no NaCl). The RBP fraction was eluted with deionized water. The pure RBP from several runs was pooled, concentrated by vacuum dialysis, and stored at −80°C under argon.

(iv) Preparation of the RBP–Sepharose affinity column. A total of 11 mg of pure RBP was used to pack a 2-mL RBP–Sepharose affinity column (1.0×2.5 cm). The coupling and packing procedures were the same as those used to prepare the TTR–Sepharose affinity column. The RBP–Sepharose affinity column was saved until used in the final purification step in the isolation of TTR from the plasma of our subjects who ingested the ^{13}C-lutein tracer.

Purification of TTR from ^{13}C-lutein-labeled plasma. *(i) Method 1.* The RBP-bound TTR fraction was purified from 250-mL samples of ^{13}C-lutein-labeled plasma collected from subjects 1–3. The RBP-bound TTR was isolated by using a combination of anion-exchange (DEAE) chromatography and ammonium sulfate precipitation, as previously described for the isolation of TTR from outdated human plasma to prepare the TTR–Sepharose affinity column. Phenyl-Sepharose chromatography was then used to dissociate the RBP–TTR complex, as previously described.

(ii) Method 2. The total TTR (free and RBP-bound) fraction was purified from the ^{13}C-lutein-labeled plasma of subject 4. Total plasma TTR was isolated by omitting the initial DEAE chromatography step. A 100-mL aliquot of plasma was subjected to ammonium sulfate fractionation and applied to a phenyl-Sepharose column (2.5×33 cm) to dissociate the RBP–TTR complex as previously described. A 1500-mL buffer gradient was used because of the larger column size, and 15-mL fractions were collected. Fractions were monitored for absorbance at 280, 330, and 450 nm. Three peaks were identified. These fractions were concentrated and analyzed by photodiode array spectrophotometry for absorbance spectra and by SDS-PAGE for purity. Peak 1, which contained TTR, was concentrated to a volume of 5 mL.

(iii) RBP–Sepharose affinity chromatography. For each of the four subjects, the partially purified TTR fraction collected from the phenyl-Sepharose column was purified to homogeneity by using the RBP–Sepharose affinity column. The protocol was the same as previously described for the purification of RBP by TTR–Sepharose affinity chromatography. The TTR fraction was eluted with deionized water and concentrated to a 0.5-mL volume by vacuum dialysis. The pure TTR was removed and the dialysis membrane was washed three times with 0.5 mL of PBS. The washings were combined with the 0.5-mL pure TTR fraction to obtain a final volume of 2 mL. The pure TTR was stored in a brown vial at −80°C under argon until analysis for ^{13}C-lutein content.

SDS-PAGE and immunoblotting. The purity of the protein fractions was analyzed by SDS-PAGE using an XCell Sure-Lock Mini-Cell, NuPage 12% Bis-Tris gels, NuPage MOPS SDS Running Buffer, NuPage LDS Sample Buffer, and Nu-Page Antioxidant, according to instructions provided by the manufacturer (Invitrogen Corp., Carlsbad, CA). Gels were stained using Coomassie Brilliant Blue G (Sigma). Immunoblotting was performed using the Mini Trans-Blot Electrophoretic Transfer Cell, Tris/Glycine Transfer Buffer (Bio-Rad, Hercules, CA), and a BA83 Pure Nitrocellulose Transfer and Immobilization membrane (Schleicher & Schuell, Inc., Keene, NH). The Perfect Protein AP Western Blot Kit was obtained from Novagen (CN Biosciences, Inc., Madison, WI). Goat antihuman prealbumin IgG (N-19, sc-8105) and alkaline phosphatase-conjugated bovine antigoat IgG (sc-2351) were obtained from Santa Cruz Biotechnology (Santa Cruz, CA). Rabbit antihuman RBP and alkaline phosphatase-conjugated goat antirabbit immunoglobins were purchased from Dako Corporation (Carpinteria, CA). BCIP/NBT Phosphatase Substrate was obtained from KPL, Inc. (Gaithersburg, MD). Pure human TTR and RBP standards were purchased from Sigma.

The protein concentration in the samples was measured at each purification step by the Bradford method. The absorbance at 595 nm was measured using an ELX 808 Automated Microplate Reader (Bio-Tek Instruments Inc., Winoosk, VT).

GC–C–IRMS analysis of the TTR extract. Each 2-mL TTR fraction was mixed with 2 mL of ethanol (0.01% BHT) followed by 4 mL of chloroform (0.01% BHT). The mixture was partitioned in a separatory funnel and the chloroform layer was saved. This partition step was repeated four times, and the chloroform fractions were combined and dried under vacuum. Unlabeled lutein (4.8 nmol) in ethanol (0.01% BHT) was added to each extract as a carrier to provide sufficient mass for HPLC purification and GC–C–IRMS analysis. The added ethanol was then dried under vacuum. The dried extract was redissolved in 50 μL of ethyl ether plus 200 μL methanol; 245 μL was injected into the HPLC system for isolation of the lutein fraction.

The HPLC system comprised the following equipment (Waters, Milford, MA): a 717Plus Autosampler with temperature control set to 5°C, two 510 solvent delivery systems, and a 996 photodiode array detector. The system was operated with Millennium[32] Chromatography Manager Software. The lutein fraction was collected from a 5-μm C_{30} 4.6×250 mm analytical column (Carotenoid Column; YMC, Wilmington, NC). Carotenoids were eluted by a linear gradient (100:0 methanol containing 0.1% ammonium acetate to 0:100 methyl *tert*-butyl ether over 30 min); the flow rate was 1 mL/min. Elution of carotenoids was monitored at 453 nm. The lutein fraction was collected, dried under vacuum, redissolved in 50 μL of ethyl

ether plus 150 µL of methanol, and repurified by injecting 195 µL into the HPLC system using the same RP-HPLC conditions. The lutein peak identities were confirmed by comparison of photodiode-array spectra with that of a commercial lutein standard (Kemin Industries, Des Moines, IA). Purified lutein was dissolved in cyclohexane and converted to thermally stable perhydro-β-carotene by hydrogenation and acid-catalyzed hydrogenolysis according to a method established in our laboratory (32). Derivatization to perhydro-β-carotene was necessary to prevent thermal degradation during GC separation prior to IRMS analysis. The perhydro-β-carotene derivatization product was dried under vacuum and stored under argon at −20°C until analyzed by GC–C–IRMS.

A 5890A Hewlett-Packard (Wilmington, DE) gas chromatograph fitted with a Fisons/VG Isotech Isochrom GC–Combustion interface to the Fisons/VG Isotech (Micromass UK Ltd., Manchester, United Kingdom) Optima Isotope Ratio mass spectrometer was used to measure the stable carbon ratio of the perhydro-β-carotene derivative of lutein. A 15 m × 0.25 mm i.d. (0.25 µm thickness) HP-1MS (J&W Scientific, Folsom, CA) fused-silica capillary column with on-column injector was used with ultrapure helium as carrier gas at a flow rate of 40 cm/s. The temperature program proceeded from 50°C, followed by a gradient of 30°C/min to 150°C, followed by a gradient of 15°C/min to 300°C. The temperature was then held at 300°C for 22 min. After injection into the GC–C–IRMS, perhydro-β-carotene was quantitatively combusted to CO_2 and H_2O. The H_2O was then removed by a chemical trap and the CO_2 gas was purified by chromatography on a Porapak QS column (4 mm i.d. × 2 m) at 60°C before entry into the dual inlet of the isotope ratio mass spectrometer. The computer-generated carbon isotope ratio measurements, expressed in delta (δ) per mil (‰) units, were used to calculate the atom% ^{13}C in each sample according to the following equation:

$$\text{atom\% } ^{13}C = \frac{(100 \times R_{PDB}) \times (\delta\,^{13}C/1000 + 1)}{1 + (R_{PDB}) \times (\delta\,^{13}C/1000 + 1)} \qquad [1]$$

where $R = {}^{13}C/{}^{12}C$ (32). The R_{PDB} represents the $^{13}C/^{12}C$ ratio for the international standard for carbon, which was obtained from the Pee Dee Belemnite formation in South Carolina, with an accepted value of $R_{PDB} = 0.0112372 \pm 0.000009$. A difference of 1‰ corresponds to a change of 0.001099 atom% ^{13}C at natural abundance (35).

RESULTS

Purity of the ^{13}C-lutein tracer. The final composition of the biosynthetic ^{13}C-lutein tracer was 96.5% lutein and 3.5% zeaxanthin based on the relative peak areas determined by using HPLC analysis (Fig. 3). The UV/vis absorbance spectrum measured by HPLC with photodiode array detection was identical to that of a commercial lutein standard (Kemin Industries, Des Moines, IA) (Fig. 4). The electron ionization (70 eV) mass spectrum shows the fragmentation of the ^{13}C-labeled lutein with a base peak at *m/z* 608.4 (Fig. 5). The molecular mass of unlabeled lutein, a C_{40} carotenoid, was 568.4. Thus, the mass
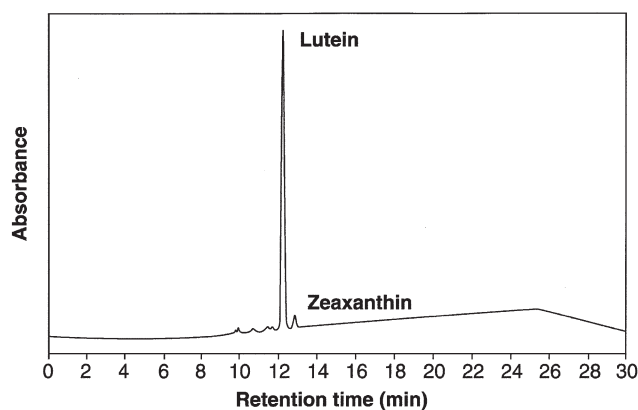
FIG. 3. HPLC chromatogram showing the high purity of the ^{13}C-lutein tracer purified from a crude lipid extract of biosynthetically ^{13}C-labeled algal biomass (Martek Bioscience, Columbia, MD).

spectral analysis was consistent with a lutein tracer in which each carbon was uniformly labeled with ^{13}C.

Purification and characterization of TTR from ^{13}C-lutein-labeled plasma. SDS-PAGE analysis of the final TTR product isolated from the RBP–Sepharose affinity column showed that TTR was purified to homogeneity (Fig. 6). The identity of the purified TTR was confirmed by immunoblot (Fig. 6).

By using method 1, which was based on initial purification of TTR as a component of the RBP–TTR complex, an average of 8.0 ± 0.4 mg of TTR was purified from each 250-mL sample of ^{13}C-lutein-labeled plasma donated by subjects 1–3 (Table 1). The mean serum RBP concentration in women was 0.048 g/L (38) or 0.012 g in a 250-mL serum sample. RBP is a 21-kDa monomeric protein; the estimated 0.012 g in our serum samples would equate to approximately 0.57 µmol (1 µmol is equivalent to 21 mg). Based on the 1:1 binding stoichiometry of RBP to TTR, we would expect approximately 0.57 µmol, or 31 mg, of RBP-bound TTR in our samples. (TTR is a 55-kDa tetrameric protein; thus, 1 µmol is equivalent to 55 mg.) On this basis, the estimated recovery of RBP-bound TTR purified by using method 1 was approximately 26%. Our isolation protocol was highly reproducible and gave
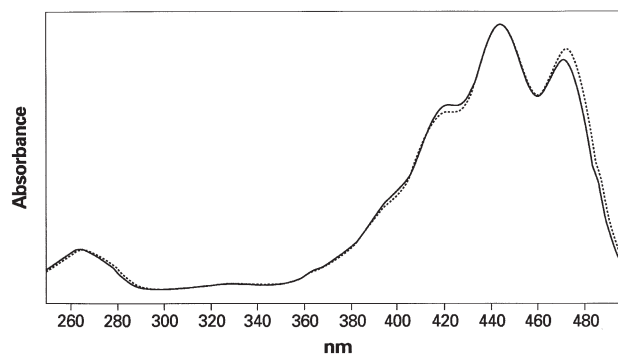
FIG. 4. Near-identical UV/vis absorbance spectra of a commercial lutein standard (reagent grade lutein, Kemin Industries, Des Moines, IA) (—) and the biosynthetic ^{13}C-lutein tracer (····).
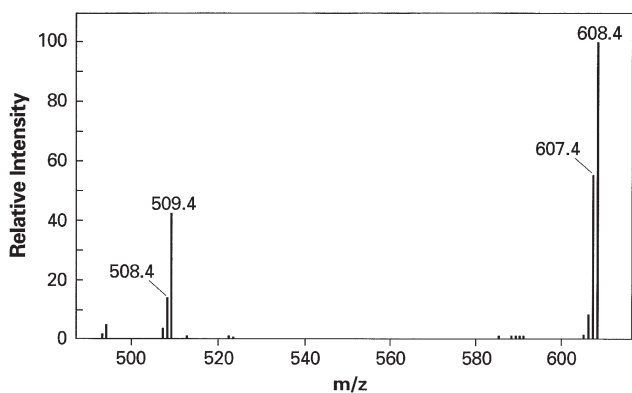
FIG. 5. Electron ionization (70 eV) MS showing fragmentation of the ^{13}C-labeled lutein to form a base peak of *m/z* 608.4. The molecular mass of unlabeled lutein, a C_{40} carotenoid, is 568.4. The mass spectrum is consistent with a lutein tracer in which each carbon is uniformly labeled with ^{13}C.

a yield comparable to that obtained with a previously published method (39).

When method 1 was used to purify RBP-bound TTR from the plasma of our subjects, we did not observe a yellow color in either the partially purified TTR fractions or the final pure TTR product. In method 2, the initial DEAE chromatography step was omitted to isolate the total plasma TTR fraction (RBP-bound and free). Each of the three fractions collected from the phenyl-Sepharose column (TTR, RBP, and an unidentified third fraction) were visibly yellow. In addition to protein absorbance at 280 nm, the TTR-containing fraction (fraction 1) showed absorbance from 380 to 500 nm, with maximal ab-

TABLE 1
Purification of Transthyretin (TTR) from ^{13}C-Lutein-Labeled Human Plasma

Fraction	Total protein[a] (mg)	
	Method 1[b]	Method 2[c]
Plasma	17,659 ± 1,299	7,540
Diethylaminoethyl chromatography	135 ± 5	—
Ammonium sulfate precipitation	84.7 ± 1.5	3,900
Phenyl-Sepharose chromatography	41.0 ± 2.6	21
RBP–Sepharose affinity chromatography	8.0 ± 0.4	4.7

[a]Protein was measured using the Bradford method.
[b]The retinol-binding protein (RBP)-bound TTR fraction was purified from 250 mL of plasma; phenyl-Sepharose chromatography was then used to dissociate the RBP–TTR complex. Yields are expressed ± SD; *n* = 3 samples.
[c]Total TTR (RBP-bound and free) was purified from a single 100-mL plasma sample; phenyl-Sepharose chromatography was then used to dissociate the RBP–TTR complex.

sorbance at 414 nm (Fig. 7). Fraction 2 (containing RBP) and fraction 3 also showed absorbance from 380 to 550 nm, but none of these protein fractions had spectra that resembled the
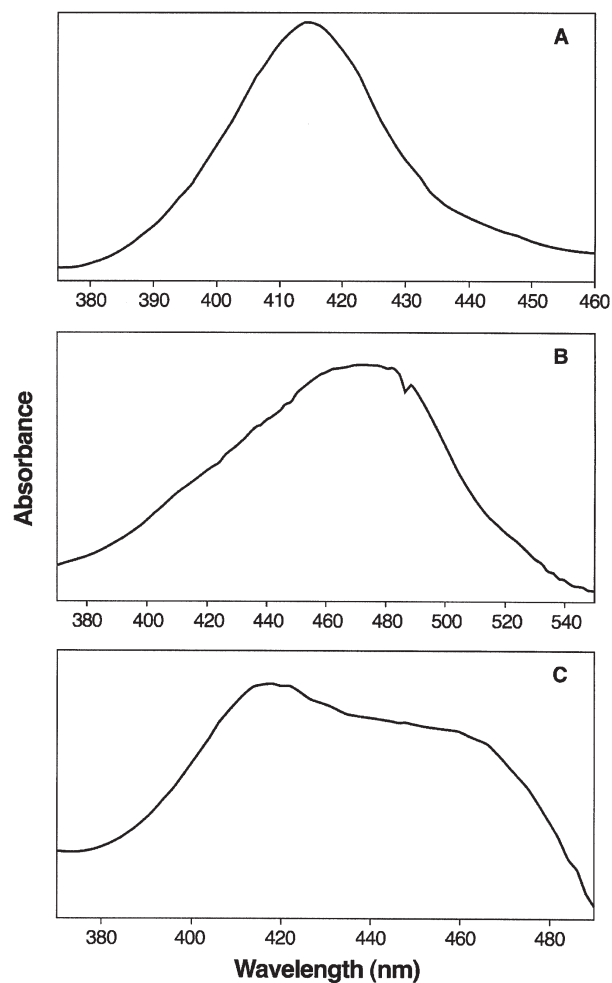
FIG. 7. Absorbance spectra of the yellow protein fractions eluted from the phenyl-Sepharose column during the purification of total TTR (RBP-bound and free) from ^{13}C-lutein-labeled human plasma: (A) the TTR-containing fraction; (B) the RBP-containing fraction; (C) unidentified third fraction. For abbreviations see Figure 2.

FIG. 6. SDS-PAGE gel (left) and immunoblot (right) of human TTR: commercial TTR standard (lanes A and C); purified TTR from human plasma (lanes B and D). Treatment of tetrameric TTR with SDS causes dissociation into 14-kDa monomers (36). The second band present in the commercial TTR standard is most likely an undissociated dimer of the 14-kDa TTR polypeptide (37). For abbreviations see Figure 2.
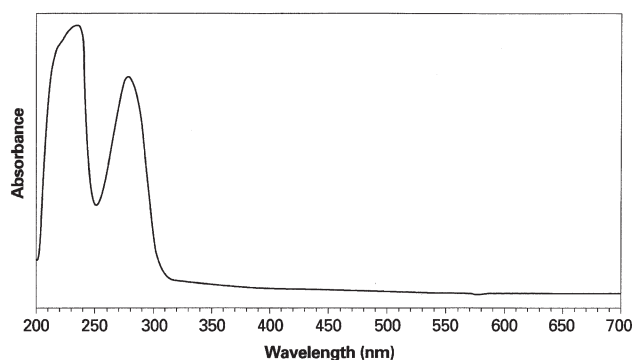
FIG. 8. UV/vis absorbance spectrum of human plasma TTR purified to homogeneity by using RBP–Sepharose affinity chromatography. There was no absorbance in the visible range to indicate the presence of carotenoid pigment. For abbreviations see Figure 2.

three-peak spectra of lutein (Fig. 4) or zeaxanthin. When the TTR-containing peak was applied to the RBP–Sepharose affinity column, the yellow color was lost. The absence of yellow color in the final pure TTR fraction was confirmed by photodiode array spectrophotometry; there was no absorbance between 400 and 500 nm in the pure TTR fraction (Fig. 8).

Analysis of ^{13}C abundance in TTR extracts. Because lutein is thermally labile, it must be converted to a heat-stable form before GC–C–IRMS analysis. To provide sufficient mass for HPLC isolation and subsequent derivatization, our chloroform extracts of TTR were spiked with unlabeled lutein. We then used catalytic hydrogenation and hydrogenolysis of the lutein fraction isolated from the TTR extracts to produce a heat-stable derivatization product, perhydro-β-carotene, suitable for GC–C–IRMS analysis (32). By using GC–C–IRMS analysis, we were able to measure the stable carbon isotope ratio (^{13}C/^{12}C) in the derivatized lutein fraction. The carbon isotope ratios (δ ^{13}C values) in the lutein fraction in the chloroform extracts of TTR purified by using method 1 were −30.57‰ (1.078 atom% ^{13}C), −29.17‰ (1.079 atom% ^{13}C), and −27.33‰ (1.081 atom% ^{13}C) for subjects 1–3, respectively. The δ ^{13}C value of the lutein fraction for subject 4, whose TTR was purified by using method 2, was −35.04‰ (1.073 atom% ^{13}C). These δ ^{13}C values were not different from the measured δ ^{13}C value for the unlabeled commercial lutein standard, which was −30.97‰ (1.077 atom% ^{13}C). Thus, there was no appreciable ^{13}C enrichment in the lutein fraction in any of the TTR extracts.

DISCUSSION

We used a uniformly labeled ^{13}C-lutein tracer and high-precision GC–C–IRMS as a high-sensitivity approach to investigate lutein as a potential ligand for TTR in human plasma. TTR was purified to homogeneity from the plasma of four subjects who were dosed daily for a 3-d period with ^{13}C-lutein. Previously, we used the high sensitivity of GC–C–IRMS to detect differences in the natural abundance of ^{13}C in lutein isolated from C$_3$ and C$_4$ plant sources (40). Despite the capability of GC–C–IRMS analysis to detect even low enrichments only slightly exceeding nat-

ural abundance, no ^{13}C-lutein enrichment was found in chloroform extracts of the purified human plasma TTR. The ^{13}C-lutein tracer was administered in a highly bioavailable emulsion identical to the formulation used in our previous tracer studies (32,41). In those studies involving a combined total of 11 subjects, the measured enrichments in small (4-mL) plasma samples collected at hourly intervals substantially exceeded the limits of detection of GC–C–IRMS analysis. Although the subjects varied considerably in the magnitude of the plasma ^{13}C-lutein response, we were readily able to quantify the plasma appearance and disappearance of ^{13}C-lutein in each subject. Thus, it is unlikely that the lack of association of ^{13}C-lutein with TTR in the present study could be attributed to poor absorption of the tracer dose. In chickens, the extent of saturation of serum TTR with lutein is estimated to be about 50% and the binding stoichiometry assumed to be a 1:1 molar ratio (20). In our human subjects, even if the saturation of plasma TTR with lutein were as low as 1% and the binding stoichiometry were a 1:1 molar ratio, the measured atom% ^{13}C in our lutein extracts analyzed by GC–C–IRMS would have exceeded 20%. The absence of ^{13}C-lutein enrichment in the chloroform extracts of TTR obtained using either of our two purification methods (methods 1 and 2) indicates that lutein is not associated with TTR in human plasma.

TTR is a tetramer of four identical subunits that form a central hydrophobic channel in which the thyroid hormones, thyroxine (T$_4$) and triiodothyronine (T$_3$), bind. TTR is one of the most strongly conserved plasma proteins (42). The similarity of amino acid sequences in chicken and human TTR is 75% overall and 100% for the central channel that contains the T$_4$-binding site (42). Although the amino acids involved in the binding of T$_4$ are completely conserved, the shape of the T$_4$-binding channel in avian and human TTR differs (43). The aspects of the cavity that enclose the inner phenolic and the outer tyrosyl rings of the hormone are narrower in avian TTR. In addition, the avian hormone-binding channel is wider at the entrance. These changes in conformation underlie the differing binding affinities of T$_3$ and T$_4$ to avian as compared with human TTR (43). Human TTR has a higher affinity for T$_4$ and a lower affinity for T$_3$ than does avian TTR. These structural changes could also potentially change the binding affinities for lutein. In contrast to the strong conservation in amino acid sequence in the core region, the NH$_2$ termini of the TTR subunits differ considerably in chickens and humans (44). The longer, more hydrophobic NH$_2$ termini of chicken TTR could change the spatial orientation of the NH$_2$ terminus with respect to the entrance to the central ligand-binding site (44). In turn, this change in conformation could influence the access and binding of thyroxine as well as that of the putative ligand, lutein. The thyroid hormones bind with their hydroxyl groups within hydrogen-bonding distance of the four serine residues at the center of the TTR tetramer (45). In contrast, the binding affinity of nonhydroxylated compounds is weak. Thus, the hydroxyl groups of lutein may account for its selective binding to chicken TTR to the exclusion of other carotenoids (20). Carotenoids are primarily transported in plasma by lipoproteins, and there are species differences in

plasma lipoprotein profiles in humans and chickens. With the exception of laying hens, in which VLDL are elevated, HDL predominate in chicken plasma (46). In humans, LDL predominate. Overall, the various species differences suggest that different ligands may associate with chicken as compared with human TTR.

For each of our four subjects, the final step in the purification of plasma TTR was RBP–Sepharose affinity chromatography. In the case of subject 4, the final purified TTR fraction included both free and RBP-bound TTR. If lutein binds only to free TTR, the affinity ligand, RBP, on the stationary phase might potentially displace lutein during the final purification step. As a result, lutein would not be detected as a TTR ligand. This scenario is unlikely for two reasons: (i) In the chicken, lutein was previously identified as a ligand for serum TTR purified by affinity chromatography on RBP–Sepharose (20), and (ii) the ligand-binding site of TTR does not participate in molecular interactions with RBP (47). The formation of the macromolecular complex of TTR with RBP stabilizes the binding of retinol to RBP (47). In contrast, the binding of T_4 to the ligand-binding site in TTR is identical in the RBP–TTR complex and in the isolated TTR protein.

When the total TTR fraction (RBP-bound and free) was isolated from the plasma of subject 4 (method 2), we observed a bright yellow color in several protein fractions, including the major TTR-containing fraction, that eluted from the phenyl-Sepharose column. The absorbance spectra of the protein fractions in the visible range resembled that of the yellow pterin derivative, 7,8-dihydropterin-6-carboxaldehyde, which was previously reported to be associated with TTR in human plasma (Fig. 7). Although we did not isolate the yellow component, TTR fractions are reported to be yellow-absorbing in the same spectral range as the purified yellow component (16). When the TTR fraction was purified to homogeneity on the RBP–Sepharose affinity column, the pure TTR was no longer yellow, as confirmed by spectral data (Fig. 8). As noted above, a potential explanation could be conformational instability and release of the yellow component upon coupling of TTR to the RBP ligand. However, this explanation was discounted since previous investigators were able to isolate the yellow component from human plasma TTR that was similarly purified by RBP–Sepharose affinity chromatography. In these previous studies, human serum was directly applied to the affinity column without initial purification (16,23,36), resulting in minor contamination of the TTR fraction with RBP and other minor impurities. The presence of RBP is reported to be important in keeping a fraction of TTR in the reduced state (36), which may be a requisite for retention of the yellow component (16). Alternatively, the yellow pigment may have associated with protein contaminants that were removed during the final purification. Each of the yellow protein fractions isolated by hydrophobic-interaction chromatography had similar absorbance in the visible spectrum (Fig. 7). Similarly, Pettersson *et al.* (16) reported a yellow color associated with low M.W. contaminants of the TTR fraction. This raises the possibility of nonspecific association.

The yellow component previously extracted from human TTR was tentatively identified as 7,8-dihydropterin-6-carboxaldehyde, which is known to be formed by oxidative degradation of dihydrofolate (23). The yellow color is enhanced upon boiling in acidic methanol (23). Ernström *et al.* (23) reported that the yellow component associated with human TTR was unstable in pure form and degraded to uncolored compounds when exposed to air. But we did not observe a loss of yellow color in our TTR fraction until application to the RBP–Sepharose affinity column.

In conclusion, we did not detect ^{13}C-lutein in association with TTR isolated from the plasma of subjects who ingested physiologically relevant amounts of ^{13}C-labeled lutein. The remarkably high concentration of xanthophylls in the central retina is almost certainly mediated by a specific binding protein(s). Recently, lutein and zeaxanthin were shown to bind specifically to membrane-associated xanthophyll-binding proteins derived from the human macula (48,49). In the soluble, cytosolic fraction of the human macula, lutein and zeaxanthin were also shown to bind tubulin, a protein component of microtubules (31). However, binding to tubulin could not explain the presence of macular pigment in the photoreceptor outer segment membranes, which do not contact microtubules (50). The transport mechanism that mediates the selective transport of the macular pigment carotenoids into their sites of concentration within the retina is an important research focus. If known, abnormalities such as those resulting from mutations or polymorphisms in genes expressing the specific transport proteins could be used to identify individuals who have increased risk of deficient macular pigment and corresponding increased risk of AMD.

ACKNOWLEDGMENTS

REFERENCES

1. Eye Diseases Prevalence Research Group (2004) Causes and Prevalence of Visual Impairment Among Adults in the United States, *Arch. Ophthalmol. 122*, 477–485.
2. Bone, R.A., Landrum, J.T., and Tarsis, S.L. (1985) Preliminary Identification of the Human Macular Pigment, *Vis. Res. 25*, 1531–1535.
3. Bone, R.A., Landrum, J.T., Friedes, L.M., Gomez, C.M., Kilburn, M.D., Menendez, E., Vidal, I., and Wang, W. (1997) Distribution of Lutein and Zeaxanthin Stereoisomers in the Human Retina, *Exp. Eye Res. 64*, 211–218.
4. Eye Disease Case-Control Group (1993) Antioxidant Status and Neovascular Age-Related Macular Degeneration, *Arch. Ophthalmol. 111*, 104–109.

5. Beatty, S., Murray, I.J., Henson, D.B., Carden, D., Koh, H., and Boulton, M.E. (2001) Macular Pigment and Risk for Age-Related Macular Degeneration in Subjects from a Northern European Population, *Invest. Ophthalmol. Vis. Sci. 42*, 439–446.

6. Bone, R.A., Landrum, J.T., Mayne, S.T., Gomez, C.M., Tibor, S.E., and Twaroska, E.E. (2001) Macular Pigment in Donor Eyes With and Without AMD: A Case-Control Study, *Invest. Ophthamol. Vis. Sci. 42*, 235–240.

7. Yeum, K.J., Booth, S.L., Sadowski, J.A., Liu, C., Tang, G., Krinsky, N.I., and Russell, R.M. (1996) Human Plasma Carotenoid Response to the Ingestion of Controlled Diets High in Fruits and Vegetables, *Am. J. Clin. Nutr. 64*, 594–602.

8. Landrum, J.T., Bone, R.A., Joa, H., Kilburn, M.D., Moore, L.L., and Sprague, K.E. (1997) A One Year Study of the Macular Pigment: The Effect of 140 Days of a Lutein Supplement, *Exp. Eye Res. 65*, 57–62.

9. Hammond, B.R., Johnson, E.J., Russell, R.M., Krinsky, N.I., Yeum, K.J., Edwards, R.B., and Snodderly, D.M. (1997) Dietary Modification of Human Macular Pigment Density, *Invest. Ophthalmol. Vis. Sci. 38*, 1795–1801.

10. Berendschot, T.T.J.M., Goldbohm, R.A., Klöpping, W.A.A., van de Kraats, J., van Norel, J., and van Norren, D. (2000) Influence of Lutein Supplementation on Macular Pigment, Assessed with Two Objective Techniques, *Invest. Ophthalmol. Vis. Sci. 41*, 3322–3326.

11. Richer, S., Stiles, W., Statkute, L., Pulido, J., Frankowski, J., Rudy, D., Pei, K., Tsipursky, M., and Nyland, J. (2004) Double-Masked, Placebo-Controlled, Randomized Trial of Lutein and Antioxidant Supplementation in the Intervention of Atrophic Age-Related Macular Degeneration: The Veterans LAST Study (Lutein Antioxidant Supplementation Trial), *Optometry 75*, 216–230.

12. Olmedilla, B., Granado, F., Blanco, I., Vaquero, M., and Cajigal, C. (2001) Lutein in Patients with Cataracts and Age-Related Macular Degeneration: A Long-Term Supplementation Study, *J. Sci. Food Agric. 81*, 904–909.

13. Landrum, J.T., and Bone, R.A. (2001) Lutein, Zeaxanthin, and the Macular Pigment, *Arch. Biochem. Biophys. 385*, 28–40.

14. Krinsky, N.I., Landrum, J.T., and Bone, R.A. (2003) Biologic Mechanisms of the Protective Role of Lutein and Zeaxanthin in the Eye, *Annu. Rev. Nutr. 23*, 171–201.

15. Johnson, E.J., Neuringer, M., Russell, R.M., Schalch, W., and Snodderly, D.M. (2005) Nutritional Manipulation of Primate Retinas. III: Effects of Lutein or Zeaxanthin Supplementation on Adipose Tissue and Retina of Xanthophyll-Free Monkeys, *Invest. Ophthalmol. Vis. Sci. 46*, 692–702.

16. Pettersson, T.M., Carlström, A., Ehrenberg, A., and Jörnvall, H. (1989) Transthyretin Microheterogeneity and Thyroxine Binding Are Influenced by Non-amino Acid Components and Glutathione Constituents, *Biochem. Biophys. Res. Commun. 158*, 341–347.

17. Ingbar, S.H. (1958) Prealbumin: A Thyroxine-Binding Protein of Human Plasma, *Endocrinology 63*, 256–259.

18. Kanai, M., Raz, A., and Goodman, D.S. (1968) Retinol-Binding Protein: The Transport Protein for Vitamin A in Human Plasma, *J. Clin. Invest. 47*, 2025–2044.

19. Hermansen, L.F., Bergman, T., Jörnvall, H., Husby, G., Ranløv, I., and Sletten, K. (1995) Purification and Characterization of Amyloid-Related Transthyretin Associated with Familial Amyloidotic Cardiomyopathy, *Eur. J. Biochem. 227*, 772–779.

20. Pettersson, T., Ernström, U., Griffiths, W., Sjövall, J., Bergman, T., and Jörnvall, H. (1995) Lutein Associated with a Transthyretin Indicates Carotenoid Derivation and Novel Multiplicity of Transthyretin Ligands, *FEBS Lett. 365*, 23–26.

21. Marusich, W.L., and Bauernfeind, J.C. (1981) Oxycarotenoids in Poultry Feeds, in *Carotenoids as Colorants and Vitamin A Precursors* (Bauernfeind, J.C., ed.), pp. 394–395, Academic Press, New York.

22. Mares-Perlman, J.A., Fisher, A.I., Klein, R., Palta, M., Block, G., Millen, A.E., and Wright, J.D. (2001) Lutein and Zeaxanthin in the Diet and Serum and Their Relation to Age-Related Maculopathy in the Third National Health and Nutrition Examination Survey, *Am. J. Epidemiol. 153*, 424–432.

23. Ernström, U., Pettersson, T., and Jörnvall, H. (1995) A Yellow Component Associated with Human Transthyretin Has Properties like a Pterin Derivative, 7,8-Dihydropterin-6-carboxaldehyde, *FEBS Lett. 360*, 177–182.

24. Dwork, A.J., Cavallaro, T., Martone, R.L., Goodman, D.S., Schon, E.A., and Herbert, J. (1990) Distribution of Transthyretin in the Rat Eye, *Invest. Ophthalmol. Vis. Sci. 31*, 489–496.

25. Inada, K. (1988) Localization of Prealbumin in Human Eye, *Jpn. J. Ophthalmol. 32*, 438–443.

26. Cavallaro, T., Martone, R.L., Dwork, A.J., Schon, E.A., and Herbert, J. (1990) The Retinal Pigment Epithelium Is the Unique Site of Transthyretin Synthesis in the Rat Eye, *Invest. Ophthalmol. Vis. Sci. 31*, 497–501.

27. Herbert, J., Cavallaro, T., and Martone, R. (1991) The Distribution of Retinol-Binding Protein and Its mRNA in the Rat Eye, *Invest. Ophthalmol. Vis. Sci. 32*, 302–309.

28. Ong, D.E., Davis, J.T., O'Day, W.T., and Bok, D. (1994) Synthesis and Secretion of Retinol-Binding Protein and Transthyretin by Cultured Retinal Pigment Epithelium, *Biochemistry 33*, 1835–1842.

29. Pfeffer, B.A., Becerra, S.P., Borst, D.E., and Wong, P. (2004) Expression of Transthyretin and Retinol Binding Protein mRNAs and Secretion of Transthyretin by Cultured Monkey Retinal Pigment Epithelium, *Mol. Vis. 10*, 23–30.

30. Bok, D., and Heller, J. (1976) Transport of Retinol from the Blood to the Retina: An Autoradiographic Study of the Pigment Epithelial Cell Surface Receptor for Plasma Retinol-Binding Protein, *Exp. Eye Res. 22*, 395–402.

31. Bernstein, P.S., Balashov, N.A., Tsong, E.D., and Rando, R.R. (1997) Retinal Tubulin Binds Macular Carotenoids, *Invest. Ophthalmol. Vis. Sci. 38*, 167–175.

32. Yao, L., Liang, Y., Trahanovsky, W.S., Serfass, R.E., and White, W.S. (2000) Use of a ^{13}C Tracer to Quantify the Plasma Appearance of a Physiological Dose of Lutein in Humans, *Lipids 35*, 339–348.

33. Monaco, H.L., Rizzi, M., and Coda, A. (1995) Structure of a Complex of Two Plasma Proteins: Transthyretin and Retinol-Binding Protein, *Science 268*, 1039–1041.

34. Berni, R., Ottonello, S., and Monaco, H.L. (1985) Purification of Human Plasma Retinol-Binding Protein by Hydrophobic Interaction Chromatography, *Anal. Biochem. 150*, 273–277.

35. Brand, W.A. (1996) High Precision Isotope Ratio Monitoring Techniques in Mass Spectrometry, *J. Mass Spectrom. 31*, 225–235.

36. Pettersson, T., Carlström, A., and Jörnvall, H. (1987) Different Types of Microheterogeneity of Human Thyroxine-Binding Prealbumin, *Biochem. 26*, 4572–4583.

37. Chang, L., Munro, S.L.A., Richardson, S.J., and Schreiber, G. (1999) Evolution of Thyroid Hormone Binding by Transthyretins in Birds and Mammals, *Eur. J. Biochem. 259*, 534–542.

38. Beetham, R., Dawnay, A., Landon, J., and Cattell, W.R. (1985) A Radioimmunoassay for Retinol-Binding Protein in Serum and Urine, *Clin. Chem. 31*, 1364–1367.

39. Peterson, P.A. (1971) Characteristics of a Vitamin A-Transporting Protein Complex Occurring in Human Serum, *J. Biol. Chem. 246*, 34–43.

40. Liang, Y., White, W.S., Yao, L., and Serfass, R.E. (1998) Use of High-Precision Gas Isotope Ratio Mass Spectrometry to Determine Natural Abundance ^{13}C in Lutein Isolated from C_3 and C_4 Plant Sources, *J. Chromatogr. A. 800*, 51–58.

41. Collins, X.H. (2003) Lutein Does Not Affect the Bioefficacy of β-Carotene Measured Using Gas Chromatography–Combustion Interfaced–Isotope Ratio Mass Spectrometry (GC–C–IRMS), Ph.D. Thesis, Iowa State University, Ames.

42. Duan, W., Achen, M.G., Richardson, S.J., Lawrence, M.C., Wettenhall, R.E.H., Jaworowski, A., and Schreiber, G. (1991) Isolation, Characterization, cDNA Cloning and Gene Expression of an Avian Transthyretin, *Eur. J. Biochem. 200*, 679–687.

43. Eneqvist, T., Lundberg, E., Karlsson, A., Huang, S., Santos, C.R.A., Power, D.M., and Sauer-Eriksson, A.E. (2004) High Resolution Crystal Structures of Piscine Transthyretin Reveal Different Binding Modes for Triiodothyronine and Thyroxine, *J. Biol. Chem. 279*, 26411–26416.

44. Richardson, S.J., Bradley, A.J., Duan, W., Wettenhall, R.E., Harms, P.J., Babon, J.J., Southwell, B.R., Nicol, S., Donnellan, S.C., and Schreiber, G. (1994) Evolution of Marsupial and Other Vertebrate Thyroxine-Binding Plasma Proteins, *Am. J. Physiol. Regul. Integr. Comp. Physiol. 266*, 1359–1370.

45. Ghosh, M., Meerts, I.A.T.M., Cook, A., Bergman, A., Brouwer, A., and Johnson, L.N. (2000) Structure of Human Transthyretin Complexed with Bromophenols: A New Mode of Binding, *Acta Crystallogr. D56*, 1085–1095.

46. Chapman, M.J. (1980) Animal Lipoproteins: Chemistry, Structure, and Comparative Aspects, *J. Lipid Res. 21*, 789–853.

47. Monaco, H.L. (2000) The Transthyretin–Retinol-Binding Protein Complex, *Biochim. Biophys. Acta 1482*, 65–72.

48. Yemelyanov, A.Y., Katz, N.B., and Bernstein, P.S. (2001) Ligand-Binding Characterization of Xanthophyll Carotenoids to Solubilized Membrane Proteins Derived from Human Retina, *Exp. Eye Res. 72*, 381–392.

49. Billsten, H.H., Bhosale, P., Yemelyanov, A., Bernstein, P.S., and Polívka, T. (2003) Photophysical Properties of Xanthophylls in Carotenoproteins from Human Retina, *Photochem. Photobiol. 78*, 138–145.

50. Rapp, L.M., Maple, S.S., and Choi, J.H. (2000) Lutein and Zeaxanthin Concentrations in Rod Outer Segment Membranes from Perifoveal and Peripheral Human Retina, *Invest. Ophthalmol. Vis. Sci. 41*, 1200–1209.

A Molecular Dynamics Study of an Archaeal Tetraether Lipid Membrane: Comparison with a Dipalmitoylphosphatidylcholine Lipid Bilayer

J.P. Nicolas*

van 't Hoff Institute for Molecular Sciences Universiteit van Amsterdam,
Nieuwe Achtergracht 166, NL-1018 WV Amsterdam, The Netherlands

ABSTRACT: Molecular dynamics simulations of an archaeal membrane made up of bipolar tetraether lipids and a dipalmitoylphosphatidylcholine (DPPC) lipid membrane were performed and compared for the first time. The simulated archaeal membrane consists of a pure monolayer of asymmetrical lipids, analogous to the main polar lipid [MPL; Swain, M., Brisson, J.-R., Sprott, G.D., Cooper, F.P., and Patel, G.B., (1997) Identification of β-L-Gulose as the Sugar Moiety of the Main Polar Lipid of *Thermoplasma acidophilum, Biochim. Biophys. Acta 1345,* 56–64] found in *T. acidophilum*, an extremophile archaeal organism. This simulated membrane lipid contains two cyclopentane rings located on one of the two aliphatic chains of the lipid. The archaeal membrane is simulated at 62°C, slightly above the optimal growth temperature of *T. acidophilum*. We compared the organization of this tetraether lipid monolayer with a DPPC bilayer simulated at 50°C, both of them being modeled in a partially hydrated state. Our results assess the singularity of the tetraether lipid organization, in particular the influence of the spanning structure on the molecular ordering within the archaeal membrane.

Paper no. L9811 in *Lipids 40*, 1023–1030 (October 2005).

Membranes define singular domains where biological processes may occur. Since this activity is related to life, membranes are not simply a protecting barrier that maintains physiological conditions (unicellular organisms, mitochondria, and so on) or keeps apart stored compounds (liposomes, chloroplasts, and the like). They also contribute to fundamental functions such as the modulation of channel activity (1), which is involved in molecular and information exchange with the surrounding of this delimited compartment. Consequently, their study at the molecular level is of great interest to fields directly related to living processes. Although most of the studied membranes today remain models made up eukaryotic lipids (2), there is now enough experimental data available in the literature to attempt to build membrane models representative of less common supramolecular assemblies such as those found in extremophile organisms (see for instance Refs. 3–6) and to investigate their original membrane properties by numerical methods.

Typically, the archaeal membrane is made of approximately 60% protein, 10% carbohydrate, and 30% ether lipid (instead of the abundant ester-lipids found elsewhere, see for instance Refs. 7 and 8 and citations therein). Archaeal lipids consist of isoprenoid alcohols linked by ether bonds to an *sn*-glycerol-1-phosphate. These phytanyl chains contain a methyl group at every fourth carbon atom in the backbone, and the ether linkage prevalent in archaeal lipids is chemically far more resistant to oxidation and high temperature than the ester bond (predominantly found in eukaryotic lipids). *In vivo*, the distribution of the membrane lipids is asymmetrical, with most of the phosphate groups pointing at the cytoplasm and the sugar moiety exposed at the outer side of the cell (9,10). However, in the case of archaeal organisms, the role of neither the head group distribution asymmetry nor the hydrophobic core asymmetry is well understood yet.

Thermoplasma acidophilum is an archaeal organism (11) able to colonize extreme media characterized by a high temperature and a low pH (12)—as one could guess from its name. The optimal growth conditions correspond to a temperature of 55–59°C and a pH range between 1 and 2 (12). Its ability to maintain physiological conditions in such an extreme environment is mainly related to its membrane properties, and consequently to the components of its lipidic barrier (3,13,14) (*T. acidophilum* having no cell wall). The peculiar membrane of *T. acidophilum* contains a rich variety of lipids, most of them (82%) polar. A large part of these lipids are bipolar tetraether lipids (3,14), the membrane being thus a single monolayer of lipid. The structure of the most abundant polar component, MPL (main polar lipid, see Fig. 1) has been recently identified (15). It is a bipolar tetraether lipid with up to four cyclopentane rings per aliphatic chain, the two hydrophilic head groups being a phosphoglycerol and a β-L-gulopyranose.

At high temperatures, the role of archaeal membranes is maintained by an increasing degree of cyclization of the aliphatic core, and the membrane composition changes toward a larger ratio of tetraether lipids vs. diether lipids (16). The number of cyclopentane rings can vary up to four per aliphatic chain at high temperature, thus maintaining the membrane fluidity, which is a prerequisite for the proper functioning of the membrane and its embedded supramolecular structures. These unique physical properties of archaeal lipids are of great interest for biotechnological and pharmaceutical applications

---

*E-mail: jpierre@science.uva.nl
Abbreviations: DPPC, dipalmitoylphosphatidylcholine; MPL, main polar lipid.

(3,17,18), and the synthesis of archaeal lipid analogs represents an exciting challenge (see for instance Ref. 19 and citations therein).

In a pioneering work (20), two different tetraether lipid membranes in vacuum were modeled and the effect of cyclopentane rings on chain packing investigated. However, very little information is given on the protocol used in their simulation studies (such as the statistical ensemble used during short molecular dynamics calculations). Moreover, from the monolayer model snapshots presented in their article, their systems seem to be either trapped in a local minimum or insufficiently equilibrated: For instance, the top of the figure shows aliphatic chains almost identical (in position), and head groups are still placed on an (almost) perfect 4 × 4 matrix, as if only the closest atoms had time to move. In addition, large gaps persist between head groups. These features are less easy to observe from the bottom of the snapshot.

In this work the first significant molecular dynamics study of a pure archaeal lipid membrane is performed, the aim being to investigate the organization of membranes made up MPL analogs. We performed the simulation of two models of hydrated membranes. The first is an archaeal membrane containing two cyclopentane rings located on one of the two aliphatic chains of the lipid molecule (named T-0–2.7 in this work; see Fig. 1 caption for explanations on the suggested nomenclature), simulated at 62°C, slightly above the optimal growth temperature of *T. acidophilum*. It is compared with the second membrane model, a dipalmitoylphosphatidylcholine (DPPC) membrane simulated at 50°C. To compare the two membrane models (DPPC bilayer and archaeal monolayer), simulations have been performed on the same time scale, which is sufficient for a correct study of the properties we are interested in. Basically, our work focuses on the effect of cyclopentane rings and spanning aliphatic chains on membrane architecture, more specifically on the hydrophobic core of the membrane. Herein, no attention has been paid to the influence of the sugar moiety variability, as experimentally observed, on physical properties of membranes. This point requires choosing a force field especially dedicated to oligosaccharide modeling and would require further work.

We do not pretend that our results can be directly related to biological archaeal membranes, but we do present evidence of properties that depend on their peculiar lipid structures. Archaeal membranes contain a large amount of proteins, which likely modulate the properties observed from a pure monolayer in a dramatic fashion.

MOLECULAR DYNAMICS

Molecular dynamics computer simulations were carried out using the DL_POLY Molecular Simulation Package (21). An all-atom model was used to describe molecules at an atomic scale using the potential energy parameter set PARM27 from the CHARMM package (22). The TIP3P water model (23) was used in all simulations. Bonds involving hydrogen were held fixed with the SHAKE algorithm (24), the SHAKE tolerance
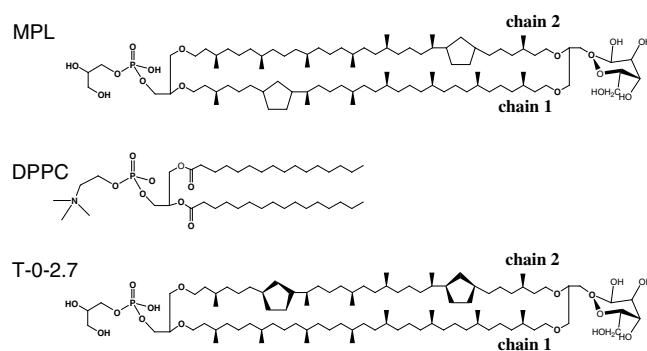
FIG. 1. One of the proposed molecular structures of a main polar lipid (MPL) from *Thermoplasma acidophilum* (15) (top); a dipalmitoylphosphatidylcholine (DPPC) lipid (center); and an MPL analog studied in this paper, T-0–2.7 (bottom). We propose a nomenclature based on the hydrophobic core structure: "T" means "tetraether lipid," "0" corresponds on chain 1 to the methyl position involved in a cyclopentane ring (in this case no methyl group is part of a ring, thus the value is 0), and "2.7" locates the two rings at the second ("2") and seventh ("7") methyls of chain 2, from one head group toward the other one. The labeling "chain 1" and "chain 2" corresponds to the nomenclature used in the reference article on MPL structure (15).

being equal to 1.0×10^{-4}. Electrostatic interactions were computed using the smooth particle mesh Ewald method (25), with a precision of 1.0×10^{-6}. Our simulations were performed in the NVT Hoover ensemble (26), i.e., with a constant number of particles (N), volume (V), and temperature (T). Simulations were run with periodic boundary conditions. All the simulations were performed using a cutoff radius of 12 Å for the van der Waals terms. The use of this statistical ensemble makes our results comparable to constant-area experimental results, based on pure membranes. A comparison with membranes from archaeal organisms would at least require a NPγT ensemble (constant normal pressure and surface tension), and the addition of a substantial amount of proteins.

We have used a three-step protocol to build the hydrated archaeal membrane model. Initially, a single lipid molecule stretched along its longer axis was pre-equilibrated in vacuum (it is worth noting that each tetraether lipid model is asymmetrical both with respect to the two different hydrophilic head groups and the stereochemistry of each side of the aliphatic chains). Then, we built our complete models by placing the lipids on a 6 × 6 grid with carbohydrate head groups forming one outer side of the membrane, and phosphate head groups the other interface, mimicking the asymmetrical topology found *in vivo* (9,10), both membrane surfaces being parallel to the *x–y* plane. The length of the simulation box along the *z* axis is chosen in such a way as to avoid any point contact between the two membrane interfaces. The dry lipid monolayer is equilibrated during a few hundred steps as the time step is gradually increased to 2 fs. Subsequently, the box is filled by adding water molecules in such a way that the system contains 36 lipid molecules and more than 2,200 water molecules, thus *ca.* 17,000 atoms and 30 water molecules per lipid head group, which corresponds to

a (not fully) hydrated membrane (27,28) with at least one layer of water molecules at each interface.

The lipid area from an MPL membrane placed under a collapse pressure at 8°C is found from surface pressure vs. molecular area experimental measurements to be equal to 73 Å² (29), where acyl chains are mainly without cyclopentane rings. With the aid of the Wilhelmy method, Elferink *et al.* (30) have studied tetraether lipids from *Sulfolobus acidocaldarius* placed under equivalent conditions, at 22°C, and found a lipid molecular area equal to 82 Å². In both cases, lipid molecules were at an air–water interface. The molecular area per lipid used in this model is reported in Table 1. Since this work is related to an archaeal lipid comparable to MPL found in *T. acidophilum*, we have chosen a T-0–2.7 lipid area close to the one measured by Strobl *et al.* (29).

Concerning the DPPC membrane, the protocol is roughly the same. First, we built a dry monolayer of 6×6 lipids. The size of the grid is set so as to achieve an area per lipid molecule equal to 61.5 Å² [close to the experimental value previously found by Nagle *et al.* (31)]. The second layer of the membrane is built by mirroring twice the initial lipid layer with respect to both the midplane of the membrane and a perpendicular plane (so that the chirality of the molecule is conserved). The equilibration period of the dry membrane following the addition of water is comparable to that of the archaeal membrane. In such a way the system contains 2×36 lipid molecules, and more than 2,000 molecules of water, thus approximately 15,000 atoms. Consequently, the DPPC lipid bilayer is modeled in the liquid-crystal state.

The two complete systems have been equilibrated for 250,000 steps with a time step of 2 fs at 50 and 62°C for the DPPC and the T-0–2.7 models, respectively. During equilibration, density profiles and energy convergence of the system have been monitored. An extra equilibration, roughly equivalent in total elapsed time to the former one, has been performed for both systems, where various force fields have been compared. Consequently, both systems were completely relaxed before the production run, as attested by the energy monitoring (data not shown). Both systems have a positive and nearly equivalent lateral pressure. After equilibration, we recorded the dynamics of the system by accumulating coordinates at an interval of 0.1 ps during a period of 0.8 ns for the DPPC bilayer, and 1 ns for the T-0–2.7 monolayer. This time scale corresponds to the one used in a previous work focusing on hydrocarbon chain properties related to fluid phase lipid bilayers (32).

TABLE 1
Simulation Box Parameters, Temperature, and Lipid Molecular Areas as a Function of the Lipid Molecular Type[a]

Lipid	*T*-0–2.7	DPPC
Temperature (°C)	62	50
L*x* = L*y* (Å)	51.6	47.1
L*z* (Å)	61.2	69.5
Molecular area (Å²⁾	74	61.6

[a]DPPC, dipalmitoylphosphatidylcholine.

RESULTS AND DISCUSSION

Mass and electronic density profiles. Mass density profiles present distributions of atoms or chemical groups along the axis perpendicular to the membrane plane. The shape of the distribution provides insights on the membrane internal organization.

Figure 2 displays the total mass density profile and its chemical group components for the two hydrated membrane models, T-0–2.7 and DPPC. Concerning the latter model, our results are consistent with data from previous simulations (33), where the force field used in this work was compared with the previous set of parameters, both developed by the CHARMM group (22). This agreement on the structural characteristics of the aliphatic domain indicates that the simulation time is sufficient to study this domain of the membrane. Compared with the PC membrane model DPPC, the total density profile of the archaeal membrane T-0–2.7 differs on at least three points: (i) the interfacial domain has a lower contribution; (ii) there is no dip in the midplane of the membrane; (iii) computed on the same time scale, the T-0–2.7 profile is much rougher.

The discrepancy noticed at the interface might be explained from the electrostatic nonbonded interaction term. Concerning
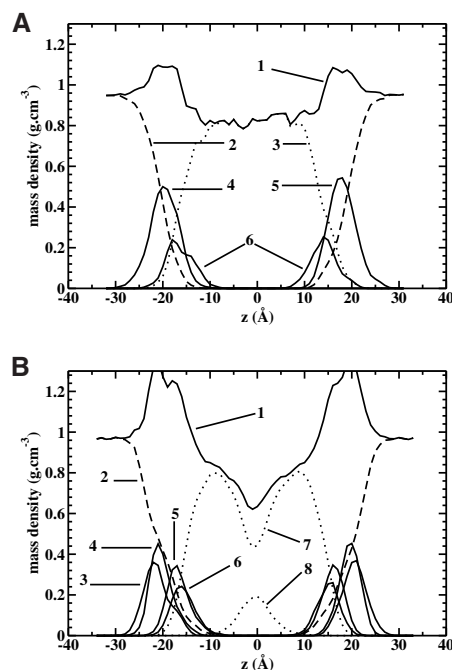
FIG. 2. Mass density profiles of the T-0–2.7 (top) and DPPC (bottom) lipid membranes, 62 and 50°C, respectively. On the tetraether lipid graph (top), the gulose (peak 5) is located on the right interface, whereas the phosphate group (peak 4) is on the left one; the two glycerol groups (peaks 6) link both the phosphate and the gulose to the two aliphatic chains (dotted line, peak 3), and water (dashed line, peak 2). The total density profile (peak 1) corresponds to the summation of all the mass density components. The representation of the total density and the water density profiles are equivalent on the phosphatidyl lipid graph (bottom). Concerning the DPPC model, peaks 3 and 4 correspond to choline and phosphatidyl groups, 5 and 6 to the glycerol and carbonyl groups, 7 and 8 to ethyl and methyl groups, which are part of the hydrophobic core. For abbreviation see Figure 1.

the PC lipids, electrostatic interactions between head group net charges are strong, owing to the zwitterionic character of the PC group (27,28), whether hydroxyl groups (–OH) from archaeal lipid head group are involved in numerous but weak hydrogen bonds. In the DPPC case these electrostatic interactions contribute to a high head group packing, whereas in the T-0–2.7 case the electrostatic forces build up a hydrogen bond network between two neighboring head groups, and between each head group and its surrounding water molecules. The absence in the total density profile of a dip in the membrane midplane is characteristic of a monolayer made of lipids with spanning aliphatic chains. A membrane made up of a macrocyclic ether lipid (34) would likely have a total density profile with a small dip in its hydrophobic core. However, since no free chain ends would be present in a pure membrane made of macrocyclic lipids, the predicted dip should be smaller compared with the one from PC membranes. The spanning geometry of the tetraether lipids contributes to another peculiarity of the density profile: All the components of the profile are represented by a rougher curve compared with the curve from the PC membrane profile (both of them being computed during the same time scale). The lipid-spanning geometry dramatically reduces the molecular dynamics related to the hydrophobic domain and thus necessitates larger simulation times to achieve comparable accuracy. Moreover, the pure lipid membranes are simulated under a positive lateral pressure, which contributes to reduce free volumes and thus molecular motions too. Consequently, the density profiles of the simulated archaeal membrane monolayers cannot be as smooth as are the profiles from PC membranes simulated at the same temperature and on the same time scale.

These discrepancies may induce a diffusion regime of small solute species in the archaeal membrane that is rather different from the diffusion process observed in the phosphatidyl membrane (35) and may lower the global diffusion across the membrane. This observation supports experimental measurements of proton diffusion through archaeal membranes (36,37), obtained from fluorescence monitoring. Those results supported the role of limited mobility of the midplane hydrocarbon region in reducing the permeability properties of the lipid membrane.

From the total mass density profile of the T-0–2.7 lipid membrane we observe two high sharp peaks, each located at the head group–water interface. They correspond to the sum of the contributions of the glycerol group, and either the phosphate or the gulose moiety, depending on which interface is represented. Although the interfaces are different in composition, the thicknesses of the two interfacial domains are comparable, both from the standpoint of the two sides of the archaeal membrane, and of the archaeal monolayer and the DPPC bilayer.

On one hand, our tetraether lipid simulations have been performed at 62°C, thus a few degrees above the optimal *T. acidophilum* growth temperature, within the liquid-crystal domain that exists above −20°C (38), and where an "appreciable membrane fluidity" should be noticeable (starting from 20°C below the growth temperature) (39,40). On the second hand, our ar-

chaeal membrane is a pure monolayer made up two-ring lipids. Lipid motions are slow compared with PC lipids, mainly owing to both the lateral methyl groups and the presence of cyclopentane rings. At time and space scales used in our simulations, this slowness dramatically precludes the observation of the experimentally evidenced membrane fluidity, but it can be used to assess the hypothesis drawn from NMR results (6) that a substantial lateral diffusion is expected from 20°C above the growth temperature.

Figure 3 displays the electronic density profiles for both the tetraether (top) and DPPC (bottom) lipid membranes (the water contribution is not represented on the graphs). As seen on the mass density profiles, the archaeal hydrophobic core is made up of a monolayer of spanning tails, compared with the bilayer geometry found in PC membranes, thus yielding a constant value of the electronic density. As we compare the contribution of each component of the interfacial domain, we notice that the glycerol distribution is slightly broader in the T-0–2.7 membrane. Moreover, this peak is asymmetrical on the phosphatidyl group side. This curve shape might be related to the presence of two cyclopentane groups on the same hydrophilic chain (chain 2). Consequently, chain 2 is shorter than chain 1, necessitating a tilt (toward the interfacial plane) of at least one glycerol group.
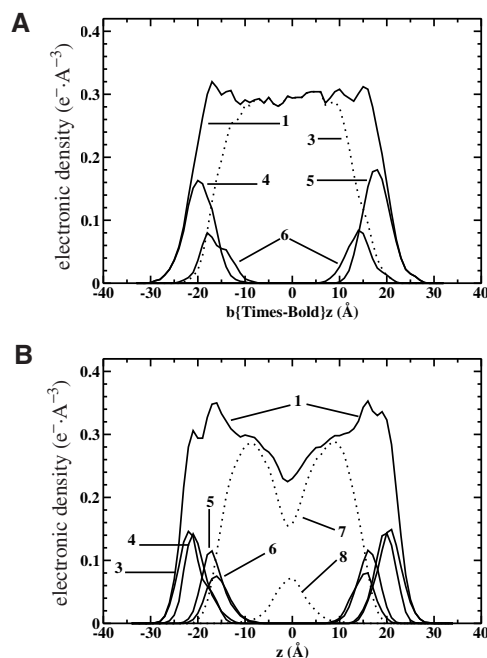
FIG. 3. Electronic density profiles of the T-0–2.7 (top) and DPPC (bottom) lipid membranes, 62 and 50°C, respectively. On the tetraether lipid graph (top), gulose (peak 5) is located on the right interface, whereas the phosphate group (peak 4) is on the left; the two glycerol groups (peaks 6) link both the phosphate and the gulose to the two aliphatic chains (dotted line, peak 3). The total density profile (peak 1) corresponds to the summation of all the electronic density components. The representation of the total density is equivalent on the phosphatidyl lipid graph (bottom). Concerning the DPPC model, peaks 3 and 4 correspond to choline and phosphatidyl groups, 5 and 6 to the glycerol and carbonyl groups, 7 and 8 to ethyl and methyl groups, which are part of the hydrophobic core. For abbreviation see Figure 1.

Owing to the relative size of the two interfacial domains (the sugar moiety is likely larger than the phosphate), motions on the phosphate side are easier.

Aliphatic chain ordering. The orientations of some moieties of the lipid molecules, such as the aliphatic chains or the head groups, can be described by the order parameter of a chain segment. In the case of the aliphatic chains, we have defined two complementary parameters. First, we have computed the orientation of carbon chains from the vector defined by the coordinates of the two carbons n and $n + 2$ belonging to the same chain. By skipping the $n + 1$ carbon, the computed orientation of a chain segment is given without the contribution of the peculiar zigzag conformation of an aliphatic chain. This approach makes direct comparisons with experiments or other calculations less obvious, but gives far better statistics. In some circumstances, it yields higher (or lower) order parameter values, compared with the $C_n - C_{n+1}$ calculation. Second, we have computed the C–H vector orientation, which can be compared with the Scd chain parameter obtained from NMR spectroscopy. The order parameter reads (Eq. 1):

$$S(z) = \frac{1}{2}\left\langle 3\cos^2\theta(z) - 1\right\rangle, \qquad [1]$$

where θ is the angle between the vector C–C or C–H and the interface normal vector. A value close to 1 corresponds to a distribution of vectors parallel to the normal of the interface, whereas a distribution of vectors parallel to the membrane plane yields an order parameter close to −0.5. When the vector angles are randomly distributed, the order parameter will be equal to 0 (although an order parameter equal to 0 may also correspond to a perfectly ordered phase, with a tilt angle distribution centered on 54.7°).

The numbering of atoms in Figures 4 and 5 starts from the midplane of the molecule, and we assign to the vector the carbon number of the atom that defines the origin of the C–H vector, or the number of the (skipped) $n + 1$ carbon located between the (n)–$(n + 2)$ carbon atoms. Only C–C vectors computed from the aliphatic backbone are shown, C–H vectors involved in cyclopentane rings not being reported in the figures.

Compared with previous works (33,41), our calculated DPPC aliphatic chain order parameters are in a good agreement, both with data derived by experiments and by other researchers' calculations. This allows further investigations on the archaeal membrane simulated under the same conditions as the DPPC bilayer, and comments on the results. MPL differs from the more classical DPPC phospholipid by the spanning geometry of the lipid within the membrane, and by the presence of methyl groups or cyclopentane rings on the aliphatic backbones, plus a few other structural features such as the ether linkage. Despite their structural discrepancies, the order parameter of DPPC lipid embedded in a membrane is similar to those of monopolar diether lipids and the cyclized macro-cyclic analogs assembled in a bilayer (34). Consequently, the study of a tetraether lipid monolayer should lead to conclusions directly related to the peculiar monolayer organization.
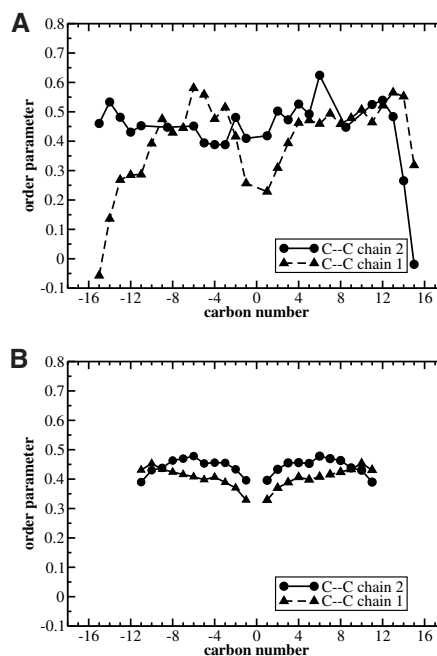
FIG. 4. Order parameter computed for each $C_n - C_{n+2}$ bonds of the hydrophobic chains for each lipid molecule: T-0–2.7 (top) and DPPC (bottom). The gulose is on the right interface, whereas the phosphate group is on the left. Numbering of bonds starts from the membrane midplane. For abbreviation see Figure 1.

Figures 4 and 5 report the C–C and C–H order parameters for each simulated membrane. As we compare the two order parameters between DPPC and T-0–2.7 membranes, we notice that the archaeal lipid membrane is on the whole much more ordered within the hydrophobic core of the membrane close to its midplane, as shown by the large value of its order parameter, whereas in the case of the DPPC membrane, large values are located on the head group side and the order parameter decreases slowly as the carbons approach the midplane. This major difference can be related both to the presence of methyl lateral groups in archaeal lipids, which act as spurs located on the chain backbone, and to the spanning geometry of lipids. Experimental results dealing with the pressure dependence of lipid mobility indicate there is no noticeable lateral diffusion in a tetraether lipid membrane at a temperature 20°C below the growth temperature (39). In our simulations, we observe a lateral lipid diffusion in neither the T-0–2.7 nor the DPPC membrane. The time scale of the simulation should be at least one order of magnitude higher than the one used in this calculation. However, the discrepancies in the shape of curves between Figures 4 and 5 suggest that local chain motions are smaller in the case of the T-0–2.7 membrane. Moreover, experimental measurements of the lateral diffusion coefficient of various lipids show that branching on lipid chains restricts aliphatic segment motions (37) and prevents kink formation (14). The organization of tetraether lipid membranes has been investigated by different experimental techniques (reviewed in Ref. 4). The bipolar lipids are tightly packed and confer to the membrane great stiffness. However, both theoretical and experimental results
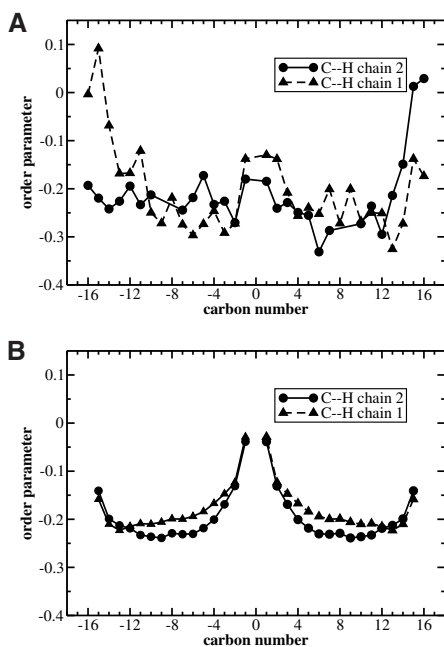
FIG. 5. Order parameter computed for each C–H bond of the hydrophobic chains for each lipid molecule: T-0–2.7 (top) and DPPC (bottom). The gulose is on the right interface, whereas the phosphate group is on the left. Numbering of bonds starts from the membrane midplane. For abbreviation see Figure 1.

FIG. 6. Orientation of the two tetraether lipid aliphatic chains relative to the membrane plane normal. Data are averaged over all the lipid molecules and over the simulation time.

suggest that the branched methyl group of the acyl chain does not contribute to this peculiar tight packing (20,40).

The C–C bonds located at the hydrophobic midplane of the lipid molecules are in some cases less oriented than the other C–C bonds. This behavior can be related to the length of the carbon chains, which depends on both the number of cyclopentane rings per chain and the conformation imposed by the stereochemistry of the carbons involved in the cyclopentane rings. Cyclization shortens the aliphatic chain (four carbons of the chain backbone are involved in each cyclopentane), thus the difference in length of two chains is directly proportional to the number of cyclopentane rings located on one of the two chains. Last, the C–C bond vector related to the cyclopentane rings (see the positions at ±8.5 and ±12.5 on the graphs) does not have a preferred orientation specific to a peculiar *cis* or *trans* ring substitution.

Moreover, the aliphatic chain orientation is perturbed by the linkage to the glycerol close to the chain ends, and more especially the chain end connected to the center of the glycerol. This suggests that small motions of both phosphate and gulose head groups induce a slight disorder in the position of the outermost hydrophobic carbons, and this disorder is consistent with experimental results. The tight packing of lipids in the membrane occurs within the hydrophobic core, the hydrophilic head groups having both a smaller cross-sectional area than the hydrophobic core and an ability to tilt and to adopt an optimal orientation depending on the lipid cross-sectional area. This might no longer be the case when one of the head groups has a cross section larger than the hydrophobic domain.
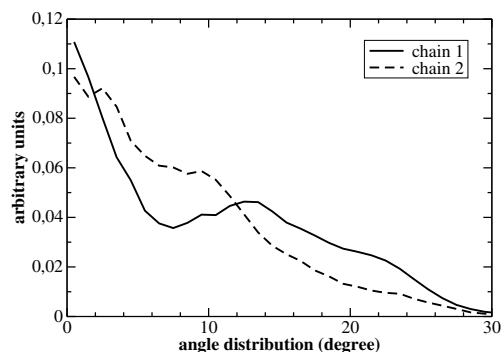
Water and lipid molecule orientations. Figure 6 reports the angle distribution between the main axis of each aliphatic chain and the normal to the membrane plane. Both of them are slightly tilted toward the interface (about 10°). Chain 2, being shortened by the presence of two cyclopentane rings, has an average position that is more vertical than chain 1, which yields a two-peak distribution. The angle distributions of chains 1 and 2 can be used to assess the hypothesis of "kink" formation in chain 1, as suggested by the order parameter of the C–C bond vectors, close to the membrane midplane. In a case of a membrane made of lipids with equivalent aliphatic chains, one could predict a tilt distribution centered on a small tilt value.

Because the two interfaces are different in composition, one could expect discrepancies in the water molecule orientation close to the interface. First, we have defined the interface position from a fit of the water density profile using an error function (see for instance Ref. 42) and then computed the orientational parameters of the dipole vector and the vector normal to the water molecule plane with respect to the membrane normal. This approach leads to the definition of an averaged position of the interface. Consequently, the distribution of water molecules located at a given distance from the monolayer is broadened. In Figure 7, the order parameters are given with respect to interfacial position: Negative distances correspond to the water molecules deeply embedded in the interfacial head group layer, and positive distances to molecules that are part of the first two solvation layers. Despite the different composition of each interface and consequently two different kinds of interactions acting on neighboring water molecules, no discrepancies are noticeable. The water molecule layer is not sufficiently broad to observe a lowering of the ordering. Water molecules close to the glucose side are involved in a hydrogen bond network, whereas on the other side, molecules close to the phosphate side interact *via* strong coulombic interactions. A further study should use a larger water layer. However, the membrane is partially hydrated with less than 10 Å of water on each interface. A fully hydrated membrane would produce water molecule order parameters vanishing as the distance from the interface is sufficiently high [about 12–14 Å (27)].
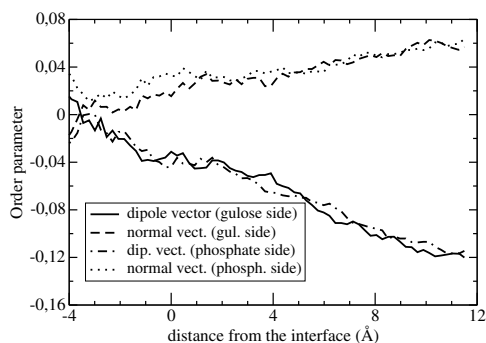
FIG. 7. Water dipole and normal vectors' orientational order parameters, at the gulose and phosphate interfaces. The orientation is computed toward the interface normal vector, and the zeroth position of the interface is defined from the fitting of the water density profile.

INTERPRETATION

Although our simulations of a tetraether lipid membrane have been performed at a temperature slightly above the growth temperature, where the lateral diffusion of lipids remains low (6), our results give an interesting insight to the organization of the aliphatic core of the membrane. Although results from the DPPC model are consistent with the literature and thus validate the simulation parameters, archaeal monolayer behaviors are rather characteristic of systems with slow dynamics. Fortunately, we focused on the hydrophobic core dynamics, which is much faster than the head group rotational dynamics.

Basically, the modeled tetraether lipid membrane can be defined as an assembly of tightly packed molecules [we have not probed in this article **u**-shaped conformations as suggested from experimental results (5)], almost parallel to the membrane normal. The molecular ordering is rather high, likely owing to both the spanning geometry of the lipid molecules and the presence of methyl groups and pentacyclic structures. In these simulations, head groups are sufficiently small (compared with the aliphatic core cross section) to play a minor role. At temperatures a few degree above the growth temperature, these membrane lipids do not exhibit a significant lateral diffusion, at least at this time scale.

Last, we would like to emphasize the large diversity of experimental results found in the literature. Numerous structures of archaeal lipids (considering both the hydrophobic core and the head group domains) have been elucidated these last few years. This proliferation of (sometimes jarring) results makes it rather difficult to draw generic conclusions and derive physicochemical properties. The present work corresponds to a theoretical approach.

ACKNOWLEDGMENTS

REFERENCES

1. Sotomayor, M., and Schulten, K. (2004) Molecular Dynamics Study of Gating in the Mecanosensitive Channel of Small Conductance MscS, *Biophys. J. 87*, 3050–3065.
2. Nagle, J.F., and Tristram-Nagle, S. (2000) Lipid Bilayer Structure, *Curr. Opin. Struct. Biol. 10*, 474–480.
3. Hanford, M.J., and Peeples, T.L. (2002) Archaeal Tetraether Lipids: Unique Structures and Applications, *Appl. Biochem. Biotechnol. 97*, 45–62.
4. Gliozzi, A., Relini, A., and Chong, P.L.G. (2002) Structure and Permeability Properties of Biomimetic Membranes of Bolaform Archaeal Tetraether Lipids, *J. Membr. Sci. 206*, 131–147.
5. Bakowsky, U., Rothe, U., Antonopoulos, E., Martini, T., Henkel, L., and Freisleben, H.J. (2000) Monomolecular Organization of the Main Tetraether Lipid from *Thermoplasma acidophilum* at the Water–Air Interface, *Chem. Phys. Lipids 105*, 31–42.
6. Jarrell, H.C., Zukotynski, K.A., and Sprott, G.D. (1998) Lateral Diffusion of the Total Polar Lipids from *Thermoplasma acidophilum* in Multilamellar Liposomes, *Biochim. Biophys. Acta 1369*, 259–266.
7. Kenneth, M.M., Jr., and Roux, B. (1996) *Biological Membranes: A Molecular Perspective from Computation and Experiment*, Birkhäuser, Boston.
8. de Rosa, M., Gambacorta, A., and Gliozzi, A. (1986) Structure, Biosynthesis, and Physicochemical Properties of Archaebacterial Lipids, *Microbiol. Rev. 50*, 70–80.
9. de Rosa, M., Gambacorta, A., and Nicolaus, B. (1983) A New Type of Cell Membrane, in Thermophilic Archaebacteria, Based on Bipolar Ether Lipids, *J. Membr. Sci. 16*, 287–294.
10. Morii, H., and Koga, Y. (1994) Asymmetrical Topology of Diether- and Tetraether-Type Polar Lipids in Membranes of *Methanobacterium thermoautotrophicum* Cells, *J. Biol. Chem. 269*, 10492–10497.
11. Woese, C.R., Kandler, O., and Wheelis, M.L. (1990) Towards a Natural System of Organisms: Proposal for the Domains Archaea, Bacteria, and Eucarya, *Proc. Natl. Acad. Sci. USA 87*, 4576–4579.
12. Darlant, G., Brock, T.D., Samsonoff, W., and Conti, S.F. (1970) A Thermophilic, Acidophilic Mycoplasma Isolated from a Coal Refuse Pile, *Science 170*, 1416–1418.
13. van de Vossenberg, J.L.C.M., Driessen, A.J.M., and Konings, W.N. (1998) The Essence of Being Extremophilic: The Role of the Unique Archaeal Membrane Lipids, *Extremophiles 2*, 163–170.
14. Albers, S.V., van de Vossenberg, J.L.C.M., Driessen, A.J.M., and Konings, W.N. (2000) Adaptations of the Archaeal Cell Membrane to Heat Stress, *Front. Biosci. 5*, 813–820.
15. Swain, M., Brisson, J.R., Sprott, G.D., Cooper, F.P., and Patel, G.B. (1997) Identification of β-L-Gulose as the Sugar Moiety of the Main Polar Lipid of *Thermoplasma acidophilum*, *Biochim. Biophys. Acta 1345*, 56–64.
16. Uda, I., Sugai, A., Itoh, Y.H., and Itoh, T. (2001) Variation in Molecular Species of Polar Lipids from *Thermoplasma acidophilum* Depends on Growth Temperature, *Lipids 36*, 103–105.
17. de Rosa, M., Morana, A., Riccio, A., Gambacorta, A., Trincone, A., and Incani, O. (1994) Lipids of the *Archaea*: A New Tool for Bioelectronics, *Biosens. Bioelectron. 9*, 669–675.
18. Gambacorta, A., Gliozzi, A., and de Rosa, M. (1995) Archaeal Lipids and Their Biotechnological Applications, *World J. Microbiol. Biotechnol. 11*, 115–131.
19. Benvegnu, T., Brard, M., and Plusquellec, D. (2004) Archaeabacteria Bipolar Lipid Analogues: Structure, Synthesis and Lyotropic Properties, *Curr. Opin. Colloid Interf. Sci. 8*, 469–479.
20. Gabriel, J.L., and Chong, P.L.G. (2000) Molecular Modeling of Archaebacterial Bipolar Tetraether Lipid Membranes, *Chem. Phys. Lipids 105*, 193–200.
21. DL_POLY 2.12 (2001) c/o Department for Computation and Information, CCLRC Daresbury Laboratory, Warrington, United Kingdom.

22. Schlenkrich, M., Brickmann, J., MacKerell, A.D., Jr., and Karplus, M. (1996) An Empirical Potential Energy Function for Phospholipids: Criteria for Parameter Optimization and Applications, in *Biological Membranes: A Molecular Perspective from Computation and Experiment*, pp. 1–31, Birkhäuser, Boston.

23. Jorgensen, W.L., Chandrasekhar, J., Madura, J.D., Impey, R.W., and Klein, M.L. (1983) Comparison of Simple Potential Functions for Simulating Liquid Water, *J. Chem. Phys. 79*, 926–935.

24. Ryckaert, J.P., Ciccotti, G., and Berendsen, H.J.C. (1977) Numerical Integration of the Cartesian Equations of Motion of a System with Constraints: Molecular Dynamics of *n*-Alkanes, *J. Comput. Phys. 23*, 327–341.

25. Essmann, U., Perera, L., Berkowitz, M.L., Darden, T., Lee, H., and Pedersen, L.G. (1995) A Smooth Particle Mesh Ewald Method, *J. Chem. Phys. 103*, 8577–8593.

26. Hoover, W.G. (1985) Canonical Dynamics: Equilibrium Phase-Space Distributions, *Phys. Rev. A. 31*, 1695–1697.

27. Lin, J.H., Baker, N.A., and McCammon, J.A. (2002) Bridging Implicit and Explicit Solvent Approaches for Membrane Electrostatics, *Biophys. J. 83*, 1374–1379.

28. Saiz, L., and Klein, M.L. (2002) Electrostatic Interactions in a Neutral Model Phospholipid Bilayer by Molecular Dynamics Simulations, *J. Chem. Phys. 116*, 3052–3057.

29. Strobl, C., Six, L., Heckmann, K., Henkel, B., and Ring, K. (1985) Physicochemical Characterization of Tetraether Lipids from *Thermoplasma acidophilum* II. Film Balance Studies on the Monomolecular Organization of the Main Glycophospholipid in Monofilms, *Z. Naturforsch. 40c*, 219–222.

30. Elferink, M.G.L., de Wit, J.G., Demel, R., Driessen, A.J.M., and Konings, W.N. (1992) Functional Reconstitution of Membrane Proteins in Monolayer Liposomes from Bipolar Lipids of *Sulfolobus acidocaldarius*, *J. Biol. Chem. 267*, 1375–1381.

31. Nagle, J.F., Zhang, R., Tristram-Nagle, S., Sun, W., Petrache, H.I., and Suter, R.M. (1996) X-ray Structure Determination of Fully Hydrated L Alpha Phase Dipalmitoylphosphatidylcholine Bilayers, *Biophys. J. 70*, 1419–1431.

32. Chiu, S.W., Clark, M.M., Jakobsson, E., Subramaniam, S., and Scott, H.L. (1999) Optimization of Hydrocarbon Chain Interaction Parameters: Application to the Simulation of Fluid Phase Lipid Bilayers, *J. Phys. Chem. B 103*, 6323–6327.

33. Feller, S.E., and MacKerrell, A.D., Jr. (2000) An Improved Empirical Potential Energy Function for Molecular Simulations of Phospholipids, *J. Phys. Chem. B 104*, 7510–7515.

34. Dannenmuller, O., Arakawa, K., Eguchi, T., Kakinuma, K., Blanc, S., Albrecht, A.M., Schmutz, M., Nakatani, Y., and Ourisson, G. (2000) Membrane Properties of Archaeal Macrocyclic Diether Phospholipids, *Chem. Eur. J. 6*, 645–654.

35. Marrink, S.J. (1994) Permeation of Small Molecules Across Lipid Membranes: A Molecular Dynamics Study, Ph.D. Thesis, University of Groningen, The Netherlands.

36. Mathai, J.C., Sprott, G.D., and Zeidel, M.L. (2001) Molecular Mechanisms of Water and Solute Transport Across Archaebacterial Lipid Membranes, *J. Biol. Chem. 276*, 27266–27271.

37. Baba, T., Minamikawa, H., Hato, M., and Handa, T. (2001) Hydration and Molecular Motions in Synthetic Phytanyl-Chained Glycolipid Vesicle Membranes, *Biophys. J. 81*, 3377–3386.

38. Ernst, M., Freisleben, H.J., Antonopoulos, E., Henkel, L., Mlekusch, W., and Reibnegger, G. (1998) Calorimetry of Archaeal Tetraether Lipid—Indication of a Novel Metastable Thermotropic Phase in the Main Phospholipid from *Thermoplasma Acidophilum* Cultured at 59°C, *Chem. Phys. Lipids 94*, 1–12.

39. Kao, Y.L., Chang, E.L., and Chong, P.L.G. (1992) Unusual Pressure Dependence of the Lateral Motion of Pyrene-Labeled Phosphatidylcholine in Bipolar Lipid Vesicles, *Biochem. Biophys. Res. Commun. 188*, 1241–1246.

40. Khan, T.K., and Chong, P.L.G. (2000) Studies of Archaebacterial Bipolar Tetraether Liposomes by Perylene Fluorescence, *Biophys. J. 78*, 1390–1399.

41. Douliez, J.P., Léonard, A., and Dufourc, E.J. (1995) Restatement of Order Parameters in Biomembranes—Calculation of C–C Bond Order Parameters from C-D Quadrupolar Splittings, *Biophys. J. 68*, 1727–1739.

42. Nicolas, J.P., and de Souza, N.R. (2004) Molecular Dynamics Study of *n*-Hexane–Water Interface: Towards a Better Understanding of the Liquid–Liquid Interfacial Broadening, *J. Chem. Phys. 120*, 2464–2469.

^{1}H and ^{13}C NMR Characterization and Stereochemical Assignments of Bile Acids in Aqueous Media

Omkar B. Ijare, B.S. Somashekar, Y. Jadegoud, and G.A. Nagana Gowda*

Centre of Biomedical Magnetic Resonance, Sanjay Gandhi Post-graduate Institute of Medical Sciences, Lucknow-226 014, India

ABSTRACT: The unconjugated bile acids cholic acid, deoxycholic acid, and chenodeoxycholic acid; their glycine and taurine conjugates glycocholic acid, glycodeoxycholic acid, glycochenodeoxycholic acid, taurocholic acid, taurodeoxycholic acid, and taurochenodeoxycholic acid; and a taurine conjugated ursodeoxycholic acid, tauroursodeoxycholic acid, were characterized through ^{1}H and ^{13}C NMR in aqueous media under the physiological pH region (7.4 ± 0.1). Assignments of ^{1}H and ^{13}C signals of all the bile acids were made using a combination of several one- and two-dimensional, homonuclear (^{1}H–^{1}H) and heteronuclear (^{1}H–^{13}C) correlations as well as spectral editing NMR methods. Stereochemical assignment of the five-membered ring of the bile acids is reported here for the first time. The complete characterization of various bile acids in aqueous media presented here may have implications in the study of the pathophysiology of biliary diseases through human biliary fluids using NMR spectroscopy.

Paper no. L9838 in *Lipids* 40, 1031–1041 (October 2005).

Bile salts constitute an important class of physiological detergents that play a key role in the solubilization of dietary fats, fat-soluble vitamins, and cholesterol (1,2). The biosynthesis of bile acids from cholesterol involves many complex enzymatic steps, of which the microsomal 7α-hydroxylation of cholesterol appears to be the rate-limiting step (3). Cholic acid (CA) and chenodeoxycholic acid (CDCA) are the primary bile acids thus synthesized from cholesterol in the liver (4). These primary bile acids usually are conjugated to glycine or taurine and are secreted in the bile (5). In addition, several other derivatives of cholic acid are present in the bile, such as glycine and taurine conjugated deoxycholic acids (DCA) (5). During enterohepatic circulation, primary conjugated bile salts are partly subjected to deconjugation and dehydroxylation by the cat-

alytic effect of anaerobic bacteria present in the gut (6) and colon (7,8). The intrinsic surface-active properties of the resulting deconjugated bile acids may have a detrimental effect on gut epithelial cells and result in a compensatory increase in the proliferation of crypt cells, which may increase the risk of colon cancer (9,10). Further, the deconjugation of bile acids may affect nutrient absorption, resulting in malabsorption syndrome (11–13). Inborn errors of bile acid metabolism and chronic cholestasis have been shown to result in abnormal bile acid excretion (14). Altered levels of some unconjugated bile acids have also been implicated in the pathogenesis of both breast and colorectal cancer (15–19). However, the pathophysiology of diseases associated with an abnormal composition of biliary biochemicals, such as unconjugated and conjugated bile acids, is not clearly understood.

The methods commonly used for the detection and quantification of bile acids in body fluids usually involve tedious steps such as extraction, hydrolysis, derivatization, and/or purification before analyses (20–25). Subsequently, the assay of conjugated bile acids is performed by enzymatic methods, GLC, or HPLC (26,27). The use of MS techniques for circumventing hitherto known limitations in detecting individual bile acids in the body fluids has continued to increase (23,28).

The technique of high-resolution NMR spectroscopy is rapidly developing as an important tool in detecting a large number of biochemicals in biofluids simultaneously without any sample pretreatment (29). This approach has immense potential in the study of dynamic variations of the bodily fluid metabolites, which has implications for the assessment of the pathophysiology of diseases and drug toxicity (30). We have recently proposed a simple method for detecting and accurately quantifying the glycine and taurine conjugated class of bile acids in human bile using ^{1}H NMR spectroscopy (31), and further work is in progress to detect individual components of conjugated and unconjugated bile acids. Unambiguous assignment of ^{1}H/^{13}C chemical shifts of various bile acids under physiological conditions is a primary requisite in identifying individual bile acids in human bile using NMR spectroscopy. Although the characterizations of many bile acids by NMR have been reported (32–36), they are essentially either partly assigned or assigned in organic solvents such as chloroform and methanol. Further, although both ^{1}H and ^{13}C chemical shift assignments of cholic and deoxycholic acids in aqueous media have been reported, there are discrepancies

---

---

in the reported assignments (37,38); in many instances, the reported values differ significantly from the actual values. Moreover, complete stereochemical assignments of the protons of the bile acids, specifically of the five-membered ring, have not been made to date. Thus, we have attempted here to characterize several unconjugated and conjugated bile acids using ^1H and ^{13}C one-dimensional (1-D) and two-dimensional (2-D) NMR in aqueous media under physiological pH (7.4 ± 0.1). These results, including the stereochemical assignments, are presented herein.

EXPERIMENTAL PROCEDURES

Sodium salts of the unconjugated bile acids CA, DCA, and CDCA, and their glycine and taurine conjugates glycocholic acid (GCA), glycodeoxycholic acid (GDCA), glycochenodeoxycholic acid (GCDCA), taurocholic acid (TCA), taurodeoxycholic acid (TDCA), taurochenodeoxycholic acid (TCDCA), and tauroursodeoxycholic acid (TUDCA), as well as deuterium oxide (99.9%) and methanol-d_4 were purchased from Sigma-Aldrich (Milwaukee, WI). Hydrochloric acid and sodium hydroxide were obtained from Qualigens Fine Chemicals (Mumbai, India). Solutions of 0.01 N DCl and 0.01 N NaOD were prepared by dissolving an appropriate quantity of HCl/NaOH in D_2O to adjust the pH of the bile salt solutions.

Bile salt solutions. Solutions of the sodium salts of bile acids CA, DCA, and CDCA were prepared by dissolving 10 mg of the respective bile acid in 0.5 mL D_2O at an alkaline pH of about 11, and the pH was then slowly brought down to 7.4 by adding 0.01 N DCl. Solutions of salts of the conjugated bile acids GCA, GDCA, GCDCA, TCA, TDCA, TCDCA, and TUDCA were prepared by dissolving 10 mg of the respective sodium salt in 0.5 mL D_2O and the pH was adjusted to 7.4 using 0.01 N NaOD. The pH of the solutions was measured using Thermo Orion model 520 A+ pH meter (Beverly, MA) after calibrating the system with standard buffers. The pH meter readings were measured without correcting for the deuterium isotope effect.

NMR experiments. NMR experiments on bile salt solutions (0.5 mL each) taken in 5-mm NMR tubes were performed on a Bruker Biospin Avance 400 NMR spectrometer (^1H frequency = 400.13 MHz, ^{13}C frequency = 100.62 MHz) at 298 K using 5-mm broad-band or broad-band inverse probe heads equipped with shielded z-gradient and XWIN-NMR software, version 3.5 (Zürich, Switzerland). A reusable capillary tube containing 35 μL of 0.375% TSP [sodium salt of 3-(trimethylsilyl)propionicacid-d_4] in D_2O was inserted into the NMR tube before obtaining NMR spectra. 1-D ^1H spectra were obtained using one pulse sequence with the residual water signal suppressed by presaturation during the relaxation delay. The parameters used were spectral width, 4800 Hz; time domain data points, 32 K; flip angle, 45°; relaxation delay, 6 s; spectrum size, 32 K points; and line broadening, 0.2 Hz. 1-D ^{13}C spectra were obtained using one pulse sequence, spin-echo FT (SEFT), and quaternary carbon detection (QCD) (39) sequences with proton decoupling using WALTZ-16 composite pulses. To study the con-

centration effect on the chemical shift, ^{13}C SEFT spectra were obtained at four different concentrations (5, 15, 30, and 50 mM) for one of the bile acids (CA). The typical parameters used for ^{13}C experiments were: spectral width, 24000 Hz; data points, 32 K; flip angle, 90°; relaxation delay, 3 s; spectrum size, 32 K points; and line broadening, 3 Hz.

Homonuclear and heteronuclear 2-D experiments, such as ^1H–^1H double-quantum filtered COSY (DQF-COSY), ^1H–^{13}C sensitivity-enhanced (by preservation of equivalent pathways using gradients) and multiplicity-edited heteronuclear single-quantum correlation (edited HSQC), and ^1H–^{13}C gradient-enhanced heteronuclear multiple bond correlation (HMBC) experiments, were performed for all the bile acids. Nuclear Overhauser enhancement spectroscopy (NOESY) experiments were performed for CA, DCA, CDCA, and TUDCA. All 2-D experiments were performed at 298 K with the residual water signal suppressed by presaturation during relaxation delay and, in the case of the NOESY experiment, the residual water signal was also suppressed during mixing time. For DQF-COSY and NOESY, a sweep width of 4800 Hz was used in both dimensions and 512 free induction decays (FID) were obtained with t_1 increments, each with 2,048 complex data points. The number of transients and the relaxation delay used were 32 and 2.5 s for DQF-COSY, and 64 and 1.5 s for NOESY, respectively. NOESY spectra were obtained at five different mixing times (200, 300, 400, 450, and 500 ms) to obtain unambiguous stereochemical assignments. Phase-sensitive data were obtained using the time-proportional phase increment method.

For ^1H–^{13}C multiplicity-edited HSQC and HMBC experiments, spectral widths of 4800 and 24000 Hz were used in the ^1H and ^{13}C dimensions, respectively. Five hundred twelve FID were collected with t_1 increments, each of 2048 data points, 32 transients, and 2-s recycle delays. Phase-sensitive data for the edited HSQC experiment were obtained using the echo–antiecho mode, whereas for the HMBC experiment, magnitude mode data were obtained. The resulting 2-D data were zero filled to 1,024 points in the t_1 dimension and double Fourier transformed after multiplying by a squared sine-bell window function shifted by π/2 along both the dimensions.

For further confirmation of the stereochemical assignments of the protons, particularly of the five-membered ring, 1-D nuclear Overhauser enhancement (nOe) experiments were also performed on CA, DCA, CDCA, and ursodeoxycholic acid (UDCA) in methanol-d_4. The nOe on the proximal protons was monitored from the difference spectrum of on- and off-resonance irradiation of H18 methyl protons. The parameters used were: spectral width, 4085 Hz; time domain data points, 32 K; flip angle, 90°; relaxation delay, 2 s; irradiation time, 3 s; spectrum size, 32 K points; and exponential line broadening, 0.3 Hz.

RESULTS

Assignment of ^1H chemical shifts. Figure 1 shows structures of the bile acids used in the present study and the numbering of
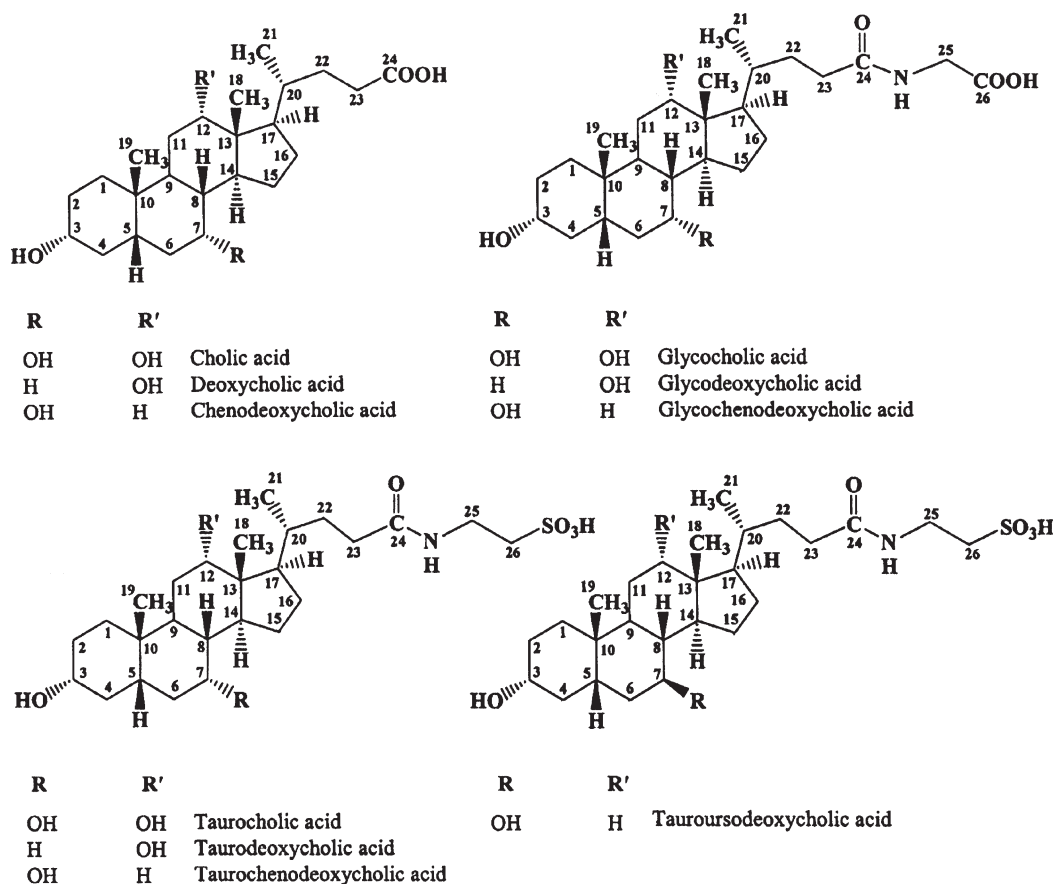
FIG. 1. Structures and numbering of ^{1}H/^{13}C of conjugated and unconjugated bile acids. The numbering of the proton(s) is same as that of the corresponding directly attached carbon. The orientations of some important substitutions are marked with respect to the plane of the ring (dashed wedge: α substitution; solid wedge: β substitution).

[1]H/^{13}C nuclei along with some stereochemical representations. [1]H spectra of all the bile acids were similar, with severe overlap of most of the signals, especially in the regions between 1.0 and 2.3 ppm. H18, H19 (both singlets), and H21 methyl signals (doublets) were, however, distinctly observed between 0.6 and 1.0 ppm in all the bile acids. The protons H3β, H7β/α, and H12β, which are geminal to the hydroxyl groups, were shifted downfield (in the range of about 3.5–4 ppm) away from rest of the signals and clearly separating from one another. In the conjugated bile acids, however, one or more of these signals overlapped with those arising from the H25 protons of the conjugated glycine or taurine (Fig. 1).

DQF-COSY spectra of all the bile acids showed cross peaks attributable to geminal proton–proton J couplings (two-bond couplings in methylene protons) as well as to vicinal (three-bond) proton–proton J couplings (Fig. 2). The intensities of the cross peaks greatly varied depending on the magnitude of the J couplings. For example, as seen in Figure 2 for CA, H3β showed strong cross peaks with H2α and H4α because of the large J couplings, whereas it showed very weak cross peaks with H2β and H4β because of the small J couplings (40). By

carefully tracing the cross peak positions along both the frequency dimensions, tentative assignments of all the cross peaks in each DQF-COSY spectrum were made. Well-separated signals of H3β, H7β/α, and/or H12β served as good starting points for making these assignments.

The multiplicity-edited HSQC spectra were immensely useful in unraveling the overlapping signals through one-bond [13]C–[1]H correlations. These 2-D spectra showed negative cross peaks for the CH and CH$_3$ groups and positive cross peaks for the CH$_2$ groups (Fig. 3). Negative peaks corresponding to three methyl groups, 18, 19 and 21, were identified based on their distinct ^{1}H signals identified from proton 1-D spectra. Subsequently, the cross peaks in the severely overlapped regions (1.0–2.3 ppm) arising from CH (negative peaks) and CH$_2$ (positive peaks) groups were distinguished based on the sign of the cross peaks. This resulted in the identification of all the CH, CH$_2$, and CH$_3$ groups for each bile acid molecule. Further, for each CH$_2$ group, two cross peaks were seen along the ^{13}C dimension, attributable to the difference in the chemical shifts of the two methylene protons (α and β). In Figure 3, these are shown by joining each pair of cross peaks by horizontal dashed lines. However, the C11 methylene group in CA, DCA, and
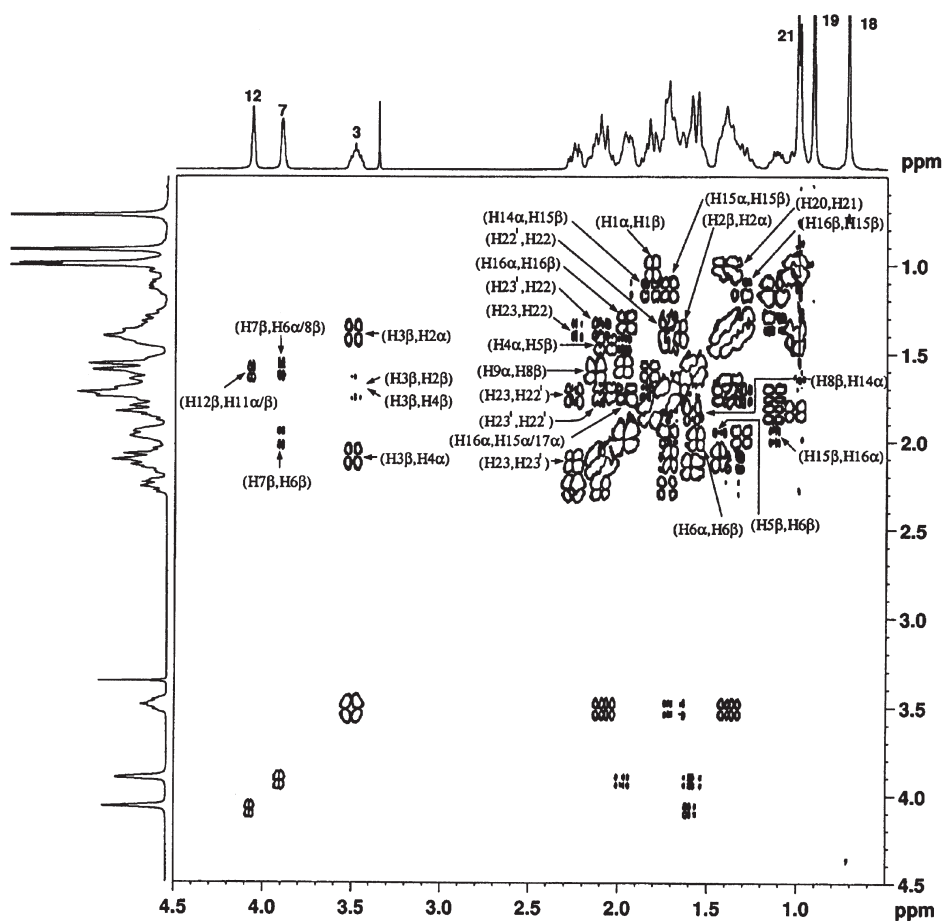
FIG. 2. ^{1}H–^{1}H double-quantum filtered COSY spectrum of cholic acid obtained on a Bruker Biospin Avance 400 MHz spectrometer, along with the stereospecific assignments of most of the cross peaks.

their conjugated derivatives (GCA, TCA, GDCA, and TDCA) showed a single cross peak, indicating that their C11 methylene protons were degenerate. Using the assignments from the edited HSQC spectra, the tentative proton assignments of the DQF-COSY spectra were confirmed for all the bile acids except the stereochemical assignment of CH$_2$ protons.

Stereochemical assignments for the ring methylene protons were made based on the relative nOe cross peak intensity in 2-D NOESY and/or 1-D nOe spectra. The nOe for the proximal protons was higher when the two protons lay on the same side of the ring; the enhancement was either absent or lower when the protons were on opposite sides of the ring. This is briefly illustrated in Figure 4 using 1-D nOe spectra for CA, DCA, CDCA, and UDCA. One can see that when the H18 methyl proton signals were irradiated, no nOe was seen for the 15α and 16α protons, indicating that H18 protons were on the opposite side of the 15α and 16α protons. On the other hand, irradiation of the H18 methyls showed distinct enhancement for H15β and H16β protons indicating that H18, H15β and H16β were all on the same side of the ring. The assignments thus

made for all the methylene protons are marked for a typical bile acid (CA) in Figure 2.

Assignment of ^{13}C chemical shifts. Carbon signals were grouped according to their multiplicity using SEFT spectra (which showed positive signals for quaternary and CH$_2$ carbons, and negative signals for CH and CH$_3$ carbons) and edited HSQC spectra (positive cross peaks for CH$_2$ carbons; negative cross peaks for CH and CH$_3$ carbons). Further, all quaternary carbons were unambiguously assigned using the spectra from QCD experiments, which showed signals from only quaternary carbons (39). Subsequently, individual assignment of all the carbons was made from the combination of multiplicity-edited HSQC and HMBC spectra. Each proton in the HMBC spectra showed cross peaks to carbons that were up to three bonds away. A typical 2-D spectrum of HMBC for the bile acid, CA is shown in Figure 5 along with most of the assignments. Figure 6 shows 1-D ^{13}C spectra for all the bile acids analyzed, marking the assignment of individual carbon signals. The maximum variation of the ^{13}C chemical shift for any carbon determined for a typical bile acid, CA, when the concentration was varied from 5–50 mM was about 0.35 ppm.
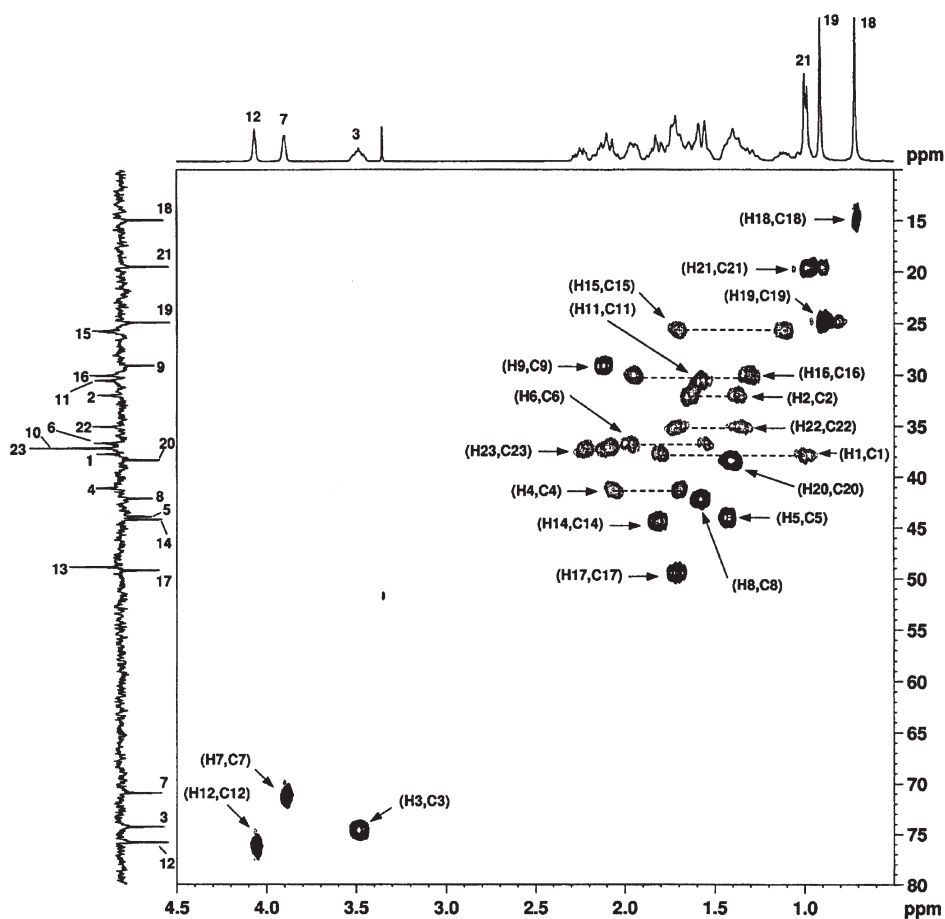
FIG. 3. Sensitivity-enhanced, multiplicity-edited [1]H-^{13}C heteronuclear single-quantum correlation spectrum of cholic acid obtained on a Bruker Biospin Avance 400 MHz spectrometer, along with the assignments of all the protons and proton-attached carbons. For clarity, CH and CH$_3$ cross peaks are shown as dark, continuous contours, whereas CH$_2$ cross peaks are shown as light, discontinuous contours. Wherever methylene protons are chemically different (nondegenerate), two distinct cross peaks were observed, corresponding to Hα and Hβ protons (each pair of cross peaks is joined by dashed lines). Traces of the one-dimensional (1-D) ^{1}H spectrum and ^{13}C spin-echo FT spectrum (CH and CH$_3$ negative and C and CH$_2$ positive) are also shown.

Complete ^{1}H and ^{13}C chemical shifts determined from the analyses of all the conjugated and unconjugated bile acids are given in Tables 1–3.

DISCUSSION

The pK_a of unconjugated bile acids is significantly high compared with conjugated bile acids (41). Therefore, unconjugated bile acids are not readily soluble in aqueous media under physiological pH, unlike conjugated bile acids. To circumvent this problem, we dissolved the unconjugated bile acids in D$_2$O after increasing the pH to about 11, and the pH was subsequently brought slowly down to 7.4. All the unconjugated bile acids and their glycine and taurine conjugates have similar structures; hence, the ^{1}H and ^{13}C spectra are similar, with several partially or severely overlapping regions. As seen from Tables 1–3, all the chemical shifts in the glycine/taurine conjugated bile acids were similar to the corresponding unconjugated bile acids except in the vicinity of conjugation, as expected, at positions C22, C23, and C24. However, depending on the pattern of substitution at the C3, C7, or C12 positions, ^{1}H and ^{13}C chemical shifts varied significantly at and in the vicinity of substitutions. The substitutions resulted in changes in the ^{13}C chemical shift of even the distant carbons by as much as 9 ppm. For example, the C17 carbon shifted downfield by about 9 ppm upon dehydroxylation at the C12 carbon position, and the C9 carbon shifted downfield by about 7 ppm upon dehydroxylation at the C7 carbon position (Tables 1–3). Thus, substitution effects considerably extended to relatively distant nuclei. Such differences in the chemical shifts may play a key role in the
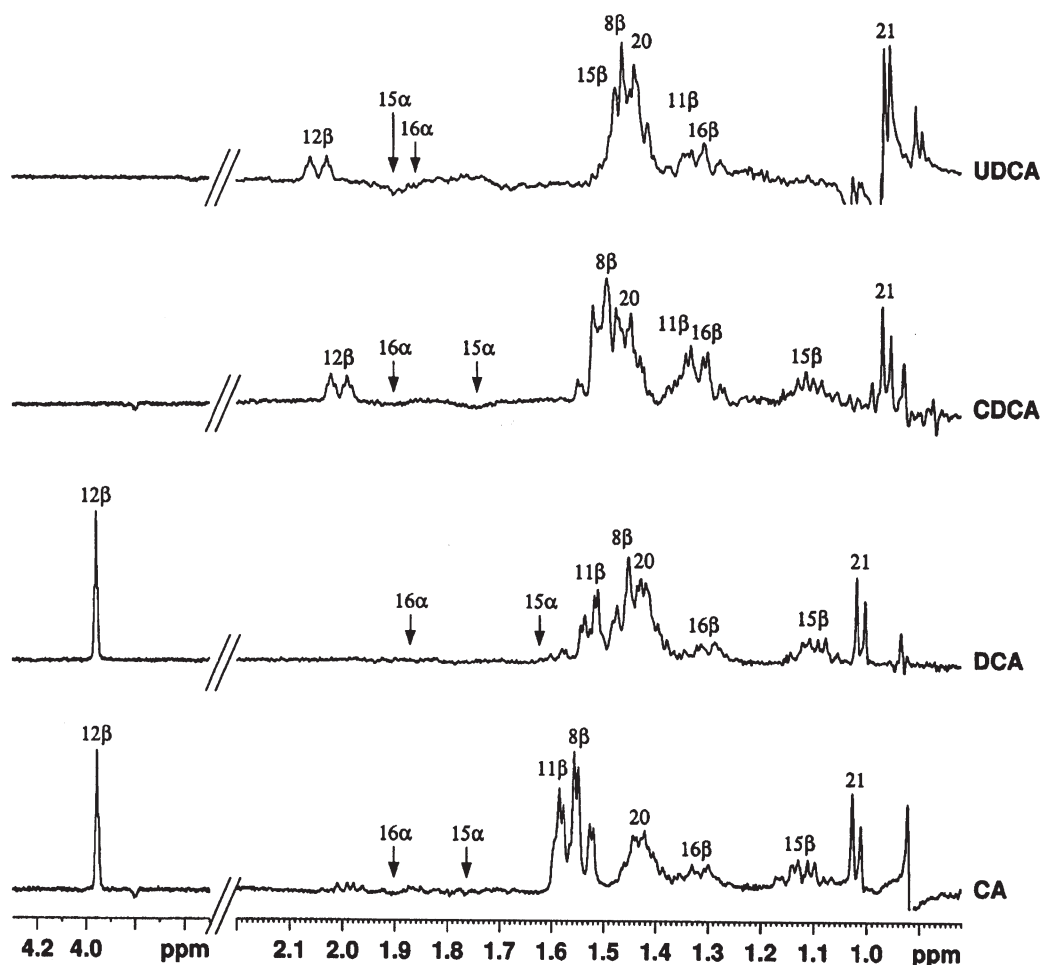
FIG. 4. Parts of 1-D nuclear Overhauser enhancement (nOe) spectra, in deuterated methanol, obtained by saturating H18 methyl protons of the bile acids cholic acid (CA), deoxycholic acid (DCA), chenodeoxycholic acid (CDCA), and ursodeoxycholic acid (UDCA). The nOe effect for H15β and H16β protons (marked as 15β and 16β), in addition to other proximal β protons (as marked), are clearly seen, indicating that these are on the same side of the ring as H18 methyl protons. However, the nOe is clearly absent for H15α and H16α protons (marked as 15α and 16α), indicating that these are on the opposite side of H18 methyl protons. For other abbreviation see Figure 3.

identification of individual bile acids in biological fluids from NMR.

Several reports have provided partial or complete assignments of ^{1}H and/or ^{13}C chemical shifts of several conjugated and unconjugated bile acids (32–36). However, these were characterized in organic solvents; hence, the chemical shifts are significantly different from those in aqueous media, obviously arising from solvent effects. In the cases in which the characterization is reported in aqueous media (CA and DCA), the assignments are either incomplete or the values differ significantly with respect to each other (37,38) and with the present study. For example, in CA, the chemical shifts of C3, C19, C21, C23, and C24 were 69.4, 17.5, 22.7, 35.4, and 185.5 ppm (37) compared with the values of 74.41, 24.92, 19.57, 37.3, and 187.24 ppm, respectively, determined in the present analysis under similar conditions. Similarly, chemical

shifts of C2, C7, C17, and C22 were 34.55, 70.31, 48.42, and 37.54 ppm (38) compared with the values of 32.05, 71.12, 49.39, and 35.11 ppm, respectively. It may be noted that the comparison of carbon chemical shifts of this bile acid obtained in the present study at different concentrations (5, 15, 30, and 50 mM) showed that the maximal variation in the chemical shift for any carbon was not more than 0.35 ppm throughout the concentration range; the concentrations included in this study covered the range below and above the CMC (38). Therefore, we ruled out that a concentration effect or micelle formation could have resulted in significant variation of the ^{13}C chemical shifts.

We have made unambiguous stereochemical assignments of the methylene protons making use of 2-D NOESY and 1-D nOe experiments. The assignment of methylene protons of all three six-membered rings of bile acids were in line with
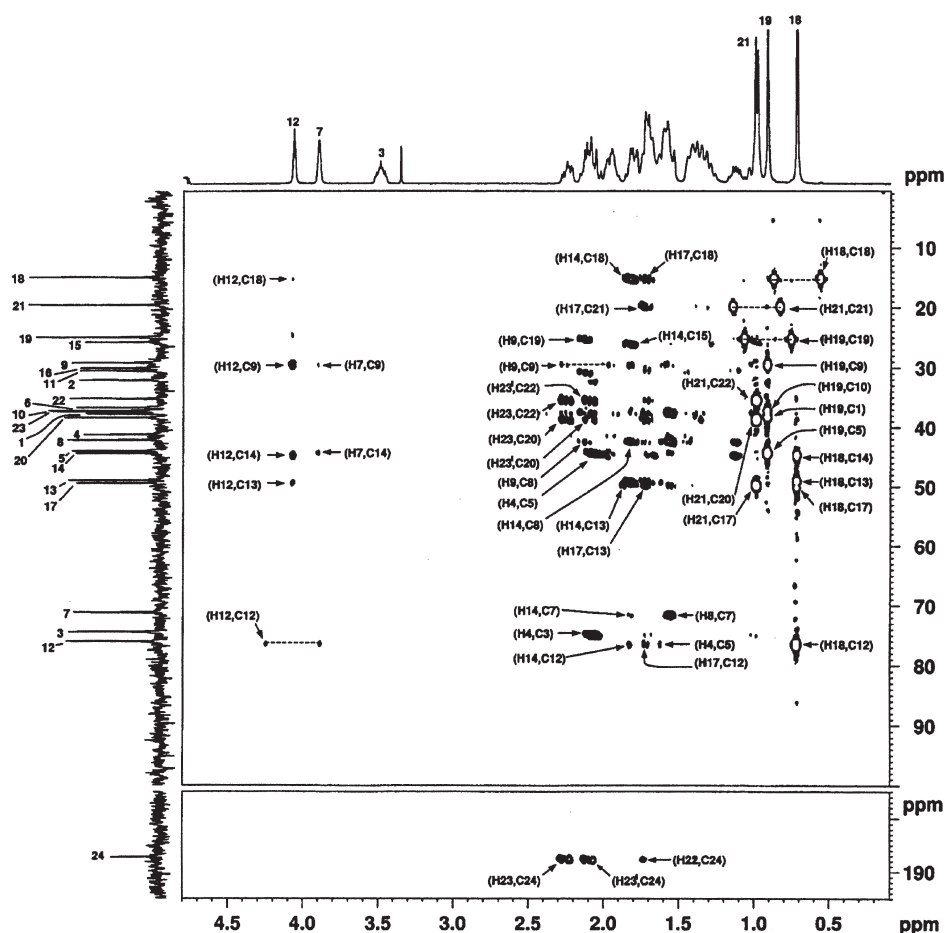
FIG. 5. Typical heteronuclear multiple-bond correlation spectrum of CA, obtained on a Bruker Biospin Avance 400 MHz spectrometer, along with the assignments of a number of cross peaks arising from one-, two-, or three-bond proton–carbon couplings. Cross peaks attributable to one-bond proton–carbon coupling for 9, 12, 18, 19, and 21 are joined by horizontal dashed lines. 1-D ¹H and ¹³C spectra are also shown on the top and left side of the 2-D spectrum, respectively.

those already reported (37). Because of the overlap of 15α/β and 16α/β protons with other signals, stereochemical assignments of the H15 and H16 methylene protons could not be made unambiguously from the spectra in aqueous media. Therefore, to confirm these assignments, we used a deuterated methanol solvent, which provided resolved signals for the H15 and H16 methylene protons. The presence of nOe for 15β and 16β and the absence of nOe for 15α and 16α upon saturation of H18 methyls clearly distinguished between the α and β protons in all the bile acids studied (Fig. 4). Our analyses revealed that H15α and H15β assignments were interchanged earlier (37). The stereochemical assignments made here on five-membered rings are further supported by recent studies on similar molecules, 17β-estradiol, 17β-hydroxyandrosta-1,4-dien-3-one, (17α,20*E*)-(*p*-trifluoromethyl-phenyl)vinylestradiol, and (17α,20*E*)-(*o*-trifluoromethyl-phenyl)vinylestradiol (42–44).

The strategies adopted for the assignments of ¹H and ¹³C chemical shifts for all the bile acids are displayed here through a set of completely assigned ¹H–¹H and ¹H–¹³C 2-D spectra for a typical bile acid, CA (Figs. 2, 3, and 5). In addition, 1-D carbon spectra are shown for all the bile acids, marking complete assignments (Fig. 6). Thus, the combined analysis of a several 1-D and 2-D spectra for each bile acid, together with 1-D and 2-D nOe studies, resulted in reliable chemical shift and stereochemical assignments.

Thus, we have presented here a complete and unambiguous analysis of ¹H and ¹³C NMR spectra of several unconjugated and conjugated bile acids that occur in biofluids using the combination of various 1-D and 2-D experiments in aqueous media near the conditions of physiological pH. In addition, for the first time, we have made unambiguous stereochemical assignments of the five-membered-ring methylene protons of H15 and H16. The characterization of bile acids is
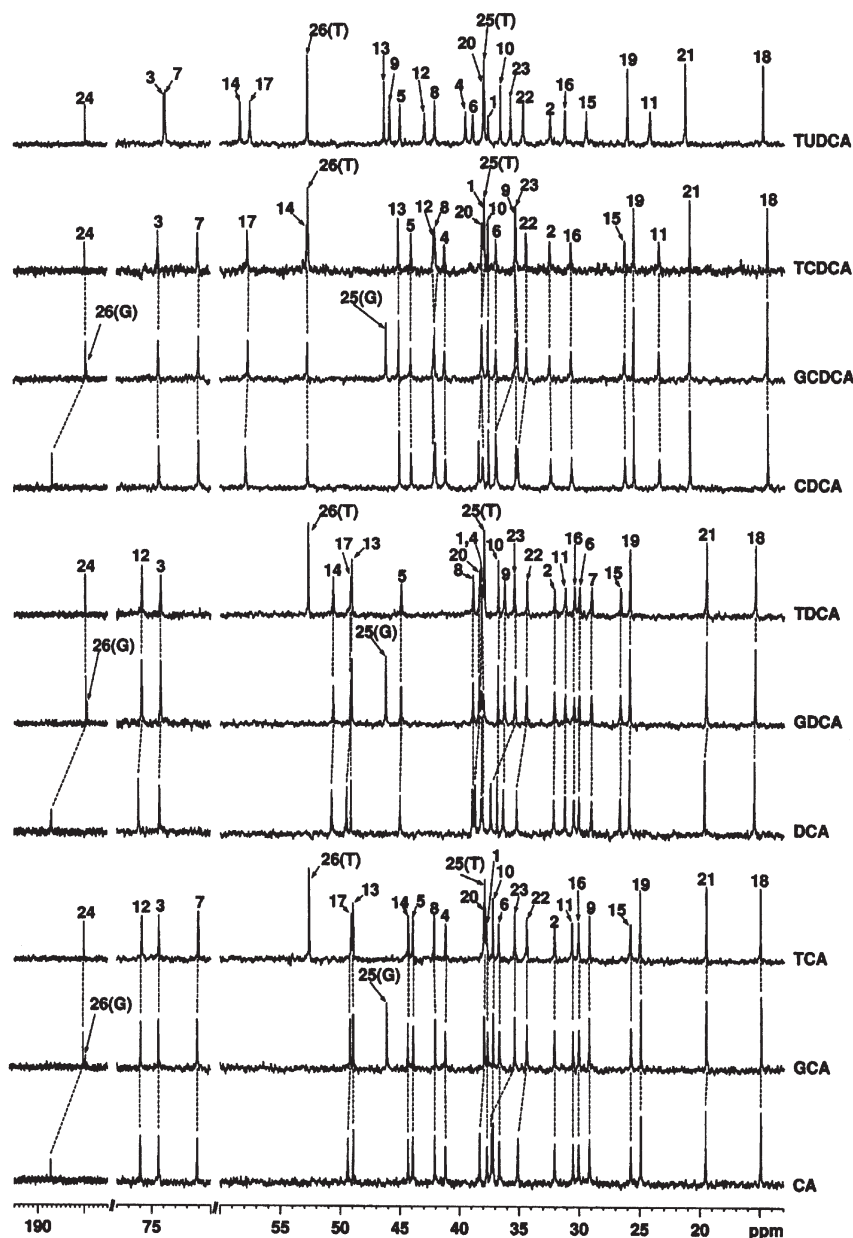
FIG. 6. 1-D ^{13}C spectra of all the bile acids characterized by NMR: CA, glycocholic acid (GCA), taurocholic acid (TCA), DCA, glycodeoxycholic acid (GDCA), taurodeoxycholic acid (TDCA), CDCA, glycochenodeoxycholic acid (GCDCA), taurochenodeoxycholic acid (TCDCA), and tauroursodeoxycholic acid (TUDCA). All the carbon assignments are marked. C25 and/or C26 chemical shifts arising from the conjugated glycine or taurine are marked as G or T in parenthesis, respectively. For other abbreviations see Figures 3 and 4.

primarily aimed at the identification of individual unconjugated and conjugated bile acids in the biofluids, such as gallbladder bile and intestinal fluids, using NMR spectroscopy. Unless reliable chemical shifts are established under physiological conditions, it is not possible to attempt identification of individual bile acids in biological fluids through NMR

spectroscopy. Therefore, we have first attempted to completely characterize both ^{1}H and ^{13}C NMR spectra of several bile acids that occur commonly in the biological fluids. The data presented herein may be invaluable for the study of the pathophysiology of diseases associated with abnormal bile acid metabolism using NMR spectroscopy.

TABLE 1
^{1}H and ^{13}C Chemical Shifts of Cholic Acid, Glycocholic Acid, and Taurocholic Acid in Aqueous Media (D$_2$O) at pH 7.4 ± 0.1

No.		Cholic acid				Glycocholic acid				Taurocholic acid		
			Proton				Proton				Proton	
	Type	Carbon	α	β	Type	Carbon	α	β	Type	Carbon	α	β
1	CH$_2$	37.69	1.80	0.99	CH$_2$	37.66	1.80	1.00	CH$_2$	37.74	1.80	0.99
2	CH$_2$	32.05	1.38	1.65	CH$_2$	32.06	1.39	1.66	CH$_2$	32.06	1.38	1.65
3	CH	74.41	—	3.48	CH	74.43	—	3.49	CH	74.39	—	3.47
4	CH$_2$	41.18	2.07	1.70	CH$_2$	41.20	2.07	1.70	CH$_2$	41.19	2.08	1.70
5	CH	43.93	—	1.44	CH	43.90	—	1.44	CH	43.95	—	1.43
6	CH$_2$	36.67	1.55	1.97	CH$_2$	36.68	1.55	1.97	CH$_2$	36.74	1.55	1.94
7	CH	71.12	—	3.89	CH	71.13	—	3.89	CH	71.04	—	3.87
8	CH	42.09	—	1.58	CH	42.06	—	1.59	CH	42.16	—	1.55
9	CH	29.17	2.13	—	CH	29.18	2.12	—	CH	29.18	2.14	—
10	C	37.19	—	—	C	37.18	—	—	C	37.22	—	—
11	CH$_2$	30.52	1.59	1.59	CH$_2$	30.54	1.59	1.59	CH$_2$	30.62	1.57	1.57
12	CH	75.98	—	4.05	CH	75.94	—	4.05	CH	75.84	—	4.03
13	C	48.93	—	—	C	48.95	—	—	C	48.96	—	—
14	CH	44.33	1.82	—	CH	44.36	1.83	—	CH	44.33	1.84	—
15	CH$_2$	25.76	1.71	1.12	CH$_2$	25.73	1.71	1.12	CH$_2$	25.78	1.72	1.09
16	CH$_2$	30.06	1.95	1.31	CH$_2$	30.04	1.96	1.29	CH$_2$	30.09	1.95	1.26
17	CH	49.39	1.72	—	CH	49.21	1.74	—	CH	49.10	1.74	—
18	CH$_3$	14.94	0.71		CH$_3$	14.91	0.71		CH$_3$	14.99	0.69	
19	CH$_3$	24.92	0.90		CH$_3$	24.90	0.91		CH$_3$	24.99	0.90	
20	CH	38.32	1.41		CH	37.95	1.44		CH	37.96	1.41	
21	CH$_3$	19.57	0.98		CH$_3$	19.50	1.00		CH$_3$	19.51	0.99	
22	CH$_2$	35.11	1.36, 1.72		CH$_2$	34.37	1.43, 1.77		CH$_2$	34.38	1.41, 1.73	
23	CH$_2$	37.30	2.23, 2.09		CH$_2$	35.29	2.36, 2.23		CH$_2$	35.39	2.32, 2.18	
24	C	187.24	—		C	180.02	—		C	180.05	—	
25					CH$_2$	46.13	3.74		CH$_2$	37.88	3.56	
26					C	179.54	—		CH$_2$	52.69	3.07	
27					NH	—	7.86		NH	—	7.96	

TABLE 2
^{1}H and ^{13}C Chemical Shifts of Deoxycholic Acid, Glycodeoxycholic Acid, and Taurodeoxycholic Acid in Aqueous Media (D$_2$O) at pH 7.4 ± 0.1

No.		Deoxycholic acid				Glycodeoxycholic acid				Taurodeoxycholic acid		
			Proton				Proton				Proton	
	Type	Carbon	α	β	Type	Carbon	α	β	Type	Carbon	α	β
1	CH$_2$	37.96	1.80	0.98	CH$_2$	38.17	1.81	0.98	CH$_2$	38.20	1.80	0.97
2	CH$_2$	32.01	1.40	1.68	CH$_2$	32.02	1.42	1.69	CH$_2$	32.02	1.40	1.67
3	CH	74.25	—	3.63	CH	74.21	—	3.63	CH	74.24	—	3.62
4	CH$_2$	38.09	1.80	1.53	CH$_2$	37.98	1.81	1.54	CH$_2$	38.12	1.80	1.52
5	CH	44.90	—	1.44	CH	44.93	—	1.44	CH	44.93	—	1.42
6	CH$_2$	29.93	1.34	1.86	CH$_2$	30.00	1.34	1.85	CH$_2$	30.01	1.31	1.84
7	CH$_2$	28.90	1.46	1.23	CH$_2$	28.99	1.45	1.23	CH$_2$	28.99	1.42	1.22
8	CH	38.81	—	1.42	CH	38.87	—	1.44	CH	38.89	—	1.42
9	CH	36.23	1.82	—	CH	36.22	1.85	—	CH	36.24	1.82	—
10	C	36.74	—	—	C	36.77	—	—	C	36.78	—	—
11	CH$_2$	31.09	1.55	1.55	CH$_2$	31.14	1.55	1.55	CH$_2$	31.21	1.53	1.53
12	CH	76.04	—	4.06	CH	75.85	—	4.05	CH	75.85	—	4.03
13	C	49.01	—	—	C	49.06	—	—	C	49.07	—	—
14	CH	50.63	1.58	—	CH	50.60	1.61	—	CH	50.63	1.59	—
15	CH$_2$	26.54	1.66	1.08	CH$_2$	26.60	1.67	1.07	CH$_2$	26.60	1.65	1.05
16	CH$_2$	30.36	1.94	1.30	CH$_2$	30.42	1.95	1.27	CH$_2$	30.42	1.92	1.22
17	CH	49.37	1.72	—	CH	49.13	1.77	—	CH	49.16	1.75	—
18	CH$_3$	15.39	0.72		CH$_3$	15.42	0.72		CH$_3$	15.42	0.70	
19	CH$_3$	25.76	0.94		CH$_3$	25.83	0.94		CH$_3$	25.84	0.92	
20	CH	38.61	1.42		CH	38.36	1.44		CH	38.33	1.42	
21	CH$_3$	19.54	0.99		CH$_3$	19.47	1.02		CH$_3$	19.51	0.99	
22	CH$_2$	35.10	1.38, 1.71		CH$_2$	34.37	1.46, 1.74		CH$_2$	34.39	1.42, 1.71	
23	CH$_2$	37.28	2.26, 2.09		CH$_2$	35.33	2.39, 2.21		CH$_2$	35.53	2.33, 2.16	
24	C	187.04	—		C	179.67	—		C	179.79	—	
25					CH$_2$	46.19	3.75		CH$_2$	37.95	3.56	
26					C	179.44	—		CH$_2$	52.69	3.07	
27					NH	—	7.83		NH	—	7.92	

TABLE 3

^1H and ^{13}C Chemical Shifts of Chenodeoxycholic Acid, Glycochenodeoxycholic Acid, Taurochenodeoxycholic Acid and Tauroursodeoxycholic Acid in Aqueous Media (D_2O) at pH 7.4 ± 0.1

		Chenodeoxycholic acid				Glycochenodeoxycholic acid				Taurochenodeoxycholic acid				Tauroursodeoxycholic acid			
				Proton				Proton				Proton				Proton	
No.	Type	Carbon	α	β	Type	Carbon	α	β	Type	Carbon	α	β	Type	Carbon	α	β
1	CH$_2$	38.11	1.87	0.99	CH$_2$	38.10	1.83	0.96	CH$_2$	38.09	1.83	1.00	CH$_2$	37.60	1.80	1.08
2	CH$_2$	32.45	1.38	1.68	CH$_2$	32.49	1.38	1.64	CH$_2$	32.48	1.37	1.66	CH$_2$	32.43	1.30	1.67
3	CH	74.43	—	3.49	CH	74.41	—	3.47	CH	74.46	—	3.48	CH	73.92	—	3.62
4	CH$_2$	41.26	2.09	1.70	CH$_2$	41.27	2.08	1.69	CH$_2$	41.30	2.08	1.70	CH$_2$	38.89	1.67	1.56
5	CH	44.14	—	1.42	CH	44.12	—	1.40	CH	44.10	—	1.41	CH	45.03	—	1.56
6	CH$_2$	36.99	1.58	1.96	CH$_2$	36.98	1.56	1.96	CH$_2$	36.96	1.57	1.96	CH$_2$	39.51	1.60	1.82
7	CH	71.06	—	3.89	CH	70.99	—	3.87	CH	71.07	—	3.87	CH	73.84	3.60	—
8	CH	42.12	—	1.49	CH	42.13	—	1.45	CH	42.11	—	1.48	CH	42.10	—	1.48
9	CH	35.34	1.83	—	CH	35.32	1.81	—	CH	35.32	1.82	—	CH	45.90	1.48	—
10	C	37.63	—	—	C	37.63	—	—	C	37.64	—	—	C	36.58	—	—
11	CH$_2$	23.45	1.52	1.30	CH$_2$	23.46	1.50	1.26	CH$_2$	23.46	1.50	1.26	CH$_2$	24.18	1.48	1.33
12	CH$_2$	42.20	1.27	2.00	CH$_2$	42.18	1.25	1.98	CH$_2$	42.19	1.28	1.96	CH	42.97	1.26	2.05
13	C	45.12	—	—	C	45.14	—	—	C	45.17	—	—	C	46.36	—	—
14	CH	52.78	1.41	—	CH	52.76	1.42	—	CH	52.80	1.41	—	CH	58.31	1.32	—
15	CH$_2$	26.30	1.72	1.10	CH$_2$	26.30	1.71	1.07	CH$_2$	26.29	1.72	1.08	CH$_2$	29.43	1.87	1.45
16	CH$_2$	30.71	1.98	1.32	CH$_2$	30.71	1.96	1.27	CH$_2$	30.73	1.97	1.27	CH$_2$	31.21	1.92	1.33
17	CH	57.92	1.24	—	CH	57.68	1.25	—	CH	57.71	1.24	—	CH	57.50	1.14	—
18	CH$_3$	14.44	0.69		CH$_3$	14.45	0.67		CH$_3$	14.43	0.67		CH$_3$	14.77	0.73	
19	CH$_3$	25.57	0.94		CH$_3$	25.57	0.92		CH$_3$	25.54	0.92		CH$_3$	26.03	0.99	
20	CH	38.46	1.44		CH	38.16	1.46		CH	38.13	1.44		CH	38.00	1.46	
21	CH$_3$	20.93	0.97		CH$_3$	20.91	0.97		CH$_3$	20.91	0.96		CH$_3$	21.25	0.99	
22	CH$_2$	35.16	1.40, 1.70		CH$_2$	34.42	1.44, 1.72		CH$_2$	34.45	1.43, 1.72		CH$_2$	34.68	1.38, 1.80	
23	CH$_2$	36.99	2.25, 2.09		CH$_2$	35.18	2.34, 2.17		CH$_2$	35.27	2.31, 2.15		CH$_2$	35.73	2.32, 2.19	
24	C	186.86	—		C	179.64	—		C	179.85	—		C	179.72	—	
25					CH$_2$	46.20	3.73		CH$_2$	37.94	3.56		CH$_2$	37.94	3.58	
26					C	179.43	—		CH$_2$	52.70	3.07		CH$_2$	52.76	3.09	
27					NH	—	7.76		NH	—	7.93		NH	—	7.98	

ACKNOWLEDGMENT

REFERENCES

1. Ikegawa, S., Okuyama, H., Oohashi, J., Murao, N., and Goto, J. (1999) Separation and Detection of Bile Acid 24-Glucuronides in Human Urine by Liquid Chromatography Combined with Electrospray Ionization Mass Spectrometry, *Anal. Sci. 15*, 625–631.
2. Tamminen, J., and Kolehmainen, E. (2001) Bile Acids as Building Blocks of Supramolecular Hosts, *Mol. 6*, 21–46.
3. Galman, C., Arvidsson, I., Angelin, B., and Rudling, M. (2003) Monitoring Hepatic Cholesterol 7α-Hydroxylase Activity by Assay of Stable Bile Acid Intermediate 7α-Hydroxy-4-cholesten-3-one in Peripheral Blood, *J. Lipid Res. 44*, 859–865.
4. Sherwin, J.E., and Sobenes, J.R. (1989) Liver Function, in *Clinical Chemistry* (Kaplan, L.A., and Pesce, A.J., eds.), pp. 359–379, C.V. Mosby, St. Louis.
5. Moseley, R.H., Bile Secretion, in *Textbook of Gastroenterology* (Yamada, T., Alpers, D.H., Owyang, C., Powell, D.W., and Silverstein, F.E., eds.), Vol. 1, pp. 383–404, J.B. Lippincott, Philadelphia.
6. Dunne, C., O'Mahony, L., Murphy, L., Thornton, G., Morrissey, D., O'Halloran, S., Feeney, M., Flynn, S., Fitzgerald, G., Daly, C., *et al*. (2001) *In vitro* Selection Criteria for Probiotic Bacteria of Human Origin: Correlation with *in vivo* Findings, *Am. J. Clin. Nutr. 73*, 386S–392S.
7. Dashkevicz, M.P., and Feighner, S.D. (1989) Development of a Differential Medium for Bile Salt Hydrolase-Active *Lactobacillus* spp., *Appl. Environ. Microbiol. 55*, 11–16.
8. Gaull, G.E., and Wright, C.E. (1987) Taurine Conjugated Bile Acids Protect Human Cells in Culture, *Adv. Exp. Med. Biol. 217*, 61–67.
9. Van Der Meer, R., Termont, D.S.M.L., and De Vries, H.T. (1991) Differential Effects of Calcium Ions and Calcium Phosphate on Cytotoxicity of Bile Acids, *Am. J. Physiol. 260*, G142–G147.
10. Van Der Meer, R., Welberg, J.W.M., Kuipers, F., Kleibeuker, J.H., Mulder, N.H., Termont, D.S.M.L., Vonk, R.J., De Vries, H.T., and De Vries, E.G.E. (1990) Effects of Supplemental Dietary Calcium on the Intestinal Association of Calcium, Phosphate and Bile Acids, *Gastroenterology 99*, 1653–1659.
11. Shindo, K., Yamazaki, R., Mizuno, T., Shionoiri, H., and Sugiyama, M. (1989) The Deconjugation Ability of Bacteria Isolated from the Jejunal Fluids in the Blind Loop Syndrome with High $^{14}CO_2$ Excretion—Using the Breath Analysis Technique and Thin-Layer Chromatography, *Life Sci. 45*, 2275–2283.
12. Tandon, B.N., Tandon, R.K., Satpathy, B.K., and Shrinivas (1977) Mechanism of Malabsorption in *Giardiasis*: A Study of Bacterial Flora and Bile Salt Deconjugation in Upper Jejunum, *Gut 18*, 176–181.
13. Tandon, B.N., Bansal, R., Kapur, B.M., and Shrinivas (1980) A Study of Malabsorption in Intestinal Tuberculosis: Stagnant Loop Syndrome, *Am. J. Clin. Nutri. 33*, 244–250.

14. Yousef, I.M., Perwaiz, S., Lamireau, T., and Tuchweber, B. (2003) Urinary Bile Acid Profile in Children with Inborn Errors of Bile Acid Metabolism and Chronic Cholestasis: Screening Technique Using Electronspray Tandem Mass-Spectroscopy, *Med. Sci. Monit. 9*, MT21–MT23.

15. Owen, R.W., Thompson, M.H., Hill, M.J., Wilpart, M., Mainguet, P., and Roberfroid, M. (1987) The Importance of the Ratio of Lithocholic Acid to Deoxycholic Acid in Large Bowel Carcinogenesis, *Nutr. Cancer 9*, 67–71.

16. Imray, C.H., Radley, S., and Davis, A. (1992) Faecal Unconjugated Bile Acids in Patients with Colorectal Cancer or Polyps, *Gut 33*, 1239–1245.

17. Owen, R.W., Dodo, M., Thompson, M.H., and Hill, M.J. (1987) Faecal Steroids and Colorectal Cancer, *Nutr. Cancer 9*, 73–80.

18. Owen, R.W., Henly, P.J., Thompson, M.H., and Hill, M.J. (1986) Steroids and Cancer: Faecal Bile Acid Screening for Early Detection of Cancer Risk, *J. Steroid Biochem. 24*, 391–394.

19. De Boever, P., Wouters, R., and Verschaeve, L. (2000) Protective Effect of the Bile Salt Hydrolase-Active *Lactobacillous reuteri* Against Bile Salt Cytotoxicity, *Appl. Microboil. Biotechnol. 53*, 709–714.

20. Wildgrube, H.J., Stockhausen, H., Petri, J., Fussel, U., and Lauer, H. (1986) Naturally Occurring Conjugated Bile Acids, Measured by High Performance Liquid Chromatography, in Human, Dog, and Rabbit Bile, *J. Chromatogr. 353*, 207–213.

21. Bloch, C.A., and Watkins, J.B. (1978) Determination of Conjugated Bile Acids in Human Bile and Duodenal Fluid by Reverse-Phase High-Performance Liquid Chromatography, *J. Lipid Res. 19*, 510–513.

22. Tietz, P.S., Thistle, J.L., Miller, L.J., and LaRusso, N.F. (1984) Development and Validation of a Method for Measuring the Glycine and Taurine Conjugates of Bile Acids in Bile by High-Performance Liquid Chromatography, *J. Chromatogr. 336*, 249–257.

23. Perwaiz, S., Tuchweber, B., Mignault, D., Gilat, T., and Yousef, I.M. (2001) Determination of Bile Acids in Biological Fluids by Liquid Chromatography–Electrospray Tandem Mass Spectrometry, *J. Lipid Res. 42*, 114–119.

24. Budai, K., and Javitt, N.B. (1997) Bile Acid Analysis in Biological Fluids: A Novel Approach, *J. Lipid Res. 38*, 1906–1912.

25. Guldutuna, S., You, T., Kurts, W., and Leuschner, U. (1993) High-Performance Liquid Chromatographic Determination of Free and Conjugated Bile Acids in Serum, Liver Biopsies, Bile, Gastric Juice and Feces by Fluorescene Labeling, *Clin. Chim. Acta 214*, 195–207.

26. Sequeira, S.S., Parkes, H.J., Ellul, J.P.M., and Murphy, G.M. (1995) *In vitro* Determination by ¹H-NMR Studies That Bile with Shorter Nucleation Times Contain Cholesterol-Enriched Vesicles, *Biochim. Biophys. Acta 1256*, 360–366.

27. Jones, M.L., Chen, H., Ouyang, W., Metz, T., and Prakash, S. (2003) Methods for Bile Acid Determination by High Performance Liquid Chromatography, *J. Med. Sci. 23*, 277–280.

28. Mim, D., and Hercules, D. (2004) Quantification of Bile Acids Directly from Plasma by MALDI-TOF-MS, *Anal. Bioanal. Chem. 378*, 1322–1326.

29. Lindon, J.C., Holmes, E., and Nicholson, J.K. (2004) Metabonomics and Its Role in Drug Development and Disease Diagnosis, *Expert Rev. Mol. Diagn. 4*, 189–199.

30. Lindon, J.C., Holmes, E., and Nicholson, J.K. (2003) So What's the Deal with Metabonomics? *Anal. Chem. 75*, 384A–391A.

31. Ijare, O.B., Somashekar, B.S., Nagana Gowda, G.A., Sharma, A., Kapoor, V.K., and Khetrapal, C.L. (2005) Quantification of Glycine and Taurine Conjugated Bile Acids in Human Bile Using ¹H NMR Spectroscopy, *Magn. Reson. Med. 53*, 1441–1446.

32. Waterhous, D.V., Barnes, S., and Muccio, D.D. (1985) Nuclear Magnetic Resonance Spectroscopy of Bile Acids. Development of Two-Dimensional NMR Methods for the Elucidation of Proton Resonance Assignments for Five Common Hydroxylated Bile Acids, and Their Parent Bile Acid, 5 β-Cholanoic Acid, *J. Lipid Res. 26*, 1068–1078.

33. Small, D.M., Penkell, S.A., and Chapman, D. (1969) Studies on Simple and Mixed Bile Salt Micelles by Nuclear Magnetic Resonance Spectroscopy, *Biochim. Biophys. Acta 176*, 178–189.

34. Maili Liu, R., Farrant, D., Lindon, J.C., and Nicholson, J.K. (1995) Two-Dimensional ¹H–¹H and ¹³C–¹H Maximum-Quantum Correlation NMR Spectroscopy with Application to the Assignment of the NMR Spectra of the Bile Salt Sodium Taurocholate, *Magn. Reson. Chem. 33*, 212–219.

35. Leibfritz, D., and Roberts, J.D. (1973) Nuclear Magnetic Resonance Spectroscopy. Carbon-13 Spectra of Cholic Acids and Hydrocarbons Included in Sodium Desoxycholate Solutions, *J. Am. Chem. Soc. 95*, 4996–5003.

36. Dominguez, C., Kreuzer, C.S., Bornet, O., Kerfelec, B., Chapus, C., and Guerlesquin, F. (2000) Interactions of Bile Salt Micelles and Colipase Studied Through Intermolecular nOes, *FEBS Lett. 482*, 109–112.

37. Bernes, S., and Geckle, J.M. (1982) High Resolution Nuclear Magnetic Resonance Spectroscopy of Bile Salts: Individual Proton Assignments for Sodium Cholate in Aqueous Solution at 400 MHz, *J. Lipid Res. 23*, 161–170.

38. Campredon, M., Quiroa, V., Thevand, A., Allouche, A., and Pouzard, G. (1986) NMR Studies of Bile Acid Salts: 2D NMR Studies of Aqueous and Methanolic Solutions of Sodium Cholate and Deoxycholate, *Magn. Reson. Chem. 24*, 624–629.

39. Nagana Gowda, G.A. (2001) One-Dimensional Pulse Technique for Detection of Quaternary Carbons, *Magn. Reson. Chem. 39*, 581–585.

40. Yang, D., Xu, X., and Ye, C. (1992) Application of HMQC to the Measurement of J(H, H) Homonuclear Coupling Constants, *Magn. Reson. Chem. 30*, 711–715.

41. Goto, J., Mano, N., and Goto, T. (2004) Development of Highly Selective Analytical Systems for Biological Substances Using Chromatography Combined with Mass Spectroscopy—With Reference to Bio-analytical Studies of Bile Acids, *Chromatography 25*, 1–8.

42. Commodari, F., Sclavos, G., Ibrahimi, S., Khiat, A., and Boulanger, Y. (2005) Comparison of 17β-Estradiol Structures from X-ray Diffraction and Solution NMR, *Magn. Reson. Chem. 43*, 444–450.

43. Ciuffreda, P., Casati, S., and Manzocchi, A. (2004) Complete ¹H and ¹³C NMR Spectral Assignment of 17-Hydroxy Epimeric Sterols with Planar A or A and B Rings, *Magn. Reson. Chem. 42*, 360–363.

44. Sebag, A.B., Hanson, R.N., Forsyth, D.A., and Lee, C.Y. (2003) Conformational Studies of Novel Estrogen Receptor Ligands by 1D and 2D NMR Spectroscopy and Computational Methods, *Magn. Reson. Chem. 41*, 246–252.

Storage Lipid Accumulation and Acyltransferase Action in Developing Flaxseed

Brent M. Sørensen[a], **Tara L. Furukawa-Stoffer**[a], **Kris S. Marshall**[b], **Erin K. Page**[b],
Zahir Mir[c], **Robert J. Forster**[c], and **Randall J. Weselake**[a,*]

[a]Department of Agricultural, Food and Nutritional Science, University of Alberta, Edmonton, Alberta T6G 2P5, Canada,
[b]Department of Chemistry and Biochemistry, University of Lethbridge, Lethbridge, Alberta T1K 3M4, Canada, and
[c]Lethbridge Research Centre, Agriculture and Agri-Food Canada, Lethbridge, Alberta T1J 4B1, Canada

ABSTRACT: Investigations of storage lipid synthesis in developing flaxseed (*Linum usitatissimum*) provide useful information for designing strategies to enhance the oil content and nutritional value of this crop. Lipid content and changes in the FA composition during seed development were examined in two cultivars of flax (AC Emerson and Vimy). The oil content on a dry weight basis increased steadily until about 20 d after flowering (DAF). The proportion of α-linolenic acid (α-18:3, $18:3\,cis\Delta^{9,12,15}$) in TAG increased during seed development in both cultivars while the proportions of linoleic acid ($18:2\,cis\Delta^{9,12}$) and saturated FA decreased. The developmental and substrate specificity characteristics of microsomal DAG acyltransferase (DGAT, EC 2.3.1.20) and lysophosphatidic acid acyltransferase (LPAAT, EC 2.3.1.51) were examined using cultivar AC Emerson. The maximal acyltransferase specific activities occurred in the range of 8–14 DAF, during rapid lipid accumulation on a per seed basis. Acyl-CoA of EPA ($20:5\,cis\Delta^{5,8,11,14,17}$) or DHA ($22:6\ cis^{4,7,10,13,16,19}$) were included in the specificity studies. DGAT displayed enhanced specificity for α-18:3-CoA, whereas the preferred substrate of LPAAT was 18:2-CoA. Both enzymes could use EPA- or DHA-CoA to varying extents. Developing flax embryos were able to take up and incorporate these nutritional FA into TAG and other intermediates in the TAG-formation pathway. This study suggests that if the appropriate acyl-CoA-dependent desaturation/elongation pathways are introduced and efficiently expressed in flax, this may lead to the conversion of α-18:3-CoA into EPA-CoA, thereby providing an activated substrate for TAG formation.

Paper no. L9792 in Lipids 40, 1043–1049 (October 2005).

The formation of TAG is known to occur *via* the Kennedy or *sn*-glycerol-3-phosphate (G3P) pathway catalyzed by membrane-bound enzymes of the endoplasmic reticulum (1–3). The pathway involves the sequential acyl-CoA-dependent acylation of the glycerol backbone beginning with G3P. The acyl-CoA used in this process are produced through the esterification of CoA to FFA, leaving the plastid (4). Further modification of the fatty acyl composition of the cytoplasmic acyl-CoA

pool may occur *via* acyl-CoA elongation in the endoplasmic reticulum, acyl-exchange between phospholipids and the acyl-CoA pool for desaturation, or through liberation of FA from phospholipids, which in turn could be re-esterified with CoA (3). The first and second acylations in the G3P pathway are catalyzed by *sn*-glycerol-3-phosphate acyltransferase (EC 2.3.1.15) and lysophosphatidic acid acyltransferase (LPAAT, EC 2.3.1.51), respectively. The phosphate group is removed prior to the final acylation, which is catalyzed by DAG acyltransferase (DGAT, EC 2.3.1.20). The level of DGAT activity in the developing seed may exert a substantial effect on the flow of carbon into TAG (5–7). Studies with developing seeds of *Brassica napus* have indicated that the activities of the three acyltransferases operating in the mainstream of TAG synthesis reach a maximum during the active phase of oil accumulation (8,9). Although TAG biosynthesis has been studied extensively in a number of oilseeds (3), investigations with flax have been limited (10–15). The current study has examined the characteristics of oil accumulation and the final two acyltransferases of the G3P pathway in developing flaxseed. Given the recent interest in developing a higher plant-based source of EPA ($cis20:5\Delta^{5,8,11,14,17}$) or DHA ($cis22:6\Delta^{4,7,10,13,16,19}$) (14,16–18), this study also examined the ability of flax acyltransferases to accommodate these nutritional FA.

EXPERIMENTAL PROCEDURES

Chemicals and reagents. [1-^{14}C]18:1 (56 mCi mmol^{-1}) and [1-^{14}C]18:2 (55 mCi mmol^{-1}) were obtained from Amersham Canada Ltd. (Baie d'Urfé, Québec, Canada). [1-^{14}C]EPA (55.6 mCi mmol^{-1}) and [1-^{14}C]α-18:3 (52 mCi mmol^{-1}) were obtained from NEN Life Science Products, Inc. (Boston, MA). [1-^{14}C]DHA (56 mCi mmol^{-1}), unlabeled FA, and most other biochemicals were obtained from Sigma-Aldrich Canada Ltd. (Oakville, Ontario, Canada) and were of the highest purity available. Radiolabeled fatty acyl-CoA thioesters were synthesized enzymatically (19). *sn*-1,2-Diolein was from Avanti Polar Lipids Inc. (Alabaster, AL). Ecolite^{TM}(+) biodegradable scintillant was from ICN Biomedicals (Irvine, CA). Fertigplatten Kieselgel 60 HPTLC plates were from E. Merck (Darmstadt, Germany). Merck Silica Gel 60 H was from VWR Canlab (Missisauga, Ontario, Canada). Inorganic salts and HPLC-grade solvents were obtained from BDH Inc. (Toronto, Ontario, Canada). Standard

---

FAME were from Nu-Check-Prep Inc. (Elysian, MN) and Sigma-Aldrich Canada Ltd.

Growth of plants. Flax (*Linum usitatissimum* L. cvs. AC Emerson and Vimy) was grown under greenhouse conditions at ambient room temperature. Seeds were planted in 10-cm diameter pots containing Metro Mix soil (Greenleaf Products Inc., Calgary, Alberta, Canada) and 3 mL Nutricote 14–14–14 fertilizer (Type 140; Greenleaf Products Inc.). Plantlets were transferred to 20-cm pots, and additional soil and fertilizer were added. The soil was watered daily and the plants were exposed to a 16 h light/8 h dark photoperiod. Individual flowers were tagged at anthesis, and the developing capsules were harvested on ice at varying days after flowering (DAF). Capsules containing the seeds were flash-frozen in liquid N_2 and stored at –80°C until needed.

Lipid extraction, TAG isolation, and FAME analysis. Approximately 0.25 g of seed was placed in a preweighed test tube at 80°C for 24 h and the net dry weight was determined. Lipids were extracted using a hexane/isopropanol method (20) to determine total lipids (TL) gravimetrically. The TL were then dissolved in hexane to give a concentration of 4 mg mL^{-1}. A 50-μL aliquot was placed in a vial and dried under N_2. A second aliquot was spotted onto a Fertigplatten Kieselgel 60 plate and developed in one ascension of hexane/diethyl ether/acetic acid (80:20:1, by vol) with TAG as a standard. The silica gel containing TAG was scraped into a second vial. Methylation was adapted from methods described by Browse *et al.* (21). To both the TL and TAG samples, 5 μL of trinonadecanoin was added as an internal standard, followed by 3 mL of methanolic HCl prepared by the method described by Christie (22). Methylation was allowed to progress overnight at 50°C. Following the addition of 0.25 mL of water, FAME were extracted twice with 5-mL portions of hexane. FAME representing TL and TAG were analyzed using a Model 5890 Hewlett-Packard gas chromatograph equipped with a J & W Scientific 30-m DB^R-23 narrowbore column (Chromatographic Specialties, Brockville, Ontario, Canada) according to the method of Pomeroy *et al.* (23). Helium was used as a carrier gas at a flow rate of 12 mL min^{-1}. After 5 min, the temperature was ramped from 180 to 230°C at a rate of 2°C min^{-1}. The retention times of peaks were compared with FAME standards. The percentages of each were determined from the ratio of peak area to the total area.

Microsome preparation. Maturing flaxseed was ground with liquid N_2 in a chilled mortar and pestle using 25 mL of grinding buffer (0.2 M Hepes-NaOH, pH 7.4, containing 0.5 M sucrose) per gram of seed. The homogenate was then centrifuged at $10,000 \times g$ for 1 h at 4°C. The supernatant was filtered through a layer of cheesecloth and spun at $100,000 \times g$ for 1 h at 4°C in an ultracentrifuge. The pellet was then resuspended in 10 mM Hepes-NaOH, pH 7.4, and spun at $100,000 \times g$ for 1 h at 4°C. The pellet was resuspended in a volume equivalent to one-tenth of the original tissue mass using 10 mM Hepes-NaOH, pH 7.4. Microsomes were divided into small aliquots, flash-frozen in liquid N_2, and stored at –80°C.

Enzyme assays and protein determination. DGAT activity was assayed based on some modifications of previous proto-

cols (24,25). The standard reaction mixture (60 μL) consisted of 0.2 M Hepes-NaOH buffer (pH 7.4) containing 0.15 mg BSA mL^{-1}, 20 mM MgSO$_4$, 330 μM *sn*-1,2-diolein in 0.2% (wt/vol) Tween 20, 15 μM [1-^{14}C] oleoyl-CoA (56 mCi mmol^{-1}), and microsomal protein (80–120 μg). The reaction was initiated by the addition of microsomes (10 μL), allowed to proceed for 60 min at 30°C in a shaking water bath, and terminated with 10 μL of 5% (wt/vol) SDS. A 50 μL aliquot of each reaction mixture was spotted directly onto a Silica Gel 60 H preparative TLC plate and allowed to air dry. The TLC plate was then developed in hexane/ether (80:20, vol/vol) with a TAG standard. Following TLC, the TAG standard was visualized with a stream of iodine. Sections of silica containing TAG were scraped into scintillation vials, combined with 5 mL Ecolite(+), and assayed for radioactivity in a liquid scintillation counter.

LPAAT activity was assayed using a method adapted from Cao *et al.* (26) and Oo and Huang (27). The standard reaction mixture (80 μL) consisted of 50 mM Tris-HCl buffer (pH 7.4) containing 40 μM lysophosphatidic acid (LPA), 1 mM MgCl$_2$, 4.5 μM [1-^{14}C]oleoyl-CoA, and 30–80 μg microsomal protein. The reaction was initiated by the addition of microsome (10 μL) and allowed to proceed for 4 min before termination with 2 mL of chloroform/methanol (1:1, vol/vol). A phase separation was induced with 1 mL of 1 M KCl in 0.2 M H$_3$PO$_4$ and the lipids were extracted. The resulting lipid sample was dissolved in 50 μL of chloroform, spotted onto a Silica Gel 60 H preparative TLC plate and developed using one ascension of chloroform/methanol/acetic acid/water (85:15:10:4, by vol) with PA as a standard. The radioactivity was determined in sections of silica gel containing radiolabeled PA using a liquid scintillation counter.

For specificity studies on DGAT and LPAAT, the radiospecific activities of the acyl-CoA were all between 50 and 60 mCi mmol^{-1}. Protein content was determined using the Bio-Rad protein microassay (Bio-Rad Laboratories, Hercules, CA) based on the Bradford procedure (28) using BSA as a standard.

Incubation of flax embryos with radiolabeled FA and analysis of labeled lipid classes. The incorporation of FA into flax lipids was monitored as described by Stymne *et al.* (13). Pods were harvested between 11 and 14 DAF, and the embryos were removed from the seeds immediately. The embryos were pooled and incubated (10 embryos per incubation) for 2 h at 30°C under incandescent light (40 μEm^{-2} s^{-1}) in 300 μL of 0.1 M potassium phosphate buffer (pH 7.4) containing 9 nmol of [1-^{14}C]free EPA or DHA (56 mCi mmol^{-1}). Following incubation, the embryos were rinsed three times with buffer. Lipid extraction was performed as already described, except the volume of reagent used was scaled down to one quarter. The final lipid residue was dissolved in 40 μL of hexane. Ten-microliter aliquots of the TL extracts were spotted, along with nonlabeled standards, onto Kieselgel 60 aluminum plates, and the TLC plates were developed with one ascension of chloroform/methanol/acetic acid/water (60:30:3:1, by vol) followed by one ascension of hexane/ether (80:20, vol/vol) to resolve polar and nonpolar species. The incorporation of radiolabeled FFA into various lipid classes was monitored by phosphorimaging (Cyclone Storage Phosphor

System, Canberra-Packard Canada Ltd., Mississauga, Ontario, Canada). The lipid classes were also assessed by charring. TLC plates containing fractionated lipids were dipped in a solution of 5% (wt/vol) $CuSO_4$ and 4% (vol/vol) H_3PO_4, and then heated at 195°C for 2 min.

RESULTS

Lipid content and FA composition of TAG during seed development. TL accumulation and FA composition of TAG during seed development were investigated in two cultivars of flax. The lipid content during seed development for the cultivars AC Emerson and Vimy under our greenhouse conditions is shown in Table 1. The TL content for both cultivars increased steadily from less than 7% of the dry weight at 8 DAF to over 30% of the dry weight at 20 DAF. A similar increase was observed for TAG as the percentage of dry weight after separating this lipid class from TL (results not shown).

FAME were generated from TAG isolated from TL samples obtained at various stages of development and analyzed by GLC. The proportion of various FA in TAG as a function of seed development is shown in Figures 1A and 1B for the cultivars AC Emerson and Vimy, respectively. The proportion of α-linolenic acid (α-18:3, $18:3cis\Delta^{9,12,15}$) increased substantially from slightly less than 25% to over 40% of TAG between 8 and 11 DAF, and then stabilized at 20 DAF. The proportion of linoleic acid (18:2, $18:2cis\Delta^{9,12}$) decreased from about 20% to 10% in the range of 10–20 DAF, concomitant with the relative increase in α-18:3. The proportion of oleic acid (18:1, $18:1cis\Delta^{9}$) also increased, but not as markedly. In AC Emerson, the proportions of stearic acid (18:0) and palmitic acid (16:0) remained relatively constant, at about 10% of TAG, throughout seed development. In Vimy, the proportion of 18:0 appeared somewhat lower than the proportion of 16:0.

DGAT and LPAAT specific activities were high during rapid lipid accumulation. Acyltransferase activities were assayed using radiolabeled acyl-CoA. Synthesis of each [1-^{14}C]acyl-CoA was monitored by TLC according to Taylor *et al.* (19) and visualized using a phosphorimager. We observed greater than 95% conversion of FA to the corresponding acyl-CoA in each case. Microsomes were prepared from developing seeds of the cultivar AC Emerson at various stages of development and were assayed for DGAT and LPAAT activity. The addition of
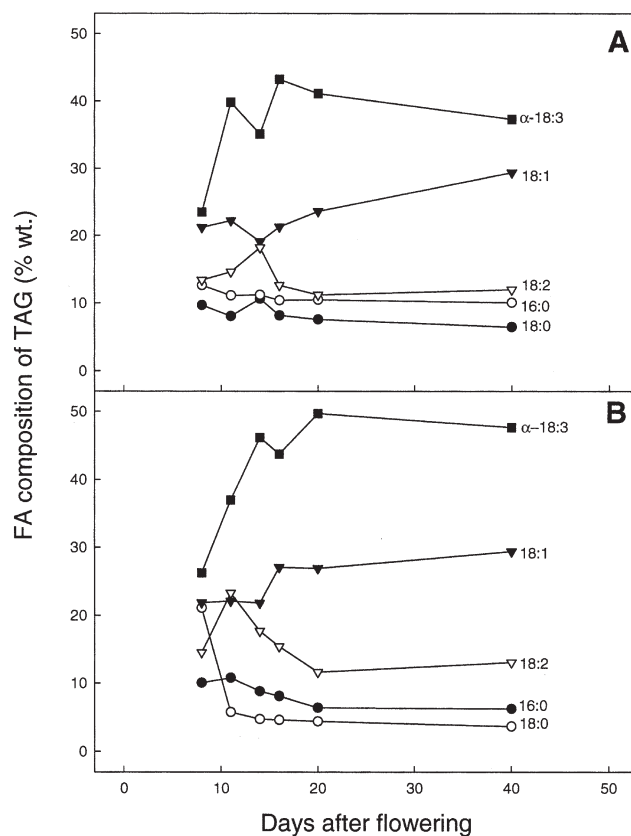
FIG. 1. FA composition of TAG from developing seeds of the cultivars AC Emerson (A) and Vimy (B).

exogenous *sn*-1,2-DAG to DGAT reaction mixtures had little effect on promoting enzyme activity. This has been observed previously in DGAT assays with microsomes prepared from developing seeds of maize (*Zea mays*) and cultures of *B. napus* (3,25). In contrast, microsomal LPAAT activity was dependent on the presence of exogenous LPA. The concentration of 40 μM LPA used in the assay of microsomal LPAAT activity was sufficient to maintain maximal enzyme activity under the experimental conditions described. High DGAT specific activity occurred between 8 and 11 DAF (Fig. 2A). The specific activity of LPAAT increased between 8 and 14 DAF, with the maximal activity displayed at 14 DAF (Fig. 2B). This was followed by a sharp decline in LPAAT specific activity between 14 and 16 DAF, and then by a gradual increase in activity at 20 DAF to the same activity observed at 8 DAF. Lipid content on a per seed basis was assessed over the range of 8–16 DAF (Fig. 2C), when acyltransferase specific activities were at the highest levels. The rate of lipid accumulation was about 60 μg/d/seed over the 8-d period.

Acyl-CoA specificity of microsomal DGAT and LPAAT activities. Microsomal DGAT and LPAAT activities were assayed using acyl-CoA consisting of various radiolabeled unsaturated FA moieties. DGAT used all of the acyl-CoA (Fig. 3), α-linolenoyl-CoA was the most effective acyl donor, and activities with 18:1-, 18:2-, and EPA-CoA were somewhat lower. DGAT activity was lowest with DHA-CoA. Microsomal

TABLE 1
Lipid Content in Developing Seeds of the Flax Cultivars AC Emerson and Vimy

	Lipid content (% dry wt)	
DAF[a]	AC Emerson	Vimy
8	6.6	4.8
11	11.3	17.2
14	21.3	21.3
16	24.6	24.0
20	33.0	34.9
40	33.0	36.8

[a]DAF, days after flowering.
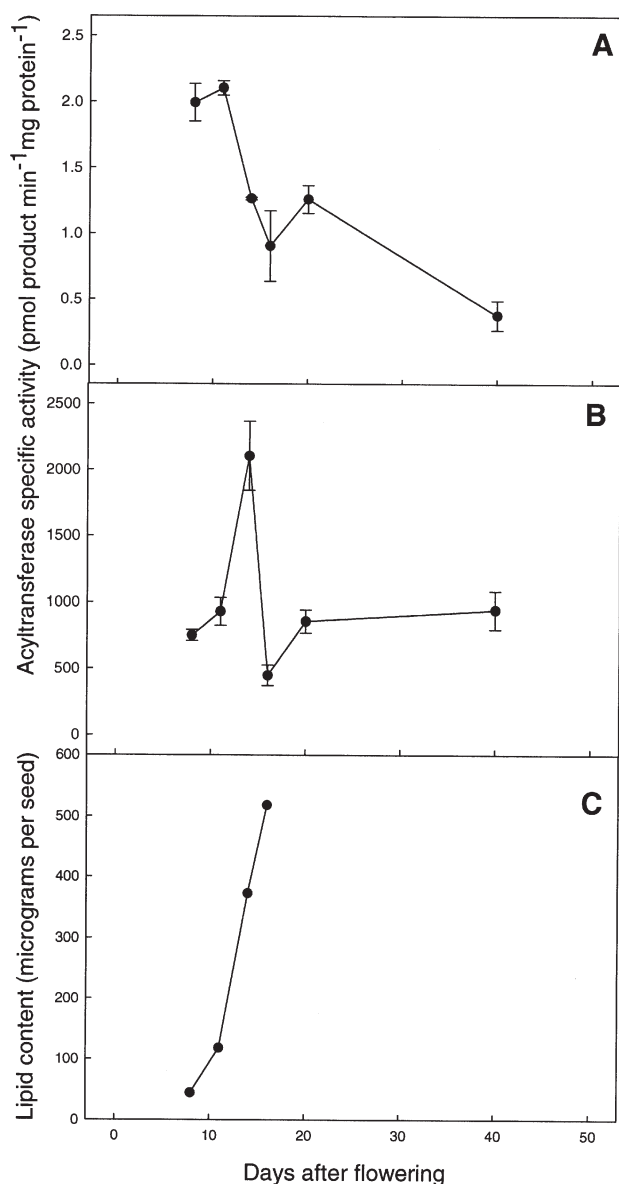
FIG. 2. Microsomal DAG acyltransferase (DGAT) activity (A) and lyosphosphatidic acid acyltransferase (LPAAT) activity (B) in developing flaxseed, and average lipid content of seed from 8–16 d after flowering (DAF) (C) (cultivar AC Emerson). For panels A and B, data points represent the mean ± SEM, *n* = 3.

LPAAT also used all of the radiolabeled unsaturated fatty acyl-CoA (Fig. 4). α-Linoleoyl-, EPA-, and DHA-CoA were all used by LPAAT at about one-third the rate of 18:2-CoA. For incubations with oleoyl-CoA, the rate of incorporation of 18:1 into TAG was about 100 times greater for LPAAT than for DGAT. LPAAT assays were conducted for a much shorter time (4 min) compared with DGAT assays (60 min) because of the apparently lower activity of DGAT in the microsomes.

Flax embryos import EPA and DHA, and incorporate the bioactive FA into glycerolipids. Developing embryos of flax were incubated with either radiolabeled EPA or DHA. A charred TLC plate is shown in Figure 5A, which depicts the
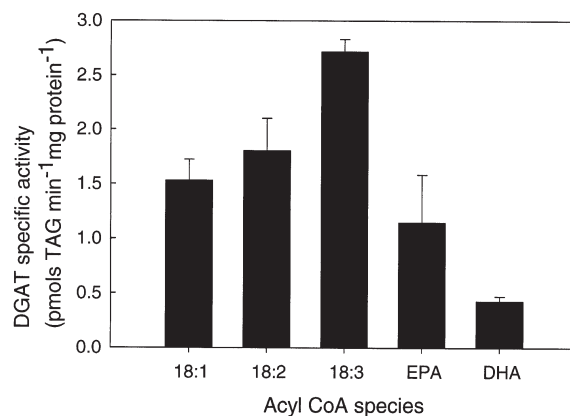
FIG. 3. Acyl-CoA specificity of microsomal DGAT activity from developing flaxseed (cultivar AC Emerson). Data points represent the mean ± SEM, *n* = 4–6. For abbreviation see Figure 2.

separation of various lipid standards, as well as the lipids that were extracted from developing flax embryos incubated with radiolabeled EPA or DHA. A phosphorimage of the radiolabeled lipid classes resolved by TLC is shown in Figure 5B. Substantial radiolabel was incorporated into PC, PA, DAG, and TAG. The level of incorporation of radiolabel in the EPA incubation into PC and PA was, however, considerably lower than for the DHA incubation.

DISCUSSION

Our observations of the lipid composition of TAG during flaxseed development were similar to earlier observations of the FA composition of the total acyl lipids of flax oil (10). Production of α-18:3 and other PUFA in oilseeds is known to occur while the acyl moieties are attached to PC (2). The availability and incorporation of α-18:3 into TAG may be facilitated by a number of processes, including the reverse reaction catalyzed by cytidine diphosphocholine: *sn*-1,2-DAG cholinephosphotransferase (EC 2.7.8.2) (15,29), acyl exchange of α-18:3 at the *sn*-2 position of PC with the acyl-CoA pool
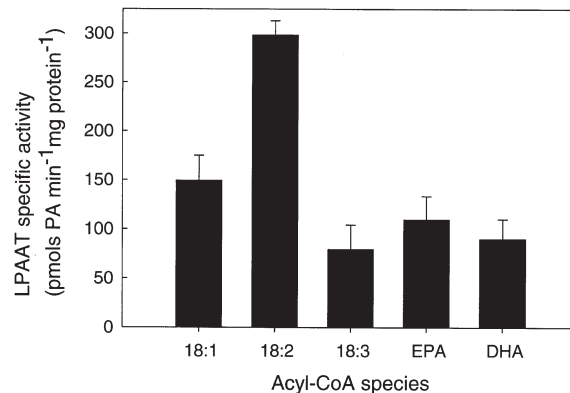
FIG. 4. Acyl-CoA specificity of microsomal LPAAT activity from developing flaxseed (cultivar AC Emerson). Data points represent the mean ± SEM, *n* = 3. For abbreviation see Figure 2.
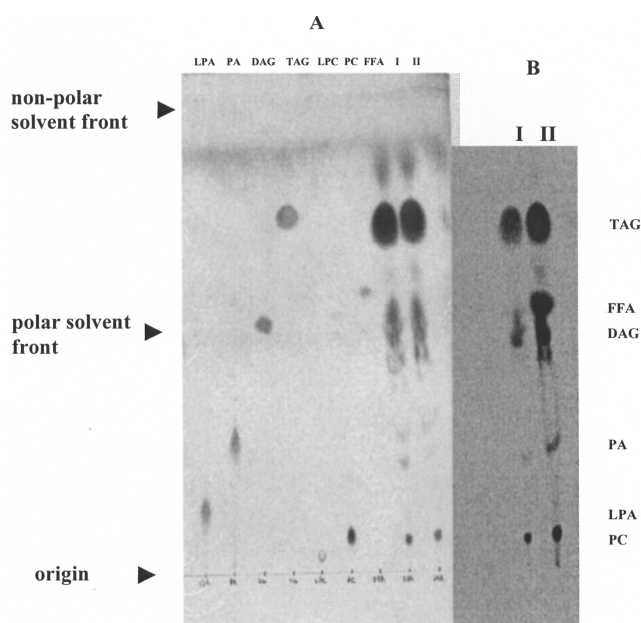
FIG. 5. Incorporation of radiolabeled EPA and DHA into various lipids of developing flax embryos (cultivar AC Emerson). Panel A represents a TLC separation of various lipid standards. Included are the lipids isolated from flax embryos, which were incubated with radiolabeled EPA (I) and DHA (II). Panel B represents a phosphorimage of radiolabeled lipids in the incubations with radiolabeled EPA (I) and DHA (II). Lipids from both EPA- and DHA-treated embryos were extracted in the same manner, and equal quantities of the final total lipid extracts were applied to the TLC plate. LPA, lysophosphatidic acid; LPC, lysophosphatidylcholine.

catalyzed by lysophosphatidylcholine acyltransferase (EC 2.3.1.23) (30), and/or transfer of α-18:3 from the *sn*-2 position of PC to *sn*-1,2,-DAG catalyzed by phospholipid:DAG acyltransferase (EC 2.3.1.158) (31,32). FFA might also be released from phospholipids by phospholipase action (32), which in turn could be converted to acyl-CoA by the catalytic action of acyl-CoA synthetase (EC 6.2.1.3).

The developmental profiles of DGAT and LPAAT specific activities indicated that high activities were associated with rapid lipid accumulation. The rate of lipid accumulation on a per seed basis over the 8–16 DAF determined in our study was similar to that reported by Jain *et al.* (33) for another cultivar of flax. In an earlier study with zygotic embryos of *B. napus*, Tzen *et al.* (8) reported that the three acyltransferases of the Kennedy pathway exhibited maximal activity during the active phase of oil accumulation. In addition, a similar developmental profile for DGAT activity was reported for seeds of both safflower and *B. napus* (9). DGAT activity observed during flaxseed development may represent the combined action of two forms of DGAT. cDNA encoding the DGAT1 isoform have been cloned using *Arabidopsis thaliana*, *B. napus*, and castor (*Ricinus communis*) (3,34–36). Two other DGAT isoforms, sharing 54% homology, were purified and cloned from *Mortierella ramanniana* (37). Homologs of the *M. ramanniana* DGAT genes, designated *MrDGAT2A* and *MrDGAT2B*, were identified in a number of oilseeds. It is also possible that

TAG formation in developing flaxseed may occur *via* acyl-CoA-independent processes such as the phospholipid:DAG acyltransferase-catalzyed reaction (31) and transfer of a fatty acyl moiety between two molecules of DAG to form TAG and MAG catalyzed by a microsomal DAG transacylase (38). The assay used in the present study, however, would have detected only acyl-CoA-dependent TAG formation activity.

The effectiveness with which flax DGAT and LPAAT use acyl-CoA of unsaturated FA suggests that these acyltransferases can easily accommodate the relatively large proportion of α-18:3 produced during seed development. Both microsomal acyltransferases could also accommodate EPA and DHA moieties. The specific activity of microsomal LPAAT, however, was over two orders of magnitude greater than that for microsomal DGAT in assays with [1-^{14}C]oleoyl-CoA. The substantially lower specific activity of DGAT compared with the *sn*-2 acyltransferase suggests that other enzymes involved directly in TAG formation, such as phospholipid:DAG acyltransferase, might also contribute to TAG accumulation in developing flaxseed. This aspect, however, remains to be investigated.

The ability of developing flax embryos to import EPA and DHA and incorporate these nutritional FA into TAG and various Kennedy pathway intermediates under *in vivo* conditions suggests that endogenous acyl-CoA synthetase used EPA and DHA as substrates and that acyltransferases used the resulting thioesters. The appearance of radiolabel in TAG and PA confirms our observations of the ability of DGAT and LPAAT to use both EPA- and DHA-CoA. The appearance of radiolabel in phospholipids may have occurred *via* processes discussed previously (i.e., conversion of DAG to PC or acyl-exchange at the *sn*-2 position of PC).

The fact that flax DGAT and LPAAT can use EPA-CoA suggests that it might be worthwhile engineering flax to produce EPA-CoA using a strategy that relies on only acyl-CoA substrates. Recently, Abbadi *et al.* (14) demonstrated that the C18Δ^9 acyl-CoA pool of developing flaxseed is similar to the FA composition of TAG. These results suggest that α-18:3-CoA would be available for further desaturation and elongation to EPA-CoA if desaturases and elongases acting only on acyl-CoA were introduced into developing flaxseed. These types of desaturases and elongases have been shown to be operative in mammalian systems (14,39–41). Interestingly, a recent study of desaturases from liverwort (*Marchantia polymorpha*) revealed a Δ^6 desaturase that appears to act on both glycerolipids and the acyl-CoA pool (42). More recently, a unicellular marine algae (*Ostreococcus tauri*) was shown to contain a Δ^6 acyl-CoA desaturase (43). The success of these proposed genetic engineering experiments, however, would depend on having access to the necessary cDNA. Future investigations might reveal additional acyl-CoA desaturases that are not restricted to the animal kingdom. Synthesis of DHA-CoA would be more complicated using the mammalian pathway, which relies exclusively on acyl-CoA substrates. In the Sprecher pathway in mammals, EPA-CoA undergoes two consecutive elongations to generate 24:5, followed by Δ^6 desaturation and one round of β-oxidation to generate 24:6, DHA-CoA

(17,40,41). Recent studies of EPA production in genetically engineered tobacco (*Nicotiana tabacum*), flax, and *Arabidopsis* implemented systems in which elongases used acyl-CoA (14,16). The desaturases used PC as a substrate. Given the ability of flax acyltransferases to use EPA- and DHA-CoA, it may also be worthwhile to consider a complementary strategy of introducing polyketide synthases from marine bacteria into this oilseed crop. These enzymes do not require α-18:3 for the synthesis of EPA- and DHA-CoA, but instead operate with a mechanism similar to bacterial FA synthase (41,44).

n-3 FA have beneficial effects in the prevention and management of cardiovascular disease, arthritis, and type 2 diabetes (45). The development of oilseed crops containing EPA and DHA in the seed oil would provide for a vegetarian source of these bioactive PUFA that is also low in saturated fat (46). The use of EPA- or DHA-CoA by flax LPAAT has important implications for the *in planta* production of molecular species of TAG with a high nutraceutical value. FA esterified at the *sn*-2 position of TAG are more readily absorbed than FA at the two other positions in TAG (47). TAG with selected FA at the *sn*-2 position have been evaluated as potential therapeutic agents in models of cancer, burn treatment, and immune dysfunction (47). Thus, genetic engineering experiments designed to incorporate EPA-/DHA-generating systems in flax should result in the accumulation of TAG with EPA or DHA moieties esterified to the *sn*-2 position, thereby enhancing the nutritional value of the oil even more.

The current study provided new information on storage lipid biosynthesis in developing flaxseed. The activities of the final two acyltransferases of the G3P pathway were coordinated with TAG accumulation during seed development and were capable of using a number of unsaturated fatty acyl-CoA, including EPA- and DHA-CoA. This was further supported by the fact that flax embryos were capable of incorporating radiolabeled EPA and DHA into TAG and other glycerolipid classes. Our study demonstrated the potential of introducing EPA- or DHA-CoA-generating systems into developing flaxseed. Engineering a system that could use α-18:3-CoA to produce EPA-CoA would be particularly attractive given the high proportions of this FA in flax. In the long term, engineering flax to produce EPA and DHA will diversify the oilseed industry by making oil with enhanced health benefits available. Future studies with developing flaxseed will be aimed at determining the extent to which the acyltransferases of TAG biosynthesis will select for EPA and DHA moieties in the presence of endogenous substrates.

ACKNOWLEDGMENTS

REFERENCES

1. Kennedy, E.P. (1961) Biosynthesis of Complex Lipids, *Fed. Proc. Am. Soc. Exp. Biol. 20*, 934–940.
2. Stymne, S., and Stobart, A.K. (1987) Triacylglycerol Biosynthesis, in *The Biochemistry of Plants* (Stumpf, P.K., ed.), Vol. 9, pp. 175–214, Academic Press, New York.
3. Weselake, R.J. (2005) Storage Lipids, in *Plant Lipids—Biology, Utilization and Manipulation* (Murphy, D.J., ed.), pp. 162–225, Blackwell Publishing, Oxford.
4. Andrews, J., and Keegstra, K. (1983) Acyl-CoA Synthetase Is Located in the Outer Membrane and Acyl-CoA Thioesterase in the Inner Membrane of Pea Chloroplast Envelopes, *Plant Physiol. 72*, 735–740.
5. Ichihara, K., Takahashi, T., and Fujii, S. (1988) Diacylglycerol Acyltransferase in Maturing Safflower Seeds: Its Influences on the Fatty Acid Composition of Triacylglycerol and on the Rate of Triacylglycerol Synthesis, *Biochim. Biophys. Acta 958*, 125–129.
6. Perry, H.J., and Harwood, J.L. (1993) Changes in the Lipid Content of Developing Seeds of *Brassica napus*, *Phytochemistry 32*, 1411–1415.
7. Perry, H.J., Bligny, R., Gout, E., and Harwood, J.L. (1999) Changes in Kennedy Pathway Intermediates Associated with Increased Triacylglycerol Synthesis in Oilseed Rape, *Phytochemistry 52*, 799–804.
8. Tzen, J., Cao, Y., Laurent, P., Ratnayake, C., and Huang, A. (1993) Lipids, Proteins, and Structure of Seed Oil Bodies from Diverse Species, *Plant Physiol. 101*, 267–276.
9. Weselake, R.J., Pomeroy, M.K., Furukawa, T.L., Golden, J.L., Little, D.B., and Laroche, A. (1993) Developmental Profile of Diacylglycerol Acyltransferase in Maturing Seeds of Oilseed Rape and Safflower and Microspore-Derived Cultures of Oilseed Rape, *Plant Physiol. 102*, 565–571.
10. Bhatia, I.S., and Sukhija, P.S. (1970) Changes in Fatty Acids of Linseed Oil (*Linum usitatissimum*) During Ripening, *Indian J. Biochem. 7*, 215–216.
11. Slack, C.R., Roughan, P.G., and Balasingham, N. (1978) Labelling of Glycerolipids in the Cotyledons of Developing Oilseeds by [1-^{14}C] Acetate and [2-^{3}H] Glycerol, *Biochem. J. 170*, 421–433.
12. Slack, C.R., and Roughan, P.G. (1978) Rapid Temperature-Induced Changes in the Fatty Acid Composition of Certain Lipids in Developing Linseed and Soya-bean Cotyledons, *Biochem. J. 170*, 437–439.
13. Stymne, S., Tonnet, M.L., and Green, A.G. (1992) Biosynthesis of Linolenate in Developing Embryos and Cell-free Preparations of High-Linolenate Linseed (*Linum usitatissimum*) and Low-Linolenate Mutants, *Arch. Biochem. Biophys. 294*, 557–563.
14. Abbadi, A., Domergue, F., Bauer, J., Napier, J.A., Welti, R., Zahringer, U., Cirpus, P., and Heinz, E. (2004) Biosynthesis of Very-Long-Chain Polyunsaturated Fatty Acids in Transgenic Oilseeds: Constraints on Their Accumulation, *Plant Cell 16*, 2734–2748.
15. Slack, C.R., Campbell, L.C., Browse, J.A., and Roughan, P.G. (1983) Some Evidence for the Reversibility of the Cholinephosphotransferase Catalysed Reaction in Developing Linseed Cotyledons *in vivo*, *Biochim. Biophys. Acta 754*, 10–20.
16. Qi, B., Beaudoin, F., Fraser, T., Stobart, A.K., Napier, J.A., and Lazarus, C.M. (2002) Identification of a cDNA Encoding a Novel C18-Δ^9 Polyunsaturated Fatty Acid-Specific Elongating Activity from the Docosahexaenoic Acid (DHA)-Producing Microalga, *Isochrysis galbana*, *FEBS Lett. 510*, 159–165.
17. Green, A.G. (2004) From α− to ω-Producing Essential Fatty Acids in Plants, *Nat. Biotechnol. 22*, 680–682.
18. Sayanova, O.V., and Napier, J.A. (2004) Eicosapentaenoic Acid: Biosynthetic Routes and the Potential for Synthesis in

Transgenic Plants, *Phytochemistry 65*, 147–158.

19. Taylor, D.C., Weber, N., Hogge, L.R., and Underhill, E.W. (1990) A Simple Enzymatic Method for the Preparation of Radiolabeled Erucoyl-CoA and Other Long-Chain Fatty Acyl-CoAs and Their Characterization by Mass Spectrometry, *Anal. Biochem. 184*, 311–316.

20. Hara, A., and Radin, N.S. (1978) Lipid Extraction of Tissues with a Low-Toxicity Solvent, *Anal. Biochem. 90*, 420–426.

21. Browse, J., McCourt, P.J., and Somerville, C.R. (1986) Fatty Acid Composition of Leaf Lipids Determined After Combined Digestion and Fatty Acid Methyl Ester Formation from Fresh Tissue, *Anal. Biochem. 152*, 141–145.

22. Christie, W.W. (1992) Preparation of Fatty Acid Methyl Esters, *INFORM 3*, 1031–1034.

23. Pomeroy, M.K., Kramer, J.K.G., Hunt, D.J., and Keller, W.A. (1991) Fatty Acid Changes During Development of Zygotic and Microspore-Derived Embryos of *Brassica napus*, *Physiol. Plant. 81*, 447–454.

24. Little, D., Weselake, R., Pomeroy, K., Furukawa-Stoffer, T., and Bagu, J. (1994) Solubilization and Characterization of Diacylglycerol Acyltransferase from Microspore-Derived Cultures of Oilseed Rape, *Biochem. J. 304*, 951–958.

25. Byers, S.D., Laroche, A., Smith, K.C., and Weselake, R.J. (1999) Factors Enhancing Diacylglycerol Acyltransferase Activity in Microsomes from Cell-Suspension Cultures of Oilseed Rape, *Lipids 34*, 1143–1149.

26. Cao, Y.Z., Oo, K.C., and Huang, A.H.C. (1990) Lysophosphatidate Acyltransferase in the Microsomes from Maturing Seeds of Meadowfoam, *Plant Physiol. 94*, 1199–1206.

27. Oo, K.C., and Huang, A.H.C. (1989) Lysophosphatidate Acyltransferase Activities in the Microsomes from Palm Endosperm, Maize Scutellum, and Rapeseed Cotyledon of Maturing Seeds, *Plant Physiol. 91*, 1288–1295.

28. Bradford, M.M. (1976) A Rapid and Sensitive Method for the Quantitation of Microgram Quantities of Protein Utilizing the Principle of Protein-Dye Binding, *Anal. Biochem. 72*, 248–254.

29. Stobart, A.K., and Stymne, S. (1985) The Interconversion of Diacylglycerol and Phosphatidylcholine During Triacylglycerol Production in Microsomal Preparations of Developing Cotyledons of Safflower (*Carthamus tinctorius* L.), *Biochem. J. 232*, 217–221.

30. Stymne, S., and Stobart, A.K. (1984) Evidence for the Reversibility of the Acyl-CoA:lysophosphatidylcholine Acyltransferase in Microsomal Preparations from Developing Safflower (*Carthamus tinctorius* L.) Cotyledons and Rat Liver, *Biochem. J. 223*, 305–314.

31. Dahlqvist, A., Ståhl, U., Lenman, M., Banaś, A., Lee, M., Sandager, L., Ronne, H., and Stymne, S. (2000) Phospholipid:Diacylglycerol Acyltransferase: An Enzyme that Catalyzes the Acyl-CoA-independent Formation of Triacylglycerol in Yeast and Plants, *Proc. Natl. Acad. Sci. USA 97*, 6487–6492.

32. Banaś, A., Dahlqvist, A., Ståhl, U., Lenman, M., and Stymne, S. (2000) The Involvement of Phospholipid:Diacylglycerol Acyltransferases in Triacylglycerol Production, *Biochem. Soc. Trans. 28*, 703–705.

33. Jain, R.K., Thompson, R.G., Taylor, D.C., MacKenzie, S.L., McHughen, A., Rowland, C.G., Tenaschuk, D., and Coffey, M. (1999) Isolation and Charaterization of Two Promoters from Linseed for Genetic Engineering, *Crop Sci. 39*, 1696–1701.

34. Hobbs, D.H., Lu, C., and Hills, M.J. (1999) Cloning of a cDNA Encoding Diacylglycerol Acyltransferase from *Arabidopsis thaliana* and Its Functional Expression, *FEBS Lett. 452*, 145–149.

35. Nykiforuk, C.L., Furukawa-Stoffer, T.L., Huff, P.W., Sarna, M., Laroche, A., Moloney, M.M., and Weselake, R.J. (2002) Characterization of cDNAs Encoding Diacylglycerol Acyltransferase from Cultures of *Brassica napus* and Sucrose-Mediated Induction of Enzyme Biosynthesis, *Biochim. Biophys. Acta 1580*, 95–109.

36. He, X., Turner, C., Chen, G.Q., Lin, J.T., and McKeon, T.A. (2004) Cloning and Characterization of a cDNA Encoding Diacylglycerol Acyltransferase from Castor Bean, *Lipids 39*, 311–318.

37. Lardizabal, K.D., Mai, J.T., Wagner, N.W., Wyrick, A., Voelker, T., and Hawkins, D.J. (2001) DGAT2 Is a New Diacylglycerol Acyltransferase Gene Family: Purification, Cloning, and Expression in Insect Cells of Two Polypeptides from *Mortierella ramanniana* with Diacylglycerol Acyltransferase Activity, *J. Biol. Chem. 276*, 38862–38869.

38. Stobart, K., Mancha, M., Lenman, M., Dahlqvist, A., and Stymne, S. (1997) Triacylglycerols Are Synthesised and Utilized by Transacylation Reactions in Microsomal Preparations of Developing Safflower (*Carthamus tinctorius* L.) Seeds, *Planta 203*, 58–66.

39. Okayasu, T., Nagao, M., Ishibashi, T., and Imai, Y. (1981) Purification and Partial Characterization of Linoleoyl-CoA Desaturase from Rat Liver Microsomes, *Arch. Biochem. Biophys. 206*, 21–28.

40. Sprecher, H. (2000) Metabolism of Highly Unsaturated n-3 and n-6 Fatty Acids, *Biochim. Biophys. Acta 1486*, 219–231.

41. Qiu, X. (2003) Biosynthesis of Docosahexaenoic Acid (DHA, 22:6-4,7,10,13,16,19): Two Distinct Pathways, *Prostaglandins Leukot. Essent. Fatty Acids 68*, 181–186.

42. Kajikawa, M., Yamato, K.T., Kohzu, Y., Nojiri, M., Sakuradani, E., Shimizu, S., Sakai, Y., Fukuzawa, H., and Ohyama, K. (2004) Isolation and Characterization of Δ^6-Desaturase, an ELO-like Enzyme and Δ^5-Desaturase from the Liverwort *Marchantia polymorpha* and Production of Arachidonic and Eicosapentaenoic Acids in the Methylotrophic Yeast *Pichia pastoris*, *Plant Mol. Biol. 54*, 335–352.

43. Domergue, F., Abbadi, A., Zähringer, U., Moreau, H., and Heinz, E. (2005) *In vivo* Characterisation of the First Acyl-CoA Δ-6-Desaturase from the Plant Kingdom, *Biochem. J. 389*, 483–490.

44. Metz, J.G., Roessler, P., Facciotti, D., Levering, C., Dittrich, F., Lassner, M., Valentine, R., Lardizabal, K., Domergue, F., Yamada, A., *et al.* (2001) Production of Polyunsaturated Fatty Acids by Polyketide Synthases in Both Prokaryotes and Eukaryotes, *Science 293*, 290–293.

45. Simopoulos, A.P. (1999) Essential Fatty Acids in Health and Chronic Disease, *Am. J. Clin. Nutr. 70*, 560S–569S.

46. Galili, G., Galili, S., Lewinsohn, E., and Tadmor, Y. (2002) Genetic, Molecular, and Genomic Approaches to Improve the Value of Plant Foods and Feeds, *Crit. Rev. Plant Sci. 21*, 167–204.

47. Stein, J. (1999) Chemically Defined Structured Lipids: Current Status and Future Directions in Gastrointestinal Diseases, *Int. J. Colorectal Dis. 14*, 79–85.

Cyanolipid-rich Seed Oils from *Allophylus natalensis* and *A. dregeanus*

P. Avato[a],*, I. Rosito[a], P. Papadia[b], and F.P. Fanizzi[b,c]

[a]Dipartimento Farmaco-Chimico, Università, I-70125 Bari, Italy, [b]Dipartimento di Scienze e Tecnologie Biologiche ed Ambientali, Università, I-73100 Lecce, Italy, and [c]Consortium C.A.R.S.O, I-70010 Valenzano, Bari, Italy

ABSTRACT: As a continuation of our study on plants of the Sapindaceae, the chemical composition of the oil extracted from seeds of *Allophylus natalensis* (Sonder) De Winter and of *A. dregeanus* (Sonder) De Winter has been investigated. The oil from both species contained approximately equal amounts of TAG and type I cyanolipids (CL), 1-cyano-2-hydroxymethylprop-2-en-1-ol-diesters, with minor amounts of type III CL, 1-cyano-2-hydroxymethylprop-1-en-3-ol-diesters. Structural investigation of the oil components was accomplished by chemical, chromatographic (TLC, CC, GC, and GC–MS), and spectroscopic (IR, NMR) means. GC and GC–MS analysis showed that C_{20} FA were dominant in the CL components of the oil from the two species (44–80% vs. 21–26% in TAG), with *cis*-11-eicosenoic acid (36–46%) and *cis* 13-eicosenoic acid (paullinic acid, 23–37%) as the major esterified fatty acyl chains in *A. natalensis* and *A. dregeanus*, respectively. *cis*-Vaccenic acid was particularly abundant (11–31%) in the CL from *A. dregeanus,* whereas eicosanoic acid (10–22%) was also a major component of CL in both species.

Paper no. L9800 in *Lipids 40,* 1051–1056 (October 2005).

Seed oils from some species of Sapindaceae have been shown to accumulate TAG and a rare class of plant lipids, the cyanolipids (CL), derived from amino acid metabolism (1–3). Four types of CL structures have been so far reported as occurring in this plant family, namely, type I, 1-cyano-2-hydroxymethyl-prop-2-en-1-ol-diester; type II, 1-cyano-2-methylprop-1-en-3-ol-ester; type III, 1-cyano-2-hydroxymethylprop-1-en-3-ol-diester; and type IV, 1-cyano-2-methylprop-2-en-1-ol-ester (4–6). CL of types I and IV are cyanogenetic.

The presence of cyanogenetic phytochemicals in nature, despite their protective physiological role for the plant, may constitute a health hazard for humans and animals. As a consequence, identification of the presence of those metabolites in food or forage plants so as to allow their removal is important.

The occurrence of CL in the plant kingdom was first reported only in a few families such as the Sapindaceae, the Hippocastanaceae, and the Boraginaceae (1,7). Reinvestigation of the last two families of plants allowed the conclusion that CL are only limited to the Sapindaceae (8). In particular, re-examination of seeds previously identified as from *Cordia verbe-*nacea (Boraginaceae) showed that they were morphologically similar to those of a sapindaceous plant, generically reported as probably belonging to the genus *Allophylus* (9). A further publication confirmed the presence of CL in two *Allophylus* species, *A. concina* and *A. occidentalis* (8). To the best of our knowledge, however, no detailed chemical study was accomplished on either the seed oils of those plants or on seed oils from other *Allophylus* species.

As a continuation of our study on the Sapindaceae (6) and in consideration of the limited and controversial data for the *Allophylus* genus, we have investigated the composition of the seed oil of *A. natalensis* (Sonder) De Winter, commonly called "dune false currant," and of *A. dregeanus* (Sonder) De Winter, the "false currant." Chemical data on the structural elucidation of the TAG and CL constituents of the oils from those plants are reported here and discussed.

EXPERIMENTAL PROCEDURES

Plant material. Seeds of *A. natalensis* (Sonder) De Winter and *A. dregeanus* (Sonder) De Winter were purchased from B & T World Seeds Paguignan sarl, France.

Oil extraction and purification. Dried, ground seeds of *A. natalensis* (6.93 g) and *A. dregeanus* (2.68 g) were extracted in a Soxhlet apparatus with refluxing petroleum ether (b.p. 40–60°C) for 6 h. Evaporation of the solvent gave a yellow oily product amounting to 1.68 g (24%) for *A. natalensis* and 0.97 g (36%) for *A. dregeanus.*

Composition of the oil was first investigated by TLC (precoated silica gel 60 F254 aluminum plates: Merck, Milan, Italy) by elution with hexane/EtOAc (9:1, vol/vol) and alternatively with benzene. Visualization of the oil components was obtained with phosphomolybdic acid reagent (10% EtOH; Sigma, Milan, Italy) followed by heating the plates at 110°C.

Individual components of the seed extracts from both plant species were separated first by column chromatography (CC) (silica gel 60 H; Merck) eluted in benzene; fractions containing mixtures of TAG and CL were submitted to a second purification by gradient elution CC in hexane/EtOAc.

Derivatization of the oil components. TAG and CL from the *Allophylus* species under investigation were subjected to a direct saponification/transmethylation according to Reference 10. About 2 mg of each sample was dissolved in 1 mL of MeOH/hexane (4:1, vol/vol) and reacted with acetyl chloride

---

*To whom correspondence should be addressed at Dipartimento Farmaco-Chimico, Università, Via Orabona 4, I-70125 Bari, Italy.
E-mail: avato@farmchim.uniba.it

Abbreviations: CC, column chromatography; CL, cyanolipids; DMOX, 4,4-dimethyloxazoline; HETCOR, ^{1}H-^{13}C heterocorrelated.

(100 µL). The reaction mixture was then heated at 100°C for 1 h. After cooling, hexane (1 mL) and K_2CO_3 (6%, 1 mL) were added to stop the reaction. The organic phase obtained was dried overnight on anhydrous Na_2SO_4.

In addition to common FAME, methyl esters of paullinic (*cis*-13-eicosenoic), *cis*- and *trans*-vaccenic, and *cis*-11-eicosenoic acids (Sigma) were used as reference compounds for GC and GC–MS analyses.

FA *tert*-butyl ester derivatives of TAG and CL were synthesized as previously described (4).

Preparation of 4,4-dimethyloxazoline (DMOX) derivatives was carried out starting from the FAME derivatives synthesized as above and then by following the procedure described in Reference 10.

GC analysis. A Carlo Erba HRGC 5160 gas chromatograph with an FID (300°C) and an on-column injector was used. Hydrogen was the carrier gas.

Analysis of FAME and FA *tert*-butyl esters of TAG and CL, as well as their DMOX derivatives, was carried out as previously described (6). GC data were processed by a Spectra Physics SP 4290 computing integrator, and results from FAME quantification are reported later in this paper.

GC–MS analysis. FAME, FA *tert*-butyl esters, and DMOX derivatives were analyzed by GC–MS with a Hewlett-Packard 6890–5973 mass spectrometer according to Reference 6.

FTIR. FTIR spectra of neat TAG and CL were recorded using NaCl cells.

NMR. Proton (^{1}H) and carbon (^{13}C) NMR spectra were recorded at 25°C on DPX400 and DRX500 Avance Bruker instruments equipped with probes for inverse detection and with *z* gradient-accelerated spectroscopy. Standard Bruker automation programs were used for 2-D NMR experiments. 2-D homonuclear COSY experiments were performed using the COSYGP (gradient-accelerated COSY) sequence. Inverse detected, standard, and long-range ^{1}H-^{13}C heterocorrelated (HETCOR) 2-D NMR spectra were obtained by using the gradient-enhanced pulse sequences INVIEAGSSI and INV4GPLRND, respectively. $CDCl_3$ was used as the solvent in all the experiments. Residual ^{1}H and ^{13}C peaks of the solvent were used as internal standards to calculate chemical shifts referred to tetramethylsilane.

RESULTS AND DISCUSSION

General. Lipid extracts obtained from the seeds of *A. natalensis* and *A. dregeanus* were first investigated by TLC. Inspection of the extract from *A. natalensis* by TLC elution in benzene revealed the presence of four different products migrating at R_f 0.70 (CL), 0.57 (TAG), 0.51 and 0.46 (TAG, CL). Similarly, TLC elution in hexane/EtOAc (9:1, vol/vol) showed the presence of four components migrating at R_f 0.60 (TAG), 0.55 and 0.51 (TAG, CL), and 0.31 (CL). The combined TLC data readily suggested the presence of two different types of CL in the oil from this plant. Previous investigations (5) showed that, in fact, the four types of natural CL can be differentially separated on TLC in the various solvent systems according to their chemical structure.

The composition of *A. dregeanus* seed oil was also inspected by TLC in the two elution systems just described and the results were similar to those obtained for *A. natalensis*; that is, the total extract was formed by TAG and two CL fractions.

Purification of the extracts from both species was accomplished by CC. A first elution in benzene of the seed oil from *A. natalensis* afforded a fraction of CL, type I (1-cyano-2-hydroxymethylprop-2-en-1-ol-diester), a fraction of pure TAG, and a mixture of TAG and CL, which was further purified by CC with hexane/EtOAc as eluent. Three fractions of TAG and one of CL, type III (1-cyano-2-hydroxymethylprop-1-en-3-ol-diester), were obtained. In total, the main isolated constituents amounted to 49% TAG, 50% CL I, and 1% CL III.
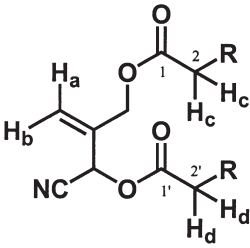
The same purification procedure was applied to the seed lipids from *A. dregeanus* and the CC separation afforded 42% TAG, 56% CL I, and 2% CL III.

Purified components from each of the two plant extracts were further characterized by chromatographic, spectroscopic, and chemical means. Similar structural results were obtained for both *A. natalensis* and *A. dregeanus* and, unless specified, the spectroscopic data reported herein equally refer to TAG and CL I and III from each of the two oils.

CL identification. IR analysis of the two CL components verified that their structures were different, as suggested by their chromatographic behavior. As expected, both CL I and CL III showed the common absorption maxima generally found in acyl lipid spectra (6), with an additional broad and double band at 1750 cm^{-1} (C=O stretching) suggesting the presence of different C=O in the molecule. Furthermore, CL III showed a typical absorption band at 2227 cm^{-1} (CN stretching), which, due to its different skeleton, was quenched in the CL type I by the effect of the oxygen atom on the same carbon as the cyano group (6).

Complete structural identification of the two CL types from *Allophylus* species was determined by ^{1}H and ^{13}C NMR analysis. Signals relative to CL I were consistent with those we previously reported in a detailed study for CL of type I, isolated from the seed oil of another sapindaceous plant, *Paullinia cupana* (6). As shown in Table 1, the CL nature of the isolated fractions from *A. natalensis* and *A. dregeanus* was revealed by the specific resonances in the ^{13}C spectra: at δ 60.87, carbon bearing the cyano function; at δ 114.88, nitrile carbon; and at δ 5.94 (^{1}H spectra), tertiary proton adjacent to the cyano group. Identification of type I CL (1-cyano-2-hydroxymethylprop-2-en-1-ol-diester) was corroborated by (i) the presence of two distinct groups of partially overlapping signals (multiple signals due to the presence of a mixture of esters of different FA) for the two C=O carbon atoms: C-1, δ 173.00 and C-1′, δ 171.47 (carbon bearing the nitrile function); and (ii) resonances at δ 135.28 (vinyl carbon), δ 120.95 (terminal vinyl carbon), and δ 62.70 (allylic carbon), which taken together, are indicative of the expected dihydroxybutenyl cyanide moiety of this structural CL type (Table 1). NMR spectra were also useful to acquire information on the fatty acyl chains esterified to the dihydroxybutenyl nitrile moiety in good agreement with data obtained by GC and GC–MS analyses (compare Tables 1 and 3).

TABLE 1
^{1}H and ^{13}C NMR Data of Cyanolipids Type I from Seed Oil of *Allophylus* Species

^{1}H	δ (J)	^{13}C	δ (J)
C**H**$_2$OCO	4.64 m^a	=**C**	135.28
C**H**-CN	5.94 s	**C**H$_2$=	120.95
CH$_2$=	5.54 H$_a$, s; 5.68 H$_b$, s	CN	114.88
C**H**$_2$C=O(O)	2.32 H$_c$, t (7.5); 2.38 H$_d$, dt (2.2;7.7)	C-1; C-1′	173.00; 171.47^b
CH$_3$, ω1	0.86 t (6.6)	C-2; C-2′	34.02; 33.77
n-CH$_2$	1.24 m	C-3; C-3′	24.54; 24.76
CH$_2$-C**H**$_2$CH$_2$-C=O	1.62, m	**C**H$_2$OCO	62.70
-C**H**$_2$-C=C-C**H**$_2$- (*cis*)	1.99 m	**C**H-CN	60.87
Olefinic (*cis*)	5.32	m CH$_3$, ω1	14.11
		CH$_2$, ω2	22.66 (18:2)
			22.68/22.69 (ω7/Sat, ω9)
		CH$_2$, ω3	31.79 (18:2)
			31.91/31.93 (ω7/Sat, ω9)
		n-CH$_2$	28.95–29.77
		-**C**H$_2$-C=C-**C**H$_2$-	27.18
		C=CH^c	129.64 (C-9 OL)
			129.80 (C-11 EI)
			129.81 (C-11 VA)
			129.85 (C-13 PA)
			129.88 (C-14 PA)
			129.91 (C-12 VA)
			129.92 (C-12 EI)
			130.03 (C-10 OL)

^{a}AB signal pattern.
^{b}Group of overlapping signals due to different acyl chains.
^{c}Identified unsaturated chains: OL, oleic; EI, *cis*-11 eicosenoic; PA, *cis*-13 eicosenoic (paullinic acid); VA, vaccenic acid.
Cyanolipid I, 1-cyano-2-hydroxymethylprop-2-en-1-ol-diesters.

Proton and carbon resonances relative to the CL III constituents of the seed oil of *A. natalensis* and *A. dregeanus* are shown in Table 2. 2-D proton-proton and proton-carbon correlations also facilitated the assignments of the relative signals. Signals at δ 114.68, nitrile carbon, and the singlet at δ 5.56, corresponding to the tertiary proton adjacent to the nitrile group, indicated that the isolated compounds were cyano derivatives. This was further supported by the signal at δ 98.60, assignable to a vinylic carbon bearing the cyano function. The downfield shift of this signal compared with the equivalent signal in the spectrum of the CL I (Table 1) and the presence of the two proton resonances at δ 4.69 and 4.87 were consistent with the different skeleton of this CL type. In particular, the latter two signals could be assigned, respectively, to the *cis,* H-4′ (δ 4.69) and *trans,* H-4 (δ 4.87) methylene protons adjacent to the oxygen atoms of the dihydroxybutenyl cyanide moiety (4). The assignment was made on the basis of chemical shifts (the nitrile group deshields the protons *cis* to it) and the magnitude of the coupling constants (the H-4 signal, at the instrument fields used, shows no measurable coupling constant in the ^{1}H NMR

spectrum, whereas H-4′ has a $^4J_{H4'-H2}$ = 1.3 Hz) (11). Further evidence came from the 2-D ^{1}H COSY spectrum where a stronger cross peak was observed between the signal of H-4′ and the vinyl proton, compared with the weaker correlation peak between H-4 and again the vinyl proton (Fig. 1).

The identification of this fraction of CL as 1-cyano-2-hydroxymethylprop-1-en-3-ol-diesters was confirmed by the presence of two extra carbon signals at δ 62.66 and 61.66, which were assigned to the two carbons C-4′ and C-4 of the dihydroxybutenyl nitrile moiety, respectively (Table 2). In the ^{1}H-^{13}C 2-D heteronuclear correlation spectrum these signals showed the expected correlations with the proton resonances at δ 4.69 (H-4′) and δ 4.87 (H-4), respectively. Moreover, ^{1}H-^{13}C long-range couplings allowed us to discriminate between the two acyl chain positions. In fact, the H-4-C5 and H-4′-C5' cross peaks are well resolved in the ^{1}H-^{13}C 2-D HETCOR long range spectrum, allowing us to identify unambiguously the acyl chains *cis* and *trans* to the nitrile functionality, respectively (Fig. 2).

The olefin region in the carbon NMR spectra was useful to

TABLE 2
¹H and ¹³C NMR Data of Cyanolipids Type III from Seed Oil of *Allophylus* Species

¹H	δ (*J*)	¹³C	δ (*J*)
C̲H₂OCO	4.69 H-4′, *d* (1.3); 4.87 H-4, *s*	C̲H-CN	98.60
C̲H–CN	5.56 *s*	C̲=, C₃	154.92
C̲H₂C=O(O)	2.349 H-6′, *t* (7.5); 2.352 H-6, *t* (7.5)	C̲N	114.68
C̲H₂–CH₂C=O(O)	1.60 *m*	C-4; C-4′	61.61; 62.66
CH₃, ω1	0.86 *t* (7.0)	C-5; C-5′	172.94; 172.57[a]
n-CH₂	1.24 *m*	C-6; C-6′	33.80; 33.97
–C̲H₂–C=C–C̲H₂– (*cis*)	1.99 *m*	C-7; C-7′	24.82; 24.77
Olefinic (*cis*)	5.33 *m*	CH₃, ω1	14.13
		CH₂, ω2	22.68 (18:2)
			22.70 (ω7, Sat, ω9)
		CH₂, ω3	31.90 (18:2)
			31.93/31.95 (ω7/Sat, ω9)
		n-CH₂	29.00–29.79
		–C̲H₂–C=C–C̲H₂–	27.23
		C=CH[b]	129.67 (C-9 OL)
			129.81 (C-11 EI)
			129.84 (C-11 VA)
			129.89 (C-13 PA)
			129.91 (C-14 PA)
			129.95 (C-12 VA)
			129.97 (C-12 EI)
			130.07 (C-10 OL)

[a]Group of overlapping signals due to different acyl chains.
[b]For abbreviatons of identified unsaturated chains see Table 1. Sat, saturated; cyanolipid III (1-cyano-2-hydroxymethyl-prop-1-en-3-ol-diesters) from *A. dregeanus* also showed signals related to linolenic (C-15, 127.31 δ; C-10, 127.97 δ; C-12, 128.49 δ; C-13, 128.42 δ; C-9, 130.42 δ; C-16, 132.16 δ) and linoleic acids (C-12, 128.09 δ; C-9, not resolved; C-10, 128.28 δ; C-13, 130.42 δ).

TABLE 3
FA Composition (wt%) of TAG and Cyanolipids[a] (CL) from *Allophylus* Species, as Measured by GC-FID Analysis of FAME

	Allophylus natalensis			*Allophylus dregeanus*		
FA	TAG	CL I	CL III	TAG	CL I	CL III
Palmitic	7.8	1.6	3.7	3.3	0.6	1.9
Palmitoleic	1.9	0.2	0.6	7.9	0.4	3.6
Stearic	1.6	0.7	1.0	1.7	0.7	1.0
Oleic	43.4	14.8	20.3	22.7	4.5	10.2
cis-Vaccenic	5.0	2.7	7.9	20.6	10.9	30.7
Linoleic	7.2	0.5	1.8	7.4	0.3	1.6
Linolenic	12.3	0.2	1.9	10.0	0.2	6.9
Eicosanoic	4.2	22.2	16.1	4.7	20.9	10.3
cis-11- Eicosenoic	14.1	46.0	36.5	6.7	22.4	10.3
cis-13-Eicosenoic	2.3	6.8	5.1	14.9	36.7	23.5
Behenic	Trace	1.4	1.4	Trace	1.1	Trace
Erucic	0.4	2.9	3.7	Trace	1.3	Trace

[a]For chemical description of CL I and CL III see Tables 1 and 2.
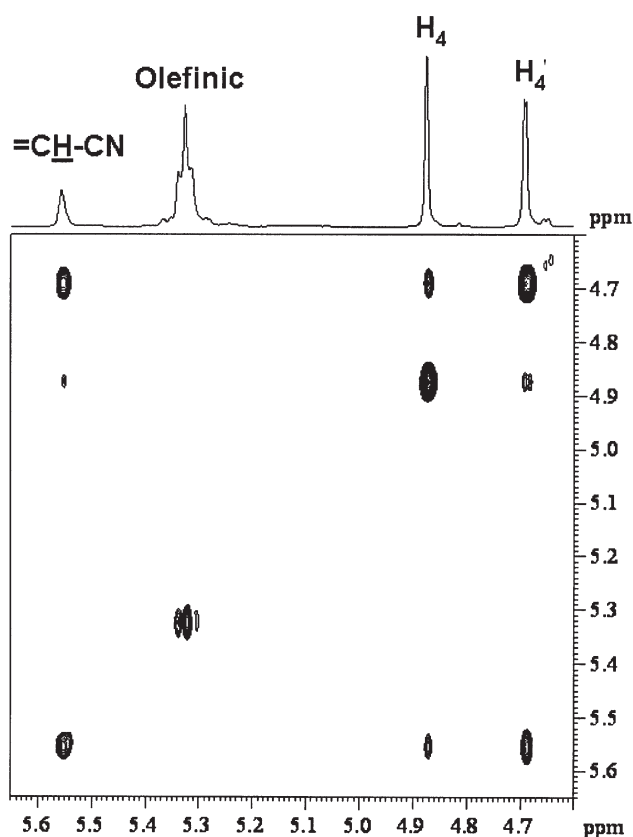
FIG. 1. Expansion of the 2-D ^{1}H COSY spectrum for cyanolipids type III from seed oil of *Allophyllus* species showing the cross peaks of the vinylic proton (=CH–CN) with H-4' (stronger), and H-4 (weaker).

FIG. 2. (A) Expansion of the [1]H-[13]C 2-D heterocorrelated spectrum of the cyanolipids type III from seed oil of *Allophyllus* species showing the H-4/C-4 and H4'/C4' cross peaks; and (B) expansion of the long-range [1]H-[13]C 2-D heterocorrelated spectrum showing cross peaks of the same protons with the carbonylic signals C5 and C5', respectively.

identify the esterified fatty acyl chains. Relative assignments are reported in Table 2.

TAG identification. TAG isolated from both species of *Allophylus* showed typical IR absorption bands consistent with previously published data for this class of compounds (6,12). NMR spectra clearly indicated that the isolated lipids were TAG. Signals relative to glycerol α- and β-carbons were present in the [1]H (*dd*, δ 4.14 and 4.29, glycerol α CH$_2$; *m*, δ 5.26, glycerol β CH) and [13]C (δ 62.30, glycerol α-carbon atoms; δ 69.11, glycerol β-carbon atom) NMR spectra. The presence of the two signals with chemical shifts at δ 173.02, C1 β chains, and at δ 173.45, C1 α chains, also corroborated that the isolated lipids were TAG (6,13,14). As for the CL, inspections of proton and carbon resonances allowed the determination of the fatty acyl chains esterified to the glycerol moiety (13–16). In agreement with GC and GC–MS data (see below), the following common major unsaturated FA were identified from the NMR spectra of the TAG fractions of *A. natalensis* and *A. dregeanus:* oleic (δ 130.23, C10; δ 129.90/129.92, C9), *cis*-vaccenic, *cis*-11-eicosenoic (δ 130.14, C12; δ 130.04, C11), *cis*-13-eicosenoic (paullinic) (δ 130.11, C14; δ 130.09, C13); linoleic (δ 130.42, C13; δ 128.10, C12; δ 130.91, C9; δ 128.30, C10), and linolenic (δ 132.16, C16; δ 127.33, C15; δ 128.43, C13; δ 128.50, C12; δ 130.42, C9; δ 127.98, C10).

FA composition. GC and GC–MS analyses were also car-

ried out for the quantification and further identification of the fatty acyl chains esterified in the TAG and CL oil fractions. FA were analyzed as their methyl, butyl, and DMOX derivatives. Reference compounds were also submitted to the same derivatization procedures and their chromatographic and spectrometric behaviors compared. Mass spectra of the above derivatives fully matched already published data (6,17–19).

FA quantification of the entire TAG fraction from both *A. natalensis* and *A. dregeanus* is reported in Table 3. In agreement with the NMR data, TAG from *A. natalensis* had a prevalence of unsaturated FA with oleic acid being by far the most abundant (43.4%). Linolenic and *cis*-11-eicosenoic acids represent other important FA. Considering the overall TAG composition, the C$_{20}$ FA—eicosanoic, *cis*-11- and *cis*-13-eicosenoic—constitute typical constituents (Table 3).

TAG from *A. dregeanus* showed a different chemical profile (Table 3). Oleic acid still represented a major FA; however, compared with *A. natalensis, A. dregeanus* produced TAG with much higher yields of *cis*-vaccenic (20.6%) and *cis*-13-eicosenoic (15.0%) acids.

As shown in Table 3, compositional differences have also been found between the esterified fatty acyl chains in the CL and the TAG from the two species of *Allophylus*. Oleic acid is still one of the abundant FA in the CL I and III (14.8 and 20.3%, respectively) from *A. natalensis*; the bulk of the fatty acyl chains is, however, represented by eicosanoic (22.2%, CL I; and 16.1%, CL III) and *cis*-11-eicosenoic (46.0%, CL I; and 36.5%, CL III) acids. Relatively higher amounts of paullinic acid are also found in the CL components from the seed oil of this species (Table 3).

As observed for the TAG fraction, CL isolated from *A. dregeanus* show a composition different from that of *A. natalensis* (Table 3), namely, they are characterized by very high amounts of C$_{20}$ FA, which in total contribute to 80% (CL I) and 44.1% (CL III). Paullinic acid is by far the most abundant, ac-

counting for 36.7 and 23.5% in the CL I and III constituents, respectively. *cis*-Vaccenic acid is the dominant FA in the CL III constituents (Table 3).

To the best of our knowledge this is the first detailed investigation on the seed oil of species belonging to the *Allophylus* genus. A previous paper (8) reported on the occurrence of CL of types II, III, and IV in the species *A. concina* and *A. occidentalis*. No chemical references were given, however.

Data here presented indicate that, as in other Sapindaceae (1), *A. natalensis* and *A. dregeanus* produce an oil that is rich in CL and, based on chemical data, the main structural types consist of CL I and III.

Previous investigations (19–22) on the total FA composition of the seed oils from members of the Sapindaceae family showed that they are very peculiar in that *cis*-vaccenic and paullinic acids are major constituents and of chemotaxonomic importance. Our previous analysis of the seed oil of *P. cupana* (6) also confirmed those findings. Data obtained in this study indicate that in general the two investigated species of *Allophylus* produce high amounts of oleic acid and C_{20} FA (Table 3). Nevertheless, among them, *A. dregeanus* represents a particularly rich source of the two rare FA, *cis*-vaccenic and paullinic acids. As already reported (6,19), C_{20} FA seem to be preferentially incorporated into the CL lipid fractions, whereas oleic acid is mostly found as a component of the TAG.

ACKNOWLEDGMENTS

REFERENCES

1. Møller, B.L., and Seigler, D.S. (1999) Biosynthesis of Cyanogenic Glycosides, Cyanolipids, and Related Compounds, in *Plant Amino Acids. Biochemistry and Biotechnology* (Singh, B.K., ed.), Marcel Dekker, New York, pp. 563–609.
2. Hegnauer, R. (1973) *Chemotaxonomie der Pflanzen*, Birkhäuser Verlag, Basel, pp. 271–287.
3. Hegnauer, R. (1990) *Chemotaxonomie der Pflanzen*, Birkhäuser Verlag, Basel, pp. 486–496.
4. Mikolajczak, K.L., Smith, C.R., Jr., and Tjarks, L.W. (1970) Cyanolipids of *Koelreuteria paniculata* Laxm. Seed Oil, *Lipids 5*, 672–677.
5. Mikolajczak, K.L., Smith, C.R., Jr., and Tjarks, L.W. (1970) Cyanolipids of *Cardiospermum halicacabum* L. and Other Sapindaceous Seed Oils, *Lipids 5*, 812–817.
6. Avato, P., Pesante, M.A., Fanizzi, F.P., and Aimbiré de Moraes Santos, C. (2003) Seed Oil Composition of *Paullinia cupana* var. *sorbilis* (Mart.) Ducke, *Lipids 38*, 773–780.
7. Seigler, D.S., Mikolajczak, K.L., Smith, C.R., Jr., and Wolff, I.A. (1970) Structure and Reactions of a Cyanogenetic Lipid from *Cordia verbenacea* DC. Seed Oil, *Chem. Phys. Lipids 4*, 147–161.
8. Seigler, D.S., and Kawahara, W. (1976) New Reports of Cyanolipids from Sapindaceous Plants, *Biochem. Syst. Ecol. 4*, 263–265.
9. Seigler, D.S. (1976) Cyanolipids in *Cordia verbenacea*. A Correction, *Biochem. Syst. Ecol. 4*, 235–236.
10. Laurent, F., and Richli, U. (1991) Location of Double Bonds in Polyunsaturated Fatty Acids by Gas Chromatography–Mass Spectrometry After 4,4-Dimethyloxazoline Derivatization, *J. Chromatogr. 541*, 89–98.
11. Rittner, R., Braibante, M.E.F., de Kowalewski, D.G., Pla, J.C., and Mazzola, E.P. (1997) ^{1}H NMR Chemical Shifts and Coupling Constants of Some 3-Monosubstituted 2-Methylpropenes, *Magn. Reson. Chem. 35*, 147–152.
12. Avato, P., Fanizzi, F.P., and Rosito, I. (2001) The Genus *Thapsia* as a Source of Petroselinic Acid, *Lipids 36*, 845–850.
13. Gunstone, F.D. (1990) ^{13}C-NMR Spectra of Some Synthetic Glycerol Esters Alone and as Mixtures, *Chem. Phys. Lipids 56*, 195–199.
14. Gunstone, F.D. (1991) ^{13}C-NMR Studies of Mono-, Di- and Tri-Acylglycerols Leading to Qualitative and Semiquantitative Information About Mixtures of These Glycerol Esters, *Chem. Phys. Lipids 58*, 219–224.
15. Gunstone, F.D., Pollard, M.R., Scrimgeour, C.M., and Vedanayagam, H.S. (1977) Fatty Acids. Part 50. ^{13}C Nuclear Magnetic Resonance Studies of Olefinic Fatty Acids and Esters, *Chem. Phys. Lipids 18*, 115–129.
16. Gunstone, F.D. ^{13}C NMR Chemical Shifts for Fatty Acids and Their Derivatives. http://www.lipid.co-uk/infores/nmr.html (accessed May, 2005)
17. Zhang, J.Y., Yu, Q.T., Liu, B.N., and Huang, Z.H. (1988) Chemical Modification in Mass Spectrometry IV—2-Alkenyl-4,4-dimethyloxazolines as Derivatives for the Double Bond Location of Long-Chain Olefinic Acids, *Biomed. Environ. Mass Spectrom. 15*, 33–44.
18. Christie, W.W., Mass Spectrometry of Fatty Acid Derivatives and Lipids. http://www.lipidlibrary.co.uk/masspec.html (accessed May, 2005)
19. Spitzer, V. (1995) GLC–MS Analysis of the Fatty Acids of the Seed Oil, Triglycerides and Cyanolipid of *Paullinia elegans* (Sapindaceae)—A Rich Source of *cis*-13-Eicosenoic Acid (paullinic acid), *J. High. Resolut. Chromatogr 18*, 413–416.
20. Hopkins, C.Y., and Swingle, R. (1967) Eicosenoic Acid and Other Fatty Acids of Sapindaceae Seed Oils, *Lipids 2*, 258–260.
21. Spitzer, V. (1996) Fatty Acid Composition of Some Seed Oils of the Sapindaceae, *Phytochemistry 42*, 1357–1360.
22. Lago, R.C.A., Simone, M.P.S.C., and Pinto, A. (2000) On the Occurrence of Cyanolipids in *Paullinia carpopodea* Cambess and *P. cupana* Kunth Seed Oils, *Acta Amazonica 30*, 101–105.

Lipid Class Distribution of Fatty Acids Including Conjugated Linoleic Acids in Healthy and Cancerous Parts of Human Kidneys

Kristina Hoffmann[a], **Jörg Blaudszun**[b], **Claus Brunken**[c], **Wilhelm-Wolfgang Höpker**[b], **Roland Tauber**[c], and **Hans Steinhart**[a,*]

[a]Institute of Biochemistry and Food Chemistry, University of Hamburg, 20146 Hamburg, Germany, and Departments of [b]Pathology and [c]Urology, General Hospital Barmbek, 22291 Hamburg, Germany

ABSTRACT: In this study the FA compositions of healthy and cancerous human renal tissues from the same patients are compared with special reference to the CLA and PUFA content. CLA was preferentially incorporated into neutral lipid compared with phospholipid classes. Its distribution profile was similar to that of monounsaturated FA, but unlike that found with 18:2n-6. Different incorporation patterns were found for individual CLA isomers. Comparing renal cell carcinoma (RCC) and healthy kidney, the total CLA content was significantly lower in the cholesterylester fraction and significantly higher in the PE and PS fractions from RCC. The most significant differences between healthy and cancerous renal tissue were in the content of t10,c12-CLA. Furthermore, the lipid class distributions of n-6 PUFA were determined, and several significant differences between RCC and healthy renal tissue were found. This is of interest, as it has been proposed that the anticarcinogenic properties of dietary CLA are associated with their interference in the metabolism of 20:4n-6. The involvement of CLA in preventing renal cancer cannot be definitively demonstrated from the design of this study, nor was it intended, but the complete determination of the FA composition of adjacent healthy and cancerous tissues may provide an insight if lipids are involved in this disease.

Paper no. L9754 in *Lipids 40*, 1057–1062 (October 2005).

Cancer of the kidney accounts for approximately 3% of all adult cancers in Western countries. Renal cell carcinomas (RCC) comprise nearly 85% of kidney cancers. This cancer occurs mainly between the ages of 50 and 70 years, and men are affected twice as often as women (1). The etiology of RCC is unknown, although epidemiological studies have suggested a relationship between the habit of smoking and RCC. Urban living, exposure to Thorotrast (a suspension of particulate radioactive ThO_2), and a family history of renal cancer are also reported risk factors (1). Furthermore, many dietary factors have been considered in relation to RCC (2). The observed relationship between the diet and cancer has raised interest in protective and physiologically active food ingredients.

The term CLA refers to a family of positional and geometric isomers of 18:2n-6 with conjugated double bonds. The main dietary sources of CLA are ruminant products, in quantities of about 0.40–1.70% of total fat (3). Several animal studies and studies *in vitro* have shown that CLA possesses anticarcinogenic properties (4,5). Studies on humans, however, are very rare and little information is available on the mechanisms of action of CLA. A number of reports provide evidence that CLA may interfere with the phospholipid (PL)-associated FA metabolism and the subsequent production of prostaglandins (6,7).

At the most fundamental level, there is a lack of understanding of the uptake of CLA into neutral lipid (NL) and PL classes. In the literature, several studies that deal with the incorporation of CLA into different types of animal tissue are described (8–12). Unfortunately, the results of animal studies cannot easily be assigned to humans because of species and tissue differences. Therefore, the primary aim of the present study was to fill this gap in our knowledge by determining the contents of CLA and n-6 PUFA in the lipid classes of healthy as well as of cancerous human renal tissues from the same patients. It was neither our intention to present a mechanistic study nor to follow a clear biological hypothesis and to provide any responses. But it is the first study at all giving basic data on lipid class distributions and CLA contents in healthy and cancerous parts of human kidneys. Based on these data and the hints that they give, mechanistic studies should be done to understand the detected differences.

MATERIALS AND METHODS

Tissue procurement. A total of 19 patients with a clinical diagnosis of renal cancer underwent radical surgery of their tumor-bearing kidneys at the Department of Urology, General Hospital Barmbek, Hamburg. A piece of cancerous as well as a piece of healthy renal tissue was removed from the nephrectomy specimen for study immediately following resection. No extrarenal or adipose tissue was included into the specimens. Tissue removal and histological diagnosis of the tumors were carried out by a pathologist at the Department of Pathology, General Hospital

---

Barmbek, Hamburg. Samples were snap-frozen and stored at −80°C until analysis. All patients gave written consent to a protocol approved by the ethics commission of the Hamburg Medical Association.

Separation of lipid classes. Total lipids were isolated from whole tissue homogenates by extracting them twice with dichloromethane/methanol (2:1, vol/vol) and once with hexane. Subsequently, separation of major PL classes was carried out according to the method described by Pietsch and Lorenz (13) with an additional step for the separation of cholesterylesters (CE). The 3-mL solid phase extraction cartridges, packed with 500 mg aminopropylsilane bound to silica gel (J.T.Baker, Philipsburg, NJ), were preconditioned with 7 mL hexane. Then the samples, containing about 40 mg of total lipid in 1.5 mL hexane, were applied and left to sink into the solid phase. Subsequently, each lipid class was eluted as follows: 3 mL of hexane for CE; 4 mL of chloroform/isopropanol (2:1, vol/vol) for TAG and cholesterol (Chol.); 8 mL of diethyl ether/acetic acid (98:2, vol/vol) for FFA; 8 mL acetonitrile/isopropanol (1:2, vol/vol) for PC and sphingomyelin (SM); 4 mL of methanol for PE; 8 mL of isopropanol/3 mol/L hydrochloric acid in butanol (7:1, vol/vol) for PS; and 2 mL of methanol/3 mol/L hydrochloric acid in butanol (9:1, vol/vol) for PI.

PC and SM were not further separated because SM is not transesterified by the base-catalyzed transesterification method used in this study. Base catalysis was chosen to ensure that no modifications of CLA isomers took place, which has been reported to occur with acid catalysis (14).

A TLC method described by Helmerich and Köhler (15) was chosen to check the quality of the lipid class separation (data not shown) and to quantify the lipid class composition of the renal tissue samples. Lipid classes were separated on 10 × 10 cm silica gel TLC plates (Merck, Darmstadt, Germany). Plates were developed with ethyl acetate/chloroform/isopropanol/methanol/45 mmol/L sodium chloride solution in water (25:25:25:10:9, by vol) for PL classes and with petroleum ether (b.p. 50–70°C)/diethyl ether/acetic acid (80:20:2, by vol) for NL classes, respectively. Bands that co-migrated with CE (cholesteryloleate), Chol., TAG (triolein), FFA (18:2n-6), PC, SM, PE, PS, and PI authentic standards (Sigma-Aldrich, Taufkirchen, Germany) were visualized by dipping the TLC plates into 0.6 mol/L cupric sulfate in 1.5 mol/L phosphoric acid and heating to 180°C for 10 min. For quantification, TLC plates showing brown spots with different color densities were converted to bitmap files (tiff-format, 8 bit grayscale, 300 dpi) by means of a flatbed scanner. Each lane of the images of the TLC plates was processed with a freely available picture evaluation program (ImageJ: http//rsb.info.nih.gov/ij/) to obtain chromatograms. The resulting peaks were integrated, and calibration was performed by using standard solutions of the lipid classes above (0.025–0.5 mg/mL).

Analysis of FA. With the exception of the FFA fraction, all lipid fractions were converted to FAME according to the method of Pfalzgraf *et al.* (16). Briefly, each lipid class was derivatized with 5% potassium methoxide in methanol (Merck-Schuchardt, Hohenbrunn, Germany) at 60°C for 15 min. The

FFA were methylated using a 2 M trimethylsilyldiazomethane solution in methanol as described previously by Hashimoto *et al.* (17). The reaction was carried out at room temperature for 30 min.

The total FAME pattern was analyzed by GC (Hewlett-Packard GC system 6890 with FID; Waldbronn, Germany) using a CP-Sil 88 capillary column (100 m × 0.25 mm i.d. with 0.2 µm film thickness; Chrompack, Middelburg, The Netherlands) (18). Inlet temperature was 200°C and detector temperature was 260°C. The oven temperature was initially 70°C and then ramped 8°C/min to 180°C, held for 10 min, ramped again 3°C/min to 235°C and held another 10 min. A volume of 2 µL was injected at a split ratio of 10:1. Hydrogen was used as carrier gas at 1.5 mL/min.

CLA isomer distribution was determined by silver ion HPLC (18,19). Separation was carried out using a Waters 515 HPLC system (Waters, Milford, MA) equipped with a Model 996 photodiode array detector. Two silver-loaded ChromSpher 5 Lipids columns (Chrompack), 5 µm particle size, 250 × 4.6 mm, were used series-wound with a mobile phase of hexane/acetonitrile (100:0.5, vol/vol) at a flow rate of 1 mL/min. Owing to their conjugated double bonds, CLA isomers can be detected at 234 nm, whereas unconjugated unsaturated FA absorb at 200 nm.

Commercial FAME standards (Sigma Chemical Co., Deisenhofen, Germany), including a mixture of CLA isomers, were used to identify and quantify sample FAME.

Statistical analysis. Data were analyzed with SPSS Statistical Software, version 11.5.2.1 (SPSS Inc., Chicago, IL). All data are expressed as mean ± SD. Statistical comparisons between healthy renal tissue and RCC were made using Student's two-tailed *t*-test for paired values ($P < 0.05$). One-way ANOVA with Scheffé, Student–Newman–Keuls, and Tukey-B as *post-hoc* tests were used to determine significant differences in FA distribution between the lipid classes studied ($P < 0.05$).

RESULTS

The 19 male and female patients studied were born between 1924 and 1957 and had a mean body mass index of 25.61 ± 2.53. They all had RCC. One patient additionally suffered familial hyperlipidemia. Table 1 shows clinical characteristics of the tumors. All clinical and anthropomorphical data were collected at the Departments of Urology and Pathology, General Hospital Barmbek, Hamburg.

First of all, the percentage lipid class distributions of the healthy as well as of the cancerous tissues were determined by TLC. The nine lipid classes—CE, Chol., TAG, FFA, SM, PC, PE, PS, and PI—were identified, and marked differences in their contents between healthy and cancerous tissue were found (Table 2). The contents of the NL classes CE, Chol., and TAG were increased in the tumor tissue owing to an increased absolute amount of these lipid classes, whereas FFA and the PL classes SM, PC, PE, PS, and PI were decreased relatively. However, due to high SD determined for most lipid classes, the changes were significant for TAG and FFA only.

TABLE 1
Clinical Characteristics of the Renal Cell Carcinomas Studied[a]

WHO (UICC) classification		No. of patients ($n = 19$)
Primary tumor		
pT1	Tumor ≤ 2.5 cm in greatest dimension, limited to the kidney	3
pT2	Tumor > 2.5 cm in greatest dimension, limited to the kidney	2
pT3a	Tumor invades adrenal gland or perinephric tissues but not beyond Gerota's fascia	7
pT3b	Tumor grossly extends into renal vein(s) or vena cava below diaphragm	5
pT4	Tumor invades beyond Gerota's fascia	2

[a]WHO, World Health Organization; UICC, Unio Internationale Contra Cancrum.

Figure 1 shows the total CLA contents of the single lipid classes from kidney and RCC. CE (1.68 ± 1.13% and 0.78 ± 0.43%, respectively) and FFA (0.98 ± 0.21% and 1.12 ± 0.37%, respectively) were found to have the highest CLA contents in both types of tissue. In general, markedly higher CLA contents were observed in the NL classes than in the PL classes. This distribution pattern shows a high similarity to the distribution pattern of the monounsaturated FA (MUFA) in sum but is completely different from the distribution patterns of the saturated FA and PUFA in sum (data not shown). In comparing RCC with healthy renal tissue, CLA content was found to be significantly decreased in the CE fraction but significantly increased in the PE and PS fractions from RCC.

To examine the distribution of CLA in renal tissue more thoroughly, the contents of single CLA isomers as percentages of the total CLA were determined. Thirteen isomers were detectable in both types of tissue: $t13,t15$-, $t12,t14$-, $t11,t13$-, $t10,t12$-, $t9,t11$-, $t8,t10$-, $t7,t9$-, $c12,t14$-, $t11,c13$-, $c11,t13$-, $t10,c12$-, $c9,t11$-, and $t7,c9$-CLA. However, the contents of the isomers $t13,t15$-, $t12,t14$-, $t11,t13$-, $t7,t9$-, $c12,t14$-, and $t11,c13$-CLA were close to the detection limit and the SD were great. For this reason, only the contents of the isomers $t10,t12$-, $t9,t11$-, $t8,t10$-, $c11,t13$-, $t10,c12$-, $c9,t11$-, and $t7,c9$-CLA are shown in Figures 2A and 2B. In addition, the PI fraction was ignored, as its CLA content is small and only a few HPLC chromatograms were analyzable.

$c9,t11$-CLA was the major isomer in all lipid classes from kidney as well as from RCC. However, the distribution pattern

TABLE 2
Percentage Lipid Class Distributions of Human Healthy and Cancerous Renal Tissue ($n = 5$)

	Content (%)	
Lipid class	Kidney	RCC[a]
Cholesterylesters	3.3 ± 0.6	19.0 ± 17.5
Cholesterol	7.2 ± 2.0	7.8 ± 2.5
TAG	7.1 ± 5.6	15.3 ± 6.1[b]
FFA	1.8 ± 0.2	1.2 ± 0.4[b]
Sphingomyelin	11.9 ± 1.6	6.8 ± 3.2
PC	32.4 ± 2.2	23.7 ± 5.5
PE	21.2 ± 1.9	16.0 ± 6.8
PS	7.8 ± 1.4	5.3 ± 2.0
PI	7.3 ± 1.8	5.6 ± 2.0

[a]Renal cell carcinoma.
[b]Significantly different from kidney ($P < 0.5$).

was different for every individual CLA isomer studied. $t10,c12$-CLA was the isomer for which the most differences between healthy and cancerous tissue were found, its content being significantly lower in the CE fraction and significantly higher in the TAG, PC, PE, and PS fractions from RCC than from healthy renal tissue. No significant variation was found for $t8,t10$-CLA.

Apart from CLA, the contents of the n-6 PUFA 18:2n-6, 20:4n-6, and 20:3n-6 were determined (Figs. 3A, 3B). The contents of 18:3n-6 were close to the detection limit and the SD were great, thus no statistical interpretation was accomplished for this n-6 PUFA, and data are therefore not shown.

For 18:2n-6, 20:4n-6, and 20:3n-6, varying distribution patterns were observed. 18:2n-6 is best incorporated into the PS fractions (37.45 ± 4.36%, human renal tissue, and 25.35 ± 7.45%, RCC tissue) and worst into the PI fractions (4.62 ± 0.70 and 4.57 ± 1.21%, respectively). In comparing the distribution patterns of 18:2n-6 and CLA, incorporation into the physiologically active membrane PL classes was found to be greater for 18:2n-6 than for CLA. 20:4n-6 and 20:3n-6 are preferentially incorporated into the PL classes of both types of tissues, the contents being highest in PE for 20:4n-6 (42.99 ± 2.72 and 46.63 ± 3.67%, respectively) and in PI for 20:3n-6 (4.62 ± 0.70 and 4.57 ± 1.21%, respectively).

Furthermore, differences between healthy and cancerous renal tissue were detected. Contents of 18:2n-6 were signifi-

FIG. 1. Contents of CLA in the tissue lipid classes from human kidney and renal cell carcinoma in percentage of total FA. Values are means ± SD ($n = 19$). Columns marked with different letters within one kind of tissue are significantly different ($P < 0.05$). Columns marked with an asterisk (*) indicate that corresponding healthy and cancerous tissues were significantly different at $P < 0.05$. CE, cholesterylester.
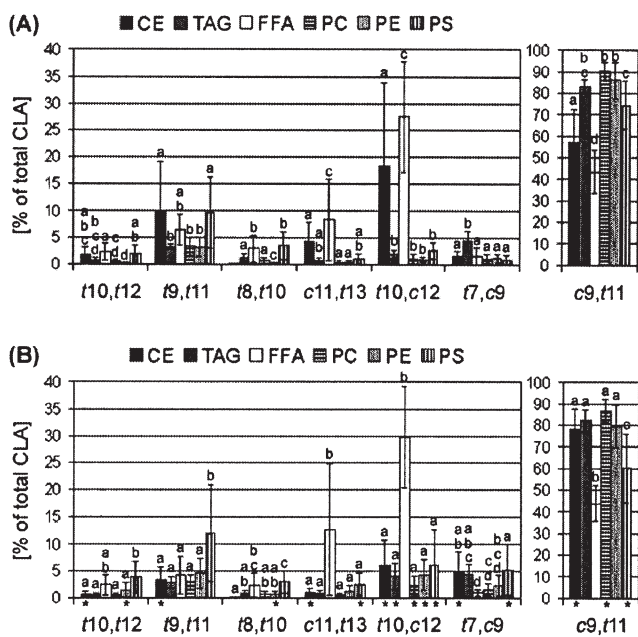
FIG. 2. Contents of single CLA isomers in the tissue lipid classes from human kidney (A) and renal cell carcinoma (B) in percentage of total CLA. Values are means ± SD (*n* = 19). Columns marked with different letters within one kind of tissue are significantly different (*P* < 0.05). Columns marked with an asterisk (*) indicate that corresponding healthy and cancerous tissues were significantly different at *P* < 0.05. For abbreviation see Figure 1.

FIG. 3. Contents of 18:2n-6, 20:4n-6, and 20:3n-6 in the tissue lipid classes from human kidney (A) and renal cell carcinoma (B) in percentage of total FA. Values are means ± SD (*n* = 19). Columns marked with different letters within one kind of tissue are significantly different (*P* < 0.05). Columns marked with an asterisk (*) indicate that corresponding healthy and cancerous tissues were significantly different at *P* < 0.05. For abbreviation see Figure 1.

cantly decreased in the FFA, PC, PE, and PS fractions from RCC. No such unique trend was found for 20:4n-6: Contents were significantly increased in the fractions TAG, PC, and PE, but significantly decreased in the fractions FFA and PS from RCC. For 20:3n-6 marked increases in content were observed in the CE, TAG, PE, and PS fractions from RCC. However, in the TAG fraction the increase was not significant.

DISCUSSION

The determination of the lipid distribution in healthy and cancerous human tissues is very difficult and for obvious reasons does not lend itself to repeated sampling. In addition, a high SD was observed in the results of the 19 patients examined in this study. Several factors contributed to the large variation, including the relatively small sample size (19 patients), differences in the tumor classification of these renal patients, differences in the nutritional (dietary) status of the patients, and differences in the renal zone sampled. Several authors have shown that there are differences in the distribution of individual lipid classes in the two renal zones, i.e., the cortex and medulla (20,21), but the FA composition of kidney lipids is mainly determined by the lipid fractions, and to a much lesser extent by the zones (21). These nutritional and compositional differences were minimized by comparing the adjacent healthy and cancerous tissue from each patient independently using a *t*-test for paired values. This approach enabled us to evaluate and com-

pare healthy and cancerous tissue specimens with the same nutritional status.

Our data show that PC and PE are the main lipid classes in healthy human kidney and that the PL classes comprise about 80% of total lipid. In the literature, contradictory results are described. Druilhet *et al.* (20) found that cortical renal lipids were composed of 58% PL and 42% NL, but the extract of normal kidney medulla contained less PL (37.7%) and more NL (62.3%). In comparison with our data, they reported markedly higher percentages of CE, Chol., and FFA, but smaller contents of TAG, SM, PC, and PE in cortical as well as medullary renal lipids. However, the results of Geers *et al.* (22), who analyzed the PL composition of kidney cortex, are in good agreement with our data on renal PL distribution.

In comparing healthy and cancerous renal tissue, marked increases in the NL classes CE, Chol., and TAG from RCC were observed. It has previously been determined that the lipid class most consistently stored in clear RCC cells is Chol., primarily in the ester form (23). Gebhard *et al.* (23) found 8-fold more total Chol. and 35-fold more CE in clear RCC than in healthy kidney. Possible explanations for the CE storage in clear RCC may be a primary abnormality in fatty acyl-CoA:cholesterol acyl transferase (ACAT, EC 2.3.1.26) activity or a reduced release of free Chol. (relative to cell content) with a secondary elevation in ACAT activity (23). Furthermore, Gebhard *et al.* (23) found a large, but variable, increase in the TAG content of clear RCC.

By determining the incorporation of CLA into the lipid classes from healthy and cancerous human renal tissue, several

characteristic features became immediately apparent. First, CLA was preferentially incorporated into the NL classes from healthy as well as from cancerous renal tissue. Second, its distribution profile resembled closely the profile of MUFA. Third, in contrast to CLA, 18:2n-6 had a very different distribution pattern, with a more substantial incorporation into PC and PS. Thus, our data demonstrate that CLA does not behave like 18:2n-6. Instead, it identifies more closely with MUFA in terms of the lipid distribution pattern. Similar results are reported for the lipid class incorporation of CLA into rat liver (9). As the tissue concentration of 18:2n-6 is higher than that of CLA, Banni *et al.* (9) speculated that the more plentiful 18:2n-6 may tend to exclude CLA from the incorporation into PL and drive it into storage as a component of NL. Alternatively, there might be discriminating controls for 18:2n-6 and CLA uptake into PL classes based on structural or biochemical determinants. Furthermore, our data show different incorporation patterns for individual CLA isomers into renal NL and PL classes.

In the literature, several studies dealing with the incorporation of CLA into several types of animal tissue are described (8–12). However, studies on humans are rare, as human tissues can only be obtained as waste products from surgeries, and systematic nutritional studies are impossible. As mentioned earlier, the results of animal studies cannot easily be assigned to humans because of species and tissue differences. Most of the studies providing data on CLA lipid class distribution in humans have focused on the analysis of serum or plasma lipids, and the results are contradictory (24–27). Shahin *et al.* (24) found the percentage CLA content was highest in plasma TAG (0.39%), followed by CE (0.26%) and PL (0.22%). The FFA fraction was found to contain very little CLA (0.06%). Mougios *et al.* (25) reported a varying distribution, the percentage CLA content being highest in serum PL (0.24%), followed by TAG (0.17%), FFA (0.17%), and CE (0.13%). There are no data on the CLA lipid class distribution in human kidney or other tissues.

In comparing RCC and healthy renal tissue, CLA content was significantly decreased in the CE fraction and slightly, but significantly, increased in the PE and PS fractions from RCC. The percentage decrease of CLA in CE is most probably the consequence of the enhanced incorporation of CE into RCC. Gebhard *et al.* (23) reported that oleate is the main form of the additional CE. However, the significantly increased CLA contents of PE and PS, even in this inconsistent collective of RCC patients studied, are of great interest, as Belury (28) suggests the anticarcinogenic effect of CLA is associated with a change in membrane PL composition, which may ultimately affect events such as oxidative stress, eicosanoid synthesis, and signal transduction pathways. It is possible that the NL pool of CLA represents a relatively inert storage form, whereas the fast turnover PL pool of CLA is biochemically more important because of its ready accessibility as a signaling molecule.

The most significant variations in content between healthy and cancerous renal tissue were found for *t*10,*c*12-CLA. Studies on the anticarcinogenic effect of individual CLA isomers are rare and contradictory. Only *c*9,*t*11- and *t*10,*c*12-CLA have been examined so far. Kim *et al.* (29) found that *t*10,*c*12-, but not *c*9,*t*11-CLA, inhibits the growth of CACO-2 colon cancer cells. In contrast, Palombo *et al.* (5) reported an antiproliferative effect for both CLA isomers in colorectal and prostatic cancer cells.

Our data on the lipid class distribution of the n-6 PUFA 18:2n-6, 20:4n-6, and 20:3n-6 are in general agreement with the data on rat renal cortical lipids previously reported (21). However, Müller *et al.* (21) did not examine individual PL classes, but PL in sum.

There were several significant differences in the PUFA content between RCC and healthy renal tissue. This was of interest since dietary CLA reportedly interferes with 20:4n-6 metabolism (6). An influence of diet on the contents of n-6 FA in kidney has already been shown for other FA than CLA. Kinsella *et al.* (30) reported that *t*,*t*-18:2n-6 at 50 and 100% of dietary fat decreased kidney size and altered its composition. The concentrations of renal Chol., PL, TAG, and CE were decreased. 18:2n-6, 20:3n-6, and 20:4n-6 were significantly depressed in lipid classes, especially in PL and CE. Swanson *et al.* (31) investigated the rate and extent of modification of FA composition of mice lung and kidney by dietary menhaden oil. The n-3 PUFA, 20:5n-3 and 22:6n-3, were rapidly incorporated into lung and kidney PL classes. A concomitant and rapid decrease in content was observed for the n-6 PUFA, 18:2n-6, 20:4n-6, and 22:5n-6.

ACKNOWLEDGMENTS

REFERENCES

1. Gospodarowicz, M.K. (1994) Kidney Cancer, in *Manual of Clinical Oncology* (Love, R.R., ed.), 6th edn., pp. 419–427, Springer-Verlag, New York.
2. Tavani, A., and La Vecchia, C. (1997) Epidemiology of Renal-Cell Carcinoma, *J. Nephrol. 10*, 93–106.
3. Fritsche, J., and Steinhart, H. (1998) Amounts of Conjugated Linoleic Acid (CLA) in German Foods and Evaluation of Daily Intake, *Z. Lebensm. Unters. Forsch. A 206*, 77–82.
4. Ip, C., Banni, S., Angioni, E., Carta, G., McGinley, J., Thompson, H.J., Barbano, D., and Bauman, D. (1999) Conjugated Linoleic Acid-Enriched Butter Fat Alters Mammary Gland Morphogenesis and Reduces Cancer Risk in Rats, *J. Nutr. 129*, 2135–2142.
5. Palombo, J.D., Ganguly, A., Bistrian, B.R., and Menard, M.P. (2002) The Antiproliferative Effects of Biologically Active Isomers of Conjugated Linoleic Acid on Human Colorectal and Prostatic Cancer Cells, *Cancer Lett. 177*, 163–172.
6. Banni, S., Angioni, E., Casu, V., Melis, M.P., Carta, G., Corongiu, F.P., Thompson, H., and Ip, C. (1999) Decrease in Linoleic Acid Metabolites as a Potential Mechanism in Cancer Risk Reduction by Conjugated Linoleic Acid, *Carcinogenesis 20*, 1019–1024.
7. Kavanaugh, C.J., Liu, K.L., and Belury, M.A. (1999) Effect of Dietary Conjugated Linoleic Acid on Phorbol Ester-Induced PGE(2) Production and Hyperplasia in Mouse Epidermis, *Nutr. Cancer 33*, 132–138.
8. Sugano, M., Tsujita, A., Yamasaki, M., Yamada, K., Ikeda, I.,

and Kritchevsky, D. (1997) Lymphatic Recovery, Tissue Distribution, and Metabolic Effects of Conjugated Linoleic Acid in Rats, *J. Nutr. Biochem. 8*, 38–43.

9. Banni, S., Carta, G., Angioni, E., Murru, E., Scanu, P., Melis, M.P., Bauman, D.E., Fischer, S.M., and Ip, C. (2001) Distribution of Conjugated Linoleic Acid and Metabolites in Different Lipid Fractions in the Rat Liver, *J. Lipid Res. 42*, 1056–1061.

10. Yang, L., Yeung, S.Y.V., Huang, Y., Wang, H.Q., and Chen, Z.-Y. (2002) Preferential Incorporation of *trans,trans*-Conjugated Linoleic Acid Isomers into the Liver of Suckling Rats, *Br. J. Nutr. 87*, 253–260.

11. Chardigny, J.M., Hasselwander, O., Genty, M., Kraemer, K., Ptock, A., and Sébédio, J.L. (2003) Effect of Conjugated FA on Feed Intake, Body Composition, and Liver FA in Mice, *Lipids 38*, 895–902.

12. Kelley, D.S., Bartolini, G.L., Warren, J.M., Simon, V.A., Mackey, B.E., and Erickson, K.L. (2004) Contrasting Effects of *t*10,*c*12- and *c*9,*t*11-Conjugated Linoleic Acid Isomers on the Fatty Acid Profiles of Mouse Liver Lipids, *Lipids 39*, 135–141.

13. Pietsch, A., and Lorenz, R.L. (1993) Rapid Separation of the Major Phospholipid Classes on a Single Aminopropyl Cartridge, *Lipids 28*, 945–947.

14. Kramer, J.K.G., Fellner, V., Dugan, M.E.R., Sauer, F.D., Mossoba, M.D., and Yurawecz, M.P. (1997) Evaluating Acid and Base Catalysts in the Methylation of Milk and Rumen Fatty Acids with Special Emphasis on Conjugated Dienes and Total *trans* Fatty Acids, *Lipids 32*, 1219–1228.

15. Helmerich, G., and Köhler, P. (2002) Simple Determination of Phospholipids with Thin Layer Chromatography (TLC), *Getreide Mehl Brot 56*, 195–197.

16. Pfalzgraf, A., Timm, M., and Steinhart, H. (1994) Gehalte von *trans*-Fettsäuren in Lebensmitteln, *Z. Ernahrungswiss. 33*, 24–43.

17. Hashimoto, N., Aoyama, T., and Shioiri, T. (1981) New Methods and Reagents in Organic Synthesis. A Simple Efficient Preparation of Methyl Esters with Trimethylsilyldiazomethane (TMSCHN$_2$) and Its Application to Gas Chromatographic Analysis of Fatty Acids, *Chem. Pharm. Bull. (Tokyo) 29*, 1475–1478.

18. Kramer, J.K.G., Cruz-Hernandez, C., Deng, Z., Zhou, J., Jahreis, G., and Dugan, M.E.R. (2004) Analysis of Conjugated Linoleic Acid and *trans* 18:1 Isomers in Synthetic and Animal Products, *Am. J. Clin. Nutr. 79 (Suppl.)*, 1137S–1145S.

19. Rickert, R., Steinhart, H., Fritsche, J., Sehat, N., Yurawecz, M.P., Mossoba, M.M., Roach, J.A.G., Eulitz, K., Ku, Y., and Kramer, J.K.G. (1999) Enhanced Resolution of Conjugated Linoleic Acid Isomers by Tandem-Column Silver-Ion High Performance Liquid Chromatography, *J. High Resolut. Chromatogr. 22*, 144–148.

20. Druilhet, R.E., Overturf, M.L., and Kirkendall, W.M. (1978) Cortical and Medullary Lipids of Normal and Nephrosclerotic Human Kidney, *Int. J. Biochem. 9*, 729–734.

21. Müller, M.M., Kaiser, E., Bauer, P., Scheiber, V., and Hohenegger, M. (1976) Lipid Composition of the Rat Kidney, *Nephron 17*, 41–50.

22. Geers, R., Christophe, A., Matthys, F., Verdonk, G., and Popelier, G. (1977) Phospholipid Analysis of Nephromas and Unaffected Cortex of Tumour-Bearing Human Kidneys, *Biochem. Soc. Trans. 5*, 1167–1169.

23. Gebhard, R.L., Clayman, R.V., Prigge, W.F., Figenshau, R., Staley, N.A., Reesey, C., and Bear, A. (1987) Abnormal Cholesterol Metabolism in Renal Clear Cell Carcinoma, *J. Lipid Res. 28*, 1177–1184.

24. Shahin, A.M., McGuire, M.K., McGuire, M.A., Ritzenthaler, K.L., and Shultz, T.D. (2003) Determination of *c*9,*t*11-CLA in Major Human Plasma Lipid Classes Using a Combination of Methylating Methodologies, *Lipids 38*, 793–800.

25. Mougios, V., Matsakas, A., Petridou, A., Ring, S., Sagredos, A., Melissopoulou, A., Tsigilis, N., and Nikolaidis, M. (2001) Effect of Supplementation with Conjugated Linoleic Acid on Human Serum Lipids and Body Fat, *J. Nutr. Biochem. 12*, 585–594.

26. Petridou, A., Mougios, V., and Sagredos, A. (2003) Supplementation with CLA: Isomer Incorporation into Serum Lipids and Effect on Body Fat of Women, *Lipids 38*, 805–811.

27. Burdge, G.C., Lupoli, B., Russell, J.J., Tricon, S., Kew, S., Banerjee, T., Shingfield, K.J., Beever, D.E., Grimble, R.F., Williams, C.M., *et al*. (2004) Incorporation of *cis*-9,*trans*-11 or *trans*-10,*cis*-12 Conjugated Linoleic Acid into Plasma and Cellular Lipids in Healthy Men, *J. Lipid Res. 45*, 736–741.

28. Belury, M.A. (1995) Conjugated Dienoic Linoleate: A Polyunsaturated Fatty Acid with Unique Chemoprotective Properties, *Nutr. Rev. 53*, 83–89.

29. Kim, E.J., Holthuizen, P.E., and Park, H.S. (2002) *Trans*10,*cis*12-Conjugated Linoleic Acid Inhibits Caco-2 Colon Cancer Cell Growth, *Am. J. Physiol. Gastrointest. Liver Physiol. 283*, G357–G367.

30. Kinsella, J.E., Yu, P.H., and Mai, J.B. (1979) Kidney Lipids: Changes Caused by Dietary 9-*trans*,12-*trans*-Octadecadienoate, *Lipids 14*, 1032–1036.

31. Swanson, J.E., Black, J.M., and Kinsella, J.E. (1987) Dietary n-3 Polyunsaturated Fatty Acids: Rate and Extent of Modification of Fatty Acyl Composition of Lipid Classes of Mouse Lung and Kidney, *J. Nutr. 117*, 824–832.

Synthesis of a Novel Series of 2-Methylsulfanyl Fatty Acids and Their Toxicity on the Human K-562 and U-937 Leukemia Cell Lines

Néstor M. Carballeira*, Carlos Miranda, Elsie A. Orellano, and Fernando A. González

Department of Chemistry, University of Puerto Rico, San Juan, Puerto Rico 00931-3346

ABSTRACT: The hitherto unknown 2-methylsulfanyldecanoic acid and 2-methylsulfanyldodecanoic acid were synthesized from methyl decanoate and methyl dodecanoate, respectively, through the reaction of lithium diisopropylamide and dimethyld-isulfide in THF followed by saponification with potassium hydroxide in ethanol. Both α-methylsulfanylated FA were cytotoxic to the human chronic myelogenous leukemia K-562 and the human histiocytic lymphoma U-937 cell lines with EC_{50} values in the 200–300 µM range, which makes them more cytotoxic to these cell lines than decanoic and/or dodecanoic acid. The cytotoxicity of the studied FA toward K-562 followed the order $2\text{-SCH}_3\text{-}12\text{:}0 > 2\text{-SCH}_3\text{-}10\text{:}0 > 10\text{:}0 > 12\text{:}0 > 2\text{-OCH}_3\text{-}12\text{:}0$, whereas toward U-937 the cytotoxicity was $2\text{-SCH}_3\text{-}10\text{:}0 > 2\text{-SCH}_3\text{-}12\text{:}0 > 12\text{:}0 > 10\text{:}0 > 2\text{-OCH}_3\text{-}12\text{:}0$. These results indicate that the α-methylsulfanyl substitution increases the cytotoxicity of the C_{10} and C_{12} FA toward the studied leukemia cell lines.

Paper no. L9820 in *Lipids 40,* 1063–1068 (October 2005).

FA at high concentrations are cytotoxic toward leukemia and melanoma cell lines (1–4). For example, a recent study established that the mitochondria from leukemic cells are more susceptible to the toxicity of FA than those from normal human lymphocytes (1). In these studies a mixture of FFA in proportions similar to the ones found in human plasma was found to trigger apoptosis (DNA fragmentation) of Jurkat (T lymphocytes) and Raji (B lymphocytes) cells, which eventually led to the loss of cell membrane integrity (necrosis). No considerable difference in toxicity between the B and T cell lines was observed, but the toxicity correlates with the carbon chain length and number of double bonds in the FA chain (2). For example, it was reported that dodecanoic acid is more cytotoxic than decanoic acid (2).

Our group has synthesized and explored the bioactivity of a novel series of naturally occurring α-methoxylated FA for some time (5). We have shown that this unusual group of FA displays comparable and, in most cases, even better antimycobacterial (e.g., $2\text{-CH}_3\text{O-}10\text{:}0$) (6), antibacterial (e.g., $2\text{-CH}_3\text{O-}16\text{:}1\Delta6$) (7), antifungal (e.g., $2\text{-OCH}_3\text{-}14\text{:}0$) (8), and, more important, antileukemic (e.g., $iso\text{-}2\text{-OCH}_3\text{-}15\text{:}0$) (9)

properties than the corresponding nonmethoxylated FA. With these properties of the α-methoxylated FA at hand, we envisioned the possibility of synthesizing and exploring the antileukemic properties of other heteroatom analogs, namely, the unknown α-methylsulfanyl FA. The benefit of changing an oxygen atom for a sulfur atom has literature precedents, since there is considerable background in the literature regarding the metabolic effects of sulfur-substituted FA, in particular the hypolipidemic effect of the 3-thia FA (10,11). A good example is tetradecylthioacetic acid (TTA), which is a lipid-lowering agent, i.e., it displays hypotriglyceridemic and hypocholesterolemic properties (11). In addition, TTA is incorporated into cell phospholipids and cannot be β-oxidized (10). Despite these intensive studies, however, it appears that nothing has been reported regarding the metabolism and cytotoxic properties of another possible family of sulfur-substituted FA, namely, the α-methylsulfanyl FA.

In this work, we describe for the first time the preparation of 2-methylsulfanyldecanoic acid (**1b**) and 2-methylsulfanyl-dodecanoic acid (**2b**) and report that these sulfur FA analogs are more cytotoxic to the leukemia K-562 and U-937 cell lines than either decanoic or dodecanoic acid. The choice of these cell lines was based on having the cells in stock in our laboratories and on having the opportunity to compare the cytotoxicity of the new acids with that of our previous database of the 2-methoxylated FA against the K-562 cell line (9).

MATERIALS AND METHODS

Instrumentation. ^1H and ^{13}C NMR spectra were recorded on either a Bruker DPX-300 or a Bruker DRX-500 spectrometer. ^1H NMR chemical shifts are reported with respect to internal Me_4Si, and chemical shifts are given in parts per million (ppm) relative to $CDCl_3$ (77.0 ppm). Mass spectral data were acquired on a GC–MS (Hewlett-Packard 5972A MS ChemStation) instrument at 70 eV, equipped with a 30 m × 0.25 mm special performance capillary column (HP-5MS) of polymethylsiloxane cross-linked with 5% phenyl methylpolysiloxane.

2-Methylsulfanylation of the FAME. The C_{10} and C_{12} methyl esters (0.10 g, 0.47–0.54 mmol) were dissolved in dry THF (2 mL) at −78°C and were added dropwise to 1.2 equiv of a THF (1.5 mL) solution of lithium diisopropylamide (LDA: prepared from diisopropylamine and *n*-butyllithium at −20°C for 15 min under nitrogen). After stirring at −78°C for 45 min, dimethyl

*To whom correspondence should be addressed at Department of Chemistry, University of Puerto Rico, P.O. Box 23346, San Juan, PR 00931-3346.
E-mail: nmcarballeira@uprrp.edu

Abbreviations: LDA, lithium diisopropylamide; TTA, tetradecylthioacetic acid.

disulfide (1.2 equiv) was added to the reaction mixture, which was further stirred for 1 h. Then, the reaction medium was treated with a saturated NH$_4$Cl solution and extracted with ether (2 × 5 mL). The organic phase was successively washed with a 0.1 M HCl solution (5–10 mL) and a saturated NaCl solution (5–10 mL) and then dried over Na$_2$SO$_4$ to afford 0.10 g (0.38–0.43 mmol) of the 2-methylsulfanyl methyl esters as colorless oils in 76–86% yields after Kugel-Rohr distillation of the impurities. The higher yield (86%) was obtained for methyl 2-methylsulfanyldecanoate.

(i) Methyl 2-methylsulfanyldecanoate. IR (neat) ν$_{max}$ 2953, 2925, 2855, 1734, 1460, 1435, 1342, 1261, 1192, 1156, 1117 cm^{-1}; ^{1}H NMR (CDCl$_3$, 300 MHz) δ 3.69 (3H, *s*, –OCH$_3$), 3.14 (1H, *dd*, *J* = 8.3 and 8.4 Hz, H-2), 2.08 (3H, *s*, SCH$_3$), 1.62 (2H, *m*, H-3), 1.22 (12H, *brs*, CH$_2$), 0.83 (3H, *t*, *J* = 6.9 Hz, CH$_3$); ^{13}C NMR (CDCl$_3$, 125 MHz) δ 172.81 (*s*, C-1), 65.72 (*q*, –OCH$_3$), 51.91 (*d*, C-2), 31.75 (*t*), 30.56 (*t*), 29.23 (*t*), 29.15 (*t*), 29.08 (*t*), 27.19 (*t*), 22.53 (*t*), 13.95 (*q*, C-10), 13.58 (*q*, –SCH$_3$); GC–MS *m/z* (relative intensity) M + 2 234 (2), M$^+$ 232 (30), 200 (13), 186 (20), 185 (18), 174 (12), 173 (100), 157 (37), 143 (13), 120 (34), 113 (2), 101 (5), 88 (14), 87 (39), 83 (18), 69 (29), 67 (11), 61 (26), 55 (32).

(ii) Methyl 2-methylsulfanyldodecanoate. IR (neat) ν$_{max}$ 2924, 2854, 1737, 1465, 1356, 1198, 1168, 721 cm^{-1}; ^{1}H NMR (CDCl$_3$, 300 MHz) δ 3.74 (3H, *s*, –OCH$_3$), 3.16 (1H, *dd*, *J* = 8.3 and 8.4 Hz, H-2), 2.06 (3H, *s*, SCH$_3$), 1.66 (2H, *m*, H-3), 1.24 (16H, *brs*, CH$_2$), 0.86 (3H, *t*, *J* = 6.9 Hz, CH$_3$); ^{13}C NMR (CDCl$_3$, 125 MHz) δ 172.92 (*s*, C-1), 65.80 (*q*, –OCH$_3$), 52.03 (*d*, C-2), 31.85 (*t*), 30.63 (*t*), 29.52 (*t*), 29.48 (*t*), 29.33 (*t*), 29.26 (*t*), 29.14 (*t*), 27.26 (*t*), 22.63 (*t*), 14.05 (*q*, C-10), 13.69 (*q*, –SCH$_3$); GC–MS *m/z* (relative intensity) M + 2 262 (1), M$^+$ 260 (21), 228 (11), 214 (18), 213 (17), 203 (5), 202 (15), 201 (100), 186 (6), 185 (45), 171 (7), 143 (9), 120 (45), 115 (4), 97 (16), 88 (14), 87 (44), 69 (23), 67 (11), 61 (28), 55 (36).

Saponification of the 2-methylsulfanyl FAME. Into a 25-mL round-bottomed flask was added the 2-methylsulfanyl methyl ester (0.050 g, 0.20–0.22 mmol) in 15 mL of 1 M KOH/ethanol and the mixture was refluxed for 1 h. The reaction mixture was then cooled to room temperature, and the ethanol was removed *in vacuo*. Hexane (15 mL) was added to the mixture, and the organic phase was washed twice with water (2 × 10 mL). The aqueous phase was then acidified with 6 M HCl and the FA extracted with ether (2 × 10 mL). The organic phase was separated, dried over Na$_2$SO$_4$, and the solvent removed *in vacuo* to afford the pure acids as colorless oils (0.030 g, 0.12–0.14 mmol) in 53–64% yield. The higher yield was obtained again for the 2-methylsulfanyldecanoic acid (**1b**).

(i) 2-Methylsulfanyldecanoic acid (1b). IR (neat) ν$_{max}$ 3478 (*br*), 2925, 2855, 1742, 1465, 1436, 1360, 1246, 1198, 1167, 722 cm^{-1}; ^{1}H NMR (CDCl$_3$, 300 MHz) δ 9.40 (1H, COO*H*), 3.44 (1H, *dd*, *J* = 7.0 and 7.2 Hz, H-2), 2.19 (3H, *s*, SCH$_3$), 1.62 (2H, *m*, H-3), 1.25 (12H, *brs*, CH$_2$), 0.88 (3H, *t*, *J* = 7.0 Hz, CH$_3$); ^{13}C NMR (CDCl$_3$, 125 MHz) δ 174.31 (*s*, C-1), 51.54 (*d*, C-2), 31.83 (*t*), 29.53 (*t*), 29.38 (*t*), 29.13 (*t*), 29.02 (*t*), 27.67 (*t*), 22.63 (*t*), 14.06 (*q*, C-10), 13.67 (*q*, –SCH$_3$); GC–MS *m/z* (relative intensity) M + 2 220 (2), M$^+$ 218 (34), 200 (3), 175

(5), 174 (12), 173 (100), 171 (24), 157 (85), 143 (4), 129 (19), 119 (3), 113 (4), 106 (84), 101 (9), 95 (6), 88 (20), 87 (15), 83 (32), 81 (14), 73 (57), 69 (56), 67 (13), 61 (46), 57 (19), 55 (49).

(ii) 2-Methylsulfanyldodecanoic acid (2b). IR (neat) ν$_{max}$ 3419 (*br*), 2922, 2851, 1707, 1459, 1378, 1260, 1111, 1022, 908, 735 cm^{-1}; ^{1}H NMR (CDCl$_3$, 300 MHz) δ 9.40 (1H, COO*H*), 3.48 (1H, *dd*, *J* = 6.9 and 7.1 Hz, H-2), 2.17 (3H, *s*, SCH$_3$), 1.65 (2H, *m*, H-3), 1.25 (16H, *brs*, CH$_2$), 0.88 (3H, *t*, *J* = 7.1 Hz, CH$_3$); ^{13}C NMR (CDCl$_3$, 125 MHz) δ 176.57 (*s*, C-1), 47.48 (*d*, C-2), 31.80 (*t*), 29.74 (*t*), 29.58 (*t*), 29.52 (*t*), 29.40 (*t*), 29.28 (*t*), 27.46 (*t*), 27.13 (*t*), 22.89 (*t*), 14.33 (*q*, C-12), 14.20 (*q*, –SCH$_3$); GC–MS *m/z* (relative intensity) M + 2 248 (1), M$^+$ 246 (26), 228 (2), 203 (4), 202 (12), 201 (85), 185 (100), 171 (4), 157 (7), 143 (4), 129 (9), 119 (3), 106 (81), 97 (23), 95 (10), 87 (14), 85 (10), 83 (29), 81 (12), 73 (48), 71 (14), 69 (32), 67 (14), 61 (36), 57 (21), 55 (48).

Cell culture. Two nonadherent cell lines were used in this study, namely, the human histiocytic lymphoma U-937 (ATCC CRL-1593), and human chronic myelogenous leukemia K-562 (ATCC CCL-243). These cells were cultured in RPMI 1640 medium that contained 10% Fetalclone III serum (K-562) or Cosmic calf serum (U-937) (Invitrogen, Inc., Carlsbad, CA) supplemented with 1% penicillin-streptomycin antibiotic solution (Sigma, St. Louis. MO). The cultures were maintained at 37°C in a humidified atmosphere of 95% air/5% CO$_2$.

Cytotoxicity assay. Cells were inoculated into 96-well microplates at $5.0 × 10^5$ cells/mL (100 μL/well) and incubated at 37°C for 24 h before treatment. Various concentrations (in DMSO) of test agents were added to the cells, followed by further incubation at 37°C for 48 h. The cells growing in suspension were fixed *in situ* with 50 μL/well of ice-cold 80% (wt/vol) aqueous TCA solution to produce a final concentration of 16% TCA (wt/vol). The plates were incubated for 90 min at 4°C after which they were washed five times with water and air-dried. A solution of 0.4% (wt/vol) sulforhodamine B in 1% (vol/vol) acetic acid was added (50 μL) to each well and incubated for 15 min at room temperature. The plates were washed five times with 1% (vol/vol) acetic acid, air-dried, and incubated with 10 mM Tris-base (pH = 10.4) with shaking for 15 min at room temperature. The absorbance at 490 nm of solubilized stain was measured on a microplate reader (MRX II; Dynex Technologies, Chantilly, VA). The concentration of FA that inhibited growth in 50% (EC$_{50}$) of the cells was calculated using the Prism Software (Graphpad, San Diego, CA) from titration curves generated from at least three independent experiments, each performed in triplicate.

RESULTS AND DISCUSSION

To the best of our knowledge, the synthesis of α-methylsulfanylated FA appears not to have been reported before; therefore, we developed an efficient synthetic procedure that would allow the preparation of a diverse series of α-methylsulfanylated analogs. We found that by starting with the corresponding methyl alkanoates, treatment of the corresponding lithium

SCHEME 1

enolates in THF with dimethyl disulfide afforded the corresponding α-methylsulfanyl FAME in 76–86% yields (Scheme 1). The reaction proceeded even better than the α-methylation of methyl alkanoates with methyl iodide: Better yields were obtained, the purification of the product was easier, and no double α-methylsulfanylation was observed. As the chain length of the FAME increased, however, the α-methylsulfanylation became more difficult, i.e., 86% yield for the C_{10} methyl ester vs. 76% yield for the C_{12} methyl ester. For this reason, in the initial studies we concentrated our efforts on the synthesis of the short-chain C_{10} and C_{12} α-methylsulfanyl FA. Final saponification with KOH in ethanol afforded the desired α-methylsulfanyl FA in 53–64% yields (Scheme 1). Therefore, in following the above-described synthetic methodology, the desired 2-methylsulfanyldecanoic acid (**1b**) and 2-methylsulfanyldodecanoic acid (**2b**) were conveniently prepared in 40–55% overall yields from the corresponding parent methyl esters.

The spectral and GC data of both the methyl 2-methylsulfanylated alkanoates and alkanoic acids deserve special mention. The methyl 2-methylsulfanylated alkanoates displayed long retention times on nonpolar gas columns (HP-5MS capillary column) in the GC analysis owing to the presence of the sulfur functionality. For example, methyl 2-methylsulfanyldecanoate possesses an ECL value of 12.94, whereas the oxygen analog, namely, methyl 2-methoxydecanoate, has an ECL value of 11.22 (6). The EI mass spectral fragmentation of the 2-methylsulfanylated FA is quite characteristic, with predominant cleavage occurring at the α-carbon atom of the carbonyl. For example, in the MS (70 eV) of 2-methylsulfanyldecanoic acid (**1b**), the base peak was observed at m/z 173 $[C_{10}H_{21}S]^+$, together with the expected McLafferty rearrangement at m/z 106 $[C_3H_6SO_2]^+$, a typical fragmentation in all of the α-methylsulfanylated FA (Fig. 1). A less common mass spectral fragmentation was observed for **1b** at m/z 157 $[M^+ - C_2H_5O_2]$ with a considerable (85%) relative abundance. The ^1H NMR spectrum of **1b** exhibited the H-2 hydrogen atom as a doublet of doublets at δ 3.44 ppm and the α-methylsulfanyl substituent as a singlet at δ 2.19 ppm. In the ^{13}C NMR spectrum of **1b,** the C-2 carbon appeared at δ 51.5 ppm, and the methylsulfanyl substituent resonated at 13.7 ppm. The C-1 carbonyl group was observed at δ 174.3 ppm in **1b**, more upfield than the 177–178 ppm absorption found for the carbonyl functionality in the ^{13}C NMR spectrum of most 2-methoxylated FA (6). These ^1H and ^{13}C NMR shifts

FIG. 1. EI-MS (70 eV) of 2-methylsulfanyldecanoic acid (**1b**).

K562 cells   U937 cells

FIG. 2. Toxicity curves for 2-methylsulfanyldecanoic acid (**1b**), 2-methylsulfanyldodecanoic acid (**2b)**, decanoic acid, and dodecanoic acid toward the two leukemia cell lines K-562 and U-937.

seem to be characteristic for saturated 2-methylsulfanylated FA and they should be useful for future reference of similar analogs.

The testing procedure described in the Materials and Methods section was followed for the acids **1b** and **2b**, and with decanoic and dodecanoic acids, to assess their effects on the two leukemia cell lines K-562 (ATCC CCL-243) and U-937 (ATCC CRL-1593) (Fig. 2). 2-Methylsulfanyldecanoic acid (**1b**) displayed an EC_{50} of 242 µM against K-562 and an EC_{50} of 310 µM against U-937, whereas decanoic acid displayed values against K-562 and U-937 of only 411 and 648 µM, respectively (Table 1). These results indicate that **1b** is about two times more cytotoxic to K-562 and U-937 than the parent decanoic acid. In contrast, 2-methylsulfanyldodecanoic acid (**2b**) possesses an EC_{50} of 213 µM against K-562 and an EC_{50} of 375

µM against U-937, whereas dodecanoic acid displayed values against K-562 and U-937 of only 589 and 516 µM (Table 1). The second set of results confirms that **2b** is also about two to three times more cytotoxic to K-562 and U-937 than dodecanoic acid. In addition to the above-mentioned FA, we also studied the cytotoxicity of the 2-methoxydodecanoic acid toward K-562 and U-937, to assess how the heteroatomic substitution of an oxygen for a sulfur atom affects the toxicity.

We have previously described the synthesis of 2-methoxydodecanoic acid (6). Unexpectedly, the 2-methoxylation decreased even further the cytotoxicity of the parent decanoic acid, to values >1000 µM, against both cell lines (Table 1). Interestingly, the cytotoxicity of the FA toward K-562 followed the order 2-SCH$_3$-12:0 > 2-SCH$_3$-10:0 > 10:0 > 12:0 > 2-OCH$_3$-12:0, whereas the order of cytotoxicity of these same

TABLE 1
Growth Inhibition (EC$_{50}$, µM) of the FA and Controls Against the Leukemia Cell Lines K-562 and U-937

Compound	EC$_{50}$ (µM), K-562	EC$_{50}$ (µM), U-937
2-Methylsulfanyldecanoic acid	242.2	309.9
	(log EC$_{50}$ = −3.61 ± 0.06)	(log EC$_{50}$ = −3.50 ± 0.09)
Decanoic acid	411.1	648.5
	(log EC$_{50}$ = −3.38 ± 0.08)	(log EC$_{50}$ = −3.18 ± 0.07)
2-Methylsulfanyldodecanoic acid	212.8	374.8
	(log EC$_{50}$ = −3.67 ± 0.07)	(log EC$_{50}$ = −3.42 ± 0.07)
Dodecanoic acid	589.3	516.5
	(log EC$_{50}$ = −3.23 ± 0.08)	(log EC$_{50}$ = −3.28 ± 0.08)
2-Methoxydodecanoic acid	>1000	>1000
Amsacrine	4.2	5.3
	(log EC$_{50}$ = −5.3 ± 0.1)	(log EC$_{50}$ = −5.2 ± 0.1)

FA toward U-937 was 2-SCH$_3$-10:0 > 2-SCH$_3$-12:0 > 12:0 > 10:0 > 2-OCH$_3$-12:0. These results clearly indicate that α-methylsulfanyl substitution increases the cytotoxicity of the C$_{10}$ and C$_{12}$ FA toward the studied cell lines. Consequently, such a functionalization should be useful for other FA to enhance the cytotoxicity toward these leukemia cell lines. However, the therapeutic potential of the α-methylsulfanylated FA remains to be elucidated.

It is important to emphasize that the 2-methylsulfanyl substitution described herein does not necessarily increase the toxicity of FA toward other biological systems. For example, following a procedure that we already described (6), we explored the inhibitory activity of the 2-methylsulfanyldecanoic acid (**1b**) toward *Mycobacterium tuberculosis* H$_{37}$Rv. We had previously shown that the 2-methoxydecanoic acid, as well as decanoic acid, inhibited *M. tuberculosis* H$_{37}$Rv (6). Interestingly, we found that acid **1b** displayed no inhibitory activity toward *M. tuberculosis* H$_{37}$Rv, i.e., minimum inhibitory concentrations exceeded 300 µM. Therefore, the 2-methylsulfanyldecanoic acid (**1b**) seems to possess some specificity toward the leukemia cell lines studied herein.

As to the mechanism of cytotoxicity displayed by these novel α-methylsulfanylated FA, we may only speculate now. Analogous to the reported mechanism of the normal-chain FA with the Jurkat and Raji cells (1), one possible mechanism of action for the α-methylsulfanylated FA is to trigger apoptosis (DNA fragmentation) followed by loss of cell membrane integrity (necrosis); indeed, the mitochondria from leukemic cells are known to be more susceptible to the toxicity of FA (2). Evidently, the α-methylsulfanyl functionality possesses advantageous properties to induce apoptosis in these FA compared with normal-chain FA. Certainly, since the sulfur atom is more polarizable than carbon, these acids are more acidic (pK_a ~ 3.7) than the corresponding parent normal-chain FA (pK_a ~ 4.8), but less acidic than the 2-methoxylated FA (pK_a ~ 3.5), and these pH differences could influence the cytotoxicity of the sulfanylated FA (12). Moreover, the α-methylsulfanylated FA are expected to be more polar than the normal-chain FA, which makes them more soluble in water, a fact that could also affect the delivery of the FA to the active site in the targets.

Another difference that needs to be addressed is the impair-

ment and/or selectivity that the α-methylsulfanyl substituent exerts on either the mitochondrial or peroxisomal β-oxidation of these FA in leukemia cells (13,14). If the α-methylsulfanylated FA are oxidized and/or metabolized more slowly than the normal-chain FA, this implies a longer half-life of these FA in the cells and more time to exert their toxic effects. For example, it has been reported that 2-methyldecanoyl-CoA, in contrast to its unbranched analog, was not oxidized by rat-liver mitochondria and purified enzymes; however, 2-methylhexadecanoyl-CoA was oxidized, although more slowly, than palmitate (13).

REFERENCES

1. Otton, R., and Curi, R. (2005) Toxicity of a Mixture of Fatty Acids on Human Blood Lymphocytes and Leukemia Cell Lines, *Toxicol. In Vitro 19*, 749–755.
2. Lima, T.M., Kanunfre, C.C., Pompeia, C., Verlengia, R., and Curi, R. (2002) Ranking the Toxicity of Fatty Acids on Jurkat and Raji Cells by Flow Cytometry Analysis, *Toxicol. In Vitro 16*, 741–747.
3. Andrade, L.N., de Lima, T.M., Curi, R., and Castrucci, A.M. (2005) Toxicity of Fatty Acids on Murine and Human Melanoma Cell Lines, *Toxicol. In Vitro 19*, 553–560.
4. Nordstrom, T., Lindqvist, C., Stahls, A., Mustelin, T., and Andersson, L.C. (1991) Inhibition of CD3-Induced Ca^{2+} Signals in Jurkat T-Cells by Myristic Acid, *Cell Calcium 12*, 449–455.
5. Carballeira, N.M. (2002) New Advances in the Chemistry of Methoxylated Lipids, *Prog. Lipid Res. 41*, 437–456.
6. Carballeira, N.M., Cruz, H., Kwong, C.D., Wan, B., and Franzblau, S. (2004) 2-Methoxylated Fatty Acids in Marine Sponges: Defense Mechanism Against Mycobacteria? *Lipids 39*, 675–680.
7. Carballeira, N.M., Emiliano, A., Hernández-Alonso, N., and

González, F.A. (1998) Facile Total Synthesis and Antimicrobial Activity of the Marine Fatty Acids (Z)-2-Methoxy-5-hexadecenoic Acid and (Z)-2-Methoxy-6-hexadecenoic Acid, *J. Nat. Prod. 61*, 1543–1546.

8. Carballeira, N.M., O'Neill, R., and Parang, K. (2005) Racemic and Optically Active 2-Methoxy-4-oxatetradecanoic Acids: Novel Synthetic Fatty Acids with Selective Antifungal Properties, *Chem. Phys. Lipids 136*, 47–54.

9. Carballeira, N.M., Cruz, H., Orellano, E.A., and González, F.A. (2003) The First Total Synthesis of the Marine Fatty Acid (±)-2-Methoxy-13-methyltetradecanoic Acid: A Cytotoxic Fatty Acid to Leukemia Cells, *Chem. Phys. Lipids 126*, 149–153.

10. Skrede, S., Sorensen, H.N., Larsen, L.N., Steineger, H.H., Hovik, K., Spydevold, O.S., and Horn, R.B.J. (1997) Thia Fatty Acids, Metabolism and Metabolic Effects, *Biochim. Biophys. Acta 1344*, 115–131.

11. Berge, R.K., Skorve, J., Tronstad, K.J., Berge, K., Gudbrandsen, O.A., and Grav, H. (2002) Metabolic Effects of Thia Fatty Acids, *Curr. Opin. Lipidol. 13*, 295–304.

12. Park, H.J. (1995) Effects of Intracellular pH on Apoptosis in HL-60 Human Leukemia Cells, *Yonsei Med. J. 36*, 473–479.

13. Mao, L.F., Chu, C., Luo, M.J., Simon, A., Abbas, A.S., and Schulz, H. (1995) Mitochondrial Beta-Oxidation of 2-Methyl Fatty Acids in Rat Liver, *Arch. Biochem. Biophys. 321*, 221–228.

14. Barbieri, B., Papadogiannakis, N., Eneroth, P., and Olding, L.B. (1995) Arachidonic Acid Is a Preferred Acetyl Donor Among Fatty Acids in the Acetylation of *p*-Aminobenzoic Acid by Human Lymphoid Cells, *Biochim. Biophys. Acta 1257*, 157–166.

COMMUNICATIONS

Kinetics of ^{14}C Distribution After Tracer Dose of ^{14}C-Lutein in an Adult Woman

Fabiana F. de Moura, Charlene C. Ho, Girma Getachew,
Sabrina Hickenbottom, and Andrew J. Clifford*

Department of Nutrition, University of California Davis, California 95616-8669

ABSTRACT: Lutein is an oxygenated carotenoid (xanthophyll) found in dark green leafy vegetables. High intakes of lutein may lower the risk of age-related macular degeneration. Current understanding of human lutein metabolism as it might occur *in vivo* is incomplete. Therefore, we conducted a feasibility study where we dosed a normal adult woman with ^{14}C-lutein (125 nmol, 36 nCi ^{14}C), dissolved in olive oil (0.5 g/kg body weight) and mixed in a banana shake. Blood, urine, and feces collected before the dose was administered served to establish baseline values. Thereafter, blood was collected for 63 d following the dose, while feces and urine were collected for 2 wk post-dose. The ^{14}C contents in plasma, urine, and feces were measured by accelerator MS. The ^{14}C first appeared in plasma 1 h after dosing and reached its highest level, ≈2.08% of dose/L plasma, at 14 h post-dose. The plasma pattern of ^{14}C did not include a chylomicrons/VLDL (intestinal) peak like that when the same subject received ^{14}C-β-carotene (a previous test), suggesting that lutein was handled differently from β-carotene by plasma lipoproteins. Lutein had an elimination half-life ($t_{1/2}$) of ≈10 d. Forty-five percent of the dose of ^{14}C was eliminated in feces and 10% in urine in the first 2 d after dosing. Quantifying human lutein metabolism is a fertile area for future research.

Paper no. L9835 in *Lipids 40,* 1069–1073 (October 2005).

Lutein, an oxygenated carotenoid (xanthophyll) more specifically classified as a dihydroxycarotenoid, is found in dark green leafy vegetables—such as kale, collard greens, and spinach—and egg yolk (1). Epidemiological studies (2,3) indicate that high intakes of lutein and its structural isomer zeaxanthin reduce the risk of age-related macular degeneration (AMD), a progressive disease that causes loss of central vision. Ingested lutein and zeaxanthin are selectively accumulated as a yellow spot at the center of the retina where they are frequently referred to as macular pigments (MP) (4).

It has been hypothesized that MP protect the retina against AMD by absorbing short-wavelength visible light and reducing chromatic aberration. MP are also thought to function as antioxidants by quenching free radicals and singlet oxygen, which are generated in the retina by the simultaneous presence of light and oxygen (5,6). Additional evidence for a key role of lutein and zeaxanthin in reducing the risk of AMD are their specific target, since lutein and zeaxanthin are located in the human rod outer segment (ROS), which is the region of the retina that is most exposed to oxidation (7).

Lutein supplementation leads to a marked increase in serum lutein levels and in total MP O.D. in humans (8–10). However, quantification of *in vivo* human xanthophyll metabolism is incomplete except for the studies that used ^{13}C- (11–13) and deuterated lutein (14). These studies found that labeled lutein first appeared in plasma at ≈4 h after dosing and reached maximal concentrations between 8 and 24 h post-dose. We used a small dose of ^{14}C-lutein, frequent blood sampling over a long period of time, and complete collection of feces and urine for 2 wk as a feasibility study to quantify lutein metabolism in an adult woman.

The fate of minute ^{14}C-tracer doses, measured by accelerator MS (AMS), is increasingly being used to quantify human micronutrient metabolism in healthy volunteers (15–17). AMS is an isotope ratio technique that measures ^{14}C/^{12}C ratios to the parts per quadrillion (10^{-15}), quantifying labeled biochemicals to attomole (10^{-18}) levels in milligram-sized samples. At attomole levels of sensitivity, the radiation exposure is negligible, allowing *in vivo* testing in healthy subjects. Furthermore, because a combustion step precedes the isotope ratio analysis, complex matrices such as urine and stool can be analyzed unprocessed.

Here we describe a feasibility study where the ^{14}C from orally administered ^{14}C-lutein was followed in plasma, feces, and urine of an adult volunteer using AMS methodology.

EXPERIMENTAL PROCEDURES

Informed written consent was obtained from a volunteer under the guidelines established by the Human Subject Review Committee. The Radiation Safety and Humans Subjects Committees of the University of California at Davis and Lawrence Livermore National Laboratories (LLNL) approved all protocols.

Biosynthesis and purification of ^{14}C-lutein. Mature spinach plants (30 d of age) were placed into an atmospherically sealed

---

*To whom correspondence should be addressed at Department of Nutrition, University of California, One Shields Ave., Davis, CA 95616-8669.
E-mail: ajclifford@ucdavis.edu

Abbreviations: AMD, age-related macular degeneration; AMS, accelerator MS; AUC, area under the concentration–time curve; AUMC, area under the moment curve; DANR, Division of Agriculture and Natural Resources at the University of California, Davis; LLNL, Lawrence Livermore National Laboratories; MP, macular pigment; MST, mean sojourn time.

plant chamber and allowed to acclimate for 2 d (18). Exposure was initiated by adding 10 mCi per day as a solution of NaH^{14}CO$_3$ to excess acid and was continued for 4 d. Labeled spinach was then harvested (~500 g).

A mass of spinach (50 g) was minced for 5 min in a 4-L bucket with 400 mL of methanol containing 100 mM mercaptoethanol. Hexane (500 mL) was then added and the suspension was filtered through glass wool and sodium sulfate; the solids were washed with hexane until they were bleached of color.

Lutein was found to reside completely in the methanol layer, which was then applied to a conditioned 15 g strong anion exchange column. None of the lutein was retained on the resin, and the total eluent from the column was saponified using 5% potassium hydroxide in methanol with pyrogallol. The saponification was conducted under argon at 23°C for 1.5 h. The sample was cooled, and 2 vol of deionized water was added.

The saponified mixture was extracted with 10 vol of 50:50 ether/hexane. This procedure was repeated three times. The volume of the extract was reduced by rotary evaporation and filtered through glass wool and sodium sulfate. The resultant material was loaded onto prepared NH$_4$ solid phase extraction columns (500 mg resin bed, 2.8 mL, aminopropyl bonded silica; Alltech, Deerfield, IL).

The column was first washed with hexane. In a second step, the column was washed with 2% 2-propanol in 75:23 hexane/ethyl acetate. Finally, in a third step, the column was washed with a 5% 2-propanol in 75:20 hexane/ethyl acetate to elute lutein. The lutein fraction was then dried under argon gas and resuspended in 50:50 acetonitrile/methylene chloride for HPLC analysis.

The purification of lutein was performed on an HPLC System (Model 1100; Agilent Technology, Palo Alto, CA) equipped with a quaternary solvent delivery system, a 200-μL loop, a thermostat-controlled column compartment, and a photodiode array detector. RP-HPLC separation was carried out using isocratic conditions of acetronitrile/methanol (80:20, vol/vol) with an UltraTracarb column (25 cm length × 10 mm i.d.; Phenomenex, Torrance, CA). The flow rate was 3 mL/min. For identification purposes, a lutein standard (Sigma, St. Louis, MO) was concomitantly injected with the lutein fraction, and the HPLC run was monitored at 445 nm. The purified lutein was dried under argon, suspended in ethanol, and its concentration determined spectroscopically at 445 nm using a molar extinction coefficient of 145×10^3 (19). The purity of lutein was >99%.

The specific activity of the lutein dose was determined by absorbance and β-scintillation counting. The lutein concentration in the pooled fraction was 62.36 μmol/L. The radioactivity found in a 50 μL sample was 0.899 nCi. Therefore, the specific activity was 0.288 Ci/mol. The accuracy was verified on two scintillation counters checked with NIST-certified ^{14}C quench standards. Figure 1 shows the chemical structure of lutein.

Dose preparation. The dose consisted of 36 nCi ^{14}C-lutein (71 μg in 1.583 g ethanol) dissolved into 32 g of olive oil (0.5 g/kg body weight). The olive oil was incorporated in a banana shake prepared with a small banana (168 g), 110 mL of skim

(all E, 3R,3'R,6'R)-β,ε- Carotene-3,3'-diol
[(3R,3'R,6'R)-Lutein]
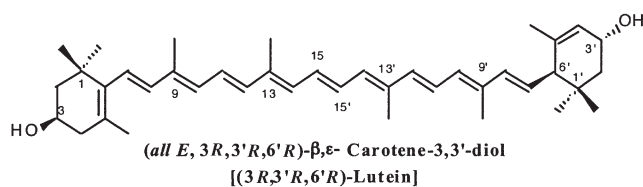
FIG. 1. Chemical structure of dietary (3R,3′R,6′R)-lutein. The systematic name of this carotenoid is followed by its common name (shown in brackets).

milk, and 2 tablespoons of sugar (~28 g). Half of the drink was combined with the dose and consumed immediately. The other half was used to rinse the container. The test meal contained 54% of the energy as fat to ensure optimal lutein absorption.

Subject, diet, and specimen collection. The subject was a 45-yr-old woman, a nonsmoker, in good health with a body mass index of 27.6 kg/m^2 (64.1 kg). Her nutrient intake was within normal ranges. The morning before the dose, a fecal and a 24-h urine collection was made and continued for 2 wk. That afternoon the subject was fitted with an intravenous catheter in her cubital median forearm vein. The patency of the catheter was maintained by flushing with 2 mL of saline right after each half hour blood draw and 2 mL of saline followed by 1 mL of heparin in between hour blood draws. All blood samples were collected into vacutainer tubes containing potassium ethylenediaminetetraacetate (K$_3$-EDTA). A baseline blood sample (10 mL) was taken just before the dose was administered. On the first day of sampling, 10 mL of blood was collected every half hour starting at time zero for the first day of the study. Collection time points were every half-hour (0–10 h), every hour (11–14 h) and then at 25, 49, 74, 98, 122, 146.5, 242.5, 290.5, 338.5, 434.5, 602.5, 650.5, 674.5, 842.5, 1178.5, and 1514.5 hours post-dose. After the first and second days of the study, blood draws were taken in the fasted state.

Specimen preparation. Plasma was separated from the red blood cells by centrifugation and stored at −75°C until needed. A 40-mL aliquot of urine collections was removed and stored at −75°C until analysis. Feces were collected in 4-mm-thick plastic bags and weighed. A volume of a 50:50 1 M potassium hydroxide and 2-propanol solution equivalent to five times the sample's mass was added to each bag. The specimen was dispersed using a Stomacher laboratory blender (Fisher Scientific: Model 3500) for 2 min at the high setting. The sealed bag was then heated for 2 h in an 80°C water bath. Following this treatment, samples were then redispersed for a second time for 2 min. The samples were returned to the 80°C water bath for another 2 h, and again dispersed for 2 min using the Stomacher. A 40-mL aliquot was then transferred to a 50 mL centrifuge tube (Falcon) that contained ≈8 mL of glass beads (6 mm, Fisher Scientific) and shaken on a Wrist-action Shaker (model 75; Burrell Scientific, Pittsburgh, PA) for at least 4 h. At this point, an aliquot of 500 μL was removed for total carbon and ^{14}C analysis. To prevent carotenoid oxidation, all procedures were conducted under yellow light.

Total carbon analysis. Total ^{12}C was assessed for each biological sample. Total carbon was measured (20) at the Division

of Agriculture and Natural Resources (DANR) at the University of California, Davis. Urine (75 μL), stool (75 μL), and plasma (25 μL) aliquots were lyophilized and sent to DANR for combustion and therefore total carbon determination.

Accelerator MS. The ^{14}C determinations were made at the Center for the Accelerator Mass Spectrometry (CAMS) at LLNL (Livermore, CA). Aliquots of plasma (25 μL), urine (75 μL), and feces (500 μL) were analyzed neat by evaporating to dryness. Then, 2 μL of tributyrin (cat. #103111, lot# 2949H, MP Biomedical, LLC, Solon, OH) was added to each dried sample to provide 1 mg of total carbon. The tributyrin used in this study had a minimal (background) level of ^{14}C radioactivity of 0.0284 Modern. A Modern is defined as 13.56 dpm per gram of carbon and is equivalent to 97.8 attomoles of ^{14}C/mg carbon or 6.11 femtoCurie/mg carbon.

Chemicals. All chemicals were checked for ^{14}C content by AMS prior to use. All solvents and other chemicals were HPLC grade. Chemicals and labware were obtained from Fisher Scientific (Santa Clara, CA), unless otherwise noted.

Calculations. A three-term exponential equation was used to describe the appearance and disappearance of ^{14}C from the plasma. The three-term exponential equation consisted of ($y = a_1e^{-b1t} + a_2e^{-b2t} + a_3e^{-b3t}$) with weighted, nonlinear least squares regression using PKAnalyst version 1.0 (MicroMath Scientific Software, Salt Lake City, UT).

The area under the plasma concentration–time curve was calculated as $AUC = \int_0^\infty y(t)dt$. The area under the moment curve was calculated as $AUMC = \int_0^\infty t \times y(t)dt$. Then we calculated the AUMC/AUC, a commonly used measure of mean sojourn time, MST.

RESULTS

The fraction of the dose of ^{14}C/L plasma by time since dose appears in Figure 2. The ^{14}C label first appeared in plasma after a 1-h delay. The maximum of ^{14}C, representing 2.08% of the dose/L plasma, was observed at 14 h (0.58 d). A poorly resolved peak (shoulder) was observed on the second day post-dose indicating that the plasma ^{14}C existed in more than a single pool. From the third to the sixty-third day the level of ^{14}C decreased gradually to baseline.

Elimination of ^{14}C in feces and urine appears in Figure 3 as the cumulative fraction of dose. Forty-five percent of the ^{14}C tracer was excreted in the feces in the first 3 collections over the period of 2 d; this amount represented the percentage of the dose that was not absorbed. An additional 3% of the dose was eliminated in the feces in the following 11 d. One-tenth of the absorbed dose was eliminated in urine during the first 14 d.

The three-term exponential equation $y(t) = -4.25e^{-1.44*(Time-T_{lag})} + 4.24e^{-1.43*(Time-T_{lag})} + e^{-0.07*(Time-T_{lag})}$ provided a good fit of the plasma ^{14}C-lutein concentration as a function of time after dose. From this equation AUC and AUMC were calculated to be 0.1929 μmol × d/L plasma and 2.55 μmol × d^2/L plasma, respectively. For ^{14}C-lutein, the ratio of AUMC/AUC, which represents the mean sojourn time (MST), was 13.22 d. The elimination half-life ($t_{1/2}$) for lutein was calculated as 9.85 d.
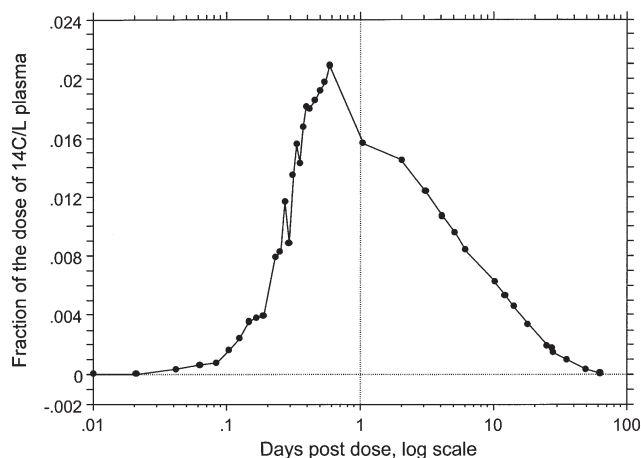
FIG. 2. The pattern of ^{14}C in plasma with time following an oral dose of ^{14}C-lutein.

DISCUSSION

In the present feasibility study, a female volunteer was found to absorb 55% of a small tracer dose of ^{14}C-lutein that was given in a banana milk shake. Our result fits well with the range of 45–54% relative bioavailability of lutein obtained from raw and processed spinach (21). These results are also in agreement with a recent finding that response to lutein from spinach is comparable to that from lutein supplements (22). However, human (23) and cell culture (24) studies have shown a significantly higher bioavailability of lutein from supplements compared with those from food. The route of elimination for the ^{14}C tracer was mainly in the feces, which represented 45% of the dose in the first 2 d. Only 10% of the dose was eliminated *via* urine. We did not find elimination/recovery data for administered lutein in the scientific literature.

The plasma ^{14}C profile in Figure 2 was expected. The 1-h delay in the first appearance of ^{14}C could represent the time for the administered lutein to reach the site of absorption from the
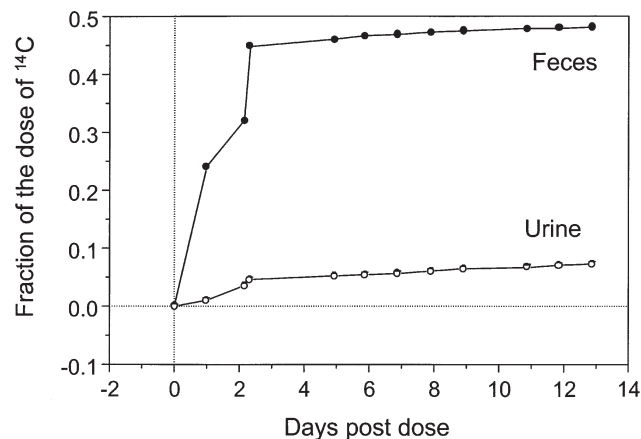
FIG. 3. Cumulative loss of ^{14}C in urine and feces as a function of time following an oral dose of ^{14}C-lutein.

intestine and be secreted in chylomicrons (25). The timing of the plasma ^{14}C peak at 14 h compares well with the 16 h peak after a lutein supplement (26), the 11 h peak after administration of ^{13}C-lutein (27,28), and the 13–24 h peak after administration of deuterated lutein (14). The mass of lutein administered in the present study was only 125 nmol compared with ≈33 μmol typical of prior studies. Our frequent plasma sampling over a relatively long time after dosing yielded a dataset consistent with the scientific literature, thus demonstrating the feasibility of our approach using AMS. Human lutein metabolism can be quantified in steady state for long periods to ensure complete equilibration of the ^{14}C-tracer with the deepest (slowest turning-over) pools that determine late-phase plasma kinetics.

The ^{14}C detected by AMS does not provide information on a specific metabolite; that can be accomplished by further characterization *via* HPLC. To further clarify the transport of lutein in circulation, a study of the distribution of the ^{14}C into the lipoproteins would be necessary. Future studies will be undertaken to determine whether the ^{14}C label is associated with lutein or its metabolite and their distribution into the lipoprotein classes.

When the same female was administered a tracer dose of ^{14}C-β-carotene (29) the absorption was 52%, a value virtually identical to the 55% for lutein. Although the percent absorption of both carotenoids was identical, each one showed a distinct ^{14}C profile in plasma (Fig. 4), indicating that the metabolisms of lutein and β-carotene differ from one another. The profile from administered ^{14}C-β-carotene had two peaks. One was ^{14}C-retinyl esters in chylomicrons + intestinal VLDL at ≈0.27 d before being taken up by liver. The other was ^{14}C-retinol bound to retinol-binding protein after release from liver at 0.5 d. The profile after ^{14}C-lutein administration did not show a pattern with a peak at 0.27 d that corresponded with chylomicrons + intestinal VLDL, indicating that lutein transport by lipoproteins differs from that of β-carotene as previously suggested (30). Finally, the use of more polar (lutein) labeled carotenoid which is located at the surface of the lipoproteins, and a polar β-carotene, located at the core, can help to clarify the similarities and differences of the metabolism and transport of other core and surface components of lipoproteins. Furthermore, ^{14}C-carotenoids can be used to label plasma lipoproteins differentially and provide important information on the metabolism of lipoproteins themselves. A lutein receptor, the scavanger receptor SR-BI, has already been reported (31); it may favor absorption of lutein over β-carotene.

Recently, Thurmann *et al.* (32) reported a $t_{1/2}$ of 5.6 d in humans. The $t_{1/2}$ of 9.9 d that we observed fits well with the $t_{1/2}$ of 12 d for zeaxanthin (33). Depletion studies reported half-lives of lutein to be 76 d (34), and 33–60 d (35). The longer half-lives obtained from those studies are a result of the depletion of lutein in tissue pools.

In conclusion, 55% of the ^{14}C-lutein dose was absorbed, and the major route of elimination was *via* feces. Also, lutein metabolism differs from that of β-carotene, and comparative study of the way that lipoproteins handle various carotenoids remains a fertile area for future research. The data presented in this feasibility study are from only one subject; therefore they should be interpreted with caution.
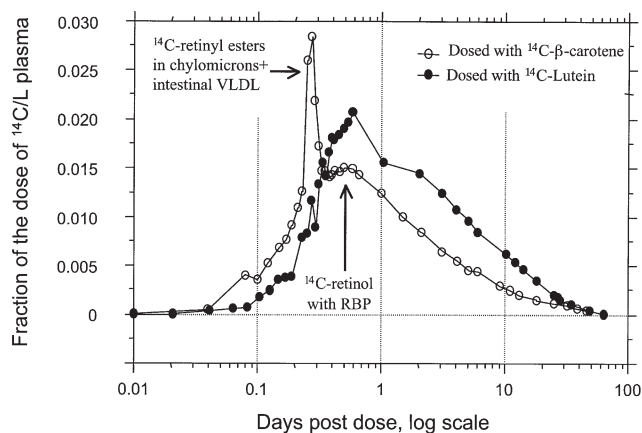
FIG. 4. Patterns of ^{14}C in plasma from oral ^{14}C-β-carotene (1 nmol) and ^{14}C-lutein (125 nmol) each in an oil-based banana cocktail to the same adult woman. Adapted from Reference 17. RBP, retinol-binding protein.

ACKNOWLEDGMENTS

REFERENCES

1. Sommerburg, O., Keunen, J.E., Bird, A.C., and van Kuijk, F.J. (1998) Fruits and Vegetables That Are Sources for Lutein and Zeaxanthin: The Macular Pigment in Human Eyes, *Br. J. Ophthalmol. 82*, 907–910.
2. Eye Disease Case–Control Study Group (1993) Antioxidant Status and Neovascular Age-Related Macular Degeneration, *Arch. Ophthalmol. 111*, 104–109.
3. Seddon, J.M., Ajani, U.A., Sperduto, R.D., Hiller, R., Blair, N., Burton, T.C., Farber, M.D., Gragoudas, E.S., Haller, J., Miller, D.T., *et al.* (1994) Dietary Carotenoids, Vitamins A, C, and E, and Advanced Age-Related Macular Degeneration. Eye Disease Case–Control Study Group, *JAMA 272*, 1413–1420.
4. Schalch, W., Dayhaw-Barker, P., and Barker, F. (1999) *The Carotenoids of the Human Retina*, CRC Press, Boca Raton, Florida.
5. Schalch, W. (1992) Carotenoids in the Retina—A Review of Their Possible Role in Preventing or Limiting Damage Caused by Light and Oxygen, in *Free Radicals and Aging* (Emerit, I., and Chance, B., eds.), pp. 280–298, Birkhauser Verlag, Basel, Switzerland.
6. Snodderly, D.M. (1995) Evidence for Protection Against Age-Related Macular Degeneration by Carotenoids and Antioxidant Vitamins, *Am. J. Clin. Nutr. 62*, 1448S–1461S.
7. Rapp, L.M., Maple, S.S., and Choi, J.H. (2000) Lutein and Zeaxanthin Concentrations in Rod Outer Segment Membranes from Perifoveal and Peripheral Human Retina, *Invest. Ophthalmol. Vis. Sci. 41*, 1200–1209.
8. Khachik, F., Beecher, G.R., and Smith, J.C., Jr. (1995) Lutein, Lycopene, and Their Oxidative Metabolites in Chemoprevention of Cancer, *J. Cell. Biochem. Suppl. 22*, 236–246.
9. Landrum, J.T., Bone, R.A., Joa, H., Kilburn, M.D., Moore, L.L., and Sprague, K.E. (1997) A One Year Study of the Macular Pigment: The Effect of 140 Days of a Lutein Supplement, *Exp. Eye Res. 65*, 57–62.

10. Bone, R.A., Landrum, J.T., Guerra, L.H., and Ruiz, C.A. (2003) Lutein and Zeaxanthin Dietary Supplements Raise Macular Pigment Density and Serum Concentrations of These Carotenoids in Humans, *J. Nutr. 133*, 992–998.

11. Liang, Y., White, W.S., Yao, L., and Serfass, R.E. (1998) Use of High-Precision Gas Isotope Ratio Mass Spectrometry to Determine Natural Abundance ^{13}C in Lutein Isolated from C_3 and C_4 Plant Sources, *J. Chromatogr. A. 800*, 51–58.

12. Yao, L., Liang, Y., Trahanovsky, W.S., Serfass, R.E., and White, W.S. (2000) Use of a ^{13}C Tracer to Quantify the Plasma Appearance of a Physiological Dose of Lutein in Humans, *Lipids 35*, 339–348.

13. Kelm, M.A., Flanagan, V.P., Pawlosky, R.J., Novotny, J.A., Clevidence, B.A., and Britz, S.J. (2001) Quantitative Determination of ^{13}C-Labeled and Endogenous β-Carotene, Lutein, and Vitamin A in Human Plasma, *Lipids 36*, 1277–1282.

14. Lienau, A., Glaser, T., Tang, G., Dolnikowski, G.G., Grusak, M.A., and Albert, K. (2003) Bioavailability of Lutein in Humans from Intrinsically Labeled Vegetables Determined by LC-APCI-MS, *J. Nutr. Biochem. 14*, 663–670.

15. Dueker, S.R., Jones, A.D., and Clifford, A.J. (1998) Protocol Development for Biological Tracer Studies, *Adv. Exp. Med. Biol. 445*, 363–378.

16. Dueker, S.R., Lin, Y., Buchholz, B.A., Schneider, P.D., Lame, M.W., Segall, H.J., Vogel, J.S., and Clifford, A.J. (2000) Long-term Kinetic Study of β-Carotene, Using Accelerator Mass Spectrometry in an Adult Volunteer, *J. Lipid Res. 41*, 1790–1800.

17. Burri, B.J., and Clifford, A.J. (2004) Carotenoid and Retinoid Metabolism: Insights from Isotope Studies, *Arch. Biochem. Biophys. 430*, 110–119.

18. Le Vuong, T., Buchholz, B.A., Lame, M.W., and Dueker, S.R. (2004) Phytochemical Research Using Accelerator Mass Spectrometry, *Nutr. Rev. 62*, 375–388.

19. Leenheer, A., Lambert, W., and Neils, H. (1992) *Modern Chromatographic Analysis of Vitamins*, 2nd edn., Marcel Dekker, New York.

20. Pella, E. (1990) Elemental Organic Analysis, *Am. Lab. 22*, 116–125.

21. Castenmiller, J.J., West, C.E., Linssen, J.P., van het Hof, K.H., and Voragen, A.G. (1999) The Food Matrix of Spinach Is a Limiting Factor in Determining the Bioavailability of β-Carotene and to a Lesser Extent of Lutein in Humans. *J. Nutr. 129*, 349–355.

22. Chung, H.Y., Rasmussen, H.M., and Johnson, E.J. (2004) Lutein Bioavailability Is Higher from Lutein-Enriched Eggs Than from Supplements and Spinach in Men, *J. Nutr. 134*, 1887–1893.

23. van het Hof, K.H., Brouwer, I.A., West, C.E., Haddeman, E., Steegers-Theunissen, R.P., van Dusseldorp, M., Weststrate, J.A., Eskes, T.K., and Hautvast, J.G. (1999) Bioavailability of Lutein from Vegetables Is 5 Times Higher Than That of β-Carotene, *Am. J. Clin. Nutr. 70*, 261–268.

24. Chitchumroonchokchai, C., Schwartz, S.J., and Failla, M.L. (2004) Assessment of Lutein Bioavailability from Meals and a Supplement Using Simulated Digestion and Caco-2 Human Intestinal Cells, *J. Nutr. 134*, 2280–2286.

25. Borel, P., Grolier, P., Armand, M., Partier, A., Lafont, H., Lairon, D., and Azais-Braesco, V. (1996) Carotenoids in Biological Emulsions: Solubility, Surface-to-Core Distribution, and Release from Lipid Droplets, *J. Lipid Res. 37*, 250–261.

26. Kostic, D., White, W.S., and Olson, J.A. (1995) Intestinal Absorption, Serum Clearance, and Interactions Between Lutein and β-Carotene When Administered to Human Adults in Separate or Combined Oral Doses, *Am. J. Clin. Nutr. 62*, 604–610.

27. Kurilich, A.C., Britz, S.J., Clevidence, B.A., and Novotny, J.A. (2003) Isotopic Labeling and LC-APCI-MS Quantification for Investigating Absorption of Carotenoids and Phylloquinone from Kale (*Brassica oleracea*), *J. Agric. Food Chem. 51*, 4877–4883.

28. Novotny, J.A., Kurilich, A.C., Britz, S.J., And Clevidence, B.A. (2005) Plasma Appearance of Labeled β-Carotene, Lutein, and Retinol in Humans After Consumption of Isotopically Labeled Kale, *J. Lipid Res. 46*, 1896–1903.

29. Lemke, S.L., Dueker, S.R., Follett, J.R., Lin, Y., Carkeet, C., Buchholz, B.A., Vogel, J.S., and Clifford, A.J. (2003) Absorption and Retinol Equivalence of β-Carotene in Humans Is Influenced by Dietary Vitamin A Intake, *J. Lipid Res. 44*, 1591–1600.

30. Clevidence, B.A., and Bieri, J. (1993) Association of Carotenoids with Human Plasma Lipoproteins, *Methods Enzymol. 214*, 33–46.

31. Reboul, E., Abou, L., Mikail, C., Ghiringhelli, O., Andre, M., Portugal, H., Jourdheuil-Rahmani, D., Amiot, M.J., Lairon, D., and Borel, P. (2005) Lutein Transport by Caco-2 TC-7 Cells Occurs Partly by a Facilitated Process Involving the Scavenger Receptor Class B Type I (SR-BI), *Biochem. J. 387*, 455–461.

32. Thurmann, P.A., Schalch, W., Aebischer, J.C., Tenter, U., and Cohn, W. (2005) Plasma Kinetics of Lutein, Zeaxanthin, and 3-Dehydro-lutein After Multiple Oral Doses of a Lutein Supplement, *Am. J. Clin. Nutr. 82*, 88–97.

33. Hartmann, D., Thurmann, P.A., Spitzer, V., Schalch, W., Manner, B., and Cohn, W. (2004) Plasma Kinetics of Zeaxanthin and 3'-Dehydro-lutein After Multiple Oral Doses of Synthetic Zeaxanthin, *Am. J. Clin. Nutr. 79*, 410–417.

34. Burri, B.J., Neidlinger, T.R., and Clifford, A.J. (2001) Serum Carotenoid Depletion Follows First-Order Kinetics in Healthy Adult Women Fed Naturally Low Carotenoid Diets, *J. Nutr. 131*, 2096–2100.

35. Rock, C.L., Swendseid, M.E., Jacob, R.A., and McKee, R.W. (1992) Plasma Carotenoid Levels in Human Subjects Fed a Low Carotenoid Diet, *J. Nutr. 122*, 96–100.

New Ceramides from *Rantherium suaveolens*

M. Habib Oueslati[a], Zine Mighri[a], H. Ben Jannet[a], and Pedro M. Abreu[b],*

[a]Laboratoire de Chimie des Substances Naturelles et de Synthèse Organique, Faculté des Sciences de Monastir, Monastir, Tunisie, and [b]REQUIMTE, Departamento de Química, Faculdade de Ciências e Tecnologia da Universidade Nova de Lisboa, 2829-516 Caparica, Portugal

ABSTRACT: A mixture of five new ceramides was isolated from the aerial parts of *Rantherium suaveolens* and characterized by spectroscopic and chemical methods. Their structures were elucidated by spectroscopic and chemical methods as (2*S*,3*S*, 4*R*,2'*R*,14*E*)-2-(2'-hydroxydocosanoylamino) - 14 - octadecene - 1,3,4-triol (**1**), (2*S*,3*S*,4*R*,2'*R*,14*E*)-2-(2´-hydroxytricosanoylamino)-14-octadecene-1,3,4-triol (**2**), (2*S*,3*S*,4*R*,2'*R*,14*E*)-2-(2'-hydroxytetracosanoylamino)- 14 - octadecene - 1,3,4 - triol (**3**), (2*S*, 3*S*,4*R*,2'*R*,14*E*) - 2 - (2' - hydroxypentacosanoylamino) - 14 - octadecene - 1,3,4-triol (**4**), and (2*S*,3*S*,4*R*,2'*R*,14*E*)-2-(2'-hydroxyhexacosanoylamino)-14-octadecene-1,3,4-triol (**5**).

Paper no. L9865 in *Lipids 40*, 1075–1079 (October 2005).

Rantherium suaveolens Desf. (Compositae), locally known as Arfej, is a perennial weedy shrub widely distributed in south Tunisia (1–3). As part of our work on bioactive substances from plant species growing in Tunisia (4–6), we have previously reported the isolation of polyacetyleneic alcohols, terpenoids, and coumarins from extracts of *R. suaveolens* (4,6). In this communication we describe the isolation of five new ceramides from the methanolic extract of *R. suaveolens* aerial parts.

EXPERIMENTAL PROCEDURES

Chromatographic and instrumental methods. Optical rotations were obtained using a PerkinElmer 241-MC polarimeter. FTIR spectra were measured on a PerkinElmer 157G IR spectrophotometer in KBr pellets. The NMR spectra were recorded on a Bruker ARX 400 NMR spectrometer (^{1}H at 400 MHz; ^{13}C at 100 MHz), using $CDCl_3$ and CD_3OD as solvents. FABMS was carried out on a Micromass Autospec spectrometer using glycerol as matrix. GC–MS was performed on an HP 5890 gas chromatograph–mass spectrometer in EI mode at 70 eV with an HP5-MS capillary column (30 m × 0.25 mm) packed with 5% diphenyl-polysiloxane/95% dimethyl-polysiloxane. Helium was used as carrier gas, and the column temperature was ramped from 80 to 250°C at 5°C/min.

Materials. Column chromatography (CC) and TLC were performed on silica gel (0.063–0.200 mm) and precoated silica gel F_{254} plates, respectively, both from Merck (Darmstadt, Germany).

Aerial parts of *R. suaveolens* were collected at Médenine (Tunisia) in May 2002, and identified by Dr. F. Harzallah-Skhiri from the Laboratoire de Biologie Végétale et Botanique, Ecole Supérieure d'Horticulture et d'Elevage de Chott Mériem, Université du Centre (Sousse, Tunisia). A voucher specimen (RS-100) is deposited at the Laboratoire de Chimie des Substances Naturelles et de Synthèse Organique, Faculté des Sciences de Monastir (Monastir, Tunisie).

Extraction and isolation. The air-dried aerial parts of *R. suaveolens* comprising leaves, stems, and flowers (2 kg) were powdered and extracted three times with 6 L of MeOH at room temperature for 3 wk (1 wk/extraction). The residue obtained after removal of the solvent *in vacuo* (316 g) was further extracted with EtOAc (2 L), and the resulting extract (32 g) was then submitted to gradient CC on silica gel by elution with petroleum ether/EtOAc (80:20–100% EtOAc) and EtOAc/MeOH (95:5–100% MeOH). The fraction representing 100% EtOAc elution (2.28 g) was subjected to silica gel CC ($CHCl_3$/MeOH 9:1, vol/vol) to yield five fractions (F_1–F_5). Recrystallization of F_3 from MeOH afforded the mixture of compounds **1–5** (26 mg), which showed a single spot on TLC plates.

Mixture 1–5. White amorphous powder; $[\alpha]^{25}_D$ = +27° (*c* = 2.0, $CHCl_3$). IR (KBr) v_{max} 3334, 3215 (OH), 2849, 2917, 1621 (N–C=O), 1544 (NH), 1466, 1277, 1021, 963, 722 cm^{-1}; ^{1}H and ^{13}C NMR data see Table 1; positive FABMS *m/z* (relative intensity, %): 710 [M_1 + H]$^+$ (1), 696 [M_2 + H]$^+$ (2), 682 [M_3 + H]$^+$ (8), 668 [M_4 + H]$^+$ (3), 654 [M_5 + H]$^+$ (2), 316 [C_3H_7–CH=CH–$(CH_2)_9$–CH(OH)–CH(OH)–CH(CH_2OH)–NH_3]$^+$ (100), 185 (12).

Acetylation of 1–5. A solution of the mixture **1–5** (8 mg) in pyridine (1 mL) was treated with acetic anhydride (1 mL) and allowed to stand overnight at room temperature. The reaction mixture was then diluted with water (5 mL) and extracted with ($CHCl_3$, 3 × 10 mL). The residue obtained from the organic phase was subjected to silica gel CC (hexane/EtOAc 7:3, vol/vol) to afford 9.8 mg of the peracetate mixture **1a–5a**. White amorphous powder; IR (KBr) v_{max} 2924, 2854, 1748 (–COCH$_3$), 1694 (N–C=O), 1532 (N–COCH$_3$), 1465, 1370, 1226, 1045; ^{1}H and ^{13}C NMR data see Table 1; positive FABMS *m/z* (relative intensity, %): 878 [M_1 + H]$^+$ (4), 864 [M_2 + H]$^+$ (4), 850 [M_3 + H]$^+$ (11), 836 [M_4 + H]$^+$ (5), 832 [M_3 – AcOH + H]$^+$ (5), 822 [M_5 + H]$^+$ (5), 818 [M_1 – AcOH + H]$^+$ (15), 804 [M_2 – AcOH + H]$^+$ (21), 790 [M_3 – AcOH + H]$^+$ (65), 776 [M_4 – AcOH + H]$^+$ (11), 763 [M_5 – AcO + H]$^+$ (16), 762 [M_5 – AcOH + H]$^+$ (35), 262 [$C_{18}H_{31}N$ + H]$^+$ (100).

*To whom correspondence should be addressed. E-mail: pma@dq.fct.unl.pt
Abbreviations: CC, column chromatography; HMBC, heteronuclear multiple bond correlation; LCB, long-chain base; MTPA, α-methoxy-α-(trifluoromethyl)phenylacetyl acid.

Table 1
^{1}H and ^{13}C NMR Spectral Data of Mixtures 1–5^a and 1a–5a^b

Position	1–5 δ_H	1–5 δ_C	1a–5a δ_H	1a–5a δ_C
1a, 1b	3.69 (*dd*, 14.4, 3.9), 3.69 (*dd*, 14.4, 4.5)	61.3	3.99 (*d*, 11.5), 4.33 (*dd*, 11.2, 6.2)	62.3
2	4.04 (*m*)	51.8	4.42 (*m*)	47.8
3	3.98 (*m*)	72.4	5.08 (*m*)	72.5
4	3.47 (*m*)	72.2	4.94 (*m*)	72.2
5a, 5b	1.36 (*m*), 1.70 (*m*)	34.7	1.69 (*m*)	32.1
6	1.36 (*m*)	25.4	1.24 (*m*)	24.8
7–12	1.20 (*m*)	29.5–32.1	1.20–1.30	28.1–31.9
13	1.90 (*m*)	33.1		
14	5.34 (*m*)	130.0	5.36 (*m*)	129.2
15	5.34 (*m*)	132.1	5.36 (*m*)	131.1
16	1.90 (*m*)	32.8	2.03 (*m*)	32.5
17	1.20 (*m*)	26.1		25.5
18	0.82 (*t*, 6.4)	14.2	0.86 (*t*, 6.4)	14.1
1′		176.1		170.8
2′	3.47 (*m*)	75.7	5.11 (*m*)	74.0
3′a, 3′b	1.36 (*m*), 1.70 (*m*)	32.8	1.82 (*m*)	32.1
4′	1.36 (*m*)	22.9	1.24 (*m*)	22.3
5′–28′	1.20 (*m*)	29.5–32.1	1.20–1.30	28.1–31.9
Terminal CH$_3$	0.82 (*t*, 6.4)	14.2	0.83 (*t*, 6.4)	14.1
NH			6.60 (*d*, 8.9)	
<u>CH$_3$</u>CO			2.01–2.17	20.7–20.9
CH$_3$<u>C</u>O				170.0–171.2

^{a}In MeOD/CDCl$_3$.
^{b}In CDCl$_3$.

*Methanolysis of **1–5***. The mixture **1–5** (12 mg) was dissolved in 1 mL MeOH containing 4 mL of 1 N HCl and refluxed for 18 h (7). The reaction mixture was neutralized with NaHCO$_3$ and extracted with hexane (3 × 10 mL). The hexane fraction was purified by silica gel CC using hexane/EtOAc (9:1, vol/vol) as eluent, to yield a 5.6 mg mixture of FAME (6), which were identified by GC–MS as methyl-2-hydroxydocosanoate {*m/z* 370 [M]$^+$ (40%)}, methyl-2-hydroxytricosanoate {*m/z* 384 [M]$^+$ (40%)}, methyl-2-hydroxytetracosanoate {*m/z* 398 [M]$^+$ (25%)}, methyl-2-hydroxypentacosanoate {*m/z* 412 [M]$^+$ (1%)}, and methyl-2-hydroxyhexacosanoate {*m/z* 424 [M]$^+$ (9%)}. [α]$^{25}_D$ = +9° (*c* = 1.4, CHCl$_3$); ^{1}H NMR (400 MHz, CDCl$_3$) δ 0.87 (*t*, *J* = 7.0 Hz, CH$_3$), 1.25 (*brs*, CH$_2$), 3.78 (*s*, OCH$_3$), 4.18 (*m*, H-2′); ^{13}C NMR (100 MHz, CDCl$_3$) δ 14.1 (CH$_3$), 22.7 (CH$_2$), 24.7 (CH$_2$), 29.3 (CH$_2$), 29.5 (CH$_2$), 31.8 (CH$_2$), 34.4 (CH$_2$), 52.4 (OCH$_3$), 70.5 (CHOH), 175.9 (CO). The MeOH/H$_2$O phase was evaporated and the residue acetylated as previously described. Purification by silica gel CC (hexane/EtOAc 6:4, vol/vol) yielded 3.8 mg of the tetraacetylated long-chain base (LCB) (2S,3S,4R,14E)-2-acetamido-1,3,4-triacetoxy-14-octadecene (**9**). White amorphous powder; [α]$^{25}_D$ = +27° (*c* = 1.5, CHCl$_3$); ^{1}H NMR (400 MHz, CDCl$_3$) δ 0.87 (*t*, *J* = 7.0 Hz, CH$_3$), 1.25–1.31 [*m*, (CH$_2$)$_n$], 2.02 (*s*, COCH$_3$), 2.04 (*s*, COCH$_3$), 2.07 (*s*, COCH$_3$), 3.99 (*d*, *J* = 11.2 Hz, H-1a), 4.33 (*dd*, *J* = 11.2, 6.2 Hz, H-1b), 4.46 (*m*, H-2), 4.93 (*d*, *J* = 9.2 Hz, H-4), 5.09 (*d*, *J* = 7.6 Hz, H-3), 5.37 (*m*, H-13, H-14), 5.98 (*d*, *J* = 8.8 Hz, NH); EI-MS (70 ev) *m/z* (relative intensity, %) 483 [M]$^+$ (5), 423 [M – AcOH]$^+$ (30), 364 [M – 2AcOH – H]$^+$ (28), 184 (57), 144 (76), 83 [C$_6$H$_{11}$]$^+$ (100).

*(R)-α-Methoxy-α-(trifluoromethyl)phenylacetyl acid (MTPA) esters of FAME (**6a**)*. To a solution of FAME (4 mg) in CH$_2$Cl$_2$ (5 mL) was added *N*,*N*-dimethylaminopyridine (0.24 mg, 0.2 μmol), dicyclohexylcarbodiimide (3.71 mg, 18 μmol), and (*R*)-MTPA (2.8 mg, 12 μmol). After heating overnight with stirring and gentle reflux, the reaction mixture was filtered, diluted with CH$_2$Cl$_2$ (25 mL), and washed with 1 M NaHCO$_3$ (2 × 20 mL). The organic layer was collected, dried over anhydrous MgSO$_4$, filtered, and concentrated *in vacuo*. The residue was purified by silica gel CC with hexane/EtOAc 9:1 (vol/vol) elution, to afford the corresponding Mosher esters. ^{1}H NMR (400 MHz, CDCl$_3$) δ 0.85 (*t*, *J* = 7.2 Hz, CH$_3$), 1.34–1.18 [*m*, (CH$_2$)$_n$], 1.57 (*m*, H-5′), 1.75 (*m*, H-4′), 1.83 (*m*, H-3′), 3.65 (*s*, OCH$_3$), 3.78 (*s*, OCH$_3$), 5.16 (*t*, *J* = 6.4 Hz, H-2′), 7.4–7.6 (5 aromatic H).

*(R)-MTPA esters of (S,R)-hydroxycaproic methyl ester (**7,8**)*. A solution of a racemic mixture of hydroxycaproic acid (12 mg) in MeOH (5 mL) was methylated with diazomethane according to a described procedure (8) and then reacted with (*R*)-MTPA, as described above, to yield the (*R*)-MTPA ester of (*S*)- and (*R*)-hydroxycaproic methyl esters (**7** and **8**, respectively). ^{1}H NMR (400 MHz, CDCl$_3$) δ 0.81 (*t*, *J* = 7.2 Hz, CH$_3$), 0.85 (*t*, *J* = 7.2 Hz, CH$_3$), 1.92–1.20 [*m*, (CH$_2$)$_n$], 3.56 (*s*, COOCH$_3$), 3.65 (*s*, COOCH$_3$), 3.74 (*s*, OCH$_3$), 3.78 (*s*, COOCH$_3$), 5.17 (*m*, H-2), 7.4–7.6 (10 aromatic H).

RESULTS AND DISCUSSION

Bioguided fractionation of the MeOH extract of *R. suaveolens* aerial parts, using the brine shrimp lethality assay (9) followed

SCHEME 1

1-5   R = H, m = 18 to 25
1a-5a   R =Ac

6   FAME, R = H
6a R = (R)-MTPA

9 Acetylated LCB
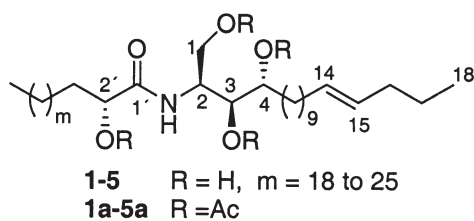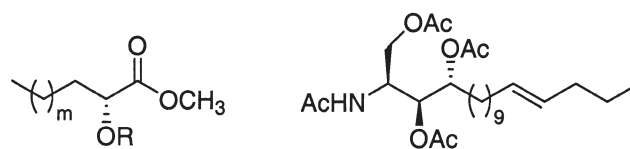
SCHEME 2

by silica gel CC of the EtOAc active fraction (ED_{50} 14 µg/mL), led to the isolation of a white solid (ED_{50} 2.3 µg/mL) whose positive-ion FABMS displayed a cluster of five 14-amu-apart quasimolecular ion peaks $[M + H]^+$ at *m/z* 710, 696, 682, 668, and 654, indicative of a mixture of homologous compounds (**1–5**) (Scheme 1). The NMR data (Table 1), including COSY, distortionless enhancement by polarization transfer, heteronuclear multiple bond connectivity, and heteronuclear multiple bond correlation (HMBC) experiments allowed the identification of a vicinal secondary diol at δ_H 3.47 (δ_C 72.2) and 3.98 (δ_C 72.4), a primary alcohol at δ_H 3.69 (δ_C 61.3) placed on a nitrogenated methine [δ_C 51.8 (δ_H 4.04)], a third secondary alcohol [δ_H 3.47 (δ_C 75.7)] vicinal to a carbonyl at δ_C 176.1, a double bond at δ_C 130.0 (δ_H 5.34) and 132.1 (δ_H 5.34), and characteristic signals for long alkyl chains [δ_H 1.25–1.40 (δ_C 14.2–33.1)]. The IR spectrum revealed the absorption bands of hydroxyls at 3334 and 3215 cm^{-1}, and a secondary amide at 1544 and 1621 cm^{-1}. The aforementioned spectral data were in good agreement with those reported for phytosphingosine-type ceramides possessing a 2-hydroxyl fatty acyl moiety (10–15). The base peak at *m/z* 316 in the FABMS, and the lack of corresponding signals differing from 14 amu suggested the occurrence of a common C-18 LCB [$C_{14}H_{27}$–CH(OH)–CH(OH) –CH(CH_2OH)–NH–] in the structures of **1–5** (15,16). The position of the double bond could be deduced from the following evidence: The methyl protons at δ 0.82 showed ^2J and ^3J HMBC correlations with carbons at δ 26.1 (C-17) and 32.8 (C-16), whereas HMBC and COSY cross signals were observed between C-16 and the olefinic proton at δ 5.34 (H-15), and between H-15 and H-16, respectively. The *E* stereochemistry of the double bond was determined on the basis of the ^{13}C NMR chemical shift of the methylene carbons adjacent to the olefinic carbons, which is observed at $\delta \approx 27$ in *Z* isomers and at $\delta \approx 32$ in *E* isomers (17,18). The acetylation of **1–5** improved the resolution of the ^1H NMR spectrum (Table 1), when compared with that of the natural mixture, allowing the separation of the methylene proton signals of the primary acetate (δ 3.99 and 4.33 ppm), as well as the multiplets displayed by the methine protons H-3 (δ 5.08), H-4 (δ 4.94), and H-2´ (δ 5.11). The nitrogen proton of **1a–5a** (Scheme 1) appeared as a doublet (*J* = 8.9) at δ 6.60, coupled to H-2 (δ 4.42). 2D NMR experiments corroborated all the assignments previously deduced for **1–5**.

The structures and configuration of acyl and alkyl chains were confirmed by the analysis of the FAME mixture **6**, and the LCB resulting from methanolysis of **1–5** (Scheme 2). The GC–MS of **6** showed the presence of five constituents, which

were identified as methyl-2-hydroxydocosanoate (*m/z* 370 $[M]^+$), methyl-2-hydroxytricosanoate (*m/z* 384 $[M]^+$), methyl-2-hydroxytetracosanoate (*m/z* 398 $[M]^+$), methyl-2-hydroxypentacosanoate (*m/z* 412 $[M]^+$), and methyl-2-hydroxyhexacosanoate (*m/z* 424 $[M]^+$). The assignment of the (R) configuration at C-2´ was concluded by comparing the methyl ester proton resonances (δ 3.65) of the (R)-MTPA esters of the FAME mixture **6a** with those of the (R)-MTPA esters of (S,R)-hydroxycaproic methyl ester (**7** and **8**) (Schemes 2 and 3). As expected from the Mosher's experiment (19–21), the chemical shift of this methyl group should be at higher field in compound **7**, due the shielding effect of the MTPA aromatic ring. Although the configuration of 2-hydroxy FA resulting from ceramide methanolysis is often determined on the basis of the sign of the corresponding optical rotation, a survey of the literature revealed several examples with *R* configuration associated either with a positive (11,13,18,22) or with a negative optical rotation (14,23–28). The method here used also allowed confirmation of the same configuration for the homologous fatty acyl chains, as evidenced by the fact that only one methyl ester peak is displayed in the ^1H NMR of mixture **6a**.

The structure of the LCB moiety was confirmed by the MS and ^1H NMR data of its peracetylated derivative **9**. The EI-MS spectrum displayed the molecular ion at *m/z* 423 corresponding to $C_{26}H_{45}O_7N$, and the base peak at *m/z* 83 $[C_6H_{11}]^+$ resulting from the β-cleavage of the double bond. The proton chemical shifts of the fragment [–CH(OAc)–CH(OAc)–CH-(CH_2OAc)–NHAc–] (see the Experimental Procedures section) are in good agreement with those reported for the tetraacetate of (2S,3S,4R) sphingosine (22), and analogs with the same configuration at C-2, C-3, and C-4 (10,29,30). The optical rotation

δ 3.65 δ 3.56 δ 3.65

6a   7   8

6a (R)-MTPA ester of FAME
7 (R)-MTPA ester of (S)-hydroxycaproic methyl ester
8 (R)-MTPA ester of (R)-hydroxycaproic methyl ester
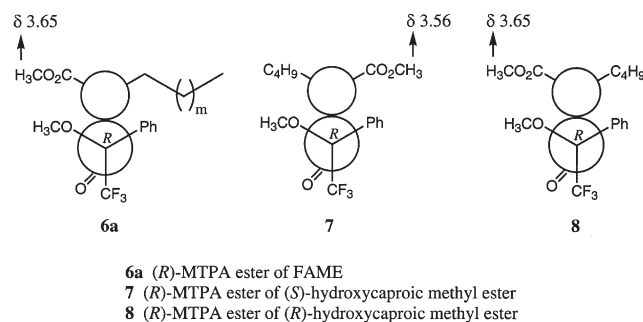
SCHEME 3

of **9** ($[\alpha]^{25}_D = +27°$) is also identical to those of natural and synthetic sphingamine tetraacetates with the same configuration (22,30,31). To the best of our knowledge, this is the first reported isolation of ceramides that comprise an LCB with a configuration 2*S*,3*S*,4*R*,14*E*.

Ceramides are key sphingolipid metabolites, which are emerging as therapeutics with clear clinical potential, owing to their role as second messengers for various cellular processes including cell cycle arrest, differentiation, senescence, apoptosis, and others (32–37). In plants, recent studies indicate that they may be involved in signal transduction, membrane stability, host–pathogen interactions, and stress responses (38). Since the ceramide bioactivity is governed by its configuration (39), the new compounds here isolated should be further studied for their biological properties to deduce possible structure–activity relationships.

ACKNOWLEDGMENT

REFERENCES

1. Alapetite, G.P. (1981) *Flora of Tunisia*, Tunisian Scientific Publications, Official Press, Republic of Tunisia, Tunis, Tunisia.
2. le Floc'h, E. (1983) *Contribution to an Ethnobotanical Study of the Tunisian Flora*, pp. 82–83, Tunisian Scientific Publications, Official Press, Republic of Tunisia, Tunis, Tunisia.
3. Issaoui, A., Kallala, A., Naffeti, M., and Akrimi, N. (1996) *Plants from South Tunisia*, Ministry of the Environment and Territorial Management, p. 174, State Secretariat of Scientific Research and Technology, Tunisia.
4. Oueslati, M.H., Ben Jannet, H., Abreu, P.J.M., and Mighri, Z. (2004) Alcools tetrahydropyraniques polyacetyleniques antibacteriens de la plante *Rantherium suaveolens* poussant dans le sud Tunisien, *J. Soc. Alger. Chim. 14*, 245–258.
5. Braham, H., Mighri, Z., Ben Jannet, H., Matthew, S., and Abreu, P.M. (2005) Antioxidant Phenolic Glycosides from *Moricandia arvensis*, *J. Nat. Prod. 68*, 517–522.
6. Oueslati, M.H., Ben Jannet, H., Abreu, P.J.M., and Mighri, Z. (2006) A New C₉ *nor*-Isoprenoid Glucoside from *Rantherium suaveolens*, *Nat. Prod. Res.*, in press.
7. Gaver, R.C., and Sweeley, C.C. (1965) Methods for Methanolysis of Sphingolipids and Direct Determination of Long-Chain Bases by Gas Chromatography, *J. Am. Oil Chem. Soc. 42*, 294–298.
8. Vogel, A. (1978) *Vogel's Textbook of Practical Organic Chemistry*, 4th edn., pp. 292, Longman, London.
9. McLaughlin, J.L. (1991) Crown Gall Tumours on Potato Discs and Brine Shrimp Lethality: Two Simple Bioassays for Higher Plant Screening and Fractionation, in *Methods in Plant Biochemistry* (Hostettman, K., ed.), Vol. 6, pp 1–32, Academic, London.
10. Krishna, N., Muralidhar, P., Kumar, M.M., Rao, D.V., and Rao, C.B. (2004) New Sphingosines from a Gorgonian, *Pseudopterogorgia australiensis* Ridley, of the Indian Ocean, *J. Nat. Prod. 67*, 1423–1425.
11. Zhan, Z.-J., and Yue, J.-M. (2003) New Glyceroglycolipid and Ceramide from *Premna microphylla*, *Lipids 38*, 1299–1303.
12. Qi, S.-H., Wu, D.-G., Zhang, S., and Luo, X.-D. (2003) A New Tetranortriterpenoid from *Dysoxylum lenticellatum*, *Z. Naturforsch. 58b*, 1128–1132.
13. Gao, J.-M., Dong, Z.-J., and Liu, J.-K. (2001) A New Ceramide from the Basidiomycete *Russula cyanoxantha*, *Lipids 36*, 175–180.
14. Loukaci, A., Bultel-Poncé, V., Longeon, A., and Guyot, M. (2000) New Lipids from the Tunicate *Cystodytes* cf. *dellechiajei*, as PLA2 Inhibitors, *J. Nat. Prod. 63*, 799–802.
15. Asai, N., Fusetani, N., Matsunaga, S., and Sasaki, J. (2000) Sex Pheromones of the Hair Crab *Erimacrus isenbeckii*. Part 1: Isolation and Structures of Novel Ceramides, *Tetrahedron 56*, 9895–9899.
16. Rubino, F.M., Zecca, L., and Sonnino, S. (1994) Characterization of Complex Mixture of Ceramides by Fast Atom Bombardment and Precursor and Tandem Mass Spectrometry, in *Mass Spectrometry*, *Biol. Mass Spectrom. 23*, 82–90.
17. Rossi, R., and Veracini, C.A. (1982) Insect Pheromone Components. Use of ¹³C NMR Spectroscopy for Assigning the Configuration of C=C Double Bonds of Monoenic or Dienic Pheromone Components and for Quantitative Determination of *Z*/*E* Mixtures, *Tetrahedron 38*, 629–644.
18. Cateni, F., Zilic, J., Falsone, G., Scialino, G., and Banfi, E. (2003) New Cerebrosides from *Euphorbia peplis*, L.: Antimicrobial Activity Evaluation, *Bioorg. Med. Chem. Lett. 15*, 4345–4350.
19. Dale, J.A., and Mosher, H.S. (1973) Nuclear Magnetic Resonance Enantiomer Reagents. Configurational Correlations *via* Nuclear Magnetic Resonance Chemical Shifts of Diastereomic Mandelate, *O*-Methylmandelate, and α-Methoxy-α-trifluoromethylphenylacetate (MTPA) Esters, *J. Am. Chem. Soc. 95*, 512–519.
20. Rasmussen, H.B., Christensen, S.B., Kvist, L.P., Kharazmi, A., and Huansi, A.G. (2000) Absolute Configuration and Antiprotozoal Activity of Minquartynoic Acid, *J. Nat. Prod. 63*, 1295–1296.
21. Seco, J.M., Quiñoá, E., and Riguera, R. (2001) A Practical Guide for the Assignment of the Absolute Configuration of Alcohols, Amines and Carboxylic Acids by NMR, *Tetrahedron: Asymmetry 12*, 2915–2925.
22. Su, B.-N., Misico, R., Park, E.J., Santarsiero, B.D., Mesecar, A.D., Fong, H.H.S., Pezzuto, J.M., and Kinghorn, A.D. (2002) Isolation and Characterization of Bioactive Principles of the Leaves and Stems of *Physalis philadelphica*, *Tetrahedron 58*, 3453–3466.
23. Liu, J.-K., Hu, L., and Dong, Z.-J. (2003) A Glucosylceramide with a Novel Ceramide and Three Ceramides from the Basidiomycete *Cortinarius umidicola*, *Lipids 38*, 669–675.
24. De Vivar, M.E.D., Seldes, A.M., and Maier, M.S. (2002) Two Novel Glucosylceramides from Gonads and Body Walls of the Patagonian Starfish *Allostichaster inaequalis*, *Lipids 37*, 597–603.
25. Costantino, V., Fattorusso, E., Mangoni, A., Di Rosa, M., Ianaro, A., and Maffia, A. (1996) Glycolipids from Sponges. IV. Immunomodulating Glycosyl Ceramides from the Marine Sponge *Agelas dispar*, *Tetrahedron 52*, 1573–1578.
26. Li, H.-y., Matsunaga, S., and Fusetani, N. (1995) Halicylindrosides, Antifungal and Cytotoxic Cerebrosides from the Marine Sponge *Halichondria cylindrata*, *Tetrahedron 51*, 2273–2280.
27. Jin, W., Rinehart, K.L., and Jares-Erijman, E. (1994) Ophidiacerebrosides: Cytotoxic Glycosphingolipids Containing a Novel Sphingosine from a Sea Star, *J. Org. Chem. 59*, 144–147.
28. Iguchi, R., Natori, T., and Komori, T. (1990) Isolation and Characterization of Acanthacerebroside B and Structure Elucidation of Related, Nearly Homogenous Cerebrosides, *Liebigs Ann. Chem.*, 51–55.
29. Sugiyama, S., Honda, M., and Komori, T. (1988) Asymmetric Synthesis of Phytosphingosine and Phytosphingosine Anhydro Base: Assignment of the Absolute Stereochemistry, *Liebigs Ann. Chem.*, 619–625.

30. Sugiyama, S., Honda, M., Higuchi, R., and Komori, T. (1991) Stereochemistry of the Four Diastereomers of Ceramide and Ceramide Lactoside, *Liebigs Ann. Chem.*, 349–356.

31. Murakami, T., and Taguchi, K. (1999) Stereocontrolled Synthesis of Novel Phytosphingosine-type Glucosaminocerebrosides, *Tetrahedron 55*, 989–1004.

32. Cremesti, A.E., and Fischi, A.S. (2000) Current Methods for the Identification and Quantitation of Ceramides: An Overview, *Lipids 35*, 937–945.

33. Kester, M., and Kolesnick, R. (2003) Sphingolipids as Therapeutics, *Pharmacol. Res. 47*, 365–371.

34. Sot, J., Goñi, F.M., and Alonso, A. (2005) Molecular Associations and Surface-Active Properties of Short- and Long-*N*-Acyl Chain Ceramides, *Biochim. Biophys. Acta 1711*, 12–19.

35. Stoica, B.A., Movsesyan, V.A., Knoblach, S.M., and Faden, A.I. (2005) Ceramide Induces Neuronal Apoptosis Through Mitogen-Activated Protein Kinases and Causes Release of Multiple Mitochondrial Proteins, *Mol. Cell. Neurosci. 29*, 355–371.

36. Azuma, H., Takao, R., Niiro, H., Shikata, K., Tamagaki, S., Tachibana, T., and Ogino, K. (2003) Total Syntheses of Symbioramide Derivatives from L-Serine and Their Antileukemic Activities, *J. Org. Chem. 68*, 2790–2797.

37. Aouali, N., Eddabra, L., Macadré, J., and Morjani, H. (2005) Immunosuppressors and Reversion of Multidrug-Resistance, *Crit. Rev. Oncol. Hematol.*, *56,* 61–70.

38. Sperling, P., and Heinz, E. (2003) Plant Sphingolipids: Structural Diversity, Biosynthesis, First Genes and Functions, *Biochim. Biophys. Acta 1632*, 1–15.

39. Jiang, H., Huang, X., Nakanishi, K., and Berova, N. (1999) Nanogram Scale Absolute Configurational Assignment of Ceramides by Circular Dichroism, *Tetrahedron Lett. 40*, 7645–7649.

REVIEW

Astonishing Diversity of Natural Surfactants: 6. Biologically Active Marine and Terrestrial Alkaloid Glycosides

Valery M. Dembitsky*

Department of Organic Chemistry and School of Pharmacy, Hebrew University, Jerusalem, Israel

ABSTRACT: This review article presents 209 alkaloid glycosides isolated and identified from plants, microorganisms, and marine invertebrates that demonstrate different biological activities. They are of great interest, especially for the medicinal and/or pharmaceutical industries. These biologically active glycosides have good potential for future chemical preparation of compounds useful as antioxidants, anticancer, antimicrobial, and antibacterial agents. These glycosidic compounds have been subdivided into several groups, including: acridone; aporphine; benzoxazinoid; ergot; indole; enediyne alkaloidal antibiotics; glycosidic lupine alkaloids; piperidine, pyridine, pyrrolidine, and pyrrolizidine alkaloid glycosides; glycosidic quinoline and isoquinoline alkaloids; steroidal glycoalkaloids; and miscellaneous alkaloid glycosides.

Paper no. L9870 in *Lipids 40*, 1081–1105 (November 2005).

Alkaloids are alkaline compounds containing nitrogen. Many of these natural products are derived from amino acids, and an enormous number of bitter, nitrogenous compounds are included in this group. More than 18,000 different alkaloids have been discovered in representatives of over 300 plant families, microorganisms, fungi, marine invertebrates, insects, amphibians, and other organisms (2–9). Alkaloids often contain one or more rings of carbon atoms, usually with a nitrogen atom in the ring. The position of the nitrogen atom in the carbon ring varies with different alkaloids and with different plant families, microorganisms, and/or invertebrates. In fact, it is the precise position of the nitrogen atom that affects the properties of these alkaloids (2–7).

Marine natural products are small- to medium-M.W. compounds produced by marine plants, invertebrates, and microorganisms that have stimulated interdisciplinary studies by chemists and biologists (10–12). Invertebrates such as sponges, soft corals, molluscs, coelenterates, and ascidians produce secondary metabolites of unusual structures; sponges and ascidians in particular produce nitrogen-containing substances, usually called "marine alkaloids." Novel classes of marine alkaloids have been found to interact with key aspects of the cell cycle, enzymes or other targets and lead to insights into new therapeutics. The study of biologically active marine alkaloids has profoundly influenced the course of discovery in fields ranging from pharmacology to oncology (11,12). State-of-the-art studies in molecular genetics, enzymology, and biochemistry address the issues of biosynthesis of marine natural products by identifying and sequencing the genes involved in transcription-translation and regulation of their cognate enzymes (5,6). The future promises heterologous expression of important marine natural products through manageable microbial fermentation (13–15).

The total synthesis of terrestrial and marine natural alkaloids aims for no less than total control of bond construction and stereochemistry of complex molecules from simple starting materials. New methods for building carbon–carbon bonds and managing heteroatom reactivity lie at the cutting edge of organic synthesis (16–20).

Alkaloid glycosides, a specific group of water-soluble terrestrial and marine natural compounds, can be subdivided into several groups, presented in this review, including: acridone, aporphine, benzoxazinoid, ergot, indole, quinoline, isoquinoline, piperidine, glycosidic lupine alkaloids, steroidal glycoalkaloids, and miscellaneous alkaloid glycosides.

ACRIDONE ALKALOIDS

Acridone alkaloids constitute a small group of natural products found exclusively in the family Rutaceae, including *Citrus, Glycosmis*, and *Severinia* species (21). They exhibit a wide range of pharmacological activities including cytotoxicity, which is presumed to be exerted by the inhibition of topoisomerase-II (22), an intracellular enzyme. These compounds, as well as their analogs and derivatives, have been tested for their antimicrobial activities and effects on mammalian cells (23). Acronycine has been tested for antitumor properties (24,25), and acronycine analogs were reported to be effective against *Trichomonas vaginalis* (26). Thirty acridone alkaloids were evaluated for their antiplasmodial activities in a rodent model (24). Seven of the alkaloids in the series had activities equivalent to that of chloroquine against *Plasmodium yoelii*. Atalaphillinine was effective as a prophylactic agent against *P. berghei* and *P. vinckie* infections in mice. Acridone alkaloids isolated from *Boenninghausenia japonica* (Rutaceae) showed antiproliferative activity against human gastric adenocarcinoma (MK-1), human uterine carcinoma (HeLa), and murine melanoma (B16F10) cells (27). The acridone alkaloid

*Address correspondence at Department of Organic Chemistry, P.O. Box 39231, Hebrew University, Jerusalem 91391, Israel.
E-mail: dvalery@cc.huji.ac.il
For the previous article in this series, see Reference 1.
Abbreviations: DIBOA, 2,4-dihydroxy-1,4-benzoxazin-3(4H)-one; SGA, steroidal glycoalkaloids; THIQM, tetrahydroisoquinolinemonoterpene.

acronycine, isolated from several *Sarcomelicope* species (Rutaceae) exhibited promising activity against a broad spectrum of solid tumors (28).

Only a few glycosides of acridone alkaloids have been isolated from the family Rutaceae. Gravacridonediol **1** and gravacridonetriol **2** were identified from a methanol extract of roots of *Ruta graveolens* (29,30), and gravacridonediol **1** also was found in *Boenninghausenia albiflora* callus tissue (31). Acridone derivatives have been identified in the extracts of the roots of *Thamnosma rhodesica* (Rutaceae) (32). This study was the first to report rhodesiacridone, one of these acridone derivatives. This novel compound showed activities against the intracellular form of the protozoan parasite *Leishmania major*, a human pathogen. Gravacridonediol **1** and 1-hydroxy-10-methylacridone exhibited activities against the intracellular form of the same parasite and the fungus *Cladosporium cucumerinum*, respectively (32). A new compound, gravacridonol monoglucoside **3**, and gravacridonediol **1** were identified from cell suspension cultures of *T. montana* grown in Gamborg B5 medium (32). The *in vitro* activities of furo[2,3b]quinoline and acridone alkaloids **4** and **5** against *Plasmodium falciparum* were evaluated by an isotopic semimicrotest. A pyran ring in the furoquinoline nucleus and 2-*O*-pyrano-glycoside substituents in the acridone nucleus improved the antimalarial activities of the compounds. These features provide a suggestion for further chemical modifications (33).
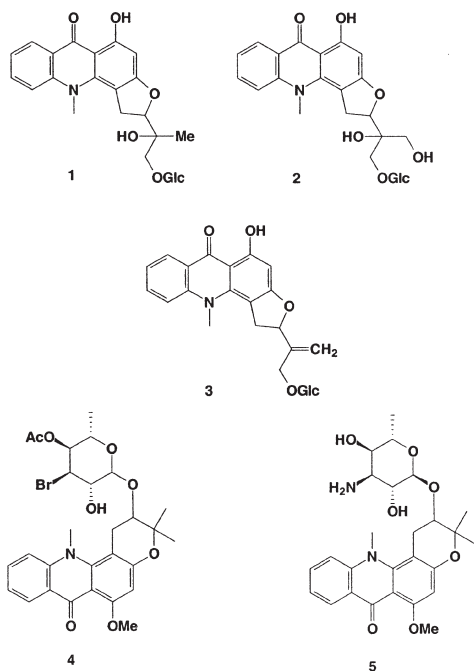
APORPHINE ALKALOID GLYCOSIDES

Aporphine alkaloids form an important group of secondary plant metabolites. They are also derived biogenetically from anthranilic acid. Some of these compounds have been used for many years in traditional medicine for the treatment of various diseases, from benign syndromes to more severe illnesses. More than 500 aporphine alkaloids have been isolated from various plant families, and many of these compounds display potent cytotoxic activities, which may be exploited for the design of anticancer agents (34).

Aporphine glycosides, stesakine-9-*O*-β-D-glucopyranoside **6** and *N*-methyl-asimilobine-2-*O*-β-D-glucopyranoside **7**, were isolated from the seeds of *Stephania cepharantha* cultivated in Japan (35). Compound **7**, previously known as floripavidine, was isolated from *Papaver floribundum* in 1976 by Russian scientists (36). Kamaline **8**, incorporating a novel urethane moiety and a glucoside unit, was isolated from *Stephania venosa* grown in India (37). Tubers of the Chinese medicinal herb *Aristolochia tuberosa* yielded two 4,5-dioxoaporphine alkaloids, 11-hydroxy-tuberosinone-*N*-β-D-glucoside **9** (also known as Zhu Sha Lian glucoside; 38) and tuberosinone-*N*-β-D-glucoside **10** (39). Aristololactam II *N*-β-D-glucopyranoside **11** (or cepharanone A *N*-β-D-glucoside) was isolated from *Aristolochia clematitis* grown in Czechia (40).
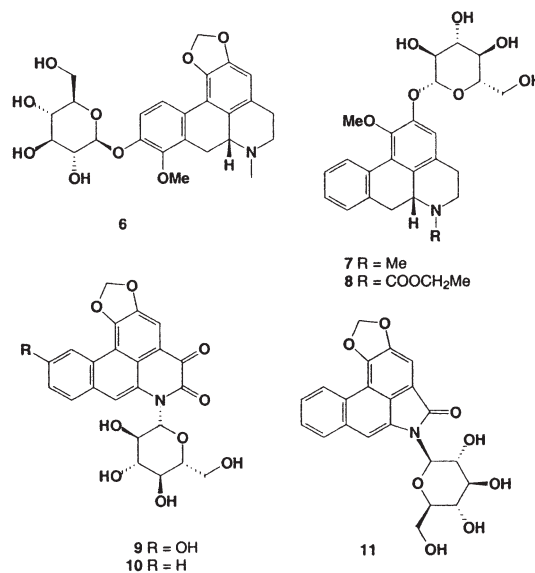
BENZOXAZINOID ALKALOID GLUCOSIDES

Benzoxazinoid acetal glucosides [having 2-hydroxy-2H-1,4-benzoxazin-3(4H)-one skeleton] are a unique class of natural products abundant in family of Gramineae, including the major agricultural crops maize, wheat, rye, and wild grasses (41). Also they are found in different species of Acanthaceae (42,43), Ranunculaceae (44), Scrophulariaceae (45), and others. Benzoxazinoids serve as important factors of host plant resistance against microbial diseases and insects and as allelochemicals and endogenous ligands. Interdisciplinary investigations by biologists, biochemists, and chemists have considered how to make agricultural use of the benzoxazinones as natural pesticides. These natural metabolites are not only constituents of a plant defense system but also part of an active allelochemical system used in the competition with other plants.

The 2-*O*-β-D-glucopyranosyl-4-hydroxy-7-methoxy-(2H)-1,4-benzoxazin-3(4H)-one **12** (alternative name: DIMBOA glucoside) isolated from blue light-illuminated maize (*Zea mays*) coleoptiles (46) plays the essential role in the phototropism of maize coleoptiles. Compounds **13–16** were obtained from monocotyledonous plants such as maize in their early growth states, which are harvested on a schedule to give optimal yield (47). These compounds have been reported to act as weight loss agents, appetite suppressants, mood enhancers, and adjunctive therapy for arthritis, sleep apnea, fibromyalgia, diabetes, and hyperglycemia. Benzoxazinoid acetal glucosides **15–19** and 7-chloro-(2*R*)-2-*O*-β-D-glucopyranosyl-2H-1,4-benzoxazin-3(4H)-one **21** have been isolated from the aerial parts of *Acanthus ilicifolius* (48). Benzoxazinoid cyclic hydroxamic acid glucosides **12–15** were identified from the genus *Aphelandra* (Acanthaceae), e.g., *A. fuscopunctata, A. squarrosa, and A. tetragona* (49). Dried seeds of *Acanthus mollis* contain 4% by dry weight of the 2,4-dihydroxy-1,4-benzoxazin-3(4*H*)-one (DIBOA) glucoside **16** (49). The results obtained showed that in all species the glucosides as well as the hydroxamic acid aglucones were present in the roots, whereas in the aerial plant parts only traces of the glucosides were detected. The phytotoxicity of DIBOA suggests that they might be involved in the allelopathic activity attributed to rye. Chinese woad, *Baphicacanthus cusia* (= *Strobilanthes cusia*, Acanthaceae), is an herbaceous plant native to northeast India, Myanmar, Thailand, and the southern part of China. Roots of *B. cusia* collected from Dinghushan (Guangdong, China) contain two alkaloids, **15** and **16** (50). The chloro-containing alkaloid glucoside, 7-Cl-DIBOA-Glc **20** as well as **15** and **16** were isolated from the aerial part of *Acanthus ebracteatus* (51). Compounds **17** and **18** were isolated from *Lamium amplexicaule*, *L. purpureum*, and *L. garganicum* belonging to Lamiaceae family (52).

12 R = OH
13 R = OMe
14 R = H

15 R = H
16 R = OH

17 R = OH, R₁ = H
18 R = H, R₁ = OH

19 R = H
20 R = OH

21
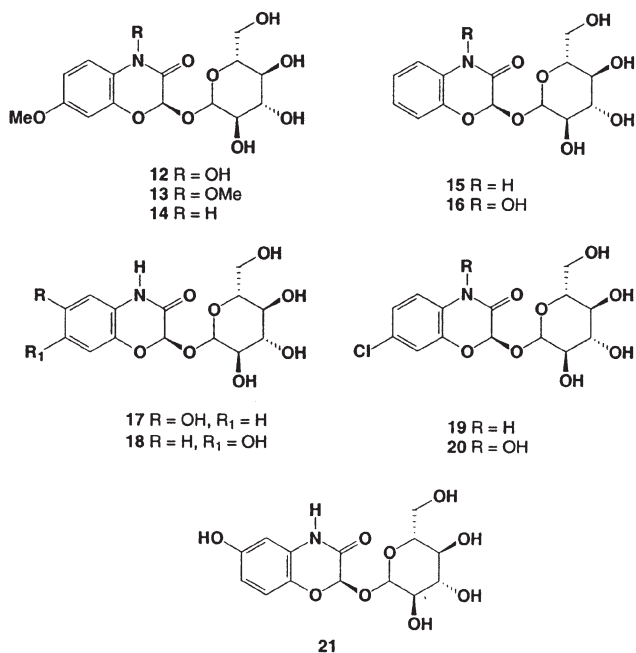
ERGOT ALKALOID GLYCOSIDES

Ergot alkaloids are one of the pharmacologically most important groups of indole alkaloids (53). These alkaloids are isolated from the dried sclerotium of the fungus *Claviceps purpurea* (Hypocreaceae) (54,55). This fungus is a parasite on rye, wheat, and other grains. Ingestion of contaminated grain, most often after the grain has been made into bread, causes ergotism, also known as the "Devil's curse" or "St. Anthony's fire;" this form of poisoning has been a problem for centuries (53). It is possible that ergot-infected grasses were produced in the first agricultural settlements of Mesopotamia around 9000 B.C., but ergot is thought to have first been mentioned around 600 B.C. by the Assyrians (55). The Roman historian Lucretius (98–55 B.C.) referred to ergotism as *Ignis sacer*, meaning Holy Fire, which was the name given to ergotism during the Middle Ages, and it was during these times that ergotism occurred frequently. Ergotism can cause convulsions, nausea, and diarrhea in mild forms, and there is some thought that an outbreak of ergotism may have been the cause of the "bewitchings" that led to the Salem witch trials in the United States in 1691. Ergotism has now been recognized as the effects of ingesting a mycotoxin, and ergotism plagues have been eliminated (56,57). However, the alkaloids derived from ergot have assumed new importance for their pharmacological properties, and ergot is produced commercially for the preparation of these alkaloids. Ergot alkaloids are used in a number of therapeutic areas including the treatment of acromegaly, blood pressure regulation, hyperprolactinemia, migraine, cerebral insufficiency, orthostatic circulatory disturbances, postpartum bleeding, Parkinsonism, uterine atonia, and others (58–62).

The first glycoside of ergot alkaloids, named elymoclavine-*O*-β-D-fructoside **22,** was isolated from a saprophytic culture of *Claviceps* sp. strain SD-58 by Floss *et al.* (63) in 1967. More recently, glycoside **22** and a new elymoclavine-*O*-β-D-fructofuranosyl-(2→1)-*O*-β-D-fructofuranoside **23** were isolated from saprophytic cultures of strains *Claviceps* sp. SD-58 and *C. purpurea* 88 EP grown on a sucrose medium (64). A submerged culture of *C. fusiformis* supplemented with chanoclavine I produced chanocalvine I *O*-β-D-fructofuranoside **24** and chanoclavine 1 *O*-β-D-fructofuranosyl-(2 → 1)-*O*-β-D-fructofuranoside **25** (65). The glycosides of ergot alkaloids **24–26** obtained by enzymatic synthesis showed strong inhibitory activity on prolactin secretion (**26**), cytotoxic activity (**27**), and potent effects against the resistant tumor cell line RAJI (**28**) (66).

22

23

24

25

26

27

28
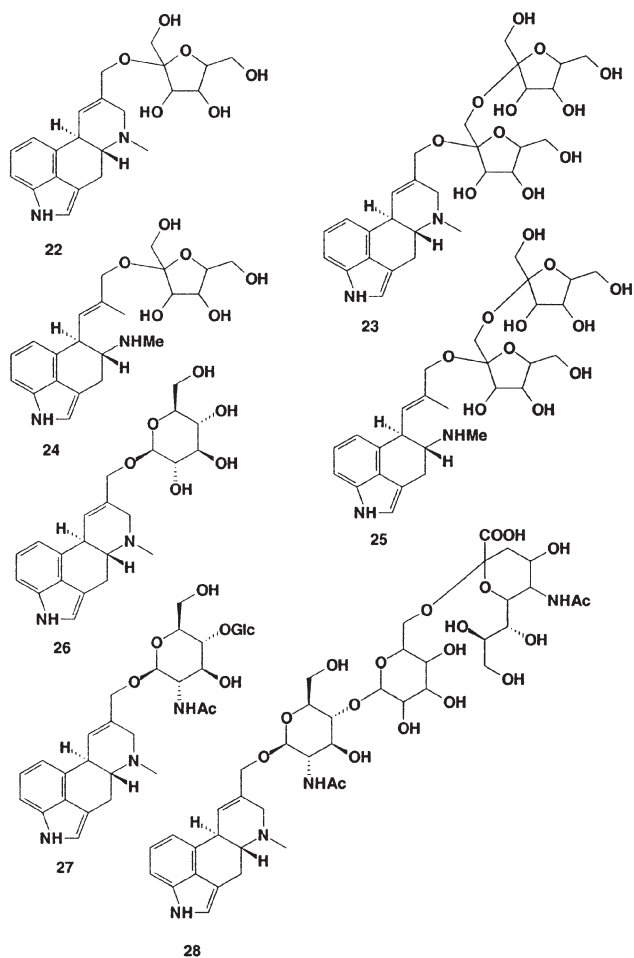
INDOLE ALKALOID GLYCOSIDES

Indole alkaloids constitute the largest group of alkaloids with double ring systems containing an indole ring. They are of interest because of their structures—often extremely complex—and their surprising physiological activities. Most contain a tryptamine unit as a readily distinguishable feature or a modified structure, and tryptamine is a precursor in the biosynthesis of many of these alkaloids. Indole alkaloids and their glycosides have been isolated from marine and terrestrial plants, algae, cyanobacteria, fungi, marine invertebrates (sponges, tunicates, bryozoans, gorgonians, sea hares), some higher animals, and a few mammals including humans. Indole alkaloids show a large spectrum of biological activities (67–69). More than 2000 indole alkaloids have been found

from the three families of Gentianales: Loganiaceae, Apocynaceae, and Rubiaceae plants. These compounds generally possess characteristic biological activities and many of them are used for medicinal purposes and as lead compounds to develop new synthetic drugs (68,69). Approximately 100 indole bases are now known (more than 20 have been identified in the last decade) that fall into the akuammiline structural category, and the chemistry and pharmacology of these have been recently reviewed (67–69).

Some simple indole glycosides have been isolated from plants. Indican **29** is one of the main secondary metabolites in *Polygonum tinctorium* and is used as precursor for the manufacture of indigo dye (70). It also is found in *Celosia argentea* from Sierra Leone (71), in Vietnamese *Indigofera* (Leguminosae family) (72), and other plant species (70). Biosynthesis of indican **29** and of its indoxyl derivatives was recently described (70). The two precursors of indigo in the woad plant, *Isatis tinctoria*, were quantified by a new spectrophotometric method involving the formation of a red adduct from indoxyl and rhodanine (73). In young leaves, approximately 24% of the dry weight the indoxyl derivatives, indoxyl-3-(5-ketogluconate): indoxyl 3-*O*-β-D-glucoside (indican **29**) and isatan B **31**, and in the ratio of approximately 3:1. Glucoindican (calanthoside A) **30** and a novel indole *S*,*O*-bisdesmoside **32** (calanthoside B) were isolated from two Oriental orchids, *Calanthe discolor* and *C. liukiuensis*, together with calaphenanthrenol, calaliukiuenoside, and the known bioactive alkaloids tryptanthrin, indirubin, and isatin (74,75). Furthermore, enzymic hydrolysis of calanthoside **32** was found to produce tryptanthrin as the main product, whereas indirubin and isatin were obtained by acid hydrolysis of calanthoside. Three new indole alkaloids, including one glycoside, named bruceolline F **33**, were isolated from the root wood of *Brucea mollis* var. *tonkinensis* (76).

5-(β-D-Glucopyranosyloxy)indole-3-acetic acid **34** was isolated from quackgrass (*Agropyron repens*) (77). Indole-3-methanol-β-D-glucoside **35** and indole-3-carboxylic acid-β-D-glucoside **36** are products of indole-3-acetic acid degradation in wheat leaf segments, and were isolated from leaves of the members of the Gramineae family (78). A new metabolite of indole-3-acetic acid was extracted from corn (*Zea mays*) seedlings and characterized as the 7-*O*-β-D-glucopyranoside of 7-hydroxy-2-oxoindole-3-acetic acid **37** (79). The results and prior work demonstrated the following catabolic route for indole-3-acetic acid in *Z. mays*: indole-3-acetic → 2-oxoindole-3-acetic acid → 7-hydroxy-2-oxoindole-3-acetic acid → 7-hydroxy-2-oxoindole-3-acetic acid glucoside.

29 R = H
30 R = Glc

31

32

33

34

35

36

37

rugosporus (85). Pyrroindomycins possess potent antimicrobial activities against methicillin-resistant *Staphylococcus aureus* and vancomycin-resistant *Enterococci*. Pyrroindomycins **43** and **44** are the first natural products that contain the highly unsaturated pyrroloindole moiety.

38 R = OMe
39 R = NH₂

40

41

42

43 R = H
44 R = Cl
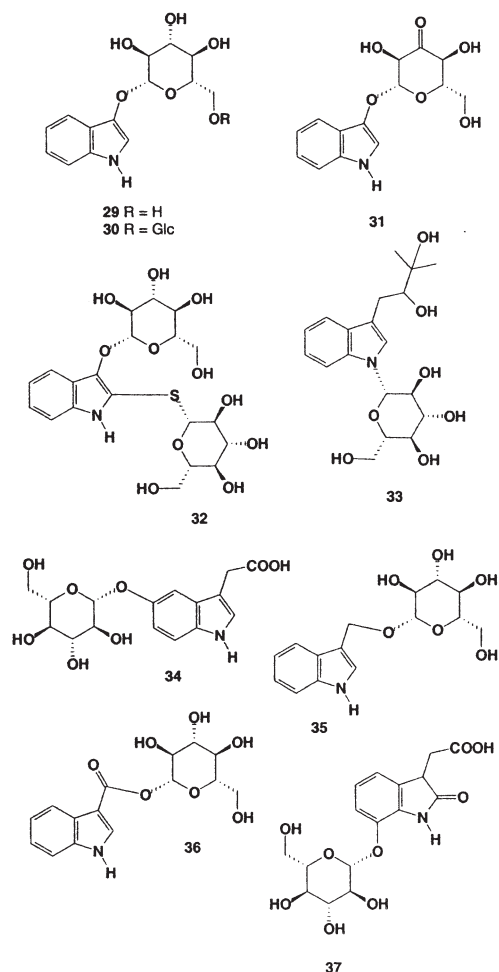
Microorganisms produce some simple indole glycosides. New indole nucleosides kahakamides A **38** and B **39** were isolated from the actinomycete *Nocardiopsis dassonvillei*, obtained from a shallow water sediment sample collected on the island of Kauai, Hawaii (80). Compounds **38** and **39** are related to the neosidomycin **40** antibiotics, a group of rare indole-N-glycosides; and **38** exhibited antimicrobial activity toward the Gram positive bacterium *Bacillus subtilis*. Neosidomycin **40**, a known antibiotic, was isolated in 1979 from a fermentation broth of *Streptomyces hygroscopicus* by Furuta *et al*. (81). Antiviral antibiotic SF-2140 **41** was obtained from the broth of *Actinomadura albolutea* (Nocardiaceae), which was isolated from soil. It showed antiviral and weak antibacterial activity against Gram-negative and Gram-positive bacteria (82,83). Two novel glycoconjugates, ethyl indole-3-lactate-*O*-β-D-glucopyranoside **42** and *p*-menth-1-ene-8,9-diol-9-β-D-glucopyranoside have been detected in Riesling wine (84).

Unusual pyrroindomycins A **43** and B **44** were isolated from fermentations of culture LL-42D005, a strain of *Streptomyces*

Rare spiro oxindole alkaloid glycosides isomitraphyllic acid-(16–1)-β-D-gluco-pyranoside **45** and mitraphyllic acid-(16–1)-β-D-glucopyranoside **46** were isolated from the leaves of *Uncaria sinensis* (86). A new glycosidic indole alkaloid, echitamidine-*N*-oxide 19-*O*-β-D-glucopyranoside **47**, was isolated from the trunk bark of *Alstonia scholaris* collected in Timor, Indonesia (87). Lyaloside **48**, a monoterpenoid glucoindole alkaloid, was isolated from the leaves of *Palicourea adusta* together with a mixture of its hydroxycinnamic acid derivatives, (*E*)-*O*-(6′)-cinnamoyl-4″-hydroxy-3″-methoxy-lyaloside **49** and (*E*)-*O*-(6′)-cinnamoyl-4″-hydroxy-3″,5″-dimethoxy-lyaloside **50**; these were separated by HPLC (88).

From the root-wood of *Brucea mollis* var. *tonkinensis* collected in China have been isolated bruceolline A **51**, bruceolline B **53** (89), and bruceolline C **52** (90).

45 46

47

48 R = H

49 R =

50 R =

51 R = Glc
52 R = H

53

leaves of *Palicourea marcgravii* (Rubiaceae) collected in Brazil (94), and extraction of leaves from the Australian tree *Ophiorrhiza acuminata* has yielded harman, lyalosidic acid, and palicoside **56** (95). Two indolic alkaloidal glucosides named naucleoside **57** and nauclecosidine **58** were isolated from the polar fraction of the stems of *Nauclea officinalis* (96). An unusual type of indole alkaloids, ophiorines A **59** and **60**, was found in the Rubiaceous plants, *Ophiorrhiza japonica* and *O. kuroiwai* (97).

54 R,R₂ = H, R₁ = Glc
55 R,R₁ = H, R₂ = Glc
56 R = Me, R₁ = H

57

58

59

60

Oleander [*Hunteria zeylanica* (Apocynaceae)] grows in Southern China and Thailand, and its leaves are used externally for the treatment of wounds and cuts. An alkaloid extracted from the leaves of *H. zeylanica* inhibited a glycine-induced chloride current using a receptor expression model of *Xenopus* oocytes (91). New glycosidic indole alkaloids, hunterioside **54** and hunterioside B **55,** were isolated from the *n*-BuOH fraction of the ethanol extracts of the stem bark of *H. zeylanica* collected in south Thailand (92), and more recently hunterioside B **55** was isolated from same tree (93). An indole alkaloid glucoside named palicoside **56** was isolated from the

Neonauclea sessilifolia (= *Nauclea sericea*), which belongs to the Rubiaceae, grows in Southeast Asia and contains many bioactive compounds. Three novel indole alkaloid glycosides, neonaucleosides A **61**, B **62**, C **63**, and rhynchophine **64** were isolated from the dried roots of *Neonauclea sessilifolia* (98). Strictosamide **65,** which has antitumor activity, was isolated from the leaves of *Nauclea orientalis* (99) and from leaves of *Sarcocephalus latifolius* (100).

61

63

62

64 R = Glc-6'-Feruloyl
65 R = Glc

eases. The occurrence of two new gluco indole alkaloids isolated from the bark of *N. diderrichii*—cadambine acid **70** and 3α-5α-tetrahydro-deoxycordifoline lactam **71**—has been reported (106).

Plants of the pantropical genus *Uncaria* have found widespread use in traditional medicine. *Uncaria* species are climbing vines with claw-like thorns (hooks). Some indole alkaloid glycosides have been isolated from this genus, including the lyaloside **48**, rhynchophine **64**, strictosamide **65**, 3β-dihydrocadambine **72**, 3β-isodihydrocadambine **73**, 3,4-dehydro-5-carboxystrictosidine **74**, carboxystrictosidine **75**, and glabratine **76** (107,108).

66

67

68 R = H
69 R = OH

70

71

72

73

74

75

76

A new β-carboline-type alkaloidal glycoside, glucodichotomine B **66,** with antiallergic activities was isolated from a Chinese natural medicine, i.e., the roots of *Stellaria dichotoma* var. *lanceolata* (101).

The plant *Psychotria correae* (syn. *Cephaelis correae)* is only described from the Cordilleras de Guanacaste and Tilarfin and from the Province of Coclé in Panama, where it grows as a small tree (102). Various *Cephaelis* species are used in the traditional medicine of Middle America, e.g., against dizziness, hallucination, dementia, and rubella (103). In the European Pharmacopoeia, preparations of C. *ipecacuanha* (=*Psychotria ipecacuanha*) are described as emetics and expectorants, and emetine, a major alkaloid from *Ipecacuanhae radix,* is used as an amoebicide (104). From extracts of the leaves and/or the roots of *Psychotria correae,* isodolichantoside **67,** the new β-carboline-type alkaloid correantoside **68**, and 10-hydroxycorreantoside **69** were isolated (105).

Nauclea diderrichii, belonging to the Rubiaceae family, grows in western and central Africa. Decoctions of the bark are widely used in folk medicine for the treatment of tropical dis-

A chlorinated alkaloid-type antibiotic, rebeccamycin **77,** which is produced by *Streptomycetes* species (109), inhibits the growth of human lung adenocarcinoma cells and produces single strand breaks in their DNA. A related antibiotic without chlorine, staurosporine **78**, produced by *Streptomyces staurosporeus*, was reported to have antifungal, hypotensive, and

antitumor activities (110). A novel brominated analog of rebec-camycin, **79**, is produced by *Saccharothrix aerocolonigenes* ATCC 39243 when grown in a defined medium containing 0.05% KBr (111). Bromorebeccamycin **79** and rebeccamycin **77** have a similar potency and activity against P388 leukemia in the murine model. Rebeccamycin **77** also was isolated from the cyanobacterium *Nocardia aerocoligenes* (112) and is a well-known topoisomerase I inhibitor.

Rebeccamycin analogs were prepared either by semisynthesis from the natural metabolite or by total synthesis. Different families of rebeccamycin analogs were obtained by modifications at the imide heterocycle, dechlorination, and substitutions on the indole moieties, modifications of the sugar residue, construction of dimers, coupling of the sugar unit to the second indole nitrogen, changing of the indolo[2,3-a]carbazole skeleton to indolo[2,3-c]carbazole, and replacement of one or both indole moieties by 7-azaindole units. The biological activities of the rebeccamycin analogs were recently reviewed (113). According to their chemical structure, the analogs can inhibit topoisomerase I and/or kinases. From the structure–activity relationships, some important rules were established. Several compounds exhibit stronger antiproliferative activities than the natural metabolite with IC$_{50}$ values in the nanomolar range. Some analogs, especially those possessing azaindole moieties, are much more selective than rebeccamycin toward the tumor cell lines tested (114).

A new indolo[3,2-b]quinoline alkaloid glycoside, jusbetonin **80**, has been isolated from the leaves of *Justicia betonica* (115). This compound is the first example of a glycosylated indolo[3,2-b]quinoline alkaloid.

Fifteen new N-glycosides of indolo[2,3-a]carbazoles, designated tjipanazoles A1, A2, B, C1, C2, C3, C4, D, E, F1, F2, G1, G2, I, and J, have been identified and are produced by the cyanobacterium *Tolypothrix tjipanasensis* (116). Tjipanazoles A1 **81** and A2 **82**, chloro-containing alkaloids, showed high antifungal activity (116). Analogs of antifungal tjipanazoles **82**–**85** were obtained by semisynthesis from rebeccamycin, an antitumor antibiotic isolated from cultures of *Saccharothrix aerocolonigenes* (117). The antiproliferative activities of the new compounds were evaluated *in vitro* against nine tumor cell lines. The effect on the cell cycle of murine leukemia L1210 cells was examined, and the antimicrobial activities against two Gram-positive bacteria, a Gram-negative bacterium, and a yeast were determined. The inhibitory properties toward four kinases and toward topoisomerase I were evaluated. The most cytotoxic compound in the series was a dinitro derivative **85** characterized as a potent topoisomerase I inhibitor.

77 R = Cl
78 R = H
79 R = Br

80

80 R = Me, R$_1$ = H
81 R = H, R$_1$ = Me

82 R = Me, R$_1$, R$_2$ = H
83 R$_1$ = Me, R, R$_2$ = H
84 R = CHO, R$_1$ = Me, R$_2$ = H
85 R$_1$ = Me, R, R$_2$ = NO$_2$
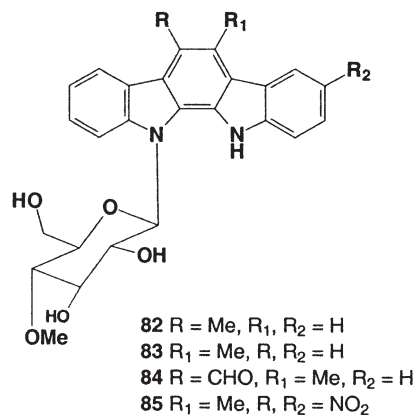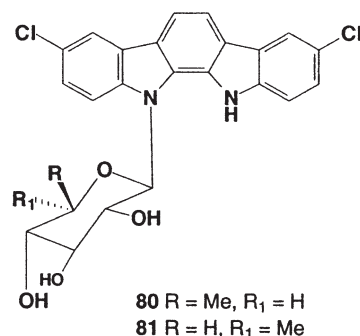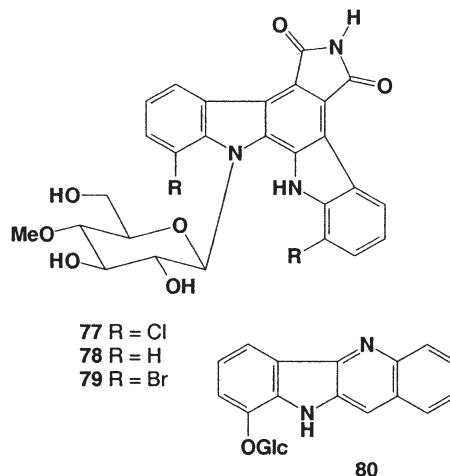
Betalains are water-soluble nitrogen-containing pigments and include the red-violet betacyanins and the yellow betaxanthins (118). Betalains accumulate in flowers, fruits, and occasionally in vegetative tissues of plants belonging to most fami-

lies of the Caryophyllales (119). Betalains and betacyanins show antioxidant and radical-scavenging activities (120).

Betanin **86** was discovered more than 45 years ago in the root of beets (*Beta vulgaris*), which are native to the Mediterranean countries (121). Phyllocactin (6′-*O*-malonyl-betanin) **87** is a well-known pigment that is isolated from flowers and fruits of the Cactaceae family (122). Red-colored plants of the family Amaranthaceae were recognized as a rich source of diverse and unique betacyanins. Gomphrenin I **88**, II **91** and **92** and other colored pigments were isolated from the Amaranthaceae family (123). Acylated betacyanins were distributed among 11 species of 6 genera, with the highest proportion occurring in *Iresine herbstii* (79.6%) and *Gomphrena globosa* (68.4%).

Lampranthins I **89** and II **90** were isolated from *Beta vulgaris* (124) and *Phytolacca americana* (125). Acylated pigment **93**, which seems to be the first betacyanin identified containing both an aliphatic and an aromatic (hydroxycinnamoyl) acyl residue, was found in *Beta vulgaris* (124). The minor pigment 2-descarboxy-betanidin **94** was found in the flowers of *Carpobrotus acinaciformis* (Aizoaceae) and the more complex compound **95** was isolated from *Bougainvillea glabra* (126). Fuller information on the chemistry of betalains and the betacyanin types of glycosidic alkaloids can be foundind in a recent review by Strack and coworkers (127).
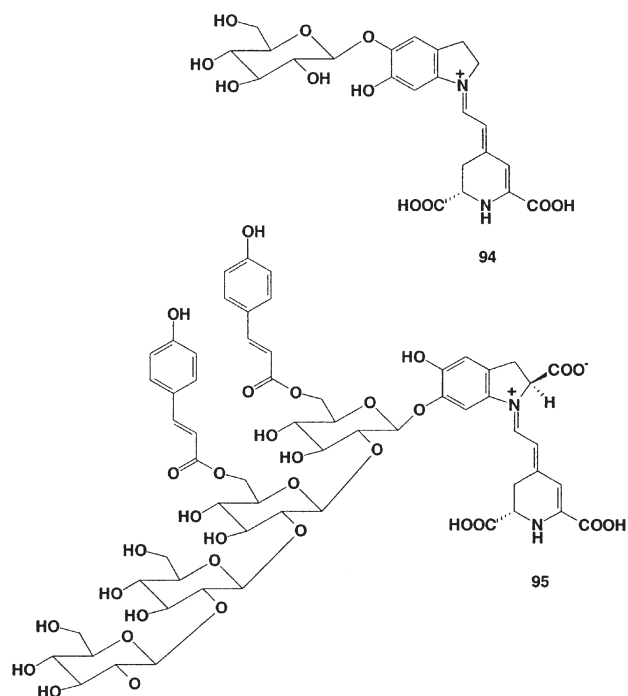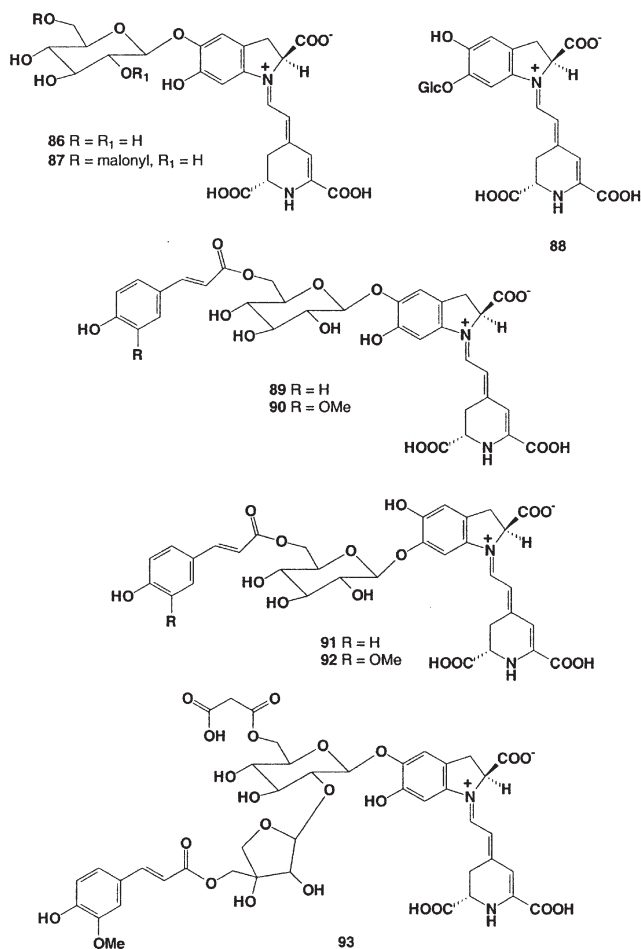
ENEDIYNE ALKALOIDAL ANTIBIOTICS

The enediyne family of alkaloidal antibiotics is characterized structurally by an enediyne core unit consisting of two acetylenic groups conjugated to a double bond or incipient double bond within a 9- or 10-membered ring (128–130). These newly discovered enediyne alkaloidal antibiotics combined unprecedented molecular structures with striking biological activities. A remarkable mechanism of action recently was proposed for these molecules to account for their phenomenal biological profiles (128–130). A few glycosides of the enediyne nitrogenous antibiotics also have been discovered.

Three new compounds of the enediyne antitumor antibiotics, shishijimicins A **96**, B, and C, have been isolated from the marine ascidian *Didemnum proliferum* (131). They encompass a novel sugar component, which is a conjugation product of a hexose and a β-carboline, attached to the calicheamicinone aglycon. Shishijimicins showed extremely potent cytotoxicity against HeLa cells, with IC_{50} values of 1.8–6.9 pM.

Kedarcidin **97**, one of the most complex and reactive of the natural enediyne antitumor agents, was isolated from the culture broth of a novel actinomycete strain L585–6 (ATCC 53650) (132). *In vivo* studies showed this natural metabolite to be extremely active against P388 leukemia and B16 melanoma. Cytotoxicity assays on the HCT116 colon carcinoma cell line result in an IC_{50} value of 1 nM. *In vitro* experiments with ΦX174, pM2 DNA, and ^{32}P-end-labeled restriction fragments demonstrate that this chromophore binds and cleaves duplex DNA with remarkable sequence selectivity, producing single-strand breaks (133).

96

97

98 R = OH, R₁ = Cl, R₂ = OMe
99 R = R₁ = R₂ = H

98 R = OH, R_1 = Cl, R_2 = OMe
99 R = R_1 = R_2 = H

100
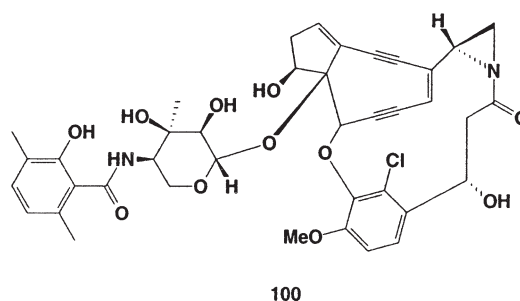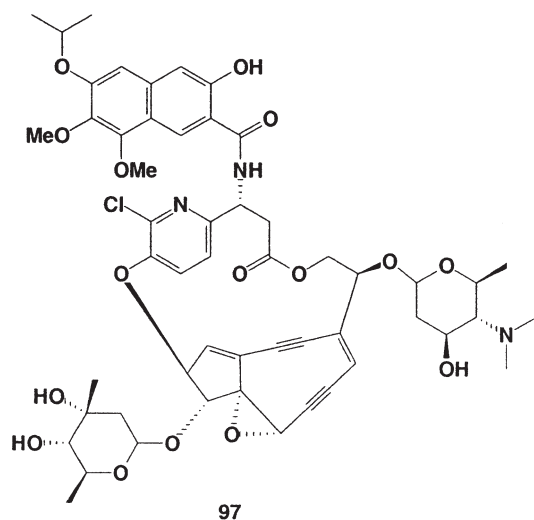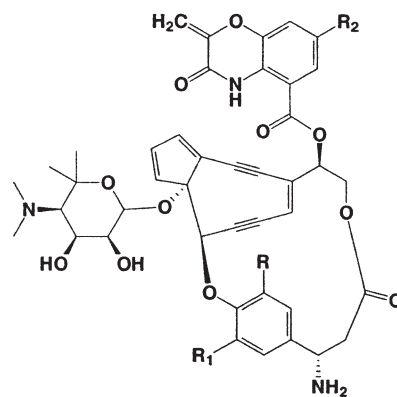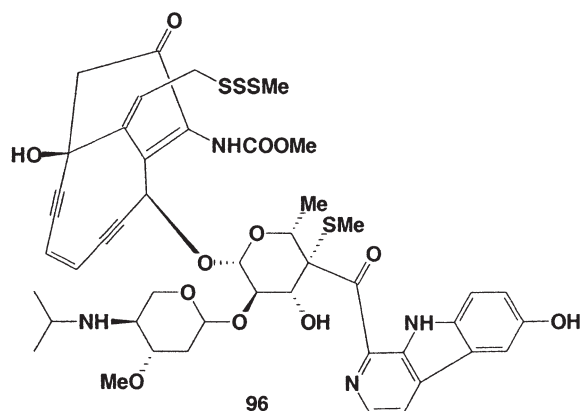
The chlorinated enediyne nitrogenous compound C-1027, **98**, a potent antitumor agent with a previously undescribed molecular architecture and mode of action, has been isolated from *Streptomyces globisporus* (134). Antibiotic C-1027, a macromolecular peptide with high cytotoxicity to cultured cancer cells, was conjugated to monoclonal antibody 3A5 and its Fab (immunoglobulin) fragment separately using SPDP (*N*-succinimidyl 3-[2-pyridyldithio]-propionamido), widely used in immunochemistry, as the linker agent. McAb 3A5, identified as IgG₁, was directed against human hepatoma BEL-7402 cells (135). The nonchlorinated analog of C-1027, **99**, also was isolated from *S. globisporus* (136).

Maduropeptin **100**, a complex of new macromolecular antitumor antibiotics, is a metabolite of *Actinomadura madurae* H710–49. The active components, maduropeptins A1, A2, and B, are acidic chromopeptides with M.W. of around 22,500 and are composed of 14 types of amino acids and an unstable chromophore. The antibiotics are active *in vitro* against Gram-positive bacteria and are highly cytotoxic to tumor cells. They produced significant prolongation of survival time of mice implanted with P388 leukemia and B16 melanoma (137).

GLYCOSIDIC LUPINE ALKALOIDS

Lupines are widely distributed across the western United States and Canada and there are many species. Most are perennial and produce a hard seed that is viable for many years. Over 100 different alkaloids have been identified in these plants, each with differing biological activities. The types and concentrations of these alkaloids vary between the species and between collections of the same species. Lupines with high alkaloid content are termed "alkaloid-rich" or "bitter" lupines; this terminology includes the majority of the western range lupines. "Alkaloid-poor" or "sweet" lupines are used for animal and human feed (138).

The majority of the more than 20 alkaloids isolated from *Lupinus* are quinolizidine alkaloids, with some piperidine and other components known lupanine and lupinine. The teratogenic alkaloid anagyrine is highest in the seeds, pods, and young leaves. The quinolizidine alkaloids implicated in lupine poisoning are found mostly in the seeds and pods. Large quantities of the plant material must be ingested in a short time to cause death. The alkaloids remain after drying, so that hay containing sufficient quantities of lupine can be toxic. General symptoms of lupine poisoning include dizziness and incoordination. Lupine seeds can be made edible by soaking and boiling the seeds in several changes of water (139). Several species of lupine (*Lupinus* spp.) are poisonous to livestock, producing death in sheep and "crooked calf disease" in cattle (140).

Quinolizidine and indolizidine alkaloids and their analogs

have been isolated from microbial, plant and animal sources, including ants, amphibians and beetles (141).

A few glycosidic lupine alkaloids have been isolated from some plant species. The (−)-(*trans*-4′-α-L-rhamnosyloxycinnamoyl)epilupinine **101** and its 3′-methoxy derivative **102** were isolated from the aerial parts of *Lupinus varius* (142). Glycosidic alkaloids **102** and **104** were isolated from the aerial parts of *L. hirsutus* (143); **103** and **105** were isolated from *L. luteus* (144).

101 R = H
102 R = OMe

103

104

105
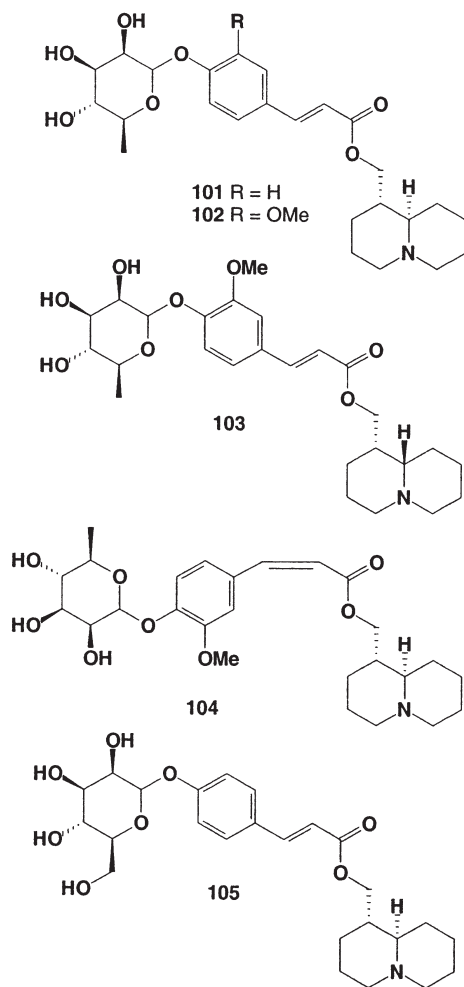
PIPERIDINE, PYRIDINE, PYRROLIDINE, AND PYRROLIZIDINE ALKALOID GLYCOSIDES

Both pyridine and piperidine alkaloids are six-membered N-heterocycles, the former being unsaturated and the latter saturated. These groups of compounds have been known for a long time (145). The best-known piperidine alkaloid, coniine, is a poison derived from the poison hemlock, *Conium maculatum*. Socrates is reputed to have been killed with a poison hemlock extract. Other well-known piperidine alkaloids include cocaine, strychnine, and atropine. Cocaine was first isolated from the plant *Erythroxylon coca* by the German chemist Friedrich Gaedcke in 1855 and named "erythroxyline." The poisonous alkaloid strychnine was the first alkaloid to be identified in

plants of the genus *Strychnos* (family Loganiaceae). Cocaine is an example of a tropane type of pyrrolidine alkaloid in which the N-heterocycle is derived from L-ornithine, an amino acid derived from glutamate. Strychnine was first discovered by French chemist Joseph-Bienaime Caenoiu and Pierre-Joseph Pelletier in 1818. Atropine, commonly known as Deadly Nightshade, was isolated from belladonna (*Atropa belladonna*) in 1831, and the use of a water-soluble salt (atropine methonitrate) was introduced into ophthalmology in 1902. A large number of piperidine-based alkaloids occur in neotropical poison frogs (Dendrobatidae), mainly as trace compounds (146).

The well-known pyridine alkaloid, nicotine, and the piperidine-pyridine alkaloid, anabasine (or neonicotine), are both found in plants from the genus *Nicotiana,* which includes cultivated, wild, and tree tobacco (147,148). Nicotine was isolated from leaves of tobacco (*N. tabacum*) in 1828, and anabasine was isolated from and *N. glauca* in 1929 (148).

Pyrrolidine alkaloids have been found in many species of the three major plant families Boraginaceae, Compositae, and Fabaceae, and are produced as well by some fungi and microorganisms. Hygrine and cuscohygrine are well-known simple pyrrolidine alkaloids isolated from natural sources (147).

Alkaloids mimicking sugars in size and shape are now believed to be widespread in plants and microorganisms. Iminosugars are monosaccharide analogs in which the ring oxygen has been replaced by an imino group. Such iminosugars inhibit the glycosidases involved in a wide range of important biological processes because of their structural resemblance to the sugar moiety of the natural substrate and the presence of the nitrogen atom mimicking the positive charge of the glycosyl cation intermediate in the enzyme-catalyzed glycoside hydrolysis. These iminosugars and their derivatives are arousing considerable attention as potential therapeutic agents and show antiviral, anticancer, antidiabetic, nematicidal, and other activities (149). The taxonomic distribution of iminosugars in plants and their biological activities has recently been reviewed (150).

Three simple iminosugars, 4-*O*-β-D-mannoside **106,** 4-*O*-β-D-mannobioside **107**, and 4-*O*-D-glucopyranosyl-1-deoxynojirimycin **108,** have been isolated from the bulbs of *Scilla sibirica* (151). Elongation of the β-mannopyranosyl chain of **106** to give **107** enhanced the inhibitory activity of α-L-fucosidase, β-glucosidase, and β-galactosidase.

A novel piperidine-type alkaloid, 2-β-D-glucopyranosyl-2-undecyl-3,5-dihydroxy-6-carboxypiperidine **109,** was isolated from *Cyclamen coum* (152), and secoiridoid glucoside LA-9 **110** was found in an extract from fruits of *Ligustrum vulgare* (153). The 3-hydroxy-5-(hydroxymethyl)-4-(methoxymethyl)-2-methylpyridine glucoside **111** was isolated from seeds of *Albizzia lucida* (154). Caerulomycin D **112**, a new metabolite from *Streptomyces caeruleus*, possessed a novel ring system (155).

Antitumor agents BE-14324 **113** and BE-14324A **114** were isolated from *Streptomyces* spp. or their mutants (156). IC$_{50}$ values of **114** on proliferation of mouse leukemia cell P388 (P388/S), its vincristine-resistant mutant P388/V, and adriamycin-resistant mutant P388/A were 1.0, 0.7, and 1.0 μg/mL, respectively.

pyrrolidine alkaloid 1,4-dideoxy-1,4-imino-D-arabinitol **120** has been identified in the leaves of bluebells (*Hyacinthoides nonscripta*) (160). The new glycoside named pisatoside **121** was isolated from *Pisum sativum* (161). A novel acaricide, gualamycin **122,** was isolated from the culture broth of *Streptomyces* sp. NK11687 (162).

106 R = H
107 R = Glc

108

109

110

111

112

113 R = Me, R₁ = Glc
114 R = CH₂OH, R₁ = H

115 R = H
116 R = Glc

117

118

119

120

121

The pyrrolidine alkaloids broussonetine A **115**, Q **116**, B **117**, K **118,** and L **119** were isolated from the branches of *Broussonetia kazinoki* Sieb (Moraceae) (157–159). ICompound **116** inhibited β-glucosidase, β-galactosidase, and β-mannosidase (157), whereas compounds **118** and **119** inhibited β-glucosidase, β-galactosidase, β-mannosidase (158); and **115** and **117** showed a strong inhibition of β-galactosidase and α-mannosidase (159). The glycosidase-inhibiting

A few pyrrolizidine alkaloid glycosides have been isolated from plant species. The highly oxygenated pyrrolizidine casuarine, its 6-*O*-α-D-glucopyranoside **123**, and 1-epi-australine 2-*O*-β-D-glucopyranoside **124** were isolated from pods of the Australian *Alexa leiopetala* (Leguminosae) (163); and a glucosidic alkaloid malaxin **125** was isolated from orchid *Malaxis congesta* (164).
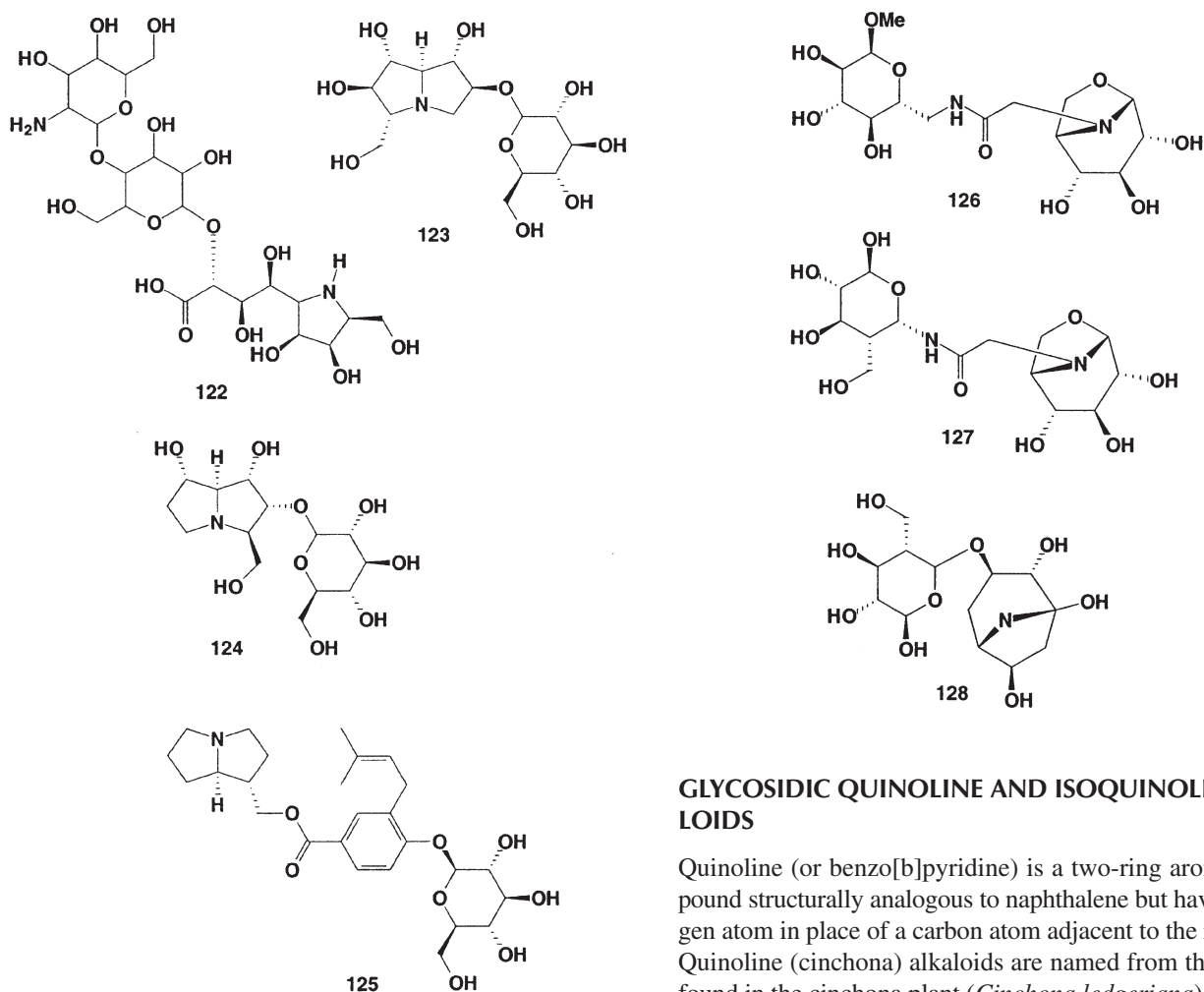
GLYCOSIDIC QUINOLINE AND ISOQUINOLINE ALKALOIDS

Quinoline (or benzo[b]pyridine) is a two-ring aromatic compound structurally analogous to naphthalene but having a nitrogen atom in place of a carbon atom adjacent to the ring fusion. Quinoline (cinchona) alkaloids are named from the quinoline found in the cinchona plant (*Cinchona ledgeriana*) and belong to the quinoline alkaloids developed in the nucleus from L-tryptophan. Quinoline alkaloids are widely used in the pharmaceutical and chemical industry (173,174). Furthermore quinine is also an important bitter agent in the beverage (soft drink) industry. Quinine has been a valuable antimalarial agent and muscle relaxant compound for more than 100 years; its isomer quinidine has been used as a cardiac depressant (antiarrhythmic agent) (175,176). Quinine is an optical isomer of quinidine. Quinoline and isoquinoline alkaloids represent one of the two largest groups of alkaloids (the other being indole alkaloids and their derivatives) and have been found in species of cyanobacteria, fungi, marine invertebrates, and amphibians (11,177–179).

The lipid extract of the marine cyanobacterium *Lyngbya majuscula* collected from Curaçao afforded two quinoline alkaloids in low yield, and one of them was glycoside **129** (180). Two new glycosidic quinoline alkaloids, **130** and **131,** were isolated from the 1-butanol extract of the aerial parts of *Echinops gmelinii* (Compositae) (181). The aerial part of *Haplophyllum perforatum* yielded a new glycoalkaloid, haplosinine **132** as well as **133** and **131** (182).

The anticancer alkaloid glycosides camptothecin 20-*O*-β-glucoside **134** and deoxypumilioside **135** have been isolated

A few tropane alkaloid glycosides from natural sources have been discovered. They have the 8-azabicyclo[3,2,1]octane nucleus, and their analogs are important for medical treatment (165). Some of the most potent tropane alkaloids are atropine, hyoscyamine, and scopolamine (166–168). These alkaloids affect the central nervous system, including nerve cells of the brain and spinal cord that control many direct body functions and the behavior of humans (169,170). Tropane alkaloids are found in many other poisonous plants of the nightshade family (Solanaceae), including henbane (*Hyoscyamus niger*), pituri (*Duboisia hopwoodii*), deadly datura (*Datura* and *Brugmansia* spp.), mandrake (*Mandragora officinarum*), and "beautiful lady" (*Atropa belladonna*), all of which were used extensively in folk medicines (170).

The occurrence and distribution of tropane and biogenetically related pyrrolidine alkaloids in 18 *Merremia* species of paleo-, neo-, and pantropical occurrence have been studied, and two tropane alkaloid glycosides **126** and **127** have been isolated (166). Calystegine B$_1$ **128** was isolated from *Nicandra physalodes* fruits (Solanaceae) (171) and from *Hyoscyamus niger* (172).

from *Mostuea brunonis* (183). The L-(+)-*N*-methylcoclaurine D-xyloside (latericine) **136** was isolated from the flowering plant *Papaver californicum* (184), and the similar alkaloid veronamine **137** was obtained from *Thalictrum fendleri* (185).

129

130 R = H
131 R = Me

132 R = Glc
133 R = H

134

135

136

137

138 R = R₁ = Me, R₂ = H
139 R = R₁ = R₂ = H
140 R = Glc, R1 = R₂ = H
141 R = H, R1 = Me, R₂ = Glc

142

143

144 R = R₁ = R₂ = H
145 R = R₂ = H, R₁ = Me
146 R = Me, R₁ = R₂ = H
147 R = H, R₁ = Me, R₂ =
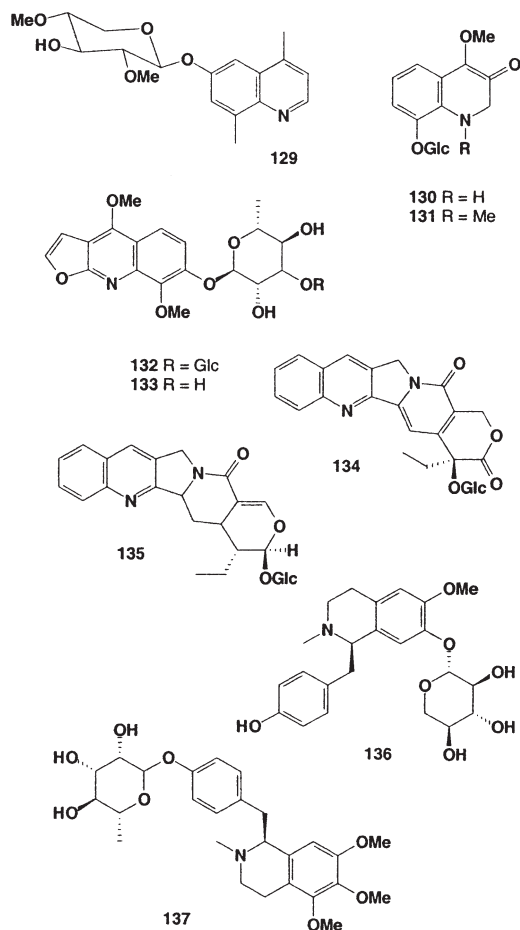
Alangiside **138** and *O*-methyl-alangiside **143** were isolated from *Alangium lamarckii* (186); demethylisoalangiside **139** and 2,11-bisglucoside **140** were obtained from the dried roots of *Cephaelis acuminata* (187). The 6-**141** and 3′-*O*-β-D-gluco-pyranosyl-alangiside **142** were isolated from dried fruits of *A. lamarckii* (188). The acylated tetrahydroisoquinoline-monoter-pene glucosides, 2′-*O*-*trans*-feruloyl-demethyl-alangiside **144** and their analogs **145**, **146,** and **147** were isolated from the fruits of *A. lamarckii* (189).
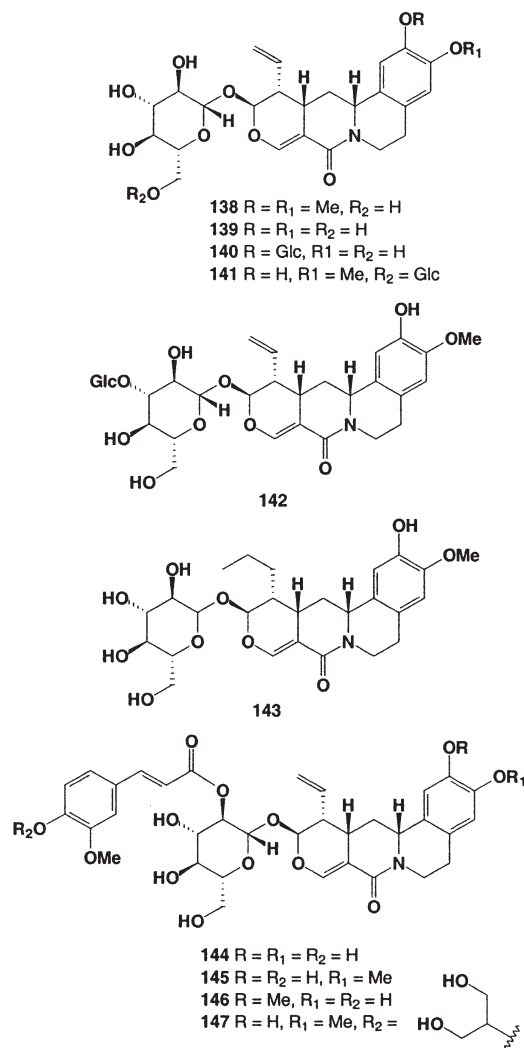
Five tetrahydroisoquinolinemonoterpene (THIQM) glyco-sides—6″-*O*-α-D-gluco-pyranosyl-ipecoside **148**, (4*R*)-4-hy-droxyipecoside **150**, (4*R*)-**151**, and (4*S*)-4-hydroxy-6,7-di-*O*-methyl-ipecosides **152** and **153**—were isolated from *Cephaelis acuminata* (187), and **148** was isolated from *Alangium lamar-ckii* (190). Two new glucosides, **154** and **155**, which possess structures different from any other known THIQM glucosides, were isolated from the fruits of *A. lamarckii* (191). Four new N-acylated THIQM glucosides, *trans*-cephaloside **156**, *cis*-

cephaloside **157**, 6-*O*-methyl-*trans*-cephaloside **158.** and 6-*O*-methyl-*cis*-cephaloside **159**, were isolated from the roots of *Cephaelis ipecacuanha* (192). Dauricoside **160**, a new glycosidal alkaloid, was isolated from the rhizomes of *Menispermum dauricum* (193). Isolated compound **160** inhibited blood-platelet aggregation induced by ADP.

Ipecac grows in the rain forests of Brazil and other parts of South and Central America. It is also cultivated to a small degree in India and Southeast Asia. Ipecac roots are used medicinally, and ipecac's major constituents are the alkaloids emetine and cephaline (194). The alkaloids have several important actions, including activation of brain centers that can induce vomiting, inhibition of the sympathetic nervous system, and inhibition of protein synthesis (195,196). Ipecac syrup is commonly used as a remedy for poisoning, to be taken following ingestion of toxic but noncaustic substances. Unusual ipecac alkaloids **161–163** were identified from extract of the dried roots of *Cephaelis acuminata* (197).

156 R = *E*, OH
157 R = *Z*, OH
158 R = *E*,OMe
159 R = *Z*,OMe

160

161 R = H, R$_1$ = OH
162 R = OH, R$_1$ = H
163 R = H, R$_1$ = OMe

148 R = Glc, R$_1$ = R$_2$ = H
149 R = R$_1$ = H, R$_2$ = Me
150 R = R$_2$ = H, R$_1$ = OH

151 α-OH
152 β-OH

153

154 α-OMe
155 β-OMe
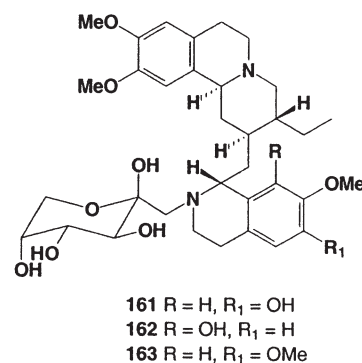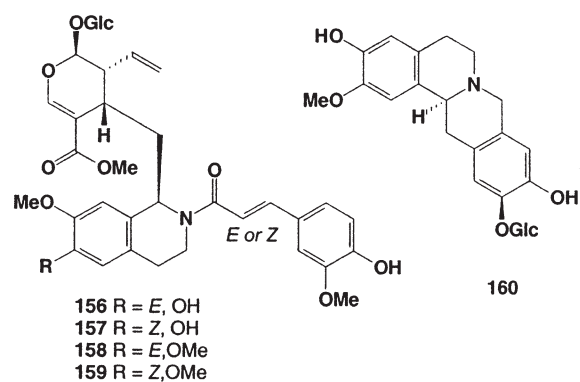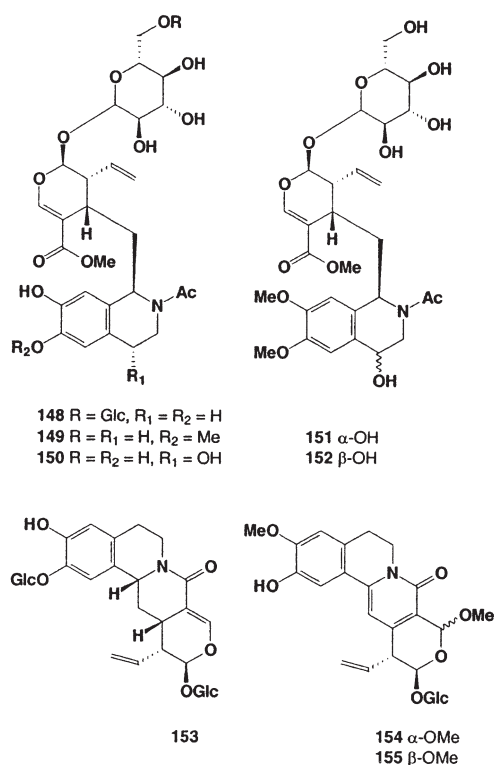
STEROIDAL GLYCOALKALOIDS

Steroidal glycoalkaloids (SGA) have been found in several vegetables: potatoes (*Solanum tuberosum*), tomatoes (*Lycopersicon esculentum*), sugar beets (*Beta vulgaris*) and fruits: apples (genus *Malus*), cherries (genus *Prunus*) and red bell peppers (*Capsicum annuum*), but mainly in the plants of the Nightshade family, particularly the potato—an everyday food for many people for more than 2000 years (198–202). Potatoes are an essential component of the diet of many humans and animals and are thus a potential source of food poisoning (199,202). The steroidal alkaloids are teratogenic, embryotoxic, and genotoxic (200,203,204) compounds with potent permeabilizing properties toward mitochondrial membranes.

Glycoalkaloids are plant steroids with a carbohydrate side chain attached to the 3-OH position, e.g., α-solanine and α-

chaconine from potatoes, α-tomatine and dehydrotomatine from tomatoes (199,200,209). Recent research has found that SGA are responsible for increasing the risk of brain, breast, lung and thyroid cancer (198,205–208). Glycoalkalois are toxic to humans; the lethal dose is 3–6 mg per kg of body mass. Structures of potato glycoalkaloids of α-solanine **164**-**167**, and of α-chaconine **168**-**171** were identified from the *Solanum tuberosum* species (199,200,209). Structures of tomato glycoalkaloids **172**-**175** isolated from *Lycopersicon esculentum* species (199,200,209) also have been determined.

Various chemical constituents isolated from different *Solanum* species include alkaloids, phenolics, flavonoids, sterols, saponins, and their glycosides were reviewed (215). Notable biological activities reported from the various species are the antioxidant activity of *S. tuberosum* and *S. lyratum*, antifertility activity of *S. xanthocarpum*, antiulcerogenic activity of *S. nigrum*, antineoplastic activity of *S. nigrum, S. dulcamara, S. capsicastrum, S. trilobatum, S. lyratum* and *S. indicum*, and the hepatoprotective activity of *S. lyratum, S. capsicastrum, S. nigrum, S. indicum*, and *S. incanum*.

164 α-Solanine, R = Gal, R₁ = Glc, R₂ = Rha
165 β1-Solanine, R =Gal, R₁ = H, R₂ = Rha
166 β2-Solanine, R = Gal, R₁ = Glc, R₂ = H
167 γ-Solanine, R = Gal, R₁ = R₂ = H
168 α-Chaconine, R = Glc, R₁ = R₂ = Rha
169 β1-Chaconine, R =Glc, R₁ = H, R₂ = Rha
170 β2-Chaconine, R = Glc, R₁ = Rha, R₂ = H
171 γ-Chaconine, R = Glc, R₁ = R₂ = H

172 α-Tomatine, R = Gal, R₁ = Glc, R₂ = Xyl, R₃ = Glc
173 β1-Tomatine, R =Gal, R₁ = Glc, R₂ = H, R₃ = Glc
174 β2-Tomatine, R = Gal, R₁ = Glc, R₂ = Xyl, R₃ = H
175 γ-Tomatine, R = Gal, R₁ = Glc, R₂ = R₃ = H

176 R = Gal, R₁ = Glc, R₂ = Man, R₃ = H
177 R = Glc, R₁ = R₂ = Rha, R₃ = Xyl

178 R = Gal, R₁ = Xyl, R₂ = Glc

179

180 R = Gal, R₁ = R₂ = Glc, R₃ = Xyl

181 R = Gal, R₁ = R₂ = Glc, R₃ = Xyl

Some new glycoalkaloids have been isolated from different plant species and their structures elucidated by physical and chemical methods. The glycoalkaloid α-solasonine **176**, extracted from Australian *Solanum sodomaeum*, showed antineoplastic activity against Sarcoma 180 in mice (ED₅₀ was 9 mg/kg) (210). Bioassay-guided fractionation of the methanol extract of the root bark of *S. arundo* led to the isolation of a steroidal glycoalkaloid, designated arudonine, **177** (211). This steroidal glycoalkaloid inhibited the growth of lettuce seedlings (*Lactuca sativa*). Glycoalkaloid **178** was extracted from the leaves of *S. lyratum* and the seeds of *Medicago hispida* and *Agrostemma githago* collected in Anhui Province of China (212). The unusual glycoalkaloid **179** has been isolated from the rhizomes of *Veratrum album* (Liliaceae) (213). Major novel steroidal alkaloid glycosides, named esculeoside A **180** and esculeoside B **181**, were first isolated from the pink color-type and the red color-type, respectively, of the ripe tomato fruits of *Lycopersicon esculentum* (213). The steroidal alkaloid glycosides, lycoperoside A **182**, B **183**, C **184**, and D **185** were isolated from tomato fruits (*L. esculentum*) (214).

182 R = Gal, R₁ = R₂ = Glc, R₃ = Xyl

183 R = Gal, R₁ = R₂ = Glc, R₃ = Xyl

184 R = Gal, R₁ = R₂ = Glc, R₃ = Xyl

185 R = Gal, R₁ = Glc

192 and vicine **193**. These glycosides hamper the development of fava beans as a worldwide food and feed crop because they cause a disease called favism in people who have an inherited absence of the enzyme glucose-6-phosphate dehydrogenase in their red blood cells (217,218).

Two monoterpene alkaloid glucosides loxylostosidine A **194** and B **195** were isolated from *Lonicera xylosteum* [European fly honeysuckle; Caprifoliaceae (219)]. Xylostosidine **196** has a similar structure and also was isolated from this plant species (220). American dwarf honeysuckle (*L. xylosteum*) was found in the states of Connecticut, Massachusetts, Michigan, Missouri, North Carolina, New Jersey, New York, and Vermont in the United States; the presence of alkaloids in North American *L. xylosteum* has not been investigated. The alkaloid isorheagenine glycoside **197** was isolated from *Papaver rhoeas* (221).
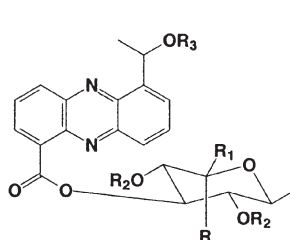
186 R = OH, R₁,R₂,R₃ = H
187 R,R₂,R₃ = H, R₁ = OH
188 R,R₂,R₃ = OAc, R₁ = H
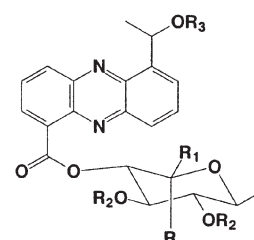
189 R = OH, R₁,R₂,R₃ = H
190 R,R₂,R₃ = H, R₁ = OH
191 R,R₂,R₃ = OAc, R₁ = H
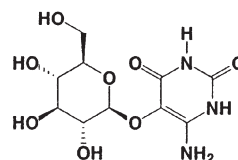
192
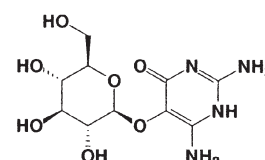
193

194 Z = β-O
195 Z = α-O

196

197

MISCELLANEOUS ALKALOID GLYCOSIDES

Fenazines **186**-**191** are a rare class of glycosidic alkaloids produced by a filamentous bacterium (isolate CNB-253, an unknown *Streptomyces* sp.) that was isolated from the shallow sediments in Bodega Bay (California) (216). Isolated compounds showed antibacterial activity.

Fava beans, *Vicia faba,* are a common human food in the Mediterranean regions of Europe. Their potential as a protein supplement for livestock is being explored in the United States and Canada. Fava beans contain the toxic glycosides covicine

Three new alkaloids, daphcalycinosidines A **198**, B **199,** and C **200** and daphcalycic acid have been isolated from the seeds of *Daphniphyllum calycinum* (222,223).

198

199

200
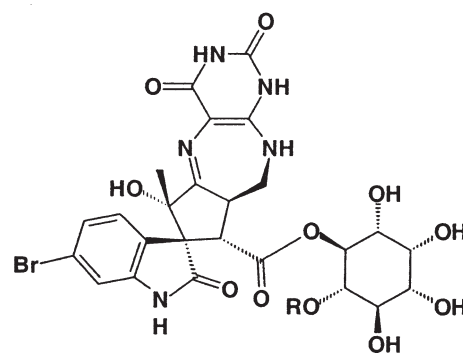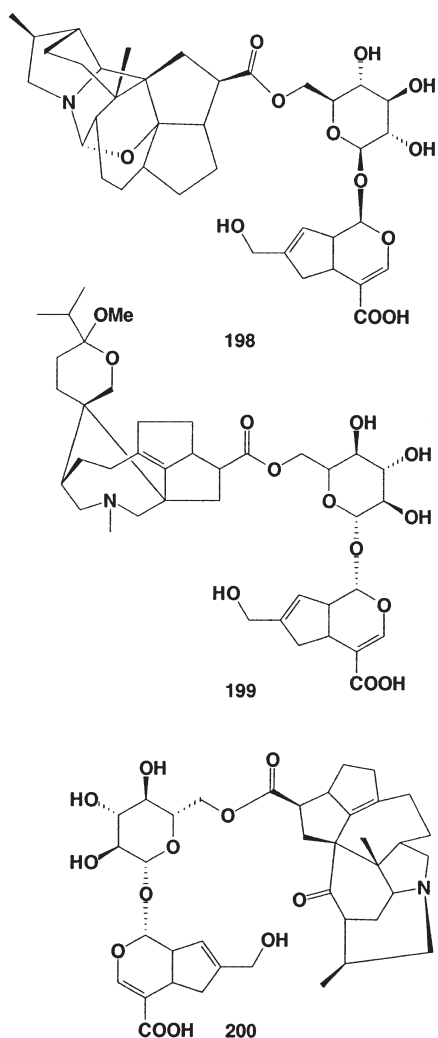
201 R = Xyl
202 R = H
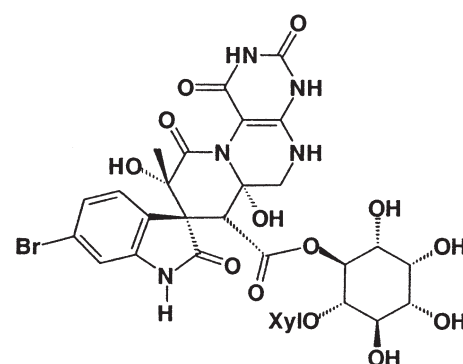
203

Neosurugatoxin **201,** which contains two sugars (myoinositol and xylopyranose) and bromine in its chemical structure, was isolated from toxic Japanese ivory shell, *Babylonia japonica* (224). Compound **201** was unstable in alkaline solution, and at 1×10^{-9} g/mL **201** inhibited the contractile response in isolated guinea pig ileum induced by 3×10^{-5} g nicotine/mL. Compound **201** also evoked mydriasis in mice at a minimum dose of 3 mg/g. The structurally related compounds prosurugatoxins **202** and surugatoxin **203** are also produced by Japanese ivory shell, and poisoning cases have been reported in Niigata, Fukui, and Shizuoka prefectures.

The methanolic extract of the stem bark of *Schumanniophyton magnificum* and schumanniofoside **204**, a chromone alkaloidal glycoside isolated from it, reduced the lethal effect of black cobra (*Naja melanoleuca*) venom in mice. This effect is greatest when the venom is mixed and incubated with the extract of schumanniofoside. It is thought that the mode of action is by oxidative inactivation of the venom (225).

In 1907, Bourquelot and Herissey (226) discovered bakankosine **205** in seeds of the Madagascarean tropical woody plant *Strychnos vacacua* (family Loganiaceae, order Gentianales). More recently, the structure of bakankosine **205** was confirmed by synthesis (227). Hypodermic injections of 0.28 g of this glycoside per kg animal were not toxic to guinea pigs. Veratramine 3-glucoside **206** and isorubijervosine **207** have been isolated from *Veratrum eschscholtzii* (228), and **207** was

isolated from *V. lobelianum* from Uzbekistan (229). The blue pigment trichotomine and the glycoside derivatives trichotomine G1 **208**, and *N,N'*-diglucopyranosyltrichotomine **209** were isolated from *Clerodendron trichotomum* fruits (230).
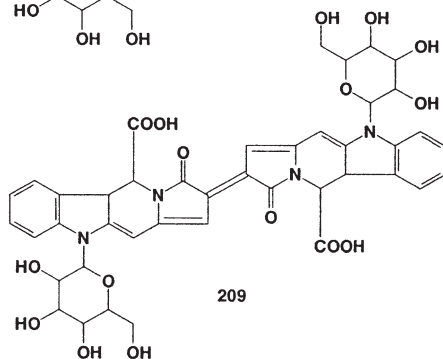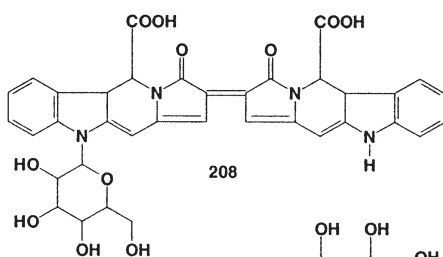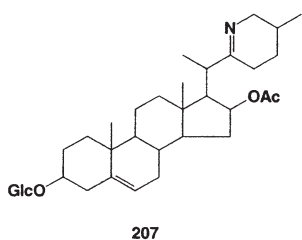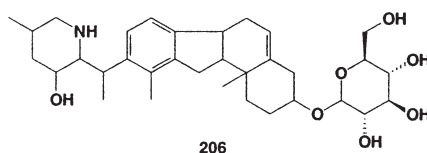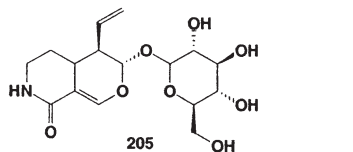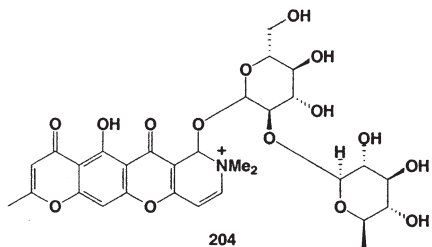
in seed-bearing plants and in berries, bark, leaves, fruits, and roots. Many alkaloids of medical importance occur in the invertebrate and plant kingdoms, and some have been synthesized. Alkaloids include the nightshade poisons, codeine, cocaine, curare, hemlock, nicotine, strychnine—a large range of dangerous chemicals. Green potato skin is full of them, and tomatoes were considered extremely poisonous in the 19th century by Europeans because of their relationship with the nightshade family until shown otherwise. Native Americans knew otherwise, of course. Alkaloids are often potent as medicines because of their high interactivity with the human body chemistry. They have a long history as local medicines known to the native peopleIt is only fairly recently that, with the ability to detail the chemistry of these substances, the pharmaceutical industry has been examining the many plants, and indeed some invertebrates, amphibian, and animals, for their alkaloids. The discovery of new sources of known biologically active alkaloids and of new alkaloids as well as their glycosides in new and already examined sources together with new structural and synthetic studies calls for periodic reviews of these important compounds.

REFERENCES

1. Dembitsky, V.M. (2005) Astonishing Diversity of Natural Surfactants. 5. Biological Active Glycosides of Aromatic Metabolites, *Lipids 40*, 869–900.
2. Raffauf, R.F. (1996) *Plant Alkaloids: A Guide To Their Discovery and Distribution*, 298 pp., Food Products Press, Binghamton, NY.
3. Harborne, J.B., Baxter, H., and Moss, G. (1998) *Phytochemical Dictionary: A Handbook of Bioactive Compounds from Plants*, 976 pp., CRC Press, Boca Raton, FL.
4. Cordell, G.A. (ed.) (1998) *Alkaloids: Chemistry and Biology*, Vol. 51, 439 pp., Academic Press, London.
5. Pelletier, S.W. (2001) (ed.), *Alkaloids: Chemical and Biological Perspectives*, Vol. 15, Pergamon, London.
6. Roberts, M.F., and Wink, M. (1998) *Alkaloids: Biochemistry, Ecology, and Medicinal Applications,* 486 pp., Kluwer Academic, Dordrecht..
7. Hesse, M. (2002) *Alkaloids: Nature's Curse or Blessing?* 400 pp., Wiley-VCH Press, Weinheim.
8. Daly, J.W. (2004) Marine Toxins and Nonmarine Toxins: Convergence or Symbiotic Organisms? *J. Nat. Prod. 67*, 1211–1215.
9. Daly, J.W. (1998) Thirty Years of Discovering Arthropod Alkaloids in Amphibian Skin, *J. Nat. Prod. 61*, 162–172.
10. Proksch, P., Ebel, R., Edrada, R.A., Wray, V., and Steube, K. (2003) Bioactive Natural Products from Marine Invertebrates and Associated Fungi, *Prog. Mol. Subcell. Biol. 37*, 117–142.
11. Dembitsky, V.M., Gloriozova, T.A., and Poroikov, V.V. (2005) Novel Antitumor Agents: Marine Sponge Alkaloids, Their Synthetic Analogs and Derivatives, *Mini Rev. Med. Chem. 5*, 319–336.
12. Kim, J., and Park, E.J. (2002) Cytotoxic Anticancer Candidates from Natural Resources, *Curr. Med. Chem. Anti-Cancer Agents 2*, 485–537.
13. Krishna, C. (2005) Solid-State Fermentation Systems. An Overview, *Crit. Rev. Biotechnol. 25*, 1–30.
14. Hashimoto, T., and Yamada, Y. (2003) New Genes in Alkaloid Metabolism and Transport, *Curr. Opin. Biotechnol. 14*, 163–168.

SUMMARY

Alkaloids are a class of compounds that typically contain nitrogen and have complex ring structures. They occur in nature

15. Kelecom, A. (2002) Secondary Metabolites from Marine Microorganisms, *An. Acad*, Bras. Cienc. 74, 151–170.
16. Danishefsky, S.J., Inoue, M., and Trauner, D. (2000) Synthesis of Immunomodulatory Marine Natural Products, *Ernst Schering Res. Found. Workshop 32*, 1–24.
17. Toyooka, N. (2001) Synthesis and Its Application to the Synthesis of Biologically Active Natural Products of New and Versatile Chiral Building Blocks, *Yakugaku Zasshi 121*, 467–479.
18. Mori, M. (2005) Development of New Synthetic Method Using Organometallic Complexes and an Application Toward Natural Product Synthesis, *Yakugaku Zasshi 125*, 51–72.
19. Delfourne, E., and Bastide, J. (2003) Marine Pyridoacridine Alkaloids and Synthetic Analogues as Antitumor Agents, *Med. Res. Rev. 23*, 234–252.
20. Cossy, J. (2005) Selective Methodologies for the Synthesis of Biologically Active Piperidinic Compounds, *Chem. Rec. 5*, 70–80.
21. Skaltsounis, A.L., Mitaku, S., and Tillequin, F. (2000) Acridone Alkaloids, in *Alkaloids* (Cordell, G.A., ed.), Vol. 54, pp. 259–377, Academic Press, London.
22. Bastow, K.F., Itoigawa, M., Furukawa, H., Kashiwada, Y., Bori, I.D., Ballas, L.M., and Lee, K.H. (1994) Antiproliferative Actions of 7-Substituted 1,3-Dihydroxyacridones; Possible Involvement of DNA Topoisomerase II and Protein Kinase C as Biochemical Targets, *Bioorg. Med. Chem. 2*, 1403–1411.
23. Fujioka, H., Nishiyama, Y., Furukawa, H., and Kumada, N. (1989) *In vitro* and *in vivo* Activities of Atalaphillinine and Related Acridone Alkaloids Against Rodent Malaria, *Antimicrob. Agents Chemother. 33*, 6–9.
24. Svoboda, G.H., Poore, G.A., Simpson, P.J., and Boder, G.B. (1966) Alkaloids of *Acronychia baueri* Schott. I. Isolation of the Alkaloids and a Study of the Antitumor and Other Biological Properties of Acronycine, *J. Pharm. Sci. 55*, 758–768.
25. Tan, P., and Auersperg, N. (1973) Effects of the Antineoplastic Alkaloid Acronycine on the Ultrastructure and Growth Patterns of Cultured Cells, *Cancer Res. 33*, 2320–2329.
26. Schneider, J., Evans, E.L., Grunberg, E., and Fryer, R.I. (1972) Synthesis and Biological Activity of Acronycine Analogs, *J. Med. Chem. 15*, 266–270.
27. Chaya, N., Terauchi, K., Yamagata, Y., Kinjo, J., and Okabe, H. (2004) Antiproliferative Constituents in Plants 14. Coumarins and Acridone Alkaloids from *Boenninghausenia japonica* Nakai, *Biol. Pharm. Bull. 27*, 1312–1326.
28. Tillequin, F., and Koch, M. (2005) Acronycine Revisited: Development of Benzo[b]acronycine Antitumor Agents, *Ann. Pharm. Fr. 63*, 35–43.
29. Reisch, J., Rozsa, Z., Szendrei, K., Novak, I., and Minker, E. (1976) Studies in the Area of Natural Product Chemistry. Part LV. Acridone Alkaloid Glucoside from *Ruta graveolens*, *Phytochemistry 15*, 240–241.
30. Kuzovkina, I.N., Al'terman, I., and Schneider, B. (2004) Specific Accumulation and Revised Structures of Acridone Alkaloid Glucosides in the Tips of Transformed Roots of *Ruta graveolens, Phytochemistry 65*, 1095–1100.
31. Kuzovkina, I.N., Rozsa, Z., Szendrei, K., and Smirnov, A.M. (1983) Alkaloids of *Boenninghausenia albiflora* Reichenb. Callus Tissue, *Rasti. Resur. (USSR) 19*, 374–378.
32. Ahua, K.M., Ioset, J.-R., Ransijn, A., Mauël, J., Mavi, S., and Hostettmann, K. (2004) Antileishmanial and Antifungal Acridone Derivatives from the Roots of *Thamnosma rhodesica*, *Phytochemistry 65*, 963–968.
33. Basco, L., Mitaku, S., Skaltsounis, A.L., Ravelomanantsoa, N., Tillequin, F., Koch, M., and Le Bras, J. (1994) *In vitro* Activities of Furoquinoline and Acridone Alkaloids Against *Plasmodium falciparum*, *Antimicrob. Agents Chemother. 38*, 1169–1171.
34. Stevigny, C., Bailly, C., and Quetin-Leclercq, J. (2005) Cytotoxic and Antitumor Potentialities of Aporphinoid Alkaloids, *Curr. Med. Chem. Anti-Cancer Agents 5*, 173–182.
35. Kashiwaba, N., Ono, M., Toda, J., Suzuki, H., and Sano, T. (2000) Aporphine Glycosides from *Stephania cepharantha* Seeds, *J. Nat. Prod. 63*, 477–479.
36. Israilov, I.A., Denisenko, O.N., Yunusov, M.S., and Yunusov, S.Y. (1976) Structure of Floripavidine, *Khim. Prirod. Soed. (USSR) 6*, 799–801.
37. Banerji, J., Chatterjee, A., Patra, A., Bose, P., Das, R., Das, B., Shamma, M., and Tantisewie, B. (1994) Kamaline, an Unusual Aporphine Alkaloid, from *Stephania venosa*, *Phytochemistry 36*, 1053–1056.
38. Zhu, D., Wang, B., Huang, B., Xu, R., Qiu, Y., Chen, X., and Quan, D. (1983) Two New Oxoaporphine Alkaloids Isolated from *Aristolochia tuberosa*. I. Structures of Tuberosinone and Tuberosinone-*N*-β-D-glucoside, *Huaxue Xuebao 41*, 74–78.
39. Zhu, D., Wang, B., Huang, B., Xu, R., Qiu, Y., and Chen, X. (1982) Two New 4,5-Dioxoaporphine Alkaloids Isolated from *Aristolochia tuberose*, *Heterocycles 17*, 345–347.
40. Kostalova, D., Hrochova, V., Pronayova, N., and Lesko, J. (1991) Constituents of *Aristolochia clematitis* L, *Chemical Papers (Czechia) 45*, 713–716.
41. Sicker, D., Frey, M., Schulz, M., and Gierl, A. (2000) Role of Natural Benzoxazinones in the Survival Strategy of Plants, *Inter. Rev. Cytol. 198*, 319–346.
42. Wolf, R.B., Spencer, G.F., and Plattner, R.D. (1985) Benzoxazolinone, 2,4-Dihydroxy-1,4-benzoxazin-3-one, and Its Glucoside from *Acanthus mollis* Seeds Inhibit Velvetleaf Germination and Growth, *J. Nat. Prod. 48*, 59–63.
43. Chatterjee, A., Sharma, N.J., Basserji, J., and Basa, S.C. (1990) Studies on Acanthaceae. Benzoxazine Glucoside and Benzoxazolone from *Blepharis edulis* Pers., *Indian J. Chem*, *Sect. B 29*, 132–134.
44. Özden, S., Özden, T., Attila, I., Kücükislamoglu, M., and Okatan, A. (1992) Isolation and Identification *via* High-Performance Liquid Chromatography and Thin-Layer Chromatography of Benzoxazolinone Precursors from *Consolida orientalis* Flowers, *J. Chromatogr. 609*, 402–406.
45. Pratt, K., Kumar, P., and Chilton, W.S. (1995) Cyclic Hydroxamic Acids in Dicotyledonous Plants, *Biochem. Syst. Ecol. 23*, 781–785.
46. Hasegawa, T., Yamada, K., Shigemori, H., Miyamoto, K., Ueda, J., and Hasegawa, K. (2004) Isolation and Identification of Phototropism-Regulating Substances Benzoxazinoids from Maize Coleoptiles, *Heterocycles 63*, 2707–2712.
47. Rosenfeld, M.J., and Forsberg, S.R. (2004) Novel Compounds for Use in Weight Loss and Appetite Suppression in Humans, U.S. Patent Appl. Publ. 38 pp., Continuation in part of U.S. Ser. No. 834,592. US A1 20040930.
48. Kanchanapoom, T., Kamel, M.S., Kasai, R., Picheansoonthon, C., Hiraga, Y., and Yamasaki, K. (2001) Benzoxazinoid Glucosides from *Acanthus ilicifolius*, *Phytochemistry 58*, 637–640.
49. Baumeler, A., Hesse, M., and Werner, C. (2000) Benzoxazinoids-Cyclic Hydroxamic Acids, Lactams and Their Corresponding Glucosides in the Genus *Aphelandra* (Acanthaceae), *Phytochemistry 53*, 213–222.
50. Xie, H., Wei, H., Yashikawa, M., Xia, N., and Wei, X. (2005) Benzoxazinoid Glucosides from *Baphicacanthus cusia*, *Biochem. Syst. Ecol. 33*, 551–554.
51. Kanchanapoom, T., Kasai, R., Picheansoonthon, C., and Yamasaki, K. (2001) Megastigmane, Aliphatic Alcohol and Benzoxazinoid Glycosides from *Acanthus ebracteatus*, *Phytochemistry 58*, 811–817.
52. Alipieva, K.I., Taskova, R.M., Evstatieva, L.N., Handjieva, N.V., and Popov, S.S. (2003) Benzoxazinoids and Iridoid Glucosides from Four *Lamium* Species, *Phytochemistry 64*, 1413–1417.

53. Barger, G. (1920) Ergot, Its History and Chemistry, *Pharmaceut. J. 105*, 470–473.

54. Flieger, M., Wurst, M., and Shelby, R. (1997) Ergot Alkaloids—Sources, Structures and Analytical Methods, *Folia Microbiol. (Praha) 42*, 3–30.

55. Van Dongen, P.W.J., and De Groot, A.N.J.A. (1995) History of Ergot Alkaloids from Ergotism to Ergometrine, *Eur. J. Obstet. Gynaecol. Reprod. Biol. 60*, 109–116.

56. Steyn, P.S. (1995) Mycotoxins, General View, Chemistry and Structure, *Toxicol. Lett. 82–83*, 843–851.

57. Pohland, A.E. (1993) Mycotoxins in Review, *Food Addit. Contam. 10*, 17–28.

58. Silerstein, S.D., and McCrory, D.C. (2003) Ergotamine and Dihydroergotamine: History, Pharmacology, and Efficacy, *Headache 43*, 144–166.

59. Inzelberg, R., Schechtman, E., and Nisipeanu, P. (2003) Cabergoline, Pramipexole and Ropinirole Used as Monotherapy in Early Parkinson's Disease: An Evidence-Based Comparison, *Drugs Aging 20*, 847–855.

60. Mucke, H. (2002) Therapies in Development for the Treatment of Migraine, *Expert Opin. Investig. Drugs 11*, 1813–1820.

61. Kren, V., and Cvak, L. (eds.) (1999) *Ergot: Genus Claviceps (Medicinal & Aromatic Plants—Industrial Profiles)*, Harwood Academic, Amsterdam.

62. Mantegani, S., Brambilla, E., and Varasi, M. (1999) Ergoline Derivatives: Receptor Affinity and Selectivity, *Farmaco 54*, 288–296.

63. Floss, H.G., Gunther, H., Mothes, U., and Becker, I. (1967) Isolation of Elymoclavin-*O*-β-ᴅ-fructoside from Cultures of Ergot, *Z. Naturforsch. [B] 4*, 399–402.

64. Flieger, M., Zelenkova, N.F., Sedmera, P., Kren, V., Novak, J., Rylko, V., Sajdl, P., and Rehacek, Z. (1989) Ergot Alkaloid Glycosides from Saprophytic Cultures of *Claviceps*. I. Elymoclavine Fructosides, *J. Nat. Prod. 52*, 506–510.

65. Flieger, M., Kren, V., Zelenkova, N.F., Sedmera, P., Novak, J., and Sajdl, P. (1990) Ergot Alkaloid Glycosides from Saprophytic Cultures of *Claviceps*, II. Chanoclavine I Fructosides, *J. Nat. Prod. 53*, 171–175.

66. Kren, V., and Martínková, L. (2001) Glycosides in Medicine: The Role of Glycosidic Residue in Biological Activity, *Curr. Med. Chem. 8*, 1313–1338.

67. Somei, M., and Yamada, F. (2005) Simple Indole Alkaloids and Those with a Non-rearranged Monoterpenoid Unit, *Nat. Prod. Rep. 22*, 73–103.

68. Dembitsky, V.M. (2002) Bromo- and Iodo-containing Alkaloids from Marine Microorganisms and Sponges, *Bioorg. Khim. (Moscow) 28*, 196–208.

69. Saxton, J.E. (1977) Indole Alkaloids, in *Alkaloids*, Vol. 7, pp. 183–246, Academic Press, London.

70. Minami, Y. (2001) Indican Metabolism in *Polygonum tinctorium*, *Kagaku To Seibutsu 39*, 202–207.

71. Sawabe, A., Nomura, M., Fujihara, Y., Tada, T., Hattori, F., Shiohara, S., Shimomura, K., Matsubara, Y., Komemushi, S., Okamoto, T., *et al.* (2001) Cosmetic Substances for Skin Depigmentation from African Dietary Leaves, *Celosia argentea* L, *Kinki Daigaku Nogaku Sogo Kenkyusho Hokoku 9*, 141–146.

72. Vu, T.T. (1999) Extraction of Glucoside (indican) from Vietnamese *Indigofera* for Indigo Blue Dyes, *Hoa Hoc Va Cong Nghiep Hoa Chat (in Vietnamese) 2*, 28–32.

73. Kokubun, T., Edmonds, J., and John, P. (1998) Indoxyl Derivatives in Woad in Relation to Medieval Indigo Production, *Phytochemistry 49*, 79–87.

74. Murakami, T., Kishi, A., Sakurama, T., Matsuda, H., and Yoshikawa, M. (2001) Chemical Constituents of Two Oriental Orchids, *Calanthe discolor* and *C. liukiuensis*: Precursor Indole Glycoside of Tryptanthrin and Indirubin, *Heterocycles 54*, 957–966.

75. Yoshikawa, M., Murakami, T., Kishi, A., Sakurama, T., Matsuda, H., Nomura, M., Matsuda, H., and Kubo, M. (1998) Novel Indole *S,O*-Bisdesmoside, Calanthoside, the Precursor Glycoside of Tryptanthrin, Indirubin, and Isatin, with Increasing Skin Blood Flow Promoting Effects, from Two *Calanthe* Species (Orchidaceae), *Chem. Pharm. Bull. (Tokyo) 46*, 886–888.

76. Ouyang, Y., Koike, K., and Ohmoto, T. (1994) Indole Alkaloids from *Brucea mollis* var. *tonkinensis*, *Phytochemistry 37*, 575–578.

77. Hagin, R.D. (1989) Isolation and Identification of 5-Hydroxyindole-3-acetic Acid and 5-Hydroxytryptophan, Major Allelopathic Aglycons in Quackgrass (*Agropyron repens* L. Beauv.), *J. Agric. Food Chem. 37*, 1143–1149.

78. Wiese, G., and Grambow, H.J. (1986) Indole-3-methanol-β-ᴅ-glucoside and Indole-3-carboxylic Acid-β-ᴅ-glucoside Are Products of Indole-3-acetic Acid Degradation in Wheat Leaf Segments, *Phytochemistry 25*, 2451–2455.

79. Nonhebel, H.M., Kruse, L.I., and Bandurski, R.S. (1985) Indole-3-acetic Acid Catabolism in *Zea mays* Seedlings. Metabolic Conversion of Oxindole-3-acetic Acid to 7-Hydroxy-2-oxindole-3-acetic Acid 7′-*O*-β-ᴅ-Glucopyranoside, *J. Biol. Chem. 260*, 12685–12689.

80. Schumacher, R.W., Harrigan, B.L., and Davidson, B.S. (2001) Kahakamides A and B, New Neosidomycin Metabolites from a Marine-Derived Actinomycete, *Tetrahedron Lett. 42*, 5133–5135.

81. Furuta, R., Naruto, S., Tamura, A., and Yokogawa, K. (1979) Neosidomycin, a New Antibiotic of *Streptomyces*, *Tetrahedron Lett. 19*, 1701–1704.

82. Ito, T., Ohba, K., Koyama, M., Sezaki, M., Tohyama, H., Shomura, T., Fukuyasu, H., Kazuno, Y., Niwa, T., and Kojima, M. (1984) A New Antiviral Antibiotic SF-2140 Produced by *Actinomadura*, *J. Antibiot. 37*, 931–934.

83. Tohyama, H., Miyadoh, S., Ito, M., Shomura, T., Ito, T., Ishikawa, T., and Kojima, M. (1984) A New Indole N-Glycoside Antibiotic SF-2140 from an *Actinomadura*. I. Taxonomy and Fermentation of Producing Microorganism, *J. Antibiot. 37*, 1144–1148.

84. Marinos, V.A., Tate, M.E., and Williams, P.J. (1992) Glucosides of Ethyl Indole-3-lactate and Uroterpenol in Riesling Wine, *Phytochemistry 31*, 2755–2759.

85. Ding, W., Williams, D.R., Northcote, P., Siegel, M.M., Tsao, R., Ashcroft, J., Morton, G.O., Alluri, M., and Abranat, D. (1994) Pyrroindomycins, Novel Antibiotics Produced by *Streptomyces rugosporus* sp. LL-42D005. I. Isolation and Structure Determination, *J. Antibiot. 47*, 1250–1257.

86. Liu, H.M., Jiang, Z., and Feng, X.Z. (1993) New Oxindole Alkaloid Glycosides from *Uncaria sinensis*, *Yaoxue Xuebao 28*, 849–853.

87. Salim, A.A., Garson, M.J., and Craik, D.J. (2004) New Indole Alkaloids from the Bark of *Alstonia scholaris*, *J. Nat. Prod. 67*, 1591–1594.

88. Valverde, J., Tamayo, G., and Hesse, M. (1999) β-Carboline Monoterpenoid Glucosides from *Palicourea adusta*, *Phytochemistry 52*, 1485–1489.

89. Ouyang, Y., Mitsunaga, K., Koike, K., and Ohmoto, T. (1995) Alkaloids and Quassinoids of *Brucea mollis* var. *tonkinensis*, *Phytochemistry 39*, 911–913.

90. Ouyang, Y., Koike, K., and Ohmoto, T. (1994) Canthin-6-one Alkaloids from *Brucea mollis* var. *tonkinensis*, *Phytochemistry 36*, 1543–1546.

91. Leewanich, P., Tohda, M., Matsumoto, K., Subhadhirasakul, S., Takayama, H., Aimi, N., and Watanabe, H. (1998) A Possible Mechanism Underlying Corymine Inhibition of Glycine-Induced Cl⁻ Current in *Xenopus* Oocytes, *Eur. J. Pharmacol. 348*, 271–277.

92. Takayama, H., Subhadhirasakul, S., Keawpradub, N., Mizuki, J., Ohmori, O., Kitajima, M., Aimi, N., Ponglux, D., and Sakai, S.-I. (1994) Structure Elucidation of the Novel Indole Alkaloids from the Three Apocynaceae Plants Growing in Southern Thailand, *Tennen Yuki Kagobutsu Toronkai Koen Yoshishu 36*, 541–548.

93. Takayama, H., Subhadhirasakul, S., Ohmori, O., Kitajima, M., Ponglux, D., and Aimi, N. (1998) Hunterioside B, a Disaccharide Carrying Monoterpenoid Indole Alkaloid, from *Hunteria zeylanica*, *Heterocycles 47*, 87–90.

94. Morita, H., Ichihara, Y., Takeya, K., Watanabe, K., Itokawa, H., and Motidome, M. (1989) A New Indole Alkaloid Glycoside from the Leaves of *Palicourea marcgravii*, *Planta Med. 55*, 288–289.

95. Nonato, M.G., Truscott, R.J.W., Carver, J.A., Hemling, M.E., and Garson, M.J. (1995) Glucoindole Alkaloids from *Ophiorrhiza acuminate*, *Planta Med. 61*, 278–280.

96. Lin, M., Li, S.Z., Liu, X., and Yu, D.Q. (1989) Structures of Two New Alkaloidal Glucosides of *Nauclea officinalis* Pierre ex Pitard, *Yaoxue Xuebao 24*, 32–36.

97. Aimi, N., Tsuyuki, T., Murakami, H., Sakai, S., and Haginiwa, J. (1985) Structure of Ophiorines A and B; Novel Type Gluco Indole Alkaloids Isolated from *Ophiorrhiza* spp, *Tetrahedron Lett. 26*, 5299–5302.

98. Itoh, A., Tanahashi, T., Nagakura, N., and Nishi, T. (2003) Two Chromone-Secoiridoid Glycosides and Three Indole Alkaloid Glycosides from *Neonauclea sessilifolia*, *Phytochemistry 62*, 359–369.

99. Erdelmeier, C.A.J., Wright, A.D., Orjala, J., Baumgartner, B., Rali, T., and Sticher, O. (1991) New Indole Alkaloid Glycosides from *Nauclea orientalis*, *Planta Med. 57*, 149–152.

100. Abreu, P., and Pereira, A. (2001) New Indole Alkaloids from *Sarcocephalus latifolius*, *Nat. Prod. Lett. 15*, 43–48.

101. Morikawa, T., Sun, B., Matsuda, H., Wu, L.J., Harima, S., and Yoshikawa, M. (2004) Bioactive Constituents from Chinese Natural Medicines. XIV. New Glycosides of β-Carboline Type Alkaloid, Neolignan, and Phenylpropanoid from *Stellaria dichotoma* L. var. *lanceolata* and Their Antiallergic Activities, *Chem. Pharm. Bull. (Tokyo) 52*, 1194–1199.

102. Burger, W., and Taylor, C.M. (1993) *Fieldiana Botany, New Series No.* 33, Flora Costaricensis, Family No. 202 Rubiaceae, p. 244, Field Museum of Natural History, Chicago.

103. Joly, L.G., Guerra, S., Septimo, R., Solis, P.N., Correa, M., Gupta, M., Levy, S., and Sandberg, F. (1987) Ethnobotanical Inventory of Medicinal Plants Used by the Guaymi Indians in Western Panama. Part I, *J. Ethnopharmacol. 20*, 145–171.

104. Di Stasi, L.C. (1995) Amoebicidal Compounds from Medicinal Plants, *Parassitologia (Brazil) 37*, 29–39.

105. Achenbach, H., Lottes, M., Waibel, R., Karikas, G.A., Correa, M.A.D., and Gupta, M.P. (1995) Alkaloids and Other Compounds from *Psychotria correae*, *Phytochemistry 38*, 1537–1545.

106. Lamidi, M., Ollivier, E., Mahiou, V., Debrauwer, R.F.L., Ekekang, L.N., and Balansard, G. (2005) Gluco-indole Alkaloids from the Bark of *Nauclea diderrichii*. ^{1}H and ^{13}C NMR Assignments of 3α-5α-Tetrahydrodeoxycordifoline Lactam and Cadambine Acid, *Magn. Reson. Chem. 43*, 427–429.

107. Endo, K., Oshima, Y., and Kikuchi, H. (1983) Part 50 in the Series on the Validity of the Oriental Medicines. Hypotensive Principles of *Uncaria* Hooks, *Planta Med. 49*, 188–190.

108. Kitajima, M., Hashimoto, K.I., and Yokoya, M. (2000) A New Gluco Indole Alkaloid, 3,4-Dehydro-5-carboxystrictosidine, from Peruvian Uña de Gato (*Uncaria tomentosa*), *Chem. Pharm. Bull. (Tokyo) 48*, 1410–1412.

109. Bush, J.A., Long, B.H., Catino, J.J., and Bradner, W.T. (1987) Production and Biological Activity of Rebeccamycin, a Novel Antitumor Agent, *J. Antibiot. 40*, 668–678.

110. Carrupt, P.-A., Testa, B., Bechalany, A., El Tayar, N., Descas, P., and Perrissoud, D. (1991) Morphine 6-Glucuronide and Morphine 3-Glucuronide as Molecular Chameleons with Unexpected Lipophilicity, *J. Med. Chem. 34*, 1272–1275.

111. Lam, K.S., Schroeder, D.R., Veitch, J.M., Matson, J.A., and Forenza, S. (1991) Isolation of a Bromo Analog of Rebeccamycin from *Saccharothrix aerocolonigenes*, *J. Antibiot. (Tokyo) 44*, 934–939.

112. Nettleton, D.E., Doyle, T.W., Krishnan, B., Matsumoto, G.K., and Clardy, J. (1985) Isolation and Structure of Rebeccamycin—A New Antitumor Antibiotic from *Nocardia aerocoligenes*, *Tetrahedron Lett. 26*, 4011–4014.

113. Prudhomme, M. (2003) Rebeccamycin Analogues as Anticancer Agents, *Eur. J. Med. Chem. 38*, 123–140.

114. Prudhomme, M. (2000) Recent Developments of Rebeccamycin Analogues as Topoisomerase I Inhibitors and Antitumor Agents, *Curr. Med. Chem. 7*, 1189–1212.

115. Subbaraju, G.V., Kavitha, J., Rajasekhar, D., and Jimenez, J.I. (2004) Jusbetonin, the First Indolo[3,2-b]quinoline Alkaloid Glycoside, from *Justicia betonica*, *J. Nat. Prod. 67*, 461–462.

116. Bonjouklian, R., Smitka, T.A., Doolin, L.E., Molloy, R.M., Debono, M., Shaffer, S.A., Moore, R.E., Stewart, J.B., and Patterson, G.M.L. (1991) Tjipanazoles, New Antifungal Agents from the Blue-Green Alga *Tolypothrix tjipanasensis*, *Tetrahedron 47*, 7739–7750.

117. Voldoire, A., Moreau, P., Sancelme, M., Matulova, M., Léonce, S., Pierré, A., Hickman, J., Pfeiffer, B., Renard, P., Dias, N., *et al.* (2004) Analogues of Antifungal Tjipanazoles from Rebeccamycin, *Bioorg. Med. Chem. 12*, 1955–1962.

118. Strack, D., Vogt, T., and Schliemann, W. (2003) Recent Advances in Betalain Research, *Phytochemistry 62*, 247–269.

119. Steglich, W., and Strack, D. (1990) Betalains, in *The Alkaloids, Chemistry and Pharmacology* (Brossi, A., ed.), pp. 1–62, Academic Press, London.

120. Cai, Y., Sun, M., and Corke, H. (2003) Antioxidant Activity of Betalains from Plants of the Amaranthaceae, *J. Agric. Food Chem. 51*, 2288–2294.

121. Saldanha, P.H., Magalhaes, L.E., and Horta, W.A. (1960) Race Differences in the Ability to Excrete Beetroot Pigment (betanin), *Nature 187*, 806.

122. Piattelli, M., and Imperato, F. (1969) Betacyanins of the Family Cactaceae, *Phytochemistry 8*, 1503–1507.

123. Cai, Y., Sun, M., and Corke, H. (2001) Identification and Distribution of Simple and Acylated Betacyanins in the Amaranthaceae, *J. Agric. Food Chem. 49*, 1971–1978.

124. Kugler, F., Stintzing, F.C., and Carle, R. (2004) Identification of Betalains from Petioles of Differently Colored Swiss Chard (*Beta vulgaris* L. ssp. *cicla* [L.] Alef. cv. Bright Lights) by High-Performance Liquid Chromatography-Electrospray Ionization Mass Spectrometry, *J. Agric. Food Chem. 52*, 2975–2981.

125. Schliemann, W., Joy, R.W., IV, Komamine, A., Metzger, J.W., Nimtz, M., Wray, V., and Strack, D. (1996) Betacyanins from Plants and Cell Cultures of *Phytolacca americana*, *Phytochemistry 42*, 1039–1046.

126. Piattelli, M., and Imperato, F. (1970) Betacyanins from *Bougainvillea*, *Phytochemistry 9*, 455–458.

127. Strack, D., Vogt, T., and Schliemann, W. (2003) Recent Advances in Betalain Research, *Phytochemistry 62*, 247–269.

128. Smith, A.L., and Nicolaou, K.C. (1996) The Enediyne Antibiotics, *J. Med. Chem. 39*, 2103–2117.

129. Dai, W.M. (2003) Natural Product Inspired Design of Enediyne Prodrugs *via* Rearrangement of an Allylic Double Bond, *Curr. Med. Chem. 10*, 2265–2283.

130. Nicolaou, K.C., Smith, A.L., and Yue, E.W. (1993) Chemistry and Biology of Natural and Designed Enediynes, *Proc. Natl. Acad. Sci. USA 90*, 5881–5888.

131. Oku, N., Matsunaga, S., and Fusetani, N. (2003) Shishijimicins A–C, Novel Enediyne Antitumor Antibiotics from the Ascidian *Didemnum proliferum*, *J. Am. Chem. Soc. 125*, 2044–2045.

132. Hofstead, S.J., Matson, J.A., Malacko, A.R., and Marquardt, H. (1992) Kedarcidin, a New Chromoprotein Antitumor Antibiotic. II. Isolation, Purification and Physico-chemical Properties, *J. Antibiot. (Tokyo) 45*, 1250–1254.

133. Zein, N., Colson, K.L., Leet, J.E., Schroeder, D.R., Solomon, W., Doyle, T.W., and Casazza, A.M. (1993) Kedarcidin Chromophore: An Enediyne That Cleaves DNA in a Sequence-Specific Manner, *Proc. Natl. Acad. Sci. USA 90*, 2822–2826.

134. Shao, R.G., and Zhen, Y.S. (1992) Antitumor Activity of New Antitumor Antibiotic C1027 and Its Monoclonal Antibody Assembled Conjugate, *Yao Xue Xue Bao 27*, 486–491.

135. Li, J.Z., Jiang, M., Xue, Y.C., and Zhen, Y.S. (1993) Antitumor Effect of the Immunoconjugate Composed of Antibiotic C1027 and Fab Fragment from a Monoclonal Antibody Directed Against Human Hepatoma, *Yao Xue Xue Bao 28*, 260–265.

136. Shen, B., and Liu, W. (2003) The *Streptomyces globisporus* Gene Cluster for Biosynthesis of the Enediyne Antitumor Antibiotic C-1027 and the Generation of Novel Variants, U.S. Pat. Appl. Publ. 119 pp., U.S. Patent 2003157654 A1 20030821.

137. Hanada, M., Ohkuma, H., Yonemoto, T., Tomita, K., Ohbayashi, M., Kamei, H., Miyaki, T., Konishi, M., Kawaguchi, H., and Forenza, S. (1991) Maduropeptin, a Complex of New Macromolecular Antitumor Antibiotics, *J. Antibiot. (Tokyo) 44*, 403–414.

138. James, L.F., Panter, K.E., Gaffield, W., and Molyneux, R.J. (2004) Biomedical Applications of Poisonous Plant Research, *J. Agric. Food Chem. 52*, 3211–3230.

139. Lopez-Ortiz, S., Panter, K.E., Pfister, J.A., and Launchbaugh, K.L. (2004) The Effect of Body Condition on Disposition of Alkaloids from Silvery Lupine (*Lupinus argenteus* Pursh) in Sheep, *J. Anim. Sci. 82*, 2798–2805.

140. Smith, R.A. (1987) Potential Edible Lupine Poisonings in Humans, *Vet. Hum. Toxicol. 29*, 444–445.

141. Michael, J.P. (2004) Indolizidine and Quinolizidine Alkaloids, *Nat. Prod. Rep. 21*, 625–649.

142. Abdel-Halim, O.B., El-Gammal, A.A., Abdel-Fattah, H., and Takeya, K. (1999) Glycosidic Alkaloids from *Lupinus varius*, *Phytochemistry 51*, 5–9.

143. Suzuki, H., Koike, Y., Takamatsu, S., Sekine, T., Saito, K., and Murakoshi, I. (1994) A Glycosidic Lupine Alkaloid from *Lupinus hirsutus*, *Phytochemistry 37*, 591–592.

144. Murakoshi, I., Toriizuka, K., Haginiwa, J., Ohmiya, S., and Otomasu, H. (1979) (−)-(*trans*-4′-β-D-Glycopyranosyloxy-3′-methoxycinnamyl)lupinine, a New Lupin Alkaloid in *Lupinus* Seedlings, *Phytochemistry 18*, 699–700.

145. Felpin, F.X., and Lebreton, J. (2004) History, Chemistry and Biology of Alkaloids from *Lobelia inflata*, *Tetrahedron 60*, 10127–10153.

146. Daly, J.W., Myers, C.W., and Whittaker, N. (1987) Further Classification of Skin Alkaloids from Neotropical Poison Frogs (Dendrobatidae), with a General Survey of Toxic/Noxious Substances in the Amphibian, *Toxicon 25*, 1023–1095.

147. O'Hagan, D. (2000) Pyrrole, Pyrrolidine, Pyridine, Piperidine and Tropane Alkaloids, *Nat. Prod. Rep. 17*, 435–446.

148. Yildiz, D. (2004) Nicotine, Its Metabolism and an Overview of Its Biological Effects, *Toxicon 43*, 619–632.

149. Asano, N. (2003) Naturally Occurring Iminosugars and Related Compounds: Structure, Distribution, and Biological Activity, *Curr. Top. Med. Chem. 3*, 471–484.

150. Simmonds, M.S.J., Kite, G.C., and Porter, E.A. (1999) Taxonomic Distribution of Iminosugars in Plants and Their Biological Activities, in *Iminosugars as Glycosidase Inhibitors* (Stütz, A.E., ed.), pp. 8–30, Wiley-VCH, Weinheim.

151. Yamashita, T., Yasuda, K., Kizu, H., Kameda, Y., Watson, A.A., Nash, R.J., Fleet, G.W.J., and Asano, N. (2002) New Polyhydroxylated Pyrrolidine, Piperidine, and Pyrrolizidine Alkaloids from *Scilla sibirica*, *J. Nat. Prod. 65*, 1875–1881.

152. Yayli, N., and Baltaci, C. (1997) A Novel Glycoside Linked Piperidine Alkaloid from *Cyclamen coum*, *Turkish J. Chem. 21*, 139–143.

153. Willems, M. (1988) A Glucosidic Alkaloid Artifact, Originated from Secoiridoid Glucosides from Fruits of *Ligustrum vulgare* L, *Arch. Pharm. (Weinheim) 321*, 357–358.

154. Orsini, F., Pelizzoni, F., Pulici, M., and Verotta, L. (1989) Isolation of a New Compounds Related to 4-Methoxypyridoxine from *Albizzia lucida*, *Gazzetta Chim. Ital. 119*, 63–64.

155. McInnes, A.G., Smith, D.G., Walter, J.A., Wright, J.L.C., Vining, L.C., and Arsenault, G.P. (1978) Caerulomycin D, a Novel Glycosidic Derivative of 3,4-Dihydroxy-2,2′-dipyridyl 6-Aldoxime from *Streptomyces caeruleus*, *Can. J. Chem. 56*, 1836–1842.

156. Oka, H., Funaishi, K., Kawamura, K., Nakajima, S., Ookura, A., Suda, H., and Okanishi, M. (1991) Antitumor Glycosides BE-14324 and Their Manufacture with *Streptomyces*, *Jpn. Kokai Tokkyo Koho*, 12 pp. Japanese Patent: JP 03081283 A2 19910405 Heisei (*in Japanese*).

157. Shibano, M., Tsukamoto, D., Fujimoto, R., Masui, Y., Sugimoto, H., and Kusano, G. (2000) Studies on the Constituents of *Broussonetia* Species. VII. Four New Pyrrolidine Alkaloids, Broussonetines M, O, P, and Q, as Inhibitors of Glycosidase, from *Broussonetia kazinoki* Sieb, *Chem. Pharm. Bull. (Tokyo) 48*, 1281–1285.

158. Shibano, M., Nakamura, S., Motoya, N., and Kusano, G. (1999) Studies on the Constituents of *Broussonetia* Species. V. Two New Pyrrolidine Alkaloids, Broussonetines K and L, as Inhibitors of Glycosidase, from *Broussonetia kazinoki* SIEB, *Chem. Pharm. Bull. (Tokyo) 47*, 472–476.

159. Shibano, M., Kitagawa, S., Nakamura, S., Akazawa, N., and Kusano, G. (1997) Studies on the Constituents of *Broussonetia* Species. II. Six New Pyrrolidine Alkaloids, Broussonetine A, B, E, F and Broussonetinine A and B, as Inhibitors of Glycosidases from *Broussonetia kazinoki* Sieb, *Chem. Pharm. Bull. (Tokyo) 45*, 700–705.

160. Watson, A.A., Nash, R.J., Wormald, M.R., Harvey, D.J., Dealler, S., Lees, E., Asano, N., Kizu, H., Kato, A., Griffiths, R.C., *et al.* (1997) Glycosidase-Inhibiting Pyrrolidine Alkaloids from *Hyacinthoides non-scripta*, *Phytochemistry 46*, 255–259.

161. Kocourek, J., Bucharova, V., Buchbauerova, V., Jiracek, V., Kostir, J.A., Kostir, J.V., Kysilka, C., Mostkova, I., Pribylova, A., Ticha, M., *et al.* (1967) Glycosides. V. Pisatoside. New Alkali-Labile, Nitrogenous β-D-Glucopyranoside of Pea (*Pisum sativum*), *Arch. Biochem. Biophys. 121*, 531–532.

162. Tsuchiya, K., Kobayashi, S., Kurokawa, T., Nakagawa, T., Shimada, N., Nakamura, H., Iitaka, Y., Kitagawa, M., and Tatsuta, K. (1995) Gualamycin, a Novel Acaricide Produced by *Streptomyces* sp. NK11687. II. Structural Elucidation, *J. Antibiot. (Tokyo) 48*, 630–634.

163. Kato, A., Kano, E., Adachi, I., Molyneux, R.J., Watson, A.A., Nash, R.J., Fleet, G.W.J., Wormald, M.R., Kizu, H., Ikeda, K., *et al.* (2003) Australine and Related Alkaloids: Easy Structural Confirmation by ^{13}C NMR Spectral Data and Biological Activities, *Tetrahedron Asymm. 14*, 325–331.

164. Leander, K., and Lüning, B. (1967) Studies on *Orchidaceae* Alkaloids. VII. Structure of a Glucosidic Alkaloid from *Malaxis congesta comb. nov. (Rchb. f.)*, *Tetrahedron Lett. 8*, 3477–3478.

165. Griffin, W.J., and Lin, D.G. (2000) Chemotaxonomy and Geographical Distribution of Tropane Alkaloids, *Phytochemistry 53*, 623–637.

166. Jenett-Siems, K., Weigl, R., Boehm, A., Mann, P., Tofern-Re-

blin, B., Ott, S.C., Ghomian, A., Kaloga, M., Siems, K., Witte, L., *et al.* (2005) Chemotaxonomy of the Pantropical Genus *Merremia* (Convolvulaceae) Based on the Distribution of Tropane Alkaloids, *Phytochemistry 66*, 1448–1464.

167. Molyneux, R.J., Gardner, D.R., James, L.F., and Steven, M. (2002) Polyhydroxy Alkaloids: Chromatographic Analysis, *J. Chromatogr. A. 967*, 57–74.

168. Dräger, B. (2002) Analysis of Tropane and Related Alkaloids, *J. Chromatogr. A. 978*, 1–35.

169. Asano, N. (2000) Water Soluble Nortropane Alkaloids in Crude Drugs, Edible Fruits and Vegetables: Biological Activities and Therapeutic Applications, *Mech. Ageing Dev. 116*, 155–156.

170. Naithani, V., Haider, S., and Kakkar, P. (2001) Plant Toxins: A Historical, Evolutionary, Economic and Toxicological Account, *J. Ecophysiol. Occupat. Health 1*, 339–364.

171. Griffiths, R.C., Watson, A.A., Kizu, H., Asano, N., Sharpo, H.J., Jones, M.G., Wormald, M.R., Fleet, G.W.J., and Nash, R.J. (1996) The Isolation from *Nicandra physalodes* and Identification of the 3-*O*-β-ᴅ-Glucopyranoside of 1α,2β,3α,6α-Tetrahydroxy-*nor*-tropane (calystegine B$_1$), *Tetrahedron Lett. 37*, 3207–3208.

172. Asano, N., Kato, A., Yokoyama, Y., Miyauchi, M., Yamamoto, M., Kizu, H., and Matsui, K. (1996) Calystegin N$_1$, a Novel Nortropane Alkaloid with a Bridgehead Amino Group from *Hyoscyamus niger*: Structure Determination and Glycosidase Inhibitory Activities, *Carbohydr. Res. 284*, 169–178.

173. Cordell, G.A. (ed). (1998) *The Alkaloids: Chemistry and Biology*, Vol. 50, Academic Press, New York.

174. Waterman, P.G. (1999) The Chemical Systematics of Alkaloids: A Review Emphasising the Contribution of Robert Hegnauer, *Biochem. Syst. Ecol. 27*, 395–406.

175. Omari, A., and Garner, P. (2004) Malaria: Severe, Life Threatening, *Clin. Evid. 11*, 1047–1057.

176. Kumar, A., Katiyar, S.B., Agarwal, A., and Chauhan, P.M. (2003) Perspective in Antimalarial Chemotherapy, *Curr. Med. Chem. 10*, 1137–1150.

177. Michael, J.P. (2004) Quinoline, Quinazoline and Acridone Alkaloids, *Nat. Prod. Rep. 21*, 650–668.

178. Von Nussbaum, F. (2003) Stephacidin B—A New Stage of Complexity Within Prenylated Indole Alkaloids from Fungi, *Angew. Chem. Int. Ed. Engl. 42*, 3068–3071.

179. Daly, J.W., Noimai, N., Kongkathip, B., Kongkathip, N., Wilham, J.M., Garraffo, H.M., Kaneko, T., Spande, T.F., Nimit, Y., Nabhitabhata, J., *et al.* (2004) Biologically Active Substances from Amphibians: Preliminary Studies on Anurans from Twenty-one Genera of Thailand, *Toxicon 44*, 805–815.

180. Orjala, J., and Gerwick, W.H. (1997) Two Quinoline Alkaloids from the Caribbean Cyanobacterium *Lyngbya majuscula*, *Phytochemistry 45*, 1087–1090.

181. Su, Y.-F., Luo, Y., Guo, C.-Y., and Guo, D.-A. (2004) Two New Quinoline Glycoalkaloids from *Echinops gmelinii*, *J. Asian Nat. Prod. Res. 6*, 223–227.

182. Rasulova, K.A., Bessonova, I.A., Yagudaev, M.R., and Yunusov, S.Y. (1987) Haplosinine, a New Furanoquinoline Glycoalkaloid from *Haplophyllum perforatum*, *Khim. Prirod. Soed. 6*, 876–879.

183. Dai, J.R., Hallock, Y.F., Cardellina, J.H., II, and Boyd, M.R. (1999) 20-*O*-β-Glucopyranosyl Camptothecin from *Mostuea brunonis*: A Potential Camptothecin Pro-drug with Improved Solubility, *J. Nat. Prod. 62*, 1427–1429.

184. Santavy, F., Maturova, M., Nemeckova, A., Schroter, H., Potesilova, B., and Preininger, H. (1960) VI. Isolation of Alkaloids from a Few Poppy Species, *Planta Med. 8*, 167–178.

185. Shamma, M., Kelly, M.G., and Podczasy, M.A., Sr. (1969) Thalictrum Alkaloids. VI. (−)-Veronamine, a Glycosidic Benzylisoquinoline, *Tetrahedron Lett. 10*, 4951–4954.

186. Shoeb, A., Raj, K., Kapil, R.S., and Popli, S.P. (1975) Alangi-side, the Monoterpenoid Alkaloidal Glycoside from *Alangium lamarckii* Thw, *J. Chem. Soc. Perkin I 13*, 1245–1248.

187. Itoh, A., Baba, Y., Tanahashi, T., and Nagakura, N. (2002) Tetrahydroisoquinolinemonoterpene Glycosides from *Cephaelis acuminata*, *Phytochemistry 59*, 91–97.

188. Itoh, A., Tanahashi, T., and Nagakura, N. (1997) Five Tetrahydroisoquinoline-monoterpene Glycosides with a Disaccharide Moiety from *Alangium lamarckii*, *Phytochemistry 46*, 1225–1229.

189. Itoh, A., Tanahashi, T., and Nagakura, N. (1996) Acylated Tetrahydroisoquinoline-monoterpene Glucosides from *Alangium lamarckii*, *Phytochemistry 41*, 651–656.

190. Itoh, A., Tanahashi, T., Tabata, M., Shikata, M., Kakite, M., Nagai, M., and Nagakura, N. (2001) Tetrahydroisoquinoline-monoterpene and Iridoid Glycosides from *Alangium lamarckii*, *Phytochemistry 56*, 623–630.

191. Itoh, A., Tanahashi, T., and Nagakura, N. (1998) Isolation of Two Unusual Tetrahydroisoquinoline-monoterpene Glucosides from *Alangium lamarckii* as Possible Intermediates in the Nonenzymic Formation of Alangimarine from Alangiside, *Heterocycles 48*, 499–505.

192. Nagakura, N., Itoh, A., and Tanahashi, T. (1993) Four Tetrahydroisoquinoline-monoterpene Glucosides from *Cephaelis ipecacuanha*, *Phytochemistry 32*, 761–765.

193. Hu, S., Xu, S., Yao, X., Cui, C.B., Tezuka, Y., and Kikuchi, T. (1993) Dauricoside, a New Glycosidal Alkaloid Having an Inhibitory Activity Against Blood-Platelet Aggregation, *Chem. Pharm. Bull. (Tokyo) 41*, 1866–1868.

194. Schmeller, T., and Wink, M. (1998) Utilization of Alkaloids in Modern Medicine, in *Alkaloids—Biochemistry, Ecology and Medicinal Applications* (Roberts, M., and Wink, M., eds.), pp. 435–459, Plenum Press, New York.

195. Artico, M. (1972) Chemotherapy of Tumors. II. Chemical Review of Natural Neoplastic Agents: Alkaloids, Their Analogs and Other Products Extracted from Plants, *Farmaco 27*, 683–712.

196. Manno, B.R., and Manno, J.E. (1977) Toxicology of Ipecac: A Review, *Clin. Toxicol. 10*, 221–242.

197. Itoh, A., Ikuta, Y., Baba, Y., Tanahashi, T., and Nagakura, N. (1999) Ipecac Alkaloids from *Cephaelis acuminata*, *Phytochemistry 52*, 1169–1176.

198. Heftmann, E. (1974) Recent Progress in the Biochemistry of Plant Steroids Other Than Sterols (saponins, glycoalkaloids, pregnane derivatives, cardiac glycosides, and sex hormones), *Lipids 9*, 626–639.

199. Maga, J.A. (1980) Potato Glycoalkaloids, *Crit. Rev. Food Sci. Nutr. 12*, 371–405.

200. Roddick, J.G. (1996) Steroidal Glycoalkaloids: Nature and Consequences of Bioactivity, *Adv. Exp. Med. Biol. 404*, 277–295.

201. Friedman, M. (2002) Tomato Glycoalkaloids: Role in the Plant and in the Diet, *J. Agric. Food Chem. 50*, 5751–5780.

202. Korpan, Y.I., Nazarenko, E.A., Skryshevskaya, I.V., Martelet, C., Jaffrezic-Renault, N., and El'skaya, A.V. (2004) Potato Glycoalkaloids: True Safety or False Sense of Security? *Trends Biotechnol. 22*, 147–151.

203. Kuc, J. (1975) Teratogenic Constituents of Potatoes, *Recent Adv. Phytochem. 9*, 139–150.

204. Wang, S., Panter, K.E., Gaffield, W., Evans, R.C., and Bunch, T.D. (2005) Effects of Steroidal Glycoalkaloids from Potatoes (*Solanum tuberosum*) on *in vitro* Bovine Embryo Development, *Anim. Reprod. Sci. 85*, 243–250.

205. Lee, K.R., Kozukue, N., Han, J.S., Park, J.H., Chang, E.Y., Baek, E.J., Chang, J.S., and Friedman, M. (2004) Glycoalkaloids and Metabolites Inhibit the Growth of Human Colon (HT29) and Liver (HepG2) Cancer Cells, *J. Agric. Food Chem. 52*, 2832–2839.

206. Skuladottir, H., Tjoenneland, A., Overvad, K., Stripp, C., Christensen, J., Raaschou-Nielsen, O., and Olsen, J.H. (2004) Does Insufficient Adjustment for Smoking Explain the Preventive Effects of Fruit and Vegetables on Lung Cancer? *Lung Cancer 45*, 1–10.

207. Mannisto, S., Dixon, L.B., Balder, H.F., Virtanen, M.J., Krogh, V., Khani, B.R., Berrino, F., Brandt, P.A., Hartman, A.M., Pietinen, P., *et al*. (2005) Dietary Patterns and Breast Cancer Risk: Results from Three Cohort Studies in the DIETSCAN Project, *Cancer Causes Control 16*, 725–733.

208. Friedman, M., Lee, K.R., Kim, H.J., Lee, I.S., and Kozukue, N. (2005) Anticarcinogenic Effects of Glycoalkaloids from Potatoes Against Human Cervical, Liver, Lymphoma, and Stomach Cancer Cells, *J. Agric. Food Chem. 53*, 6162–6169, 8420.

209. Friedman, M. (2004) Analysis of Biologically Active Compounds in Potatoes (*Solanum tuberosum*), Tomatoes (*Lycopersicon esculentum*), and Jimson Weed (*Datura stramonium*) Seeds, *J. Chromatogr. A. 1054*, 143–155.

210. Cham, B.E., Gilliver, M., and Wilson, L. (1987) Antitumor Effects of Glycoalkaloids Isolated from *Solanum sodomaeum*, *Planta Med. 53*, 34–36.

211. Fukuhara, K., Shimizu, K., and Kubo, I. (2004) Arudonine, an Allelopathic Steroidal Glycoalkaloid from the Root Bark of *Solanum arundo* Mattei, *Phytochemistry 65*, 1283–1286.

212. Ye, W.-C., Wang, H., Zhao, S.-X., and Che, C.-T. (2001) Steroidal Glycoside and Glycoalkaloid from *Solanum lyratum*, *Biochem. Syst. Ecol. 29*, 421–423.

213. Fujiwara, Y., Takaki, A., Uehara, Y., Ikeda, T., Okawa, M., Yamauchi, K., Ono, M., Yoshimitsu, H., and Nohara, T. (2004) Tomato Steroidal Alkaloid Glycosides, Esculeosides A and B, from Ripe Fruits, *Tetrahedron 60*, 4915–4920.

214. Yahara, S., Uda, N., Yoshio, E., and Yae, E. (2004) Steroidal Alkaloid Glycosides from Tomato (*Lycopersicon esculentum*), *J. Nat. Prod. 67*, 500–502.

215. Amir, M., and Kumar, S. (2004) Possible Industrial Applications of Genus *Solanum* in Twenty-first Century: A Review, *J. Scient. Indust. Res. 63*, 116–124.

216. Pathirana, C., Jensen, P.R., Dwight, R., and Fenical, W. (1992) Rare Phenazine L-Quinovose Esters from a Marine Actinomycete, *J. Org. Chem. 57*, 740–742.

217. Vural, N., and Sardas, S. (1984) Biological Activities of Broad Bean (*Vicia faba* L.) Extracts Cultivated in South Anatolia in Favism Sensitive Subjects, *Toxicology 31*, 175–179.

218. Lattanzio, V., Bianco, V.V., Crivelli, G., and Miccolis, V. (1983) Variability of Amino Acids, Protein, Vicine and Convicine in *Vicia faba* (L), *J. Food Sci. 48*, 992–993.

219. Chaudhuri, R.K., Sticher, O., and Winkler, T. (1981) Structures of Two Novel Monoterpene Alkaloid Glucosides from *Lonicera xylosteum* L, *Tetrahedron Lett. 22*, 559–562.

220. Chaudhuri, R.K., Sticher, O., and Winkler, T. (1980) Xylostosidine: The First of a New Class of Monoterpene Alkaloid Glycosides from *Lonicera xylosteum*, *Helv. Chim. Acta 63*, 1045–1047.

221. Nemeckova, A., Cross, A.D., and Santavy, F. (1967) Occurrence of Isorheagenine Glycoside, *Naturwissenschaften 54*, 45.

222. El Bitar, H., Nguyen, V.H., Gramain, A., Sévenet, T., and Bodo, B. (2004) Daphcalycinosidines A and B, New Iridoid-Alkaloids from *Daphniphyllum calycinum*, *Tetrahedron Lett. 45*, 515–518.

223. El Bitar, H., Nguyen, V.H., Gramain, A., Sevenet, T., and Bodo, B. (2004) New Alkaloids from *Daphniphyllum calycinum*, *J. Nat. Prod. 67*, 1094–1099.

224. Kosuge, T., Tsuji, K., and Hirai, K. (1982) Isolation of Neosurugatoxin from the Japanese Ivory Shell, *Babylonia japonica*, *Chem. Pharm. Bull. (Tokyo) 30*, 3255–3259.

225. Akunyili, D.N., and Akubue, P.I. (1986) Schumanniofoside, the Antisnake Venom Principle from the Stem Bark of *Schumanniophyton magnificum* Harms, *J. Ethnopharmacol. 18*, 167–172.

226. Bourquelot, E., and Herissey, H. (1907) Bakankosine, a New Glucoside Hydrolyzed by Emulsin, Found in the Seeds of a *Strychnos* from Madagascar, *Compt. Rend. Acad. Sci. Paris 144*, 575–577.

227. Tietze, L.F. (1976) Iridoids. VII. Synthesis and Structural Proof of Bakankosine, *Tetrahedron Lett. 29*, 2535–2538.

228. Klohs, M.W., Draper, M.D., Keller, F., Malesh, W., and Petracek, F.J. (1953) Alkaloids of *Veratrum eschscholtzii*. I. The Glycosides, *J. Am. Chem. Soc. 75*, 2133–2135.

229. Taskhanova, E.M., and Shakirov, R. (1981) *Veratrum lobelianum* Alkaloids, *Khim. Prirod. Soed. (USSR) 3*, 404–405.

230. Iwadare, S., Shizuri, Y., Sasaki, K., and Hirata, Y. (1974) Isolation and Structure of Trichotomine and Trichotomine G_1, *Tetrahedron 30*, 4105–4111.

9-trans,11-trans-CLA: Antiproliferative and Proapoptotic Effects on Bovine Endothelial Cells

Kuan-Lin Lai, Armida P. Torres-Duarte, and Jack Y. Vanderhoek*

Department of Biochemistry and Molecular Biology, The George Washington
University School of Medicine, Washington, DC 20037

ABSTRACT: Endothelial cell function can be influenced by nutrition, especially dietary FA and antioxidants. One class of dietary FA that is found in meat and dairy products derived from ruminant animals is conjugated linoleic acids (CLA). We have examined the effects of several CLA isomers on endothelial cell proliferation. $9t,11t$-CLA was the only isomer that inhibited bovine aortic endothelial cell (BAEC) [^{3}H]methylthymidine incorporation (I_{50} = 35 μM), and this antiproliferative effect was time-dependent. A small decrease (20%) in cell number was observed only at the highest concentration (60 μM) tested. The $9c,11t$-, $9c,11c$-, $10t12c$-, and $11c,13t$-CLA isomers did not exhibit any antiproliferative effects over a 5–60 μM concentration range. α-Tocopherol and BHT decreased BAEC proliferation, but pretreatment of cells with either of these antioxidants substantially attenuated the antiproliferative effect of $9t,11t$-CLA. No difference in lipid peroxidation, as measured by the thiobarbituric acid assay for malondialdehyde, was observed on treatment of endothelial cells with either $9t,11t$- or $9c,11t$-CLA. However, a 43% increase in caspase-3 activity was observed after incubating BAEC with $9t,11t$-CLA, suggesting that the antiproliferative effect of this isomer is partially due to an apoptotic pathway. In contrast to the above results with normal endothelial cells, these five CLA isomers all inhibited proliferation of the human leukemic cell line THP-1, with the $9t,11t$ isomer again being the most (I_{50} = 60 μM) effective. These results confirm that different CLA isomers have different inhibitory potencies on the proliferation of normal and leukemic cells.

Paper no. L9777 in *Lipids 40*, 1107–1116 (November 2005).

The endothelium [or the endothelial cell (EC) monolayer] constitutes a dynamic interface between the vessel wall and bloodstream and plays a central role in the maintenance of vascular homeostasis. Injury to the endothelium leads to altered function and may be a critical event in the initiation of atherosclerosis. To overcome this endothelial dysfunction, replacement of EC and re-endothelialization is required; EC proliferation is one mechanism to reestablish the integrity of the vascular intima.

PUFA, including fish oil EPA and DHA, reportedly modulate proliferation of a number of different cells, both normal (including EC) and cancerous (1–5). Conjugated linoleic acid, a class of dietary PUFA characterized by the presence of a conjugated diene system, has attracted considerable attention because its physiological effects include the reduction of breast, colon and prostate cancers; arteriosclerosis; diabetes; and body mass fat and the modulation of immune function (6).

CLA is a group of positional and geometric isomers of linoleic acid. Most of these isomers are synthesized by rumen bacteria and are found in meat and dairy products. Studies have shown that CLA reduces cell proliferation and induces apoptosis in a large number of cancer cell lines (7–17). However, only a few reports have examined the effects of CLA on cell proliferation of normal cells such as rat EC and hepatocytes and human skin fibroblasts and umbilical vein EC (7,12,18,19). A number of mechanisms have been proposed to explain the antiproliferative effects of CLA, including increased lipid peroxidation, modulation of lipid metabolism, and alteration of signal transduction (6,7). Furthermore, the proapoptotic action of CLA has been shown to involve reactive oxygen species and caspase activation (9,13,20).

Most *in vivo* and *in vitro* studies involving CLA have used isomeric mixtures in which the major components were $9c,11t$- and $10t,12c$-CLA, the former being the predominant isomer found in nature. Since other purified isomers have become commercially available, it has become possible to delineate the physiological activities of each isomer. Studies that used purified CLA isomers have tended to focus on the effects of $9c,11t$- and $10t,12c$-CLA, but several reports also have tested the $9c,11c$- and $9t,11t$ isomers (13,16,20).

In view of our recent work on the effects of certain CLA isomers on various cells involved in the cardiovascular system (21,22), we decided to examine the effects of five pure CLA isomers on the proliferation of normal, adherent EC. In addition, we also tested the effects of these isomers on a contrasting system involving tumor-like cells grown in suspension, i.e., THP-1, a human monocytic leukemia cell line.

MATERIALS AND METHODS

$9c,11t$-, $9c,11c$-, $9t,11t$-, $10t,12c$-, and $11c,13t$-CLA were purchased from Matreya LLC (Pleasant Gap, PA). Bovine aortic EC (BAEC) were obtained from the Coriell Institute for Medical Research (Camden, NJ) and the human THP-1 cells from the American Type Culture Collection (Manassas, VA). BHT, EC growth supplement, FA-free BSA, NAD, lactic dehydrogenase, and α-tocopherol were purchased from Sigma-Aldrich

---

*To whom correspondence should be addressed at Dept. of Biochemistry and Molecular Biology, The George Washington University School of Medicine, 2300 Eye St., N.W., Washington, DC 20037. E-mail: bcmjyv@gwumc.edu
Abbreviations: BAEC, bovine aortic endothelial cell; EC, endothelial cell; FBS, fetal bovine serum; LDH, lactate dehydrogenase; MDA, malondialdehyde.

Corp. (St. Louis, MO). DMEM/F12 and RPMI-1640 media were bought from Mediatech Inc. (Herndon, VA), and Whatman GF/C glass microfilters (25 mm) were obtained from Fisher Scientific (Suwanee, GA). [^{3}H]Methylthymidine was purchased from American Radiolabeled Chemicals (St. Louis, MO) and FBS from Gibco Invitrogen (Carlsbad, CA). Econosafe liquid scintillation cocktail was obtained from Research Products International Corp. (Mt. Prospect, IL).

Cell culture. Initially, 6.6×10^4 BAEC (passages #8 and 9) in 4 mL DMEM/F12 media containing 15% FBS, EC growth supplement (20 μg/mL), heparin (50 μg/mL), and penicillin-streptomycin (1000 IU, 1 mg/mL) were plated in 60×15 mm tissue culture dishes for 24 h to allow the cells to attach to the dishes. CLA-BSA complexes were prepared as previously described (21) and added to the cells. In some experiments, cells were pretreated with either BHT, α-tocopherol, or indomethacin for 4 h prior to the addition of CLA-BSA complexes. T-75 flasks (4×10^5 cells/20 mL/flask) were used for the caspase and malondialdehyde (MDA) experiments. THP-1 cells were grown in RPMI-1640 (containing L-glutamine and 10% FBS) in 60×15 mm culture dishes.

Cell proliferation experiments. Triplicate dishes containing BAEC were pulsed for 4 h with 1 μCi/dish [^{3}H]methylthymidine prior to cell harvest. After removal of the growth medium and washing, the cells were trypsinized in trypsin-EDTA and harvested (after 24, 48, or 72 h) using a 12-sample Millipore 1225 Sampling manifold and GF/C glass microfilters. After washing the filters, they were transferred to liquid scintillation vials, suspended in Econosafe scintillation cocktail, and counted in a Beckman LS 3801 liquid scintillation counter. Duplicate dishes containing BAEC were used for cell counting and viability assays. After trypsinization, a 50 μL cell aliquot was counted in a Z1 Coulter Particle Counter (Beckman Coulter Inc., Miami, FL). Cell viability was assessed by determining lactate dehydrogenase (LDH) release into the medium (23). A 0.1 mL cell supernatant sample was treated with 48 mM lactate and 5 mM NAD, and NADH formation was measured at 340 nm. Absorbance data were expressed as the percentage of LDH release from control cultures treated with 0.2% Triton X-100. THP-1 cells were grown in suspension for 72 h and were either pulsed for 4 h prior to harvest with 1 μCi/dish [^{3}H]methylthymidine (cell proliferation, in triplicate) or not (cell counting, in duplicate). Cells were harvested directly on GF/C microfilters and counted for radioactivity incorporation.

Caspase-3 activity and lipid peroxidation measurements. BAEC (passage #10) were grown in the absence or presence of CLA/BSA for 72 h as described above. After removal of the control or CLA-containing medium and washing, the cells were then harvested and counted. For the caspase-3 experiments, the cells were lysed in lysis buffer [50 mM HEPES, pH 7.4, 5 mM 3-[(3-cholamidopropyl)dimethylammonio]-1-propanesulfonate , and 5 mM DTT] for 20 min on ice, followed by three liquid nitrogen freeze-thaw cycles, 1–2 s sonication, and centrifugation at $14,000 \times g$ for 10 min at 4°C. Caspase-3 activity in the cell lysates was determined using a fluorometric caspase-3 assay kit (Sigma-Aldrich Corp., Mil-

waukee, WI) following the manufacturer's instructions with a Wallac 1420 microplate fluorometer set at an excitation wavelength of 360 nm and emission of 460 nm. Caspase-3 activity was monitored every 10 min for 1 h, and the results are expressed as pmol 7-amino-4-methylcoumarin released/min/mL sample. Lipid peroxidation was monitored by measuring MDA levels (24). After harvesting, the cells were disrupted by the addition of 2 mL of 20% TCA. After addition of 1 mL of 0.67% thiobarbituric acid, the mixture was heated at 100°C for 20 min and, after cooling, centrifuged at $12,000 \times g$ for 10 min. The absorbance was measured at 532 nm, and the concentration of MDA was calculated by using a standard curve generated from 1,1,3,3-tetraethoxypropane and an extinction coefficient of 153,000.

Statistical analysis. Data were analyzed by one-way ANOVA and Student's *t*-test.

RESULTS

The effect of incubating various CLA isomers with BAEC for 72 h on cell growth, as measured by [^{3}H]methylthymidine incorporation, is shown in Figure 1A. Compared with the vehicle control, only 9*t*,11*t*-CLA decreased cell proliferation over a concentration range of 5–60 μM whereas the 9*c*,11*c*-, 9*c*,11*t*-, 10*t*,12*c*,- and 11*c*,13*t*-CLA isomers were relatively ineffective. Similarly, only the 9*t*,11*t*-CLA reduced the BAEC numbers under these experimental conditions (Fig. 1B). Thus 60 μM 9*t*,11*t*-CLA reduced [^{3}H]methylthymidine incorporation by 72 ± 21% (relative to control, *n* = 12) and reduced cell number by 22 ± 20% (*n* = 12). To determine whether the growth-inhibitory effects of 5–60 μM 9*t*,11*t*-CLA were toxic to the BAEC, LDH release into the medium through membrane leakage was evaluated as an indicator of cytotoxicity. No statistically significant differences in LDH release between these concentrations of 9*t*,11*t*-CLA-treated cells and untreated controls were observed (results not shown). The time course of the 9*t*,11*t*-CLA effect is shown in Figure 2 and indicates that the same maximal inhibition of cell growth was observed at 48 and 72 h.

Since a number of studies had shown that antioxidants and cyclooxygenase inhibitors can affect cell growth (24–26), we examined whether these agents could influence the 9*t*,11*t*-CLA-induced decrease in BAEC cell proliferation. Treatment of BAEC with the antioxidant α-tocopherol (7.5 μM) resulted in a 80% (*n* = 4) decrease in [^{3}H]methylthymidine incorporation and a 45% decrease in cell number. A 37% increase in LDH release (relative to untreated controls) was observed with this concentration of α-tocopherol (results not shown). When BAEC were pretreated for 4 h with this concentration of α-tocopherol followed by the addition of 20–60 μM 9*t*,11*t*-CLA, the inhibitory effect of CLA was reduced (Fig. 3). Thus, 7.5 μM α-tocopherol decreased the inhibitory effectiveness of 60 μM CLA on the residual ability of BAEC to proliferate from 79 to 18%. Similar results were obtained with 30 μM α-tocopherol (results not shown). The presence of CLA did not result in any additional LDH release other than that observed with α-tocopherol alone. Using BHT as the antioxidant also resulted in a dose-dependent decrease of cell
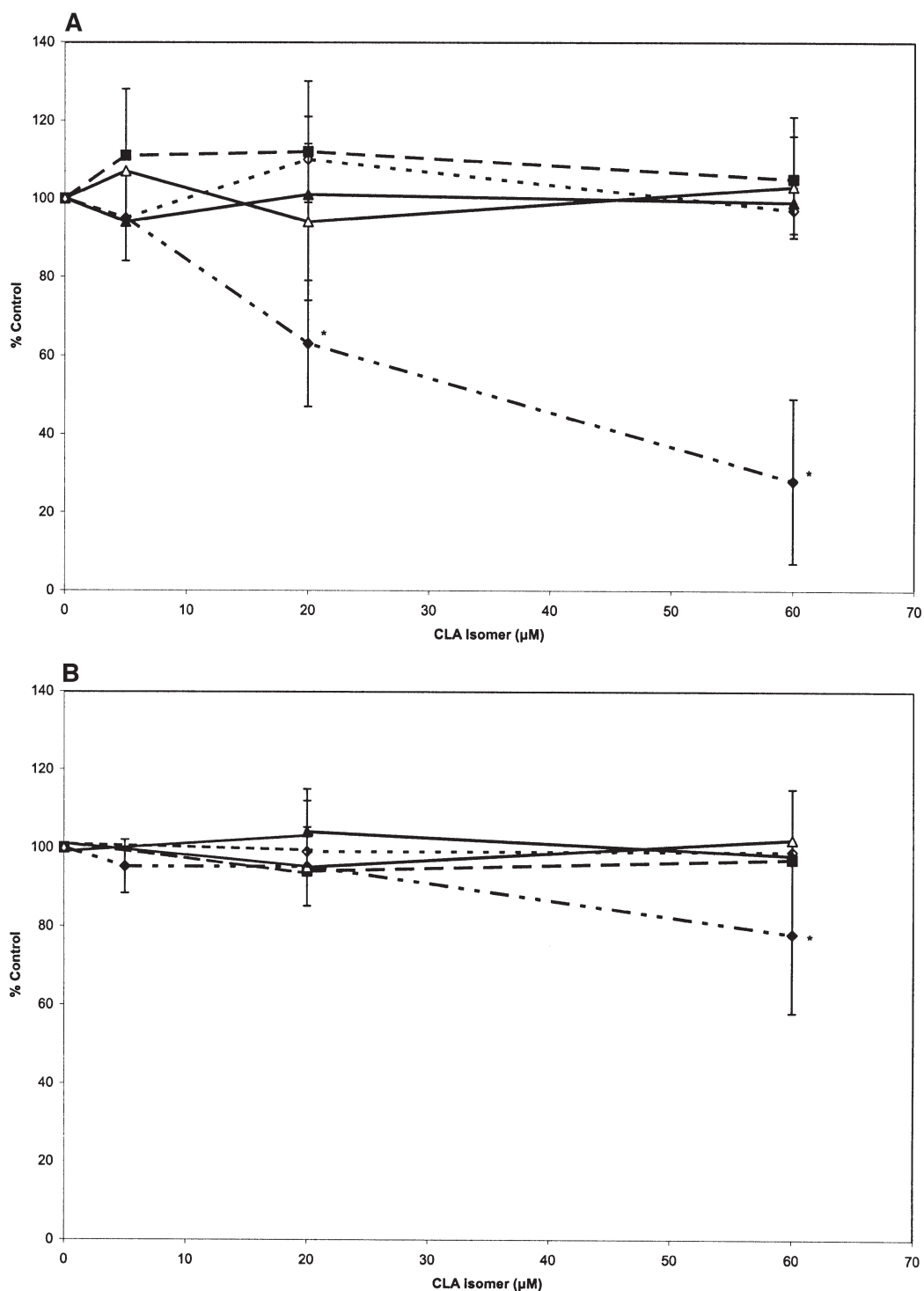
FIG. 1. Effect of different CLA isomers on cell proliferation and cell numbers of bovine aortic endothelial cells (BAEC). Cells were plated and after 24 h were supplemented with either vehicle or different concentrations of CLA isomers complexed with 1% BSA. (A) Cell proliferation was measured 72 h after supplementation by the addition of 1 μCi/dish of [³H]methylthymidine for the last 4 h of culture. Under these conditions, [³H] incorporation into control cells (vehicle instead of CLA) averaged 1.59 ± 1.17 nCi/dish (*n* = number of separate experiments = 8). The results of triplicate dishes containing CLA isomers are given as % control. Values are mean ± SD. (B) Cell numbers were measured in duplicate dishes after 72 h using the same protocol as described in (A) except no [³H]methylthymidine was added. Control dishes contained 1.7 ± 0.33 x 10⁶ cells (*n* = 8) after 72 h. ◆, 9*t*,11*t* (part A, B: *n* = 12, 14); ■, 9*c*,11*t* (*n* = 4, 5); △, 9*c*,11*c* (*n* = 5, 4); ▲, 10*t*,12*c* (*n* = 4, 5); ◇, 11*c*,13*t* (*n* = 4, 4). *P < 0.01 when compared with control without CLA. Error bars represent SD.
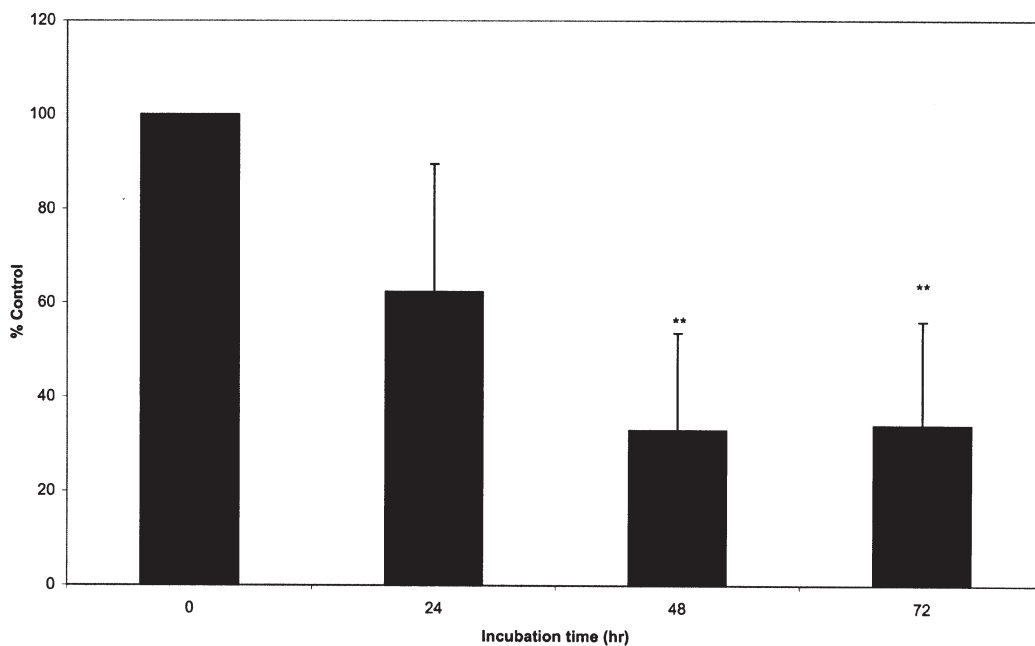
FIG. 2. Time course of the antiproliferative effect of 9*t*,11*t*-CLA on BAEC. Cells were incubated with or without 60 μM 9*t*,11*t*-CLA/BSA for 24, 48, or 72 h. Cell proliferation was measured as described in the legend of Figure 1. Control cells incorporated 3.0 ± 2.2, 2.9 ± 2.3, and 2.6 ± 1.5 nCi/dish after 24, 48, and 72 h, respectively. Results are mean ± SD (*n* = 3 separate experiments). **$P < 0.05$ when compared with control without CLA. For abbreviation see Figure 1.
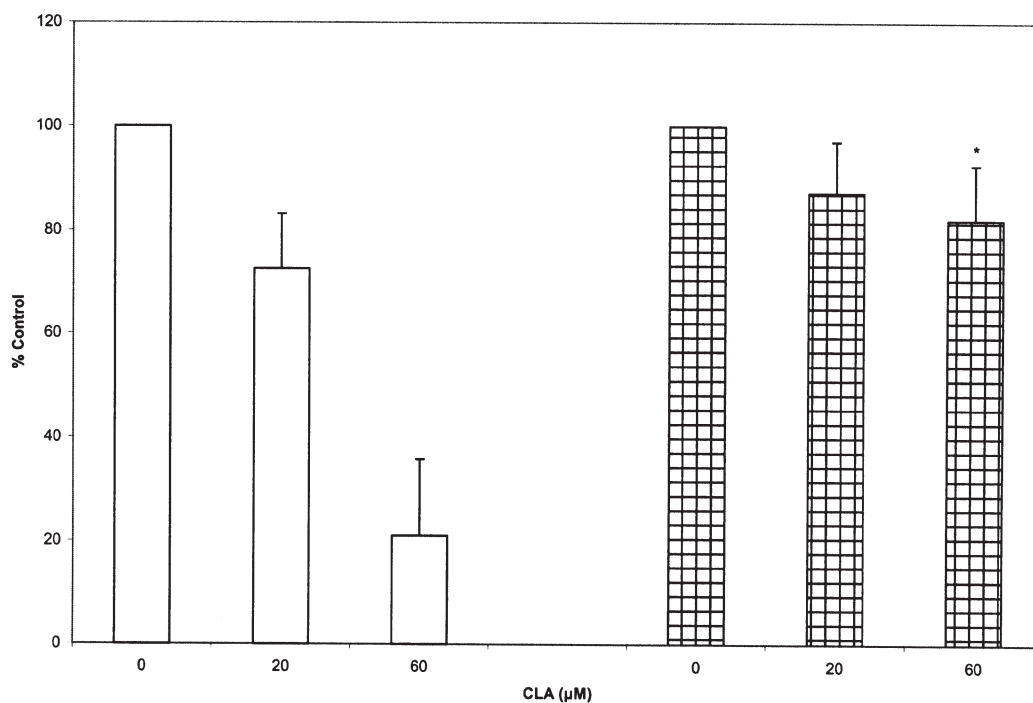
FIG. 3. Protective effect of α-tocopherol on the antiproliferative effect of 9*t*,11*t*-CLA on BAEC. BAEC were preincubated with or without 7.5 μM α-tocopherol for 4 h followed by the addition of either vehicle/BSA (control) or different concentrations of 9*t*,11*t*-CLA/BSA. After 72 h, cell proliferation and cell numbers were measured as described in the legend of Figure 1. Under these conditions, [³H] incorporation into control cells in the absence or presence of α-tocopherol averaged 0.56 ± 0.18 and 0.11 ± 0.037 nCi/dish (*n* = 4), respectively, and the corresponding cell numbers averaged 1.9 ± 0.43 x 10⁶ and 1.0 ± 0.27 x 10⁶. Open bars, no α-tocopherol; hatched bars, with 7.5 μM α-tocopherol. Results are mean ± SD (*n* = 4 separate experiments). *$P < 0.01$ when compared with CLA alone. For abbreviation see Figure 1.
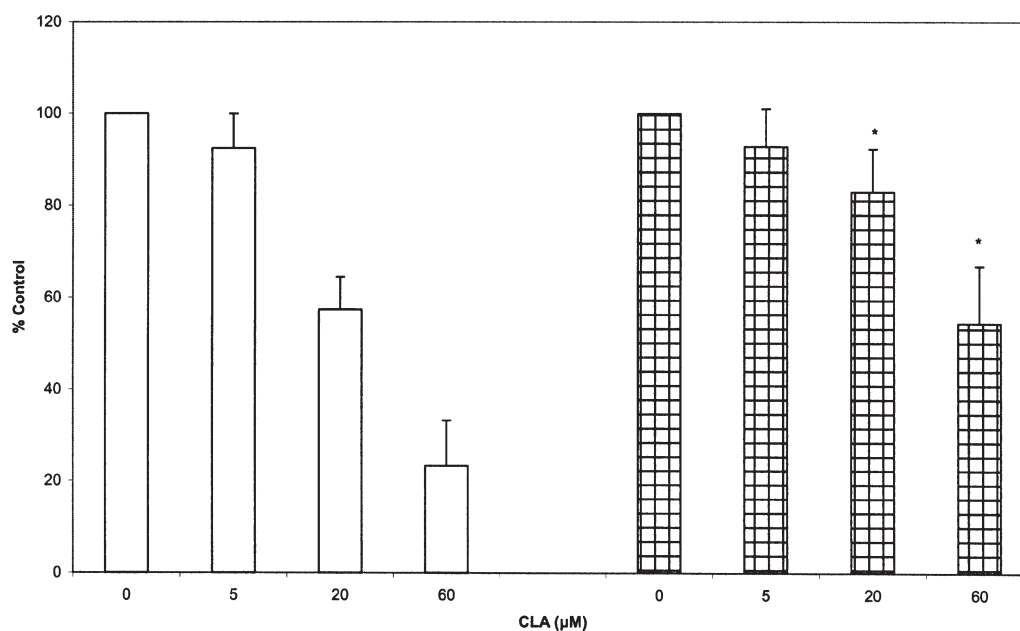
FIG. 4. BHT effect on the antiproliferative effect of 9*t*,11*t*-CLA on BAEC cell growth and cell number. BAEC were preincubated with or without 20 μM BHT for 4 h followed by the addition of either vehicle/BSA (control) or different concentrations of 9*t*,11*t*-CLA/BSA complexes. After 72 h, cell proliferation and cell numbers were measured as described in the legend of Figure 1. Under these conditions, [³H] incorporation into control cells in the absence or presence of BHT averaged 2.14 ± 0.91 and 0.22 ± 0.017 nCi/dish (*n* = 6), respectively, and the corresponding cell numbers averaged 2.1 ± 0.29 x 10⁶ and 1.1 ± 0.49 x 10⁶. Open bars, no BHT, hatched bars, with 20 μM BHT. Results are mean ± SD (*n* = 6 separate experiments). *P < 0.01 when compared with CLA alone. For abbreviation see Figure 1.

proliferation and cell number. For example, 20 μM BHT decreased [³H]methylthymidine incorporation by 90% (*n* = 6) and cell number by 47% and increased LDH release by 30%. When BAEC were pretreated with 20 μM BHT, the inhibitory effects of 9*t*,11*t*-CLA on the residual proliferative ability of BAEC (as measured by [³H]methylthymidine incorporation) were partially but significantly reduced. At 20 and 60 μM 9*t*,11*t*-CLA, BHT decreased the inhibitory effects from 43 and 77% of control (respectively) to 17 and 45% (*n* = 6, *P* < 0.01) (Fig. 4). No additional LDH release was observed in the presence of both BHT and CLA. A pretreatment with 5 μM BHT did not result in any significant change in the inhibitory effect of 9*t*,11*t*-CLA (results not shown). These results suggested that lipid peroxidation was involved with the 9*t*,11*t*-CLA-induced reduction of BAEC proliferation. To evaluate lipid peroxidation, cellular MDA levels were measured in BAEC treated with either 9*t*,11*t*- or 9*c*,11*t*-CLA, using the latter isomer as a control since it had no effect on BAEC proliferation (Fig. 1). As shown in Figure 5, no change in MDA formation (relative to untreated cells) was observed for cells treated with 9*t*,11*t*-CLA whereas a 68 ± 46% (*n* = 3) increase in MDA formation was observed with the 9*c*,11*t*-CLA isomer. However, when corrections were made for the different cell numbers obtained after treatment with these CLA isomers, no significant differences in increased MDA production were observed, [9*t*,11*t*-CLA, 145 ± 16% (*n* = 3) vs. 9*c*,11*t*-CLA, 159 ± 56%]. Pretreating BAEC with 10 μM indomethacin, a cy-

clooxygenase inhibitor, for 4 h before incubating BAEC with 5–60 μM 9*t*,11*t*-CLA had no effect on cell proliferation (results not shown).

To determine whether the 9*t*,11*t*-CLA-induced decrease in BAEC cell proliferation and cell number was due to an induction of apoptosis, caspase-3 activity was monitored since activation of this enzyme has been used as a biochemical marker for cells undergoing apoptosis. BAEC were treated with 60 μM of either 9*t*,11*t*- or 9*c*,11*t*-CLA for 72 h followed by measurement of caspase-3 activity of the cell lysates. The results in Figure 6 show that a 43% increase in caspase-3 activity was observed after treatment with 9*t*,11*t*-CLA compared with a 24% decrease obtained with the 9*c*,11*t* isomer.

To compare the above-described effects of CLA isomers on proliferation of adherent normal EC with nonadherent leukemia cells, we assessed the effects of these five CLA isomers on the growth of the human monocytic leukemia THP-1 cells. As illustrated in Figure 7A, 20 μM of each of these isomers inhibited [³H]methylthymidine incorporation 17–27% whereas 60 μM decreased incorporation 37–53%. Although the 9*t*,11*t*-CLA was the most potent isomer (53%), the differences in inhibitory potency between the isomers were not statistically significant. Similarly, at a CLA concentration of 60 μM, the 9*t*,11*t*-isomer was also the most effective in decreasing cell numbers after 72 h (30%). The other CLA isomers decreased THP-1 cell numbers in the16–24% range (Fig. 7B).
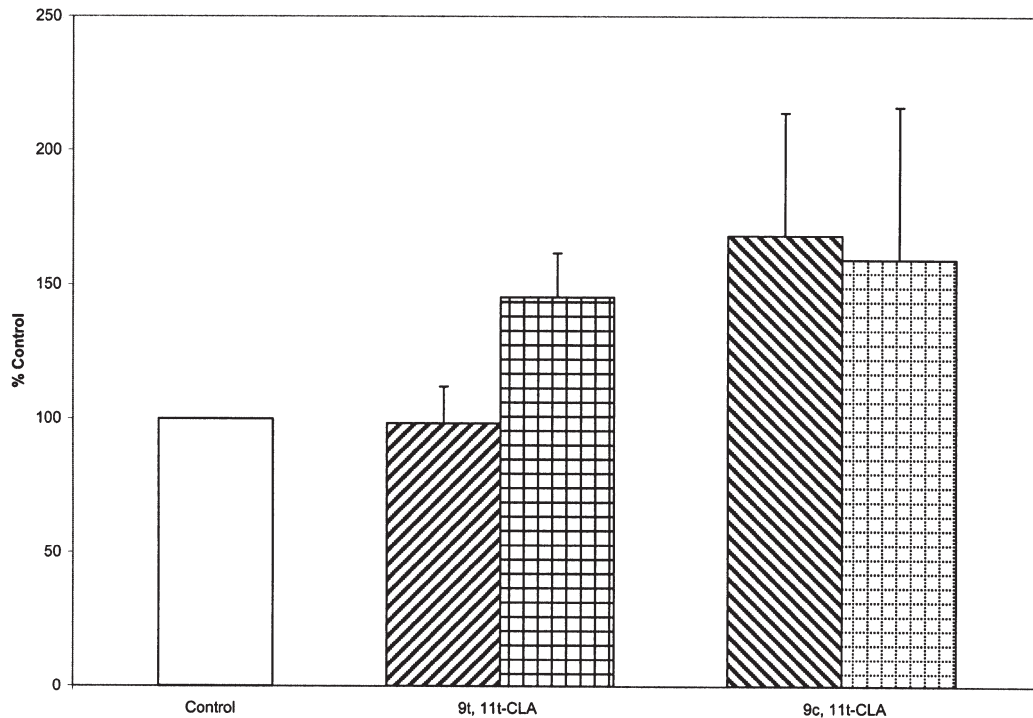
FIG. 5. Malondialdehyde (MDA) formation on BAEC treated with either 9*t*,11*t*-CLA or 9*c*,11*t*-CLA. BAEC were incubated for 72 h without (vehicle/BSA, control) or with 60 μM of either 9*t*,11*t*-CLA or 9*c*,11*t*-CLA/BSA complexes. After 72 h, the cells were isolated, disrupted with TCA followed by the addition of thiobarbituric acid. MDA and cell numbers were determined as described in the Materials and Methods section. Control cells produced 0.40 ± 0.081 nmol MDA/sample. Cross-hatched columns have been corrected for cell number. Results are mean ± SD (*n* = 3 separate experiments). For other abbreviation see Figure 1.

DISCUSSION

A number of reports have appeared that have examined the antiproliferative effects of several CLA isomers on various tumor cells (7–17). In general, 9*c*,11*t*- and 10*t*,12*c*-CLA were found to reduce the proliferation of human breast, colorectal, liver, lung, stomach and prostate tumor lines as well as several leukemia cell lines. In contrast, few studies have focused on the effects of CLA on normal cells. These two CLA isomers reduced cell growth in rat mammary EC and hepatocytes but had no effects on human skin fibroblasts and human umbilical vein EC (7,12,18,19). Most of these studies used CLA isomeric mixtures or pure 9*c*,11*t*- and/or 10*t*,12*c*-CLA. Only three reports have appeared that tested the antiproliferative effects of an additional isomer, either the 9*c*,11*c*- or 9*t*,11*t*-CLA (13,16,20). The present study compares the effects of all five CLA isomers that are commercially available in pure form at this time on the proliferation of both normal, adherent cells (BAEC) and a leukemic cell line grown in suspension (THP-1).

Cis, trans isomers constitute the major (86–93% of total isomers) CLA isomer class found in dairy and beef products (27–29). The 9*c*,11*t*-CLA represented more than 70% of this class whereas the next most abundant isomer in this group, 7*t*,9*c*-CLA, amounted to only 10%. The most abundant *trans, trans* component was 9*t*,11*t*-CLA, which represented 1.5–3.7% of the total CLA isomers and was present to a slightly greater

extent than the 10*t*,12*c*-CLA isomer (28,29). Although the 9*t*,11*t*-CLA isomer was a minor component of the CLA pool in foods, two recent reports indicate that this isomer is a major CLA constituent in tissue lipids. Thus Petridou and coworkers (30) reported that 9*t*,11*t*- and 9*c*,11*t*-CLA were the main CLA isomers in serum isolated from women (each represented 41% of the CLA total) (30). We also found that these isomers were the two major CLA isomers in platelet lipids (17 and 33% of the total respectively) (22). Huang and coworkers (31) reported that the plasma CLA level in healthy men was 7 μM (31); thus one can calculate that the 9*t*,11*t*-CLA concentration would be in the 1–3 μM range. Since local concentrations could easily be 10-fold higher, the effective levels of 9*t*,11*t*-CLA used in our study (20–60 μM) should be physiologically attainable (32). Our results show that only the 9*t*,11*t*-CLA decreased BAEC growth (I_{50} = 35 μM) and that the other isomers tested, including the more abundant ones found in dairy and beef foodstuffs, did not appreciably affect proliferation even at 60 μM. However, all five CLA isomers attenuated THP-1 cell proliferation, with the 9*t*,11*t*-isomer again the most potent isomer (I_{50} = 60 μM). The inhibitory differences between the isomers were not statistically significant except that the least effective isomer was 11*c*,13*t*-CLA. Furthermore our results suggest that normal cells may be much less sensitive to the antiproliferative effects of certain CLA isomers than tumor cells, although more comparative studies are needed to confirm this hypothesis and
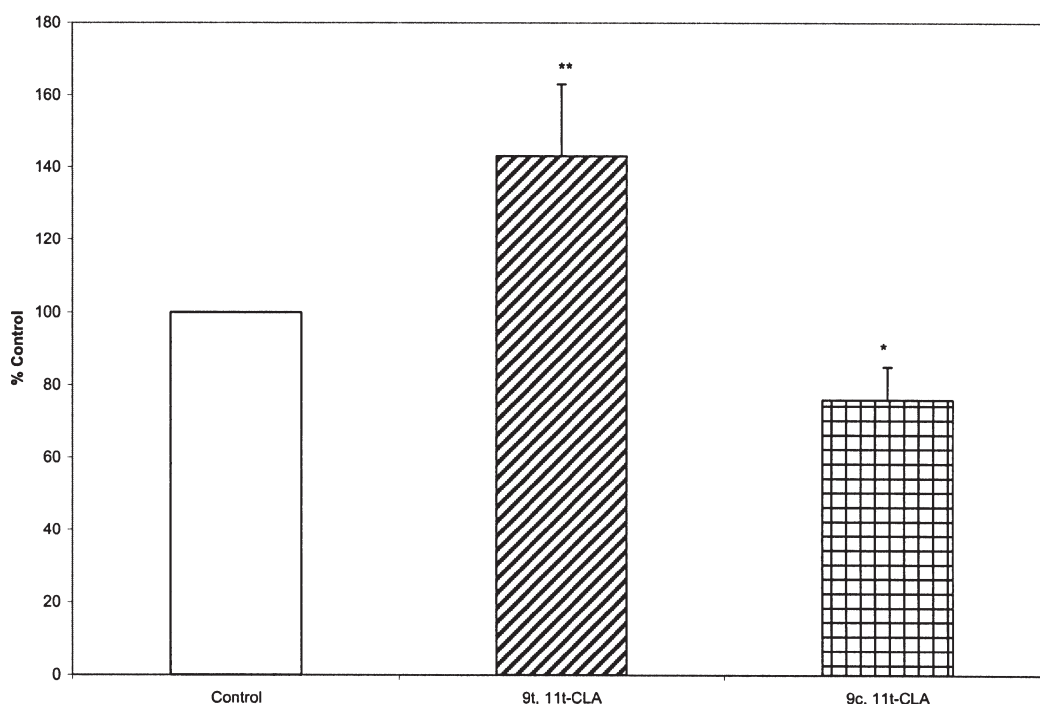
FIG. 6. Effect of 9t,11t-CLA and 9c,11t-CLA on caspase-3 activity in BAEC. Cells were treated for 72 h without (vehicle/BSA, control) or with 60 μM of either 9t,11t-CLA or 9c,11t-CLA/BSA complexes. After 72 h, the cells were isolated and then lysed; caspase-3 activity was then determined as described in the Materials and Methods section. Results have been corrected for cell number and are expressed as the mean ± SD ($n = 4$ separate experiments). Control cells released 20 ± 4.0 pmol 7-amino-4-methylcoumarin/min/mL sample. *$P < 0.01$, **$P < 0.05$ when compared with control without CLA. For abbreviation see Figure 1.

whether these CLA isomers can be used as anticancer agents. This would agree with the report by Begin and coworkers (2) that certain PUFA were much more antiproliferative and cytotoxic to human cancer cells than to normal human fibroblasts and normal animal cells.

Our data indicate that 9t,11t-CLA inhibited cell proliferation to a greater extent than it decreased cell number, and this difference was also observed with α-tocopherol and BHT. Since thymidine incorporation, an indicator of DNA synthetic activity, is only measured during a 4-h window just before cell harvest, the antiproliferative effects of this CLA isomer and these antioxidants would only affect a small subset of cells that is actively dividing during this time period. On the other hand, cell number measurements represent a cumulative effect over 72 h. This could explain why different results were obtained by these different assays. Our observations that both BHT and α-tocopherol decreased BAEC proliferation differ from other reports on the effects of these antioxidants on EC. Several studies indicated that BHT and/or α-tocopherol stimulated EC proliferation (33–35) whereas another stated that α-tocopherol had no effect (36). One possible explanation for these differences is that EC from different sources were used in these studies, i.e., EC derived from fetal calf thoracic aorta (34), porcine pulmonary arteries (33), and human umbilical cords (35,36), and that the antioxidants affected these EC differently. Recently, α-tocopherol was reported to in-

hibit human mastocytoma cell proliferation (37). Our finding that the antiproliferative effect of 9t,11t-CLA could be partially overcome by either BHT or α-tocopherol is similar to earlier observations that α-tocopherol could reverse the antiproliferative effects of arachidonic and eicosatrienoic acids on smooth muscle cells, fibroblasts, and medial cells (24,38). On the other hand, neither of these antioxidants was able to restore decreased cell proliferation in HepG2 hepatoma cells induced by a 1:1 mixture of 9c,11t- and 10t,12c-CLA isomers (11). Although the antioxidants inhibited BAEC proliferation by 80–90%, our results indicate that the presence of these antioxidants decreased the antiproliferative effect of 9t,11t-CLA. This protective (but not additive) effect of the antioxidants on the residual proliferative ability of the cells suggested the generation of oxidant species in the antiproliferative effect of 9t,11t-CLA as was noted by Bergamo and coworkers (20).

A number of oxidant intermediates and products are generated during cell proliferation, some of which are derived from lipid peroxidation including peroxy radicals and MDA. However, this oxidant is probably not a MDA precursor since we observed no differences in MDA formation on treatment of BAEC with the antiproliferative 9t,11t-CLA and the ineffective 9c,11t-isomer. Furthermore, since prostaglandins such as PGE$_2$ have been reported to stimulate cell proliferation in certain cancer cells and angiogenesis (25,39), our results showing
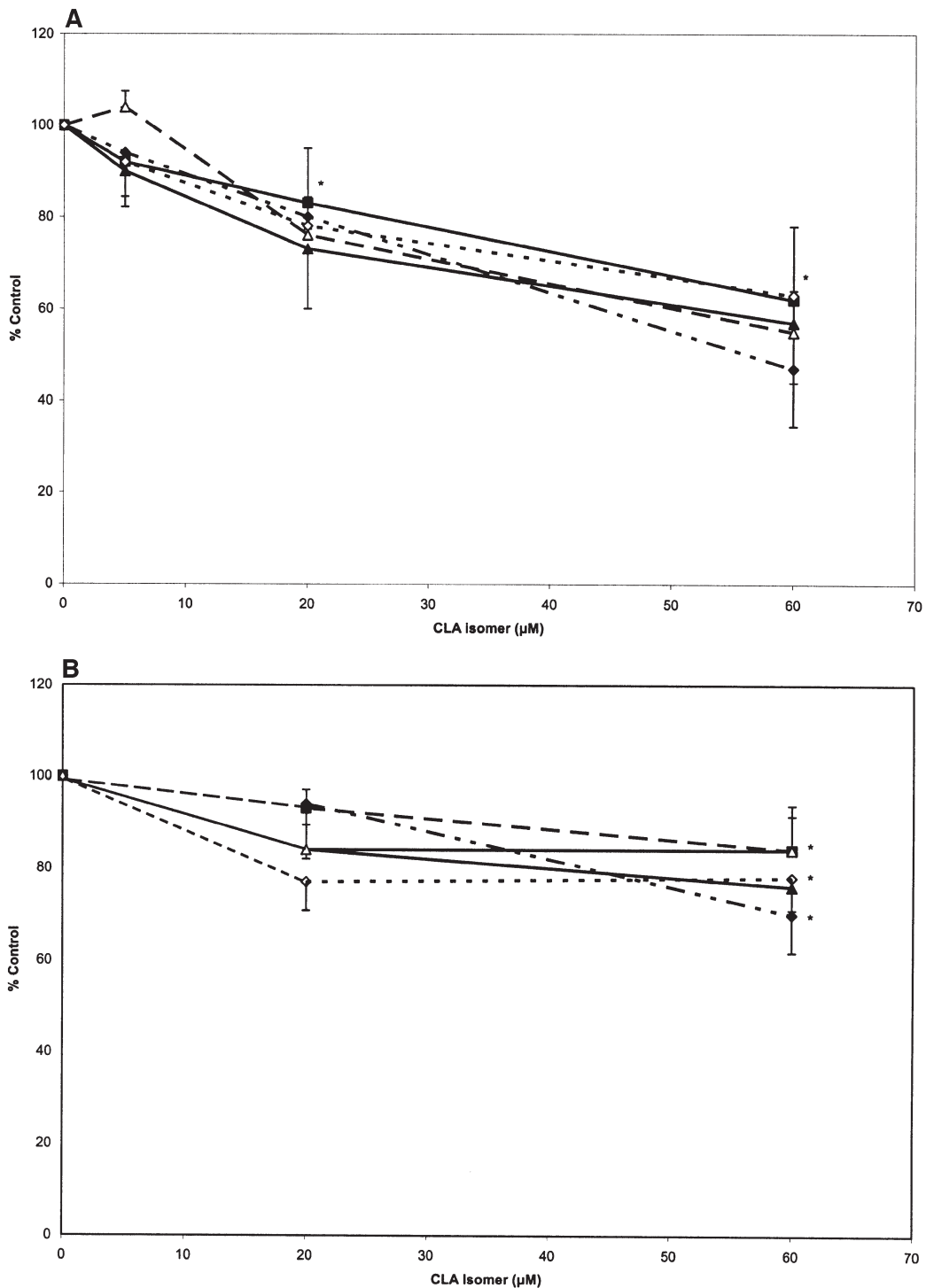
FIG. 7. Effect of different CLA isomers on cell proliferation and cell numbers of THP-1 leukemia cells. Cells were grown for 24 h and were then supplemented with either vehicle or different concentrations of CLA isomers complexed with 1% BSA. (A) 72 h after vehicle or CLA supplementation, cell proliferation was measured by the addition of 1 μCi/dish of [^{3}H]methylthymidine for the last 4 h of culture. Under these conditions, [^{3}H] incorporation into control cells (vehicle instead of CLA) averaged 1.26 ± 0.38 nCi/dish (*n* = 5). The results of triplicate dishes are given as % control. Values are mean ± SD (*n* = 4 separate experiments). (B) Cell numbers were measured in duplicate dishes after 72 h using the same protocol as described in (A) except no [^{3}H]methylthymidine was added. Control dishes contained 0.8 ± 0.076 x 10^6 cells after 72 h. ◆, 9*t*,11*t*; ■, 9*c*,11*t*; △, 9*c*,11*c*; ▲, 10*t*,12*c*; ◇, 11*c*,13*t*. *P < 0.01 when compared with control without CLA.

that the cyclooxygenase inhibitor indomethacin had no effect on the antiproliferative effect of 9*t*,11*t*-CLA indicated that prostaglandins were probably not involved in this process.

A number of studies have reported that several CLA isomers induced apoptosis *via* activation of caspase-3. Thus 9*c*,11*t*- and 10*t*,12*c*-CLA enhanced the caspase-3 activity in SW480, HT-29, and MIP-101 human colon cancer cell lines; dRLh-84 rat hepatoma cells; and human Jurkat T cells (12,13,19,32). Depending on the cell system, incubation times (6–96 h), and CLA concentrations (10–200 μM), activity increases from 20 to 400% were observed. In Jurkat T cells, the 9*c*,11*t*-CLA was the most effective isomer (fivefold increase) and the 9*t*,11*t*-isomer the least effective (twofold increase) when the cells were treated with the CLA isomer at 200 μM for 24 h (20). In the present study, comparable numbers were obtained, as we found that 60 μM 9*t*,11*t*-CLA increased caspase-3 activity 43% in BAEC after 72 h. However, with BAEC and our experimental conditions, a 24% decrease in caspase-3 activity was observed with the 9*c*,11*t*-isomer. These results suggest that when a CLA isomer exhibits antiproliferative properties, this is associated with induction of apoptosis as indicated by increased caspase-3 activity.

Thus, the present study provides evidence that 9*t*,11*t*-CLA, but not 9*c*,11*t*-CLA, inhibits proliferation of BAEC, and this antiproliferative effect involves the activation of the proapoptotic caspase-3 as well as oxidant species that are not precursors to MDA. Nor did 9*c*,11*c*-, 10*t*,12*c*-, and 11*c*,13*t*-CLA inhibit BAEC proliferation, but all five CLA isomers exhibited antiproliferative effects on THP-1 leukemia cells.

REFERENCES

1. Huttner, J.J., Gwebu, E.T., Panganamala, R.V., Milo, G.E., Cornwell, D.G., Sharma, H.M., and Geer, J.C. (1977) Fatty Acids and Their Prostaglandin Derivatives: Inhibitors of Proliferation in Aortic Smooth Muscle Cells, *Science 197*, 289–291.
2. Begin, M.E., Das, U.N., Ells, G., and Horrobin, D.F. (1985) Selective Killing of Human Cancer Cells by Polyunsaturated Fatty Acids, *Prostaglandins Leukot. Med. 19*, 177–186.
3. Sagar, P.S., and Das, U.N. (1995) Cytotoxic Action of *cis*-Unsaturated Fatty Acids on Human Cervical Carcinoma (HeLa) Cells *in vitro*, *Prostaglandins Leukot. Essent. Fatty Acids 53*, 287–299.
4. Pakala, R., Pakala, R., Sheng, W.L., and Benedict, C.R. (1999) Serotonin Fails to Induce Proliferation of Endothelial Cells Preloaded with Eicosapentaenoic Acid and Docosahexaenoic Acid, *Atherosclerosis 145*, 137–146.
5. Nano, J.L., Nobili, C., Girard-Pipau, F., and Rampal, P. (2003) Effects of Fatty Acids on the Growth of Caco-2 Cells, *Prostaglandins Leukot. Essent. Fatty Acids 69*, 207–215.
6. Wahle, K.W.J., Heys, S.D., and Rotondo, D. (2004) Conjugated Linoleic Acids: Are They Beneficial or Detrimental to Health? *Prog. Lipid Res. 43*, 553–587.
7. Schonberg, S., and Krokan, H.E. (1995) The Inhibitory Effect of Conjugated Dienoic Derivatives (CLA) of Linoleic Acid on the Growth of Human Tumor Cell Lines Is in Part Due to Increased Lipid Peroxidation, *Anticancer Res. 15*, 1241–1246.
8. Durgam, V.R., and Fernandes, G. (1997) The Growth Inhibitory Effect of Conjugated Linoleic Acid on MCF-7 Cells Is Related to Estrogen Response System, *Cancer Lett. 116*, 121–130.
9. O'Shea, M., Stanton, C., and Devery, R. (1999) Antioxidant Enzyme Defence Responses of Human MCF-7 and SW480 Cancer Cells to Conjugated Linoleic Acid, *Anticancer Res. 19*, 1953–1960.
10. Igarashi, M., and Miyazawa, T. (2000) Newly Recognized Cytotoxic Effect of Conjugated Trienoic Fatty Acids on Cultured Human Tumor Cells, *Cancer Lett. 148*, 173–179.
11. Igarashi, M., and Miyazawa, T. (2001) The Growth Inhibitory Effect of Conjugated Linoleic Acid on a Human Hepatoma Cell Line, HepG2, Is Induced by a Change in Fatty Acid Metabolism, but Not the Facilitation of Lipid Peroxidation in the Cells, *Biochim. Biophys. Acta 1530*, 162–171.
12. Yamasaki, M., Chujo, H., Koga, Y., Oishi, A., Rikimaru, T., Shimada, M., Sugimachi, K., Tachibana, H., and Yamada, K. (2002) Potent Cytotoxic Effect of the *trans*10, *cis*12 Isomer of Conjugated Linoleic Acid in Rat Hepatoma dRLh-84 Cells, *Cancer Lett. 188*, 171–180.
13. Palombo, J.D., Ganguly, A., Bistrian, B.R., and Menard, M.P. (2002) The Antiproliferative Effects of Biologically Active Isomers of Conjugated Linoleic Acid on Human Colorectal and Prostatic Cancer Cells, *Cancer Lett. 177*, 163–172.
14. Kim, E.J., Holthuizen, P.E., Park, H.S., Ha, Y.L., Jung, K.C., and Park, J.H. (2002) *Trans*-10,*cis*-12-Conjugated Linoleic Acid Inhibits Caco-2 Colon Cancer Cell Growth, *Am. J. Physiol. Gastrointest. Liver Physiol. 283*, G357–G367.
15. Luongo, D., Bergamo, P., and Rossi, M. (2003) Effects of Conjugated Linoleic Acid on Growth and Cytokine Expression in Jurkat T Cells, *Immunol. Lett. 90*, 195–201.
16. Agatha, G., Voigt, A., Kauf, E., and Zintl, F. (2004) Conjugated Linoleic Acid Modulation of Cell Membrane in Leukemia Cells, *Cancer Lett. 209*, 87–103.
17. Ochoa, J.J., Farquharson, A.J., Grant, I., Moffat, L.E., Heys, S.D., and Wahle, K.W.J. (2004) Conjugated Linoleic Acids (CLAs) Decrease Prostate Cancer Cell Proliferation: Different Molecular Mechanisms for *cis*-9, *trans*-11 and *trans*-10, *cis*-12 Isomers, *Carcinogenesis 25*, 1185–1191.
18. Ip, M.M., Masso-Welch, P.A., Shoemaker, S.F., Shea-Eaton, W.K., and Ip, C. (1999) Conjugated Linoleic Acid Inhibits Proliferation and Induces Apoptosis of Normal Rat Mammary Epithelial Cells in Primary Culture, *Exp. Cell Res. 250*, 22–34.
19. Moon, E.J., Lee, Y.M., and Kim, K.W. (2003) Antiangiogenic Activity of Conjugated Linoleic Acid on Basic Fibroblast Growth Factor-Induced Angiogenesis, *Oncol. Rep. 10*, 617–621.
20. Bergamo, P., Luongo, D., and Rossi, M. (2004) Conjugated Linoleic Acid-Mediated Apoptosis in Jurkat T Cells Involves the Production of Reactive Oxygen Species, *Cell. Physiol. Biochem. 14*, 57–64.
21. Torres-Duarte, A.P., and Vanderhoek, J.Y. (2003) Conjugated Linoleic Acid Exhibits Stimulatory and Inhibitory Effects on Prostanoid Production in Human Endothelial Cells and Platelets, *Biochim. Biophys. Acta 1640*, 69–76.
22. Al-Madaney, M.M., Kramer, J.K.G., Deng, Z., and Vanderhoek, J.Y. (2003) Effects of Lipid-Esterified Conjugated Linoleic Acid Isomers on Platelet Function: Evidence for Stimulation of Platelet Phospholipase Activity, *Biochim. Biophys. Acta 1635*, 75–82.
23. Ulmer, D.D., Vallee, B.L., and Wacker, W.E. (1956) Metalloenzymes and Myocardial Infarction. II. Malic and Lactic Dehydrogenase Activities and Zinc Concentrations in Serum, *N. Engl. J. Med. 255*, 449–456.
24. Gavino, V.C., Miller, J.S., Ikharebha, S.O., Milo, G.E., and Cornwell, D.G. (1981) Effect of Polyunsaturated Fatty Acids and Antioxidants on Lipid Peroxidation in Tissue Cultures, *J. Lipid Res. 22*, 763–769.
25. Lee, P.P.H., and Ip, M.M. (1992) Regulation of Proliferation of Rat Mammary Tumor Cells by Inhibitors of Cyclooxygenase and Lipoxygenase, *Prostaglandins Leukot. Essent. Fatty Acids 45*, 21–31.
26. Sheng, H., Shao, J., Kirkland, S.C., Isakson, P., Coffey, R.J.,

Morrow, J., Beauchamp, R.D., and Dubois, R.N. (1997) Inhibition of Human Colon Cancer Cell Growth by Selective Inhibition of Cyclooxygenase-2, *J. Clin. Invest. 99*, 2254–2259.

27. Rickert, R., Steinhart, H., Fritsche, J., Sehat, N., Yurawecz, M.P., Mossoba, M.M., Roach, J.A.G., Eulitz, K., Ku, Y., and Kramer, J.K.G. (1999) Enhanced Resolution of Conjugated Linoleic Acid Isomers by Tandem-Column Silver-Ion High Performance Liquid Chromatography, *J. High Resolut. Chromatogr. 22*, 144–148.

28. Fritsche, J., Rickert, R., and Steinhart, H. (1999) Formation, Contents and Estimation of Daily Intake of Conjugated Linoleic Acid Isomers and *trans*-Fatty Acids in Foods, in *Advances in Conjugated Linoleic Acid Research Vol. 1* (Yurawecz, M., Mossoba, M.M., Kramer, J.K.G., Pariza, M.W. and Nelson, G.J., eds.), pp. 378–396, AOCS Press, Champaign, Illinois.

29. Parodi, P.W. (2003) Conjugated Linoleic Acid in Food, in *Advances in Conjugated Linoleic Acid Research Vol. 2* (Sebedio, J.L., Christie, W.W., and Adlof, R., eds), pp. 101–122, AOCS Press, Champaign, Illinois.

30. Petridou, A., Mougios, V., and Sagredos, A. (2003) Supplementation with CLA: Isomer Incorporation into Serum Lipids and Effect on Body Fat of Women, *Lipids 38*, 805–811.

31. Huang, Y.C., Luedecke, L.O., and Shultz, T.D. (1994) Effect of Cheddar Cheese Consumption on Plasma Conjugated Linoleic Acid Concentrations in Men, *Nutr. Res. 14*, 373–386.

32. Miller, A., Stanton, C., and Devery, R. (2002) *Cis*-9,*trans*-11- and *trans*-10,*cis*-12-Conjugated Linoleic Acid Isomers Induce Apoptosis in Cultured SW480 Cells, *Anticancer Res. 22*, 3879–3888.

33. Hennig, B., Biossonneault, G.A., Fiscus, L.J., and Marra, M.E. (1988) Effect of Vitamin E on Oxysterol- and Fatty Acid Hydroperoxide-Induced Changes of Repair and Permeability Properties of Cultured Endothelial Cell Monolayers, *Internat. J. Vit. Nutr. Res. 58*, 41–47.

34. Kuzuya, M., Naito, M., Funaki, C., Hayashi, T., Yamada, K., Asai, K., and Kuzuya, F. (1991) Antioxidants Stimulate Endothelial Cell Proliferation in Culture, *Artery 18*, 115–124.

35. Totzke, G., Metzner, C., Ulrich-Merzenich, G., Ko, Y., Sachinidis, A., and Vetter, H. (2001) Effect of Vitamin E and Vitamin C on the DNA Synthesis of Human Umbilical Arterial Endothelial Cells, *Eur. J. Nutr. 40*, 121–126.

36. Huang, N., Lineberger, B., and Steiner, M. (1988) α-tocopherol, a Potent Modulator of Endothelial Cell Function, *Thromb. Res. 50*, 547–557.

37. Kempná, P., Reiter, E., Arock, M., Azzi, A., and Zingg, J.M. (2004) Inhibition of HMC-1 Mast Cell Proliferation by Vitamin E. Involvement of the Protein Kinase B Pathway, *J. Biol. Chem. 279*, 50700–50709.

38. Miller, J.S., Gavino, V.C., Ackerman, A., Sharma, H.M., Milo, G.E., Geer, J.C., and Cornwell, D.G. (1980) Triglycerides, Lipid Droplets and Lysosomes in Aorta Smooth Muscle Cells During the Control of Cell Proliferation with Polyunsaturated Fatty Acids and Vitamin E, *Lab. Invest. 42*, 495–506.

39. Form, D.M., and Auerbach, R. (1983) PGE_2 and Angiogenesis, *Proc. Soc. Exp. Biol. Med. 172*, 214–218.

Intake of Conjugated Eicosapentaenoic Acid Suppresses Lipid Accumulation in Liver and Epididymal Adipose Tissue in Rats

Tsuyoshi Tsuzuki[a,*], **Yuki Kawakami**[b], **Yoshihiro Suzuki**[b], **Renpei Abe**[b], **Kiyotaka Nakagawa**[b], and **Teruo Miyazawa**[b]

[a]Department of Food Management, School of Food, Agricultural and Environment Sciences, Miyagi University, Sendai 982-0215, Japan, and [b]Food & Biodynamic Chemistry Laboratory, Graduate School of Agricultural Science, Tohoku University, Sendai 981-8555, Japan

ABSTRACT: It has been reported that consumption of CLA and EPA alters lipid metabolism. CLA contains conjugated double bonds, and EPA is an n-3 PUFA. Based on the possibility that a molecule with both of these structures might have interesting physiological effects, we prepared conjugated FA from EPA by alkaline isomerization and examined the effects of the conjugated EPA (CEPA) on lipid metabolism in rats. Rats were fed by oral gavage every day for 4 wk with 200 mg of FA including linoleic acid, EPA, CLA, or CEPA. Compared with other groups, rats fed CEPA showed a significant weight loss in epididymal adipose tissue and significant decreases in the levels of liver TAG and total cholesterol (TC), indicating reduced accumulation of lipid in the liver and adipose tissue. The plasma levels of TAG, TC, FFA, and tumor necrosis factor-α in rats fed CEPA were reduced, as was the activity of the FA synthesis system in the liver, whereas the FA-β-oxidation system was activated by CEPA. These results suggest that intake of CEPA suppresses lipid accumulation in the liver and epididymal adipose tissue while increasing lipid catabolism in rats.

Paper no. L9815 in *Lipids 40*, 1117–1123 (November 2005).

A total caloric intake characterized by an excessive consumption of lipid in the absence of increased energy expenditure leads to obesity (1). Obesity is evidenced as an excessive increase in white adipose tissue, and it provides the basis for so-called lifestyle-related diseases such as diabetes mellitus, hyperlipidemia, and arteriosclerosis. Accumulation of TAG, which constitute the majority of dietary lipids, causes changes in liver function and is strongly associated with the development of pathological conditions such as fatty liver, hyperlipidemia, and obesity (2). Therefore, prevention of lipid accumulation in white adipose tissue and the liver would be useful in preventing lifestyle-related diseases.

Recent studies have reported that CLA (18:2), a group of FA isomers with conjugated double bonds, has an antiobesity effect due to suppression of body fat accumulation (3–6). However, there are a number of reports disclaiming the antiobesity effect of CLA in humans (7). Several geometric isomers of CLA are found in natural products; these isomers are especially abundant in ruminant-derived oils and fats such as beef tallow and milk fat (8). Other than antiobesity effects, CLA has been reported to have various physiological actions, such as anticancer and antiarteriosclerosis effects (8–12), but because the CLA content in natural oils and fats is only about 1%, it would be difficult to use them as CLA-containing functional lipids. Thus, CLA-containing oils and fats resulting from alkaline isomerization of plant oils such as safflower oil are currently available as commercial products (7,9).

In addition to CLA, other conjugated FA occur naturally in plant seeds and marine algae (13–15), but their properties have not been widely explored. Our previous reports on the physiological functions, metabolism, analysis, and oxidative stability of conjugated FA other than CLA (16–22) indicated that their *in vitro* and *in vivo* tumoricidal effects are stronger than those of CLA (18,19,22). We have also found that rats fed FA containing conjugated triene systems convert them to FA with conjugated dienes (16,21). These studies have been facilitated by the development of analytical methods in which isomerization of conjugated FA is avoided and the FA are stabilized against oxidation (17,20).

These findings are of interest, but the metabolism effects of conjugated FA other than CLA remain unclear. Furthermore, consumption of highly unsaturated n-3 FA such as EPA (5Z,8Z,11Z,14Z,17Z-20:5) has been reported to improve lipid metabolism (23). In this study, we speculated that a highly unsaturated n-3 FA with conjugated double bonds might have interesting physiological effects, perhaps including increased lipid catabolism. To examine this possibility, we prepared conjugated EPA (CEPA) from EPA by alkaline isomerization and determined its physiological effects in rats. Positive controls were a CLA preparation with reported antiobesity effect and EPA. To evaluate the antiobesity effect, the weights of body and white adipose tissue were measured. In addition, the plasma concentrations of leptin, tumor necrosis factor (TNF)-α, and FFA secreted from the white adipose tissue were measured. To evaluate the influence on *in vivo* lipid metabolism, the lipid composition of liver and plasma and the lipid-metabolizing enzyme activity of the liver were measured. As a result, we show that CEPA suppresses lipid accumulation in the liver and adipose tissue and increases lipid catabolism to a greater

extent than linoleic acid (LA), CLA, and EPA. CEPA is not found in the mammals not fed this FA. Thus the intake of CEPA might be effective in preventing obesity.

EXPERIMENTAL PROCEDURES

Materials. EPA (90% purity) was donated by Bizen Chemical (Okayama, Japan). Safflower oil and CLA (80% purity) were obtained from Rinoru Oil Mills (Nagoya, Japan).

Preparation of safflower oil FA. After being bubbled with nitrogen gas for 15 s, 90 mg of safflower oil was saponified with 15 mL of 0.3 N KOH in 90% methanol at 37°C for 2 h to produce safflower oil FA (16,17). Once the reaction mixture was cooled to room temperature, it was added to 5 mL of 90% methanol and 15 mL of hexane, and the mixture was vigorously shaken. The methanolic aqueous layer was further washed twice with 15 mL of hexane to exclude the nonsaponified material. The recovered washed methanolic aqueous layer was added to 9 mL of 6 N HCl, and the FA were then extracted with hexane (2 × 15 mL). The combined hexane extracts were evaporated under a nitrogen stream, and the concentrate was passed through Sep-Pak Silica (Waters, Milford, MA) with 10 mL of hexane/diethyl ether (95:5, vol/vol) as the eluent to collect the safflower oil FA.

Preparation of CEPA. CEPA was prepared from EPA by alkaline isomerization, using the AOAC method with slight modifications (19,24). EPA (1 g) in a test tube (100-mL vol) was mixed with 10 mL of potassium hydroxide at a concentration of 21% (w/w) in ethylene glycol. Nitrogen gas was bubbled through the mixture, and the tube was then screw-capped and allowed to stand for 5 min at 180°C. The reaction mixture was cooled, and 10 mL of methanol was added. The mixture was acidified to below pH 2 with 20 mL of 6 N HCl, and, after dilution with 20 mL of distilled water, the conjugated FA was extracted with 50 mL of hexane. The hexane extract was washed with 30 mL of 30% methanol and with 30 mL of distilled water before being evaporated under a nitrogen gas stream. The concentration of the conjugated FA was determined by UV/vis spectrophotometric analysis by using a Shimadzu UV-2400PC (Shimadzu, Kyoto, Japan). The spectrophotometric readings confirmed the presence of conjugated FA (25) and showed that about 90% of the EPA had been isomerized to a variety of CEPA. After being purged with nitrogen gas, CEPA was stored at –20°C.

Animals and treatment. Male Sprague-Dawley rats (4 wk of age) were obtained from Japan SLC (Hamamatsu, Japan). Commercial diet (MF) used for animal trials was purchased from Oriental Yeast Co., Ltd. (Chiba, Japan) and had the following approximate composition (g/kg diet): carbohydrate, 544; protein, 236; fat, 53; fiber, 29; moisture, 77; ash, 61. The energy content of the commercial diet was 360 kcal/100 g diet (21). FA composition of the commercial diet was 16:0 (15%), 16:1 (1%), 18:0 (3%), 18:1 (26%), 18:2 (47%), 18:3 (4%), 20:1 (1%), 20:5 (1%), 22:1 (1%), and 22:6 (1%). The nature of the conjugated double bonds in the conjugated FA samples prepared as described above was determined by UV/vis spectrophotometric analysis, and these data are summarized in

TABLE 1
FA Composition of the Dietary Oil Mixtures

	LA[a]	CLA[b]	EPA[c]	CEPA[d]
		(%)		
16:0	8.1	9.3	2.1	2.2
18:0	2.9	4.7	0.8	1.1
18:1n-9	16.3	14.6	14.5	12.7
18:2n-6	71.8	10.3	21.4	17.0
CLA				
9*Z*,11*E*	—	24.0	—	—
10*E*,12*Z*	—	25.8	—	—
Others	—	10.2	—	—
20:5n-3	—	—	60.0	5.5
CEPA				
Diene	—	—	—	33.6
Triene	—	—	—	20.3
Tetraene	—	—	—	4.6
Pentaene	—	—	—	1.5
Other	0.9	1.1	1.2	1.5

[a]Safflower oil FA.
[b]Safflower oil FA: CLA = 13:87 (vol/vol).
[c]Safflower oil FA: EPA = 28:72.
[d]Safflower oil FA: Conjugated EPA (CEPA) = 22:78. CLA was donated by Rinoru Oil Mills. CEPA was prepared from EPA by the AOAC method (19,24). 9*Z*,11*E*, 9*Z*,11*E*-18:2; 10*E*,12*Z*, 10*E*,12*Z*-18:2; Diene, conjugated diene; Triene, conjugated triene; Tetraene, conjugated tetraene; Pentaene, conjugated pentaene.

Table 1. The prepared test oils contained the main FA as 60% of the total FA content, based on GC and UV/vis spectrophotometry (Table 1). The GC conditions were described previously (16,20,21). The test oils were prepared as follows: LA oil was prepared with only safflower oil FA; CLA oil, with safflower oil FA and CLA (safflower oil FA/CLA = 13:87, vol/vol); EPA oil, with safflower oil FA and EPA (safflower oil FA/EPA = 28:72, vol/vol); and CEPA oil, with safflower oil FA and CEPA (safflower oil FA/CEPA = 22:78, vol/vol). The test oils were stored at −20°C until they were fed to the animals. After acclimation to a commercial diet for 1 wk, rats were randomly divided into four groups according to the administered test oils: safflower oil FA supplement (LA group, *n* = 8); 60% CLA supplement (CLA group, *n* = 8); 60% EPA supplement (EPA group, *n* = 8); and 60% CEPA supplement (CEPA group, *n* = 8). Two hundred milligrams of test oil per rat was administered daily by oral gavage. The amount of 200 mg/d in rats is equal to about 0.8–1% of dietary intake (21–23 g/d) (16). The lipid content of the commercial diet is 5.1%. So, the lipid intake is about 6% in this study; this does not represent a high-fat diet. The antiobesity effect of CLA appears at about 0.5–1% of the diet, according to past reports (3–6). So, the dietary intake of CEPA was adjusted to about 0.5% in this study. Oral administration was selected because the conjugated FA are easily oxidized (20) and because it was important to keep the dietary intake of the conjugated FA constant. Two rats were housed in each cage in a temperature- and humidity-controlled room with light cycles of 12 h on and 12 h off. Animals were given free access to commercial diets and distilled water. All procedures were performed in accordance with the Animal Experiment Guidelines of Tohoku University.

Sample preparation and measurements of diet intake, body weight, and tissue weight. During the 4-wk test period, the diet intake was measured in each group. The diet was given in the same feeding box as for powdered diets except with an inside lid. The feeding box was fixed so that the rat could not damage or alter it. The diet intake was determined by weighing the feeding box every day and calculating the decrement of diet. During the test period, body weight was measured in each group every week. At the end of the 4-wk test period, the rats were weighed, and blood samples were collected following decapitation. The liver, spleen, kidney, lung, heart, and epididymal adipose tissue were removed and weighed. Blood was treated with EDTA, and the plasma was isolated by cold centrifugation at $1,000 \times g$ for 15 min at 4°C, as previously reported (16,18,19). Tissues and plasma were stored at −30°C until use.

Assays for leptin, TNF-α, FFA, insulin, and glucose concentrations in plasma. The leptin concentration in plasma was determined with a rat leptin EIA (Enzyme Immuno Assay) kit (Immuno-Biological Laboratory. Co., Ltd., Gunma, Japan), TNF-α with a rat TNF-α ultrasensitive ELISA kit (BioSource International, Inc., Camarillo, CA), and insulin with a rat insulin ELISA kit (Shibayagi Ltd., Gunma, Japan), according to the manufacturer's protocol in each case. The glucose and FFA contents were measured enzymatically with commercial kits supplied by Wako Pure Chemical Industries (Tokyo, Japan), again according to the manufacturer's protocol.

Lipid determination. TAG and total cholesterol (TC) in plasma and liver were measured using commercially available enzyme kits (TAG Test Wako and Total Cholesterol Test Wako) according to the manufacturer's protocol. Phospholipid (PL) content in plasma and liver was determined using the method described by Bartlett (26).

Assays of enzyme activity in liver. FA synthase (FAS) activity in the liver was determined spectrophotometrically from the rate of malonyl-CoA-dependent NADPH oxidation (27). Malic enzyme (ME) activity in liver was determined as previously described (28). FAS and ME activities were expressed as nmol of NADPH/min/mg protein. Acyl-CoA oxidase (ACO) activity in liver was measured from the rate of palmitoyl-CoA-dependent H_2O_2 production coupled with dichlorofluorescein oxidation, as described by Small *et al.* (29), and expressed as nmol of dichlorofluorescein/min/mg protein. The protein concentration in liver was determined using a DC Protein Assay kit (Bio-Rad Laboratories, Hercules, CA), with BSA used as the standard.

Statistical analysis. Statistical analysis was performed using one-way ANOVA, followed by a Newman–Keule's test for multiple comparisons among several groups. A difference was considered to be significant at $P < 0.05$.

RESULTS

CLA has only conjugated diene structures, whereas CEPA has diene, triene, and other structures (Table 1). Each rat was fed 200 mg of the test oil once every day for 4 wk. The diet plus

200 mg of the test oil in rat is equivalent to a 6% fat diet, which is not a high-fat diet and is within the normal limits of rat dietary lipid content. The conjugated FA accounted for an average of 0.5% of the daily intake of the rats, and all animals in all the groups showed favorable growth during the experimental period. The amount of diet intake was 22.9 ± 2.1 g/d in the LA group, 21.9 ± 2.3 g/d in the CLA group, 22.3 ± 1.8 g/d in the EPA group, and 20.1 ± 2.3 g/d in the CEPA group (mean ± SD, $n = 8$). There was no significant difference in the average dietary intake during the test period. The average body weight in the CEPA group was significantly lower than those in the other groups at the end of the test period, and was 89% of that in the LA group (Fig. 1). To clarify the basis for the effect of CEPA, several tissues were weighed, but no significant differences in the heart, lung, liver, spleen, and kidney weights were found among the four groups (Table 2). However, the weight of epididymal adipose tissue, a visceral white adipose tissue, was significantly lower in the CEPA group than in the other groups, and was only 45% of that in the LA group (Table 2). Therefore, the body weight decrease in the CEPA group appeared to be due to a decrease in the white adipose tissue weight.

To explain the decrease in the white adipose tissue weight, changes in the plasma levels of the antiobesity hormone leptin, of TNF-α, which is known to induce insulin resistance, and of FFA were measured. No significant difference in the plasma leptin level was found among the four groups (Fig. 2). In contrast, the TNF-α level in the CEPA group was significantly lower than those in the other groups, and was only 20% of that in the LA group. The TNF-α level in the CLA group was also significantly lower than in the LA group, showing a decrease to 57% of the level in the LA group. The FFA level in the CEPA group was significantly lower than in the LA and CLA groups, with a decrease to 72% of that in the LA group. And, the FFA level in the CEPA group was in the decreasing tendency compared with the EPA group. The FFA levels in the CLA and EPA groups were 80 and 74%, respectively, of the level in the LA group, a significant decrease. These results suggest that CEPA prevents the ac-
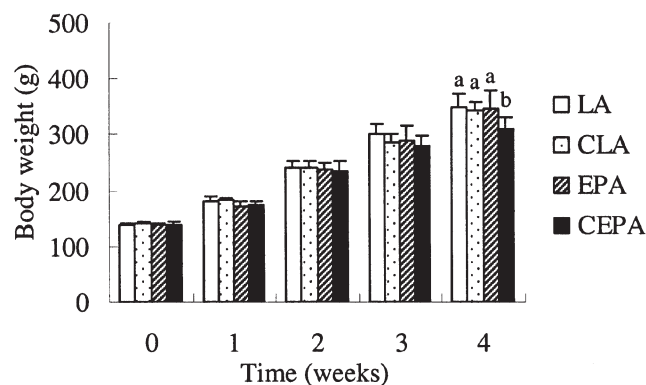
FIG. 1. Effects on body weight of rats fed conjugated FA for 4 wk. Values are mean ± SD ($n = 8$). [a,b]Means at a given time point with different superscripts are significantly different at $P < 0.05$. LA, linoleic acid; CEPA, conjugated EPA.

TABLE 2
Effects of CEPA on Weight of Selected Organs of Rats[a]

	LA	CLA	EPA	CEPA
	(g/100 g body weight)			
Heart	0.33 ± 0.03	0.33 ± 0.02	0.33 ± 0.02	0.34 ± 0.02
Lung	0.40 ± 0.04	0.40 ± 0.06	0.39 ± 0.07	0.42 ± 0.03
Liver	4.97 ± 0.37	5.05 ± 0.22	5.00 ± 0.50	5.21 ± 0.27
Spleen	0.18 ± 0.02	0.19 ± 0.02	0.21 ± 0.04	0.18 ± 0.03
Kidney	0.67 ± 0.04	0.68 ± 0.04	0.68 ± 0.08	0.69 ± 0.06
Epididymal adipose tissue	2.81 ± 0.56[a]	2.15 ± 0.69[b]	2.37 ± 0.38[a,b]	1.27 ± 0.29[c]

[a]Values are mean ± SD (*n* = 8). [a,b,c]Means in a row with different superscripts are significantly different at *P* < 0.05. For abbreviations see Table 1.

cumulation of white adipose tissue in rats. To examine this further, the lipid composition (the levels of TAG, TC, and PL) was determined in the plasma and liver. The plasma TAG levels in the CEPA group were significantly lower than those in the other groups, showing a decrease to 73% of the level in the LA group (Table 3). The plasma TAG levels in the CLA and EPA groups were also significantly decreased to 86 and 90%, respectively, of the level in the LA group. The plasma TC levels in the CLA, EPA, and CEPA groups were significantly decreased to 88, 87, and 83%, respectively, of that in the LA group (Table 3), and the plasma PL levels in the CEPA group were significantly decreased to 81% of the level in the LA group (Table 3). The lipid composition in the liver showed similar behavior to that in plasma, with decreased levels in the CEPA group (Table 3). The liver TAG levels in the CEPA group were significantly lower than in the other groups, and were decreased to 65% of that in the LA group (Table 3). The liver TAG levels in the CLA and EPA groups were also significantly decreased to 86 and 90%, respectively, of that in the LA group, and the liver TC levels in the EPA and CEPA groups were significantly decreased to 91 and 89%, respectively, of the level in the LA group. There were no significant differences in liver PL levels among the four groups.

The lipid composition data suggest that CEPA reduces liver and plasma lipid levels and prevents lipid accumulation (particularly TAG) in the liver by influencing FA metabolism enzymes in the liver. To examine changes in FA metabolism in the liver, the activities of FA-synthesizing enzymes such as FA synthetasesynthase (FAS) and ME and the FA β-oxidation enzyme ACO were measured (Fig. 3). FAS and ME activities in the CEPA group were significantly reduced to 69 and 87%, respectively, of the activities in the LA group. In contrast to the activities of FA-synthesizing enzymes, ACO activity showed the opposite tendency, with the CEPA group showing significant increases in ACO activity to 190% of that in the LA group. These results indicate that CEPA reduces the FA-synthesis system and promotes the FA β-oxidation system. Overall, the results show that CEPA inhibits lipid accumulation in rat liver and adipose tissue.

DISCUSSION

In this study, the effects of CEPA on lipid metabolism in rats were examined, and the effects were compared with those in-

duced by LA, CLA, and EPA. We were able to show for the first time that CEPA, an n-3 PUFA containing conjugated double bonds, suppresses fat accumulation in the liver and adipose tissue and increases lipid catabolism.

The body weight in the CEPA group after 4 wk of administration was significantly decreased compared with the other groups (Fig. 1), and we therefore examined which organ was influenced by CEPA. The weight of epididymal adipose tissue in the CEPA group was significantly lower than that in other groups (Table 2), whereas there were no significant differences in the heart, lung, liver, spleen, and kidney weights among the
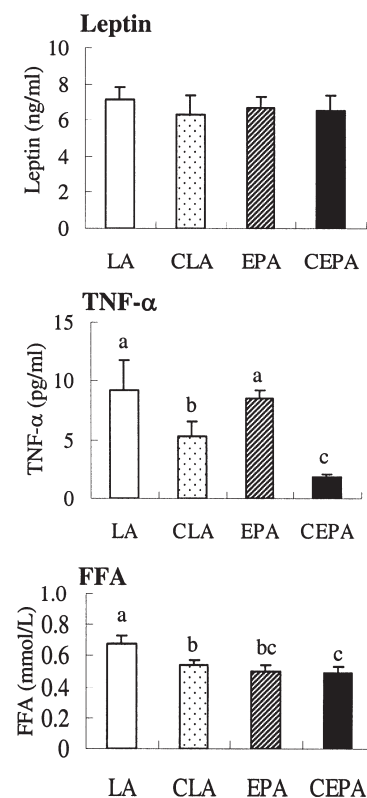
FIG. 2. Leptin, tumor necrosis factor-α (TNF-α), and FFA concentrations in plasma of rats fed conjugated FA for 4 wk. Values are mean ± SD (*n* = 8). [a,b,c]Means in a panel with different superscripts are significantly different at *P* < 0.05. For abbreviations see Figure 1.

TABLE 3
Effects of FA Intake on the Plasma and Liver Lipids of Rats[a]

		LA	CLA	EPA	CEPA
Plasma	TAG	2.23 ± 0.20^a	1.91 ± 0.16^b	2.01 ± 0.18^b	1.62 ± 0.16^c
(μmol/mL)	TC	2.97 ± 0.25^a	2.60 ± 0.31^b	2.58 ± 0.26^b	2.46 ± 0.27^b
	PL	3.16 ± 0.44^a	$2.77 \pm 0.30^{a,b}$	$3.07 \pm 0.46^{a,b}$	2.57 ± 0.25^b
Liver	TAG	45.3 ± 2.28^a	39.1 ± 3.09^b	41.1 ± 3.40^b	29.5 ± 4.54^c
(μmol/g)	TC	8.95 ± 0.49^a	$8.61 \pm 0.46^{a,b}$	8.15 ± 0.69^b	7.92 ± 0.54^b
	PL	14.1 ± 2.28	14.1 ± 3.68	12.4 ± 2.67	13.9 ± 2.65

[a]Values are mean ± SD ($n = 8$). TC, total cholesterol; PL, phospholipid; for other abbreviations see Table 1. [a,b,c]Means in a row with different superscripts are significantly different at $P < 0.05$.

four groups (Table 2). Hence, it appears that CEPA administration inhibits expansion of rat adipose tissue. To explain this phenomenon, the blood levels of leptin, TNF-α and FFA were measured, since these molecules are secreted from adipocytes. Leptin is an antiobesity hormone that is closely associated with progression of obesity (30), since its function is to promote energy metabolism, whereas TNF-α is known to cause insulin resistance and FFA decrease energy metabolism and consequently oppose the function of leptin (31–34). In this study, there were no significant differences in the plasma leptin levels among the four groups, but the TNF-α and FFA levels in the CEPA group were significantly decreased compared with the other groups (Fig. 2). Adipocytes are known to accumulate lipids intracellularly and to secrete large amounts of TNF-α and FFA (31,35). Hence, CEPA may prevent adipocyte growth.

The activities of the liver FA-synthesis enzymes FAS and ME were also significantly reduced by CEPA administration, whereas the activity of ACO, the rate-limiting enzyme in FA β-oxidation in the liver, was significantly enhanced by CEPA (Fig. 3). These results indicate that CEPA has an effect on fat accumulation in the liver and adipose tissue, largely through reduction of FA synthesis and promotion of FA catabolism through the liver β-oxidation system. Transcription of the ACO gene is regulated by ligand-induced transcription factors referred to as peroxisome proliferator-activated receptors (PPAR) (36,37). Fibrates and thiazolidinedione derivatives (antidiabetic drugs) are known to be ligands for PPAR, and highly unsaturated FA and their metabolites, eicosanoids, are endogenous ligands (38–41). In addition to ACO, the transcription of various enzymes related to catabolism and utilization of FA, such as mitochondrial β-oxidation system enzymes, enzymes involved in acyl-CoA-synthesis, and lipoprotein lipases, is activated by PPAR to suppress fat accumulation (37). CLA have been reported to act as high-affinity ligands for PPAR and to activate PPARα in the regulation of lipid metabolism (42–44). Therefore, CEPA may also regulate lipid metabolism through this mechanism, and may have a higher affinity for PPAR than CLA has. However, a recent study has shown that in PPARα-knockout mice and wild-type mice fed a CLA-containing diet, the genes related to hepatic lipid metabolism respond similarly, suggesting that PPARα may not be of importance in CLA-induced regulation of lipid metabolism (45). Therefore, conjugated FA may regulate lipid metabolism by a PPARα-independent mechanism, through which CEPA controls adipocyte expansion, promotes leptin function, and decreases lipid deposition in the body.

CEPA showed stronger effects than CLA in the present study, suggesting that the conjugated double-bond structure has an influence on these effects. We have previously reported that lipids with a conjugated triene structure had a stronger tumoricidal effect than conjugated diene lipids, and that the effect was influenced by the structure of the conjugated double bonds (17,18). As shown in Table 1, CEPA contains conjugated triene and tetraene structures, suggesting that lipids containing such structures may have a stronger antiobesity effect than those with conjugated dienes. The combination of conjugated double bonds and n-3 FA in CEPA had a stronger effect on fat accumulation than CLA and EPA; hence, CEPA reduced the secretion of TNF-α and FFA from white adipose tissue, reduced hepatic
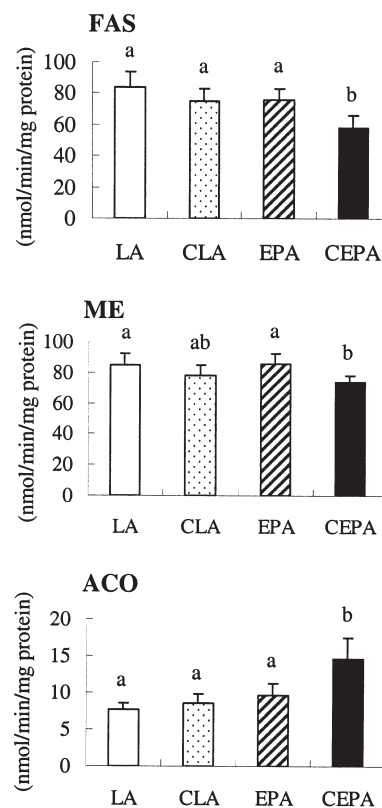
FIG. 3. Activity of enzymes in FA metabolism in the liver of rats fed conjugated FA for 4 wk. Values are mean ± SD ($n = 8$). [a,b]Means in a panel with different superscripts are significantly different at $P < 0.05$. FAS, FA synthase; ME, malic enzyme; ACO, acyl-CoA oxidase. For other abbreviations see Figure 1.

FA synthesis, lowered blood TAG and TC levels, and suppressed the accumulation of fat in the liver and adipose tissue. These results suggest that CEPA may have antiobesity effects in humans, although further studies of the observed effects and safety will be of importance. CLA made by isomerizing safflower oil and corn oil with alkali is sold as a health food supplement (7). Therefore, if CEPA made from the alkaline isomerization of EPA is found to be safe and without toxic side effects, CEPA might also be suitable as a health food supplement. Based on the present research in rats, humans would need to consume about 5 g CEPA a day as a health food supplement to see any effect. Therefore, it is also necessary to examine the effects of lower doses.

REFERENCES

1. Bray, G.A., and Popkin, B.M. (1998) Dietary Fat Intake Does Affect Obesity! *Am. J. Clin. Nutr. 68*, 1157–1173.
2. Sharadi, Y., and Eldad, A. (2000) Nonalcoholic Fatty Liver Disease Is Associated with Hyperlipidemia and Obesity, *Am. J. Med. 109*, 171.
3. Park, Y., Albright, K.J., Storkson, J.M., Liu, W., Cook, M.E., and Pariza, M.W. (1999) Changes in Body Composition in Mice During Feeding and Withdrawal of Conjugated Linoleic Acid, *Lipids 34*, 243–248.
4. Tsuboyama-Kasaoka, N., Takahashi, M., Tanemura, K., Kim, H.J., Tange, T., Okuyama, H., Kasai, M., Ikemoto, S., and Ezaki, O. (2000) Conjugated Linoleic Acid Supplementation Reduces Adipose Tissue by Apoptosis and Develops Lipodystrophy in Mice, *Diabetes 49*, 1534–1542.
5. Berven, G., Bye, A., Hals, O., Blankson, H., Fagertun, H., Thom, E., Wadstein, J., and Gudmundsen, O. (2002) Safety of Conjugated Linoleic Acid (CLA) in Overweight or Obese Human Volunteers, *Eur. J. Lipid Sci. Technol. 102*, 455–462.
6. Kreider, R.B., Ferreira, M.P., Greenwood, M., Wilson, M., and Almada, A.L. (2002) Effects of Conjugated Linoleic Acid Supplementation During Resistance Training on Body Composition, Bone Density, Strength, and Selected Hematological Markers, *J. Strength Cond. Res. 16*, 325–334.
7. Larsen, T.M., Toubro, S., and Astrup, A. (2003) Efficacy and Safety of Dietary Supplements Containing CLA for the Treatment of Obesity: Evidence from Animal and Human Studies, *J. Lipid Res. 44*, 2234–2241.
8. Ha, Y.L., Grimm, N.K., and Pariza, M.W. (1987) Anticarcinogens from Fried Ground Beef: Heat-Altered Derivatives of Linoleic Acid, *Carcinogenesis 8*, 1881–1887.
9. Gaullier, J.M., Halse, J., Hoye, K., Kristiansen, K., Fagertun, H., Vik, H., and Gudmundsen, O. (2005) Supplementation with Conjugated Linoleic Acid for 24 Months Is Well Tolerated by and Reduces Body Fat Mass in Healthy, Overweight Humans, *J. Nutr. 135*, 778–784.
10. Ip, C., Chin, S.F., Scimeca, J.A., and Pariza, M.W. (1991) Mammary Cancer Prevention by Conjugated Dienoic Derivative of Linoleic Acid, *Cancer Res. 51*, 6118–6124.
11. Ip, C., Singh, M., Thompson, H.J., and Scimeca, J.A. (1991) Conjugated Linoleic Acid Suppresses Mammary Carcinogenesis and Proliferative Activity of the Mammary Gland in the Rat, *Cancer Res. 54*, 1212–1215.
12. Lee, K.N., Kritchevsky, D., and Pariza, M.W. (1994) Conjugated Linoleic Acid and Atherosclerosis in Rabbits, *Atherosclerosis 108*, 19–25.
13. Badami, R.C., and Patil, K.B. (1981) Structure and Occurrence of Unusual Fatty Acids in Minor Seed Oils, *Prog. Lipid Res. 19*, 119–153.
14. Lopez, A., and Gerwick, W.H. (1987) Two New Icosapentaeinoic Acids from the Temperate Red Seaweed *Ptilota filicina* J. Agardh, *Lipids 22*, 190–194.
15. Mikhailova, M.V., Bemis, D.L., Wise, M.L., Gerwick, W.H., Norris, J.N., and Jacobs, R.S. (1995) Structure and Biosynthesis of Novel Conjugated Polyene Fatty Acids from the Marine Green Alga *Anadyomene stellate*, *Lipids 30*, 583–589.
16. Tsuzuki, T., Igarashi, M., Komai, M., and Miyazawa, T. (2003) A Metabolic Conversion of 9,11,13-Eleostearic Acid (18:3) to 9,11-Conjugated Linoleic Acid (18:2) in the Rat, *J. Nutr. Sci. Vitaminol. (Tokyo) 49*, 195–200.
17. Igarashi, M., Tsuzuki, T., Kambe, T., and Miyazawa, T. (2004) Recommended Methods of Fatty Acid Methylester Preparation for Conjugated Dienes and Trienes in Food and Biological Samples, *J. Nutr. Sci. Vitaminol. (Tokyo) 50*, 121–128.
18. Tsuzuki, T., Tokuyama, Y., Igarashi, M., and Miyazawa, T. (2004) Tumor Growth Suppression by α-Eleostearic Acid, a Linolenic Acid Isomer with a Conjugated Triene System, *via* Lipid Peroxidation, *Carcinogenesis 25*, 1417–1425.
19. Tsuzuki, T., Igarashi, M., and Miyazawa, T. (2004) Conjugated Eicosapentanoic Acid Inhibits Transplanted Tumor Growth *via* Membrane Lipid Peroxidation in Nude Mice, *J. Nutr. 134*, 1162–1166.
20. Tsuzuki, T., Igarashi, M., Iwata, T., Yamauchi-Sato, Y., Yamamoto, T., Ogita, K., Suzuki, T., and Miyazawa, T. (2004) Oxidation Rate of Conjugated Linoleic Acid and Conjugated Linolenic Acid Is Slowed by Triacylglycerol Esterification and α-Tocopherol, *Lipids 39*, 475–480.
21. Tsuzuki, T., Tokuyama, Y., Igarashi, M., Nakagawa, K., Ohsaki, Y., Komai, M., and Miyazawa, T. (2004) α-Eleostearic Acid (9Z11*E*13*E*-18:3) Is Quickly Converted to Conjugated Linoleic Acid (9Z11*E*-18:2) in Rats, *J. Nutr. 134*, 2634–2639.
22. Tsuzuki, T., Tanaka, K., Kuwahara, S., and Miyazawa, T. (2005) Synthesis of the Conjugated Trienes 5*E*,7*E*,9*E*,14*Z*,17*Z*-Eicosapentaenoic Acid and 5*Z*,7*E*,9*E*,14*Z*,17*Z*-Eicosapentaenoic Acid, and Their Induction of Apoptosis in DLD-1 Colorectal Adenocarcinoma Human Cells, *Lipids 40*, 147–154.
23. Hun, C.S., Hasegawa, K., Kawabata, T., Kato, M., Shimokawa, T., and Kagawa, Y. (1999) Increased Uncoupling Protein2 mRNA in White Adipose Tissue, and Decrease in Leptin, Visceral Fat, Blood Glucose, and Cholesterol in KK-A^y Mice Fed with Eicosapentaenoic and Docosahexaenoic Acids in Addition to Linolenic Acid, *Biochem. Biophys. Res. Commun. 259*, 85–90.
24. Helrich, K. (ed.) (1990) Acids (polyunsaturated) in Oil and Fats, in *Official Methods of Analysis of the Association of Official Analytical Chemists*, 15th edn., pp. 960–963, Association of Official Analytical Chemists, Arlington, VA.
25. Pitt, G.A.J., and Morton, R.A. (1957) Ultra-violet Spectrophotometry of Fatty Acids, *Prog. Chem. Fats Other Lipids 4*, 227–278.
26. Bartlett, G.R. (1957) Colorimetric Assay Methods for Free and Phosphorylated Glyceric Acids, *J. Biol. Chem. 226*, 497–509.
27. Nepokroeff, C.M., Lakshmanan, M.R., and Porter, J.W. (1975) Fatty Acid Synthase from Rat Liver, *Methods Enzymol. 37*, 37–44.
28. Ochoa, S., Mehler, A.H., and Kornberg, A. (1948) Biosynthesis of Dicarboxylic Acids by Carbon Dioxide Fixation. I. Isolation and Propeties of an Enzyme from Pigeon Liver Catalyzing the Reversible Oxidate Decarboxylation of *l*-Malic Acid, *J. Biol. Chem. 174*, 979–1000.
29. Small, G.M., Burdett, K., and Connock, M.J. (1985) A Sensitive Spectrophotometric Assay for Peroxisomal Acyl-CoA Oxidase, *Biochem. J. 227*, 205–210.
30. Friedman, J.M., and Halaas, J.L. (1998) Leptin and the Regulation of Body Weight in Mammals, *Nature 395*, 763–770.
31. Okuno, A., Tamemoto, H., Tobe, K., Ueki, K., Mori, Y., Iwamoto,

K., Umesono, K., Akanuma, Y., Fujiwara, T., Horikoshi, H., *et al*. (1998) Troglitazone Increases the Number of Small Adipocytes in Obese Zucker Rats: Possible Mechanism of the Amelioration of Insulin Resistance, *J. Clin. Invest. 101*, 1354–1361.

32. Roden, M., Price, T.B., Perseghin, G., Petersen, K.F., Rothman, D.L., Cline, G.W., and Shulman, G.I. (1996) Mechanism of Free Fatty Acid-Induced Insulin Resistance in Humans, *J. Clin. Invest. 97*, 2859–2865.

33. Hawkins, M., Barzilai, N., Liu, R., Hu, M., Chen, W., and Rossetti, L. (1997) Role of the Glucosamine Pathway in Fat-Induced Insulin Resistance, *J. Clin. Invest. 99*, 2173–2182.

34. Hotamisligil, G.S., and Spiegelman, B.M. (1994) Tumor Necrosis Factor α: A Key Component of the Obesity–Diabetes Link, *Diabetes 43*, 1271–1278.

35. Tsigos, C., Kyrou, I., Chala, E., Tsapagas, P., Stavridis, J.C., Raptis, S.A., and Katsilambros, N. (1999) Circulating Tumor Necrosis Factor Alpha Concentrations are Higher in Abdominal Versus Peripheral Obesity, *Metabolism 48*, 1332–1335.

36. Osmundsen, H., Bremer, J., and Pedersen, J.I. (1991) Metabolic Aspects of Peroxisomal β-Oxidation, *Biochim. Biophys. Acta 1085*, 141–158.

37. Schoonjans, K., Staels, B., and Auwerx, J. (1996) Role of the Peroxisome Proliferator-Activated Receptor (PPAR) in Mediating the Effects of Fibrates and Fatty Acids on Gene Expression, *J. Lipid Res. 37*, 907–925.

38. Forman, B.M., Chen, J., and Evans, R.M. (1997) Hypolipidemic Drugs, Polyunsaturated Fatty Acids, and Eicosanoids Are Ligands for Peroxisome Proliferator-Activated Receptors α and δ, *Proc. Natl. Acad. Sci. USA 94*, 4312–4317.

39. Lehmann, J., Moore, L.B., Smith-Oliver, T.A., Wilkison, W.O., Willson, T.M., and Kiewer, S.A. (1995) An Antidiabetic Thiazolidinedione Is a High Affinity Ligand for Peroxisome Proliferator-Activated Receptor γ (PPARγ), *J. Biol. Chem. 270*, 12953–12956.

40. Murakami, K., Tobe, K., Ide, T., Mochizuki, T., Ohashi, M., Akanuma, Y., Yazaki, Y., and Kadowaki, T. (1998) A Novel Insulin Sensitizer Acts as a Coligand for Peroxisome Proliferator-Activated Receptor-α (PPAR-α) and PPAR-γ, *Diabetes 47*, 1841–1847.

41. Kliewer, S.A., Sundseth, S.S., Jones, S.A., Brown, P.J., Wisely, G.B., Koble, C.S., Devchand, P., Wahli, W., Willson, T.M., Lenhard, J.M., *et al.* (1997) Fatty Acids and Eicosanoids Regulate Gene Expression Through Direct Interactions with Peroxisome Proliferator-Activated Receptor α and γ, *Proc. Natl. Acad. Sci. USA 94*, 4318–4323.

42. Moya-Camarena, S.Y., Heuvel, J.P.V., Blanchard, S.G., Leesnitzer, L.A., and Belury, M.A. (1999) Conjugated Linoleic Acid Is a Potent Naturally Occurring Ligand and Activator of PPARα, *J. Lipid Res. 40*, 1426–1433.

43. Belury, M.A., and Vanden Heuvel, J.P. (1999) Modulation of Diabetes by Conjugated Linoleic Acid, in *Advances in Conjugated Linoleic Acid Research Volume 1* (Yurawecz, M.P., Mossoba, M.M., Kramer, J.K.G., Parisa, M.W., and Nelson, G.J., eds.), AOCS Press, Champaign, pp. 404–411.

44. Evans, M., Park, Y., Pariza, M., Curtis, L., Kuebler, B., and McIntosh, M. (2001) *Trans*-10,*cis*-12 Conjugated Linoleic Acid Reduces Triglyceride Content While Differentially Affecting Peroxisome Proliferator Activated Receptor γ2 and aP2 Expression in 3T3-L1 Preadipocytes, *Lipids 36*, 1223–1232.

45. Peters, J.M., Park, Y., Gonzalez, F.J., and Pariza, M.W. (2001) Influence of Conjugated Linoleic Acid on Body Composition and Target Gene Expression in Peroxisome Proliferator-Activated Receptor α-Null Mice, *Biochim. Biophys. Acta 1533*, 233–242.

Biochemical, Functional, and Histochemical Effects of Essential Fatty Acid Deficiency in Rat Kidney

Anísio Francisco Soares[a], Rosa Cristina Santiago[b], Maria Luíza Martins Aléssio[a],
Bernard Descomps[c], and Carmen de Castro-Chaves[a],*

[a]Departamentos de Fisiologia-Farmacologia and [b]Histologia-Embriologia, Universidade Federal de Pernambuco, 50670-901,
Recife, Pernambuco, Brazil, and [c]Laboratoire de Atherogénèse et Nutrition Humaine, Université Montpellier I, Montpellier, France

ABSTRACT: The present study was designed to examine the effects of EFA deficiency (EFAD) on biochemical, functional, and structural aspects of the kidney in growing and adult rats fed a normal or EFAD diet for 9 wk after weaning. Food and fluid intake (FI), urine volume, and Na^+ and K^+ excretions were measured weekly from weeks 4 to 8 by placing the rats in individual metabolic cages for 24 h. At week 9, Li^+ and a 5% water load, respectively, were administered at 14 and 1.5 h prior to glomerular and proximal tubular function studies, as assessed by 3-h creatinine (C_{Cr}) and Li^+ (C_{Li+}) clearances. Hematocrit and urine volume; serum and urine [Cr], [Li^+], [Na^+], and [K^+]; and renal FA distribution were also measured. Data [corrected to 100 g/body weight (bw) and presented as means ± SEM] were significant, at $P \leq 0.05$. Despite a similar ingestion of solids from weeks 4 to 7 (weeks 7 to 10 of life), the rats on the EFAD diet showed a decreased body weight from week 5. From weeks 4 to 8, FI and urine volume were similar for both groups, but the FI increased at week 6 in the EFAD group; 24-h Na^+ and K^+ excretions were similar at all weeks, except for an increase in the EFAD group for both ions at week 7. In the EFAD group, C_{Cr} and C_{Li+} decreased by 27 and 56.3%, respectively (385.7 ± 33.4 vs. 280 ± 21.1, and 21.0 ± 2.1 vs. 9.2 ± 1.1 µL/min/100 g; $n = 9$ vs. 10), the latter result suggesting increased proximal reabsorption. The 3-h Na^+ and K^+ excretions were similar, but the Li^+ decreased (0.78 ± 0.06 × 10^{-2} vs. 0.32 ± 0.03 × 10^{-2} µeq/min/100 g) in the EFAD group, giving additional support to the suggestion. Renal structure was normal and similar for both groups, but the EFAD group showed a more prominent proximal tubule brush border, together with heavier periodic acid–Schiff staining in all specimens from weeks 5 to 9. In the EFAD group, FA of the n-9 and n-7 series were higher, but most of the n-6 series were lower as a percentage of total lipids in the medulla and cortex. Medullary levels of 20:4n-6 were maintained, 22:4n-6 declined twice, arachidonic acid was maintained, and 20:5n-3 was lower. The EFAD diet affected glomerular function, proximal tubular structure and function, and FA distribution in the rat kidney.

Paper no. L8915 in *Lipids* 40, 1125–1133 (November 2005).

The development of a deficiency disease as a result of the rigid restriction of dietary fat emphasizes the importance of the dietary lipid supply (1). Besides being precursors of eicosanoids, long-chain PUFA also regulate membrane fluidity and permeability, modulate the activity of membrane-bound receptors, and may influence membrane enzymes, thus affecting signal transduction and transport activities (2,3). In turn, the eicosanoids regulate the renal vasculature status (4). In studies in mice (5) and rats (6), the kidney has been shown to be more resistant than the liver to the depletion of arachidonic acid induced by an EFA-deficient (EFAD) diet (7). However, the cited study showed that in the kidney cortex and medulla, arachidonic acid (AA) levels were altered. In the same publication, PI was shown to be the main source of protaglandin production in response to receptor-mediated agonists. Also, the n-6 family of FA, which are associated with cholesterol in the plasma and adrenals, participated in prostaglandin vascular and cellular metabolism (2). EFA deficiency (EFAD) is characterized by a decrement in the n-6 and n-3 FA families and by an accumulation of the n-9 FA family (7). Moreover, prostaglandin levels are decreased in renal tissue with EFAD (8,9). Since one of the kidney functions is body homeostatic (10–12), EFAD renal dysfunction would be expected to affect body homeostasis. There are, however, few studies relating the biochemical and structural changes to the functional effects of EFAD on the kidney. One of these studies showed that male and female 80-d-old rats on a fat-free diet since weaning presented, along with skin-related abnormalities, bloody urine (1) and many renal structural changes, the most striking of which were tubular cell calcification, necrotic areas in the medulla, and a variable extent of epithelial degeneration and fatty changes by hematoxylin-eosin and Mallory's aniline blue stainings (13). In another investigation, prostaglandin depletion was induced in adult rats after 7 d of fasting and with 4 d on 10% dextrose instead of water, followed by 14 d on an EFAD diet (14). Other studies were conducted at the end of the depletion period on both awake and anesthetized rats, as well as after supplementation with 0.5 g/d of linoleic acid (LA) for 5 d (14). The blood

pressure (BP), renal blood flow, and glomerular filtration rate (GFR) were not different between the control and EFAD anesthetized rats. No difference was depicted between the 24-h GFR, urine volume (V), Na$^+$ excretion (U$_{Na^+}$V), and K$^+$ excretion (U$_{K^+}$V) in either group of awake rats, whereas prostaglandin E$_2$ (PGE$_2$) excretion decreased in the deficient rats (113 vs. 22 ng/24 h). The V and U$_{Na^+}$V were lower following a Na$^+$ load in the deficient rats either in the awake (5-h) or anesthetized (2-h) state. The awake, deficient rats were less able to excrete the given oral water load and the intraperitoneal K$^+$ one, respectively, at 5 and 2 h, and 0.9% saline substitution for drinking water during 9 d disclosed high BP in the EFAD rats from day 3. The LA supplementation normalized not only the high BP but also the ability to excrete water and Na$^+$ loads in the awake, deficient rats, and urinary PGE$_2$ returned to control values within 4 d (14).

Another study measured the GFR of 50-, 70-, 90-, and 200-d-old anesthetized female rats, fasted for 24 h, that were fed a control or EFAD diet from weaning, and whose mothers had been on the same diet regimen 10 d before delivery and also during lactation (15). The control diet used soybean lipids, whereas the EFAD diet was obtained using hydrogenated lard. GFR and plasma urea increased at day 50 and deteriorated thereafter, with higher plasmatic levels of creatinine (Cr), urea, and Na$^+$ as well as lower total protein and altered histology (15). An EFAD-simulated state occurred in cultured Madin–Darby canine kidney (MDCK) cells, an *in vitro* experimental model for the renal distal tubule cell (16). MDCK cells grown in FBS had an increased cholesterol/phospholipid ratio attributable to a 50% decrease in phospholipid content as well as a reduced number of hemicysts, which were seen under electron microscopy to be much flatter than their counterparts, with a surface less dense in microvilli and mitochondria (16).

The aforementioned studies have shown a lack of agreement in the GFR values or between the GFR and the Na$^+$ and K$^+$ excretions for diverse models of deficiency induction with animals at different ages, of different sexes, and in different states. These facts prompted the present study in which the anesthetized rat model, with its secondary effects on cardiac, respiratory, and renal function, was avoided (17). Functional and structural studies were carried out to measure the weight gain, ingestion of solids (SI), fluid intake (FI) and excretion, and Na$^+$ and K$^+$ urinary excretions of awake growing and young adult rats on either diet, from weaning at 21 d of age. These studies were followed by renal GFR and proximal tubular function (PTF) measurements at week 9 on the diets, as well as with cortical and medullary phospholipid FA distribution measurements to determine diet effectiveness in inducing EFAD in these rats.

EXPERIMENTAL PROCEDURES

Animals and diets. All animals grew and were kept at 22 ± 3°C, 65 ± 5% RH, and a 12-h dark/light cycle at the Physiology Department, Universidade Federal de Pernambuco, with free access to food and water. The parent Wistar rats were fed a commercial pellet food and mated for 10 d. From pregnancy con-

TABLE 1
FA Composition of EFA Control (EFAC) and Deficient (EFAD) Diets

FA	EFAC 5% (corn oil)		EFAD 5% (coconut oil)	
	% of FA	% of diet	% of FA	% of diet
8:0	—	—	6.4	0.32
10:0	—	—	7.4	0.37
12:0	—	—	51.0	2.55
14:0	1.4	0.07	18.0	0.90
16:0	11.4	0.57	8.4	0.42
18:0	2.9	0.15	8.0	0.40
18:1n-9	26.2	1.31	0.5	0.02
18:2n-6	54.0	2.70	0.2	0.01
18:3n-3	1.0	0.05	—	—
20:0	0.2	0.01	—	—
20:1n-9	0.1	0.01	—	—
22:0	0.2	0.01	—	—
24:0	0.2	0.01	—	—

firmation to weaning, each mother and 8 male offspring were housed in the same cage. From weaning and for the following 9 wk, the offspring (4 per cage) had free access to water and to a diet with either an adequate level of EFA (control, EFAC) or a very low level of EFA (deficient, EFAD), thus establishing two experimental groups. The FA source of the EFAC was corn oil, with adequate levels of 18:2n-6 and 18:3n-3, and for the EFAD it was hydrogenated coconut oil, providing 0.01% of 18:2n-6 and being almost free of 18:3n-3 FA (18). The diet composition is shown in Table 1.

Protocols. (i) Body weight (bw) plus 24-h SI, FI, urine excretion, and Na$^+$ and K$^+$ excretions in awake, unrestrained growing and young adult rats fed EFAC and EFAD diets after weaning. All animals were weighed weekly after weaning. After being adapted to the individual metabolic cage (IMC), 12 rats on EFAC and 12 on EFAD went weekly to the IMC between weeks 4 and 8 on either diet in the awake, unrestrained state, with urine collection for 24 h. Animals and food were weighed before and after the 24-h period, with the difference in food weight being considered the SI (g/100 g/24 h). The amount of water in the IMC container at the end of the period was subtracted from the initial volume, giving the FI (mL/100 g/24 h). V was measured at the end of this period (mL/100 g/24 h). Na$^+$ and K$^+$ urinary concentrations (μeq/mL) were determined (Na$^+$-K$^+$-Li$^+$ analyzer; Medica Corp., Bedford, MA) and multiplied by V, yielding the respective urinary excretions, U$_{Na^+}$V and U$_{K^+}$V (μeq/100 g/24 h).

(ii) Renal GFR and PTF studies for 3 h in awake, unrestrained young adult rats fed EFAC and EFAD diets for 9 wk after weaning. During week 9 on either diet, 10 EFAC and 9 EFAD rats received LiCl (0.06 meq/100 g body bw) and a 5-mL/100 g bw water expansion, respectively, at 14 and 1.5 h before the experiment. They were then placed in the IMC for 3 h, during which time their urine was collected and their food and fluids restricted. At the end of this period, a final hematocrit was taken and the rats were decapitated for blood collection. GFR was measured by Cr clearance, (C$_{Cr}$) = ([Cr]$_u$ × V)/[Cr]$_p$ (in μL/min/100 g bw), where [Cr]$_u$ and [Cr]$_p$ are, respectively, the urinary and plasmatic Cr concentrations (in mg/dL) and V is the

urine volume (in μL/100 g/min) (19–21). [Cr] was measured kinetically and analyzed automatically (Cobas-Mira; Roche, Basel, Switzerland), based on Jaffé's reaction. The PTF was assessed by Li$^+$ clearance (C_{Li+}, in μL/min/100 g), using the above formula (19–21).

Formulae. The following formulae were used to calculate (i) the fractional proximal Na$^+$ reabsorption: $(FrP_{Na+}R) = (FL_{Na+} - D_{Na+}D) \times (FL_{Na+}) \times 100$, in % (where FL_{Na+} is the sodium filtered load); (ii) the distal Na$^+$ delivery: $(D_{Na+}D) = C_{Li+} \times [Na^+]_{plasma}$, in μeq/min/100 g; (iii) the fractional distal Na$^+$ reabsorption-I: $(FrD_{Na+}R\text{-I}) = (D_{Na+}D - [Na^+]_{urine}) \times V/(D_{Na+}D \times 100)$; and (iv) the fractional distal Na$^+$ reabsorption-II: $(FrD_{Na+}R\text{-II}) = (D_{Na+}D - [Na^+]_{urine}) \times V/FL_{Na+} \times 100$ (19–21).

Statistics for functional studies. Results are expressed as 100 g/bw and presented as means ± SEM. Paired and unpaired Student's *t*-tests and ANOVA for repeated measures, complemented by Scheffé's *F*-test, were used for statistical analyses. Differences were considered significant when $P \leq 0.05$.

(i) Renal structural and histochemical studies. Weekly, between weeks 4 and 9 on either diet, 2 rats from each group were decapitated and their kidneys were processed for structural and histochemical studies. Briefly, the kidneys were cut sagitally, fixed in Bouin's solution for 24 h, and kept in 70% ethanol until processing; the tissue was then dehydrated, cleared, impregnated, and embedded in paraffin and cut into 6-μm slices; specimens were stained with hematoxylin-eosin and Gomori's trichromic for structural analysis and by the periodic acid–Schiff (PAS) reaction for histochemical analysis (22).

(ii) Renal phospholipid FA composition in the cortex and medulla from EFAC and EFAD rats. In week 9 on either diet, another 5 rats from each group were decapitated and their kidneys were removed surgically. The cortex and medulla were dissected over ice, washed rapidly in ice-cold 0.9% NaCl, and homogenized in 10 mM Tris-HCl-1 mM EGTA buffer. The homogenate was centrifuged at $12,000 \times g$ for 30 min at 4°C (RC2-B, Sorvall). The pellet was resuspended in 50 mM Tris-HCl buffer and a total lipid extract was prepared (23). After separating the phospholipids by a Sep-Pack® procedure (24), transmethylation was carried out (25). FAME analyses were performed using a gas chromatograph (Shimadzu, model GC14B) equipped with a SUPELCOWAX (Supelco, Bellefonte, PA) glass capillary column (60 m × 0.25 mm, film thickness of the bonded phase 0.25 μm). Injector and detector temperatures were 250°C. The column starting temperature of 130°C was gradually increased to 245°C at a rate of 2.5°C/min for 10 min. The carrier gas (H_2) pressure was set at 240 kPa with a flow rate of 2 mL/min. A standard FAME mixture was used to identify the FAME by their retention times (Sigma, St. Louis, MO). Nonconventional FA (20:3n-9, 22:3n-9, 22:4n-6, 22:5n-6) were previously authenticated in lipid extracts from EFAD rats (26). FA data are presented as mean ± SD. Statistical comparisons used ANOVA, with the differences being considered significant when $P \leq 0.05$.

RESULTS

Body weight and 24-h SI, FI, urine excretion, and Na$^+$ and K$^+$ excretions in awake, unrestrained, growing and young adult rats fed an EFAC or EFAD diet after weaning. Body weights were similar for the two groups from weeks 1 to 4 on both diets, but from week 5 on, the bw of the EFAD group were lower (Fig. 1A), in spite of having SI similar to the EFAC group and regardless of having a higher SI than the EFAC group at week 8 (Fig. 1B). The FI was similar between the groups at all weeks (Fig. 1C) except for an episodic increase at week 6 in the EFAD group (9.1 ± 0.7 vs. 12.7 ± 1.0 mL/100 g/24 h, EFAC vs. EFAD; $P < 0.05$, $n = 12$ for both) that was not reflected in urine excretion (4.3 ± 0.8 vs. 6.7 ± 1.0 mL/100 g/24 h, EFAC vs. EFAD; $n = 12$ for both). V was not different in either group across all the study weeks (Fig. 1D). Urinary Na$^+$ (Fig. 1E) and K$^+$ (Fig. 1F) excretions were similar for both groups at weeks 5, 6, 8, and 9, but increased in the EFAD group at week 7.

Renal GFR and PTF studies for 3 h in awake, unrestrained young adult rats fed an EFAC or EFAD diet for 9 wk after weaning. The final hematocrit (49.00 ± 2.10 vs. 48.50 ± 2.20%, $n = 10$ vs. 9, EFAC vs. EFAD) and final plasma [Cr] (4.6 ± 0.2 × 10^{-2} vs. 4.9 ± 0.1 × 10^{-2} mg/mL), [K$^+$] (5.96 ± 0.20 vs. 5.35 ± 0.47 μeq/mL), [Li$^+$] (0.38 ± 0.02 vs. 0.37 ± 0.04 μeq/mL), and [Na$^+$] (140.30 ± 1.30 vs. 139.70 ± 1.14 μeq/mL) were similar for both groups at week 9 on the diets. V did not differ between the groups, but C_{Cr} and C_{Li+} (Table 2) were lower in the EFAD group, whose Na$^+$ (0.42 ± 0.08 vs. 0.48 ± 0.08 μL/min/100 g, EFAC vs. EFAD) and K$^+$ (23.89 ± 4.44 vs. 17.94 ± 2.11 μL/min/100 g, EFAC vs. EFAD) clearances were not different from the EFAC. Li$^+$ excretion decreased in the EFAD, whereas Na$^+$ and K$^+$ excretions did not differ from those of the EFAC group (Table 2). $FrP_{Na+}R$ increased in the EFAD rats, whereas the $D_{Na+}D$ and the $FrD_{Na+}R$-I and -II decreased (Table 2).

Renal structural and histochemical studies at growth and in the young adult. Renal structure, assessed by hematoxylin-eosin staining, was normal and similar for both groups during all weeks under study. The parenchyma/framework relation, assessed by Gomori's trichromic staining, was maintained in the cortex and medulla for both groups, from week 4 until week 9 on either diet. In the EFAD group, a more prominent and heavier PAS-stained proximal tubule brush border was found in all specimens from weeks 4 to 9.

Phospholipid FA compositions in the renal cortex and medulla from EFAC and EFAD rats. In decreasing order, arachidonic (20:4n-6), stearic (18:0), and palmitic (16:0) acids were the main renal cortical and medullary FA for both groups (Table 3). Comparisons between the two groups revealed that the phospholipid FA distribution had been modified by the EFAD diet: FA of the n-7 and n-9 families were higher in the cortex and medulla; cortical and medullary n-6 FA levels were dramatically lower, mainly for 18:2n-6, 20:3n-6, and 22:4n-6; and AA levels were maintained in the medulla but decreased in the cortex (Table 3). The latter observation should be considered together with the greater decline of 22:4n-6 from the medulla to the cortex (−1.04 vs. –0.51%, respectively). The
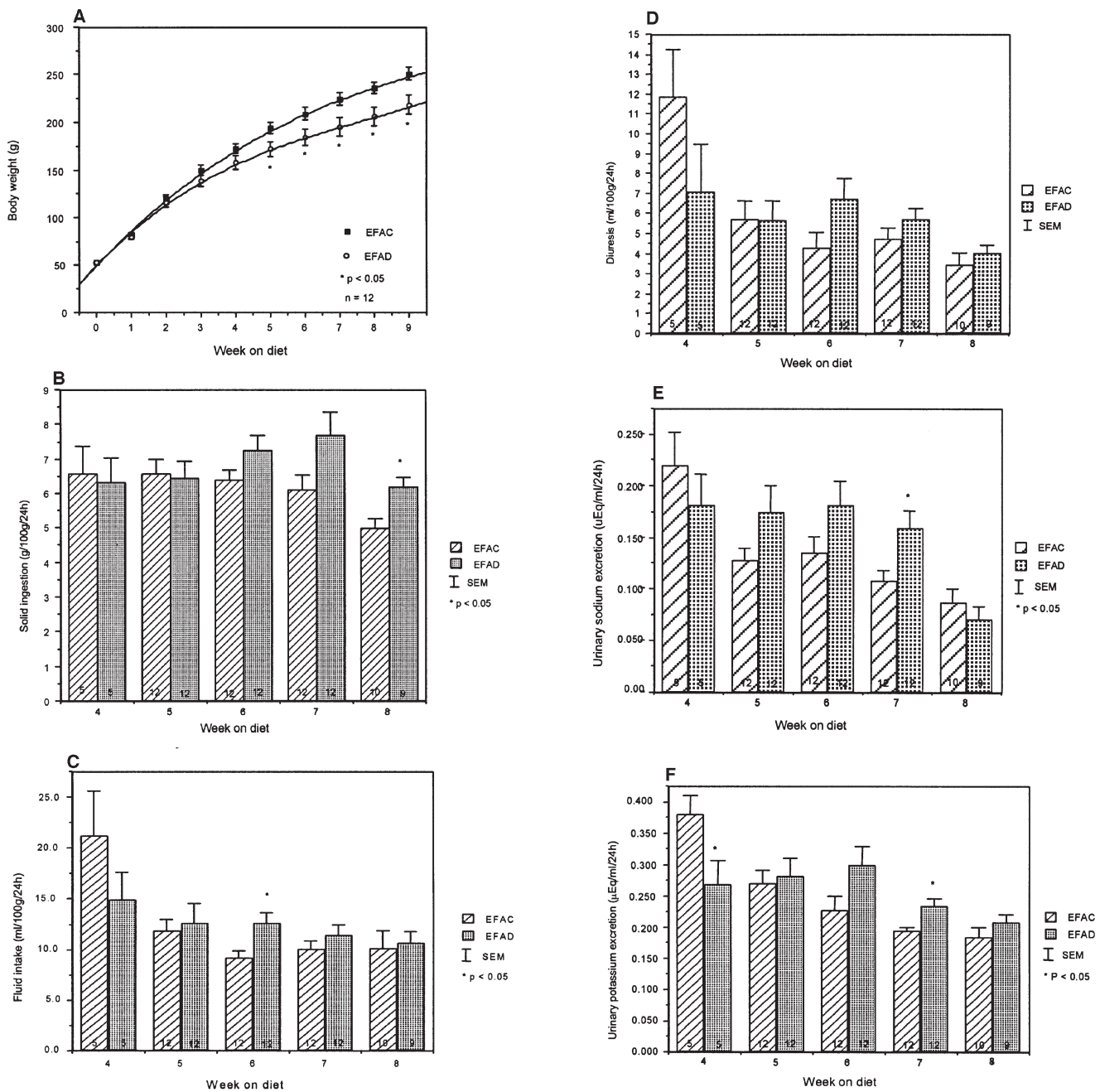
FIG. 1. Weekly effects of EFA control (EFAC) or deficient (EFAD) diet for 9 wk from weaning on awake, unrestrained rats. (A) Body weight; (B) 24-h ingestion of solids; (C) 24-h fluid intake; (D) 24-h diuresis; (E) 24-h urinary sodium excretion; (F) 24-h urinary potassium excretion. *$P \leq 0.05$.

paradoxically higher medullary level of 22:5n-6 and the lower ratio of 22:6n-3/22:5n-6 in EFAD rats indicates a tendency toward an n-3 FA deficiency (27), confirmed by the lower medullary 20:5n-3 levels.

DISCUSSION

All animals were kept under similar conditions after weaning, except for the dietary FA. They were adapted to the IMC, remaining there only for the study hours to avoid chronic social isolation, with the associated psychosocial stress and the chronic, adrenal-dependent elevation of BP seen in otherwise normotensive rats (17). The EFAD diet altered the FA distribution of the phospholipid FA in the two main renal regions. The FA profiles shifted to an EFAD pattern, shown by significantly higher sums of either the n-7 or n-9 FA families. Particularly 16:1n-7 and 20:3n-9, which are good indices of EFAD (27), were drastically affected (Table 3). AA was found to be preserved in the kidney cortex of animals on an EFAD diet (7). AA levels were maintained in the renal medulla but showed a decrease in the renal cortex in the EFAD rats (Table 3). However, these apparently conflicting results could be attributed to

TABLE 2
Urine Volume (V); Creatinine, Li^+, Na^+, and K^+ Clearances (C_{Cr}, C_{Li^+}, C_{Na^+}, and C_{K^+}); Li^+, Na^+, and K^+ Excretions ($U_{Li^+}V$, $U_{Na^+}V$, and $U_{K^+}V$); Fractional Proximal Na^+ Reabsorption ($FrP_{Na^+}R$,); Distal Na^+ Delivery ($D_{Na^+}D$); and Fractional Distal Na^+ Reabsorptions-I and -II ($FrD_{Na^+}R$-I and -II) on Awake, Unrestrained Adult Rats Fed an EFAC or EFAD Diet for 9 wk from Weaning[a]

Parameter	EFAC ($n = 10$)	EFAD ($n = 9$)
V (μL/min/100 g)	14.43 ± 1.15	12.11 ± 0.66
C_{Cr} (μL/min/100 g)	385.69 ± 33.39	280.10* ± 21.15
C_{Li^+} (μL/min/100 g)	20.97 ± 2.09	9.16* ± 1.12
C_{Na^+} (μL/min/100 g)	0.42 ± 0.08	0.48 ± 0.08
C_{K^+} (μL/min/100 g)	23.89 ± 4.44	7.94 ± 2.11
$U_{Li^+}V$ (μeq/min/100 g)	$0.78 ± 0.06 × 10^{-2}$	$0.32* ± 0.03 × 10^{-2}$
$U_{Na^+}V$ (μeq/min/100 g)	$5.99 ± 1.12 × 10^{-2}$	$6.68 ± 1.07 × 10^{-2}$
$U_{K^+}V$ (μeq/min/100 g)	$14.11 ± 2.59 × 10^{-2}$	$9.21 ± 0.98 × 10^{-2}$
$FrP_{Na^+}R$ (%)	94.40 ± 0.56	96.65* ± 0.39
$D_{Na^+}D$ (μeq/min/100 g)	2.95 ± 0.31	1.28* ± 0.16
$FrD_{Na^+}R$-I (%)	98.05 ± 0.25	93.89* ± 1.35
$FrD_{Na^+}R$-II (%)	5.49 ± 0.55	3.19* ± 0.40

[a]n = number of experiments; *$P \le 0.05$. For other abbreviations see Table 1.

the different deficiency inductions. The 22:4n-6 is involved in maintaining AA homeostasis by retroconversion to 20:4n-6 (28), and levels in the medulla were about twice that in the cortex. The finding that medullary mobilization was twofold that of the cortex (a change of −1.02 vs. −0.51%, respectively) confirmed the role of 22:4n-6. The increase in 22:5n-6 levels in EFAD rats is paradoxical since these animals lack 18:2n-6 (Table 3), but this finding has been reported previously as a response to n-3 FA deficiency (29). The n-3 FA deficiency was reproduced in our experiments: The 20:5n-3 levels were lower in the EFAD rats and there was also a decrease in the 22:6n-3/22:5n-6 ratio. Although rats from both groups showed a progressive and similar weight gain from weeks 4 to 7 of life (weeks 0 to 4 on the diets), the EFAD rats gained less weight from week 8 until adulthood (Fig. 1A), thus replicating the re-

sults from other studies (15,18,30). Food ingestion for the EFAD group was similar to that of the EFAC group up to week 7, but increased at week 8 (Fig. 1B), pointing to factors other than decreased food consumption for their lower growth rate. Accordingly, a greater metabolic energy requirement has been used to explain the growth retardation in EFAD rats, mainly due to thermogenesis secondary to transdermal water loss (30). If this had been the case in the present study, however, an increased FI would have been seen with the EFAD rats. Moreover, the similarity in FI and excretion between the two groups of rats points to their ability to maintain their respective water balances (10,11). Na^+ and K^+ 24-h excretions were also similar between the groups at all weeks, except for an episodic increase for both ions in EFAD rats at week 7, which returned to normal at week 8 (Figs. 1E, 1F). Usually, the Na^+ excretion reflects ingestion (10,11); thus, the results indicate the Na^+ balance was maintained in the EFAD rats. The similarity between blood and plasma values shows the same physical condition for the EFAC and EFAD rats. C_{Cr} has been used to measure GFR in the awake state, including in humans (19–21). The EFAC values of C_{Cr} (385.7 ± 33.4 μL/min/100 g) are in agreement with other control studies: 275 ± 30 μL/min/100 g (19) and 306.7 ± 9.3 μL/min/100 g (29). The EFAD had a 27.4% decrease in C_{Cr} (Table 2), a result similar to anesthetized rats at the same age with a slightly different deficiency induction (15). The GFR decrement could be due to various factors, including eicosanoids (4), but such a study is beyond the scope of this paper.

The proximal tubule is the main nephron segment involved in NaCl and water reabsorption (10). C_{Li^+} is an accepted indirect method for measuring PTF, with antidiuretic hormone inhibition, and it has been particularly useful in renal function studies on the awake state (19–21,31). The C_{Li^+} decrement (Table 2) in the EFAD group could be due to the 27.4% less fluid provided for reabsorption by the lower GFR or to an en-

TABLE 3
Effect of an EFAD Diet on the Relative FA Composition (% of total FA) of Phospholipids from the Renal Medulla and Cortex (mean ± SD)[a]

| FA	Renal medulla		Renal cortex	
	Control	EFAD	Control	EFAD
16:0	17.5 ± 0.39	16.24 ± 0.14*	18.64 ± 0.52	16.88 ± 0.20**
16:1n-9	0.19 ± 0.02	0.46 ± 0.02**	0.15 ± 0.01	0.49 ± 0.02**
16:1n-7	0.70 ± 0.06	2.01 ± 0.08**	0.53 ± 0.02	1.93 ± 0.04**
18:0	19.19 ± 0.97	17.53 ± 0.54	20.79 ± 0.79	21.12 ± 1.88
18:1n-9	8.07 ± 0.59	9.68 ± 0.42*	5.93 ± 0.50	8.29 ± 0.37**
18:1n-7	2.89 ± 0.15	3.51 ± 0.06**	2.25 ± 0.07	3.30 ± 0.12**
18:2n-6	8.44 ± 0.42	5.21 ± 0.37**	8.72 ± 0.27	5.65 ± 0.29**
20:3n-9	ND	2.50 ± 0.15**	ND	2.76 ± 0.18**
20:3n-6	0.78 ± 0.04	0.38 ± 0.05**	0.74 ± 0.05	0.50 ± 0.05**
20:4n-6	27.86 ± 1.56	28.28 ± 0.41	29.33 ± 0.17	25.54 ± 1.01*
20:5n-3	0.18 ± 0.02	0.08 ± 0.03**	0.14 ± 0.02	0.11 ± 0.02
22:4n-6	1.46 ± 0.06	0.42 ± 0.03**	0.83 ± 0.01	0.32 ± 0.03**
22:5n-6	0.55 ± 0.02	0.84 ± 0.01**	0.69 ± 0.03	0.85 ± 0.05*
22:6n-3	0.72 ± 0.02	0.83 ± 0.02	0.92 ± 0.04	0.81 ± 0.05
Σn-9	10.31 ± 0.77	13.57 ± 0.51**	7.76 ± 0.80	12.46 ± 0.75**
Σn-7	3.59 ± 0.14	5.52 ± 0.27**	2.78 ± 0.70	5.23 ± 0.35**
22:6n-3/22:5n-6	1.26 ± 0.13	0.98 ± 0.07*	1.36 ± 0.10	0.95 ± 0.02**

[a]ND, not present in detectable amounts; *$P \le 0.05$; **$P \le 0.01$. For abbreviations see Table 1.
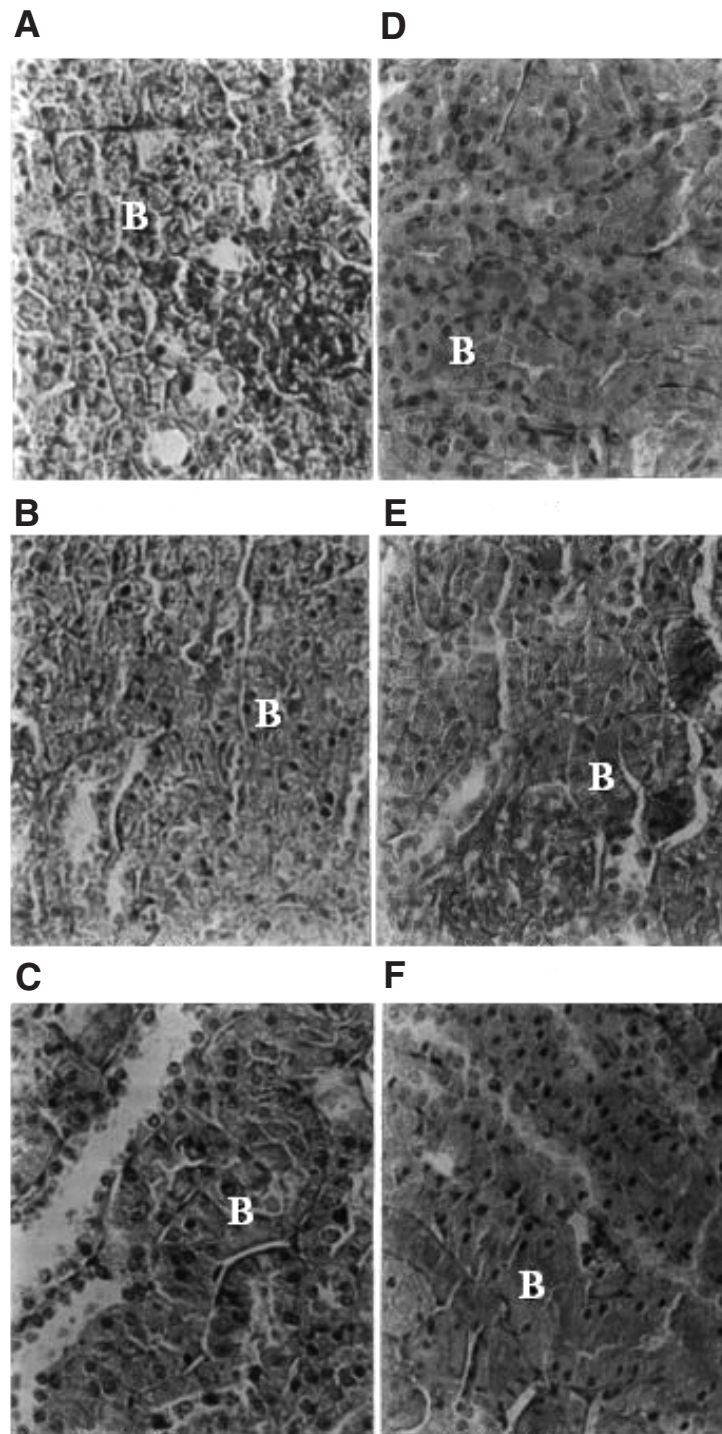
FIG. 2. Micrographs of rat kidney cortical regions from week 4 to week 6 on EFAC or EFAD diets from weaning. Note the proximal convoluted tubule and more prominent and heavily periodic acid–Schiff (PAS)-stained brush border (B) in EFAD rats and nonprominent and normally stained brush border in EFAC rats. (A) EFAC, week 4; (B) EFAC, week 5; (C) EFAC, week 6; (D) EFAD, week 4; (E) EFAD, week 5; (F) EFAD, week 6. Obj. 40×, periodic acid–Schiff (PAS) reaction. For other abbreviations see Figure 1.

hanced proximal tubular reabsorption, and even to a combination of both. The EFAD group's C_{Li^+} decrement of 56.3% strongly suggests addition of effects. The decreased Li^+ excretion, due to increased reabsorption, gives further support to this hypothesis. In spite of the GFR decrement in the EFAD group,

the Na^+ and K^+ 3-h excretions did not differ between the two groups. Normally, the GFR decrement results in diminished water and electrolyte excretion (11). Assuming an enhanced proximal tubular reabsorption in the EFAD group, we would expect a lower excretion, but the nephron segments beyond the
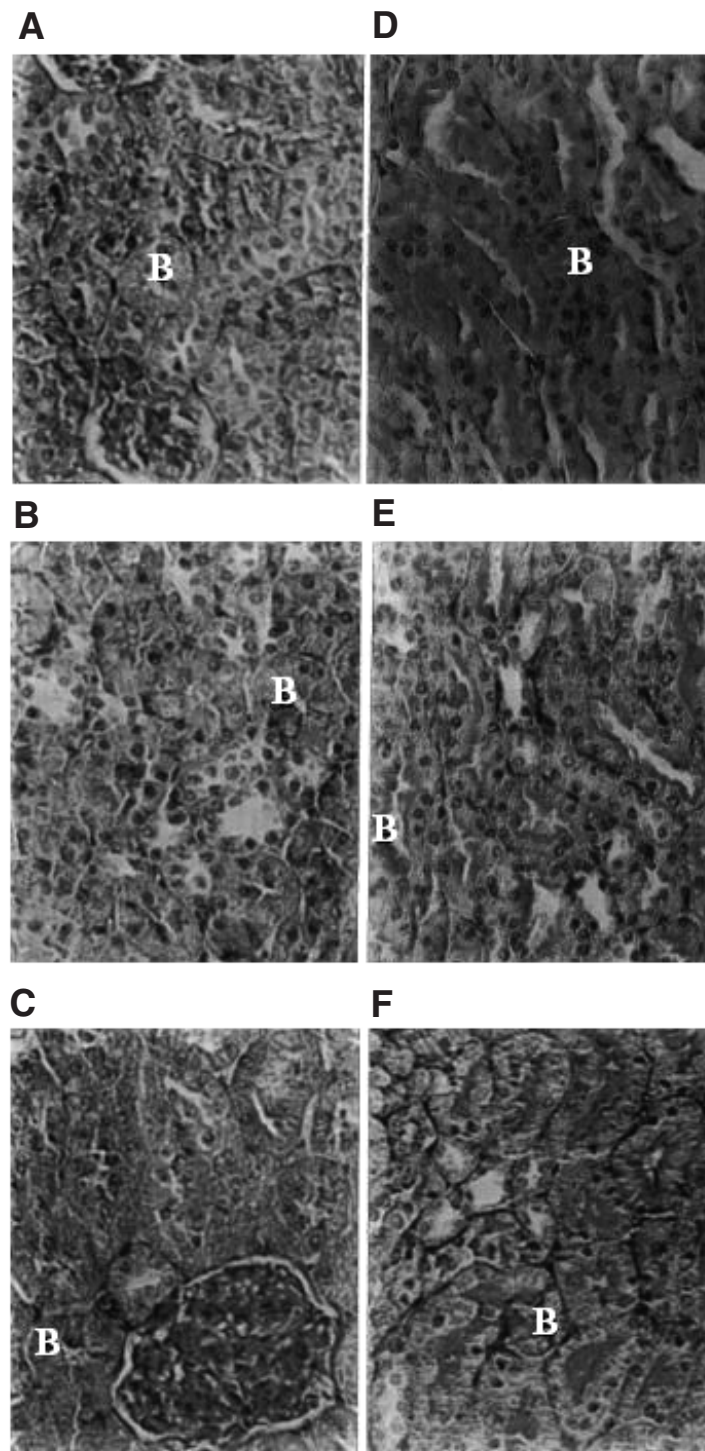
FIG. 3. Micrographs of kidney cortical regions from week 7 to week 9 of rats on EFAC or EFAD diets from weaning. Note the proximal convoluted tribute and more prominent and heavily PAS-stained brush border (B) in EFAD rats and nonprominent and normally stained brush border in EFAC rats. (A) EFAC, week 7; (B) EFAC, week 8; (C) EFAC, week 9; (D) EFAD, week 7; (E) EFAD, week 8; (F) EFAD, week 9. Obj. 40×, PAS reaction. For abbreviations see Figures 1 and 2.

Henle loop are capable of compensating by reabsorbing less and excreting normal amounts of water and electrolytes to maintain the body balance (10), as also occurred with the EFAD group.

Tubulo-glomerular feedback (11), is capable of being disrupted, i.e., through decreased GFR with increased tubular func-

tion and vice versa. The first case occurs in diminished effective circulatory volume and/or Na^+ depletion (10). The brush border was more prominent, occupying a larger area and consequently resulting in an increased proximal tubular reabsorption, possibly in a homeostatic maneuver to confront the chronic GFR decrement. The $FrP_{Na^+}R$ was related to the filtered load and to the

$D_{Na^+}D$, respectively, and was directly dependent on the decreased C_{Cr} and C_{Li^+} of the EFAD group. The lower $D_{Na^+}D$ was probably due to the C_{Li^+} decrement in the EFAD rats. The $FrD_{Na^+}R$-I and -II were both related to the lower $D_{Na^+}D$ of the EFAD group.

Unlike the structural renal findings in rats on a fat-free diet (13), this study was unable to detect differences in kidney structure between the EFAC and EFAD by hematoxylin-eosin and Gomori's trichromic staining. This divergence in results could be due to the relatively different protocols: older vs. younger rats; diets differing in lipid quality and quantity, and also in protein content. The more prominent and heavier PAS-stained brush border found in EFAD rats could be due to increased amounts of glycides, which specifically react with PAS (Figs. 2, 3), but the heavier staining at the glycocalyx could also be at the glycolipid site. Another possibility is cell elaboration of more microvilli to increase the absorptive surface area of the cell, although the distal MDCK EFAD cell findings cannot be totally applied to the proximal cell (16). The histochemical data not only provide further support for the hypothesis of chronically enhanced proximal tubular reabsorption in the EFAD rats but also shed some light on the etiology of proximal tubular reabsorption. Interestingly, the maintainance of AA levels in the EFAD renal medulla and their decrement in the cortex provided an opportunity to consider the renal function data under conditions in which the renal potency of eicosanoid synthesis had been maintained in the medulla but not in the cortex. Indeed, some parameters were related exclusively to the renal cortex: The glomerular filtration rate and the proximal tubular function, measured by C_{Cr} and C_{Li^+}, respectively, were depressed, whereas Na^+ and K^+ clearances and excretions (the last at either 24 or 3 h, which also have medullary renal transport) were not.

The dietary intake of adequate amounts of EFA and their subsequent efficient intestinal absorption are necessary for good health from the beginning of life as an embryo. The kidney is one of the systems involved in maintaining homeostasis by controlling the volume and the constitution of the body. Therefore, any disturbances resulting in EFA deficiency could cause impaired kidney function. An EFAD diet not only slowed the growth rate, but also decreased the glomerular function, increased proximal tubular function, altered renal structure and histochemistry, and modified the cortical and medullary FA composition in the kidneys of awake, unrestrained, growing young adult rats.

ACKNOWLEDGMENTS

REFERENCES

1. Burr, G.O., and Burr, M.M. (1929) A New Deficiency Disease Produced by the Rigid Exclusion of Fat from the Diet, *J. Biol. Chem. 82*, 345–367.
2. Bezard, J., Blond, J.P., Bernard, A., and Clouet, P. (1994) The Metabolism and Availability of Essential Fatty Acids in Animal and Human Tissues, *Reprod. Nutr. Dev. 34*, 539–568.
3. Ballabriga, A. (1994) Essential Fatty Acids and Human Tissue Composition. An Overview, *Acta Paediatr. Suppl. 402*, 63–68.
4. Imig, J.D. (2000) Eicosanoid Regulation of the Renal Vasculature, *Am. J. Physiol. 279*, F965–F981.
5. Werner, A., Havinga, R., Bos, T., Bloks, V.W., Kuipers, F., and Verkade, H.J. (2005) Essential Fatty Acid Deficiency in Mice Is Associated with Hepatic Steatosis and Secretion of Large VLDL Particles, *Am. J. Physiol. Gastrointest. Liver Physiol. 288(6)*, G1150–G1158.
6. Moriguchi, T., Lim, S.Y., Greiner, R., Lefkowitz, W., Loewke, J., Hoshiba, J., and Salem, N., Jr. (2004) Effects of an n-3-Deficient Diet on Brain, Retina, and Liver Fatty Acyl Composition in Artificially Reared Rats, *J. Lipid Res. 45(8)*, 1437–1445.
7. Lefkowith, J.B., Flippo, V., Sprecher, H., and Needleman, P. Paradoxical Conservation of Cardiac and Renal Arachidonate Content in Essential Fatty Acid Deficiency, *J. Biol. Chem. 260*, 15736–15744.
8. Dunham, E.W., and Balasingam, M. (1978) Effects of Essential Fatty Acid Deficiency on Prostaglandin Synthesis and Fatty Acid Composition in Rat Renal Medulla, *Lipids 13*, 892–897.
9. Choi, J.H. (1998) Dietary Restriction as a Modulator of Age-Related Change in Rat Kidney Prostaglandin Production, *J. Nutr. Health Aging 2*, 167–171.
10. Knox, F.G., and Granger, J.P. (1992) Control of Sodium Excretion: An Integrative Approach, in *Handbook of Physiology* (Windhager, E.E., ed.), Vol. 1, Section 8, Chapter 21, pp. 927–967, Oxford University Press, New York.
11. Kurokawa, K. (1998) Tubuloglomerular Feedback, Its Physiological and Pathophysiological Significance, *Kidney Int. 54*, S71–S74.
12. Harris, R.C., Wang, J.L., Cheng, H.F., Zhang, M.Z., and McKanna, J.A. (1998) Prostaglandins in Macula Densa Function, *Kidney Int. 54*, S49–S52.
13. Borland, V.G., and Jackson, C.M. (1931) Effects of a Fat-Free Diet on the Structure of the Kidney in Rats, *Arch. Pathol. 11*, 687–708.
14. Cox, J.W., Rutecki, G.W., Francisco, L.L., and Ferris, T.F. (1982) Studies of the Effects of Essential Fatty Acid Deficiency in the Rat, *Circ. Res. 51*, 694–702.
15. Hjelte, L., Larsson, M., Alvestrand, A., Malmborg, A.S., and Strandvik, B. (1990) Renal Function in Rats with Essential Fatty Acid Deficiency, *Clin. Sci. 79*, 299–305.
16. Stoll, L., and Spector, A. (1995) A Functional and Ultrastructural Effect of Essential Fatty Acid Deficiency in Kidney Epithelial Cells, *Lipids 30*, 1093–1103.
17. Mills, D.E., Huang, Y.S., Narce, M., and Poisson, J.P. (1994) Psychosocial Stress, Catecholamines, and Essential Fatty Acid Metabolism in Rats, *Soc. Exp. Biol. Med. 205*, 56–61.
18. Soares, M.C.F., Aléssio, M.L., Léger, C.L., Bluert, M.T., Clauser, H., Enjalbert, A., Kordon, C., and Wandscheer, D.E. (1995) Effect of Essential Fatty Acid Deficiency on Membrane Fatty Acid Content and Growth Hormone Stimulation of Rat Pituitaries During Postnatal Development, *J. Lipid Res. 36*, 1401–1406.
19. Garcia, W.E., Gontijo, J.A., and Figueiredo, J.F. (1991) Clearance de Lítio como Método de Avaliação do Manuseio Tubular de Sódio em Ratos Acordados Estudados em Gaiolas Metabólicas, *J. Bras. Nefrol. 13*, 89–94.
20. Levinski, N.G., and Lieberthal, W. (1992) Clearance Techniques, in *Handbook of Physiology* (Windhager, E.E., ed.), Vol.

1, Section 8, Chapter 5, pp. 227–247, Oxford University Press, New York.

21. Thomsen, K. (1990) Lithium Clearance as a Measure of Sodium and Water Delivery from Proximal Tubules, *Kidney Int. 37*, S10–S16.

22. Vialli, M. (1955) Techinica per l'uso Contemporaneo in Histochimica dell Alcian Blue e della Reazione di Hotchkiss, *Arch. Zoo. Ita. 40*, 399–407.

23. Folch, J., Lees, M., and Sloane Stanley, G.H. (1957) A Simple Method for the Isolation and Purification of Total Lipids from Animal Tissues, *J. Biol. Chem. 226*, 497–509.

24. Juaneda, P., and Rocquelin, G. (1985) Rapid and Convenient Separation of Phospholipds and Non-phosphorus Lipids from Rat Heart Using Silica Cartridges, *Lipids 20*, 239–240.

25. Berry, J.F., Cevallos, W.H., and Wade, R.R. (1965) Lipid Class and Fatty Acid Composition of Intact Peripheral Nerve During Wallerian Degeneration, *J. Am. Oil Chem. Soc. 42*, 492–500.

26. Alessio, M.L., Wandscheer, D.E., Soares, M.C., Clauser, H., Enjalbert, A., Kordon, C., and Leger, C.L. (1992) Effect of an Essential Fatty Acid Deficiency on the Phospholipid Composition in Anterior Pituitary Membranes, *Biochem. Biophys. Res. Comm. 183*, 1047–1055.

27. Mead, J.F. (1957) The Metabolism of Essential Fatty Acids. VI. Distribution of Unsaturated Fatty Acids in Rats on Fat Free and Supplemented Diets, *J. Biol. Chem. 277*, 1025–1034.

28. Longmuir, K.J. (1987) Biosynthesis and Distribuition of Lipids, *Curr. Topics Membr. Transp. 29*, 129–174.

29. Van Houwelingen, A.C., Foreman-van Drongelen, M.M., Nicolini, U., Nicolaides, M.D., Kester, A.D., and Hornstra, G. (1996) Essential Fatty Acid Status of Plasma Phospholipids: Similar to Postnatal Values Obtained at Comparable Gestational Ages, *Early Hum. Dev. 46*, 141–152.

30. Phinney, S.D., Clarke, S.D., Odin, R.S., Moldawer, L.L., Blackburn, G.L., and Bistrian, B.R. (1993) Thermogenesis Secondary to Transdermal Water Loss Causes Growth Retardation in Essential Fatty Acid-Deficient Rats, *Metabolism 42*, 1022–1026.

31. Amaro, C.R.P.R., Padovani, C.R., Gontijo, J.A.R., and Figueiredo, J.F. (1997) Avaliação da função tubular proximal utilizando o clearance de lítio no tratamento pela ciclosporina a em ratos, *J. Bras. Nefrol. 19*, 369–375.

Parathyroid Hormone Stimulates Phosphatidylethanolamine Hydrolysis by Phospholipase D in Osteoblastic Cells

Amareshwar T.K. Singh[a], Michael A. Frohman[b], and Paula H. Stern[a,*]

[a]Department of Molecular Pharmacology and Biological Chemistry, Northwestern University Feinberg School of Medicine, Chicago, Illinois 60611-3008, and [b]Department of Pharmacology and the Center for Developmental Genetics, University Medical Center at Stony Brook, Stony Brook, New York 11794-5140

ABSTRACT: Parathyroid hormone (PTH) and phorbol-12,13-dibutyrate (PDBu) stimulate phospholipase D (PLD) activity and PC hydrolysis in UMR-106 osteoblastic cells {Singh, A.T., Kunnel, J.G., Strieleman, P.J., and Stern, P.H. (1999) Parathyroid Hormone (PTH)-(1–34), [Nle^{8,18},Tyr^{34}]PTH-(3–34) Amide, PTH-(1–31) Amide, and PTH-Related Peptide-(1–34) Stimulate Phosphatidylcholine Hydrolysis in UMR-106 Osteoblastic Cells: Comparison with Effects of Phorbol 12,13-Dibutyrate, *Endocrinology 140*, 131–137}. The current studies were designed to determine whether ethanolamine-containing phospholipids, and specifically PE, could also be substrates. In cells labeled with ^{14}C-ethanolamine, PTH and PDBu treatment decreased ^{14}C-PE. In cells co-labeled with ^{3}H-choline and ^{14}C-ethanolamine, PTH and PDBu treatment increased both ^{3}H-choline and ^{14}C-ethanolamine release from the cells. Choline and ethanolamine phospholipid hydrolysis was increased within 5 min, and responses were sustained for at least 60 min. Maximal effects were obtained with 10 nM PTH and 50 nM PDBu. Dominant negative PLD1 and PLD2 constructs inhibited the effects of PTH on the phospholipid hydrolysis. The results suggest that both PC and PE are substrates for phospholipase D in UMR-106 osteoblastic cells and could therefore be sources of phospholipid hydrolysis products for downstream signaling in osteoblasts.

Paper no. L9504 in *Lipids 40*, 1135–1140 (November 2005).

Phospholipase D (PLD) is activated by a number of extracellular signaling factors including growth factors, neurotransmitters, and hormones (1,2). PLD-mediated phospholipid hydrolysis modulates membrane composition and produces second messenger molecules (3). It plays a key role in cellular signaling processes leading to cytoskeletal organization, vesicle trafficking, and cell proliferation and differentiation. Previously, we demonstrated that parathyroid hormone (PTH) stimulates PC breakdown and PLD activity, as assessed by transphosphatidylation, in UMR-106 osteoblastic cells (4). We have also shown that calcium, mitogen-activated protein kinase (MAPK), small G proteins, and Gα12/Gα13 heterotrimeric G proteins are involved in regulation of the PTH-stimulated PLD activity (5,6). In the latter studies, transphosphatidylation of ethanol, a process directly mediated by PLD, was used as an indicator of PLD activity. Comparisons between results of experiments in which either PC hydrolysis or transphosphatidylation was assayed revealed that the PTH- or phorbol-12,13-dibutyrate (PDBu)-stimulated effects, as measured by transphosphatidylation, were greater than those from PC hydrolysis. These data suggested that additional phospholipid species might be involved in the actions of PTH and PDBu. PE is another major phospholipid component of biological membranes. Kiss and Anderson (7) have shown that phorbol ester stimulates PE hydrolysis in leukemic HL-60, NIH 3T3, and BHK-21 cells. Nakamura *et al.* (8) determined that both PC and PE are substrates for PLD activity in bovine kidney. However, in other studies, PLD1 and PLD2 showed little (9) or no (10) activity on PE. An N-acylPE-hydrolyzing PLD also has been identified in mammalian cells (11,12). To address the question of whether ethanolamine-containing phospholipids, and specifically PE, could be hydrolyzed in addition to PC in response to PTH or PDBu in UMR-106 cells, we determined the effects of PTH and PDBu on hydrolysis of PE as well as hydrolysis of PC in dual-labeled UMR-106 cells.

EXPERIMENTAL PROCEDURES

Materials. UMR-106 osteoblastic cells were purchased from American Type Culture Collection (Manassas, VA). PTH was from Bachem (Torrance, CA). PDBu was from Sigma Chemical Co. (St. Louis, MO). [Methyl-^{3}H]choline chloride was from Amersham (Arlington Heights, IL), and [2-^{14}C]ethan-1-ol-2-amine hydrochloride was from Amersham Biosciences (Piscataway, NJ). Dominant negative PLD constructs were generated as previously described (13).

Cells. UMR-106 osteoblastic cells were cultured to confluence in DMEM with 15% heat-inactivated horse serum and 100 U/mL K-penicillin G at 37°C in a 5% CO$_2$ environment. Cells from passages 16–18 were used. For experiments, cells were then seeded at 500,000 cells per well in sterile 6-well plates and allowed to attach for 24 h.

PC or PE hydrolysis. To assess PC or PE hydrolysis, UMR-106 cells were incubated for 48 h with [methyl-^{3}H]choline chloride (0.25 µCi/mL) and [2-^{14}C]ethanolamine hydrochloride (0.1

*To whom correspondence should be addressed at Department of Molecular Pharmacology and Biological Chemistry, Northwestern University Feinberg School of Medicine, 303 E. Chicago Ave., Chicago, IL 60611-3008.
E-mail: p.stern@northwestern.edu

Abbreviations: PDBu, phorbol-12,13-dibutyrate; PLD, phospholipase D; PTH, parathyroid hormone.

µCi/mL). Radioactivity in PC and PE reached a plateau by this time point. After the labeling, cells were washed with DMEM and then incubated in 2 mL serum-free DMEM containing 20 mM HEPES buffer and 0.1% BSA in the absence or presence of either PTH or PDBu. Following incubation at the indicated times and concentrations, media were quickly removed, and radioactivity in the media was determined by dual channel scintillation spectrometry.

To determine the specificity of the incorporation of the choline and ethanolamine labels, ^3H and ^{14}C were determined in both the choline and ethanolamine released into the medium. A 20 µL aliquot of the medium was spotted on a TLC plate. Choline and ethanolamine were separated using 0.5% NaCl/CH$_3$OH/NH$_4$OH (50:50:5) and visualized by exposing the plate to iodine. The plates were autoradiographed for 2 wk at −80°C. The choline ($R_f = 0.14$) and ethanolamine ($R_f = 0.5$) bands were scraped and counted by liquid scintillation.

To determine whether PE was affected by the treatments, cells were labeled with ^{14}C-ethanolamine, treated with PTH or PDBu for 60 min, and then scraped into ice-cold methanol. The lipids were then extracted. The organic phase was dried under N$_2$, re-equilibrated in 100 µL CHCl$_3$/CH$_3$OH (9:1), and 50 µL was spotted on a TLC plate. PE ($R_f = 0.54$) was separated using CHCl$_3$/CH$_3$OH/NH$_4$OH (65:25:5) as the running solvent. Samples were spiked with a PE standard (1-palmitoyl-2-oleoyl-*sn*-glycero-3-phosphoethanolamine; Avanti Polar Lipids, Alabaster, AL). The PE standard was visualized with iodine and radioactivity in the band determined.

Transfection. 0.5 µg each of pcDNA$_3$ (parental vector), dn PLD1 or dn PLD2 were precomplexed with Lipofectamine Plus® reagent (Life Technologies, Rockville, MD) in OPTI-MEM (Gibco BRL, Gaithersburg, MD) in the absence of an-

tibiotics and serum. Cells were incubated with the constructs for 3 h at 37°C in a 5% CO$_2$ atmosphere, after which 1 mL of OPTI-MEM medium containing 5% FBS and 1% penicillin/streptomycin was added to each of the culture dishes. Medium was changed after 6 h, and incubation continued until 48 h.

Transphosphatidylation. Cells were labeled with [^{14}C]-palmitic acid (0.25 µCi/mL) for the final 24 h of the incubation with the constructs described above. Cells were washed and then treated with PTH for 30 min in DMEM containing 20 mM HEPES, 0.1% BSA, and 1% absolute ethanol. To terminate the reaction, media were quickly removed, and 1 mL ice-cold methanol was added to cells. Cells were scraped into chloroform and lipids extracted using the method of Folch *et al.* (14). The extract containing lipids was dried under nitrogen, lipids were re-equilibrated in 100 µL CHCl$_3$/CH$_3$OH (9:1), of which 50 µL was spotted on a TLC plate, and a 10-µL aliquot was used to determine total lipid radioactivity. Phosphatidylethanol ($R_f = 0.57$) was separated from the total lipid fraction by TLC using CHCl$_3$/CH$_3$OH/CH$_3$COOH (70:10:2) as the running solvent. A 1,2-dipalmitoyl-*sn*-glycero-3-phosphoethanol standard was run concurrently. Lipids were visualized by exposure to iodine vapor. For autoradiography, TLC plates were incubated at −70°C for 72 h. The phosphatidylethanol bands were scraped, and radioactivity was determined by liquid scintillation counting. The ^{14}C radioactivity recovered in phosphatidylethanol at the end of the treatments was expressed as the percentage of total ^{14}C lipid radioactivity.

Statistics. The graphs in this paper display data from single experiments. For each experiment, unless otherwise indicated in the figure legend, each single treatment was repeated in three separate wells, and the means ± SE of the responses to the treat-
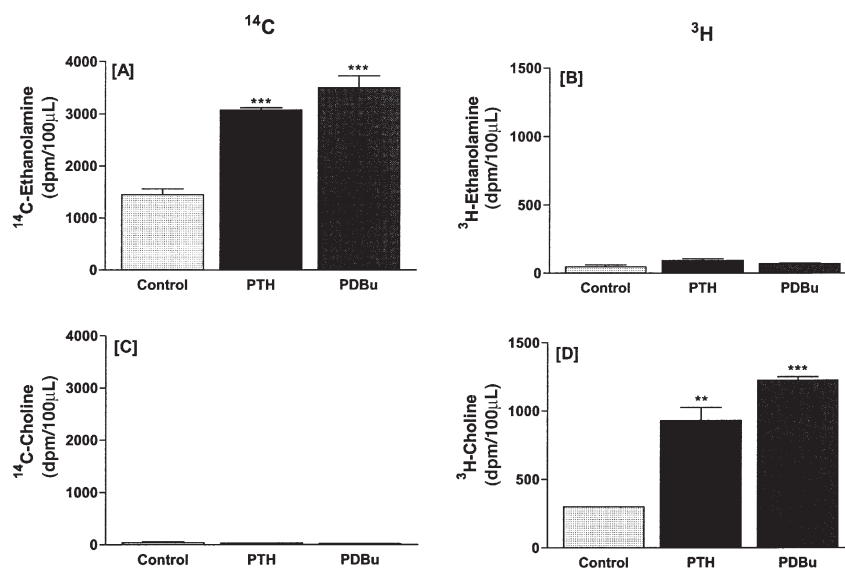
FIG. 1. Parathyroid hormone (PTH: 10 nM) and phorbol-12,13-dibutyrate (PDBu: 500 nM) stimulate the production of labeled ethanolamine (A) and choline (D) from ^{14}C-ethanolamine-labeled (A, B) and ^3H-choline-labeled (C,D) phospholipids in UMR-106 osteoblastic cells. Incubation time was 60 min. Results are mean ± SE of triplicate determinations for each treatment. **$P < 0.01$, ***0.001 vs. respective controls.
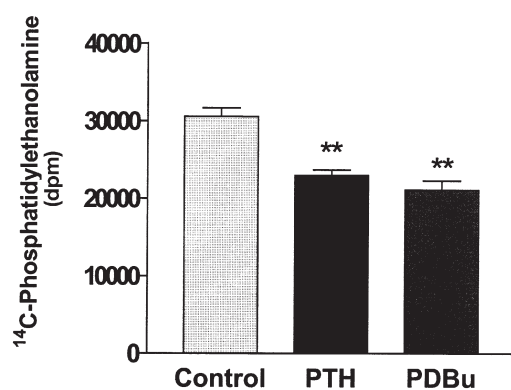
FIG. 2. PTH (10 nM) and PDBu (500 nM) decrease ^{14}C-PE in UMR-106 cells. Incubation time was 60 min. Results are the mean ± SE of triplicate determinations for each treatment. **$P < 0.01$ vs. respective controls. For abbreviations see Figure 1.

ments were calculated. Statistical significance was determined by one-way ANOVA and Tukey post-test (15).

RESULTS AND DISCUSSION

To determine whether both PC and ethanolamine-containing phospholipids were serving as substrates for PLD activity stimulated by the agonists, UMR-106 cells were dual-labeled with [methyl-^{3}H]choline chloride and [2-^{14}C]ethanolamine hydrochloride, and phospholipid hydrolysis was assessed as described in the Experimental Procedures section. In an experiment designed to test this (Fig. 1), media from the incubations were chromatographed to determine whether any of the ^{3}H-choline label appeared in the ethanolamine and, conversely, whether any of the ^{14}C-ethanolamine label appeared in the choline. Treating the cells with PTH (10 nM) or PDBu (500 nM) increased medium ^{14}C-ethanolamine (Fig. 1A) and ^{3}H-choline (Fig. 1D). The labeling was selective, in that there was no significant ^{3}H label in the ethanolamine fraction (Fig. 1B) and no significant ^{14}C label in the choline fraction (Fig. 1C). For subsequent experiments, media were not fractionated, and ^{14}C and ^{3}H were used as indicators of ethanolamine-containing phospholipids and PC hydrolysis, respectively.

To determine whether PE was hydrolyzed in response to treatment with PTH (10 nM) or PDBu (500 nM), ^{14}C-ethanolamine-labeled lipids were separated by TLC as described in the Experimental Procedures section. Treatment for 60 min with either agonist resulted in a significant decrease in radioactive PE (Fig. 2).

To confirm that the effects on lipid hydrolysis were mediated through PLD, cells were transfected with catalytically inactive constructs of PLD1 or PLD2 that previously have been used successfully as putative dominant negatives (16–18). Both PLD1 and PLD2 constructs were used, since both isoforms are present in the UMR-106 cells (5). pcDNA3 served as a control for transfection. Effects of PTH were then determined. Initial experiments were carried out to confirm that the constructs inhibited PTH-stimulated transphosphatidylation. Data from a representa-
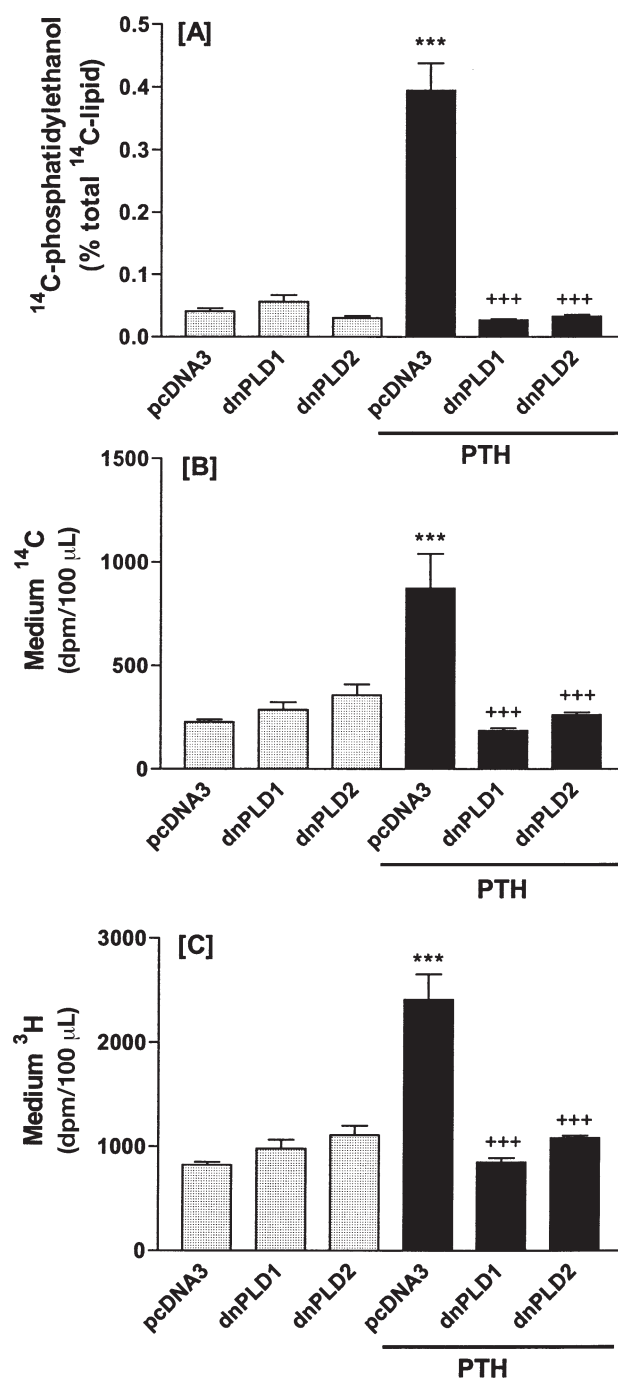

FIG. 3. Dominant negative phospholipase D1 and D2 constructs (generated as described in Ref. 13) inhibit PTH-stimulated transphosphatidylation (A) and hydrolysis of ethanolamine-containing phospholipids (B) and PC (C) in UMR-106 cells. Incubation time was 30 min. Results in panel A are the mean ± SE of duplicate measurements for each treatment. Results in panels B and C are the mean ± SE of triplicate determinations for each treatment. ***$P < 0.001$ vs. pcDNA3; +++$P < 0.001$ vs. PTH. For abbreviation see Figure 1.

tive experiment are shown (Fig. 3A). The constructs inhibited PTH-stimulated hydrolysis of ethanolamine-containing phospholipids (Fig. 3B) and PC (Fig. 3C), indicating that the effects on phospholipid hydrolysis were mediated through PLD.
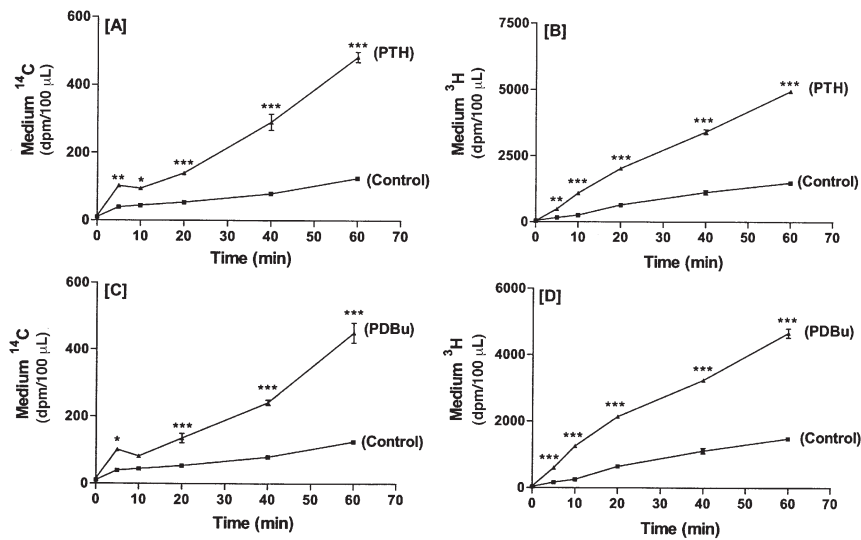
FIG. 4. Time course of 10 nM PTH- (A,B) or 500 nM PDBu- (C,D) stimulated release of radioactive hydrolysis products from UMR-106 cells dual-labeled with ^{14}C-ethanolamine and ^{3}H-choline. Results are mean ± SE of triplicate determinations for each treatment. *$P < 0.05$, **$P < 0.01$, ***$P < 0.001$ vs. respective controls. For abbreviations see Figure 1.
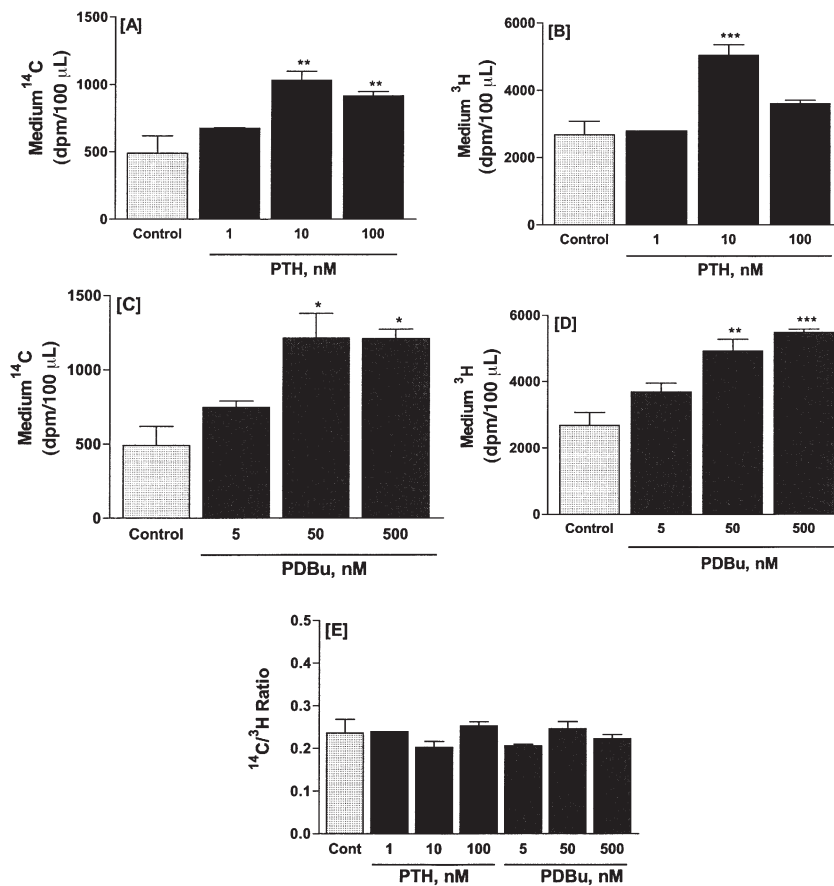
FIG. 5. Dose response of PTH (A,B) or PDBu (C,D) effects on the release of radioactive hydrolysis products from UMR-106 cells dual-labeled with ^{14}C-ethanolamine and ^{3}H-choline. Incubation time was 30 min. Results are mean ± SE of triplicate determinations for each treatment. *$P < 0.05$, **$P < 0.01$, ***$P < 0.001$ vs. respective controls. The ratio of ^{14}C to ^{3}H radioactivity, which was unaffected by the stimulators, is presented in panel E.

In time course experiments, 10 nM PTH (Fig. 4A,B) and 500 nM PDBu (Fig. 4C,D) elicited significant increases in ^{14}C and ^{3}H radioactivity at time points as early as 5 min. Responses increased progressively and were sustained for up to 60 min. In dose-response experiments at the 30-min time point (Fig. 5), effects of PTH on ^{14}C release were maximal at 10 nM and remained elevated at 100 nM (Fig. 5A). PTH (1–100 nM) elicited a biphasic effect on ^{3}H release, with significant effects at 10 but not 100 nM (Fig. 5B). PDBu (5–500 nM) (Fig. 5C,D) elicited dose-dependent increases, with significant stimulation of phospholipid hydrolysis obtained with 50 nM PDBu and no further increase with 500 nM. These dose-related effects of PTH and PDBu were replicated in other experiments. The ratios of ^{14}C to ^{3}H were not significantly different in control and treated groups (Fig. 5E), indicating that the treatments did not affect the relative rates of ^{3}H-choline and ^{14}C-ethanolamine release.

In view of the emerging role of PLD in signal transduction, it is important to identify the phospholipid pools that can serve as substrates. A number of investigators have reported the hydrolysis of PC by PLD (19). Although this pathway is well established, it is now clear that PE is also a potential source of signaling molecules in cells stimulated with phorbol esters and agonists (20). Activation of PLD in NIH3T3 fibroblasts by phorbol ester (21), ATP or GTP (22), hormones (23), and oxidative stimuli (24) had been shown to correlate with hydrolysis of PE. The present results, in particular the observation that dominant negative alleles of PLD1 and PLD2 block agonist-stimulated PE hydrolysis, suggest that PE is a direct target for hydrolysis by PLD in response to PTH in UMR-106 cells. PLD1 had been shown previously to hydrolyze PE *in vitro* with limited efficiency in comparison with PC (9); this is the first study, however, that links PLD1 and PLD2 action *in vivo* with PE hydrolysis. PE and PC are differently distributed within the plasma membrane, with PE being more predominant in the inner leaflet (25). This differential distribution could result in distinct functions being mediated by PC and PE hydrolysis.

In summary, PTH and PDBu stimulated PLD-dependent generation of ^{3}H-choline and ^{14}C-ethanolamine in UMR-106 cells. Effects on phospholipid hydrolysis were time- and dose-dependent. The findings are likely to be relevant to PTH effects in osteoblastic cells. Phospholipid hydrolysis generates the signaling molecules PA and DAG, and our previous studies have shown that both of these are increased in response to PTH (26). The current results suggest that PE, in addition to PC, may serve as a phospholipid source of these mediators of downstream signaling in UMR-106 osteoblastic cells

ACKNOWLEDGMENT

REFERENCES

1. Exton, J.H. (1997) New Developments in Phospholipase D, *J. Biol. Chem. 272*, 15579–15582.

2. McDermott, M., Wakelam, M.J., and Morris, A.J. (2004) Phospholipase D, *Biochem. Cell Biol. 82*, 225–253.

3. Cockcroft, S. (2001) Signalling Roles of Mammalian Phospholipase D1 and D2, *Cell. Mol. Life Sci. 58*, 1674–1687.

4. Singh, A.T., Kunnel, J.G., Strieleman, P.J., and Stern, P.H. (1999) Parathyroid Hormone (PTH)-(1–34), [Nle^{8,18},Tyr^{34}]PTH-(3–34) Amide, PTH-(1–31) Amide, and PTH-Related Peptide-(1–34) Stimulate Phosphatidylcholine Hydrolysis in UMR-106 Osteoblastic Cells: Comparison with Effects of Phorbol 12,13-Dibutyrate, *Endocrinology 140*, 131–137

5. Singh, A.T., Bhattacharyya, R.S., Radeff, J.M., and Stern, P.H. (2003) Regulation of Parathyroid Hormone-Stimulated Phospholipase D in UMR-106 Cells by Calcium, MAP Kinase, and Small G Proteins, *J. Bone Miner. Res. 18*, 1453–1460.

6. Singh, A.T., Gilchrist, A., Voyno-Yasenetskaya, T., Radeff-Huang, J.M., and Stern, P.H. (2005) Gα_{12}/Gα_{13} Subunits of Heterotrimeric G Proteins Mediate Parathyroid Hormone Activation of Phospholipase D in UMR-106 Osteoblastic Cells, *Endocrinology 146*, 2171–2175.

7. Kiss, Z., and Anderson, W.B. (1989) Phorbol Ester Stimulates the Hydrolysis of Phosphatidyethanolamine in Leukemic HL-60, NIH 3T3, and Baby Hamster Kidney Cells, *J. Biol. Chem. 264*, 1483–1487.

8. Nakamura, S., Kiyohara, Y., Jinnai, H., Hitomi, T., Ogino, C., Yoshida, K., and Nishizuka, Y. (1996) Mammalian Phospholipase D: Phosphatidylethanolamine as an Essential Component, *Proc. Natl. Acad. Sci. USA 93*, 4300–4304.

9. Pettitt, T.R., McDermott, M., Saqib, K.M., Shimwell, N., and Wakelam, M.J. (2001) Phospholipase D1b and D2a Generate Structurally Identical Phosphatidic Acid Species in Mammalian Cells, *Biochem. J. 360*, 707–715.

10. Hammond, S.M., Altshuller, Y.M., Sung, T.-C., Rudge, S.A., Rose, K., Engebrecht, J., Morris, A.J., and Frohman, M.A. (1995) Human ADP-Ribosylation Factor-Activated Phosphatidylcholine-Specific Phospholipase D Defines a New and Highly Conserved Gene Family, *J. Biol. Chem. 270*, 29640–29643.

11. Okamoto, Y., Morishita, J., Tsuboi, K., Tonai, T., and Ueda, N. (2004) Molecular Characterization of a Phospholipase D Generating Anandamide and Its Congeners, *J. Biol. Chem. 279*, 5298–5305.

12. Okamoto, Y., Morishita, J., Wang, J., Schmid, P.C., Krebsbach, R.J., Schmid, H.H., and Ueda, N. (2005) Mammalian Cells Stably Overexpressing N-Acylphosphatidylethanolamine-Hydrolysing Phospholipase D Exhibit Significantly Decreased Levels of N-Acylphosphatidylethanolamines, *Biochem. J. 389*, 241–247.

13. Sung, T.-C., Roper, R.L., Zhang, Y., Rudge, S.A., Temel, R., Hammond, S.M., Morris, A.J., Moss, B., Engebrecht, J., and Frohman, M.A. (1997) Mutagenesis of Phospholipase D Defines a Superfamily Including a Trans-Golgi Viral Protein Required for Poxvirus Pathogenicity, *EMBO J. 16*, 4519–4530.

14. Folch, L., Lees, M., and Sloane Stanley, G.H. (1957) A Simple Method for the Isolation and Purification of Total Lipids from Animal Tissues, *J. Biol. Chem. 226*, 497–509.

15. Tukey, J.W. (1949) Comparing Individual Means in the Analysis of Variance, *Biometrics 5*, 99–114.

16. Vitale, N., Caumont, A.S., Chasserot-Golaz, S., Du, G., Wu, S., Sciorra, V.A., Morris, A.J., Frohman, M.A., and Bader, M.F. (2001) Phospholipase D1: A Key Factor for the Exocytotic Machinery in Neuroendocrine Cells, *EMBO J. 20*, 2424–2434.

17. Huang, P., Altshuller, Y.M., Hou, J.C., Pessin, J.E., and Frohman, M.A. (2005) Insulin-Stimulated Plasma Membrane Fusion of Glut4 Glucose Transporter-Containing Vesicles Is Regulated by Phospholipase D1, *Mol. Biol. Cell 16*, 2614–2623.

18. Du, G., Huang, P., Liang, B.T., and Frohman, M.A. (2004) Phospholipase D2 Localizes to the Plasma Membrane and Reg-

ulates Angiotensin II Receptor Endocytosis, *Mol. Biol. Cell 15*, 1024–1030.

19. Billah, M.M., and Anthes, J.C. (1990) The Regulation and Cellular Functions of Phosphatidylcholine Hydrolysis, *Biochem. J. 269*, 281–291.

20. Hii, C.S.T., Edwards, Y.S., and Murray, A.W. (1991) Phorbol Ester-Stimulated Hydrolysis of Phosphatidylcholine and Phosphatidylethanolamine by Phospholipase D in HeLa cells. Evidence That the Basal Turnover of Phosphoglycerides Does Not Involve Phospholipase D, *J. Biol. Chem. 266*, 20238–20243.

21. Kiss, Z., Rapp, U.R., Pettit, G.R., and Anderson, W.B. (1991) Phorbol Ester and Bryostatin Differentially Regulate the Hydrolysis of Phosphatidylethanolamine in Ha-ras- and raf-Oncogene-Transformed NIH 3T3 cells, *Biochem. J. 276*, 505–509.

22. Kiss, Z., and Anderson, W.B. (1990) ATP Stimulates the Hydrolysis of Phosphatidylethanolamine in NIH 3T3 Cells. Potentiating Effects of Guanosine Triphosphates and Sphingosine, *J. Biol. Chem. 265*, 7345–7350.

23. Kiss, Z. (1992) Differential Effects of Platelet-Derived Growth Factor, Serum and Bombesin on Phospholipase D-Mediated Hydrolysis of Phosphatidylethanolamine in NIH 3T3 Fibroblasts, *Biochem. J. 285*, 229–233.

24. Natarajan, V., Taher, M.M., Roehm, B., Parinandi, N.L., Schmid, H.H., Kiss, Z., and Garcia, J.G. (1993) Activation of Endothelial Cell Phospholipase D by Hydrogen Peroxide and Fatty Acid Hydroperoxide, *J. Biol. Chem. 268*, 930–937.

25. Verkleij, A.J., and Post, J.A. (2000) Membrane Phospholipid Asymmetry and Signal Transduction, *J. Membr. Biol. 178*, 1–10.

26. Radeff, J.M., Singh, A.T., and Stern, P.H. (2004) Role of Protein Kinase A, Phospholipase C and Phospholipase D in Parathyroid Hormone Receptor Regulation of Protein Kinase C α and Interleukin-6 in UMR-106 Osteoblastic Cells, *Cell Signal. 16*, 105–114.

Lipid Malabsorption Persists After Weaning in Rats Whose Dams Were Given GLP-2 and Dexamethasone

Claudiu Iordache[a], Laurie A. Drozdowski[a], M. Tom Clandinin[a], Gary Wild[b], Zoe Todd[a], and Alan B.R. Thomson[a,*]

[a]Nutrition and Metabolism Group, Department of Medicine, University of Alberta, Edmonton, Alberta, Canada, and [b]Department of Anatomy and Cell Biology, McGill University, Montreal, Québec, Canada

ABSTRACT: Glucagon-like peptide-2 (GLP-2) enhances intestinal growth and absorption in mature animals, and glucocorticosteroids (GC) increase the sugar and lipid uptake in adult animals. However, the role of GC and GLP-2 in the ontogeny of lipid absorption is unknown. We hypothesized that GLP-2 and the GC dexamethasone (DEX), when administrated to rat dams during pregnancy and lactation, would enhance lipid uptake in the offspring. Rat dams were treated in the last 10 d of pregnancy and during lactation with GLP-2 [0.1 µg/g/d subcutaneous (sc)], DEX (0.128 µg/g/d sc), GLP-2 + DEX, or a placebo. Sucklings were sacrificed at 19–21 d of age, and weanlings were sacrificed 4 wk later. Lipid uptake was assessed using an *in vitro* ring uptake method. Although DEX and GLP-2 + DEX increased the jejunal mass, the jejunal lipid uptake was unchanged. In contrast, GLP-2, DEX, and GLP-2 + DEX reduced the ileal lipid uptake in suckling and weanling rats. This reduction was not due to alterations in intestinal morphology or to changes in fatty acid-binding protein abundance, but it was partially explained by an increase in the effective resistance of the intestinal unstirred water layer. In sucklings, DEX dramatically reduced the jejunal lipid uptake to levels similar to those seen in weanlings, such that the normal ontogenic decline in lipid uptake was not observed. Giving dams GLP-2 or DEX during pregnancy and lactation reduced lipid uptake in the offspring, and this persisted for at least 1 mon. The impact this may have on the nutritional well-being of the animal in later life is unknown.

Paper no. L9663 in *Lipids 40*, 1141–1148 (November 2005).

The ontogeny of the intestinal tract includes all the events involved in the development and maturation of the gut. This complex process involves morphological maturation with the transition from the endodermal tube to the villous-crypt architecture and functional maturation of the digestive and absorptive functions, as well as the barrier properties of the mucosa (1–3). The digestive functions exhibit age-dependent alterations in the absorption of nutrients during the suckling and weaning period (4). These variations are due to alterations of abundance and/or activities of the transporters and digestive enzymes, as well as to changes in the permeability of the brush border membrane (BBM) (2,4–6).
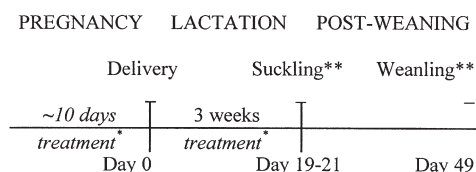
Intestinal lipid uptake involves both passive diffusion and protein-mediated transport (7). The uptake of lipids is higher in suckling rats than in adult rats, possibly because of their increased BBM permeability as well as the more efficient metabolism of fat (8,9). The ontogeny of lipid absorption has not been studied extensively. Glucagon-like peptide-2 (GLP-2) enhances the absorption of sugars in adult animals (10–12), but whether this peptide influences the intestinal absorption of lipids is not known. In adult rats, glucocorticosteroids (GC) increase the uptake of both sugars and lipids (13–15). GC may need to be given to pregnant and lactating mothers for health reasons, and it is not known whether this affects lipid absorption in their offspring, whether any possible effect continues in the offspring after GC are discontinued, or whether the effects of GC can be modified if the dams are given GLP-2. Accordingly, this study was undertaken to determine (i) the influence of GLP-2, dexamethasone (DEX), and GLP-2 + DEX, when administered to pregnant and lactating rat dams, on the intestinal *in vitro* uptake of FA and cholesterol in their suckling offspring; (ii) whether alterations in the uptake of lipids are due to variations in the intestinal morphology or mass, or to changes in selected lipid-binding proteins in the cytosol of the enterocytes; and (iii) whether these changes persist a month later in postweaning animals.

MATERIALS AND METHODS

Animals. The principles for the care and use of laboratory animals observed in the conduct of this study were approved by the Canadian Council on Animal Care and by the Council of the American Physiological Society. All experiments were approved by the Animal Ethics Board, University of Alberta. Eight 1-wk-old pregnant Sprague Dawley rats were obtained from Bio Science Animal Services, University of Alberta. The dams were randomized into four groups and received treatment with GLP-2, DEX, GLP-2 + DEX, or a placebo. Treatment was started 10 d before delivery and was continued until the animals were 19–21 d of age. DEX was administered in a dose of 0.128 µg/g body weight/d subcutaneously (sc) once per day at 7:00 PM. GLP-2 was administered in a dose of 0.1 µg/g body weight/d sc twice per day at 7:00 AM and 7:00 PM. The regimen used for the DEX + GLP-2 group was DEX 0.128 µg/g

PREGNANCY   LACTATION   POST-WEANING

Delivery   Suckling**   Weanling**

~*10 days*   3 weeks
*treatment**   *treatment**
Day 0   Day 19-21   Day 49

FIG. 1. Experimental design. *Glucagon-like peptide-2 (GLP-2), dexamethasone (DEX), GLP-2 + DEX, and a placebo were administered during pregnancy and lactation. **Uptake studies were performed at days 19–21 ("suckling") and at day 49 ("weanling").

body weight/d sc once per day at 7:00 PM plus GLP-2 0.1 μg/g body weight/d sc twice per day at 7:00 AM and 7:00 PM. The placebo group received 0.9% saline sc in a volume equal to the volume of GLP-2 administered daily per rat (depending on the weight of the dams, the volume ranged from 0.32 to 0.46 mL), twice per day at 7:00 AM and 7:00 PM.

After delivery, the offspring were downsized to 12 pups and were housed with their dams; there were 2 dams and 24 pups in each group. At weaning, 8 offspring per group ("sucklings") were sacrificed for the uptake studies and 8 per group were sacrificed for morphological analysis and immunohistochemistry (Fig. 1). The remaining postweaning animals ("weanlings") were sacrificed for uptake studies at 7 wk of age.

The animals were housed at a temperature of 21°C and each day were exposed to 12 h of light and 12 h of darkness. During the suckling period, the offspring received only the dam's milk. The weanlings were housed in pairs, and water and food were supplied *ad libitum*. The dams and the weanlings were fed a standard rat chow (PMI #5001; Nutrition International LLC, Brentwood, MO). The diets were nutritionally adequate, providing for all known essential nutrient requirements. Body weights were recorded at the time of weaning and then weekly for the next 4 wk.

Uptake studies. (i) Probe and marker compounds. The [14C]-labeled probes included cholesterol (0.05 mM) and six FA (0.1 mM): lauric acid (12:0), palmitic acid (16:0), stearic acid (18:0), oleic acid (18:1), linoleic acid (18:2), and linolenic acid (18:3). The labeled and unlabeled probes were supplied by Amersham Biosciences Inc. (Baie d'Urfe, Québec, Canada). The lipid probes were prepared by solubilizing them in 10 mM taurodeoxycholic acid (Sigma, St. Louis, MO) in Krebs-bicarbonate buffer, with the exception of 12:0, which was solubilized in only Krebs-bicarbonate buffer. [3H]Inulin was used as a nonabsorbable marker to correct for the adherent mucosal fluid volume (16).

(ii) Tissue preparation. Eight animals per treatment group were sacrificed by an intraperitoneal injection of Euthanyl® (sodium pentobarbital, 240 mg/100 g body weight). The whole length of the small intestine was rapidly removed and rinsed with 150 mL cold saline. The intestine was divided into two parts: The proximal half of the intestine beginning at the ligament of Treitz was termed the "jejunum," and the distal half was termed the "ileum." A 2-cm piece of each segment of jejunum and ileum was gently scraped with a glass slide. The mucosal scrapings and the remaining intestinal wall were dried overnight in an oven at 55°C. The percentage of the intestinal wall comprising mucosa was then calculated. The remaining intestine was everted and cut into small rings of approximately 2–4 mm each. These intestinal rings were immersed in preincubation beakers containing Krebs buffer (pH 7.2) at 37°C, bubbled with oxygen plus bicarbonate (O_2-CO_2, 95:5 vol/vol), and allowed to equilibrate for 5 min (17). Uptake was initiated by the timed transfer of the tissue rings from the preincubation buffer to a 5-mL plastic vial containing [3H]inulin and [14C]-labeled lipids in Krebs buffer bubbled with oxygen plus bicarbonate that had been equilibrated to 37°C in a shaking water bath. The intestinal rings were incubated in the lipid substrates for 5 min.

(iii) Determination of uptake rates. The rate of lipid uptake was terminated by pouring the vial contents onto filters on an Amicon vacuum filtration manifold that was maintained under suction, followed by washing the intestinal rings three times with ice-cold saline. The tissue rings were then placed on a glass slide and dried overnight in an oven at a constant temperature of 55°C. The dry weight of the tissue was determined, and the tissue was transferred to scintillation-counting vials. The samples were saponified with 0.75 M NaOH, scintillation fluid was added, and radioactivity was determined by means of an external standardization technique to correct for variable quenching of the two isotopes (16). The rates of lipid uptake were determined as nmol of substrate absorbed per 100 mg dry weight of the mucosa per minute (Jm, nmol·100 mg mucosal tissue^{-1}·min^{-1}).

Morphological analysis. To determine the morphological characteristics of the intestine, vertical sections were prepared from the jejunum and from the ileum. Hematoxylin and eosin-stained slides were prepared from paraffin blocks. Crypt depth, villous height, villous width, and villous width at half height were measured using the program MetaMorph 5.05r (Universal Imaging Corporation, Downingtown, PA). The group means were obtained based on 10 villi and 20 crypts per slide, with a minimum of 4 animals in each group.

Immunohistochemistry. The jejunal and ileal tissues were embedded in paraffin, and 4- to 5-μm sections were mounted on glass slides. The sections were heated and placed immediately in xylene (2× for 5 min each), followed by absolute ethanol (2× for 2 min each), and were then rinsed with tap water. The slides were incubated in a hydrogen peroxide/methanol solution and rinsed with tap water. They were then rehydrated, and the tissue was encircled on the slides with a hydrophobic slide marker (PAP pen; BioGenex, San Ramon, CA). The slides were incubated for 15 min in blocking reagent (20% normal goat serum), followed by primary antibody to the intestinal FA-binding protein (I-FABP) or to the liver FA-binding protein (L-FABP) for 30 min. Both antibodies were a generous gift from Dr. Luis B. Agellon, University of Alberta. The slides were incubated in LINK® and LABEL®, and with DAB® solution (BioGenex). The slides were then washed, stained in hematoxylin, dehydrated in absolute ethanol, and cleared in xylene. The slides were photographed, and the area labeled with antibody was determined using Metamorph 5.05r. The results were expressed as the ratio of the area that was antibody-positive to

TABLE 1
Intestinal Characteristics of Suckling Rats of Dams Injected Through Pregnancy and Lactation with Glucagon-like Peptide-2 (GLP-2), Dexamethasone (DEX), or GLP-2 + DEX[a]

	Control	GLP-2	DEX	GLP-2 + DEX
Jejunum				
Mucosa (mg/cm)	1.8 ± 0.3	2.7 ± 0.7	4.1 ± 0.5*	3.8 ± 0.2*
Remaining intestinal wall (mg/cm)	1.8 ± 0.3	2.5 ± 0.8	1.2 ± 0.2	0.9 ± 0.1
Total weight (mg/cm)	3.6 ± 0.3	5.2 ± 0.7	5.4 ± 0.6	4.7 ± 0.2
% Mucosa	50.6 ± 5.1	53.1 ± 9.7	76.9 ± 4.0*	79.8 ± 2.2*
Ileum				
Mucosa (mg/cm)	1.5 ± 0.3	2.1 ± 0.2	2.8 ± 0.7	1.9 ± 0.3
Remaining intestinal wall (mg/cm)	1.9 ± 0.3	1.2 ± 0.2	1.6 ± 0.5	1.5 ± 0.3
Total weight (mg/cm)	3.5 ± 0.3	3.3 ± 0.2	4.4 ± 0.6	3.4 ± 0.2
% Mucosa	44.8 ± 5.8	64.8 ± 5.0	61.8 ± 9.0	55.9 ± 8.0

[a]Values are expressed as mean ± SEM, $n = 8$. *Values are significantly different from controls ($P \leq 0.05$ by one-way ANOVA). The treatments include GLP-2 (0.1 µg/g twice a day), DEX (0.128 µg/g once a day), and GLP-2 + DEX at those doses, given during pregnancy and lactation. The suckling animals were sacrificed on days 19–21.

the total area. Statistical analyses were based on a minimum of four villi per animal and four animals per group.

Statistical analyses. The results were expressed as mean ± SEM. The statistical significance of the differences between the four groups was determined by ANOVA and the Student–Newman–Keuls test. Significant differences between sucklings vs. weanlings were determined using a Student's *t*-test. Statistical significance was accepted as $P \leq 0.05$.

RESULTS

Body and intestinal weights, and villous morphology. There was no significant difference in body weight gain (g/d) among the dams used in the control, GLP-2, DEX, or GLP-2 + DEX groups (data not shown). There were also no differences in the body weights of the suckling or weanling rats in these four groups.

Compared with controls, sucklings whose pregnant and lactating dams were given DEX or GLP-2 + DEX had increased jejunal mucosal weight and an increase in the percentage of the jejunal wall comprising mucosa (Table 1). There were no changes in the ileum. GLP-2 by itself had no effect on the characteristics of the jejunum or ileum. In weanlings, GLP-2, DEX, or GLP-2 + DEX had no effect on the weight of the jejunal or ileal mucosa, the weight of the intestine, or the percentage of the intestinal wall comprising mucosa (Table 2).

In sucklings, GLP-2 increased the ileal villous height compared with controls (data not shown). The weanling rats of dams exposed to the placebo, GLP-2, DEX, or GLP-2 + DEX 1 mon previously showed no difference in jejunal or ileal morphology between the treatment groups.

Lipid uptake. Because of the effect of DEX and GLP-2 + DEX on the jejunal weights (Table 1) and morphology of the suckling rats, the rate of lipid uptake was expressed on the basis of mucosal mass (Jm, mmol·100 mg mucosa^{-1}·min^{-1}).

In sucklings, GLP-2 reduced the ileal uptake of 12:0, 18:1, and 18:2, whereas DEX reduced the jejunal uptake of 12:0 and

TABLE 2
Intestinal Characteristics of Weanling Rats of Dams Injected Through Pregnancy and Lactation with GLP-2, DEX, or GLP-2 + DEX[a]

	Control	GLP-2	DEX	GLP-2 + DEX
Jejunum				
Mucosa (mg/cm)	8.7 ± 2.0	8.9 ± 1.3	8.8 ± 0.8	8.5 ± 1.1
Remaining intestinal wall (mg/cm)	1.0 ± 0.1	1.2 ± 0.16	0.9 ± 0.1	1.0 ± 0.2
Total weight (mg/cm)	10.0 ± 2.0	10.1 ± 1.2	9.7 ± 0.8	9.5 ± 0.9
% Mucosa	87.9 ± 2.5	89.7 ± 2.3	90.0 ± 1.9	87.7 ± 2.6
Ileum				
Mucosa (mg/cm)	7.9 ± 1.2	10.5 ± 2.1	8.8 ± 0.7	8.3 ± 0.6
Remaining intestinal wall (mg/cm)	0.7 ± 0.1	1.0 ± 0.2	0.8 ± 0.1	0.9 ± 0.1
Total weight (mg/cm)	8.6 ± 1.1	11.5 ± 2.0	9.5 ± 0.6	9.2 ± 0.6
% Mucosa	89.8 ± 2.6	89.8 ± 2.8	91.3 ± 1.8	89.9 ± 1.5

[a]Values are expressed mean ± SEM, $n = 8$. None of these differences was statistically significant tested by one-way ANOVA. The treatments included GLP-2 (0.1 µg/g twice a day), DEX (0.128 µg/g once a day), and GLP-2 + DEX at those doses, given during pregnancy and lactation. The weanling animals were sacrificed 28 d after weaning. For abbreviations see Table 1.

TABLE 3
Effect of Treating Dams During Pregnancy and Lactation on the Jejunal and Ileal Uptake (Jm) of Lipids in Suckling Rats[a]

| | FA | mean ± SEM | | | |
		Control	GLP-2	DEX	GLP-2 + DEX
Jejunum	12:0	62.7 ± 10.4	53.7 ± 9.4	18.2 ± 4.0*	28.9 ± 4.2*
	16:0	4.7 ± 0.5	4.5 ± 0.6	2.4 ± 0.5	3.2 ± 0.7
	18:0	5.0 ± 0.7	5.5 ± 0.8	2.4 ± 0.2*	2.9 ± 0.5*
	18:1	3.7 ± 0.5	3.55 ± 0.7	1.7 ± 0.3	3.0 ± 0.6
	18:2	3.5 ± 0.6	4.5 ± 1.9	1.6 ± 0.2	1.2 ± 0.3
	18:3	2.0 ± 0.3	2.7 ± 0.4	2.0 ± 0.5	2.6 ± 0.3
	Chol	1.7 ± 0.3	3.3 ± 0.8	1.7 ± 0.3	1.1 ± 0.2
Ileum	12:0	98.9 ± 16.4	58.2 ± 5.7*	24.7 ± 10.2*	46.4 ± 5.5*
	16:0	5.6 ± 0.9	8.2 ± 1.2	2.5 ± 0.3	4.2 ± 0.8
	18:0	10.1 ± 1.6	6.8 ± 0.8	3.0 ± 1.4*	4.3 ± 0.6*
	18:1	12.8 ± 2.4	2.5 ± 0.5*	4.4 ± 1.9*	5.6 ± 0.6*
	18:2	9.8 ± 1.8	3.8 ± 0.5*	2.1 ± 0.4*	4.9 ± 1.3*
	18:3	4.7 ± 0.6	5.2 ± 0.8	3.4 ± 0.4	4.1 ± 0.5
	Chol	2.8 ± 0.5	2.8 ± 0.5	2.0 ± 0.4	1.0 ± 0.1*

[a]Values are mean ± SEM, $n = 8$. *Values are significantly different from controls ($P \leq 0.05$ by one-way ANOVA). Jm: uptake rate calculated based on mucosal weight (nmol 100 mg^{-1} mucosal weight min^{-1}). The treatments included GLP-2 (0.1 µg/g twice a day), DEX (0.128 µg/g once a day), and GLP-2 + DEX at those doses, given during pregnancy and lactation. The suckling animals were sacrificed on days 19–21. Chol, cholesterol; for other abbreviations see Table 1.

18:0 and the ileal uptake of 12:0, 18:0, 18:1, and 18:2 (Table 3). The combination of GLP-2 + DEX also reduced the jejunal uptake of 12:0 and 18:0, and reduced the ileal uptake of 12:0, 18:0, 18:1, 18:2, and cholesterol.

In weanlings, GLP-2 had no effect on the jejunal uptake of lipids but reduced the ileal uptake of 12:0 and 18:3 and increased the uptake of 18:2 (Table 4). DEX reduced the jejunal uptake of 18:1 and the ileal uptake of 12:0, 18:1, and 18:3. GLP-2 + DEX reduced the ileal uptake of 12:0 and 18:1.

The uptake of lipids was generally lower in the jejunum and ileum of weanling, as compared with suckling, control rats, or those given GLP-2 or GLP-2 + DEX (Tables 3, 4). In those given DEX, the jejunal uptake of lipids was similar in sucklings and in weanlings, and was lower in the ileum of weanlings than sucklings.

Immunohistochemistry. There were no differences between sucklings and weanlings in the abundance of I-FABP or L-FABP in the jejunum or ileum of the control animals (Table 5). GLP-2, DEX, and GLP-2 + DEX had no effect on the abundance of I- or L-FABP in suckling or weanling rats, except for a lower abundance of I-FABP in the ileum of weanlings whose dams received GLP-2 + DEX.

TABLE 4
Effect of Treating Dams During Pregnancy and Lactation on the Jejunal and Ileal Uptake (Jm) of Lipids in Weanling Rats[a]

| | FA | mean ± SEM | | | |
		Control	GLP-2	DEX	GLP-2 + DEX
Jejunum	12:0	17.8 ± 1.5	17.3 ± 1.7	12.9 ± 1.9	12.3 ± 2.1
	16:0	1.6 ± 0.1	1.8 ± 0.1	1.4 ± 0.2	1.6 ± 0.3
	18:0	1.5 ± 0.8	1.9 ± 0.2	1.9 ± 0.2	1.0 ± 0.1
	18:1	1.5 ± 0.2	1.7 ± 0.1	1.2 ± 0.1*	1.4 ± 0.1
	18:2	1.2 ± 0.1	1.6 ± 0.1	1.4 ± 0.2	1.3 ± 0.2
	18:3	1.3 ± 0.2	1.5 ± 0.1	1.4 ± 0.2	1.1 ± 0.1
	Chol	0.9 ± 0.1	1.1 ± 0.2	1.1 ± 0.1	0.7 ± 0.1
Ileum	12:0	21.0 ± 1.6	14.0 ± 0.1*	13.8 ± 1.8*	15.0 ± 1.3*
	16:0	1.2 ± 0.1	1.4 ± 0.1	1.3 ± 0.1	0.9 ± 0.1
	18:0	1.3 ± 0.1	1.6 ± 0.2	1.0 ± 0.1	1.1 ± 0.1
	18:1	1.3 ± 0.1	1.1 ± 0.1	0.9 ± 0.2*	0.8 ± 0.1*
	18:2	0.9 ± 0.1	1.4 ± 0.2*	0.8 ± 0.1	1.1 ± 0.1
	18:3	1.2 ± 0.1	0.8 ± 0.1*	0.8 ± 0.1*	1.0 ± 0.1
	Chol	1.0 ± 0.1	1.0 ± 0.2	1.1 ± 0.1	0.7 ± 0.1

[a]Values are mean ± SEM, $n = 8$. *Values are significantly different from controls ($P \leq 0.05$ by one-way ANOVA). Jm: uptake rate calculated based on mucosal weight (nmol 100 mg^{-1} mucosal weight min^{-1}). The treatments included GLP-2 (0.1 µg/g twice a day), DEX (0.128 µg/g once a day), and GLP-2 + DEX at those doses, given during pregnancy and lactation. The weanling animals were sacrificed 28 d after weaning. For other abbreviations see Tables 1 and 3.

TABLE 5
I-FABP and L-FABP Abundance in the Ileum of Offspring Whose Mothers Received Treatment During Pregnancy and Lactation[a]

	Control	GLP-2	DEX	GLP-2 + DEX
I-FABP				
Suckling	78.3 ± 3.6	71.4 ± 4.7	76.7 ± 2.6	66.0 ± 3.3
Weanling	72.2 ± 4.7	65.1 ± 3.0	67.8 ± 3.7	58.0 ± 0.9*
L-FABP				
Suckling	64.9 ± 2.2	67.8 ± 5.7	58.5 ± 3.2	60.9 ± 5.5
Weanling	59.0 ± 3.4	60.7 ± 4.0	62.0 ± 2.3	55.3 ± 3.0

[a]Protein abundance was determined by immunohistochemistry. Values are pixels per area and are expressed as mean ± SEM, $n = 8$. *Values are significantly different from controls ($P \leq 0.05$ by one-way ANOVA). The treatments included GLP-2 (0.1 µg/g twice a day), DEX (0.128 µg/g once a day), and GLP-2 + DEX at those doses, given during pregnancy and lactation. The sucklings were sacrificed on days 19–21 and the weanlings were sacrificed 28 d after weaning. I-FABP, intestinal FA-binding protein; L-FABP, liver FA-binding protein; for other abbreviations see Table 1.

DISCUSSION

GLP-2 has a proabsorptive effect in adult rats and in humans (18,19). However, treating pregnant and lactating dams with GLP-2 reduced the ileal uptake of some long-chain FA (LCFA) in both the suckling and weanling offspring (Tables 3, 4). This unexpected decline was partially due to the enhanced resistance of the intestinal unstirred water layer (UWL) (16), as the uptake of lauric acid (12:0) was also reduced.

In adult rats, GLP-2 has a trophic effect on the intestine (20,21). In sucklings, GLP-2 increased the ileal villous height (data not shown), whereas the mucosal weight did not change (Table 1). However, this effect did not persist past the weaning period (data not shown), suggesting that the effect of GLP-2 on intestinal morphology was short-lived. GLP-2 may exert its influence on the suckling animals by increasing intestinal proliferation or decreasing apoptosis. Indeed, in adult animals, GLP-2 has an antiapoptotic (21) and trophic effect (20,21). We did not specifically measure apoptosis or proliferation; nonetheless, the reduction in lipid uptake seen with GLP-2 clearly could not be explained by changes in the animals' body weight or by enhancement of the intestinal weight.

The GLP-2-secreting "L" cells are more abundant in the distal than in the proximal small intestine (22,23). However, in adult rats the prominent trophic effects of systemically administered GLP-2 are observed in the jejunum (24), and the receptors for GLP-2 (GLP-2R) are more abundant in the jejunum than in the ileum (25). Thus, the lack of stimulating effect of GLP-2 on the jejunal uptake of lipids was unlikely to be due to a lack of GLP-2R.

It is important to stress that in this study, GLP-2 was given to pregnant and lactating mothers. Whether GLP-2 crosses the placenta or passes through the mammary gland into the mother's milk is not known. Furthermore, any GLP-2 that might come into the intestinal lumen with the mother's milk might possibly be digested, although breast milk may delay this process (26,27).

The inhibitory effect of GLP-2 on lipid uptake into the ileum may not be a direct effect of GLP-2, but rather be due to some other mediator such as the hepatocyte growth factor, fibroblast growth factor, platelet-derived growth factor, or granulocyte colony-stimulating factor (28–31). Whether these trophic factors are released in response to GLP-2 administration is unknown. We speculated that GLP-2 influenced the secretion of one or more of these factors, which may thereby have indirectly inhibited lipid uptake.

When budesonide or prednisone was given directly to 21-d-old rats for 4 wk, the lipid uptake was enhanced (13). In contrast, DEX reduced the ileal lipid uptake in suckling and weanling rats (Tables 3, 4). This effect likely occured during pregnancy, since DEX given during lactation enhanced lipid uptake in the offspring (32). The decline in lipid uptake with DEX was also associated with an increase in the jejunal mucosal mass in sucklings (Table 1), although changes in the jejunal villous morphology were found only in weanlings (data not shown). Thus, the inhibitory effects of DEX on lipid uptake were not due to atrophy of the intestine, unlike the situation in adult rats in which DEX induced atrophy in the intestine (33,34).

We had anticipated that the suckling and weanling rats would lose weight when given DEX, as DEX has a catabolic effect on the whole body when given to adult rats (33,35). However, DEX given to pregnant and lactating dams (0.128 µg/g body weight per day for 30 d) had no effect on the body weights of the offspring. Clearly, the effect of GC on the intestine of adult animals was different from that in the newborn. Furthermore, the malabsorption of lipids in the ileum was not sufficient to cause weight loss. This may have been because lipid absorption in the proximal intestine remained sufficient to maintain body weight, or because the absorption of other macronutrients was enhanced in a compensatory manner.

The mechanism for the decline in lipid uptake with DEX as well as with GLP-2 could not be explained by alterations in the abundance of the two cytosolic FABP that were measured. There was no change in the abundance of I-FABP or L-FABP in suckling or weanling animals, although in the ileum of weanlings given GLP-2 + DEX there was a decline in I-FABP abundance (Table 5). Others have also reported that changes in I-FABP do not necessarily mimic alterations in the intestinal lipid uptake (36,37). There are several other lipid-binding proteins in the BBM or enterocyte cytosol (such as caveolin-1, the scavenger receptor class B type I, the plasma membrane-FABP,

the FA transporter, the FA transport protein-4, the cholesterol transport protein, and the ileal lipid-binding protein) (38–40). It is possible that our treatments with GLP-2 and DEX reduced the abundance of these proteins, thereby reducing the lipid uptake.

It is likely that the effect of GC on the intestine of the offspring was a direct effect, because DEX injected into the mother crosses the placenta (41,42) and also passes into her milk (43–45). GC may influence intestinal absorption by reducing proliferation and enhancing apoptosis (33,46–48), as well as by modifying gene transcription through their effects on nuclear receptors (49,50). GC also reduce the effects of trophic peptides such as the hepatocyte growth factor and epidermal growth factor (47,48,51), so part of the effect of DEX may have been indirect. As was the case for GLP-2, GC also did not have an effect on intestinal lipid-binding proteins (Table 5). This agrees with results from previous studies using GC (13,14).

The combination of GLP-2 + DEX also reduced the ileal LCFA uptake, consistent with the effects of GLP-2 alone and DEX alone (Tables 3, 4). However, there was clearly no obvious additive or synergistic effect, as might have been anticipated because of the permissive effect of steroids on peptides such as GLP-2, which act *via* cAMP (52). Again, this change in lipid uptake could be explained in part by an increase in the effective resistance of the UWL (Tables 3, 4), but was not explained by alterations in the intestinal weights or morphology (Tables 1, 2). Treatment with GLP-2 + DEX decreased the ileal I-FABP abundance in weanlings (Table 5). This may partially explain the decrease in lipid uptake in weanlings, but it does not explain the decline in uptake in sucklings or the decline in uptake in weanlings given GLP-2 alone or DEX alone.

Under physiological conditions, lipids are preferentially absorbed in the jejunum (53,54). In our experiment the decline in lipid uptake with GLP-2, DEX, and GLP-2 + DEX was observed largely in the ileum. The ileum is also known to be more adaptable than the jejunum to alterations in nutrient load, or following intestinal resection (55–57). It is therefore possible that the distal small intestine is more responsive to GLP-2, DEX, and GLP-2 + DEX because of the lower baseline levels of lipid uptake, or perhaps because of its greater adaptive capabilities.

To determine whether the changes seen in the suckling rats persisted 4 wk after injections with GLP-2 or DEX were discontinued, we first needed to know what effect age had on lipid uptake. When comparing suckling with weanling rats given a placebo (Tables 3, 4), we found a consistent decline in the jejunal and ileal uptake of LCFA. Other studies have shown a fall in the absorption of lipids with weaning (8,9). This fall was probably due to a lower permeability of the BBM in adults as compared with sucklings, possibly as the result of a fall in BBM fluidity (58,59). Luminal lipids may be important to set the level of fat absorption (60). Therefore, the fall in lipid uptake may be the result of the usual decrease in the dietary fat content and the increase in the carbohydrate content that occurs when an animal is weaned from milk (a high-fat diet) onto chow (a high-carbohydrate diet).

In animals given DEX, the age-associated decline in lipid uptake into the jejunum was not observed (Tables 3, 4). This was likely due to the reduction in lipid uptake seen in suckling animals in response to DEX, a reduction that was much greater than that achieved by the other treatments. As a result, the uptake levels were similar to those seen in weanlings, and a decline was therefore not observed in these animals. DEX may have prematurely reduced lipid uptake levels in the sucklings to levels comparable to those seen postweaning. This may have important nutritional implications, as suckling animals consume breast milk, which is high in fat. A down-regulation of lipid uptake, particularly at this critical age, may result in lipid malabsorption and compromised nutritional status.

Nonetheless, the results found in weanlings appear to be late effects of GLP-2, DEX, and GLP-2 + DEX (Table 4). That there are late effects of early nutrition has long been appreciated (61). For example, changing the type of lipids in the diets of pregnant or lactating dams modifies the normal ontogeny of intestinal absorption (62–64). The late effects observed in our experiments could be the result of a reprogramming of the normal ontogenic process. This raises the possibility that giving GLP-2 or DEX to the pregnant and lactating mother may have a lasting effect on lipid uptake in her offspring. How long this lipid malabsorption lasts, or whether there are other persistent and deleterious effects on lipid metabolism are unknown.

In summary, GLP-2, DEX, and GLP-2 + DEX given to pregnant and lactating rat dams reduced the ileal uptake of LCFA in suckling and weanling offspring (Tables 3, 4). This malabsorption of lipids was not due to alterations in body weight, intestinal morphology, or the abundance of two cytosolic lipid-binding proteins. This lipid malabsorption persisted after the treatments had been stopped, but the importance of this effect on the nutritional welfare of the animal in later life is unknown.

REFERENCES

1. Henning, S.J. (1987) Functional Development of the Gastrointestinal Tract, in *Physiology of the Gastrointestinal Tract* (Johnson, L.R., ed.), pp. 285–300, Raven Press, New York.
2. Henning, S.J., Rubin, D.C., and Shulman, R.J. (1994) Ontogeny of the Intestinal Mucosa, in *Physiology of the Gastrointestinal Tract* (Johnson, L.R., ed.), pp. 571–599, Raven Press, New York.
3. Paulsen, D.B., Buddington, K.K., and Buddington, R.K. (2003) Dimensions and Histologic Characteristics of the Small Intestine of Dogs During Postnatal Development, *Am. J. Vet. Res. 64*, 618–626.
4. Sanderson, I.R., and Walker, W.A. (2000) *Development of the Gastrointestinal Tract*, BC Decker, Hamilton, Ontario.
5. Buddington, R.K., and Malo, C. (2003) Postnatal Development of Nutrient Transport in the Intestine of Dogs, *Am. J. Vet. Res. 64*, 635–645.
6. Nanthakumar, N.N., Dai, D., Newburg, D.S., and Walker, W.A. (2003) The Role of Indigenous Microflora in the Development of Murine Intestinal Fucosyl- and Sialyltransferases, *FASEB J. 17*, 44–46.
7. Besnard, P., and Niot, I. (2000) Role of Lipid Binding Protein in Intestinal Absorption of Long Chain Fatty Acids, in *Fat Digestion and Absorption* (Cristophe, A.B., and De Vriese, S., eds.), pp. 96–118, AOCS Press, Champaign.

8. Flores, C.A., Hing, S.A., Wells, M.A., and Koldovsky, O. (1989) Rates of Triolein Absorption in Suckling and Adult Rats, *Am. J. Physiol. 257*, G823–G829.

9. Frost, S.C., Clark, W.A., and Wells, M.A. (1983) Studies on Fat Digestion, Absorption, and Transport in the Suckling Rat. IV. *In vivo* Rates of Triacylglycerol Secretion by Intestine and Liver, *J. Lipid Res. 24*, 899–903.

10. Cheeseman, C.I., and Tsang, R. (1996) The Effect of GIP and Glucagon-like Peptides on Intestinal Basolateral Membrane Hexose Transport, *Am. J. Physiol. 271*, G477–G482.

11. Cheeseman, C.I. (1997) Upregulation of SGLT-1 Transport Activity in Rat Jejunum Induced by GLP2 Infusion *in vivo*, *Am. J. Physiol. 273*, R1965–R1971.

12. Cheeseman, C.I., and O'Neill, D. (1998) Basolateral D-Glucose Transport Activity Along Crypt-Villus Axis in Rat Jejunum and Upregulation by Gastric Inhibitory Peptide and Glucagon-like Peptide 2, *Exp. Physiol. 83*, 605–616.

13. Thiesen, A., Wild, G.E., Keelan, M., Clandinin, M.T., Agellon, L.B., and Thomson, A.B. (2002) Locally and Systemically Active Glucocorticosteroids Modify Intestinal Absorption of Lipids in Rats, *Lipids 37*, 159–166.

14. Thiesen, A. (2002) Steroids, Dietary Lipids, Resection and Intestinal Adaptation, Ph.D. Thesis, University of Alberta, Edmonton.

15. Thiesen, A., Wild, G.E., Tappenden, K.A., Drozdowski, L., Keelan, M., Thomson, B.K.A., McBurney, M.I., Clandinin, M.T., and Thomson, A.B.R. (2003) The Locally Acting Glucocorticosteroid Budesonide Enhances Intestinal Sugar Uptake Following Intestinal Resection in Rats, *Gut 52*, 252–259.

16. Westergaard, H., and Dietschy, J.M. (1974) Delineation of the Dimensions and Permeability Characteristics of the Two Major Diffusion Barriers to Passive Mucosal Uptake in the Rabbit Intestine, *J. Clin. Invest. 54*, 718–732.

17. Perin, N., Keelan, M., Jarocka-Cyrta, E., Clandinin, M.T., and Thomson, A.B. (1997) Ontogeny of Intestinal Adaptation in Rats in Response to Isocaloric Changes in Dietary Lipids, *Am. J. Physiol. 273 (3, Pt. 1)*, G713–G720.

18. Scott, R.B., Kirk, D., MacNaughton, W.K., and Meddings, J.B. (1998) GLP-2 Augments the Adaptive Response to Massive Resection in Rat, *Am. J. Physiol. 275*, G911–G921.

19. Jeppesen, P.B., Hartmann, B., Thulesen, J., Graff, J., Lohmann, J., Hansen, B.S., Tofteng, F., Poulsen, S.S., Madsen, J.L., Holst, J.J., and Mortensen, P.B. (2001) Glucagon-like Peptide 2 Improves Nutrient Absorption and Nutritional Status in Short-Bowel Patients with No Colon, *Gastroenterology 120*, 806–815.

20. Drucker, D.J., Ehrlich, P., Asa, S.L., and Brubaker, P.L. (1996) Induction of Intestinal Epithelial Proliferation by Glucagon-like Peptide 2, *Proc. Natl. Acad. Sci. USA 93*, 7911–7916.

21. Drucker, D.J. (2003) Glucagon-like Peptides: Regulators of Cell Proliferation, Differentiation, and Apoptosis, *Mol. Endocrinol. 17*, 161–171.

22. Kieffer, T.J., and Habener, J.F. (1999) The Glucagon-like Peptides, *Endocr. Rev. 20*, 876–913.

23. Burrin, D.G., Petersen, Y., Stoll, B., and Sangild, P. (2001) Glucagon-like Peptide 2: A Nutrient-Responsive Gut Growth Factor, *J. Nutr. 131*, 709–712.

24. Brubaker, P.L., and Drucker, D.J. (2002) Structure–Function of the Glucagon Receptor Family of G Protein-Coupled Receptors: The Glucagon, GIP, GLP-1, and GLP-2 Receptors, *Recept. Channels 8*, 179–188.

25. Munroe, D.G., Gupta, A.K., Kooshesh, F., Vyas, T.B., Rizkalla, G., Wang, H., Demchyshyn, L., Yang, Z.J., Kamboj, R.K., Chen, H., *et al*. (1999) Prototypic G Protein Coupled Receptor for the Intestinotrophic Factor Glucagon-like Peptide 2, *Proc. Natl. Acad. Sci. USA 96*, 1569–1573.

26. Rao, R.K., Philipps, A.F., Williams, C.S., McCracken, D.M., and Koldovsky, O. (1998) Luminal Stability of Insulin-like

Growth Factors I and II in Developing Rat Gastrointestinal Tract, *J. Pediatr. Gastroenterol. Nutr. 26*, 179–185.

27. Fellah, A.M., Philipps, A.F., Gillespie, T.J., Galo, J.R., and Dvorak, B. (2001) Degradation of Insulin-like Growth Factors in Small Intestine of Suckling Rats, *Regul. Pept. 98*, 19–25.

28. Calhoun, D.A., Lunoe, M., Du, Y., Staba, S.L., and Christensen, R.D. (1999) Concentrations of Granulocyte Colony-Stimulating Factor in Human Milk After *in vitro* Simulations of Digestion, *Pediatr. Res. 46*, 767–771.

29. Calhoun, D.A., Lunoe, M., Du, Y., and Christensen, R.D. (2000) Granulocyte Colony-Stimulating Factor Is Present in Human Milk and Its Receptor Is Present in Human Fetal Intestine, *Pediatrics 105*, 392–397.

30. Calhoun, D.A., Gersting, J.A., Lunoe, M., Du, Y., and Christensen, R.D. (2001) Transfer of Recombinant Human Granulocyte Colony Stimulating Factor (rhG-CSF) from the Maternal to the Fetal Circulation Is Not Dependent upon a Functional G-CSF-Receptor, *Placenta 22*, 609–612.

31. Sukhotnik, I., Siplovich, L., Krausz, M.M., and Shiloni, E. (2003) Peptide Growth Factors and Intestinal Adaptation in Short Bowel Syndrome, *Isr. Med. Assoc. J. 5*, 184–187.

32. Iordache, C., Drozdowski, L., Clandinin, T., Wild, G., Todd, Z., and Thomson, A.B. (2004) Dexamethasone plus Glucagon-like Peptide 2 Given to Lactating Rat Dams Has a Late Effect on Intestinal Lipid Uptake in the Weanling Offspring, *J. Parenter. Enteral, Nutr. 28*, 355–363.

33. Park, J.H., McCusker, R.H., Mohammadpour, H., Blackwood, D.J., Hrbek, M., and Vanderhoof, J.A. (1994) Dexamethasone Inhibits Mucosal Adaptation After Small Bowel Resection, *Am. J. Physiol. 266*, G497–G503.

34. Kritsch, K.R., Huss, D.J., and Ney, D.M. (2000) Greater Potency of IGF-I than IGF-I/BP-3 Complex in Catabolic Parenterally Fed Rats, *Am. J. Physiol. 278*, E252–E262.

35. Rooman, R., Koster, G., Bloemen, R., Gresnigt, R., and van Buul-Offers, S.C. (1999) The Effect of Dexamethasone on Body and Organ Growth of Normal and IGF-II-Transgenic Mice, *J. Endocrinol. 63*, 543–552.

36. Agellon, L.B., Toth, M.J., and Thomson, A.B. (2002) Intracellular Lipid Binding Proteins of the Small Intestine, *Mol. Cell. Biochem. 239*, 79–82.

37. Vassileva, G., Huwyler, L., Poirier, K., Agellon, L.B., and Toth, M.J. (2000) The Intestinal Fatty Acid Binding Protein Is Not Essential for Dietary Fat Absorption in Mice, *FASEB J. 14*, 2040–2046.

38. Smart, E.J., Graf, G.A., McNiven, M.A., Sessa, W.C., Engelman, J.A., Scherer, P.E., Okamoto, T., and Lisanti, M.P. (1999) Caveolins, Liquid-Ordered Domains, and Signal Transduction, *Mol. Cell. Biol. 19*, 7289–7304.

39. Schulthess, G., Werder, M., and Hauser, H. (2000) Receptor Mediated Lipid Uptake at the Small Intestinal Brush Border Membrane, in *Fat Digestion and Absorption* (Cristophe, A.B., and De Vriese, S., eds.), pp. 60–95, AOCS Press, Champaign.

40. Thomson, A.B.R., Clandinin, M.T., Drozdowski, L., Woudstra, T., and Wild, G. (2003) Barrier Function in Lipid Absorption, in *Encyclopedia of Gastroenterology*, Elsevier Academic Press, New York.

41. Munson, L.P. (1995) *Principles of Pharmacology: Basic Concepts & Clinical Applications*, Chapman & Hall, New York.

42. Reece, E.A. (1995) *Handbook of Medicine of the Fetus & Mother*, Lippincott, Philadelphia.

43. Angelucci, L., Patacchioli, F.R., Scaccianoce, S., Di Sciullo, A., Cardillo, A., and Maccari, S. (1985) A Model for Later-Life Effects of Perinatal Drug Exposure: Maternal Hormone Mediation, *Neurobehav. Toxicol. Teratol. 7*, 511–517.

44. Grosvenor, C.E., Picciano, M.F., and Baumrucker, C.R. (1993) Hormones and Growth Factors in Milk, *Endocr. Rev. 14*, 710–728.

45. Pacha, J. (2000) Development of Intestinal Transport Function

in Mammals, *Physiol. Rev. 80*, 1633–1667.

46. Batt, R.M., and Scott, D.J. (1982) Response of the Small Intestine Mucosa to Oral Glucocorticosteroids, *Scand. J. Gastroenterol. 74*, 75–88.

47. Croxtall, J.D., Choudhury, Q., and Flower, J. (2000) Glucocorticosteroids Act Within Minutes to Inhibit Recruitment of Signaling Factors to Activated EGF Receptors Through a Receptor-Dependent, Transcriptional-Independent Mechanism, *Br. J. Pharm. 130*, 289–298.

48. Croxtall, J.D., van Hal, P.T.W., Choudhury, Q., Gilroy, D.W., and Flower, J. (2002) Different Glucocorticoids Vary in Their Genomic and Non-genomic Mechanism of Action in A549 Cells, *Br. J. Pharm. 135*, 511–519.

49. Bamberg, C.M., Bamberg, A.M., DeCastro, M., and Chrousos, G.P. (1996) Molecular Determinants of Glucocorticoid Receptor Function and Tissue Sensitivity to Glucocorticosteroids, *Endocr. Rev. 17*, 245–261.

50. Sheppard, K.E. (2002) Nuclear Receptors. II. Intestinal Corticosteroid Receptors, *Am. J. Physiol. 282*, G742–G746.

51. Skouteris, G.G., and Schroder, C.H. (1996) The Hepatocyte Growth Factor Receptor Kinase-Mediated Phosphorilation of Lipocortin-1 Transduces the Proliferating Signal of the Hepatocyte Growth Factor, *J. Biol. Chem. 271*, 27266–27273.

52. Michel, M.C., Knapp, J., and Ratjen, H. (1994) Sensitization by Dexamethasone of Lymphocyte Cyclic AMP Formation: Evidence for Increased Function of the Adenylyl Cyclase Catalyst, *Br. J. Pharmacol. 113*, 240–246.

53. Shiau. Y.-F. (1987) Lipid Digestion and Absorption, in *Physiology of the Gastrointestinal Tract* (Johnson, L.R., ed.), pp. 584–586, Raven Press, New York.

54. Meddings, J.B. (1988) Lipid Permeability of Rat Jejunum and Ileum: Correlation with Physical Properties of the Microvillus Membrane, *Biochim. Biophys. Acta 943*, 305–314.

55. Thompson, J.S., Quigley, E.M., and Adrian, T.E. (1999) Factors Affecting Outcome Following Proximal and Distal Intestinal Resection in the Dog: An Examination of the Relative Roles of Mucosal Adaptation, Motility, Luminal Factors, and Enteric Peptides, *Dig. Dis. Sci. 44*, 63–74.

56. Thompson, J.S., and Ferguson, D.C. (2000) Effect of the Distal Remnant on Ileal Adaptation, *J. Gastrointest. Surg. 4*, 430–434.

57. Thomson, A.B.R., Drozdowski, L., Iordache, C., Vermeire, S., Clandinin, M.T., and Wild, G. (2003) Small Bowel Review: Diseases of the Small Intestine, *Dig. Dis. Sci. 48*, 1546–1599.

58. Schwarz, S.M., Hostetler, B., Ling, S., Mone, M., and Watkins, J.B. (1985) Intestinal Membrane Lipid Composition and Fluidity During Development in the Rat, *Am. J. Physiol. 248*, G200–G207.

59. Hubner, C., Lindner, S.G., Stern, M., Claussen, M., and Kohlschutter, A. (1988) Membrane Fluidity and Lipid Composition of Rat Small Intestinal Brush-Border Membranes During Postnatal Maturation, *Biochim. Biophys. Acta 939*, 145–150.

60. Thomson, A.B., Keelan, M., Garg, M., and Clandinin, M.T. (1987) Spectrum of Effects of Dietary Long-Chain Fatty Acids on Rat Intestinal Glucose and Lipid Uptake, *Can. J. Physiol. Pharmacol. 65*, 2459–2465.

61. Ferraris, R.P., and Diamond, J.M. (1989) Specific Regulation of Intestinal Nutrient Transporters by Their Dietary Substrates, *Annu. Rev. Physiol. 51*, 125–141.

62. Thomson, A.B.R., Keelan, M., Garg, M., and Clandinin, M.T. (1989) Evidence for Critical-Period Programming of Intestinal Transport Function: Variations in the Dietary Ratio of Polyunsaturated to Saturated Fatty Acids Alters Ontogeny of the Rat Intestine, *Biochim. Biophys. Acta 1001*, 302–315.

63. Jarocka-Cyrta, E., Perin, N., Keelan, M., Wierzbicki, E., Wierzbicki, T., Clandinin, M.T., and Thomson, A.B. (1998) Early Dietary Experience Influences Ontogeny of Intestine in Response to Dietary Lipid Changes in Later Life, *Am. J. Physiol. 275*, G250–G258.

64. Perin, N., Jarocka-Cyrta, E., Keelan, M., Clandinin, T., and Thomson, A. (1999) Dietary Lipid Composition Modifies intestinal Morphology and Nutrient Transport in Young Rats, *J. Pediatr. Gastroenterol. Nutr. 28*, 46–53.

Immediate No-Flow Ischemia Decreases Rat Heart Nonesterified Fatty Acid and Increases Acyl-CoA Species Concentrations

Daniel Maoz[a], Ho-Joo Lee[a], Joseph Deutsch[a,b],
Stanley I. Rapoport[a], and Richard P. Bazinet[a],*

[a]Brain Physiology and Metabolism Section, National Institute on Aging, National Institutes of Health,
Bethesda, Maryland 20892, and [b]Department of Medicinal Chemistry, David R. Bloom Center for Pharmacy,
The Hebrew University School of Pharmacy, Jerusalem, Israel

ABSTRACT: Tissues changes in FA metabolism can occur quite rapidly in response to ischemia and may require immediate microwave fixation to determine basal concentrations. The present study aimed to quantify the effects of immediate no-flow ischemia on concentrations of individual nonesterified FA (NEFA) and acyl-CoA species in the rat heart. Male CDF 344 rats were anesthetized and decapitated either 5 min prior to being microwaved (5.5 kW, 3.4 s, twice) to produce ischemia or microwaved prior to decapitation (nonischemic). Hearts were then removed and used to measure the concentrations of acyl-CoA species and FA in several lipid classes. The ischemic heart total NEFA concentration was significantly lower than that in the nonischemic heart (11.9 vs. 19.0 nmol/g). Several individual NEFA concentrations were decreased by 31–85%. Ischemic heart total long-chain acyl-CoA concentrations (21.0 nmol/g) were significantly higher than those in nonischemic hearts (11.4 nmol/g). Increased concentrations of individual acyl-CoA species occurred in palmitoyl-CoA, stearoyl-CoA, oleoyl-CoA, and linoleoyl-CoA. Concentrations of short-chain acetyl-CoA and β-hydroxy-β-methylglutaryl-CoA were also two- to threefold higher in ischemic hearts than in nonischemic hearts. The FA concentration in TG and phospholipids generally did not differ between the groups. Decreases in concentrations of individual FA and increases in acyl-CoA species during no-flow ischemia occur very rapidly within the heart. Although it is not clear how these alterations contribute to the pathogenesis of ischemia, it is evident that future studies attempting to quantify basal levels of these metabolites could use microwave fixation.
Paper no. L9834 in *Lipids 40*, 1149–1154 (November 2005).

Ischemia can be defined as a mismatch between energy supply and demand (1). A narrower, more practical definition in clinical settings is reduced blood flow to tissues. Under normal physiological conditions in the heart, FA serve as the main energy source (2,3) and as signaling molecules (4). Ischemia causes major alterations in lipid metabolism (see discussion below) that manifest as a depletion of some metabolites and accumulation of others. Because of the importance of FA in heart energy metabolism and signaling, some of these alterations in FA metabolism are believed to potentiate ischemic injury (5,6).

FA β-oxidation is rapidly inhibited with the onset of ischemia (7). This leads to a rapid accumulation of total long-chain (>12 carbon) acyl-CoA in the heart (1,8). In the brain, it is known that only the arachidonoyl (20:4n-6)-CoA level increases in response to ischemia (9,10). To the best of our knowledge individual heart acyl-CoA alterations in response to ischemia have not been reported. The precursors of heart long-chain acyl-CoA are nonesterified FA (NEFA), which originate from plasma or from cellular esterified lipid pools. Increases in heart individual NEFA concentrations have been reported in low-flow ischemia models, but this accumulation is much slower than the increase in total long-chain acyl-CoA (7,11,12).

Low-flow ischemic and isolated perfusion models have been used to study FA metabolism in the heart (13–15). Because no-flow models do not have a plasma/cellular exchange of FA and metabolites, they allow for a better understanding of intact isolated cardiac tissue metabolism in response to ischemia. Because alterations in FA metabolism are quite rapid, we used a previously published global ischemic no-flow model to better understand early alterations of FA metabolism in the heart (9,10,16–18). Early alterations may help explain alterations at longer time intervals and thus may elucidate their role in ischemic injury (2,3). We also extended a novel method for measuring individual long-chain acyl-CoA in the brain to those in the heart to characterize changes in individual long-chain acyl-CoA during no-flow ischemia (19). Whereas rapid microwave fixation has been used extensively in measuring basal lipid concentrations in the brain because it prevents artifacts from postdecapitation ischemia and residual enzyme activity during homogenization, it has not been used in the heart to measure acyl-CoA (9,16,18,20–26). Although variations of this method have been used to quantify heart acyl-CoA concentrations, the effect of ischemia on these concentrations has not been assessed (24,27,28). This method, combined with the measurement of individual FA concentrations in other pools, provides a novel approach to understanding the early regulation of FA metabolism during ischemia and may help to identify new therapeutic targets.

*To whom correspondence should be addressed at Brain Physiology and Metabolism Section, NIA, NIH; 9000 Rockville Pike, Bldg. 9, Rm. 1s 126, Bethesda, MD 20892. E-mail: rbazinet@mail.nih.gov

Abbreviations: 14:0, myristic acid; 16:0, palmitic acid; 18:0, stearic acid; 18:1n-9, oleic acid; 18:2n-6, linoleic acid; 20:4n-6, arachidonic acid; 22:6n-3, docosahexaenoic acid; CoASH, free CoA; HMG-CoA, β-hydroxy-β-methylglutaryl-CoA; NEFA nonesterified fatty acid.

METHODS AND MATERIALS

Chemicals. HPLC grade heptane, toluene, and isopropanol were purchased from EM Science (Gibbstown, NJ). Ammonium sulfate, glacial acetic acid, and diethyl ether were purchased from Mallinckrodt (Paris, KY). Reagent grade chloroform and methanol were from Mallinckrodt (Phillipsburg, NJ). HPLC grade acetonitrile was obtained from Fisher Scientific (Fair Lawn, NJ). Potassium phosphate, 2,2,4-trimethyl-pentane, and CoA standards were from Sigma-Aldrich (St. Louis, MO). Perchloric acid was purchased from Aldrich Chemicals (Milwaukee, WI).

Animals and tissue extraction. The study was conducted according to National Institutes of Health guidelines (Publication no. 80-23) and approved by the National Institute of Child Health and Human Development Animal Care and Use Committee. Male CDF-344 rats, weighing 200–250 g (Charles River; Wilmington, MA) were used. Rats were acclimatized for 5–7 d in an animal facility in which the temperature, humidity, and light cycle were controlled, and had *ad libitum* access to food (NIH-31 diet) and water. They were anesthetized with sodium pentobarbital (2.5 mg/kg, i.p.) (Abbott Laboratories, North Chicago, IL) prior to being allocated to either an ischemic or a nonischemic (control) group. Nonischemic rats were microwaved (5.5 kW, 3.4 s; Cober Electronics, Stamford, CT) to abruptly stop metabolism (9), decapitated, and the remaining carcass was microwaved a second time (5.5 kW, 3.4 s). This process rapidly "cooks" the heart, denaturing its proteins. Rats in the ischemic group were decapitated and after exactly 5 minutes were microwaved (5.5kW, 3.4 s, twice). Five minutes was chosen as this has been previously used for the brain and represents a reasonable estimate of the total time it would take from death to freezing of the heart with conventional methods. The heart continued to beat for less than 30 s in the decapitated animal. The heart was excised, separated into halves, across the midcoronal plane, and rinsed extensively in ice-cold phosphate buffered saline to remove excess blood. Tissue was then frozen in −60°C *n*-methylbutane and placed on dry ice prior to storage at −80°C.

Lipid extraction and chromatography. Total lipids were extracted from half of each heart according to the method of Folch (29). A known amount of free heptadecaenoic acid (17:0) was added as an internal standard to the total lipid extract for quantification of NEFA. TG, NEFA, and phospholipids were separated from total lipid extracts by TLC on silica gel plates (Whatman, Clifton, NJ) and separated using a mixture of heptane/diethylether/glacial acetic acid (60:40:2 by vol) (30). Bands were visualized with 6-*p*-toluidine-2-naphthalenesulfonic acid under UV light and scraped into a test tube containing toluene. A known amount of di-17:0-PC was added to the TG and phospholipid scrapings prior to methylation for quantification. FAME were formed by heating the scrapings in 1% H_2SO_4 in methanol at 70°C for 3 h. FAME were then separated on a 30 m × 0.25 mm i.d. capillary column (SP-2330; Supelco, Bellefonte, PA) using GC with an FID (Model 6890N; Agilent Technologies, Palo Alto, CA). Runs were initiated at

80°C, with a temperature gradient to 160°C (10°C/min) and 230°C (3°C/min) in 31 min, and held at 230°C for 10 min. Peaks were identified by comparison with retention times of FAME standards. FA concentrations (nmol/g tissue) were calculated by proportional comparison of GC peak areas to areas of the internal standards.

Acyl-CoA measurements. Long-chain acyl-CoA were measured in the heart according to the method of Deutsch with slight modifications (19). The heart was sliced thinly over dry ice, weighed, and along with a known amount of 17:0-CoA as an internal standard, placed in a 15-mL conical vial prior to sonicating the tissue in 25 mM potassium phosphate. Isopropanol (2 mL) was added to the vial and the homogenate was sonicated again. Saturated ammonium sulfate (0.25 mL) was added and the sample was lightly shaken by hand. Acetonitrile (4 mL) was added and the sample was vortexed for 10 min prior to centrifugation. The upper phase was extracted and 10 mL of 25 mM potassium phosphate was added. Each sample was run three times through an activated oligonucleotide purification cartridge (Applied Biosystems, Foster City, CA), washed with 10 mL of 25 mM potassium phosphate, and eluted with 400 μL isopropanol/1 mM glacial acetic acid (75:25 vol/vol). Samples were dried under nitrogen and reconstituted in 100 μL isopropanol/1 mM glacial acetic acid (75:25 vol/vol) for HPLC analysis. Acyl-CoA species were separated using HPLC (Beckman, Fullerton, CA) with a Symmetry C-18 5-μm column (250 × 4.6 mm; Waters-Millipore Corp., Milford, MA), and UV absorbance was measured at 260 and 280 nm with a System Gold 168 dual wavelength detector. Conditions were set to a 1 mL/min gradient system composed of (A) 75 mM potassium phosphate and (B) 100% acetonitrile. The gradient started with 44% B and 66% A, and was then increased to 49% B over 25 min and then to 70% B over 5 min; it remained at 70% B for 9 min and returned to 44% over 4 min, and was held there for 4 min (end of run). Concentrations of acyl-CoA species (nmol/g wet weight) were identified according to the retention times of authentic standards and measured using peak area analysis (32 Karat, version 5.0; Beckman Coulter, Fullerton, CA) from HPLC chromatograms.

Short-chain acyl-CoA were extracted according to the method of Deutsch with slight modifications (31). Hearts were sliced over dry ice and weighed, and a known amount of propionyl-CoA (internal standard) and 6% perchloric acid were added to the sample prior to homogenization followed by sonication. This step was followed by vortexing the samples and centrifugation at 1050 × *g* for 5 min. The liquid phase was extracted and 75 mM potassium phosphate was added. Each sample was manually passed twice through an activated oligonucleotide purification cartridge. The cartridge was then washed with 75 mM potassium phosphate and the short-chain acyl-CoA were eluted with 4% isopropanol in 25 mM potassium phosphate containing 16% methanol. The samples were stored at −80°C until analyzed by HPLC. The above-mentioned processes were carried out over ice and all the solutions were ice-cold. HPLC conditions were a 1 mL/min gradient system composed of (A) 75 mM potassium phosphate and (B) 100%

acetonitrile. The gradient started with 4% B; it was increased to 7% B over 5 min and then to 9% B over 4 min, then returned to 4% B over 1 min and remained at 4% B for 4 more min. It was then increased to 12% B over 1 min and then to 20% B over 10 min. Afterward, it was increased to 60% B over 2 min and then reduced to 4% B over 2 more min, where it was held for 16 min. Peaks were identified by comparing the retention times with those of purchased acyl-CoA standards, with the exception of glutathione CoA (see next paragraph). The peak areas were integrated using 32 Karat, version 5.0 (Beckman Coulter) software, and short-chain acyl-CoA were identified according to the retention times of authentic standards. Concentrations (nmol/g heart wet weight) were calculated by the proportional comparison of HPLC peak areas to the area of the propionyl-CoA internal standard.

Reduced glutathione-CoA was prepared by the anhydride method using oxalyl chloride (32). In a glass test tube containing reduced glutathione (Sigma) and methylene chloride (1 mL), an equimolar amount of oxalyl chloride was added and incubated at room temperature for 2 h with occasional stirring. After 1 h, the methylene chloride solution was dried under a steady stream of nitrogen at 45°C and redissolved in *t*-butanol. The dissolved oxalyl glutathione anhydride was mixed with CoA to form reduced glutathione-CoA.

Statistics. Unpaired, two-tailed *t*-tests were used to compare means between ischemic and nonischemic animals (v. 9.0; SAS, Cary, NC) and statistical significance was taken as $P \leq$ 0.05. Data are presented as means ± SD.

RESULTS

NEFA. The total measured NEFA concentration of the ischemic heart was 33% lower than that of the nonischemic heart ($P <$ 0.001) (Table 1). There was no statistical difference in myristic acid (14:0) concentrations between the ischemic and nonischemic heart. Concentrations of all other measured NEFA, palmitic acid (16:0), stearic acid (18:0), oleic acid (18:1n-9), linoleic acid (18:2n-6), 20:4n-6, and DHA (22:6n-3), were significantly lower (32, 31, 46, 73, 68, and 85% for 16:0, 18:0, 18:1n-9, 18:2n-6, 20:4n-6, and 22:6n-3, respectively) in the ischemic heart, compared with the nonischemic heart.

Long-chain acyl-CoA. Total measured long-chain acyl-CoA were significantly higher (84%) in the ischemic heart compared with the nonischemic heart (Table 2). The concentrations of saturated CoA species, 16:0-CoA and 18:0-CoA, were 75 and 146% higher in the ischemic heart compared with the nonischemic heart. The concentration of 18:1n-9-CoA was 88% higher in the ischemic heart than in the nonischemic heart. The concentration of 18:2n-6-CoA was the only other measured polyunsaturated CoA species that was significantly higher in the ischemic heart compared with the nonischemic heart (71%). Consistent with a previous report, 22:6n-3-CoA was not detected (28).

TG and phospholipids. There was no difference in the measured TG total FA concentration between the ischemic and nonischemic heart (16390 ± 5279 vs. 13210 ± 2855 nmol/g for the ischemic and nonischemic heart, respectively, $P = 0.18$). In

addition, there were no changes in individual TG FA concentrations, except for 18:0, which was significantly higher in the ischemic heart (2203 ± 318) compared with the nonischemic heart (1427 ± 234 nmol/g, $P < 0.001$). There was also no significant difference in the phospholipid total FA concentrations, or in any individual esterified FA concentration.

Short-chain acyl-CoA. Measured, total short-chain acyl-CoA concentrations did not differ between the two groups (74.9 ± 16.8 vs. 66.7 ± 16.5 nmol/g in the ischemic vs. nonischemic heart). The glutathione-CoA level was significantly lower (46%) in the ischemic heart compared with the nonischemic heart (Table 3). There was no significant difference in

TABLE 1
Nonesterified FA (NEFA) Concentration of Nonischemic and Ischemic Rat Hearts[a]

FA	Nonischemic (nmol/g wet weight)	Ischemic (nmol/g wet weight)
Myristic acid (14:0)	1.69 ± 0.38	2.05 ± 1.07
Palmitic acid (16:0)	6.27 ± 1.48	4.23 ± 0.64 **
Stearic acid (18:0)	3.91 ± 0.57	2.70 ± 0.40 ***
Oleic acid (18:1n-9)	2.59 ± 0.64	1.39 ± 0.37 ***
Linoleic acid (18:2n-6)	2.35 ± 0.74	0.65 ± 0.11 ***
Arachidonic acid (20:4n-6)	0.48 ± 0.21	0.15 ± 0.06 ***
Docosahexaenoic acid (22:6n-3)	0.35 ± 0.25	0.05 ± 0.02 *
Sum of FA	19.03 ± 3.05	11.90 ± 1.64 ***

[a]Data are mean ± SD, $n = 8$ samples per group. *$P < 0.05$, **$P < 0.01$, ***$P < 0.001$ vs. nonischemic.

TABLE 2
Long-Chain Acyl-CoA Concentration of Nonischemic and Ischemic Rat Hearts[a]

FA	Nonischemic (nmol/g wet weight)	Ischemic (nmol/g wet weight)
Myristoyl-CoA (14:0-CoA)	0.63 ± 0.36	0.90 ± 0.35
Palmitoyl-CoA (16:0-CoA)	3.25 ± 1.84	5.67 ± 1.20 **
Stearoyl-CoA (18:0-CoA)	1.83 ± 0.68	4.52 ± 1.98 **
Oleoyl-CoA (18:1n-9-CoA)	3.16 ± 1.42	5.94 ± 2.19 **
Linoleoyl-CoA (18:2n-6-CoA)	1.99 ± 1.11	3.41 ± 1.07 *
Arachidonoyl-CoA (20:4n-6-CoA)	0.54 ± 0.17	0.54 ± 0.32
Sum of acyl-CoA	11.40 ± 5.09	20.98 ± 6.53 **

[a]Data are mean ± SD, $n = 8$ samples per group. *$P < 0.05$, **$P < 0.01$ vs. nonischemic.

TABLE 3
Short-Chain Acyl-CoA Concentration of Nonischemic and Ischemic Rat Hearts[a]

FA	Nonischemic (nmol/g wet weight)	Ischemic (nmol/g wet weight)
Glutathione-CoA	8.97 ± 2.85	4.84 ± 1.62 **
CoASH	47.98 ± 18.24	41.76 ± 14.71
HMG-CoA	0.80 ± 0.29	1.52 ± 0.53 **
Acetyl-CoA	8.97 ± 3.55	26.76 ± 8.85 ***

[a]Data are mean ± SD, $n = 8$ samples per group. **$P < 0.01$, ***$P < 0.001$ vs. nonischemic. CoASH, free CoA; HMG-CoA, β-hydroxy-β-methylglutaryl-CoA.

the free CoA (CoASH) concentration in the ischemic vs. non-ischemic heart. β-Hydroxy-β-methylglutaryl-CoA (HMG-CoA) was 89% higher in the ischemic rat heart compared with the nonischemic heart. The acetyl-CoA concentration was 198% higher in the ischemic heart compared with the nonischemic heart.

DISCUSSION

Several myocardial lipid pools are significantly altered in various ischemic models (5,8,13,33). In general, these models differ from that of the current study with respect to the use of different species and the degree and duration of ischemia. In the current study, we examined the immediate stages of no-flow ischemia to better understand this process. Ischemic alterations related to lipid metabolism are due to the cessation of oxygen-consuming processes (i.e., β-oxidation, oxidative respiration) leading to an accumulation of intermediate products from the affected processes. The 197% higher acetyl-CoA concentration in the ischemic rat heart in the current study is consistent with a decrease in oxidative respiration. It has been reported that total long-chain acyl-CoA levels increase shortly after the onset of ischemia (1,8). Our results show for the first time that increases in some individual long-chain acyl-CoA are of a magnitude of 71–146%. The total measured CoA (acyl and free) were higher in ischemic hearts (97.8 ± 18.6) compared with nonischemic hearts (78.1 ± 13.1, $P < 0.05$, data not shown). Although this result may explained by a rapid increase in CoA synthesis, as seen in other models (34,35), it would be important to measure other CoA sources to further test this hypothesis.

The role of long-chain acyl-CoA accumulation in ischemic damage and/or protection is not yet clear (5). Their amphiphilic characteristics are thought to damage membranes and activate lysosomes (13,36,37). In addition, long-chain acyl-CoA have been shown to inhibit adenine nucleotide translocase (38) and Na-K-ATPase (39). Nevertheless, there is evidence that these adverse effects may not occur *in vivo*, mainly due to compartmentalization of the long-chain acyl-CoA (5,33). Conversely, the accumulation of long-chain acyl-CoA in ischemia may also have a protective role. This has been attributed to their ability to facilitate opening of the KATP channel, which results in potassium efflux from the cell followed by reduced contractility and therefore reduced energy requirements (40,41).

Individual NEFA concentrations decreased by 31–85% (excluding 14:0). Several groups have reported that NEFA actually increased during ischemia (1,33). However, these later studies measured NEFA after 45 min to 1 h of ischemia (7,11). Studies of shorter duration (10-min ischemia) also showed that NEFA did not increase (11,42) and some NEFA were even decreased (11). NEFA are supplied to the heart from either exogenous (plasma NEFA and possibly lipoproteins) or endogenous (TG and phospholipids) sources (3,12). Since we used a no-flow model, the supply from exogenous sources could be excluded. Therefore, it seems likely that in our model, NEFA were activated by an acyl-CoA synthetase prior to any alterations in TG or phospholipid metabolism. The decrease in

NEFA was roughly proportional to the increase in long-chain acyl-CoA, further supporting this notion. Unlike the brain, which accumulates predominantly 20:4n-6 and 20:4n-6-CoA during ischemia, increases in the heart FA and acyl-CoA species are more proportional (9,21). During brain ischemia (unlike the heart), glutamate is released, causing an increase in the activities of the 20:4n-6 selective calcium-dependent cytosolic and secretory phospholipase A_2, thus releasing 20:4n-6 from neural membranes (43,44).

TG are a prominent storage pool and the main NEFA source in the absence of exogenous (plasma) NEFA (3,45). NEFA contribute most of the myocardial energy supply under normal physiological conditions (2). In the current study, there was no statistically significant change in cardiac FA TG concentrations after 5 min of no-flow ischemia (except for 18:0). These results are broadly consistent with publications suggesting that TG do not change during early ischemia (7,11) but accumulate following prolonged (30- to 60-min) ischemia (46–48). Similarly, we found no effect of ischemia on the FA concentrations of esterified phospholipid FA. Similar to TG, changes in heart phospholipids are believed to occur over several hours of ischemia (49).

Previous work in low-flow models suggests that CoASH levels decrease during ischemia (13), whereas in our study there was a nonsignificant 23% decrease. A possible explanation for this discrepancy might be that low-flow models continue to provide NEFA as a substrate for acyl-CoA synthetases, resulting in a larger depletion in heart CoASH. In our study, acetyl-CoA levels were almost threefold higher in the ischemic group. A low-flow pig heart ischemic model demonstrated a transient increase in acetyl-CoA over the first minute, followed by a decrease and stabilization to one-third of its original concentration (50). Because acetyl-CoA does enter the tricarboxylic acid cycle during ischemia, it is possible that it is being shunted toward cholesterol synthesis or other pathways, thus explaining the observed increase in HMG-CoA concentration in the ischemic rat heart (51,52). An increase in the amount of acetyl-CoA would also be expected to produce malonyl-CoA, causing inhibition of carnitine palmitoyl transeferase-1 and further inhibition of β-oxidation (51,52).

No-flow heart ischemia can be viewed as a state of cessation of oxygen-demanding processes while at the same time the energy (ATP) level is sufficient to maintain many of the nonoxygen-based pathways. One of these energy-demanding pathways is the activation of NEFA to fatty acyl-CoA (requiring one mole of ATP per mole of acyl-CoA formed) (53,54), which continues to take place despite ischemia. This is possible, as during ischemia, heart ATP and creatine phosphate concentrations are slowly depleted over time (11,50,55).

In summary, the onset of changes in FA metabolism in the no-flow ischemic model of the heart are quite rapid and vary in magnitude between lipid classes and individual acyl species. They do not necessarily reflect changes observed in long-term ischemia and low-flow models. How these changes relate to the pathophysiology of ischemia and whether they can be targeted for the treatment of ischemia remain to be explored. Future investigations attempting to quantify basal heart NEFA and acyl-

CoA (but not phospholipid or TG) concentrations should take into consideration that tissues that are not rapidly fixed could be altered. Microwaving the heart of living animals is one method of rapidly fixing the tissue to prevent artifacts in acyl-CoA and NEFA from residual enzyme activity after ischemia and during the homogenization process. A better understanding of the true basal concentration of these lipids will be useful in understanding their role in a variety of models.

REFERENCES

1. Neely, J.R., and Feuvray, D. (1981) Metabolic Products and Myocardial Ischemia, *Am. J. Pathol. 102*, 282–291.
2. Saddik, M., and Lopaschuk, G.D. (1991) Myocardial Triglyceride Turnover and Contribution to Energy Substrate Utilization in Isolated Working Rat Hearts, *J. Biol. Chem. 266*, 8162–8170.
3. Lewin, T.M., and Coleman, R.A. (2003) Regulation of Myocardial Triacylglycerol Synthesis and Metabolism, *Biochim. Biophys. Acta 1634*, 63–75.
4. Van Bilsen, M., and Van der Vusse, G.J. (1995) Phospholipase-A_2-Dependent Signalling in the Heart, *Cardiovasc. Res. 30*, 518–529.
5. Hutter, J.F., and Soboll, S. (1992) Role of Fatty Acid Metabolites in the Development of Myocardial Ischemic Damage, *Int. J. Biochem. 24*, 399–403.
6. de Groot, M.J., Coumans, W.A., Willemsen, P.H., and van der Vusse, G.J. (1993) Substrate-Induced Changes in the Lipid Content of Ischemic and Reperfused Myocardium. Its Relation to Hemodynamic Recovery, *Circ. Res. 72*, 176–186.
7. van der Vusse, G.J., Prinzen, F.W., van Bilsen, M., Engels, W., and Reneman, R.S. (1987) Accumulation of Lipids and Lipid-Intermediates in the Heart During Ischaemia, *Basic Res. Cardiol. 82* (*Suppl. 1*), 157–167.
8. Eaton, S. (2002) Control of Mitochondrial β-Oxidation Flux, *Prog. Lipid Res. 41*, 197–239.
9. Deutsch, J., Rapoport, S.I., and Purdon, A.D. (1997) Relation Between Free Fatty Acid and Acyl-CoA Concentrations in Rat Brain Following Decapitation, *Neurochem. Res. 22*, 759–765.
10. Rabin, O., Deutsch, J., Grange, E., Pettigrew, K.D., Chang, M.C., Rapoport, S.I., and Purdon, A.D. (1997) Changes in Cerebral Acyl-CoA Concentrations Following Ischemia-Reperfusion in Awake Gerbils, *J. Neurochem. 68*, 2111–2118.
11. van Bilsen, M., van der Vusse, G.J., Willemsen, P.H., Coumans, W.A., Roemen, T.H., and Reneman, R.S. (1989) Lipid Alterations in Isolated, Working Rat Hearts During Ischemia and Reperfusion: Its Relation to Myocardial Damage, *Circ. Res. 64*, 304–314.
12. Corr, P.B., Gross, R.W., and Sobel, B.E. (1984) Amphipathic Metabolites and Membrane Dysfunction in Ischemic Myocardium, *Circ. Res. 55*, 135–154.
13. Whitmer, J.T., Idell-Wenger, J.A., Rovetto, M.J., and Neely, J.R. (1978) Control of Fatty Acid Metabolism in Ischemic and Hypoxic Hearts, *J. Biol. Chem. 253*, 4305–4309.
14. Trach, V., Buschmans-Denkel, E., and Schaper, W. (1986) Relation Between Lipolysis and Glycolysis During Ischemia in the Isolated Rat Heart, *Basic Res. Cardiol. 81*, 454–464.
15. Henderson, A.H., Most, A.S., Parmley, W.W., Gorlin, R., and Sonnenblick, E.H. (1970) Depression of Myocardial Contractility in Rats by Free Fatty Acids During Hypoxia, *Circ. Res. 26*, 439–449.
16. Deutsch, J., Rapoport, S.I., and Rosenberger, T.A. (2002) Coenzyme A and Short-Chain Acyl-CoA Species in Control and Ischemic Rat Brain, *Neurochem. Res. 27*, 1577–1582.
17. Bazinet, R.P., Rao, J.S., Chang, L., Rapoport, S.I., and Lee, H.J. (2005) Chronic Valproate Does Not Alter the Kinetics of Do-cosahexaenoic Acid Within Brain Phospholipids of the Unanesthetized Rat, *Psychopharmacology (Berlin) 182*, 180–185.
18. Bazinet, R.P., Lee, H.J., Felder, C.C., Porter, A.C., Rapoport, S.I., and Rosenberger, T.A. (2005) Rapid High-Energy Rapid Microwave Fixation Is Required to Determine the Anandamide (*N*-arachidonoylethanolamine) Concentration of Rat Brain, *Neurochem. Res. 30*, 597–601.
19. Deutsch, J., Grange, E., Rapoport, S.I., and Purdon, A.D. (1994) Isolation and Quantitation of Long-Chain Acyl-Coenzyme A Esters in Brain Tissue by Solid-Phase Extraction, *Anal. Biochem. 220*, 321–323.
20. Anton, R.F., Wallis, C., and Randall, C.L. (1983) *In vivo* Regional Levels of PGE and Thromboxane in Mouse Brain: Effect of Decapitation, Focused Microwave Fixation, and Indomethacin, *Prostaglandins 26*, 421–429.
21. Bazan, N.G., Jr. (1970) Effects of Ischemia and Electroconvulsive Shock on Free Fatty Acid Pool in the Brain, *Biochim. Biophys. Acta 218*, 1–10.
22. Bosisio, E., Galli, C., Galli, G., Nicosia, S., Spagnuolo, C., and Tosi, L. (1976) Correlation Between Release of Free Arachidonic Acid and Prostaglandin Formation in Brain Cortex and Cerebellum, *Prostaglandins 11*, 773–781.
23. Deutsch, J., Kalderon, B., Purdon, A.D., and Rapoport, S.I. (2000) Evaluation of Brain Long-Chain Acylcarnitines During Cerebral Ischemia, *Lipids 35*, 693–696.
24. Golovko, M.Y., and Murphy, E.J. (2004) An Improved Method for Tissue Long-Chain Acyl-CoA Extraction and Analysis, *J. Lipid Res. 45*, 1777–1782.
25. Miller, J.M., Jope, R.S., Ferraro, T.N., and Hare, T.A. (1990) Brain Amino Acid Concentrations in Rats Killed by Decapitation and Microwave Irradiation, *J. Neurosci. Methods 31*, 187–192.
26. Kurooka, S., Hosoki, K., and Yoshimura, Y. (1972) Some Properties of Long Fatty Acyl-Coenzyme A Thioesterase in Rat Organs, *J. Biochem. (Tokyo) 71*, 625–634.
27. Tardi, P.G., Mukherjee, J.J., and Choy, P.C. (1992) The Quantitation of Long-Chain Acyl-CoA in Mammalian Tissue, *Lipids 27*, 65–67.
28. Molaparast-Saless, F., Shrago, E., Spennetta, T.L., Donatello, S., Kneeland, L.M., Nellis, S.H., and Liedtke, A.J. (1988) Determination of Individual Long-Chain Fatty Acyl-CoA Esters in Heart and Skeletal Muscle, *Lipids 23*, 490–492.
29. Folch, J., Lees, M., and Sloane Stanley, G.H. (1957) A Simple Method for the Isolation and Purification of Total Lipides from Animal Tissues, *J. Biol. Chem. 226*, 497–509.
30. Skipski, V.P., Good, J.J., Barclay, M., and Reggio, R.B. (1968) Quantitative Analysis of Simple Lipid Classes by Thin-Layer Chromatography, *Biochim. Biophys. Acta 152*, 10–19.
31. Grange, E., Deutsch, J., Smith, Q.R., Chang, M., Rapoport, S.I., and Purdon, A.D. (1995) Specific Activity of Brain Palmitoyl-CoA Pool Provides Rates of Incorporation of Palmitate in Brain Phospholipids in Awake Rats, *J. Neurochem. 65*, 2290–2298.
32. Deutsch, J., Rapoport, S.I., and Rosenberger, T.A. (2003) Valproyl-CoA and Esterified Valproic Acid Are Not Found in Brains of Rats Treated with Valproic Acid, but the Brain Concentrations of CoA and Acetyl-CoA Are Altered, *Neurochem. Res. 28*, 861–866.
33. van der Vusse, G.J., Glatz, J.F., Stam, H.C., and Reneman, R.S. (1992) Fatty Acid Homeostasis in the Normoxic and Ischemic Heart, *Physiol. Rev. 72*, 881–940.
34. Fisher, M.N., Robishaw, J.D., and Neely, J.R. (1985) The Properties and Regulation of Pantothenate Kinase from Rat Heart, *J. Biol. Chem. 260*, 15745–15751.
35. Robishaw, J.D., and Neely, J.R. (1985) Coenzyme A Metabolism, *Am. J. Physiol. 248*, E1–E9.
36. Brecher, P. (1983) The Interaction of Long-Chain Acyl CoA with Membranes, *Mol. Cell. Biochem. 57*, 3–15.

37. Katz, A.M., and Messineo, F.C. (1981) Lipid–Membrane Interactions and the Pathogenesis of Ischemic Damage in the Myocardium, *Circ. Res. 48*, 1–16.

38. Shrago, E. (1978) The Effect of Long Chain Fatty Acyl CoA Esters on the Adenine Nucleotide Translocase and Myocardial Metabolism, *Life Sci. 22*, 1–5.

39. Owens, K., Kennett, F.F., and Weglicki, W.B. (1982) Effects of Fatty Acid Intermediates on Na$^+$-K$^+$-ATPase Activity of Cardiac Sarcolemma, *Am. J. Physiol. 242*, H456–H461.

40. Schulze, D., Rapedius, M., Krauter, T., and Baukrowitz, T. (2003) Long-Chain Acyl-CoA Esters and Phosphatidylinositol Phosphates Modulate ATP Inhibition of KATP Channels by the Same Mechanism, *J. Physiol. 552*, 357–367.

41. Liu, G.X., Hanley, P.J., Ray, J., and Daut, J. (2001) Long-Chain Acyl-Coenzyme A Esters and Fatty Acids Directly Link Metabolism to K(ATP) Channels in the Heart, *Circ. Res. 88*, 918–924.

42. Prinzen, F.W., Van der Vusse, G.J., Arts, T., Roemen, T.H., Coumans, W.A., and Reneman, R.S. (1984) Accumulation of Nonesterified Fatty Acids in Ischemic Canine Myocardium, *Am. J. Physiol. 247*, H264–H272.

43. Balsinde, J., Winstead, M.V., and Dennis, E.A. (2002) (Phospholipase A$_2$ Regulation of Arachidonic Acid Mobilization, *FEBS Lett. 531*, 2–6.

44. Bazan, N.G., Allan, G., and Rodriguez de Turco, E.B. (1993) Role of Phospholipase A$_2$ and Membrane-Derived Lipid Second Messengers in Membrane Function and Transcriptional Activation of Genes: Implications in Cerebral Ischemia and Neuronal Excitability, *Prog. Brain Res. 96*, 247–257.

45. Olson, R.E., and Hoeschen, R.J. (1967) Utilization of Endogenous Lipid by the Isolated Perfused Rat Heart, *Biochem. J. 103*, 796–801.

46. Straeter-Knowlen, I.M., Evanochko, W.T., den Hollander, J.A., Wolkowicz, P.E., Balschi, J.A., Caulfield, J.B., Ku, D.D., and Pohost, G.M. (1996) ^{1}H NMR Spectroscopic Imaging of Myocardial Triglycerides in Excised Dog Hearts Subjected to 24 Hours of Coronary Occlusion, *Circulation 93*, 1464–1470.

47. Bruce, T.A., and Myers, J.T. (1973) Myocardial Lipid Metabolism in Ischemia and Infarction, *Recent Adv. Stud. Cardiac Struct. Metab. 3*, 773–780.

48. Burton, K.P., Buja, L.M., Sen, A., Willerson, J.T., and Chien, K.R. (1986) Accumulation of Arachidonate in Triacylglycerols and Unesterified Fatty Acids During Ischemia and Reflow in the Isolated Rat Heart. Correlation with the Loss of Contractile Function and the Development of Calcium Overload, *Am. J. Pathol. 124*, 238–245.

49. Chien, K.R., Han, A., Sen, A., Buja, L.M., and Willerson, J.T. (1984) Accumulation of Unesterified Arachidonic Acid in Ischemic Canine Myocardium. Relationship to a Phosphatidylcholine Deacylation-Reacylation Cycle and the Depletion of Membrane Phospholipids, *Circ. Res. 54*, 313–322.

50. Salem, J.E., Saidel, G.M., Stanley, W.C., and Cabrera, M.E. (2002) Mechanistic Model of Myocardial Energy Metabolism Under Normal and Ischemic Conditions, *Ann. Biomed. Eng. 30*, 202–216.

51. McGarry, J.D., Leatherman, G.F., and Foster, D.W. (1978) Carnitine Palmitoyltransferase I. The Site of Inhibition of Hepatic Fatty Acid Oxidation by Malonyl-CoA, *J. Biol. Chem. 253*, 4128–4136.

52. Lopaschuk, G.D., and Gamble, J. (1994) The 1993 Merck Frosst Award. Acetyl-CoA Carboxylase: An Important Regulator of Fatty Acid Oxidation in the Heart, *Can. J. Physiol. Pharmacol. 72*, 1101–1109.

53. Hisanaga, Y., Ago, H., Nakagawa, N., Hamada, K., Ida, K., Yamamoto, M., Hori, T., Arii, Y., Sugahara, M., Kuramitsu, S., *et al.* (2004) Structural Basis of the Substrate-Specific Two-Step Catalysis of Long Chain Fatty Acyl-CoA Synthetase Dimer, *J. Biol. Chem. 279*, 31717–31726.

54. Waku, K. (1992) Origins and Fates of Fatty Acyl-CoA Esters, *Biochim. Biophys. Acta 1124*, 101–111.

55. Opie, L.H. (1976) Effects of Regional Ischemia on Metabolism of Glucose and Fatty Acids. Relative Rates of Aerobic and Anaerobic Energy Production During Myocardial Infarction and Comparison with Effects of Anoxia, *Circ. Res. 38*, I52–I74.

Synthesis of Dihydroperoxides of Linoleic and Linolenic Acids and Studies on Their Transformation to 4-Hydroperoxynonenal

Claus Schneider[a], William E. Boeglin[a], Huiyong Yin[a,b], Donald F. Stec[b], David L. Hachey[a], Ned A. Porter[b], and Alan R. Brash[a],*

[a]Department of Pharmacology, Vanderbilt University Medical School, and
[b]Department of Chemistry, Vanderbilt University, Nashville, Tennessee 37232

ABSTRACT: The cytotoxic aldehydes 4-hydroxynonenal, 4-hydroperoxynonenal (4-HPNE), and 4-oxononenal are formed during lipid peroxidation *via* oxidative transformation of the hydroxy or hydroperoxy precursor fatty acids, respectively. The mechanism of the carbon chain cleavage reaction leading to the aldehyde fragments is not known, but Hock-cleavage of a suitable dihydroperoxide derivative was implicated to account for the fragmentation [Schneider, C., Tallman, K.A., Porter, N.A., and Brash, A.R. (2001) Two Distinct Pathways of Formation of 4-Hydroxynonenal. Mechanisms of Nonenzymatic Transformation of the 9- and 13-Hydroperoxides of Linoleic Acid to 4-Hydroxyalkenals, *J. Biol. Chem. 275*, 20831–20838]. Both 8,13- and 10,13-dihydroperoxyoctadecadienoic acids (diHPODE) could serve as precursors in a Hock-cleavage leading to 4-HPNE *via* two different pathways. Here, we synthesized diastereomeric 9,12-, 10,12-, and 10,13-diHPODE using singlet oxidation of linoleic acid. 8,13-Dihydroperoxyoctadecatrienoic acid was synthesized by vitamin E-controlled autoxidation of γ-linolenic acid followed by reaction with soybean lipoxygenase. The transformation of these potential precursors to 4-HPNE was studied under conditions of autoxidation, hematin-, and acid-catalysis. In contrast to 9- or 13-HPODE, neither of the dihydroperoxides formed 4-HPNE on autoxidation (lipid film, 37°C), regardless of whether the free acid or the methyl ester derivative was used. Acid treatment of 10,13-diHPODE led to the expected formation of 4-HPNE as a significant product, in accord with a Hock-type cleavage reaction. We conclude that, although the suppression of 4-H(P)NE formation from monohydroperoxides by α-tocopherol indicates peroxyl radical reactions in the major route of carbon chain cleavage, the dihydroperoxides previously implicated are not intermediates in the autoxidative transformation of monohydroperoxy fatty acids to 4-HPNE and related aldehydes.

Paper no. L9855 in *Lipids 40*, 1155–1162 (November 2005).

Oxidative cleavage of polyunsaturated fatty acids during lipid peroxidation gives rise to a diverse array of aldehydes with considerable bioactivity (1–3). Among the most prominent and well-studied are the cytotoxic aldehydes 4-hydroxynonenal (4-HNE), 4-hydroperoxynonenal (4-HPNE), 4-oxononenal, and 4-hydroxyhexenal (4–8). As the free aldehydes, these products can deplete cellular GSH through adduct formation leading to apoptosis (9). They also have the potential to interfere with cell cycle events and to manipulate protein expression (10,11). Membrane phospholipids and LDL carrying short-chain aldehydes esterified to the PC head group have been shown to promote entry of monocytes into the vessel wall (12,13). In the progression of atherosclerosis, they can also serve as potent ligands for the macrophage scavenger receptor CD36, actively promoting uptake of the oxidized lipids and ultimately leading to the transformation of macrophages into foam cells (14). Therefore, insights into the mechanisms of aldehyde formation during lipid peroxidation can advance our understanding of the etiology of atherogenesis and other diseases associated with oxidative stress. Notwithstanding this significance for mammalian pathophysiology, the precise chemical mechanisms responsible for carbon chain cleavage and aldehyde formation during lipid autoxidation have yet to be determined.

A chemical mechanism for carbon chain cleavage of hydroperoxy fatty acids is the Hock rearrangement (15,16). Although this reaction generally requires catalysis by acid, it could mechanistically account for formation of the aldehyde fragments observed during autoxidation of hydroxy- and hydroperoxy fatty acids. We have shown before that the 13-hydroperoxy group of 13S-hydroperoxyoctadecadienoic acid (HPODE) is not involved in the cleavage of the C9–C10 carbon bond during transformation of 13S-HPODE to 4S-HPNE (17). Therefore, we proposed the formation of a 10,13-dihydroperoxide intermediate that could undergo a Hock-type of cleavage reaction to explain the retention of chirality of the hydroperoxy group during transformation (17). Assuming a similar mechanism, an equivalent 10-hydroperoxy-13-hydroxy intermediate could account for the observed cleavage of 13S-hydroxyoctadecadienoic acid (HODE) into 4S-HNE (18). In the case of 13-HPODE, two intermediates that theoretically could Hock-fragment into 4-HPNE are the 10,13- and 8,13-dihydroperoxides of linoleic acid (Fig. 1). Starting with 13-HPODE, the common initiating step for the two pathways suggested in Figure 1 is a hydrogen abstraction at C8 leading to a delocalized radical that is oxygenated to the hydroperoxide at

*To whom correspondence should be addressed at Dept. of Pharmacology, Vanderbilt University, 23rd Ave. at Pierce, Nashville, TN 37232-6602.
E-mail: alan.brash@vanderbilt.edu

Abbreviations: CID collision-induced dissociation; HETE, hydroxyeicosatetraenoic acid; HODE, hydroxyoctadecadienoic acid; H(P)NE, 4-hydro(pero)xy-2*E*-nonenal; HPODE, hydroperoxyoctadecadienoic acid; HPOTE, hydroperoxyoctadecatrienoic acid.

either carbons 10 or 8, yielding either a 10,13- or a 8,13-dihydroperoxide. From there, the two pathways diverge. In pathway A, 10,13-diHPODE is proposed to Hock-cleave between carbons 9 and 10 directly yielding 4-HPNE and 9-oxononanoic acid (Fig. 1) (17). In the second pathway that is newly proposed here, 8,13-diHPODE is projected to Hock-cleave between carbons 8 and 9 to yield a 10-carbon enol, 5-hydroperoxydeca-1,3*E*-dien-1-ol, or the tautomeric aldehyde, 5-hydroperoxy-3*E*-decenal (Fig. 1, pathway B). This enol is presumed to be highly unstable and is subject to immediate oxygenation at C2 resulting in decarboxylation to give 4-HPNE and formic acid. Here we synthesized several isomeric dihydroperoxide derivatives of C_{18} unsaturated fatty acids and studied their potential toward transformation into 4-HPNE under various conditions.

EXPERIMENTAL PROCEDURES

Synthesis of HPODE substrates. 13*S*-HPODE was synthesized using soybean lipoxygenase (type V; Sigma, St. Louis, MO) as described before (19). DiHPODE methyl esters were synthesized by singlet oxidation of methyl linoleate (15,20). Methyl linoleate, 1 g, and 1 mg of methylene blue were dissolved in 25 mL of methanol and transferred to a photochemistry apparatus equipped with a water cooling jacket, an oxygen gas supply, and a 500 W halogen lamp. The reaction was set up in a cold room at 4°C and allowed to proceed for 15 h. For sample workup, a 10-mL aliquot of the crude reaction was diluted with the same volume of methanol, and 10 mL of water was added in 1-mL aliquots while vortexing. The solution was loaded onto five 1-g C18 Mega Bond Elut cartridges (Varian), and seven 2-

mL fractions each were collected upon elution with MeOH/water 80:20 (vol/vol). Aliquots (5 µL) of the fractions were analyzed by UV spectroscopy to monitor product elution. The second fraction contained products with only end absorbance in the UV, and these were further separated by RP-HPLC using a Waters Symmetry C18 column (0.46 × 25 cm; Waters, Milford, MA) eluted with MeOH/water 70:30 (vol/vol) at a flow rate of 1 mL/min and with UV detection at 205 nm. Six peaks of isomeric diHPODE methyl esters were collected and extracted with methylene chloride. The products were stored in MeOH at −20°C until further use.

Synthesis of 8,13-dihydroperoxy-6Z,9Z,11E-octadecatrienoic acid. γ-Linolenic acid methyl ester, 200 mg, and α-tocopherol, 600 mg, were dissolved in 10 mL of methylene chloride (21). The mixture was transferred to a 1-L round-bottomed flask, the solvent was evaporated, and the residue was flushed with oxygen. Autoxidation was carried out at 37°C for 5 d with daily flushing with oxygen. The reaction mixture was then fractionated on a 25-g silica open bed column at 4°C. The column was eluted with 500 mL hexane/ethyl acetate (100:2.5, vol/vol) and 500 mL hexane/ethyl acetate (100:5, vol/vol). The 100:5 fractions were pooled and evaporated. The sample was injected on RP-HPLC using a Waters Symmetry C18 7-µm column (1.9 × 30 cm) eluted with acetonitrile/water (70:30, vol/vol) at a flow rate of 10 mL/min with UV detection at 205 nm. Five fractions were collected, evaporated to approximately half volume under a stream of nitrogen, and extracted with methylene chloride. The first and second peaks, containing the bis-allylic hydroperoxides, were hydrolyzed using KOH as described below. Both products were reacted with soybean lipoxygenase in a UV
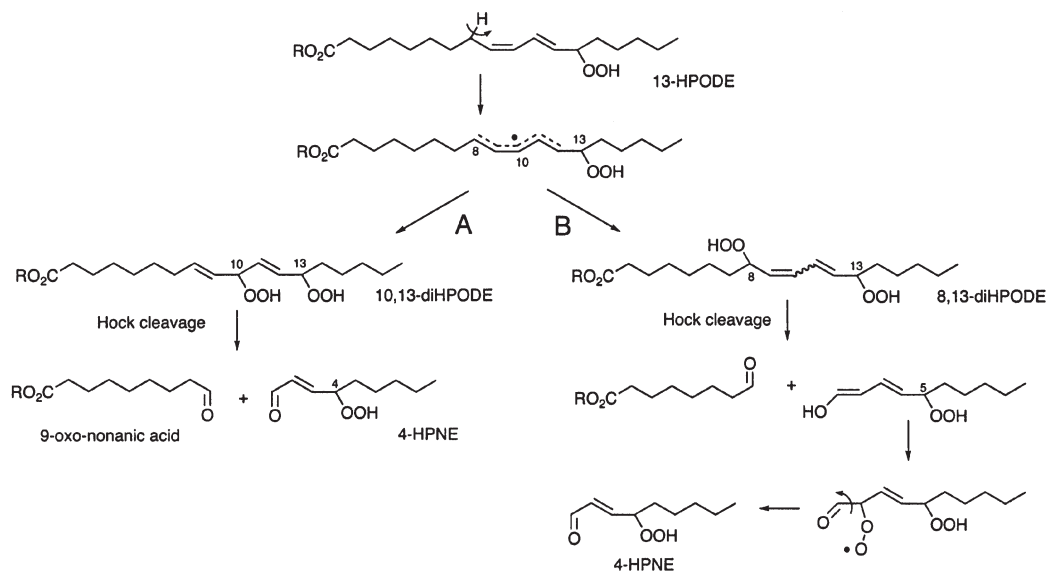
FIG. 1. Two mechanistic hypotheses on the transformation of 13-hydroperoxyoctadecadienoic acid (HPODE) to 4-hydroperoxy-2*E*-nonenal (HPNE) *via* Hock cleavage of 10,13-diHPODE and 8,13-diHPODE intermediates. In mechanism (A), C8 hydrogen abstraction is followed by trapping of the carbon-centered radical at C10, formation of the hydroperoxide, and Hock cleavage of the C9–C10 carbon bond to form 4-HPNE and 9-oxononanoic acid. In (B), an 8,13-diHPODE is formed that cleaves into 8-oxo-octanoic acid and a 10-carbon dienol product that is prone to oxygenation at C2. Loss of formic acid from the intermediate peroxyl radical yields 4-HPNE. R is H or CH_3.

cuvette. Only the product in the first RP-HPLC peak reacted with the enzyme and was therefore identified as the bis-allylic 8-hydroperoxide (the second peak containing the 11-hydroperoxide does not react with soybean lipoxygenase).

8-Hydroperoxy-6Z,9Z,12Z-octadecatrienoic acid, 500 µg, was dissolved in 50 mL of 100 mM K_2HPO_4 buffer at room temperature. Several 10-µL portions of soybean lipoxygenase (type V; Sigma) were added over the course of 1 h, and aliquots of the reaction were monitored in the UV for the increase in absorbance at 235 nm. When no further increase in absorbance was observed, the mixture was acidified to pH 6 using 1 N HCl and KH_2PO_4. Products were extracted using methylene chloride and washed with water twice. 8,13-Dihydroperoxy-6Z,9Z,11E-octadecatrienoic acid was isolated by HPLC using a Whatman Partisil 5 µm column eluted with hexane/isopropanol/HOAc (100:4:0.1, by vol) at a flow rate of 1 mL/min and UV detection at 235 nm. The product was used immediately for autoxidation reactions.

Hydrolysis of diHPODE methyl esters. For hydrolysis of methyl esters, the substrates (0.5–1 mg) were placed in 3 mL of methanol, and 300 µL of methylene chloride was added. KOH (3 mL of a 1 M solution) was added, and the mixture was vortexed vigorously and sonicated. After standing at room temperature for 30 min, the reaction was placed on ice and the following cold reagents were added for extraction: 4.5 mL of methylene chloride, 1.5 mL 1 M KH_2PO_4, and 2.5 mL of 1 N HCl, bringing the pH to 6. The organic layer was washed with water twice and evaporated to dryness. The residue was dissolved in 1 mL methanol. RP-HPLC analyses were used to determine completeness of the hydrolysis.

Autoxidation reactions. Hydroperoxide substrates, 1 or 5 µg, were transferred to 1.5-mL plastic reaction tubes and evaporated from solvent. The tubes were placed in an oven at 37°C for the time indicated. After the reaction, 30 µL of column solvent was added, and the entire mixture was injected on RP-HPLC with diode array detection (model 1100; Agilent, Palo Alto, CA). For RP-HPLC a Waters Symmetry C18 column (0.46 × 25 cm) was eluted with acetonitrile/water/HOAc (60:40:0.01, by vol) at a flow rate of 1 mL/min. Some of the reactions were analyzed using methanol/water/HOAc (75:25:0.01, by vol) at a flow rate of 1 mL/min as the mobile phase. The decomposition of 13S-HPODE and 13S-HPODE methyl ester (5 µg for each data point) was quantified by comparing the remaining peak height (235 nm) after autoxidation relative to the initial peak height of the starting material. 4-HPNE was quantified by comparison of the peak height at 220 nm with a standard curve of 4-HNE (5–100 ng) injected on RP-HPLC.

Hematin reaction. 10,13-DiHPODE, 2 µg, was dissolved in 50 µL of water. A freshly prepared hematin solution in 1 mM NaOH was added to a final concentration of 5 µM. The mixture was incubated at room temperature for 5 min and then extracted using the Bligh and Dyer method (22). The entire reaction was injected on a Waters Symmetry C18 column (0.46 × 25 cm) eluted with acetonitrile/water/HOAc (60:40:0.01, by vol) at a flow rate of 1 mL/min and monitored using a diode array detector.

GC–MS and LC–MS. For GC–MS analysis, the crude frac-

tion from the open bed column containing the diHPODE methyl esters was reduced using $NaBH_4$. The products were separated using a Beckman Si 5 µm column (0.46 × 25 cm; Beckman, Fullerton, CA) eluted with hexane/isopropanol (100:3, vol/vol) at a flow rate of 1 mL/min with UV detection at 205 nm. The collected products were converted to the trimethylsilyl ethers by treatment with *N,O*-bis(trimethylsilyl) trifluoroacetamide in pyridine. For GC–MS a Thermo Finnigan DCQ system was used equipped with an Rtx-1701 fused-silica capillary column (17 m × 0.25 mm i.d.; Restek Corp., Bellefonte, PA). Samples were injected at 150°C, and after 1 min the temperature was programmed to 300°C at 10 or 20°C/min.

LC–MS was performed using a Thermo Finnigan LC Quantum instrument. A Waters Symmetry C18 column (0.46 × 25 cm) was eluted with MeOH/H_2O/HOAc (75:25:0.01, by vol, containing 0.15 mM $AgBF_4$) at 1 mL/min, and the column effluent was split in a 5:1 ratio into a UV detector (205 nm) and the electrospray ionization interface. The heated capillary ion lens was operated at 220°C. Nitrogen was used as a nebulization and desolvation gas. The electrospray potential was held at 4 kV. Source-induced dissociation was set at –10 eV. Mass spectra were acquired over the mass range *m/z* 100–600 at 2 s/scan. Collision-induced dissociation (CID) was performed at –15 eV.

NMR spectroscopy. ^{1}H and H,H-COSY NMR spectra were recorded in benzene-d_6 on a Bruker Avance DRX 400 MHz or 500 MHz spectrometer. Chemical shifts are reported relative to δ = 7.24 ppm for the residual protons.

9,12-Dihydroperoxy-10E,13E-octadecadienoic acid methyl ester (**1**). ^{1}H NMR, C_6D_6, 400 MHz; δ 7.57, *s*, 1H, OOH; δ 7.31, *s*, 1H, OOH; δ 5.89, *dd*, *J* = 15.8/6.5 Hz, 1H, H13; δ 5.80, *m*, 2H, H14, H10; δ 5.59, *dd*, *J* = 15.5 Hz/7.0 Hz, 1H, H11; δ 4.89, *dd*, *J* = 6.6 Hz, 1H, H12; δ 4.34, *q*, *J* = 6.7 Hz, 1H, H9; δ 3.43, *s*, 3H, OCH_3; δ 2.19, *t*, *J* = 6.5 Hz, 2H, H2; δ 1.99, *q*, *J* = 6.7 Hz, 2H, H15. EI-MS, methyl ester, TMS-ether: *m/z* 73 (100, rel. abundance), 259 (33), 223 (30), 155 (27), 211 (16), 313 (15), 380 (6), 439 (2), 455 (1).

9,12-Dihydroperoxy-10E,13E-octadecadienoic acid methyl ester (**5**). ^{1}H NMR, C_6D_6, 400 MHz; δ 7.50, *s*, 1H, OOH; δ 7.40, *s*, 1H, OOH; δ 5.87, *dd*, *J* = 15.7 Hz/6.7 Hz, 1H, H13; δ 5.77, *m*, 2H, H14, H10; δ 5.56, *dd*, *J* = 15.5 Hz/7.1 Hz, 1H, H11; δ 4.88, *dd*, *J* = 6.8 Hz, 1H, H12; δ 4.33, *q*, *J* = 6.8 Hz, 1H, H9; δ 3.44, *s*, 3H, OCH_3; δ 2.17, *t*, *J* = 7.4 Hz, 2H, H2; δ 1.99, *q*, *J* = 6.6 Hz, 2H, H15. EI-MS, methyl ester, TMS-ether: 73 (100), 259 (32), 223 (30), 155 (26), 211 (16), 313 (14), 380 (5), 439 (2), 455 (1).

10,13-Dihydroperoxy-8E,11E-octadecadienoic acid methyl ester (**2**). ^{1}H NMR, C_6D_6, 400 MHz; δ 7.51, *s*, 1H, OOH; δ 7.47, *s*, 1H, OOH; δ 5.89, *dd*, *J* = 15.8 Hz/6.2 Hz, 1H, H9; δ 5.85, *dd*, *J* = 15.4 Hz/6.8 Hz, 1H, H12; δ 5.76, *dt*, *J* = 15.8 Hz/7.0 Hz, 1H, H8; δ 5.59, *dd*, *J* = 15.5 Hz/7.1 Hz, 1H, H11; δ 4.89, *dd*, *J* = 6.6 Hz, 1H, H10; δ 4.35, *q*, *J* = 6.6 Hz, 1H, H13; δ 3.43, *s*, 3H, OCH_3; δ 2.16, *t*, *J* = 7.4 Hz, 2H, H2; δ 1.97, *dt*, *J* = 6.8 Hz, 2H, H7. EI-MS, methyl ester, TMS-ether: 73 (100), 173 (53), 309 (15), 297 (10), 399 (9), 237 (6), 380 (5), 439 (2), 455 (1).

10,13-Dihydroperoxy-8E,11E-octadecadienoic acid methyl ester (**6**). ^{1}H NMR, C_6D_6, 400 MHz; δ 7.55, *s*, 1H, OOH; δ 7.48, *s*, 1H, OOH; δ 5.88, *dd*, *J* = 15.8 Hz/6.6 Hz, 1H, H9; δ 5.78, *dd*,

J = 15.6 Hz/7.2 Hz, 1H, H12; δ 5.74, *dt*, *J* = 15.0 Hz/7.0 Hz, 1H, H8; δ 5.57, *dd*, *J* = 15.6 Hz/7.1 Hz, 1H, H11; δ 4.89, *dd*, *J* = 6.8 Hz, 1H, H10; δ 4.34, *q*, *J* = 6.6 Hz, 1H, H13; δ 3.43, *s*, 3H, OCH₃; δ 2.16, *t*, *J* = 7.4 Hz, 2H, H2; δ 1.96, *dt*, *J* = 7.0 Hz, 2H, H7. EI-MS, methyl ester, TMS-ether: 73 (100), 173 (56), 309 (15), 297 (10), 399 (9), 237 (6), 380 (5), 439 (2), 455 (1).

10,12-Dihydroperoxy-8*E*,13*E*-octadecadienoic acid methyl ester (**3**). ¹H NMR, C₆D₆, 400 MHz; δ 7.62, *s*, 1H, OOH; δ 7.53, *s*, 1H, OOH; δ 5.74–5.64, *m*, 2H, H8, H14; δ 5.48, *m*, 2H, H9, H13; δ 4.68, *dt*, *J* = 7.1 Hz/6.8 Hz, 2H, H10, H12; δ 3.43, *s*, 3H, OCH₃; δ 2.17, *t*, *J* = 7.3 Hz, 2H, H2; δ 2.03–1.93, *m*, 6H, H15, H11, H7. EI-MS, methyl ester, TMS-ether: 73 (100), 185 (72), 237 (44), 129 (41), 271 (31), 323 (27), 380 (4), 413 (1), 455 (<1), 470 (<1).

10,12-Dihydroperoxy-8*E*,13*E*-octadecadienoic acid methyl ester (**4**). ¹H NMR, C₆D₆, 400 MHz; δ 7.62, *s*, 1H, OOH; δ 7.48, *s*, 1H, OOH; δ 5.80–5.64, *m*, 2H, H8, H14; δ 5.50, *m*, 2H, H9, H13; δ 4.62, *m*, 2H, H10, H12; δ 3.43, *s*, 3H, OCH₃; δ 2.33, *ddd*, *J* = 14.3 Hz/7.4 Hz, 1H, H11a; δ 2.17, *t*, *J* = 7.2 Hz, 2H, H2; δ 1.97, *m*, 4H, H15, H7; δ 1.74, *ddd*, *J* = 14.4 Hz/6.0 Hz, 1H, H11b. EI-MS, methyl ester, TMS-ether: 73 (100), 185 (82), 237 (45), 129 (44), 271 (38), 323 (28), 380 (4), 413 (1), 455 (<1), 470 (<1).

8,13-Dihydroperoxy-6*Z*,9*Z*,11*E*-octadecatrienoic acid. ¹H NMR, CDCl₃, 400 MHz; δ 6.64, *dd*, *J* = 14.8 Hz/11.7 Hz, 1H, H10; δ 6.22, *m*, 1H, H9; δ 5.72, *m*, 2H, H11, H12; δ 5.61, *dd*, *J* = 8.9 Hz, 1H, H7; δ 5.43, *dd*, *J* = 9.9 Hz, 1H, H8; δ 5.37, *t*, *J* = 9.8 Hz, 1H, H6; δ 4.42, *m*, 1H, H13.

RESULTS

Formation of 4-HPNE from 13S-HPODE and from 13S-HPODE methyl ester. We compared the time course of formation of 4-HPNE during autoxidation of the free acid and the methyl ester derivative of 13*S*-HPODE to investigate the influence of the carboxylate group on the carbon chain cleavage reaction. Aliquots of both substrates (5 μg each) were autoxidized separately for 1, 2, 3, and 4 h and analyzed by RP-HPLC. As shown in Figure 2, the rate of decay of the free acid 13*S*-HPODE was about twice as fast as the rate of the methyl ester in these experiments. Nevertheless, their efficiency in formation of 4-HPNE was comparable, since about 50% decay of 5 μg of either HPODE precursor led to the accumulation of about 15 ng 4-HPNE (1.2% molar yield).

When a mixture of 5 μg each of 13*S*-HPODE and 13*S*-HPODE methyl ester was autoxidized, both decayed at the same rate (Fig. 2C). This rate was intermediate compared with the rates observed in the separate reactions, implying that the different rates observed in the separate reactions were due to a difference in the abundance of initiating radicals in the substrate preparations. Thus, 13*S*-HPODE and the methyl ester of 13*S*-HPODE are equally efficient precursors to 4-HPNE formation.

Synthesis of linoleic acid dihydroperoxides. The 9,12-, 10,12-, and 10,13-dihydroperoxides were synthesized by singlet oxidation of linoleic acid methyl ester. Initial separation on a C18 Bond Elute cartridge gave a pooled fraction of the

polar dihydroperoxides that was resolved from the monohydroperoxides. This mixture was injected on analytical RP-HPLC, and six peaks with end absorbance in the UV were detected (products **1**—**6**) (Fig. 3A). The same HPLC system was used for semipreparative isolation of the six dihydroperoxide products. An aliquot of the crude sample was reduced with NaBH₄ and resolved using straight-phase HPLC (Fig. 3B), and the individual dihydroxy methyl ester products were reacted to the TMS ether derivatives and analyzed by GC–MS in the EI mode. The MS fragmentation patterns were used to define the location of the hydroxy groups along the carbon chain. Together with the ¹H NMR data, the six peaks were identified as the diastereomers of the 9,12- (**1** and **5**), 10,12- (**3** and **4**), and 10,13- (**2** and **6**) dihydroperoxides of linoleic acid methyl ester (Fig. 3C). The absolute configuration of the hydroperoxide groups in the different isomers was not determined. For use in
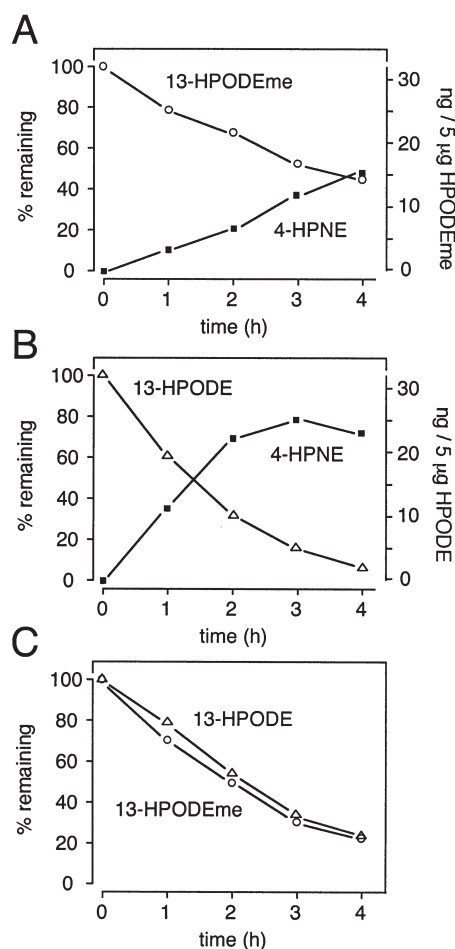

FIG. 2. Time course of transformation of 13*S*-HPODE and 13*S*-HPODE methyl ester (me) into 4-HPNE. Five micrograms each per time point of (A) 13*S*-HPODE methyl ester, (B) 13*S*-HPODE, and (C) a mixture of both were autoxidized at 37°C for the time indicated. The decay of 13*S*-HPODE methyl ester (○), 13*S*-HPODE (△), and the formation of 4-HPNE (■) was quantified using RP-HPLC and comparison of the peak heights. The mean of two independent experiments with virtually identical results is shown. For other abbreviations see Figure 1.
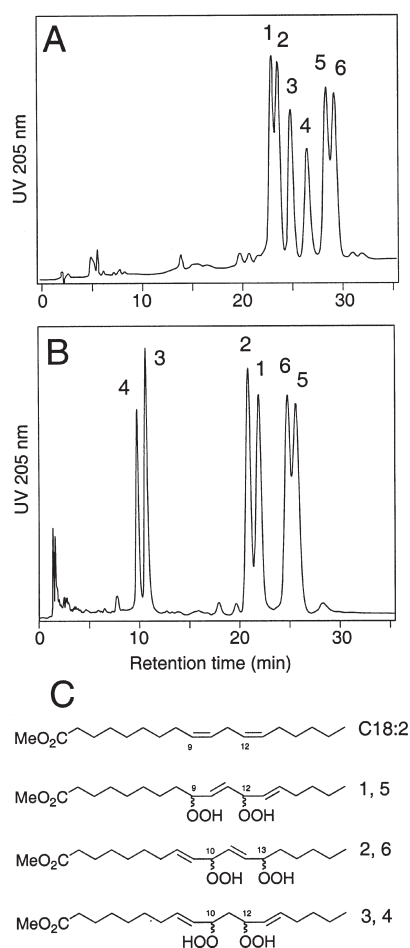
FIG. 3. HPLC analysis of diHPODE methyl esters **1–6** synthesized by singlet oxidation of linoleic acid methyl ester. DiHPODE methyl esters were prepared by singlet oxidation of linoleic acid methyl ester as described in the Experimental Procedures section. (A) RP-HPLC analysis of a crude fraction of diHPODE methyl esters using a Waters Symmetry C18 column (0.46 × 25 cm; Waters, Milford, MA) eluted with MeOH/water 70:30 (vol/vol) at a flow rate of 1 mL/min; (B) SP-HPLC analysis of a crude fraction of diHPODE methyl esters after reduction with NaBH$_4$. A Beckman Ultrasphere Si 5 μm column (0.46 × 25 cm; Beckman, Fullerton, CA) was eluted with hexane/isopropanol (100:3, vol/vol) at a flow rate of 2 mL/min. Both chromatograms were recorded at 205 nm. (C) The products are: **1** and **5**, 9,12-diHPODEme; **2** and **6**, 10,13-diHPODEme; **3** and **4**, 10,12-diHPODEme. For abbreviations see Figures 1 and 2.

some of the autoxidation reactions, the methyl esters were hydrolyzed to the free acids using a protocol for mild hydrolysis to avoid degradation of the hydroperoxide groups.

Autoxidation of 10,13-diHPODE and 9,12-diHPODE. 10,13-DiHPODE (**2** or **6**) is a potential precursor to autoxidative formation of 4-HPNE, whereas 9,12-diHPODE (**1** or **5**) was used for comparison as substrate that is assumed not to form 4-HPNE on cleavage (Fig. 1) (17). Aliquots (5 μg) of the methyl ester derivatives of both diHPODE were autoxidized as a dry lipid film at 37°C for 1, 2, and 3 h, and then analyzed by RP-HPLC with diode array detection. The reaction conditions were similar to those used before in the transformation of 13-
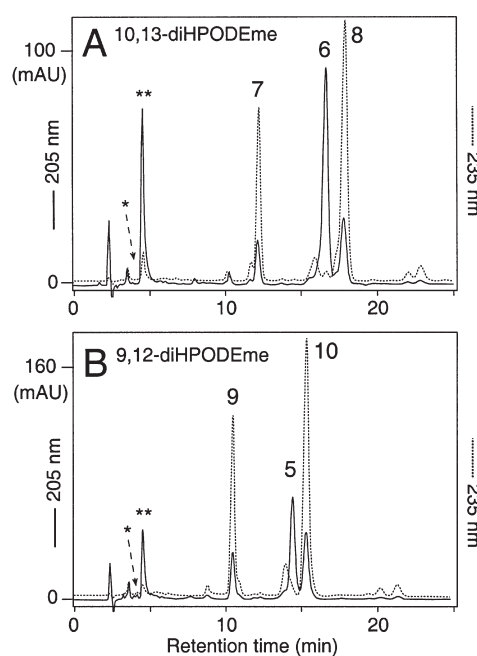
FIG. 4. Autoxidation of the methyl ester derivatives of 10,13-diHPODE **6** and 9,12-diHPODE **5**. (A) 5 μg 10,13-diHPODE (methyl ester, **6**) and (B) 5 μg 9,12-diHPODE (methyl ester, **5**) were autoxidized as a dry film at 37°C for 3 h and analyzed by RP-HPLC with diode array detection. The reactions were analyzed using a Waters Symmetry C18 column (0.46 × 25 cm) eluted with methanol/water/HOAc (75:25:0.01, by vol) at a flow rate of 1 mL/min. A product with retention time and UV spectrum similar to 4-HPNE was not detected in either of the reactions. The single asterisk (*) marks the retention time of 4-HPNE. The double asterisk (**) marks a solvent artifact peak. Solid line, UV 205 nm; dashed line, UV 235 nm. For abbreviations see Figures 1 and 2; for manufacturer see Figure 3.

HPODE to 4-HPNE, and 15-hydroxyeicosatetraenoic acid (HETE) to 4-HNE (17,18). Figure 4 shows a representative HPLC analysis after 3 h of autoxidation. Both the 10,13- and the 9,12-dihydroperoxides rearranged each into two products **7**, **8**, and **9**, **10**, respectively, with identical UV spectra that were characteristic of *trans,trans*-conjugated diene chromophores (λ_{max} = 231 nm) (17,23). The products were further analyzed using LC-coordination (Ag$^+$) ion spray-MS (24). LC-MS revealed molecular adduct ions [M + Ag$^+$] of *m/z* 465 and 467 for the 9,12- and 10,13-diHPODE (methyl ester) starting compounds as well as for each of the two main metabolites, respectively. This is compatible with a M.W. of 358 (methyl ester derivative) and implies that both allylic diHPODE rearranged into a pair of diastereomeric conjugated diHPODE.

On CID in the presence of Ag$^+$, the 10,13-diHPODE (methyl ester **6**, *m/z* 465) gave two main fragments at *m/z* 293 and 305, resulting from a Hock-fragmentation of the C9–C10 and C10–C11 carbon bonds, respectively. Two less abundant fragments were found at *m/z* 347 and 377 representing cleavage of the C12–C13 and C13–C14 bonds, respectively. This fragmentation pattern is therefore compatible with the hydroperoxy groups located at carbons 10 and 13. The conjugated rearrangement products **7** and **8** gave identical mass spectra
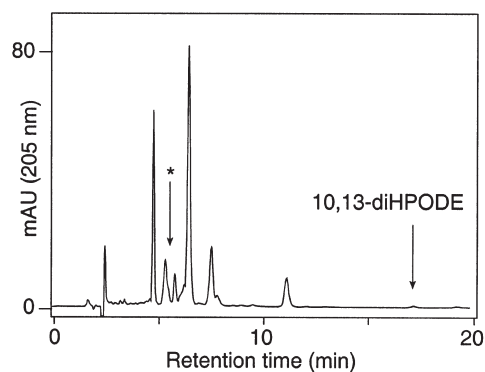
FIG. 6. Hematin-catalyzed transformation of 10,13-diHPODE **2**. 10,13-DiHPODE **2**, 2 µg, was dissolved in 50 µL of water and treated with 5 µM hematin at room temperature for 5 min. Following extraction, the entire reaction was injected on RP-HPLC using conditions as in Figure 3 and diode array detection. The asterisk marks the retention time of 4-HPNE. For abbreviations see Figure 1.

FIG. 5. Acid-catalyzed transformation of the methyl ester derivatives of 10,13-diHPODE **2** and 9,12-diHPODE **1**. (A) 10,13-DiHPODE methyl ester **6**, 2 µg dissolved in 5 µL methanol, was treated with 1.5 µL 1 N HCl at 37°C for 1 h. (B) 9,12-diHPODE methyl ester **5**, 2 µg, was treated as in (A). For RP-HPLC analysis a Waters Symmetry C18 column (0.46 × 25 cm) was eluted with acetonitrile/water/HOAc (60:40:0.01, by vol) at a flow rate of 1 mL/min and monitored using a diode array detector. The chromatograms shown were recorded at UV 205 nm. The asterisk (*) in panel (B) marks a product eluting at about the retention time of 4-HPNE but with a different UV spectrum. For abbreviations see Figure 1; for manufacturer see Figure 3.

with a main product ion at *m/z* 279 resulting from a Hock-fragmentation of the C8-C9 bond, indicating a hydroperoxy group at C8. The product ion *m/z* 377 was also found in both spectra, indicating the presence of the 13-hydroperoxide group. The fragmentation patterns together with the UV data indicate that the main transformation products **7** and **8** of 10,13-diHPODE (methyl ester) are a pair of diastereomeric 8,13-dihydroperoxy-9*E*,11*E*-octadecadienoic acid methyl esters.

CID of the 9,12-diHPODE (methyl ester **5**, *m/z* 465) gave a major product ion at *m/z* 293. A product ion *m/z* 293 was also obtained by CID of the two conjugated rearrangement products **9** and **10**. In each of the three spectra, *m/z* 293 is derived from Hock-cleavage of the C9–C10 carbon bond, also indicating the presence of a 9-hydroperoxy group in the rearrangement products. In contrast to the 9,12-diHPODE starting material, the rearrangement products **9** and **10** showed a product ion of *m/z* 391 resulting from cleavage of the C14–C15 bond indicating the presence of a 14-hydroperoxy group. Thus, the two rearrangement products **9** and **10** of 9,12-diHPODE (methyl ester) were identified as a pair of diastereomeric 9,14-dihydroperoxy-10*E*,12*E*-octadecadienoic acid methyl esters. Products **7**–**10** are the methyl ester equivalents to the free acid products that had been isolated before as transformation products during autoxidation of 13-HPODE and 9-HPODE, respectively (17).

In the autoxidation reactions, neither the 10,13- nor the 9,12-diHPODE (methyl ester) formed a product with retention

time and UV spectrum similar to 4-HPNE (or 4-HNE) (Fig. 4). The autoxidation reactions were repeated in the presence of equimolar amounts of linoleic acid or 15*S*-HETE (to have a free carboxylate group in the reaction and to efficiently generate peroxyl radicals) and also with the 10,13-diHPODE free acid after hydrolysis of the methyl ester. Neither of the substrates or reaction conditions led to detectable formation of 4-HPNE in the HPLC analyses.

Acid-catalyzed transformation of 10,13-diHPODE and 9,12-diHPODE. To the dry lipid film of the 10,13- and 9,12-diHPODE, respectively, was added 1.5 µL of 1 N HCl immediately before the autoxidation. After 1 h of incubation at 37°C, the reactions were analyzed directly using RP-HPLC with diode array detection (Fig. 5). Under the strongly acidic conditions, the 10,13-diHPODE (methyl ester) gave a prominent cleavage product that was identical in retention time and UV spectrum with an authentic standard of 4-HPNE (Fig. 5A). As judged by the UV/diode array analyses, 4-HPNE was the major detectable transformation product formed on acid-catalyzed transformation of 10,13-diHPODE (methyl ester) (8% molar yield). The 9,12-diHPODE (methyl ester) gave two tentative cleavage products, and as expected, both products were different from 4-HPNE. The earlier product had a UV spectrum similar to 4-HPNE (λ_{max} 219 nm) but eluted 0.5 min earlier (Fig. 5B). The smaller peak differed in the UV spectrum and eluted just after 4-HPNE.

Treatment of 10,13-diHPODE with hematin. Hematin has been shown to induce the rearrangement of fatty acid hydroperoxides into epoxyalcohols and other hydroxy and keto derivatives (23,25). We therefore tested its ability to induce cleavage of the dihydroperoxide into aldehyde fragments. The free acid 10,13-diHPODE, 2 µg (product **6**), was dissolved in 50 µL of water and treated with 5 µM hematin at room temperature for 5 min. In pilot experiments, this concentration of hematin was found to be sufficient to degrade 5 µg of 15*S*-hydroperoxyeicosatetraenoic acid under similar conditions within 5 min. RP-HPLC analysis confirmed that this treatment was sufficient to transform the dihydroperoxide substrate **6** completely into sev-
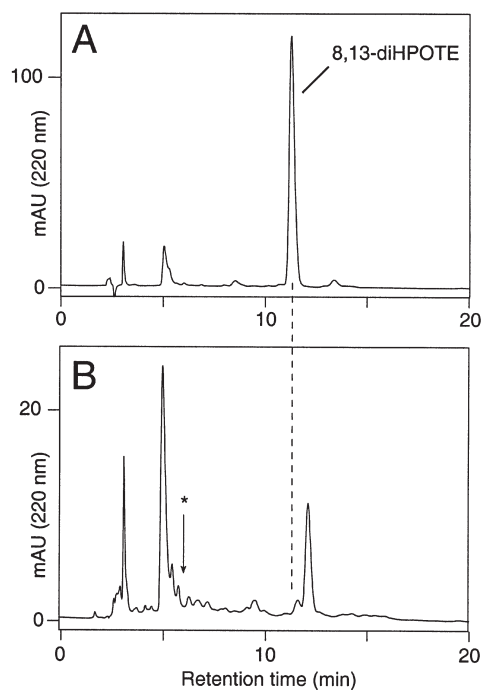
FIG. 7. Autoxidation of 8,13-dihydroperoxyoctadecatrienoic acid (di-HPOTE). Aliquots of 8,13-diHPOTE, 2 μg each, were analyzed (A) before and (B) after 90 min of autoxidation at 37°C as a dry lipid film. The reactions were analyzed using a Waters Symmetry C18 column (0.46 × 25 cm) eluted with methanol/water/HOAc (70:30:0.01, by vol) at a flow rate of 1 mL/min with monitoring using a diode array detector. The chromatograms shown were recorded at 220 nm. The asterisk (*) marks the retention time of 4-HPNE. For other abbreviation see Figure 1; for manufacturer see Figure 3.

eral products of differing polarity (Fig. 6). Neither 4-HPNE nor 4-HNE was detected among these or the less abundant products, indicating that hematin does not induce the Hock-type cleavage required for formation of these aldehydes.

Synthesis of 8,13-dihydroperoxy-6Z,9Z,11E-octadecatrienoic acid (8,13-diHPOTE). 8,13-DiHPOTE was synthesized by first generating the bis-allylic 8-hydroperoxy-6Z,9Z,12Z-octadeca-trienoic acid methyl ester using vitamin E-controlled autoxida-tion of γ-linolenic acid methyl ester (21). A 300% excess (w/w) of α-tocopherol was sufficient to trap the bis-allylic 8- and 11-hydroperoxides as abundant products during autoxidation (26). Following isolation of the 8-hydroperoxide by HPLC and hy-drolysis of the methyl ester, the second hydroperoxy group at C13 was introduced by reaction with soybean lipoxygenase. Since soybean lipoxygenase shows chiral discrimination for a hydroxy group at the C5 carbon relative to the position of oxy-genation (Brash, A.R., unpublished observations), only one pos-sible diastereomer was formed in the enzymatic reaction. The final product, 8,13-dihydroperoxy-6Z,9Z,11*E*-octadecatrienoic acid, appeared to be very labile and required HPLC purification immediately prior to the autoxidation experiments.

Autoxidation of 8,13-diHPOTE. Aliquots of 8,13-di-HPOTE, 2 μg each, were autoxidized as a dry film for 30, 60, and 90 min and analyzed by the RP-HPLC method with diode array detection (Fig. 7). The 8,13-diHPOTE rapidly degraded

over the course of 90 min, but 4-HPNE was not detected among the transformation products.

DISCUSSION

We have previously proposed a mechanism that could account for the retention of chirality in the autoxidative transformation of 13*S*-HPODE into 4*S*-HPNE, and, likewise, for the transfor-mation of the hydroxy analog, 13*S*-HODE, into 4*S*-HNE, again with retention of the configuration (17,18). Here we have tested a crucial step of this mechanism together with a new proposal also routed through dihydroperoxides as the key intermediate (Fig. 1). Both mechanisms entail a Hock cleavage of a suitable dihydroperoxide leading to two aldehyde fragments. One of our main conclusions from the studies reported here is that di-hydroperoxides of linoleic acid are not intermediates in the au-toxidative pathway leading from 13*S*-H(P)ODE to 4*S*-H(P)NE. In using our standard autoxidation conditions (under which both 9- and 13-HPODE give rise to 4-HPNE), the synthesized 10,13- and 8,13-dihydroperoxides were not transformed into 4-HPNE in any detectable yield.

In fact, under autoxidation conditions, the 10,13-diHPODE rearranged to the thermodynamically more stable conjugated 8,13-diHPODE. The likely pathway entails facile conversion of the 10-hydroperoxide to a 10-peroxyl radical. The 10-peroxyl is then readily cleaved to a carbon radical and molecular oxygen (β-fragmentation), followed by rotation of the carbon chain into the *trans* configuration, reoxygenation at C-8, and trapping as the 8,13-diHPODE (17). This rearrangement is particularly favored when the peroxyl resides in a bis-allylic carbon, C-10 in this ex-ample. The 8,13-diHPODE with a *trans,trans* conjugated diene is found as an autoxidation product from 13-HPODE, and it likely arises *via* formation of a C-10 peroxyl, rather than a 10-hydroperoxide. Study of the on-off rates for molecular oxygen onto the different positions of an activated pentadiene radical shows that the off reaction (β-fragmentation) at the bis-allylic position is 5000 times faster than at the 1- and 5-positions (26). This means that the bis-allylic hydroperoxide is unlikely to be detectable unless in the presence of an efficient peroxyl trapping agent such as α-tocopherol.

The Hock reaction is catalyzed by protic or Lewis acids and involves migration of one of the alkyl groups to the protonated hydroperoxy oxygen followed by loss of water. The resulting hemiacetal is unstable, adds back water, and hydrolyzes into the two fragments (15,16). Hock cleavage of alkyl hydroper-oxides can also occur by thermal decomposition in the GC in-jection port (27), or it can be induced by the presence of silver ions in LC–MS (24). In accord with the proposed mechanism of Hock cleavage, we found that 10,13-diHPODE is trans-formed into 4-HPNE when a small amount of acid is present in the autoxidation reactions. The observed cleavage is compati-ble with the Hock mechanism and shows that the proposed pathway is a conceivable possibility under certain experimen-tal conditions.

Under our standard autoxidation conditions of a thin film of hydroperoxide starting material, 13-HPODE is observed to

cleave between the 9,10 and the 12,13 carbons to give rise to C9 and C12 4-hydroperoxyalkenals, respectively, and 9-HPODE also gives C9 and C12 products through directly equivalent reactions (17). Addition of 5% α-tocopherol was observed to block the 9,10 cleavage from 13-HPODE (and the equivalent reaction from 9-HPODE), yet formation of aldehyde products resulting from a chain cleavage next to the hydroperoxide was still observed (17). The α-tocopherol-insensitive route to 4-hydroperoxyalkenals has yet to be explained, and under these conditions a Hock cleavage remains as a theoretical possibility, accounting for a slow rate of aldehyde formation over time without the catalytic acceleration by acid.

Finally, we have shown that the methyl ester derivative of 13-HPODE is an equally efficient precursor for 4-HPNE formation as the free acid 13-HPODE. Therefore, the fatty acid carboxylate does not act as the "acid" catalyzing a Hock reaction. We conclude that the significance of using the methyl ester derivatives compared with the free carboxylate of the fatty acid starting materials is mechanistically negligible because both show similar product patterns during autoxidation. A free carboxylate group or another form of acid catalysis is not required for H(P)NE formation. This was shown here for the methyl esters but can equally be expected for cholesterol esters, phospholipids, and other physiologically relevant esters of polyunsaturated fatty acids.

ACKNOWLEDGMENT

REFERENCES

1. Benedetti, A., Comporti, M., and Esterbauer, H. (1980) Identification of 4-Hydroxynonenal as a Cytotoxic Product Originating from the Peroxidation of Liver Microsomal Lipids, *Biochim. Biophys. Acta 620*, 281–296.
2. Benedetti, A., Esterbauer, H., Ferrali, M., Fulceri, R., and Comporti, M. (1982) Evidence for Aldehydes Bound to Liver Microsomal Protein Following CCl_4 or $BrCCl_3$ Poisoning, *Biochim. Biophys. Acta 711*, 345–356.
3. Esterbauer, H., Schaur, R.J., and Zollner, H. (1991) Chemistry and Biochemistry of 4-Hydroxynonenal, Malonaldehyde and Related Aldehydes, *Free Radic. Biol. Med. 11*, 81–128.
4. Lee, S.H., and Blair, I.A. (2000) Characterization of 4-Oxo-2-nonenal as a Novel Product of Lipid Peroxidation, *Chem. Res. Toxicol. 13*, 698–702.
5. Lee, S.H., and Blair, I.A. (2001) Oxidative DNA Damage and Cardiovascular Disease, *Trends Cardiovasc. Med. 11*, 148–155.
6. Uchida, K. (2003) 4-Hydroxy-2-nonenal: A Product and Mediator of Oxidative Stress, *Prog. Lipid Res. 42*, 318–343.
7. Bacot, S., Bernoud-Hubac, N., Baddas, N., Chantegrel, B., Deshayes, C., Doutheau, A., Lagarde, M., and Guichardant, M. (2003) Covalent Binding of Hydroxy-Alkenals 4-HDDE, 4-HHE, and 4-HNE to Ethanolamine Phospholipid Subclasses, *J. Lipid Res. 44*, 917–926.
8. Je, J.H., Lee, J.Y., Jung, K.J., Sung, B., Go, E.K., Yu, B.P., and Chung, H.Y. (2004) NF-κB Activation Mechanism of 4-Hydroxyhexenal *via* NIK/IKK and P38 MAPK Pathway, *FEBS Lett. 566*, 183–189.
9. West, J.D., Ji, C., Duncan, S.T., Amarnath, V., Schneider, C., Rizzo, C.J., Brash, A.R., and Marnett, L.J. (2004) Induction of Apoptosis in Colorectal Carcinoma Cells Treated with 4-Hydroxy-
10. 2-nonenal and Structurally Related Aldehydic Products of Lipid Peroxidation, *Chem. Res. Toxicol. 17*, 453–462.
10. Dianzani, M.U. (2003) 4-Hydroxynonenal from Pathology to Physiology, *Mol. Aspects Med. 24*, 263–272.
11. Nakashima, I., Liu, W., Akhand, A.A., Takeda, K., Kawamoto, Y., Kato, M., and Suzuki, H. (2003) 4-Hydroxynonenal Triggers Multistep Signal Transduction Cascades for Suppression of Cellular Functions, *Mol. Aspects Med. 24*, 231–238.
12. Watson, A.D., Leitinger, N., Navab, M., Faull, K.F., Horkko, S., Witztum, J.L., Palinski, W., Schwenke, D., Salomon, R.G., Sha, W., *et al.* (1997) Structural Identification by Mass Spectrometry of Oxidized Phospholipids in Minimally Oxidized Low Density Lipoprotein That Induce Monocyte/Endothelial Interactions and Evidence for Their Presence *in vivo, J. Biol. Chem. 272*, 13597–13607.
13. Subbanagounder, G., Leitinger, N., Schwenke, D.C., Wong, J.W., Lee, H., Rizza, C., Watson, A.D., Faull, K.F., Fogelman, A.M., and Berliner, J.A. (2000) Determinants of Bioactivity of Oxidized Phospholipids. Specific Oxidized Fatty Acyl Groups at the *sn*-2 Position, *Arterioscler. Thromb. Vasc. Biol. 20*, 2248–2254.
14. Podrez, E.A., Poliakov, E., Shen, Z., Zhang, R., Deng, Y., Sun, M., Finton, P.J., Shan, L., Febbraio, M., Hajjar, D.P., *et al.* (2002) A Novel Family of Atherogenic Oxidized Phospholipids Promotes Macrophage Foam Cell Formation *via* the Scavenger Receptor CD36 and Is Enriched in Atherosclerotic Lesions, *J. Biol. Chem. 277*, 38517–38523.
15. Frimer, A.A. (1979) Reaction of Singlet Oxygen with Olefins—Question of Mechanism, *Chem. Rev. 79*, 359–387.
16. Gardner, H.W., and Plattner, R.D. (1984) Linoleate Hydroperoxides Are Cleaved Heterolytically into Aldehydes by a Lewis Acid in Aprotic Solvent, *Lipids 19*, 294–299.
17. Schneider, C., Tallman, K.A., Porter, N.A., and Brash, A.R. (2001) Two Distinct Pathways of Formation of 4-Hydroxynonenal. Mechanisms of Nonenzymatic Transformation of the 9- and 13-Hydroperoxides of Linoleic Acid to 4-Hydroxyalkenals, *J. Biol. Chem. 276*, 20831–20838.
18. Schneider, C., Porter, N.A., and Brash, A.R. (2004) Autoxidative Transformation of Chiral ω6 Hydroxy Linoleic and Arachidonic Acids to Chiral 4-Hydroxy-2*E*-nonenal, *Chem. Res. Toxicol. 17*, 937–941.
19. Brash, A.R., and Song, W.-C. (1996) Detection, Assay, and Isolation of Allene Oxide Synthase, *Methods Enzymol. 272*, 250–259.
20. Neff, W.E., Frankel, E.N., and Weisleder, D. (1982) Photosensitized Oxidation of Methyl Linolenate. Secondary Products, *Lipids 11*, 780–790.
21. Brash, A.R. (2000) Autoxidation of Methyl Linoleate: Identification of the Bis-allylic 11-Hydroperoxide, *Lipids 35*, 947–952.
22. Bligh, E.G., and Dyer, W.J. (1959) A Rapid Method of Total Lipid Extraction and Purification, *Can. J. Biochem. Physiol. 37*, 911–917.
23. Hamberg, M. (1983) A Novel Transformation of 13-L$_s$-Hydroperoxy-9,11-octadecadienoic Acid, *Biochim. Biophys. Acta 752*, 191–197.
24. Havrilla, C.M., Hachey, D.L., and Porter, N.A. (2000) Coordination (Ag^+) Ion Spray-Mass Spectrometry of Peroxidation Products of Cholesteryl Linoleate and Cholesteryl Arachidonate: High-Performance Liquid Chromatography–Mass Spectrometry Analysis of Peroxide Products from Polyunsaturated Lipid Autoxidation, *J. Am. Chem. Soc. 122*, 8042–8055.
25. Dix, T.A., and Marnett, L.J. (1985) Conversion of Linoleic Acid Hydroperoxide to Hydroxy, Keto, Epoxyhydroxy, and Trihydroxy Fatty Acids by Hematin, *J. Biol. Chem. 260*, 5351–5357.
26. Tallman, K.A., Pratt, D.A., and Porter, N.A. (2001) Kinetic Products of Linoleate Peroxidation: Rapid β-Fragmentation of Nonconjugated Peroxyls, *J. Am. Chem. Soc. 123*, 11827–11828.
27. Frankel, E.N., and Gardner, H.W. (1989) Effect of α-Tocopherol on the Volatile Thermal Decomposition Products of Methyl Linoleate Hydroperoxides, *Lipids 24*, 603–608.

Conversion of Linoleic Acid into Novel Oxylipins by the Mushroom *Agaricus bisporus*

Mayken W. Wadman[a], Guus van Zadelhoff[a], Mats Hamberg[b], Tom Visser[c], Gerrit A. Veldink[a],*, and Johannes F.G. Vliegenthart[a]

[a]Department of Bio-organic Chemistry, Utrecht University, 3584-CH, Utrecht, The Netherlands,
[b]Department of Physiological Chemistry, Karolinska Institutet, SE-171 77 Stockholm, Sweden, and
[c]Department of Vibrational Spectroscopy, Utrecht University, 3584-CA, Utrecht, The Netherlands

ABSTRACT: Oxylipins are associated with important processes of the fungal life cycle, such as spore formation. Here, we report the formation of FA metabolites in *Agaricus bisporus.* Incubation of a crude extract of lamellae with linoleic acid (18:2) led to the extensive formation of two oxylipins. They were identified as 8(*R*)-hydroxy-9*Z*,12*Z*-octadecadienoic acid (8-HOD) and 8(*R*),11(*S*)-dihydroxy-9*Z*,12*Z*-octadecadienoic acid (8,11-diHOD) by using RP-HPLC, GC–MS, IR, GC–MS analysis of diastereomeric derivatives, and ^{1}H NMR and ^{13}C NMR spectroscopy. Neither compound has been reported before in *A. bisporus.* Oleic (18:1), α-linolenic (18:3n-3), and γ-linolenic (18:3n-6) acids were converted into their 8-hydroxy derivatives as well, and 18:3n-3 was further metabolized to its 8,11-diol derivative. Reactions with [U-^{13}C]18:2 demonstrated that the compounds 8-HOD and 8,11-diHOD were formed from exogenously supplied 18:2. When [U-^{13}C]8-HOD was supplied, it was not converted into 8,11-diHOD, indicating that it was not an intermediate in the formation of 8,11-diHOD. When a crude extract of *A. bisporus* was incubated under an atmosphere of $^{16}O_2$/$^{18}O_2$, the two hydroxyl groups of 8,11-diHOD contained either two ^{18}O atoms or two ^{16}O atoms. Species that contained one of each isotope could not be detected. We propose that the formation of the 8,11-dihydroxy compounds occurs through either an 8,11-endoperoxy, an 8-peroxo free radical, or an 8-hydroperoxy intermediate. In the latter case, the reaction should be catalyzed by dioxygenase with novel specificity.

Paper no. L9807 in *Lipids 40*, 1163–1170 (November 2005).

The metabolism of FA is a central feature in all biological systems, including animals, plants, and fungi. An important class of enzymes involved in FA metabolism is the dioxygenases, which include lipoxygenases, prostaglandin H synthases, and linoleate diol synthases (1). Lipoxygenases are nonheme-iron-containing proteins that catalyze the regio- and stereospecific insertion of oxygen in PUFA with one or more 1*Z*,4*Z*-pentadiene systems, thus forming 1(*S*)-hydroperoxy-2*E*,4*Z*-pentadiene derivatives. Secondary metabolites of these hydroperoxides have a wide variety of functions. Prostaglandin H synthases are ferric heme proteins that exist in vertebrates and presumably in corals (2). They catalyze two sequential reactions: (i) the double dioxygenation and cyclization of arachidonic acid by forming an endoperoxide function and (ii) the reduction of the remaining hydroperoxide (3). The reaction products are involved in a variety of biological functions. Linoleate diol synthases contain heme-iron and have two related enzyme activities, namely, (i) the dioxygenation of the C_8 of 18:2 (linoleic acid) and (ii) the isomerization of the hydroperoxide group into 7,8-dihydroxy linoleic acid. This 7,8-linoleate diol synthase has been reported only in fungi, and its amino acid sequence is homologous to prostaglandin H synthases (1,4).

Despite the enormous number (over 1.5 million) of known species in the fungal kingdom, fungal FA metabolism has received relatively little attention. In several species, lipoxygenases have been reported that have activities similar to the plant and mammalian enzymes (5–9). However, some of the dioxygenating enzymes and intermediates differ remarkably from the FA metabolites present in plants and mammals. For instance, the lipoxygenase that is proposed to catalyze the formation of 1-octen-3-ol, the typical mushroom flavor, has an unusual specificity. It should convert the pentadiene system into a 4-hydroperoxy-1*Z*,5*E* pentadiene derivative, but the mechanism of this reaction is still unclear (10,11). Also, a nonheme-manganese lipoxygenase has been reported that converted the pentadiene system into a 3(*S*)-hydroperoxy-1*Z*,4*Z* pentadiene derivative (12).

A growing number of oxygenated FA and their secondary metabolites are being identified as products of fungal FA metabolism. Also, fungal dioxygenases seem to possess novel specificities compared with their plant and mammalian counterparts. As part of a study on fungal FA metabolism, we have carried out an investigation into the capacity of *Agaricus bisporus* to transform polyunsaturated long-chain FA.

MATERIALS AND METHODS

Materials. All chemicals used were commercially obtained and were of analytical grade. 18:1 (oleic acid, 99% pure), 18:2 (99% pure), 18:3n-3 (α-linolenic acid, 99% pure), 18:3n-6 (γ-linolenic acid, 99% pure), and Z-vaccenic acid (11Z-octadecenoic acid, 99% pure) were obtained from Sigma (St. Louis, MO). [U-^{13}C]18:2 (99% pure) was obtained from Isotec (Matheson Trigas, Irving, TX). Solutions of 30 mM FA were stored in methanol under N_2 at −20°C until use. 2(*S*)- and 2(*R,S*)-hydroxynonanoic acids as well as 2(*S*)- and 2(*R,S*)-hydroxy-1,9-nonanedioic acids were purchased from Larodan Fine Chemicals (Malmö, Sweden). Cysteine, glutathione, and glutathione peroxidase were purchased from Acros (Fairlawn, NJ) and Sigma. $^{18}O_2$ (500 mL) was 99.51% pure.

Three types of mushrooms (*A. bisporus, Lentinus edodes*, and *Pleurotus ostreatus*) were purchased from a local supermarket and stored at 4°C until use. An additional three types (*Piptoporus betulinus, Tricholoma fulvum*, and *Tricholoma flavovirens*) were picked in a local forest and identified on the guidance of a fungi handbook.

Preparation of crude extracts of lamellae. Lamellae were separated from the cap and homogenized directly with 1 mL buffer (50 mM sodium phosphate, pH 6.5)/g lamellae in a commercial Waring blender and centrifuged at 4°C, $2500 \times g$, for 20 min. The supernatant (crude extract) was filtered through cheesecloth and used immediately or after boiling in a water bath for 10 min as a control for enzyme activity.

Extraction and purification of FA products. Typically, 4 mL phosphate buffer (50 mM, pH 6.5) was mixed with 1 mL crude extract, rigorously stirred, and incubated with 120 μM substrate for 30–45 min at room temperature under a continuous flow of O_2. In some cases, cysteine (250 μM) or glutathione (1 mM) and glutathione peroxidase (2 or 8 U/mL) were added at the start of the incubation. For the large-scale production of 18:2 metabolites, reactions were carried out with 100 mL crude extract and 400 mL phosphate buffer. Incubations under an atmosphere of $^{16}O_2/^{18}O_2$ were carried out after repeated evacuation and purging of the reaction vessel containing the dissolved substrate with nitrogen. The experimental atmosphere had an $^{18}O_2/^{16}O_2$ ratio of either 6:1 (vol/vol) or 3:2 (vol/vol). FA and reaction products were recovered directly by solid-phase extraction (SPE; Oasis HLB, 200 mg; Waters, Milford, MA). The eluate was concentrated under N_2 and analyzed by RP-HPLC. Analysis by GC–MS of the reaction products as trimethylsilyl (TMS) ethers of methyl derivatives was performed as described previously (13). The FA methylation reagent was diazomethane. For GC–MS analysis, samples were analyzed before and after hydrogenation. Endogenously present oxylipins were extracted from frozen mushrooms according to the method of Bligh and Dyer using dichloromethane instead of chloroform (14).

Characterization of FA products. IR spectral analysis was carried out by means of diffuse reflectance (DRIFT) spectroscopy. Samples were prepared by slowly evaporating a few droplets of the concentrated eluate at 40°C onto powdered KBr

in a DRIFT cup. Similarly, solutions of methyl 18:1 and methyl 18:2 in methanol were used for reference purposes. Blank KBr exposed to a few droplets of pure methanol was used as the background. After evaporation, the cups were transferred to a DRIFT accessory (Spectra-tech) in a Perkin-Elmer-2000 FTIR spectrometer. Spectra were recorded by accumulating 25 scans at an optical resolution of 4 cm^{-1}. All spectra were converted into Kubelka–Munk units prior to interpretation.

^{1}H NMR spectra were recorded at 300 K with a Bruker AMX 500 (500 MHz) spectrometer; δ_H values are given in ppm relative to the signal for internal TMS ($\delta_H = 0$, CDCl$_3$). 2-D ^{1}H-^{1}H total correlation spectroscopy (TOCSY) (mixing times 7 and 100 ms) and ^{1}H-^{13}C heteronuclear single quantum correlation (HSQC) spectra were recorded at 300 K with a Bruker AMX 500 (500 and 126 MHz).

Stereoconfiguration of the reaction products from 18:2 was determined by the formation of methyl (−)-menthoxycarbonyl (MC) derivatives followed by oxidative ozonolysis and methyl esterification (15). Methyl 8(*R*),11(*S*)-dihydroxy-9Z,12Z-octadecadienoic acid (8,11-diHOD, approx. 1 mg) was dissolved in ethyl acetate (3 mL) and stirred for 20 min under hydrogen gas in the presence of palladium-on-calcium carbonate (5 mg) (12). An aliquot of the partially hydrogenated material was derivatized with trimethylchlorosilane (trimethylchlorosilane/hexamethyldisilazane/pyridine 1:1:5, by vol), and the resulting TMS ethers of methyl derivatives were analyzed by using GC–MS. GC was performed with a Hewlett-Packard model 5890 gas chromatograph equipped with a methylsilicone capillary column (length, 25 m; film thickness, 0.33 μm; Agilent Technologies, Wilmington, DE). Helium was used as the carrier gas at a flow rate of 25 cm/s. For analysis of the methyl MC derivatives, the start temperature was either 190°C and increased by 2°C/min (analysis of methyl MC 2-hydroxynonanoates) or 210°C and increased by 3°C/min (analysis of dimethyl MC 2-hydroxy-1,9-nonanedioates). Under the conditions used, the MC derivative of methyl 2(*S*)-hydroxynonanoate eluted with a shorter retention time (11.80 min) compared with the corresponding derivative of the methyl 2(*R*)-hydroxy compound (11.94; separation factor, 1.01). In the same way, the MC derivative of dimethyl 2(*S*)-hydroxy-1,9-nonanedioate eluted with a shorter retention time (11.56 min) than the MC derivative of the dimethyl 2(*R*)-hydroxy compound (11.67 min; separation factor, 1.01). GC–MS of the methyl MC derivatives was carried out with a Hewlett-Packard model 5970B mass selective detector connected to a Hewlett-Packard model 5890 gas chromatograph equipped with a 5% phenylmethylsiloxane capillary column (12 m; film thickness, 0.33 μm; Agilent Technologies). The start temperature was 120°C and was increased by 10°C/min.

RESULTS

RP-HPLC analysis. A crude extract of the lamellae of *A. bisporus* was incubated with 18:2, and the reaction mixture was extracted with SPE and analyzed by RP-HPLC. A typical HPLC chromatogram is shown in Figure 1. Incubation with 18:2 resulted in two large peaks and a smaller one appearing in
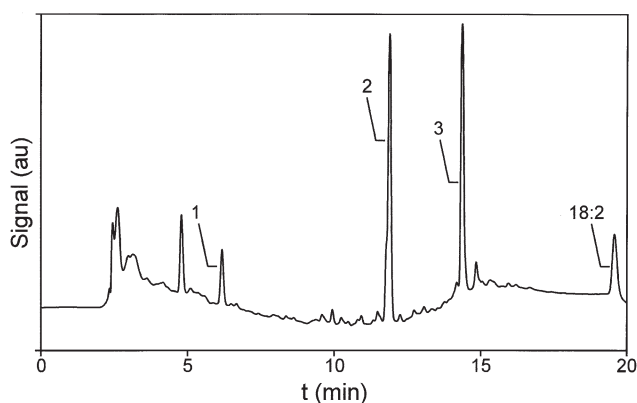
FIG. 1. RP-HPLC chromatogram (λ = 200 nm) of the reaction of a crude extract of *Agaricus bisporus* lamellae and linoleic acid (18:2). Indicated are peak 1 [10-oxo-8*E*-decenoic acid (10-ODA)], peak 2 [8,11-diHOD, 8(*R*),11(*S*)-dihydroxy-9*Z*,12*Z*-octadecadienoic acid (8,11-diHOD)], and peak 3 [8(*R*)-hydroxy-9*Z*,12*Z*-octadecadienoic acid (8-HOD)], the major FA metabolites. RP-HPLC analysis and purification of the FA products was carried out on a Cosmosil 5C18-AR (5 μm; 250 × 4.6 mm i.d.; Nacalai Tesque, Kyoto, Japan) reversed-phase column using a gradient system [solvent A: methanol/water/acetic acid (50:50:0.01, by vol); solvent B: methanol/water/acetic acid (95:5:0.01, by vol)] with the following gradient program: 100% solvent A for 1 min, followed by a linear increase of solvent B up to 100% within 10 min, and finally an isocratic postrun at 100% solvent B for 10 min. The flow rate was 1 mL/min.

the HPLC chromatogram. Peak 2 (Fig. 1) had a retention time of 11.9 min, and peak 3 (Fig. 1) had a retention time of 14.5 min. Both had absorbance at 200 nm. Peak 1 (Fig. 1), at a 6.1

min retention time, contained a compound with λ_{max} at 220 nm, characteristic of a conjugated oxo-ene in methanol. Reference compounds of dihydroxy FA reaction products had retention times of 11–12 min, whereas the monohydroxy FA references eluted between 13 and 15 min.

Minor amounts of regioisomeric, dihydroxy, and monohydroxy FA were also separated in the subsequent GC–MS analysis of the RP-HPLC peaks. Several had a λ_{max} at 234 nm, characteristic of a conjugated diene dissolved in methanol.

GC–MS. Dihydroxy and monohydroxy FA reaction products were fractionated on HPLC and after derivatization were further investigated with GC–MS. Structures of oxygenated FA were deduced from the spectra of the TMS ethers of methyl hydroxy and dihydroxy compounds. In some cases, reaction products were also hydrogenated.

(i) Analysis of monohydroxy FA. In the GC chromatogram of the hydrogenated monohydroxy FA as TMS ethers of methyl derivatives, one prominent peak was present. The MS identified it as a TMS ether of the methyl of 8-hydroxyoctadecanoate in view of the prominent fragment at *m/z* 245, which was produced by cleavage between C_9 and C_8 toward the carboxylic headgroup (Table 1).
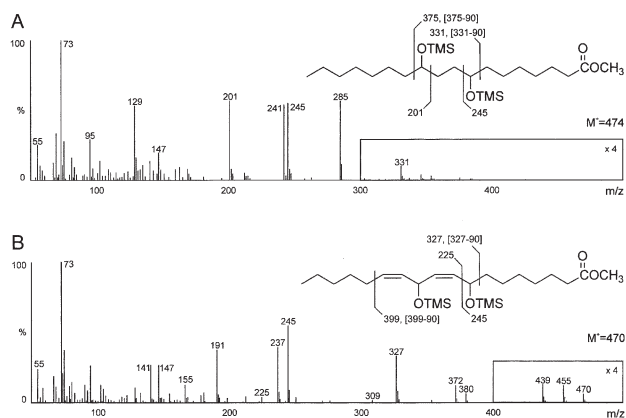
GC–MS analysis of the corresponding nonhydrogenated monohydroxy FA as TMS ethers of methyl derivatives revealed that the TMS ether of methyl 8-hydroxyoctadecanoate was derived from the TMS ether of methyl 8-hydroxy-9,12-octadecadienoate (Table 1). Thus, the monohydroxy FA, peak 3 (Fig. 1), was identified as 8-hydroxy-9,12-octadecadienoic acid (16).

Furthermore, minor amounts (5–10% as estimated from the

TABLE 1
Characteristic Mass Fragments of (hydrogenated) Trimethylsilyl (TMS) Ethers of Methylated *Agaricus bisporus* Metabolites of 18:2 (mass fragment; relative abundance)[a]

	Hydrogenated (*m/z*)		Nonhydrogenated (*m/z*)		
Mass identity	8-HOD	8,11-diHOD	8-HOD	8,11-diHOD	8-HOM
M^+	386 (<1)	—	382 (< 1)	470 (< 1)	384 (< 1)
$M^+ - CH_3$	371 (<1)	—	367 (1)	455 (1)	369 (1)
$M^+ - CH_3O$	355 (1)	—	—	439 (1)	353 (< 1)
$M^+ - CH_3OO$	339 (3)	—	335 (< 1)	—	337 (2)
$M^+ - TMSOH$	—	384 (<1)	292 (7)	380 (8)	294 (3)
F1	245 (44)[a]	375 (<1)[b]	271 (4)[c]	399 (< 1)[d]	245 (30)[a]
F1 – TMSOH	—	285 (57)	—	309 (3)	—
F2	243 (28)[e]	331 (3)[f]	239 (27)[g]	327 (35)[h]	241 (10)[i]
F2 – TMSOH	—	241 (54)	—	237 (42)	151 (27)
F3	—	245 (55)[a]	—	245 (58)[a]	—
F3 – TMSOH	—	—	—	—	—
F4	—	201 (58)[j]	—	—	—
F4 – TMSOH	—	—	—	—	—
TMS^+	73 (100)	73 (100)	73 (100)	73 (100)	73 (100)

[a]GC–MS analyses were performed under conditions similar to those described in the legend to Figure 2. [a]Cleavage between C_8 and C_9; $TMSO^+ = CH-(CH_2)_6-COOCH_3$. [b]Cleavage between C_{11} and C_{12}; $TMSO^+ = CH-(CH_2)_2-(TMSO-CH)-(CH_2)_6-COOCH_3$. [c]Cleavage between C_{10} and C_{11}; $^+CH=CH-(TMSO-CH)-(CH_2)_6-COOCH_3$. [d]Cleavage between C_{13} and C_{14}; $^+CH=CH-(TMSO-CH)-CH=CH-(TMSO-CH)-(CH_2)_6-COOCH_3$. [e]Cleavage between C_7 and C_8; $TMSO^+ = CH-(CH_2)_9-CH_3$. [f]Cleavage between C_7 and C_8; $TMSO^+ = CH-(CH_2)_2-(TMSO-CH)-(CH_2)_6-CH_3$. [g]Cleavage between C_7 and C_8; $TMSO^+ = CH-CH=CH-CH_2-CH=CH-(CH_2)_4-CH_3$. [h]Cleavage between C_7 and C_8; $TMSO^+ = CH-CH=CH-(TMSO-CH)-CH=CH-(CH_2)_4-CH_3$. [i]Cleavage between C_7 and C_8; possibly $TMSO^+ = CH-(CH_2)_3-CH=CH-(CH_2)_4-CH_3$. [j]Cleavage between C_{10} and C_{11}; $TMSO^+ = CH-(CH_2)_6-CH_3$. 8-HOD, 8(*R*)-hydroxy-9*Z*,12*Z*-octadecadienoic acid; 8,11-diHOD, 8(*R*),11(*S*)-dihydroxy-9*Z*,12*Z*-octadecadienoic acid; 8-HOM, 8-hydroxy-octadecaenoic acid.

FIG. 3. Structures of the main products of the incubations of 18:2 with *A. bisporus*: 8-HOD and 8,11-diHOD. For abbreviations see Figure 1.

FIG. 2. MS and fragmentation patterns of (A) the trimethylsilyl (TMS) ether of fully hydrogenated methyl 8,11-diHOD, and (B) the TMS ether of methyl 8,11-diHOD. GC–MS analysis was performed on a Carlo Erba gas chromatograph 8060 equipped with a Fisons MD800 MassLab spectrometer equipped with a column (30 m AT-1 × 0.25 mm × 0.25 μm; Alltech, Deerfield, IL). The column temperature was held at 140°C for 2 min, then allowed to rise from 140 to 280°C at 6°C/min, and then held at this temperature for 2 min. MS was performed in positive ion EI mode over a mass range of 50–500 Da and electron ionization at 70 eV. For abbreviations see Figure 1.

peak intensity by GC–MS) of other monohydroxides, namely, the TMS ether of methylated 10-hydroxy-8*E*,12*E*-octadecadienoic acid (10-HOD), the TMS ether of methyl 9-hydroxy-10*E*,12*Z*-octadecadienoate, and the methylated TMS ether of 13-hydroxy-9*Z*,11*E*-octadecadienoate (data not shown), were observed in the GC chromatogram as a portion of RP-HPLC peak 3. Interestingly, another monohydroxy compound, namely, 8-hydroxy-octadecaenoic acid (8-HOM), was identified by GC–MS of the TMS ether of its methyl derivative (Table 1). Originally, the compound contained two double bonds (9*Z* and 12*Z*). One double bond (9*Z*) appeared to be hydrogenated by an *A. bisporus* homogenate. Most likely, the remaining double bond was still 12*Z*.

(ii) Analysis of dihydroxy FA. Hydrogenated dihydroxy FA as TMS ethers of methyl derivatives were separated by using GC, and one dominant peak was present in the chromatogram. The MS showed four ion peaks stemming from cleavages around the two oxygenated C atoms, thereby indicating the presence of a TMS ether of methyl 8,11-dihydroxyoctadecanoate (Table 1, Fig. 2) Comparison of spectra from the hydrogenated and nonhydrogenated samples showed that the TMS ether of methyl 8,11-dihydroxyoctadecanoate was derived from the TMS ether of methyl 8,11-dihydroxy-9,12-octadecadienoate. This was evidenced by the molecular ion at *m/z* 470 and by the characteristic fragments resulting from cleavage around the double bonds and the oxygenated C atoms (Table 1, Fig. 2). Thus, the major dihydroxy FA product in peak 2 (Fig. 1) proved to be 8,11-dihydroxy-9,12-octadecadienoic acid.

In addition, small amounts (5–10% as estimated from peak intensity on GC–MS) of 8,9-dihydroxy-10,12-octadecadienoic acid and 8,13-dihydroxy-9,11-octadecadienoic acid were formed (data not shown).
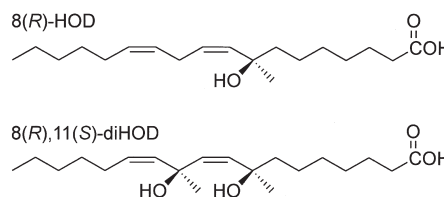
Furthermore, peak 1 (Fig. 1) was characterized by using GC–MS as its methyl ester. Its MS was compared with reported data, and the compound was identified as 10-oxo-8*E*-decenoic acid (10-ODA) (17,18).

IR spectroscopy. The *Z* configuration of the double bonds in methyl 8-hydroxy-9,12-octadecadienoate as well as in methyl 8,11-dihydroxy-9,12-octadecadienoate was proved by DRIFT spectroscopy analysis. Both compounds exhibited absorption bands characteristic of the *Z* configuration, i.e., a =C–H stretching vibration around 3005 cm^{-1}, a C=C stretching at 1655 cm^{-1}, and a =C–H out-of-plane bending vibration at about 690 cm^{-1}. In agreement with this assignment, bands typical of an *E* double-bond geometry at 3025, 1675, and 965 cm^{-1} were absent in the spectra of both products.

Steric analysis. Stereoconfiguration of the hydroxyl groups in 8-hydroxy-9*Z*,12*Z*-octadecadienoic acid and in 8,11-dihydroxy-9*Z*,12*Z*-octadecadienoic acid were analyzed as the methyl MC derivatives of the FA.

(i) Steric analysis of methyl 8-hydroxy-9Z,12Z-octadecadienoate. Methyl 8-hydroxy-9,12-octadecadienoate (approx. 0.5 mg) was derivatized with MC chloride and the MC derivative was isolated by TLC. The material obtained was subjected to oxidative ozonolysis, and the methyl-esterified product was analyzed by GC. A main peak was observed that coeluted with the MC derivative of dimethyl 2(*R*)-hydroxy-1,9-nonanedioate, whereas less than 3% of the 2(*S*)-derivative was present. Accordingly, C$_8$ of the degraded oxylipin had an *R* configuration (Fig. 3).

(ii) Steric analysis of methyl 8,11-dihydroxy-9,12-octadecadienoate. Methyl 8,11-dihydroxy-9*Z*,12*Z*-octadecadienoate was partially hydrogenated and analyzed as its TMS ether derivative. Four main peaks were observed, designated A–D. Peak A (12.55 min; 49%) corresponded to the TMS ether of the starting methyl 8,11-dihydroxyoctadecadienoate, whereas peak D (13.06 min, 11%) was due to the fully hydrogenated derivative, i.e., the TMS ether of methyl 8,11-dihydroxyoctadecanoate. The mass spectra of peak B (12.68 min; 20%) showed prominent ions at *m/z* 373 [M$^+$ − (CH$_2$)$_6$CH$_3$], 329 [M$^+$ − (CH$_2$)$_6$COOCH$_3$], 283 [373 − TMSOH], and 239 [329 − TMSOH] that originated from the TMS ether derivative of methyl 8,11-dihydroxy-9-octadecenoate. Peak C (12.80 min; 20%) showed ions at *m/z* 457 [M$^+$ − CH$_3$], 245 [TMSO$^+$ = CH–(CH$_2$)$_6$COOCH$_3$], and 199 [TMSO$^+$ = CH–CH=CH-(CH$_2$)$_4$CH$_3$; base peak] and represented the TMS ether derivative of methyl 8,11-dihydroxy-12-octadecenoate. The above-mentioned mixture of FFA was con-

TABLE 2
Relevant Resonances in the ^{1}H NMR Spectrum of Methyl 8-HOD^a

CDCl$_3$ δ		Coupling constant ^{3} (J = Hz)	Protons	Assignment
0.90	*t*	(H18, H17) = 6.9	3H	C18**H$_3$**^{b}
1.36	*m*		14H	C4**H$_2$**C5**H$_2$**C6**H$_2$**C7**H$_2$** and C15**H$_2$**C16**H$_2$**C17**H$_2$**
1.61	*m*		2H	C3**H$_2$**
2.07	*d,t*	(H14, H13) = 7.2	2H	C14**H$_2$**
		(H14, H15) = 7.2		
2.31	*t*	(H2, H3) = 7.6	2H	C2**H$_2$**
2.85	*m*		2H	C11**H$_2$**
3.67	*s*		3H	OC**H$_3$**
4.46	*dt*	(H8, H9) = 8.3	1H	C8**H**
		(H8, H7) = 6.4		
5.40	*m*		4H	C9**H**C10**H**C11H$_2$C12**H**C13**H**

^{a}The spectrum was recorded at 500 MHz, in CDCl$_3$, and assigned by using 2-D ^{1}H-^{1}H total correlation spectroscopy and ^{1}H-^{13}C heteronuclear single-quantum correlation (500 and 126 MHz, CDCl$_3$). ^{13}C resonances: δ = 133.0 (C-9), δ = 131.2 (C-13), δ = 130.7 (C-10), δ = 127.3 (C-12), δ = 67.8 (C-8), δ = 51.6 (OCH$_3$), δ = 37.5 (C-7), δ = 34.2 (C-2), δ = 31.7 (C-16), δ = 29.3 (C-4, C-5, C-15), δ = 27.3 (C-14), δ = 26.1 (C-11), δ = 25.2 (C-6), δ = 25.0 (C-3), δ = 22.1 (C-17), δ = 14.1 (C-18). ^{b}The protons involved are printed in boldface type. For abbreviation see Table 1.

verted into MC derivatives, fractionated by TLC, and subjected to oxidative ozonolysis. The methyl-esterified product was analyzed by GC. Peaks were observed coeluting with the MC derivative of methyl 2(*S*)-hydroxynonanoate [less than 3% of the 2(*R*)-isomer] and with the MC derivative of dimethyl 2(*R*)-hydroxy-1,9-nonanedioate [less than 3% of the 2(*S*)-isomer], respectively. The former component was formed by cleavage of the double bond of methyl 8,11-dihydroxy-9-octadecenoate, and the latter fragment was from methyl 8,11-dihydroxy-9-octadecenoate and also from unhydrogenated methyl 8,11-dihydroxy-9,12-octadecadienoate. We concluded that C$_{11}$ of the degraded oxylipin had an *S* configuration and that C$_8$ had an *R* configuration (Fig. 3).

Thus, the two main metabolites from the reaction of 18:2 with a crude extract of *A. bisporus* lamellae were identified as 8(*R*)-hydroxy-9Z,12Z-octadecadienoic acid (8-HOD) and 8(*R*),11(*S*)-dihydroxy-9Z,12Z-octadecadienoic acid (8,11-diHOD), respectively.

^{1}H NMR and ^{1}H-^{13}C HSQC spectra. The identification of methyl 8-HOD and methyl 8,11-diHOD was further confirmed by recording ^{1}H NMR, ^{1}H-^{1}H TOCSY, and ^{1}H-^{13}C HSQC spectra (Tables 2, 3).

The question arose whether the formation of these compounds was specific to *A. bisporus*. Therefore, we randomly tested several other mushroom species. In all species, one or both of these metabolites were formed as well: Upon 18:2 incubation, *P. betulinus*, *T. fulvum*, *T. flavovirens, L. edodes*, and *P. Ostreatus* formed 8-HOD, as identified by RP-HPLC and GC–MS. *Tricholoma fulvum* and *L. edodes* formed both 8-HOD and 8,11-diHOD, as evidenced by RP-HPLC and GC–MS.

Enzyme characteristics. Boiling the crude extract prior to incubation resulted in a complete loss of activity. In the corresponding RP-HPLC chromatogram, peaks 1, 2, and 3 disappeared completely (data not shown). Since the energetically unfavorable *Z* configuration was retained and the product was chiral, it is likely that 8-HOD and 8,11-diHOD were formed by an

TABLE 3
Relevant Resonances in the ^{1}H NMR Spectrum of Methyl 8,11-diHOD^a

CDCl$_3$δ		Coupling constant ^{3} (J = Hz)	Protons	Assignment
0.90	*t*	(H18, H17) = 6.6	3H	C18**H$_3$**^{b}
1.37	*m*		14H	C4**H$_2$**C5**H$_2$**C6**H$_2$**C7**H$_2$** and C15**H$_2$**C16**H$_2$**C17**H$_2$**
1.61	*m*		2H	C3**H$_2$**
2.07	*m*		2H	C14**H$_2$**
2.31	*t*	(H2, H3) = 7.5	2H	C2**H$_2$**
3.67	*s*		3H	OC**H$_3$**
4.46	*dt*	(H8, H9) = 6.8	1H	C8**H**
		(H8, H7) = 6.4		
5.31	*dd*	(H11, H12) = 7.8	2H	C11**H**
		(H11, H10) = 7.8		
5.53	*m*		4H	C9**H**C10**H**C11H$_2$C12**H**C13**H**

^{a}The spectrum was recorded under the same conditions as described at Table 2. ^{13}C resonances: δ = 134.9 (C9), δ = 133.1 (C13), δ = 130.7 (C10, C12), δ = 68.0 (C8), δ = 63.9 (C11), δ = 51.6 (OCH$_3$), δ = 36.9 (C7), δ = 34.0 (C2), δ = 31.6 (C16), δ = 29.3 (C4, C5, C15), δ = 27.5 (C14), δ = 25.2 (C6), δ = 24.6 (C3), δ = 22.3 (C17), δ = 14.2 (C18). ^{b}The protons involved are printed in boldface type. For abbreviation see Table 1.

enzymatic reaction. Their syntheses were found to occur in the eluate after filtration through a 0.22-µm filter. Therefore, we expected that 8-HOD and 8,11-diHOD were formed by a cytosolic enzymatic reaction (19).

Minute amounts (about 1 au by RP-HPLC) of endogenous 8-HOD and 8,11-diHOD were present in mushrooms extracts obtained by the method of Bligh and Dyer (14). Directly after blending and centrifugation, only minor amounts (around 10 au on RP-HPLC) of the metabolites were present. In a reaction without added substrate, 8-HOD and 8,11-diHOD were also formed (around 60 au on RP-HPLC) but to a lesser extent than in a reaction with added substrate (about 100 au on RP-HPLC) and arose from the presence of free endogenous 18:2. Incubation with [U-^{13}C]18:2 showed that products represented a mixture of converted 18:2 from endogenous and exogenous sources. The conversion of exogenously supplied 18:2 was about 60% of the total conversion, as judged by the ratio of ^{13}C-labeled fragments to unlabeled fragments by using GC–MS.

Incubation with [U-^{13}C]18:2 was performed to study the connection between 18:2 and its metabolites. Analysis by GC–MS showed that incubation with [U-^{13}C]18:2 resulted in the formation of labeled 8-HOD, labeled 8,11-diHOD, and labeled 8-HOM. Also, unlabeled 8-HOD, 8,11-diHOD, and 8-HOM were formed. Incubation with labeled [U-^{13}C]8-HOD resulted in the formation of labeled and unlabeled 8-HOM; however, only unlabeled 8,11-diHOD could be detected. This indicates that 8-HOD was most likely not an intermediate in the formation of 8,11-diHOD. To evaluate whether 8,11-diHOD may be formed through a hydroperoxy or endoperoxy intermediate, experiments were carried out in the presence of a reducing agent (250 µM cysteine or 1 mM glutathione and glutathione peroxidase, 2 or 8 U/mL). In such a reducing environment, hydroperoxides and endoperoxides are reduced to hydroxides, but the amount and the ratio 8-HOD to 8,11-diHOD remained unchanged. Also, during time-based experiments (t = 0, 2, 4, 6, 8, 10, 15, 20, 25, and 30 min), no change in the ratio of 8-HOD to 8,11-diHOD was observed. When 8,11-diHOD was isolated and characterized after incubation under an atmosphere of $^{16}O_2/^{18}O_2$, the hydroxyl groups of 8,11-diHOD contained either two atoms of ^{16}O or two atoms of ^{18}O. Species containing one of each isotope could not be detected. This finding indicated that the two hydroxyl groups were derived from the same molecule of gaseous oxygen. Therefore, the intermediate in the formation of 8,11-diHOD was possibly an 8,11-endoperoxy, an 8-peroxo free radical, or an 8-hydroperoxy intermediate. However, experiments in the presence of a reducing agent failed to confirm the presence of such intermediates.

Substrate requirements for the 8- and 8,11-hydroxylating activity were studied by adding various substrates to the homogenate and analyzing the reaction products by using RP-HPLC and GC–MS. 18:1, 18:3n-3, and to a limited extent 18:n-6 were converted into 8-hydroxylated derivatives. However, Z-vaccenic acid was not metabolized. Only 18:3n-3 was also converted into 8,11-dihydroxy-9,12,15-octadecatrienoic acid (8,11-diHOT). Apparently, a 9Z double bond, with no other

double bond toward the carboxylic headgroup, is necessary for the 8- and 8,11-hydroxylating activity.

DISCUSSION

The main finding of the present study was the formation of novel oxygenated products from 18:2 when incubated with a crude extract of *A. bisporus* lamellae. The major reaction products were two oxylipins, identified as 8-HOD and 8,11-diHOD. Analysis by using IR showed that all double bonds had remained in the *Z* configuration. Steric analysis showed that the hydroxyl group at the C_8 position in 8-HOD and 8,11-diHOD had an *R* configuration and that the hydroxyl group at C_{11} in 8,11-diHOD had an *S* configuration. These identifications were further confirmed by ^{1}H NMR and ^{1}H-^{13}C HSQC spectra. Repeating the reaction with [U-^{13}C]18:2 demonstrated that these compounds were formed from exogenously supplied linoleic acid. A crude extract supplied with [U-^{13}C]8-HOD did not convert it into 8,11-diHOD. This suggests that 8-HOD, as such, was not an intermediate in the formation of 8,11-diHOD. Incubating a crude extract of *A. bisporus* under an atmosphere of $^{16}O_2/^{18}O_2$ showed that the two hydroxyl groups of 8,11-diHOD contained either two ^{18}O atoms or two ^{16}O atoms. We propose that this reaction occurs through 8,11-endoperoxy, 8-peroxo free radical, or 8-hydroperoxy intermediates, involving a novel dioxygenase. The conversion of the intermediate is probably too fast to be trapped by a reducing agent.

The formation of 8-HOD has previously been observed in several instances, namely, the ascomycete *Gaeumannomyces graminis*, a pathogen of agricultural crops (4,16); in the oomycete *Leptomitus lacteus*, a sewage fungus (20); in the basidiomycete *Laetisaria arvalis*, a soil fungus (21); in the ascomycete *Magnaportha grisea*, which causes rice blast disease (22), and in the ascomycete *Aspergillus nidulans*, a seed-infesting fungus (23). Upon incubation with 18:2, 8-HPOD, 8-HOD, and 7(*S*),8(*S*)-dihydroxy-9Z,12Z-octadecadienoic acid (7,8-diHOD) were the major reaction products formed by *G. graminis* and *M. grisea*. This activity was assigned to a 7,8-linoleate diol synthase that dioxygenates 18:2 into 8-HPOD and either isomerizes this into 7,8-diHOD or reduces it to 8-HOD (24). This linoleate diol synthase differs from lipoxygenase in that it contains heme-iron and abstracts the monoallylic hydrogen from the C_8 of 18:2. This process is energetically less favorable than the abstraction of allylic hydrogen at C_{11} (25). Molecular oxygen is then inserted antarafacially at C_8 with no change of the position of the double bonds (26). Lipoxygenase abstracts a hydrogen from the allylic C_{11} of OD and inserts a molecular oxygen at C_9 or C_{13} with the formation of *Z/E* conjugated double bonds. Unlike lipoxygenases, the 7,8-linoleate diol synthase has two secondary activities, i.e., isomerization or reduction of the hydroperoxide formed in the first step. *Aspergillus nidulans* produced 8-HOD, 5(*S*),8(*R*)-dihydroxy-9Z,12Z-octadecadienoic acid (5,8-diHOD), and the lactone of 5,8-diHOD from 18:2 (23,27). The mechanism of this reaction has not yet been described. In a *L. lacteus* homogenate, it was demonstrated that a portion of 8,11-diHOD was among the

many dioxygenase and monooxygenase products present (20).

It is possible that, in analogy to 7,8-diHOD in *G. graminis* and *M. grisea,* 8,11-diHOD in *A. bisporus* is formed by 8,11-linoleate diol synthase, which forms and isomerizes an 8-hydroperoxy intermediate. Another possibility is that, in analogy with prostaglandin H synthases, an 8,11-endoperoxy intermediate is formed that in a second step is reduced to two hydroxyl groups. However, the occurrence of such intermediates has yet to be demonstrated.

Interestingly, in other studies on mushroom FA metabolism, 10-HOD was found to be the most prominent metabolite (11). In these studies 10-HOD was derived from 10-HPOD, the proposed intermediate in the formation of 1-octen-3-ol, and 10-ODA (10,17). In our experiments we detected only minor amounts of 10-HOD and 10-ODA. This indicates that this pathway is active, but much less so than the pathway forming 8,11-diHOD. It remains as the subject of further studies whether a connection exists between the formation of 8-HOD and 8,11-diHOD, and 1-octen-3-ol and 10-ODA.

In *A. nidulans* 8-HOD acts as a sporulation hormone (27–29); 8-HOD (in some papers termed psiBα), and 5,8-diHOD (also known as psiCα) stimulated ascospore (sexual) and inhibited conidia (asexual) development. The lactone of 5,8-diHOD (or psiAα) had the opposite effect. In *L. arvalis,* 8-HOD (or laetisaric acid) was reported to possess antifungal properties by inducing rapid hyphal lysis of soil plant pathogens, including *Rhizoctonia solani, Phythium ultimum, Fusarium oxysporum*, and *Mucor globusus* (30). The functions of 8-HOD and 7,8-diHOD in *G. graminis* and *M. grisea* and 8-HOD and 8,11-diHOD in *A. bisporus* have still to be established. It is interesting to note that when added to human white blood cells *in vitro*, 8-HOD attenuated leukotriene B$_4$ formation (31).

The results presented here extend previous studies performed on the formation of oxylipins in fungi in general and *A. bisporus* in particular. This is the first time that extensive formation of 8-HOD and 8,11-diHOD is reported and that a complete structural elucidation, including stereoconfiguration, is described. We demonstrated the formation of these compounds in several different mushroom families, indicating that these kinds of oxylipins may be general to fungal species. To facilitate characterization of this novel dioxygenating activity, more detailed experiments are required, most importantly, the isolation, purification, and cloning of the enzyme.

ACKNOWLEDGMENTS

REFERENCES

1. Hornsten, L., Su, C., Osbourn, A.E., Garosi, P., Hellman, U., Wernstedt, C., and Oliw, E.H. (1999) Cloning of Linoleate Diol Synthase Reveals Homology with Prostaglandin H Synthases, *J. Biol. Chem. 274*, 28219–28224.
2. Varvas, K., Jarving, I., Koljak, R., Valmsen, K., Brash, A.R., and Samel, N. (1999) Evidence of a Cyclooxygenase-Related Prostaglandin Synthesis in Coral. The Allene Oxide Pathway Is Not Involved in Prostaglandin Biosynthesis, *J. Biol. Chem. 274*, 9923–9929.
3. Funk, C.D. (2001) Prostaglandins and Leukotrienes: Advances in Eicosanoid Biology, *Science 294*, 1871–1875.
4. Brodowsky, I.D., Hamberg, M., and Oliw, E.H. (1992) A Linoleic Acid (8*R*)-Dioxygenase and Hydroperoxide Isomerase of the Fungus *Gaeumannomyces graminis*. Biosynthesis of (7*S*,8*S*)-Hydroxylinoleic Acid and (7*S*,8*S*)-Dihydroxylinoleic Acid from (8*R*)-Hydroperoxylinoleic Acid, *J. Biol. Chem. 267*, 14738–14745.
5. Li, D., Lui, Z., and Lu, J. (2001) Purification and Characterization of Lipoxygenase from the Thermophilic Fungus *Thermomyces lanuginosus*, *Mycol. Res. 105*, 190–194.
6. Kuribayashi, T., Kaise, H., Uno, C., Hara, T., Hayakawa, T., and Joh, T. (2002) Purification and Characterisation of Lipoxygenase from *Pleurotus ostreatus*, *J. Agric. Food Chem. 50*, 1247–1253.
7. Bisakowski, B., Atwal, A.S., and Kermasha, S. (2000) Characterization of Lipoxygenase Activity from a Partially Purified Enzymic Extract from *Morchella esculenta*, *Process Biochem. 36*, 1–7.
8. Perraud, X., Kermasha, S., and Bisakowski, B. (1999) Characterization of a Lipoxygenase Extract from *Geotrichum candidum*, *Process Biochem. 34*, 819–827.
9. Filippovich, S., Rybakov, Y., Afanasieva, T., Bachurina, G., Lukina, G., Ezhova, I., Nosova, A., Artjushkina, T., Sineokii, S., and Kristskii, M. (2001) Characterisation of Lipoxygenase from Fungi of the Genus *Mortierella*, *Appl. Microbiol. Biotechnol. 37*, 473–479.
10. Wurzenberger, M., and Grosch, W. (1984) The Formation of 1-Octen-3-ol from the 10-Hydroperoxide Isomer of Linoleic Acid by a Hydroperoxide Lyase in Mushrooms (*Psalliota bispora*), *Biochim. Biophys. Acta 794*, 25–30.
11. Matsui, K., Sasahara, S., Akakabe, Y., and Kajiwara, T. (2003) Linoleic Acid 10-Hydroperoxide as an Intermediate during Formation of 1-Octen-3-ol from Linoleic Acid in *Lentinus decadetes*, *Biosci. Biotechnol. Biochem. 67*, 2280–2282.
12. Hamberg, M., Su, C., and Oliw, E. (1998) Manganese Lipoxygenase. Discovery of a Bis-allylic Hydroperoxide as Product and Intermediate in a Lipoxygenase Reaction, *J. Biol. Chem. 273*, 13080–13088.
13. van Zadelhoff, G., Veldink, G.A., and Vliegenthart, J.F. (1998) With Anandamide as Substrate Plant 5-Lipoxygenases Behave like 11-Lipoxygenases, *Biochem. Biophys. Res. Commun. 248*, 33–38.
14. Bligh, E.G., and Dyer, W.J. (1959) A Rapid Method of Total Lipid Extraction and Purification, *Can. J. Med. Sci. 37*, 911–917.
15. Hamberg, M. (1971) Steric Analysis of Hydroperoxides Formed by Lipoxygenase Oxygenation of Linoleic Acid, *Anal. Biochem. 43*, 515–526.
16. Brodowsky, I.D., and Oliw, E.H. (1992) Metabolism of 18:2(n-6), 18:3(n-3), 20:4(n-6) and 20:5(n-3) by the fungus *Gaeumannomyces graminis*: Identification of Metabolites Formed by 8-Hydroxylation and by ω2 and ω3 Oxygenation, *Biochim. Biophys. Acta 1124*, 59–65.
17. Wurzenberger, M., and Grosch, W. (1982) The Enzymic Oxidative Breakdown of Linoleic Acid in Mushrooms (*Psalliota bispora*), *Z. Lebensm. Unters. Forsch. 175*, 186–190.
18. Mau, J.L., Beelman, R.B., and Ziegler, G.R. (1993) Preparation, Purification and Identification of 10-Oxo-trans-8-decenoic Acid (ODA) from the Cultivated Mushroom, *Agaricus bisporus*, *J. Food Biochem. 16*, 371–388.
19. Song, W.C., and Brash, A.R. (1991) Purification of an Allene Oxide Synthase and Identification of the Enzyme as a Cytochrome P-450, *Science 253*, 781–784.

20. Fox, S.R., Akpinar, A., Prabhune, A.A., Friend, J., and Ratledge, C. (2000) The Biosynthesis of Oxylipins of Linoleic and Arachidonic Acids by the Sewage Fungus *Leptomitus lacteus*, Including the Identification of 8*R*-Hydroxy-9*Z*,12*Z*-octadecadienoic Acid, *Lipids 35*, 23–30.

21. Brodowsky, I.D., and Oliw, E.H. (1993) Biosynthesis of 8*R*-Hydroperoxylinoleic Acid by the Fungus *Laetisaria arvalis*, *Biochim. Biophys. Acta 1168*, 68–72.

22. Cristea, M., Osbourn, A.E., and Oliw, E.H. (2003) Linoleate Diol Synthase of the Rice Blast Fungus *Magnaporthe grisea*, *Lipids 38*, 1275–1280.

23. Mazur, P., Meyers, H.V., Nakanishi, K., El-Zayat, A.A.E., and Champe, S.P. (1990) Structural Elucidation of Sporogenic Fatty Acid Metabolites from *Aspergillus nidulans*, *Tetrahedron Lett. 31*, 3837–3840.

24. Brodowsky, I.D., Zhang, L.Y., Oliw, E.H., and Hamberg, M. (1994) Linoleic Acid 8*R*-Dioxygenase and Hydroperoxide Isomerase of the Fungus *Gaeumannomyces graminis*, *Ann. N. Y. Acad. Sci. 744*, 314–316.

25. Su, C., and Oliw, E.H. (1996) Purification and Characterization of Linoleate 8-Dioxygenase from the Fungus *Gaeumannomyces graminis* as a Novel Hemoprotein, *J. Biol. Chem. 271*, 14112–14118.

26. Hamberg, M., Zhang, L.Y., Brodowsky, I.D., and Oliw, E.H. (1994) Sequential Oxygenation of Linoleic Acid in the Fungus *Gaeumannomyces graminis*: Stereochemistry of Dioxygenase and Hydroperoxide Isomerase Reactions, *Arch. Biochem. Biophys. 309*, 77–80.

27. Tsitsigiannis, D.I., Zarnowski, R., and Keller, N.P. (2004) The Lipid Body Protein, PpoA, Coordinates Sexual and Asexual Sporulation in *Aspergillus nidulans*, *J. Biol. Chem. 279*, 11344–11353.

28. Calvo, A.M., Hinze, L.L., Gardner, H.W., and Keller, N.P. (1999) Sporogenic Effect of Polyunsaturated Fatty Acids on Development of *Aspergillus* spp, *Appl. Environ. Microbiol. 65*, 3668–3673.

29. Champe, S.P., and El-Zayat, A.A.E. (1989) Isolation of a Sexual Sporulation Hormone from *Aspergillus nidulans*, *J. Bacteriol. 171*, 3982–3988.

30. Bowers, W.S., Hoch, H.C., Evans, P.H., and Katayama, M. (1986) Thallophytic Allelopathy: Isolation and Identification of Laetisaric Acid, *Science 232*, 105–106.

31. Vasange-Tuominen, M., Perera-Ivarsson, P., Shen, J., Bohlin, L., and Rolfsen, W. (1994) The Fern *Polypodium decumanum*, Used in the Treatment of Psoriasis, and Its Fatty Acid Constituents as Inhibitors of Leukotriene B4 Formation, *Prost. Leuk. Ess. Fatty Acids 50*, 279–284.

Inhibition of 12- and 15-Lipoxygenase Activities and Protection of Human and Tilapia Low Density Lipoprotein Oxidation by I-Tiao-Gung (*Glycine tomentella*)

Tsui-Yao Chen[a,b], Ming-Shi Shiao[c], and Bonnie Sun Pan[a,*]

[a]Food Science Department, National Taiwan Ocean University, Keelung, Taiwan, 202, Republic of China,
[b]Food Science Department, National I-Lan University, I-Lan, 260 Taiwan, Republic of China, and
[c]Department of Medical Research and Education, Veterans General Hospital-Taipei, 111, Taiwan, Republic of China

ABSTRACT: I-Tiao-Gung, *Glycine tomentella*, has been used extensively as a traditional herbal medicine to relieve physical pain, but its bioactivity has not been studied systematically. Ninety-five percent ethanol extracts of *G. tomentella* (GT-E) showed antioxidant activity in human plasma by prolonging the lag phase (+T_{lag}) of Cu^{2+}-induced LDL oxidation and were dose dependent. The +T_{lag} of LDL combined with 3.2 μg/mL GT-E was similar to that with 2.0 μM (*ca.* 0.5 μg/mL) Trolox. A similar inhibitory effect was found toward tilapia plasma LDL. In addition, GT-E inhibited tilapia thrombocyte (nucleated platelet) 5-, 12-, and 15-lipoxygenase (LOX). The IC_{50} values were 0.43, 0.72, and 0.42 μg/mL, respectively, whereas the IC_{50} values for nordihydroguaiaretic acid (NDGA) on 5-, 12-, and 15-LOX were 2.3, 1.6, and 1.7 μg/mL, respectively. The IC_{50} value for cyclooxygenase-2 (COX-2) inhibition by GT-E was 42.0 μg/mL, whereas the IC_{50} value by indomethacin as a positive control was 0.61 μg/mL. The prevention of LDL oxidation and the dual inhibition of LOX and COX-2 are indicative of the possible roles of I-Tiao-Gung in antiatherosclerosis and anti-inflammation.

Paper no. L9794 in *Lipids 40*, 1171–1177 (November 2005).

Recent studies have demonstrated that atherosclerosis is a complex, chronic inflammatory disease progressing from fatty lesions to fibrous and unstable plaques. It is the major underlying cause of most coronary artery diseases (1). LDL oxidation is actively involved in the initiation and progression of atherogenesis (2–4). Modified or oxidized LDL is taken up by the scavenger receptors of monocyte-derived macrophages, gradually leading to the formation of foam cells and fibrous plaques (5).

Several oxidizing enzymes including 15-lipoxygenase (15-LOX) and myeloperoxidase are involved in LDL oxidation (6–10). Mammalian 15-LOX preferentially oxidizes LDL cholesterol esters, forming a specific pattern of oxygenation products (6). A specific 15-LOX inhibitor is able to limit monocyte-macrophage enrichment of atherosclerotic lesions. It attenuates the development of fibrofoamy and fibrous plaque lesions in the absence of changes in the concentration of total cholesterol or lipoprotein cholesterol (11).

Cyclooxygenase-2 (COX-2), being an inducible protein, elevates in concentration in inflamed tissues (12,13). Nonsteroidal anti-inflammatory agents achieve their therapeutic effects *via* the inhibition of COX-2 to reduce the formation of prostanoids in affected tissues (14,15). In addition, arachidonic acid is converted to other metabolites by 5-lipoxygenase (5-LOX), which is found in cells involved in inflammatory responses (16). It catalyzes the production of the unstable compound of 5-hydroperoxyeicosatetraenoate and its conversion to leukotriene B_4 (LTB_4) or *via* a series of reactions to the cysteinyl leukotrienes LTC_4, LTD_4, and LTE_4. Among these compounds, LTB_4 is the most significant in inflammatory responses. Elevated levels of LTB_4 have been found in blood and joint fluids from patients with rheumatoid arthritis (17). New strategies, notably the dual inhibition of COX-2 and 5-LOX, have been considered (15).

Antioxidants such as probucol, vitamins E and C, and polyphenols have been used to inhibit LDL oxidation *in vitro* and to significantly arrest atherogenesis in rabbits, hamsters, mice, and nonhuman primates *in vivo* (18). I-Tiao-Gung radices of *Glycine tomentella* Hayata and *Flemingia philipinesis* of the Leguminosae have been used extensively as an herbal medicine in Taiwan and mainland China to treat rheumatism, gout, arthritis, and body aches (19,20), indicative of its anti-inflammatory activities. These two strains of I-Tiao-Gung are cultured in Taiwan for their claimed bioactivities. However, except for one report on the hypolipidemic effects of I-Tiao-Gung in the hamster (20) and our previous paper on the major bioactive compounds identified (daizein, daidzin, malonyldaizin, genistin, and glycitin; Ref. 21), no other experimental evidence has been reported in the literature.

The purpose of this study was to verify the long-claimed anti-inflammatory activity of I-Tiao-Gung and to assess its potential effect on atherosclerosis using human recombinant COX-2 (hCOX-2), the LOX of tilapia thrombocytes (the nucleated platelets of fish) (22,23), and the Cu^{2+}-induced oxidation of tilapia LDL as indicators. In addition, the lipoproteins

---

of poikilothermic animals such as fish contain high levels of PUFA, which are susceptible to oxidative modifications. The possible use of tilapia as an animal model to study the preventive effects of herbal compounds on atherosclerosis is also evaluated.

MATERIALS AND METHODS

I-Tiao-Gung, the dried radix of *Glycine tomentella* Hayata (GT), was purchased from Kimnen, Taiwan. Fifty grams of dried roots was powdered by a silent cutter, then added to 95% ethanol at a ratio of 1:10 (wt/vol) and refluxed for 2 h at 75°C. The suspension was filtered to separate the solvent extract from the solid material and refluxed again. The solvent extracts were combined, the ethanol was removed under vacuum, and the extract was then freeze-dried to a powder (GT-E), which was dissolved in methanol for chromatographic analysis following the method reported in our previous paper (21). The RP-HPLC chromatogram of the GT-E used in this study is shown in Figure 1. Blood samples were obtained by venipuncture with a blood collection needle and BD vacutainer containing sodium heparin (Becton Dickinson, Franklin Lakes, NJ) from apparently normal lipidemic students not given vitamin supplements after an overnight fast. The whole blood was centrifuged (1000 × g) at room temperature for 10 min to remove the red blood cells. Plasma samples were collected into polypropylene tubes and stored at 4°C for use within a week.

LOX were isolated from the thrombocytes of tilapia (*Oreochromis niloticus*) according to the procedure of Pan *et al.* (22). The whole blood of tilapia was drawn by caudal puncture with heparinized syringes. The erythrocytes were removed by centrifugation at 4°C, 100 × g, for 10 min. The thrombocyte pellets were isolated by centrifugation at 4°C, 600 × g, for 20 min. After careful removal of the plasma, the thrombocyte pellet was resuspended in sterile 0.05 M phosphate buffer (pH 7.4), which was used as the thrombocyte LOX solution.

hCOX-2 and hydroxyl eicosatetraenoic acids (HETE) were purchased from Cayman (Ann Arbor, MI). Arachidonate, α-tocopherol, 6-hydroxy-2,5,7,8-tetramethyl-chroman-2-carboxylic acid (Trolox), and nordihydroguaiaretic acid (NDGA) were purchased from Sigma (St. Louis, MO). The protein assay reagent was purchased from Bio-Rad (Richmond, CA). All chemicals were of analytical grade.

Determination of the inhibition of LOX. The tilapia thrombocytes resuspended in sterile 0.05 M phosphate buffer (pH 7.4) at 20 mg protein/mL were assayed using the Bradford procedure (24) to determine LOX activity (25). Thrombocyte suspensions (0.1 and 0.79 mL) of 0.05 M phosphate buffer (pH 7.0) containing 0.04% Tween 20 and different concentrations of GT-E or NDGA (0.1 mL and 100 mM) and arachidonic acid dissolved in 95% ethanol (10 μL) were added and mixed, then incubated for 15 min at 25°C. The hydroperoxy FA formed were reduced to the corresponding hydroxyl compounds (HETE) by addition of sodium borohydride. The mixture was acidified to pH 3 with 3 N HCl to terminate the reaction. The hydroxyl FA were extracted with 3 mL of ethyl acetate. The
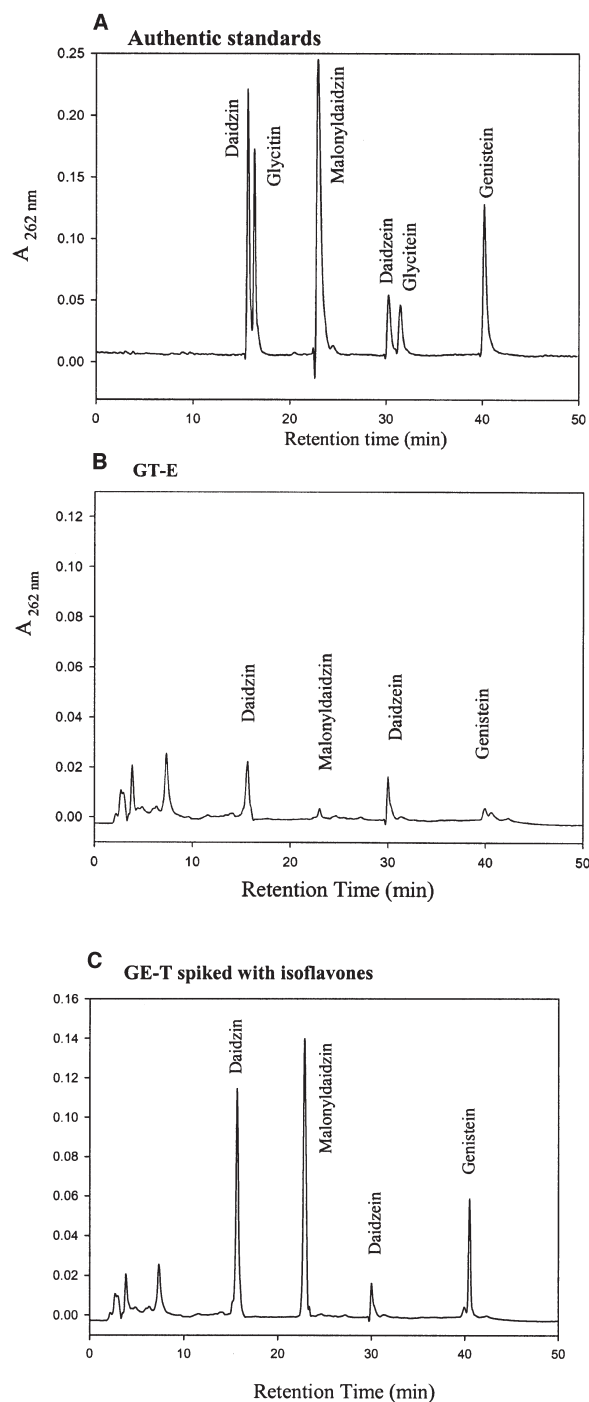
FIG. 1. RP-HPLC chromatograms of (A) isoflavone authentic standards, (B) a 95% ethanol extract of I-Tiao-Gung (GT-E), and (C) GT-E spiked with the authentic compounds daidzin, malonyldaidzin, and genistein, chromatographed on a Luna C18 column (250 × 4 mm, 5 μm particle size; Phenomenex, Torrance, CA), eluted with mobile phase A (0.1% acetic acid aqueous solution) and mobile phase B (0.1% acetic acid in acetonitrile) using the following gradient program: 0–5 min isocratic of 15% B; 5–31 min, linearly increased to 31% of B; 31 min, and then to 35% in 8 min. The system was recycled to 15% B at the end of 45 min. The flow rate was 1.0 mL/min for the first 5 min, then increased to 1.5 mL/min for the next 40 min. The UV absorbance was monitored at 262 nm (Waters 490E programmable multiwavelength detector; Waters, Milford, MA).

solvent was removed under vacuum, and the residues were reconstituted in 0.2 mL of methanol/water (2:1 vol/vol). Aliquots of this solution were injected into a reversed-phase high-performance liquid chromatograph with a Luna C18 column (250 × 4 mm, 5 µm particle size; Phenomenex, Torrance, CA), using a solvent system of methanol/water/acetic acid (85:15:0.1, by vol) at a flow rate of 1 mL/min. The absorbance at 234 nm was monitored during the run with a Waters 490 E programmable multiwavelength detector (Milford, MA). The retention times and peak areas of HETE were compared with those of standards to identify the LOX isozymes and calculate their activities. The same chromatograph, coupled with a diode array detector (SPD-M10A; Shimadzu, Tokyo, Japan), was used to record the UV spectra of the thrombocyte-catalyzed products of HETE isomers. The similarities between the HETE products and the corresponding authentic standards were analyzed using Class-M10A software, version 1.64 (Shimadzu, Tokyo, Japan).

LDL isolation. LDL was obtained by ultracentrifugation of the human and tilapia blood plasma from a density range of $1.019 < d < 1.063$ (adjusted with NaBr) (26). The LDL was extensively dialyzed, while avoiding light for 24 h, against 5 mM phosphate buffer containing 125 mM NaCl (pH 7.4) at 4°C and was used within 3 d.

Cu^{2+}-*induced LDL oxidation.* The concentration of dialyzed LDL was adjusted to 0.15 mg cholesterol/mL. The kinetics of LDL oxidation were determined by monitoring the change in absorbance at 232 nm (ΔA_{232nm}) and was carried out in a 96-well microliter plate (Spectramax 190; Maxline Microplate Reader System Devices, Sunnyvale, CA) at 25°C (26). A 100-µL aliquot of LDL in each well was preincubated with GT-E or Trolox for 30 min. The final volume in each well was adjusted to 240 µL with PBS. LDL oxidation was initiated by adding 0.125 mM $CuSO_4$ (10 µL) to reach a final volume of 250 µL. The ΔA_{232nm} vs. time showed three consecutive phases: a lag phase, a propagation phase, and a decomposition phase. The lag phase was defined as the intercept of the tangent drawn to the steepest segment of the propagation phase to the horizontal axis (26).

RESULTS

Inhibition of 5-LOX and hCOX-2. Inhibitors of hCOX-2 and 5-LOX activities may exhibit anti-inflammatory effects (12,13,16). Tilapia thrombocytes acting on arachidonic acid resulted in three products, i.e., 5-, 12-, and 15-HETE, indicating that the tilapia thrombocytes had three forms of LOX activity (Fig. 2). Rainbow trout thrombocytes have also shown three derivatives from LOX-catalyzed reactions (27). Since tilapia, mullet, and rainbow trout thrombocytes have all shown 5-,12-, and 15-LOX activities (Table 1; Ref. 27), tilapia thrombocytes could be used as a source of LOX for *in vitro* experiments (Table 2). 5-LOX was inhibited by GT-E (IC$_{50}$, 0.43 µg/mL). The inhibition by GT-E was more efficient than that by NDGA, the LOX inhibitor used as a positive control (IC$_{50}$, 2.3 µg/mL). The inhibition of hCOX-2 activity by GT-E (IC$_{50}$, 42.0 µg/mL) was less potent than that by indomethancin. Daidzein is the
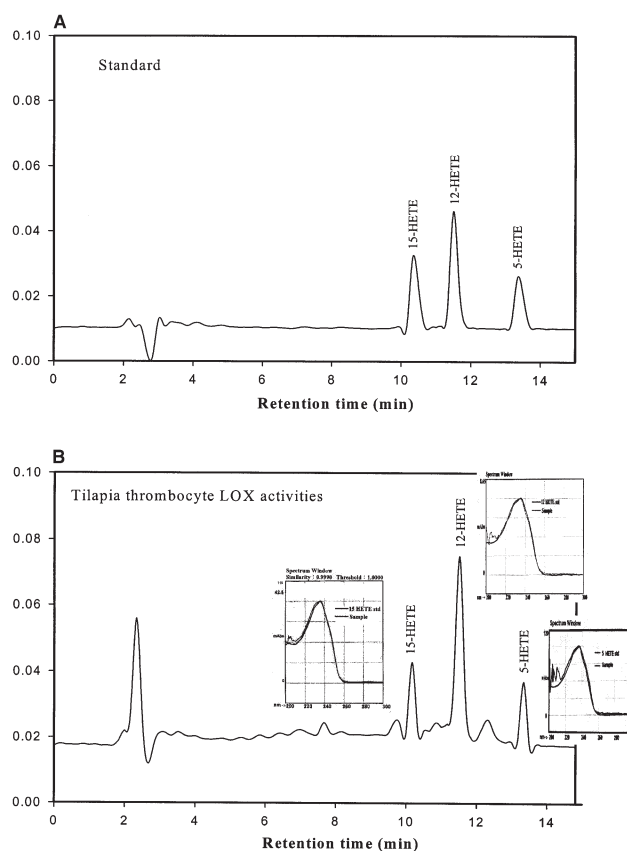
FIG. 2. RP-HPLC chromatograms of arachidonate derivatives catalyzed by authentic standards of hydroxyl eicosatetraenoic acids (HETE) (A) and tilapia thrombocyte lipoxygenases (LOX) (B).

major isoflavone in GT-E (21), and a GT-E concentration of 42.0 µg/mL would be equivalent to 165 µM of daidzein. The inhibitory efficiency of GT-E was 1% that of the positive control indomethacin (IC$_{50}$, 0.61 µg/mL = 1.7 µM), but its efficacy in inhibiting 5-LOX activity was 4.5 times higher than that of the positive control NDGA. Thus, GT-E was a more potent inhibitor of 5-LOX activity than of hCOX-2 activity.

Inhibition of 12-LOX and 15-LOX. GT-E also had inhibitory effects on 12- and 15-LOX activities (IC$_{50}$ of 0.72 and 0.42 µg/mL, respectively) and was thus more potent than NDGA in the assay (Table 2). An *in vivo* test is currently underway using GT-E as a feed ingredient for normal and stressed tilapia to examine their physiological responses. This is perhaps the first study in which fish are used as a model to assay for the inhibitory effect of an herbal extract on LOX activities and the possible role of the herb in preventing LDL oxidation and atherosclerotic lesions.

Prolongation of the lag phase in LDL oxidation. In this study, GT-E was found to inhibit 12- and 15-LOX, which play important roles in mediating that LDL oxidation that leads to the pathogenesis of atherosclerosis (8,10). The efficacy of GT-E in inhibiting LDL oxidation was also evaluated. Both human and tilapia plasma LDL were used for Cu^{2+}-induced oxidation. ΔA_{232nm} was measured to indicate the amount of diene conjugates formed

TABLE 1
Lipoxygenases (LOX) Observed in the Blood Components of Fish

Fish	Blood component	LOX activities (pmol/min/mg protein)			Ref
		5-HETE	12-HETE	15-HETE	
Tilapia	Thrombocytes	30.5	200.0	36.9	This study
Rainbow trout[a]	Thrombocytes	3.2[b]	6.7	0.9[c]	27
Grey mullet	Thrombocytes	139.0	2817.0	94.8	22
	Erythrocytes	1.1	4.2	0.3	22
	Plasma	2.0	27.8	1.4	22

[a]Rainbow trout thrombocytes (approx. 1×10^7 cells) were incubated with 0.1 μM platelet-activating factor (C-18) at 18°C for 20 min. The LOX products were expressed as ng/L $\times 10^7$ cells (27).
[b]Determined as leukotrine B_4.
[c]Determined as LXA_4.

from oxidized PUFA in LDL oxidation. Oxidation appeared in three phases: a lag phase, a propagation phase, and a decomposition phase (Fig. 3). GT-E prolonged the lag phase of the Cu^{2+}-induced oxidation of human plasma LDL to a greater extent than did the positive control, 2.0 μM Trolox (Fig. 3). This Trolox concentration was equivlent to 0.5 μg/mL, calculated on the basis of Trolox having a M.W. of 264 g/mol. On the same weight-concentration basis, GT-E was less effective than Trolox. It showed about 15.5% the efficacy of the latter in prolonging the lag phase of LDL oxidation (Fig. 4). GT-E was found to consist of the hydrophilic antioxidant components previously identified as genistein, daidzein, daidzin, and malonyldaidzin (21), as shown in the RP-HPLC chromatogram in Figure 1. These isoflavones may have functions similar to those of Trolox in conserving the naturally occurring antioxidants enclosed in LDL particles and thus delaying oxidation.

Similarly, GT-E extended the lag phase of tilapia plasma LDL oxidation (Fig. 3). The lag time prolonged by GT-E showed dose-dependent correlations with both human LDL (r^2 = 0.98) and tilapia LDL (r^2 = 0.99) (Fig. 4). The slope of tilapia LDL oxidation was more gradual than that of human LDL oxidation, indicating that GT-E was less effective in protecting tilapia LDL than human LDL from oxidation. Therefore, tilapia LDL may serve as a rapid *in vitro* test model for screening the effectiveness of antioxidants in prolonging the lag phase of Cu^{2+}-induced LDL oxidation.

Reduction of the propagation rate of LDL oxidation. The oxidation rate in the propagation phase of Cu^{2+}-induced oxidation of human LDL is shown in Figure 3. The increased concentration of GT-E added to the human LDL assay mixture decreased the oxidation rate during the propagation phase (re-
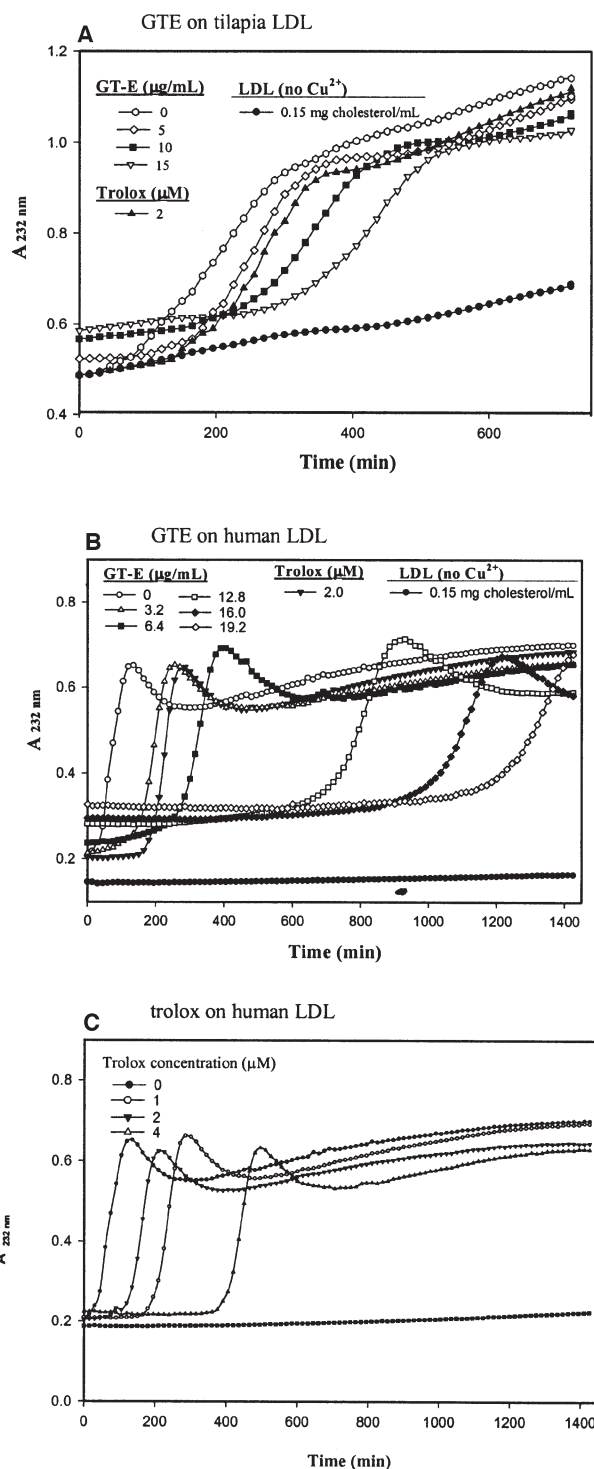
duced slope) and also decreased the maximal formation of diene conjugates during the decomposition phase. The reduction in oxidation rate was proportional to the concentration of GT-E added. Trolox did not change the rate of oxidation in the propagation phase, compared with the rate when neither GT-E nor Trolox was added (Fig. 3). Since Trolox is a hydrophilic antioxidant, it probably could not readily enter the LDL particles. The fact that GT-E reduced the LDL oxidation rate illustrated that it was more hydrophobic than Trolox, thus enabling the herb to be more accessible to LDL particles and protecting the endogenous tocopherol or PUFA in the human LDL particles from oxidation.

A similar effect was found for tilapia LDL oxidation (Fig. 3), the rate of which was about 20% (2.6×10^{-3} vs. 1.32×10^{-2}) that of human LDL when the GT-E concentration was 0. When a 2.0-μM concentration of Trolox was added to tilapia LDL, the oxidation rate was 2.6×10^{-3}, in contrast to 1.3×10^{-2} for human LDL. There was again a fivefold difference in oxidation rates between human and tilapia LDL. Since Trolox is hydrophilic, one possible explanation for this observation is that GT-E probably had better access to the tilapia LDL particles than to the human LDL particles. Thus, the tilapia had a higher concentration of GT-E in the LDL and was able to conserve more endogenous tocopherol in the LDL particles. Current analyses have shown the tocopherol concentration in tilapia LDL to be higher than that in human LDL. An *in vivo* study showed that tilapia fed a diet containing GT-E for 3 mon had higher α-tocopherol concentrations in the LDL than those fed a control diet (unpublished data), indicating that the oxidation rate of LDL is dependent on its conservation of antioxidants.

TABLE 2
Inhibitory Effects on the Activities of Human Recombinant Cyclooxygenase-2 (hCOX-2) and Tilapia Thrombocyte LOX by I-Tiao-Gung Ethanolic Extracts (GT-E) in Comparison with Indomethacin and Nordihydroguaiaretic Acid (NDGA) as Positive Controls

Agent	IC$_{50}$ (μg/mL)			
	5-LOX	12-LOX	15-LOX	hCOX-2[a]
GT-E	0.43 ± 0.32	0.72 ± 0.33	0.42 ± 0.28	42.0 ± 10.2
NDGA	2.3 ± 0.3	1.6 ± 0.3	1.7 ± 0.3	
Indomethacin				0.61 ± 0.15

[a]Cited from Reference 21.

FIG. 4. Correlation between GT-E concentration and prolongation of the lag phase ($+T_{lag}$) of Cu^{2+}-induced oxidation of LDL from human and tilapia using Trolox as a positive control. For other abbreviation see Figure 1.

dation did not show a peak in A_{232nm} before approaching the decomposition phase (Fig. 3B). The difference between the oxidation pattern of tilapia LDL and that of human LDL suggests that the unsaturated FA in human LDL were more susceptible to degradation after the formation of hydroperoxy diene conjugates than were those of tilapia. In the human LDL, the maximum $\Delta A_{232\,nm}$ decreased with an increase in the GT-E concentration, perhaps due to the longer lag phase with GT-E.

DISCUSSION

In our previous study (21), GT-E showed great potential for scavenging free radicals and inhibiting free-radical-mediated lipid oxidation, an early event in biomolecular damage that may cause DNA damage in the later stages. The free radicals that form easily under high oxidative stress result in lipofusins, which are the cross-linked products of free radicals to proteins or DNA (28). An accumulation of lipofusin in the tissues or organs may destroy the biological functions of DNA. In this study, GT-E was found to inhibit LDL oxidation and the oxidative enzymes LOX and COX-2. This antioxidant potential of GT-E may have pharmacological or nutraceutical applications in the future.

COX-2 and 5-LOX activities are involved in inflammation (14,15). Many COX-2 or 5-LOX inhibitors have been developed as drugs to treat inflammation (15,17); however, some COX-2 inhibitors have been withdrawn from the market (29), indicating a need for a COX-2 inhibitor free of side effects. On the other hand, zileuton, a 5-LOX inhibitor, exhibited a more antinociceptive effect on inflammatory pain in acetic acid-induced writhing in mice than did rofecoxib, a COX-2 inhibitor (30). This study demonstrated that GT-E is a natural dual inhibitor of both 5-LOX and COX-2 and is more potent toward 5-LOX. This explains why I-Taio-Gung has a long history as an effective herbal medicine for the treatment of physical pain. What the traditional herbalists did not know was the potential preventive effects of I-Tiao-Gung on atherosclerosis.

FIG. 3. Inhibitory effect of GT-E on Cu^{2+}-induced LDL oxidation: (A) tilapia LDL; (B) human LDL; (C) Trolox. For abbreviation see Figure 1.

Reduction in the maximal formation of conjugated dienes. The absorption at 232 nm wavelength (A_{232nm}) was monitored to reflect the formation of conjugated dienes caused by the oxidation of PUFA in LDL. After the A_{232nm} reached a maximum, it then dropped to the decomposition phase. Tilapia LDL oxi-

To further elucidate the biological effects of GT-E, an animal study or a model system that can provide an *ex vivo* evaluation is essential. The tilapia thrombocytes displayed 5-, 12-, and 15-LOX activities using arachidonate as a substrate, thus offering a good system for the *ex vivo* evaluation of LOX inhibitory activities. In addition, tilapia is a poikilothermic animal that is easy to handle in aquaria for *ex vivo* or *in vivo* tests. Using a tilapia model in this study, we found GT-E to be more efficient than the positive control NDGA in inhibiting 5-LOX activity.

GT-E was also found to inhibit 12- and 15-LOX activities simultaneously. An earlier study showed that inhibiting the mammalian reticulocyte 15-LOX-1 reduced atherosclerosis in the 12/15-LOX gene (similar to the rabbit and human reticulocyte 15-LOX) in knockout mice (7). Also, attenuating 12- and 15-LOX expression decreased LDL oxidation. 12/15-LOX and apoE double-knockout mice exhibited fewer arterial lesions than did apoE-deficient mice with a functional 12-LOX gene (7). In addition, 12(*S*)-HETE, a product of 12/15-LOX, increased the adhesion of monocytes to human endothelial cells *in vitro*, indicating the involvement of 12/15-LOX in inflammation (31). The inhibition of 12-LOX also reduced cancer cell proliferation and induced apoptosis in human gastric cancer cells (32). Still more *in vivo* studies are needed to confirm the claimed bioactivities of I-Tiao-Gung.

Even though plants such as the soybean exhibit 15-LOX activity, the protein sequence and predicted structure of soybean 15-LOX are very different from those of mammalian 15-LOX (33). (−)-Epicatechin and the fraction of procyanidin dimers prepared from the seeds of *Theobroma cacao* inhibited rabbit 15-LOX but were not inhibitory toward soybean 15-LOX (34). Since tilapia is a vertebrate whose taxonomy is closer to that of mammals, the primary structure of tilapia LOX is expected to be more closely related to that of mammals.

Many scientific studies have used fish as an animal model, including respiratory and cardiovascular research on cell culture as well as pharmacological and genetic studies (35). LDL from trout was incubated and determined using ΔA_{232nm} as an index for conjugated diene formation (36), and a pattern similar to that of human LDL oxidation showing three stages of oxidation (a lag phase, a propagation phase, and a decomposition phase) was observed. This study also indicates that LDL oxidation in tilapia was similar to that in humans but that tilapia LDL oxidized more easily.

Since fish are less costly to raise and maintain than are mammalian, avian, reptilian, or amphibian systems, it may save time and reduce costs to use fish as a model for screening bioactive herbal materials that are protective against oxidative modifications, endothelial dysfunction, and inflammation that lead to the pathogenesis of atherosclerosis (32). Many potential antioxidants from herbs, vegetables, and fruits that are able to inhibit LDL oxidation *in vitro* have shown antiatherosclerotic effects in rabbits, transgenic mice, and nonhuman primates *in vivo* (37,38). Here, we to propose that tilapia can be used as an animal model, not to replace the established mammalian models, but to use them for preliminary screening of their potential

bioactivities in the search for anti-inflammatory and antiatherosclerotic herbs, nutraceuticals, and pharmaceuticals.

REFFERENCES

1. Ross, R. (1999) Atherosclerosis: An Inflammatory Disease, *N. Engl. J. Med. 340*, 115–126.
2. Steinberg, D. (1997) Low Density Lipoprotein Oxidation and Its Pathobiological Significance, *J. Biol. Chem. 272*, 20963–20966.
3. Schumacher, M., Eber, B., Tatzber, F., Kaufmann, P., Esterbauer, H., and Klein, W. (1992) LDL Oxidation and Coronary Atherosclerosis, *Lancet 16*, 1183–1186.
4. Mertens, A., and Holvoet, P. (2001) Oxidized LDL and HDL: Antagonists in Atherothrombosis, *FASEB J. 15*, 2073–2084.
5. Ross, R. (1993) The Pathogenesis of Atherosclerosis: A Perspective for 1990s, *Nature 362*, 801–809.
6. Belkner, J., Stender, H., and Kuhn, H. (1998) The Rabbit 15-Lipoxygenase Preferentially Oxygenates LDL Cholesterol Esters, and This Reaction Does Not Require Vitamin E, *J. Biol. Chem. 273*, 23225–23232.
7. Cyrus, T., Witztum, J.L., Rader, D.J., Tangirala, R., Fazio, S., Linton, M.F., and Funk, C.D. (1999) Disruption of the 12/15-Lipoxygenase Gene Diminishes Atherosclerosis in Apo E-Deficient Mice, *J. Clin. Invest. 103*, 1597–1604.
8. Fujita, H., Saito, F., Sawada, T., Kushiro, T., Yagi, H., and Kanmatsuse, K. (1999) Lipoxygenase Inhibition Decreases Neointimal Formation Following Vascular Injury, *Atherosclerosis 147*, 69–75.
9. Yamashita, H., Nakamura, A., Noguchi, N., Niki, E., and Kuhn, H. (1999) Oxidation of Low Density Lipoprotein and Plasma by 15-Lipoxygenase and Free Radicals, *FEBS Lett. 445*, 287–290.
10. Harats, D., Shaish, A., George, J., Mulkins, M., Kurihara, H., Levkovitz, H., and Sigal, E. (2000) Overexpression of 15-Lipoxygenase in Vascular Endothelium Accelerates Early Atherosclerosis in LDL Receptor-Deficient Mice, *Arterioscler. Thromb. Vasc. Biol. 20*, 2100–2105.
11. Bocan, T.M., Rosebury, W.S., Mueller, S.B., Kuchera, S., Welch, K., Daugherty, A., and Cornicelli, J.A. (1998) A Specific 15-Lipoxygenase Inhibitor Limits the Progression and Monocyte-Macrophage Enrichment of Hypercholesterolemia-Induced Atherosclerosis in the Rabbit, *Atherosclerosis 136*, 203–216.
12. Seibert, K., Zhang, Y., Leahy, K., Hauser, S., Masferrer, J., Perkins, W., Lee, L., and Isakson, P. (1994) Pharmacological and Biochemical Demonstration of the Role of Cyclooxygenase-2 in Inflammation and Pain, *Proc. Natl. Acad. Sci. USA 91*, 12013–12017.
13. Harada, Y., Hatanaka, K., Kawamura, M., Saito, M., Ogino, M., Majima, M., Ohno, T., Yamamoto, K., Taketani, Y., Yamamoto, S., *et al.* (1996) Role of Prostaglandin H Synthase-2 in Prostaglandin E_2 Formation in Rat Carrageenan-Induced Pleurisy, *Prostaglandins 51*, 19–33.
14. Kurumbail, R.G., Stevens, A.M., Gierse, J.K., McDonald, J.J., Stegeman, R.A., Pak, J.Y., Gildehaus, D., Miyashiro, J.M., Penning, T.D., Seibert, K., *et al.* (1996) Structural Basis for Selective Inhibition of Cyclooxygenase-2 by Anti-Iinflammatory Agents, *Nature 384*, 644–648.
15. Bertolini, A., Ottani, A., and Sandrini, M. (2001) Dual Acting Anti-inflammatory Drugs: A Reappraisal, *Pharmacol. Res. 44*, 437–450.

16. Bonnet, C., Bertin, P., Trèves, R., and Rigaud, M. (1995) Lipoxygenase Products and Expression of 5-LOX and FLAP in Human Synovial Cells, *Prostaglandins 50*, 127–135.

17. Sharon, P., and Stenson, W.F. (1984) Enhanced Synthesis of Leukotriene B-4 by Colonic Mucosa in Inflammatory Bowel Disease, *Gastroenterology 86*, 453–460.

18. Chisolm, G.M., and Steinberg, D. (2000) The Oxidation Modification Hypothesis of Atherogenesis: An Overview, *Free Radic. Biol. Med. 28*, 1815–1826.

19. Chen, C.R. (1979) *Dictionary of Chinese Medicine*, p. 46, World Book, Taipei, Taiwan.

20. Ko, Y.J., Wu, Y.W., and Lin, W.C. (2004) Hypolipidemic Effect of *Glycine tomentella* Root Eextract in Hamsters, *Am. J. Chin. Med. 32*, 57–63.

21. Pan, B.S., Kuo, Y.Y., Chen, T.S., and Liu, Y.C. (2005) Anti-oxidative and Anti-inflammatory Activities of Two Different Species of a Chinese Herb I-Tiao-Gung, *Life Sci. 77*, 2830–2839.

22. Pan, B.S., Hsu, H.H., Chen, S., and Chen, H.M. (1999) Effects of α-Tocopherol on Lipoxygenase-Catalyzed Oxidation of Highly Unsaturated Fatty Acid, in *Proceedings of the 3rd International Conference on Food Science & Technology*, pp. 76–85, Institute of Food Technologists, Chicago.

23. Stokes, E.E., and Firkin, B.G. (1971) Studies of the Peripheral Blood of the Port Jackson Shark (*Heterodontus portusjacksoni*) with Particular Reference to the Thrombocyte, *Br. J. Haematol. 20*, 427–435.

24. Bradford, M.M. (1976) A Rapid and Sensitive Method for the Quantitation of Microgram Quantities of Protein Utilizing the Principle of Protein-Dye Binding, *Anal. Biochem. 72*, 744–748.

25. Berger, M., Schwarz, K., Thiele, H., Reimann, I., Huth, A., Sabine Borngraber, S., Kuhn, H., and Thiele, B.J. (1998) Simultaneous Expression of Leukocyte-Type 12-Lipoxygenase and Reticulocyte-Type 15-Lipoxygenase in Rabbits, *J. Mol. Biol. 278*, 935–948.

26. Kleinveld, H.A., Hak-Lemmers, H.L.M., Stalenhoef, A.F.H., and Demacker, P.N.M. (1992) Improved Measurement of Low-Density-Lipoprotein Susceptibility to Copper-Induced Oxidation: Application of a Short Procedure for Isolating Low Density Lipoprotein, *Clin. Chem. 38*, 2066–2072.

27. Lloyd-Evans, P., Barrow, S.E., Hill, D.J., Bowden, L.A., Rainger, G.E., Knight, J., and Rowly, A.F. (1994) Eicosanoid Generation and Effects on the Aggregation of Thrombocytes from the Rainbow Trout, *Oncorhynchus mykiss*, *Biochim. Biophys. Acta 1215*, 291–299.

28. Kikugawa, K., Beppu, M., Sato, A., and Kasai, H. (1997) Separation of Multiple Yellow Fluorescent Lipofusin Components in Rat Kidney and Their Characterization, *Mech. Ageing Dev. 97*, 93–107.

29. Bombardier, C., Laine, L., Reicin, A., Shapiro, D., Burgos-Vargas, R., Davis, B., Day, R., Ferraz, M.B., Hawkey, C.J., Hochberg, M.C., *et al.* (2000) Comparison of Upper Gastrointestinal Toxicity of Rofecoxib and Naproxen in Patients with Rheumatoid Arthritis, *N. Engl. J. Med. 343*, 1520–1528.

30. Singh, V.P., Patil, C.S., and Kulkarni, S.K. (2005) Differential Effect of Zileuton, a 5-Lipoxygenase Inhibitor, Against Nociceptive Paradigms in Mice and Rats, *Pharmacol. Biochem. Behav. 81*, 433–439.

31. Hatley, M.E., Strinvasan, S., Reilly, K.B., Bolick, D.T., and Hedrick, C.C. (2003) Increased Production of 12/15 Lipoxygenase Eicosanoids Accelerates Monocyte/Endothelial Interactions in Diabetic db/db Mice, *J. Biol. Chem. 278*, 25369–25375.

32. Wong, B.C.U., Wang, W.P., Cho, C.H., Fan, X.M., Lin, M.C.M., Kung, H.F., and Lam, S.K. (2001) 12-Lipoxygenase Inhibition Induced Apoptosis in Human Gastric Cancer Cells, *Carcinogenesis 22*, 1349–1354.

33. Kuhn, H., and Thiele, B.J. (1999) The Diversity of the Lipoxygenase Family, *FEBS Lett. 449*, 7–11.

34. Schewe, T., Sadik, C., Klotz, L.O., Yoshimoto, T., Kuhn, H., and Sies, H. (2001) Polyphenols of Cocoa: Inhibition of Mammalian 15-Lipoxyogenase, *Biol. Chem. 382*, 1687–1696.

35. Bolis, C.L., Piccolella, M., Valle, A.Z.D., and Rankin, J.C. (2001) Fish as Model in Pharmacological and Biological Research, *Phamacological Res. 44*, 265–280.

36. Froystad, M.K.M., Volden, V., Berg, T., and Gjoen, T. (2002) Metabolism of Oxidized and Chemically Modified Low Density Lipoproteins in Rainbow Trout-Clearance *via* Scavenger Receptors, *Dev. Comp. Immunol. 26*, 723–733.

37. Wu, U.J., Hong, C.Y., Lin, S.J., Wu, P., and Shiao, M.S. (1998) Increase of Vitamin E Content in LDL and Reduction of Atherosclerosis in Cholesterol-Fed Rabbits by a Water-Soluble Antioxidant-Rich Fraction of *Salvia miltiorrhiza*, *Arterioscler. Thromb. Vasc. Biol. 18*, 481–486.

38. Sadik, C.D., Sies, H., and Schewe, T. (2003) Inhibition of 15-Lipoxygenases by Flavonoids: Structure-Activity Relations and Mode of Action, *Biochem. Pharmacol. 65*, 773–781.

METHOD

4-Hydroxy-3-methoxycinnamate Esters of Milkweed Oil: Synthesis and Characterization

Rogers E. Harry-O'kuru*

New Crops and Processing Technology Research Unit, National Center for Agricultural
Utilization Research, ARS, USDA, Peoria, Illinois 61604

ABSTRACT: The common milkweed (*Asclepias syriaca* L.) is a new industrial crop. Its seed oil (TAG) is highly polyunsaturated. In the search for novel applications for milkweed seed oil, the olefinic groups in the TAG were oxidized to polyhydroxy TAG *via* epoxidation and subsequent epoxy ring-opening reactions. These polyhydroxy TAG exhibit unique industrially desirable emulsoid properties in water. Esterification of the secondary polyhydroxy functionalities of the TAG derivatives of the oil with *trans*-4-hydroxy-3-methoxycinnamic acid (ferulic acid) has resulted in the development of novel cinnamate esters of milkweed oil. These cinnamates are also obtainable via direct ring-opening of the epoxy TAG intermediate with ferulic acid. Among the interesting characteristics of the ester derivatives is their UV radiation-absorbing property.

Paper no. L9809 in *Lipids 40*, 1179–1183 (November 2005).

For a new industrial crop to achieve economic success, its components must have unusual properties that set it apart for new markets. Such markets are usually small-volume, value-added niches. The higher-value products give incentives to the farmer to undertake the initial capital investment necessary to cultivate the new crop. The situation for the common milkweed (*Asclepias syriaca* L.) would have presented a double impediment to commercialization because this species is viewed as a nuisance by most farmers who have encountered it in their crop fields or in the range. But in spite of its image, milkweed in recent years has again become a new industrial crop because of market demand for its floss (fiber) in hypoallergenic pillows and comforters. Interestingly, the floss is the same component of the seed that made milkweed a strategic material during World War II (1). But a one-product crop is hardly profitable. Fortunately for milkweed, the increasing demand for the fiber has led to an accumulation of seed and pod hulls, which has resulted in studies to explore possible uses for the seed components and the hulls. To generate new uses for the seed oil, which is 25–30% by weightt of the seed, we have successfully converted the polyolefinic TAG of milkweed oil (Table 1) to the oxiranes and polyhydroxy TAG (2). In seeking further diversification of the nonfood industrial application for the oil, we have also explored conversion of the TAG intermediates

TABLE 1
FA Composition of Milkweed (*Ascepias syriaca*) Oil[a]

Acid type	% Content	Acid type	% Content
Oleic	31.0 (Δ^9, Δ^{11})	Palmitoleic	9.6 (Δ^9, $\Delta^{9,12}$)
Linoleic	50.5	Palmitic	5.7
Linolenic	1.2	Stearic	2.5

[a]From Reference 2.

(epoxy and polyhydroxy forms) into estolides. Estolides have been identified as naturally occurring in some seed oils especially those from species having a monohydroxy functional group in the acyl chain of the TAG (3–7). The synthesis of ricinoleic acid estolides had earlier been reported by Achaya (8). But it was the application of carbocation chemistry that enabled estolides to be prepared on a pilot scale from unsaturated carboxylic acids that have no hydroxyl functional groups (9). Mechanistically, unlike the traditional condensation reaction between an alcohol moiety of an acyl chain and a free carboxylic acid to form estolides, a larger-scale estolide reaction depends on the initial generation of an electrophile at one end of a C=C bond as a result of protonation of the double bond by a Brønsted acid catalyst. The resulting electrophile then accepts an electron pair from the carboxyl OH of a neighboring carboxylic acid moiety thus forming the estolide. Overall the reaction is an addition across a C=C bond by the –OH moiety of a carboxylic acid. These reactions have only been successful with monounsaturated carboxylic acids (10–12). Compton and coworkers (13) used lipase-catalyzed transesterification of soybean oil with ferulic acid ethyl ester to produce UV-absorbing glycerides. The present study reports the novel synthesis of a UV-absorbing estolide by condensation of milkweed polyhydroxy TAG with *trans*-4-hydroxy-3-methoxycinnamic acid (ferulic acid) to give the cinnamate ester of the intact TAG. This ester is also accessible by direct ring-opening of milkweed epoxy TAG with 4-hydroxy-3-methoxycinnamic acid in the presence of a Lewis acid catalyst.

MATERIALS AND METHODS

Materials. Crude, cold-pressed milkweed oil was obtained from Natural Fibers Corporation (Ogallala, NE). Activated acid clay (Bentonite) was obtained from Harshaw/Filtrol Clay Products Division, (Jackson, MS). Sample centrifugation was performed using a Beckman Coulter centrifuge, model J2-HS (Beckman Coulter, Inc., Fullerton, CA). Formic acid, 96% was

obtained from Fisher Scientific (Chicago, IL); hydrogen peroxide, 50% in water, and anhydrous $ZnCl_2$ powder were from Aldrich Chemical Company (St. Louis, MO). ^{1}H and ^{13}C NMR spectra were obtained on a Bruker ARX-400 with a 5-mm dual proton/carbon probe (Bruker Spectrospin, Billerica, MA); the internal standard used was tetramethylsilane. Specific rotation $[\alpha]^{20}_D$ values were measured on a PerkinElmer Polarimeter model 341 (PerkinElmer, Norwalk, CT).

Viscosity measurements. Viscosity measurements were determined in a Temp-Trol viscosity bath (Precision Scientific, Chicago, IL) using Cannon-Fenske viscometers for transparent liquids (Cannon Instrument Company, State College, PA) in accordance with AOCS Official Method Tq 1a-64 (14). The size of the Cannon-Fenske viscometer used was number 400 (378E) or 300. The cleaned dry tube was loaded at room temperature with the sample oil and placed in its holder in the constant-temperature bath. The sample was allowed to equilibrate for 10 min at 40°C or 15 min at 100°C before the sample was suctioned into the lower bulb until the meniscus just overshot the mark above the lower bulb. The suction was removed and the meniscus adjusted to the mark. The sample was allowed to flow at the same time the stop clock was started. The duration (in seconds) it took the meniscus to reach the mark below the bulb multiplied by the tube constant gave the viscosity of the fluid. The measurement was replicated for reproducibility.

FTIR spectrometry. Test samples of the reaction products were pressed between two NaCl discs (25 × 5 mm) to give thin transparent oil films for analysis by FTIR spectrometry. Spectra were measured on a Bomem Arid Zone FTIR spectrometer (Bomem MB-Series; Bomem, Québec, Canada) equipped with a deuterated triglycine sulfate detector. Absorbance spectra were acquired at 4 cm^{-1} resolution and signal-averaged over 32 scans. Interferograms were Fourier-transformed using cosine apodization for optimal linear response. Spectra were baseline corrected and normalized to the methylene peak at 2927cm^{-1}

Methods. (i) Synthesis of epoxy TAG. Refined milkweed oil [186.8 g, 212.1 mmol, iodine value (IV) = 111.4] was placed in a 500-mL three-necked jacketed flask equipped with a mechanical stirrer and heated to 40.5°C. Formic acid (96%, 12.0 g, 25.0 mmol, ~0.3 equiv/mol of C=C) was added and the mixture stirred to homogeneity. Hydrogen peroxide (50%, 70.0 g, 57.4 mL, 4.75 equiv) was added slowly. At the end of the hydrogen peroxide addition, the temperature was raised to 70°C and vigorous stirring was continued for 7 h. The heat source was then removed; the reaction mixture was allowed to cool and was then transferred to a separatory funnel with ethyl acetate as diluent. The material was washed with saturated NaCl (150 mL × 2) followed by saturated Na_2CO_3 (25 mL) in 100 mL more NaCl solution. At about pH 7.5, the organic phase was then washed with deionized water. The organic layer was separated from a turbid aqueous phase, dried over Na_2SO_4, and concentrated *in vacuo* at 60°C to remove the solvent. The yield of epoxy TAG was 188 g (92.3%), and the measured kinematic viscosities were as follows: 1208.95 cSt at 40°C and 81.3 cSt at 100°C, that is, a viscosity index of 18.8 cSt/°C, IV = 1.79. Specific rotation $[\alpha]^{20}_D$ = +0.18° (0.065, CH_2Cl_2). FTIR (film

on NaCl) cm^{-1}: 2967 *s*, 2935 *v-s*, 2876 *s*, 2863 *v-s*, 1754 *v-s*, 1474 *s*, 1393 *m-s*, 1241 *s*, 1187 *s*, 1124 *m-s*, 1021 *m*, 845 *d (m)*, 726 *w-m*. ^{1}H NMR ($CDCl_3$) δ (ppm): 5.25 *m* (residual olefinic), 4.29 *dd* (*J* = 4.3, 11.9 Hz, 2H), 4.14 *dd* (*J* = 5.9, 11.9 Hz, 2H), 3.1 *m* (2H), 2.96 *m* (2H), 2.89 *m* (2H), 2.3 *m* (6H), 1.75–1.25 *m* (72), 0.87 *m* (9). ^{13}C NMR ($CDCl_3$) δ: 173.1, 172.7 (–OC=O), 68.87 (–HCO–), 62.02 (–CH_2O–), 57.10 (HC–O– epoxy), 57.05 (HC–O– epoxy), 56.91 (HC–OC), 56.85 (CO–C), 56.63 (C–O–C), 56.55 (COC), 54.25 (COC), 54.09 (–C–O–C–), 34.06 (–CH_2–), 33.90 (–CH_2–), 31.79 (–CH_2), 31.61 (–CH_2), 29.63 (–CH_2), 29.47 (–CH_2), 29.28 (–CH_2–), 29.23 (–CH_2), 29.15 (–CH_2), 29.12 (–CH_2), 28.92 (CH_2), 28.88 (–CH_2–), 27.83 (–CH_2–), 27.77 (CH_2), 27.75 (–CH_2), 27.16 (–CH_2), 26.88 (CH_2), 26.55 (–CH_2), 26.52 (–CH_2), 26.08 (–CH_2–), 24.73 (–CH_2–), 22.51 (–CH_3), 13.93 (–CH_3).

(ii) Synthesis of polyhydroxy TAG. In a 1-L jacketed flask, as in above setup, was placed reprocessed milkweed oil (648.0 g, 735.7 mmol). The oil was stirred vigorously at 40°C, and formic acid (90.4%, 62.2 g, 1.22 mol) was added in one portion followed by a slow (dropwise) addition of H_2O_2 (50%, 203.0 g, 2.98 mol). At the end of peroxide addition, the temperature was increased to 70°C. After 15 h, the heat source was removed but stirring was continued, allowing the reaction mixture to cool to room temperature; stirring was stopped and the separated aqueous phase was removed. Deionized water (300 mL) was added followed with 6 M HCl (100 mL). The nearly colorless sludge was stirred at 70°C overnight. The cream-colored product was transferred into a separatory funnel using ethyl acetate as diluent. The aqueous layer was discarded and the organic phase was washed sequentially with saturated brine, then saturated $NaHCO_3$ until a pH of 7.5 in the wash water was achieved, followed with deionized water. Ethanol was added to facilitate separation of the phases. After removal of the aqueous layer, the product was concentrated *in vacuo* at 70°C to yield 711.6 g (92.1%) of the polyhydroxyl TAG with an IV = 14 compared with an IV of 114 in the starting milkweed oil. The measured kinematic viscosities were: 2332.5 cSt at 40°C and 75.53 cSt at 100°C, that is, a viscosity index of 37.6 centistokes/°C. Specific rotation $[\alpha]^{20}_D$ = +0.37°. FTIR (film on KBr) cm^{-1}: 3636–3168 *b*, 2927 *vs*, 2856 *vs*, 1743 *vs*, 1463 *s*, 1378 *m*-s, 1240 *m-s*, 1173 *vs*, 1097 *s*, 881 *w*, 725 *w-m*. ^{13}C NMR ($CDCl_3$) δ: 173.2, 172.8 (–O_2C–), 84.60 (HCO), 83.00 (COH), 82.50 (HCO), 82.00 (COH), 80.50 (COH), 74.40 (HCO), 73.82 (HCO), 73.20 (–HC–O), 68.82 (–OCH_2–), 62.04 (–OCH_2–), 34.75 (–CH_2–), 34.48 (–CH_2–), 34.10 (–CH_2–), 33.94 (–CH_2–), 33.54 (–CH_2–), 31.79 (–CH_2–), 31.61 (–CH_2–), 30.47 (–CH_2–), 29.64 (–CH_2–), 29.56 (CH_2), 29.47 (CH_2), 29.42 (CH_2), 29.31 (CH_2), 29.26 (CH_2), 29.21 (CH_2), 29.17 (CH_2), 29.05 (CH_2), 28.91 (CH_2), 25.58 (CH_2), 25.26 (–CH_2–), 24.76 (–CH_2–), 22.61 (CH_2), 22.56 (CH_2), 22.45 (–CH_2–), 14.08 (–CH_3).

(iii) Synthesis of milkweed cinnamate from the polyhydroxy TAG. Milkweed polyhydroxy TAG (34.40 g, 32.74 mmol), glacial acetic acid (150 mL), ferulic acid (45.0 g, 231.7 mmol), HCl (12.1 M, 4.5 mL), and ethyl acetate (250 mL) were placed in a 1-L three-necked round-bottomed flask equipped with a

mechanical stirrer. The contents of the reaction flask were stirred and heated to gentle reflux. Progress of the reaction was monitored by TLC (hexanes/ethyl acetate: 1:1 vol/vol) on pre-coated silica gel. After 48 h the reaction mixture was allowed to cool to room temperature, diluted with more ethyl acetate, and transferred into a separatory funnel. The solution was washed with deionized water (300 mL × 4) to remove most of the acetic acid. The organic phase was then washed with saturated disodium hydrogen phosphate solution and deionized water until the washings were about pH 7. The red-tinged organic solution was dried over anhydrous Na_2SO_4 and concentrated *in vacuo* to give a crude product (64.0 g, 93.1% yield). The crude product was purified by a vacuum LC (VLC) technique on silica gel with hexanes/ethyl acetate (1:1) as the eluting solvent. The yield of the desired fraction i.e., without free ferulic acid) was 44.50 g (64.7%) based on the hexaferuloyl estolide. R_f values on normal-phase silica gel were 0.36, 0.42, and a major band 0.57, compared with 99% ferulic acid, which gave two spots of R_f 0.18 and 0.21; $[\alpha]^{20}_D = +0.12°$ (0.05, CH_2Cl_2). UV absorbance maxima were at 322.5 and 294.5 nm. FTIR (film on NaCl) cm^{-1}: 3554 (phenolic OH stretch) *b*, 3014 (=C–H) *w*, 2967 (CH_3 asym.) *s*, 2939 (–CH_2– asym.) *vs*, 2876 (CH_3 sym.) *s*, 2863 (–CH_2—sym. stretch) *vs*, 1753 (–OC=O TAG) *vs*, 1714 (–OC=O feruloyl) *m*, 1640 (–C=C– alkene puckering) *m*, 1612, 1523 (–C=C– arom. breathing mode) *m-s*, 1465 (–CH_2– deformation) *m-s*, 1375 (–CH_3 umbrella effect) *m*, 1277 (–COC– ester) *m*, 1251 (–COC– ester) *w*, 1185 (–OCH–CHO–) *m-s*, 1042 (C–CH_2O– stretch) *w*. ^{1}H NMR ($CDCl_3$) δ: 7.64 *d* (*J* = 15.9Hz, *trans* H–C=C–H, 2H), 7.08 *dd* (*J* = 8.2 Hz, arom. *ortho* coupling, 2H), 7.05 *d* (*J* = 2.0 Hz, arom. *meta* coupling, 2H), 6.93 *d* (*J* = 8.2 Hz, arom. *ortho* coupling 2H), 6.30 *d* (*J* = 15.9 Hz, *trans* –C=C–H coupling, 2H), 4.26 *q* (*J* = 14.3 Hz, 7H), 4.19 *q* (*J* = 14.3 Hz, 7H), 3.88 *s* (–OCH_3, 9H), 2.31 *t* (*J* = 7.5 Hz, 7H), 2.11 *m* (8H), 1.62 *m* (8H), 1.33 *m* (90H), 0.90 *t* (*J* = 7.0 Hz, 9H). ^{13}C NMR ($CDCl_3$) δ: 173.9 (4 overlapping lines C=O), 170.7 (2 lines C=O), 167.4 (C=O), 148.0 (ipso arom.), 146.0 (ipso arom.), 144.7 (arom.), 127.1 (arom.), 123.1, 115.7, 114.8, 109.4 (arom.), 75.12 (–OCH–), 74.85 (–OCH–), 73.05 (–OCH–), 72.45 (–OCH–), 69.22 (–OCH–), 68.79 (–OCH–), 64.56 (–H_2CO–), 60.43 (–CH_2O–), 60.25 (–CH_2O–), 56.00 (–OCH_3), 34.97 (–CH_2–), 34.74 (–CH_2–), 34.40 (–CH_2–), 32.00 (–CH_2–), 31.89 (–CH_2–), 31.82 (–CH_2–), 31.72 (–CH_2–), 31.32 (–CH_2–), 31.28 (–CH_2), 29.76 (–CH_2–), 29.72 (–CH_2–), 29.66 (–CH_2–), 29.58 (–CH_2–), 29.52 (–CH_2–), 29.42 (–CH_2–), 29.33 (–CH_2–), 29.28 (–CH_2–), 29.22 (–CH_2–), 29.13 (–CH_2–), 29.08 (–CH_2–), 28.90 (–CH_2–), 26.65 (–CH_2–), 26.60 (–CH_2–), 26.34 (–CH_2–), 25.62 (–CH_2–), 25.35 (–CH_2–), 25.06 (–CH_2–), 25.03 (–CH_2–), 24.98 (–CH_2–), 22.76 (–CH_2–), 22.72 (CH_2), 22.62 (–CH_2–), 22.55 (–CH_2–), 21.12 (–CH_2–), 21.03 (–CH_2–), 14.43 (–CH_3), 14.32 (–CH_3), 14.11 (–CH_3).

Synthesis of 4-hydroxy-3-methoxycinnamate estolide from milkweed epoxy TAG. Milkweed epoxy TAG (20.90 g, 21.8 mmol), ferulic acid (26.77 g, 137.9 mmol), and anhydrous $ZnCl_2$ (0.80 g) were placed in a 500-mL reaction flask fitted

with a mechanical stirrer and a reflux condenser. Toluene (200 mL) was added and the reaction mixture stirred and heated to reflux. After 24 h the reaction was cooled to room temperature and then transferred into a separatory funnel with ethyl acetate as diluent. The solution was washed with saturated sodium bicarbonate followed with deionized water. The organic phase was dried (Na_2SO_4) and concentrated *in vacuo* to remove all traces of toluene. The semisolid mass was extracted with ethyl acetate (100 mL × 3) and the extract concentrated to give 25.00 g of a reddish syrup. VLC purification of the crude product over silica gel (hexanes/ethyl acetate, 1:0–1:1 as solvent) gave 18.40 g (40.3% yield) from combined fractions (fractions 5–35) of cinnamoyl estolide of the TAG. The later fractions were ~1:2 mixtures of the estolide and unreacted ferulic acid. The purified compound is a viscous, reddish syrup that is visibly blue under long and short UV wavelengths and gives UV spectral band maxima at 322.5 nm (intense) and a weaker absorption band at 297.0 nm. $[\alpha]^{20}_D = 0.29°$ (0.04, CH_2Cl_2) compared with ferulic acid $[\alpha]^{20}_D = +0.50°$ (0.01, EtOH). FTIR (film on NaCl) cm^{-1}: 3557 *bm*, 2969 *vs*, 2939 *vs*, 2876 *s*, 2863 *vs*, 1753 *vs*, 1714 *w*, 1640 *m-s*, 1612 *m-s*, 1523 *s*, 1472 *s*, 1394 *m-s*, 1279 *s*, 1179 *bs*, 1040 *m-s*, 846 *m*, 820 *m*. ^{1}H NMR ($CDCl_3$) δ: 7.58 *d* (*J* = 15.92Hz, 1H, *trans* coupling aromatic side chain), 7.03 *dd* (*J* = 8.1 Hz, *ortho-* and 1.9 Hz, *meta*-coupling, 1H), 7.01 *d* (*J* = 1.9 Hz, 1H, *meta* coupling), 6.87 *d* (*J* = 8.1 Hz, *ortho*, 1H), 6.26 *d* (*J* = 15.9 Hz *trans* coupling aromatic side chain, 1H), 4.22 *q* (*J* = 14 Hz, 2H), 4.09 *m* (5H), 3.88 *s* (–OCH_3), 2.25 *t* (*J* = 7.0 Hz, 4H), 2.07 *m* (3H), 2.01 *s* (3H), 1.58 *m* (3H), 1.26 *m* (56H), 0.85 *t* (*J* = 7.5 Hz, 9H). ^{13}C NMR ($CDCl_3$) δ: 173.3, 173.2, 172.8, 170.6 (–O_2C–), 148.4 (ipso), 147.0 (ipso), 146.5 (ipso), 126.7 (arom.), 123.4 (arom.), 123.2 (arom.), 114.9 (arom.), 114.0 (arom.), 109.4 (arom.), 73.87 (–CHO–), 68.89 (–CHO–), 62.08 (–CH_2O–), 57.23 (–OCH_3), 57.17 (–OCH_3), 57.01 (–OCH–), 56.95 (–CHO–), 56.73 (–CHOC), 56.66 (–CHO–), 55.91 (–CHO–), 54.35 (–CHO–), 54.19 (–CHO–), 34.12 (–CH_2–), 34.02 (–CH_2–), 34.00 (–CH_2–), 33.96 (–CH_2–), 31.91 (–CH_2–), 31.84 (–CH_2–), 31.76 (–CH_2–), 31.65 (–CH_2–), 29.68 (–CH_2–), 29.64 (–CH_2–), 29.60 (–CH_2–), 29.55 (–CH_2–), 29.53 (–CH_2–), 29.51 (–CH_2–), 29.46 (–CH_2–), 29.42 (–CH_2–), 29.34 (–CH_2–), 29.29 (–CH_2–), 29.45 (–CH_2–), 29.20 (–CH_2–), 29.18 (–CH_2–), 29.16 (–CH_2–), 29.09 (–CH_2–), 29.07 (–CH_2–), 29.04 (–CH_2–), 28.97 (–CH_2–), 28.94 (–CH_2–), 27.88 (–CH_2–), 27.86 (–CH_2–), 27.81 (–CH_2–), 27.78 (–CH_2–), 27.19 (–CH_2–), 26.90 (–CH_2–), 26.59 (–CH_2–), 26.57 (–CH_2–), 26.55 (–CH_2–), 26.46 (–CH_2–), 26.44 (–CH_2–), 26.23 (–CH_2–), 26.12 (–CH_2–), 24.84 (–CH_2–), 24.81 (–CH_2–), 24.79 (–CH_2–), 24.77 (–CH_2–), 24.76, 22.67, 22.65 (–CH_2–), 22.55 (–CH_2–), 22.48 (–CH_2–), 14.09 (–CH_3), 14.06 (–CH_3), 13.98 (–CH_3).

RESULTS AND DISCUSSION

Epoxy TAG. The oxiranes of the common milkweed TAG were prepared as described above (Scheme 1) by oxidation of the C=C bonds of the TG using performic acid made *in situ*

Epoxidation of Milkweed Oil
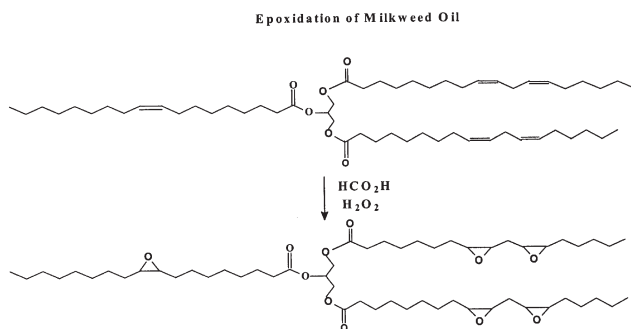
SCHEME 1

(2,15–18). FTIR spectroscopic analysis of the isolated product showed an absorption band characteristic of the –CH–O–CH– stretch of the disubstituted epoxy TAG, that is, a doublet at 824–842 cm^{-1}. The spectrum also showed disappearances of the prominent H–C= stretching mode (3018 cm^{-1}) as well as the C=C breathing or puckering modes (1654 cm^{-1}) of the parent olefin. The ^{13}C NMR distortionless enhancement proton transfer experiment of this intermediate clearly indicated four epoxy units with eight methine carbon resonances at 57.10, 57.05, 56.91, 56.85, 56.63, 56.55, 54.25, and 54.09 ppm. This spectral region was transparent in the starting TAG.

Polyhydroxy TAG. The polyhydroxy TAG was synthesized in two ways. In one approach, the isolated oxirane was ring-

opened in aqueous mineral acid (HCl) followed by ethyl acetate extraction from the aqueous phase (Scheme 2). The preferred approach was a one-pot reaction starting with the purified milkweed oil oxidation followed in sequence by ring-opening of the intermediate epoxy moieties and final isolation of the polyhydroxy TAG. Although the physical characteristics of this compound have been described elsewhere (2), the main spectroscopic feature observed is its diagnostic broad IR absorption band (3636–3168 cm^{-1}), which is characteristic of hydrogen-bonded OH stretching frequencies. The derivative of this spectrum shows four well-separated sharp bands corresponding to the symmetric (2863 cm^{-1}) and the asymmetric (2938 cm^{-1}) stretching modes of the –CH$_2$–; the bands corresponding to the symmetric and asymmetric stretching vibrational modes for the –CH$_3$ moieties are 2876 and 2967 cm^{-1}, respectively. The other major features of this spectrum are the very strong ester carbonyl absorption at 1759 cm^{-1}, the –CH$_2$– deformation at 1473 cm^{-1}, the strong –C–C–O– stretch at 1192 cm^{-1}, and the disappearance of the –C–O–C– stretch of the epoxy TAG. Confirming the presence of secondary hydroxyl carbons on the alkyl chains as a result of epoxy ring-opening, eight low-field resonance lines (84.60, 83.00, 82.50, 82.00, 80.50, 74.30, 73.82, and 73.20 ppm) corresponding to these carbons were observed in the ^{13}C NMR spectrum of this compound.

4-Hydroxy-3-methoxycinnamate estolides of Asclepias

Syntheses of Cinnamate Estolides of Milkweed Oil

R = H, feruloyl-
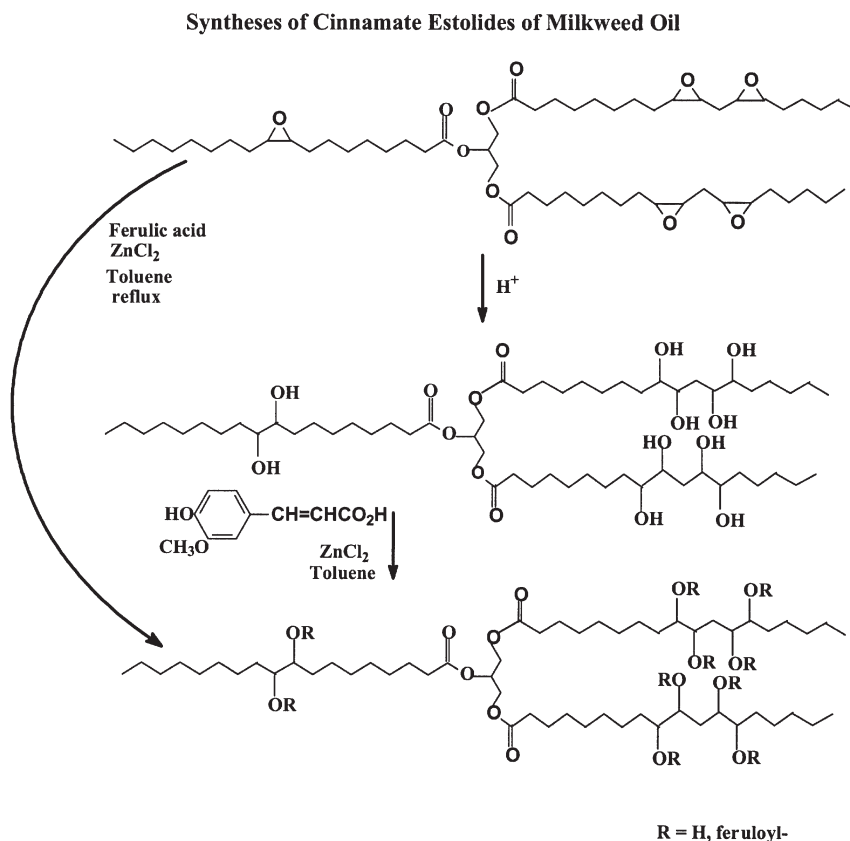
SCHEME 2

TAG. Native milkweed oil is not amenable to direct estolide synthesis because of the polyunsaturated nature of these TAG. A different reaction path was therefore necessary to convert the oil to suitable platforms such as the oxirane and polyhydroxy derivatives. A condensation reaction between the polyhydroxy TAG and ferulic acid catalyzed by concentrated HCl in HOAc and EtOAc gave the estolide in 48 h. A better catalyst for this purpose, however, is the Lewis acid, anhydrous $ZnCl_2$, which gives the product in about one-third of the above reaction time using toluene as solvent. The analogous reaction with tetrahydroxy jojoba wax catalyzed by $ZnCl_2$ goes to completion in 10–13 h relative to HCl catalysis (18). The IR features noticed in the purified estolide are additional bands (3014, 1640, 1612, and 1523 with a weak absorbance at 1714 cm^{-1}). The 3014 cm^{-1} absorption band corresponds to the = C–H stretch, whereas the breathing modes of the aromatic rings are evident at 1612 and 1523 cm^{-1}. The band at 1640 cm^{-1} is assignable to the puckering mode of the alkene moiety of the feruloyl species, and the weaker band at 1714 cm^{-1} is attributable to the conjugated ester –C=O function of the estolide. The estolide is also achievable *via* a direct epoxy TAG ring-opening reaction with ferulic acid under $ZnCl_2$ catalysis. The number of cinnamate moieties incorporated in the latter reaction is usually much lower than could be achieved with the polyhydroxy TAG under the same reaction conditions. Using either approach, the estolide obtained shows the same characteristics which in addition to having good lubricity, strongly absorbs both long and short UV wavelengths. The UV spectra show greater absorption intensity for the product derived from the epoxy TAG than that from the polyhydroxy starting material. This is understandable in terms of the extent of reaction obtained when $ZnCl_2$ is used as catalyst at the reflux temperature of toluene (solvent) compared with the concentrated HCl-catalyzed reaction of the polyhydroxy TAG in refluxing ethyl acetate. This property of strong UV absorbance at very low concentrations makes these TAG derivatives valuable materials that offer effective protection against the increasingly damaging effects of the sun's UV rays. We have previously shown with *trans*-4-hydroxy-3-methoxycinnamate derivatives of jojoba oil that the relative intensities of the absorption band maxima between (360 and 260 nm) could be modulated in favor of the shorter-wavelength band (297.5 nm) if desired, while maintaining the same spectral range (18).

ACKNOWLEDGMENTS

REFERENCES

1. Berkman, B. (1949) Milkweed—A War Strategic Material and a Potential Industrial Crop for Sub-marginal Lands in the United States *Econ. Bot. 3*, 223–239.

2. Harry-O'kuru, R.E., Holser, R.A., Abbott, T.P., and Weisleder, D. (2002) Synthesis and Characterization of Polyhydroxy Triglycerides from Milkweed Oil, *Ind. Crops Prod. 15*, 51–58.

3. Kleiman, R., Spencer, G.F., Earle, F.R., Nieschlag, H.J., and Barclay, A.S. (1972) Tetra-acid Triglycerides Containing a New Hydroxy Eicosadienoyl Moiety in *Lesquerella auriculata* Seed Oil, *Lipids 7*, 660–665.

4. Payne-Wahl, K., Plattner, R.D., Spencer, G.F., and Kleiman, R. (1979) Separation of Tetra-, Penta- and Hexaacyl Triglycerides by High-Performance Liquid Chromatography, *Lipids 14*, 601–604.

5. Madrigal, R.V., and Smith, C.R., Jr. (1982) Estolide Triglycerides of *Trewia nudiflora*, *Lipids 17*, 650–655.

6. Payne-Wahl, K., and Kleiman, R. (1983) Quantitation of Estolide Triglycerides in *Sapium* Seeds by High-Performance Liquid Chromatography with Infrared Detection, *J. Am. Oil Chem. Soc. 60*, 1011–1012.

7. Plattner, R.D., Payne-Wahl, K., Tjarks, L.W., and Kleiman, R. (1979) Hydroxy Acids and Estolides from Triglycerides of *Heliophila amplexicaulis* L.f. Seed Oil, *Lipids 14*, 576–579.

8. Achaya, K.T. (1971) Chemical Derivatives of Castor Oil, *J. Am. Oil Chem. Soc. 48*, 758–763.

9. Erhan, S.M., Kleiman, R., and Isbell, T.A. (1993) Estolides from Meadowfoam Oil Fatty Acids and Other Monounsaturated Fatty Acids, *J. Am Oil Chem, Soc. 70*, 461–465.

10. Isbell, T.A., and Kleiman, R. (1994) Characterization of Estolides Produced from Acid-Catalyzed Condensation of Oleic Acid, *J. Am. Oil Chem. Soc. 71*, 379–383.

11. Harry-O'kuru, R.E., Isbell, T.A. and Weisleder, D. (2001) Synthesis of Estolide Esters from *cis*-9-Octadecenoic Acid Estolides, *J. Am. Oil Chem. Soc. 78*, 219–222.

12. Isbell, T.A., and Kleiman, R. (1996) Mineral Acid-Catalyzed Condensation of Meadowfoam Fatty Acids into Estolides, *J. Am. Oil Chem. Soc. 73*, 1097–1107.

13. Compton, D.L., Laszlo, J.A., and Berhow, M.A. (2000) Lipase-Catalyzed Synthesis of Ferulate Esters, *J. Am. Oil Chem. Soc. 77*, 513–519.

14. AOCS (1997) *Official Methods and Recommended Practices of the AOCS,* 5th edn*.,* Method Tq 1a-64, AOCS Press, Champaign.

15. Findley, T.W., Swern, D., and Scalan, J.T. (1945) Epoxidation of Unsaturated Fatty Materials with Peracetic Acid in Glacial Acetic Acid, *J. Am. Chem. Soc. 67*, 412–414.

16. Chadwick, A.F., Barlow, D.O., D'Adieco, A.A., and Wallace, J.G. (1958) Theory and Practice of Resin-Catalyzed Epoxidation, *J. Am. Oil Chem. Soc. 35*, 355–358.

17. Page-Xatart-Pares, X., Bonnet, C., and Morin, O. (2000) Synthesis of New Derivatives from Vegetable Oil Methyl Esters *via* Epoxidation and Oxirane Ring Opening, in *Recent Developments in the Synthesis of Fatty Acid Derivatives* (Knothe, G., and Darksen, J.T.P., eds.), pp. 141–156, AOCS Press, Champaign.

18. Harry-O'kuru, R.E., Mohamed, A., and Abbott, T.P. (2005) Synthesis and Characterization of Tetrahydroxyjojoba Wax and Ferulates of Jojoba Oil, *Ind. Crops Prod. 22*, 125–133.

The Fate and Intermediary Metabolism of Stearic Acid

Harini Sampath[a] and James M. Ntambi[b],*

[a]Departments of Nutritional Sciences and [b]Departments of Nutritional
Sciences and Biochemistry, University of Wisconsin, Madison, Wisconsin, 53706

ABSTRACT: Coming from the Greek for "hard fat," stearic acid represents one of the most abundant FA in the Western diet. Otherwise known as *n*-octadecanoic acid (18:0), stearate is either obtained in the diet or synthesized by the elongation of palmitate, the principal product of the FA synthase system in animal cells. Stearic acid has been shown to be a very poor substrate for TG synthesis, even as compared with other saturated fats such as myristate and palmitate, and in human studies stearic acid has been shown to generate a lower lipemic response than medium-chain saturated FA. Although it has been proposed that this may be due to less efficient absorption of stearic acid in the gut, such findings have not been consistent. Along with palmitate, stearate is the major substrate for the enzyme stearoyl-CoA desaturase, which catalyzes the conversion of stearate to oleate, the preferred substrate for the synthesis of TG and other complex lipids. In mice, targeted disruption of the stearoyl-CoA desaturase-1 (SCD1) gene results in the generation of a lean mouse that is resistant to diet-induced obesity and insulin resistance. SCD1 also has been shown to be a key target of the anorexigenic hormone leptin, thus underscoring the importance of this enzyme, and consequently the cellular stearate-to-oleate ratio, in lipid metabolism and potentially in the treatment of obesity and related disorders.

Paper no. L9785 in *Lipids 40*, 1187–1191 (December 2005).

STEARATE: STRUCTURE AND SOURCES

Stearate was first described by Michel Eugene Chevreul in 1823 in his studies on fats and oils and is one of the most abundant saturated FA in the Western diet (1). Stearic acid is also denoted as *n*-octadecanoic acid or as 18:0, as it is composed of 18 carbons with no double bonds. Although it is found in small quantities in seed and marine oils, major sources of this long-chain saturated fat include milk fats, which can contain 5 to 15% stearate, as well as lard and cocoa and shea butters, which can contain from 10–35% stearate. Stearic acid is also a large constituent in hydrogenated fats and oils.

Apart from dietary sources, stearate can also be endogenously synthesized from acetyl-CoA molecules (Fig. 1). The biotin-containing acetyl-CoA carboxylase (ACC) catalyzes the irreversible conversion of the two-carbon acetyl-CoA to the three-carbon intermediate, malonyl-CoA. Malonyl-CoA then serves as the precursor for the endogenous synthesis of FA *via* the FA synthase (FAS) multienzyme complex. In bacteria and yeast, FAS exists as seven or two separate polypeptides, respectively, that are tightly associated in one large complex. In mammals, the reactions of the FAS system are catalyzed by individual domains of a single large polypeptide that also includes an acyl carrier protein (ACP) domain (2,3). The large protein functions as a 480 kDa homodimer to carry out seven cycles of sequential condensation, reduction, and dehydration reactions to form the 16-carbon saturated FA, palmitate. Although small amounts of stearate are sometimes formed through the actions of FAS, chain elongation generally stops at 16 carbons, and the palmitate is released from the ACP moiety (2,3). Further elongation generally occurs through the actions of microsomal elongases to form stearate (Fig. 1).

Six different isoforms of FA elongase (Elovl) have been identified in the mouse, rat, and human genomes (3–6). Elovl1-1 (Ssc1) and Elovl-6 [LCE, fatty acid elongase (FACE), rElo2] have been shown to elongate saturated and monounsaturated FA (3,7,8). Elovl-2 (Ssc2) acts on 20- to 22-carbon PUFA, whereas Elovl-5 (FAE1, Relo1, Helo1) has a wide range of substrates from 16 to 22 carbons long (7,8). 16:0-CoA has been shown to be a substrate for Elovl-1 and Elovl-6 and is converted to 18:0-CoA by these FA elongases (7–10).
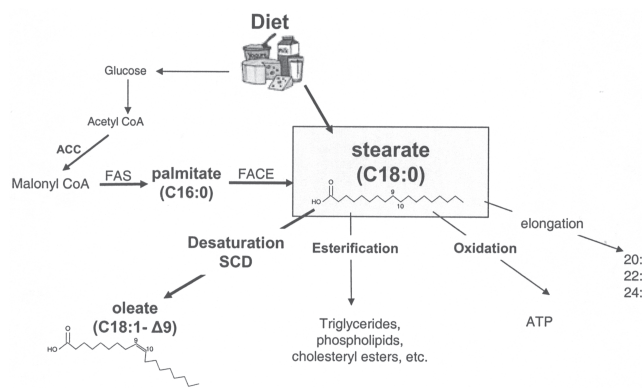
FIG. 1. Synthesis and fate of stearic acid. Stearate can either be obtained from the diet or be synthesized *de novo* in the body through the actions of acetyl-CoA carboxylase (ACC) and the FA synthase (FAS) enzyme complex and through elongation of palmitate by FA elongases (FACE). Once it has been formed, stearate can undergo various fates including further elongation, oxidation, and esterification to form complex lipids or desaturation by the enzyme stearoyl-CoA desaturase (SCD) to form the monounsaturated FA, oleate.

REGULATION OF STEARATE SYNTHESIS

The pathway of the synthesis of stearate and other FA is highly regulated. The compartmentalization of FA synthesis and oxidation in the cytosol or mitochondria, respectively, allows for reciprocal regulation of these two processes. Also, while the product of FA breakdown is acetyl-CoA, *de novo* synthesis of FA is not a simple reversal of this catabolic process. Instead, the formation of the three-carbon intermediate, malonyl-CoA, is a requisite step in FA synthesis (2). Furthermore, the enzymes involved in the synthesis of stearate are all highly regulated by dietary, hormonal, and physiological changes.

In general, insulin, glucose, 3,5,3′-triiodothyronine, and glucocorticoids have all been shown to induce *de novo* lipogenesis (DNL), whereas long-chain PUFA, epinephrine, and glucagon have been shown to suppress DNL (11–13). There is also considerable evidence for the transcriptional regulation of enzymes of *de novo* FA synthesis, including FAS and Elovl-6 through the actions of the lipogenic transcription factor, sterol-regulatory element-binding protein (SREBP) (3,7,9,10,14).

SREBP are a family of helix-loop-helix transcription factors that were first identified through their ability to bind to a sterol response element found on genes involved in cholesterolgenesis. Three isoforms of SREBP have thus far been identified; SREBP-1a and SREBP-1c regulate genes of lipid synthesis, whereas SREBP-2 has been shown to be involved in cholesterol homeostasis. SREBP-1a and -1c are both transcribed from the same gene locus and differ only at their N-termini; SREBP-2 is encoded by a separate gene. SREBP1c is the major isoform in rodent and human liver and is now recognized as a key regulator of FA and TG synthesis (14,15).

SREBP are initially synthesized as large proteins (125 kDa) anchored to the endoplasmic reticulum membrane with two membrane-spanning domains and with their C-terminal end bound to the SREBP-cleavage activating protein (SCAP). In response to cellular signals such as decreased sterol levels, the SREBP–SCAP complex moves to the Golgi apparatus, where it undergoes two proteolytic events, giving rise to the smaller (65 kDa), mature form of the SREBP protein (14,15). This proteolytic cleavage then results in the transit of the mature form of the protein to the nucleus, where it binds to *cis*-elements termed sterol regulatory elements (SRE) in the promoters of target genes and induces transcription of a variety of genes involved in cholesterol, TG, and FA synthesis; these include ACC and FAS as well as stearoyl-CoA desaturase-1 (SCD1), which converts stearate (18:0) to oleate (18:1n-9) (14–17).

Mice overexpressing SREBP in the liver have been shown to accumulate lipids in their liver as a result of increased expression of lipogenic genes. However, the majority of FA in the livers of these transgenic mice tend to be 18 carbons long rather than 16 carbons long, suggesting that the FA elongase responsible for the synthesis of stearate from palmitate is also upregulated by SREBP (3). Indeed, it was recently shown that Elovl-6, also known as FACE, is upregulated in SREBP transgenic mouse livers (7,10,18). It has since been described that Elovl-6 specifically utilizes 12- to 16-carbon saturated and monounsat-

urated FA in the liver as substrates. Elovl-6 is also upregulated in leptin-deficient ob/ob mice that have markedly higher hepatic SREBP levels (10). Elovl-6 expression was also shown to be upregulated by agonists of the liver X receptor (LXR) (10), a nuclear receptor that is a strong activator of SREBP-1c transcription.

FATE OF STEARATE

Once stearate has been synthesized in the cell, it can undergo several different fates (Fig. 1) depending on various factors such as the energy charge of the cell, hormonal signals, and so forth. Under conditions of low energy charge, the enzyme carnitine palmitoyl transferase-1 transports stearate to the mitochondria, where it is oxidized (19). Alternately, under conditions of high energy charge, such as after a meal, stearate can be directly esterified to form complex lipids for storage. However, it has been shown that stearate is a very poor substrate for esterification (20). On the other hand, stearate can be desaturated by the actions of the enzyme stearoyl-CoA desaturase to form oleate (18:1n-9), which has been shown to be the preferred substrate for complex lipid synthesis (21). Alternately, stearate can be further elongated to form other long-chain saturated FA (Fig. 1).

DESATURATION: STEAROYL-CoA DESATURASES

In mammalian cells, stearate is rapidly acted on by the enzyme stearoyl-CoA desaturase and is converted to its monounsaturated product, oleate. SCD is the rate-limiting enzyme in the synthesis of monounsaturated FA from their saturated FA precursors. SCD introduces a single double bond between carbons 9 and 10 of the saturated FA and shows high substrate specificity for palmitate and stearate, converting them to palmitoleate and oleate, respectively (21,22).

The genes for SCD have been identified and cloned from several species, including yeast, *Caenorhabditis elegans*, hamster, sheep, rat, mouse, and human. Four different isoforms of the enzyme have been identified in the mouse, whereas two different isoforms have thus far been identified in the human (21,22). In the mouse, SCD1 is the major isoform expressed in white adipose tissue, brown adipose tissue, and the meibomian, Harderian, and preputial glands. It is also dramatically induced in the liver upon high-carbohydrate feeding (21,22). The presence of four different isoforms of SCD in the mouse is partially explained by differential tissue distribution of the various isoforms. However, it is also becoming apparent that these various SCD isoforms may differ in terms of their substrate specificities. It has been suggested, for instance, that although SCD1 and SCD2 may show greater specificity toward the desaturation of stearate (23,24), SCD3 may prefer palmitate as a substrate (25,26). Support for these hypotheses comes from studies using the SCD1 knockout (SCD1−/−) mouse model, which, due to a targeted mutation of the SCD1 gene, exhibits complete loss of SCD1 expression and activity. However, microsomes from the Harderian glands of SCD1−/− mice retain the ability

to desaturate 16:0-CoA, whereas their ability to desaturate 18:0-CoA is reduced by over 90% (21,24). This suggests that SCD1 may prefer stearate over palmitate as a substrate. Studies in the preputial glands of SCD1−/− mice have revealed that although SCD1 and SCD3 activities are virtually absent, SCD2 expression is not attenuated. At the same time, microsomes from the preputial glands of SCD1−/− mice exhibit greater desaturase activity toward 18:0-CoA compared with 16:0-CoA, suggesting that SCD2 prefers stearate as a substrate (21,25). Treatment of SCD1−/− mice with testosterone increases SCD3 expression in preputial glands, concomitantly increasing 16:1n-7 levels; this suggests that the SCD3 isoform may prefer 16:0-CoA as a substrate (21,25). The substrate specificity of the newly identified SCD4, if any, is yet to be determined. These differences in tissue specific expression as well as substrate specificity may provide additional levels of regulation in determining the lipid composition of the cell, thereby regulating diverse cellular processes.

IS STEARATE FUNCTIONALLY DIFFERENT FROM OTHER SATURATED FATS?

In general, saturated fat has been recognized as deleterious to the health because of its hypercholesterolemic and atherogenic effects. Hence, the recommended dietary intake of saturated fat has been set at less than 10% of the total daily fat intake. Because of this generalized recommendation, stearate has been grouped with other saturated FA simply due to its chemical structure. However, there is evidence that the effects of stearate are considerably different from the effects of shorter-chain saturated FA such as laurate, myristate, and palmitate (20,27–31).

The early work of Keys *et al.* (28) and Hegsted *et al.* (29) established that, unlike laurate, myristate, and palmitate, stearate does not raise plasma cholesterol levels. More recently, it has been shown in hamsters that although diets high in laurate, myristate, or palmitate increase plasma cholesterol by depressing LDL receptor activity and increasing the rate of LDL production, stearate does neither and is in fact associated with a hypocholesterolemic response (32). In humans, stearate has been shown to be as potent as oleate at reducing plasma LDL levels (33). Furthermore, our studies with the SCD1−/− mouse have revealed that despite their inability to desaturate stearate into oleate, there is no significant accumulation of stearate in the tissues of SCD1−/− animals even when substantial amounts of stearate are added to their diets (34). Dietary oleate, on the other hand, is able to partially rescue the hypolipidemic profile of SCD1−/− mice (34), suggesting that stearate may not necessarily mediate the hypertriglyceridemic effect associated with saturated FA.

Several hypotheses have been proposed for why stearate may behave differently from its shorter-chain saturated FA counterparts. First, stearate has been shown to be a very poor substrate for TG and cholesteryl ester formation (20,31). It has been suggested that stearate, because of its chain length and saturated nature, is not absorbed efficiently (35). However, studies in humans show that absorption of stearic acid and its

metabolizable energy are only marginally lower than those of other FA and are probably insufficient to explain its differential effects on plasma lipoprotein responses (36,37).

It has also been suggested that the effects of stearate may in fact be mediated by its desaturation into oleate, catalyzed by the enzyme SCD (38). Ongoing studies on the role and regulation of SCD will no doubt be key to understanding whether the conversion of stearate to oleate mediates the intracellular effects of stearic acid.

CELLULAR STEARATE-TO-OLEATE RATIOS: CLINICAL IMPLICATIONS

Oleate, the product of SCD, has been shown to be the preferred substrate for the synthesis of TG, cholesteryl esters, and DAG (21). It is abundant in the diet and can be obtained from various sources including animal and vegetable fats. Despite this, the SCD enzyme is subject to various forms of regulation by dietary, hormonal, and environmental factors (22), suggesting an important role for the maintenance of the cellular ratio of stearate to oleate. Indeed, the cellular ratio of oleic to stearic acids has been shown to play a role in various conditions by effecting changes in membrane fluidity and signal transduction that can, in turn, regulate cell growth and differentiation (39–42). In general, changes in SCD expression affect the FA composition of membrane phospholipids, TG, and cholesteryl esters and may thus have an impact on diseases of lipid metabolism including obesity, diabetes, and cardiovascular disease. For instance, murine hypertriglyceridemia has been shown to be well correlated with hepatic SCD activity, and consequently plasma 18:1/18:0 ratios. Furthermore, in human subjects, a low-fat, high-carbohydrate diet was found to cause an increase in the plasma 18:1/18:0 ratio, and this increase was larger in subjects exhibiting a hypertriglyceridemic response to the diet compared with those whose TG levels were lower (43).

More recently, it has also been shown that stearate may also play a role in regulating gene transcription (44). Lin *et al.* (44) have shown that saturated FA, including stearate, are involved in the activation of SREBP, and consequently of lipogenic target genes. This activation requires the transcriptional coactivator PGC-1β and also involves concurrent coactivation of the nuclear receptor LXRα.

Further understanding of the potential role of SCD activity, and therefore of the stearate–oleate ratio in the cell, has come from studies in the SCD1 knockout mouse model, as described in the Desaturation: Stearoyl-CoA Desaturases section. SCD1−/− mice have very low hepatic TG and cholesteryl ester accumulation and decreased whole-body adiposity (45,46). SCD1−/− mice also display decreased lipogenic gene expression as well as increased metabolic rates and lipid oxidation (22,45,47,48). SCD1−/− mice are protected from diet-induced obesity, suggesting that the loss of SCD activity in this mouse model may protect them from hypertriglyceridemia as well as hepatic steatosis (34,47,48). Given the high degree of correlation between atherosclerosis and cardiovascular disease and HDL and LDL ratios, these findings in the SCD1−/− mice are of potential clinical significance.

Furthermore, SCD1−/− mice display greater insulin sensitivity compared with their wild-type littermates and are resistant to diet-induced obesity (49,50). Recently, SCD1 has also been shown to be a downstream target of the anorexigenic hormone leptin (51), suggesting a potentially prominent role for this enzyme in the regulation of appetite and body weight, as well as in insulin sensitivity.

CONCLUSION

As conditions such as obesity reach epidemic proportions, lipid-induced disorders such as hepatic steatosis, hypertriglyceridemia, cardiovascular disease, and insulin resistance have moved to the forefront of public health concerns. Given the severity of this epidemic, there is mounting interest in identifying modifiable risk factors, especially dietary components, that may contribute to the progression or prevention of lipid-induced diseases. Although saturated fats have generally been considered to be prolipogenic and proatherogenic, it seems likely that stearic acid is unique in its effects on plasma lipids as compared with other saturated FA. Stearate is known to be a poor substrate for TG and cholesteryl ester synthesis; this may explain why, unlike laurate, myristate, or palmitate, stearate is generally not associated with a hypercholesterolemic response. Stearate is rapidly converted to oleate by the enzyme SCD, which is subject to various levels of regulation by hormonal, dietary, and physiological factors. Recent studies using the SCD1−/− mouse model have revealed several important aspects of the potential role that the cellular stearate-to-oleate ratio may play in conditions such as obesity and insulin resistance. Further studies will be important in deciphering the specific effects of intracellular stearate in the progression or attenuation of lipid-induced disease.

ACKNOWLEDGMENTS

REFERENCES

1. Spady, D.K., Woollett, L.A., and Dietschy, J.M. (1993) Regulation of Plasma LDL-Cholesterol Levels by Dietary Cholesterol and Fatty Acids, *Annu. Rev. Nutr. 13*, 355–381.
2. Towle, H.C., Kaytor, E.N., and Shih, H.M. (1997) Regulation of the Expression of Lipogenic Enzyme Genes by Carbohydrate, *Annu. Rev. Nutr. 17*, 405–433.
3. Wang, Y., Botolin, D., Christian, B., Busik, J., Xu, J., and Jump, D.B. (2005) Tissue-Specific, Nutritional, and Developmental Regulation of Rat Fatty Acid Elongases, *J. Lipid Res. 46*, 706–715.
4. Leonard, A.E., Pereira, S.L., Sprecher, H., and Huang, Y.S. (2004) Elongation of Long-Chain Fatty Acids, *Prog. Lipid Res. 43*, 36–54.
5. Moon, Y.A., and Horton, J.D. (2003) Identification of Two Mammalian Reductases Involved in the Two-Carbon Fatty Acyl Elongation Cascade, *J. Biol. Chem. 278*, 7335–7343.
6. Prasad, M.R., Nagi, M.N., Ghesquier, D., Cook, L., and Cinti, D.L. (1986) Evidence for Multiple Condensing Enzymes in Rat Hepatic Microsomes Catalyzing the Condensation of Saturated, Monounsaturated and Polyunsaturated Acyl Coenzyme A, *J. Biol. Chem. 261*, 8213–8217.
7. Moon, Y.A., Shah, N.A., Mohapatra, S., Warrington, J.A., and Horton, J.D. (2001) Identification of a Mammalian Long Chain Fatty Acyl Elongase Regulated by Sterol Regulatory Element-Binding Proteins, *J. Biol. Chem. 276*, 45358–45366.
8. Inagaki, K., Aki, T., Fukuda, Y., Kawamoto, S., Shigeta, S., Ono, K., and Suzuki, O. (2002) Identification and Expression of a Rat Fatty Acid Elongase Involved in the Biosynthesis of C18 Fatty Acids, *Biosci. Biotechnol. Biochem. 66*, 613–621.
9. Horton, J.D., Shah, N.A., Warrington, J.A., Anderson, N.N., Park, S.W., Brown, M.S., and Goldstein, J.L. (2003) Combined Analysis of Oligonucleotide Microarray Data from Transgenic and Knockout Mice Identifies Direct SREBP Target Genes, *Proc. Natl. Acad. Sci. USA 100*, 12027–12032.
10. Matsuzaka, T., Shimano, H., Yahagi, N., Yoshikawa, T., Amemiya-Kudo, M., Hasty, A.H., Okazaki, H., Tamura, Y., Iizuka, Y., Ohashi, K., *et al.* (2002) Cloning and Characterization of a Mammalian Fatty Acyl-CoA Elongase as a Lipogenic Enzyme Regulated by SREBP, *J. Lipid Res. 43*, 911–920.
11. Kersten, S. (2001) Mechanisms of Nutritional and Hormonal Regulation of Lipogenesis, *EMBO Rep. 2*, 282–286.
12. Jump, D.B., and Clarke, S.D. (1999) Regulation of Gene Expression by Dietary Fat, *Annu. Rev. Nutr. 19*, 63–90.
13. Sampath, H., and Ntambi, J.M. (2004) Polyunsaturated Fatty Acid Regulation of Gene Expression, *Nutr. Rev. 62*, 333–339.
14. Brown, M.S., and Goldstein, J.L. (1997) The SREBP Pathway: Regulation of Cholesterol Metabolism by Proteolysis of a Membrane-Bound Transcription Factor, *Cell 89*, 331–340.
15. Osborne, T.F. (2000) Sterol Regulatory Element-Binding Proteins (SREBPs): Key Regulators of Nutritional Homeostasis and Insulin Action, *J. Biol. Chem. 275*, 32379–32382.
16. Kim, J.B., Sarraf, P., Wright, M., Yao, K.M., Solanes, G., Lowell, B.B., and Spiegelman, B.M. (1998) Nutritional and Insulin Regulation of Fatty Acid Synthetase and Leptin Gene Expression Through ADD1/SREBP1, *J. Clin. Invest. 101*, 1–9.
17. Shimano, H., Yahagi, N., Amemiya-Kudo, M., Hasty, A.H., Osuga, J., Tamura, Y., Shionoiri, F., Iizuka, Y., Ohashi, K., Harada, K., *et al.* (1999) Sterol Regulatory Element Binding Protein-1 as a Key Transcription Factor for the Nutritional Induction of Lipogenic Enzyme Genes, *J. Biol. Chem. 274*, 35832–35839.
18. Inagaki, K., Aki, T., Fukuda, Y., Kawamoto, S., Shigeta, S., Ono, K., and Suzuki, O. (2002) Identification and Expression of a Rat Fatty Acid Elongase Involved in the Biosynthesis of C18 Fatty Acids, *Biosci. Biotechnol. Biochem. 66*, 613–621.
19. Foster, D.W. (2004) The Role of the Carnitine System in Human Metabolism, *Ann. N. Y. Acad. Sci. 1033*, 1–16.
20. Pai, T., and Yeh, Y.Y. (1997) Stearic Acid Modifies Very Low Density Lipoprotein Lipid Composition and Particle Size Differently from Shorter-Chain Saturated Fatty Acids in Cultured Rat Hepatocytes, *Lipids 32*, 143–149.
21. Ntambi, J.M., and Miyazaki, M. (2004) Regulation of Stearoyl-CoA Desaturases and Role in Metabolism, *Prog. Lipid Res. 43*, 91–104.
22. Ntambi, J.M., Miyazaki, M., and Dobrzyn, A. (2004) Regulation of Stearoyl-CoA Desaturase Expression, *Lipids 39*, 1061–1065.
23. Kim, Y.C., Gomez, E., Fox, B.G., and Ntambi, J.M. (2000) Differential Regulation of the Stearoyl-CoA Desaturase Genes by Thiazolidinediones in 3T3-L1 Adipocytes, *J. Lipid Res. 41*, 1310–1316.
24. Miyazaki, M., Kim, H.J., Man, W.C., and Ntambi, J.M. (2001) Oleoyl-CoA Is the Major *de novo* Product of Stearoyl-CoA De-

saturase 1 Gene Isoform and Substrate for the Biosynthesis of the Harderian Gland 1-Alkyl-2,3-diacylglycerol, *J. Biol. Chem. 276*, 39455–39461.

25. Miyazaki, M., Gomez, E.F., and Ntambi, J.M. (2002) Lack of Stearoyl-CoA Desaturase-1 Function Induces a Palmitoyl-CoA Δ6 Desaturase and Represses the Stearoyl-CoA Desaturase-3 Gene in the Preputial Glands of the Mouse, *J. Lipid Res. 43*, 2146–2154.

26. Watts, J.L., and Browse, J. (2000) A Palmitoyl-CoA-Specific Δ9 Fatty Acid Desaturase from *Caenorhabditis elegans*, *Biochem. Biophys. Res. Commun. 272*, 263–269.

27. Bonanome, A., Bennet, M., and Grundy, S.M. (1992) Metabolic Effects of Dietary Stearic Acid in Mice: Changes in the Fatty Acid Composition of Triglycerides and Phospholipids in Various Tissues, *Atherosclerosis 94*, 119–127.

28. Keys, A., Anderson, J.T., and Grande, F. (1965) Serum Cholesterol Response to Change in the Diet. IV. Particular Saturated Fatty Acids in the Diet, *Metabolism 14*, 776–787.

29. Hegsted, M.D., McGandy, R.B., Meyers, M.L., and Stare, F.J. (1965) Quantitative Effects of Dietary Fat on Serum Cholesterol in Man, *Am. J. Clin. Nutr. 17*, 281–295.

30. Kris-Etherton, P.M., Derr, J., Mitchell, D.C., Mustard, V.A., Russell, M.E., McDonnell, E.T., Salabsky, D., and Pearson, T.A. (1993) The Role of Fatty Acid Saturation on Plasma Lipids, Lipoproteins and Apolipoproteins: I. Effects of Whole Food Diets High in Cocoa Butter, Olive Oil, Soybean Oil, Dairy Butter, and Milk Chocolate on the Plasma Lipids of Young Men, *Metabolism 42*, 121–129.

31. Pai, T., and Yeh, Y.Y. (1996) Stearic Acid Unlike Shorter-Chain Saturated Fatty Is Poorly Utilized for Triacylglycerol Synthesis and β-Oxidation in Cultured Rat Hepatocytes, *Lipids 31*, 159–164.

32. Woollett, L.A., Spady, D.K., and Dietschy, J.M. (1992) Regulatory Effects of the Saturated Fatty Acids 6:0 Through 18:0 on Hepatic Low Density Lipoprotein Receptor Activity in the Hamster, *J. Clin. Invest. 89*, 1133–1141.

33. Bonanome, A., and Grundy, S.M. (1988) Effect of Dietary Stearic Acid on Plasma Cholesterol and Lipoprotein Levels, *N. Engl. J. Med. 318*, 1244–1248.

34. Miyazaki, M., Dobrzyn, A., Man, W.C., Chu, K., Sampath, H., Kim, H.J., and Ntambi, J.M. (2004) Stearoyl-CoA Desaturase 1 Gene Expression Is Necessary for Fructose-Mediated Induction of Lipogenic Gene Expression by Sterol Regulatory Element-Binding Protein-1c-Dependent and -Independent Mechanisms, *J. Biol. Chem. 279*, 25164–25171.

35. Jones, P.J., Pencharz, P.B., and Clandinin, M.T. (1985) Whole Body Oxidation of Dietary Fatty Acids: Implications for Energy Utilization, *Am. J. Clin. Nutr. 42*, 769–777.

36. Bonanome, A., and Grundy, S.M. (1989) Intestinal Absorption of Stearic Acid After Consumption of High Fat Meals in Humans, *J. Nutr. 119*, 1556–1560.

37. Olubajo, O., Marshall, M.W., Judd, J.T., and Adkins, J.T. (1986) Effects of High- and Low-Fat Diets on the Bioavailability of Selected Fatty Acids, Including Linoleic Acid, in Adult Men, *Nutr. Res. 6*, 931–955.

38. Pai, T., and Yeh, Y.Y. (1997) Desaturation of Stearate Is Insufficient to Increase the Concentrations of Oleate in Cultured Rat Hepatocytes, *J. Nutr. 127*, 753–757.

39. Ntambi, J.M. (1995) Cellular Differentiation and Dietary Regulation of Gene Expression, *Prostaglandins Leukot. Essent. Fatty Acids 52*, 117–120.

40. Casimir, D.A., Miller, C.W., and Ntambi, J.M. (1996) Preadipocyte Differentiation Blocked by Prostaglandin Stimulation of Prostanoid FP2 Receptor in Murine 3T3-L1 Cells, *Differentiation 60*, 203–210.

41. Sun, Y., Hao, M.M., Luo, Y., Liang, C.P., Silver, D.L., Cheng, C., Maxfield, F.R., and Tall, A.R. (2003) Stearoyl-CoA Desaturase Inhibits ATP-Binding Cassette Transporter A1-Mediated Cholesterol Efflux and Modulates Membrane Domain Structure, *J. Biol. Chem. 278*, 5813–5820.

42. Kasai, T., Ohguchi, K., Nakashima, S., Ito, Y., Naganawa, T., Kondo, N., and Nozawa, Y. (1998) Increased Activity of Oleate-Dependent Type Phospholipase D During Actinomycin D-Induced Apoptosis in Jurkat T Cells, *J. Immunol. 161*, 6469–6474.

43. Attie, A.D., Krauss, R.M., Gray-Keller, M.P., Brownlie, A., Miyazaki, M., Kastelein, J.J., Lusis, A.J., Stalenhoef, A.F., Stoehr, J.P., Hayden, M.R., *et al*. (2002) Relationship Between Stearoyl-CoA Desaturase Activity and Plasma Triglycerides in Human and Mouse Hypertriglyceridemia, *J. Lipid Res. 43*, 1899–1907.

44. Lin, J., Yang, R., Tarr, P.T., Wu, P.H., Handschin, C., Li, S., Yang, W., Pei, L., Uldry, M., Tontonoz, P., *et al*. (2005) Hyperlipidemic Effects of Dietary Saturated Fats Mediated Through PGC-1β Coactivation of SREBP, *Cell 120*, 261–273.

45. Ntambi, J.M., Miyazaki, M., Stoehr, J.P., Lan, H., Kendziorski, C.M., Yandell, B.S., Song, Y., Cohen, P., Friedman, J.M., and Attie, A.D. (2002) Loss of Stearoyl-CoA Desaturase-1 Function Protects Mice Against Adiposity, *Proc. Natl. Acad. Sci. USA 99*, 11482–11486.

46. Miyazaki, M., Kim, Y.C., Gray-Keller, M.P., Attie, A.D., and Ntambi, J.M. (2000) The Biosynthesis of Hepatic Cholesterol Esters and Triglycerides Is Impaired in Mice with a Disruption of the Gene for Stearoyl-CoA Desaturase 1, *J. Biol. Chem. 275*, 30132–30138.

47. Ntambi, J.M., and Miyazaki, M. (2003) Recent Insights into Stearoyl-CoA Desaturase-1, *Curr. Opin. Lipidol. 14*, 255–261.

48. Dobrzyn, A., and Ntambi, J.M. (2005) Stearoyl-CoA Desaturase as a New Drug Target for Obesity Treatment, *Obes. Rev. 6*, 169–174.

49. Rahman, S.M., Dobrzyn, A., Dobrzyn, P., Lee, S.H., Miyazaki, M., and Ntambi, J.M. (2003) Stearoyl-CoA Desaturase 1 Deficiency Elevates Insulin-Signaling Components and Down-regulates Protein-Tyrosine Phosphatase 1B in Muscle, *Proc. Natl. Acad. Sci. USA 100*, 11110–11115.

50. Rahman, S.M., Dobrzyn, A., Lee, S.H., Dobrzyn, P., Miyazaki, M., and Ntambi, J.M. (2005) Stearoyl-CoA Desaturase 1 Deficiency Increases Insulin Signaling and Glycogen Accumulation in Brown Adipose Tissue, *Am. J. Physiol. Endocrinol. Metab. 288*, E381–E387.

51. Cohen, P., Miyazaki, M., Socci, N.D., Hagge-Greenberg, A., Liedtke, W., Soukas, A.A., Sharma, R., Hudgins, L.C., Ntambi, J.M., and Friedman, J.M. (2002) Role for Stearoyl-CoA Desaturase-1 in Leptin-Mediated Weight Loss, *Science 297*, 240–243.

Dietary Stearic Acid and Risk of Cardiovascular Disease: Intake, Sources, Digestion, and Absorption

Penny M. Kris-Etherton[a,b,*], Amy E. Griel[a,b], Tricia L. Psota[a,b], Sarah K. Gebauer[a,b], Jun Zhang[a], and Terry D. Etherton[a,c]

Departments of [a]Nutritional Sciences, [b]Integrative Biosciences, and [c]Dairy and Animal Science, The Pennsylvania State University, University Park, Pennsylvania 16802

ABSTRACT: Individual FA have diverse biological effects, some of which affect the risk of cardiovascular disease (CVD). In the context of food-based dietary guidance designed to reduce CVD risk, fat and FA recommendations focus on reducing saturated FA (SFA) and *trans* FA (TFA), and ensuring an adequate intake of unsaturated FA. Because stearic acid shares many physical properties with the other long-chain SFA but has different physiological effects, it is being evaluated as a substitute for TFA in food manufacturing. For stearic acid to become the primary replacement for TFA, it is essential that its physical properties and biological effects be well understood.

Paper no. L9894 in *Lipids 40*, 1193–1200 (December 2005).

Individual FA have distinctive biological effects and physical properties. Differences in chain length and degree of saturation/unsaturation account for the unique characteristics of dietary FA. FA are provided in the diet in a wide array of different fats that vary appreciably in their FA profile. Thus, the FA composition of the diet reflects the fat sources that are included in the diet. Moreover, the FA profile of the diet can be modified by inclusion of different fats. In the context of food-based dietary guidance designed to decrease saturated FA (SFA) and *trans* FA (TFA) and to ensure adequate intake of unsaturated FA, specific fats are recommended, and others are targeted for reduction.

Stearic acid, a unique long-chain SFA, has emerged as a candidate to use as a substitute for TFA in food manufacturing. It has the requisite physical attributes that a solid fat imparts and seems to have little effect on important risk factors for cardiovascular disease (CVD). If stearic acid is to become the conventional replacement for TFA, it is important that we have a good understanding of its biological effects on a variety of metabolic systems. This must be assessed in terms of likely intake levels due to substituting stearic acid for TFA. The complexity of this is underscored by the need to understand biological effects of synthesized fats that contain stearic acid in dif-

*To whom correspondence should be addressed at Department of Nutritional Sciences, The Pennsylvania State University, S-126 Henderson Bldg., University Park, PA 16802. E-mail: pmk3@psu.edu

Abbreviations: CHO, carbohydrate; CSFII, Continuing Survey of Food Intakes by Individuals; CVD, cardiovascular disease; DGAC, Dietary Guidelines Advisory Committee; FVIIa, activated factor DG, diglyceride; VII; HDL-C, HDL-cholesterol; kcal, calories; LDL-C, LDL-cholesterol; MG, monoglyceride; MUFA, monounsaturated FA; NHANES, National Health and Examination Surveys; SFA, saturated FA; TC, total cholesterol, TFA, *trans* FA; TG, triglyceride.

ferent positions on the glycerol backbone of the triglyceride (TG) molecule. Specifically, where stearic acid is located (i.e., at the *sn*-1, *sn*-2, *sn*-3 position) could be an important determinant of its health effects. In addition, the overall FA compositional change of the modified fats must be considered when assessing their health effects. The purpose of this paper is to review our current understanding of dietary intake, food sources, and digestion and absorption of stearic acid. In addition, we will review studies that have been conducted to assess the effect of stearic acid on major risk factors for CVD.

DIETARY CONSUMPTION AND FOOD SOURCES OF STEARIC ACID

Based on data from the Continuing Survey of Food Intakes by Individuals (CSFII) survey, the average intake of stearic acid is 5.2 g/d for women and 8.1 g/d for men, representing 9.2 and 9.4% of total fat for women and men, respectively (1). The dietary consumption of stearic acid has gradually declined from 1987 [3.3% total calories (kcal)] to 1996 (2.9% total kcal). This decrease has been accompanied by similar decreases in total SFA (13.2 to 11.3% total kcal), total monounsaturated FA (MUFA) (14 to 12.5% total kcal), and total PUFA (7.2 to 6.4% total kcal) (1). Data from the National Health and Examination Surveys (NHANES I, NHANES II, NHANES III, NHANES 1999–2000) indicate that the percentage of kcal from total fat has decreased from 36.9 to 32.8% ($P < 0.01$) for men and from 36.1 to 32.8% ($P < 0.01$) for women between 1971 and 2000 (2). These reductions in the percentages of kcal from fat reflect an increase in total kcal consumed (2,450 to 2,618 kcal for men and 1,542 to 1,877 kcal for women; $P < 0.01$), and a corresponding increase in carbohydrate intake (42.4 to 49.0% kcal for men and 44.8 to 49.7% kcal for women). Data from NHANES I, NHANES II, NHANES III, and NHANES 1999–2000 indicate that the absolute intake of total fat has increased among women (6.5 g; $P < 0.01$) and decreased among men (5.3 g; $P < 0.01$) from 1971 to 2000. Thus, although the absolute intake of fat has remained relatively stable, the percentage of dietary fats has decreased owing to an increase in total kcal and carbohydrate intake.

Dietary stearic acid intake ranks second among the SFA consumed in the United States, accounting for 25.8% of SFA intake and 2.9% of total kcal (1). Palmitic acid is the predominant SFA consumed in the United States (56.3%) (Fig. 1) (3).
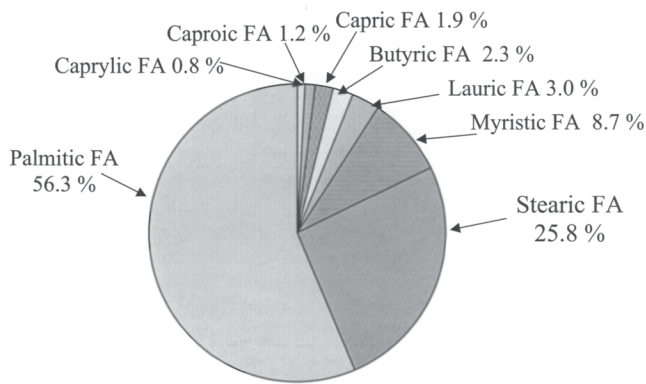
FIG. 1. Percentage of total saturated fat for various FA.

TABLE 1
Stearic Acid from Selected Food Groups: Mean Intakes (g) for Men and Women, >20 yr

Food group	Men	Women
Grain products	1.99	1.33
Vegetables	0.62	0.39
Fruits	0.01	0.01
Milk/milk products	1.36	0.94
Meat, poultry, fish	2.96	1.66
Eggs	0.26	0.16
Legumes	0.12	0.08
Fats and oils	0.49	0.36
Nuts and seeds	0.08	0.05
Sugars and sweets	0.21	0.18
Beverages	0.01	<0.005

Sources of dietary SFA are (i) meat, poultry, fish, eggs, dairy (60%), (ii) grains, vegetables, fruits, sweets, all others that are prepared with fats (30%), and (iii) fats and oils (10%). The food groups that account for the greatest intake of stearic acid for men and women are meat, poultry, and fish and grain products (Table 1) (1). Since 1980, the average annual per capita consumption of meat has decreased from 136.7 to 119.5 pounds (62.0 to 54.2 kg) in 2004 (4). This decrease in the consumption of red meat may account for a reduction in the consumption of dietary stearic acid. Specific fats that are rich sources of stearic acid include cocoa butter, lard, beef tallow and butter (Fig. 2) (5).

Given its unique physical characteristics and properties, stearic acid is currently being considered as a replacement for TFA in the food supply. Current dietary guidelines recommend that intake of TFA be kept as low as possible (≤1% of calories) for all population groups. This recommendation put forth by the 2005 Dietary Guidelines Advisory Committee (DGAC) (6) is supported by seven recent publications, a systematic, extensive review of the evidence collected by the Institutes of Medicine (20 controlled trials and 11 epidemiologic studies), and the analysis of evidence conducted by the National Cholesterol Education Program Adult Treatment Panel III Report Committee. Based on CSFII data from 1989 to 1991, the estimated

mean TFA intake for the U.S. population ages 3 and older was 2.6% of calories (7). Industrial sources of TFA account for 80% of intake, whereas 20% comes from animal sources. Elaidic acid (*t*-18:1) is the predominant TFA found in many partially hydrogenated fats and is produced in the deodorization of vegetable oils. These industrial sources of TFA are commonly found in commercially prepared baked products, fried foods, and margarine. Meat and dairy products contain the naturally occurring TFA vaccenic acid and CLA.

GENERAL DIGESTION AND ABSORPTION OF STEARIC ACID

The major lipids in the diet are TG, which are the carriers of dietary FA. These lipids must be hydrolyzed and emulsified before they can be absorbed (8). The first step in hydrolysis, initiated by lingual and gastric lipases, results in the formation of DG and FFA. Approximately 10–30% of dietary fat is hydrolyzed in the stomach before moving to the duodenum, where the majority of TG digestion occurs (9). Pancreatic lipase is secreted into the duodenum, where it is activated by colipase, and
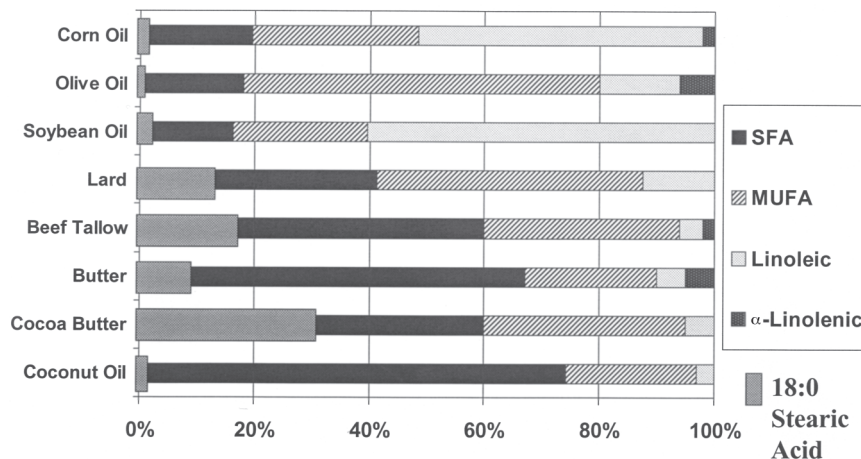

FIG. 2. FA content of common fats and oils.

TABLE 2
Positional Distributions of FA (mol%) in TG[a]

		FA (mol%)			
	Position	Palmitic (16:0)	Stearic (18:0)	Oleic (18:1)	Linoleic (18:2)
Seed oils					
Peanut	1 and 3	14 and 11	5 and 5	59 and 57	18 and 10
	2	1	Trace[b]	58	39
Soybean	1 and 3	14 and 13	6 and 6	23 and 28	48 and 45
	2	1	Trace	21	70
Maize	1 and 3	18 and 13	3 and 3	27 and 31	50 and 51
	2	2	Trace	26	70
Cocoa butter	1 and 3	34 and 37	50 and 53	12 and 9	1 and —
	2	2	2	87	9
Animal fats					
Human	1 and 3	42 and 19	15 and 6	27 and 57	6 and 11
	2	10 and —	2	55	4
Cattle	1 and 3	41 and 22	17 and 24	20 and 37	4 and 5
	2	17	9	41	5
Pig	1 and 3	10 / -	30 and 7	51 and 73	6 and 8
	2	72	2	13	3
Milk products					
Cow	1 and 3	36 and 5	15 and 1	21 and 23	1 and 2
	2	33	6	14	3

[a]Adapted from Kubow (29).
[b]Trace, <1 mol%.

acts to hydrolyze TG. Pancreatic lipase preferentially hydrolyzes the FA in the *sn*-1 and *sn*-3 positions of the TG while leaving the FA in the *sn*-2 position, thus producing 2-monoglyceride (MG) and FFA as the products (10). Some further hydrolysis of the MG occurs, with less than 25% of dietary TG being completely hydrolyzed to glycerol and three FA (8). Bile acids emulsify the products into soluble micelles, which are carried to the brush border of the enterocyte and taken up *via* facilitated diffusion. In the enterocyte, TG are resynthesized and are transported in chylomicrons to lymph where they are carried to the blood stream.

As reviewed by Kritchevsky (11), early animal studies demonstrated that stearic acid or TG rich in stearic acid were absorbed less efficiently than other SFA such as lauric, myristic, and palmitic acids. Studies in animals have shown that stearic acid esterified on the *sn*-1 and *sn*-3 positions of glycerol has limited bioavailability (12,13). Mattson *et al.* (14) have demonstrated in rats that stearic acid is well absorbed when located in the *sn*-2 position of the TG, but only 55% is absorbed when located in the *sn*-1 or *sn*-3 position with two oleates on the TG. Furthermore, stearic acid located in both the *sn*-1 and *sn*-3 positions resulted in only 37% absorption (14). A study in rats comparing the digestibilities of increasing amounts of dietary corn oil (2% stearic acid) and cocoa butter (34% stearic acid) reported significantly lower digestibility coefficients for cocoa butter vs. corn oil (15). Digestibility coefficients for 5, 10, and 20% corn oil were 92.7 ± 0.9, 96.9 ± 0.1, and 96.3 ± 0.2%, respectively, whereas coefficients for cocoa butter at the same levels of intake were 58.8 ± 0.5, 60.3 ± 1.4, and 71.7 ± 1.3%, respectively.

More recent studies have reported that stearic acid is generally well absorbed. A randomized study in free-living healthy men comparing the digestibility of moderate amounts of cocoa butter (30.7 g/d) with that of corn oil demonstrated that there were no significant differences in fecal weight, fecal fat, or defecation frequency between the two treatments (16). A study conducted by Denke and Grundy (17) in men demonstrated that oleic acid was 99% absorbed, palmitic acid was 96–97% absorbed, and stearic acid was 90–94% absorbed. Furthermore, a comparison of stearic acid and palmitic acid metabolism using stable-isotope tracer methods indicates that absorption of stearic acid is not significantly different from palmitic acid (18). The most recent study conducted to date that evaluated the absorption of stearic acid reported that stearic acid absorption was less ($P < 0.0002$) than that of palmitic acid (94% vs. 97%, respectively); absorption of other FA studied (lauric, myristic, oleic, linoleic, and *trans* 18:1 monomers) was higher ($P < 0.001$; >99%) than that of stearic and palmitic acids (19).

INFLUENCE OF POSITION OF STEARIC ACID IN TG ON DIGESTION AND ABSORPTION

A high proportion of SFA is usually found in the *sn*-2 position in many animal fats. In most vegetable-derived fats, SFA primarily occupies the *sn*-1 and *sn*-3 positions, whereas the *sn*-2 position is enriched with unsaturated FA (Table 2) (20–29). It has been hypothesized that the position of the FA on the glycerol backbone is more important than the overall saturation of TG in affecting the level of postprandial lipemia. Test fats prepared by using randomization (18:0 or 16:0 in the *sn*-2 position) indicated lower TG levels than when presented in the *sn*-1 or *sn*-3 position (30–32).

In the manufacturing process used to synthesize fats, positioning changes of FA on the glycerol backbone of TG can be

achieved by several techniques, leading to increased SFA and stearic acid in the *sn*-2 position. One way is to interesterify natural or fractionated oils and fats. Interesterification involves the redistribution and interchange of FA within and between the TG molecules. Interesterification does not result in formation of TFA. Generally, interesterification is used to change the m.p. of oils, fats, and mixtures. Chemical interesterification produces a complete positional randomization of acyl groups in TG molecules. In contrast, enzymatic interesterification uses lipases as a catalyst and results in more selective interesterification (33).

In contrast to the naturally occurring sources of fats used in the above studies, synthetic randomized stearic acid-rich fat substitutes have been reported to result in low fat digestibility and high stearic acid excretion. In the study conducted by Sanders *et al.* (34), 17 subjects consumed 50 g of fat as either natural cocoa butter or randomized cocoa butter to test the differences in postprandial lipemia changes. After randomization of the fats, the proportion of oleic acid in the *sn*-2 position of the chylomicron TG was reduced from 67.4 to 35.9 mol% and resulted in an increase in the proportion of stearic acid in the *sn*-2 position from 9.2 to 25.4 mol%. Compared with the unrandomized cocoa butter, the randomization resulted in the reduction of the postprandial plasma TG area under the curve by 41% ($P < 0.01$). At 3 h after the fat intake, the plasma concentrations of TG, 16:0, 18:0, and 18:1 were 26, 18, 34, and 19% lower, respectively.

These results are consistent with data from Berry and Sanders (35). The investigators compared the results of consumption of 50 g of cocoa butter with 50 g of randomized 18:0-rich fat derived from sunflower oil (43 mol 18:0/100 mol in the *sn*-2 position). The randomized fat led to a significantly lower postprandial lipemia; at 4 h the serum concentration of 18:0 was 70% lower than that with cocoa butter.

In contrast to the naturally occurring sources used in the above studies, a synthetic randomized stearic acid-rich fat substitute, SALATRIM, has been reported to result in a low fat digestibility and high stearic acid excretion (36). SALATRIM is composed of structured TG containing long-chain FA, predominantly stearic acid, and the short-chain aliphatic acids acetic, propionic, and butyric acids. In a clinical trial determining the absorption of stearic acid using SALATRIM, subjects were assigned to either an 1800 kcal/d diet or a 2500 kcal/d based on sex, body weight, and age, and were given one of two doses of SALATRIM, providing 27.4 and 34.2 g/d of stearic acid, respectively. The absorption of stearic acid was 72.4 and 63.5% on the 1800 kcal diet and 2500 kcal diet, respectively. In addition, subjects consuming SALATRIM exhibited an increase in stearic acid excretion. These results suggest that the position of stearic acid in structured TG effects the absorption of stearic acid.

The differences between the digestion and absorption of natural fats and randomized fats might occur for the following reasons. During the test fat preparation, randomization led to a marked decrease in the proportion of the symmetrical TG molecules and increases in the proportions of asymmetrical TG

(34). In addition, interesterification increased the proportion of trisaturated TG as well. The consequences of randomization were that the high m.p. of TG was elevated. Thus, TG containing stearic acid in the *sn*-2 position were not efficiently absorbed or else their release into the circulation was delayed (33). As absorption is affected by the position of FA on the TG molecule, alteration of the postprandial lipid response would be expected.

PHYSIOLOGICAL CONSEQUENCES OF STEARIC ACID

Early feeding studies conducted by Keys *et al.* (37,38) and Hegsted *et al.* (39) demonstrated that SFA elevate serum total cholesterol (TC) and subsequently increase CVD risk. Data from these studies were used to develop predictive equations to establish the hypercholesterolemic effects of SFA. More recently, regression analyses have been used to develop equations that predict the effects of SFA, MUFA, and PUFA on different lipoprotein classes [e.g., LDL-cholesterol (LDL-C) and HDL-cholesterol (HDL-C)] (40,41), as well as TC levels (37–39). These studies have demonstrated that stearic acid has no effect on TC, LDL-C, and HDL-C levels (42), when compared with myristic acid, lauric acid, and palmitic acid (43). A recent meta-analysis of 60 controlled trials determined the effects of different SFA relative to carbohydrate (CHO) on serum lipids and the TC/HDL-C ratio (44). Stearic acid and lauric acid both reduced the ratio due to slight decreases in TC or increases in HDL-C, respectively; myristic and palmitic acids had little effect on the ratio due to similar increases in both TC and HDL-C. Furthermore, stearic acid, myristic acid, lauric acid, and palmitic acid significantly reduced TG levels by approximately 0.017 mmol/L ($P < 0.001$) (44).

The evidence base presented in the meta-analysis by Mensink *et al.* (44) clearly demonstrates that stearic acid has a neutral effect on lipids and lipoproteins, when replacing CHO in the diet. Clinical trials have demonstrated that when stearic acid is substituted for CHO and oleic acid at 5 and 13% of total energy, respectively, lipids and lipoproteins are not affected (45,46). Controlled feeding studies have shown that stearic acid intakes, ranging from 9.3 to 40% of total energy, tend to decrease plasma TC (47–51) and LDL-C (17,47,49,51) levels when compared with baseline levels and diets in which palmitic acid is substituted for stearic acid. Consistent with the change in LDL-C, two studies demonstrated that diets with stearic acid contributing 9.3 and 36% of energy significantly decreased plasma levels of apolipoprotein B by 10 and 18%, respectively, in comparison with values at baseline (49), and after a diet rich in palmitic acid (36% of total energy) (48). However, when stearic acid contributed 9.3% of energy, lipoprotein(a) also significantly increased when compared with baseline levels (49). This increase is consistent with those found in other studies that evaluated the effects of stearic acid on fasting (52,53) and postprandial (54) lipoprotein(a) levels compared to diets rich in palmitic acid. The effects of stearic acid on HDL-C and TG levels are less consistent, with some demonstrating beneficial effects (55), adverse effects (49), or no effects (45–47,50,56). Following stearic acid in-

takes at 5% of total energy, the HDL-C level was 0.08 ± 0.03 mmol/L higher ($P < 0.01$) and the TG level was 0.06 ± 0.03 mmol/L lower ($P < 0.05$), compared with stearic acid intakes at 2.2% of total energy (55). However, when stearic acid contributed 9.3% of total energy, HDL-C decreased by 11% (49).

Postprandial lipemia and the activation of thrombotic factors during the postprandial state are associated with an increased risk of CVD. The effects of a high-fat meal on postprandial lipids and thrombotic factors have been evaluated extensively. Specifically, a stearic acid-rich meal increases postprandial lipemia, as measured by the area under the curve for plasma TG concentrations, but to a lesser extent than oleic (30), elaidic (30), and palmitic acids (30,57). The concentration of activated factor VII (FVIIa), a vitamin K-dependent coagulation factor, and the coagulation activity of factor VII tend to increase during the postprandial state following a stearic acid-rich meal (30,57,58). However, FVIIa increases, to a lesser extent, after a stearic acid-rich meal in comparison with a meal rich in oleic acid (30) or palmitic acid (57).

The evidence on the effects of stearic acid on hemodynamic measures is conflicting. Epidemiologic data from the Multiple Risk Factor Intervention Trial indicates that the serum level of cholesterol ester stearic acid is inversely associated with diastolic blood pressure among middle-aged men at high risk of coronary heart disease (60). Each SD increase of serum level of cholesterol ester stearic acid (0.2%) was associated with a decrease of 1.4 mm Hg (95% confidence interval, −2.5 to −0.2 mm Hg) (60). In another study, each SD increase in the proportion of stearic acid in serum cholesterol esters was associated with significant improvement in left ventricular diastolic function, as measured by Doppler echocardiograph, by 0.10 units ($r = −0.29$, $P < 0.05$) in healthy men (61). Controlled clinical trials have shown that diets with stearic acid contributing 8 and 13% of energy have no effect on blood pressure in patients with diabetes mellitus (45) or normotensive men and women (62), respectively.

There is minimal evidence about the effects of stearic acid on inflammatory markers. One study has shown that when stearic acid contributes 11% of total energy (39% energy from fat, 46% energy from CHO, and 15% energy from protein), plasma fibrinogen concentrations are significantly elevated 4.4% in comparison with a CHO-rich diet [31% energy from fat (3% from stearic acid), 54% energy from CHO, and 15% energy from protein]. Plasma levels of C-reactive protein, interleukin-6, and E-selectin were unchanged when stearic acid provided 11% of energy in the diet compared with the CHO diet that provided 3% of energy from stearic acid (63). This study also demonstrated that when stearic acid and TFA are each substituted for 4% of energy from CHO {39% energy from fat [7% from stearic acid (4% from substitution, 3% naturally occurring)], 46% energy from CHO, and 15% energy from protein} plasma levels of fibrinogen, C-reactive protein, interleukin-6, and E-selectin were unchanged (63). Although fibrinogen levels were increased when stearic acid contributed 11% of total energy, this intake level is well above the current intake level (3% of total energy) (1). All markers of inflammation were unaffected at the lower intake level of stearic acid (7% of total energy), which is also above current intake.

Epidemiologic data from the Atherosclerosis Risk in Communities study has shown that diabetes incidence is positively associated with the proportion of stearic acid in plasma phospholipids (64). In patients with diabetes, 13.7 ± 1.2% of FA in plasma phospholipids was stearic acid; whereas stearic acid contributed 13.2 ± 1.1% of FA in plasma phospholipids in patients without diabetes ($P < 0.01$). The percentage of total SFA in plasma phospholipids was higher in patients with diabetes (64). Clinical trials have shown that measures of glucose metabolism, such as the insulin sensitivity index and glucose effectiveness in healthy women (46) and fructosamine, glycosylated hemoglobin (HbA1c), and fasting blood glucose in patients with type 2 diabetes (45), are unaffected by diets rich in stearic acid (5 and 13% of total energy, respectively).

Although stearic acid consistently has been shown to have neutral effects on lipids and lipoproteins, the effects of stearic acid on thrombosis, inflammation, and hemodynamic pathways are less clear. Owing to limited evidence regarding the effects of stearic acid and other 18-carbon FA on hemostatic function, oxidation, and inflammation, recent research cautions against exchanging stearic acid for other FA in the diet at this time (56). Furthermore, the effects of increasing dietary stearic acid, as a substitute for TFA, need further evaluation since these emerging markers of CVD risk are of potential concern (65).

ESTIMATING THE PROJECTED INCREASE IN DIETARY STEARIC ACID

Given our current understanding of the biological effects of stearic acid, and the fact that it is being considered as a substitute for TFA, it is important to estimate what the increase of stearic acid would be in the diet when substituted for *trans* fats. The following is a simulation that presents a projected estimate of how much stearic acid would increase in the diet if it were the sole FA substitute for TFA. Based on NHANES IIII data for males of all ages (consuming 2,666 cal/d), *trans* fat intake is 6.1 g/d (2.03% of calories). The DGAC 2005 Report estimated that the lower threshold of intake for TFA is 1% of total calories (because the process of deodorization of oils creates a small amount of TFA) (66). Thus, substituting the other 1% of TFA calories with stearic acid correspondingly would increase stearic acid intake by 3 g. The current stearic acid consumption is 8.2 g/d. Thus, a one-for-one substitution of the "1%" TFA with stearic acid intake and addition of this to the current stearic acid intake (8.2 g/d) would result in a stearic acid intake of 11.2 g/d, or 3.7% of calories. If twice the amount of stearic acid was needed to substitute for every one unit of *trans* fat, then stearic acid intake would be 14 g/d, or 4.7% of calories. At the upper end of *trans* fat intake (66), which is 3.2% of calories, if stearic acid were fully substituted for *trans* fat at a daily calorie level of 2,666, this would result in an intake of stearic acid of about 17 g/d (8.2 g from usual diet and 9 g from *trans* fat substitution). If twice the amount of stearic acid was needed to be substituted for every one unit of *trans* fat (at an intake of

3.2%), then stearic acid intake would be 26 g/d, or 9% of calories. Even at this extreme intake (which is not realistic because other fat sources likely also will be substituted for *trans* fat), it is unlikely that any adverse effects of this level of stearic acid would be observed. This is based on the report by Baer *et al.* (63) in which consumption of about 38 g of stearic acid per day increased fibrinogen, but 24 g/d had no effect. Collectively, these simulations assume that all *trans* fat is substituted by stearic acid, an assumption that it is not likely to occur. Nonetheless, this estimation provides a reasonable perspective of the extreme to which stearic acid intake might change. Based on this, it is clear that the increased intake is in the range where adverse effects are not likely.

CONCLUSION

Based on the available evidence about the biological effects of stearic acid, we propose that it is a viable candidate as a replacement for *trans* FA. It is clear that stearic acid is uniquely different from other long-chain SFA. It does not raise TC and LDL-C levels. However, the effects on other markers of CVD risk, such as hemostatic factors and inflammation, remain unclear. With respect to its absorption, recent studies with naturally occurring fats and oils have demonstrated that absorption is relatively similar to other SFA, whereas structured/synthesized lipids containing stearic acid may exhibit reduced absorption. Different food applications have different fat needs, including liquid fats for frying (e.g., French fries, chicken) and solid fats for bakery products (e.g., pastry crust, cookies) and snacks (e.g., crackers and chips). Stearic acid can replace *trans* FA in fats that are used to produce some of these foods. Consequently, stearic acid would be increased in the food supply and diet; however, even when considering extremes in its inclusion in the diet, stearic acid intake would change less than twofold. More research is needed to achieve a comprehensive understanding of the health effects of increasing dietary stearic acid. A small increase appears not to have any adverse effects on CVD risk factors and, in fact, stearic acid may indirectly have positive health effects as a consequence of replacing *trans* FA in the diet.

REFERENCES

1. USDA, Agricultural Research Service (2005) Data Tables: Intakes of 19 Individual Fatty Acids: Results from the 1994–1996 Continuing Survey of Food Intakes by Individuals, USDA, Beltsville, MD. http://www.barc.usda.gov/bhnrc/foodsurvey/home.htm (accessed November 10, 2005).
2. Centers for Disease Control and Prevention (2004) Trends in Intake of Energy and Macronutrients—United States, 1971–2000, in *MMWR 53*, 80–82.
3. Ervin, R.B., Wright, J.D., Wang, C.Y., and Kennedy-Stephenson, J. (2004) Dietary Intake of Fats and Fatty Acids for the United States Population: 1999–2000, *Adv. Data* (November 8), 1–6.
4. National Cattleman's Beef Association (2005) Average Annual Per Capita Consumption of Meat, http://www.beef.org (accessed November 10, 2005).
5. USDA, Agricultural Research Service (2002) USDA National Nutrient Database for Standard Reference, Release 15, Nutrient Data Laboratory Home Page, http://www.nal.usda.gov/fnic/foodcomp (accessed November 10, 2005).
6. Dietary Guidelines Advisory Committee (2005) Report of the Dietary Guidelines Advisory Committee on the *Dietary Guidelines for Americans*, *2005*, Departments of Health and Human Services and Agriculture, U.S. Government Printing Office, Washington, DC.
7. Allison, D.B., Egan, S.K., Barraj, L.M., Caughman, C., Infante, M., and Heimbach, J.T. (1999) Estimated Intakes of *trans* Fatty and Other Fatty Acids in the US Population, *J. Am. Diet. Assoc. 99*, 166–174; Quiz 175–176.
8. Murray, R., Granner, D., Mayes, P., and Rodwell, V. (2003) *Harper's Illustrated Biochemistry*, 26th edn., McGraw-Hill Medical, New York.
9. Mu, H., and Høy, C.E. (2004) The Digestion of Dietary Triacylglycerols, *Prog. Lipid Res. 43*, 105–133.
10. Mattson, F.H., and Volpenhein, R.A. (1964) The Digestion and Absorption of Triglycerides, *J. Biol. Chem. 239*, 2772–2777.
11. Kritchevsky, D. (1994) Stearic Acid Metabolism and Atherogenesis: History, *Am. J. Clin. Nutr. 60*, 997S–1001S.
12. Carroll, K.K. (1958) Digestibility of Individual Fatty Acids in the Rat, *J. Nutr. 64*, 399–410.
13. Clarke, S.D., Romsos, D.R., and Leveille, G.A. (1977) Differential Effects of Dietary Methyl Esters of Long-Chain Saturated and Polyunsaturated Fatty Acids on Rat Liver and Adipose Tissue Lipogenesis, *J. Nutr. 107*, 1170–1181.
14. Mattson, F.H., Nolen, G.A., and Webb, M.R. (1979) The Absorbability by Rats of Various Triglycerides of Stearic and Oleic Acid and the Effect of Dietary Calcium and Magnesium, *J. Nutr. 109*, 1682–1687.
15. Apgar, J.L., Shively, C.A., and Tarka, S.M., Jr. (1987) Digestibility of Cocoa Butter and Corn Oil and Their Influence on Fatty Acid Distribution in Rats, *J. Nutr. 117*, 660–665.
16. Shahkhalili, Y., Duruz, E., and Acheson, K. (2000) Digestibility of Cocoa Butter from Chocolate in Humans: A Comparison with Corn-Oil, *Eur. J. Clin. Nutr. 54*, 120–125.
17. Denke, M.A., and Grundy, S.M. (1991) Effects of Fats High in Stearic Acid on Lipid and Lipoprotein Concentrations in Men, *Am. J. Clin. Nutr. 54*, 1036–1040.
18. Emken, E.A. (1994) Metabolism of Dietary Stearic Acid Relative to Other Fatty Acids in Human Subjects, *Am. J. Clin. Nutr. 60*, 1023S–1028S.
19. Baer, D.J., Judd, J.T., Kris-Etherton, P.M., Zhao, G. and Emken, E.A. (2003) Stearic Acid Absorption and Its Metabolizable Energy Value Are Minimally Lower than Those of Other Fatty Acids in Healthy Men Fed Mixed Diets, *J. Nutr. 133*, 4129–4134.
20. Christie, W.W. (1985) Structure of the Triacyl-*sn*-glycerols in the Plasma and Milk of the Rat and Rabbit, *J. Dairy Res. 52*, 219–222.
21. Brockerhoff, H., and Yurkowski, M. (1966) Stereospecific Analyses of Several Vegetable Fats, *J. Lipid Res. 7*, 62–64.
22. Christie, W.W., Moore, J.H., Lorimer, A.R., and Lawrie, T.D. (1971) The Structures of Triglycerides from Atherosclerotic Plaques and Other Human Tissues, *Lipids 6*, 854–856.
23. Brockerhoff, H., Hoyle, R.J., and Wolmark, N. (1966) Positional Distribution of Fatty Acids in Triglycerides of Animal Depot Fats, *Biochim. Biophys. Acta 116*, 67–72.
24. Noble, R.C., Christie, W.W., and Moore, J.H. (1971) Diet and the Lipid Composition of Adipose Tissue in the Young Lamb, *J. Sci. Food Agric. 22*, 616–619.
25. Christie, W.W., and Moore, J.H. (1970) A Comparison of the Structures of Triglycerides from Various Pig Tissues, *Biochim. Biophys. Acta 210*, 46–56.

26. Christie, W.W., and Moore, J.H. (1972) The Structures of Adipose Tissue and Heart Muscle Triglycerides in the Domestic Chicken (*Gallus gallus*), *J. Sci. Food Agric. 23*, 73–77.

27. Breckenridge, W.C., Marai, L., and Kuksis, A. (1969) Triglyceride Structure of Human Milk Fat, *Can. J. Biochem. 47*, 761–769.

28. Walker, R.W., Barakat, H., and Hung, J.G. (1970) The Positional Distribution of Fatty Acids in the Phospholipids and Triglycerides of *Mycobacterium smegmatis* and *M. bovis* BCG, *Lipids 5*, 684–691.

29. Kubow, S. (1996) The Influence of Positional Distribution of Fatty Acids in Native, Interesterified and Structure-Specific Lipids on Lipoprotein Metabolism and Atherogenesis, *J. Nutr. Biochem. 7*, 530–541.

30. Sanders, T.A., de Grassi, T., Miller, G.J., and Morrissey, J.H. (2000) Influence of Fatty Acid Chain Length and *cis/trans* Isomerization on Postprandial Lipemia and Factor VII in Healthy Subjects (postprandial lipids and factor VII), *Atherosclerosis 149*, 413–420.

31. Sanders, T.A., Oakley, F.R., Cooper, J.A., and Miller, G.J. (2001) Influence of a Stearic Acid-Rich Structured Triacylglycerol on Postprandial Lipemia, Factor VII Concentrations, and Fibrinolytic Activity in Healthy Subjects, *Am. J. Clin. Nutr. 73*, 715–721.

32. Yli-Jokipii, K., Kallio, H., Schwab, U., Mykkanen, H., Kurvinen, J.P., Savolainen, M.J., and Tahvonen, R. (2001) Effects of Palm Oil and Transesterified Palm Oil on Chylomicron and VLDL Triacylglycerol Structures and Postprandial Lipid Response, *J. Lipid Res. 42*, 1618–1625.

33. Berry, S.E., and Sanders, T.A. (2005) Influence of Triacylglycerol Structure of Stearic Acid-Rich Fats on Postprandial Lipaemia, *Proc. Nutr. Soc. 64*, 205–212.

34. Sanders, T.A., Berry, S.E., and Miller, G.J. (2003) Influence of Triacylglycerol Structure on the Postprandial Response of Factor VII to Stearic Acid-rich Fats, *Am. J. Clin. Nutr. 77*, 777–782.

35. Berry, S.E.E., and Sanders, T.A.B. (2003) Postprandial Lipaemia Induced by Cocoa Butter Compared with an Inter-Esterified Blend of Totally Hydrogenated and Unhydrogenated High Oleic Sunflower Oil, *Proc. Nutr. Soc. 62*, 41A.

36. Finley, J., Klemann, L., Leveille, G., Otterburn, M., and Walchak, C. (1994) Caloric Availability of SALATRIM in Rats and Humans, *J. Agric. Food Chem. 42*, 495–499.

37. Keys, A., Anderson, J.T., and Grande, F. (1957) Prediction of Serum-Cholesterol Responses of Man to Changes in Fats in the Diet, *Lancet 273*, 959–966.

38. Keys, A., Anderson, J.T., and Grande, F. (1965) Serum Cholesterol Response to Changes in the Diet. IV. Particular Saturated Fatty Acids in the Diet, *Metabolism 14*, 776–787.

39. Hegsted, D.M., McGandy, R.B., Myers, M.L., and Stare, F.J. (1965) Quantitative Effects of Dietary Fat on Serum Cholesterol in Man, *Am. J. Clin. Nutr. 17*, 281–295.

40. Mensink, R.P., and Katan, M.B. (1992) Effect of Dietary Fatty Acids on Serum Lipids and Lipoproteins. A Meta-analysis of 27 Trials, *Arterioscler. Thromb. 12*, 911–919.

41. Hegsted, D.M., Ausman, L.M., Johnson, J.A., and Dallal, G.E. (1993) Dietary Fat and Serum Lipids: An Evaluation of the Experimental Data, *Am. J. Clin. Nutr. 57*, 875–883.

42. Yu, S., Derr, J., Etherton, T.D., and Kris-Etherton, P.M. (1995) Plasma Cholesterol-Predictive Equations Demonstrate That Stearic Acid Is Neutral and Monounsaturated Fatty Acids Are Hypocholesterolemic, *Am. J. Clin. Nutr. 61*, 1129–1139.

43. Muller, H., Kirkhus, B., and Pedersen, J.I. (2001) Serum Cholesterol Predictive Equations with Special Emphasis on *trans* and Saturated Fatty Acids. An Analysis from Designed Controlled Studies, *Lipids 36*, 783–791.

44. Mensink, R.P., Zock, P.L., Kester, A.D., and Katan, M.B. (2003) Effects of Dietary Fatty Acids and Carbohydrates on the Ratio of Serum Total to HDL Cholesterol and on Serum Lipids and Apolipoproteins: A Meta-analysis of 60 Controlled Trials, *Am. J. Clin. Nutr. 77*, 1146–1155.

45. Storm, H., Thomsen, C., Pedersen, E., Rasmussen, O., Christiansen, C., and Hermansen, K. (1997) Comparison of a Carbohydrate-Rich Diet and Diets Rich in Stearic or Palmitic Acid in NIDDM Patients. Effects on Lipids, Glycemic Control, and Diurnal Blood Pressure, *Diabetes Care 20*, 1807–1813.

46. Louheranta, A.M., Turpeinen, A.K., Schwab, U.S., Vidgren, H.M., Parviainen, M.T., and Uusitupa, M.I. (1998) A High-Stearic Acid Diet Does Not Impair Glucose Tolerance and Insulin Sensitivity in Healthy Women, *Metabolism 47*, 529–534.

47. Bonanome, A., and Grundy, S.M. (1988) Effect of Dietary Stearic Acid on Plasma Cholesterol and Lipoprotein Levels, *N. Engl. J. Med. 318*, 1244–1248.

48. Tholstrup, T., Marckmann, P., Jespersen, J., and Sandstrom, B. (1994) Fat High in Stearic Acid Favorably Affects Blood Lipids and Factor VII Coagulant Activity in Comparison with Fats High in Palmitic Acid or High in Myristic and Lauric Acids, *Am. J. Clin. Nutr. 59*, 371–377.

49. Aro, A., Jauhiainen, M., Partanen, R., Salminen, I., and Mutanen, M. (1997) Stearic Acid, *trans* Fatty Acids, and Dairy Fat: Effects on Serum and Lipoprotein Lipids, Apolipoproteins, Lipoprotein(a), and Lipid Transfer Proteins in Healthy Subjects, *Am. J. Clin. Nutr. 65*, 1419–1426.

50. Nestel, P.J., Pomeroy, S., Kay, S., Sasahara, T., and Yamashita, T. (1998) Effect of a Stearic Acid-Rich, Structured Triacylglycerol on Plasma Lipid Concentrations, *Am. J. Clin. Nutr. 68*, 1196–1201.

51. Snook, J.T., Park, S., Williams, G., Tsai, Y.H., and Lee, N. (1999) Effect of Synthetic Triglycerides of Myristic, Palmitic, and Stearic Acid on Serum Lipoprotein Metabolism, *Eur. J. Clin. Nutr. 53*, 597–605.

52. Tholstrup, T., Marckmann, P., Vessby, B., and Sandstrom, B. (1995) Effect of Fats High in Individual Saturated Fatty Acids on Plasma Lipoprotein[a] Levels in Young Healthy Men, *J. Lipid Res. 36*, 1447–1452.

53. Hornstra, G., van Houwelingen, A.C., Kester, A.D., and Sundram, K. (1991) A Palm Oil-Enriched Diet Lowers Serum Lipoprotein(a) in Normocholesterolemic Volunteers, *Atherosclerosis 90*, 91–93.

54. Tholstrup, T., and Samman, S. (2004) Postprandial Lipoprotein(a) Is Affected Differently by Specific Individual Dietary Fatty Acids in Healthy Young Men, *J. Nutr. 134*, 2550–2555.

55. Kris-Etherton, P.M., Derr, J.A., Mustad, V.A., Seligson, F.H., and Pearson, T.A. (1994) Effects of a Milk Chocolate Bar Per Day Substituted for a High-Carbohydrate Snack in Young Men on an NCEP/AHA Step 1 Diet, *Am. J. Clin. Nutr. 60*, 1037S–1042S.

56. Thijssen, M.A., and Mensink, R.P. (2005) Small Differences in the Effects of Stearic Acid, Oleic Acid, and Linoleic Acid on the Serum Lipoprotein Profile of Humans, *Am. J. Clin. Nutr. 82*, 510–516.

57. Mennen, L., de Maat, M., Meijer, G., Zock, P., Grobbee, D., Kok, F., Kluft, C., and Schouten, E. (1998) Factor VIIa Response to a Fat-Rich Meal Does Not Depend on Fatty Acid Composition: A Randomized Controlled Trial, *Arterioscler. Thromb. Vasc. Biol. 18*, 599–603.

58. Mitropoulos, K.A., Miller, G.J., Martin, J.C., Reeves, B.E., and Cooper, J. (1994) Dietary Fat Induces Changes in Factor VII Coagulant Activity Through Effects on Plasma Free Stearic Acid Concentration, *Arterioscler. Thromb. 14*, 214–222.

59. Thijssen, M.A., Hornstra, G., and Mensink, R.P. (2005) Stearic, Oleic, and Linoleic Acids Have Comparable Effects on Markers of Thrombotic Tendency in Healthy Human Subjects. *J. Nutr.*

135, 2805–2811.

60. Simon, J.A., Fong, J., and Bernert, J.T., Jr. (1996) Serum Fatty Acids and Blood Pressure, *Hypertension 27*, 303–307.

61. Steer, P., Millgard, J., Sarabi, D.M., Basu, S., Vessby, B., Kahan, T., Edner, M., and Lind, L. (2002) Cardiac and Vascular Structure and Function Are Related to Lipid Peroxidation and Metabolism, *Lipids 37*, 231–236.

62. Zock, P.L., Blijlevens, R.A., de Vries, J.H., and Katan, M.B. (1993) Effects of Stearic Acid and *trans* Fatty Acids Versus Linoleic Acid on Blood Pressure in Normotensive Women and Men, *Eur. J. Clin. Nutr. 47*, 437–444.

63. Baer, D.J., Judd, J.T., Clevidence, B.A., and Tracy, R.P. (2004) Dietary Fatty Acids Affect Plasma Markers of Inflammation in Healthy Men Fed Controlled Diets: A Randomized Crossover Study, *Am. J. Clin. Nutr. 79*, 969–973.

64. Wang, L., Folsom, A.R., Zheng, Z.J., Pankow, J.S., and Eck-feldt, J.H. (2003) Plasma Fatty Acid Composition and Incidence of Diabetes in Middle-Aged Adults: The Atherosclerosis Risk in Communities (ARIC) Study, *Am. J. Clin. Nutr. 78*, 91–98.

65. Danesh, J., Lewington, S., Thompson, S.G., Lowe, G.D., Collins, R., Kostis, J.B., Wilson, A.C., Folsom, A.R., Wu, K., Benderly, M., *et al.* (2005) Plasma Fibrinogen Level and the Risk of Major Cardiovascular Diseases and Nonvascular Mortality: An Individual Participant Meta-analysis, *JAMA 294*, 1799–1809.

66. U.S. Food and Drug Administration and Center for Food Safety and Applied Nutrition (2003) Food Labeling: *Trans* Fatty Acids in Nutrition Labeling, Nutrient Content Claims, and Health Claims, *Federal Register 68*, 41434–41506.

Effects of Stearic Acid on Plasma Lipid and Lipoproteins in Humans

Ronald P. Mensink*

Department of Human Biology, Nutrition and Toxicology Research Institute
Maastricht (NUTRIM), Maastricht University, Maastricht, The Netherlands

ABSTRACT: More than 40 years ago, saturated FA with 12, 14, and 16 carbon atoms (lauric acid, myristic acid, and palmitic acid) were demonstrated to be "hypercholesterolemic saturated FA." It was further concluded that the serum total cholesterol level would hardly be changed by isocaloric replacement of stearic acid (18:0) by oleic acid (*cis*-18:1n-9) or carbohydrates. These earlier studies did not address the effects of the various FA on the serum lipoprotein profile. Later studies found that the hypercholesterolemic saturated FA increase serum total cholesterol levels by raising concentrations of both the atherogenic LDL and the antiatherogenic HDL. Consequently, the ratio of total to HDL cholesterol will hardly change when carbohydrates replace these saturated FA. Compared with other saturated FA, stearic acid lowers LDL cholesterol. Studies on the effects on HDL cholesterol are less conclusive. In some, the effects on HDL cholesterol were comparable to those of palmitic acid, oleic acid, and linoleic acid, whereas in others a decrease was observed. This may suggest that in this respect the source of stearic acid is of importance, which needs however further study. From all these studies, however, it can be concluded that stearic acid may decrease the ratio of total to HDL cholesterol slightly when compared with palmitic or myristic acid. Without doubt, the effects of stearic acid are more favorable than those of *trans* monounsaturated FA.

Paper no. L9817 in *Lipids 40*, 1201–1205 (December 2005).

More than 40 years ago, Keys and colleagues (1) demonstrated that saturated FA with 12, 14, and 16 carbon atoms (lauric acid, myristic acid, and palmitic acid) are the so-called hypercholesterolemic saturated FA. This means that iso-caloric replacement of carbohydrates by these FA increases serum total cholesterol concentrations. Furthermore, serum total cholesterol level is hardly changed by isocaloric replacement of stearic acid (18:0) for oleic acid (*cis*-18:1n-9) or carbohydrates. From another series of well-controlled studies, Hegsted and coworkers (2) also concluded that stearic acid, oleic acid, and carbohydrates had comparable effects on serum total cholesterol concentrations. In addition, they suggested that, in particular, myristic and to a lesser extent palmitic acid were hypercholesterolemic. These earlier studies did not, however, address the effects of stearic acid on the serum lipoprotein profile, which is important in view of the opposing relationships of LDL and HDL cholesterol with cardiovascular risk. The aim of this review therefore is to summarize findings from well-controlled studies on the effects of stearic acid on serum lipids and lipoproteins in humans.

HUMAN STUDIES ON THE EFFECTS OF STEARIC ACIDS ON SERUM LIPIDS AND LIPOPROTEINS

In 1990, Grande *et al.* (3) published a study of the effects of stearic and palmitic acids on serum total cholesterol concentrations in man. Thirty healthy men were given four different diets. Three of these diets were rich in stearic acid. One of the three diets was made from cocoa butter, whereas the other two diets were made by randomization of palm oil, totally hydrogenated soybean oil, olive oil, and safflower oil. The fourth diet was rich in palmitic acid. The three stearic acid-rich diets produced nearly identical serum total cholesterol concentrations, which were lower than those on the diet rich in palmitic acid. It was further concluded that cocoa butter did not contain any special cholesterol-lowering substance.

Bonanome and Grundy (4) studied the effects of liquid-formula diets rich in stearic acid, palmitic acid, and oleic acid in 11 male subjects. The fat that was high in stearic acid was made by hydrogenation of soybean oil. This hydrogenated oil, which consisted of 90% stearic acid, was hydrolyzed and randomly interesterified with high-oleic safflower oil. In the end, the experimental fat consisted of nearly 43% stearic acid. In the diet that was high in palmitic acid, palm oil was the only source of fat. High-oleic acid safflower oil was used for the diet high in oleic acid. Compared with the diet high in palmitic acid, the diets rich in stearic acid and oleic acid lowered serum total and LDL cholesterol concentrations. No effects on other lipoproteins were found, although it should be noted that HDL cholesterol concentrations were lowest on the diet high in stearic acid. Intestinal absorption of palmitic acid, stearic acid, and oleic acid in the three dietary periods varied between 97 and 100%.

Denke and Grundy (5) examined the influence of beef tallow and cocoa butter, two fats high in stearic acid, on the serum lipoprotein profile. In addition, butterfat and olive oil were examined. The liquid-formula diets were given in random order for 3 wk to 10 middle-aged men. Butterfat raised serum total and LDL cholesterol concentrations the most, while concentrations were the lowest on olive oil. Levels were intermediate on the two diets rich in stearic acid. No effects on HDL cholesterol were found. Serum TAG concentrations on the olive oil diet were significantly lower than those on the beef diet. In addition,

*Address correspondence to Dept. of Human Biology, NUTRIM, Maastricht University, Universiteitssingel 50, 6229 ER Maastricht, The Netherlands.
E-mail: R.Mensink@HB.UNIMAAS.NL

fecal excretion of the FA was studied. It was reported that 90–94% of the stearic acid, 96–97% of the palmitic acid, and 99% of the oleic acid were absorbed.

In another well-controlled trial with 56 subjects Zock and Katan (6) compared the effects of stearic acid with those of *trans* monounsaturated FA and linoleic acid. Fats for the stearic acid-rich diet were produced by interesterification of a mixture of fully hydrogenated high-linoleic acid sunflower oil with high-oleic acid sunflower oil and high-linoleic acid sunflower oil. A fat high in *trans* monounsaturated FA was made by isomerization of high-oleic acid sunflower oil. The isomerized fat was mixed with high-oleic acid-rich oil. Sunflower oil was the main source for the preparation of the diets rich in linoleic acid. The results showed that stearic acid and *trans* monounsaturated FA had comparable effects on the serum lipoprotein profile. Compared with linoleic acid, these two FA increased total and LDL cholesterol and decreased HDL cholesterol. In addition, the stearic acid-rich diet increased serum concentrations of TAG slightly.

In 18 normocholesterolemic young men, Kris-Etherton *et al.* (7) examined the effects of whole-foods prepared with different test fats. The diet high in stearic acid was made from cocoa butter, the diet high in oleic acid from olive oil, the diet high in linoleic acid from soybean oil, and the diet high in saturated FA from butter. Cocoa butter lowered serum LDL cholesterol when compared with butter. Concentrations, however, were the lowest on the diet high in linoleic acid. Sunflower oil also decreased TAG. No effects on HDL were observed.

Tholstrup and colleagues (8) studied the effects of shea butter, of palm oil, and of a mixture of palm kernel oil plus high-oleic sunflower oil in 15 young men. Shea butter is a fat commonly used in some African countries that is rich in stearic and oleic acids: 42 and 45% of total FA, respectively. Stearic acid is exclusively at the *sn*-1 position of the TAG molecule. The other two fats were rich, respectively, in palmitic acid and in lauric acid plus myristic acid. Serum total, LDL, and HDL cholesterol concentrations were the lowest on the fat high in stearic acid. Serum TAG concentrations did not differ between the three diets.

Dougherty *et al.* (9) found that stearic acid lowered serum total and LDL cholesterol when compared with palmitic acid. Serum HDL cholesterol and TAG concentrations were comparable between the two diets. In this study with 10 middle-aged males, shea butter was used for the preparation of fat high in stearic acid, and palmitic acid was used for the production of a fat high in palmitic acid.

To compare the effects of stearic acid and *trans* monounsaturated FA on serum lipoproteins, Aro *et al.* (10) fed 80 volunteers two different diets. The diet high in stearic acid was made by interesterification of a mixture of fully hydrogenated sunflower oil and of sunflower oils rich in oleic or linoleic acids. Compared with the diet high in *trans* FA, the diet high in stearic acid lowered LDL cholesterol and TAG but increased HDL cholesterol.

In a small study with only 6 young healthy men, Hunter *et al.* (11) compared the effects of stearic acid, oleic acid, and linoleic acid on serum lipoproteins. Stearic acid in the test fat

was positioned at the *sn*-1 and/or s*n*-3 position. Serum lipid and lipoprotein concentrations did not differ significantly among the three diets, probably due to the limited number of subjects that participated in the study.

In a large study with 50 volunteers, Judd *et al.* (12) examined the cholesterolemic effects of six different diets. One diet was specifically enriched with stearic acid and another diet in stearic acid plus *trans* monounsaturated FA. The other diets were rich in a mixture of saturated FA, carbohydrates, oleic acid, or *trans* monounsaturated FA. A high-stearate fat was made from a randomized mixture of completely hydrogenated soybean oil, coconut oil, canola oil, and ethyl myristate. Stearic acid lowered LDL cholesterol when compared with *trans* FA but increased it relative to oleic acid. Differences in concentrations among the other diets did not reach statistical significance. For HDL cholesterol, concentrations were the lowest on the diets rich in stearic acid and *trans* FA. TAG concentrations were also slightly elevated in the diet high in stearic acid.

These studies clearly show that stearic acid lowers the atherogenic LDL cholesterol concentrations when compared with lauric acid, myristic acid, palmitic acid, and *trans* monounsaturated FA. In fact, effects of stearic acid on LDL cholesterol are comparable to those of oleic acid. For HDL cholesterol, results are less conclusive. Several studies suggest that stearic acid slightly lowered HDL cholesterol when compared with the other saturated FA and *cis*-unsaturated FA (4,6,8,9,11,12), although differences did not always reach statistical significance (4,11). Other studies, however, could not demonstrate an effect of stearic acid on HDL cholesterol (5,7). There is no obvious explanation for the discrepant findings. It can be speculated that the source of stearic acid is important.

Studies of the effects of stearic acid have been limited by the composition of available oils and fats. In some experiments, cocoa butter and shea butter have been used as major sources of stearic acid. Other studies, however, have used synthetic fats. Most of these fats were made by fully hydrogenating oils rich in linoleic acid, which were then randomly interesterified with other oils and fats. The advantage of this approach is that fats with any desired FA composition can be made. In addition, it is possible to avoid the presence of tristearate, which is poorly absorbed due to its high m.p. A potential disadvantage is that in tailor-made fats about one-third of the stearic acid is situated at the *sn*-2 position. In shea and cocoa butters, stearic acid is mainly located at the *sn*-1 or *sn*-3 position. For palmitic acid, there is no strong evidence that TAG structure determines plasma lipid concentrations (13). For stearic acid, this question has never been studied systematically. Table 1 shows that in all studies with synthetic fats stearic acid slightly lowered HDL cholesterol. Of the studies that used natural fats, shea butter decreased HDL cholesterol (8,9), whereas effects were less evident in the two studies that have used cocoa butter and beef tallow (5,7). Thus, the question remains open whether TAG structure or source of fat is important to the effects of stearic acid fats on HDL cholesterol.

Finally, it should be noted that effects of stearic acid on HDL cholesterol were more favorable than those of *trans* monounsaturated FA (6,10).

TABLE 1
Dietary Stearic Acid and Serum Lipid and Lipoprotein Concentrations: Results from Well-Controlled Intervention Trials

Authors	No. of men/women	Design[a]	Days of test period	Test diet[b]	Main source for stearic acid	FA composition[c] (% of daily energy intake) S — Total	S — C16	S — C18	M	P	T	Lipid or lipoprotein[d] (mmol/L) TC	LDL-C	HDL-C	TAG
Grande et al., 1970 (3)	30:0	X	18	I	Diet I: cocoa butter;	18.8		9.9	11.1	2.5		5.25[a,b]			1.24
				II	Diets II and IV: totally hydrogenated soybean oil,	18.8		9.5	11.2	2.6		5.15[c]			1.38[a]
				III		16.9		2.2	11.6	3.8		5.61[b,c,d]			1.14[a,b]
				IV	reesterified with palm oil, olive oil and safflower oil	17.4		12.2	11.9	3.5		4.99[a,d]			1.37[b]
Bonanome and Grundy, 1988 (4)	11:0	X	21	I	Fully hydrogenated soybean oil,	19.9	3.2	16.5	15.2	3.2		4.47[a,b]	2.84[a,b]	1.03[a]	1.46
				II		19.6	17.3	1.8	14.9	3.7		5.22[a]	3.62[b]	1.09[a,b]	1.45
				III	reesterified with high-oleic acid safflower oil	3.1	2.1	0.8	30.6	4.7		4.68[b]	3.07[b]	1.13[b]	1.38
Denke and Grundy, 1991 (5)	10:0	X	21	I	Diet I: cocoa butter	23.2	10.0	13.2	13.6	<3.0		5.14	3.82[b]	0.87	1.21
				II		8.0	6.8	1.2	25.8	<3.0		4.88[a,b]	3.62[c]	0.87	1.13[a]
				III	Diet IV: beef tallow	25.4	10.0	4.0	8.4	<3.0		5.61[a]	4.24[a,b,c,d]	0.87	1.25
				IV		18.8	12.4	7.6	16.4	<3.0		5.48[b]	4.03[a,d]	0.94	1.39[a]
Zock and Katan, 1992 (6)	26:30	X	21	I	Fully hydrogenated sunflower oil,	20.1	5.7	11.8	16.3	4.3	0.3	4.89[a]	3.00[a]	1.41	1.04[a]
				II		11.0	5.8	2.8	15.7	12.5	0.1	4.74[a,b]	2.83[a,b]	1.47	0.95[a]
				III	reesterified with sunflower oils rich in oleic and linoleic acids	10.3	4.8	3.0	15.6	4.2	7.7	4.90[a]	3.07[b]	1.37	1.00
Kris-Etherton et al., 1993 (7)	18:0	X	26	I	Cocoa butter	20.9	9.3	11.4	13.2	2.1		4.27[a,b,c]	2.67[a,b,c]	1.16	0.98[a]
				II		6.0	4.5	1.4	27.2	2.3		3.93[b,d,f]	2.38[b,d]	1.24	0.95[b]
				III		6.3	4.5	1.7	10.1	17.8		3.59[c,e,f]	2.15[c,e]	1.16	0.82[a,b,c]
				IV		21.0	9.3	4.5	10.1	1.7		4.55[a,d,e]	2.92[a,d,e]	1.16	0.99[c]
Tholstrup et al., 1994 (8)	15:0	X	21	I	Shea butter	15.7	1.7	13.6	15.7	2.7		3.18[a,b]	2.18[a]	0.86[a,b]	0.70
				II		18.1	15.8	1.8	14.3	4.3		4.08[a,c]	2.96[b]	0.99[a,c]	0.73
				III		20.2	2.9	1.1	14.4	2.3		4.42[b,c]	3.06[a,b]	1.19[b,c]	0.74
Dougherty et al., 1995 (9)	10:0	X	40	I	Shea butter	10.8	2.4	7.3	9.5	7.9	0.6	4.40[a]	3.10[a]	0.80	1.10
				II		9.1	7.2	1.5	9.5	7.0	1.0	4.70[a]	3.30[a]	0.90	1.10
Aro et al., 1997 (10)	31:49	//	35	C	Fully hydrogenated sunflower oil,	13.8		3.6	12.2	3.4	0.8	4.71	2.89[a]	1.42[a]	0.96[a]
				I	reesterified with sunflower oils rich in oleic and linoleic acids	15.0		9.3	12.2	3.5	0.4				
				II		7.1		2.6	12.5	2.9	8.7	4.80	3.06[a]	1.36[a]	1.09[a]
Hunter et al., 2000 (11)	6:0	X	14	I, II, III	Tailor-made fat with stearic acid at the sn-1,3-positions	17.6	3.8	13.0	13.9	4.5		3.76	2.79	0.96	0.54
						6.8	3.8	2.3	25.0	4.4		3.91	3.12	1.06	0.52
						7.3	4.3	2.3	14.4	14.4		3.71	2.58	1.04	0.51
Judd et al., 2002 (12)	50:0	X	35	I	Fully hydrogenated soybean oil,	20.9	6.9	10.9	10.5	4.4	0.3	4.78[a,b,c]	3.10[a]	1.16[a,b]	1.13[a,b]
				II		16.9	6.9	6.9	10.6	4.3	4.2	4.98[c,d,e]	3.32[b,c,d]	1.17[c,d,e]	1.06[c]
				III	reesterified with coconut oil, canola oil, and ethyl myristate	20.7	10.0	2.7	10.5	4.2	0.2	4.96[f,g]	3.21[e,f,g]	1.30[d,e,f,g,h]	0.97[b]
				IV		12.7	5.7	2.9	10.5	3.8	0.2	4.72[d,f,h]	3.05[b,e,h]	1.20[a,l,f]	1.03[d]
				V		12.7	5.7	2.9	17.6	3.8	0.1	4.59[a,e]	2.95[a,c,f,i]	1.24[b,c,g,i,j]	0.88[a,c,d,e]
				VI		12.9	7.6	2.8	10.6	4.0	8.3	4.99[b,h,i]	3.36[d,g,h,i]	1.16[a,b]	1.02[e]

[a]X, Cross-over or Latin square design; //, parallel design.
[b]C, Control diet. Lipid values are corrected for differences between groups when on the control diets.
[c]S, Saturated FA; M, monounsaturated FA; P, PUFA; T, trans FA; Total, total saturated FA; C16, palmitic acid; C18, stearic acid.
[d]TC, Total cholesterol; LDL-C, LDL cholesterol; HDL-C, HDL cholesterol. Values sharing a common superscript are significantly different ($P < 0.05$).

EFFECTS OF STEARIC ACIDS ON SERUM LIPIDS AND LIPOPROTEINS: RESULTS OF A META-ANALYSIS

Estimates of the effects of dietary FA on the serum lipoprotein profile can be obtained in several ways. One approach is to exchange isocalorically within one study a particular FA for another FA or for carbohydrates. These studies have been discussed above. The number of diets, however, that can be examined within one experiment is limited. In addition, results may vary between experiments because of differences in the experimental designs. Another approach is to carry out a meta-analysis, in which the results from many independent experiments are combined with statistical techniques. In this way, it is possible to estimate the mean change in serum lipoprotein levels for a group of subjects when 1% of the energy from carbohydrates is replaced by an isocaloric amount of a particular FA. Two years ago, we published such a meta-analysis (14). The studies (those that were included) had to meet certain criteria. First, food intake of the participants had to be controlled thoroughly, with dietary FA being the sole variable. Thus, energy intake, cholesterol intake, and dietary fiber intake had to be constant throughout the study. Second, the experimental design used had to eliminate the effect of nonspecific drifts of the outcome variables with time. This can be achieved by feeding the different diets side-by-side (parallel design), or by giving the diets to the volunteers in random order (cross-over or Latin square design). Third, dietary periods had to be at least 14 d, which is sufficiently long for serum lipids to reach a new steady-state situation. Fourth, only studies with healthy persons who did not suffer from disturbances of lipid metabolism or diabetes were included. Finally, diets that had been specifically enriched in the very long chain n-3 PUFA (fish oils) were excluded, as these FA have specific effects on the serum lipoprotein profile.

In the end, we identified 35 studies that had reported intakes of individual saturated FA. In these studies, 91 different diets were fed. The effects of stearic acid on LDL cholesterol were found to be very similar when compared with carbohydrates. Relative to other saturated FA (lauric acid, myristic acid, and palmitic acid) and *trans* monounsaturated FA, however, stearic acid lowered LDL cholesterol (Table 2). A comparable picture was obtained for HDL cholesterol. Lauric acid strongly increased HDL cholesterol, but the effects decreased with increasing chain length. Again, *trans* monounsaturated FA had the most unfavorable outcome. In this meta-analysis, the effects of the individual FA on the total to HDL cholesterol ratio, which also predicts the risk for coronary heart disease, also were estimated. It was found that lauric acid favorably decreased this ratio relative to carbohydrates. This ratio was less affected by the other three saturates, although it was somewhat more favorable for stearic acid than for myristic and palmitic acids. When compared with carbohydrates, all saturated FA decreased TAG concentrations to the same extent. Effects of monounsaturated FA and PUFA on TAG concentrations were also more favorable than those of carbohydrates.

An important question, of course, is whether the assumed estimates for the effects of the individual FA are appropriate. This can be tested by applying these estimates to an experiment that was not part of the meta-analysis. Recently we finished a study (Mensink, R.P., and Cardone, K., unpublished data) in which the effects of two semisolid fats were compared. One fat was high in palmitic acid. For the other fat, about 34% of the palmitic acid (calculated as the percentage of the experimental fat) was replaced for 9% stearic acid, 18% oleic acid, and nearly 4% *trans* FA. Experimental fats provided about 17% of total energy. For LDL a decrease of −0.23 mmol/L was predicted, whereas a decrease of −0.34 mmol/L was observed. For HDL, these values were, respectively, −0.03 and −0.06 mmol/L. This shows that these formulas are not conclusive, but do give a valuable indication of the expected effects.

TABLE 2
Estimated Effects for the Change in Serum Lipids and Lipoproteins for a Group of Subjects When 1% of Energy in the Diet from Carbohydrates Is Replaced Isocalorically by a Particular FA[a]

FA		Total cholesterol (mmol/L)	LDL cholesterol (mmol/L)	HDL cholesterol (mmol/L)	Total to HDL cholesterol ratio	TAG (mmol/L)
Stearic acid	Change	−0.010	−0.004	+0.002	−0.013	−0.017
	95% CI	−0.026 to 0.006	−0.019 to 0.011	−0.001 to 0.006	−0.030 to 0.003	−0.024 to −0.010
Lauric acid	Change	+0.069	+0.052	+0.027	−0.037	−0.019
	95% CI	0.040 to 0.097	0.026 to 0.078	0.021 to 0.033	−0.057 to −0.017	−0.028 to −0.011
Myristic acid	Change	+0.059	+0.048	+0.018	−0.003	−0.017
	95% CI	0.036 to 0.082	0.027 to 0.069	0.013 to 0.023	−0.026 to 0.021	−0.027 to −0.006
Palmitic acid	Change	+0.041	+0.039	+0.010	+0.005	−0.017
	95% CI	0.028 to 0.054	0.027 to 0.051	0.007 to 0.013	−0.008 to 0.019	−0.023 to −0.011
Trans-monounsaturates	Change	+0.031	+0.040	0.000	+0.022	0.000
	95% CI	0.020 to 0.042	0.020 to 0.060	−0.007 to 0.006	0.005 to 0.038	−0.012 to 0.012
Cis-monounsaturates	Change	−0.006	−0.009	+0.008	−0.026	−0.019
	95% CI	−0.012 to 0.000	−0.014 to −0.003	0.005 to 0.011	−0.035 to −0.017	−0.024 to −0.014
Cis-polyunsaturates	Change	−0.021	−0.019	+0.006	−0.032	−0.026
	95% CI	−0.027 to −0.015	−0.025 to 0.013	0.003 to 0.009	−0.042 to −0.022	−0.031 to −0.020

[a]Data are derived from Reference 13. CI, confidence interval.

CONCLUSION

Effects of stearic acid on LDL cholesterol levels are more comparable to those of oleic acid than to those of the cholesterol-raising saturated FA or *trans* monounsaturated FA. Stearic acid may slightly decrease HDL when compared with other saturated FA but may have a more favorable effect on the total to HDL cholesterol ratio. To what extent these findings can be translated into cardiovascular risk depends, of course, on the effects of stearic acid on other cardiovascular risk markers. Finally, it is not clear whether TAG structure or source of fat is of importance to explain the effects of stearic-acid fats on HDL cholesterol.

REFERENCES

1. Keys, A., Anderson, J.T., and Grande, F. (1965) Serum Cholesterol Response to Changes in the Diet. IV. Particular Saturated Fatty Acids in the Diet, *Metabolism 14*, 776–786.
2. Hegsted, D.M., McGandy, R.B., Myers, M.L., and Stare, F.J. (1965) Quantitative Effects of Dietary Fat on Serum Cholesterol in Man, *Am. J. Clin. Nutr. 17*, 281–295.
3. Grande, F., Anderson, J.T., and Keys, A. (1970) Comparison of Effects of Palmitic and Stearic Acids in the Diet on Serum Cholesterol in Man, *Am. J. Clin. Nutr. 23*, 1184–1193.
4. Bonanome, A., and Grundy, S.M. (1988) Effect of Dietary Stearic Acid on Plasma Cholesterol and Lipoprotein Levels, *N. Engl. J. Med. 318*, 1244–1248.
5. Denke, M.A., and Grundy, S.M. (1991) Effects of Fats High in Stearic Acid on Lipid and Lipoprotein Concentrations in Men, *Am. J. Clin. Nutr. 54*, 1036–1040.
6. Zock, P.L., and Katan, M.B. (1992) Hydrogenation Alternatives: Effects of *trans* Fatty Acids and Stearic Acid Versus Linoleic Acid on Serum Lipids and Lipoproteins in Humans, *J. Lipid Res. 33*, 399–410.
7. Kris-Etherton, P.M., Derr, J., Mitchell, D.C., Mustad, V.A., Russell, M.E., McDonnel, E., Salabsky, D., and Pearson, T.A. (1993) The Role of Fatty Acid Saturation on Plasma Lipids, Lipoproteins, and Apoproteins: I. Effects of Whole Food Diets High in Cocoa Butter, Olive Oil, Soybean Oil, Dairy Butter, and Milk Chocolate on the Plasma Lipids of Young Men, *Metabolism 42*, 121–129.
8. Tholstrup, T., Marckmann, P., Jespersen, J., and Sandström, B. (1994) Fat High in Stearic Acid Favorably Affects Blood Lipids and Factor VII Coagulant Activity in Comparison with Fats High in Palmitic Acid or High in Myristic Acid, *Am. J. Clin. Nutr. 59*, 371–377.
9. Dougherty, R.M., Allman, M.A., and Iacono, J.M. (1995) Effects of Diets Containing High or Low Amounts of Stearic Acid on Plasma Lipoprotein Fractions and Fecal Fatty Acid Excretion of Men, *Am. J. Clin. Nutr. 61*, 1120–1128.
10. Aro, A., Jauhiainen, M., Partanen, R., Salminen, I., and Mutanen, M. (1997) Stearic Acid, *trans* Fatty Acids, and Dairy Fat: Effects on Serum and Lipoprotein Lipids, Apolipoproteins, Lipoprotein(a), and Lipid Transfer Proteins of Healthy Subjects, *Am. J. Clin. Nutr. 65*, 1419–1426.
11. Hunter, K.A., Crosbie, L.C., Weir, A., Miller, G.J., and Dutta-Roy, A.K. (2000) A Residential Study Comparing the Effects of Diets Rich in Stearic Acid, Oleic Acid, and Linoleic Acid on Fasting Blood Lipids, Hemostatic Variables and Platelets in Young Healthy Men, *J. Nutr. Biochem. 11*, 408–416.
12. Judd, J.T., Baer, D.J., Clevidence, B.A., Kris-Etherton, P., Muesing, R.A., and Iwane, M. (2002) Dietary *cis* and *trans* Monounsaturated and Saturated FA and Plasma Lipids and Lipoproteins in Men, *Lipids 37*, 123–131.
13. Zock, P.L., de Vries, J.H., de Fouw, N.J., and Katan, M.B. (1995) Positional Distribution of Fatty Acids in Dietary Triglycerides: Effects on Fasting Blood Lipoprotein Concentrations in Humans, *Am. J. Clin. Nutr. 61*, 48–55.
14. Mensink, R.P., Zock, P.L., Kester, A.D.M., And Katan, M.B. (2003) Effects of Dietary Fatty Acids and Carbohydrates on the Ratio of Serum Total to HDL Cholesterol and on Serum Lipids and Apolipoproteins: A Meta-analysis of 60 Controlled Trials, *Am. J. Clin. Nutr. 77*, 1146–1155.

Influence of Dietary Saturated Fatty Acids on the Regulation of Plasma Cholesterol Concentration

Michaelann S. Wilke and M. Thomas Clandinin*

Alberta Institute for Human Nutrition, University of Alberta, Edmonton, Alberta, Canada T6G 2H1

ABSTRACT: The specific effects of individual fatty acids (FA) on plasma cholesterol levels, in the range habitually consumed by humans, is not usually presented by the literature. Conclusions have been made regarding the cholesterolemic effect of individual FA, even though these FA cannot be tested individually. It appears that FA balance of the diet may be more important than individual FA intakes. Variation in plasma cholesterol response to diet is influenced by many factors, such as gene–nutrient interactions. The effect on human health of current processes used in the food industry that are certain to change dietary fat composition and TG structure is yet to be fully explored. Some of the relevant research regarding dietary fat and plasma cholesterol levels is reviewed.

Paper no. L9808 in *Lipids* 40, 1207–1213 (December 2005).

First, research "proved" that total fat and cholesterol in the diet influenced plasma cholesterol levels. Then it was "shown" that saturated fats were more important in this role. Now it is well accepted that individual FA have differing effects on plasma cholesterol levels. Specific effects, within the context of the range of intake of humans, are less clear. Much of the literature in this area reflects the effect of fat types and amounts in many different animal models that may not be relevant to the human situation. Even when the research is simply exploring the mechanism underlying an effect, it is not known whether the same effect occurs in humans, especially when considering fat intake in the normal range. Data reflecting what FA Americans habitually consume are difficult to find. According to data for the U.S. population from the National Health and Nutrition Examination Survey 1999–2000 (Table 1) (1), the average intake of the three largest contributors of dietary FA appears to be around 6% of energy for each of palmitic (16:0) and linoleic (18:2n-6) acid and not more than 3% of energy for stearic (18:0) acid.

Knowing the range of intake for these FA may be more important in designing studies relevant to the human dietary situation. Computer analysis of baseline 7-d food records from 30 free-living subjects indicated ranges of total fat intake from 18.8 to 54.0%en (percentage of total dietary energy),

saturated FA intake from 6.4 to 15.7%en, and PUFA intake from 2.4 to 5.7%en (Wilke, M.S., Ryan, E.A., French, M.A., Jumpsen, J., Goh, Y.K., and Clandinin, M.T., unpublished data). These are wide ranges, but not nearly as wide or variable as the animal data from the literature used to test the effect of various FA on plasma cholesterol levels (2). These data also show that actual intake can differ considerably from recommendations for fat intake. Consuming an undesirable balance of FA may have effects on an individual's plasma cholesterol levels, platelet aggregation, and coronary heart disease risk (3).

Whereas information on specific FA may be scarce, general data on total and saturated fat intake are available (4,5). Some epidemiological studies have collected longer-term food intake data to examine the relationship between fat intake and plasma cholesterol or disease occurrence. For instance, the Nurse's Health study compared quintiles of dietary fat intake and coronary heart disease risk. At the lowest quintile, median PUFA intake was 4.1%en, and in the highest quintile it was 7.4%en. A good indication of average intake range (for women) can be taken from these data. For the lowest and highest quintiles of total fat and saturated FA, median intake was 28.3 and 44.0%en, and 10.1 and 17.6%en, respectively. These results, not surprisingly, show an inverse relation between polyunsaturated fat intake and coronary heart disease risk. The data also indicated that saturated fat intake was not related to risk, although the PUFA/saturated FA ratio was inversely related (6). Examining the effect of the intake of one type of fat does not demonstrate the effect of dietary

TABLE 1
Estimated FA Intake of Americans (1999–2000)[a]

		16:0	18:0	18:2
Both sexes/all ages[b]		6.2	2.8	6.0
Men	20–39 yr	6.2	2.8	5.8
	40–59 yr	6.0	2.8	5.9
	60+ yr	6.0	2.8	6.1
Women	20–39 yr	6.1	2.8	6.2
	40–59 yr	6.0	2.8	6.3
	60+ yr	6.0	2.7	6.5

[a]Data from the National Health and Nutrition Examination Survey 1999–2000 for U.S. population based on 24-h recall and coded to USDA's Survey Nutrient Database (versions 1994–96 and 1998) (1). Values represent means as percentage of energy, assuming fat intake at 33% of energy.
[b]Excludes nursing infants and children.

*To whom correspondence should be addressed at Alberta Institute for Human Nutrition, 231A General Services Bldg., University of Alberta, Edmonton, Alberta, Canada T6G 2H1. E-mail: tclandin@ualberta.ca

Abbreviations: %en, percentage of total dietary energy; 12:0, lauric acid; 14:0, myristic acid; 16:0, palmitic acid; 18:0, stearic acid; 18:2n-6, linoleic acid; apo, apolipoprotein.

fat balance, whereas the polyunsaturated/saturated FA ratio may provide a better indication of the balance of FA in the diet consumed.

THE LITERATURE

The conclusions made in the literature indicating that consumption of saturated FA increases plasma cholesterol or LDL cholesterol levels are difficult to accept when one examines individual research studies. Frequently, formulation of such conclusions is complicated further by research that does not report FA analysis of the diets fed. Some studies report the type of oil used, which does not necessarily demonstrate the FA composition of the diets. Furthermore, in other studies the diets to be tested were designed by adding a specific type of oil or an oil blend to rat chow. This not only increases the fat intake of the animals, substantially reducing the intake of other essential nutrients, but also results in variable FA composition.

Even when the data include analysis of dietary FA composition, assessing the effect of one FA is difficult. To test the effect of one FA, another acid, often linoleic acid (18:2n-6), must be altered. Changes in diet are made through substitutions; therefore, the levels of fat and cholesterol vary in the diets fed. A common substitution is saturated fat for polyunsaturated fat, or the effects of saturated FA at different levels of polyunsaturated FA may be tested. A study using guinea pigs tested the effect of fat saturation on LDL metabolism, but the levels of 18:2n-6 in the diets compared in the study (15.1% fat by weight) were deficient in the olive oil ("high in monounsaturated fat;" 7.3% 18:2n-6) and lard ("high in saturated fat;" 10.7% 18:2n-6) diets and very high in the corn oil diet ("high in polyunsaturated fat;" 48.4% 18:2n-6) (7). Consequently, it was not surprising that the olive oil diet had effects on many aspects of LDL metabolism that were not different from the lard diet since both had <4%en coming from 18:2n-6. A study in cebus monkeys showed that when consumption of 18:2n-6 is low (3–4%en), an increase in consumption of 14:0 or 16:0 increases total cholesterol levels (8). In cebus and rhesus monkeys, when 18:2n-6 was low (3–4%en) in a cholesterol-free/low-14:0 diet, high 16:0 intake had no effect on LDL cholesterol. This study demonstrated no effect on lipoproteins in rhesus monkeys, but effects were observed in cebus monkeys (9). Further research in rhesus monkeys showed that reducing fat intake by decreasing 16:0 lowered LDL cholesterol more than decreasing 12:0 + 14:0 (10). When testing the effect of saturated FA in animal diets, enough 18:2n-6 is sometimes fed to "prevent deficiency." However, the deficient state is rarely seen in adult humans, particularly in areas of the world where cardiovascular disease prevention is important. Saturated FA need to be tested at the same levels of fat and at logical levels of other FA compared with the FA in question. It was shown in both hamsters and cynomolgus monkeys that when 18:2n-6 intake was high (10.5%en), substituting 4%en of 18:0 for 16:0 did not increase total cholesterol or LDL cholesterol or result in
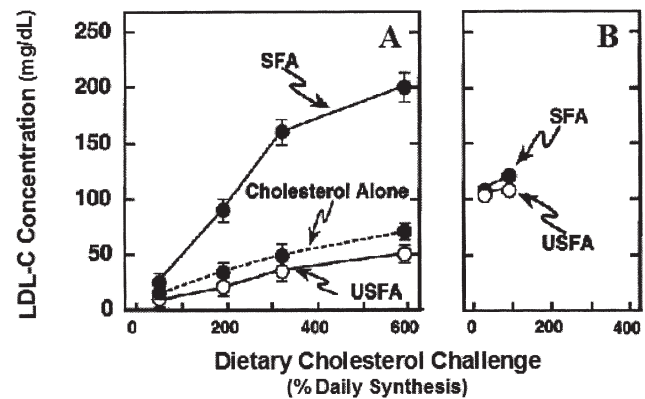

FIG. 1. The dependency of FA effects on LDL cholesterol concentration on the level of dietary cholesterol intake (42). This diagram shows the absolute concentration of LDL cholesterol achieved in hamsters (A) or humans (B) fed predominantly saturated FA (SFA) or unsaturated FA (USFA) under circumstances in which the amount of cholesterol in the diet was varied. This diagram was originally constructed using data from two sources (16,17). In the hamster diets, the SFA diet was hydrogenated coconut oil and tripalmitin added to the USFA diet (16). The human SFA diets consisted of 4.5%en vs. 9.5%en 18:2n-6 (17).

observable lipoprotein changes (11,12). Animal research suggests that stearate (18:0) may be more hypocholesterolemic than 12:0, 14:0, or 16:0. In rats, for example, the addition of 18:0 to coconut oil decreased total cholesterol by about 15% in both plasma and liver (13). When compared with other interesterified fats, fat that is high in dietary 18:0 lowers total cholesterol in hamsters, perhaps due to a difference in fat absorption (14).

Each study in the literature has to be examined closely to identify reliable conclusions about the effect of specific FA on plasma cholesterol levels. Conclusions generalized from results that are complicated by diet and animal model used cannot be accepted as relevant without careful consideration. The animal model needs to be considered in relation to its unique response to dietary factors. For example, some animal models such as the hamster are used to reflect what is referred to as "cholesterol-sensitive individuals" and then results may be extrapolated to all humans by review articles and the common rhetoric.

It is important when comparing the effect of one FA to another on plasma cholesterol levels that the other dietary FA be kept equal. The amount of cholesterol in the diet also needs to be considered. Many animals only respond to dietary saturated FA when cholesterol is present in the diet. From the literature, it would appear that at higher cholesterol intakes, saturated FA increase LDL cholesterol (15) (Fig. 1). However, on further examination of the data, these diets are not comparable on the basis of saturated FA intake alone. For instance, a high saturated fat diet tested in the hamster (Fig. 1A) consisted of hydrogenated coconut oil and tripalmitin added to the unsaturated fat (USFA) diet (16). The comparison of saturated fat (SFA) to USFA in humans (Fig. 1B) consisted of 4.5%en 18:2n-6 compared with intakes of 9.5%en 18:2n-6
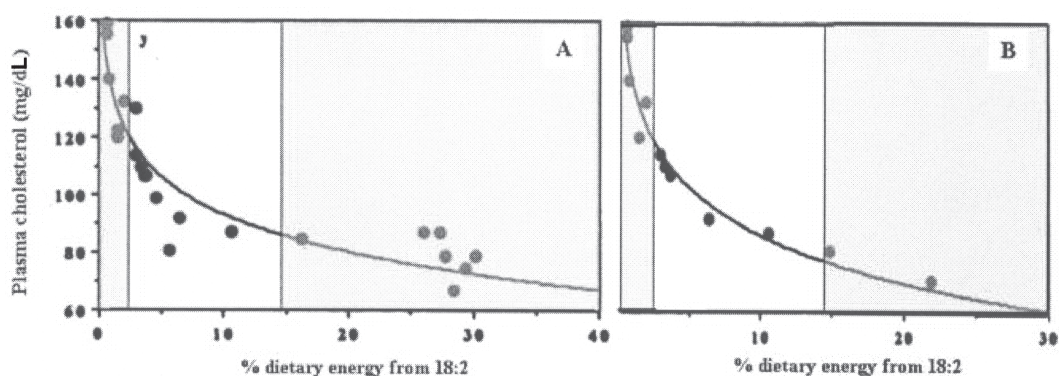
FIG. 2. Plasma cholesterol response to dietary 18:2n-6 is nonlinear in the gerbil. (A) Decreasing 18:2n-6 raises total cholesterol independent of 14:0 intake [when dietary 14:0 was low and relatively constant, 0.13–1.08%en; $y = 136.5 - 43.1*\log(x)$ $R^2 = 0.861$]. (B) Response of plasma cholesterol to dietary 18:2n-6 [when dietary 14:0 + 16:0 was relatively high and constant, 7.8–11.8%en; $y = 149.9 - 54.5*\log(x)$ $R^2 = 0.951$]. The range of intake typical for humans has been highlighted to show what could be interpreted as a more linear relationship (adapted from Ref. 2).

(17). Clearly, the effect attributed to higher saturated fat and cholesterol in the diet may be a consequence of lower intake of 18:2n-6.

It has been proposed that 18:2n-6 has a "threshold effect," above which saturated FA may not have an effect on plasma cholesterol levels. In many animal studies, high vs. low 16:0 or 18:0 is commonly 18:2n-6 deficient vs. 18:2n-6-adequate. Furthermore, many high saturated fat comparisons often are low in 18:2n-6 and high in 14:0. Perhaps this is why all saturated FA have been labeled hypercholesterolemic even though all available evidence indicates that individual saturated FA have quite different effects on plasma cholesterol.

SATURATED FA COMPARISONS AND THRESHOLD EFFECTS

A threshold effect of 18:2n-6 was proposed by Hayes and Khosla (8) whereby 16:0 does not affect LDL cholesterol in normocholesterolemic subjects when dietary 18:2n-6 levels are above a "threshold" of 6%en. It has also been suggested that the plasma cholesterol response to 18:2n-6 intake is not linear (Fig. 2). On closer examination of this response curve, the cholesterol response appears linear in the range of 18:2n-6 intake that may be applicable to humans.

In a series of well-controlled studies, we examined the effect of exchanging dietary FA on cholesterol response. The first of these was a 21-d crossover feeding study involving healthy male subjects. This study demonstrated that consumption of high amounts of 16:0 (12%en) did not affect serum total cholesterol and LDL cholesterol if the amount of 18:2n-6 in the diet was also at recommended levels (8–9%en). Interestingly, in observing individual values (Fig. 3), it can be concluded that dietary PUFA level may determine whether a subject can be labeled hypercholesterolemic or normocholesterolemic (18). Further, fractional synthesis rates of cholesterol were unaffected, suggesting no relationship between the

endogenous synthesis of cholesterol and dietary 16:0 content. In a similar experiment involving hyperlipidemic subjects, total cholesterol and LDL cholesterol also were unaffected by high dietary 16:0 at high levels of dietary 18:2n-6 (data not shown) (19). This was not true for *trans* FA, where exchanging 16:0 from palm olein for partially hydrogenated fat resulted in higher plasma total cholesterol, LDL cholesterol, and endogenous synthesis of free cholesterol. Contrary to the previous studies in which HDL levels were unaffected by the dietary fat exchanges, exchanging palm olein for hydrogenated fat also decreased HDL cholesterol levels (20). It is now generally recognized that individual saturated FA are either neutral or increase HDL cholesterol when replacing mono- or polyunsaturated fats in the diet. In contrast, small amounts of *trans* FA (from hydrogenation) increase plasma
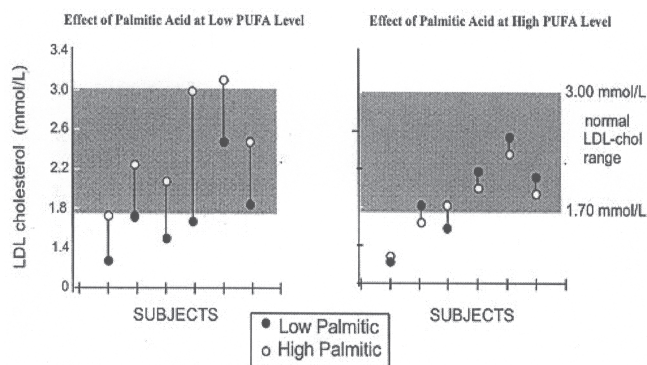
FIG. 3. Individual variation in response to diet. Four diets were formulated to provide combinations of high and low levels of palmitic acid at high and low levels of linoleic acid. Subjects received each of the diet treatments for 21 d, followed by washout periods of 21 d in a crossover design. The data indicated that serum total cholesterol and LDL cholesterol levels were not significantly affected by the high level of palmitic acid when diets also contained a high level of linoleic acid (18).

TABLE 2
Total Fat, PUFA, Saturated FA, and Monounsaturated FA Intakes as Percentage of Energy at Varying Levels of Energy from Dietary Linoleic Acid[a]

	Diet no.							
	1	2	3	4	5	6	7	8
Diet component[b]	10	8.5	7.5	6.5	5.5	4.5	3.5	2.5
Energy (kcal)	3104	2984	2964	2906	2954	2956	2888	2964
Total fat (%en)	30.9	30.3	30.1	29.8	29.6	30.1	29.5	29.2
PUFA (%en)	10.5	8.9	8.0	7.0	5.9	4.9	4.0	2.9
18:2[b]	10.0	8.5	7.5	6.6	5.5	4.5	3.5	2.5
SFA (%en)	12.0	11.9	11.7	11.9	11.9	11.5	12.1	13.0
16:0[c]	10.1	10.0	10.1	10.1	10.0	9.9	10.0	10.4
18:0	1.1	1.1	1.2	1.2	1.2	1.3	1.3	1.5
MUFA (%en)	7.3	8.0	9.2	9.5	10.1	12.7	12.2	11.7
Cholesterol (mg)	98.0	107.9	101.3	101.4	104.5	104.5	113.0	124.9

[a]Data from Reference 21.
[b]Healthy subjects received each diet treatment, designed to consist of varying amounts of linoleic acid [18:2n-6; percentage of total dietary energy (%en)] for 21 d, followed by washout periods of 7 d in a crossover design.
[c]Palmitic acid (16:0) was fed at 10%en in conjunction with decreasing levels of 18:2n-6 to determine whether a threshold level of 18:2n-6 prevented 16:0 from being hypercholesterolemic. SFA, saturated FA; MUFA, monounsaturated FA.

levels of LDL cholesterol and decrease HDL cholesterol regardless of which fat is replaced by it, thereby resulting in a less desirable lipid profile.

To determine whether a threshold level of 18:2n-6 prevents high 16:0 intake from being hypercholesterolemic, a subsequent experiment examined cholesterol response to high dietary 16:0 (10%en) intake in combination with decreasing levels of 18:2n-6 (Table 2). In this study, healthy subjects followed each diet for 21 d in a crossover design. The results showed that total plasma cholesterol levels increased as the percentage of energy in the diet from 18:2n-6 decreased. It was found that there may be a threshold effect of 18:2n-6, because high 16:0 intake was less hypercholesterolemic if dietary 18:2n-6 was greater than 4.5%en (Fig. 4) (21). It can be concluded that individual saturated FA, and specifically 16:0, may be conditionally hypercholesterolemic depending on the dietary intake of 18:2n-6.

VARIATION IN INDIVIDUAL RESPONSES

Response to diet, and specifically the response of plasma cholesterol to dietary fat amount and composition, is variable and dependent on many factors. Some aspects of animal studies uniquely contribute to this difficulty in interpretation. First, the range of species used in the research makes analysis of the information almost impossible. In investigating plasma cholesterol response to dietary fat, variation exists not only between different animal models (i.e., monkeys, guinea pigs, gerbils, hamsters, rats, rabbits, pigs), but also between species of primates (i.e., monkeys: cebus, rhesus, cynomolgus, vervet) and within strains of the same species (i.e., hamsters: F1B or CR Golden Syrian) (22). Many animal models vary in their response to dietary fat amount and type, and the responses may

also differ depending on the presence of or total amount of cholesterol in the diet.

There are several key differences in cholesterol metabolism between animals and humans. In general, cholesterol synthesis in humans is more tightly controlled, in that synthesis and absorption are able to coordinate to regulate the amount of cholesterol in body pools. This is why many animal models respond adversely to any added dietary cholesterol, whereas in the majority of humans, the effect of dietary cholesterol on plasma cholesterol level is small (reviewed in Ref. 23). Lipoprotein structure and function also vary depending on which animal model is used. As opposed to LDL in humans, HDL is the main carrier of cholesterol in most animals. Even guinea pigs, which carry cholesterol in LDL (24), have differences from humans in their lipoprotein metabolism.

In humans, results can be more variable than in animal studies, perhaps due in part to the inability to tightly control environmental influences and genetic differences. Even though changes in the dietary fat used in animal studies is generally more extreme, the variation in other dietary influences in human studies can be much greater due to the availability of a variety of foods and to other contributors to eating behavior and choice. Further, analysis of diet by 1-d food records/recalls does not accurately capture this variation or provide the basis to statistically identify all relevant factors. The errors in estimating FA intake by this methodology are often extremely high (25).
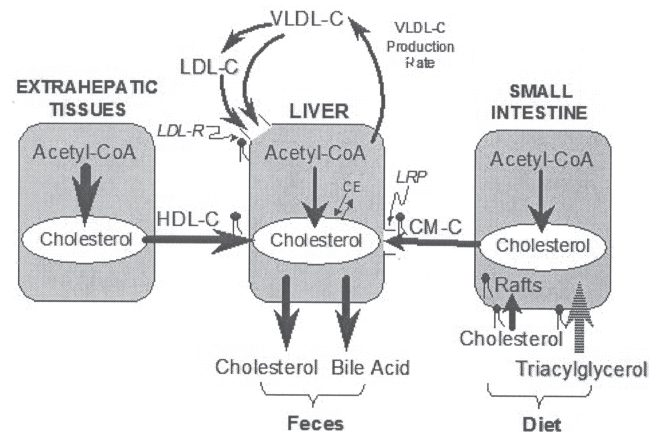
As technology and our knowledge of lipoprotein metabolism increase, our understanding of the "traditional causes" of individual variation is expanding. Factors known to affect plasma cholesterol levels include body mass index, age, gender, menopausal status, and baseline LDL cholesterol levels. In addition to, and perhaps in concert with, these more overt
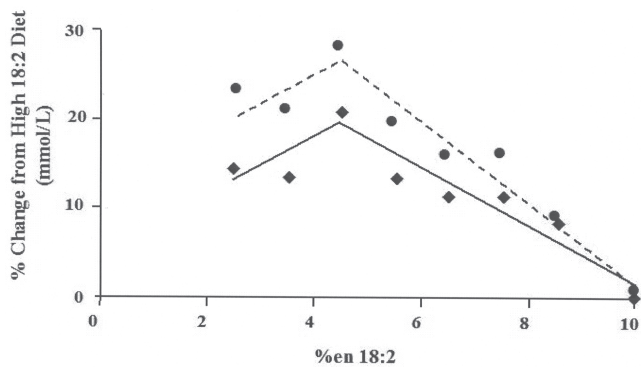
FIG. 4. Mean change in total cholesterol and LDL cholesterol when consuming a high SFA diet at different 18:2n-6 intakes. The effect of dietary intake of high palmitic acid levels (10%en) on plasma cholesterol levels was assessed in combination with decreasing levels of 18:2n-6 in healthy subjects. The data indicated that high levels of palmitic acid were not hypercholesterolemic if intake of linoleic acid was greater than 4.5% of energy (21). ($\bullet$---) LDL cholesterol, R^2 = 0.37 and 0.95; ($\blacklozenge$—) total cholesterol, R^2 = 0.63 and 0.91, respectively.

FIG. 5. Major pathways for the acquisition of movement of cholesterol among major tissue compartments of the body (15). The liver controls LDL cholesterol metabolism, through either the production or clearance of lipoproteins. When plasma cholesterol levels are normal, absorption from the intestine and synthesis in the liver and extrahepatic tissues is balanced with clearance by mostly receptor-dependent mechanisms. If there is expansion of cholesterol pools in the body and liver receptors are down-regulated, plasma LDL cholesterol levels increase. FA influence LDL cholesterol levels by up-regulating or down-regulating LDL receptor activity, differences in absorption of FA and cholesterol, or likely through both owing to changes in lipid constituents in rafts involved in uptake from the brush border membrane of the enterocytes. CM-C, chylomicron cholesterol; HDL-C, HDL cholesterol; LDL-C, LDL cholesterol; VLDL-C, VLDL cholesterol; LDL-R, LDL receptor; CE, cholesterol ester; LRP, LDL receptor-related protein; ✝, highly influenced by phospholipids' FA composition.

phenotypic characteristics are differences in genotype. For example, having particular genes can make an individual more susceptible to certain diseases: Specific gene polymorphisms are known to make an individual more likely to display a cholesterolemic response to diet. Aside from inborn errors of metabolism that may cause severe alterations in how fat and cholesterol are metabolized, there are subtle differences in genes that are directly or indirectly involved in lipoprotein metabolism. It is not yet possible to know all of the genetic variation influencing cholesterol response to diet; however, advances are being made in this area (reviewed in Ref. 26), and some gene–nutrient interactions are to be noted. For example, the apolipoprotein (apo) E genotype, specifically the ε4 allele, has been implicated in influencing the cholesterolemic response to diet (27). A study examining the effects of synthetic-source saturated TAG indicated that apoE phenotype partially explained a strong cholesterolemic response to 16:0 in the diet at very low levels of 18:2n-6 (28). ApoA-I genotype, particularly the G/A polymorphism, may increase responsiveness of LDL cholesterol to dietary saturated FA changes (29). Genes involved in FA transport may also contribute. Intestinal FABP2 has two variants (A54 and T54) that may account for some of the interindividual variation in response to diet. The T54 variant seems to result in a greater response of plasma fasting LDL cholesterol and apoB levels to dietary soluble fiber (30) and in differences in postprandial lipemia after intake of fat having varied FA composition (31).

Adding to the difficulty of assessing cholesterolemic response to individual dietary FA is the possible contribution of TAG structure. The position that is held by a particular FA on the glycerol molecule may play a role in some of the physiological effects of dietary fat. There is some evidence that TAG structure has an effect on how FA are absorbed, reassembled into TAG, transported, stored, and even incorporated into other lipids (i.e., phospholipids) (reviewed in Ref. 32). There

are many different TAG stereoisomers in dietary fat; however, some trends exist in the specific positional distribution of individual FA in native oils and fats. For instance, most of the 16:0 in human milk fat is esterified at the *sn*-2 position and 18:2n-6 at the *sn*-1 and -3 positions on the glycerol molecule, whereas in vegetable oils and other fats 16:0 is primarily in the *sn*-1 and -3 positions and the unsaturated FA such as 18:2n-6 are esterified at the *sn*-2 position. The exception to this is lard, where 16:0 is also predominantly in the *sn*-2 position. Lard is often interesterifed, ultimately rearranging its native structure. This is important, as it appears that the stereospecific structure of dietary TAG is largely conserved during absorption. Previous research indicated that the breakdown products of fat reassembled in enterocytes are mainly as 2-MAG and unesterified FA from the *sn*-1 and -3 positions (33). This may subsequently influence downstream metabolic processes that are difficult to predict and not fully explained at this time. How FA, DAG, phospholipids, and cholesterol esters of different compositions incorporate into and affect the function of lipid rafts, cell signaling, and membrane transporters is a complicated area that is just beginning to be explored. In fact, there are still many questions to be answered regarding the absorption and transport of FA. It is speculated that cholesterol esterification specificity may be due in part to the absorption of free cholesterol into the enterocyte followed by esterification using 2-MAG absorbed from dietary TAG.

Interestingly, a study in formula-fed piglets demonstrated that feeding a synthesized TAG (with a rearrangement of FA vs. a palm olein formula) resulted in higher 16:0 and lower long-chain polyene incorporation into LDL phospholipids and cholesteryl esters (34). Human infants fed synthesized TAG formula vs. human milk also showed preservation of the dietary TAG structure and subsequent alterations in lipoprotein metabolism, such as lower plasma HDL cholesterol and higher apoB concentrations (35). Studies in adult humans have similarly shown conservation of *sn*-2 TAG structure and incorporation into plasma lipoprotein TAG and cholesterol ester (36). The effects of specific dietary TAG structure on FA use in the body and subsequent cholesterolemic response are yet to be fully elucidated.

SUMMARY AND CONCLUSIONS FROM THE LITERATURE

As we have previously noted, "On a food composition basis there is clearly a relationship between the intakes of different fatty acids; hence, one might argue that each are not independent variables in any statistical analysis" (37). It is simply not possible to test the effect of each FA on plasma cholesterol levels individually. The literature considers the effect of each FA separately, even though they must be tested in concert. If energy from fat is to be kept constant, there is no instance whereby one FA can be tested without being at the expense of another. However, more important than the amount of a particular FA is the overall FA balance. Most countries where coronary heart disease is prevalent have populations that eat too much *trans* fat, sometimes in combination with high saturated fat and/or low linoleic acid and/or n-3 FA. Intake of highly saturated fat should be reduced in the context of balance, but how low this needs to be usually remains unaddressed. A minimal amount may be necessary for optimal health. FA exert effects at the cell membrane, which reflect dietary FA composition and ultimately result in changes in membrane function (38). It seems obvious that the optimal function of receptors, binding proteins, transporters, apoproteins, and enzymes requires a balanced FA composition in the phospholipids and/or lipid rafts of the cell, mitochondria, or lipoprotein surface. These all contribute to the control of body cholesterol pools and regulation of LDL cholesterol metabolism (Fig. 5). This is also why it is important to test FA at levels within the range typical for human intake.

WHAT IS THE CURRENT ISSUE?

The food industry requires palatable, shelf-stable fats for use in food manufacturing processes. Given that the shift away from saturated fat to partially hydrogenated fats for this purpose has proven unfavorable to human health, solutions are needed. Adding what appears to be noncholesterolemic saturated FA, such as stearic acid, back into food is one possibility. However, this may seem less desirable to food companies because stearic acid may not have the physical properties

required. It would also be listed under the saturated fat portion of the label, and this may affect perceptions of the healthfulness of a product. For this reason, practices such as interesterification are being used to change dietary fat characteristics and FA composition to reflect a more desirable FA profile. Interesterification involves the randomization of FA on the glycerol backbone to achieve this goal. For instance, interesterifying a highly unsaturated oil with an oil containing high amounts of saturated FA allows the resulting mixture to have more of the desired properties. This can be achieved through chemical or enzymatic means; however, the properties and FA composition depend on the combination of oils/fats used in the process and the procedure used. Although it results in lower *trans* FA formation than partial hydrogenation (39), there may be additional effects in which the health consequences cannot be predicted at this time. Thus far, limited human research on the effects of interesterified oils on blood lipids has not shown adverse effects (reviewed in Ref. 40). Therefore, it would appear that interesterification aids in achieving the goals of both desirable fat characteristics and FA composition. It would also appear to have a different effect on the positional structure of blood lipids from that of *trans* or saturated fats. However, it should be noted that not all interesterified fats are the same and therefore should not be categorized as such. Rearrangement of TAG has the potential to produce over a thousand stereoisomers, most of which are not normally found in human food. The time intervals between the introduction of new components/processing procedures for use in food, the research that indicates the possible health effects from its consumption, and the establishment of regulations to protect the public can be lengthy. For instance, the first major study in humans to show definitively that *trans* FA were detrimental to plasma cholesterol profiles was in 1990 (41). It has taken 15 years for the regulatory climate in North America to take this issue seriously. How long will it take for researchers to discover the health effects of new synthetic TAG? One can hope that new technology and knowledge gained from past experience in saturated and *trans* FA research will expedite answers to this question.

REFERENCES

1. Ervin, R.B., Wright, J.D., Wang, C.Y., and Kennedy-Stephenson, J. (2004) Dietary Intake of Fats and Fatty Acids for the United States Population: 1999–2000, *Adv. Data* (Nov. 8), 1–6.
2. Pronczuk, A., Khosla, P., and Hayes, K.C. (1994) Dietary Myristic, Palmitic, and Linoleic Acids Modulate Cholesterolemia in Gerbils, *FASEB J. 8*, 1191–1200.
3. de Lorgeril, M., Salen, P., Martin, J.L., Monjaud, I., Delaye, J., and Mamelle, N. (1999) Mediterranean Diet, Traditional Risk Factors, and the Rate of Cardiovascular Complications After Myocardial Infarction: Final Report of the Lyon Diet Heart Study, *Circulation 99*, 779–785.
4. Kennedy, E.T., Bowman, S.A., and Powell, R. (1999) Dietary-Fat Intake in the U.S. Population, *J. Am. Coll. Nutr. 18*, 207–212.
5. Centers for Disease Control and Prevention (2004) Trends in Intake of Energy and Macronutrients—United States, 1971–2000, *MMWR 53*, 80–82.
6. Oh, K., Hu, F.B., Manson, J.E., Stampfer, M.J., and Willett, W.C.

(2005) Dietary Fat Intake and Risk of Coronary Heart Disease in Women: 20 Years of Follow-up of the Nurses' Health Study, *Am. J. Epidemiol. 161*, 672–679.

7. Fernandez, M.L., Lin, E.C., and McNamara, D.J. (1992) Regulation of Guinea Pig Plasma Low Density Lipoprotein Kinetics by Dietary Fat Saturation, *J. Lipid Res. 33*, 97–109.

8. Hayes, K.C., and Khosla, P. (1992) Dietary Fatty Acid Thresholds and Cholesterolemia, *FASEB J. 6*, 2600–2607.

9. Khosla, P., and Hayes, K.C. (1992) Comparison Between the Effects of Dietary Saturated (16:0), Monounsaturated (18:1), and Polyunsaturated (18:2) Fatty Acids on Plasma Lipoprotein Metabolism in Cebus and Rhesus Monkeys Fed Cholesterol-free Diets, *Am. J. Clin. Nutr. 55*, 51–62.

10. Khosla, P., Hajri, T., Pronczuk, A., and Hayes, K.C. (1997) Decreasing Dietary Lauric and Myristic Acids Improves Plasma Lipids More Favorably Than Decreasing Dietary Palmitic Acid in Rhesus Monkeys Fed AHA Step 1 Type Diets, *J. Nutr. 127*, 525S–530S.

11. Ramamoorthy, L., Gupta, S.V., and Khosla, P. (2000) Effects of Exchanging 4%en Between Dietary Stearic and Palmitic Acid on Hamster Plasma Lipoprotein Metabolism, *Int. J. Food Sci. Nutr. 51 (Suppl.)*, S51–S59.

12. Gupta, S.V., and Khosla, P. (2001) Palmitic and Stearic Acids Similarly Affect Plasma Lipoprotein Metabolism in Cynomolgus Monkeys Fed Diets with Adequate Levels of Linoleic Acid, *J. Nutr. 131*, 2115–2120.

13. Rao, R., and Lokesh, B.R. (2003) TG Containing Stearic Acid, Synthesized from Coconut Oil, Exhibit Lipidemic Effects in Rats Similar to Those of Cocoa Butter, *Lipids 38*, 913–918.

14. Imaizumi, K., Abe, K., Kuroiwa, C., and Sugano, M. (1993) Fat Containing Stearic Acid Increases Fecal Neutral Steroid Excretion and Catabolism of Low Density Lipoproteins Without Affecting Plasma Cholesterol Concentration in Hamsters Fed a Cholesterol-Containing Diet, *J. Nutr. 123*, 1693–1702.

15. Dietschy, J.M. (1997) Theoretical Considerations of What Regulates Low-Density-Lipoprotein and High-Density-Lipoprotein Cholesterol, *Am. J. Clin. Nutr. 65*, 1581S–1589S.

16. Spady, D.K., and Dietschy, J.M. (1988) Interaction of Dietary Cholesterol and Triglycerides in the Regulation of Hepatic Low Density Lipoprotein Transport in the Hamster, *J. Clin. Invest. 81*, 300–309.

17. Fielding, C.J., Havel, R.J., Todd, K.M., Yeo, K.E., Schloetter, M.C., Weinberg, V., and Frost, P.H. (1995) Effects of Dietary Cholesterol and Fat Saturation on Plasma Lipoproteins in an Ethnically Diverse Population of Healthy Young Men, *J. Clin. Invest. 95*, 611–618.

18. Clandinin, M.T., Cook, S.L., Konard, S.D., and French, M.A. (2000) The Effect of Palmitic Acid on Lipoprotein Cholesterol Levels, *Int. J. Food Sci. Nutr. 51 (Suppl.)*, S61–S71.

19. Clandinin, M.T., Cook, S.L., Konrad, S.D., Goh, Y.K., and French, M.A. (1999) The Effect of Palmitic Acid on Lipoprotein Cholesterol Levels and Endogenous Cholesterol Synthesis in Hyperlipidemic Subjects, *Lipids 34 (Suppl.)*, S121–S124.

20. Sundram, K., French, M.A., and Clandinin, M.T. (2003) Exchanging Partially Hydrogenated Fat for Palmitic Acid in the Diet Increases LDL-Cholesterol and Endogenous Cholesterol Synthesis in Normocholesterolemic Women, *Eur. J. Nutr. 42*, 188–194.

21. French, M.A., Sundram, K., and Clandinin, M.T. (2002) Cholesterolaemic Effect of Palmitic Acid in Relation to Other Dietary Fatty Acids, *Asia Pac. J. Clin. Nutr. 11 (Suppl. 7)*, S401–S407.

22. Dorfman, S.E., Smith, D.E., Osgood, D.P., and Lichtenstein, A.H. (2003) Study of Diet-Induced Changes in Lipoprotein Metabolism in Two Strains of Golden-Syrian Hamsters, *J. Nutr. 133*, 4183–4188.

23. McNamara, D.J. (2000) Dietary Cholesterol and Atherosclerosis, *Biochim. Biophys. Acta 1529*, 310–320.

24. Fernandez, M.L., and McNamar, D.J. (1989) Dietary Fat-Mediated Changes in Hepatic Apoprotein B/E Receptor in the Guinea Pig:

Effect of Polyunsaturated, Monounsaturated, and Saturated Fat, *Metabolism 38*, 1094–1102.

25. Beaton, G.H., Milner, J., Corey, P., McGuire, V., Cousins, M., Stewart, E., de Ramos, M., Hewitt, D., Grambsch, P.V., Kassim, N. *et al.* (1979) Sources of Variance in 24-hour Dietary Recall Data: Implications for Nutrition Study Design and Interpretation, *Am. J. Clin. Nutr. 32*, 2546–2559.

26. Corella, D., and Ordovas, J.M. (2005) Single Nucleotide Polymorphisms That Influence Lipid Metabolism: Interaction with Dietary Factors, *Annu. Rev. Nutr. 25*, 341–390.

27. Sarkkinen, E., Korhonen, M., Erkkila, A., Ebeling, T., and Uusitupa, M. (1998) Effect of Apolipoprotein E Polymorphism on Serum Lipid Response to the Separate Modification of Dietary Fat and Dietary Cholesterol, *Am. J. Clin. Nutr. 68*, 1215–1222.

28. Snook, J.T., Park, S., Williams, G., Tsai, Y.-H., and Lee, N. (1999) Effect of Synthetic Triglycerides of Myristic, Palmitic, and Stearic Acid on Serum Lipoprotein Metabolism, *Eur. J. Clin. Nutr. 53*, 597–605.

29. Mata, P., Lopez-Miranda, J., Pocovi, M., Alonso, R., Lahoz, C., Marin, C., Garces, C., Cenarro, A., Perez-Jimenez, F., de Oya, M. *et al.* (1998) Human Apolipoprotein A-I Gene Promoter Mutation Influences Plasma Low Density Lipoprotein Cholesterol Response to Dietary Fat Saturation, *Atherosclerosis 137*, 367–376.

30. Hegele, R.A., Wolever, T.M., Story, J.A., Connelly, P.W., and Jenkins, D.J. (1997) Intestinal Fatty Acid-Binding Protein Variation Associated with Variation in the Response of Plasma Lipoproteins to Dietary Fibre, *Eur. J. Clin. Invest. 27*, 857–862.

31. Dworatzek, P.D., Hegele, R.A., and Wolever, T.M. (2004) Postprandial Lipemia in Subjects with the Threonine 54 Variant of the Fatty Acid-Binding Protein 2 Gene Is Dependent on the Type of Fat Ingested, *Am. J. Clin. Nutr. 79*, 1110–1117.

32. Hayes, K.C. (2001) Synthetic and Modified Glycerides: Effects on Plasma Lipids, *Curr. Opin. Lipidol. 12*, 55–60.

33. Small, D.M. (1991) The Effects of Glyceride Structure on Absorption and Metabolism, *Annu. Rev. Nutr. 11*, 413–434.

34. Innis, S.M., and Dyer, R. (1997) Dietary Triacylglycerols with Palmitic Acid (16:0) in the 2-Position Increase 16:0 in the 2-Position of Plasma and Chylomicron Triacylglycerols, but Reduce Phospholipid Arachidonic and Docosahexaenoic Acids, and Alter Cholesteryl Ester Metabolism in Formula-Fed Piglets, *J. Nutr. 127*, 1311–1319.

35. Nelson, C.M., and Innis, S.M. (1999) Plasma Lipoprotein Fatty Acids Are Altered by the Positional Distribution of Fatty Acids in Infant Formula Triacylglycerols and Human Milk, *Am. J. Clin. Nutr. 70*, 62–69.

36. Zock, P.L., de Vries, J.H., de Fouw, N.J., and Katan, M.B. (1995) Positional Distribution of Fatty Acids in Dietary Triglycerides: Effects on Fasting Blood Lipoprotein Concentrations in Humans, *Am. J. Clin. Nutr. 61*, 48–55.

37. Clandinin, M.T., and Wilke, M.S. (2001) Do *trans* Fatty Acids Increase the Incidence of Type 2 Diabetes? *Am. J. Clin. Nutr. 73*, 1001–1002.

38. Clandinin, M.T. (1976) Fatty Acid Composition Changes in Mitochondrial Membranes Induced by Dietary Long Chain Fatty Acids, *FEBS Lett. 68*, 41–44.

39. Alpaslan, M., and Karaali, A. (1998) The Interesterification-Induced Changes in Olive and Palm Oil Blends, *Food Chem. 61*, 301–305.

40. Hunter, J.E. (2001) Studies on Effects of Dietary Fatty Acids as Related to Their Position on Triglycerides, *Lipids 36*, 655–668.

41. Mensink, R.P., and Katan, M.B. (1990) Effect of Dietary *trans* Fatty Acids on High-Density and Low-Density Lipoprotein Cholesterol Levels in Healthy Subjects, *N. Engl. J. Med. 323*, 439–445.

42. Dietschy, J.M. (1998) Dietary Fatty Acids and the Regulation of Plasma Low Density Lipoprotein Cholesterol Concentrations, *J. Nutr. 128*, 444S–448S.

Overview of Hemostatic Factors Involved in Atherosclerotic Cardiovascular Disease

William B. Kannel*

Boston University School of Medicine/Framingham Heart Study, Framingham, Massachusetts

ABSTRACT: Hemostatic factors associated with the development of cardiovascular disease (CVD) include fibrinogen, von Willebrand factor, tissue plasminogen activator (tPA) antigen, plasminogen activator inhibitor-1 (PAI-1), and factor VII. Each SD increment of these increases the association by 24–30%. Most hemostatic factors are intercorrelated with inflammatory markers [e.g., C-reactive protein (CRP)] and LDL cholesterol. Fibrinogen seems the most fundamental hemostatic risk factor for CVD. The Framingham Study reaffirms the significant linear risk factor trends across fibrinogen tertiles ($P < 0.001$) for age, body mass index, smoking, diabetes mellitus, total cholesterol, HDL cholesterol, and TG in both sexes. Fibrinogen may also directly increase CVD risk because of its role in platelet aggregation, plasma viscosity, and fibrin formation. Fibrinogen is also an acute-phase reactant that is elevated in inflammatory states. Fibrinogen mediates the thrombogenic effect of other risk factors. Fibrinogen levels increase with the number of cigarettes smoked and quickly fall after smoking cessation. This rapid fibrinogen decline may be a mechanism for CVD risk reduction after smoking cessation. Weight loss is accompanied by reduced fibrinogen. The correlation between fibrinogen and LDL cholesterol suggests that lipid-imposed CVD risk is mediated partly through fibrinogen. Hyperreactive platelets of diabetics may result in part from their increased fibrinogen. Elevated fibrinogen and CRP of unstable angina suggest an acute-phase reaction. Prevalence, case-control, angiographic, and echocardiogram investigations incriminate hemostatic and inflammatory markers as strong independent risk factors for initial and recurrent CVD. Framingham Study data indicate that each SD increase in fibrinogen imposes a 20% independent increment in risk. It may be concluded that fibrinogen and CRP determination may be useful screening tools to identify individuals at added risk for thrombotic complications of CVD.

Paper no. L9745 in *Lipids 40*, 1215–1220 (December 2005).

This review of hemostatic factors is promoted by the great interest in probing beyond established cardiovascular disease (CVD) risk factors to gain further insights into the atherogenic process and its clinical manifestations. Thrombogenic risk factors and markers of inflammation are under intense investigation for the prediction of initial and recurrent atherosclerotic CVD events. Vascular disease is caused by many factors acting in concert. Several processes promote atherogenesis, which eventuates in clinical events by conditions that produce arterial vascular occlusions (1). Research indicates that lipids and blood pressure remain as the critical ingredients that promote the long-term development of atherosclerosis, that cigarette smoking acts additionally as a precipitating factor, and that diabetes effects include several atherogenic pathophysiological mechanisms. Each of these factors is used to estimate coronary heart disease (CHD) risk.

New risk factors under investigation may provide clues to pathogenesis and sometimes improve our ability to predict CVD. The utility of novel risk factors for predicting initial CVD events should be assessed in terms of the incremental risk they impose after consideration of the core set of risk factors, which include age, sex, blood pressure, total cholesterol or LDL cholesterol (LDL-C), HDL cholesterol (HDL-C), smoking, and type 2 diabetes mellitus. This criterion is often not met in new investigations because relatively large data sets and extended follow-up are required to ensure that novel factors such as thrombogenic and inflammatory markers improve multivariable assessment of vascular disease risk (2).

HEMOSTATIC FACTORS

A number of hemostatic and inflammatory factors are important promoters of occlusive atherogenic disease (2). Inflammatory markers such as the leukocyte count, serum amyloid A, and C-reactive protein (CRP) are the chief markers that were investigated in the population setting in relation to initial vascular outcomes (2). A high-normal leukocyte count is associated with increased CVD risk. Unfortunately, leukocyte counts need to be determined on fresh specimens, and current cigarette smoking can increase leukocyte counts, limiting the utility of the test. Also, like the CRP with which it is highly correlated, it is not specific for vascular disease (3). Meta-analysis by Danesh *et al.* (4) of seven studies estimates a 1.4-fold excess CHD risk for an elevated leukocyte count (compared with the bottom third of the distribution). Numerous studies have found an association between CRP and development of CVD (Fig. 1). Prospective studies of asymptomatic persons comparing people with low-tertile CRP with those having top tertile values suggest a risk factor-adjusted odds ratio of 1.8 [95% confidence interval (CI) 1.6–2.0] for CHD among healthy

*Address correspondence at Boston University School of Medicine/Framingham Heart Study, 73 Mt. Wayte Ave., Framingham, MA 01702-5827. E-mail: billkannel@yahoo.com

Abbreviations: BMI, body mass index; CHD, coronary heart disease; CI, confidence interval; CRP, C-reactive protein; CVD, cardiovascular disease; HDL-C, HDL cholesterol; LDL-C, LDL cholesterol; PAI-1, plasminogen activator inhibitor-1; RR, relative risk, risk ratio; tPA, tissue plasminogen activator.
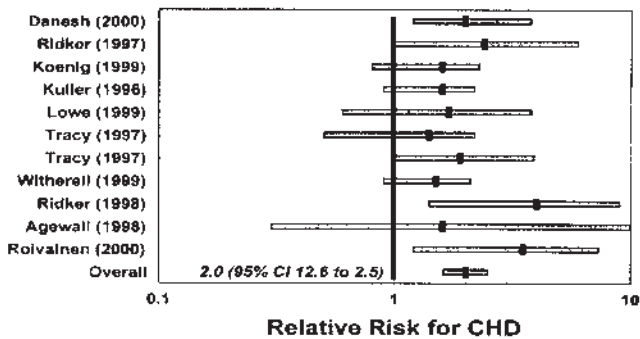
FIG. 1. C-Reactive protein and coronary heart disease (CHD), relative risk (top vs. bottom tertile). Prospective: persons without cardiovascular disease (CVD) at baseline. CI, confidence interval. Adapted with permission from Reference 4.

TABLE 1
Meta-analysis of Long-Term Prospective Studies of Inflammatory Markers as Predictors of Coronary Heart Disease (CHD) in Healthy or Prior CHD Subjects[a]

Inflammatory marker	Risk factor adj. risk ratio[b]
Fibrinogen (18 studies)	1.8 (1.6–2.0)
C-Reactive protein (7 studies)	1.7 (1.4–2.1)
Leukocyte count (7 studies)	1.4 (1.3–1.5)
Albumin (decreased, 8 studies)	1.5 (1.3–1.7)

[a]From Reference 4.
[b]Values within parentheses are confidence intervals.

persons or those with prior CHD (4). Because of their significant independent effect, inflammatory biomarkers merit consideration for incorporation into CHD risk estimation algorithms (Table 1). However, inflammatory and hematologic markers are not currently included among the set of factors used to estimate multivariable CVD risk in the population setting (2).

HEMOSTATIC RELATION TO OTHER CVD RISK FACTORS

Hemostatic variables are related to established CVD risk factors. The association of hemostatic variables with CVD risk factors and prevalent CVD was investigated in the prospective cohort PRIME Study of myocardial infarction in men aged 50–59 yr (5). Fibrinogen was found to increase with age, smoking, waist/hip ratio, and LDL-C level. It decreased in relation to educational level, physical activity, alcohol intake, and HDL-C level.

Factor VII increased with body mass index (BMI), waist/hip ratio, and TG, HDL-C, and LDL-C levels. Plasminogen activator inhibitor-1 (PAI-1) increased with BMI, waist/hip ratio, TG level, alcohol intake, and cigarette smoking and decreased with physical activity. Standard CVD risk factors were estimated to explain 8% of the variance in fibrinogen, 9% of the variance in factor VII, and 26% of the variance in PAI-1. The statistically significant ($P < .001$) CVD odds ratio for one SD in fibrinogen was 1.31 (CI 1.20–1.42) and for PAI-1 1.38 (CI 1.27–1.49) (Table 2).

Recent investigation of fibrinogen by the Framingham Study also demonstrates its interrelationship with numerous cardiovascular risk factors (6). With the immunoprecipitation method, there were significant linear trends across fibrinogen tertiles ($P < 0.001$) for age, BMI, smoking, diabetes mellitus, total cholesterol, HDL-C, and TG in men and women (Table 3). Also, fibrinogen levels were higher among subjects with CVD compared with those without disease. The unadjusted mean fibrinogen concentration for men was 354 ± 5.46 among those with CVD and 319 ± 2.32 mg/dL for those without disease ($P < 0.001$). The unadjusted mean fibrinogen concentrations for women were also higher among those with CVD (370 ± 9.04 vs. 316 ± 2.23 mg/dL, $P < 0.001$). In both men and women,

TABLE 2
Association of Hemostatic Factors, Cardiovascular Disease (CVD) Risk Factors (RF), and CVD: The PRIME Study[a]

Hemostatic factor	Variance explained	RF increase	RF decrease
Fibrinogen	8%	LDL-C	HDL-C
Odds for CVD per			
SD increase: 1.31		W/H ratio	Physical activity
SD		Age	Education
		Smoking	Alcohol
Factor VII	9%	BMI	
		TG	
		W/H ratio	
		HDL-C	
		LDL-C	
PAI-1	26%	BMI	Physical activity
Odds for CVD per		W/H ratio	
SD increase: 1.38		Diabetes	
		Alcohol	
		TG	
		Smoking	

[a]From Reference 5. HDL-C, HDL cholesterol; W/H ratio, waist to hip ratio; BMI, body mass index; LDL-C, LDL cholesterol; PAI-1, plasminogen activator inhibitor-1.
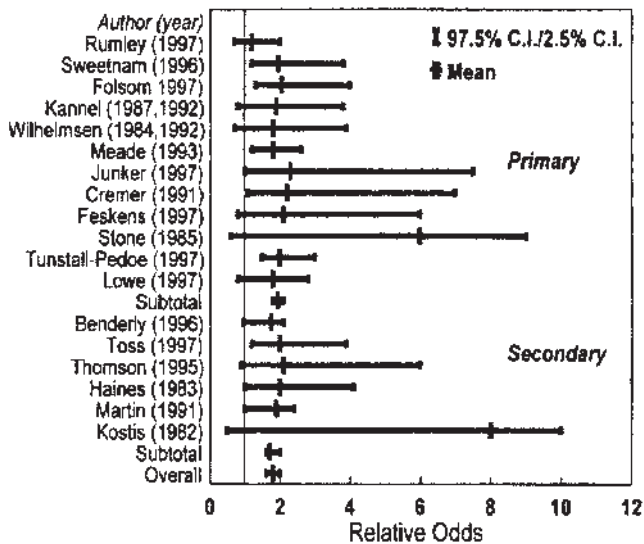
FIG. 2. Fibrinogen and CHD meta-analysis (top vs. bottom third). For abbreviations see Figure 1. Adapted with permission from Reference 4.

after adjustment for age, BMI, smoking, diabetes mellitus, total cholesterol, and TG, fibrinogen remained significantly higher in cases: 333 ± 5.16 vs. 322 ± 2.00 mg/dL in men, and 336 ± 7.25 vs. 319 ± 1.89 mg/dL in women) ($P = 0.035$ and $P = 0.018$) for men and women, respectively.

FIBRINOGEN AND CVD

Starting in the 1970s, elevated fibrinogen levels were shown to be a major independent risk factor for various heart disease and stroke outcomes in several population studies (Fig. 2) (7,8). CVD, CHD, and all-cause mortality were all increased in pa-

tients of both sexes who had higher fibrinogen concentrations, and this excess mortality persisted after adjusting for the standard risk factors. Higher fibrinogen levels enhanced the CHD risk of patients with hypertension, cigarette smokers, and people with diabetes. In an early meta-analysis of 18 studies, Danesh and colleagues (4) compared the top third of the distribution with the bottom third and found higher fibrinogen to be related to a relative risk of 1.8 (95% CI 1.6–2.0) for CHD.

Plasma fibrinogen is a consistent risk factor for coronary disease in prospective studies, but there are fewer data on its relationship to development of stroke and peripheral artery disease. The Framingham Study found that fibrinogen is related to subsequent occurrence of stroke and peripheral artery disease as well as coronary disease (9) (Fig. 3). Each SD increment in fibrinogen was associated with an increased risk of CHD and peripheral artery disease of 20% in men and 30% in women, whereas in stroke the increase noted was 10% in each sex (Table 4). A prospective relationship to stroke [relative risk (RR) 1.52] was also found in the Edinburgh Artery Study in multivariate analysis adjusting for cigarette smoking, LDL-C, systolic blood pressure, and ischemic heart disease (10). This investigation also found that tissue plasminogen activator (tPA) antigen and fibrin D-dimer were independently related to risk of stroke (RR 1.69 and 1.96, respectively).

Because fibrinogen is established as an independent risk factor for cardiovascular events and is also associated with traditional cardiovascular risk factors, it seems likely that elevation of fibrinogen may be a pathway by which these risk factors exert their effect. Fibrinogen strongly affects blood rheology, coagulation, and platelet aggregation, suggesting that it may be on the causal pathway for certain risk factors to promote thrombosis. It is also an acute-phase reactant that is increased in inflammatory states and has direct effects on the vessel wall (11).

TABLE 3
Association of Fibrinogen with Traditional CVD Risk Factors[a]

	Fibrinogen tertiles		
	Low ($n = 418$)	Mid ($n = 418$)	High ($n = 420$)
Men			
Age	52.3 (±0.50)	56.7 (±0.49)	58.6 (±0.46)
BMI	27.2 (±0.18)	28.6 (±0.22)	29.0 (±0.22)
Smoking	13.4%	18.2%	24.8%
Diabetes mellitus	3.1%	9.3%	14.0%
Total cholesterol	193.7 (±1.60)	201.9 (±1.55)	204.5 (±1.70)
HDL-C	46.5 (±0.56)	43.8 (±0.56)	38.3 (±0.48)
TG	116.3 (±3.53)	152.6 (±3.96)	213.2 (±7.10)
	Low ($n = 459$)	Mid ($n = 459$)	High ($n = 458$)
Women			
Age	51.4 (±0.45)	55.6 (±0.46)	58.3 (±0.43)
BMI	24.5 (±0.19)	26.5 (±0.22)	29.5 (±0.30)
Smoking	13.1%	20.9%	22.9%
Diabetes mellitus	0.9%	3.3%	9.6%
Total cholesterol	198.4 (±1.65)	207.7 (±1.75)	220.0 (±1.79)
HDL-C	61.4 (±0.68)	56.2 (±0.70)	50.3 (±0.72)
TG	101.0 (±2.35)	130.0 (±2.96)	188.2 (±7.61)

[a]Values are mean (±SE) for continuous parameters. For every risk factor, a linear trend across fibrinogen tertiles is significant ($P < 0.001$). BMI, body mass index; for other abbreviations see Tables 2 and 3.
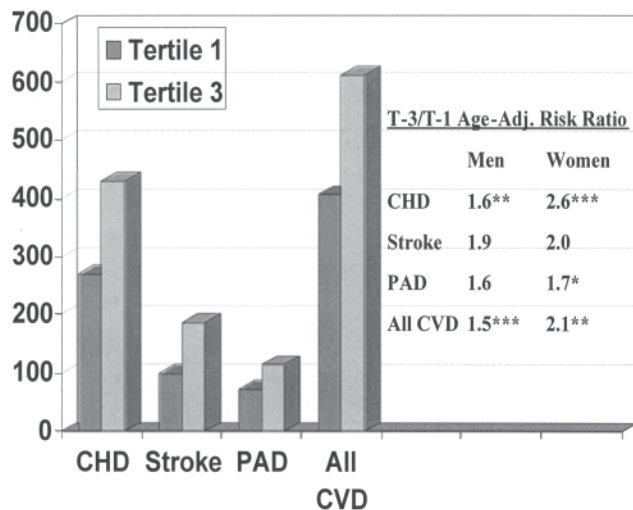
FIG. 3. Risk of CVD events by fibrinogen levels (Framingham study). T-3, third tertile; T-1, first tertile; PAD, peripheral artery disease; for other abbreviations see Figure 1.

The association of fibrinogen with traditional CVD risk factors and its independent contribution to CVD incidence suggest that it may play a mechanistic role by which the risk factors exert their effect (Table 5). For example, the increased risk of CVD and stroke associated with smoking may be mediated in part through fibrinogen (12). Fogari *et al.* (13) found that fibrinogen levels increased with the number of cigarettes smoked. Fibrinogen levels also quickly fall after smoking cessation, suggesting that this rapid fall in level may be a mechanism for the reduction in cardiovascular risk after smoking cessation.

Elevation in fibrinogen level may also be a mechanism by which obesity increases the risk of CVD. A reduction in BMI after a low-calorie diet for 6 mon is accompanied by a fall in fibrinogen level (14).

The strong relationship between fibrinogen and LDL-C level suggests that the increased risk of CVD associated with elevated LDL levels may be mediated in part through fibrinogen. Fibrinogen influences the risk of CHD at any level of LDL-C. The Prospective Cardiovascular Munster (PROCAM) study found that individuals who had LDL and fibrinogen levels in the highest tertile had a 6.1-fold increase in coronary risk

compared with those in the lowest tertile (15). The event rate was significantly lower when fibrinogen levels were in the lowest tertile even though LDL remained in the highest tertile. Evidently, elevated LDL-C imposes an ominous CHD risk when accompanied by a high fibrinogen level (Fig. 4).

Like fibrinogen, statins that reduce both LDL-C and CRP appear to have a variable influence on CHD outcomes depending on the CRP level. Patients with a low CRP after statin therapy experience better clinical outcomes of myocardial infarction or CHD mortality than those with higher CRP, regardless of resultant LDL-C on treatment (17).

Thompson and colleagues (18) found fibrinogen to be a strong predictor of coronary events in patients with angina pectoris. In those subjects with high total cholesterol, a high fibrinogen level conferred added risk compared with those with low fibrinogen. Patients in the highest fibrinogen quintile had 3 times the risk of a coronary event as those in the lowest quintile.

Subjects with diabetes mellitus have been found to have hyperreactive platelets. This platelet hyperreactivity may result in part from increased fibrinogen levels associated with diabetes because fibrinogen acts as a cross bridge between platelets. Poor diabetic control also has been particularly associated with higher levels of fibrinogen and other hemostatic variables (19).

The optimal fibrinogen assay for risk stratification is uncertain. In the Framingham Study the immunoprecipitation test showed a stronger association with CVD than the Clauss method, suggesting that it may be a preferred screening tool to identify individuals at increased thrombotic risk of CVD (6).

INFLAMMATORY MARKER–LIPID INTERACTION

The impact of LDL-C on the risk of CVD is augmented by the presence of an inflammatory marker such as CRP. In a population sample of postmenopausal women who had no heart disease at baseline, occurrence of myocardial infarction, cardiac death, and restenosis after percutaneous coronary intervention was augmented by an increase in CRP at all levels of LDL-C (20). The combination of elevations of both has more ominous implications than elevation of either alone (Fig. 5). This resembles the impact of a combination of elevated LDL-C accompanied by increased fibrinogen, which is also an acute-phase reactant as well as a thrombogenic risk factor.

TABLE 4
Risk of Cardiovascular Events by Increment of Fibrinogen in the 18-yr Follow-up to the Framingham Study[a]

CVD event	18-yr rate per 1000		Increment per SD increase	
	Men	Women	Men (%)	Women (%)
CHD	430	296	20**	30***
Stroke	187	224	10	10
PAD	113	68	20	30*
All CVD	611	514	20***	20**

[a]From Reference 9. *P < 0.05, ** P < 0.01, ***P < 0.001. PAD, peripheral artery disease; for other abbreviations see Tables 1 and 2.

TABLE 5
Fibrinogen: Mechanism for the Influence of CVD Risk Factors[a]

- Fibrinogen increases with number of cigarettes smoked and quickly falls on quitting. May be a mechanism for rapid CVD risk reduction after smoking cessation (13).
- Dietary reduction of BMI is accompanied by a fall in fibrinogen (14).
- LDL-C is strongly related to fibrinogen and fibrinogen influences CHD risk at any level of LDL-C (15).
- Platelet hyperreactivity is associated with elevated fibrinogen in diabetics. Poor diabetic control is associated with higher levels of fibrinogen and other hemostatic variables.
- Low reported physical activity and low aerobic power are associated with high plasma fibrinogen concentration in newly diagnosed type 2 diabetes (16).

[a]For abbreviations see Tables 1–3.

FIBRINOLYTIC FACTORS

Fibrinolytic factors have also been linked to initial and recurrent CHD, but less information is available (21,22). Nevertheless, strong evidence from some large observational epidemiological studies has linked hemostatic variables to future risk of myocardial infarction and stroke. A variety of markers of a procoagulatory tendency have been identified that appear to be associated with development of atherothrombotic events in most vascular beds. These include elevated fibrinogen, factor VII, factor VIII, and von Willebrand factor; platelet hyperaggregation; and increased plasma D-dimer. Decreased fibrinolytic capacity characterized by increased PAI-1 activity and decreased tPA has also been prospectively incriminated (21).

HOMOCYSTEINE AND FIBRINOLYTIC POTENTIAL

Elevated homocysteine consistently has been found to be associated with increased risk of CVD, but the mechanism responsible is not clear. Since thrombosis plays an important role in the development of atherosclerotic plaques and in precipitating acute coronary events, the Framingham Study tested the hypothesis that elevated homocysteine increases CVD risk by raising the potential for thrombus development (23). Hemostatic means of 3,216 Framingham Offspring Study participants were measured and examined in relation to homocysteine levels. A higher level of homocysteine was found to be associated with increases in PAI-1, tPA antigen, von Willebrand factor, and level of fibrinogen. Significant associations between homocysteine and PAI-1 and tPA antigen persisted after adjustment for covariates, leading to the suggestion that increased

homocysteine is associated with an impaired fibrinolytic potential. This offers the possibility that folic acid or other therapies that lower homocysteine may decrease excess risk by reducing the thrombotic tendency, but this hypothesis remains unproven.

SUMMARY

Atherosclerotic cardiovascular events are commonly manifested *via* a thrombotic event. The process of clotting involves coagulation, limited and controlled by anticoagulation, and the counterbalancing process of fibrinolysis, limited by antifibrinolysis.

Thrombosis clearly precipitates the acute clinical manifestations of coronary, cerebrovascular, and peripheral artery disease. The role of hemostatic factors in the development of the underlying atherosclerotic lesions has been difficult to prove (24). It is possible that the association between hemostatic factors and CVD may be due to confounding by other risk factors or may result from the disease rather than causing it. It may also act as part of a causal pathway that requires interaction with other CV risk factors or already existing atherosclerotic disease. Furthermore, there are issues about measurement of hemostatic factors that still need to be resolved.

Nevertheless, studies have strongly incriminated a number of coagulation factors such as fibrinogen, factor VII, factor VIII, and platelet aggregability in the thrombotic complications of CVD. Fibrinolytic factors also have been implicated, including tPA activator, PAI-1, lipoprotein(a), and plasminogen or global fibrinolytic activity. Of these, only fibrinogen is sup-
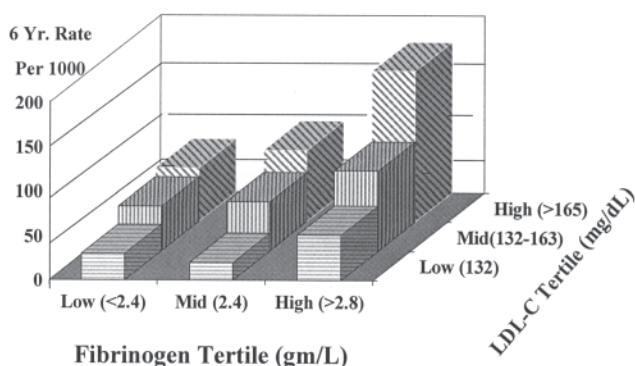
FIG. 4. Risk of CHD by fibrinogen and LDL-C (15). LDL-C, LDL cholesterol; for other abbreviation see Figure 1.
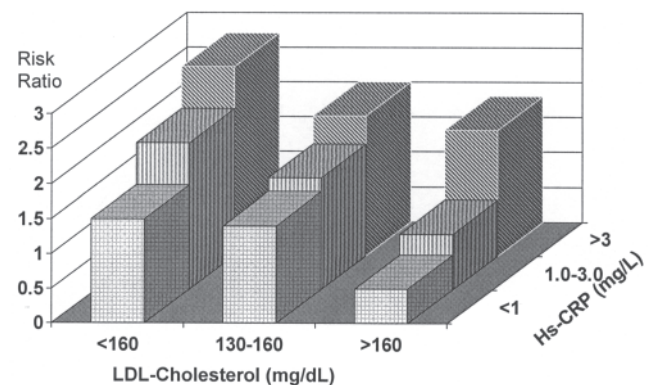
FIG. 5. Relative risk of CVD events by hs-CRP and LDL-C (20). Hs-CRP, high-sensitivity C-reactive protein. For other abbreviations see Figure 1 and 4.

ported not only by strong but also by consistent evidence of a causal connection to CVD.

REFERENCES

1. Fuster, V., Badimon, L., and Chesebro, J.H. (1992) The Pathogenesis of Coronary Artery Disease and the Acute Coronary Syndromes, *N. Engl. J. Med. 326*, 242–250.
2. Wilson, P.W.F. (2004) CDC/AHA Workshop on Markers of Inflammation and Cardiovascular Disease. Application to Clinical and Public Health Practice in Asymptomatic Patients: A Background Paper, *Circulation 110*, e568–e571.
3. Ernst, E., Hammerschmidt, D.E., Bagge, U., Matrai, A., and Dormandy, J.A. (1987) Leukocytes and the Risk of Ischemic Diseases, *J. Am/ Med. Assoc. 257*, 2318–2324.
4. Danesh, J., Collins, R., Appleby, P., and Peto, R. (1998) Association of Fibrinogen, C-Reactive Protein, Albumin or Leukocyte Count with Coronary Heart Disease; Meta-analyses of Prospective Studies, *J. Am. Med. Assoc. 279*, 1477–1482.
5. Scarabin, P.Y., Aillaud, M.F., Amouyel, P., Evans, A., Luc, G., Ferrieres, J., Arveiler, D., and Juhan-Vague, I. (1998) Association of Fibrinogen, Factor VII and PAI-1 with Baseline Findings Among 10,500 Male Participants in a Prospective Study of Myocardial Infarction—The PRIME Study. Prospective Epidemiological Study of Myocardial Infarction, *Thromb. Haemost. 80*, 749–756.
6. Stec, J.J., Silbershatz, H., Tofler, G.H., Matheney, T.H., Sutherland, P., Lipinska, I., Massaro, J.M., Wilson, P.W.F., Muller, J.E., and D'Agostino, R.B. (2000) Association of Fibrinogen with Cardiovascular Risk Factors in the Framingham Offspring Population, *Circulation 102*, 1634–1638.
7. Ernst, E., and Resch, K.L. (1993) Fibrinogen as a Cardiovascular Risk Factor: A Meta-analysis and Review of the Literature, *Ann. Intern. Med. 118*, 956–963.
8. Kannel, W.B., Wolf, P.A., Castelli, W.P., and D'Agostino, R.B. (1987) Fibrinogen and Risk of Cardiovascular Disease. The Framingham Study, *J. Am. Med. Assoc. 258*, 1183–1186.
9. Kannel, W.B. (1997) Influence of Fibrinogen on Cardiovascular Disease, *Drugs 54*, 32–40.
10. Smith, F.B., Lee, A.J., Fowkes, F.G.R., Price, J.F., Rumley, A., and Lowe, G.D.O. (1997) Hemostatic Factors as Predictors of Ischemic Heart Disease and Stroke in the Edinburgh Artery Study, *Arterioscler. Thromb. Vasc. Biol. 17*, 3321–3325.
11. Catanzaro, J.A., and Suen, R. (1996) Clinical Laboratory Indicators of Cardiovascular Disease Risk, *Alt. Med. Rev. 1*, 185–194.
12. Athukorala, T.M., and Ranjini, L.P. (1991) Lipid Patterns and Fibrinogen Levels of Smokers and Non-smokers, *Ceylon Med. J. 36*, 98–101.
13. Fogari, R., Zoppi, A., Marasi, G., Vanasia, A., and Villa, G. (1994) Associations Between Plasma Fibrinogen Levels and Cardiovascular Risk Factors in Hypertensive Men, *J. Cardiovasc. Risk 1*, 341–345.
14. Ditschuneit, H.H., Flechtner-Mors, M., and Adler, G. (1995) Fibrinogen in Obesity Before and After Weight Reduction, *Obesity Res. 3*, 43–48.
15. Heinrich, L., Balleisen, L., Schulte, H., Assmann, G., and van de Loo, J. (1994) Fibrinogen and Factor VII in the Prediction of Coronary Risk: Results of the PROCAM Study in Healthy Men, *Arterioscler. Thromb. 14*, 54–59.
16. Vanninen, E., Laitinen, J., and Uusitupa, M. (1994) Physical Activity and Fibrinogen Concentration in Newly Diagnosed NIDDM, *Diabetes Care 17*, 1031–1038.
17. Ridker, P.M., Cannon, C.P., Morrow, D., Rifai, N., Rose, L.M., McCabe, C.H., Pfeffer, M.A., and Braunwald, E., Pravastatin or Atorvastatin Evaluation and Infection Therapy—Thrombolysis in Myocardial Infarction 22 (PROVE IT—TIMI 22) Investigators (2005) C-Reactive Protein Levels and Outcomes After Statin Therapy, *N. Engl. J. Med. 6, 352*, 20–28.
18. Thompson, S.G., Kienast, J., Pyke, S.D., Haverkate, F., and van de Loo, J.C. (1995) Hemostatic Factors and the Risk of Sudden Death in Patients with Angina Pectoris. European Concerted Action on Thrombosis and Disabilities Angina Pectoris Study Group, *N. Engl. J. Med. 332*, 635–641.
19. el Khawand, C., Jamart, J., Donckier, J., Chatelaine, B., Lavenne, E., Moriau, E., and Buysschaert, M. (1993) Hemostasis Variables in Type 1 Diabetic Patients Without Demonstrable Vascular Complications, *Diabetes Care 16*, 1137–1145.
20. Ridker, P. (2003) Clinical Application of C-Reactive Protein for Cardiovascular Disease Detection and Prevention, *Circulation 107*, 363–369.
21. Ridker, P.M., Vaughan, D.E., Stampfer, M.J., Manson, J.E., and Hennekens, C.H. (1993) Endogenous Tissue-type Plasminogen Activator and Risk of Myocardial Infarction, *Lancet 341*, 1165–1168.
22. Koenig, W. (1998) Haemostatic Risk Factors for Cardiovascular Diseases, *Eur. Heart J. 19* (*Suppl. C*), C39–C43.
23. Tofler, G.H., D'Agostino, R.B., Jacques, P.F., Bostom, A.G., Wilson, P.W., Lipinski, I., Mittleman, M.A., and Selhub, J. (2002) Association Between Increased Homocysteine Levels and Impaired Fibrinolytic Potential: Mechanism for Cardiovascular Risk, *Thromb. Haemost. 88*, 799–804.
24. Pearson, T.A., LaCava, J., and Weil, H.F. (1997) Epidemiology of Thrombotic-Hemostatic Factors and Their Association with Cardiovascular Disease, *Am. J. Clin. Nutr. 65*, 1674S–1682S.

Influence of Stearic Acid on Postprandial Lipemia and Hemostatic Function

Thomas A.B. Sanders* and Sarah E.E. Berry

Nutritional Sciences Research Division, King's College London, London SE1 9NH, England

ABSTRACT: It has been suggested that fats rich in stearic acid may result in exaggerated postprandial lipemia and have adverse effects on hemostatic function. The effects of test meals containing different saturated and monounsaturated FA were compared in healthy subjects in a series of studies to investigate this hypothesis. Stearic acid, when present as cocoa butter, resulted in similar postprandial lipemia and factor VII activation compared with a meal containing high-oleic sunflower oil. Stearic acid when presented as shea butter or as randomized stearate-rich TAG resulted in decreased postprandial lipemia and decreased postprandial activation of factor VII. Stearic acid-rich test meals did not result in impaired fibrinolytic activity compared with either a low-fat meal or a meal high in oleate. The difference in responses between the different stearic acid-rich fats appears to be due to varying solid fat contents of the fats at 37°C.

Paper no. L9830 in *Lipids 40*, 1221–1227 (December 2005).

Stearic acid (18:0) appears to have effects similar to oleic acid (18:1n-9) on fasting plasma lipoprotein concentrations (1) and therefore may not have an adverse effect on the risk of cardiovascular disease. However, little consideration has been given to its acute postprandial effects. More than 25 years ago, Zilversmit (2) observed that impaired clearance of chylomicron remnants was associated with an increased risk of atherothrombotic disease. An intake in excess of 15 g of TAG containing long-chain FA ($\geq C_{14}$) results in postprandial lipemia. The extent of postprandial lipemia strongly depends on the fat content of individual meals but is also influenced by age, gender, and physical activity. Exaggerated postprandial lipemia is associated with accelerated atherosclerosis, and chylomicron remnants can result in foam cell formation and be atherogenic. Postprandial lipemia may also increase the risk of coronary thrombosis by increasing factor VII coagulant activity ($FVII_c$) and plasminogen activator inhibitor type-I (PAI-1) activity and impairing endothelial function. The mechanisms by which postprandial lipemia may affect the risk of atherothrombotic disease have been reviewed elsewhere (3).

Phan *et al.* (4) proposed, on the basis of animal studies, that chylomicrons enriched in stearic acid may persist longer in the circulation. Studies conducted in animals also found that injection of stearic acid induced thrombosis, and this has led to the view that stearic acid is thrombogenic (5). Few systematic studies have been conducted on the influence of stearic acid on postprandial lipemia and thombogenesis.

The Northwick Park Heart Study first reported an association between elevated $FVII_c$ and increased risk of fatal ischemic heart disease (6). Subsequent studies showed $FVII_c$ to be positively associated with serum cholesterol and TAG concentrations. A relationship between total fat intake and $FVII_c$ was reported, and a reduction in fat intake resulted in a marked decline in $FVII_c$. An association was found between the proportion of stearic acid in plasma FFA and $FVII_c$ (7,8). Stearic acid and the *trans* FA elaidic acid (18:1 *trans*), but not oleic acid (9), were found to increase $FVII_c$ activation *in vitro*, and stearic acid has been postulated to activate factor XII, and hence $FVII_c$, by forming a negatively charged contact surface on TAG-rich lipoproteins.

$FVII_c$ is a functional assay of factor VII (FVII) activity that depends on the concentration of the zymogen ($FVII_{ag}$) and the concentration of FVII circulating in the activated form ($FVII_a$). $FVII_a$ increases 3–4 h following a high-fat meal and remains elevated for several hours without any change in $FVII_{ag}$. Our research over the past 10 years was specifically designed to test the hypothesis that saturated FA, particularly stearic acid and *trans* FA, have adverse effects on postprandial lipemia and hemostatic function (10–17).

EXPERIMENTAL PROCEDURES

Human subjects were recruited from among the staff and student population of King's College London. The subjects were healthy, and exclusion criteria included a history of cardiovascular disease, diabetes, a body mass index of <20 or >35 kg/m², plasma cholesterol of >7.8 mmol/L (302 mg/dL), plasma TAG of >3 mmol/L (267 mg/dL), current use of antihypertensive or lipid-lowering medication, and a self-reported intake of alcohol of greater than 28 units/wk (1 unit = 10 mL ethanol). Fasting plasma lipoprotein lipid concentrations, body weight, blood pressure, blood cell count, and liver function were confirmed to be within the prescribed limits prior to subjects' entry into the study. All studies involved a crossover design, and subjects were randomized to the different treatment sequences using an orthogonal Latin-square design with at least 1 wk between treatments.

Subjects were asked to avoid foods high in fat the day preceding each test meal and to fast overnight from 2200h. Fasting

*To whom correspondence should be addressed at Nutritional Sciences Research Division, King's College London, Franklin-Wilkins Bldg., 150 Stamford St., London SE1 9NH, England. E-mail: Tom.Sanders@kcl.ac.uk

Abbreviations: FVII, factor VII; $FVII_a$, activated form of FVII; $FVII_c$, factor VII coagulant activity; $FVII_{ag}$, FVII zymogen measured as antigen; iAUC, integrated area under the curve; MCT, medium-chain triacylglycerols; PAI-1, plasminogen activator inhibitor type-I; tPA, tissue plasminogen activator.

venous blood samples were obtained between 0800 and 1000 h the following morning. The test meal was consumed within 15 min, and further venous blood samples were taken at varying hourly intervals postprandially, usually for up to 6 h. Following the 3-h blood sample, subjects received a standardized lunch (1.7 MJ) consisting of fresh fruit and a low-fat yogurt (less than 1 g of fat). To control physical activity levels, subjects were asked to refrain from alcohol or strenuous exercise, including cycling and any sporting activity, on the day prior to the test meal and on the day of the test meal. Smokers were not excluded from the studies. The subjects received a modest financial reimbursement for their participation in the study. The study protocol was reviewed and approved by the College Research Ethics Committee, and all participants gave written informed consent.

Test meals. In our earliest studies we compared test meals providing 90 g of fat in which we varied approximately 40% of the fat intake with different saturated and monounsaturated FA. In later studies the test meals provided a lower amount of fat (50 g) and were provided as a muffin and a milkshake. In the first study reported here (13), we compared fats enriched in medium-chain TAG (MCT), palmitic, stearic, elaidic (18:1 *trans*), and oleic (18:1n-9) acids, with an isoenergetic low-fat diet in 16 young healthy male and female subjects. In a subsequent study (14), we compared a high-oleate meal in which the fat was derived from high-oleate sunflower oil with meals enriched in stearic acid-rich fats (cocoa butter and a structured stearic-rich TAG; SALATRIM™ type 23SO, Cultor Foods, Ardsley, NY) in 35 middle-aged and mildly hypercholesterolemic subjects (18 women and 17 men, aged 40–60 yr). We then compared native (unrandomized) cocoa butter vs. randomly interesterified (randomized) cocoa butter in 17 healthy men aged 38 ± 10 yr (15). As a follow-up to this study, a comparison was made in 6 male subjects between unrandomized cocoa butter and a randomized stearic acid-rich TAG made from a blend of totally hydrogenated and unhydrogenated high-oleic sunflower oil (18). More recently, we compared native (unrandomized) with randomly interesterified (randomized) shea butter in 16 men and unrandomized shea butter with high-oleic sunflower oil in 13 of these men.

Collection and handling of blood samples. In the first three studies, venous blood samples were collected using the vacutainer technique with the minimal compression necessary to display the vein. In the later studies, venous blood samples were collected using an indwelling venous cannula. Blood for lipid analysis was collected in tubes containing dipotassium EDTA, and plasma was separated by centrifugation at 4°C for 15 min at $1500 \times g$. Chylomicrons were separated by ultracentrifugation from the 3-h blood sample, and plasma lipoprotein concentrations were determined from unfrozen plasma kept at 4°C, within 48 h of blood collection. For determination of plasma $FVII_c$, $FVII_a$, $FVII_{ag}$, PAI-1, and D-dimer, 4.5 mL of blood was collected into 0.5 mL of 38 g/L trisodium citrate solution at room temperature and centrifuged at $1500 \times g$ for 15 min at 20°C. A 4.5-mL blood sample for the tissue plasminogen activator (tPA) assay was collected into precooled tubes containing 0.5 mL of 0.5 mol/L citrate buffer, pH 4.0, which

resulted in a final pH of 5.5. Plasma was separated by centrifugation at $1500 \times g$ for 15 min at 4°C. All plasma samples were snap frozen in liquid nitrogen and stored at −70°C until analyzed. Blood samples were processed within 1 h of blood collection.

Analytical methods. Plasma TAG concentrations were determined by enzymatic assay. Lipids were extracted from the chylomicrons with chloroform/methanol (1:1 vol/vol), and the TAG fraction was isolated by TLC on silica gel G plates developed in hexane/diethyl ether/glacial acetic acid (80:20:2 by vol). The composition of the FA in the *sn*-2 position of the test fats and the chylomicron TAG fraction was determined by specific enzymatic hydrolysis followed by separation of the 2-MAG by TLC and analysis of their FA by GLC as methyl esters.

NMR analysis of the test fats was undertaken using a QP20+ pulsed NMR instrument (Oxford Instruments Ltd., Oxfordshire, United Kingdom). Samples were measured in duplicate at five temperatures (32, 37, 42, 47, and 52°C). A standard preconditioning procedure for fats showing the polymorphism was followed on all samples. The samples were melted at 80°C and held at 60°C for 5 min, followed by storage in a water bath at 26°C for 40 h. Prior to analysis, the samples were equilibrated for 90 min at 0°C and then at the measurement temperatures for 60 min. Plasma $FVII_c$ was measured by a one-stage semi-automated bioassay using rabbit-brain thromboplastin (Diagen, Thame, Oxon, United Kingdom) and a FVII-deficient substrate plasma prepared as described elsewhere (19). Plasma $FVII_a$ was measured according to the bioassay method described by Morrissey *et al.* (20). Plasma $FVII_{ag}$ was determined using an ELISA (Novo Nordisk, Copenhagen, Denmark). Plasma D-dimer concentration was measured by ELISA (Chromogenix AB, Mölndal, Sweden), and tPA and PAI-1 activities were determined by chromogenic assay (Chromogenix AB).

Statistical analyses. Statistical analyses of the data were carried out using two-factor repeated-measures ANOVA models. Where there were significant changes with time, postprandial values were compared with fasting values. The values following the different meals were compared using the deviations from fasting values to allow for any baseline differences, and diet × time interactions were included in these models. Data for plasma TAG was log-transformed prior to statistical analysis. Where the *F* values were significant ($P < 0.05$), the statistical significance of specific contrasts was tested. All pairwise testing was adjusted for multiple comparisons using a Bonferroni correction factor.

RESULTS

Table 1 shows the nutrient composition of the test meals used in the first study, and Figure 1 shows the effects of the different test meals on the postprandial changes in plasma TAG concentrations. The response to the meal was monophasic, and the maximal increase in plasma TAG concentrations at 3 h was significantly greater after the oleate, elaidate, and palmitate than after the stearate ($P < 0.001$, $P < 0.01$, $P < 0.01$, respectively),

TABLE 1
**Nutritional Composition of the Test Meals[a] Used to Compare Different Saturated and Monounsaturated FA**

	Oleate	Elaidate	Stearate	Palmitate	MCT	Low fat
Energy (MJ)	5.2	5.2	5.2	5.2	5.2	5.2
Protein (% energy)	12	12	12	12	12	12
Carbohydrate (% energy)	23	23	23	23	23	81
Fat (% energy)	65	65	65	65	65	7
Fiber (g)	8	8	8	8	8	8
Fat (g)	90	90	90	90	90	10
8:0 (g)	0	0	0	0	*19.1*	0
10:0 (g)	0	0	0	0	*18.6*	0
16:0 (g)	3.7	3.7	6.2	*36.9*	2.2	0.4
18:0 (g)	3.8	7.1	*35.6*	3.8	1.9	0.4
18:1 *trans* (g)	0.1	*34.1*	0	0.3	0	0
18:1n-9 *cis* (g)	*68.6*	30.8	34.3	34.3	34.4	7.6
18:2n-6 (g)	8.2	8.6	7.9	8.6	8.6	0.9

[a]From Reference 13. The italicized numbers show the fat exchanges between test meals. MCT, medium-chain TAG.

MCT ($P < 0.001$, $P < 0.01$, $P < 0.01$, respectively), and low-fat (all $P < 0.001$) meals. To compare the lipemic response, the integrated area under the curve (iAUC) was calculated. The iAUC was significantly lower after the MCT meal compared with the oleate, elaidate, and palmitate meals ($P < 0.001$, $P < 0.001$, $P < 0.01$, respectively) and was significantly lower after the stearate meal than after the oleate and elaidate meals ($P < 0.001$, $P < 0.05$, respectively).

Table 2 shows the FA composition of the different test fats used to compare two stearic acid-rich fats (SALATRIM and cocoa butter) and a high-oleic sunflower oil (oleate). The high stearic acid meals provided between 11 and 16 g stearic acid. Figure 2 shows the changes in serum TAG concentrations at 3 and 6 h following the test meals. The postprandial increased in serum TAG was markedly lower following the randomized stearic acid-rich TAG (SALATRIM) but was similar between the meals rich in cocoa butter and high-oleic sunflower oil. Because part of the effect of SALATRIM could be mediated by its high content of very short chain FA, we decided to compare the effects of meals providing randomized or unrandomized cocoa butter (Fig. 3). Postprandial lipemia was significantly lower following the randomized cocoa butter. We then decided to confirm our initial observation that the randomized stearic acid-rich TAG, as used in the first study (13), resulted in decreased postprandial lipemia by comparing a test meal containing 50 g of this fat with 50 g of unrandomized cocoa butter (Fig. 4). As predicted, the randomized stearic acid-rich TAG resulted in a decreased postprandial rise in plasma TAG. Finally, we compared 50 g of randomized shea butter with 50 g of unrandomized shea butter and found that both forms of shea butter led to only a modest increase in postprandial lipids (data not shown). We confirmed that unrandomized shea butter resulted in decreased lipemia by comparing a test meal containing 50 g unrandomized shea butter with a test meal consisting of 50 g high-oleic sunflower oil (Fig. 5). We found that the FA in the *sn*-2 position of the dietary TAG was conserved in the same position on absorption (Fig. 6). Although, we initially

believed that the differences between the responses to the fats were due to the different proportions of symmetrical and asymmetrical TAG, this did not hold true for shea butter. On investigation of the physical properties of the test fats, the extent of postprandial lipemia induced by the different stearic acid-rich
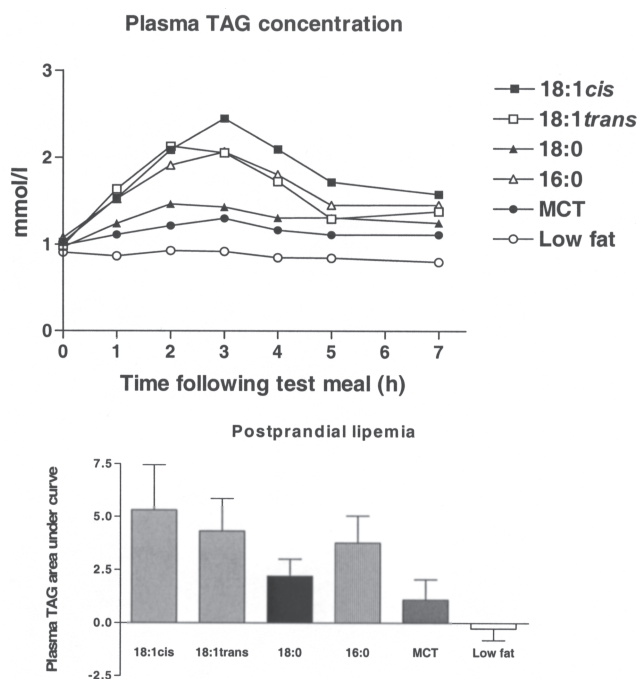
FIG. 1. Mean plasma TAG concentration (mmol/L) and postprandial lipemia (mean values with 95% confidence interval) measured as the areas under the curve following high-fat (90 g) test meals with different saturated and monounsaturated FA compared with a low-fat (10 g) test meal (data from Ref. 13). Repeated-measures ANOVA showed a significant effect of meal × time interaction ($P < 0.0001$). Postprandial lipemia was significantly lower after the medium-chain TAG (MCT) meal compared with the oleate, elaidate, and palmitate meals ($P < 0.001$, $P < 0.001$, $P < 0.01$, respectively) and significantly lower after the stearate meal than after the oleate and elaidate meals ($P < 0.001$, $P < 0.05$, respectively).

TABLE 2
Analyzed FA Content (g) of the Test Meals[a]

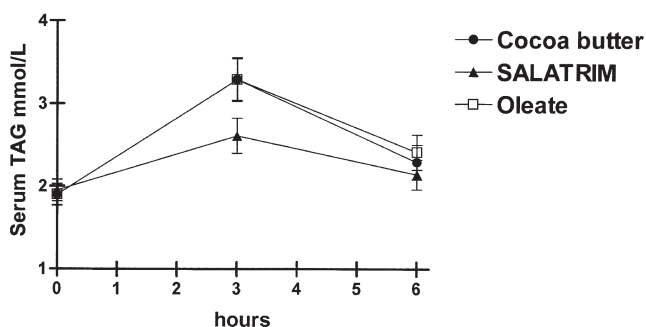|	Oleate	Randomized stearic acid-rich TAG	Cocoa butter
Acetic (2:0)	0	6.3	0
Propionic (3:0)	0	0.8	0
Palmitic (16:0)	2.2	3.1	8.4
Stearic (18:0)	1.8	16.1	11.2
Oleic (18:1n-9)	37.9	11.5	21.7
Linoleic (18:2n-6)	5.2	5.8	5.8

[a]From Reference 14.

fats appeared to be related to the proportion of solid fat measured by NMR at 37°C (Fig. 7).

Hemostatic function. Table 3 shows the changes in $FVII_c$ and $FVII_a$ following the test meals in the first study (13). $FVII_c$ increased following all high-fat test meals, especially those rich in palmitate, oleate, and elaidate compared with the low-fat meal. However, the increase in $FVII_a$ was lower following the stearate and MCT meals compared with the oleate meal. In the second study (14), $FVII_c$ and $FVII_a$ increased to the same extent following test meals rich in high-oleate sunflower oil or unrandomized cocoa butter but did not increase significantly following test meals containing the randomized stearic acid-rich TAG (Fig. 8). In a later study (15), we showed that ingestion of randomized cocoa butter resulted in a much smaller increase in postprandial TAG and activation of FVII than found with cocoa butter. No adverse effects on the fibrinolytic activity of test meals containing stearic acid-rich fats were found (Tables 4 and 5). However, PAI-1 activity tended to fall through the day regardless of treatment, and tPA tended to rise.

DISCUSSION

The studies reported here were specifically designed to demonstrate the adverse effects of stearic acid on postprandial lipemia and hemostatic function. We were unable to find any evidence


FIG. 2. Geometric mean ± SE in serum TAG following test meals rich in cocoa butter stearic acid randomized TAG (SALATRIM[TM]; Cultor Foods, Ardsley, NY) or high-oleic sunflower oil (oleate) in 18 women and 17 men, aged 40–60 yr (data from Ref. 14). There was a significant diet × time interaction ($P = 0.002$) for the analyses of the deviations of serum TAG from fasting values. The increase in serum TAG was significantly lower after the structured TAG meal than after the oleate and cocoa butter meals at 3 h ($P < 0.0001$ for both) and at 6 h ($P = 0.04$, $P = 0.001$, respectively).
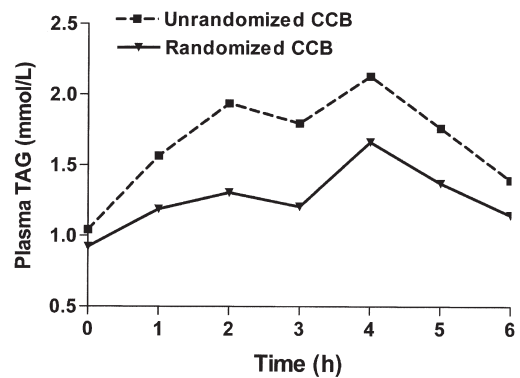
FIG. 3. Mean ± SE plasma TAG in 17 healthy men after consuming test meals containing either 50 g randomized or 50 g unrandomized cocoa butter (CCB). Data taken from Reference 15. The areas under the curve are significantly different from each other ($P < 0.01$); randomized: 267 arbitrary units (95% confidence interval: 210, 314); unrandomized: 447 arbitrary units (95% confidence interval: 338, 557).
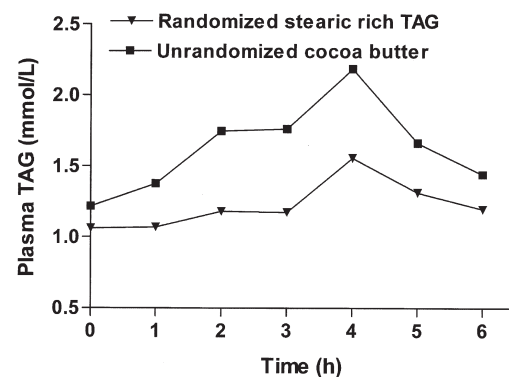
FIG. 4. Mean ± SE plasma TAG in 6 healthy men following test meals containing 50 g randomized stearic acid-rich TAG and 50 g cocoa butter. The areas under the curve were significantly different ($P = 0.006$): randomized stearic acid-rich TAG, geometric mean 54.9 (95% confidence interval: 19.8, 152.3); unrandomized cocoa butter, geometric mean 164.0 (95% confidence interval: 96.0, 280.3).
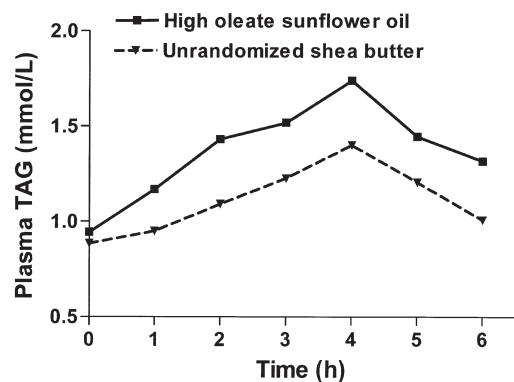
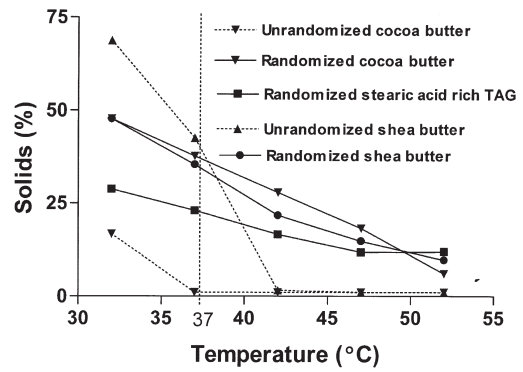**FIG. 5.** Geometric mean ± SE plasma TAG in 13 healthy men after consuming test meals containing either 50 g unrandomized shea butter or 50 g high-oleate sunflower oil. The areas under the curve were significantly different $P = 0.017$: unrandomized shea butter, geometric mean 86.8 (95% confidence interval: 49.8, 151.3); high-oleate sunflower oil, geometric mean 162.7 (95% confidence interval: 111.4, 237.7).
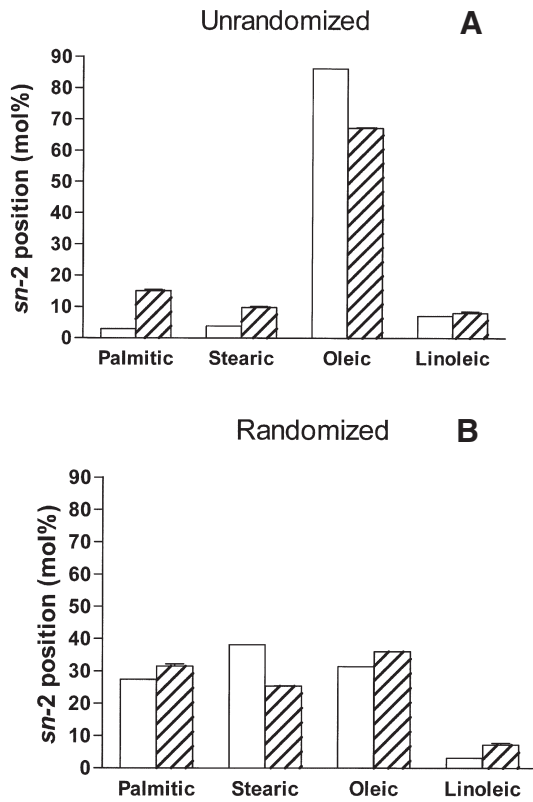
FIG. 6. Composition of palmitic, stearic, oleic, and linolenic acids in the *sn*-2 position of the chylomicron TAG (with 95% confidence intervals) compared with the proportions in unrandomized and randomized cocoa butter (from Ref. 15).

FIG. 7. Solid fat content of stearic acid-rich fats measured at different temperatures using low-resolution NMR.

FVII activation than other fats. However, our findings indicate that there is considerable variability in the response to different stearic acid-rich fats. Initially, we proposed that these differences may be due to the TAG structure. It was clearly evident that FA in the *sn*-2 position in the dietary fat were conserved in this position on absorption. This is in agreement with a report by Summers *et al.* (21), who also observed that the presence of stearic acid in the *sn*-2 position did not affect its subsequent rate of clearance. We found that shea butter, which consists predominantly of 1,3-distearoyl-2-oleoylglycerol, led to significantly less postprandial lipemia than high-oleate sunflower oil. Randomization of shea butter did not appreciably alter the postprandial response. When we undertook measurements of the proportion of solids at 37°C by low-resolution NMR, we found that this was strongly predictive of the extent of postprandial lipemia. Since completing this work, Tholstrup *et al.* (22,23) have published data confirming that randomized stearic acid-rich TAG result in less postprandial lipemia compared with oleic acid and a lower activation of FVII$_a$ (compared only with *trans* 18:1). They were also unable to find any adverse effects

to support the view that stearic acid-rich fats had adverse effects compared with oleic acid-rich fats. Indeed, our data suggest that oleic acid-rich fats result in more pronounced postprandial lipemia than other fats and in a greater postprandial increase in

TABLE 3
Effect of High-Fat (90 g) Test Meals with Different Saturated and Monounsaturated FA^a on Indices of Factor VII Coagulant Activity (FVII$_c$) and Factor VII Activated Concentration (FVII$_a$) Compared with an Isoenergetic Low-Fat Test Meal (10 g fat) in 16 Healthy Subjects (5 females, 11 males)^b

|	Low fat	MCT	Palmitate	Stearate	Elaidate	Oleate
FVII$_c$ (%)						
Fasting	112 ± 8.0	104 ± 6.9	105 ± 5.4	111 ± 6.9	110 ± 7.2	111 ± 6.9
3 h	104 ± 7.0	116 ± 7.1*	113 ± 7.2*	109 ± 7.3	118 ± 7.4	118 ± 6.7
7 h	99 ± 6.8*	113 ± 8.1	112 ± 6.9*	114 ± 8.2	121 ± 7.4*,†	124 ± 7.4*,†
FVII$_a$ (ng/mL)						
Fasting	1.4 ± 0.15	1.1 ± 0.14	1.3 ± 0.16	1.4 ± 0.13	1.4 ± 0.13	1.4 ± 0.18
3 h	1.4 ± 0.16	1.7 ± 0.33*	2.1 ± 0.39*,†	1.9 ± 0.24*	2.1 ± 0.24*,†	2.4 ± 0.44*,†
7 h	1.4 ± 0.19	1.5 ± 0.27	2.1 ± 0.33*	1.9 ± 0.26*	2.0 ± 0.19*	2.7 ± 0.56†,‡,§

^{a}From Reference 13.
^{b}Mean values ± SE. Repeated-measures ANOVA data for FVII$_c$ and FVII$_a$ showed a significant meal × time interaction ($P < 0.001$). *$P < 0.05$: Compared with fasting value in the same column; Dunnett's multiple-comparison test. †$P < 0.05$: Compared with the corresponding value after the low-fat meal; Dunnett's multiple-comparison test. ‡$P < 0.05$: Compared with the corresponding value after the MCT meal; Bonferroni's multiple-comparison test. §$P < 0.05$: Compared with the corresponding value after the stearate meal; Bonferroni's multiple-comparison test. For other abbreviations see Table 1.

TABLE 4
Effect of High-Fat (90 g) Test Meals with Different Saturated and Monounsaturated FA on Indices of Fibrinolytic Activity Compared with an Isoenergetic Low-Fat Test Meal (15 g fat) in 16 Healthy Subjects (5 females, 11 males)[a]

	Low fat	MCT	Palmitate	Stearate	Elaidate	Oleate
tPA (IU/min)						
Fasting	3.1 ± 0.57	3.0 ± 0.50	3.7 ± 0.60	3.0 ± 0.57	3.4 ± 0.64	2.7 ± 0.54
3 h	3.7 ± 0.67	3.2 ± 0.57	3.3 ± 0.56	3.6 ± 0.63	3.1 ± 0.55	3.5 ± 0.51
7 h	3.2 ± 0.65	2.7 ± 0.42	3.7 ± 0.60	3.6 ± 0.69	2.9 ± 0.54	3.5 ± 0.55
PAI-1 (IU/min)						
Fasting	10.3 ± 1.60	7.7 ± 1.42	10.4 ± 1.60	11.7 ± 5.58	9.7 ± 5.95	12.1 ± 1.92
3 h	8.1 ± 1.20	8.6 ± 0.82	7.3 ± 1.09	6.9* ± 3.36	8.1 ± 4.05	6.8* ± 0.66
7 h	7.7 ± 0.96	8.6 ± 1.11	7.6 ± 1.02	6.4* ± 5.37	7.5 ± 3.05	8.0* ± 1.39
D-dimer (µg/L)						
Fasting	117 (64–235)	134 (39–210)	114 (41–186)	107 (78–209)	145 (53–198)	91 (62–223)
3 h	115 (63–226)	121 (41–178)	103 (44–221)	97 (53–164)	121 (78–234)	90 (36–217)
7 h	102 (57–258)	105 (42–203)	108 (52–201)	78 (38–156)	118 (38–186)	108 (45–216)

[a]Mean values ± SE for tissue plasminogen (tPA) and plasminogen activator inhibitor type 1 (PAI-1) activities and the median and range for D-dimer concentration. Repeated-measures ANOVA. There was a significant time effect for tPA ($P < 0.05$) but no significant meal or meal × time interaction. There was a significant diet × time interaction for PAI-1 ($P = 0.03$). No values within the same row are significantly different from each other ($P > 0.05$). *$P < 0.05$: Compared with fasting values in the same column; Dunnett's multiple-comparison test.
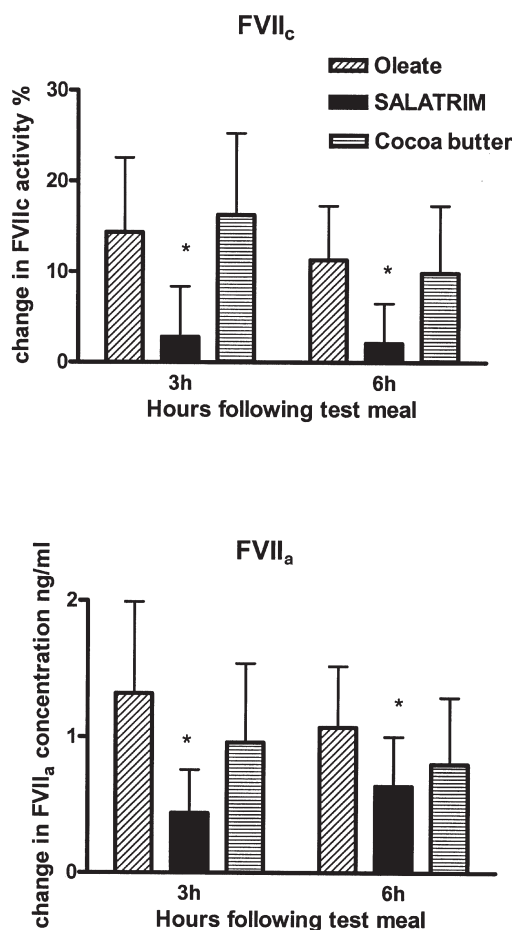
FVII$_c$

FIG. 8. Mean changes ± 95% confidence interval in factor VII coagulant activity (FVII$_c$) and activated factor VII concentration (FVII$_a$) from fasting following test meals rich in cocoa butter stearic acid randomized TAG (SALATRIM) or high-oleic sunflower oil (oleate) in 18 women and 17 men, aged 40–60 yr (data taken from Ref. 14). *$P < 0.05$ compared with high-oleate sunflower and cocoa butter test meals.

TABLE 5
tPA and PAI-1 Activities and D-Dimer Concentrations Following Two Stearate-rich Test Meals[a] Compared with an Oleate-rich Test Meal in 35 Male and Female Subjects[b]

	Oleate	SALATRIM	Cocoa butter
tPA activity (IU/mL)			
Fasting	1.54 ± 1.40	1.57 ± 1.58	1.72 ± 1.46
3 h	2.51 ± 1.40*	2.39 ± 1.58	2.75 ± 1.21*
6 h	1.95 ± 1.40	2.46 ± 1.40	2.32 ± 1.11
PAI-1 (IU/mL)			
Fasting	10.5 ± 6.0	10.3 ± 6.1	10.3 ± 5.3
3 h	6.6 ± 2.5*	5.4 ± 4.5*	6.4 ± 3.7*
6 h	8.3 ± 3.8*	6.6 ± 3.5*	7.0 ± 3.3*
D-Dimer (µg/L[c])			
Fasting	228.1 ± 98.1	244.7 ± 115.0	254.7 ± 101.9
3 h	225.9 ± 99.4	244.7 ± 119.9	252.1 ± 103.4
6 h	225.9 ± 106.2	257.2 ± 115.8	244.6 ± 97.8

[a]From Reference 14. For abbreviations see Table 4.
[b]Geometric mean values ± SD. Two-factor repeated-measures ANOVA showed a significant time main effect for tPA ($P < 0.0001$) and for PAI-1 ($P < 0.0001$). There were no significant differences between meals or meal × time interactions. *$P < 0.05$: Compared with fasting values; Dunnett's multiple-comparison test.
[c]$n = 32$.

of stearic acid-rich fats on fibrinolytic activity. Taken together, these data refute the hypothesis that stearic acid-rich fats have adverse effects on postprandial lipemia, fibrinolytic, and FVII$_c$ activities. However, further research is needed to clarify the effects of these and other lipids on endothelial function.

REFERENCES

1. Mensink, R.P., Zock, P.L., Kester, A.D., and Katan, M.B. (2003) Effects of Dietary Fatty Acids and Carbohydrates on the Ratio of Serum Total to HDL Cholesterol and on Serum Lipids and Apolipoproteins: A Meta-analysis of 60 Controlled Trials, *Am. J. Clin. Nutr. 77*, 1146–1155.
2. Zilversmit, D.B. (1979) Atherogenesis: A Postprandial Phenomenon, *Circulation 60*, 473–485.

3. Sanders, T.A. (2003) Dietary Fat and Postprandial Lipids, *Curr. Atheroscler. Rep. 5*, 445–451.

4. Phan, C.T., Mortimer, B.C., Martins, I.J., and Redgrave, T.G. (1999) Plasma Clearance of Chylomicrons from Butterfat Is Not Dependent on Saturation: Studies with Butterfat Fractions and Other Fats Containing Triacylglycerols with Low or High Melting Points, *Am. J. Clin. Nutr. 69*, 1151–1161.

5. Hoak, J.C. (1997) Fatty Acids in Animals: Thrombosis and Hemostasis, *Am. J. Clin. Nutr. 65*, 1683S–1686S.

6. Meade, T.W., Ruddock, V., Stirling, Y., Chakrabarti, R., and Miller, G.J. (1993) Fibrinolytic Activity, Clotting Factors, and Long-Term Incidence of Ischaemic Heart Disease in the Northwick Park Heart Study, *Lancet 342*, 1076–1079.

7. Girelli, D., Olivieri, O., Arigliano, P.L., Guarini, P., Bassi, A., and Corrocher, R. (1996) Influences of Lipid and Non-lipid Nutritional Parameters on Factor VII Coagulant Activity in Normal Subjects: The Nove Study, *Eur. J. Clin. Invest. 26*, 199–204.

8. Mitropoulos, K.A., Miller, G.J., Martin, J.C., Reeves, B.E., and Cooper, J. (1994) Dietary Fat Induces Changes in Factor VII Coagulant Activity Through Effects on Plasma Free Stearic Acid Concentration, *Arterioscler. Thromb. 14*, 214–222.

9. Mitropoulos, K.A., Reeves, B.E., and Miller, G.J. (1993) The Activation of Factor VII in Citrated Plasma by Charged Long-Chain Saturated Fatty Acids at the Interface of Large Triglyceride-rich Lipoproteins, *Blood Coagul. Fibrinolysis 4*, 943–951.

10. Oakley, F.R., Sanders, T.A., and Miller, G.J. (1998) Postprandial Effects of an Oleic Acid-rich Oil Compared with Butter on Clotting Factor VII and Fibrinolysis in Healthy Men, *Am. J. Clin. Nutr. 68*, 1202–1207.

11. Sanders, T.A., Miller, G.J., de Grass, T., and Yahia, N. (1996) Postprandial Activation of Coagulant Factor VII by Long-Chain Dietary Fatty Acids, *Thromb. Haemost. 76*, 369–371.

12. Sanders, T.A., de Grass, T., Miller, G.J., and Humphries, S.E. (1999) Dietary Oleic and Palmitic Acids and Postprandial Factor VII in Middle-Aged Men Heterozygous and Homozygous for Factor VII R353Q Polymorphism, *Am. J. Clin. Nutr. 69*, 220–225.

13. Sanders, T.A., de Grass, T., Miller, G.J., and Morrissey, J.H. (2000) Influence of Fatty Acid Chain Length and *cis/trans* Isomerization on Postprandial Lipemia and Factor VII in Healthy Subjects (postprandial lipids and factor VII), *Atherosclerosis 149*, 413–420.

14. Sanders, T.A., Oakley, F.R., Cooper, J.A., and Miller, G.J. (2001) Influence of a Stearic Acid-rich Structured Triacylglyc-erol on Postprandial Lipemia, Factor VII Concentrations, and Fibrinolytic Activity in Healthy Subjects, *Am. J. Clin. Nutr. 73*, 715–721.

15. Sanders, T.A., Berry, S.E., and Miller, G.J. (2003) Influence of Triacylglycerol Structure on the Postprandial Response of Factor VII to Stearic Acid-rich Fats, *Am. J. Clin. Nutr. 77*, 777–782.

16. Sanders, T.A., Oakley, F.R., Crook, D., Cooper, J.A., and Miller, G.J. (2003) High Intakes of *trans* Monounsaturated Fatty Acids Taken for 2 Weeks Do Not Influence Procoagulant and Fibrinolytic Risk Markers for CHD in Young Healthy Men, *Br. J. Nutr. 89*, 767–776.

17. Sanders, T.A., Berry, S.E., and Miller, G.J. (2003) Influence of Triacylglycerol Structure on the Postprandial Response of Factor VII to Stearic Acid-rich Fats, *Am. J. Clin. Nutr. 77*, 777–782.

18. Berry, S.E., and Sanders, T.A. (2005) Influence of Triacylglycerol Structure of Stearic Acid-rich Fats on Postprandial Lipaemia, *Proc. Nutr. Soc. 64*, 205–212.

19. Miller, G.J., Stirling, Y., Esnouf, M.P., Heinrich, J., van de Loo, .J., Kienast, J., Wu, K.K., Morrissey, J.H., Meade, T.W., Martin, J.C. *et al.* (1994) Factor VII-Deficient Substrate Plasmas Depleted of Protein C Raise the Sensitivity of the Factor VII Bioassay to Activated Factor VII: An International Study, *Thromb. Haemost. 71*, 38–48.

20. Morrissey, J.H., Macik, B.G., Neuenschwander, P.F., and Comp, P.C. (1993) Quantitation of Activated Factor VII Levels in Plasma Using a Tissue Factor Mutant Selectively Deficient in Promoting Factor VII Activation, *Blood 81*, 734–744.

21. Summers, L.K., Fielding, B.A., Herd, S.L., Ilic, V., Clark, M.L., Quinlan, P.T., and Frayn, K.N. (1999) Use of Structured Triacylglycerols Containing Predominantly Stearic and Oleic Acids to Probe Early Events in Metabolic Processing of Dietary Fat, *J. Lipid Res. 40*, 1890–1898.

22. Tholstrup, T., Sandström, B., Bysted, A., and Hølmer, G. (2001) Effect of 6 Dietary Fatty Acids on the Postprandial Lipid Profile, Plasma Fatty Acids, Lipoprotein Lipase, and Cholesterol Ester Transfer Activities in Healthy Young Men, *Am. J. Clin. Nutr. 73*, 198–208.

23. Tholstrup, T., Miller, G.J., Bysted, A., and Sandström, B. (2003) Effect of Individual Dietary Fatty Acids on Postprandial Activation of Blood Coagulation Factor VII and Fibrinolysis in Healthy Young Men, *Am. J. Clin. Nutr. 77*, 1125–1132.

Influence of Stearic Acid
on Hemostatic Risk Factors in Humans

Tine Tholstrup*

The Research Department of Human Nutrition, Centre of Advanced Food Research,
The Royal Veterinary and Agricultural University, Frederiksberg, Denmark

ABSTRACT: Stearic acid has been claimed to be prothrombotic. Elevated plasma factor VII coagulant activity (FVIIc) may raise the risk of coronary thrombosis in the event of plaque rupture. Fibrinogen, an acute-phase protein, is necessary for normal blood clotting; however, elevated levels of fibrinogen increase the risk of coronary heart disease (CHD). Here I report the results of three controlled, human dietary intervention studies, which used a randomized crossover design to investigate the hemostatic effects of stearic acid-rich test diets in healthy young men. A diet high in stearic acid (shea butter) resulted in a 13% lower fasting plasma FVIIc than a high palmitic acid diet, and was 18% lower than a diet high in myristic and lauric acids ($P = 0.001$) after 3 wk of intervention. The stearic acid-rich test fat increased plasma fibrinogen concentrations slightly compared with the myristic–lauric acid diet ($P < 0.01$). When investigating the acute effects of fatty meals, those high in stearic acid (synthesized test fat) resulted in a smaller postprandial increase in FVII than those high in *trans* and oleic FA, indicating a smaller increase in activated FVII after ingesting stearic acid compared with fats high in monounsaturated FA, probably caused by lower postprandial lipemia. Thus, the present investigations did not find dietary stearic acid to be more thrombogenic, in either fasting effects compared with other long-chain FA, or in acute effects compared with dietary unsaturated FA, including *trans* monounsaturated FA. The slightly increased effect on fasting plasma fibrinogen may be biologically insignificant, but it should be investigated further.

Paper no. L9816 in *Lipids 40*, 1229–1235 (December 2005).

Stearic acid, a long-chain dietary saturated FA (SFA), is known to have unique beneficial effects because, unlike other long-chain SFA, it has a neutral or lowering effect on plasma cholesterol (1). However, to determine whether stearic acid is a healthy alternative to SFA and *trans* FA, which increase cholesterol, it is relevant to study its effects on other important risk factors for coronary heart disease (CHD). It has repeatedly been suggested that long-chain SFA, especially stearic acid, have thrombogenic effects. The idea that long-chain FA are thrombogenic originates from studies performed in the 1960s, when it was shown that

stearic acid, added as sodium salts to the blood *in vitro*, accelerated thrombus formation (2). Others reported that injections of unbound long-chain SFA into the systemic circulation of dogs was followed by massive thrombosis and sudden death (3). Later, when focusing on the thrombogenic effects of SFA in a population comparison, Renaud *et al.* (4) demonstrated that stearic acid was correlated with clotting activity and platelet aggregation. However, platelet aggregation was measured by *in vitro* methods and the results are not considered applicable to the situation *in vivo*. In contrast, valid methods exist to measure key hemostatic variables affecting blood clot formation and the dissolution of blood clots. Figure 1 illustrates blood coagulation and fibrinolysis with particular reference to factors (boldfaced) of the pathways included in this paper. Normally, the hemostatic system is finely balanced between fibrin formation and dissolution. However, during atherothrombosis it may become unbalanced, with excessive fibrin formation. Factor VII (FVII) appears to play a major role in basal thrombin generation (5) and thereby in thrombus formation. We report the results of FVII coagulant activity (FVIIc), which measures the zymogen (inactivated form of the protein), and the activated FVII (FVIIa), which is normally approximately 1%. Plasma FVIIc has been reported to be

Coagulation and fibrinolysis
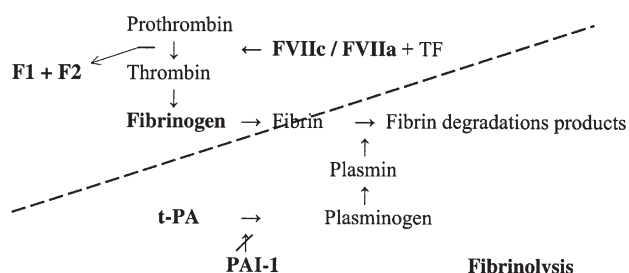
FIG. 1. Blood coagulation and fibrinolysis, an overview of part of the coagulation cascade and fibrinolytic system. Parameters investigated in the studies reported in this paper are highlighted. F1+2, prothrombin fragment 1 + 2; FVIIa, activated factor VII; FVIIc, factor VII coagulant activity; t-PA, tissue plasminogen activator; PAI-1, plasminogen activator inhibitor type-1.

---

*Address correspondence at the Research Department of Human Nutrition, LMC, The Royal Veterinary and Agricultural University, Rolighedsvej 30, DK 1958–Frederiksberg, Denmark. E-mail: tth@kvl.dk

Abbreviations: CHD, coronary heart disease; CRP, C-reactive protein; F1+2, prothrombin fragment 1 + 2; FVII, factor VII; FVIIa, activated factor VII; FVIIag, total protein concentrations of FVII; FXag, concentration of factor X; O, oleic acid; PAI-1, plasminogen activator inhibitor type-1; protein Cag, concentration of protein C; SFA, saturated fatty acid; t-PA, tissue plasminogen activator.

strongly and independently associated with the risk of CHD in middle-aged men (6), although this relation have not been observed in several more recent prospective studies (7–10). Nevertheless, the possibility cannot be discounted that a high peak FVIIc in the postprandial period, caused by activation of FVII (11), may temporarily raise the risk of serious coronary thrombosis in the event of rupture of an atheromatous plaque. Moving further downstream in the coagulation cascade (Fig. 1), thrombin converts fibrinogen to fibrin, which is deposited in strands that trap erythrocytes and form the clot. Elevated fibrinogen is a coagulation factor and a marker of inflammatory reaction (7,12,13). Fibrinogen is strongly associated with CHD. It increases blood viscosity and stimulates platelet aggregation (14) and smooth muscle cell proliferation (15). Plasma fibrinogen concentration is affected by age, smoking, body mass index, and alcohol consumption (16).

With regard to dissolution of the blood clot, the primary initiator of fibrinolysis is tissue plasminogen activator (t-PA), which, when bound to fibrin, activates plasminogen to plasmin, which in turn cleaves fibrin and breaks up the blood clot. Overall, low levels of t-PA may increase the risk of subsequent CHD. However, the major regulator of fibrinolysis is plasminogen activator inhibitor type-1 (PAI-1) (17). High PAI-1 concentrations have been associated with CHD (18–20).

This paper includes the results of three different intervention studies investigating the effect of stearic acid test fats (natural or synthesized) on coagulation and fibrinolysis in healthy men.

SUBJECTS AND METHODS

We report the results of three studies focusing on fasting, postprandial, and background effects, respectively. All the studies were performed as controlled dietary intervention studies with a crossover design. The effects of stearic acid were investigated after either 3–4 weeks of intervention in the fasting phase (study I), postprandially 2, 4, 6, and 8 h after intake of fatty meals (study II), or postprandially after 3 wk of intervention (study III). The subjects of the studies were healthy young men, aged 20–30 yr. Intervention periods or days were separated by washout periods (3–8 wk). Habitual diet was assessed by 7-d weighed food records prior to inclusion. We investigated the effects of three different types of stearic acid test fats: shea butter, a natural source of stearic acid (Fig. 2) (study I) (21); interesterified synthetic fat (Fig. 3) (study II) (22); or milk fat, in which the FA composition was modified by purposefully designed feeding of the dairy cows (Table 1) (study III) (24), respectively. Test fats were incorporated into one or more of the following items: bread, rolls, cakes, vegetable dishes, mashed potatoes, sausages, or fish patés.

Blood analyses. Plasma FVIIc (% standard) was assessed by a one-stage clotting assay as described previously (21,22), and plasma FVIIa was measured by a one-stage clotting assay using a soluble mutant recombinant tissue factor that possessed cofactor activity for FVIIa but failed to support the activation of FVII (22). Total protein concentrations of FVII (FVIIag)
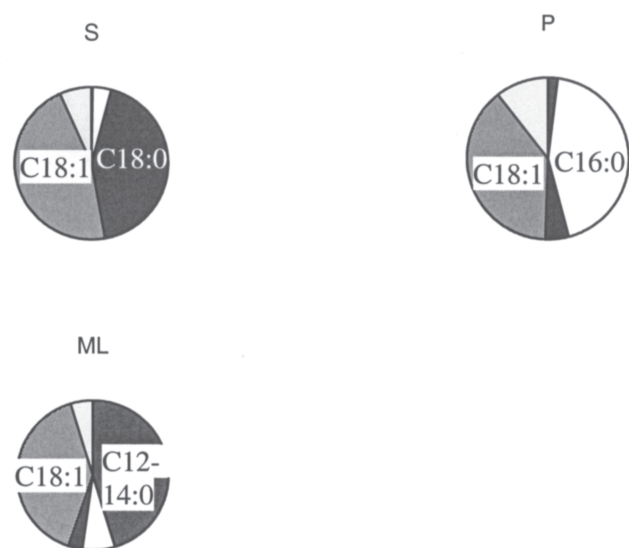
FIG. 2. Analyzed proportion of the major FA in the three test fats used in the intervention study (study I; Ref. 1). S, high in stearic acid, produced from shea butter (nuts from the shea butter tree, *Butyrospermum parkii* Sapotacae), refined and rinsed with acetone, containing 6.9% nonglycerides; P, high in palmitic acid, from palm oil (Palmitex, Aarhus Olie A/S, Aarhus, Denmark); ML, high in both myristic and lauric acids, from a mixture of palm kernel oil and high-oleic sunflower oil (21).
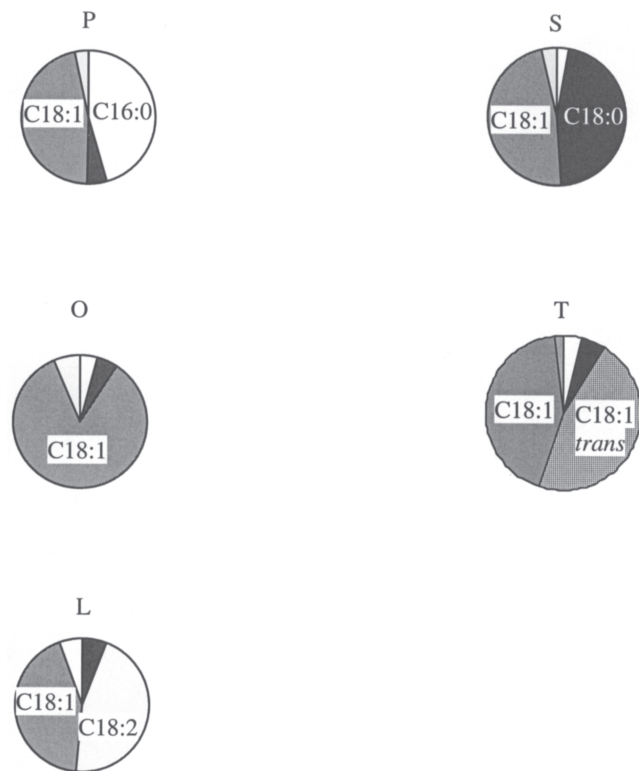
FIG. 3. Analyzed proportion of the major FA in the five interesterified test fats used in the intervention study (II). O, rich in oleic acid; T, rich in *trans* FA; L, rich in linoleic acid; for other abbreviations see Figure 2 (22).

TABLE 1
Content of the Major FA in the Test Milk[a]

FA	% FA of total FA	
	Modified milk fat (M)	Danish milk fat (D)
4:0–10:0	8.7	10.7
12:0	2.9	4.1
14:0	10.7	12.1
16:0[b]	21.1	36.8
18:0	**10.9**	**7.2**
18:1 *trans*	6.4[c]	1.1[d]
18:1n-9	**25.0**	**15.3**

[a]Analyzed by GLC. The boldfaced values indicate the content of stearic and oleic acids in the two test milks.
[b]16:0 also includes the branched isoforms typical of milk fat.
[c]The two major *trans* isomers are 18:1n-7 and 18:1n-8, about 2% of each.
[d]The major *trans* isomer is 18:1n-7.

were assessed by an ELISA, the protein concentrations of protein C (protein Cag) and C-reactive protein (CRP) were measured by ELISA methods, the protein concentration of factor X (FXag) was measured by rocket immunoelectrophoretic methods, fibrinogen and albumin were determined by immunologic methods, and the *in vivo* generation of thrombin was assessed by measuring prothrombin fragment 1 + 2 (F1+2) by a commercially available ELISA method (23).

The plasma t-PA activity and PAI-1 antigen concentration were assessed by commercial enzyme-linked immunosorbent assays, and the plasma PAI-1 antigen was assessed by a chromogenic assay (22).

Ethics. The protocol and the aim of the studies were fully explained to the subjects, who gave their written consent. The Scientific Ethics Committee of the municipalities of Copenhagen and Frederiksberg approved the research protocols of the different studies.

RESULTS

Effects in the fasting state. Study I: stearic acid from shea butter, 3 wk of intervention. Plasma FVIIc was significantly reduced after giving shea butter, with high amounts of stearic acid, compared with the diets high in palmitic acid, high in myristic + lauric acids, and the habitual diet (Fig. 4) (21). To elucidate the mechanisms behind the effect of stearic acid on FVIIc, we investigated the effects of the coagulation cascade on some proteins (FVIIag, FXag, and protein Cag). All decreased after receiving stearic acid (Table 2) (23), indicating that the observed decrease in FVIIc was due to a decrease in the amount of protein and had no effect on the activity state of the protein. F1+2, a sensitive marker of activation of the coagulation system produced during the conversion of prothrombin to thrombin, was reduced, and plasma fibrinogen was slightly increased after receiving stearic acid compared with myristic–lauric acids (Table 2) (23). However, the acute-phase proteins CRP and albumin were not affected differently by receiving stearic acid (Table 2). In addition, the fibrinolytic parameters were not affected differently.

Effects in the fasting state. Study III: milk fat increased in stearic (and oleic acid), 4 wk of intervention, fasting values.
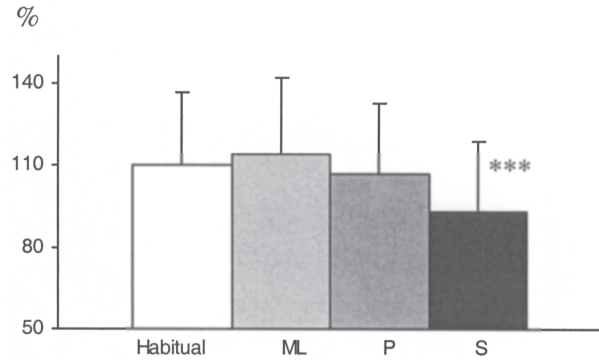
FIG. 4. Plasma mean FVIIc% + median (Q_{50} values) after 3 wk on an S, P, or ML diet. ***$P < 0.001$ compared with others (21). For abbreviations see Figure 2.

Milk fat with an increased content of stearic acid did not result in any differences in FVIIc and the fibrinolytic parameters (24).

Effects in the postprandial state. Study II: meals high in stearic acid. Stearic acid (30–38 g) in a synthesized interesterified test fat (Fig. 3) resulted in a lower FVIIa than did *trans* FA and a lower FVIIc than did oleic acid ($P < 0.02$) (diet × time interaction) (Figs. 5a, 5b) (22). For comparison, we included the responses in FFA and lipemia (Figs. 5e, 5f) (22). Although the response pattern of FVII and plasma TAG was rather similar, the increase in FVIIa was not significantly associated with the level of lipemia. No other differences were observed in the hemostatic variables.

Effects of the background diet. Study III: modified milk fat. Postprandial FVIIc was increased less after a meal (with 1.2 g milk fat/kg body weight) of modified milk fat (FA composition shown in Table 1) on day 21 of the intervention period compared with a meal with ordinary Danish milk fat (Fig. 6) (24). No other differences were observed.

DISCUSSION

Effects in the fasting state. When stearic acid was given as shea butter, we observed a uniform decline in FVIIc compared with

TABLE 2
Hemostatic Variables[a]

Variable	Diet ML	Diet S
FVII:Ag (%)	90 (71–97)	80** (50–91)
FX:Ag (%)	91 (79–96)	87* (76–95)
Protein C:Ag (%)	96 (88–122)	83* (74–105)
F1+2 (nmol/L)	1.00 (0.78–1.09)	0.90** (0.71–0.99)
CRP (mg/L)	0.42 (0.18–0.91)	0.39 (0.04–0.67)
Albumin (g/L)	30.6 (29.0–31.1)	30.1 (29.2–31.0)
Fibrinogen (g/L)	2.6 (2.4–2.7)	2.8** (2.7–3.1)

[a]Median values ($n = 15$) (25–75% percentile) after 3 wk on a diet high in myristic and lauric acid (ML) or rich in stearic acid (S). FVII:Ag, factor VII protein concentration; FX:Ag, factor X protein concentration; protein C:Ag, protein C protein concentration; F1+2, prothrombin fragment 1 + 2; CRP, C-reactive protein. *$P < 0.05$, **$P < 0.01$ (Wilcoxon).
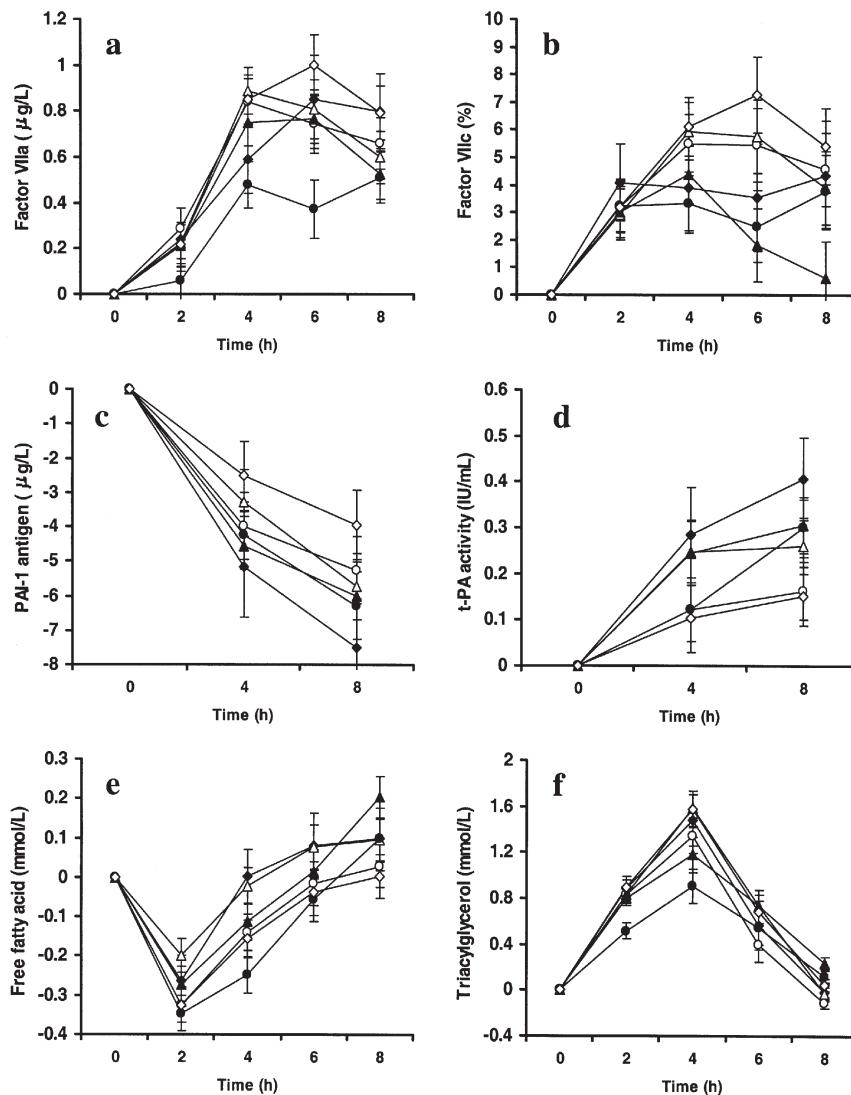
FIG. 5. Least-squares mean (± SE) changes in FVIIa (a) and FVIIc (b) 2, 4, 6, and 8 h after in-take and in PAI-1 (c) antigen and t-PA (d) activity 4 and 8 h after intake of test meals rich in palmitic acid (P, ▲; $n = 16$), stearic acid (S, ●; $n = 16$), oleic acid (O, △; $n = 16$), *trans* FA (T, ◇; $n = 15$), and linoleic acid (L, ○; $n = 16$). For comparison we included data for the change in free FA (e) and plasma TAG (f) 2, 4, 6, and 8 h after intake of test meals rich in the same fats. Data for 0 h are fasting values; other values are postprandial. For details of the FA compo-sition of the test fats, see Figure 3. The overall repeated-measures ANOVA for FVIIa was $P = 0.053$; that for S vs. P was $P = 0.017$. The overall repeated-measures ANOVA for FVII:c was $P = 0.018$; that for S vs. O was $P = 0.012$, and that for S vs. P was $P = 0.021$. For abbreviations see Figures 1–3.

test fats high in palmitic (15%) and myristic–lauric acid (18%) (Fig. 4) (21). The reduction in FVIIc indicated a decrease in procoagulant activity, because the decrease in other proteins of the coagulation cascade (i.e., FVIIag and FXag) was accompa-nied by a decrease in F1+2, which is formed during the con-version of prothombin to thrombin (23). The lower FVIIc after a high-stearic test fat agrees with results by a single study in which a high stearic acid test fat (synthetic hardened canola, high-oleic sunflower oil) decreased FVIIc compared with base-line values (25), whereas the decrease in FVIIc after giving stearic acid was not significantly lower than after giving

palmitic acid. However, our results disagreed with findings by Mutanen and Aro (26), who found no differences between the effects of stearic acid, dairy fat, or *trans* fat. A study with 9 par-ticipants also showed no drop in FVIIc after giving stearic acid compared with oleic and linoleic acids (27), probably because of a lack of statistical power. It is not clear what caused the dif-ference in the effects of stearic acid between our study and that of Mutanen and Aro. It could be that we served higher amounts of stearic acid (14 E% vs. 9 E% in their study). Our control diets were very well matched and compliance was extremely high, as the participants were followed very thoroughly, which
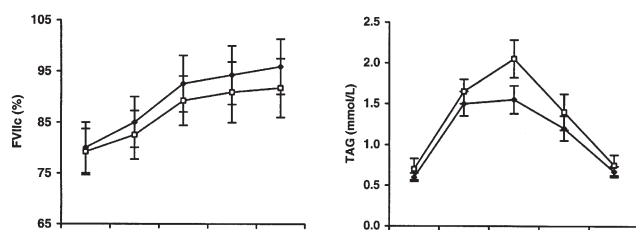
FIG. 6. Plasma FVII and TAG in fasting samples (0 h) and in samples collected (2,4,6,8 h) after intake of a high-fat breakfast (with the same FA composition as the intervention diet) on day 21 of the test period. Diet with modified milk fat (M, □), a diet containing Danish milk fat (D, ◆). FVIIc values are medians and 25–75 percentile ranges; values for plasma TAG are means ± SEM, $n = 18$ (24). For other abbreviations see Figure 1.

may not have been possible in the much larger Finnish study with a parallel design. Also, the nature of the stearic acid test fat may have played a role. We investigated shea butter, which has a high concentration of nonglyceride components. This may have affected FVIIc, whereas the other study included a synthetic fat, margarine with stearic acid. However, the existence of a specific effect of nonglyceride components is not supported by the results of Kelly *et al.* (25), who observed a reduction in FVIIc after giving a synthetic stearic acid test fat. Thus, for the time being, we can conclude only that stearic acid may decrease FVIIc, whereas the nonglyceride components may also play a role.

Another finding in our study was a slight increase in plasma fibrinogen after giving stearic acid compared with myristic–lauric acids, in agreement with the slight but uniform increase in fibrinogen found by others (26,28). We observed a 7% increase in fibrinogen (2.6–2.8 0.2 g/L) after 15E% of stearic acid compared with myristic–lauric acids (23). Mutanen and Aro (26) reported a 4% increase (3.49–3.63 = 0.14 g/L) after giving 9E% of stearic acid compared with a baseline with dairy fat, and Baer *et al.* (28) found a 6% increase (2.71–2.86 = 0.15 g/L) after giving 8E% stearic acid compared with oleic acid, a 4% increase (2.74–2.86 = 0.12 g/L) compared with *trans* FA, and a 6% increase (2.68–2.86 = 0.18 g/L) compared with a test fat containing lauric, myristic, and palmitic acids. In our study, the increase in fibrinogen was not accompanied by an increase in plasma CRP, an acute-phase protein and a marker of inflammation (29), or by a decrease in albumin. Although fibrinogen is an independent risk marker of CHD (30), the mechanism by which stearic acid increases fibrinogen is not understood. In addition, the role of fibrinogen has not been fully elucidated. The increasing effect on fibrinogen after giving stearic acid observed in most studies is small and results from very high amounts of stearic acid. Although this effect may be biologically insignificant, it warrants further investigation.

Effects in the postprandial state. We focused on postprandial effects, because plasma TAG after a meal may represent a procoagulative state by promoting FVII activation and increasing plasma PAI-1.

We observed a lower increase after stearic acid in FVIIc compared with oleic acid (22). In addition, there was a smaller increase in FVIIa with stearic acic than after the intake of *trans* FA (22). Our results are in agreement with findings by Sanders *et al.* (31), who also reported a lower FVIIc after the intake of stearic acid. However, Mennen *et al.* (32) did not find a specific effect of stearic acid when compared with palmitic, linoleic, or linolenic acid. We tested the effects of high amounts of synthesized interesterfied stearic test fats (30–38 g of stearic acid) (22,31), as did Sanders' group, whereas only half the amount of stearic acid (the source of stearic acid was not reported) was served by Mennen *et al.* (32). Thus, factors such as the amounts of fat and m.p. (higher for synthesized interesterfied fats) may have caused the difference in results. We suggest that the capacity to absorb stearic acid may be somewhat impaired or delayed when large amounts are eaten. In addition, stearic acid in synthetic fats (random esterification) may be less completely and more slowly absorbed (33).

Effects of the background diet (study III). Surprisingly, we observed a slightly lower increase in postprandial FVIIc after a load (1.2 g milk fat/kg body weight) with higher stearic and oleic acids and a lower content of palmitic and myristic acids. Because plasma TAG and FVII activation is somewhat linked, and the decrease in FVIIc observed in our study was accompanied by an increased plasma TAG, we suggest that the attenuating effect after giving the modified test fat was an effect of the background diet (which in this case was the intervention diet with the modified milk fat) and not an effect of the FA composition of the meal. Our finding is in line with the suggestion that FVIIc may be affected more by habitual dietary FA than FA of the acute test meal. A background diet high in olive oil has been shown to affect postprandial FVIIc in two different studies (34,35). Thus, a background diet with stearic and oleic acid may attenuate postprandial FVII activation. However, further investigation is required to determine the role of stearic acid *per se*.

SUMMARY

Shea butter high in stearic acid decreased fasting FVIIc compared with fats high in palmitic and myristic–lauric acids. Whether the effect was due to stearic acid *per se* or the nonglyceride components remains to be established. Stearic acid in a synthethic randomized fat attenuates postprandial activation of FVII compared with some other FA, oleic acid, and *trans* FA.

OVERALL CONCLUSIONS

Dietary stearic acid was not more thrombogenic than unsaturated FA, including *trans* FA, in the postprandial state. Fat high in stearic acid was not more thrombogenic than that containing other long-chain SFA. The slight increasing effect on fasting plasma fibrinogen may be biologically insignificant; however, this should be investigated further.

FURTHER RESEARCH

The effect of stearic acid on FVIIc should be investigated further to determine whether the decrease in FVIIc was an effect of stearic acid *per se* or an effect of the nonglyceride components of the test fat. The effect of stearic acid in natural sources compared with synthetic fats on fasting FVIIc should be elucidated further. It would also be relevant to investigate whether stearic acid in the background diet has some beneficial attenuating effects on postprandial FVIIc. Finally, new end points related to the effect of stearic acid on CHD, such as inflammatory markers, atherosclerotic progression, and plaque stability, should be included.

ACKNOWLEDGMENTS

REFERENCES

1. Bonanome, A., and Grundy, S.M. (1988) Effect of Dietary Stearic Acid on Plasma Cholesterol and Lipoprotein Levels, *N. Engl. J. Med. 319*, 1244–1248.
2. Connor, W.E., Hoak, J.C., and Warner, E.D. (1963) Massive Thrombosis Produced by Fatty Acid Infusion, *J. Clin. Invest. 42*, 860–866.
3. Wilson, L.W., Powers, D., and Soloff, L.A. (1965) The Hemodynamic Effects of Infusions of Long Chain Saturated Fatty Acids into Dogs, *Am. J. Med. Sci. 249*, 75–78.
4. Renaud, S., Dumont, E., Godsey, F., Suplisson, A., and Thevenon, C. (1979) Platelet Functions in Relation to Dietary Fats in Farmers from Two Regions of France, *Thromb. Haemost. 40*, 518–531.
5. Bauer, K.A., Kass, B.L., Cate, H., Hawiger, J.J., and Rosenberg, R.D. (1990) Factor IX Is Activated *in vivo* by the Tissue Factor Mechanism, *Blood 76*, 731–736.
6. Meade, T.W., Ruddock, V., Stirling, Y., Chakrabarti, R., and Miller, G.J. (1993) Fibrinolytic Activity, Clotting Factors, and Long-Term Incidence of Ischaemic Heart Disease in the Northwich Park Heart Study, *Lancet 342*, 1076–1079.
7. Folsom, A.R., Wu, K.K., Rosamund, W.D., Sharrett, A., Richey, P.H., and Chambles, L.E. (1997) Prospective Study of Hemostatic Factors and Coronary Heart Disease: The Atherosclerosis Risk in Communities (ARIC) Study, *Circulation 96*, 1102–1108.
8. Junker, R., Heinrich, J., Schulte, H., van de Loo, J., and Assmann, G. (1997) Coagulation Factor VII and the Risk of Coronary Heart Disease in Healthy Men, *Arterioscler. Thromb. Vasc. Biol. 17*, 1539–1544.
9. Tracy, R.P., Arnold, A.M., Ettinger, W., Fried, L., Meilahn, E., and Savage, P. (1999) The Relationship of Fibrinogen and Factors VII and VIII to Incident Cardiovascular Disease and Death in the Elderly: Results from the Cardiovascular Health Study, *Arterioscler. Thromb. Vasc. Biol. 19*, 1776–1783.
10. Cooper, J.A., Miller, G.J., Bauer, K.A., Morrissey, J.H., Meade, T.W., Howarth, D.J., Barzegar, S., Mitchell, J.P., and Rosenberg, R.D. (2000) Comparison of Novel Hemostatic Factors and Conventional Risk Factors for Prediction of Coronary Heart Disease, *Circulation 102*, 2816–2822.
11. Silveira, A., Karpe, F., Blombäck, M., Steiner, G., Walldius, G., and Hamsten, A. (1994) Activation of Coagulation Factor VII During Alimentary Lipemia, *Arterioscler. Thromb. 14*, 60–69.
12. Meade, T.W., Mellows, S., Brozovic, M., Miller, G.J., Chakrabarti, R.R., North, W.R., Haines, A.P., Stirling, Y., Imeson, J.D., and Thompson, S.G. (1986) Haemostatic Function and Ischaemic Heart Disease: Principal Results of the Northwich Park Heart Study, *Lancet 2 (8506)* 533–537.
13. Danesh, J., Collins, R., Appleby, P., and Peto, R. (1998) Association of Fibrinogen, C-Reactive Protein, Albumin, or Leukocyte Count with Coronary Heart Disease: Meta-analyses of Prospective Studies, *JAMA 279*, 1477–1482.
14. Schneider, D.J., Taatjes, D.J., Howard, D.B., and Sobel, B.E. (1999) Increased Reactivity of Platelets Induced by Fibrinogen Independent of Its Binding to the IIb-IIIa Surface Glycoprotein: A Potential Contributor to Cardiovascular Risk, *J. Am. Coll. Cardiol. 33*, 261–266.
15. Fatah, K., Hamsten, A., Blomback, B., and Blomback, M. (1992) Fibrin Gel Network Characteristics and Coronary Heart Disease: Relations to Plasma Fibrinogen Concentration, Acute Phase Protein, Serum Lipoproteins and Coronary Atherosclerosis, *Thromb. Haemost. 68*, 130–135.
16. Folsom, A.R. (1999) Fibrinogen and Cardiovascular Risk Markers, *Blood Coagul. Fibrinolysis 10 (Suppl. 1)*, S13–S16.
17. Kohler, H.P., and Grant, P.J. (2000) Plasminogen-Activator Inhibitor Type I and Coronary Artery Disease, *N. Engl. J. Med. 342*, 1792–1801.
18. Hamsten, A., Walldius, G., Dahlén, G., Johansson, B., and Faire, U.D. (1986) Serum Lipoproteins and Apolipoproteins in Young Male Survivors of Myocardial Infarction, *Atherosclerosis 59*, 223–235.
19. Geppert, A., Beckmann, R., Graf, S., Hornykewyez, S., Lang, I., Schuster, E., Binder, B.R., and Huber, K. (1995) Tissue-Type Plasminogen Activator and Type-1 Plasminogen Activator Inhibitor in Patients with Coronary Heart Disease-Relations to Clinical Variables and Cardiovascular Risk Factors, *Fibrinolysis 9*, 109–113.
20. De Bono, D. (1994) Significance of Raised Plasma Concentrations of Tissue-Plasminogen Activator and Plasminogen Activator Inhibitor in Patients at Risk from Ischemic Heart Disease, *Br. Heart J. 71*, 504–517.
21. Tholstrup, T., Marckmann, P., Jespersen, J., and Sandström, B. (1994) Fat High in Stearic Acid Favorably Affects Blood Lipids and Factor VII Coagulant Activity in Comparison with Fats High in Palmitic Acid or High in Myristic and Lauric Acids, *Am. J. Clin. Nutr. 59*, 371–377.
22. Tholstrup, T., Miller, G.J., Bysted, A., and Sandstrom, B. (2003) Effect of Individual Dietary Fatty Acids on Postprandial Activation of Blood Coagulation Factor VII and Fibrinolysis in Healthy Young Men, *Am. J. Clin. Nutr. 77*, 1125–1132.
23. Bladbjerg, E.M., Tholstrup, T., Marckmann, P., Sandström, B., and Jespersen, J. (1995) Dietary Changes in Fasting Levels of Factor VII Coagulant Activity (FVII:C) Accompanied by Changes in Factor VII Protein and Other Vitamin K-Dependent Proteins, *Thromb. Haemost. 73*, 239–242.
24. Tholstrup, T., Marckmann, P., Hermansen, J.E., Hølmer, G., and Sandström, B. (1999) Effect of Modified Dairy Fat on Fasting

and Postprandial Haemostatic Variables in Healthy Young Men, *Br. J. Nutr. 82*, 105–113.

25. Kelly, F.D., Sinclair, A.J., Mann, N.J., Turner, A.H., Abedin, L., and Li, D. (2001) A Stearic Acid-rich Diet Improves Thrombogenic and Atherogenic Risk Factor Profiles in Healthy Males, *Eur. J. Clin. Nutr. 55*, 88–96.

26. Mutanen, M., and Aro, A. (1997) Coagulation and Fibrinolysis Factors in Healthy Subjects Consuming High Stearic or *trans* Fatty Acid Diets, *Thromb. Haemost. 77*, 99–104.

27. Hunter, K.A., Crosbie, L.C., Horgan, G.W., Miller, G.J., and Dutta-Roy, A.K. (2001) Effect of Diets Rich in Oleic Acid, Stearic Acid and Linoleic Acid on Postprandial Haemostatic Factors in Young Healthy Men, *Br. J. Nutr. 86*, 207–215.

28. Baer, D.J., Judd, J.T., Clevidence, B.A., and Tracy, R.P. (2004) Dietary Fatty Acids Affect Plasma Markers of Inflammation in Healthy Men Fed Controlled Diets: A Randomized Crossover Study, *Am. J. Clin. Nutr. 79*, 969–973.

29. Ridker, P.M., Rifai, N., Rose, L., Buring, J.E., and Cook, N.R. (2002) Comparison of C-Reactive Protein and Low-Density Lipoprotein Cholesterol Levels in the Prediction of First Cardiovascular Events, *N. Engl. J. Med. 347*, 1557–1565.

30. Danesh, J., Whincup, P., Walker, M., Lennon, L., Thomson, A., Appleby, P., Rumley, A., and Lowe, G.D. (2001) Fibrin D-Dimer and Coronary Heart Disease: Prospective Study and Meta-analysis, *Circulation 103*, 2323–2327.

31. Sanders, T.A., de Grassi, T., Miller, G.J., and Morrissey, J.H. (2000) Influence of Fatty Acid Chain Length and *cis/trans* Isomerization on Postprandial Lipemia and Factor VII in Healthy Subjects (postprandial lipids and factor VII), *Atherosclerosis 149*, 413–420.

32. Mennen, L., de Maat, M., Meijer, G., Zock, P., Grobbee, D., Kok, F., Kluft, C., and Schouten, E. (1998) Factor VIIa Response to a Fat-rich Meal Does Not Depend on Fatty Acid Composition: A Randomized Controlled Trial, *Arterioscler. Thromb. Vasc. Biol. 18*, 599–603.

33. Sanders, T.A., Oakley, F.R., Cooper, J.A., and Miller, G.J. (2001) Influence of a Stearic Acid-rich Structured Triacylglycerol on Postprandial Lipemia, Factor VII Concentrations, and Fibrinolytic Activity in Healthy Subjects, *Am. J. Clin. Nutr. 73*, 715–721.

34. Roche, H.M., Zampelas, A., Knapper, J.M.E., Webb, D., Brooks, C., Jackson, K.G., Wright, J.W., Gould, B.J., Kafatos, A., Gibney, M.J., *et al.* (1998) Effect of Long-Term Olive Oil Dietary Intervention on Postprandial Triacylglycerol and Factor VII Metabolism, *Am. J. Clin. Nutr. 68*, 552–560.

35. Larsen, L.F., Bladbjerg, E.M., Jespersen, J., and Marckmann, P. (1997) Effects of Dietary Fat Quality and Quantity on Postprandial Activation of Blood Coagulation Factor VII, *Arterioscler. Thromb. Vasc. Biol. 17*, 2904–2909.

ARTICLES

Mitochondrial Cholesterol Transport: A Possible Target in the Management of Hyperlipidemia

E.A. Hall[a], S. Ren[a,d], P.B. Hylemon[b], K. Redford[d],
A. del Castillo[c], G. Gil[c], and W.M. Pandak[a,d,*]

Departments of [a]Internal Medicine, [b]Microbiology and Immunology, and [c]Biochemistry, Virginia Commonwealth University,
and [d]Department of Internal Medicine, McGuire Veterans Affairs Medical Center, Richmond, Virginia 23249

ABSTRACT: Sterol 27-hydroxylase (CYP27A1) may defend cells against accumulation of excess cholesterol, making this enzyme a possible target in the management of hyperlipidemia. The study objective was to analyze cholesterol homeostatic responses to increases in CYP27A1 activity in HepG2 cells and primary human hepatocytes. Increasing CYP27A1 activity by increasing enzyme expression led to significant increases in bile acid synthesis with compensatory increases in HMG-CoA reductase (HMGR) activity/protein, LDL receptor (LDLR) mRNA, and LDLR-mediated cholesterol uptake. Under these conditions, only a small increase in cellular 27-hydroxycholesterol (27OH-Chol) concentration was observed. No changes were detected in mature sterol regulatory element-binding proteins (SREBP) 1 or 2. Increasing CYP27A1 activity by increasing mitochondrial cholesterol transport (i.e., substrate availability) led to greater increases in bile acid synthesis with significant increases in cellular 27OH-Chol concentration. Mature SREBP 2 protein decreased significantly with compensatory decreases in HMGR protein. No change was detected in mature SREBP 1 protein. Despite increasing 27OH-Chol and lowering SREBP 2 protein concentrations, LDLR mRNA increased significantly, suggesting alternative mechanisms of LDLR transcriptional regulation. These findings suggest that regulation of liver mitochondrial cholesterol transport represents a potential therapeutic strategy in the treatment of hyperlipidemia and atherosclerosis.

Paper no. L9848 in *Lipids 40*, 1237–1244 (December 2005).

With its ability to metabolize cholesterol (Chol) to the regulatory oxysterol 27-hydroxycholesterol (27OH-Chol) and its wide distribution in many different organs and tissues, mitochondrial sterol 27-hydroxylase (CYP27A1) has long been thought to play a major role in the regulation of cholesterol homeostasis, and more specifically, in the general defense of cells against cholesterol accumulation. In hepatocytes the 27-hydroxylation of cholesterol/sterol intermediates by mitochondrial CYP27A1 represents an important step in both the "acidic" and the "neutral" pathways of bile acid biosynthesis. CYP27A1-mediated 27-hydroxylation of cholesterol is the initial step in the "acidic" pathway, whereas in the "neutral" or "classic" pathway, CYP27A1-mediated 27-hydroxylation of sterol intermediates occurs as a later step following 7α-hydroxylation (1).

Our laboratory has shown that transport of cholesterol to the inner mitochondrial membrane represents an important regulatory step in the degradation of cholesterol to 27OH-Chol by CYP27A1. Moreover, CYP27A1 activity and, subsequently, intracellular 27OH-Chol levels and bile acid synthesis *via* the acidic pathway can be increased through overexpression of the mitochondrial cholesterol transporter, StAR (steroidogenic acute regulatory protein), both in human, rat, and mouse hepatocytes *in vitro* (2) and in the rat and mouse *in vivo* (3). A regulable StAR-like mitochondrial cholesterol transporter has now been identified in these same hepatic cell lines as well as in whole liver tissue (4).

In a number of cell types, the addition of micromolar concentrations of exogenous oxysterols (i.e., 25-hydroxycholesterol, 27-hydroxycholesterol, etc.) has been shown to reduce the levels of HMG-CoA reductase (HMGR; i.e., rate-determining step of cholesterol biosynthesis) mRNA, protein, and specific activity, as well as LDL-receptor (LDLR) mRNA levels and LDLR-mediated cholesterol uptake (5,6). More specifically, sterols have been shown not only to lower the transcriptional activity of HMGR, but also to independently increase the rate of protein degradation (7,8). Based on these observations, it was hypothesized that circulating 27OH-Chol is a potent feedback regulator of cholesterol homeostasis (9,10). In support of this hypothesis, subsequent studies have shown that increasing 7α-hydroxylation of 27OH-Chol by CYP7B1 (oxysterol 7α hydroxylase) eliminated the ability of 27OH-Chol to down-regulate cholesterol biosynthesis (11). However, these additional findings also led to the contrasting hypothesis that 27OH-Chol may in fact have little or no impact on cholesterol biosynthesis in cells (i.e., hepatocytes) where it can be rapidly converted to the cholest-5-ene,3β,7α,27-triol (by microsomal CYP7B1) and subsequently to bile acids.

The current study was conducted to determine whether an increase in hepatic CYP27A1 activity that resulted in increased cholesterol metabolism and higher hepatic 27OH-Chol levels could alter cellular cholesterol homeostasis in a manner that would have therapeutic implications in the management of atherosclerosis and hyperlipidemia. CYP27A1 specific activity

was increased in HepG2 cells in one of two ways: by adeno-viral-mediated overexpression of CYP27A1 or by adenoviral-mediated overexpression of the mitochondrial cholesterol transporter, StAR. Increasing CYP27A1 expression increased the 27-hydroxylation of cholesterol and the production of bile acids with little change in cellular 27OH-Chol levels. However, these changes still elicited significant changes in hepatic cholesterol homeostasis (increasing HMGR protein/activity; increasing LDLR mRNA and uptake of cholesterol). By increasing the transport of cholesterol to the inner mitochondrial CYP27A1, cells were able to increase cellular 27OH-Chol levels while at the same time increasing bile acid synthesis even further. Under these conditions, the changes observed in cholesterol metabolism, synthesis, and uptake suggested that hepatic mitochondrial cholesterol transport could be a target in management of hypercholesterolemia (increasing cholesterol metabolism, decreasing HMGR protein, and increasing LDLR mRNA levels).

EXPERIMENTAL PROCEDURES

Materials. HepG2 cells were obtained from the American Type Culture Collection (ATCC; Rockville, MD). Primary human hepatocytes were obtained from a National Institutes of Health-approved facility (Liver Tissue Procurement Distribution System, University of Minnesota, Minneapolis, MN). All cell culture materials were obtained from Gibco BRL (Grand Island, NY) unless otherwise specified. The cesium chloride (CsCl), agarose, and RNA ladder used to size mRNA were also purchased from Gibco BRL. FBS was obtained from BioWhittaker (Walkersville, MD). Tissue culture flasks were purchased from Costar Corp. (Cambridge, MA). Chemicals used in this research were obtained from Sigma Chemical Co. (St. Louis, MO) or Bio-Rad Laboratories (Hercules, CA) unless otherwise specified. All solvents were obtained from Fisher (Fair Lawn, NJ) unless otherwise indicated. All radionucleotides as well as the Aquasol solution were purchased from DuPont NEN (Boston, MA). Enhanced chemiluminescence (ECL) reagents were purchased from Amersham Biosciences (Piscataway, NJ). Waters Silica Sep-Paks were obtained from Waters Corporation (Milford, MA). β-Cyclodextrin was purchased from Cyclodextrin Technologies Development Inc. (Gainesville, FL). Testosterone and 27OH-Chol were obtained from Research Plus Inc. (Bayonne, NJ). LK6 20×20 cm TLC plates were purchased from Whatman Inc. (Clifton, NJ). Mevalonate was obtained from Aldrich Chemical Co. (Milwaukee, WI). Nylon membranes were purchased from Micron Separation Inc. (Westborough, MA). Ammonium persulfate was obtained from Amresco (Solon, OH). Nonfat dry milk was purchased from Carnation (Glendale, CA). DiI (1,1′-dioctadecyl-3,3,3′,3′-tetramethyl-indocarbocyanine perchlorate), labeled LDL/HDL, and unlabeled LDL/HDL were obtained from Intracel Corporation (Rockville, MD). Mevinolin was obtained from Merck Research Laboratories (Rahway, NJ). The HMGR mouse monoclonal antibody was prepared in our laboratory with A9 Mouse Hybridoma cells obtained from the ATCC. The mouse monoclonal IgG sterol regulatory element binding protein (SREBP) 2 was prepared in our laboratory with IgG-1D2 Mouse Hybridoma cells obtained from ATCC. The mouse monoclonal IgG SREBP 1 was purchased from BD PharMingen (San Jose, CA). The secondary antibody [goat anti-mouse or rabbit IgG-horseradish peroxidase (HRP) conjugate] was also purchased from Bio-Rad Laboratories. The human StAR cDNA probe and polyclonal antibody were generous gifts from Dr. J.F. Strauss (University of Pennsylvania, Philadelphia, PA) (12).

Generation, propagation, and purification of recombinant adenovirus encoding rat CYP27A1 and control virus CMV[+1]. Recombinant replication-defective adenoviruses Ad-CMV[+1] (control virus), Ad-CMV-CYP27A1, and Ad-CMV-StAR were generated as described previously (13).

Cell culture and adenovirus infection. HepG2 cells were grown in MEM containing nonessential amino acids, 0.03 M $NaHCO_3$, 10% FBS, 1 mM L-glutamine, 1 mM sodium pyruvate, and 1% penicillin/streptomycin; and incubated at 37°C in 5% CO_2. Where indicated, 10% LPDS (lipoprotein-deficient serum) was substituted for 10% FBS. Primary human hepatocytes were isolated and plated as described previously (14,15) in the presence of 0.1 M dexamethasone. Cells were grown in 162 cm^2 (25 mL) tissue culture flasks until they were 80–90% confluent. They were then infected for 48 h [HepG2 cells—multiplicity of infection (MOI) of 1; primary human hepatocytes—MOI of 10) with Ad-CMV-CYP27A1, Ad-CMV-StAR, or Ad-CMV[+1] as described previously (13). A virus-free control was maintained for each experiment. Cells (control, control virus, CYP27A1, and StAR infected) were harvested for the isolation of mitochondria, microsomes, cytosol, nuclear extract, and RNA.

Primary human hepatocytes. Primary human hepatocytes were purchased from an NIH-approved facility (Liver Tissue Procurement Distribution System, University of Minnesota). Cells were obtained from a random sampling of males and females 18–69 yr of age. Experiments were performed as cells became available to corroborate findings in experiments conducted in HepG2 cells.

Cell fractionation. Mitochondria and microsomes were isolated from cell culture as described previously (16,17). Nuclear extract was isolated from cell culture as described by Wang *et al.* (18).

Enzymatic activity. CYP27A1 specific activity was assayed by the method of Petrak and Latario (19), with modifications as previously described (13). CYP27A1 activities were expressed as percentage of control values. Microsomal HMGR specific activity was assayed by the method of Shefer *et al.* (20) and expressed as percentage of control values.

Quantification of CYP27A1, LDLR, and HMGR mRNA levels. Methods for the isolation of RNA and the determination of mRNA levels by Northern blotting have been described previously (21). The CYP27A1 cDNA probe used has been described previously (22). The HMGR cDNA probe used in these experiments was the same as the probe used by Day *et al.* (23). The LDL cDNA probe (pLDLR3) was obtained from ATCC (Manassas, VA).

Bile acid and 27OH-Chol synthesis. Labeled bile acids and 27OH-Chol were extracted from both media and cells using the method of Folch *et al.* (24). Bile acid biosynthesis was measured as the conversion of [^{14}C]cholesterol to [^{14}C]-labeled bile acids (25). [^{14}C]27OH-Chol was isolated from the cell extract or media CHCl$_3$ phase on TLC (hexane/isopropanol/glacial acetic acid; 95:3:2 by vol). [^{14}C]27OH-Chol (R_f = 0.19) and [^{14}C]cholesterol (R_f = 0.36) bands were scraped from the TLC plates, and radioactive counts were obtained using a Beckman Liquid Scintillation Counter. The concentration of 27OH-Chol was calculated as a percentage of the cholesterol substrate to correct for possible loading errors. Both bile acid biosynthesis rates and 27OH-Chol concentrations for infected samples were expressed as a percentage of control values.

Western blot analysis of protein. Mitochondrial, microsomal, and nuclear extract proteins (30 µg) were separated on a 10% SDS-polyacrylamide denaturing gel according to the method of Laemmli (26). Following electrophoresis, proteins were electrophoretically transferred overnight to Immobilon-P membranes using a Bio-Rad Mini Trans Blot Electrophoretic Transfer cell. The membranes were then blocked for 90 min (25°C) in blocking buffer (PBS, pH 7.4, 0.1% Tween, 5% nonfat dry milk). Mitochondrial proteins were then incubated for 90 min (25°C) or overnight (4°C) with a rabbit StAR polyclonal IgG (1:12,000). Microsomal proteins were incubated overnight (4°C) with a mouse HMGR monoclonal IgG (1:100). Nuclear extract proteins were incubated for 90 min (25°C) with a mouse SREBP 2 monoclonal IgG (1:100) or a mouse SREBP 1 monoclonal IgG (1:1000). After washing, a secondary antibody (goat antirabbit IgG-HRP conjugate, 1:3000 for StAR, goat antimouse IgG-HRP conjugate, 1:3000 for HMG-CoA reductase and 1:10,000 for SREBP) was added to the blocking solution (25°C, 1 1/2 h). After washing, the protein bands were detected using the Amersham ECL plus Kit.

Spectrofluorescence analysis of DiI-lipoprotein uptake. Uptake of DiI-LDL into HepG2 cells was determined by the method of Teupser *et al.* (27) with the following modifications. Cells were maintained throughout the experiment in media optimal for cell viability (see *Cell cultures and adenovirus infection* section). All incubations were performed in duplicate, and fluorescence was measured in a Spectrafluor Plus (Tecan US, Inc., Research Triangle Park, NC).

Statistics. Results are reported as mean ± SE, where possible. Statistical significance was determined where appropriate by Student's *t*-test.

RESULTS

Data from our laboratory have shown that CYP27A1 mRNA, protein levels, and specific activity increase significantly ($P \le$ 0.02) in HepG2 cells 48 h following infection with the recombinant replication deficient adenovirus encoding the CMV-driven full-length CYP27A1 gene (Ad-CMV-CYP27A1) (data not shown; see Ref. 13). No changes were observed in CYP27A1 mRNA, protein levels, or specific activity in cells infected with a control virus (Ad-CMV[+1]).

The data in Table 1 show the effects of increasing CYP27A1 specific activity on the rates of bile acid synthesis in HepG2 cells and in primary human hepatocytes. In HepG2 cells, bile acid synthesis was increased 50% above control values in cells infected with Ad-CMV-CYP27A1 (i.e., overexpressing CYP27A1) and 169% above control values in cells infected with the Ad-CMV-StAR (i.e., overexpressing StAR increased substrate availability) ($P \le 0.02$). In primary human hepatocytes, bile acid synthesis was increased 73% above control values following overexpression of CYP27A1 and 514% above control values following overexpression of StAR ($P \le 0.02$) (Table 1). No change in the rates of bile acid synthesis was observed in cells infected with the control virus (Ad-CMV[+1]).

The cellular 27OH-Chol levels in control HepG2 cells were 0.60 ng/10^6 cells (137 nM). Following CYP27A1 gene overexpression, little increase was seen the in cellular 27OH-Chol (116% increase; $P \le 0.02$; Table 2). However, HepG2 cells in

TABLE 1
Bile Acid Synthesis Rates Following Infection with Ad-CMV-CYP27A1 or Ad-CMV-StAR[a]

Adenovirus	HepG2	1° Human
Ad-CMV-CYP27A1	150[b] ± 4%	177[b] ± 33%
Ad-CMV-StAR	269[b] ± 7%	614[b] ± 180%

[a]Data are expressed as percentage of controls (no virus; mean ± SE) ($n = 6$). No significant differences in bile acid synthesis rates were observed between hepatocytes receiving no virus and hepatocytes infected with the control virus (Ad-CMV[+1]; data not shown). Ad, adenovirus; CMV, cytomegalovirus; CYP27A1, sterol 27-hydroxylase; StAR, steroidogenic acute regulatory protein.
[b]$P \le 0.02$.

TABLE 2
StAR Protein, Cellular 27OH-Chol Concentration, HMGR mRNA/Protein, and LDRL mRNA Following Infection with Ad-CMV-CYP27A1 and Ad-CMV-StAR[a–c]

StAR protein	Cellular [27OH-Chol]	HMGR mRNA	HMGR protein	LDLR mRNA	
239[b] ± 6%	116[b] ± 4%	101[c] ± 3%	145[b] ± 7%	173[b] ± 10%	Ad-CMV-CYP27A1
897[b] ± 159%	197[b] ± 19%	81[b] ± 2%	66[b] ± 6%	282[b] ± 62%	Ad-CMV-StAR

[a]Data are expressed as percentage of controls (no virus; mean ± SE) ($n = 6$). No significant differences were observed between hepatocytes that received no virus and hepatocytes infected with control virus (Ad-CMV[+1]; data not shown). 27OH-Chol, 27-hydroxycholesterol; HMGR, HMG-CoA reductase; LDLR, LDL-receptor; for other abbreviations see Table 1.
[b]$P \le 0.02$.
[c]$P \le 0.800$.
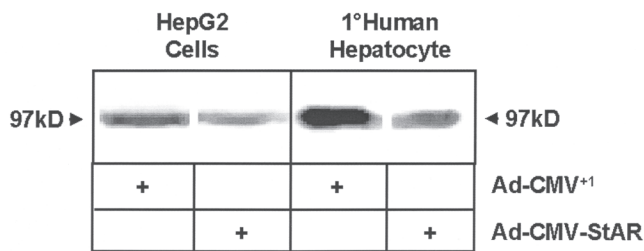
FIG. 1. HMGR protein levels in HepG2 cells and primary (1°) human hepatocytes following infection with Ad-CMV-StAR. Representative Western blot showing HMG-CoA reductase protein levels in HepG2 cells and 1° human hepatocytes following infection for 48 h with Ad-CMV[+1] or Ad-CMV-StAR. HMGR, HMG-CoA reductase; Ad, adenovirus; CMV, cytomegalovirus; StAR, steroidogenic acute regulatory protein; kD, kilodalton.

which the mitochondrial cholesterol transporter StAR had been overexpressed showed a 97% increase in cellular 27OH-Chol levels ($P \leq 0.02$; Table 2). No changes in 27OH-Chol levels were observed in cells infected with the control virus (Ad-CMV[+1]).

HMGR protein levels increased significantly in HepG2 cells following overexpression of CYP27A1 (45% increase; $P \leq 0.006$; Table 2). As previously observed, trends in HMGR specific activity correlated directly with trends in protein levels (183% increase; $P \leq 0.02$; data not shown). In cells infected with Ad-CMV-StAR, HMGR protein levels were significantly decreased (34% decrease; $P \leq 0.001$; Table 2, Fig. 1). Select studies performed in primary human hepatocytes also showed a significant decrease in HMGR protein levels following overexpression of StAR (Fig. 1). No change in HMGR protein or specific activity was observed in cells infected with the control virus (Ad-CMV[+1]).

LDLR mRNA levels were found to be increased (between 1.7- and 2.8-fold) in HepG2 cells following infection with both Ad-CMV-CYP27A1 and Ad-CMV-StAR ($P \leq 0.001$; Table 2). No increase in LDLR mRNA was observed in cells infected with the control virus, Ad-CMV[+1]. The increase in LDLR mRNA levels was correlated with an 18–24% increase in LDLR cholesterol uptake ($P \leq 0.001$; data not shown). Significant ($P \leq 0.01$) increases in HDL cholesterol uptake were also observed (10%; data not shown).

Although LDLR mRNA increased significantly ($P \leq 0.001$), HMGR mRNA ($P \leq 0.8$) levels remained unaffected with increasing CYP27A1 expression (Table 2). Furthermore, increasing expression of CYP27A1 did not affect mature SREBP 1 or 2 protein levels (Fig. 2A, B). Overexpression of StAR protein, however, repressed HMGR mRNA and protein levels (Table 2), changes that were correlated with the intracellular increase in 27OH-Chol levels and the decrease in mature SREBP 2 protein levels (Fig. 2B).

To confirm that the HepG2 cell cultures were standardized and responding as previously observed, we altered culture conditions to those known to change mature SREBP 2 protein levels. As previously observed, severely depleting cellular choles-
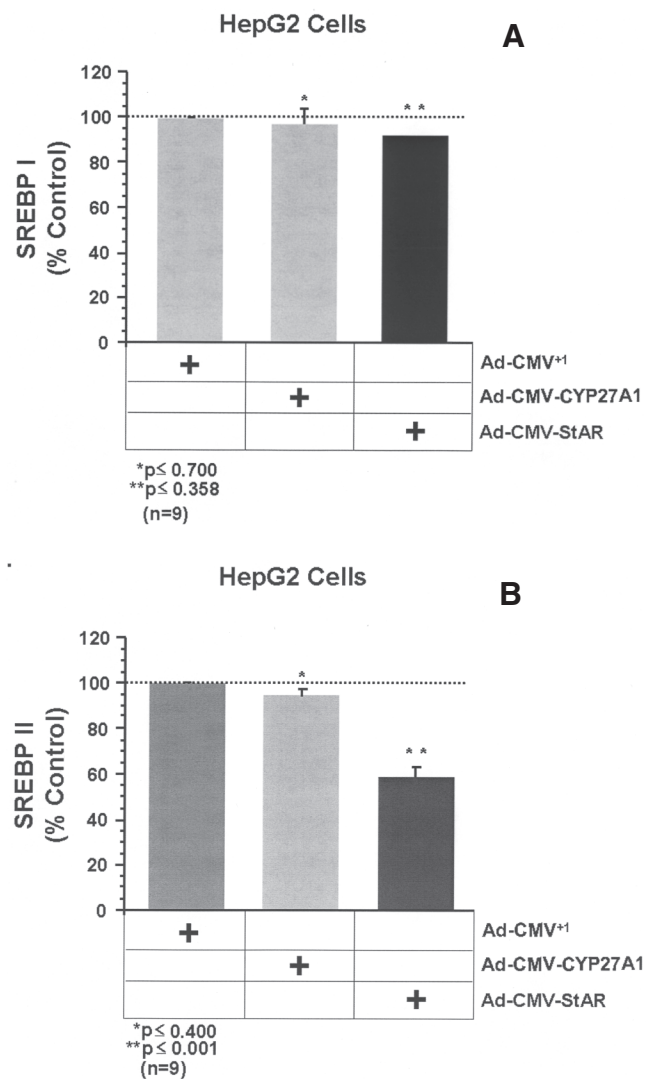
FIG. 2. Western analysis: mature sterol regulatory element-binding protein (SREBP) 1 (A) and SREBP 2 (B) protein in HepG2 cells following infection with Ad-CMV-CYP27A1 or Ad-CMV-StAR. Data are expressed as percentage of controls (no virus; mean ± SE). No differences were observed between hepatocytes receiving no virus and those infected with control virus (Ad-CMV[+1]). CYP27A1, sterol 27-hydroxylase; for other abbreviations see Figure 1.

terol levels *via* the addition of LPDS and/or mevinolin (HMGR inhibitor) significantly increased mature SREBP 2 protein levels in HepG2 cells (Fig. 3A). Addition of micromolar concentrations of 27OH-Chol to cells maintained in LPDS resulted in significant decreases in mature SREBP 2 protein levels (Fig. 3A). When 27OH-Chol + cholesterol (1:10 ratio) were added to the cells, results similar to those stated above were observed (data not shown). Selective studies showed that the above changes in mature SREBP 2 protein levels were associated with changes in HMGR protein (Fig. 3B) and LDLR mRNA (Fig. 3C) levels. These findings are consistent with previously described responsiveness to cholesterol depletion and oxysterol addition (5,6).
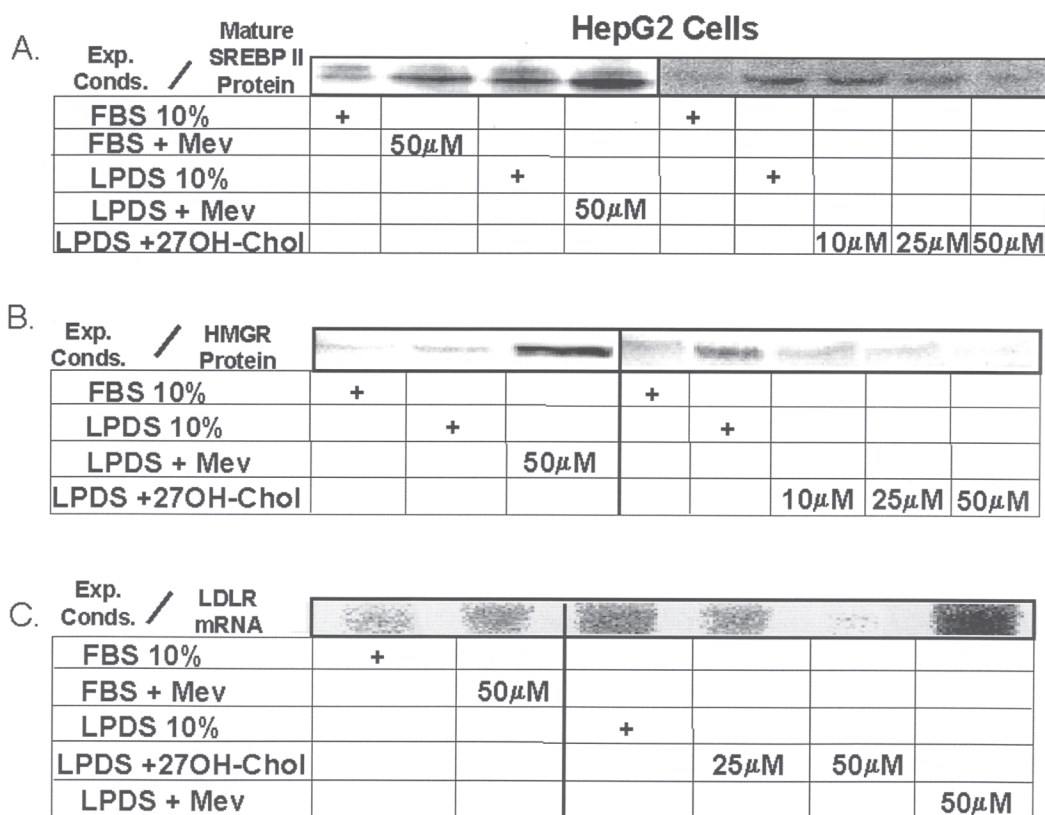
FIG. 3. Western analysis: Mature SREBP 2 protein, HMGR protein, and LDLR mRNA levels in HepG2 cells following changes in culture media. Media conditions (see Methods): 10% FBS; mevinolin (Mev); 10% lipoprotein deficient serum (LPDS); Mev + LPDS-containing media; and 27-hydroxycholesterol (27OH-Chol) + LPDS-containing media. For other abbreviations see Figures 1 and 2.

DISCUSSION

The metabolism of cholesterol to 27OH-Chol by CYP27A1 is believed to play several roles in the maintenance of cholesterol homeostasis. The oxidation of cholesterol not only decreases cholesterol content but also drastically reduces the half-life of the molecule, directing it toward more water-soluble and excretable metabolites, i.e., oxysterols and bile acids. Furthermore, oxysterols are known activators/repressors of gene transcription (5,6,9). In addition to their ability to aid in the solubilization of lipids in the intestine and gall bladder, bile acids function as regulatory molecules, regulating the expression of hundreds of genes through at least two well-described means: activation of specific nuclear receptors (28–30) and of cell signaling pathways (31–35).

In theory, increasing CYP27A1-mediated cholesterol metabolism could lead to lower serum cholesterol levels *in vivo*. This hypothesis is supported by baboon and mouse models in which the females of the species have been shown to have lower serum cholesterol in direct association with higher CYP27A1 activity than their male counterparts. Preliminary observations from our laboratory have shown that female mice exhibiting lower serum cholesterol have not only higher CYP27A1 activity but also increased levels of the mitochondr-

ial cholesterol transport protein, StAR (Pandak, W.M., and Ren, S., unpublished data); these findings are supportive of the hypothesis that an up-regulated acidic pathway initiated by mitochondrial cholesterol delivery could play an important role in cholesterol homeostasis.

Recent *in vivo* observations in knockout and transgenic mouse models have not been entirely supportive of 27OH-Chol as a regulatory oxysterol (36,37). Lack of a cerebrotendinous xanthomatosis (CTX)-like phenotype in CYP27A1 knockout mice has been used to support the belief that CYP27A1 is not an important regulator of cholesterol homeostasis. However, Honda *et al.* (38,39) have since shown that 25-hydroxylated bile alcohols are more efficiently metabolized in Cyp27$^{-/-}$ mice than in CTX patients, at least in part accounting for their lack of a human-like phenotype. Interestingly, lower rates of bile acid synthesis, higher rates of cholesterol synthesis, and increased mortality due to feeding an atherogenic diet have been observed in a Cyp27$^{-/-}$ strain (37). Additional studies in the same strain showed a 40–45% increase in adrenal and liver size, a 2.5-fold increase in whole body cholesterol synthesis, decreased rates of bile acid synthesis, and a decrease in the bile acid pool size (40). Therefore, although the classic human CTX-like phenotype was not apparent in Cyp27$^{-/-}$ mice, these observations demonstrated a phenotype supportive of a role for

the acidic pathway in the regulation of lipid homeostasis. In a transgenic mouse model, CYP27A1 overexpression led to a five– to ninefold increase in serum 27OH-Chol levels without significant detectable changes in total serum cholesterol or rates of cholesterol synthesis (36). Under these conditions, total body cholesterol homeostasis appeared to be unchanged. However, as mentioned by the authors, changes in key regulatory parameters in individual tissues were not determined. The lack of predicted changes in cholesterol metabolism in this model has yet to be adequately explained.

The design of this study differs from previous models attempting to explore the regulatory role of CYP27A1. In contrast to previous *in vitro* trials in which 27OH-Chol levels were increased by *exogenous* addition, this study was designed to determine the transitory effects of increasing the delivery of cholesterol to the mitochondria, and the effects of its subsequent metabolism. This model, in which intracellular cholesterol is depleted through increased mitochondrial metabolism, provided a unique opportunity to study the interplay between cholesterol and acidic pathway metabolites in the regulation of cholesterol homeostasis.

In the current study, compensatory changes in cellular cholesterol homeostasis occur in HepG2 cells following an increase in CYP27A1 activity as mediated *via* increased enzyme expression and increased mitochondrial cholesterol transport. More specifically, up-regulation of endogenous cholesterol metabolism led to significant changes in LDLR mRNA levels and uptake of LDL cholesterol. Whereas increased endogenous cholesterol metabolism following increased CYP27A1 expression was also correlated with up-regulation of HMGR protein and activity levels, the overriding inhibitory changes observed in HMGR that occurred following StAR overexpression (i.e., increasing mitochondrial cholesterol transport) seemed to correlate with the cell's ability to increase intracellular 27OH-Chol levels (Table 1).

Overexpression of both StAR and CYP27A1 increased cholesterol metabolism as evidenced by a significant increase in the rates of bile acid biosynthesis (Table 1). As expected, this decrease in intracellular cholesterol concentration led to increased LDLR gene transcription, as well as compensatory increases in LDL cholesterol uptake. As shown previously and again in this study (Fig. 3A–C), the addition of relatively high (μM) concentrations of exogenous 27OH-Chol to HepG2 cells led to a marked decrease in both the mature form of SREBP 2 and in LDLR mRNA. Interestingly, in the present study, with nanomolar increases in endogenously generated 27OH-Chol and decreases in mature SREBP 2 protein following StAR overexpression, LDLR mRNA and LDL uptake increased in HepG2 cells (Fig. 3). These changes support the presence of additional cholesterol-responsive controls capable of regulating sterol-mediated LDLR gene transcription. These findings and this hypothesis are not entirely original, as Makar *et al.* (41) also found a potentially novel mechanism of regulating LDLR gene transcription that appeared as sterol regulatory element-1 (SRE-1)-*dependent* and SREBP-*independent* in the Jurkat T cell line. The findings of this study are also consistent

with those of Winegar *et al.* (42). Given these observations, it is plausible to hypothesize that low levels of *endogenously* generated 27OH-Chol may elicit differing effects on cholesterol homeostatic mechanisms from that of higher concentrations of the same hydroxylated sterol or its metabolites. It is equally plausible to suggest that under conditions where more physiologic levels of 27OH-Chol are present, in contrast to its effects on HMGR, 27OH-Chol has little direct inhibitory effect on the transcriptional/translational control of the LDLR.

SREBP 1 and 2 are regulators of multiple enzymes responsible for the coordinated regulation of the biosynthesis of cholesterol and FA. Changes in SREBP 2 regulation have been found to closely follow changes in the mRNA levels of genes encoding enzymes of cholesterol synthesis, whereas the regulation of SREBP 1 seems to parallel more closely that of mRNA levels for genes encoding enzymes for FA synthesis (43). Not unexpectedly, given the interdependence of the cholesterol and fatty synthesis pathways, a similar responsiveness in SREBP 1 and SREBP 2 levels frequently has been observed under many experimental conditions. A coordinated responsiveness in SREBP 1 and 2, however, was not observed in this study. Of note is that HepG2 cells, like many cultured cells, contain predominantly the more constitutive SREBP 1a isoform and not the more responsive SREBP 1c (43). Furthermore, although a weak activator of cholesterol synthesis, SREBP 1c is primarily responsive for and activates genes required for FA synthesis. Therefore, in contrast to SREBP 2, a sterol-responsive, relatively selective activator of genes of cholesterol synthesis, it would not be surprising for SREBP 1 protein levels (i.e., predominance of SREBP 1a), as determined in this study, to not be found significantly altered with the increase in 27OH-Chol levels observed following StAR overexpression. Therefore, the differences observed in the SREBP responsive HMGR following CYP27A1 vs. StAR overexpression appear to reflect an SREBP 2 response to the greater increase in 27OH-Chol levels seen following StAR overexpression. In summary, these findings suggest the existence of additional sterol responsive controls in the regulation of LDLR and in the maintenance of cholesterol homeostasis. Furthermore, this study suggests that mitochondrial cholesterol transport plays a significant role in the regulation of cholesterol homeostasis and could represent a target in the management of atherosclerosis and hyperlipidemia.

ACKNOWLEDGMENTS

REFERENCES

1. Pikuleva, I.A., Babiker, A., Waterman, M.R., and Bjorkhem, I. (1998) Activities of Recombinant Human Cytochrome P450c27 (CYP27) Which Produce Intermediates of Alternative Bile Acid Biosynthetic Pathways, *J. Biol. Chem. 273*, 18153–18160.
2. Pandak, W.M., Ren, S., Marqeus, D., Hall, E., Redford, K.,

Mallonee, D., Bohdan, P., Heuman, D., Gil, G., and Hylemon, P.B. (2002) Transport of Cholesterol into Mitochondria Is Rate-Limiting for Bile Acid Synthesis *via* the Alternative Pathway in Primary Rat Hepatocytes, *J. Biol. Chem. 277*, 48158–48164.

3. Ren, S., Hylemon, P.B., Marques, D., Gurley, E., Bodhan, P., Hall, E., Redford, K., Gil, G., and Pandak, W.M. (2004) Overexpression of Cholesterol Transporter StAR Increases *in vivo* Rates of Bile Acid Synthesis in the Rat and Mouse, *Hepatology 40*, 910–917.

4. Hall, E.A., Ren, S., Hylemon, P.B., Rodriguez-Agudo, D., Redford, K., Marques, D., Kang, D., Gil, G., and Pandak, W.M. (2005) Detection of the Steroidogenic Acute Regulatory Protein, StAR, in Human Liver Cells, *Biochim. Biophys. Acta 1733*, 111–119.

5. Ellsworth, J.L., Carlstrom, A.J., and Deikman, J. (1994) Ketoconazole and 25-Hydroxycholesterol Produce Reciprocal Changes in the Rate of Transcription of the Human LDL Receptor Gene, *Biochim. Biophys. Acta 1210*, 321–328.

6. Schroepfer, G.J., Jr. (2000) Oxysterols: Modulators of Cholesterol Metabolism and Other Processes, *Physiol. Rev. 80*, 361–554.

7. Moriyama, T., Wada, M., Urade, R., Kito, M., Katunuma, N., Ogawa, T., and Simoni, R.D. (2001) 3-Hydroxy-3-methylglutaryl Coenzyme A Reductase Is Sterol-Dependently Cleaved by Cathepsin L-Type Cysteine Protease in the Isolated Endoplasmic Reticulum, *Arch. Biochem. Biophys. 386*, 205–212.

8. Tam, S.P., Brissette, L., Ramharack, R., and Deeley, R.G. (1991) Differences Between the Regulation of 3-Hydroxy-3-methylglutaryl-Coenzyme A Reductase and Low Density Lipoprotein Receptor in Human Hepatoma Cells and Fibroblasts Reside Primarily at the Translational and Post-translational Levels, *J. Biol. Chem. 266*, 16764–16773.

9. Axelson, M., Larsson, O., Zhang, J., Shoda, J., and Sjovall, J. (1995) Structural Specificity in the Suppression of HMG-CoA Reductase in Human Fibroblasts by Intermediates in Bile Acid Biosynthesis, *J. Lipid Res. 36*, 290–298.

10. Bjorkhem, I., Andersson, O., Diczfalusy, U., Sevastik, B., Xiu, R.J., Duan, C., and Lund, E. (1994) Atherosclerosis and Sterol 27-Hydroxylase: Evidence for a Role of This Enzyme in Elimination of Cholesterol from Human Macrophages, *Proc. Natl. Acad. Sci. USA 91*, 8592–8596.

11. Martin, K.O., Reiss, A.B., Lathe, R., and Javitt, N.B. (1997) 7 α-Hydroxylation of 27-Hydroxycholesterol: Biologic Role in the Regulation of Cholesterol Synthesis, *J. Lipid Res. 38*, 1053–1058.

12. Christenson, L.K., and Strauss, J.F., III (2000) Steroidogenic Acute Regulatory Protein (StAR) and the Intramitochondrial Translocation of Cholesterol, *Biochim. Biophys. Acta 1529*, 175–187.

13. Hall, E., Hylemon, P., Vlahcevic, Z., Mallonee, D., Valerie, K., Avadhani, N., and Pandak, W. (2001) Overexpression of CYP27 in Hepatic and Extrahepatic Cells: Role in the Regulation of Cholesterol Homeostasis, *Am. J. Physiol. Gastrointest. Liver Physiol. 281*, G293–G301.

14. Arakane, F., Kallen, C.B., Watari, H., Foster, J.A., Sepuri, N.B., Pain, D., Stayrook, S.E., Lewis, M., Gerton, G.L., and Strauss, J.F., III (1998) The Mechanism of Action of Steroidogenic Acute Regulatory Protein (StAR). StAR Acts on the Outside of Mitochondria to Stimulate Steroidogenesis, *J. Biol. Chem. 273*, 16339–16345.

15. Pandak, W.M., Schwarz, C., Hylemon, P.B., Mallonee, D., Valerie, K., Heuman, D.M., Fisher, R.A., Redford, K., and Vlahcevic, Z.R. (2001) Effects of CYP7A1 Overexpression on Cholesterol and Bile Acid Homeostasis, *Am. J. Physiol. Gastrointest. Liver Physiol. 281*, G878–G889.

16. Stravitz, R.T., Vlahcevic, Z.R., Russell, T.L., Heizer, M.L., Avadhani, N.G., and Hylemon, P.B. (1996) Regulation of Sterol 27-Hydroxylase and an Alternative Pathway of Bile Acid Biosynthesis in Primary Cultures of Rat Hepatocytes, *J. Steroid Biochem. Mol. Biol. 57*, 337–347.

17. Vlahcevic, Z.R., Stravitz, R.T., Heuman, D.M., Hylemon, P.B., and Pandak, W.M. (1997) Quantitative Estimations of the Contribution of Different Bile Acid Pathways to Total Bile Acid Synthesis in the Rat, *Gastroenterology 113*, 1949–1957.

18. Wang, X., Sato, R., Brown, M.S., Hua, X., and Goldstein, J.L. (1994) SREBP-1, a Membrane-Bound Transcription Factor Released by Sterol-Regulated Proteolysis, *Cell 77*, 53–62.

19. Petrack, B., and Latario, B.J. (1993) Synthesis of 27-Hydroxycholesterol in Rat Liver Mitochondria: HPLC Assay and Marked Activation by Exogenous Cholesterol, *J. Lipid Res. 34*, 643–649.

20. Shefer, S., Hauser, S., Lapar, V., and Mosbach, E.H. (1972) HMG CoA Reductase of Intestinal Mucosa and Liver of the Rat, *J. Lipid Res. 13*, 402–412.

21. Pandak, W.M., Li, Y.C., Chiang, J.Y., Studer, E.J., Gurley, E.C., Heuman, D.M., Vlahcevic, Z.R., and Hylemon, P.B. (1991) Regulation of Cholesterol 7α-Hydroxylase mRNA and Transcriptional Activity by Taurocholate and Cholesterol in the Chronic Biliary Diverted Rat, *J. Biol. Chem. 266*, 3416–3421.

22. Su, P., Rennert, H., Shayiq, R.M., Yamamoto, R., Zheng, Y.M., Addya, S., Strauss, J.F., III, and Avadhani, N.G. (1990) A cDNA Encoding a Rat Mitochondrial Cytochrome P450 Catalyzing Both the 26-Hydroxylation of Cholesterol and 25-Hydroxylation of Vitamin D_3; Gonadotropic Regulation of the Cognate mRNA in Ovaries, *DNA Cell Biol. 9*, 657–667.

23. Day, R., Gebhard, R.L., Schwartz, H.L., Strait, K.A., Duane, W.C., Stone, B.G., and Oppenheimer, J.H. (1989) Time Course of Hepatic 3-Hydroxy-3-methylglutaryl Coenzyme A Reductase Activity and Messenger Ribonucleic Acid, Biliary Lipid Secretion, and Hepatic Cholesterol Content in Methimazole-Treated Hypothyroid and Hypophysectomized Rats After Triiodothyronine Administration: Possible Linkage of Cholesterol Synthesis to Biliary Secretion, *Endocrinology 125*, 459–468.

24. Folch, J., Lees, M., and Sloane-Stanley, G.H. (1957) A Simple Method for the Isolation and Purification of Total Lipides from Animal Tissues, *J. Biol. Chem. 226*, 497–509.

25. Kubaska, W.M., Gurley, E.C., Hylemon, P.B., Guzelian, P.S., and Vlahcevic, Z.R. (1985) Absence of Negative Feedback Control of Bile Acid Biosynthesis in Cultured Rat Hepatocytes, *J. Biol. Chem. 260*, 13459–13463.

26. Laemmli, U.K. (1970) Cleavage of Structural Proteins During the Assembly of the Head of Bacteriophage T4, *Nature 227*, 680–685.

27. Teupser, D., Thiery, J., Walli, A.K., and Seidel, D. (1996) Determination of LDL- and Scavenger-Receptor Activity in Adherent and Non-adherent Cultured Cells with a New Single-Step Fluorometric Assay, *Biochim. Biophys. Acta 1303*, 193–198.

28. Chiang, J.Y. (2002) Bile Acid Regulation of Gene Expression: Roles of Nuclear Hormone Receptors, *Endocr. Rev. 23*, 443–463.

29. Chiang, J.Y. (2003) Bile Acid Regulation of Hepatic Physiology: III. Bile Acids and Nuclear Receptors, *Am. J. Physiol. Gastrointest. Liver Physiol. 284*, G349–G356.

30. Chiang, J.Y. (2004) Regulation of Bile Acid Synthesis: Pathways, Nuclear Receptors, and Mechanisms, *J. Hepatol. 40*, 539–551.

31. Fang, Y., Han, S.I., Mitchell, C., Gupta, S., Studer, E., Grant, S., Hylemon, P.B., and Dent, P. (2004) Bile Acids Induce Mitochondrial ROS, Which Promote Activation of Receptor Tyrosine Kinases and Signaling Pathways in Rat Hepatocytes, *Hepatology 40*, 961–971.

32. Qiao, L., Studer, E., Leach, K., McKinstry, R., Gupta, S., Decker, R., Kukreja, R., Valerie, K., Nagarkatti, P., El Deiry, W. *et al.* (2001) Deoxycholic Acid (DCA) Causes Ligand-Independent Activation of Epidermal Growth Factor Receptor

(EGFR) and FAS Receptor in Primary Hepatocytes: Inhibition of EGFR/Mitogen-Activated Protein Kinase-Signaling Module Enhances DCA-Induced Apoptosis, *Mol. Biol. Cell 12*, 2629–2645.

33. Qiao, L., Yacoub, A., Studer, E., Gupta, S., Pei, X.Y., Grant, S., Hylemon, P.B., and Dent, P. (2002) Inhibition of the MAPK and PI3K Pathways Enhances UDCA-Induced Apoptosis in Primary Rodent Hepatocytes, *Hepatology 35*, 779–789.

34. Qiao, L., Han, S.I., Fang, Y., Park, J.S., Gupta, S., Gilfor, D., Amorino, G., Valerie, K., Sealy, L., Engelhardt, J.F. *et al.* (2003) Bile Acid Regulation of C/EBPβ, CREB, and c-Jun function, *via* the Extracellular Signal-Regulated Kinase and c-Jun NH$_2$-Terminal Kinase Pathways, Modulates the Apoptotic Response of Hepatocytes, *Mol. Cell. Biol. 23*, 3052–3066.

35. Rao, Y.P., Studer, E.J., Stravitz, R.T., Gupta, S., Qiao, L., Dent, P., and Hylemon, P.B. (2002) Activation of the Raf-1/MEK/ERK Cascade by Bile Acids Occurs *via* the Epidermal Growth Factor Receptor in Primary Rat Hepatocytes, *Hepatology 35*, 307–314.

36. Meir, K., Kitsberg, D., Alkalay, I., Szafer, F., Rosen, H., Shpitzen, S., Avi, L.B., Staels, B., Fievet, C., Meiner, V. *et al.* (2002) Human Sterol 27-Hydroxylase (*CYP27*) Overexpressor Transgenic Mouse Model. Evidence Against 27-Hydroxycholesterol as a Critical Regulator of Cholesterol Homeostasis, *J. Biol. Chem. 277*, 34036–34041.

37. Rosen, H., Reshef, A., Maeda, N., Lippoldt, A., Shpizen, S., Triger, L., Eggertsen, G., Bjorkhem, I., and Leitersdorf, E. (1998) Markedly Reduced Bile Acid Synthesis but Maintained Levels of Cholesterol and Vitamin D Metabolites in Mice with Disrupted Sterol 27-Hydroxylase Gene, *J. Biol. Chem. 273*, 14805–14812.

38. Honda, A., Salen, G., Matsuzaki, Y., Batta, A.K., Xu, G., Leitersdorf, E., Tint, G.S., Erickson, S.K., Tanaka, N., and Shefer, S. (2001) Side Chain Hydroxylations in Bile Acid Biosynthesis Catalyzed by CYP3A Are Markedly Up-Regulated in *Cyp27$^{-/-}$* Mice but Not in Cerebrotendinous Xanthomatosis, *J. Biol. Chem. 276*, 34579–34585.

39. Honda, A., Salen, G., Matsuzaki, Y., Batta, A.K., Xu, G., Leitersdorf, E., Tint, G.S., Erickson, S.K., Tanaka, N., and Shefer, S. (2001) Differences in Hepatic Levels of Intermediates in Bile Acid Biosynthesis Between Cyp27$^{-/-}$ Mice and CTX, *J. Lipid Res. 42*, 291–300.

40. Repa, J.J., Lund, E.G., Horton, J.D., Leitersdorf, E., Russell, D.W., Dietschy, J.M., and Turley, S.D. (2000) Disruption of the Sterol 27-Hydroxylase Gene in Mice Results in Hepatomegaly and Hypertriglyceridemia. Reversal by Cholic Acid Feeding, *J. Biol. Chem. 275*, 39685–39692.

41. Makar, R.S., Lipsky, P.E., and Cuthbert, J.A. (2000) Multiple Mechanisms, Independent of Sterol Regulatory Element Binding Proteins, Regulate Low Density Lipoprotein Gene Transcription, *J. Lipid Res. 41*, 762–774.

42. Winegar, D.A., Salisbury, J.A., Sundseth, S.S., and Hawke, R.L. (1996) Effects of Cyclosporin on Cholesterol 27-Hydroxylation and LDL Receptor Activity in HepG2 Cells, *J. Lipid Res. 37*, 179–191.

43. Horton, J.A., and Shimomura, I. (1999) Sterol Regulatory Element-Binding Proteins: Activators of Cholesterol and Fatty Acid Biosynthesis, *Curr. Opin. Lipidol. 10*, 143–150.

Effect of Dietary n-6 and n-3 Polyunsaturated Fatty Acids on Peroxidizability of Lipoproteins in Steers

Valérie Scislowski[a], Dominique Bauchart[a], Dominique Gruffat[a],
Paul-Michel Laplaud[b], and Denys Durand[a],*

[a]Institut National de la Recherche Agronomique (INRA), Research Unit on Herbivores, Nutrients and Metabolisms Group,
Research Centre of Clermont-Ferrand/Theix, 63122 Saint Genès-Champanelle, France, and
[b]Institute National de la Santé et de la Recherche Médicale (INSERM), Unit 551, CHU Pitié-Salpetrière, Paris, France

ABSTRACT: The susceptibility of major plasma lipoproteins to lipoperoxidation was studied in relation to the FA composition of their neutral and polar lipids in steers given PUFA-rich diets. Two trials used, respectively, 18 ("sunflower" experiment, S) or 24 ("linseed" experiment, L) crossbred Salers × Charolais steers. Each involved three dietary treatments over a 70-d period: a control diet (CS or CL diets) consisting of hay and concentrate, or the same diet supplemented with oilseeds (4% diet dry matter) fed either as seeds (SS or LS diets) or continuously infused into the duodenum (ISO or ILO diets). Compared with control diets, ISO and ILO treatments tended to decrease the resistance time of LDL and HDL classes to peroxidation, mainly owing to the enrichment of their polar and neutral lipids with PUFA. With diets SS and LS, sensitivity of major lipoprotein classes (LDL, light and heavy HDL) was not affected because ruminal hydrogenation of dietary PUFA decreased their incorporation into lipoparticles. ISO and ILO treatments induced a more important production of conjugated dienes and hydroperoxides generated by peroxidation in the three lipoprotein classes due to the higher amounts of PUFA esterified in lipids of the core and the hydrophilic envelope of particles. The production of malondialdehyde (MDA) increased in steers fed linseed supplements, indicating that MDA production did not occur with linoleic acid provided by sunflower oil supplements. Thus, plasma peroxidation of PUFA generates toxic products in steers fed diets supplemented with PUFA and can be deleterious for the health of the animal during long-term treatment.

Paper no. L9661 in *Lipids 40*, 1245–1256 (December 2005).

The FA composition of the diet plays a key role in disease prevention and health in humans. Hence, a number of scientific authorities have proposed recommendations regarding the intake of total fat, saturated FA (SFA), monounsaturated FA (MUFA), and n-6 and n-3 PUFA in the general population (1–3). According to these recommendations, the contribution of total fat and SFA to dietary energy intake should not exceed 0.35 and 0.10 of total intake, respectively, the PUFA/SFA ratio should be close to 0.45, and the n-6 PUFA/n-3 PUFA ratio should be less than 4 (3). However, the amounts of PUFA, and especially n-3 PUFA, ingested by most subjects are much lower than the recommended levels. These latter PUFA are only present in small amounts in the diets of persons in most developed countries, because the consumption of lipids from fish, seed oils, and green vegetables in the latter is considerably less than the consumption of animal lipids (essentially milk and beef) (4).

Beef is generally characterized by a low intramuscular fat content (5% of fresh tissue) where total FA are mainly represented by SFA and MUFA (47 and 42%, respectively) to the detriment of PUFA (4%) (5). One of the most convenient strategies to increase PUFA deposition in beef lipids is to provide a PUFA supplement to ruminant diets using oilseeds (6–8). Moreover, PUFA concentrations in ruminant tissues can be efficiently raised by feeding dietary PUFA that are physically protected from bacterial hydrolases and hydrogenases present in the rumen (6,9).

However, before their deposition in muscle tissues, dietary PUFA are absorbed by the small intestine and recycled in blood mainly as TG-rich lipoprotein (TGRLP) particles. At this stage, PUFA become preferential targets for the action of free radicals that induce an oxidative stress. This type of stress is facilitated if an imbalance occurs between the respective amounts of PUFA (which can be attacked by free radicals) and antioxidant systems (involved in PUFA protection against free radicals). In humans, such an oxidative stress is known to be influential in pathological conditions such as cancer, cardiovascular diseases, cataracts, and diabetes (1,4). Oxidatively modified LDL have been identified as a key factor in the initiation and progression of atherosclerosis (1,4). Conversely, HDL appear to have a protective effect through their ability to decrease the intensity of lipid peroxidation in LDL (10). In the bovine, the susceptibility of lipoproteins to peroxidation is still unknown, especially regarding HDL despite the fact that these particles represent the main class of plasma lipoproteins (>80% of total lipoproteins) (11).

The aim of this study therefore was to determine the susceptibility to lipid peroxidation of the main lipoprotein classes (LDL, light and heavy HDL) in fattening steers given PUFA-rich diets. Thus, this work (i) compared the extent of the peroxidation process of PUFA in animals fed, respectively, n-6 PUFA (from extruded sunflower seeds) and n-3 PUFA (from

---

extruded linseeds), and (ii) evaluated the efficiency of the protection of dietary PUFA against ruminal biohydrogenation obtained by direct PUFA infusion into the proximal duodenum.

EXPERIMENTAL PROCEDURES

Animals and experimental diets. (i) "Sunflower" experiment. A total of 18 crossbred Charolais × Salers steers (454 ± 20 d old; live weight: 528 ± 36 kg) were assayed for an experimental period of 70 d. To cope with experimental constraints and to minimize the variability between animals, six groups of three animals were constituted (one of each diet) according to their initial live weight and their pre-experimental daily weight gain. In each group, each of the animals was subsequently randomly assigned to one of three diets. These diets were either (i) a control diet (Control Sunflower, CS; $n = 6$) consisting in 540 g naturalgrass hay and 460 g concentrate mixture per kg on a dry matter (DM) basis. The average composition of the concentrate mixture was 575 g corn seed, 240 g soybean meal, 120 g dehydrated alfalfa, 20 g cane molasses, 25 g urea, and 20 g vitamin and mineral mixture per kg DM; (ii) a "sunflower seed" diet (SS, $n = 6$), consisting in crushed sunflower seeds added to the control diet (4% of diet DM); and (iii) an "infused sunflower oil" diet (ISO, $n = 6$), consisting in the control diet supplemented with 4% (of diet DM) of sunflower oil continuously infused into the proximal duodenum through a chronic cannula. The respective values for DM content and the FA composition of each of the three diets are given in Tables 1 and 2, respectively.

(ii) "Linseed" experiment. For this purpose, a total of 24 crossbred Charolais × Salers steers (412 ± 33 d old; live weight: 536 ± 33 kg) were assayed during an experimental period of 70 d. In a design similar to that described for the "Sunflower" experiment, eight groups of three animals were constituted according to their initial live weight and pre-experimental daily weight gain, and each animal in each group was then randomly assigned to one of three different diets. These diets were either (i) a control diet (Control Linseed, CL; $n = 8$) consisting in 450 g natural-grass hay and 550 g concentrate mixture per kg DM

TABLE 1
Mean Dry Matter (DM) Concentration and DM Composition of Control Diets (CS and CL) or of the Same Control Diets Supplemented with Extruded Sunflower Seed (SS) and Extruded Linseed (LS) or with the Corresponding Sunflower Oil (ISO) or Linseed Oil (ILO) Directly Infused into the Proximal Duodenum

Diet	Sunflower experiment			Linseed experiment		
	CS	SS	ISO	CL	LS	ILO
DM (g/kg feed)	915	917	918	915	925	919
Composition of DM (g/kg)						
Organic matter	935	936	895	937	939	904
Net energy value[a]	0.85	0.85	0.86	0.85	0.90	0.87
Crude protein	188	181	180	189	190	176
Lipid	36.7	73.6	70.2	40.7	75.3	79.1
FA	20.0	54.8	51.5	26.8	53.5	60.6

[a]Feed units for maintenance and meat production.

TABLE 2
FA Composition (wt% total FAME) of Diets and Mean Total FA Intake (g/d) in Fattening Steers Given Control Diets or the Same Control Diets Supplemented with Extruded Sunflower Seed and Extruded Linseed or with the Corresponding Sunflower Oil or Linseed Oil Directly Infused into the Proximal Duodenum[a]

FA (%)	Sunflower experiment			Linseed experiment		
	CS	SS	ISO	CL	LS	ILO
14:0	1.4	0.5	0.6	0.6	0.3	0.3
16:0	20.8	11.0	11.1	20.3	12.3	11.0
18:0	2.4	3.7	3.4	2.8	3.2	2.8
18:1	12.8	20.5	19.3	20.5	17.4	17.4
18:2n-6	30.2	52.2	52.0	37.7	25.0	22.8
18:3n-3	21.3	7.6	8.3	9.9	38.3	42.1
20:2n-6	2.5	0.8	0.8	2.2	0.9	0.8
20:3n-6	2.2	0.7	0.7	2.1	ND	0.8
22:5n-6	2.3	0.7	0.8	ND	ND	ND
Sum of						
SFA	25.2	16.0	15.9	24.9	16.4	14.6
MUFA	14.9	21.2	20.4	21.0	17.7	17.7
n-6 PUFA	37.7	54.6	54.5	42.8	27.3	24.6
n-3 PUFA	22.5	8.2	9.1	11.8	39.2	42.8
Mean total FA intake (g/d)	134	372	347	225	468	514

[a]SFA = saturated FA; MUFA = monounsaturated FA; ND = not detectable; for other abbreviations see Table 1.

whose composition was the same as the one used in the "Sunflower" experiment; (ii) a "linseed" diet (LS, $n = 8$), consisting in extruded linseed added to the control diet (4% of diet DM); and (iii) an "infused linseed oil" diet (ILO, $n = 8$), consisting in the control diet supplemented with 4% (of diet DM) linseed oil continuously infused into the proximal duodenum through a chronic cannula. The respective DM content and FA composition of these three diets are given in Tables 1 and 2, respectively.

In both experiments, during the pre-experimental period (1 mon), the animals received a basal diet composed of a 50% natural-grass hay and 50% concentrate mixture. Diets were formulated weekly to meet protein and energy requirements as well as feed intake capacity of growing animals, using the "IN-RAtion" micro computer program (12).

During the first week of the experiment, animals given SS, LS, ISO, and ILO diets were adapted progressively to lipid supplements using diets containing 2% of DM as lipids. To determine separately the effect of the lipid supplement, steers assigned to ISO and ILO diets received sunflower and linseed meals in amounts equal to those provided by the corresponding seeds in diets SS and LS.

In both experiments, the three animals in each group were managed in pair-feeding conditions to reach a daily weight gain of 1.0–1.2 kg.

Isolation of plasma lipoprotein classes. At the end of the experimental period (day 70) and immediately before the morning meal, blood samples (500 mL) were collected from the jugular vein on Na_2-EDTA, Na-azide and merthiolate (final concentration 3 mM, 0.01%, and 0.001%, respectively). Plasma was separated by centrifugation at $600 \times g$ for 10 min at 15°C. Na_2-EDTA was then added to the plasma at a final concentration of 0.1 g/mL to stop the peroxidation processes that may have been initiated during manipulation. TG-rich lipoproteins (TGRLP) were then isolated from plasma by ultracentrifugal flotation at the density limit ($d < 1.006$ g/mL) defined for the bovine by Bauchart *et al.* (13). Ultracentrifugation was performed in a Centrikon T-2060 ultracentrifuge equipped with the TFT 38-70 fixed-angle rotor (Kontron Analysis Division, Zurich, Switzerland). Since the resulting bottom fractions (i.e., plasma samples deprived of TGRLP) could not be treated immediately, these were stored in the dark at −20°C under a nitrogen flux until subsequent treatment and analysis.

Isolation of major lipoprotein classes, i.e., LDL (1.019 < d < 1.060 g/mL), light HDL (1.060 < d < 1.091 g/mL), and heavy HDL (1.091 < d < 1.180 g/mL), was performed as follows: the $d < 1.006$ g/mL centrifugation bottom fractions were thawed at 4°C in the dark and submitted to a sequential ultracentrifugal flotation according to the density limits defined by Bauchart *et al.* (13). Lipoprotein fractions were then dialyzed in the dark at 4°C in a 200-fold volume of degassed 0.01 M PBS (pH 7.4) changed every 12 h for 36 h. To discard free radicals, dialysis membranes were previously incubated for 15 min in a boiling solution of 27 mM Na_2-EDTA and then rinsed in distilled water. Since dialysis treatment had suppressed Na-EDTA, dialyzed lipoproteins (without any additional antioxidant substances) were used immediately for the measurement of their relative susceptibility to lipoperoxidation.

Kinetics of conjugated diene (CD) generation by PUFA peroxidation. The susceptibility of plasma lipoproteins to peroxidation was first determined by monitoring the kinetic parameters of CD generation. These CD were produced, following induction of the peroxidation process using copper salts, according to the method of Esterbauer *et al.* (14) and adapted to bovine samples by Scislowski *et al.* (15) using data reported by Ziouzenkova *et al.* (16). Therefore, FA oxidation in each lipoprotein class, previously diluted in degassed PBS (0.25 mg/mL), was induced at 37°C by a freshly prepared 5 µM aqueous copper chloride solution. Absorbance of CD was continuously recorded at 234 nm using a Uvikon 923 double-beam spectrophotometer (Kontron Analysis Division). The kinetics of CD generation was divided into three phases from which three parameters were calculated as described by Esterbauer *et al.* (14): (i) length of the lag phase (L_p) corresponding to the resistance time of PUFA against oxidation, (ii) maximal rate of peroxidation (R_{max}) during the propagation chain reaction, and (iii) maximal amount of CD (CD_{max}) accumulated at the end of the propagation phase. R_{max} and CD_{max} values were expressed in nmol CD/min/mg lipoprotein and in nmol CD/mg lipoprotein, respectively, by using the value of 29,500 M^{-1} cm^{-1} for the molar absorptivity of CD at 234 nm as calculated by Esterbauer *et al.* (14).

Kinetics of lipoperoxides (LPO) and TBARS generated by PUFA peroxidation. Lipoproteins diluted in degassed PBS (1.5 mg/mL) were incubated for 12 h at 37°C with a freshly prepared 5 µM aqueous copper chloride solution. One milliliter of oxidized lipoprotein fraction was collected every hour, and the oxidation chain reaction was stopped by adding 0.27 mM Na_2-EDTA. Each fraction was maintained in the dark at 4°C until analysis for total LPO and malondialdehyde (MDA).

LPO assay. LPO were determined according to the method of El-Saadani *et al.* (17). Briefly, 100 µL of the oxidized lipoprotein solution was mixed with 1 mL of the iodide color reagent and then kept 30 min in the dark at ambient temperature before LPO determination at 365 nm. Concentration of LPO was calculated using 24,600 M^{-1} cm^{-1} for the molar absorptivity of I_3 at 365 nm.

TBARS assay. MDA production was measured as described by Buege and Aust (18). Briefly, 500 µL of oxidized lipoprotein solution was mixed with 1 mL of reagent [15% TCA (wt/vol); 0.375% thiobarbituric acid (wt/vol); 0.25 N hydrochloric acid] and then heated for 15 min in a boiling water bath. After cooling and centrifugation at $1,200 \times g$ for 10 min, the concentration of MDA present in the supernatant was determined by spectrophotometry at 535 nm. TBARS were determined using a standard curve of MDA equivalents generated by the acid hydrolysis of 1,1,3,3-tetraethoxypropane, as described by Wallin *et al.* (19).

Lipid and protein analysis of lipoprotein classes. Concentrations of the different lipid classes [free cholesterol (FC), cholesteryl esters (CE), TG, and phospholipids] of LDL and of light and heavy HDL were determined enzymatically as previously described by Leplaix-Charlat *et al.* (20). Total cholesterol

(TC) and FC were measured using the cholesterol reagent kit supplied by Biotrol Diagnostic (Chennevières-lès-Louvres, France). CE were then calculated using the following relationship: $(TC - FC) \times 1.68$. TG content was determined using the reagent kit PAP 1000 (ref. A 00970; BioMérieux, Charbonnières-les-Bains, France). Phospholipids were determined by the enzymatic method of Trinder using the 150 kit PAP (ref. 61491; BioMérieux). Total polar lipids (PL) and neutral lipids (NL) correspond to the sums of phospholipids + FC and TG + CE, respectively.

Concentration of total protein in lipoprotein class was determined by the colorimetric method of the bicinchoninic acid protein assay reagent (Pierce, Rockford, IL), as previously described by Leplaix-Charlat *et al.* (20).

Chemical analysis of FA in PL and NL of lipoprotein classes. Total lipids of LDL, light HDL and heavy HDL fractions were extracted according to the method of Folch *et al.* (21). Their two main components, phospholipids and neutral lipids (CE and TG), were prepared from total lipids by semipreparative TLC using glass plates covered with delipidated Kieselgel. Total FA were extracted from PL and NL and converted into FAME according to the method described by Bauchart and Aurousseau (22).

The FA compositions of PL and NL were determined by GLC (Peri 2001; Perichrom, Saulx les Chartreux, France) with a CP-Sil 88 glass capillary column (100 m length, 0.25 mm i.d.). GLC conditions were as follows: oven temperature was programmed for 70°C for 30 s, 70 to 175°C at a rate of 20°C/min, 175°C for 25 min, then 175 to 215°C at a rate of 10°C/min, and finally 215°C for 41 min; injector and detector temperatures were 235 and 250°C, respectively; hydrogen was the carrier gas (H_2 flow: 1.1 mL/min) in conditions of split injection (1:50). FA were identified by comparing their retention times with those of FA standards (Supelco, St-Germain-en-laye, Cedex, France). Chromatographic signals were analyzed using the Winilab II software Chromatography Data System (Perichrom).

The peroxidation index (PI) estimates the concentration of bisallylic hydrogen atoms present in unsaturated FA. It thus represents an index of the susceptibility of unsaturated FA to oxidation. PI was calculated from the equation reported by Nagyova *et al.* (23): PI = (% dienoic × 1) + (% trienoic × 2) + (% tetraenoic × 3) + (% pentaenoic × 4) + (% hexaenoic × 5).

Statistical analysis. In both the sunflower and linseed experiments, data concerning lipid and protein concentrations and chemical FA composition of lipids in each lipoprotein class obtained were analyzed in a simple factorial arrangement in a six and eight randomized group design, respectively, by ANOVA using the GLM procedure of SAS (24). When the diet effect was declared statistically significant ($P < 0.05$), the respective means of the three groups were compared using the Student's *t*-test of SAS. The same procedure was used to realize the statistical treatment of values of parameters calculated by the CD method.

Data concerning LPO and TBARS production in the medium, as determined every hour for 12 h, were used in repeated-measurements for each of the six and eight randomized

groups of animals, respectively. The statistical method was ANOVA according to the GLM (generalized linear model) procedure of SAS (Cary, NC). When the main factors (diet effect and time effect) were considered statistically significant ($P < 0.05$), treatment means were compared between the three groups and/or between the kinetic points, respectively, using the Student's *t*-test of SAS. When the diet × time interaction was statistically significant ($P < 0.05$), the significance of the main factors was not taken into account, and treatment mean values were compared for each kinetic point by the Student's *t*-test of SAS.

RESULTS

Lipoprotein analysis. (i) Sunflower experiment. In control steers, total LDL ($1.018 < d < 1.060$ g/mL), light HDL ($1.060 < d < 1.091$ g/mL), and heavy HDL ($1.091 < d < 1.180$ g/mL) accounted for 14, 54, and 28% of total plasma lipoproteins, respectively (Table 3). With the SS diet (nonprotected n-6 PUFA supplement), the respective plasma levels of LDL and light HDL increased significantly (1.5× and 1.4×, respectively), but the respective proportions of NL and PL remained constant in the three lipoprotein classes.

As regards NL, the PUFA/SFA ratio increased by about 1.5× in all three lipoprotein classes ($P < 0.05$) owing to the higher proportion of n-6 PUFA (1.2× for LDL and light HDL, $P < 0.05$) and a concomitant decrease in SFA (−20%).

For its part, the PUFA/SFA ratio for PL remained approximately constant in both LDL and light HDL because the small increase in n-6 PUFA was compensated by a parallel decrease in n-3 PUFA (Table 3). Infusion of sunflower oil into the duodenum (ISO treatment) led to a large increase in the plasma concentration of LDL (4.3×, $P < 0.05$) as well as in the value of the PUFA/SFA ratio for NL (2–2.4×) in the three lipoprotein classes. A similar increase in the PUFA/SFA ratio was noted in PL in both LDL and heavy HDL (1.6×, $P < 0.05$) when compared with that of control steers.

The value of PI tended to increase with diet SS and especially with the diet ISO, but the substitution of n-3 for n-6 PUFA minimized the enrichment of lipoparticles in double bonds (Table 3).

(ii) Linseed experiment. As observed in the sunflower experiment, administration of the linseed supplement (diet LS) increased the respective plasma levels of two lipoprotein classes (1.9× for LDL, $P < 0.05$; 1.5× for light HDL, $P < 0.05$) (Table 4). We simultaneously observed an increased proportion of n-3 PUFA in NL (3× for LDL and light HDL, $P < 0.05$; and 2.3× for heavy HDL, $P < 0.05$) and, to a lower extent, in PL of LDL and light HDL (1.8×, $P < 0.05$). As with the n-6-rich dietary supplement (diet SS), the n-3-rich diet provided by extruded linseed (diet LS) decreased the SFA content in NL (−19%) and PL (−9%) only in the LDL fraction (Table 4). This led to a decrease of n-6 PUFA in NL (−25 to −30%) of the three lipoprotein classes and also of PL of LDL and heavy HDL (−20%, $P < 0.05$). These changes in FA composition did not result in higher PUFA/SFA values compared with the control (Table 4).

TABLE 3
Chemical Composition (mean wt%) and Concentration (mg/dL) of the Major Lipoprotein Classes Isolated from Plasma in Fattening Steers Fed the Control Diet or the Same Control Diet Supplemented with Extruded Sunflower Seed or with the Corresponding Sunflower Oil Directly Infused into the Proximal Duodenum[a]

	CS	SS	ISO	SEM	P
LDL (1.018 < d < 1.060 g/mL)					
Lipoprotein concentration (mg/dL plasma)	44[a]	66[b]	187[c]	7.42	0.0001
Neutral lipids (% total lipid)	38	38	38	0.64	NS
SFA	33.3[a]	26.0[b]	23.1[b]	0.5	0.0005
MUFA	15.7[a]	16.3[a]	7.6[b]	0.9	0.0162
n-6 PUFA	44.9[a]	52.8[b]	67.2[c]	1.1	0.0005
n-3 PUFA	5.7[a]	4.5[a,b]	1.9[b]	0.5	0.0463
PUFA/SFA	1.5[a]	2.2[b]	3.0[c]	0.1	0.0005
PI	65.1[a]	71.1[a,b]	76.5[b]	1.4	0.0389
Polar lipids (% total lipid)	31	32	34	0.59	NS
SFA	43.9	45.0	42.7	0.5	NS
MUFA	18.7[a]	18.8[a]	8.0[b]	0.3	0.0001
n-6 PUFA	24.6[a]	30.9[b]	47.1[c]	1.0	0.0002
n-3 PUFA	11.7[a]	4.9[b]	2.1[b]	0.9	0.0096
PUFA/SFA	0.8[a]	0.8[a]	1.2[b]	0.1	0.0017
PI	65.9[a]	44.2[b]	53.0[a,b]	2.8	0.0490
Light HDL (1.060 < d < 1.091 g/mL)					
Lipoprotein concentration (mg/dL plasma)	168[a]	230[b]	309[c]	4.81	0.0001
Neutral lipids (% total lipid)	34	35	37	0.44	NS
SFA	17.1[a]	13.6[b]	11.6[b]	0.6	0.0253
MUFA	19.8[a]	15.6[b]	5.7[c]	0.5	0.0001
n-6 PUFA	52.5[a]	64.2[b]	81.4[c]	1.1	0.0001
n-3 PUFA	10.1[a]	6.6[b]	1.4[c]	0.4	0.0003
PUFA/SFA	3.7[a]	5.3[b]	7.3[c]	0.3	0.0071
PI	86.1[a]	87.6[a]	99.4[b]	1.6	0.0278
Polar lipids (% total lipid)	31	30	32	0.55	NS
SFA	50.2	44.8	42.7	2.0	NS
MUFA	18.0[a]	18.9[a]	9.5[b]	0.5	0.0003
n-6 PUFA	24.0[a]	31.3[a]	46.1[b]	1.9	0.0086
n-3 PUFA	7.5[a]	4.5[b]	1.4[c]	0.5	0.0064
PUFA/SFA	0.7	0.8	1.1	0.1	NS
PI	44.6[a]	44.1[a]	50.7[b]	2.6	NS
Heavy HDL (1.091 < d < 1.180 g/mL)					
Lipoprotein concentration (mg/dL plasma)	88	116	121	3.65	NS
Neutral lipids (% total lipid)	27	29	31	0.85	NS
SFA	22.6	17.7	14.3	2.2	NS
MUFA	16.0[a]	14.4[b]	7.0[c]	1.1	0.0321
n-6 PUFA	51.3[a]	58.2[a]	76.0[b]	2.3	0.0124
n-3 PUFA	10.1	9.7	2.7	1.6	NS
PUFA/SFA	2.8	4.3	6.7	0.8	NS
PI	84.5	94.2	93.1	6.3	NS
Polar lipids (% total lipid)	27	25	25	0.72	NS
SFA	49.3[a]	43.7[b]	41.1[b]	0.7	0.0057
MUFA	17.5[a]	19.9[b]	9.8[c]	0.4	0.0002
n-6 PUFA	26.6[a]	29.2[b]	45.9[c]	0.7	0.0001
n-3 PUFA	6.3	7.0	3.1	1.0	NS
PUFA/SFA	0.7[a]	0.8[b]	1.2[c]	0.1	0.0008
PI	47.0	52.6	54.7	3.0	NS

[a]Results are expressed as mean ± SEM. [a,b,c]Values with different superscripts differ significantly (P < 0.05). PI, peroxidation index; NS, not significant; for other abbreviations see Tables 1 and 2.

As in the sunflower experiment, duodenal infusion of linseed oil intensified the effects noted with the linseed treatment. Higher levels of plasma lipoproteins were observed, especially for LDL (4.6×, P < 0.05), in which NL and PL were intensively enriched in n-3 PUFA (9× and 3.6×, respectively; P < 0.05) and simultaneously depleted in SFA. This led to an important increase of the PUFA/SFA ratio in NL of LDL (10×, P < 0.05)

and, to a lower extent, in the HDL fractions (2×, P < 0.05). A similar increase of the PUFA/SFA ratio was noted in PL for all lipoprotein classes (1.3×, P < 0.05) (Table 4).

Measured PI values were 1.2 times higher for the NL of all lipoproteins in animals given extruded linseed (diet LS), and were also 1.2 times higher in NL and PL of all lipoprotein classes in animals given linseed oil by duodenal infusion.

TABLE 4
Chemical Composition (mean wt%) and Concentration (mg/dL) of the Major Lipoprotein Classes Isolated from Plasma in Fattening Steers Fed the Control Diet or the Same Control Diet Supplemented with Extruded Linseed or with the Corresponding Linseed Oil Directly Infused into the Proximal Duodenum[a]

	CL	LS	ILO	SEM	P
LDL (1.018 < d < 1.060 g/mL)					
Lipoprotein concentration (mg/dL plasma)	69[a]	129[b]	318[c]	23.7	0.0001
Neutral lipids (% total lipid)	41	41	42	0.80	NS
SFA	42.7[a]	34.5[b]	8.5[c]	1.2	0.0001
MUFA	9.0[a]	14.6[a]	2.8[b]	1.1	0.0046
n-6 PUFA	41.2[a]	31.1[b]	42.8[a]	1.4	0.0174
n-3 PUFA	5.0[a]	16.1[b]	44.9[c]	0.9	0.0001
PUFA/SFA	1.1[a]	1.4[a]	10.8[b]	0.4	0.0001
PI	63.3[a]	77.3[b]	142.4[c]	2.5	0.0001
Polar lipids (% total lipid)	27[a]	29[b]	31[b]	0.82	0.0026
SFA	43.8[a]	39.8[b]	37.4[b]	0.7	0.0098
MUFA	15.4[a]	21.7[b]	12.4[a]	0.9	0.0048
n-6 PUFA	34.0[a]	27.1[b]	30.9[c]	0.6	0.0052
n-3 PUFA	4.9[a]	8.9[b]	17.4[c]	0.6	0.0001
PUFA/SFA	0.9[a]	0.9[a]	1.3[b]	0.1	0.0004
PI	67.9[a]	68.1[a]	82.8[b]	1.7	0.0090
Light HDL (1.060 < d < 1.091 g/mL)					
Lipoprotein concentration (mg/dL plasma)	195[a]	288[b]	352[c]	19.2	0.0001
Neutral lipids (% total lipid)	34[a]	36[b]	39[c]	0.80	0.0009
SFA	16.3	14.8	15.5	2.4	NS
MUFA	8.3	10.5	5.7	1.0	NS
n-6 PUFA	65.0[a]	44.0[b]	40.7[b]	1.7	0.0005
n-3 PUFA	9.0[a]	27.9[b]	36.4[b]	2.1	0.0015
PUFA/SFA	5.0	5.4	9.3	1.5	NS
PI	98.2	114.4	126.5	4.7	NS
Polar lipids (% total lipid)	25	26	25	0.40	NS
SFA	43.0	39.9	39.3	0.9	NS
MUFA	16.0[a]	20.2[b]	12.4[c]	0.3	0.0001
n-6 PUFA	32.3	26.7	29.4	0.8	NS
n-3 PUFA	6.2[a]	10.8[b]	16.5[c]	0.3	0.0001
PUFA/SFA	0.9[a]	1.0[b]	1.2[b]	0.1	0.0192
PI	71.2[a]	74.4[b]	81.1[b]	0.7	0.0008
Heavy HDL (1.091 < d < 1.180 g/mL)					
Lipoprotein concentration (mg/dL plasma)	111[a]	121[a,b]	149[b]	11.7	NS
Neutral lipids (% total lipid)	29	29	30	0.90	NS
SFA	18.8[a]	16.7[a]	12.1[b]	0.6	0.0046
MUFA	8.2[a]	10.8[b]	3.7[c]	0.4	0.0001
n-6 PUFA	59.7[a]	45.6[b]	41.7[c]	0.6	0.0001
n-3 PUFA	10.6[a]	24.9[b]	41.7[c]	0.9	0.0001
PUFA/SFA	3.8[a]	4.4[a]	7.1[b]	0.3	0.0036
PI	102.3[a]	116.3[b]	137.4[c]	1.7	0.0001
Polar lipids (% total lipid)	21	22	22	0.69	NS
SFA	41.4[a]	41.8[a]	37.1[b]	0.5	0.0048
MUFA	16.6[a]	20.5[b]	13.4[c]	0.5	0.0015
n-6 PUFA	32.5[a]	25.6[b]	30.0[a,b]	0.5	0.0006
n-3 PUFA	6.6[a]	9.5[a]	17.3[b]	0.6	0.0001
PUFA/SFA	1.0[a]	0.9[a]	1.3[b]	0.1	0.0006
PI	72.8[a]	70.4[a]	83.6[b]	1.3	0.0049

[a]Results are expressed as mean ± SEM. [a,b,c]Values with different superscripts differ significantly ($P < 0.05$). For abbreviations see Tables 1–3.

CD generated by PUFA peroxidation in lipoproteins. (i) Sunflower experiment. In animals receiving the SS diet, the length of the lag phase (L_p) observed for light and heavy HDL tended to decrease [−25%, not significant (NS)] compared with the control group (Table 5), whereas the oxidation rate (R_{max}) increased by about 1.4× in the two HDL subclasses ($P < 0.05$).

The maximum amount of CD generated (CD_{max}) tended to increase in HDL and decrease in LDL, although these changes did not reach statistical significance. With the ISO diet, the L_p decrease in HDL was more pronounced (−45%, NS), and respective increases in R_{max} ($P < 0.05$) and in CD_{max} (NS) were higher than those observed with the SS diet.

TABLE 5
Susceptibility of the Main Lipoprotein Classes to *in vitro* Copper-Induced Peroxidation in Fattening Steers Fed Control Diet (*n* = 6) or the Same Control Diet Supplemented with Sunflower Seed (*n* = 6) or with Sunflower Oil Infused into the Duodenum (*n* = 6)[a]

	Sunflower experiment				
	CS	SS	ISO	SEM	*P*
LDL (1.018 < *d* < 1.060 g/mL)					
L_p (min)	10.4	10.4	11.8	1.7	NS
R_{max} (nmol CD/mg LDL/min)	1.3[a]	1.6[a]	3.5[b]	0.4	0.0028
CD_{max} (nmol CD/mg LDL)	63.0	55.3	82.9	9.8	NS
Light HDL (1.060 < *d* < 1.091 g/mL)					
L_p (min)	16.4	11.6	9.9	3.1	NS
R_{max} (nmol CD/mg LDL/min)	2.3[a]	3.4[a]	4.6[b]	0.5	0.0118
CD_{max} (nmol CD/mg LDL)	69.0	78.6	102.3	12.8	NS
Heavy HDL (1.091 < *d* < 1.180 g/mL)					
L_p (min)	6.1	4.7	2.9	1.3	NS
R_{max} (nmol CD/mg LDL/min)	2.4[a]	3.3[b]	4.0[c]	0.2	0.0025
CD_{max} (nmol CD/mg LDL)	75.9	80.6	98.7	13.3	NS

[a]Results are expressed as mean ± SEM. [a,b,c]Values with different superscripts differ significantly (*P* < 0.05). L_p, time of the lag phase; R_{max}, maximal rate of peroxidation; CD_{max}, maximum amount of conjugated dienes (CD); for other abbreviation see Table 3.

(ii) Linseed experiment. Similarly to the results obtained with the SS diet, addition of linseed in the diet tended to decrease the L_p in LDL and light HDL (−12%, NS) compared with the control diet (Table 6). Oil infusion increased the R_{max} in LDL (1.9×, *P* < 0.05) and light HDL (1.3, *P* < 0.05) and increased by 1.2 the CD_{max} in the three lipoprotein classes (*P* < 0.05 in LDL and heavy HDL).

LPO generated by PUFA peroxidation in lipoproteins. (i) Sunflower experiment. In control steers, production of LPO did not increase in LDL during the 12 h of the peroxidation assay (Fig. 1A). On the other hand, when steers were given extruded sunflower seeds (diet SS), LPO production in LDL was 3.7 and 6 times higher than in control animals at T_6 (*P* < 0.05) and at T_{12} (*P* < 0.05), respectively. In animals given sunflower oil by infusion into the duodenum, a higher production of LPO was

already noted at T_2 in LDL (4×, *P* < 0.05) and continued to increase at T_{12} (8.2×, *P* < 0.05) compared with control animals. More pronounced effects of sunflower oil supplements were shown in light HDL (Fig. 1B), but these effects were less marked with heavy HDL (Fig. 1C).

(ii) Linseed experiment. In control steers, and as already noted in the sunflower experiment, LPO production increased only in heavy HDL at T_{12} (35 nmol LPO/mg HDL) (Figs. 1C, 2C). Contrary to what was observed in heavy HDL, production of LPO in LDL (Fig. 2A) and in light HDL (Fig. 2B) increased considerably (especially after T_8), in animals given linseed oil infused into the duodenum (ILO treatment) (*P* < 0.05 vs. control and LS animals).

TBARS generated by PUFA peroxidation in lipoproteins. (i) Sunflower experiment. In LDL (Fig. 1D), light HDL (Fig. 1E),

TABLE 6
Susceptibility of the Main Lipoprotein Classes to *in vitro* Copper-Induced Peroxidation in Fattening Steers Fed Control Diet (*n* = 8) or the Same Control Diet Supplemented with Linseed (*n* = 8) or with Linseed Oil Infused into the Duodenum (*n* = 8)[a]

	Linseed experiment				
	CL	LS	ILO	SEM	*P*
LDL (1.018 < *d* < 1.060 g/mL)					
L_p (min)	12.5	10.7	10.0	2.1	NS
R_{max} (nmol CD/mg LDL/min)	1.4[a]	1.5[a]	2.7[b]	0.2	0.0047
CD_{max} (nmol CD/mg LDL)	90.7[a]	90.7[a]	114.7[b]	6.2	0.05
Light HDL (1.060 < *d* < 1.091 g/mL)					
L_p (min)	14.3	12.7	10.0	1.3	NS
R_{max} (nmol CD/mg LDL/min)	2.6[a]	2.9[a]	3.5[b]	0.2	0.0112
CD_{max} (nmol CD/mg LDL)	96.8	95.3	114.1	6.6	NS
Heavy HDL (1.091 < *d* < 1.180 g/mL)					
L_p (min)	5.3[a]	9.6[b]	6.2[a,b]	0.7	NS
R_{max} (nmol CD/mg LDL/min)	2.1[a,b]	1.8[a]	2.3[b]	0.2	NS
CD_{max} (nmol CD/mg LDL)	70.0[a]	60.5[a]	84.4[b]	4.6	0.008

[a]Results are expressed as mean ± SEM. [a,b,c]Values with different superscripts differ significantly (*P* < 0.05). For abbreviations see Tables 1, 3, and 5.
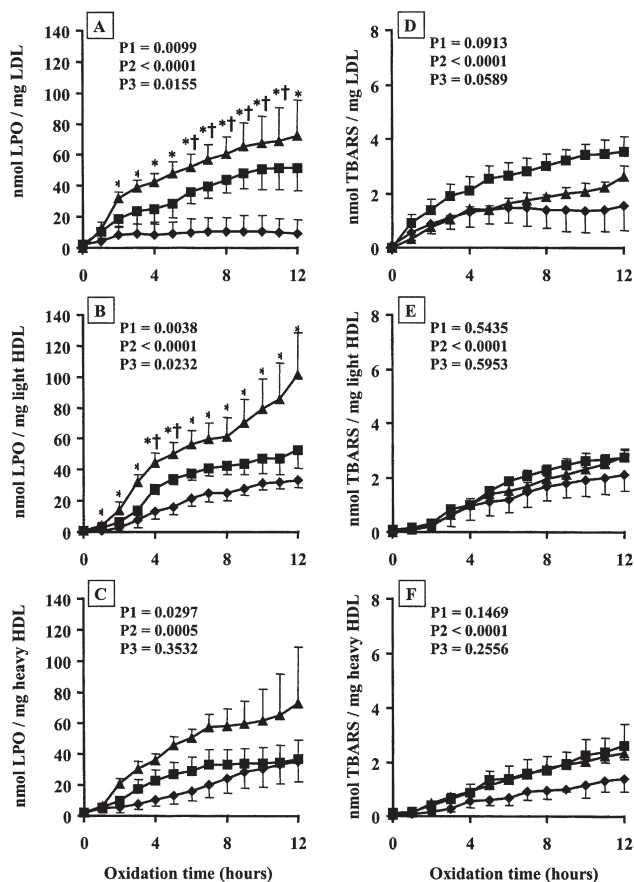
FIG. 1. Production of lipoperoxides (nmol LPO/mg lipoprotein) (A, B, and C) and TBARS (nmol TBARS/mg lipoprotein) (D, E, and F) for 12 h following copper-induced lipoperoxidation of lipoparticles LDL, light HDL, and heavy HDL, in fattening steers fed control diets (CS, ♦, $n = 6$) or the same control diet supplemented with sunflower seeds (SS, ■, $n = 6$) or with sunflower oil infused into the duodenum (ISO, ▲,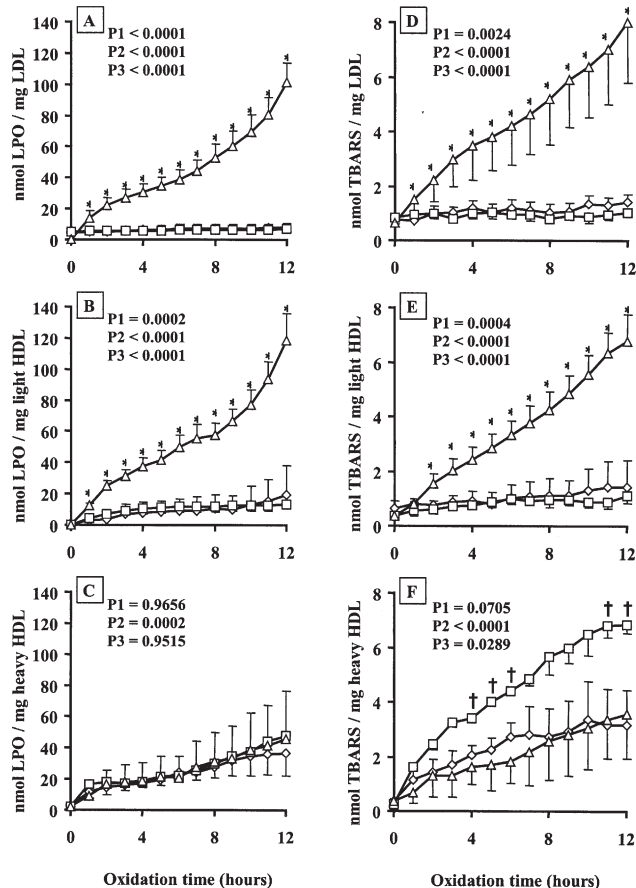 $n = 6$). Results are expressed as mean ± SE and are analyzed by ANOVA for repeated measures. P1: treatment effect; P2: time effect; P3: treatment × time interaction. * indicates statistically significant differences among diets ISO and CS, and ✝ indicates statistically significant differences among diets SS and CS ($P < 0.05$) at a specific time point.

FIG. 2. Production of lipoperoxides (nmol LPO/mg lipoprotein) (A, B, and C) and TBARS (nmol TBARS/mg lipoprotein) (D, E, and F) for 12 h following copper-induced lipoperoxidation of lipoparticles LDL, light HDL, and heavy HDL, in fattening steers fed control diets (CL, ◇, $n = 8$) or the same control diet supplemented with linseed (LS, □, $n = 8$) or with linseed oil infused into the duodenum (ILO, △, $n = 8$). Results are expressed as mean ± SE and are analyzed by ANOVA for repeated measures. P1: treatment effect; P2: time effect; P3: treatment × time interaction. * indicates statistically significant differences among diets ILO and CL and ✝ indicates statistically significant differences among diets LS and CL ($P < 0.05$) at a specific time point.

and heavy HDL (Fig. 1F) classes, the time effect was significant ($P < 0.0001$) indicating a production of TBARS (MDA) during the 12 h of peroxidation with the three diets. On the other hand, no significant differences resulting from administration of the diets were noted in the three lipoprotein classes although in LDL, the level of TBARS tended (treatment effect P1 = 0.0913) to be higher with the SS diet compared with those observed with the CS and ISO diets (Fig. 1D).

(ii) Linseed experiment. Generally, the effects of lipid supplementation were more pronounced here than in the sunflower experiment. In steers fed the control diet, production of TBARS increased only in heavy HDL (Fig. 2F), a result consistent with that already noted for LPO production (Fig. 2C). In both LDL (Fig. 2D) and light HDL (Fig. 2E), the production of TBARS increased considerably (5× at T_{12}, $P < 0.05$) in animals given duodenally infused linseed oil. As regards heavy

HDL (Fig. 2F), PUFA peroxidation increased TBARS production significantly only in the case of a comparison between the LS treatment and the control diet (1.7× and 2.2× at T_4 and T_{12}, respectively, $P < 0.05$).

DISCUSSION

The objective of this work was to determine how changes in the lipid and FA composition of the main lipoprotein classes in fattening steers given PUFA-rich diets can favor lipoperoxidation processes in these particles. Part of the originality of this work lay in the experimental protocol allowing comparison of the metabolic effects of dietary PUFA provided by extruded oil seeds (PUFA exposed to ruminal biohydrogenation) or by the corresponding oils continuously infused into the proximal duodenum (PUFA totally protected from ruminal hydrogenation).

Two experiments were conducted simultaneously, one using sunflower oil rich in n-6 PUFA and the other using linseed oil rich in n-3 PUFA.

Resistance of bovine lipoproteins to lipoperoxidation. The relative susceptibility of the major classes of lipoproteins to lipoperoxidation can be efficiently compared in our animals by *in vitro* induction of PUFA peroxidation using a copper salt and subsequent kinetic analysis of CD production, as previously described in humans by Esterbauer *et al.* (14). Determination of the resistance time (lag phase) before the initiation of CD production showed that duodenal infusion of n-3 PUFA decreased specifically the capacity of LDL and light HDL fractions to resist the lipoperoxidation process, whereas infusion of n-6 PUFA produced a similar effect exclusively in light and heavy HDL. In both cases, such an alteration in the resistance of lipoproteins to peroxidation was related to a higher content in peroxidizable PUFA present in both PL and NL. Indeed, such lipoprotein enrichments in PUFA probably led to an imbalance between PUFA and antioxidant systems in favor of an oxidative stress. Our results are in agreement with previous data obtained in both humans (25) and rats (26) and show a positive correlation between a higher sensitivity of LDL to peroxidation and a high PUFA content of their lipids. Conversely, a strong negative correlation could be observed between the lag time and the FA unsaturation index in LDL particles. Shorter lag times previously were reported for LDL in humans given a dietary long-chain n-3 PUFA supplement derived from fish oil (27–30), an n-6 PUFA supplement from high-linoleic safflower oil (31), or a diet supplemented with sunflower oil (32). Finally, similar results were noted in rats given an n-6 PUFA supplement (33).

The higher resistance of lipoproteins to the peroxidation process induced by copper salts observed in our steers given seed compared with those receiving an oil infusion could mainly be explained by the intense activity of biohydrogenation of dietary PUFA (about 80 and 92% for linoleic and linolenic acids, respectively) catalyzed by bacterial enzymes during their transit in the rumen (34). Such an alteration of the dietary PUFA absorbable by the small intestine consequently led to a minimal increase in the PUFA/SFA ratio of NL and/or PL, thus explaining the low impact of such dietary supplements on the susceptibility of lipoproteins to peroxidation.

A possible hypothesis to explain the lack of effect of the n-6 PUFA-rich diets on the resistance to oxidation of LDL particles is a selective distribution, in the different lipoprotein classes, of α-tocopherol provided by sunflower seed supplements (35). This hypothesis was in agreement with some characteristics of the plasma transport of this lipophile antioxidant as part of lipoproteins (36) and especially of the more lipid-rich of these particles. Thus, in humans given a dietary safflower oil supplement (rich in n-6 PUFA), plasma transport of α-tocopherol was more associated with LDL and HDL_2 (a counterpart of bovine light HDL) than with HDL_3 (a counterpart of bovine heavy HDL) (31).

Moreover, we have shown that n-3 PUFA supplements, especially given to steers in unprotected form (linseed), resulted in an unexpectedly higher resistance of heavy HDL to peroxidation. Since n-3 PUFA are very sensitive to peroxidation (29,30), this higher resistance of bovine heavy HDL suggests a protective effect of antioxidants provided by linseed, which are dominated by secoisolariciresinol diglycoside, a water-soluble lignan (37). The high protein content of these HDL particles (about 50%) probably favored lignan adsorption onto the HDL envelope, but the mechanism by which this lignan would preferentially protect heavy HDL against peroxidation is still unclear. The higher resistance of heavy HDL to peroxidation associated with the administration of a linseed supplement could also be explained by an enrichment of PL and NL in MUFA since a beneficial effect of these FA in LDL protection was demonstrated in humans given an olive oil-based diet (38).

With all diets considered in the present experiment, bovine heavy HDL appeared to be generally more sensitive to peroxidation than LDL and light HDL particles, since the corresponding lag phase duration was about two times shorter than that noted in other lipoproteins. This higher sensitivity of bovine heavy HDL to a pro-oxidant agent was previously observed in human HDL_3 (31). One may hypothesize that the different physical characteristics of heavy HDL particles, such as their smaller size (93–120 Å) compared with that of light HDL (120–150 Å) and LDL (190–250 Å) (11) and/or the higher rigidity of their hydrophilic envelope (39) plays a role. Such physical characteristics would reduce their surface area available for the solubilization of lipophilic antioxidants (40) and the solubility and the depth of penetration of antioxidants (41), respectively. Consequently, copper ions bound to HDL particles appear to be more efficient in promoting peroxidation than those bound to LDL (42). Finally, HDL are known to be the major carriers of plasma lipid hydroperoxides (43), which contribute to accelerate the initiation of peroxidation reactions *via* the peroxyl and alkoxyl radical generation in response to copper reduction.

Intensity of peroxidation reactions in bovine lipoproteins. Our experiments clearly demonstrated that incorporation of dietary PUFA provided by an infusion of linseed oil or sunflower oil favored production of LPO and MDA, products derived from PUFA peroxidation, in bovine plasma lipoproteins. The higher production of CD observed indicates an increased frequency of collisions between the Cu-generated lipid radicals and the surrounding PUFA in lipoproteins. Such a relation has been already shown in humans fed sunflower oil (38). It was then related to the value of the PI: This latter parameter indeed accurately reflects the degree of unsaturation of FA and estimates the concentration of bisallylic hydrogen atoms able to interact with free radicals (23). This could explain why the production of CD in lipoproteins tended to be higher in steers given linseed oil (18:3n-3) than in steers given sunflower oil (18:2n-6). Our results are in agreement with the previously shown twofold higher peroxidizability of linolenate compared with linoleate (44). Conversely, the increase in the PUFA content of lipids in lipoproteins of steers given extruded seeds was probably insufficient to increase FA peroxidizability in these lipoproteins, as already observed in humans fed safflower oil (31).

Biochemical reactions involved in lipid peroxidation can occur both in the hydrophilic envelope and in the hydrophobic core of lipoproteins, thus leading to the generation of phospholipid and CE hydroperoxides, respectively (41). Compared with phospholipids, CE are physically more susceptible to peroxidation because of their localization in the inner core of lipoproteins where a higher fluidity of lipids favors the propagation of free radicals (45,46). This probably explains the higher production of LPO observed in the light HDL of our steers receiving oil infusions, a situation where lipoproteins were enriched in CE exhibiting a high PUFA content. Similarly, the higher rigidity of heavy HDL compared with LDL and light HDL in steers (39) can, at least partly, explain the lower production of LPO in these particles.

Lipid peroxidation in lipoproteins is known ultimately to generate various aldehydes, including MDA, arising from the cleavage of LPO (47). In our steers assigned to duodenal infusion of linseed oil (rich in 18:3n-3), the TBARS test revealed a high production of MDA during LDL and light HDL peroxidation. A similar phenomenon was observed with duodenal infusion of sunflower oil (rich in 18:2n-6), despite a higher production of LPO in this latter situation. Such a discrepancy between the consequences of the peroxidation of n-6 and n-3 PUFA in bovine lipoproteins, already reported for human LDL (27), may at least partly depend on the amount and the position of the double bonds in the main FA of the dietary oil. Indeed, only peroxidation of PUFA with more than two double bonds (such as linolenic acid) can generate MDA since this product can be produced only when the peroxidation reaction occurs on the double bond in the β-position (48). Such a specificity of the TBARS test indicates that MDA detection may erroneously imply the lack of peroxidation reaction. Pertinent analysis of lipid peroxidation reactions needs to take into account several markers representative of each level of the process, which is what we have done in this work.

From a physiological point of view, the higher sensitivity of lipoproteins to the lipoperoxidation process observed in steers given high-PUFA diets indicates for the first time that bovine fed this type of diet may become more sensitive to the oxidative shocks that can be induced by different key events of animal life (reproduction, weaning, intensive growth, transport, slaughter) (49). This higher peroxidizability of bovine lipoproteins implies considerable alteration of the physicochemical properties of lipoproteins (50) thus possibly inducing high cytotoxicity (51) due to a defect in lipoprotein recognition by lipoprotein receptors, affinity of peroxidized lipids for scavenger receptors in macrophages (27), and a disturbing effect on cellular cholesterol homeostasis (52). Peroxidative modifications of HDL particles, which represent 80% of total lipoproteins in steers (11), may impair their capacity to bind to cell receptors and reduce their effectiveness to promote cellular lipid efflux (53), thus considerably impairing their role in reverse cholesterol transport.

Any injuries to cells and/or lipoproteins can alter various animal functions such as fertility or growth rate and may have negative consequences on bovine carcass and meat quality (49). Thus, in the bovine, dietary PUFA-rich lipid supplements must be administered in a form where these FA are totally protected against ruminal biohydrogenations, with a concomitant dietary supplementation in antioxidant compounds to inhibit free radical attacks of PUFA during their transport in blood by lipoprotein particles.

ACKNOWLEDGMENTS

REFERENCES

1. Roche, H.M. (1999) Unsaturated Fatty Acids, *Proc. Nutr. Soc. 58*, 397–401.
2. Simopoulos, A.P. (2001) n-3 Fatty Acids and Human Health: Defining Strategies for Public Policy, *Lipids 36* (*Suppl.*), S83–S89.
3. Legrand, P., Bourre, J.M., Descomps, B., Durand, G., and Renaud, S. (2001) Lipides, in *Apports nutritionnels conseillés pour la population française,* 3rd edn. (TEC and DOC edition), pp. 63–82, Lavoisier, Paris.
4. Williams, C.M. (2000) Dietary Fatty Acids and Human Health, *Ann. Zootech. 49*, 165–180.
5. Moloney, A.P., Mooney, M.T., Kerry, J.P., and Troy, D.J. (2001) Producing Tender and Flavoursome Beef with Enhanced Nutritional Characteristics, *Proc. Nutr. Soc. 60*, 221–229.
6. Clinquart, A., Micol, D., Brundseaux, C., Dufrasne, I., and Istasse, L. (1995) Utilisation des matieres grasses chez les bovins à l'engraissement, *INRA Prod. Anim. 8*, 29–42.
7. Wood, J.D., Enser, M., Fisher, A.V., Nute, G.R., Richardson, R.I., and Sheard, P.R. (1999) Manipulating Meat Quality and Composition, *Proc. Nutr. Soc. 58*, 363–370.
8. Scollan, N.D., Choi, N.J., Kurt, E., Fisher, A.V., Enser, M., and Wood, J.D. (2001) Manipulating the Fatty Acid Composition of Muscle and Adipose Tissue in Beef Cattle, *Br. J. Nutr. 85*, 115–124.
9. Scollan, N.D., Enser, M., Gulati, S.K., Richardson, I., and Wood, J.D. (2003) Effects of Including a Ruminally Protected Lipid Supplement in the Diet on the Fatty Acid Composition of Beef Muscle, *Br. J. Nutr. 90*, 709–716.
10. Mackness, M.I., Durrington, P.N., and Mackness, B. (2000) How High-Density Lipoprotein Protects Against the Effects of Lipid Peroxidation, *Curr. Opin. Lipidol. 11*, 383–388.
11. Bauchart, D. (1993) Lipid Absorption and Transport in Ruminants, *J. Dairy Sci. 76*, 3864–3881.
12. Micol, D., Robelin, J., and Agabriel, J. (1989) Growing and Finishing Cattle, in *INRAtion. Microcomputer Program of Ration Formulation for Ruminant Livestock* (Agabriel, J., Champciaux, P., and Espinasse, C., eds.), Agrilog, Cergy, France.
13. Bauchart, D., Durand, D., Laplaud, P.M., Forgez, P., Goulinet, S., and Chapman, M.J. (1989) Plasma Lipoproteins and Apolipoproteins in the Preruminant Calf, *Bos* spp: Density Distribution, Physicochemical Properties, and the *in vivo* Evaluation of the Contribution of the Liver to Lipoprotein Homeostasis, *J. Lipid Res. 30*, 1499–1514.
14. Esterbauer, H., Striegl, G., Puhl, H., and Rotheneder, M. (1989) Continuous Monitoring of *in vitro* Oxidation of Human Low Density Lipoprotein, *Free Radic. Res. Commun. 6*, 67–75.
15. Scislowski, V., Durand, D., Mouty, D., Motta, C., Laplaud, M., and Bauchart, D. (2000) Fluidité et susceptibilité à la peroxydation des lipoprotéines du bouvillon recevant des rations enrichies en huile de tournesol, *Nutr. Clin. Metab. 14*, 151.

16. Ziouzenkova, O., Gieseg, S.P., Ramos, P., and Esterbauer, H. (1996) Factors Affecting Resistance of Low Density Lipoproteins to Oxidation, *Lipids 31 (Suppl.)*, S71–S76.

17. El-Saadani, M., Esterbauer, H., El-Sayed, M., Goher, M., Nassar, A.Y., and Jurgens, G. (1989) A Spectrophotometric Assay for Lipid Peroxides in Serum Lipoproteins Using a Commercially Available Reagent, *J. Lipid Res. 30*, 627–630.

18. Buege, J.A., and Aust, S.D. (1978) Microsomal Lipid Peroxidation, *Methods Enzymol. 52*, 302–310.

19. Wallin, B., Rosengren, B., Shertzer, H.G., and Camejo, G. (1993) Lipoprotein Oxidation and Measurement of Thiobarbituric Acid Reacting Substances Formation in a Single Microtiter Plate: Its Use for Evaluation of Antioxidants, *Anal. Biochem. 208*, 10–15.

20. Leplaix-Charlat, L., Bauchart, D., Durand, D., Laplaud, P.M., and Chapman, M.J. (1996) Plasma Lipoproteins in Preruminant Calves Fed Diets Containing Tallow or Soybean Oil With and Without Cholesterol, *J. Dairy Sci. 79*, 1267–1277.

21. Folch, J., Lees, M., and Sloane Stanley, G.H. (1957) A Simple Method for the Isolation and Purification of Total Lipides from Animal Tissues, *J. Biol. Chem. 226*, 497–509.

22. Bauchart, D., and Aurousseau, B. (1981) Postprandial Lipids in Blood Plasma of Preruminant Calves, *J. Dairy Sci. 64*, 2033–2042.

23. Nagyova, A., Krajcovicova-Kudlackova, M., and Klvanova, J. (2001) LDL and HDL Oxidation and Fatty Acid Composition in Vegetarians, *Ann. Nutr. Metab. 45*, 148–151.

24. SAS/STAT (1987) *Guide for Personal Computers*, SAS Institute, Cary, NC.

25. Kontush, A., Hubner, C., Finckh, B., Kohlschutter, A., and Beisiegel, U. (1994) Low Density Lipoprotein Oxidizability by Copper Correlates to Its Initial Ubiquinol-10 and Polyunsaturated Fatty Acid Content, *FEBS Lett. 341*, 69–73.

26. Lu, Y.-F., and Lu, S. (2002) Influence of Dietary Fat Saturation on Lipid Peroxidation of Serum and Low Density Lipoprotein in Rats, *Nutr. Res. 22*, 463–472.

27. Suzukawa, M., Abbey, M., Howe, P.R., and Nestel, P.J. (1995) Effects of Fish Oil Fatty Acids on Low Density Lipoprotein Size, Oxidizability, and Uptake By Macrophages, *J. Lipid Res. 36*, 473–484.

28. Sorensen, N.S., Marckmann, P., Høy, C.E., van Duyvenvoorde, W., and Princen, H.M. (1998) Effect of Fish-Oil-Enriched Margarine on Plasma Lipids, Low-Density-Lipoprotein Particle Composition, Size, and Susceptibility to Oxidation, *Am. J. Clin. Nutr. 68*, 235–241.

29. Stalenhoef, A.F., de Graaf, J., Wittekoek, M.E., Bredie, S.J., Demacker, P.N., and Kastelein, J.J. (2000) The Effect of Concentrated n-3 fatty Acids Versus Gemfibrozil on Plasma Lipoproteins, Low Density Lipoprotein Heterogeneity and Oxidizability in Patients with Hypertriglyceridemia, *Atherosclerosis 153*, 129–138.

30. Finnegan, Y.E., Minihane, A.M., Leigh-Firbank, E.C., Kew, S., Meijer, G.W., Muggli, R., Calder, P.C., and Williams, C.M. (2003) Plant- and Marine-Derived n-3 Polyunsaturated Fatty Acids Have Differential Effects on Fasting and Postprandial Blood Lipid Concentrations and on the Susceptibility of LDL to Oxidative Modification in Moderately Hyperlipidemic Subjects, *Am. J. Clin. Nutr. 77*, 783–795.

31. Schnell, J.W., Anderson, R.A., Stegner, J.E., Schindler, S.P., and Weinberg, R.B. (2001) Effects of a High Polyunsaturated Fat Diet and Vitamin E Supplementation on High-Density Lipoprotein Oxidation in Humans, *Atherosclerosis 159*, 459–466.

32. Nielsen, N.S., Pedersen, A., Sandstrom, B., Marckmann, P., and Høy, C.E. (2002) Different Effects of Diets Rich in Olive Oil, Rapeseed Oil and Sunflower-Seed Oil on Postprandial Lipid and Lipoprotein Concentrations and on Lipoprotein Oxidation Susceptibility, *Br. J. Nutr. 87*, 489–499.

33. Fremont, L., Gozzelino, M.T., Franchi, M.P., and Linard, A. (1998) Dietary Flavonoids Reduce Lipid Peroxidation in Rats Fed Polyunsaturated or Monounsaturated Fat Diets, *J. Nutr. 128*, 1495–1502.

34. Doreau, M., and Ferlay, A. (1994) Digestion and Utilisation of Fatty Acids by Ruminants, *Anim. Feed Sci. Technol. 45*, 379–396.

35. Scislowski, V., Bauchart, D., Gruffat, D., Laplaud, P.M., and Durand, D. (2005) Effects of Dietary n-6 or n-3 Polyunsaturated Fatty Acids Protected or Not Against Ruminal Hydrogenations on Plasma Lipids and Their Susceptibility to Peroxidation in Fattening Steers, *J. Anim. Sci. 40*, 2162–2174.

36. Cohn, W., Gross, P., Grun, H., Loechleiter, F., Muller, D.P., and Zulauf, M. (1992) Tocopherol Transport and Absorption, *Proc. Nutr. Soc. 51*, 179–188.

37. Prasad, K. (1997) Hydroxyl Radical-Scavenging Property of Secoisolariciresinol Diglucoside (SDG) Isolated from Flaxseed, *Mol. Cell. Biochem. 168*, 117–123.

38. Kratz, M., Cullen, P., Kannenberg, F., Kassner, A., Fobker, M., Abuja, P.M., Assmann, G., and Wahrburg, U. (2002) Effects of Dietary Fatty Acids on the Composition and Oxidizability of Low-Density Lipoprotein, *Eur. J. Clin. Nutr. 56*, 72–81.

39. Scislowski, V., Durand, D., Gruffat-Mouty, D., Motta, C., and Bauchart, D. (2004) Linoleate Supplementation in Steers Modifies Lipid Composition of Plasma Lipoproteins but Does Not Alter Their Fluidity, *Br. J. Nutr. 91*, 575–584.

40. Sunesen, V.H., Weber, C., and Holmer, G. (2001) Lipophilic Antioxidants and Polyunsaturated Fatty Acids in Lipoprotein Classes: Distribution and Interaction, *Eur. J. Clin. Nutr. 55*, 115–123.

41. Cazzola, R., Cervato, G., and Cestaro, B. (1999) Variability in α-tocopherol Antioxidant Activity in the Core and Surface Layers of Low- and High-Density Lipoproteins, *J. Nutr. Sci. Vitaminol. (Tokyo) 45*, 39–48.

42. Thomas, M.J., Chen, Q., Zabalawi, M., Anderson, R., Wilson, M., Weinberg, R., Sorci-Thomas, M.G., and Rudel, L.L. (2001) Is the Oxidation of High-Density Lipoprotein Lipids Different Than the Oxidation of Low-Density Lipoprotein Lipids? *Biochemistry 40*, 1719–1724.

43. Bowry, V.W., Stanley, K.K., and Stocker, R. (1992) High Density Lipoprotein Is the Major Carrier of Lipid Hydroperoxides in Human Blood Plasma from Fasting Donors, *Proc. Natl. Acad. Sci. USA 89*, 10316–10320.

44. Cosgrove, J.P., Church, D.F., and Pryor, W.A. (1987) The Kinetics of the Autoxidation of Polyunsaturated Fatty Acids, *Lipids 22*, 299–304.

45. Yoshida, Y., Ito, N., Shimakawa, S., and Niki, E. (2003) Susceptibility of Plasma Lipids to Peroxidation, *Biochem. Biophys. Res. Commun. 305*, 747–753.

46. Chancharme, L., Therond, P., Nigon, F., Zarev, S., Mallet, A., Bruckert, E., and Chapman, M.J. (2002) LDL Particle Subclasses in Hypercholesterolemia. Molecular Determinants of Reduced Lipid Hydroperoxide Stability, *J. Lipid Res. 43*, 453–462.

47. Esterbauer, H., Jurgens, G., Quehenberger, O., and Koller, E. (1987) Autoxidation of Human Low Density Lipoprotein: Loss of Polyunsaturated Fatty Acids and Vitamin E and Generation of Aldehydes, *J. Lipid Res. 28*, 495–509.

48. Dahle, L.K., Hill, E.G., and Holman, R.T. (1962) The Thiobarbituric Acid Reaction and the Autoxidations of Polyunsaturated Fatty Acid Methyl Esters, *Arch. Biochem. Biophys. 98*, 253–261.

49. Aurousseau, B. (2002) Les radicaux libres dans l'organisme des animaux d'élevage: Conséquences sur la reproduction, la physi-

ologie et la qualité de leurs produits, *INRA Prod. Anim. 15*, 67–82.

50. Zarev, S., Bonnefont-Rousselot, D., Jedidi, I., Cosson, C., Couturier, M., Legrand, A., Beaudeux, J.L., and Therond, P. (2003) Extent of Copper LDL Oxidation Depends on Oxidation Time and Copper/LDL Ratio: Chemical Characterization, *Arch. Biochem. Biophys. 420*, 68–78.

51. Morel, D.W., Hessler, J.R., and Chisolm, G.M. (1983) Low Density Lipoprotein Cytotoxicity Induced by Free Radical Peroxidation of Lipid, *J. Lipid Res. 24*, 1070–1076.

52. Salonen, J.T. (2000) Markers of Oxidative Damage and Antioxidant Protection: Assessment of LDL Oxidation, *Free Radic. Res. 33* (*Suppl.*), S41–S46.

53. Bonnefont-Rousselot, D., Motta, C., Khalil, A.O., Sola, R., La Ville, A.E., Delattre, J., and Gardès-Albert, M. (1995) Physicochemical Changes in Human High-Density Lipoproteins (HDL) Oxidized by Gamma Radiolysis-Generated Oxyradicals. Effect on Their Cholesterol Effluxing Capacity, *Biochim. Biophys. Acta 1255*, 23–30.

Analogs of Squalene and Oxidosqualene Inhibit Oxidosqualene Cyclase of *Trypanosoma cruzi* Expressed in *Saccharomyces cerevisiae*

Simonetta Oliaro-Bosso, Maurizio Ceruti, Gianni Balliano, Paola Milla, Flavio Rocco, and Franca Viola*

Dipartimento di Scienza e Tecnologia del Farmaco, Università di Torino, 10125 Turin, Italy

ABSTRACT: Recently, a number of inhibitors of the enzyme oxidosqualene cyclase (OSC; EC 5.4.99.7), a key enzyme in sterol biosynthesis, were shown to inhibit in mammalian cells the multiplication of *Trypanosoma cruzi*, the parasite agent of Chagas' disease. The gene coding for the OSC of *T. cruzi* has been cloned and expressed in *Saccharomyces cerevisiae*. The expression in yeast cells could be a safe and easy model for studying the activity and the selectivity of the potential inhibitors of *T. cruzi* OSC. Using a homogenate of *S. cerevisiae* cells expressing *T. cruzi* OSC, we have tested 19 inhibitors: aza, methylidene, vinyl sulfide, and conjugated vinyl sulfide derivatives of oxidosqualene and squalene, selected as representative of different classes of substrate analog inhibitors of OSC. The IC_{50} values of inhibition (the compound concentration at which the enzyme is inhibited by 50%) are compared with the values obtained using OSC of pig liver and *S. cerevisiae*. Many inhibitors of pig liver and *S. cerevisiae* OSC show comparable IC_{50} for *T. cruzi* OSC, but some phenylthiovinyl derivatives are 10–100 times more effective on the *T. cruzi* enzyme than on the pig or *S. cerevisiae* enzymes. The expression of proteins of pathogenic organisms in yeast seems very promising for preliminary screening of compounds that have potential therapeutic activity.

Paper no. L9864 in *Lipids 40*, 1257–1262 (December 2005).

Sterols are eukaryotic membrane components that are necessary to support cell growth and differentiation. Sterol biosynthesis is a well-established chemotherapeutic target in pathogenic eukaryotes, such as fungi (1,2). The final product of the sterol biosynthetic pathway in fungi is the 24-alkyl sterol ergosterol. Ergosterol or similar 24-alkyl sterols are also the final products of the sterol synthetic pathway of some pathogenic protozoa including *Trypanosoma* species. These organisms cannot completely substitute these sterols with the cholesterol biosynthesized in host mammalian cells and need to synthesize at least some of their own distinctive sterols (3–5). This dependence on sterols suggests that sterol biosynthesis inhibitors may be useful antiprotozoal drugs.

The sterol biosynthetic pathway (Fig. 1) offers many potential targets for therapeutic purposes. Many effective antifungal drugs already in use act by inhibiting different enzymes of sterol biosynthesis; the allylamine antifungal drug terbinafine inhibits squalene epoxidase (6), and azole drugs such as ketoconazole and itraconazole are inhibitors of lanosterol C_{14}-demethylase (7). The activity of these inhibitors can be explained as a consequence either of depletion of the ergosterol or of accumulation of toxic intermediates or side products. In addition to the antifungal activity, some of these compounds
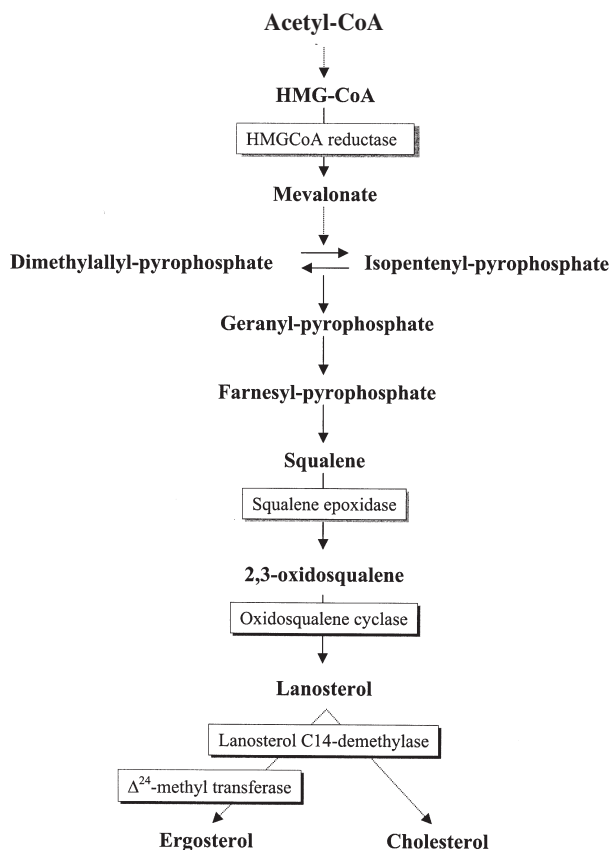
FIG. 1. Schematic representation of sterol biosynthetic pathways. The end products (ergosterol and cholesterol) are typical for fungi and animals, respectively. In the boxes are shown the enzymes cited in the text as targets for antimicrobial drugs.

---

*To whom correspondence should be addressed at Dipartimento di Scienza e Tecnologia del Farmaco, Via P. Giuria, 9-10125 Torino, Italy.
E-mail: franca.viola@unito.it

Abbreviations: IC_{50}, inhibitor concentration reducing enzymatic activity by 50%; OSC, oxidosqualene cyclase.
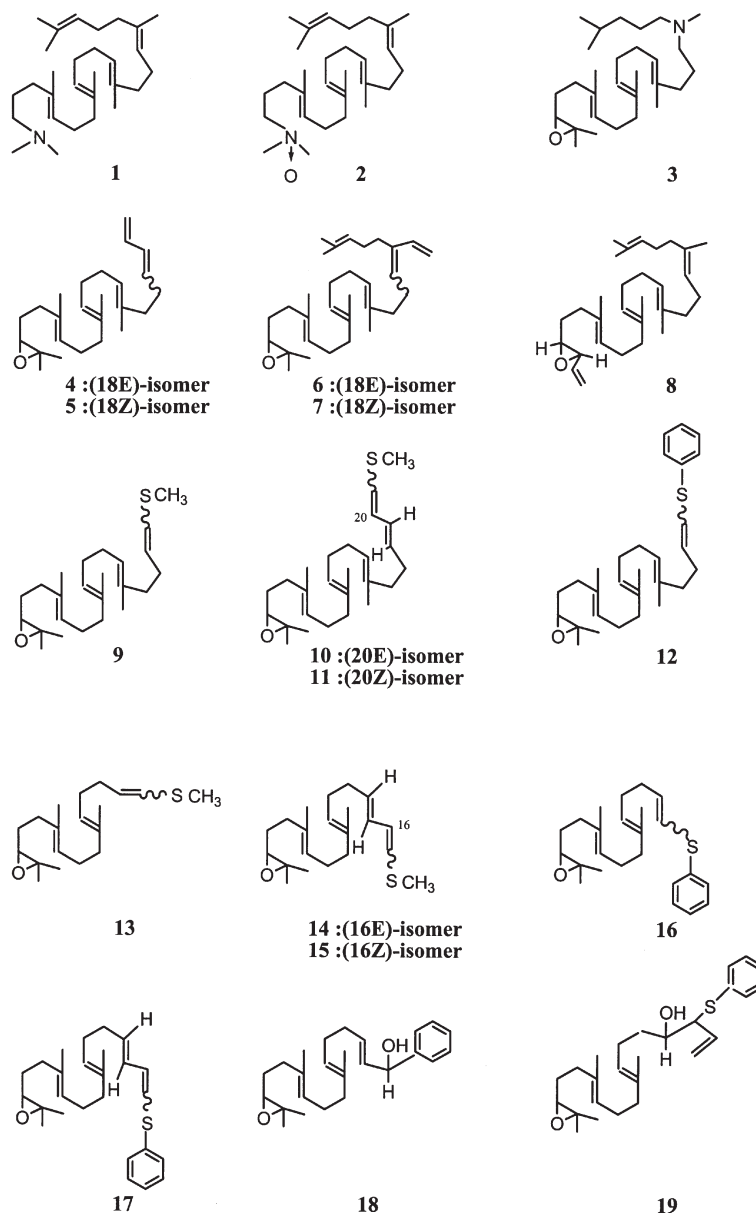
FIG. 2. Squalene and 2,3-oxidosqualene derivatives tested as inhibitors of *Trypanosoma cruzi* oxidosqualene cyclase.

were shown to inhibit the growth of *Trypanosoma* and other kinetoplastid parasites (8). Kinetoplastid parasites have also been shown recently to be susceptible to inhibitors of squalene synthase (9,10) and oxidosqualene cyclase (11,12).

The enzyme oxidosqualene cyclase (OSC; EC 5.4.99.7), which catalyzes the formation of the first cyclic precursor of sterols, is considered a good target for the inhibition of sterol biosynthesis in both humans and fungi. Many inhibitors, designed on the basis of the complex cyclization mechanism of OSC (13), are active on the enzyme and have been investigated as potential cholesterol-lowering or antifungal drugs (1,2,13). The recent crystallization of human OSC as a complex with the

potent inhibitor RO48–8071 opens the way to new structure-based studies of the cyclization mechanism (14).

We have designed and tested against mammalian and fungal OSC many acyclic substrate analogs modified either to mimic the high-energy carbocationic intermediates (compounds **1**–**3** of Fig. 2) or to bear reactive functions able to interact with the active site residues, as the methylidene (compounds **4**–**8**), vinyl sulfide (compounds **9**, **12**, **13**, **16**), conjugated vinyl sulfide (compounds **10**, **11**, **14**, **15**, **17**), hydroxysulfide (compound **19**), or hydroxyphenyl derivatives (compound **18**) (15–20). OSC of different origins can have significantly different susceptibilities to the inhibitors, showing

the possibility of selective inhibition (19,20). Therefore, it would be worth testing the activity of these inhibitors on the OSC of the pathogen protozoon *Trypanosoma cruzi*, which recently has been shown to be susceptible to pyridinium ion-based inhibitors and to some umbelliferone aminoalkyl derivatives (11,12). *Trypanosoma cruzi*, like other pathogenic protozoa, is difficult to culture for an extensive, preliminary screening of the many available, effective inhibitors of OSC. Recently, the gene coding for the OSC of *T. cruzi*, a lanosterol synthase, has been cloned and expressed in *Saccharomyces cerevisiae* (21). The enzyme expressed in the yeast cells could be a safe and easy model for a preliminary study of the activity and the selectivity of the potential inhibitors of *T. cruzi* OSC.

In this paper we report the activity of different types of substrate analogs as inhibitors of the *T. cruzi* OSC expressed in *S. cerevisiae* cells. Basically, three types of inhibitors were studied: analogs of the carbocationic intermediates, as the aza-squalenes (15,18); oxidosqualene derivatives bearing a conjugated methylidene group, designed as affinity-labeling inhibitors (16,22); and vinyl sulfide, and conjugated vinyl sulfide derivatives of oxidosqualene, very effective inhibitors of yeast OSC (17,19,20), (Fig. 2).

MATERIALS AND METHODS

Materials, substrates, and test compounds. All the components of buffers and culture broths were obtained from Sigma-Aldrich (Milan, Italy) unless otherwise specified.

The substrate of OSC, 2,3-oxidosqualene, was synthesized as previously described (23). The labeled [^{14}C]-(3*S*)2,3-oxidosqualene was obtained through biological synthesis by incubating a pig liver S_{10} supernatant with *R,S*[2-^{14}C]mevalonic acid (55 mCi/mmol, 2.04 GBq/mmol) (Amersham Pharmacia Biotech, Buckinghamshire, United Kingdom), in the presence of the OSC inhibitor U-14266A (24), as previously described (19). [2-^{14}C]Acetate (50 mCi/mol) was obtained from Amersham Pharmacia Biotech. The synthesis of the inhibitors tested (compounds **1–19** of Fig. 2) has been described elsewhere (16,17,19,20,23,25,26). The identity and purity of inhibitors was checked by TLC, ^{1}H NMR and mass spectra before testing the inhibition of *T. cruzi* OSC.

Strains of S. cerevisiae and culture conditions. SMY8pBJ1.21 strain, expressing the OSC of *T. cruzi*; SMY8pSM61.21, expressing the wild-type yeast OSC; and SMY8pSM60.21, expressing the *Arabidopsis thaliana* OSC obtained by transformation of lanosterol synthase mutant strain of *S. cerevisiae* SMY8 (*MATα erg7::HIS3 hem1::TRP1 ura3–52-trpl-Δ63 leu2–3.112 his3-Δ200 ade2* Gal$^+$) were kindly provided by Professor S.P.T. Matsuda [Department of Chemistry and Biochemistry and Cell Biology, Rice University, Houston, TX (21,27,28)]. All strains were grown in a YPD culture broth (yeast extract 1%, peptone 2%, dextrose 2%) containing hemin (0.013 mg/mL) and ergosterol (0.02 mg/mL). Hemin had to be added to the growth medium since the SMY8 strains contains a mutation (hem1::TRP1) affecting heme biosynthesis. The presence of a

heme mutant background is necessary for the viability of lanosterol synthase mutants in aerobic conditions (27). OSC expression was induced in YPG broth (yeast extract 1%, peptone 2%, galactose 2%) containing hemin (0.013 mg/mL). All strains were preserved in 40% glycerol at –80°C.

Enzymatic assays. The activity of OSC was assayed in cell-free homogenates obtained from cultures grown to late exponential phase in YPG at 30°C. The cells were centrifuged at $3000 \times g$ for 10 min and the homogenates prepared by lysing the cell wall with lyticase (2 mg/g wet cells in 1.2 M sorbitol, 0.02 M KH_2PO_4, pH 7.4, for 60 min at 30°C). The spheroplasts obtained after lysis were sedimented at $3000 \times g$ for 10 min, washed twice with 1.2 M sorbitol, 0.02 M KH_2PO_4 and homogenized with a Potter device in 10 mM MES/TRIS buffer, containing 0.2 mM EDTA and 1 mM PMSF, pH 6.9. Proteins in the homogenate were quantified with the Protein Assay Kit SIGMA, based on the method of Lowry, modified by Peterson (29). The homogenates could be used fresh or after storage at –80°C for several months. The OSC activity was assayed by incubating the homogenate in the presence of the labeled [^{14}C]-(3*S*)-2,3-oxidosqualene (1000 cpm) diluted with unlabeled (*R,S*)2,3-oxidosqualene to a final concentration of 25 μM. Cold and labeled substrates and inhibitors, when present, were added as solutions in $CHCl_3$ to test tubes in the presence of Tween-80 (0.2 mg/mL of final volume) and Triton X-100 (1 mg/mL of final volume). The solvent was evaporated under nitrogen. The substrate and inhibitors were dissolved in 50 μL of MES/TRIS buffer, containing 0.2 mM EDTA, pH 6.9 and the amount of homogenate necessary to obtain a 20% substrate transformation was added and diluted to a final volume of 250 μL buffer. After 30 min of incubation at 35°C in plugged tubes, the enzymatic reaction was stopped by adding 1 mL of KOH in methanol (10% wt/vol) and heating at 80°C for 30 min in a water bath. After extracting with 2 mL of petroleum ether, the solvent was evaporated and the extract was dissolved in a small amount of CH_2Cl_2 and spotted on TLC plates (Alufolien Kieselgel 60F254; Merck, Darmstadt, Germany) using *n*-hexane/ethyl acetate (85:15, vol/vol) as developing solvent. The conversion of the labeled substrate into labeled lanosterol was analyzed by a System 200 Imaging Scanner (Hewlett-Packard, Palo Alto, CA); the counts were collected for 5 min, and the percentage of transformation was calculated by integration. For the K_m determinations different final concentrations of substrate (1–200 μM) were used and the incubation times arranged to obtain percentages of transformation not exceeding 10% (to keep safely within the range of linear relationship between product formation and time of reaction). The values of the enzymatic rate obtained at the different substrate concentrations were fitted by a nonlinear regression method to the Michaelis–Menten equation to calculate the K_m (30).

IC_{50} values (the concentration of inhibitor that reduces the enzymatic conversion by 50%) were calculated by nonlinear regression analysis of the residual activity vs. the log of concentrations of inhibitors. The values in the table are the means of two separate experiments each in duplicate.

RESULTS

Inhibition of T. cruzi OSC in cell-free homogenate of SMY8pBJ1.21 strain. To screen the inhibitors we used a homogenate of cells of the SMY8pBJ1.21 strain grown to late exponential phase. The *T. cruzi* OSC, known to partition between the cytosolic lipid bodies and the microsomes (31), was highly expressed in these cells. Detergents are needed to ensure the access of the apolar substrate and inhibitors to the enzyme in the lipid bodies and in the membranes and were used according to previous experiences (15,16,32). The enzyme activity was evaluated by radiometric scanning of thin-layer chromatograms of the organic extract of incubation mixtures. In our experimental conditions (plugged test tubes with no NADPH added), the only labeled peaks detected corresponded to cold standards of 2,3-oxidosqualene and lanosterol. No label was found in the 4-desmethylsterol region.

The specific activity, expressed as nmol of lanosterol formed, was 4 nmol/h/mg of proteins. The value of K_m, calculated by a nonlinear regression method, was 66 ± 13.5 μM.

To check the reliability and suitability of this homogenate for inhibition studies, we determined that the K_m values of the *S. cerevisiae* and *A. thaliana* enzymes expressed in the same host were, respectively, 30 ± 14.2 and 91 ± 29.6 μM, in agreement with the data reported for these enzymes using different enzymatic preparations (33,34). Therefore, the OSC expressed in transformed SMY8 cells have the same affinity for the substrate previously determined and seem suitable for testing inhibitors and comparing the results with those previously obtained with OSC of different origin.

All the inhibitors assayed, illustrated in Figure 2 and listed in Table 1, are substrate analogs already tested on mammalian and fungal OSC and were chosen as the more representative of different classes of compounds designed to inhibit OSC by different mechanisms. Prior to testing the inhibition of *T. cruzi* OSC, compound **1** was tested with the *S. cerevisiae* OSC expressed in yeast, compounds **12** and **16** were tested with pig liver enzyme. The IC$_{50}$ values determined and found to be the same as those reported in References 18 and 20, respectively.

Table 1 shows the IC$_{50}$ values obtained with some aza and methylidene derivatives of the substrate and with a series of vinyl and conjugated sulfide derivatives of truncated oxidosqualene. The activities are compared with those obtained previously by using detergent-solubilized microsomes prepared from pig liver and *S. cerevisiae* cells. The azasqualene derivatives are the 2-aza-2,3-dihydrosqualene **1**, its N-oxide **2**, and the 19-azasqualene **3** (25,26). The OSC of *T. cruzi* and of pig liver are inhibited similarly by 2-aza derivatives **1** and **2**, but not by 19-aza derivative **3**, which is a 30 times less effective inhibitor of *T. cruzi* enzyme. The methylidene derivatives **4**, **6**, **7**, and **8** show comparable activities against the *T. cruzi* and pig liver enzyme whereas compound **5** is five times less effective on *T. cruzi* OSC. As already observed for mammalian enzyme, the isomers of inhibitor with the same configuration as the substrate are at least 10 times more effective (16). The presence of a vinyl function in position 2 as in the *trans* 2-

vinyl-2-oxido-1,1-bisnorsqualene **8**, as already observed in pig and *S. cerevisiae* OSC, is not effective for inhibition (18).

Compounds **9–19** of Table 1 are vinyl and conjugated sulfide derivatives of truncated oxidosqualene (17,19,20). The *T. cruzi* OSC seems specifically inhibited by all the phenyl derivatives tested, i.e., compounds **12**, **16**, **17**, **18**, and **19**. The IC$_{50}$ values for these derivatives are in the range 70–600 nM, or 10 to 100 times lower than the IC$_{50}$ found in pig liver OSC. Furthermore, the corresponding methyl derivatives **9**, **13**, **14**, and **15**, which are very active in pig and *S. cerevisiae* (19,20), are less effective on *T. cruzi* OSC. The major difference is observed with compound **9**, showing, with *T.cruzi*, a 30 times larger IC$_{50}$ than with *S. cerevisiae*. Compounds **13** and **16** were also tested with the OSC of *A. thaliana*, expressed in the yeast strain SMY8pSM60.21. The IC$_{50}$ of both compounds were similar, 4.5 and 2 μM, respectively. IC$_{50}$ of phenyl derivatives **12**, **16**, **17** and **19**, tested with the OSC of *S. cerevisiae* expressed in a SMY8-derived strain (SMY8pSM61.21) were in complete accordance with the data shown in Table 1, obtained previously (18,20) with a wild-type *S. cerevisiae* (33).

DISCUSSION

We used a mutant strain of *S. cerevisiae* expressing the OSC of the pathogen protozoon *T. cruzi* to test a series of OSC inhibitors, with the aim of determining the susceptibility of this

TABLE 1

Inhibition of *Trypanosoma cruzi* OSC Expressed in SMY8pBJ1.21 Yeast Strain by Aza, Methylidene, and Vinyl and Dienic Sulfide Derivatives of Substrate Compared with IC$_{50}$ Previously Obtained with OSC from Pig Liver and *Saccharomyces cerevisiae*

	IC$_{50}$ (μM)[b]		
Compound[a]	OSC *T. cruzi*	OSC Pig liver[c]	OSC *S. cerevisiae*[c]
1	0.8	0.15	10.0
2	4.0	3.3	16.0
3	50.0	1.7	35.0
4	5.5	3.5	1.5
5	100.0	20.0	15.0
6	2.0	4.0	5.0
7	0.2	0.4	1.0
8	100.0	100.0	50.0
9	1.7	1.0	0.05
10	>100	1.2	0.4
11	>100	1.0	0.9
12	0.09	7.0	1.0
13	18.0	5.0	1.5
14	12.0	3.6	6.0
15	10.0	2.6	2.0
16	0.07	7.0	10.0
17	0.6	20.0	12.0
18	0.15	9.0	>100
19	0.5	7.5	40.0

[a]For structures of these compounds see Figure 2.
[b]Values are the means of two separate experiments, each with duplicate incubations. The maximal deviations from the mean were less than 10%.
[c]See References 16–20. OSC, oxidosqualene cyclase; IC$_{50}$, inhibitor concentration reducing enzymatic activity by 50%.

enzyme to different types of OSC inhibitors and possibly identifying specific inhibitors. OSC can be considered a promising target to inhibit the multiplication of pathogenic microbes, but, unlike some targets for sterol inhibition, such as Δ^{24} methyl transferase, OSC also is present in the mammalian cells. Specificity for the pathogen enzyme is consequently an important prerequisite for inhibitors.

We have tested 19 inhibitors, selected as representative of different classes of inhibitors. The azasqualene derivatives, which were designed as analogs of the high-energy carbocationic intermediates generated at C-2 after the opening of the oxiranic ring, or at C-19, after the closure of the fourth ring, have been well studied as inhibitors of mammalian and fungal OSC (15,25,26). From the comparison of the IC$_{50}$ obtained with the *T. cruzi* and with the pig and *S. cerevisiae* OSC, these compounds do not show specificity for the *T. cruzi* enzyme, probably because the mechanism of the initial step of the cyclization is very conserved in all the OSC (13). The closure of the last ring and the rearrangement are probably differently controlled in different OSC, as the 19-aza-derivative is very active only against pig liver OSC. The 29-methylidene derivatives **4–7**, previously shown to be time-dependent inhibitors (16,22), similarly lack specificity.

The most selective inhibition of *T. cruzi* OSC was found in the series of vinyl-thio-derivatives. The design of these compounds was based on the hypothesis that a partial cyclization of these compounds in the active site of the enzyme, because of the excellent properties of the sulfur in stabilizing the electron-deficient α-carbon, owing to its good π- and σ-donor properties, could generate carbocationic intermediates that were more stable and more able to interact strongly with nucleophilic amino acid residues. Our previous results showed that a methyl sulfide derivative, such as compound **9**, is a very effective inhibitor of *S. cerevisiae* OSC and a time-dependent inhibitor of pig OSC, whereas phenyl sulfide derivatives, such as **16**, **17**, and **19**, are poor inhibitors of both pig and yeast OSC (17,19,20). The *T. cruzi* OSC seems to be specifically inhibited by all the phenyl derivatives tested (compounds **12**, **16–19**). On the basis of these results, we initially speculated that the inhibition could be ascribed to specific π-π interaction of the aromatic derivatives with the Tyr540 of *T. cruzi* (21), which in the other lanosterol synthases is substituted for a conserved threonine residue. A tyrosine is conserved at this position in cycloartenol synthase (35,36), the plant enzyme converting oxidosqualene into cycloartenol, the precursor of plant sterols. The type of amino acid present in this position seems catalytically relevant for determining the final product of cyclization. Mutagenesis experiments have shown that the T/Y substitution causes a loss of accuracy in determining the final product of cyclization. A *S. cerevisiae* T384Y mutant produces substantial amounts of parkeol and lanost-24-ene-3β,9α-diol in addition to lanosterol (35), and the Y410T mutant of *A. thaliana* does not form cycloartenol, but rather lanosterol and 9β-lanosta-7,24-dien-3β-ol (36). To test the hypothesis that Tyr540 determines inhibitor specificity, we studied the inhibition of compounds **13** and **16** using a homogenate of a SMY8pSM60.21 strain expressing the OSC of *A. thaliana*.

In contrast to our hypothesis, both the methyl and the phenyl derivatives showed similar IC$_{50}$, respectively, 4.5 and 2 μM. Therefore, the specificity of the aromatic derivatives for the *T. cruzi* OSC may result from more complex differences between the two active sites, allowing different interactions with the inhibitors and possibly relating to the mechanism of control of the rearrangement and of the formation of the final product (37).

In conclusion, our results show that the homogenate of a yeast strain expressing enzymes of pathogenic organisms can be used for a preliminary screening of compounds potentially active against eukaryotic pathogenic organisms in totally safe conditions. The aromatic vinyl-thio-derivatives of the substrate of OSC are very promising candidates for the inhibition of sterol biosynthesis in *T. cruzi* and possibly related pathogens, and could also be considered as models for the design of new inhibitors.

REFERENCES

1. Mercer, E.I. (1991) Sterol Synthesis Inhibitors: Their Current Status and Modes of Action, *Lipids 26*, 584–597.
2. Abe, I., and Prestwich, G.D. (1999) Squalene Epoxidase and Oxidosqualene Lanosterol Cyclase—Key Enzymes in Cholesterol Biosynthesis, in *Comprehensive Natural Products Chemistry. Isoprenoid Including Carotenoids and Steroids* (Cane, D., ed.), Vol. 2, pp. 267–298, Elsevier, Oxford, United Kingdom.
3. Urbina, J.A. (1997) Lipid Biosynthesis Pathways as Chemotherapeutic Targets in Kinetoplastid Parasites, *Parasitology 114*, S91–S99.
4. Coppens, I., and Courtoy, P.J. (1995) Exogenous and Endogenous Sources of Sterols in the Culture-Adapted Procyclic Trypomastigotes of *Trypanosoma brucei*, *Mol. Biochem. Parasitol. 73*, 179–188.
5. Contreras, L.M., Vivas, J., and Urbina, J.A. (1997) Altered Lipid Composition and Enzyme Activities of Plasma Membranes from *Trypanosoma (Schizotrypanum) cruzi* Epimastigotes Grown in the Presence of Sterol Biosynthesis Inhibitors, *Biochem. Pharmacol. 53*, 697–704.
6. Ryder, N.S., Stuetz, A., and Nussbaumer, P. (1992) Squalene Epoxidase Inhibitors: Structural Determinants for Activity and Selectivity of Allylamines and Related Compounds, in *Regulation of Isopentenoid Metabolism* (Nes, W.D., Parish, E.J., and Trzaskos, J.M., eds.), pp. 192–204, American Chemical Society, Washington, DC.
7. Vanden Bossche, H., Marichal, P., Coene, M.-C., Willemsens, G., Le Jeune, L., Cools, W., and Verhoeven, H. (1992) Cytochrome P450-dependent 14α-Demethylase: Target for Antifungal Agents and Herbicides, in *Regulation of Isopentenoid Metabolism* (Nes, W.D., Parish, E.J., and Trzaskos, J.M., eds.), pp. 219–230, American Chemical Society, Washington, DC.
8. Docampo, R., and Schmuñis, G.A. (1997) Sterol Biosynthesis Inhibitors: Potential Chemotherapeutics Against Chagas Disease, *Parasitol. Today 13*, 129–130.
9. Urbina, J.A., Concepcion, J.L., Rangel, S., Visbal, G., and Lira,

R. (2002) Squalene Synthase as Chemotherapeutic Target in *Trypanosoma cruzi* and *Leishmania mexicana*, *Mol. Biochem. Parasitol. 125*, 35–45.

10. Orene Lorentes, S., Gomez, R., Jimenez, C., Cammerer, S., Yardley, V., de Luca-Fradley, K., Croft, S.L., Ruiz-Perez, L.M., Urbina, J., Gonzalez Pacanowska, D., *et al.* (2005) Biphenylquinuclidines as Inhibitors of Squalene Synthase and Growth of Parasitic Protozoa, *Bioorg. Med. Chem. 13*, 3519–3529.

11. Buckner, F.S., Griffin, J.H., Wilson, A.J., and Van Voorhis, W.C. (2001) Potent Anti-*Trypanosoma cruzi* Activities of Oxidosqualene Cyclase Inhibitors, *Antimicrob. Agents Chemother. 45*, 1210–1215.

12. Oliaro-Bosso, S., Viola, F., Matsuda, S., Cravotto, G., Tagliapietra, S., and Balliano, G. (2004) Umbelliferone Aminoalkyl Derivative as Inhibitors of Oxidosqualene Cyclase from *Saccaromyces cerevisiae, Trypanosoma cruzi,* and *Pneumocystis carinii*, *Lipids 39*, 1007–1012.

13. Abe, I., Rohmer, M., and Prestwich, G.D. (1993) Enzymatic Cyclization of Squalene and Oxidosqualene to Sterol and Triterpenes, *Chem. Rev. 93*, 2189–2206.

14. Thoma, R., Schulz-Gasch, T., D'Arcy, B., Benz, J., Aebi, J., Dehmlow, H., Hennig, M., Stihle, M., and Ruf, A. (2004) Insight into Steroid Scaffold Formation from the Structure of Human Oxidosqualene Cyclase, *Nature 432*, 118–122.

15. Viola, F., Brusa, P., Balliano, G., Ceruti, M., Boutaud, O., Schuber, F., and Cattel, L. (1995) Inhibition of 2,3-Oxidosqualene Cyclase and Sterol Biosynthesis by 10- and 19-Azasqualene Derivatives, *Biochem. Pharmacol. 50*, 787–796.

16. Ceruti, M., Rocco, F., Viola, F., Balliano, G., Milla, P., Arpicco, S., and Cattel, L. (1998) 29-Methylidene-2,3-oxidosqualene Derivatives as Stereospecific Mechanism-Based Inhibitors of Liver and Yeast Oxidosqualene Cyclase, *J. Med. Chem. 41*, 540–554.

17. Viola, F., Balliano, G., Milla, P., Cattel, L., Rocco, F., and Ceruti, M. (2000) Stereospecific Synthesis of *trans*-Vinyldioxidosqualene and β-Hydroxysulfide Derivatives, as Potent and Time-Dependent 2,3-Oxidosqualene Cyclase Inhibitors, *Bioorg. Med. Chem. 8*, 223–232.

18. Viola, F., Ceruti, M., Cattel, L., Milla, P., Poralla, K., and Balliano, G. (2000) Rationally Designed Inhibitors as Tools for Comparing the Mechanism of Squalene-Hopene Cyclase with Oxidosqualene Cyclase, *Lipids 35*, 297–303.

19. Ceruti, M., Balliano, G., Rocco, F., Milla, P., Arpicco, S., Cattel, L., and Viola, F. (2001) Vinyl Sulfide Derivatives of Truncated Oxidosqualene as Selective Inhibitors of Oxidosqualene and Squalene Hopene Cyclases, *Lipids 36*, 629–636.

20. Rocco, F., Oliaro-Bosso, S., Viola, F., Milla, P., Roma, G., Grossi, G., and Ceruti, M. (2003) Conjugated Methyl Sulfide and Phenyl Sulfide Derivatives of Oxidosqualene as Inhibitors of Oxidosqualene and Squalene-Hopene Cyclases, *Lipids 38*, 201–207.

21. Joubert, B.M., Buckner, F.S., and Matsuda, S.P.T. (2001) Trypanosome and Animal Lanosterol Synthases Use Different Catalytic Motifs, *Org. Lett. 3*, 1957–1960.

22. Xiao, X., and Prestwich, G.D. (1991) 29-Methylidene-2,3-oxidosqualene: A Potent Mechanism-Based Inactivator of Oxidosqualene Cyclase, *J. Am. Chem. Soc. 113*, 9673–9678.

23. Ceruti, M., Balliano, G., Viola, F., Cattel, L., Gerst, N., and Schuber, F. (1987) Synthesis and Biological Activity of Azasqualenes, bis-Azasqualenes and Derivatives, *Eur. J. Med. Chem. 22*, 199–208.

24. Field, R.B., Holmund, C.E., and Whittaker, N.F. (1979) The Effects of the Hypocholesteremic Compound 3 β-(β-dimethylaminoethoxy)-androst-5-en-17-one on the Sterol and Steryl Ester Composition of *Saccharomyces cerevisiae*, *Lipids 14*, 741–747.

25. Duriatti, A., Bouvier-Navé, P., Benveniste, P., Schuber, F., Delprino, L., Balliano, G., and Cattel, L. (1985) *In vitro* Inhibition of Animal and Higher Plants 2,3-Oxidosqualene-Sterol Cyclases by 2-Aza-2,3-dihydrosqualene and Derivatives, and by Other Ammonium-Containing Molecules, *Biochem. Pharmacol. 34*, 2765–2777.

26. Ceruti, M., Rocco, F., Viola, F., Balliano, G., Grosa, G., Dosio, F., and Cattel, L. (1993) Synthesis and Biological Activity of 19-Azasqualene 2,3-Epoxide as Inhibitor of 2,3-Oxidosqualene Cyclase, *Eur. J. Med. Chem. 28*, 675–682.

27. Corey, E.J., Matsuda, S.P.T., Baker, C.H., Ting, A.Y., and Cheng, H. (1996) Molecular Cloning of a *Schizosaccharomyces pombe* cDNA Encoding Lanosterol Synthase and Investigation of Conserved Tryptophan Residues, *Biochem. Biophys. Res. Commun. 219*, 327–331.

28. Hart, E.A., Hua, L., Darr, L.B., Wilson, W.K., Pang, J., and Matsuda, S.P.T. (1999) Directed Evolution to Investigate Steric Control of Enzymatic Oxidosqualene Cyclization. An Isoleucine-to-Valine Mutation in Cycloartenol Synthase Allows Lanosterol and Parkeol Biosynthesis, *J. Am. Chem. Soc. 121*, 9887–9888.

29. Peterson, G.L. (1977) A Simplification of the Protein Assay Method of Lowry *et al.* Which Is More Generally Applicable, *Anal. Biochem. 83*, 346–356.

30. Duggleby, R.G. (1981) A Nonlinear Regression Program for Small Computers, *Anal. Biochem. 110*, 9–18.

31. Milla, P., Viola, F., Oliaro-Bosso, S., Rocco, F., Cattel, L., Joubert, B.M., LeClair, R.J., Matsuda, S.P.T., and Balliano, G. (2002) Subcellular Localization of Oxidosqualene Cyclases from *Arabidopsis thaliana, Trypanosoma cruzi*, and *Pneumocystis carinii* Expressed in Yeast, *Lipids 37*, 1171–1176.

32. Milla, P., Athenstaedt, K., Viola, F., Oliaro-Bosso, S., Kohlwein, S.D., Daum, G., and Balliano, G. (2002) Yeast Oxidosqualene Cyclase (Erg7p) Is a Major Component of Lipid Particles, *J. Biol. Chem. 277*, 2406–2412.

33. Balliano, G., Viola, F., Ceruti, M., and Cattel, L. (1988) Inhibition of Sterol Biosynthesis in *Saccharomyces cerevisiae* by *N,N*-Diethylazasqualene and Derivatives, *Biochim. Biophys. Acta 959*, 9–19.

34. Taton, M., Benveniste, P., and Rahier, A. (1992) Inhibition of 2,3-Oxidosqualene Cyclases, *Biochemistry 31*, 7892–7898.

35. Meyer, M.M., Segura, M.J.R., Wilson, W.K., and Matsuda, S.P.T. (2000) Oxidosqualene Cyclase Residues That Promote Formation of Cycloartenol, Lanosterol, and Parkeol, *Angew. Chem. Int. 39*, 4090–4092.

36. Herrera, J.B.R., Wilson, W.K., and Matsuda, S.P.T. (2000) A Tyrosine-to-Threonine Mutation Converts Cycloartenol Synthase to an Oxidosqualene Cyclase That Forms Lanosterol as Its Major Product, *J. Am. Chem. Soc. 122*, 6765–6766.

37. Segura, M.J.R., Lodeiro, S., Meyer, M.M., Patel, A.K., and Matsuda, S.P.T. (2002) Directed Evolution Experiments Reveal Mutation at Cycloartenol Synthase Residue His477 That Dramatically Alter Catalysis, *Org. Lett. 4*, 4459–4462.

Fatty Acid and Hydroxy Acid Adaptation in Three Gram-Negative Hydrocarbon-Degrading Bacteria in Relation to Carbon Source

Mohamed Soltani, Pierre Metzger*, and Claude Largeau

Centre National de la Recherche Scientifique (CNRS) UMR 7618,
Ecole Nationale Supérieure de Chimie de Paris, 75231 Paris cedex 05, France

ABSTRACT: The lipids of three gram-negative bacteria, *Acinetobacter calcoaceticus, Marinobacter aquaeolei,* and *Pseudomonas oleovorans* grown on mineral media supplemented with ammonium acetate or hydrocarbons, were isolated, purified, and their structures determined. Three pools of lipids were isolated according to a sequential procedure: unbound lipids extracted with organic solvents, comprising metabolic lipids and the main part of membrane lipids, OH⁻-labile lipids (mainly ester-bound in the lipopolysaccharides, LPS) and H⁺-labile lipids (mainly amide-bound in the LPS). Unsaturated FA composition gave evidence for an aerobic desaturation pathway for the synthesis of these acids in *A. calcoaceticus* and *M. aquaeolei,* a nonclassic route in gram-negative bacteria. Surprisingly, both aerobic and anaerobic pathways are operating in the studied strain of *P. oleovorans.* The increase of the proportion of saturated FA observed for the strain of *P. oleovorans* grown on light hydrocarbons would increase the temperature transition of the lipids for maintaining the inner membrane fluidity. An opposite phenomenon occurs in *A. calcoaceticus* and *M. aquaeolei* grown on solid or highly viscous C_{19} hydrocarbons. The increases of FA $< C_{18}$ when the bacteria were grown on *n*-nonadecane, or of *iso*-FA in cultures on *iso*-nonadecane would decrease the transition temperature of the lipids, to maintain the fluidity of the inner membranes. Moreover, *P. oleovorans* grown on hydrocarbons greatly decreases the proportion of β-hydroxy acids of LPS, thus likely maintaining the physical properties of the outer membrane. By contrast, no dramatic change in hydroxy acid composition occurred in the other two bacteria.

Paper no. L9810 in *Lipids 40,* 1263–1272 (December 2005).

Most microorganisms adapt their membrane lipid composition to environmental changes, such as temperature stress or contact with organic substances, so as to keep the membrane fluidity at a constant value (1,2). To stabilize the fluidity of the membranes (a phenomenon known as homeoviscous adaptation) (3), there are two main mechanisms in bacteria: a *cis-trans* isomerization of unsaturated FA (4–7) and the variation of the saturated to unsaturated FA ratio (8). Hence, growth of a strain of the hydrocarbon-degrading bacterium *Pseudomonas oleovorans* on octane induces the isomerization of *cis* monounsaturated FA into *trans* FA (5). This change in favor of FA exhibiting higher m.p. counterbalances the decrease of the transition temperature of the membrane lipids induced by the intercalation of short-chain alkanes in the phospholipid bilayer.

The effect of hydrocarbons on the FA composition of phospholipids in several hydrocarbon-degrading bacteria has been investigated for many years (9–11). By contrast, little is known about the influence of environmental changes on the composition of other bacterial lipids, such as lipopolysaccharides (LPS), the major components of the outer leaflet of the outer membrane of gram-negative bacteria. LPS consist of three domains: an O-antigen polysaccharide attached to an amphiphilic lipid A *via* a core oligosaccharide (12). Lipids A generally contain four 3-hydroxy alkanoate residues attached to a glucosamine disaccharide backbone, two *via* ester links and two *via* amide bonds. Furthermore, alkanoic acids as well as 2-hydroxy or 3-hydroxy acids can be attached *via* ester bonds to the hydroxyl groups of these hydroxy alkanoates. Recent work with *Marinobacter hydrocarbonoclasticus* has shown that this gram-negative bacterium can incorporate β-hydroxy acids derived from the hydrocarbons fed to the organism into LPS as long as their steric hindrance and geometry do not markedly differ from those of 3-hydroxy-dodecanoic acid, the highly predominating hydroxy acid in LPS of this bacterium (13–15).

The aim of the present work was to determine the influence of aliphatic hydrocarbons on the lipid composition of three gram-negative bacteria: *Pseudomonas oleovorans,* which can grow on medium-chain hydrocarbons, C_6 to C_{12} (16); *Acinetobacter calcoaceticus* (17,18), which degrades long-chain hydrocarbons, C_{16} to C_{33}; and *M. aquaeolei,* recently isolated from a Vietnamese oil-producing well, which is known to degrade *n*-hexadecane and crude oils (19). This latter bacterium belongs to a rapidly expanding genus whose species exhibit hydrocarbonoclastic properties (20–23).

As previously outlined (15), this type of study has geochemical applications in evaluating the impact of hydrocarbon pollution on organic matter in sediments and in particular on the organic matter from prokaryotic origin. Hence, to apply the analytical procedure to sediments, which are often resistant to the extraction of total lipids, a sequential extraction procedure leading to three lipid pools has to be used (13,24). A first extraction of the dry cells with organic solvents affords the so-called unbound lipids that correspond to metabolic lipids and to the main part of phospholipids, as recently demonstrated (15). At this point of the protocol, LPS are not extracted from the bacterial

biomass. To obtain the ester-bound (OH⁻ labile) and amide-bound (H⁺ labile) acids of LPS, which are the main lipoconjugates in gram-negative bacteria, basic and acid treatments of the extracted biomass are performed successively.

EXPERIMENTAL PROCEDURES

Chemicals. Silica gel (70–230 mesh) was from Merck Eurolab (Lyon, France). FA standards were purchased from Sigma-Aldrich (L'Isle d'Abeau, France) and Larodan (Malmö, Sweden). An etheral solution of diazomethane was prepared from Diazald® (Sigma-Aldrich) according to an Aldrich procedure (Technical Information Bulletin AL-180). Dimethyl disulfide (DMDS) and pyrrolidine were from Merck (Darmstadt, Germany).

n-Octane and 2-methyl-heptane (To avoid any confusion with 2,2,4-trimethyl-pentane, the *iso*-octane used for the definition of octane number, the *iso* terminology is not used for 2-methyl-heptane) were obtained from Acros (Noisy-le-Grand, France; purity 99%). *n*-Nonadecane was obtained from Fluka (L'Isle d'Abeau, France; purity 99%). *iso*-Nonadecane was prepared by catalytic hydrogenation of *cis*-2-octadec-7-ene (Lancaster, Bischleim, France; purity 98%) in the presence of Rh/C 5% (Acros) in heptane, and then purified as previously described (15).

Cultures. The bacteria investigated in this study were obtained from the Culture Collection of Institut Pasteur (Paris, France): *A. calcoaceticus* 66.33, *M. aquaeolei* 106100 T, and *P. oleovorans* 59.11 T. Cells were grown at 25°C in 3-L Erlenmeyer flasks containing 750 mL of an appropriate culture medium supplemented with ammonium acetate (4 g/L) or hydrocarbons (1 g/L). For *M. aquaeolei*, a synthetic seawater medium was used (14); *P. oleovorans* (25) and *A. calcoaceticus* (9) were grown on mineral media. The tested hydrocarbons were *n*-nonadecane and *iso*-nonadecane with *M. aquaeolei* and *A. calcoaceticus*, and *n*-octane and 2-methyl-heptane with *P. oleovorans*. The pH of each culture medium was adjusted to 7.5–7.8 before autoclaving. The growth was monitored by measuring the O.D. at 450 nm with a Varian DMDS 90 UV-vis spectrophotometer. The biomasses were harvested at the late exponential growth phase by centrifugation at $12,000 \times g$ for 15 min at 4°C, washed twice with 30 mL of synthetic medium, and freeze-dried.

Isolation of lipids. The protocol used for the sequential extraction of the lipids has been previously reported (15). Briefly, the dry biomass was extracted with chloroform/methanol (2:1, vol/vol), with stirring at room temperature. This extract was transesterified at 0°C in methanol/KOH (0.1 M); then the reaction mixture was acidified to pH 1 and extracted with diethyl ether/heptane. The product was then purified using silica gel column chromatography; a first elution with heptane furnished the unmetabolized hydrocarbons, and elution with diethyl ether/methanol (4:1, vol/vol) gave the unbound lipids. The transesterification of the solvent-extracted biomass in methanol/KOH 1 M under reflux furnished the OH—labile lipids, and finally the acid hydrolysis of the residual biomass in aqueous 4 M HCl under reflux gave the H⁺-labile lipids.

Derivatization and GC–MS. Generally, the treatment of lipids by a methanol/KOH solution furnishes predominantly methyl esters and variable proportions of FA. To complete the esterification, the transesterified lipid fractions were treated by an etheral solution of diazomethane, until the characteristic yellow color of diazomethane persisted. Acids released by acid hydrolysis were esterified in a similar way by diazomethane. Alcohols and hydroxy acid methyl esters were analyzed as trimethylsilyl (TMSi) ethers (26). A standard of *iso*-C$_{19}$ primary fatty alcohol was prepared by reduction of the corresponding FAME with LiAlH$_4$ as previously described (15). DMDS adducts were prepared by an I$_2$ reaction (27), and N-acyl pyrrolidides were prepared by direct treatment of methyl esters with pyrrolidine/acetic acid (28). *Cis*- and *trans*-isomers of monounsaturated FA were identified *via* their *threo*- and *erythro*-DMDS adducts, respectively, considering that the derivative from a *cis*-isomer elutes first on GC columns containing nonpolar phases (29). Lipids were analyzed by GC–MS (70 eV) with a Hewlett-Packard HP 6890 gas chromatograph coupled with an HP 5973N mass spectrometer (Agilent Technology). The chromatograph was equipped with a J&W Scientific (Massy, France) DB-5MS fused-silica column (30 m × 0.25 mm) coated with 95% polydimethylsiloxane and 5% phenylsiloxane (film thickness 0.25 µm). The temperature program was from 100 to 300°C (4°C/min).

RESULTS

Quantitative data. In the three bacteria, the unbound lipids dominated, ranging from 59 (*P. oleovorans* grown on *n*-octane) to 75% (*A. calcoaceticus* grown on ammonium acetate or *iso*-nonadecane, and *M. aquaeolei* grown on *iso*-nonadecane) of total lipids, whereas the OH⁻-labile lipids varied between 14 (*A. calcoaceticus* grown on ammonium acetate) and 27% (*P. oleovorans* grown on *n*-octane), and the H⁺ lipids varied between 4 (*A. calcoaceticus* grown on *n*-nonadecane) and 16% (*P. oleovorans* grown on 2-Me-heptane) of total lipids (Table 1).

Cultures of P. oleovorans. The compositions of the lipids extracted from the cultures of *P. oleovorans* on ammonium acetate, *n*-octane and 2-Me-heptane are listed in Table 2. Data in Table 3 summarize the main trends observed for the distribution of FA in unbound lipids of *P. oleovorans* according to the carbon source. FA highly predominated in the unbound lipids, with even carbon-numbered compounds highly dominating in the ammonium acetate and *n*-octane cultures. Culture on ammonium acetate principally led to unsaturated FA (mainly *n*-18:1(11*c*) and *n*-16:1(9*c*), whereas the cultures on *n*-octane and 2-Me-heptane mainly furnished saturated FA (Tables 2 and 3). Moreover, oleic acid, *n*-18:1(9*c*) was abundant in the culture on *n*-octane, but it was not detected in the culture on ammonium acetate. Low proportions of cyclopropane FA and *trans*-unsaturated FA were also detected.

In the OH⁻-labile lipids of the ammonium acetate culture, saturated FA (*n*-12:0 dominant) and β-hydroxy acids (*n*-10:0 major) were dominant, whereas the β-hydroxy acids became minor products in the cultures on hydrocarbons (Table 2).

TABLE 1
Abundance of Lipid Pools Isolated from *Acinetobacter calcoaceticus, Marinobacter aquaeolei*, and *Pseudomonas oleovorans* Cultivated on Different Carbon Sources

Bacteria/	Cell yield[a]	Total lipids	Lipid		
Carbon sources	(mg/L)	(% of dry cells)	Unbound	OH⁻-labile	H⁺-labile
A. calcoaceticus					
$CH_3CO_2NH_4$	853	2.8	75	14	10
n-$C_{19}H_{40}$	697	6.8	73	23	4
i-$C_{19}H_{40}$	352	6.2	75	18	7
M. aquaeolei					
$CH_3CO_2NH_4$	628	5.3	72	24	4
n-$C_{19}H_{40}$	319	7.0	67	25	8
i-$C_{19}H_{40}$	283	6.1	75	20	5
P. oleovorans					
$CH_3CO_2NH_4$	ND[b]	ND	74	16	10
n-C_8H_{18}	ND	ND	59	27	14
2-Me-C_7H_{15}	ND	ND	61	23	16

[a]Dry weight (free of nonmetabolized hydrocarbons).
[b]ND, not determined owing to the presence of mineral salts in addition to the lyophilized cells.

β-Hydroxy acids were markedly abundant in the H⁺-labile lipid pool isolated from the culture on ammonium acetate, with *n*-12:0 dominant and low amounts of its higher (*n*-13:0 and *n*-14:0) and lower (*n*-10:0 and *n*-11:0) homologs. Their proportions decreased in the cultures on *n*-octane and 2-Me-heptane. In the cultures on hydrocarbons, appreciable proportions of FA, mainly saturated (palmitic acid dominant), were present.

Cultures of A. calcoaceticus. Data concerning the cultures of *A. calcoaceticus* on ammonium acetate, *n*-nonadecane, and *iso*-

nonadecane are listed in Table 4. The FA, β-hydroxy acids (*n*-12:0 excepted), and fatty alcohols present in the unbound lipids appeared to relate rather well to the structure of the carbon source, with straight-chain compounds (acetate and *n*-nonadecane), or *iso* (on *iso*-nonadecane), and even-numbered (on acetate) or odd-numbered (on *n*- and *iso*-nonadecanes) predominating (Table 5). For instance, whereas FA of the ammonium acetate culture were mainly composed of *n*-18:1(9*c*), *n*-16:1(9*c*), and *n*-16:0, those predominating in the *iso*-nonadecane culture

TABLE 2
FA, Hydroxy Acid, and Fatty Alcohol Composition[a] of the Three Lipid Pools[b] Isolated from *P. oleovorans* grown on $CH_3CO_2NH_4$, and *n*-C_8 and 2-Me-C_7 Alkanes

	Unbound			OH⁻-labile			H⁺-labile		
Lipids	$CH_3CO_2NH_4$	n-C_8H_{18}	2-Me-C_7H_{15}	$CH_3CO_2NH_4$	n-C_8H_{18}	2-Me-C_7H_{15}	$CH_3CO_2NH_4$	n-C_8H_{18}	2-Me-C_7H_{15}
FA	*97.6*	*88.7*	*85.9*	*60.1*	*88.9*	*85.9*	*5.3*	*25.9*	*26.0*
Saturated FA	*18.3*	*47.7*	*56.9*	*47.1*	*52.7*	*40.2*	*4.7*	*21.0*	*25.4*
n-12:0	0.1	1.6	2.2	32.7	16.2	0.7	—[c]	0.1	0.6
n-16:0	15.7	27.9	27.3	11.8	22.0	23.7	2.2	9.8	14.8
n-17:0	0.1	1.1	7.9	0.6	0.4	8.5	0.2	0.8	1.6
n-18:0	1.8	9.0	6.9	1.1	1.7	4.1	1.3	5.1	3.8
Cyclopropane FA	*6.0*	*3.6*	*2.1*	*0.7*	*1.4*	*3.5*	—	*3.2*	—
17 Cycl (9,10)	4.8	2.4	1.5	0.5	1.0	2.6	—	2.1	—
Unsaturated FA	*73.3*	*37.4*	*26.9*	*12.3*	*34.8*	*42.2*	*0.6*	*1.7*	*0.6*
n-16:1(9*c*)	12.3	6.6	1.7	1.5	6.5	9.6	—	0.3	—
n-16:1(9*t*)	3.1	0.3	0.1	0.7	3.4	2.4	—	Trace	—
n-17:1(9*c*)	—	Trace	7.0	—	0.2	7.9	—	—	—
n-17:1(9*t*)	—	—	0.6	—	0.1	0.2	—	—	—
n-17:1(8*c*)	—	—	7.3	—	—	Trace	—	—	—
n-17:1(8*t*)	—	—	0.4	—	—	—	—	—	—
n-18:1(11*c*)	55.6	8.3	1.4	8.5	15.2	11.5	0.3	1.4	0.6
n-18:1(11*t*)	2.3	0.7	Trace	0.4	2.5	0.3	0.3	Trace	—
n-18:1(9*c*)	—	21.5	5.9	0.2	4.7	3.2	—	—	—
β-Hydroxy acids	*Trace*	*Trace*	*Trace*	*38.6*	*2.8*	*7.3*	*91.5*	*68.7*	*64.6*
n-10:0	—	—	—	36.0	2.4	0.3	0.4	3.7	0.8
n-11:0	—	—	—	—	Trace	Trace	0.3	0.6	Trace
n-12:0	Trace	Trace	Trace	2.6	0.4	7.0	90.0	63.8	61.0
Fatty alcohols	*1.6*	*7.5*	*7.5*	*0.9*	*1.0*	*5.0*	*1.9*	*5.0*	*7.1*
n-16:0,1-OH	0.8	5.3	5.0	0.4	0.6	1.3	1.0	3.1	4.0
Other	*0.8*	*3.8*	*6.6*	*0.4*	*7.3*	*1.8*	*1.3*	*0.4*	*2.3*

[a]Only the compounds accounting for more than 5% in at least one pool, or those playing a role regarding metabolism or lipid adaptation are detailed.
[b]Expressed as the percentage of total lipids for the considered pool.
[c]—, not detected. For other abbreviations see Table 1.

TABLE 3
Main Properties of FA from Unbound Lipids and Hydroxy Acids from Lipopolysaccharides (LPS) in *P. oleovorans* in Relation to the Carbon Source

Lipids[a]	$CH_3CO_2NH_4$	$n\text{-}C_8H_{18}$	$2\text{-Me-}C_7H_{15}$
ΣFA of unbound lipids (wt% of the pool)	98	89	86
Saturated *n*-FA	18	44	56
cis-Unsaturated *n*-FA	68	36	23
trans-Unsaturated *n*-FA	5	1	1
Even carbon-numbered *n*-FA	91	78	50
n-FA	92	82	83
iso-FA	—[b]	2	1
Total unsaturated FA	73	37	27
Cyclopropane FA	6	4	2
Total FA > C_{16}	66	44	42
β-Hydroxy acids in OH⁻-labile lipids			
Total (wt% of the pool)	39	3	7
% of β-OH *n*-10:0	93	86	4
β-Hydroxy acids in H⁺-labile lipids			
Total (wt% of the pool)	92	69	65
% of β-OH *n*-12:0	98	93	94

[a]In this table, the compounds not detailed in Table 2 are taken into account.
[b]—, not detected. For other abbreviation see Table 1.

were *i*-19:1(9) and *i*-17:0. On the whole, cultures on ammonium acetate and *n*-nonadecane led to dominant straight-chain unsaturated FA series, whereas the one on *iso*-nonadecane gave mainly *iso* saturated FA series (Table 5). Moreover, the proportion of unsaturated FA decreased after culturing on *iso*-nonadecane. Low amounts of *trans*-unsaturated FA were only detected in the cultures on *n*-nonadecane and *iso*-nonadecane (data not shown). In bacteria grown on *n*-nonadecane, two C_{19} primary fatty alcohols (a saturated and a monounsaturated, *n*-19:1(10),1-OH), and one secondary (*n*-19:0,2-OH) were identified. By contrast, *iso*-nonadecane furnished only two saturated primary fatty alcohols (*i*-19:0,1-OH and 2-Me-18:0,1-OH).

In the OH⁻-labile lipids, short-chain *n*-FA predominated in the ammonium acetate (*n*-12:0) and *n*-nonadecane cultures (*n*-12:0 and *n*-11:0), whereas in the *iso*-nonadecane culture *iso* and straight-chain series of saturated FA were equally represented. Unsaturated FA related rather well to the structure of the carbon source. In both series of α- and β-hydroxy acids, *n*-12:0 predominated (Table 4). Variable amounts of higher (*n*-13:0 and *n*-14:0) and lower (*n*-10:0 and *n*-11:0) homologs were also present and in rather substantial amounts in the case of the culture on *n*-nonadecane.

By contrast, β-hydroxy acids were highly dominant in the H⁺-labile lipids, especially in the cultures on hydrocarbons, whereas α-hydroxy acids became minor constituents. Fatty alcohols were important constituents of both OH⁻- and H⁺-labile lipids from the acetate culture (*n*-16 and *n*-18 primary alcohols; up to 34.9% of the H⁺-labile lipids), whereas they were side products in the same pools of the cultures on hydrocarbons.

Cultures of M. aquaeolei. The compositions of the three lipid pools isolated from the cultures on ammonium acetate, *n*-and *iso*-nonadecane are shown in Table 6. FA highly dominated the unbound lipids of the three cultures. In the unbound lipid pool, the chemical structure of FA was rather well related to that of the carbon source, as also observed for *A. calcoaceti-*

cus. In the ammonium acetate culture, the main FA were, in descending order, *n*-16:0, *n*-18:1(9*c*), *n*-16:1(7*c*), and *n*-16:1(9*c*), whereas in the culture on *n*-nonadecane they were *n*-17:0, *n*-17:1(9*c*), *n*-15:0, and *n*-16:1(7*c*), and in the one on *iso*-nonadecane, *i*-17:0, *n*-18:1(9*c*), *i*-17:1(9), and *i*-15:0. In addition, a minor series of midchain-branched FA structurally related to the carbon source was also detected. It was composed mainly of 10-Me-16:0 and 10-Me-18:0 (not shown in the table) FA in the ammonium acetate culture, 10-Me-17:0 FA in the *n*-nonadecane culture, and a mixture of midchain methyl-branched derivatives of *i*-15:0, *i*-17:0, and *i*-19:0 FA in the *iso*-nonadecane culture. Moreover, unsaturated FA were in higher amounts in the ammonium acetate culture than in those on hydrocarbons (Table 7). Low amounts of alcohols derived from alkane oxidation were present, with predominance of the saturated primary fatty alcohol. In addition, β-hydroxy acids structurally related to the fed alkanes were identified: 3-OH-*n*-19:0, or 3-OH-*i*-19:0.

In the OH⁻-labile lipids, the straight-chain series dominated, with *n*-12:0 FA dominant in the cultures on ammonium acetate and *iso*-nonadecane, and *n*-17:0 in the culture on *n*-nonadecane (Tables 6 and 7). β-Hydroxy acids were abundant in this pool, with 3-OH-*n*-12:0 predominating in the culture on ammonium acetate, and accompanied by variable proportions of some lower and higher homologs. In the culture on *iso*-nonadecane *i*-13:0 β-hydroxy acid was detected in low amount. Rather similar profiles of β-hydroxy acids were observed in the H⁺-labile lipids (Table 6), except in the case of the culture on *iso*-nonadecane, which furnished 3-OH-*i*-13:0 as the sole hydroxy *iso*-acid.

DISCUSSION

This study shows that the three gram-negative bacteria grow as well as on straight-chain hydrocarbons as on *iso*-alkanes. The growth of *A. calcoaceticus* and *M. aquaeolei* on *iso*-nonade-

TABLE 4
FA, Hydroxy Acid, and Fatty Alcohol Composition[a] of the Three Lipid Pools[b] Isolated from *A. calcoaceticus* Grown on $CH_3CO_2NH_4$, and *n*-C_{19} and *iso*-C_{19} Alkanes

Lipids	Unbound			OH⁻-labile			H⁺-labile		
	$CH_3CO_2NH_4$	*n*-$C_{19}H_{40}$	*i*-$C_{19}H_{40}$	$CH_3CO_2NH_4$	*n*-$C_{19}H_{40}$	*i*-$C_{19}H_{40}$	$CH_3CO_2NH_4$	*n*-$C_{19}H_{40}$	*i*-$C_{19}H_{40}$
FA	*89.4*	*95.3*	*97.3*	*50.1*	*46.3*	*37.8*	*10.4*	*1.3*	*1.5*
Saturated FA	*37.4*	*35.6*	*57.6*	*40.2*	*34.1*	*25.7*	*8.8*	*1.3*	*1.5*
n-10:0	—[c]	—	—	1.2	5.3	—	0.3	—	—
n-11:0	—	—	—	—	7.1	—	Trace	—	—
n-12:0	0.2	—	—	24.5	12.6	8.4	1.4	—	—
n-15:0	0.5	8.1	—	0.7	2.9	—	0.2	Trace	—
i-15:0	—	Trace	5.9	—	—	2.5	—	—	—
n-16:0	34.8	2.8	2.4	9.4	1.1	3.8	5.6	0.4	1.5
i-16:0	—	—	5.9	—	—	1.2	—	—	—
n-17:0	0.1	23.1	—	Trace	4.1	—	0.3	0.1	—
i-17:0	—	Trace	41.1	—	—	9.8	—	—	—
Unsaturated FA	*52.0*	*59.7*	*39.7*	*9.9*	*12.2*	*12.1*	*1.6*	—	—
n-16:1(9*c*)	20.2	0.4	1.7	2.2	Trace	2.3	0.2	—	—
n-17:1(9*c*)	0.4	17.7	—	—	4.0	—	—	—	—
n-17:1(9*t*)	—	0.4	—	—	—	—	—	—	—
n-17:1(8*c*)	—	23.0	—	—	3.7	—	—	—	—
n-17:1(7)	—	2.2	—	—	—	—	—	—	—
i-17:1(9*c*)	—	—	2.0	—	—	0.3	—	—	—
i-17:1(9*t*)	—	—	0.2	—	—	—	—	—	—
n-18:1(9*c*)	30.5	5.4	—	7.4	1.4	—	1.4	—	—
n-19:1(9)	—	5.7	—	—	0.8	—	—	—	—
i-19:1(9)	—	—	30.5	—	—	8.1	—	—	—
α-*Hydroxy acids*	—	—	*0.5*	*13.9*	*19.7*	*27.3*	*2.4*	*0.9*	*Trace*
n-11:0	—	—	—	—	1.2	Trace	—	Trace	—
n-12:0	—	—	0.5	13.9	17.0	26.9	2.4	0.9	Trace
n-13:0	—	—	—	—	1.1	0.4	—	Trace	—
β-*Hydroxy acids*	*0.2*	*0.2*	*0.2*	*20.4*	*31.6*	*30.8*	*50.4*	*93.8*	*95.9*
n-11:0	—	Trace	—	Trace	5.9	0.4	—	1.5	—
n-12:0	0.2	0.1	0.1	19.4	22.6	29.2	17.4	51.3	36.4
n-13:0	—	—	Trace	0.3	2.3	0.6	2.1	26.8	6.4
n-14:0	Trace	Trace	—	0.5	0.3	0.6	30.9	14.0	51.8
n-15:0	—	—	—	—	Trace	—	—	0.2	1.3
n-19:0	—	0.1	—	—	Trace	—	—	—	—
i-19:0	—	—	0.1	—	—	—	—	—	—
Fatty alcohols	*2.7*	*3.1*	*0.7*	*13.1*	*1.0*	*0.5*	*34.9*	*0.2*	*0.5*
n-16:0,1-OH	1.2	0.1	0.2	4.9	0.3	0.3	12.4	0.1	0.5
n-18:1,1-OH	1.1	—	—	5.8	0.4	—	15.7	—	—
n-19:0,1-OH	—	1.5	—	—	0.1	—	—	—	—
n-19:0,2-OH	—	0.2	—	—	Trace	—	—	—	—
n-19:1(10),1-OH	—	1.1	—	—	—	—	—	—	—
i-19:0,1-OH	—	—	0.3	—	—	Trace	—	—	—
2-Me-18:0,1-OH	—	—	0.1	—	—	—	—	—	—
Other	*7.7*	*1.3*	*1.3*	*2.3*	*1.4*	*3.6*	*1.9*	*3.8*	*2.1*

[a]Only the compounds accounting for more than 5% in at least one pool, or those playing a role regarding metabolism or lipid adaptation are detailed.
[b]Expressed as the percentage of total lipids for the considered pool.
[c]—, not detected. For other abbreviations see Table 1.

cane induced the production of very high proportions of *iso* FA, in contrast to the culture of *P. oleovorans* on 2-Me heptane. This ability of *M. aquaeolei*, in addition to the high efficiency of *M. hydrocarbonoclasticus*, *M. squalenivorans*, and some other *Marinobacter* species for degrading a wide range of hydrocarbons (15,21,23,30), emphasizes the remarkable adaptation of the members of this genus for degrading hydrocarbons. FA profiles of *M. aquaeolei* and *A. calcoaceticus* may become typical of gram-positive bacteria, i.e., with high proportions of branched FA (31), when they grow on *iso*-alkanes, as recently shown with *M. hydrocarbonoclasticus* (15).

The presence of 10-methyl FA in the unbound lipids of *M. aquaeolei* grown on ammonium acetate, previously detected in a culture on a complex medium (19), confirms that these FA can be no longer considered as characteristic of bacteria of the genus *Desulfobacter* (32), nor as indicator of a hydrocarbonoclastic activity when detected in sediments (11).

An important feature of *A. calcoaceticus* and of species of this genus is the accumulation of wax esters when the bacterium is grown on nitrogen-deficient media (17,33). Wax esters were not detected in unbound lipids, probably due to the abundance of ammonium salts in the present culture media. In

TABLE 5
Main Properties of FA from Unbound Lipids and Hydroxy Acids from LPS in *A. calcoaceticus* in Relation to the Carbon Source

Lipids[a]	$CH_3CO_2NH_4$	$n\text{-}C_{19}H_{40}$	$i\text{-}C_{19}H_{40}$
ΣFA of unbound lipids (wt% of the pool)	89	95	97
Saturated *n*-FA	37	37	2
Unsaturated *n*-FA	52	63	2
Even carbon-numbered *n*-FA	88	12	4
n-FA	89	95	4
iso-FA	—[b]	Trace	93
Total unsaturated	52	60	40
Total FA < C_{18}	57	81	63
α- and β-Hydroxy acids in OH⁻-labile lipids			
Total α-hydroxy (wt% of the pool)	14	20	27
% of α-OH *n*-12:0	100	86	98
Total β-hydroxy (wt% of the pool)	20	32	31
% of β-OH *n*-12:0	95	71	95
β-Hydroxy acids in H⁺-labile lipids			
Total (wt% of the pool)	50	94	96
% of β-OH *n*-12:0	34	55	38
% of β-OH *n*-14:0	61	15	54

[a]In this table, the compounds not detailed in Table 4 are taken into account.
[b]—, not detected. For other abbreviations see Tables 1 and 3.

this culture, appreciable proportions of primary fatty alcohols, *n*-16:0 and *n*-18:1, were detected in the OH⁻-labile lipids and even more in the H⁺-labile lipid pool. The nature of the corresponding esters is presently unknown, and the only linkage imaginable for the H⁺-labile fatty alcohols could be of a glycosidic type, i.e., sensitive to acidic conditions (34).

Hydrocarbon metabolism. Both *A. calcoaceticus* and *M. aquaeolei* metabolize *n*-nonadecane and *iso*-nonadecane mainly *via* oxidation to primary alcohols (Fig. 1): (i) In the case of *iso*-nonadecane, the oxidation occurs mainly on the less-hindered terminal methyl group (Fig. 1). The identification of minor amounts of *i*-18:0 and *i*-16:0 FA in the cultures on *iso*-nonadecane (data not shown) indicated that another route, *via* the α-oxidation pathway, also occurred (Fig. 1). (ii) Subterminal oxidation is a minor route for the degradation of *n*-nonadecane in these two bacteria. (iii) As recently observed in *M. hydrocarbonoclasticus* (15), the derived *n*-nonadecan-2-ol was likely oxidized to *n*-C18:0 FA *via* a Bayer–Villiger type reaction (35). (iv) The desaturation of *n*-nonadecane and/or *n*-nonadecan-1-ol, could then give *n*-nonadecen-1-ols, with unsaturations at position 9, 10, and 11, depending on the bacterium.

In the cultures of *P. oleovorans*, none of the possible intermediates of hydrocarbon oxidation were identified. The oxidation pathway of medium chain-length *n*-alkanes (C_6 to C_{12}) to the corresponding primary alcohols and further oxidations to acids then entering the β-oxidation cycle is, however, well established (36).

FA biosynthetic pathways. In terms of FA biosynthesis, the three bacteria exhibit unexpected behaviors. Indeed, it is generally admitted that bacteria synthesize unsaturated FA by *de novo* synthesis, through the anaerobic pathway *via cis*-decenoic acid 10:1(3*c*) and successive elongations to palmitoleic acid, 16:1(9*c*) and *cis*-vaccenic acid, 18:1(11*c*). By contrast, in animals and some microorganisms, desaturation occurs after lipid biosynthesis, through the aerobic pathway, by FA desaturation

to produce mainly palmitoleic, 16:1(9*c*), and oleic, 18:1(9*c*), acids (37–39). Regarding *A. calcoaceticus* and *M. aquaeolei*, the clear predominance of oleic acid relative to *cis*-vaccenic acid, whatever the substrate, bears evidence of the aerobic pathway. The existence of long alkyl-chain desaturases is confirmed by the identification of *n*-nonadecen-1-ols when the two bacteria are grown on *n*-nonadecane. The ability to desaturate saturated FA occurs typically in mycobacteria and corynebacteria (39), but it is much less widely distributed in gram-negative bacteria (40,11); this pathway notably has been reported in another strain of *A. calcoaceticus* (41). Although the multifunctional enzyme system producing unsaturated FA in actinomycetes is now well known, the aerobic desaturase system operating in the gram-negative bacteria is presently unknown. By comparison, the biosynthesis of unsaturated FA in *P. oleovorans* appears more complex, with both aerobic and anaerobic pathways coexisting in this strain. Over two decades ago, Wada *et al.* (42) demonstrated such a coexistence in a *Pseudomonas* and presumed that many bacteria of this genus would exhibit this property. In the present case, unsaturated FA are synthesized *via* the anaerobic route in the presence of ammonium acetate, but both pathways operate in presence of hydrocarbons. These results suggest that in this strain of *P. oleovorans*, *n*-octane and 2-methyl heptane, or their oxidized derivatives, would partially inhibit the synthesis of *cis*-decenoic acid 10:1(3*c*), the intermediate in the biosynthesis of palmitoleic and *cis*-vaccenic acids *via* the anaerobic pathway.

Adaptation of FA composition. In response to exposure to light hydrocarbons, *P. oleovorans* adapts the FA composition of the unbound lipids essentially by decreasing the proportion of *cis*-unsaturated FA, when compared with results obtained when culturing the organism on ammonium acetate, and by increasing the proportion of saturated FA. This strategy is different from the one adopted by another strain of *P. oleovorans*

TABLE 6

FA, Hydroxy Acid, and Fatty Alcohol Composition[a] of the Three Lipid Pools[b] Isolated from *M. aquaeolei* Grown on CH₃CO₂NH₄, and *n*-C₁₉ and *iso*-C₁₉ Alkanes

Lipids	Unbound			OH⁻ labile			H⁺-labile		
	$CH_3CO_2NH_4$	$n\text{-}C_{19}H_{40}$	$i\text{-}C_{19}H_{40}$	$CH_3CO_2NH_4$	$n\text{-}C_{19}H_{40}$	$i\text{-}C_{19}H_{40}$	$CH_3CO_2NH_4$	$n\text{-}C_{19}H_{40}$	$i\text{-}C_{19}H_{40}$
FA	*97.5*	*93.1*	*96.4*	*55.9*	*37.7*	*45.2*	*6.0*	*22.1*	*36.7*
Saturated FA	*42.4*	*50.9*	*59.7*	*37.1*	*24.9*	*33.2*	*5.3*	*20.4*	*27.2*
n-12:0	Trace	—[c]	0.3	14.1	1.8	15.6	Trace	4.0	—
n-15:0	0.1	10.4	0.1	0.2	0.1	0.2	0.3	Trace	0.1
i-15:0	Trace	0.1	9.5	Trace	0.1	0.5	Trace	—	5.2
n-16:0	31.6	3.0	5.5	17.3	3.9	2.2	2.6	3.8	4.7
n-17:0	0.1	29.6	Trace	0.1	13.4	0.5	0.3	3.2	0.5
i-17:0	—	—	33.5	—	—	6.6	—	—	9.1
10-Me-16:0	1.7	1.0	Trace	0.8	0.1	—	Trace	0.2	1.6
8,15-Me₂-16:0	—	—	1.5	—	—	—	—	—	0.8
10,15-Me₂-16:0	—	—	3.0	—	—	—	—	—	0.1
10-Me-17:0	Trace	3.5	—	—	1.2	—	—	0.4	—
i-19:0	—	—	2.0	—	—	1.6	—	—	1.2
10,17-Me₂-18:0	—	—	0.3	—	—	—	—	—	0.1
Unsaturated FA	*55.1*	*42.2*	*36.7*	*18.8*	*12.8*	*12.0*	*0.7*	*1.7*	*9.5*
n-16:1(9*c*)	8.7	2.3	1.6	0.4	0.8	0.3	Trace	0.3	0.5
n-16:1(7*c*)	17.7	5.6	3.2	7.1	1.8	0.5	0.2	0.7	1.1
n-17:1(9*c*)	0.2	17.8	—	Trace	1.2	0.3	—	0.5	—
i-17:1(9*c*)	—	—	11.5	—	—	1.9	—	—	2.8
n-18:1(11*c*)	3.4	0.1	0.1	0.5	0.1	Trace	0.1	Trace	0.1
n-18:1(9*c*)	25.0	3.4	15.3	9.3	0.8	3.0	0.4	0.1	4.5
n-19:1(9*c*)	—	1.0	Trace	—	0.3	0.1	—	—	—
i-19:1(9*c*)	—	—	2.0	—	—	—	—	—	—
β-Hydroxy acids	*Trace*	*0.1*	*0.3*	*42.5*	*56.6*	*50.9*	*91.6*	*74.5*	*58.9*
n-10:0	—	—	—	0.5	Trace	0.4	0.1	—	0.2
n-11:0	—	Trace	—	0.1	11.2	0.6	0.1	13.9	0.5
n-12:0	Trace	Trace	0.2	41.9	36.0	47.4	90.7	52.5	55.8
n-13:0	—	—	—	Trace	7.4	0.2	0.1	6.8	0.2
i-13:0	—	—	—	—	—	2.0	—	—	2.2
n-14:0	—	—	—	—	—	0.5	0.6	Trace	—
n-19:0	—	0.1	—	—	Trace	—	—	—	—
i-19:0	—	—	0.1	—	—	Trace	—	—	—
Fatty alcohols	*0.7*	*1.2*	*0.6*	*0.5*	*0.3*	*0.1*	*1.3*	*1.0*	*1.8*
n-19:0,1-OH	—	0.6	—	—	0.1	—	—	Trace	—
n-19:0,2-OH	—	Trace	—	—	—	—	—	—	—
n-19:1(11),1-OH	—	Trace	—	—	—	—	—	—	—
n-19:1(10),1-OH	—	0.3	—	—	—	—	—	—	—
n-19:1(9),1-OH	—	0.1	—	—	—	—	—	—	—
i-19:0,1-OH	—	—	0.1	—	—	Trace	—	—	Trace
Other	*1.8*	*5.6*	*2.8*	*1.1*	*6.4*	*3.8*	*1.1*	*2.4*	*2.6*

[a]Only the compounds accounting for more than 5% in at least one pool, or those playing a role regarding metabolism or lipid adaptation are detailed.
[b]Expressed as the percentage of total lipids for the considered pool.
[c]—, not detected. For other abbreviation see Tables 1 and 3.

grown on *n*-octane (5). In analyzing membrane lipids isolated by extraction with chloroform/methanol, just as in the present study, the authors observed a pronounced increase in the proportion of *trans*-unsaturated FA, and in the mean acyl chain length. These changes resulted in an increase in the transition temperature of membrane lipids, closely related to the stereochemistry of the acyl chains, allowing maintenance of the membrane fluidity in response to the exposure to *n*-octane. It can be assumed that in the present strain, the significant increase of saturated FA and decrease of unsaturated FA have a similar effect. It must be stressed that the change in FA synthesis activity, i.e., the synthesis of oleic acid instead of *cis*-

vaccenic acid, is not related to homeoviscous adaptation, since these acids show almost identical transition temperatures (43).

Growing *A. calcoaceticus* and *M. aquaeolei* on *n*-nonadecane, which is solid at room temperature, affected their FA composition. In addition to the influence on the predominance of even or odd carbon-numbered FA, one observes in both bacteria a moderate increase of the proportions of FA shorter than C_{18}. This trend is accompanied by a slight increase in the proportions of unsaturated FA for *A. calcoaceticus*, whereas a slight decrease occurred for *M. aquaeolei*. Although the net result of these changes on the transition temperature of membrane lipids is difficult to appreciate in the case of *M. aquaeolei*, it can be

TABLE 7
**Main Properties of FA from Unbound Lipids and Hydroxy Acids from LPS in *M. aquaeolei*
in Relation to the Carbon Source**

Lipids[a]	$CH_3CO_2NH_4$	$n\text{-}C_{19}H_{40}$	$i\text{-}C_{19}H_{40}$
ΣFA of unbound lipids (wt% of the pool)	98	93	96
Saturated *n*-FA	40	46	7
Unsaturated *n*-FA	55	42	20
Even carbon-numbered *n*-FA	95	15	27
n-FA	96	88	28
iso-FA	Trace	0.1	61
Total unsaturated	55	42	37
Total FA < C_{18}	65	83	70
β-Hydroxy acids in OH^--labile lipids			
Total (wt% of the pool)	42	57	51
% of β-OH *n*-12:0	99	64	93
β-Hydroxy acids in H^+-labile lipids			
Total (wt% of the pool)	92	74	59
% of β-OH *n*-12:0	99	70	95

[a]In this table, the compounds not detailed in Table 6 are taken into account. For abbreviations see Tables 1 and 3.

assumed that they induce a decrease of the transition temperature in those of *A. calcoaceticus*. Even more marked changes occurred when these two bacteria grew on *iso*-nonadecane, which is highly viscous at room temperature. Thus, in *A. calcoaceticus* the proportion of branched FA sharply increased. This supremacy of *iso*-FA is accompanied by an important decrease in the proportion of unsaturated FA and a reduction in straight-chain FA. Similar but less marked trends were seen in *M. aquaeolei*. These observations suggest that an increase of the proportions of *iso*-branched FA in *A. calcoaceticus* and *M.*

aquaeolei plays a physiological role similar to the one of *cis*-unsaturated FA, likely leading to a decrease in the transition temperature of the lipids (44). Such changes in response to the exposure to long-chain hydrocarbons are opposite to those occurring in *P. oleovorans* grown on light hydrocarbons. In one way, they are rather similar to FA adaptation resulting from a cold stress, as in *Escherichia coli* (45) or in the psychrophilic bacterium *Shewanella gelidimarina* (46).

Adaptation of hydroxy acid composition in LPS. The hydrocarbons provided to the bacteria exert quantitative and (or)
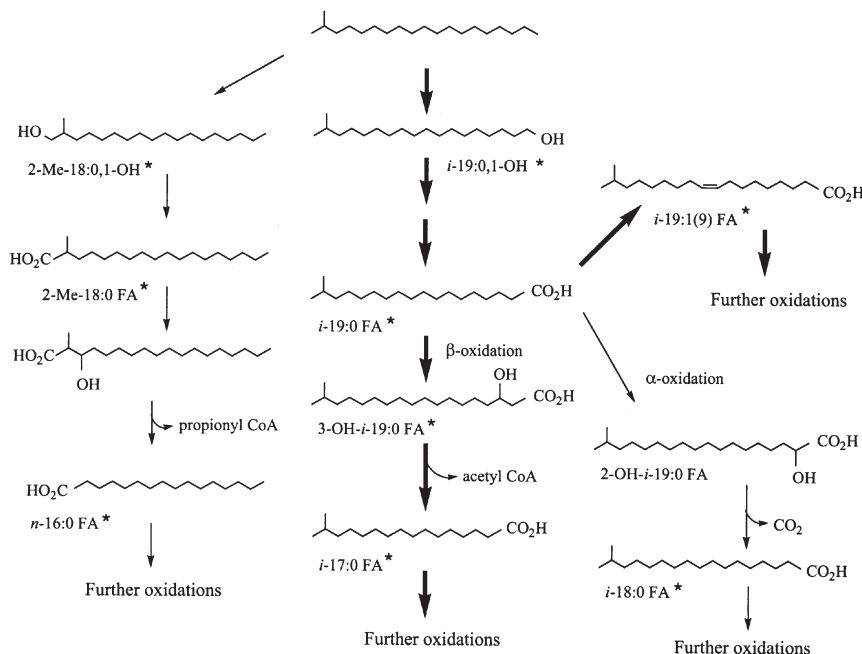
FIG. 1. Metabolic pathways of *iso*-nonadecane in *Acinetobacter calcoaceticus*. Compounds identified in the lipid extracts are indicated by an asterisk (*). The predominant pathways are shown by arrows in bold.

qualitative influences on the composition of hydroxy acids, depending on the bacterium and the physical properties of the substrate. Thus, in *P. oleovorans*, grown on light hydrocarbons, ester-linked β-hydroxy acids were reduced in comparison with the amount observed in the standard culture. By comparison, amide-linked β-hydroxy acids were less affected. Such a phenomenon is rather similar to the one recently observed in the Antarctic psychrotrophic bacterium *P. syringae* when submitted to temperature variations (47). In this case, it was shown that the bacterium decreases the proportion of β-hydroxy acids in LPS in response to an increase in temperature. The hydroxy groups of these acids would probably act as a methyl branching in FA of the cytoplasmic membrane, by causing perturbations in the hydrophobic region of LPS. In the present cases, the decrease of β-hydroxy acids in LPS would help to maintain the homeoviscosity of the outer membrane in contact with fluid hydrocarbons.

Marineobacter aquaeolei exhibits variations of β-hydroxy acid composition rather similar to those recently observed in *M. hydrocarbonoclasticus* cultivated on various hydrocarbons (15). LPS of these two bacteria comprise β-hydroxy dodecanoic acid as the main ester- and amide-linked hydroxy acid in standard cultures. Both species incorporate appreciable proportions of 3-OH-*n*-11:0 and 3-OH-*n*-13:0 acids in LPS when they are grown on *n*-nonadecane. By comparison, β-hydroxy acids derived from an *iso*-alkane are poorly accepted, likely owing to steric hindrance of the *iso* group.

Acinetobacter calcoaceticus exhibits a more complex composition of hydroxy acids in relation to the presence of two isomer series in LPS, exhibiting α and β hydroxy groups (48). When the bacterium was grown on hydrocarbons, variable but low proportions of ester-linked 2-OH-*n*-11:0, 2-OH-*n*-13:0, 3-OH-*n*-11:0, and 3-OH-*n*-13:0 can be incorporated in LPS. In the same way, the proportions of the amide-bound 3-OH-*n*-13:0 greatly increased, especially in the culture on *n*-nonadecane. By contrast, hydroxy *iso*-acids are not incorporated in LPS of *A. calcoaceticus*. This high specificity regarding the chain length and the methyl branching is thought to be due to the existence of hydrocarbon rulers in acyl transferases responsible for the *O*-acyl and *N*-acyl transfers in lipid A biosynthesis (49–51).

REFERENCES

1. Heipieper, H.J., and de Bont, J.A.M. (1994) Adaptation of *Pseudomonas putida* S12 to Ethanol and Toluene at the Level of Fatty Acid Composition of Membranes, *Appl. Environ. Microbiol. 60*, 4440–4444.
2. Suutari, M., and Laakso, S. (1994) Microbial Fatty Acids and Thermal Adaptation, *Crit. Rev. Microbiol. 20*, 285–328.
3. Sinensky, M. (1974) Homeoviscous Adaptation—A Homeostatic Process That Regulates the Viscosity of Membrane Lipids in *Escherichia coli*, *Proc. Natl. Acad. Sci. USA 71*, 522–525.
4. Diefenbach, R., Heipieper, H.J., and Keweloh, H. (1992) The Conversion of *cis* into *trans* Unsaturated Fatty Acids in *Pseudomonas putida* P8: Evidence for a Role in the Regulation of Membrane Fluidity, *Appl. Microbiol. Biotechnol. 38*, 382–387.
5. Chen, Q., Nijenhuis, A., Preusting, H., Dolfing, J., Janssen, D.B., and Witholt, B. (1995) Effects of Octane on the Fatty Acid Composition and Transition Temperature of *Pseudomonas oleovorans* Membrane Lipids During Growth in Two-Liquid-Phase Continuous Cultures, *Enzyme Microb. Technol. 17*, 647–652.
6. Pedrotta, V., and Witholt, B. (1999) Isolation and Characterization of the *cis-trans*-Unsaturated Fatty Acid Isomerase of *Pseudomonas oleovorans* GPo12, *J. Bacteriol. 181*, 3256–3261.
7. Heipieper, H.J., Meinhardt, F., and Segura, A. (2003) The *cis-trans* Isomerase of Unsaturated Fatty Acids in *Pseudomonas* and *Vibrio*: Biochemistry, Molecular Biology and Physiological Function of a Unique Stress Adaptative Mechanism, *FEMS Microbiol. Lett. 229*, 1–7.
8. Cronan, J.E., Jr., and Gelmann, E.P. (1975) Physical Properties of Membrane Lipids: Biological Relevance and Regulation, *Bacteriol. Rev. 39*, 232–256.
9. Makula, R., and Finnerty, W.R. (1968) Microbial Assimilation of Hydrocarbons. I. Fatty Acids Derived from Normal Alkanes, *J. Bacteriol. 95*, 2102–2107.
10. King, D.H., and Perry, J.J. (1975) The Origin of Fatty Acids in the Hydrocarbon Utilizing Microorganism *Mycobacterium vaccae*, *Can. J. Microbiol. 21*, 85–89.
11. Doumenq, P., Acquaviva, M., Asia, L., Durbec, J.P., Le Dréau, Y., Mille, G., and Bertrand, J.-C. (1999) Changes in Fatty Acids of *Pseudomonas nautica*, a Marine Denitrifying Bacterium, in Response to *n*-Eicosane as Carbon Source and Various Culture Conditions, *FEMS Microbiol. Ecol. 28*, 151–161.
12. Wilkinson, S.G. (1988) Gram-Negative Bacteria, in *Microbial Lipids* (Ratledge, C., and Wilkinson, S.G., eds.), Vol. 1, pp. 299–488, Academic Press, London.
13. Lattuati, A., Metzger, P., Acquaviva, M., Bertrand, J.-C., and Largeau, C. (2002) *n*-Alkane Degradation by *Marinobacter hydrocarbonoclasticus* SP 17: Long Chain β-Hydroxy Acids as Indicators of Bacterial Activity, *Org. Geochem. 33*, 37–45.
14. Aubert, E., Metzger, P., and Largeau, C. (2004) Incorporation of 1-Chlorooctadecane into FA and β-Hydroxy Acids of *Marinobacter hydrocarbonoclasticus*, *Lipids 39*, 81–85.
15. Soltani, M., Metzger, P., and Largeau, C. (2004) Effects of Hydrocarbon Structure on Fatty Acid, Fatty Alcohol, and β-Hydroxy Acid Composition in the Hydrocarbon-Degrading Bacterium *Marinobacter hydrocarbonoclasticus*, *Lipids 39*, 491–505.
16. Baptist, J.N., Gholson, R.K., and Coon, M.J. (1963) Hydrocarbon Oxidation by a Bacterial Enzyme System. I. Products of Octane Oxidation, *Biochim. Biophys. Acta 69*, 40–47.
17. Makula, R., Lockwood, P., and Finnerty, W. (1975) Comparative Analysis of the Lipids of *Acinetobacter* Species Grown on Hexadecane, *Can. J. Microbiol. 121*, 250–258.
18. Lal, B., and Khanna, S. (1996) Degradation of Crude Oil by *Acinetobacter calcoaceticus* and *Alcaligenes odorans*, *J. Appl. Bacteriol. 81*, 355–362.
19. Huu, N.B., Denner, E.B.M., Ha, D.T.C., Wanner, G., and Stan-Lotter, H. (1999) *Marinobacter aquaeolei* sp. nov., a Halophilic Bacterium Isolated from a Vietnamese Oil-Producing Well, *Int. J. Syst. Bacteriol. 49*, 367–375.
20. Gauthier, M.J., Lafay, B., Christen, R., Fernandez, L., Acquaviva, M., Bonin, P., and Bertrand, J.-C. (1992) *Marinobacter hydrocarbonoclasticus* gen. nov., a New, Extremely Halotolerant, Hydrocarbon-Degrading Marine Bacterium, *Int. J. Syst. Bacteriol. 42*, 568–576.
21. Díaz, M.P., Grigson, S.J.W., Peppiatt, C.J., and Burgess, J.G. (2000) Isolation and Characterization of Novel Hydrocarbon-Degrading Euryhaline Consortia from Crude Oil and Mangrove Sediments, *Mar. Biotechnol. 2*, 522–532.
22. Rontani, J.-F., Mouzdahir, A., Michotey, V., Caumette, P., and Bonin, P. (2003) Production of a Polyunsaturated Isoprenoid

Wax Ester During Aerobic Metabolism of Squalene by *Marinobacter squalenivorans* sp. nov, *Appl. Environ. Microbiol. 69*, 4167–4176.

23. McGowan, L., Herbert, R., Ward, A., and Muyzer, G. (2002) A Comparative Study of Hydrocarbon Degradation of Putative *Marinobacter* sp. Isolated from Different Mat Systems, in *Proceeding of the MATBIOPOL Meeting, Role of Microbial Mats in Bioremediation of Hydrocarbon Polluted Coastal Zones* (Caumette, P., ed.), Barcelona, 12–16 February 2002, pp. 269–274, University of Pau, France.

24. Goossens, H., de Leeuw, J.W., Rijpstra, W.I.C., Meyburg, G.J., and Schenk, P.A. (1989) Lipids and Their Mode of Occurrence in Bacteria and Sediments: I. A Methodological Study of the Lipid Composition of *Acinetobacter calcoaceticus* LMD 79-41, *Org. Geochem. 14*, 15–25.

25. Schwartz, R.D. (1973) Octene Epoxidation by a Cold-Stable Alkane-Oxidizing Isolate of *Pseudomonas oleovorans*, *Appl. Microbiol. 25*, 574–577.

26. Kates, M. (1986) *Techniques of Lipidology*, 2nd edn., pp. 344–345, Elsevier, Amsterdam.

27. Scribe, P., Pepe, C., Barouxis, A., Fuche, C., Dugant, J., and Saliot, A. (1990) Détermination de la Position de l'Insaturation des Monoènes par Chromatographie en Phase Gazeuse Capillaire-Spectrométrie de Masse des Dérivés Diméthyl-Disulfures: Application à l'Analyse d'un Mélange Complexe d'Alcènes, *Analusis 18*, 284–288.

28. Anderson, B.A., and Holman, R.T. (1974) Pyrrolidides for Mass Spectrometric Determination of the Position of the Double Bond in Monounsaturated Fatty Acids, *Lipids 9*, 185–190.

29. Christie, W.W. (1999) Structural Analysis of Fatty Acids, in *Advances in Lipid Methodology* (Christie, W.W., ed.), Vol. 4, pp. 119–169, The Oily Press, Dundee.

30. Doumenq, P., Aries, E., Asia, L., Acquaviva, M., Artaud, J., Gilewicz, M., Mille, G., and Bertrand, J.-C. (2001) Influence of *n*-Alkanes and Petroleum on the Fatty Acid Composition of a Hydrocarbonoclastic Bacterium: *Marinobacter hydrocarbonoclasticus* Strain 617, *Chemosphere 44*, 519–528.

31. Kaneda, T. (1991) *Iso-* and *anteiso*-Fatty Acids in Bacteria: Biosynthesis, Function, and Taxonomic Significance, *Microbiol. Rev. 55*, 288–302.

32. Parkes, R.J., Dowling, N.J.E., White, D.C., Herbert, R.A., and Gibson, G.R. (1993) Characterization of Sulphate-Reducing Bacterial Populations within Marine and Estuarine Sediments with Different Rates of Sulphate Reduction, *FEMS Microbiol. Ecol. 102*, 235–250.

33. Fixter, L.M., Nagi, M.N., McCormack, J.G., and Fewson, C.A. (1986) Structure, Distribution and Function of Wax Esters in *Acinetobacter calcoaceticus*, *J. Gen. Microbiol. 132*, 3147–3157.

34. Dembitsky, V.M. (2004) Astonishing Diversity of Natural Surfactants: 1. Glycosides of Fatty Acids and Alcohols, *Lipids 39*, 933–953.

35. Ratledge, C. (1978) Degradation of Aliphatic Hydrocarbons, in *Developments in Biodegradation of Hydrocarbons* (Watkinson, R.J., ed.), Vol. 1, pp. 1-46, Applied Science, London.

36. van Beilen, J.B., Wubbolts, M.G., and Witholt, B. (1994) Genetics of Alkane Oxidation by *Pseudomonas oleovorans*, *Biodegradation 5*, 161–174.

37. Rock, C.O., and Cronan, J.E. (1996) *Escherichia coli* as a Model for the Regulation of Dissociable (type II) Fatty Acid Biosynthesis, *Biochim. Biophys. Acta 1302*, 1–16.

38. Schweizer, E., and Hofmann, J. (2004) Microbial Type I Fatty Acid Syntheses (FAS): Major Players in a Network of Cellular FAS Systems, *Microbiol. Mol. Biol. Rev. 68*, 501–517

39. Schweizer, E. (1989) Biosynthesis of Fatty Acids and Related Compounds, *in Microbial Lipids* (Ratledge, C., and Wilkinson, S.G., eds), Vol. 2, pp. 3–50, Academic Press, New York.

40. Ghaneker, A.S., and Nair, P.M. (1973) Evidence for the Existence of an Aerobic Pathway for Synthesis of Monounsaturated Fatty Acids by *Alcaligenes faecalis*, *J. Bacteriol. 114*, 618–624.

41. Kabelitz, N., Santos, P.M., and Heipieper, H.J. (2003) Effect of Fatty Alcohols on Growth and Degree of Saturation of Membrane Lipids in *Acinetobacter calcoaceticus*, *FEMS Microb. Lett. 220*, 223–227.

42. Wada, M., Fukunaga, N., and Sasaki, S. (1989) Mechanism of Biosynthesis of Unsaturated Fatty Acids in *Pseudomonas* sp. Strain E-3, a Psychrotrophic Bacterium, *J. Bacteriol. 171*, 4267–4271.

43. Gunstone, F.D., Harwood, J.L., and Padley, F.B. (1994) *The Lipid Handbook* (2nd ed.), Chapman & Hall, London.

44. Russel, N.J., and Fukunaga, N. (1990) A Comparison of Thermal Adaptation of Membrane Lipids in Psychrophilic and Thermophilic Bacteria, *FEMS Microbiol. Rev. 75*, 171–182.

45. Morein, S., Anderson, A.-S., Rilfors, L., and Lindblom, G. (1996) Wild-Type *Escherichia coli* Cells Regulate the Membrane Lipid Composition in a Window Between Gel and Non-lamellar Structures, *J. Biol. Chem. 271*, 6801–6809.

46. Nichols, D.S., Olley, J., Garda, H., Brenner, R.R., and McMeekin, T.A. (2000) Effect of Temperature and Salinity Stress on Growth and Lipid Composition of *Shewanella gelidimarina*, *Appl. Environ. Microbiol. 66*, 2422–2429.

47. Kumar, G.S., Jagannadham, M.V., and Ray, M.K. (2002) Low-Temperature-Induced Changes in Composition and Fluidity of Lipopolysaccharides in Antartic Psychrotrophic Bacterium *Pseudomonas syringae*, *J. Bacteriol. 184*, 6746–6749.

48. Wollenweber, H.W., Seydel, U., Lindner, B., Luderitz, O., and Rietschel, E.T. (1984) Nature and Location of Amide-Bound (*R*)-3-Acyloxyacyl Groups in Lipid A of Lipopolysaccharides from Various Gram-Negative Bacteria, *Eur. J. Biochem. 145*, 265–272.

49. Williamson, J.M., Anderson, M.S., and Raetz, C.R.H. (1991) Acyl-Acyl Carrier Protein Specificity of UPD-GlcNAc Acyl-Transferases from Gram-Negative Bacteria: Relationship to Lipid A Structure, *J. Bacteriol. 173*, 3591–3596.

50. Wyckoff, T.J., Lin, S., Cotter, R.J., Dotson, G.D., and Raetz, C.R.H. (1998) Hydrocarbon Rulers in UDP-*N*-acetylglucosamine Acyltransferases, *J. Biol. Chem. 273*, 32369–32372.

51. Sweet, C.R., Preston, A., Tolands, E., Ramirez, S.M., Cotter, R.J., Maskell, D.J., and Raetz, C.R.H. (2002) Relaxed Acyl Chain Specificity of *Bordetella* UDP-*N*-acetylglucosamine Acyltransferases, *J. Biol. Chem. 277*, 18281–18290.

Lipolysis of Different Oils Using Crude Enzyme Isolate from the Intestinal Tract of Rainbow Trout, *Oncorhynchus mykiss*

Jesper R. Gøttsche[a,*], Nina S. Nielsen[b], Henrik H. Nielsen[b], and Huiling Mu[a]

[a]Biochemistry and Nutrition Group, BioCentrum, and [b]Department of Seafood Research, Danish Institute for Fisheries Research, Technical University of Denmark, 2800 Kgs. Lyngby, Denmark

ABSTRACT: Crude enzyme isolate was prepared from the intestine of rainbow trout. Positional specificity of the crude enzyme isolate was determined from both 1(3)- and 2-MAG products after *in vitro* lipolysis of radioactive-labeled triolein. The ratio of 2-MAG/1(3)-MAG was 2:1, suggesting that the overall lipase specificity of the enzyme isolate from rainbow trout tended to be 1,3-specific; however, activity against the *sn*-2 position also was shown. *In vitro* lipolysis of four different unlabeled oils was performed with the crude enzyme isolate. The oils were: structured lipid [SL; containing the medium-chain FA (MCFA) 8:0 in the *sn*-1,3 positions and long-chain FA (LCFA) in the *sn*-2 position], DAG oil (mainly 1,3-DAG), fish oil (FO), and triolein (TO). MCFA were rapidly hydrolyzed from the SL oil. LCFA including n-3 PUFA were, however, preserved in the *sn*-2 position and therefore found in higher amounts in 2-MAG of SL compared with 2-MAG of FO, DAG, and TO. Lipolysis of the DAG oil produced higher amounts of MAG than the TAG oils, and 1(3)-MAG mainly was observed after lipolysis of the DAG oil. The positional specificity determined and the results from the hydrolysis of the different oils suggest that n-3 very long-chain PUFA from structured oils may be used better by aquacultured fish than that from fish oils.

Paper no. L9783 in *Lipids 40*, 1273–1279 (December 2005).

The aquaculture industry currently uses more than 70% of the global supply of fish oil; however, the industry is still expanding rapidly. Since fisheries are not anticipated to grow, a future shortage of fish oil is expected; thus, the requirement of aquaculture is estimated to reach close to 100% of the world's total production of fish oil by the year 2010 (1). Substitution of fish oil by alternative oils, e.g., vegetable oil, may have no deleterious effect on the growth of some fish species (2–4). However, vegetable oils do not contain n-3 very long chain PUFA (VLC-PUFA). Reduced content of healthy n-3 VLCPUFA, such as EPA and DHA, in Atlantic salmon and rainbow trout fed vegetable oils has been reported, resulting in reduced availability of VLCPUFA for consumers (2,3). An approach to solve this problem may be to use structured lipids (SL) in fish feed.

In mammals, improved absorption of long-chain FA (LCFA) from SL containing medium-chain FA (MCFA) in the primary positions and LCFA in the *sn*-2 position has been observed in comparison with conventional long-chain TAG (5). This is a result of fast hydrolysis of the MCFA in the primary positions by the 1,3-specific pancreatic lipase. However, only limited information is available regarding the positional specificity of lipases in fish, since specificity has been investigated in only a few fish species so far, with contradictory results. Leger and Bauchart (6) reported preferential 1,3-positional specificity of partly purified pancreas lipase from rainbow trout; 1,3-specificity was also reported for crude material and partly purified cod lipase (7). In contrast, nonspecific lipase activities were reported in anchovy, striped bass, pink salmon (8), and Arctic charr (9). Another increasing problem in fish aquaculture is the increased fat content due to a diet high in lipids. DAG oil already was shown to reduce fat accumulation in animals and humans (10,11); therefore, DAG oil may be an interesting oil with respect to fish feed in the future. At present, no literature describes the hydrolysis of either MCFA from SL or DAG oil by fish lipases. Therefore, it is important to obtain knowledge about the lipolytic digestive system in fish to design fats for improving incorporation of the n-3 VLCPUFA into fillets (instead of utilization as energy) and reducing fat accumulations.

SL and DAG oil were used in fish feed for rainbow trout to explore the effects of these oils on incorporation of n-3 VLC-PUFA in fillets and accumulation of fat (12). The objectives of this study were (i) to determine the positional specificity of digestive lipases in crude enzyme isolate from the intestinal tract of rainbow trout and (ii) to investigate the effect of the crude enzyme isolate on hydrolysis of oils with different structures. To imitate the "digestive system" in the intestine, we used a crude enzyme isolate so that no enzymes, coenzymes, or bile acids that could affect the overall positional specificity would be lost during purification steps.

MATERIALS AND METHODS

Chemicals. Triolein (TO, >99%), sodium taurocholate (99%), CaCl$_2$, Tris-HCl, 2,7-dichlorofluorescein, pancreatic lipase (E.C. 3.1.1.3, type IV), and colipase were purchased from Sigma (St. Louis, MO). Copper acetate, ortho-phosphoric acid

---

(85%), boron trifluoride (14% in methanol), boric acid, NaOH, NaCl, K$_2$CO$_3$, and TLC plates (Silica gel 60) were from Merck (Darmstadt, Germany). Internal standards (>99%) were tridecanoic acid, monotridecanoin glyceride, ditridecanoin glyceride, and tritridecanoin glyceride (Nu-Chek-Prep Inc., Elysian, MN) and 1,2-ditridecanoyl-*sn*-glycero-3-phosphocholine (Avanti Polar Lipids Inc., Alabaster, AL). All solvents, acetone (Kebo Laboratory A/S, Albertslund, Denmark), heptane (Rathburn Chemicals, Walkerburn, Scotland), ethanol and acetic acid (Merck), chloroform, and methanol (Labscan, Dublin, Ireland) were HPLC grade. Fish oil (FO) was anchovy oil from Peruvian anchovies (Denofa AS, Gamle Frederikstad, Norway), and the DAG oil was obtained from Japan (Kao, Tokyo, Japan). Specific SL was produced by enzymatic interesterification of anchovy oil and caprylic acid with the procedure described previously (13). Radioactive-labeled TO [9,10-^{3}H(N), 52.6 Ci/mmol] was purchased from PerkinElmer (Boston, MA); the scintillation liquid Ultima Gold^{TM} was from Bioscience (Meriden, CT).

Analysis of acylglycerol compositions of oils. SL and DAG oils were analyzed by normal-phase HPLC using ELSD. TAG, 1,3- and 1,2(2,3)-DAG, and MAG were separated on a Hypersil silica column (l = 10 cm, i.d. = 2.1 cm, particle size = 5 µm; Thermo Hypersil-Keystone, Bellefonte, PA) using heptane (A) and heptane/ethyl acetate/2-propanol/acetic acid (B) = 80:10:10:1 (by vol). Solvent B was increased from 2 to 35% over 10 min at a flow rate of 0.50 mL/min, further to 98% over 1 min, and maintained for 6 min before reverting to 2%, all at a flow rate of 1 mL/min (14). Calibration curves were constructed and results are given in weight percentage (wt%) of total lipids.

Analysis of FA compositions of oils. KOH-catalyzed methylations of experimental oils were performed at room temperature (15). FAME were analyzed by GC (Hewlett-Packard 5890 Series II Gas Chromatograph) using an SP-2380 column (60 m × 0.25 mm i.d.; Supelco, Bellefonte, PA). Conditions were as follows: injector temperature 270°C, FID 270°C, helium carrier gas at 1.2 mL/min (column flow), and injector split ratio 1:11. The initial column temperature was 70°C (maintained 5 min); step 1: 15°C/min to 160°C; step 2: 1.5°C/min to 200°C and held for 15 min; step 3: 30°C/min to 225°C and maintained for 10 min. FAME were identified by comparing their retention times with those of known standards (Nu-Chek-Prep Inc.) and methyl esters of well-characterized FO.

Analyses of FA compositions in the sn-2 position of oils. Oils were partially degraded by Grignard degradation as described by Becker *et al.* (16). 2-MAG spots were scraped off and methylated with a modified boron trifluoride-catalyzed method (17). Briefly, TAG were saponified for 5 min at 80°C with 1 mL 0.5 M NaOH in methanol and converted to FAME using 1 mL 14% boron trifluoride/methanol solution and 0.5 mL 0.1% hydroquinone in methanol for 2 min at 80°C. FAME were extracted with 2 × 0.5 mL heptane after addition of 2 mL of 0.73% NaCl solution. The combined heptane phases were washed with 1 mL weakly basic saturated NaCl solution (40 g NaCl and 150 mg K$_2$CO$_3$/100 mL water). FAME were ana-

lyzed as described above. The closed system and the lack of solvent evaporation were used to ensure quantitative analysis of MCFA.

Preparation of the crude enzyme isolate. Three rainbow trout (*Oncorhynchus mykiss*), 800–1000 g, were killed by a blow to the head. The fish had been fed commercial fish feed (ECOLIFE 19, 4.5 mm; BioMar A/S, Brande, Denmark). The gastrointestinal system was cut out and immediately frozen in liquid nitrogen. After thawing, the content of the pylorus region of the foregut, the midgut, and the hindgut was isolated, freeze-dried, and kept at –80°C until use. Analyses were performed with a pooled fraction from three trout.

Analysis of lipids in the crude enzyme isolate. The lipids in the crude enzyme isolate were extracted by the method of Folch *et al.* (18). Lipids were dissolved in chloroform/methanol (95:5, vol/vol) and applied onto TLC plates. The plates were developed with chloroform/isopropanol/acetic acid (95:5:1, by vol) and visualized under UV light after spraying with 2,7-dichlorofluorescein. TAG, DAG, MAG, FFA, and phospholipid (PL) spots were quantitatively scraped off and corresponding internal standards containing 13:0 FA were added. Boron trifluoride-catalyzed methylation followed by GC analysis was carried out as described above.

Test of the standard assay system for hydrolysis of oils. In vitro lipase hydrolysis of oils with crude enzyme isolate was performed using the method described by Martin *et al.* (19) with modifications. The standard assay system used comprised 10.0 mg of oil, 62.0 mg crude enzyme isolate from rainbow trout intestine, and 3.0 mL buffer solution consisting of CaCl$_2$ (0.18 g/L) and sodium taurocholate (0.1 g/L) in 0.5 M Tris/HCl (pH 7.7). Initially, the assay system was tested for possible acyl migration by investigating the effect of hydrolysis time (5 and 30 min), importance of fast extraction (immediately and after 20 min), and the influence of stopping the hydrolysis with diluted HCl, NaOH, or chloroform. To test the assay, 2-MAG was added instead of oil and no crude enzyme isolate was used, whereas all other reagents were the same as described above.

Results of the acyl migration test in the assay system were used to define the parameters in the standard assay system that was used for determination of specificity. Buffer, 1 and 2 mL, respectively, was added to the oil and the crude enzyme isolate and sonicated 2 min each (20°C). Both solutions were heated for 2 min at 37°C in a water bath. Lipolysis was started by adding the enzyme solution to the sonicated solution of oil under vigorous stirring at 37°C. The reaction was stopped after 1.5 min by adding 2 mL chloroform. Total lipid was instantly extracted with a further 1 mL chloroform and applied to a boric acid-impregnated TLC plate that was developed 2 × 35 min in chloroform/acetone (90:10, vol/vol) [modified from Becker *et al.* (16)]. 1(3)- and 2-MAG spots were visualized by spraying with 2,7-dichlorofluorescein in anhydrous ethanol, quantitatively scraped off, and methylated as previously described for analysis of FA compositions in the *sn*-2 position of oils.

Assay of hydrolysis of radioactive-labeled TO. The above-mentioned standard assay system was used for *in vitro* hydrolysis of TO with crude enzyme isolate. Radioactive-labeled TO (0.82

μg, corresponding to 0.925 MBq) was mixed with 10.0 mg unlabeled TO. Visualization was performed by spraying with copper acetate in phosphoric acid (8% wt/vol) followed by 20 min carbonization of the lipid at 160°C. To determine the specificity of the crude enzyme isolate, 1(3)- and 2-MAG spots were quantitatively scraped off and mixed with 7.0 mL of scintillation liquid. [³H]Monoolein was quantified using scintillation counting (Tri-Carb 2100TR; Packard, Meriden, CT). The extent of oil hydrolysis was determined after lipolysis of radioactive-labeled TO by separation of lipid classes as described for analysis of lipids in crude enzyme isolate. Spots were visualized and quantified as described above for radioactive-labeled 1(3)- and 2-MAG.

Assay for hydrolysis of different unlabeled oils. Different oils (10.0 mg of FO, SL, DAG, and TO) were hydrolyzed *in vitro* with the crude enzyme isolate. Lipids were extracted with chloroform and separated on boric acid-impregnated TLC plates; both 1(3)- and 2-MAG were scraped off and methylated. All procedures were the same as described for the standard assay system.

Statistics. Results were expressed as means ± SEM. Differences among groups were tested using one-way ANOVA, and significant differences were analyzed using Tukey's multiple comparison test. All statistical analyses were performed using Graphpad Prism v. 3.0 (Graphpad Software, San Diego, CA).

RESULTS

Investigation of acyl migration. No 1-MAG was observed when the hydrolysis time was 5 min, when the lipids were extracted immediately at pH 7.7. However, a trace amount of 1-MAG was detected when the hydrolysis time was 30 min followed with direct extraction or when the hydrolysis time was 5 min and the sample was left 20 min in the water bath before extraction. A trace amount of 1-MAG was also visible when the hydrolysis was stopped with either diluted HCl or NaOH (solution pH below 2 or over 12).

Analyses of lipids in the crude enzyme isolate. Total lipid content of the crude enzyme isolate was 12.8 wt% and was distributed among different lipid classes as follows (wt%): FFA, 58.8 ± 1.9; PL, 14.1 ± 0.3; TAG, 13.2 ± 0.3; DAG, 10.3 ± 0.2; and MAG, 3.6 ± 0.1. TLC also showed trace amounts of sterols (not determined). FA compositions of the determined lipid classes showed higher levels of 14:0, 16:0, and 18:0 in DAG and MAG compared with TAG (Table 1). In contrast to saturated FA (SFA), the levels of PUFA were lower in DAG and MAG compared with TAG. MCFA (8:0) were not detected in any of the lipid classes from the crude enzyme isolate.

Determination of positional specificity of digestive lipases in the crude enzyme isolate. Positional specificity of the crude enzyme isolate was determined using radioactive-labeled TO, to exclude the lipid contribution from the isolate itself. The scintillation results showed that 0.8% of radioactive-labeled TO was recovered as MAG, 33% of the produced MAG was 1(3)-MAG, and 67% was 2-MAG (Fig. 1). This indicated an overall specificity toward 1- and 3-ester bonds in TAG, but activities for hydrolysis of FA from the *sn*-2 position were also

TABLE 1
**FA Composition[a] of Lipid Classes in Crude Enzyme Isolate from Intestine of Rainbow Trout (mol%)**

FA	TAG	DAG	MAG	FFA	PL
8:0	ND	ND	ND	ND	ND
14:0	11.4	17.7	15.5	6.4	6.5
16:0	25.0	38.0	35.3	21.1	23.8
16:1n-7	7.2	5.5	6.7	7.0	1.9
18:0	4.7	6.2	7.0	4.9	5.9
18:1n-9	11.7	7.6	7.7	13.3	5.2
18:1n-7	3.0	2.5	3.9	2.4	2.3
18:2n-6	3.0	1.5	1.3	3.7	6.9
18:3n-3	1.3	0.7	0.5	1.6	0.7
20:1n-9	2.8	2.3	3.1	2.1	0.8
18:4n-3	1.1	0.5	0.3	2.0	0.4
22:1n-11	2.6	1.6	2.3	2.3	0.2
20:4n-3	0.6	0.3	0.2	1.0	0.3
20:5n-3	4.0	1.5	0.7	8.2	4.7
22:5n-3	1.2	0.6	0.3	2.2	0.9
22:6n-3	9.2	5.4	4.9	9.7	13.0
Others	11.3	8.0	10.2	12.1	26.4
Total n-3	17.4	9.0	6.8	24.6	20.1

[a]Data represent the mean of two determinations. TLC also showed trace amounts of sterols (not determined). PL, phospholipids; ND, not detected.

observed. The extent of hydrolysis was estimated from the recovery of other lipid classes (recovery percentage of radioactive-labeled TO): TAG, 88.4 ± 1.3; DAG, 5.6 ± 0.2; MAG, 0.8 ± 0.06; FFA, 2.7 ± 0.03; total 97.5 ± 1.1 (3 determinations).

Analyses of oils. FO and SL oils contained only TAG. The DAG oil consisted of (wt%): 50% 1,3-DAG, 27% 1,2(2,3)-DAG, and 23% TAG. The FA compositions of total acylglycerols and in the *sn*-2 position of experimental oils are shown in Table 2. The FO oil had a higher content of n-3 VLCPUFA, especially in primary positions, compared with the SL oil. On the other hand, the SL oil was characterized by a high content of MCFA (8:0) in primary positions, whereas the level of EPA and DHA in the *sn*-2 position was slightly lower than for FO. The DAG oil was constituted mainly of oleic acid and linoleic acid distributed almost equally among *sn*-positions.

Lipolysis of different unlabeled oils with the crude enzyme isolate. Four different oils (SL, DAG, FO, and TO) were lipolyzed with the crude enzyme isolate. Furthermore, a blank (without added oil) was hydrolyzed as the reference. The
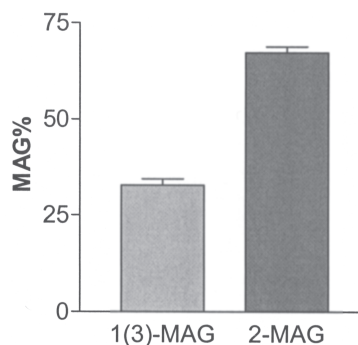
FIG. 1. Distribution of 1(3)- and 2-MAG after lipolysis of radioactive-labeled triolein with crude enzyme isolate (means ± SEM, *n* = 4).

TABLE 2
FA Composition[a] of Total Acylglycerols and in the *sn*-2 Position of Experimental Oils (mol%)

FA	FO Oil	FO sn-2	SL Oil	SL sn-2	DAG Oil	DAG sn-2
8:0	ND	ND	47.6	4.8	ND	ND
14:0	8.9	17.1	5.0	14.9	0.1	ND
16:0	19.5	25.4	9.8	23.7	3.3	3.6
16:1n-7	7.1	8.8	3.3	8.1	0.1	0.2
18:0	3.4	0.7	1.0	0.8	1.1	1.2
18:1n-9	9.8	3.8	3.3	3.9	36.3	35.4
18:1n-7	2.5	1.0	0.8	1.0	2.2	2.7
18:2n-6	1.3	1.1	0.6	1.1	46.2	46.7
18:3n-3	1.1	1.1	0.5	1.0	5.5	5.6
20:1n-9	2.0	1.4	0.6	1.1	0.5	0.4
18:4n-3	2.7	2.3	1.9	2.4	ND	ND
22:1n-11	3.2	0.5	1.3	0.5	ND	ND
20:4n-3	0.7	0.4	0.4	0.4	ND	ND
20:5n-3	11.8	8.6	6.0	7.9	ND	ND
22:5n-3	1.5	2.8	1.0	2.4	ND	ND
22:6n-3	10.6	17.1	8.8	15.2	ND	ND
Others	13.6	8.2	7.9	10.8	2.2	4.0
Total n-3	28.4	32.3	18.6	29.3	5.4	5.6

[a]Values are the mean of two determinations for FA composition in oil and three determinations for *sn*-2. FO, fish oil; SL, structured lipid; for other abbreviation see Table 1.

amounts of 1(3)- and 2-MAG products after lipolyses of oils with the crude enzyme isolate were calculated and are shown in Table 3. A similar amount of 1-MAG was obtained for the oils and the blank, except a significantly higher amount of 1-MAG was obtained for the DAG oil ($P < 0.001$). The lipolysis of the DAG oil also produced more 2-MAG than FO and the blank ($P < 0.05$). The MAG produced after hydrolysis of DAG oil was enriched with FA; 18:1n-9, 18:1n-7, 18:2n-6, and 18:3n-3, which originated from the DAG oil (Table 3). Lipolysis of the SL oil produced more 2-MAG than did FO and the

blank, and only twice as much 8:0 was observed in 1-MAG compared with 2-MAG in the SL products. Another interesting result for hydrolysis of the SL oil was a higher level of n-3 PUFA (18:4n-3, 20:5n-3, and 22:5n-3) in the 2-MAG products compared with all other oils ($P < 0.05$); however, DHA was significantly higher only in SL compared with the FO oil and the blank ($P < 0.05$). Lipolysis of the TO oil resulted in nearly the same amounts of 1(3)- and 2-MAG as the blank; however, the level of 18:1n-9 was higher in 2-MAG compared with that of FO, SL, and the blank ($P < 0.05$).

The ratios of 1(3)-MAG/2-MAG obtained after lipolysis of oils and the blank are shown in Figure 2. The DAG oil increased the ratio compared with the blank, and all TAG oils decreased the ratio compared with the blank ($P < 0.05$). Moreover, the ratio of 1(3)-MAG/2-MAG for FO and SL was significantly lower than for TO ($P < 0.05$).

DISCUSSION

Investigation of acyl migration. Acyl migration is a side reaction that can mask the specificity of the lipase, as the amounts of lipolysis products [1(3)- and 2-MAG] formed the basis of specificity determination in the present study. A shift of acyl groups happens with extreme ease; procedures involving heat, acids, or bases should especially be avoided according to Thomas *et al.* (20). The standard assay system used for *in vitro* hydrolysis of oils was initially tested for possible acyl migration in MAG. We found that both pH and time significantly influenced acyl migration in the standard assay system; therefore, we decided to reduce the hydrolysis time as much as possible (1.5 min) and stop the reaction without adding acid or base but with chloroform, which was also used for instant extraction of the lipolytic products.

Analysis of lipids in crude enzyme isolate. FFA constituted

TABLE 3
Amounts[a] of 1(3)- and 2-MAG Products After Lipolysis of Oils with Crude Enzyme Isolate (μg MAG/10.0 mg oil/62.0 mg crude enzyme isolate)

MAG	FO 1(3)-MAG	FO 2-MAG	SL 1(3)-MAG	SL 2-MAG	DAG 1(3)-MAG	DAG 2-MAG	TO 1(3)-MAG	TO 2-MAG	Blank 1(3)-MAG	Blank 2-MAG
8:0	ND	ND	6.8 ± 0.3	3.5 ± 0.1	ND	ND	ND	ND	ND	ND
14:0	50.1 ± 1.9	54.7 ± 1.3[A,B]	60.2 ± 2.8	63.8 ± 2.5[A]	55.2 ± 5.3	45.8 ± 3.8[B]	60.4 ± 3.4	55.4 ± 1.5[A,B]	56.3 ± 1.4	53.3 ± 0.9[AB]
16:0	135.7 ± 4.8	77.1 ± 1.0	165.5 ± 9.9	90.0 ± 4.8	165.4 ± 13	77.8 ± 6.1	160.8 ± 8.7	75.9 ± 2.1	162.0 ± 4.2	80.4 ± 3.9
16:1n-7	17.4 ± 0.9	30.5 ± 1.0	20.2 ± 1.2	35.8 ± 1.8	18.0 ± 1.4	28.6 ± 2.4	18.1 ± 1.0	29.6 ± 0.8	18.8 ± 0.9	30.0 ± 1.1
18:0	42.7 ± 1.7	4.7 ± 0.2	53.2 ± 3.2	4.9 ± 0.2	52.6 ± 3.1	6.3 ± 0.4	50.7 ± 3.0	4.0 ± 0.2	51.2 ± 1.5	5.2 ± 1.1
18:1n-9	26.6 ± 1.4[c]	28.9 ± 0.6[C]	31.8 ± 2.0[b,c]	33.4 ± 2.3[C]	160.2 ± 8.9[a]	71.7 ± 5.0[A]	41.4 ± 3.9[b]	50.9 ± 3.7[B]	30.7 ± 1.8[b,c]	29.5 ± 0.9[C]
18:1n-7	19.8 ± 0.9[b]	3.7 ± 0.1[B]	24.7 ± 1.6[b]	4.4 ± 0.4[B]	31.9 ± 2.2[a]	6.4 ± 0.6[A]	23.6 ± 1.6[b]	3.8 ± 0.1[B]	24.3 ± 0.9[b]	3.7 ± 0.1[B]
18:2n-6	3.3 ± 0.2[b]	8.2 ± 0.3[B]	3.7 ± 0.2[b]	9.5 ± 0.6[B]	152.6 ± 9.4[a]	64.2 ± 4.2[A]	3.2 ± 0.2[b]	7.8 ± 0.3[B]	3.7 ± 0.3[b]	8.5 ± 0.5[B]
18:3n-3	2.0 ± 0.1[b]	3.6 ± 0.1[B]	2.4 ± 0.1[b]	4.4 ± 0.3[B]	20.8 ± 1.2[a]	10.8 ± 0.7[A]	2.0 ± 0.2[b]	3.4 ± 0.1[B]	2.3 ± 0.1[b]	3.7 ± 0.3[B]
20:1n-9	17.8 ± 0.4	4.9 ± 0.4	23.0 ± 1.3	6.0 ± 0.9	23.2 ± 1.6	5.5 ± 0.4	21.4 ± 2.1	5.4 ± 0.5	22.8 ± 1.0	4.5 ± 0.1
18:4n-3	1.3 ± 0.1	4.3 ± 0.2[B]	1.4 ± 0.1	6.2 ± 0.3[A]	0.5 ± 0.3	3.3 ± 0.2[C]	0.4 ± 0.4	3.3 ± 0.1[C]	0.6 ± 0.3	3.4 ± 0.2[C]
22:1n-11	13.1 ± 0.4[b]	6.2 ± 1.3	17.6 ± 0.6[a,b]	8.0 ± 2.0	17.6 ± 1.3[a,b]	4.4 ± 0.8	15.2 ± 2.5[a,b]	6.9 ± 1.1	20.3 ± 1.0[a]	3.1 ± 0.2
20:4n-3	0.5 ± 0.5	2.0 ± 0.1	1.4 ± 0.1	2.4 ± 0.3	0.4 ± 0.4	1.9 ± 0.2	0.4 ± 0.4	1.9 ± 0.1	1.2 ± 0.1	1.9 ± 0.1
20:5n-3	3.5 ± 0.2[a]	9.3 ± 0.9[B]	3.4 ± 0.1[a]	15.0 ± 1.2[A]	2.5 ± 0.1[b]	8.2 ± 0.5[B]	2.0 ± 0.3[b]	7.5 ± 0.5[B]	2.4 ± 0.2[b]	7.8 ± 0.7[B]
22:5n-3	ND	3.5 ± 0.4[B]	ND	5.9 ± 0.5[A]	ND	4.0 ± 0.2[B]	ND	3.5 ± 0.3[B]	ND	3.5 ± 0.3[B]
22:6n-3	9.6 ± 1.1	42.0 ± 4.6[B]	12.1 ± 1.6	68.1 ± 7.6[A]	13.2 ± 2.1	48.2 ± 4.7[A,B]	9.1 ± 2.1	45.9 ± 2.2[A,B]	16.4 ± 0.7	40.9 ± 3.4[B]
Total	404.9 ± 15[b]	328.7 ± 13[B]	508.3 ± 27[b]	417.0 ± 30[A,B]	810.4 ± 5[a]	431.6 ± 32[A]	474.0 ± 29[b]	346.8 ± 8.5[A,B]	487.2 ± 15[b]	321.4 ± 7.6[B]

[a]Data represent the means ± SEM of three measurements. TO, triolein; for other abbreviations see Tables 1 and 2. Values in the same row with different superscripts are significantly different ($P < 0.05$); small letters are used for comparison of 1-MAG and capital letters for 2-MAG among the groups.
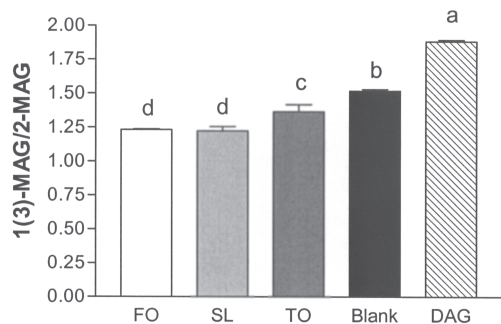
FIG 2. Ratios of 1(3)-MAG/2-MAG after lipolysis of 10.0 mg oil with 62.0 mg crude enzyme isolate (means ± SEM, $n = 3$). FO, fish oil (anchovy); SL, structured lipid; TO, triolein; DAG, DAG oil. Blank, hydrolysis without oil (only contribution from crude isolate). Means with different letters are significantly different at $P < 0.05$.

58.8 wt% of the lipids in the crude enzyme isolate from the intestinal tract of rainbow trout, suggesting extensive digestion of the lipids in fish feed. Comparison of the FA composition in TAG with DAG and MAG showed higher levels of SFA (14:0, 16:0, and 18:0) in DAG and MAG (Table 1). The levels of 14:0 and 16:0 were lower in MAG than in DAG; however, the level of 18:0 was higher in MAG. These results indicate preferred digestion of 14:0 and 16:0 compared with 18:0 in the intestinal tract of rainbow trout. Similar results have been reported previously, as SFA were preferred during the digestion by intestinal lipase from Arctic charr in the order 12:0, 14:0, and 16:0, whereas 18:0 was resistant to digestion (9).

In contrast to SFA, the levels of PUFA were lower in DAG and MAG than in TAG (Table 1), indicating preferred digestion of PUFA compared with SFA. This was also supported by the composition of the FFA fraction, as the levels of PUFA were higher in the FFA fraction than in acylglycerols whereas the levels of SFA were lower in FFA than in acylglycerols. Our results are consistent with previous reports on efficiently hydrolyzed PUFA compared with the SFA and less unsaturated FA by enzymes, for example, purified lipase, from the hepatopancreas of red sea bream (21), crude preparation of bile salt-dependent lipase from leopard shark (22), and crude enzyme mixtures from the intestines of salmon and rainbow trout (23).

Determination of the positional specificity of digestive lipases in crude enzyme isolate. According to Jensen *et al.* (24), positional specificity should be ascertained before studying topics such as FA specificity. Positional specificity can be determined by lipolyses of TO, olive oil, 2,3-dioleoylbutanediol, synthetic TAG, and the like. A distribution of 33% 1(3)-MAG and 67% 2-MAG was observed in the present study, when radioactive-labeled TO was hydrolyzed with the crude enzyme isolate. Thus, specificity for primary esters dominated even though considerable activity also was found for the esters in the *sn*-2 position. The result of the present study is in accordance with previous results reported by Leger and Bauchart (6) and Leger *et al.* (25), who observed dominating 1,3-specificity after hydrolyses of synthetic TAG when a partly purified pancreatic lipase from rainbow trout was used. Although many different experimental designs as well as determination methods

have been used for determination of the specificity of enzymes from fish that may complicate comparison of results, it is likely that a variation in positional specificity among different fish species exists. For instance, nonspecific lipase activity was found in anchovy, striped bass, pink salmon (8), and Arctic charr (9), whereas Gjellesvik *et al.* (7,26) reported 1,3-specificity for cod lipase. The present study demonstrates an alternative method for determination of positional specificity using a crude enzyme isolate; hence, no enzymes, coenzymes, or bile acids were lost during purification steps that could influence the overall positional specificity. For shark lipase, a fourfold greater stimulation of activity was measured with natural bile salts of the shark compared with pure sodium taurocholate (22). Therefore, the "digestive system" in the intestine is imitated better with a crude enzyme isolate, resulting in more putative overall positional specificity.

Hydrolysis of different unlabeled oils with the crude enzyme isolate. Four different oils (SL, DAG, FO, and TO) were hydrolyzed *in vitro* with the crude enzyme isolate. Analyses of lipid classes in the crude enzyme isolate showed that acylglycerols, especially DAG and MAG, might have contributed to the analyzed values of MAG when the hydrolysis time was only 1.5 min. Therefore, a blank (hydrolysis performed without addition of oil) was included to determine the ratio of 1(3)- and 2-MAG in the crude enzyme isolate in the assay. However, we cannot exclude the possibility that variation may exist for the contribution of lipids from the crude enzyme isolate during the lipolyses of the oils and the blank.

In mammals, structured lipids have been observed to improve the absorption of LCFA in comparison with conventional long-chain TAG (5). The SL oil was designed to investigate whether it was possible to improve the incorporation of long-chain n-3 PUFA in fillets of trout; it contained MCFA in the *sn*-1,3 positions and long-chain PUFA in the *sn*-2 position. The results showed a fast hydrolysis of MCFA in the primary positions, since only twice the amount of MCFA was found in 1(3)-MAG compared with 2-MAG (Table 3), in spite of the fact that 10 times more MCFA was incorporated in SL oil (TAG) than in the *sn*-2 position of the SL oil (Table 2). As a consequence of rapid hydrolysis of MCFA, a significantly higher level of n-3 PUFA was observed in the 2-MAG fraction of SL compared with the other oils and the blank. If the investigated *in vitro* lipolysis of the crude enzyme isolate is similar to lipolysis in rainbow trout, the use of n-3 VLCPUFA in trout may be improved. However, increased incorporation of n-3 VLCPUFA was not observed in a trout-feeding experiment executed in parallel to the present study using the same SL (12). The reason may be that the oils have enough time to be efficiently hydrolyzed in rainbow trout in the presence of specific as well as nonspecific lipases. It cannot be excluded, however, that different mechanisms of absorption and resynthesis exist between rainbow trout and mammals that might also have affected the use of n-3 VLCPUFA.

The release of FA during hydrolysis of capelin oil with both human and cod pancreatic bile salt-dependent lipase was shown to be dependent on incubation temperature (27). Temperature

optima of 36 and 37°C were already shown for lipolysis with crude preparations from leopard shark (22) and cod (28), respectively. To ensure sufficient production of MAG in 1.5 min, the present study was also performed at 37°C.

The amount of MAG produced from lipolysis was highest for the DAG oil, which principally can be explained by the presence of only two ester bonds in the molecule, as only one bond has to be cleaved to produce MAG. It has been shown that DAG oil containing mainly 1,3-DAG decreased postprandial hyperlipidemia and reduced diet-induced obesity compared with TAG (10), and it was suggested that the absorption and metabolism of DAG oil differ from that of TAG owing to the lack of 2-MAG after hydrolysis of DAG oil in the intestine (11). Our results showed that the DAG oil was rapidly hydrolyzed to mainly 1(3)-MAG.

In contrast to SL and DAG oils, TO and the FO were hydrolyzed slower, resulting in only small changes in the amounts of MAG products compared with the blank. The FO initially contained more n-3 PUFA, e.g., EPA and DHA, than the SL oil. However, less 2-MAG containing n-3 PUFA was observed from FO than from SL after lipolysis. The trend of slow hydrolysis of FO is also prevalent for several other FA, although the trend was not significant according to the statistics used here, with three replicates. Hydrolysis of unlabeled TO was in agreement with observations for radioactive-labeled TO, since twice as much 2-MAG as 1(3)-MAG was produced compared with the blank.

Lipolysis of the unlabeled oils influenced the ratio of 1(3)-MAG/2-MAG differently, as all TAG oils lowered the ratio whereas the DAG oil increased the ratio compared with the blank (Fig. 2). That can be explained by the fact that lipolysis of DAG oil (mainly 1,3-DAG) with 1,3-positional specific enzyme produces more 1(3)-MAG than 2-MAG, hence an increased ratio of 1(3)-MAG/2-MAG. Owing to the preferred 1,3-positional specificity of the crude enzyme isolate, an increased amount of 2-MAG was expected for all the TAG oils, hence a lower ratio of 1(3)-MAG/2-MAG. It seems that more MAG [both 1(3)- and 2-MAG] were obtained after hydrolysis of SL in comparison with the blank owing to the fast hydrolysis of MCFA, whereas less 2-MAG was obtained for FO compared with the blank. However, the differences were not significant. The lower ratio of 1(3)-MAG/2-MAG observed for SL oils and FO compared with TO may be explained by the different FA composition of the oils.

In conclusion, the present study presents an alternative method for determining the positional specificity of fish lipases. The results show the existence of 1,3-specificity of lipases in crude enzyme isolate from rainbow trout. The overall 1,3-specificity is similar to mammalian pancreatic lipase, even rainbow trout have considerable lipase activity toward the *sn*-2 position of TAG. Both DAG and SL oils are hydrolyzed faster than FO and TO. MCFA in primary positions of the SL oil are rapidly hydrolyzed, whereas VLCPUFA are enriched in the 2-MAG fraction.

REFERENCES

1. International Fishmeal and Fish Oil Organization. (2005) Sustainability of Fishmeal and Oil Supply, http://www.iffo.org.uk/tech/sterling.htm (accessed December 2005).
2. Caballero, M.J., Obach, A., Rosenlund, G., Montero, D., Gisvold, M., and Izquierdo, M.S. (2002) Impact of Different Dietary Lipid Sources on Growth, Lipid Digestibility, Tissue Fatty Acid Composition and Histology of Rainbow Trout, *Oncorhynchus mykiss*, *Aquaculture 214*, 253–271.
3. Bell, J.G., McGhee, F., Campell, P.J., and Sargent, J.R. (2003) Rapeseed Oil as an Alternative to Marine Fish Oil in Diets of Post-Smolt Atlantic Salmon (*Salmo salar*): Changes in Flesh Fatty Acid Composition and Effectiveness of Subsequent Fish Oil "Wash Out," *Aquaculture 218*, 515–528.
4. Izquierdo, M.S., Obach, A., Arantzamendi, L., Motero, D., Robaina, L., and Rosenlund, G. (2003) Dietary Lipid Sources for Seabream and Seabass: Growth Performance Tissue Composition and Flesh Quality, *Aquacult. Nutr. 9*, 397–407.
5. Ikeda, I., Tomari, M., Sugano, S., Watanabe, S., and Nagata, J. (1991) Lymphatic Absorption of Structured Glycerolipids Containing Medium-Chain Fatty Acids and Linoleic Acid, and Their Effect on Cholesterol Absorption in Rats, *Lipids 26*, 369–373.
6. Leger, C., and Bauchart, D. (1972) Hydrolyse de Triglycerides par le Systeme Lipasique du Pancreas de Truite (*Salmo gairdneri* Rich.). Mise en Evidence d'un nouveau Type de Specificite d'Action, *Acad. Sci. Paris Ser. D*, 2419–2422.
7. Gjellesvik, D.R., Lombardo, D., and Walther, B.T. (1992) Pancreatic Bile Salt Dependent Lipase from Cod *(Gadus morhua)*: Purification and Properties, *Biochim. Biophys. Acta 1124*, 123–134.
8. Patton, J.S., Nevenzel, J.C., and Benson, A.A. (1975) Specificity of Digestive Lipases in Hydrolysis of Wax Esters and Triglycerides Studied in Anchovy and Other Selected Fish, *Lipids 10*, 575–583.
9. Olsen, R.E., Henderson, R.J., and Ringø, E. (1998) The Digestion and Selective Absorption of Dietary Fatty Acids in Arctic Charr, *Salvelinus alpinus*, *Aquacult. Nutr. 4*, 13–21.
10. Tada, N. (2004) Physiological Actions of Diacylglycerol Outcome, *Curr. Opin. Clin. Nutr. Metab. Care 7*, 145–149.
11. Flickinger, B.D., and Matsuo, N. (2003) Nutritional Characteristics of DAG Oil, *Lipids 38*, 129–132.
12. Nielsen, N.S., Gøttsche, J.R., Holm, J., Xu, X., Mu, H., and Jacobsen, C. (2005) Effects of Structured Lipids Based on Fish Oil on the Growth and Fatty Acid Composition in Rainbow Trout *(Oncorhynchus mykiss)*, *Aquaculture 250*, 411–423.
13. Xu, X., Mu, H., Høy, C.-E., and Adler-Nissen, J. (1999) Production of Specially Structured Lipids by Enzymatic Interesterification in a Pilot Enzyme Bed Reactor: Process Optimization by Response Surface Methodology, *Fett/Lipid 101*, 207–214.
14. Mu, H., Kalo, P., Xu, X., and Høy, C.-E. (2000) Chromatographic Methods in the Monitoring of Lipase-Catalyzed Interesterification, *Eur. J. Lipid Sci. Technol. 102*, 202–211.
15. Christopherson, S.W., and Glass, R.L. (1969) Preparation of Milk Fat Methyl Esters by Alcoholysis in an Essential Nonalcoholic Solution, *J. Dairy Sci. 52*, 1289–1290.

16. Becker, C.C., Rosenquist, A., and Hølmer, G. (1993) Regiospecific Analysis of Triacylglycerols Using Allyl Magnesium Bromide, *Lipids 28*, 147–149.

17. Hamilton, S., Hamilton, R.J., and Sewell, P.A. (1992) Extraction of Lipids and Derivative Formation, in *Lipid Analysis—A Practical Approach* (Hamilton, S., and Hamilton, R.J., eds.), pp. 13–64, Oxford University Press, Oxford, United Kingdom.

18. Folch, J., Lees, M., and Sloane-Stanley, G.H. (1957) A Simple Method for the Isolation and Purification of Total Lipids from Animal Tissue, *J. Biol. Chem. 226*, 497–509.

19. Martin, J.C., Caselli, C., Broquet, S., Juaneda, P., Nour, M., Sébédio, J.L., and Bernard, A. (1997) Effect of Cyclic Fatty Acid Monomers on Fat Absorption and Transport Depends on Their Positioning Within the Ingested Triacylglycerol, *J. Lipid Res. 38*, 1666–1679.

20. Thomas, A.E., Scharoun, J.E., and Ralston, H. (1965) Quantitative Estimation of Isomeric Monoglycerides by Thin-Layer Chromatography, *J. Am. Oil Chem. Soc. 42*, 789–792.

21. Iijima, N., Tanaka, S., and Ota, Y. (1998) Purification and Characterization of Bile Salt-Activated Lipase from the Hepatopancreas of Red Sea Bream, *Pagrus major*, *Fish Physiol. Biochem. 18*, 59–69.

22. Patton, J.S., Warner, T.G., and Benson, A.A. (1977) Partial Characterization of the Bile Salt-Dependent Triacylglycerol Lipase from the Leopard Shark Pancreas, *Biochim. Biophys. Acta 486*, 322–330.

23. Halldorsson, A., Kristinsson, B., and Haraldsson, G.G. (2004) Lipase Selectivity Toward Fatty Acids Commonly Found in Fish Oil, *Eur. J. Lipid Sci. Technol. 106*, 79–87.

24. Jensen, R.G., deJong, F.A., and Clark, R.M. (1983) Determination of Lipase Specificity, *Lipids 18*, 239–252.

25. Leger, C., Bauchart, D., and Flanzy, J. (1977) Some Properties of Pancreatic Lipase in *Salmo gairdnerii* Rich: K_m, Effects of Bile Salts and Ca^{2+}, Gel Filtrations, *Comp. Biochem. Physiol. B, Biochem. Mol. Biol. 57*, 359–363.

26. Gjellesvik, D.R., Raae, A.J., and Walther, B.T. (1989) Partial-Purification and Characterization of a Triglyceride Lipase from Cod (*Gadus morhua*), *Aquaculture 79*, 177–184.

27. Gjellesvik, D.R. (1991) Fatty Acid Specificity of Bile Salt-Dependent Lipase: Enzyme Recognition and Super-Substrate Effects, *Biochim. Biophys. Acta 1086*, 167–172.

28. Lie, Ø., and Lambertsen, G. (1985) Digestive Lipolytic Enzymes in Cod (*Gadus morrhua*): Fatty Acid Specificity, *Comp. Biochem. Physiol. B, Biochem. Mol. Biol. 80*, 447–450.